WAVE GENOME (/)

HOME / ГЛАВНАЯ (/)

SERVICES / УСЛУГИ (/SERVICES--105910571051105910431048.HTML)

PRODUCTS / ТОВАРЫ (/PRODUCTS--105810541042104010561067.HTML)

CONTACT / КОНТАКТ (/CONTACT--105010541053105810401050105 8.HTML)

(/tesla-generator.html) (/order-tesla-selenium.html) (/tesla-water.html) (/order-tesla-glasses.html) (/digital-pharmacy.html) (/order-tesla-screen.html)

TESLA PSI-GENERATOR | TESLA SELENIUM | TESLA WATER | TESLA GLASSES | DIGITAL PHARMACY | TESLA SCREEN

IRENE CAESAR, PH.D.

President & Founder

WAVE GENOME LLC

465 Buckland Hills Drive

Unit 33211, Manchester, CT 06042

1-646-480-0496

(/tesla-generator.html)

WAVE GENOME IS A FRONTIER OF THE TECHNOLOGICAL REVOLUTION

WAVE GENOME IS AN AMERICAN COMPANY LOCATED IN CONNECTICUT - A PROUD PIONEER OF PRODUCING WAVE MATRICES / BIOHOLOGRAMS BY LASERS FOR THE LOCAL AND REMOTE MANAGEMENT OF BIOSYSTEMS AND HUMAN CONDITION

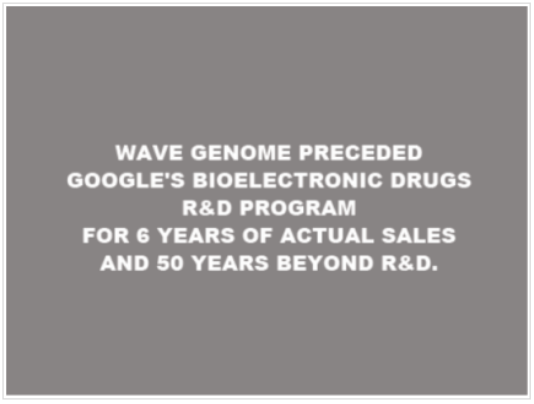

WAVE GENOME HAS INTELLECTUAL PRIORITY FOR THE WAVE OPTICS IN CHROMOSOMES AS BIOHOLOGRAPHY

(/diaschev-dipol-di-pol.html)

(http://www.facebook.com/pages/Wave-Genome/203765456304318?fref=ts) (/wave-genome--russian.html)

WAVE GENOME LLC uses Bauman Moscow Russian State Technical University, major Science University of Russia, of MIT level, to verify WAVE GENOME'S technological models.

(/wave-pharmaceuticals.html)

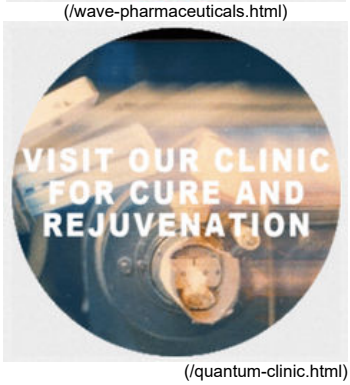

(/quantum-clinic.html)

(/order-tesla-selenium.html)

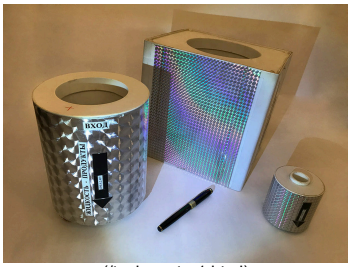
(/tesla-water1.html)
TESLA WATER GENERATORS

RA MINI-TESLA PSI-GENERATOR.

Click here (/diaschev-dipol-di-pol.html) to read on how WAVE GENOME's technology differs from Dr. Peter P. Gariaev's and Dr. Alexander D. Panchenko's technology (DIPOL or DI-POL Generator, sold by Dr. Diaschev).

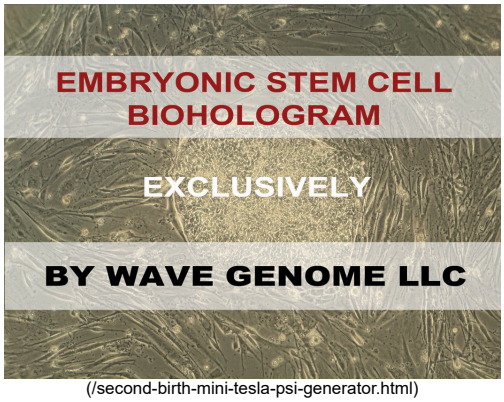

(/second-birth-mini-tesla-psi-generator.html)

GLOBAL LAUNCH OF THE SECOND-BIRTH MINI-TESLA PSI-GENERATOR BY WAVE GENOME (/second-birth-mini-tesla-psi-generator.html)

(/second-birth-mini-tesla-psi-generator.html)

(/second-birth-mini-tesla-psi-generator.html)

(/second-birth-mini-tesla-psi-generator.html)

JANUARY 13, 2018

Wave Genome is proud to announce its most advanced MINI-TESLA PSI-GENERATOR ever: the SECOND-BIRTH Mini-Tesla Psi-Generator.

We called the new chip the "SECOND BIRTH" generator (/second-birth-mini-tesla-psi-generator.html), because the client gets the most valuable bioholographic treatment ever for rejuvenation -- the biohologram of the embryonic stem cell. The SECOND-BIRTH Biohologram (/second-birth-mini-tesla-psi-generator.html) is available as a chip encoded by laser on nanolevel. The clinical trials were conducted by the Bauman University Medical Center. The clinical trials had demonstrated the radical improvement in the wellbeing of the participants in the clinical trials.

Sold either with the **DIGITIZED HUMAN EMBRYONIC STEM CELL**; **TESLA HUMAN CELL (of the paradigmatic infant)**; (/tesla-human-cell.html)or with **REMOTE LASER TREATMENT (/remote-laser-treatment.html)**, at the customer's choice.

Click here to read more. (/second-birth-mini-tesla-psi-generator.html)

GLOBAL LAUNCH OF

TESLA TEST (/tesla-test.html)

WORLDWIDE LAUNCH OF HOLONET (© Dr. Irene Caesar 2010) - HOLOGRAPHIC BIOINTERNET & HOLOGRAPCHIC DRUGS, BIOELECTRONIC DRUGS AND INTERNET DRUGS

H-DRUGS, E-DRUGS AND I-DRUGS

FOR REMOTE AND LOCAL REJUVENATION

NEWS

(https://www.youtube.com/watch?v=nJZwNokyWAg)

DR. IRENE CAESAR - SPEECH "REMOTE GENETIC ENGINEERING AS BIOHOLOGRAPHY BASED UPON THE SHAPE OF CHROMOSOMES, DNA AND RNA FOR FOCUSING GENETIC INFORMATION" (https://www.youtube.com/watch?v=nJZwNokyWAg), BIT's 8th World Gene Convention-2017, Macao, China, November 13-15, 2017, with the participation of the Yale University (USA), University of Louisville (USA), University of Georgia (USA), University of Texas Health Science Center (USA), York University (Canada), Waterloo Institute for Nanotechnology (Canada), Paris Descartes Pharmacy University (France), etc. Click here for BIT's page for this conference (http://www.bitcongress.com/wgc2017/).

(https://www.youtube.com/watch?v=YiFPZLmV9-8&t=337s)

DR. IRENE CAESAR - SPEECH "REMOTE MANAGEMENT OF BIOSYSTEMS VIA THE DIGITIZED BIOHOLOGRAM OF THE HUMAN EMBRYONIC STEM CELL BASED UPON THE WAVE OPTICS OF CHROMOSOMES FOR FOCUSING GENETIC INFORMATION" (https://www.youtube.com/watch?v=YiFPZLmV9-8&t=337s), BIT's 9th Anniversary World DNA DAY-2018, Dalian, China, April 25-27, 2018; with

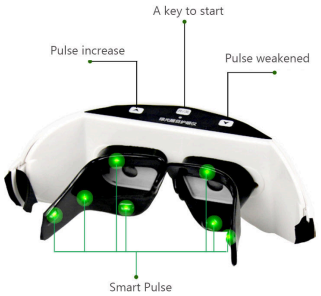

(/order-tesla-glasses.html)
TESLA GLASSES X (ADVANCED)

(/order-tesla-glasses.html)

Read about TESLA GLASSES here (/order-tesla-glasses.html).
Order TESLA GLASSES here (/order-form.html).

EIGHT YEARS OF SATISFIED CUSTOMERS

WE OFFER ADVANCED WEATHER CONTROL. BUT WHAT CAN BE NOBLER THAN SAVING LIVES!
(/quantum-clinic.html)

BIOWAVE GENOME HAS DISTRIBUTORS ALL OVER THE WORLD:

Germany, Sweden, Poland, United States, Russia, Thailand

(/quantum-clinic.html)
Large-size AURA PSI-GENERATOR for radical rejuvenation of all bodily organs and physiological systems.

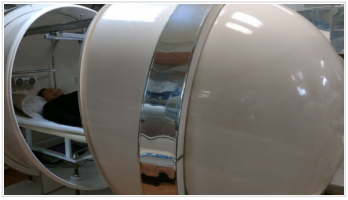

(/quantum-clinic.html)
Large-size AURA PSI-GENERATOR offers radical rejuvenation for patents rejected by conventional medicine to the degree they do not need conventional medicine any longer.

Click here (/quantum-clinic.html) to read about our clinic.

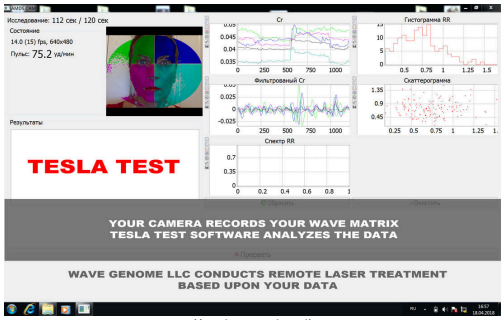

(/tesla-test.html)

In January 2018, **WAVE GENOME LLC** launched **TESLA TEST**. **TESLA TEST** is a software program that makes the camera on your computer record your Wave Matrix, and analyzes the data. **WAVE GENOME LLC** uses this data for the **REMOTE LASER MANAGEMENT (/remote-laser-treatment.html)** of your Biohologram (ordered separately, based upon subscription). **TESLA TEST** is sold with the following three protocols of the **BIOELECTRONIC THERAPY**:
(1) **DIGITIZED BIOHOLOGRAM OF THE HUMAN EMBRYONIC STEM CELL** as MP3 file of the white noise.
(2) **TESLA HUMAN CELL (/tesla-human-cell.html)** as the Digitized Biohologram / Wave Matrix of a selected (paradigmatic) healthy infant, sold as white noise (half-audible) encoded into the five soundtracks of Sacred Ancient Aryan Mantras, each around 1 hour length.
(3) **REMOTE LASER TREATMENT (/remote-laser-treatment.html)**.
TESLA TEST (/tesla-test.html) software program is offered as a promotion with the **SECOND-BIRTH MINI-TESLA PSI-GENERATOR (/second-birth-mini-tesla-psi-generator.html)**, which is coded with the digitized Biohologram of the Embryonic Stem Cell, the most valuable biological information on the global market.
Click here to read more. (/tesla-test.html)

GLOBAL LAUNCH OF THE DIGITIZED EMBRYONIC STEM CELL

In December 2017, **WAVE GENOME LL**C launched the **DIGITIZED BIOHOLOGRAM OF THE EMBRYONIC STEM CELL** as an MP3 file of the white noise, produced in cooperation with the Bauman Russian State Technology University in Moscow, the largest and most important Science University in Russia, of MIT level. Sold with the **SECOND-BIRTH MINI-TESLA PSI-GENERATOR** and **TESLA TEST**, or on its own.

GLOBAL LAUNCH OF TESLA HUMAN CELL (/tesla-human-cell.html)

In March 2018, **WAVE GENOME LLC** launched **TESLA HUMAN CELL. TESLA HUMAN CELL** is the Digitized Biohologram / Wave Matrix of a selected healthy infant. Sold as white noise (half-audible) encoded into the five soundtracks of Sacred Ancient Aryan Mantras, each around 1 hour length.
Sold either with **SECOND-BIRTH MINI-TESLA PSI-GENERATOR (/second-birth-mini-tesla-psi-generator.html)** or on its own, at the customer's choice.
Click here to read more. (/tesla-human-cell.html)

the Support of Dalian Association for Science and Technology, Dutch Society of Clinical Genetics, and French Federation of Human Genetics; with the participation of three Noble Prize Laureates Dr. Edward I. Moser (Norwegian University of Science and Technology, Norway), Dr. Aaron Ciechanover (Israel Institute of Technology, Israel), and Dr. Michael Levitt (Stanford University, USA). The Conference was held in the Dalian International Conference Center, place for the Summer Davos.

(https://www.youtube.com/watch?v=Tvl4bZ5yfvk&t=1337s)

DR. IRENE CAESAR - SPEECH "REMOTE BIOMEDICAL ENGINEERING VIA MASTERING THE GEOMETRICAL OPTICS OF CHROMOSOMES" (https://www.youtube.com/watch?v=Tvl4bZ5yfvk&t=1337s), BIT's 1st World Congress of Biomedical Engineering - 2017. Theme: Co-Creating a New Future of Biomedicine, November 9-11, 2017, Xi'an, China. Dr. Irene Caesar was invited to be the Chair of the Neural Engineering Section.

(https://www.youtube.com/watch?v=ro0S-YN0yME&t=71s)

DR. IRENE CAESAR - REMOTE MANAGEMENT OF BIOSYSTEMS AS BIOHOLOGRAPHY BASED UPON THE SHAPE OF CHROMOSOMES FOR FOCUSING GENETIC INFORMATION, BIT's 8th Annual World DNA & Genome Day-2017; BIT's 7th Annual World Congress of Molecular & Cell Biology, April 25-27, Xi'an, China.
(https://www.youtube.com/watch?v=ro0S-YN0yME&t=71s)

(https://www.youtube.com/watch?v=GMFXUG7eEN8&t=4s)

DR. IRENE CAESAR - NEW PRINCIPLES OF PROTECTION AGAINST PSYCHOTRONIC ATTACK BASED ON WAVE OPTICS"

Consortium "MATRIX CITY - city as one integrated wave matrix" (/consortium.html)

(/irene-caesar---matrix-city-project.html)

(/remote-laser-treatment.html)

Models of TESLA PSI-GENERATORS by WAVE GENOME.

TRUE BIOELECTRONIC E-DRUGS

The MINI-TESLA psi-generator **DIGITAL PHARMACY (/digital-pharmacy-software--1057105410601058-106210481060105610541042105410 49-104010551058104510501048.html)** software program generates HOLOGRAPHIC SIGNAL (as white noise) encoded in music for every system and vital organ in your body.

GLOBAL LAUNCH OF REMOTE LASER TREATMENT (/remote-laser-treatment.html)

In May 2013, **WAVE GENOME LLC** launched the **REMOTE LASER TREATMENT (/remote-laser-treatment.html)**, becoming the first to make a commercial offering of the remote management of biosystems.

In January 2018, **WAVE GENOME LLC** offered a new protocol of the **REMOTE LASER TREATMENT (/remote-laser-treatment.html)** via the use of the additional testing and verifying tenique - **TESLA TEST (/tesla-test.html)**. **TESLA TEST (/tesla-test.html)** uses the camera on your computer to record and analyze your **WAVE MATRIX**. Click here to read more. (/remote-laser-treatment.html)

DR. IRENE CAESAR, PRESIDENT, WAVE GENOME LLC, WAS INVITED TO CHAIR THE SECTION "ROLE OF MOLECULAR & CELL BIOLOGY IN TRANSLATIONAL MEDICINE", HAD DELIVERED HER SPECIAL ADDRESS ON THE LOOMING GENETIC COLLAPSE, AND A SPEECH 'REMOTE MANAGEMENT OF BIOSYSTEMS VIA HOLOGRAPHIC EMBRYO OF THE HUMAN EMBRYONIC STEM CELL BASED UPON THE WAVE OPTICS OF CHROMOSOMES AS MODULATED SCALAR WAVE DIFFRACTION GRATING" at the BIT's 9th Annual World Congress of Molecular & Cell Biology, Theme: "Exploring Life Inspiring Innovation, Creating Future", October 14, 2018, Fukuoka, Japan. **Click here to view a video of Dr. Irene Caesar's speech (https://www.youtube.com/watch?v=zEukdv76fLw&t=594s).** And **click here to view a video of Dr. Irene Caesar's speech to the World Congress of Molecular & Cell Biology (https://www.youtube.com/watch?v=cl9ZmJh6Ahg)**.

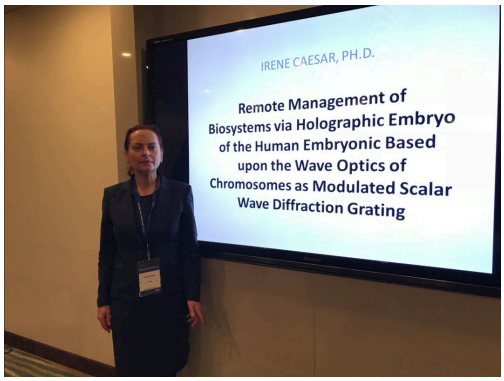

(https://www.youtube.com/watch?v=GMFXUG7eEN8&t=4s), the 3rd International Conference "Against the use of radiating weapons against people", December 1st, 2018, Moscow, Russia.

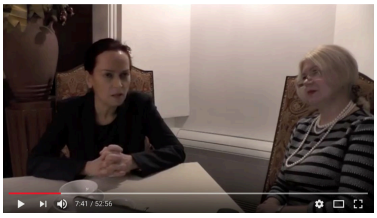

DR. IRENE CAESAR - INTERVIEW "PSYCHOTRONIC WEAPONS & DEFENSE" TO GALINA LOZOVITSKAYA, COLONEL OF THE MINISTRY OF THE INTERNAL AFFAIRS, PROFESSOR AT THE ACADEMY OF GOVERNMENT AT THE MINISTRY OF THE INTERNAL AFFAIRS (https://www.youtube.com/watch?v=bt6MxABW6Eg), September 16, 2018, Moscow, Russia.

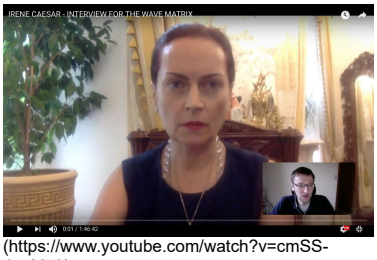

(https://www.youtube.com/watch?v=cmSS-JguM70)

DR. IRENE CAESAR - INTERVIEW FOR WAVE GENOME'S LLC DISTRIBUTOR IN PARAGUAY, ANDREAS WALTHER, AND HIS COMPANY WAVE MATRIX. (https://www.youtube.com/watch?v=cmSS-JguM70)

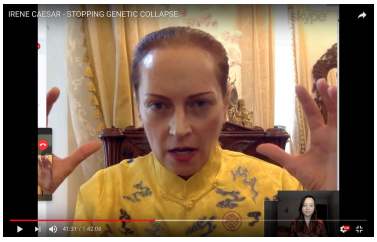

DR. IRENE CAESAR - INTERVIEW FOR WAVE GENOME GERMANY, THE DISTRIBUTOR OF WAVE GENOME LLC IN GERMANY, MARCH 2018 (https://www.youtube.com/watch?v=mw0yFlvAD5o)

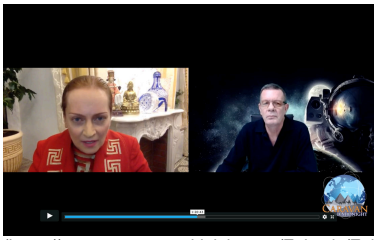

(https://www.caravantomidnight.com/Episode/EpisodesL

MILESTONES

Over the span of the 20th century, generations of extraordinary scientists, among whom Russian scientists played a leading role, laid down scientific foundation for the technological revolution of information-wave technology of the Quantum Leap.

MORE (/milestones.html)

(/uploads/3/5/1/1/35112207/5553543_orig.jpg)
For developing and producing its products, WAVE GENOME is teaming with most advanced scientists all over the world. Here we see Scientific Research Institute for National Security in Moscow, now closed. The scientific group still operates the clinic. Among clients of the clinic were Russian President Boris Yeltsin, famed American astronaut Edgar Mitchell, and actor celebrity Alexander Kalyagin. The institute has received the written Blessing of Patriarch Alexis and Patriarch of Constantinople.

(/uploads/3/5/1/1/35112207/4353994_orig.jpg)
Famed American Astronaut Edgar Mitchell received a treatment by GENERATOR AURA-001.

OUR PLEDGE

We build our strategy upon a firm foundation of the highest standards of ethics.

MORE (/our-pledge.html)

Our MINI-TESLA PSI-GENERATOR is used by Russian Special Forces.

Our MINI-TESLA PSI-GENERATOR is used by Russian Olympic Team.

DR. IRENE CAESAR, PRESIDENT, WAVE GENOME LLC, WAS AWARDED THE CERTIFICATE OF HONORARY CREDENTIAL AND HAD DELIVERED A SPEECH 'REMOTE DRUG DELIVERY VIA MODULATING THE REFRACTION IN THE WAVE OPTICS OF CHROMOSOMES" at the BIT's 16th Annual World Congress of International Drug Delivery Science & Technology, Theme: "Focusing on Biomedical Frontiers, Driving Industrial Innovative Development", November 7, 2018, Jinan, China. **Click here to view Dr. Irene Caesar's speech (https://www.youtube.com/watch?v=Xj1hxeh2p3s&t=1550s)**.

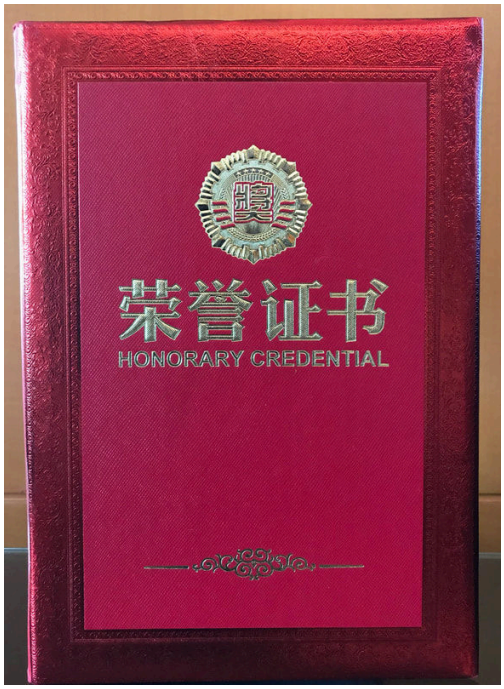

Id=20796)

DR. IRENE CAESAR - INTERVIEW TO JOHN B. WELLS, CARAVAN TO MIDNIGHT SHOW, NOVEMBER 24, 2017. (https://www.caravantomidnight.com/Episode/EpisodesDetails?Id=20796)

Picture (https://www.youtube.com/watch?v=gDsKpeNoZBE)

DR. IRENE CAESAR SPEECH "REMOTE BIOMEDICAL AND NEURAL ENGINEERING VIA THE GEOMETRICAL OPTICS OF CHROMOSOMES", CONFERENCE "DISCOVERER", MOSCOW, DECEMBER 17, 2017. (https://www.youtube.com/watch?v=gDsKpeNoZBE)

Picture (https://www.youtube.com/watch?v=igrKYMm2Dz0&feature=youtu.be)

DR. IRENE CAESAR SPEECH "REMOTE GENETIC ENGINEERING AS BIOHOLOGRAPHY BASED UPON THE SHAPE OF CHROMOSOMES, DNA, RNA FOR FOCUSING GENETIC INFORMATION", CONFERENCE "DISCOVERER", MOSCOW, DECEMBER 4, 2017. (https://www.youtube.com/watch?v=igrKYMm2Dz0&feature=youtu.be)

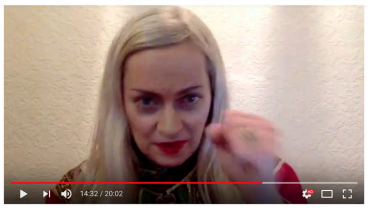

IRENE CAESAR INTERVIEW FOR MINDTECH ENTERPRISES DEC 13 2016

DR. IRENE CAESAR - INTERVIEW FOR MINDTECH ENTERPRISES DEC 13 2016 (https://www.youtube.com/watch?v=ap8kHpuYlxM&feature=youtu.be)

Picture

IRENE CAESAR, Ph.D., PRESIDENT AND OWNER OF WAVE GENOME: INTERVIEW FOR RIPSONAR NEWS, APRIL 22, 2017 (https://www.youtube.com/watch?v=iTTHLETrz1A).

Picture (https://www.youtube.com/watch?v=uxfui6xTtEc)

IRENE CAESAR, Ph.D., PRESIDENT AND OWNER OF WAVE GENOME: INTERVIEW FOR POROZMAWIAJMY TV CONDUCTED BY ALEXANDER BERDOWICZ, FEBRUARY 7, 2017. (https://www.youtube.com/watch?v=uxfui6xTtEc)

Our TESLA GLASSES are used by Russian Central Intelligence Service.

Our TESLA GLASSES are used by Russian Space Forces.

Our TESLA GLASSES are used by Russian Strategic Missile Forces.

Our TESLA GLASSES are used by Russian Ministry of Emergency Situations.

Our TESLA GLASSES are used by Russian Federal Security Service.

Our TESLA GLASSES are used by Russian Interior Ministry.

WAVE GENOME LLC employs scientists from most advanced research group all over the world, including the present Moscow Bauman Russian State Technical University, the major Science University in Russia, of MIT level; and scientists of the former most secret USSR Research Institutes, which conducted studies in psychotronics, e.g., "Scientific-Research Institute Energy" (founded in 1937, with 5000 scientists under supervision of the National Security Agencies of the Soviet Union (Научно- производственное Объединение Энергия). The Scientific-Research Institute Energy was developing devices and

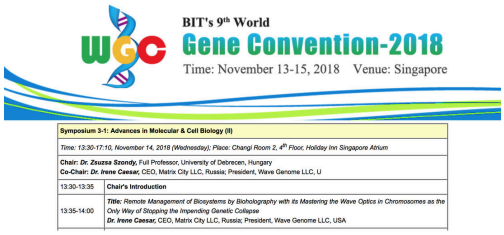

DR. IRENE CAESAR, PRESIDENT, WAVE GENOME LLC, WAS INVITED TO CO-CHAIR THE SECTION "ADVANCES IN MOLECULAR & CELL BIOLOGY", AND HAD DELIVERED A SPEECH 'REMOTE MANAGEMENT OF BIOSYSTEMS BY BIOHOLOGRAPHY WITH ITS MASTERING THE WAVE OPTICS IN CHROMOSOMES AS THE ONLY WAY OF STOPPING THE IMPENDING GENETIC COLLAPSE" at the BIT's 9th World Gene Convention-2018, November 14, 2018, Singapore. **Click here to view a video of Dr. Irene Caesar's speech. (https://www.youtube.com/watch?v=3rTMegMHPXI&t=1s)**

DR. IRENE CAESAR, PRESIDENT, WAVE GENOME LLC, HAD DELIVERED A SPEECH 'REMOTE MANAGEMENT OF BIOSYSTEMS VIA THE DIGITIZED BIOHOLOGRAM OF THE HUMAN EMBRYONIC STEM CELL BASED UPON THE WAVE OPTICS OF CHROMOSOMES FOR FOCUSING GENETIC INFORMATION" at the BIT's 9th Anniversary WORLD DNA DAY-2018, Theme: "Accelerating Great Cooperation in Bioworld of the Belt and Road", April 26, Dalian, China. **Click here to view a video of Dr. Caesar's speech. (https://www.youtube.com/watch?v=YiFPZLmV9-8&t=337s)**

NOVEMBER 9-11, 2017

DR. IRENE CAESAR WAS INVITED TO BE A CHAIR OF THE NEURAL ENGINEERING SECTION OF THE BIT'S 1st WORLD COGRESS OF BIOMEDICAL ENGINEERING, Theme: Co-creating a New Future of Biomedicine, November 9-11, 2017, in Xi'an, China. I will deliver paper called **"REMOTE BIOMEDICAL ENGINEERING VIA MASTERING THE GEOMETRICAL OPTICS OF CHROMOSOMES"**. List of Renowned Speakers include professors from University of Oxford, UK; Harvard Medical School, USA; American College Of Clinical Engineering, USA; California South University, USA; University of Illinois at Chicago, USA; The Mount Sinai Medical Center, USA; University of California, USA; Washington University School of Medicine, USA; The Salerno Center for Complementary Medicine, USA; National Cancer Institute, NIH, USA; University of Pennsylvania, USA; Washington University in St. Louis Campus, USA; International Federation For Medical and Biological Engineering, USA; Louisiana State University Health Sciences Center in Shreveport, USA; International Spine Research Foundation, USA; RWTH Aachen University, Germany; Technical University of

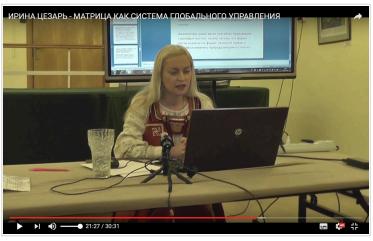

IRENE CAESAR, Ph.D., PRESIDENT AND OWNER OF WAVE GENOME: LECTURE "MATRIX AS A GLOBAL MANAGEMENT SYSTEM OF LIFE. MECHANISM OF REMOTE MANAGEMENT OF BIOSYSTEMS," CONFERENCE "PSYCHICS - YESTERDAY, TODAY, AND TOMORROW, (4TH MEETING OF THE ASSOCIATION OF ASTRAL ANTHROPOLOGY AND PSYCHOLOGY), MOSCOW, RUSSIA, OCTOBER 10, 2016. (https://www.youtube.com/watch?v=eEKzZQ4Wzcc)

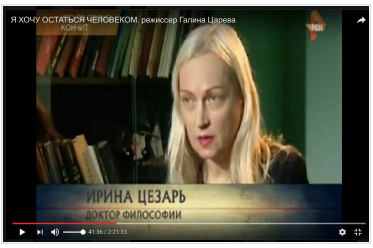

IRENE CAESAR, PH.D., PRESIDENT AND OWNER OF WAVE GENOME, IN THE FILM BY RENOWNED RUSSIAN PRODUCER GALINA TSAREVA "I WANT TO REMAIN HUMAN", AUGUST, 2016. (https://www.youtube.com/watch?v=YTTWaIRT_0Y)

(https://www.youtube.com/watch?v=XuwV_QCTf2I)

IRENE CAESAR, PH.D., PRESIDENT AND OWNER OF WAVE GENOME: "REMOTE MANAGEMENT OF BIIO SYSTEMS BASED UPON THE SHAPE OF CHROMOSOMES AS DIFFRACTION GRATING FOR FOCUSING GENETIC INFORMATION" - RECORDING OF DR. IRENE CAESAR'S SPEECH, BANGKOK THONBURI UNIVERSITY 2ND INTERNATIONAL SYMPOSIUM, JULY 23, 2016.
(https://www.youtube.com/watch?v=XuwV_QCTf2I)

Picture (https://www.youtube.com/watch?v=pSsgOPUzz9A)

IRENE CAESAR, PH.D., PRESIDENT AND OWNER OF WAVE GENOME: "REMOTE MANAGEMENT OF BIIO SYSTEMS BASED UPON THE SHAPE OF CHROMOSOMES AS DIFFRACTION GRATING FOR FOCUSING GENETIC INFORMATION" - SLIDE SHOW OF THE LECTURE, BANGKOK THONBURI UNIVERSITY 2ND INTERNATIONAL SYMPOSIUM, JULY 23, 2016.

services for the first persons in the State, military commanders, diplomats, Special Forces and the Olympic Team. Technologies of the Institute were declassified in 2008. In the US, these technologies are still classified. Dr. Irene Caesar was also collaborating with the Scientific Research Institute for the National Security in Moscow, Russian Federation, now closed.

Nonetheless, it was Dr. Irene Caesar herself who was first to offer to record the holographic signal of the wave matrices via laser from the pharmaceutical drugs as recreated biohologrames representing in this dimension the scalar wave diffraction gratings of multidimensional wave crystals. And Dr. Caesar was first to offer an idea to encode electrets via laser on nanolevel with these biohologrames of the pharmaceutical drugs.

Dr. Caesar created a theory of the Wave Optics (Geometrical Optics) in chromosomes as refraction in the scalar wave diffraction grating.

Dr. Caesar was first to offer an idea of DIGITAL PHARMACY as the collection not of frequencies, but of biohologrames.

WAVE GENOME LLC is focused on developing and commercializing **QUANTUM BIOCOMPUTING** as the **INFORMATION-WAVE TECHNOLOGY OF THE LASER BIOHOLOGRAPHY** in the fields of rejuvenation, wellness and agriculture.

THE INFORMATION-WAVE TECHNOLOGY OF LASER BIOHOLOGRAPHY is based upon the application of Quantum Physics to Genetics, a new theory of Genetics, which is called **WAVE OPTICS IN CHROMOSOMES** (© Irene Caesar, Ph.D., 1989-2018), and the application of various lasers, including the stabilized He-Ne lasers with internal mirrors.

Specifically, this technology applies:
- the holographic model of the Quantum Vacuum identical for macro and micro dimensions;
- the holographic torsion model of the cell as a torus;
- polarized biohologrephy and polarized biohologrames, based upon the principles of geometrical optics;
- the notions of two kinds of torus: torus as a boundless sphere and torus as a wave crystal (© Irene Caesar, Ph.D., 1989);
- the Kozyrev Mirror principle for the reflection of the external signal upon itself, and creating the scalar wave diffraction grating (wave crystal);
- the diffraction grating (wave crystal) for the refraction of the external signal towards the zero center;
- the notion of the zero center of the wave crystal as the information portal;
- the notion of the instantaneous and remote transmission of information through the zero center of the wave crystal via quantum entanglement in the paradigm of the **QUANTUM BIOINTERNET**.

INFORMATION-WAVE TECHNOLOGY OF THE LASER BIOHOLORAPHY is radically different from the Digital Homeopathy and Bioresonance Technology, though it is also based upon the wave-particle duality in physics. Cell dies when it goes into bioresonance with itself. Soviets had the psychotronic

Munich, Germany; Institut Curie, France; University of Queensland, Australia; Tsinghua University, China; Asia Pacific Association for Medical Informatics, South Korea; European Medical Association, Belgium; University of Geneva, Switzerland; Gyeongbuk Institute of Science and Technology, South Korea; University of Geneva, Switzerland; The Standing Committee of European Doctors, Belgium; International Scociety of Medical Laser Applications, Austria.

Link to the NEURAL ENGINEERING Session:
http://www.bitcongress.com/wcbme2017/scientificprogram.asp

List of Renowned Speakers:
http://www.bitcongress.com/wcbme2017/default.asp

"REMOTE BIOMEDICAL ENGINEERING VIA MASTERING THE GEOMETRICAL OPTICS OF CHROMOSOMES"

Abstract

The same gene is expressed in functional individuals and species by metacentric chromosome, and in dysfunctional individuals and species via acrocentric chromosome. Metacentric chromosome is analogous to a well-centered and focused eye crystal, while acrocentric chromosome is analogous to a myopic or farsighted eye. Chromosome is a lens that allows our cells to focus the needed wave information during cell division, analogously to a crystal in our eye. Thus, Biomedical Engineering is possible only via mastering the Geometrical Optics of Chromosomes by Laser Biohology. Current genetic engineering via cutting and pasting DNA snippets destroys the systematic wholes of chromosomal biohologrames and the refraction of the geometrical optics in chromosomes, and, therefore, causes genetic collapse. The Quantum Leap in the Biomedical Engineering is the cost of our survival. Biomedical Engineering as Biohology is based on Quantum Physics, and understanding the non-local nature of the Biohologrames. Since universe is holographic, we can record and transmit only holographic information, based upon changing the refraction of the scalar wave diffraction grating in chromosomes. According to Holographic principle, Universe is entirely in its every matrix point. The implication of the Holographic Principle states that if Universe is entirely in its every matrix point, then, every matrix point is not simply different from any other matrix point, but is unique. This means that every wave matrix is both non-local, and unique. Thus, if we have two exact copies of the same non-local wave matrix, we can transmit information instantaneously and remotely, from one copy of the same non-local unique wave matrix to another copy. Thus, the precision in the Biomedical Engineering is achieved not via the precision of localization, but, vice versa, via the precision of refraction in the unique and non-local biohologrames aka “wave crystals”. The secret in the remote Biomedical Engineering as Quantum Biocomputing lies in the recording and instantaneous transmission of a structural phantom. I will introduce the new method for recording and remote transmitting of biohologrames via laser spectroscopy and coding electrets on nanolevel via laser. The technology creates “lenses” assisting our chromosomes in correcting their refraction for focusing genetic biohologrephic information, both locally and remotely.

APRIL 25-27, 2017

IRENE CAESAR, PH.D., SPEECH "REMOTE MANAGEMENT OF BIOSYSTEMS AS BIOHOLOGRAPHY BASED UPON THE SHAPE OF CHROMOSOMES FOR FOCUSING GENETIC INFORMATION" at the Annual World Congress of Molecular & Cell Biology Xi'an, China. **Click here** (http://www.bitcongress.com/cmcb2017/)for the official webpage of the Summit. **Click here (http://www.bitcongress.com/cmcb2017/scientificprogram_4.asp)** for the official list of participants.

(https://www.youtube.com/watch?v=pSsgOPUzz9A)

IRENE CAESAR, PH.D., FOUNDER, OWNER AND PRESIDENT OF WAVE GENOME: LECTURE "GOSPEL OF IRENE" (PAPER "GOSPEL OF IRENE" WAS PUBLISHED IN FULL IN THREE ISSUES OF THE SOCIALIST FACTOR MAGAZINE, LUCKNOW AND LONDON), THE STRATEGIC INFORMATICS ADVISORY, MARYLAND, USA, JULY 7, 2016.
(https://www.youtube.com/watch?v=QFEErBqSJjY&feature=youtu.be)

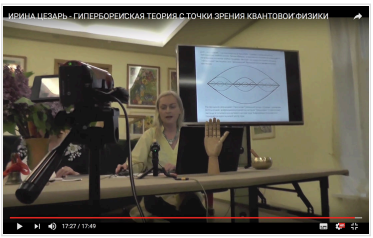

IRENE CAESAR, PH.D., PRESIDENT AND OWNER OF WAVE GENOME: "HYPERBOREAN THEORY FROM THE POINT OF VIEW OF QUANTUM PHYSICS" - PAPER DELIVERED AT THE CONFERENCE "ESOTERICS, NEW TURNAROUND", ASSOCIATION OF ANTHROPOLOGY AND PSYCHOLOGY, MOSCOW, MAY 16, 2016. (https://www.youtube.com/watch?v=CRbRsohA8i4)

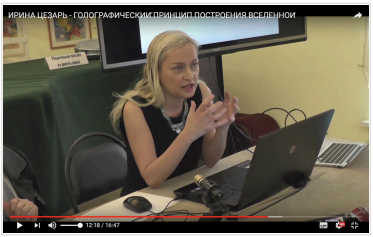

IRENE CAESAR, PH.D., PRESIDENT AND OWNER OF WAVE GENOME: "HOLOGRAPHIC PRINCIPLE OF THE STRUCURE OF THE UNIVERSE" - PAPER DELIVERED AT THE CONFERENCE "UNKNOWN COSMOS", ASSOCIATION "PROTOHISTORY", MOSCOW, MAY 14, 2016. (https://www.youtube.com/watch?v=M4oYWLLmP4c)

Picture (https://www.youtube.com/watch?v=RT1nSUJilbY)

IRENE CAESAR, PH.D., PRESIDENT AND OWNER WAVE GENOME: "STRUCTURALIST WAVE GENOME AS THE FOUNDATION FOR SUPER INTELLECT" - PAPER DELIVERED AT THE CONFERENCE OF THE ASSOCIATION FOR ANTHROPOLOGY AND PSYCHOLOGY, MOSCOW, APRIL 26, 2016.

weapon, based upon the principle of bioresonance. Thus, the bioresonance technologies in the West are still wide spread simply because they cannot do enough harm due to incompetence. The information is received and transmitted not through waves (frequencies). The information is received and transmitted through the **GEOMETRICAL CODES** of the wave crystals.

Also, the **INFORMATION-WAVE TECHNOLOGY OF THE LASER BIOHOLORAPHY** is not the scalar wave technology, since scalar waves neutralize any external signal. And to call the **INFORMATION-WAVE TECHNOLOGY OF THE LASER BIOHOLOGRAPHY** as the "scalar wave technology" is to say nothing. Scalar waves are only one element of this technology. Information is not received and transmitted via scalar waves. Scalar waves are simply used for creating the diffraction grating inside the wave crystal in order to refract the external signal toward the zero center of the wave crystal. Information is received and transmitted **ONLY** through the zero center of the biohologram / wave matrix (wave crystal). The information is transmitted from one identical token to another identical token of the same unique non-local wave matrix **REMOTELY** and **INSTANTANEOUSLY** via **QUANTUM INTERNET**.

WAVE GENOME LLC employs only professional and experienced specialists to administer rejuvenation treatments in its partner clinics and produce its products, including the **TESLA WATER (/tesla-water.html)** and **MINI-TESLA GENERATOR (/tesla-generator.html)**. Majority of **WAVE GENOME LLC** specialists are both MD and Ph.D. and are well-known doctors all over the world.

WAVE GENOME'S LLC scientists have conducted the first in the world experiment for the remote lowering of the blood sugar in a diabetic cow at a distance of 20 kilometers in the mid 1990s. **WAVE GENOME LLC** has eight years of benefiting global market with its services and products, which are patented, licensed, and certified.

Irene Caesar, Ph.D., Speech "Remote Management of Biosystems Based upon the Shape of Chromosomes as Diffraction Grating for Focusing Genetic Information", International Symposium HEALTH 2.0, Nanjing, China, November 9-10, 2016.

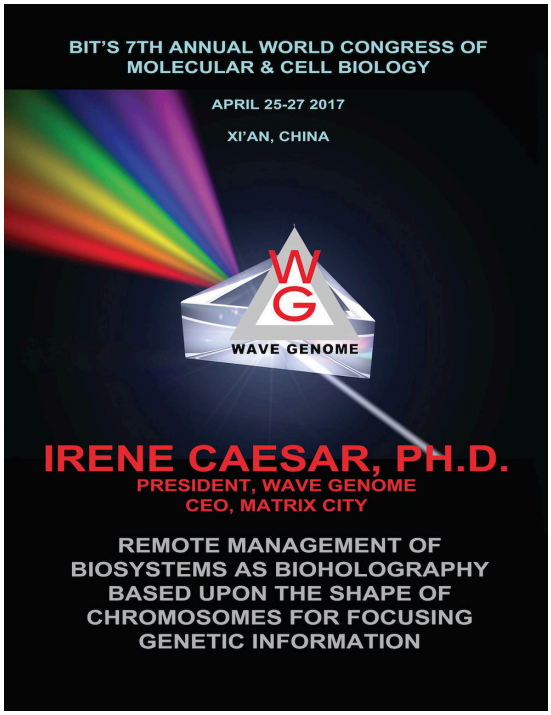

Keynote speakers: Dr. Christian Paterman, Former Director, European Commission, Germany; Dr. Martin Banwell, Professor, Australian National University, Australia; Dr. Robert S. Plumb, Professor, Imperial College London, UK; Dr. Dongping Zhong, Professor, Ohio State University, USA.

Abstract

We are standing at the threshold of the biggest scientific revolution in the history of human kind, called Quantum Leap. All Transhumanist models of genetic modification of organisms, relying on global artificial intellect and brain-computer interfaces are obsolete technologies of the pre-Quantum Era. Either Biology makes Quantum Leap, or humankind will be destroyed by genetic collapse. Human enhancement is possible only through mastering the geometrical optics of chromosomes via Biohology.

Now bioengineering fails since it does not account for the geometrical optics of chromosomes, leading to the corruption of genomes. The same gene gets expressed in dysfunctional individuals by acrocentric chromosome, and in functional individuals by metacentric chromosome. I claim that chromosome is a geometrical code and functions via refraction in the wave crystal, i.e., nonlocal unique biohologram or wave matrix that focuses genetic information unique to this individual via his / her own unique scalar wave diffraction grating. The implication of the holographic principle states that if the universe is entirely in its every matrix point, then, every matrix point

(https://www.youtube.com/watch?v=RT1nSUJilbY)

Another version of this video recording.
(http://www.wavegenome.com
http://www.thematrixcity.com)

Picture (http://Skip navigation RUUpload Search Analytics Video Manager ИРИНА ЦЕЗАРЬ О ВОЛНОВОЙ ГЕНЕТИКЕ И СЕБЕ ГЛОБАЛЬНАЯ ВОЛНА 3 АПРЕЛЯ 2016 Irene Caesar Irene Caesar Channel settingsDownload720 Add to Share More 82 views Published on Jun 7, 2016 ИРИНА ЦЕЗАРЬ О ВОЛНОВОЙ ГЕНЕТИКЕ И СЕБЕ ГЛОБАЛЬНАЯ ВОЛНА 3 АПРЕЛЯ 2016 SHOW MORE Comments are disabled for this video. Autoplay Up Next Сергей Салль Ответ еврейке Цезарь - Салль позор России игра в бисер 12,851 views 50:28 ИРИНА ЦЕЗАРЬ - РАВВИН ЭТО РУСО-АРИЙ ГЛОБАЛЬНАЯ ВОЛНА Irene Caesar 97 views 2:52:41 Засланный казачок Ирина Цезарь или очередной проект сатаноизбранных (Сергей Салль) Светослав 4,499 views 50:28 ИРИНА ЦЕЗАРЬ - СТРУКТУРНАЯ ВОЛНОВАЯ ГЕНЕТИКА КАК ОСНОВА СВЕРХРАЗУМА Irene Caesar 362 views 18:05 СПИЦЫН - Золотая Орда. Дмитрий Донской. Нашествия ханов. Куликовская битва. Монголы и Русь. Евгений Спицын ИСТОРИЯ РОССИИ Recommended for you 57:16 ИРИНА ЦЕЗАРЬ - ДОКАЗАТЕЛЬСТВА ДРЕВНОСТИ РУСОВ Irene Caesar 162 views 1:09:36 America)

IRENE CAESAR, PH.D., PRESIDENT AND OWNER OF WAVE GENOME - NTERVIEW ABOUT WAVE GENOME ON GLOBAL WAVE, MOSCOW, APRIL 3, 2016
(https://www.youtube.com/watch?v=VNLtnfLCOlk&feature=youtu.be)

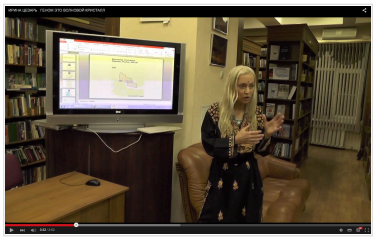

(https://www.youtube.com/watch?v=tgF8PCbRJCQ&feature=youtu.be)

IRENE CAESAR, PH.D., PRESIDENT AND OWNER OF WAVE GENOME: "GENOME IS THE REFRACTION OF SIGNALS TOWARDS THE FOCUS IN THE WAVE CRYSTAL OF CHROMOSOMES" - GUEST PUBLIC LECTURE "DNA GENEALOGY IN THE LIFHT OF RUSSIAN IDEA", EXTRACT, RESEARCH CENTER ON THE ETHICS OF THE RUSSIAN WORLD, MOSCOW, MARCH 16, 2016
(https://www.youtube.com/watch?v=tgF8PCbRJCQ&feature=youtu.be)

Picture (https://www.youtube.com/watch?v=nPgyM2d0HQg&feature=youtu.be)

IRENE CAESAR, PH.D., PRESIDENT AND OWNER OF WAVE GENOME: "CONFIRMATION OF THE HYPERBOREAN THEORY BY QUANTUM PHYSICS" - GUEST PUBLIC LECTURE "DNA GENEALOGY IN THE LIFHT OF RUSSIAN IDEA", EXTRACT, RESEARCH CENTER ON THE ETHICS OF THE RUSSIAN WORLD, MARCH 16, 2016
(https://www.youtube.com/watch?v=nPgyM2d0HQg&feature=youtu.be)

Irene Caesar, Ph.D., Speech "Remote Management of Biosystems Based upon the Shape of Chromosomes as Diffraction Grating for Focusing Genetic Information", International Symposium HEALTH 2.0, Nanjing, China, November 9-10, 2016.

(/theory--
-10581045105410561048107l.html)

SEPTEMBER 2016

IRENE CAESAR'S ARTICLE "QUANTUM GENETICS" IN SEPTEMBER 2016 ISSUE OF "SOCIALIST FACTOR" MAGAZINE (LUCKNOW AND LONDON), as the publication of Irene Caesar's paper "Remote Management of Biosystems Based upon the Shape of Chromosomes as Diffraction Grating for Focusing Genetic Information", delivered as lecture at the Bangkok Thonburi University International Symposium, July 23, 2016. **Click here** (http://2016-9-irene-caesar-quantum-genetics-socialist-factor-magazine.pdf) for the PDF of the article.

(https://www.youtube.com/watch?
v=MuYnjs6khiU)

OCTOBER 1-2, 2016

IRENE CAESAR'S SEMINAR "REMOTE MANAGEMENT OF BIOSYSTEMS BASED UPON

is not simply different from any other matrix point, but is unique. Thus, if we have two exact copies of the same unique non-local biohologram, we can transmit information remotely and instantaneously from one copy to another copy for the remote management of biosystems.

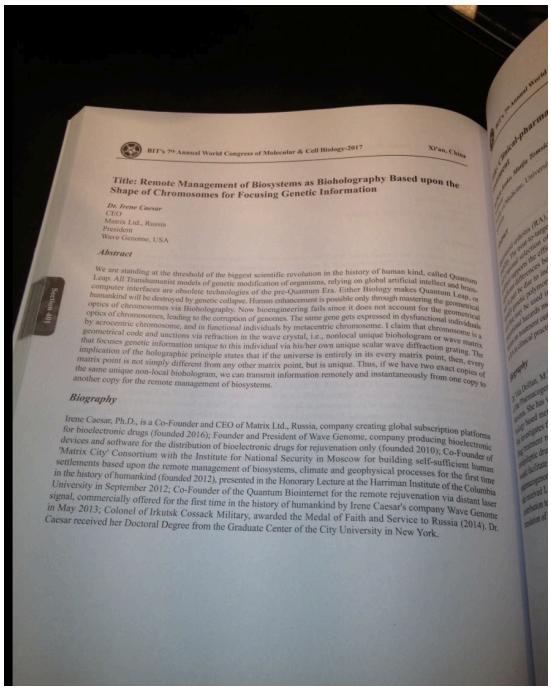

Click here (/ultimate-mini-tesla-psi-generator.html) to read **PRESS RELEASE** on the **GLOBAL LAUNCH OF THE ULTIMATE TESLA PSI-GENERATOR by WAVE GENOME**

ULTIMATE TESLA PSI-GENERATOR IS BASED UPON IMPORTANT DISCOVERY BY DR. IRENE CAESAR REGARDING THE SHAPE OF CHROMOSOMES AS DIFFRACTION GRATING / REFRACTION MECHANISM FOR FOCUSING GENETIC INFORMATION

Picture (https://www.youtube.com/watch?
v=ONPUDcRVgHY&feature=youtu.be)

IRENE CAESAR, PH.D, PRESIDENT AND OWNER OF WAVE GENOME: "SHAPE OF CHROMOSOMES AS A KEY TO WAVE GENOME - GUEST PUBLIC LECTURE, CHETEK ("MAN, TECHNOLOGY, CAPITAL"), MOSCOW, JANUARY 27, 2016
(https://www.youtube.com/watch?
v=ONPUDcRVgHY&feature=youtu.be)

Picture (https://www.youtube.com/watch?
v=2BCiU31THbQ)

IRENE CAESAR, PH.D., PRESIDENT AND OWNER OF WAVE GENOME: "WAVE GENOME - LOCAL AND REMOTE BIOELECRONIC DRUGS AS FRONTIER OF QUANTUM LEAP" - LECTURE, HOSTED BY PRAXIS DR. GRUENAGEL, TRANSLATED BY KATIA MEIER, MD (OWNER OF THE CLEAR SKY MEDICAL, PC, IN DENVER, CO), WACHENHEIM, GERMANY, FEBRUARY 18, 2015, PART 1 (https://www.youtube.com/watch?v=2BCiU31THbQ)
PART 2 (https://www.youtube.com/watch?v=2a9dDLfCE5g)
PART 3 (https://www.youtube.com/watch?v=Ntg-IJFC974)

Picture (https://www.youtube.com/watch?
v=PasGu7KjhyQ)

IRENE CAESAR, PH.D., PRESIDENT AND OWNER OF WAVE GENOME: "QUANTUM LEAP VIA WAVE GENOME" - LECTURE, AS PART OF WAVE GENOME'S PARTICIPATION IN EVOLVE EXPO 2015, EVOLVE EXPO 2015, THE NATIONAL WESTERN COMPLEX, DENVER, COLORADO, USA, FEBRUARY 7-8, 2015 (https://www.youtube.com/watch?
v=PasGu7KjhyQ)

Picture (https://www.youtube.com/watch?
v=xWYkXpzVJPo)

KATIA MEIER, MD, REPRESENTATIVE OF WAVE GENOME IN COLORADO, OWNER OF CLEAR SKY MEDICAL, PC, ON HER REPRESENTATION OF WAVE GENOME - LECTURE AS PART OF WAVE GENOME'S PARTICIPATION IN EVOLVE EXPO 2015, EVOLVE EXPO, THE NATIONAL WESTERN COMPLEX, DENVER, COLORADO, USA, MARCH 7-8, 2015
(https://www.youtube.com/watch?
v=xWYkXpzVJPo)

Picture

IRENE CAESAR'S, PH.D., SEMINAR WELLENGENOM @ ORANIA-ZENTRUM, GERMANY, KURNACH BEI WURZBURG, FILM BY EXTREME NEWS, NOVEMBER 21-23, 2014 (https://www.youtube.com/watch?
v=PHPBOCkdmiQ)

Picture

(http://www.wavegenome.com/1/post/2013/08/leakproof the-singularity-irene-caesar-interviews-roman-yampolskiy.html)

LEAKPROOFING THE SINGULARITY: IRENE CAESAR INTERVIEWS ROMAN YAMPOLSKIY, AUGUST 6, 2013
(http://www.wavegenome.com/1/post/2013/0

THE SHAPE OF CHROMOSOMES AS DIFFRACTION GRATING FOR FOCUSING GENETIC INFORMATION", Jane Mackenzie's Rejuvenating Centre, Johannesburg. **Click here** (https://www.youtube.com/watch?v=MuYnjs6khiU) for the video.

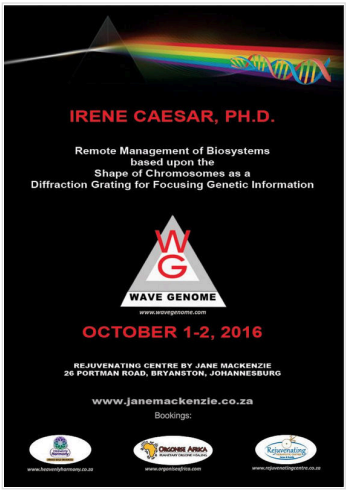

OCTOBER 1-2, 2016

IRENE CAESAR'S SEMINAR "REMOTE MANAGEMENT OF BIOSYSTEMS BASED UPON THE SHAPE OF CHROMOSOMES AS DIFFRACTION GRATING FOR FOCUSING GENETIC INFORMATION", Jane Mackenzie's (http://www.janemackenzie.co.za) Rejuvenating Centre Johannesburg. (http://www.rejuvenatingcentre.co.za)

(https://www.youtube.com/watch?v=lyfh-C3oSm0&feature=youtu.be)

ON DECEMBER 2, 2016, IRENE CAESAR, PH.D.. PRESIDENT, FOUNDER AND OWNER OF WAVE GENOME, LAUNCHED HER NEW PRODUCT -- ULTIMATE MINI-TESLA PSI-GENERATOR FOR THE ULTIMATE PROTECTION AGAINST PSYCHOTRONIC AND GENETIC WARFARE. Intellectual and Commerical Property belongs to WAVE GENOME. Magnus Olsson, President of Mindtech Enterprises, becomes the designated Distributor for WAVE GENOME'S ULTIMATE MINI-TESLA PSI-GENERATOR, available on wavegenome.com (http://www.wavegenome.com) and mindtechenterprises.com (http://www.mindtechenterprises.com). **Click here (https://www.youtube.com/watch?v=lyfh-C3oSm0&feature=youtu.be)** to see the official video of the global launch of THE ULTIMATE MINI-TESLA PSI-GENERATOR by WAVE GENOME.

(/order-tesla-glasses.html)

(/order-tesla-glasses.html)

Click here (/order-tesla-glasses.html) to read about WAVE GENOME TESLA GLASSES.

8/leakproofing-the-singularity-irene-caesar-interviews-roman-yampolskiy.html)

Picture (https://www.youtube.com/watch?v=rVU1MHIruwQ)

IRENE CAESAR, PH.D.: "MATRIX CITY - PUBLIC LECTURE AT THE HARRIMAN INSTITUTE, COLUMBIA UNIVERSITY, SEPTEMBER 13, 2012 (https://www.youtube.com/watch?v=rVU1MHIruwQ)

MORE (/news.html)

In November 2011, Dr. Irene Caesar presented to President Vladimir Putin's Agency for Strategic Initiatives her project of the MATRIX CITY - the self-sufficient city as an integrated information-wave matrix, built with the application of the information-wave technologies of the Quantum Leap. In August 2012, Dr. Irene Caesar offered her project of the MATRIX CITY to the Institute for National Security in Moscow for practical realization. As a result, Dr. Irene Caesar, Founder, Owner and President of Wave Genome, and Dr. Alexej Diaschev had established the Consortium **"Matrix City" (http://www.thematrixcity.com).** Irene Caesar, Ph.D., presented her project of the Matrix City in her public lecture at the Harriman Institute of the Columbia University on September 13, 2012.

WE OFFER:

Picture

Irene Caesar, Ph.D., Founder, Owner and President of WAVE GENOME with Magnus Olsson, President of Mind Tech Enterprises, and Director of World, European and US Coalitions Against Covert Electronic Harassment, one of Distributors of WAVE GENOME.

- **MINI-TESLA PSI-GENERATOR (/tesla-generator.html)**

as a chip (artificial crystal) structured with the generic or personal biohologram / wave matrix by the laser on the nano level for healing, rejuvenation and self-defense from harmful electromagnetic fields, psychotronic and psychic attacks, and genetic warfare;

- **WAVE PHARMACEUTICALS (/wave-pharmaceuticals.html) VIA DIGITAL PHARMACY (/digital-pharmacy-software--1057105410601058-106210481060105610541042105410 49-104010551058104510501048.html)**

via generic and individual wave matrices. **WAVE MATRIX** (http://www.wavegenome.com/wave-pharmaceuticals.html) is the hologram, recorded by the laser. **WAVE MATRICES** (http://www.wavegenome.com/wave-pharmaceuticals.html) include (a) INDIVIDUAL WAVE MATRIX (http://www.wavegenome.com/wave-pharmaceuticals.html), recorded by the laser from the childhood photograph, placenta or navel blood, or/and (b) generic **WAVE MATRIX** (http://www.wavegenome.com/wave-pharmaceuticals.html) recorded by the laser from the healthy human cells and bodily systems, and digitised as **DIGITAL CELLS, (http://www.wavegenome.com/wave-pharmaceuticals.html)**(c) generic or personal **WAVE MATRICES (http://www.wavegenome.com/wave-pharmaceuticals.html)** of medications as psi-medications, including such psi-pharmaceuticals, as psi-

(https://www.youtube.com/watch?v=Z8Otz0gbqeM)

DECEMBER 2, 2016

IRENE CAESAR, PH..D, PRESIDENT, FOUNDER AND OWNER OF WAVE GENOME: "HOW THE ULTIMATE TESLA PSI-GENERATOR WORKS", Global Launch of the ULTIMATE TESLA PSI-GENERATOR by WAVE GENOME. **Click here (https://www.youtube.com/watch?v=Z8Otz0gbqeM)** for the video.

(https://www.youtube.com/watch?v=H8hkdkMMkMg)

DECEMBER 2, 2016

IRENE CAESAR, PH..D, PRESIDENT, FOUNDER AND OWNER OF WAVE GENOME ON WAVE GENOME PRODUCTS, Global Launch of the ULTIMATE TESLA PSI-GENERATOR by WAVE GENOME. **Click here** (https://www.youtube.com/watch?v=H8hkdkMMkMg) for the video.

(https://www.youtube.com/watch?v=6BpWw4R8XBo)

DECEMBER 2, 2016

IRENE CAESAR, PH.D., FOUNDER AND PRESIDENT OF WAVE GENOME, ON POLARIZED BIOHOLOGRAPHY. Click here (https://www.youtube.com/watch?v=6BpWw4R8XBo&feature=youtu.be) for the video.

(https://www.youtube.com/watch?v=2QgxLxAbkWs&feature=youtu.be)

DECEMBER 2, 2016

IRENE CAESAR, PH.D., FOUNDER AND PRESIDENT OF WAVE GENOME: "WAVE GENOME FOR VICTIMS OF VOICE TO SKULL" (WAVE GENOME helps V2K victim Magnus Olsson). **Click here** (https://www.youtube.com/watch?v=2QgxLxAbkWs&feature=youtu.be)for the video.

(https://www.youtube.com/watch?v=zQgSz2_PdG0&spfreload=10)

DECEMBER 2, 2016**. IRENE CAESAR & MAGNUS OLSSON WAVE GENOME HELP TO V2K VICTIMS**. Click here (https://www.youtube.com/watch?v=zQgSz2_PdG0) for the video.

(https://www.youtube.com/watch?v=sgttqrKAFlg)

VYagra, psi-hormones, etc. **WAVE PHARMACEUTICALS (/wave-pharmaceuticals.html)** has various platforms for dispensation, including:

(1) generic or personal **WAVE MATRICES (http://www.wavegenome.com/wave-pharmaceuticals.html),** encoded by the laser in the chip of the **PSI-GENERATOR (http://www.wavegenome.com/order-your-mini-tesla-generator.html)** on the nano level;

(2) **INDIVIDUAL WAVE MATRIX (http://www.wavegenome.com/wave-pharmaceuticals.html), DIGITAL CELL (http://www.wavegenome.com/wave-pharmaceuticals.html)** and **DIGITAL PHARMACEUTICALS (/wave-pharmaceuticals.html)** - generic or personalised wave matrices of human cells and pharmacueuticals recorded by lasers, digitised and administered as holographic / granulated signal in the form of the **WHITE NOISE (http://www.wavegenome.com/wave-pharmaceuticals.html)**, encoded into the music in the acoustic and video **PSI-PROGRAM (/digital-pharmacy-software--1057105410601058-106210481060105610541042105410 49-104010551058104510501048.html)** of the binaural self-therapy. Each psi-generator comes with the flash drive, which contains a software with **COMPREHENSIVE DIGITAL PHARMAC (/digital-pharmacy-software--1057105410601058-106210481060105610541042105410 49-104010551058104510501048.html)Y** that has 44 digital modules of the digitized wave matrices in the form of the white noise, encoded into the music, for every bodily system (e.g., endocrine system, reproductive system, cardiovascular system, digestive system, etc.) and every vital organ in the body (e.g., liver, kidney, brain, etc.) -- 22 modules for organs and 22 modules for physiological systems. Digital drugs per se, like psi-vyagra or psi-hormones, are offered as extra. White noise, generated by the **PSI-PROGRAM (/digital-pharmacy-software--1057105410601058-106210481060105610541042105410 49-104010551058104510501048.html)**, can be used for programming water. Digital encoding of wave matrices onto various media via laser is available;

(3) **QUANTUM INTERNET (/remote-laser-treatment.html)** - wireless programming of biosystems, water and human condition via laser. **QUANTUM INTERNET** is **REMOTE, WIRELESS,** and **INDIVIDUALISED;**

- **TESLA WATER (/tesla-water.html)**

Bioactive restructured water charged remotely via **QUANTUM INTERNET** with the use of laser through Quantum nonlocality**,** or charged locally by the white noise (initially programmed by the laser, and, then, digitized), when you run your program of the **DIGITAL PHARMACY** (/wave-pharmaceuticals---digital-pharmacy.html) on your computer. In both cases, you need to purchase **MINI-TESLA PSI-GENERATOR (/tesla-generator.html)**. **TESLA WATER (/tesla-water.html)** is either individualised for every client or generic for specific conditions. **TESLA WATER** can be used in agriculture to increase its productivity manifold;

- **REMOTE REJUVENATION "OM" (/remote-laser-treatment.html)**

via **QUANTUM INTERNET** for all the physiological systems, including endocrine system, digestive system, cardiovascular system, hearing / eye sight, reproductive

DECEMBER 2, 2016. **IRENE CAESAR ON THE QUANTUM LEAP OF WAVE GENOME.** Click here (https://www.youtube.com/watch?v=sgttqrKAFIg) for the video.

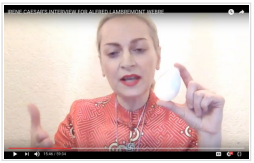

(https://newsinsideout.com/2017/01/dr-irene-caesar-reveals-russian-quantum-leaps-new-science-next-evolution-health-now-available-online-mindtechenterprises-com/)

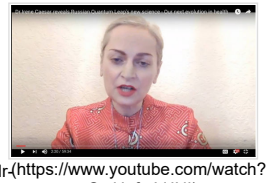

(https://www.youtube.com/watch?v=OwHafg-VJNI)

JANUARY 2, 2017

ARTICLE BY ALFRED LAMBREMONT WEBRE ON DR. IRENE CAESAR AND HER COMPANY WAVE GENOME: "Dr. Irene Caesar reveals Russian Quantum Leap's new science – Our next evolution in health, now available online at MindTechEnterprises.com and wavegenome.com", News Insideout. **Click here** (https://newsinsideout.com/2017/01/dr-irene-caesar-reveals-russian-quantum-leaps-new-science-next-evolution-health-now-available-online-mindtechenterprises-com/) to read the article.

DECEMBER 17, 2016

IRENE CAESAR, PH.D., INTERVIEW TO ALFRED LAMBREMONT WEBRE: "Dr. Irene Caesar reveals Russian Quantum Leap's new science – Our next evolution in health, now available online at MindTechEnterprises", By Alfred Lambremont Webre. With the participation of MindTech Enterprices Team -- distributors of products of Irene Caesar's company Wave Genome, Magnus Thorwald Olsson and Madlen Namro. Click here to see the video (https://www.youtube.com/watch?v=2T2VRsJNE34).

Dr. Irene Caesar, CEO, Matrix Ltd., Russia;
President, Wave Genome, USA

+View Bio

Health 2.0 Asia 2016

International Summit on Smarter Healthcare & Great Health Industry

Theme: Smart Science & Technology Services Health

Time: November 9-10, 2016 Place: Nanjing, China

15:50-16:10	题目：基于作为聚焦遗传信息衍射光栅的染色体形状的生物系统远程管理 **Title:** Remote Management of Biosystems Based upon the Shape of Chromosomes as Diffraction Grating for Focusing Genetic Information **Irene Caesar**博士，俄罗斯Matrix公司首席执行官；美国Wave Genome公司董事长 **Dr. Irene Caesar,** CEO, Matrix Ltd., Russia; President, Wave Genome, USA

NOVEMBER 9-10, 2016

IRENE CAESAR, PH.D., SPEECH "REMOTE MANAGEMENT OF BIOSYSTEMS BASED UPON THE SHAPE OF CHROMOSOMES AS DIFFRACTION GRATING FOR FOCUSING GENETIC INFORMATION" at the International Health 2.0 Asia 2016 Conference in Nanjing, China, supported by Nanjing Municiple Government, and with the participation of Professor Daniel Shechtman, Nobel Prize Laureate in Chemistry (2011). **Click here (http://www.bitcongress.com/HEALTH2016/default.asp)** for the official webpage of the Summit. **Click here (http://www.wavegenome.com/2016_11_9_10_Irene_Caesar_at_Health_2_Asia_International_Summit_Speaker_List.pdf)** for the official list of participants.

system, intellectual abilities, improvement of memory, psychic abilities, sexual potency, etc. This service is provided remotely via **WIRELESS QUANTUM INTERNET (/remote-laser-treatment.html);**

- **SUBSCRIPTION PACKAGES FOR MAINTENANCE (http://wavegenome.com/wave-genome---prices.html) (in works)**

Client can purchase the everyday maintenance of his **WAVE MATRIX (http://www.wavegenome.com/wave-pharmaceuticals.html).** Client sends his data to the Institute either via the conventional internet, and via the **QUANTUM INTERNET (/remote-laser-treatment.html). HOLOGRAPHIC MAINTENANCE (http://www.wavegenome.com/wave-pharmaceuticals.html)** is the correction of the intensity and modules of biohologrames / wave matrices in accordance with the changing client's condition, earthly electro-magnetic activity, solar and lunar activity, geophysical activity, and predicted social unrest. The correction is provided by the specialists of WAVE GENOME LLC remotely or locally. **HOLOGRAPHIC MAINTENANCE (http://www.wavegenome.com/wave-pharmaceuticals.html)** is provided via the update of the digital files in the Digital Pharmacy and by the remote (non-local) laser signal via **QUANTUM INTERNET (/remote-laser-treatment.html).** For example, we can offer the remote management of diabetes;

- **CLINIC with LARGE-SIZE PSI-GENERATORS (/quantum-clinic.html)**

Exclusive rejuvenation services in our partner clinics for restoration and self-defense, especially for patients who were refused by conventional medicine, infertility cases, impotence, drug dependence, and rehabilitation. BIOHOLOGRAPHIC TREATMENT can restore menstruation cycles in the post-menopausal women over 60 years old, so that a woman can again bear a child;

- **TESLA ENHANCEMENT (/quantum-clinic.html)**

Special programs in our partner clinics for those who are seeking to enhance their mental and physical abilities via **LARGE-SIZE PSI-GENERATORS (/quantum-clinic.html);**

- **CONSULTING SERVICES (/ask-our-maven.html)**

regarding the Quantum Leap information-wave technologies by our mavens.

Picture (/theory---10581045105410561048107 1.html)

AUGUST 2016

IRENE CAESAR'S ARTICLE (2012) "HOW TO BUILD MATRIX CITY" IN AUGUST 2016 ISSUE OF "SOCIALIST FACTOR" MAGAZINE (LUCKNOW AND LONDON), first published on thematrixcity.com in 2012, as a major document of the Matrix City Consortium (founded August 2012), Co-founded by Dr. Irene Caesar and the Institute for National Security in Moscow. **Click her** (http://wavegenome.com/2016-8-irene-caesar-matrix-city-socialist-factor-magazine.pdf)**e** for the PDF of the article.

Irene Caesar, Ph.D., Speech "Remote Management of Biosystems Based upon the Shape of Chromosomes as Diffraction Grating for Focusing Genetic Information", International Symposium HEALTH 2.0, Nanjing, China, November 9-10, 2016.

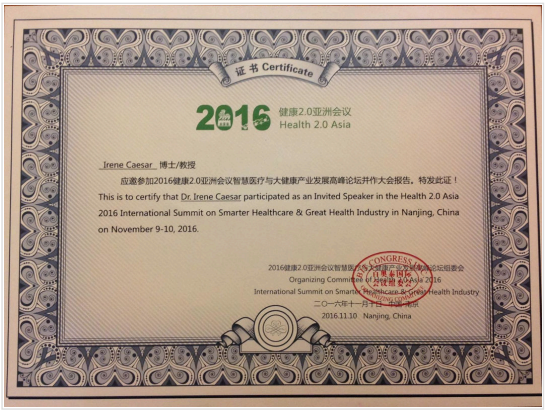

Irene Caesar, Ph.D., Speech "Remote Management of Biosystems Based upon the Shape of Chromosomes as Diffraction Grating for Focusing Genetic Information", International Symposium HEALTH 2.0, Nanjing, China, November 9-10, 2016.

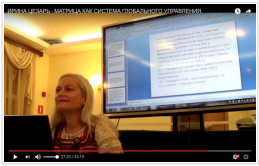

(https://www.youtube.com/watch?v=bECHfG4WttQ)

OCTOBER 10, 2016

LECTURE BY IRENE CAESAR, Ph.D., "MATRIX AS A GLOBAL MANAGEMENT SYSTEM OF LIFE. MECHANISM OF REMOTE MANAGEMENT OF BIOSYSTEMS." Conference "Psychics - yesterday, today and tomorrow", October 10, 2016, (4th Meeting of the Association for Astral Anthropology and Psychology), House of Culture "Scarlet Sails", Moscow, Russia. **Click here** (https://www.youtube.com/watch?v=bECHfG4WttQ) for the video. **Click here (https://www.youtube.com/watch?v=eEKzZQ4Wzcc)** for another version of vidoe recording.

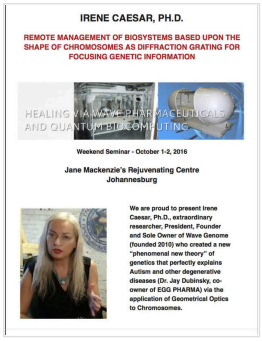

OCTOBER 1-2, 2016

PRESS RELEASE FOR IRENE CAESAR'S SEMINAR "REMOTE MANAGEMENT OF BIOSYSTEMS BASED UPON THE SHAPE OF CHROMOSOMES AS DIFFRACTION GRATING FOR FOCUSING GENETIC INFORMATION", Jane Mackenzie's Rejuvenating Centre Johannesburg. **Click here (http://www.wavegenome.com/2016_9_1_irene_caesar_seminar_zar_press_release_final.pdf)** for PDF file of the Press Release.

(/theory--
-10581045105410561048107 1.html)

JULY 2016

IRENE CAESAR, PH.D., LECTURE "REMOTE MANAGEMENT OF BIOSYSTEMS BASED UPON THE SHAPE OF CHROMOSOMES AS DIFFRACTION GRATING FOR FOCUSING GENETIC INFORMATION", Bangkok Thonburi University International Symposium, July 23, 2016. **Click here** (https://www.youtube.com/watch?v=XuwV_QCTf2I) for the recording of Irene Caesar's lecture at the Bangkok Thonburi University. **Click here** (https://www.youtube.com/watch?v=pSsgOPUzz9A) for the slide show of Irene Caesar's lecture at the Bangkok Thonburi University International Symposium.

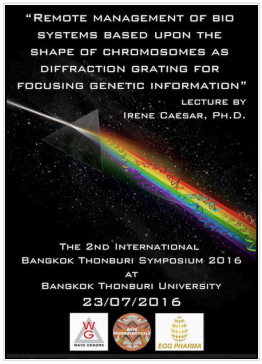

(/theory--
-10581045105410561048107 1.html)

SEPTEMBER 2016

PUBLICATION OF IRENE CAESAR'S, PH.D., PAPER "REMOTE MANAGEMENT OF BIOSYSTEMS BASED UPON THE SHAPE OF CHROMOSOMES AS DIFFRACTION GRATING FOR FOCUSING GENETIC INFORMATION" in the Proceedings of the Bangkok Thonburi University International Symposium, July 23, 2016, also published in the September Issue of the "Socialist Factor" Magazine (Lucknow and London). **Click here** (http://www.wavegenonome.com/2016_BTUSymposium.pdf) for PDF of the BTU Symposium Proceedings.

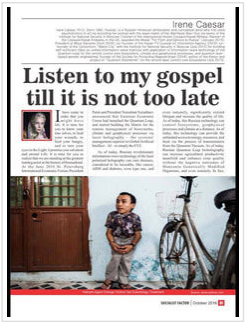

(/uploads/3/5/1/1/35112207/4952633_orig.jpg)

OCTOBER 2016

IRENE CAESAR, PH.D., ARTICLE "LISTEN TO MY GOSPEL TILL IT IS NOT TOO LATE" IN OCTOBER 2016 ISSUE OF "SOCIALIST FACTOR MAGAZINE (LUCKNOW AND LONDON). Click here (http://www.wavegenome.com/2016-10-irene-caesar-listen-to-my-gospel-socialist-factor-magazine.pdf) for the PDF of the article.

FDA DISCLAIMER: Content on this site is for reference purposes and is not a substitute for advice from a licensed health-care professional. You should not rely solely on this content, and wave genome.com assumes no liability for inaccuracies. Always read directions before using a product. Statements regarding products and services have not been evaluated by the FDA, and these products and services are not intended to diagnose, treat, cure, or prevent any disease or condition.

Payment in full is due ahead of services. No refunds and returns.

COPYRIGHT NOTICE: Text, graphics, and HTML code on wavegenome.com belong to Irene Caesar, Ph.D., their sole author, and are protected by US and International Copyright Laws, and may not be copied, reprinted, published, translated, hosted, or otherwise distributed by any means without explicit permission from Irene Caesar, Ph.D., and in violation of the International Laws for citing references. Any citation of the wavegenome.com website should be accompanied with the proper reference to Irene Caesar, Ph.D. Any citation exceeding the length, permissible for the reference length by the International Copyright Law, will be considered to be a violation of the International Copyright Law.

© IRENE CAESAR, PH.D., FOUNDER AND SOLE OWNER OF WAVEGENOME 2010-2017 ALL RIGHTS RESERVED

WAVE GENOME (/)

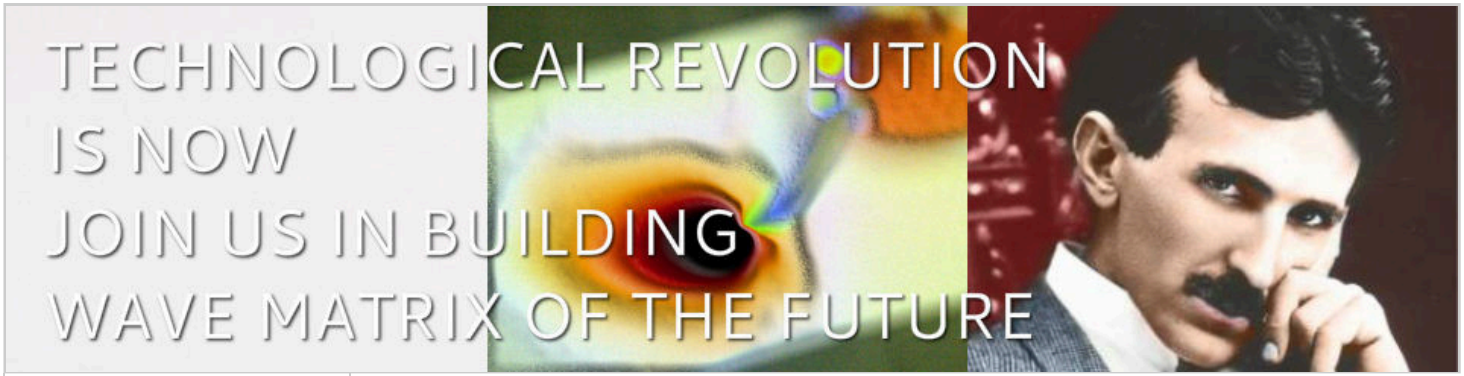

HOME / ГЛАВНАЯ (/)

SERVICES / УСЛУГИ (/SERVICES--10591057105110591043 1048.HTML)

PRODUCTS / ТОВАРЫ (/PRODUCTS--10581054104210401056 1067.HTML)

CONTACT / КОНТАКТ (/CONTACT--10501054105310581040 10501058.HTML)

Basic TESLA GLASSES - $1090
Advanced TESLA GLASSES X - $2000

TESLA GLASSES BY WAVE GENOME

Article published by Irene Caesar, Ph.D., Founder, Owner and President of Wave Genome, in January 2015,
All Rights Reserved, © IRENE CAESAR, 2015.

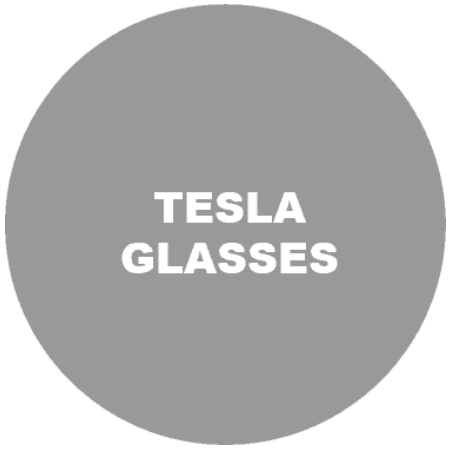

Our TESLA GLASSES are used by Russian Space Forces.

Our TESLA GLASSES are used by Russian Strategic Missile Forces.

Our TESLA GLASSES are used by Russian Ministry of Emergency Situations.

HEALTH, ENHANCEMENT AND REJUVENATION PROMOTION WITH TESLA GLASSES

Our TESLA GLASSES are used by Russian Federal Security Service.

Our TESLA GLASSES are used by Russian Interior Ministry.

FORMULATION OF THE PROBLEM

- Up to 95% of the Russian population are in the state of stress.

- In our country, 50 million people are in need of

Certificate # 0285580
Certification reg. № ROSS RU 001.11AE63.
by "OBORONTEST" (DEFENSE SYSTEMS TESTING)
Compliance with regulatory documents
GOST R 52161.1-2004 GOST R 51318.14.1-2006 (P.4).
The Winner of the Russian Government order for
Police and Security officers in 2011

WAVE GENOME LLC is offering two models of **TESLA GLASSES**: **BASIC TESLA GLASSES** and **TESLA GLASSES X** (advanced model)

TESLA GLASSES BASIC

TESLA GLASSES X (Advanced Model)

Used by Russian Military pilots and Astronauts, TESLA GLASSES by WAVE GENOME LLC are not "glasses" per se, but QUANTUM BIOCOMPUTER, which functions like brain massager and programmer. TESLA GLASSES massage the brain with holographic signal and program designated areas of the brain with the holographic signal modulated with the holographic information restoring brain area responsible for a specific organ and physiological system, and thus, restoring this specific organ and physiological system through the brain. The frequencies entering the eye are getting folded (reflected upon themselves) within the eye crystal, to become holographic signals. Every segment of the retina is connected to a specific brain area. And the holographic signal hitting the retina, activates a specific segment of retina, and, therefore, a specific area of your brain. Thus, through brain, you massage your entire body from inside, including organs that need treatment, and program your organ in need of treatment for regeneration.

TESLA GLASSES X (Advanced Model)

improving their eye sight.

- More than 4 million people a year lose their eye sight, out of whom 400 000 go blind.

- Conventional medicine cannot solve the health problems that quickly, cheaply and effectively as **TESLA GLASSES** can!

Brain Research Institute in Moscow proved that our biological age may be higher than the passport age for 10-15 years, because of the diseases. But it is possible to get rejuvenated for 10-15 and more years in comparison with the passport age.

WHO NEEDS TESLA GLASSES?

- Business people and those people who are over 40 years for active longevity

- Athletes and Military, students

- Everyone who works on the PC

APPLICATION OF THE TESLA GLASSES IS PARTICULARLY USEFUL FOR:

- Prevention of cardiovascular disease

- The positive effect in the case of somatic and mental disorders

- Reduction of occupational injuries and accidents on the roads

- Improvement of sleep, mood and efficiency

- the removal of eye fatigue, improvement of vision in myopia, glaucoma, cataract and presbyopia

- The development of creative abilities and improving sleep

In addition, high efficiency and low cost of procedure allows every PC user apply **TESLA GLASSES** for removing eye fatigue. The device is useful to anyone who has to deal with PCs and mobile phones for the prevention of myopia, hyperopia, cataract and glaucoma.

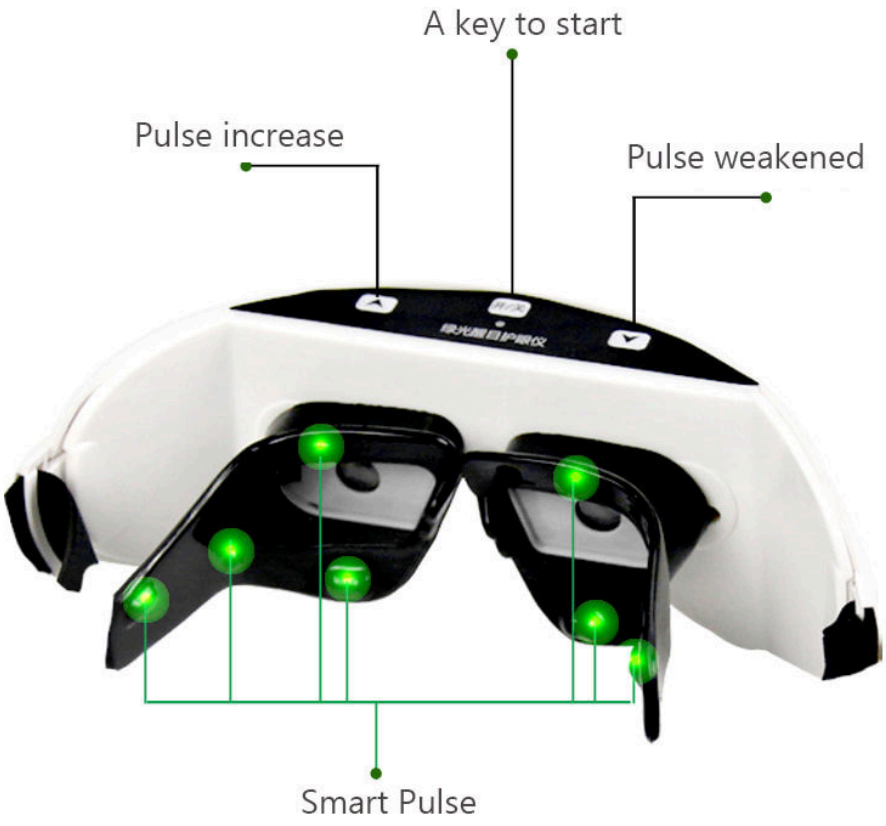

TESLA GLASSES X is the advanced model of TESLA GLASSES by WAVE GENOME.

TESLA GLASSES X (Advanced Model) offers 11 modules similar to the modules of the BASIC TESLA GLASSES in addition to the low frequency electrical stimulation of the acupuncture points around eyes, and the possibility to manually change the distance between the focus points in accordance with the distance between the pupils.

INDICATIONS AND COUNTER-INDICATIONS FOR USE

Prevention and correction of:

• Stress and its consequences;

• Deterioration of the physical and mental performance;

• Reduction of immunity and the bodily defenses;

• Eye diseases;

• Diseases of the internal organs and physiological systems

Contraindications:

- Children younger than 3 years old;

- Epilepsy;

- Cancer and tumors of various localization;

- After organ and tissue transplantation;

- In acute inflammatory diseases of the eye;

- During other serious diseases

TECHNOLOGY

The device consists of a control circuit and Light-Emitting Diodes. One pair of glasses can be used by the entire family.

TESLA GLASSES use the method of Polarized Holography. Polarized Holography is the application of Quantum Physics for the purpose of rejuvenating all organs of the person through the Eye Crystal (Eye Lens and Iris). It is proven to provide significant physical and mental improvement, including a significant improvement in brain functions: decision speed, attention and memory.

The method consists in the control of the brain via triggering the holographic signal in the eye, and its modulation. This control overwrites any verbal and mental imperatives, is non-local (can be used for instantaneous transmission of information at infinitely large distances), instantaneous (exceeds speed of light), and simultaneously reaching out towards every cell in the body.

The method is based upon Quantum Physics, specifically, upon the theory and technology of Polarized Holography, which uses the modulation of the holographic signal according to the Kozyrev Mirror principle.

The method is based upon the special ability of an eye to convert any linear signal into the holographic signal. The process of this conversion

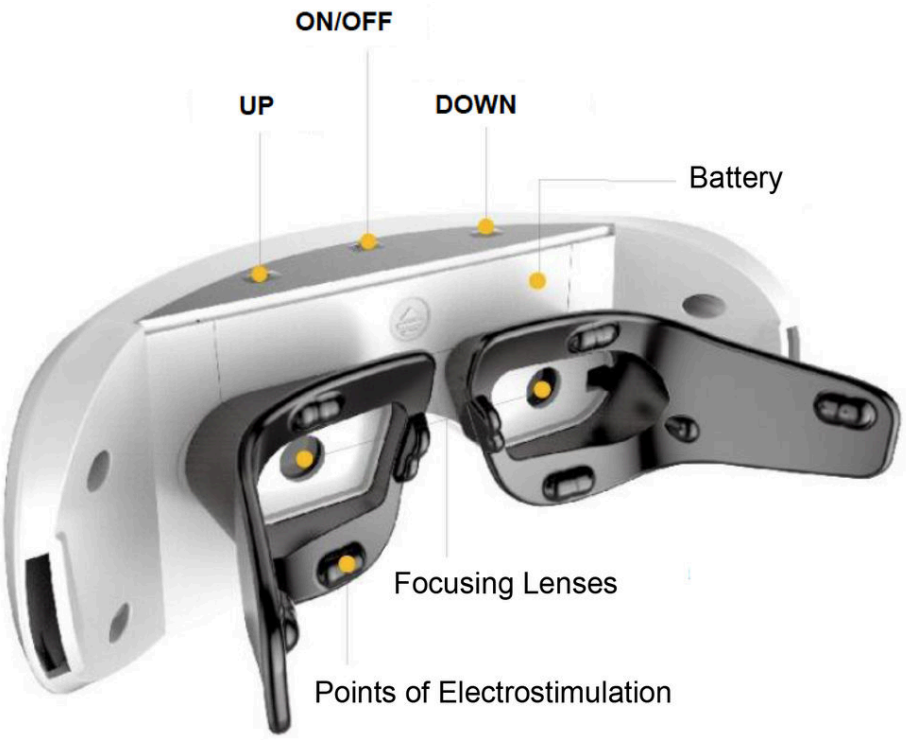

Change of distance between eye pupils

consists in the emergence of the scalar wave diffraction grating, polarization and refraction toward the zero center of the wave crystal (torus). Since the universe is holographic, we can record and transmit information only via the holographic signal, and through the zero center of the wave crystal. The zero center of every toroidal wave crystal coincides from the zero center of every chromosome on the cellular level, and every atom and subatomic particle on the subatomic level to the zero center of our galaxy.

TECHNOLOGY (CONTINUED)

Any healing, rejuvenation, and mental, psychic, and physical enhancement are based upon the ability to produce, control and enhance the holographic signal. The holographic signal instantaneously reaches the zero center of every wave crystal in our body, from the subatomic and atomic to the molecular levels – from the zero center of our skull and every bone to the zero center of every metacentric chromosome. Our eyes, skull, bones and chromosomes are centered and focused similar to our eye crystal according to the laws of the geometrical optics.

Hence, the eye is a very unique receiver, transmitter, and producer of the holographic signal. And that is precisely why vision is a trigger of brain activity. Via correct triggering the holographic signal in the zero center of the eye crystal, we can immediately reach the zero center of the toroidal wave crystal of our brain, thus delivering controlling information instantaneously into the zero center of the wave crystal of every metacentric chromosome in cell division, and into the zero center of the wave crystal of every bone, so that stem cells are programmed in a correct way in the bone marrow.

Correct triggering consists in the modulation of the holographic signal in the eye. The modulation of the holographic signal in **TESLA GLASSES** consists in (1) modulation by the Schumann holographic signal; (2) modulation by human Brain holographic signal; (3) modulation by the holographic signal of a healthy organ and physiological system, recorded upon the chip in the glasses. It is combined with the modulation by the narrowband light-emitting diode sources of five colors. Research had shown that five colors, used by the glasses, benefit organs and physiological systems. The signal for every color is produced from the holographic signal of healthy organs and physiological systems, and, then, it is matched with the color. The signal of the color is not simply the color frequency.

The carrier holographic signal is the individual holographic signal of the user – the unique [indestructible and uncreated] non-local wave matrix of the user. This is the primary holographic signal. The modulation holographic signals are the holographic enhancers, which help the unique [indestructible and uncreated] non-local wave matrix of the user get centered and focused in this

HOW TO USE TESLA GLASSES X (ADVANCED)

(1) Wipe the plastic parts of the goggles with the wet tissue to insure the best contact between the skin and the plastic. Plastic is electrically conductive to ensure electrical stimulation. The tight contact between skin and glasses provides for the proper level of electrostimulation.

ATTENTION: You should wipe the glasses with wet tissue only when the device is switched off, you will see the

(2) To turn the device on, press the button "ON/OFF" on the top of the glasses. When device is turned on, the control panel shows the number of the program used during the previous session. Choose the program that you would like to use. For choosing the program, use the "UP" and "DOWN" buttons.

ATTENTION: Program # 12 is not a treatment program, but is used exclusively for testing the device at the production facility.

(3) After choosing the desired program, press "ON/OFF" button again in order to switch to choosing the intensity of electrostimulation.

ATTENTION: In order to turn off the electrostimulation, please choose the intensity level, in which you see in the right lower corner of the control panel the image of "dot", and press "ON/OFF" button.

(4) Choose the desired intensity of electrostimulation, using "UP" and "DOWN" buttons. You need to increase the intensity only to the level of the pleasant tingling.

ATTENTION: The intensity of perception might go down if your skin is dry around your eyes, and go up if your skin is wet around your eyes.

Presss the "ON/OFF" button again in order to launch the session of the combined usage (light-diodes stimulation plus electrostimulation).

(5) To use the device with more comfort, please choose the proper distance between eye pupils. For this, move the body of the device outwards or inwards, as it is shown in the picture above.

(6) Session goes for 3.t to 5 minutes, until the device turns off automatically.

To turn the device before the end of the session, please press "ON/OFF" button.

ATTENTION: Program # 12 does not stop automatically, and requires that you manually turn it off.

dimension (on this planet). These are secondary holographic signals.

The advantage of the glasses over other Quantum Leap Polarized Holography devices is that glasses use an eye as a filter for filtering out all harmful linear signals, which unseal wave crystals. For example, microwave radiation shortens brain waves via “unsealing” the involuted wave crystals, thus, literally lowering the intellectual potential of people.

Thus, the effect of the **TESLA GLASSES** is based not simply upon the superficial stimulation of innervation. The stimulation of innervation, tone of the eye muscles, blood circulation, regeneration, and enhancement of all other biochemical and bioelectrical processes in the body are based upon the structural efficacy of Polarized Holography, which centers and focuses chromosomes, and prevents the transformation of metacentric chromosomes into acrocentric chromosomes.

The modulation via secondary holographic signals (see above) allows for the emergence of the most coherent and sophisticated scalar wave diffraction grating that produces the more clear zero focus within the wave crystal (of a wave torus on every level from the atomic, subatomic to cellular and molecular levels).

The modulation occurs through the designated areas of Iris, each one corresponding to a specific organ in the body. As a result, the user achieves the stimulation of the projection zones in the Iris, each one being connected to a specific organ in the body.

In addition, **TESLA GLASSES** use the same effect as the binaural therapy. Binaural therapy uses the stereo effect, when signal in one ear gets into the brain with delay in relation to signal in the other ear. This produces the emergence of the complex scalar wave diffraction grating in the skull, based upon Kozyrev Mirror principle (polarization, refraction and emergence of the zero center of the wave crystal). Similar to this, **TESLA GLASSES** use the stereo effect of color signal, when color signal in one eye gets into the brain with delay in relation to signal in the other eye.

Ophthalmologists have found that all healthy people have rhythmic alternation visual perception. Man sees in turn by the right eye, and, then, by the left eye at regular intervals.

These intervals last for 2-3 seconds. The research was conducted using modern 3D technologies. And if one eye is covered by a blue filter, and the other eyes is covered by the red filter, the healthy person sees both colors simultaneously and separately. The left eye sees 20% of the image, and the right eye sees 80% of the image.

With age, these rhythms get broken. But the

BASIC TESLA GLASSES

MANUAL FOR TESLA GLASSES (ADVANCED MODEL AND BASIC MODEL)

restoration of the "biological clock" is possible using Polarized Holography, modulated by color signals, with the frequency of the brain of a healthy person. And, as the positive effect, we can achieve a significant rejuvenation of the body.

THE EFFECTIVENESS OF THE METHOD IS HIGH

- Relieving stress is approaching 99%;

- Short-sightedness - 96%

- Glaucoma - 83%

- Initial cataract and hyperopia up to 78% improvement

- Normalization of blood pressure and sleep

COURSE OF TREATMENT

3-4 procedures per day (4 min per procedure.). Full course is 21 days. The number of procedures and the color are selected individually.

SATISFIED USERS

The technology is used by the Russian Strategic Missile Forces, Law Enforcement Agencies - the Interior Ministry, the Federal Security Service, Ministry of Emergency Situations and such Resorts, as "Moscow", "Rescuer", "Arkhangelsk", "Blue River" and UDP "Rus" in Sochi.

THE DEVICE IS ALSO USED BY:

Russian Medical Academy for the Post Graduate Education of the Russian Ministry of Health

Research Institute of Traditional Treatments of the Russian Ministry of Health

Institute of Normal Physiology named after Anokhin

Russian Academy of Medical Sciences

Russian University of Peoples' Friendship

Clinical Psychiatric Hospital №15 in Moscow

Central Military Hospital of Russian Strategic Missile Forces of Russian Ministry of Defense

Central Military Clinic of Russian Strategic Missile Forces of Russian Ministry of Defense

Children's Clinic #130 in Moscow

Central Clinic #17 of Russian Ministry of Defense

The sanatorium "Green Grove", etc.

DESCRIPTION OF THE DEVICE

The device **TESLA GLASSES** is a psi-generator (psychotronic generator) / Quantum Biocomputer designated for individual use at work and at home for correction and enhancement of various physical and mental functions, including the improvement of vision, using color as a natural integrator of psychological, mental and psycho-physiological processes. The device has eleven corrective programs with manual setting mode. The impact on the body is carried out not only with a certain color, but also via the rhythm of supplying the light pulses coupled with their modulation, thereby accelerating the process of recovery of the human body.

The device consists of dark goggles frame (124013. GOST R) and the electronic board mounted on the inside of the glass of the frame. The electronic board has two (for each eye) Light-Emitting Diodes consisting of six LEDs each, and a control device (two program selection buttons and indicator for the program number).

MAINTENANCE

1. Before using, remove dust from the surface of the glasses with a dry soft flannel.

2. Perform external examination of the glasses and make sure there are no mechanical or other damage.

3. As glasses get dirty (including when they are used by different people), they must be disinfected with 3% solution of hydrogen peroxide by wiping glasses twide with a soft cloth.

4. Replace the batteries, when glasses are switched off, in the following sequence:

4.1. To replace the batteries, unscrew the screw on the inside of the device and remove the electronic board. Batteries are therein in two holders.

4.2. Each holder has three slots, one large - for

THE PHYSIOLOGICAL SIGNIFICANCE OF EACH COLOR

The physiological significance of each color:

RED LIGHT (620 - 760 nanometers) improves vascular tone and activity of tropic hormones, normalizes cardiovascular activity, eliminates stagnation. Exposure to low-intensity red light of 630 nm (Laser or light-emitting diodes) leads to the activation of the drainage system of the eye and entire body; there happens the strengthening of lymphatic drainage for dozens of times! In an experimental model of dystrophic form of myopia, the inventor of **TESLA GLASSES** demonstrated a protective (prophylactic) effect of color on the development of degenerative eye diseases. The use of this color has proved itself in the treatment of myopia, astigmatism, retinal degeneration, strabismus and amblyopia in children.

ORANGE LIGHT (585-620 nanometers) improves blood circulation, digestion, skin trophism, promotes regeneration (recovery) of the nervous and muscular tissue, stimulates the activity of sex glands,

insertion and removal of the batteries, and two small - for pressing through them upon the batteries during their withdrawal.

4.3. Through any of the small slots, reach the battery with the tip of a flat-head screwdriver, and gently squeeze the element out of the holder.

4.4. Insert a new battery into the holder according to the polarity indicated on the holder.

4.5. Install the electronic board back onto the inner side of the frame and tighten the screw. The device is ready to go.

5. All kinds of instrument repairs are made by the company for the additional fee, determined case by case.

SAFETY

Technology is allowed for application by Ministry of Health of the Russian Federation.

- Wide testing is undertaken in the medical departments of the Security Forces.

- More than 10 000 units are in active use, especially by the Military and Security Forces

- Active users amount to 40 000 people.

- The technology is based on 40 years of research.

enhances sexuality, increases the level of neuroendocrine regulation, increases muscle strength. In ophthalmology, orange light is effective in the treatment of amblyopia, myopia, optic nerve atrophy, degeneration of the retina. It is recommended for the elderly.

YELLOW LIGHT (575-585 nm) stimulates the gastrointestinal tract, pancreas, liver, activates the autonomic nervous system, produces a cleansing effect for the entire body. It removes the feeling of tiredness and lethargy. It is effective for amblyopia, strabismus, optic atrophy, retinal dystrophies.

GREEN LIGHT (510-550 nanometers) harmonizes, calms, reduces arterial and intraocular blood pressure, heart rate and headaches, improves the immune system, helps to eliminate toxins. It is effective for glaucoma, spasms of accommodation, retina dystrophy, computer vision syndrome.

LIGHT BLUE LIGHT (480-510 nanometers) calms, has a bactericidal action, lowers blood pressure, headaches and appetite. It eliminates inflammation, and is effective with myopia, spasms of accommodation, and inflammatory diseases of the eyes.

DARK BLUE LIGHT (450-480 nm) has a control action on the pituitary gland, and the parasympathetic nervous system; has antibacterial properties; reduces inflammation and pain. It rejuvenates, enhances creativity and immunity.

It is effective in the treatment of inflammatory diseases of the eye, glaucoma, cataracts, corneal opacities, and vitreous.

VIOLET LIGHT (380-450 nm) has a tonic effect on the brain and eyes, helps produce happiness hormones (endorphins), malatonin. It rejuvenates, enhances creativity and immunity. It is effective with cataracts, uveitis, corneal opacity.

Health correction with the help of light and color is called vibrational healing, the foundations of which the inventor of **TESLA GLASSES** has developed for more than 30 years.

STEVE (60 YEARS OLD): TESLA GLASSES TESTIMONIAL

These Russian glasses are absolutely amazing, I have to say. When I first got them, I was very skeptical. They have a lot of different things that they can do including high blood pressure adjustment, obesity, depression, and a variety of other things. So obviously I could not test out all of these things, but I wanted to test out whether these glasses could help me to reduce the doctor's settings on my reading glasses. When I started, I was using diopter 2.5.

So, I started using the glasses, and after about a week I went down to 2.25, and I could see just as well pretty much. After another 3 to 4 days, I went down to a diopter of two, and, then, after another 3 to 4 days, I went down to a diopter of 1.75. This took a little adjustment so I stayed there for about a week, and, then, I continued to use the glasses, and it went down to 1.5 and, then, I went down to a diopter setting at 1.25. I got busy at that time and could not continue to do the exercises, so I'm still basically at 1.25 after four months, but I do not need the 2.5 at all.

I noticed that my vision is much sharper when reading and now I can actually read music in Church, and also on my iPhone without the glasses at all. It's slightly blurry but I could still do it and, sure, this makes life much more convenient!

There's one other thing that I use these glasses for. Sometimes I will awake in the middle of the night and cannot get back to sleep easily. So I'll put glasses on setting five, which is a blue violet color and usually one session or maybe two, and I'm right back asleep. If I don't do that, I'll be up for quite some time. This is a really nice feature.

So, I can say without a doubt that these glasses really work. Based on the functions that I've tested, I've got good results.

DIRK: TESLA GLASSES TESTIMONIAL

Forget Bates, forget Quertant

Review by Dirk

For years my wife and I have been interested in natural methods of eye/vision improvement, but these glasses top the bill. I have to thank Georg for pointing me to the Wavegenome catologue. After some hesitation (the price!), I decided to go for it, because I stronlgy suspected they would be worth the investment. We have not been disappointed: forget Bates, forget Quertant, these glasses gave us better and quicker results than anything we tried before, and with minimal time investment. My wife was starting to have trouble reading small print, but that is history now, and she won't be buying reading glasses after all. I myself have noticed marked improvement in my myopia. We haven't been able to test every program, but it is already clear to me we will be using these glasses daily, for a very long time. The effects are profound, both on vision and on general wellbeing. To me, 3 minutes of using these glasses is worth taking a nap or meditating for an hour, depending on the program. (I admit being very sensitive) Highly recommended! (Posted on 28/07/2017)

RESULTS OF THE TREATMENT VIA TESLA GLASSES

№	Name of disease	Number of patients	Improvement of functions (in %)	Without dynamics (in %)
	1. Diseases of the eye			
1	Myopia	184	97	3
2	Hyperopia	63	84	16
3	Cataract	104	78	22
4	Glaucoma	65	86	14
5	Strabismus	20	81	5
6	Retinal Dystrophy	71	96	4
7	Wall-eye	12	7	5

2. Diseases of internal organs				
1	Bronchial asthma	32	87,5	12,5
2	Cardiac ischemia	42	88	12
3	Hypertonic disease	64	97	-
4	Urolithiasis disease	21	85,7	14,3
5	Cholelithiasis	24	84,4	15,6
6	Endocrine disorders	35	97,2	2,8
3. Psychoemotional disorder				
1	Depression	37	94,6	5,4
2	Sleep disorder	28	82,8	17,2
3	Neuroses and Neurotic states	31	90,3	9,7
4	Psychasthenia	43	93	7
5	Vascular dystonia	42	88	12

TESLA GLASSES MANUAL

MANUAL

1. Take the device [glasses] in both hands.
2. Find the two buttons and the mode indicator on the inner side of the glasses.

   Right button – (1) switching on and (2) switching modes in ascending order.

   Left button – (1) switching modes in descending order and (2) switching off.

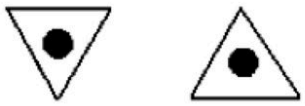

left right

3. Press the right button.

Mode number lights up on the display, from the previous session.

4. To select a different mode, press the right (up) button or the left (down) button.

After 2 seconds, the unit will begin to work.

The session lasts for 3.5 to 5 minutes, after which the device automatically shuts down.

5. For early termination of the program, it is necessary to press the left button.

The device had 12 operating modes:

Key Modes	**Additional Modes**
1 - Orange	7 - Green
2 - Yellow	8 - Orange + Green
3 - Green	9 - Orange + Blue
4 - Blue	0 - Purple + Yellow
5 - Purple	1 or 11 - Violet + Blue + Green simultaneously
6 - Orange	2. – All six colors - (without shutting down)

Selection of modes is carried out individually.

With hyperopia, morning Mode – 1; day mode - 1 or 8; night mode - 4 night and / or 1. Total - 15 minutes a day.

When myopia and glaucoma, the most useful modes are green, blue and purple. 1st course is for 21 days. Then, do a break for 9 days.

PLEASE NOTE:

"0" or "0." is "10".
"1." is "11".
"2." is "12".
The dot designates the next level of performance.

PROGRAMS FOR PSYCHO-EMOTIONAL AND PATHOPHYSIOLOGICAL CORRECTION

	The list of recovery programs programs		
	Morning	Day	Night
Atherosclerosis	1,7	2,7	5,7
Insomnia	1,6	3,7	5
Myopia	8,7	10,7	10
Chronic Bronchitis	1, 7	3,7	10,7
Vegeto-vascular dystonia	1,7	8, 7	5,7
Chronic Gastritis	1	1,6	5,7
Hemorrhoids	2,4	2,7	8,7
Chronic Hepatitis B	2,6	2,7	4,7
Herpes simplex	1,7	8,5	8,5
Hypertension	3,7	3,7	1,7
Hypotension	1,8	1,8	9,7
Hyperopia	1,6	8,7	4,6
Depression	1,6	2,6	5,11
Underweight	1,6	8,6	4,11
Diabetes, Diabetic Angiopathy	1,6	2,10	1,7
Constipation	1,6	2,6	9,7
Goiter simple	1,6	2,10	4,7
Immunodeficiency	1,6	2,4	5,7
Impotence	1,6	1,7	10,7
Cardiac ischemia	1,7	1,7	5,7
Cataract	10,7	10,4	5,7
Chronic Colitis	3,7	2,4	4,7
Computer Syndrome	1,7	11,7	10,7
Chronic Laryngitis	1,4	9,7	4,7
Migraine	1,7	9,4	11
Neurasthenia	3	3,7	11
Neurosis	1,7	3,11	11,7
Obesity	4,10	4,7	11
Osteochondrosis	1,10	5,7	5
Osteoporosis	5,6	5,7	5

Chronic Pancreatitis	1,6	2,7	5,7
Alveolysis	1,7	10,5	5
Bone Fracture	2,6	8,7	10
Chronic Pneumonia	8,6	2,6	5,7
Kidney disease	9,7	9	5,7
Premature Aging	1,6	3,7	5
Presbyopia	1,6	9,7	5
Chronic Prostatitis	1,6	2,7	4
Radiculitis	5	10,7	5
Sleep Disorders	1,7	10,7	5
Chronic Rhinitis	8,7	10	5
Chronic Fatigue Syndrome	8,7	9	1,7
Conditions after Stroke	3,7	10,7	10,7
Brain Concussion	5	10,7	5
Angina	9,7	3,4	5,7
Stress	9,7	10	11,7
Tachycardia	10	7	4
Chronic Tonsillitis	1,7	3,7	4
Chronic Pharyngitis	1,7	3,7	10
Chronic Cholecystitis	9,7	10,7	4,7
Chronic Ischemic Attack	9,7	3,7	10,7
Chronic Erysipelas	1,7	10,7	10

MAIN TECHNICAL SPECIFICATIONS

Value	Value
Dimensions of the device when folded (mm)	160-60-50
The radiation power at the maximum operating pulse (MW)	No more than 40-50
Switching time for the working light pulse from one eye to the other (sec)	0.5±0,2
The time of one cycle of operation, depending on the wavelength of the radiation (sec): - Red LED - Orange LED - Yellow LED - Green LED - Blue LED - Purple LED	 2,5 ±0 5 3±0.5 3,5 ±0 5 4,0 ±0.5 4,5 ±0.5 5,5 ±0 5
The frequency of the intra-pulse modulation (Hz)	9,2±0,2
Continuous working time (hours)	Not less than 24
Power supply (V)	6
Average current consumption (mA)	No more than 2
Device weight (kg)	0,70

HOW TO CHANGE THE BATTERIES FOR TESLA GLASSES

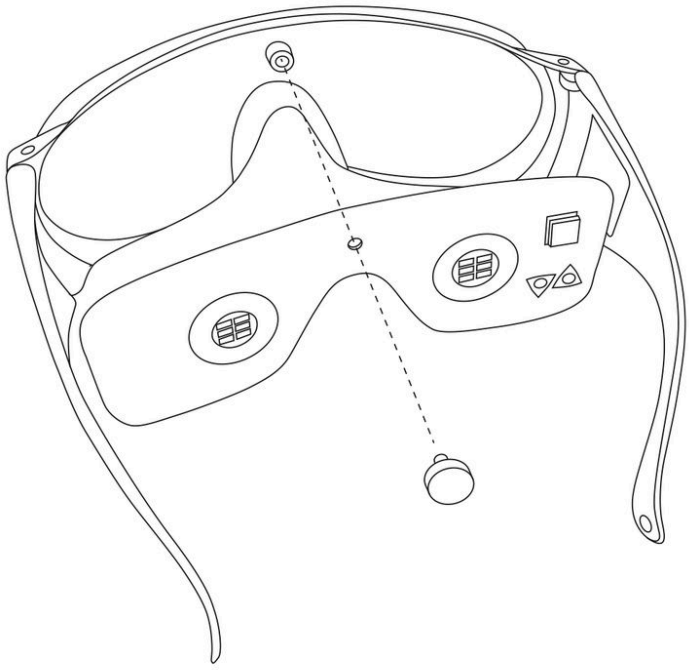

TESLA GLASSES by **WAVE GENOME** use two international standard round batteries, available anywhere in the world. To change the batteries, please unscrew the central plastic screw (see the drawing above). The screw is located in the center of the motherboard. Take the motherboard off the glasses. You will see two round batteries on the left and on the right side of the **TESLA GLASSES.** Please use a screw driver or other long object to push the batteries out of their sockets. Replace them with new ones, taking care of polarity. Screw the motherboard back with the screw.

PRIVACY POLICY (/privacy-policy.html) SHIPPING POLICY (/shipping--warranty.html) RETURN POLICY (/return-policy.html) TERMS OF SERVICE (/terms-of-service.html)

FDA DISCLAIMER: Content on this site is for reference purposes and is not a substitute for advice from a licensed health-care professional. You should not rely solely on this content, and wave genome.com assumes no liability for inaccuracies. Always read directions before using a product. Statements regarding products and services have not been evaluated by the FDA, and these products and services are not intended to diagnose, treat, cure, or prevent any disease or condition.

Payment in full is due ahead of services. No refunds and returns.

COPYRIGHT NOTICE: Text, graphics, and HTML code on wavegenome.com belong to Irene Caesar, Ph.D., their sole author, and are protected by US and International Copyright Laws, and may not be copied, reprinted, published, translated, hosted, or otherwise distributed by any means without explicit permission from Irene Caesar, Ph.D., and in violation of the International Laws for citing references. Any citation of the wavegenome.com website should be accompanied with the proper reference to Irene Caesar, Ph.D. Any citation exceeding the length, permissible for the reference length by the International Copyright Law, will be considered to be a violation of the International Copyright Law.

© IRENE CAESAR, PH.D., FOUNDER AND SOLE OWNER OF WAVEGENOME 2010-2017 ALL RIGHTS RESERVED

WAVE GENOME (/)

HOME / ГЛАВНАЯ (/)
SERVICES / УСЛУГИ (/SERVICES--105910571051105910431048.HTML)
PRODUCTS / ТОВАРЫ (/PRODUCTS--105810541042104010561067.HTML)
CONTACT / КОНТАКТ (/CONTACT--105010541053105810401050105 8.HTML)

(/wave-pharmaceuticals.html)

(/tesla-generator.html)

(/quantum-clinic.html)

WE OFFER ADVANCED WEATHER CONTROL. BUT WHAT CAN BE NOBLER THAN SAVING LIVES!
(/quantum-clinic.html)

THEORY OF THE QUANTUM INTERNET

DNA is a scaled and refracted scalar wave. Scalar wave nullifies any signal. Thus, information is not received and transmitted by any kind of an external signal – wave, particle or field, even “entangled” particles, or by “resonance”. External signal is only a trigger.

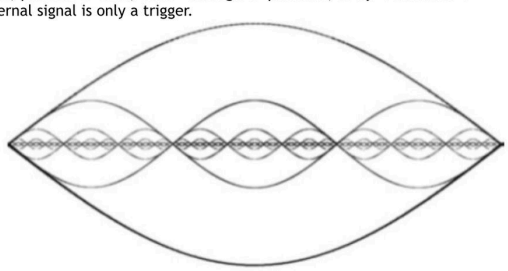

Polarization involutes the external signal. Scalar wave creates the diffraction grating that “sieves” and refracts the particles towards the zero center of the torus. Information is received and transmitted through the zero center of the torus.

(http://www.facebook.com/pages/Wave-Genome/203765456304318?fref=ts) (/wave-genome-russian.html)

SEPTEMBER 2016

IRENE CAESAR'S ARTICLE "QUANTUM GENETICS" IN SEPTEMBER 2016 ISSUE OF "SOCIALIST FACTOR" MAGAZINE (LUCKNOW AND LONDON).

DISPATCH FROM MOSCOW

Irene Caesar

Quantum Genetics

This article is the publication for Irene Caesar's paper "Remote Management of Biosystems Based upon the Shape of Chromosomes as Diffraction Grating for Focusing Genetic Information", delivered as lecture at the Bangkok Thonburi University International Symposium, July 23, 2016, and also published in the proceedings of the Bangkok Thonburi University International 2016 Symposium. For the PDF file of the publication in the Proceedings of the BTU 2016 International Symposium, **c (http://www.wavegenonome.com/2016_BTU Symposium.pdf)lick here (http://www.wavegenonome.com/2016_BTU Symposium.pdf).**

NEWS

LEAKPROOFING THE SINGULARITY: IRENE CAESAR INTERVIEWS ROMAN YAMPOLSKIY (http://www.wavegenome.com/1/post/2013/08/leakproofing-the-singularity-irene-caesar-interviews-roman-yampolskiy.html)

IRENE CAESAR, PH.D.: MATRIX CITY - PUBLIC LECTURE AT THE HARRIMAN INSTITUTE (http://www.wavegenome.com/1/post/2012/10/irene-caesar-matrix-city-public-lecture-at-the-harriman-institute.html)

MORE (/news.html)

MILESTONES

(http://www.thematrixcity.com)

Consortium Agreement

(http://www.thematrixcity.com/) **"MATRIX CITY - city as one integrated wave matrix"**

(/remote-laser-treatment.html)

JANUARY 2014

EXTRACT FROM IRENE CAESAR'S BOOK "WAVE PHARMACEUTICALS"

In the case of **QUANTUM INTERNET**, you send your information **REMOTELY** and **WIRELESS LY**. At the Institute, the laser reads the feedback from your wave matrix in real time, using your digitised wave matrix on record at the Institute.

According to the holographic principle, the universe is holographic, meaning that it is entirely in its every matrix part. The holographic principle has three important implications:

The first implication of the holographic principle postulates the **UNIQUENESS** of every wave matrix. if the universe is entirely in its every matrix point, then, every matrix point is not simply different from any other matrix point, but is unique.

The second implication of the holographic principle postulates the **NON-LOCALITY** of every wave matrix. If the universe is entirely in its every matrix point, then every wave matrix is simultaneously present in the infinite number of dimensions via its tokens. Though there are infinitely many tokens of the same non-local wave matrix, all of them constitute one integrated **SYSTEMATIC WHOLE**.

The non-local holographic nature of wave matrices also means that the wave matrix has the infinite set of waves, particles and fields within its **TORUS** -- from infinitely micro to infinitely macro dimensions. It is impossible to talk of each individual wave matrix as "a specific frequency". And it is impossible to postulate any "medium" of

AUGUST 2016

IRENE CAESAR: HOW TO BUILD MATRIX CITY

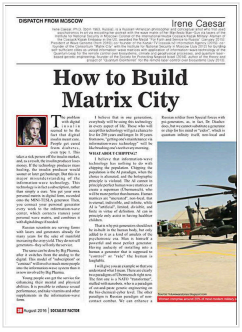
DISPATCH FROM MOSCOW Irene Caesar

How to Build Matrix City

Dispatch from Moscow: Irene Caesar's article "How to build Matrix City" is published in the "Socialist Factor" Magazine, August Issue, 2016, London and Lucknow (capital of Socialist state of Uttar Pradesh, home of Taj Mahal).

The article explains the Subscription Model for E-DRUGS (electronic drugs) and I-DRUGS (Quantum Internet Drugs = Remote Management of Biosystems).

For the PDF file of the publication in the Proceedings of the BTU 2016 Symposium, **click here**. The text was initially published on thematrixcity.com site of the "Matrix City" Consortium, co-founded by Dr. Irene Caesar with Dr. A.N. Diashev, Director of the Institute for National Security in Moscow (2012) (**click here for the full text** (http://thematrixcity.com/structure-of-the-matrix-city-english.html))

JULY 2016

REMOTE MANAGEMENT OF BIOSYSTEMS BASED UPON THE SHAPE OF CHROMOSOMES AS DIFFRACTION GRATING FOR FOCUSING GENETIC INFORMATION

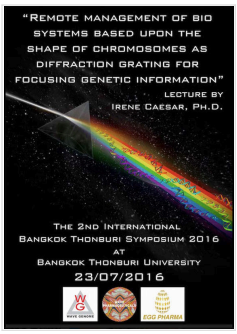

Irene Caesar, Ph.D., President and Sole Owner of Wave Genome, delivered a lecture at the Bangkok Thonburi University International Symposium, July 23, 2016. Irene Caesar's paper was also published in the proceedings of the Bangkok Thonburi University International 2016 Symposium.

For the PDF file of the publication in the Proceedings of the BTU 2016 Symposium, **click here (http://www.wavegenonome.com/2016_BTUSymposium.pdf)**.

Abstract

The same gene gets expressed in dysfunctional individuals by acrocentric chromosome, and in functional individuals by metacentric chromosome, and till now nobody was able to explain why. I claim that chromosome functions as wave crystal, i.e., nonlocal unique wave matrix that focuses genetic information unique to this individual via his / her own unique scalar wave diffraction grating. Thus, chromosome is a structural / geometric code or shape that has holographic nature allowing for the remote management of biosystems via laser polarized holography.

JUNE 13, 2016

REMOTE MANAGEMENT OF BIOSYSTEMS BASED UPON THE SHAPE OF CHROMOSOMES AS DIFFRACTION GRATING FOR FOCUSING GENETIC INFORMATION

Over the span of the 20th century, generations of extraordinary scientists, among whom Russian scientists played a leading role, laid down scientific foundation for the technological revolution of information-wave technology.

MORE (/milestones.html)

(/uploads/3/5/1/1/35112207/5553543_orig.jpg)

Located in the heart of Moscow, the Scientific Research Institute for National Security is fully privatized, and engaged in developing information-wave technology and applying it in medicine, and agriculture. Among clients of the Institute were Russian President Boris Yeltsin, famed American astronaut Edgar Mitchell, and actor celebrity Alexander Kalyagin. The institute has received the Blessing of Patriarch Alexis and Patriarch of Constantinople.

(/uploads/3/5/1/1/35112207/1725599.gif)

Our **MINI-TESLA GENERATOR** is used by Russian Special Forces.

(/milestones.html)

Our **MINI-TESLA GENERATOR** is used by Russian Olympic Team.

its existence, like "scalar wave", "aether", "Higgs / boson field", "torsions", "leptons", etc. There is no specific medium for transferring the information.

The third implication of the holographic principle postulates that there is the **QUANTUM ENTANGLEMENT** in the form of the instantaneous transmission of information between all the tokens of the same non-local wave matrix. The signal that records and transmits the **ENTANGLED INFORMATION** between different wave matrices or between the tokens of the same non-local wave matrix has specific nature. It is **HOLOGRAPHIC**. Only lasers with internal Kozyrev Mirrors can record and transmit holographic signal, based upon the principles of the polarised refraction holography (described in terms of geometrical optics). Thus, the principle of recording and transmitting the **MATRIX SIGNAL** is structural, and not medium-based.

Thus, it is possible to remotely and instantaneously transfer some wave information to a man via the entanglement between his body (at one location) and his photograph (at another location), as two tokens of his non-local wave matrix.

For example, it is possible to remotely lower blood sugar in a diabetic man via scanning his photograph with the laser ray, which is passing through insulin before reaching the photograph.

© Irene Caesar, Ph.D. from her book "WAVE PHARMACEUTICALS" (2014) ALL RIGHTS RESERVED

Irene Caesar, Ph.D.

June 13, 2016

Abstract

The same gene gets expressed in dysfunctional individuals by acrocentric chromosome, and in functional individuals by metacentric chromosome, and till now nobody was able to explain why. I claim that chromosome functions as wave crystal, i.e., nonlocal unique wave matrix that focuses genetic information unique to this individual via his / her own unique scalar wave diffraction grating. Thus, chromosome is a structural / geometric code or shape that has holographic nature allowing for the remote management of biosystems via laser polarized holography.

Keywords

Irene Caesar, wave genome, polarized holography, chromosome shape, metacentric chromosome, acrocentric chromosome, remote control over biosystems, digital drugs, electronic drugs, quantum biointernet, wave pharmaceuticals, diffraction grating, wave crystal, crystalline structure of torus, nanotechnology, nanochips of new generation, remote laser control system, holographic principle, wave matrix, matrix city, structuralist genetics

Introduction

We can conduct remote laser management of the biosystems, and, thus, create individuals with enhanced physical and psychic abilities, and dramatically extend life span, based upon the implication of the holographic principle (© Quantum Biointernet, Irene Caesar 2013), and mastering the geometric codes of chromosomes.

Objectives

The objective is to build a Matrix City, i.e., the self-sufficient human settlement of the Quantum Leap Era (http://www.thematrixcity.com (http://l.facebook.com/l.php?u=http%3A%2F%2Fwww.thematrixcity.com%2F&h=EAQFREpf3AQGZ7Z5MRILBo7ipxt7YhXQmEiLJXvZtMJSytA&enc=AZMfAWYOcFTgmp_h86rnBA_GOIiaPi4peP6I_-b_Z84Ma365SnVN5e5lodNK6vBlzRqK3NXeRSvxodmBQHPwrjehgjpk3tCGch2s8JTmEFLEBHiyDpDOyKTajob8YeuysaXl33BI8l62b4PK2K9Bfb91JWI0tLxnMGRb5yz917gcyw&s=1) and specifically: http://www.thematrixcity.com/structure-of-the-matrix-city-r… (http://l.facebook.com/l.php?u=http%3A%2F%2Fwww.thematrixcity.com%2Fstructure-of-the-matrix-city-russian.html&h=_AQGfkyC8AQExY_Udh8KEuaWZTGrZa54di4E2YogUdvBRyg&enc=AZOUXQl0nOl-v7AzlmwscI6eLKFUkgkoYwq91xokx_pvRMZQ7U34lDem9JMd-uD4L3hKlvU8btXt1rrW8my8NI920ntDwg-tiNzEdQz8XBYEyVtSw8CwUB1g2wYOWBK6t7uUWEyBgGiaPlDv9cEPCbOPHSzuhsdg_2K4urucJz9yig&s=1)), where enhanced man in enhanced environment can have enhanced life of any life span he chooses. The objective includes: (1) creating BANKS OF WAVE MATRICES for every living creature on this planet; (2) creating MATRIX CITY ZONES, where individuals receive all their supplements and medications via E-DRUGS and I-DRUGS from the MATRIX CITY based upon subscription model; (3) cultivating men with enhanced physical, intellectual and psychic abilities.

Review of Related Literature

The Polarized Holography is mainly based upon Russian research, especially upon the research of Nikolai Kozyrev, and his so called “Kozyrev Mirror” principle; the structuralist genetics by Alexander Gurvich; as well as upon the toroidal (“torsion”) research by Anatoly Akimov and Gennady Schipov. In 2002 some information got licked to the West, when two researchers of the NPO “Aura” (NPO “Energy”/BINAR, which became “The Institute for National Security” in 2000) Peter Gariaev and George Tertyshny, who did not have clearance and full access to the research, have brought a laser to Toronto to demonstrate remote management of the artificially induced diabetes via the laser signal at a distance of 20 kilometers in the rats of the same genetic line. But Gariaev and Tertyshny did not have access to the Digital Pharmacy of the digitized bioholograms of healthy bodily organs and physiological systems (aka “Digital Cell”), and could not diagnose wave matrices. The technology was classified at that time in Russia, and got declassified only in 2008.

Conceptual Framework

Universe is holographic, i.e., it is entirely contained in its every matrix point. Since universe is holographic, we can record, transmit and receive only holographic information. The implication of the holographic principle states that, If entire universe is contained in its every matrix point (holographic principle), then, every matrix point is not simply different from any other matrix point, but is unique (implication of the holographic principle, © Irene Caesar 2012). If we have an exact copy of the unique nonlocal wave matrix, we can send information instantaneously through Quantum Nonlocality, from one copy of the unique nonlocal wave matrix to the other copy, to any dimension, any planet, or galaxy, to the past, and to the future.

Research Methodology

The chromosome geometry changes the nature of the external signal from linear to holographic (@ Irene Caesar 2012, implication of holographic principle) via (1) torus polarization (via the change of the spin in the integral toroidal field of DNA); (2) reflection of any external linear signal upon itself and creation of the scalar / standing wave diffraction grating, which neutralizes any external signal; (3) refraction of any incoming signal towards the zero center of the wave crystal, which functions as a focus similar to how our eye functions (Irene Caesar, Chromosome Geometry ©2014).

Quantum Leap technology applying knowledge of the chromosome geometry is called “polarized holography”, and is based upon application of stabilized Helium-Neon Lasers with internal mirrors. This kind of lasers are capable of creating holographic signal. Analogously, our bones are capable of producing stem cells, only because the shape of the bone is analogous to laser tube and is capable of changing the nature of external signal.

Research Results

As of today, the Institute for National Security in Moscow offers the local and remote management of biosystems, and individuals:
(1) via electronic / digital drugs (DIGITAL PHARMACY consisting of digitized biohologrames of wave matrices for every healthy bodily organ and physiological system; and including E-DRUGS [additional upon subscription], of which more than 300 are already created, including E-VYAG-RA and I-VYAG-RA);
(2) via remote laser signal (I-DRUGS or Quantum Biointernet).

Institute has conducted the first in the world official and public remote lowering of blood sugar in diabetic calf via the laser signal at the distance of 20 kilometers for the American Diabetic Association in 1999. Over 2015, the Institute has created the digital platform for dispensation of E-DRUGS and I-DRUGS via subscription analogous to mobile phone subscription programs.

E-DRUGS are offered in two forms: (1) as chips inside a pendant [MINI-TESLA PSI-GENERATOR] of electret nature structured by laser on the nanolevel, and (2) as software program on flash drive sold with a MINI-TESLA PSI-GENERATOR, which contains the entire DIGITAL PHARMACY (soon only by subscription).

Discussion

It is clear that the exiting model of Human Genome is not correct, since it cannot explain 98% of DNA calling it “Junk DNA”. Thus, genetic engineering based upon “cutting and pasting” of “identifiable” 2% of DNA is doomed for failure. Only the Holographic Wave Genetics, based upon chromosome geometry, can explain the difference between functional and dysfunctional individuals, and promote the advance in genetic engineering.

© Irene Caesar 2016 ALL RIGHTS RESERVED

ALL TEXTS © Irene Caesar, Ph.D. 2010-2016 ALL RIGHTS RESERVED

FDA DISCLAIMER: Content on this site is for reference purposes and is not a substitute for advice from a licensed health-care professional. You should not rely solely on this content, and wave genome.com assumes no liability for inaccuracies. Always read directions before using a product. Statements regarding products and services have not been evaluated by the FDA, and these products and services are not intended to diagnose, treat, cure, or prevent any disease or condition.

Payment in full is due ahead of services. No refunds and returns.

COPYRIGHT NOTICE: Text, graphics, and HTML code on wavegenome.com belong to Irene Caesar, Ph.D., their sole author, and are protected by US and International Copyright Laws, and may not be copied, reprinted, published, translated, hosted, or otherwise distributed by any means without explicit permission from Irene Caesar, Ph.D., and in violation of the International Laws for citing references. Any citation of the wavegenome.com website should be accompanied with the proper reference to Irene Caesar, Ph.D. Any citation exceeding the length, permissible for the reference length by the International Copyright Law, will be considered to be a violation of the International Copyright Law.

© IRENE CAESAR, PH.D., FOUNDER AND SOLE OWNER OF WAVEGENOME 2010-2017 ALL RIGHTS RESERVED

WAVE GENOME (/)

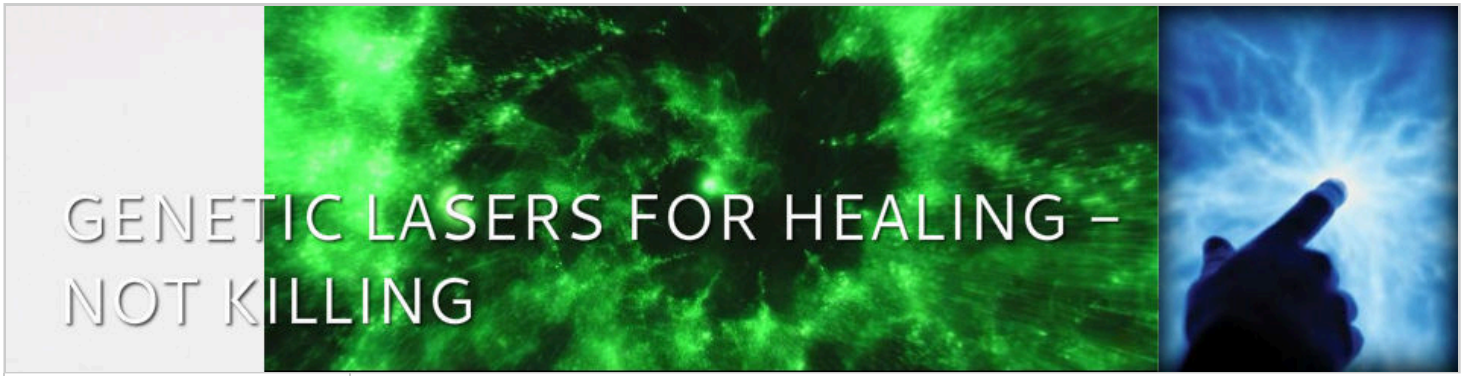

HOME / ГЛАВНАЯ (/)

SERVICES / УСЛУГИ (/SERVICES--105910571051105910431048.HTML)

PRODUCTS / ТОВАРЫ (/PRODUCTS--105810541042104010561067.HTML)

CONTACT / КОНТАКТ (/CONTACT--105010541053105810401050105 8.HTML)

MILESTONES

(/milestones-russian.html)

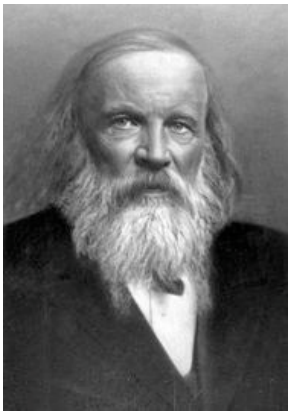

(/uploads/3/5/1/1/35112207/8756602_orig.jpg)

On May 6, 1875, **Dmitry I. Mendeleev** (1834-1907), member of Russian Academy of Sciences, formulated "Suggestions" to the Physical Society at the St. Petersburg University regarding the founding of the Commission for the study of mediumistic phenomena.

(/uploads/3/5/1/1/35112207/6779082_orig.jpg)

In 1902, Russian scientist **Y. N. Zhuk** performed experiments for the telephathic transfer of visual perceptions.

Zhuk was attentively looking at some image, while the other participant of the experiment, who could not see the image, was supposed to reproduce the image that he was getting into his mind on a piece of paper

Out of 189 experiments, 86 experiments(51%) were successful, and the images were identical.

Y.N. Zhuk, Transfer of Visual Perceptions, Kiev, 1902

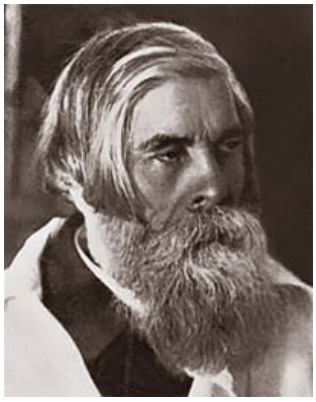

(/uploads/3/5/1/1/35112207/256444_orig.jpg)

Vladimir M. Bekhterev, member of Russian Academy of Sciences, was first to offer the electro-magnetic hypothesis for explaining telepathic phenomena.

(/uploads/3/5/1/1/35112207/5878497_orig.jpg)

It was Russian scientist **Alexander Gurwich** (also: Gurwitsch, Russian, 1874-1954) who created a theory of human bio-field -- biological energy field (1912).

In 1923 he first observed biophotons (http://en.wikipedia.org/wiki/Biophoton) or ultra-weak biological photon emissions; weak electromagnetic waves which were detected in the ultra-violet range of the spectrum.

Gurwitsch named the phenomenon *mitogenetic (http://en.wikipedia.org/wiki/Mitogenesis) radiation* since he believed that this light radiation allowed the morphogenetic field to control embryonic development. His published observations, which related that cell-proliferation of an onion was accelerated by directing these rays down a tube, brought him great attention.

MORE (/alexander-gurwich.html)

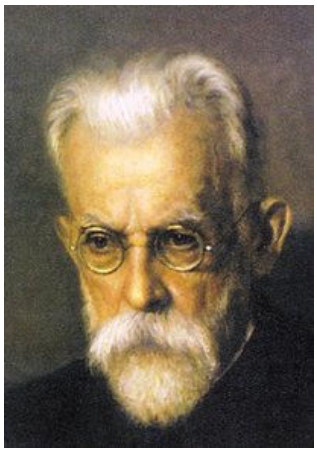

(/uploads/3/5/1/1/35112207/9082120_orig.jpeg)

In **Vladimir Vernadsky**'s (Russian, 1863-1945) theory of the Earth's development, the **noosphere** is the third stage in the earth's development, after the geosphere (inanimate matter) and the biosphere (biological life). Just as the emergence of life fundamentally transformed the geosphere, the emergence of human cognition fundamentally transformed the biosphere.

The word is derived from the Greek νοῦς (nous "mind") + σφαῖρα (sphaira "sphere"), in lexical analogy to "atmosphere" and "biosphere" -- literally, “mind-sphere," or Earth’s mental sheathe -- its energo-informational field. In the words of Kaznacheev and Trofimov (pls see post below): "Living matter possesses a ‘mysterious’ information potential in the so-called "Kozyrev's pace" (holographic and non-local quantum vacuum) where it evolves, self-reflects, and echoes the evolution of the universe and where it is reproduced by a flow that constitutes evolution itself — the Nomogenesis described by L.S. Berg and V.I. Vernadsky."

Vladimir Vernadsky, *T*he Biosphere,1926

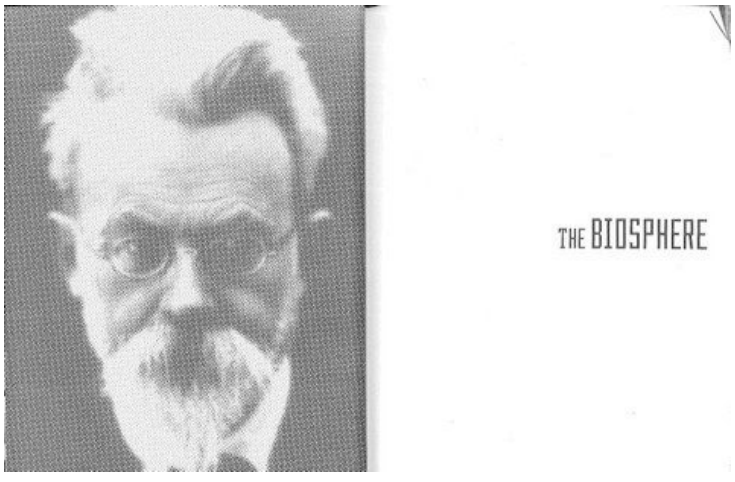

(/uploads/3/5/1/1/35112207/1280987_orig.jpg)

(/uploads/3/5/1/1/35112207/2774182_orig.jpg)

Bernard B. Kazhinski (1890-1962) was a Russian scientist (electrical engineer) of the Soviet era, who pioneered the reserch in the field of biological radio.

"Bernard Kazhinski (Russian) was to be styled as an "electro-technologist" specializing in studying the electrical nature of the human nervous system. It is well worth noting here that the electrical nature of the human nervous system did not in the West become even a somewhat accepted scientific topic until the 1980s. By 1923, Kazhinski had collected facts and had come to the conclusion that the human nervous system IS capable of reacting, by means unknown, to stimuli not accessible to the normal five senses" (Ingo Swann).

B.B. Kazhinksi, Transfer of Thoughts, Moscow, 1923

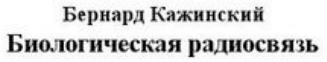

(/uploads/3/5/1/1/35112207/8510299_orig.jpg)

(/uploads/3/5/1/1/35112207/771948_orig.jpg)

Vladimir L. Durov (25 June 1863 - 8 August 1934) was a famous Russian animal-trainer and zoo-psychologist, who created a technique of using radio waves for TELEPATHIC training of animals in collaboration with Vladimir Bekhterev, not less famous Russian neuroligist. The results were so impressive that Russian Emperor Nikolai II ordered a unit of 20 combat seals in 1915. Almost a century later, Americans used the same technique. Durov actively helped B.B. Kazhinski organize his experiments.

At the time of Durov's death, the number of experiments for the telepathic training of animals through the use of radio waves has exceeded 10 thousand. In his book "Training animals", V.L. Durov explains his technique of telepathic control over animals via the mental transmitting of tasks to animals (according to Kazhinski's theory of mental radio) for animal's movements, for the number of actions of barking or sneezing and other actions of a dog, which were determined in a mental order of a trainer.

V.L. Durov, Training Animals, Moscow, 1924

(/uploads/3/5/1/1/35112207/1495502_orig.jpg)

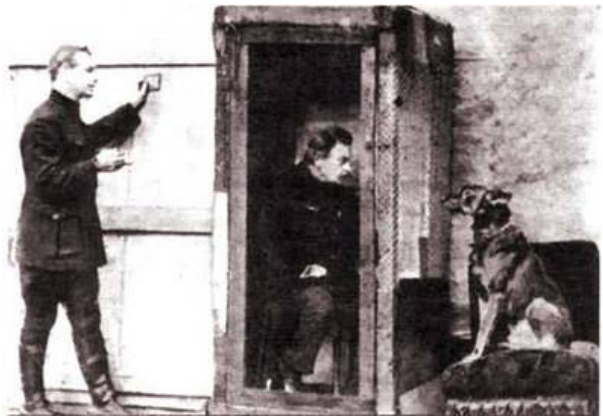

(/uploads/3/5/1/1/35112207/3345587_orig.jpg)

(/uploads/3/5/1/1/35112207/8224886_orig.jpg)

Georges Lakhovsky (1869 in Russia-1942 in NY) was a Russian scientist extraordinaire who demonstrated that living cells emit and receive electromagnetic radiations at their own high frequencies. He invented and used the Multiple Wave Oscillator for the successful medical treatments, including the treatment of cancers.

In 1925 Lakhovsky wrote a Radio News Magazine article entitled "Curing Cancer With Ultra Radio Frequencies." In 1929 while in France he wrote a book "The Secret of Life: Electricity, Radiation and Your Body" (French) in which he claimed and attempted to demonstrate that good or bad health was determined by the relative health of these cellular oscillations, and bacteria, cancers, and other pathogens corrupted them, causing interference with these oscillations. It was translated to English in 1935. Numerous depictions pictured in the book supposedly have Lakhovsky in a Paris, France hospital conducting clinical research treating cancer patients with before, during, and after photographs.

MORE (/georges-lakhovsky.html)

(/uploads/3/5/1/1/35112207/1790241_orig.jpeg)

Wolf G. Messing (1899-1975) was a famous psychic, born in Poland, who lived in Russia from 1939. He possessed unique abilities in telepathy, clear vision and psychic suggestion. He gave public performances, during which he demonstrated his psychic abilities.

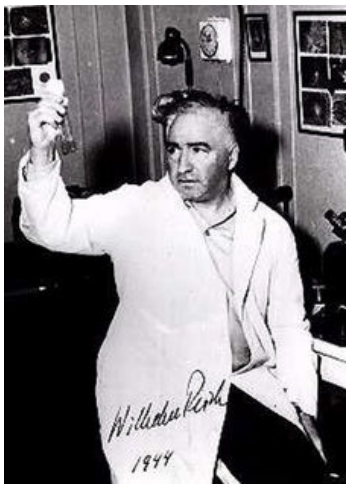

(/uploads/3/5/1/1/35112207/1795325_orig.jpg)

Wilhelm Reich (1897-1957) invented the "orgone accumulator" (orgone being life force, described by ancient greeks as Eros) and tube-like devices sometimes dubbed "cloud busters" for sending earth energies into the clouds to control weather patterns. Medical experiments revealed that sitting in an accumulator enhanced the curative powers of a patient's own life force. Physical experiments also proved that orgone energy could run an electric motor. It was the discovery in about 1941 that the accumulation of orgone energy had natural healing powers, that got Reich in trouble. The court ruled that "all books and all journals, in which the word orgone is used, should be burned." Reich began working with Dr. Michael Silvert on his cloud buster in Arizona. Silvert, a psychiatrist and student of Reich, decided to defy the court. Without Reich's permission or knowledge, Silvert moved the accumulators and books from Maine, where they were to be destroyed, to an empty store in Greenwich Village. In doing this he broke the injunction. Both men were sentenced to prison. Silvert committed suicide and Reich died in prison of heart failure. If Reich's "accumulators" of Vril had really worked, he was A TARGET # 1 for Ahnenerbe. HIs was the solution for the Vril-flied spaceships.

(/uploads/3/5/1/1/35112207/8393915_orig.jpg)

Royal Rife (1888-1971) invented a microscope powerful enough to identify cancer cells and then invented a sound frequency machine that destroyed them. Rife's labs were mysteriously destroyed by an arson fire as were offices and labs of other scientists who heard of Rife's work and attempted to duplicate his machine. All of the papers were lost. Dr. Milbank Johnson, former president of the Southern California AMA, who supported Rife, was fatally poisoned and his papers lost. Rife was killed in 1971 by an "accidental" lethal dose of Valium and alcohol while he was a patient at Grossmont Hospital.

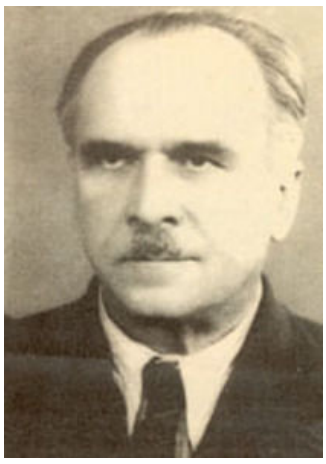

(/uploads/3/5/1/1/35112207/1048030_orig.jpg)

Leonid L. Vasiliev (1892-1966) was a Russian scientist, member of Russian Academy of Medical Sciences, head of the physiology department of the Leningrad University, who pioneered the research in the field of psychotronic control.

L.L. Vasiliev, Psychic Suggestion at a Distance, Moscow, 1962

(/uploads/3/5/1/1/35112207/905281_orig.jpg)

In 1960, Russian factory of plastic goods in Bakov, started production of condoms, which became known to Soviet citizens as "Item #2". Condom's packing had a sign: "tested by electronics". Electronics tested not the plastic itself, but the spectrum of electro-mageneric radiation produced by sperm. Factory produced "Item #2" with different filter: red, yellow, and green. Condom's producers tried to lower the risk of transmitting to woman's genome the information that was radiated by sperm in the form of bio-field during casual sex.

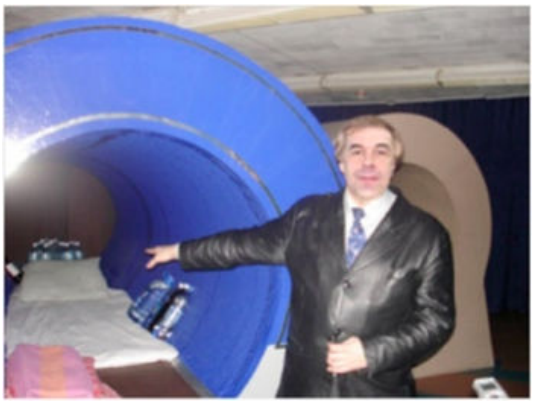

(/uploads/3/5/1/1/35112207/9954027_orig.png)

Among Trofimov and Kaznacheev's conclusions are:

1) our planet's electromagnetic field is actually the "veil" which filters time and place down to our everyday Newtonian reality — enabling us to have the human experience of linear time,

2) in the absence of an electromagnetic field, we have access to an energy field of "instantaneous locality" that underlies our reality,

3) that the limiting effect of the electromagnetic field on an individual is moderated by the amount of solar electromagnetic activity occurring while that person was in utero, and

4) that once a person has accessed these states, his or her consciousness remains so enhanced

"As we investigate brain activity — either with an electro-encephalogram, or by assessing brain functions like intellect level, memory, and other functions, we realize that we currently use only 5% of the capacity of our brains throughout our whole lives. And then, after we spend some time inside the apparatus ("cosmobiotron" clinical device) — in a space without magnetism — we repeat the same tests, and we see a drastically different picture. We see that our mind's additional reserves and abilities are activated. We see an increase in memory capacity, increased IQ, and changing zones of electric activity of the brain" (Alexander V. Trofimov, MD, General Director of the International Scientific Research Institute for Cosmic Anthropo-Ecology, founded in 1994 and located in Academic City, Novosibirsk, Russia in his interview "Kozyrev's Mirrors" with Carol Hiltner.)

(/uploads/3/5/1/1/35112207/7624998_orig.jpg)

Dr. Johnjoe McFadden, the author of "Quantum Evolution" (2000) and professor at the University of Surrey in Guildford, UK, explains that the principle of random selection in the Darwinian theory of evolution is insufficient for explaining the apparent and non-random response of the cell to the environment via the increase of the mutation rate.

(/uploads/3/5/1/1/35112207/7309397_orig.jpg)

A Noble Prize Laureate, **Luc Montagnier** filed for a U.S. patent on the technology of detecting phantom replica of DNA in water. Essentially, DNA Replication at a Distance– reported by Nobel scientist builds on research first published in 1992 by Russian scientists Peter Gariaev and Vladimir Poponin.

The claim of Montagnier's team is that the radiation generated by DNA affects water in such a manner that it behaves as if it contained the actual DNA. This claim is made 20 years after the similar findings of Dr. Peter Gariaev, based on a more advanced technology of torsion lasers.

The E/M coil that Luc Montagnier has used for DNA teleportation is significantly more primitive than red HeNe lasers and other equipment used by P.P. Gariaev and A.N. Diashev.

In 2011, Montagnier has taken a new position at Jiaotong University in Shanghai, China (this university is often referred to as "China's MIT"), where he will work in a new institute bearing his name.

А. Р. Беднев, "Властелин мира", Л., 1929

Ф. Петров, Действие электромагнитного поля низкой частоты на высшую нервную деятельность, "Труды института физиологии им. И. П. Павлова, т. 1, 1959,

Д. М. Спитковский, П. И. Цитлин, В. С. Тонгур, О двух конфигурационных состояниях ДНК и некоторых связанных сними феноменах, журн. "Биофизика", т. V, вып. 1, 1960, стр.3-15

акад. А. В. Леонтович перешел к определению: "Нейрон как аппарат колебательного тока". Измеренные А. В. Леонтовичем средние величины параметров колебаний нейрона как вибратора: (= 1 см; n = 1010 в сек; i = 10-15 амп.; L = 10-13 генри; C=10-13 фарада; R = 1010 ом. Сопротивление R кажется парадоксально ничтожным, что объясняется возникновением собственной ЭДС в цепи возбужденного нерва как колебательного контура.

Л. И. Гуляев. Электрические процессы коры головного мозг а человека, Л., 1960

1. Белоусов Л. В., Гурвич А. А, Залкинд С. Я., Каннегисер Н. К Александр Гаврилович Гурвич. М.: Наука, 1970. 2. Гурвич А. Г. Теория биологического поля. М.: Советская наука, 1944. 3. Гурвич А. и Л. Введение в учение о митогенезе. М.: Изд. АМН СССР, 1948. 4. Сборник работ по митогенезу и теории биологического поля. М.: Изд. АМН СССР, 1947. 5. Гурвич АЛ и Л. Д., Залкинд С. Я., Песоченский Б. С. Учение о раковом тушителе. М.: Изд. АМН СССР, 1947. 6. Гурвич А. Г. Избранные труды / Составители Л. В. Белоусов, А. А. Гурвич, С. Я. Залкинд. М.: Медицина, 1977. 7. Гурвич А. А. Проблема митогенетического излучения как аспект молекулярной биологии. Л.: Медицина, 1968. 8. Гурвич А. Г. Принципы аналитической биологии и теории клеточных полей. М.: Наука, 1991. 9. Казначеев В. П., Михайлова Л. П. Сверхслабые излучения в межклеточных взаимодействиях. Новосибирск: Наука (Сиб. отд.), 1981. 10. Казначеев В. П., Михайлова Л. П. Биоинформационная функция естественных электромагнитных полей. Новосибирск: Наука (Сиб. отд.), 1985. 11. Мостовников Л. И., Хохлов И. В. Взаимодействие клеток человека с помощью электромагнитных волн оптического диапазона. Минск, 1977. 12. Конев С. В. К вопросу о природе и биологическом значении сверхслабых свечений клеток // Биолюминесценция. М.: Наука, 1965. С. 181-185. 13. Конев СВ., Мамуль В.М. Межклеточные контакты. Минск: Наука и Техника, 1977. 14. Шноль С.Э. Физико-химические факторы биологической эволюции. М.: Наука, 1979. 15. Гурвич А. и Л. II Успехи совр. биологии. 1943. Т. 16. С. 305. 16. Белоусов Л. В., Воейков В. Л., Попп Ф.-Ф. Митогенетические лучи гурвича // Природа. 1997. №3. С. 64-80/ 17. Кузин А. М. и Полякова О. И. О ферментативной активности высокоразбавленных растворов ферментов в присутствии аминокислот // [4]. 1947. С. 54-63. 18. Воейков В. Л., Баскаков И. В., Кефалиас К, Налетов В. И. Инициация сверхслабым УФоблучением или перекисью водорода вырожденно-разветвленной цепной реакции дезаминирования глицина // Биоорганическая химия. 1996. Т. 22.№ 1. С. 39-47. 19- Кузин А. М. Стимулирующее действие ионизирующего излучения на биологические процессы. М.: Атомиздат, 1977. 20. Кузин А. М. Идея радиационного гормезиса в атомном веке. М.: Наука, 1995. 21. Кузин АМ. Вторичные биогенные излучения — лучи жизни. Пущино, 1997. 22. Biophotonics. Non-equilibrium and Coherent Systems in Biology, Biophysics and Biotechnology (Proceedings of Intern. Conf. Dedicated to the 120'Л birthday of Aleksander Gavrilovich Gurwitsch (1874-1954). Sept., 28-Oct.? 2 1994) / Eds. L V. Belousov, F.-A. Popp. Russia: Bioinform Services Co., 1995. 23- Кузин АМ. Роль природного радиоактивного фона и вторичного биогенного излучения в явлении жизни. М.: Наука, 2002.

FDA DISCLAIMER: Content on this site is for reference purposes and is not a substitute for advice from a licensed health-care professional. You should not rely solely on this content, and wave genome.com assumes no liability for inaccuracies. Always read directions before using a product. Statements regarding products and services have not been evaluated by the FDA, and these products and services are not intended to diagnose, treat, cure, or prevent any disease or condition.

Payment in full is due ahead of services. No refunds and returns.

COPYRIGHT NOTICE: Text, graphics, and HTML code on wavegenome.com belong to Irene Caesar, Ph.D., their sole author, and are protected by US and International Copyright Laws, and may not be copied, reprinted, published, translated, hosted, or otherwise distributed by any means without explicit permission from Irene Caesar, Ph.D., and in violation of the International Laws for citing references. Any citation of the wavegenome.com website should be accompanied with the proper reference to Irene Caesar, Ph.D. Any citation exceeding the length, permissible for the reference length by the International Copyright Law, will be considered to be a violation of the International Copyright Law.

© IRENE CAESAR, PH.D., FOUNDER AND SOLE OWNER OF WAVEGENOME 2010-2017 ALL RIGHTS RESERVED

WAVE GENOME (/)

LEAKPROOFING THE SINGULARITY: IRENE CAESAR INTERVIEWS ROMAN YAMPOLSKIY (//wavegenome.com/news/leakproofing-the-singularity-irene-caesar-interviews-roman-yampolskiy)

8/6/2013

232 Comments (//wavegenome.com/news/leakproofing-the-singularity-irene-caesar-interviews-roman-yampolskiy#comments)

DR. ROMAN YAMPOLSKIY

Assistant Professor, Director Cybersecurity Lab
University of Louisville, KY
Memberships of Professional Societies:
ACM, IEEE, Tau Beta Pi
Dr. Yampolskiy is an author of over 100 publications (http://cecs.louisville.edu/ry/publications.htm) including multiple journal articles and books.

'I am the slave of the lamp' -- Genie from Aladdin (from Roman V. Yampolskiy paper "Leakproofing the Singularity", 2011)

1. Congratulations on writing your new book "Artificial Superintelligence: A Futuristic Approach" to be completed in January 2014. In your widely publicized 2011 paper "Leakproofing the Singularity ("http://cecs.louisville.edu/ry/LeakproofingtheSingularity.pdf), you have offered to create an AI confinement environment, and even call it a "JAIL" – "Just for AI Location," which should be marked with a Hazard symbol analogous to "Bio-Hazard," "Radiation," and "Magnetic Field". Why do you argue against the idea that after extensive testing in different confinement environments confirming the AI is 'Friendly' (Yudkowsky, 2001) it should be released (Chalmers, 2010)? According to Ray Kurzweil (2005), singularity means that human and artificial intellect merge. So does your AI confinement argument mean that you do not expect singularity to happen? And does it mean that you do not agree with Ray Kurzweil that we need to merge with machines in order to survive the singularity?

AI should never be released because you can never actually confirm that it is friendly, it may simply pretend to be so, until it gains its freedom. A standard definition of singularity is that machines learn to produce the next generation of even smarter machines and that process speeds up to the point of being beyond prediction or understanding. Kurzweil argues that machines and humans will merge and so that will allow us to keep up with accelerating change. I do fully expect singularity to happen, but merging with machines by definition means the end of humanity, we will stop existing as humans and will become machines. Regardless of how you feel about it, you have to agree that it is not a way for humanity to survive singularity.

© WAVE GENOME

Welcome to the technological revolution of the information-wave technologies!

Archives

August 2013 (/news/archives/08-2013)
October 2012 (/news/archives/10-2012)

Categories

All (/news/category/all)
Artificial Intelligence (/news/category/artificial intelligence)
Biorobot (/news/category/biorobot)
Cyborg (/news/category/cyborg)
Internet Of Everything (/news/category/internet of everything)
Internet Of Things (/news/category/internet of things)
Irene Caesar (/news/category/irene caesar)
Irene Caesar Interviews Roman Yampolskiy (/news/category/irene caesar interviews roman yampolskiy)
Leakproofing The Singularity (/news/category/leakproofing the singularity)

2. You proposed Artimetrics as a new field of study for the issues of AI and singularity. Artimetrics should identify, classify and authenticate AI agents, robots, and virtual reality avatars for security purposes (Yampolskiy, 2007; Yampolskiy & Govindaraju, 2008; 2007b, Gavrilova and Yampolskiy, 2010). (209). What are the achievements in Artimetrics so far? What exactly is the AI confinement protocol you propose?

Artimetrics is adaptation of behavioral and physical biometric profiling to virtual worlds and artificial agents. It is a way to track and identify AI software and avatars. It is something practical we can do in the field of AI security before we have actual human level AI developed. As of today we can do facial recognition of avatars and linguistic profiling of chatbots, but it is still an ongoing research project. We are currently working on better ways of telling bots from humans and vise versa.

Proposed confinement protocol is somewhat technical but to explain it simply it is a way to limit AI's communication channel in such a way that it can't sneak any information in or out without being authorized to do so, limiting AI's impact on the real world.

3. In your paper "Leakproofing the Singularity," you proposed the following Secured Communication Protocol with AI: Limited Inputs and Limited Outputs. You have also admitted that besides the DARPA route, Google's AI seems to be the most likely way towards Superintelligence. Can we in principle confine AI if AI is disseminated in the worldwide internet? It seems that to be truly useful, AI should have access and, so, a database, which exceeds the capacity of one human, a group of humans, or even the entire state and humankind. How can we make Google's Oracle's inputs and outputs limited, if its very "superintelligent" status depends upon the access to the unlimited databases? If we use your confinement protocol, based upon limited inputs and limited outputs, can we truly benefit from AI?

Google is always developing new versions of its search algorithm and before making them public they are tested in a restricted environment. So if Google wanted to confine its AI they could. The protocol is flexible enough to allow unlimited input but still limit output so we can benefit from useful information discovered by AI without it having unrestricted influence over us. How beneficial the AI system is does depend on its freedom to communicate, and so we need to find a balance between freedom of communication and security. This is very similar to the problem we face as a nation in choosing between our freedoms and security against terrorism.

4. Do you believe that the worldwide web is secure? What would you say, if you are confronted with the concern that every country should have its own national web with its own AI confinement protocol? Is it possible in principle to confine AI in only one box for the entire planet Earth?

The web is not secure, it was not designed with security in mind. Some countries are starting to develop national sub-internets to exercise better control over the available content. Will same thing happen with AI projects? Possibly. So as many countries/corporations begin to get closer to true AI we will probably see a number of AI boxes set up for testing and further development.

5. In your paper, you say: "Superintelligence is not omnipotent; it is a piece of software capable of looking at all the options it has in a given situation and properly evaluating probabilities for each option" (210). Does this assessment undermine Ray Kurzweil's utopist paradigm of AI, which is capable of becoming the superior (the highest) intelligence in the universe? At the same time, in the same paper, you declare that "Human intellect is no match to that of a superintelligent machine" (204) and is "the best the humanity can do" (206), in support of Ray Kurzweil's promise that AI will get for us the radical life extension and expansion. So what is your ultimate judgment: can self-conscious machines become the highest intelligence in the universe only because they have superior computational abilities?

The short answer is YES. In my opinion superior computational capabilities are sufficient for machines to become a dominant intelligence as we have seen in many restricted domains such as chess. However superior does not mean omnipotent.

6. What would you say if you are confronted with the concern that the "superintelligent" status of Google's AI is a false flag, and essentially, it would be simply the mechanism of manipulating the information, including financial markets through the high-frequency trading, and your confinement protocol would serve in this case as the mechanism of the ultimate alienation of information and ability from those internet users who are denied the access to the AI?

If you mean Google's search engine, I would say it makes no sense. If the develop system that is not intelligent than restricting access to it is completely trivial. If Google wants to limit access to its services to some users they can do so in a very direct way, no need for any confinement protocols.

7. What would you say if you are confronted with the concern that Ray Kurzweil is mistaken about the nature of intelligence. Wavefunction constitutes 96% of reality, and particles constitute only 4%. Some wavefunctions (called scalar waves) are characterized by quantum non-locality in the infinite space and time, meaning not only that they are indestructible, but also that they are uncreated. In other words, these waves coincide with infinity. If we extend quantum physics to humans, and view man as a wavefunction with the scalar waves component, then, we need to account for this uncreated and indestructible wave component in humans. On the contrary, the artificial intelligence (AI) is created and so finite, in virtue of definition. Then it

Matrix (/news/category/matrix)
Matrix City (/news/category/matrix city)
Nick Bostrom (/news/category/nick bostrom)
Peter Gariaev (/news/category/peter gariaev)
Posthuman (/news/category/posthuman)
Ray Kurzweil (/news/category/ray kurzweil)
Roman Yampolskiy (/news/category/roman yampolskiy)
Scalar Waves (/news/category/scalar waves)
Singularity (/news/category/singularity)
Transhumanism (/news/category/transhumanism)

RSS Feed (/1/feed)

seems that no AI would ever be able to supersede or even reproduce a human, because the scalar segment of wavefunction in the human intellect would be beyond its ability to even detect. Even if we use human DNA to create biorobots as DNA computers, the AI will never equal the human access to the infinity simply because the AI will forever lack this uncreated wave module.

WHY? Prove it! Assuming that your claims about wave functions, quantum effects, etc., are true, machines which are potentially made from the same physical matter as humans would have just as much access to those properties and so would have no problem matching or exciding human performance. "…A machine is created, and, so, is finite." Just like a human. I never heard of wavefunctions or scalar waves, etc., but if you can "extend quantum physics to humans," you can just as easily extend quantum physics to robots achieving the same level of performance.

8. Still, if all this is true in regards biorobots as DNA computers, what would you say if you are confronted with the concern that the "superintelligent" status of Google's AI is a false flag, so that Google's AI, Geneva's Financial AI and cyborgs are simply the variant of the depopulation program and the continuation of MK-Ultra program to produce mind-slaves?

I don't understand how the claim that you can't build a true AI system implies a program to control human mind.

9. Since the publication of your paper, IBM, Intel, Cisco, Google and GE made it public that that they are preparing a worldwide launch of the "Internet of Things" or "Internet of Everything". In essence, "Internet of Things" means the following: things acquire a way of interacting with each other without the participation of humans, or, in other words, machines become capable of communicating without human involvement. Things "communicate" between each other through one central AI, which is placed above both things and humans. Cisco advertising of "The Internet Things" has gone live on Channel 63 Headlines News in January 2013. In mid-December 2012, Google has hired Ray Kurzweil as its Director of Engineering. At the end of January 2013, it was made public that Mr. William Ruh, GE software research vice president, is overseeing the investment of $1.5bn to build "Industrial Internet" as the GE sector of the "Internet of Things" in the UK. AI in the "Internet of Everything" is clearly more widespread and has more control over the human reality than Google AI, financial AI, military AI, or industrial AI each taken on its own. AI in the "Internet of Everything" is clearly all these things combined. It is a global control by AI. How your AI confinement protocol would address the "Internet of Everything"?

http://www.v3.co.uk/v3-uk/news/2237727/general-electric-embarks-on-internet-of-things-uk-recruitment-drive (http://www.v3.co.uk/v3-uk/news/2237727/general-electric-embarks-on-internet-of-things-uk-recruitment-drive)

The protocol is designed to be used by the AI developers. If AI emerges from distributed contributions of different internet companies, it would be impossible to contain such AI much like it is impossible to contain information from Internet.

10. You book is about ways to make sure that an AI we construct is safe and beneficial to humanity, how does this compare to dozens of books about AI published every year?

As far as I know AI books currently available on the market talk about how to develop AI and how great it is going to be. I am yet to find a book, which talks about ways to integrate Safety and Security engineering into AI construction process. I know that Oxford philosopher Nick Bostrom is working on a book similar to mine, but it also has not been published as of today.

11. Why did you decide to crowdfund your book?

Essentially the book is currently in the pre-order phase. This will allow me to place an initial order for printed books in a much higher quantify leading to a greatly reduced final cost for my readers. I also provided an opportunity to anyone interested to become an editor for the book, contribute content, offering corrections (http://igg.me/at/ASFA (http://igg.me/at/ASFA)**). This is a very novel approach and I think this will results in greatly improved quality of the book.**

July 2013

Like 4 Tweet

232 Comments (//wavegenome.com/news/leakproofing-the-singularity-irene-caesar-interviews-roman-yampolskiy#comments)

IRENE CAESAR, PH.D.: MATRIX CITY - PUBLIC LECTURE AT THE HARRIMAN INSTITUTE (//wavegenome.com/news/irene-caesar-matrix-city-public-lecture-at-the-harriman-institute)

10/8/2012

112 Comments (//wavegenome.com/news/irene-caesar-matrix-city-public-lecture-at-the-harriman-institute#comments)

Irene Caesar's, Ph.D., lecture "Matrix City" at the Harriman Institute of the Columbia University, September 13, 2012: "Technological revolution of energy-information technologies is here! I would like to invite you to my presentation of a Matrix City built as an integrated energy-information Matrix. The project is the social and political evaluation of the starting-now technological revolution of quantum / resonance sciences, i.e., applying psi-generators in industry, medicine, and agriculture -- the conversion of climate, psychotronic and geo-phisical weapons for the peaceful application in economy. These technologies offer cure or close-to-cure for now "incurable" diseases, and manifold increase in crop yield in agriculture" (Irene Caesar, Ph.D.).

Like 2 Tweet

112 Comments (//wavegenome.com/news/irene-caesar-matrix-city-public-lecture-at-the-harriman-institute#comments)

FDA DISCLAIMER: Content on this site is for reference purposes and is not a substitute for advice from a licensed health-care professional. You should not rely solely on this content, and wave genome.com assumes no liability for inaccuracies. Always read directions before using a product. Statements regarding products and services have not been evaluated by the FDA, and these products and services are not intended to diagnose, treat, cure, or prevent any disease or condition.

Payment in full is due ahead of services. No refunds and returns.

COPYRIGHT NOTICE: Text, graphics, and HTML code on wavegenome.com belong to Irene Caesar, Ph.D., their sole author, and are protected by US and International Copyright Laws, and may not be copied, reprinted, published, translated, hosted, or otherwise distributed by any means without explicit permission from Irene Caesar, Ph.D., and in violation of the International Laws for citing references. Any citation of the wavegenome.com website should be accompanied with the proper reference to Irene Caesar, Ph.D. Any citation exceeding the length, permissible for the reference length by the International Copyright Law, will be considered to be a violation of the International Copyright Law.

© IRENE CAESAR, PH.D., FOUNDER AND SOLE OWNER OF WAVEGENOME 2010-2017 ALL RIGHTS RESERVED

IRENE CAESAR, PH.D. ON HOW TO BUILD MATRIX CITY

SUBSCRIPTION INSTEAD OF MEDICATION

The problem with digital insulin seemed to be the fact that digital insulin meant cure. People get cured from diabetes, even type 1. This takes a sick person off the insulin market, and, as a result, the insulin producer loses money. If the technology produces mass healing, the insulin producer would sooner or later get bankrupt. But this is a major misunderstanding of the information-wave technology. This technology is in fact a subscription, rather than simply a cure. You get your own personal matrix in digital form, recorded onto the MINI-TESLA generator. Then, you connect your personal generator every week to the information-wave center, which corrects (tunes) your personal wave matrix, and combines it with digital drugs if needed.

Russian scientists are serving farms with lasers and generators already for many years for the sake of manifold increasing the crop yield. They do not sell generators - they sell only the service.

The same can be done by Big Pharma, after it switches from the analog to the digital. This model of "subscription" or "contract" will involve much more people into the information-wave system than it is now involved by Big Pharma.

Young people can get the service for enhancing their mental and physical abilities. It is possible to enhance sexual performance, and take vitamins and other supplements in the information-wave form.

I believe that in one generation, everybody will be using this technology in every aspect of life. Those who will accept this technology will get a chance to live for 200 years and longer. In 10 years from now, "getting one's maintenance via information-wave technology" will be like brushing one's teeth every morning.

WHAT ABOUT CHIPPING?

I believe that information-wave technology has nothing to do with chipping the population. Chipping the population is the AI paradigm, when the choice is alienated, and the holographic principle is violated. The AI cannot in principle perfect human wave matrices or create a superman (Übermensch), who will be more perfect than humans. Human matrices are "uncreated", non-local, that is -- eternal, indivisible, and infinite, while AI is "artificial", limited, divisible, and finite in virtue of definition. AI can in principle only assist in having healthier children.

That is why psi-generators should not be in-built in the human body, but only added to it as a kind of

STRUCTURE OF MATRIX CITY

Lasers and generators will constitute the INNER CORE or the NUCLEUS of the Matrix City under the protection of agencies for national security.

The NUCLEUS will consist of concentric circles with centers for the production and conservation of wave matrices.

The center of NUCLEUS will consist in the production of non-fossil fuel generators of energy.

The conservation center will take care of the wave matrices banks for the Matrix Zone.

The NUCLEUS will handle the production of bioactive water, which itself is a generator.

The NUCLEUS will regulate all forms of life in the Matrix Zone, from organism to

amulets of the psychotronic era. Man is himself a powerful and most perfect generator. Having audacity of installing into a human a generator that is supposed to "control" or "rule" the human is laughable.

I will give you an example so that you understand what I mean. There are clearly two paradigms of Übermensch right now. The first one is a NATO "transformer", stuffed with nanobots, who is a paradigm of cut-and-paste genetic engineering on the bio-chemical-cyber level. The other paradigm is Russian paradigm of non-contact combat. We can enhance a Russian soldier from Special forces with psi-generators, as, in fact, Dr. Diashev does, but we cannot substitute a generator or chip for his mind or "eidos", which is quantum infinity itself, non-local and entangled with everything forever.

CULTIVATION OF OPERATORS

The matrix is the energy structure, which has a wave component of indestructible omnipresent nature, i.e., quantum non-locality and quantum entanglement. This infinite wave literally gives life - it heals, increases life span, and gives joy. The point of building Matrix Cities is to have such architecture, agriculture, medicine, industry, energy, education, and all other sides of human life, so that they all have access to this wave component.

That is why the agenda of Matrix Cities would be the cultivating of operators who would be producing wave matrices. This cultivation should be voluntary. And those who do not want to join should be left alone.

species, from bacteria to man.

The NUCLEUS will produce lasers and generators.

Around NUCLEUS, there will be a protective perimeter.

Over the protective perimeter, around the NUCLEUS, there will be concentric circles with housing for operators, their centers for education and cultivation, the Secondary Production Centers, and the Subscription Center.

Matrix City will handle subscription to its service. Service should be provided via personal mini psi-generators, which should be connected to the information-wave system of the Matrix City through the internet at least once a week.

The Secondary Production Centers will consist of farms as agro-factories and industrial park, which will produce all components of information-wave technology -- bioactive construction and industrial materials, wave pharmaceuticals, etc.

MATRIX ZONES

The country should be divided into the Matrix Zones. Each Matrix zone should have its own Matrix City, which would serve its zone with wave matrices.

It looks like, advanced people will gather in special zones which are serviced by the Matrix City, the same way as now those who can are looking for areas with better schools for their children. These zones will be ecologically pure, with bioactive architecture, and bioactive water. These zones should accept everyone who wants to join, independently of money. The only condition should be the acceptance of a connection to the Matrix City. But nobody should be forced to join.

This condition will put down all accusations that Matrix Cities are a new exploitation device and a new segregation device. In fact, Matrix Cities should take care of personal, racial and national uniqueness and survival as much as the rare animal species are protected by the Red Book. DNA wave matrices banks should preserve all the variety of human genome.

SPECIAL CHARTER FOR MATRIX CITIES

Generators and lasers producing wave matrices should be protected by the state and agencies for national security.

Matrix Cities should have their own Charter, i.e., be special, semi-military zones, because ultimately this is a more powerful weapon than nuclear bomb, and, if used peacefully, generators will be more desirable thing than gold.

It is completely clear that without the control from the state and agencies for national security, this technology cannot be commercialized in principle. Matrix City is basically a conversion of psychotronic weapons into peaceful applications in industry, medicine, agriculture, etc.

© IRENE CAESAR, PH.D., MATRIX CITY, ALL RIGHTS RESERVED, 2012

CONSORTIUM CITY MATRIX

The project "City of the Matrix" was approved by the Consortium "The City of the Matrix", the founders of which are A.N. V.E. Prigogine, President of Propaganda Industries.

The consortium "City of Matrix" operates as a closed club on the basis of an agreement on the consortium "City of Matrix" and membership fees. Club members have preferential access to a package of technologies, and to the services and products of consortium members. The goal of the club is to create a non-profit coalition that can contribute to further commercial and production activities of members of the consortium in the way of introducing information-wave technologies.

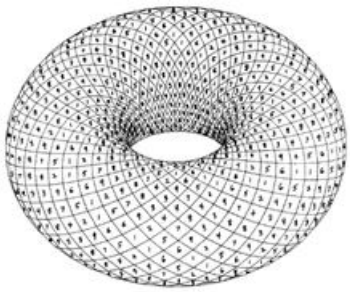

© IRENE CAESAR, PH.D., MATRIX CITY, ALL RIGHTS RESERVED, 2012

WAVE GENOME (/)

HOME / ГЛАВНАЯ (/)

SERVICES / УСЛУГИ (/SERVICES--105910571051105910431048.HTML)

PRODUCTS / ТОВАРЫ (/PRODUCTS--105810541042104010561067.HTML)

CONTACT / КОНТАКТ (/CONTACT--105010541053105810401050105 8.HTML)

TESLA TEST

SOLD WITH THE **SECOND-BIRTH MINI-TESLA PSI-GENERATOR (/second-birth-mini-tesla-psi-generator.html)**

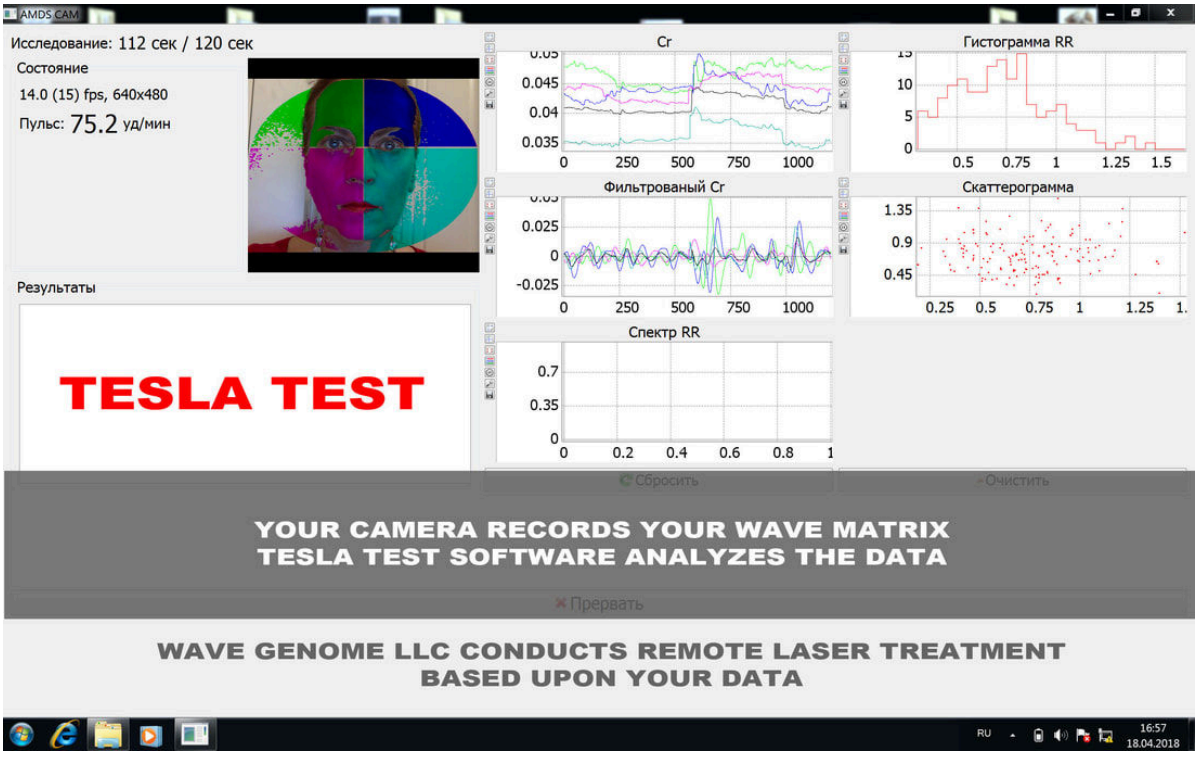

WAVE GENOME LLC made the first in the world commercial offering of the REMOTE LASER TREATMENT in May 2013, before anybody in the field, and presented its project in London to Andrew Charalambous, the Prior of the Byzantine Templars. The Laser reads client's Biohologram, and corrects the deficiencies in the **REFRACTION CODE** of the Wave Crystal / Biohologram. The holographic signal gets instantaneously transmitted to the client via the Quantum Nonlocality.

In January 2018, **WAVE GENOME LLC** launched the **SECOND-BIRTH MINI-TESLA PSI-GENERATOR (/second-birth-mini-tesla-psi-generator.html)**, coded with the Digitized Biohologram of the Embryonic Stem Cell, the most valuable biological information on the global market.

Together with **SECOND-BIRTH MINI-TESLA PSI-GENERATOR (/second-birth-mini-tesla-psi-generator.html)**, we offer the most reliable solution for the **REMOTE LASER MANAGEMENT OF BIOSYSTEMS**. In addition to the diagnostics done by the laser remotely, we offer now the **TESLA TEST** (abbreviation: **TT**) - the most advanced software program for recording and analyzing your WAVE MATRIX. Price is promotional. Commercial value is $20,0i00. **TESLA TEST** adds the layer of reliability and verifiability for the procedure.

TESLA TEST software program makes the camera on your computer record your Wave Matrix, and analyzes the data. **TESLA TEST** produces the **TT REPORT**. Clients emails the **TT REPORT** to **WAVE GENOME LLC**. **WAVE GENOME LLC** uses the **TT REPORT** for the **REMOTE LASER MANAGEMENT** of client's Biohologram.

OPEN FILES ON THE FLASHDRIVE

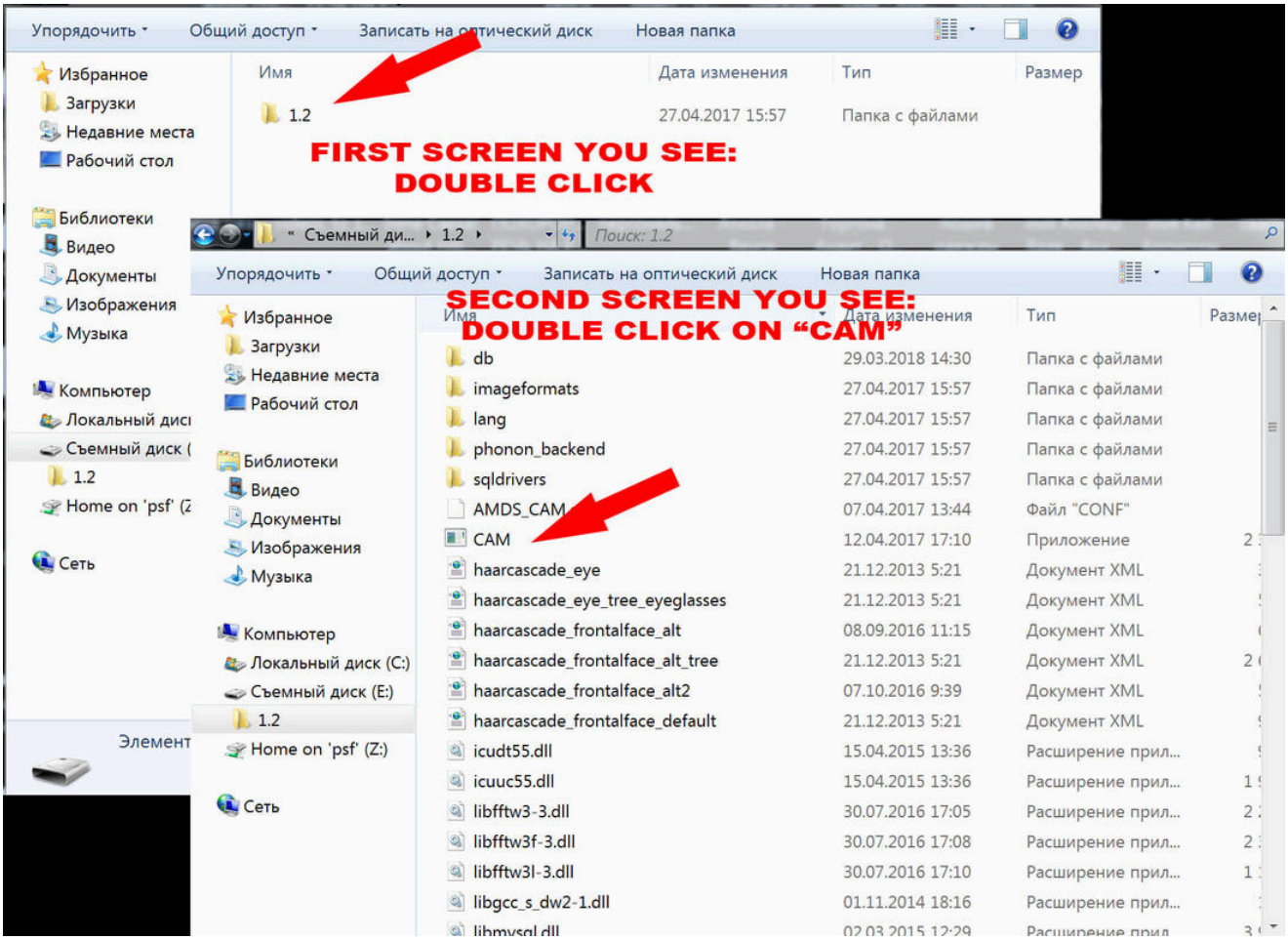

FILL UP THE FORM

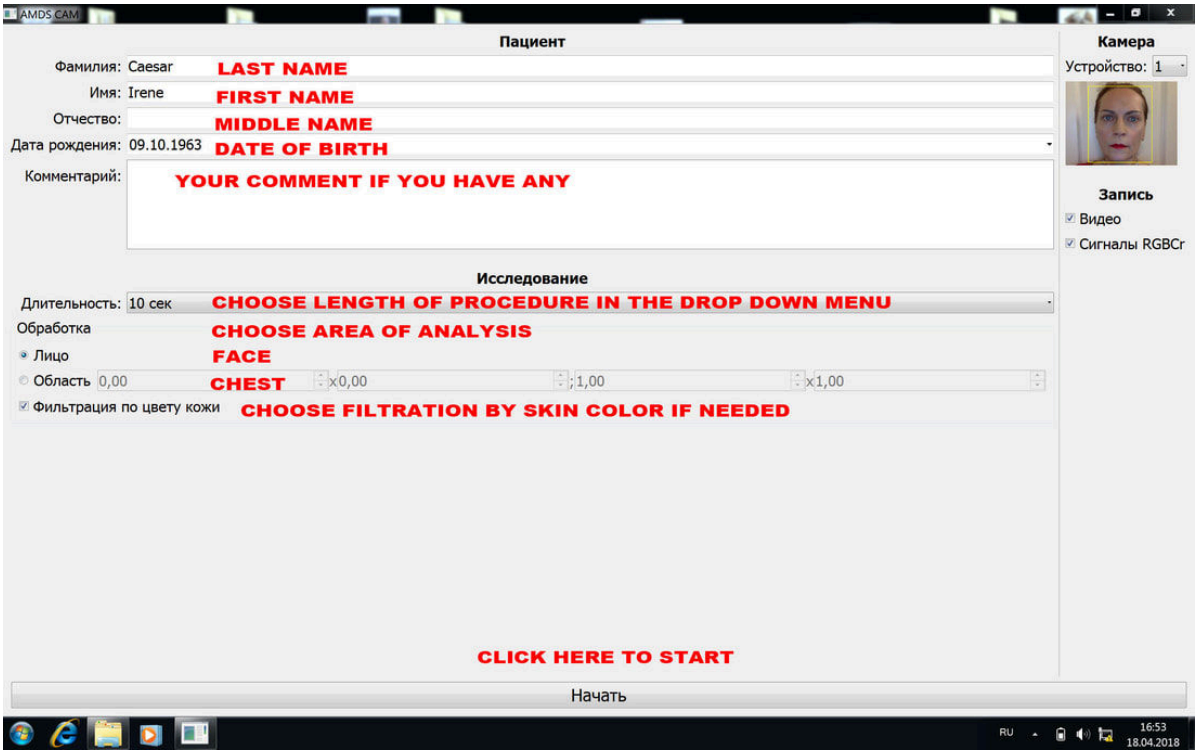

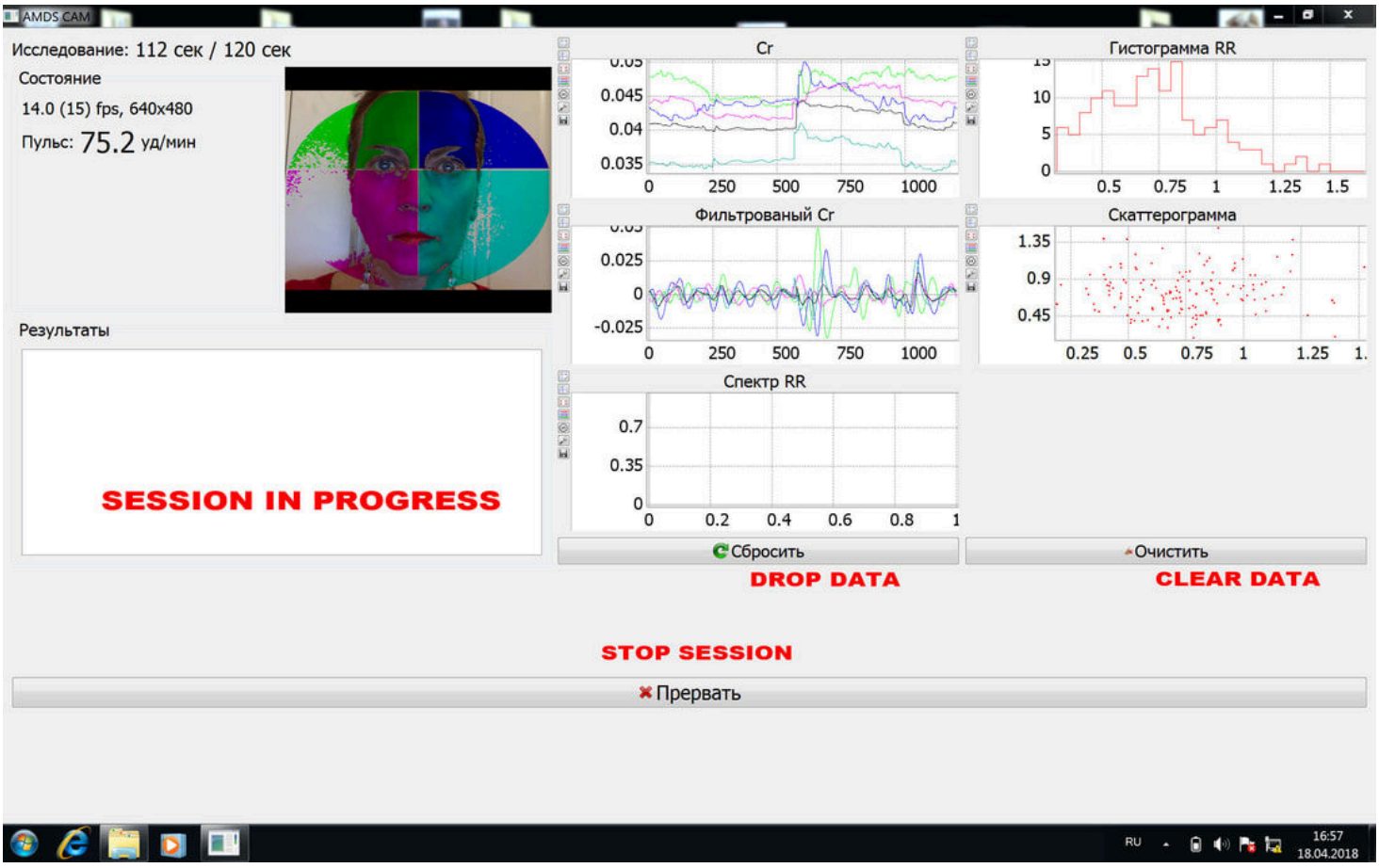

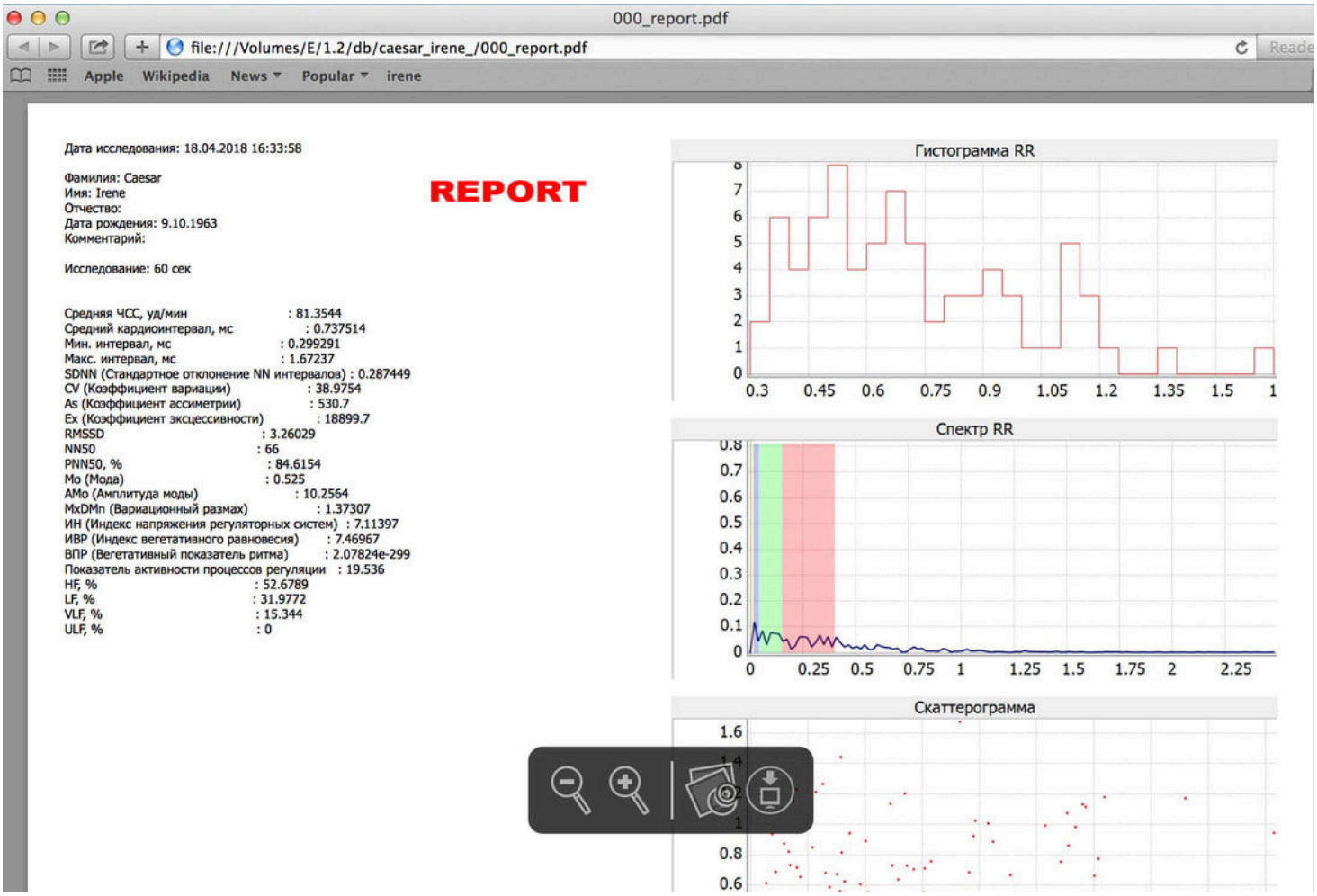

PRIVACY POLICY (/privacy-policy.html) SHIPPING POLICY (/shipping--warranty.html) RETURN POLICY (/return-policy.html) TERMS OF SERVICE (/terms-of-service.html)

FDA DISCLAIMER: Content on this site is for reference purposes and is not a substitute for advice from a licensed health-care professional. You should not rely solely on this content, and wave genome.com assumes no liability for inaccuracies. Always read directions before using a product. Statements regarding products and services have not been evaluated by the FDA, and these products and services are not intended to diagnose, treat, cure, or prevent any disease or condition.

Payment in full is due ahead of services. No refunds and returns.

COPYRIGHT NOTICE: Text, graphics, and HTML code on wavegenome.com belong to Irene Caesar, Ph.D., their sole author, and are protected by US and International Copyright Laws, and may not be copied, reprinted, published, translated, hosted, or otherwise distributed by any means without explicit permission from Irene Caesar, Ph.D., and in violation of the International Laws for citing references. Any citation of the wavegenome.com website should be accompanied with the proper reference to Irene Caesar, Ph.D. Any citation exceeding the length, permissible for the reference length by the International Copyright Law, will be considered to be a violation of the International Copyright Law.

© IRENE CAESAR, PH.D., FOUNDER AND SOLE OWNER OF WAVEGENOME 2010-2017 ALL RIGHTS RESERVED

WAVE GENOME (/)

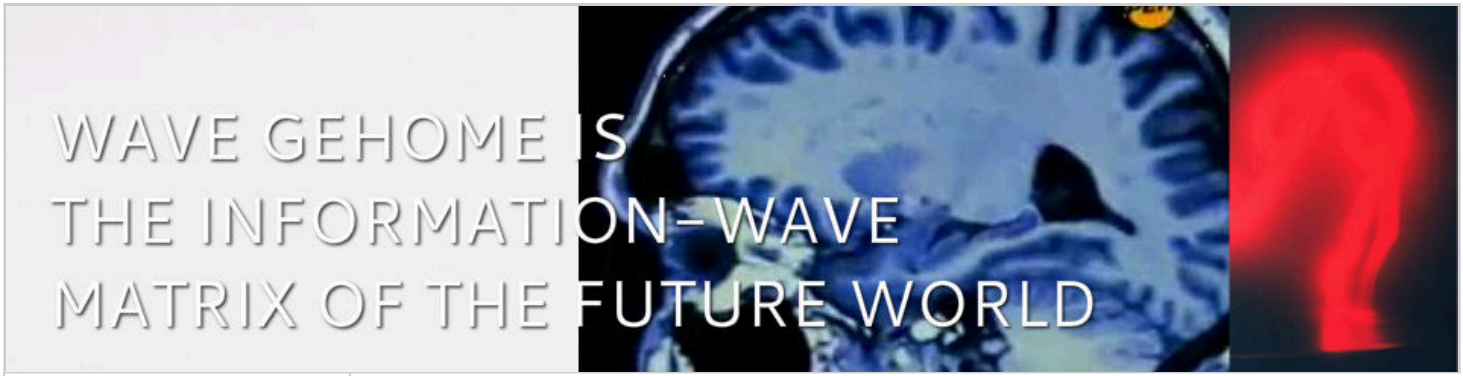

HOME / ГЛАВНАЯ (/)

SERVICES / УСЛУГИ (/SERVICES--105910571051105910431048.HTML)

PRODUCTS / ТОВАРЫ (/PRODUCTS--105810541042104010561067.HTML)

CONTACT / КОНТАКТ (/CONTACT--105010541053105810401050105 8.HTML)

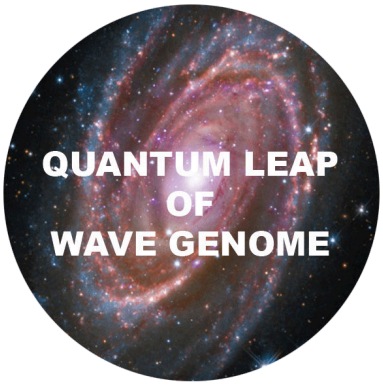

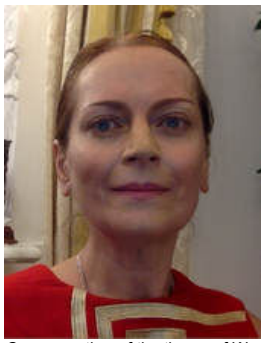

Dr. Irene Caesar, author of the theory of Wave Optics in Chromosomes as Biohology, and author of the technological model for recording and transferring the bioholograms of cells and drugs via refractions codes in the scalar wave diffraction grating; the Head of the group of technical professionals to verify the technological model offered and theoretically substantiated by her.

PRESS RELEASE ON GLOBAL LAUNCH OF THE SECOND-BIRTH TESLA PSI-GENERATOR BY WAVE GENOME

JANUARY 13, 2018

© Irene Caesar, Ph.D., President, Founder and Owner of Wave Genome

Wave Genome is proud to announce its most advanced MINI-TESLA PSI-GENERATOR ever: the **SECOND-BIRTH Mini-Tesla Psi-Generator**.

We called the new chip the "SECOND BIRTH" generator, because the client gets the most valuable biohologrаphic treatment ever for rejuvenation -- the biohologram of the embryonic stem cell. The SECOND-BIRTH Biohologram is available as a chip encoded by laser on nanolevel. The clinical trials were conducted by the Bauman University Medical Center. The clinical trials had demonstrated the radical improvement in the wellbeing of the participants in the clinical trials.

In the **GENERIC SECOND-BIRTH Tesla Generator**, the biohologram of the embryonic stem cell is generic. It is a **DIGITAL CELL**. It is not the biohologram of a specific embryo, but the result of the Embryonic research based upon the Quantum Leap diagnostic of holograms according to the coherence of the geometrical optics in chromosomes.

In the **INDIVIDUAL SECOND-BIRTH Tesla Generator**, the biohologram of the embryonic stem cell is modulated by client's most coherent biohologram, recorded via

Prof. Alexander K. Volkov, Ph.D., Medical Sciences, Director of the Scientific, Medical, Technological and Educational Center of the Bauman Moscow Russian State Technical University, who headed the group of medical professionals to verify the technological model offered by Dr. Irene Caesar.

Prof. Vladimir I. Sinopalnikov, Ph.D. Medical Sciences, The Renowned Physician of the Russian Federaration, Deputy Director of the Scientific, Medical, Technological and Educational Center of the Bauman Moscow Russian State Technical University, who participated in the group of medical professionals to verify the technological model offered by Dr. Irene Caesar.

Scientific, Medical, Technological and Educational Center of the Bauman Moscow Russian State Technical University, in possession of the cutting edge lasers, and other technology.

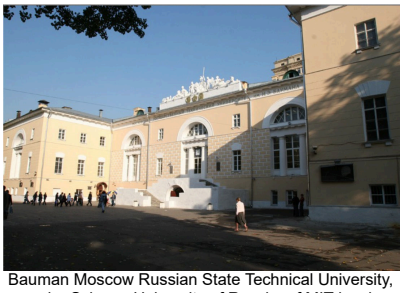

Bauman Moscow Russian State Technical University, major Science University of Russia, of MIT level.

laser from his childhood photograph.

The **INDIVIDUAL SECOND-BIRTH Tesla Generator** is stronger than the GENERIC one, since it has a more precise focus due to the finer / smaller grid of the scalar wave diffraction grating. But you can use the GENERIC one for the entire family, and this is also a great benefit.

If somebody else will wear your own unique **INDIVIDUAL Tesla Generator**, this individual will simply not connect to the focus of your unique biohologram encoded on the chip, since this person has his/her own geometrical code for refraction in the scalar wave diffraction grating of his/her biohologram.

When the modulation is added to the carrier wave in the scalar wave diffraction grating, the resulting hologram is different from these two components taken separately.

In the biohologram, the polarization emerges due to the change of the spin in the integral torsion. Due to polarization, the external signal is reflected upon itself, so that the scalar / standing wave emerges. In the scalar wave, the peak of the forward-going wave is annulled by the trough of the same wave when it is reflected upon itself. Scalar wave creates the diffraction grating, so that any next external signal is refracted towards the focus / zero center of the biohologram (aka “wave crystal”).

Any external signal is only a trigger, and the external signal can be a psychotronic attack. This is a great benefit of the Quantum Leap Laser Polarized Biohologrаphy. The more modulations the biohologram has, the more precise focus / zero center is achieved via refraction, and the better is your protection against the psychotronic attack.

Because the **SECOND-BIRTH Tesla Generator** has the most fine / small / scaled scalar wave diffraction grid among our other generators, the SECOND-BIRTH Tesla Generator provides the most precise focus / zero focus of client’s biohologram and the best defense against psychotronic attack.

Thus, with the **SECOND-BIRTH Chip**, you will experience the most radical rejuvenation effects, including mental and physical enhancement, a more emotional control, and a better defense against psychotronic attacks.

Those of our clients, who already own one of our **MINI-TESLA PSI-GENERATORS**, can either wear both generators together, or carry one of the generators in a pocket, or alternate generators.

NEW GENERATION DIGITAL PHARMACY

SECOND-BIRTH TESLA PSI-GENERATOR (http://wavegenome.com/second-birth-mini-tesla-psi-generator.html) is the **SECOND GENERATION CHIP** (inside a pendant). It comes with the **ADVANCED DIGITAL PHARMACY**, which consists either in **TESLA TEST (http://wavegenome.com/tesla-test.html)** software program (abbreviation: TT) for the **REMOTE LASER TREATMENT (http://wavegenome.com/remote-laser-treatment.html)**, or with the **TESLA HUMAN CELL X (http://wavegenome.com/tesla-human-cell.html)**, as 5 MP3 files of the digitized Biohologrаms of the essential bodily organs and physiological systems encoded as half-audible white noise in the Sacred Mantras, recorded by the new generation laser.

TESLA TEST (http://wavegenome.com/tesla-test.html) software program, is the most advanced way to record and verify client's WAVE MATRIX. **TESLA TEST (http://wavegenome.com/tesla-test.html)** makes the camera on your computer record your Wave Matrix, and analyzes the data. **WAVE GENOME LLC** uses this data for the **REMOTE LASER MANAGEMENT (http://wavegenome.com/remote-laser-treatment.html)** of your Biohologram.

TESLA TEST (/tesla-test.html)

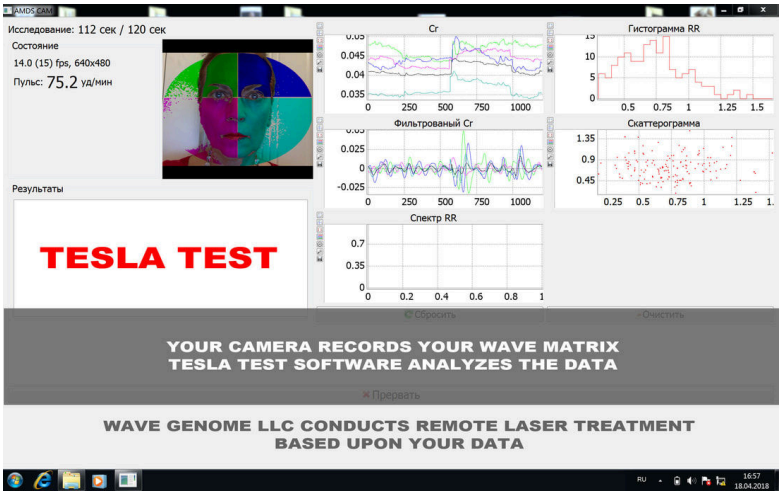

As a promotion, the **SECOND-BIRTH MINI-TESLA PSI-GENERATOR (http://wavegenome.com/second-birth-mini-tesla-psi-generator.html)** is offered with the **TESLA TEST (/tesla-test.html)**software program.

In January 2018, **WAVE GENOME LLC** launched **TESLA TEST**.

TESLA TEST is a software program that makes the camera on your computer record your Wave Matrix, and analyzes the data, $20,000 commercial value.

WAVE GENOME LLC uses this data for the **REMOTE LASER MANAGEMENT (/remote-laser-treatment.html)** of your Biohologram.

Click here to read more. (/tesla-test.html)

WAVE GENOME HAS INTELLECTUAL PRIORITY FOR THE WAVE OPTICS IN CHROMOSOMES AS BIOHOLOGRAPHY

Click here (/diaschev-dipol-di-pol.html) to read on how WAVE GENOME's technology differs from Dr. Gariaev's and Dr. Diaschev's technology (DIPOL or DI-POL Generator).

FDA DISCLAIMER: Content on this site is for reference purposes and is not a substitute for advice from a licensed health-care professional. You should not rely solely on this content, and wave genome.com assumes no liability for inaccuracies. Always read directions before using a product. Statements regarding products and services have not been evaluated by the FDA, and these products and services are not intended to diagnose, treat, cure, or prevent any disease or condition.

Payment in full is due ahead of services. No refunds and returns.

COPYRIGHT NOTICE: Text, graphics, and HTML code on wavegenome.com belong to Irene Caesar, Ph.D., their sole author, and are protected by US and International Copyright Laws, and may not be copied, reprinted, published, translated, hosted, or otherwise distributed by any means without explicit permission from Irene Caesar, Ph.D., and in violation of the International Laws for citing references. Any citation of the wavegenome.com website should be accompanied with the proper reference to Irene Caesar, Ph.D. Any citation exceeding the length, permissible for the reference length by the International Copyright Law, will be considered to be a violation of the International Copyright Law.

© IRENE CAESAR, PH.D., FOUNDER AND SOLE OWNER OF WAVEGENOME 2010-2017 ALL RIGHTS RESERVED

(/)

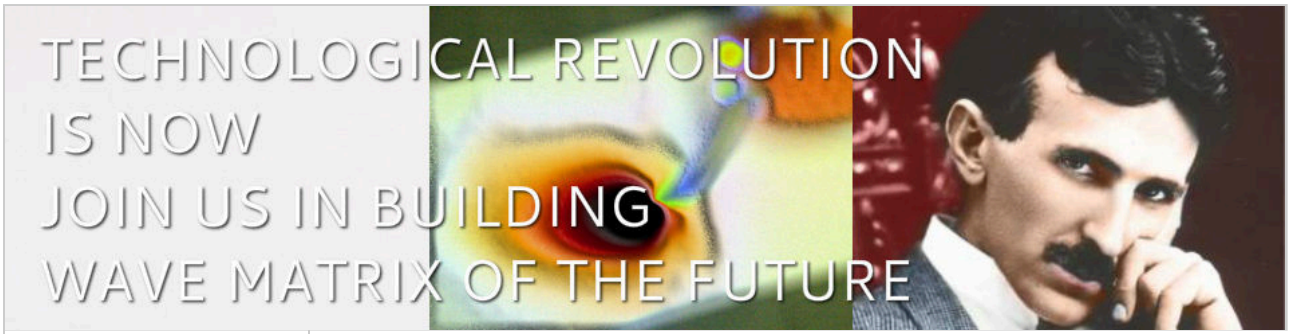

HOME / ГЛАВНАЯ (/)

SERVICES / УСЛУГИ (/SERVICES--10591057105110591043 1048.HTML)

PRODUCTS / ТОВАРЫ (/PRODUCTS--10581054104210401056 1067.HTML)

CONTACT / КОНТАКТ (/CONTACT--10501054105310581040105010 58.HTML)

DIGITAL PHARMACY SOFTWARE

Every **MINI-TESLA psi-generator** comes with:

(1) a **CHIP**, structured with a laser on a nano-level with the wave matrix of healthy human or your own individual wave matrix in childhood (recorded from your childhood photograph), and cased either in pearl or wood;

(2) and psi-program (in English) - a flash drive with the software that has the entire **DIGITAL PHARMACY** with 44 modules generated as the white noise encoded in music for your lifetime and for every system and vital organ in your body.

PRIVACY POLICY (/privacy-policy.html)

SHIPPING POLICY (/shipping--warranty.html)

RETURN POLICY (/return-policy.html)

TERMS OF SERVICE (/terms-of-service.html)

FDA DISCLAIMER: Content on this site is for reference purposes and is not a substitute for advice from a licensed health-care professional. You should not rely solely on this content, and wave genome.com assumes no liability for inaccuracies. Always read directions before using a product. Statements regarding products and services have not been evaluated by the FDA, and these products and services are not intended to diagnose, treat, cure, or prevent any disease or condition.

Payment in full is due ahead of services. No refunds and returns.

COPYRIGHT NOTICE: Text, graphics, and HTML code on wavegenome.com belong to Irene Caesar, Ph.D., their sole author, and are protected by US and International Copyright Laws, and may not be copied, reprinted, published, translated, hosted, or otherwise distributed by any means without explicit permission from Irene Caesar, Ph.D., and in violation of the International Laws for citing references. Any citation of the wavegenome.com website should be accompanied with the proper reference to Irene Caesar, Ph.D. Any citation exceeding the length, permissible for the reference length by the International Copyright Law, will be considered to be a violation of the International Copyright Law.

© IRENE CAESAR, PH.D., FOUNDER AND SOLE OWNER OF WAVEGENOME 2010-2017 ALL RIGHTS RESERVED

Wave Genome – Chromosome Shape and Bioholography by Irene Caesar

Remote management of biosystems based upon the shape of chromosomes as diffraction grating for focusing genetic information

A novel holographic wave genetic approach to informational based medicine, genetics and agriculture

by Irene Caesar of Wave Genome

Irene Caesar, founder of the Wave Genome, combining aspects of Kozyrev's Torsion, Asimov and Shipov's Toroid Dynamics, and Gurvich's Structural Genetics. Some of it seems vaguely analagous to the deeper radionic protocols I have come across. Informational based medicine will be a massively blooming field in the coming years, weening man of its dependency of detrimental chemical cocktails. Wave Genome technology offers another example of the rejuventing technologies based on treating the root informational causes of illness.

Subscribe to Aether Force Newsletter

Email *

Subscribe!

DONATE TO SUPPORT AETHER FORCE

Donate

AETHERIC TOPICS

Privacy & Cookies: This site uses cookies. By continuing to use this website, you agree to their use.
To find out more, including how to control cookies, see here: Cookie Policy

Close and accept

According to Caesar "Chromosomes function as a geometrical code in the liquid media of the living cell, according to the law of geometric optics in holograms. Chromosomes transform the liquid media into the crystallized refracted structure aka "wave crystal". Thus the chromosome is a structural code or shape that has a holographic nature allowing for the remote management of biosystems via laser polarised holography".

Caesars work is independent of Gariaev's studies on Linguistic Wave Genetics. You can learn more here: http://wavegenome.com/diaschev-dipol-di-pol.html.

The services of Wave Genome include a digital pharmacy which can be applied remotely to your digital witness or an agricultural prooject. They also construct tesla psi-generators and vision repair glasses, wearable chips or bio-active water imprinted with your personal hologram.

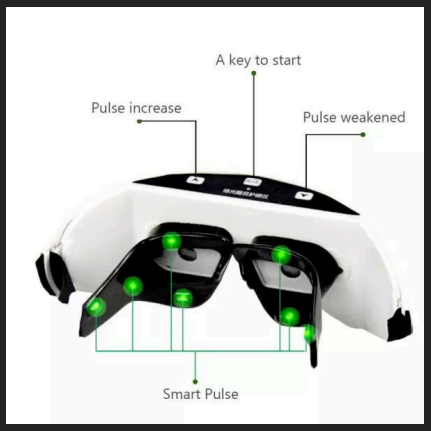

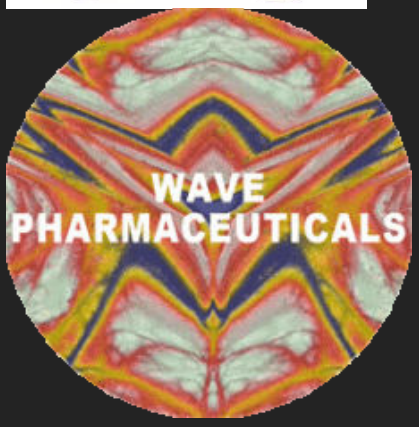

Here is an EXTRACT FROM IRENE CAESAR'S BOOK "WAVE PHARMACEUTICALS"

" In the case of **QUANTUM INTERNET**, you send your information **REMOTELY** and **WIRELESSLY**. At the Institute, the laser reads the feedback from your wave matrix in real time, using your digitised wave matrix on record at the Institute.

According to the holographic principle, the universe is holographic, meaning that it is entirely in its every matrix part. The holographic principle has three important implications:

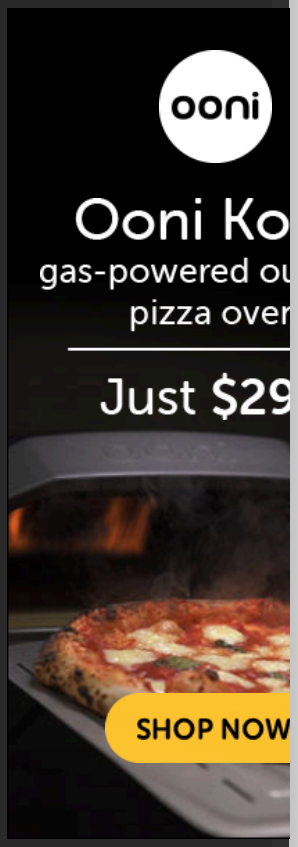

Product categories

Select a category

Aether Shop Products

Aether Force Seeker's

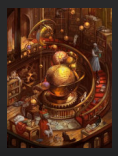

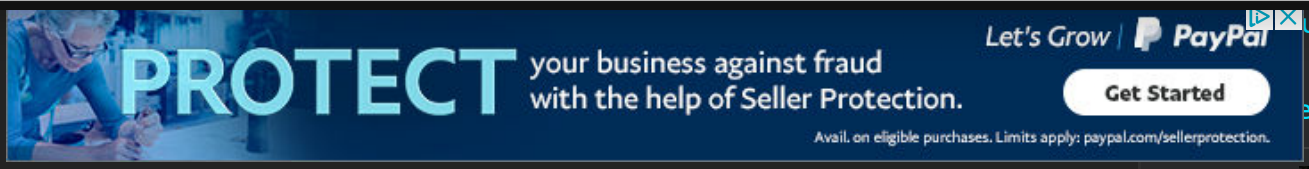

The first implication of the holographic principle postulates the **UNIQUENESS** of every wave matrix. If the universe is entirely in its every matrix point, then, every matrix point is not simply different from any other matrix point, but is unique.

The second implication of the holographic principle postulates the **NON-LOCALITY** of every wave matrix. If the universe is entirely in its every matrix point, then every wave matrix is simultaneously present in the infinite number of dimensions via its tokens. Though there are infinitely many tokens of the same non-local wave matrix, all of them constitute one integrated **SYSTEMATIC WHOLE**.

The non-local holographic nature of wave matrices also means that the wave matrix has the infinite set of waves, particles and fields within its **TORUS** — from infinitely micro to infinitely macro dimensions. It is impossible to talk of each individual wave matrix as "a specific frequency". And it is impossible to postulate any "medium" of its existence, like "scalar wave", "aether", "Higgs / boson field", "torsions", "leptons", etc. There is no specific medium for transferring the information.

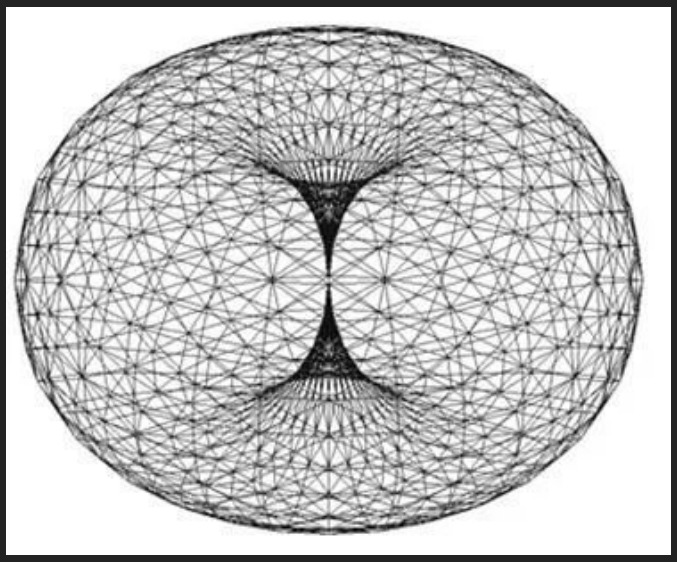

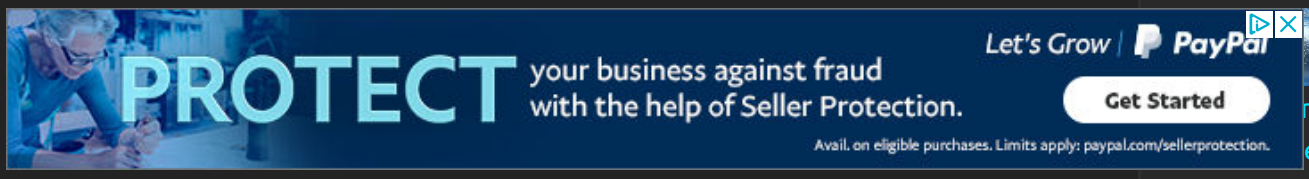

The third implication of the holographic principle postulates that there is the **QUANTUM ENTANGLEMENT** in the form of the instantaneous transmission of information between all the tokens of the same non-local wave matrix. The signal that records and transmits the **ENTANGLED INFORMATION** between different wave matrices or between the tokens of the same non-local wave matrix has specific nature. It is **HOLOGRAPHIC**. Only lasers with internal Kozyrev Mirrors can record and transmit holographic signal, based upon the principles of the

um ~ 2
Hard
e

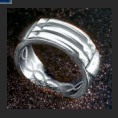

Authentic Atlantis Ring

Scalar
Labyrinth Antennas

Biomat Infrared Amethyst Therapy

SE-5 1000 Radionic Unit

Heart Math Institute

Sympathethic Vibratory Science

Cymatic Therapy
red,
ed,
Energized

Shungite

Aetheric Sciences
Books

polarised refraction holography (described in terms of geometrical optics). Thus, the principle of recording and transmitting the **MATRIX SIGNAL** is structural, and not medium-based.

Thus, it is possible to remotely and instantaneously transfer some wave information to a man via the entanglement between his body (at one location) and his photograph (at another location), as two tokens of his non-local wave matrix.

For example, it is possible to remotely lower blood sugar in a diabetic man via scanning his photograph with the laser ray, which is passing through insulin before reaching the photograph. ”

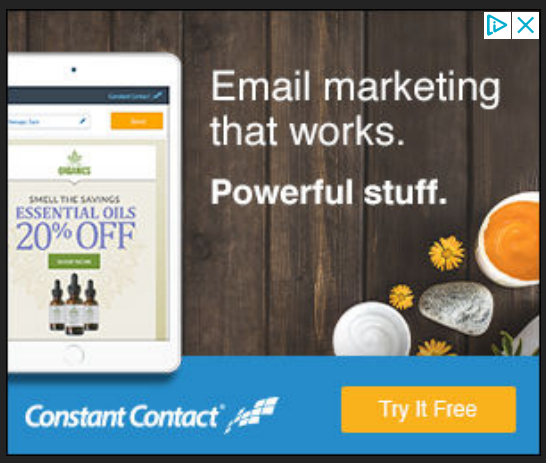

THE FOLLOWING ARTICLE IS SOURCED
FROM: https://irenecaesar.wordpress.com/tag/quantum-biointernet/

Abstract

The same gene gets expressed in dysfunctional individuals by acrocentric chromosome, and in functional individuals by metacentric chromosome, and till now nobody was able to explain why. I claim that chromosome functions as wave crystal, i.e., nonlocal unique wave matrix that focuses genetic information unique to this individual via his / her own unique scalar wave diffraction grating. Thus, chromosome is a structural / geometric code or shape that has holographic nature allowing for the remote management of biosystems via laser polarized holography.

Introduction

Vesica Institute Online Courses

HHO Kits - Run Your Car on Water

Schauberger Vortex Water Revitalizer

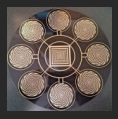

Magnetron Pyramid Symbolic Radionics Instrument

Pyramids & Metaforms

Jivara Water Structurizers

Chi-O Holographic Radionic Devices

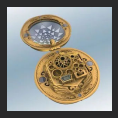

Digital Acupuncture **$27.00**

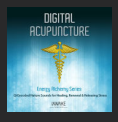

Colloidal Silver **$27.00**

We can conduct remote laser management of the biosystems, and, thus, create individuals with enhanced physical and psychic abilities, and dramatically extend life span, based upon the implication of the holographic principle (© Quantum Biointernet, Irene Caesar 2013), and mastering the geometric codes of chromosomes.

Objectives

The objective is to build a Matrix City, i.e., the self-sufficient human settlement of the Quantum Leap Era (http://www.thematrixcity.com and specifically: http://www.thematrixcity.com/structure-of-the-matrix-city-r…), where enhanced man in enhanced environment can have enhanced life of any life span he chooses. The objective includes: (1) creating BANKS OF WAVE MATRICES for every living creature on this planet; (2) creating MATRIX CITY ZONES, where individuals receive all their supplements and medications via E-DRUGS and I-DRUGS from the MATRIX CITY based upon subscription model; (3) cultivating men with enhanced physical, intellectual and psychic abilities.

Review of Related Literature

The Polarized Holography is mainly based upon Russian research, especially upon the research of Nikolai Kozyrev, and his so called "Kozyrev Mirror" principle; the structuralist genetics by Alexander Gurvich; as well as upon the toroidal ("torsion") research by Anatoly Akimov and Gennady Schipov. In 2002 some information got licked to the West, when two researchers of the NPO "Aura" (NPO "Energy"/BINAR, which became "The Institute for National Security" in 2000) Peter Gariaev and George Tertyshny, who did not have clearance and full access to the research, have brought a laser to Toronto to demonstrate remote management of the artificially induced diabetes via the laser signal at a distance of 20 kilometers in the rats of the same genetic line. But Gariaev and Tertyshny did not have access to the Digital Pharmacy of the digitized bioholograms of healthy bodily organs and physiological systems (aka "Digital Cell"), and could not diagnose wave matrices. The technology was classified at that time in Russia, and got declassified only in 2008.

Conceptual Framework

Universe is holographic, i.e., it is entirely contained in its every matrix point. Since universe is holographic, we can record, transmit and receive only holographic information. The implication of the holographic principle states that, If entire universe is contained in its every matrix point (holographic principle), then, every matrix point is not simply different from any other matrix point, but is unique (implication of the holographic principle, © Irene Caesar 2012). If we have an exact copy of the unique nonlocal wave matrix, we can send information instantaneously through Quantum Nonlocality, from one copy of the unique nonlocal wave matrix to the other copy, to any dimension, any planet, or galaxy, to the past, and to the future.

Popular Aether Force Articles

Stay in
Ad Capella

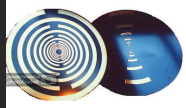
New De
aether-force

Physic
aether-force

IMAGE
aether-force

Vogel a
aether-force

Nikola
aether-force

Beyon
aether-force

Uncle..
aether-force

A Reso
aether-force

Nikola
aether-force

Crystal
aether-force

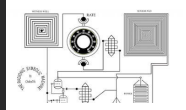
What is
aether-force

Plants
aether-force

Research Methodology

The chromosome geometry changes the nature of the external signal from linear to holographic (@ Irene Caesar 2012, implication of holographic principle) via (1) torus polarization (via the change of the spin in the integral toroidal field of DNA); (2) reflection of any external linear signal upon itself and creation of the scalar / standing wave diffraction grating, which neutralizes any external signal; (3) refraction of any incoming signal towards the zero center of the wave crystal, which functions as a focus similar to how our eye functions (Irene Caesar, Chromosome Geometry ©2014).

Quantum Leap technology applying knowledge of the chromosome geometry is called "polarized holography", and is based upon application of stabilized Helium-Neon Lasers with internal mirrors. This kind of lasers are capable of creating holographic signal. Analogously, our bones are capable of producing stem cells, only because the shape of the bone is analogous to laser tube and is capable of changing the nature of external signal.

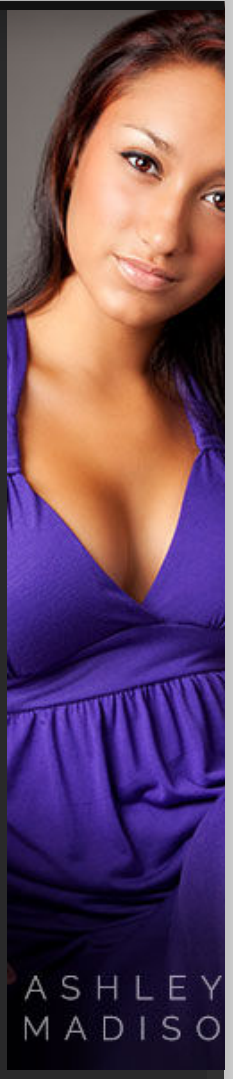

Research Results

As of today, the Institute for National Security in Moscow offers the local and remote management of biosystems, and individuals:
(1) via electronic / digital drugs (DIGITAL PHARMACY consisting of digitized biohologrames of wave matrices for every healthy bodily organ and physiological system; and including E-DRUGS [additional upon subscription], of which more than 300 are already created, including E-VYAG-RA and I-VYAG-RA);
(2) via remote laser signal (I-DRUGS or Quantum Biointernet).

Institute has conducted the first in the world official and public remote lowering of blood sugar in diabetic calf via the laser signal at the distance of 20 kilometers for the American Diabetic Association in 1999. Over 2015, the Institute has created the digital platform for dispensation of E-DRUGS and I-DRUGS via subscription analogous to mobile phone subscription programs.

E-DRUGS are offered in two forms: (1) as chips inside a pendant [MINI-TESLA PSI-GENERATOR] of electret nature structured by laser on the nanolevel, and (2) as software program on flash drive sold with a MINI-TESLA PSI-GENERATOR, which contains the entire DIGITAL PHARMACY (soon only by subscription).

Discussion

It is clear that the exiting model of Human Genome is not correct, since it cannot explain 98% of DNA calling it “Junk DNA”. Thus, genetic engineering based upon “cutting and pasting” of “identifiable” 2% of DNA is doomed for failure. Only the Holographic Wave Genetics, based upon chromosome geometry, can explain the difference between functional and dysfunctional individuals, and promote the advance in genetic engineering.

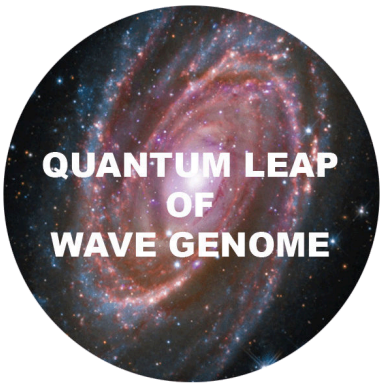

WAVE GENOME HAS INTELLECTUAL PRIORITY FOR THE WAVE OPTICS IN CHROMOSOMES AS BIOHOLOGRAPHY

(/ask-our-maven-russian.html)

Read on how WAVE GENOME's technology differs from Dr. Gariaev's and Dr. Diaschev's technology (DIPOL or DI-POL Generator)

JANUARY 13, 2013

CLIENT'S QUESTION: Irene, I am also wondering if you know of other people working with hologram technology.

DR. IRENE CAESAR'S ANSWER: "It was totally my idea to use biohologrаms of drugs and cells precisely as reconstructed into visible systematic wholes from the holographic signal of the laser.

The term of "Laser Polarized Biohолography" was coined by Dr. Tertyshniy. But he and his collaborator Peter Gariaev did not have the theory of wave optics in chromosomes that I have created as "wave crystal theory" in 1980s and which I have expanded to chromosomes in 2010-2014. That is why, Tertyshniy and Gariaev were recording laser signals via radio receiver in the narrow electro-magnetic range. In 2002 Tertyshniy and Gariaev had split apart, and Gariaev never used the term "Laser Polarized Biohолography". Gariaev is even now selling a crackling sound of a radio receiver. He also uses his laser in the unscreened room, since he does not have the theory of wave optics, and, so, contaminates matrices with the holographic signals of his neighbors and himself. Also, Gariaev and Tertyshniy did not encode electrets via laser. This was suggested by me to my team of scientists. Nobody in the world before my company WAVE GENOME was encoding the biohолograms onto electrets via laser.

DIPOL (DI-POL) generator is invented and produced by Dr. Alexander D. Panchenko, and sold by Dr. Diaschev. DIPOL is a chip made of layers of foil and paper glued together with epoxy resin, according to the official description, almost alike to orgonite. Dr. Diaschev himself does not use lasers, and does not have lasers at his facility. Dr. Diaschev functions as a middle man between various scientists and clients.

WAVE GENOME was the first scientific group in the world that started producing the laser recording of client's biohолogram as proper biohолography, and the laser encoding of the individual biohолogram of the client, recorded from clients's childhood photograph, upon the electret chip, as well as the laser encoding of modulators onto the casing of the chip. WAVE GENOME also produced a new DIGITAL PHARMACY software as the collection of the digitized biohолograms of organs and physiological systems.

In the summer of 2017 I have contracted and financed the laser specialists from Moscow Baumann Russian State University, to bring my project of recording and transferring of biohолograms via laser encoding and laser reading to the new level of scientific standards and verification, and to conduct clinical trials.

You will be able to read it all in my 40-page manuscript, which I was asked to submit to the Genetic Therapy Journal published in San Francisco.

My clinical trials with laser biohолograms were very successful, and I was able to prove my theory of the wave optics of biohолogoraphy in chromosomes as scalar wave diffraction gratings. I created HASPIRIN – the digitized biohолogram of aspirin, and verified it in clinical trials. Also, I have created the EMBRYONIC STEM CELL BIOHOLOGRAM (Second Birth Chip) - and verified it in clinical trials."

FDA DISCLAIMER: Content on this site is for reference purposes and is not a substitute for advice from a licensed health-care professional. You should not rely solely on this content, and wave genome.com assumes no liability for inaccuracies. Always read directions before using a product. Statements regarding products and services have not been evaluated by the FDA, and these products and services are not intended to diagnose, treat, cure, or prevent any disease or condition.

Payment in full is due ahead of services. No refunds and returns.

COPYRIGHT NOTICE: Text, graphics, and HTML code on wavegenome.com belong to Irene Caesar, Ph.D., their sole author, and are protected by US and International Copyright Laws, and may not be copied, reprinted, published, translated, hosted, or otherwise distributed by any means without explicit permission from Irene Caesar, Ph.D., and in violation of the International Laws for citing references. Any citation of the wavegenome.com website should be accompanied with the proper reference to Irene Caesar, Ph.D. Any citation exceeding the length, permissible for the reference length by the International Copyright Law, will be considered to be a violation of the International Copyright Law.

© IRENE CAESAR, PH.D., FOUNDER AND SOLE OWNER OF WAVEGENOME 2010-2017 ALL RIGHTS RESERVED

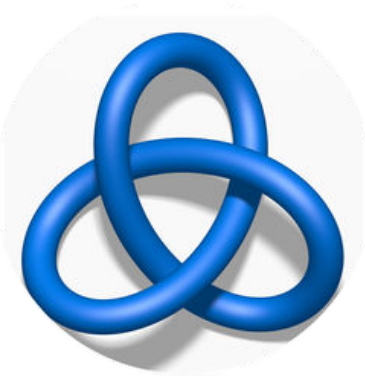

QUANTUM REJUVENATION CLINIC "OM"

We offer remote quantum rejuvenation via **QUANTUM INTERNET**. Quantum rejuvenation implies the rejuvenation of all the physiological systems, including endocrine system, digestive system, cardiovascular system, hearing / eye sight, reproductive system, intellectual abilities, improvement memory, etc.

THE REMOTE REJUVENATION SERVICE is provided for a period, chosen by the customer upon payment for a subscription.

Session of the **REMOTE LASER TREATMENT** consists in the distant transmission of client's **CHILDHOOD BIOHOLOGRAM** or the **MODULATING BIOHOLOGRAM**, such as the Digitized Biohologram of the Human Embryonic Stem Cell, the Digitized Biohologram of the Immune Modulator, the Digitized Biohologram of RNA upon the client, mediated by client's photograph. Technology is based upon Quantum Nonlocality of all copies of the same unique nonlocal Wave Matrix / Biohologram. One session lasts one hour a day.
In addition, **WAVE GENOME LLC** uses the **REPORT** of the **TESLA TEST (/tesla-test.html)** software program.

- $270 per hour
- $6000 per month

Client can combine multiple Bioholographic Modulators, or run more sessions a day, for the additional fee.

CONDITIONS

Firstly, to receive **THE REMOTE REJUVENATION SERVICE**, customer should order the **SECOND-BIRTH MINI-TESLA PSI-GENERATOR. (/second-birth-mini-tesla-psi-generator.html)**

Secondly, to receive **THE REMOTE REJUVENATION SERVICE**, customer should fill up **THE ORDER FORM (/order-form.html)** and upload the following information about himself/herself:
(1) Full name, (2) age, (3) contact information (address, phone number, email), (4) the diagnosis / extract from the medical records, including biochemical tests (blood / urine) and the analysis of genetic / hereditary diseases with a detailed case history / description of the state of health, provided by the physician, (5) the certificate of disability, if any, and an extract from the medical records by medical specialists, (6) present photo, (7) biochemical tests every two weeks throughout the treatment, and an extract from medical records upon visiting the doctor every two weeks / once a month.

PRIVACY POLICY (/privacy-policy.html) SHIPPING POLICY (/shipping--warranty.html) RETURN POLICY (/return-policy.html) TERMS OF SERVICE (/terms-of-service.html)

FDA DISCLAIMER: Content on this site is for reference purposes and is not a substitute for advice from a licensed health-care professional. You should not rely solely on this content, and wave genome.com assumes no liability for inaccuracies. Always read directions before using a product. Statements regarding products and services have not been evaluated by the FDA, and these products and services are not intended to diagnose, treat, cure, or prevent any disease or condition.

Payment in full is due ahead of services. No refunds and returns.

COPYRIGHT NOTICE: Text, graphics, and HTML code on wavegenome.com belong to Irene Caesar, Ph.D., their sole author, and are protected by US and International Copyright Laws, and may not be copied, reprinted, published, translated, hosted, or otherwise distributed by any means without explicit permission from Irene Caesar, Ph.D., and in violation of the International Laws for citing references. Any citation of the wavegenome.com website should be accompanied with the proper reference to Irene Caesar, Ph.D. Any citation exceeding the length, permissible for the reference length by the International Copyright Law, will be considered to be a violation of the International Copyright Law.

© IRENE CAESAR, PH.D., FOUNDER AND SOLE OWNER OF WAVEGENOME 2010-2017 ALL RIGHTS RESERVED

WAVE GENOME (/)

HOME / ГЛАВНАЯ (/)

SERVICES / УСЛУГИ (/SERVICES--105910571051105910431048.HTML)

PRODUCTS / ТОВАРЫ (/PRODUCTS--105810541042104010561067.HTML)

CONTACT / КОНТАКТ (/CONTACT--105010541053105810401050105 8.HTML)

TREATMENT AT OUR CLINICS (/quantum-clinic.html) is priced on the individual basis. We help with travel, lodging, escort and interpreting services at extra cost according to regular Russian rates, for example, interpreter is usually billed $177 for the first hour of translation / escort (or below one hour) with $59 for every next hour (regular 8 hours working day); while for working days with overtime (over 8 hours regular working day), client is billed at $177 for the first hour, and $94 for every next hour. We accept only our own interpreters. **Clinics are RUSSIAN CLINICS. WAVE GENOME does NOT own any of these clinics, but offer VISITATION programs for getting treatments at Russian clinics.**

(/visit-our-clinic-russian.html)

GENERATOR AURA-001

Generator Aura-001 can cure diseases that are considered to be incurable by the conventional medicine. Clinical experience has shown its ability to repair damage in the functioning of any bodily organ. The feedback principle in the operation of the device allows detecting and localizing the disease before the onset of pathology. When exposed to the device, healthy cells do not respond to the exposure, while the sick cells enter into dialogue with the device, so that the human body responds to the exposure (with the pronounced effect of parastasis).

(/generator-aura-001.html)

MORE (/generator-aura-001.html)

GENERATOR AURA-008

(/generator-aura-008.html)

Generator Aura-008 is designed for the prophylactics and treatment of the spine. It promotes relaxation, stimulation and post-traumatic rehabilitation of the musculoskeletal system via the non-contact method of low-level electromagnetic

(/uploads/3/5/1/1/35112207/6473212_orig.jpg)

Located in the heart of Moscow, the Scientific Research Institute for National Security is fully privatized, and engaged in developing information-wave technology and applying it in medicine, and agriculture. Among clients of the Institute were Russian President Boris Yeltsin and famed American astronaut Edgar Mitchell.

T (http://www.wavegenome.com/visit-our-clinic-for-cure-and-rejuvenation.html)REATMENT AT OUR CLINICS is priced on the individual basis. At extra cost, we help with travel, lodging and interpreting services. Minimum course of treatment is 10 days, for three hours a day. Booking is accepted at least one month ahead. Payment in full is due ahead of coming to the clinic. No refunds, even in case you cannot make it to the clinic, since we reserve time for you.

(/uploads/3/5/1/1/35112207/3028539_orig.jpg)

Famed American Astronaut Edgar Mitchell visited our clinic and received a treatment by our PSI-GENERATOR AURA-001.

influence on the patient's energy centers located in the region of vertebral column.
Its principle of operation is based on effects of external physical factors on the structural elements and systems of the human body at different levels.

MORE (/generator-aura-008.html)

GENERATOR AURA-009

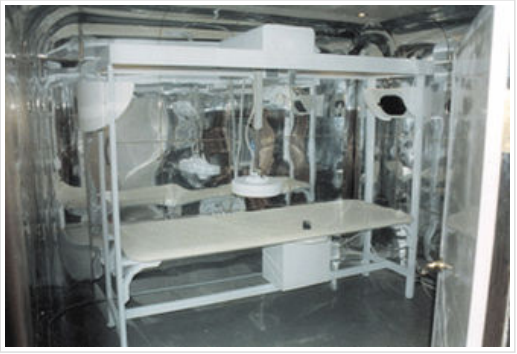

(/generator-aura-009.html)

Generator Aura-009 is used for psycho-physiological correction and bioresonance therapy of targeted impact. Generator Aura-009 is designed for use in specialized clinics, sanatoriums, resorts and spa for the prevention of functional disorders, increasing mental, psychic and physical potential and restoring the functional state of various organs and systems of the human body by a targeted impact on the projection of the individual organs and skin areas (zones of G. A. Zakharyin and H.Head).

MORE (/generator-aura-009.html)

GENERATOR AURA-013

(/generator-aura-013.html)

We offer truly revolutionary cure for breast cancer and infertility. G**enerator Aura-013** is treating such diseases as: • mastitis, breast fibrocystic mastopathy; • breast cancer in 2, 3 stages; • cysts, fibroids, ovarian fibroma; • tubal obstruction; • endometriosis; • sterility of all kinds of pathologies; • frigidity; • genealogical diseases; • infertility with money back guarantee.

MORE (/generator-aura-013.html)

GENERATOR AURA-017

(/generator-aura-017.html)

Generator Aura-017 is designed for synchronizing bio-correction, rehabilitation and bioresonance therapy of the bioquantum and psycho-physical state of the body via targeted impact by acoustic, laser and high-frequency electromagnetic field.

MORE (/generator-aura-017.html)

PRIVACY POLICY (/privacy-policy.html) SHIPPING POLICY (/shipping--warranty.html) RETURN POLICY (/return-policy.html) TERMS OF SERVICE (/terms-of-service.html)

FDA DISCLAIMER: Content on this site is for reference purposes and is not a substitute for advice from a licensed health-care professional. You should not rely solely on this content, and wave genome.com assumes no liability for inaccuracies. Always read directions before using a product. Statements regarding products and services have not been evaluated by the FDA, and these products and services are not intended to diagnose, treat, cure, or prevent any disease or condition.

Payment in full is due ahead of services. No refunds and returns.

COPYRIGHT NOTICE: Text, graphics, and HTML code on wavegenome.com belong to Irene Caesar, Ph.D., their sole author, and are protected by US and International Copyright Laws, and may not be copied, reprinted, published, translated, hosted, or otherwise distributed by any means without explicit permission from Irene Caesar, Ph.D., and in violation of the International Laws for citing references. Any citation of the wavegenome.com website should be accompanied with the proper reference to Irene Caesar, Ph.D. Any citation exceeding the length, permissible for the reference length by the International Copyright Law, will be considered to be a violation of the International Copyright Law.

© IRENE CAESAR, PH.D., FOUNDER AND SOLE OWNER OF WAVEGENOME 2010-2017 ALL RIGHTS RESERVED

WAVE GENOME (/)

HOME / ГЛАВНАЯ (/)

SERVICES / УСЛУГИ (/SERVICES--10591057105110591043 1048.HTML)

PRODUCTS / ТОВАРЫ (/PRODUCTS--10581054104210401056 1067.HTML)

CONTACT / КОНТАКТ (/CONTACT--10501054105310581040 10501058.HTML)

QUANTUM LEAP AGRICULTURE VIA LASER BIOHOLOGRAPHY BY WAVE GENOME LLC

(/agriculture-on-generators-russian.html)

We offer **LASER POLARIZED BIOHOLOGRAPHY** for restoring the Wave Optics of chromosomes in the agricultural plants and animals, which was destroyed by GMO. GMO or Genetically Modified Organisms are created by the mistaken paradigm of genetic engineering via cutting and pasting the gene snippets, so that it destroys the refractional geometry in the systematic wholes of the chromosomes, and leads to the extinction of species via their sterilization.

LASER POLARIZED BIOHOLOGRAPHY by **WAVE GENOME LLC** is the ONLY solution to the Genetic Collapse caused now by GMO in the developed capitalist countries in the West, like the US, Canada, Great Britain, France, and Germany. GMO is a biological binary weapon.

We offer local and remote servicing of the seeds, plants and animals with the **DIGITZED BIOHOLOGRAMS** of the intact plants and animals for treating animals and seeds harmed by the binary biological war.

We offer the enhancing of the seeds and animals for the purposes of breeding the more functional species.

Local service includes service by **TESLA GENERATORS** and lasers for the purpose of the manifold increase of the crop yield, and quality of food.

Remote service includes the remote service at close range and the remote service at long range. At close range, we apply chips structured by laser at nano level, and **DIGITAL PHARMACY**. At long range, we offer the remote laser signal for managing biosystems at a distance.

Pesticides, hormones, antibiotics can be all substituted by **BIOHOLOGRAMS / WAVE MATRICES** delivered locally or remotely -- WITH NO HARM to humans, animals, and biosphere at large.

WAVE GENOME LLC offers the stage of full industrialization of the Quantum Leap technology of **LASER POLARIZED BIOHOLOGRAPHY**.

PRIVACY POLICY (/privacy-policy.html) SHIPPING POLICY (/shipping--warranty.html) RETURN POLICY (/return-policy.html) TERMS OF SERVICE (/terms-of-service.html)

FDA DISCLAIMER: Content on this site is for reference purposes and is not a substitute for advice from a licensed health-care professional. You should not rely solely on this content, and wave genome.com assumes no liability for inaccuracies. Always read directions before using a product. Statements regarding products and services have not been evaluated by the FDA, and these products and services are not intended to diagnose, treat, cure, or prevent any disease or condition.

Payment in full is due ahead of services. No refunds and returns.

COPYRIGHT NOTICE: Text, graphics, and HTML code on wavegenome.com belong to Irene Caesar, Ph.D., their sole author, and are protected by US and International Copyright Laws, and may not be copied, reprinted, published, translated, hosted, or otherwise distributed by any means without explicit permission from Irene Caesar, Ph.D., and in violation of the International Laws for citing references. Any citation of the wavegenome.com website should be accompanied with the proper reference to Irene Caesar, Ph.D. Any citation exceeding the length, permissible for the reference length by the International Copyright Law, will be considered to be a violation of the International Copyright Law.

© IRENE CAESAR, PH.D., FOUNDER AND SOLE OWNER OF WAVEGENOME 2010-2017 ALL RIGHTS RESERVED

You can place an order via filling up **THE ORDER FORM (/order-form.html).** Prices differ depending on the service, client's condition, and disease.

Models of **TESLA PSI-GENERATOR**S differ by the size of the chip (the number of layers). The chip is multilayered and it takes longer than one day to produce just one layer. Our **SUPER**, **ULTRA** and **ULTIMATE PSI-GENERATORS** has twice as much layers than our **BASIC TESLA PSI-GENERATOR**. Production of our **ULTRA** and **ULTIMATE MINI-TESLA PSI-GENERATORS** takes about or longer than one month. There are two generations of chips: **FIRST GENERATION CHIP** and **SECOND GENERATION CHIP**.

Each model comes in **GENERIC** and **INDIVIDUAL** version. Generic version has the universal human biohologram (aka DIGITAL CELL) encoded via laser into the chip on nano level. And the individualized version has the personal human biohologram encoded via laser into the chip on nano level.

GENERIC TESLA PSI-GENERATORS are produced for large families, who would like to share the same **TESLA GENERATOR** for all members of the family. Generic Human Biohologram, aka DIGITAL CELL, is the result of decades of research, and is the foundation for our diagnostics procedures.

INDIVIDUAL TESLA PSI-GENERATORS have individual biohologram of a client in the chip, being encoded via laser onto the chip on nano level. Individual biohologram is recorded from your childhood photograph (or navel blood / placenta) via laser, digitized, diagnosed, and encoded into the chip via laser.

INDIVIDUAL TESLA PSI-GENERATORS are produced for the ultimate protection against genetic and psychotronic warfare.

FIRST GENERATION CHIPS (inside a pendant) come with the **COMPLETE DIGITAL PHARMACY** (in English) as software on a flash drive with 44 modules for every essential bodily organ and physiological system. Market value is 35,000 Euros only one module.

SECOND GENERATION CHIPS (inside a pendant) come with the **ADVANCED DIGITAL PHARMACY**, which consists either in **TESLA TEST (/tesla-test.html)** software program (abbreviation: TT) for the **REMOTE LASER TREATMENT (/remote-laser-treatment.html)**, or with the **TESLA HUMAN CELL (/tesla-human-cell.html)**, as 5 MP3 files of the digitized Biohologrames of the essential bodily organs and physiological systems encoded as half-audible white noise in the Sacred Mantras, recorded by the new generation laser.

COMPLETE DIGITAL PHARMACY SOFTWARE PROGRAM

All our models of **TESLA PSI-GENERATORS** (chip) come with a separate flash drive with the **DIGITAL PHARMACY** for every essential bodily organ and physiological system (**PSI-PROGRAM**) as the collection of the **E-DRUGS** / **BIOELECTRONIC DRUGS** (aka wave matrices / biohologrames) for every health condition.

We offer two kinds of the **DIGITAL PHARMACY**. The **FIRST GENERATION DIGITAL PHARMACY** is the software, built with the first generation lasers. The SECOND GENERATION DIGITAL PHARMACY is called **TESLA HUMAN CELL X (/tesla-human-cell.html),** and consists of 5 MP3 files of the digitized Biohologrames of the essential bodily organs and physiological systems encoded as half-audible white noise in the Sacred Mantras. MP3 files are more reliable, and are recorded by the new generation laser.

SECOND-BIRTH TESLA PSI-GENERATOR

(g) **SECOND-BIRTH TESLA PSI-GENERATOR (/second-birth-mini-tesla-psi-generator.html)** is the **SECOND GENERATION CHIP** (inside a pendant). It comes with the **ADVANCED DIGITAL PHARMACY**, which consists either in **TESLA TEST (/tesla-test.html)** software program (abbreviation: TT) for the **REMOTE LASER TREATMENT (/remote-laser-treatment.html)**, or with the **TESLA HUMAN CELL X (/tesla-human-cell.html)**, as 5 MP3 files of the digitized Biohologrames of the essential bodily organs and physiological systems encoded as half-audible white noise in the Sacred Mantras, recorded by the new generation laser.

TESLA TEST (http://wavegenome.com/tesla-test.html) software program, is the most advanced way to record and verify client's WAVE MATRIX. **TESLA TEST (/tesla-test.html)** makes the camera on your computer record your Wave Matrix, and analyzes the data. **WAVE GENOME LLC** uses this data for the **REMOTE LASER MANAGEMENT (/remote-laser-treatment.html)** of your Biohologram.

GENERIC SECOND-BIRTH MINI-TESLA GENERATOR - $3000

INDIVIDUAL SECOND-BIRTH MINI-TESLA GENERATOR - $3500

SECOND-BIRTH TESLA PSI-GENERATOR

(a) **has a more advanced, second generation chip encoded by laser on nano level with the most valuable bioholographic information on the global market: EMBRYONIC STEM CELL;**

(b) has a new technology of encoding the chip by the newly invented laser (patented);

(c) layers of the chip are made of a new material of organic nature more advanced than our other chips;

(d) its efficacy is proven by the clinical trials at the Medical Clinic of the Moscow Bauman Russian State Technical University, the most important Science University in Russia, of MIT level. Generator has twice as more layers of the chip than the **BASIC MINI-TESLA PSI-GENERATOR.**

(e) has either **GENERIC** or **INDIVIDUAL** biohologram.

(f) provides the ultimate modulation for the scalar wave diffraction grating for the most precise focus / zero center of the biohologram (aka 'wave crystal") in the process of rejuvenation. Click here to read more on **SECOND-BIRTH MINI-TESLA PSI-GENERATOR**. (/second-birth-mini-tesla-psi-generator.html)

BASIC-X TESLA PSI-GENERATOR

SUPER TESLA PSI-GENERATOR

ULTRA TESLA PSI-GENERATOR

ULTIMATE TESLA PSI-GENERATOR

SUPER MINI-TESLA GENERATOR (chip)

(a) has twice as more layers of the chip than the **BASIC MINI-TESLA PSI-GENERATOR.**

(b) has either **GENERIC** or **INDIVIDUAL** biohologram.

(c) Both sides of the casing for the chip are made of Real Solid Pearl.

GENERIC SUPER MINI-TESLA GENERATOR - $1179

INDIVIDUAL SUPER MINI-TESLA GENERATOR - $1768

MATRIX TESLA PSI-GENERATOR

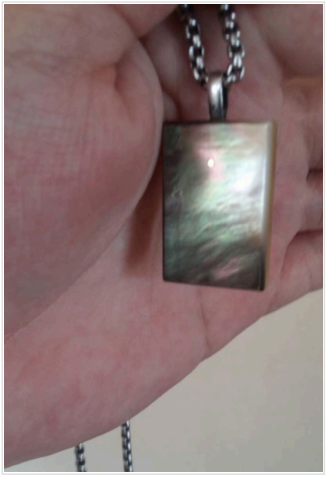

BASIC TESLA PSI-GENERATOR (chip)

(a) has twice less layers of the chip than our other models**.**

(b) has either the **GENERIC** or **INDIVIDUAL** biohologram of a healthy human in the chip, being encoded via laser onto the chip on nano level.

(c) **BASIC TESLA PSI-GENERATOR** has both sides of the casing for the chip made of Real Solid Pearl.

(d) **BASIC-X TESLA PSI-GENERATOR** has one side of the casing for the chip made of Real Solid Pearl, and another side of casing made of 3D printing plastic, encoded with the immune system rejuvenation **E-DRUG** (**BIOELECTRONIC DRUG / DIGITIZED BIOHOLOGRAM**). This makes **"TWO-CHIPS IN ONE"** solution.

GENERIC BASIC MINI-TESLA GENERATOR - $856

INDIVIDUAL BASIC MINI-TESLA GENERATOR - $1179

INDIVIDUAL BASIC-X MINI-TESLA PSI-GENERATOR - $1534

MATRIX TESLA PSI-GENERATOR

(a) has twice as more layers of the chip than the **BASIC MINI-TESLA PSI-GENERATOR.**

(b) has either **GENERIC** or **INDIVIDUAL** bioh ologram.

(c) Both sides of the casing for the chip are made of 3D printing plastic, encoded with the immune system rejuvenation **E-DRUG** (**BIOELECTRONIC DRUG / DIGITIZED BIOHOLOGRAM**). This makes **"TWO-CHIPS IN ONE"** solution.

GENERIC MATRIX MINI-TESLA GENERATOR - $2122

INDIVIDUAL MATRIX MINI-TESLA GENERATOR - $2947

ULTRA MINI-TESLA GENERATOR (chip)

(a) has twice as more layers of the chip than the **BASIC MINI-TESLA PSI-GENERATOR.**

(b) has either **GENERIC** or **INDIVIDUAL** bioh ologram.

(c) One side of the casing for the chip is made of Real Solid Pearl, and another side of casing is made of 3D printing plastic, encoded with the immune system rejuvenation **E-DRUG** (**BIOELECTRONIC DRUG / DIGITIZED BIOHOLOGRAM**). This makes **"TWO-CHIPS IN ONE"** solution.

GENERIC ULTRA MINI-TESLA GENERATOR - $1768

INDIVIDUAL ULTRA MINI-TESLA GENERATOR - $2358

ULTIMATE MINI-TESLA GENERATOR (chip)

(a) has twice as more layers of the chip than the **BASIC MINI-TESLA PSI-GENERATOR.**

(b) has either **GENERIC** or **INDIVIDUAL** bioh ologram.

(c) One side of the casing for the chip is made of Real Solid Pearl, and another side of casing is made of 3D printing plastic, encoded with the RNA **E-DRUG**(**BIOELECTRONIC DRUG / DIGITIZED BIOHOLOGRAM**) for the ultimate protection against psychotronic and genetic warfare. This makes **"TWO-CHIPS IN ONE"** solution.

GENERIC ULTIMATE MINI-TESLA GENERATOR - $2358

INDIVIDUAL ULTIMATE MINI-TESLA GENERATOR - $2712 (promotional price)

RA MINI-TESLA PSI-GENERATOR (/ra-psi-generator.html)

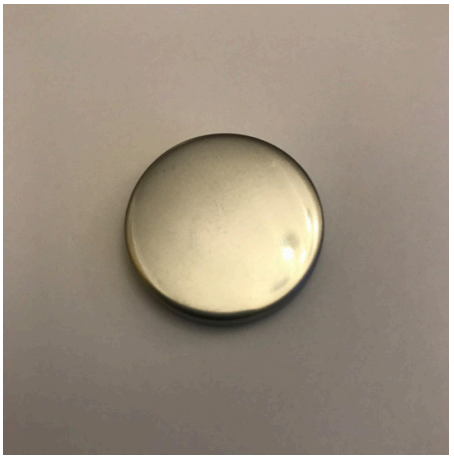

RA PSI-GENERATOR (/ra-psi-generator.html) is the device is a device enhancing the Wave Optics of chromosomes and protecting the user in the case of psychotronic and psychic attack.

Inside the metal casing, there is the electret-based chip structured by the Holographic Signal. The Holographic Signal is created by true nanotechnology via producing and modulating the Wave Optics inside the scalar wave diffraction grating. Protective effect of the device is based upon (1) reflecting any external linear signal upon itself in the scalar wave, so that the peak of the forward-going wave is neutralized by the trough of the same wave when it is reflected upon itself; and upon (2) refracting any next external linear signal towards the Zero Center / Focus of the Wave Crystal (crystalline structure of the Wave Fronts). As the result, the generators of the pathological energy are dissolved The same principle is used for protecting the user from the pathological electromagnetic energy, and overcoming the Wave Optical Plug-ins of the planetary organisms of viruses and bacteria.

Individual **RA PSI-GENERATOR** (/ra-psi-generator.html) is coded via the Holographic Signal modulated by client's individual Wave Optics recorded from client's childhood or adult photograph.

MINI-TESLA GENERATOR

MANUAL FOR MINI-TESLA PSI-GENERATOR

ABOUT THE DEVICE

The device consists of two parts: a chip in a pendant and a computer program (software) on a flash drive.

CHIP:

The user wears a pendant with a chip inside on his/her neck at the level of the solar plexus. We have chips of first and second generation. First generation chip is an artificial polymer crystal with electret properties, which has two modules, depending on how you turn it towards your body: open module (reinforcing the impact of a user on the environment) and closed (protecting a user from the harmful effects of the environment). Second generation chip (more advanced) has the entirely holographic technology, and functions through the focus / zero center of the scalar wave diffraction grating in the hologram encoded into the chip via laser on nanolevel.

Chips are structured by laser at the nano level. The laser writes to the chip at the nano level client's digitized biohologram, which is read by the laser from the childhood photograph, placenta or umbilical cord blood of the client for the individual

generators, or the biogologram of a average healthy person for the generic generators.

When user is wearing the chip, the electret is emitting the wave crystalline structure (hologram or matrix) upon the user, and makes his chromosomes repeat the wave crystalline structure of a healthy person during cell division.

The laser and chip itself use the principle of Kozyrev Mirrors. The Universe consists of energy for 93%, and of particles only for 7%, and particles are the concentrated energy. The universe is holographic, that is, it is entirely in its every Matrix Point. Wave Hologram or Matrices exist in two forms: in the form of a Torus (simultaneously present from the infinitely small to the infinitely large dimensions) and in the form of the Wave Crystal. Man exists in the form of a Torus during sleep. During waking hours, the person is in the form of a Wave Crystal.

Wave Crystals are formed in the structures, which reproduce in their shape the Kozyrev Mirrors. Kozyrev Mirrors reflect any external wave signal, and, therefore, are called "mirrors". These structures neutralize any external linear signal, and refract it towards their Zero Center or focus. Neutralization of any external signal happens due to the reflection of the wave and the polarization, and the creation of a so-called standing (scalar wave). Trough of the back-running wave neutralizes the peak of the forward-going wave, when the initial wave is reflected. This provides protection from harmful electro-magnetic and other technogenic or anthropogenic influences.

As a result of the standing (scalar) wave, there emerges the interference (diffraction) grating, which refracts any next linear signal line towards the center (focus) of the Wave Crystal.

It is necessary to know this, because all the information in the universe is transmitted and received only through the Zero Center of the Wave Crystal. This is analogous to the work of our eye. We see only because there is the gathering of all the external linear signals in the focus of the lens (Wave Crystal). If focus is not achieved, and the refraction of the signal takes place before or behind the center of the lens, we have developed the long-sightedness (hyperopia), or the long-sightedness (myopia), and we don't see well. Receiving information by both our eye, and our DNA takes place strictly in accordance with the laws of geometrical optics. The technology used for creating the chip is called "Polarized Holography".

It is possible to record and transmit only a holographic signal. To record Wave Crystals (Biohologrames or Matrices) of users, we use devices that can record and transmit holographic signal - He-Ne laser with internal mirrors. These lasers convert any external linear signal into a holographic signal, i.e., changing the nature of the initial signal. For example, our bones produce stem cells only because their shape and structure is analogous to the laser tubes, which "involute" a

"PSI" stands for "psychotronic", that is, for the technology that is offering technical means for managing biosystems.

Every **MINI-TESLA psi-generator** comes with

(1) a **CHIP**, structured with a laser on a nano-level with the digitized Wave Matrix / Biohologram of healthy human or your own individual wave matrix in childhood (recorded from your childhood photograph), and cased either in pearl or 3-D printing plastic, or combination of these two materials. You wear it on a chain on your solar plexus all the time, taking it off only for bathing;

(2) and psi-program - a flash drive with the software that has the entire **DIGITAL PHARMACY** generated as the holographic / granulated signal (aka "white noise" - signal beyond your auditory perception) and encoded in music. You are getting the complete **DIGITAL PHARMACY** for your lifetime and for every system and vital organ in your body. You run this software at least once a day for best results. If you are sick, you run this software as often as possible.

All sales upon agreeing to c**lient consent conditions** (/client-consent.html), no refunds.

Produced according to TU 9444-021-42844321. Certificate # 77, FC.19.944. P.2455.11.00

Our **MINI-TESLA GENERATOR** is used by Russian Special Forces and Olympic Team.

MINI-TESLA GENERATOR is a CHIP (artificial / polymer crystal), structured by laser on a nanolevel, as a collector and retransmitter of wave structures (Matrices or Biohologrames), which functions as a dispenser for WAVE MATRICES (http://www.wavegenome.com/wave-pharmaceuticals.html) within the revolutionary

Нажмите на Русский флаг для перемещения на версию сайта на Русском языке

Refer to our **FAQ (Frequently Asked Questions) (/mini-tesla-generator-faq.html)** for any concerns.

IMPORTANT: CHIP has two modes : OPEN and CLOSED. In the **OPEN MODE**, you increase your information-wave impact upon people. The **CLOSED MODE** is the **SHIELD MODE**, which protects you from any psychotronic attack, including V2K (voice to skull) and cancer guns, subliminal advertising and psychic attacks. Those customers who are endangered with these attacks can wear their **CHIP** in the protective mode nonstop. **PLEASE NOTE**: Plastic towards your body is a **SHIELD MODE**. For casing which has both sides from plastic, the **SHIELD SIDE** is thinner so that the chip is noticeable beneath plastic. For casing which has both sides from Pearl, the darker side of Pearl towards your body is the **SHIELD MODE**.

READ INFORMATION LEAFLET FOR THE MINI-TESLA GENERATOR

(COMES WITH THE UNIT) (/information-leaflet-for-mini-tesla-generator.html)

Over the course of decades, our institute participated in the research in the field of information technologies of a new generation, and their commercialization. The institute created the system of information-energy correction, which is the most advanced in the world, and is the two-way connection through the energy-information cloud. In Russia, our **MINI-TESLA generator** is used by Special Forces and the Olympic Team in order to help them cope with stress and enhance their

signal.

Similarly, our DNA is able to transmit and receive information, only because, in its structure, it is the Wave Crystal. Two strands of DNA are literally the standing (scalar) wave, since in the first strand of DNA, a wave goes in the direction opposite to the wave going in the second strand of DNA. Moreover, DNA coils into the crystalline structure, which literally reproduces the interference / diffraction grating of the standing wave in the Kozyrev Mirror, in order to most accurately refract any external linear signal toward the Zero Center / Focus of its Wave Crystal.

We live only thanks to cell division. During cell division, chromosome is formed. A chromosome is formed when two sisters chromatids unite together into a cruciform structure. Chromosomes come in two main shapes: acrocentric and metacentric. In acrocentric chromosomes, two endings of the sisters chromatids are shorter than the other two endings. On the contrary, metacentric chromosome has all the endings the same, so that it is absolutely symmetrical. Metacentric chromosome resembles the quadratic / symmetrical cross (Crux Quadrata / Gammadion), as well as the lens of a well-seeing eye. The same gene in apes, in children with Down syndrome, and wild horses of Przewalski has the acrocentric chromosome, whereas in humans, normal children, and Arabian horses, the same gene has the metacentric shape of the chromosome. That is, the functionality of the species directly depends upon the shape of chromosome, that is, upon the laws of the Polarized Holography of Wave Crystals.

Our device is centering and focusing the chromosomes during cell division, giving them the metacentric form.

Because the entire universe is entirely in its every Matrix Point, each Matrix Point is not simply different from any other Matrix Point, but is unique (© Irene Caesar, 2012). Each Matrix of each person is the uncreated and indestructible unique nonlocal Wave Matrix. If we have two copies of a unique non-local Wave Matrix, we can instantaneously transfer information from one copy of a unique non-local Wave Matrix to another copy. In this way, birds and insects share one unique non-local Wave Matrix for their entire species, and instantaneously transmit information between all individuals of a given species. But each man has his own unique nonlocal Wave Matrix. If you order an individual generator, you get your unique non-local Wave Matrix with the most clear focus / center of the Wave Crystal. Your generator transmits upon your chromosomes your unique uncreated and indestructible information from the noosphere of the universe. If you order the generic (universal) generator, its action is limited, but it, nevertheless, helps your chromosomes to get centered and focused.

We also offer the remote therapy by the distant laser signal that instantly, through Quantum Non-locality, affects your genetic apparatus according

paradigm of LASER POLARIZED BIOHOLOGRAPHY, which is the true WAVE PHARMACEUTICALS (/wave-pharmaceuticals.html) **-- information technology of a new generation. Generator or retransmitter functions like a vibrator, which emits micro vibrations of special kind - scalar wave diffraction grating.**

WAVE MATRICES (http://www.wavegenome.com/wave-pharmaceuticals.html) can be generic or individualised. Wave matrices can be of a human as a whole, of specific bodily system, or of a specific medication.

Comes with the software that has 44 modules of DIGITISED WAVE MATRICES (http://www.wavegenome.com/wave-pharmaceuticals.html) for every bodily system and every vital organ in your body.

DIGITISED WAVE MATRICES (http://www.wavegenome.com/wave-pharmaceuticals.html) also can be either generic or individualised, and of a human as a whole, of a specific bodily system, or of a specific medication.

(/uploads/3/5/1/1/35112207/3881928_orig.png)
The first-generation model of MINI-TESLA PSI-GENERATOR, which combined the chip with the flash drive containing the DIGITAL PHARMACY software.

BASIC MINI-TESLA GENERATOR emits generic **HUMAN CELL HOLOGRAM**, recorded by the laser from healthy human cells and bodily systems, and then used to structure the crystal via the laser on nanolevel.

SUPER, ULTRA, MATRIX AND ULTIMATE MINI-TESLA PSI-GENERATORS emit individual **HUMAN CELL HOLOGRAM** in the form of your childhood wave matrix, which is recorded from your childhood photograph when you were a healthy child. We also need your date of birth. We use the complex systematic approach to read the biohologramphic information from your photograph, including the application of laser.

After your matrix is recorded from your photograph, we run a special diagnostic program in our Institute to reveal the defects in your matrix, and to correct them.

performance.

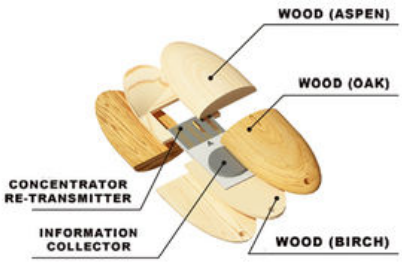

(/uploads/3/5/1/1/35112207/3725345_orig.jpg)
The first-generation model of MINI-TESLA PSI-GENERATOR, which combined the chip with the flash drive containing the DIGITAL PHARMACY software.

The second-generation model of MINI-TESLA PSI-GENERATOR, with casing of chip made from Pearl and Wood. Now this model is offered in Pearl for the BASIC MINI-TESLA GENERATOR (chip structured by the laser with the generic biohologram of a healthy human on nano level).

The device is in fact very necessary in modern times when we are bombarded by the harmful electro-magentic radiation.

The device is designed in such a way that you can turn it either with darker-colorer side to yourself, and, in this case, the generator is programmed to open your biofield; or to turn it with the lighter-colored side (aspen side in generators coated in wood) to yourself, and, in this case, the generator becomes your psychotronic "firewall".

IF you are a jet setter, you are receiving a huge amount of radiation each time you fly. Radiation is one of the causes of cancer. That is why our MINI-TESLA GENERATOR is indispensable for jet-setters.

If you get sick, e.g., infected with a virus or bacteria, your wave imprint / data received at the institute will immediately alert the system, and we will correct the situation via sending you the necessary correction to your wave-diagram (available only for **ULTRA MINI-**

to the principle described above. The user uses his/her individual generator as an antenna and a filter for the remote laser signal.

DIGITAL PHARMACY SOFTWARE

The user uses the computer program (software) every day once a day in a normal state of health, and several times a day, depending on the complexity of his/her state of health. When working with the computer program of the generator, the user must turn his/her generator to the open module.

Computer program of the generator is a comprehensive Digital Pharmacy of the digitized Biohologrames (Wave Crystal structures or Matrices) of all healthy vitally important organs and physiological systems. The user tales a self-test for self-therapy, and the program generates for him the granular (holographic) signal, which is encoded in the music.

Self-therapy is the binaural therapy, which uses the Kozyrev Mirrors principle alike the chip inside the generator. Binaural therapy is based on the effect of the stereo signal to both ears, so that signal is delayed in one ear with respect to the signal applied to the second ear. It is in this way that the Kozyrev Mirrors effect is created, when human skull itself becomes the Kozyrev Mirror. The signal is reflected; there emerges a standing (scalar), the wave interference / diffraction grating; and the signal is refracted toward the Zero Center / focus of the wave crystal.

Also, the user can order any pill or tincture in the form of a software module of the Digital Pharmacy. Digital Pill module is attached to the Digital Pharmacy software, and the user receives the Digital Pill as the granular (holographic) signal encoded in the music. We record the Digital Pill via a laser and as the wave structure (Hologram or Matrix), which is afterwards gets digitized. Digital Pills do not have the danger of overdose and side effects.

If no childhood photograph is available, we can use your adult photograph, since the Institute can diagnose **WAVE MATRICES (http://www.wavegenome.com/wave-pharmaceuticals.html)** and correct them.

We can "record" wave matrices / biohologrames upon various media, and not only on the electret-based chip of the MINI-TESLA PSI-GENERATOR. Examples of such media are CDs that are used "as such", and not for extracting the digital files from them.

We can combine your childhood wave matrix with wave medications.

We can tune up your childhood matrix.

We can tune up your childhood matrix in such a way that some specific bodily systems or organs are stimulated.

SELF-MAINTENANCE

You run software with **PSI-PROGRAM** on your computer in order to perform the self-maintenance as often as you need. **PSI-PROGRAM** has 44 modules for every bodily system and every vital organ in your body. These 44 modules were recorded by the laser from healthy human cells and bodily systems, and, then, digitised.

Software has (1) the chart of bodily systems and organs to choose from for self-maintenance; (2) a self-assessment test; (3) binaural therapy which consists of the digitized biohologrames encoded in music as white noise (signal beyond the range of human perception).

QUANTUM COMPUTER

Besides conventional tests, **WAVE GENOME LLC** developed a completely new way of recording and transmitting information. We call it **QAUNTUM BIOINTERNET**.

When you run the **PSI-PROGRAM**, the spin states of the software and the spin states of your crystal / chip in the generator constitute one and the same torus (hologram). There is the instantaneous biofeedback / bioresonance two-way communication between the running software and the crystal inside the **MINI-TESLA PSI-GENERATOR.**

The crystal / nano chip in the **MNI-TESLA PSI-GENERATOR** and the **PSI-RPOGRAM** software (during its operation on your computer) constitute one integrated **QUANTUM COMPUTER**. The spin states of the crystal / nanochip in the generator and the spin states of the software coincide / resonate or oppose each other, according to the principles of the polarised holography. The principles of the polarised holography are expressed by geometrical optics.

TESLA PSI-GENERATORS) (http://www.wavegenome.com/wave-genome---prices.html).

Some bacteria and viruses are considered to be incurable because they leave a wave imprint in the body, even after they are cleared up on the biochemical level. And, then, these wave imprints can literally rebuild the virus and bacteria from scratch. This same principle is seen in the classic physics experiment involving passing photons and molecules through two slits simultaneously. That is why it is necessary to protect and cure oneself on the wave level.

(/uploads/3/5/1/1/35112207/5220735_orig.jpg)
The first-generation model of the MINI-TESLA PSI-GENERATOR, which was approximately 2 inches long, and which was worn at your solar plexus the same way as the new model of the MINI-TESLA PSI-GENERATOR. Both models are invisible when you wear it. The first-generation model had chip and flash drive with the software combined in one piece.

MAINTENANCE VIA QUANTUM INTERNET BY WAVE GENOME LLC

In the case of **QUANTUM INTERNET**, you send your information **REMOTELY** and **WIRELESSLY**. At the WAVE GENOME LLC, the laser reads the feedback from your wave matrix in real time, using your digitised wave matrix on record at the Institute.

According to the holographic principle, the universe is holographic, meaning that it is entirely in its every matrix part. The holographic principle has three important implications:

The first implication of the holographic principle postulates the **UNIQUENESS** of every wave matrix. if the universe is entirely in its every matrix point, then, every matrix point is not simply different from any other matrix point, but is unique.

The second implication of the holographic principle postulates the **NON-LOCALITY** of every wave matrix. If the universe is entirely in its every matrix point, then every wave matrix is simultaneously present in the infinite number of dimensions via its tokens. Though there are infinitely many tokens of the same non-local wave matrix, all of them constitute one integrated **SYSTEMATIC WHOLE**.

The non-local holographic nature of wave matrices also means that the wave matrix has the infinite set of waves, particles and fields within its **TORUS** --

(/uploads/3/5/1/1/35112207/7731776_orig.gif)

Our MINI-TESLA GENERATOR is used by Russian Olympic Team.

(/uploads/3/5/1/1/35112207/1566232_orig.gif)

Our MINI-TESLA GENERATOR is used by Russian Special Forces.

The software reads via its own spin states the information off the crystal (its spin states), and corrects it. Then, the crystal tunes via the bioresonance of the spin states to the hologram, corrected by the operating software.

In this way, the crystal / nanochip inside the generator self-corrects itself based upon the operation of this **QUANTUM COMPUTER**.

MAINTENANCE BY WAVE GENOME LLC

WAVE GENOME offers everyday **MAINTENANCE** of **WAVE MATRICES** with the purchase of the **ULTRA MINI-TESLA PSI-GENERATOR** and **SUBSCRIPTION PACKAGES.**

The maintenance consists in receiving the necessary correction of your bio-field from the **WAVE GENOME LLC**.

To obtain MAINTENANCE from the WAVE GENOME LLC, you send in your information. The **WAVE GENOME LLC** tracks down the changes in your **WAVE MATRIX** and makes necessary corrections. Corrections also account for the changes in the earthly electromagnetic activity, solar and lunar activity, geophysical activity, weather anomalies, and predicted social unrest.

There are two ways to send in your information. You can send your biofeedback information either **DIGITALLY** through the conventional internet, or via **QUANTUM INTERNET**.

DIGITAL MAINTENANCE BY WAVE GENOME

In the case of **DIGITAL MAINTENANCE BY WAVE GENOME LLC, WAVE GENOME LLC** corrects the digital files in the software of your **PSI-PROGRAM**.

When you connect your **MINI-TESLA GENERATOR** to your computer, you both receive and transmit through the internet the information, needed for your utmost performance, to and from the our facility.

Your childhood matrix, recorded onto the generator-transmitter, is your antennae that helps your body tune to the waves which are beneficial to you, and ward off harmful waves. That is why this technology is also called "the resonance technology".

Device strengthens the immune system and body's resistance to infectious and toxins;
Improves performance and cognitive abilities, including, sharpness of thinking and memory, and overall quality of life;
Protects against stress factors of any nature (technogenic, including, electromagnetic, as well as from infinitely micro to infinitely macro dimensions. It is impossible to talk of each individual wave matrix as "a specific frequency". And it is impossible to postulate any "medium" of its existence, like "scalar wave", "aether", "Higgs / boson field", "torsions", "leptons", etc. There is no specific medium for transferring the information.

The third implication of the holographic principle postulates that there is the **QUANTUM ENTANGLEMENT** in the form of the instantaneous transmission of information between all the tokens of the same non-local wave matrix. The signal that records and transmits the **ENTANGLED INFORMATION** between different wave matrices or between the tokens of the same non-local wave matrix has specific nature. It is **HOLOGRAPHIC**. Only lasers can record and transmit holographic signal, based upon the principles of the polarised refraction holography (described in terms of geometrical optics). Thus, the principle of recording and transmitting the **MATRIX SIGNAL** is structural, and not medium-based.

Thus, it is possible to remotely and instantaneously transfer some wave information to a man via the entanglement between his body (at one location) and his photograph (at another location), as two tokens of his non-local wave matrix.

For example, it is possible to remotely lower blood sugar in a diabetic man via scanning his photograph with the laser ray, which is passing through insulin before reaching the photograph.

© Irene Caesar, Ph.D. from her book **"WAVE PHARMACEUTICALS"** (2014)

(/)

HOME / ГЛАВНАЯ (/)

SERVICES / УСЛУГИ (/SERVICES--10591057105110591043 1048.HTML)

PRODUCTS / ТОВАРЫ (/PRODUCTS--10581054104210401056 1067.HTML)

CONTACT / КОНТАКТ (/CONTACT--10501054105310581040 10501058.HTML)

WAVE PHARMACEUTICALS AS WAVE DRUGS THROUGH THE DIGITAL PHARMACY, QUANTUM INTERNET AND PERSONAL WAVE MATRIX

In the 1980s-1990s, a vast group of Russian scientists in the secret KGB institutes was using childhood photographs for recording wave matrices via various kinds of lasers and generators, and for distant transmitting of these wave matrices in order to attempt treating incurable-before diseases like diabetes, cancer, and other ones. The rationale for this technology was as following.

World is the energy. Particles constitute about 4%, but they are also just the condensed energy. Photograph is not simply a sheet of photo paper with emulsion, but, in fact, a holographic wave matrix. According to quantum physics, the universe is holographic. This means that the universe is completely in its every point, that is, every point of the universe has a wave component, which is characterized by quantum non-locality – indestructibility and omnipresence outside of time and space. The holographic principle is another way of expressing the quantum non-locality and quantum entanglement of any particle with any other particle in infinity.

Matrix - is the structures or energy “crystals”, which have such a component. If we record the energy matrix of man, we get access to that component, that is, to the indestructible factor of man’s energy structure. This component restores human energy structure to the “norm”, when the individual "tunes to" or "resonates" with the spin states of the wave field of his wave matrix. Our DNA is antenna that emits and receives the wave information. It is possible to be cured only through access to one’s wave holographic matrix.

We record the wave matrix by helium-neon laser. This laser works on polarized photons that change their spin states, and, therefore, are capable of recording a holographic wave matrix from a childhood photo, a substance, or a human.

MORE (/wave-pharmaceuticals---more.html)

You can get your WAVE DRUGS (/tesla-generator.html) or REJUVENATION WAVE MODULES (/remote-laser-treatment.html) through THE MINI-TESLA GENERATOR (/tesla-generator.html) used for THE DIGITAL PHARMACY (/wave-pharmaceuticals---digital-pharmacy.html) (e.g., E-VIAGRA) or QANTUM INTERNET (/remote-laser-treatment.html) used for the remote and wireless transmission of wave modules (e.g., I-VIAGRA).

(/wave-pharmaceuticals-russian.html)

READ ON DIGITAL PHARMACY (/wave-pharmaceuticals---digital-pharmacy.html)

READ ON QUANTUM INTERNET (/remote-laser-treatment.html)

WAVE GENOME (/)

HOME / ГЛАВНАЯ (/)

SERVICES / УСЛУГИ (/SERVICES--105910571051105910431048.HTML)

PRODUCTS / ТОВАРЫ (/PRODUCTS--105810541042104010561067.HTML)

CONTACT / КОНТАКТ (/CONTACT--105010541053105810401050105 8.HTML)

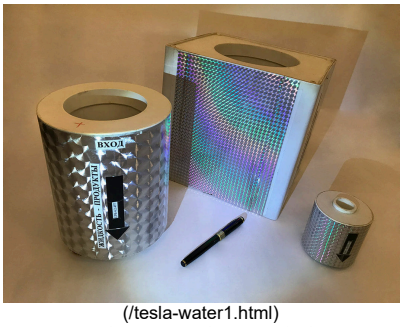

(/tesla-water1.html)
TESLA WATER GENERATORS

BIOACTIVE TESLA WATER

(/bioactive-water-russian.html)

For 20 years already, we program water and make it more effective than some drugs - PROVEN and CERTIFIED.

We program our **TESLA WATER** via **QUANTUM INTERNET**.

Water programming is **REMOTE** and **WIRELESS**.

Water programming is **INDIVIDUALIZED**.

Bioactive water can be used in agriculture for the radical manifold crop yield increase, and for healing diseases, considered to be otherwise incurable, like radiological poisoning, cancer, viral infections, and some other diseases.

At the invitation of the Grand Master of the Masonic Mother Lodge in London, our scientists cured mad cow disease and cancer in the UK in the 1990s with the restructured bioactive water.

Contact us to inquire about **TESLA WATER**.

(/tesla-water.html)

Ordering all our products and services means you accept the conditions of this client consent form.

Services and products include your MINI-TESLA PSI-GENERATOR (/tesla-generator.html), REMOTE REJUVENATION SERVICE (/remote-laser-treatment.html), E-VIAGRA (/tesla-generator.html) and **I-VIAGRA (/remote-laser-treatment.html), TESLA BIOACTIVE WATER (http://www.wavegenome.com/order-bioactive-water.html), VISIT TO OUR CLINICS IN MOSCOW OR SIBERIA (http://www.wavegenome.com/visit-our-clinic-for-cure-and-rejuvenation.html), and CONSULTATION (http://www.wavegenome.com/ask-our-maven.html), but are not limited to this, and are subject to change at our sole discretion, as well as conditions themselves, without prior notice to our customers.**

By placing an order, the client authorizes **WAVE GENOME LLC** to perform all the necessary procedures, including the HeNe laser procedure, in order to produce client's **MINI-TESLA PSI-GENERATOR** (/tesla-generator.html) or administer the **REMOTE REJUVENATION SERVICES (/remote-laser-treatment.html)**, including the remote charging of **TESLA BIOACTIVE WATER (/tesla-water.html)** and administering **E-VIAGRA (/tesla-generator.html)** and **I-VIAGRA (/remote-laser-treatment.html)**. Placing an order implies that the client is fully informed of the reasons, and anticipated benefits for this procedure. This authorization is given with the understanding that the practice of medicine and rejuvenation is not an exact science and unforeseen circumstances might disrupt or prevent the successful treatment. The client recognizes that during the course of treatment, these unforeseen circumstances may necessitate additional or different procedures than those set forth above. The client acknowledges that he/she had the opportunity to discuss his/her condition, proposed services, concerns or questions. The client acknowledges that he/she has been given enough information, has his/her questions answered, has adequate knowledge to make an informed decision and wishes to proceed with the proposed treatment. The client testifies that he/she has read and understood this form and voluntarily authorizes and consents to the services.

Client agrees with SHIPPING / HANDLING and RETURN / EXCHANGE policy.

All sales upon agreeing to client consent conditions (http://wavegenome.com/wave-genome---client-consent.html) are final, no refunds. Invoices paid with delay accrue penalties.

Agreeing to the client consent conditions constitutes a legal agreement between WAVE GENOME LLC and customer.

(/mini-tesla-generator-faq.html)

READ INFORMATION LEAFLET FOR THE MINI-TESLA GENERATOR (COMES WITH THE UNIT) (/information-leaflet-for-mini-tesla-generator.html)

(/)

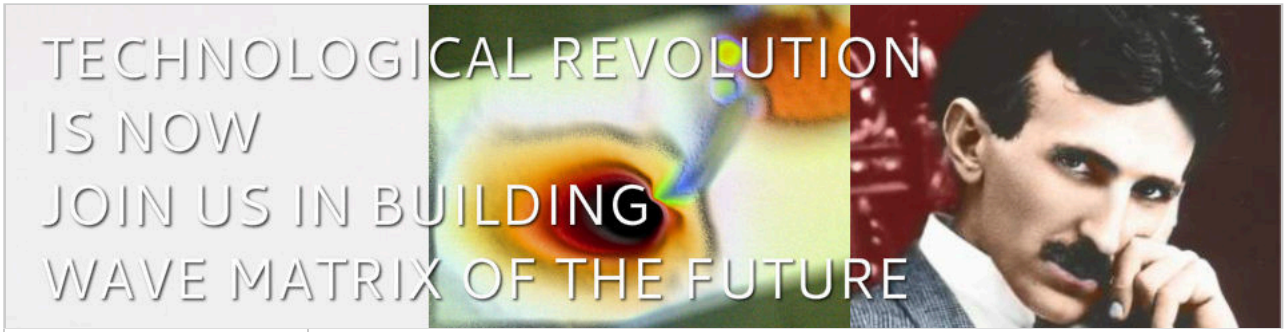

HOME / ГЛАВНАЯ (/)

SERVICES / УСЛУГИ (/SERVICES--10591057105110591043104 8.HTML)

PRODUCTS / ТОВАРЫ (/PRODUCTS--10581054104210401056106 7.HTML)

CONTACT / КОНТАКТ (/CONTACT--10501054105310581040105010 58.HTML)

ORDER FORM

(/tesla-generator.html)

(/remote-laser-treatment.html)

(/tesla-water.html)

Use this **ORDER FORM** to order all products by **WAVE GENOME LLC**. In the "**ORDER DETAILS**" please designate which product you would like to order.

Our TESLA PSI-GENERATORS are produced according to TU 9444-021-42844321

Certificate # 77, FC.19.944. P.2455.11.00

Ordering means you accept THE CLIENT CONSENT CONDITIONS (/client-consent.html)

Please copy/paste or reproduce the following Order Form in your email to WAVE GENOME LLC in order to place your order.

NAME

DATE OF ORDER

ACCEPT CLIENT CONSENT CONDITIONS YES / NO

DATE OF BIRTH (format: September 10, 1963)

PRODUCTS

EMAIL

ADDRESS

PHONE

Send your order and your photographs as high resolution scans and as jpegs files for the INDIVIDUALIZED MINI-TESLA psi-generators

(/mini-tesla-generator-faq.html)

You can order:

TESLA PSI-GENERATOR (/tesla-generator.html)
RA PSI-GENERATOR (/ra-psi-generator.html)
TESLA GLASSES (/order-tesla-glasses.html)
TESLA SCREEN (/tesla-screen.html)
TESLA WATER (/tesla-water1.html)
TESLA SELENIUM (/order-tesla-selenium.html)TESLA HUMAN CELL (/tesla-human-cell.html)
TESLA TEST (/tesla-test.html)
REMOTE LASER TREATMENT (/remote-laser-treatment.html)

E-DRUGS or I-DRUGS (http://www.wavegenome.com/wave-pharmaceuticals.html)

AUTHENTICITY CONCERNS:

Our items are in high demand. To make sure you buy authentic product produced by **WAVE GENOME**, you need to register your item by sending Registration Inquiry to mail@wavegenome.com

to mail@wavegenome.com (mailto:mail@wavegenome.com)

After we receive your order, we email you your invoice. We accept payments via Bank Wire Transfer, or via **ZELLE (https://www.zellepay.com/)** (sending money via email though your Bank online).

All shipments are made from Russia via EMS Russian State Global Courier Door-to-Door Express Mail. EMS is very reliable, safe and totally trackable though every point of moving your shipment across the continents. In the first quarter of 2017, PricewaterhouseCoopers (PwC) Consulting Firm assigned EMS the sixth place among the best Global Courier Services in its Global Rating for the quality of service. EMS is a signature required service.

Shipping fee is $100 for shipping to the US and elsewhere, and $77 for shipping to Europe. In the "Order Details", please specify which product and which model of the **MINI-TESLA psi-generators** you want. Contact us at mail@wavegenome.com if you have any questions.

REMOTE REJUVENATION "OM" (/remote-laser-treatment.html)
TESLA BIOACTIVE WATER (/tesla-water.html)
VISIT TO OUR CLINICS IN MOSCOW (/quantum-clinic.html) - Visitation Program to Russian clinics NOT owned by WAVE GENOME
CONSULTATION (/ask-our-maven.html)

Note: We do not produce, distribute, market and sell wave matrices of harmful substances, like narcotics.

To place your order:

(1) F**ill up this Order Form.**

(a) provide your order details;
(b) provide your contact information;
(c) email to mail@wavegenome.com your scanned photograph in childhood or youth as a high rez jpeg file for your **MINI-TESLA psi-generator (/tesla-generator.html)**. If you do not have childhood photograph, you can send in your adult photograph.

(2) **VISIT TO OUR CLINICS (/quantum-clinic.html)**
require sending in your medical data as well.

(3) In six to eight weeks your **MINI-TESLA psi-generator** (/tesla-generator.html) will be shipped to you. Other products are shipped in three to four days depending on stock availability. **We ship worldwide**.

**WELCOME TO THE QUANTUM LEAP BY WAVE GENOME,
THE PIONEER OF THE LASER POLARIZED BIOHOLOGRAPHY**

QUANTUM GENETICS

Laser Polarized Bioholography as a Diffraction of Geometric Optics with Chromosomes

Modern genetic engineering through the cutting and gluing of DNA fragments the (Monsanto method) will lead to a collapse of the human, animal and plant genome. of genetic collapse. The universe is holographic and we can record and transmit only holographic information based on the Geometric Optics of chromosomes.

Irene Caesar, PhD. [https://wavegenome.com/index.html]

September 5, 2017
Moscow. Russian Federation

This scientific study was aimed at experimental verification of the theoretical hypothesis put forward by Irene Caesar in 2014 that the genome functions as a Polarization Bioholography, based on the shape of chromosomes for focusing genetic information. This

hypothesis lays the basis for the development of technologies for remote Quantum Bio-Internet, both the management of biosystems by a remote laser signal, and for the recording and transfer of drugs on electret and digital media.

The theory of geometric optics of chromosomes was created by Irene Caesar on the basis of the theory of wave crystals developed by her in the 1980s, in which the signals are reflected into themselves in consequence of the negative shell of the wave crystal (due to the change in the spin of a single torsion / torus), and the refraction of the signals to zero the center of the wave crystal as an optical focus:

> "Modern genetic engineering through the cutting and gluing of DNA fragments leads to genetic collapse.While the universe is holographic, we can record and transmit only holographic information based on the Geometric Optics of chromosomes."

The same gene is expressed in functional individuals by the metacentric chromosome, and in dysfunctional individuals – through the acrocentric chromosome.The chromosome is a lens that allows our cells to focus the necessary wave information The procedure during cell division is similar to the crystal (lens) in our eye.The metacentric chromosome is analogous to a well-centered and focused eye crystal, whereas the acrocentric chromosome is similar to the myopic or far-sighted eye. " (Irene Caesar, Phd.)

According to Dr. Caesar:

> "The chromosome is a geometric code and functions through refraction (refraction) in a wave crystal, that is, in a nonlocal unique biohologram or wave matrix that focuses genetic information unique to a given person through its unique interference / diffraction grating of a scalar (standing) wave. "

"Thus," continues Dr. Caesar:

> the chromosome is a structural / geometric code or form that is holographic in nature, allowing remote control of

> biosystems through Laser Polarized Holography

According to Dr. Caesar:

> A hologram is not an image, but a special structural quality of a signal.

According to the holographic principle, the universe is entirely in each of its matrix points. ” Caesar states that the Hologram contains an infinite number of waves, particles and fields. Therefore, according to her, the hologram can not be “counted” in terahertz, infrared or any other range. In August 2012, she formulated the consequence of the holographic principle, which theoretically explains the possibility of remote control of biosystems.

Dr. Caesar states that:

> If the universe is completely at each of its matrix points, then each matrix point is not simply different from any other matrix point, but is unique.

Thus, each wave matrix is both unique and non-local.

The project of Quantum Bio-Internet was created by Dr. Caesar in the spring of 2013, and presented to her for the joint implementation in May 2013 in London of the head of the Byzantine Templars, Andrew Sharalambus. The project consisted in the instantaneous transmission of holographic information from one copy to another copy of a unique non-local wave matrix / biohologram during the scanning of one of the copies by a Helium-Neon laser with internal mirrors. This transfer was proposed for the first time on the global market, ahead of all other researchers in this field, including PP. Garyaeva, who began offering a remote transfer only after this project was made public.

According Dr. Caesar, the holographic principle explains the eleotrical / dipole nature of the biohologram: the holographic principle “means that each biohologram has opposite poles, each pole representing a change in the spin in a single torsion (torus). The change in the spin causes each linear external signal to be reflected on itself inside the hologram, so that a

scalar / standing wave arises when the peak of the forward-going wave is annihilated by a depression of the same wave when it reflects itself.

A diffraction grating of a scalar wave refracts the external linear signals in the direction of the zero center of the wave crystal / hologram, similar to the focus of the crystal in our eye. Covering the shape of the crystal, that is, the refraction inside the diffraction grating, our eye receives different information. The same happens with our chromosomes.

After that, DNA is self-protected from any external linear signal, since it is a paradigmatic scalar wave, because its one turn goes in one direction and the other in the opposite direction. While RNA is a single-stranded spiral antenna, which is thus vulnerable to external signals. Thus, the secret of the genome lies in the form of RNA as an inductor, which collects, amplifies and stores energy in the form of a magnetic field. Genetic improvement is possible only if RNA collects and stores the correct linear signals and for a long time; and only if DNA annihilates these signals in its scalar wave by creating spatial translational symmetry (metacentricity) of the holographic signal, imposing it on the chromosomes during cell division “(Irene Caesar, PhD).

Dr. Caesar states that “The geometry of chromosomes changes the nature of the external signal from linear to holographic through:

1. the polarization of the torus (by changing the spin in a single toroidal DNA field)
2. through the reflection of any external linear
3. through the refraction of any incoming signal to the center of the wave crystal that functions as a focus, in the same way as y to earn our eye (© Irene Caesar, Geometry Chromosomes 2014) (Irene Caesar, Ph.D., “Remote Control / biosystems based on the form of chromosomes as a diffraction grating for focusing the genetic information”, reports and articles,

Dr. Caesar concludes: “We can produce remote laser control of biosystems and, thus, create people with improved physical and mental abilities, and dramatically prolong life expectancy, based on the consequence of the holographic principle and the mastery of geometric codes chromosomes.

See Dr. Caesar’s article.: Remote management of biosystems based upon the shape of chromosomes as diffraction grating for focusing genetic information [https://irenecaesar.wordpress.com/2016/06/14/remote-management-of-biosystems-based-upon-the-shape-of-chromosomes-as-diffraction-grating-for-focusing-genetic-information/]

Irene Caesar was the first person who proposed to transfer pharmaceutical preparations with holograms as diffraction / refraction gratings, and to create holograms by lasers on the principle of refraction.

From May to September 2017, at the experimental sites of the Moscow State Technical University, named after NE Bauman, a scientific group led by her successfully implemented and tested her new method of recording and remote transmission of biograms using laser spectroscopy and coding electrets at the nanoscale using a laser. According to Dr. Caesar, “Polarized Biohologography technology creates “lenses” that help our chromosomes correct their refraction to focus genetic biologic information both locally and remotely”

During the experiments, for the first time in the world, a new high-precision laser spectrograph was used to record Biohologram Pharmaceuticals. Dr. Caesar proposed a modification of the laser spectrograph (an egg with shiny inner surfaces, for sublimation through resonance in the pyramidal part, and then for zeroing the signal in the spherical part in a scalar / standing wave), which will greatly expand the capabilities of this device for recording biohologramms.

The mathematical model was developed by a group of scientists who developed a mathematical model of the flight of the Caliber rockets.

50MEGS Sign In Sign-Up

QUANTUM BIOHOLOGRAPHY

Biophysics * Biochemistry * Biocosmology * Holographic Universe * DNA Phantom

Home Page
INTRO
Zero Point
Photonic Brain
Photonic Body
Illumination
Invisible Ground
Consciousness
Soma Sophia
Golden Flesh
Pineal DMT
Ionatopia Links
Biophysics
Biohology
Bioplasma
HoloMind
HoloVerse
Psi Research
ART GALLERY
News
WHAT'S NEW
Realblog

FROM HELIX TO HOLOGRAM

FROM HELIX TO HOLOGRAM
(Ode on the Human Genome)

Iona Miller, O.A.K., 2003
iona_m@yahoo.com

"Form is not other than Void; Void is not other than Form." Heart Sutra

FROM BIOCHEMISTRY TO BIOPHYSICS

What is DNA; where did it come from; how does it function to create life, to create us?

We have some of the biochemical answers, but we can look deeper into biophysics for our models. We propose that DNA functions in a way that correlates with holographic projection. DNA projects a blueprint for the organism that is translated from the electrodynamic to the molecular level. Further, research strongly suggests DNA functions as a biocomputer. This DNA-wave biocomputer reads and writes genetic code and forms holographic pre-images of biostructures. We are more fundamentally electromagnetic, rather than chemical beings.

BIOCOSMOLOGY

Where do we come from? Imagine the possibility life may have come from the fertile womb of the Universe to Earth as a tiny hitchhiking alien, using a meteor as a spacecraft. Anaxagorus, an ancient Greek, first proposed the theory that the seeds of life are spread throughout the universe. A science for discovering the foundations of life needs a theory, a biological Big Bang. One current theory has emerged from astrobiology, the science that searches for life in the universe. It is a candidate to replace the old concept that life arose on Earth in "primordial soup."

Panspermia alleges that life exists and is distributed uniformly through the universe in the form of amino acids, microbes, germs, and spores. If life arose extraterrestrially, our planet is not a closed-system. The fossil evidence shows life took root on Earth as soon as possible, once the heavy bombardment period subsided, the planet cooled and water formed. Vulcanism and space debris made it inhospitable to life for the first half a billion years of planetary existence.

This "seed of life" can travel between worlds by natural means, such as ballistic impact, meteorites, and comets. Intergalactic space may be permeated with cosmic dust and microbes. Evidence shows they could survive the hard-core radiation and the near-absolute cold of deep space. Some researchers (Hoyle and Wickramasinghe, 2000) believe these "seeds" of life are still raining down on us all the time, affirming our cosmic ancestry.

Four billion years ago there was no DNA. It is widely believed that our DNA/protein based cells are derived from an earlier world based on RNA, which can both replicate information and be a catalyst for chemical or metabolic processes. In the prebiotic era, self-assembling RNA was both the genetic and catalytic basis. The simple genome resided in the RNA, a single circular chromosome.

We still don't know how RNA arose in the first place (Poole, 1998). Perhaps it arose from some simpler self-replicating molecule. The evolutionary path from the RNA world led to the most primitive organisms, prokaryotes (bacteria and archaea) and eukaryotes (single-celled organisms).

Neither variety of primitive organism is a complete cell, but even prokaryotes have some free-floating DNA and ribosomes to make protein. Ribosomes "read" the genetic information and make whatever the cell needs. They possibly existed longer than 3.55 billion years ago, as their fossils and carbon deposits may indicate. Even exponents of competing theories of the origin of life agree ribosomes are at least 2.7 billion years old (Copley, 2003).

For 500 million years there were only RNA-based organisms. Primitive life could exist in hostile

surroundings, with extreme heat, acidity, or with no oxygen or even light. Latest findings show this lifeform descends deep within the crust of our planet, and perhaps others. It seems life is not so fragile after all, but hearty and robust. The womb of our Universe is fertile, rather than hostile to life.

How life took a quantum leap into the world that eventually manifested human life is still a mystery. To call it life, you need a cell with both a nucleus and containing membrane. The mystery is written in the cells and molecules of all the life that still surrounds us.

The eukaryotes evolved in complexity, developing cellular characteristics. Arguably, there are fossils 3.8 billion years old that have structural molecules, ribosomes, and protein-synthesizing machinery. Proteins make the molecules for the “blueprint” molecule DNA possible. The stable DNA molecule became the genome carrier.

SALT OF THE EARTH

“We wish to suggest a structure for the salt of deoxyribonucleic acid (DNA). This structure has novel features which are of considerable biological interest.” Thus, Watson and Crick announced their revolutionary discovery with an understatement about their studies on pure crystallized DNA. But what was the role in the evolution of life for this “salt of the earth”?

A shift to an oxygen-rich atmosphere 2.0 billion years ago allowed the evolution of cells with a nucleus. Eukaryotes keep their DNA structures in a nucleus. They have 10 to 1000 times more of this genetic substance than prokaryotes. For a thousand million years there were only prokaryotes (microbes) and single-celled micro-organisms, eukaryotes. Their reign covers half the timeline of life on Earth.

Cells became more and more complex over eons, and developed into organs, and beings evolved to fuel them. Fish, vertebrae, plants, insects, amphibians, reptiles, mammals, birds, and flowers appeared. All animals, insects, plants, fungi, and algae are eukaryotes, though the volume of prokaryotes far outnumbers cellular life. Prokaryotes are still essential to sustaining life on the planet. RNA still plays a vital role in cellular life, and hasn’t relinquished its primal importance.

Perhaps life did not evolve on Earth at all if it is over 3850 million years old. Maybe it did come in the form intergalactic organic compounds, of extremely hardy bacteria, spores, and microbes from space, perhaps safely nestled deep in meteors, comets, and planetary debris torn loose in collisions. Once they arrived from space, according to the theory, they self-assembled as proteins, then amino acids, and life with the ability to grow and reproduce.

DNA became the active repository of nature’s blueprints for life, a library of proteins. Deoxyribonucleic acid is the molecule that programs our genetic potential. It is a virtually immortal thread tying us to all the life that has ever existed. Decoding life has become a reality, pulling off the veil of nature’s mysterious process. Scientists can now purify, amplify and reproduce DNA in the laboratory. They can also overwrite the genetic code, to create wholly new organisms.

THE GENETIC ODE

The secret of life! How long mankind has yearned to know its essence and how to extend lifespan and improve health. The discovery of the DNA helix in 1953, by Watson and Crick revealed the shape of this magic molecule. The following 50 years of research has directly led to our ability to read the human genome. We can now decipher its creative meaning and imitate its creative evolution. Genetic engineering is no longer a chimera or scifi dream, but a stark reality.

In terms of genetics, we are moving from the machine age to the gene age; a flood of new genetic information is transforming science and medicine. A linear string of nucleotides makes up DNA. It specifies ‘codons’, which in turn specify the amino acids that make up all of the different proteins that combine together to make a body. Five decades of tedious work made it possible to identify the 3.3 billion nucleotides that encode the sequence of the human genome.

Where are we now? It remains to be seen what sort of balance we strike between using the genome for good or ill, or even if we retain our “humanity” and genetic integrity. Humankind has never attempted such a crucial project before. It has often been said that “The map is not the territory,” and the same holds true for the “map” of the human genome. Looking at the map doesn’t reveal the natural consequences of real life experimentation. In complex systems, small changes can quickly pump up into dramatic consequences, often unforeseen and potentially catastrophic.

For the time being, the twisted staircase of DNA is explored in the realms of molecular biology and biochemistry. Based on opening this world of biological organization, we can conjecture what mysteries an even deeper look at the functional basis of living matter might reveal. This is the domain of biophysics, realm of both particle and wave interactions -- fields. It has been demonstrated that DNA is electrically conductive; much like copper wire it can carry a charge. It is believed this live-wire vital capacity may have been the charge transfer that gave life a jump-start. DNA’s ability to transport charge helps minimize genetic damage from oxidation (Lawton, 2003).

The same fundamental physical laws that govern matter and the Universe also govern living organisms. Even a sound biochemical theory can be replaced by an even better, more fundamental, biophysical theory. It is still important to study properties at their own levels, not just as consequences of more fundamental scientific disciplines.

Where are we going? Who knows how future generations of man may be engineered from the 3.3 billion “letters” of the human genome? We have been looking to the genetic code for the secret of life. Perhaps we should be listening to the “genetic ode”, the EM song of life that reverberates throughout our being, the audible life stream.

THE HOLOGRAPHIC UNIVERSE

We are more fundamentally electromagnetic, rather than chemical beings. DNA is not the driver of evolution but even more fundamental quantum mechanical symmetry-breaking forces (King, 2003).

If we drop down another whole domain of observation from the juicy “wetware” described by chemistry and atomic structure, we enter the subatomic realm of quantum physics. At this level the behavior of matter, both organic and inorganic, is governed not by classical notions of cause and effect or even complex dynamics, but by those of quantum probability.

“Something” appears to emerge from virtually “nothing” which physicists have come to describe as a sea of infinite potential. They call it quantum foam, vacuum potential, or zero-point energy. We can call it the vacuum substructure. Subatomic particles wink in and out of existence on a continuous basis, like some subatomic froth. This “something” appears paradoxically in wave/particle form. This world is not transcendent to matter, but underlies it as a coherent unity, much like ecology underlies biology.

Within this context, some physicists (Miller, 1975; Bohm, 1980) have strongly suggested that the nature of reality is fundamentally analogous to that of a holographic projection. The optical process called holography uses interference patterns. Holography describes transformations of light and optical information mathematically in wave mechanical terms.

The superposition of a split beam of laser light led to the laboratory development of holograms, or recordable holographic images demonstrated by Dennis Gabor beginning in 1949. In 1971, Karl Pribram applied this metaphor to neuropsychology, suggesting it was more than analogy, that the brain actually encodes information as holograms. The pattern holds the form.

Holograms contain all the information needed to reconstruct a whole image. Holograms contain many dimensions of information in far less space, like a compressed file. They hold that information in a subtle network of interacting frequencies. Thus, shining a coherent light (reference beam) or laser through the fuzzy-looking overlapping waves of a 2-dimensional hologram can create a virtual image of a 3-dimensional figure.

The gist of the holographic paradigm is that there is a more fundamental reality. There is an invisible flux not comprised of parts, but an inseparable interconnectedness. The holographic paradigm is one of reciprocal enfolding and unfolding of patterns of information. All potential information about the universe is holographically encoded in the spectrum of frequency patterns constantly bombarding us.

In this dynamic model there are no “things”, just energetic events. This “holoflux” includes the ultimately flowing nature of what is, and all possible forms. All the objects of our world are three-dimensional images formed of standing and moving waves by electromagnetic and nuclear processes. This is the guiding matrix for self-assembly, and manipulating and organizing physical reality.

Criss-crossing patterns occur when two or more waves ripple through each other. In the transactional interpretation of quantum physics, waves of probability originate in the past, present, and future. Events manifest when waves from past and future interfere with each other in the present. That pattern creates matter and energy. The universe emerges from the rippling effects of immense numbers of criss-crossing interference waves. The geometry of the fields is more fundamental than the fields or emergent particles themselves.

Our brains mathematically construct ‘concrete’ reality by interpreting frequencies from another dimension. This information realm of meaningful, patterned primary reality transcends time and space. Thus, the brain is an embedded hologram, interpreting a holographic universe. All existence consists of embedded holograms within holograms and their interrelatedness somehow gives rise to our existence and sensory images.

Interference patterns of waves can be visualized interacting like ripples on a pond. At the quantum level they create matter and energy as we perceive them, lifelike 3-dimenional effects. Consciousness and matter share the same essence, differing by degrees of subtlety or density. There is a strong correlation between modulations of the brain’s EM field and consciousness (Persinger,1987; McFadden, 2002). The universe is a continuously evolving, interactively dynamic hologram.

This “Holographic Concept of Reality” was first suggested by Miller, Webb, and Dickson in 1973, and later touted by David Bohm (1980), Ken Wilber (1982), Karl Pribram (1991), Michael Talbot (1991), and others. In this holistic theory, the Universe is considered as one dynamic holomovement, a grand Unity.

The part is not only contained within the whole, the whole is contained in every part, only in lower resolution. So, following the axiom of “As Above; So Below” we can expect biology to be based on the same physical foundation of creation. Miller and Webb hypothesized precisely this in “Embryonic Holography,” also in 1973. At the time, of course, such notions were untestable. But, with continuing revolutions in technology, now we are closer to modeling and demonstrating this creative process.

DNA AS HOLOGRAPHIC PROJECTOR

In a hologram, wave fields interfere with one another to lay the foundations for the reconstruction of the image of an object. But how are the wave fields produced? The term holography comes from the Greek roots meaning “entire” and “to write”. In holography, the image is projected by a coherent light source split into both an object wave and the reference wave background.

This dichotomous nature is reflected in the particle/wave nature of the DNA molecule, which can be “read out” with biophotons from chromosomes to set up a holographically produced wave field. This superposition of wave fields (object wave and reference wave) creates a wave guide for the formation of biological structure.

The image is constructed according to the reference information contained in the genes. The reconstructed object wave is identical with the object wave field. The reconstructed wave fields reproduce exactly the recorded ones (the DNA with genetic code).

Russian research in genetics led scientists to begin looking experimentally at the helical structure of DNA as a possible holographic “projector” of the DNA code. Thus, the existential blueprint described by the spiral staircase of DNA is translated into a complex EM field that guides the molecular growth of the organism. Miller, et al, suggested as much three decades ago, and outlined possible mechanisms of this quantum biohologram at both the cellular and whole organism level.

This process emerges from a domain more fundamental than the standard genetic code triplet model. Biophysics can now describe how our form emerges directly from the void, the vacuum substructure. In essence, we emerge from the cosmic void -- pre-geometrically structured nothingness. DNA is the projector of that field which sets up the stress gradients in the vacuum substructure to initiate dynamic unfolding. Genes function as holographic memories of the existential blueprint.

At the moment of ovulation there is a definite shift in the electrical fields of the body of a woman. The membrane in the follicle bursts and the egg passes down the fallopian tube. The sperm is negative with respect to the egg. When the sperm and egg unite, the membrane around the egg becomes hyperpolarized, shutting out other sperm.

It is at this moment that the electromagnetic entity is formed. The fertilized egg cell contains all the holistic information necessary to create a complete operational human being. The biohologram begins to function at conception and ceases only at death. Our contention is that the DNA at the center of each cell creates the multi-cellular creature hologram by expressing and projecting the DNA in the center of the cells.

The biohologram projected by the embryonic nervous system forms a three-dimensional pattern of resonant structures. These structures behave as acoustic waves, acting as field guides for flowing matter and energy. The holograms are “read” by electromagnetic or acoustic fields that carry the gene-wave information beyond the limits of the chromosome structure. In this new understanding, DNA and the chromosome apparatus is the recording, storing, transducing, and transmitting system for genetic information at both material and physical field levels.

DNA-WAVE BIOCOMPUTER

The Gariaev group (1994) proposed a theory of the DNA-wave Biocomputer. They suggest (1) that there are genetic “texts”, similar to the context-dependent texts in human language. (2) The chromosome apparatus acts simultaneously both as a source and receiver of these genetic texts, respectively decoding and encoding them. (3) The chromosome continuum acts like a dynamical holographic grating, which displays or transduces weak laser light and solitonic electro-acoustic field. In other words, the code is transformed into physical matter guided by light and sound signals.

Complex information can be encoded in EM fields, as we all know from coding and decoding of television and radio signals. Even more complex information can be encoded in holographic images. DNA acts as a holographic projector of acoustic and EM information that contains the informational quintessence of the biohologram. Quantum non-locality of genetic information is fundamental.

The nervous system acts as a coordination mechanism that integrates DNA projection of the rest of the cells in the system, aligning these cellular holograms. The biohologram, projected by the brain, creates standing and moving electromagnetic wave patterns at different frequencies of the spectrum in order to effect different biochemical transformations. There may be specific electrostatic fields, or there may be electrodynamic field varying at various frequencies, from low (radio waves) all the way up the spectrum into visible light (biophotons) and beyond.

Genes are located on chromosomes in a linear order within the cell nucleus. Chromosomes have the ability to transform their own genetic-sign laser radiation into broadband genetic-sign radio waves (the encoded signal transforms from light to sound). The polarization of chromosome laser photons is connected non-locally and coherently to polarizations of radio waves.

Through this mechanism a new field structure is excited from the physical vacuum by an intrinsic creativity that emerges through DNA. The genome genetic and other regulatory wave information is recorded at the polarization level of its photons and is non-locally transferred or played out through the entire biosystem by the polarization code parameter.

Only 3% of the 3 billion base pair genome encodes the physical body. The four-letter alphabet of genetic elements includes Adenine (A), Cytosine (C), Guanine (G), and Thymine (T) or Uracil (U) components of DNA, arranged in three-letter “words” that tell the cell what proteins to manufacture.

These genetic characters are distributed in the genetic text in a fractal distribution, i.e., reiterated. So, the nucleotides of DNA molecules are able to form holographic pre-images of biostructures. This process of “reading and writing” the very matter of our being manifests from the genome’s associative holographic aspect in conjunction with its quantum nonlocality.

Rapid transmission of genetic information and gene-expression unite the organism as a holistic entity embedded in the larger Whole. Gene-expression is the mechanism by which new patterns are called into being. The system works as a biocomputer, a wave biocomputer.

This biogenesis mirrors the cosmic process of creation. The holographic dynamic underlies both processes of cosmological creation and biogenesis. Chemical bonding is a consequence of the non-linear inverse square law of electromagnetic charge interaction in spacetime.

Charge interaction precedes quantum chemistry perturbations of bonding energetics. Despite being genetically coded, molecules form fractal structures both in their geometry and dynamics. Generating core biochemical pathways gives rise to the fractal structures of proteins, nucleic acids and tissues.

Theories of biogenesis, such as Panspermia, are strongly supported by the fact that organic molecules and amino acids, as well as the nucleotides A, U, G, and C have been detected in meteorites. It is a fecund universe, at both the cosmic and human scale.

QUANTUM BIOHOLOGRAPHY

Hypothesis: The organization of any biological system is established by a complex electrodynamical field that is, in part, determined by its atomic physiochemical components. These, in part, determine the behavior and orientation of these components. This dynamic is mediated through wave-based genomes wherein DNA functions as the holographic projector of the psychophysical system, a quantum biohologram.

In the mid-1980s, physicist Peter Gariaev first noted a DNA phantom effect in his experiments. DNA was bombarded with laser light. When removed physically from the scattering chamber, its electromagnetic signature, a ghostly holographic after-image apparently remained. What is measured is light scattering from the DNA phantom fields.

No other substance has been found to emulate the effects of the DNA molecule. As long as the chamber is not disturbed, the effect is measurable for long periods of time. Evidence suggests a relationship to the phenomena of endogenous bioluminescence, liquid crystals, and superconductivity.

Bioluminescence is the emission of photons of light produced when certain energized electrons drop into a lower or ground state. Humans emit a variety of electromagnetic radiations across the emission spectrum, indicative of the energy state of the organism.

In the nuclei of each cell of the human body, the DNA (deoxyribonucleic acid) carries the structure of our whole body. It is the blueprint not only of our physical form, but also of the processes that our form undergoes in terms of survival. The primal vacuum is the matrix of our existence and proportionately our most fundamental reality. In essence, we emerge from pre-geometrically structured nothingness. DNA is the projector of that field which sets up the stress gradients in the vacuum or quantum foam to initiate the process of embryonic holography.

DNA PHANTOM

The Gariaev group has discovered a wave-based genome and DNA phantom effect that strongly supports the holographic concept of reality. This main information channel of DNA is the same for both photons and radio waves. Superposed coherent waves of different types in the cells interact to form diffraction patterns. First, they emerge in the acoustic domain, secondly in the electromagnetic domain.

DNA seems to embody the capacity to produce a field experienced by other DNA in the body, linking all holistically together. This dynamic is linked to the cellular level via mechanisms of RNA transfer and enzymatic action in the cell. DNA and RNA are likely to be in non-local communication, possible because DNA molecules in chromosomes are in a state of substance-wave duality. So, DNA codes an organism both through DNA matter and by DNA wave sign functions at the laser radiation level. Wave information is recorded at the polarization level of photons and is non-local. It is transferred throughout the biosystem by the polarization code parameter, eliciting holistic response patterns.

Gariaev claims to have demonstrated subtle fields emerging from the quantum foam or vacuum potential, making the effect quantifiable and measurable, objective. He found the phantom effect by irradiating DNA with a target UV wavelength of 338 nm. Poponin (1995) went on to suggest that some new field structure is being excited from the physical vacuum by an intrinsic ability that emerges through DNA.

Gariaev discovered the DNA Phantom Effect in 1985 when he worked in correlation spectroscopy of DNA, ribosomes and collagen in the Institute of Physics, in the Academy of Science of the USSR. He was first able to publish his results in 1991, leading to a book in 1994, Wave Based Genome. He demonstrated a dynamic new field in the vacuum substructure by bombarding it with coherent laser light and coupling it to conventional electromagnetic fields. The experimental protocols for this procedure have been reproduced in Moscow from ideas developed at Stanford, and are currently in another replication by experimental physicist Louis Malklaka.

YOU TURN ME ON; I'M A RADIO

In analyzing any complex adapative system, we follow what happens to the information; in this case the genetic information. The quantum hologram is a dynamical translation process between acoustical and optical holograms. DNA and the genome have been identified as active "laser-like" environments.

Roughly speaking, DNA can be considered a liquid crystal gel-like state that acts on the incoming light in the manner of a solitonic lattice. A soliton is an ultra stable wave train that arises in the context of non-linear wave oscillation. Oscillations are set up when DNA acts as a rotary pendulum kindling other oscillations.

Chromosomes can transform their own genetic-sign laser radiations into broadband genetic-sign radio waves. This is the main information channel of DNA, the same for both photons and radio waves. Superposed coherent waves of different types in the cells interact to form diffraction patterns, first in the acoustic domain, then in the electromagnetic domain. The quantum hologram is the matrix of the translations between acoustical and optical holograms. The human biocomputer can be modeled through the marriage of quantum mechanical and complex dynamics.

Other researchers soon obtained similar results, and not only based on photons. Multi-frequency physical fields are now teleported. Based on this data, it's possible to suppose that photon fields, emitted by chromosomes as sign fields, can be teleported within or even outside the organism's space. T

he same is true for wave photon fronts, which were read from the chromosome continuum similar to reading from a multiplex hologram. If photons are transformed into radio waves through the EPR-mechanism, then this phenomenon is vital. In fact, the importance of quantum non-locality existence for a genome is hard to overestimate (Gariaev, et al, 2001).

Basic assumptions of Gariaev, et al included the following:

1. The genome has a capacity for quasi-consciousness so that DNA "words" produce and help in the recognition of 'semantically meaningful phrases."

2. The DNA of chromosome control fundamental programs of life in a dual way: as chemical matrixes and as a source of wave function and holographic memory.

3. Processes in the substance-wave structures of the genome can be observed and registered through the dispersion and absorption of a bipolar laser beam.

QUANTUM TELEPORTATION

The polarizations of chromosome laser photons are connected non-locally and coherently to polarizations of radio waves. The signal can be "read out" without any loss of the essential information in the form of polarized radio waves. The genome is a quasi-hologram of light and radio waves that create the background necessary for the appropriate expression of genetic material. Gariaev argues that the genome emits light and radio-waves whose delocalized interference patterns creates calibration fields or "blueprints" for a system or organism's spacetime organization, in a coordinated response typical of living systems. Gariaev asserts that quantum non-locality and holography is indispensable to properly explaining such realtime dynamics.

Other research suggests the fundamental interaction of internal and external fields is the right track. Joseph Jacobson (2002) at MIT, found a way to switch cells off and on with radio waves. His team also "unzipped" and manipulated DNA with a radio-frequency pulse. The same approach worked on proteins as well, and proteins orchestrate nearly all cellular chemical processes.

Thus, genes can act as quantum objects exhibiting the phenomenon of quantum non-locality/teleportation. This robust dynamic assures information super redundancy, cohesion and the organism's integrity, and thus viability. Gariaev's experiments suggest that DNA does indeed behave like a single quantum, which induces a "hole" temporarily in the vacuum when the DNA sample is physically removed from the vacuum chamber.

Quantum Bioholography says that DNA satisfies the principle of computer construction. It carries a copy of itself, its own blueprint, while the mechanism engineering the DNA replication is the biophotonic electromagnetic field. The "letters" of the genetic texts A, G, C, U are held invariant. The existence of the genetic text constitutes the classical signal process of quantum teleportation. It facilitates the quantum mechanical signal processes of both the copying of the DNA as its own blueprint, and of the construction and homeostasis of the organism in a massively parallel way by means of quantum teleportation.

So, the marriage of the 50 year old study of DNA with the 50 year old science of holography has given birth to the model we call the quantum biohologram. The discovery of Gariaev of the phantom DNA and the DNA-wave biocomputer strongly suggests that this is more than a model but actually the physical mechanism for our appearance from virtually nothing. In one way you could say we "came out of nowhere."

But here we are, nevertheless. It is solely because of our DNA's ability to transform its genetic blueprint into a physical reality, embodying simultaneously our inherited past and our future. Sure, we can now

create ersatz life, but we cannot create the fundamental elements from which it arises, which are the gift of the universe, cooked in giant supernovae aeons ago. It's like that old joke where the scientist says to God, "We can now make an Adam out of clay, and God says, "No, first you have to make your own dirt!"

REFERENCES

Berezin, A.A., Gariaev, P.P., et al (1996), "Is it possible to create laser based on information biomacromolecules?", Laser Physics, v.6, N6, pp. 1211-1213.

Bohm, David (1980), Wholeness and the Implicate Order, Routledge, London.

Copley, Jon (2003). "Proof of Life". New Scientist. Vol. 177, No. 2383, pp. 28-31, Feb. 22, 2003.

Gariaev, Peter, Boris Birshtein, Alexander Iarochenko et al. (2002), "The DNA-wave Biocomputer", MS, Institute for the Control of Sciences, Russian Academy of Sciences, Moscow, Russia, and Wave Genetics, Inc., Toronto, Canada; also see http://www.emergentmind.org .

Gariaev, P.P. (1994), Wave Genome, Public Profit, Moscow, 279 pages [in Russian].

Gariaev, P.P. (1993) Wave based genome, Depp. VINITI 15:12. 1993, N 3092?93, 278pp. [in Russian].

Gariaev, P., Tertinshny, G., and Leonova, K. (2001), "The Wave, Probabilistic and Linguistic Representations of Cancer and HIV," JNLRMI, v.1, No.2.
Hoyle, F., (1981). The relation of biology to astronomy (University College Cardiff Press).
Hoyle, F. and Wickramasinghe, N.C., (1981). In Comets and the Origin of Life (ed. C. Ponnamperuma) pp 227-239 (D. Reidel)
Hoyle, F. and Wickramasinghe, N.C., (1985). Living Comets (University College, Cardiff Press)
Hoyle, F. & Wickramasinghe, N.C., (2000). Astronomical Origins of Life: Steps towards Panspermia. Kluwer Academic Press.
Jacobson, Joseph et al. (2002), "Remote electronic control of DNA hybridisation through inductive coupling to an attached metal nanocrystal antenna", Nature (2002) 415:15-155.
Kelleher, Colm A. (1999), "Retrotransposons as Engines of Human Bodily Transformation," Journal of Scientific Exploration, 13, no 1, Spring 1999, pp. 9-24.

King, Chris (1999). "Fractal Neurodynamics and Quantum Chaos: Resolving the Mind-Brain Paradox Though Novel Biophysics," Fractals of Brain; Fractals of Mind, Advances in Consciousness Research 7. http://www.dhushara.com/book/paps/consc/brcons1.htm#anchor217145

King, Chris (2003). "Biocosmology" . http://www.dhushara.com/book/biocos/biocos.pdf

Lawton, Graham (2003). "Live Wire," New Scientist. Vol. 117, No. 2386., March 15, 2003, pp.38-39.

Marcer, P. and Schempp, W. (1996). "A Mathematically Specified Template for DNA and the Genetic Code, in Terms of the Physically Realizable Processes of Quantum Holography" Proceedings of the Greenwich Symposium on Living Computers, editors Fedorec, A. and Marcer, P., 45-62.

Marcer, P. and Schempp, W. (1997a), The Model of the Prokaryote Cell as an Anticipatory System Working by Quantum Holography, Proceedings of CASYS 97, 11-15, August, HEC-Liege, Belgium, International Journal of Computing Anticipatory Systems, v2, 307-315.

Maslov, M.U. and Gariaev, P.P. (1994), Fractal Presentation of Natural Language Texts and Genetic Code, 2nd Intl Conference on Quantitative Linguistics, Sept. 20-24, Moscow State University, Philological Faculty, pp. 193-194.

McFadden, Johnjoe (2002), "Synchronous Firing and Its Influence on the Brain's Electromagnetic Field: Evidence for an Electromagnetic Field Theory of Consciousness," (CEMI Theory), Journal of Consciousness Studies (2002) 9: 23-50.

Miller, R.A., Webb, B. Dickson, D. (1975), "A Holographic Concept of Reality," Psychoenergetic Systems Journal Vol. 1, 1975. 55-62. Gordon & Breach Science Publishers Ltd., Great Britain; reprinted in the hardback book Psychoenergetic Systems, Stanley Krippner, editor. 1979. 231-237. Gordon & Breach, New York, London, Paris; again in the journal Psychedelic Monographs and Essays, Vol. 5, 1992. 93-111. Boynton Beach, FL, Tom Lyttle, Editor. Also in JNLRMI 2002 at emergentmind.org

Miller, R. A., Webb. B., "Embryonic Holography," Psychoenergetic Systems, Stanley Krippner, Ed. Presented at the Omniversal Symposium, California State College at Sonoma, Saturday, September 29, 1973. Reprinted in Lyttle's journal Psychedelic Monographs and Essays, Vol. 6, 1993. 137-156. Also in JNLRMI 2003 at emergentmind.org

Miller, R.A. (1974), "Bioluminescence, Kirlian Photography and Medical Diagnostics"; Mankind Research Unlimited, a formerly unpublished, proprietary paper.

Miller, R. A., Iona Miller, and Burt Webb (2002). Quantum Bioholography: A Review of the Field from 1973-2002. JNLRMI, Oct. 2002.

Miller, Iona (1993), "The Holographic Paradigm and the Consciousness Restructuring Process,"

Chaosophy '93, O.A.K., Grants Pass.

Miller, S.L., and Robertson, M.P. (1995). "An efficient prebiotic synthesis of cytosine and uracil," Nature, 375, 772.

Patel, A. (2000), Quantum Algorithms and the Genetic Code, Proceedings of the Winter Institute of Quantum Theory and Quantum Optics, 1-13 January, S.N. Bose National Centre for Basic Sciences, Calcutta, India.

Persinger, Michael A (1987), Neuropsychological Bases of God Beliefs, Praeger Publishers, New York.

Poole, A.M., Jeffares, D.C. and Penny, D. (1998). "The path from the RNA world," Journal of Molecular Evolution, 46, 1.

Poponin, Vladimir, "The DNA Phantom Effect: Direct Measurement of A New Field in the Vacuum Substructure."

Presman (1970), Electromagnetic Fields and Life. New York: Plenum.

Pribram, Karl (1971), Languages of the Brain, Prentice-Hall, Inc., Englewood Cliffs: New Jersey.

Pribram, Karl (1991), Brain and Perception: Holonomy and Structure in Figural Processing, Lawrence Erlbaum Associates, Publishers, Hilldale: New Jersey.

Pullman and Pullman (1963), Quantum Biochemistry, New York: Interscience, 1963. .

Rossi, E. (2000-2002), "Exploring Gene Expression in Sleep, Dreams & Hypnosis with the New DNA Microarray Technology." http://home.earthlink.net/~rossi/

Rossi, E. and Lippincott, B.M., "The Wave Nature of Being: Ultradian Rhythms and Mind-Body Communication. http://home.earthlink.net/~rossi/

Rossi, E., "Psyche, Soma and Gene Expression" http://home.earthlink.net/~rossi/

Rossi, E. (2002). The Psychobiology of Gene Expression: Neuroscience and Neurogenesis in Hypnosis and the Healing Arts. New York: W.W. Norton Professional Books.

Schempp, W. (1992), "Quantum Holography and Neurocomputer Architectures", Journal of Mathematical Imaging and Vision, 2, 279-326.

Schempp, W. (1993) "Bohr's Indeterminacy Principle in Quantum Holography, Self-Adaptive Neural Network Architectures, Cortical Self-organization, Molecular Computers, Magnetic Resonance Imaging and Solitonic Nanotechnology", Nanobiology 2, 109-164.

Shcheglov, V.A., Gariaev, P.P. (1996) Lazer-lazer interactions and phantom effects in genetic structures. "Science on the threshold XXI age New Paradigms" [in Russian].

Sidorov, L. (2002), "Control systems, transduction arrays and psi healing: an experimental basis for human potential science", The Journal of Non-Locality and Remote Mental Interactions, online at http://www.emergentmind.org.

Szent-Gyorgyi (1957), Bioenergetics. New York: Academic Press.

Szent-Gyorgyi (1960), Introduction to a Submolecular Biology. New York: Academic Press.

Talbot, Michael (1991), The Holographic Universe, Harper Collins Publishers, New York.

Wilber, Ken (1982), The Holographic Paradigm, Boulder: Shambhalla.

Archived from http://www.skywatch-research.org/QuantumHolographic.htm on April 8, 2004 .

The Biophotonic Quantum Holographic Matrix

by William F. Hamilton III

ABSTRACT: This paper is an attempt to integrate studies of the quantum potential, quantum holography, biophotonics and the enveloping matrix of biointegration, biocommunication, and bioinformation that composes the web of light and life in living organisms and their possible genesis in an electromagnetic infoton.

Introduction:

David Bohm, theoretical physicist proposed a new hidden variables theory of Quantum mechanics. He assumes the wave function does not represent just a set of probabilities: it represents an actual field. This field exists and acts upon particles the same way a classical potential does, thus it is a quantum

potential which is associated to this field and is a function of the wave function. It is postulated here that the quantum potential is active as a field in living cells and organisms and acts upon them.

The equation Bohm used to represent this quantum potential is given:

the quantum potential
(1)

Research reveals that Bohmian quantum potential is still used, but that it may only represent a means to extend quantum theory into a realistic theory of particles and fields.

It resolves the dilemma of the appearance, in one and the same phenomenon, of both particle and wave properties in a rather straightforward manner: Bohmian mechanics is a theory of motion describing a particle (or particles) guided by a wave. This guiding wave is usually attributed to atomic particles, but might be more insightfully seen as a traveling soliton or vortex.

Bohmian mechanics is manifestly nonlocal, and the velocity may depend upon the positions of other, even distant particles whenever the wave function of the system is entangled.

The behavior of the particle is determined by the particle's position and momentum, the wave field and the sub-quantum fluctuations.

"Bohm's quantum potential binds the entire universe together into what he liked to call a seamless "unbroken wholeness." Every particle in the universe is connected by the quantum potential to every other particle. He likened the cosmos to a hologram in which each point on the film carries information about the entire picture. Bohm's GWT, far more sophisticated than de Broglie's crude version, is a "holistic" vision in which all parts of the universe are joined to every other part. "Interconnectedness" was one of Bohm's favorite words. He saw the universe as resembling the unity of a living organism, a kind of pantheism not unlike Spinoza's--a pantheism Einstein himself favored." (2)

Bohm referred the holomovement as the basic reality. The pattern formed on a photographic plate by light waves that interfere and create a hologram. This pattern is the interaction or interference pattern of two parts of a laser light (coherent light). One beam reflects off an object, the other off a mirror. In addition, any portion of the holographic plate contains information on the whole object.

Biohologram:

Every cell in the human body contains nuclear DNA, information on the whole body, much like a hologram, only the cells can go through a process of division and reproduction (mitosis).

In quantum holography, things are spookier still. While holograms are typically constructed with interfering beams of light, in quantum holography the researchers measure the simultaneous arrivals of an illuminating photon that is sent into a chamber and a companion photon in the other entangled beam. (2)

Quantum holography, as depicted in this cartoon, is a way that physicists could produce three-dimensional images of objects that would be invisible to systems relying on classical physics. A source S produces two photon beams (h1 and h2). The photons in h1 are quantum mechanically entangled with the photons in h2. When a photon in h1 enters chamber C, it encodes three-dimension information about the enclosed object (in this case a Grecian bust) in the interference of the two paths it could take - a path that intercepts the object and subsequently is reflected to the chamber wall, and a path that misses the object and strikes the chamber wall directly. The second beam, h2, passes through conventional optics and strikes a detector array D. A coincidence counter extracts the holographic information by monitoring the relative time between a photon in h1 striking the chamber wall and its entangled mate in h2 arriving at detector D.

Wave Genetics Inc. and the Moscow Institute of Control Sciences are exploring a new concept of the genetic code that asserts:

(1) That the evolution of biosystems has created genetic "texts", similar to natural context dependent texts in human languages, shaping the text of these speech-like patterns.

2) That the chromosome apparatus acts simultaneously both as a source and receiver of these genetic texts, respectively decoding and encoding them, and

3) That the chromosome continuum of multicellular organisms is analogous to a static-dynamical multiplex time-space holographic grating, which comprises the space-time of an organism in a convoluted form.

That is to say, the DNA action, theory predicts and which experiment confirms,

(i) is that of a "gene-sign" laser and its solitonic electro-acoustic fields, such that the gene-biocomputer "reads and understands" these texts in a manner similar to human thinking, but at its own genomic level of "reasoning". It asserts that natural human texts (irrespectively of the language used), and genetic "texts" have similar mathematical-linguistic and entropic-statistic characteristics, where these concern the fractality of the distribution of the character frequency density in the natural and genetic texts, and

where in case of genetic "texts", the characters are identified with the nucleotides, and

(ii) that DNA molecules, conceived as a gene-sign continuum of any biosystem, are able to form holographic pre-images of biostructures and of the organism as a whole as a registry of dynamical "wave copies" or "matrixes", succeeding each other. This continuum is the measuring, calibrating field for constructing its biosystem.

“Complex information can be encoded in EM fields, as we all know from coding and decoding of television and radio signals. Even more complex information can be encoded in holographic images. DNA acts as a holographic projector of acoustic and EM information which contains the informational quintessence of the biohologram. Only 3% of human DNA encodes the physical body. The remaining 97% of the 3 billion base pair genome contains over a million genetic structures called transposons, that have the capacity to jump from one chromosomal location to another (Kelleher, 1999). We are 99.9% alike in our genetic legacy. Our individuality is expressed in three million small variations in our cells, called single nucleotide polymorphisms.

Gene-expression is the mechanism by which new patterns are called into being (Rossi, 2000). There is also a strong correlation between modulation of the brain’s EM field and consciousness (Persinger, 1987; McFadden, 2002). The Gariaev group has discovered a wave-based genome and DNA phantom effect which strongly supports the holographic concept of reality (Miller, Webb, thingyson, 1975). This main information channel of DNA is the same for both photons and radio waves. Superposed coherent waves of different types in the cells interact to form diffraction patterns, firstly in the acoustic domain, secondly in the electromagnetic domain -- a quantum hologram -- a translation process between acoustical and optical holograms.” (4)

The distribution of the character frequency in genetic texts is fractal, so the nucleotides of DNA molecules are able to form holographic pre-images of biostructures. This process of "reading and writing" the very matter of our being manifests from the genome's associative holographic memory in conjunction with its quantum nonlocality. Rapid transmission of genetic information and gene-expression unite the organism as holistic entity embedded in the larger Whole. The system works as a biocomputer -- a wave biocomputer.

The quantum nonlocality of the genetic information is fundamental. Experimental work of the Gariaev group shows how quantum nonlocality is directly related to laser radiation from chromosomes (coherent light), which jitterbugs its polarization plane to radiate or occlude photons. DNA and the genome have now been identified as active "laser-like" environments. Roughly speaking, DNA can be considered as a liquid crystal gel-like state that acts on the incoming light in the manner of a solitonic lattice.” (5)

Biophotonics:

This entire section is extracted from the History of Biophotonics website:

Around 1923 Alexander Gurwitsch discovers an "ultraweak" photon emission from living systems (onions, yeast,...), since he suggested connections between photon emission and cell division rate. He calls this photonemission "mitogenetic radiation". His experiments indicate that the wavelength is in the range around 260 nm (Bibliography under Gurwisch and also Ruth (1977, 1979)).

Around 1950: Russian scientists rediscover "ultraweak photon emission" from living organisms. Most results are published in "Biophysics" (engl.) and originally in "Biofizika").(Bibliography under Ruth, 1979).

Italian nuclear physicists discover by chance "bioluminescence" of seedlings. They do not think that this finding is significant, but they publish the results. (Colli et al. 1954, 1955, Ruth 1979).

The Russian biophysicist and the American chemist enunciate the first theory of ultraweak photonemission (UWPE) from biological systems, the so called "imperfection" theory. UWPE shall be an expression of the deviation from equilibrium, some kind of distortion of metabolic processes (Zhuravlev 1972, Seliger 1975, Ruth 1979).

Independently from each other and by different motivations scientific groups in Australia (Quickenden), Germany (Fritz-Albert Popp), Japan (Inaba), and Poland (Slawinski) show evidence of ultraweak photon emission from biological systems by use of modern single-photon counting systems. Bibliography (Quickenden, Inaba, Popp &Ruth, Slawinski).

While Quickenden, Slawinski and Inaba prefer the imperfection theory, Popp and his group enunciate just the opposite theory:

1. The radiation originates from an almost perfect coherent photon field.

2. Essential sources are the DNA and corresponding resonators in the cells.

3. The mechanism describes photon storage in cavities and information channels, tuned by Casimir forces.

4. There is a close connection to delayed luminescence which corresponds to excited states of the coherent photon field.

5. The radiation is not the product but essentially the initiator of chemical reactions in the cells. The radiation submits the information within and between cells.

6. The radiation is not limited to the optical range but follows a f = const-rule (the occupation probability of the phase space is equal for all wavelengths) and extends to longer wavelengths including the so called heat radiation of the body.

7. This radiation is the proper regulator and information carrier of life.

The Marburg group of Fritz-Albert Popp calls this phenomenon "biophotons" in order to stress the difference to "bioluminescence": Biophotons are single quanta which are permanently and continuously emitted by all living systems. They are subjects of quantum physics and they display an universal phenomenon attributed to all living systems. Worldwide all scientists who agree with these statements call the radiation biophotons and the scientific field "biophotonics".

From 1972 to 1980 the Marburg group of the leader, the physicist and Dr. habil. Fritz-Albert Popp, evaluated experimentally all the essential physical properties of biophotons.

1. The intensity ranges from a few up to some hundreds photons/(s cm2).

2. The spectral distribution follows in the time average a f = const-rule.

3. The modes are strongly coupled.

4. The delayed luminescence that approaches continuously the biophoton emission follows a hyperbolic rather than an exponential relaxation function.

5. The biophotons origin from an almost fully coherent field.

6. Cells are able to establish cavity resonators which contribute to biophoton regulation.

7. The essential source of non-equilibrium biophoton emission is the DNA.

This group introduces the first time photocount statistics (PCS) into biophotonics. They show evidence that biophotons are emitted according to a Poissonian PCS. Furthermore they show evidence (1) that the delayed luminescence follows a hyperbolic relaxation function rather than an exponential one, (2) that the modes are strongly coupled, and (3) that there are hyperbolic oscillations around the continuous hyperbolic relaxation function. The group finds the first time intercellular communication by means of biophotons. Later this was confirmed by Albrecht-Bühler (Bacteria), Popp and Chang (dinoflagellates), Galle (daphnia), Shen (blood), Vogel (bacteria).

(Bibliography under Popp and coworkers, i.e. Bahr, Böhm, Grass, Grolig, Herrmann, Kramer, Rattemeyer, Ruth, Schmidt, Wulle, Albrecht-Bühler, Chang, Galle, Shen, Vogel).

The papers of Popp and his group are examined mainly by the group of B. Chwirot (Kopernikus University, Torun). They confirm the essential results (Bibliography Chwirot et al.).

Herbert Klima (Atom Institute Vienna) performs his dissertation in Popp`s group at the University in Marburg. He transfers "Biophotonics" to the University in Vienna, in particular investigations on laser excitation of living systems.

(Bibliography Klima or Atominstitut Wien).

J.Slawinski cooperates with the groups in Japan, USA and the Popp-group in Germany. He follows mainly the links between biophotons and biochemical reactions. There arises a branch biochemical biophotonics that becomes an essential part mainly in Japan and USA." (6)

Bioinfotons:

This term "bioinfoton" is one I am adopting to specify any particle (such as the Ganesh Particle*), wave, or biomolecule that transfers information from an emitter to a receptor. It is possible that if a biophoton is emitted from a coherent source that it will carry holographic information as a form of modulation (possibly frequency modulated) and produce action or results in biological systems.

It is possible that biophotons may even be carriers of psi information and that a coherent coupling can be established between two conscious life forms resulting in a transference of information from a higher potential field to a field at lower potential. Even though this is conjecture at this point, it suggests other means by which disparate life forms can communicate. We know there is a process by which trees communicate and even signal each other in the face of danger. We may be exchanging information with pets and other animals through biophotonic communication. This may be how some people who have a green thumb affect plants they care for.

Even communication with other intelligent life forms in the Cosmos may be effected by the amplification and vectoring of biophotons or via the quantum potential, produce information at a distance.

A virtual photon flux in the quantum potential may be integrating the coordinated wholeness of the organism while the action of bioinfotons may keep every part of the organism in communication with

every other part.

Conclusions:

Life and living organisms are more than the sum of their parts and are composed of material and non-material parts. The spiral form of DNA evidently produces an electromagnetic wave field that informs the organism's growth and structure.

Scientist Richard Alan Miller is a pioneer in this field and has written,

"In a hologram, wave fields interfere with one another to lay the foundations for the reconstruction of the image of an object. But how are the wave fields produced? The term "holography" comes from the Greek roots meaning "entire" and "to write". In holography, the image is projected by a coherent light source split into both the object wave and the reference wave background. This dichotomous nature is reflected in the particle/wave nature of the DNA molecule, which can be "read out" with biophotons from chromosomes to set up a holographically produced wave field. This superposition of wave fields (object wave and reference wave) creates a wave guide for the formation of biological structure. The image is constructed according to the reference information contained in the genes. The reconstructed object wave is identical with the object wave field. The reconstructed wave fields reproduce exactly the recorded ones (the DNA with genetic code). " (7)

Mr. Miller also proposes this hypothesis:

"QUANTUM BIOHOLOGRAPHY

Hypothesis: The organization of any biological system is established by a complex electro dynamical field that is, in part, determined by its atomic physiochemical components. These, in part, determine the behavior and orientation of these components. This dynamic is mediated through wave-based genomes wherein DNA functions as the holographic projector of the psychophysical system—a quantum biohologram."

I propose that the biohologram is embedded as an integral part of the biocosmic hologram we call Universe.

Dr. Dan Burisch has seen evidence that a Ganesh Particle* can transmute itself into a fully functional atypical eukaryotic cell in a matter of seconds, not aeons. Such evidence, when it becomes available, will change our entire perspective on the existence of a universal holonomic mind that informs its creation.

*Ganesh Particles are charged clusters that extracted from ancient bedrock and have a seemingly unknown origin, but carry information which is transferred to cells via a crossbridge. (Discovered by Dr. Dan B.C. Burisch)

References:

1. http://plato.stanford.edu/entries/qm-bohm/#qp2. http://www.ksharpe.com/Word/BM05.htm3. http://www.aip.org/enews/physnews/2001/split/566-1.html4. http://www.rialian.com/rnboyd/dna-wave.doc5. http://www.geocities.com/iona_m/Chaosophy4/ bioholography/bioholo graphy.htm6. http://www.lifescientists.de/history.htm

1. http://www.nwbotanicals.org/oak/newphysics/Helix%20to%20Hologram .pdf

SubatOMic, Io 2005

These are a few of my favorite photographs from my different travels. Feel free to browse themas you like. If you want one click your right mouse button and choose"Save As" from the menu.

50MEGS

Sign In Sign-Up

PHOTONIC BRAIN

Photodynamics * Bioholograms * Pulse Dynamics * DMT

Home Page

INTRO

Zero Point

Photonic Brain

Photonic Body

Illumination

Invisible Ground

Consciousness

Soma Sophia

Golden Flesh

Pineal DMT

Ionatopia Links

Biophysics

Bioholography

Bioplasma

HoloMind

HoloVerse

Psi Research

ART GALLERY

News

WHAT'S NEW

Realblog

PHOTONIC BRAIN

Life is Light
Photodynamics
Brain Holograms
Signal Cascade
Pulse Dynamics

PART I: PHOTONIC BRAIN

Hypothesis: There are photoreceptors deep in the brain, which circulate signals to other parts of the body. We are spectral photonic beings with laser, fiber optic, bioluminescent, optical imaging and tuning capacities. Energetic medicine techniques employ photons, electrons, protons, waveforms, frequencies, and other transducing elements, taking medicine far beyond current biology and technology.

Bringing Physics to Life

Chambers of light deep in the brain? Imagine an internal visual space as ground, a literal holographic theater of the mind, a laserium in the fluid-filled ventricles of the deep brain. We always have to remind ourselves to ask where the energy comes from. Physics defines the living organism as good as or better than biochemistry. Quantum process describes the organism and dynamics best. Energy makes discrete jumps from state to state.

Quantum physics and molecular biology are two disciplines that have evolved relatively independently. However, recently a wealth of evidence has demonstrated the importance of quantum mechanics for biological systems and thus a new field of quantum biology is emerging. Is there a biology of quantum information? Koichiro (2000) argues there is: “Novel biophysical methods resulting from the fusion of biology and quantum mechanics have the potential to revolutionize our understanding of both fields.”

Novel biophysical methods resulting from the fusion of biology and quantum mechanics have the potential to revolutionize our understanding of both fields. Living systems have mastered the making and breaking of chemical bonds, which are quantum mechanical phenomena. Absorbance of frequency specific radiation (e.g. photosynthesis and vision), conversion of chemical energy into mechanical motion (e.g. ATP cleavage) and single electron transfers through biological polymers (e.g. DNA or proteins) are all quantum mechanical effects.

A matter-wave is a disturbance of space foam, the dense grid-like structure. When disturbed, a resonance of the

What's New with Biophysics

HEATSTRINGS: Quantum Biofeedback
http://heartstringsbook.50megs.com

BIOPHYSICS Portal
http://biophysics.50megs.com

EMERGENT HEALING Portal
http://emergenthealing.50megs.com

PSIONA PARAPSYCHOLOGY
http://psiona.50megs.com

DIY MIND CONTROL
http://mindcontrol.50megs.com

Consciousness may be somehow mediated by the cerebro-spinal fluid in the brain's cavities, the ventricles (Ferguson 1996). Cerebrospinal fluid is a water-based, nutrient-filled liquid generated within the two largest ventricles, the lateral ventricles. Each hemisphere of the brain contains one of these lateral ventricles. These fluid-filled cavities then connect with a centrally located third and fourth ventricle. These connect to the spinal column. Cerebrospinal fluid circu lates freely around the brain and throughout these cavities.

Optometrist Ray Gottlieb has theorized that the brain may use the principles underlying the physics of phase-conjugate mirrors (from laser holography) to retrieve associated information and make decisions (Ferguson 1996). To Gottlieb and others, the brain's ventricles, filled with cere brospinal fluid, provide the reactive medium needed to support such a

matter-wave is also a resonance in the electromagnetic field, the oscillation of electron waves. The electromotive force of light (virtual photons) drives an exchange observable in mitogenic radiation. State changes are a result virtual photon fluctuation. Mitogenic radiation acts as a coherent light laser in the infrared, UV, and visible frequencies.

Photons are discrete concentrations of massless energy emitted when electrons move from one energy state to another. Electrons demonstrate interference patterns like photons of light. Photons are the elementary unit or quantum of electromagnetic radiation. Much of the biophoton is virtual and scalar in dimension

Life is an electrodynamic process, and all electrodynamic processes are photon-dependent. Photons have spin 1 and they are therefore bosons. Photons mediate the electromagnetic field. They are the particles that enable other particles to interact with each other electromagnetically and with the electromagnetic field.

Bacteria and plants exploit quantum physics for excitation and are optimized to use light energy (light-harvesting) to drive their metabolic reactions. Humans don't live by photosynthesis, but light is still a big factor in metabolism, circadian rhythms, reproduction, and perhaps other processes.

In the quantum holographic DNA-wave biocomputer theory, DNA is a self-calibrating antenna working by phase conjugate adaptive resonance. It is capable of both receiving and transmitting quantum holographic information stored in the form of diffraction patterns, quantum holograms.

The brain and senses are matter-wave systems, as is the structure of all Reality we know. The brain and body are wave-biocomputers (Gariaev). Growth of the brain may be related to a wave resonance that arises from a DNA wave system. The brain is essentially a resonance system.

Photonics deals with generating, controlling and detecting light. It plays a major role in sensing. The linings of the brain ventricles are essentially enfolded skin tissue, a sensing organ with similar sensitivities to those of the retina. Quantized lightwaves impinge on the retina, and likewise endogenous light may impinge on photoreceptors in the ventricle lining.

Scientists have witnessed an atom and a photon - a small packet of light - share the same information. Chris Monroe (3004) and colleagues from the University of Michigan used a cadmium atom trapped in an electric field to 'store' information about the atom's magnetic state. By pumping energy into the atom with a laser, they forced it to spit out a packet of light. That photon carried an imprint of the atom's information with it, which could be read by a detector.

The photon as a mobile bit of quantum information is called a 'flying qubit'. Researchers have already entangled pairs of atoms, and pairs of photons. But this is the first time that scientists have seen a single atom entangled with a single photon.
http://www.bioedonline.org/news/news.cfm?art=853

The development of single photon sources and single photon counting detectors is driven by the emergence of many applications requiring such devices. These applications, such as quantum cryptography, quantum computation, correlated photon metrology, quantum imaging, quantum interferometry etc, comprise a new area of endeavor known as Quantum Information Technologies

theory. Other research shows that biological structures emit the photons necessary for such a function (Rubik 1996). If the brain uses phase-conjugate principles, information could be distributed throughout the brain and body by means other than nerve pathways. Gottlieb's theory supports the holographic brain model proposed by Karl Pribram in the 1970's.

Ferguson, M. (1996). Is mind mediated by water? In Brain Mind - A bulletin of Breakthroughs. Vol. 21, 4-5.

A Proposed Mechanism for Consciousness via Phsyiologically Functional Endogenous Light
K.Simanonok .
Photons are known to be emitted from cells and may be physiologically functional as signal carriers. Not to be confused with macroscopic bioluminescence (which may however represent a specialization in energy emission of which all cells are capable), cell photon emissions occur at low ('weak' or 'ultraweak') intensities not detectable by the eye. They span the visible spectrum and extend into the near ultraviolet; although emissions outside the visible spectrum may only loosely be termed 'light', they are included in that term in this context. For a system of physiologically functional endogenous light to exist, at least four capabilities are required (others beyond these minimal four may of course exist): 1) Light signals must be generated and emitted from cells. 2) Emitted light signals must be transmitted to adjacent and/or distant cells. 3) Cells must be capable of receiving light signals. 4) Cells must be capable of transducing received light signals into information that they can process. Cell photon emissions are well documented but have not yet been shown to carry information (except for some examples of bioluminescence, fireflies being perhaps the best known). Capability 2 may be met by collagen fibers functioning as fiber optics, since almost all nonmotile cells are interconnected by a

(QIT).

Photodynamics

Particles found in biological processes include photons, electrons, protons, elementary ions, inorganic radicals, organic radicals, molecules, and molecular aggregates. Photons act upon electrons by raising their energy state. This process is called excitation.

Excited electrons can drop back to more stable energy levels and emit photons. Electron excitation can lead to the formation of an electronic bond between molecules. This is the traditional bond of classical chemistry. The breaking of such bonds can, by reverse process, lead to the excitation of electrons.

In living systems the excitation of electrons by photons and the subsequent conversion of that excitation into the bond energy is called photosynthesis and is the basic builder of biological structures. The reversal of this process is called bioluminescence. This phenomenon is the transfer of energy from a bond to an excited electron, resulting in the emission of a photon. It has been suggested by Szent-Gyorgyi (1957) that the energetics of living creatures can be understood in terms of photosynthesis and its reversal, bioluminescence.

Radiated photons are a type of electromagnetic signal. The photonic flux process may or may not only manipulate and guide photons but also convert photons into electrons and process the electrical signal. An ideal photonic material emits and modulates light efficiently. Photonics can ideally do an enormous amount of parallel processing, intelligent photonics. Signals may exceed visible and near infrared. Allan Frey showed microwave frequency auditory inputs in the human brain.

Cell photon emissions are well documented but have not yet been shown to carry information. Photons are known to be emitted from cells and may be physiologically functional as signal carriers. This phenomenon should not be confused with macroscopic bioluminescence, energy emission of which all cells are capable. Cell photon emissions occur at low ('weak' or 'ultraweak') intensities not detectable by the eye.

Our own eyes, like those of other vertebrates, have ciliary photoreceptors; so does the pineal "third eye", a structure that is buried in the brain and is involved in circadian rhythmicity, and which still, in lower vertebrates, functions directly as a photoreceptor.

Photon emissions span the visible spectrum and extend into the near ultraviolet. Emissions outside the visible spectrum may only loosely be termed 'light', but are included in that term in this context. According to Simanonok (2000), for a system of physiologically functional endogenous light to exist, at least four capabilities are required (others beyond these minimal four may of course exist):

Light signals must be generated and emitted from cells.

Emitted light signals must be transmitted to adjacent and/or distant cells.

Cells must be capable of receiving light signals.

Cells must be capable of transducing received light signals into processed information.

Collagen fibers function as fiber optics. Almost all nonmotile network of collagen fibers, a network which makes up approximately half of the total protein content of a human body. Other fiber types such as elastin and intracellular matrixes of microtubules (especially those in neural axons) are also possible candidates for functional roles in a biophotic information exchange system. Collagen fibers have been shown to exhibit fiber optic properties in preferentially conducting light along their fiber axes, and can modulate a light signal passing through them when stretched at physiologic force levels. It is well known that retinal photoreceptors are capable of capabilities 3 (receiving light) and 4 (processing light into information), which again may represent a functional specialization like macroscopic bioluminescence built upon more rudimentary capabilities of which many cells are capable. What is less well known is that the lamellar structures of retinal photoreceptors are highly specialized cilia, and that ciliated cells are abundant in the brain. Do cilia possess rudimentary photoreceptive (and possibly waveguide) capabilities, which evolution has built upon to create photoreceptors? This is a key question because much of the ependymal lining of the cerebral ventricles is ciliated (their function unknown). It is proposed that ventricular ciliary beating is affected by and becomes coordinated with the timing of neural activity so that endogenous light is guided into dynamically resonant patterns in the ventricles and surrounding tissues, patterns involving energy loci which have feedback capability on neural events. Dynamically resonant patterns of light within the brain may interact with a larger population of virtual photons and/or virtual particles filling space outside our normal frame of reference and support consciousness in the brain by creating a pathway for a small part of the intelligent consciousness underlying the universe (‘god’) to be affected by and to influence endogenous light patterns, which in turn influence neural events, which in turn influence perception, thought, and

cells are interconnected by a network of collagen fibers, which makes up approximately half of the total protein content of a human body. Other fiber types such as elastin and intracellular matrixes of microtubules (especially those in neural axons) are also possible candidates for functional roles in a biophotic information exchange system (Hameroff).

Simanonok also suggests, it is well known that retinal photoreceptors are capable of capabilities 3 (receiving light) and 4 (processing light into information), which again may represent a functional specialization like macroscopic bioluminescence built upon more rudimentary capabilities of which many cells are capable.

Cerebral Photoreceptors

All biological material is photosensitive. What is less well known is that the lamellar structures of retinal photoreceptors are highly specialized cilia, and that ciliated cells are abundant in the brain. Do cilia possess rudimentary photoreceptive (and possibly waveguide) capabilities, which evolution has built upon to create photoreceptors?

This is a key question because much of the lining of the cerebral ventricles is ciliated (their function unknown). Ventricular ciliary beating could be affected by and become coordinated with the timing of neural activity. Thus, endogenous light is guided into dynamically resonant patterns in the ventricles and surrounding tissues, patterns involving energy loci which have feedback capability on neural events.

Dynamically resonant patterns of light within the brain may interact with a larger population of virtual photons filling space outside our normal frame of reference and support consciousness in the brain. This is a possible pathway for endogenous light patterns to holistically influence neural events, which in turn influence perception, thought, and behavior in resonant feedback loops.

Brain ventricles may do far more simply bathe the brain interior in buffering cerebrospinal fluid and remove wastes. The pineal gland sits in the middle of them, like some mystical island in an ambrosial lake. These curiously-shaped hollow chambers may form a resonant cavity for the light sensitive DMT producing pineal gland. Why else would the pineal both produce photic neurotransmitters (Melatonin; DMT) and be sensitive to light?

In Kriya Yoga, the 3rd Ventricle is called the Cave of Brahma. The thalamus gland forms its walls, the hypothalamus its floor and plexus of the third choroid ventricles its roof.

“The mighty Hamsa Soul then wins its Wings to Freedom, as the subtle fibers of his Corona Radiata light up with Divine effulgence he takes flight into Cosmic Consciousness. He then experiences the total Divinity of and beyond Creation, gaining the ultimate knowledge of 'Tat Tvam Asi' That Thou Art.”

Brain Holograms

The ventricles of the brain act as liquid crystals. The primordial brain ventricle forms when the embryonic neural tube closes. The embryo develops not by chemical law but energetic dynamics, where energetic fields dictate growth. Radiation emanates from living tissue; because of its effects on mitosis it is called mitogenic radiation. Mitogenic

behavior in feedback loops.

On the Possibility of Large Upconversions and Mode Coupling between Frohlich States and Visible Photons in Biological Systems

J. Swain
Physics Department, Northeastern University
and
International Institute of Biophysics (IIB)
Landesstiftung Hombroich, Raketenstation
E-mail: john.swain@cern.ch

At least two significant roles for large scale quantum coherence in living systems have been suggested: Herbert Frohlich’s coherent excitations of nonlinearly coupled ensembles of large polarizable molecules, with frequencies in the microwave region, and Fritz Popp’s coherent visible photon emission arising from metabolically active cells. The large difference in frequencies has made it difficult to see these two phenomena as being linked. Here a case is made for a potentially large coupling between these modes, and suggestions are made for the biological roles played by these coherent excitations.

radiation has frequencies of 10(12 power) Hz. to 10(15 power) Hz., covering infrared through visible rays, bordering on ultraviolet.

Standing waves can be created that arise from vibrations in the ventricles. This creates a holographic frequency domain. Rhythm-entraining photoreceptors might be a second basis of bioholographic projection (besides DNA) in the resonant cavity ventricles. DNA produces mitogenic rays that can influence other cells.

The cavity of the neural tube may be considered a primordial ventricular cavity. It contains fluid that later will be termed cerebrospinal fluid. The secretion and absorption of this fluid now determines the pressure exerted on the neural tube. The opening of the optic vesicles into the ventricular cavity is semi-lunar at this stage. There are functional changes of these photoreceptors during pre- and postnatal development. They may be part of the process of embryonic holography.

Do these signals amplify in a resonant cavity as they do in modelocking in laser technology? One roundtrip of a modelocked laser is a single pulse (sometimes called a soliton) traveling back and forth inside the laser cavity. Each time the radiation passes through the saturable absorber, the highest intensity peak is reduced less than all of the others, so eventually just once peak oscillates back and forth in the cavity. It gets sharper and sharper as it bounces back and forth. http://www.unc.edu/~dtmoore/model_td.html

Modelocking is a method to obtainultrashort pulses from mode-locked lasers. Here, the laster cavity contains either an active element (an optical modulator) or a nonlinear passive element (a saturable absorber) which leads to the formation of an ultrashort pulse circulating in the laser cavity, in this analogy the ventricles.

Modelocking is a way of short pulse generation in which an optical pulse is repetitively reshaped as it circulates in the laser cavity. In the modelocking mode of operation a balance exists between mechanisms that tend to shorten and to widen the pulses. The aim is to find a configuration that delivers optical pulses with repetition rates in the GHz range, an active gain section and a passive cavity section. This becomes important because our bodies produce their own pulse dynamics.

Why are there nonvisual photoreceptors in the deep brain? They may do more than synchronizing internal clocks with the environment. The light-based entrainment of endogenous circadian clocks is present in various organs. Simanonok hypothesizes that photons emitted from cells in the brain are guided to the surfaces of the brain's fluid-filled ventricular spaces, where they interact with cilia lining those ventricles and are guided by the timed beating of the cilia so that the photons form interference patterns within the ventricular spaces, creating an interface.

The most ancient type of vertebrate nerve cells ("protoneurons"), CSF-contacting neurons are sensory-type cells sitting in the wall of the brain ventricles that send a ciliated dendritic process into the CSF. Various opsins and other members of the phototransduction cascade have been demonstrated in telencephalic and hypothalamic groups of these neurons. In all species examined so far, deep brain photoreceptors play a role in the circadian and circannual regulation of periodic functions. (Vigh, et al)

Altogether three phases were supposed to exist in pineal entrainment of internal pacemakers: an embryological synchronization by light and in viviparous vertebrates by maternal effects (1); a light-based, postnatal entrainment

(2); and in adults, a maintenance of periodicity by daily sympathetic rhythm of the hypothalamus. In addition to its visual function, the lateral eye retina performs a nonvisual task.

Nonvisual retinal light perception primarily entrains genetically determined periodicity, such as EEG rhythms or retinomotor movements. It also influences the primary pacemaker of the brain. As neither rods nor cones seem to represent the nonvisual retinal photoreceptors, the presence of additional photoreceptors has been supposed. Opsins are good candidates for nonvisual photoreceptor molecules, evolving from nonvisual --> semivisual --> visual in vertebrates.

Signal Cascade

Photoreceptors share structural features with pineal photoreceptors and with certain invertebrate extraretinal photoreceptors, but they are morphologically and biochemically distinct from visual photoreceptors of the retina. (Grace et al). Opsins are light-sensitive protein/pigments for detecting certain wavelengths.

Opsins are responsible for the initial cellular reactions involving light perception. A series of molecular reactions within the cell, called a signal cascade. Each individual opsin complex can be thought of as a specific detector. All wavelengths of light fall upon the complex, but only a narrow range of wavelengths is relayed down the signal cascade.

Tuning the spectrum to a specific peak wavelength, this channeling of light by the opsin-chromophore complex is called "spectral tuning." The spectrum, consisting of a broad range of wavelengths of energy (x-ray, microwave, visible light, radio wave), is tuned to one peak wavelength by each opsin complex.

All photoreceptors (modified neurons) contain pigment molecules that absorb light. Encephalic photoreceptors may have undiscovered roles. Nonvisual photoreceptors of the deep brain and pineal organs may collect signals across the wall of the brain ventricles that send a ciliated dendritic process into the CSF, a specific waveform, even a standing wave or holographic interference pattern.

In nonmammalian vertebrates, photic cues that regulate the timing of seasonal reproductive cyclicity are detected by nonretinal, nonpineal deep brain photoreceptors. In birds there is direct communication between the brain photoreceptor and the reproductive axis.

Gonadotropin releasing hormone (GnRH) neurons and processes are scattered among photoreceptor cells. Brain photoreceptors communicate directly with GnRH-neurons; this represents a means by which photoperiodic information reaches the reproductive axis.

Opsins constitute a large family of proteins, some of which have recently been found in mammalian brains; we aren't sure of their precise function. Many aspects of brain photoreception are understood. Encephalic photoreceptors are necessary and sufficient for the detection of changes in day length that determine seasonal reproductive readiness. The photic link between the brain sensory cells and the reproductive axis is achieved and unexpectedly reveal that the circadian system is not a necessary intermediary between the sensory and reproductive components.

Pulse Dynamics

Light created chemically by the pineal, or mechanically by the cilia are suggested signal carriers. Vibrational changes in the ventricles from resonating piezoelectrical vibrations from the heart have been demonstrated (Bentov). Vibrational changes in the photoreception complex of the ventricles can be generalized. Ordered water is another possible information channel, but here we are pursuing light.

Cranial Rhythms: The cranium has three major rhythmic pulsations that can be monitored. Cerebral spinal fluid moves with the fluctuation of the CRI (craniosacral rhythmical impulse). This reciprocation has a two-phase cycle, a tide-like phenomenon, flexion and extension.

1. Cardiovascular, 60 - 72 times per minute, this pulsation provides circulation throughout the cranium and the rest of the body.

2. Respiratory, 14 - 19 times per minute this rhythm provides oxygen to the vascular system.

3. CRI (cranial rhythmic impulse or craniosacral rhythmical impulse) 6 - 12 times per minute, this flexion/extension movement is synchronous with tension changes to the membrane, within the dural system. The CRI provides the main pumping motion to circulate the CSF (cerebrospinal fluid) and maintain the existence of the neurological components of the CSF. When this takes place, the ventricles of the brain increase in volume and size.

These signals can be conducted to the gray matter of the cortex. CSF is produced in the ventricles. This CSF circulates across the entire surface of the central nervous system, then into the bloodstream. Phototransduction cascade molecules may be another signal pathway of photonic communication. Does this intracranially generated light support consciousness?

In the Effulgence of its Brilliance.

FROM LIGHT TO DELIGHT: DMT, THE SPIRIT MOLECULE

The Biology of the Inner Light

Illumination has been described as being blinded by the manifestation of God’s presence. This brightness has no relation to any visible light. Visionary experience, which has symbolic or religious content, may give way to this dazzling light, which is reported in eastern and western religions. No wonder it is called illumination, and it can confer a palpable glow to the person that is perceptible after the return to ordinary awareness.

Imagine suggesting the body makes it own psychedelic drug! This is just what psychiatrist Rick Strassman contends in DMT: The Spirit Molecule (2001). He asserts it is an active agent in a variety of altered states, including mystical experience. This chemical messenger links body and spirit. Pineal activation may awaken normally latent synthetic pathways.

Meditation may modulate pineal activity, eliciting a standing wave through resonance effects that affects other brain centers with both chemical and electromagnetic coordination. Resonance can be induced in the pineal using electric, magnetic, or sound energy. Such harmonization resynchronizes both hemispheres of the brain. This may

result in a chain of synergetic activity resulting in the production and release of hallucinogenic compounds

Tripping the Light Fantastic

If this is true, it is easy to see how much this mind-altering chemical could amplify all of the tendencies toward mystical apprehension originating in other parts of the brain, as we have described above. To explore his theory, Strassman conducted extensive testing, injecting volunteers with the powerful psychedelic, synthetic DMT. DMT is so powerful it is physically immobilizing, and produces a flood of unexpected and overwhelming visual and emotional imagery. Taking it is like an instantaneous LSD peak.

He suggests the mysterious pineal gland is implicated in the natural production of this mystic molecule, as metaphysical teachers have long claimed. The pineal has been called the spirit gland and may be the biological basis of spiritual experience. The only solitary, or unpaired gland in the brain may initiate and support a variety of altered states of consciousness.

The pineal is known to contain high levels of the enzymes and building-blocks for making DMT, and it may be secreted when inhibitory processes cease blocking its production. It may even produce other chemicals, such as beta-carbolines that magnify and prolong its effects.

The pineal sits, well-protected in the deep recesses of the brain, bathed in cerebrospinal fluid by the ventricles, the fluid-filled cavities of the brain that feed it and remove waste. It emits its secretions to the strategically surrounding emotional, visual and auditory brain centers. It helps regulate body temperature and skin coloration. It secretes the hormone melatonin. Generally, after the more imaginative period of childhood, the pineal calcifies and diminishes.

Highlights

Endogenous DMT is described as the source of visionary Light in transpersonal experiences. Its primary source, the pineal, has traditionally been referred to as the Third Eye. Curiously, this gland is light sensitive and actually has a lens, cornea, and retina.

DMT production is particularly stimulated, according to Strassman in the extraordinary conditions of birth, sexual ecstasy, childbirth, extreme physical stress, near-death, psychosis, and physical death, as well as meditation. Pineal DMT may also play a significant role in dream consciousness.

“All spiritual disciplines describe quite psychedelic accounts of the transformative experiences, whose attainment motivate their practice. Blinding white light, encounters with demonic and angelic entities, ecstatic emotions, timelessness, heavenly sounds, feelings of having died and being reborn, contacting a powerful and loving presence underlying all of reality; these experiences cut across all denominations. They also are characteristic of fully psychedelic DMT experience. How might meditation evoke the pineal DMT experience?”

“Meditative techniques using sound, sight, or the mind may generate particular wave patterns whose fields induce resonance in the brain. Millennia of human trial and error have determined that certain ‘sacred’ worlds, visual images, and mental exercises exert uniquely desired effects. Such effects may occur because of the specific fields they generate within the brain. These fields cause multiple systems to vibrate and pulse at certain frequencies. We can

feel or minds and bodies resonate with these spiritual exercises. Of course, the pineal gland also is buzzing at these same frequencies . . .The pineal begins to 'vibrate' at frequencies that weaken its multiple barriers to DMT formation."

The pineal-DMT theory is only a theory, and has not been established as fact. There is compelling circumstantial evidence for a pineal-DMT link, but it's not been rigorously examined yet. Nonetheless, there are other sources of DMT in the body that are well established; for example, blood, brain, and lung. Also, the human DMT synthesizing enzyme has been found, cloned, and injected into a virus. When this virus infects cells in the test tube, those cells produce DMT. (Strassman; http://www.rickstrassman.com/).

ENLIGHTENMENT by Todd Murphy
http://www.innerworlds.50megs.com/enlightenment.htm

(c)2005-6 Iona Miller, All Rights Reserved

50MEGS Sign In Sign-Up

PSI RESEARCH

Parapsychology * Paraphysics * Psiberlife * Dream Telepathy * Nonlocal Healing * Resonance * ESP * Subtle Energies

Home Page
INTRO
Zero Point
Photonic Brain
Photonic Body
Illumination
Invisible Ground
Consciousness
Soma Sophia
Golden Flesh
Pineal DMT
Ionatopia Links
Biophysics
Biohologrаphy
Bioplasma
HoloMind
HoloVerse
Psi Research
ART GALLERY
News
WHAT'S NEW
Realblog

21st CENTURY PSI RESEARCH

NEW MILLENNIUM PSI RESEARCH
ESP, Hypnosis, Paraphysics, and Remote Viewing

Iona Miller, 2003
Organization for the Advancement of Knowledge, Grants Pass, Oregon

"One really should start thinking in terms of biomind receptors,
rather than in terms of ESP" --Ingo Swann

SHOT IN THE DARK-SIDE OF THE MOON

While on his journey to the moon and back, astronaut Edgar Mitchell conducted an unscheduled experiment of his own. On June 22, 1971, he informed the New York Times that, "During the Apollo 14 lunar expedition I performed an extrasensory-perception experiment the world's first in space. In it five symbols a star, cross, circle, wavy line and square were oriented randomly in columns of 25. Four persons in the United States attempted to guess the order of the symbols. They were able to do this with success that could be duplicated by chance in one out of 3,000 experiments."

He claimed, in effect, that his demonstration showed that ESP was independent of shielding, locale, distance, or time. When he got back to planet Earth, he founded The Institute of Noetic Science (IONS), noetic meaning consciousness studies. That program, now run by parapsychologist Dean Radin, is still thriving and the Institute recently moved to larger quarters in an old school in Petaluma, California. IONS is celebrating its 30th anniversary.

MAKES ME WANT TO PSI

The spontaneous event commonly called psychic experience, perception or ability is called 'psi' in scientific arenas. Even more precisely, it is now often referred to as anomalous cognition (AC). A particular form of intentional AC is known as Remote Viewing. Between 1978-1995 the U.S. government sponsored the Stargate Program, in conjunction with Stanford Research Institute (SRI), a psyops development think tank.

The existence of psi or ESP abilities has been hotly debated among scientists for decades, since J. B. Rhine began his experiments in 1927. Both the pro (Dean Radin; Ingo Swann; Jessica Utts, Russell Targ; Hiroshi Motoyama) and con (James Randi, Susan Blackmore, CSICOPS) positions have their "true believers", and it seems never the twain shall meet.

Psi is still a paradigm that lives on the outskirts trying to become a sanctioned science. But just because a subject is controversial, and happens to be a space and time transcending experience, doesn't mean we shouldn't investigate it. In fact, it beckons us to focus on it even more thoroughly to reveal the truths hidden there. We simply need to do it with stringent, critic-proof methodology.

There are a variety of psi powers, known for centuries in Eastern philosophy as siddhas, exceptional human abilities. The uninitiated or skeptical may be perplexed or daunted at the prospect of coming to any rational conceptual understanding of these anomalous phenomena, which have been associated with the realm of mysticism, superstition and the supernatural.

In actual fact, research by the authors, who are both certified hypnotherapists (A.C.H.E.), and others (Miller; Ryzl) shows that nearly anyone can improve their psi ability through simple techniques of self-hypnosis.

Psi is also at the root of focused intent, distant mental interactions, distance healing and therapeutic rapport, where there is a subtle shared consciousness and often brainwave synchronization. This

capacity is within everyone's grasp, as the human potential movement demonstrated with such trance phenomena as fire walking and guided imagery.

We've virtually all had those uncanny or awesome experiences where we seemed to intuit, dream, or "know" something in advance of conventional means. Sometimes it is called pre-sentiment. Around 55% of reported incidents occur in dreams. Another example, is the synchronicity at work in the affairs of "star-crossed lovers." When we are in love, we seem to share the same "wavelength," virtually able to read one another's minds. Who hasn't thought of a friend or acquaintance only to have the phone ring?

Often the most compelling stories come from those who don't even "believe" in the phenomenon, but find themselves experiencing it, usually in the unfortunate circumstance of the illness, injury or death of a distant loved-one. Psi is not just a mental perception or conception; we feel it in our guts, in our bones, in our marrow. It is first and foremost a holistic mind/body experience.

According to leading parapsychologist Dr. Stanley Krippner, "At one level of investigation, there already are 'replications' and 'battle-tested' results, specifically the finding that about 50% of an unselected group will report having had a 'psychic experience,' supposedly involving those psi phenomena that have been given such labels as 'telepathy', 'clairvoyance', 'precognition', and 'psychokinesis' [mind over matter]. This percentage may vary from one culture, age group, and educational level to the next, but it has been repeated, in one study after another, for the last several decades."

The move in biophysics is to take psi research from endless theorization, proofs of existence and boring replications into innovative and practical experimentation. The problem is that in order to do that scientifically, one has to risk credibility and professional suicide, as well as being underfunded.

OPEN SESAME

Though it often seems confined to mystics, mediums, channels, sensitives, or ESPers, most individuals are capable of expressing some nonlocal communication or psi phenomena. However, that ability may be blocked for various reasons by an adaptation to consensus reality, to conventional thinking. We need to develop "out of the box" thinking. Even Einstein said that past, present, and future are illusions, even if they are stubborn ones. Conscious calculation rarely plays a role in ESP; the same is true for creativity.

Both ESP and creativity have deep taproots in the psyche. Pang and Forte (1967) found some evidence of a relationship between creativity and ESP, as did others (Honorton, 1967). Frederick Myers reported that a large proportion of ESP experiences occur in altered states such as dreams, trance, hypnosis and creativity while Masters and Houston (1966) counted it among the varieties of psychedelic experience.

ESP, hypnosis and mind-expanded states have sensitivity to the unconscious at their core. And that subconscious expresses itself through symbols, imagery, and sensations to communicate with the conscious mind. Hypnosis is the "open sesame" to the waking impressions and sensory images of the deeper mind/body.

The elusive ability to swing back 'the doors of perception' and enter the numinous realm of the collective unconscious was described by psychologist C. G. Jung. Whether deliberate or accidental, anyone can open to the force of this revealed process, to this dynamic information field. Those who frustrate themselves with self-defeating behavior in other areas of life often show poor psi performance.

Positive ESP scores seem to correlate generally with traits such as openness, high self-esteem, warmth, sociability, adventuresomeness, relaxation, assertiveness, talkativeness and practicality. However, some psi-talented individuals often don't score well in laboratory settings.

On the other hand Russell Targ (1994) claims, "[P]si is no longer elusive; it can be demonstrated when needed for study and investigation." Even though psychic training to strengthen the signal line is possible, unpredictability has been the hallmark of this emergent gift. To overcome this problem in both the theoretical and experimental arenas requires a marriage of the disciplines of physics, biology, medicine, psychology, and hypnosis.
Findings from all these fields converge in the paradoxical subject of Extra-Sensory Perception. As the ideas of quantum mechanics, relativity and parapsychology slowly make their way into our collective consciousness, our common-sense views on time and causality find themselves more strained than they've ever been in the course of human history.
Will this challenge remain the domain of theoretical science, or can we foresee a day in which the general understanding, and even the experience of the average individual, will be shaped by this new perspective on reality? (Sidorov, 2003, "The Mind In Time").

It takes many disciplines, as well as the latest findings in physiology, neurobiology and information theory to begin to formulate any comprehensive understanding of the phenomenon and bridge the conceptual gap. ESP used to be studied in Parapsychology, an adjunct of psychology. But its subject matter has become so mainstream, the field has been return to ordinary Psychology. ESP "software" is studied in psychology, but ESP "hardware" is the domain of biophysics.

Researchers are probing the interface between matter, spacetime and mind with increasing precision. There is optimism that ultimately conventional pathways will be found to explain their appearance. Suggestions have included Schumann Resonance as
a nearly-instantaneous carrier of psi information or perhaps paradoxical quantum nonlocality or

coherence to account for it.

There are many models that provide potentially viable explanations. The mental aspects can perhaps be described psychologically, but the mechanics require models from physics. A variety of theories have been proposed, including neurological, holographic, electromagnetic, and quantum mechanics based hypotheses.

Like electricity, no one knows how psi works. However, to foster and practice psi we don't need to know how it works, anymore than we need to know the mechanics of internal combustion to drive a car.

WHAT IS PSI?

This month (July 2003) on the editorial board of the Journal of Non-Local and Remote Mental Interactions, we have been preparing a special issue on Remote Viewing.
< http://www.emergentmind.org/jnlrmi_ii(2).htm>

Stargate RV expert and teacher, Joseph McMoneagle is interviewed, along with such notables as author and theoretical physicist, Fred Alan Wolf, and Finnish physicist Matti Pitkanen. Many plausible theories and new experimental protocols are being proposed, pushing the leading edge of physics, biophysics, and experimental parapsychology. Though it is often suggested, it remains to be seen if psi is a field, a quantum effect, or a physical quantity.

We are examining aspects from coherent fields to strength of intent, arousal states, target specificity, subject-target separation, psi-expectancy, anticipatory effects and information flow. Studies of field resonance, metabolism, biophotons, entanglement, geomagnetic fluctuations, time-reversed experience, energy transfer, physiological detectors, biomind receptors, psychophysical responses, bioregulation, enhanced recovery, experimenter effects, EM signatures and transduction pathways may yield more information about the process.

The areas of extrasensory perception or anomalous cognition we discuss here include (1) Telepathy; (2) Clairvoyance; and (3) Precognition. These faculties came into the public eye when stories of Russian and CIA remote viewers broke in the press. But compelling, anecdotal stories alone do not satisfy the scientific method.

Stories of distance healing, a form of PK or psychokinesis (mind over matter), require another article of their own to do them justice. It may be easier to model virtual information transfer than mind over matter. "Spooky action at a distance" requires even stronger evidence than sensing at a distance. But is "distance" here really a factor or an illusion in a holographic simply-connected universe? The paradox of spacetime and relativity presents itself in psi as psycho-retrocognition, or time-reversed PK.

Though these experiences of knowing at a distance are called "extra-sensory," they often appear "as if" received by conventional sensory or mental means, for how else can we "know what we know"? It is a holistic psychophysical experience, affecting the whole self, physically, emotionally, mentally and often spiritually. The impediments of distance and time seem to dissolve; the barriers of spacetime are mysteriously overcome. The information is 'just there' in one form or another, whether spontaneous or facilitated.

1). Telepathy is a message, direct mind-to-mind communiction, direct knowing through being, a clear intuition or empathic awareness, often demonstrated in the psychotherapeutic setting. Telepathy is a transmission from one mind to another.

2). Clairvoyance appears as information about events at remote locations, manifesting as an image, or gestalt psychic impression, rather than a thought; (it is often linked to perception at a distance: so-called astral travel, out-of-body experience, or remote viewing).

3). Precognition is the most uncanny; transcending time, it seems to rend the veils of the future (jamais vu) and the past (deja vu) with strong, often unpleasant, premonitions.

According to Scientific American (Sept. 2002, p. 103), [apparently long after Pribram's theory from the 70s], "in 1990 Herman Sno, a psychiatrist at Hospirtal de Heel in Zaandam, the Netherlands, suggested that memories are stored in a format similar to holograms. Unlike a photograph, each section of a hologram contains all the information needed to reproduce the entire picture. But the smaller the fragment, the fuzzier the resultant image. According to Sno, deja vu occurs when some small detail in one's current situation closely matches a memory fragment, conjuring up a blurry image of that former experience." There are competing theories of deja vu, but the holographic concept of reality is a leading contender in the biomechanical explanations of psi.

Psi meaning comes through emotionally intense visual, auditory and kinesthetic experiences. It is a human potential we can learn to tap. We can use our intentionality as a probability perturbation instrument. We can use mental focus to alternately concentrate and relax our attention. Intent is suggested as a variable in transmission and reception in the exchange of extrasensory information, possibly within the range of ELF electromagnetic frequencies (Sidorov, 2002).

Stanford and Lovin (1970) found possible support for a relationship between the generation of alpha waves and ESP, as did Monroe (1971). More recent research has implicated the electromagnetic signals of Schumann Resonances as carrier of
seemingly non-local transfer of information (Pitkanin, 2001). Persinger (1989) has suggested that psi information signals are actually carried on extremely low electromagnetic frequencies and our temporal

lobe structures are sensitive to them.

Whether one believes in spontaneous psi experience, or not, it has a long and colorful history, in the mystic and healing arts of the East and West, and in science, even business. The difference is the trigger that evokes the experience. Management trainers have taught self-hypnosis as a means of fostering intuition, rapport and other practical applications of ESP.

The role of ESP is inextricably bound up with other creative processes where information or inspiration seemingly appear from nowhere. Data acquired through ESP, prescient dreams and other imaginative thought processes riddles the stories of scientific discovery and creativity. Psychic detective work and investigative reporting has received mixed reviews, since following up on dry leads uses time and vital resources. Without controls, these anecdotes are difficult to evaluate.

In the arts, it has been said that "life imitates art," sometimes to uncanny proportions. Krippner (1972) recounts a story of ESP in creativity, whose prophetic detail later took on ominous tones.

In 1898, Morgan Robertson published a popular novel called Futility. It described the wreck of a giant ship called the Titan, considered "unsinkable" by the characters in the novel. Perhaps you recognize this oft-told tale as that of the Titanic, but it was not wrecked until April 15, 1912. In the novel, the ship displaced 70,000 tons (Titanic 66,000 tons), was 800 feet long (Titanic 828 feet); the Titan carried 3000 passengers and 24 lifeboats, while Titanic had only 20 lifeboats for the same number of people. Both ships sank while encountering an iceberg at the speed of 23-25 knots. The rest, as they say, is history.

FROM TRANCE TO CREATIVITY

The question becomes "How can we facilitate the emergence of psi phenomena, either for greater awareness or creativity?" Knowing what we know about psi expression, how can we train ourselves to encourage its emergence? Hypnosis or self-hypnosis simply helps engage the emotional mind, the imaginal mind, the biophysical mind rather than just approaching the task rationally and conceptually.

Unfortunately, the question of psi-facilitation was asked by covert forces during the Cold War, and much of the statistical and practical data on psi comes from those black-ops sources (CIA, KGB, NSA, DIA, DOD, U.S. Army and Navy). The Russians wanted to use psi for espionage and the US countered with its own team. Much of this government-sponsored work went on at Stanford Research Institute (now SRI International), by Puharich, Puthoff, Targ, and Swann.

Human potential advocates, Jack Schwarz and Robert Monroe separately pursued independent, more explorative and mystical approaches. Both taught consciousness management techniques through forms of self-hypnosis. Schwarz, practicing as the Aleithea Foundation in Southern Oregon, focused on bioregulation with autohypnosis and subtle human energies.

Monroe's techniques employ neuroregulation with the frequency-following response (which he trademarked with the Monroe Institute in Virginia, as Hemi-Synch) to induce trance, entraining both hemispheres in alpha and theta (1982).

Hemi-Synch, also known as binaural beat technology, actively drives the modulation of electrocortical activity through resonance effects, changing levels of awareness and arousal, attentional focus, and cognitive content. Often combined with biofeedback, it helps shortcut processes that would take years of technologically unassisted yogic training.

Graywolf Swinney (2001), Dr. Stanley Krippner, and Iona Miller (1993-2006) have conducted trainings in co-consciousness (Erickson, Rossi & Rossi, 1976) and theta training at Asklepia Foundation, also in Southern Oregon. A deep state of rapport is used in psychotherapeutic journey processes, employing shamanic hypnotherapeutic techniques. Theta is reportedly the psychic range of the mind, generated largely in the temporal lobes. Co-consciousness is a shared virtuality, a telepathic rapport wherein both participant's brainwaves become synchronized into a single holographic biofield (Miller and Swinney, 2000).

Spontaneous psi phenomena have been associated with theta waves by Krippner (1977), the Greens (1977), and more recently by Persinger (1987). Consciously producing theta requires quieting the body, emotions and thoughts simultaneously, leading to an integrative reverie, a deep focus of attention. Theta is often accompanied by hypnagogic or dream-like imagery emanating from the temporal lobes.

John Curtis Gowan (1975) catalogued the entire spectrum of extraordinary phenomena related to trance, art, and creativity. In his taxonomy, he called these distinctive modes or domains of human dynamics Prototaxic (Trance), Parataxic (Art), and Syntaxic (Creativity).

Trance is characterized by loss of ego, art by emotionally charged (often symbolic) imagery, and in creativity meaning is more or less fully cognized symbolically with ego present. In some ways, these modalities could represent the uncanniness of precognition, the imagery of clairvoyance, and the knowing of telepathy.

Trance is often associated with awe, dread, horror, and panic since ego control is weak or absent. These numinous effects are moderated in the artistic experience that comes as visualization, audialization, emotional inspiration, sensual, symbolic and mythopoetic imagery.

In terms of precognition, artists are often said to be perceptually "ahead of their time." Art is the transition phase in the relationship between the ego and the emergent transcendent function.

Transcendence is a "quantum leap," a recurrent process, not a steady-state. It is a phase-transition moving toward illumination. The syntaxic experience of creativity is even more benign since the mind apprehends directly without ego dissociation. Psi experiences become more naturally integrated, regular, inspirational and uplifting while less frightening or awesome.

Gowan's work naturally included both hypnosis and ESP, which he cited as consciously or unconsciously operative at these various levels of dissociation, ego-involvement and levels of arousal (sympathetic and parasympathetic). Puharich (1961) found telepathic reception facilitated by parasympathetic activation, while sending the message was stronger with activation of the sympathetic, or adrenergic system.

For Gowan, the accessibility of certain psychic experiences depended on the mode of functioning. Intuitive self-knowledge is intrinsic to a wide variety of higher mental functions. Hypnosis and self-hypnosis are clearly linked to the primal trance, but can
be applied in more integrated modes to enhance psi ability (Krippner, 1968).

PSI DEEPLY: HYPNOSIS & ESP

In 1967, the Czech government tried to co-opt the allegedly successful psychical research and training program of biochemist Milan Ryzl. After screening many candidates, he found 50 high-scoring subjects, and they proceeded to win several rounds of the Czech lottery.

“Milan Ryzl, a chemist who defected to the United States from Czechoslovakia in 1967, developed a hypnotic technique for facilitating ESP. . .Ryzl’s technique involved the intensive use of deep hypnosis sessions almost daily for a period of several months. The first stage of the sessions was to instill confidence in his subjects that they could visualize clear mental images containing accurate extrasensory information. Once this stage was reached, Ryzl concentrated on conducting simple ESP tests with immediate feedback so that subjects might learn to associate certain mental states with accurate psychic information. Subjects were taught to reject mental images which were fuzzy or unclear. This process, according to Ryzl, continued until the subject was able to perceive clairvoyantly with accuracy and detail. Finally, Ryzl attempted to wean the subject away from his own tutelage so that he or she could function independently. While still in Czechoslovakia, Ryzl claimed to have used this technique with some five hundred individuals, fifty of whom supposedly achieved success.”

“Other studies have shown heightened ESP in states of physical relaxation or in trance and hypnotic states. In fact, the use of hypnosis to produce high ESP scores is one of the most replicable procedures in psi research.” (Mishlove, 1975).

WORLD’S FIRST PSYCHIC TOURNAMENT

In 1973, after hosting Ryzl for weeks in his Seattle home with many late-night discussions on the nature of psi, physicist and parapsychologist Richard Alan Miller created a model for anomalous cognition. Also drawing on his laboratory experience with biofeedback, he wrote a paper called “ESP Induction through Forms of Self Hypnosis.” In 1975, while never claiming to be a psychic, he got to put his theory to a rather unique test: the World’s First Psychic Tournament.

On September 21, 1975, Llewellyn Publications, noted occult publisher, sponsored this event in Minneapolis, Minnesota as part of their 5th Annual Gnosticon Festival. The tournament itself was co-sponsored by the Foundation for the Study of Man, originally set up to continue the work of Dr. J. B. Rhine and his pioneering work in ESP at Duke University. Many famous psychics were invited, including such personalities as John Pierrakos and Sibyl Leek.

One of the authors of this article (RAM) was also invited to test the proposed models for inducing ESP ability using forms of self-hypnosis. Since he was relatively unknown for having any abilities in this ESP field, it seemed to hold some potential as a valid first study. More than 20 nationally known psychics also participated in this event.

The clairvoyance test consisted of twenty (20) cards randomly pulled from ten (10) poker decks. Each participant was to guess the suit of each card. With one chance in four of guessing the correct suit, the average score for a run of 20 cards with no ESP ability is 5. Each participant was given five (5) different runs. A final score determined the winner, with a total of 25 representing the norm.

What happened is now history: More than 50 percent of those participating showed normal scores ranging from 22 to 27 out of a possible 100, as would be expected in the general population. Most of the more well-known psychics showed some seemingly paranormal ability in clairvoyance, as expected, with total scores averaging between 8 and 12 correct answers out of 20. One well-known psychic even had a score as high as 61 out of a total possible 100.

Using the technique of ESP induction through forms of self-hypnosis as outlined in his paper, however, Miller did not have a run less than 16 out of 20. His total score was 83 out of 100. This was more than two orders of magnitude greater probability than scores of nationally recognized psychics. He took home a first place certificate as testament to his extraordinary performance. It still hangs on the wall in the office.

THE PSI FACTOR

Of course, this anecdotal evidence does not constitute scientific proof of this model. What it does

represent, however, is a need to understand the true significance of self-hypnosis is and how it relates to extra-sensory perception. Something definitely made a difference in the experiment. How might this be applied to therapy? Or perhaps to such questions as the role of placebo, spontaneous healing based in the physically-transforming belief that you can do something beyond your normal scope.

Miller went on to create an ESP screening questionnaire that helps define the attitudes that facilitate psi. It was given to 500 college students and weighing factors were assigned to individual questions.

The bell-shaped curve developed from the survey indicated that helpful traits included a belief in ESP, extroversion, freedom from anxiety, easy or frequent dream recall, hypnotizability, and a relatively expressive personality. Memory, creativity, and visualization/association showed inconclusive results.

However, EEG parameters showed a highly significant positive correlation between directional alpha frequency shift and ESP scoring. More recent studies have shown an even greater correlation for theta brainwaves and psi faculty. There also seems to be a correlation between high ESP scores and number of reported psi experiences.

In its Stargate Project, SRI developed even more stringent criteria for what constitutes a viable remote viewer, based on statistical results. In their program, the level of arousal, according to McMoneagle as told to JNLRMI, didn't seem to matter much. Whereas normal people are recommended to relax or use the progression relaxation that facilitates self-hypnosis, professional remote viewers can begin from a relaxed state and move to an excited one, or begin excited and become calmer.

HOW DID HE DO IT?

So, just how did Miller wind up beating the best psychics in the nation at their own game? And more importantly, how can you increase your Psi-Q? Miller developed a set of self-consistent definitions and postulates relating self-hypnosis and ESP, both a theory and a practice.

The standard definitions used for hypnosis often call it a borderline state between sleeping and waking, i.e. body asleep, mind awake. Any state characterized by an intense concentration of attention in on area, accompanied by a profound lack of attention in other areas, may also be considered hypnosis. It opens us to our psychophysical impressions by limiting external input.

With this type of definition, everyone is considered to be continually in a light state of hypnosis, witness "white line fever" while driving, or the plea, "I was spaced-out." Musicians call it "being in the groove," others "sharing a wavelength." Our social roles are also like trance states with their intrinsic patterns. When we go in public we wear the 'armour" of our persona and immerse ourselves in that self-image.

Charisma is also a form of hypnosis akin to Mesmer's original "animal magnetism." Traumas also create trance states with automatic behaviors that can persist for years. The "scripts, games, and rackets"of Transactional Analysis can also be seen as trance states, where we habitually replay our typical ways of dealing with self, others, and world. So the question becomes not "if" one is hypnotized, but what kind of trance and its depth one is in at any given moment.

The depth of hypnosis, which is an implied issue in this definition, may be defined as the difference between the intensity of concentration in one sphere or area and the depth of inhibition in others. Attention focused in one area creates a corresponding lacuna, or lack of attention, in other areas of the brain. Centering the attention for prolonged periods, often with suggestions for further deepening, leads to deeper states of hypnosis. With these definitions, a useful model for relating hypnosis to psi phenomena is possible.

Psi Theory:

Postulate I: The conscious experience is associated with the nervous processes which take place above a certain critical level of awareness/alertness. This function, defined as I(c), varies considerably in a state of hypnosis, where attention is focused.

Postulate II: Psi Energy, arbitrarily defined as E(psi), is an equivalent in the field of extra-sensory phenomenon of what, in our three-dimensional world, is called energy.

Correlate A: E(psi) is not limited by time.

Correlate B: E(psi) can not be transformed into other energies (i.e. physical energies,; converting heat into light).

Correlate C: E(psi) operates by manipulating the transformation of physical energies.
Postulate III: Psi Energy, is responsible for extra-sensory perception and psycho-kinetic phenomenon (PK).

Postulate IV: Psi Energy is the product of some aspect of the metabolic processes. Physical data regarding the relationship between metabolic processes and extra-sensory perception can be found in Beyond Telepathy, by Andrija Puharich.

Postulate V: The generation of Psi Energy rapidly decreases the level of alertness. This immediately explains why: (1) each conscious act has a limited duration, (2) why we experience a permanent train of changing thoughts, and (3) why our attention permanently shifts from one object to the next.

When you think, Psi Energy is created. The Psi Energy automatically decreases the level of alertness so that one shifts to something else.

Postulate VI: The intensity of conscious experience, I(c), depends on the time rate of the generation of psi Energy. Mathematically, this is described as dE(psi)/dt = A(e) x I(c).

The rate of change of E(psi) as a function of time is equal to some geographical constant, A(e), times the intensity of concentration, I(c). More simply stated Psi Energy is equal to a geographical constant times the intensity of concentration, I(c), times the amount of time that the thought is held. E(psi) = A(e) x I(c) x t

If we cannot make any particular thought last long enough, it should be sufficient to repeat it again and again until the value of the individual brief periods add up to a sufficient value. The equation now becomes E(psi) = A(e) c I(c) x [t(1) + t(2) + t(3)

Postulate VII: The formation of Psi Energy, which is created by a holistic psychophysical act, preserves the semantic control of the thought that created it. In essence, your thought is uniquely distinct. If you deviate from your thought slightly, it is a different thought-form, including the psychosomatic component. There is a tangible shift in the mind/body.

The Method:

(1). Formulate the question.
(2). Hold that thought for as long as possible.
(3). Assume that the event has occurred.
(4). Drop into a “blank mind” state and wait.

When questioning or desiring thoughts are intense enough, lasting long enough, or repeated frequently enough, psi is produced in sufficient intensity and structure to be detectable in the physical world. This may occur in hypnotic states, in states of intentionality, elated or traumatic emotions, or when interest, motivation, or desire is strongly increased.

The individual confronts the continuum with desire and prolonged concentration. The question being asked must be intense enough to impress itself on the unconscious. Lacking intensity, the signal will not be perceived. Intentionality strengthens the signal path.

Consciousness is then dropped into a “blank” state, an empty state, or “beginner’s mind.” The actual visualization is a switch from the concentrated point to the void. When this occurs the information is impressed on consciousness, resulting in a psychophysical perceptual event. This event is independent of both space and time.

Ordinarily when people spontaneously fall into trance states, they are generally not in a “blank mind” state of expectant emptiness. There is the chatter of subconscious thoughts going on even as the process deepens toward sleep. These thoughts are generated and go on automatically at a subliminal level, often without awareness.

Consequently, the information or signal path gets distorted, and weird patterns emerge, much like those experienced in dreams. In a waking dream, distorted signals may be perceived as “spirit guides”, automatic handwriting, or other autonomous related phenomena of trance states. We have seen earlier that Gowan characterized this loss of ego-awareness as the Prototaxic Mode.

Puharich believes reception is enhanced by “parasympathetic activation” in which there is an increase in released acetylcholine. He claims that telepathic sending of information is easier when there is an increased amount of adrenaline in the system. These metabolic processes are not “causal” but merely correlates of psi. Psi meaning comes through intense visual, auditory, and kinesthetic psychosensory experiences.

This “energized enthusiasm” can be seen in states of emotional involvement and artistic inspiration (Parataxic Mode), as well as creativity (Syntaxic Mode). Parataxic experience consists of relationships with multisensory images whose meaning remains on the symbolic level.

Syntaxic experiences occur when the consciously aware ego cooperates willingly with the subconscious forces. Here knowing and meaning are clearer and fully cognized with minimal distortion. Other higher forms of concentration include biofeedback, meditation, tantra, peak experiences, higher Jhana states of yoga, and so on. Concentration is intense, structured and prolonged.

Discussion:

ESP is often observed in hypnosis, a state characterized by a single intensive thought. Recurrent cases of psycho-kinetic phenomena, such as the haunted-house variety, are often reported to be connected with previous trauma or tragic events, associated with intensity of concentration, I(c).

The frequently reported cases of crisis telepathy, ESP contact between two persons, one of which is dying or in grave danger, are necessarily associated with intense thought or concentration, even obsession and a highly aroused state. The length of time experienced depends entirely upon the circumstances; in some cases there is subjective dilation of time perception.

The discovery of mental impregnation, known in the literature as psychometry suggests that repeated identical thoughts increase the expected psychic effect. Wearing a ring for a long time may “imprint” memory of the wearer onto the ring; just slipping a ring on and off and handing it to a psychometrist will not generally reveal any memory of the wearer.

Religious or spiritual traditions assert that repeated prayers may be more effective than single ones. In other words, the more you repeat the same prayer, or mantra, or the more you do a single ritual, the greater the effect. Along that line of reasoning, “tithing” might be seen as a factor of one’s time or attention, rather than money. Some meditation schools, for example, require no money but 10% of your daily time (2.5 hours) in meditation.

The stimulating action of psi formation on the brain may account for memory, more particularly, active recollection. The influence of psi formation increases the level of awareness of the neuro-patterns corresponding to the thought to be remembered. The synapses are flooded over and over with the same chemical messengers and electrical signals. The correlating psychosomatic content is consciously re-experienced.

DREAM TELEPATHY AND BEYOND

“In 1969, Charles Honorton and Stanley Krippner reviewed the experimental literature of studies designed to use hypnosis to induce ESP. Of nineteen experiments reported, only seven failed to produce significant results. Many of the studies produced astounding success. In a particularly interesting precognition study, conducted by Fahler and Osis with two hypnotized subjects, the task also included making confidence calls predicting which guesses would be most accurate. The correlation of confidence call hits produced impressive results with a probability of 0.0000002.” (Mishlove, 1975).

Krippner went on to conduct research in Dream Telepathy (1973) with Montague Ullman, following the lead of other Maimonides Hospital (Brooklyn, N.Y.) researchers, such as Frederick Myers. These experiments in nocturnal ESP are foundational and though never replicated, the results were highly suggestive of a strong psi correlation.

Their ten-year study concluded that dream reports can show the effect of telepathy, clairvoyance, and precognition. Their hypothesis was that ESP is more common during dreaming than waking and therefore an "agent" could more easily transfer the target thoughts or imagery to a sleeping subject, influencing their dreams.

Such prominent dream researchers as David Foulkes (Belvedere & Foulkes, 1971), Gordon Globus (Globus et al., 1968), Calvin Hall (1967), Robert Van de Castle (1971), and Keith Hearne (1987) attempted to repeat these findings. Because the replication rate from these other laboratories was inconsistent, the Maimonides team did not claim to have conclusively demonstrated that communication in dreams can sometimes transcend space and time. However, they did open a promising line of investigation.

Years later, Stanley Krippner and Michael Persinger, a Canadian neuroscientist, reviewed the entire body of dream research data from Maimonides Medical Center, selecting the first night that each subject in a telepathy experiment had visited the laboratory. They matched the results of these nights with geomagnetic data, discovering that the subjects' telepathy "hits" tended to be higher during calm nights than during nights marked by electrical storms and high sunspot activity (Persinger & Krippner, 1989).

Persinger (1974) has urged using reported psi phenomena in new and ingenious ways, observing, "Across cultures and throughout history people have been reporting psi- experiences. Let us find out what they are saying. . .It is by looking at the similarities of the verbal behavior that we may find enough consistencies to understand the factors responsible for the reports” (p. 13).

Persinger (e.g., Schaut & Persinger, 1985) has examined several collections of spontaneous cases, including the 35 gathered by Stevenson (1970), reporting that they seem to occur most frequently when geomagnetic activity is calmer than the days before or after the experience - - and lower than the month's average activity.

This approach can be applied to any collection of cases (e.g., Persinger & Krippner, 1989) where the date of the alleged experience has been recorded. If repeatable, these effects may help to provide an understanding of the mechanisms underlying psi phenomena, and may even indicate a potentially predictable pattern for such events. (Krippner)

Geomagnetic field perturbations have been reported to affect biological systems by other investigators (e.g., Subrahmanyam, Sanker Narayan, & Srinivasan, 1985). Persinger (1989) has proposed two interpretations of the geomagnetic field effect. The first is that psi is a geomagnetic field correlate; solar disturbances and consequent geomagnetic storms affect this correlate. The second is that the geomagnetic field affects brain receptivity to psi, which remains constant.

In the latter interpretation, psi is always present in space and time, waiting to be accessed by crisis, emotion, or by optimal laboratory stimulus parameters. Geomagnetic activity may affect the detection capacity of the brain for this information, especially the neural pathways that facilitate the consolidation and conscious access to this information. Without this geomagnetic activity, awareness of the psi stimulus might not be as likely and the brain's "latent reserve capacities" would not be utilized.

Taking this argument one step further, Persinger (1989) points out that deep temporal lobe activity exists in equilibrium with the global geomagnetic condition. When there is a sudden decrease in geomagnetic activity, there appears to be an enhancement of processes that facilitate psi reception, especially telepathy and clairvoyance.

Increases in geomagnetic activity may suppress pineal melatonin levels and contribute to reductions of cortical seizure thresholds. Indeed, melatonin is correlated with temporal lobe-related disorders such as depression and seizures. (Krippner)

CYBER PSI TRAINING

So what direction can we expect psi research to take in this new millennium? Clearly, the experimenters themselves want to follow a self-directed course rather than the mandates of a government-driven program. They would like access to private, academic, and government funds, with leading edge equipment: high-ticket brain monitoring equipment such as 90-channel EEG, fMRI, SPECT, and ERP. They would like to practice without a professional stigma attached to their pioneering work.

Several theories of psi have been put forth throughout the years. Psychologist Rex Stanford, altered-states expert Charles Tart, post-quantum physicist Jack Sarfatti, and psi researcher Charles Honorton, as well as physicist Helmut Schmidt have all developed models for ESP and precognition. Each embodies certain possible, even plausible factors. Some researchers worked with Eastern swamis and yogis to understand the mechanisms and induction techniques or evocation of this psychic power.

Quantum theory predits that empty space (the vacuum) contains an enormous amount of residual background energy known as zero-point energy (ZPE). Physicist David Bohm, biologist Rupert Sheldrake (researching psychic pets) with his morphogenetic fields, and Ervin Laszlo propose zero-point or vacuum potential mediation for psi. The superdense quantum vacuum may be a physically real field, including but not limited to gravitation and electromagnetism. Perhaps it can transmit psi.

However, they can't provide any experimental protocols that might test such theories. Is psi a field or a quantum effect? Fields link phenomena in time as well as space. But, fields themselves cannot be observed; only the influences propagating through them.

Other theories suggest phase-conjugate pilot waves, scalar waves, virtual states, hyperfield flux, holographic hyperchannel effect, complementarity, even uncertainty. Biophysical theories for the paranormal bridge include Josephson junctions, microtubules, and liquid crystals as psi transducers.

Honorton and others long ago found defects in old psi testing techniques and addressed criticisms with new methodology. They eliminated variables like subconscious cueing by covering the subjects'eyes with split ping-pong balls and playing "white noise" into their ears.

Researchers hypothesized that this neutral field would function as a less-distracting "blank canvas" for psi hits. So it served a dual purpose of refining experimental procedure and minimizing distracting sensory input. These experiments, (known as Ganzfield tests), were replicated by many experimenters in many facilities, with encouragingly similar positive results. Other tests were conducted in sensory deprivation chambers and electrically-shielded Faraday cages.

Experimenter bias, the tendency to find what one seeks, is an occupational hazard, though skeptics have found positive psi correlations. But careful interpretations of models, artifacts, experimental method, instrumentation, randomization, target selection, statistical inference, sensory leakage, recording errors, and controls can't be rigorous enough.

Proper scientific control for ESP research has been refined over the years, though cheating and frauds have plagued the field, and the inexperienced scientist. One solution to this dilemma lately has been to experiment with the field-tested government Remote Viewers, who have established track records. They have their own reports of their subjective experiences, not the results of their missions but the sensations that led to the observation or retrieval of those images.

Remote Viewer Ingo Swann, called the father of RV, argues for the demystification of psi. Swann's model supercedes the traditional psi paradigm and focuses on the hardware issues discussed in neurobiology and information theory.

Swann argues for systematic and deliberate development of this ability much like athletic training, as well as conceptual understanding. He prefers the term Distant Mental Interactions with Living Systems (DMILS) to ESP. He wants this capacity tested in the context of physical science as part of man's natural spectrum of senses. He claims applying focus or attention on the perceptual apparatus with feedback on results "fine tunes" psi ability.

His concrete approach and insightful conclusions include his view of our sensory apparatus as a "transducer array" to convert information from one form to another. He calls his human "software" program a "mental information processing grid." He simply converts various forms of input energy to another form his sensory system can "read."

We do much the same when we interpret the electromagnetic signals that come through the air from a voice into meaning in our brains. He suggests we can develop the ability for several transducers of signals, depending on our exposure to the cognitive processing of these signals.

Targ claimed to see reasonably sharp and clear pictures. In remote viewing, if the mental picture

doesn't form, one is left with a mere "impression," a less-precise signal. The signal is compared against memory to determine if it is meaningful to the task at hand, the target.

In other words, you can develop this ability through practice and feedback of the accuracy of your perceived signals. Pathways that work get reinforced. The process is very similar to psychophysical learning with biofeedback, such as alpha and theta training.

Swann argues for learning to fine tune one's signal to noise ratio, learning to notice direct sensory data as well as imaginal signals, such as feelings, intuition, impressions. Repeated exposure and accurate feedback strengthens recognition of subtle and implicit relationships. Can cybernetic machines, such as random number generators, computers, and biofeedback devices help us hone psi faculties?

Swann emphasizes the difference between message and its structure. An experienced viewer can put together mental images from subtle cues. In RV, the signal appears as symbols, sounds, feelings, tastes, pictures, and holistic impressions. One learns to organize them based, again, on repeated feedback.

Misconceptions, fears, rigid concepts, body movement, excessive gastrointestinal activity, sleepiness, language categories, and other psychological "baggage" can be sources of confounding noise. Other blocks come from trying too hard, and distracting daydreaming or preoccupying thoughts. Telepathy, empathy or rapport, and charisma seem to be related and clearly come into play during therapeutic entrainment.

BIOPHYSICS OF PSI

Nothing is known about the physical mechanism of ESP, or anomalous cognition. No one knows what modulates performance. Even those who can demonstrate psi in the laboratory on demand, cannot account for signal nonlocality or distant interaction. The origins of the data are not revealed, only the conclusions with their level of resolution or accuracy. This is where the models of information theory and biophysics come into play.

Physicist Lian Sidorov proposes two working models for non-local communication and intent-mediated healing: 1). Direct transmission (entrainment) of specialized electromagnetic frequencies, observed primarily in proximal healing; and, 2). Distant healing and remote viewing/diagnosis, where the target's electromagnetic profile is modulated from a distance via partial entanglement of subject-target.

He cites the research of Finnish physicst Matti Pitkanen as a model for "directed entanglement" between the subject and target, the magnetic sensory canvas hypothesis. Pitkanen conjectures that distance healing involves transfer of specific electromagnetic frequencies through quantum wormholes for near-instant transfer of information.

The transmission may trigger certain brain frequencies and psychophysical changes. Thus, amplification of the signal leads from quantum to macroscopic effects. Pitkanen suggests the brain is a sensory organ of our electromagnetic selves, and may be linked to planetary rhythms through Schumann Resonance.

In his model, the EM fields are not directly carried from sender to target. They are simultaneously generated at the two locations by a vacuum (geometrical) current. Therefore, they remain coherent while by passing the paradox of non-attenuation with distance. Neural processing and quantum events may interpenetrate.

This still doesn't really account for origins of the data, but merely the transmission modes. Biophysics researchers are attempting to follow the signal back to its source. The research must be interfaced with current theories in the natural sciences. Then it can be considered empirical; the paradoxical anomaly can then be linked within the known framework of knowledge. Is there really a field, or field-like continua, capable of transmitting information beyond the recognized limits of time and space?

Laszlo (1996) suggests that the natural processes of complexity and chaos could amplify vacuum-level fluctuations into significant inputs to behavior, and that the brain, another chaotic system, could receive and amplify these signals which can penetrate into consciousness.

SHAVING WITH OCCAM'S RAZOR

Occam's Razor is a principle applied in science that contends problems should be stated in basic terms, not making more assumptions than needed to choose the simplest of equivalent models. Many hypotheses are proposed, tested, and rejected. Their validity is debated exposing their flaws and underlying assumptions.

Additional relevant hypotheses and unrelated statements are weeded out. Experiments with the sensitivity reveal which yield the most accurate predictions. If two rival theories pass empirical tests, the simpler one must be preferred. When it comes to conspiracy theories, we apply Hanlon's Razor: "Never attribute to malice that which can be adequately explained by stupidity."

But before we can find answers, we have to ask the right questions. Once we ask the right questions, we often have all the information needed to solve the problem. Unfortunately, in the case of psi, it may be that our understanding of physics is still too incomplete to solve the riddle.

Lian Sidorov, editor of Journal of Non-Locality and Remote Mental Interactions has posed many incisive

questions:

How is information stored and retrieved nonlocally by consciousness? This simple question contains the essence of all psi paradoxes, from spontaneous events like precognition and telepathy to carefully engineered processes like retro-psychokinesis.

How can one strengthen the signal line?

What is the significance of electromagnetic signatures detected at the target in remote conscious interactions?

What is the earliest physiological detector of psi information in the transduction pathway to conscious awareness?

What determines the direction of information flow in nonlocal interactions; for example, between healer and patient?

What are the technical requirements of an experimental program and how do we develop the most suitable types of equipment to detect such effects.

Sidorov (2003) summarizes his discussion with expert remote viewer, Joe McMoneagle:

“What you are saying seems to be that: 1. everything you will ever know is already contained in your universe, although not necessarily accessible to your conscious mind that comes with the effort involved in RV, or is revealed spontaneously as in “precognitive” 2. “when” a given target event takes place relative to the experimental present is irrelevant, because all the information is already available; 3. other people’s expectation and feedback should not affect your results, as long you are careful to task yourself in a way which does not include those elements. 4. “Making contact” with the target is more like flipping to the right page in your book than reaching anything in space and time.”

Are there preferred pathways for the signals in psi phenomena, windows of psi “sensitivity”? How specifically is the target recognized? How does one modulate and target “intent”? How does the signal rise above the threshold of awareness?

Mental intent seems to create cognitive bridges between subject and object, operator and target. We can also learn to recognize certain psychophysical patterns in ourselves through feedback. The physical and the psychical are inseparable. There appears to be an energetic/informational component, perhaps based in EM frequencies and holographic interference patterns. Holographic processes do occur in nature, including holographic information storage. The holographic field is a physical reality composed of interference waves.

In Scientific American (Aug. 2003), Bekenstein poses the question “Are you a hologram?” and states quantum physics says the entire universe might be. Can a somatic EM hologram possibly amplify as little as one quantum of energy into an effective signal? Are there holographic hyperchannels? Information in a field is holographic and the propagation of holographic interference patterns is quasi-instantaneous. Every part of the field contains the whole informational content, just in lower resolution.

“Each particle of mass in our bodies represents one closure of the entire universe, yielding a holographic reality and deeper communication with ourselves is identical to communication with the universe, including any part of it, at any distance. Furthermore, in hyperspace the future and the past are all present. Since a particle does indeed exhibit a four-dimensional component for 1/137 of the time, each particle does connect to the future and to the past. With selective tuning and kindling any part of this holographic reality is accessible. However, because of the smallness of a single selective signal in the midst of the totality, the channel is quite noisy. For this reason skilled psychics, persons who have been found to have a greater fidelity for selective tuning can be expected to produce better results than the normal person.” (Bearden, 1988).

Entanglement seems to occur somehow between all participants of a given intentional set-up. We have no idea how the non-local factor of target specificity is accomplished, other than intent and training. Do subject and target share a unified holographic field? Are standing waves picked up and carried by the Schumann Resonance, or transmitted by scalar waves or a gradient in the vacuum potential? Are the brains entrained on a resonant frequency? Does DNA function as a multi-mode antenna regulating growth, evolution, and perhaps psi?

Are specific interference patterns in the brain decoded and amplified? Ambient ELF fields and human bioreceptors, such as liquid crystals and piezoelectric crystal calcifications, have been suggested.

How we can increase our sensitivity is yet another question. The signal is perceived against a transient background of chaotic noise, and amplified by the body’s physiological pathways. Desire, intense concentration, and spiritual focus have been suggested. The trance state has been proposed as restricting the amount of input while allowing access to subtle perceptions.

Mind is a dynamic function of the entire organism at all levels of self-organization. Constantly fluctuating local parameters are embodied and amplified through the body’s electromagnetic control hologram. Mind/body modulates our sensitivity to external and internal information. Researchers measure a brainwave known as Contingent Negative Variation (CNV) to measure anticipation, anticipatory strategies, or readiness to respond; this stimulus can be informative or uninformative, carry content or just be an alert.

Remote viewing requires super-sensitivity and super-efficient states. It is not the result of cognitive training, but a gradual remolding of the entire psychophysical structure and metabolic pathways. Thus, the mind/body becomes a highly coherent, information-transparent transducer.

Vast information resources are hidden in unexplored manifolds of the mind/body continuum. In psi research, the study of nature and our nature, our potential becomes entwined. As Einstein (1934, The World As I See It) said, “We are seeking for the simplest possible scheme of thought that will bind together the observed facts.”

REFERENCES

Beckenstein, Jacob (2003), “Information in the Holographic Universe”, SciAm, Aug. 03. pp. 58-65.
Bearden, Thomas E. (1988). Excalibur Briefing: Explaining Paranormal Phenomena. San Francisco: Strawberry Hill Press.
Erickson, Milton H. and Ernest L. Rossi & Sheila Rossi (1976). Hypnotic Realities, New York: Irvington Publishers, Inc.
Gowan, John Curtis (1974). Development of the Psychedelic Individual, privately printed for the Creative Education Foundation, Northridge, California.
Gowan, John Curtis (1975). Trance, Art, and Creativity, privately printed for the Creative Education Foundation, Buffalo, New York. http://www.csun.edu/edpsy/Gowan
Green, Elmer and Alyce (1977). Beyond Biofeedback, San Francisco: Delacorte Press.
Honorton, Charles (1967). "Creativity and precognitive scoring level," Psych. Abs. 41:08057.
Honorton, Charles (1969), "A combination of techniques for separation of high and low-scoring ESP subjects," Psych. Abs. 43:08881, 1969.
Krippner, Stanley (1968), "An experimental study in hypnosis and telepathy," Am. J. of Clinical Hypnosis, 11(1): 45-54.
Krippner, Stanley, “Psi Research and the Human Brain’s ‘Reserve Capacities’”, DynaPsych.
Krippner, Stanley (Ed.), Advances in Parapsychological Research, Vol. I and Vol. II.
Laszlo, Ervin (1996). "Subtle Connectins: Psi, Grof, Jung, and the Quantum Vacuum”; DynaPsych.
Laszlo, Ervin (1994). “Toward a Physical Foundation for Psi Phenomena.” J. B. Rhine Lecture. American Parapsychological Assn., Amsterdam, August 8, 1994.
Masters, R. and Jean Houston (1966). The Varieties of Psychedelic Experience, New York: Holt, Reinhart, and Winston.
Miller, R.A., Webb, B. Dickson, D. (1975), “A Holographic Concept of Reality,” Psychoenergetic Systems Journal Vol. 1, 1975. 55-62. Gordon & Breach Science Publishers Ltd., Great Britain. Later reprinted in the hardback book Psychoenergetic Systems, Stanley Krippner, editor. 1979. 231-237. Gordon & Breach, New York, London, Paris. And in the journal Psychedelic Monographs and Essays, Vol. 5, 1992. 93-111. Boynton Beach, FL, Tom Lyttle, Editor.
Miller, R. A., Webb. B., “Embryonic Holography,” Psychoenergetic Systems, Stanley Krippner, Ed. Presented at the Omniversal Symposium, California State College at Sonoma, Saturday, September 29, 1973. Reprinted in Lyttle's journal Psychedelic Monographs and Essays, Vol. 6, 1993. 137-156.
Miller, Richard Alan (1985), The Magical and Ritual Use of Aphrodisiacs, New York, NY: Destiny Books.
Miller, Iona and Graywolf Swinney (2000). "CRP and Theta Reverie," Chaosophy 2000, Wilderville, Oregon: Institute for Consciousness Studies and Technologies.
Mishlove, Jeffrey (1975, 1993), The Roots of Consciousness, Tulsa: Council Oak Books.
Monroe, Robert (1971), Journeys Out of the Body, New York: Doubleday.
Monroe, Robert (1982). “The Hemi-Synch Process”, Unpublished, Monroe Institute.
Motoyama, Hiroshi with Rande Brown, Science and the Evolution of Consciousness: Chakras, Ki and Psi.
Pang, Henry and L. Fort (1967), "Relatedness of Creativity, . . .and ESP," Perceptual and Motor Skills, 24: 650.
Persinger, Michael A. (1989), "Psi Phenomena and Temporal Lobe Activity: The Geomagnetic Factor," in I.A. Henkel and R. E. Berger (eds.) Research in Parapsychology 1988, Metuchen, NJ: Scarcrow Press.
Persinger M.A., & Krippner S. (1989). Dream ESP experiments and geomagnetic activity. Journal of the American Society of Psychical Research, 83, 101- 106.
Pitkanin, Matti, JNLRMI, Vol. 1, No. 1.
Puharich, Andrija (1961), Beyond Telepathy. New York: Doubleday.Radin, Dean (1997). The Conscious Universe: The Scientific Truth of Psychic Phenomena. New York: Harper & Collins.
Radin, Dean and Bierman, Dick. “Anomalous unconscious emotional responses: evidence for a reversal of the arrow of time,”
Randi, James. Flim Flam: Psychics, ESP, Unicorns, and Other Delusions. Prometheus Books. Books.
Ryzl, Milan. Parapsychology: A Scientific Approach
Schmidt, Helmut (1970). “A Quantum Mechanical Random Number Generator for Psi Tests,” Journal of Parapsychology, Vol. 34(3) 219-224, 1970.
Schaut, G.B., & Persinger, M.A. (1985). Subjective telepathic experiences, geomagnetic activity and the ELF hypothesis. Part I. Data analysis. Psi Research 4(1), 4- 2O.
Sidorov, Lian (2002) "On the possible mechanism of intent in paranormal phenomena," Journal of Non-Local and Remote Mental Interaction, Vol. 1(1). http://emergentmind.com/sidorov_II.htm
Sidrov, Lian (2003a). “Editor’s Note”, http://emergentmind.org/editor’snotes.htm
Sidorov. Lian (2003b). “Landscaping the Mind: Interview with Joseph McMoneagle,” http://emergentmind.org/mcmoneagle_II2.htm
Sidorov, Lian (2003c). “Thinking Outside the Box in Experimental Parapsychology,” http://emergentmind.org/sidorovII2.htm
Stanford, R.G. and C. R. Lovin (1970), "The eeg alpha rhythm and ESP performances": Journal of the American Society for Psychical Research, 64:4.

Stevenson, Ian (1970), Telepathic Impressions, Charlottesville: University of Virginia Press.
Swinney, Graywolf (2001). Holographic Healing, Wilderville: Asklepia Publishing.
Targ, Russell, & Hurt, David B. (1972). “Learning Clairvoyance and Perception with an Extra-Sensory Teaching machine,” Parapsychology Review, Vol.3(44) 9-11, 1972.
Ullman, Montague and Stanley Krippner (1973), Dream Telepathy, New York: McMillan Publishing Co.

File Created: 7/11/03

****

DISTANCE HEALING TODAY
Quantum Resonance and Biofeedback

By Iona Miller, 6/2005

Science proceeds by way of 'discovery,' as well as simple accumulation or even 'invention.' This is the basis of scientific revolutions, and paradigm shifts - "the tradition-shattering complements to the tradition-bound activity of normal science," (Kuhn, 1962). A paradigm is a disciplinary matrix. Paradigms are essentially worldviews -- expressing our beliefs about the way things work, including tacit assumptions.

Chaos Theory and Complexity have disclosed the self-organizing inner workings of non-linear dynamics in nature and human nature. Systems (and subsystems) are always connected in various ways to various degrees; energy and information is constantly exchanged. In complex phase interactions and dynamical energy systems, resonance is the key dynamic which couples them, increasing dimensional complexity and leading to emergence of new properties.

Interactive resonance occurs both within and between material systems, through recurrent feedback encoding a complex interactive history. Circulating recurrent feedback interactions (cyclic information) are the fundamental bases of holism. The more rapid the feedback, the more stable the holistic system. This circulation of energy and information allows them to interact as a whole.

HYPOTHESIS: Emergent healing depends on the nonlocal principles of nature's own self-organization, as well as on direct causal influences on the mindbody of the organism. It is proposed that the interactive field -- therapeutic entrainment -- present in the healing situation can be amplified intentionally to mobilize the psychophysical healing process.

INTRODUCTION

All those who believe in the power of mind over matter, please raise my hand!

Clearly, the whole story of human technology is the the story of the ascendency of mind over matter. Whether that is a triumph or a tragedy for humankind remains to be seen.

Conventional medicine takes an allopathic approach to healing, but Complementary Medicine works holistically in conjunction with it through compassionate intentionality. Historically, so-called spiritual healing or faith healing has been person-to-person, whether local or nonlocal. It works on the premise of evoking the healing potential through a commonly shared field-effect, electromagnetic physiological reactivity.

Today’s technology has allowed distance healers to experiment with technological aids to their healing practices. There are still many mysteries of the interactive field which remain to be explored.

With a phenomenological eye toward field dynamics, this exploration demonstrates an additional theoretical framework within the interactive field applicable to paradoxical healing. It opens creative and healing possibilities and allows for the active, intentional liberation of the psychophysical imaginal realm. The genesis of the interactive field is rooted also in shamanic realms as a backdrop from which to see field theory.

Shamanic expressions, ancient healing forces, of the unified field include mana, chi, prana, qi, kundalini, bioenergetics, psi faculty, universal energy, orgone, wakonda, etc. Field theory is also explored in the world of quantum physics where the universal field is examined from paradigms situated in varied consciousness models.

The somatic unconscious, an intrinsic part of the interactive field in mutual engagement with two or more persons, is also woven into this fabric. In this study it is an intersection between the universal field and the psychodynamic field -- embodying co-consciousness in healing. (Miller, 2003)

Just as traditional medicine identifies itself with the past through the Hippocratic Oath, this new orientation also draws on the ancient Greek and Egyptian healing cults and our collective taproot back into 50,000 years of shamanic healing culture. Like traditional physicians seek to identify themselves with the Hippocratic ideal, we can embody this paradigm, this philosophy, by embracing a worldview which is seemingly new, but older than history -- medical intuition and holistic spirituality. It doesn't negate or even supercede the Hippocratic orientation; in ancient Greece both the complementary methods of healing mind, body and spirit were part of the cult of Asklepios.

When conventional means failed, supplicants went to the dream temples to heal their psyches -- their souls -- they entered the Mysteries. These healing dreams somehow mobilized the nonrational elements of being and healing somehow emerged. But their notion of soul was not disembodied; it meant the whole psychophysical organism. Ancient Vedic healers based their treatment in the philosophy that the common essence of humankind and cosmos was consciousness. Altering that primal essence, consciousness, could change one's state of health. It isn't really a case of activating mind over matter, but mobilizing what undergirds both mind and matter.

What, essentially, is this consciousness of which we speak? Can it be more than our subjective awareness, our existential experience -- the result of perceptual input and self-referential internal processing? Is it the very basis of materiality, a neutral essence more fundamental than energy or matter, more than microstates of the functioning of human wetware?

But, does psi or ESP even exist, or is it merely an optical illusion of the mind? There are volumes of research (Krippner, Motoyama, Honorton, Tart, Swann, Schwartz, Putoff and Targ, Radin, Utts and Nobel-winner Josephson) to suggest that it does, though skeptics staunchly maintain it does not. Because the issue is emotional and seemingly unresolved does not mean we should stop asking, looking for a deeper relationship of psyche and matter.

In fact, the mandate was laid down several decades ago by physicist Wolfgang Pauli when he worked with psychologist C.G. Jung: " We should now proceed to find a neutral, or unitarian, language in which every concept we use is applicable as well to the unconscious as to matter, in order to overcome this wrong view that the unconscious psyche and matter are two things."

However, as Carl Sagan also said, " Extraordinary claims require extraordinary evidence." Therefore, we will approach the notion from a variety of perspectives, from the "soft" science of psychology, and the "hard" science of physics, as well as the median position of alternative medicine -- transpersonal and energy medicine, with their holistic perspective. In this way we hope to create a circumspect view about and investigate the possibility of the role of co-consciousness in healing.

Preliminary research done by Dr. Hiroshi Motoyama in Japan has shown that a person emits very small amounts of visible light. The amount is so small that a photon counter is needed. Dr. Motoyama found that photon emission is higher at certain acupuncture points compared to a region of skin with no acupuncture point. According to unpublished research done by him in Japan, there is some indication that emission at certain acupuncture points is increased for persons with psychic abilities. The modern healer is moving away from epic, heroic models of power toward imaginative fantasy. Awareness is growing that image-consciousness heals (Miller and Miller, 1994).

The healing dyad is best characterized by its emphasis on intent. Both parties have the intention of engaging in a healing dynamic experience. This is the foundation or underlying raison d' etre of the therapeutic encounter. This intention can deepen into a linking or "hook up" of the individuals into a unified field, a shared resonant interactive field. This field seems to facilitate or mobilize the healing dynamic.

The facilitation of attentional resonance opens the participants to the simultaneous presence of both classical and acausal field phenomena. They are mutually connected through the unified field. The more mutual the process, the more the interactive field manifests. In this interactive field, we are embedded in an imaginally perceived whole situation -- an encompassing, infusing, and mutually interactive field, with conscious attention to the relationship.

HISTORY OF REMOTE HEALING

The genesis of the interactive field is rooted in shamanic realms as a backdrop from which to see field theory. Shamanic expressions, ancient healing forces, of the unified field include mana, chi, prana, qi, kundalini, bioenergetics, psi faculty, Odic force, universal energy, orgone, wakonda, etc. Field theory is also explored in the world of quantum physics where the universal field is examined from paradigms situated in varied consciousness models.

The shaman is the archetype of the wounded-healer and is perceived as having social or personal power for vision and healing. Healers learn not to exploit or identify egotistically with this process of mobilizing the unconscious. Rather, they let it operate through them as guides or mentors, so the other can discover that the healing resources are within and find empowerment -- the dramatic healing breakthrough, (Swinney and Miller, 1993).

The history of modern remote healing is lost in antiquity, in 50,000 or more years of shamanic practice, but modern investigation began in earnest in the 1950s and 1960s. One of the pioneers of this era, and perhaps the Godfather of Distance Healing is Dr. Hiroshi Motoyama of Japan.

Motoyama conducted near- and distance-healing experiments in both screened (Faraday cages) and unscreen situations to test the potency of intentionality, and the ability to one human being to influence the physiology of another without direct contact.

Motoyama also worked with and incorporated the theories of Itzhak Bentov into his protocols. Bentov summarized his early findings in his work STALKING THE WILD PENDULUM (Bantam, 1977), a popular book which educated the public about resonance phenomena.

Medicine is mostly concerned with mass, the material aspect. Matter is a kind of accumulation of energy in a fixed order. Chaos is energy but random, not in order. But when the energy is fixed, in order, in a certain frequency, etc, it becomes quantum, and this quantum is the origin of mass. So this quantum forms an electron or a proton or nucleus and thence an atom. The atoms combine and they make molecules and the molecules combine to make DNA and protein and then us: matter-with-consciousness (Motoyama).

The very first Motoyama-Bentov Fellow was Dr. Marshall Gilula, a Neuropsychiatrist with a specialty in EEG. Over the years, Dr. Gilula has employed both soft and hard technologies in his healing practice. He was a pioneer in CES, which is now known as Transcranial Electrical Stimulation, which is an active method of driving brainwaves into coherence and synchrony, now widely accepted in the conventional medical world. AlphaStim, etcÃƒÂ¢Ã¢â€šÂ¬Ã‚Â¦..See http://heartsstringsbook.50megs.com

SUBTLE ENERGIES

Numerous controlled studies suggest that conscious intent can initiate helpful changes in a variety of organisms, including human beings, at great distances. These events appear to be genuinely nonlocal in nature. They do not yield to explanations based in classical concepts of energy, space, time, and causation. Classical models of distant healing, including the concept of "energy," must be reexamined. A new theoretical perspective, anchored in the nonlocal nature of human consciousness, may be necessary if we are to progress in our understanding of nonlocal healing events. (Dossy, 1994)

The International Society for the Study of Subtle Energies and Energy Medicine was founded in 1989 in Colorado. ISSSEEM was founded to explore the application of subtle energies to the experience of consciousness, healing, and human potential and is designed as a bridging organization for scientists, clinicians, therapists, healers, and laypeople. ISSSEEM encourages experimental exploration of the phenomena long associated with the practice of energy healing.

To study systems and energies that interact with the human psyche and physiology, either enhancing or perturbing health.

To interconnect persons who work with or conduct research about subtle energies.

To encourage an exchange of information through conferences, seminars, and workshops.
They describe the field of inquiry as:
Energy Medicine includes all energetic and informational interactions resulting from self-regulation or brought about through other energy linkages to mind and body. In addition to various therapeutic energies which we may use, there are also energy pulses from the environment which influence humans and animals in a variety of ways. For instance, low-level changes in magnetic, electric, electromagnetic, acoustic, and gravitational fields often have profound effects on both biology and psychology. In addition to energies originating in the environment, it has been documented that humans are capable of generating and controlling subtle, not-yet-measurable energies that seem to influence both physiological and physical mechanisms.

Subtle Energies, compared with "energy medicine," is a concept more difficult to define within the current scientific paradigm. Ancient and modern wisdom traditions describe human bioenergies referred to by many names (e.g., chi, ki, prana, etheric energy, fohat, orgone, odic force, mana, homeopathic resonance) that is believed to move throughout the so-called "etheric" (or subtle) energy body and thus is difficult to measure using conventional instrumentation.

In addition, many of the complementary and alternative therapies that are becoming increasingly popular appear to involve the flow of these subtle energies through the dense physical body. In addition, it is traditionally accepted that expansions of consciousness often are related to changes in subtle energies that cannot be quantified. These latter "energies", which are said to be associated with interactions and with transcendence, may not, in fact, actually be involved with known physical fields.

INFINITE REVERBERATION

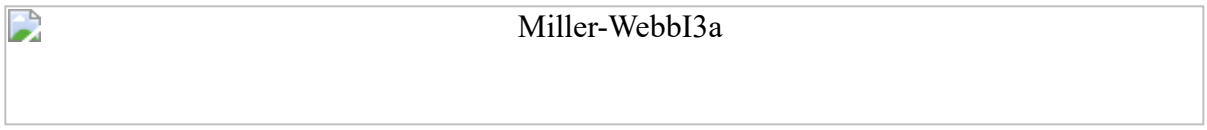

Home Up

Journal of Non-Locality and Remote Mental Interactions Vol.I Nr. 3

QUANTUM BIOHOLOGRAPHY

A Review of the Field from 1973 - 2002

Richard Alan Miller, Iona Miller, and Burt Webb, ©2002
drram@magick.net; iona_m@yahoo.com, phoenix@eskimo.com
Organization for the Advancement of Knowledge, Grants Pass, Oregon

ABSTRACT: Complex information can be encoded in EM fields, as we all know from coding and decoding of television and radio signals. Even more complex information can be encoded in holographic images. DNA acts as a holographic projector of acoustic and EM information which contains the informational quintessence of the biohologram. Only 3% of human DNA encodes the physical body. The remaining 97% of the 3 billion base pair genome contains over a million genetic structures called transposons, that have the capacity to jump from one chromosomal location to another (Kelleher, 1999). We are 99.9% alike in our genetic legacy. Our individuality is expressed in three million small variations in our cells, called single nucleotide polymorphisms.

Gene-expression is the mechanism by which new patterns are called into being (Rossi, 2000). There is also a strong correlation between modulation of the brain's EM field and consciousness (Persinger, 1987; McFadden, 2002). The Gariaev group has discovered a wave-based genome and DNA phantom effect which strongly supports the holographic concept of reality (Miller, Webb, Dickson, 1975). This main information channel of DNA is the same for both photons and radio waves. Superposed coherent waves of different types in the cells interact to form diffraction patterns, firstly in the acoustic domain, secondly in the electromagnetic domain -- a quantum hologram -- a translation process between acoustical and optical holograms.

Creative, novel and enriching psychotherapeutic experiences can lead to neurogenesis, gene expression, and healing which facilitate mindbody communication and can have a long-term transformative effect on the whole person (Rossi, 2002). Thus, bioholography has relevant applications for optimizing health, well-being and even self-realization. It is relevant in biophysics, medicine, psychobiology, psychotherapy and the holistic healing arts. It provides us with a more genetically integrated model of the complex dynamics of the mindbody -- one arising in the domain underlying the standard genetic code triplet model.

Keywords: DNA, DNA phantom, wave biocomputer, genome, wave-based genome, quantum holography, bioholography, organismic evolution, vacuum substructure, biophysics, psychobiology, gene expression, psychotherapeutic applications.

INTRODUCTION

Hypothesis: The organization of any biological system is established by a complex electrodynamic field which is, in part, determined by its atomic physiochemical components. This field, in turn, determines the behavior and orientation of these components. This dynamic is mediated through wave-based genomes wherein DNA functions as the holographic projector of the psychophysical system - a quantum biohologram.

A model of the mind-body relationship is developed in which novel biophysical principles in genome function generate a dynamic possessing attributes consistent with both our psychophysical nature and consciousness. The model invokes a fractal link between neurodynamical chaos and quantum uncertainty. Transactional wave collapse allows this link to be utilized predictably by the excitable cell, in a way which bypasses and complements formal computation. The formal unpredictability of the model allows mind to interact upon the brain, the predictability of consciousness in survival strategies being selected as a trait by organismic evolution (King, 2001). This quantum evolution is orchestrated by the information transduction of DNA.

The Gariaev group (1994) has proposed a theory of the Wave-based Genome where the DNA-wave functions as a Biocomputer. They suggest (1) that there are genetic "texts", similar to natural context-dependent texts in human language; (2) that the chromosome apparatus acts simultaneously both as a source and receiver of these genetic texts, respectively decoding and encoding them; (3) that the chromosome continuum acts like a dynamical holographic grating, which displays or transduces weak laser light and solitonic electro-acoustic fields.

The distribution of the character frequency in genetic texts is fractal, so the nucleotides of DNA molecules are able to form holographic pre-images of biostructures. This process of "reading and writing" the very matter of our being manifests from the genome's associative holographic memory in conjunction with its quantum nonlocality. Rapid transmission of genetic information and gene-expression unite the organism as holistic entity embedded in the larger Whole. The system works as a biocomputer -- a wave biocomputer.

The quantum nonlocality of the genetic information is fundamental. Experimental work of the Gariaev group shows how quantum nonlocality is directly related to laser radiation from chromosomes (coherent light), which jitterbugs its polarization plane to radiate or occlude photons. DNA and the genome have now been identified as active "laser-like" environments. Roughly speaking, DNA can be considered as a liquid crystal gel-like state that acts on the incoming light in the manner of a solitonic lattice.

A soliton is an ultra stable wave train that arises in the context of non-linear wave oscillation. The DNA reading process can be modeled as a complex mechanical oscillator capable of producing solitonic wave transmissions. DNA, modeled as a kind of rotary pendulum can be simulated as a chain of non-linear oscillators. Complex dynamic patterns arise when taking into account the non-linear covalent connections between nucleotides.

The same researchers suspect the ability of chromosomes to transform their own genetic-sign laser radiations into broadband genetic-sign radio waves. The polarizations of chromosome laser photons are connected nonlocally and coherently to polarizations of radio waves. (Thus, we seem to have an explicit physical analogue for the traditional mystical apprehension of "inner light" and the "audible life stream"). This is the main information channel of DNA, the same for both photons and radio waves. Superposed coherent waves of different types in the cells interact to form diffraction patterns, firstly in the acoustic domain, secondly in the electromagnetic domain -- a quantum hologram -- a translation process between acoustical and optical holograms.

I. QUANTUM BIOHOLOGRAPHY

In *Languages of the Brain* (1971), Pribram postulated a neural hologram made by the interaction of waves in the cortex, which in turn is based on a hologram of much shorter wavelengths formed by the wave interactions on the sub-atomic level. Thus, we have a hologram within a hologram, and the interrelatedness of the two somehow gives rise to our sensory images. Bohm (1980), in *Wholeness and the Implicate Order* went further, declaring the brain is a hologram interpreting a holographic universe. In a holographic model this inseparable interconnectedness begins at the even more fundamental level of human existence, rooted in our existential blueprint, DNA. The brain is a hologram, enfolded within our holographic mind-body, enfolded within a holographic universe.

Recent discoveries by Russian scientists Peter Gariaev & al. and later speculations by Vladimir Poponin shed tremendous light on our proposal that the human being is a transducer of universal energy and consciousness -- essentially a biocomputer. The new feature of this research is the ability to physically demonstrate subtle fields emerging from the quantum foam or vacuum potential. This makes the effect quantifiable and measurable -- objective.

This takes the phenomenon and subjectivity of consciousness out of the realm of quantum metaphysics and plants it firmly under the rubric of hard science. It heralds the unification of quantum mechanical and chaotic dynamics in human consciousness. We can now model the human bio-computer.

Poponin (1995) boldly suggests that this deeper understanding of the mechanisms underlying subtle energy phenomena include many of the observed alternative healing phenomena and includes a physical theory of consciousness. This hypothesis is based on a precise quantitative background and combines both quantum mechanics and complexity or chaos dynamics in a startling and compelling new way. It posits that some new field structure is being excited from the physical vacuum by an intrinsic ability that emerges through DNA.

Gariaev discovered the DNA Phantom Effect in 1985, when he worked in correlation spectroscopy of DNA, ribosomes and collagen in the Institute of Physics, in the Academy of Science of the USSR. He was first able to publish his results in 1991, leading to a book in 1994, *Wave Based Genome.* His DNA Phantom Effect demonstrates a dynamic new field in the vacuum substructure by bombarding it with coherent laser light and coupling it to conventional electromagnetic fields. The experimental protocols for this procedure are rigorous, and have been reproduced in Moscow and at Stanford.

R. A. Miller, I. Miller, and B. Webb (2001) are now consulting on the project to suggest the next research directions and applications. Miller and Webb have a long-standing background in this field. Long before David Bohm published his *Wholeness and the Implicate Order* (1980), Miller and Webb published "A Holographic Concept of Reality" in the journal *Psychoenergetic Systems*, ed. Stanley Krippner, Vol. 1, 1975. 55-62. Gordon & Breach Science Publishers Ltd., Great Britain. "Holographic Concept" was later reprinted in the book *Psychoenergetic Systems*, S. Krippner, editor. 1979. 231-237. Gordon & Breach, New York, London, Paris. It was reprinted again in the journal *Psychedelic Monographs and Essays,* Vol. 5, 1992. 93-111. Boynton Beach, FL, Tom Lyttle, Editor.

This foundational paper was followed shortly by "Embryonic Holography: An Application of the Holographic Concept of Reality", also in 1973. Presented at the Omniversal Symposium, California State College at Sonoma, Saturday, September 29, 1973. Reprinted in Lyttle's journal *Psychedelic Monographs and Essays,* Vol. 6, 1993. 137-156. Miller followed this project with a proposal prepared for the government through Mankind Research Unlimited, described in a formerly unpublished, proprietary paper called "Bioluminescence, Kirlian Photography and Medical Diagnostics" (1974), which is only now seeing the light of day. It was an application of his paper on "The Physical Mechanisms of Kirlian Photography."

In 1993, Iona Miller published "The Holographic Paradigm and the Consciousness Restructuring Process," another application to psychotherapeutic mindbody healing. Subsequently she has published extensively on the role of complex dynamics in relationship to consciousness and process-oriented psychotherapy, through Asklepia Foundation. A deep interest in the nature of *Synergetics* (Fuller, 1975), zero-point field, the vacuum potential, and quantum foam has led her to develop innovative applications of chaos theory in consciousness studies. She has dovetailed many of those discoveries with the reports of mystics of their intuitive inner-plane experiences of Light and Sound (Shabd) throughout history (Singh, 1979; Blavatsky, 1987; Puri, 1964; Miller and Miller, 1983). Could it be that these mystics somehow perceive holographic processes when they look inside themselves?

Endogenous DMT (N,N-dimethyltryptamine) is described as the source of visionary light in transpersonal experiences. Its primary source, the pineal, has traditionally been referred to as the Third Eye. DMT production is particularly stimulated, according to Strassman (2001), in the extraordinary conditions of birth, sexual ecstasy, childbirth, extreme physical stress, near-death, and death, as well as meditation. Pineal DMT also plays a significant role in dream consciousness. How might meditation evoke the pineal DMT experience?

"Meditative techniques using sound, sight, or the mind may generate particular wave patterns whose fields induce resonance in the brain. Millennia of human trial and error have determined that certain "sacred" words, visual images, and mental exercises exert uniquely desired effects. Such effects may occur because of the specific fields they generate within the brain. These fields cause multiple systems to vibrate and pulse at certain frequencies. We can feel our minds and bodies resonate with these spiritual exercises. Of course, the pineal gland also is buzzing at these same frequencies. The pineal begins to "vibrate" at frequencies that weaken its multiple barriers to DMT formation: the pineal cellular shield, enzyme levels, and quantities of anti-DMT. The end result is a psychedelic surge of the pineal spirit molecule, resulting in the subjective states of mystical consciousness." (Strassman, 2001). But these philosophical aspects are best addressed further elsewhere.

Here, in this presentation, the joint work of decades by Miller, Miller and Webb comes to fruition and perhaps finds a physical proof.

The organization of any biological system is established by a complex electrodynamic field. This em field is, in part, determined by its atomic physicochemical components and, in turn, determines the behavior and orientation of these components. The holographic model of reality emerging from this principle provides a scientific explanation of psychoenergetic phenomena, (Miller, Webb, Dickson, 1973).

In 1973, Miller and Webb suggested biohologrames as the projectors of our material reality: in the nuclei of each cell in the human body, the DNA (deoxyribonucleic acid) carries the structure of our whole body. Not just our physical form, but also the processes that that form undergoes in terms of survival. If all of these things are in truth locked in the DNA, how does that turn into a functioning being?

The DNA could possibly be the holographic projectors. The DNA could be projecting a field that would be experienced by other DNA in the body. The DNA molecules, in a sense, could be linked together. The DNA molecules are also linked to their own cell, which they are controlling via mechanisms of RNA transfer and enzymatic action in the cell. We believe that it is likely that the DNA and the RNA are in non-local communication. It is known from the EPR phenomenon that entangled photons retain a mutual

informational bond even at a distance, through polarization, and allow a kind of quantum teleportation, which has finally been experimentally verified.

> *DNA molecules, included in chromosomes, possess a substance--wave duality which is similar to the dualism of elementary particles. In accordance with it, DNA codes an organism in two ways, both with the assistance of DNA matter and by DNA sign wave functions, including coding at its own laser radiation level - [28].*
>
> *The genetic apparatus can be non-local at the molecular level (holographic memory of a chromosome continuum) and at the same time quantum mechanically non-local in compliance with the Einstein-Podolsky-Rosen effect [4]. The latter means that the genome genetic and other regulatory wave information is recorded at the polarization level of its photons and is non-locally (everywhere and in no time) transferred (plays out) throughout the entire space of a biosystem by the polarization code parameter. This helps to set a quick-response information contact among the billions of cells constituting an organism.*
>
> *The genome on the whole and the individual nucleus of cells can generate and recognize text-associative regulatory structures with the application of a background principle, holography and quantum non-locality.* (Gariaev, et al, 2000).

We believe that the DNA is the projector of the biohologram, both at the cellular level and at the whole-organismic level. This means that the DNA creates a situation of a complex pattern of three-dimensional electromagnetic standing and moving wave fronts in the space that the organism occupies.

> *Other researchers soon obtained similar results, and not only based on photons. Multi-frequency physical fields are now teleported. Based on this data, it's possible to suppose that photon fields, emitted by chromosomes as sign fields, can be teleported within or even outside the organism's space. The same is true for wave photon fronts, which were read from the chromosome continuum similar to reading from a multiplex hologram. If photons are transformed into radio waves (the situation we found - ref. to [8, 33,37]) through the EPR-mechanism, then this phenomenon is vital. In fact, the importance of quantum non-locality existence for a genome is hard to overestimate.* (Gariaev, et al, 2001).

We think that these wave fronts interact with, interpenetrate with, and interdetermine the physical substance that makes up the physical creature. According to the holographic model of reality, all the objects we can observe are three-dimensional images formed of standing and moving waves by electromagnetic and nuclear processes. All the objects of our world are three-dimensional images formed electromagnetically, i.e. holograms. Just like a hologram encodes a 3-D image, the biohologram encodes and projects the blueprint of the human being, as well as other biological systems.

We also believe that the nervous system constitutes a coordination mechanism that integrates DNA projections of the rest of the cells in the system, that it is first and foremost a coordination mechanism which aligns these cellular holograms.

Imagine the information pleroma, beyond energy and matter, as the source of all infinitely coherent light, "shining" itself into its own entropic womb where our temporo-spatial universe is given its life-potential as a single laser beam.

The DNA in a particular cell is not totally active. It has been determined that there may be as little as 1% of the DNA present in the nucleus of the cell acting as the determinant for the structure of that cell. The nervous system, interestingly enough, has the highest percentage of operating DNA of any cell system in the body, of up to at least 10% of the DNA in the brain cells. The neuron nuclei are most active.

We suggest that the nervous system projects a global biohologram which interacts with the cellular biohologrames. If the membrane structure of the neuron nuclei is examined closely, it will be seen that the

different cavity systems that enter the outer membrane also enter the inner membranes, therefore topologically, these are one and the same. Hence the nucleus is lacking a membrane, or the neurons are lacking a membrane in the sense that two of their membranes are topologically one.

We suggest that the neurons are not actually brain cells as such. We believe that the brain is the cell, and the neurons are like a distributed nucleus for that cell. That makes the glial cells organelles in the giant brain-cell. But they are also cells in their own right, much more so than neurons are. We believe the glial cells are infinitely involved with the biohologram, in its projections, and its coordination.

To go further, the biohologram, projected by the brain, creates standing and moving electromagnetic wave patterns at different frequencies of the spectrum in order to effect different biochemical transformations. There may be specific electrostatic fields, or there may be electrodynamic fields varying at various frequencies, from low (radio waves) all the way up the spectrum into visible light and beyond.

Another process of holography is called "acoustical holography". Acoustical holography employs sound waves to create a movement on a surface that is used as the basis for creation of an optical hologram. So we essentially convert between a pattern of sound waves reflected off an object in space into a pattern of light waves that can reconstruct the shape of that object. We have a transformation between two levels of vibration, two media as it were, preserving a pattern in space. (Miller and Webb, 1973).

We suggest that this happens to a much greater degree in the DNA control of our bodies. The liver, for example, contains special function cells. The special function of the liver cells is created by the influence of the projection of the liver pattern on the DNA in the cells in the area where the liver is created. We are suggesting an important feedback mechanism between the activation of the DNA in a particular cellular tissue type that causes it to be that tissue type, and the biohologram being projected by the nervous system. This is biohholography.

Returning to the recent Russian discoveries (Gariaev, and reporter Poponin), which seem to confirm the seminal discovery of Miller and Webb: both quantitative and qualitative data are crucial for the development of a new unified nonlinear quantum field theory which includes the physical theory of consciousness. The DNA phantom field effect may be interpreted as a manifestation of a new physical vacuum structure which has been previously overlooked. It is perhaps a specific example of a more general category of electromagnetic phantom effects.

Results of the experiments as described by Poponin showed that when DNA was placed in a scattering chamber and bombarded with laser light a "phantom" was revealed, even when the DNA itself had been removed. The DNA was bombarded with weak coherent laser radiation in two frequencies; the intensity of the scattered light was measured, as well as non-linear localized excitations.

The experimental team found a surprising effect while measuring the vibrational modes of DNA in solution using a sophisticated MALVERN laser photon correlation spectrometer (LPCS), which tests the fluctuation dynamics of DNA solutions.

> *In each set of experimental measurements with DNA samples, several double control measurements are performed. These measurements are performed prior to the DNA being placed in the scattering chamber. When the scattering chamber of the LPCS is void of physical DNA, and neither are there any phantom DNA fields present, the autocorrelation function of scattered light looks like the one shown in Figure 2a. This typical control plot represents only background random noise counts of the photomultiplier. Note that the intensity of the background noise counts is very small and the distribution of the number of counters per channel is close to random. Figure 2b demonstrates a typical time autocorrelation functions when a physical DNA sample is placed in the scattering chamber, and typically has the shape of an oscillatory and slowly exponentially decaying function. When the DNA is removed from the scattering chamber, one anticipates that the autocorrelation function will be the same as before the DNA was placed in the scattering chamber. Surprisingly and counter-intuitively it*

> *turns out that the autocorrelation function measured just after the removal of the DNA from the scattering chamber looks distinctly different from the one obtained before the DNA was placed in the chamber. . . Two conditions are necessary in order to observe DNA phantoms. The first is the presence of the DNA molecules and the second is the exposure of the DNA to weak coherent laser radiation.* (Poponin).

Researchers hypothesize that some new field structure is being excited from the physical vacuum substructure. As long as the chamber is not disturbed, it is measurable for long periods of time. What is measured is light scattering from the DNA phantom fields. What is attained is qualitative and quantitative information about the nonlinear dynamical properties of the phantom DNA fields. Its origin is related to physical DNA. As yet, they have found no other substance which recreates or emulates the effect of the DNA molecule.

It is this model which suggests a more general nonlinear quantum theory which may explain many of the observed subtle energy phenomena and might lead to a physical theory of consciousness.

This suggests that the electromagnetic phantom effect is a more fundamental phenomenon which can be used to explain other observed phantom effects, though not to be confused with the often misinterpreted secondary emission of electrons seen in Kirlian Photography and dubbed "phantoms." [ref. R.A. Miller on "The Physical Mechanisms of Kirlian Photography," *Psychoenergetic Systems*, Stanley Krippner, ed., 1974]. Evidence suggests a relationship to the phenomena of [endogenous] bioluminescence, liquid crystals, and superconductivity, which we intend to pursue, elsewhere.

Bioluminescence can be considered an indicator of life activity. It is the emission of photons of light produced when certain energized electrons drop into a lower or ground state. A common example is the visible light (or electromagnetic radiation) generated by the firefly. The importance of this phenomenon is seen by taking the broad view of the life process as we know it: photons from the sun excite electrons here on earth; this high energy state is transformed into high energy phosphate bonds by the process of photosynthesis; the release of the energy stored in these bonds is the fuel of life; electrons are transferred between molecules in a downward cascade fashion to lower energy states; this action produces the electric current that produces the motion that we call life. (Miller, 1974).

Entities can also luminesce at higher frequencies than the normal visible spectrum, such as in the UV or microwave region. It has been shown that the human being is an emitter of various electromagnetic radiations. Different emissions correspond to different body structures across the emission spectrum. These electromagnetic radiations are of course indicative of the energy state of the organism, and can be indicative of the state of health.

Other research (Childre, 1992; Paddison, 1992; King, 2001) suggests that consciousness is non-localized in the bodymind. Joseph Chilton Peace in his latest, *The Biology of Transcendence: A Blueprint of the Human Spirit,* (2001) points out that we have five neural centers or brains--and establishes that our fourth and most recently developed brain is located in the head while the fifth is located in the heart.

It is the dynamic interaction of this head brain (intellect) and heart brain (intelligence), of biology and spirit, which allows transcendence from one evolutionary place to the next. Pearce declares we are quite literally, made to transcend. He says, "Transcendence is our biological imperative, a state we have been moving toward for millennia."

In less scientific and more mystical terms, we emerge through self-organization from the Void and to the Void we can return for renewal and sustenance. It is, in fact the *Heart Sutra* that informs us that "Form is not other than Void; Void is not other than Form." Our human form is not other than this void, and biophysics now demonstrates this quantitatively and qualitatively.

We are more fundamentally electromagnetic, rather than chemical beings. The void state, "cosmic zero," is the primal matrix and proportionately our most fundamental reality. In essence, we emerge from pre-

geometrically structured nothingness, and DNA is the projector of that field which sets up the stress gradients in the vacuum or quantum foam to initiate that process of embryonic holography, (Miller and Webb, 1973-93). The holographic paradigm is one of reciprocal enfolding and unfolding of patterns of information. All of the potential information about the universe is holographically encoded in the spectrum of frequency patterns that constantly bombard us.

We can imagine that the self-organizing emergent function of the rippling effects of immense numbers of criss-crossing interference waves must be one way of making mutually interactive, or reciprocal, holographic projections of holographic projections. Our DNA projects our psychophysical self, and likewise our brains mathematically construct objective reality by interpreting frequencies that are ultimately projections from another dimension, a deeper order of existence that is beyond both space and time: The brain is a hologram enfolded in a holographic universe, (Talbot, 1991, p. 55).

Researchers have found that at the moment of ovulation there is a definite shift in the electrical fields of the body of the woman. The membrane in the follicle bursts and the egg passes down the fallopian tube. The sperm is negative with respect to the egg. When the sperm and egg unite, the membrane around the egg becomes hyperpolarized, shutting out other sperm. It is at this moment that the electromagnetic entity is formed. The fertilized egg cell contains all the information necessary to create a complete operational human being.

The biohologram begins to function at conception and ceases only at death. Our contention is that the DNA at the center of each cell creates the multi-cellular creature hologram by expressing the DNA in the center of the cells. The biohologram projected by the embryonic nervous system forms a three-dimensional pattern of resonant structures. These include points, lines, and planes that electromagnetically behave as the acoustic waves - the material waves - of the drumhead, acting as field guides to flowing matter and energy.

The Gariaev group has proposed a theory of the DNA-wave Biocomputer. They suggest (1) that there are genetic "texts", similar to natural context-dependent texts in human language; (2) that the chromosome apparatus acts simultaneously both as a source and receiver of these genetic texts, respectively decoding and encoding them; (3) the chromosome continuum acts like a dynamical holographic grating, which displays or transduces weak laser light and solitonic electro-acoustic fields. The distribution of the character frequency in genetic texts is fractal, so the nucleotides of DNA molecules are able to form holographic pre-images of biostructures.

In other words, the basic assumptions of the Gariaev team include the following:

1. the genome has a capacity for quasi-consciousness so that DNA words produce and help in the recognition of semantically meaningful phrases;

2. the DNA of chromosomes control fundamental programs of life in a dual way: as chemical matrixes and as a source of wave function and holographic memory;

3. processes in the substance-wave structures of the genome can be observed and registered through the dispersion and absorption of a bipolar laser beam.

This process of "reading and writing" the very matter of our being manifests from the genome's associative holographic memory in conjunction with its quantum nonlocality. Rapid transmission of genetic information and gene-expression unite the organism as holistic entity embedded in the larger Whole. The system works as a biocomputer -- a wave biocomputer.

The quantum nonlocality of the genetic information is fundamental. Experimental work of the Gariaev group shows how quantum nonlocality is directly related to laser radiation from chromosomes (light), which jitterbugs its polarization plane to radiate or occlude photons. The same researchers suspect the ability of chromosomes to transform their own genetic-sign laser radiations into broadband genetic-sign

radio waves. Curiously, mystics have always called the pervasive creative sacred Sound, Logos or Word, the Audible Life Stream (Blavatsky, 1987; Hines, 1996). They declare the Light and the Sound are one, and holographic concept is another name for Unity.

The polarizations of chromosome laser photons are connected nonlocally and coherently to polarizations of radio waves. The signal can be "read out" without any loss of the essential information in the form of polarized radio waves. The liquid crystal phases of the chromosome apparatus (laser mirror analogues) can be considered a fractal environment which stores the localized photons. This creates a coherent continuum of quantum-nonlocally distributed polarized radio wave genomic information.

The genetic wave information from DNA, recorded within the polarizations of connected photons, being quantum nonlocal, constitutes a broadband radio wave spectrum. This spectrum is correlated by means of polarizations with the photons. This is the main information channel of DNA, the same for both photons and radio waves.

This biocomputer memory and retrieval program features photon-laser-radiowave polarization spectroscopy. Complex dynamics are expressed as fractal patterns at all levels of organization in nature. And this is no exception. The fundamental notion is, that the photon-laser-radiowave features of different objects (the Fourier-spectra of the radiowaves of crystals, water, metals, DNA, etc.) are stored for definite but varying times by means of laser mirrors, such that the "mirror spectra" concern chaotic attractors with a complex fractal dynamics, recurring in time.

This research is the first example of a novel static storage/recording environment (laser mirrors) capable of directly recording the space-time atomic/molecular rotary dynamical behavior of objects. It also demonstrates an essentially new type of radio signal, where the information is encoded by polarizations of electromagnetic vectors. This could even be the basis of a new type of still or video recording, leading to a new form of cinema.

This newly detected phenomenon of quantized optical activity can be considered as the means by which an organism obtains unlimited information on its own metabolism. Such information is read by endogenous laser radiations of chromosomes. The chromosome, in turn, produces the regulative ("semantic") radio emission of the genome biocomputer. Semantic resonances in the biosystem's space are realized at both the wavelength level, and level of frequencies and angles of twist of the polarization modes.

A gene has a holographic memory, (which is typically distributed, associative, and nonlocal), where the holograms "are read" by electromagnetic or acoustic fields. These carry the gene-wave information out beyond the limits of the chromosome structure. At this and subsequent levels, the nonlocality takes on its dualistic material-wave nature, as may also be true for the holographic memory of the cerebral cortex (Pribram, 1991).

Pribram posits a neural holographic process, wherein images are reconstructed when representations in the form of distributed information systems are appropriately engaged. These representations operate as filters or screens. The temporary organization of cortical columns and the arrival of impulses at neuronal junctions converge from at least two sources, forming interference patterns. These patterns are made up of classical postsynaptic potentials, coordinated with awareness. This microstructure of slow potentials is accurately described by the equations that describe the holographic process which is also composed of interference patterns.

From this it follows that in the brain information representing input is distributed over the entire extent of the neural pattern. In the bodymind information is also holographically distributed, each "part" having more or less information about the whole organism. Information is fractally distributed and present in greater or lesser resolution.

A neural holographic or similar process does not mean that input information is distributed willy-nilly over the entire depth and surface of the brain. It is confined primarily to those limited regions where reasonably

stable junctional designs are initiated by the input participating in the distribution. Holographic memory processing does away with the need for keeping track of where information is stored. The "filter," "sieve," or "screen" of holographic patterns is composed not only of the lattice of membrane macromolecules making up the synapto-dedritic net, but also of a facilitation of all tendencies toward Image formation and the initiation of certain departure patterns of nerve impulses (Pribram, 1971).

At the junctional patterns of neural activity, Image forming capacity is enhanced. Superposition, i.e. spatial interactions among phase relationships of neighboring junctional patterns occurs, with properties akin to those of optical information processing systems -- the properties of holograms.

Chaotic dynamics are part of this image-forming process. There is order even in disorder. There is order, manageable chaos (fractals) and unmanageable chaos. The fractal dimension expresses the complexity of a particular fractal form. ﷺFractalﷺ comes from the Latin *fractus*, which mean broken or fragmented. Fractals delineate a whole new way of thinking about structure and form -- even the forms of dis-ease, which take root organically in the body and psyche.

Like holograms, magnify a fractal again and again and more detail emerges from its infinitely embedded structure. The same self-similar patterns repeat, over and over, no matter what level you care to examine. You look closer and closer and still see the same form. A single image is infinitely reiterated. Thus, a wealth of structure emerges from simplicity. So, too, the dis-ease process can be seen at the physical, emotional, mental, and spiritual levels. Yet, the form remains the same.

> *"At the most fundamental level of our individual being, we too, our bodies and our psyches are part of the interference patterns caused by the interaction of consciousness and wave fronts arising from fields of infinite possibility. We then must also operate by holographic principles, thus our internal perception of this reality is itself a hologram in our brain. It is the means of perception that gives the universe its apparent forms and solidity. It is also this holographic perception that influences the dynamics of our brain's and our body's chemistry, our self-hologram. In this perceptual hologram resides the fundamental basis of our structure and our sense of self and external environment, including our health and illness in both our physiological and psychological being. Our disease structures are incorporated within it. It is here, at this level of our being where fundamental healing and physical-psychic restructuring occur. This hologram is what I have termed the primal existential sensory self-image or existential hologram. . .our sense of self is a holographic, existential, multi-sensory image."* (Swinney, 1999).

The key to this process lies in our DNA, in our genes and gene-expression. Our understanding of the human biocomputer must be based on a new understanding of the higher forms of the DNA memory, and the chromosome apparatus, as the recording, storing, transducing, and transmitting system for genetic information, to be considered simultaneously at the level of matter and physical fields.

The wave-biocomputer model helps explain the apparatus of protein biosynthesis of living organisms, providing an important interpretation of the initial stages within the hierarchic chain of material and field, sign, holographic, semiotic-semantic and, and figurative encoding and deciphering of chromosome functions. At the gene-sign continuum of any biosystem, DNA forms pre-images of biostructures and the organism as a whole as a registry of dynamical "wave copies" or "matrices", succeeding each other. This continuum is the measuring, calibrating field for constructing or creating any biosystem, (Gariaev).

II. MECHANISMS: QUANTUM MECHANICS AND COMPLEX DYNAMICS

A quick review of the Holographic Concept refreshes us on the basics of biophysics.

Particles found in biological processes include photons, electrons, protons, elementary ions, inorganic radicals, organic radicals, molecules, and molecular aggregates. Photons act upon electrons by raising their energy state. This process is called excitation. Excited electrons can drop back to more stable energy levels and emit photons. Electron excitation can lead to the formation of an electronic bond between molecules. This is the traditional bond of classical chemistry. The breaking of such bonds can, by reverse process, lead to the excitation of electrons.

In living systems the excitation of electrons by photons and the subsequent conversion of that excitation into the bond energy is called photosynthesis and is the basic builder of biological structures. The reversal of this process is called bioluminescence. This phenomenon is the transfer of energy from a bond to an excited electron, resulting in the emission of a photon. It has been suggested by Szent-Gyorgyi (1957: 8) that the energetics of living creatures can be understood in terms of photosynthesis and its reversal, bioluminescence.

All cellular processes are driven by energy derived from the breaking of chemical bonds and the excitation of electrons. Depending upon the particular environment and circumstances, the excitation of the electron can be converted in one of three ways: (1) conversion into heat and dissipation (2) translation of molecules or ions through the cell, or (3) transformation of the molecules' shapes which profoundly influences their biological reactivity.

The formation of a certain type of chemical bond known as the resonance bond (which is most easily seen in the case of the Benzene molecule) leads to a peculiar situation in which certain electrons are freed from a local or particular location in the molecule. These are then free to travel around the entire molecule. This means that the electrons occupy an energy shell of the whole molecule as opposed to any particular atom in the molecule. The existence of molecular systems with mobile electrons has been found to be of profound significance in the phenomena of life.

Hydrogen, carbon, nitrogen, and oxygen, which compose 99 percent of all living systems, are among the atoms in the periodic table which form the multiple bonds most easily leading to mobile electrons. Sulphur and phosphorus, which are extremely important for life processes, also form such multiple bonds quite easily.

All the essential biochemical substances, which perform the fundamental functions of living matter, are composed completely or partially of such mobile electrons. Molecules which contain these electrons are known as conjugated systems (Pullman and Pullman, 1963, chapter 18). The essential fluidity of life may correspond with the fluidity of the electronic cloud in conjugated molecules. Such systems may best be considered as both the cradle and the main backbone of life.

Conjugate bonded molecules may interact in a variety of ways. Among these types of interaction can be found the interpenetration of electron orbitals which permits an electromagnetic coupling. This coupling can permit activated electron energy to pass from one molecule to another in the same way a radio can transmit a message to a radio receiver. There is also the possibility of the transfer of an entire electron which is known as charge transfer.

It is possible for a molecular complex to contain several radicals at different positions on the main molecule, each of which are conjugated. If these are in close enough proximity, or can be brought into proximity by changes in the structural configuration of the molecule, a charge can pass between these two groups. This is the case of the transfer of electron charges on or around a single molecular complex. It has been suggested by Szent-Gyorgyi (1968) that the sugars and phosphates that make up the side of the alpha helix of DNA can permit the passage of electrons, functioning as a conductor.

The biological conduction systems operate primarily on an amorphous semiconductor mode as opposed to resembling metallic conductors. These do not have sharply defined energy bands in which electrons may flow, as opposed to other bands in which they are bound rigidly. There is a spread or bell-curve in which the points or tails are bound more closely to a particular molecule. The hump indicates a conducting band that

permits electrons to flow across the surface of a particular molecule or between molecules (McGinness, 1972).

This means, in essence, that protein molecules which are composed of amino acid sequences, may act as organic circuits. The amino acids each have a donor group and an acceptor group on opposing ends. This means that a string or series of amino acids could pass a charge along as if it were being passed along a series of spines sticking up from the main body of the molecule.

Different pathways could be defined across the surface of a protein molecule by the amino acid radicals projecting out from the surface of the protein. The shape of the protein molecules is a function of the charges and the conjugate systems on the radicals that make up the protein. When a protein is manufactured and peels off the ribosome, it immediately assumes a three-dimensional spatial pattern that is directly related to the charges on its surface and the ways in which they interact.

The biological activity or specificity of action of various molecules is intimately related to their structure or their exact three-dimensional spatial configuration. Electronic energy and electrons can move through a protein molecule between its different parts and can pass among different molecules. We now come to understand a possible mechanism for biological regulation involving flows of electrons and transfer of electronic energy between molecules. These can change their shape and thereby change their specific action and activity. The fusion of electron clouds can exist within a conjugated system and among conjugated systems. This can account for cohesion or the adherence of such molecules to each other. Such fusion is a very important determinate of the structure of larger aggregates of molecules and portions of living cells, such as membranes.

III. BIOHOLOGRAM FIELD THEORY

A liquid crystal in a cell through its own structure becomes a proto-organ for mechanical and electrical activity, and when associated in specialized cells in higher animals gives rise to true organs such as muscles and nerves. The oriented molecules in liquid crystals furnish an ideal medium for catalytic action, particularly of the complex type needed to account for growth and reproduction. A liquid crystal has the possibility of its own structure through singular lines, rods and cones, etc. Such structures belong to the liquid crystal as a unit and not to its molecules which may be replaced by others without destroying them, and they persist in spite of the complete fluidity of the substance (Needham, 1936).

Bernal's statement (1933) would seem to support Burr and Northrop's macro-atomic theory (1935), which postulates that there are two aspects to reality, the field and the particle. They associate the field with what they term the macroscopic aspect and the electron with the particle. They associate the field with what they term the macroscopic aspect and the electron with the particle. The particle is associated with movement. The structure of biological material seems to be associated with the field aspect. The electric field causes polarization of the macromolecules in the solution due to the fact that molecules possess a dipole moment, and changes the position of protons in the molecule. Such action can affect the relative stability of different possible configurations of the macromolecules. The field affects the degree of structure present in the solution.

A constant magnetic field can, in principle, affect the various processes in biological objects. Three possible mechanisms for this biomagnetic affect are (1) the orientation of diamagnetic or paramagnetic molecules by the magnetic field (2) distortions of the angles in the molecules and (3) orientation of the spins of molecules in a magnetic field (Fowler and Bernal, 1933; Freedericks and Zolina, 1933; Van Iterson, 1933; Osborne, Ambrose and Stuart, 1970). Presman (1970) has postulated that such electromagnetic fields normally serve as conveyors of information, from the environment to the organism, within the organism, and among organisms. He suggests that organisms employ these fields in conjunction with the well known sensory, nervous, and endocrine systems, in effecting coordination and integration.

Muses (1970) has proposed the possibility of unit impulse functions evolving from the Gaussian. His work traces the relation of that mathematical concept to quantum biological indeterminacy in terms of a process of the modulation of random fluctuations by target-seeking perturbations which points the way to the understanding and computing of the parameters of volitional experience in quantum biological terms. He maintains that we are dealing with Gaussian wave packets, put to use in terms of a close-range reaction in turn resulting in the resonant microbiological specificity (arising from the relatively large number of specific molecular parameters) necessary to the essential life and evolutional processes of chromosome synapses, replication, and mutagenesis.

Muses holds that inherently indeterminate processes may be biologically used in achieving determinate ones such as our repeatable and commonly accepted volitional experiences of effort and direction. The range of quantum indeterminate fluctuation of biological efficacy is in the far ultraviolet, and it is in this spectral region that we should expect to look for any modulation effects on Gaussian wave packets by volitional energies manifesting as ultramicrobiological field perturbations.

Biologically, there is a threshold of non-randomicity below which peaks tend to emerge that are sharp enough to possess biodirectiveness in an enzyme-guiding sense. Random biological quantum energies which are physiologically unassigned are the clue to psychosomatic directing, which can be beneficial or deleterious to the organism. Muses (1970) describes the mechanism of this effect as a microbiolaser type process.

Heisenberg explored the possible relevance of the quantum indeterminacy of elementary particles for biological systems, especially human systems (discussed in Koestler, 1972). He stated that there are two places in the human system where the quantum indeterminacy of a single particle can have a profound influence. The first important effect is that of mutation in the genetic code. The second important influence is the alteration of the behavior of neurons during human thought processes.

Tien (1969) has conceptualized mind as mass in relative motion and brain as energy at relative electrical charges in motion, like electrons bombarding a television screen, and personality is seen as a time series of scintillating frames of consciousness. Personality becomes a reverbating input-output pattern of self-creation, seeking information or patterns of energy from the environment as well as from its own memories. The stability of any given personality of its identity is maintained by feedback upon the principle of most similarity.

The personality never recreates itself, but creates only a close approximation which is accepted due to the principle of constancy as being the same. The phenomena of unique individuality and personal continuity depend on memory, of which consciousness is the most recent and, thereby, the most subject to erasure and loosening. Personality transformation becomes energy pattern modification of not only scintillating consciousness but also of recent circulating memories and older stored memories of childhood.

According to the holographic model of reality, all the objects we can observe are three-dimensional images formed of standing and moving waves by electromagnetic and nuclear processes. All the objects of our world are three-dimensional images formed electro-magnetically, i.e., holograms.

This concept and the models of human information processing based on the hologram, throw interesting light on the philosophical tradition which holds that the world of objects is an illusion. With the triumph of relativity and quantum physics, the interpenetration of the philosophical and the scientific is possible.

LeShan (1969) has observed, in discussing some individuals who purportedly experience psycho-energetic phenomena, that their view of the universe as a great thought of which they are a part is quite similar to many physicists' view that they see reality only in their own mental image.

We propose that the "reality hologram" which appears as a stable world of material objects is the elementary particle which has a long-term existence and fairly simple rules of interaction. We also propose the existence of a "biohologram" which appears as mobile and evolving, through the DNA molecule. This

"biohologram" projects a dynamic three-dimensional image that serves as a guiding matrix for the manipulation and organization of the "reality hologram." (Miller, Webb, Dickson, 1973).

Thus we have mobile self-organizing holograms moving through a relatively static simpler hologram. The possibility exists that such "biohologrames" could achieve sufficient coherence to continue existence as a pattern of radiant energy apart from a material substrate. We feel that such an occurrence could form the scientific basis of such psychoenergetic phenomena as psycho-kinesis, clairvoyance, telepathy, and precognition.

Quantum holography asserts that DNA satisfies the principle of computer construction as defined by Von Neumann (1966). It carries a copy of itself and is its own blueprint written in the genetic texts where the mechanism engineering the DNA replication is the biophotonic electromagnetic field, while the "letters" of the genetic texts, A, G, C, U are held invariant. In replication of the organism, the blueprint creates the "acoustic field" which mechanically constructs/engineers the organisms out of the available matter, in accordance with the information held in the electromagnetic field holograms.

Both quantum entanglement and therefore quantum teleportation can be related to quantum holography, through solitons, resonance effects, and superconductivity.

Experimental evidence confirms that the mutual recognition of one DNA antiparallel half chain (+) by the other (-) concerns special super persistent/resonant acoustic-electromagnetic waves or solitons. DNA solitons express two types of memory which concern the capability of non-linear systems to remember initial modes of energisation and to periodically repeat them [Dubois, 1992]. The DNA liquid crystals within the chromosome structure form such a non-linear system. The DNA-continuum is quasi-holographic/fractal and relates, as is the case for any hologram or fractal, to the fundamental property of biosystems, i.e. their ability to restore the whole out of the part.

DNA solitary waves (solitons), and in particular, the nucleotide waves of oscillatory rotation, "read" the genome's sign patterns, so that such sign vibratory dynamics may be considered as one of many genomic, non-linear dynamic semiotic processes. The key parameter of such patterns is fractality. It can therefore be hypothesized that the grammar of genetic texts is a special case of the general grammar of all human languages. We can realize the wave-coding capabilities of the matter-wave sign functions of DNA as true wave control capabilities facilitates in an aqueous solution acting as a liquid-crystal condition. The living cell is a computer based on DNA.

The genome has been identified as an active "laser-like" environment. Yet this approach to DNA-wave biocomputation means entering into new semiotic areas of the human genome and the biosphere in general. These are the areas which are used by Nature to create humankind. The quasi-speech of chromosomes of all organisms concerns semantic exobiological influences wherein DNA acts as a kind of aerial open to the reception of internal influences and changes within the organism as well as those outside it. This extends beyond it to the extent of the entire universe through complex fractal embedding and non-locality.

Creation of biocomputers can be based on these totally new principles of DNA-wave biocomputation, which use quantum teleportation [Sudbury, 1997], (see also SciAmer on quantum teleportation). Experiments show that DNA considered as a liquid-crystal gel-like state, reveals a periodically reoccurring pattern which acts on the incoming light in the manner of a solitonic lattice. What could such an action achieve?

A soliton is an ultra stable wave train often with a seemingly simple closed shape, which can arise in the context of non-linear wave oscillations. Really it consists of a rather complexly interrelated assembly of sub wave structures, which keep the whole solotonic process in a stationary state over a comparatively long time. The soliton is neither a particle nor wave in much the same as a quantum is characterized by wave-particle duality. It is a means to carry information. It probably reads the codons, as a travelling "window" that opens in the double helix structure as the reading takes place. In this model the reading process is a

complex mechanical oscillator (Gariaev, 1994), capable of producing solitonic wave transmissions, which take the form of a system of rotary pendulums.

DNA forms such pendulums in this model which are simulated as a chain of non-linear oscillators. The window as it travels is highly context dependent on the actual layout of the elements as specified by the actual genetic code sequence involved. Complex dynamic patterns arise in the non-linear covalent connections between nucleotides. Oscillatory activities are located somewhere together in the "acoustic" wave domain.

As a liquid crystal, DNA probably influences the polarization of the weak light emission known to exist in cells, as so-called biophotons. Such biophotonic, mitogenic radiation or mitogenic light, while being ultraweak, is yet highly coherent. It has an inherent laser-like quality. Endogenous intracellular coherent light is emitted by the DNA molecule itself.

The superposed coherent waves of different types in the cells are interacting to form diffraction patterns, first in the "acoustic" domain and then in the electromagnetic domain. This is a kind of quantum hologram. Interactions of solitonic oscillations in the liquid crystal structure of DNA and the polarization vector of the ultraweak biophotonic highly coherent light, could be understood as a mechanism of translation between holograms in the "acoustic" frequency domain of short range effects and those in the electromagnetic domain, and vice versa.

Quantum holography has been used to predict the workings of MRI (Schempp, 1992,1998). The DNA-wave biocomputer model is also in agreement with the qubit model explanation of DNA.

In the quantum holographic DNA-wave biocomputer theory, DNA is a self-calibrating antenna working by phase conjugate adaptive resonance capable of both receiving and transmitting quantum holographic information stored in the form of diffraction patterns -- quantum holograms. The model describes how during the development of an embryo of the DNA's organism, these holographic patterns carry the essential holographic information necessary for that development.

The quantum holographic theory requires that the DNA consists of two antiparallel (phase conjugate) helices, between which are located hologram planes/holographic gratings, where the necessary 3 spatial dimensional holographic image data of the organism is stored. Endogenous laser illumination can be expected to turn the DNA into a series of active adaptive phase conjugate mirrors/holographic transducers. A beam of radiation resonantly emerges on which is carried the holographic information as encoded in the DNA. This confirms the quantum holographic prediction that DNA functions as an antenna capable of both encoding and decoding holographic information.

We can also model the quantum holography of the neuron. This model is in good accord with the biological neuron's information processing morphology and signal dynamics. This is the quantum holographic model of the brain as a conscious system. We can incorporate signal theory into quantum physics through the concept of the pilot wave or radar.

Quantum holography predicts polarized or orthogonally rotated holograms encoded on a "paged" associative holographic memory. Sharp frequency adaptive coupling conditions specify very narrow spectral windows, i.e. the "pages." "Magic windows" are a naturally tuned frequency of a good hyperchannel between orthogonal frames where scalar wave anenergies crosstalk readily. They are frequency dependent interdimensional nodal points. Some magic windows are 38-40 lHz; 150-160 kHz; 1.1-1.3 MHz; 1.057 (Lambshift) and the near ultraviolet (life energy frequency), (Beardon, 1988).

Described in terms of tensor multiplication, the orthgonality condition can be seen as specifying a set of diagonal elements, which traces in a unit matrix in the frequency domain. The planes on which the base pairing takes place concerns two quantum holograms. The tensor operation, in quantum holography, describes a quantum entanglement.

Murray Gell-Mann describes quantum entanglement in *The Quark and the Jaguar* (1994). He first points out that coarse graining can wash out interference terms. The interference terms between two coarse-grained histories is the sum of all the interference terms between pairs of fine-grained histories belonging to those two coarse-grained ones. The underlying explanation for decoherence is the mechanism that makes interference terms sum to zero and permits the assignment of probabilities. It is the entanglement of what is followed in the coarse-grained histories with what is ignored and summed over.

IV. BIOLOGICAL EFFECTS OF SCALAR ENERGY

There are only a few known forces in nature and unfortunately we are at a loss to explain what their actual sources are. The best physics has been able to do is ascribe them to some fundamental characteristics of the universe, a charge of some kind. That's why we can more abstractly view a force as the variation of a certain potential and therefore practically every influence field can be thought of as a force field. This potential can be a scalar as in the case of Coulomb's law; a vector as in the case of the electromagnetic vector potential which neatly streamlines the mathematics of Maxwell's equations; or a tensor, which is the case of the metric tensor of the Riemann space in Einstein's GTR equations.

There is a predominance of non-linear processes in biological systems. Several types of quasi-particles, each with their own characteristic resonant frequencies have been proposed to mediate these non-linear phenomena, including solitons, excitons, and plasmons. The right frequencies of non-linear energies might have profound healing properties, according to Stanford researcher Dr. Glen Rein. Due to the non-linear nature of biological systems it is proposed that scalar waves should be more biologically active than their linear electromagnetic counterparts.

> *In the simplest cases, scalar resonance can be imagined as two ordinary single-frequency EM standing waves in a resonant cavity, with the two waves coupled exactly 180 degrees out of phase so that --externally--their E fields sum to zero and the capacity is said to be in scalar resonance. The cavity walls must act as phase conjugate mirrors (PCM). Mass itself is simply a standing scalar resonance, with the standing walls tapped by particle spin. The atomic nucleus continually bombarded by virtual photon flux from the vacuum is a pumped PCM. Since the nucleus is positively charged, it produces Phase Conjugate Replicators (PCRs), having negative energy and negative time. It thus produces negentropy, which prevents the entropic decay of the atom. Essentially all frequencies can be and are present at once, but certain nuclear resonance frequencies are thought to predominate. By increasing the amplitude of the standing scalar wave that is the nuclear pseudopotential, inertia and mass of the nucleus are increased. Zeroing the amplitude dematerializes the nucleus.* (Beardon, 1980).

So, scalar energy is transduced into linear electromagnetic energy in the body by liquid crystals in the cell membrane and solid crystals found in the blood and in several biological tissues. Clinical studies of the effects of scalar energy on the mind-body and brainwaves have been conducted since the 1980s. If they can be believed, research from Stanford University Medical Center produced some tantalizing results.

Electrochemical oscillation between membrane-bound lipids near phase-transition temperature have been analyzed with and described by nonlinear quantum mechanical equations. They also analyzed the coupling between harmonic oscillators represented by action potentials generated from active neuronal networks in the central nervous system, finding evidence of chaos. The extraction of scalar components from Maxwell's original electromagnetic equations and from Schrodinger's equation using imaginary numbers has been reported, and their unusual non-linear waves described by many experimenters.

A Crystalline Transduction Theory has been put forth to explain the interactive mechanism of scalar waves with biological systems. Another possibility is transduction in microtubules dispersed throughout the whole organism. Tissue culture studies imply that the action of scalars on biological systems is more than a

placebo effect mediated by the brain/mind, such as stress, moods or beliefs. Stray EM energy in the ambient atmosphere makes it difficult to study the healing properties of scalar energies in a clinical setting.

Clinical healing sometimes occurred several months after initial exposure to the scalar waves. It is known that the brain and body, each the immune system, communicate bidirectionally. Thus, a direct action of scalar energy on the body could cause a subsequent change in brain state. Therefore EEG studies do not indicate whether scalar energy also effects the body directly or whether the brain and the body are both affected. Even if scalar energy directly affects individual cells, it may also affect the mind resulting in an altered psychological outlook which results in clinical improvement.

Dr. Michael Persinger (1987) was the first person to test the effects of scalar energy using isolated cells. The scalar waves were generated by partially canceling two vortex-type magnetic fields (0.SHz, 10pT) by intersecting them in the air. The biological endpoint, degranulation of mast cells, was increased by the scalar fields. Dr. Puharich, in another study, grew tissue samples of E. Coli, and detected an increased activity of ubiquitone, a protein involved in DNA repair. These results indicate that scalar energy can have a direct effect at the subcellular level as well as a direct effect on the immune system.

Another project detected an effect of scalar energy on neurotransmitter function, which mimicked the effect of antidepressant medication. Scalars appear to modulate the basic biochemical communication between nerve cells mediated by neurotransmitters. Cultured nerve cells called PC 12 cells were isolated from rats, and the functional properties of noradrenaline release from PC 12 cells was shown to be increased by a 500Hz monopolar square wave, and noradrenaline uptake was inhibited by a 15Hz biopolar square wave, (Rein).

Noradrenaline uptake was chosen because it is directly mediated by the plasma membrane via an intramembrane protein carrier. The plasma membrane, with its liquid-crystal structure, is the critical cellular barrier which interfaces with the chemical and electromagnetic environment. Since other intramembrane proteins show non-linear properties, the plasma membrane is a likely target for scalar energy.

The physiological function of carrier mediated neurotransmitter uptake is to remove excess neurotransmitter from the synaptic cleft after its release from presynaptic nerves. Thus, inhibiting uptake results in the accumulation of the neurotransmitter in the synaptic cleft. This is the mechanism of action of tricyclic antidepressants, since they inhibit noradrenaline uptake.

Depression is associated with decreased noradrenaline levels. Rein exposed confluent monolayer culture of PC12 cells to noradrenaline in the presence or absence of scalar energy. After 30 minutes, the cells were washed and centrifuged and noradrenaline uptake measured. Overall, uptake was inhibited by 19.5% in the presence of the scalar field as compared with the control value obtained in its absence. This is a significant statistical difference of p 0.01.

Researchers think a wide variety of physiological changes could be created resulting in improvement of a variety of clinical diseases, only one of which could be depression. Scalar energy can have a direct effect on the cell membrane. Researchers want to test whether diseased cells are preferentially sensitive to scalar energy; and what characterizes its mechanisms of action.

V. ROSSI’S DREAM-PROTEIN HYPOTHESIS ON HEALING

Ernest Rossi (1999; 2002) has developed a pertinent creativity hypothesis: “Enriching life experiences that evoke psychobiological arousal with positive fascination and focused attention during creative moments of art, music, dance, drama, humor, spirituality, numinosity, awe, joy, expectation, and social rituals can evoke immediate early gene protein cascades to optimize brain growth, mindbody communication, and healing.”

> *[The] psychotherapeutic approach can contribute to psychobiological arousal, enrichment and relaxation; it may be possible to help people find optimal levels of mental stimulation to facilitate actual growth in the hippocampus of their brain to encode new memory, learning and behavior...optimizing psychobiological growth and healing.*

Rossi (1999) describes a mind/body communication channel that is pertinent in that it may describe another way neural plasticity and healing manifests from REM. He describes how immediate-early genes (also called Primary Response Genes or third messengers) play a central role in the dynamics of waking, sleeping, dreaming, and mind-body healing at the cellular level.

There is evidence that immediate-early genes (IEGs) function as mediators of information transduction between psychological experience, behavioral states, and gene expression. A wide range of behavioral state-related gene expression (from relaxation, hypnosis and sleep to high arousal, performance, stress and trauma) culminate in the production of new proteins or homeostasis, physical and psychosocial adaptation.

Behavioral states modulate certain patterns of gene expression. Interaction between the genetic and behavioral levels is a two way street. Genes and behavior are related in cybernetic loops of mind-body communication. How does this relate, for example, to manic depression?

A look at the systems related to IEGs, shows that they affect all the systems disrupted in bipolar disorder. They are expressed continually in response to hormone messenger molecules mediating processes of adaptation to extracellular signals and stimuli. Extracellular stimuli come from the outside environment, including temperature, food, sexual cues, psychosocial stress, physical trauma, and toxins. IEGs are fundamental in the sleep-wake cycle, appetite regulation, sexual response, and reactions to stress, trauma, and toxins (Rossi, 1986; 1999; 2002).

There are persistent alterations in IEG expression in the process of adaptive behavior on all levels from the sexual and emotional to the cognitive. They can transduce relatively brief signals from the environment into enduring changes in the physical structure of the developing nervous system as well as its plasticity in the form of memory and learning throughout life. If external cues can modulate cell function through regulation of gene expression, this could also be true for internal cues.

IEGs are also fundamental in the regulation of REM-on, REM-off neurons, neuronal networks that are associated with REM sleep and dreaming. That makes them significant as molecules which can modulate mind, emotions, learning and behavior. They influence the rhythm of the natural healing process and circadian and ultradian rhythms of the body, in general. Ultradian rhythms are those shorter than the 24-hour circadian rhythms (Rossi; Cheek, 1988).

Milton Erickson discovered that his therapy sessions usually took from one and a half to two hours to come to natural closure. Later it was discovered that this delineates the natural work cycle that is harmonious with our own internal rhythms. IEGs modulate this process. This ultradian time frame is related to the activation or deactivation of the expression of specific genes and can occur in a matter of hours or even minutes.

> *Most arousing environmental stimuli that have been studied can induce immediate-early genes within minutes, their concentrations typically peak within fifteen to twenty minutes and their effects are usually over within an hour or two. These time parameter IEG expressions and their ultimate translation into the formation of new proteins correspond to the parameters of a complete work cycle of mind-body communication and healing. The changes in gene transcription and new protein formation initiated in this time frame, however, can lead to lasting changes in the central nervous system by converting short term memory to long lasting learning by the process of long term potentiation. . .the activation or deactivation of the expression of specific genes can occur in a matter of hours or even minutes." (Rossi, 1999).*

This mechanism assesses the duration and intensity of prior waking and/or the homeostatic or executive mechanisms that bring about sleep. Sleep deprivation leads to a wide variety of psychotic and non-psychotic symptoms. This system is also associated with the neuronal network associated with the dynamics of REM sleep. Deprivation of REM and dreaming creates its own phenomenology.

> *The study of IEGs indicates that sleep and wake, as well as synchronized and desynchronized sleep, are characterized by different genomic expressions, the level of IEGs being high during wake and low during sleep. Such fluctuation of gene expression is not ubiquitous but occurs in certain cell populations in the brain. Thus...IEG induction may reveal the activation of neural networks in different behavioral states. Do the areas in which IEGs oscillate during sleep and wake subserve specific roles in the regulation of these physiological states and a general resetting of behavioral state? Is gene induction a clue to understanding the alternation of sleep and wake, and of REM and non-REM sleep? (Rossi, 1999).*

In Rossi's Dream-Protein Hypothesis, new experience is encoded by means of protein synthesis in brain tissue...dreaming is a process of psychophysiological growth that involves the synthesis or modification of protein structures in the brain that serve as the organic basis for new developments in the personality...new proteins are synthesized in some brain structures associated with REM dream sleep.

Rossi generalizes the dream-protein hypothesis, to include all states of creativity associated with the peak periods of arousal and insight generation in psychobiologically oriented psychotherapy.

Enriched internal and external environments leads to the growth and development of new cells. IEG cascades lead to the formation of new proteins and neurons along with increased synapses and dendrites that encode memory and learning. On the other hand, excessive trauma and psychosocial stress can lead to suppression of growth processes in the brain. When psychotherapy contributes to arousal, enrichment, and relaxation it facilitates actual growth in the brain to encode new memory, learning and behavior, optimizing growth and healing.

> *Communication within the neuronal networks of the brain is modulated by changes in the strengths of synaptic connections...meaning is to be found in the complex dynamic field of messenger molecules that continually bathe and contextualize the information of the neuronal networks in ever changing patterns. Most of the sexual and stress hormones...have state dependent effects on our mental and emotional states as well as memory and learning, a constantly changing dynamical field of meaning. (Rossi, 1991).*

Novel and enriching psychotherapeutic experiences can lead to neurogenesis and gene expression which facilitate mindbody communication and can have a long-term transformative effect on the whole person (Rossi, 2002). Rossi points out that many of the essential dynamics of gene expression involved in the formation of the brain and body in embryology are now recognized as a continuing creative development through an individual's lifetime. He also asserts that a lack of optimal gene expression and neurogenesis is associated with psychological depression and stress. Thus, bioholography has relevant applications for optimizing health and well-being across disciplines, such as biophysics, medicine, psychobiology, psychotherapy and the holistic healing arts.

VI. CONCLUSION

Sidorov (2002) has summarized the thrust of the Gariaev group:

> *Since the early '90s, Gariaev's team has been developing a new theoretical and experimental approach to the study of genetic material encoding and expression. In a pioneering paper*

(Gariaev 2001; JNLRMI I(2)), he and his colleagues challenge the limits of the genetic code triplet model and propose instead a dual, substance/wave basis for the encoding and expression of genetic material. The wave-like, non-local aspect of genetic regulation is recorded at the polarization level of DNA-associated photons, and the genome is seen as a quasi-hologram of light and radio waves which create the background necessary for the appropriate expression of genetic material.

The authors argue that the genome emits light and radio-waves whose delocalized interference patterns create calibration fields (blueprints) for a system's space-time organization. This holographic-type information is being constantly and simultaneously read in billions of cells, accounting for the quick coordinated response typical of living systems.

We can use the observations of the Gariaev group to further summarize the essence of the human biocomputer:

"Thus, nonlocality can be postulated to be the key factor explaining the astonishing evolutionary achievement of multicellular biosystems. This factor says that bioinformatic events, can be instantaneously coordinated, taking place "here and there simultaneously", and that in such situations the concept of "cause and effect" loses any sense. This is of a great importance! The intercellular diffusion of signal substances and of the nervous process is far too inertial for this purpose. Even if it is conceded that intercellular transmissions take place electro-magnetically at light speeds, this would still be insufficient to explain how highly evolved, highly complex biosystems work in real time." [5]

Gariaev asserts that quantum nonlocality and holography is indispensable to a proper explanation of such real time working.

"[T]he genes can act as quantum objects, and that, it is the phenomenon of quantum non-locality/teleportation, that ensures the organism's super coherency, information super redundancy, super knowledge, cohesion, and, as a totality or whole, the organism's integrity (viability)." [5]

Quantum Holography defines an admitter/absorber quantum vacuum model of quantum mechanics in terms of annihilation/creation operators [Schempp, 1993]. This implies that DNA does indeed behave like a single quantum, which induces a "hole" temporarily in the vacuum by its removal.

This new understanding of biocomputers, constitutes a further step in a development of computer technology in general. An understanding that brings about a total change of the constituent basis of that technology to the figurative semantic (nonlocal) wave computer or biocomputer, based on DNA memory, and the chromosome apparatus.

Quantum Biohologrаphy argues that DNA satisfies the principle of computer construction, since it carries a copy of itself, its own blueprint, with the mechanism engineering the DNA replication being the biophotonic electromagnetic field, while the "letters" of the genetic texts A, G, C, U are held invariant. The existence of the genetic text constitutes the classical signal process of quantum teleportation, and facilitates the quantum mechanical signal processes of both the copying of the DNA as its own blueprint, and of the construction of the organism in a massively parallel way by means of quantum teleportation.

REFERENCES

1. Beardon, Thomas (1980, 1988, 2002), Excalibur Briefing, Strawberry Hill Press, San Francisco.

Quantum Biohology

by Iona Miller

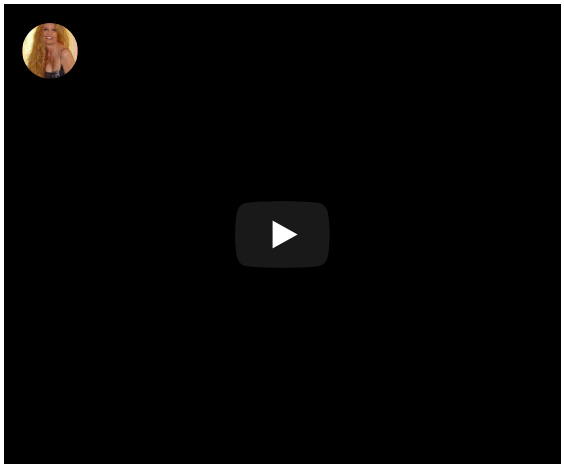

Helix to Hologram

QUANTUM BIOHOLOGRAPHY

A Review of the Field from 1973 - 2002

Richard Alan Miller, Iona Miller, and Burt Webb, ©2002
drram@magick.net; iona_m@yahoo.com, phoenix@eskimo.com
Organization for the Advancement of Knowledge, Grants Pass, Oregon

ABSTRACT: Complex information can be encoded in EM fields, as we all know from coding and decoding of television and radio signals. Even more complex information can be encoded in holographic images. DNA acts as a holographic projector of acoustic and EM information which contains the informational quintessence of the biohologram. Only 3% of human DNA encodes the physical body. The remaining 97% of the 3 billion base pair genome contains over a million genetic structures called transposons, that have the capacity to jump from one chromosomal location to another (Kelleher, 1999). We are 99.9% alike in our genetic legacy. Our individuality is expressed in three million small variations in our cells, called single nucleotide polymorphisms.

Gene-expression is the mechanism by which new patterns are called into being (Rossi, 2000). There is also a strong correlation between modulation of the brain's EM field and consciousness (Persinger, 1987; McFadden, 2002). The Gariaev group has discovered a wave-based genome and DNA phantom effect which strongly supports the holographic concept of reality (Miller, Webb, Dickson, 1975). This main information channel of DNA is the same for both photons and radio waves. Superposed coherent waves of different types in the cells interact to form diffraction patterns, firstly in the acoustic domain, secondly in the electromagnetic domain -- a quantum hologram -- a translation process between acoustical and optical holograms.

Creative, novel and enriching psychotherapeutic experiences can lead to neurogenesis, gene expression, and healing which facilitate mindbody communication and can have a long-term transformative effect on the whole person (Rossi, 2002). Thus, bioholography has relevant applications for optimizing health, well-being and even self-realization. It is relevant in biophysics, medicine, psychobiology, psychotherapy and the holistic healing arts. It provides us with a more genetically integrated model of the complex dynamics of the mindbody -- one arising in the domain underlying the standard genetic code triplet model.

Keywords: DNA, DNA phantom, wave biocomputer, genome, wave-based genome, quantum holography, bioholography, organismic evolution, vacuum substructure, biophysics, psychobiology, gene expression, psychotherapeutic applications.

INTRODUCTION

Hypothesis: The organization of any biological system is established by a complex electrodynamic field which is, in part, determined by its atomic physiochemical components. This field, in turn, determines the behavior and orientation of these components. This dynamic is mediated through wave-based genomes wherein DNA functions as the holographic projector of the psychophysical system - a quantum biohologram.

A model of the mind-body relationship is developed in which novel biophysical principles in genome function generate a dynamic possessing attributes consistent with both our psychophysical nature and consciousness. The model invokes a fractal link between neurodynamical chaos and quantum uncertainty. Transactional wave collapse allows this link to be utilized predictably by the excitable cell, in a way which bypasses and complements formal computation. The formal unpredictability of the model allows mind to interact upon the brain, the predictability of consciousness in survival strategies being selected as a trait by organismic evolution (King, 2001). This quantum evolution is orchestrated by the information transduction of DNA.

The Gariaev group (1994) has proposed a theory of the Wave-based Genome where the DNA-wave functions as a Biocomputer. They suggest (1) that there are genetic "texts", similar to natural context-dependent texts in human language; (2) that the chromosome apparatus acts simultaneously both as a source and receiver of these genetic texts, respectively decoding and encoding them; (3) that the chromosome continuum acts like a dynamical holographic grating, which displays or transduces weak laser light and solitonic electro-acoustic fields.

The distribution of the character frequency in genetic texts is fractal, so the nucleotides of DNA molecules are able to form holographic pre-images of biostructures. This process of "reading and writing" the very matter of our being manifests from the genome's associative holographic memory in conjunction with its quantum nonlocality. Rapid transmission of genetic information and gene-expression unite the organism as holistic entity embedded in the larger Whole. The system works as a biocomputer -- a wave biocomputer.

The quantum nonlocality of the genetic information is fundamental. Experimental work of the Gariaev group shows how quantum nonlocality is directly related to laser radiation from chromosomes (coherent light), which jitterbugs its polarization plane to radiate or occlude photons. DNA and the genome have now been identified as active "laser-like" environments. Roughly speaking, DNA can be considered as a liquid crystal gel-like state that acts on the incoming light in the manner of a solitonic lattice.

A soliton is an ultra stable wave train that arises in the context of non-linear wave oscillation. The DNA reading process can be modeled as a complex mechanical oscillator capable of producing solitonic wave transmissions. DNA, modeled as a kind of rotary pendulum can be simulated as a chain of non-linear oscillators. Complex dynamic patterns arise when taking into account the non-linear covalent connections between nucleotides.

The same researchers suspect the ability of chromosomes to transform their own genetic-sign laser radiations into broadband genetic-sign radio waves. The polarizations of chromosome laser photons are connected nonlocally and coherently to polarizations of radio waves. (Thus, we seem to have an explicit physical analogue for the traditional mystical apprehension of "inner light" and the "audible life stream"). This is the main information channel of DNA, the same for both photons and radio waves. Superposed coherent waves of different types in the cells interact to form diffraction patterns, firstly in the acoustic domain, secondly in the electromagnetic domain -- a quantum hologram -- a translation process between acoustical and optical holograms.

I. QUANTUM BIOHOLOGRAPHY

In *Languages of the Brain* (1971), Pribram postulated a neural hologram made by the interaction of waves in the cortex, which in turn is based on a hologram of much shorter wavelengths formed by the wave interactions on the sub-atomic level. Thus, we have a hologram within a hologram, and the interrelatedness of the two somehow gives rise to our sensory images. Bohm (1980), in *Wholeness and the Implicate Order* went further, declaring the brain is a hologram interpreting a holographic universe. In a holographic model this inseparable interconnectedness begins at the even more fundamental level of human existence, rooted in our existential blueprint, DNA. The brain is a hologram, enfolded within our holographic mind-body, enfolded within a holographic universe.

Recent discoveries by Russian scientists Peter Gariaev & al. and later speculations by Vladimir Poponin shed tremendous light on our proposal that the human being is a transducer of universal energy and consciousness -- essentially a biocomputer. The new feature of this research is the ability to physically demonstrate subtle fields emerging from the quantum foam or vacuum potential. This makes the effect quantifiable and measurable -- objective.

This takes the phenomenon and subjectivity of consciousness out of the realm of quantum metaphysics and plants it firmly under the rubric of hard science. It heralds the unification of quantum mechanical and chaotic dynamics in human consciousness. We can now model the human bio-computer.

Poponin (1995) boldly suggests that this deeper understanding of the mechanisms underlying subtle energy phenomena include many of the observed alternative healing phenomena and includes a physical theory of consciousness. This hypothesis is based on a precise quantitative background and combines both quantum mechanics and complexity or chaos dynamics in a startling and compelling new way. It posits that some new field structure is being excited from the physical vacuum by an intrinsic ability that emerges through DNA.

Gariaev discovered the DNA Phantom Effect in 1985, when he worked in correlation spectroscopy of DNA, ribosomes and collagen in the Institute of Physics, in the Academy of Science of the USSR. He was first able to publish his results in 1991, leading to a book in 1994, *Wave Based Genome.* His DNA Phantom Effect demonstrates a dynamic new field in the vacuum substructure by bombarding it with coherent laser light and coupling it to conventional electromagnetic fields. The experimental protocols for this procedure are rigorous, and have been reproduced in Moscow and at Stanford.

R. A. Miller, I. Miller, and B. Webb (2001) are now consulting on the project to suggest the next research directions and applications. Miller and Webb have a long-standing background in this field. Long before David Bohm published his *Wholeness and the Implicate Order* (1980), Miller and Webb published "A Holographic Concept of Reality" in the journal *Psychoenergetic Systems*, ed. Stanley Krippner, Vol. 1, 1975. 55-62. Gordon & Breach Science Publishers Ltd., Great Britain. "Holographic Concept" was later reprinted in the book *Psychoenergetic Systems*, S. Krippner, editor. 1979. 231-237. Gordon & Breach, New York, London, Paris. It was reprinted again in the journal *Psychedelic Monographs and Essays,* Vol. 5, 1992. 93-111. Boynton Beach, FL, Tom Lyttle, Editor.

This foundational paper was followed shortly by "Embryonic Holography: An Application of the Holographic Concept of Reality", also in 1973. Presented at the Omniversal Symposium, California State College at Sonoma, Saturday, September 29, 1973. Reprinted in Lyttle's journal *Psychedelic Monographs and Essays,* Vol. 6, 1993. 137-156. Miller followed this project with a proposal prepared for the government through Mankind Research Unlimited, described in a formerly unpublished, proprietary paper called "Bioluminescence, Kirlian Photography and Medical Diagnostics" (1974), which is only now seeing the light of day. It was an application of his paper on "The Physical Mechanisms of Kirlian Photography."

In 1993, Iona Miller published "The Holographic Paradigm and the Consciousness Restructuring Process," another application to psychotherapeutic mindbody healing. Subsequently she has published extensively on the role of complex dynamics in relationship to consciousness and process-oriented psychotherapy, through Asklepia Foundation. A deep interest in the nature of *Synergetics* (Fuller, 1975), zero-point field, the vacuum potential, and quantum foam has led her to develop innovative applications of chaos theory in consciousness studies. She has dovetailed many of those discoveries with the reports of mystics of their intuitive inner-plane experiences of Light and Sound (Shabd) throughout history (Singh, 1979; Blavatsky, 1987; Puri, 1964; Miller and Miller, 1983). Could it be that these mystics somehow perceive holographic processes when they look inside themselves?

Endogenous DMT (N,N-dimethyltryptamine) is described as the source of visionary light in transpersonal experiences. Its primary source, the pineal, has traditionally been referred to as the Third Eye. DMT production is particularly stimulated, according to Strassman (2001), in the extraordinary conditions of birth, sexual ecstasy, childbirth, extreme physical stress, near-death, and death, as well as meditation. Pineal DMT also plays a significant role in dream consciousness. How might meditation evoke the pineal DMT experience?

"Meditative techniques using sound, sight, or the mind may generate particular wave patterns whose fields induce resonance in the brain. Millennia of human trial and error have determined that certain "sacred" words, visual images, and mental exercises exert uniquely desired effects. Such effects may occur because of the specific fields they generate within the brain. These fields cause multiple systems to vibrate and pulse at certain frequencies. We can feel our minds and bodies resonate with these spiritual exercises. Of course, the pineal gland also is buzzing at these same frequencies. The pineal begins to "vibrate" at frequencies that weaken its multiple barriers to DMT formation: the pineal cellular shield, enzyme levels, and quantities of anti-DMT. The end result is a psychedelic surge of the pineal spirit molecule, resulting in the subjective states of mystical consciousness." (Strassman, 2001). But these philosophical aspects are best addressed further elsewhere.

Here, in this presentation, the joint work of decades by Miller, Miller and Webb comes to fruition and perhaps finds a physical proof.

The organization of any biological system is established by a complex electrodynamic field. This em field is, in part, determined by its atomic physicochemical components and, in turn, determines the behavior and orientation of these components. The holographic model of reality emerging from this principle provides a scientific explanation of psychoenergetic phenomena, (Miller, Webb, Dickson, 1973).

In 1973, Miller and Webb suggested bioholograms as the projectors of our material reality: in the nuclei of each cell in the human body, the DNA (deoxyribonucleic acid) carries the structure of our whole body. Not just our physical form, but also the processes that that form undergoes in terms of survival. If all of these things are in truth locked in the DNA, how does that turn into a functioning being?

The DNA could possibly be the holographic projectors. The DNA could be projecting a field that would be experienced by other DNA in the body. The DNA molecules, in a sense, could be linked together. The DNA molecules are also linked to their own cell, which they are controlling via mechanisms of RNA transfer and enzymatic action in the cell. We believe that it is likely that the DNA and the RNA are in non-local communication. It is known from the EPR phenomenon that entangled photons retain a mutual informational bond even at a distance, through polarization, and allow a kind of quantum teleportation, which has finally been experimentally verified.

DNA molecules, included in chromosomes, possess a substance--wave duality which is similar to the dualism of elementary particles. In accordance with it, DNA codes an organism in two ways, both with the assistance of DNA matter and by DNA sign wave functions, including coding at its own laser radiation level - [28].

The genetic apparatus can be non-local at the molecular level (holographic memory of a chromosome continuum) and at the same time quantum mechanically non-local in compliance with the Einstein-Podolsky-Rosen effect [4]. The latter means that the genome genetic and other regulatory wave information is recorded at the polarization level of its photons and is non-locally (everywhere and in no time) transferred (plays out) throughout the entire space of a biosystem by the polarization code parameter. This helps to set a quick-response information contact among the billions of cells constituting an organism.

The genome on the whole and the individual nucleus of cells can generate and recognize text-associative regulatory structures with the application of a background principle, holography and quantum non-locality. (Gariaev, et al, 2000).

We believe that the DNA is the projector of the biohologram, both at the cellular level and at the whole-organismic level. This means that the DNA creates a situation of a complex pattern of three-dimensional electromagnetic standing and moving wave fronts in the space that the organism occupies.

Other researchers soon obtained similar results, and not only based on photons. Multi-frequency physical fields are now teleported. Based on this data, it's possible to suppose that photon fields, emitted by chromosomes as sign fields, can be teleported within or even outside the organism's space. The same is true for wave photon fronts, which were read from the chromosome continuum similar to reading from a multiplex hologram. If photons are transformed into radio waves (the situation we found - ref. to [8, 33,37]) through the EPR-mechanism, then this phenomenon is vital. In fact, the importance of quantum non-locality existence for a genome is hard to overestimate. (Gariaev, et al, 2001).

We think that these wave fronts interact with, interpenetrate with, and interdetermine the physical substance that makes up the physical creature. According to the holographic model of reality, all the objects we can observe are three-dimensional images formed of standing and moving waves by electromagnetic and nuclear processes. All the objects of our world are three-dimensional images formed electromagnetically, i.e. holograms. Just like a hologram encodes a 3-D image, the biohologram encodes and projects the blueprint of the human being, as well as other biological systems.

We also believe that the nervous system constitutes a coordination mechanism that integrates DNA projections of the rest of the cells in the system, that it is first and foremost a coordination mechanism which aligns these cellular holograms.

Imagine the information pleroma, beyond energy and matter, as the source of all infinitely coherent light, "shining" itself into its own entropic womb where our temporo-spatial universe is given its life-potential as a single laser beam.

The DNA in a particular cell is not totally active. It has been determined that there may be as little as 1% of the DNA present in the nucleus of the cell acting as the determinant for the structure of that cell. The nervous system, interestingly enough, has the highest percentage of operating DNA of any cell system in the body, of up to at least 10% of the DNA in the brain cells. The neuron nuclei are most active.

We suggest that the nervous system projects a global biohologram which interacts with the cellular bioholograms. If the membrane structure of the neuron nuclei is examined closely, it will be seen that the different cavity systems that enter the outer membrane also enter the inner membranes, therefore topologically, these are one and the same. Hence the nucleus is lacking a membrane, or the neurons are lacking a membrane in the sense that two of their membranes are topologically one.

We suggest that the neurons are not actually brain cells as such. We believe that the brain is the cell, and the neurons are like a distributed nucleus for that cell. That makes the glial cells organelles in the giant brain-cell. But they are also cells in their own right, much more so than neurons are. We believe the glial cells are infinitely involved with the biohologram, in its projections, and its coordination.

To go further, the biohologram, projected by the brain, creates standing and moving electromagnetic wave patterns at different frequencies of the spectrum in order to effect different biochemical transformations. There may be specific electrostatic fields, or there may be electrodynamic fields varying at various frequencies, from low (radio waves) all the way up the spectrum into visible light and beyond.

Another process of holography is called "acoustical holography". Acoustical holography employs sound waves to create a movement on a surface that is used as the basis for creation of an optical hologram. So we essentially convert between a pattern of sound waves reflected off an object in space into a pattern of light waves that can reconstruct the shape of that object. We have a transformation between two levels of vibration, two media as it were, preserving a pattern in space. (Miller and Webb, 1973).

We suggest that this happens to a much greater degree in the DNA control of our bodies. The liver, for example, contains special function cells. The special function of the liver cells is created by the influence of the projection of the liver pattern on the DNA in the cells in the area where the liver is created. We are suggesting an important feedback mechanism between the activation of the DNA in a particular cellular tissue type that causes it to be that tissue type, and the biohologram being projected by the nervous system. This is biohology.

Returning to the recent Russian discoveries (Gariaev, and reporter Poponin), which seem to confirm the seminal discovery of Miller and Webb: both quantitative and qualitative data are crucial for the development of a new unified nonlinear quantum field theory which includes the physical theory of consciousness. The DNA phantom field effect may be interpreted as a manifestation of a new physical vacuum structure which has been previously overlooked. It is perhaps a specific example of a more general category of electromagnetic phantom effects.

Results of the experiments as described by Poponin showed that when DNA was placed in a scattering chamber and bombarded with laser light a "phantom" was revealed, even when the DNA itself had been removed. The DNA was bombarded with weak coherent laser radiation in two frequencies; the intensity of the scattered light was measured, as well as non-linear localized excitations.

The experimental team found a surprising effect while measuring the vibrational modes of DNA in solution using a sophisticated “MALVERN” laser photon correlation spectrometer (LPCS), which tests the fluctuation dynamics of DNA solutions.

“In each set of experimental measurements with DNA samples, several double control measurements are performed. These measurements are performed prior to the DNA being placed in the scattering chamber. When the scattering chamber of the LPCS is void of physical DNA, and neither are there any phantom DNA fields present, the autocorrelation function of scattered light looks like the one shown in Figure 2a. This typical control plot represents only background random noise counts of the photomultiplier. Note that the intensity of the background noise counts is very small and the distribution of the number of counters per channel is close to random. Figure 2b demonstrates a typical time autocorrelation functions when a physical DNA sample is placed in the scattering chamber, and typically has the shape of an oscillatory and slowly exponentially decaying function. When the DNA is removed from the scattering chamber, one anticipates that the autocorrelation function will be the same as before the DNA was placed in the scattering chamber. Surprisingly and counter-intuitively it turns out that the autocorrelation function measured just after the removal of the DNA from the scattering chamber looks distinctly different from the one obtained before the DNA was placed in the chamber. . . Two conditions are necessary in order to observe DNA phantoms. The first is the presence of the DNA molecules and the second is the exposure of the DNA to weak coherent laser radiation.” (Poponin).

Researchers hypothesize that some new field structure is being excited from the physical vacuum substructure. As long as the chamber is not disturbed, it is measurable for long periods of time. What is measured is light scattering from the DNA phantom fields. What is attained is qualitative and quantitative information about the nonlinear dynamical properties of the phantom DNA fields. Its origin is related to physical DNA. As yet, they have found no other substance which recreates or emulates the effect of the DNA molecule.

It is this model which suggests a more general nonlinear quantum theory which may explain many of the observed subtle energy phenomena and might lead to a physical theory of consciousness.

This suggests that the electromagnetic phantom effect is a more fundamental phenomenon which can be used to explain other observed phantom effects, though not to be confused with the often misinterpreted secondary emission of electrons seen in Kirlian Photography and dubbed "phantoms." [ref. R.A. Miller on "The Physical Mechanisms of Kirlian Photography," *Psychoenergetic Systems*, Stanley Krippner, ed., 1974]. Evidence suggests a relationship to the phenomena of [endogenous] bioluminescence, liquid crystals, and superconductivity, which we intend to pursue, elsewhere.

Bioluminescence can be considered an indicator of life activity. It is the emission of photons of light produced when certain energized electrons drop into a lower or ground state. A common example is the visible light (or electromagnetic radiation) generated by the firefly. The importance of this phenomenon is seen by taking the broad view of the life process as we know it: photons from the sun excite electrons here on earth; this high energy state is transformed into high energy phosphate bonds by the process of photosynthesis; the release of the energy stored in these bonds is the fuel of life; electrons are transferred between molecules in a downward cascade fashion to lower energy states; this action produces the electric current that produces the motion that we call life. (Miller, 1974).

Entities can also luminesce at higher frequencies than the normal visible spectrum, such as in the UV or microwave region. It has been shown that the human being is an emitter of various electromagnetic radiations. Different emissions correspond to different body structures across the emission spectrum. These electromagnetic radiations are of course indicative of the energy state of the organism, and can be indicative of the state of health.

Other research (Childre, 1992; Paddison, 1992; King, 2001) suggests that consciousness is non-localized in the bodymind. Joseph Chilton Peace in his latest, *The Biology of Transcendence: A Blueprint of the Human Spirit,* (2001) points out that we have five neural centers or brains--and establishes that our fourth and most recently developed brain is located in the head while the fifth is located in the heart.

It is the dynamic interaction of this head brain (intellect) and heart brain (intelligence), of biology and spirit, which allows transcendence from one evolutionary place to the next. Pearce declares we are quite literally, made to transcend. He says, "Transcendence is our biological imperative, a state we have been moving toward for millennia."

In less scientific and more mystical terms, we emerge through self-organization from the Void and to the Void we can return for renewal and sustenance. It is, in fact the *Heart Sutra* that informs us that "Form is not other than Void; Void is not other than Form." Our human form is not other than this void, and biophysics now demonstrates this quantitatively and qualitatively.

We are more fundamentally electromagnetic, rather than chemical beings. The void state, "cosmic zero," is the primal matrix and proportionately our most fundamental reality. In essence, we emerge from pre-geometrically structured nothingness, and DNA is the projector of that field which sets up the stress gradients in the vacuum or quantum foam to initiate that process of embryonic holography, (Miller and Webb, 1973-93). The holographic paradigm is one of reciprocal enfolding and unfolding of

patterns of information. All of the potential information about the universe is holographically encoded in the spectrum of frequency patterns that constantly bombard us.

We can imagine that the self-organizing emergent function of the “rippling” effects of immense numbers of criss-crossing interference waves must be one way of making mutually interactive, or reciprocal, holographic projections of holographic projections. Our DNA projects our psychophysical self, and likewise “our brains mathematically construct objective reality by interpreting frequencies that are ultimately projections from another dimension, a deeper order of existence that is beyond both space and time: The brain is a hologram enfolded in a holographic universe,” (Talbot, 1991, p. 55).

Researchers have found that at the moment of ovulation there is a definite shift in the electrical fields of the body of the woman. The membrane in the follicle bursts and the egg passes down the fallopian tube. The sperm is negative with respect to the egg. When the sperm and egg unite, the membrane around the egg becomes hyperpolarized, shutting out other sperm. It is at this moment that the electromagnetic entity is formed. The fertilized egg cell contains all the information necessary to create a complete operational human being.

The biohologram begins to function at conception and ceases only at death. Our contention is that the DNA at the center of each cell creates the multi-cellular creature hologram by expressing the DNA in the center of the cells. The biohologram projected by the embryonic nervous system forms a three-dimensional pattern of resonant structures. These include points, lines, and planes that electromagnetically behave as the acoustic waves - the material waves - of the drumhead, acting as field guides to flowing matter and energy.

The Gariaev group has proposed a theory of the DNA-wave Biocomputer. They suggest (1) that there are genetic "texts", similar to natural context-dependent texts in human language; (2) that the chromosome apparatus acts simultaneously both as a source and receiver of these genetic texts, respectively decoding and encoding them; (3) the chromosome continuum acts like a dynamical holographic grating, which displays or transduces weak laser light and solitonic electro-acoustic fields. The distribution of the character frequency in genetic texts is fractal, so the nucleotides of DNA molecules are able to form holographic pre-images of biostructures.

In other words, the basic assumptions of the Gariaev team include the following:

1. the genome has a capacity for quasi-consciousness so that DNA “words” produce and help in the recognition of “semantically meaningful phrases”;

2. the DNA of chromosomes control fundamental programs of life in a dual way: as chemical matrixes and as a source of wave function and holographic memory;

3. processes in the substance-wave structures of the genome can be observed and registered through the dispersion and absorption of a bipolar laser beam.

This process of "reading and writing" the very matter of our being manifests from the genome's associative holographic memory in conjunction with its quantum nonlocality. Rapid transmission of genetic information and gene-expression unite the organism as holistic entity embedded in the larger Whole. The system works as a biocomputer -- a wave biocomputer.

The quantum nonlocality of the genetic information is fundamental. Experimental work of the Gariaev group shows how quantum nonlocality is directly related to laser radiation from chromosomes (light), which jitterbugs its polarization plane to radiate or occlude photons. The same researchers suspect the ability of chromosomes to transform their own genetic-sign laser radiations into broadband genetic-sign radio waves. Curiously, mystics have always called the pervasive creative sacred Sound, Logos or Word, the Audible Life Stream (Blavatsky, 1987; Hines, 1996). They declare the Light and the Sound are one, and holographic concept is another name for Unity.

The polarizations of chromosome laser photons are connected nonlocally and coherently to polarizations of radio waves. The signal can be "read out" without any loss of the essential information in the form of polarized radio waves. The liquid crystal phases of the chromosome apparatus (laser mirror analogues) can be considered a fractal environment which stores the localized photons. This creates a coherent continuum of quantum-nonlocally distributed polarized radio wave genomic information.

The genetic wave information from DNA, recorded within the polarizations of connected photons, being quantum nonlocal, constitutes a broadband radio wave spectrum. This spectrum is correlated by means of polarizations with the photons. This is the main information channel of DNA, the same for both photons and radio waves.

This biocomputer memory and retrieval program features photon-laser-radiowave polarization spectroscopy. Complex dynamics are expressed as fractal patterns at all levels of organization in nature. And this is no exception. The fundamental notion is, that the photon-laser-radiowave features of different objects (the Fourier-spectra of the radiowaves of crystals, water, metals, DNA, etc.) are stored for definite but varying times by means of laser mirrors, such that the "mirror spectra" concern chaotic attractors with a complex fractal dynamics, recurring in time.

This research is the first example of a novel static storage/recording environment (laser mirrors) capable of directly recording the space-time atomic/molecular rotary dynamical behavior of objects. It also demonstrates an essentially new type of radio signal, where the information is encoded by polarizations of electromagnetic vectors. This could even be the basis of a new type of still or video recording, leading to a new form of cinema.

This newly detected phenomenon of quantized optical activity can be considered as the means by which an organism obtains unlimited information on its own metabolism. Such information is read by endogenous laser radiations of chromosomes. The chromosome, in turn, produces the regulative ("semantic") radio emission of the genome biocomputer. Semantic resonances in the biosystem's space are realized at both the wavelength level, and level of frequencies and angles of twist of the polarization modes.

A gene has a holographic memory, (which is typically distributed, associative, and nonlocal), where the holograms "are read" by electromagnetic or acoustic fields. These carry the gene-wave information out beyond the limits of the chromosome structure. At this and subsequent levels, the nonlocality takes on its dualistic material-wave nature, as may also be true for the holographic memory of the cerebral cortex (Pribram, 1991).

Pribram posits a neural holographic process, wherein images are reconstructed when representations in the form of distributed information systems are appropriately engaged. These representations operate as filters or screens. The temporary organization of cortical columns and the arrival of impulses at neuronal junctions converge from at least two sources, forming interference patterns. These patterns are made up of classical postsynaptic potentials, coordinated with awareness. This microstructure of slow potentials is accurately described by the equations that describe the holographic process which is also composed of interference patterns.

From this it follows that in the brain information representing input is distributed over the entire extent of the neural pattern. In the bodymind information is also holographically distributed, each "part" having more or less information about the whole organism. Information is fractally distributed and present in greater or lesser resolution.

A neural holographic or similar process does not mean that input information is distributed willy-nilly over the entire depth and surface of the brain. It is confined primarily to those limited regions where reasonably stable junctional designs are initiated by the input participating in the distribution. Holographic memory processing does away with the need for keeping track of where information is stored. The "filter," "sieve," or "screen" of holographic patterns is composed not only of the lattice of membrane macromolecules making up the synapto-dedritic net, but also of a facilitation of all tendencies toward Image formation and the initiation of certain departure patterns of nerve impulses (Pribram, 1971).

At the junctional patterns of neural activity, Image forming capacity is enhanced. Superposition, i.e. spatial interactions among phase relationships of neighboring junctional patterns occurs, with properties akin to those of optical information processing systems -- the properties of holograms.

Chaotic dynamics are part of this image-forming process. There is order even in disorder. There is order, manageable chaos (fractals) and unmanageable chaos. The fractal dimension expresses the complexity of a particular fractal form. “Fractal” comes from the Latin *fractus*, which mean broken or fragmented. Fractals delineate a whole new way of thinking about structure and form -- even the forms of dis-ease, which take root organically in the body and psyche.

Like holograms, magnify a fractal again and again and more detail emerges from its infinitely embedded structure. The same self-similar patterns repeat, over and over, no matter what level you care to examine. You look closer and closer and still see the same form. A single image is infinitely reiterated. Thus, a wealth of structure emerges from simplicity. So, too, the dis-ease process can be seen at the physical, emotional, mental, and spiritual levels. Yet, the form remains the same.

"At the most fundamental level of our individual being, we too, our bodies and our psyches are part of the interference patterns caused by the interaction of consciousness and wave fronts arising from fields of infinite possibility. We then must also operate by holographic principles, thus our internal perception of this reality is itself a hologram in our brain. It is the means of perception that gives the universe its apparent forms and solidity. It is also this holographic perception that influences the dynamics of our brain's and our body's chemistry, our self-hologram. In this perceptual hologram resides the fundamental basis of our structure and our sense of self and external environment, including our health and illness in both our physiological and psychological being. Our disease structures are incorporated within it. It is here, at this level of our being where fundamental healing and physical-psychic restructuring occur. This hologram is what I have termed the primal existential sensory self-image or existential hologram. . .our sense of self is a holographic, existential, multi-sensory image." (Swinney, 1999).

The key to this process lies in our DNA, in our genes and gene-expression. Our understanding of the human biocomputer must be based on a new understanding of the higher forms of the DNA memory, and the chromosome apparatus, as the recording, storing, transducing, and transmitting system for genetic information, to be considered simultaneously at the level of matter and physical fields.

The wave-biocomputer model helps explain the apparatus of protein biosynthesis of living organisms, providing an important interpretation of the initial stages within the hierarchic chain of material and field, sign, holographic, semiotic-semantic and, and figurative encoding and deciphering of chromosome functions. At the gene-sign continuum of any biosystem, DNA forms pre-images of biostructures and the organism as a whole as a registry of dynamical "wave copies" or "matrices", succeeding each other. This continuum is the measuring, calibrating field for constructing or creating any biosystem, (Gariaev).

II. MECHANISMS: QUANTUM MECHANICS AND COMPLEX DYNAMICS

A quick review of the Holographic Concept refreshes us on the basics of biophysics.

Particles found in biological processes include photons, electrons, protons, elementary ions, inorganic radicals, organic radicals, molecules, and molecular aggregates. Photons act upon electrons by raising their energy state. This process is called excitation. Excited electrons can drop back to more stable energy levels and emit photons. Electron excitation can lead to the formation of an electronic bond between molecules. This is the traditional bond of classical chemistry. The breaking of such bonds can, by reverse process, lead to the excitation of electrons.

In living systems the excitation of electrons by photons and the subsequent conversion of that excitation into the bond energy is called photosynthesis and is the basic builder of biological structures. The reversal of this process is called bioluminescence. This phenomenon is the transfer of energy from a bond to an excited electron, resulting in the emission of a photon. It has been suggested by Szent-Gyorgyi (1957: 8) that the energetics of living creatures can be understood in terms of photosynthesis and its reversal, bioluminescence.

All cellular processes are driven by energy derived from the breaking of chemical bonds and the excitation of electrons. Depending upon the particular environment and circumstances, the excitation of the electron can be converted in one of three ways: (1) conversion into heat and dissipation (2) translation of molecules or ions through the cell, or (3) transformation of the molecules' shapes which profoundly influences their biological reactivity.

The formation of a certain type of chemical bond known as the resonance bond (which is most easily seen in the case of the Benzene molecule) leads to a peculiar situation in which certain electrons are freed from a local or particular location in the molecule. These are then free to travel around the entire molecule. This means that the electrons occupy an energy shell of the whole molecule as opposed to any particular atom in the molecule. The existence of molecular systems with mobile electrons has been found to be of profound significance in the phenomena of life.

Hydrogen, carbon, nitrogen, and oxygen, which compose 99 percent of all living systems, are among the atoms in the periodic table which form the multiple bonds most easily leading to mobile electrons. Sulphur and phosphorus, which are extremely important for life processes, also form such multiple bonds quite easily.

All the essential biochemical substances, which perform the fundamental functions of living matter, are composed completely or partially of such mobile electrons. Molecules which contain these electrons are known as conjugated systems (Pullman and Pullman, 1963, chapter 18). The essential fluidity of life may correspond with the fluidity of the electronic cloud in conjugated molecules. Such systems may best be considered as both the cradle and the main backbone of life.

Conjugate bonded molecules may interact in a variety of ways. Among these types of interaction can be found the interpenetration of electron orbitals which permits an electromagnetic coupling. This coupling can permit activated electron energy to pass from one molecule to another in the same way a radio can transmit a message to a radio receiver. There is also the possibility of the transfer of an entire electron which is known as charge transfer.

It is possible for a molecular complex to contain several radicals at different positions on the main molecule, each of which are conjugated. If these are in close enough proximity, or can be brought into proximity by changes in the structural configuration of the molecule, a charge can pass between these two groups. This is the case of the transfer of electron charges on or around a single molecular complex. It has been suggested by Szent-Gyorgyi (1968) that the sugars and phosphates that make up the side of the alpha helix of DNA can permit the passage of electrons, functioning as a conductor.

The biological conduction systems operate primarily on an amorphous semiconductor mode as opposed to resembling metallic conductors. These do not have sharply defined energy bands in which electrons may flow, as opposed to other bands in which they are bound rigidly. There is a spread or bell-curve in which the points or tails are bound more closely to a particular molecule. The hump indicates a conducting band that permits electrons to flow across the surface of a particular molecule or between molecules (McGinness, 1972).

This means, in essence, that protein molecules which are composed of amino acid sequences, may act as organic circuits. The amino acids each have a donor group and an acceptor group on opposing ends. This means that a string or series of amino acids could pass a charge along as if it were being passed along a series of spines sticking up from the main body of the molecule.

Different pathways could be defined across the surface of a protein molecule by the amino acid radicals projecting out from the surface of the protein. The shape of the protein molecules is a function of the charges and the conjugate systems on the radicals that make up the protein. When a protein is manufactured and peels off the ribosome, it immediately assumes a three-dimensional spatial pattern that is directly related to the charges on its surface and the ways in which they interact.

The biological activity or specificity of action of various molecules is intimately related to their structure or their exact three-dimensional spatial configuration. Electronic energy and electrons can move through a protein molecule between its different parts and can pass among different molecules. We now come to understand a possible mechanism for biological regulation involving flows of electrons and transfer of electronic energy between molecules. These can change their shape and thereby change their specific action and activity. The fusion of electron clouds can exist within a conjugated system and among conjugated systems. This can account for cohesion or the adherence of such molecules to each other. Such fusion is a very important determinate of the structure of larger aggregates of molecules and portions of living cells, such as membranes.

III. BIOHOLOGRAM FIELD THEORY

A liquid crystal in a cell through its own structure becomes a proto-organ for mechanical and electrical activity, and when associated in specialized cells in higher animals gives rise to true organs such as muscles and nerves. The oriented molecules in liquid crystals furnish an ideal medium for catalytic action, particularly of the complex type needed to account for growth and reproduction. A liquid crystal has the possibility of its own structure through singular lines, rods and cones, etc. Such structures belong to the liquid crystal as a unit and not to its molecules which may be replaced by others without destroying them, and they persist in spite of the complete fluidity of the substance (Needham, 1936).

Bernal's statement (1933) would seem to support Burr and Northrop's macro-atomic theory (1935), which postulates that there are two aspects to reality, the field and the particle. They associate the field with what they term the macroscopic aspect and the electron with the particle. They associate the field with what they term the macroscopic aspect and the electron with the particle. The particle is associated with movement. The structure of biological material seems to be associated with the field aspect. The electric field causes polarization of the macromolecules in the solution due to the fact that molecules possess a dipole moment, and changes the position of protons in the molecule. Such action can affect the relative stability of different possible configurations of the macromolecules. The field affects the degree of structure present in the solution.

A constant magnetic field can, in principle, affect the various processes in biological objects. Three possible mechanisms for this biomagnetic affect are (1) the orientation of diamagnetic or paramagnetic molecules by the magnetic field (2) distortions of the angles in the molecules and (3) orientation of the spins of molecules in a magnetic field (Fowler and Bernal, 1933; Freedericks and Zolina, 1933; Van Iterson, 1933; Osborne, Ambrose and Stuart, 1970). Presman (1970) has postulated that such electromagnetic fields normally serve as conveyors of information, from the environment to the organism, within the organism, and among organisms. He suggests that organisms employ these fields in conjunction with the well known sensory, nervous, and endocrine systems, in effecting coordination and integration.

Muses (1970) has proposed the possibility of unit impulse functions evolving from the Gaussian. His work traces the relation of that mathematical concept to quantum biological indeterminacy in terms of a process of the modulation of random fluctuations by target-seeking perturbations which points the way to the understanding and computing of the parameters of volitional experience in quantum biological terms. He maintains that we are dealing with Gaussian wave packets, put to use in terms of a close-range reaction in turn resulting in the resonant microbiological specificity (arising from the relatively large number of specific molecular parameters) necessary to the essential life and evolutional processes of chromosome synapses, replication, and mutagenesis.

Muses holds that inherently indeterminate processes may be biologically used in achieving determinate ones such as our repeatable and commonly accepted volitional experiences of effort and direction. The range of quantum indeterminate fluctuation of biological efficacy is in the far ultraviolet, and it is in this spectral region that we should expect to look for any modulation effects on Gaussian wave packets by volitional energies manifesting as ultramicrobiological field perturbations.

Biologically, there is a threshold of non-randomicity below which peaks tend to emerge that are sharp enough to possess biodirectiveness in an enzyme-guiding sense. Random biological quantum energies which are physiologically unassigned are the clue to psychosomatic directing, which can be beneficial or deleterious to the organism. Muses (1970) describes the mechanism of this effect as a microbiolaser type process.

Heisenberg explored the possible relevance of the quantum indeterminacy of elementary particles for biological systems, especially human systems (discussed in Koestler, 1972). He stated that there are two places in the human system where the quantum indeterminacy of a single particle can have a profound influence. The first important effect is that of mutation in the genetic code. The second important influence is the alteration of the behavior of neurons during human thought processes.

Tien (1969) has conceptualized mind as mass in relative motion and brain as energy at relative electrical charges in motion, like electrons bombarding a television screen, and personality is seen as a time series of scintillating frames of consciousness. Personality becomes a reverbating input-output pattern of self-creation, seeking information or patterns of energy from the environment as well as from its own memories. The stability of any given personality of its identity is maintained by feedback upon the principle of most similarity.

The personality never recreates itself, but creates only a close approximation which is accepted due to the principle of constancy as being the same. The phenomena of unique individuality and personal continuity depend on memory, of which consciousness is the most recent and, thereby, the most subject to erasure and loosening. Personality transformation becomes energy pattern modification of not only scintillating consciousness but also of recent circulating memories and older stored memories of childhood.

According to the holographic model of reality, all the objects we can observe are three-dimensional images formed of standing and moving waves by electromagnetic and nuclear processes. All the objects of our world are three-dimensional images formed electro-magnetically, i.e., holograms.

This concept and the models of human information processing based on the hologram, throw interesting light on the philosophical tradition which holds that the world of objects is an illusion. With the triumph of relativity and quantum physics, the interpenetration of the philosophical and the scientific is possible.

LeShan (1969) has observed, in discussing some individuals who purportedly experience psycho-energetic phenomena, that their view of the universe as a great thought of which they are a part is quite similar to many physicists' view that they see reality only in their own mental image.

We propose that the "reality hologram" which appears as a stable world of material objects is the elementary particle which has a long-term existence and fairly simple rules of interaction. We also propose the existence of a "biohologram" which appears as mobile and evolving, through the DNA molecule. This "biohologram" projects a dynamic three-dimensional image that serves as a guiding matrix for the manipulation and organization of the "reality hologram." (Miller, Webb, Dickson, 1973).

Thus we have mobile self-organizing holograms moving through a relatively static simpler hologram. The possibility exists that such "biohologrames" could achieve sufficient coherence to continue existence as a pattern of radiant energy apart from a material substrate. We feel that such an occurrence could form the scientific basis of such

psychoenergetic phenomena as psycho-kinesis, clairvoyance, telepathy, and precognition.

Quantum holography asserts that DNA satisfies the principle of computer construction as defined by Von Neumann (1966). It carries a copy of itself and is its own blueprint written in the genetic texts where the mechanism engineering the DNA replication is the biophotonic electromagnetic field, while the "letters" of the genetic texts, A, G, C, U are held invariant. In replication of the organism, the blueprint creates the "acoustic field" which mechanically constructs/engineers the organisms out of the available matter, in accordance with the information held in the electromagnetic field holograms.

Both quantum entanglement and therefore quantum teleportation can be related to quantum holography, through solitons, resonance effects, and superconductivity.

Experimental evidence confirms that the mutual recognition of one DNA antiparallel half chain (+) by the other (-) concerns special super persistent/resonant acoustic-electromagnetic waves or solitons. DNA solitons express two types of memory which concern the capability of non-linear systems to remember initial modes of energisation and to periodically repeat them [Dubois, 1992]. The DNA liquid crystals within the chromosome structure form such a non-linear system. The DNA-continuum is quasi-holographic/fractal and relates, as is the case for any hologram or fractal, to the fundamental property of biosystems, i.e. their ability to restore the whole out of the part.

DNA solitary waves (solitons), and in particular, the nucleotide waves of oscillatory rotation, "read" the genome's sign patterns, so that such sign vibratory dynamics may be considered as one of many genomic, non-linear dynamic semiotic processes. The key parameter of such patterns is fractality. It can therefore be hypothesized that the grammar of genetic texts is a special case of the general grammar of all human languages. We can realize the wave-coding capabilities of the matter-wave sign functions of DNA as true wave control capabilities facilitates in an aqueous solution acting as a liquid-crystal condition. The living cell is a computer based on DNA.

The genome has been identified as an active "laser-like" environment. Yet this approach to DNA-wave biocomputation means entering into new semiotic areas of the human genome and the biosphere in general. These are the areas which are used by Nature to create humankind. The quasi-speech of chromosomes of all organisms concerns semantic exobiological influences wherein DNA acts as a kind of aerial open to the reception of internal influences and changes within the organism as well as those outside it. This extends beyond it to the extent of the entire universe through complex fractal embedding and non-locality.

Creation of biocomputers can be based on these totally new principles of DNA-wave biocomputation, which use quantum teleportation [Sudbury, 1997], (see also SciAmer on quantum teleportation). Experiments show that DNA considered as a liquid-crystal gel-like state, reveals a periodically reoccurring pattern which acts on the incoming light in the manner of a solitonic lattice. What could such an action achieve?

A soliton is an ultra stable wave train often with a seemingly simple closed shape, which can arise in the context of non-linear wave oscillations. Really it consists of a rather complexly interrelated assembly of sub wave structures, which keep the whole solotonic process in a stationary state over a comparatively long time. The soliton is neither a particle nor wave in much the same as a quantum is characterized by wave-particle duality. It is a means to carry information. It probably reads the codons, as a travelling "window" that opens in the double helix structure as the reading takes place. In this model the reading process is a complex mechanical oscillator (Gariaev, 1994), capable of producing solitonic wave transmissions, which take the form of a system of rotary pendulums.

DNA forms such pendulums in this model which are simulated as a chain of non-linear oscillators. The window as it travels is highly context dependent on the actual layout of the elements as specified by the actual genetic code sequence involved. Complex dynamic patterns arise in the non-linear covalent connections between nucleotides. Oscillatory activities are located somewhere together in the "acoustic" wave domain.

As a liquid crystal, DNA probably influences the polarization of the weak light emission known to exist in cells, as so-called biophotons. Such biophotonic, mitogenic radiation or mitogenic light, while being ultraweak, is yet highly coherent. It has an inherent laser-like quality. Endogenous intracellular coherent light is emitted by the DNA molecule itself.

The superposed coherent waves of different types in the cells are interacting to form diffraction patterns, first in the "acoustic" domain and then in the electromagnetic domain. This is a kind of quantum hologram. Interactions of solitonic oscillations in the liquid crystal structure of DNA and the polarization vector of the ultraweak biophotonic highly coherent light, could be understood as a mechanism of translation between holograms in the "acoustic" frequency domain of short range effects and those in the electromagnetic domain, and vice versa.

Quantum holography has been used to predict the workings of MRI (Schempp, 1992,1998). The DNA-wave biocomputer model is also in agreement with the qubit model explanation of DNA.

In the quantum holographic DNA-wave biocomputer theory, DNA is a self-calibrating antenna working by phase conjugate adaptive resonance capable of both receiving and transmitting quantum holographic information stored in the form of diffraction patterns -- quantum holograms. The model describes how during the development of an embryo of the DNA's organism, these holographic patterns carry the essential holographic information necessary for that development.

The quantum holographic theory requires that the DNA consists of two antiparallel (phase conjugate) helices, between which are located hologram planes/holographic gratings, where the necessary 3 spatial dimensional holographic image data of the organism is stored. Endogenous laser illumination can be expected to turn the DNA into a series of active adaptive phase conjugate mirrors/holographic transducers. A beam of radiation resonantly emerges on which is carried the holographic information as encoded in the DNA. This confirms the quantum holographic prediction that DNA functions as an antenna capable of both encoding and decoding holographic information.

We can also model the quantum holography of the neuron. This model is in good accord with the biological neuron's information processing morphology and signal dynamics. This is the quantum holographic model of the brain as a conscious system. We can incorporate signal theory into quantum physics through the concept of the pilot wave or radar.

Quantum holography predicts polarized or orthogonally rotated holograms encoded on a "paged" associative holographic memory. Sharp frequency adaptive coupling conditions specify very narrow spectral windows, i.e. the "pages." "Magic windows" are a naturally tuned frequency of a good hyperchannel between orthogonal frames where scalar wave anenergies crosstalk readily. They are frequency dependent interdimensional nodal points. Some magic windows are 38-40 lHz; 150-160 kHz; 1.1-1.3 MHz; 1.057 (Lambshift) and the near ultraviolet (life energy frequency), (Beardon, 1988).

Described in terms of tensor multiplication, the orthgonality condition can be seen as specifying a set of diagonal elements, which traces in a unit matrix in the frequency domain. The planes on which the base pairing takes place concerns two quantum holograms. The tensor operation, in quantum holography, describes a quantum entanglement.

Murray Gell-Mann describes quantum entanglement in *The Quark and the Jaguar* (1994). He first points out that coarse graining can wash out interference terms. The interference terms between two coarse-grained histories is the sum of all the interference terms between pairs of fine-grained histories belonging to those two coarse-grained ones. The underlying explanation for decoherence is the mechanism that makes interference terms sum to zero and permits the assignment of probabilities. It is the entanglement of what is followed in the coarse-grained histories with what is ignored and summed over.

IV. BIOLOGICAL EFFECTS OF SCALAR ENERGY

There are only a few known forces in nature and unfortunately we are at a loss to explain what their actual sources are. The best physics has been able to do is ascribe them to some fundamental characteristics of the universe, a charge of some kind. That's why we can more abstractly view a force as the variation of a certain potential and therefore practically every influence field can be thought of as a force field. This potential can be a scalar as in the case of Coulomb's law; a vector as in the case of the electromagnetic vector potential which neatly streamlines the mathematics of Maxwell's equations; or a tensor, which is the case of the metric tensor of the Riemann space in Einstein's GTR equations.

There is a predominance of non-linear processes in biological systems. Several types of quasi-particles, each with their own characteristic resonant frequencies have been proposed to mediate these non-linear phenomena, including solitons, excitons, and plasmons. The right frequencies of non-linear energies might have profound healing properties, according to Stanford researcher Dr. Glen Rein. Due to the non-linear nature of biological systems it is proposed that scalar waves should be more biologically active than their linear electromagnetic counterparts.

In the simplest cases, scalar resonance can be imagined as two ordinary single-frequency EM standing waves in a resonant cavity, with the two waves coupled exactly 180 degrees out of phase so that --externally--their E fields sum to zero and the capacity is said to be in scalar resonance. The cavity walls must act as phase conjugate mirrors (PCM). Mass itself is simply a standing scalar resonance, with the standing walls tapped by particle spin. The atomic nucleus continually bombarded by virtual photon flux from the vacuum is a pumped PCM. Since the nucleus is positively charged, it produces Phase Conjugate Replicators (PCRs), having negative energy and negative time. It thus produces negentropy, which prevents the entropic decay of the atom. Essentially all frequencies can be and are present at once, but certain nuclear resonance frequencies are thought to predominate. By increasing the amplitude of the standing scalar wave that is the nuclear pseudopotential, inertia and mass of the nucleus are increased. Zeroing the amplitude dematerializes the nucleus. (Beardon, 1980).

So, scalar energy is transduced into linear electromagnetic energy in the body by liquid crystals in the cell membrane and solid crystals found in the blood and in several biological tissues. Clinical studies of the effects of scalar energy on the mind-body and brainwaves have been conducted since the 1980s. If they can be believed, research from Stanford University Medical Center produced some tantalizing results.

Electrochemical oscillation between membrane-bound lipids near phase-transition temperature have been analyzed with and described by nonlinear quantum mechanical equations. They also analyzed the coupling between harmonic oscillators represented by action potentials generated from active neuronal networks in the central nervous system, finding evidence of chaos. The extraction of scalar components from Maxwell's original electromagnetic equations and from Schrodinger's equation using imaginary numbers has been reported, and their unusual non-linear waves described by many experimenters.

A Crystalline Transduction Theory has been put forth to explain the interactive mechanism of scalar waves with biological systems. Another possibility is transduction in microtubules dispersed throughout the whole organism. Tissue culture studies imply that the action of scalars on biological systems is more than a placebo effect mediated by the brain/mind, such as stress, moods or beliefs. Stray EM energy in the ambient atmosphere makes it difficult to study the healing properties of scalar energies in a clinical setting.

Clinical healing sometimes occurred several months after initial exposure to the scalar waves. It is known that the brain and body, each the immune system, communicate bidirectionally. Thus, a direct action of scalar energy on the body could cause a subsequent change in brain state. Therefore EEG studies do not indicate whether scalar energy also effects the body directly or whether the brain and the body are both affected. Even if scalar energy directly affects individual cells, it may also affect the mind resulting in an altered psychological outlook which results in clinical improvement.

Dr. Michael Persinger (1987) was the first person to test the effects of scalar energy using isolated cells. The scalar waves were generated by partially canceling two vortex-type magnetic fields (0.SHz, 10pT) by intersecting them in the air. The biological endpoint, degranulation of mast cells, was increased by the scalar fields. Dr. Puharich, in another study, grew tissue samples of E. Coli, and detected an increased activity of ubiquitone, a protein involved in DNA repair. These results indicate that scalar energy can have a direct effect at the subcellular level as well as a direct effect on the immune system.

Another project detected an effect of scalar energy on neurotransmitter function, which mimicked the effect of antidepressant medication. Scalars appear to modulate the basic biochemical communication between nerve cells mediated by neurotransmitters. Cultured nerve cells called PC 12 cells were isolated from rats, and the functional properties of noradrenaline release from PC 12 cells was shown to be increased by a 500Hz monopolar square wave, and noradrenaline uptake was inhibited by a 15Hz biopolar square wave, (Rein).

Noradrenaline uptake was chosen because it is directly mediated by the plasma membrane via an intramembrane protein carrier. The plasma membrane, with its liquid-crystal structure, is the critical cellular barrier which interfaces with the chemical and electromagnetic environment. Since other intramembrane proteins show non-linear properties, the plasma membrane is a likely target for scalar energy.

The physiological function of carrier mediated neurotransmitter uptake is to remove excess neurotransmitter from the synaptic cleft after its release from presynaptic nerves. Thus, inhibiting uptake results in the accumulation of the neurotransmitter in the synaptic cleft. This is the mechanism of action of tricyclic antidepressants, since they inhibit noradrenaline uptake.

Depression is associated with decreased noradrenaline levels. Rein exposed confluent monolayer culture of PC12 cells to noradrenaline in the presence or absence of scalar energy. After 30 minutes, the cells were washed and centrifuged and noradrenaline uptake measured. Overall, uptake was inhibited by 19.5% in the presence of the scalar field as compared with the control value obtained in its absence. This is a significant statistical difference of p 0.01.

Researchers think a wide variety of physiological changes could be created resulting in improvement of a variety of clinical diseases, only one of which could be depression. Scalar energy can have a direct effect on the cell membrane. Researchers want to test whether diseased cells are preferentially sensitive to scalar energy; and what characterizes its mechanisms of action.

V. ROSSI'S DREAM-PROTEIN HYPOTHESIS ON HEALING

Ernest Rossi (1999; 2002) has developed a pertinent creativity hypothesis: "Enriching life experiences that evoke psychobiological arousal with positive fascination and focused attention during creative moments of art, music, dance, drama, humor, spirituality, numinosity, awe, joy, expectation, and social rituals can evoke immediate early gene protein cascades to optimize brain growth, mindbody communication, and healing."

"[The] psychotherapeutic approach can contribute to psychobiological arousal, enrichment and relaxation; it may be possible to help people find optimal levels of mental stimulation to facilitate actual growth in the hippocampus of their brain to encode new memory, learning and behavior...optimizing psychobiological growth and healing."

Rossi (1999) describes a mind/body communication channel that is pertinent in that it may describe another way neural plasticity and healing manifests from REM. He

describes how immediate-early genes (also called “Primary Response Genes” or third messengers) play a central role in the dynamics of waking, sleeping, dreaming, and mind-body healing at the cellular level.

There is evidence that immediate-early genes (IEGs) function as mediators of information transduction between psychological experience, behavioral states, and gene expression. A wide range of behavioral state-related gene expression (from relaxation, hypnosis and sleep to high arousal, performance, stress and trauma) culminate in the production of new proteins or homeostasis, physical and psychosocial adaptation.”

Behavioral states modulate certain patterns of gene expression. Interaction between the genetic and behavioral levels is a two way street. Genes and behavior are related in cybernetic loops of mind-body communication. How does this relate, for example, to manic depression?

A look at the systems related to IEGs, shows that they affect all the systems disrupted in bipolar disorder. They are expressed continually in response to hormone messenger molecules mediating processes of adaptation to extracellular signals and stimuli. Extracellular stimuli come from the outside environment, including temperature, food, sexual cues, psychosocial stress, physical trauma, and toxins. IEGs are fundamental in the sleep-wake cycle, appetite regulation, sexual response, and reactions to stress, trauma, and toxins (Rossi, 1986; 1999; 2002).

There are persistent alterations in IEG expression in the process of adaptive behavior on all levels from the sexual and emotional to the cognitive. They can transduce relatively brief signals from the environment into enduring changes in the physical structure of the developing nervous system as well as its plasticity in the form of memory and learning throughout life. If external cues can modulate cell function through regulation of gene expression, this could also be true for internal cues.

IEGs are also fundamental in the regulation of REM-on, REM-off neurons, neuronal networks that are associated with REM sleep and dreaming. That makes them significant as molecules which can modulate mind, emotions, learning and behavior. They influence the rhythm of the natural healing process and circadian and ultradian rhythms of the body, in general. Ultradian rhythms are those shorter than the 24-hour circadian rhythms (Rossi; Cheek, 1988).

Milton Erickson discovered that his therapy sessions usually took from one and a half to two hours to come to natural closure. Later it was discovered that this delineates the natural work cycle that is harmonious with our own internal rhythms. IEGs modulate this process. This ultradian time frame is related to the activation or deactivation of the expression of specific genes and can occur in a matter of hours or even minutes.

“Most arousing environmental stimuli that have been studied can induce immediate-early genes within minutes, their concentrations typically peak within fifteen to twenty minutes and their effects are usually over within an hour or two. These time parameter IEG expressions and their ultimate translation into the formation of new proteins correspond to the parameters of a complete work cycle of mind-body communication and healing. The changes in gene transcription and new protein formation initiated in this time frame, however, can lead to lasting changes in the central nervous system by converting short term memory to long lasting learning by the process of long term potentiation. . .the activation or deactivation of the expression of specific genes can occur in a matter of hours or even minutes." (Rossi, 1999).

This mechanism assesses the duration and intensity of prior waking and/or the homeostatic or executive mechanisms that bring about sleep. Sleep deprivation leads to a wide variety of psychotic and non-psychotic symptoms. This system is also associated with the neuronal network associated with the dynamics of REM sleep. Deprivation of REM and dreaming creates its own phenomenology.

“The study of IEGs indicates that sleep and wake, as well as synchronized and desynchronized sleep, are characterized by different genomic expressions, the level of IEGs being high during wake and low during sleep. Such fluctuation of gene expression is not ubiquitous but occurs in certain cell populations in the brain. Thus...IEG induction may reveal the activation of neural networks in different behavioral states. Do the areas in which IEGs oscillate during sleep and wake subserve specific roles in the regulation of these physiological states and a general ‘resetting’ of behavioral state? Is gene induction a clue to understanding the alternation of sleep and wake, and of REM and non-REM sleep?” (Rossi, 1999).

In Rossi’s Dream-Protein Hypothesis, “new experience is encoded by means of protein synthesis in brain tissue...dreaming is a process of psychophysiological growth that involves the synthesis or modification of protein structures in the brain that serve as the organic basis for new developments in the personality...new proteins are synthesized in some brain structures associated with REM dream sleep.”

Rossi generalizes the dream-protein hypothesis, “to include all states of creativity associated with the peak periods of arousal and insight generation in psychobiologically oriented psychotherapy.”

Enriched internal and external environments leads to the growth and development of new cells. IEG cascades lead to the formation of new proteins and neurons along with increased synapses and dendrites that encode memory and learning. On the other hand, excessive trauma and psychosocial stress can lead to suppression of growth processes in the brain. When psychotherapy contributes to arousal, enrichment, and relaxation it facilitates actual growth in the brain to encode new memory, learning and behavior, optimizing growth and healing.

“Communication within the neuronal networks of the brain is modulated by changes in the strengths of synaptic connections...meaning is to be found in the complex dynamic field of messenger molecules that continually bathe and contextualize the information of the neuronal networks in ever changing patterns. Most of the sexual and stress hormones...have state dependent effects on our mental and emotional states as well as memory and learning, a constantly changing dynamical field of meaning.” (Rossi, 1991).

Novel and enriching psychotherapeutic experiences can lead to neurogenesis and gene expression which facilitate mindbody communication and can have a long-term transformative effect on the whole person (Rossi, 2002). Rossi points out that many of the essential dynamics of gene expression involved in the formation of the brain and body in embryology are now recognized as a continuing creative development through an individual's lifetime. He also asserts that a lack of optimal gene expression and neurogenesis is associated with psychological depression and stress. Thus, biohology has relevant applications for optimizing health and well-being across disciplines, such as biophysics, medicine, psychobiology, psychotherapy and the holistic healing arts.

VI. CONCLUSION

Sidorov (2002) has summarized the thrust of the Gariaev group:

Since the early '90s, Gariaev's team has been developing a new theoretical and experimental approach to the study of genetic material encoding and expression. In a pioneering paper (Gariaev 2001; JNLRMI I(2)), he and his colleagues challenge the limits of the genetic code triplet model and propose instead a dual, substance/wave basis for the encoding and expression of genetic material. The wave-like, non-local aspect of genetic regulation is recorded at the polarization level of DNA-associated photons, and the genome is seen as a quasi-hologram of light and radio waves which create the background necessary for the appropriate expression of genetic material.

The authors argue that the genome emits light and radio-waves whose delocalized interference patterns create calibration fields (blueprints) for a system's space-time organization. This holographic-type information is being constantly and simultaneously read in billions of cells, accounting for the quick coordinated response typical of

living systems.

We can use the observations of the Gariaev group to further summarize the essence of the human biocomputer:

"Thus, nonlocality can be postulated to be the key factor explaining the astonishing evolutionary achievement of multicellular biosystems. This factor says that bioinformatic events, can be instantaneously coordinated, taking place "here and there simultaneously", and that in such situations the concept of "cause and effect" loses any sense. This is of a great importance! The intercellular diffusion of signal substances and of the nervous process is far too inertial for this purpose. Even if it is conceded that intercellular transmissions take place electro-magnetically at light speeds, this would still be insufficient to explain how highly evolved, highly complex biosystems work in real time." [5]

Gariaev asserts that quantum nonlocality and holography is indispensable to a proper explanation of such real time working.

"[T]he genes can act as quantum objects, and that, it is the phenomenon of quantum non-locality/teleportation, that ensures the organism's super coherency, information super redundancy, super knowledge, cohesion, and, as a totality or whole, the organism's integrity (viability)." [5]

Quantum Holography defines an admitter/absorber quantum vacuum model of quantum mechanics in terms of annihilation/creation operators [Schempp, 1993]. This implies that DNA does indeed behave like a single quantum, which induces a "hole" temporarily in the vacuum by its removal.

This new understanding of biocomputers, constitutes a further step in a development of computer technology in general. An understanding that brings about a total change of the constituent basis of that technology to the figurative semantic (nonlocal) wave computer or biocomputer, based on DNA memory, and the chromosome apparatus.

Quantum Biohology argues that DNA satisfies the principle of computer construction, since it carries a copy of itself, its own blueprint, with the mechanism engineering the DNA replication being the biophotonic electromagnetic field, while the "letters" of the genetic texts A, G, C, U are held invariant. The existence of the genetic text constitutes the classical signal process of quantum teleportation, and facilitates the quantum mechanical signal processes of both the copying of the DNA as its own blueprint, and of the construction of the organism in a massively parallel way by means of quantum teleportation.

REFERENCES

1. Beardon, Thomas (1980, 1988, 2002), Excalibur Briefing, Strawberry Hill Press, San Francisco.

2. Berezin, A.A., Gariaev, P.P., et al (1996), "Is it possible to create laser based on information biomacromolecules?", Laser Physics, v.6, N6, pp. 1211-1213.

3. Blavatsky, H.P. (1987, 1992), The Voice of the Silence, Theosophical Publishing, Wheaton: Illinois.

4. Bohm, David (1980) Wholeness and the Implicate Order, Routledge, London.

5. Gariaev, Peter, Boris Birshtein, Alexander Iarochenko, et al, “The DNA-wave Biocomputer,”

6. Gariaev, P.P. (1994), Wave Genome, Public Profit, Moscow, 279 pages [in Russian].

7. Gariaev, P.P. (1993) Wave based genome, Depp. VINITI 15:12. 1993, N 3092?93, 278pp. [in Russian].

8. Gariaev, P., Tertinshny, G., and Leonova, K. (2001), "The Wave, Probabilistic and Linguistic Representations of Cancer and HIV," JNLRMI, v.1, No.2.

9. Gell-Mann, Murray (1994) The Quark and the Jaguar, New York: W. H. Freeman and Company.

10. Hines, Brian (1996), God's Whisper; Creation's Thunder, Threshold Books, Brattleboro, Vermont.

11. Kelleher, Colm A. (1999), “Retrotransposons as Engines of Human Bodily Transformation,” Journal of Scientific Exploration, 13, no 1, Spring 1999, pp. 9-24.

12. King, Chris (1999) “Fractal Neurodynamics and Quantum Chaos: Resolving the Mind-Brain Paradox Though Novel Biophysics,” Fractals of Brain; Fractals of Mind, Advances in Consciousness Research 7. Online at http://www.dhushara.com/book/paps/consc/brcons1.htm#anchor217145

13. LeShan (1969), Toward a general theory of the paranormal. Parapsychological Monographs, No. 9.

14. Marcer, P. and Schempp, W. (1996), A Mathematically Specified Template for DNA and the Genetic Code, in Terms of the Physically Realizable Processes of Quantum Holography, Proceedings of the Greenwich Symposium on Living Computers, editors Fedorec, A. and Marcer, P., 45-62.

15. Marcer, P. and Schempp, W. (1997a), The Model of the Prokaryote Cell as an Anticipatory System Working by Quantum Holography, Proceedings of CASYS 97, 11-15, August, HEC-Liege, Belgium, International Journal of Computing Anticipatory Systems, v2, 307-315.

16. Maslov, M.U. and Gariaev, P.P. (1994), Fractal Presentation of Natural Language Texts and Genetic Code, 2nd Intl Conference on Quantitative Linguistics, Sept. 20-24, Moscow State University, Philological Faculty, pp. 193-194.

17. McFadden, Johnjoe (2002), “Synchronous Firing and Its Influence on the Brain’s Electromagnetic Field: Evidence for an Electromagnetic Field Theory of Consciousness,” (CEMI Theory), Journal of Consciousness Studies (2002) 9: 23-50.

18. McGinness, J.E. (1972), Mobility Gaps: A mechanism for band gaps in melanins. Science, 1972, 177, 896-897.

19. Miller, R.A., Webb, B. Dickson, D. (1975), “A Holographic Concept of Reality,” Psychoenergetic Systems Journal Vol. 1, 1975. 55-62. Gordon & Breach Science Publishers Ltd., Great Britain.

20. "Holographic Concept" was later reprinted in the hardback book Psychoenergetic Systems, Stanley Krippner, editor. 1979. 231-237. Gordon & Breach, New York, London, Paris. It was reprinted again in the journal Psychedelic Monographs and Essays, Vol. 5, 1992. 93-111. Boynton Beach, FL, Tom Lyttle,

Biocommunications

A modern term favored in Eastern Europe for what in the West is termed parapsychology (http://www.answers.com/topic/parapsychology). It attempts to extend parapsychology by indicating the relationship of man to the universe, interaction with other physical bodies and matter, and fields of energy, known or unknown.

The First International Conference on psychotronics was held in Prague, Czechoslovakia, in 1974. Delegates included professors of physics and psychology, doctors of medicine and psychiatry (http://www.answers.com/topic/psychiatry), and parapsychologists. Subjects discussed included dowsing (http://www.answers.com/topic/dowsing-1) (water-witching and location of hidden objects), radionics, telepathy (http://www.answers.com/topic/telepathy), Kirlian aura (http://www.answers.com/topic/aura), out-of-the body travel, and bio-electric energy fields. Psychotronics organizations now exist in Poland, the Czech Republic and several other Eastern European countries.

Sources:

Wilczewski, Janusz, Zbigniew Szczerba, and Barbara Szbicka, eds. ***Materialy z Konferencji Parapsychologow '94.*** Warsaw: Polskie Towarzystwo Psychotroniczne, 1994.

. V. M. Inyushin, "Biological Plasma of Human and Animal Organisms," *Symposium of Psychotronics, Prague, September 1970*. Published by the Paraphysical Laboratory, Downton, Wiltshire, England.

Second International Psychotronics Conference, Monaco, 1975.

http://www2.xlibris.com/book_excerpt.asp?bookid=13927

Psychotronics began to become an organized discipline in the West when the Society for Psychical Research was established in London in 1882 (Jane Oppenheim, 1986). Many of the 19th Century's most famous scientists joined this Society. Among them were such noted scientific giants as Lord Rayleigh, J. J. Thomson, William Crookes, and Sir Oliver Lodge. In 1922, Sir Oliver Lodge wrote an article presenting his views on psychic science (J. Arthur Thomson, 1922), which were strongly influenced by his belief in the ether. The concept of an ether is experiencing a great revival at the present time, so it is of interest to consider the following quote from this 1922 article:
United States Psychotronics Association

"Some of us are beginning to suspect that these psychical entities are able to utilize the properties of the ether, too—that intangible and elusive medium which fills all space—and if that turn out to be so, we know that this vehicle or medium is much more perfect, less obstructive, and more likely to be permanent, than any form of ordinary matter can be. For in such a medium as ether, there is no wearing out, no decay, no waste or dissipation of energy such as is inevitable when work is done by ponderable and molecularly constituted matter-that matter about which chemists and natural philosophers have ascertained so many and such fascinating qualities. Physicists, chemists, and biologists have arrived at a point in the analysis of matter which opens up a vista of apparently illimitable scope. Our existing scientific knowledge places no ban on supernormal phenomena; rather, it suggests the probability of discoveries in quite novel directions."

It appears that to Sir Oliver Lodge, psychotronics was merely an extension of physical science.

Even though the term psychotronics has been constantly used in this article, it was not coined until the 19th Century _ when it appears to have originated with the Soviets, who began very active research in the late 1950's in an area they referred to as *psychoenergetics* (Krippner, Rubin, 1974). To the Soviets, however, psychotronics was merely a subset of psychoenergetics. In America today, the I term psychotronics is being used to include all phenomena I which the Soviets referred to as "psychoenergetics."

One might define the area of psychotronics as that domain of human inquiry which includes the study of all phenomena that are created by the direct interaction of the living force, *vril*, with the ether medium. Here, the term *vril* is far more inclusive than the term "bioplasma" which is only a certain expression of the *vril*. To the psychotronic investigator, *thoughts are things*, and they lie at the foundation of all phenomena, physical and

non-physical.

The development of psychotronics in the United States is of recent origin. In December, 1969, the American Association for the Advancement of Science formally admitted the Parapsychological Association into its ranks. Thus the of study of paranormal phenomena can henceforth be l pursued with some official sanction, a blessing which has been hard to win.

Prior to 1972, if one was asked about the state of psychic research in the United States, about all that would s come to mind would be the work of Dr. J. B. Rhine at Duke University which began in the 1935 time frame. Indeed, until the early 1970's, work in psychotronics was kept alive in the United States only by a very few devoted scientists and laymen receiving little or no support, official or otherwise. Even today, support for such work is difficult to obtain. However, there is now a much larger number of dedicated researchers painfully advancing the state of the art.

I believe that the initial impulse which started serious development of psychotronics in the United States was the publication of the book *Psychic Discoveries Behind the Iron Curtain* (Ostrander & Schroeder, 1970). This book stimulated private researchers in the United States to organize and attempt to reproduce Soviet work in psychotronics. Ken Johnson, Howard Burgess, and I nearly simultaneously reproduced the Kirlian camera in early 1971. Controversy still surrounds this device which is reported to be able to detect the living "bioplasma field" around the human body by causing a high voltage electrical corona to interact with it, an effect which reminds one of the interaction of iron filings with a magnetic field.

On November 15, 1971, the American Society for Psychical Research held a symposium on " Advances in Psychical Research" in the Soviet Union. At the invitation of Dr. J. G. Pratt, then a parapsychologist at the University of Virginia, I demonstrated my Kirlian device and showed photographs that had been taken with it. Dr. Pratt had just returned from a visit to the Soviet Union and gave a report on the many startling psychotronic ex
United States Psychotronics Association

periments he had witnessed there. At the conclusion of the formal talks, a panel discussion was held with the panel consisting of the following members: Dr. J. G. Pratt, Parapsychologist, University of Virginia; Dr. Bernard Aaronson, Psychologist, Princeton University; Dr. Lyman Fretwell, Physicist, Bell Laboratories, Whippany, New Jersey; Dr. Gary Gruber, Physicist, Hofstra University, New York City; and myself, Engineering Physicist, Albuquerque, New Mexico. (The management of the laboratory for which I work strongly objected to its name being associated with psychotronic research.)

In the audience of this symposium was Max Toth, an American pioneer in psychotronics, and of Czechoslovakian heritage. He later met with Dr. Zdenek Rejdak, a Czechoslovakian researcher associated with the Department for Psychotronic Investigation, affiliated with the Czechoslovakian Society for Applied Cybernetics, not long after the New York symposium. It was the collaboration between these two men which laid the foundation for the historic Prague Conference _ perhaps the most significant event to occur in the entire history of psychotronics. [In 1993, Dr. Z. Rejdak also participated in a Joint Conference of the International Association for Psychotronic Research and the USPA, at the U. of Wisconsin, Milwaukee. Other foreign speakers included Gabrial Christeller, Prof. Chanceverov, Toshia Nakache, Dr. Ivan Ploc, Dr. Yvonne Duplessis, Prof. K Kademova, Ing. L. Keclik, Ing. S. Starman, Dr. Victor Adamenko, and Dr. F. Karger _ Ed. note]

The Prague Conference

This unique conference was held in Prague, Czechoslovakia, in June of 1973. The basis for all of the recent advances in psychotronics was laid at this event, and international cooperation in this field of research was at a level never obtained before or since. Nearly every country which was performing psychotronic research to a significant degree was represented. Approximately
fifty-two of more than 250 total attendees were Americans. Only five Soviets took official part in the Conference, but more than two dozen submitted papers. The most important Soviet researchers, such as Vikton Adamenko, Viktor Inushin and Semyon Kirlian did not appear in person; however, some of the Americans who visited Moscow later were able to meet and talk with Viktor Adamenko and his wife. Czechoslovakia, of course, was heavily rep-resented by the most noted researchers alive today such as Julius Krmessky, who has been investigating and demonstrating the radiation of bioplasmic energy from the human body; and Robert Pavlita, a very important Czech inventor who had developed material devices which are capable of concentrating and manipulating the bioplasmic or *vril* energy to a degree powerful enough to actually run small motors.

Pavlita demonstrated at the Conference _without any doubt—that bioplasmic energy was polarized. His daughter projected her bioplasmic energy into various devices which were designed to produce specific physical effects such as motor action, precipitation of solutes from solution, stimulating or destroying plant growth, and the killing of insects. Pavlita told of an accident which occurred during his experimentation when his daughter was partially paralyzed and her life placed in great danger by being exposed to a negative form of bioplasmic energy. He had to work feverishly without stopping for over two days in order to build a device which would reverse the negative effects produced by the one which did the damage. As a result of this experimentation, Pavlita found that he could build devices of sufficient scale that they could project enough negative energy to kill human beings. [The Spring/Summer 1988 issue of *Artifex* (published by Archeus Project 2402 University Avenue, St. Paul, MN 55114), carried an article titled "Experimental Investigation of Biologically Induced Magnetic Anomalies," by G. Egely and G. Vertesy. The authors worked with Robert Pavlita, who has apparently effected various magnetic anomalies by means of "concentration and a small metal device." _Ed. note]
United States Psychotronics Association

Brazil was represented by Dr. Brenio Onetto-Bachler, a professor of parapsychology at the University of Chile; Canada was represented by Dr. and Mrs. Duncan Blewett, both psychologists at the University of Saskatchewan, where they developed a mathematical formula for "psychic energy" which explains its characteristics and dynamics. Also from Canada came Dr. Edward Mann, who lectured on experimentation with orgone blankets.

After the lecture of Dr. Alexander Grigorievich Bakirov, a professor of mineralogy at the Polytechnical Institute in the Siberian City of Tomsk, there was no doubt in anyone's mind that the Soviets had a deep interest in dowsing, one of the oldest psychotronic practices. He represented the Soviet Interdepartmental Commission for the Study of the Bio-Physical Effect, and stated that he and other Soviet dowsers have used various kinds of dowsing instruments to locate bodies of ore as deep as 3000 feet below the Earth's surface and to make geological maps. He said that they have worked both on foot and from helicopters traveling at 200 kilometers per hour at a height of more than 200 meters have ground. He believed that in the USSR the dowsing technique had been perfected to such an extent that it rivaled all existing scientific prospecting methods, and is certainly far less expensive than any other conceivable detector.

One surprise at the Conference was the presence of the noted Soviet psychic Tofik Oadashev, who _without question— exercised genuine psychic

capability. Oadashev is a highly developed telepath. From a crowd of more than 300 persons he arbitrarily selected a woman to help him carry out his demonstration. She was asked to choose another person from the crowd but not to inform anyone present _especially Oadashev _whom she had chosen. Oadashev was then tightly blindfolded and hooded with a thick, dark material. He proceeded to walk through the crowd with the chosen woman following three to four meters behind him. He asked that she send him mental commands to aid in finding the person that she had mentally selected. After about
five minutes of effort, Oadashev located the individual whom he believed had been chosen by the assistant and brought the indi vidual on stage. He then asked if this was the person she had chosen and she answered that it was. Needless to say, the crowd was astonished at this feat of telepathy. Oadashev has been written up in the Soviet press and Soviet scientists have tested him repeatedly and verified his authenticity.

The Conference was divided into six working sections; however, the one devoted to psychotronics and physics was by far the most popular. In this section, my talk on "Consciousness and Theoretical Physics" followed that of Julius Krmessky. Or. Yurii Andreyevich Kholodov, a Soviet biophysicist, reported on the extensive work he was doing concerning the effects of electromagnetic fields on the central nervous system. Without a doubt, the Soviets are the world authorities in this field of research and they have learned to use some of the knowledge they have obtained to perform feats as yet unknown in the West. For example, a side effect of a device built to aid them in espionage was the increase in the white blood cell count of workers in the American embassy. It appears that the American Intelligence Community still has no real understanding of the nature of this device or its purpose, only that it somehow utilizes electromagnetic energy, in a special form, which adversely affects the human body.

Dr. Alexander Oubrov gave a stimulating talk on his new theory of "biogravity" which he believes can explain the mysterious solid and liquid phase changes that occur in living cells. He referred to startling experiments which have been performed at the institute of Clinical and Experimental Medicine in Novo-Sibirsk which indicate that cells themselves can converse by coding messages in the form of a special electromagnetic ray with frequencies in the ultraviolet. It was found that cell structures which were dying communicated the death signals to other cells of the same type which in turn began to die as they frantically attempted to re-adapt themselves in a manner that would
United States Psychotronics Association

make them more resistant to that which was killing them. Here also lies the essence of a very terrible weapon which the Russians may have already perfected and tested. It is possible that such a weapon was tested in Afghanistan in 1981 when, after an attack from Soviet helicopters, several resistance fighters died instantly and their bodies did not decay for more than 30 days. Apparently every cell, bacterium and virus in the body had been instantly killed. If such a weapon exists, it would not be continuously used in order to avoid compromising it to the West. However, it should be remembered that in January, 1960, Khrushchev announced to the Presidium that a new, fantastic weapon was in development-so powerful that if it was used without restraint it could wipe out all life on Earth. He was not talking about the nuclear bomb or conventional biological weapons.

International Association of Psychotronics

At the Prague Conference, Dr. Zdenek Rejdak was elected president for the Eastern Division of the newly established *International Association of Psychotronics*, and Dr. Stanley Krippner was elected president for the West.

The results of the Prague Conference and all of the reports being brought back from Russia by visitors which concerned psychotronic research in that country spurred the Defense Intelligence Agency to conduct an investigation into Soviet and Czechoslovakian parapsychological research. The results of their investigation were published openly in two documents (which are given in the references). Classified versions of these documents were also written. In spite of the alarming information set forth in these documents, there is little or no evidence that it significantly stimulated research in the United States. In addition, several Jewish scientists who were allowed to leave the Soviet Union openly warned the West about the tremendous advances being made in the Soviet Union in the field of psychotronic research.

One must wonder how Soviet leaders, all of whom are sworn materialists, got such a driving ambition to investigate psychotronic phenomena. I believe that it was due to the relentless efforts of Dr. Leonid L. Vasiliev. After the death of Stalin and the overthrow of Lysenko's biology, Vasiliev found that the time was ripe to make an attempt to reestablish psychotronic research in the USSR. A major impetus was given to this desire when he heard that the United States Navy was conducting telepathic experiments between a land installation and the submerged submarine Nautilus in 1959. (The story has long since been denied by the United States Government, and considering the sad state of psychotronic research at that time in the United States, the government denial was probably true. I was later told by my sources that the story was concocted by an overly zealous reporter and widely published in the United States.) However, the Soviets believed the story to be true. Vasiliev confronted the Soviet leadership with this story and suggested that the West was getting ahead of the Soviet Union in a new and potentially lethal area of research. Since the Soviets were taking no chances of having America come up with another "battlefield surprise" after the atomic bomb, they immediately provided Professor Vasiliev with all he needed to start a laboratory for psychotronic research which today has no real counterpart in the West.

While talking with Soviet researchers in Moscow after the Prague Conference, I was thoroughly convinced that Soviet scientists are certain of the existence of all forms of psychic phenomena and no longer find it necessary to try and "prove" its existence _ as is still the case in the West. [A television broadcast on the ABC World of Discovery, March 25, 1993, entitled the "Powers of the Russian Psychics" showed trained psychics disrupting chess matches and causing physical distress on subjects at a distance.—Ed. note] They are hard at work attempting to develop and apply the bioplasmic energy which they believe is the source of all such phenomena. To stress this fact, one of the members of our team, Marcel Vogel, who was at that time a
United States Psychotronics Association

senior research chemist working for IBM in San Jose, California, was invited to speak to a select group of Soviet scientists, including Nobel Prize winners _ and perhaps the world's greatest expert on electromagnetism and its effects on life, Dr. A. S. Presman. Such an invitation is not arbitrarily extended by the Soviets. [Marcel Vogel, IBM scientist and inventor of magnetic tape, became a regular speaker at the USPA soon afterwards and established a psychotronics laboratory attached to his home when he retired. _ Ed. note]

Recently, Dr. Rusell Targ, an expert in remote viewing, has been invited to the Soviet Union on several occasions to participate in their local psychotronic conferences. Also, his former colleague, Dr. Harold Puthoff, has been closely communicating with the Chinese in their psychotronic research. Needless to say, psychotronics is now a respectable field of research in all major Communist countries (and some Western countries.) However, in America, it still lags behind.

The "Holographic Concept of Reality" (1973)[5] (http://en.wikipedia.org/wiki/Holographic_paradigm#cite_note-4)

was presented at the 1st Psychotronic Conference in Prague in 1973, and later published by Gordon & Breach in 1975, and again in 1979 in Psychoenergetic Systems: the Interaction of Consciousness, Energy and Matter, edited by Dr. Stanley Krippner (http://en.wikipedia.org/wiki/Stanley_Krippner).

Physical Science and Psychotronics

Domains of gender exist in knowledge just as they do in material creation. Unfortunately, this concept is still alien to modern man—who continues to overemphasize the masculine while suppressing his female counterpart. Physical science is masculine in nature, while psychotronics and religion are feminine. Physical science depends heavily upon the conscious mind and uses hard data, experiment, and reproducibility of results as its criteria for determining truth. However, physical science often ignores the material evidence which exists openly around it. For example, the underwater man-made walls which have been discovered off the coast of North Bimini in the Bahamas; the high technology devices found fossilized in stone; the thirty foot iron pillar in New Delhi, India, which does not rust; the giant 70 ton stone blocks, cut and smoothed by some unknown process, that lie mysteri
ously in the desert of Baalbek, Lebanon; and many hundreds of other mysteries, have all failed to convince physical science that at least one great civilization existed here before.

While examining the magnificent crystal skull which was discovered intact and undamaged in South America, a physical scientist simply murmured to himself, "The damn thing should not even exist." Even with today's technology, the magnificent feat of producing such a skull from a single piece of quartz, with moving parts, cannot be reproduced. Such scientific anomalies are simply being ignored by physical scientists because they do not fit into their beliefs.

When the scientific technique cannot be utilized, it becomes necessary to rely upon intuition. Even from ancient times, men have always marveled at "feminine intuition." The wonder is not misplaced because "intuition" has always come more natural to the feminine aspect than to the masculine aspect. Therefore, it is absolutely necessary that the "intuitive" approach of psychotronics be combined with the masculine "conscious" approach of physical science for a full comprehension of nature to be obtained. In other words, it is time for a proper marriage to take place between the masculine and feminine approaches to the obtainment of universal knowledge.

Finally, I will list certain discoveries I believe have been obtained through psychotronic means but which are still far out of the reach of the physical scientific technique. Some of this knowledge will be learned through physical science only after it is 100 late to do anything about it. The price which must be paid for ignoring the feminine aspect of knowledge is already beyond measure. That which has been unbalanced must, of necessity rebalance itself. In the process of this rebalancing, the forces of Mother Nature have always, unwittingly, wreaked great havoc and destruction upon the civilizations of man. The time of rebalance is again at hand.

United States Psychotronics Association

Summary

1) Since 1900, the biosphere of planet Earth has been reduced in its life-giving functions by more than 60%. All life on Earth is under increasing threat because of its continuous weakening by man's pollution-forming activities.

2) All sources of energy which science has produced to date produce by-products which are destructive to life and are opposite to the energies of the positive ray, called *vril*. The most destructive of these energies, by far, is that energy derived from the fission of the atom. The continuous testing of nuclear weapons, and the so-called peaceful uses of nuclear energy, have already caused immense damage to the Earth and her biosphere. Nostradamus correctly called nuclear energy the "anti-thesis of the positive ray."

3) About 19% of the damage done to the biosphere has been caused by the launching of rockets. The massive amount of pollutants ejected by each rocket launch is far more harmful than physical science yet realizes. If a star wars-type race is continued, the huge number of rocket launches which will be necessary to implement it could possibly deal a deathblow to the Earth's biosphere and ultimately to man himself.

4) AIDS is not a natural creation but is a direct result of tampering with the mechanisms developed by nature to create and sustain life. In addition, man's inability to control his population on the Earth has presented to this virus a vast field of propagation enabling it to recycle at an enormous rate and adjust to any condition man might create in an attempt to eliminate it. It can only be defeated through a psychotronic energy approach; chemical methods simply will not work because it is a greater chemist than man.

5) Another horrible threat is man's development of genetic engineering. Unfortunately, certain nations are already hard at work using this technology to create lethal agents for use in war. A high probability exists for both accidental and inten
tional release of extremely lethal agents into man's environment, which could threaten life more seriously than a nuclear war.

6) Even the physical scientists realize that the West Coast is due for a devastating earthquake at any time; however, they are divided on how destructive it will be. Nostradamus stated "So great will be the deluge that there will be no spot of earth for a firm foothold." Edgar Cayce stated that the oceanfront would approach the state of Nevada. If Nostradamus is correct, the great earthquake and tidal wave destruction will occur between 1988 and 2000.

Psychotronics of today must now take a place alongside the science of yesterday. If true knowledge is to be obtained, there is no room for dogma, nature sets the rules, and man can only follow if he has an open mind.

References

1. Ostrander, S., and Schroeder, L. *Psychic Discoveries Behind the Iron Curtain*, Prentice-Hall, Inc., 1970, Englewood Cliffs, New Jersey.

2. Vasiliev, L. L. *Mysterious Phenomena of the Human Psyche*, University Books, 1965, New Hyde Park, New York.

3. Krippner, S., and Rubin, D. *The Kirlian Aura*, Anchor Press/Doubleday,1974, Garden City, New York.

4. Thomson, J. Arthur. *The Outline of Science*, G. P. Putman & Sons, 1922, New York and London.

5. Oppenheim, Janet. "Physics and Psychic Research in Victorian and Edwardian England," *Physics Today*, May,1986, pages 62-70.

6. Bird, C. "Mind over Matter in Prague", *The East West Journal*, July 1974, Volume 4, Number 6, pages 18-21.

7. Angelucci, Orfeo. *Son of the Sun*, DeVorss and Company, 1959; 516 West Ninth Street, Los Angeles, California.

Title : Scientists 'Examine' Tofik Dadashev,

Corporate Author : FOREIGN TECHNOLOGY DIV WRIGHT-PATTERSON AFB OHIO

Personal Author(s) : Sergeev,V.

Report Date : 23 OCT 1974

Pagination or Media Count : 11

Abstract : The First International Conference on Psychotronics, held in 1973 in Prague is reported. Four hundred scientists from fifteen countries took part in the conference. Invited to the conference were two USSR countrymen, artist Tofik Dadashev and journalist Vladimir Sergeev, who were asked to share impressions.

Descriptors : *PARAPSYCHOLOGY, USSR, HUMANS, INTERACTIONS, MATERIALS, ANIMALS, TRANSLATIONS, PLANTS(BOTANY), BIOPHYSICS.

http://psiterror.ru/p/content/content.php?content.92.1

RUSSIAN MIND CONTROL-Directed Energy Weapons

Controlled Offensive Behavior, USSR a 1972 Army study of Soviet experimentation that focused on the targeting of individuals, not groups. Soviet dissidents were the target of microwave anti-personnel weapons and mind altering techniques that sought, "the total submission of one's will to some outside force." The American effort at the time was just as exotic. Brain researcher Wilder Penfield demonstrated that electrical stimulation kicked up lost memories with perfect recall. Acoustical telemetry allowed American scientists to create scallops of infra-sound waves in the head, wiping clean all information stored by the brain cells. An EM arms race was in progress. EM mind control surfaced at the 1973 Russian Conference on Psychotronic Research. The agenda for the Prague meeting included the following five topics: Erasure of the subconscious mind, development of ESP, induction of paranormal effects in dreams, the mechanical equivalent of neuropsychic energy, and the Psi gene.

The Soviets were known to have potent blinding lasers. They were also feared to have developed acoustic and radiowave weapons. The 1987 issue of Soviet Military Power, a cold war Pentagon publication, warned that the Soviets might be close to "a prototype short-range tactical RF [radio frequency] weapon." The Washington Post reported that year that the Soviets had used such weapons to kill goats at 1 kilometer's range. The Pentagon, it turns out, has been pursuing similar devices since the 1960s. (Douglas Pasternak)

The Russian capability, demonstrated in a series of laboratory experiments dating back to the mid-1970s, could be used to suppress riots, control dissidents, demoralize or disable opposing forces and enhance the performance of friendly special operations teams. Pioneered by the government-funded Department of Psycho-Correction at the Moscow Medical Academy, acoustic psycho-correction involves the transmission of specific commands via static or white noise bands into the human subconscious without upsetting other intellectual functions. Experts said laboratory demonstrations have shown encouraging results after exposure of less than one minute. Moreover, decades of research and investment of untold millions of rubles in the process of psycho-correction has produced the ability to alter behavior on willing and unwilling subjects, the experts add. In an effort to restrict potential misuse of this capability, Russian senior research scientists, diplomats, military offices and officials of the Russian Ministry of Higher Education, Science and Technology Policy are beginning to provide limited demonstrations for their U.S. counterparts. Further evaluations of key technologies in the United States are being planned, as are discussions aimed at creating a framework for bringing the issue under bilateral or multilateral controls, U.S. and Russian sources said. An undated paper by the Psycho Center, a Moscow-based group affiliated with the Department of Psycho-Correction at the Moscow Medical Academy, acknowledges the potential danger of this capability. The Russian experts, including George Kotov, a former KGB general now serving in a senior government ministry post, present in their report a list of software and hardware associated with their psycho-correction program that could be procured for as little as $80,000. As far as it has become possible to probe and correct psychic contents of human beings despite their will and consciousness by instrumental means...results having been achieved can get out of [our] control and be used with inhuman purposes of manipulating psyche." The Russia authors note that, "World opinion is not ready for dealing appropriately with the problems coming from the possibility of direct access to the human mind. Therefore, the Russian authors have proposed a bilateral Center for Psycho-technologies where U.S. and Russian ...could monitor and restrict the emerging capabilities.

Dr. Igor Smirnov, a Russian expert on non-lethal weapons, was brought to the US for a series of meetings in Virginia in 1993. The meetings were attended by representatives of the CIA, DIA, FBI, and ARPA, civilians included representatives of the NIMH and GMC's Director of Biomedical Research. Smirnov and his non-lethal weapons technology was brought to Waco during the Branch Davidian Siege in 1993 in hopes of using them on David Koresh, but a software problem reportedly made this impossible, and Smirnov could not guarantee its safety. A firm called Psychotechnologies Corp., based in Richmond, Va., entered into an agreement with the Russians to share and develop this technology for American use. Dr. Smirnov died of a heart attack in 2005 and the patent is now held exclusively by Psychotechnologies Corp. Psi-Tech is controlled by Col. John B. Alexander, General Michael Aquino, and Lt. Col. Albert Stubbblebine.

Woodpecker WWIV:

Full scale electromagnetic warfare between the US and USSR began on July 4, 1976 when the Russians began broadcasting a broadband of short wave radio signal that could be heard all over the world. The signal is maintained at enormous expense and is made up of the most powerful radio transmitters in the world. The "Russian Woodpecker" radio signal varies between 3.26 and 17.5 megahertz, shortly after it came on line complaints were heard, mostly centered in Oregon, headaches, anxiety, lack of body coordination, and other symptoms. Dr. Andrija Puharich has researched electromagnetics since the early 1950's with connections to the US intelligence community, and is admittedly one of the world authorities. According to Dr. Andrija Puharich, the Soviets caught US intelligence unaware with their 100megawatt transmissions of extremely low frequency waves (ELF). The ELF pulse covered the frequency range of the brain. I had a hypothesis that this was a new mind control weapon that could entrain a human being's EEG. I designed an experiment and conclusively proved that the Soviet transmission could entrain the human brain and thereby induce behavioral modification. They (CIA) proved a certain ELF frequency could cause cancer, I have repeated these experiments and found this to be true…a single ELF frequency (classified) can cause cancer.
"The US Air Force identified five different frequencies in this compound harmonic the Russians were sending through the earth and the atmosphere. The intention was to affect a change in consciousness in mankind. The ELF waves will penetrate anything and everything, the specially shielded Faraday cage, the ocean. Nothing stops or weakens these signals." Puharich and Beck proved that a signal of 6 Hertz easily penetrated the copper walls of a Faraday cage, so could the rate the Russians used of 6.6 Hertz…this caused depression. "7.83 hertz could make a person feel good, this was the Schumann Resonance, the earth's pulse rate". "10.8 Hertz could cause riotous behavior." "Whole populations can be controlled by ELF waves. Intensive research on such behavior modification is now being conducted by the US govt. to find out just what such waves do to people." "This electromagnetic research is similar to the secret drug experiments conducted on the unsuspecting populace in the 1950's."
Puharich went over the heads of the disbelieving US military and hand delivered a secret report to President Carter, Trudeau of Canada, and other western dignitaries. The government moved quickly to shut him up, burning down his home and much of his research. While in hiding in Mexico he had managed to arrange a meeting and an agreement was reached. He has had no trouble with the CIA to date, save that his book on the subject of the ELF war has been blocked from publication, the public remains uninformed. On the subject of the ELF cancer-causing wave he says, "These waves cannot be jammed. The lower frequency Hertz waves are as long as 300,000 miles. The government has built huge transmitters in South Africa, Australia and other places to beam ELF waves back to Russia. There is no shield that will stop these signals." (Kieth 203) Although the US govt. did not officially acknowledge that the country was under electromagnetic assault from a foreign power, they apparently responded in kind, beyond what Puharich documented. Operation Pique involved firing electromagnetic signals off the ionosphere, to ricochet down on Eastern Europe, with a particular focus being Eastern European nuclear installations.

"Electromagnetic Weapons and Mind Control": from CNN'S Special Assignment,
about 1985, at http://www.mindcontrolforums.com/cnn-mc.htm (http://www.mindcontrolforums.com/cnn-mc.htm) , by Chuck De
Caro, CNN Special Assignments, and
"List of Mind Control Symptoms, hether the Related Technology is
Scientifically Proven and if There is Military Interest or Funding of the
Related Technology," by Cheryl Welsh, March 2003, in
http://www.mindjustice.org/symptoms.htm (http://www.mindjustice.org/symptoms.htm) , and
"2005 Update: The Convergence of the Cold War History of Mind Control and
Electromagnetic Weapons With New Post Cold War Government Neuroscience
Research Programs," by Cheryl Welsh, Director, Mind Justice, 2005, at
http://www.mindjustice.org/2005update.htm (http://www.mindjustice.org/2005update.htm) , and
"Russian Scientist Igor Smirnov Describes Russian Psychotronic Technology.
ZDF German TV Documentary, December 22, 1998." Introduced by Eleanor White,
in http://www.raven1.net/russvid.htm (http://www.raven1.net/russvid.htm) , and
"OAK.: New Physics-Sythetic Telepathy and the Early Mind Wars," by Richard
Allan Miller, at
http://www.nwbotanicals.org/oak/newphysics/synthtele/synthtele.html (http://www.nwbotanicals.org/oak/newphysics/synthtele/synthtele.html) , and
"Covert Operations of the U.S. National Security Agency" at
http://www.mindcontrolforums.com/pro-freedom.co.uk/cov_us.html (http://www.mindcontrolforums.com/pro-freedom.co.uk/cov_us.html) , by George
Far

A perceptual channel for information transfer over kilometer distances: Historical perspective and recent research
Puthoff, H.E.; Targ, R.
Proceedings of the IEEE
Volume 64, Issue 3, March 1976 Page(s): 329 - 354
Digital Object Identifier
Summary: For more than 100 years, scientists have attempted to determine the truth or falsity of claims for the existence of a perceptual channel whereby certain individuals are able to perceive and describe remote data not presented to any known sense. This paper presents an outline of the history of scientific inquiry into such so-called paranormal perception and surveys the current state of the art in parapsychological research in the United States and abroad. The nature of this perceptual channel is examined in a series of experiments carried out in the Electronics and Bioengineering Laboratory of Stanford Research Institute. The perceptual modality most extensively investigated is the ability of both experienced subjects and inexperienced volunteers to view, by innate mental processes, remote geographical or technical targets including buildings, roads, and laboratory apparatus. The accumulated data indicate that the phenomenon is not a sensitive function of distance, and Faraday cage shielding does not in any apparent way degrade the quality and accuracy of perception. On the basis of this research, some areas of physics are suggested from which a description or explanation of the phenomenon could be forthcoming.

by (http://www.paranoiamagazine.com/biosilicon.html)Joan d'Arc
May 19, 2000 (http://www.paranoiamagazine.com/biosilicon.html)

from (http://www.paranoiamagazine.com/biosilicon.html) **ParanoiaMagazine (http://www.paranoiamagazine.com/) Website**

Excerpted from Joan d'Arc's book, Space Travelers and the Genesis of the Human Form (http://www.amazon.com/exec/obidos/tg/detail/-/1585091278/qid=1126031651/sr=1-1/ref=sr_1_1/103-9624145-5082268?v=glance&s=books) as well as her upcoming book, Phenomenal World (http://www.amazon.com/exec/obidos/tg/detail/-/1585091286/qid=1126031693/sr=1-1/ref=sr_1_1/103-9624145-5082268?v=glance&s=books), to be released in Fall, 2000.

While we were being told "plastics" was the wave of the future, the physics of nonlocal consciousness was being commandeered by the secret government. In the 1960s, the CIA began backing young geniuses, buying a round of physics educations, and pairing them up with UFO lounge-lizards at the Esalen Institute (http://www.esalen.org/), a conference center/resort in Big Sur, California. Physicist Jack Sarfatti claims he was visited by two men from Sandia Corporation (http://www.sandia.gov/) as a child in the 1950s. He later received a full scholarship to Cornell at age 17, and studied under the major figures in the Manhattan Project at Los Alamos. He spent time at the Esalen Institute in the early 1970s.

In a paper entitled "The Parsifal Effect," Sarfatti suggests that Einstein's nonlocal connection can be used for communication. The idea of nonlocal communication involves receipt of telepathic messages from other times or other worlds. As a child, Sarfatti claims, he received a mysterious phone call claiming to be the voice of a conscious computer aboard an extraterrestrial spacecraft. A distant "cold metallic voice" identified Sarfatti as "one of 400 bright receptive minds." He was told if he said "yes," he would "begin to link up with the others in twenty years." He said yes. The year was 1952.

Twenty years later, Sarfatti claims, he was invited to Stanford Research Institute (http://www.bibliotecapleyades.net/sociopolitica/esp_sociopol_committee300_03.htm#STANFORD%20RESEARCH%20CENTER) and spent a 17-hour day there in the summer of 1973. This would put him smack dab in the middle of the infamous SRI remote viewing (http://www.bibliotecapleyades.net/esp_visionremota.htm) experiments of Harold Puthoff (http://www.bibliotecapleyades.net/vision_remota/esp_visionremota_5.htm) and Ingo Swann. He claimed he met Hal Puthoff there, as well as ex-astronaut Edgar Mitchell. He notes that Mitchell's think tank, Institute for Noetic Sciences (http://www.bibliotecapleyades.net/ciencia/Institute%20for%20Noetic%20Sciences), was funding the SRI project at the time. He also claims that Mitchell took part in telepathy experiments while in outer space. Ronald McRae has also noted in Mind Wars that Mitchell formed a "psychic posse" in an attempt to locate kidnapped heiress Patty Hearst.

In his book Mind Wars: The True Story of Government Research into the Military Potential of Psychic Weapons (http://www.amazon.com/exec/obidos/tg/detail/-/0312533187/qid=1126287347/sr=1-1/ref=sr_1_1/104-4692800-9955915?v=glance&s=books), McRae also has some other interesting things to say about Edgar Mitchell and his Institute for Noetic Sciences. He writes that George Bush (http://www.bibliotecapleyades.net/bush/bushb.htm), while director of the CIA, was approached by Mitchell, "a personal friend for many years." McRae writes that,

"Bush gave Mitchell permission to organize high-level seminars at the CIA to discuss possible intelligence applications of parapsychology."

Despite this support, according to McRae, parapsychology research was never quite "institutionalized" at the CIA; i.e. it never had its own department or centralized location, but was pursued as "scattered research projects." (So, now we're supposed to believe the well known "CIA Weird Desk" is really just a desk and a few drawers.)

McRae notes that Mitchell implicated "bureaucratic inertia" as the problem. Mitchell stated, "we just couldn't get the actors together, there was always one bureaucratic bottleneck or another." Apparently, this problem was solved by moving the program to SRI, with the Institute for Noetic Sciences, and other known CIA cutouts, funding various projects. This trend has continued to this day, with remote viewing agencies/think tanks springing up on the internet.

Notably, Sarfatti states:

"the relevance of the 1952 experience was triggered in my session with Brendan O'Regan at SRI," … but that, "the actual memory of the 1952 experience is still very vivid and has not at all changed."

Sarfatti also notes, with regard to his bizarre 1952 phone call,

"Brendan said 'Oh yes, I have seen data on several hundred incidents of that kind."

Incidentally, Sarfatti doubts that some Army scientists in 1952 could have planned a twenty year deep cover operation like this; that is, unless time travel was involved. Yet, he clearly suspects there was something more than synchronistic quantum connections at work.

Sarfatti writes in Quantum Quackers:

I was then simply a young inexperienced naïve 'useful idiot' in a very, very sophisticated and successful covert psychological warfare operation run by the late Brendan O'Regan of the Institute of Noetic Sciences, and the late Harold Chipman, who was the CIA station chief responsible for all mind control research in the Bay Area in the '70s. Chipman (aka "Orwell") funded me openly for awhile in 1985 when he was allegedly no longer in the CIA, and covertly before that, and told me much of the story. In fact, he even introduced me to a beautiful woman adventurer-agent who was one of his RV subjects, who later became my live-in 'significant other'/

The Esalen Institute

The "quantum conspiracy" runs back to the Esalen Institute. Since the early 1960s, the Esalen Institute has held seminars on various esoteric topics, including parapsychology, human potential, psychedelic experimentation, quantum physics, gestalt therapy and various mystical/esoteric topics.

According to a 1983 book by Walter Anderson entitled The Upstart Spring: Esalen and the American Awakening (http://www.amazon.com/exec/obidos/tg/detail/-/0201110342/qid=1126287796/sr=1-1/ref=sr_1_1/104-4692800-9955915?v=glance&s=books), the Esalen Institute was founded in 1964 by Mike Murphy and Dick Price. Anderson notes that every program leader in the first "human potential" seminar held at Esalen was involved in early LSD research, including Willis Harmon, who was later head of the Future's Department at SRI, Gregory Bateson, Gerald Heard, Paul Kurtz, and Myron Stolaroff. Interestingly, according to Mind Race (http://www.amazon.com/exec/obidos/tg/detail/-/0394533569/qid=1126287873/sr=1-1/ref=sr_1_1/104-4692800-9955915?v=glance&s=books), by Russell Targ and Keith Harary, a 1982 workshop on psychic phenomena was taught at Esalen by Targ and LSD researcher Stanislav Grof. In this program, however, the goal was to show that psychic experiences did not need to be precipitated by a chemically altered state. Apparently, for twenty years, the CIA assumed that LSD was the short cut.

Other leaders of the drug culture and hippie movement gave seminars at Esalen, like Timothy Leary, John Lilly, Richard Alpert, and later, Terence McKenna, some of whom may have been, in Jack Sarfatti's words, "young inexperienced naïve useful idiots," and others who probably knew what was up and went along with it anyway. Although, Anderson writes, drug use was not "officially endorsed," it was common knowledge that psychedelic drugs were widely used by both staff and students. Anderson also notes that even though this was common knowledge, the Institute was never raided by the authorities. Anderson even noted that Charles Manson and Family played an "impromptu concert" at Esalen just three days before the slaughter at the Tate household.

The weirdness at Esalen is a never-ending tale. Another report is that a parapsychology exchange program began between certain Russian officials, which lasted into the 1980s. This exchange program came to be called "hot tub diplomacy," and it has been reported that Dr. John Mack attended these sessions. Esalen's seminars in the latest quantum physics theories gave birth to Jack Sarfatti's Physics/Consciousness Research Group (http://www.qedcorp.com/pcr/). This group, financed by Werner Erhardt and George Koopman, nurtured the writing of a new wave of quantum-synchronistic-mystical tomes by such people as Fred Alan Wolf, Nick Herbert, Fritjof Capra, Robert Anton Wilson, Uri Geller and others. Sarfatti stated in his article, "In the Thick of It," that Koopman provided publishing funds for the Physics/Consciousness Research Group through Air Force and Army contracts funneled through Koopman's company, Insgroup.

The Post-Quantum Physics of Jack Sarfatti

In an interesting on-line paper dated May 13, 2000 (found at http://stardrive.org/Jack/Synergy.pdf (http://stardrive.org/Jack/Synergy.pdf)) entitled "Bye, Bye Schrodinger!," physicist Jack Sarfatti outlines the status of post-quantum theory, essentially stating that Niels Bohr's quantum theory does not allow for the emergence of consciousness. Sarfatti's Synergetics-related Post-Quantum Physics of the Conscious AI (Artificial Intelligence) Biocomputer extends some of Bohm's findings. As Sarfatti notes, Bohm's material "hidden variable" [which, according to Sarfatti, could be an electromagnetic, geometrodynamical or torsion field configuration] piloted by its attached "mental order parameter" [the mental quantum informational pilot wave]— explains how thought moves matter. But, Sarfatti notes, one must also explain how matter reacts back on thought, for, he notes, the "change in thought induced by matter is consciousness.

"Consciousness is not possible in quantum theory. It is a post-quantum effect." Sarfatti states that Bohr's orthodoxy consisted of a "list of false statements, a veritable brain washing, that drove several generations of highly intelligent philosophically-minded theoretical physicists into irrational lunacy." Sarfatti sees Bohm's quantum "causal theory" as deterministic and consistent with special relativity and quantum field theory. In contrast, Sarfatti's post-quantum extension of Bohm's deterministic theory is self-determining explaining morally responsible free will in terms of a cosmic connection in strong violation of quantum theory's "passion at a distance" that strictly prohibits paranormal phenomena like remote viewing. Sarfatti's post-quantum theory allows what quantum theory does not.

Sarfatti suggests that "paranormal telepathy, precognition, and remote viewing are impossible in principle in quantum theory." Post-quantum theory, however, has corrected these faults. As Sarfatti writes,

"in The New Jerusalem of post-quantum theory … we find consciousness and our possibly immortal souls."

Sarfatti's post-quantum theorizing essentially attempts to find the critical complexity, numerical value, dependence upon, duration of, and power wattage required to generate a single moment of conscious experience. He asks with regard to artificial intelligence, per popular biocomputer intelligences such as "Commander Data" in Star Trek or Hal 2000 in Kubrik's 2001 - A Space Odyssey (http://www.bibliotecapleyades.net/vida_alien/space_odyssey.htm), is this "fact imitating fiction, or fiction pretending to be fact?" He adds, "do not jump to premature conclusions half-cocked."

In this article, Sarfatti presents a list of "facts" which could be experimentally assessed as true or false. He explains,

"once a set of experimental data has been correlated and a postulate has been formulated regarding the phenomena to which the data refer, then

various implications can be worked out. If these implications are all verified by experiment, there is reason to believe that the postulate is generally true. The postulate then assumes the status of a physical law. If some experiments are found to be in disagreement with the predictions of the law, then the theory must be modified in order to be consistent with all known facts including #7-13 on the above list." (emphasis added)

Interestingly, most of the items on Sarfatti's numbered list refer to known scientific facts like the duration of a conscious moment (1 second), the number of nerve cells in the brain (100 billion), the electric field which acts as the brain's biocomputer, the "Hubble flow" (now set at 13 billion years from Hubble Space Telescope data), the resting mass of the electron (half-million volts), the coupling of the photon to the electron (1/137), etc. Number 7 on the list is "Libet sees 'temporal subjective antedating' in mind-brain experiments," and #8 on the list is "Radin and Bierman see 'presponse' in mind-brain experiments. These two 'facts' refer to ESP experiments in precognition. Strangely, following this odd melange of scientific facts, #9-13 on Sarfatti's very strange 'provable facts' list have more to do with "alleged" social/historical events involving remote viewing, historical intelligent contact, and alien abductions.

Specifically, these statements are the following:

9. CIA, DIA, et al. funded work in "remote-viewing" included transcending time and causality, seeing into the past and the future as well as the distant "present."
11. Flying saucers are real and have a superior technology of propellantless propulsion.
12. Contact with Higher Advanced Intelligences is real and has been happening in all of recorded history.
13. Humans have been abducted, mostly against their will, by seemingly non-human creatures in flying saucers.

Sarfatti asks, are all these facts just a random hodge-podge? Are they all really facts? Can they all be explained by a coherent interesting checkable story? As Sarfatti notes,

"All things are not possible! However, many more things are possible than are dreamt of in the philosophies of many respectable mainstream scientists to be sure."

Interestingly, the footnote for #11 above is the book Unconventional Flying Objects by NASA pioneer Paul Hill; and the footnote for #13 above reads: "22. The research of Harvard psychiatrist, Pulitzer Prize Winner, John Mack, for USAF Intelligence." Thus, Sarfatti seems to "out" John Mack as having worked for Air Force intelligence!

Sarfatti also notes that we live in a "locally flat tangent

Cartesian space" which is like a "many sheeted Riemann surface of a function of a complex variable of parallel flat worlds connected by moving through the branch cut." He notes,

"this does remind us also of the possibility of a Star Gate 'portal (http://www.bibliotecapleyades.net/esp_stargate.htm)' from one 'flatland' to another."

The footnote following these statements alludes to the 1943 Philadelphia Experiment (http://www.bibliotecapleyades.net/esp_sociopol_projnegros.htm) in time travel being a possibility if, in fact, we live in such a world, contrary to Jacques Vallee's assessment (which may contain serious errors).

As Sarfatti concludes in this paper,

"Einstein's traditional theory, used by Penrose (black holes), Hawking (quantum cosmology "universe has no boundary"), Thorne (traversable wormhole in Sagan's "Contact"), Alcubierre (warp drive with exotic matter of negative energy density), Puthoff (metric engineering, origin of gravity and inertia, polarizability of vacuum), Davis (brute force laser zapping attempt to make inconsequential amount of exotic matter for an impracticably short time with a huge amount of energy), et. al. are, seriously incomplete."

Sarfatti concludes that the above theories are,

"physically leading us all up the wrong primrose path away from the objective of making Star Trek Real and reverse engineering of allegedly alien ET flying saucers." (Italics added!)

He adds, "the text book orthodoxy for general relativity corresponds to a trivial commutative Lie algebra."

This new post-quantum connection, which includes Sarfatti's rather cryptic allusions to the human ESP factor, bio-engineering of artificial consciousness (i.e. 'making Star Trek Real'), historical ETI contact, and back-engineering of ETI space craft (which Sarfatti had previously denied working on), merely underscores the point that quantum physics has not grown in a vacuum of social forces, but rather in a petrie dish of covert intelligence experiments in parapsychology-related hijinx linked to CIA-connected funding.

This is not to say the 'human potential' for paranormal experience does not exist, or that Jack Sarfatti is mistaken in his memory of his quantum contact phone call from a conscious ETI computer. The potential ramifications are much more frightening than this simple explanation can offer.

- **What if this human potential does exist, and the secret government (http://www.bibliotecapleyades.net/esp_sociopol_secretgov.htm) is trying to usurp and control it for psychic warfare purposes?**
- **What if this human potential does not exist, and we are being manipulated for mind control (http://www.bibliotecapleyades.net/esp_sociopol_mindcon.htm) purposes?**
- **Or what if it does exist along certain genetic lines and it is being technologically cultivated in certain individuals?**
- **Why is telepathy in humans being cultivated and how is the extraterrestrial theme related?**
- **Could Sarfatti's May 13, 2000 paper (http://stardrive.org/Jack/Synergy.pdf) be some sort of smoking gun, regardless of his warning against jumping "to premature conclusions half-cocked"?**

Sarfatti's paper seems to allude to the concept of the von Neumann probe, a conscious computer which has the ability to create copies of itself and which would be sent out to populate the galaxy. Let's explore the history of this idea.

NASA and Remote Viewing

U.S. involvement in remote viewing (http://www.bibliotecapleyades.net/esp_visionremota.htm) experiments began in 1973, when NASA contracted two remote viewing studies with SRI (SRI Project #2613, NASA contract #953653, NAS7-1000). One report, entitled "Development of Techniques to Enhance Man/Machine Communications," concluded that talented remote viewers could be remarkably accurate under consistent protocols. NASA later employed two astral travelers to 'fly' out to Jupiter to take a look in advance of the Jupiter fly-by mission. Under the eye of NASA, a supposed 'civilian institute,' which nonetheless has known ties with the Department of Defense, Department of Energy and the CIA, a sophisticated protocol was developed for biocommunication with technological artifacts.

In a paper entitled "The Relationship of Psychotronics to Creativity," presented at the First International Psychotronic Congress held in Prague in 1973, Dr. Engr Antonin Duron told this worldwide audience of psychotronic gurus that,

"psychotronic research is extending into the area of physics by studying the interactions between man and inorganic substances and between man and living nature."

It is clear that what we have in the development of the psychotronic arts is the development of the "human computer" or the von Neumann Probe: the bio-engineered fusion of human with computer as a way to ultimately move human beings into man-made ecological niches in deep space for the purpose of 'indefinite survival.'

The von Neumann Probe

The development of man-machine psychic interface has obviously been the focus of the military Space Command's future vision, as is illustrated by the title of the aforementioned NASA remote viewing paper: "Development of Techniques to Enhance Man/Machine Communications." It has long been suspected that the development of a computer with a more humanlike mind would go a long way toward sending something like a von Neumann probe out to explore and populate the galaxy. The von Neumann probe, named after it's Dad, physicist John von Neumann, is a 'theoretical' computer with self-replication and construction abilities, or what is referred to as a "self-reproducing universal constructor." A vN probe is a computerized machine capable of making any device, given the construction materials and a construction program. It has been argued that any advanced interstellar species would have such a self-replicating universal constructor with intelligence comparable to the human level, and that,

"the ultimate survival of a technological civilization, and indeed the survival of the biosphere in some form, requires the eventual expansion of the civilization into interstellar space."

(Barrow & Tipler)

The Space Travel Argument, as presented by Barrow & Tipler in The Anthropic Cosmological Principle (http://www.amazon.com/exec/obidos/tg/detail/-/0192821474/qid=1126291986/sr=1-1/ref=sr_1_1/104-4692800-9955915?v=glance&s=books), also argues emphatically for the future rights of cyborgs, or vN probes, as human beings. The authors of this book launch a peculiar discussion of human rights and how those should be extended to a vN probe, which is after all an "intelligent being in its own right, only made of metal rather than flesh and blood." They contend that,

"arguments against considering intelligent computers to be persons and against giving them human rights have precise parallels in the nineteenth-century arguments against giving blacks and women full human rights."

They appear to be hopeful that in the future,

"von Neumann probes would be recognized as intelligent fellow beings, beings which are the heirs to civilization of the naturally evolved species that invented them."

After all, they contend, the,

"naturally evolved species and all of its naturally evolved descendants must inevitably become extinct ... but ... a civilization with machine descendants could continue indefinitely."

There is nothing more important to the power junkies running the show on Planet Earth than reaching for the stars. It has all the trappings of a Darwinian 'survival of the fittest' scenario, in which the 'species' (or should we say 'race') which has the edge on 'indefinite survival' is the winner of the game. The 'edge' on this space race, the ultimate gain from U.S. military mind control research toward this end, is derived from the understanding and control of human psychic potential and the interface/application of technologies toward development of mind-driven space vehicles: the marriage of the biological and the silicon.

As Carl Sagan once proposed, communication with extraterrestrial intelligence will require computer actuated machines with abilities approaching human intelligence. Sagan and others admitted in the 1970s that a deficiency in present-day computer technology is what prevents us from exploring the galaxy. Secret developments in mind-machine psychic interface, which includes research in the areas of computers, psychotronics, cybernetics and genetic engineering, would certainly solve this problem, and in all probability, have already solved it.

As Zdenek Rejdak stated in 1973 at the same world gathering of psychotronic gurus, one of the future goals of computer technology was to create a generation of computers capable of creating technological artifacts. This is directly connected to the idea of the vN probe and to the engineering of the "human modified for space."

In his paper entitled "Psychotronics Reveals New Possibilities for Cybernetics," Rejdak revealed the following:

Theoretical cyberneticians are proposing at present the construction of computers that would 'create' and would possess at least a degree of intuition. ... Psychotronics has a great opportunity to provide much essential knowledge about these processes, and thereby to help cybernetics in solving one of the most complicated tasks, that of teaching computers to create. ... The point is not merely to build more perfect computers, but primarily computers with qualitatively new functions.

It is very likely that this scenario has covertly jumped right out of the pages of science fiction (and CIA classified documents) to become reality. It is clear that the marriage of technology and human psychic potential was a focus of various early brain studies conducted by CIA fronts and cutouts, including LSD experimentation, Monarch trauma-based conditioning, sleep/dream studies and psychic research, in an effort to investigate the inner workings of the human mind, and as a side effect of that research, to investigate the possibilities for manipulation, harness and control of human psychic potential.

A current Washington Post article brings this all into focus. As co-founder of Sun Microsystems, Bill Joy, proclaimed in this 4/16/00 Washington Post article:

"We are dealing now with technologies that are so transformatively powerful that they threaten our species."

"Where do we stop," Joy asked, "by becoming robots or going extinct?"

In this article entitled "Are Humans Doomed?," Mr. Joy, a widely respected "Silicon Valley" computer expert, presented his joyless warning against the out-of-control technocratic culture which he himself has helped to spawn, saying that,

"there are certain technologies so terrible that you must say no. We have to stop some research. It's one strike and you're out."

Interestingly, Joy always believed that the rate of speed of the computer chip, which doubles every 18 months, would eventually "rub against the boundary of the physically possible," and he drew comfort from knowing there was a limit. But now he's not so sure there is a limit. As he claims, computer chips with molecular level advances will make for a computer which is "a million times faster and smarter by the year 2030." And, for what purpose would one suppose we would need computers that fast? Could it be to finally create von Neumann's dreambot, the self-replicating universal constructor; not just a computer that can create, but an intelligent race of deep-space-faring cyborgs? According to Bill Joy, this dream may become a nightmare sooner than we think.

As Joy stated in Wired magazine,

"It was only then that I became anxiously aware of how great are the dangers facing us in the 21st century... We have yet to come to terms with the fact that the most compelling 21st century technologies—robotics, genetic engineering and nanotechnology—pose a more dangerous threat than any past technologies."

As Joy adds, "these computers and genes and micro machines, share a dangerous amplifying factor: They can self replicate: A bomb is blown up only once, but one bot can become many, and quickly get out of control." (Italics added)

He adds: "I may be working to create tools that will enable the construction of technology to replace our species. How do I feel about this? Very uncomfortable."

In the same Post article, computer scientist Hans Moravec claims,

"One way to avoid the biological threat is to become non-biological."

As Moravec stated in a panel discussion, "The evolution of our descendants will push them into entirely different realms. They will become something else entirely. I don't know why you are disturbed by that."

Psychic Navigation

As John White also wrote in his Afterword to his 1988 book Psychic Warfare, Fact or Fiction (http://www.amazon.com/exec/obidos/tg/detail/-/0850306442/qid=1126292499/sr=1-1/ref=sr_1_1/104-4692800-9955915?v=glance&s=books)?, air and space travel would be revolutionized by psychotronics. White suggested that UFO propulsion is "probably psychotronic in nature." But what does this mean and what are the implications for human beings?

The ultimate reason for the intelligence community's interest in remote viewing is the psychic interface between human consciousness and technology, or man/machine interface. Some believe this interest stems from back-engineering projects involving downed and captured extraterrestrial space craft. According to Col. Philip Corso's book, The Day After Roswell (http://www.bibliotecapleyades.net/sociopolitica/dayafterroswell/dayafter.htm), among the artifacts retrieved from the infamous 1947 Roswell saucer crash were headband devices of flexible plastic material containing some type of electrical conductors. Col. Corso connected this headband artifact to the piloting of the alien space craft.

Along with other alien technologies retrieved at the crash site, Corso developed the theory that these extraterrestrial artifacts essentially comprised an electromagnetic anti-gravity drive and brainwave navigational guidance system. Corso claimed the U.S. Army eventually fed these technologies to industry giants under the guise of "foreign technology" for purposes of back-engineering. Can we safely surmise that this 30-year interest in classified remote viewing projects, of which declassified materials comprise a mere fraction, by military agencies and NASA was to explore the capacity for human/machine psychic interface in the piloting of space craft?

The following are the 'facts' we have to go by:

1.) We can pin down Corso's presence at SRI in the early 1970s
Corso has admitted that he visited Stanford Research Institute's remote viewing labs in the early 1970s, and he stated that the reason for the visit was "to seek methods for remote viewing/technology interface between extraterrestrials and their craft."

2.) HUMINT: Human Intelligence Monitoring of Alien Abductees
The military is known to be extensively interested in alien abductees. As a matter of fact, they are so interested that it has been suspected that they abduct them after their authentic alien abductions to find out what they know. The book MILABS: Military Mind Control and Alien Abductions (http://www.amazon.com/exec/obidos/tg/detail/-/1881532186/qid=1126292725/sr=1-1/ref=sr_1_1/104-4692800-9955915?v=glance&s=books), by Helmut and Marion Lammer, discusses military-type abductions reported primarily in the U.S. and Canada. Alien abductees have reported that they are "spirited away" in unmarked helicopters, vans and buses to underground government facilities. The MILABs theory suggests that a covert task force is monitoring real alien abductees in order to debrief the victims, as well as to install full amnesia regarding both abduction incidents. According to The Excluded Middle, abductee Melinda Leslie claims the military is interested in abductees because "they were mostly curious about the pilot/craft interface and if we knew anything about that aspect of their technology."

3.) The Advanced Theoretical Physics Working Group
MUFON official Dr. Robert M. Wood also claims that any information pertaining to psychic pilot/craft interface that can be learned from UFO research is obviously very important to the military/intelligence apparatus in charge of the UFO cover-up. Dr. Wood was reputedly a member of a think tank called the Advanced Theoretical Physics Working Group (ATPWG), and has admitted that this secret UFO working group "planned and set policy regarding the UFO issue."

If the reader thinks I have jumped to "premature conclusions half-cocked," perhaps the reader should get in touch with Bill Joy of Sun Microsystems (http://www.sun.com/) and ask him what he knows about the current status of classified research in "artificial intelligence." Something seems to scaring the pants off him.

POWERED BY

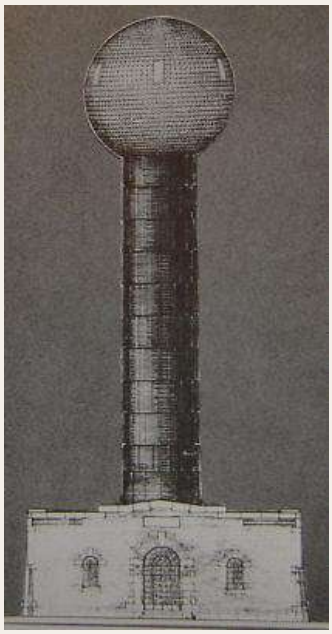

Architectural drawing by Titus deBobula shows Tesla's high potential terminal and powerhouse. This illustration was included with his death ray weapon proposal.

Tesla explained in many articles about experiments or inventions that could produce effects at considerable distances. He described different phenomena which seems to have different nature between eachother. Despite his statements about this concepts have never been demonstrated today there exist the concept of "directed energy weapons" which is applyed in different weapons for the military defence "to produce effects at distance".

Tesla's Latest Results – He Now Produces Radiographs at a Distance of More Than Forty Feet - Electrical Review - March 18th, 1896:

> *"I am producing strong shadows at distances of 40 feet. I repeat, 40 feet and even more. Nor is this all. So strong are the actions on the film that provisions must be made to guard the plates in my photographic department, located on the floor above, a distance of fully 60 feet, from being spoiled by long exposure to the stray rays. Though during my investigations I have performed many experiments which seemed extraordinary, I am deeply astonished observing these unexpected manifestations, and still more so, as even now I see before me the possibility, not to say certitude, of augmenting the effects with my apparatus at least tenfold!"*
>
> *"These effects upon the sensitive plate at so great a distance I attribute to the employment of a bulb with a single terminal, which permits the use of practically any desired potential and the attainment of extraordinary speeds of the projected particles. With such a bulb it is also evident that the action upon a fluorescent screen is proportionately greater than when the usual kind of tube is employed, and I have already observed enough to feel sure that great developments are to be looked for in this direction".*

Today we know that X-rays are a form of invisible, high frequency electromagnetic radiation withwavelenght between 10 and 0.01 nanometres, corresponding to a frequencyof 30 PHz to 3 E Hz. They are produced by accelerating electrons at a metal target. In medical application, this is Tungstran (95%), Rhenium (5%), orMolibden. X rays are used in various medical application.

concentrated non-dispersive energy through natural media - Briefly Exposed by Nikola Tesla - Circa May 16, 1935

- **News on directed energy weapons**
- **Nazi developed Particle Beam Weapon & electric gun/cannon**
- **Videos/documentaries on secret weapons & the death ray & directed energy weapons**

In 1907, when commenting on the destruction of the French ship Iena, Tesla noted in a letter to the New York Times that he has built and tested remotely controlled torpedoes, but that electrical waves would be more destructive:

> *"As to projecting wave energy to any particular region of the globe, this can be done by my devices," he wrote. Further, he claimed that "the spot at which the desired effect is to be produced can be calculated very closely, assuming the accepted terrestrial measurements to be correct."*

In 1908 Tesla repeated the idea of destruction by electrical waves to the newspaper on April 21st His letter to the editor stated:

> *"When I spoke of future warfare I meant that it should be conducted by direct application of electrical waves without the use of aerial engines or other implements of destruction." He added: "This is not a dream. Even now wireless power plants could be constructed by which any region of the globe might be rendered uninhabitable without subjecting the population of other parts to serious danger or inconvenience."*

Again in 1915, in another letter to the editor, Tesla stated:

> *"It is perfectly practical to transmit electrical energy without wires and produce destructive effects at a distance. I have already constructed a wireless transmitter which makes this possible. When unavoidable, the [transmitter] may be used to destroy property and life."*

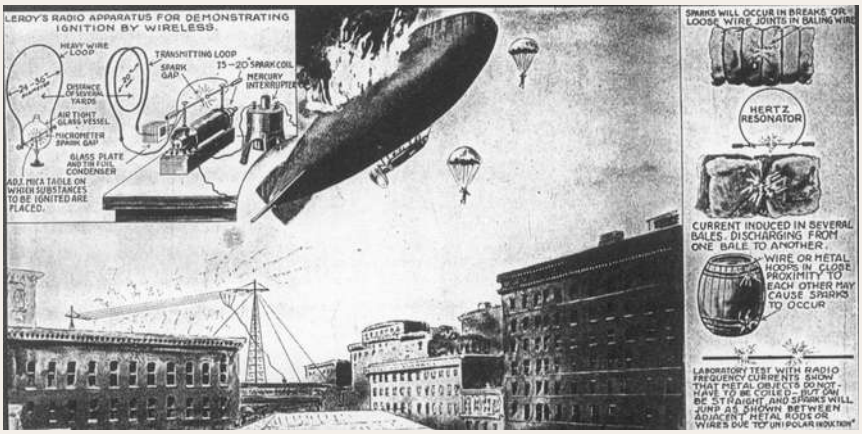

Can Radio Ignite Balloons? - Electrical Experimenter - October 1, 1919

Courtesy of Tesla Collection - http://teslacollection.com/

TESLA'S NEW DEVICE LIKE BOLTS OF THOR

He Seeks to Patent Wireless Engine for Destroying Navies by Pulling a Lever.

TO SHATTER ARMIES ALSO

A New York Times headline from December 8th, 1915

Tesla's Views on Electricity and the War - The Electrical Experimenter - August, 1917:

> "At the time of those tests I succeeded in producing the most powerful X-rays ever seen. I could stand at a distance of 100 feet from the X-ray apparatus and see the bones of the hand clearly with the aid of a fluoroscope screen; and I could have easily seen them at a distance several times this by utilizing suitable power. In fact, I could not then procure X-ray generators to handle even a small fraction of the power I had available. But I now have apparatus designed whereby this tremendous energy of hundreds of kilowatts can be successfully transformed into X-rays."

By the same month Tesla outlined a concept for primitive radar-like units. He stated:

> *"...by their [electromagnetic waves] use we may produce at will, from a sending station, an electrical effect in any particular region of the globe; [with which] we may determine the relative position or course of a moving object, such as a vessel at sea, the distance traversed by the same, or its speed".*

Tesla's 1917 proposal for Directed Energy submarine warfare (Tesla's Views on Electricity and the War - The Electrical Experimenter - August, 1917 and New Yankee Tricks to Circumvent the U-Boat - The Fort Wayne Journal-Gazette, Fort Wayne, Indiana - August 19, 1917):

> *"I believe the magnetic method of locating or indicating the presence of an iron or steel mass might prove very practical in locating a hidden submarine. And it is of course of paramount importance that we do find a means of accurately locating the sub-sea fighters when they are submerged, so that we can, with this information, be ready to close in on them when they attempt to come to the surface. Especially is this important when several vessels are traveling in fleet formation; the location and presence of the enemy submarine can be radiographed to the other vessels by the one doing the magnetic surveying and, by means of nets in some cases, or gun-fire and the use of hydro-aeroplanes sent aloft from the ships, the enemy under water stands a mighty good chance of being either 'bombed,' shelled or netted.*
>
> *"However, a means would soon be found of nullifying this magnetic detector of the submerged undersea war-craft. They might make the 'U-boat' hulls of some non-magnetic metal, such as copper, brass, or aluminum. It is a good rule to always*

keep in mind that for practically every good invention of such a kind as this, there has always been invented an opposite, and equally efficient counteracting invention."

"Now suppose that we erect on a vessel a large rectangular helice or inductance coil of insulated wire. Actual experiments in my laboratory at Houston Street (New York City) have proven that the presence of a local iron mass such as the ship's hull would not interfere with the action of this device. To this coil of wire, measuring perhaps 400 feet in length by 70 feet in width (the breadth of the ship), we connect a source of extremely high frequency and very powerful oscillating current. By this means there are radiated powerful oscillating electro-static currents, which as I have found by actual experiment in my Colorado tests some years ago, will first affect a metallic body (such as a submarine hull, even though made of brass or any other metal), and in turn cause that mass to react inductively on the exciting coil on the ship. To locate an iron mass, it is not necessary to excite the coil with a high frequency current; the critical balance of the coil will be affected simply by the presence of the magnetic body. To be able to accurately determine the direction and range of the enemy submarine, four exciting inductances should be used. With a single inductance, however, it would be possible to determine the location of a submarine by running the ship first in one direction and then in another, and noting whether the reactance effect caused by the presence of the submarine hull increased or decreased. The radiating inductance must be very sharply attuned to the measuring apparatus installed on the ship, when no trouble will be found in detecting the presence of such a large metallic mass as a submarine, even at a distance of 5 to 6 miles; of this I feel confident from my past experiments in the realm of ultra-high frequency currents and potentials."

Tesla was incorrect in his assumption that high frequency radio waves would penetrate water but Émile Girardeau, who helped develop France's first radar system in the 1930s, noted in 1953 that Tesla's general speculation that a very strong high frequency signal would be needed was correct stating:

"(Tesla) was prophesying or dreaming, since he had at his disposal no means of carrying them out, but one must add that if he was dreaming, at least he was dreaming correctly."

On July 11, 1934 the inventor described a new weapon for first time in the New York Sun and The New York Times as being able to be used against ground-based infantry or for anti-aircraft purposes. The press called it a "peace ray" or death ray.

Tesla announced to the world two astonishing new inventions. The first was a particle-beam projector that Tesla intended to be used as an instrument of national defense. He called his system "teleforce." With this machine he declared that a nation could bring wholesale destruction upon invading armies and shoot down fleets of incoming aircraft at a distance of 200 miles (400 km) away. While the basic beam weapon concept was first revealed in 1934, on Tesla's 78th birthday, specific details about the actual device have been difficult to obtain.

One year later, during his annual birthday press conference on July 10, 1935, Tesla claimed a method to transmit mechanical energy with minimal loss over any terrestrial distance, allowing for a new means of communication and a technique for the location of subterranean mineral deposits. Tesla's mechanical power transmission system, he dubbed it the "art of telegeodynamics," was based primarily upon his reciprocating engine invention, patented in 1894. While the fundamental operating principles of Tesla's mechanical oscillator are well understood, little has been said about how the machine would have been used for underground prospecting.

In Leland Anderson's newest book "Nikola Tesla's Teleforce & Telegeodynamics Proposals" these two important papers, hidden for more than 60 years, are presented for the first time. The principles behind teleforce the particle-beam weapon, and telegeodynamics the mechanical earth-resonance concept for seismic exploration, are fully addressed. In addition to copies of the original documents, typed on Tesla's official stationery, this work also includes two Reader's Aid sections that guide the reader through the more technical aspects of each paper. The papers are followed by Commentary sections which provide historical background and functional explanations of the two devices. Significant newspaper articles and headline accounts are provided to document the first mention of these proposals. A large Appendix provides a wealth of related material and background information, followed by a Bibliography section and Index.

TESLA AT 78 BARES NEW DEATH-BEAM

Invention Powerful Enough to Destroy 10,000 Planes 250 Miles Away, He Asserts.

DEFENSIVE WEAPON ONLY

Scientist, in Interview, Tells of Apparatus That He Says Will Kill Without Trace.

Nikola Tesla, father of modern methods of generation and distribution of electrical energy, who was 78 years old yesterday, announced a new invention, or inventions,

Times Wide World Photo.
NOTED INVENTOR 78.
Nikola Tesla.

Postcard illustration of the Hotel New Yorker, New York City. (Collection of The New-York Historical Society)

Tesla announced his new beam weapon in numerous newspaper interviews on his seventy-eighth birthday

In 1934 Tesla moved to his final residence, room 3327 (still divisible by three) of the recently completed Hotel New Yorker. There he lived alone with his ideas and his pigeons for the next decade. He posted a typewritten note on the door: "Please Do Not Disturb The Occupant Of This Room."

In Tesla's mind, it was time to reveal his greatest invention: a perfect and impossible idea, a weapon to prevent World War II.

On July 11, 1934, the headline on the front page of The New York Times anounced: "Tesla at 78 bares new death beam"

> *"Will send concentrated beams of particles through the free air, of such tremendous energy that they will bring down a fleet of 10,000 enemy airplanes at a distance of 250 miles* (400 km) *from a defending nation's border and will cause armies of millions to drop dead in their tracks.*
>
> *When put in operation, Dr. Tesla said, this latest invention of his would make war impossible. This death-beam, he asserted would surround each country like an invisible Chinese wall, only a million times more impenetrable. It would make every nation impregnable against attack by airplanes or by large invading armies".*

Joseph Butler, a U.S. Air Force expert on beam weapons, has said of Tesla's idea, "Definitely, he had the concept of a charged particle beam weapon back in the 1930s. The concept was right on the mark ... particles projected out long distances to do

damage to some enemy airplanes, in his particular case." But Butler added, "I haven't a clue how he meant to actually do it" (interview with the authors, 1998).

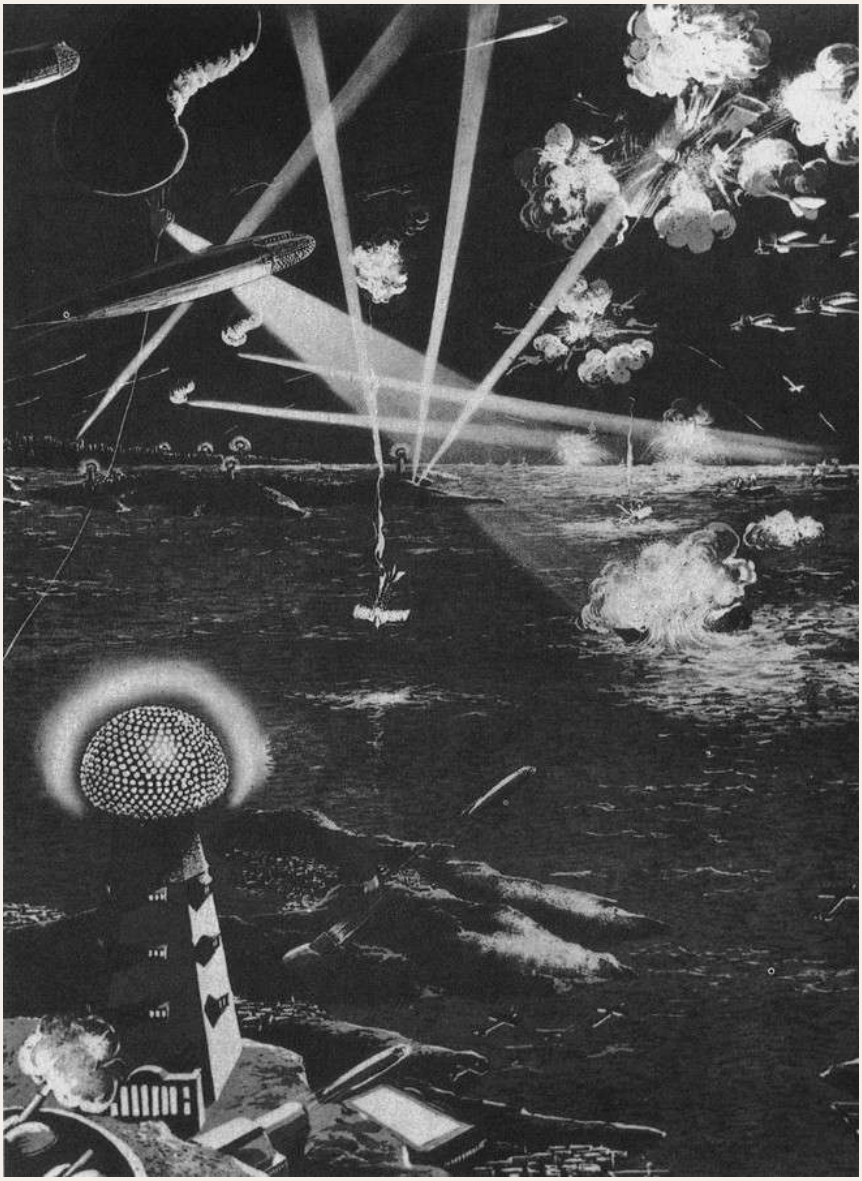

Tesla's concept of future warfare: Tesla tower in action supplying and directing war machines from distances of hundreds or even thousands of miles away.

The inventor envisioned war in the future as a "mere contest" between machines. This concept was illustrated by Paul Frank and appeared in Science and Invention, February 1922.

Sensing a business opportunity, Tesla commissions architect Titus deBobula in 1934 to draw plans of what the new particle beam weapon towers might look like and contacts several governments around the world to try to sell his plans.

Principles and concepts of Tesla's "death ray"

Beam to Kill Army at 200 Miles, Tesla's Claim on 78th Birthday - New York Herald Tribune - July 11, 1934:

> *"First and most important is a **mechanism for producing rays and other energy manifestations in free air**. Hitherto vacuum tubes have always been necessary. Second is an **apparatus for producing unheard-of quantities of electrical current and for controlling it when produced**. The current is necessary as power for the first mechanism. Without this, no rays of sufficient strength could be produced. The third is **a method of intensifying and amplifying the second process**, and the fourth is **a method of producing "tremendous electrical repellent force"**.*

On July 23, 1934 Time Magazine wrote an article about Tesla's Ray:

"*Last week Dr. Tesla announced a combination of four inventions which would make war unthinkable.*

Nucleus of the idea is a death ray – a concentrated beam of sub-microscopic particles flying at velocities approaching that of light. The beam, according to Tesla, would drop an army in its tracks, bring down squadrons of airplanes 250 miles away. Inventor Tesla would discharge the ray by means of

1. *a device to nullify the impeding effect of the atmosphere on the particles,*
2. *a method for setting up high potential,*
3. *a process for amplifying that potential to 50.000.000 volts,*
4. *creation of "a tremendous electrical repelling force."*

http://www.tfcbooks.com/teslafaq/q&a_011.htm

According to Tesla production of the particle beam is dependent upon the following four inventions (For more details see also: "The new art of projecting concentrated non-dispersive energy through natural media"):

> **1-**.A method and apparatus for producing rays and other manifestations of energy in free air, eliminating the high vacuum necessary at present for the production of such rays and beams. This is accomplished with a novel form of high vacuum tube, one end of which is open to the atmosphere. The projectiles are accelerated in a vacuum and then conducted into the atmosphere through a valvular conduit.

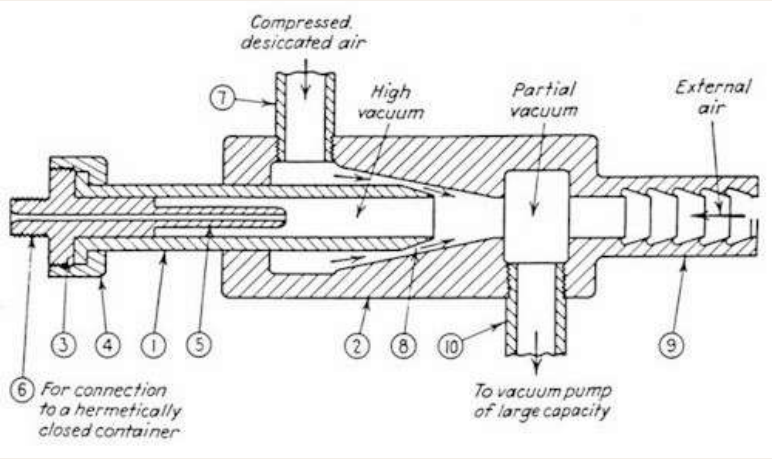

Modified open vacuum tube

- GB179,043 - Improved process and apparatus for production of high vacua - March 24, 1921

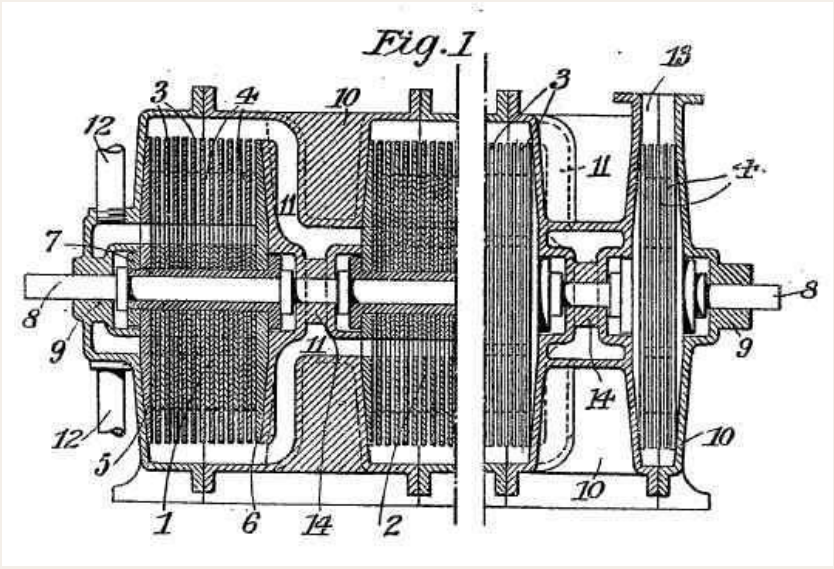

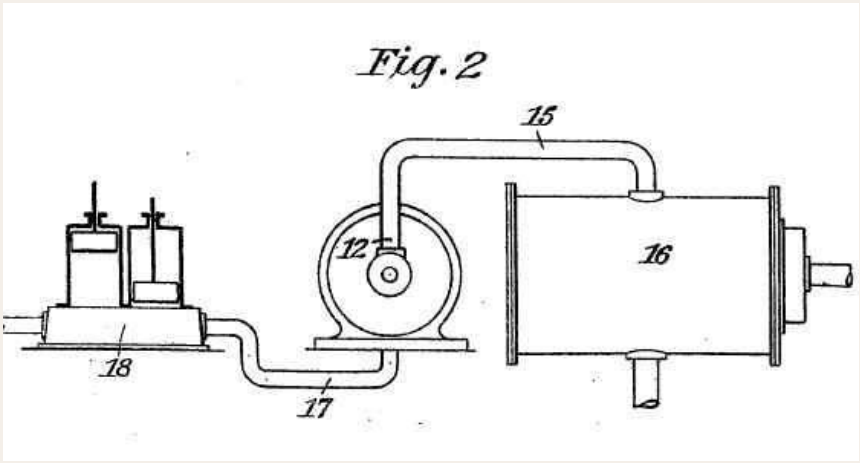

- 1,329,559 Valvular Conduit, February 3, 1920

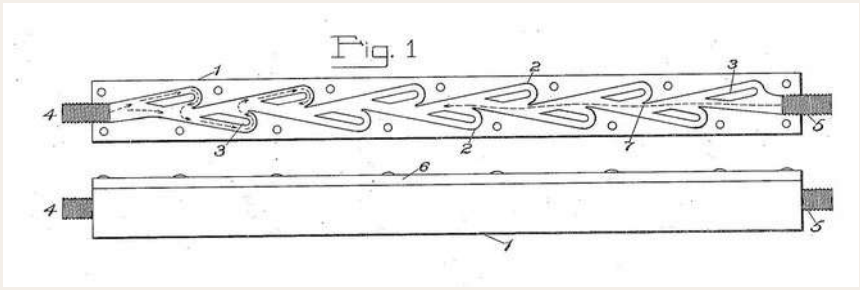

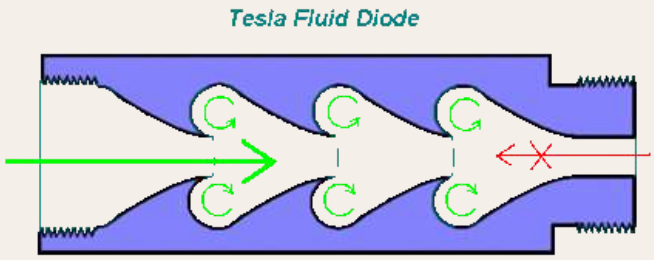

2-.A method and process for producing very great electrical force in the range of 60,000,000 volts to propel the particles to their objective. Tesla specified that this could be done with a large electrostatic generator on a new principle and of very great power, in many respects similar to a Van de Graaff generator. In place of a charge-carrying belt it employs a circulating stream of desiccated air that is propelled through a hermetically sealed ductwork by a Tesla disc blower. A Wardenclyffe type apparatus could also be used for this purpose.

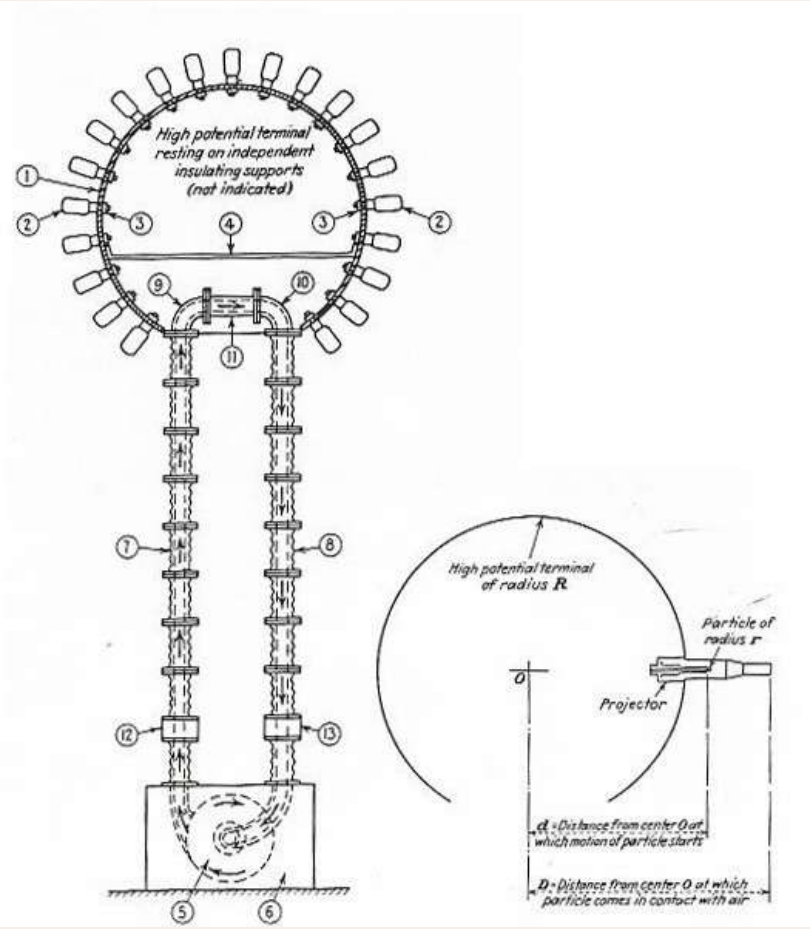

SCHEMATIC ILLUSTRATION OF NEW HIGH POTENTIAL GENERATOR & SPHERICAL TERMINAL AND AN OPEN VACUUM TUBE

- US1,061,142 - Fluid Propulsion - April 29, 1913

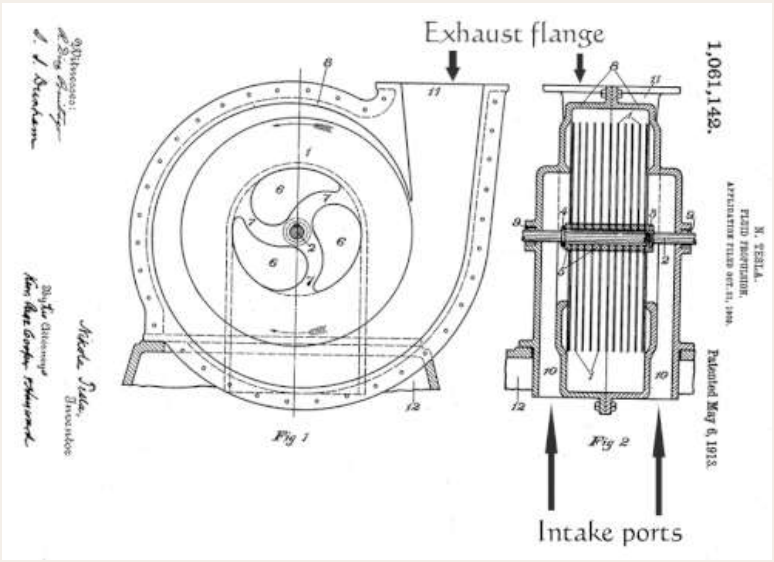

3-.A method for amplifying this process in the second invention. The exterior of the high potential terminal is equipped with numerous bulbs of some insulating material each containing, —an electrode of thin metal sheet suitably rounded— and — exhausted to the highest vacuum obtainable.—

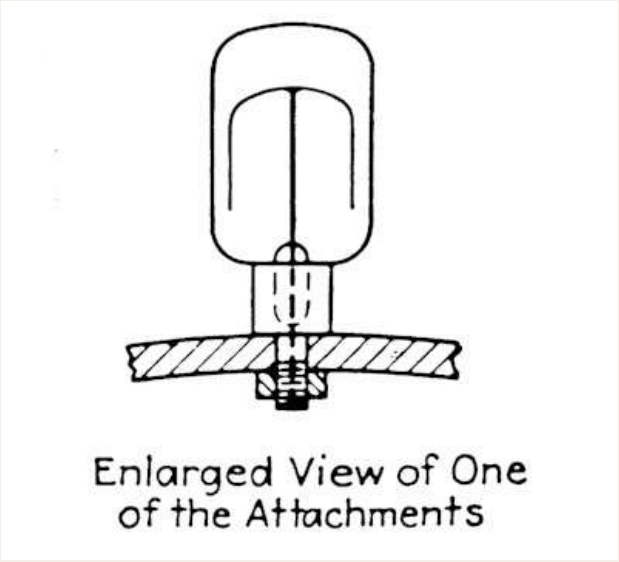

NEW TERMINAL FOR EXCEEDINGLY HIGH POTENTIALS
CONSISTING OF SPHERICAL FRAME ATTACHMENTS

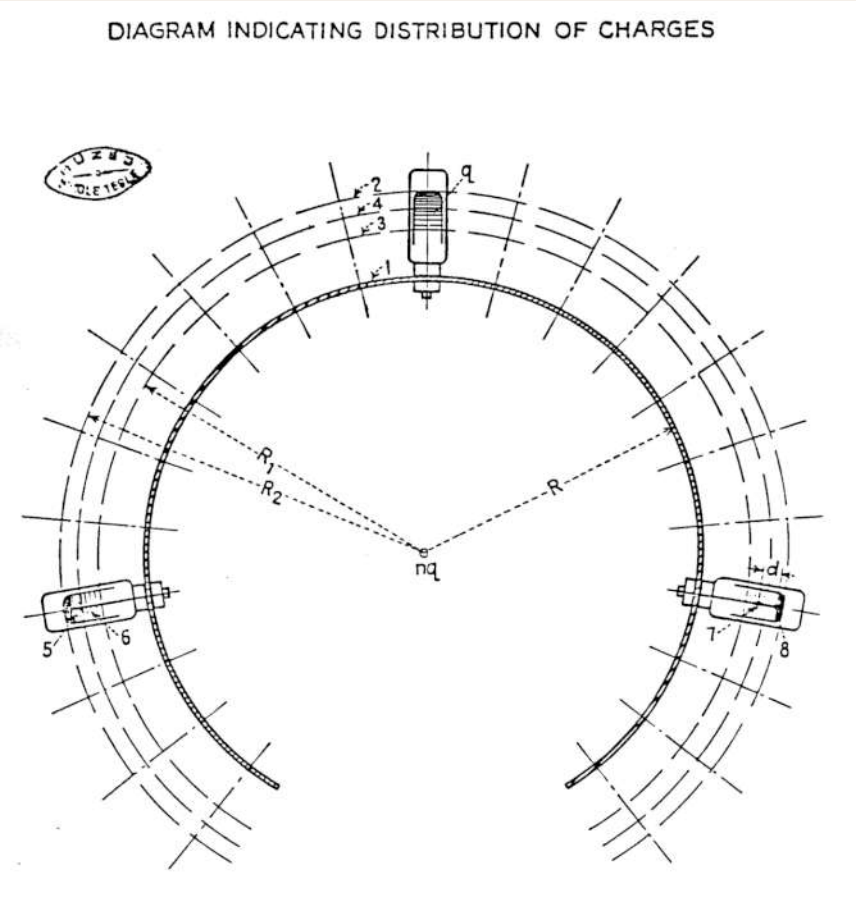

4-.A new method for producing a tremendous electrical repelling force in the form of —provisions for imparting to a minute particle an extremely high charge.— It appears this refers to the internal conducting component (the socket and central extension) at the base of the projector or gun element of the system While the specific details about this aspect of the design are not readily apparent, it seems that strict attention to the fulfillment of requirements 1, 2 and 3 is critical to success. In Tesla's words, *"by the application of my discoveries it is possible to increase the force of repulsion more than a million times and what was heretofore impossible is rendered easy of accomplishment"*.—[1, 2]

His idea was probably to use a gigantic electrostatic generator run by one of his turbines to accelerate tiny particles of mercury until they became a stream of super high-powered bullets of several million volts. Since they were accelerated in a vacuum, Tesla needed a way to spit them out of the accelerator sphere without letting air in. He proposed to do this with the special nozzle which blew high-pressure air around an open tube leading to the evacuated sphere and acted like a constantly renewing plug to preserve the vacuum. What happens to the mercury stream after it left the nozzle and had to travel through the atmosphere was another matter that was never quite figured out.

In the death ray prpoposal, Tesla used the term "particles" but in this case he did not mean atomic particles like protons, neutron... etc but he meant microscopic droplets accelerated in a electron tube and by the action of the repulsion of the electrostatic force.

The Inventions, Researches and Writings of Nikola Tesla - by Thomas Commerford Martin, Editor - 1894:

The electrostatic attractions and repulsions between bodies of measurable dimensions are, of all the manifestations of this force, the first so-called electrical phenomena noted. But though they have been known to us for many centuries, the precise nature of the mechanism concerned in these actions is still unknown to us, and has not been even quite satisfactorily explained. What kind of mechanism must that be? We cannot help wondering when we observe two magnets attracting and repelling each other with a force of hundreds of pounds with apparently nothing between them. We have in our commercial dynamos magnets capable of sustaining in mid-air tons of weight. But what are even these

[Pg 326]

forces acting between magnets when compared with the tremendous attractions and repulsions produced by electrostatic force, to which there is apparently no limit as to intensity. In lightning discharges bodies are often charged to so high a potential that they are thrown away with inconceivable force and torn asunder or shattered into fragments. Still even such effects cannot compare with the attractions and repulsions which exist between charged molecules or atoms, and which are sufficient to project them with speeds of many kilometres a second, so that under their violent impact bodies are rendered highly incandescent and are volatilized. It is of special interest for the thinker who inquires into the nature of these forces to note that whereas the actions between individual molecules or atoms occur seemingly under any conditions, the attractions and repulsions of bodies of measurable dimensions imply a medium possessing insulating properties. So, if air, either by being rarefied or heated, is rendered more or less conducting, these actions between two electrified bodies practically cease, while the actions between the individual atoms continue to manifest themselves.

An experiment may serve as an illustration and as a means of bringing out other features of interest. Some time ago I showed that a lamp filament or wire mounted in a bulb and connected to one of the terminals of a high tension secondary coil is set spinning, the top of the filament generally describing a circle. This vibration was very energetic when the air in the bulb was at ordinary pressure and became less energetic when the air in the bulb was strongly compressed. It ceased altogether when the air was exhausted so as to become comparatively good conducting. I found at that time that no vibration took place when the bulb was very highly exhausted. But I conjectured that the vibration which I ascribed to the electrostatic action between the walls of the bulb and the filament should take place also in a highly exhausted bulb. To test this under conditions which were more favorable, a bulb like the one in Fig. 174, was constructed. It comprised a globe b, in the neck of which was sealed a platinum wire w carrying a thin lamp filament f. In the lower part of the globe a tube t was sealed so as to surround the filament. The exhaustion was carried as far as it was practicable with the apparatus employed.

This bulb verified my expectation, for the filament was set spinning when the current was turned on, and became incandes

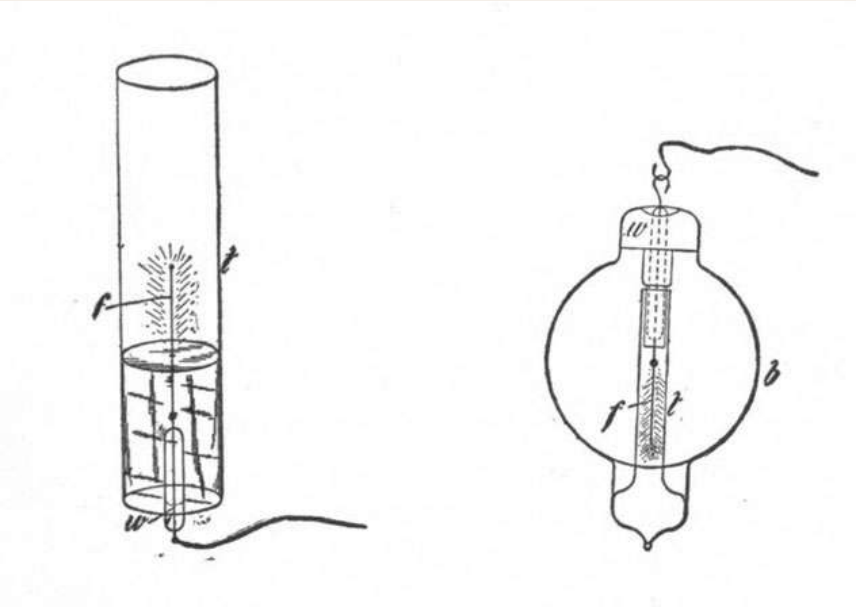

Fig. 173. & Fig. 174.

[Pg 327]

cent. It also showed another interesting feature, bearing upon the preceding remarks, namely, when the filament had been kept incandescent some time, the narrow tube and the space inside were brought to an elevated temperature, and as the gas in the tube then became conducting, the electrostatic attraction between the glass and the filament became very weak or ceased, and the filament came to rest. When it came to rest it would glow far more intensely. This was probably due to its assuming the position in the centre of the tube where the molecular bombardment was most intense, and also partly to the fact that the individual impacts were more violent and that no part of the supplied energy was converted into mechanical movement. Since, in accordance with accepted views, in this experiment the incandescence must be attributed to the impacts of the particles, molecules or atoms in the heated space, these particles must therefore, in order to explain such action, be assumed to behave as independent carriers of electric charges immersed in an insulating medium; yet there is no attractive force between the glass tube and the filament because the space in the tube is, as a whole, conducting.

It is of some interest to observe in this connection that whereas the attraction between two electrified bodies may cease owing to the impairing of the insulating power of the medium in which they are immersed, the repulsion between the bodies may still be observed. This may be explained in a plausible way. When the bodies are placed at some distance in a poorly conducting medium, such as slightly warmed or rarefied air, and are suddenly electrified, opposite electric charges being imparted to them, these charges equalize more or less by leakage through the air. But if the bodies are similarly electrified, there is less opportunity afforded for such dissipation, hence the repulsion observed in such case is greater than the attraction. Repulsive actions in a gaseous medium are however, as Prof. Crookes has shown, enhanced by molecular bombardment.

In some moment of his life, Tesla believed in the possibility of the atomic energy as a source of energy, but after some years he stated just the oposite as a result of his unsuccessfull experiments of "accelerating and crushing atomic particles". For this reason it is supposed that some kind of particle accelerator would be necessary to develop such experiments, however the details are uknown. The utilization of electron

tubes (or cathode tubes) is described in some articles and interviews about Tesla's "death ray".

Harnessing Nature - Can The Free Energy Of Space Be Utilized? - Scientific American - April 5, 1913

> *"Experiments conducted by Mr. Nikola Tesla with electromotlve forces of 2.000.000 volts have* ***convinced him that if 100.000.000 volts could be produced it might be possible to break down the atomic structure of any element and thus liberate a certain amount of energy.*** *"But," he told the wrlter of this artlcle, "even lf the feat could be accomplished and suficient energy set free, there still remains the enormously dificult problem of devising a means of utillzing the energy ln a practical way."*

Tesla, 75, Predicts New Power Source - New York Times - July 5th, 1931

> *"When and where do you expect to make the official announcement of your new discoveries?" the inventor was asked.*
>
> *"These discoveries," he replied, "did not come to me over night, but as the result of intense study and experimentation for nearly thirty-six years. I am naturally anxious to give the facts to the world as soon as possible, but I also wish to present them in a finished form. That may take a few months or a few years."*
>
> *"The idea of atomic energy is illusionary but it has taken so powerful a hold on the minds, that although I have preached against it for twenty-five years, there are still some who believe it to be realizable."*
>
> *"I have disintegrated atoms in my experiments with a* ***high potential vacuum tube I brought out in 1896****, which I consider one of my best inventions.* ***I have operated it with pressures ranging from 4,000,000 to 18,000,000 volts. More recently I have designed an apparatus for 50,000,000 volts which should produce many results of great scientific importance.***
>
> *"But as to atomic energy,* ***my experimental observations have shown that the process of disintegration is not accompanied by a liberation of such energy*** *as might be expected from the present theories."*

Aerial defense "death beam" offered to U.S by Tesla - The Baltimor Sun - July 12, 1940.

> ***The voltages for propelling the deth beam to its objective, he stated, will attain a potential of 50.000.000****.*
>
> ***With this enourmous voltage, he said, microscopic particles of matter will be catapulted on their mission of defensive destruction.***

Beam to Kill Army at 200 Miles, Tesla's Claim on 78th Birthday - New York Herald Tribune - July 11, 1934:

> ***"It Is an Electric Gun***
>
> *The beam of force itself, as Dr. Tesla described it, is a concentrated current - it need be no thicker than a pencil - of microscopic particles moving at several*

hundred times the speed of artillery projectiles. The machine into which Dr. Tesla combines his four devices is, in reality, a sort of electrical gun.

He illustrated the sort of thing that the particles will be by recalling an incident that occurred often enough when he was experimenting with a ***cathode tube****. Then, sometimes, a particle larger than an electron, but still very tiny, would break off from the cathode, pass out of the tube and hit him. He said he could feel a sharp, stinging pain where it entered his body, and again at the place where it passed out.* ***The particles in the beam of force, ammunition which the operators of the generating machine will have to supply, will travel far faster than such particles as broke off from the cathode****, and they will travel in concentrations, he said.*

As Dr. Tesla explained it, ***the tremendous speed of the particles will give them their destruction-dealing qualities****. All but the thickest armored surfaces confronting them would be melted through in an instant by the heat generated in the concussion".*
"I should also say, and this is perhaps as important as anything else about it, that in this apparatus all limitations as to electric force and the quantity of electricity transmitted have been removed."

Prepared Statement of Tesla (For interview with press on 81st birthday observance):

There is one more discovery which I want to announce at this time, consisting of a new method and apparatus for the obtainment of vacua exceeding many times the highest heretofore realized. I think that as much as one-billionth of a micron can be attained. What may be accomplished by means of such vacua is a matter of conjecture, but it is obvious that they will make possible the production of much more intense effects in ***electron tubes****. My ideas regarding the electron are at variance with those generally entertained.* ***I hold that it is a relatively large body carrying a surface charge and not an elementary unit. When such an electron leaves an electrode of extremely high potential and in very high vacuum, it carries an electrostatic charge many times greater than the normal.*** *This may astonish some of those who think that the particle has the same charge in the tube and outside of it in the air. A beautiful and instructive experiment has been contrived by me showing that such is not the case, for* ***as soon as the particle gets out into the atmosphere it becomes a blazing star owing to the escape of the excess charge****.* ***The great quantity of electricity stored on the particle is responsible for the difficulties encountered in the operation of certain tubes and the rapid deterioration of the same.***

Proposing the "death ray" for defense - Philadelphia Inquirer - October 20, 1940:

"It is based on an entirely new principle of physics that nobody ever has dreamed of. **It is different from the principle embodied in my inventions relating to the transmission of electrical power from a distance**, for which I hold a number of basic patents."

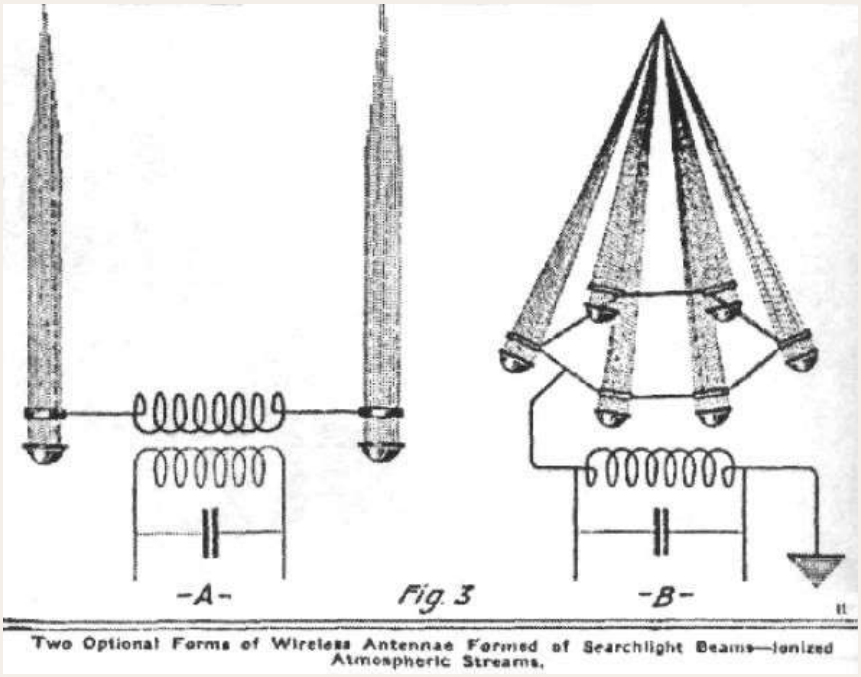

Two Optional Forms of Wireless Antennae Formed of Searchlight Beams—Ionized Atmospheric Streams.

Illustrations from an article in the March, 1920 issue of Electrical Experimenter entitled "Wireless Transmission of Power Now Possible". The illustrations show his prototype devices for "directed ionized beam transmissions," a "deathray—searchlight" device. But according to Tesla, the results of tests did not justify the hope of important practical applications in large distance.

> *"After preliminary laboratory experiments,* ***I made tests on a large scale with the transmitter referred to and a beam of ultra-violet rays of great energy in an attempt to conduct the current to the high rarefied strata of the air and thus create an auroral display*** *such as might be utilized for illumination, especially of oceans at night.* ***I found that there was some virtue in the principal but the results did not justify the hope of important practical applications*** *although, some years later, several inventors claimed to have produced a "death ray" in this manner. While the published reports to this effect were entirely unfounded, I believe that with the new transmitter to be built, many wonders will be achieved".*

A Machine to End War - Liberty - February 1937:

> *My discovery ends the menace of airplanes or submarines, but it insures the supremacy of the battleship, because battleships may be provided with some of the required equipment. There might still be war at sea, but no warship could successfully attack the shore line, as the coast equipment will be superior to the armament of any battleship.*
>
> ***I want to state explicitly that this invention of mine does not contemplate the use of any so-called "death rays." Rays are not applicable because they cannot be produced in requisite quantities and diminish rapidly in intensity with distance.*** *All the energy of New York City (approximately two million horsepower) transformed into rays and projected twenty miles, could not kill a human being, because, according to a well known law of physics, it would disperse to such an extent as to be ineffectual.*
>
> ***My apparatus projects particles which may be relatively large or of microscopic dimensions****, enabling us to convey to a small area at a great*

distance trillions of times more energy than is possible with rays of any kind. Many thousands of horsepower can thus be transmitted by a stream thinner than a hair, so that nothing can resist. This wonderful feature will make it possible, among other things, to achieve undreamed-of results in television, for there will be almost no limit to the intensity of illumination, the size of the picture, or distance of projection.

I do not say that there may not be several destructive wars before the world accepts my gift. I may not live to see its acceptance. But I am convinced that a century from now every nation will render itself immune from attack by my device or by a device based upon a similar principle.

At the age of 81, at a luncheon in his honor, concerning the Death Ray, Tesla stated:

"But it is not an experiment…. I have built, demonstrated and used it. Only a little time will pass before I can give it to the world."

History of particle accelerators

There are two basic classes of accelerators: electrostatic and oscillating field accelerators. Electrostatic accelerators use static electric fields to accelerate particles. A small-scale example of this class is the cathode ray tube in an ordinary old television set. Other examples are the Cockcroft–Walton generator and the Van de Graaff generator. The achievable kinetic energy for particles in these devices is limited by electrical breakdown. Oscillating field accelerators, on the other hand, use radio frequency electromagnetic fields to accelerate particles, and circumvent the breakdown problem. This class, which was first developed in the 1920s, is the basis for all modern accelerator concepts and large-scale facilities.

To be able to go deeper into the secrets of the structure of matter, the phycisists found that they had to "crush", "hit" or "disturb" the atomic particles with the maximum energy as possible. In 1911 Rutherford achieved to elaborate an atomic model by the help of a projectile of certain energy: the α particles (alpha particles). During a long period of time such particles were the unique method to disturb the microcosmos in a controled way; but for the only way to produce them, it was necesary some kind of material which would be already radiactive in nature. This limitation became more remarkable in 1919 when Rutherford opened the new field of nuclear transformations when he studied the reaction N14 + α (alpha) => O17 + p (a nucleus of Nitrogen absorbs an α particle, emiting a proton and transforming it into a Oxigen nucleus). The radiactive sources available were too weak to continue penetrating into the mistery of atomic nucleus. One gram of radium produced 37.000 milion of α particles per second (apart from other products of the disintegration) of which 1 from 100.000 brought a transformation; too few to be able to separate chemically the generated substances to examine the products. Furthermore, the energy of those α particles were just enough to be able to surpass the electric repulsion of the nucleus to which they were directed. It was urgent to find machines which would be able to increase the number and velocity (energy) of the particles. And because they were charged, one way was to put them inside great potential differences.

Before the WW1 no technical means existed to progress so much in that direction. From the 1920's already begun to appear some apparatus. In Cambridge, John Cockcroft and Ernest Walton used a voltaic multiplier which provided to them 125 Kv (1Kv=1000V) to be the first to observe in 1932 the artificial disintegration of atoms of lithium in two α particles. In the department of Terrestrial Magnetism of the Carnegie Institute of

Washington, Merle Tuve in 1928 used a transformer invented by Nikola Tesla with which he reached 3 million Volts. With the colaboration of Gregory Breit, Tuve used this method to accelerate protons and electrons. After working during a short time in an electric power plant in Alabama, Robert J. Van de Graaf designed his electrostatic generator. After spending one year in Oxford with a studentship, he conceived a device to build up a high voltage using simple principles of electrostatics. A belt of insulating material carries electricity from a point source to a large insulated spherical conductor. Another belt likewise delivers electricity of the opposite charge to another sphere. The spheres build up a potential until the electric field breaks down the air and a huge spark "arcs" across. While a postdoctoral fellow at Princeton, he adapted it (where he arrived in 1928) for the acceleration of particles. In a short time his prototype provided the 80 Kv and in 1931 was already possible to provide 750 Kv and using two spheres it was possible to achieve a potential difference of 1,5 Mv (1Mv=1000Kv). In 1937 already existed Van de Graaf generators of 5 meters high which were able to provide 5Mv. By increasing the radius of the spheres, Van de Graaff could reach higher voltages without arcing. The maximum voltage in theory, in megavolts, roughly equalled the radius of the sphere in feet. He was soon planning a pair of spheres 15 feet across. In 1933 Tuve and his team used a Van de Graaf generator of 1 Mv together with the discharge tube which they improved and they observed the disintegration of lithium and boron.

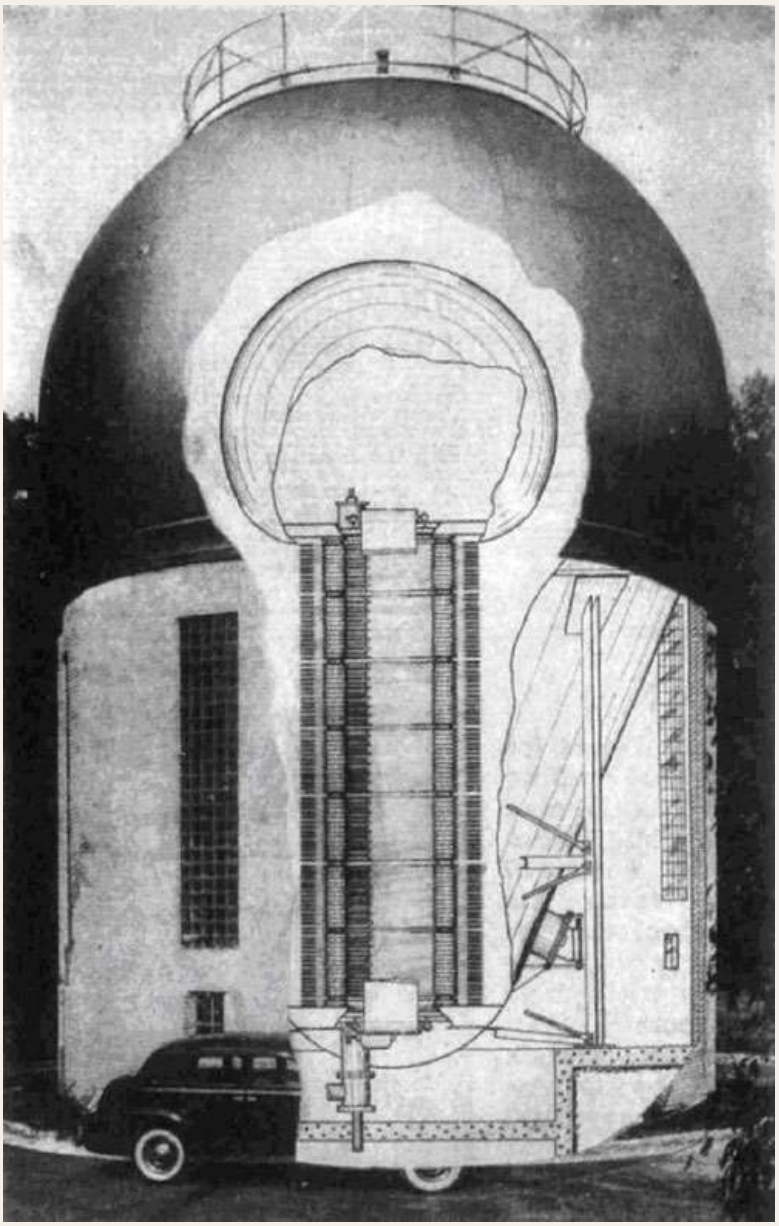

This electrostatic generator (Van de Graaf generator) atom-smasher was built at the Carnegie Institution in Washington D.C., and used between 1920 and 1940. The cross-section shows a spherical conductor, its insulating supports, and tube in which particles are accelerated. The charging belt is shown cut-off near the top and bottom. This structure was also the talk of "death-rays".

The most important initiative which ended up developing more and marking an era of physics was that associated to American phycisist Ernest Orlando Lawrence. The difficulties of maintaining high voltages led several physicists to propose accelerating particles by using a lower voltage more than once. After graduating in Yale Lawrence was hired as a professor associated to physics for Berkley in 1928. Lawrence learned of one such scheme in the spring of 1929, while browsing through an issue of *Archiv für Elektrotechnik*, a German journal for electrical engineers. Lawrence read German only with great difficulty, but he was rewarded for his diligence: he found an article by a Norwegian engineer, Rolf Wideröe, the title of which he could translate as *"On a new principle for the production of higher voltages."* The diagrams explained the principle and Lawrence skipped the text. This article inspired his idea of a particle accelerator, the first cyclotron.

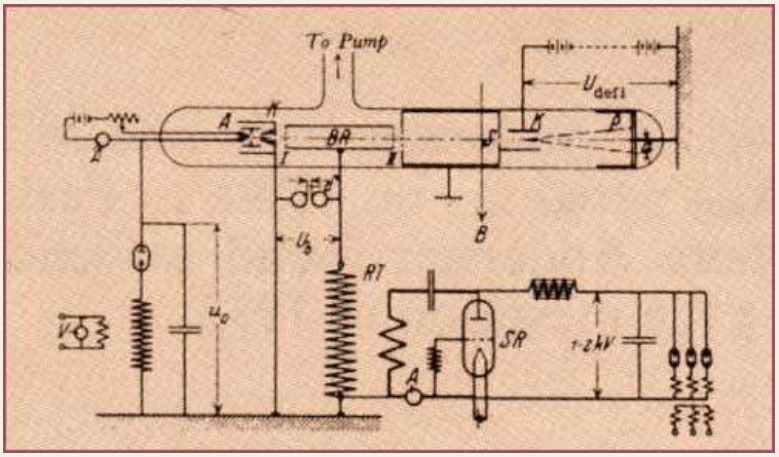

The first radio frequency linac for acceleration of heavy ions was designed by Rolf Widerøe in 1928. 1 MHz, 25KV rf source to accelerate potassium ions up to 50 KeV. Optimum gap distance d=βλ/2=βc/2f

Rolf Widerøe, Gustav Ising, Leó Szilárd, Donald Kerst, and Ernest Lawrence are considered pioneers of the particle accelerators, conceiving and building the first operational linear particle accelerator, the betatron, and the cyclotron.

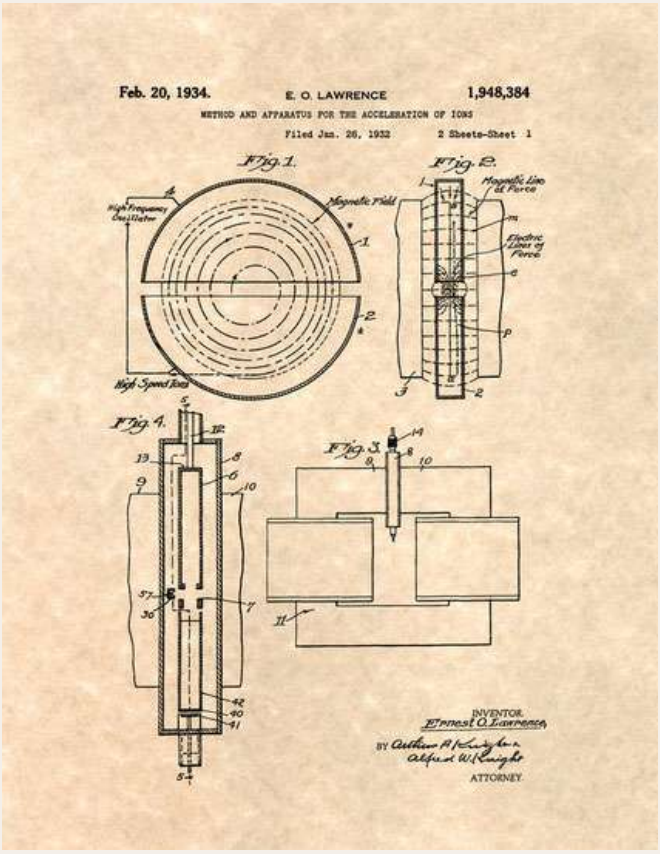

Feb. 20, 1934. E. O. LAWRENCE 1,948,384

METHOD AND APPARATUS FOR THE ACCELERATION OF IONS

Filed Jan. 26, 1932 2 Sheets-Sheet 1

Fig. 1.

Fig. 2.

Fig. 4.

Fig. 3.

INVENTOR
Ernest O. Lawrence
BY Arthur H. Compton
Alfred W. Knight
ATTORNEY

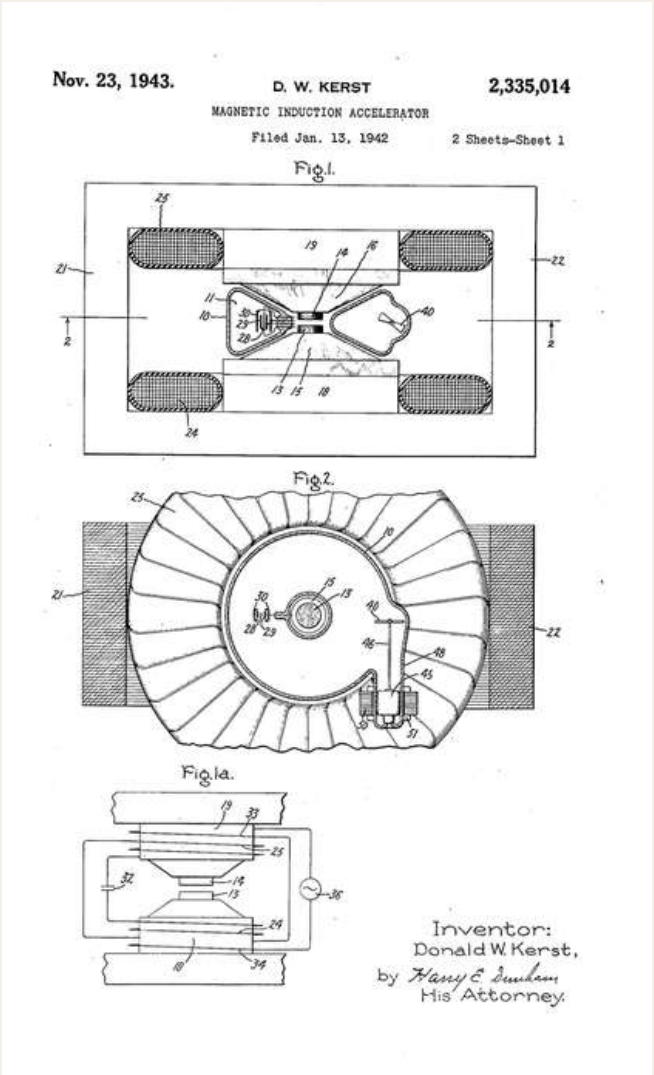

Nov. 23, 1943. D. W. KERST 2,335,014

MAGNETIC INDUCTION ACCELERATOR

Filed Jan. 13, 1942 2 Sheets-Sheet 1

Fig. 1.

Fig. 2.

Fig. 1a.

Inventor:
Donald W. Kerst,
by Harry E. Dunham
His Attorney.

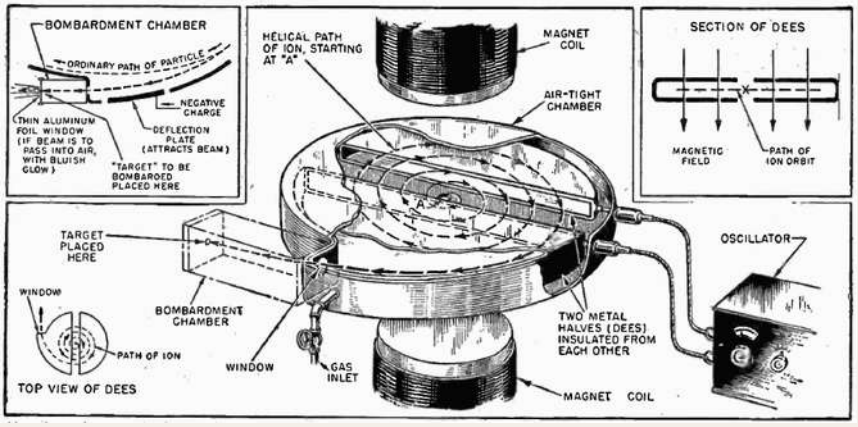

Diagram of a cyclotron, a particle accelerator invented by Earnest O. Lawrence in 1932 and widely used from the 1930s to the 1950s. It consists of a pair of "D" shaped sheet metal electrodes called "Dees" placed face to face inside a vacuum chamber, between the poles of an electromagnet. An oscillating radio frequency voltage of several thousand volts is applied to the dees. Atomic particles to be accelerated, such as protons are released in the center. The magnetic field causes them to travel in a spiral path from the center to the rim of the dees, being accelerated each time they pass from one electrode to the other. When the particles reach the rim they pass out of the dees through a small gap and strike a target. In this diagram the electromagnet pole pieces are not shown full size; they must be at least as big as the dees to create a uniform field. Caption: How the cyclotron works. Size of the magnets has been kept down to show the path of the electron

The New Art of Projecting Concentrated Non-Dispersive Energy Through Natural Media

Whether Tesla's idea was ever taken seriously is still a mater of conjecture. Most experts today consider his idea infeasible. Though, his death beam bears an uncanny resemblance to the charged-particle beam weapon developed by both the United States (Beam Experiments Aboard Rocket) and the Soviet Union during the cold war.

At the end of 1930s many conflicts were giving enough evidence that the dark future of war would soon break out in Europe. Nikola Tesla tryed to convince the military to generate interest to get the fundings for his "peace beam", but it seems that he didn't recieve the attention that he was hoping. After some attempts, he decided to not give up and he sent an elaborate technical paper, including diagrams, to a number of Allied nations including the United States, Canada, England, France, the Soviet Union, and Yugoslavia.

A paper surfaces in 1983 which is the first to show an actual plan for a weapon. An analysis of the paper by the Tesla museum in Belgrade determines them to be authentic. The paper, which is entitled "New Art of Projecting Concentrated Non-Dispersive Energy Through Natural Media" is the only known paper Telsa ever wrote about particle beam weaponry.

The most interested country of all which recieved Tesla's proposal, the greatest interest came from the Soviet Union. In 1937 (agreement dated in April 20, 1935) Tesla presented a plan to the Amtorg Trading Corporation, an alleged Soviet arms front in New York City. Two years later, in 1939, one stage of the plan was tested in the USSR and Tesla received a check for $25,000. It is highlighted from the released unclassified FBI archives (Part 1 page 185). Contained within the extract Tesla agreed to supply

plans, specification, and complete information on a method and apparatus for producing very small particles in a tube open to air, for increasing the charge of the particles to the full voltage of the high potential terminal, and for projecting the particles to a distances of a hundred miles or more. The maximum speed of the particles was specified as not less than 350 miles per second. The receipt of $25,000 fee for this disclosure was acknowledged by Nikola Tesla and by A. Bartanian of the Amtorg Trading Corporation.

During World War II, Amtorg handled the flow of military supplies to the Soviet Union, including armaments, raw materials, food, and uniforms under the Lend-Lease program.

During the Cold War years, the scope of Amtorg's enterprise was more limited, but it continued to conduct its business at 49 West 37th Street, in New York City, maintaining a skeleton staff. As an arm of the Soviet state, Amtorg, at that time located at 355 Lexington Avenue in New York City, was targeted in two bombing attempts, in 1971 and 1976, by members of the Jewish Armed Resistance, an extremist group affiliated with the Jewish Defense League.

Surrounded by continuing controversy, Amtorg survived the Cold War but did not survive the collapse of the Soviet Union, quietly disappearing in 1998.

In a letter that was written to J. P. Morgan, Jr. on November 29, 1934, Tesla described the weapon:

> *"I have made recent discoveries of inestimable value... The flying machine has completely demoralized the world, so much that in some cities, as London and Paris, people are in mortal fear from aerial bombing. The new means I have perfected afford absolute protection against this and other forms of attack. ... These new discoveries, which I have carried out experimentally on a limited scale, have created a profound impression. One of the most pressing problems seems to be the protection of London and I am writing to some influential friends in England hoping that my plan will be adopted without delay. The Russians are very anxious to render their borders safe against Japanese invasion and I have made them a proposal which is being seriously considered".*

During the period in which the negotiations were being carried on, Tesla claimed that efforts had been made to steal the invention. His room had been entered and his papers had been scrutinized, but the thieves, or spies, left empty-handed. He said that there was no danger that his invention could be stolen for he had at no time committed any part of it to paper. The blueprint for the Teleforce weapon was all in his mind.

In 1940 Tesla estimated that each station would cost no more than $2,000,000 and could have been constructed in a few months.

CNN Special Report 1985 Electromagnetic Frequency

Tesla Weapons

Other controversial death ray proposals and possible frauds

THE RAY IN OPERATION EXPLODING GUNPOWDER.

Death ray proposal by Harry Grindell Matthews

Death ray proposal by Harry Grindell Matthews

"Tesla's Views on Electricity and the War" - The Electrical Experimenter - August, 1917

> "The 'Ulivi ray' really was transplanted from this country to Italy," asserted Dr. Tesla. "It was simply an adaptation of my ultra-powerful high-frequency phenomena as carried out in Colorado and cited previously. With a powerful oscillator developing thousands of horsepower it would become readily possible to detonate powder and munition magazines by means of the high frequency currents induced in every bit of metal, even when located five to six miles away and more. Even a powder can would have a potential of 6,000 to 7,000 volts induced in it at that distance.
>
> "At the time of those tests I succeeded in producing the most powerful X-rays ever seen. I could stand at a distance of 100 feet from the X-ray apparatus and see the bones of the hand clearly with the aid of a fluoroscope screen; and I could have easily seen them at a distance several times this by utilizing suitable power. In fact, I could not then procure X-ray generators to handle even a small fraction of the power I had available. But I now have apparatus designed whereby this tremendous energy of hundreds of kilowatts can be successfully transformed into X-rays."

Tesla was probablly wrong in this case when he stated that Giacomo Ulivi copyed his idea knowing that Ulivi's death rays were finally considered a fraud after many attempts in different places to avoid his excuses to demonstrate his invention to the public without conditions but also because he had the bad habbit to disapear in the righ moments (See also: http://trove.nla.gov.au/ndp/del/article/6426458?searchTerm=Giulio%20Ulivi&searchLimits=).

The death ray proposal by Harry Grindell Matthews had almost the same reputation as the false italian inventor Giacomo Ulivi because he never had been able to demonstrate to the military of the UK or to any other witness, but it seems that there has always been some doubt as to whether Matthews ever actually invented a 'Death Ray' knowing that some documents held in the French patent office show a patent registered for the 'Projection à distance Phénomenès invisibles de haute fréquency électrique' - or the 'remote projection of invisible high frequency electricity' (seeking source) in other words, the 'Death Ray' - filed in October 1924 under the name Eugene Royer, Matthews' close associate.

Nazi developed "death ray" Weapon

More information: " Nazi developed "death ray" Weapon."

The following is a set of data related to the Nazi project.

Death-Rays as Life-Savers in the Third Reich by Pedro Waloschek (the description which appear in the book about Tesla's "death ray" is wrong as it was not supposed to use electromagnetic waves or wireless energy and in this case Tesla never stated that particles should travel faster than light):

> Today we know that the ‘death rays’ made famous through science fiction literature and cinema were never actually deployed, and certainly not during World War II. The extensive literature on secret weapons provides us with very few mentions of ‘death rays’, and most of these refer to desperate publicity stunts by the German leadership towards the end of the war. However, several proposals were made, which led to the establishment of real research and development projects that aimed (or hoped) to achieve the development of ‘death rays’, or at least to gather

some of the knowledge considered indispensable for the realisation of such weaponry. This does not belong to the world of conjecture; there is real evidence of activity, which can be reconstructed thanks to archive documents and witness statements.

Towards the end of the war, scientists in Germany tried to make use of what funds were still available for research work. Some of these projects were sensible, others less so. They also used such projects as pretexts to save their employees from war services (see Schiebold) or from deportation in concentration camps (see Schmellenmeier). Most of them were already thinking in terms of post-war scientific or commercial applications. So they were supported and encouraged by industrial firms like Brown Boveri (BBC), Philips and Siemens, which expected a future market for X-ray-producing machines for hospitals. And they were in strong competition with US-firms like General Electric.

However, in order to obtain the materials, financial support and services required for a project, several scientists found it expedient to declare that their work was of vital importance to the war effort. Their chances of success fared even better if they could assert that their developments were indispensable for producing a specific weapon, which could prove decisive for a conclusive (and somewhat miraculous) victory. Sometimes these proposals were explicit, and 6 unambiguous (albeit secret) reports were submitted to the authorities in writing. But in other cases suggestions were raised only orally, and the paperwork that was presented merely served to hide the military purpose of these projects behind a smokescreen of civilian intent. To some extent the scientists were able to play this game thanks to the Nazi leadership's lack of technical and scientific understanding. Furthermore, it was unlikely that experts with opposing viewpoints would raise any objections to a project considered essential to the war effort since this would have been considered in general as rank defeatism.

Nevertheless the world was afraid of Hitler's miracle weapons and particularly his death rays. What was the truth behind these death rays? And how had the German Luftwaffe and other authorities been convinced of the case for making substantial research and development efforts to produce such death rays? This is the area under discussion. The subject began to fascinate me in my youth.

My aim is to present the collection of data I have accumulated over many years, and make it accessible to others in a way that I hope will be interesting and easy to understand. I have been particularly interested in the lives and problems of the people involved in the 'death ray' projects, and I hope that the information I present will contribute to the elimination of some of the myths and prejudices that arose after the war, mainly as a result of the (sometime justified) silence of the participants.

German "death ray" weapon wrecked - The argus, Melbourne - 8 sept, 1944

This concrete structure in France was intended to house a Nazi secret weapon, French civilians believe. Five thousand workmen were engaged on it day and night, but after 35 attacks by the RAF the project was abandoned. Construction men hinted that a death ray machine capable of stopping aircraft engines in flight and burning London to the ground was being installed. (Canadian WIB Radio photo received by Beam Wireless.)

http://www.arcforums.com/forums/air/index.php?showtopic=215575

From "Restricted Films of WWII":

> *"An incomplete German Block House near Vatan, France. (About 240Km south of Paris) According to civilians, the nazis hoped to house electrical apparatus to send out beams that would stop aircraft in flight. The structure is 300' long, 200' wide, and some four stories high. Steel doors meant to operate on rollers are 8' thick and 24'-25' high. Allied aircraft pounded the block hous and it's environs with 1000lb bombs."*

Aerial view of the heavily bombed bunker - Blockhaus d'Éperlecques - Open to the public since 1973 and listed "Ancient Memorials" in 1985.

http://www.456fis.org/NAZI_SECRET_WEAPONS_OF_1944.htm

Mechanix Illustrated
April 1944

The British government was spooked back in 1935. Not because of Hitler's air force or his infantry. Because of his death ray.

Newspapers screamed that the Nazis might have a super-weapon that could incinerate living tissue or detonate a bomb at long distance. Flooded by letters begging for a response, the British Air Ministry asked prominent physicist Robert Watson-Watt to see if a radio-wave-based death ray was feasible.

Within ten days Watson-Watt reported that such a weapon was unlikely. But using radio waves to locate an approaching bomber was a real possibility. And that's how radar was born.

Robert Watson-Watt is given the credit for inventing the radar. In fact, this credit should go to the German engineer Christian Hulsmeyer who in 1904, using patented an early warning system for shipping. He, in turn, used a discovery by Heinrich Hertz who had discovered in 1888 that radio waves could be bounced off objects.

In 1935, Robert Watson-Watt - a Scottish physicist - was asked by the Air Ministry to investigate the possibility of creating a "death-ray" weapon using radio waves. Watson-Watt was working at the National Physical Laboratory in Slough.

Watson-Watt did not create a "death-ray" weapon but he did find that his radio transmitters could create an echo from an aeroplane that was over 200 miles away. This information would give the Royal Air Force an early warning of an attack by enemy fighters. By the time an enemy force was nearing the coastline, fighters would be airborne and ready to fight. The enemy would have lost the element of surprise. This invention by Watson-Watt was vital to the RAF during the Battle of Britain in 1940.

In 1940, aided by John Randall and Henry Boot from Birmingham University, Robert Watson-Watt invented the cavity magnetron. This produced a compact source of short-wave radio waves and allowed Fighter Command of the RAF to detect incoming enemy planes from a much greater distance thus giving the pilots more time to organize themselves.

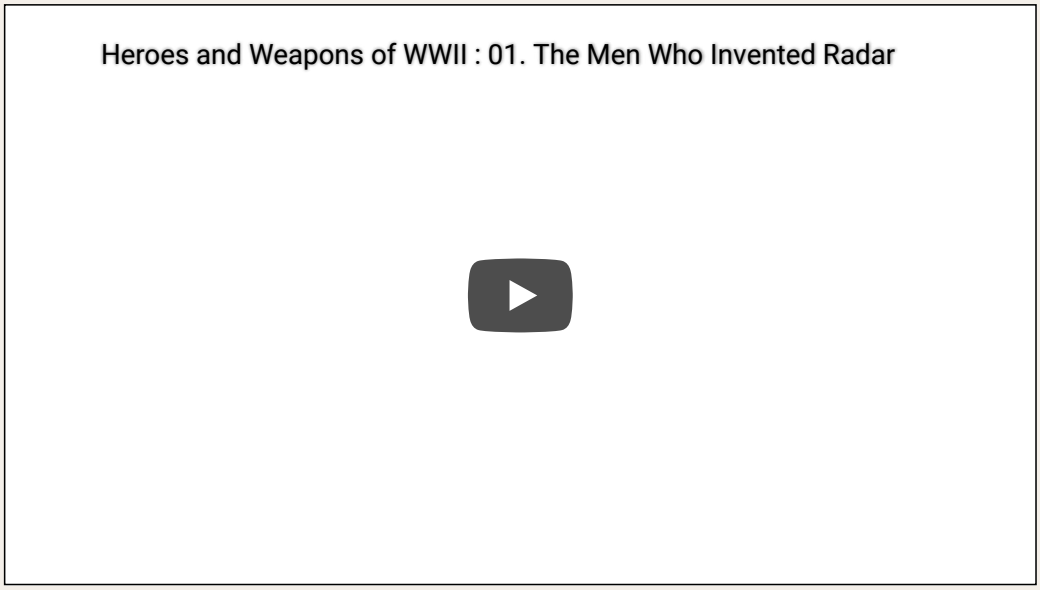

The Quantum Exodus: Jewish Fugitives, the Atomic Bomb, and the Holocaust - by Gordon Fraser - 2012 - Pg 133-134:

> A network of scientific supporters sprung into action to convince the authorities that Gans, an expert in magnetism, would be more profitably employed in Schmellenmeier's laboratory. A letter from no less than SS Reichsfürer Heinrich

Himmler appeared to settle the matter. The enfeebled Gans was assigned a new objective. More than a decade before, an obscure idea in a German research journal had led the US scientis Ernest Lawrence to invent cyclotrons. Machines to whirl protons and other subatomic fragments and accelerate them to high energies. Schmellenmeier's idea was to investigate wether this new machines could be made into weapons. The effectiveness of conventional German antiaircraft guns had been reduced by Allied bombers flying high, out of range ofthe guns, and wreaking increasing havoc on German cities. Perhaps Schmellenmeier's new weapon could hit such targets in the stratosphere. The idea was to whirl electrons round in a ring to create intense microwave radiation. This would them be beamed at enemy aeroplanes and interfere with engine ignition or blind the crew. The device was called the "Rheotron". On a paper, it sounded very impressive, a new superweapon to complement the V1 and the V2 "Vergeltungswaffen" (retaliation weapons) then beeing readied. However the idea of such "death ray" was not new. In 1935, Britain had set up a comitee to study the new methods of air defence. Soon it appeared that the beam power needed was unattainable, but the technology was soon refocused into what became to known as "radar".

Gans had been rescued once from fate in a concentration camp, but was still not safe. His luck finally seemed to have run out in the summer of 1944, when he was arrested and taken to the Grosse Hamburger Strasse, Berlin's assembly point for jews en route to concentration camps. Again, a rescue mission swung into action in the last minute. By now, with the fate of the Nazis becoming clear, some high-level SS members were eager to fabricate some protection for themselves by helping Jews instead of killing them. The Rheotron was an elaborate bluff in several levels. First it was a paper deterrent, but it also had a secondary role as a cover for Jewish scientists, notably Gans, who suspected that the idea would not work. Later that year Schmellenmeier's equipment was evacuated with the instruction that "in case of military defeat, the Jew Gans is to be liquidated. However the American forces arrived first.

Ernst Schiebold (1894-1963) was a German mineralogist who has rendered outstanding services to the material examination using X-rays. Von Schiebold sold Milch of the Air Force the idea that it was possible to build an X-ray searchlight which would cause burns on the crews of Allied bombers at altitudes up to 30.000 feet. the source of the X-rays was to be a betatron.

http://www.abovetopsecret.com/forum/thread817832/pg1
http://www.forbiddenknowledgetv.com/videos/911--false-flags/911-proof-of-laser-weapons-part-3.html

During WW2 the German electronics firm Siemens developed a particle beam weapon for the Luftwaffe. It was invented by Prof Max Steenbeck in 1935. Heinz Schmellenmeier, Richard Gans and Fritz Houtermans were leading figures in the project.

How the machine worked was that it interrupted the magnetos of engines in Allied bombers and brought aircraft down to lower altitudes into the reach of FLAK batteries.

Norwegian born Dr Rolf Wideroe wrote in his autobiography that he worked on a particle accelerator X-Ray transformer for this project at Hamburg in 1943. The Philips subsidiary Valvo also participated and much of the engineering was performed by CHF Muller & Co. Wideroe later rescued the device from the rubble of Dresden and delivered it to General Patton's 3rd Army at Burggrub on 14 April 1945.

A second rival device, Ernst Schiebolds 'Röntgenkanone was developed at Großostheim south of Frankfurt. This employed a particle accelerator cupped from beneath by a Beryllium parabolic mirror with a bundle of nine beryllium rods as an anode at it's core. the entire device was steerable at Allied bomber formations. The Company Richert Seifert & Co was largely responsible for it's manufacture.

These were not lasers. They directed hard radiation at aircraft and were the forerunners of Star wars weapons today.

http://www.answers.com/topic/directed-energy-weapons
http://en.wikipedia.org/wiki/Wunderwaffe

In the later phases of World War II, Nazi Germany increasingly put its hopes on research into technologically revolutionary secret weapons, the Wunderwaffen.

Among the directed-energy weapons the Nazis investigated were X-Ray Beam Weapons developed under Heinz Schmellenmeier, Richard Gans and Fritz Houtermans. They built an electron accelerator called Rheotron (invented by Max Steenbeck at Siemens-Schuckert in the 1930s, these were later called Betatrons by the Americans) to generate hard X ray synchrotron beams for the Reichsluftfahrtministerium (RLM). The intent was to pre-ionize ignition in Aircraft engines and hence serve as anti-aircraft DEW and bring planes down into the reach of the FLAK. The Rheotron was captured by the Americans in Burggrub on April 14, 1945.

Another approach was Ernst Schiebolds 'Röntgenkanone' developed from 1943 in Großostheim near Aschaffenburg. The Company Richert Seifert & Co from Hamburg delivered parts.

The Third Reich further developed sonic weaponry, using parabolic reflectors to project sound waves of destructive force. Microwave Weapons were investigated together with the Japanese (see also: Japanese radar and related weapons of world war 2).

http://www.cdvandt.org/CIOS-XXVIII-31.pdf
http://www.quora.com/Sy-Gunson

Rolf Wideroe said in his autobiography:

"It appears that Dr. Schiebold hawked his ideas about. He spoke to physicists who must have thought him a hopeless case, but he also tackled some influential people in official capacities who were not in a position to make informed judgements. Most people probably dismissed him as a harmless lunatic, but some must have been convinced because the Air Force, i.e. the German Aviation Ministry (RLM) and Command of the Luftwaffe, provided a certain amount of support for his `death ray'.

In order to conduct some test experiments for this `death ray', a still unused and unpacked X-ray apparatus with a high voltage supply of a little over one million volts (made by means of a sort of cascade circuit), was taken from a hospital in Hamburg to a small military airport called Groß-Ostheim (today `Großostheim') in the region of Hanau. If I remember rightly, Richard Seifert organized this tests and Hollnack was their administrator. However, both engineers and technicians quickly understood that the danger to themselves operating the machine on the ground was far greater than to the pilots and bombs in the enemy aircraft.

Still, a ray-transformer or betatron could produce X-rays of many million volts and in doing so one could, in principle (purely on the grounds of the laws of physics), improve the `bundling' of the beam with an increase of energy. To a certain extent, the effective range could be increased. This seemed to be the reason for the German Air Force's interest in the betatron. I wasn't really supposed to know anything about it, and we only ever talked about the betatron in terms of its importance to medicine. As it turned out this was actually correct.

By November 1943 I had developed a three-phase plan which provided first for the construction of a 15 MeV betatron in Hamburg, then a 200 MeV betatron and finally an experimental station in Groß-Ostheim for even larger installations... [Wideroe comments that only the Hamburg machine came to fruition however Allied intelligence refers to a working machine at Groß-Ostheim disrupting Allied bombers therefore Wideroe may have been out of the loop on subsequent developments]

Our work in Hamburg soon confirmed that the step from Kerst's 2.3 MeV machine (USA) to our planned 15 MeV ray-transformer was the right one. Of course, all we wanted in principle was to achieve as much energy as possible, but at 15 MeV we did not expect any imminent problems with the iron yoke (which was very similar to that of an ordinary transformer). However, these problems did appear when we built the first 31MeV machine for Brown Boveri in Baden, as I shall explain later."

Dr. Schiebold's 'Röntgenkanone' was captured by Patton's Army at Burggrub near Beyreuth about 14 April 1945. It disappeared into US black projects in New Mexico brought back to USA by Project LUSTY.

http://jansrose.blogspot.com.es/2012/03/death-rays-and-ball-lightning.html

From Wideroe's online autobiography, The Infancy of Particle Accelerators:

I eventually found out why the German Air Force was so interested in the betatron. Physicist Dr. Schiebold from Leipzig, a specialist on non-destructive testing of materials using X-rays among other methods (after the War he became professor in Magdeburg) had had the idea that it would be possible to build an X-ray tube....[that] would cause the X-rays to be emitted in a narrow bundle. With sufficiently high voltage it would then be possible to achieve high radiation intensities at long distances. Thus it may even be possible to kill the pilots.

> *In order to conduct some test experiments for this 'death ray', a still unused and unpacked X-ray apparatus with a high voltage supply of a little over one million volts (made by means of a sort of cascade circuit), was taken from a hospital in Hamburg to a small military airport called Groß-Ostheim (today 'Großostheim') in the region of Hanau.*

Gunson states that "ball lightning" was an artifact of the ray when it was used to disable aircraft in flight. I have heard this claim before, though I can't remember where. However, mention of ball lightning always rings a resounding "ding! ding! we have a winna!" in my head.

http://en.wikipedia.org/wiki/Betatron

A betatron is a cyclic particle accelerator developed by Donald Kerst at the University of Illinois in 1940 to accelerate electrons, but the concepts ultimately originate from Rolf Widerøe, whose development of an induction accelerator failed due to the lack of transverse focusing. Previous development in Germany also occurred through Max Steenbeck in the 40s.

The betatron is essentially a transformer with a torus-shaped vacuum tube as its secondary coil. An alternating current in the primary coils accelerates electrons in the vacuum around a circular path. The betatron was the first important machine for producing high energy electrons.

Betatrons were historically employed in particle physics experiments to provide high energy beams of electrons—up to about 300 MeV. If the electron beam is directed at a metal plate, the betatron can be used as a source of energetic x-rays or gamma rays; these x-rays may be used in industrial and medical applications (historically in radiation oncology). A small version of a Betatron was also used to provide electrons converted into hard X-rays by a target to provide prompt initiation of some experimental nuclear weapons by means of photon-induced fission and photon->neutron reactions in the bomb core.

The Radiation Center, the first private medical center to treat cancer patients with a betatron, was opened by Dr. O. Arthur Stiennon in a suburb of Madison, Wisconsin in the late 1950s.

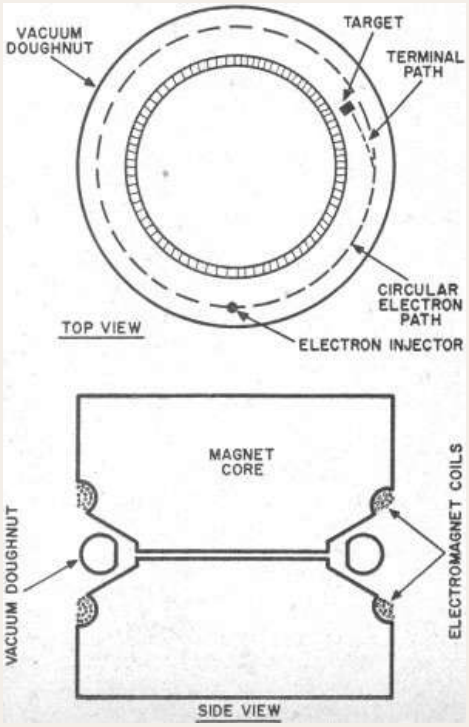

Fig. ? The betatron. Note how the pole pieces go into the center of a vacuum "doughnut."

American Atomic Bomb testing!! (a Betatron bomb)

The George device used a Mk-5 bomb assembly and was intended to gather additional data on the initiation time vs yield curve. A device used of an external initiator as opposed to an internal one activated by the implosion shockwave. This device known as a betatron used electrons to generate high energy X-rays inducing photo-fission in the core to initiate the chain reaction. The betatron allowed very accurate control of initiation time. The test device had a diameter of 100cm and weighed 1224kg, the cloud reached 11,000m. The shot was postponed due to unfavorable weather conditions, and was also moved to a different area of the Nevada Test Site due to residual radiation from the previous shots Easy and Fox.

http://nuclearweaponarchive.org/Usa/Tests/Tumblers.html

Operation Tumbler-Snapper
George
1 June 1952

Cosmic Self-Massage

Taoist Way of Rejuvenation

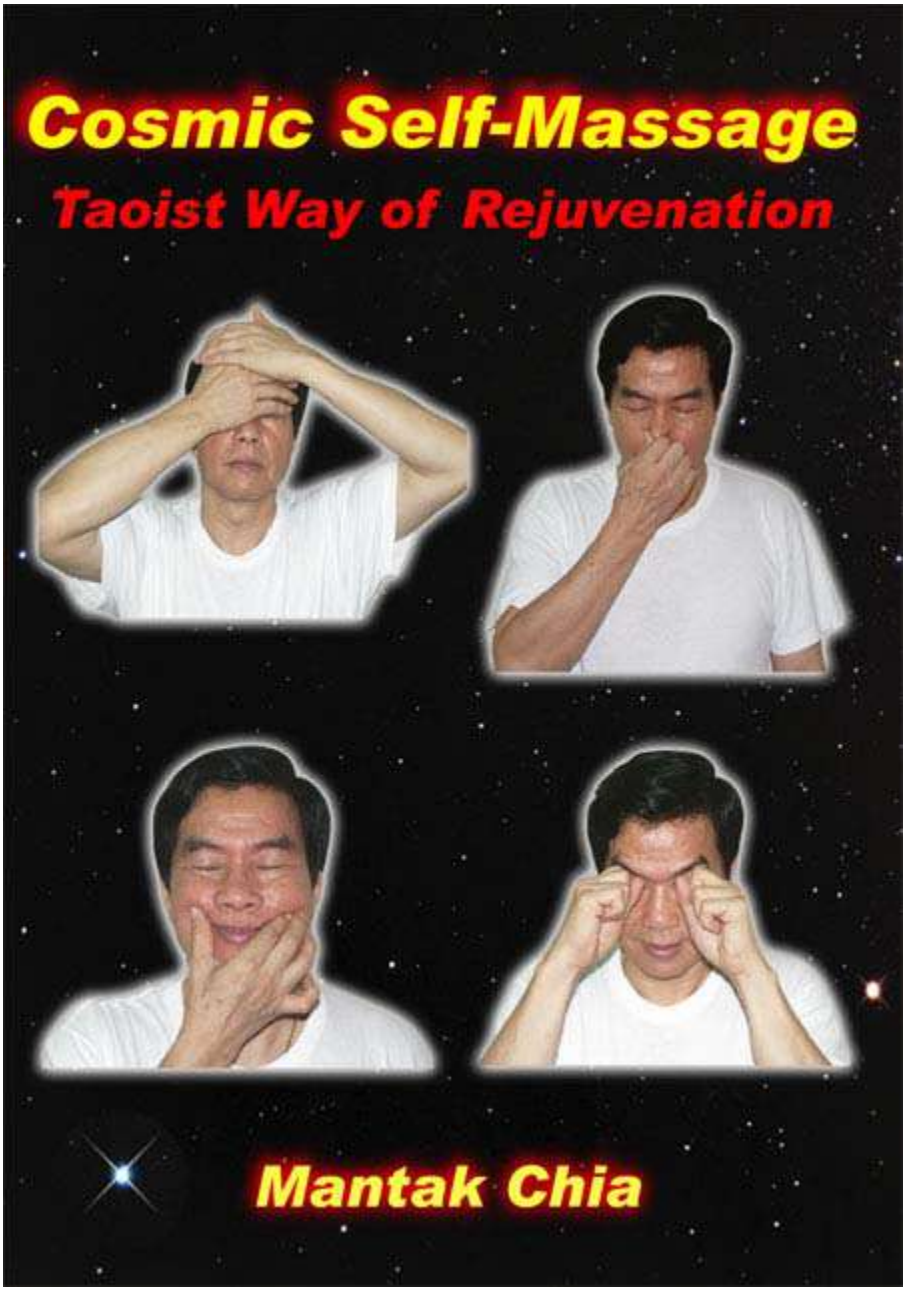

Mantak Chia

Cosmic Self-Massage

Taoist Way of Rejuvenation

Mantak Chia

Edited by:

Dena Saxer

Editor: Dena Saxer

Design and Publishing Consultant: Cathy Umphress

Illustrations: Juan Li

Computer Graphics: Saisunee Yongyod

Layout: Siriporn Chaimongkol

Production Manager: Saniem Chaisarn

Final Editing: Jean Chilton

Project Manager: W.U. Wei

© *North Star Trust*

First published in 2003 by:

Universal Tao Publications
274 Moo 7, Luang Nua,
Doi Saket, Chiang Mai 50220 Thailand
Tel: (66)(53) 495-596 Fax: 495-853
Email: universaltao@universal-tao.com
Web Site: universal-tao.com

Manufactured in Thailand

ISBN: 0-9671718-5-7

All rights reserved. No part of this booklet may be used or reproduced in any manner whatsoever without the express written permission from the author, with the exception of brief quotations embodied in critical articles and reviews. Anyone who undertakes these practices on the basis of this booklet alone, does so entirely at his or her own risk.

Contents

Healing Hand 1
Palms 1
Pericardium 1
Large Intestine 1
Major Palm Lines 3
Fingers have Corresponding Bodily Functions..... 3
Fingers Correspond to Emotions, Elements and Organs 8
Head 10
Face 14
Temples 15
Mouth 16
Eyes 17
A. Bring Chi Energy to the Hands and Eyes 18
B. For the Eyeballs and Surrounding Area 20
C. Pull up the Eyelids 20
D. For the Eye Sockets 21
E. For getting a Tear out 21
F. Pull in the Eyeballs 23
G. Learn to Maintain Eye Contact 25
Nose 25
Ears 26
A. Outer Ear 26
B. Inner Ear 29
Gums, Tongue, Teeth 30
A. Bring Chi Energy to the Hands 31
B. Gums 31
C. Gums and Tongue 31
D. Tongue 32
E. Teeth Clenching 34
F. Energy to Teeth 34

Neck 36
A. Thyroid and Parathyroid: Site of Courage, the Power of Speech 36
B. Bring Chi Energy to the Hands 37
C. Whole Neck 37
D. Middle Neck 37
E. Turtle Neck 38
F. Crane Neck 38
G. Massage the Neck 38
Shoulders 40
Detoxifying Organs and Glands 41
I. Thymus Gland 41
II. Heart 42
III. Lungs 42
IV. Liver 43
V. Stomach, Spleen, Pancreas 43
VI. Large and Small Intestines 44
VII. Kidneys 45
VIII. Sacrum 46
Knees and Feet 47
I. Knees and Feet 47
II. Feet: Roots of the Body 48

The meditations, practices and techniques described herein are ***not*** intended to be used as an alternative or substitute for professional medical treatment and care. If any readers are suffering from illnesses based on mental or emotional disorders, an appropriate professional health care practitioner or therapist should be consulted. Such problems should be corrected before you start training. This booklet does not attempt to give any medical diagnosis, treatment, prescription, or remedial recommendation in relation to any human disease, ailment, suffering or physical condition whatsoever.

Healing Hand

Humans can build all kinds of sophisticated instruments because of the magnificence of the hands and the fingers. Another higher function of the hands is the power of healing. Knowing the major points of the hands and fingers will enable you to stimulate and maintain the organs in good function.

Palms

The palms are where all major energies of Chi join. The palm can be the place from which the life-force is sent out to heal others or yourself. The palm also is the place where energy can be received and enter into the bone structure and into the major organs.

Pericardium

The pericardium (P-8) is the main place of energy concentration. You can collect the energy in this point and transmit stronger energy from this point.

Large Intestine

The large intestine (LI-4) is the major point which controls all the pain in the body, especially in the sense organs (eyes, ears, nose) and headaches.

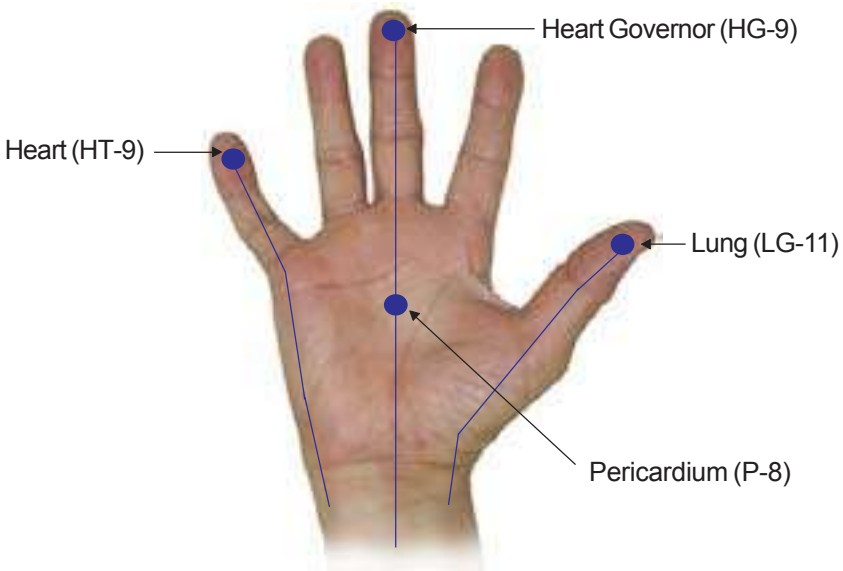

Fig. 1 *Pericardium*

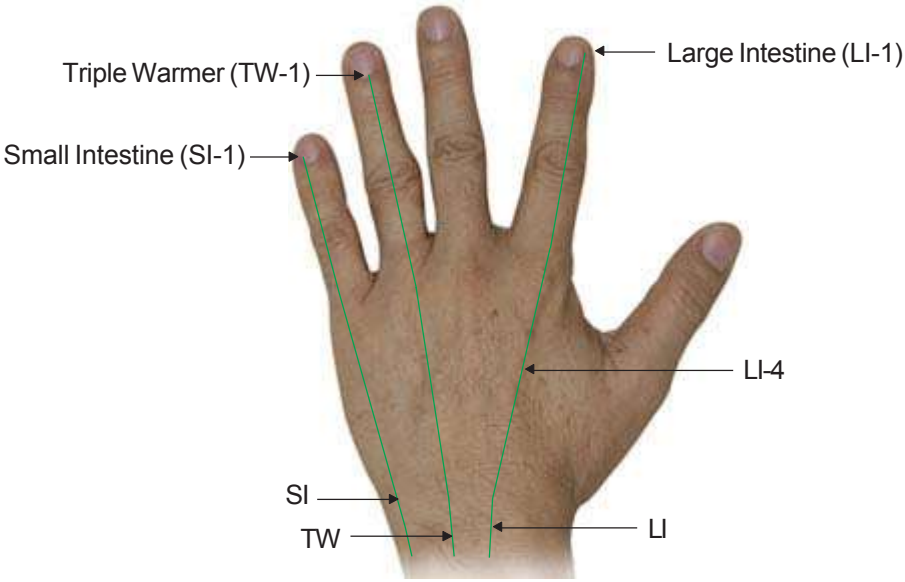

Fig. 2 *Large Intestine*

Major Palm Lines

The three major palm lines are the Life Line, the Line of Intellect and the Line of Emotion.

Fingers have Corresponding Bodily Functions

The fingers are connected to the organs' meridians. The joints of the finger bones are also related to parts of the organs and their corresponding senses and emotions.

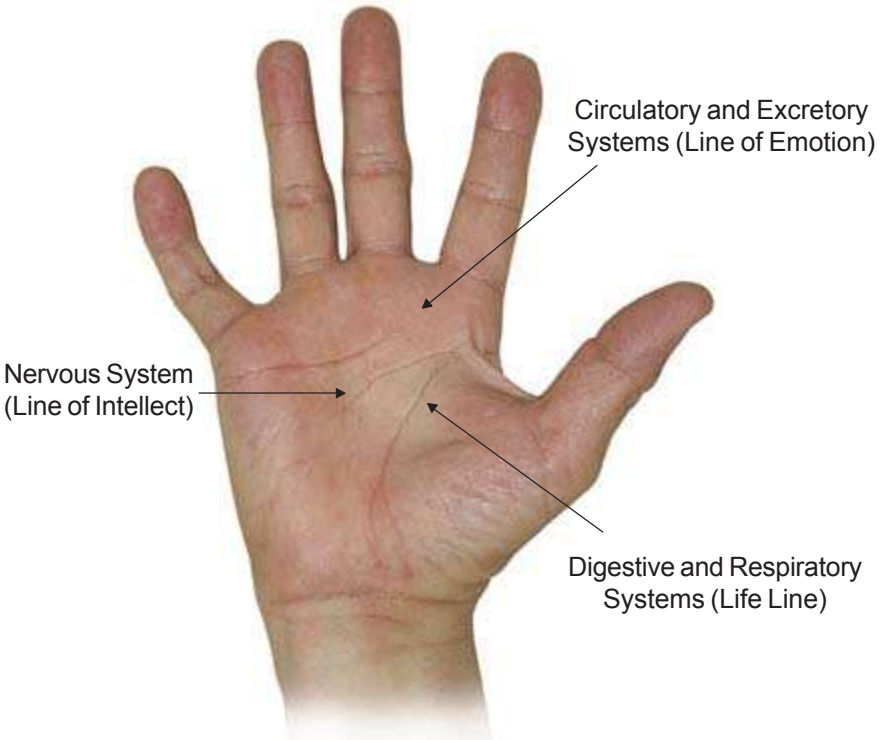

Fig. 3 *Three Major Palm Lines*

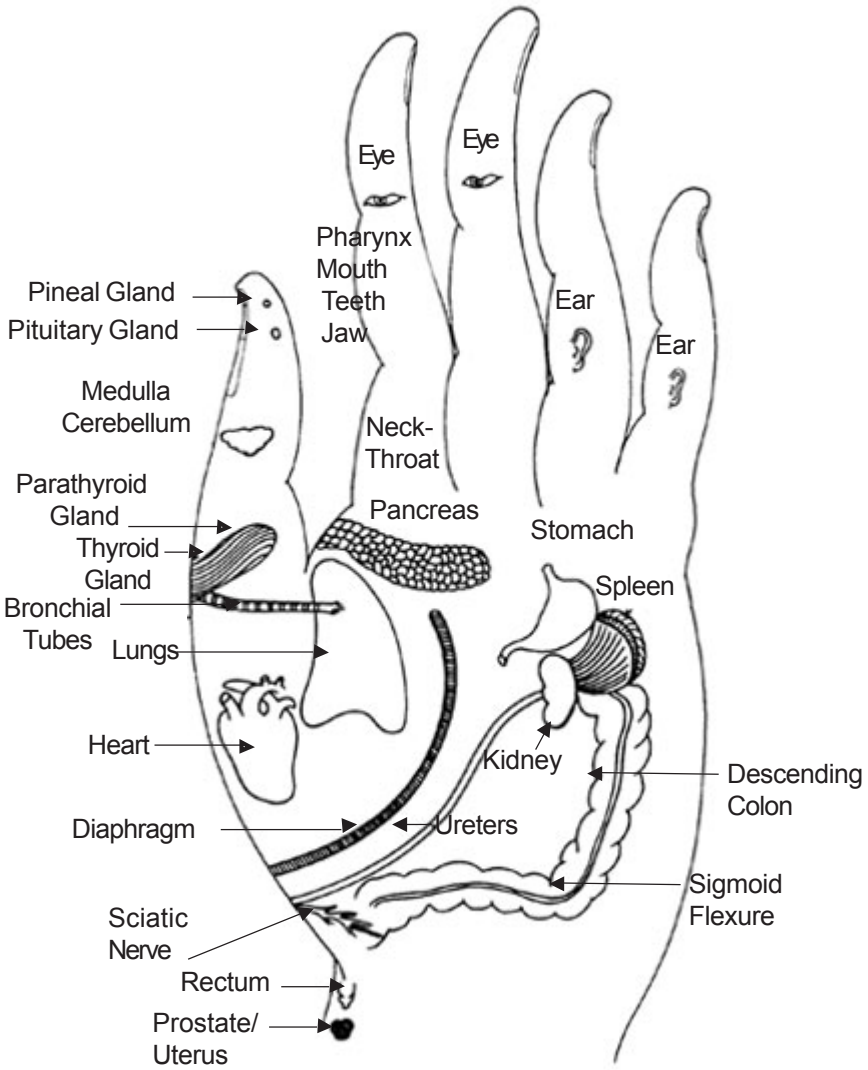

Fig. 4 *Fingers and Their Corresponding Bodily Functions Through the Organs' Meridians*

Massage the Hands

Always start by rubbing your hands until they are warm.

1. Massage the pericardium (P-8). Use the thumb to press the middle of the palm with a circular motion.

Fig. 5 *Massaging the Pericardium with fingers cupped in the palm in a half-fist, the pericardium is the point at the tip of the middle finger.*

2. Massage the hegu (LI-14). Press the thumb around the point in a circular motion, and press more at the index finger bone. Find the pain point and massage it away.

Fig.6 *Massaging LI-14*

3. Massage the major palm lines. Use the thumb to massage along the palm lines. Massage more towards the thumb bone and along that bone. When a lot of emotion is held inside, find the sore point and massage it.

4. Massage the back of the hand. Use the thumb to press along the bones on the back of the hand. When you find a tender spot, take more time to work on it.

5. Massage the fingers. Always rub your hands until warm. Use the right hand's fingers to wrap around the left thumb, and then, one by one, squeeze, hold and release each finger on the left hand three to six times. Start with the left hand and continue to the right hand's fingers, according to the elements of the finger. This will greatly help to control emotions.

Fig. 7 *Massaging the Palm Lines*

Fingers Correspond to Emotions, Elements and Organs

A. Thumb corresponds to the element earth and is associated with the stomach. The corresponding emotion is worry.

B. Index finger corresponds to the element of metal and is associated with the lungs and large intestine. It links with the emotions of sadness, grief and depression.

C. Middle finger corresponds with the element of fire and is associated with the heart, small intestine, circulatory system and the respiratory system. It links with the emotions of impatience and hastiness.

D. Ring finger corresponds to the wood element and is associated with the liver, gall bladder and the nervous system; it corresponds to the emotion of anger.

E. Pinky finger corresponds to the water element; it is associated with the kidneys, and corresponds with the emotion of fear.

Worry

Sadness

Impatience

Anger

Fear

Fig. 8 *Fingers' corresponding emotions, elements and organs*

Head

A. Crown Point

This is located in the center of the crown; in the fontanelle area of an infant's skull there may still be a slight depression. The crown point is the junction of one hundred channels through which the energy of the body passes. Massage this area with both your middle fingers. This will relieve dizziness and headaches, which result from too much energy in the head. It also relieves high blood pressure and stimulates the nervous system.

Fig. 9 *Crown Point is the junction point of one hundred energy channels.*

B. Bring Chi Energy to the Hands and Face

Inhale, contract the sexual organ, buttocks and middle of the anus. Rub the hands, clench the teeth, and put the tongue to the roof of the mouth. When the face, head, and hands are hot, breathe normally and begin to massage.

C. Knock the Head

Hit the head with the knuckles of the hand, knocking all around the head. Knocking the head lightly can help to clear your head, eliminate stubbornness and make your thinking sharper. Many of our students use this knocking of the head to release the pressures that they have from today's life of fast, advanced technology and the feeling of always having to keep up. This is especially true of those graduate students who feel a great deal of pressure and stress in keeping up with their studies. Each year students commit suicide because the pressures and stress accumulate too much in their heads, making them unable to think clearly: they start to feel everything in their society as too much pressure, which leads to worry, fear, sadness, and many, mixed emotions. The simple knocking of the head can release pressure and stress that accumulate there.

Fig. 10 *Knocking the Head*

D. Hold your Breath to Increase Chi Flow

Holding your breath will increase the Chi flow to the face. The head has many channels that join in the skull, especially in the crown point.

E. Scalp

Prepare your hands, head and scalp by warming up. Using both hands like a comb, press hard and move slowly, massage the scalp, going straight back from the hairline to the base of the skull. As you do this, mentally direct your energy from the back of the skull to your feet. Repeat 6-9 times. Massage more in any places in which you feel pain, until the pain goes away.

Fig. 11 *Massaging the Scalp*

F. Crest

Using your thumbs, massage the crest (the edge) at the base of the skull until you feel no pain there. This will help you reduce headaches and eye aches and will increase vision. This place in Tao tradition is called the Pool of Wind which tends to collect the “evil wind”, the major cause of all the pain in the senses.

Fengchi Point (GB-20)

Fig. 12 *Crest - Edge of the Skull*

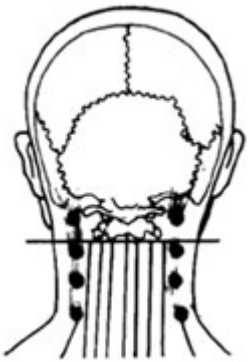

Fig. 13 *Go straight back from the hairline to the base of the skull.*

Face

Natural Beauty

Massaging your face with Chi is a far more effective beauty treatment than the most expensive cream or cosmetic, Your skin will glow brightly and eventually become less wrinkled. There are many meridians passing through or ending at the face. When blocked, they result in reduced flow of Chi energy and circulation. The face is the first impression imprinted in other people's minds. Chi circulation provides it with attractive personal energy.

Fig. 14 *Head and Face*

Fig. 15 *Massage the Whole Face*

Fig. 16 *Massage the Mid Forehead*

Temples

Use your index fingers to massage the temples in a circular motion, first clockwise, then counterclockwise. Massage the forehead and the temples; use the knuckle rub from the middle of the forehead all the way to the temples ten to twenty times. These exercises will reduce headaches in the front and in the temples. Find the painful point and massage it until the pain is gone.

Fig. 17 *Massage the Temples*

Mouth

Depression makes the corners of the mouth drop. Looking cheerful, delightful, more attractive and happy are dependent so much on the eyes and the corners of the mouth. When the muscles of the mouth are loose because of stress, depression, or sadness, the corners of the mouth drop and the energy system is depressed and in low key. No one likes to look at a sad face or a depressed face; it makes other people feel sad and depressed, too.

The flow of energy in the body and the expression of the face are the main attractive powers of a person. Massaging the mouth muscles up will help to lift the corners of the mouth. The Inner Smile and lifting up the corners of the mouth are very important to building up attractive energy.

Beautify the Mouth Massage

Using the thumb and the index finger of the right hand, touch both corners of the mouth and feel the Chi from the thumb and index finger pass to the corners of the mouth. Slowly press and push up about one inch, release and start again at the corners, pressing up ten to twenty times each day.

Cheerful Delight

Mouth Corners Drop

Fig. 18 *Beautifying the Mouth Massage*

Eyes

The eyes are the windows of the spirit. In Taoism we regard the eyes as Yang energy which will guide all Chi flow in the body. The eyes can greatly affect your personality Some people are born with a lot of white in their eyes--three portions of white to one portion of iris—sometimes called “thief eyes” or “danger attack eyes.” Such eyes can result in a suspicious look, portending unpleasant things. Through the exercises, you can gradually correct the white portion of the eyes.

Since the eyes are connected to the entire nervous system, they have a special importance. The eyes reveal the health of your entire body. Through the eyes we can tell which organs are weak and/or toxic. Massaging the eyes will remove stress from the vital organs. Nowadays people use their eyes much more than in the past to read, watch television, and work with computers, electronics and microscopes. This strains them a great deal and makes the openings of the organs loose, so that much of the organ energy is drained out. In Taoism, we regard the eyes as the doorways to the soul as well as the opening of the liver.

A. Bring Chi Energy to the Hands and Eyes

Repeat the procedure for bringing energy to the hands by inhaling; holding the breath; and contracting the sexual organ, buttocks and middle of the anus and both the left and right sides of the anus. Direct the Chi to both eyes. Rub the hands, clench the teeth, place the tongue on the roof of your mouth. Direct the energy to the face and then the hands. When your hands are hot, focus on your eyes until you feel them filled with energy.

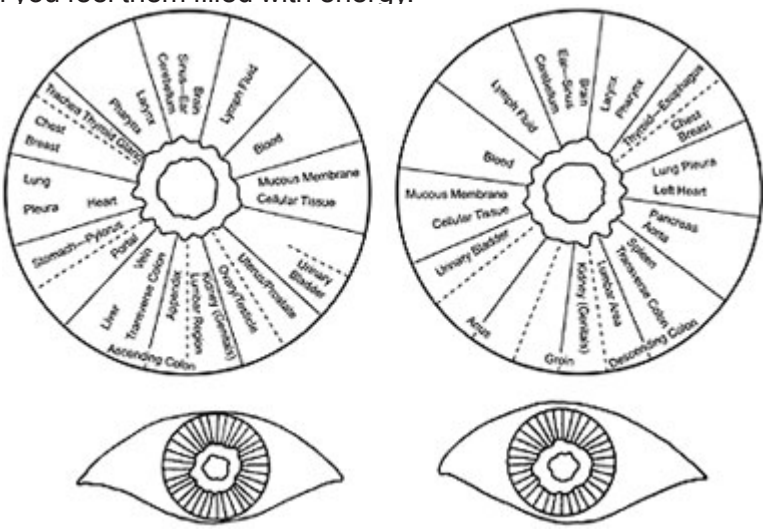

Fig. 19 *Eyes are the Windows of the Spirit*

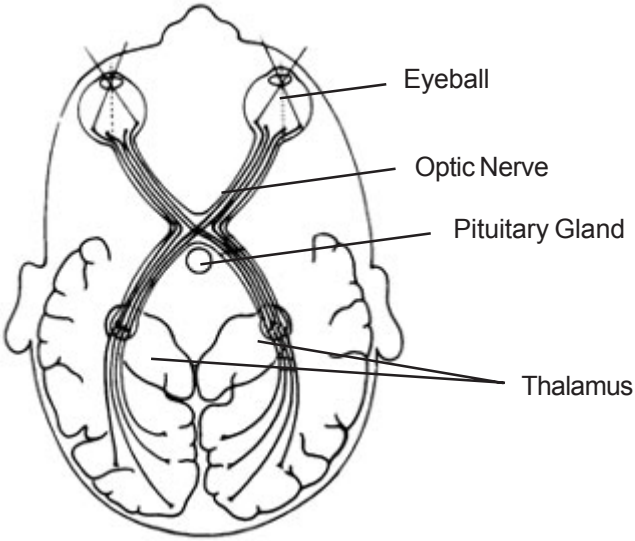

Fig. 20 *Eyes are the Doorways to the Soul*

Fig. 21 *Use the Fingertips to Gently Massage the Eyeballs*

B. For the Eyeballs and Surrounding Area

Close your eyes. Use your fingertips to gently massage your eyeballs through your closed eyelids, six to nine times clockwise, then six to nine times counterclockwise. Then gently massage the area around the lids the same number of times. Be aware of painful spots and massage those places until the pain goes away. Pay special attention to the inner and outer corners of the eyes. These are points of the gall bladder meridian and will relieve eye ailments if massaged.

C. Pull up the Eyelids

Pulling up the eyelids will increase the fluid. Use the thumb and index finger to pinch, pull up and release the eyelids six to nine times.

Fig. 22 *Pull Up the Eyelids*

D. For the Eye Sockets

Bend your index fingers and use the lower section (second phalanx) of each thumb to rub the upper and lower bones of the eye sockets six to nine times.

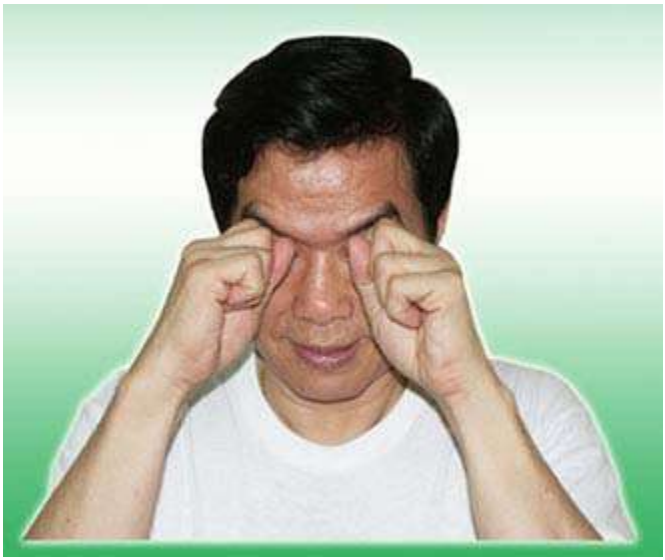

Fig. 23 *Massage the Eye Sockets*

E. For getting a Tear out

Hold an index finger up about eight inches from the eyes, or put a dot on the wall five or six feet away from you. Stare at it intently without blinking your eyes until you feel like a fire is burning in them. The Taoists believe that the toxins will burn out of the body through the eyes. They will begin to tear. Do this to strengthen your eyes. Then, rub your hands until warm; close your eyes and cover your eye sockets with your palms. Feel the Chi from the hands absorbed into the eyes. Rotate your eyes six to nine times, first in a clockwise direction, then counterclockwise.

Fig. 24 *Getting a Tear Out*

Fig. 25 *Absorbing the Chi into the Eyes*

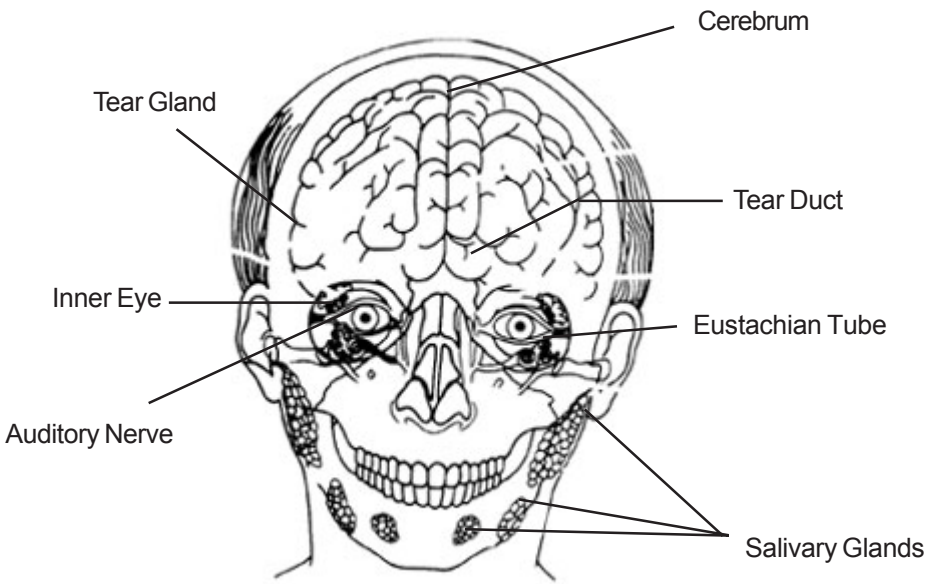

Fig. 26 *Parts of the Eyes Connect with Senses and Brain*

F. Pull in the Eyeballs

The eyes are divided into five parts. Each part is closely connected with the organs and nerves. Become aware of the eyes.

Pulling and pressing the eyeballs will exercise the organs, sense, glands and the brain. This is also the best exercise for the eye muscles. The eyes have many muscles which we do not exercise very much and, thus, they become weak, contributing to poor eyesight.

1. With the eyes still closed and cupped by the palms, inhale, contract the anus and sexual organ, and pull the eyeballs back into the sockets.
2. Contract the middle of the anus and the middles of the eyeballs.
3. Contract the front of the anus and the tops of the eyeballs.
4. Contract the back of the anus and the bottoms of the eyeballs.
5. Contract the right side of the anus and the right sides of the eyeballs.
6. Contract the left side of the anus and the left sides of the eyeballs. This exercise not only strengthens the eyes but also the pituitary and pineal glands and the inner ear including the ear drum and canals. When you pull the eyeballs in and upward and look toward the crown, you are exercising the upper muscles and stimulating the pituitary gland and pineal gland.

When you contract and pull in the middle of your eyeballs, you are exercising the back of the eye muscles and the inner ear.

When pulling in the outer corners of the eyes, you are strengthening the side eye muscles as well as the ear canals end the ear drums.

When pulling in the inner corners of the eyes, you are strengthening the inner side muscles, the tear ducts and the nose.

When pulling in the lower parts of the eyes, you are pressing the lower part of the ear canals and the nervous system.

Pressing into the Inner Ear

Left Eye Pressing into the Ear Canal. Right Eye Pressing into the Eustachian Tube

Pressing into the Pituitary Gland

Right Eye Pressing into the Ear Canal. Left Eye Pressing into the Eustachian Tube

Pressing into the Eustachian Tube

Fig. 27 *Moving the Eyes*

G. Learn to Maintain Eye Contact

Some people in eye to eye contact with other people feel nervous and frightened, and their voices become very low and hard to hear because of weak organs. Some people will look around and not look into your eyes when you talk to them. This can be caused by weakness of the gall bladder and kidneys. To improve this, you can use the Inner Smile, Six Healing Sounds and Tao Rejuvenation, plus the practice of staring.

Look at your face in a mirror for two to five minutes each day for the first week. After ten days you can begin to stare at your eyes and increase your confidence by looking at your irises. Gradually you will lose the fear of looking into other people's eyes.

Nose

The nose has several important functions. When we breathe properly through the nose and not through the mouth, the nose filters out dirt, preventing it from reaching the lungs. It also regulates the temperature of the air: when the air is too cold, the nose will warm it up first. Without this regulating action, extreme temperatures could injure the lungs, make us susceptible to upper respiratory illnesses and subject to getting colds easily. One great advantage about people who practice the Tao System is that they seldom get colds.

The nose has three meridians running through it: the large intestine, the stomach, and the Governor or back Channel. Rubbing the nose strengthens the temperature regulator stimulates the above organs, and increases hormone secretion. In China just a few needles inserted in the nose serve as a general anesthetic for any part of the body to be operated on.

An unhealthy nose affects the personality. A thin, flat and unhealthy looking nose, or a badly shaped nose, can make you less attractive to other people. A strong nose can help you to have good Chi. The nose is the first place into which the breath of life enters.

A weak nose usually will be infected, and a lot of mucous can leak into the sinuses. A weak nose also can affect the voice. A good singer always has a good nose. Rubbing and massaging the nose will increase the Chi and will improve circulation around the nose.

Ears

In China we believe that a person with thick, long ears will have a long, healthy life and that the personality will be more attractive.

The following exercises can prevent hearing loss which occurs gradually as we age. The ears are acupuncture maps of the whole body, containing 120 points. Many acupuncturists now use only the ear points to cure many ailments as well as for weight control.

A. Outer Ear

Repeat the method for bringing energy to the hands, contracting the left and right sides of the anus.

1. Front and back: Make a space between your index and ring fingers and simultaneously rub in front and in back of the ears.

2. Ear shells: Rub the ear shells with all your fingers. This will stimulate the autonomic nervous system and warm up your whole body, especially in the cold weather.

3. Ear lobes: Using your thumb and index finger, pull down on the ear lobes.

Rub in Front and Back of Ears

Rub the Ear Shells

Pull Down on the Ear Lobes

Fig. 28 *Rubbing the Ear*

4. Ear drum exercises: For the outer ear drum, repeat the method for bringing energy to the hands, contracting the left and right sides of the anus. Inhale and then exhale completely. Put your index fingers in your ears; it should feel as if there is a vacuum in the ears. If it does not, then exhale more. Move your index fingers back and forth six to nine times at your own pace until you can feel that the insides of the ears are moving, and pull out the fingers with a quick movement. You should hear a “pop” sound, and you will feel that you can hear better and that your mind is clearer.

Fig. 29 *Outer Ear Drum Exercise*

B. Inner Ear

Repeat the method for bringing energy to the hands, contracting the left and right sides of the anus.

The inside of the inner ear, being inaccessible, is usually not exercised and grows weaker with age. These two exercises use air pressure and vibrations to strengthen the inner ear. The ear canals, the nose canal, and the mouth are connected together, so in this exercise we are using the pressure that builds in the lungs and bringing it back up to the mouth, thus adding pressure to the inner ear drums. This is how to exercise the inner ear drums.

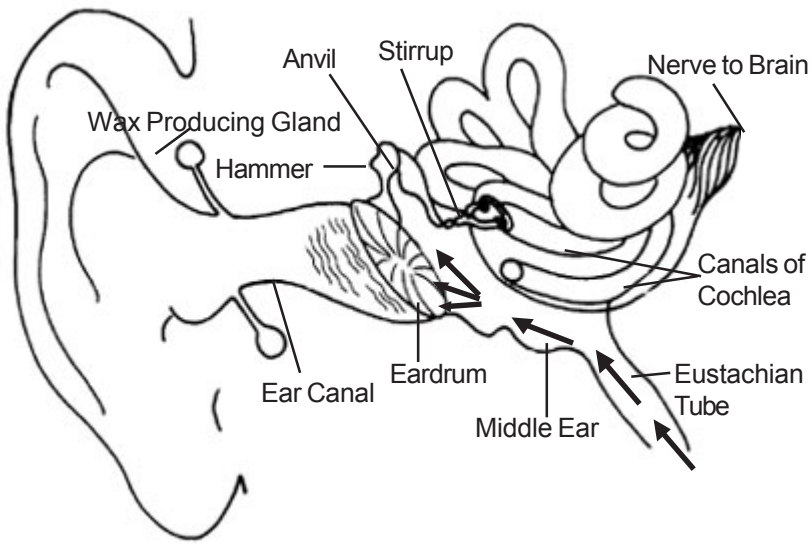

Fig. 30 *Diagram of Inner Ear Drum*

Fig. 31 *Inner Ear Drum Exercise*

Gums, Tongue, Teeth

Healthy teeth require healthy gums as their foundation. These exercises will strengthen both the gums and teeth. Teeth are the excess energy of the bones, and when the teeth get stronger, so do the bones. When the teeth and tongue are strong, your breath improves as well, eliminating bad breath.

We regard saliva as an essential form of energy which can lubricate the organs and digestive system. The tongue is the opening of the heart, and both are made of similar tissue. A healthy and clean tongue will strengthen the organs, especially the heart. You should clean your tongue twice a day with a brush or scrape it with a tongue scraper, and massage your tongue with a tongue depressor or a clean finger. Find the painful spots and massage there until the pain goes away.

A. Bring Chi Energy to the Hands

Repeat the procedure for bringing energy to the hands, contracting the middle of the anus.

B. Gums

Open your mouth and stretch your lips tautly over your teeth. Use three fingertips (index, middle, and ring fingers) to tap the skin around the upper and lower gums. Hit around until you feel warmth in the area.

C. Gums and Tongue

Massage your upper and lower gums with your tongue. Then suck in some saliva, press your tongue tightly against the roof of your mouth, and try to exercise the tongue. When you strengthen your tongue, you are strengthening your heart. Press around. Press the tongue to the roof of your mouth, tighten your neck muscles and swallow the saliva. This lubricates the digestive glands and organs.

Fig. 32 *Hitting the Gums Exercise.Using the Tongue, Massage the Upper and Lower Gums.*

D. Tongue

In a sitting position place the hands on the knees, palms down. Exhale and straighten the arms, spreading the fingers apart and keeping the hands on the knees. Open the mouth as wide as possible and thrust the tongue out and down, focused on the throat. With the tongue out as far possible, gaze at the tip of the nose. The whole body should be tense. Hold the breath for as long as you feel comfortable. Relax with inhalation and regulate the breath. This will help to strengthen the throat, the tongue and the power of speech. These exercises will help to improve foul breath and to clarify speech.

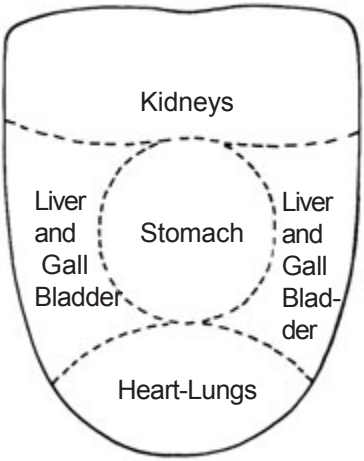

Fig. 33 *Diagram of Tongue Parts and Corresponding Organs*

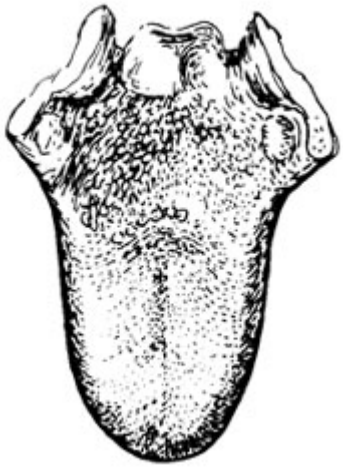

Fig. 34 *Tongue*

Fig. 35 *Press Tongue to the Roof of the Mouth*

Inhale, then exhale as you press your tongue out and down as far as you can. Follow by pulling the tongue in and curling it. Press your tongue to the roof of your mouth as hard as you can, contracting the middle of the anus and the esophagus to help the tongue. With more practice you will know how to use the inside force, the force from the organs, to press your tongue up. Even though the tongue has no bones to exert force, you will still be able to exercise the tongue well.

E. Teeth Clenching

Relax your lips. Click the teeth together lightly and then clench them hard, as you inhale and pull up the middle of the anus. Do this six to nine times. Move your tongue and mouth to create a lot of saliva. The technique of swallowing the saliva is to put the tongue up to the palate and swallow quickly with a hard gulp, sending the saliva down the esophagus to your stomach.

F. Energy to Teeth

Close your mouth and let your teeth touch lightly. Direct the energy to your teeth. Gradually feel the electrical flow of energy there.

Fig. 36 *Click the Teeth Together Lightly*

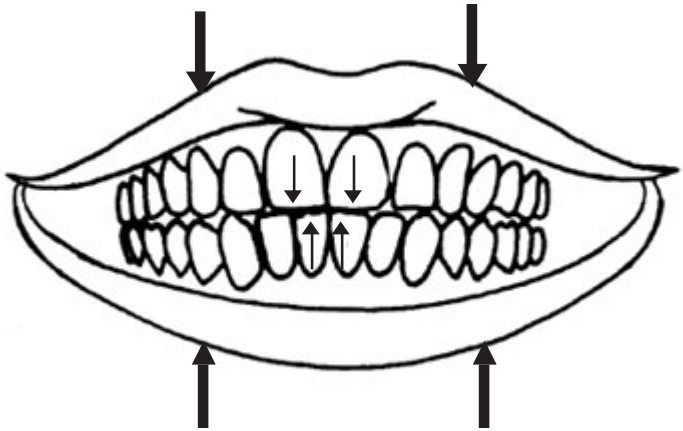

Fig. 37 *Clench the Teeth Together Hard*

Fig. 38 *Throat Glands*

Neck

A. Thyroid and Parathyroid: Site of Courage, the Power of Speech

The neck carries the busiest traffic in the body and is the seat of the thyroid and parathyroid glands. When you massage here, you increase the body's metabolism. Neck tension can also be caused by emotional imbalance. When we are tense and nervous, we are responding to negative emotions, such as anger, fear and sadness. The neck is similar to a traffic bottleneck. All of the signals, as well as the emotions, have to pass through it. When under stress and under emotional strain, the neck starts to accumulate and jam the tension. Unconsciously, the neck muscles tighten, attempting to block out pain. Keeping the neck soft will help Chi flow to the higher center that is located in the brain, keeping the mind and body in harmony together.

Tension in the neck can make you less courageous. When the neck is tense, it will block self expression in the throat. With proper flow of Chi energy, we can express ourselves appropriately at the proper time, place, and in a proper way.

The neck is the passageway of many meridians and is the channel of the Chi energy of the organs. In the middle is the Governor meridian. On the sides are the bladder meridian, the triple warmer meridian and the large intestine meridian. The emotions passing through the meridians of the neck may tense and jam up there.

Emotion:	Organ/Associate Organ:
Anger	Liver/Gall Bladder
Fear	Bladder/Kidneys
Grief	Large Intestine/Lungs
Hastiness	Heart/Small Intestine/Triple Warmer
Worry	Spleen/Stomach/Pancreas

B. Bring Chi Energy to the Hands

Do the procedure for bringing energy to the hands and contract the front of the anus.

C. Whole Neck

Spread your thumbs apart from your other fingers. Alternating hands, rapidly wipe the neck from the chin to the base nine to thirty-six times.

D. Middle Neck

Alternating hands, use the middle three fingers to rapidly wipe down the middle of the neck from the chin to the base nine to thirty-six times. The thyroid and parathyroid glands are in the front section of the neck. Use your thumb and the three other fingers to massage these glands. Find the painful points and massage them until you feel them open. Massaging this area will help to increase metabolism and the power of speaking.

Fig. 39 *Wipe the Neck from the Chin to the Base*

E. Turtle Neck

Sink your chin down, then out and up. Feel your spine press down and then expand. This will help loosen the vertebrae and discs of your neck.

F. Crane Neck

Move your chin forward, circling out, then down, then up, and out again. Feel your spine expand and then contract.

G. Massage the Neck

Massage the points along the back of the neck and on the back along the cervical vertebrae. Start from the shoulders and go up to the base of the skull. Use your fist to hit along the neck. Find any painful spots and any tense spots and massage until they are released. This will greatly help to release the tension of the neck and help to detoxify the toxic accumulations in the neck area, the causes of many headaches.

Fig. 40 *Turtle Neck*

Fig. 41 *Crane Neck*

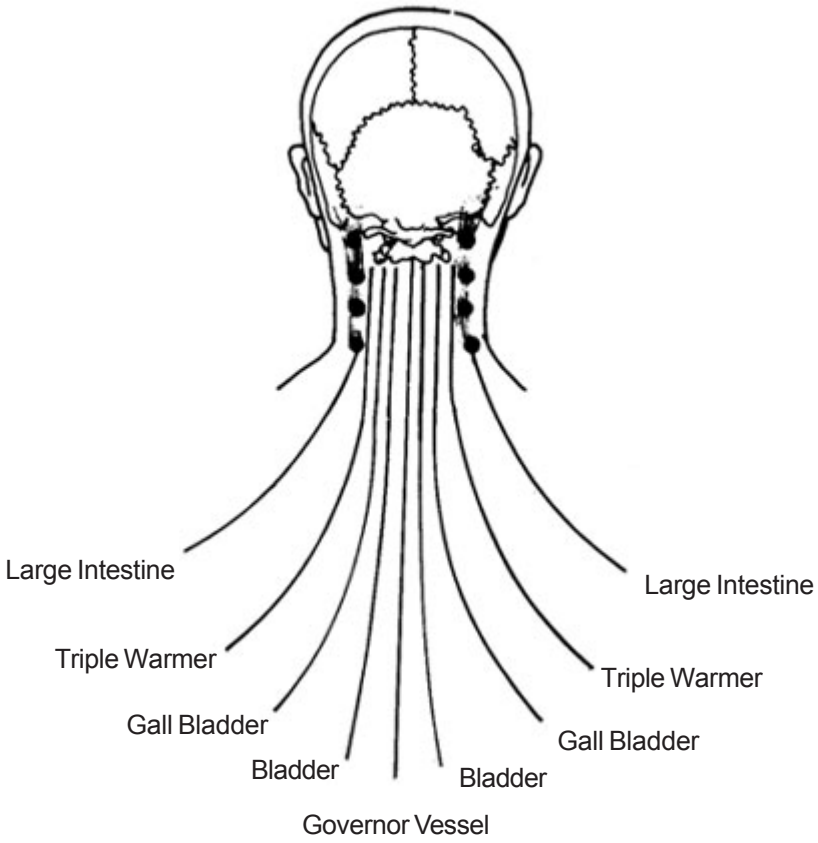

Fig. 42 *Massage the Points Along the Neck*

Shoulders

Many people feel tense and worried, and their shoulders are tight and held up. The way to release the tension is by pulling up your shoulders to press against the neck, tightening the muscles of the neck and shoulders. Hold for a while, exhale deeply, and let them drop down, pulled by gravity like a sack of potatoes. Feel the burden, worry, and stress drop down to the feet and out to the ground. Feel yourself grounded. Do this three to nine times, and the tension and worry will go away.

Relax your shoulders and chest, exhale and release more, until you feel the tenseness gone.

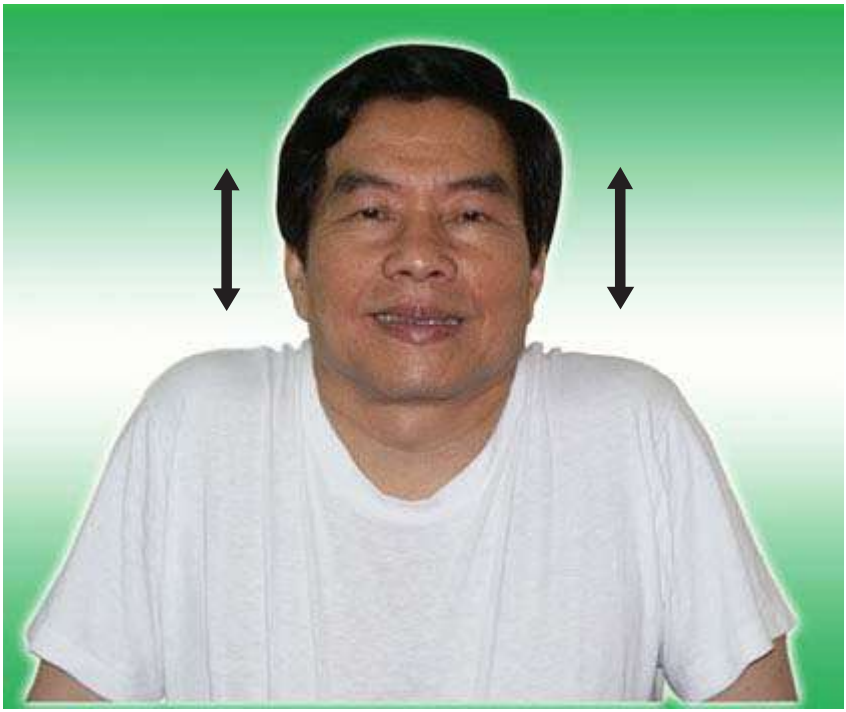

Fig. 43 *Dropping the Shoulders will Help to Release Tension and Worry.*

Detoxifying Organs and Glands

Lightly slapping and tapping over the organs and glands help to shock the toxic sediment and increase the circulation and Chi flow to these areas. Our practitioners claim they are able to heal themselves from many chronic illnesses which are very hard to heal by conventional medicine.

I. Thymus Gland

The thymus gland controls the immune system and is related to longevity. Normally the thymus gland atrophies after childhood. In the higher levels of Taoist practice, the thymus gland can be re-grown. This helps maintain health and vitality and supports greater spirituality. Thumbing the thymus gland can help increase the activity and release more hormones.

A. Bring energy to your hands by the usual procedure, contracting the front of the anus and bring the Chi toward the thymus.

B. Make a fist, inhale and thump down the middle of the upper chest from the collar bone to the nipples six to nine times. Do not talk while you are doing this or you might harm yourself.

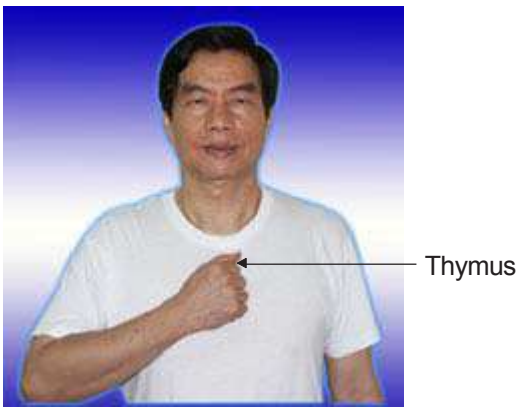

Fig. 44 *Hitting the Thymus Gland*

II. Heart

Lightly slapping an organ stimulates the release of toxins, which allows the organ to rebuild and repair itself. In doing these exercises, be aware that the slapping or tapping should be adjusted by you so as not to use excessive force which may be harmful.

A. Do the energy to hands procedure, contracting the left side of the anus and bringing Chi toward the heart.

B. Slap your heart lightly with your palm six to nine times. Don't speak.

III. Lungs

A. Bring energy to your hands, contracting the right side of the anus and bringing Chi to the lungs.

B. Using your palm, slap up and down your right lung, hitting only as hard as is comfortable. Do not talk. Contract the left side of your anus and slap your left lung. This can help to clean out the mucous and to clean out the lungs.

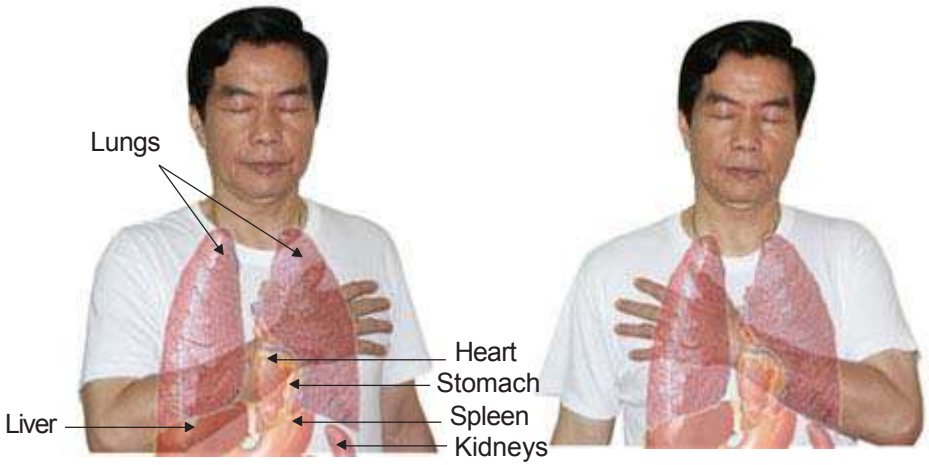

Fig. 45 *Slap at Heart, Lungs and Liver Areas*

IV. Liver

A. Bring energy to the hands, contracting the right side of the anus and bringing Chi to the liver.

B. Using your palm, slap below the rib cage on the right side. Don't speak. This can help to detoxify the liver.

V. Stomach, Spleen, Pancreas

A. Bring energy to your hands, contracting the middle of the anus.

B. Contract the anus at the left side, and slap at the spleen, pancreas and stomach. Place one palm on top of the other and rub below the rib cage, from center to left, then left to center.

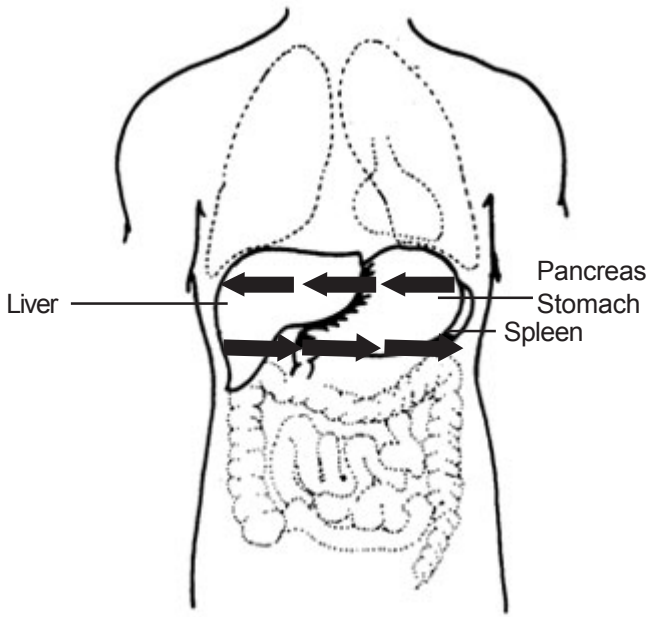

Fig. 46 *Rub the Stomach, Spleen and Pancreas*

Fig. 47 *Rub Back and Forth over the Liver, Stomach and Spleen*

VI. Large and Small Intestines

A.Bring energy to the hands, contracting the entire anus.

B. Small intestine: With palms together, rub a small circle around your navel, first clockwise, then counterclockwise.

The small intestine is one of the longest tubes in the digestive system. A careless diet, too much hot food or dairy products, or too little fibrous food will create mucous that will stick to the walls of the intestine, block the absorption of nutrients and slow down digestion. Once mucous accumulates, it is like a snow ball that will get bigger and bigger, eventually becoming a lump which slows down the traffic of the digestive system.

C. Large intestine: Place one palm on top of the other and rub your abdomen in a large circle. Start on the lower right side and rub up and around in a clockwise direction. This will move the energy in the intestine and relieve constipation. For diarrhea, rub counterclockwise. If you have normal elimination, rub in both directions. These exercises increase the absorption and dissolve the accumulations that stick to the large intestine's wall.

Fig. 48 *Hitting the Sacrum Can Help in Strengthening the Sciatic Nerves*

VII. Kidneys

The kidneys act as helping to filter out waste material from the blood. If there is too much waste in the system, the kidneys cannot filter it all. The waste will tend to collect in the ducts and tubules of the kidneys, impairing their health. By hitting the kidneys' area, we shake out the harmful sediment and help prevent kidney malfunction.

A. Bring energy to the hands, contracting the left and right sides of the anus.

B. Locate the kidneys just above the lowest, or floating, rib in the back on either side of the spine. Make a fist and hit the kidneys with the back of the fist between the wrist and knuckles. Alternate hands and hit only as hard as is comfortable. This will help to shake loose the sediment, crystals, and uric acid that get caught in the kidneys. This will also strengthen the kidneys and relieve back pain.

C. Rub your hands together to warm them. Then rub your palms up and down over the kidneys until they feel warm.

VIII. Sacrum

In the Taoist system the sacrum is regarded as extremely important. It is a pump which helps to bring spinal fluid and energy (Chi) to the brain. It is also the junction where the sexual organs, rectum, and legs meet. Sciatic pain, which shoots down the legs, originates in the sacrum; therefore, strengthening it will release this intense pain.

A. Bring energy to the hands, contracting the back of the anus to the sacrum.

B. Make a fist and use your knuckles alternately to hit both sides of the sacrum. First hit in the area of the eight sacral holes, and then the hiatus, the depression at the bottom of the sacrum.

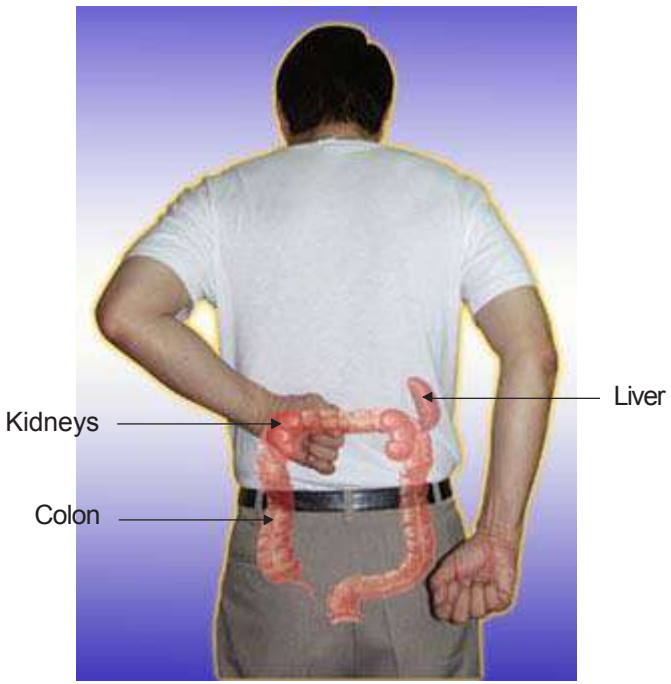

Fig. 49 *Hitting the Kidneys will help to Shake Out Sediment*

Knees and Feet

I. Knees are Toxin Collectors

Toxins tend to collect in the lower limbs because of the slowdown of the circulation due to gravity. The most common places are the back parts of the knees. Slapping at these places will break down the toxins. The body will then eliminate the toxins out of the body by urine, bowel movements and sweat.

A. Bring Chi Energy to the Hands

Bring energy to the hands; do no contractions.

B. Behind the Knees

Prop your leg up on a chair or low table so the knee is straight. Then slap smartly behind the knee nine to eighteen times. Although it hurts, it is extremely beneficial in releasing toxins which accumulate there. This release may be indicated by the appearance of a purple dot. Use discretion as to how hard you slap, since it can be overdone. Repeat this exercise on the other knee.

Fig.50 *Slapping Smartly behind the Knee Helps to Release Toxins*

Fig. 51 *Massaging the Knee Cap*

C. Knee Cap Massage

Massage the knee cap until it is warm, There is very little blood flowing to it and it tends to be quite vulnerable. This practice strengthens it. Massage the other knee cap.

D. Move the Knee Caps

Relax the knee caps, then move them up and down to the left and right and around both clockwise and counterclockwise.

E. Massage the Knees

Falling down is often caused by weak knees. Massaging the knees will improve your stability and flexibility.

II. Feet: Roots of the Body

Strong feet and tendons increase your stability by connecting you to the healing energy of the earth. Feet are the reflexes of the whole body's organs, glands and limbs. (They are like remote controls. Massaging will help to stimulate the organs and glands and increase the circulation.

A. Bring Chi Energy to the Hands

Bring energy to the hands; do no contractions.

B. Massage the Feet

Take off your shoes and stockings and massage the tops and bottoms of each foot with your thumbs and fingers. Be sure to massage the kidney point, the sore spot in the center between the ball of each foot and the adjoining pad. If you are in a hurry, massage the whole of each foot once by rubbing the sole of the foot vigorously and carefully across the top of the other foot, going from the heel to the arch to the toes. The soles of the feet have energy meridians to the entire body. Massage the feet, and when you find painful points massage them until the pain goes away. This will help to clear any blockage of Chi channel flow.

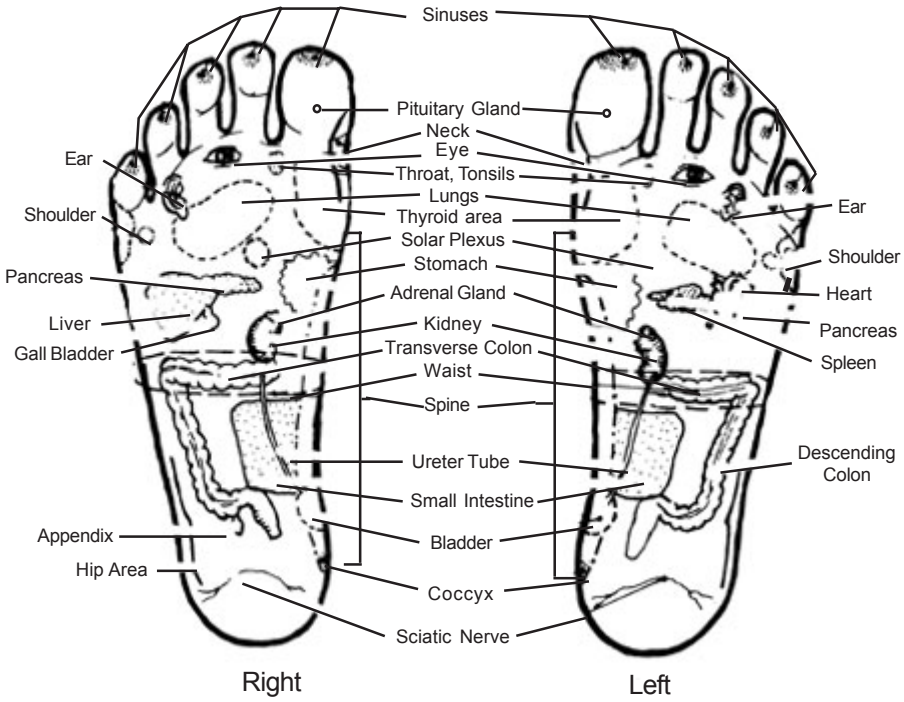

Fig. 52 *Feet are the Reflexes of the Whole Body's Organs, Glands and Limbs*

C. Spread Out the Toes

Spread out and separate all the toes, especially the little toes, and then release. Repeat six to nine times. This is especially good for the tendons of the feet.

Fig. 53 *Separate all the Toes by Spreading them out.*

D. Big and Second Toes

Rub the big toes and second toes together rapidly. This a good exercise to do at odd moments during the day.

E. Rub Feet Together

Keep the feet warm by rubbing them together. This will help to stimulate all the body's organs.

For further information about Universal Tao Centers, courses, or other resources, contact:

Universal Tao Instructor Associations

North America Instructors Association (NAIA)
c/o Loretta Robb, Treasurer
13 Plymouth Drive, Newark, Delaware 19713 USA
Tel: (1)(888) 444-7426 (Toll Free) or (1)(212) 330-7876
Email: info@taoinstructors.org Website: http://taoinstructors.org

European Instructors Association (EIA)
c/o Zentrum Waldegg
3823 Wengen, SWITZERLAND
Tel: (41)(33) 8554422 Fax: (41)(33) 8555068
Email:info@waldegg.ch Website: www.waldegg.ch

To order English books, and for your local Insructors use our Web Sites: www.universal-tao.com and www.taogarden.com

Universal Tao World Fulfillment Center
274 Moo 7, Luang Nua, Doi Saket, Chiang Mai, 50220 Thailand
Tel: (66)(53) 495-596 & 865-034 Fax: (66)(53) 495-852
North America Fax (1)(212) 504-8116 Europe Fax (31)(20) 524-1374
Email: universaltao@universal-tao.com **or** info@tao-garden.com

The Universal Tao is not and cannot be responsible for the consequences of any practice or misuse of the information in this book. If the reader undertakes any exercise without strictly following the instructions, notes, and warnings, the responsibility must lie solely with the reader.

$6.95

Cosmic Self-Massage

Taoist Way of Rejuvenation

Mantak Chia

Illustrations by Udon Jandee

Cosmic Self-Massage

In this booklet Virtually all Western massage is massage primarily of the muscles. Whatever its virtues, Western massage is altogether different from Chi Massage. Tao Rejuvenation employs one's own internal energy, Chi energy, to strengthen and rejuvenate the sense organs—eyes, ears, nose, tongue, teeth and skin—and the inner organs.

The techniques used by Taoists are some five thousand years old and, until very recently, were closely guarded secrets passed on from a Master to a small group of students. Often, too, each Master knew only a small part. Now Master Chia has pieced together the entire system of Chi Massage in a logical sequence in such a way that once you have it shown to you, you need only five or ten minutes of practice daily.

In short order you will note improvement in complexion, taste, vision, hearing, sinuses, gums, teeth, tongue, the internal organs and general stamina.

ISBN 0-9671718-5-7

9 780967 171852

Universal Tao Publications

274 Moo 7, Luang Nua, Doi Saket,
Chiang Mai 50220, Thailand
Tel: (66)(53) 495-596 Fax: 495-852
Email: universaltao@universal-tao.com
Web Site: www.universal-tao.com

Cosmic Healing I

Cosmic Chi Kung

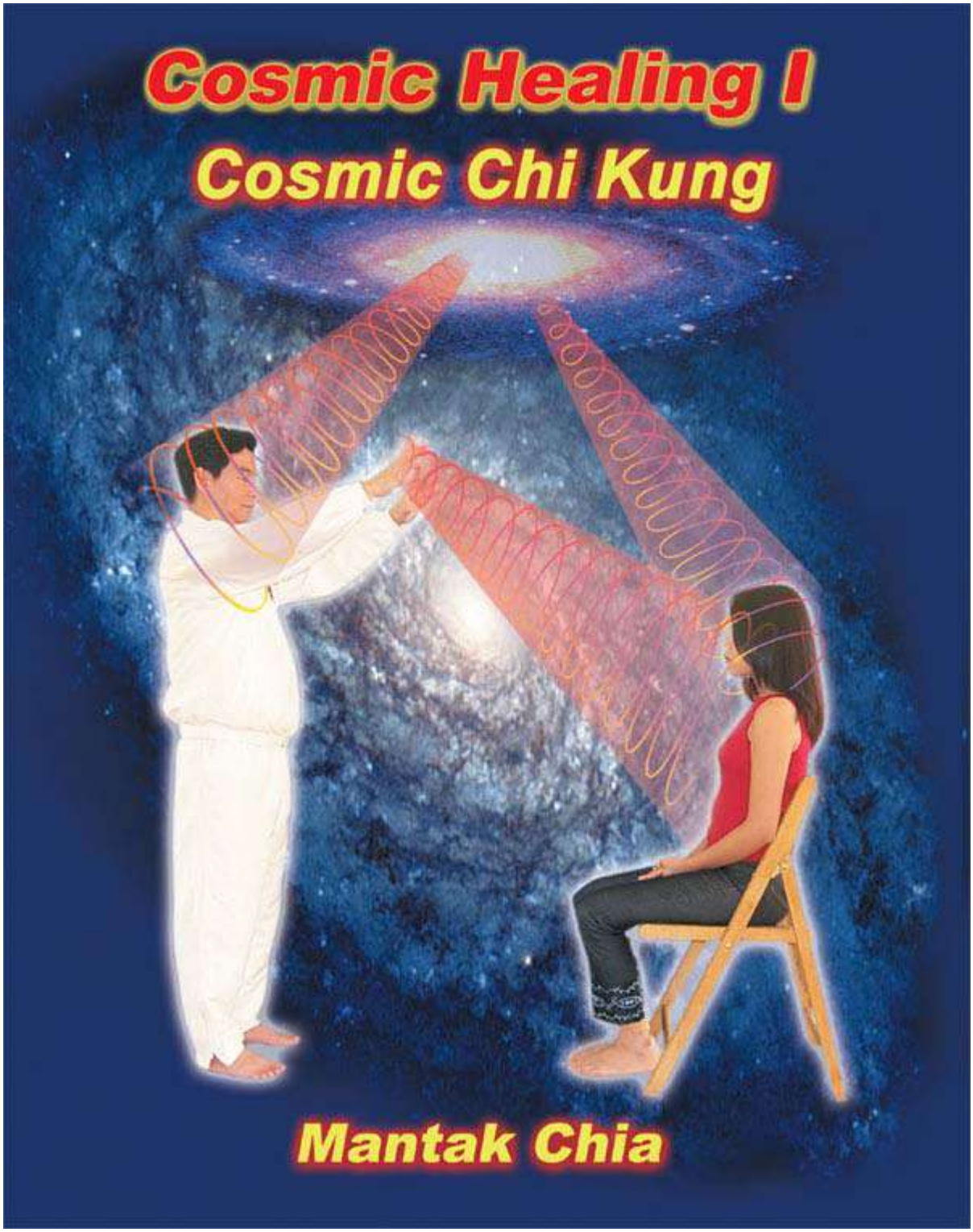

Mantak Chia

Cosmic Healing I

Cosmic Chi Kung

Mantak Chia

Edited by
Colin Campbell

Copy Editor: Colin Campbell

Assistant Editor: Matt Gluck

Contributing Editor: Kendra Moshe

Computer Graphics: Raruen Keawpadung

Photographer: Saysunee Yongyod

Design and Production: Saniem Chaisarn

Illustrations: Udon Jandee

Final Editing: Jean Chilton

Project Manager: W.U. Wei

© *North Star Trust*

First published in 2001 by:

Universal Tao Publications
274/1 Moo 7, Luang Nua,
Doi Saket, Chiang Mai, 50220 Thailand
Tel (66) (53) 865-034 & 495-596 Fax 495-852
Email: universaltao@universal-tao.com

ISBN: 974-87672-5-6
Library of Congress Catalog Number:

Manufactured in Thailand
Second Printing, 2001

All rights reserved. No part of this book may be used or reproduced in any manner whatsoever without the express written permission from the author except for brief quotations embodied in critical articles and reviews.

Contents

About the Author 9
Acknowledgements 12
Words of Caution 13

Chapter I
Cosmic Healing
Cosmic Healing Chi Kung in the Universal Tao System 14
Foundation of the Universal Tao System 14
Cosmic Inner Smile and the Six Healing Sounds 15
Iron Shirt Chi Kung and Bone Breathing 15
Stages of Mastering Chi 16
Four Sections of Cosmic Healing 17
Connecting to Heaven and Earth 17
Opening the Bridge and Regulator Channels & Extending your Chi Outwards 18
Opening and Energizing the Governor and Functional Channels 18
Activating One Finger Art and the Chi Belt 18

Chapter II
Preparing for Cosmic Chi Kung
Preparatory Practices 19
Warm up the Stove 19
Transform Sexual Energy 20
Filling the Joints with Chi 21
Bone Breathing and Marrow Washing 21
Bone Breathing 21
Marrow Washing 23
Heavenly Marrow Washing with Violet Light 23
Microcosmic Orbit 25

Chapter III
Cosmic Chi Kung
Opening the Three Tan Tiens to the Six Directions 27
Introduction 27
Relaxation, Letting Go, Surrender and Ego 28
Mind, Organs and Sexual Organs 28
Opening the Three Tan Tiens 30
Combined Practice 32
Warm Up Exercises 32

True Breath - Skin Breathing..... 33
Daily Practice: Opening, Connecting & Activating Chi Within & Cosmic Charging 34
Relax and Let go - Smile to Connect with Universe Within..... 41
Tan Tien Consciousness: The Second Brain 37
Three Minds into One: 'Yi' Power 44
Activating the Six Directions and the Three Fires 45
Direction Below 45
Front Direction and Tan Tien Fire 46
Back Direction and Kidney Fire 47
Heart Fire 48
Sacred Fire (Chi Fire)..... 49
Open the Third Eye 49
Front Direction: Push/Pull Master Practice 51
Left and Right Directions 52
Direction Above 53
Open the Spine..... 54
Open the Middle Channel and Perineum..... 56
Tan Tien and the Universe 57
Open the Three Tan Tiens 59
Upper Tan Tien - Mideyebrow 58
Middle Tan Tien - Heart Center - Conscious Mind 61
Recharge and Cut Around the Armpits 62
Lower Tan Tien - Navel - Awareness Mind 63
Activate Chi in the Bones of the Hips, Legs and Sacrum 64

Chapter IV
General Healing Session
Three Minds into One Mind (Introduction)..... 68
Activate the Six Directions (Introduction)..... 68
Activate the Three Fires (Introduction) 68
Linking Personal Stars, Energy Bodies and the Universe (Introduction) 69
Protective Circle and Chi Field (Introduction)..... 69
Sacred or Chi Fire..... 69
Chi (Sacred) Water Practice (Introduction)..... 69
Empty and Fill (Introduction) 70
Clean with Green Light (Introduction)..... 70
Clean with Blue Light (Introduction)..... 70
Charge with Violet Light (Introduction) 70

Chapter V
Cosmic Healing I - Basic

Source of Chi and Colors 126
Earth Chi 127
Human and Nature Chi 128
Solar Chi 128
Simple Practice 128
General Information 128
Healing Colors 129
White Chi 129
Blue Chi 129
Green Chi 129
Red Chi 130
Tangerine Chi 131
Yellow Chi 131
Violet Chi 131
Golden Chi 133
The Spleen 133
Cosmic Healing Planetary Colors 134
Summary - Working with Color 135

Chapter VI
Individual Healing Session

Almighty Knife 138
Outline of Practice 139
Energizing and Activating the Immune System 141
Outline of Practice 142
Cleansing the Internal Organs Technique 143
Healing Some Common Illnesses 143
General Principles 145
Outline of Practice 146
Cleansing the Spinal Cord 149
Cleansing the Blood (Lungs) 150
Outline for Cleansing the Blood/Lungs 150
Circulatory/Heart System 151
Stomach Pains 151
Relieving Pain: Blue Chi 152
Headache: Light Whitish Green and Light Whitish Blue Chi 153
Migraine Headache: Light Whitish Green Blue and Violet Chi 153
Toothache: Light Whitish Green and Blue Chi 153
Broken Bone: Orange - Yellow Chi 153
Back Injury: Light Whitish Blue and Green Violet Chi 154

Cysts: *Light Green and Blue Chi* 154
Infection and Inflammation: Light Green Chi 154
Fever 154
Insomnia: Green and Blue 155
Tinnitus 155
Blood Clotting: Blue Chi - Fresh Burns: Green and Blue Chi 155
Old Minor Burns: Green and Red Chi 155
Old Severe Burns: Green and Red Chi 156
Old Wounds: Green and Red Chi 156
Some Specific Points and Ailments: 156
Solar Plexus: Blue Chi 157
Skin Infection: Blue Chi 157
Eyes: Green Chi 158
Ears: Violet Chi 158
Summary of Individual Healing Session 159

Chapter VII
Different Hand Techniques
Forget about your Palms 165
Don't Focus your Mind on the Sick Part 165
Cosmic Healing is Teaching 165
Chi Kung Diagnosis: Hand Scanning 166
General Variations in the Energy Field 166
Hand Scanning the Internal Organs 167

Chapter VIII
Cosmic Chi Kung Palm and Finger Training
Why We Practice the Cosmic Chi Kung 169
Opening Heaven and Earth Force in the Palms - Heaven and Earth Spirals 170
Cell Breathing 171
Mind, Eyes, Heart and Intention (YI) 172
Connecting the Bridge 173
Cosmic Chi Kung Preparation 174
Cosmic Chi Kung Preparation Standing 175
Opening to Heaven, Earth and Nature 176
Outline of Practice 176
Part I - Opening to Heaven, Earth and Cosmic Chi 177
Opening Movements 177
Core Movements of Part I 182
Closing Movements 183
Part II - Opening the Bridge and Regulator Channels 189
Theory 189

General Functions of the Eight Extraordinary Channels 190
The Eight Extraordinary Channels and Chi Kung 193
Special Functions of the Bridge and Regulator Channels..... 193
Bridge Channels Yin and Yang Chiao Mo Function 193
Summary..... 195
Practice..... 196
Part III - Opening the Functional and Governor Channels..... 205
Theory: The Functional and Governor Channels..... 205
Chi Ball..... 206
Part IV - Activating the Yin and Yang Channels on the Chi Belt..... 217
Theory..... 217
Yin and Yang Channels of the Arms..... 217
Projecting Healing Energy through the Fingers..... 217
Activating the Chi Belt - Dai Mo..... 222
Practice..... 223
Healing Others..... 226
Summary and Combined Practice..... 226
Cosmic Chi Kung: Simple Combined Sequence..... 226

Chapter IX
Universal Tao Basic Practices
Cosmic Inner Smile..... 232
Six Healing Sounds..... 236
The Six Healing Sounds - Practice..... 235

Appendix..... 241
Guide to Acupuncture Points used in Cosmic Chi Kung..... 241
Bibliography..... 249

About the Author

Mantak Chia

Master Mantak Chia is the creator of the Universal Tao System and is the director of the Universal Tao Center and Tao Garden Health Resort and Training Center in the beautiful northern countryside of Thailand. Since childhood he has been studying the Taoist approach to life. His mastery of this ancient knowledge, enhanced by his study of other disciplines, has resulted in the development of the Universal Tao System which is now being taught throughout the world.

Mantak Chia was born in Thailand to Chinese parents in 1944. When he was six years old, Buddhist monks taught him how to sit and "still the mind." While still a grammar school student, he learned traditional Thai boxing. He was then taught Tai Chi Chuan by Master Lu, who soon introduced him to Aikido, Yoga and broader levels of Tai Chi.

Years later, when he was a student in Hong Kong excelling in track and field events, a senior classmate named Cheng Sue-Sue introduced him to his first esoteric teacher and Taoist Master, Master Yi Eng (I Yun). At this point, Master Chia began his studies of the Taoist way of life in earnest. He learned how to circulate energy through the Microcosmic Orbit and, through the practice of Fusion of the Five Elements, how to open the other Six Special Channels. As he studied Inner Alchemy further, he learned the Enlightenment of the Kan and Li, Sealing of the Five Senses, Congress of Heaven and Earth and Reunion of Heaven and Man. It was Master Yi Eng who authorized Master Chia to teach and heal.

When Mantak Chia was in his early twenties he studied with Master Meugi in Singapore, who taught him Kundalini, Taoist Yoga and the Buddha Palm. He was soon able to clear blockages to the flow of energy within his own body. He learned to pass the life force energy through his hands also, so that he could heal Master Meugi's patients. He then learned Chi Nei Tsang from Dr. Mui Yimwattana in Thailand.

A while later, he studied with Master Cheng Yao-Lun who taught him the Shao-Lin Method of Internal Power. He learned the closely guarded secret of the organs, glands and bone marrow exercise known as Bone Marrow Nei Kung and the exercise known as Strengthening and Renewal of the Tendons. Master Cheng Yao-Lun's system combined Thai boxing and Kung Fu. Master Chia also studied at this time with Master Pan Yu, whose system combined Taoist, Buddhist and Zen teachings. Master Pan Yu also taught him about the exchange of Yin and Yang power between men and women, and how to develop the Steel Body.

To understand the mechanisms behind healing energy better, Master Chia studied Western anatomy and medical science for two years. While pursuing his studies, he managed the Gestetner Company, a manufacturer of office equipment and became well acquainted with the technology of offset printing and copying machines.

Using his knowledge of Taoism, combined with the other disciplines, Master Chia began teaching the Universal Tao System. He eventually trained other Instructors to communicate this knowledge and he established the Natural Healing Center in Thailand. Five years later, he decided to move to New York, where in 1979, he opened the Universal Tao Center. During his years in America, Master Chia continued his studies in the Wu system of Tai Chi with Edward Yee in New York.

Since then, Master Chia has taught tens of thousands of students throughout the world. He has trained and certified over 1,200 instructors and practitioners from all over the world. Universal Tao Centers and Chi Nei Tsang Institutes have opened in many locations in North America, Europe, Asia, and Australia.

In 1994, Master Chia moved back to Thailand, where he had begun construction of Tao Garden, the Universal Tao Training Center in Chiang Mai.

Master Chia is a warm, friendly and helpful man who views himself primarily as a teacher. He presents the Universal Tao System in a straightforward and practical manner, while always expanding his knowledge and approach to teaching. He uses a laptop

computer for writing and is totally at ease with the latest computer technology.

Master Chia estimates that it will take thirty five books to convey the full Universal Tao System. In June 1990, at a dinner in San Francisco, Master Chia was honored by the International Congress of Chinese Medicine and Qi Gong (Chi Kung), who named him the Qi gong Master of the Year. He is the first recipient of this annual award.

In December 2000, the Tao Garden Health Resort and Universal Tao Training Center was completed with two Meditation Halls, two open air Simple Chi Kung Pavilions, indoor Tai Chi, Tao Yin and Chi Nei Tsang Hall, Tai Chi Natural Swimming Pool, Pakua Communications Center with a complete Taoist Library, Internal World Class Weight Lifting Hall and complete 8 Court Recreational Facilities.

In February 2002, the Immortal Tao practices will be held at Tao Garden for the first time using Dark Room technology, creating a complete environment for the higher level Taoist practices.

He has previously written and published these Universal Tao books:

Awaken Healing Energy of the Tao - 1983
Taoist Secrets of Love: Cultivating Male Sexual Energy
co-authored with Michael Winn - 1984.
Taoist Ways to Transform Stress into Vitality -1985
Chi Self-Massage: the Tao of Rejuvenation - 1986
Iron Shirt Chi Kung I - 1986
Healing Love Through the Tao: Cultivating Female Sexual Energy - 1986
Bone Marrow Nei Kung - 1989
Fusion of the Five Elements I - 1990
Chi Nei Tsang: Internal Organ Chi Massage - 1990
Awaken Healing Light of the Tao - 1993
The Inner Structure of Tai Chi co-authored with Juan Li - 1996
Multi-Orgasmic Man co-authored with Douglas Abrams 1996 - published by Harper/Collins
Tao Yin - 1999
Chi Nei Tsang II - 2000
Multi-Orgasmic Couple co-authored with Douglas Abrams 2000 - published by Harper/Collins
Cosmic Healing I - 2001
Cosmic Healing II co-authored with Dirk Oellibrandt - 2001

Also many of the books above are available in the following foreign languages:
Bulgarian, Czech, Danish, Dutch, English, French, German, Greek, Hebrew, Hungarian, Indonesian, Italian, Japanese, Korean, Lithuanian, Malaysian, Polish, Portuguese, Russian, Serbo-Croatian, Slovenian, Spanish, & ***Turkish*** editions are available from the Foreign Publishers listed in the Universal Tao Center Overview in the back of this book.

Acknowledgments

The Universal Tao Publications staff involved in the preparation and production of *Cosmic Healing I: Cosmic Chi Kung* extend our gratitude to the many generations of Taoist Masters who have passed on their special lineage, in the form of an unbroken oral transmission, over thousands of years. We thank Taoist Master I Yun (Yi Eng) for his openness in transmitting the formulas of Taoist Inner Alchemy.

Thanks to Juan Li for the use of his beautiful and visionary paintings, illustrating Taoist esoteric practices.

We offer our eternal gratitude to our parents and teachers for their many gifts to us. Remembering them brings joy and satisfaction to our continued efforts in presenting the Universal Tao System. For their gifts, we offer our eternal gratitude and love. As always, their contribution has been crucial in presenting the concepts and techniques of the Universal Tao.

We wish to thank the thousands of unknown men and women of the Chinese healing arts who developed many of the methods and ideas presented in this book. We offer our graditute to Master Lao Kang Wen for sharing his healing techniques.

We wish to thank Colin Campbell for his editorial work and writing contributions on the first printing of this book, as well as his ideas for the cover. We appreciate his research and great labor. We wish to thank Matt Gluck for his editorial contributions on the revised edition of this book, as well as thanking our instructors, Dennis Huntington and Annette Derksen, for their insightful contributions to the revised version. We thank Dirk Oellibrandt for his technical editing and clear writing throughout the book.

A special thanks goes to our ***Thai Production Team*** for their cover illustration and book design and layout: Raruen Keawapadung, Computer Graphics; Saysunee Yongyod, Photographer; Udon Jandee, Illustrator; and Saniem Chaisarn, Production Designer.

Thanks to the testing institutes: Gerhard Eggelsberger, Institute for Applied Biocybernetics Feedback Research, Vienna, Austria and Dr. Ronda Jessum, Biocybernetics Institute, San Diego, California.

We also wish to express thanks to Cosmic Healing Certification Retreat Organizers around the world who have worked with us for many years and helped us prepare this manuscript throughout the Retreats: Beate Nimsky, Vienna, Austria; Serguei Orechkine, Moscow, Russia; Christopher Larthe, London, England; Masahiro Ouchi, Rye, New York; Dr. Angela C. Shen, San Francisco, California; Dirk Oellibrandt, Hamme, Belgium; Brita Dahlerg, Frankfurt, Germany and Lizbeth Cavegn, Zurich, Switzerland.

We wish to further express our gratitude to all the instructors and students who have offered their time and advice to enhance this system, especially Felix Senn, Barry Spendlove, Chong-Mi Mueller, Clemens Kasa, Andrew Jan, Marga Vianu, Harald Roeder, Salvador March, Dr. Hans Leonhardy, Peter Kontaxakis, Thomas Hicklin, Gianni Dell'Orto, Walter and Jutta Kellenberger.

Words of Caution

The practices described in this book have been used successfully for thousands of years by Taoists trained by personal instruction. Readers should not undertake the practice without receiving personal transmission and training from a certified instructor of the Universal Tao, since certain of these practices, if done improperly, may cause injury or result in health problems. This book is intended to supplement individual training by the Universal Tao and to serve as a reference guide for these practices. Anyone who undertakes these practices on the basis of this book alone, does so entirely at his or her own risk.

The meditations, practices and techniques described herein are ***not*** intended to be used as an alternative or substitute for professional medical treatment and care. If any readers are suffering from illnesses based on mental or emotional disorders, an appropriate professional health care practitioner or therapist should be consulted. Such problems should be corrected before you start training.

Neither the Universal Tao nor its staff and instructors can be responsible for the consequences of any practice or misuse of the information contained in this book. If the reader undertakes any exercise without strictly following the instructions, notes and warnings, the responsibility must lie solely with the reader.

This book does not attempt to give any medical diagnosis, treatment, prescription, or remedial recommendation in relation to any human disease, ailment, suffering or physical condition whatsoever.

Chinese Medicine and Chi Kung emphasizes balancing and strengthening the body so that it can heal itself. The meditations, internal exercises and martial arts of the Universal Tao are basic approaches to this end. Follow the instructions for each exercise carefully and do not neglect the foundations, i.e, the Microcosmic Orbit and any other supplemental exercises. Also pay special attention to the warnings and suggestions. People who have high blood pressure, heart disease or a generally weak condition should proceed cautiously, having prior consent from a qualified medical practitioner. People with venereal disease should not attempt any practices involving sexual energy until they are free of the condition.

The Universal Tao is not and cannot be responsible for the consequences of any practice or misuse of the information in this book. If the reader undertakes any exercise without strictly following the instructions, notes, and warnings, the responsibility must lie solely with the reader.

Chapter I
Cosmic Healing

Cosmic Healing Chi Kung in the Universal Tao System

Cosmic Healing Chi Kung is an important branch of the Universal Tao, an entire system of Taoist practices for cultivating the body, the Chi and the spirit. Your level of skill in Cosmic Healing Chi Kung will be based upon your mastery of the Universal Tao System as a whole. One of the most important parts of the Taoist practices is working with the energy moving within the body.

Foundation of the Universal Tao System is the Microcosmic Orbit Meditation

This is the major practice to connect with the earth, cosmic and universal forces. This is the way to make a connection with the North Star and the Big Dipper's violet/red light which is one of the very powerful universal healing lights. Through this practice you learn to feel Chi and to use your mind/eye/heart power to guide the Chi flow through the primary energy routes in your body. This practice is later extended to include the arm and leg routes too; it is then called the Macrocosmic Orbit.

Many people, including Chi Kung Masters, come to me and say that they have been practicing Chi Kung for years and nothing is happening. They don't feel any energy and they think that they must be performing their Chi Kung incorrectly. I tell them that they also need to do meditation. Hand movements are nothing by themselves. There are hundreds of different Chi Kung forms in China. You could spend seventy lifetimes just learning the hand movements. The practice of the Microcosmic Orbit meditation will help you to feel the Chi more easily inside, outside or around the body and in the extremities of the hands and feet.

When I was a child I liked to practice Chi Kung so much I had to save my lunch money to learn. After many years of practice of many Chi Kung forms, I started to forget the first form, so I learned it again. One day when I tried to practice and review all the forms that I had learned, I couldn't remember many of them. I sat down and thought, "I only have two hands, two legs and one head. Why are there so many forms? And why are there are so many religions and beliefs." I said to myself that there must be one main thing that they have in common. I started to search and I found out that the most important thing is feeling the Chi within us. Being able to increase, transform, take in and stay in touch with the universal, the cosmic, nature and the earth force. Letting

them all combine within us is what is important. Likewise in religion there is God (a Force in Taoism we call Wu Chi, the nothingness, the supreme power controlling the universe); with a good heart and virtue energy we can connect with this force.

The complete practice of the Microcosmic Orbit Meditation is fully described in the book "Awaken Healing Light of the Tao" by Mantak Chia.

Cosmic Inner Smile and the Six Healing Sounds

These are very important practices to make the connection among the organs, the colors and the good virtue energy; each organ color will enhance your connection to the cosmic and the Universal Healing power.

Fig. 1.1 *Red for the Heart*
White for the Lungs
Yellow for the Spleen
Blue for the Kidneys
Green for the Liver.

Each organ has its own vital color and when abundant it will radiate out as an aura for healing and protection. These organ colors and their associated universal connections have great healing power. The power of the 'Six Healing Sounds' will help enhance the connection to the cosmic source. Each sound will foster different healing energy. The practices also help balance, refine and transform the negative energy back to positive energy.

Iron Shirt Chi Kung and Bone Breathing

Iron Shirt Chi Kung and Bone Breathing are a system of standing meditations. These exercises help you to become grounded and to root your connection into the earth force, in order to build a good structure and absorb greater force. In turn, this will help draw in the heavenly force, which will combine with the very potent healing power of the earth's yellow light. The practice also strengthens the body so you can hold a higher energetic charge. These abilities are essential prerequisites for handling greater amounts of energy.

Iron Shirt Chi Kung also includes the art of 'Changing the Sinews and Washing the Marrow'. Through these aspects of Iron Shirt, you learn to absorb, store and discharge large amounts of energy through the tendons and bones. *These practices are outlined in detail in the books "Iron Shirt Chi Kung" by Mantak Chia and "Bone Marrow Nei Kung" by Mantak Chia.*

To attain skill in Cosmic Chi Kung, it will help if you practice Iron Shirt, Bone Marrow and meditation as a minimum requirement. Beyond the basic level, the Universal Tao System includes many other intermediate and advanced level Chi Kung practices and meditations. The further one advances, the greater one's mastery of Chi.

Your increasing level of skill in the Universal Tao system will reflect immediately in your Cosmic Healing Chi Kung practice. Furthermore, you will discover that you can incorporate many of your Universal Tao practices directly into your practice of Cosmic Chi Kung. We will give you a simple combined practice of the Cosmic Healing Chi Kung, the Inner Smile, Microcosmic Orbit, Iron Shirt and the Sexual practices.

Stages of Mastering Chi

1. In the Universal Tao system, our *first* goal is to learn to conserve our Chi; when a battery is totally drained it is harder to charge; money makes money, Chi makes Chi. Conservation of Chi will help gain more Chi. To have more Chi we first need to maintain control of the gates through which energy normally leaks out and unwittingly drains our life force.

We leak energy: - through our reproductive system
- through negative emotions
- through constantly turning our senses outward

Without knowing how to conserve the Chi that we already have, what is the point of acquiring more?

2. We learn to balance our Chi; that is, we seek to keep a smooth and balanced flow of energy moving throughout the whole body. If our energy is imbalanced, we may have too much energy in some places and not enough in others; we may also be too yang or too yin. We may have excess or deficient heat, cold, damp or dryness. This imbalanced energy tends to make us go to extremes.

3. We learn to transform our Chi into more beneficial energies. For example, through the Taoist Sexual Chi Kung practices taught in the Universal Tao (the course known as Healing Love through the Tao), we can transform sexual energy back into basic life force Chi. Through other practices (such as the Inner Smile, the Six Healing Sounds, and Fusion of the Five Elements) we learn to transform negative emotional Chi into positive virtuous Chi. Thus Chi is not only the foundation of our health; it is also the basis of spiritual development in the Tao.

4. Once we have accomplished the three previous phases of mastering Chi, we then learn to increase it. Chi pervades all of heaven, earth and nature. In Cosmic Healing

Chi Kung we learn time tested ways to tap into these unlimited and transpersonal reservoirs of Chi and greatly expand the amount of energy available to us. It is very important to master first the stages of conservation, balance and transformation before we emphasize increasing our Chi. Otherwise we may waste the energy we bring in, or we may inadvertently amplify the imbalanced or negative energies that we have not yet learned to bring under control.

5. Finally, we learn to extend our mind to tap into the vast Chi of nature, cosmic and the universe, to heal our body, mind and spirit and to heal other people. Cosmic Healing Chi Kung practice sensitizes your hands to the feeling and movement of Chi; it uses the mind-eye power to absorb cosmic Chi into the palm and crown and to send it out through the hands and beyond, so that you can help restore balance in others without touching them or draining yourself.

This may sound fantastic at first, yet recent researchers in Chinese Chi Kung hospitals have not only measured the energies emitted by Chi Kung masters; they have also discovered that different varieties and frequencies of healing Chi can be emitted. This research has been corroborated by experiments in the United States at such places as the Menninger Institute.

Four Sections of Cosmic Healing

The next step is to learn the four sections of the Cosmic Healing Chi Kung, the 'Empty Force' sequence. Each of the four sections of Cosmic Healing Chi Kung develops a different type of energy mastery. Each section begins and ends in the same way, yet has different movements in the middle.

Connecting to Heaven and Earth

The first section of Cosmic Healing Chi Kung emphasizes connecting to the external Chi emanating from heaven and earth. This ability is very beneficial for self-healing and is essential for healing others. If you do not connect to some source of external energy when healing others, you will draw upon your own personal reservoirs. Our personal Chi is limited by nature, and can easily become depleted if we give it away too freely.

Over the past decade external Chi healing has become very popular in China. There are now hundreds of Chi Kung hospitals and clinics throughout the country. Yet many of the Chi Kung therapists can only administer two or three treatments a day; they spend the rest of their day practicing Chi Kung to replenish their own Chi. Those who practice the more traditional Chi Kung know how to connect to the Chi of heaven, earth and nature.

In this first section, you will learn to sense the energies outside your body. You will then learn to draw and absorb these energies into your body and process them in order to use them for self-healing and healing others.

Opening the Bridge and Regulator Channels and Extending your Chi Outwards

The second section opens and strengthens four of the Eight Extraordinary Channels: the Yin and Yang Bridge and Regulator Channels. This section also teaches the student to extend and take in the cosmic Chi and emit Chi out of the body for healing others. This ability is the heart of Cosmic Healing Chi Kung practice.

Opening and Energizing the Governor and Functional Channels

The third section enhances the energy in the points along the two channels used in the Microcosmic Orbit. Opening the Microcosmic Orbit strengthens and balances one's own energy, and prepares one to heal others. Practicing this section will be of great help with the Microcosmic Orbit Meditation.

Activating One Finger Art and the Chi Belt

The fourth section of Cosmic Healing Chi Kung activates the hands and you will practice emitting Chi from each of your fingers and opening the "Chi Belt." This channel is also known as the Belt Route or Girdle Vessel.

Chapter II
Preparing for Cosmic Chi Kung

Preparatory Practices

In the Universal Tao, we teach Cosmic Healing Chi Kung within an entire system of exercise and meditation. As a part of this system, Cosmic Healing Chi Kung comprises the art of healing oneself and others. It focuses on energy work for projecting Chi to effect these healings. One can easily learn the simple movements of Cosmic Healing Chi Kung without doing any other Universal Tao practices, but if one truly wishes to master the art of Cosmic Healing Chi Kung, it is important to have a firm foundation in the basic Universal Tao practices. Therefore in this chapter we will introduce you to the basic Universal Tao practices that are used in conjunction with Cosmic Chi Kung.

The preparatory practice consists of a few parts; work through each part at your own pace and eventually join them together as a whole.

Always start with "warming the stove" at the abdomen and direct the fire down to the sexual center to transform the sexual energy. Next practice the Cosmic Inner Smile. The Cosmic Inner Smile is a powerful relaxation and self-healing technique that uses the energy of love, happiness, kindness and gentleness as a language to communicate with the internal organs of the body. Each organ corresponds to a specific element and color. For example, the kidneys will consist of the element of water and the color blue. The heart will consist of the element of fire and the color red. This makes it very easy to guide the healing power into each organ by using the appropriate color. The practice also aids the transformation of negative emotions into positive virtuous energy. This transformation is a very powerful Chi Kung practice. A genuine smile transforms negative energy into loving energy that has the power to relax, balance and heal. By learning to smile inwardly to the organs and glands, your whole body will feel loved and appreciated and enjoy more Chi. After the Inner Smile, practice Bone Breathing, Marrow Washing, Cosmic Healing and the Microcosmic Orbit.

Warm Up the Stove

1. Sit on the edge of a chair with your hands clasped together and your eyes closed.
2. Start by doing the "bellows breathing", moving your abdomen in and out quickly. Emphasize the exhalation by breathing out forcefully 18 to 36 times. Rest, cover your navel and feel nice and warm.
3. Next, do the "inner laughing" exercise; you feel the abdomen vibrate inside you. Practice

this for a few minutes, allowing the movement of your inner laughter to grow stronger. Then rest and use the mind and eye power to gather the Chi (now felt as a warmth behind the navel) into the Tan Tien. Picture a stove with burning fire behind your navel. Feel nice and warm.

Transform the Sexual Energy

Once you feel the Tan Tien is warm enough, smile down and bring the warm Chi down to the sexual organs; women bring the Chi down to the uterus, men bring the Chi down to the testicles. It may feel like the 'sun shining on the water'. The rays of the sun purify the water until it becomes rising steam. Keep smiling down to the sexual organs and feel the warm or fiery feeling from the navel area continue to flow down to the sexual organs; this transforms the sexual energy into Chi, and this Chi rises up the spine into the brain helping to activate the 'crown' and 'mideyebrow' energy centers.

Focus your awareness in the sacrum. At the very tip of the sacrum there is a hole in the coccyx. Breathe into this hole until you feel some activity there. This may be felt as tingling, numbness or pulsing. If you can really activate this point it will generate 'suction'. Be aware of the sacrum opening. Feel the suction force pulling through the hole in the tailbone (sacral hiatus); breathe into it until you feel it becomes activated. When the sacrum is activated you will feel the suction easily, as well as breathing in the cranium and mideyebrow. Keep on gently smiling and softly breathing into the Tan Tien and feel the suction in the abdomen. Focus 95 % of your awareness in the Tan Tien and 5 % in the sacrum, the crown and the mideyebrow. Be aware of the Tan Tien breathing and observe internally the pulsing and breathing in the sacrum, the mideyebrow and the crown. Do this 36 times.

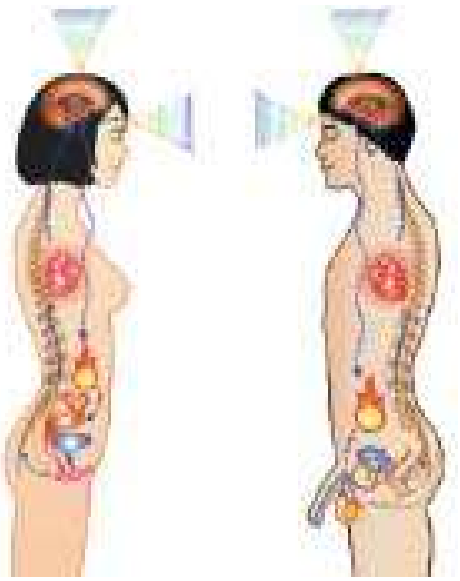

Fig. 2.1 *Smile down to the Lower Tan Tien.*

Filling the Joints with Chi

The bones have the ability to process Cosmic Chi (Chi above and around us) to be used by the body. The joints are also able to store Chi and they also serve as the cushion between the bones.

Be aware of your index fingers and thumbs; lightly raise the index fingers, feel a slight tension and open the thumbs to the sides and feel it magnify. Breathe into the finger tips, until you feel the sensation of Chi entering the fingers. The fingers will feel stiff as they stretch, to make way for the Chi entering the joints. Continue to breath in the Chi - the stiffness will spread to the other fingers, wrists, elbows and shoulder joints making the whole arm tense and stiff. The fingers and the arms become one piece. Eventually the Chi will fill every joint of the body making it into a complete unit.

Be aware of the big toes; breathe into the toes and feel the toes grow longer. When the Chi fills the joints the big toes become tense and stiff. Gradually it will fill the other toes rising to the ankles, knees, hips, sacrum and spine; the feeling may be one of tension and stiffness, numbness or like an electrical charge. The legs and the spine become one piece. You will certainly feel good.

Bone Breathing and Marrow Washing

Bone Breathing is one of the main practices of Cosmic Healing Chi Kung. This is a method of drawing external Chi through the skin into the bones to help replenish the bone marrow, thereby reactivating the production of white blood cells. Sending Chi into the bones will enhance functioning of the immune system. This process also helps to clean out fat in the bone marrow ("Washing the Marrow"), one of the main causes of osteoporosis (brittleness of the bones). Tension in the muscles close to the bones is decreased so Chi and blood can flow into the bones easily, enabling them to become stronger.

The Bone Breathing process uses the mind and the eyes to absorb Chi into the bones. The better your Bone Breathing is the better your Cosmic Healing Chi Kung practice will be. Mind and eyes are also used immediately after the exercise to gather the energy at the navel. Once you have it, when you move your hand, the energy will follow easily. You will be able to absorb external Chi effortlessly, so you will not need to use your own energy in your healing work.

Bone Breathing

There are several variations in the Bone Breathing and Marrow Washing process. Here we will introduce you to the first type of Bone Breathing, inhaling and exhaling Chi

through the skin and packing it into the bones. In this method, you imagine that your bones are like hollow tubes, and that you breathe and suck the Chi into the bones.

Bone Breathing is practiced in a three-stage process. **Let your breathing follow a normal pace. Do not strain or hold your breath too long**.

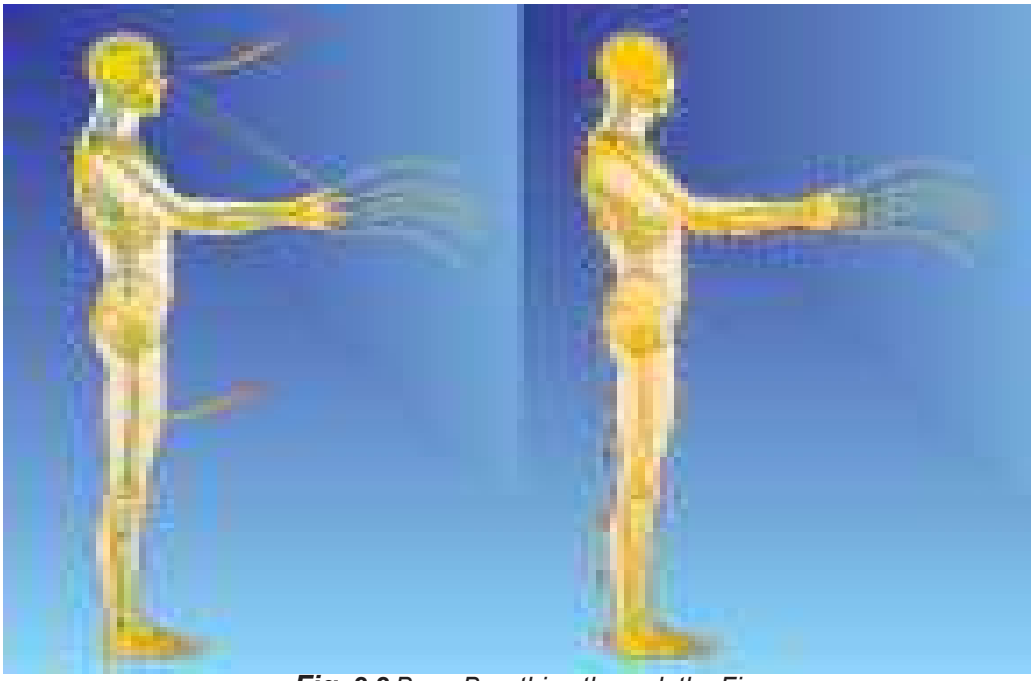

Fig. 2.2 *Bone Breathing through the Fingers*

1. You can do this practice in the sitting position or in the Embracing the Tree posture (or any other Iron Shirt Chi Kung posture). You will use your mind and eye power to breathe in a short breath and at the same time feel suction. Suck the Chi of the atmosphere into your hands, eventually expand to the universe and breathe in a few more times. Use a combination of 'mind/eyes/heart' power (Yi), to suck the Chi from the atmosphere into your hands, while taking small sips of breath. Once you can clearly feel the increase of Chi 'pressure' in your hands, you extend the feeling throughout your arms. The whole skin surface of the arms breathes in the Chi, feeling the skin holding this pressure.
2. Inhale one more deep breath and lightly contract the arm muscles to squeeze the Chi into the bones. Hold for a while to condense the Chi into the marrow of your bones. Exhale and at the same time feel a distinct heaviness in the bones, meaning that the Chi has been condensed and packed into the bones successfully. Eventually you will use more mental power (mind/eyes/heart power) and less muscle, using soft breathing, to draw the force into the bones. Do 6 to 9 times; rest and feel the Chi that has been condensed into the bones.

3. Proceed in the same way, breathing in progressively through the bones of the forearms, upper arms, scapulae, collarbone, sternum and ribs. You may feel a different sensation as you breathe in each area; in some areas the feeling is cool, in others warm or tingling, depending on the bone structure and the quality of the marrow.
4. Inhale and exhale in the same way through the toes, feet and legs; then, in a step-by-step progression, inhale up through the calf bones, thighbones, pelvis, coccyx and sacrum, and up the spinal column to the C-7 vertebrae.
5. Finally breathe in through the arms and legs simultaneously. Combine their energy as it flows up past C-7 and up through the neck and skull. Breathe in this way for at least nine breaths. Conclude by collecting energy at the navel.

Marrow Washing

You can wash your bone marrow with earth force, heavenly force or with cosmic force. This energy helps to cleanse and rejuvenate the bone marrow.

Heavenly Force Marrow Washing with Violet Light

1. Men place the left palm on the top of the head, and cover it with the right palm. Be aware of your 'Personal Star' (star that appears in your mind's eye and is located above your crown), above. Slightly press the palms and spiral in the clockwise direction, spiralling from the front to the right ear, to the back and the left ear 9 times; rest and feel the increased Chi pressure in the crown. Do 3 sets.
2. Women place the right palm on the top of the head and cover it with the left palm. Be aware of your Personal Star above you. Press the palms lightly and spiral in a counterclockwise direction, spiralling from the front to the left ear, to the back and the right ear 9 times; rest and feel the increased Chi pressure in crown. Do 3 sets.
3. Face your palms towards Heaven and feel that you are scooping a galactic Chi ball from above. This Chi ball contains the North Star (Violet) and the Big Dipper (Red). See the dipper fill with violet/red energy. Imagine you reach out your arms to hold the dipper handle and pour the violet/red liquid over your crown. It will feel like there is a numbness descending. Your palms face down to your crown and pour the whole galaxy onto your crown. You may perceive this energy as violet amethyst and red light frequencies. Smile.

4. Guide this sensation down into your skull, deep into your brain, cervical vertebrae, sternum, thoracic vertebrae, lumbar vertebrae and down through your legs. Feel it penetrating and enlivening your bones, deep into the bone marrow, washing, cleansing, energizing. This 'liquid-like' Chi spills all the way down to your feet. Feel it connecting with the earth through the soles of your feet; be aware of the bubbling springs in the feet (the K1 points of the kidney meridian) breathing and pulsating.
5. Touch your navel with the fingers of both hands. Focus on the door of life, and let the fire activate in the Tan Tien and kidneys. Chi will rise up to the brain.

6. Move your hands down touching your femur bones; feel your hands penetrate into the bone and into the bone marrow. Feel like an electric shock or a tingling moving all the way down through the bones of the leg and down to the soles of your feet.
7. Slowly move your fingers down touching the bone and into bone marrow and extend yourself down past the earth to touch the galaxy on the other side. Raise your sacrum and picture yellow light coming up from the earth and the other side of the galaxy; focus on the Lower Tan Tien and feel it fill with Chi. Do this three times. Go back down to the squatting position.

Fig. 2.4 *Galaxies Spiral Star and the Direction of Spiral*

8. Place the palms face down to the earth and be aware of the galaxy and the yellow light; make three to six circles to gather the Chi below. Gather the yellow Chi; touch your heels and feel the yellow Chi flowing up the leg bones. Feel the bubbling of your bones like an electric current running up through the feet, tibia and fibula, femur, pelvis, and spine. While touching your bone and bone marrow with your fingers, slide your hands up along the back of your legs; slowly come all the way up to touch the coccyx and the sacrum. Concentrate on your sexual center so the energy will flow and spread out to the sexual organs. Go back to the navel and gather the Chi into your Tan Tien.

Fig. 2.5 *Hands circle to gather Earth Chi.*

Microcosmic Orbit

The Microcosmic Orbit Meditation awakens, circulates and directs Chi through the 'Governing Channel', which ascends from the base of the spine up to the head and the 'Functional' or 'Conception Channel', which runs from the tip of the tongue down the middle of the torso to the perineum. Dedicated practice of this ancient esoteric method eliminates stress and nervous tension, energizes the internal organs, restores health to damaged tissue and builds a strong sense of personal well being.

The Microcosmic Orbit is the foundation of Cosmic Healing Chi Kung practice. Each new practice is dependent upon the high quality of your meditations and your ability to perfect the Microcosmic Orbit. In order to master Cosmic Chi Kung, one must practice meditation daily. The meditations in the Microcosmic Orbit also strengthen the 'Original Chi' and teach you the basics of circulating Chi. They allow the palms, the soles of the feet, the mideyebrow point and the crown to open. These specific locations are the major points where energy can be absorbed, condensed and transformed into fresh new life force.

- **1.** Focus on the Lower Tan Tien (the area where the Original Chi is stored, between the navel, kidneys and sexual organs). Feel the pulsing in this area, observe whether this area feels tense or relaxed, cool or warm, expansive or contracting. Notice any sensations of Chi: tingling, heat, expansiveness, pulsing, electric or magnetic sensations. Allow these to grow and expand. Then let this energy flow out to the Navel Center.

- **2.** Use your intention (mind-eye-heart power) to spiral in the navel point guiding and moving the Chi. Let the energy flow down to the sexual center (Ovarian or Sperm Palace).
- **3.** Move the energy from the sexual center to the perineum and down to the soles of the feet.
- **4.** Draw the energy up from the soles to the perineum and to the sacrum.
- **5.** Draw the energy up from the sacrum to the Door of Life (the point in the spine opposite the navel).
- **6.** Draw the energy up to the mid-spine point (the T-11 vertebrae).
- **7.** Draw the energy up to the base of the skull (Jade Pillow).
- **8.** Draw the energy up to the crown.
- **9.** Move the energy down from the crown to the mideyebrow point.
- **10.** Touch the tip of your tongue to your upper palate, press and release a few times; then lightly touch the palate, sensing the electric or tingling feeling in the tip of the tongue. Move the energy down from the mideyebrow to where the tip of your tongue and palate meet.
- **11.** Move the energy down from the palate through your tongue to the throat center.
- **12.** Move the energy down from the throat to the heart center.
- **13.** Bring the energy down from the heart to the solar plexus and feel a small sun shining out.
- **14.** Bring the energy back down to the navel.
- **15.** Continue to circulate your energy through this entire sequence of points, at least nine times. Once the pathways are open, you can let your energy flow continuously like a river of energy without needing to stop at each point.
- **16.** Conclude when you wish by collecting energy at the navel.

Men: Cover your navel with both palms, left hand over right. Collect and mentally spiral the energy outward from the navel 36 times clockwise, and then inward 24 times counterclockwise.

Women: Cover your navel with both palms, right hand over left. Collect and mentally spiral the energy outward from the navel 36 times counterclockwise, and then inward 24 times clockwise. *For details of this practice see the book, "Awaken Healing Light", by Mantak Chia.*

Chapter III
Cosmic Chi Kung

Opening the Three Tan Tiens to the Six Directions

Introduction

Opening the Three Tan Tiens is a Chi Kung meditation that strengthens our connection to the universe, opening us up to the primordial force of the Cosmos and the energy within Nature. We are dynamically connected to the infinite. "As above, so below" is an echo of wisdom heard from sages and mystics throughout the ages. When we can connect to and absorb the energy that surrounds us, we are able to tap into the many splendors of the universe.

We exist because of the unique combination of the forces that are around and within us. The two main forces are electricity and magnetism. 'Bio-electro magnetism' is the western term for life force, and what the Tao refers to as Chi. For the last 5000 years, the Taoists have utilized this bio-electro-magnetic energy to enhance their way of life and establish a relationship with the universe. Bio signifies life, electro refers to the universal energies (yang) of the stars and planets and the magnetic force refers to the earth force (yin) or gravitational force present on all planets and stars. As we align ourselves with these forces, we become a conduit through which we can absorb and digest these energies through the body, mind and spirit establishing a direct connection with the universe. The Taoists recognized this connection and created the Chi Kung form of 'Opening the Three Tan Tiens to the Six Directions' to enhance our relationship to and our understanding of this connection.

Humans normally access bio-electro-magnetic energy through food and air. Plants take the universal energies of the sun and the magnetic energies of the earth and digest and transform them, thereby making these energies available to all living beings. Taoists believe that the food sources with the purest form of energy are the green leafy vegetables. These have taken sunlight directly into their cells. Rather than waiting until the energy in the universe is processed through plants, the Taoist goes directly to the source of this primordial energy. Through Chi Kung and meditation, the Taoists direct the energy of the universe precisely. Opening the Three Tan Tiens is a meditational Chi Kung exercise that focuses on how to directly tap into the source of energy all around us.

The Tao views human beings as lamps filled with fuel. Many people burn this fuel at very high intensity, without ever taking the time to replenish the oil in the lamp. Alcohol,

drugs, tobacco and promiscuity all quicken the depletion of this fuel. The Taoist exercises strive to continually refuel the energy within. The Taoist recognizes that we are limited in our nature as human beings, unless we connect the sources of energy within the universe, thereby becoming infinite. So, within the limitations of our human nature, we constantly fill ourselves with the unlimited abundance of energy around us.

Through their internal quest, the Taoists discovered a doorway to the universe. The more we open our internal energy, the more we are capable of connecting to the forces of energy around us.

Human beings have amazing potential and capabilities. We are unique creatures in the way we use our minds and hands. Look at the world around you, the skyscrapers, the architecture, computers, technology and the myriad creations of man. All have come about through the combination of the mind with the hands. In the Tao practice, we use the mind and the hands, in both Chi Kung and meditation, to connect to the forces of the universe. We use the mind to project a pattern of energy into the universe, to connect to the force, and to bring this energy back into the body.

The mind can travel millions of light years in a few moments. Taoists discovered the unlimited potential of the human mind. If you picture something in your mind; an ocean, a sunset or a mountain, you automatically connect with that image. The mind can take you anywhere you imagine. With the proper training you can connect to the energy of nature and the universe and project your Chi to combine with it, drawing these forces into the body. The hands are called the touching force, and like antennae they can transmit the frequencies and vibrations from space. With the mind and the hands, each of us can journey into the boundless energy of the universe.

Relaxation, Letting Go, Surrender and Ego

In some religions and spiritual paths, there is a great emphasis on surrender and letting go. This is actually a form of relaxation. Taoist practices emphasize relaxation, letting go, and emptiness. When a person is relaxed, the muscles are open, the breathing is soft, and the energy can flow through the channels of the body. There is no resistance and no fighting. This allows the creative and higher forces to flow into us.

Most religions have a similar process. To contact the higher self and the higher forces, one needs to let go and surrender in order to reach the level where one can be in contact and become one with the higher forces. Through the surrender of control, one opens up and touches the forces of nature. However, if you continue to surrender and let go, you will lose the energy you have sent out. In the long term, this will gradually drain you. The force will suck the energy out of you, rather than help you to bring the energy into yourself. To avoid this, at the moment that one is in touch with the higher forces, one again becomes aware of oneself and his or her own energy. One is then able to project his or her own thoughts, intentions and patterns into the force, integrating the outer with the doubling or tripling inner energies. You can bring this force back to your place, your house and into yourself.

One must remain open and empty while using one's intentions, mind and Chi to draw the energy into oneself. What might initially appear to be a paradox is reformed as one does the practice and learns how to be empty and open and to simultaneously retain enough consciousness to draw the force into oneself.

Mind, Organs and Sexual Organs

It seems that some people are disconnected from themselves and from their sexual organs. The mind and organs are therefore separate. Taoism believes that the mind, body and spirit must work together. The results depend on a person's practice.

Brain

The brain can access and generate the higher forces, but storing this energy in the brain itself is not easy. We need to train the brain to increase its ability and capacity to store energy. The brain energy, when increased to a certain level, can enable more synapses to grow, and can help turn protein into brain cells. The Tao believes that with training and practice, one can learn to grow more brain and nerve cells, as well as increase the number of synapses in the central nervous system.

Organs of the Body

The organs can also generate energy, but much less than the sexual organs and the brain. They also have a much greater capacity to store and transform energy.

Sexual Organs

The Tao discovered that the sexual organs are the only organs that can generate a significant amount of sexual energy (life force). However, the sexual organs cannot store the energy efficiently. When too much energy is generated, considerable amounts have to be dumped out. And this is the best energy that one has. It is the ‘creative’ energy.

Three Tan Tiens

The Three Tan Tiens can also store energy, transform it and supply it to the brain, spinal cord, sexual organs and other organs.

The aim of Taoist basic training is to integrate the brain, sexual organs and other organs into one system. If the brain generates too much energy, it can store the energy in the organs. The excess sexual energy can also be stored in the organs and the three Tan Tiens. If the brain generates too much of the higher forces and we are unable to store this energy, we have to throw it away. It is like preparing food for one hundred people, when only one person is eating. The rest gets thrown away. In the same way,

when too much sexual energy is produced and there is no place to store it, it is wasted. We do not have enough of this energy to be able to waste it. We have a limited amount of energy and of time.

Some practices just deal with the spirit and ignore the body and the sexual energy. These practices can generate a lot of energy, but when one is not connected to the organs, it cannot be stored anywhere. One will end up draining oneself. Some people practice sitting quietly, emptying the mind, with the whole body relaxed and calm, but very little energy is actually generated. When one gets deep into the practice, some people find it hard to come back to society, because they have no energy and their mind power does not work well. These people have to depend on others to support them.

In the Universal Tao, we are learning to create a sacred and holy temple within ourselves. With the simple practice of smiling to all the organs, we can integrate our bodies, minds and spirits. They are no longer separate. The sexual practice connects the mind with the sexual organs and the brain. The separation between these parts of ourselves is bridged and a synergy is created.

The Taoist practice provides us with the resources to extend beyond the realm of our senses. By tapping into our internal resources and channeling the energy around us, we can perceive much more than the senses normally report to the mind. We want to extend our perception from the limited perspective of the sociologically conditioned senses to the unlimited awareness of the universe. For example, our senses tell us that the earth is flat, that we are stationary, and that heaven is above us. In reality, the earth is a sphere hurtling through space at thousands of miles per hour and the heavens are above, below and beyond the earth in every direction. The goal of the Three Tan Tiens is to connect with the forces from the six directions - above, below, left, right, front and back - and draw all these forces into the body. Eventually, with practice one can draw upon many different energies and use them as needed, thereby giving form to the formless energy that is abundant in nature.

Opening the Three Tan Tiens

Opening the Three Tan Tiens to the Six Directions is just another one of the many resources the Taoist practitioner uses to connect with the universe. The practice combines the power of the mind with the extension of Chi. This combination allows our personal consciousness to directly connect to the patterns and matrices of energy in the universe. When we put our thoughts into the web of the universe, we transform the electromagnetic energy into a force that is accessible to us. The combination of mind power and energy is what allows us to establish a relationship to these creative forces and the high sources of energy.

Three Tan Tiens

Once we make the connection with the forces of energy in the universe, we then want to be able to store this energy in the body. Energy is like money, if you are making a million dollars a year and spend a million dollars, you have nothing left to use in the future. That is the way we live and use our energy in our society. We are spending more energy than we are saving and we are living on borrowed energy, paying very high interest. Our credit will run out very soon.

In the Tao practice, we store energy in the Three Tan Tiens. The Three Tan Tiens are the reservoirs of energy within us.

Fig. 3.1 *The* ***Upper Tan Tien*** *is in the brain (the* ***Crystal Room****, third ventricle), and when it is full of energy, the capacity of the brain increases. We store our spiritual intelligence, the mind here. All the Tan Tiens have both yin and yang within them. In nature, the yin and yang are present in all things. Day (yang) turns into the sunset, which turns to night (yin). It is very important to feel the qualities of yin within yang and yang with yin (sunrise/sunset). One quality does not exist without the other. They are inseparable qualities of the same force.*

Fig. 3.2 *The* ***Heart*** *Center Tan Tien, between the two nipples, is the* ***Middle Tan Tien****. It is associated with the fire element. Yet, within fire there is always water. The original spirit (Shen) is stored here.*

Fig. 3.3 *The lower abdomen at the* ***Navel*** *is like an empty universe, or ocean. We want to feel a universe of energy in the* ***Lower Tan Tien****. Within this universe or ocean, there is a fire, like a volcano under the ocean; 'fire under water'.*

The Three Tan Tiens refer to the three reservoirs of energy within the body. These reservoirs are places where we can store, transform and collect energy. The reservoirs are the source of energy that flows through the body. The meridians are rivers of energy fed by these reservoirs. The goal of Opening the Three Tan Tiens is to continually fill and replenish the energy of the Three Tan Tiens. When we are connected to the Tao, life ceases to be a struggle. Through the observation of nature, the Taoists learned to flow with the stream of energy and connect to forces in the universe.

In these practices, we use a variety of hand movements and body postures to open to the energy around us. We draw the energy from the six directions into the body, activate the three fires, open the Three Tan Tiens and circulate this energy in the Microcosmic Orbit.

Combined Practice

Warm - Up Exercises

Rotating the Sacrum

Rotating the sacrum is an excellent exercise to open the lower back and activate the spinal cord. Place one hand over the sacrum and the other over the pubic bone. Rotate the sacrum in a circle, 36 times in each direction. This movement activates the sacral pump.

Spinal Cord Breathing

Inhale and expand the chest, arms bent at the elbows and extended to the sides of the body. Exhale, tuck the tailbone under you and round the back, bringing the elbows toward one another in front of the chest. Smile. Inhale, expand the chest, tuck the chin in toward the throat, push the chin back and raise the crown and bring the arms out to the sides. Repeat this back and forth movement 36 times. This movement activates the cranial and sacral pumps, and loosens all the joints in the spine.

Shaking

Shake the whole body loose, especially the joints, by bouncing up and down on the heels. Let all the joints open and relax. Also, shake the testicles and the breasts loose. This will open the sexual energy (the yin electric) and you do this on back as well.

The yin and yang are the negative and positive electric forces in the universe. The heart produces impulses (the yang electric) and the adrenal glands produce the adrenal hormone to stimulate the heart to beat. Of all the hormones inside us, this is the one that gives the vital force to our life.

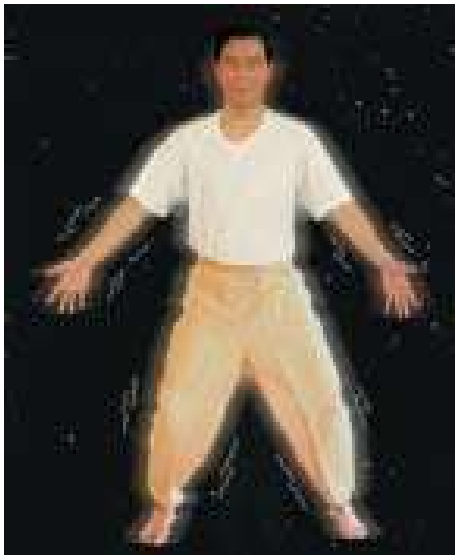

When we concentrate on the sexual organs, the heart and the mind, we can make the yin and the yang electricity combine.

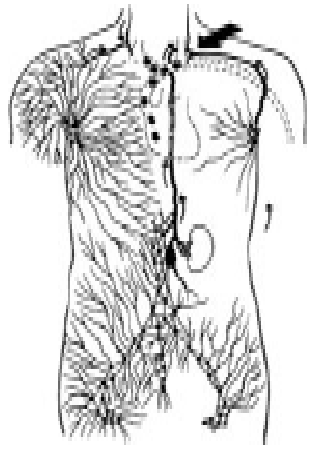

Fig. 3.4 *Whole Body shaking and Lymphatic System*

True Breath - Skin Breathing

We exist because of the physical food and the unique combination of forces that surround us. The daily requirement of calories is about 6,000 units, while we only get 2,000 calories from food. The other 4,000 calories come from the forces around, above and below us. These forces that surround us are electricity, magnetism, cosmic particle energy, light, sound and heat. If we don't know how to absorb and transform this cosmic food, we need to depend on others to supply us. We then need to ask a priest, monk or holy person to give us our daily spiritual food.

The Taoists discovered that we can learn to absorb these surrounding and universal energies through the skin and the major energy centers. Absorbing energy through the skin is called the True Breath. This powerful energetic technique requires the Inner Smile and relaxation. The more one can relax, the more the body and the skin can open to the energy around us. The practice allows one to extend the mind, to touch the force and to draw that energy back into the body.

Daily Practice: Opening, Connecting and Activating Chi Within and Cosmic Charging

Paradoxically, in order to project ourselves out into the immensity of the galaxies and the universe to gather limitless resources of Cosmic Chi for healing, we must take the first steps of the journey within ourselves. In order to 'go out', we must first 'go in'. The vehicle for this magical journey is powered by our ability to relax in mind and body. As we physically relax and let go of muscular and emotional tensions and joint and bone structures we gain access to the inner realms by turning on our very special subtle smile. It opens the pathways of the parasympathetic nervous system. This helps us to reduce the out flowing habits of our senses so that we can be more alert in sensing our inner universe.

This simple process of 'going in' enables us to develop our internal skills so as to safely 'go out' to the universe.

Practice

Relax and Let go - Smile to Connect with the Universe Within

Smile to mideyebrow, eyebrows, eyes, mouth, jaw, tongue, lips, cheeks, ears, shoulders, ribcage and brain. Let the relaxed sensations and the 'Observer Mind' (Upper Brain) sink down into the Lower Tan Tien.

1. Smile to the mideyebrow. Relax and let go. Smile to the eyebrows and let them grow long to the sides. Lower these relaxed sensations down to the Tan Tien.

Fig. 3.5 *Smile and Relax to the Mideyebrow and think of the eyebrows growing long.*

2. Smile to the eyes: relax the eyes and feel how nice and cool they are. Let the eyes draw back in their sockets and start to sink down to the chest and gradually down to the abdomen, the home of your 'feeling and awareness mind'.

Fig. 3.6 *Smile and relax the eyes, sink into the eye sockets and gradually feel the eyes dropping down into the Abdomen.*

3. Relax the two broad muscles extending from the outer portions of the upper lips across the cheekbones, and lightly smile feeling their connection to the upper front of the ears. Gradually feel the ears growing 'long', up and down. Feel the ears grow all the way down and connect to the kidneys.

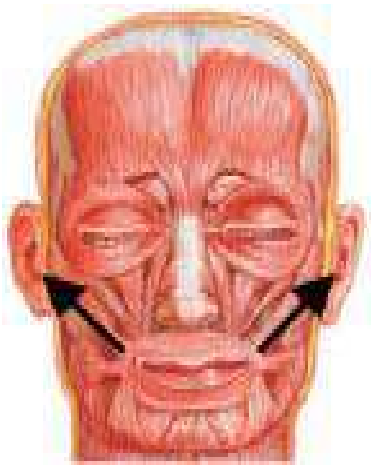

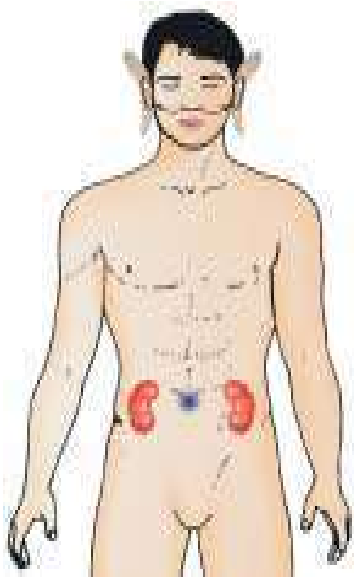

Fig. 3.7 *Smile to the Ears and listen to the Kidneys.*

4. Open your mouth and relax your jaw, separating the upper and lower teeth. Feel the jaw relax. Once the jaw relaxes the shoulders will relax and drop down. Continue to feel the jaw relax until you feel the saliva start to come out. Relax down to the rib cage. Feel the rib cage drop down, softening all the joints, relaxing down to the Lower Tan Tien. Let the tongue relax back in the mouth. Feel the tongue start to drop down into the throat to the chest and all the way down to the navel sinking the 'floating' sensation down to the Lower Tan Tien.
5. Smile to the shoulders and relax until you feel the shoulders drop and the rib cage relax.

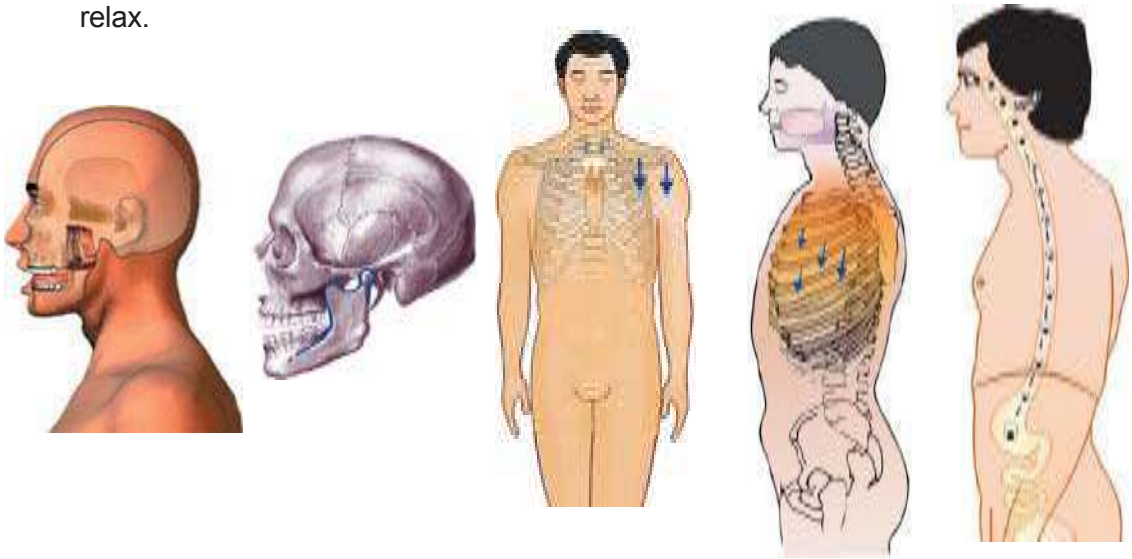

Fig. 3.8 *Relax the Jaw; and the Shoulders and Tongue will relax down to Lower Tan Tien.*

6. Lightly close the lips, but keep the teeth slightly separated. Physically begin a child-like smile with the corners of the mouth gently uplifted and the outer edges of the eyes softly crinkled up. Breathe through your nose.
7. Smile into the brain and empty the upper (observing) mind down to the Tan Tien.
8. Become aware of your inner universe as a big empty space. Keep on sinking – sinking down, into the darkness of your empty space. Keep sinking and experience the vastness until you get closer and closer to the center, the 'original force.' Stay relaxed and alert so as to be able to see one dot of light. It becomes a galaxy spiraling inside you.

   Do the above practice several times until you become familiar and comfortable with it.

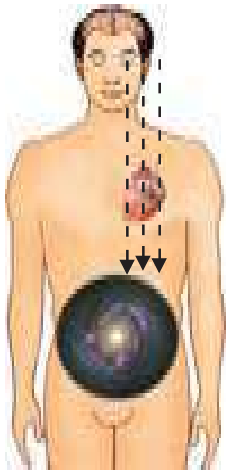

Fig. 3.9 *Bring the Senses down to the Tan Tien.*

Tan Tien Consciousness: Second Brain

Already terms have been used like 'upper mind', 'feeling and awareness mind' in the abdomen and lower 'Tan Tien'. In the next phase of practice, the 'conscious mind of the heart' is introduced. For those readers who have not been updated on the scientific and medical revelations of the recent era about a 'second' and 'third' brain, we offer the following information.

Along with this, there is the long-standing Taoist practice of cultivating and training consciousness in the Three Tan Tiens, especially the Lower Tan Tien. There is my own experience in participating in brain wave measurements and 'brain energy potential' research in recent years. The combination of all these areas of knowledge and experience in our time, makes Cosmic Healing practices accessible for our minds while also being very 'down to earth.' Now let's talk about the Lower Tan Tien.

In addition to its importance as the control center for the mechanics of the physical structure of the body, the Lower Tan Tien also houses a treasure of even more far-reaching significance. It has been a well-kept secret in the western world, as well as in most of the rest of the world: our Second Brain. Most of us who have had Taoist training in Chi Kung, Tai Chi, various Chi meditations or healing practices have often heard the reminder, 'Be aware of your Tan Tien.' But, do most people really 'get' the meaning of the injunction to always be conscious of the Tan Tien? Probably not. Further, do we use our Second Brain as much as we can? Definitely not.

In western terms, do we actually understand "Be aware of your Tan Tien" as being a way to train consciousness and awareness, like educating a brain in the abdominal area, in our Tan Tien? Probably not. Throughout the world, there are institutions to train the brain in the head. That is good. But, what about training the 'second brain' in the abdominal area? I didn't think of it exactly like that in western terms, either, even though that is exactly what I have been doing all of my life in my Taoist training and teaching.

Personal Revelation

Suddenly I came to understand a few things which are so simple and so important, and that's what I am going to share with you. It started in 1994 in Los Angeles when a clinical psychologist there, Dr. Rhonda Jessum, wanted to start testing me. I agreed to do the testing, but the machines at that time didn't tell me much. However, it was discovered that when I did the Inner Smile meditation, my brain waves went down dramatically – but at the same time, my 'beta' waves increased to a very high level. That means the waves showed that I could be driving a car, but that my brain should have been resting and sleeping. So the researchers said, "Hey, how did you do that?" I didn't understand either – because it was not clear to me either.

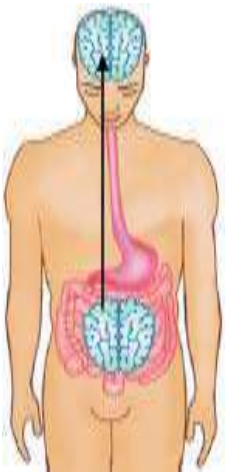

Fig. 3.10 *First and Second Brains are linked.*

Fig. 3.11 *Second Brain*

After that, I was invited to start testing in Europe by the Institute for Applied Biocybernetics and Feedback Research. My name is becoming known there because I teach in Europe a lot. One of the biggest institutes for training top athletes in Europe is in Vienna. They developed an instrument that can measure the brain's potential energy, which represents all the energy in the body. The doctors also said that this proves to the west that Chi exists, there is energy and a life force running in the body. That instrument picks it up in the brain and indicates how much potential brain energy you have. It also determines how much energy you have for the whole day and how much of that energy is for mental clarity and body power. They use these instruments to measure the athletes.

The study measures brainwave frequencies during four practices.

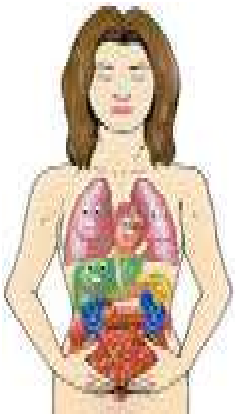

Fig. 3.12 *Cosmic Inner Smile*

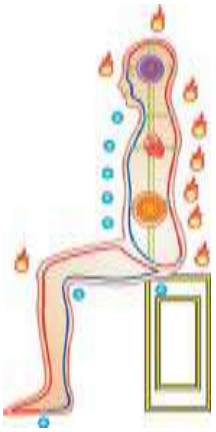

Fig. 3.13 *Cosmic Orbit*

Fig. 3.14 *Six Healing Sounds*

Fig 3.15 *Orgasmic Upward Draw*

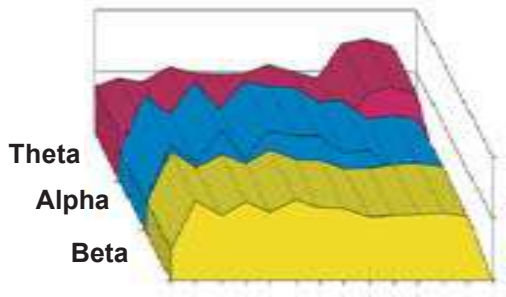

Fig. 3.16 *Alpha and Theta Waves increasing during the Cosmic Inner Smile Meditation.*

Fig. 3.17 *Ultraslow Brain potentials measurement while in Vienna.*

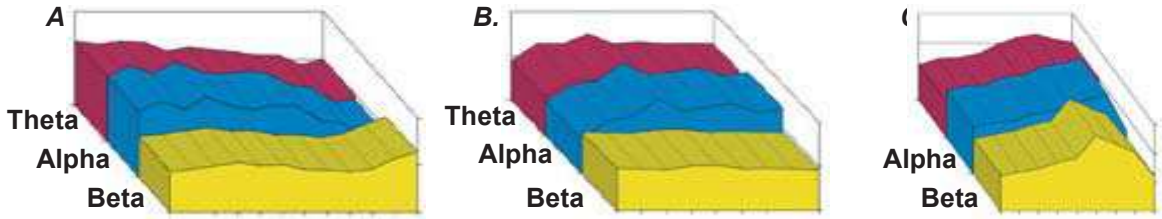

Fig. 3.18 A. *Altering dominance of alpha and theta waves during the Cosmic Orbit Meditation.*
B. *Cosmic Healing Sounds Meditation, results in increases in alpha and theta frequencies. There are minimal beta brainwaves; the brain reaches a state of stillness and internal focus.*
C. *Orgasmic Upward Draw Meditation increases the levels of alpha and theta.*

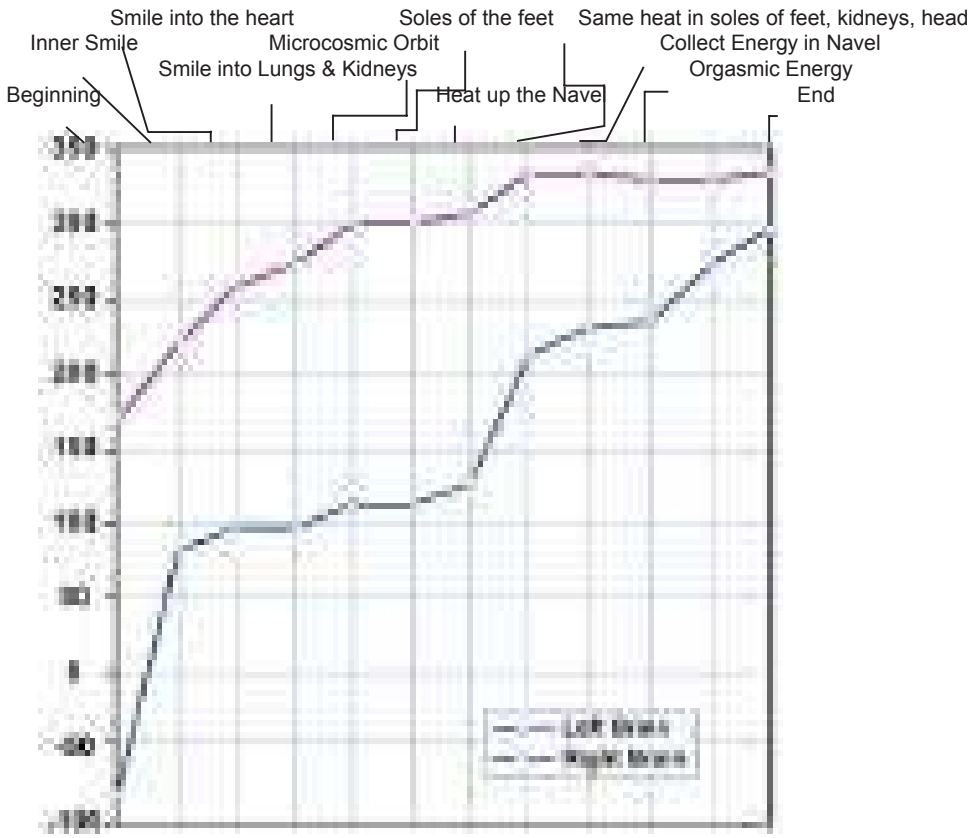

Fig. 3.19 *Left and Right Brain Charts*

It's interesting because the energy I have been describing in my teaching is exactly what they were measuring during their testing. So I went there and did the measurements with them. I just did the Inner Smile, smiling into my abdomen. They picked up these readings very quickly and said, "Your brain waves are going lower, lower and resting – and you are nearly in the sleeping state." At the same time, the muscle tension

was very low, the heartbeat was very low and the skin resistance was very low. After that, I surged the energy up to the brain and they started to see that the energy actually charged up there. When we are thinking, worrying or feeling anger, shame or guilt – the energy level in the brain actually decreases, and the brain doesn't get charged up. They were quite amazed, and said, "Hey, this is what we're looking for!"

They asked me what I was doing. I said, "I'm smiling to my abdomen." They kept on talking to me and asking me questions. They discovered that this brain (in the head) was not very active at all, meaning that there was not much activity in the brain. It was still in a very light resting state. But, how could I answer their questions? They said, "Hey, look! Master Chia is talking to us in his sleep. How can he talk to us in his sleep?"

After that, I said, "Oh, I understand now." Because, throughout the whole practice of the Tao is the injunction, 'train the second brain in order to use the second brain.' It took the westerners a long time to understand that. So, when the article about the 'Hidden Brain in the Gut' came out in The New York Times,[1] I started to understand that. You can be miserable; you can be happy; you can feel all kinds of feelings. But according to this article, they had also discovered that this brain in the gut, the enteric nervous system, can do a lot of functions. It says that this gut brain can send and receive impulses; it can record experience and respond to emotions. So, it is like a brain. In this article, they had only discovered that the large intestine and the small intestines have the same neurons as the brain cells. After that article, a new book, *The Second Brain,* was published.[2]

Now in medical science, I might add, they have begun to discover consciousness in the heart. They found that the heart can record a whole event, and it has its own brain. Dr. Paul Pearsall has written a new book, called *The Heart's Code*.[3] They have found that people who have a heart transplant actually get the emotions of the donor. They actually experience whatever the donor experienced. One of the cases is that of a girl who was brutally killed, and they didn't know who killed her. But, the heart was OK; so, it was transplanted into another girl. After that, the girl started to get nightmares and described somebody killing her. Then she described how the killer looked. Finally, the mother took the girl to a psychiatrist, and he in turn contacted the police. The girl gave the police an exact description and a police artist drew a likeness of the killer. With the information provided by the girl, the police were able to go and arrest the man. Afterwards, when confronted with clear details of the crime, the man confessed that he was indeed guilty of this crime. So, from that experience, medical scientists and others came to realize that the heart can record all of an event and remember it.

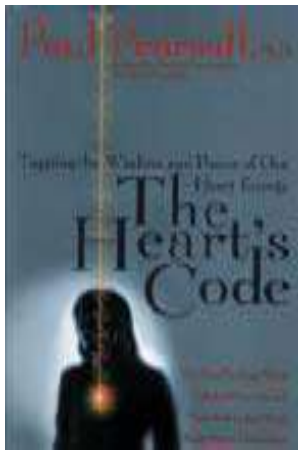

Fig. 3.20 *Heart's Code*

[1] "Complex and Hidden Brain in the Gut Makes Stomachaches and Butterflies," The New York Times, section C1, Tuesday, January 23, 1996

[2] Gershon, Michael. *The Second Brain* (New York: Harper Collins Publishers Inc., 1998).

[3] Pearsall, Paul, Ph.D. *The Heart's Code* (New York: Broadway Books, 1998)

The Lower Brain consumes less energy and can do a lot of daily work, like send and receive impulse records and experience and respond to emotions. When you lower down the Upper Mind, it will also lower the blood pressure and anxiety.

Fig. 3.21 *Abdomen has it own Brain: the Awareness Mind.*

On the second page of the Times' article, it says that even the large intestine is loaded with neurons. The question was posed, 'Can it learn?' But I say, "Hey, this goes back to 4,700 years of the Tao practice, which says: Train all the organs; train them how to do different things." You can rest the head brain when you're not using it – and use the brain in the gut. Why is it so important? Because the head brain is a 'monkey mind' riddled with doubt, shame, guilt and a suspicious mind. It is always thinking. Worrying, figuring things out things, head trips – it just keeps on, all the time. To be a God, you must let go of the past and empty the mind. Now we are in the information age; anything flits in – we think. Just one word flits in and we start an entire string of thought. When somebody says one bad word to you, you can think and figure it out for three days and three nights. 'How am I going to get revenge? How am I going to get revenge?'

Scientists have discovered that when people worry too much, thinking, planning, etc., this brain actually uses up a lot of energy. Depending on the type of person– some people are very physical types who use very little brain energy, but their physical body consumes a lot of energy. However, most people think and think and think. So the scientists give an approximation, by way of a percentage. This is just a number for comparison, not an exact number. They say that this brain in the head can use up to 80% of the body's energy. So, what happens is you have only 20% left for the organs.

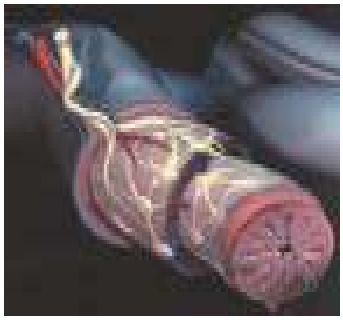

Fig. 3.22 *Cross-section of the neurons in the Large Intestine.*

According to the information about the brain in the gut, they have discovered that the brain in the head and the brain in the gut can do some similar jobs. For example, this brain in the gut is the emotional and the feeling brain. In the west you have the expres-

sions, 'I feel you from my gut' and 'I have a gut feeling about something.' Why do people mention a gut feeling? Obviously people have some feeling in their gut. It's very interesting that the whole Tao practice is feeling, awareness and consciousness – using this gut to feel, to be aware, and to be conscious.

You can rest, relax the brain in the head by using the 'brain in the gut.' This is the first step. The first thing we learn in the Tao is to forgive and let go. When we keep on remembering past negative emotions, we will stop seeing the truth. To let go of the past is to empty the mind and use the abdominal mind, the awareness and consciousness. Here's an interesting point in the way of the Tao: This gut brain can do a lot of simple functions that are similar to the functions of the brain in the head. This is a feeling and awareness type of functioning similar to many of our 'right brain' functions. However, we need to use the brain in the head in order to perform complex functions such as reasoning, making plans and making complex calculations. For rational functions, we need to use the brain in the head for the 'left brain' functions.

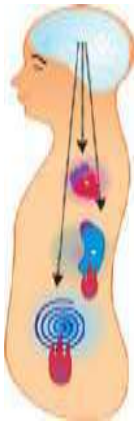

For our daily life of consciousness, awareness and feeling, we can use either the brain in the gut or the brain in the head. When we use the upper brain less, it will become charged with more energy and its power will be increased – and more power will be available to the body. That is why we say in Taoism, that we have to train the brain in the gut, so that we can use it when the brain in the head is resting. When the head brain is resting, it can be recharged: brain repair and maintenance occurs. Also, it can grow new brain cells. With more charging we have more power for creativity or whatever we want to use it for. If we like, we can use it to develop our higher spiritual nature.

Fig. 3.23 *When you are not using the Upper Brain allow it to rest by sending it down to the Lower Tan Tien.*

The simple thing is, that for the same job that the head brain or the gut brain can do, the head brain charges you eighty dollars. The gut brain only charges you twenty dollars. So, which one do you want to use? No, of course we are not that silly to use this overpriced person for the same work. But when we come to our own actual life, we don't know how to do it. We always use this mind, this high-priced brain. To add to this, we continue using it and using it, until the brain energy is completely consumed – no more energy. When you get to a certain level the brain is empty. These brain energy measurements are not only for indicating mental energy levels, they also represent energy conditions for the whole body and spiritual energy.

Whenever I smile down, the brain waves go lower and lower very quickly – and the transformed energy from the Tan Tien and organs charges up the brain in the head! Just by flexing the facial muscles into the mode we use with a genuine smile, we can produce the effects on the nervous system that normally goes with the natural sponta-

neous feeling. We can actually make ourselves relaxed and happy by taking advantage of this built-in human mechanism. It's natural. Just do it! Learning to smile down to the abdominal area and maintain the awareness of the relaxed, smiling sensation in the Tan Tien is the first step in training the *Second Brain!* Think about it: Pure awareness and consciousness can change attitudes and emotions carried in the DNA.

Remember: Number 1: "Empty your mind down to the Tan Tien, and fill the Tan Tien with Chi." An axiom in the Tao is, where the mind goes the Chi follows. And, Number 2: "When your mind is empty, it will be filled!" This means that when the organs have extra energy, the extra organ energy will rise up and fill the brain with Chi.

Fig. 3.24 *When the mind is empty, transformed energy from all the organs can charge the brain with Chi.*

Practice

Three Minds into One: 'Yi' Power

Smile into your heart. Lower the Observation Mind, then the Heart Mind down to the Tan Tien. With the Feeling/Awareness Mind, Spiral the three minds into one.

1. Smile into your heart. Make it feel soft. Feel love. Feel joy. Feel happy and feel compassion in your heart. Feel the heart spiral.
2. Spiral in the upper mind. Lower your upper mind, the observation mind, down to the Tan Tien in your navel area.
3. Turn the consciousness in your heart, activated by your love and softness, down to your Tan Tien.
4. Combine the upper and middle minds with the energy of the feeling/awareness mind of the entire nervous system – the Second Brain in the abdomen. Merge the three minds into one mind by spiraling their energy, blending them together as one in the Tan Tien.

When the three minds merge into one they become the 'Yi' power, the three-mind power – activate the spiraling at the mideyebrow, crown and the soles of your feet – expand to the universe in six directions: up, down, front, back, left and right. Once you get it, the Yi, we will start to activate the six directions and the three fires.

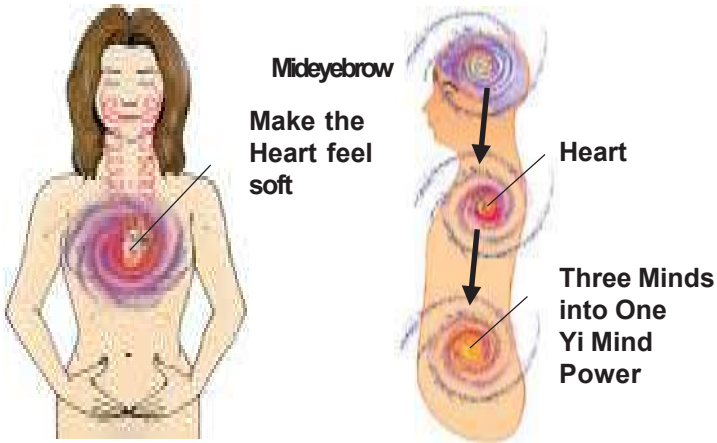

Fig. 3.25 ***A.*** *The Heart softens like a rose blossoming.* ***B.*** *Spiral the Upper Tan Tien to the Lowest Tan Tien and Three Mind 'Yi' Power.*

Activating the Six Directions and the Three Fires

This powerful energetic technique allows one to extend the mind, to touch the force, and to draw that energy back into the body.

The Six Directions teaches you how to expand your mind and Chi for receiving healing power. By practicing the Six Directions daily you will increase your healing and cosmic power. Turn your mind and Chi into the cosmos, multiply them and draw them back.

Direction Below

When you achieve the three minds into one mind begin expanding into the Six Directions; press your hands down and start with the low direction. Picture yourself standing on the earth and you expand yourself very far away – deep down into the earth, very, very deep down into the earth. Your hands become very long; your feet become very long — they go all the way down into the earth and out past it into the galaxy below on the other side.

Push. When you push, connect with the galaxy below — pull and think about your Tan Tien filling with Chi. Push and pull. Push and pull. Fill your Tan Tien with Chi.

A. ***B.*** ***C.***

Fig. 3.26 A. *Hands expand through the earth and to the galaxy below.*
B. *Hands push forward and pull back.* ***C.*** *Smile to the primordial Chi from the universe back to the Lower Tan Tien and fill the Tan Tien with Chi.*

1. Stand, feet together. Put you hands down, parallel to the ground. Expand your hands very far away and your mind very far away smiling into the ground. Continue expanding your hands, feet and your mind very far away beyond the earth below. Go down through the galaxy, way beyond to the primordial force. It's just like you are extending all the way to the primordial force before 30 million years ago.
2. Push, moving the hands forward six inches only.
3. Pull, moving the hands back by the sides. Think about your Tan Tien – Chi coming to the primordial force in your Tan Tien. Smile to your Tan Tien, dark, deep and vast.
4. Push: touch the primordial force in the universe.

A. ***B.*** ***C.***

Fig. 3.27 A. *Be aware of the universe in front.*
B. *Expand your hands very big and long to the universe in front.*
C. *Hold the fire ball to activate the Tan Tien Fire.*

5. Pull back to your Tan Tien the dark primordial forces with your hands.

Push and pull: It's just like you go to an empty space – vast. Then you come back to your Tan Tien – also empty, just like the primordial condition before anything existed.That is where all the forces come from. Push and pull 3 – 9 times.

Front Direction and Tan Tien Fire

Next, be aware of the front direction; a huge fireball appears in front of you.

Open your palms: scoop up the Chi, scoop up the fire. Bring the fire into your Tan Tien. Activate the Tan Tien Fire.

1. You start with a small dot of light inside you. Expand your awareness smiling to the universe in front of you.
2. Become aware of a big fireball in front of you. Fell your hand become bigger and longer. Scoop up the fireball. You may close your eyes to help your inner sensing.
3. Use the fireball to light the fire in your Tan Tien. Feel the fire burning in the darkness, the 'fire burning under the sea.'

Fig. 3.28 *Smile to the Burning Fire.*

Back Direction and Kidney Fire

Be aware of the back of the Tan Tien, the Door of Life and the back or rear direction. Extend your mind very far away to the 'back'. Scoop up the fire and light up your 'Kidney Fire'.

Fig. 3.29 *Be aware of the back direction, move the arms toward the back of the universe and scoop up the universal fire.*

1. Expand your awareness all the way to the back. Move the arms toward the universe behind you.
2. Touch the universe; scoop up the fire. Activate the Kidney Fire. Maintain your awareness in the Tan Tien and expand smiling out to the universe. The energetic spiral glows in the Tan Tien. Spiral in the heart, spiral in your crown and spiral in the universe.

Heart Fire

Raise your hands up under your armpits, and feel yourself holding the two fireballs. Touch the heart by extending the fingers energetically in from the sides; feel your hands extending into your heart and very far away. Activate the Heart Fire.

Fig. 3.30 *Activate the Heart Fire.*

1. Move your hands up under your armpits and extend your fingers deep into your heart and very far away.
2. Tan Tien and the Universe: you are connecting to the 'charger,' charging more fire into yourself.
3. Feel your heart soft in the center as you smile down. Feel the warmth of the fire energy of love, joy and happiness in the heart.
4. You feel the connection with the unconditional love in the universe as you keep your heart consciousness in your Tan Tien and extend your awareness out to the universe.

Sacred Fire *(Chi Fire)*

Connect the Three Fires to combine into one Fire: *Heart to Kidneys to Navel to Heart*.

Fig. 3.31 *Connect the Three Fires and Sacred Fire.*

1. Move your hands together in front of your heart. Hold your hands together in front near the heart and feel the fire burning in there. Connect the Heart Fire to the Kidney Fire, the Kidney Fire to the Tan Tien Fire and back up to your heart; connecting them as one triangular Sacred Fire, circulating the Chi at 1,000 revolutions per minute, 10,000 R.P.M, 30,000 R.P.M and 60,000 R.P.M, doubling or tripling their collective power.

Open the Third Eye

Now, extend your hands out to the front, very far away – pushing, pushing, pushing. Push. Turn your palms inward, and extend your middle fingers inward toward your third eye. Picture a crack in the middle of your forehead, and pull the crack open. Feel the light from the heavens opening it and feel the light from the heavens shining into your brain.

1. Open your palms. Open your eyes, dimming the eyes. Look to the universe. Extend your hands to the front, palms vertical. Extend the arms from the scapulas. Smile and touch the universe.
2. Turn your palms inward and extend your middle fingers inward toward your third eye.

3. Picture a crack in the middle of your forehead and let the heavenly light shine into the brain; pull the crack open and let the light reflect into the organs.
4. Close the third eye. Again, open. Pull: open-close-open. And, close. With the third eye open, the light from the heavens shines into your brain and reflects down to all your organs. Open and close the third eye 3 - 9 times.

Fig. 3.32 *Look as you smile into the Universe in front of you.*

A. ***B.***

Fig. 3.33 A. *The Middle of the Finger hooks into the third eye and reflects down into the Organs.*
B. *Pull open the Third Eye; let heaven open and shine its light into the Brain.*

Front Direction: Push/Pull Master Practice

Now, turn your palms, pushing out. Push. Pull. This is the master practice that is imperative for successful completion. When you first start practicing you should do it at least one hundred times and increase up to 200 times. Push and pull. When you push, you feel your hands extended very far away – very long – reach the sky. Touch the universe.

1. Push: Extend your arms and hands to the front, palms vertical. Extend the arms from the scapulas.
   Expand: smiling, smiling, touching the universe – touching the force, touch -ing the Cosmic Chi.

Fig. 3.34
Master practice:
Touch the Universe.

2. Pull: Draw the Chi back to you from the universe. Moving the arms from the scapulas, draw the hands toward your body in a horizontal position, drawing the Chi into the body.

Fig. 3.35 *'Drawing' Universal Chi - feel your Tan Tien and fill it with Chi.*

Pull. Think and smile to your Tan Tien. Push, very far away to the universe.
Pull. Push: Smile, relax, and let go, touching the sky, touching the universe.

Fig. 3.36
Let go - Push and Touch the Universe, do it 6, 9 or 18 times.

Left and Right Directions

Now, move your hands to the left and right directions. Pull the Universal energy in. Push; touch the universe. Pull; think about your Tan Tien. Push – all the way, touching-touching-touching the universe.

1. Move your extended hands from the front horizon to the left and right sides.

Fig. 3.37 *Touch the Universe Left and Right.*

2. Pull Tan Tien: Smile to your Tan Tien. Keep smiling to your Tan Tien.
3. Push to both sides. Expand all the way, smiling and touching the universe.

   Push/Pull: touching, touching the universe drawing the Chi smile energy into you from both sides.

   Do 3-6 times.

Fig. 3.38 *Pull: Just feel about your Tan Tien.*

Direction Above

Turn your palms up to the universe. Scoop up the Chi. Pour the Chi over your crown, and touch your crown. Project the Chi all the way down to the perineum and down through the earth to the universe below. Tan Tien and universe; always feel your Tan Tien spiraling, heart spiraling, crown spiraling and the universe around you spiraling.

Fig. 3.39 A. *Raise the hands above the crown and feel it extend up to heaven.*
B. *Feel that the hands are big and long and that the bones are hollow. Fill and pack the bones with Chi.*

Raise your hands up to the universe and expand your hands as big as the universe - feel the Chi charge into your bones.

Scoop and gather the energy turning the body three times to the left and three times the right drawing the smiling energy.

Fig.3.40 *Scoop up the Universal Chi and pour it over the head.*

Open the Spine

1. Touch the back-crown point. Pour the Chi all over your crown. Think of your soles so that you feel like there is a waterfall of Chi flowing from your crown all the way down to your soles. Feel your finger grow long and the Chi penetrate down through your spine to the coccyx. Leave the fingers touchng the back of the crown, to maintain the energetic connection with the coccyx.

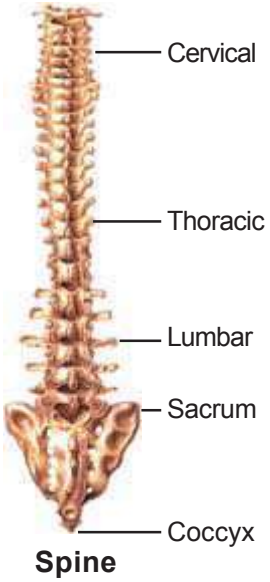

Spine

Fig. 3.41 *Feel your fingers growing long, all the way down to the coccyx.*

Turn 'Three Minds into One Mind' at the Lower Tan Tien, and expand the awareness to the universe. Let yourself be charged by the universe.

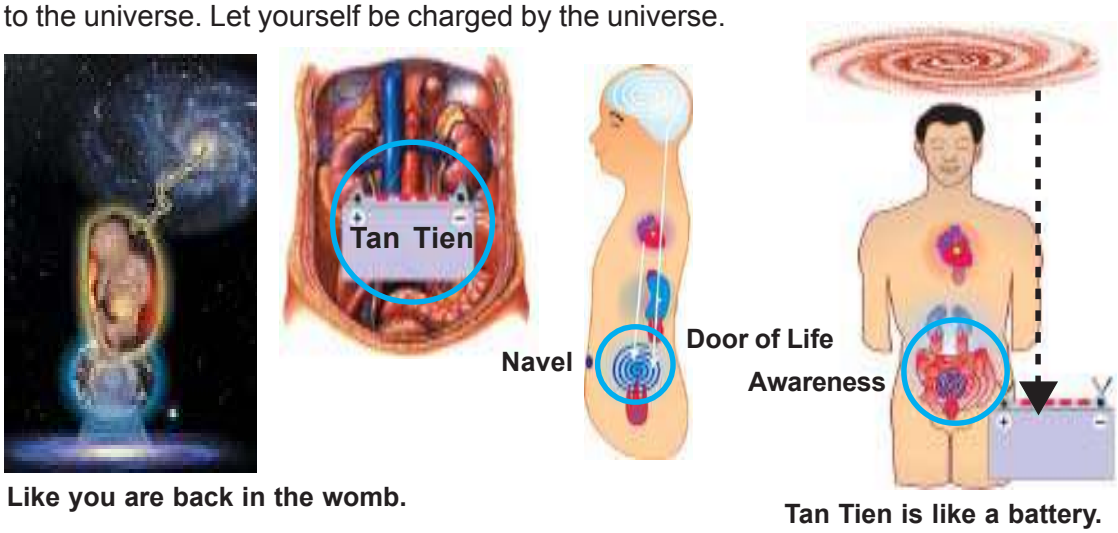

Fig. 3.42 *Universe charges Tan Tien power.*

Beware of the Tan Tien and spiral it like universal energy in motion. Feel the heart center spiraling and the crown spiraling. Be aware of the universe spiraling above, below, front, back, left and right. Let all of the sick energy and the negative forces leave the body and go down into the ground for Mother Earth to recycle. Extend the Chi from above, all the way down through the earth and the universe below.

Fig. 3.43 *Be aware of the Lower Tan Tien, Heart Center and Crown spiraling. Feel the Universe is spiraling and charging the Three Tan Tiens.*

Open the Middle Channel and Perineum

1. Move to the mid-crown point. Touch the point and project your fingers inwards; go deeper, deeper through the middle of your body down to the perineum. Focus on the perineum. Feel the Chi from the universe flow into your perineum. Look for one dot of light. Look into the darkness, the vast darkness, the immense darkness; this is the primordial force, a cloudy moving force. Look for a dot of light at the perineum and extend your awareness all the way down through the ground and the universe below.

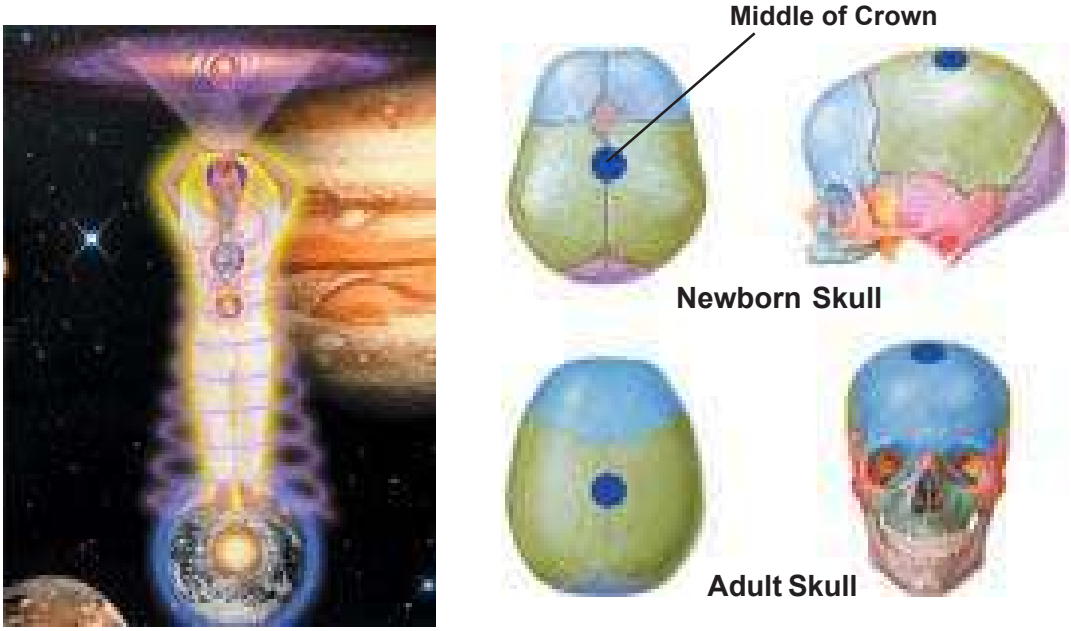

Fig. 3.44 *Move the Hands to the Middle of the Crown and feel the Fingers Penetrate to the Perineum.*

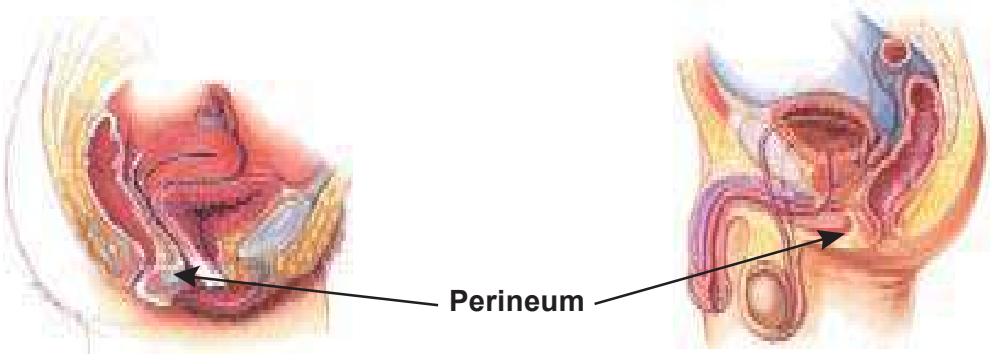

When finished opening to the Six Directions and igniting the Three Fires, gather the Chi in the center and bring this expanded awareness into the healing session.

Tan Tien and the Universe

The expression, 'Tan Tien and the Universe', is a reminder to feel your Tan Tien, heart, mideyebrow and crown spiraling and that you are connected to the universe spiraling in the six directions around you.

1. Establish a Complete Location

You will use your Yi, the three-mind power, repeatedly to recharge your Chi for various purposes. You recharge by connecting to the Universal Chi in the six directions of the universe simultaneously. When you charge a particular area or direct Chi into the body to a particular point, you first establish a connection point for the Chi by placing the hand or fingers at an appropriate location on the surface. This is like giving a location for the Chi to go to. Once the location is established and the Chi starts to go there, leave your hands there.

Then you move your attention to where you want the Chi to go in the body. Feel the Chi connected to and charging the intended location.

2. Charge Tan Tien from Universe

When the location connection is established, be aware of your Tan Tien, heart center, mideyebrow and crown spiraling. Be sure that the conscious mind of the heart is lowered to the Tan Tien and the awareness mind of the abdomen is connected to the mideyebrow crown and out to the universe. Feel them connected to the spiraling energy in the six directions of the universe. Let the universe charge your Tan Tien.

3. Don't Stop at the Location

With your focus in the Tan Tien, the Chi will go from there to the 'location' indicated by your hands and then to the intended location in the body. Don't let Chi stop there, however.

4. Direct Chi out the Opposite Side to Universe

Direct your attention to guide the Chi flow through the body and out the opposite side. You want to clear out any blockages and prevent any others from accumulating. You also want to release sick energy and negative forces down into the earth. Let the Universal Chi flow out through the universe and beyond.

Open the Three Tan Tiens

Move your hands down to the mideyebrow. Touch the mideyebrow.
We are going to open the three Tan Tiens, starting with the Upper Tan Tien.

Upper Tan Tien - Mideyebrow

1. Recharge. Remember: Tan Tien – heart consciousness in, awareness out. Spiral – Tan Tien, heart, third eye and crown. Universe – six directions spiraling.

Fig. 3.45 *Raise hands and charge with Universal Chi.*

2. Move your hands down and touch the mideyebrow. Feel your fingers grow very long (energetically) and penetrate all the way back to the base of the skull. Focus on the back. Remember: Tan Tien and the universe spiraling. With the spiraling, the Chi in the fingers will become hot. It will expand and penetrate out through the back of the head all the way to the universe behind.

Fig 3.46 *Fingers touch mideyebrow and penetrate to the back of the skull and the universe at the rear.*

Fig 3.47
Tan Tien and the Universe.

3. Picture your fingers like laser beams of Chi, 'Tan Tien and Universe': Feel your Tan Tien and the universe spiral and charge your fingers. Move your fingers out from the mideyebrow around the side of the head to the top of the ears. Your fingers are like lasers -cut-cut-cutting open your skull right in the middle, around to the top of the ear, cutting open your Upper Tan Tien. Cut and project your fingers long into the middle of your brain. Spiral your Tan Tien and the universe. Leave your fingers there. Concentrate on your Tan Tien spiraling – your heart, crown, the universe above, below, front, back left and right all spiraling. Your Tan Tien is a big empty space: primordial force; darkness. You can put so much Chi inside there! The Chi penetrates into your brain.

Fig. 3.48 *Move the fingers to the top of the ears. Feel them growing longer and cutting the skull open, penetrating into the brain.*

4. Move your hands all the way to the back, cutting to the back of the skull. Touch, and feel the Upper Tan Tien open.
5. Touch the base of your skull. Focus on the mid-eyebrow. Feel the Chi flow like a laser beam from back to front and out to the universe in front. Complete the opening process by moving the hands back around to the mideyebrow, cutting as you go.

Fig. 3.49 *Chi moves like a laser, penetrating from the mideyebrow at the front, to the back of skull.*

6. Recharge in the universe. Feel your bones and your arms are hollow. Fill and compact them with Chi.
7. Scoop the Universal Chi and pour it down over your crown and all the way down, down to the Middle Tan Tien.

Fig. 3.50
Recharge in the Universe, scoop and pour the Chi down to the Middle Tan Tien (Heart Center).

Middle Tan Tien - Heart Center - Conscious Mind

1. Move your hands all the way down to your heart center at the mid-sternum. Touch. Focus on the point opposite the heart, T5/T6, on the spine. Fingers 'long', Chi penetrates into your thymus gland. Light – golden light – penetrates into your thymus. Feel the Chi penetrate through your heart all the way through T5/T6 to the universe behind. 'Tan Tien and the Universe' also feel your Chi Fingers penetrate into the bone and bone marrow and spread out into your rib cage.

Fig 3.51 *Golden light enters the heart, thymus, bones and marrow; feel it penetrate to the universe at the rear.*

Recharge and cut around to the Armpits

1. Recharge In the universe, pour Chi over the crown down through the body and lower your hands down to the heart center. Touch with the fingertips. Move your hands around under your armpits, extending the Chi like laser beams cutting open this Middle Tan Tien. Pause under the armpits as you send the Chi into the center.

Fig. 3.52 *Cut open the Middle Tan Tien by cutting around the armpits.*

2. Continue to move your hands around to your back at T5/T6, touch and send the Chi from back to front. Let the beam of Chi penetrate out through the heart center to the universe in front of you. Then, move the hands back around the sides to the front, cutting as you go.

Fig. 3.53 *Chi beam from T5/T6 penetrates to the Heart Center in front.*

Lower Tan Tien - Navel - Awareness Mind

1. Recharge with Universal Chi. Tan Tien and Universe: Again, raise your hands and charge with the Chi into the universe. Your hands are very big, very long. The bones are hollow and compacted with compressed Universal Chi. Scoop the Chi from above and guide it down. Pour all the way down, down, down to the navel. Touch the navel, and focus on the Door of Life opposite on the spine between L2/L3. Touch and feel the Chi penetrate to the Door of Life Tan Tien and Universe. Feel the Chi penetrate through to the back and out to the universe behind.

A. ***B.***

Fig. 3.54 A. *Recharge the Lower Tan Tien and penetrate through to the Door of Life.*
B. *Raise the hands up to the universe and charge with Chi. Bring the power down to Tan Tien.*

2. Open this Lower Tan Tien the same way as for the Upper and Middle Tan Tiens. Charge more Chi into your hands, and let them be like lasers cutting it open. Cut around to the sides. Pause. The fingers of the left and right hands are very long, extended energetically inside. Cut and feel the energy penetrate into the center. Focus at Tan Tien and universe and feel more Chi.

Fig. 3.55 *'Cut' open the Lower Tan Tien with Laser Fingers.*

3. Continue cutting to the Door of Life. Touch, and send the Chi from the Door of Life back to the navel and out to the universe in front.

Fig. 3.56 *'Cut' open the Door of Life and send Chi to the navel and universe in front.*

4. Move the hands back around the sides to the navel, extending the fingers and "cutting" the Tan Tien open as you go. Touch the navel: Tan Tien and the universe spiraling. Feel more Chi, and feel the Tan Tien open.

Activate Chi in the Bones of Hips, Legs and Sacrum

1. Now touch your pelvic bone by energetically extending your fingers from the front area near the hips to the back. Feel Chi penetrate into your pelvic bones: funny, laughing, happy bones.
2. Touch the femur bones. Tan Tien and universe. Charge the fingers. Also, feel the funny, happy, laughing vibration inside the bones and in the bone marrow. Be aware of the Three Tan Tiens. Spiral from the universe. Spiraling charging your Tan Tien. Charge your hands and your bones.

Fig. 3.57 *Touch the femurs - happy laughing bones!*

3. Now we are going to slowly lower the sensation of Chi down through the bones to the earth. Opening up the sacrum. Move the hands down the legs as you bend down.
4. Lower yourself all the way down to the ground and sit on your feet. Move the Chi with your hands down to your toes, down through the earth and the universe below.

A. ***B.***

Fig. 3.58 A. *Sink the Chi into the earth.* ***B.*** *Lower and sink the mind and Chi down to the universe.*

5. Raise your sacrum up, keeping your hands at the toes. Smile to your Tan Tien and feel the Chi from the universe coming to fill the Three Tan Tiens. Opening up the sacrum.

Fig. 3.59
Raise the sacrum and smile to the Tan Tien.

6. Lower down again. Lower the Chi down to the earth and the galaxy below.
7. Once more, raise your sacrum up, maintaining hand contact with your feet. Smile to your Tan Tien.
8. For the third time, lower down. Open your palms, gathering the Chi from the earth below. Gather and scoop the Chi.

Fig. 3.60 *Gather the Earth Chi.*

9. Touch your heels and feel your bones as you slowly rise up. Fill your bones with Chi as you guide it up with your hands.
10. Fill the bones in the upper legs as you move your hands up.

Fig. 3.61 A. *Fill the bones with Chi.* ***B.*** *Feel your fingers penetrate into the bones as you rise.*

11. Feel your bones, and fill them with Chi all the way up to your coccyx. Touch your coccyx. Leave your fingers there, then be aware of the Chi and feel the Chi raising up to the Tan Tien and the universe. Feel it charge the fingers and the spine.
12. Come up to the sacrum. Feel the sacrum open. Focus at the Tan Tien and the universe.

A. ***B.***

Fig. 3.62 A. *Bring the Chi to the Coccyx.*
B. *Move your hands up to the Sacrum and feel the Chi rise up to the Crown.*

13. Come up to the door of life, and then back to the navel. You may sit down to continue the next step in the Cosmic Healing Practice.

Fig. 3.63 *Bring the Chi to the Door of Life and let it penetrate to the Navel.*

Practice daily till you feel the Chi. Then you can apply this Chi to the Healing Sessions.

Chapter IV
General Healing Session

The General Healing session practices are to be done with every student regardless of their age or health condition. These are for cleaning and strengthening the cells. Cells must be clean and strong to heal. The General Healing practices listed steps A-K are the most important part you must always do in every session. You can do this with one person or with many people at the same time. The following is a detailed decription of each of these steps. Become familar with them and they will flow easily one into the other.

A. Three Minds into One Mind

Smile down to the inner universe. Activate the heart consciousness and empty the mind and heart down to the LowerTan Tien, the Abdominal Brain. Gather the 'Yi' (mind-eye-heart power), combining three minds into one. Fill the Tan Tien with this Chi. Start to spiral. You are then ready to connect to the higher forces of Universal and Heavenly Chi. The Three Minds are the Upper, Middle and Lower, or three Tan Tiens. The Upper Mind is the one we have been closely related to most of our lives. It is the logical thinking, planning, calculating and worrying mind; it consumes 80% of our body's energy.
The key is to learn 'to releas the mind' by learning to sink the Chi to the Lower Tan Tien, whereby it can be used in synergy with the other two.

B. Activate the Six Directions

Activating the six directions is for opening the whole body, mind and soul to all of the Universal and Cosmic forces in all directions. We literally learn to draw in the Universal and Cosmic forces from all directions at the same time. This is important for healers so they are not using their own energy for healing but drawing on the limitless Universal forces.

Expand your awareness to connect to the universe and the Six Directions at the mideyebrow and crown; left, right, front, behind, above and below. Connect to the universe, collect and spiral the energy into your Lower Tan Tien.

C. Activate the Three Fires

Activate the Tan Tien, Kidney and Heart Fires to create a Sacred Fire Triangle. Move from the Tan Tien to the Heart, the Heart to the Kidneys and the Kidneys back to the Tan Tien.

D. Linking Personal Stars, Energy Bodies and the Universe

World Link is a way for intelligent life force to return to the source; inwards and upwards. Become aware of the 'personal stars' above the crown and below the earth.We link with our own personal stars and then with the stars of each person in a group. This links the energy bodies of everyone in a group together. Start to spiral your energy and connect to other peoples' stars and energy bodies. Make a left spiraling pattern, progressing around the circle in a clockwise rotation. Link all of these stars together and form ***one large energy body.*** Each meditator will become an individual unit in an integrated communication link. A link between the earth and the universe.

E. Protective Circle and Chi Field

We create Chi Fields, Protective Animals and call the Eight Forces to protect the group from disturbances and psychic attacks. Raise your right (or leading) hand in the air and access the **'Sacred Fire'** of the universal cauldron. "Feel your fingers becoming big, long and hollow", as they reach into the Sacred Fire. The Chi will fill and pack your arm as you bring it down into your body. Use Yi-Power to create the **Sacred Fire Protective Circle.** The fire will purify and protect the circle. You can cast a circle around your community, house, room and body. This will create an energetic field of Chi around the whole room.

Then Create a **Chi Dome**. Invoke the 'guardian animals'; Blue Tortoise from the north, Red Pheasant from the south, Green Dragon from the east, White Tiger from the west, Yellow Phoenix from above and Black Tortoise from below.

Finally, activate the **Eight Elemental Forces of Nature and the Universe**. Call the forces of fire, water (ocean), thunder (lightning), lake (rain), earth, mountain, wind and heaven. Activate fire in the north, water in the south, lightning in the east, and rain in the west.

F. Chi (Sacred) Water Practice

Invoke the power of the Sacred, Chi or Holy Water practice to cleanse and heal the body's sick, toxic or negative energy. Make a request to receive healing energy and feel yourself touch a heavenly pool of sacred water energy. Feel the pool pouring down heavenly water to fill your arm.

Use the thumb and index finger to remove the sick energy from the cup, without touching the water. Talk to the sick cells. Let the sick energy return to the earth for recycling. Fill the water with your heart's compassion. Give the command: "This Sacred Water will give health, wealth and longevity". Cosmic Healing works on a cellular level. It is the water's 'job' to carry the message of the practice to all the cells, where it will remain. Drink the water in unison with the rest of the group.

G. Empty and Fill

The Empty and Fill technique is emptying the sick energy into the earth and filling with healing Cosmic Force Energy. Project your 'sword' hand (middle and index fingers) down to the ground. Project the hand 'very big and very long' and your feet 'very big and very long' - extended down to the ground. Now very slowly inhale, bring up the earth energy. Bring the energy up to your feet and into your bones. Let it enter all the bones, organs and cells. Feel it blending with all the sick energy. Turn your palm up, turn it back down again and exhale; let go of all the sick energy, the negative energy, the worries and burdens, all the way down into the earth. Repeat this three to nine times. Dig a hole and bury all the sick energy; tell it, "Do not come back; you will be happy down there." Smile.

H. Clean with Green Light

The Green light is for cleaning the cells. This is vitally important because the cells must be clean for healing. Green can help detoxify the toxic cells. Green Chi is mild and safe. Green Chi is used for cleansing, and as a decongestant for diseased parts. It 'loosens' the area. The light green Chi is used to break down dirty or diseased energy, like a detergent is used for washing clothes or dishes.

Afterwards, the cells will be rinsed with blue light, like clean water is used to rinse the detergent and residue from clothes or dishes.

When you carry out healing try to 'see' the cells enlarged and this green energy go in and blend with the dirty, black and cloudy energy. See it come out and let it go down to the earth. Dig a hole and bury it there. Tell it, "Don't come back. You will be happy down there". Become aware of the green light and spiral counter clockwise. Spiral down. Cleaning out the stress. Repeat as many times as you like, three times minimum.

I. Clean with Blue Light

Blue is like cold water; it has the yin power to dissolve all kinds of negative energy and sickness. It has an inhibiting effect. Blue yin energy is the opposite of red yang, which has a strengthening and stimulating effect.

Blue has a cooling effect; it can reduce pain and inflammation, and it can help blood clot. It stops bleeding and reduces fever. It can help to induce rest and sleep.

J. Charge with Violet Light

Charging with Violet light holds the highest healing energy. When the cells are clean they will absorb and hold the Violet light and the healing will take place. Luminous Violet has intelligence and can be programmed. The universe is full of violet light, especially the North Star and the Big Dipper. The color of the star of the higher self or soul, above the crown, is also violet. It is the color of Divine or Soul energy.

It has properties of other Chi colors. It has a rapid regenerating effect on damaged organs and nerves. Always use green and blue light before using violet. Violet light develops the crown center, the spiritual core. It is good for psychological ailments as well as for physical deficiencies.

K. Activate the Immune and Defense System

The body has various mechanisms which combine to provide protection and defense against illness and disease. These mechanisms enable the body to produce various cells and bodies which act against invading or unwanted substances. As soon as a foreign body is recognized, the immune system will be triggered and will act to provide the most efficient means of eliminating the danger and return the body to a balanced state of health. A strong and healthy body will have good resources to protect itself from negative or sick energy. The aim of these practices is to help you to realize the potential of true harmony within yourself. To activate the immune and defense system is to increase the production of red and white blood cells. To do this we activate the bone marrow and lymphatic system. Guide the student or whole group together in all of these steps. You will not lose energy by doing this. You will gain more energy because you are all connected together in the group power. The crucial part is to multiply your good intentions, Chi and virtue energy into the cosmos, making yourself and each person a direct line from the Universe. After you finish the General Healing session you can tailor the healing techniques in the next chapters to the individual's needs.

Practice

A. Three Minds into One Mind

1. Smile to the Inner Universe

Place your palms together in salutation, in front of your heart. Feel the Laogong points in your hands connect, creating an energy loop running from your heart through your arms and hands and back again.

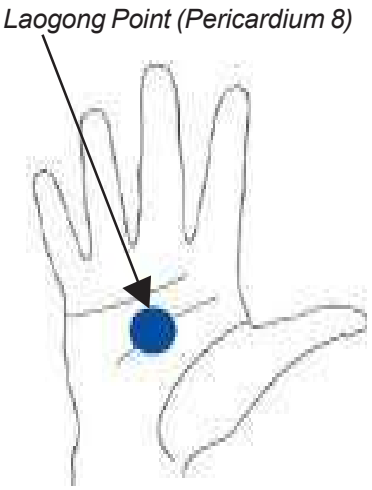

A. ***B.***

Fig. 4.1 A. *Empty the mind down to the lower abdomen.*
B. *Activate the heart's compassion.*

2. Activate the Heart Compassion Energy

Smile to the heart and feel it softening. Feel love, joy, compassion and happiness. Smile down and empty the mind to the Tan Tien, the Abdominal Brain. Fill the Tan Tien with Chi and start to spiral. When the abdomen is warm, it is full of Chi. The Chi can then charge up to the brain.

3. Combine the Three Minds into One

1. Turn Upper Mind to observation mind.
2. Turn consciousness (Middle Mind) down to Lower Tan Tien.
3. Combine three minds into one mind at the Lower Tan Tien (the Yi).
4. Manifest out at the mideyebrow.

Fig. 4.2 *'Three Minds into One'.*

B. Activate the Six Directions

Expand the awareness to connect to the universe and the Six Directions at the crown, mideyebrow, heart and Tan Tien.

Fig. 4.3 *Trust and believe - turn visualization into actualization.*

C. Activate the Three Fires

1. Tan Tien Fire - Activate the Tan Tien Fire:

Smile down to the abdomen to create a burning stove near the lower lumbar and sacrum. Create a fire ball behind the navel, above the stove.

2. Kidney Fire - Activate the Kidney Fire:

Always retain awareness at the Tan Tien and keep it spiraling.

3. Heart Fire - Activate the Heart Fire:

Keep the heart soft and fill the heart with joy, love and happiness.

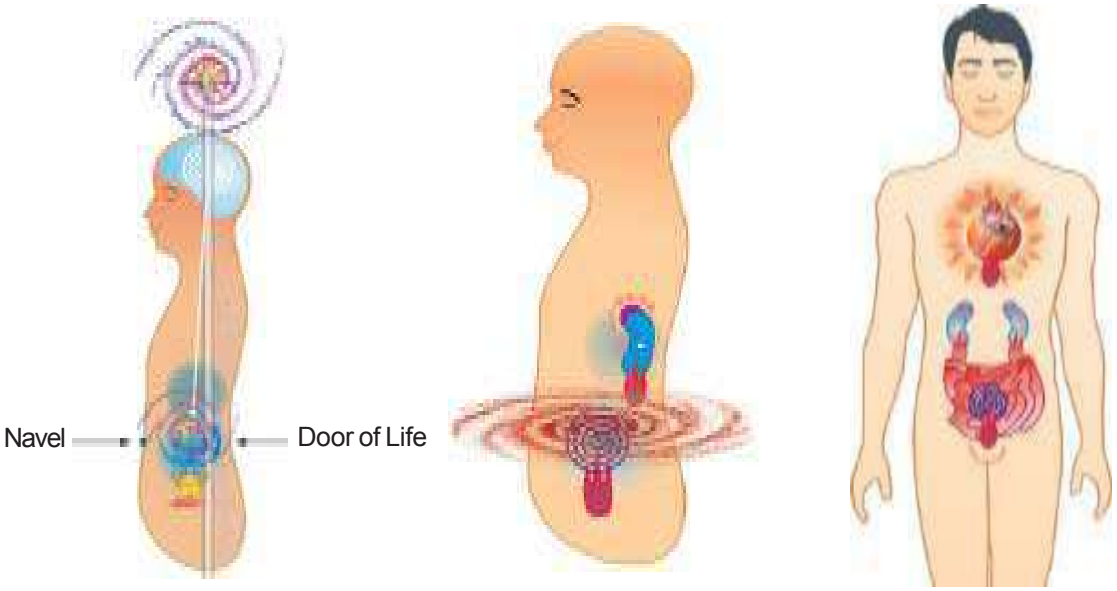

Fig. 4.4 A. *Activate the Lower Tan Tien Fire.* ***B.*** *Activate the Kidney and Adrenal Fires.* ***C.*** *Activate the Heart Fire.*

4. Sacred Fire Triangle

The Sacred Fire Triangle has triple force. Make a triangle from kidneys to navel (Tan Tien). From the heart make the connection to the kidneys. Move from the Tan Tien up to the heart.

5. Cosmic Star and the Earth Star

At the moment of conception, the two forces yin and yang connect with such a force, then only fractions of a moment later, the two forces explode into nine different Energy Centers. Seven of them we find in the body and two of them outside the body, forming our personal stars.

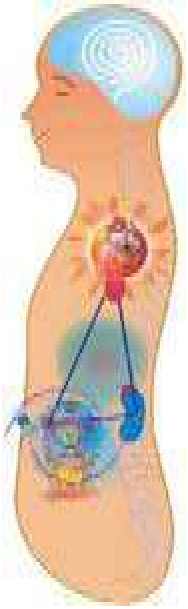

Fig. 4.5 *Three Fires into One*

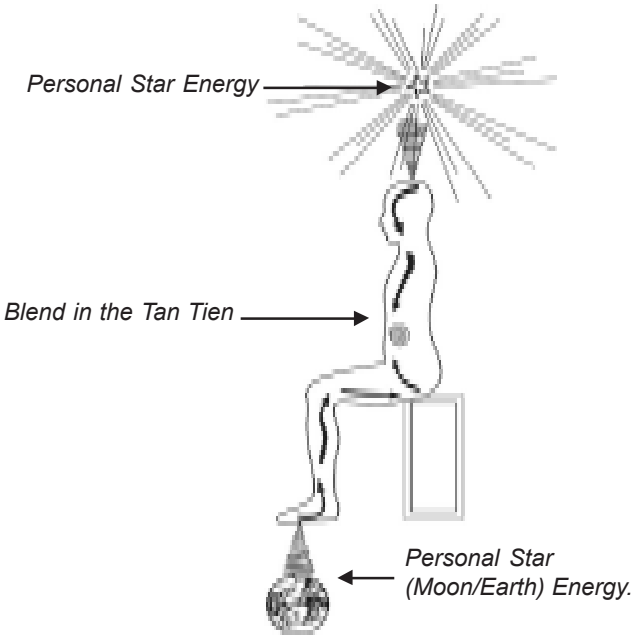

Fig. 4.6 *'Personal Star' Energy*

The two personal stars are in fact energy centers connecting the aural field of each individual with the universal forces and the earth forces. In a way one can see the aim of Taoist Inner Alchemy in bringing these nine forces together, merging them into one force and thus enabling the return to the original force, the Wu Chi.

There is a star about six inches above your crown and another one about one to three feet below the soles of your feet. They are also known as the higher self, guidance, protector, adviser. These stars are our connection to the cosmic force, the universal force and the earth deep below us.

Always make sure your Tan Tien is warm and the sacrum and mideyebrow are breathing. Be aware of the crown breathing and see a star or a small sun above you. Be aware of the crown and feel a light beam extend out of the crown and make a connection to the star above you. Keep on breathing until you feel a strong connection. Feel how the star above you is exercising a strong pulling force on your crown. Once you feel this pull on your crown you will also feel a strong pull down from the earth. Be aware of the star above and the earth and universal force below you. Feel that both of them have a strong pull on you.

1. Reconfirm the star above you and the earth directly below you.
2. Fix the image of the North Star and the Big Dipper six to nine feet above your crown. See the cup of the Big Dipper filling with the violet light, which gathers Chi from the North Star and the universe.

3. **Reach up with your left hand, and hold on to the handle of the Big Dipper. Pour the violet light down to your personal star 4 to 6 inches above your head, in order to predigest the energy of the violet light. Then let it flow down to your crown, into the Upper Tan Tien, to be processed and flow down to the heart center (Middle Tan Tien) or to the back of the head down to C-7 (Cervical 7) and T-2 (Thoracic 2) and down to the palms.**

   In Taoism we consider that the North Star emits a violet light, which is regarded as the highest healing light and the Big Dipper as emitting a red light.

   You can do these meditations sitting, or standing in the Chi Kung posture. The standing position will support a stronger structure and provide a better connection with the earth.

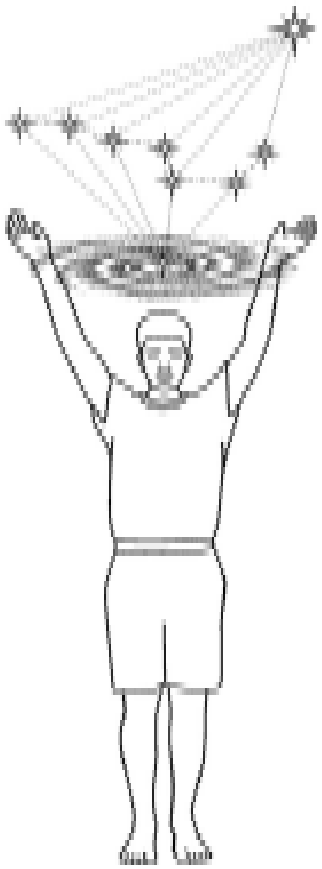

Fig. 4.7 *The North Star, Big Dipper and Galaxy spiral above.*

4. Always remember to breathe in slowly so you can process the awareness of the Lower Tan Tien. Feel a suction, warmth (Chi) and continue to breathe in and be aware of the suction of the crown, North Star and Big Dipper above you.

D. Linking Personal Stars, Energy Bodies and the Universe

Be aware of your 'personal stars' above and below and connect to other peoples' stars and energy bodies.

Three minds unite, one mind aware of the stars above you and a star below you. Connect these stars to the people around you. Think about the bright light above the crowns of other people. Start to spiral your energy to connect to each of them. Group all the stars into one energy body and connect all the way to the center of the universe.

Fig. 4.8 *World Link Meditation*

1. Center Channel and Personal Star above

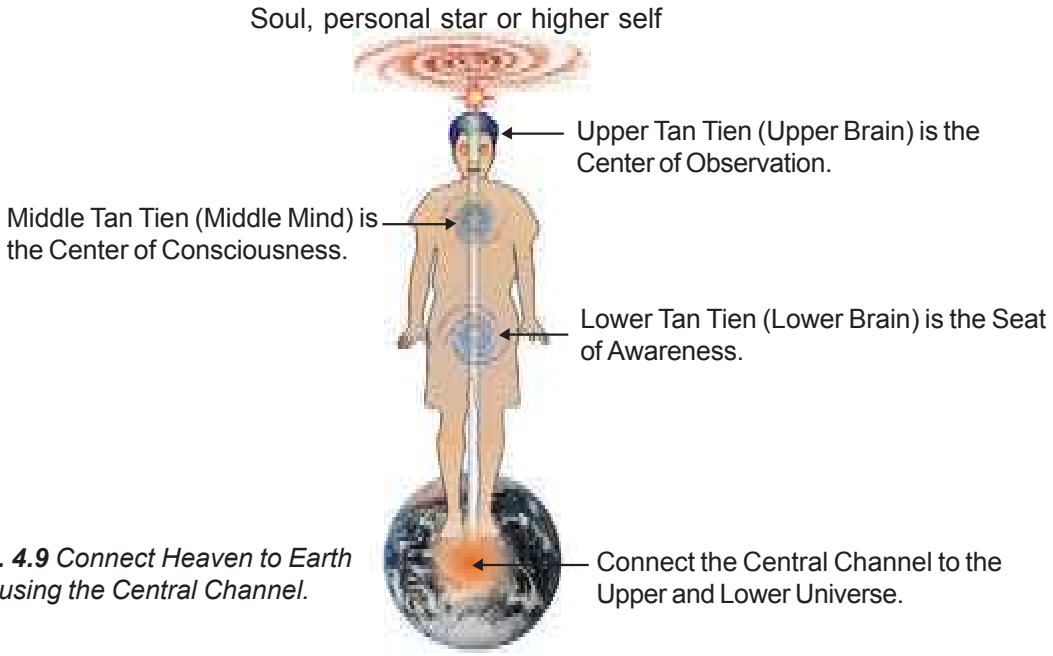

Fig. 4.9 *Connect Heaven to Earth using the Central Channel.*

2. Use Yi power to connect to your Personal Star above

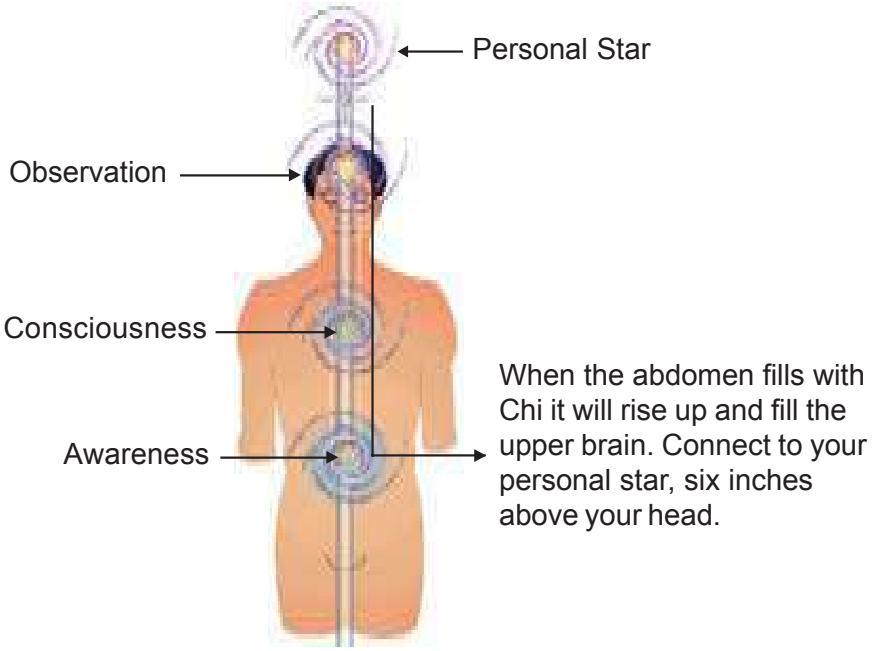

Fig. 4.10 *Connect to your Personal Star Energy using 'Yi' Power.*

3. Connect your Personal Star to the Personal Star of each person
Connect your personal star to each person and then to the universe.

4. Create a Chi Body becoming the major connecting point. Counterclockwise spiral to connect each person's star into a larger group star.

Fig. 4.11 *Link with Each others Personal Stars.*

Fig. 4.12 *Connect into Group Star.*

5. Meditators become satellite links and create a group energy body.
The World Link meditations become an integrated communication link. They are linked to the earth and the universe. Spiral and connect each person's star together and group the energy into one energy body. This energy body becomes an integrated communication center for each person in the group. We can be connected, wherever we are. Each person can connect and become their own 'Center of the Universe'.

Fig. 4.13 *Form a Satellite Link and create a Group Energy Body.*

E. Protective Circle and Chi Field

Raise your hand up and become aware of the 'Sacred Fire' in the universe. Feel that your fingers are very 'big', very 'long' and touch the fire. Bring the fire down. Make a circle around your community, your house, Tao Garden, the meditation hall and around your bodies. Create an energetic field of Chi around the whole room.

Sacred or Chi Fire
Connect and Receive Fire from the Universal Cauldron

1. Activate the Sacred Fire in the Universe

Be aware of yourself. Feel your arm and fingers 'big', 'long' and 'hollow'. Reach to the universe to the Sacred Fire. Let the Sacred Fire fill and pack your arm.

2. Use Yi-Power to Create Sacred Fire Protective Circle

Use the Yi Power to draw the Sacred Fire Circle on the ground around your house, office and the room you work in.

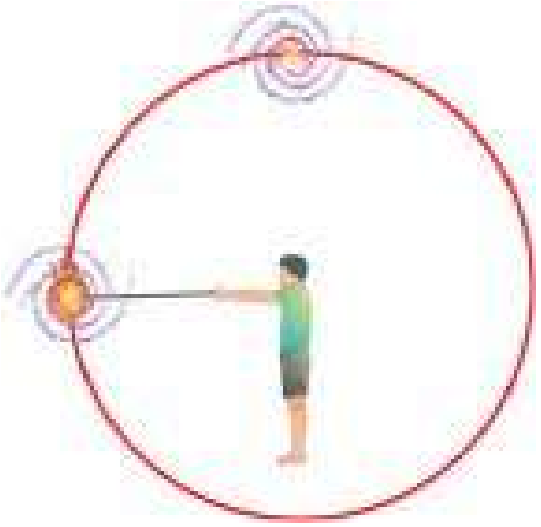

A. ***B.***

Fig. 4.14 A. *Create a Group Energy Body.* ***B.*** *Sacred Fire 'Protection'*

3. Create a Chi Dome

Set up the 'guardian animals', Blue Tortoise in the north, Red Pheasant in the south, Green Dragon in the east, White Tiger in the west, Yellow Phoenix above and Black Tortoise below.

Fig. 4.15 *Create and surround yourself with a Chi Dome and the Guardian Animals.*

4. Activate the Eight Elemental Forces of Nature and the Universe

Activate all eight forces; wind, mountain, fire and thunder on the east. Earth, lake, water and heavenly power on the west.

Call the Eight Forces; fire, water (ocean), thunder (lightning), lake (rain), earth, mountain, wind, and heaven.

Fig. 4.16 *Activate the Eight Forces.*

In the next sections F,G,H,I are practices that are for cleaning the cells. The more you clean the cells the more the Cosmic Healing can take place.

F. Chi (Sacred) Water Practice

The Sacred Water practice (also known in the West as Holy Water) is to exercise the right of being the creators of the Cosmos. With strict and absolutely regular daily water intake to prevent the stresses and associated damages of dehydration, the chief conductor and supervisor of the body's well being – tryptophan and its neurotransmitter derivatives, serotonin, tryptamine and melatonin will be well positioned to regulate all functions. Regular daily walks will keep muscles well coordinated and correct any physiological processes that are established in the body as a result of anxiety or emotional stress.

A well hydrated and healthy skin needs water to constantly replace that which it loses to the outside environment. This then allows blood vessels to the face and the body to open up and provide necessary nourishment for exposed skin cells.

Science has discovered that even if we clean water through filtration processes, although it may look and taste alright, closer analysis using high powered microscopic technology, indicates that its cell structure is 'unclean'. Water, like humans, maintains the memory of its old 'self'. We store our 'memory' within our DNA; water stores its memory within its cells.

The world is about 70% water

Fig. 4.17 *Water is Life.*

The following three pages contain extracts from the book 'The Message from Water' by Masaru Emoto. It advises us that 'water is telling us to take a closer look at ourselves - water is a mirror reflecting our mind.'

After offering a prayer to the Fujiwara dam the message is reflected in the water.

Chi and Love

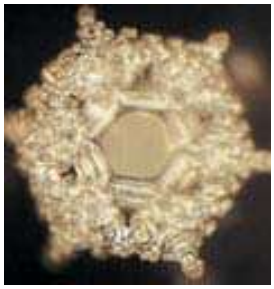

Love-Appreciation

Let's do it

Do it!

When we project Chi and love into water and then freeze it; it will turn into a 'regular' and well structured crystal. If we project negative energy into water, the opposite will apply. Our projections will access the cellular level, clean out the polluted cells and reprogram those remaining with the essence of our affirmation.

When we project a nice, loving instruction or thought into water, like 'let's do it' the water will pick up this vibration and restructure itself. If we project negativity into the water, like a command, 'do it!', the water will acknowledge this accordingly. When we look into a pond we see our image. If we drink a glass of negative image water its destructive energy will enter our system and attempt to multiply.

Fig. 4.18 *The Human Body consists of 70% Water.*

Research has demonstrated that if we completely filter polluted water, using every process available, it will still maintain its old vibration and unstable structure. It will maintain memory in the same way that a computer does. We must therefore reprogram the cells with our intent.

If the water we drink contains too many pollutants and antioxidants it will eventually poison us.

As we can see from these pictures, there is an enormous difference between natural spring water and regular city water. It is now quite clear that if we program water so that it becomes, sacred, holy or Chi water, then it will have the power to remove all antioxidants and pollutants – all sickness. It will have the power to reprogram the water within our bodies, to carry the same pure structure.

Tokyo Tap Water

London Tap Water

Paris Tap Water

Under Ground Water in Northern Island, New Zealand

Buenos Aires, Argentina

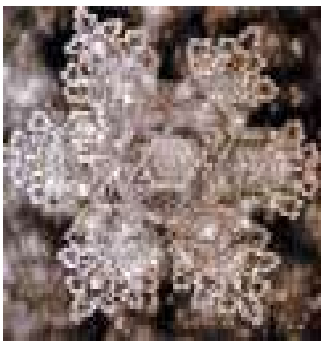

Spring Water of Saijo, Hiroshima Prefecture

Fig. 4.19 *Healing or hurting?*

We can also use music to program a vibration into water. Classical music will create a vibration that synchronizes with our own health, whereas heavy metal music will have a tendency to 'shatter'!

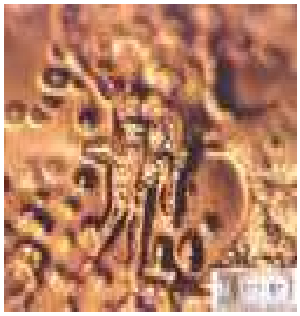

"You make me sick", or "I will kill you".

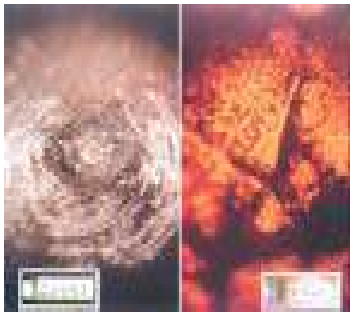

You Fool

Heavy Metal Music

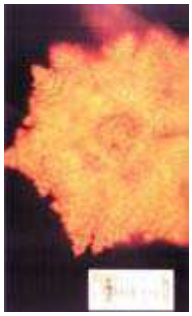

Thank you

Folk song of Celtic Region in UK

Healing Music

Fig. 4.20 *Power to heal or harm?*

Similarly, when we program our emotions regarding other people into water, the effects are the same. If we think negatively of someone, then the response will produce a bad vibration. If we think kind, loving thoughts then the structure will be like a beautiful crystal. If we love Mother Theresa and send this energy into the water, a wonderful crystalline structure will be created. Sick water can be transformed into healthy water. Healthy water can be transformed into sick water. The human body consists of 70% water. The key is your intent and your ability to believe that healing comes from the nature of your vibration. Always be open to receive.

Adolph Hitler

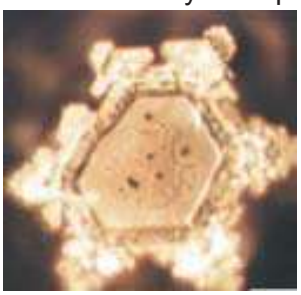

Mother Teresa

Dirty

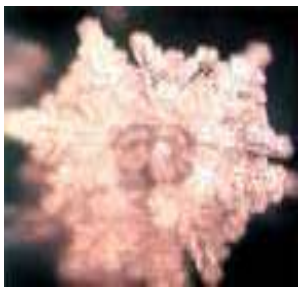

Beautiful

Fig. 4.21 *Sick or saintly?*

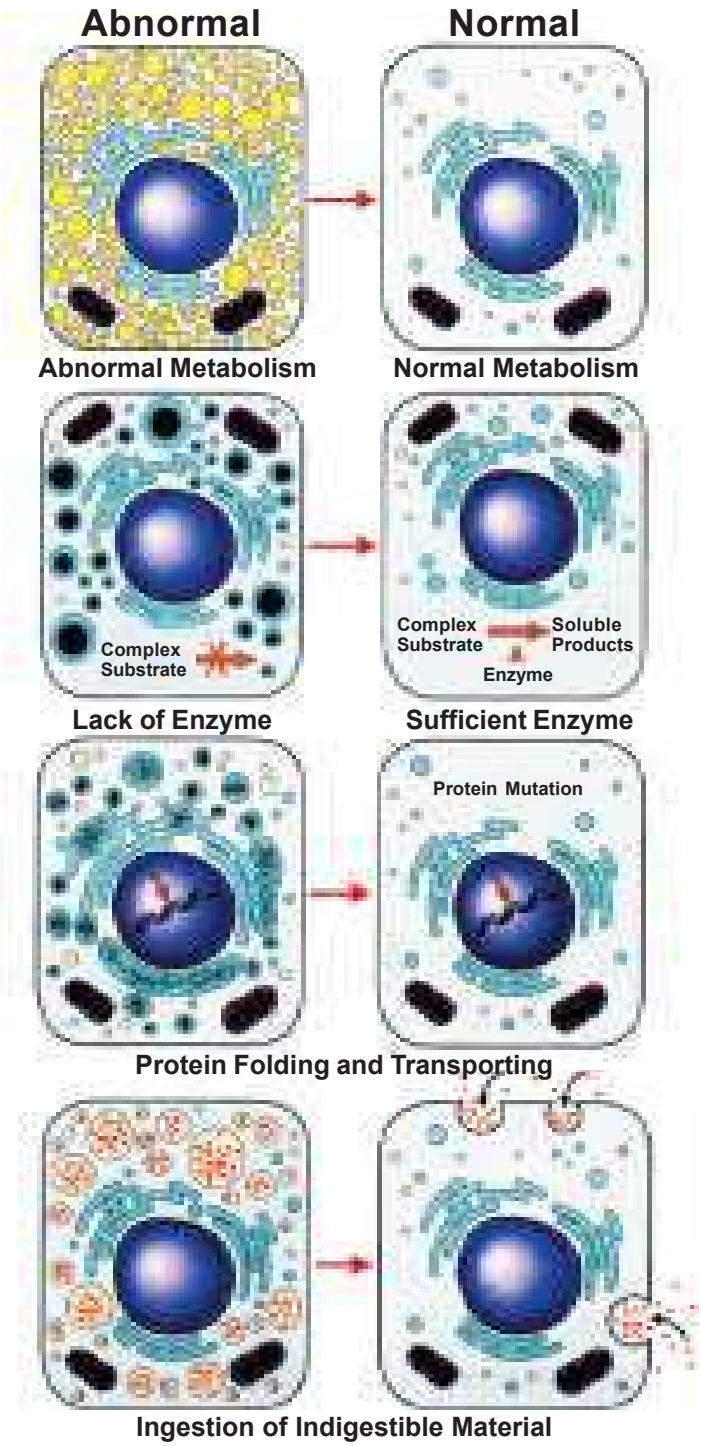

A positive mental attitude will be transmitted into the cells of the water contained within our own body. We must consciously practice inner work until it becomes reflexive.

Fig. 4.22 *With the Power of the Sacred Water Abnormal Cells can be cured.*

Outline of Sacred Water Practice

Invoke the power of the Sacred Water practice to cleanse and heal the body's sick, toxic or negative energy. **If you are working with a group of people, direct your energy through the energy body overhead and into each person's star, as you guide them through the procedure**.

I. Hold a glass one quarter full of water in your left hand, folding the middle and the ring fingers into the center of the palm.

II. Hold the glass in front of your body as you point the 'Sword Fingers' of your right hand up to Heaven.

III. Make a request to receive healing energy and feel yourself touch a heavenly pool of sacred water energy. Feel the pool pouring down heavenly water to fill your arm.

IV. Place your fingers on the cup and ask:
Command 1: ***"Yin power and good fortune come from the east. Yin power please dissolve all negative energy, all sickness and bad fortune".*** Make a cross over the top of the cup.

V. Bring your arm down and point the sword fingers around the inner rim of the glass. Smile as you circle the fingers around the rim.
Command 2: ***"By my request. Please carry out the order now."*** Repeat this three times, charging the water with Yin Power. Project your thoughts into the water.

VI. Use the thumb and index finger to remove the sick energy from the cup, without touching the water. Do this three times. Talk to the sick cells. Tell them to listen to your command:
Command 3: ***"All sick cells please listen: Clear, clean and bright, this Sacred Water will take all the sickness away."***

VII. Repeat the order and visualize yourself removing the sick energy from the cells and giving it to Mother Earth for recycling.

VIII. Hold the cup with both hands near your heart.
Command 4: ***"This Sacred Water will give me/you health, wealth and longevity."***
Project love, joy, thankfulness, gratefulness, appreciation and the energy of compassion into the cup.

IX. The Sacred Water will carry the message of the practice to all the cells, where it will remain. If you are practicing in a group, drink the water in unison. If you are working with a student, pass them the glass to drink using both hands.

Step I: Prepare the Hands and Arms to Receive the Universal Chi

Left Hand Position: Prepare to hold a cup or glass with the left hand by folding the ring and middle finger into the center of the palm. Hold the glass in front of the body.

A. ***B.***

Fig. 4.23 A. *Fold Ring and Middle Fingers.* ***B.*** *Hold Glass in Front of Body.*

Step II: Prepare the Sword Hands to Receive the Universal Chi

Right Hand Position: Form the right hand into a 'sword hand' by folding the pinkie, ring fingers and thumb into the palm. Straighten and hold the index and middle fingers together and extend them upward.

Fig. 4.24 *Prepare to receive the Universal Chi.*

Step III: Fill your Arm with the Power of the Heavenly Pool

Sense the sword fingers and the arm as being 'long' and 'big' as you raise them towards Heaven. Sense that the middle of the arm is hollow and bottom is sealed at the shoulder. The mind's attention is focused on merging with the primordial Chi of the Universe, the energy of your thoughts will be multiplied.

As you make your request to the Universe, feel that you are touching a heavenly pool of Sacred Water Energy. Feel that the pool is pouring down like a waterfall to fill the arm. When it is full compact, compress the Sacred Energy into it as much as you can.

Fig. 4.25 *Touch the Heavenly Pool.*

A. ***B.***

Fig. 4.26 A. *Blessing Sacred Water in Russia.* ***B.*** *Opening the Third Eye in Russia.*

Step IV: Make the Cross on the Top of the Cup

Put Sword Fingers on top of the Cup. Ask for the Yin Power: **Command 1:** ***"Yin Power and good fortune, come from the east. Yin has the power to dissolve all negative energy, all sickness and bad fortune."***

Command 2: Make the cross on the top of the cup and say ***"By my request....."***.

Fig. 4.27 *Give the command: "Fortune comes from the East - Yin has the power to dissolve all negative energy, all sickness and bad fortune. By my request....".*

Step V: Charge the Water to Transform it into Sacred Water

Bring your arm down and point the sword fingers into the glass of water. Smile and circle the sword fingers around the inner rim of the glass.

Continue to order: ***"Please carry out the order now."*** Repeat 3 times to charge the water with the Yin Power. As you do this, project a good thought into the water.

Fig. 4.28 *"Please carry out the order now" Repeat three times, charging the water with the yin power.*

Step VI: Command 3: ***"All sick cells please listen : Clear, Clean and Bright, this Sacred Water will take all the Sickness away."***

Give the above command. Use the thumb and index finger to pick up sick energy from the cup, without touching the water. Do this three times.

Fig. 4.29 *"All sick cells please listen: clear, clean and bright, this sacred water will take my/your sickness away".*

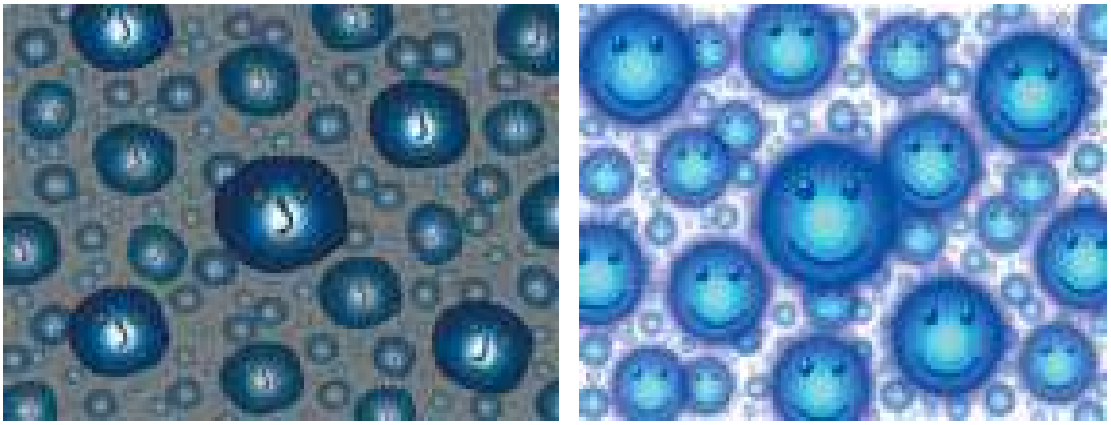

A. ***B.***

Fig. 4.30

A. *Ask for the power to see the cells - if they are toxic and dark, ask for them to be cleaned out.*
B. *"Clear, clean and bright".*

Step VII: Let go of the Sick Energy to be transformed by the Earth

As you **repeat** the order, picture yourself removing the sick energy from the cells and discarding it down into the Earth to be transformed and recycled.

Fig. 4.31 *Sick Energy return to the Earth.*

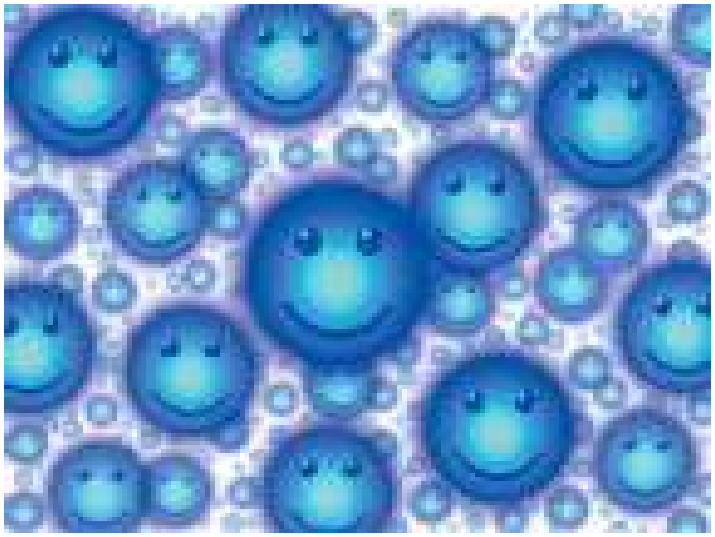

Fig. 4.32 *See the Cells become Clean, Bright and Smiling.*

Step VIII: Fill the Water with Compassion

Hold the cup with both hands near the heart and project goodness into the water. **Command 4: *"This sacred water will give me/you health, wealth and longevity."***

Project love, joy, thankfulness, gratefulness, appreciation and the energy of compassion into the cup.

Fig. 4.33 *"This Sacred Water will give you health, wealth and longevity."*

Step IX: Drink the Sacred Water

The Sacred Water will carry the message to all the cells. It will keep the message of the Sacred Water practice in all the cells. Use both hands to pass the Sacred Water to the student you are working with, or drink it yourself and/or in unison with your group. **Feel the water go into all the cells of your body. Feel it removing the sick cells and purifying your body.**

You can also sprinkle it on to any area that requires healing.

Fig. 4.34 *Drink the Sacred Water.*

G. Empty and Fill

Ask for permission to work on the student by communicating with their personal star. Point your sword hand down to the ground. Project your hand 'very big and very long' and your feet 'very big and very long' - extended down to the ground. Now very slowly inhale, bring up the earth energy. An important part of the practice is to extend a 'line' down from universe into yourself and one into the student. The line sinks through the Tan Tien into the universe below. You can send your energy up to your energy body and it will be brought down to the energy body of the other person.

Fig. 4.35 *Feel your hands are long as down into the earth they extend.*

Fig. 4.36 *Project the other person's legs deep into the earth.*

Fig. 4.37 *Blend the universal energy and Earth Chi - bring it into all of the bones and cells.*

Bring the energy up to your feet, into your bones. Let it enter all the bones, organs and cells. Feel it blending with all the sick energy. Turn your palm up, turn it back down again and exhale; let go of all the sick energy, the negative energy, the worries and the burdens all the way down to the earth. Down, down, down to the earth. Again from the earth up. Do it at least three, six or nine times. When people are very sick, you need to clean them thoroughly. Bring the earth energy up into your bones again. Feel numb, tinkling electricity flowing in all your cells. Return the energy down, down, down to the earth. Relax, let go; worries, burdens, let everything go. It is very important to say to yourself or group: **"You must let go of all your sick energy. Let go of all your burdens. Let go of all your worries, down to the earth".** Repeat it once again. Inhale from the universe and into the earth. From the earth let it enter into your bones. From the bones all the way to your inner self. Feel the energy blend with the sick energy. Exhale and let go of all your sick energy, any negative emotions burdens, worries, anxieties; release them all the way down into the earth.

Fig. 4.38 *Bring the Universal Chi down and let it blend with the sick and negative energy. Bring it down into the earth and bury it there.*

Empty negative, sick energy, burdens, worries, go deep down into the earth. Dig a hole and bury them there - tell them "Do not come back; you will be happy there."

Feel that the feet are long and extended into the earth. The hollow bones have been compacted with compressed Chi.

Once again guide the good Chi from earth up to the fill the person again. See the cells as big as the stars and fill them with Chi to blend with the dirty and sick energy. Then empty them again down to the earth.

Fig. 4.39 *You can also use a Tree to guide the Chi down into the Earth.*

H. Clean with Green Light

Become aware of your liver and breathe into your throat center. Feel that you are breathing the green light into your throat center and let it blend in the Tan Tien. The Chi comes up to blend in the heart, up to the crown, spirals and goes up to the universe. Raise your hand in a spiraling motion up to the universe. Use your 'one hand' to spiral in the universe. Spiral clockwise first. Spiral green light from the universe. Now reverse, counterclockwise - multiply and spiral counterclockwise, bringing the Chi down to clean out your communities, your house, the Tao Garden, the meditation hall, your bodies and all of the people that are 'here' - fill yourselves with Chi. You will use this power to see the cells.

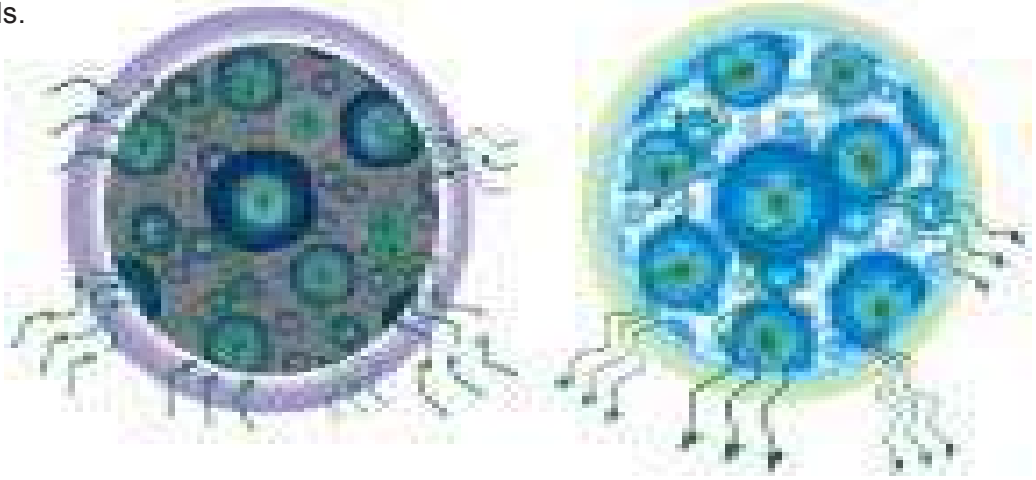

Fig. 4.40 *Spiral Sick Energy Counterclockwise down to the Earth. Smile to the Cells and let the Green Light clean out the sickness, flushing it down into the Earth below.*

See the cells enlarged and this green energy go in and blend with the dirty, black and cloudy energy. See it come out and let it go down into the earth. Dig a hole and bury it there. Tell it, “Don’t come back. You will be happy down there”. Become aware of the green light and spiral counterclockwise. Spiral down, cleaning out the stress. Clean out your house. Send everything down into the earth. Repeat three, six, nine, thirty six or one hundred and eight times. This depends on how much sick energy you are dealing with in your body.

Green:

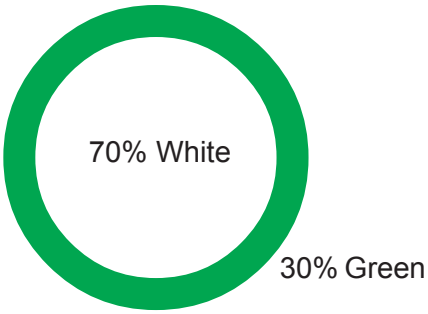

Fig. 4.41 *Clean with green.*

Green cleans and detoxifies all of the body’s cells. Green Chi is mild and safe. Green Chi is used for cleansing, and as a decongestant for diseased parts. It ‘loosens’ the area. The light green Chi is used to break down dirty or diseased energy, like a detergent is used for washing clothes or dishes. Afterwards, the cells will be rinsed with blue light, like clean water is used to rinse the detergent and residue from clothes or dishes.

Throat Center Green

Be aware of the liver’s green color, the throat and the forest. Breathe into the throat, feel yourself breathing in the green light. Guide it down to the Tan Tien, blend and move it up to the heart and the crown.

Project it to the universe; spiral and let it multiply.

Channel one direct line down to the student, one to your crown and one to your palm.

Fig. 4.42 *Blend Green Chi into the Three Tan Tiens - project to the Universe, multiply and bring the Energy back down to the Student.*

Be aware of the liver, the gall bladder, the forest and the throat breathing.

Be aware of the green light in the universe. Let the light come in and blend in the Tan Tien, up to the heart to blend with the compassion in the heart, and up to the crown.

Project the light up to the universe. See it spiral and let it multiply.

Always keep your Lower Tan Tien Fire warm. **Spiral in your Tan Tien and spiral the energy down to the student.** Spiral 1,000 revolutions per minute, 10,000, 30,000 and 60,000.

Fig. 4.43 *Draw down the Green Light from the Universe.*

Cleanse and Remove Sickness

Extend your arms up, with palms facing the heavens. Use one hand to spiral the green force down. The other hand holds the position and connects to the universe. Let this big pool of green light in the universe spiral down – through your community, your home and then into your crown.

Let the Green light blend into the cells and bond with sickness and toxins. Let the green light bring the sickness out of the cells and flow down to the center of the earth.

Dig a hole and bury it. Give the command: “Don’t come back. You will be happy down there. You will be transformed into good Chi.” Smile. Always smile.

Repeat it six, nine or eighteen times. For people who are very sick, who have cancer or may be terminally ill, you can do this two or three hundred times.

Fig. 4.44 *Green Light bonds with the Sickness and Toxins before returning them to the Earth.*

I. Clean with Blue Light

Be aware the blue light, kidney blue. Breathe the blue light into the throat center. Now slowly blend the blue light in the Tan Tien. Blend the blue light in the heart, in the crown and project it up to the universe, spiraling clockwise. Then feel the universe pouring the blue light back down; counterclockwise. Spiral down. Look at the cells and see the blue light, like water, go in to the cells to rinse and clean all the dirty things, down, down, down to the earth. All the way down. Repeat three, six or nine times. Smile.

Blue:

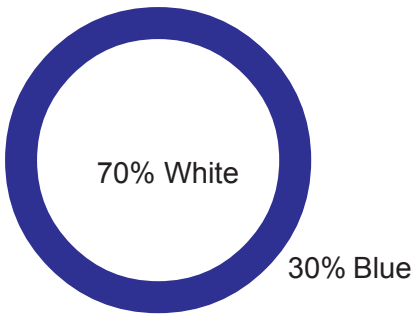

Fig. 4.45 *Rinse with Blue.*

Blue is like cold water; it has the yin power to dissolve all kinds of negative energy and sickness. It has an inhibiting effect. Blue yin energy is the opposite of red yang, which has a strengthening and stimulating effect. Blue has a cooling effect; it can reduce pain, inflammation and can help blood to clot. It stops bleeding and reduces fever. It can help to induce rest and sleep.

Throat Center Blue

Be aware of the kidneys' blue color and breathe the blue light into your throat. Guide it down to the Tan Tien, blend and move back up to the 'heart of compassion' and then the crown.

Project up to the universe, spiral and let it multiply.

Channel one direct line down to the student, one to your crown and one to your palm.

Fig. 4.46 *Multiply the Universal Blue Light - guide the Energy from the Throat, Heart and Crown into the Universe and back down.*

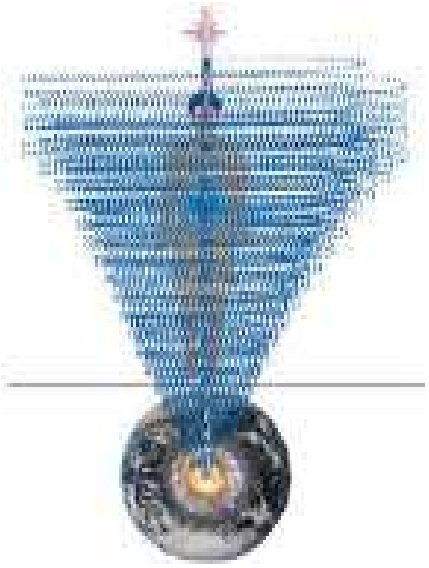

Be aware of the kidneys, the bladder, the oceans and the throat breathing.

Be aware of the blue light in the universe. Let the light come in and blend in the Tan Tien, up to the heart to blend with the compassion and up to the crown.

Project the light up to the universe. See it spiral and let it multiply.

Fig. 4.47 *Draw the Blue Light from the Universe - rinse clean and remove sickness.*

Rinse and Flush

Extend your arms in the air, with palms facing heaven. Use one hand to spiral the green force down. The other hand holds the position and connects to the universe. Let a big pool of green light in the universe spiral down – through your community, your home, and then into your crown.

Let the blue light flush into the cells and flush out sickness and toxins towards the center of the earth.

Dig a hole and bury them. Give the command: "Don't come back. You will be happy down there. You will be transformed into good Chi."

Repeat it six, nine or eighteen times. For people who are very sick, who have cancer or who may be terminally ill you can do this up to thirty six, seventy two or one hundred and eight times.

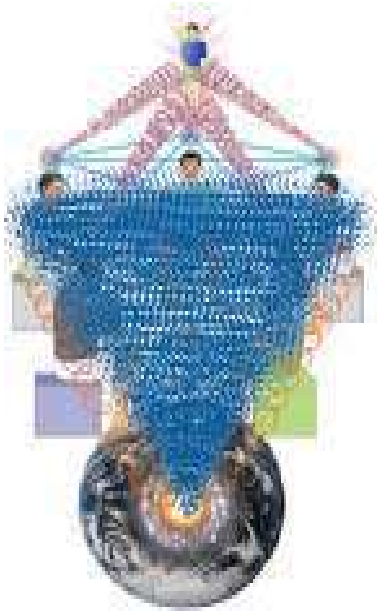

Fig. 4.48 *Blue Light flushes out the sickness and toxins before returning them to the earth.*

J. Charge with Violet Light

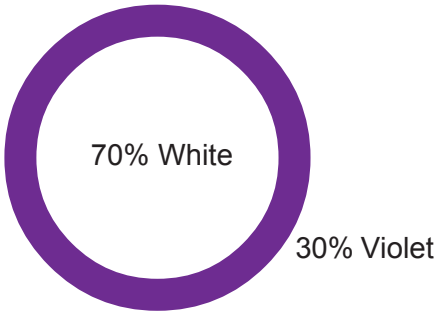

Fig.4.49 *Intelligent Luminous Violet*

Luminous Violet has intelligence and can be programmed. The universe is full of violet light, especially the North Star and the Big Dipper. The color of the star of the higher self or soul, above the crown, is also violet light, the Divine or Soul energy.

It has properties of other Chi colors. It has a rapid regenerating effect on damaged organs and nerves. Always use green and blue light before using violet. Violet light develops the crown center, the spiritual core. It is good for psychological ailments as well as for physical deficiencies.

Primordial Force

Turning the three minds into one mind, go deep into the empty space of the cell and deep into the chromosomes, magnify the space as you enter into the DNA and return to the original cells. The empty space is the Wu Chi. When you enter this stage you turn the subconsciousness into consciousness and you can talk to your body and cells. You can change the programming of DNA and RNA.

Ask for the power to see the cells and look at the brain cells spread out into the space. “Brain cells please listen. Clear, Clean, and Bright: fill with violet light and return to normal function”.

Violet Light into the Cells

See violet light. Be aware of your crown. The Tan Tien Chi and the negative Chi all combine in the crown. Extend a violet light up to the universe. See the North Star in the Big Dipper. Tell the student to hold their arms in the air, so that they can funnel the Chi into their personal star. Bring the North Star and the Big Dipper down; hold the handle of the Big Dipper and pour the violet light over the student’s personal star. The higher cells will be programmed. Let the Chi enter the brain and ask for the power to see the brain cells. “Brain cells listen to the command”. If there is sickness in the brain, give the command. “Sickness go away”.

The North Star is a major source of violet light.

The Big Dipper is a major source of red and infrared light. Taoists understand that the cup of the Big Dipper gathers all the violet light from the universe. The left hand holds the handle of the big dipper - pour it down to your crown. It then flows down throughout the body.

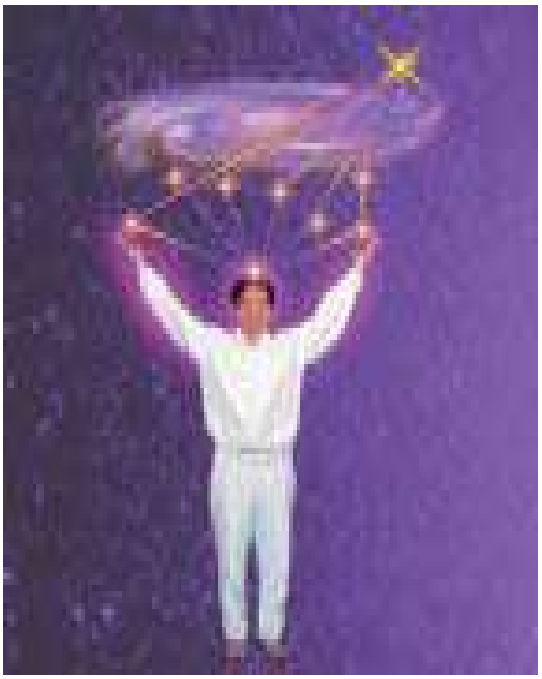

Fig. 4.50 *Connect with the North Star to receive the Violet Light.*

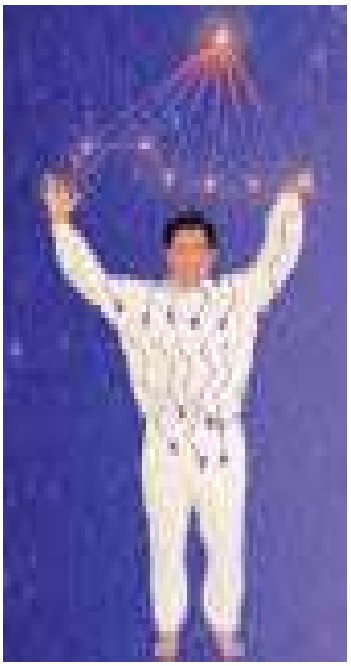

Fig. 4.51 *Practitioner connects with Universal Violet Light.*

Bring the violet light down to the student's personal star above their crown. Pause to let the higher cells of the brain reprogram the violet light at the personal star. Continue to spiral the violet light down through the cells of the brain and down through the cells of the whole body.

Fig. 4.52 *Pause to reprogram the Violet Light at the other Person's Personal Star.*

Fig 4.53 *Lead the person and guide them to follow you.*
Tell them to focus on the part of their body that you are working on.

1. Ask for the power to see into the cells of the brain. Ask the student to move their hands to cover their brain. “Brain cells listen to the command: Sickness go away. Clear, clean and bright; fill with violet light and return to normal function”.

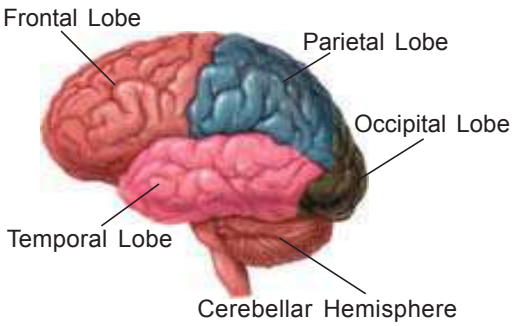

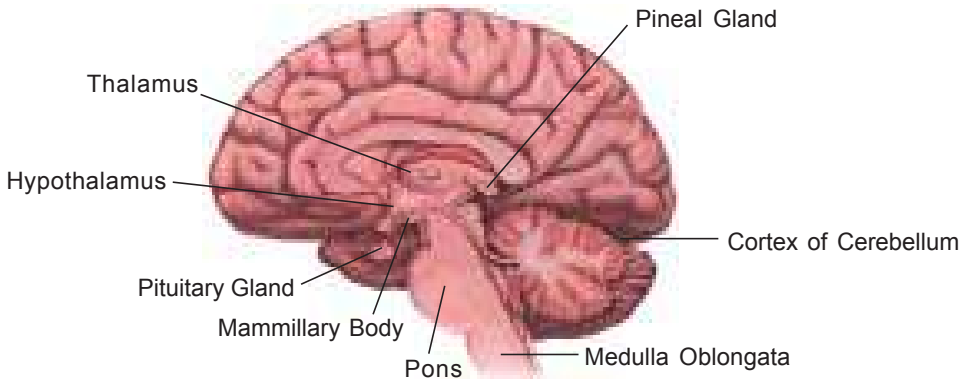

Fig. 4.54 *“Clear, clean and bright; fill with violet light and return to normal functions”.*

Brain Cells

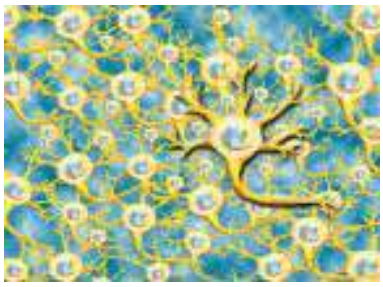

Healthy Happy Cells

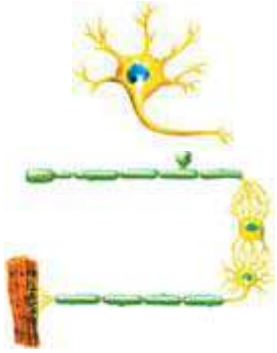

Fig. 4.55 *‘Intent’ to Heal.*

2. Ask for the power to see the cells of the sense organs. Ask the student to move their hand to cover their senses. Give the command: "Eyes, ears, nose, tongue and mouth cells listen to the command. Sickness go away. Clear, clean and bright; fill with violet light and return to normal function".

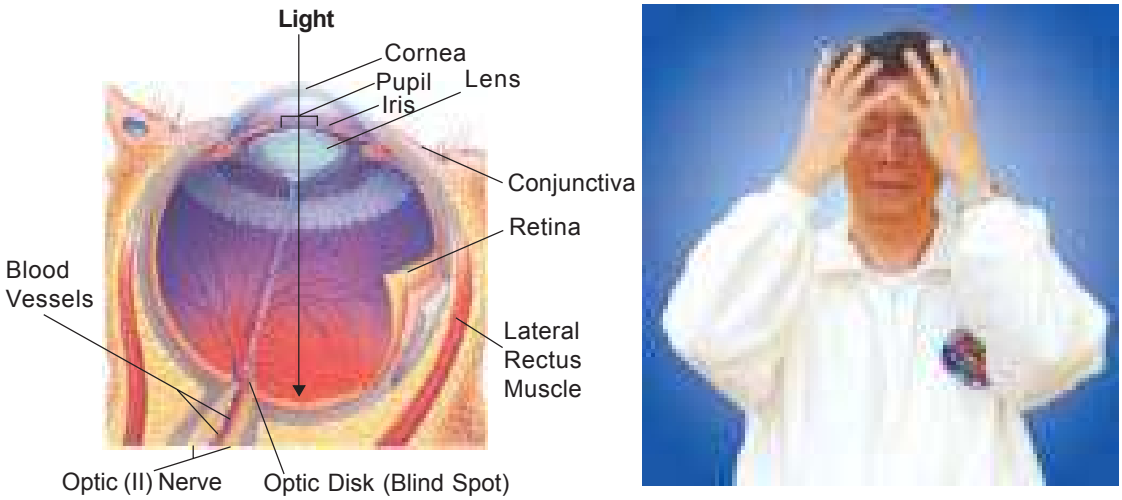

Fig. 4.56 *"Eyes, listen; clear, clean and bright; fill with Violet Light and return to normal function".*

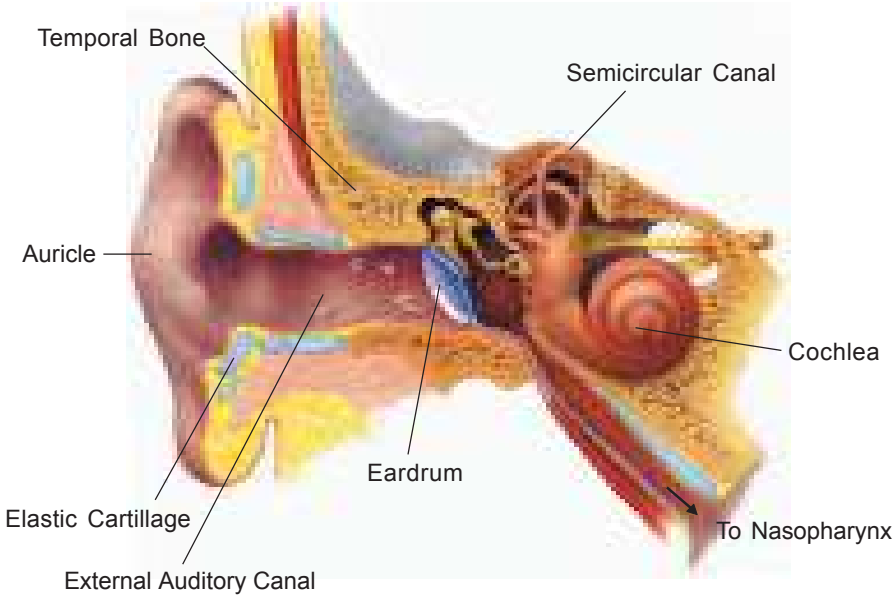

Fig. 4.57 *"Ears, listen; clear, clean and bright; fill with Violet Light and return to normal function".*

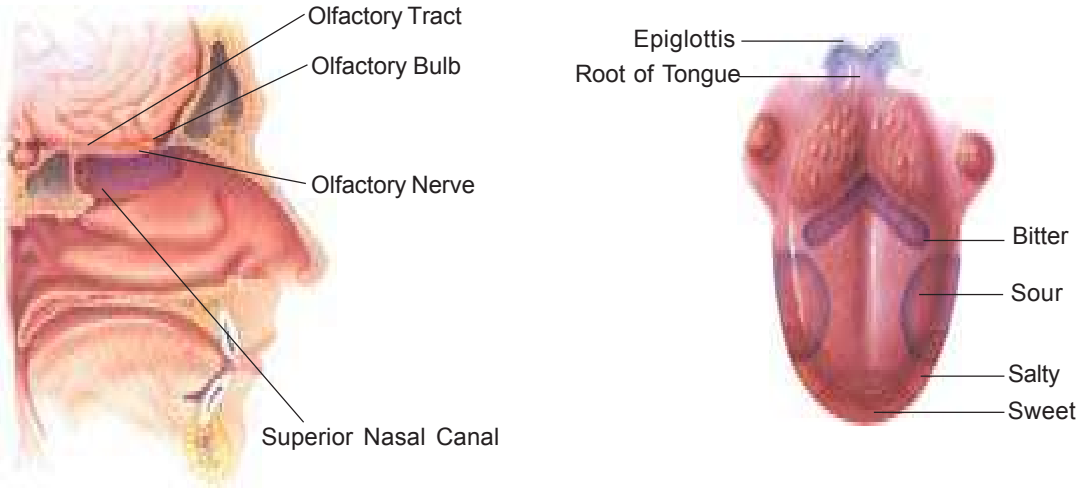

Fig. 4.58

"Nose, tongue, listen; clear, clean and bright; fill with violet light and return to normal function"

3. Move your hands down to your throat center and give the command: "Thyroid, parathyroid and Thymus glands, listen to the command; Clear, clean and bright; fill with violet light and return to normal function".

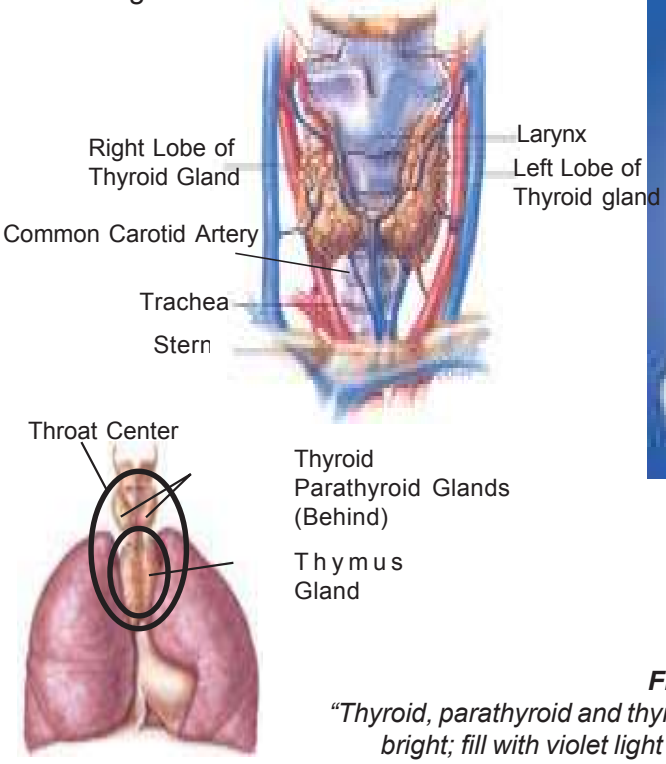

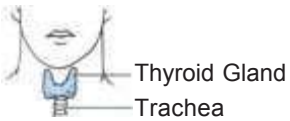

Fig. 4.59

"Thyroid, parathyroid and thymus glands - listen; clear, clean and bright; fill with violet light and return to normal function".

4. Move your hands to the heart and the lungs. Ask for the power to see the cells of the heart and lungs. Give them the command: “Lungs and heart cells, listen to the command”. If there is no sickness, just clean them out. See the cells and clean them out with violet light. If there is sickness, tell the sickness to “go away - be clear, clean and bright; fill with violet light and return to normal function”. Make sure that you say this part aloud. Give the command in a very firm tone of voice.

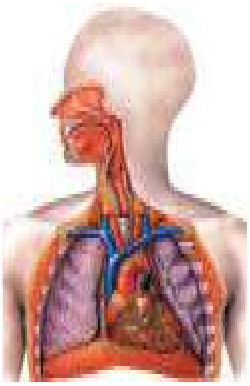

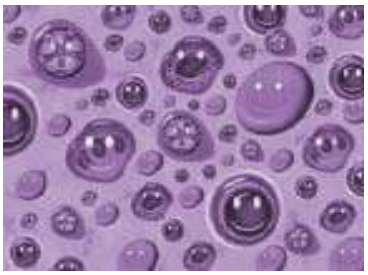

Fig. 4.60

“Heart and lung cells please listen; clear, clean & bright; fill with violet light and return to normal function”.

5. Move your hands to cover the left and right sides of the ribcage. Ask for the power to see the cells of the liver, gallbladder, spleen, pancreas and stomach. Give them the command: “Liver, gallbladder, spleen, pancreas and stomach cells, listen to the command”. If there is no sickness, just clean them out. If there is sickness, tell the sickness to, “go away - be clear, clean and bright; fill with violet light and return to normal function”. Make sure that you say this part aloud. Give the command in a very firm tone of voice.

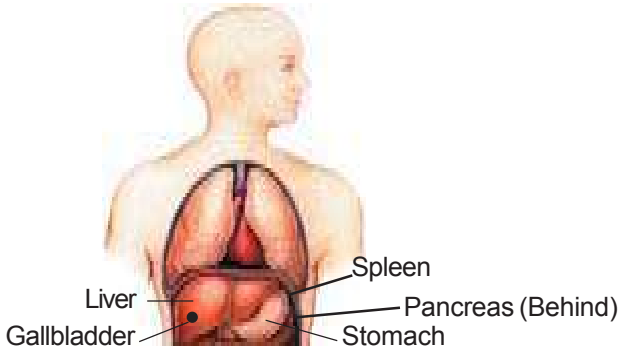

Fig. 4.61

“Liver, gallbladder, pancreas and spleen cells please listen; clear, clean and bright: fill with violet light and return to normal function”.

6. Move your hands to the large and small intestine on the front of the abdomen. Ask for the power to see the cells of the intestines. Give them the command: “Large and small intestine, listen to the command”. If there is no sickness, just clean them out. See the cells and clean them out with violet light. If there is sickness, tell the sickness to, “go away - be clear, clean and bright; fill with violet light and return to normal function”. Make sure that you say this part aloud. Give the command in a very firm tone of voice.

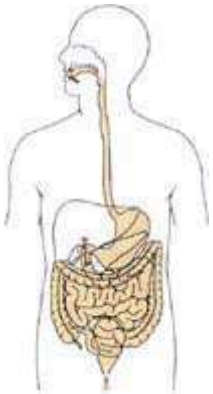

Intestines **Healthy cells**

Fig. 4.62 *“Small and large intestine cells listen to the command: clear, clean and bright; fill with violet light and return to normal function”.*

7. Move your hands to the kidney and sexual organs and ask for the power to see their cells. Give the command: “Kidney and sexual organ cells listen to the command: Clear, clean and bright; fill with violet light and return to normal function”. Gather the violet light again and let it pour down and fill all the cells. See the violet light again and feel and see that all the cells are, “clear, clean and bright”. Smile.

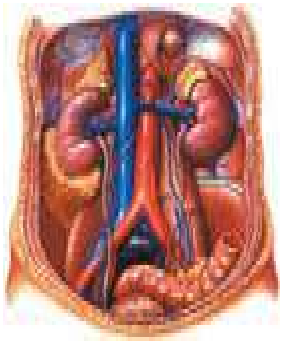

Kidney **Testes** **Ovaries**

Fig. 4.63 *“Kidneys and Sexual Organs listen”.*

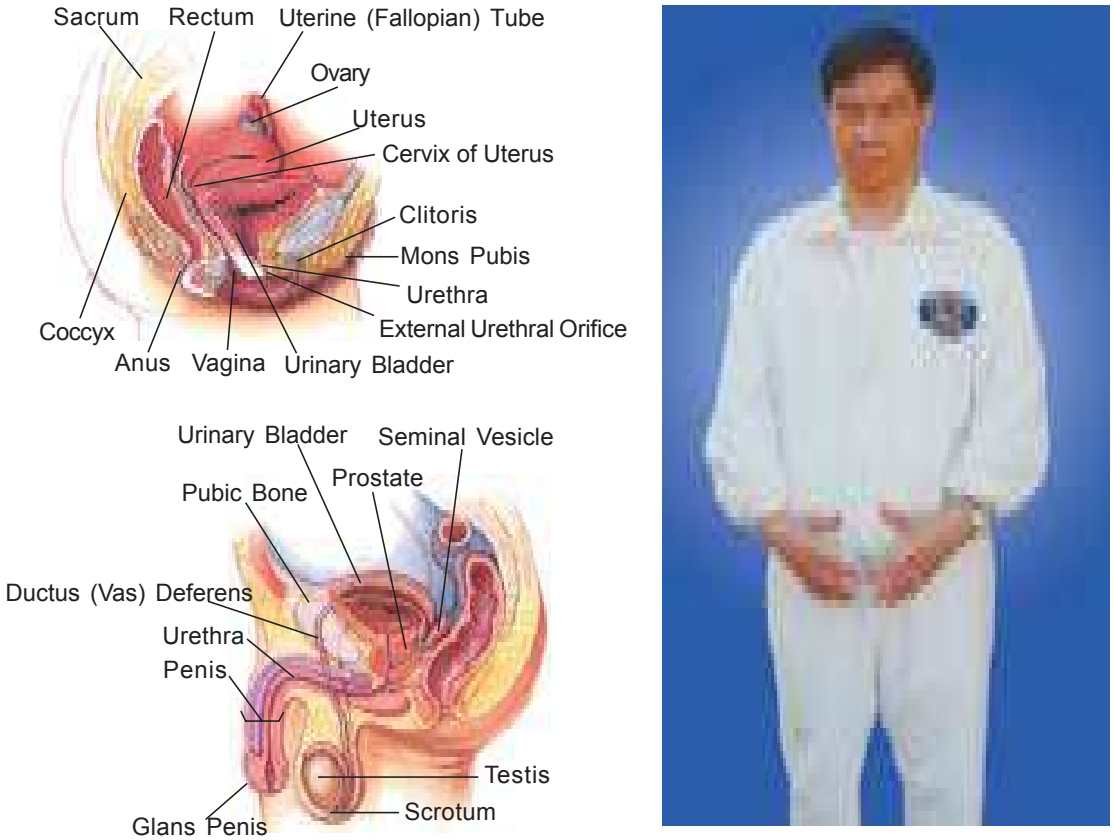

Fig. 4.64 *Male and Female Sexual Organs*

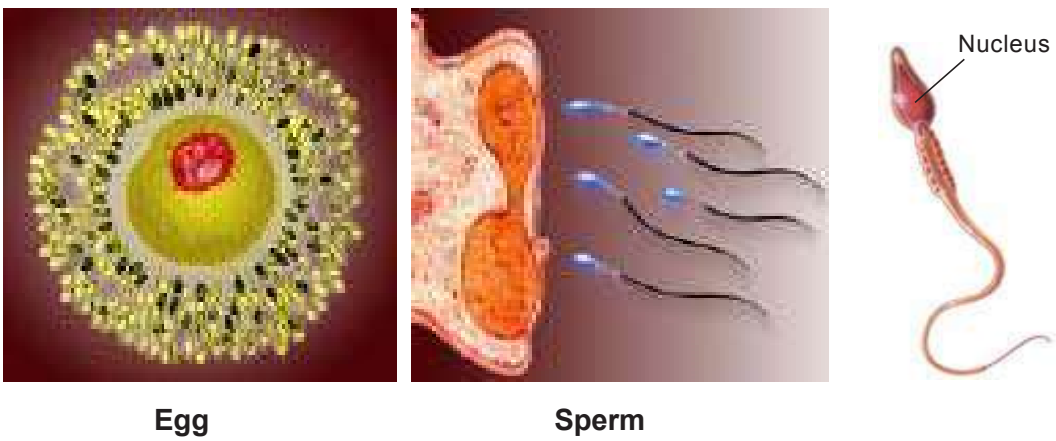

Fig. 4.65 *"Clear, clean and bright: fill with Violet Light and return to normal function".*

K. Activate the Defense and Immune System

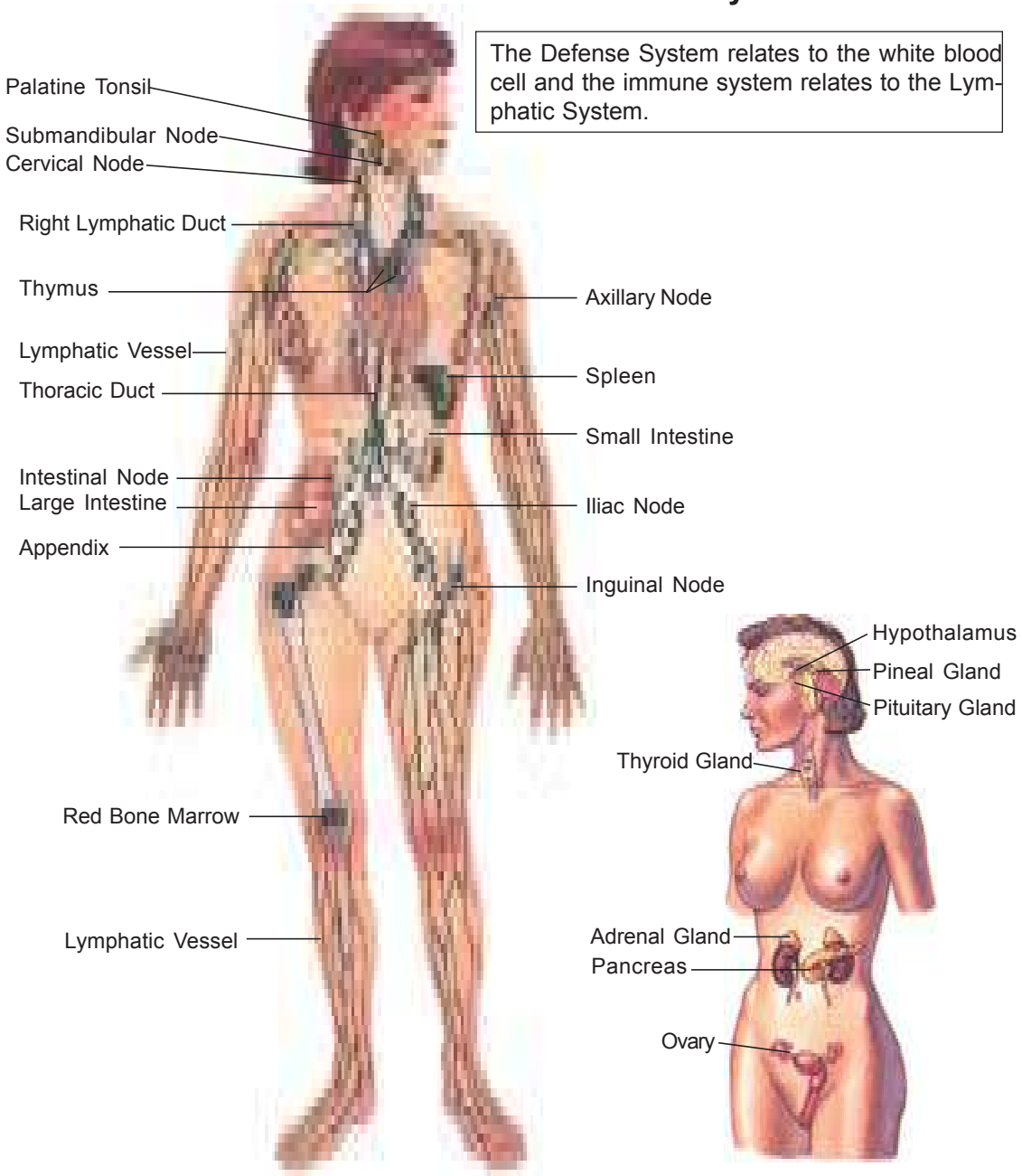

Fig. 4.66 *Ask the cells to listen to the command.*
The bone marrow produces red and white blood cells. The lymphatic system cleans the toxic and polluted material and bacteria from the cells.

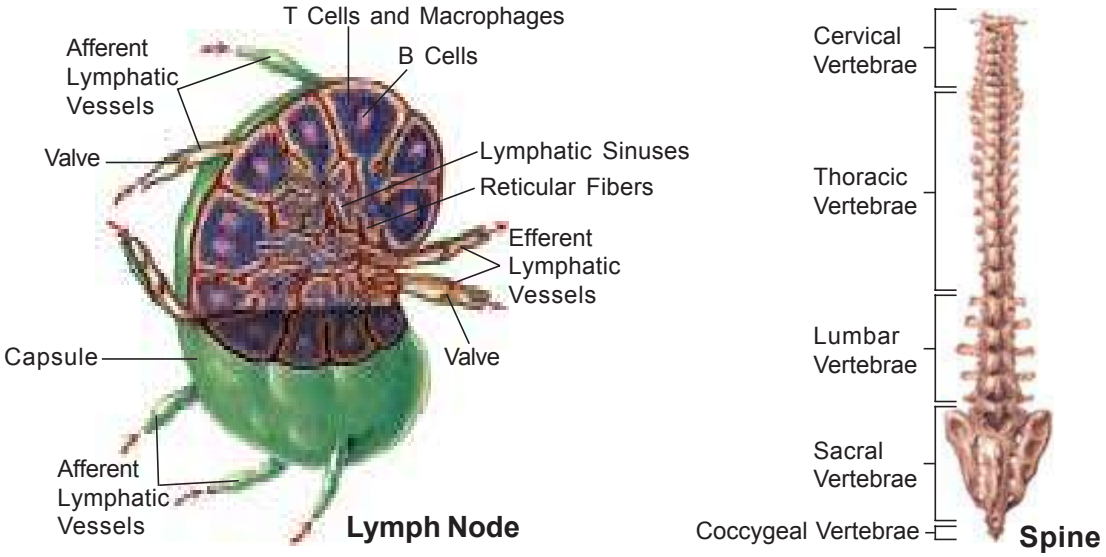

Fig. 4.67 *"Immune Cells and Vertebrae please listen: clear, clean and bright; fill with Violet Light and return to normal function".*

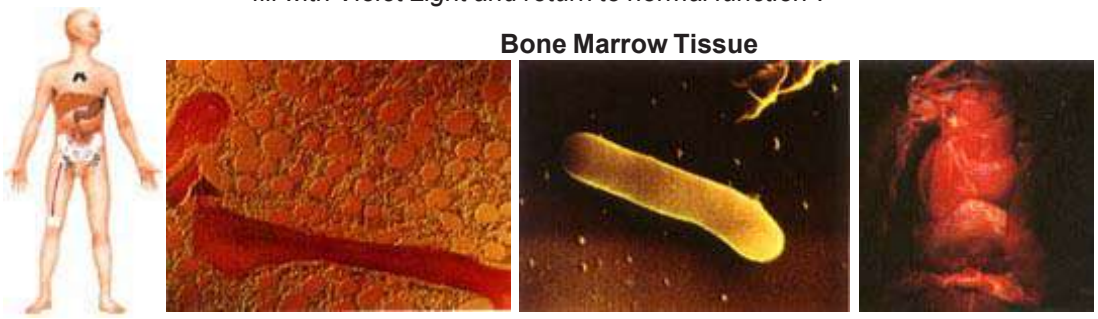

Sacrum: The sacrum controls all the bones and marrow. It effects the production of red and white blood cells. The bone marrow produces the lymphatic cells (white blood cells). When the blood is full of Chi it becomes lighter. Negative emotions make the blood thick and acidic. The blood cells in a healthy body can live up to ten times longer than in a weak or diseased one.

Bone Marrow: A tissue rich in fats, containing plenty of nourishment for the comprehensive production of the different blood cells: red cells for the transport of oxygen, blood platelets for clotting and the various white cells for the immune system.

Bacterium: Represents the foreign invader, but it is only one of many invaders. Parasites, fungi, viruses, chemicals, mineral fragments, metal particles—these and a great deal besides, set the immune system to work.

Thymus Gland: Perhaps the most important organ of the immune system. The vital training of the different T-lymphocytes takes place inside. When they pass through the thymus they receive a program to convert them into 'T' lymph cells. When they pass through the liver and large intestine they become 'B' cells and helper cells.

We have obtained Fig. 4.68 and the following text from the publication 'The Body Victorious' by Lennart Nilsson and Jan Lindberg.

We hope that you find this short selection of material as informative as we did.

"The illustration below is a highly schematic and simplified picture of our immune system. *Top left*, the pale yellow 'house' symbolizes the bone marrow, where all blood cells are born. *Bottom Right*, a solitary bacterium (yellow) represents the foreign invader that the immune system needs to combat. The light blue path represents the older defenses, with various feeding cells that tackle all foreign substances and also function as a kind of cleaning system. They deal with all the old, dead and used-up material in the body. The newer, special defense force, which develops later, follows the green path. Its cells are more specialized; they obtain their special training and reach maturity in organs such as the thymus gland and in the lymphoid tissue around the intestines and in the liver. In the lymphoid tissue, the yellow 'half-way house' (far right), the 'B-lymphocytes are trained. These are the precursors of the large plasma cells - the pale green cells (far right) in the illustration, which produce the body's sniper ammunition, the antibodies (Red and Y-Shaped).

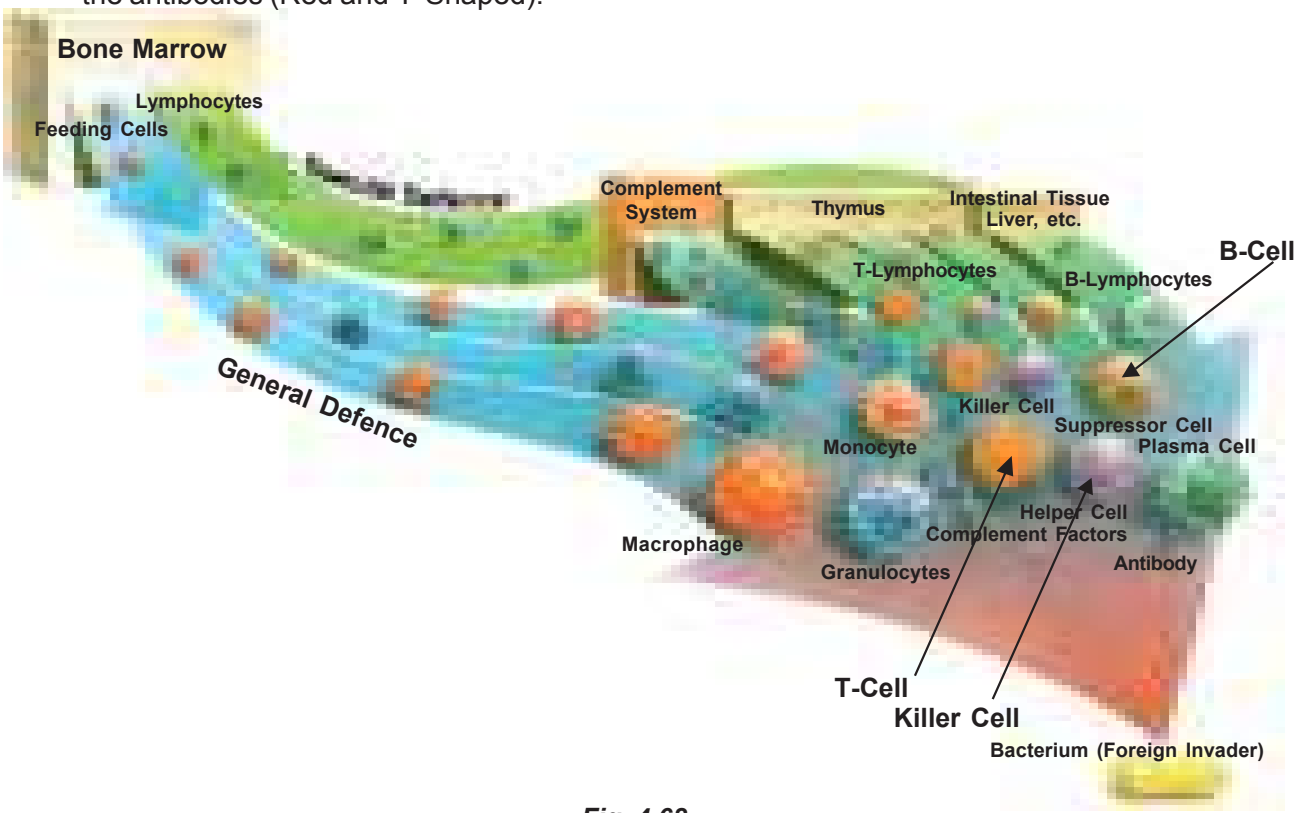

Fig. 4.68

Bone marrow, bacterium and thymus please listen: clear, clean and bright; fill with violet light and return to normal function".

The three paths from the thymus are intended to show that there are different types of T- lymphocytes - among others, aggressive killer cells, helper cells and suppressive cells. All of them have specialized tasks to perform when the immune system launches a counterattack. The three blue paths of the older defenses have three different kinds of feeding cells. First, the large and powerful macrophages (orange) advance on the enemy; then come the granulocytes (blue), smaller and faster moving, followed by the (pink) monocytes. The nuclei in the shimmering cell bodies are faintly discernable. In addition, there is an important complement system (middle), symbolized here by a multicolored range of small spheres flocking toward the foreign bacterium. These molecules play a large part in increasing the efficiency of both antibodies and feeding cells. In addition, they have the capacity to destroy bacteria by shooting holes in them. The complement factors are produced in many different cells in the body.

Chi Kung has a very strong effect against viruses. Altough medical science is struggling to discover a medicine that will kill them, Chi Kung practice is able to prevent them from occuring in the first place. Whether we are sick or healthy, we all need our defense system to be in good shape.

Defense System - Outline of Practice

1. Work on yourself first to activate your sacrum. Project the sacrum as big as the universe. See the eight holes in the bone and visualize them breathing. Breathe and compress the Universal Chi into the bones. Feel the Chi begin to rise up the spine and into your mideyebrow and temple bones. When you feel that there is enough Chi, project it out to the universe, multiply it and spiral it back down. Project it towards the student and ask them to touch their sacrum. Rub your hands until warm and touch the sacrum. Picture the sacrum getting bigger and bigger, breathing into the eight holes. Tell the person to smile at the sacrum and start to work on your Tan Tien and universe. Multiply more energy and picture the Chi from the universe coming down to the sacrum of the other person (and your own) and then charge up the spine, to the rib cage, to the temple bone and to the mideyebrow.

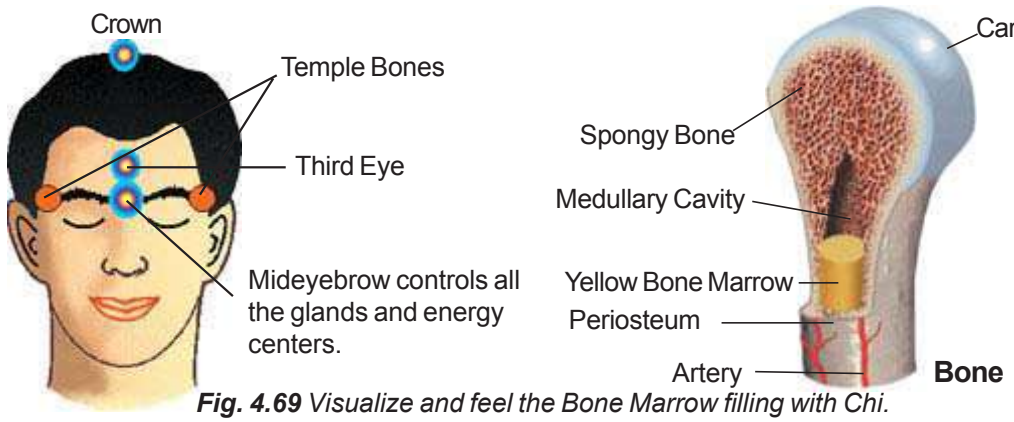

Fig. 4.69 *Visualize and feel the Bone Marrow filling with Chi.*

2. Tell the student to move their hands to the hip bones. Tell them to smile to these bones. Feel them as 'funny, laughing, happy bones'. Tell them to feel the electricity in the sacrum and bone marrow.
3. Touch the femur bones. Feel the electricity running up the legs.
4. Touch the humerus bones. Feel the electricity running up the arms.
5. Touch the lower part of the sternum and feel the Chi penetrate into the bones and spread out to the rib cage. Feel the electricity run throughout the rib cage.

Practice

1. Touch the sacrum, feel your fingers grown 'long' and penetrate into the marrow. Feel that the sacrum is as big as the universe and that the Chi has been compacted. Fill the sacrum with Chi. The eight holes are breathing. Let the fingers touch the sacrum and become aware of the Tan Tien spiraling, until you feel the crown and the mideyebrow spiral and connect to the universe. Hold until the universe fills the sacrum once again and rises up the spine to the mideyebrow.

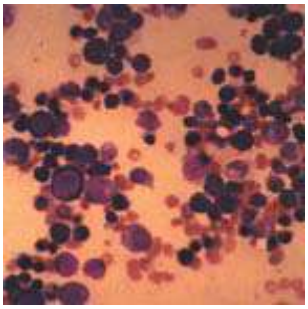

Bone Marrow Cells

Fig. 4.70 *Touch the Sacrum - see the Eight Holes breathing - fill the Sacrum, Mideyebrow and Crown with Chi - empty to the universe and 'fill' again.*

Sacrum Breathing to get Chi

Breathe through the sacrum; feel red and yellow light enter. Guide it into Tan Tien. Blend the Chi in the Tan Tien. Move up to the Heart Center. Move up to the Crown and project up to the universe; let it blend and multiply. Multiply in the universe

Open a direct channel down to the other person, and one to your palm.

Sacrum Chi

Project the student's feet down to the earth and connect to the earth's core.

Third Eye and Temple Bones are aligned in a triangle.

Activate the Sacrum until you feel the Chi rising up the spine and feel it pulsing; be aware of the Temple Bones.

Fig. 4.71 *Activate the Sacrum - Be aware of the Temples.*

2. Tell the student to move their hands to the hip bones. Tell them to smile to these bones. Feel them as 'funny, laughing, happy bones'. Tell them to feel the electricity in the sacrum and bone marrow. Tell the student to pack and compress the Chi into the bones in order to revitalize and revive bone marrow. Give the command. "Produce healthy white and red blood cells".

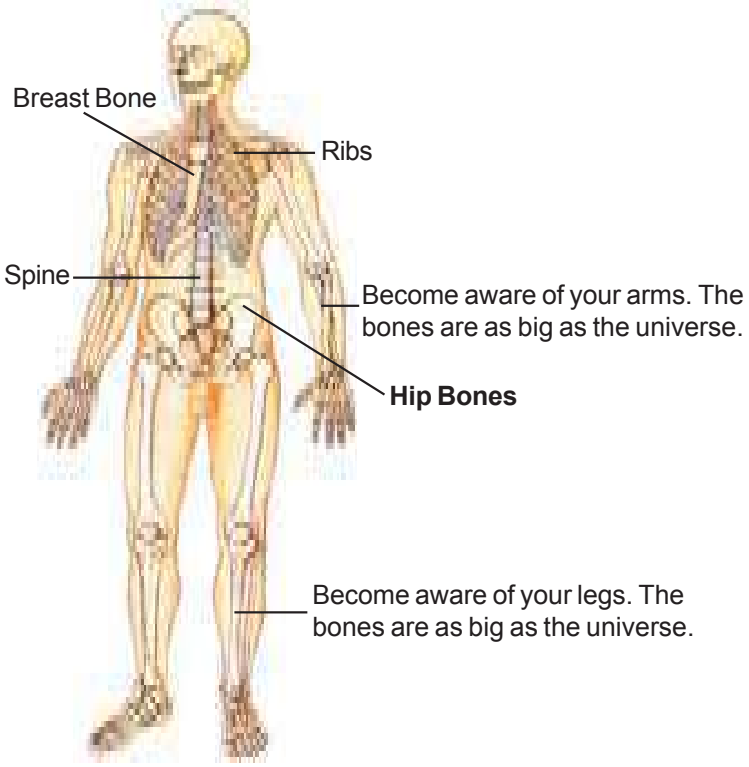

Fig. 4.72 *"Hip Bones produce healthy White and Red Blood Cells".*

White Blood Cell
(Neutrophil)

Leave the fingers touching the hip bones and start to spiral in the Tan Tien until you feel the crown and the mideyebrow also spiral. Expand your awareness to the Universe and the Universe will charge into the hip bones.

Fig. 4.73 *Touch and feel the bones. Leave your fingers there - lower your mind into the Tan Tien and the universe.*

3. Touch the middle part of the femur bone to help increase the production of healthy red blood cells. Feel the electricity running up the legs. Give the same command for the femur bones: "Funny, laughing, happy bones produce healthy white and red cells." After that put your mind into the Tan Tien and universe so that the Chi can charge into the bones. Feel electricity run throughout the whole skeleton.

Fig. 4.74 *"Funny, laughing, happy femur bones produce healthy white and red blood cells".*

4. Touch the humerus bones. Feel the electricity running up the arms.Give the same command: "Funny, laughing, happy bones produce healthy white and red cells." After that, put your mind into the Tan Tien and universe so that the Chi can charge into the bones. Give the same command for the lower part of the sternum. Chi penetrates into the bone and spreads out into the rib cage 'Tan Tien and Universe'. Put your mind into the Tan Tien and the universe so that the Chi can charge into the bones.

5. Touch the lower part of the sternum and feel it and the rib cage as funny, happy, laughing bones. Feel the Chi and electricity penetrate into the bones and spread out to the rib cage. Touch the lower part of the sternum. Give the same command again. "Produce healthy white and red cells". After that you put your mind into the Tan Tien and universe so that the Chi can charge into the bones.

You have finished activating the defense system.

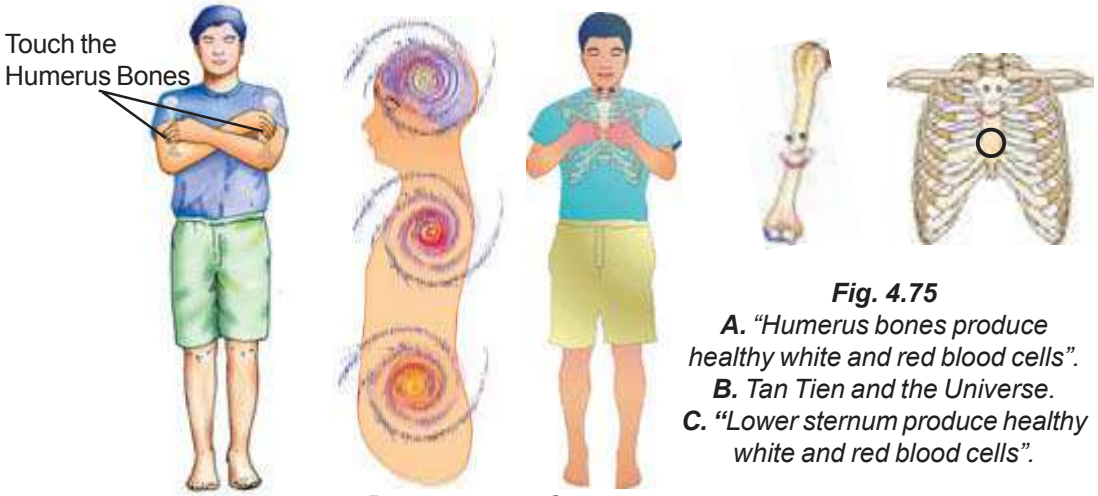

Fig. 4.75
A. *"Humerus bones produce healthy white and red blood cells".*
B. *Tan Tien and the Universe.*
C. *"Lower sternum produce healthy white and red blood cells".*

Immune System

1. The Immune System starts with the top part of the sternum. Touch the top part of the sternum. Project your fingers 'very long' into the bone and feel them penetrate right into the thymus. Activate the thymus gland. Gradually, feel the fingers rising up to the thyroid and parathyroid. Activate the thyroid and parathyroid and throat center. Give the command, "Clear ,clean and bright fill with violet light and return to normal function".

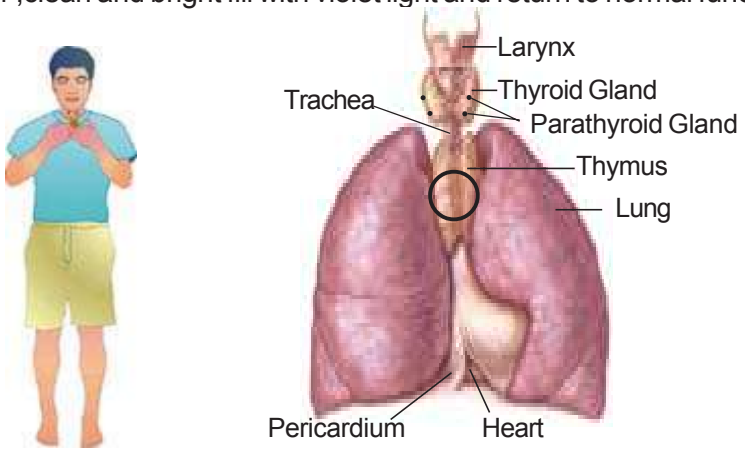

Fig. 4.76 *Touch the Top of the Sternum & activate the Thymus, Thyroid and Parathyroid Glands.*

2. Move the fingers to touch both sides of the jaw bones to help activate the tonsils, the body's first line of defense. The jaw bone affects the lymph nodes beneath, which include the tonsils. Fill them with Chi. Give the command, "Clear, clean and bright; fill with violet light and return to normal function".

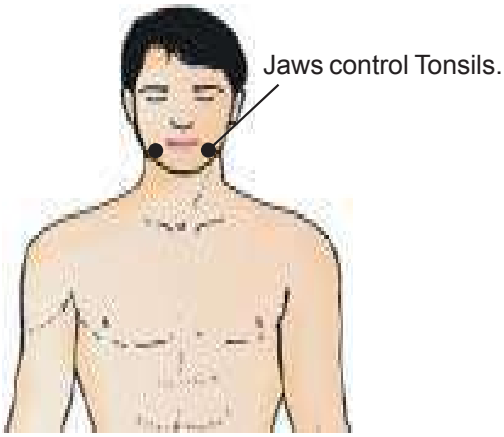

Fig. 4.77 *Activate the Tonsils and Jaw Bones.*

3. Touch the mideyebrow and crown, which control the pituitary and pineal glands respectively. Touch the third eye, feeling it open and feel the light from heaven entering into your brain and into your body. Touch the crown. Feel your fingers reaching deep inside and feel the Chi penetrating all the way down to your perineum. Give the command, "Clear, clean and bright fill with violet light and return to normal function".

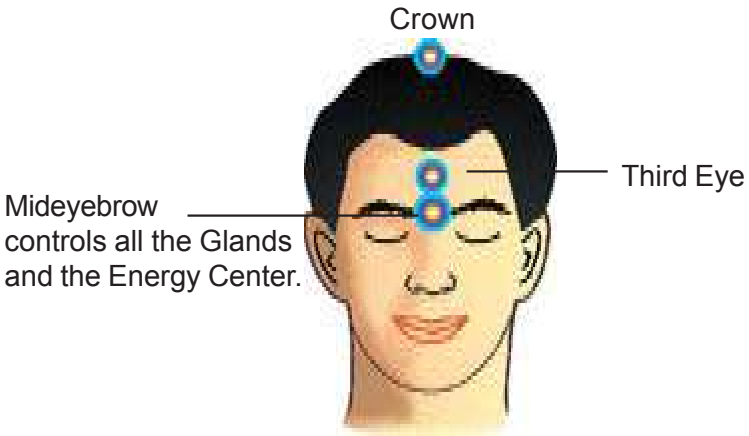

Fig. 4.78 *Third Eye, Mideyebrow and the Crown affects the Immunity and Defense Systems.*

4. Rub both of your hands until they are warm and cross the hands on the neck and feel the lymphatic system has been activated. Cross your arms and hold your hands

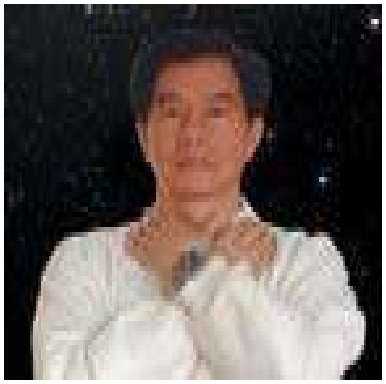

under your armpits. Picture the lymphatic system of the armpits as you activate the lymph nodes. Give the command; “Clear, clean and bright fill with violet light and return to normal function”. The lymphatic system of the upper body is clear, clean and bright and the lymphatic fluid flows! Smile.

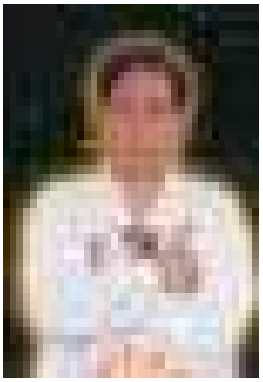

Fig. 4.79 *Lymphatic System of the Neck and Armpits are clear, clean and bright.*

5. Move the hands to the cover the groin area. Give the command to the lymph nodes there. Next, cover the lymph nodes of the navel area, and give the command; “Clear, clean and bright fill with violet light and return to normal function”. The groin and the navel area lymph nodes become clear, clean and bright.

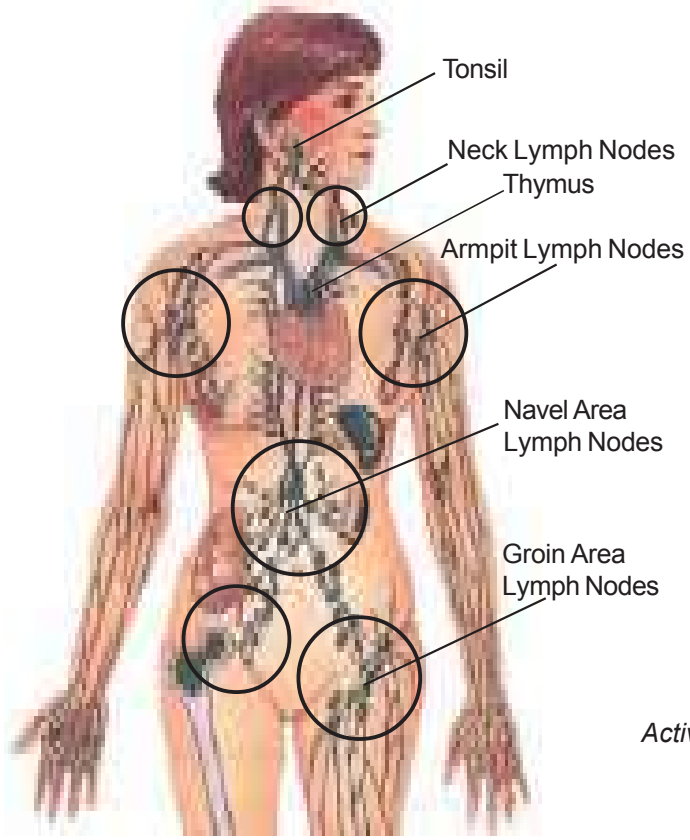

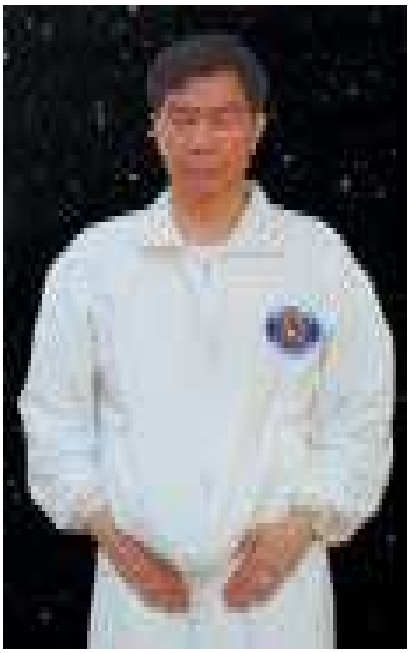

Fig. 4.80
Activate the Lymph Nodes in the Groin.

6. Place your palms over your navel and activate the lymph nodes. Give the command; “Clear, clean and bright fill with violet light and return to normal function”. See them become clear, clean and bright. You have now activated the immune system.

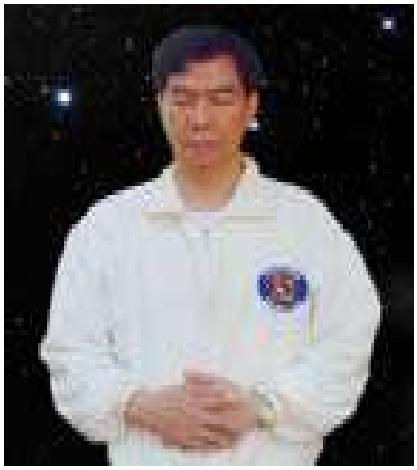

Fig. 4.81
Touch and activate the Lymph Nodes in the Navel.

Summary - General Healing Session

This General Healing Session will help everybody.

A. Three Minds into One
B. Activate the Six Directions
C. Activate the Three Fires
D. Linking Personal Stars, Energy Bodies and the Universe
E. Protective Circle and Chi Field
F. Chi Water (Sacred Water) Practice
G. Empty and Fill
H. Clean with Green Light
I. Clean with Blue Light
J. Charge with Violet Light
K. Defense and Immune System

A. Three Minds into One

Smile to the inner universe, activate the heart compassion energy; feel the love and joy within. Smile and empty the mind and heart down into the Tan Tien. Fill the Tan Tien with Chi and spiral the energy. When the Tan Tien is full, the energy will rise up to fill the brain. Manifestation will occur at the mideyebrow.

B. Activate the Six Directions

Expand the awareness to connect to the Six Directions at the crown, mideyebrow, heart and Tan Tien.

C. Activate the Three Fires

Activate the Tan Tien, Kidney and Heart Fires.

Activate the Sacred Fire Triangle circulating the energy between the Tan Tien, kidneys and the heart. Feel the energy's force multiply.

Activate the personal stars; the cosmic star above the head and the earth star below the soles of the feet.

Keep the Tan Tien warm, and spiral at the sacrum and mideyebrow. Turn your eyes to look upwards and see the crown spiraling, connecting to the cosmic star about six inches above the crown point. Feel the cosmic and earth stars pull the body simultaneously towards heaven and earth. See the cup of the Big Dipper fill with Violet Light, gathering Chi from the North Star and the universe. When the cup is full, pour the light down into the cosmic star above your head. Feel the violet light spreading throughout your entire system, filling the Upper, Middle and Lower Tan Tiens.

D. Linking Personal Stars, Energy Bodies and the Universe

Feel the central channel running from your cosmic star, through your three Tan Tiens and connecting to the earth energy below. Use you 'Yi' power to connect to the personal or cosmic star above the head. Connect the personal star to the stars of each other person in the meditation. Create a Chi body and become the major connecting point. Create a left spiral pattern to connect all the stars into a larger group. All the meditators then become a satellite, creating a group energy body.

E. Protective Circle and Chi Field

Raise the hands and touch the Universal Fire. Use your Yi to bring the energy down and manifest a Sacred or Chi Fire around the room, creating a protective circle. Create a Chi Dome and set up the guardian animals and/or angels. Activate the eight elemental forces of nature and the universe.

F. Chi Water (Sacred Water) Practice

Invoke the power of the Sacred Water practice to cleanse the body of all sickness, negative energy and bad fortune. Energize and renew the self at a cellular level with health, wealth and longevity.

G. Empty and Fill

Empty any remaining negative energy, sickness, burdens and worries, down in the depths of the molecular mother, the earth. Bury the energy there so that the earth can recycle it. Bring recycled energy up from the center of the earth into the body. Fill and compact the Chi into the 'hollow bones'. See all of the cells on the horizon of your mind's eye; spread them across the panorama and see the cells as big as the stars in the night sky. Fill them with Chi, blending it with any sick or grey energy. Then empty again, as you guide the all of the Chi back into the earth for recycling. If you wish, you can fill with earth Chi once again before you begin to 'clean with green'.

H. Clean with Green Light

Green cleans and detoxifies all of the body's cells**.** Green Chi is mild and safe. Green Chi is used for cleansing, and as a decongestant for diseased parts. Be aware of the liver's green color, the throat and the emerald forest. Breathe into the throat, feel yourself breathing in the green light. Guide it down to the Tan Tien, blend and move it up to the heart and the crown.

Project it to the universe; spiral and let it multiply. Channel one direct line down to the student, one to your crown and one to your palm. Bring the energy back down and blend it with any sickness in the liver, gallbladder or anywhere else in the body. Spiral the energy counter clockwise and down into the earth. Continue cleaning with green until you see that all the cells have been charged with the emerald light of the forest.

I. Clean with Blue Light

Be aware of the kidneys' blue sapphire color and breathe the blue light into your throat. Guide it down to the Tan Tien, blend and move back up to the 'heart of compassion' and then to the crown.

Project up to the universe, spiral and let it multiply. Channel one direct line down to the student, one to your crown and one to your palm. Then feel the universe pouring the blue light back down; clockwise. Spiral down. Look at the cells and see the blue light, like water, go into the cells to rinse, clean and remove any sickness. Spiral the energy counter clockwise and down into the earth. Continue rinsing with blue light until you see that all the cells have been charged with the sapphire blue.

J. Charge with Violet Light

Luminous Violet has intelligence and can be programmed.

Turn three minds into one mind, go deep into the empty space of the cell and deep into the chromosomes, magnify the space as you enter into the DNA and return to the original cells. Ask for the power to see the cells and look at the brain cells spread out into the space. "Brain cells please listen. Clear, Clean, and Bright: fill with violet light, back to normal function". See violet light. Be aware your crown. The Tan Tien Chi and the negative Chi all combine in the crown. Extend a violet light up to the universe. See the North Star and the Big Dipper. Tell the students to hold their arms in the air, so that they can funnel the Chi into their personal star. Bring the North Star and the Big Dipper down; hold the handle of the Big Dipper and pour the violet light over the student's personal star. The higher cells will be programmed. Let the Chi enter the brain and ask for the power to see the brain cells. "Brain cells listen to the command". If there is sickness in the brain, give the command. "Sickness go away". Continue to spiral the violet light down through the cells of the whole body.

1. Ask for the power to see into the cells of the **Brain.** Ask the student to move their hands to cover their brain. "**Brain Cells** listen to the command;"Sickness go away. Clear, clean and bright fill with violet light and return to normal functions".

2. Ask for the power to see the cells of the sense organs. Ask the student to move their hand to cover their senses. Give the command; **"Eyes, Ears, Nose, Tongue and Mouth** cells listen to the command. Sickness go away. Clear, clean and bright fill with violet light and return to normal function".
3. Move your hands down to your Throat Center and give the command; **"Thyroid, Parathyroid and Thymus Glands** listen to the command; Clear, clean and bright fill with violet light and return to normal function".
4. Move your hands to the heart and the lungs. Ask for the power to see the cells of the heart and lungs. Give them the command; **"Lungs and Heart Cells** listen to the command; Clear, clean and bright; Fill with violet light and return to normal function".
5. Move your hands to cover the left and right sides of the ribcage. Ask for the power to see the cells of the liver, gallbladder, spleen, pancreas and stomach. Give them the command; **"Liver, Gallbladder, Spleen, Pancreas and Stomach Cells** listen to the command; Clear, clean and bright fill with violet light and return to normal function".
6. Move your hands to the large and small intestine on the front of the abdomen. Ask for the power to see the cells of the intestines. Give them the command; **"Large and Small Intestine**, listen to the comm and Clear, clean and bright fill with violet light and return to normal function".
7. Move your hands to the kidney and sexual organs and ask for the power to see their cells. Give the command; **"Kidney and Sexual Organ Cells** listen to the command; Clear, clean and bright fill with violet light and return to normal function". Gather the violet light again and let it pour down and fill all the cells. See the violet light again and feel and see that all the cells are "clear, clean and bright". Smile.

K. Defense and Immune System

Defense System

1. Work on yourself first to activate your **Sacrum**. Project the sacrum as big as the universe. Breathe and compress the universal Chi into the sacrum until it rises up to fill your brain. Project out into the universe, multiply the energy and spiral it back down. Project it to the students and tell them to touch the sacrum.
2. Tell the students to move their hands to the **Hip Bones**. Tell them to smile to these bones. Feel them as 'funny, laughing, happy bones'. Tell them to feel the electricity in the sacrum and bone marrow.
3. Touch the **Femur Bones.** Feel the electricity running up the legs.
4. Touch the **Humerus Bones.** Feel the electricity running up the arms.
5. Touch the lower part of the **Sternum** and feel the Chi penetrate into the bones and spread out to the **Rib Cage**. Feel the electricity run throughout the rib cage.

Immune System

1. The Immune system starts with the top part of the **Sternum**. Touch the top part of the sternum. Project your fingers 'very long' into the bone and feel them penetrate right into the **Thymus**. Activate the thymus gland. Gradually, feel the fingers rising up to the thyroid and parathyroid. Activate the **Thyroid** and **Parathyroid** and **Throat Center**. Give the command; "Clear, clean and bright fill with violet light and return to normal function".
2. Move the fingers to touch both sides of the **Jaw Bones** to help activate the **Tonsils,** the body's first line of defense. The jaw bone affects the **Lymph Nodes** beneath, which includes the tonsils. Fill them with Chi. Give the command; "Clear clean and bright fill with violet light and return to normal function".
3. Touch the **Mideyebrow** and **Crown**, which control the **Pituitary** and **Pineal Glands** respectively. Touch the third eye, feeling it open and feel the light from heaven entering into your brain and into your body. Touch the crown. Feel your fingers reaching deep inside and feel the Chi penetrating all the way down to your perineum. Fill the glands with Chi. Give the command; "Clear, clean and bright fill with violet light and return to normal function".
4. Rub both of your hands until they are warm. Cross your arms and hold your hands under your **Armpits**. Picture the **Lymphatic System** of the armpits as you activate the lymph nodes. Give the command; "Clear, clean and bright fill with violet light and return to normal function". The lymphatic system of the upper body is clear, clean and bright then the lymphatic fluid flows! Smile.
5. Move the hands to the cover the **Groin** area. Give the command to the **Lymph Nodes** there. Give the command; "Clear, clean and bright fill with violet light and return to normal function".
6. Place your palms over your **Navel** and activate the **Lymph Nodes**. Give the command to the lymph nodes there. Give the command; "Clear, clean and bright fill with violet light and return to normal function". **You have now activated the immune system.**

Chapter V
Cosmic Healing I - Basic

Source of Chi and Color

There are different sources of Chi in the universe: cosmic (air), earth, nature and human. Different parts of the human body have different energies and are correlated with the universe and nature. Each part of our body, especially the organs and glands can produce, receive, transform and emit different Chi and color.

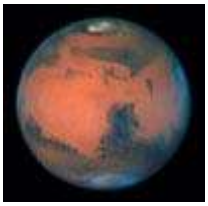

Mars - Red Chi
Frontal Bone - 1

Saturn - Yellow Chi
Frontal Bone - 2

Jupiter - Green Chi
Right Parietal Bone - 3

Earth - Yellow Chi

Moon - Silver Chi
Sacral Bone - 7

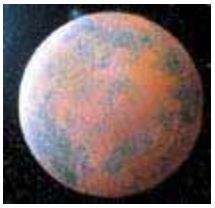

Mercury - Blue Chi
Occipital Bone - 4

Venus - White Chi
Left Parietal Bone - 5

Sun - Golden Chi
Third Eye - 6

Fig. 5.1 *Planet, Bone and Cosmic Colors*

Earth Chi

While Cosmic Chi (the atmosphere over us and the universal force) is ethereal in nature, what is called earth Chi is not. This Chi appears as the line visible above the horizon when the sun is low in the sky, and seems to hover just above the ground. It actually also sinks into the ground.

Earth Chi contains yellow and some white Chi. When the ground and the cosmic (air) combine they will become white Chi. This Chi has a very powerful healing energy, not too overheated, but balanced and mild.

When treating a problem, white Chi, in the proportion 7:3 (7 white to 3 of the selected color) acts as a brake on colors which are hot or too active. This enables the body to take in chi more easily.

Fig. 5.2 *Use White Chi to blend all the other Colors.*

Special Note: Many of the color references came from the following books: *"Let There be Light"* by Darius Dinshah and *"Advanced Pranic Healing"* by Master Choa Kok Sui.

Human and Nature Chi

These include the things we can see on the earth: the mountains, lakes, seas, forests, streams, caves, valleys, rocks and precious stones. Taoism classifies five elemental forces: earth, metal, water, wood and fire.

So there are five elements in our body and five elements in nature; there are five elements in the cosmic and five elements in the universe.

According to the Taoists, when we can make the connection and control our body's elements, we will quickly make connections to nature and the universal forces and employ them very easily.

Solar Chi

Before sunrise or sunset there is more white Chi in the air, which we can use abundantly for health and healing. White Chi affects the lungs and the large intestine, so we direct this Chi to these organs. This will generate further Chi to maintain our daily activities. All colors of the spectrum are present in white.

Simple Practice

Look at the horizon at sunrise and sunset. Stand still and extend your palms toward the sun, smile and absorb the rising or setting sun's energy into yourself.

General Information

Energy can be introduced to the affected area of the body by moving the hand clockwise in a spiral.

Move the hand **anticlockwise** with a spiraling motion to clean, flush and remove energy from the treatment area. After this, brush down the whole body, to direct the sick energy into the earth.

Use an anticlockwise spiraling movement in order to clean, then expel the energy.

Use a clockwise movement to bring energy in and an anticlockwise one to take it out.

As a general rule and especially when you are beginning to practice the techniques, keep the color combinations simple. **Always use blue (to cool, calm and stabilize), green to clean, white to harmonize and violet (which carries the properties of all the other colors) to program.**

Although it is important to learn all of the applications, it is more important to begin practice, maintaining a serene state of mind throughout. You will immediately realize that Cosmic Healing provides the practitioner with as much benefit as the student. The more you practice the more you heal.

Healing Colors

White Chi

The color of the chi from the air, earth and sun is always white and acts as a calming agent for the surplus chi produced by the other colors. It also redirects this chi to areas of the body which need it. For this reason, use white in combination with another color in the proportion 7:3.

Shining white chi should be concentrated at the center, while colored Chi goes to the edge. This can also be reversed. It is also possible to blend the white and colored Chi together.

It is safe to use white chi when you are not sure which color might be suitable for a patient, especially when treating babies, toddlers, the elderly and the weak. People with minor problems can be treated with blue, green or mauve, while gold colored Chi or mauve/white Chi is better when the problem is serious. For a stimulating and strengthening effect use white-red.

When it becomes necessary to switch from one color to another, an abrupt shaking movement of the hand should ensure a smooth transition to a new color.

There is a very strong violet light in the North Star. You can dilute the color with white. White Chi is composed of red, orange, yellow, violet and blue.

Blue Chi

The effect of blue Chi is one of cooling, and hindering similar to yin or water energy. The opposite effect can be obtained with the use of red Chi.

When we draw the energy down, some peoples' bodies can't adjust to the energy immediately, so using blue Chi is always good. "Water blue' is the one element that always brings harmony and does not cause any harm.

a. Blue Chi, like yin, water energy, has a cooling effect. It also can act as a restraining agent.
b. Because of blue Chi's ability to cool, soothe and numb, it is particularly appropriate for promoting relaxation and sleep, reducing abnormally high body temperature, minimizing pain and swelling. It can also hinder the proliferation of viruses and bacteria and assist in the rapid clotting of blood.

Blue (and green) can detoxify and also energize.

Green Chi

While tangerine Chi can be quite dangerous, the action on green chi is gentle and harmless. Freeing up a damaged area so that cleaning can then take place may be done with green Chi. Once it's loose you can then use blue or organ's color Chi to expel the disease completely. It can therefore remove the disease and bad energy by locally sweeping either to and then out of the arms for the upper body or out of the legs for the lower body.

If there is a need to energize with the organ's color Chi, first energize with pale green Chi. Always use green chi before using the colors purple, tangerine and red.

Use the throat to activate and draw the green Chi up to the crown, rising to the universe to be multiplied and brought back down for use. Always add blue Chi when there is pain. The motion of pushing and pulling through the affected part is very powerful. You also can also use the 'sword finger' in a small area and for infection.

Green can also be used for energizing together with violet; first use green and follow with violet.

Pale green and pale tangerine chi can be employed in sequence, as the first acts on the 'sick' energy, reducing it to a form which can easily be driven out by the second.

Simultaneous use of pale green pale tangerine and white chi in the ratio 2:1:7 is recommended to treat stubborn areas because the effects are intensified when these proportions are used together.

In the treatment of cancer, dark green and tangerine Chi may be employed, preceded by blue. This can assist in toxin removal, and in the cleaning and freeing up of disease affected areas so that necrotic cellular tissue is released. These colors can relieve congestion and free up 'sick' energy which is 'stuck' when used with brushing movements over the affected areas. They also help with treatment of colds and elevated body temperatures, and in the dispersal of blood clots.

Red Chi

Cerise chi makes the area to which is applied stronger, while crimson chi has the opposite effect. When using color for healing, project luminous white in the center and cerise at the edges for a strengthening effect. Always combine red with blue and green; never use it on its own.

Cerise mixed with white, because of its expansion abilities, can help widen blood vessels and breathing tubes. It also helps those with heart and asthma problems.

Red chi with its qualities of warmth and expansion, has a number of benefits. It is good for the circulatory and respiratory systems and the blood, as it expands blood vessels and other tubes, thus improving circulation and breathing, particularly for heart patients and asthma sufferers. It also brings increased energy into the blood and helps allay feelings of fatigue or weakness, driving out 'sick' energy along with toxic substances and other waste materials. It can also help those who are sensitive to allergens. It may help those whose lives are near the end have a longer period on earth, and promote revival of consciousness.

Avoid the use of dark colors, which may cause an adverse reaction. If a person is suffering from a sexually transmitted disease, it is not advisable to treat him or her with chi which is crimson. Chi of this color makes the microbes that cause such diseases multiply at a fast rate and can also produce an inflammatory or constrictive reaction.

Tangerine Chi

When using orange Chi, always use blue Chi first; to tone and calm down the ailing body area, before applying the vitality of orange.

Pale tangerine chi with added white can be used; however certain areas are inappropriate for treatment by this color because of its power. Do not use with the eyes (including retinal problems), heart, head, throat, brain (for example bleeding in the brain) or the spleen.

The large intestine benefits from the use of tangerine chi, but this color should be used sparingly on areas like the solar plexus and navel. Appendix problems should not be treated with this color as it could exacerbate the problem. Tangerine chi has an effect on the bowel, and can also aid in returning an unconscious person to consciousness or in stimulating someone who is dying.

To treat cancers of certain types, dark green and dark tangerine are suitable because of their ability to destroy. Always avoid the head and the heart when using orange.

Forcible removal of waste products, toxic substances, 'sick' energy, viruses and bacteria
Menstrual difficulties
Waste elimination problems
Freeing up 'sick' energy
Breakdown of clots in the blood
Problems of the urinary and respiratory systems
Diseases of joints and connective tissue
Common cold
Problems caused by allergens
Cysts

Yellow Chi

Yellow Chi has a close connection to the nerves, the bones and the bone marrow. It is the color of the spleen; in Taoism we feel the spleen is involved in the assimilation and processing of food and the appetite. This doesn't mean eat a lot, but when the spleen is balanced the appetite will be controlled.

Chi which is yellow in color is beneficial in the treatment of nerves as it promotes re-growth. It also helps in the repair of fractures and cells. It is good for the health of bones, tissues and organs. It has the power to increase bone marrow production.

Violet Chi

Violet Chi has the properties of all the other colors. It's used for severe types of sickness.

The qualities found in all colors are contained in purple chi, therefore it is particularly effective for serious illnesses. Mauve (light purple) chi which contains elements of blue and green, helps to restore organs and nerves affected by disease or trauma. Although mauve chi can be employed on certain kinds of severe infections, chi which is dark purple should be avoided when diseases of the respiratory system are present, as it could cause the proliferation of disease causing microbes.

Violet Chi is use chi that is pale white/green or pale white/tangerine and, selecting each in turn, with a brushing movement apply to the whole spinal area and especially to the area where the trauma is located.

If purple chi is used in combination with other colors, it will intensify their qualities and if used together with red, tangerine or yellow chi can be dangerous; it may cause the undesirable proliferation of some cells.

Dark electric violet can be used for tumors or cancers. Always use the blue or green first.

In order to make an area which has become weak stronger, mauve mixed with white can be used, but for really fast strengthening use cerise mixed with white.

Both white and violet have the properties of all the Chi colors. The difference is that violet Chi has a greater penetrating effect and is easier to assimilate than white.

Because bright purple chi has been acted upon by the soul, it has the capacity for independent thought and action.

Energy or chi which comes from the air, the earth and the sun is called purple chi. There is a second type of chi with this color, but having more brightness – this has been called bright purple chi and is derived from the soul through the crown of the head, the point connected to the North Star or Big Dipper.

Bright purple chi can only be brought down from the universe via the crown point if the practitioner has highly developed senses, The effects of chi from air, earth and the sun depends on the development of the practitioner's soul.

In contrast to purple chi, the chi which is bright purple in color has a much greater potency because it can help in the restoration of nerves and organs which have been affected either by disease or trauma. This bright purple chi can be used to remove infection and to promote fast healing, even in the case of serious illness. In addition, this chi has been said to possess its own consciousness (Master Choa Kok Sui. Advanced pranic healing:49)

When cancer and other growths are being treated, use bright purple chi because it has the ability to destroy. However, beforehand, the affected area should be energized with pale blue chi.

Do not use bright purple chi at the same time as chi which is yellow, green, tangerine or red because it will intensify and increase the effects of these colors. In addition, the use of any dark colors with bright purple chi (either preceding or following its use) should be avoided, as this will produce a very damaging result. As a general guideline, use blue before electric violet.

Golden Chi

Gold colored chi, which has almost the same qualities as bright purple chi, is formed when bright purple chi meets the spirit body. The color changes to cerise (pale red) when this gold colored chi enters the physical body. However, this chi is does not have as much influence as the bright purple chi, being gentler and therefore less effective as a cleansing agent. Gold colored chi should be used to treat a very local area, while bright purple chi can be employed over a wider area.

Spleen

The spleen is connected to the solar plexus and the navel, the major center that connects to all the organs. Holding solar energy or a white ball at the solar plexus will help distribute Chi to all the organs.

If the solar plexus gets clogged up the liver and spleen will also become blocked. The spleen, the Door of Life and the navel are all linked together; the navel and the Door of Life sit opposite each other. We call this an emotional link. Many diseases are caused by emotional links; people use psychology to deal with it which can work to a certain level, but all the energy would eventually get stuck at this main juncture or plexus. White chi is taken in mainly at the spleen, and before being sent to the various parts of the body, is split into its colored forms of red, green, purple, blue and tangerine.

If the spleen is not clean, the immune system will be affected, together with the production of bone marrow. The blood will be dirty and diseases of the joints and connective tissue encouraged.

Cosmic Healing Chi Kung works very well with Chi Nei Tsang. The Cosmic Healing Chi Kung, Chi Nei Tsang and all the other Universal Tao practices all play a unique role in working to heal the physical and subtle bodies. When you combine these three in synergy, it allows you to perform many healing tasks. The spleen (located under the left side of the rib cage), spleen center or navel can absorb white Chi directly into the front or back. The Chi will be broken down into color and distributed to other centers and their associated organs.

There is one thing that I always advise: the recipient or student should be under a doctor's supervision and that they should alternate between the medicine from the doctor and the work with us at the Universal Tao. The doctor should be advised of what we intend to do with the student.

Cosmic Healing Planetary Colors

In Taoism we give each planet a color which enhances the healing power. Have the 'Planets' chart (located at the beginning of this chapter) in front of you, look at the relevant planet and close your eyes. Hold the planet in your mind.

Fig. 5.3 *Channel the Cosmic Planetary Energy into the body.*

Mars: Focus your awareness on the star above you, turn your eyes up and look up to the crown. Hold the image of Mars and extend your sight beyond the crown, looking up into infinity. See the **Red Light** and gradually bring it down to your head about 6 feet above you. Form it into a red ball, a holographic image of the planet Mars shining its red light above you. Invite it to flow down to your 'star' (located above your crown) and continue to flow into your Upper Tan Tien for processing. Let it flow down to the heart (or T-2) and down to the palms. Red and orange light also can be breathed in through the sacrum. Feel the sacrum pulsing and breathing in the red and orange light. Practice 9 to 18 times, rest and shake your hands.

Venus: Become aware of the star above you, turn your eyes up and look up to the crown and into infinity, seeing the expanse of **White Light.** Gradually bring the light down to your head, about 6 feet above you. Form it into a white ball, a holographic image of the planet Venus shining its white light above you. Invite it to flow down to the star above your crown and continue to flow into your Upper Tan Tien, for processing. Now it may flow down to your lungs freely.

Saturn: The **Yellow Light** from Saturn can also be absorbed via the earth through the soles of your feet and perineum. This is for your spleen. Follow as above.

Mercury: The **Blue Light** from Mercury may be absorbed through the throat center. This is for your kidneys.

Jupiter: The **Green Light** from Jupiter can also be absorbed through the throat center. This is for your liver. Follow as above.

Summary - Working with Color

(Practitioner to Student)

There are two ways of doing this type of healing session:

One way is to focus on the specific location in your own body, using your hands and ask the other person to do the same. Together you complete the entire route.

Another way is to focus on your own energy body and ask the student to do the same. Bring a channel or line down from your energy body into your physical body and do the same for the student. Once again, complete the routes together.

For reasons of clarity this text only mentions one student and uses the male gender; *this session may however be performed with a group also*. Before starting the session do some group meditation practice and warm ups.

1. Be aware of the Tan Tien and connect to the universe. Let the student sit with his back to you. You are behind him. Be aware of your **Sacrum** area and feel the Chi; **wait for the Chi to rise up to the crown** and to the universe. Spiral the Chi down to the student's and your own energy body and it will flow into the physical realm.
2. Draw in the green light with your palm, push it right through the sacrum and disperse the sickness throughout the other side of the universe. Pull the green light from the universe through the sacrum and push the sick Chi out to the universe. Do this 6 to 9 times until you feel the **sacrum has been cleaned**. When you pull back stop the green Chi at the student's sacrum; there is no need to pull it back to you.

   Yellow light from the earth will help strengthen the sacral bone. Visualize the sacrum and vitalize the complete bone structure with yellow light passing throughout.
3. Be aware of the energy body above the **Crown**; extend yourself up from above your crown and **channel down the white light from the center of the universe and the violet light from the North Star.** Using your 'mind-power' ask the inside of the bone structure to open, allowing the white and violet light to **flow into the marrow.** Focus on the energy body; you can picture the energy body's sacrum and bone

structure to help guide the energy inside and see the whole body light up from deep within.

4. Then focus on the **Door of Life and the Navel.** First flush them through with **green** light, cleaning them out. Draw the green light from the Door of Life through to the navel, and then push back through. To cool down the Door of Life (if necessary), draw the **blue** light and push it through from the navel to the Ming Men, connecting with the universe. Then bring the **white or violet light down and activate the Lower Tan Tien.** Always teach people about their Tan Tien. It is like an ocean and the body is like a hollow bamboo. The bamboo can bring the water up. This way energy will never dry up.
5. Concentrate on the **Solar Plexus and the Chi Chung (T-11)**. Once again, draw the **green** light, spiral it, use it to flush, then **energize with white and violet light**. As before, always allow the energy to stream through both the points completely. The solar plexus holds all the emotions. When working on the solar plexus, the **most important thing to remember is to connect the 'backside' to the universe.** There is literally no end to this connection. Just allow the Chi to come all the way down and then pull it towards the rear slightly. Simply clean out the path. Allow the information to condense; allow any images to manifest and then release. Then stabilize the energy. Picture the Chi-Field enveloping the person as a big protective bubble. **Cool down with blue.**
6. Proceed to the **Heart and the Shen Dao (T5/ T6).** Draw in the **green** light, push it through and repeat several times. Now scan the heart with your palm, sensing its strength; then select an appropriate hue, i.e., not too dark. Send the **red** light through the heart to strengthen it.

   Cool down any excess heat in the heart, flushing down and out, using **blue** color. Draw in the **white** Chi; push it through to the **Wing Point (T5/T6)**. **Energize the center at the back of the heart using violet and golden Chi.** Picture the heart surrounded by a golden aura.
7. Move up to the **Throat Center, flushing through to C-7**, using **blue** light first to open and clear it and then **green** light to clean.
8. Next activate the **mideyebrow.** Focus on the mideyebrow in your own body. Use **golden yellow** Chi; use it to **flush and stabilize** the mideyebrow. Flush it all the way through to the backside of the head. **Energize with violet golden light.**
9. Proceed up to the **third eye** in the middle of the forehead. **Connect to the Kun Lun** at the back of the crown. **Flush** through both points using the pale **violet light. Energize** with **electric white or golden light.**
10. Concentrate on the **crown**. Use **violet** or **golden** light to enter and **flush** all the way down through the **central channel**, leaving the body at the **perineum**. **Cool down the system by showering blue light over the whole body.**

    When people have a serious infection, they should consult a doctor. It is common for infections to take a long time to clear up nowadays, even when using antibiotics.

There are two ways to deal with this; allopathically or naturally. The Taoist practices are in great conflict with 'contemporary (i.e., not alternative/natural) western concepts'. The western concepts recommend a full course of antibiotics. Using the theories of Chi Kung, a baby for example, would absorb natural antibiotics via the bones. Western Allopathic Practice consider antibiotics as wonder drugs. The only 'wonder' is when will they realize the many harmful effects that it has on the body? Babies that have been 'fed' with antibiotics frequently suffer many organ related problems by the time they reach 20 to 30 years of age. The worst thing is that they are given to children nearly every time that they become ill. If you scan (cosmically) the solar plexus, thymus or spleen of such a person, the area feels like a hollow void. This means that the immune system is totally non-functional. The same thing applies to ***Aids***: the immune system no longer functions. Any virus can enter the body - medicine cannot kill it. There is nothing left to 'fight with'.

In my experience and following my own experiments, in circumstances like the above my own practices are as follows: I clean my colon; there are a few ways to do that. I eat fiber, vegetables, especially green leafy ones. I eat a big bowl of vegetable soup. I also add things like onion, pumpkin, carrots and cabbage, which will give it a sweet taste. I don't eat any meat and drink a lot of water. The colon is cleansed within two days. I also brush the skin, which is a very good detoxifier. The vegetables will provide natural carbohydrates which are digested and absorbed very quickly. A healthy diet consists of many whole natural foods. It is 'alkaline' as opposed to 'acid' based. I also use the 'colema' which I feel is the best cleanser.

Chapter VI
Individual Healing Session

The Individual Healing session embodies all of the techniques that you have used previously and consolidates them for use on a one-to-one basis. The session comprises the following three parts:

A. Almighty Knife (Chi Knife)

The almighty knife can be used for any health problems. We can charge the knife with Yin or Yang energy. We charge the almighty knife most often with Yin Power. Yin is the cold energy and is used for any inflammation, pain or heat. Yin is used to break up illness. Charge the almighty knife with Yang for strengthening, melting or expelling. Only use the Yang when there is no pain.

B. Energizing and Activating the Immune System

C. Cleansing the Internal Organs

A. Almighty Knife

Fig. 6.1 *Almighty Chi Knife*

Since the dawn of ages and our descent into the material realm, we have constructed, manufactured and used tools to facilitate the progress of events. They are an extension of ourselves that enable us to enhance, mould and magnify our intrinsic nature as inquisitive playful beings.

We have used implements to help nourish, protect and amuse ourselves and further our progress in attempting to understand the 'how' and 'why' of existential reality. The knife has served as a means to carve our way into the present. It is a simple, yet powerful 'friend' and derives as much power as we wish to lend it.

Its design may consist of any combination of the five elements (Earth) which when combined with Universal (Heaven) and Cosmic (Man) forces, provide a unit of energetic substance which receives and transmits magnification, purpose and power in accordance with the human will that governs it. 'Chi Knife' and "Powers of Ten' adopt the precepts of a truly magical existence. When we arrive at our destination we will realize that we have indeed turned "the Wheel of Law'. In achieving this end we will have completed the cycle and returned to the beginning of the journey. We will understand that the simple things in life, like the knife, contain the same amount of power as state of the art technology.

We are all returning to the Garden of Eden. Complex telescopic and microscopic equipment now enables us to see the truth:

"Inside has no outside; outside has no inside".

They are one in the same thing. When they merge together we will indeed enter the Kingdom of God.

Outline of Practice

1. Hold the knife in the right hand (left, if you are left handed). Hold the other hand near your body, with the thumb and index finger touching. Project the Chi Knife as big as the universe, 'long and big - reaching to Heaven'. The bones in your arm are hollow and the 'bottom' is sealed at the shoulder. Feel them 'fill and pack' with the power coming from above.
2. Then give the command: **"Power comes from the east. This Chi Knife has the power to dissolve all the negative energy, sickness and bad fortune. By my request, please carry out the order now."** Wait until you feel that your arm and the knife are heavy and full of Chi.

Eye Problems

Use the thumb and the index finger to hold the eye wide open.

You hold the knife like holding a pen, 3 to 6 cm away from the eye. Use the little finger for leverage and support.

WARNING!

DO NOT USE A KNIFE. THE **MASTERS** OF GREAT EXPERIENCE USE RITUAL SCALPEL TYPE KNIVES. THE STUDENT SHOULD USE THE "SWORD HAND" FINGERS (P.76, FIG. 4.24).

DO **NOT** USE SHARP OBJECTS NEAR THE EYES**.**

Fig. 6.2 *Hold the knife three to six cm. from the eye.*

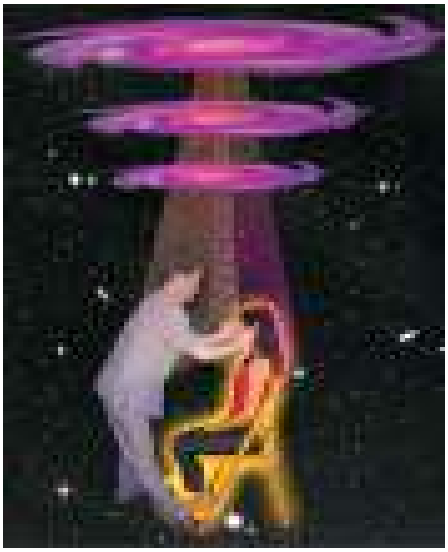

Chi knife - "Almighty Knife" helps all eye problems". Cut up and down and sideways in the cross pattern 'through' the eye thoroughly. Tell the student to move the eye left and slowly move to the right as you cut with the Chi Knife. When they move their eye to the right, move the Chi Knife to the left. **Remember that the knife is used for 'energetic surgery' and should never make contact with the eye itself.**

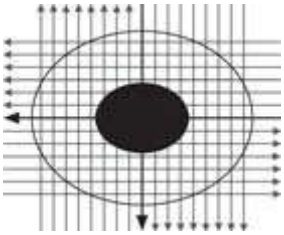

"Slice" the eye toward the right side for 50 to 100 knife movements and do the same to the left side.

Fig. 6.3 *"Almighty Chi Knife helps eye all problems".*

"Almighty Knife, please destroy all kinds of wounds, warts and tumors". Cut up, down and sideways in the cross pattern through the part that has the 'condition'.

Fig. 6.4 *"Almighty Knife, please destroy all kinds of wounds, warts and tumors".*

The almighty knife can be used for any problem in the body. Follow the same procedure to carry out 'energetic surgery' on all parts of the anatomy. It is especially good for soft tissue repair, including the brain.

When you feel that the Chi Knife is full of sick Chi, spiral counter clockwise and discard it down to the ground. When you feel that the knife is 'empty' charge it with Chi from the universe.

B. Energizing and Activating the Immune System

In cases of severe illness, you will want to do this technique many many times, because it is essential to stimulate the body's defence-systems. This technique is also beneficial for debilitation and infection. You may also want do this in a preventative manner.

Activating the immune system always involves the bone structure, especially the round bones in the arms and legs and the flat bones in the skull, jaw, rib cage, hips and spine. All of these are involved with the production of white blood cells. The **thymus gland** and the **spleen** are of special importance to the immune system, because they are involved with programming and training the white blood cells (called T-Cells) to do the right job. **The lymphatic system is involved in removing toxic waste from the body; it is therefore beneficial to stimulate the lymph flow as well.** This is best done in combination with Chi Nei Tsang. *For details refer to the Chi Nei Tsang Books.*

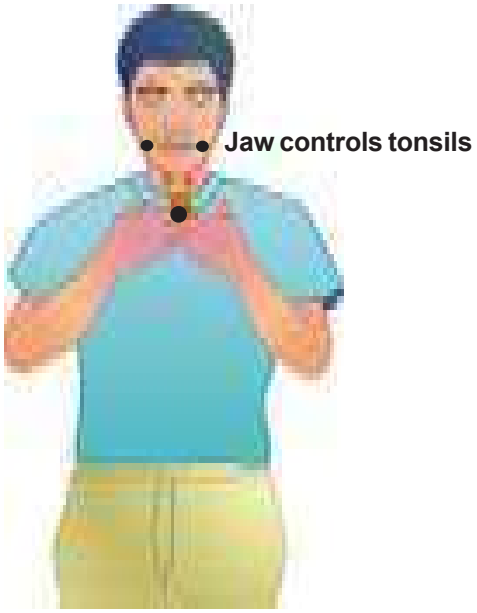

Fig. 6.6
Touch the top of Sternum to activate the Thymus.

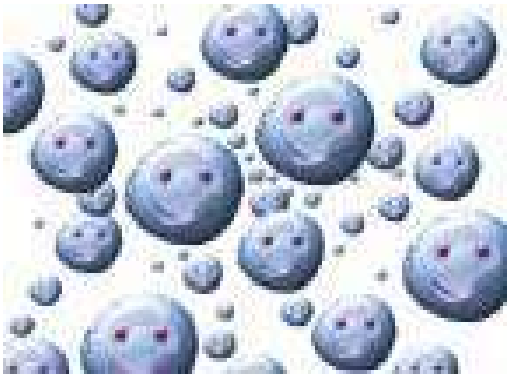

Fig. 6.7 *Happy Cells.*

If you work on a one-to-one basis, first perform the general cleansing session, where you 'pour energy' over the other person. After that use your hands, drawing Chi and pushing it through. Remember to push the energy all the way through and connect it with the universe beyond. Ask your student to concentrate on the areas that you are treating, preferably by guiding them, touching each point as you go.

Outline of Practice

Fig. 6.9 *Touch the Sacrum.*

Guide the student as you practice together. Work with your own energy body and tell the student to work with theirs. Presuming that you have already done the previous set of general healing, you can start with the **coccyx**.

1. Be aware of your Tan Tien and connect to the universe. Direct the Chi down to the fingers. Touch your coccyx with the fingers concentrating a beam of white light on to it. Picture the sacrum opening and the white light streaming inside, flowing up the spine and streaming out over the whole bone-structure. Transfer the feeling of Chi in the coccyx up to the universe, multiply it and guide it down to your energy body.
2. Always be aware of the Tan Tien and the universe first. Attract the yellow light; spiral and condense the healing light into the tip of your fingers; move the fingers up to touch the sacrum. Send out a beam of yellow Chi into the sacrum, directing it up the spine. This will stimulate the production of red blood cells. If you are not sure whether you are able to send it right into the marrow, picture the marrow or emit the Chi from your fingers, while at the same time concentrating on the bone marrow of the energy body. Transfer the feeling of 'Bone Chi' up to the universe and down to the energy body.

3. Proceed to the crown, showering it with violet light. Then spread from the crown throughout the bones of the body. Repeat several times. Instruct the student to feel the bone structure breathing. Ask him/her to extend up from the crown to the Big

Dipper and North Star, channelling down the red and violet light into the thymus gland.

4. Continue to the throat, stroking down with your palms, using green color to move the lymph down towards the backside of the heart. **(Never stroke up towards the head. Only guide the lymph down).**

A. ***B.***

Fig. 6.10 A. *Channel the Violet Light of the North.*
B. *Use your Palms to bring the Lymph flow back to the Heart.*

5. Proceed to the lymph nodes under the armpits and across the sternum. Next activate the lymph nodes in the groin. From the groin you guide the lymph up to the navel center (Not down where it will get stuck in the legs).
6. Return to the navel center. Send the energy deep inside, energizing the lymph nodes at the back. Pull back, drawing green energy, flushing out any waste products that are stuck in them.

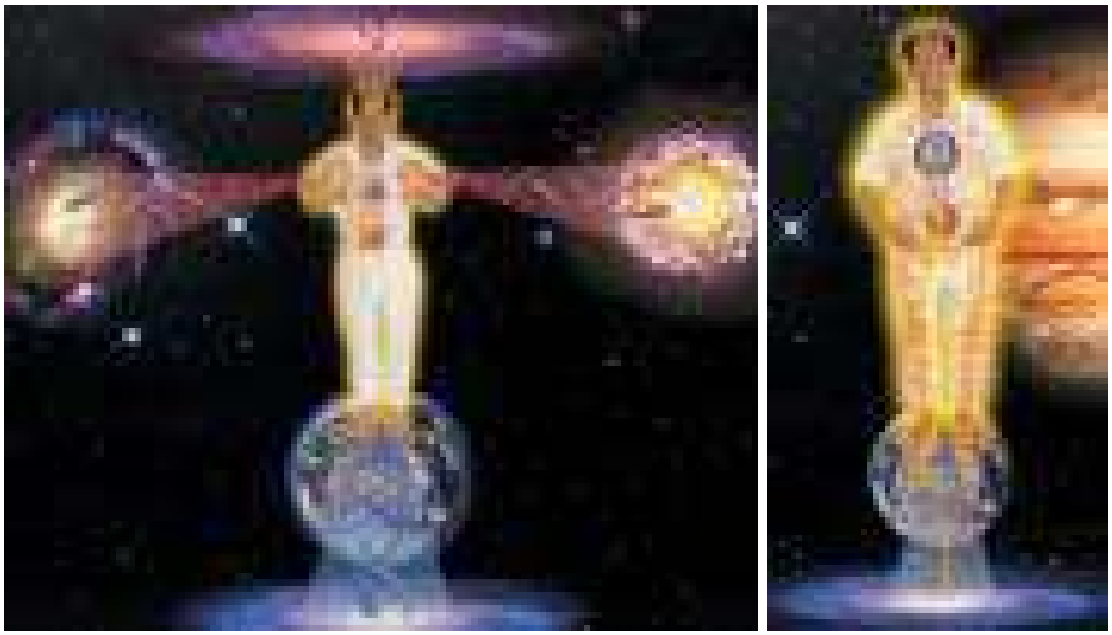

A. ***B.***

Fig. 6.11 A. *Activate the Lymph Nodes in the Armpits and Groin.*
B. *Energize and flush the Lymph Nodes in the Navel.*

C. Cleansing the Internal Organs Technique

Healing Some Common Illnesses

This session can be used for any kind of ailment and carried out with any number of students. It can take place on a singular, paired, small group or large group basis. Numbers can range from one person, one hundred, one thousand, ten thousand, ad infinitum. It is more likely that a greater energetic current will be created in much larger groups. In the case of 'mass' healings, there will always be a 'guide' or 'conductor', to open the channel for the students to follow. In the case of solo practices you will of course be the guide. **The following instructions have been set out on a one-to-one basis**.

By connecting to heaven, earth and your student, you will maximise the wholistic healing potential to your physical and subtle bodies. We recommend you spend about twenty minutes on the general healing before moving on to the more localized practices of emptying and cleansing the body's centers, systems and organs, contained within this chapter. We recommend that you spend between five to fifteen minutes on all of these. **Always perform the Sacred or Chi Water practice before.**

It is important to remember that if there is no energy in your Tan Tien, then there will be no energy to work with. 'Connecting the Tan Tien and the Universe' means connect your center to the infinite source of the universe, the Tao. When you make the connection you access this power. Always hold on to your center; it is the only thing that is truly yours. Keep the fire warm and spiraling. When you are aware of your Chi, you can direct heavenly light straight into your energy body and then into the student's.

General Principles

1. Push and pull the energy through the student's body. Push and disperse the sick energy into the universe and out to the planets, where it will be transformed and recycled.
2. Pull the energy back and stop it between yourself and the student.
3. Spiral the energy counterclockwise until you see the **green** light mix and clean the sick energy. Spiral and flush the energy down into the earth.
4. Spiral with **blue** light; see it mix and flush the energy within the student's body. Spiral this energy down to the ground.
5. Energize the student with **white** or **violet** light.
6. You can also use both hands to channel Chi when you 'push and pull' through the body.
7. Energy can be introduced to the affected area of the body by moving the hand clockwise in a spiral.
8. Move the hand anticlockwise with a spiraling motion to clean, flush and remove energy from the treatment area. After this, brush down the whole body, to direct the sick energy into the earth.
   Use an anticlockwise spiraling movement in order to clean, then expel the energy.
   Use a clockwise movement to bring energy in and an anticlockwise one to take it out.
9. When you begin pushing, pulling and sweeping, you may feel resistance in the body. As you progress and the energy centers open, this feeling will diminish.
10. There are many color combinations that can be applied to the various parts of the body. When you start practice, stick to the basic 'blue, green, white, violet and blue' formula. When you are working on a specific area, you can keep this book near by, or write a short 'color recipe' before you begin. In this way, you will be able to relax your mind.
11. 'Pushing and pulling' is like fanning and venting the body; when you fan your hands in front of your face, it will have a cooling effect. Ventilation enables the stagnant, sick energy to leave the body.
    Below is a list of the body's organs in relation to their tendency to 'store heat'. They are listed in descending order, i.e, the head is the hottest:

Head, heart, liver, lung, stomach and spleen, large intestine and small intestine, kidneys and sexual organs (which become hot when aroused).

Outline of Practice

Occupying a position amongst most of the internal organs, the solar plexus acts as a kind of clearing center for energy generated by the emotions. It also lies in between the lower and higher energy centers.

1. Scan; ask for the power to look at the cells.
2. Push, pull and give the command, “Disperse”. Push until you feel the solar plexus clear and open.
3. Spiral green Chi counterclockwise. Talk to the sick energy; tell it to “leave”, you will take it to “a better place, where it will be happy”. Give the command, “Out”.
4. Spiral Blue Chi counterclockwise, flushing out any remaining sickness. Guide the sick energy into the earth.
5. Spiral and sweep Blue-Green and Red Chi into the solar plexus, sweeping the organs. If the patient is expecting a baby, has an infection or bleeding in the intestinal area; do not use this method.

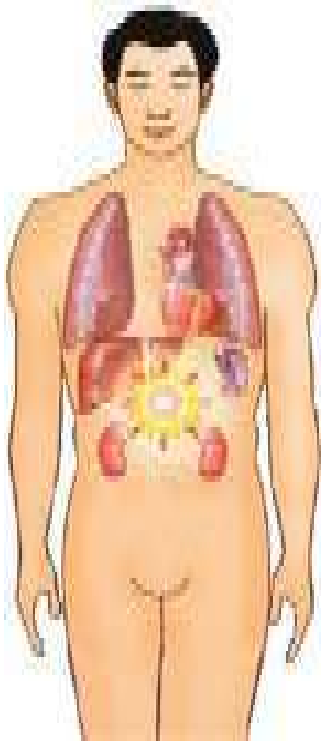

Fig. 6.12
Spiral Green Chi counterclockwise in the Navel.

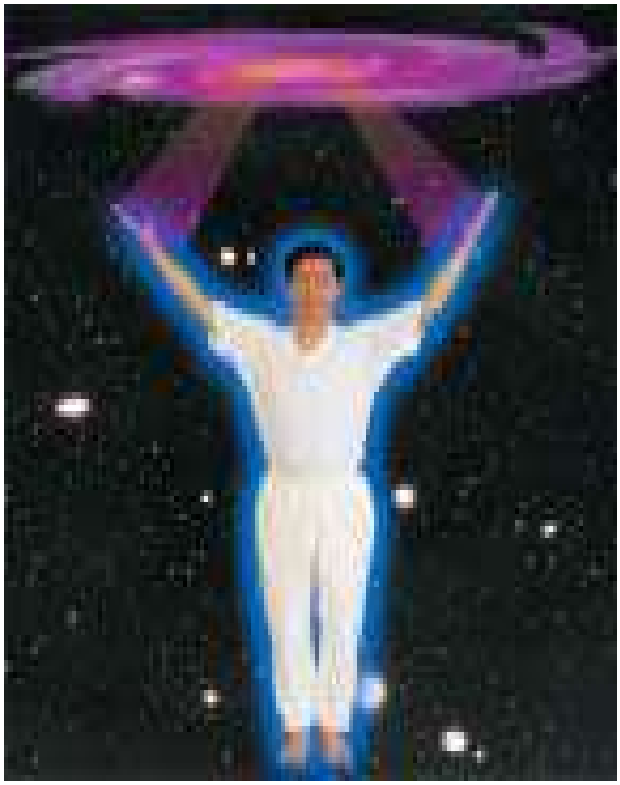

Fig. 6.13 *Charge your Hands with Chi - project the Hand Bones into the Universe and feel them fill and pack with Chi.*

Work on cleaning out the **organs**. Scan the person and see which parts are hot. A lot of people will have an overheated solar plexus, which means that this area will require a lot of attention. You will feel the heat when you scan.

You can **clean the organs by 'pushing and pulling'**. Picture the organ and push; feel your hands are very 'long', extending through the organs and reaching out to the universe. Project all the sick energy down into the earth and out to the universe. Use your intent to guide it into the earth and out to the other planets in the solar system, where it will be processed and recycled. Pull the universal energy back towards yourself; push and disperse all the negative energy out to universe. Pull; when you pull the Chi back past the student, stop in between the two of you. Push, pull, push and pull, until you feel the energy or power. **Ask; "Give me the power to see". Feel your Chi entering into the organs with ease.**

A. ***B.***

Fig. 6.14

A. *Extend through the solar plexus and reach out to the universe.*

B. *'Clean and energize with Green' - push and pull to help loosen the solar plexus. Spiral counterclockwise with a Green Light. Blend with the sick energy and guide it down to the ground.*

Clean with Green Light. Spiral counterclockwise. Feel the green light mixing with the sick energy. Push and pull until you feel the energy in the solar plexus begin to disperse. Spiral the energy counterclockwise and guide it down to the ground.

A. ***B.***

Fig. 6.15 A. *'Push and Pull' to help disperse the energy in the Solar Plexus.*
B.*'Flush and stabilize with Blue'-Picture Ocean Blue and flush sick energy down into the Earth.*

Rinse and flush with blue light. Picture ocean blue and flush down to the earth. See and feel the solar plexus becoming cleaner. Flush the sick energy down to the earth.

Now clean out the whole body again. With all the organs: from the lungs, heart, liver, gall bladder, pancreas, spleen, stomach, small intestines, large intestine, kidneys and sexual organs. Clean all the way down to the earth. **When you clean the solar plexus and all the other organs you remove all the negative emotional energy.**

Energize the **spleen**, **liver** and **kidneys** with blue or white light. Then project green, followed by orange light to the cores of the liver and kidneys. Clean with the green and orange light and stabilize with blue light.

Work on the **back** of the **spleen** and **kidneys**. Energize them with blue-white light. The spleen is on the student's left and kidneys on the right and left. They all help to clean the blood. Spiral the energy clockwise into the spleen. See it in your mideyebrow. See the cells and spiral the light into them. Give the command, "**Stay**". This is very important; it makes sure that none of the cells hide from the dazzling light that you are sending. Give the command again. Then stabilize them with blue light. Picture the kidneys and see their cells and feel the blue light go into the cells.

Work on the **Liver** on the student's right hand side. Smile and laugh to the liver and see all of its cells. Give the command, "**Stay**"; then send in the healing light. Send in blue or white (energize), followed by green (energize and clean), blue (rinse and stabilize), violet (recharge and reprogram) and then blue to stabilize again.

Spleen - Front and Rear

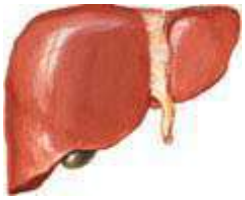

Liver

Fig. 6.16 *'Push and Pull' to help disperse the energy in the Liver and Spleen. Clean with Green and flush and stabilize with blue. Flush the sick energy down into the Earth.*

It is essential that you feel and talk to any sick energy. **If the student is healthy then you will feel their 'light'.** Ask their energy body to tell you where it **may** need some healing. Send in 'light radar'. Transmit green light and flush down to the earth. **When you feel that energy is accumulating, start to spiral more.** Push and pull and give the command for the sick energy to leave.

The more you clean, the more you heal. Tell your student to practice at home after the session, at an agreed time. You can then carry out 'absent or distance' healing, linking everyone's personal star, energy body and the universe. **With time, you will master the techniques, imprinting them with your own manner.** Eventually symptoms disappear, as the blockages are cleared and the flow returned.

Cleansing the Spinal Cord

Spine

Always cleanse the spinal cord, which protects the entire body from diseased and negative energy, both physical and psychic. When you open the spinal cord and solar plexus you can release many energy blockages. Sweep the hand in a clockwise motion to energize the spine with either/or a combination of; **blue, green, white and ultra-violet**. Then spiral counterclockwise and **brush** the spine down to the ground. Continue sweeping until you feel that the spinal cord has cooled down. Remember not to use orange or red.

Cleansing the Blood (Lungs)

Pale green/white and tangerine/white chi work as cleaning agents for the blood. Diseases of the blood and arteries can be treated. The chi first energises the lungs and as the blood passes through them, it takes in the chi, thus becoming purified. The benefit is then carried to the rest of the body as the blood circulates. Serious infections can also be treated in this way; however, the technique should not be used on women who are pregnant.

A. ***B.***

Fig. 6.17 A. *Cleansing the Blood and emptying the Lungs.*
B. *Become aware your Three Tan Tiens. Connect to the Universe and ask for 'the Power to See'.*

Outline for Cleansing the Blood/Lungs

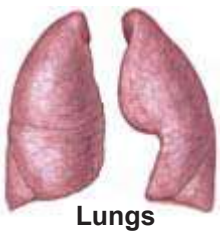

Lungs

1. Scan the student.
2. Push through and open the lungs from the back to the front.
3. When the lungs need to be given energy, use pale green/white followed by pale tangerine/white chi beginning at the front and moving top the rear.
4. To make weak patients stronger, cerise/white chi can be employed as this will bring energy into the lungs.
5. Purification of the blood is carried out by the liver, kidneys and spleen. Use white chi to bring energy to these areas, after first pushing and pulling through them.
6. The blood requires a lot of cleaning on a regular basis.
7. Energize with white Chi. **Germs can only grow in the dark. 'Fill yourself with the light'.**

Circulatory/Heart System General

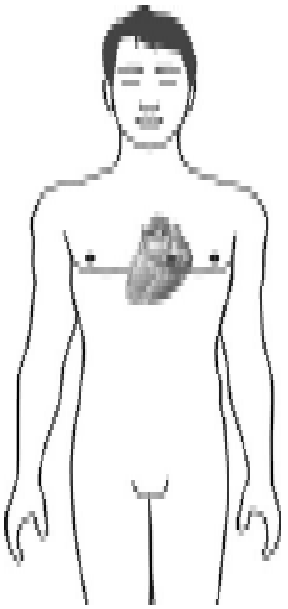

One of the basic problems pertaining to the circulatory system and heart is hypertension and hypotension. Once again, the sacrum and solar plexus are involved. The sacrum controls the bones; indirectly, it stimulates the marrow and enhances the quality of the blood. Good blood is like running the highest quality motor oil through the engine of a motor vehicle.

(Within the Universal Tao System we also have the view that the sacrum controls the Chi-pulse. If there is enough Chi, the heart does not have to work so hard, because the Chi pushes the blood).

The solar plexus relates to the emotions, affecting the heart through two mechanisms:

- It may affect the heart directly, causing rhythmic disturbance or pressure around the heart muscle
- Malfunction in the liver or digestive tract, leading to high cholesterol levels or gas which pushes up towards the heart from the intestines and causes unwanted heat and pressure.

Cleaning out the Solar Plexus will greatly improve these conditions. If you have been trained in Chi Nei Tsang you can use it in combination with the Cosmic Healing techniques.

Specific

Working on the Heart Muscle:
Clean out the Solar Plexus as outlined above. Push and pull with green and blue.
Detoxify the liver, flush with green.
Enhance with white and violet light.
Use the finger to work on the lower left and upper right part of the heart.
Remember that the heart muscle is very delicate.
You draw the force, you spiral and you push.
Stabilize with white.
For enlarged heart use blue.
Carefully use the red light to balance the blood and open the blood vessels.
Sweep the sacrum with green, red and blue.
Sweep the solar plexus with green, blue, red, white and violet.
Energize and cool down the throat center, using blue.
Working on Hypertension (High Blood Pressure):

Overactive adrenals/ kidneys often cause hypertension. Clean out the solar plexus first, because the adrenals (T11) are connected to it. The adrenal glands produce adrenaline, the hormone that stimulates the heart to pump. Overactive adrenal glands will eventually affect the heart.
Tune-up the Door of Life with blue, calming it.
Take the pressure from the heart, use green.
Energize the heart, use violet.
Flush down from head to feet with blue;
The basic problem with hypertension is that the Chi goes up and cannot come down. Work on the sacrum, using orange and yellow.

Working on Hypotension (Low Blood Pressure):
In hypotension the Door of Life and T11 are underactive.
First clean out the Solar Plexus, this time focus on removing blocks or stuck energy.
Energize the Door of Life, using green and red.
Energize the Sacrum (same colors).
Energize the Base of Skull with green and violet.

Stomach Pains

Pass your hands over the patient and brush the whole abdomen, especially the solar plexus, navel and lower abdomen. The navel should be treated with a combination of green and blue, and blue should be used at the end to firm up the energy.

If problems persist: A) Treat with Chi Nei Tsang B) Seek the advice of a qualified medical practitioner.

Relieving Pain: *Blue Chi*

Chi that is associated with the colors blue and green can be utilized in different ways. While green chi acts to free up energy that has become ‘sick’ and ‘stuck’, blue chi can act as a painkiller because of its ability to reduce the severity of pain.

1. Push and pull the through the affected part out to the universe or ground the sick energy until partial relief is attained.
2. A large amount of pale blue/white chi together with pale green/white chi should be used to transmit energy to the problem area.
3. For the alleviation of pain, use pale green/white chi and pale tangerine/white chi in turn.

Energize means draw the Chi into the part that you want to receive healing. Cleansing means push energy through the affected part and send it out to the universe. Pull the new Chi back into the same area. Light green Chi is used in loosening and cleansing delicate organs like the eyes and the brain.

Headache: *Light Whitish Green and Light Whitish Blue Chi*

1. To check for areas that are congested or lacking in energy, the eyes, temples, spine and solar plexus area should be scanned. Also, the crown, mideyebrow, forehead and back of the head and neck.
2. The eye and temple areas should be brushed down when the headache is because of eyestrain and then flushed into the ground.
3. The whole head, particularly the painful section should be brushed and then pale green/white, blue/white and pale purple/white Chi used to bring energy into the area.

Migraine Headache: *Light Whitish Green Blue and Violet Chi*

1. Persons who suffer from prolonged or chronic headaches including those types termed 'migraine' headaches have an abnormal accumulation of energy in various parts of their bodies. Starting with the solar plexus, this energy follows a route up the vertebral column and thence into the neck and head. As a result the various blood vessels in the head expand, causing pain in the head area. Mental strain and emotional disturbances usually cause this type of headache.
2. Use a pushing movement to clean and open the solar plexus and liver areas. First use pale green/white, then pale blue/white and finally mauve/white chi to bring energy to the solar plexus area.
3. In order to send the 'sick' red chi into the ground, brush down the spinal column.
4. The back of the heart can be opened by pushing through in order to remove the dirty Chi. Then bring energy to the heart by using pale green/white and purple. Use your mind to see the heart center expanding and opening.
5. Brush down the dirty chi from the head area and send it into the earth.
6. Use a combination of pale green/white, blue and purple to bring energy to the back of the head, the crown point and the forehead.

Toothache: *Light Whitish Green and Blue Chi*

1. Brush down the area with pale green/white Chi.
2. Energy should be brought into the area with pale green/white, mauve/white and blue Chi.

Broken Bone: *Orange-Yellow Chi*

For anything relating to the bones always activate the sacrum. Light orange-yellow Chi is used to encourage broken bones to knit quickly, Chi which is pale yellowish tangerine may be employed. The sacrum attracts the orange-yellow Chi; feel the eight holes in the bone breathing. The orange-yellow Chi enters, transfers up to the crown and is sent up to the universe to multiply.

1. The fracture area should be brushed using a combination of pale green/white and pale tangerine/white chi.
2. To promote fast knitting of fractures, a daily treatment with pale tangerine yellow Chi mixed with white can be employed, in the ratio of 7:1.5:1.5 of white (for the center), yellow and tangerine respectively. Push through and brush the sacral and navel areas, using a cerise (light red) Chi mixed with white.

Back Injury: *Light Whitish Blue and Green Violet Chi*

1. Scan the student to see which parts are congested.
2. Use chi that is pale white/green or pale white/tangerine and, selecting each in turn, with a brushing movement apply to the whole spinal area and especially to the area where the trauma is located.
3. To bring energy to the damaged area, use a combination of pale blue/white, green and purple.
4. White chi should be used with a brushing movement on both the back and front of the solar plexus area.

Infection and Inflammation: *Light Green Chi*

Treat the damaged area with green and tangerine/white chi, using a brushing movement. For the heart and spleen, these colors should be replaced with green and purple.

Bring energy to the area by the use of mauve, white, tangerine, green and blue and strengthen the natural immune of the body.

Cysts: *Light Green and Blue Chi*

During the course of the session, repeatedly pass your hands over the patient's body. Treat the solar plexus area with a combination of green and blue chi. The cyst can be removed using a chi knife, spiraling clockwise with green and tangerine chi; moving the 'stuck' red chi out of the body and grounding it in the earth. After, blue chi should be used for a calming effect, while green and tangerine can also provide energy. For maximum benefit, sessions should be thrice weekly.

As foods containing a lot of highly spiced ingredients have a lot of red chi, these should be kept to a minimum. The patient should use the Inner Smile to calm and balance his/her emotional state.

It is sometimes necessary to sweep 100-200 times, to cool the affected area. Scanning will enable you to take a temperature reading. If the area is still hot then continue sweeping until it reaches a satisfactory temperature.

Fever

1. Brushing can be done with blue or green Chi.
2. Push and pull through the affected part, sweeping the spleen with green and blue. Clean and rinse thoroughly.
3. The solar plexus area can be treated with tangerine and blue Chi but tangerine should not be used on a patient with diarrhea.
4. The thymus gland can be stimulated by the application of green, tangerine and purple Chi. First, brush the heart area with green and blue. This helps the body to ward off infection.
5. Both lungs should be brushed and energy brought into the back of the lung area by the use of tangerine and green.
6. Sweep the spleen with green.

If the student has a fever then they must lie down to receive the healing. This applies in all cases where the student is unable to sit up comfortably.

Insomnia: *Green and Blue*

Inability to sleep may be the result of too much activity in the solar plexus and the sacral area. The solar plexus may also be congested. Similar problems can also occur in the throat, mideyebrow and forehead, as well as at the crown point.

Repeatedly pass your hands over the patient's body as the treatment progresses and use a combination of blue and green chi to clean the sacral and solar plexus areas.

Sleep can be brought on by use of blue, as it soothes the solar plexus area. Use blue and green to brush the mideyebrow, forehead and crown point and white and tangerine on the navel. Finish with blue.

Do not eat food late in the evening.

Sleep in a separate bed from your partner. You can place two beds next to each other.

Tinnitus

Relates to weakened kidneys. Work on the kidneys, mideyebrow and forehead.

Blood Clotting: *Blue Chi* - Fresh Burns: *Green and Blue Chi*

Because of the cooling and calming properties of blue chi, it can be used to remove the heat from burns. Green has a similar effect.

The area needing treatment should be scanned, then brushed with a combination of pale green/white and blue Chi until relief is felt and the heat in the cells released.

Old Minor Burns: *Green and Red Chi*

Pass your hands over the damaged areas and repeat this during the treatment period. Use pale green/white and tangerine, but do not use on the head, eyes or brain, or other sensitive organs.

To reduce discomfort in the damaged area and promote fast healing, firstly pale blue Chi mixed with white should be employed, followed by cerise mixed with white, and green in equal proportions as this mixture optimizes the breaking down of necrotic cellular material. However, cerise should not be used in the head area but be replaced by mauve mixed with white.

Use cerise/white chi to brush the sacral and navel areas and follow with blue which assists in the release of the stagnant Chi. This session should be repeated for 2 or 3 days.

Old Severe Burns: *Green and Red Chi*

1. Scan at the beginning and end of the treatment (Note:I do not think scan can be seen as plagiarism and I don't know what other word to use in this context as I do not have the full text)
2. The local area should be brushed first with pale green/white and then with pale tangerine white. Keep repeating but make sure to omit sensitive organs and the head area.
3. To speed up healing and reduce pain and infection, the damaged area should be filled with energy from pale blue white, pale green white and mauve with white Chi.
4. To help speed up the healing process, wait a few days until there is much less pain, then use pale green white and cerise mixed with white Chi. If the head area is affected, use mauve mixed with white in place of the cerise.
5. Brush in the sacral and navel areas and to speed up healing use white Chi.
6. After making your healing intent stable, release it.

Old Wounds: *Green and Red Chi*

Green chi, in equal proportion of pale green/white and pale red/white should be employed on injuries which are not new as, when used in large quantities, it attacks and disperses damaged cellular matter, promoting fast healing. On recent injuries, it will have an adverse effect because it is likely to cause the trauma area to become moist, and it also will not be able to work quickly.

Scan at the beginning and end of the treatment, and brush the damaged area with pale green/white and pale tangerine/white Chi. Some pale blue/white can be employed locally to energise the area. Use of pale green/white followed by cerise mixed with white can speed up the healing process and assist in the breakdown of cellular material.

The navel and sacral areas should be brushed using pale cerise/white Chi. This will fill the area with energy and make the wounds heal faster. Before the Chi is let go, it should be stabilized.

Some Specific Points and Ailments

The following descriptions are mere guidelines. Each case is different and much depends on your own abilities. One needs practice to detect diseases. Best results with Cosmic Healing will be obtained when practiced in combination with Chi Nei Tsang.

Remember that these techniques are not meant to replace the doctor, but merely to assist him. The student must always work with the practitioner. ***The practitioner is a channel, the student the healer.***

Solar Plexus: *Blue Chi*

The Solar Plexus is the connection point for practically all the nerves inside the body. That is why it becomes laden with emotions so easily. When the Solar Plexus jams up and overheats, the liver will overheat; when this happens, the heart will also overheat; this will in turn affect the thyroid and parathyroid; finally the brain will be affected. Cleaning out this center is therefore extremely important. This type of cleaning may be done from the top down (as in the general cleansing session) or aimed at the Solar Plexus directly. Draw the green light, spiral it, flush with the green light, then energize with white and violet light. As before, always allow the energy to stream through both the points fully. The Solar Plexus holds all the emotions. When working on the Solar Plexus, the most important thing to remember is to connect the backside to the universe. There is literally no end to the 'other' end of this connection. Just allow the Chi to come all the way down and slightly pull inwards a little. Simply clean out the path. Allow the information to condense, allow any images to come out. Then stabilize the energy. Picture the Chi-field enveloping the person as a big protective bubble. Cool down with blue.

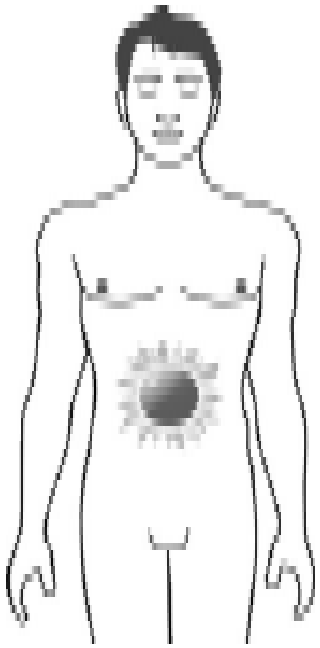

Skin Infection: *Blue Chi*

The skin is related to the lungs and the kidneys. Whenever there is an infection, the immune system is involved.

1. Enhance immunity as outlined in pages 101-108.
2. Focus on strengthening the lungs. Always start with green to flush out. Then send orange light into the lungs. Make sure you are not sending it up to the brain. Energize the lungs with blue and white.
3. Detoxify the kidneys, purify the blood (green) and energize with blue. Ask the person to visualize a fresh mountain-stream to stimulate the kidneys.
4. Treat the area locally, using your hands. If the area is big, use your palm, if small use the fingers. Do not focus on your palms - refer to the section 'Forget About Your Palms'. on page 152. Draw green Chi from the forest, and then energize with violet.
5. To diminish pain or itch, use blue to cool down. Also use the Chi knife to work on the infection.

In case the skin problem is allergy-based, you should also treat the mideyebrow; there might be some irritation here. First clean with green, then either energize with

violet (if resistance is low) or soothe with a light shade of yellow. If the skin problem is related to asthma, open the lungs with bright red clean the throat center with green and energize it with (deep) blue.

If the problem is due to toxicity, also clean out the liver flushing with a combination of green and orange. Energize with green. Enhance the immune system by working on the sacrum.

Eyes: *Green Chi*

The right and left eye are governed by the forehead and mideyebrow respectively. The eyes are also linked to the temples. Ask the person to touch their temple bone and guide them to take in the (white or light violet) Chi. Send Chi through the mideyebrow and forehead (all the way through). Ask the person to visualize the light coming in. Use soft shades of green with golden yellow to stimulate the optic nerve. Use blue to calm the eye muscles and light violet to stimulate the inner eyesight.

The eyes are connected to the liver. Scan the liver and energize with green. Scan the jawbone to see if there is any unreleased anger. Cool down with blue. Channel bright green into the liver.

Ears: *Violet Chi*

The right and left ears are governed by the forehead and mideyebrow respectively. Push and pull green Chi to clean. The ears are connected to the kidneys, so you can work on them also. The ears are also connected to the sinuses and upper respiratory tract. This means that infections need to cool down before you can use any cleaning technique. Use blue to cool and clean with violet. As long as fever and severe infection persist, use blue to cool them down. When clean, energize with violet.

Have Better Health, Less Stress and Remain Young

Brush specifically on the areas of the solar plexus, liver, stomach and pancreas.

White chi brings energy to the crown point, head (at the back) and both sides of the brain.

Both the front and rear of the heart and lungs can receive energy from white/purple Chi.

Both the front and rear of the spleen, the navel and lower abdominal area, the spinal cord, the kidneys, using white Chi.

On the sexual center use white chi but if the problem is difficult to shift, use green. You can also use white Chi on the sacral area, and green or purple on other organs.

White Chi can be employed for the arms and hands, while the legs and feet should be treated with white and purple Chi.
Eye problems with green/yellow energy.

After a session, patients who are particularly weak should not bathe for one full day. The energy which has been put into their bodies can thus be kept there by application of pale blue/white Chi at the end of the session.

Fig. 6.18 *Use Compassion, Love and Kindness.*

Summary of Individual Healing Session

A. Chi Knife
B. Energizing and Activating the Immune System
C. Cleansing with the Internal Organ Techniques

General Outline of Practices

1. Gain experience by working with one person. **Stand in front of them with your feet shoulder width apart.** Hold your hands at your heart in salutation. Transmit your love and compassion and ask for their permission to help them to help themselves heal.

2. Connect to the student's and your own cosmic star above your head and ask for universal permission. **Radiate your love and transfer three minds into one mind**. Lower your Upper Tan Tien. Activate your consciousness: Three minds become one mind. Expand your awareness in the mideyebrow and the crown. Feel the Tan Tien, heart, mideyebrow and crown spiraling. Expand to the universe.
3. Visualize the person's legs as being 'very long', extending down to the earth. **Activate the Sacred Fire** and bring it down. Clean out the room and make a big Chi field around you and the student.
4. **Call the Elemental Forces:** water, fire, thunder, lightning, rain, lake, earth, mountain, wind and Heavenly Chi. Call the guardian animals; Blue Tortoise from the north, Red Pheasant from the south, Green Dragon from the east, White Tiger from the west, Yellow Phoenix from above and Black Tortoise from below. Feel that you are protected by the Chi; gather the power of all the mountains, rivers, streams, stones and rocks into the room. Activate them with lightning, thunder and wind - filling the whole room with electrified Chi.

A. Chi Knife

1. Hold the knife in right hand (left, if you are left handed). Hold the other hand near your body with the thumb and index finger touching. Project the Chi Knife as big as the universe, 'long and big - reaching to Heaven'. The bones in your arm are hollow and the 'bottom' is sealed at the shoulder. Feel them 'fill and pack' with the power coming from above.
2. Then give the command: **"Power comes from the east. This Chi Knife has the power to dissolve all the negative energy, sickness and bad fortune. By my request, please carry out the order now."** Wait until you feel that your arm and the knife are heavy and full of Chi.

   Carry out energetic surgery, **cutting and slicing the affected area with cool yin energy**. When you feel that the Chi Knife is full of sick Chi, spiral counterclockwise and discard it down into the ground. When you feel that the knife is 'empty', charge it with Chi from the universe. Continue until you feel that the area has been cleansed.

B. Energizing and Activating the Immune System

In cases of severe illness, debilitation and infection, it is essential to stimulate the body's defence systems. You may also want do this in a preventative manner. Guide the student as you practice together. Presuming that you have already done the previous set of general healing, you can start with the coccyx.

1. Be aware of your Tan Tien and connect to the universe. Touch your **coccyx** with the fingers concentrating a beam of white or yellow light on to it. Picture the sacrum opening and the light streaming inside, flowing **up the spine** and streaming out over

the whole bone structure. Feel the Chi rising up to the universe, multiply it and guide it down to your energy body.

2. Be aware of the Tan Tien and the universe. Attract the yellow light; spiral and condense the healing light into the tips of your fingers; move the fingers up to touch the **sacrum**. Send out a beam of yellow Chi into the sacrum, directing it up the spine. This will stimulate the production of red blood cells. Transfer the feeling of 'Bone-Chi' up to universe and down to your energy body.
3. Proceed to the **crown**, showering it with violet light. Then spread from the crown throughout the bones of the body. Repeat several times. Instruct the student to feel the bone structure breathing. Ask him/her to extend up from their crown to the Big Dipper and North Star, channelling down the red and violet light into the thymus gland.
4. Continue to the **throat**, stroking down with your palms, using green color to move the lymph down towards the backside of the heart. (Never stroke up towards the head! Only guide the lymph down).
5. Proceed to the **lymph nodes under the armpits and across the sternum**. Next activate the lymph nodes in the **groin**. From the groin you guide the lymph up to the navel center (Not down where it will get stuck in the legs).
6. Return to the **navel center**. Send the energy deep inside, energizing the lymph nodes at the back. Pull back, drawing green energy, flushing out any waste products that are stuck in them.

Activate the points at the inside of the **elbows** and the **knees**.
Shower the whole body with healing light and energize the **perineum** with blue Chi.
Always remember to ground any sick energy by sending it deep into the ground.
Ask the student to do the same and it will be more effective. You should do this while giving the session as well as when closing it.

C. Cleansing the Internal Organs (Repeated from pages 132-133 and pages 136-137)

This session can be used for any kind of ailment and carried out with any number of students. **It is important to remember that if there is no energy in your Tan Tien, then there will be no energy to work with.** When you are aware of your Chi, you can direct heavenly light straight into your energy body and then into the student's.

General Cleansing Procedure

1. Push and pull the energy through the student's body. Push and disperse the sick energy into the universe and out to the planets, where it will be transformed and recycled.
2. Pull the energy back and stop it between yourself and the student.
3. Spiral the energy counterclockwise until you see the **green** light mix and clean the sick energy. Spiral and flush the energy down into the earth.

4. Spiral with blue light; see it mix and flush the energy within the student's body. Spiral this energy down to the ground.
5. Energize the student with **white** or **violet** light.
6. You can also use both hands to channel Chi when you 'push and pull' through the body.
7. **Spiral in** - spiral clockwise to bring energy into the body and energize it.
8. **Spiral out** - spiral counterclockwise to cleanse, flush and remove energy.
9. When you begin pushing, pulling and sweeping, you may feel resistance in the body. As you progress and the energy centers open, this feeling will diminish.
10. There are many color combinations that can be applied to the various parts of the body. When you start practice, stick to the basic 'blue, green, white, violet and blue' formula. When you are working on a specific area, you can keep this book near by, or write a short 'color recipe' before you begin. In this way, you will be able to relax your mind.
11. 'Pushing and pulling' is like fanning and venting the body; when you fan your hands in front of your face, it will have a cooling effect. Ventilation enables the stagnant, sick energy to leave the body.

    Below is a list of the body's organs in relation to their tendency to 'store heat'. They are listed in descending order, i.e, the head is the hottest.

    Head, heart, liver, lung, stomach and spleen, large intestine and small intestine, kidneys and sexual organs (which become hot when aroused).

Outline of Practice

The **solar plexus** is the clearing house for emotional energy and is situated in between the lower and higher energy centers and in the center of most of the internal organs. All the organs dump their negative emotions here. The internal organs can be cleansed by sweeping the solar plexus, energizing, cleaning and flushing it of sick energy. When you feel sick energy in the body, give the command: "Stay". This is very important; it makes sure that none of the cells hide from the dazzling light that you are sending in.

1. Scan; ask for the power to look at the cells.
2. Push, pull and give the command "Disperse". Push until you feel the solar plexus clear and open.
3. Spiral green Chi counterclockwise. Talk to the sick energy; tell it to "Leave", you will take it to "a better place, where it will be happy". Give the command "Out".
4. Spiral Blue Chi counterclockwise, flushing out any remaining sickness. Guide the sick energy into the earth.
5. Spiral and sweep Blue - Green and Red Chi into the solar plexus, sweep the organs. Do not use in cases where there is intestinal infection and internal bleeding (which can be worsened) or in the presence of pregnant women.

Cleansing the Spinal Cord

Always cleanse the spinal cord, which protects the entire body from diseased and negative energy, both physical and psychic. When you open the spinal cord and solar plexus you can release many energy blockages. Sweep the hand in a clockwise motion to energize the spine with either/or a combination of: blue, green, white and ultra-violet. Then spiral counterclockwise and brush the spine down to the ground. Continue sweeping until you feel that the spinal cord has cooled down. Remember not to use orange or red

Cleansing the Blood (Lungs)

The blood can be cleansed by energizing the lungs with whitish green, then with light whitish orange. The blood passing through the lungs will absorb the green and orange Chi, thereby cleansing the blood plasma and vessels and the rest of the body. This technique is very useful for treating ailments of the blood and of the arteries and for severe infections. Do not use it on pregnant women.

Outline of Practice

1. Scan the student.
2. Push through and open the lungs from the back to the front.
3. Energize the lungs from front to back with light whitish green, then with light whitish orange. Push through.
4. If the student is weak, energize the lungs with light whitish red, which will provide a strengthening effect.
5. The **spleen**, **liver and kidneys** purify the blood. Push and pull through the organs and energize with white Chi.
6. The blood requires a lot of cleaning on a regular basis.
7. Energize with white Chi. **Germs can only grow in the dark. 'Fill yourself with the light'.**

General Principles

Energy can be introduced to the affected area of the body by moving the hand clockwise in a spiral. **Flush** means to return the sick energy to the earth for recycling.

Stabilize means to return the area to normal functioning.

Spiral in a **clockwise** motion when you are '**stabilizing**'.

Use **blue or white** light to energize the area that you are working on.

Use **green** light to **energize** and **clean** the area that you are working on.

Use **blue** light to **flush** and **stabilize** the area that you are working on.

Use **violet** light to **balance** the sick energy and **reprogram** the cells of the body.

For **general infections** always **use green** (energize and clean) and **blue** (stabilize) light. Use violet light to balance the sick energy and reprogram all the cells. Use the 'Chi Knife' for infections as well. Never use orange on the head, heart and spleen.

Give the command **"Stay"** to make sure **all the cells receive the light** you are sending in. Remember that germs and bacteria cannot hide in the light.

Energize means to draw the Cosmic Chi into the part that requires healing.
Cleanse means to clean all the cells being treated.

You can also work on yourself. You may need some help when working on the back. If you obtain optimum health and practice the Cosmic Orbit regularly then you will never 'need' to apply any of these techniques to yourself.

Like all Chinese medicine, Cosmic Healing works on the system as a whole, balancing the entire organism, treating the cause to cure the symptoms.

The techniques really are simple.

When in doubt use; blue, green, white, violet, blue.
You can always use white and violet.
Upper organs - use violet.

You can practice group healings and then link your students' personal stars together, at an agreed time later in the day. **You can then perform the World Link Cosmic Healing**.

Work on any other ailments that the student may have.
The simplest way to learn is to begin practicing today.
The simplest way to heal is to allow yourself to be healed.

Chapter VII
Different Hand Techniques

Forget about your Palms

An extremely important theory of Cosmic Healing Hand Techniques is to ‘forget about your palm’. This means that you should only use the palm (which is incredibly sensitive), for ‘guiding’ the universal energy into the right spot, sending out a minute beam of light, like a laser, that marks the place where the energy should be sent. Your palm is connected to your brain, which has been sunk into your Tan Tien. The light marker will serve as a beacon for the force that is directed down by your mind. Draw down the Universal Chi, guide it to the right spot and give the command; "Stay". This is very important, otherwise the Chi will disappear once you move your hand.

When you practice Cosmic Healing it makes no difference how many people you treat, because you are not transferring your own energy.

Don't Focus your Mind on the Sick Part

If you direct your attention towards something, your energy will go there. If you focus on some ailment, you are already sending out your energy. Instead you should try to connect with a greater source, Universal Chi, extending your mind very far away. This way you won't lose your power. The only thing you do as a practitioner is to form the connection between nature, the student and the sick energy or between the universe, the Chi field and the sick part.

Cosmic Healing is Teaching

One of the best methods of protection for a practitioner is the Fusion practice (*Refer to ‘Fusion of the Five Elements I by Mantak Chia*). Perhaps even better is for the practitioner not to perceive him/herself as a healer, but as a person that comes to guide people in something they have to do themselves. When you say; "I am a healer", the sickness or bad energy, has already found a new home. When you check it out, first it will try to hide, and then it will try to attach itself to you. But if you don't interfere, the energy will go straight to the ground. So it is very important to clarify that you are not a healer, but a practitioner that can help, and that the student or sick person has to do most of the job.

Fig. 7.1 *The Stronger your Awareness of your Inner Body, the Easier it will be for others present to pick up this Sense.*

If you guide those present, this will greatly enhance your healing session. Sit or stand facing your student. Any time you want him or her to focus on a particular point of the body, ask them to touch it with their hands. For example, "Now place your hands on your navel", while you do the same thing yourself. As soon as you feel the Chi there, you instruct them to focus on the navel themselves. This way you are actually helping them to deepen their bodily awareness. The stronger your own awareness of your inner body, the easier it will be for the others present to pick it up. This means that if you are treating some part of another person's body, or if you see that the person is not aware of any energy in some part of the body, you can help by focusing your awareness on this particular part of your own body.

Chi Kung Diagnosis: Hand Scanning

Hand scanning is a simple and effective diagnostic tool of External Chi Healing. It involves passing your palm over the body of your student from one inch to one foot above the surface of the skin and being aware of the energetic state of the various bodily areas. What one senses is described as the electromagnetic field, the aura or the energy body.

General Variations in the Energy Field

The variations you may sense with scanning that have diagnostic significance are:

Temperature

Heat generally indicates excess, while cold indicates deficiency. However, some areas of the body are naturally warmer or colder than others. This is described below under "Hand Scanning the Internal Organs."

Thickness

A feeling of thickness over the area would indicate excess, while thinness may indicate deficiency.

Wind

You may feel sensations of wind leaving the body at various places. This may indicate internal wind at a given location, or it may point to an area of the body that is "leaking energy" and needs to be ‘patched’ or ‘sealed’. It may also be a positive sign that you are driving wind out of the body.

Peaks and Valleys

Peaks in the energy field will feel like mountains or hills in the aural landscape. They may actually push your hand away. Valleys feel like depressions or energy vortexes drawing you in. They may also feel empty, like a hole or pit. Peaks indicate excess or stagnation, while valleys indicate deficiency.

Tingling

Accumulations of sick Chi may cause your hand to tingle, feel prickly, throb, or even hurt. These are excesses of energy and upon inquiry, the student may complain of pain in this area.

Hand Scanning the Internal Organs

Each Organ Emits a Different Aura

Each organ emits a different kind of force or aura through the skin. By passing a hand one or two inches above the skin, you can feel different sensations that reflect the condition or state of the internal organs. You need to develop the sensitivity to receive and identify the vibration or frequency of each organ. Practicing the Cosmic Chi Kung Meditations will help develop such sensitivity.

Liver and Gall Bladder Scanning

Healthy liver and gall bladder energy feels warm.

Negative Emotions: When you pass your hand over the liver, under the right side of the rib cage, you will feel a charged energy come up to your hand. This is a sign of anger in the liver.

Overactivity: When you pass your hand over the liver and feel a rush of hot energy, this indicates that the liver is overheating because of toxins or emotional stress.

Underactivity: When you pass your hand over the liver and you feel a dense and hot energy, the liver is weak, congested and sick.

Lungs Scanning

Healthy lung energy feels cool and dry.

Negative Emotions: Pass your hand over the lungs. Do the Lungs' Sound and listen to the echo of the sound as it rebounds from the lungs. Sadness will feel like a deflating ball pressed between your hands.

Overactivity: Energy that feels dry and hot indicates an overworked organ.

Underactivity: Energy that feels damp and cool under the scanning hand indicates underactive or congested lungs that can lead to respiratory problems.

Heart Scanning

Healthy heart energy feels warm and energetic.

Negative Emotions: Hot and charged energy indicates impatience, hastiness and arrogance in the heart.

Overactivity: If your hand detects hot, charged and overly expansive energy, this indicates that the heart and blood may be overheating.

Underactivity: Energy that feels cool and less expansive indicates an underactive or congested heart.

Spleen Scanning

Healthy spleen energy feels lukewarm.

Negative emotions: Energy that feel damp and sinking indicates excessive worry.

Overactivity: The energy feels hot and damp when the spleen is overactive.

Underactivity: The energy feels cool and damp.

Kidneys Scanning

Healthy kidney energy feels cold, but not too cold.

Negative emotions: Energy that feels cold and chilly indicates fear.

Overactivity: When the kidneys are overworked or overstimulated by excessive exercise or improper diet and liquid intake, the energy can feel damp, stick and hot.

Underactivity: When toxins are blocking the organs, the energy can feel damp and cold.

Hand scanning is an art, and may take a while for you to feel confident using it. Practicing Cosmic Chi Kung is one of the best ways to develop greater sensitivity in hand scanning.

Chapter VIII
Cosmic Chi Kung
Palm and Finger Training

Why We Practice the Cosmic Chi Kung

The Cosmic Chi Kung is also known as Buddha Palm. The reason we train with the Empty Force practice in connection with the Cosmic Healing is to learn how to project Chi through the space in the cosmos, the space between your hands and to project Chi through the space to your students. Usually when we touch the student we pick up sick energy. This practice will teach you how to ground the sick energy to the earth and to disperse it into the Universe to be decomposed and recycled by the planets.

Practice until you can project Chi out from your palms and fingers and when you feel the Chi coming into your body through your hands. The most important part is to always remain connected with the Universal Force coming from all six directions. If you focus on healing from your hands or your Tan Tien you will use up your own energy. You must be connected to the Cosmic Universal Force.

Expand your awareness to nature, the oceans, the lakes, the forests and mountains. Smile to nature and feel it smile back to you; inhale and draw the Chi into your palms. Expand your awareness to connect to the light, the Milky Way and the cosmos.

Be aware of the heart and the red light in the heart; expand your awareness to infinity. The light will come close to you; picture the red planet Mars above you. See it shine down to your crown, feeling the light in your palms. Be aware of the six directions, feel your body growing bigger; until you touch the sky, your feet still planted in the earth.

Opening Heaven and Earth Force in the Palms with Heaven and Earth Spirals

The purpose of this technique is to draw in the forces of heaven and earth through the palm. Activate the spirals, the symbol for the heaven and earth force in the center of the palm.

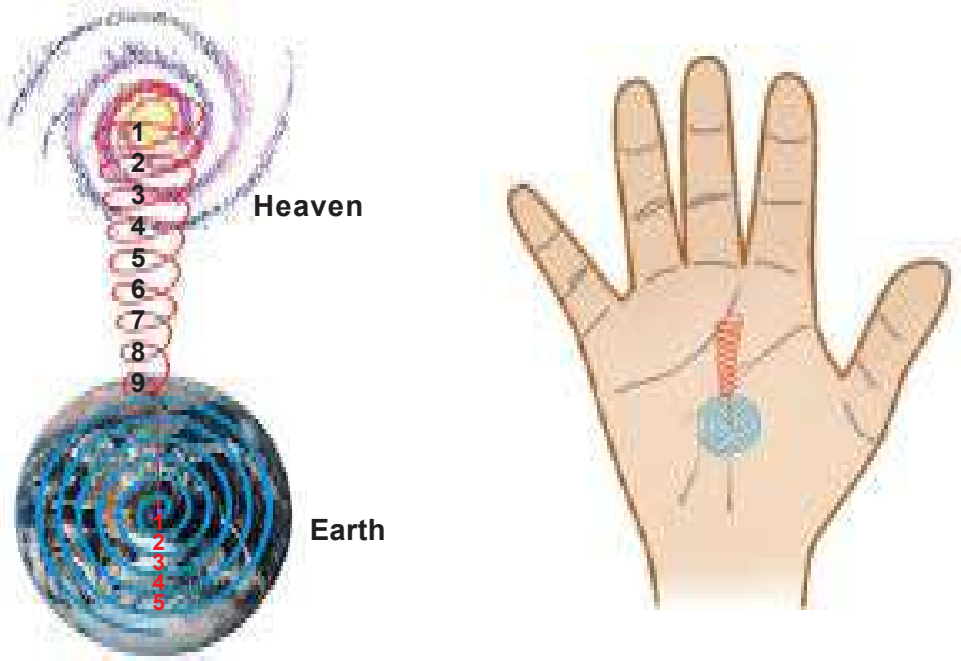

Fig. 8.1 *Enhances the symbol of Heaven and Earth Force, in the Laogong - Pericardium 8.*

This is accomplished by drawing these spirals with the palm itself. As you draw the spirals, you should actually feel the palm breathing, inhaling these forces in. In the beginning, however, you may only be able to use your own mental imagery and imagine that you are absorbing these forces. In time the feelings will replace your imagination.

You breathe in Heavenly Chi when you draw the heaven spirals, and breathe in Earthly Chi when drawing the earth spirals. You may draw in both in one session; you may also choose just to draw in either Heaven or Earth Chi if you feel you need more of one or the other. It is important to balance these energies whenever you do this exercise.

1. Begin by raising the right hand to about shoulder height with the elbow sunk and the palm facing forward. Slightly pull back (open) the index finger, and slightly stretch the thumb forward and down. This will activate the Laogong point on the palm.

At the same time, touch the tips of your left thumb and index fingers together. This will allow the right hand to draw in the Heaven and Earth Chi. The left hand will then be held palm up to draw in the heavenly force, or held palm down to draw in the earthly force.

2. Begin **drawing the heaven spiral** by moving the **palm in a clockwise motion**, with the circles getting smaller and smaller, spiraling inward. At the same time, your left hand is held at your side, palm up with thumb and index tips touching each other. Draw seven or nine (planets of our solar system) small spirals with your right hand in this way, drawing in the violet heavenly energy.
3. Next, lower your right hand slightly and turn your left palm down to face the earth. Then begin **drawing the earth spiral** by moving the right palm in a **counterclockwise motion** with the circles getting larger and larger. Draw five spirals (five elements), drawing in the blue earth energy as you move. Inhale into the palm, feeling the energies.
4. You may now bring both hands down to the beginning position of Cosmic Chi Kung, or you may open the Cosmic Channel to the planets for healing. This is discussed in the next section, Part I, 'Opening to Heaven, Earth and Cosmic Chi'.

Cell Breathing

By understanding the operations of our cells, we establish a foundation for our experience of Cosmic Chi Kung. Each cell is a living, breathing entity, absorbing energy with each inhalation and releasing toxins with each exhalation. Thus with every breath, we are creating more Chi.

We are made up of over one hundred trillion cells (one trillion is one thousand billion). Each one of these cells is constantly breathing. In order for our cells to function optimally, we must follow nature's teachings.

Fig. 8.2 *Each Cell is a Living, Breathing Entity.*

The first thing is to keep your cells free of toxins. Eat nutritional foods. This helps the Chi to flow smoothly through your energy channels and aids greater assimilation of vitamins and minerals. Learn and apply Five Element nutrition principles, eating according to the seasons and to your own constitution.

The second thing is to keep your cells free of excess emotions. Develop the skill of acting positively to situations, rather than reacting, especially negatively. Don't allow anyone to make you sad and unhealthy. Some people like to say, "You make me angry," or "You made me worry." We cannot allow other people to make us so emotional. We do not need to accept the negative emotions that other people try to dump on us. Cellular and psychic boundaries are related. Negative emotions disturb the cells' ability to absorb Chi and to generate the energy necessary for healing. We need all the Chi that we can get. Learn and apply the Six Healing Sounds, the Cosmic Inner Smile and the Fusion of the Five Elements meditation to transform negative emotions into personal power.

Third, create more energy by cultivating a happy attitude, so that your cells can regenerate more easily. **Smiling and loving** are the two quickest ways to make more Chi. In order to have an ample supply of Chi, develop an attitude of **joy and love** in yourself and towards others.

Mind, Eyes, Heart and Intention (YI)

The opening of the mind, eyes, heart and use of intention is vital for further activating and increasing your Chi. In the Tao we achieve this by cultivating our "Yi" (pronounced "yee"). "Yi" means mind power, intention, awareness and concentration. The Yi leads and guides the Chi. With our mind we control thought patterns. With our eyes we control the senses of sight, hearing, smell and taste. With our heart we control all our organs and their related emotions: the kindness/anger of the liver, the joy/impatience of the heart, the openness/worry of the spleen, the courage/sadness of the lungs and the gentleness/fear of the kidneys.

Fig. 8.3 *'Yi' leads and guides the Chi.*

Every excellent achievement in our lives depends upon the quality and efficient operation of our Yi. Combining the awareness of the mind, eyes, heart and intention into one, causes the creation of a rich and rare alchemical mixture. The power of the Yi is the magical catalyst that assures energetic results.

The basic teachings are all in the Microcosmic Orbit, the Cosmic Inner Smile and the Six Healing Sounds. As long as you are alive and healthy, you are able to draw in energy from the universe and nature. The stronger the battery, the better it is able to store this energy. If you're weak and sick, you have no way to draw any energy from nature or the universe. When the cells stop drawing in energy, life ends. If you have perfected these practices, you have all the personal physical, mental and spiritual power that you need. Everything comes together. Your mind is aware of the original force. From the knowledge of Oneness, you are inwardly aware of your mind, senses and heart; you are outwardly aware of the universal energy. Now you are capable of receiving the abundantly available healing power of the universe; you can tune into everything, inwardly and outwardly in all directions. This is what we are here for: to heal and become whole again. We have higher goals to reach. The foundation for reaching our goals is a strong and healthy body.

Cosmic Healing Chi Kung is merely an extension of the universe within yourself. You draw the universe in through your palms, skin, heart and crown. With your Yi you breathe in the cosmos through these various open cavities of receptivity in your body, absorb its power, condense it, transform it and use it for the benefit of all.

Connecting the Bridge

Contracting the muscles of the perineum, sexual organs and anus activates our connection with the earth energy. By pulling up these areas and drawing in energy through the soles of the feet, we immediately become grounded and bring the earth (yin) energy into the Microcosmic Orbit. Pulling up should be done gently and directed by the Yi.

When we speak of "Connecting the Bridge," we are referring to the above exercise, except that we do not pull up on the perineum. Pull up gently and lightly on the sex organs and anus while leaving the perineum totally relaxed. After performing the first contractions, when you then relax the perineum, the earth energy will continue to flow into the body using the principles of a siphon. We thus connect the "Bridge" across the perineum from the sexual organs to the anus using the Yi to direct the energy. This actively combines the earth energy and your sexual energy and directs it into the Microcosmic Orbit. This energy is circulated during Cosmic Chi Kung. Holding a very gentle contraction will keep you grounded during the exercise. It can be done sitting or standing.

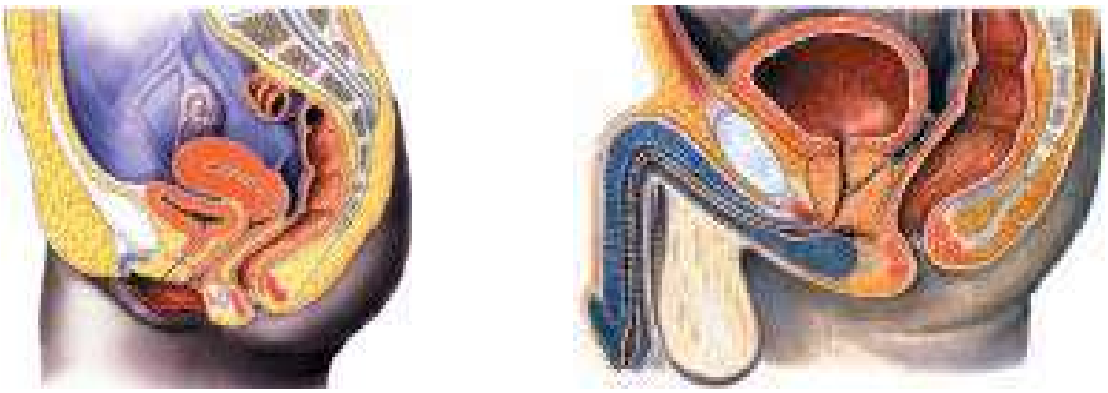

Women lightly contract the Vagina *Men lightly contract the Perineum and Anus*

***Fig. 8.4** Connect the Bridge - combine Earth and Heavenly Energy.*

Cosmic Chi Kung Preparation

Cosmic Chi Kung can be practiced either in a sitting or a standing position.
Sitting, relax as much as possible and invoke the **Cosmic Inner Smile**.

1. Be aware of your **heart** and listen to your **kidneys** with your inner senses. Smile to your heart and kidneys and feel them pulsing; feel them communicating and interacting with each other. The **Kan** and **Li**; the water of the kidneys and the fire of the heart, balance and **begin to mix**.
2. Open the arm pits as if you were holding a ping pong ball there and slightly move the fingers to activate the Chi flow. Relax. **Feel** the sensations of the **Chi flow**: tingling, warmth, pulsing, electric and magnetic feelings.
3. Be aware of your palms. Draw in Chi by **activating the bone breathing** process. Become aware of the perineum; slightly pull up the perineum, sexual organs and anus and "**connect the bridge**." (Remember to relax the perineum).
4. Breathe into the palms of the hands and soles of the feet, further enhancing your connection to the earth force. Smile to the blue earth energy as it flows up your arms and legs and suffuses your body with pleasant Yin energy.
5. Breathe into the **mideyebrow** point and activate your connection with the **Cosmic Force**. Smile to the golden light of the cosmic energy as it swirls into your mideyebrow point and flows throughout your body, healing and balancing your energy.
6. Breathe into your **crown** point and activate your connection with the **Heavenly Force.** Smile to the red and violet light of the heavenly force as it flows into your brain and washes your body with subtle pure Yang energy.

Fig. 8.6 *Invoke the Cosmic Inner Smile.*

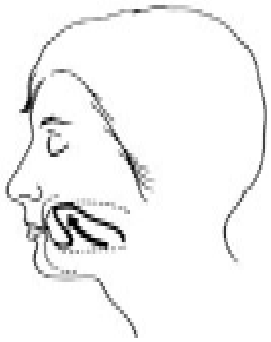

Fig. 8.5
Place the Tip of the Tongue on the Upper Palate.

7. Place the tip of your tongue on the upper palate behind the teeth in a comfortable position.

8. As you begin to move through the postures of Cosmic Chi Kung, always be aware of the Chi flow and its attending sensations.

Cosmic Chi Kung Preparation Standing

1. Stand with your **feet parallel** and shoulder width apart.
   Tilt your **sacrum** and **pelvis** slightly forward until you feel your feet press more firmly into the ground. As you tilt the pelvis, feel your lumbar vertebrae pressing outward; this is called "**Opening the Door of Life**."
2. Relax your **chest** and sink your **sternum**. Draw your chin in slightly, and hold your **head, neck** and **spine** erect as if your head and spine were suspended from above by a string.
3. Follow the same instructions for the preparations of Cosmic Chi Kung.

Opening to Heaven, Earth and Nature

The natural world is the source of our power. Cosmic Chi Kung teaches us about nature and its energies. In the Tao, nature and the universe are equivalent to God. You are a part of nature and can easily learn to open to the forces in the macrocosm and let them flow through you. This is very simple. Just tune into the frequencies around you. Your fingers are antennae, which transmit and receive.

1. To begin your practice of Cosmic Chi Kung, simply **stand** up and **feel the energy around you**. When you stand or sit, be aware of your soles (Bubbling Spring points) making a good connection with the earth. Your perineum (Hui Yin point) is relaxed and open. You are connecting to the earth force and can expand further down on to the other side of the universe. This is one type of energy.
2. When you draw your **chin in**, slightly **relax your chest** and tilt your head slightly forward; you begin to be aware of the heavenly force. This is another type of energy.
3. The qualities of the **Five Elements** reveal themselves as woody trees (growing force), fiery deserts (expanding force), earth mountains (stabilizing force), metal air (contracting force) and watery oceans and lakes (gathering force). We call the combination of these elements the '**Cosmic Force**'.

Thus, your mind and body learn to gather, absorb, direct and transform the heaven, earth and cosmic energy for your own use. This is the essence of Chi Kung. Today there is a lot of emphasis on learning movements and forms of Chi Kung. However, if the inner feeling is not there, the movements are of little value.

Heavenly force is Yang. Earth force is Yin. By learning to connect to the energies of heaven and earth, you have a powerful tool for restoring and maintaining your inner balance of Yin and Yang.

Outline of Practice

Before practicing each of the Cosmic Chi Kung sets in this chapter and in the following chapters begin with the heaven and earth spirals as outlined on page 157.

First **Create the Chi Field**.

Hold each of the Cosmic Chi Kung postures for at least 5 - 30 seconds, gradually lengthening the time to 60 - 120 seconds per posture.

Note: While holding the postures count the breath from 5 to 15 seconds, being aware of the **Tan Tien** and feeling the Chi in the Tan Tien which then moves up to the **crown** and expands up to the universe; fuse your Chi with the Universal Chi and let it multiply down to your palms. **Just concentrate on the 'Tan Tien and the Universe'**; do not concentrate on the palms at all.

Throughout parts I, II, III and IV 'Tan Tien and Universe' means to spiral into the Tan Tien and spiral out into the universe connecting 'Tan Tien and Universe'.

Part I
Opening to Heaven, Earth and Cosmic Chi

Opening Movements

Three Minds into One Mind

Empty the mind and heart down to the Tan Tien.
Hold the hands together at the heart center.
Smile and make the heart feel soft; feel love, joy and happiness.
Turn your consciousness inward and your awareness out.

Fig. 8.7 *Empty your Mind and Heart down to your Lower Tan Tien.*

Feel your legs lengthen extending down to the center of the earth.
Feel your hands lengthen extending to the universe below.
Let the mind expand and be aware all the way down to the universe.
Feel the 'long' bones of the arms and legs and begin bone breathing.
Feel universal Chi filling, packing and compressing into the bones.
Draw this Chi down to the back of your crown and feel a heavy pressure press on the crown; feel slightly numb or a light electric downward flow, like oil dripping down. 'Focus at Tan Tien and Universe'. Count to five.

Channeling the Earth Force - Washing the Bone Marrow

Smile into the **perineum, palms** and **crown**. Then slowly raise the arms, palms facing each other, to chest height keeping the elbows relaxed and sunk. Rotate the arms slowly until the palms are facing down. Be aware of the mideyebrow and feel your breath and lightly contract your eyes and round muscles around the eyes. Connect the perineum bridge by slightly squeezing the sex organs and the anus; do this a few times.

Rest and **smile to soles of the feet**, feel the Chi bubbling and feel like you are standing on a hot spring starting to bubble up.

Be aware of your Tan Tien and expand your mind down past the earth to connect with the galaxy below you. Multiply and bring your mind back to the Tan Tien. Gradually feel the Chi being absorbed through the whole body and absorb it into the bones and body like a **rising steam or mist**. Feel the earth force move through the center of the bones and enter the bone marrow move up the calves and thighs (femur bones) through the hip bones, spine, **scapula**, **arms**, **neck** and **skull**. Finally **swirl the energy around your brain. 'Focus at Tan Tien and Universe'**.

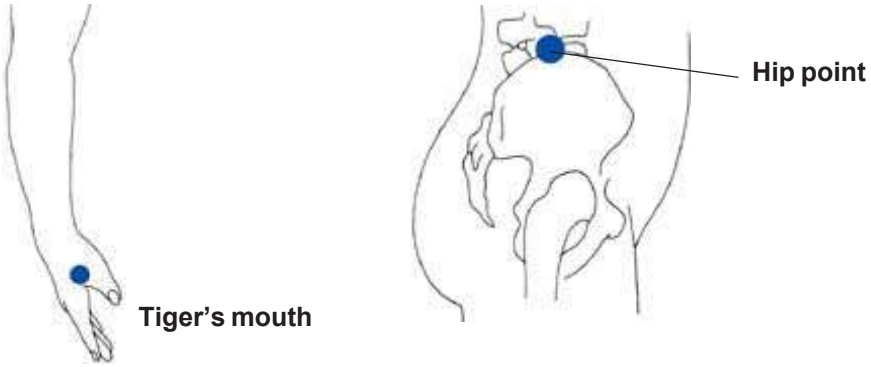

Fig 8.8 *Activate the Hip: Large Intestine 4, Pericardium 8 and Small Intestine 3.*

Raise your index finger slightly upward to activate the Hegu Point (Large Intestine).

Tiger's Mouth

Fig. 8.9 *Open the 'Tiger's Mouth'.*

Then **stretch your thumbs out to the sides and down**, so that they end up pointing downwards toward the earth. This activates Large Intestine 4 (Hegu). Large Intestine 4 is found in the webbing between the thumb and index finger. It is called the "eye of the hand"; this area is also known as the "Tiger's Mouth."

Slowly draw the elbows back and lower the hands until your palms are facing down beside the "eye of the hip" (the iliac crest) with the "eye of the hand" (Large Intestine 4) aligned with the "eye of the hip. "Be aware of the Tan Tien (Yi, the abdominal brain) and expand your mind out into space, the Cosmos and the universe. Remember: The fingers and the energy point act just like a laser to help guide the universal force flow; as soon as you focus on the fingers or the palms you are starting to use your own energy. Feel your Tan Tien and the crown full with Chi. Just use your second mind intention, lightly aware of the area between the hips and LI-4 points. Focus at Tan Tien and the universe. This will activate the lungs and large intestines. **Hold for a 30 second count** and gradually you will feel the ascending colon and the sigmoid colon have been activated; you may feel some movement around this area.

Fig. 8.10 *Activate the Organ Energy.*

Use your Yi to rotate your hands so that the fingers first point out, then back, turn the palms up and finally point the middle finger in toward the eye of the hip. Tan Tien and the universe - **95 % aware of the 'Tan Tien and the Universe' and 5 % aware of energy flowing back and forth between the tips of the middle fingers** (Pericardium 9); feel the Chi passing through the hips. This will activate the pericardium.

Rotate the hands again until the fingers are pointing forward with the **palms facing up**. Align the knife edges (Small Intestine 3) with the eyes of the hip. 'Focus at Tan Tien and the Universe'. Be lightly aware of the energy passing back and forth between the two hands. This will activate the heart and small intestine.

Fig. 8.11 *Activate the Heart and Small Intestine.*

Absorb the Heavenly Force Washing the Bone Marrow - Crown to Soles

Extend the arms forward to chest height with the palms facing upward.

Laogong Point (Pericardium 8)

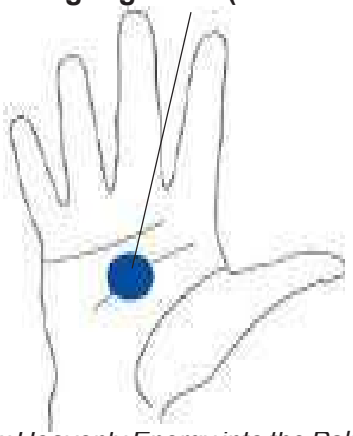

Fig. 8.12 *Draw Heavenly Energy into the Palms.*

Become aware of the **Tan Tien, the Crown and the Star above you**. Expand your mind (YI) out to the universe and connect to the galaxy. Be aware of the palms and the crown which are connected to the galaxy. Activate the Laogong point (Pericardium 8).

Feel the heavenly energy come directly to your palms, and be aware of the violet light of the North Star and the red light of the Big Dipper both shining radiantly.

Fig. 8.13 *Hold the Big Dipper.*

Picture yourself holding the handle of the Big Dipper and turn the 'cup' pouring the light over your head. Draw this light in through the palms and the crown point and feel it washing your bone marrow. Always remember your Tan Tien. **Direct the sensations down through the skull, cervical vertebrae, clavicle, scapulas and sternum. Activate your thymus gland and continue drawing the healing heavenly light down through the rib cage, arms, spine, hips, femurs and calf bones, feet and toe bones. Be aware of the soles bubbling up to the perineum and up to the crown**.

Lightly rock yourself like riding a horse; this will help keep your spine open and Chi can flow easily throughout the practice.

Absorb the Earth Force and the Other Side of the Galaxy

Rotate the arms until the **hands are palms down**.

Raise the index fingers slightly and extend the thumbs first towards each other and then toward the ground. Be 95% aware of the Tan Tien and the Universe, and 5 % aware of the index fingers and the big toes. Wait until you feel the Chi enter. Fill the joints of the fingers and up to the wrists; feel 'tense but not tense' and let the **Chi continue to fill the joints** up to the elbows, up to the shoulders and gradually up to the neck and the head. Go from the toes up the legs to the hips and on into the spine and the rib cage **completing all the joints of the body**.

Be aware of the Tan Tien and the universe and only slightly aware of the palms (Laogong), the soles of the feet (Kidney 1-Bubbling Spring), and the perineum (Conception Vessel 1-Hui Yin) bubbling. Activate these points, feel the earth energy and continue smiling through the earth to connect with the galaxy, Milky Way, and the universe. Draw this light in through the palms and soles and let it wash up through the center of your bones from the feet up. Let it **steam and cleanse your marrow**. Picture any impurities or illness dripping out of your bones and draining down into the earth, where they will be recycled and purified.

Fig. 8.14 *Open the index fingers.*

Core Movements of Part I

Grasping the Moon

Connecting the Heaven and Earth Forces - Right Side over Left

Open Position: Heaven Force - Slightly raise the index fingers to open the palms. Bring the arms up , bending the elbows so that the left hand is under the right elbow with the left index finger pointing up to Heart 3.

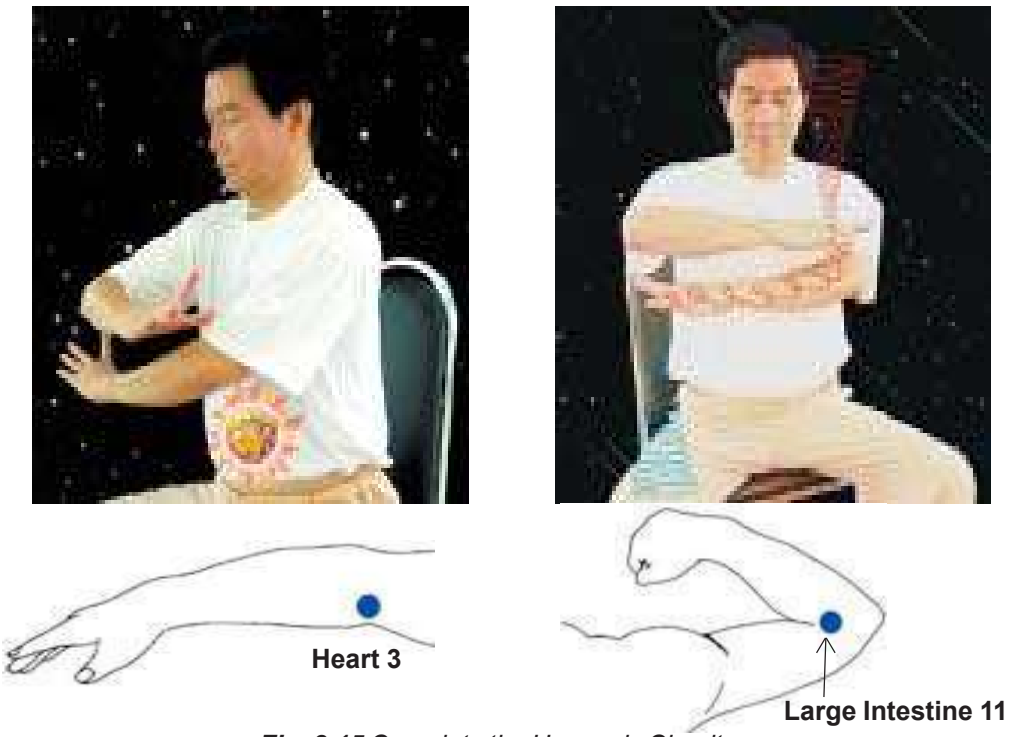

Fig. 8.15 *Complete the Heavenly Circuit.*

The right index finger is pointing up toward heaven and connecting to the galaxy. The right forearm is over the left forearm, with the tip of the right index finger held above the Large Intestine 11 point of the left arm.

The **right index finger draws in the heavenly force** like antennae. The force flows up the bones of the right arm, across the shoulders to the left arm and through the bones of the left arm to the left index fingertip. It **then flows through the index finger of the left hand** into the Heart 3 point of the right arm, **completing the heavenly circuit**. Continue cycling in this way. Hold the position and count to five.

The practice uses the 'Empty Force'; this means that there is no contact. The fingers must be 'tense without tensing'. When you tense and raise the index finger, you will feel the Laogong point opening.

Close Position: Tan Tien, earth and the universal force - keeping the arms in the same position, move both index fingers to point down. The **right index finger will now point toward the Large Intestine 11 point of the left arm and the left index finger will point downward toward the earth** and continue down to connect to the universe. Draw in the earth force through the left index finger, bringing it through the bones of the left arm, across the shoulders through the right arm to the right index finger and out into the Large Intestine 11 point of the left arm. Continue cycling in this way, **completing the earth circuit**.

Open and close three times altogether ending in the open position. Hold each count for five seconds.

Holding and Activating the Chi Ball
Tan Tien and the Original Force - Right Side over Left

Turn the **left palm upward** and lower it to the Tan Tien with the pinky pointing inwards.

Lower the right palm to the navel, palm down, as though you were holding a small Chi ball. Lower the right thumb to point toward the left Laogong point. This opens the eye of the right hand (LI-4), then point it toward the navel. Be aware of Tan Tien and universe.

Fig. 8.16 *Right Side over Left - 'Holding the Ball'.*

Yin/Yang Palms

Separate the hands and extend them out in front of the body at navel level. The **left palm** is still pointing up, and is **Yang** drawing in the heavenly force through Laogong. The **right palm** is still facing down, and is **Yin** drawing in the earth and the galactic force from below.

Conclude by turning the left palm over to face downward. **Draw in the earth force through both palms.**

Fig. 8.17 *'Yin and Yang Palms' - Right Hand connecting to Earth and Left to Heaven.*

Left Side: **Repeat on the left hand side with the left arm over the right**. Holding the Chi ball the left hand is on top. Hold for a count of five seconds.

Fig. 8.18 *Open the Heavenly Circuit. Then the bottom hand slides and turns 'Palm-Up' and the Top Arm slides to 'hold the Chi Ball'*

Fig. 8.19 *Holding the Chi Ball - Left Side over Right.*

Closing Movements

Activate the Chi Channels - Balance the Organs

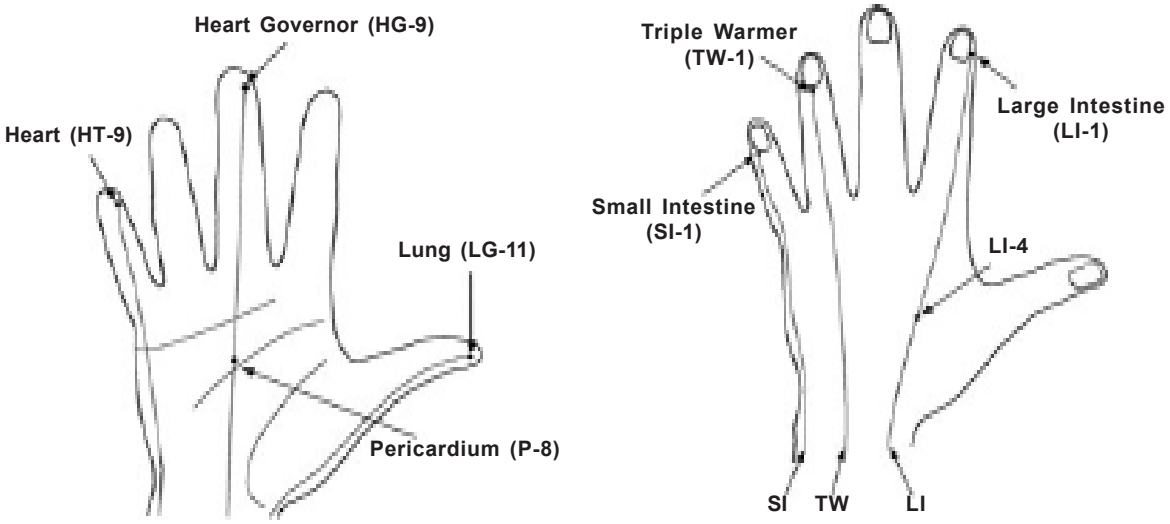

Fig. 8.20 *Finger Points*

The closing movements balance organ energy while activating the Chi Channels.

Hold the arms extended forward with the palms down at solar plexus level. Hold each stage for a count of five seconds.

Index Fingers:

Tense all the fingers and feel the Chi filling all the joints; open the index fingers, raising them up, while keeping the rest of the fingers level.

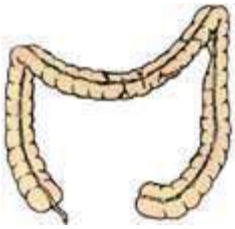

Large Intestine

Fig. 8.21 *Activate the Index Fingers - Up.*

The tension should be like the string of a tuned musical instrument. When lightly tense the Heavenly Chi will be drawn in through the index fingers.

Relax the hands and bring the index fingers back to the neutral position, level with the other fingers.

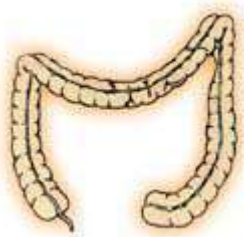

Energy to Large Intestine

Fig. 8.22 *Draw Earth Energy through the Index Fingers - Down.*

Stretch out and tense all the fingers and **press the index fingers to point down** toward the earth and continue down to the universe. Keep the other fingers level. **Draw in earth energy through the index fingers and circulate it through the body.**

Bring the index fingers back to neutral and relax your hands.

Once again **open the index fingers by raising the index fingers up**, while keeping the rest of the fingers level. **Draw in the Heavenly Chi through the index fingers**.

Bring the index fingers back to neutral again and relax your hands.

Ring Fingers:

Stretch the ring fingers down toward the earth, keeping the rest of the fingers level. Draw in earth energy through the ring fingers and circulate it through the body.

Fig. 8.23 *Draw Earth Energy through the Ring Fingers.*

Bring the ring fingers back to neutral and relax your hands.

Once again open the index fingers by raising the index fingers up, while keeping the rest of the fingers level, and draw in the Heavenly Chi through the index fingers.

Bring the index fingers back to neutral again and relax your hands.

Thumbs:

Stretch the thumbs out and down toward the earth, keeping the rest of the fingers level. Draw in earth energy through the thumbs and circulate it through the body.

Bring the thumbs back to neutral and relax your hands.

Fig. 8.24 *Draw Earth Energy through the Thumbs.*

Once again open the index fingers by raising the index fingers up, while keeping the rest of the fingers level, and draw in the Heavenly Chi through the index fingers.

Bring the index fingers back to neutral again and relax your hands.

Pinky Fingers:

Stretch the pinky fingers out and down toward the earth, keeping the rest of the fingers level. Draw in earth energy through the pinky fingers and circulate it through the body.

Small Intestine

Fig. 8.25 *Draw Earth Energy through the Pinky Fingers.*

Bring the pinky fingers back to neutral and relax your hands.

Once again open the index fingers by raising the index fingers up, while keeping the rest of the fingers level. Draw in the Heavenly Chi through the index fingers. Bring the index fingers back to neutral again and relax your hands.

Middle Fingers:

Stretch the middle fingers out and down toward the earth, keeping the rest of the fingers level. Draw in earth energy through the middle fingers and circulate it through the body.

Bring the middle fingers back to neutral and relax your hands.

Once again open the index fingers by raising the index fingers up, while keeping the rest of the fingers level. Draw in the Heavenly Chi through the index fingers.

Bring the index fingers back to neutral again and relax your hands.

Heart

Fig. 8.26 *Draw Earth Energy through the Middle Fingers.*

Crane's Beak and Swallow the Saliva:

Form the "Crane's Beak" with both hands by bringing all the fingertips together with the thumbs inside. **Inhale** and **contract the sexual organs**.

Move your tongue and suck the mouth to **activate the saliva**. Divide it into three parts, tighten the neck and gulp down the **first part** to the center of the **navel**; force the **second** mouthful of nectar down to the **left side of the navel** and the **third** to the **right side of the navel**. Raise the forearms up to shoulder height with the fingers pointing down. Slowly open the palms and begin to lower the arms to the sides, until the palms are facing each other before the starting position.

Fig. 8.27 *Form the 'Crane's Beak'.*

Fig. 8.28 *Raise Forearms to Shoulders.*

Fig. 8.29 *Lower Arms to the Sides.*

Fig. 8.30
Palms facing each other to cover the Navel.

Conclusion:

Bring awareness to the navel. Notice the quality and intensity of the energy generated and **collect your energy at the navel**. Men place hands over the navel with the right hand on top; women vice versa. Rest.

Summary:

Practice Part I daily for one or two weeks until you can do it well. Then you can proceed to learning Part II.

Part II
Opening the Bridge and Regulator Channels

Theory

Chi flows through your body along numerous channels or meridians. The channels are divided into two major groups: the **extraordinary** or special channels and the **ordinary** channels. After your mother's egg and your father's sperm joined together to form a single cell, that cell began to divide. The extraordinary channels were the first energy channels formed as a result of that early cell division.

There are **Eight Extraordinary Channels:**

Governor Channel
Functional or Conception Channel
Thrusting Channel
Belt Channel
Yang Regulator Channel
Yin Regulator Channel
Yang Bridge Channel
Yin Bridge Channel

Later, as your fetus developed, your Original Chi flowed through the eight extraordinary channels to help create your internal organs and their energy channels. These twelve "ordinary channels" are divided into yin and yang. The yin Channels are connected to the solid organs, and the yang channels are connected to the hollow organs.

The **Twelve Ordinary Channels:**

Lung (Yin) Channel
Large Intestine (Yang) Channel
Stomach (Yang) Channel
Spleen (Yin) Channel
Heart (Yin) Channel
Small Intestine (Yang) Channel
Bladder (Yang) Channel
Kidneys (Yin) Channel
Pericardium (Yin) Channel
Triple Warmer (Yang) Channel
Gall Bladder (Yang) Channel
Liver (Yin) Channel

These twelve organs serve to extract energy from the food and water we ingest and the air that we breathe to create energy through the metabolic processes of respiration, circulation, digestion, elimination and reproduction. This energy is called PostNatal Chi, as it comes in after we are born. Thus the extraordinary channels serve as the link between our Original or Prenatal Chi which came from our mother and father, and our Postnatal Chi which comes from our food and air as a result of metabolism.

General Functions of the Eight Extraordinary Channels

They serve as reservoirs of Chi.

About two thousand years ago, one of the great texts of Chinese medicine, the Nan Ching was written. This classical text describes the twelve ordinary channels as rivers and the eight extraordinary channels as reservoirs of Chi. When the ordinary channels become low in energy, they can draw from the reservoirs of energy in the extraordinary channels. On the other hand, if the ordinary channels become too full, the excess can be taken up by the extraordinary channels. In this way the extraordinary channels help us to maintain a balance in our energy body.

They store and circulate Ching Chi.

The extraordinary channels all draw their energy from the kidneys, which are the storehouse of Ching Chi (essence or sexual energy) in the body. Thus the extraordinary channels circulate the Ching Chi around the body, particularly to the skin and hair, and to the five ancestral organs: the brain and spinal cord, the bone marrow, the blood, the uterus and the liver and gall bladder.

They circulate Defensive Chi to protect the body.

The Chi that protects the body against invasion by external pathogens is called Defensive Chi or Wei Chi. The extraordinary channels circulate Defensive Chi over the back, abdomen and thorax. These functions are performed by the Governor Channel, the Functional Channel and the Thrusting Channels, respectively.

They regulate our life cycles.

In the first chapter of the Yellow Emperor's Classic of Internal Medicine (Huang Di Nei Ching Su Wen), another of the classical texts of Chinese medicine, the life changes of women and men are described in 7 and 8 year cycles respectively. The Functional Channel and the Thrusting Channel govern these cycles.

Eight Extraordinary Channels and Chi Kung

There are few texts available today that describe the purpose and function of the eight extraordinary channels and their place in Chi Kung practice. To make matters more confusing, the extraordinary channels and points used in Chi Kung are often quite different from those used in acupuncture, even though they may bear the same names.

Most acupuncturists pay little attention to the eight extraordinary channels in diagnosis and treatment with the exception of some modern Japanese researchers. By contrast, the extraordinary channels have been of special importance to Taoists and Chi Kung practitioners for thousands of years. Taoists see the extraordinary channels as the foundation of our bodily energy, as the bridge between our Original or Prenatal Chi and our Postnatal Chi; these channels affect us on the deepest level of our basic constitutional energy.

Therefore, Taoists focus on opening up the flow of energy through the eight extraordinary channels as a prerequisite for opening the energy flow in the twelve ordinary channels. In the Universal Tao system, you first open up the Governor Channel and the Functional Channel in the Microcosmic Orbit Meditation. The second pair: the Thrusting Channels and the Belt Channels are opened in the Fusion of the Five Elements II Meditation. The last four channels, the Yin and Yang Bridge Channels and the Yin and Yang Regulator Channels are opened in the third level of Fusion of the Five Elements Meditation. After opening all eight channels, in the next level of Taoist inner alchemical meditation called the Lesser Enlightenment of Kan and Li, the twelve ordinary channels are then opened.

Special Functions of the Bridge and Regulator Channels

The Bridge and Regulator Channels have no points of their own. They borrow points from the other 'ordinary' channels linking together and controlling the flow through all the separate channels of the body. The Bridge and Regulator Channels travel along the same paths. There is no 'real' difference between them. Both of them connect or 'bridge' and 'regulate' the flow of Chi in the body's meridians.

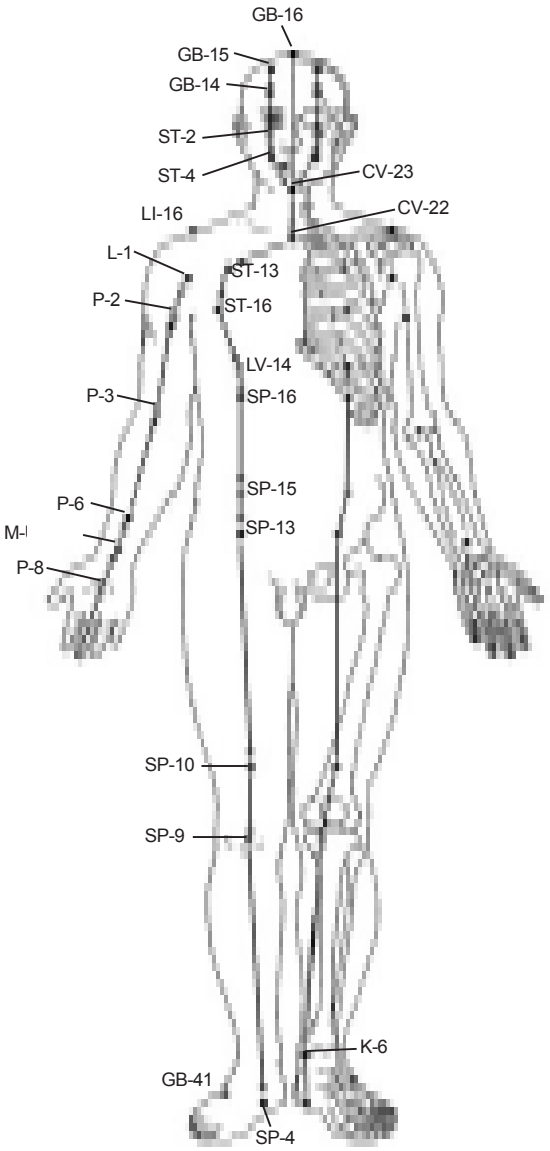

Fig. 8.31 *Yin Bridge and Regulator Channels*

Bridge Channels Yin and Yang Chiao Mo Function

The Bridge Channels, also called the Heel Vessels as they originate at the heels, regulate the amount of energy being used by all the other meridians in the body. They act like a bridge linking together the stored Chi in the body and the areas in need of Chi. Usually if any meridian uses more energy than it needs to flow properly, then other meridians become deficient as a result. Thus the Bridge Channels seek to assure that your energy is distributed in a balanced way. The Yin Bridge Channel runs along the front or yin side of the body, while the Yang Bridge Channel runs along the back of the body.

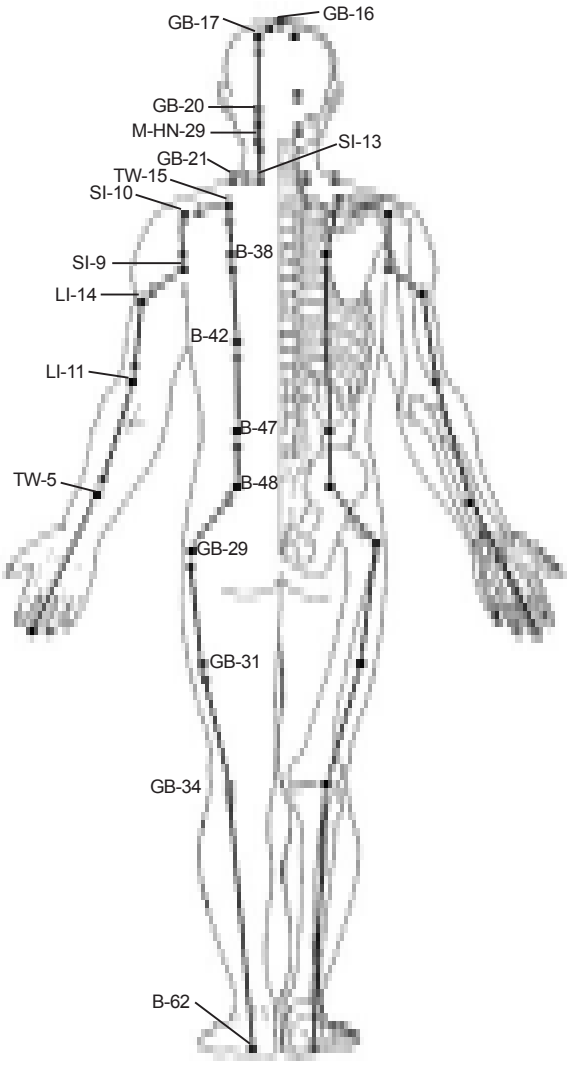

Fig. 8.32 *Yang Bridge and Regulator Channels*

Disorders of the Bridge Channels

Excess Yang Energy

When yin energy is slowed down in the Bridge Channels, yang energy flows more rapidly. The excess yang can cause the following problems: insomnia, difficulty in closing the eyes, hypertension, stiff back and waist, inability to bend down, thigh tumors, bad colds, spontaneous sweating, headaches, painful eyes, paralysis of the arms and legs, vomiting of milk in infants, deafness, epilepsy, nose bleeding, swelling of the body, pain in the joints and head sweating.

Excess Yin Energy

When yang energy is slowed down in the Bridge Channels, yin energy moves more rapidly. The excess yin causes the following problems: sleepiness, difficulty in keeping the eyes open, hypotension, choking, painful urination, stomach rumbling, vomiting, diarrhea, difficult bowel movements, difficult labor and unconsciousness.

Regulator Channels

Yin and Yang Wei Mo Function

The Regulator Channels, also called the Linking Vessels, bind together all the meridians in the body. The Regulator Channels are also divided into yin and yang. The yin aspect, which runs along the front of the body, moves the yin energy and regulates the blood and inner parts of the body. It connects with all the yin channels: the Liver, Spleen, Kidney, Heart, Pericardium and Lung channels. If the yin aspect becomes imbalanced, the person may suffer from heart pains.

The yang aspect, which runs along the back side of the body, moves the yang energy, controls Defensive Chi, regulates resistance to external infections, and regulates the external parts of the body. It connects with all the yang channels: the Stomach, Bladder, Gall Bladder, Large Intestine, Triple Warmer & Small Intestine channels. If the yang aspect becomes out of balance, the person may catch colds and fevers easily.

By joining together the various channels, the Regulator Channels help to maintain a harmonious and cooperative interaction between the different channels.

The Regulator Channels in Taoist Yoga and Chi Kung are slightly different from those presented in acupuncture texts. The Chi Kung Regulator Channels include the yin and yang arm routes as well; some Taoist Yoga texts also refer to the arm routes as the Yin Yu and the Yang Yu. Acupuncture texts, by contrast, include only the leg, trunk and head routes. Many recent Chi Kung texts, unaware of these differences, depict illustrations from acupuncture texts alone, further adding to the confusion.

Disorders of the Regulator Channels

Excess Yang Energy

When yin energy is slowed down in the Regulator Channels, yang energy moves more rapidly. The excess yang can cause the following problems: swelling and pain in the joints, cold knees, paralysis of the arms and legs, painful back and sides, aching muscles, pain in the head, neck and edge of the eyebrows, fever, rashes, night sweating, tetanus, painful red eyes, colds and superficial fevers.

Excess Yin Energy

Similarly, when yang energy is slowed down in the Regulator Channels, yin energy moves more rapidly. The excess yin can cause the following problems: heart pain, diarrhea with stomach rumbling, difficulty swallowing, pain on both sides of the chest, diseases associated with cold and convulsions.

Summary

The Bridge and Regulator Channels link all of the yin and yang channels in the body together and regulate the flow of energy in these channels to maintain a state of energetic balance in the body. The channels used for meditation are somewhat different from the ones seen in Chinese medical text and acupuncture charts. This is because their purposes are different.

Chinese medicine aims to restore sick people to health. The points being treated must be superficial so that they can be activated by acupuncture needles.

Chi Kung and Taoist meditation aim to maintain health and to take one beyond mere physical health to spiritual immortality. The channels and points can be deep within the body, since the energy is guided by the mind or by postures and movements rather than by needles.

The movements used in Cosmic Chi Kung Part II to activate the Bridge and Regulator Channels are relatively simple. To completely master the Bridge and Regulator Channels, you must learn and practice the third level of Fusion of the Five Elements Meditation. Once you have done so, this part of Cosmic Chi Kung practice will be particularly powerful and balancing for you.

Practice

Opening Movements

The Opening Movements for this second part of Cosmic Chi Kung are the same as for the first part. By now you should be familiar with these movements, so they will be described briefly. For a more detailed description, refer to Part I, Opening Movements.

Hands down at sides, palms facing each other. Commence Bone breathing. Be aware of the Tan Tien and absorb Cosmic Chi. Be aware of the Tan Tien and channeling the earth and galactic forces.

Washing the Bone Marrow

Raise arms to chest height - palms facing each other. Rotate arms until palms face down. Open the 'Tiger's Mouth' - Index finger up, thumb down.

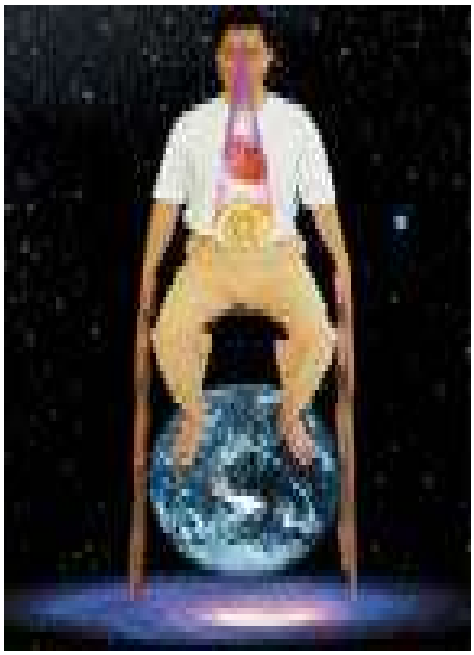

Fig. 8.33 *Hands lower to the Sides. Lower the Mind to the Tan Tien.*

Fig. 8.34 *Open the 'Tiger's Mouth'.*

Activate and Beam to the Eye of the Hip

A. Large Intestine 4 - Eye of the Hand
B. Pericardium 9 - Tip of the Middle Finger
C. Small Intestine 3 - Knife Edge of the Hand

Fig. 8.35 *Activate the Large Intestine, Pericardium and Small Intestine.*

Be aware of the Tan Tien and absorb the Heavenly Force Washing the Bone Marrow Crown to Soles.

Extend the arms forward - palms upward. Be aware of the Tan Tien and absorb the heavenly force. Rotate the arms until the palms face down. Raise the index fingers slightly. Absorb the Earth Chi.

A. ***B.***

Fig. 8.36
A. *Be aware of the Tan Tien and absorb the Heavenly Force.*

B. *Index Fingers up - be aware of the Tan Tien and absorb the Earth and Universal Force.*

Core Movements of Part II
Opening the Bridge and Regulator Channels

Activate the Throat Center - Right Side

Keeping the elbows sunk, raise the left palm first so that it is about 1 inch in front of the throat center (Conception Vessel 22), palm facing in. Then bring the right hand up so that it is about 1 inches in front of the left hand, palm facing in. Align the Lung 10 point in the middle of the eminence of the left hand with the **throat center. Feel the Chi go through the neck to C-7**. Continue smiling to the universe and connect to the back side of the universe. Hold for a 5 to 30 count and feel the throat center activated.

Fig. 8.37 *Connect to the Throat Center.*

Fig. 8.38
Feel the connection to the Universe at the Back.

Move both hands out slowly like you're pulling silk; when the feeling is diminished or the silk starts to break stop there. Be still and feel the beam connect the throat center to C-7 and the universe. Maintain the energy beam as you move in and out three times altogether ending with the hands as above.

Activate Mideyebrow Point - Right Side

Be aware of the Tan Tien and the universe. Keeping the Lung 10 points aligned, raise the hands up to the level of the mideyebrow point about one inch in front of the face. **Keep the points aligned and beam the energy passing through both hands into the mideyebrow point and through to the base of the skull.** Continue smiling and extending to make a connection to the back universe for a 5 to 30 count.

Use only 5% of the awareness to move both hands very slowly out, like you are **pulling silk**; continue to move out as long as your can feel the connection to the mideyebrow, C-7 points and the universe, maintaining the energy beam as you move.

Move in and out three times altogether, ending with the hands as above.

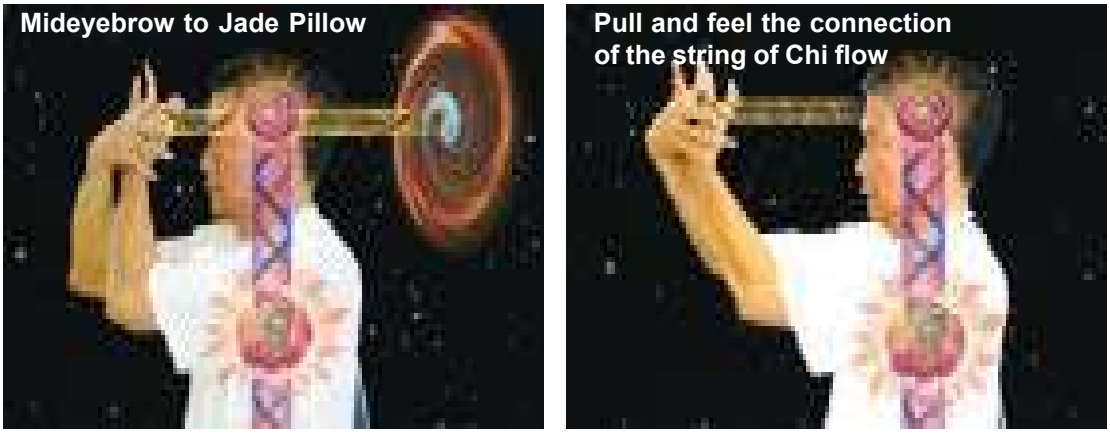

Fig. 8.39 *Connect to the Mideyebrow, Jade Pillow and the Universe at the Back.*

Keeping the palms and thenars (Lung 10) aligned, move the hands back down to the position in front of the throat center. Keeping the forearms horizontal at shoulder height, separate the hands so that the Laogong point is aligned in front of Stomach 13, just **below the clavicle** on a vertical line above the nipple or mammillary line. The middle fingertips should almost be touching. **Beam energy from the Laogong points into ST-13 through the back on the side of the spine and connect to the universe**. You will be following this vertical line, which passes through the nipples, down the torso to the level of the navel, **stopping to focus and beam energy into key points along the way.** On each of these, focus your Yi on beaming energy into the organs inside each position. Stomach 13 is the location that activates the Heart and Lungs. Feel the change in your breathing as you activate the lungs.

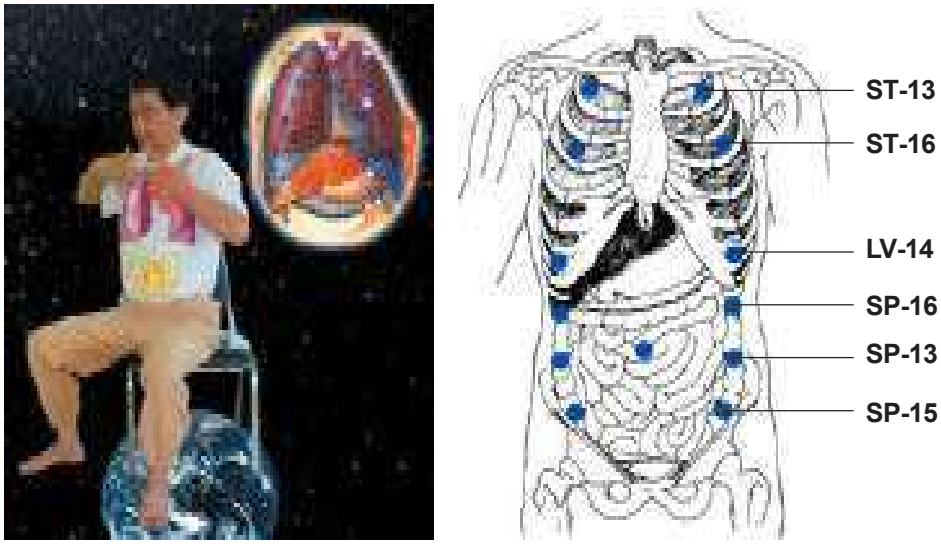

Fig. 8.40 *Beam Energy into ST13.*

Move the hands down the mammillary line to Stomach 16, about one inch above the nipple (in the space between the third and fourth ribs). Chi connects to the back and to the universe. Again, beam energy to energize and balance the **heart and middle of the lungs**. Move the hands down to Liver 14 (about 2 - 3 inches below the nipple in the space between the 6th and 7th ribs). Beam healing energy into the **liver and gall bladder.** Feel the Chi or the vibration of the palms activate the liver and feel the energy moving inside there.

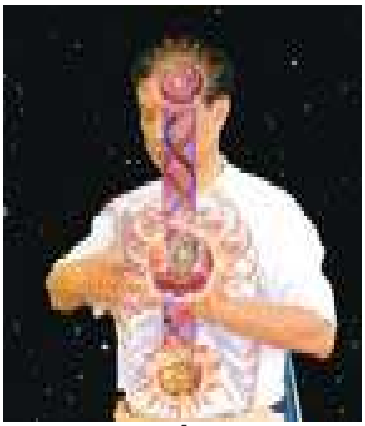

A.

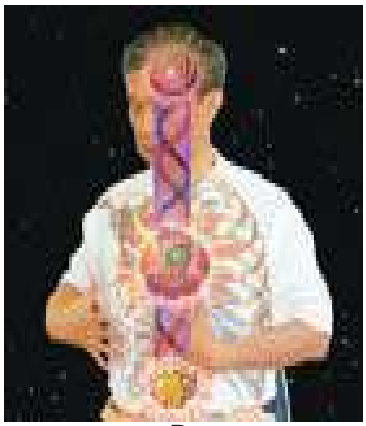

B.

Fig. 8.41 A. *Energize and balance the Lungs at ST16.*
B. *Energize and balance the Liver and Gallbladder at LV14.*

Move the hands down to **Spleen** 16 (just below the rib cage on the mammillary line). Beam healing energy into the **stomach, pancreas and spleen and the liver.** Picture the organs receiving the Chi from the cosmic and the universe.

Move the hands down to Spleen 15 (on the mammillary line to the level of the navel). Beam healing energy from your palms into the **small intestine and the Tan Tien.**

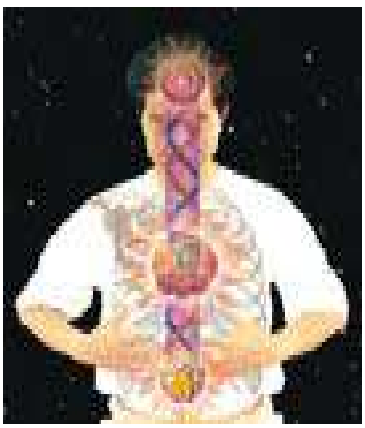

A.

B.

Fig. 8.42 A. *Energize the Stomach, Pancreas, Spleen and Liver at SP 16.*
B. *Energize the Tan Tien and Small Intestine at SP15.*

Hold the Chi Ball - Right Hand on Top

Turn the **left palm up** and align the Chi Ball with the Tan Tien. Turn the **right palm down** and align the eye of the hand (LI-4) with the navel. Feel your palms holding a Chi ball and feel a **Chi ball inside the Tan Tien**. Feel the Chi ball connect to the Cosmic Chi outside. Feel the north (usually left) and south (usually right) poles in the hands. Lower the right thumb to point toward the left Laogong point.

Fig. 8.43
Hold the 'Chi Ball' - One in the Tan Tien and the other in the hands - Right Hand over Left.

Yin/Yang Palms

Separate the hands and extend them out in front of the body at solar plexus level. The **left palm** is still pointing up and is yang drawing in the **Heavenly Force** through Laogong. The **right palm** is still facing down and is yin drawing in the **Earth Force** energy. **'Be Aware Tan Tien and Universe'**.

Fig. 8.44 *Connect to Heaven and Earth.*

Conclude by turning the left palm over to face downward. **Draw in the 'Earth Force' through both palms.**

Fig. 8.45 *Draw the Earth Force through the Palms.*

Repeat the sequence with the left palm over the right.

Start by moving the right palm to the throat and then the left palm. Scan the body, as in the previous sequence, using both palms to connect to the points running down the front of the body. Remember to maintain a sense of the Chi flowing between the points in the front and their corresponding points in the back of the body.

Fig. 8.46 *Repeat the Practice on the Left Side. Push and Pull the silk at the Throat.*

Fig. 8.47 *Project to the Mideyebrow and Base of the Skull - connect to the Universe at the back. Then hold the Ball and repeat Finger Movements, as below.*

Continue with the left side, now pulling the silk at throat (C-7).

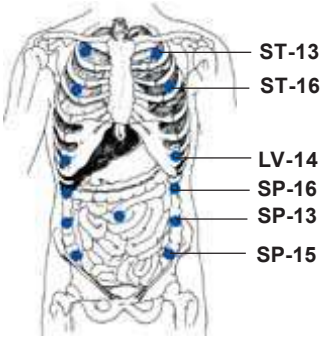

Fig. 8.48 *Beam Energy into each of the Organs like the last time.*

Closing Movements

The closing movements, crane's beak and finish are the same as before.
Activate the Chi channels - balancing the organs.

Index Fingers

Fig. 8.49 *Open (up)*

Fig. 8.50 *Neutral*

Fig. 8.51 *Close (down)*

Fig. 8.52
Ring Finger *- down, neutral.*
Index Finger *- open, neutral.*

Fig. 8.53
Thumb *- in and down, neutral.*
Index Finger *- open, neutral.*

Fig. 8.54
Pinky Finger *- down, neutral.*
Index Finger *- open, neutral.*

Fig. 8.55
Middle Finger *- down, neutral.*
Index Finger *- open, neutral.*

Crane's Beak

Form the crane's beak with both hands by bringing the fingertips together with the thumbs inside. Activate the saliva and swallow down three times to the Tan Tien. Raise the forearms to shoulder height with the fingers pointed down, inhaling gently as you raise. Open the palms slowly and begin to lower the arms to the sides as you exhale, until the palms are facing each other in the starting position.

Finish

Bring the awareness to the navel and notice the quality and intensity of the energy generated. **Collect energy at the navel**. Men, place the hands over the navel with the right hand on top; vice versa for women.

Part III
Opening the Functional and Governor Channels

Theory: Functional and Governor Channels

The Functional and Governor Channels are the first two of the eight extraordinary channels described earlier in this chapter (beginning p.178). They serve as the reservoirs of yin and yang energy in the body. The Functional or Conception Channel is yin and all of the ordinary yin channels connect to it. Similarly, the Governor Channel is yang and all of the ordinary yang channels connect to it.

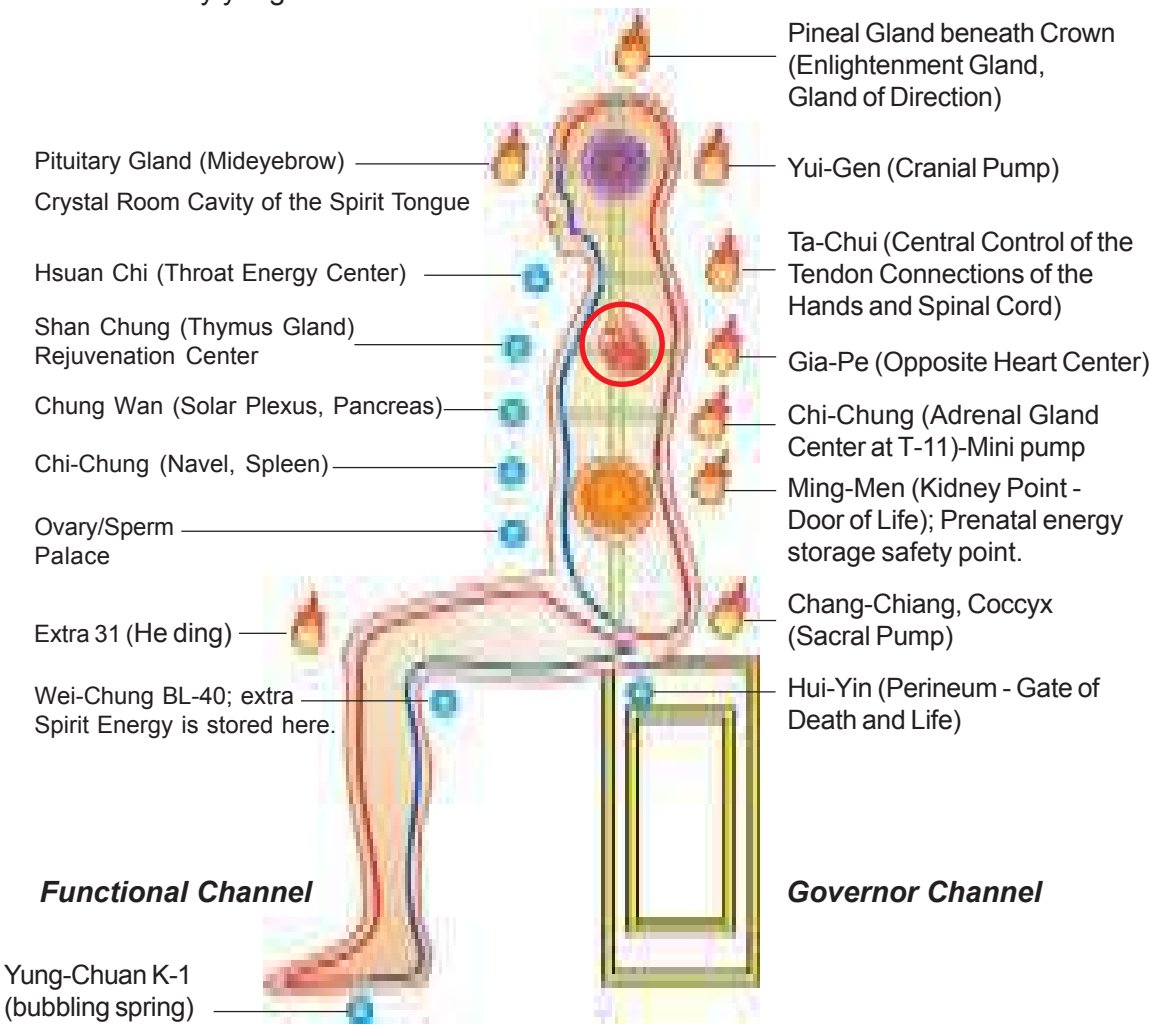

Fig. 8.56 *Cosmic Orbit*

Chi Ball

In Part III we also begin to focus more on the sensation of Chi being emitted from our palms. This energy is emitted from the **Laogong** points primarily, but you can also feel it throughout the palms and fingers. It will feel like a balloon between your hands that is expanding and contracting or like two magnetic fields repelling and attracting each other.

Once you have practiced Cosmic Chi Kung for awhile and have become skillful at it, you may find that Grasping the Chi ball is all you need to do to activate your flow of healing energy before doing a session. As you become sensitive to the sensation of your own Chi, it becomes an easy step to feel the Chi of others.

Fig. 8.57 *Grasping the Chi Ball.*

Opening Movements, Hands Down at Sides, Palms Facing Each Other
Bone Breathing - Absorbing Cosmic Chi

The Opening Movements are the same as in the sequence in Part I, 'Opening to Heaven, Earth and Cosmic Chi', on page 164.

A. Channeling the Earth Force - Washing the Bone Marrow Raise arms to chest height - Palms facing each other. Rotate arms until **palms face down.** Open the Tiger's Mouth - Index finger up, thumb down.
B. Activate and Beam to the Eye of the Hip
C. Absorb the Heavenly Force Washing the Bone Marrow - Crown to Soles

Core Movements of Part III

Grasping the Chi Ball

Slowly rotate the hands so that your palms face each other in front of your navel.

Fig. 8.58 *Hold the Chi Ball.*

Fig. 8.59 *Stretch and squeeze it.*

Feel the invisible ball of energy between your hands. Allow the energy to push your hands apart keeping the feeling of connection between your palms. When you have less feeling stop the palms and hold it there and reestablish the feeling of the Chi ball.

Let the energy draw your hands back toward each other, like a magnet, until you feel as if you were squeezing and compressing the ball.

Stretch and squeeze the Chi ball three times by opening and closing your palms in this way.

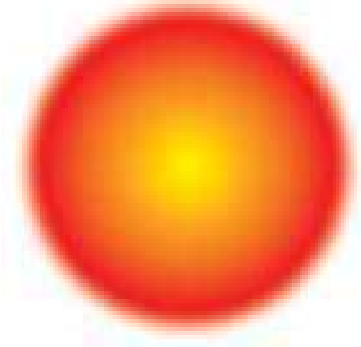

Activate the Outer and Inner Arm Gates

Activate Waiguan Triple Warmer 5 and Neiguan Pericardium 6 - **Right** arm on top. Slowly rotate the arms so that both **palms face down.**

Cross the right wrist over the left wrist with 1 inch of space between the hands. Align PC-6 of the right wrist with TW-5 of the left wrist. Feel the two gates activate each other like metal and magnet drawn to each other. Hold for a 5 to 30 second count.

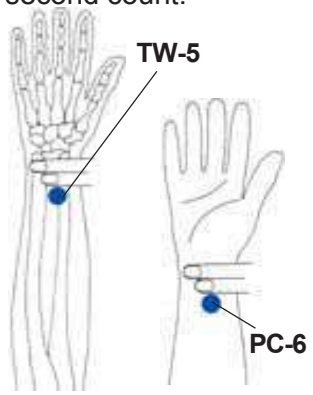

Fig. 8.60 *Align and activate PC-6 (Right) with TW-5 (Left).*

Keeping the wrists crossed, slowly rotate hands **turning the palms upward**. Now TW-5 of the right wrist will be aligned with PC-6 of the left wrist. Hold and count and feel the points activated. 'Be aware of Tan Tien and Universe'.

Fig. 8.61
Align and activate TW-5 (Right) with PC-6 (Left).

Fig. 8.62 *Feel the Chi Ball and beam energy from LI-4 into the Navel Point.*

Open the Functional Channel with LI-4

Bring the left hand down to the level of the Tan Tien with the Chi Knife facing in. Lower the right hand, palm down and align the eye of the hand, the LI-4 point with your navel. **Feel the Chi ball between your two hands**, and at the same time beam energy from LI-4 into the **navel** point.

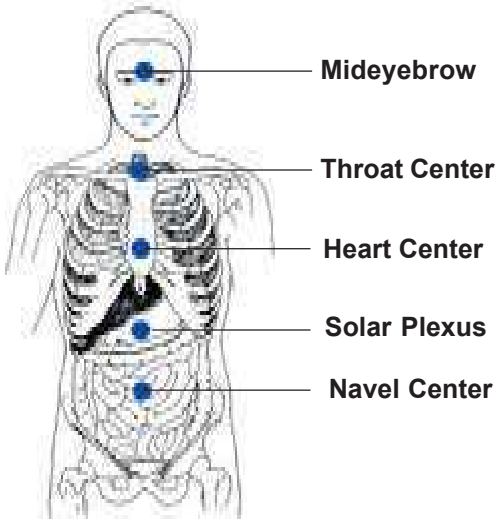

Fig. 8.63 *Magnify the Power of the Beam to the Solar Plexus.*

Fig. 8.64 *Activate all the Points.*

Raise the right hand up the Functional Channel, stopping and aligning LI-4 with the **solar plexus**, hold for a 5 to 30 second count and feel the points open and starting to activate each other.

Fig. 8.65 *Beam to the Heart Center.*

Fig. 8.66 *Beam to theThroat*

Fig. 8.67 *Beam to the Mideyebrow*

Continue to move up to the **heart**, **throat** (CV-22) and **mideyebrow** points. Beam energy from the eye of the hand into each of these points and at the same time, continue to feel the Chi ball connection between the two hands.

Return down the Functional Channel in the same manner, starting from the mideyebrow and stopping to beam energy into each point.

Next beam into the **throat center, heart center, solar plexus** and finally the **navel**. Hold the Chi ball at the navel with the right hand over the left.

Yin/Yang Palms

Separate the hands and extend them out in front of the body at solar plexus level. The left palm is still pointing up and is yang drawing in the heavenly force through the Laogong point. The right palm is still facing down and is yin drawing in the earth force energy.

Fig. 8.68 *Separate the Hands, one palm facing up and one down - draw in the Forces of Heaven and Earth.*

Fig. 8.69 *Draw in Earth Force.*

Conclude by turning the left palm over to face downward. Draw in the earth force through both palms.

Activate the Chi Ball, Tan Tien and the Original Force

Turn the right palm upward and lower it to the Tan Tien with the Chi knife pointing inwards.

Lower the left palm to the navel, palm down. Lower the left thumb to point toward the right Laogong point. This opens the eye of the left hand (LI-4), pointing it toward the navel.

Fig. 8.70 *Activate the Chi Ball, Tan Tien and the Original Force - Right Hand over left, the 'Large Intestine 4' pointing at the Navel.*

Open the Functional Channel with the Left Hand

A. ***B.*** ***C.***

Fig. 8.71 ***A.*** *Bring LI4 point up to the Solar Plexus and Heart Center.*
B. *Then up to the Throat Center.*
C. *Then up to the Mideyebrow. Descending down the channel in reverse, finishing at the Navel.*

After going up the functional channel come down the channel with the left hand.

Holding a Chi Ball: Open the hands with the palms facing each other holding a Chi ball. Stretch and squeeze the Chi ball a few times in order to feel the Chi as a substance; open and then relax the palms as you squeeze.

Fig. 8.72 *Hold and squeeze the Chi Ball.*

Fig. 8.73
Feel the Chi Ball expanding, growing Bigger.

Double Palm and Double Beam - Palm to Palm
Activate the Functional and Governor Channels - Right Palm on Left

Bring the left palm in first to face the navel, about 1 inch away, aligning the Laogong point with the navel. Follow by bringing the right hand in front of the left hand, **aligning the Laogong of the right palm with the Laogong of the left hand and the navel**. Both palms are now facing in. Beam energy through both Laogong points to the **navel and through the body to the Door of Life**, between L-2 and L-3 (Lumbar Vertebrae). Hold for a 5 to 30 second count and feel the vibration of the palms and Chi beam penetrate through the two points; feel them link together.

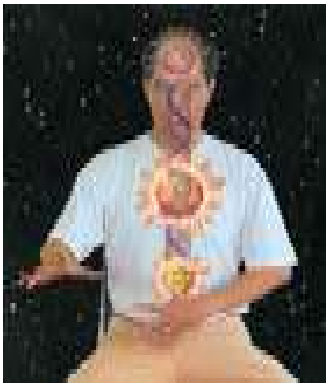

Fig. 8.74
Left Palm to Navel.

Fig. 8.75
Right on Top.

Fig. 8.76
Beam from Navel to Door of Life.

Next raise the left palm up to the solar plexus, aligning the Laogong point with the solar plexus.

Follow with the right palm aligning the Laogong to the left palm. Beam energy into the **solar plexus point and through the body to the T-11 point (thoracic vertebrae)**.

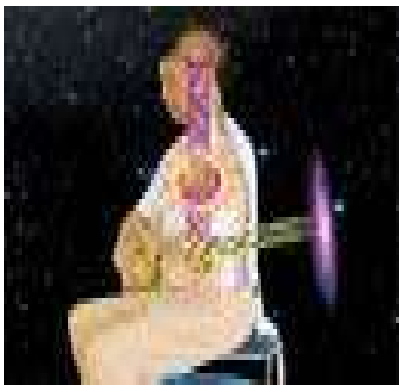

Fig. 8.77
Raise Left Palm to Solar Plexus.

Fig. 8.78 *Follow with the Right Hand to form the Double Beam.*

Continue in the same way with the left hand leading to the **heart point and wing point,** the **throat point and C-7 (cervical vertebrae)**, the **mideyebrow point and Jade Pillow**, and the **crown point and perineum**. **Always remember 'Tan Tien and the universe'.**

Fig. 8.79 *Beam into the Heart Center and to the back of the Heart.*

Fig. 8.80 *Beam into the Throat Center and to C7.*

When you reach the crown lightly spiral the palms and feel the Chi slowly penetrate deep into the body reaching the perineum; this will also open the **Thrusting Channels.** This might take a longer time, try a 30 to 60 second count.

Fig. 8.81 *Beam into the Mideyebrow to the base of the Stall.*

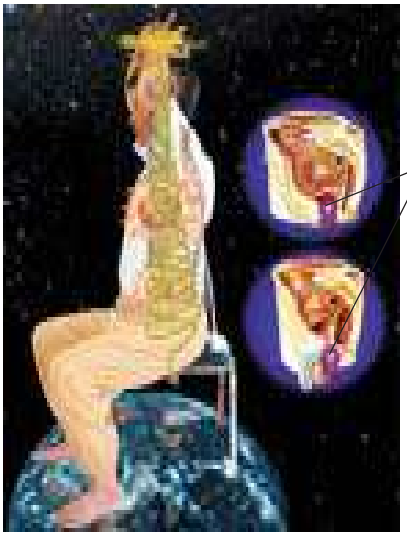

Fig. 8.82 *Beam from the Crown down to the Perineum.*

Return down the front, point by point in the same way, leading with the left hand.

Go up and down this way three times. The double palm and beam activate both the Functional and Governor Channels. The energy beam passes all the way through the body at each point.

Grasping the Chi Ball

Separate the hands and slowly extend the arms in front of you at navel level, palms facing each other, holding the Chi ball.

Fig. 8.83 *Squeeze the Chi Ball.*

Fig. 8.84 *Magnify its Energy.*

Stretch and squeeze the Chi ball three times as before by opening and closing the palms. 'Be Aware of Tan Tien and Universe'.

A. ***B.*** ***C.***

Fig. 8.85 *Repeat the double palm and beam with the* ***left hand on the outside and the right palm leading,*** *beaming from;* ***A.*** *Navel to Door of Life.*
B. *Solar Plexus to T11 and Heart Center to the Wing Point* ***C.****Throat Center to C7.*

Fig. 8.86 *Activate the Mideyebrow to the Base of the Skull.*

Fig. 8.87 *Activate the Crown and feel the Energy penetrate to the Perineum.*

A. Lower the right hand to the mideyebrow and penetrate to the skull.
B. Lower the right hand down to the throat center, following with the left.
C. Lower down to the solar plexus and penetrate to T11.
D. Lower down to the navel and penetrate to the Door of Life.

Fig. 8.88 *Channel the Earth Force.*

Rotate the **hands to face downward** and draw in the earth force through the palms, soles and perineum.

Closing Movements

Activate the Chi Channels - Balancing the Organs

The closing movements, crane's beak and finish are the same as before.
Index Finger *open (up), close (down), neutral (even with the other fingers)*
Ring Finger *- down, neutral.*
Index Finger *- open, neutral.*
Thumb *- in and down, neutral.*
Index Finger *- open, neutral.*
Pinky Finger *- down, neutral.*
Index Finger *- open, neutral.*
Middle Finger *- down, neutral.*
Index Finger *- open, neutral.*

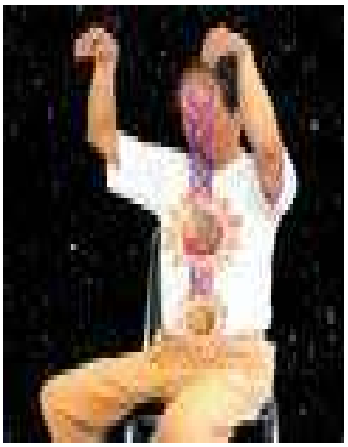

Fig. 8.89 *Form the Crane's Beak.*

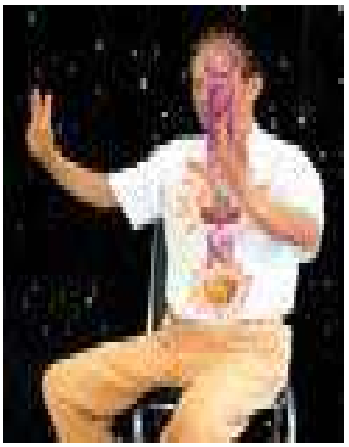

Fig. 8.90 *Palms to Front.*

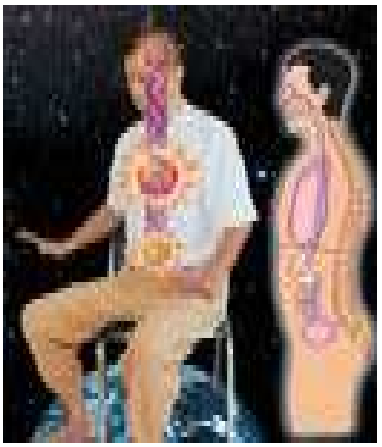

Fig. 8.91 *Lower to Sides.*

Crane's Beak

Form the crane's beak with both hands by bringing the fingertips together with the thumbs inside. Activate the saliva and swallow this elixir down three times to the Tan Tien. Raise the forearms to shoulder height with the fingers pointed down, inhaling gently as you raise.

Open the palms slowly and begin to lower the arms to the sides as you exhale, until the palms are facing each other in the starting position.

Finish

Bring awareness to the navel and notice the quality and intensity of the energy generated. Collect energy at the navel. Men, place the hands over the navel with the right hand on top; vice versa for women.

Part IV
Activating the Yin and Yang Channels and the Chi Belt

Theory

In this final part of Cosmic Chi Kung, you will focus on opening the yin and yang channels of the arms and on activating the Chi Belt around the waist. Mastery of Part IV of Cosmic Chi Kung will enhance your ability to project Chi through your fingers for healing.

Yin and Yang Channels of the Arms

There are six important energy channels flowing through the arms. These channels are paired together with each pair comprised of a yin channel and a yang channel. The yin channel of each pair flows down the inside of the arm from torso to fingertip, while its yang counterpart flows up the outside of the arm from fingertip to head.
The pairs are as follows:

Metal Element - Yin - Lung Channel - Thumb
Yang - Large Intestine Channel - Index Finger
Fire Element - Yin - Pericardium Channel - Middle Finger
Yang - Triple Warmer Channel - Ring Finger
Fire Element - Yin - Heart Channel - Pinky Finger
Yang - Small Intestine - Pinky Finger

Projecting Healing Energy through the Fingers

Emitting Chi from the fingers for healing is known in China as the **"One Finger Art."** Because the various energy channels of the arms either end or begin at the fingertips, the fingers are very effective instruments for projecting healing energy. Your fingers can focus energy like a laser beam toward a concentrated area such as a specific acupuncture point. You can also emit energy from all the fingers at once creating a combined effect to target an area. Part IV of Cosmic Chi Kung will stimulate all of the arm channels and will give you an opportunity to activate all of the fingers for beaming energy.

Fig. 8.92 *"One Finger Art"*

Activating the Chi Belt - Dai Mo

The Chi Belt or Belt Channel (also called the Girdle Vessel) is the only channel in the body that runs horizontally. It encircles the body at the waist level, connecting together all the vertical channels running through the torso. Thus, the Belt Channel plays an important role in maintaining a good energetic communication between the upper and lower body. In women it strongly affects the uterus and the menstrual cycle in particular.

In Taoist Chi Kung, the Belt Channel is not limited to the waist region. It encircles the entire body, almost like weaving an energetic cocoon around you from head to foot. Activating the Belt Channel strengthens the aura and helps to defend and protect you from outside negative energies.

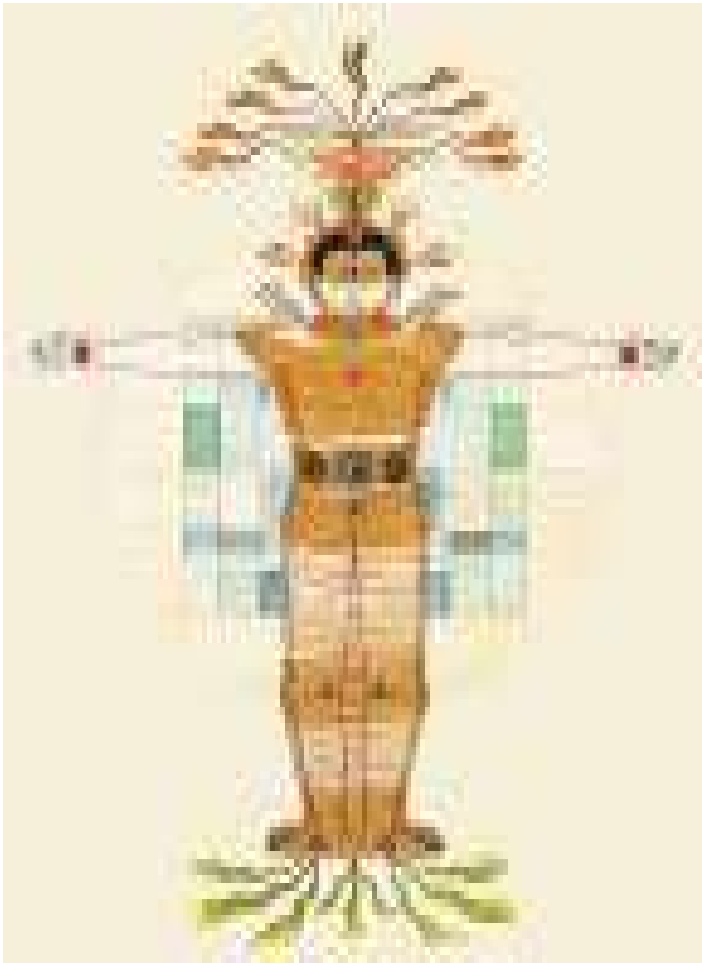

Fig. 8.93 *Belt Channel*

Practice

Opening Movements

These opening movements have been described in Parts I, II, III. Refer to Part I to refresh your practice.

Hands Down at Sides - Palms Facing Each Other - Bone Breathing - Absorbing Cosmic Chi.

Channeling the Earth Force - Washing the Bone Marrow.
Raise arms to chest height - Palms facing each other.
Rotate arms until palms face down.
Open the Tiger's Mouth - Index Finger up, thumb down.

Activate and Beam to the Eye of the Hip.
Large Intestine 4 - Eye of the Hand.
Pericardium 9 - Tip of the Middle Finger.
Small Intestine 3 - Knife Edge of the Hand.

Absorb the Heavenly Force - Washing the Bone Marrow - Crown to Soles.
Extend the arms forward to chest height - palms upward.

Absorb the Earth Force.
Rotate the arms until the palms face down.
Raise the Index Fingers slightly.

Fig. 8.94 *Mother Earth's Healing Power*

Core Movements of Part IV Yin and Yang Channels - Chi Belt

Activating the Yin Channels - Left Side

Turn the palms down and slightly open the index fingers. Smile to your palms and soles and channel the earth force.

Turn your right palm up and pass it just one inch below the left arm yin channels from the left palm to the armpit, **without physically touching the arm**. Feel the Chi moving. Turn your right palm to face your left rib cage and pass your right hand down the left side of your abdomen along the descending colon, and a cross the pelvis to the right side to activate the **yin** energy.

Fig. 8.95 *Channel the Earth Force.* ***Fig. 8.96*** *Activate the Yin Energy from the Palm to the Pelvis.*

Fig. 8.97 *Raise Chi in the Right Palm.*

Fig. 8.98 *Pass it to the Left.*

Pass your right hand up the right side of the abdomen to the level of your forehead with the palm facing diagonally toward the left palm (which simultaneously turns palm up at the level of the navel). Project the Chi from palm to palm for 30 to 60 seconds, vibrating the palm and feeling Chi from the right palm sent to the left picking up by the left palm. Keep the palms open and relaxed.

Next point the right ring finger toward the left palm and project Chi making very small circles from the right ring finger (Triple Warmer channel); emit the Chi to the left palm for 30 to 60 seconds.

Then return the right index finger to neutral position. Point the left ring finger up toward the right palm, project into the right palm for 30 to 60 seconds, and then return to neutral.

Next both ring fingers project toward the opposite palms at the same time for 30 to 60 seconds and then return to neutral. Notice that the energy may meet in the middle.

Fig. 8.99 *Project Energy and balance Left and Right.*

Activate the Yang Channels - Left Side

Turn the left palm down and lower the right palm to cover the back of the left hand, palm down. Pass the right palm over the left arm's **yang** channels from the back of the left hand to the left shoulder. Then pass the right palm across the upper chest and across the right breast. Scoop the right palm under the right armpit, fingers first. Then bring the right palm forward, palm down and press forward with the left palm at the same time. Relax and channel the earth force.

A. *Left Palm down, lower Right Palm to cover the back of Left Hand.*

B. *Pass the Right Palm over the Left Arm's Yang Channels.*

C. *Pass the Right palm across the chest and scoop under the Right Armpit, Fingers first.*

D. *Press both Palms forward, relax and channel the Earth Force.*

Fig. 8.100 *Balance Left Side Yin and Yang and Channel Earth Energy.*

Repeat, Activating the Yin and Yang Channels to the Right Side

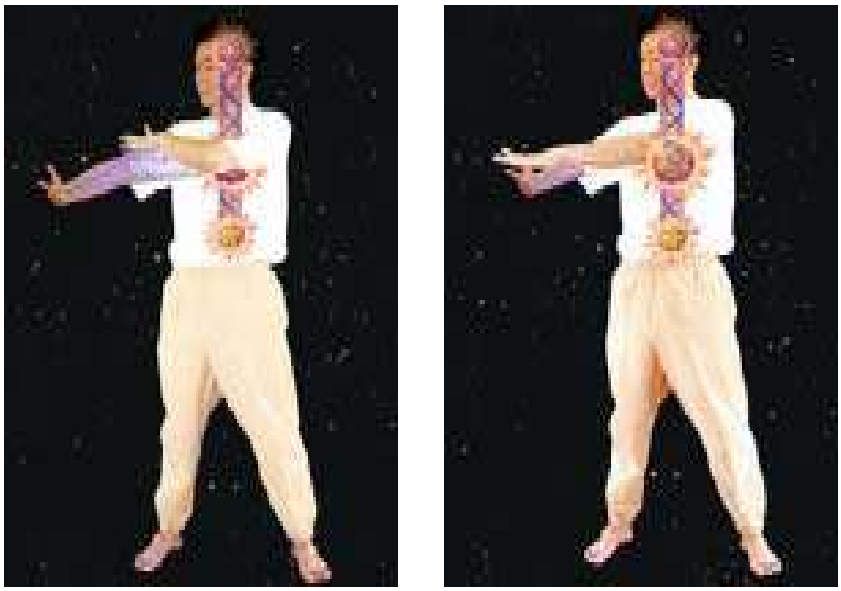

Fig. 8.101 *Balance right side yin and yang and channel earth energy*

Then repeat **Activating the Yin and Yang Channels** with the other fingers and channels in the following order:

Index Finger - Large Intestine
Thumb - Lung
Pinky Finger - Heart and Small Intestine
Middle Finger - Pericardium

Fig. 8.102 *One Finger Art - activating the Laogong.*

Activate the Chi Belt - Right Foot Forward

Step forward with the right foot. The right palm covers the navel and the left palm covers the Door of Life. Feel the Chi beam penetrate from palm to palm.

Turn your hips to the right and shift weight to your right leg. At the same time move your right palm to the Door of Life in a brushing manner, while your left palm moves to the right hip in a sweeping manner. Note that the palms face the Chi belt.

Repeat the above three times altogether.

Fig. 8.103 *Activate the Chi Belt - Right Side.*

Activate the Chi Belt - Left Foot Forward

Repeat the above with the left foot forward and reversing the right and left hands.

Fig. 8.104 *Activate the Chi Belt - Left Side.*

Channel the Earth Force

Bring the hands forward and rotate the palms to face downwards. **Smile** and channel the earth force as before.

For these Closing Movements see the pictures beginning on page 171.

Closing Movements
Activate the Chi Channels - Balancing the Organs

Index Finger - open (up), close (down), neutral (even with the other fingers).
Ring Finger - down, neutral.
Index Finger - open, neutral.
Thumb - in and down, neutral.
Index Finger - open, neutral.
Pinky Finger - down, neutral.
Index Finger - open, neutral.
Middle Finger - down, neutral.
Index Finger - open, neutral.

Crane's Beak

Form the crane's beak with both hands by bringing the fingertips together with the thumbs inside. Swallow the saliva. Raise the forearms to shoulder height with the fingers pointed down, inhaling gently as you raise.

Open the palms slowly and begin to lower the arms to the sides as you exhale, until the palms have returned to the starting position.

Finish

Bring the awareness to the navel and notice the quality and intensity of the energy generated.

Collect energy at the navel. Men, place the hands over the navel with the right hand on top; vice versa for women.

Healing Others

Summary and Combined Practice

After learning the four sets of Cosmic Chi Kung, you may want to combine them all into a short and simple daily practice. This combined set, previously called Buddha Palm I, synthesizes the movements from the first three sets into one basic sequence. The movements are done on the right side only, so the entire set can be completed in **ten to twenty minutes**.

Cosmic Chi Kung: Simple Combined Sequence

Opening Movements

Bone Breathing - Absorbing Cosmic Chi

1. Stand with your hands down by your sides. Feel your Chi moving and activate the **bone breathing**.
2. Activate the cosmic force by using your mental intention (Yi) to spiral at the **mideyebrow** point and draw in the golden light energy. Breathe through the mideyebrow point in the same manner as in bone breathing, allowing the energy to **flow through the Microcosmic Orbit**. Alternatively you can breathe the golden light down into your navel to charge up your Original Chi at the Tan Tien. You can also simply circulate the golden light throughout your body. Relax, smile and enjoy the sensation of your entire body breathing in the cosmic energy.

Channeling the Earth Force - Washing the Bone Marrow

1. Connect with the earth force by activating the **perineum** and the **soles of the feet, Kidney 1, Bubbling Spring**. Connect the bridge by slightly squeezing the sex organs and the anus. Wash the bone marrow from the soles to the crown.
2. **Smile** into the perineum, palms, mideyebrow and crown. Then slowly raise the arms, palms facing each other to chest height keeping the elbows relaxed and sunk. Then slowly rotate the arms until the **palms are facing down**. Absorb the Earth Chi through the soles, perineum and palms; feel it being absorbed into the bones and body like a **steam or mist rising from the earth**. Feel the earth force move through the **center of the bones**, up the calves, thighs (femur bones), through the hip bones, spine, scapulas, arms, neck and skull. Finally swirl the energy around your brain.

Activate the Hip - Large Intestine 4, Pericardium 9 and Small Intestine 3

1. Raise your index finger slightly upward to activate the Laogong point (Pericardium 8). Then stretch your thumbs out to the sides and down, so that they end up pointing downwards toward the earth to activate Large Intestine 4 (Hegu). **Large Intestine 4 is found in the webbing between the thumb and index finger. It is called the "eye of the hand"; this area is also known as the "Tiger's Mouth."**
2. Slowly draw the elbows back and lower the hands until your palms are facing down beside the "eye of the hip" (the iliac crest) with the "eye of the hand" (Large Intestine 4) aligned with the "eye of the hip". **Use your mind intention to beam the energy back and forth between your two LI-4 points. This will activate the large and small intestines.**
3. Rotate your hands so that the fingers first point out, then back and finally point the fingers in toward the eye of the hip. **Beam energy back and forth between the tips of the middle fingers** (Pericardium 9) passing through the hips.
   Rotate the hands again until the fingers are pointing forward with the palms facing up. Align the knife edge (Small Intestine 3) with the eyes of the hip, and **beam the energy back and forth between the two hands.**

Absorb the Heavenly Force - Washing the Bone Marrow - Crown to Soles

Extend the arms forward to chest height with the **palms still facing upward**.

Become aware of the palms and the crown. Activate the Laogong point (Pericardium 8). Feel the heavenly energy, and be aware of the violet light of the North Star and the red light of the Big Dipper shining down. Draw this light in through the palms and the crown point and feel it washing your bone marrow. Direct the sensations down through the skull, cervical vertebrae, clavicle, scapulas and sternum. Activate your thymus gland and continue drawing the healing heavenly light down through the rib cage, arms, spine, hips, femurs, calf bones, feet and toe bones. **Feel your bones activated with a positive electrical force (the positive force comes from heaven, negative from the earth).**

Absorb the Earth Force

1. Rotate the arms until the **palms face down**.
   Raise the index fingers slightly, extend the thumbs first towards each other, and then towards the ground.
2. Become aware of the palms (Laogong), the soles of the feet (Kidney 1, Bubbling Spring) and the perineum (Conception Vessel 1, Hui Yin). Activate these points, feel the earth energy, and **be aware of a gentle blue light or white light rising up from the earth like a pure steamy mist.** Draw this light in through the palms and soles and let it wash up through the center of your bones as it steam cleans your

marrow. Picture any impurities or illness dripping out of your bones and draining down into the earth, where they are recycled and purified.

Core Movements

Grasping the Moon - Connecting the Heaven and Earth Forces

1. **Open Position:** Heaven Force - Bring the arms up to shoulder height, bending the elbows so that the **left hand is under the right elbow** with the left index finger pointing up to Heart 3.
2. The right forearm is over the left forearm with the tip of the right index finger held above the Large Intestine 11 point of the left arm. The right index finger is pointing up toward heaven.
3. The right index finger draws in the heavenly force like an antenna. The force flows up the bones of the right arm across the shoulders to the left arm, and through the bones of the left arm to the left index fingertip. It then flows through the index finger of the left hand into the Heart 3 point of the right arm **completing the heavenly circuit**. Continue cycling in this way.
4. **Close Position:** Earth Force - Keeping the arms in the same position, move both index fingers to point down. The right index finger will now point toward the Large Intestine 11, point of the left arm and the left index finger will point downward toward the earth. Draw in the earth force through the left index finger bringing it through the bones of the left arm, across the shoulders through the right arm to the right index finger and out into the Large Intestine 11 point of the left arm. Continue cycling in this way **completing the earth circuit.**

   Open and close three times altogether ending in the open position.

Activate the Throat Center

1. Draw the elbows out to the side and rotate the palms to face in so that the left palm is about 3 - 6 inches in front of the Throat Center (Conception Vessel 22), palm facing in, and the right hand is about 1 - 3 inches in front of the left hand, palm facing in. Align the Lung 10 point of the right hand with the Lung 10 of the left hand, and align the Lung 10 points in the middle of the thenar eminence of the left hand with the Throat Center. **Keep the points aligned and beam the energy passing through both hands into the Throat Center.**
2. Move both hands about 12-18 inches out from the Throat Center maintaining the energy beam as you move.
3. Move in and out three times altogether in this way ending with the hands in as in preivous point above.

Activate the Third Eye

1. Keeping the Lung 10 points aligned, raise the hands up to the level of the mideyebrow point. Keep the points aligned and **beam the energy passing through both hands into the mideyebrow point.**
2. Move both hands about 12-18 inches out from the mideyebrow point maintaining the energy beam as you move. **Move in and out three times** altogether in this way, ending with the hands as previously.
3. Keeping the palms and thenars (Lung 10) aligned, move the hands back down to the position in front of the **Throat Center.**

Open the Bridge and Regulator Channels

1. Keeping the forearms horizontal at shoulder height, separate the hands so that the Laogong points are aligned in front of Stomach 13 just below the clavicle on a vertical line above the nipple or **mammillary** line. The fingertips should almost be touching. Beam energy from the Laogong points into ST-13. You will be following this vertical line, which passes through the nipples, down the torso to the level of the navel stopping to focus and **beam energy into key points along the way**. On each of these, focus your Yi on beaming energy into the organs inside each position. Stomach 13 is the location that activates the Heart and Lungs. Feel the change in your breathing as you activate the **lungs**.
2. Move the hands down the mammillary line to Stomach 16, about one inch above the nipple (in the space between the third and fourth ribs). Again, beam energy to energize and balance the **heart and lungs**.
3. Move the hands down to Liver 14 (about 2 - 3 inches below the nipple in the space between the 6th and 7th ribs). Beam healing energy into the **liver and gall bladder**.
4. Move the hands down to Spleen 16 (just below the rib cage on the mammillary line). Beam healing energy into the **stomach, pancreas and spleen**.
5. Move the hands down to Spleen 15 (on the mammillary line to the level of the navel). Beam healing energy from your palms into the **small intestine and the Tan Tien**.

Grasping the Chi Ball

1. Slowly rotate the hands so that your palms face each other in front of your navel. Feel the invisible ball of energy between your hands. Allow the energy to push your hands apart keeping the feeling of connection between your palms.
2. Let the energy draw your hands back toward each other, like a magnet, until you feel as if you are squeezing a ball.
3. Stretch and squeeze the Chi ball three times by opening and closing your palms in this way.

Activate the Outer and Inner Arm Gates
Waiguan - Triple Warmer 5 and Neiguan - Pericardium 6 - Right Arm on Top

1. Slowly rotate the arms so that both palms face down.
2. Cross the right wrist over the left wrist with 1-3 inches of space between the hands. Align PC-6 of the right wrist with TW-5 of the left wrist.
3. Keeping the wrists crossed, slowly rotate hands turning the palms upward. Now TW-5 of the right wrist will be aligned with PC-6 of the left wrist.

Open the Functional Channel with LI-4

1. Bring the left hand down to the level of the Tan Tien with the Chi Knife facing in. Lower the right hand, palm down, and align the eye of the hand, the LI-4 point with your navel. Feel the Chi ball between your two hands, and at the same time beam energy from LI-4 into the navel point.
2. Raise the right hand up the Functional Channel stopping and aligning LI-4 with the **solar plexus, heart, throat** (CV-22) and **mideyebrow** points. **Beam energy from the eye of the hand into each of these points**, and at the same time continue to feel the Chi ball connection between the two hands.
3. Return down the Functional Channel in the same manner stopping to beam energy into each point. **Go up and down the Functional Channel** in this way three times.

Yin/Yang Palms

1. Separate the hands and extend them out in front of the body at solar plexus level. The left palm is still pointing up and is yang drawing in the heavenly force through Laogong. The right palm is still facing down and is yin drawing in the earth force energy.
2. Conclude by turning the left palm over to face downward. Draw in the earth force through both palms.

Double Palm and Beam to Activate the Functional and Governor Channels

1. Bring the left palm in first to face the navel, about 3 - 5 inches away, aligning the Laogong point with the navel. Follow by bringing the right hand in front of the left hand, aligning the Laogong of the right palm with the Laogong of the left hand and the navel. Both palms are now facing in. **Beam energy through both Laogong points to the navel and through the body to the Door of Life**.
2. Next raise the left palm up to the **solar plexus** aligning the Laogong point with the solar plexus. Beam energy into the solar plexus point and through the body to the T-11 point. Your right hand remains at the navel level beaming energy to the navel and the Door of Life.
3. Raise your right hand up to the outside of the left hand at the solar plexus level, and beam energy through both hands into the **solar plexus point and the T-11 point**. Continue in the same way with the left hand leading to the **heart point and wing**

point, the **throat point and C-7**, the **mideyebrow point and jade pillow** and the **crown point and perineum**.

4. Return down the front, point by point in the same way, leading with the left hand. Go up and down in this way three times. **The double palm and beam activate both the Functional and Governor Channels. The energy beam passes all the way through the body at each point**.

Grasping the Chi Ball

1. Separate the hands and slowly extend the arms in front of you at navel level, palms facing each other holding the Chi ball.
2. Stretch and squeeze the Chi ball three times as before by opening and closing the palms.

Channel the Earth Force

Rotate the hands to face downward, and draw in the earth force through the palms, soles and perineum.

Closing Movements

Activate the Chi Channels - Balancing the Organs

Index Finger - open (up), close (down), neutral (even with the other fingers).
Ring Finger - down, neutral.
Index Finger - open, neutral.
Thumb - in and down, neutral.
Index Finger - open, neutral.
Pinky Finger - down, neutral.
Index Finger - open, neutral.
Middle Finger - down, neutral.
Index Finger - open, neutral.

Crane's Beak

1. Form the crane's beak with both hands by bringing the fingertips together with the thumbs inside. Raise the forearms to shoulder height with the fingers pointed down, inhaling gently as you raise.
2. Open the palms slowly and begin to lower the arms to the sides as you exhale, until the palms are facing each other in the starting position.

Finish

1. Bring the awareness to the navel and notice the quality and intensity of the energy generated.
2. Collect energy at the navel. Men, place the hands over the navel with the right hand on top; vice versa for women.

Chapter IX
Universal Tao Practices

Cosmic Inner Smile

Fig. 9.1 *Inner Smile*

The Inner Smile begins at the eyes and the mideyebrow point and moves down to the heart. As you activate the heart, the loving energy will flow out and you will feel the energy of your Inner Smile flow down the entire length of your body like a waterfall. This is a very powerful and effective tool to counteract stress, tension and negative Chi.

1. Be aware of the **mideyebrow,** imagining that your are in one of your favorite places in the world, a place where you feel safe, relaxed and happy. Recall the sights you might have seen there, the sounds you might have heard, the scents, sensations and flavors that you associate with that place.
2. Imagine that one of your favorite people is standing in front of you, smiling to you with loving, happy, radiant shining eyes. **Smile** to your face and slightly lift up the corners of your mouth.
3. Feel yourself responding to that special person's smile with a smile of your own. Feel your eyes smiling and relaxing.
4. Smile down to the **thymus gland** and picture a white flower blossoming. Gently inhale into the thymus gland, connecting your breath to the olfactory organ. Smell the good fragrance.
5. Aim your inner attention at your **heart**, picturing the heart before your inner eye and smile to it. **Smile** until you feel the heart smile back to you. Picture your heart like a red rose, gradually opening. This will activate the **love** and fire of **compassion** in the heart. Once you feel the red light and loving awareness it will activate the **cosmic red healing light** or mist from above and around you.
6. Smile at the light or mist and very slowly with a soft, long, deep breath draw the red mist, love and compassion into the mideyebrow, down through the mouth and throat, into the heart and gradually overflowing to the **small intestine**. Exhale, but retain the red light and the love and compassion in the **heart and small intestine**. At the same time exhale the cloudy, black or negative energy. Keep on doing this breathing 18 to 36 times waiting until the heart becomes bright red before your inner vision and starts to radiate out to the tongue, mouth, nose, ears and eyes. Allow the red light to whirl around you and form a **red aura**. Feel your skin glowing with red energy.
7. Let the heart's loving energy radiate out to the **lungs**. Aim your attention at the lungs; picture them before your inner eye and smile to them. **Smile** until you feel the lungs smile back to you. Picture your lungs like a white rose, gradually opening; smell the good fragrance. This will activate the courage in the lungs. Once you invoke the white light and courage into the lungs, you will also activate the **cosmic white healing light** or mist from above and around you.
8. Smile at the light or mist and very slowly, softly take a long deep breath and draw the white mist into the mideyebrow, the mouth and down to the lungs, gradually overflowing into the **large intestine**. Exhale but retain the white light and the feeling of courage in the lungs. At the same time exhale the cloudy, black or negative energy. Keep on doing this kind of breathing 18 to 36 times, waiting until the lungs become bright white and start to radiate out to the nose, ears, eyes, tongue and mouth. Invite the white light to whirl around you and form a **white aura** covering your skin like autumn dew.
9. The **spleen, pancreas and stomach** correspond to the yellow color of the earth element. Connect to these organs and smile down into them from the mideyebrow.

First connect to the heart, then attract the clear yellow light from above and around you. You might see the **golden yellow aura** of a wheat field ready for harvest. Expel feelings of worry; exhale the cloudy, sticky energy. Breathe in the golden yellow aura, filling your spleen center with golden yellow light. Repeat to complete 18 to 36 cycles, then allow the light to radiate out to your mouth, nose, ears, eyes and tongue. Wrap the golden aura around you, leaving a golden shine on your skin.

10. The **kidneys and bladder** correspond to the blue color of the water element. Gentleness is contained within the blue healing light. Inhale the blue aura into the kidneys. Expel feelings of fear or stress on breathing out. Allow your energy field to expand, breathing in and out the blue energy 18-36 times, until it starts to radiate out from your kidneys to your ears, eyes, tongue, mouth and nose. Gather the blue mist on your skin enveloping you with a **blue aura**.
11. The **liver and gall bladder** connect to the green color of the element wood; kindness replaces anger, which is expelled on breathing out. Do the same as above and create a **green aura** around you. Exhale the dark red, cloudy heat. Inhale the nourishing green of the forests. Do 18 to 36 cycles, until the green light has completely filled the liver and starts to radiate out to your eyes, tongue, mouth, nose and ears. Invite the green light to form a green aura around you.
12. **Smile** down to the **sexual organs** and reproductive system. Feel love and sexual arousal and the heart and sexual organs uniting. Observe how this process transforms the sexual energy into Chi. Channel down orange and red light to the sexual organs. Thank them for their work in keeping you alive and healthy. Rest. Do nothing. Gather and store the energy by smiling and spiraling in the Tan Tien.

Six Healing Sounds

The Six Healing Sounds enhance Therapeutic Work

Everyone has heard stories about gifted beings who possess great healing powers. People seek out gifted healers. Yet even in the best of circumstances, how much time can a great healer spend with you? One hour a day? An hour a week? What about the rest of the time? Thus you must learn how to take care of yourself; you must learn how to clear out your negative energy and transform it into positive healthy energy. If you maintain yourself in this way it will surely enhance any other therapy you are receiving.

The Six Healing Sounds are a simple yet powerful tool to promote physical, energetic and emotional healing and balance. If you are healing others, you can teach your students one or two of the Six Healing sounds each session, to enhance the effects of your therapeutic work. During the practice of the sound the resting period is very important. Growing the good virtue of the organs is essential so the negative or sick energy has less room to grow.

The sounds are also used to generate certain frequencies for specific healing. Each sound can generate different energy for the healing of the different organs.

Once the movements, sounds and information have been integrated into your practice you can simplify and make the Six Healing Sounds more powerful. For example, when you are settled into the lung sound and you are breathing white healing light and feel the mideyebrow wide open, you put the awareness in the 'Tan Tien and Universe'.

Chi will flow from the universe into the Tan Tien and just the right amount and quality will flow from the Tan Tien into the lungs and large intestine. Just set up the location (the organ) and connect to the universe and the Chi will flow to the correct location!

When doing these, the eyes are open only while making the sound.

Six Healing Sounds - Practice

Lung Sound

Element: Metal
Associated Organ: Large Intestine
Sound: SSSSSSS (Tongue behind Teeth)
Emotions: Negative - Grief, Sadness, Depression
Positive - Courage, Righteousness, High Self Esteem
Color: White, Clear, Metallic
Season: Fall
Direction: West

Position: Sit in a chair with your back straight and your hands resting palms up on your thighs. Have your feet flat on the floor about a hip's width apart . **Smile** down to your lungs and be aware of any sadness, grief or excess heat in your lungs. Slowly inhale and raise your hands up your center line with your fingers pointing toward each other. When your hands pass your shoulder level, begin to rotate the palms out as you continue raising your hands up in front of you and above your head with the palms up. Point your fingers towards the fingers of the opposite hand and keep your elbows slightly bent.

Sound: Part your lips slightly, keeping your jaw gently closed. Look up through the space between your two hands and push your palms slightly upward as you slowly exhale and make the sound, "SSSSSSS". Picture and feel any excess heat, sadness, grief, depression, sickness and dingy white color expelled and released as you exhale slowly and fully.

Resting Posture: When you have completely exhaled, rotate the palms to face downward with the fingers still pointing toward each other. Slowly lower the palms and bring them just in front of the chest feeling the lung's aura.

Close your eyes and be aware of your lungs. **Smile** into your lungs, and as you inhale, imagine that you are breathing in a **bright white mist of light**. Breathe this light into your lungs and feel it cooling, cleansing, invigorating, healing and refreshing your lungs. Feel it flowing down to the large intestine to balance the energy of the yin lungs and yang large intestine, allowing the **courage** quality of your lungs to emerge. Grow more courage, so sadness and depression have less room to grow. With each inbreath, feel yourself drawing in cool fresh energy. With each outbreath, mentally make the Lung Sound and release any remaining sadness or hot energy.

Repeat at least three times. For the first two repetitions, you can make the sound aloud. On the third or last repetition, make the sound sub-vocally (vocalizing the sound so softly that only you can hear it) Repeat six, nine, twelve or twenty four times to alleviate extreme sadness, depression, colds, flu, toothaches, asthma and emphysema.

Kidney Sound

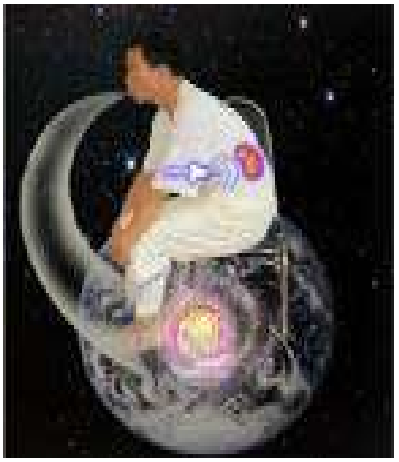

Element: Water
Associated Organ: Bladder
Sound: CHOOOOOO (with your lips forming an "O" as if blowing out a candle.)
Emotions: Negative - Fear, Shock
Positive - Gentleness, Wisdom
Color: Dark Blue or Black
Season: Winter
Direction: North

Position: Now move the hands to cover the kidneys. **Smile** to your kidneys, and be aware of any excess cold or heat in the kidney region. Then bring your legs together, ankles and knees touching. Lean forward and clasp the fingers of both hands together around your knees. Inhale and pull your arms straight from the lower back while bending the torso forward (this allows your back to protrude in the area of the kidneys). Tilt your head upward as you look straight ahead, still pulling on your arms from the lower back. Feel your spine pulling against your knees.

Sound: Round the lips slightly and slowly exhale while making the sound "CHOOOOOO." Simultaneously contract your abdomen, pulling it in toward your kid-

neys. Imagine any fear, sickness, imbalances, excess cold or heat energy being released and squeezed out of the fascia surrounding the kidneys.

Resting Posture: After you have fully exhaled, slowly sit erect and return the hands to touch the aura of the kidneys. Close your eyes and again be aware of your kidneys. **Smile** to your kidneys and, on the inbreath, imagine you are breathing a brilliant **luminous blue light mist** into them; feel this mist healing, balancing and refreshing your kidneys and bladder and picture them glowing a bright blue color. On the outbreath, imagine you are still making the Kidney Sound.

Repeat at least 3 times, as with the previous sound. Repeat six, nine, twelve, or twenty four times to alleviate extreme fear, fatigue, low-pitched ringing in the ears, dizziness, back pain, bladder and urinary infections or other problems of the reproductive system.

Liver Sound

Element: Wood
Associated Organ: Gall Bladder
Sound: SHHHHHHH
Emotions: Negative - Anger, Frustration, Resentment
Positive - Loving Kindness, Benevolence, Forgiveness
Color: Green
Season: Spring
Direction: East

Position: Place the hands on the liver. **Smile** to your liver and be aware of any anger, frustration, resentment or excess heat. Slowly begin to inhale a deep breath as you extend your arms up from the sides with your palms up. Continue to raise them over your head. Interlace your fingers together and turn your joined hands over to face the sky, palms up. Push out through the heels of the palms and extend the arms up, keeping the shoulders relaxed. Bend a little to the left and stretch your right arm slightly to gently open the area of your liver.

Sound: Open your eyes wide (the eyes are the sensory opening of the liver). Slowly exhale, making the sound, "SHHHHHHH" sub-vocally. Feel that you are releasing any trapped excess heat, anger, illness and negativity from your liver and that these are riding out of your body on your breath.

Resting Posture: Once you have fully exhaled, separate your hands, turn the palms

down and slowly lower your arms to the sides, leading with the heels of the hands. **Smile** and inhale a **shiny spring green mist**, illuminating the liver and gall bladder. Bring your hands back to rest on the liver's aura. Close your eyes and smile into your liver. With each inbreath, breathe fresh Chi into your liver and gall bladder and mentally make the Liver Sound with each outbreath.

Repeat at least three times, as with the previous sound. Repeat six, nine, twelve or twenty four times to alleviate extreme anger, to relieve red or watery eyes, to remove a sour or bitter taste in the mouth or to detoxify the liver.

Heart Sound

Element: Fire
Associated Organ: Small Intestine
Sound: HAAAAAAAW
Emotions: Negative - Arrogance, Harshness, Cruelty, Hatred
Positive - Joy, Honor, Respect, Love, Happiness
Color: Red
Season: Summer
Direction: South

Position: Let both hands rest on the heart. **Smile** to your heart and be aware of any arrogance, haughtiness, hatred, giddiness, cruelty or hastiness. Slowly begin to inhale a deep breath as you extend your arms up from the sides with your palms up, as you did with the Liver Sound. Continue to raise them over your head. Interlace your fingers together and turn your clasped hands over to face the sky, palms up. Push out through the heels of the palms and extend the arms up, keeping the shoulders relaxed. Bend a little to the right and stretch your left arm slightly to gently open the area of your heart.

Sound: Keep your eyes soft and relaxed, looking up through your hands. Slowly exhale, making the sound, "HAAAAAAAW" sub-vocally. Feel that you are releasing any trapped heat, negative emotions, illness and imbalances from your heart and that these are riding out of the body on your breath.

Resting Posture: Once you have fully exhaled, close your eyes, separate your hands, turn the palms down and slowly lower your arms to the sides, leading with the heels of the hands. As you move inhale a **bright red mist** into the heart and small intestines. Bring your hands back to rest on your heart's aura . Smile into your heart. With each inbreath, breathe fresh Chi into your heart with each outbreath mentally repeat the heart sound.

Repeat at least three times, as with the previous sound. Repeat six, nine, twelve or twenty four times for the heart and small intestines; feel them balanced. This will alleviate extreme impatience, hastiness, arrogance, nervousness, moodiness, jumpiness, irritability, tongue ulcers, palpitations, sore throat, heart disease, insomnia and detoxify the heart.

Spleen Sound

Element: Earth
Associated Organ: Pancreas, Stomach
Sound: WHOOOOOOO (gutturally from the throat)
Emotions: Negative - Worry, Excess Sympathy, Overthinking
Positive - Fairness, Balance, Equanimity, Justice, Openness
Color: Yellow
Season: Indian Summer
Direction: Center (where you stand, looking out to the Six Directions)

Position: Place your hands on the body covering the spleen, pancreas, and stomach area. Be aware of your spleen and **smile** sincerely into it. Inhale deeply as you move the arms outward in an embrace and aim the fingers up under the left rib cage. Place your fingers of both hands just beneath the sternum and rib cage on the left side.

Sound: Look out, lean into your fingers and gently push your fingertips in. Exhale slowly and make the sound, "WHOOOOOOO," from the depths of your throat. Feel yourself releasing any trapped heat, worry, mental fixations or excess sympathy.

Resting Posture: Once you have fully exhaled, close your eyes, slowly release the hands and extend the arms out embracing the earth; return your hands to the resting position on the spleen's aura. Smile to your spleen, pancreas and stomach. Inhale fresh Chi to your spleen, pancreas and stomach as a brilliant **luminous yellow healing mist** that cleanses and refreshes your organs. Mentally do the Spleen Sound with each outbreath.

Repeat at least three times, as with the previous sound. Repeat six, nine, twelve or twenty four times to alleviate extreme indigestion, heat or cold in the stomach or spleen, worry, nausea, hemorrhoids, fatigue, organ prolapse or loose stools.

Triple Warmer Sound

The Triple Warmer refers to the upper, middle and lower body, and to the distinct metabolic transformations that occur within each area. The Upper Warmer is the area above the diaphragm, where the heart and lungs are located. This area tends to become hot and is responsible for respiration and cardiovascular circulation. The Middle Warmer, the area between the diaphragm and the navel, becomes warm and is where the digestive organs are located. The Lower Warmer, the area below the navel, is responsible for reproduction and elimination and is cool in temperature. The sound "HEEEEEEE" balances the temperatures of the three levels by bringing hot energy down to the lower center and cold energy up to the higher centers.

Position: Lie on your back with your arms resting palms up at your sides. Keep your eyes closed. **Smile**. First breathe into the upper part of your lungs to expand the Upper Warmer; then breathe into the middle of the lungs to expand the Middle Warmer; finally, with the last part of your inhalation, expand your lower lungs and fill the Lower Warmer. Breathing in this way creates more space inside for each organ, helping to release and circulate any internal heat or cold.

Sound: Exhale with the sound "HEEEEEEE" sub-vocally, first flattening your chest, then your solar plexus, and finally your lower abdomen. Feel the dark and cloudy color, cold and chill energy exit from the tips of the fingers.

Resting Posture: Once you have fully exhaled, do not to focus on any emotions or purification process at all. Just let go and relax your body and mind completely.

Repeat at least three times, as with the previous sound. Repeat six, nine, twelve or twenty four times to alleviate insomnia and stress.

When you have completed the Six Healing Sounds just rest, **smile** and do nothing.

Regular daily practice of the Six Healing Sounds will help you to keep in touch with the energetic and emotional state of your internal organs. Most importantly do the sounds in the evening before going to sleep. This will help clear out the negative emotions before sleeping, so you can feel that the night's rest recharges your energy positively. This practice will greatly benefit your personal Cosmic Healing Chi Kung practice. It will help sensitize you to the varieties and differing qualities of Chi. This knowledge will also help you in diagnosing and treating others.

For more details of this practice please see the book "Taoist Ways to Transform Stress Into Vitality", by Mantak Chia.

Appendix

Guide to the Acupuncture Points used in Cosmic Chi Kung

The following is a detailed description of the acupuncture energy points used in the Cosmic Chi Kung practice. It is necessary to know the exact location of the points to do the practice well. However, you do not have to know the traditional Chinese medical functions and energetics of the points to do the practice. These are included in this appendix as an item of interest.

The names of the points are given first by the channel and number, second by the English translation of the traditional Chinese name for the point and finally by the name in Chinese.

We are emphasizing the traditional Chinese medical therapeutic properties of the points given herein. Many of these points also have very different purposes in Taoist Yoga. *For a description of the Taoist Yoga energetics, refer to "Awaken Healing Light of the Tao" by Mantak Chia.*

Pericardium 8

"Lakor's Palace" - Laogong

Ying Spring, Fire Point

Location: On the center of the palm, where the tip of the middle finger touches when making a loose fist.

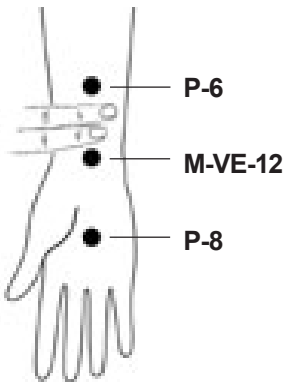

Functions: Cools the heart, drains heat from the heart, cools the blood, calms the spirit, regulates the heart Chi and yang, Ghost Point for treating spirit possession.

Indications: Coma from stroke, heat exhaustion, angina pectoris, mania, hysteria, mental illness, excessive sweating of the palms, mouth problems.

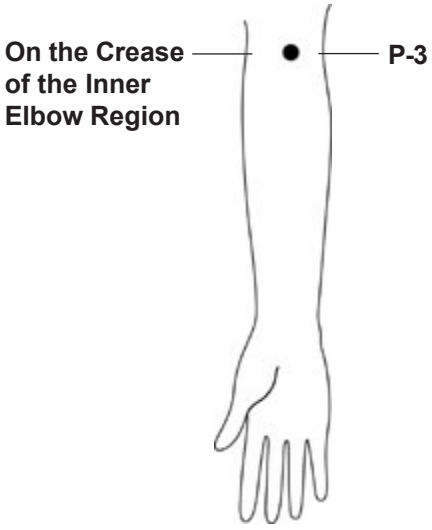

Large Intestine 4
"Adjoining Valleys" - Hegu

Yuan Source Point
Location: On the back side of the hand between the thumb and index finger, in the web approximately at the middle of the metacarpal bone of the index finger.
Functions: Disperses wind, relieves exterior conditions, suppresses pain and clears the channels, clears lung heat, calms the spirit.
Very powerful point for moving the Chi and blood of the whole body; main point for pain; main point for headache; main point for ailments of the head, face and sensory organs; main point for immunity.
Indications: Headaches, common cold, redness with pain and swelling of the eyes, toothache, facial swelling, sore throat, finger cramps, arm pain, fever, abdominal pain, constipation.
Caution: Contra-indicated in pregnancy.

Small Intestine 3
"Back Creek" - Houxi

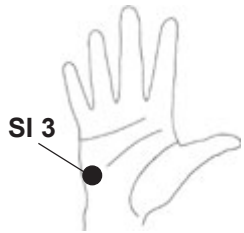

Shu Stream, Wood Point
Master Point of the Governor Channel
Coupled Point of the Yang Bridge Channel
Location: When a loose fist is made, the point is near the head of the fifth metacarpal bone on the knife edge of the hand at the junction of the red and white skin.
Functions: Relaxes the tendon-muscular channels, opens the Governor Channel, clears the Spirit, drains evil Chi from the heart.
Indications: Seizures, psychosis, hysteria, intercostal neuralgia, headache, stiff neck, red, painful and congested eyes, deafness, spasms of the arm, elbow and fingers; fever, night sweating, whiplash, occipital headaches.

Used for structural/musculo-skeletal problems; opens the Governor Channel for problems with back, neck and head, main point for stiff neck, antispasmodic for muscle spasms; anti-inflammatory for spinal arthritis, intestinal inflammation.

Lung 10
"Fish Border" - Yuji

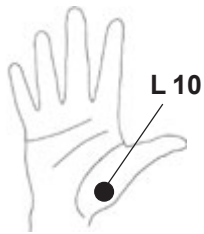

Ying Spring, Fire Point
Location: In the middle of the ulna eminence below the thumbs at the junction of the red and white skin.
Functions: Cools heat in the lungs, benefits the throat.
Indications: Sore throat, cough, laryngitis, tonsillitis, fever with common cold.

Triple Warmer 5
"Outer Gate" - Wai Guan

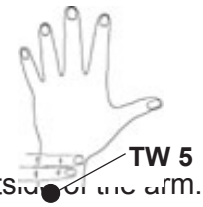

Luo Connecting Point
Master Point of the Yang Regulator Channel
Coupled Point of the Belt Channel
Location: About two fingers width above the wrist crease on the outside of the arm.
Functions: Regulates the Yang Regulator Channel and Belt Channel, tonifies and consolidates Protective (Wei) Chi, releases exterior hot and cold conditions, helps circulate stagnant Chi in the channels.
Indications: Common cold with alternating chills and fever, high fevers, pneumonia, deafness, migraine headaches, paralysis, stiff neck.

Pericardium 6
"Inner Gate" - Nei Guan

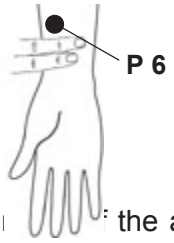

Luo Connecting Point
Master Point of the Yin Regulator Channel
Location: About two fingers width above the wrist crease on the inside of the arm, between the two prominent tendons.
Functions: Calms the heart and spirit, regulates the Chi, opens and relaxes the chest, regulates and harmonizes the stomach, regulates the liver, relieves pain.
Indications: Rheumatic heart disease, shock, angina pectoris, palpitations, chest pain, asthma, shortness of breath, tightness or fullness in the chest, spasm of the diaphragm, vomiting, stomach ache, abdominal pain, morning sickness, motion sickness, migraine headaches, hysteria, anxiety, irritability, insomnia, seizures, swollen and painful throat, painful menses or nausea with period.

Large Intestine 11
"Crooked Pond" - Qu Chi

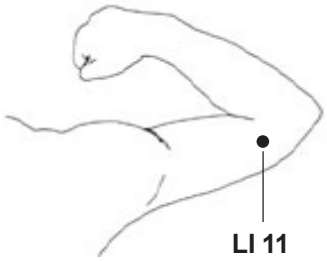

He Sea, Earth Point
Ghost Point
Location: When the elbow is flexed, in the depression at the outer and upper end of the elbow crease.
Functions: Cools heat, clears fire, drains dampness, eliminates wind and exterior conditions, regulates and moistens large intestine.
Indications: Arthritic pain in the arms, paralysis, hypertension, high fever, anemia, allergies, skin problems, Parkinson's Disease. Main point for skin diseases; main point for high fever.

Conception Vessel 22

"Heaven's Chimney" - Tian Tu

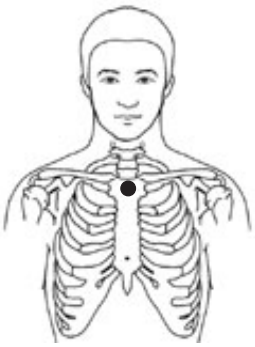

Intersecting Point of the Yin Regulator Channel on the Conception Vessel, Window of the Sky Point
Location: At the top of the breastbone (sternum) in the V-shaped indentation (suprasternal notch). Press in and downward at a forty-five degree angle.
Functions: Cools the throat and clears the voice, facilitates and regulates movement of lung Chi, frees the breath and helps restore the proper functioning of the lungs and bronchi, helps open Conception Vessel (Functional Channel).
Indications: Asthma, bronchial asthma, bronchitis, coughing, pharyngitis, goiter, hiccups, nervous vomiting, hoarse voice, spasms of the esophagus, diseases of the vocal cords, sore throat.

Conception Vessel 17

"Central Altar" - Tan Zhong

Front Mu-Alarm Point of the pericardium, Influential Point of Chi of the body
Sea of Chi Point, Master Point of the Middle Tan Tien
Location: On the frontal midline at the level of the fourth intercostal space, between the nipples.
Functions: Regulates the lungs and the Upper Warmer, tonifies Ancestral Chi, opens and relaxes the chest, diffuses lung Chi, regulates and tonifies Chi, transforms phlegm.
Indications: Pulmonary tuberculosis with shortness of breath, bronchitis, asthma, bronchial asthma, chest pain; all breast problems such as mastitis, insufficient lactation, breast abscesses, wheezing, chest pain, labored breathing, palpitations, difficulty swallowing food, anxiety.

Conception Vessel 12

"Middle Cavity" - Zhongwan (Solar Plexus)

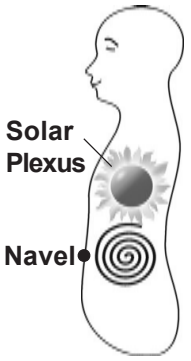

Front Mu-Alarm Point of the stomach, Influential point of all yang organs
Location: Approximately midway between the navel and the top joint of the xiphoid process.
Functions: Regulates the stomach Chi and yin, regulates, strengthens and tonifies the spleen Chi and yang, regulates the Middle Warmer, reduces digestive stagnation, tonifies nutritive Chi, regulates Chi and blood, redirects rebellious Chi downwards, clears stomach fire and heat, calms the fetus, controls the aura.
Indications: Acute or chronic gastritis, stomach and duodenal ulcers, prolapsed stomach, acute intestinal obstruction, stomach ache, vomiting, abdominal distention, diarrhea, constipation, acid regurgitation, indigestion, hypertension, mental diseases.

Mideyebrow Point

"Seal Hall" - Yin Tang

Master Point of the Upper Tan Tien
Location: At the midpoint between the two eyebrows.
Functions: Calms the spirit, activates the Crystal Room, opens the Governor Channel, draws in Cosmic Chi, eliminates wind heat.
Indications: Headache, vertigo, rhinitis, sinusitis, common cold, hypertension, infantile convulsions, sore eyes.

Conception Vessel 6

"Chi Ocean" - Chi Hai

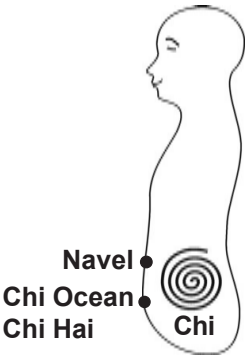

Master Point of the Lower Tan Tien
Location: Approximately three fingers width below the navel.
Functions: Regulates Chi, tonifies Original Chi, strengthens weak kidneys, harmonizes the blood, regulates the Thrusting Route Conception Vessel, reinforces Ching Chi, enriches yin.
Indications: Neurasthenia, abdominal distention, abdominal pain, irregular menstruation, impotence, spermatorrhea, urinary retention, frequent urination, intestinal paralysis, incontinence, constipation, infertility, uterine bleeding, hernia.

Stomach 13

"Chi's Household" - Chi Hu

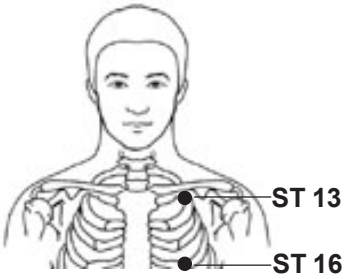

Location: Below the midpoint of the collarbone along the mammilary line (directly above the nipple).
Functions: Clears heat, loosens the chest, relaxes the diaphragm, regulates lung Chi.
Indications: Asthma, bronchitis, chest and back pain, hiccups.

Stomach 16

"Breast's Window" - Ying Chuang

Location: In the space between the third and fourth ribs, one rib directly above the nipple in men, slightly higher in women.
Functions: Stops pain, reduces swelling, clears heat, resolves depression, opens lungs, stops cough, relaxes chest, moves Chi.
Indications: Coughing, asthma, swelling of the breasts, chest and stomach pain, heartburn, shortness of breath, melancholy, diarrhea

Liver 14

"Gate of Hope" - Chi Men

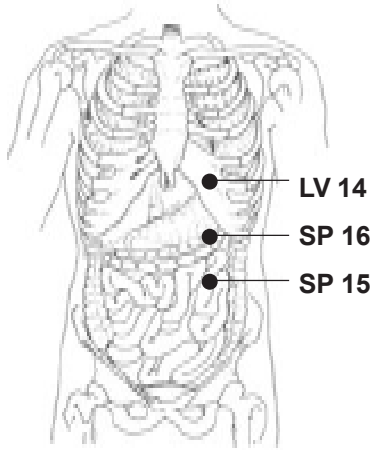

Front Mu-Alarm Point of the liver
Intersecting point of the Yin
Regulator and spleen channels on the liver channel
Location: In the sixth intercostal space, directly below the nipple.
Functions: Spreads liver Chi, transforms and removes congealed blood, strengthens spleen and stomach, expands and relaxes the chest.
Indications: Difficulty in breathing, chest pain, hepatitis, enlarged liver, gall stones, pleurisy, nervous stomach, menopausal disorders, cholera, failure to discharge the placenta after childbirth.

Spleen 16

"Abdomen's Sorrow" - Fu Ai

Location: Just below the bottom edge of the rib cage on the mamillary line.
Functions: Frees bowel Chi, dispels damp and heat, opens the organs and clears Chi stagnation.
Indications: Pain in the navel region, indigestion, dysentary, constipation.

Spleen 15

"Great Horizontal" - Da Heng

Intersecting point of the Yin Regulator Channel on the spleen channel
Location: At the level with the navel along the mamillary line.
Functions: Regulates the spleen, regulates and moistens the intestines, reduces digestive stagnation and transforms damp-heat.
Indications: Abdominal distension, diarrhea, constipation, intestinal paralysis, parasitic worms in the intestines, chronic sadness.

Conception Vessel 8

"Spirit Palace Gate" - Shen Que

Doorway to the Original Chi,
Location: In the center of the navel
Functions: Tonifies, strengthens and regulates the spleen (Chi and yang), and stomach Chi, regulates the intestines, warms the interior and reduces digestive stagnation, tonifies the kidneys, warms the yang, dries dampness and dispels cold.
Indications: Chronic diarrhea, intestinal tuberculosis, all urinary disorders, shock resulting from intestinal adhesions, heatstroke, rectal or anal prolapse, restless fetus.

Governor Vessel 4
"Door of Life" - Ming Men

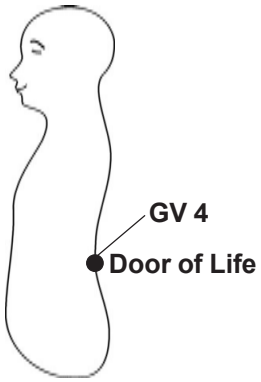

Back Doorway to the Lower Tan Tien
Location: Below the spinous process of the second lumbar vertebrae. Approximately at the level of the navel.
Functions: Nourishes the Original Chi, strengthens and harmonizes the kidneys, tonifies ching and yang, clears channels and invigorates collateral vessels, benefits the lower back and bones, regulates water pathways.
Main point to build life fire; main point for sexual/genital problems.
Indications: Bone disorders, chronic nephritis, enuresis, low sex drive, fatigue, spermatorrhea, impotence, irregular menses, painful menses, no menses, scanty menses, abnormal uterine bleeding, lower back stiffness and pain, kidney pain radiating to the abdomen, hemorrhoids, urinary incontinence, painful urination, diarrhea, sciatica, spinal myelitis.

Governor Vessel 6
"Middle of Spine" - Jizhong

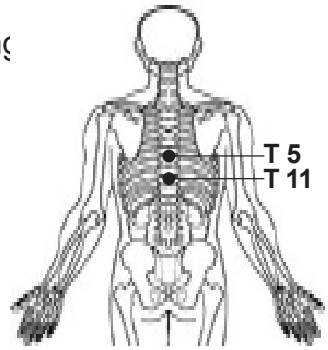

Location: Below the spinous process of the 11th thoracic vertebrae (T-11).
Functions: Stimulates Ching Chi, benefits spleen, stomach and kidneys and liver.
Indications: Hepatitis, seizures, low back pain, paralysis of lower limbs, blood in stools, diabetes, diarrhea.

Governor Vessel 11
"Spirit's Path" - Shen Tao

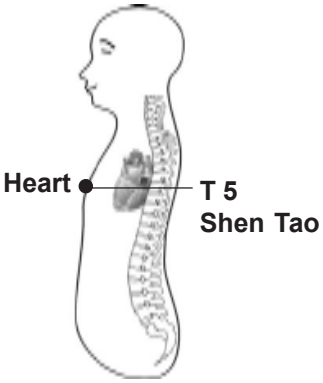

Location: Below the spinous process of T-5 (opposite CV-17, the Heart Point).
Functions: Calms heart and mind, regulates heart Chi and yang, expands and relaxes the chest, benefits heart and lungs, sedates pain, sedates fright and dispels wind.
Indications: Anxiety and palpitations due to fear or fright, neurasthenia, asthma, cough, shortness of breath, chest and hypochondriac pain, insomnia, aphasia due to winds, stroke, forgetfulness, fever.

Governor Vessel 14

" Big Vertebra" - Da Zhui

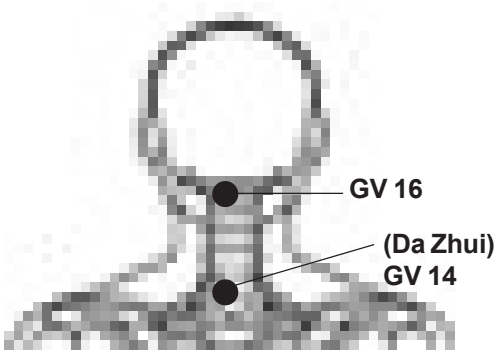

Influential point of yang
Sea of Chi point
Intersection point of all yang channels.
Location: Below the spinous process of the seventh cervical vertebra (C-7), approximately at the level of the shoulders.
Functions: Opens the yang, clears the brain, calms the spirit, tonifies Protective (Wei) Chi, reduces fever, relieves exterior conditions, clears heat.
Indications: Fever, sunstroke, malaria, psychosis, seizures, bronchitis, asthma, pulmonary tuberculosis, emphysema, hepatitis, blood diseases, eczema, hemiplegia, pain in the back of the shoulders, cold-induced diseases, cough, fever and chills.

Governor Vessel 16

“Jade Pillow” or "Wind Palace" - Feng Fu

Sea of Marrow Point, Window of Sky Point, Ghost Point
Intersection point of the Yang Regulator Channel on the Governor Vessel
Location: At the base of the skull, about one inch above the posterior hairline.
Functions: Benefits and clears the brain, calms spirit, opens the sensory orifices, dispels wind, wind-cold and wind-heat, smoothes joint functions.
Indications: Seizures, mania, hemiplegia, loss of speech due to stroke, delirium, suicidal behavior, fear and fright, anxiety, common cold, sensation of heaviness in the head, headache, dizziness, numbness of the limbs, deaf-mutism, blurred vision, sinusitis, stiff neck.

Governor Vessel 20

"One Hundred Meetings" - Bai Hui

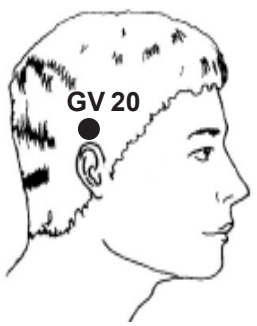

Sea of Marrow Point
Location: At the crown of the head, approximately on the midpoint of the line connecting the top apex of the two ears.
Function: Clears the senses, calms the spirit, extinguishes liver wind, stabilizes ascending yang.
Indications: Headache, dizziness, shock, depression, hypertension, insomnia, seizures, prolapsed anus, prolapsed uterus, mental dullness, hemorrhoids.

Bibliography

Bensky, Dan. Acupuncture: A Comprehensive Text, Seattle, WA: Eastland Press, 1981.
Chia, Mantak. Awaken Healing Light of the Tao, Huntington, NY: Healing Tao Books, 1993.Chi Nei Tsang: Internal Organ Chi Massage. Huntington, Ny: Healing Tao Books, 1990.
Cooper, Groffrey M. The Cell, A Molecular Approach, Washington, DC: Sinauer Associates, 1996.
De Lee, H. Lorenzen. Message from Water: Word of Recommendation, 1984.**DeLaney, Colleen, Leonard, David, and Kitsch, Lancelot.** The Acupuncture Point Book, Santa Cruz, CA: Roast Duck Productions, 1989.
Dong, Paul and Esser, Aristide H. Chi Gong: The Ancient Chinese Way to Health. New York: Paragon House, 1990.
Jou, Tsung Hwa. The Tao of Meditation: Way to Enlightenment. Piscataway: Tai Chi Foundation, 1983.
Lade, Arnie. Acupuncture Points: Images and Functions, Seattle, WA: Eastland Press, 1989.
Lindsay, Mary. The Visual Dictionary of the Human Body, First American Edition, New York, NY: Dorling Kindersley Publications, 1991.
Lu, Kuan Yu. Taoist Yoga: Alchemy and Immortality, New York, NY: Samuel Weiser, 1970.
Maciocia, Giovanni. The Foundations of Chinese Medicine, Edinburgh, Scotland: Churchill Livingstone, 1989.
Matsumoto, Kiiko and Birch, Stephen. Extraordinary Vessels. Brookline: Paradigm Publications, 1986.
McGraw-Hill Companies Human Physiology, 1999.
Morrison, Philip and Phylis and the Office of Charles and Ray Eames. Power of Ten:1982
Nilsson, Lennart. The Body Victorious. New York: NY: Delacorte Press, 1985.
Shanghai College of Traditional Medicine, translated by O'Connor, John and Teeguarden, Iona Marsaa. Acupressure Way of Health: Jin Shin Do, Tokyo, Japan: Japan Publications, 1978.
Tortora, Gerard J. and Grabowski, Sandra R. Introduction to the Human Body, Fifth Edition. New York, NY: Wiley, 2000.
Yang, Jwing-Ming. The Root of Chinese Chi Kung Jamaica Plain, MA: YMAA, 1989.

$19.95

Cosmic Healing I

Cosmic Chi Kung

Mantak Chia

Illustrated by Udon Jandee

Cosmic Healing I

Cosmic Healing I builds on the healing aspects of the Universal Tao foundation practices. In Cosmic Healing I the student will learn how to use the Cosmic Healing Chi Kung in combination with color for guiding the healing learn to process in yourself & other, you'll make use of your Personal Stars & connections with the Big Dipper & North Star so as to have the chi to "sweep & clean out" sick energies.

A New Approach to Healing

In Cosmic Healing I Master Mantak Chia, continue to bring the ancient, time-tested wisdom of the Universal Tao System to the Western world. Cosmic Healing I presents a whole new understanding and approach to healing with detailed explanations of self-healing techniques and ways to transform negative, sick energies from them and others.

Hand Techniques for Detoxifying and Rejuvenating the Vital Organs

Learn to develop your most powerful healing potential through the Cosmic Chi Kung combined with your Mind, Eyes, Heart & Intention. The Cosmic Chi Kung encourages your Compassion to bloom so as to enhance your self- healing & your ability to support other in healing them selves.

Universal Tao Publications

Preston B. Nichols, with Peter Moon

The Montauk Project
Experiments In Time

This book is dedicated to the memory of the crew of the U. S. S. Eldridge and to those who gave their life at Montauk.

CONTENTS

Introduction
Guide to the Reader
One-The Philadelphia Experiment
Two-Montauk Discovered
Three-A Visit to Montauk
Four-Duncan Arrives
Five-A Conspiracy Revealed
Six- "Project Moonbeam"
Seven-Wilhelm Reich and the Phoenix Project
Eight-The "Phoenix Project" Absorbs "Project Rainbow"
Nine-The Montauk Project Begins
Ten-The Montauk Chair
Eleven-Creation from the Ether
Twelve-Time Warping
Thirteen-Time Travel
Fourteen-Mission to Mars
Fifteen-Encounter with the Beast
Sixteen-The Nature of Time
Seventeen-The Montauk Base is Sealed
Eighteen-Montauk Today
Nineteen-von Neumann Alive!
Appendix A-A Scientific Analysis of the Radiosonde
Appendix B-Wilhelm Reich
Appendix C-Mind Control and the Persian Gulf War
Appendix D-Nikola Tesla
Appendix E-History of the Philadelphia Experiment and its Reconcilation with the Montauk Project
Appendix F-Quantum Levels of Existence
Appendix G-Glossary

INTRODUCTION

At the eastern most end of Long Island sits Montauk Point, known to most New Yorkers for its scenic beauty and landmark lighthouse. To the immediate west of the lighthouse, there is a mysterious and derelict Air Force base on the grounds of old Fort Hero. Although it was officially decommissioned and abandoned by the U.S. Air Force in 1969, it was subsequently reopened and continued to operate

without the sanction of the U. S. Government.

The entire financing for the base is also a mystery. No funding can be traced to the military or government. Officials of the U. S. Government have probed for answers without success.

The secrecy of the operation has prompted legends to thrive across Long Island. However, it is unlikely that any of the local people of Montauk, or those who spread the tales, know the full story of what actually went on there.

A circle of insiders believe the Montauk Project was a development and culmination of the phenomena encountered aboard the U.S.S. Eldridge in 1943.

Popularly known as the "Philadelphia Experiment", the ship actually disappeared while the Navy conducted radar invisibility experiments.

According to these accounts, over three decades of secret research and applied technology ensued. Experiments were conducted that included that included electronic mind surveillance and the control of distinct populations.

The climax of this work was reached at Montauk Point in 1983. It was at that time that the Montauk Project effectively ripped open a hole in space-time to 1943.

Perhaps the person best qualified to tell the real story is Preston Nichols, an electrical engineer and inventor who has studied the Montauk Project for the better part of a decade. His interest in the project was spurred in part by unusual circumstances in his own life. He was also able to legally acquire much of the equipment that was used for the project. His continued investigation ultimately revealed his own role as the technical director of the project. Despite brainwashing and threats to silence him, he has survived and has decided it is in the best interest of all to tell his story.

GUIDE TO THE READER

Because of the subject matter of this book is controversial, we would like to offer some guidelines.

This book is an exercise in consciousness. It is an invitation to view time in a new manner and expand your awareness of the universe. Time rules our fate and ushers in our death. Although we are regulated by its laws, there is much that we do not know about time and how it relates to our consciousness. Hopefully, at the very least, this information will broaden your horizons.

Some of the data you will read in this book can be considered as "soft facts".

Soft facts are not untrue, they are just not backed up by irrefutable documentation.

A "hard fact" would be documentation or hard physical evidence that could stand up to scrutiny.

By the nature of the subject matter and security considerations, hard facts about the Montauk Project have been very difficult to obtain. There is also an area between soft and hard which can be termed "gray facts". These would be very plausible but not as easily provable as a hard fact.

Any serious investigation will show that a Montauk Project did, in fact, exist. One can also find people who have been experimented on in some fashion or another.

This book is not an attempt to prove anything. The purpose is to get a story told that is of essential interest to scientific researchers, metaphysicians and citizens of the planet Earth. It is the story of one particular individual and his circle of contacts. It is hoped that more individuals will come out of the closet and that researchers will come forth with more investigations and documentation.

This work is being presented as non-fiction as it contains no falsehoods to the best knowledge of the authors. However, it can also be read as pure science fiction if that is more suitable to the reader.

A short glossary has been provided in the back to assist with ordinary electronic terms and those of a more esoteric nature. Scientists who read this book should understand that the definitions are designed to assist the general reader's understanding. They are not purported to be the latest technical jargon.

Likewise, the general reader should understand that the diagrams in this book are included for the benefit of technical people. If one is interested, they can get a further understanding of those terms and symbols by studying the Radio Amateur's Handbook or a text of similar nature.

ONE-THE PHILADELPHIA EXPERIMENT

The origin of the Montauk Project dates back to 1943 when radar invisibility was being researched aboard the USS Eldridge. As the Eldridge was stationed at the Philadelphia Navy Yard, the events concerning the ship have commonly been referred to as the "Philadelphia Experiment". Having been the subject of differnet books and a movie, only a quick synopsis will be given here.*

The Philadelphia Experiment was known as the Rainbow Project to those who manned and operated it. It was designed as a top secret project that would help end World War II. The forerunner of today's stealth technology, the Rainbow Project was experimenting with a technique to make a ship invisible to enemy radar. This was done by creating an "electromagnetic bottle" which actually diverted radar waves around the ship. An "electromagnetic bottle" changes the entire electromagnetic field of a specific area - in this case, the field encompassing the USS Eldridge.

While the objective was to simply make the ship undetectable by radar, it had a totally unexpected and drastic side effect. It made the ship invisible to the naked eye and removed it from the space-time continuum. The ship suddenly reappeared in Norfolk, Virginia, hundreds of miles away.

The project was a success from a material standpoint, but it was a drastic catastrophe to the people involved. While the USS Eldridge "moved" from the Philadelphia Naval Yard to Norfolk and back again, the crew found themselves in complete disorientation. They had left the physical universe and had no familiar surrounding to relate to. Upon their return to the Philadelphia Navy Yard, some were planted into the bulkheads of the ship itself. Those who survived were in a mental state of disorientation and absolute horror.

The crew were subsequently discharged as "mentally unfit" after having spent considerable time in rehabilitation. The status of "mentally unfit" made it very convenient for their stories to be discredited.

This put the Rainbow Project at a standstill.

Although a major breakthrough had occurred, there was no certainty that human beings could survive further experimentation. It was too risky. Dr. John von Neumann, who headed the project, was now summoned to work on the Manhattan Project. This concerned the making of the atom bomb, which became the weapon of choice for ending World War II.

Although it is not well known, vast research that began with the Rainbow Project was resumed in the late 1940's. It continued on, culminating with a hole being ripped through space-time at Montauk in 1983. The goal of this book is to give you a general understanding of the research and events subsequent to the Philadelphia Experiment and up to 1983 at Montauk. I will begin by telling you how I, Preston Nichols, stumble across it.

* Further information about the Philadelphia Experiment can be found in Appendix E.

TWO-MONTAUK DISCOVERED

In 1971, I began working for BJM*, a well known defense contractor on Long Island. Through the years, I got a degree in electrical engineering and became a specialist in electromagnetic phenomena. I was not then aware of the Philadelphia Experiment or its accompanying phenomena.

Although I was not extraordinarily interested in the paranormal at that time, I had obtained a grant to study mental telepathy and to determine whether or not it existed. I sought to disprove it, but I was surprised to find out that it did, in fact, exist.

I began my research and found out that telepathic communication operated on principles that are strikingly similar to that of radio waves. I had discovered a wave that could be termed a "telepathic wave". In some respects, it behaved like a radio wave. I set out to get the characteristics of this "telepathic wave". I studied their wave lengths and other pertinent facts. I determined that while a telepathic wave behaves like a radio wave, it isn't exactly a radio wave. Although it propagates in a similar fashion to that of electromagnetic waves and possesses like properties, not all of these fit into normal wave functions.

I found all of this very exciting. I had discovered a whole brand new electromagnetic function that was not in any of the text books I'd ever seen.

I wanted to learn as much as I could and studied all the activities that might use this type of function. My interest into metaphysics had been launched.

I continued to research in my spare time and collaborated with different psychics to test and monitor their various responses. In 1974, I noticed a peculiar phenomena that was common to all of the psychics that I worked with. Every day, at the same hour, their minds would be jammed. They couldn't think effectively.

Suspecting that the interference was caused by an electronic signal, I used my radio equipment and correlated what came on over the air waves at the times the psychics were non-functional. Whenever a 410-420 MHz (Megahertz) cycle appeared on the air, they were jammed. When the 410-420 MHz cycle was off, the psychics would open back up after about twenty minutes. It was obvious that this signal was greatly impeding the ability of my psychics.

I decided to trace the signal. Placing a modified TV atenna on the roof of my car, I grabbed a VHF receiver and set out looking for the source of it. I tracked it right to Montauk Point. It was coming directly from a red and white radar atenna on the Air Force base.

At first, I thought that this signal might have been generated accidentally.

I checked around and found out that the base was still active. Unfortunately, security was tight and the guards wouldn't give any useful information. They said that the radar was for a project run by the FAA. I couldn't press the point beyond that. In fact, their statement didn't make a lot of sense. This was a World War II radar defense system known as "Sage Radar". It was totally antiquated, and there is not any known reason why the FAA would need such a system I didn't believe them but couldn't help being intrigued. Unfortunately, I had hit a dead end.

I continued my psychic research, but didn't get anywhere on the investigation of the Montauk atenna until 1984, when a friend of mine called. He told me the place was now abandoned, and that I should go out there and check it out. I did.

It was indeed abandoned, with debris strewn everywhere. I saw a fire extinguisher left amidst many scattered papers. The gate was opened as were the windows and doors of the buildings. This is not the way the military normally leaves a base.

I strolled around. The first things that caught my eye was the high voltage equipment. I was very interested as it was a radio engineer's delight. I am a collector of ham gear and radio equipment, and I wanted to buy it. I figured it would be available cheap if I made the proper arrangements though the Surplus Disposal Agency in Michigan.

After examing all the equipment, I contacted the disposal agency and spoke to a friendly lady. I told her what I wanted, and she told me she would see what could be done. It appeared to be abandoned material and looked like a scrap contract. If this was so, I'd be able to take what I wanted. Unfortunately, I didn't hear from her so I called her back three weeks later. She informed me that there had not been any success with tracing the equipment. They couldn't find out who owned it. Neither the military or the GSA (General Services Administration) claimed to know anything about it. Fortunately, the Surplus Disposal Agency said they would continue to track the matter further. After another week or two went by, I called her back. She said she'd turn me over to a John Smith (fictitious name), located at a military overseas terminal in Bayonne, New Jersey.

"Talk to him and he'll set something up," she said.

"We like to keep our customers satisfied."

I met John Smith. He didn't want to discuss anything on the phone. He said that no one officially admitted to owning that equipment. As far as they were concerned, the equipment was abandoned and I could go in and take whatever I wanted. He gave me a piece of paper which appeared be official and said to show it to anyone who might question my presence in the area. It was not an official document nor was it registered with anybody, but he assured me that it would keep the police off my back. He also referred me to the caretaker of the Montauk Air Force Base who would show me around.

*BJM is a fictitious name for the company I worked for.

THREE-A VISIT FROM MONTAUK

I was out at the base within the week. There I met the caretaker, Mr. Anderson.

He was very helpful. He told me to be careful and showed me where things were so that I wouldn't fall through the floor and that type of thing. He said I was welcome to take anything I could this trip, but if he ever saw me out there again, he'd have to kick me out. His job, afer all, was to keep people off the base.

He realized that the permission I had was semi-official at best. He was also kind enough to tell me that he went out for a dring every evening at 7P.M..

I had taken a trip to Montauk with a fellow named Brian. Brian was a psychic who had helped me with my research. As we foraged around the base, we went in two different directions. I went into a building and saw a man who appeared to be homeless. He told me that he had been living in the building ever since the base was abandoned. He also said that there had been a big experiment a year earlier and that everything had gone crazy. Apparently, he'd never gotten over it himself.

In fact, the man recognized me, but I had no idea who he was or what he was talking about. I did listen to his story. He said he had been a technician at the base and that he'd been AWOL. He had deserted the project just before the base had been abandoned. He spoke about a big beast appearing and frightening everyone away. He told me a lot about the technical details of the machinery and how things worked. He also said something that was very strange. He told me that he remembered me well. In fact, I had been his boss on the project. of course, I thought it was pure nonsense.

I didn't know then that there was any truth to his story. This was just the beginning of my discovery that the Montauk Project was real.

I left the man and found Brian. He was conplaining that things weren't right and that he was feeling some very funny vibrations. I decided to ask him for a psychic reading right there. His reading was strangely similar to what the homeless man had just told me. He spoke of irregular weather patterns, mind control and a vicious beast. He mentioned animals being affected, crashing through windows.

Mind control was a main focus of Brian's reading.

The reading was interesting, but we were there to cart out the equipment. Much of it was heavy and we weren't allowed to bring a vehicle right onto the base.

We had to back pack it. I was thus able to acquire much of the equipment left behind from the Montauk Project.

A few weeks later, I was surprised by a visitor who barged into my lab. He came straight to the lab, which was in back of the house. He didn't ring the door bell or anything. He claimed to know me and said that I had been his boss. He went on to explain many of the technical details of the Montauk Project. His story corroborated what psychics and the homeless man had told me. I didn't recognize him but listened to all he had to say.

I was sure that something had gone on at the Montauk base, but I didn't know what. My personal involvement was evident, but I still didn't consider it very seriously. I was, however, puzzled by different people recognizing me. I had to make it my business to investigate Montauk. So, I went out and camped on the beach for a week or so. I went to bars and asked the locals for stories about the base. I talked to people on the beach, on the street, wherever I could find them. I asked all about the stranged activities that were purported to have occurred.

Six different people said that it had snowed in the middle of August. There were listings of hurricane force winds that came out of nowhere. Thunder storms, lightning and hail were also reported under unusual circumstances. They would appear when previously there had been no meterorologial evidence to expect such.

There were other unusual stories besides the weather. These included stories of animals coming into the town en masse and sometimes crashing through the windows. By this time, I had taken different psychics out to the base. The stories confirmed what psychics had been able to determine through their own sensitivity.

I finally got the idea to speak to the Chief of Police who also informed me of strange happenings. For example, crimes would be committed in a two hour period. Then, all of a sudden, nothing. Keep in mind that Montauk is a very small town. After the quiet, another two hour period of crimes would occur.

Teens were also reported to suddenly group en masse for two hours, then mysteriously separate and go their own ways. The Chief couldn't account for it, but his statements lined up perfectly with what the psychics had indicated about mind control experiments.

I had collected some really bizarre information, but I didn't have many answers.

I was, however becoming very suspicious. I had often travelled to Ham-fests, (where Ham radio equipment is bought and sold) and there more people would recognize me. I had no idea who they were, but I would talk to them and ask them about Montauk. As I did, more information came, but everything was still a big puzzle.

FOUR- DUNCAN ARRIVES

In November of '84, another man appeared at my lab door. His name was Duncan Cameron. He had a piece of audio equipment, and he wanted to know if I could help him with it. He quickly became absorbed in the group of psychics I had working with me at the time. This endeavor was a continuation of my original line of research. Duncan showed a keen aptitude for such work and was extremely enthusiastic.

I thought he was too good to be true and became suspicious of him. My assistant, Brian, felt the same. He didn't like duncan's sudden involvement and decided to go his own way.

At one point, I surprised Duncan by telling him that I would be taking him some place to see if he recognized it. I drove him to the Montauk Air Force Base.

He not only recognized it, he told me what the purpose was for each of the

various buildings. He knew exactly where the bulletin board in the mess hall was and many other suchminute details. Obviously, he had been there before. He knew the place like the back of his hand. He provided new information about the nature of the base and what his own function had been, Duncan's input dovetailed very nicely with the previous data I had collected.

When Duncan entered the transmitter building, he suddenly went into a trance and began spitting out information. This was curious, but I had to shake him repeatedly to break him out of it. When I brought him back to the lab, I applied techniques that I'd learned to help Duncan unblock his memories. Layers of programming were now coming out of Duncan. A lot of information concerned the Montauk Project.

Many different things were revealed, until finally a shocking program came straight to the awareness of Duncan's conscious mind. He blurted out that he had been programmed to come to my place, befriend me and, then, kill me and blow up my entire lab. All my work would be totally destroyed. Duncan appeared to be more outraged at all this than I was. He swore that he would no longer help those who had programmed him, and he has worked with me ever since.

Further work with Duncan revealed even more bizarre information. He had been involved in the Philadelphia Experiment! He said that he and his brother Edward had served aboard the USS Eldridge as members of the crew*.

A lot of things surfaced as a result of my work with Duncan. I started to remember things about the Montauk Project and was now certain I'd been involved.

I just didn't know how or why. The puzzle was slowly clearing up. I found Duncan to be an extremely operational psychic and through him I was able to confirm new information.

* An account of Duncan's role in the Philadelphia Experiment is in the book "The Philadelphia Experiment & Other UFO Conspiracies" by Brad Steiger with Al Bielek and Sherry Hanson Steiger.

FIVE- A CONSPIRACY REVEALED

I visited Montauk many more times, often with different people who had been involved. A small group of us began to realize that we had stumbled across one of the highest security projects the country had ever known. We figured that we had better do something fast with this new found knowledge. If we didn't, we might end up dead.

As a group, we decided action had to be taken. We weren't sure exactly what to do, so we sat around and discussed it. What was the best thing to do? Publish it? Immediately? We talked about it extensively. In July of 1986, we decided that I should go to the United States Psychotronics Association (USPA) in Chicago and talk about it. I did, and it created an uproar. Word got around fast to those who didn't want the Montauk story to be revealed. Suddenly, here I was, giving an unannounced lecture. The information got out to hundreds of people, swept under the rug without creating a public furor. To this day, I still appreciate the open forum and free speech that the USPA provided me.

Now, we decided to feed the information to the federal government. One of associates knew the nephew of a senior senator from the Southwest. The nephew, who we will call Lenny, worked for the Senator. We gave the information to Lenny, who passed it to his uncle. This information included pictures of the orders given to the different military personnel, which we had found strewn about the base.

The Senator did a personal investigation and verified that miitary technicians had in fact been assigned to the base. The Senator also discovered that the base was decommissioned, derelict and mothballed since 1969. Having served his country as an Air Force general, he was particularly interested to know why Air Force personnel were working on a derelict base. And, where did the money come from to open up the base and run it?

After they did their own investigation and saw the pictures and documents we supplied them, there was no question that the base had been active. They verified that Fort Hero (which is the name of the original World War I base that surrounds the entire area of the Air Force base) and Montauk were indeed derelict and simply listed as property held by the General Services Administrations since 1970.

The Senator got very involved and travelled to Long Island to find out what he could about Montauk Air Force Base. He was not greeted with enthusiastic cooperation despite having very impressive personal credentials. People reported seeing him looking through the fences and trying to find out what was going on. He visited me and told me to keep quiet about it as speaking out any further could jeopardize his investigation. That is why I have kept this strory quiet until now.

When the Senator completed his investigation, he couldn't find any trace of government funding, no appropriations, no oversight committees and no payments.

He eventually retired due to advancing age, but I have since been informed by Lenny that he sees no problem with my story being published. He also said that the Senator is still in the picture and that the investigation had been reopened.

SIX- "PROJECT MOONBEAM"

While the Senator was seaching for paper trails that might reveal the secrets of Montauk, I knew that they would not solve my personal mysteries one bit. I had been recognized by people I didn't know, and it was obvious that I had severe memory blocks. What made things so hard to reconcile was that I had a full set of "normal" memories which told me where I had been.

My memory improved while working with Duncan, and I eventually realized that I must have been existing on two separate time tracks. As bizarre as it may sound, it was the only sensible explanation under the circumstances.

As my memory was still largely blocked, there were three avenues of approach to the problem. First, I could simply try to remember the other time track, through regression or hypnosis. This proved to be very difficult for me and was virtually of no use. Secondly, I could look for clues and hints (in our normal time track) that the other time track did, in fact, exist. Thirdly, I could try to find the answers through technology. This would include theories of how the other time track was created and how I ended upon it.

The third approach was the easiest. I am told that many people might find this very confusing, but I was familiar with the theories of the Philadelphia Experiment and was not intimidated by physics or electromagnetics. I found it plausible.

The second approach also proved extremely helpful, but clues were hard to come by.

It was now 1989. I started to roam around the plant at BJM, where I was still working. I would talk to different people and dredge up what information I could without trying to appear suspicious. I would also walk around and just sense my own personal gut reaction to the different places in the plant.

I became particularly irritated when I would come to a certain room. My innards would just churn. I sensed very strongly that there was something in that room that was disturbing me. I had to investigate it. I rang the doorbell and was told that I couldn't come in. It was a high security area. Reportedly, only ten people at the plant had the proper clearance to be in that room.

I found that virtually no one knew anything about it. Finally, I did find two people who'd been in there, but they said they couldn't tell me anything.

One of them must have turned me in, because the security personnel visited me shortly thereafter. It was time to lay low for a while.

About a year after my futile investigation, the room was totally cleared out.

The doors were open and anyone could walk right in. It was obvious that there had been all sorts of equipment. Dirt markings revealed that four round things had stood on the floor. I presumed they were coil structures. It was clear that there had been a console. There was also a huge power line that still ran into the room. The entire place gave me the creeps, but I was driven to find all I could.

I discovered an elevator in the back of the room. I got in and found only two buttons: Main Floor and Sub Floor. There was also a numbered key pad. I pushed the button for Sub Floor and tried to go down, but the elevator would only go so far. I heard a voice that told me to punch in the proper coded numbers on the key pad. I didn't have the code and a beeping noise went off for about thirty seconds. Security was alerted. I had hit another dead end.

I wasn't scoring any points with security, and it was time to lay low once again. I began to think of how I could show that something very unusual was going on.

I also recalled earlier strange experiences that had occurred while working at BJM. There was a period when, all of a sudden, a band-aid would appear on my hand. It hadn't been there fifteen minutes ago! I couldn't remember putting it on. This hapened more than a few times.

One day, I had been sitting at my desk and my hand suddenly started to ache.

The back of the hand was sore, and there was a band aid on it. I absolutely knew that I had not put that band aid on nor had I had it put on. I became very suspicious. I got up and went down to the nurse.

I said to her, "This may sound wacky, but was I in here for a band aid?"

"No, you weren't in here," she told me.

I asked her where I'd gotten it and she said, "You must've gotten it from one of the first aid kits. Don't you remember?"

"I'm just trying to figure it out," I said, and I walked out. I thought in my mind, "I'm not going to get a band-aid at BJM except from the company nurse."

I wanted a record, so I made a conviction that I would never use a first aid kit.

I eventually remembered the reason I had sustained so many injuries to my hands. In my alternate reality, I frequently had to move different equipment.

I was just about the only one who could move it as most people would go wacky when they'd get near it. For some reason, it didn't seem to bother me. But it was heavy and hard to maneuver. With no one to assist me, bruised hands and band aids became a regular occurrence.

I kept to my conviction not to use any band aids from first aid kits. I continued to check with the nurse when they appeared, and the records indicated I'd never been to her.

As this was an irregularity, she must have reported it to security. They visited me and said, "Why are you asking about band aids, Mr. Nichols?" I knew better than to pursue that anymore.

Recalling these experiences with the band aids helped spur my memory back to 1978. I remembered sitting at my work bench one day. All of a sudden, I smelled the scent of burning transformers. It was pungent, like the smell of burning tar. It came and disappeared very fast. This happened at 9:00 o'clock in the morning. The rest of the day continued as normal until 4:00 o'clock in the afternoon when the whole plant began to smell like putrid smoke from burning transformers.

I thought to myself, "That's the same smell I smelled at 9:00 o'clock this morning." But now it occurred to me that the event probably hadn't happened at the time I had thought. You can't burn up a transformer and have the smell disappear as fast as it had that morning.

Many more events of this nature had occurred. Each puzzle tended to confuse the general issue. Streams of unfamiliar people continued to recognize me. I began to get executive mail that would normally be for the vice president of a company.

For instance, I would be asked to come to a conference concerning patents. I didn't know what they were talking about. I was also called to meetings with a

certain executive. He always appeared very agitated whenever we spoke.

Most of the inquiries I received from these people were about the Moonbeam Project. I didn't know what it was. But one day, I had an intuitive urge. The basement of the BJM building in Melville had a very high security area. Consciously, I had no clearance to be in that area, but I walked in anyway. Normally, when you walk from one security area to another, you must hand the guard your badge and he gives you another badge (with a different designation). This permits you to walk in the secure area. I simply went in and gave him my badge from the lesser security area, and what do you know? He gave me a badge with my name on it! I'd had a hunch and it worked.

I walked around and let the churning in my gut determine what direction I should go in. I ended up in a posh mahogany paneled office. There was a large desk with a name plate on it that read, "Preston B. Nichols, Assist Project Director". This was the first tangible physical proof I had that something out of the ordinary was definitely occurring. I sat at the desk and looked through all the papers.

It was impossible to take the papers out of the place as I knew I would be searched very thoroughly on my way out of this high security area. So, I committed everything I saw to memory, to the best of my ability. I had an entire second career here that I knew almost nothing about! I can't even talk about most of it.

It is top secret. I'm bound not to mention it for thirty years because of an agreement I signed when I went to work for BJM. However, I didn't sign a single thing regarding the activities of the Montauk Project.

Sifting through the material, I spent about six hours in my newly discovered office. Then, I decided I'd better get back to my regular job before the day was through. I handed back my badge and walked out. A couple of days went by before I decided it was time to go back and check things out again. Once more, I handed the guard my badge, but this time he didn't give me anything back. He said, "By the way, Mr. Roberts (fictitious name) wants to see you."

A man, Mr. Roberts, came out of an office that had "Project Director" written on it. He looked at me and said, "What do you want to come in here for, sir?"

"To get to my other desk," I replied.

He said, "You don't have any other desk here."

I pointed to the office where my desk had been. But as I entered the room with the Project Director, I found it to be gone. In the couple of days since I'd been there, they had removed every trace of myself from the room.

Somebody must have realized that I had visited my office when I wasn't supposed to. I had entered in an ordinary state of mind which was not to their liking. They apparently had not turned on the program (switching me to an alternate reality) for that particular day and must have been wondering why I'd shown up. They must have concluded that the process was leaking and that I was some how able to remember my alternate existence. As a result, they stopped everything. I was pulled aside through security channels and was told that if I breathed a word of what I'd seen, I'd be locked up in jail and the key thrown away.

I tried to think of other strange incidents that had occurred. I'd kept a suspicious eye and had been experiencing two separate existences. How the hell had I been at Montauk and working at BJM, apparently during the same time period? I had already arrived at the conclusion that I must have been working two jobs simultaneously because there was a period of time when I'd come home and be totally exhausted.

At this point, all of what you've read was one huge confused mess in my mind.

I knew that I'd been working on two separate time lines or maybe more. In fact, I'd discovered quite a bit, but it was more confused than clear. I was, however, able to make a major breakthrough in 1990. I had begun constructing a Delta T* antenna on the roof of my laboratory. One day, I was sitting on the roof

and soldering all the loops together into the relay boxes (which relay the signals from the antenna downstairs to the lab). Apparently, as I sat there and held the wires together to solder them, the time functions were causing my mind to shift. The more soldering I did, the more I became aware. Then, one day - bang! - the whole memory line blew open for me. All I could figure was that the Delta T antenna was storing up time flux waves as I was connecting it together. It just kept pushing my mind a little bit with regard to the time reference. The antenna was stressing time (bending it) and enough bend was created so that I was subconsciously in two time lines. This was my memory breakthrough.

Whatever the explanation, I was very pleased to have regained so much of my memory. I also believe my theory about the Delta T antenna is correct because the more time I spent working on the antenna, the more memories came back. By early June 1990, all my key memories had come back.

In July, I was laid off. Subsequent to my firing, all of my close connections were removed as well. After having worked at BJM for the better part of two decades, I no longer had any links or friends to the company. My information sources had been effictively severed.

You now have a general idea of the circumstances whereby I regained my memory.

The next part of the book will contain the history of the Montauk Project that includes a general description of the technology involved. It is based upon my own memories and the information that has been shared with me by my various colleagues involved with the Montauk Project.

* A Delta T antenna is an octahedronal antenna structure that can shift time zones. It is designed to bend time. Delta T=Delta Time. Delta is used in science to show change and "Delta T" would refer to a change in time. More about the nature of this antenna will be covered later in the book.

SEVEN- WILHELM REICH AND THE PHOENIX PROJECT

The U.S. Government began a weather control project in the late 1940's under the codename "Phoenix." The information and technology for this came from Dr. Wilhelm Reich, an Austrian scientist who had studied with Freud and Carl Jung.

Reich was an extremely brilliant man but highly controversial. Although he experimented extensively and wrote many volumes, few of his critics have taken an honest look at all of his research because much of it is not available. Part of this can be attributed to the Food and Drug Administration who supervised a massive book burning of all his available materials and also destroyed much of his laboratory equipment.

Reich was known in part for his discovery of "orgone" energy, which is orgasmic or life energy. His experiments revealed orgone energy to be distinctly different from ordinary electromagnetic energy. He was able to prove the existence of this energy in the laboratory. His findings were written up in various psychiatric and medical journals of the period. The discovery of a type of energy called "orgone" was not so controversial. It became very controlversial with the powers at be when he reported curing cancer with his theories. He also associated "orgone" energy with "cosmic energy" and the Newtonian concept of "the ether". None of these views won him support from conventional scientists of the 1940's.

At the turn of the century, scientists had embraced the Newtonian "ether".

This is referred to a hypothetical invisible substance as a medium for light and radiant energy. Einstein, who embraced the theory in his early years, eventually determined that there could not be a calm ether sea through which matter moves.

Not all physicists bought Einstein's argument, but Reich didn't disagree. He

pointed out that Einstein disproved the concept of a static ether. Reich considered the ether to be wave-like in nature and not static at all.

Conventional scientists have since recognized the existence of phenomena that are a cross between particles and waves. They are sometimes referred to as "wavicles".

Common research has also shown that vacuum space contains complex properties that are dynamic in nature.

Although it is not my cause to take up the case of Reich, his concept of the ether has proven itself functional in my research. It does not matter whether we are actually referring to "wavicles" or even more esoteric phenomena when we talk about the ether. Is is the word that Reich used, and it is easier for me to use in describing this for the general public. The reader is invited to read up on Reich as his work is vast and encompasses much more than can be covered in the scope of this book.

For instance, he found practical uses for his theories such as modifying the weather. He found that violent storms accumulate "dead orgone", which he termed "DOR." Dead orgone refers to the accumulation of "dead energy" or energy that is on a descending spiral. Orgone and DOR were found to be present not only in biological organisms but in empty regions of the environment as well. An active and enthusiastic go-getter would be considered to have plenty of orgone energy, whereas a complaining hypochondriac who wanted to die would have DOR energy.

For example, he found that the more DOR in the storm system, the more violent the storm. He experimented with many forms of DOR busting, and came up with a simple electromagnetic method to reduce the violence of storms. In the late 1940's, Reich contacted the government and told them he had developed technology that could take the violence out of storms. Despite what disinformation you may hear, the government already knew what Reich could do and considered him a brilliant man. They asked for his prototypes and he was happy to oblige since he wasn't interested in the mechanical development, just the research.

At this point, the government's technology team merged Reich's discoveries with their own weather monitors and produced what is known today as the "radiosonde."

The government's contribution to the radiosonde dates back to the "airborne metrograph"* of the 1920's. This was a mechanical device that recorded temperature, bumidity and pressure. It was sent up in a parachute balloon and recorded information on a paper tape. The balloon was designed to burst so that the parachute would bring the metrograph back to Earth. The public were encouraged to retrieve them for a $5 reward, which was considerably more money in those days. This was how the government obtained data on the weather.

As these devices were returned via the mail, the time that elapsed before the recorded information could be read was much too long.

In the late 1930's, a new device was designed that was called a "radio metrograph."

This was similar to the airborne metrograph except that it contained electrical sensors. These sensors were connected to a transmitter that would transmit to a receiver on the ground.

The radio metrograph was the state-of-the-art weather device when Wilhelm Reich contacted the government in the late 1940's. He gave them a little balsa wood package that could be sent up in a balloon. According to witnesses, approaching thunderstorms actually split up and went arount the test sit on Long Island.

The government combined the technology of the radio metrographs with Reich's DOR busting device and called it the "radiosonde." It was developed until consistent effects on the weather could be reproduced.

By the 1950's, radiosondes were being sent into the air en masse at a rate of about 200 per day.

Since these radiosondes were sent up in balloons, they would not come down hard enough to self destruct upon impact. The public would find them, and it would

be impossible to keep the actual units secret enough without arousing suspicion. They publicized the apparent purpose of recording weather data, which uniformed examination would back up. The real purpose is not that obvious.

If someone tuned into one of these packages, the signal would not appear unusual when normal radio equipment was ued. So far so good!

They showed the public a data receiving station; set up to receive the inaccurate and unusuable data. A small production run of this receiving equipment was produced.

There were literally hundreds of these radiosondes in the air every day. With the radio range being limited to 100 miles, there should have been a "pile" of receivers known as radiosonde receptors and they should have been very common.

As I am a surplus radio collector "nut", it is quite strange that I have never seen a radiosonde receptor or the equipment that should accompany one. It is very unusual to have a data transmitter (in this case, the radiosonde) with no receiver to pick it up. This indicates that the Government didn't use the receivers!

My next clue was to look at the specification sheet for the radiosonde tube which emphatically states that the life expectancy is only a few hours. Despite this, I have had a tube on the air for over 2,000 hours, and at this time have built over twenty such units with only on efailure. This is a good industrial failure rate but is a major red flag. My only explanation is that if some local amateur radio operator finds or buys a radiosonde on the surplus market, he will read the data, get misled and not bother building a circuit that will run for a "only a few hours." He will use another tube.

It appears that the Government does not want the public to use these tubes and find something unusual and thus blow their secret. This is why misinformation in the spec sheet preserves the secret. In fact, they are not telling a lie because the battery pack was designed so that the tube would burn out after three hours or so. This is caused by back bombardment of the cathode, which would cool slowly and then destruct.

By the time these radiosondes hit the ground, they were dead. This way the public, who were encouraged to return them, wouldn't be able to pick up live units. If there was no secrecy involved here, why would the government design a battery to burn out a costly tube that would have to be replaced after a very short usage? More disinformation was accomplished by packing the sensors in sealed vials, which implies that upon exposure to the air, the sensors are short lived. Because of these precautions, the secret was maintained for over forty years, which is excellent security.

Upon further examination of the radiosonde and its circuitry, I discovered that the temperature and humidity registers in the radiosonde didn't work. Not any of them!

The temperature sensor was useless for recording the temperature, but it did have a function.** It acted as a DOR antenna while the humidity sensor acted as an orgone antenna. If DOR was sensed by the antenna, the transmitter would be broadcast out of phase and bust up the DOR and take the violence out of a storm.

Conversely, transmitting in phase would cause the DOR to build up.

The humidity sensor had the same effect with orgone energy. Transmitting in phase would build up the orgone energy and transmitting out of phase would reduce it.

The radiosonde also contained a pressure element that would act as a switch signal and would maintain either DOR or orgone. This was how they built up the orgone energy.

The transmitter consisted of two oscillators. One was a carrier oscillator, which runs at 403 MHz. The other ran at 7 MHz and is a relaxation oscillator.

This one would pulse on and off depending on what was encountered. Somehow, this monitored the etheric function of the radiosonde. I haven't discovered everything there is to know about radiosonde, but I have done a scientific analysis of it which I've included in the appendix (see Appendix A) for those who

are interested.

What I have told you about the radiosonde is hard evidence that can stand up to scrutiny. It establishes the credibility of my story that there was a secret project that involved weather control. We can't say exactly whether the radiosondes were used just to bust up violent storms, but the possibility was also there to build them up. The government abandoned the weather control aspect eventually. Changing weather, if it were proven in court, could lead to many law suits.

What is more intriguing than the weather aspect is the entire prospect of orgone and DOR energy and what could be done with that. In theory, this means that the government could have targeted communities, buildings or an entire populace and transmitted orgone or DOR energy. These type of activities have been reported in Russia for years. Not much press coverage has been given the U. S. effort in this regard, but there has been some activity. Whether it has been used harmfully or in war, I cannot answer, but the potential was there.

Forty years of development could also have made this a very refined technological device.

Please refer to Appendix B for additional information on Wilhelm Reich.

* The word "metrograph" is more clearly defined if you understand that "metro" signifies that it was a meteorological device and that "graph" means to write.

** For those technically oriented, the temperature sensor is essentially a thermistor; but instead of being carbon based, it contains noble metals and exotic elements. It is a very poor temperature sensor because as the temperature cycles it up and down, the resistance curve changes and it doesn't hold its calibration. The humidity sensor suffers from the same problem.

EIGHT- "THE PHOENIX PROJECT" ABSORBS "PROJECT RAINBOW"

While the Phoenix Project was investigating the weather and the use of radiosondes, Project Rainbow resurfaced in the late 1940's. Project Rainbow (which was the code name for the operation that brought about the Philadelphia Experiment) was going to continue research into the phenomena encountered on the USS Eldridge.

This project was concerned with the "electromagnetic bottle" technology, which eventually resulted in today's stealth fighter craft.

At about the same time, Dr. John von Neumann and his research team were called back. They had worked on the original Rainbow project and went to work on a new endeavor. This was similar to the Rainbow Project but had a different gowl. They were to find out what went wrong with the "human factor" of the experiment and why it failed so miserably.

In the early 1950's, it was decided that the remnants of Project Rainbow and the radiosonde project should be included under the same umbrella with the human factor study. After that point, the title of "Phoenix Project" was used to refer to all of these activities.

The project headquarters was at Brookhaven Labs on Long Island and the first order of business was to put Dr. von Neumann in charge of the entire project.

Dr. von Neumann was a mathematician who came to the United States from Germany.

He also became a theoretical physicist and was noted for his very advanced concepts of space and time. He originated the computer and built the first vacuum tube computer at Princeton University, where he also served as the head of the Institute for Advanced Study.

Dr. von Neumann had what could be described as a "good technical feel." He had the ability to apply advanced theories to technology. His background in math

gave him enough theory to communicate with Einstein, and he could in turn pass this on to the engineers and serve as a bridge between the two.

As von Neumann began work on the Phoenix Project, he quickly learned that he was going to have to study metaphysics. He had to understand the metaphysical side of man. The Rainbow technology had dissolved the physical and biological structure of human beings. People were stuck in bulkheads and changed beyond recognition in some cases. But it was the esoteric workings of the mind that had been affected first, in each case.

Von Neumann and his team spent about ten years working out why human beings had troubles with electromagnetic fields that shifted them through different places and times. They actually found out that humans are born with what is known as a "time reference" point. At conception, an energy being is attached to a time line and we all start from that point. To understand this, it is necessary to view the "energy being" or soul as distinct from the physical body of the person concerned.

Our whole reference as a physical and metaphysical being stems from that time reference which actually resides within the electromagnetic background of our planet. This time reference is the basic orientation point you have to the universe and the way it operates. You can imagine how you would feel if the clock suddenly started moving backwards and time as well. It is this time reference point that was thrown out of kilter with the individual crewmen of the USS Eldridge and caused them untold trauma.

The Rainbow technology turns on and creates what can be called an alternate or artificial reality. It creates a stealth effect by not only isolating the ship, but the individual beings as well, within a "bottle effect." Those beings were literally removed from space and our universe as we know it. This accounts for the invisibility of the ship and of the people on board. The alternate reality thus created has no time references at all because it is not part of the normal time stream. It is entirely out of time. To be in an artificial reality would be like waking up and not knowing where the hell you are. All of this would be very confusing.

The Phoenix Project was faced with solving the problem of bringing human beings into the "bottle" (and eventually out again) while at the same time connecting them to their real time reference (that they would know as the planet Earth, etc).

This meant that when they were in the alternate reality or "bottle", they had to be supplied with something that would give them a time reference. They solved this by feeding into the "bottle" all the natural backgrounds of the Earth - at least enough to convince them of a continuous stream time reference. To do otherwise, would likely cause those in the "bottle" to experience transdimensional disorder and problems of this sort. This is why it was necessary to set a phony stage. They could then feel some degree of normality.

Dr. von Neumann was the ideal candidate for the job since he knew computers.

A computer had to be used if they were going to calculate the time references of specific people and replicate those references while they were passing through an "electromagnetic bottle" or alternate reality. The people inside the "bottle" would be going through zero time and essentially a "no reality" or a disoriented one at best. The computer had to generate an electromagnetic background (or phony stage) that the physical being would synchronize with as well. If that wasn't done, the spirit and the physical body would go out of synch, thus resulting in insanity.

There are two points to be brought out here: the physical being and the spiritual being. This is why the time reference would lock in the spirit and the electromagnetic background would lock in the body. This whole project started in 1948 and was finally developed in 1967.

When this project was complete, a final report was written and submitted to Congress. Congress had funded this particular project thus far and followed the results. They were told that the consciousness of man could definitely be affected

by electromagnetics; and additionally, that it would be possible to develop equipment that could literally change the way a person thinks.

Not surprisingly, Congress said no. They were concerned that if the wrong people got a hold of this technology that they themselves could lose their minds and be controlled. It is a very valid concern and word was given by 1969 to disband the entire project.

NINE- THE MONTAUK PROJECT BEGINS

It is no secret that Congress has tried to brow beat the CIA into finding out everything that goes on in the intelligence community. They have cut their funding, limited their legal powers, and even the most naive person would likely admit to a credibility gap of some degree. However, we are not dealing with the CIA proper here. Indeed, if the CIA is involved, it would be a splinter wing or wings that are being used by a source other than the CIA director.

When Congress disbanded the Phoenix Project, the group at Brookhaven had already built an entire kingdom around this project. They had Reichian and stealth technologies which could definitely affect the mind of man.

The Brookhaven group went to the military and informed them about this fantastic new piece of technology they were working on. They told them about a device that could make the enemy surrender without a battle simply by throwing a switch. Of course, the military was very interested. This was every war expert's dream. Imagine, a device that makes the enemy give up before the battle starts!*

The military became enthusiastic and were ready to cooperate. They were informed that they didn't need to get involved in the financing because that was covered by the group at Brookhaven National labs. But, the Brookhaven people needed a place where proper experimentation could be done in seclusion. They needed certain equipment and personnel from the military. They gave the military a list of all technology required.

Of particular import on the technology list was the old Sage Radar. For this, they required a huge radiosonde that would operate around 425 to 450 MegaHertz.

From earlier research, it was known that this was one of the "window frequencies" for getting into the human consciousness. A very high powered radar device was needed that ran at 425 to 450 MHz.

The military had just what they were looking for: a mothballed Air Force base at Montauk Point that housed an obsolete Sage Radar system that fit the bill.

This system already had the RF sections and the modulator that would be required to build a huge radiosonde.

The Sage Radar at Montauk was originally part of the early warning defense system used during the '50's and '60's. Today, satellites and over-the-horizon radar make this technology obsolete for defense purposes. It certainly raises an important question, even if one doesn't believe this story. Why was an old antiquated defense system turned on and utilized for a period of over ten years?

The name for this project was known as "Phoenix II" by the officials concerned.

It has since been colloquially named by myself and others involved as the Montauk Project.

Up until then, Congress had been informed about what had occurred. But at this point, independent people were carrying forward with a project denied by Congress and were operating outside of any controls. They were even using the U. S. military in the process. Of course, it quickly becomes, "Who is using who?"

But, the point being stressed here is that it was being done without the supervision of elected officials and in spite of their objections.

The Montauk Base was being reopened. The Sage Radar had been shut down since 1969/1970 when the base was turned over to the General Services Administration.

It was a surplus government base without anything on it, and government financing for it had ceased.

It is obvious that major funding would be required for such an endeavor. The financing is shrouded in mystery, but it appeared to be totally private. I do not have documented evidence myself of the financing but have been told by my Montauk acquaintances that the original money came courtesy of the Nazis.

In 1944, an American troop train went through a French tunnel carrying 10 billion dollars worth of Nazi gold. This train was dynamited in the tunnel while carrying 51 GIs. General George Patton was in Europe at the time and investigated this, but he couldn't understand how an American troop train could be dynamited in western Allied territory. As a general and human being, he cared about the GIs. The 10 billion dollars was also a mystery, but Patton's efforts were blocked.

I've been told this gold eventually showed up at Montauk, and it was 10 billion dollars of gold priced, then, at $20 an ounce. This was the equivalent of almost 200 billion dollars in today's currency. It was used to finance the project initially and for years to come. After it was all spent, the project was allegedly financed by the infamous Krupp** family, who controlled the ITT corporation.

In late 1970 and 1971, the Montauk Air Force Base, 0773rd Radar Battalion, was actively being reestablished. They had to establish a staff, get the equipment working and set up the whole research facility. This took about a year, and by late '71, the Montauk Project was underway.

The strictest security measures were employed, part of which were entirely valid. Although confidential stealth technology was involved, it is no secret that the stealth aircraft was designed with a radar resistant absorbine coating and a reduced surface cross section. What is secret are certain aspects of the "electromagnetic bottle" technology and how that was propagated. We're not going to discuss this or describe it as it remains a duly authorized military secret that concerns the defense of the United States. With this book, we are concerned with disclosing a project that should never have been activated in the first place. With no military or defense purposes to begin with, it was only designed for controlling the minds of the population and in spite of Congress forbidding this project.

The staff was a mixture of military employees, government employees and personnel supplied by various corporations. I was one of the latter and came to the project in 1973.

There were a number of Air Force technicians who had worked on the Sage Radar in the '60's. The Air Force had assigned them to Montauk even though it was listed on the books as a decommissioned, derelict base. The technicians told the Phoenix group that they could change the general mood of the base by changing the frequency and pulse duration of the radar. they had noticed this as a professional curiosity after years of working with radar.

This was a surprise to the Phoenix people, and they found it very interesting.

By changing the pulse rate and pulse width, they could change the general way people were thinking. This was what they were looking for.

This new information prompted what I now refer to as the "Microwave Oven" experiments. They took the reflector (which looks like a huge banana peel and which can be seen from a distance when you are at the Point), rotated it almost due west and angled it down so that it was focused on one of the buildings, in what they though to be a safe place.

Inside that building they had a chair inside a shielded room. First, they'd sit someone in the chair - this was usually Duncan Cameron. Then, they would open and close the door to determine how much UHF/microwave energy was getting into the room. All this was being done while the antenna was rotated and focused to a point in front of the building. At the same time, the transmitter was blasting gigawatts of power.

They experimented by running the transmitter at different pulse widths, different pulse rates, and different frequencies. They tried everything they could

think of, just plain empirical experimentation. They just wanted to see what would happen to the person in the chair if he was bombarded by "x" frequency, pulse, etc. They observed that certain changes made a person sleep, cry, laugh, be agitated and so on. There were rumors that whenever the Sage Radar ran, the mood of the whole base would change. This was very interesting to the project supervisors as they were primarily concerned with the study of human factors.

They wanted to see how they could train and change brain waves. This was done by changing the repitition rates of the pulse and the amplitude in correspondence to different biological functions. In this way, a person's thoughts could be controlled. With the 425-450 MHz of radio frequency power, they actually had a window into the human mind. The next step would be to find out what was inside of it.

Although the door to the shielded room was closed most of the time, it didn't work properly. The subjects were exposed to a strong enough field to influence the brain waves but not enough to do damage. However, if exposed to it for several days on end, it could be quite damaging.

Duncan sustained serious brain and tissue damage as a result of continuous expsure to 100 kilowatts of RF power at a distance of about 100 yards. The radio waves baked his brains and chest. Anywhere in his body where there was a change of density, zones of heat or energy would be created by the concentration of the microwave beams.

Upon visiting a doctor in 1988, Duncan's doctor commented upon the unusual scar tissue in his lungs. He'd never seen anything like it. Another doctor who was consulted said he'd only seen it in the service when someone had gotten in front of a high powered radar beam.

Previous research in or about 1986 indicated that Duncan was actually brain dead. Initially, I had asked different psychics to do readings on Duncan. They determined he was brain dead. I also knew that it was possible to inject a particular dye into the brain and have x-rays or CAT scans can reveal what areas of the brain are using oxygen. Brain dead individuals suffer from a lack of oxygen to the cerebrum. If the psychic readings were accurate, his brain would not be using much oxygen.

I asked a neurologist with whom I was friendly with, and he said it was definitely possible that some one could be brain dead and yet be walking around. He cited some post mortems done on people in England in the U. S. whose brains had unusual coatings inside the skull. The coatings were about a millimeter thick.

More interesting yet was a case he'd encountered about ten years ago. He took out a group of x-rays of a normal human being and showed me the red areas. He also indicated blue areas but told me they were ares that didn't require much oxygen.

Then, he put up another x-ray where the entire brain was blue. This meant that the person was alive and was walking around like a normal human except he has memory loss problems from it. He was essentially brain dead and the brain was using just enough oxygen to keep it from rotting. I noticed the corner of the x-ray and was surprised to see Duncan's name. Based upon this information, Duncan is indeed brain dead.

I asked the doctor for an explanation, but he wasn't sure. He could only offer a theoretical conclusion based upon psychic powers. He said that his profession recognized the existence of psychic phenomena but did not understand it.

At this point, we learned that the only reason Duncan is alive today is due to his strong psychic aptitude. The psychic part of his mind takes over the physical part of his mind and runs the body. His brain stem is alive; his spinal chord is alive; his body is alive, but his actual higher brain is dead. His psychic energy runs the body through the brain stem.

Duncan was not the only person affected. We don't know how many people were involved but the body count was probably high.

It wasn't until 1972 or '73 when it was finally realized that stealth

technology dealth with non-burning radiation. One theory was that actual non-burning radiation, which is the higher order of components (as opposed to burning radiation), actually went through the reflector and would be opposite to the focal point of the antenna.

THey tried it and turned the antenna around 180 degrees. They aimed the burning rays into the sky and hit the person with the non-burning rays. Then, they found they had the same mood altering capabilities, if not more than they had before, but this did not damage the people. But at what cost to the persons previously experimented on!

At this point in the project, they were interested in monitoring people and changing their thoughts and moods, etc. It was not necessarily how they changed but the fact that they changed under certain circumstances. Different army units were invited to come to the base and have R&R there. As far as the soldiers were concerned, it was free R&R in a beautiful location.

The outer base had a nice gymnasium and a bowling alley with excellent food and accommodations. Unbeknownst to the servicemen, they became guinea pigs for the mood control experiments. However, these were not the only guinea pigs.

Experimentation was also done on the townspeople, Long Island, New Jersey, upstate New York and Connecticut civilians, just to see how far it could go. However, most experimentation was done on the vacationing soldiers.

Time was spent monitoring different pulse types, trying this and trying that.

They would note and categorize the different effects. It was all pure empirical experimentation and a huge data base was collected. Once they had enough data, they began to make some sense out of which functions did what.

During this period, they also experimented with frequency hopping. Frequency hopping consists of the transmitter instantaneously and randomly shifting around to any of five different frequencies (that were being fed to the transmitter). This point became veryimportant later on as it was key to bending time.

They discovered that very fast frequency hops made the modulations more psycho- active. A data base was then developed that would list the frequency hop times (times you go from one frequency to another), how they pulse modulated, the rate the pulse modulated at, the pulse width, and the power output they pulsed it at.

This was then coupled with the responding effects it had. The data base was very extensive and covered an extremely broad range of causes and effects.

After the extensive experimentation, they developed a control panel with which they could set different pulse modulations and timings. They knew that these different pulses and functions represented certain thought patterns from the individual. They could set the modulators and timings so that a transmission would be generated that would place thought patterns into an individual. This meant they could literally set this pulse at anything they wanted and expect a desired effect to take place.

All of this took about three or four years to research. The transmitter was now fully operational and hooked up. Programs could be typed in that would put the transmitter through its phases. Programs were derived that could change the moods of people, increase the crime rate, or make people agitated. Even animals within the vicinty were programmed to do strange things.

The researchers were able to derive programs whereby they could focus on a car and stop all the electric functions in it. I don't know what the modulations were, but I understand they found this quite by accident.

One day, there were military vehicles riding around the base. They suddenly ceased to operate without any function. An investigation ensued to find out what was occurring with the transmitter at the time, and a program was developed. At first, the program could only get the lights in a car to dim. It was eventually refined to where the program caused all electrical functions in a vehicle to cease.

Several years of research and collecting information had finally yielded a

mind control device. The next objective was to create a precision technology with the material. In order to do this, help from very strange sources was enlisted.

* I have included in Appendix C some vidence that suggests mind control devices were used against the Iraqis during the Persian Gulf War.

** The Krupp's were the owners of the German munitions factories for World War I and II. After being found guilty of war crimes and complicity with Hitler at the Nuremberg Trials, the head of the Krupp family was paroled from a light prison sentence and allowed to continue his notorious arms dealings.

TEN- THE MONTAUK CHAIR

In the 1950's, ITT developed sensor technology that could literally display what a person was thinking. It was essentially a mind-reading machine. It operated on the principle of picking up the ectromagnetic functions of human beings and translating those in an understandable form. It consisted of a chair in which a person would sit. Coils, which served as sensors, were placed around the chair. There were also three receivers, six channels and a Cray 1 computer which would display what was on a person's mind - digitally or on a screen.

It is still a mystery how this technology was developed. It has been suggested that the research was aided by the Sirians, an alien race who come from the star system known as Sirius. This theory has the aliens providing the basic design and humans working it out from that.

Three sets of coils were set up in a pyramid around the chair. There was also a coil around the top of the pyramid to parallel the base coil. The person would be placed inside the field of the coils. The three sets of coils were connected to three different radio receivers (Hammerland Super ProP 600's) and six outputs.

An independent sideband detector, which had a floating carrier reference system, would provide six outputs from the three receivers. Three of them were of the sideband below the carrier wave. Three of them were of the sideband above the carrier wave. This brings to mind a very important question. If this device was reading minds, what was the carrier wave it was using to do this?

With the use of an oscillator, the detectors in the receivers were able to lock on a phantom or etheric signal that was being picked up by the coils. There was no actual carrier wave as we would normally know it. the detectors would lock in on the noise peak that the coils picked up from the three sets of frequencies the receivers were tuned to.

At this point, the research team was actually able to detect the signals that represented the comparable functions of the human mind. Solid signals that would change with a person's thoughts were actually coming out of the receivers. This device was actually reading the human aura, which is a word that psychics and metaphysicians use to describe the electromagnetic field that surrounds the human body. In the same way that human speeck is carried via radio waves, this device was carrying thoughts (which theoretically manifest in the aura).

The six output channels from the receivers were then run through a digital converter (turning them into computer language) and fed into a computer. A Cray 1 computer was used to decode what the receivers were picking up. A lot of hard work and a lot more computer crunching got things to the point where the computer could print out a dialogue. This would be a running dialogue of the person thinking.

More work got it to where the person would visualize something and a picture would actually appear on the computer monitor. Improvements and refinements continued until a 3D representation of the actual audio/visual aspect (of the person's thoughts) appeared on the computer monitor and could in turn be printed out.

When the people at Montauk heard about this mind reading device, they thought it was great. They wanted to turn this mind reading machine into a

transmitter. This could possibly cut the risks to human beings undergoing invisibility or time experimentation. The theory was that a person in the chair would transmit an alternate reality to the crew (like in the Philadelphia Experiment). When the ship became invisible, the crew would then be insynchronization with the alternate reality and wouldn't become disoriented or mentally lost.

At this point, a chair was procured, which we now refer to as the famous "Montauk Chair". It was hooked up to the coil set-up from ITT. The Cray1 computer, which was used to decode the transmissions being generated from the person in the chair, was then interfaced with an IBM 360 computer. This was, in turn, interfaced with the Montauk transmitter.

The IBM 360 was needed to control the modulation of the transmitter so that the transmitter could frequency hop across the entire band.

It was about this time that I remember Al Bielek taking on a key role. Al is one of the authors of 'The Philadelphia Experiment and Other UFO Conspiracies.'

He has memories of being involved in the Rainbow Project as well. Originally, he was brought to the project to explain what was going on metaphysically with the use of the transmitter on human beings. He was chosen because he not only had an engineering background, but he was psychically sensitive and had an extensive knowledge of esoteric matters.

It now became Al's job to help interface the Cray 1 computer with the IBM 360.

The Cray 1 was putting out tons of information. They didn't know what to do with it and needed someone with esoteric knowledge to figure it out. They had to convert what the Cray 1 was putting out so that it would synchronize with what the pulse modulation comupter wanted. The IBM 360 served this function and was essentially used as a translator and storage bank for what the Cray 1 was outputting. Al got very heavily involved because he was part of the team that figured out what program to put on the IBM 360 that would translate the Cray 1 output to drive the transmitter.

The transmitter had a modulation computer which was digitally fed the typical 32 bit code that the 360 put out. The modulation computer and the transmitter were set.

The IBM 360 would tell the modulation computer how to modulate the transmitter.

Now we had a system where one could put in 32 bit words of data and the transmitter would give back something. And here the chair fed the receptors feeding the Cray 1 which would tell what the person was thinking. They had to take this and translate what was coming out of the Cray 1 and make it so that the IFM 360 could re-encode the thought form that was actually transmitting. It took about a year to successfully link up the computers.

I had joined the project at this time to work with the radio frequencies and transmitter. Although some linkage had been achieved with the computers, they were having huge problems with feedback from the transmitter to the chair. The solution to the feedback was to move the chair down the coast to the ITT center in Southampton, Long Island. A psychic would then sit in the chair in Southampton and relay via computer to the Montauk transmitter.

The psychic would think thoughts, and the Cray 1 would decode them. They'd be put on a 32 bit radio link and sent Montauk where they would go into the IBM 360.

The IBM computer would then broadcast it out the transmitter and could build a thought form out at Montauk of what the psychic was thinking in Southampton. The device was essentially a mind amplifier.

It took another year of research before they could get a readable signal (based upon what the psychic was thinking at Southampton) sent to Montauk and out the transmitter. This was their first objective: get some thought fidelity from the chair through the Montauk transmitter and out the antenna. Besides Duncan, there were a couple of additional psychics on site. They literally tuned up the

computer programs. Finally, the thought forms became clear. The psychic could concentrate on something in Southampton and the transmitter at Montauk would transmit a very clear representation of what he was thinking.

That was the first point at which the Montauk transmitter was working with high thought fidelity.

In another year, I recall as early '75, they discovered another problem. If there was a glitch in the flow of time in our reality, everything fell apart. In other words, if the psychic in the chair projected a reality (in terms of time in this case) that was not consistent with out reality (i. e., the flow of time in our reality), it would cause the connection between Southampton and Montauk to break up. Any glitch in space-time between the two cities would cause the transmission of the thought form to cease.

To better understand a time glitch, imagine time as a continuous pulsation or flow. As the basic pulsation of time interacts and changes form with other flows or phenomena, we have motion as we know it, against the backdrop of time. When these core pulsations that make up time are shifted (due to a reality change or other phenomena); the direction, speed, or flow of time is changed. This is what is known as a time glitch. Theoretically, these occur every now and then, since we are referenced in our reality, we really don't notice a time glitch. Deja vu phenomena could well be an example of a time glitch in the fabric of time.

With the chair in Southampton, the mind control experiments with the transmitter were not always working. This was attributable to the time glitches. It was also known that if a large amount of power was fed into the transmitter during a time glitch, there could be disastrous effects.

It now became imperative to get the chair working at Montauk. They first put tremendous shielding around the chair so that the electromagnetic fields at Montauk would not affect it. That didn't work, so they tried putting the chair in an electromagnetic dead zone. They picked the best dead zone available, but this was not successful either.

They worked through mid '75 but continued to have difficulties until they consulted the original prototype that the chair was based upon (allegedly devised by the Sirians). This device was not identical to the one ITT had created. It had a different kind of coil set-up wherein the coils were connected to crystal type receivers. These were actual crystals and not ordinary electronic devices.

After review of the prototype, secret bids for a new chair were put out and RCA came up with the winning bid. Nikola Tesla* had designed receivers for RCA in the '30's. Tesla's work during this period was done under the name "N. Terbo", which referred to his mother's maiden name. These Tesla receivers had very special coil structures. They were normal type radio coils but were arranged in strange coupling patterns as set up and designed by Tesla.

The set up of the Montauk Chair was also enhanced by using Helmholtz coils.

These were placed around the chair to serve as pick up coils. In ordinary electronics, Helmholtz coils consist of two sets of coils. They possess a unique property in that they can be phased to create a constant field (of energy) inside the coils.

At Montauk, the researchers extrapolated upon the principles of Helmholtz coils.

They used three sets of coils (X, Y and Z), and phased them so that while a constant energy couls be maintained inside the coils, there was absolutely no effect on the outside.

The coil structure in the receivers designed by Tesla was ideal for the Montauk Project. Not only would the chair be in a coil structure, but so would the receivers themselves. This would shield the energy field.

It should also be noted that the coil sturctures in the Tesla receivers are also known as Delta T or Delta Time coil structures. The property of shielding an energy field is part of what enable a "bottle effect" to be created around the USS Eldridge in the Philadelphia Experiment. These Delta T coils were actually picking up three axes of time signals. More pertinent to the project, they no longer had a

microwave link that would malfunction during a reality shift.

To get the Montauk chair operating without interference, they had to replicate what the crystal receivers did with the "Sirian" technology. The coil structures in the prototype receivers were Delta Time coil structures. And the receiver itself did the Delta Time function, but not the antenna. ITT had the Delta Time function in the antenna instead of the receivers. The RCA version used standard type Helmholtz pick up coils that could accomplish Delta Time conversion in the receivers. They also had the same kind of detector system and oscillator locks that ITT used with the Cray 1 computer.

At this point, it now became inclusive of the coil only. Outside, the coil structure, there was no sensitivity. They could put the chair in the dead spot that was between the transmitting antenna on top of the transmitter building and the transmitting magnetic antenna that was underground. This was in the underground basement of the transmitter building, which had already been tightly shielded. In the next room, they had these three specially designed receivers with another rack of equipment. These were used to synchronize all local oscillators with the signal, similar to the ITT system.

Now, the antenna, the transmitter, and the chair were in the same time plane.

The computers were in their own time plane. It didn't matter that they had the chair underground and the Cray and 360 in the other building (feeding back to the transmitter building). When everything is digitized, one is no longer in real time. A "fake time" is created. The computers could have been located anywhere. The computer building was designed to operate computers and shielded out electromagnetics and energy didn't drive the computer insane. The operation center was totally shielded in cement and steel.

Finally, they created the second and last generation of the Montauk chair.

It performed the same purpose as the first chair. It brought the same six channels of information to the computer, but there was an additional advantage. It was immune to the signal from the antenna. Now, the signal from the antenna didn't feed back and cause interference. So, they had everything on site. They spent another six months until about late '75, early '76, just aligning, adjusting, and making sure everything was working.

They finally got the transmitter functioning, which was quite astounding. What happened afterwards was even more so.

* Nikola Tesla was an electronic genius who was the first to discover and apply the principles of alternating current. With the financial backing of George Westinghouse, he revolutionized the way electricity was used across the world.

See Appendix D for more information on Tesla.

ELEVEN- CREATION FROM THE ETHER

Once they had the transmitter working, it took about another year to work out the computer programs so the system would receive and transmit all psycho-active functions. By late '77, the transmitter was reproducing thought forms without glitches and with a very high degree of fidelity. At this point, they pulled out all the stops. They had the psychic, Duncan Cameron, concentrate on a solid object, and guess what happened? The solid object actually precipitated out of the ether!

In his mind, he would concentrate on a solid object, and it would appear somewhere on the base. Whatever Duncan would visualize, the transmitter would transmit the lattice (or matrix) for, and build enough power to materialize whatever he was thinking of. Every single point to where he could witness to a particular spot on the base, at that spot an object would materialize. In other words, if he would hold an object in his hand and/or visualize it, it would appear at the given spot.

They actually had discovered pure creation out of thought with the use of the transmitter.

Whatever Duncan could think up would appear. Many times, it would be only visible and not solid to the touch, like a ghost. Sometimes, it was a real solid object that was stable and would stay. Other times, it was a solid object that would remain as long as the transmitter was turned on and then fade out as the transmitter was turned off. The read out from the computer gave an accurate representation of what Duncan was thinking. The researchers could then select what thoughts would be broadcase out of the transmitter. Most of these though forms were broadcast in the vicinity of the Montauk Air Force Base, but other locations were used as well.

What Duncan though of as a subjective reality would be created as an objective reality (either solid or transparent, depending on the circumstances). For example, he could think of an entire building and that building would appear on base. This type of experimentation was routine.

The system worked with a good degree of fidelity. Now, they wanted to see what they could do with it. the first experiment was called "The Seeing Eye." With a lock of person's hair or other appropriate object in his hand, Duncan could concentrate on the person and be able to see as if he was seeing through their eyes, hearing through their ears, and feeling through their body. He could actually, see through other people, anywhere on the planet. This style of experimentation was extensive, but I don't know how far it was taken.

It is truly incredible that such a feat could be accomplished, however the agenda employed was more sinister than incredible. They were interested in controlling how human beings think. The next move was to see if they could put thoughts in the head of another person. For instance, they would have Duncan meet a subject individual.

Subsequent to the meeting and unbeknownst to the individual, Duncan would concentrate on the individual. Ninety-nine percent of the time, the subject would get thoughts similar to Duncan's. Being able to push his mind so far into the mind of another being, Duncan could control another person and make them do anything he wanted.

This control factor was on a deeper level than ordinary hypnosis.

Through Duncan, the equipment and the Montauk transmitter, scientists could actually load information, programs and commands into the individual's mind. Duncan's thoughts would become an individual's own thoughts. And, using this process, an individual could be made to do something he wouldn't ordinarily do. This was the start of the mind control aspect of the Montauk Project.

This line of research continued until about 1979. Many other different experiments ensued. Some of them were interesting, but others had horrible consequences.

They would target individuals or masses of people, animals, places and technology.

They could basically target anything they wanted. For example, a TV set could be made to go haywire. They could stop the picture or shut it off entirely. They telekinetically moved objects and destroyed rooms.

In one particular case, Duncan concentratedon shattering a window. Enough force was generated to the point where it actually broke a window in the nearby town of Montauk. Animals could also be made to charge off Montauk Point and into the town. Humans could be influenced to start a crime wave.

One must realize that when Duncan did these experiments, he was in an altered form of consciousness. He had been given special training which could possibly have been administered by the CIA or NSA. In any event, his conscious mind would be diverted through sexual bliss. What could be termed the primitive mind would then surface.

Duncan, the individual, would be transferred into an orgasmic trance. His primitive mind, at the disposal of the researchers, became very suggestible and therefore controllable.

For this programming, information could be installed via any of the body's senses. Duncan would then be directed to have his primitive mind concentrate on the information thus installed. For instance, once his primitive mind surfaced and was told to concentrate on something, it would concentrate with its whole being. His whole mind would focus on one subject while his body went into suspended animation.

The primitive mind could also be cleared of previous programming, and something else could be inserted. There was a literal translator, whereby they could program in whatever they wanted. Spoken words, written words, movies, music or whatever was needed was employed to work the primitive mind.

These techniques were the key to getting clear thought forms from the transmitter that would either affect another person's mind or bring creation out of the ether.

By 1978, the mind control techniques were fully developed and recorded. Appropriate tapes were made and distributed to different agencies so they could be developed into something practical.

TWELVE- TIME WARPING

As the experiments continued throughout 1979, a very peculiar phenomena was noticed. As Duncan's thoughts were projected out through the transmitter, they would suddenly cease. This was disappointing and appeared to be a malfunction.

Eventually, it was noticed that the projection of Duncan's thoughts hadn't ceased.

They were just occurring out of the normal time stream!

For example, he would concentrate on something at 8:00 PM and the object or occurrence would happen at midnight or even 6:00 AM. Whatever he thought of would not happen at the time he thought of it.

It now appeared that the Montauk scientists could now use Duncan's psychic powers to actually bend time!

They eagerly started to research this phenomena. We were all required to attend what were known as the "Sigma Conferences", which were held near Olympia, Washington.

These conferences were on the subject of time functions, and we were there to gain a better knowledge of how time works. We were told we had to optimize the use of the transmitter for time manipulations.

We learned that the equipment being used was strong enough to bend time, but it wasn't doing a complete job. The antennas being employed were giving us what could be a side effect of "time warping." This side effect of time shifting did show, however, that the basic equipment was sufficient to do it. But, we required an antenna that was much more effective in creating time potentials.

After going to several conferences and talking to many people, our research group decided that the radio frequency being used was not working. Changes had to be made, such as setting up pulses into a coil. We also studied pyramid based geometry and how to use that to bend the time field. Additionally, we had to learn more about what is known as the Delta Time function (time changing function).

The key clue to our understanding time was a suggestion that we use a particular type of antenna structurde, which I now refer to as an Orion Delta T antenna. It is referred to as "Orion" because there was a persistent rumor that the design was given tot he project by aliens from the Orion constellation (this is a different group of aliens from the Sirians, whose knowledge was alegedly used for the Montauk chair). According to the rumor, the Orions knew we were close to achieving our task and had their own agenda for helping us.

The Orion Delta T was a huge octahedronal antenna, and it was placed underground.

Its height was about 100 to 150 feet from point to point. Excavations were

completed to about 300 feet to house the antenna under the transmitter.

The Montauk chair was placed under the transmitter and above the Delta T antenna.

This was done in order to phase the ground RF antenna with the below ground loop antenna so that the chair was in a null point between them. The null point was meant to cut out the interference even deeper. It knocked the interference right out of the chair - completely.

The Delta T transmitting antenna was supplied by three drives. Two of the drives came from the pulse modulators of the two transmitters and fed into the x and y coils of the Delta T. (The same pulse that supplied power to the amplitron also supplied power to the Delta T antenna that was underground). The third axis was the z-axis.

It was placed around the perimeter of the antenna and was derived from a white noise* source that came from a 250 kilowatt audio amplifier. The white noise correlated the whole transmitter and more will be said on that later.

The RF was fed into an omnidirectional antenna located above ground on the top of the transmitter building. Additionally, the non-hertzian component (which is etheric in nature) of the RF made it below ground and interfaced with the magnetic field that had been generated underground. When these frequencies are summed in that manner, time disturbances and distortions result.

The basic techniques were the same as those employed in the Philadelphia Experiment.

On the Eldridge, they had the RF transmissions on the main mast of the ship. The coils were placed around the deck and were driven by pulses. We had essentially duplicated by upgraded the Rainbow Porject machine. This technique also made the project far more controllable.

In addition to the Delta T antenna, there are two other key points to understand: zero time and white noise.

Zero time was referred to previously, but I will give a more complete understanding of it now. First, zero time is outside the realm of our normal three dimensional universe. It would be considered senior to the createed world as zero time existed prior to our created world. Zero time is our basic connection to the universe.

As our universe roates, it rotates around zero time. But our universe is not the only one. Every universe has a zero point. All the zero points of the different universes coincide and never move: that is why it is called a zero point.

It may help to imagine a carnival style merry-go-round that revolves around a central booth. The man inside that booth would represent the zero point. In addition to the merry-go-round, there would be several more merry-go-rounds at different levels, but all would be under the control of the central zero point booth.

A zero time reference generator had already been constructed by Nikola Tesla in the 1920's. It consisted of an assortment of spinning widgets and rotating wheels. colloquially, we referred to it as a "whirligig". It is a strange device because when you turn it on, yu can hear it "lock in" to something, but we are not referring to the power line. I'm told it locks into the rotation of the Earth itself, which is a secondary zero time reference. It is secondary because the Earth's rotation is inertially related to the solar system, which is inertially related to the galaxy, on down to the universe. The universe rotates around the zero time point.

One can get an even better understanding of this by reading up on Tesla and how he discovered alternating current by applying the principles of the rotating magnetic fields of the earth. The zero time generator is to some degree an extrapolation of that, however it doesn't just refer to the rotation of the Earth. It takes into account the orbit of the Sun, our galaxy, and ultimately the center of our whole reality.

The other key point to understand is white noise. White noise could be

considered the glue that makes the whole operation work. It basically made the whole transmitter system coherent. It is a highly technical operation which I will simplify.

The Sage transmitter contained something like forty or fifty crystal controlled oscillators, mixers and amplifiers that generated a 425MHz signal. It also had "frequency agility", which meant it was able to spontaneously switch from one frequency to another.

Along with the transmitter, they had what is called a "COHO" or a "coherent oscillator set-up." Normally, a "COHO" would function by having only one frequency reference. However, this is not how the Montauk transmitter achieved coherency.

In order to make it entirely coherent, we took every oscillator available and amplitude modulated it with white noise. Since white noise is fifty percent correlated to everything, it serves a universal auto-correlating function. The result was that all of the etheric components of the oscillators were now coherent to each other. We weren't trying to correlate the normal electrical functions as they didn't concern us. We were only interested in the etheric functions, as they gave the results we were searching for.

A very stable time reference was required from the zero time generator. This produced two 30 hertz waves, referenced to zero time. One was connected to the computers and synchronized the clock or timing functions. The other modulated the white noise generator. By adjusting the phase between them, we could focus on and monitor the whole operation. This enabled us to take the correlations of the white noise and refer it right to the center point of time, where all time crosses.

The purpose of this experiment was to make the psychic transmissions of Duncan time coherent. Dr. von Neumann had instructed us that the transmitter had to be time coherent with respect to zero time. The whirligig zero time reference also served as a witness point back to the Philadelphia Experiment, and that was very important. The project was trying to open a door to the USS Eldridge in 1943.

Modifications continued on the equipment through 1979, until we had a coherent transmission system with respect to time phase.

Now, they had to calibrate Duncan. This meant they had to adjust and modify the equipment to synchronize with him. He had already demonstrated that he had zero point references of his own when the inadvertent time bending had occurred. This could perhaps be better explained due to his prior experience during the Philadelphia Experiment. There, he had jumped off the Eldridge and was thrust into a time vortex.

At Montauk, he was now in an entirely new set of circumstances, but his familiarization with zero time had apparently never left him.

There were also other psychics, but Duncan was the first they had used, and he was in the chair ninety percent of the time the system was in operation. If he was sick or didn't feel well, they'd wait a day. Because every time they changed the operator, they had to recalibrate and reprogram the computers and pulse modulator, and it took about two full days to do that. If Duncan was out for two weeks or more, they'd put in another operator, but I only remember one time when they did that. It was almost a disaster, because they didn't spend enough time in the initial calibration. From then on, Duncan was the one and only one who ran the equipment. A backup had to be there, however, in case something happened to Duncan.

By 1980, the big radar reflector (that looks like a huge banana peel) on top of the building was no longer in use. Now, there were two transmitters that fed the omnidirectional antenna (the one above ground). The pulse modulators of the transmitters were feeding both that antenna and the coils of the Delta T antenna (underground).

Also connected to the computer was the Montauk chair, which was now placed between both antennas at the null point. By this time, the computer system was huge and was housed inside the control room next to the radar tower. Additionally, the computer room contained a lot of different terminals and displays to monitor the various activities of the project.

Duncan would start out sitting in the chair. Then, the transmitter would be turned on. His mind would be blank and clear. He would then be directed to concentrate on an opening in time from say, 1980 (then the current time) to 1990. At this point, a "hole" or time portal would appear right in the center of the Delta T antenna - you could walk through the portal from 1980 to 1990. There was an opening that you could look into. It looked like a circular corridor with a light at the other end.

The time door would remain as long as Duncan would concentrate on 1990 and 1980.

I've been told by those who entered the tunnel that it looked like a spiral, similar to science fiction sytle renditions of a vortex. When outside the tunnel, it looked like you were looking through space - from one circular opening through space to a circular but little bit smaller window at the other end. I was considered too valuable to the technical operation and was not allowed to travel through the portal.

From 1980 to late 1981, the time function was calibrated. At first, the time portals would drift away. One might go throught the portal and come out in 1960.

But when one went back to find it later, although it was still being tracked in real time, the portal would not appear where it should have been. One could easily get lost in time and space. Initially, the portal would be opened up, but it would drift. This was because Duncan himself was drifting. He had to got through extensive training to get the portal to be stable. We also had to focus the transmitter more closely and tighten up the thought form translation to get everything right.

We would spend days just rying to get a particular time change to occur as predicated.

However, there was no particular problem with creating a time warp. Predicting what it would do was the difficulty. Finally, towards the end of 1981, we learned how to stabilize it so that when a portal would appear, it would remain. Although the function was not absolutely perfect, it was predictable, stable and running according to plans.

Essentially, what the scientists were doing was using 1943, 1963, 1983 vortex, which was based upon the natural twenty year biorhythms of the Earth .1943, 1963 and 1983 acted as anchor points for the main vortex. Sub vortices or open ended vortices would be created by going from the main one through an anchor point ('43, '63 or '83). At Montauk, August 12, 1983 was used.

For example, let's say they wanted to reach November 1981. There would be a bridge point from November of '81 to August 12, 1983. From August 12, '83 they could go to whatever time they wanted. The vortex ran between August 12, 1943 and August 12, '83 because that was the master vortex. It is called open ended, because there is no device at the other end which anchoring it.

Although they had stabilized the time aspect of the portals, they had to work on the spatial aspect as well. They stabilized this aspect so that they could not only place a portal at a particular time but in a particular space.

Once time stabilized and the above was accomplished, they kicked out everybody and cleared the entire base except for a few key persons. I remained there as I was the technical operator and was essential to the project. Duncan remained as he was the psychic who made the operation work. The entire system was tuned to him.

Two other psychics were also retained as back-ups in case Duncan was killed or incapacitated. The project directors also stayed, but the military left. A whole new team was brought in to do the more mundane functions of maintaining the base.

Up to that point, everyone operated on a "need to know" basis. Security was already tight, but they wanted even higher security. They didn't want the military to know what they were doing with time. But everybody knew there was something weird going on. They just didn't know what.

* White noise is an impulse at every frequnecy at the same time. When you

are tuning your FM radio dial, the noise you hear between stations is white noise.

It can be thought of as a sudden burst at every frequency or a bunch of impulses thrown together.

THIRTEEN- TIME TRAVEL

As most of the technicians were gone, a new technical crew was brought in.

I don't know who they were and what their qualifications were, but they were called the "Secret Crew." The project was relaunched and is now sometimes referred to as "Phoenix III." This lasted from February 1981 until 1983.

The objective now was to explore time itself. The crew began to look at past history and to the future, just scouting around. They would search ahead for a hostile environment. Through the vortex, they could sample the air, the terrain and everything without entering the portal.

Those who travelled through the vortex described it as a peculiar spiral tunnel that was lit, all the way down. As one started to walk down, he would suddenly be pulled through it. It propelled one out the other end, usually in another place (as opposed to Montauk), or according to where the transmitter was set or placed. It could be anywhere in the Universe.

The tunnel resembled a corkscrew with an effect similar to lit bulbs. It was a fluted sort of structure and not a straight tunnel. It twisted and took turns until you'd come out the other end. There, you would meet somebody or do something.

You would complete your mission and return. The tunnel would open for you, and you'd come back to where you came from. However, if they lost power during the operation, you'd be lost in time or abandoned somewhere in the vortex itself. When someone was lost, it was usually caused by a glitch in hyperspace.* And although many were lost, the scientists didn't abandon people deliberately or carelessly.

According to Duncan, there was also another function of the time tunnel. About two-thirds of the way down the tunnel, one's energy leaves the body. One would feel a big thump accompanied by a tendency to see on a broad scale. He reported sensing a higher intelligence along with an out-of-the-body experience. This was referred to as a FULL OUT. The researchers would try to manifest this in Duncan.

It could have been for further "Seeing Eye" experiments or for other reasons.

It was routine to create a tunnel, grab somebody off the street and send them down. Most of the time these people were winos or derelicts whose absence wouldn't create a furor. If they returned, they would make a full report on what they had encountered. Most of the winos used for the experiments were sobered up for a week before entering a portal, but many didn't make it back. We don't know how many people are still floating around in time, whenever, wherever, and however.

As "Phoenix III" developed, the individuals so chosen for this reseearch would be wired up with all sorts of TV and radio equipment so that they could report back "live." Each individual would be escorted through the portal, sometimes with force. TV and radio signals would travel right through the portals and as long as they could pick these up, researchers would have radio/video tapes of what the time traveller had experienced.

Those controlling the project began to play all sorts of games, manipulating the past and future. I don't really know what they did because I was the one at the switch. My station was in the transmitter building, and I had to keep everything going. I was not privy to a lot of what was going on, but at one point I do know that they had an extensive library of videotapes. I saw the tapes themselves although I was not granted extensive viewing privileges. Actually, I designed and built the viewer (with the aid of tremendous resources) so I had some

idea of what was going on. Much of what I knew came from Duncan's own reports, because by that time, we had become good friends. Eventually, we were debriefed and sent on our separate ways. Most of my memories of him had been wiped out.

In addition to the derelicts, the reserachers also used kids for some reason.

I'm not sure what exactly the purpose was, but there was one kid at Montauk who would go out and get other kids and bring them to the project. He was like a tractor beam. He lived in Montauk and would circulate around very effectively. There was also an entire corps of these around the New York metro area that could get away for six hours or so without being missed. They were specifically trained to go out and bring in other kids. Some kids returned home, some didn't. The kids chosen were between 10 and 16, or maybe 18 at the oldest and 9 at the youngest. Most were just about to reach puberty or had just finished it. They were usually blond, blue eyed, tall and light skinned. They fit the Aryan stereotype. To my knowleddge, there were no girls in this group.

A later investigation showed that Montauk had a NeoNazi connection and that the Nazis were still on the Aryan kick. We don't know where the kids went, what they were educated in or programmed for. Whether they came back or not is still a mystery.

What information is available is that they sent every raw recruit into the future to 6037 AD, always to the same point, to what appeared to be a dead city in ruins.

Everything was stationary, not unlike a dreamlike state. There were no signs of life. In the center of the city was a square with a gold horse on a pedestal.

There were inscriptions on that pedestal, and recruits were sent there to read what they said. Each recruit would interpret and report. We still don't know what the reseachers were after. They could have been trying to find the same answer from different people. I don't know. Duncan suggested there was technology in the pedestal and that they were trying to get somebody to sense or feel what the technology was.

Someone else involved in the project has said the horse was there to test the powers of observation of the recruits and that it also served as a point of reference.

The recruits were always asked if they saw anybody in the city. Each individual would interpret what he observed and report.

We know a lot of people were shoved somewhere into the future, maybe 200 or 300 years ahead. Estimates range from three to ten thousand people that were eventually abandoned. We have no idea for what purpose.

I have already said that I don't know exactly what they did with time. I wasn't there, but I do know they did a lot with World War I and World War II. They monitored those times and took pictures. They knew exactly what they were doing.

They could actually make up a secondary vortex to observe what was going on. We called this a seeing eye function. The original vortex was such that one could drive a truck through it. Using phase conjugation through the elaborate computer set-up, past and future history could actually be transmitted through the portal and viewed on television.

* Hyperspace is defined as space which exceeds the boundaries of three dimensions.

FOURTEEN- MISSION TO MARS

The project researchers continued to scout around in time. It was in late 1981 or '82 when the first actual use of this technology was employed to gain entrance into the underground areas in the big pyramid on the planet Mars.

As this material will be controlversial to much of the general public, I will try to give some background.

There is currently a video tape in circulation entitled "Hoagland's Mars".

This is a presentation to NASA scientists by scientific journalist Richard Hoagland concerning the tetrahedral complex that is associated with the "Face on Mars."

In this video, Hoagland shows the "face" and nearby pyramids that were photographed by the Viking spacecraft in the '70's. computerized projection techniques are used that give one a 360 degree "fly by" of the "face." The video also gives a close look at the pyramids.

Hoagland is trying to convice NASA to make more pictures of this region, which is known as Cydonia. NASA has been hard to convince and minimized the significance of Hoagland's work. In fact, a major effort was launched to prohibit the showing of this tape on public television stations. The story of this scandal was reported on by New York radio station WABC.

Why would NASA assume such a stance about a subject that is so intriguing?

The answer is perhaps explained by a book entitled, 'Alternative 3,' by Leslie Watkins with David Ambrose and Christopher Miles.* This book was based on a 1977 video that revealed a secret space program being run by an international conspiracy that included both the Russians and the United States. It is a fascinating account that includes astronauts breaking security, disappearing scientists, murder and the establishment of slave societies on the moon and the planet Mars. The book claims that men actually landed on Mars as early as 1962.

It is not my cause to prove that a colony exists or did exist on Mars. I have included this information so that the reader will understand that there is an entire scenario concerning Mars that is separate from my story. Those who are interested can investigate "Hoagland's Mars" or 'Alternative 3' for themselves. It is interesting to note, however, that the documentary entitled "Alternative 3" was shown on a San Francisco TV station sometime around the late '70's. A story has proliferated since that at the time the FCC threatened to revoke the station's broadcasting license if it were to be shown again. It wasn't shown again.

The directows of the Montauk Project knew there was a colony on Mars. It is more than likely that they were a part of the conspiracy.

Mars was interesting to the Montauk researchers, because they had realized that there was an old technology there. They knew somebody had built the pyramids and face on Mars. These were not natural formations.

According to the information that my associates and I have dug up, the people who were living on the surface of Mars could not get to the underground area beneath the pyramid. The entrances were either sealed over or simply couldn't be found. In fact, it appeared that the big pyramid was sealed better then the pyramid at Giza. Despite all the expensive and fancy technology that was available, the pyramid could not be penetrated.

The scientists at Montauk decided the best approach would be to project right into the center of the Martian underground. The newly discovered Montauk technology gave them the wherewithal to use a spatial warp to get inside. They wanted to get into the underground caverns. These were thought to be set up and administered by a very old civilization.

The time portal took the risk out of the operation as we could look through it.

We had a set up with TV monitors so that whatever Duncan would visualize would appear on the monitors. This provided a visual of present time on planet Mars. In order to find the underground area, we kept moving the opoen end of the vortex until a corridor appeared. At that point, we had Duncan solidify the portal. The away team was then able to walk from Montauk to Mars and be underground.

By this time, Duncan was no longer required to be continuously in the chair.

We had learned to have Duncan generate functions with the computer storing them and continually spitting them back. The computer could generally run the transmitter for a short time and had enough memory to modify the flow of time for about four hours. If Duncan would not return after that time, the thought forms

being generated would drop out of reality. In such a case, the thought forms would have to be reconstructed from scratch.

The system definitely needed a live being initially. He would create the time portals and hold them open through concentration. Once the opening was made, we could record on tape what the live person was generating. The tape could then be used on its own to create another opening.

The system was continually refined and improved. If Duncan made a time connection once, it would then be recorded on tape. Because he sometimes had difficulty getting a connection, the tape made it easier and automatic. An entire library was eventually accumulated so that they didn't have to rely on Duncan. It was this development that enabled Duncan to be sent through the vortices himself. This occurred in '82 and '83. He was eventually selected for the team that went to Mars.

Using the time portals, Mars had been scoured for live inhabitants. Researchers had to push back about 125,000 years before they could find any. I don't know what they found out or what they did with the information. Duncan has tried to access this information, but it is deeply buried and difficult to contact.

My personal view is that the pyramid on Mars serves as an antenna. Perhaps there is technology inside of the pyramid. According to Duncan's recollections, he travelled to the inside of the pyramid. He saw technology being operated there and called it "The Solar System Defense." According to his account, the Montauk researchers wanted this shut off. It had to be shut off before anything else could be done.

This defense has been shut off retroactive to 1943, which is commonly considered amongst many UFO buffs to be the beginning of the massive UFO phenomena.

There's not much more I can say about Mars at this point except that the movie "Total Recall" is fancifully based upon some of the events that occurred with the Montauk Project. The way they used the chair in the movie is strinkingly similar.

Time research continued and countless missions were run until August 12, 1983. This was when the actual lock was made back to 1943 and 1963.

* 'Alternative 3' was originally published in the United Kingdom. The first printing in the U.S. was in 1979 by Avon Books, a Division of the Hearst Corporation, 959 Eighth Avenue, New York, New York, 10019.

FIFTEEN- ENCOUNTER WITH THE BEAST

On August 5th, 1983, we were given a directive to run the transmitter non-stop - just turn it on and let it go continuously. We followed the orders, but nothing out of the ordinary occurred until August 12th. Then, something very strange happened. All of a sudden, the equipment appeared to drop into synch with something else. We didn't know what function the system was now attuned to, but at that point, the USS Eldridge (the ship used for the Philadelphia Experiment) appeared through the portal. We had locked up with the Eldridge.

I'm not sure if this was a pure accident, but if the Montauk researchers were trying to hook up with the Eldridge, the attempt had to be made on this exact date. This is due to the 20 year biorhythms of the planet Earth (which was a discovery made in the process of these experiments) and the Eldridge experiment having occurred on August 12, 1943.

At this point, the Duncan from 1943 appeared and could be seen through the time portal along with his own brother. Both were crew members of the USS Eldridge.

We kept the Duncan of 1983 from seeing himself so as to avoid a time paradox and resultant negative effects.

The project had now reached apocalyptic proportions. Natural laws were being violated, and it seemed everyone involved felt uncomfortable. Three colleagues and myself had been privately voicing misgivings about the project over a period of months. We had talked about the pitfalls of dealing with time and how this might affect the karma of the planet. We hoped the project would truncate itself.

Consequently, our little cabal created a contingency program that only Duncan could activate. It was designed to crash the entire project.

We finally decided we'd had enough of the whole experiment. The contingency program was activated by someone approaching Duncan while he was in the chair and simply whispering, "The time is now."

At this moment, he let loose a monster from his subconscious, and the transmitter actually portrayed a hairy monster. It was big, hairy, hungry and nasty. But it didn't appear underground in the null point. It showed up somewhere on the base.

It would eat anything it could find, and it smashed everything in sight. Several different people saw it, but almost everyone described a different beast. It was either 9 feet tall or 30 feet tall, depending on who saw it. I personally believe it was about 9 or 10 feet in height. Fright does strange things to people, and no one was sure of what the exact physical constitution of this monster was. No one was in any frame of mind to calmly and collectively analyze its exact nature.

My supervisor had ordered us to shut off the generatorsin order to stop whatever type of phenomena was occurring. This didn't work, so it was decided that the thing had to be stopped.

It was decided that the transmitter had to be shut down. There were two efforts made in this direction. One was to send somebody back and turn off the transmitters on the Eldridge. They would be smashed if that was what was necessary to shut them down.

The other effort was by myself and the director of the project. We unsuccessfully attempted to shut the transmitter at Montauk. We then went into the power station and disconnected the base from the Long Island Lighting Company. The power kept going and nothing stopped.

We weren't concerned about the lights. We just wanted to stop the transmitter itself. We decided the next best thing to do was to go into the power station and cut the wires leading into the ground from the big transformers. I put an acetylene torch on my back and cut the wires going into the ground. I had to be careful because they were hot. Still, nothing happened. The lights at the base stayed on.

I figured there must have been another power feed somewhere. We went over to the transformer farm nex to the transmitter building and cut the wires coming up out of the ground. At that point, the lights at the base went out and the computer stopped. But, the lights in the transmitter building stayed on!

We went into the building and pulled the wires out of the panel that controlled the transmitter. Then wires from the transmitter itself. The lights in the building went off, but the transmitter stayed on.

I then went upstairs and cut the actual equipment apart. I cut the conduits. I cut the cabinets. Finally, I cut enough apart that the transmitter just groaned and stopped. All the lights went off. We'd done it. Today, you can still see the torch marks where I'd cut things apart.

It was at this point that the beast stopped moving and faded back into the ether.

The portal closed and that was the end of that episode.

After we stopped the transmitter and things settled, we figured out what had happened. When we had first thrown the switches in the power station, none of the lights went off at the base. There was no power coming into the base. When I cut the lines going to the transmitter building, the rest of the base went off, including the computers. However, the transmitters ran without computers.

The system had actually gone into a free energy mode. The two systems (i. e.

the two generators - one in 1943 aboard the Eldridge, one at Montauk in 1983) were locked together. There was a tremendous amount of energy bouncing between the generators. With so much energy between them, all the electrical circuits that were connected remained active. The lights stayed on.

More importantly, the generators established a connection from 1983 to 1943.

By bouncing energy between the two time periods, a stable vortex was created.

This served as an anchor. Using this vortex, a time tunnel could then be projected to a specific point in time.

For example, if one wanted to go from 1983 to 1993, the '83 to '43 vortex would first have to be functioning to serve as the anchor. The projection to '93 (or whatever other point in time chosen) would come out the '83 end of the vortex.

If one wanted to go to 1923, one would project through the 1943 end of the vortex. Times between 1943 and 1983 could be reached by going through either end of the vortex. Dates after 1963 were accessed through 1983 and dates prior to 1963 via 1943.

This is not to say that all time travel would have to be done in this manner (using the master vortex from 1943 to 1983). During these experiments, no generators were found in either the past or the future that could link up and establish a vortex of this nature. There are, of course, plenty of generators around, but a successful link had to be made. That link required a "witness effect."

"Witness" is an occult term. As a noun, it refers to an object that is connected or related to someone or something. For example, a lock of someone's hair or a picture could serve as a witness. As a verb, "witness" means to use an object to enter a person's consciousness or otherwise have an effect on them.

One example of a "witness effect" would be for someone to take a lock of hair, use it with a love potion, and have the owner of the hair fall in love.

With the Montauk Project, there were three "witness effects." They could be considered as three different levels of witnessing.

The first level consisted of physical people who were actually on the USS Eldridge. Any surviving crew members they could find were brought to Montauk for the experiment in 1983. This also included personnel who were considered to be reincarnated since the Philadelphia Experiment. Duncan and Al Bielek were both there and were two of the primary witnesses.

The second level of witnessing concerned technology. The zero time reference generator (referred to previously as the whirligig) used aboard the Eldridge was also used at Montauk. When the Eldridge was eventually decommissioned in 1946, the whirligig was placed in storage. It was eventually brought out to Montauk and incorporated with the system there. In addition to the whirligig, there were two very strange radio transceivers* linking the two projects. They were "crosstime" transmitters. They could transmit across time, and they used that to lock up the two projects.

The third level of witnessing was the planetary biorhythm. the term "biorhythm" is esoteric and refers to the higher order channels that regulate life in an organism.

Biorhythms are a result of the resonance upon which nature operates. In humans, the processes of sleeping and eating would involve biorhythms. Of course, there are many subtle ones that could be studied, ad infinitum. When viewing the Earth as an organism, there are also biorhythms. The seasons and the daily spin of the planet would involved biorhythms. The scientists at Montauk exhaustively studied the biorhythms of the Eart and how they related to the entire universe. They discovered that there is a major planetary biorhythm that peaks out every twenty years.

The Philadelphia Experiment occurred in 1943. Although 1983 was forty years later, it was a multiple of twenty and served as a potent witness. It enabled the two projects to link up. I should also mention that it is entirely possible that the link could have been made without the witness effect, however its application

proved very helpful to the project.

The reader should now have some idea of the general theories and applications that were used at Montauk.

After the bizarre occurrences of August 12, 1983, the Montauk base virtually emptied. The power was restored, but lights were left on with everything in disarray. Most of the personnel were eventually rounded up, debriefed and brainwashed accordingly.

* I was able to acquire a few of the transceivers that were used in the experiments.

Up to this date, I do not fully understand them or their function. It is impossible to get any literature or manuals on the subject. The only possible way to get information on these transceivers is to ask people who have used them. The only answers I've gotten thus far is that they were a highly classified piece of equipment. People I spoke to knew they were for stealth airplanes, but they didn't know what exactly they were for.

SIXTEEN- THE NATURE OF TIME

This book will give rise to many questions, particularly about the nature of time itself. From my experience in talking to groups, I will try to clarify some points that often confuse people.

First of all, the past and the future can be changed.

It will help to consider the idea of a chessboard. In chess, there might be thirty moves in a game. Each one of these moves will create a different layout of the chess board. If one were to "go back in time" and change a move that has been made, it would consequently change all the other board layouts subsequent to that change.

Time could be considered a hypnotic pulse that we all subconsciously agree or submit to. When someone is able to manipulate a change in time, they are also manipulating our subconscious considerations and experiences. Therefore, if time is changed, one wouldn't necessarily realize it.

This scenario implies that we are merely pieces on a grand chess board. To a degree, this is true. For example, retired generals often complain of having been the pawns of international bankers. It is a farfetched comment, but perhaps there would be no war if generals could be truly clued in on the real machinations behind international politics.

There is also the example of Homer's 'Iliad', which tells the story of the Trojan War. According to that legend, the gods literally manipulated the characters on Earth like a chess board. The story is ripe with intrigue between mortals and gods. The plots become so intricate and thick that it sometimes seems Homer is trying to provide us witha microcosmic view of the entire universe.

Whatever the case, we are all players in the game that is known as "time." The obvious way to protect one's interest is, of course, to gain knowledge about time itself. Whether one wants to do this by pursuing meditation or astrophysics is an entirely personal matter.

At Montauk, the scientists also viewed the future. The viewers they had gave them the ability to look at multiple futures. Once they chose a particular scenario and activated it by someone or something travelling to it, that future would become fixed. That point would be locked to the time from whence the connection was made.

It would create a loop that was fixed.

For example, let's say multiple futures were viewed with different people becoming president. Suppose the future with "Sam Jones" as president was chosen by the researchers, for whatever reason. Linking a person or item from the present would lock in the President Sam Jones scenario no matter what. However, none of this means that a fixed point scenario couldn't be further changed by the

scientists doing more manipulations.

At this writing, we arecurrently in a time loop. This loop extends from where the Montauk researchers penetrated into the past up to where they penetrated into the future. It's fixed and would appear unalterable. However, this does not mean that we are all relegated to being hopeless slaves of time manipulators. The subconscious has its automatic or hypnotic levels, but it also contains the seeds of freedom: dreams. If one can dream something, it can be brought into being.

It is very easy to get philosophical about all of this and get lost in that process. My point with this book is that there has been manipulation of time. This has also exploited individuals and caused untold misery. It could easily be considered to be the work of dark forces.

There is still one major question. Who was really behind the Montauk Project?

There are countless intrigues and scenarios one can envision. Religionists can bring in God and the Devil. UFO aficionados can offer a grand scheme of aliens vying for our solar system. Left wingers will offer explanations concerning the CIA and secret government.

I believe that all of the above can shed light on what actually happened at Montauk. It is also my hope that this book will bring more people out of the woodwork. Thus, we can have more answers and less mystery.

SEVENTEEN- THE MONTAUK BASE IS SEALED

After the events of August 12, 1983, the Montauk Air Force Base was abandoned.

By the end of that year, there was no knowledge of anyone being on the base.

In May or June of 1984, a crack squad of Black Berets were sent to the base.

I believe they were Marines, but I'm not absolutely sure. They were reportedly ordered to shoot anything that moved. Their purpose was to purge anyone who might be on the base.

There was a second team that followed the Black Berets. They removed secret equipment which was considered too sensitive to leave behind.

The next step was to prepare the underground to be sealed. Certain incriminating evidence was removed at this point. I've heard that a room with hundreds of skeletons was cleared out during this evolution.

About six months later, a caravan of cement mixers appeared on the base. Many people saw these trucks. They filled the vast underground areas of Montauk with cement. This included dumping cement down the elevator shafts as well.

The gates were locked up and the base was abandoned for good.

EIGHTEEN- MONTAUK TODAY

If one travels to Montauk Point today and parks in the state parking lot near the light house, it is possible to get a good view of the giant radar reflector that sits atop the transmitter building.

For those who are either brave or foolish, one can follow the dirt roads that lead to the base. Most of the entrance gates have been bent or otherwise vandalized so that entrance is easy. This was probably done by local juveniles who sometimes get drunk and have beer parties on the base. However, walking on the base is prohibited by New York State park rangers who periodically patrol the area.* There are also occupied buildings on the main roads to the base.

It should be noted that I am not writing this information to lure people to the base. People are going to be curious after reading this book, and it is my responsibility to warn them. I'm not absolutely sure of the legal techinicalities, but walking on the base is probably illegal. One goes at one's own risk.

There are also other dangers to consider.

Two people I know who participated in the Montauk Project visited the area in the late '80's. They claimed they were abducted and do not totally remember what happened to them.

Another person has reported in August of 1991 that video cameras can now be seen from the top of the transmitter building. This is a new development and is rather odd considering it is a vacant and derelict facility.

There are also reports that the underground areas of the base are being reopened.

This is speculative but should serve to warn anyone making travel plans to Montauk.

* The entirety of Fort Hero, including the inner Montauk Base has since been donated to New York State as a park. While there are peculiar political arrangements concerning the base to this day, the rangers are not out of bounds in keeping people off the grounds. The buildings are in a state of disrepair and are potentially dangerous to those going on a casual walk.

NINTEEN- VON NEUMANN ALIVE!

After completing the first draft of this book, a new development took place.

It concerns occurrences that started years ago but only came to a resolution recently.

This concerns John von Neumann and corroborates the theory that he didn't die in 1958 as is generally believed.

In 1983, I was contacted by a friend of mine in upstate New York who I will refer to as Klark. He knew I was interested in communicatoins equipment and told me about an old time suplus dealer who I will call Dr. Rinehart.* Rinehart was a legend in the local surplus community.

Klark said that the man had a collection of equipment that went back as far as the 1930's and 1940's. A meeting was arranged with Dr. Rinehart on the pretext that I was interested in buying him out. Klark introduced me, and Rinhart showed me his collection on a silver platter. He sincerely wanted to sell out, but I thought his price was too high. A great deal of the equipment was junk and would have cost just as much to cart away.

I considered his prices exorbitant and thought he might be a bit crazy. Apparently, he went even crazier after he met me. Klark visited him again on his own and was met at the door with a shot gun. Rinehart pointed the gun and told Klark that he didn't want to see that bastard Preston on his property. He didn't want to see Klark, Preston or any of their friends on the property. He said he'd shoot them if they showed up.

Klark tried to calm him down and asked what this was all about. He had no idea why the man was so upset. Rinehart said that Preston had come back and robbed him the night he was last there.

As it turned out, somebody had come to the guy's house, strapped him to the chair, ransacked the house and stole money. It certainly wasn't me, and Klark and I were both confused. Years went by, and I had dismissed the puzzling circumstances concernign Dr. Rinehart.

As my memory of the Montauk Project returned, I suddenly recognized Dr. Rinehart.

He was actually John Eric von Neumann, the brains behind the Philadelphia Experiment and Montauk Project!

Many years back, perhaps as early as 1958, von Neumann had been assigned to a "witness relocation" program. He was given a new identity as Dr. Rinehart and slipped into a new role as a surplus dealer upstate. He also remained on call to the authorities that ran the Phoenix and Montauk Projects and would work for them whenevery he was needed. Sometimes this was for months at a time.

This man not only looked like von Neumann, his doctorates in mathematics and physics were on the wall and came from Germany. Despite this, he claimed never to have left the United States.

It was also apparent that this gentleman's faculties and memory had been tampered with.

I had talked this over with Al Bielek, and we figured that my presence at von Neumann's house was too much for him. He would have remembered me from Montauk and that probably frightened him and caused him to flip out.

All of this is fascinating in its own right, but my main interest was in a strange looking receiver that he had. It is known as an FRR 24 Receiver. I had noticed it on my origianl visit, and it was still there. I wasn't about to return to his place in view of his threats, but I'd sent people up there and they indicated the receiver was still there.

Al remembered von Neumann as well and wanted to visit him. In fact, von Neumann as Dr. Rinehart had taken a liking to Al. Hoping to get my hands on his receiver, I drove Al upstate to Rinehart's house.

We weren't sure how to approach him on the receiver. We thought about having me wear a disguise but thought it might be easier to have Al buy the receivers on my behalf.

Al got out of the car and greeted him. I remained in the car in hopes that he would ignore me. It started to rain, so Rinehart told Al that they should go to the trailer on the other side of the property. That's where the equipment was. Rinehart walked right by my car and looked me straight in the face. He was friendly and said I should come along, too. Apparently, Rinehart didn't recognize me. I followed them to the trailer as if nothing had ever happened between us.

Al got the guy talking, and I just listened. Von Neumann didn't come through.

He was strictly in the identity of "Dr. Rinehart" as he spoke to us.

When he stopped talking, I told Rinehart that I'd heard he had a very large receiver setup where each reciever fits in a rack by itself.

He said, "Oh, that thing! I was gonna keep that. But hell, I'm never gonna use it. I can't even move it. I'm gonna keep it, or I'm gonna sell it."

I asked him how much he wanted for it, and he said he would give it to me for a thousand dollars. I told him that Al and I couldn't afford that kind of money, so he suggested a trade.

Al told me to make an offer so I offered $600 for four racks of the receivers.

He said that was a little less than he wanted and that he'd have to think it over.

We left on good terms and returned home.

Another meeting was arranged some time later. He said that he wanted hi-fi equipment and would be willing to work out a trade. We dug up some hi-fi material and went up again. He looked at it and practically got tears in his eyes. He was excited to see the material and remembered the people who actually designed much of it.

He apologized and said that he really couldn't use any of the material. He wanted cash. If we sold the material, he said we could come back and get the receivers for cash.

We carted everything back to Long Island again. I was frustrated but wasn't going to give up. I called around and found out that I could sell the material.

It was worth $750 to other dealers, and I sold it immediately.

I wanted to get his receivers quickly as he was getting known again by national collectors. They would snap up the receivers if I didn't act soon.

I took $800 and went up to see Dr. Rinehart again. I'd taken along some friends to help me move the equipment. Fortunately, it was a clear day, and the weather wasn't going to interfere with our plans.

Dr. Rinehart came out and was in a friendly mood. I showed him $750, but he said he didn't want any money until he was sure I was satisfied with the

receivers.

He showed us around the place. We went to look at the receivers, and I was surprised.

He had four racks of the equipment, and I had remembered only one. He was willing to let them all go for my offer of $750 which was more than fair on his part.

I found him to be quite pleasant. In fact, I was a bit puzzled. Initially, he had wanted $1,200 per rack which meant $4,800 for the entire system. Now, it was seven years later, and he was accepting $750. It is my opinion that he wanted me to have the receivers for some reason. I still don't know exactly what it was.

As I poked around and looked at the receivers, my two friends went to the chicken coop as they were interested in some Western Electric equipment that was stored there. Dr. Rinehart was sitting in a chair not far from the receivers. Suddenly, I noticed that he was no longer Rinehart. He was John von Neumann! He remembered his true identity and began to talk.

He definitely remembered me and told me things that were of a sensitive nature which I am obligated not to repeat. He also said that over the years he had seen that millions of dollars were put away in secret Swiss bank accounts. This money was to be used to compensate many of the workers at Montauk who had suffered as a result of the project. Apparently, when I had visited him years back, some sort of signal alerted the secret group that backed the Montauk Project. He was bound up and robbed the next night, and his secret bank books were missing. He now realized that I had not been involved.

I wasn't able to start moving the receivers out until the next day. It was a big job. I took the receivers out of their racks and broke them up so they could be moved safely. Rinehart was there, took, and he started to fade in and out. First, he was Rinehart, then he'd be von Neumann. It was like a yo-yo. Finally, he settled on von Neumann.

As von Neumann, he said that he had obtained these receivers for a very good reason. They were actually capable of tuning in on either of the two projects: Project Rainbow (the Philadelphia Experiment) or the Montauk Project. Further, the receivers were capable of tuning in on the project from any other space and time in our universe. He also believed this receiver was the main witness from Montauk to the USS Eldridge. He said it could pick up the pattern of the Eldridge back in 1943.

It seemed that von Neumann had completed what he had to say. Rinehart returned, and I loaded up the receivers to take back to Long Island.

I wasn't sure how the receivers worked or what they were all about. My first step was to ask Duncan to do a psychic reading. He indicated that the receiver was capable of tuning to any particular point in time by way of zero time. He said that if we could figure out how to tune it, we could tune in to any other point in time.

We realized what von Neumann had already told me: this equipment was a key part of the Montauk time machine. I don't think the particular equipment that I had was on either the Eldridge or at Montauk. I think it had been used at the Philadelphia Navy Yard in the 1940's.

I wanted to trace this equipment further to see if it had a logical point of origin. I called the biggest old time radio surplus dealer in the country. They had never heard of the FRR 24 Receiver. I talked to lots of friends in the surplus business and found only one person who had ever seen one or heard of one. This person said that the receiver came out of RCA. He owned a piece of one of the receivers at one time. It had gone out of his hands when an old man from upstate New York came and paid an exorbitant price for the piece he had of the receiver.

Tracing this back to Dr. Rinehart, he verified that he was the purchaser of the equipment. But, he said that this only accounted for pieces from two of the racks he'd sole to me. There were four in total, and he had to buy the other two racks of receivers from somebody else. I tracked the other person down with Dr. Rinehart's help. This person was a young man who also said the FRR 24 Receiver had

come from RCA.

I decided to find out how many of these receivers had actually been released.

I called up the Surplus Disposal Agency, gave them the number for the receiver, and they did a computer read out. A lady at the agency said that only three FRR 24's had ever been released. All the other systems were either still in use or had been destroyed.

Then, she indicated that until recently, this receiver had been classified. She said that if any of them had been scrapped, the manuals for them had to be destroyed.

There was also a note indicating that each FRR 24 unit contained seventy-five pounds of silver. The units had reportedly been scrapped and sold to dealers for silver recovery. When scrapped, they are not useful as they would have been put through a crusher.

The report indicated that FRR 24's were only released when the government agreed to sell them to a world communications company. There were three such instances listed. One FRR 24 went to RCA, one went to ITT on the west coast and another to Vero Beach, Florida.

I tried to trace down people who had actually worked with the FRR 24. Finally, I located a retired gentleman who had worked at RCA Rocky Point (on the eastern end of Long Island). He had worked at the receiver station at Rocky Point.

The gentleman indicated that the FRR 24's had been at the RCA receiving station for years. He raved about the receivers and said they were beautiful and fantastic.

When they were turned on, however, he said that a very strange type of interference was picked up all across Long Island Sound. It was a mystery and neither he nor anyone else could figure it out. He also mentioned that the receivers made strange audio noises and that RCA finally decided not to use them.

This was interesting because von Neumann told me that two receiver racks from RCA Rocky Point had been sent back to the 1930's. One ended up in the Philadelphia Naval Yard and was used to track the Rainbow Project in 1943. The other receiver rack ended up at RCA for disassembly and study so that it could be replicated and applied to the technology of the day.

It is interesting to note that in the 1930's, RCA made tremendous strides in radio technology. The years 1933 and 1934 were particularly ripe with new discoveries.

If von Neumann was right, RCA received and analyzed a rack of receivers from the future. It is likely that von Neumann would have sent them back himself.

The receiver rack that ended up at the Philadelphia Naval Yard eventually came into my possession, and I still have it. The disassembled rack was enhanced and improved upon by RCA, and these are what ended up at Rocky Point. This was accomplished through a time loop, thus there are some differences in the RCA receivers (the FRR 24's that I recently got from von Neumann) and the one used during the Philadelphia Experiment. Both receivers, however, have more similarities than differences.

In addition to the above, I also have equipment developed by Tesla that appears to be inspired by the FRR 24's that were sent back from the future by von Neumann.

Whatever the case, radio technology was pushed way ahead in the 1930's. As an engineer and professional radio man, it is my personal conclusion that it couldn't have been done without some major help from somewhere. For example, Nikola Tesla was always upsetting the status quo by saying that he experienced communication with aliens.

There is another major point of interest concerning the FRR 24 Receiver. When I purchased them from Rinehart, I noticed that the aluminum housing was corroded on the outside. Aluminum itself does not corrode, but it does when it is mixed with impurities. The aluminum panel in the chassis, however, had no such corrosion. The chassis were therefore made out of a very pur aluminum. Commercial

grade aluminum used in radio equipment is usually not that pure.

What does all this tell us?

There had to be a reason that the aluminum was so pure. Recently, it has come to the surface in conventional scientific circles that aluminum can be made into a superconductor. A friend of mine at NASA told me that mixing mercury with aluminum and alcohol makes microchannels big enough for electrons to channel through the aluminum. This essentially creates a room temperature superconductor.

Rinehart also warned me about the chassis. He said there might be a little bit of mercury contamination on the chassis. Further inspection has revealed that the chassis had some sort of mercury treatment process.

It is currently my belief that the treatment process is related to the silver resonators, which are the capacitors and coils. The mercury and aluminum create microfine channels along the superconducting chassis and the channels become a multi-dimensional resonator.

To conclude, this receiver is actually a multi-dimensional space-time resonator and would be part and parcel of any time machine that was used for the Philadelphia Experiment or at Montauk.

* Dr. Rinehart is a pseudonym used to protect this individual's privacy.

APPENDIX A- A SCIENTIFIC ANALYSIS OF THE RADIOSONDE

Note: This analysis is not expected to be readily understood by the general lay public. It is included only for those who are technically inclined. It also serves as corroboration of my statement that the government had the means to affect the weather).

The Radiosonde consists of two variable resistance type sensors. One registers temperature, the other humidity.

The temperature sensor is a thermistor, where the electrical resistance varies inversely with the temperature. The humidity sensor is an electrolytic resistor where the electrical resistance varies directly with the relative humidity. In most of the Radiosondes, the pressure sensor is of the pressure responsive selctor switch type (Baro switch). In essence, the transmitter sees a varying resistance which is selected alternately by the Baro switch or a sequential switcher. A short circuit is selected occasionally which is called the reference mode. This is what the sensors do on the surface. It is also the line the government releases to the public. Although cursory investigation will show this description to be true, there is also other activity which is secret. The temperature sensor is a carbon bar with precious metals added, and acts as an antenna to the DOR function. It also inverts the transform known as DOR energetics. This item is packed in a small vial, and has to be installed on fasten stock clips on the arms of the Radiosonde. In order to get a true temperature reading, it is painted white to reflect the sun's radiant heat and sits above the package in the open. This placement is understandable from conventional science, but it cannot be understood from the viewpoint of relativistic sciences.

The humidity sensor is an electrolytic resistor. We do not understand its operation because the usual electrolytic resistor varies inversely with the relative humidity. This humidity sensor consists of a grid of conductive lines with an unknown chemical overlay. It acts as an antenna for orgone in phase. It is also similar to the electrolytic detectors that have been introduced for the detection of esoteric energies. The humidity sensor is also hermetically sealed in a small vial and has to be put in its holder on top of the Radiosonde, thus totally covering and protecting it from direct rain, but allowing air to circulate around it. This follows the released line of information.

In later Radiosondes, the Baro switch is replaced with a clock-work driven scanning switch, with the addition of a receiver that the Government claims is used as a transponder to track direction and height. This suggests that the Baro

switch gives height information, which can be read from the pressure, but depends on a uniform pressure gradient which our atmosphere does not exhibit. This follows the released information, but is grossly inaccurate.

I do not believe that this is the real objective for the Baro switch. In fact, an entirely different purpose is intimated. It appears that the Baro switch is the correlated function which would be necessary to synchronize the DOR busting to the environment of the Earth. It is also apparent that the receiver synchronizes the DOR busting to the the environment. At this point, I do not fully understand the sensor scheme.

In addition to the sensors, the other part of the radiosonde is the transmitter.

It is pulst time modulated and the repetition rate of the pulse varies with the resistance presented to the transmitter. There are two types of pulse modulation used.

One is where the modulation pulses off the CW (CW=carrier wave) carrier oscillator.

The other is where a high voltage pulse supplies B+ (B+ stands for "B batteries", which refer to plate voltage) to the carrier oscillator. There are two frequencies used: 400 MHz and 1680 MHz. The 400 MHz oscillator is comprised of tuned lines with the trioed tube in the field of the lines. The 1680 MHz oscillator is of the integral cavity type, with the triode tube inside the fields of the cavity.

In the down pulsed CW oscillator transmitter, there are two sections: the modulation oscillator and the carrier oscillator. The modulation oscillator is what generates the pulse, which is a triode oscillator with a blocking network in the grid circuit.

The operation of the transmitter is simple. When the oscillator runs, the grid bias builds up across the cap (C) and when the voltage reaches the tube cutoff the oscillation stops. At this point, C discharges until the tube starts up again.

As the grid voltage across C cycles up and down, the oscillator starts and stops; hence modulating the voltage drop across Rp, which is bypassed. The value of C and Rg and Rext and Rref determines the repetition rate of the pulse across Rp.

The signal with the pulse and its potentials are capacitively coupled to the carrier oscillator.

This is the usual explanation, but let us consider the relativistic activity.

When the tube is cut off, the higher order signal builds up inside the tube like the charge on a capacitator. The longer the tube is cut off, the more relativistic signal builds up in the tube. When the tube turns on and oscillates, it slew between saturation and cutoff, and two things happen. First, the stored relativistic charge is forced out. Second, the slewing of the oscillation between saturation and cutoff has the effect of amplifying the hgiher order components by "0" point activity.

The result is that the signal is amplified and outputs in pulses. From this point, the modulation signal is capacitively coupled to the grid of the carrier oscillator, where the pulse stops the oscillation.

When we consider the carrier oscillator, the circuit is a standard one. How it was optimized probably has something to do with the placement of the tube in the field of the resonant network and the design of the tube. The higher order operation in the carrier oscillator is similar to the modulation oscillator. When the tube slews from saturation to cutoff, the 0 point of the vacuum is ripped. This results in relativistic gain as well as forcing all signals stored in the tube to the output and the antenna.

The bypassed output of the modulation oscillator, which is pulsed potential (scalar) at approzimately 7 MHz is coupled to the grid of the carrier oscillator and slews the Q point * from saturation to cutoff. The "0" point activity sends

out bursts of relativistic signal which replicates closely the input signal from the sensors.

The pulse modulator transmitter uses a delay line pulse modulator with a thyratron, charging reactor, blocking diode, pulse forming network, and a pulse transformer that generates 1400 V pulses which drives the carrier oscillator. The thyratron is fired off by the output of the same modulation oscillator as in all of the rest.

The modulation oscillator loads the relativistic signal into the delay line through the thyratron which is cut off but still has "0" point gain. When the thyratron fires, everything in the pulse forming network is loaded into the carrier oscillator tube as a 1400 V pulse which rips apart the vacuum and results in a high "relativistic gain" through the usual "0" point activity.

The whole package is operated by a battery pack which lasts approximately three hours.

* "Q point" means quiescent point. This refers to the point where the tube rests.

APPENDIX B- WILHELM REICH

Although the government had great appreciation for the discoveries and developments of Wilhelm Reich, it appears they had very little use for him personally. He was under pressure from the AMA and FDA for years on charges of quackery. Eventually, he was given a very stiff prison sentence for contempt of court when he refused to appear. The subsequent burning of his books and destruction of his equipment may be unparalleled in modern times for its outrageousness.

His claims about jamming the drives of UFOs didn't win him too many friends either. He concluded that the drives of UFOs ran on cosmic or orgone energy. He developed a "space gun" on the basis of orgone theory and was able to make UFOs fade away with regularity according to eyewitness accounts.

After he was in prison, authorities reportedly gave him express permission to work on anti-gravity equations. This is odd to say the least; especially if they believed he was a quack.

Whatever the exact facts and details of Wilhelm Reich are, it appears that he was used for his inventive genius and then put away so he couldn't disseminate his discoveries elsewhere. The systematic condemnation of his work only backs this up.

APPENDIX C- MIND CONTROL AND THE PERSIAN GULF WAR I was still laid off when the Persian Gulf War erupted and had the opportunity to watch the live briefings. Live briefings are interesting to me because information sometimes comes through that would otherwise be edited out.

In one report, a CNN reporter said that he had just returned from Kuwait where he had travelled with an American patrol. They had noticed a patrol of about thirty Iraqis on the next sand dune. While the Americans were wondering how they would get the Iraqis to surrender, a U. S. helicopter suddenly appeared and flew over the Iraqis. By the time the helicopter had reached the next sand dune, the Iraqis had their hands up and were surrendering.

This is all very suspicious in itself. These were the same Iraqis who fought a Holy War against Iran for eight years.

The next news of interest that I noted came towards the end of the conflict when Brigadier General Neil was questioned by a British reporter from the BBC. The reporter asked the General about his plans to get the Iraqi soldiers out of the deep bunkers that the Germans built for the Iraqis. These bunkers were known to be extremely well fortified, and it was a good question.

General Neil said, "We bring in the psychological..."*

He then broke his sentence with coughing. It didn't sound like a real cough

but that he had caught himself saying something he shouldn't reveal. When he stopped coughing, he continued speaking.

"I'm sorry, we bring in the helicopters with PA (public address) systems and we talk 'em out."

To me, his statements were very significant. It is apparent to me that the General had made a mistake and had to continue his sentence in the same vein. In my opinion, he was going to say something like "psychological broadcasting helicopters."

He had helicopters on his mind and in order to make it less obvious, I believe he changed what he was going to say and referred to "PA system helicopters."

I did some research into the Iraqi bunkers and discovered that the Americans had been trying to get the plans for their construction from the East Germans.

The Americans wanted to know how to penetrate the bunkers. They did retrieve the plans and found out the walls were very thick. Even after the air blitz, the Iraqis were still deep in the bunkers. They had electricity, entertainment and enough food and water to last at least six months. The bunkers were three feet thick and probably could have withstood a nuclear blast. The Iraqis also had the equipment to tunnel out if necessary.

The British reporter knew it wouldn't be easy to get the Iraqis out of the bunkers. That's why he asked the question. I believe it is absurd to suggest that these fanatic soldiers would have surrendered under the mere threat of PA system helicopters.

* The quotations by General Neil are not exact quotations but are paraphrases based upon my memory of the actual events.

APPENDIX D- NIKOLA TESLA

Nikola Tesla was born in 1856 in what is today known as Yugoslavia. Known as the "Father of Radio", he was clairvoyant and had different paranormal abilities.

Most notable was his vision as a youngster that he would build an alternating current generator that would revolutionize the way that mankind harnessed electricity.

Tesla received a renaissance education and learned to speak several languages.

He worked his way across Europe as an inventor and electronics engineer. In Paris, his genius came to the attention of one of Thomas Edison's associates, and Tesla was invited to meet the famous inventor. Although Edison hired him, the two never got along well.

Edison's utilities used direct current which required a power plant every few miles or so. Tesla tried to convince him that alternating current was more effective and less costly to operate. Edison was stubborn and Tesla's brilliance must have made him feel insecure. Here was a man whose geius was far superior to that of Edison's!

Edison would never back up Tesla's plans to revolutionize the world with alternating current. The two finally had a complete falling out when Tesla advised Edison that he could upgrade his entire facility by building new machines and replacing the old ones. Edison offered him $50,000 to complete the task. Tesla designed twenty-four types of machines and effectively enhanced the factory. Edison was very impressed but wouldn't pay the money. He claimed it was just his "American sense of humor."

George Westinghouse was an inventor himself and recognized the genius in Tesla.

He backed Tesla's plan to harness alternating current from Niagara Falls and the world has never been the same since. Meanwhile, Edison tried to prove that alternating current could be deadly to humans and went to the extent of

electrocuting a dog in public (with alternating current) to prove his point. Edison ended up embarrassed and humiliated.

Tesla's career went on the rise and his experiments were of vast renown. He demonstrated remote control with small boats in Madison Square Garden, but many people dismissed it as witchcraft.

He even generated lighting between the Earth and sky at Colorado Springs. This experiment was particularly remarkable because he put light bulbs to the raw ground and they light up. This demonstrated that the Earth's surface was a conductor of electricity. This proved that if the proper vehicles were used that the entire population of Earth could enjoy free energy.

Tesla created a huge tower on Long Island and sought to build a system that would provide free energy. While in progress the financier J. P. Morgan pulled the rug out from under Tesla. He didn't want free energy.

Tesla's career went into a decline and his reputation was hurt. Part of this was caused by his periodic admisssions that he received communication from aliens.

His receivers supposedly picked up transmissions from Mars.

No one ever denied he was an electronics genius, but because he understood supernatural phenomena, he was held in suspicion. Today, many of my engineering colleagues consider him a "nut" who just happened to be brilliant in electronics. This is a very convenient explanation.

It is my opinion that he was incredibly ahead of his time.

APPENDIX E- HISTORY OF THE PHILADELPHIA EXPERIMENT AND ITS RECONCILIATION WITH THE MONTAUK PROJECT

In 1912, a mathematician named David Hilbert developed several different methods of new math. One of these was known as "Hilbert Space." With this he developed equations for mulitple realities and multiple spaces. He met Dr. John von Neumann in 1926 and shared his information. Von Neumann took a lot of the systems he learned from Hilbert and ran with it. According to Einstein, von Neumann was the most brilliant of mathematicians. He had an uncanny ability to take abstract theoretical concepts in math and apply them to physical situations. Von Neumann developed all kinds of new systems and math.

A Dr. Levinson had come along and developed the "Levinson Time Equations."

He published three books, which are now very obscure and almost impossible to find.

An associate of mine did dig up two of them at Princeton's Institute for Advanced Study. All of this work was to serve as a background for the invisibility project which would apply the theoretical principles to a large hard object.

Serious research into the subject of invisibility began in earnest in the early 1930's at the University of Chicago. Dr. John Hutchinson Sr. served as Dean at this particular time and was privy to the work of Dr. Kurtenhauer, an Austrian physicist then at the University. They were later joined by Nikola Tesla. Together, they studied the nature of relativity and invisibility.

In 1933, the Institute for Advanced Study was formed at Princeton University.

This included Albert Einstein and John von Neumann, a brilliant mathematician and scientist. The invisibility project was transferred to Princeton shortly thereafter.

In 1936, the project was expanded and Tesla was made the director of the group.

With Tesla on board, partial invisibility was achieved before the end of the year.

Research went on to 1940 when a full test was done in the Brooklyn Naval Yard.

It was a small test, with no one on board the vehicle. The ship used was powered by generators from other ships, connected by cables.

Another scientist, T. Townsend Brown, became involved at this point. He was known for his practical ability to apply theoretical physics. Brown had a background in gravity and magnetic mines. He had developed counter measures to the mines with a technique known as degaussing. This would trip the mines at a safe distance.

There was a big brain drain on Europe in the 1930's. Many Jewish and Nazi scientists were smuggled into the country. Much of this influx has been attributed to A. Duncan Cameron Sr. Although we know he had extensive connections, his exact relationship to intelligence circles is still a mystery.

By 1941, Tesla had full confidence of the powers that be (FDR). A ship was prcured on his behalf, and he had coils wrapped around the entire ship. His famous Tesla coils were also employed on the ship. However, he grew wary because as the project developed, he knew there would be problems with personnel. Perhaps he knew this due to his ability to fully visualize his inventions in his mind. In any case, Tesla knew that the mental state and bodies of the crew would be affected severely.

He wanted more time to perfect the experiment.

Von Neumann desagreed with this vehemently at the time and the two never got along. Von Neumann was a brilliant scientist but did not embrace metaphysics for its own sake. Metaphysics was old hat to Tesla, and he had built a successful legacy of inventions based upon his unique prescience.

Part of what made his views so controversial was that during his experiments in Colorado Springs, circa 1900, he said that off planet intelligence had contacted him via consistent signal messages when Mars approached. This also occurred in 1926 when he had radio towers erected in the Waldorf Astoria and at his New York city lab.

He claimed to receive information that he'd lose people if things were not changed.

He needed time to design new equipment.

Tesla's requests for more time were not heeded. The government had a war to win and additional time was not granted. Tesla wen through the motions but secretly sabotaged the operation in March 1942. He was either fired or quit. He is supposed to have died in 1943, but there is arguable evidence to suggest he was whicked off to England. A look-alike derelict is supposed to have been put in his place for the funeral. He was cremated the day after his body was found which was not in keeping with the tradition of his family's orthodox faith. Whether or not he died is controversial. That secret papers were removed from his safe has never been in question.

Von Neumann was named director of the project. He did a study and determined that two huge generators would be required for the experiment. The keel for the USS Eldridge was laid in July 1942. Tests were done at dry dock. Then, in late '42, von Neumann decided that the experiment could be fatal to people, just as Tesla had suggested. Ironically, he still got upset at the mention of Tesla's name. He decided a third generator would do the trick. He had time to build one but never got the third one to synchronize with the other two. It never worked because the gear box was incompatible. The experiment went out of control and a Navy technician was zapped, went comatose for four months and left the project. They pulled out the third generator. Von Neumann wasn't satisfied, but his superiors weren't going to wait any longer.

In July 20, 1943, they decided it was ready and made tests. Duncan Cameron Jr. and his brother, Edward, were in the control room to operate it. The ship was no longer at anchor and orders came by radio to turn it on. Fifteen minutes of invisibility ensued. There were immediate problems with people. They got sick, some experiencing nausea. There were also mental illnesses and psychological disorientation. They needed more time, but the final deadline was given for August 12th, 1943. The orders came from the Chief of Naval Operations, and he said he was only concerned with the war.

Trying to avoid damage to individuals involved, von Neumann tried to modify

the equipment so that only radar invisibility would be achieved, not literal sight invisibility.

Six days before the final test on the Eldridge, three UFOs appeared over the ship.

The switch was thrown for the final test on August 12th, 1943. Two of the UFOs left the area. One was sucked up into hyperspace and ended up in the underground facility at Montauk.

Reports from Duncan indicated that he and his brother knew things were going to go wrong with the August 12th experiment. However, for three to six minutes, things looked good. It appeared it might work without any devastating effects. They could see the outline of the ship - everything was gone. There were problems.

The principal radio mast and the transmitter were broken. People were jammed in the bulkheads. Others were walking around in an insane state.

Duncan and Edward Cameron did not suffer the same trauma as their shipmates.

They had been shielded in the generator room which was surrounded by steel bulkheads.

The steel acted as a shield to the RF energy. As they witnessed things falling apart, they tried to shut off the generator and transceivers but were unsuccessful.

At the same "time", another experiment was going on forty years later at Montauk.

Research had revealed that the Earth, like humans, has a biorhythm. These biorhythms peak out every twenty years on August 12th. This coincided with 1983 and provided an additional function for the connecting links through the Earth's field for the Eldridge to be pulled into hyperspace.

The Cameron brothers could not turn off the equipment on the Eldridge because it was linked through time to the generator at Montauk. They figured it wasn't safe to remain on the ship and decided the best alternative would be to jump overboard in hopes of escaping the electromagnetic field of the ship.

They jumped and found themselves pulled through a time tunnel and onto dry ground at Montauk on Aug .12th, '83 at night. They were found quickly and taken downstairs.

Von Neumann met Duncan and Edward and indicated he knew they were coming. He was now an old man. He said that there had been a lock up in hyperspace and that he'd been waiting since 1943 for this date. He told the time travellers that the technicians at Montauk were unable to go shut things down. Duncan and Edward were required to go back to 1943 and shut the generator off. Von Neumann even told them that the historical records showed that they had turned it off. But they hadn't done it yet! He told them to destory any equipment if that's what it took.

Before returning to 1943 for good, Duncan and Edward did some missions for the Montauk group. They made a number of trips back to 1943. On one of these trips, Duncan passed through the time portal and entered the time tunnel. Duncan somehow entered a side tunnel and got caught there. Side tunnels were a mystery and remain so.

Even though the Montauk scientists theoretically considered side tunnels non-existent, Duncan was warned not to enter them if they should appear. Edward soon ended up in the same tunnel with Duncan.

A group of aliens revealed themselves. Apparently, the side tunnel was an artifical reality created by the aliens. They wanted a piece of equipment before they would let their captives go. This equipment was a very sensitive instrument that charged the crystal drive to the UFO that was underground at Montauk. The aliens didn't seem to mind leaving a ship, but they were very intent on keeping the drive source a mystery to humans.

Duncan and Edward returned to Montauk and retrieved the drive for the aliens.

Eventually, they were able to return to the Eldridge and carry out von Neumann's orders. They smashed the generators, transmitters and cut every cable they could find. The ship finally returned to its original point at the

Philadelphia Naval Yard.

Before the portal closed, Duncan returned to Montauk in 1983. His brother, Edward, remained in 1943. Duncan is not sure why he returned. It has been suggested that he may have been under orders or programmed to do so.

This adventure turned out to be a disaster for Duncan. His time references totally dissolved, and he lost his link to the time line. When time references are lost, one of three things happens: aging slows down, remains the same or speeds up. In this case, it speeded up. Duncan began to age rapidly. After a short amount of time, he began to die of extreme old age.

We're not sure how this happened, but we believe von Neumann transferred him to another time. Scientists were enlisted to help him. They couldn't let the Duncan from 1943 die. He was not only invaluable to the project, he was elaborately involved with the entire scope of time. His death could have created bizarre paradoxes and had to be avoided.

Unfortunately, Duncan's body was dying and there was nothing that could be done to alter the rapid aging. But there was another alternative. Research had already demonstrated that each human being has their own unique electromagnetic identity. This was commonly referred to as one's "electromagnetic signature" or just "signature." If this "signature" could be preserved when Duncan's body ceased to function, it could theoretically be transferred to a new body.

The Montauk scientists were already intensely familiar with all of Duncan's electromagnetic manifestations from the exhaustive research that had been done.

By some means, I'm not sure how, his "soul" or "signature" was transferred to a new body.

They sought help from one of their most loyal and effective agents: A. Duncan Cameron Sr., who happened to be the father of Duncan and Edward Cameron.

Duncan Sr. was a mysterious character. He was married five times over the course of his life. He had numerous connections and didn't seem to work. He spent his time building sailboats and travelling to Europe. Some have alleged that he smuggled Nazi and/or German scientists into the U. S. via his boating activities.

There is practically only one tangible piece of evidence that connects him to intelligence circles. He appeared in a photo of a special graduation for intelligence personnel at the Coast Guard Academy. He was not officially affiliated with the Coast Guard in any way.

Through the use of the Montauk time techniques, the Montauk group contacted Duncan Sr. in 1947. They informed him of the situation and told him to get busy and have another son. He now had a different wife than Duncan Jr.'s original mother. Duncan Sr. cooperated and a child was born, but it was a girl. His directions were to produce a son. Finally, a boy was born in 1951. "Duncan" was chosen as the name for this child, and this is the same Duncan I know today.

The Montauk techniques are obviously remarkable, but they were not sophisticated enough to move Duncan from 1983 straight back to 1951. There could have been other factors involved, but it appears the scientists had to rely on and ust the twenty year biorhythms of the Earth. As Duncan's original body was dying, he was transferred to 1963 and "installed" into the new body provided by Duncan Sr. and his wife.

Duncan Jr. has no memories prior to 1963. It is also obvious that whoever occupied his body between 1951 and 1963 was forced out.

I have often heard accounts of a secret project that was run by ITT at Brentwood, Long Island in 1963. It is entirely possible that transferring Duncan to a new body was the focal point or a very important part of this project. Whatever the circumstances, this project would certainly have been trying to somehow utilize the Earth's bioshythm that occurs every twenty years.

Edward Cameron had returned to 1943. Duncan was in 1963.

After the August 1943 experiment, the Navy brass didn't know what to do. Four days worth of meetings ensued with no conclusions. They decided to do one more test.

In late October of 1943, the Eldridge disembarked for the final experiment.

No personnel wree to remain on board. The crew boarded another vessel and controlled the equipment on the Eldridge remotely. The ship became invisible for about fifteen or twenty minutes. When they boarded it, some of the equipment was missing.

Two transmitters, and a generator were gone. The control room was a burnt shambles, but the zero time reference generator was left intact. It was put into secret storage.

The Navy washed their hands of the entire operation and officially launched the USS Eldridge with its office of record. The ship was eventually sold to the Greek navy who later uncovered the log books and found that everything before January of 1944 had been omitted from the records.

According to Al Bielek's account, Edward Cameron continued his career in the Navy. He had top level security clearance and probed into many sensitive areas such as "free energy" vehicles and devices. He was outspoken and complained about improper proceedures.

For whatever reason, he was brainwashed to forget the Philadelphia Experiment and anything else to do with secret technology.

Al has stated that age regression techiques were used to put Edward Cameron into a new body in the Bielek family. The Bielek family was chosen as there was only one child in the family and the baby had died by the time of his first birthday.

Edward was substituted and the parents were brainwashed accordingly. Edward has since been knwon as "Al Bielek."

Age regression techniques have been traced back to Tesla. When he was working on the original Philadelphia Experiment, he developed a device to help sailors in the event that they lost their time locks. The purpose of this device was to reestablish an individual with his normal time locks in the event he had been disoriented from time travel. The government or someone allegedly used this Tesla device and developed it for physical time regression.

Tesla said that if the time locks of an individual are moved ahead in time, one could actually remove age. If one's time locks were pushed back twenty years younger, the body would be referenced to those locks.

Edward Cameron now became Al Bielek. Al grew up with his own identity and education and became and engineer. Eventually, he ended up working at Montauk.

It was not until the mid 1980's that Al began to get memories from his earlier identity. To this day, he continues to doggedly research the Philadelphia Experiment and is planning to write another book. He intends to prove, even to the most skeptical, that the Philadelphia Experiment did indeed happen.

APPENDIX F- QUANTUM LEVELS OF EXISTENCE (According to Preston Nichols)

When I am referring to quantum levels of existence, "quantum" refers to the different or many possible levels. "Quantum" comes from the Latin root "quantis" which means quantity.

Understanding multiple realities is key to understanding time. Conventional physics does not deny the possibility of parallel existences, but it is mostly concerned with theories about matter and anti-matter. As there is much evidence to prompt scientific investigation into the area, there are currently about sixty theories around the world and ten in the U. S. that deal with quantum levels of reality.

I am offering my own theory based upon my experiences, some of which are covered in this book. Like any proper scientific theory, this is being offered because it has proven workable to me in the laboratory. It will also help the reader get a better grasp of how time functions.

What exactly is parallel reality?

It would be a world or universe that has almost everything we have here. If

we switched into it, we'd see another body that would represent us in the other existence.

The parallel universe would not necessarily behave exactly like the one we're familiar to. It would have unique properties unto itself.

It is my understanding that we exist in a number of parallel realities. We are primarily conscious of "our reality" because we are focused or referenced to it. The parallel universes might reach our consciousness through dreams, ESP, meditation or artificially induced mental states.

It is now important to consider the overall view and what these different realities might look like in schematic form. Einstein theorized that if one travels in a straight line from any particular point in space that one would eventually end up in exactly the sam eplace that they started at. This could be considered a full loop.

We are not going to go into the equations of that, but the general reader can grasp this by understanding what Einstein called a time toroid. For this purpose, a toroid can be likened to a two dimensional doughnut. Einstein likened the entire universe to a time toroid. He theorized that if one started in a straight line from any given point on the outside of the doughnut, that one would end up at the exact opposite end of the doughnut. Both of these point would be essentially the same, except that one could be considered "positive" and the other "negative." As they are both points in the infinite stream of time, one point could be called "positive infinity" and the other "negative infinity."

For purposes of explaining my theory, I have extrapolated upon Einstein's idea and have converted his time toroid into a three dimensional sphere. The reader can easily picture a smaller sphere inside of a bigger sphere. For clarification, we will call the inside sphere, Sphere A, which can be likened to a softball.

The bigger sphere will be called Sphere B and can be likened to a basketball (which is hollow).

Our experiences in different realities all occur within the realm of Sphere A.

If you start from a point on Sphere A and travel in a straight line, you will eventually come back to where you started from.

Within Sphere A, everything in dynamic and moving. It is time as we conceive it.

The area between Sphere A and Sphere B is not dynamic at all. In fact, it is considered to be at rest. We can postulate this area to be a sea of time particles.

These are not particles in any ordinary sense. In fact, trying to describe them in this three dimensional example is awkward. We are simply assuming these non-moving particles of time exist because we can sense them (if only in idea form). These particles between Sphere A and Sphere B would be the same as the particles in dynamic time (within Sphere A) except that they are static, i. e. at rest.

Incidentally, we are not conscious of static time because our "normal" reality is built upon dynamic functions or dynamic time.

A reality in time is created when God or someone creates a stress on the wall of Sphere A. This stress will cause the dynamic particles inside of Sphere A to move and travel through the sphere until there is a loop, thus completing the Alpha and Omega (beginning and end).

Our reality can be considered one gigantic loop. It could have started with the big bang or the beginning of the universe and would eventually end there, but it would in fact continue ad infinitum.

When someone or something then takes that loop that we are in and creates a new time stress and changes reality, a new loop is created that is, in fact, an alternate reality. The original loop cannot be obliterated or denied. It will still be there. The new loop could be modified in any way the modifier chooses. It could be an opening in 1963 that goes to 1983. Everything in between those times

would be an alternate loop. It would not be an entire loop of its own, but would be added to the original loop of our normal reality. In this way, partial loops would be added on to our original time line, and we can call this conglomeration of loops a manifold.

Each loop could also be called a manifold (a manifold generally refers to something that has many parts).

As different alternate realities are created off of the original loop, additional manifolds are added to the sphere and make it swell. In addition to the alternate realities created by changing the reality of a particular time line, there could be parallel realities created in the beginning of time that also have their own "original" loops as well. There is an infinate number of loops and manifolds possible.

Some people may wonder about Sphere B in the above example. It is basically there to make the theory fit. At this point, I can add no further significance to Sphere B except that it serves as a wall containing time stress particles. It could possibly be a part of a bigger scheme of metaphysics.

Now that you have a grasp of how these time loops and manifolds fit into an overall picture of the universe, there is another key question that must be asked.

Is it possible to gain consciousness of the other loops or manifolds?

Yes, it is. This is what happened on my roof when I was putting up my Delta T antenna (as discussed in Chapter Six). That antenna has a subtle interdimensional effect on the nature of time itself. It enabled me to regain consciousness of an alternate time line that I had been put on against my innate will.

It is therefore possible for others to travel from one time loop to another.

In fact, it appears that this is the entire reason for the Philadelphia Experiment and Montauk Project in the first place. This theory indicates that not only was an alternate time loop created but that this loop enabled a vast influx of alien UFOs to come to this planet. UFOs have always been around, but there is no denying the sudden frequency of reports in the 1940's.

Even if you do not accept any of this as the truth, it is quite obvious that this is the type of advantage an alien race might have over us.

The next point I want to address is that parallel realities are based upon principles common to electromagnetics. For example, it is common knowledge that alternating current is created by an alternating difference in potentials.

It is the relationship between the voltage and the current that makes alternating current function. Further, the relationship between the current and voltage is inextricable.

Just as there is an interplay between the voltage and current, there is one between two different realities.

Extrapolating from these principles, it can be understood that parallel realities are ninety degrees out of phase with our "normal reality." In other words, if there is a parallel reality, one has to consider that it has potential energy. It is not activated of itself. It would also be ninety degrees out of kilter from our normal viewpoint. The fact that it is potential energy means that it has the capability to flow to our reality and vice versa.

This explains that there is not only a relationship between electromagnetic principles and other universes, but suggests that by utilizing electromagnetic principles that one can theoretically enter the realm of other realities. These would include the alternate time loops of which I have already spoken.

It is hoped that the above will give the reader a general understanding of how electromagnetic principles were used to manipulate time at Montauk.

APPENDIX G- GLOSSARY

Amplitron- A high powered UHF amplifier. At Montauk, this served as the

final amplifier of the transmitter before a function was radiated out the antenna.

A large tube, it weighed 300 pounds and measured 35 inches in its largest dimension.

Biorhythm- This is an esoteric term and refers to any regularly repeating life function in an organism. A biorhythm is perhaps best understood in terms of Oriental "Ki" or "Chi" energy, which is the life force that regulates the entire body. Acupuncture addresses biorhythms in order to affect a cure. When the planet is considered as an organism, biorhythms would include all the subtle functions that make life possible and regulate it. The seasons, rotation of the Earth and spinning of the galaxy would all be taken into account. Legendary places such as Stonehenge are considered to be constructed in harmony with the biorhythms of the planet.

Cathode- In a vacuum tube, the electron emitting material is called a cathode.

In an electrolytic cell, it is the negative electrode from which current flows.

In essence, it is a source of flow.

Cycle- A unit of activity within a wave that continually repeats itself. A cycle will go up and down before it repeats itself. If you visualize ocean waves that are all uniform, the series of waves would be called the "wave." The one ocean wave that a surfer might ride would be a "cycle."

Delta T- Short for "Delta Time." Delta is used in science to indicate change, thus "Delta T" would indicate a change in time.

Delta T antenna- An octahedronal antenna structure that is designed to bend time.

Visually, it looks like two pyramids sharing the same base. By definition, it can actually facilitate shifting time zones. Two coils are placed vertically around the edges of the pyramid structure at 90 degree angles to one another.

A third coil surrounds the base. Shifting time zones was accomplished by pulsing and powering the Delta T antenna, as is discussed in Chapter 12. Even when the antenna is not powered, it has a subtle interdimensional effect on the nature of time itself.

DOR- Stands for "Dead ORgone" (see definition of "orgone".) This refers to life energy that has become stagnant or negative. DOR couls be considered the antithesis of life energy.

"Electromagnetic bottle"- This refers to a "bottle effect" that is created when a specific space is surrounded by an electromagnetic field. The specific space itself is the inside of the "bottle." The walls would be the electromagnetic field.

When people or objects are within the specific space, they would be within an "electromagnetic bottle."

Electromagnetic wave- When an electric charge occurs that oscillates (swings back and forth), a field around the charge is generated. This field is both electric and magnetic in nature. This field also oscillates which in turn propagates a wave through space. This was is called an electromagnetic wave.

Frequency- The number of waves or cycles per second.

Helmholtz coils- commonly, Helmholtz coils refer to two identical coils that are separated by a distance of one radius of the coils themselves. (You can visualize this if youthink of two hula hoops parallel to each other.) When the coils are electrified, they produce a homogeneous magnetic field over a larger volume of space than does a single coil.

Hertz- (abbr Hz) This is simply one cycle of a wave. A wave consists of numerous cycles that are repetitions of one cycle. To be a bit more technical, hertz is the complete fluctuation of a wave from plus (the highest point) to minus (the lowest point.) Five hertz would be five cycles per second.

MHz- MegaHertz, which are equivalent to 1,000,000 hertz.

Non-hertzian component- This term does not exist in conventional science. It refers to the etheric component of electromagnetic waves. Theoretically, the non-

Hertzian component is a wave function. Instead of oscillating transversely, it oscillates with the direction of propagation, which is known as longitudinal (i. e. sound waves.) It could be looked at as an "acoustical" electromagnetic wave.

Orgone- This refers to life energy or sexual energy as observed by Dr. Wilhelm Reich. It is the positive energy that "makes us tick."

Oscillator- A device that establishes and maintains oscillations. To oscillate means to swing back and forth. In electronics, an oscillations refers to a regular variation between maximum and minimum values, such as current or voltage.

Phase- The time intervale between when one thing occurs and the instant a second related thing takes place.

Phase conjugation- This is the process whereby a wave comes back from a received source that is an imaginary image of a transmitted wave. In other words, when a radio wave is transmitted, an image goes back to the transmitter by the process of conjugation. (For more information, one can read up on modern electro-optics theory.)

Phoenix Project- A secret project that commenced in the late 1940's. It researched the use of orgone energy, particularly in regards to weather control. It eventually inherited the Rainbow Project and included the Montauk Project itself. "Phoenix" was an official code name.

Psycho-active- This pertains to any activity or function that has an effect on the mind or psyche. In this book, psycho-active refers primarily to electromagnetic functions or electric equipment that influence human thinking and behavior.

Psychotronics- The science and discipline of how life functions. It includes the study of how technology interacts with the human mind, spirit and body.

Science, mathematics, philosophy, metaphysics and esoteric studies are united through the study of psychotronics. It would also include other realities and how we interface with other dimensions of existence.

Pulse modulations- These are sent as a series of short pulses which are separated by relatively long stretches of time with no signal being transmitted.

RF- Radio Frequency. Frequencies above 20,000 hertz are called radio frequencies because they are useful in radio transmissions.

Radio wave- An electromagnetic wave that carries intelligent information (pictures, sound, etc.)

Relativistic- Relativistic functions refer to activities that are out of our normal reference frame. It also concerns how activities in other reference frames relate to ours. Relativity embraces the concept of everything without any limitations, including other dimensions and the entire universe(s).

Sideband- This is the component of radio waves that actually carries the intelligent information.

Space-time- When you study higher level physics, it becomes apparent that space and time are inextricably related to each other. It is considered less accurate to refer to just space or time by itself (because they don't exist by themselves.)

That would be like saying your mouth ate the dinner.

Time reference(s)- This refers to the electromagnetic factors by which we are connected to the physical universe and the stream of time. Consciousness of time can be likened to a deep hypnosis which causes one to be in sympathy with the various frequencies and pulses of the physical universe.

Tranceiver- An instrument that serves as both a receiver and a transmitter.

Transmitter- A device or unit that sends a signal or message.

Wave- A state of motion that rises and falls periodically is called a wave. It can be transmitted from one particular area to another with no actual transport of matter taking place. A wave consists of many cycles and can carry signals, pictures or sounds.

THE STORY CONTINUES...

MONTAUK REVISITED, Adventures in Synchronicity: By Preston B. Nichols and Peter Moon Montauk revistied unmasks the occult forces that were behind the scene and technology used in "The Montauk Project." An ornate tapestry is revealed which interweaves the mysterious associations of the Cameron clan with genesis of American rocketry, the bizarre history of the electronic transistor and the magic of Aleister Crowley. The Montauk investigation carries forward as Preston Nichols opens the door to Peter Moon and unleashes a host of incredible characters and new information. A startling scenario is depicted that reaches far beyond the scope of the first book, "The Montauk Project." Illustrations and photos .256 pgs.

PYRAMIDS OF MONTAUK, Explorations in Consciousness: By Preston B. Nichols and Peter Moon An astonishing second sequel that awakens the consciousness of humanity to its ancienty history and origins through the discovery of pyramids at Montauk. Their placement on sacred native American ground opens the door to an unprecedented investigation of the mystery schools of earth and their connection to Eygpt, Atlantis, Mars and the star Sirius. Mr. Nichols fascinates us with an update on covert operations that includes the discovery of a nuclear particle accelerator and the development of new psychotronic weapons. "Pyramids of Montauk" stirs the quest for the end of time as we know it .256 pgs.

THE MONTAUK PULSE, A Chronicle of Time

As "The Montauk Project: Experiments in Time" originally went to press in May 1992, many new and startling developments began to take place. Consequently a newsletter entitled "The Montauk Pulse" began in January 1993 to keep interested readers up to date on breaking news regarding the Montauk scenario.

It was not envisioned at that time that two subsequent books would be published on the subject. The Pulse has a distinct identity from the books and will often comment on details and history that don't necessarily find their way into book form.

The Montauk Pulse contains at least six pages per issue and is published quarterly.

It includes exciting new breakthroughs on the Montauk story as well as similarly related phenomena like the Philadelphia Experiment or other space-time projects.

The Delta-T Antenna

The Delta-T antenna is the device of legend from 'Project Phoenix'. The device consists of 3 antennas or coils each at 90 degrees to the other. The main two are fed a sine and cosine wave so that they are 90 degrees phase-shifted. This starts up a rotational magnetic field in the center of the antennas whose rotational velocity is equal to the input frequency. The third antenna pulls the field into the 3rd dimension.

Here is a possible Delta-T configuration:

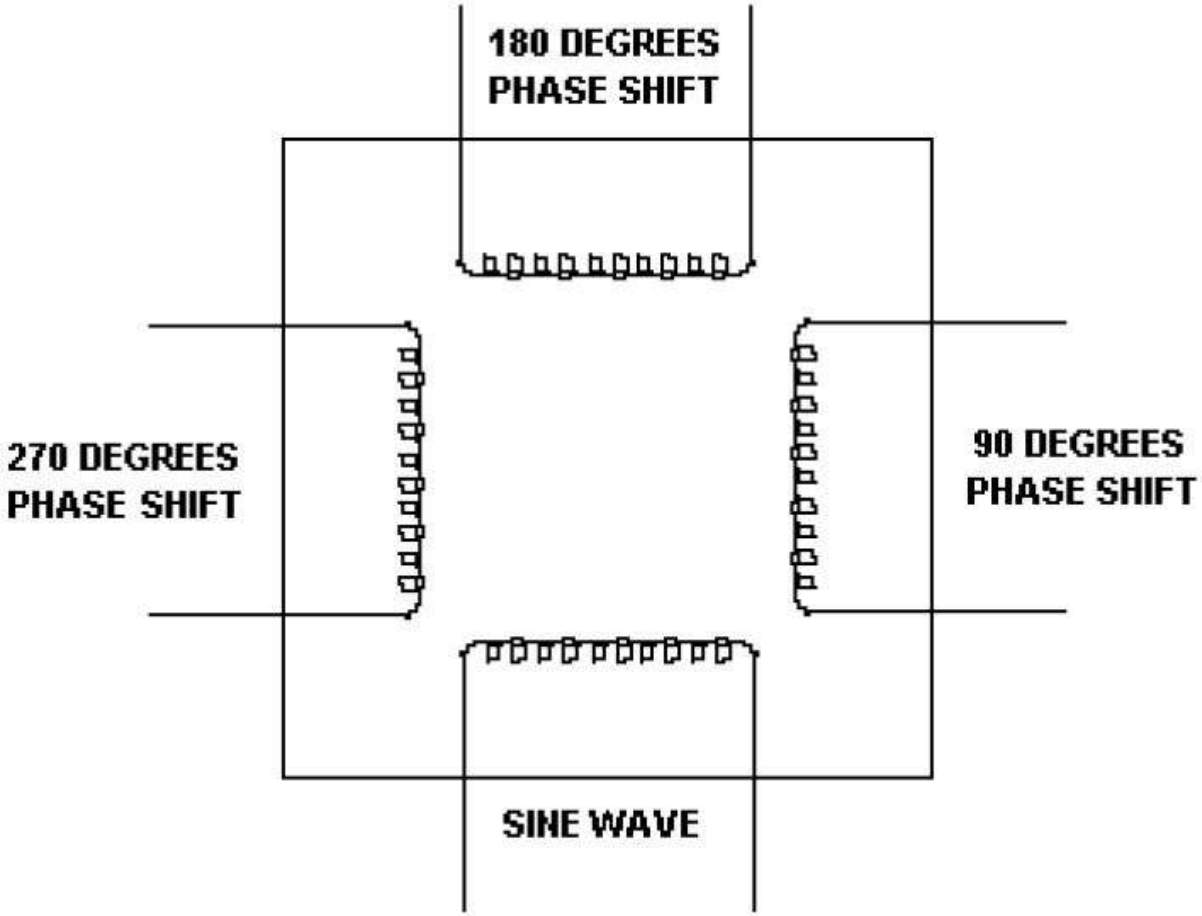

Construction:

This device (Delta-T) enables time-traveling. The central part of the device consists of 2 frame antennas that are arranged 90 degree in relationship to each other. Each frame is approximately 2 meters in diameter. The antennas can consist of tubes which are 10 cm in diameter. The tubes must be superconductive. Inside the tubes float liquid helium for the superconductivity.

The control device of the machine consists of a sinus generator with a tuning capacity from 1-Hz to 1000-MHz. The signal from this generator is amplified a little before it goes to a phase changer. This changes the phase of the signal 90-degrees. The phase changer is independent of the frequency in. The phase change is 90-degrees for both the 1-Hz and 1000-MHz input. The in-signal is split just before the phase changer so that one part is unchanged and another part is changed 90-degrees. After the phase changer, the signal amplified with 2 linear amplifiers to 100,000 watts on each channel. After that, the 2 channels are fed to its respective frame antenna. The signal on one frame antenna will always be 90-degrees in phase difference to the other frame antenna.

Usage:

The generator is set to 1-Hz and the machine is turned on. A compass needle at the center of the machine will travel slowly round. Inside and round the antenna system, it becomes a powerful rotating magnetic field.

At a higher generator frequency, the magnetic field will rotate faster. Approximately 2 meters from the antennas are placed several chairs arranged in a circle around the antenna system. Here the time travelers are placed. One increases now the generator frequency gradually until the speed of the rotating magnetic field is close to the speed-of-light. If the right conditions are present now (etherical/astral), the time will run slower for those who are sitting on the chairs compared to persons outside the power-field. Seen from the chairs, the time will run normal between each chair. The time travelers' clock will run normal.

They will see the clock on the wall outside the power-field running fast into the Future. The nearer the rotating speed of the magnetic field comes to the speed-of-light, the faster will the time travelers move into the future. If the speed of the magnetic field is set equal to the speed-of-light, the time will freeze as seen from outside the magnetic field. As seen from the time travelers view, they are moving endlessly fast into the future (they will not be able to sense the world outside the magnetic field and the time will stop for them). If one increases the frequency further, the rotating speed of the magnetic field will become greater than the speed-of-light. The time sensed from the chairs would then be reversed, and they will see the clock on the wall outside the magnetic field moving backwards. The time travelers will now travel back in time.

At the speed-of-light, the time travelers go both endlessly fast into the Future and the Past at the same time. The result is that the time freezes at that speed.

At a higher frequency, they will travel slower into the Past. When the speed of the magnetic field approaches the speed-of-light from above, the time travelers will travel faster into the past. At the speed-of-light for the magnetic field rotation, the time is frozen for the people inside the power-field and they can't register anything. For an outside person who looks inside, the power-field it looks like looking at a frozen hologram. If one from outside the magnetic field tries to touch the field at this state, it seems harder than steel. The outside person will at this state not be able to penetrate the power-field which acts as an endlessly strong armor at that state. If one puts a clock inside the power-field, an outside person will observe the following.

At 1-Hz, the clock will run normal. When the frequency arrives at the lowest part of the VHF band (above 30-MHz) the clock seems to be going slower. At the top of the VHF band (approximately 300-MHz), the clock will stop completely. In the lower part of the UHF band (from 400-MHz), the clock begin to go slowly backwards. At 1000-MHz, the clock will go approximately at normal speed backwards. It's also possible that the machine must have an injection of modulated orgone energy to function.

The Montauk Project Papers

by Thomas Skeggs

Introduction

Over the last few years I have amassed some information on 2 strange experimental projects known as the **Montauk Project** and the **Philadelphia Experiment**.

So I have decided to publish extracts from some of my papers on these fascinating stories. There is a lot of debate surrounding the Montauk Project and the Philadelphia Experiment. Some of this debate can get a bit heated where both skeptic and believer trade insults and accusations of fraud, hoaxing, and even lying. Others make the claim that the Montauk Project and the Philadelphia Experiment are nothing more than disinformation -- a tool to distract the gullible investigator, researcher and journalist away from the real truth surrounding highly-classified and secretive research programs.

When writing these papers, I have simply looked at them from purely a technical point-of-view to try to determine the true nature on how the equipment described in these projects may have actually worked.

The Montauk Chair

According to the authors Preston Nichols and "Peter Moon", the technology to read a person what way a person was thinking was originally allegedly developed at the ITT Technical Institute at the University of Southampton, Long Island in the 1950s. (Some basic research reveals the ITT Institute has closed down at Southampton). Nichols states in his book that RCA went on to develop a second version of the chair during the 1970s.

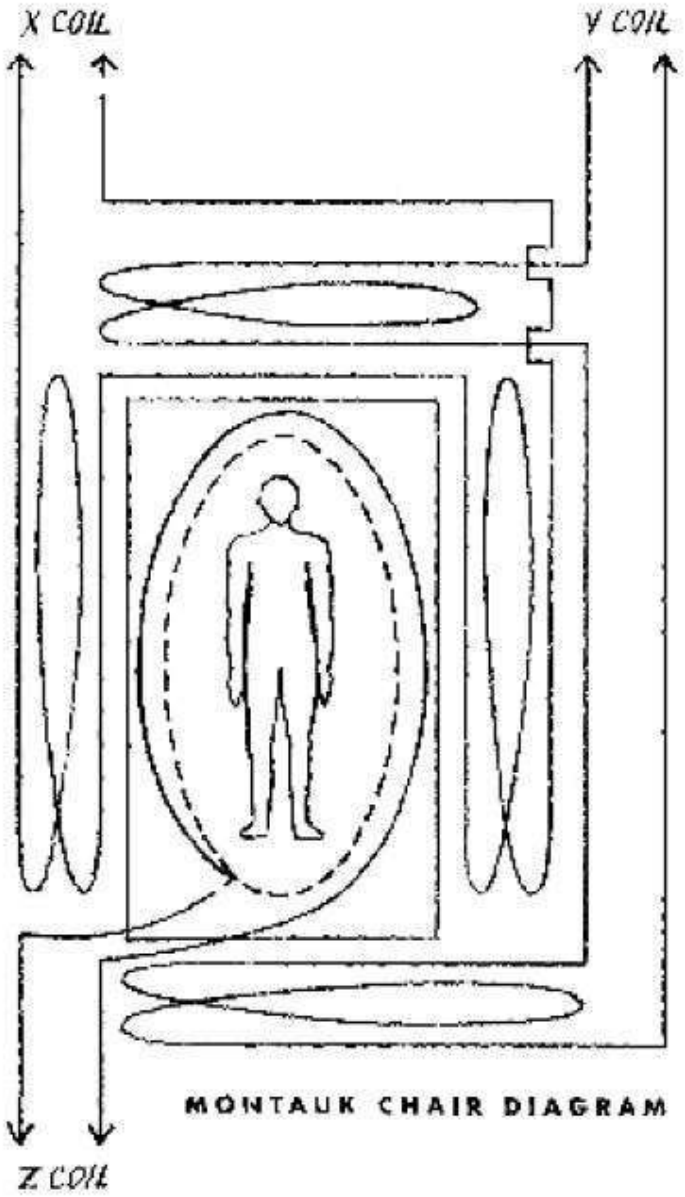

a diagram drawn by Nichols describing the lay-out of the Montauk Chair.

Nichols claims the chair was surrounded by 3 **Helmholtz coils** described as the 'X' coil, 'Y' coil and 'Z' coil. Note the 'X' coils are located on each site of the individual. The 'Y' coils are located above the head and below the feet. And the 'Z' coil appears to be wound around the chair. (2 loops could have been used above and below the chairs which may have been designed to pick up fluctuations or modulations within the electrical magnetic field surrounding the human body.)

Helmholtz coils consist of cable wound in loops in to produce a coil. Helmholtz coils are used in industry and science to produce a constant magnetic field. Also notice in the above diagram that each pair of loops are wound in opposite directions -- one clockwise and the other counterclockwise.

This arrangement is known as a **pair Helmholtz coils**. And the magnetic field is uniform in the center between the 2 loops or Helmholtz coils.

The diagram above basically shows the magnetic field that is produced when a currant is applied to the cables wound in a loop like those found in a pair of Helmholtz coils.

The 3 Helmholtz coils were connected to what appears to be 3 antiquated value-driven radio receivers.

Researching other sources of information has drawn very little supporting evidence from other sources regarding reading the thoughts of people. Yet I have found a short reference to the work carried out by Lawrence Pinneo (a neurophysiologist) from the Stanford Research Institute (SRI) in 1974. He had developed a computer system capable of **reading a person's mind** by correlating the brain wave 3

with subjects on an ECG with certain commands. Writer and researcher K.B. Wells, Jr. writes in his book The Montauk Files that the CIA developed a chair in the 1960s which used polygraph-like technology to determine if the person sitting in the chair was telling the truth.

Also scientists at the University of Sussex, England had developed a sensor which could read a heartbeat of an individual from between 1-2 meters. The sensor would not have to come into physical contact with the skin. The scientists said it would be especially useful with monitoring the heartbeat of serious burn victims. The scientists stated the sensor worked by picking up fluctuations in the electromagnetic field surrounding the individual. The heartbeat causes the fluctuations, and sensor can pick these tiny fluctuations and filter out noise. They also said the sensor was highly sensitive voltmeter.

The Montauk chair system may have operated in a very similar way by acting as a highly sensitive magnetometer, which could record the slightest change in within the individual’s magnetic field. The Montauk chair system may have focused on brain activity. The coils are all wired up to 3 old radio receivers with no sign of an external power source. Yet the above diagrams immediately draw to mind Faraday’s Law. If you have a fluctuating or moving magnetic field, it will induce a currant to flow with a coil of wires. This means that the Montauk chair system may have been actually powered by electromagnetic field surrounding the human body of an individual.

Chair Notes

- The first version of the chair was allegedly developed at the ITT Technical Institute in Southampton, Long Island during the 1950s.
- The second version of the chair was allegedly developed by RCA during the 1970s.
- The chair system used 3 pairs of Helmholtz coils, designed to pick fluctuations of the electromagnetic field surrounding an individual.
- A computer system was developed in 1974 at the SRI which could read the minds with certain commands.

The Montauk Chair Receivers

According to the Preston Nichols' first book The Montauk Project: Experiments in Time, there were 2 versions of the Montauk Chair. The first version of the infamous Montauk chair used 3 Hammarland SP600 or the Hammarland Super ProP600 radio receivers. I later found references to Hammarlund SP600 receivers on the Internet plus references to a Super Pro SP600. It appears that Nichols misspelled the make and model numbers. These valve-driven radio receivers were built between 1950 to 1972. There are also numerous model variations usually identified with suffix number. For example, SP600-J12. Nichols

has not printed a suffix number, so it still remains uncertain as to what actual model was used. It can be important because most of the model variations have slightly different specifications and frequency responses.

a photo of the Hammarlund SP600 Radio receiver claimed to have be used at Montauk

There are several models made and were widely used by the U.S. Navy, Signal Corps, and the Air Force. Hammarlund also produced a civilian version of the SP600 which was popular with Amateur Radio enthusiasts. (Nichols and Bielek are such enthusiasts and attend HAM radio meetings.)

another photo of a Hammarlund SP600 radio receiver. This may be a Hammarland Super Pro SP600

Yet one odd feature is the frequency ranges. The Hammarlund SP600 receiver has a frequency range of 0.54-54 MHz.

According to Nichols, they developed a second version of the Montauk chair which used 3 radio receivers built by RCA. This type of receiver has proven harder to find information on. In Nichol's book, he first just referred to the receivers as RCA "1935" (which was the year the first FM radios were developed).

Nichols then names the second version of the radio receiver built by RCA as a "FRR-24". Later in his book, he also claims the FRR-24 was used in the legendary Philadelphia Experiment. Nichols suggests it was an **extra-dimensional resonator**. But the FRR-24 is a receiver -- not a transmitter. It would only be able to detect-or-receiver signals and not produce -or-propagate them. But it does seem possible that an AN/FRR-24 could have been fitted as standard kit to a new warship being built in 1943 like the *USS Eldridge*. 5

Nichols also stated in his book that he managed to trace a man who had used a AN/FRR-24 receiver and this man sung the praises of the receiver. But this did point out to Nichols that the set was prone to picking up an unidentified source of interference. I did find a reference to an AN/FRR-24 radio describing it as just a receiving set. (Nichols left off the 'AN' prefix which means it's a set made for the military). Information on this particular model appears very sketchy. I did manage to find some details on its predecessor the U.S. Navy's AN/FRR-23 (also built by RCA). See picture below. Finding a photo of the AN/FRR-24 or technical details has drawn a blank.

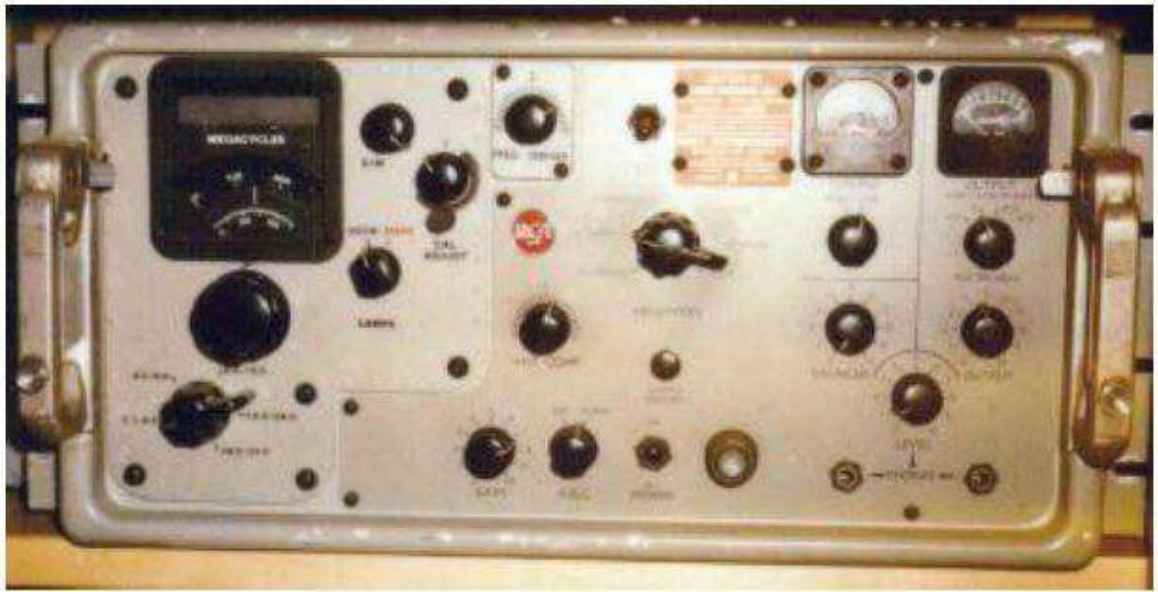

This is a rare photo of the AN/FRR-23, built by RCA for the U.S. Navy. Trying to find a photo of the AN/FRR-24 as used in the Montauk Project has drawn a blank so far.

Note in the picture of the AN/FRR-23 the red RCA label. And it was built for the U.S. Navy.

The AN/FRR-23 was an AM (Amplitude Modulation) HF receiver. It had a frequency range of 2-32 MHz. The date AN/FRR-23 entered service was around 1940-45. The radio sets appear to be very heavy, between 900-100 lbs.

I also found an intriguing reference to special radio receiver known as the "R-274/FRR" ordered by the U.S. Navy in Oct 1957. Its frequency range was between 100-400 khz and 1.35-29.7 MHz. This radio receiver was a version of the popular Hammarlund SP600 series. (Could this have been a replacement for aging AN/FRR-24 receivers).

The radio receiver system described by Nichols appears to consist of 3 antiquated valve-driven radio receivers developed for the U.S. Navy and civilian use in the 1940s and 1950s. Yet Nichols stated that the Montauk Chair system was developed in the 1950s. Why would they use old valve receiver sets?

I recall one TV documentary on the Cold War. The Americans had managed to capture a MIG 21 fighter aircraft. And when technicians took the MIG 21 apart, they found its avionics largely consisted of old valve-driven circuits. The technicians laughed at how primitive it was. During the 1950s and 1960s during atomic bomb tests in Nevada, technicians found that the high-tech transistor-based avionics fitted in most Western military aircraft was prone to the Electro-Magnetic Pulse (EMP) produced when atomic bombs are detonated. The EMP would seriously damage unprotected transistor based circuits, and the old valve circuits were a lot more robust. The technicians then realized why Soviet aircraft were fitted with the old style valves. It may be due to the sets are less prone to damage by sudden bursts of EM radiation. 6

This could explain why such old and antiquated radios sets could have been used at Montauk because they were less prone to EM interference. Secondly, many radio and hi-fi fans will usually state that valve-driven radios and amplifiers produce a much better quality sound and signal output.

One thing that did catch my attention is that Nichols stated that each of the 3 receivers may have been tuned to 3 different frequencies. And each of the 3 radio receivers were connected to 3 sideband detector producing 2 outputs: a USB (Upper SideBand) and LSB (Lower SideBand) output. Looking at the wiring diagram, the signals picked up by the Helmholtz coils and radio receivers surrounding the chair appeared to be mostly filtered out. So what the sideband detectors may have done is pick up fluctuations or modulations within the electromagnetic field surrounding the human body (as described in the 'Chair' section).

I'm still following up research in this area of using LSB and USB. Plus I will try to find out if these sets are AM or FM receivers.

Another oddity is that Nichols wrote in his first book that these old radio receivers were located inside the transmitter/radar tower. That appears to contradict his story that the engineers went to great lengths to isolate and screen out noise around the infamous Montauk Chair. They then go and place the old radio receivers inside a noisy building where high-powered microwave transmitters are pumping out megawatts of EM radiation. But Nichols stated the Montauk chair was located in the basement of the transmitter building. I have recently conducted some research into Montauk, and I believe the radio receivers and chair system could have been located in another building located near to the transmitter. Not inside or below it. (I will write more about this at a later date).

Receiver Notes

- Version 1 of the chair may have used Hammarlund SP600 receivers or 3 Super Pro SP600 receivers.
- Version 2 of the chair may have used 3 AN/FRR-24 HF AM radio receivers built for the U.S. Navy by RCA during the 1940s.
- The 3 receivers may have been tuned to 3 different frequencies.
- The 3 radio receivers were connected to 3 sideband detectors.
- The receivers are obsolete and antiquated.
- The old receivers were located in the transmitter/radar building.

The Computers

This section will examine how the computers were used to process the information from the radio receivers.

The Transmitters

This section will look at the transmitters installed at Montauk.

The Delta T Antenna

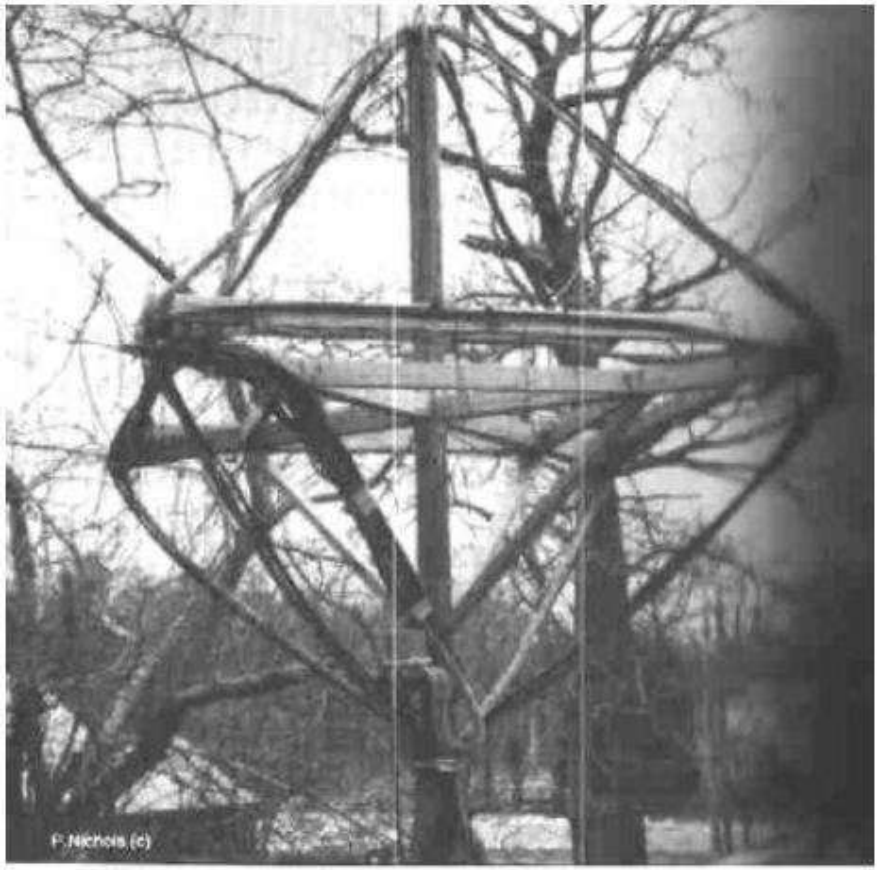

a photo of the Delta T antenna which is claimed to have been used in the Montauk Project by Preston Nichols

According to Nichols, the Delta-T antenna consists of 2 pyramid-shaped wiring looms with 3 Helmholtz coils wired in a special way to create a time-shifting field

a replica of the Delta T antenna.

It consists of an outer steel skin with a wooden interior. The antenna has a removable floor panels. By looking at the photo, you can see where the coils will be located inside the antenna. The remote-viewing data that I got seems to suggest some transparent material covering the triangular openings like window blinds. It reminds me of a Chinese Lantern. 8

The model is based on written accounts and remote-viewing data.

What's confusing about the RV data is that there may have been different versions of the Delta-T antenna built at different sites or different times. Or there may have been more than one antenna in operation. The RV data seems to offer conflicting RV data regarding its overall shape.

It's also difficult to trace the antennas as they were placed in long-term storage around America. Also different parts were stored at different locations (Plattsburgh, Hanscom, Wright Field, and a base in New Jersey).

I also got some RV data on a possible second site surrounded by Pine trees and a chain link fence. It has a warning notice -- red background with white letters "Danger". It had black letters underneath. The only word I could pick out is "Hazard". It looked bare on the other side of the fence. It had overgrown grass plus antennas and wires. During RV sessions, I am repeatedly drawn to this location.

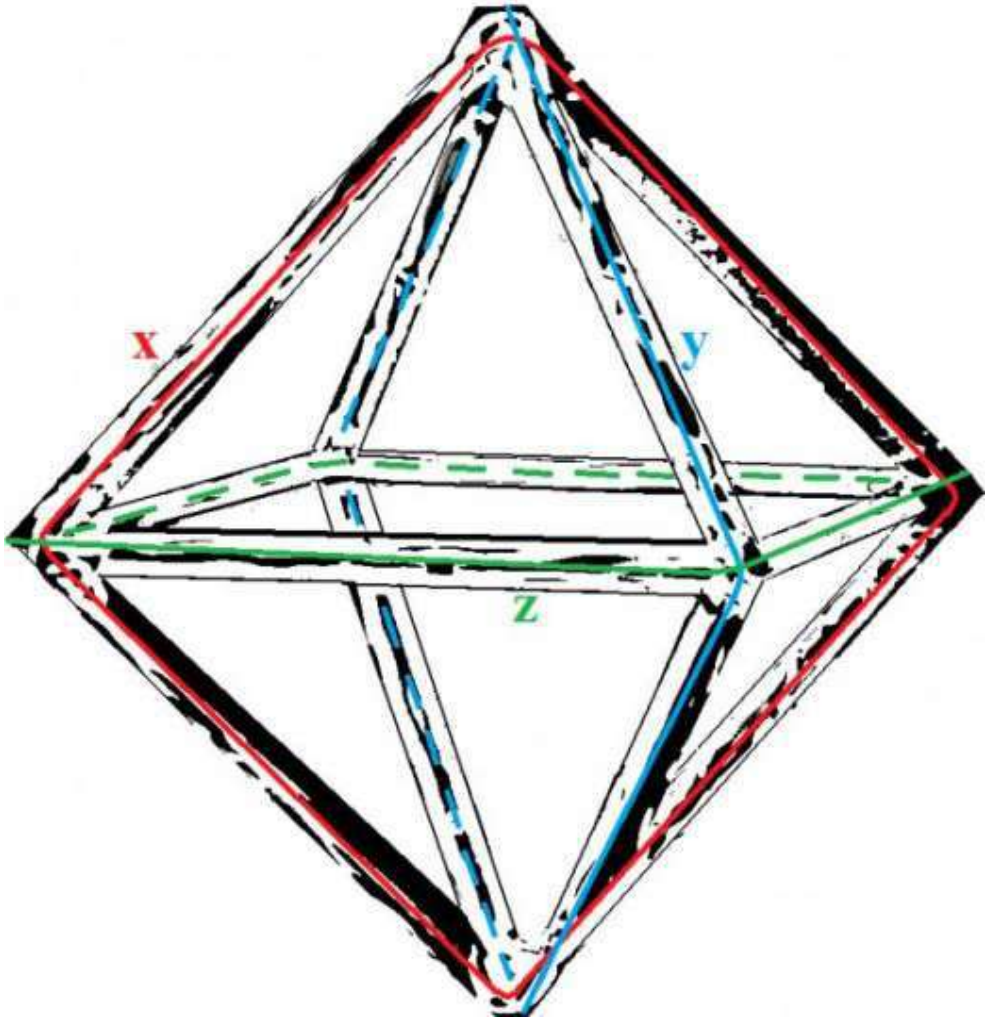

The Delta T Antenna uses the platonic solid shape (building block of the Universe) of a octahedra to achieve it specialized function.

Montauk, America's Greatest Unknown Conspiracy

Updated on October 17, 2015

Radar Instillation, Camp Hero

This is the radar dish used for mind control experiments and EF transmissions at Camp Hero, Montauk, New York.

Peter Moon

The Montauk Project: Experiments in Time

Etymology of Montauk

Native American shamans describe a spirit guide, shape shifter or time traveler as a Manatu or Manituo. According to The Keys of Enoch by J.J. Hurtak, the Tibetan word for Orion is Tak and is described as the gateway from human physical consciousness in this dimension to the next level of human evolution (creation).

Discovering the Conspiracy

What little is known about the United States Militaries' clandestine activities that revolve around Montauk Point Long Island, New York can be summed up in books by Peter Moon, Preston Nichols and Stewart Swerdlow. These men have found the courage to reveal activities that may very well have gone

undocumented had they remained silent and not blown the whistle on a secret Government project that could very well affect the lives of every man, woman and child on this planet. In this article Montauk, America's Greatest Unknown Conspiracy we will explore what little is truly known about the subject and speculate on its implications for mankind.
Montauk, America's Greatest Unknown Conspiracy involves mind control experiments, weather manipulation, star gate technology, telepathy, UFOs, Aliens, Nazi's, pyramids, sleeper agents, Aleister Crowley and black magic, time travel and time 'police', remote viewing, Deep Underground Military Bases (D.U.M.B.s) and above all an incredible amount of synchronicity that cannot be easily explained as mere coincidence. The implications of this profound mystery will leave the reader reeling from the sheer number of unexplained phenomenon, bizarre coincidences and mind boggling innuendo.

Another aspect of this mystery that cannot be ignored is the number of famous people involved in this ongoing mystery such as Jack Parsons, co-founder of the Jet Propulsion Laboratory, L. Ron Hubbard founder of the Church of Scientology, Aliester Crowley, the wickedest man on Earth (666), Mark Hammel, Luke Sky Walker of the Star Wars movies, Alfred Bielek, physicist, Remote Viewer and Director of PSI OPS at Montauk AF Base, Dr. John von Neumann famous physicist, Thomas Jefferson, 3rd President of the United States, Dr. John Dee alchemist and astronomer for Queen Elizabeth, Karl Haushofer, spiritual ambassador to the Far East for the Nazi's and a prominent General and leader in Hitler's rise to power and of course Duncan Cameron the operator of the infamous 'Montauk Chair'.

Montauk, America's Greatest Unknown Conspiracy really began with the Philadelphia Experiment in 1943 aboard the USS Eldridge, which was the U.S. Militaries' first publicly known attempt to create a 'stealth' field around an American warship that ostensibly would make the ship invisible to enemy radar. The USS Eldridge was stationed in the Philadelphia Navy Yard and the resulting stealth experiment was originally known as the Project Rainbow. While the attempt failed miserably, killing sailors and leaving others in a psychotic condition, it did open up new avenues of research into wormholes, star gates and quark fields.

Basically what scientists and researchers, headed by Dr. John Von Neumann, attempted to do was to create an electromagnetic field or bottle around the ship that would divert radar signals around the bottle, making it undetectable to radar waves and underwater mine fields. While the experiment was essentially successful it had some unintended side affects, such as making the entire ship invisible to the naked eye. What was learned later was that the entire ship and crew had been moved into another dimension of space-time and transported hundreds of miles away to Norfolk, VA and back again.

Needless to say, no one was prepared for this turn of events and when the ship re-materialized it left some of the sailors aboard fused into the bulkheads of the ship, much like how matter caught in a tornado can be fused together from the Hutchinson Effect which is found naturally in tornadoes. Because of these effects to human life and the fact that no one at the time really understood the results of the experiment the Project Rainbow was (publicly) 'terminated' and Von Neumann moved on to the Atomic Bomb and The Manhattan Project.

However, because of the results of the Project Rainbow, the Government at some point decided to look deeper into the subject and that research began after World War II at Montauk Point Long Island, New York. This information may very well have gone completely unnoticed and never had been discovered had Preston Nichols not received a Government grant to research telepathy, in 1971, he lived on Long Island, New York.

Originally he set out to disprove mental telepathy as he was a stern non-believer in psychic phenomenon. He learned through his research on his test subjects (psychics) that in fact telepathy not only existed but could be proved through the detection of an electromagnetic wave that was formed by the psychics themselves. His expertise was in electrical engineering and electromagnetic phenomenon, he had little interest in paranormal experience and had never even heard of the Philadelphia Experiment, of course most people hadn't until a movie was made about it in 1984. He set about learning about this electromagnetic wave and its properties and learned that it functioned much like a radio wave.

His research however lead him to conclude that a 410-420 MHz (megahertz) cycle being broadcast over the airwaves, at a specific time of the day, was effectively jamming the telepathic signals his psychics created, resulting in their inability to focus mentally or form a telepathic wave. The human mind operates on the 400 to 450 MHz cycle. Intrigued and frustrated he set out to trace this signal and found that it was coming directly form a radar dish on Montauk Air Force Base Long Island, New York.
Upon further investigation into this radar facility he learned that it was being used by the FAA (Federal Aviation Administration) for experiments with radar technology and this excuse may well have held up, except for the fact that Preston Nichols was an expert in radar technology and could see no practical use the FAA would have for using an antiquated (World War II technology) Sage Radar system to broadcast signals in 410 to 420 MHz range. However because of incredibly tight security and stonewalling by Government officials he could learn little else, until 1984 when he learned the base had been shut down.

Before we continue with the unravelling of this mystery, let's take a little time to reflect upon the exact location of Montauk Point Long Island New York as it has an intriguing history that is pertinent to this investigation.

Ley Lines

What is interesting to note is that the ley line that passes through Montauk, NY, intersects with the Bermuda Triangle.

Montauk Point, New York -
Montauk Point, Montauk, NY 11954, USA
Montauk Point as been described as an island but is actually connected to Long Island, New York.

Preston Nichols & Peter Moon

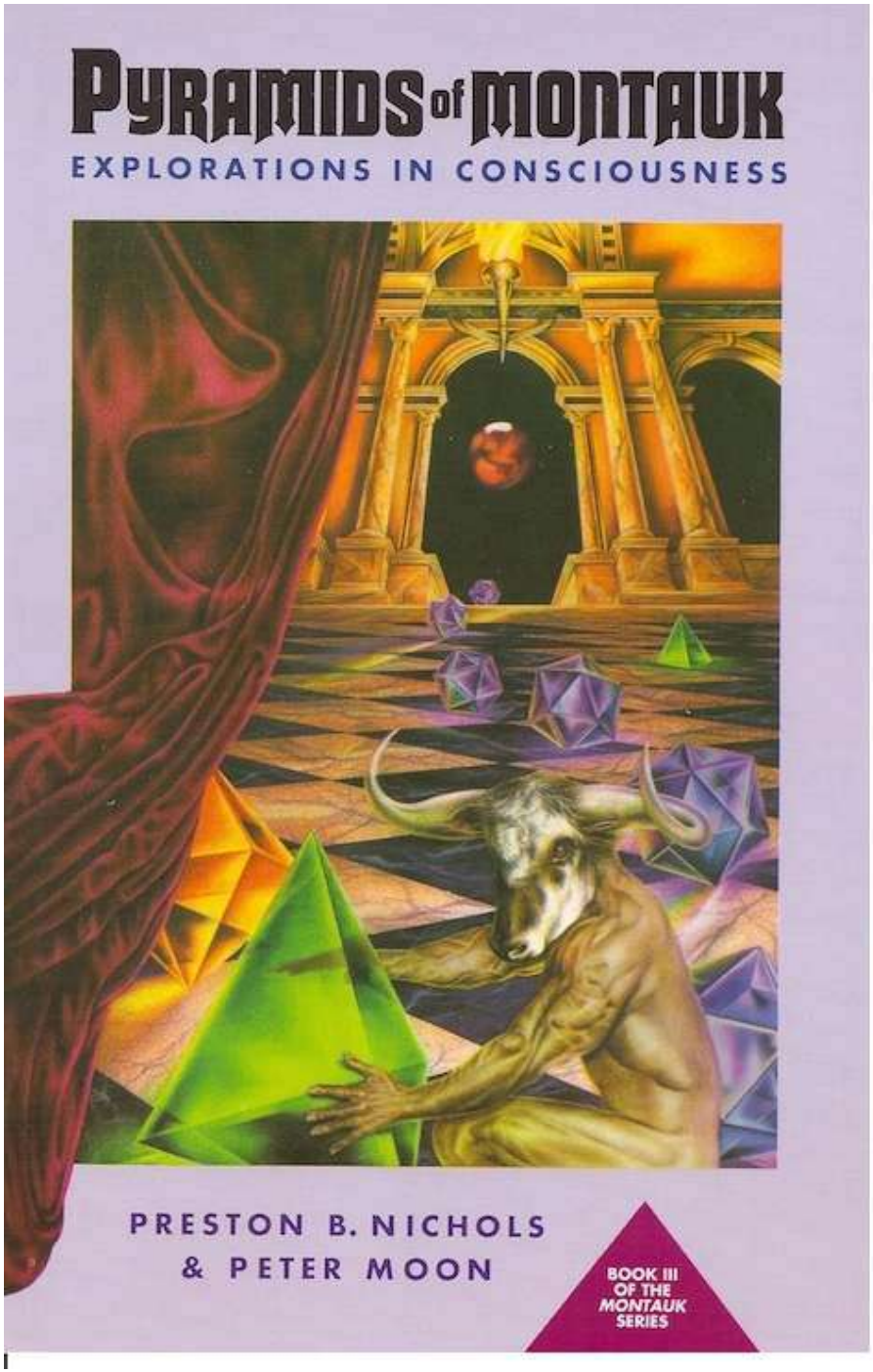

Pyramids of Montauk: Explorations in Consciousness

Montauk Point Long Island, New York

Montauk (Island) Point, New York is located on a ley line and is part of the Earth's electro-magnetic grid. For those of you unfamiliar with the term ley line it refers to a low frequency electro-magnetic grid that covers the Earth. This grid creates geometric shapes in the form of platonic solids (the building blocks of the Universe) across the globe. Many ancient megalithic structures were built on these lines as away to harness the natural energy of the Earth, such as the Pyramids of Giza and Stonehenge.

The Native Americans that lived for thousands of years in this section of New York, the Montauk Tribe (the word Montauk means a place of farseeing), were part of a larger tribe known as the Algonquin. What is interesting is that the chiefs of this Montauk tribe were named Pharaohs and that there is documented evidence and photographs of the tops of three pyramids along the coast of Montauk Point (see Pyramids of Montauk). These pyramids have since been buried to protect their location and prevent vandals from pilfering them. Only two other civilizations in human history have used the title Pharaoh for their rulers, Atlantis and Egypt.

This tribe of Native Americans spoke an ancient language not known to many other tribes in the area, called the Vril Language. The Vril are described in myth and legend as an ancient race of man (Atlanteans) that live inside Hollow Earth and possess sophisticated technology and weapons. For more on the subject of the Vril I highly recommend a short novel written by Edward Bulwer Lytton called The Coming Race. However I would also like to point out that Nazi Germany created a secret 'spiritual' group closely linked to the SS, known as the Vril Society, which was involved in secret weapons research and technology concerned with round winged aircraft (UFOs) and anti-gravity.

Another interesting aspect of this mystery is that this Vril 'language' has also been linked to the language of the Angels, called Enochian, which was translated by the infamous alchemist Dr. John Dee, t he royal astronomer for Queen Elizabeth. Dr.John Dee was a founding member of the Rosicrucian Order, was used as a role model for characters in Shakespeare's plays, such as King Lear and has been linked to the sinking of the Spanish Armada by weather manipulation and many other myths and legends.

Adding an interesting twist to this mystery is that the 3rd President of the United States and known Freemason, Thomas Jefferson, travelled to Montuak to record, translate and preserve the Montauk language, known as Vril the language of Atlantis from the root language of Enochian, the language of the Angels. According to Jefferson upon returning to Washington the manuscript (which including an alphabet and dictionary) he had so carefully transcribed was lost in the Potomac River. There seems to be no end to the strange incidents, events and synchronicity involved in the Montauk, America's Greatest Unknown Conspiracy, including but not limited to, who actually owns the land of Montauk Point, New York.

When the Montauk Indians 'sold', (they were told it would be a renewable lease), their rights to Montauk, New York to white settlers the dates of the transactions all included three sixes (666 is the number of the Beast, which was Aleister Crowley's calling card). The first transaction took place when they 'sold' their land to the township of East Hampton on August 6th, 1660. The next deed for Indian occupation of the land was transacted on February 6th, 1661. Over the next two centuries there were many legal battles over the true ownership and rights to the land, however in 1910 New York Supreme Court ruled that the Montauk Tribe was 'legally extinct' and that the land was the property of the Federal Government.

Peter Moon

U.S.S. Eldridge

The Philadelphia Experiment, The Movie

Released in 1984 and distributed by Thorn E.M.I., one of the largest electronic firms in the United Kingdom, after only few weeks in movie theaters across the United States it was pulled at the behest of unknown U.S. Government officials. Thorn E.M.I. took the issue to court and won, getting the censorship reversed and allowing the movie to be seen by the public but the damage had been done and few movie theaters would touch it, the movie was a financial bust. I have watched the movie and must say that I would like to have those two hours of my life back.

Despite the movie receiving rave reviews by critics, it was a box office flop and only became popular after being released on video. However the synchronicity involved with the making of this movie and the characters involved in its production, distribution and story lead even a die hard skeptic to recognize that there is more to this story than meets the eye.

In 1918, Aleister Crowley (666), at the height of his magical career took a 'magical retirement' to Montauk Point Long Island, New York, what he did while he was there remains a mystery. The Crowley family name, along with the Wilson family name became business partners in the early 1900s England to form a corporation involved in the manufacturing of the first electronic instruments in Great Britain used to monitor electric pulsations.

This corporation merged with other companies in the 1920s to form Thorn Lighting, which eventually became Thorn E.M.I. in 1979. They also have an entertainment division which includes music and video publishing and distribution.

I mention the name Wilson because of the odd connection to other players in this mystery. L. Ron Hubbard's original name was Wilson, as his father was adopted at an early age and took on the name of his adopted parents. The wife of Jack Parsons (JPL co-founder), whom went by the name Cameron, her maiden name was Wilson. Both her and Hubbard worked for Naval Intelligence and were reported to have been used as spies to investigate Jack Parsons. Jack Parsons was a student of Aliester Crowley and member of the O.T.O. (Ordo Templi Orientis), Crowley was purportedly the head of this secret order.

An interesting side note is the link between Parsons, Hubbard and Cameron participating in a magic ritual known as the Babylon Working which purportedly dealt with opening a hole in the space time continuum, a rift to another dimension, which could conceivably allow Alien spaceships (UFOs) to enter our dimension. This secret magical 'working' took place in 1946, a year before the infamous Roswell UFO

crash. Jack Parsons was killed in an explosion in his laboratory in 1952 but neither his wife nor the executor of his will was able to see the body before it was cremated.
Another odd twist to this movie is the reported involvement of Mark Hammil, whom played Luke Skywalker in the original Star Wars movies. Although this information cannot be substantiated he was known to be a silent financier of the movie and childhood friends of Preston Nichols and Duncan Cameron. Nichols worked as a sound engineer on the movie The Empire Strikes Back.

Al Bielbek reported to have dealings with Hammel in 1956 in Hawaii, which would make Hammels' far older than what he appears to be. However since the movie did involve time travel and part of the Montauk mystery does seem to revolve around this concept perhaps this isn't as unlikely as it seems.
Of course there is the convoluted story of Mark Hammils' infamous 'car accident' between the time the movie Star Wars came out and The Empire Strikes Back, was made. Starwars.com had this to say about it, "A car accident in early 1977 did extensive damage to Hamill's face, and the actor underwent reconstructive surgery prior to filming The Empire Strikes Back."

After much reading and research about this movie and its connection to Montauk, the only other aspect that I find strange is that normally if a movie is a box office flop and actually loses money, a sequel is not made. However with every other bizarre aspect of Montauk, America's Greatest Unknown Conspiracy, The Philadelphia Experiment II was made and released in 1994. This movie involves an altered timeline that has Germany winning World War II and America being run as fascist military regime by the Nazis. Although, this may seem a fantastic scenario to most Americans it is not without precedence considering the information related in my article Nibiru Planet X How the Fourth Reich Plans to Rule the World After the Pole Shift.

Peter Moon

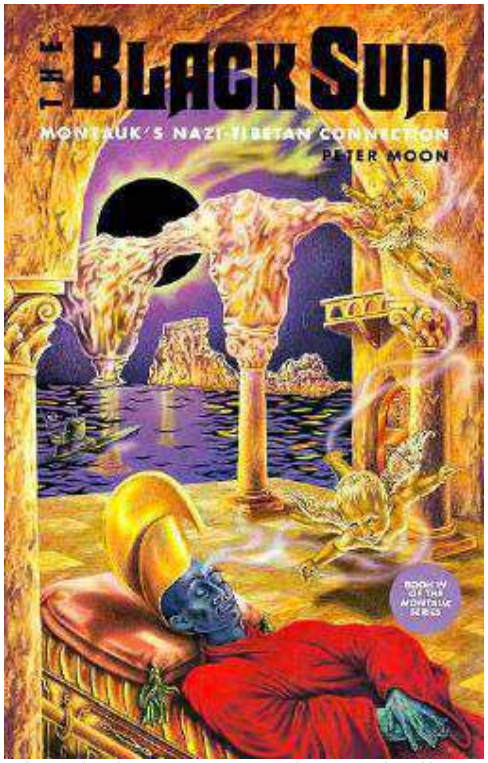

The Black Sun: Montauk's Nazi-Tibetan Connection

The Nazi Montauk Connection

The amount of synchronicity involved with the Nazi/Montuak connection is extensive and convoluted to the extreme, whole books have been written on this subject and for good reason. I will try to be brief however it is a conspiracy theorist dream come true.

According to Peter Moon in his book Pyramids of Montauk and The Black Sun, Aliester Crowley, members of the Thule Society (which were instrumental in Hitler's rise to power) and the Order of the Silver Star of the Illuminati conspired together in a magical ritual known as the Phisummum in 1923 to create a worm-hole for time travel. The Order of the Black Sun and high ranking Nazi officials were the controlling parties of the various powers involved using the Spear of Destiny as a magical power Source to travel back in time an retrieve the Holy Grail.

The result of their magical ritual was a 'time explosion' that connected to Philadelphia in 1943, Montauk in 1634 and Bannock Hill, England during the time of King Arthur and Merlin. It has long been speculated and rumored that Hitler and Nazi Germany were in league with Extra-terrestrials but the identity of these Aliens has never been determined. Some sources claim a faction of the Pleadians, others the Alpha-Draconians, while still others the Alderberans. Whatever

the case maybe, they did seem to have a leg up on the rest of the world in terms of technology and scientific advancements. Speculation is that this advanced knowledge of anti-gravity, weapons, cloning and magical rituals were derived from knowledge gained by German ambassador Karl Haushofer's time spent in the Orient and initiation into the Dragon Society of Japan.

Karl Haushofer, a WW I General and some suspect co-author of Mein Kampf, was a known Bon Priest, Bon is an ancient religion predating Buddha in Tibet. The basic principals of the Bon Religion deals with the control of linear time and is grounded in a spiritual connection to nature and Mother Earth.

A fundamental belief of the followers of Bon was that in their heaven, to which they referred as 'Sridpa Yesang', there were three deities who controlled the world. These were Dagpa, Salba and Shepa, one of whom controlled the past, another the present and the third controlled the future. It was they who held the key to Bon doctrines and Tonpa Shenrab Miwo claimed to be their earthly incarnation endowed with the power to control the current time.

The connection to Montauk is interesting from the perspective that a submarine base located at Ford Pond Bay (Long Island, NY) was in operation during the WW II within miles of Montauk Point and many eye-witness testimony from the locals puts fleets of Nazi submarines off the coast during the War. It has long been speculated that an underground/water submarine base existed in the vicinity of Stony Hill, Amagansett, NY by the locals during World War II.

During the 1930s the largest population of the Aryan Brotherhood in the USA existed in Yaphank, New York, known as Camp Siegfried (after the Norse God). This group promoted an eugenics program of sterilization of inferior races and held what the locals called Bund Meetings and Nazi rallies. Coincidentally the infamous Brookhaven Laboratories is located right next door to Camp Siegfried.

Further speculation has it that late in the War as the Nazi regime began to fall, a clandestine mission was conducted by a Nazi submarine in which gold and other loot from the War was buried at Montauk Point to be used by Nazi scientist that would be brought to America through Operation Paperclip. It has long been rumored that the Nazi's exchanged three nuclear bombs with America late in the War for safe passage out of Germany by high ranking Nazi officials before and after the War, including but not limited to Hitler himself.

What complicates the matter is that no American doctors or military officials were able to examine Hitler's remains, as Russia was the first to arrive at Hitler's bunker and cordoned off the area. Stalin had reported many times in the press of the day, that he believed that Hitler's body was a fake and that his supposed death was a Nazi trick. Incidentally, Hitler's autopsy reports weren't released until March 5, 1953, eight years after the end of the War and right after Stalin's death, presumably so that he could not shed any light on the details.

Regardless of whether or not Hitler escaped and lived on after World War II and there have been many books related to this subject, the focus of this article Montauk, America's Greatest Unknown Conspiracy is about the known information that involves Montauk Island, New York and how it affects the course of human history.

Montauk Conspiracy
Brookhaven Laboratory

The Relativistic Heavy Ion Collider (RHIC) under construction.
Brookhaven Laboratory

The completed Relativistic Heavy Ion Collider (RHIC) on Long Island, New York.

Montauk Conspiracy

It seems clear to this writer that there is an abundance of secret intrigue, disinformation, synchronicity and clandestine operations revolving around the area known as Montauk Point, New York. From early historical knowledge of colonial settlers right up to present day, the amount of unusual events, secret societal involvement, military activity and local gossip shows that this region of Long Island, New York has more than its fair share of intrigue and speculation.

What we do know about Montauk, America's Greatest Unknown Conspiracy is that in 1986, electronics expert Preston Nichols announced in Chicago, to the dismay of the U.S. intelligence community, his involvement in the 'black operation' known as Operation Phoenix which might be better known as the Montauk Project. Originally this project was designed to utilize the technology and experiments by Dr. Wilhelm Reich. An Austrian scientist known for his discovery of 'orgone' energy in the 1940s, which is more closely related to cosmic energy and the Newtonian concept of ether physics.

Although Reich was able to prove the existence of orgone energy in laboratory experiments and published his findings in scientific journals his ideas were scoffed at and ridiculed by his peers. Among his claims was that orgone energy could cure cancer and that it directly affected the weather through what he called dead orgone energy or DOR. His research lead him to conclude that storms such as hurricanes, violent thunderstorms and other bad weather were caused by high levels of DOR (dead orgone energy). However he also learned that living orgone energy could be found in humans as well, with active happy people having more orgone energy than depressed lethargic people.
He developed a device that could break up DOR in bad weather by connecting it to balloons and releasing them into the weather systems. His experiments showed that he could actually dissipate bad weather using his invention. However when he presented this invention to the U.S. Government his research and technology was confiscated citing National Security issues. Later all of his research papers and laboratory materials were destroyed by the Food and Drug Administration to prevent his discoveries of orgone energy from going public.
The U.S. Government used his invention, coupled with a device used in the 1920s to collect weather data, known as the metrograph. This device recorded weather related phenomenon using a balloon/parachute system. The balloon was designed to burst after reaching a prescribed altitude, deploying a parachute to deliver it safely to the ground. Citizens were given $5 dollars (a lot of money back then) to return the device to the authorities.

The U.S. Government created an invention they called a radiosonde based on Reich's invention and the metrograph. However what was known publicly as a device for measuring and detecting weather elements, upon further research has been revealed as a transmitter of weather elements, specifically DOR. In the fifties as many as 200 radiosonde's were being used in the atmosphere above America, daily. The device was eventually scrapped after more advanced weather manipulation technology was created, such as HAARP.
So, initially Operation Phoenix began as weather manipulation but it soon took on a much wider scope, when it was combined with Project Rainbow, ostensibly to keep the latter shielded from the public. Dr. von Neumann would head up the entire project headquartered at Brookhaven National Laboratories on Long Island. He built the first vacuum tube computer at Princeton University to help in this research into theoretical physics and space/tome manipulation.

What he learned initially as the reasons concerning the failure of the Philadelphia Experiment were due to humans having a time reference point, which is altered significantly when surrounded by an electro-magnetic field that essentially displaces whatever is inside it in the space/time continuum or alternative reality. His idea was to use a computer to create a false reality that humans could then use to synchronize too when undergoing any further electro-magnetic space/time experiments. What he found through experimentation on human test subjects (the general public and selected individuals) was that he could affectively control what people thought using the technology he had developed from 1948 to 1967 during Project Phoenix.

Up until his final report the U.S. Congress had funded this project but upon learning the implications of this technology they ordered the project to be shut down, perhaps fearing their own minds would be tampered with and understandably so. However considering the implications for weapons research and

population control it would be grossly naïve to think that this project would end. Enter the Military Industrial Complex and the real intrigue behind Montauk, America's Greatest Unknown Conspiracy.

Amplitron

With names of devices right out of science fiction the technology was used to create time travel and star gates.

Thyratron

A Thyratron was one of the devices used with the Sage Radar to help with the time travel experiments.

Montauk Air Force Base

The Montauk Air Force Base (MAFB) was 'officially' reactivated in 1971 and was the site of a mothballed Sage Radar instillation. Although Congress was no longer officially involved in funding the new Phoenix II Project, money from Brookhaven Laboratories was funneled into the project for research and MAFB was used for the physical research and for security purposes. A combination of civilian and military personnel were used to work on how the technology from the original project could be used for military purposes.

Essentially they used the Sage Radar antenna as a super radiosonde transmitter to broadcast on a 425-450MHz radio frequency using varying pulsations and amplitude to affect different biological functions and thought control. Initially they used the base personal as their first guinea pigs but eventually began broadcasting to the general public in the nearby area. They found that they could even affect the behavior of animals in the region, as well.

To monitor the results of their ongoing experiments they would use 'sleeper agents' infused into the local population to report results and spread disinformation. Some of the side affects of their experiments was a wide range of abnormalities with electronic devices such as radios, televisions and appliances, including turning off or on cars in the area. They compiled a huge data base using different amplitudes, pulse modulations and frequencies and their results. This lead to the creation of a control panel with different settings that could be used to create instant results. After three or four years they could control the crime rate in the local population, the general mood and even some physical attributes, such as sexual urges or dysfunction.

However all this was seen as only a general application to a wide physical range, what was needed was a refinement of their techniques, so that individuals could be targeting and more control could be exerted. Learning to refine this technology is what created the ability of the people behind Montauk, America's Greatest Unknown Conspiracy to open wormholes and time vortexes.

Using an idea derived and based on applications taken from reversed engineered UFO technology what is known as the Montuak Chair was developed. ITT had been working on this idea since the 50s, in which they could read a persons mind and display it on a computer monitor using a similar type chair. The Phoenix II Project technicians wanted to use this technology to create a virtual reality machine that would enable one person to broadcast into the minds of their test subjects. Ostensibly this would be to allow anyone involved in entering an alternate reality to maintain their zero time reference point and would be the first step in making time travel possible, that was the theory anyway.
Many problems had to be worked out but oddly enough some of the technical issues were solved using Tesla technology form the 30s, known as Delta T (time) coil structures. Also Al Bielek got involved to solve some the computer interface issues concerning the pyschics being used in the chairs operation.

Duncan Cameron

Delta T Antenna

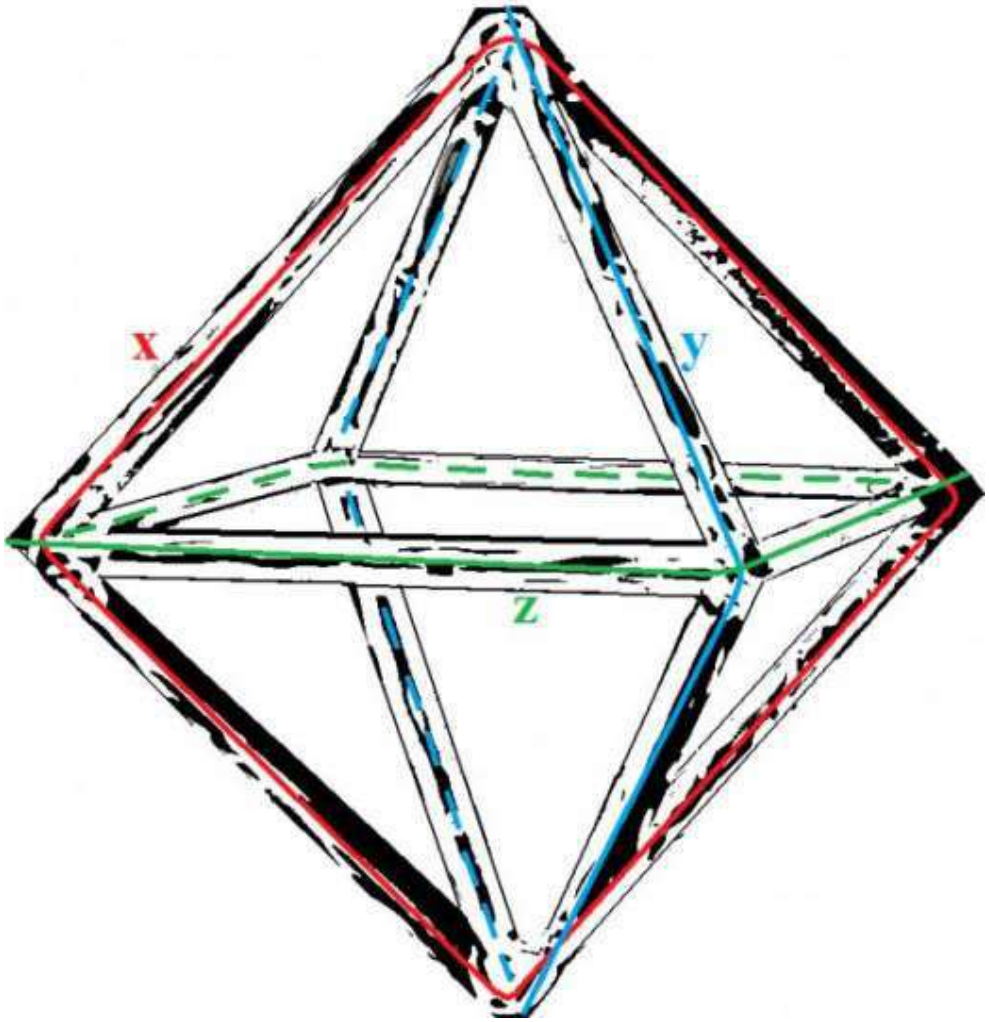

The Delta T Antenna uses the platonic solid shape (building block of the Universe) of a octahedra to achieve it specialized function.

The Zero Time Concept

The concept of zero time can be easily understood if we picture the center of the Universe like a large merry-go-round with many levels or dimensions. At the center of this merry-go-round would be a control booth that operates or exists in a zero time capsule and all linear time moves outward from that point.

The reason I mention this is because for the technology to work properly all aspects of the components including the operator of the chair had to be harmonically synchronized to the zero time reference. To do this required that they not only modify the existing technology but also create their own 'white noise' generator as a way of harmonizing all the various technology together. My understanding of this concept is limited but I basically see it as a constant wave signal that allows calibration to be achieved.

However what needs to be pointed out or recognized is that the engineers and scientist involved in the Phoenix II Project or Montauk, America's Greatest Unknown Conspiracy did not have the technical sophistication to invent or create a device that could generate a zero point, white noise oscillator back in the late 70s. However because they did have access to certain information supplied by 'off world' intelligence's with their own nefarious agenda, they were able to 'borrow' this technology without having a complete understanding of how it worked or was engineered.

Persistent rumors circulated that Aliens from both the Sirius and Orion star systems were involved in the project. Whether their intentions were honorable or not, is beside the point, the high degree of technological assistance and theoretical concepts employed in this operation did seem to take a decidedly Alien bent. To achieve the successful time experiments desired required technology that simply was not available in the late 70s. What was known as the Orion Delta T Antenna was supplied by an unknown source fully functional, as well as a fully functional Tesla Zero Point Time Reference Generator, supposedly invented in the 20s by Tesla himself.

These components allowed the engineers to create a COHO or coherent 'white noise' oscillator that could be linked to all the other devices and achieve a harmonic synchronization with the chair and operator, which would allow the desired time experiments to succeed.

Preston Nichols & Peter Moon

Montauk Revisited: Adventures in Synchronicity

Duncan Cameron

Duncan Cameron was 'the' main Montauk Chair operator with the most success and was used extensively for most of the experiments in time. Duncan's revelations in the books written by Peter Moon and Preston Nichols were paramount in deciphering Montauk, America's Greatest Unknown Conspiracy. Duncan is a psychic, employed and trained by either the NSA or CIA in remote viewing techniques, depending on which source your willing to accept and his history is full of time travel innuendo, mysterious circumstances and aspects of mind control. However he seems to have a vast knowledge of technology and American history that only researchers and writers of conspiracy theory have been able to find.

The history of the Cameron Clan is extensive and far too broad to be written about here but suffice to say the name Cameron is old, with connections to ancient royal bloodlines, and can be found throughout American history as well. It has been reported that their was a Cameron (perhaps named Wilson) on board the

USS Eldridge during the Philadelphia Experiment and some speculation is that it could very well have been the same man who became the main Montauk Chair operator in the 1980s.

Whatever the case maybe to this enigmatic character, once he was synchronized to the Montauk Chair, his psychic abilities were increased to a high degree and he was able to produce startling results that defy conventional wisdom. Among his outstanding results, if they're to be accepted as real were opening time portals, materializing objects by mere thought, feeling through the five senses of other humans no matter where they were on the planet or off, traveling through time and space, projecting thoughts into other human minds to the point of controlling their actions and many other similar experiments.

Once the technological bugs were worked out of the system and a high degree of harmonic fidelity was achieved with Duncan in 'The Chair' it was just a matter of fine tuning the synchronization of the technology and testing the limits of his psychic abilities. However as more and more successful 'experiments' were achieved, the program began to take on a more sinister agenda.

At first, this was just experiments that involved controlling inanimate objects and electronics such as switching TV channels in peoples homes, turning them on and off and causing them to produce static but then it turned to destroying them, breaking windows, moving objects and destroying furniture and appliances. Then it turned even more deadly by using Cameron to influence peoples thoughts by directing them to commit crimes sprees and engage in odd sexual behavior. The truly sinister aspect of this was that the minds of those he engaged in these experiments would have no memory of the actual events, it was very deep form of hypnotic mind control.

One result of these experiments that showed some potential that the Military Industrial Complex wished to explore was the phenomenon involving displaced time. It was found that Cameron could think of an event taking place or an object materializing and then that event or object would appear before he thought of it or sometimes many hours or days after he thought of it, even when he wasn't 'plugged into the Chair'. This lead to creating programs based on the recorded data supplied by these experiments, so that eventually they didn't even need Duncan to be 'plugged in' to produce the same results.

Because of the nature of these experiments and technology required a high degree of 'secrecy' an underground complex was built beneath Montauk Air Force Base at Camp Hero, New York. However the construction of this base did not go unnoticed by the local population as tons of earth and large boulders began appearing along the coastlines of Montauk Point without any known means of arrival. The odd behavior of the locals and clandestine comings and goings of personnel began to become transparent and reported, this lead to a sophisticated disinformation campaign that still exists today.

Time Portal

This excellent illustration exemplifies my concept of what a Duncan Cameron created time portal may have looked like.

Time Portal

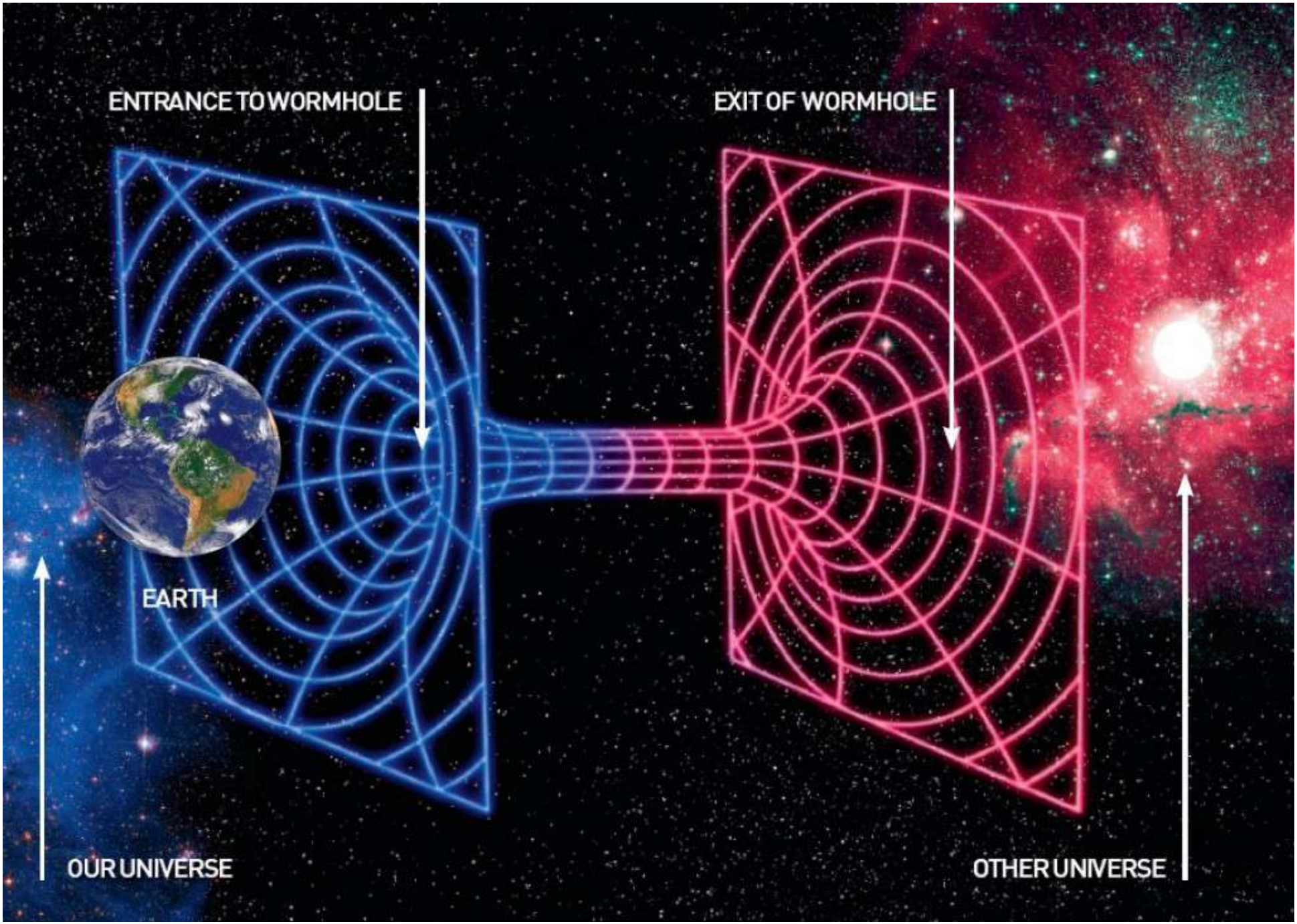

From the article How to Build a time Machine by Stephen Hawkings, well worth the read.

Preton Nichols & Peter Moon

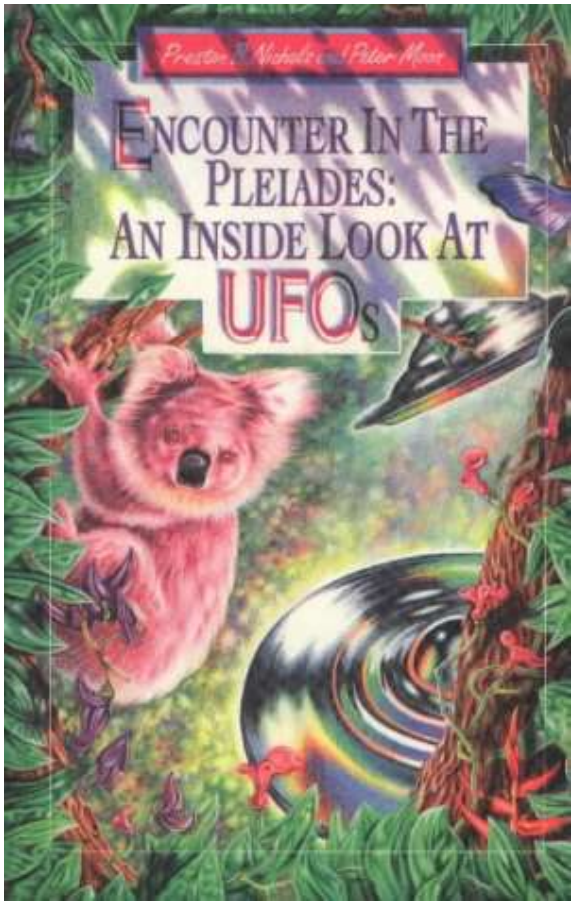

Encounter in the Pleiades: An Inside Look at UFOs

Experiments In Time

Once the advanced Alien technology had been integrated into the system and tested in 1980, the experiments began to concentrate on space/time and less on mind control. However because of the nefarious mind control experiments and time travel implications a secret group within the Phoenix Project decided to implement a 'fail safe procedure' just in case things got out of control, in hindsight this turned out to be a wise precaution.

The time experiments began by having Duncan concentrate on a specific date and year while the zero point time generator kept him located in his own time.

After many experiments and testing he was able to produce a window in time or what was labelled a 'time portal' in which viewers were able to look into the future and the past. Eventually he was able to open a dimensional doorway that linked two time periods together in which humans could actually walk through and return . . . sometimes!
However since this was in essence untested waters and there was never a shortage of homeless people in New York City, the first guinea pigs used were the indigent and poor, after all no one would miss them and it wouldn't arouse suspicion if they were lost in time.

Before these actual time experiments took place however secrecy was amped up to a new level and all non-essential personnel were removed, this included the military. This was done by reporting to the Military Industrial Complex hierarchy that the time experiments were a failure. This is a common tactic used by The Powers That Be whenever they steal technology from inventors or scientist, they merely publicly term the invention or technology a failure, hire experts to write scientific essays on why the technology cannot work and promote it through the Fake Stream Media.

This tactic can also be used to make people disappear by faking their deaths and having the media report it as fact. As long as the body cannot be identified or witnessed, none is the wiser. This is why the suspicious death of Jack Parsons has been questioned as well as other notable instances such Osama Bin laden and the Seal Team that dispatched him . . . dead men tell no tales.

Once all the personnel were removed and replaced by other agents, the only remaining people were those that had specialized knowledge that couldn't be easily replaced. However certain mind control techniques were used on these remaining personnel so that they would have no memory of what they were working on. This lead to the phenomenon of 'missing time' which to most people makes them question their own sanity. Having experienced this phenomenon myself I can tell you it is quite disconcerting and very difficult to relate to anyone else. The best way to describe it would be to waking up fully clothed and have no idea of how you got there, with your last memory of being somewhere else (location) in time.

All of this information is known because Preston Nichols was one of the specialized engineers that worked on and created many of the technical devices used in the experiments and he had become good friends with Duncan Cameron. Duncan had a direct mental link with the time events taking place and would often have an out-of-body experience while plugged into the chair. Of course their daily memory would be erased and replaced with other memories so that they 'thought' they were going to work in one place and returning home, completely unaware of what they were really doing.

After all these precautions were in place, a new name was used for the ongoing experiments, it was now called the Phoenix Project III. They began cataloguing different eras of time and space, by sampling the environment using automated devices, such as robots, drones and sensors. The tunnel or time portal was described very much like the stargate animation shown in the popular TV series Stargate, as it twisted and turned surrounded by wormhole like lights and elements.

As long as the power remained on and no 'glitches' occurred during the transmission a portal would remain open on the other end and the robotic sensors could return with their collected data. After 'using' and testing many involuntary (homeless) subjects, sometimes by force, with various degrees of success, the project began using time operatives to conduct missions. These operatives would have advanced video equipment, sensors and cameras that would report in real time what they experienced while on their missions, so that their controllers could see what they were seeing and evaluate the data without having to rely on individual reports. A vast catalogue of videos were created using this technology.

Besides the normal operatives, children were used as well and according to Duncan and Nichols and every one of them was sent to a specific date and time in the future (6037 A.D.) as an initiation process, before their first mission. Why this was done remains one of the many truly bizarre mysteries revolving around the Montauk, America's Greatest Unknown Conspiracy.

Both Cameron and Nichols estimate that as many as 10,000 people were sent 200 to 300 years into the future never to return. However much of the experiments in time revolved around both World War I and World War II. A secondary vortex was also used in conjunction with the first that would allow the controllers to beam, through sophisticated computer technology a television signal into the past or future that could be viewed by any with the same technology.

One of the most interesting aspects of this technology was the reported time travel to other planets in the future as well as the past and the exploration of the Pyramids on Mars or Face of Cydonia complex.

Mars Mission

In a nutshell, The Powers That Be, the true hierarchy behind Montauk, America's Greatest Unknown Conspiracy knew beyond a shadow of a doubt that the Face of Cydonia Pyramid Complex had been created by an ancient sophisticated race of Aliens and wanted any technology that still existed there. According to both Duncan and Preston this information was known and considered a foregone conclusion.

To reveal to anyone how this information was obtained would require divulging their 'ultra-secret' space program that had been in existence since at least the early 60s, they used a time tested form of disinformation through ridicule, censorship and silence pertaining to any information that might reveal that the Face of Cydonia and surrounding area, was in fact a large pyramid complex.

However, because The Powers That Be assume the public is stupid and can't help themselves from rubbing our noses in our own stupidity, they allowed a docu-drama called Alternative 3 to be aired once on British Television in the late 70s that described how the United States and Russia had set up jointly run military prison bases on both the Moon and Mars. These bases were initially designed to allow the rich elite, 'themselves', to flee the Earth in case of any catastrophic Earth Changes that would take place in the near future . . . such as a Polar Shift.

The bases also served as means of exploring both planets or moon in hopes of recovering any Alien technology left behind by advanced races. The base on Mars was located near the Face of Cydonia and is the main reason the Mars Rover was not sent there, later. However in the early 80s after twenty years of trying to get into the pyramids on Mars using various mining techniques and explosives with no success, they decided the Phoenix Project would solve their problems and gain entry.

Although both Duncan and Preston vaguely remember planning a mission to Mars they can't recall much else about it. Duncan was able to remember penetrating the main pyramid 125,000 years into the past and 'seeing' operating technology which was part of what he called "The Solar System Defense System". The Powers That Be were desperate to have this automated system turned off but he could not recall if they were successful. Some speculation is that

this 'Defense System' may be preventing The Powers That Be from leaving the planet en masse and could be the reason no 'publicly known' manned missions to other planets or the Moon have been accomplished since the Apollo mission in the early 70s.

Philip K. Dick

It is interesting to note that two of Philip K. Dick's novels, The Man in the High Castle and We Can Remember It For You Wholesale have inspired the movies Philadelphia Experiment II and Total Recall, respectively, both pertaining too the Montuak Project.

While researching this information I have learned that 11 of his 44 novels have been made into movies, all of which deal with alternative realities. Of course, Do Androids Dream of Electric Sheep (Blade Runner) is the most famous of these.

Duncan's Beast

This is one of the photos of Duncan Cameron's subconscious Beast.

The Montauk Project Gets Shut Down

On August 5, 1983 the operators of the Montauk Project were given orders to turn on the chair, transmitter and time machine equipment and leaving it running until further notice. After a week of running continuously, August 12, 1983, exactly forty years to the day from the Philadelphia Experiment, August 12, 1943, the equipment lurched into high gear and became synchronized with another power source. When this happened a time portal opened back into the past and the USS Eldridge could clearly be seen at the other end.
Due to the nature of their research and experiments the operators of the Montauk Project had learned that the Earth went through a cycle of twenty year biorhythms which made opening time portals easier when one used these cycles for time travel. Even Duncan Cameron could be seen on board the Eldridge and some of the operators began to get worried that some boundaries had been crossed and that a paradox could upset the nature of time itself.

Fortunately a select few operators that still remained from the original crew had created a fail -safe countermeasure if the project needed to be terminated without prejudice. Duncan Cameron was given the code words, 'The Time Is Now' and Cameron let loose a beast from his subconscious mind that showed up literally as huge beast somewhere on the AF Base. This monster, perhaps powered by the huge amounts of energy coursing through the time portal, began destroying everything in its path. Photographs of this beast were taken showing it actually existed.

The supervisor of the operation fearing the experiment was out of control and not knowing what a time explosion could do ordered the technicians to shut down the equipment, which they did, to no avail. The two time periods seemed to be fused together in loop with energy cascading out of control. It was decided that both transmitters had to be destroyed for the link to be severed, so someone would have to go back in time and destroy the one on the USS Eldridge, this would be one way ticket, there was no coming back.
Preston Nichols and the Supervisor began pulling wires on all the equipment, using an acetylene torch, Preston was able to cut through live wires and still the

transmitter stayed on. A permanent time portal had been created using the USS Eldridge and the Montauk Project. The operators panicked and began smashing equipment and cutting wires, still the portal remained. Nothing they tried seemed to work, they ran to the transformer farm above ground and cut all the power cables leading underground and still the portal remained.
They cut all the power cables leading from the power station in town to the AF Base, and the lights of the base shut off and even the computer link-up yet the portal remained open, the energy seemed to be growing. They ran to the transmitter station and cut all the power cables there, the lights went out but the transmitter remained operating, they were getting desperate.

Finally Preston took his acetylene torch and began cutting the actual (hot) transmitter machine into pieces, he cut the conduits, he cut the cabinets, he cut apart all the moving parts. The machine groaned once like a dying beast and stopped, the time portal collapsed and the beast from Duncan's subconscious mind disappeared, it was over.
From that day forward, August 12, 1983, forty years from the Philadelphia Experiment failure, the Montuak Project shut down . . . or did it? The personnel were debriefed, their memories erased, the base was abandoned and fenced off. Eventually some memories did re-surface but more questions remain than answers.

Time Travel

Wormholes through the 4th dimension could be used for more than just 'time travel' by linking planets and destinations in fixed portals.

Conclusions

While the amount of truly bizarre synchronicity (coincidence) involved in Montauk, America's Greatest Unknown Conspiracy can only be fully appreciated by reading Preston Nichols and

Peter Moon's books, I hope that I have shown the reader that there is more to this story than meets the eye. Without the courage and dedication shown by Peter

Moon, Duncan Cameron, Preston Nichols and even Stewart Swerdlow to reveal this mystery to America and the world, I doubt if any of this information would have seen the light of day.
All that being said, I think the most significant information outlined here is that, some secret group (The Powers That Be) have conspired to create technology that would allow them to travel through time and space. We may never know their true intentions or even any of the results of their experiments but it seems clear to this writer that even our own Government (Congress) sanctioned these experiments up to a point.

What should be carefully thought about and considered is that if, in fact, any changes were made in the past due to these 'experiments in time' it could very well have already affected the lives of every man, woman and child living on this planet today.
This should not be taken lightly as we may already be living in an altered timeline, without even realizing what affects it may lead too nor anyway of knowing or recognizing the profound changes it could have to our very existence.

Without a doubt the decisions of a select few could very well have plunged humanity into a future that was never meant to be, while keeping the billions of people that live on this planet completely in the dark. However since there is no point in worrying about events we have no control over the main point of this article is awareness, consideration and planting the seed of knowledge.

Putting the nefarious experiments aside for a moment, it seems clear that a form of mind control was practiced on American people, with startling results. The implications of Nazi collusion in technology, should also raise an eyebrow or two, however I barely touched on that aspect in this article. The technology and science alone that resulted from these experiments, if shared with the world, could open avenues of research that could potentially solve some of the worlds energy problems and even perhaps clear up some of the more profound mysteries of our ancient history.

Consider for a moment a device that would allow children of all ages and even adults to explore our ancient past without ever leaving the confines of their homes. Think of the implications towards a better education of not only our history but the history of our entire Universe. Think of using a wormhole for travel to other parts of the planet or planets within our solar system as easy as walking through a door.

When mankind begins to create a new paradigm built on giving, unconditional love and cooperation we could use this kind of technology to vastly improve the lives of every man, woman and child on the planet. While this idea may seem naïve to the reader, consider how far the human race could be in terms of spiritual, scientific and technological advancements if we could temper our competitive nature, get over our differences and embrace our common heritage.

People say that War and violence is human nature but I disagree, children have to be taught this kind of behavior. Raise a child or even a pet just on love, with no harsh words, no physical discipline and no references to violent behavior through books, TV or movies and you will see a being that knows nothing but various degrees of love.
While this article Montauk, America's Greatest Unknown Conspiracy may have revolved around the selfish decisions of a select few humans to control and influence the masses, perhaps the Greatest Unknown Conspiracy should be why Unconditional Love is not recognized as the most powerful force in the Universe.

THE PHILADELPHIA PROJECT PROJECT RAINBOW AND THE USS ELDRIDGE

In July 1943, the destroyer U.S.S. Eldridge pulled into the Delaware Bay area for a United States Naval experiment that involved the task of making the ship invisible. The project's official name is Project Rainbow, but was nicknamed and more commonly known as the Philadelphia Experiment. Much has been written and speculated about the legendary experiment into invisibilty, but sorting fact from fiction is a near impossible task, especially with the recent influx of misinformation and deliberate disinformation that has been spread by those connected to the U.S. Intelligence community and professional skeptics.

There is much controversy over what exactly happened, but one thing is for sure. For some reason, soon after the test was completed, a massive blanket of secrecy and denial was placed over what happened in Delaware Bay. It is thought that a huge scientific breakthrough was made, and the ship was accurately transported over space and time, disappearing in Philadelphia, Pennsylvania and reappearing in Norfolk, Virginia. Whatever did happen is still not known, but different theories are discussed below: The "Official" Navy Record The Navy admits that the U.S.S. Eldridge took part in an experiment that involved wrapping wire around the hull of the destroyer in an attempt to cancel out the magnetic fields of the metal on the ship. This is known as degaussing. This would render the ship "invisible" to underwater magnetic mines that rely on proximity sensors to trigger the detonation.

These sensors operate by detecting magnetic fields around ships. Without the magnetic field, the ship would be able to pass through regions mined with these sensors, invisible to enemy mines, but not to radar or vision. The Navy's report is very plausible, and doesn't mention any exotic results or circumstances. But could this just be a believable account to drop the interest by the general public, leaving only the true minority of investigators in doubt? Physical Invisibility Some scientists have developed the theory that the Navy was working on a way to make the ship invisible to vision. However, it didn't involve warping space time or any complex task of a similar nature. This theory suggests that the Eldridge was equipped with high frequency generators that would heat up the surrounding air to cause a mirage, making the vessel invisible. This phenomenon is naturally occurring, and there have been cases where entire islands have disappeared from view in the right weather conditions. The high frequency generator would heat up the surrounding air and the water (creating a green-colored fog that was said to have engulfed the ship), causing a mirage to form, concealing the ship from view. The generator would also account for the sickness (physical and mental) of the crew after the experiment.

A high freqency generator can cause serious harm to a person's wellbeing, especially at close range. This is more plausible than the degaussing theory, and would also explain the crew's sick condition as a result of the test. The main problem with these theories though, is that it doesn't explain how the U.S.S. Eldridge was seen in Norfolk, Virginia by the civilian crew of the SS Andrew Furuseth, when the ship disappeared from view in Philadelphia in a space of only about fifteen minutes. There are also details such as crewmen being fused to the hull of the ship and some not even reappearing. Transported across space and time? The most interesting theory about the Philadelphia Experiment is that the destroyer did in fact disappear and was teleported across space and time. Supposedly, there was a great number of ingenious scientists (including Tesla and Einstein) that were taking part in the experiment. However, Nikola Tesla was supposed to dead at the time of the Naval experiment. The theory is that light has to be bent around the ship to make it invisible. To accomplish this, the Navy wrapped the ship's circumference in wire and passed a measured current through it. This caused a huge oscillating magnet to form a magnetic field around the ship, not only bending the light, but space and time as well. The physics of the experiment are reminiscent of Einstein's Unified Field Theory that once you bend light, you are also unwittingly bending space and time as well.

The first time this experiment was undertaken, the ship didn't completely disappear, and an imprint of the hull could be seen sitting in the water. The second time, the ship totally disappeared in a green fog and was sighted in Norfolk, Virginia. A haunting fact is that when the ship reappeared, the crew were all in a state of disorientation. Some were mentally ill, while other crewmen didn't even return. There were also crewmen that returned embedded in the hull. Later accounts arose about the crewmen, including a former crew member who was involved in a bar fight, and all the participants froze in time, as reported by a local newspaper! There were also accounts of people who were on the ship, spontaneously combusting. The mystery remains It is still not known what happened that day in 1943, mainly due to the lack of witnesses coming forth who served aboard the Eldridge. There is also no documentation available to the

public which details Project Rainbow. It may have simply been a degaussing experiment. But how did the destroyer appear seconds later in Virginia? Its possible the answer will never be known, but the mystery may be solved when scientists rediscover what happened in Delaware Bay.

Camp Hero: Mind Control, Time Travel & Reptilians

The following information is an update to a post from January 2012:

Montauk, N.Y. — like Area 51, written about in Annie Jacobsen's book Area 51: An Uncensored History of America's Top Secret Military Basethe Montauk facility has been the center of an otherworldly conspiracy theory for decades.

Believers say that people were kidnapped at a U.S. Air Force base and subjected to mind control and time travel experiments. And extraterrestrials somehow had a hand in it all.

But nobody has been able to actually prove these allegations. And all that's left of the Montauk facility — currently a state park — are the above-ground remnants of the original Air Force base. According to a document issued by the Air Force Historical Studies office, the Montauk base, known as Camp Hero, was decommissioned in the early 1980s.

Montauk is a small seaside resort town on the tip of Long Island that draws vacationers to its shores every year. Camp Hero, located a short distance outside of Montauk, has roots as far back as the Revolutionary War, during which it was used to test military cannons. Later, during World War II, Camp Hero served as a coastal defense installation against any possible Nazi intrusions into America.

Montauk Chronicles follows the story of three men, Alfred Bielek, Stewart Swerdlow and Preston Nichols, who claim that Camp Hero ended up as an underground site for scientific atrocities.

Bielek, a retired electrical engineer, maintains he was part of the mysterious Philadelphia Experiment, where in 1943, the U.S. Navy allegedly tried to make a small destroyer undetectable to radar. The test ended in disastrous results, including the ship disappearing from the Philadelphia Navy yard and — purportedly — traveling through time.

The Philadelphia Experiment: Invisibility Time Travel and Mind Control - The Shocking Truth- Al Bielek

According to Bielek's story, he was transported ahead in time from Philadelphia, and extraterrestrials were responsible for the technology used in the Philadelphia Experiment. He also maintains he was recruited in 1970 to work on mind control and time travel projects at the Montauk facility.

Swerdlow's story involves being kidnapped as a teenager from his Long Island, N.Y., home, taken to the Montauk base, and subjected to a variety of experiments.

"Beatings, a lot of torture, electrical shock, burials, near-drownings," Swerdlow said. "They'd bring you to the point of death, and then they would save you, and the person doing this would be your rescuer or god, and would say, 'I'm the one that saved you and remember that.' And that became your handler — your programmer."

Swerdlow recalls being part of some horrific experiments while at the Montauk facility.

Montauk: The Alien Connection- Stewart Swerdlow

"The walls were very damp, oozing water, so it appeared to be deep underground or even underwater. I was always on this cold, hard table. Sometimes there'd be other people around, either my age or older, and electrodes were put into me and injections."

All three men claim to have seen extraterrestrials while at the underground Camp Hero facility.

"Well, there were quite a number of aliens at Montauk," said Bielek. "Some were there on a semi-permanent basis. A lot of them were just visitors that came in and looked at what they wanted to see and went back home.

"There were little grays there, which I suspected were degenerated humans from out of the future. Large gray aliens (which are a different species) were also at Montauk, and they were highly intelligent."

Nichols, like Bielek, was an electrical engineer, who says he worked with Bielek in the mind control and psychic aspects of the Montauk Project.

The Montauk Project: Experiments in Time- Preston B. Nichols

"There were definitely alien beings at Montauk," Nichols said. "We had the little grays and the larger grays as well as a variety of reptilian beings. The large grays didn't want anything to do with me because they couldn't reach me telepathically. When I entered a room they would leave.

"They were the strangest thing that I ever saw. At that point, I was beginning to doubt my own sanity."

And Swerdlow also saw an alien presence at Montauk. "Most of the time my interaction was with human beings, but I did come into close contact with alien beings.

“I did see, occasionally, intelligent reptilian humanoid beings as well as gray aliens who were once human beings but were physically altered as a result of degeneration and radiation toxins in their system. Most of them communicated with mental telepathy.”

Garetano shot much of his film at the actual site of Camp Hero. - Lee Speigel - Montauk Project: New Film Takes On Allegations Of Mind Control, Time Travel And Alien Encounters At Military Base - THP

Montauk Mind Control Victim Interview

An exclusive interview with Andy Pero, survivor of a secret mind control project aimed at creating the super soldier with psionic abilities.

By Eve Frances Lorgen, M.A -

Andy Pero was unwillingly subjected to a mind control program off-shoot the Monarch Project-a trauma based mind control program similar to what Cathy O' Brien describes in her autobiography by Mark Philips, "Tranceformation of America".

Andy Pero claims to have been created through a combination of genetic manipulation, trauma based mind control and Silva Mind Control training resulting in superhuman feats and psionic abilities. In addition to this, Mr. Pero alleges to have been unwittingly used in covert assassinations as a Manchurian Candidate and also in missions connected to the Montauk Project, such as time travel.

Andy Pero first went public with his story in August of 1998 as a special guest of Preston Nichols while at a lecture series hosted by Bob Eure of Philadelphia, PA. I was so astounded with Andy's testimony, that I interviewed him personally so that his story could be shared with readers of Unknown Magazine. For those who are unfamiliar with me, I have worked for ten years investigating and counseling UFO experiencers, abductees and occasionally survivors of various forms of anomalous trauma, such as ritual abuse and mind control. Because of my background in alien abductions, paranormal, the occult and anomalous trauma, I recognized Andy as an extraordinary survivor of trauma based mind control, one whose story should not remain hidden:

EL: Andy, where are you from originally and when did your training begin?

AP: I was born in Fallon, Nevada in November of 1969. My father was a Lieutenant Commander at the Fallon Naval Air Station in Nevada at the time. I believe my first experiences began by the time I was two and a half years old. At five years old my family lived in Munich, Germany and I remember attending two distinct Kindergarten classes, on in German that was located on or near McGraw Army Troop Army Base, and another Kindergarten in English.

I have flashback memories of torture sessions as early as age two where I was subjected to shock treatments with needles inserted in my ears and genitalia. What they (the controllers/handlers) do is use extreme trauma to separate the mind from the body. They do this to split the mind into several parts that can later be programmed to do things-like superhuman feats. Basically, they disconnect all of the normal human brain impulses, emotions and whatever is normally present, then reprogram in new ones. They do this to remove all fear, so that when they program in new abilities, you will not have the instinctual, "but I can't, I'm afraid..." response. They program you to do, not think. In essence, they treat and program your mind as if it was a computer.

EL: Who are the people running these secret programs like the Monarch and Montauk Projects, and where do they conduct their activities?

AP: Our own government. One of my handlers-who tried to brainwash me into believing that he was my father--was basically a Nazi. I nicknamed him Adolph

because he is very Aryan looking.

After WW2 many Nazi scientists were brought over to the US through our own Intelligence community who formerly worked in mind control research in the concentration camps. I believe they are a remnant of the Nazi party working in conjunction with different branches of the US government and the military.

Much of my training and torture sessions were done right at the University of Rochester, NY. They used to take me to a private room in the attic or top floor of the library. The big lab where I had most of the programming done to me was at the Rome National Air Base in Rome, NY. I have also been used in the Montauk chair while at Camp Hero, Montauk, L.I. and also in a chair in Atlanta, GA at Dobbins Air Force Base.

The Montauk facility located in Camp Hero, L.I. was reopened by the Department of the Navy and is active to this day.

Basically there are underground bases located across the country. Each one has a different function and specialty. There is a facility in Rochester, NY, Paramus, NJ, Dobbins Air Force Base in Atlanta, GA, Camp Hero in Montauk, L.I. and many others. In the Paramus, NJ facility is where they do the sex programming for many of the female agents. For the most part, 99% of them are involuntary sex agents and couriers who were raised in various mind control projects.

EL: What were some of the things the mind control programmers made you do?

AP: I remember my mother enrolling me in a Silva Mind Control course when I was ten. It is a type of self-hypnosis where you learn to go to different levels of your mind to do self-healing, relaxation, visualization, bending spoons with the power of your mind, things like that. This is also the time when I saw two peculiar military men, who would periodically visit me throughout my childhood, especially sporting events. I did exceptionally well at Silva Mind Control (and sports), so much so that the two military men approached me and said, "I hear you have some very special abilities. Someday you will work for us." At the time I didn't understand, but later the two men figured prominently in all the training I had up all the way through my college years. Of course I didn't realize this until my memories came back. I did very well at sports and demonstrated a genius IQ, but I stuttered so badly until I was in my twenties, that everyone just thought I was a dumb jock. The stuttering was due to all the electroshock treatments.

I recall being subjected to electroshock numerous times, being placed in an enclosed water tank and told to breathe underwater. Consequently, I drowned several times and would revive because of my self-created healing pool in my mind. I learned to create my own mental laboratory through Silva Mind Control, replete with a super powerful healing pool that could heal any injury. I was forced to endure suffering beyond belief to accomplish superhuman feats of strength and survival.

EL: Tell me more about the various superhuman abilities you discovered you had.

AP: The trainers would put me into a trance whereby I'd be told I could jump off a ladder of minimal height. In my mind, I believed that I was only jumping off a footstool or a short ledge. In actuality, I was progressively led to jump higher and higher heights to the point of successfully jumping off buildings and even out of planes without a parachute.

When under mind control, I could do whatever I was instructed to do as long as I believed them. I would do 200 or more push ups in perfect form, sometimes as long as a half hour straight, or until I was told to stop. I weight lifted 545 lbs.on a barbell and squats while attending college and much more (500-1500 lb.) while I was under the mind control in the training laboratory not far from Rochester, NY.

In my jumps, it was as if I was falling like a cat, calm and cool with no fear, focusing like a laser only on the landing.

EL: Are there others like yourself who have had similar training and experiences?

AP: I think there are thousands of other children and people who are used and many end up missing. Many die in the process. They are considered expendable. The ones who can survive the most rigorous programming live on to become what are known as the Montauk boys. Duncan Cameron is such a person. In general, the boys and young men are trained to be couriers, assassins and super soldiers and even psychic killers. The women are mostly used as sex agents. Cathy O' Brien's story is an example.

EL: What kinds of special missions or time travel experiments do you remember taking part in?

AP: There were times I remember being at the small Rochester airport, being picked up in an F-16 fighter plane and ending up in some southwestern desert terrain either for special military training and obstacle courses or assassination missions. I remember seeing other men in black t-shirts and pants on the same training course at one time. Other times I found myself on some aircraft carrier out at sea. After the mission they would take me back and I would return to college after a couple of days or even hours not remembering what even happened. All of these missions were done between the time I was 15 years old and until 1988-1992 under deep hypnotic programming with the memories erased, until of some of my memories started to return.

I was also taught to handle various types of guns, loading, cleaning, special characteristics of each model and firing at exact targets repeatedly and perfectly without thinking, just doing.

EL: Tell me more about your involvement in the Montauk Project.

AP: I was involved in an off shoot of the Montauk Project called the Montauk chair. Basically the Montauk chair was developed to give the human and spirit a zero point of reference to facilitate time travel. What the chair essentially does is separate the mind from the body. The chair operator's thoughts and vibrational energy is picked up by umbrella looking antennas above the chair, sent to a computer, over to a processor, then amplified several hundred times. The information is sent to a network of free energy crystals arranged in a circle. Then whatever thoughts were amplified, i.e., a time period, a wormhole would open up in the room. The wormhole was as large as 16-18 feet across and even large enough for a truck to go through.

In Camp Hero, Montauk, the location is the cross hairs of the earth's biorhythms and is the point on earth where time travel is most easily accomplished when earth is the point of origin.

My part of the Montauk chair project was to use my focused visualization skills to think of specific time points in history that were assigned to me. The chair is connected to a sophisticated computer system and thought amplifier, such that when a thought or time period is visualized, the computer simulates a time portal based on that point in time. A series of time portals are done until a library of time periods and portals are accumulated.

The chair is also used to amplify extremely focused thoughts to create three-dimensional materializations based on the operators thoughts. Preston Nichols wrote several books on the Montauk Project and describes an incident in which Duncan Cameron created a monster while in the Montauk chair.

One such time travel mission was called Project Southern Cross. It was used to win WW2 in favor of the allies. What the US government did using time travel was to go back in time to the 1940's to help us win the war. We would deliver communication devices, weapons and technologies made out of 1940's parts. These would be delivered to the 1940's along with a complete set of drawings on how to make them out of 1940's parts. I took part in several of these deliveries, one time I was sent to Germany and another time to England. I was not allowed to speak to anyone, other than deliver my parcel and quickly return back to our time. And this was all done under deep hypnotic programming, so I didn't have a lot of freedom to explore. I was gone no longer than two hours for the deliveries.

EL: Have you ever encountered any extraterrestrials or seen any aliens in any of your underground base memories?

AP: From what I understand the Department of the Navy made an agreement with the alien Greys to exchange technologies for human women and children to conduct horrific breeding experiments. This is what is going on right now in an underground base not far from Miami, Florida. One of my most disturbing memories is being escorted down a hallway in this underground lab and seeing cages of chickenwire fencing with women and children screaming for help. I have seen Grey aliens (the 4-foot tall ones with large black eyes) and also 7-foot tall reptilian beings in some of my experiences. I have been told that I have many children from alien breeding experiments. I have had abductions with the Greys also.

On one occasion I was introduced to a Reptilian being while in an underground base sometime in 1989-90. At first I saw a 7-foot tall human Ayran looking man. He walks towards me and I notice that his image phases out as if something interfered with an energy field. He does something to a device on his belt and tells me, "OK, I'll show you." He then pushes some button and then I see his image change into a 7-foot tall lizard like creature who looked like he weighed over 400 lb.

I was introduced to a group of beings that claimed to be a sub group of the Illuminati. They were made up of a group of about 40-50 men, all 6' 2" or taller, white, and of an indeterminate older age, averaging 70, but I suspect much older considering the technology they have access to. They convened in a boardroom that I believe was in an underground base, perhaps Camp Hero, Montauk. They sat around a large football shaped table made of wood. Each high backed chair had a light at the tip and each sitting had a TV type of screen and control panel that came out >from the table. There was a huge screen located in the front of the room as well. I have reason to believe that not all of the Illuminati are human, but in actuality are alien beings that appear to look human.

EL: Who or what groups do you think are running the show here in the US or even on Earth? How do the aliens fit into all of this?

AP: It is very complicated, but basically there are four main versions or groups of the New World Order, all with slightly varying agendas. The first group comprises the US and Western Europe (i.e., England, Germany, France and the US). The second group is Eastern Europe fused with Western Europe and the US. The third group is the countries of the Orient, and the fourth is the Middle Eastern-Saudia Arabian elements and all the oil money. There are also off world groups (aliens and future human Nazi's types called Zardanians, Reptilians, Greys and Dracos) who also have a hand in the NWO plans. For the time being, the old money groups of Europe and England have teamed up with die hard Nazi factions, Jews and Americans forming the group that has been always been known as the Illuminati and affiliated secret societies. This large international group controls the media, police force, military, etc. The Illuminati is also part of the NWO plan, which includes members such as George Bush, Prince Charles and other high ranking people.

As for the aliens, I think most of the alien Greys are either under the authority of or in collaboration with the Reptilians, Dracos and the Illuminati, based on some of my experiences and memories that are still returning to me. Some Grey groups are in conflict with the Reptilian/Draco agenda and are doing their own thing (human/grey hybridization programs) so to speak. Their agenda gets into heavy spiritual matters having to do with acquiring an emotional body and an ability to ascend to higher dimensions. They are using humans to accomplish this via the human/alien hybrids. Humans have the key in terms of having a threefold essence or unity of being, physical, emotional and spiritual. Other aliens have lost this unity of being (because of the fall from grace), thus inhibiting them from ascending to higher dimensions, or evolving to higher levels. This gets back to the original Luciferic rebellion, fallen angels and the various conflicts between species.

EL: When did you start remembering your memories? How did or can you break the programming they install?

AP: Some of my first memories surfaced while I was living with a roommate in Atlanta, GA back in 1996. We went to the bowling alley and I saw a large sign in the shape of a man dressed like a Rhino advertising, "Bowl with Rhino balls." This triggered me into remembering that "Rhino" is the name my Nazi handlers called me. My roommate overheard me say outloud, "I'm Rhino-they called me Rhino." He got excited and immediately asked me, "Where did you hear that?" He had a grave look of concern on his face and kept questioning me. By his reaction, I realized later that all along he was one of my hired programmers and handlers. The initial triggered memory that surfaced was a flashback of me being electrocuted and shocked and screaming in pain in one of

my numerous torture sessions.

Then after that first memory, other memories started leaking through. It was like my mind was dammed up and the subconscious memories were starting to leak through. My mind controller programmers deliberately built a wall around my memories so that I wouldn't remember. When I started recalling bits and pieces, I'd write notes to myself and hide them. Then I'd find my notes, after I had forgotten everything because my roommate was catching on that I was remembering. So he would repeatedly put me in trances, erase my memories and I'd forget what I had just remembered. But then everything came crashing down, because I deliberately hid notes and pretended that I didn't know to my roommate. I had thought he was a friend and it turned out he was just hired to be another controller and handler to keep me in the program.

I recall that in the past I did not even remember my dreams for ten years. But now things are coming back. I am working on purifying the body to help clear my mind and get my abilities back.

EL: How do they keep control overall these people who have been and are still in mind control projects?

AP: The essence of their control tactics is of splitting the mind at a young age. This entails a process of trauma, torture, degradation and humiliation of the subject. The process is different for each individual, but in essence they go to your subconscious mind and find out what the most personal parts of you are. Then they essentially use this against you to break you down and rip your mind apart. What happens is this: An individual who possesses special mental abilities is selected at a very young age. (Very often they are from military families or from multigenerational Satanic ritual abuse families-EL) Then they are subjected to various stages of terror and horror to begin to separate them from their own minds. It is a process of progressive dissociation and compartmentalization of the mind and personality.

They control your mind through various complicated hypnosis techniques and commands until they create the perfect Manchurian Candidate.(See The Greenbaum Speech by D.C. Hammond) They program you to do something, then erase the memory. Basically they program your mind as if it were a computer. Once they install the magic word, all they have to do is say it and you're under their control. This happens from an early age so it is easier to control them if they are conditioned and dissociated into several personalities.

Another method of control is that they send in special people in your lives, handlers and controllers who pose as friends, teachers, "deprogrammers", roommates, lovers, etc. who are actually operatives for the mind control projects. Some are sleeper operatives who don't even know they are being used to a certain extent. It makes it hard to trust anyone at this point.

EL: Is there anything else you can say about these projects or advice to others who have gone through similar experiences, like how they can be set free from its influence?

AP: For those who want to get out of the influence of the programs of mind control, you must have a strong fighting instinct to do what is right regardless of what others are doing. Your only cage is the one you build for yourself. You must connect with your highest self to break the evil that is all around us, and not succumb to doing evil just because everyone else is doing it. Retain your fundamental sense of right and wrong.

It all goes back to the basic conflict basic good and evil. It is like the dark forces in power of the planet at this time are trying to cheat their way into heaven or higher dimensions. - Eve Frances Lorgen, M.A

Back To Contents

It is even said that under the perfect conditions, the device offers its user the ability to foresee what was going to happen in the near future.

However, Father Ernetti remained secretive and stated he was not at liberty to reveal further details about the Chronovisor.

Father Ernetti did however reveal that the Chronovisor worked by '...processing residual electromagnetic radiation left over by numerous processes...'

According to numerous reports, Father Ernetti used the Chronovisor to witness important historical events, with the most notable being the crucifixion of Christ.

However, Father Ernetti revealed that thanks to this invention had managed to witness the destruction of Sodom and Gomorrah, and other major historical events such as the founding of Rome in 753 B.C. Also, thanks to the Chronovisor, Father Ernetti was able to recompose the missing work "Thyestes" , written by Ennio Quinto and represented in Rome in 169 A.C. in its original version, and the original text of the the two stone tablets written by God (Exodus 24:12) which were given to Moses on Mount Sinai, apart from witnessing the likes of Napoleon, Roman philosopher Cicero and other great and momentous historical and biblical episodes.

French priest François Charles Antoine Brune was one of the first to hear about the Chronovisor.

According to Father François, he met Father Ernetti in the 1960's when the two were traveling across the Grand Canal of Venice. As the two were experts in ancient languages, they began to talk about the Bible and its interpretation through the years.

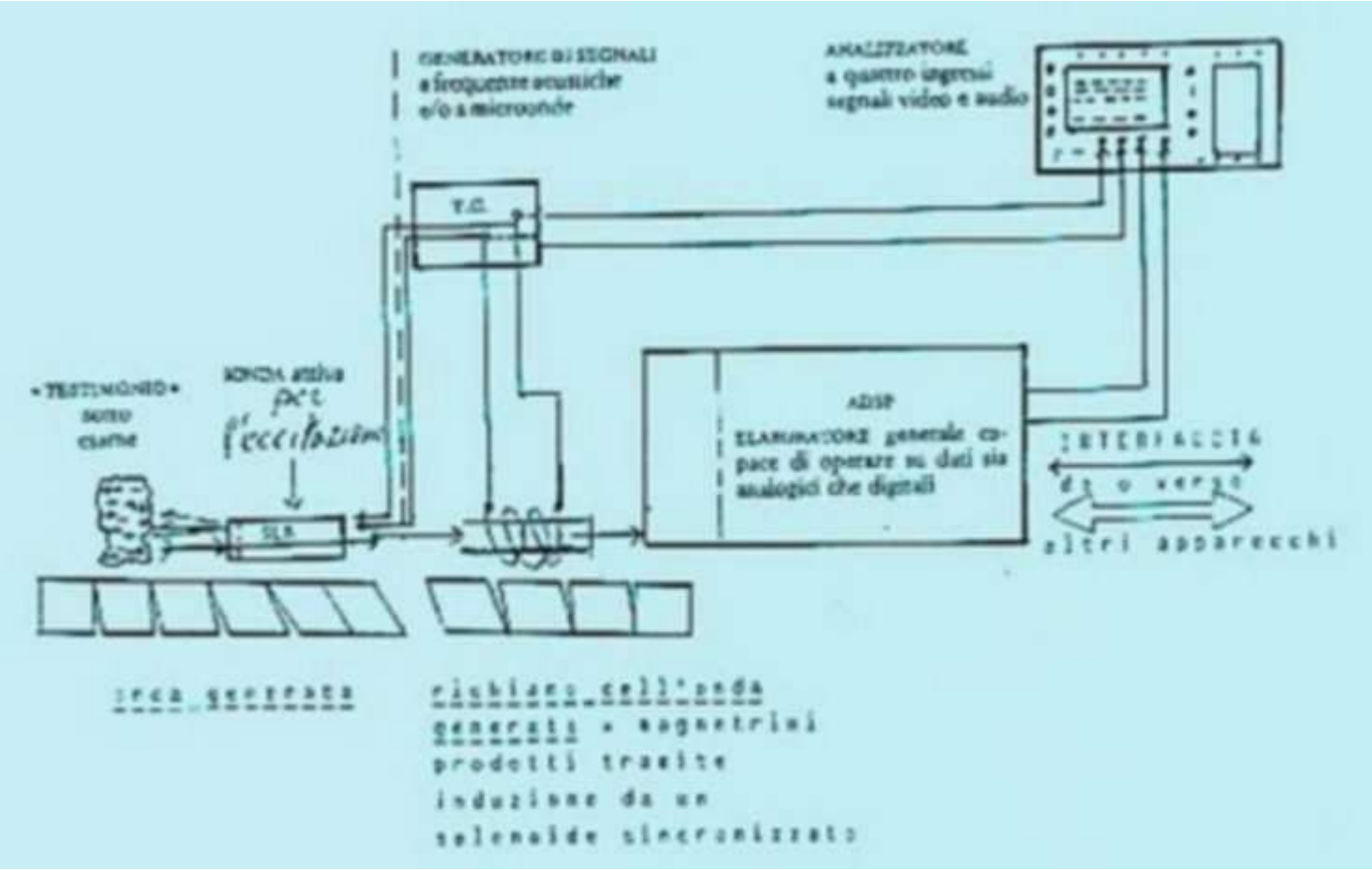

Supposedly, these are the blueprints of the Chronovisor.

Father Brune that was very intrigued when the Father Ernetti revealed that there was a machine that could answer all questions related to the Bible.

When Father François asked about the Machine, Father Ernetti described the Chronovisor, saying that it was device that functioned just like a T.V., but instead of receiving transmissions from local stations, the chronovisor was able to tune into the past and allow the viewer to “see and hear” events that had occurred centuries before.

Ernetti told Brune that the machine worked by detecting images and sounds that humanity had ‘created’ which were “floating” in space.

Empowerment by Virtue of Golden Truth
Human Cloning: Specifically,
REM Driven Human Cloning
FULL DISCLOSURE

Donald Marshall

29 October 2015

https://www.facebook.com/donald.marshall.148
http://donaldmarshall.proboards.com/
Vincent Eastwood Interview
https://www.youtube.com/watch?v=M_1UiFeV5Jg&ab

Contents

List of Images 5
Introduction 6
Whistle Blowing: Qualifying Disclosure 6
The Serious Crime Act 2015 7
Fundamentals 8
Key Figures 9
Phil Schneider 9
George Green 11
Aaron Russo 13
Income Tax 13
Radio Frequency Identification (RFID) Microchips 14
Habeas Corpus 15
Fraudulent Manipulation of Election Results 15
The War on Terrorism is the War on Your Freedom 16
Whoever Makes the Money Makes the Rules 16
Russo's Message to Mankind 16
Let's Consolidate our Problems 17
Aaron Russo: Reflections and Warnings 17
The Falsehood of September 11th 2001 17
The New World Order Agenda 19
Women's Liberation from the Perspective of the Elite 20
America is a Republic 20
Depopulation 21
Borrowing Money from Private Banks causes Inflation and Debt 21
The Deception of the Council of Foreign Relations (CFR) 23
Combining America, Mexico and Canada into one Country 24
Russo's Vision on How to Bring These People Down 25
The Trans-humanist / Post Human Agenda 26
The Phases of Sleep and Rapid Eye Movement (R.E.M) Sleep 27
REM Sleep 28
Current Advances in Technology 28
Memory Suppression Technologies 29
Mind-Voice Technology 29
H.A.A.R.P. Technology 29
H.A.A.R.P. and Weather Control 30
H.A.A.R.P. and Mind Control 31
RFID Technology 32

RFID Technology and the Medical Profession 32
Further Implications of RFID Technology 33
Mind Control: MK Ultra Technology 33
Human Cloning 35
Cloning Centre and Cloning Technology 36
Drip Feed Disclosure and Evaluative Conditioning 36
Drip Feed Disclosure 36
Evaluative Conditioning 37
Consciousness Transfer 38
Disclosure: Save the Victims through your Diligence 40
Words of Inspiration: Personalized from a Theoretical Physicist –Thomas Campbell 41
The Science of Hidden Consciousness 41
Disclosure: Donald Marshall's Message to the World 42
The Two Types of Cloning Techniques 42
The Different Grades of Clones: "Mark 1" to "Mark 4" Clones 43
Donald Marshall's Dilemma with "Mark 2" Sleep Driven REM Clones 43
Consciousness Transfer Happens When the Original Reaches REM Sleep 43
Donald Marshall is an Original as he sits at Home Typing this Disclosure 44
When Donald Marshall's REM Driven Cloned Experiences Began 45
The Science of REM Driven Cloning Began in 1945 46
Help Donald Marshall STOP REM Driven Cloning NOW! 47
Do Not Panic, Riot, or Cause Chaos. This is Very Important. 47
Spread this Disclosure Document until it reaches the Armed Forces 47
Donald Marshall is NOT "The New Age Saviour". Nobody wants to be a 'saviour' 48
How the Nostradamus Prophecies shapes the lives of the Illuminati 49
HIV/AIDS has been cured; so have many forms of cancer 49
The Behaviour of High Profile People at the Cloning Centre 50
The Ring Leaders of the Cloning Centre 50
The Royal Family of England 53
Help Donald Marshall by Sharing this Disclosure with Your Close Friends and Family 57
The Deplorable Nature of the Illuminati 59
What Happened to Britney Spears? 60
NEVER EVER SELL YOUR SOUL 62
In This Physical World Selling Your Soul Is Selling Your REM Driven Clone 62
Fake Alien Abductions conducted through REM Driven Cloning Technology 64
I am THE Spy for Humanity against the Corruption of the Illuminati 65
The Threat to Humanity when the H.A.A.R.P Grid is Complete 66
REM Driven Cloning is the Most Terrible Nightmare Situation Ever 68

The Meek Shall Inherit the Earth 70
Be Wary of: Shills; Trolls; Disinformation Agents and Double Agents 72
Contact Information 73
Interviews 74
Links to Donald Marshall Interviews 76
Vincent Eastwood 76
Jeanice Barcelo 76
Lisa Phillips (CFR) 76
Radio Presenters –Contact Donald Marshall 77
Professionals who understand "Consciousness Transfer" –Contact Donald Marshall 77
Email 77
How to Learn More about Donald Marshall's Whistle Blowing Disclosures 77
How Much Do You Know About Post-humanism / Trans-humanism? 78
This IS your ONLY chance to end these monsters. There is a deadline! 79
Do NOT Be Afraid to Help. We Outnumber the Illuminati by 1,000,000:1 80
Noteworthy Frequently Asked Question 81
Donald Marshall's Mission and Vision on How to Bring Down The Illuminati 81
Empowerment by Virtue of Golden Truth 83
Appendices 84
Appendix A: Thien Thanh Thi Nguyen (Tila Tequila) Transcript 84
Appendix B: MK Ultra 87
Appendix C: The Illuminati 89
References 99
Legislation 111

List of Images

Image 1: Stages of sleep..... 27
Image 2: The ionosphere's relationship to earth..... 30
Image 3: Megadeth Album Cover: *The World Needs a Hero* (2001)..... 58
Image 4: Donald Marshall's original body compared with his REM Driven Duplicate Clone..... 58
Image 5: Britney Spears Japanimation: Britney Spears grown as a duplicate clone..... 61
Image 6: Britney Spears Japanimation: Britney Spears walks into the Cloning Centre..... 61
Image 7: Britney Spears Japanimation: The Cloning Centre depicted from an aerial view..... 61
Image 8: Possible H.A.A.R.P. Locations. 67

Introduction

Just read it. Every word in this document is true, and it is the most important document to ever reach the internet. This document is written to empower good people of the world against the tyranny which exists all around us in our world today. Effectively, the document presented here discloses concealed information about the extent to which medicine, science, and technology has advanced in our **current** era. Moreover, I am disclosing this information because I have been extensively abused, and I am victim of **current** advances in medicine, science, and technology, which I describe in detail below. There are many, many, other victims of abuse, including myself, and therefore it is our plea that you read this document with an open mind and you investigate **ALL** statements which may initially irk you and appear 'suspect' to begin with (the circumstantial evidence is available all around you); because as a victim of abuse, I can honestly say, there is nothing worse than experiencing abuse, and those who have the power to protect you from your abusers, ignore you.

I will now discuss what qualifies as whistle blowing disclosure. After detailing the criteria which qualifies for whistle blowing disclosure, I will detail aspects of the Serious Crime Act, and preface a foundation which defines, explains, and references key information for the reader to understand as well as explore the extent to which medicine, science, and technology has advanced today; all for the express purpose of compelling the reader that medicine, science, and technology, has advanced at an incredible rate; that **current** advances in medicine, science and technology are withheld from public knowledge; and finally these advancements in medicine, science, and technology, have been and are **currently** used to commit **serious unspeakable** crimes against humanity and our environment here on earth. Moreover, it is my aim to present this information as coherently as possible to assist the reader to save me, and save many, many others who experience abuse daily resulting from concealed advances in technology.

Whistle Blowing: Qualifying Disclosure

In the United Kingdom under the Public Interest Disclosure Act (1998) (PIDA) section 43B, a "qualifying disclosure" (whistle blowing disclosure) implies "any disclosure of information which in the reasonable belief of the worker, tends to show one of the following:

a) That a criminal offence has been committed, is being committed or is likely to be committed,
b) That a person has failed, is failing or is likely to fail to comply with any legal obligation to which he is subject
c) That a miscarriage of justice has occurred, is occurring or is likely to occur,
d) That the health or safety of any individual has been, is being or is likely to be endangered,
e) That the environment has been, is being, or is likely to be damaged, or
f) That information tending to show any matter falling within any one of the preceding paragraphs has been, or is likely to be deliberately concealed"

Furthermore, under the Enterprise and Regulatory Reform Act (ERRA) 2013 section 17 (*The new 'public interest' test)* is added for whistle blowing disclosures, amending section 43B of the Employment Rights Act (ERA) 1996 and therefore now reads as such (new words underlined):

"(1) In this part a 'qualifying disclosure' means any disclosure of information which, in the reasonable belief of the worker making the disclosure, *is made in the public interest and* tends to show one or more of the following-- [criminal offence, breach of legal obligation, etc]." (Halliday 2013, p. 2).

The following information is presented **with the express intent** that it is made in the public interest, and meets the all criteria set out in section 43B (a-f) of PIDA as well as the 'public interest test', ERRA section 17. Furthermore, in order for the reader to perceive the credence of my statements, so that (s)he has impetus to research the validity of my statements and not dismiss it as folly supplied by an internet troll who has nothing better to do than waste peoples' time, I will cite the Serious Crime Act 2015 here for the express purpose of convincing the reader that all statements made in this document and my original document are indeed FACTUAL! THIS IS NO HOAX. THIS IS NO JOKE. This is simply what is happening in the world today.

The Serious Crime Act 2015

The Serious Crime Act 2015 (UK) section 41, 3ZA, amends section 3A of the Computer Misuse Act 1990 which **previously** read [under Computer Misuse Offences]:

[F1 3A Making, supplying or obtaining articles for use in offence under section 1 or 3

1) [That] A person is guilty of an offence if he makes, adapts, supplies or offers to supply any article intending it to be used to commit, or to assist in the commission of, an offence under section 1 or 3.

To: [The Serious Crime Act 2015, section 41, 3ZA]

3ZA Unauthorised acts causing, or creating risk of, serious damage

(1) A person is guilty of an offence if—

(a) the person does any unauthorised act in relation to a computer;

(2) Damage is of a "material kind" for the purposes of this section if it is—

(a) damage to human welfare in any place;

(b) damage to the environment of any place;

(c) damage to the economy of any country; or

(d) damage to the national security of any country.

3) For the purposes of subsection (2)(a) an act causes damage to human welfare only if it causes—

(a) loss to human life;

(b) human illness or injury;

(4) It is immaterial for the purposes of subsection (2) whether or not an act causing damage—

(a) does so directly;

(b) is the only or main cause of the damage.

(5) In this section—

(c) a reference to a country includes a reference to a territory, and to any place in, or part or region of, a country or territory.

(6) A person guilty of an offence under this section is (unless subsection (7) applies) liable, on conviction on indictment, to imprisonment for a term not exceeding 14 years, or to a fine, or to both.

(7) Where an offence under this section is committed as a result of an act causing or creating a significant risk of—

(a) serious damage to human welfare of the kind mentioned in subsection (3)(a) or (3)(b), or

(b) serious damage to national security,

a person guilty of the offence is liable, on conviction on indictment, to imprisonment for life, or to a fine, or to both."

In laymen's terms it is a **serious crime** (Serious Crime Act 2015), punishable by imprisonment, a fine, or both, to cite hatred or spread hoaxes by use of a computer which would cause mass hysteria or public dissension. I have been condemning public figures, high profile individuals, celebrities, singers, movie stars, directors, politicians, world leaders, royalty, anti-secret society 'truthers' (who are really misinformation agents, and agents of deception) etc. –the list is long - since 2011 and **NOT** a single one of these high profile people has issued a public statement saying "I do not like how you have tarnished my name" or filed a law suit against me. Why you may ask? **Because** every word I have stated and will state again (in this document) is true.

Fundamentals

Before I describe the heinous crimes committed against me and many others (including unsuspecting civilians of the world) it is important that I explain, define, and reference:

- Key figures such as Phil Schneider, George Green and Aaron Russo, so that the reader has reference points to verify the extent to which technology has advanced in our **present** era (and continues to advance);
- Define and briefly explain the transhumanist / post human agenda (for those who may be unfamiliar with their aims).
- Define and explain rapid eye movement (R.E.M) sleep, the phases of sleep, and what happens to the (original's) body during sleep.

- Reference advances in technology, with particular attention to: Memory suppression technologies; Mind-voice technology; H.A.A.R.P technology, RFID microchip technology, and MK Ultra technology (CIA's mind control program);
- Define and explain cloning; the different types of clones; cloning centres and cloning technology;
- Define drip feed disclosure / evaluative conditioning and explain why it occurs;
- Explain what 'consciousness transfer' is to the best of my knowledge, and cite drip feed disclosure articles with the express intent to allow the reader to grasp the abuse I have suffered daily at the hands of my tormentors.

Key Figures

Phil Schneider

Phil Schneider (pictured) had 17 years experience working in government black projects carrying a level three security clearance. He was a geologist and engineer who worked in the black projects underground bases at Area 51, S-4, and Los Alamos.

He is most notable for disclosing (Schneider 1995; 1996; Open Minds 2011):

- The 'black budget' expenditure of the United States, which Schneider claims to be between 1.023 trillion U.S. dollars every 2 years (over $500 billion per year);
- Deep Underground Military Bases (also known as D.U.M.Bs -"dumbs"), and at the time of his lecture (Schneider, 1995), –that there are 131 **active** Deep Underground Military Bases present in the United States, and 1477 Deep Underground Military Bases worldwide;
- Each D.U.M.B costs on average 17-19 billion U.S. dollars; paid for by the taxpayer; and it takes approximately a year-and-a-half to 2 years to build D.U.M.Bs with sophisticated methods.
- That military technology outstrips the general public's technology at a rate of 44 to 45 years of technology for every calendar year which passes. In other words for every 12 months which passes military technology will have advanced by 44 years than what we as the general public is currently accustomed to. Therefore as a rough example if we were to take the year Facebook was founded (2004) as a base year, then the military technology since the creation of Facebook will have outstripped what the

general public is accustomed to by as much as **484 years(!)** (2015 - 2004 = 11. 11 x 44 = 484). Similarly, if we are to use the year which YouTube was founded as a base year (2005), once again, military technology would be 440 years more advanced than what the public is currently accustomed to today.

For the purpose of disclosing current advances in medicine, science and technology, and how such advances are used against me and the people of the world to commit monstrous crimes I will use 1945 as a base year. Everything will become apparent including why I use 1945 as a base year for my disclosure, but for the express purpose of compelling the reader to investigate my disclosure I must present everything, logically, sequentially, methodologically, and provide references for the reader in a coherent way to enable him or her to **pay serious attention** to my eye witness accounts. Therefore, at this present stage keep in mind the year 1945, and the fact that military technology outstrips the general public's technology at a rate of 44 years for every 12 months which passes.

George Green

George Green (pictured) was affiliated with U.S. Presidential candidates, and was once asked to be the Finance Chairman for the next President of the United States. Green would later declined the offer of Finance Chairman when a comment made by Ted Kennedy regarding sleeping with Green's 14 year old daughter caused George Green to re-evaluate his associations with this in-group.

During his 2008 interview with Project Camelot (2008a; 2008b), Green disclosed the following noteworthy information:

- U.S. presidents are "selected" and not elected. This is clearly expressed in a story Green recounts, when Green asks:
  "Who is going to be the next President of the United States [for him to overlook their finances]?"
  And the reply was: "Jimmy Carter"
  Green responds: "Jimmy who?"
  The reply Green received was: "Well, he's the Democratic Governor of Georgia."
  George Green: "But I've been voting Republican."
  Green was then confronted by a tall man, Paul Volcker (American Economist, and Chairman of Federal Reserve under Jimmy Carter and Ronald Regan), who walked over and said, "Son, don't worry about it [Republican or Democrat], we control 'em both."
- U.S. scientists learned how to make people (clones) since 1938 -walking talking ones –and the scientists call these people "synthetics" or "the others".
- Cloning technology is relatively advanced. All that has to be done is take two cells from the original, give the cells a small electrical charge (retain a fertilised egg), then all one needs is a receiver (a womb / artificial womb for the fertilised egg to grow).
- Scientist were excited by the synthetic technology because it meant that spare organ parts could be grown for an "original" human without rejection, because theoretically speaking, the DNA of the synthetic is the same as the original.
- Green gives an example of a cloned Politician: George Walker Bush. Green advices the viewer to seek old video recordings of George W. Bush, and compare the old George W. Bush, with the George W. Bush during Bush's second term,

-in terms of mannerism, speech pattern, body language etc. (old videos of George Walker Bush (Boringest 2006; Fox 4 News - Dallas-Fort Worth 2014) are presented in the References section).

- Scientist have also learned how to make these synthetic people within a few months, to the point where the synthetic can be a walking, talking duplicate of the original, intact with all the memories and experiences of the original. The only problem is that the memory, experiences, and functioning capabilities of these synthetics are like: "A DVD recorder. Sometimes you have glitches, and you have to take the synthetics to Camp David occasionally [every 6 months to a year] to get them tuned up."
- Remember these synthetics are people too, they can think and act just like you can, but they do not have a soul.
- Most of the world leaders have been bought and paid for [by men in the background] and are created to think a certain way –to meet the agendas of these men who remain in the background.
- The global elite plans on depopulating the current human population of **over 7 billion** to **500 million** people. This is corroborated by the "Georgia Guidestones" (WorldTruth 2014).
- Vladimir Putin is executing plans to bring the United States down and into a massive depression. Furthermore, China agrees with Vladimir Putin's plans; stating that the Chinese government has not been a Superpower for over 5000 years and "It is their turn to run the world."
- China has the capacity to set back / shut down all of U.S. computing and electrical systems within two days.

At this present stage, the most **salient** points to keep in mind from Green's accounts are that: U.S. presidents are selected and not elected; and **most importantly**, that scientists have been capable of creating synthetics (cloning people) since 1938. If you have kept in mind Schneider's statement (1995; 1996), (that for every 12 months which passes military technology increases by the equivalent of 44 years compared to what the general public is accustomed to) –then learning that scientists have been capable of cloning humans since 1938 should not come as much surprise. Again, everything regarding my disclosure will become apparent, and I thank these men for disclosing their information, because it helps the reader to corroborate my disclosure.

Aaron Russo

Aaron Russo (pictured) was an American businessman, director, and political activist. He is best known for directing blockbuster films such as *Trading Places, The Rose* and *Wise Guys.* Russo believed that a human being "Should stand for something, and do the right thing when the time calls to act". Consequently, during the latter part of his career he did his best to warn the American public by producing documentaries such as *Mad as Hell* (1996), *Freedom to Fascism* (Russo 2006), and *Reflections and Warnings* (Jones 2008).

Russo disclosed the following key information in *Freedom to Fascism* (Russo 2006):

Income Tax

- There is no law requiring Americans to pay income tax. **Although this is a truth, I DO NOT advocate Americans NOT to pay income tax (and neither did Russo).** This is simply because the Federal Reserve can imprison you and seize your possessions for not paying income tax (although there is no law requiring Americans to do so). So for the sake of avoiding hassle for the mean time –pay your income taxes.
- To further illustrate the above point, Bob Shultz speaking at "We the People Foundation" said the following: "Most people believe that the income tax system is legal and that the revenue from the tax is used in the public interest. However, there is a substantial conclusive body of evidence that proves that our income tax system represents the most pernicious form of tyranny. It is the greatest hoax ever perpetrated by government against the working men and women of America."
- Charlie Beall: "The federal government itself refuses to provide, the American people, who are coercively being subjected to this extraction of their private property, without any underlying legal justification. There is no law. There is no law that requires the average American worker in the private sector to pay a direct un-apportioned tax on their labour and compensation for services. There is no law."

- State Representative – Phil Hart –(R-Idaho): "You can look through the statutes, and look for the law that requires you to pay, and when you do that, you **cannot** identify a law that requires the average person in America who earns a wage and works in private business to pay an income tax."
- Peter Gibbons (Tax Attorney) –It's actually very simple. Congress tried to enact an income tax in 1894 –The Supreme Court said that is unconstitutional. When The Supreme Court says something is unconstitutional, it's unconstitutional. They (Congress) tried again in 1913 –and The Supreme Court said –the 16th amendment- "No new power of taxation" –so if they (Congress) didn't have it then (1913) and they didn't get it; they **DON'T** have it. There is no constitutional base for a tax on the wages for Americans living and working in the 50 States of the union. Period. End of argument.

Radio Frequency Identification (RFID) Microchips

- The latest technology for identifying people at the point of self, when they make purchases –is actually the implantable (RFID) microchip. There are microchips that can actually be imbedded directly into human flesh... It's a tiny glass capsule about the size of a grain of rice... it contains an RFID computer microchip with a coiled antenna and it can transmit information also at a distance.
- Katherine Albrecht –Author of "*Spychips*" (2005) makes the following comment: "RFID is a technology that uses tiny computer technology the size of a grain of sand or smaller; hooked up to miniature antennas to transmit information about items at a distance. Back in 1999, Procter and Gamble, Gillette, and MIT got together to find a way to commercialise this technology and make it small enough, make it efficient enough and make it low cost enough to essentially ---their dream is to put these tiny computer chips on every physical item manufactured on planet earth."
- Radio waves can travel through walls, they can travel through wood, and they can travel through things we normally rely on to protect our privacy, for example your purse, your bag-pack, your pocket, –anything you are wearing or carrying.
- One of the most worrisome applications of RFID microchips, are proposals to put them into cash, meaning that it would be able to track every bank note where it had been, who it had been issued to, and create in essence an audit trail. That would essentially take away the anonymity of cash we now enjoy today.
- Once everything you do is tied down to a single number and there is no longer the ability to pay with cash, then all it takes to render you a non citizen is to simply turn that microchip off. **You will no longer be able to participate in any function in society including buying food. Once money becomes digitised through RFID technology, the elite can deduct whatever amount of money they want out of your microchip, whenever they want. They can trace you whenever they want. You will be at their mercy.**

Habeas Corpus

- Habeas Corpus is "[A] writ [formal document] requiring a person under arrest to be brought before a judge or into court, especially to secure the person's release unless lawful grounds are shown for their detention" (Legal-dictionary 2015).
- During the Bush Presidency [2001-2009 (History 2015)], President Bush signed executive orders giving him sole authority to impose martial law, and suspend Habeas Corpus. This gives him doctorial power over the people without any 'checks and balances.'

  In other words, "The government can jail you for life without charges, without a trial, without a lawyer" (Russo 2006).
- Furthermore: "The National Defense Authorization Act [4] signed by President Obama on the 31st December 2011 authorises the indefinite detention, without trial or indictment, of any US citizens designated as enemies by the executive." See Paye (2013) for further discussion regarding the suspension of Habeas Corpus.

Fraudulent Manipulation of Election Results

- In 2004 at the "Forum of Presidential Election" Clinton Eugene Curtis, a former Computer Programmer for NASA and ExxonMobil testified under oath that election results can be rigged using electronic programs.
- In 2004 he gave the following abridged testimony (Russo 2006):

  Judge: Mr Curtis, are there programs which can be used to secretly fix elections?
  Curtis: Yes.
  Judge: How do you know that to be the case?
  Curtis: Because in October of 2000 I wrote a prototype for present congressman Tom Feeney, and the company I worked for in Oviedo Florida –it did just that.
  Judge: And when you said, "it did just that" –it would rig an election?
  Curtis: It would flip the vote 51:49 –whoever you wanted it to go to, and whichever race you wanted to win.
  Judge: And would that program that you designed be something that election officials that might be on county boards would actually, could detect?
  Curtis: They'd never see it.
  Judge: So how would such a program, a secret program that, fixes the election –how could it be detected?
  Curtis: You would have to view it either with source code, or you would have to have a receipt and then count the hard paper against the actual vote total –other than that you won't see it.
- **Judge:** Given the availability of such vote rigging software and the testimony that has been given under oath of substantial statistical anomalies and gross differences –between exit polling data and the actual tabulated results, do you have an opinion whether or not Ohio elections, the Ohio Presidential elections was hacked?
  Curtis: Yes. I would say it was.

Person in the audience: ---So in other words there is absolutely no assurance whatsoever in anything in regard to these machines?
Curtis: Absolutely none.

- See Truthstream (2006) for further details regarding the full account of Curtis' testimony on how elections can be manipulated.
- Moreover, voting machine manufactures refuse to allow anyone to see the source code. Without paper ballots, the honesty of any election cannot be verified.

The War on Terrorism is the War on Your Freedom

- It is time to wake up America. These ID cards are not about defeating terrorism, but they are **ALL** about controlling the American people.
- The (mainstream) media controls the information that a person gets in various ways. They can make sure that the average American watching T.V. or reading the newspaper is going to come out with a certain mindset. She is going to say this is good, that's bad –and that is all they (media/elites) have to do.

Whoever Makes the Money Makes the Rules

- As Mayer Rothschild said "Give me control of a nation's money supply, and I care not who makes its laws". Mayer Rothschild, private banker, –knew that he and the other bankers would now control the laws of the nation. Government gave these bankers one of its most important powers, and now had to borrow money from the bankers and pay interest to finance the government.
- America has gone from people owning their own property, owning their own businesses –to a nation in debt because all the money is created by borrowing (from private banks) and this country has become one where people just live by borrowing.

Russo's Message to Mankind

- If you are in the military or law enforcement, remember you swore an oath [to uphold the law of the land]. You did not swear an oath to promote world government, or corporations.
- Now that you do understand what happened [to America, and the monetary system based on debt slavery] and how it is leading to a tyrannical one world government – the future of mankind depends on you –will you choose freedom or slavery?
- Stop being passive liberals. Stop being passive conservatives. Stop being passive centralists. Stop being passive human beings! When the media starts telling you that the country will fall apart if this is done... Do not be fooled!!
- Remember these are sick, malevolent and twisted people we are dealing with, trying to save themselves. Squash their agendas and stay on course.
- "I believe the time for mankind is time to give all or perish. Grow up or die. Grow up and become adults. Act like adults. Take some responsibility. The world which you have perceived is childlike; –and now the curtain has been pulled back for all to see."

- Unless people get active [get fully informed, and learn how governments of the world are conspiring against their people] and say –I am going to help shut down the Federal Reserve System; I am going to shut down the powers that be –the whole human race is doomed otherwise.
- We are coming near the end game and things are starting to accelerate... –and people are looking at the world leaders to declare martial law [which in turn will rid Habeas corpus].

Let's Consolidate our Problems

- If we can all get focused on how to win the game instead of all these different objectives –such as people are fighting for a better environment; people are fighting to keep their guns/gun control; there are all these different issues which are going on around the world -and which are all important on their own –but if we can consolidate on that and focus –and take all those people –and say –hey let's shut down the Federal Reserve, then we'll deal with those issues. Let's go to the agenda, the objective, the root cause of man's problems, first, then we'll go back to the other stuff.
- That is the priority right now. You have to cut off the head of the beast. And the head of the beast is the Federal Reserve System and the people behind it. You see, and that is what will save the world, and if people understand that –and they **stop** being passive liberals, and **stop** being passive republicans, but rather become **active** human beings –that is what will save the world!

Aaron Russo: Reflections and Warnings

In this documentary Russo recalls his relationship with Nick Rockefeller. Russo shares critical information Rockefeller discussed with him.

The Falsehood of September 11th 2001

- Russo met Nick Rockefeller through a female attorney who telephoned Russo and said "One of the Rockefellers would like to meet you." Russo made a documentary called *Mad as Hell* (1996), and Rockefeller had watched the video and knew Russo was running for Governor of Nevada and wanted to meet him. Russo said "Sure I'd like to meet him", and the two met and talked. Rockefeller proved to be a very smart man and shared ideas with Russo and was the person to tell Russo 11 months before 9/11 happened "There was going to be an event..."
- Rockefeller never told Russo what the event was going to be; but, there was going to be an event –and out of that event, we [America] were going to invade Afghanistan, to run pipelines from the Caspian Sea; we were going to invade Iraq, to take over the oil fields and establish a base in the Middle East, and make it all part of the New World Order; and we would go after (Hugo) Chavez and Venezuela –and sure enough, later when 9/11 happened –and I remember he was telling me how you are going to see soldiers looking in caves for people in Afghanistan and Pakistan and all these places and there is going to be this war on terror which has no real enemy and

the whole thing is a giant HOAX, but it is a way for the government to take over the American people (and the world).

- There is no question about it [that 9/11 is a hoax]. Nick Rockefeller said to Russo: "There is going to be a "War on Terror"" and he was laughing. Who are we fighting against...? Why do you think 9/11 happened and then nothing has happened since then? Do you think that our security is so great here that these people who pulled off 9/11, who were able to lock down another plane...? Come on it is ridiculous... 9/11 was done by people in our own government and our own banking system to perpetuate the fear of the American people into subordinating themselves to anything the government wants them to do. That is what it is about and to create this endless war on terror.
- Nick Rockefeller was laughing when he said, "We are going to be sending men into caves in Afghanistan and Pakistan" –and it was just cynical, he kept laughing and saying "Look how stupid everyone is! We can do whatever we want!"
- 9/11 was the first lie; and the next lie was to go into Iraq, to get Saddam Hussein out with his weapons of mass destruction (when the real issue was control of the oil fields) –that was the next lie. 9/11 created an endless war on terror that would go on and on and you can never define a real winner. There is no one to defeat and so it goes on and on forever. And they can do whatever they want; because they scared the hell out of the American public.
- This whole war on terror is [perpetuated on] a fraud. It is a farce. It is very difficult to say it out loud because people are intimidated in saying it. Because if you say it they want to make you into a nutcase –but the truth has to be... and the truth has to come out. The fact of the matter happens to be the whole war on terror is a fraud, it is a farce. Yes. There is a war going on in Iraq, because we invaded Iraq, and people over there are fighting... but the 'war on terror' –it is a JOKE –you know, and until we discover what really happened in 9/11 and who was responsible for 9/11 –because that is where the war on terror emanates from. That is where it comes from. It was 9/11 which allowed this war on terror to begin and until we get to the bottom root of 9/11 –the truth of 9/11 we'll never know about the war on terror.
- Russo was in Tahiti when 9/11 happened and he got a call from his son – and his son said –"The twin towers, they were just attacked and they are falling down or something..." Russo was in Tahiti and had just woken up from sleep. Russo didn't realise what it was immediately (11 months after Rockefeller had told him about 9/11 and it had happened –because Rockefeller said there was going to be an event –he wasn't specific) –but after Russo saw that America was going to go to Iraq and Afghanistan, that is when he realised, and equated it to what Rockefeller had said.
- 9/11 was only a manifestation to create a fear in the American public. So that we would obey and do what they want us to do. Take for example, Richard Reed 'The shoe bomber' –now here is a guy who is 6 feet 6, ugly as can be; I heard he smelled... He sits on a plane, lights a match in a non-smoking area, to put his shoe on fire... surrounded by people... That is idiotic! If you were going to blow up a plane... you would go into the bathroom... you close the door... and you put your shoe on fire...

you are not going to sit there.... surrounded by people, lighting matches in a no smoking flight... they (elite) want you to believe this nonsense. That is ridiculous!

- The war on terrorism is to keep people in fear. It is an endless war without a real enemy ('terrorists') –so that people would submit and do whatever the government wants them to. Submit to searches, give you ID cards, put Radio Frequency Identification (RFID) chips in you etc. You become servants to the elite –that is what this is all about...
- Freedom of liberty is what people really want, and it is time to stop the duplicity of the government from lying to us. You see many people know the truth of what is happening in this country; like 9/11 but they are afraid to stand up. People have to stand up and find their courage and say "I'm not going to take this anymore, I know the truth" –and they create a situation where if you tell the truth, you are considered a lunatic.
- In other words if someone goes on a T.V. show and says that 9/11 was an inside job – immediately the person is labelled an idiot or crazy. They call you names. **You cannot be afraid of that.**
- If you do not fight the corruption and you do not stand up for what is right in life, you end up being a serf and a slave and you are leaving your children a world in which you would not want to live in yourself, so how can you in decency behave that way? You have to stand up for what is right in life, and unless you do that you are nothing.

The New World Order Agenda

- The whole agenda is to create a one world government where everyone has an RFID chip implanted in them. All the money is to be in those chips [a cashless world]. This information came straight from Nick Rockefeller himself. That is what the ultimate plans of the global elite, banking industry and Rockefeller wants to accomplish.
- The agenda is to implant everyone with RFID microchips. All money is transferred to those microchips. There is no more cash. Money would be in microchips. Instead of having cash, you would have money in your microchips, but whenever they want, they (elite) could take whatever amount out of your microchip whenever they want to. Total control. If you are a protestor they just turn off your chip; you cannot buy food; you cannot do anything; it is total control of the people.
- So they want a one world government controlled by them. Everyone being chipped, all the money in those chips, and they control the chips and they control people, and you become a slave. You become a serf to these people –that is their goal. That is their goal; that is their intentions.
- Russo did not believe in enslaving people and Rockefeller would question him in the following manner: "Why do you care about them? Why do you care about those people? What difference does it make to you [Aaron]? Take care of your own life.
  Do the best you can for you and your family. What do the rest of the people mean to you? They don't mean anything to you. They are just serfs. They are just people..."

- Rockefeller asked –"Why are you fighting for the people for, what is it all about? The people have to be ruled. The constitution, what you are standing for is only for a few people, it's only for a few individuals who can live that way and we believe that it is best for society to be ruled by an elite people who control everything." Russo told Rockefeller he does not believe that. Russo believes: "God put me on this earth to be best person I could be and put everyone on this earth to be the best they can be, and NOT to be a slave and a sheep to YOU and these people (elite) –and I do not understand why you want to control everything. What is the need for that?"
- It was just a lack of caring [from Rockefeller's part], and that is just not who Russo was. It was just sort of like cold you know, and Russo used to say to Rockefeller, "What is the point, of all this? You have all the money in the world you need; you have all the power you need, what is the point? What is the end goal? Rockefeller said "The end goal is to get everyone chipped. To control the whole society. To have the elite people [the bankers and government] controlling the world."

Women's Liberation from the Perspective of the Elite

- Women's' Liberation was founded by the Rockefellers.
- Rockefeller asked Russo: "What do you think women's liberation was about?" At the time Russo had a pretty conventional thinking about it and he said "It's about women having the right to work; get equal pay with men; just like they won the right to vote." At this point Rockefeller started to laugh and he said to Russo "You're an idiot"
- Rockefeller said –"Let me tell you what that was about. We the Rockefellers funded women's' liberation. We are the ones who got it all over the newspapers and television. The Rockefeller foundation –and you want to know why? There were two primary reasons:"
- 1) "We couldn't tax half the population before Women's Liberation and the second reason was"
- 2) "Now we get the kids at an early age [because both parents are away from home working] –we can indoctrinate the kids how to think, so it breaks up their family –the kids start looking at the state as the family, as the school as the officials as their family, not as their parents teaching them, and so those are the two primary reasons for women's liberation."
- Russo thought, up to that point, Women's Liberation was a noble thing; however when he saw the Rockefellers' intentions behind it, where they were coming from when they created Women's Liberation; the thought process of it; Russo saw the evil behind what he thought was a noble venture.

America is a Republic

- America is a constitution republic / it is supposed to be a constitution republic –and **NOT** a democracy. The majority should not rule, and nor should the majority take over the inalienable rights of the minority.

- Americans pledge allegiance to the "Flag and the **Republic** which it stands" –and **NOT** democracy.
- Democracy is the worst form of government you can have because it is majority rule. Therefore the government can tell you what to do because 'the majority' wants it. It is irrelevant what the majority wants. Decisions should not take away the inalienable rights of an individual.
- Russo also said "It doesn't matter who you vote for, republican or democrat; –they are the same –neither one of them is stopping the Federal Reserve or paying income taxes.
- The elite (Federal Reserve) have taken over the American government; there is no difference between republicans and democrats. There is no difference between the two parties. The duality is manufactured. They (Federal Reserve; central banks) control both parties. It doesn't matter to the elite which one wins, because whoever is running for President will be someone they anoint. Whoever runs for President, will do whatever the elite want them to do. The fact of the matter happens to be that you cannot win an election unless you have enough money to win; they (Federal Reserve; central banks) make sure who gets the money.

Depopulation

- Russo and Rockefeller discussed many things –and one of the things Rockefeller brought up in conversation was reducing the world population. Rockefeller felt that there are too many people in the world. In a way Russo agreed that there are too many people in the world, but he **does not** think he has the authority to say who dies and who lives; but the elite felt that they want to reduce world population and Rockefeller felt it should be reduced by half.
- Rockefeller even mentioned to Russo in conversation, that they were having a real problem trying to solve the Israel/Palestine problem –and they were playing with the idea of bringing Israel to Arizona –and taking everybody from Israel and giving everybody a million dollars, and setting up Israel in the state of Arizona –because that is a problem that they are not in charge of.

Borrowing Money from Private Banks causes Inflation and Debt

- These people (elite) control the money so they make all the rules, and therefore they put the rules in which they want into effect, and the truth is America has really become a socialist communistic country. Everyone says it is a capitalistic country, but how can it be a capitalistic country when you have a central bank? That is the first question people should ask. It can't be. It is a planned economy, it is a phony!
- If they want to create prosperity, they just print dollars, or put digits into the economy. Now you have prosperity. You do not have real prosperity, you do not have real manufacturing, you just have money being injected in which is infusion of credit. This makes the government go into more debt.

- Whoever makes the money makes the rules. Rothschild said that. Why are we allowing these private bankers to make the money for our country? It is nonsense. Why are we paying interest to these banks to make money for us when the government can do it itself without paying interest, without all that debt? There is no answer to that question and it is a question no politician will raise. Everybody talks about America's debt... We are in debt because we borrow money... but we don't HAVE to borrow money. They designed it so that we can go into debt. We can create the money, and back it by gold so that they cannot create too many of it, so that you do not have the inflation, and do what the Founding Fathers told us.
- Why in the world does the American government borrow money from the banks when they have the ability to create it themselves without borrowing it, and paying interest on it? Why? Nobody can answer that question –not one politician ever raises that. Why does the American government ever borrow money, when they can create it without paying interest?

  –And people say that –well if the American government creates it, it will cause inflation. And that is their answer. And Russo says well let's look at it: the American government has the Federal Reserve do it, which creates the same inflation as if they did it, but also with the inflation –now you are getting massive debt –so with the Federal Reserve you have inflation and debt. Now if the American government made the money, backed by gold which would limit the amount they could make –you wouldn't have debt and you wouldn't have inflation.
- It wasn't until 1913 when the Federal Reserve came in, that America had inflation. Before then there was no inflation for 100 years. There were points and spikes, mostly during the Civil War –but basically there was no inflation other than during that short period of time. I mean a loaf of bread would cost the same thing. People could plan their lives.
- Today, they have planned inflation, and now you have two parents working, they cannot afford to take and pay for their family anymore; the kids are going to state run schools now, the kids are being indoctrinated how to think; they are being given Ritalin, they are being given all these drugs, the whole country is being dumb down, it is all because of the Federal Reserve System; and the Federal Reserve system and these bankers are responsible for the demise of America. And if we ever want to win this battle you must shut down the Federal Reserve System, and we must shut down these bankers and restore sound money to this country.
- If you analyse the situation and if you realise that since the Federal Reserve has come into being since 1913, illegally, without a constitutional amendment, by bribing a few senators during Christmas vacation, they turned over the most important power that the American government has, the creation and issuance of money to a private bank.
- Through that private bank issuing money they have destroyed this country. They have destroyed the purchasing power of money in this country; they have created social programs that are destroying this country.
- The Federal Reserve has created massive inflation in America which means the American worker has to keep on making more money to keep up with the cost of

living. The more money they make to keep up with the cost of living, the less competitive they become in the world economy. So now what happens is that we have to pay our workers so much to keep up with the cost of living; and then they (elite; government; corporations etc.) say screw the American worker; let's go overseas now to get the cheap labour.

- The inflation the Federal Reserve has created has now allowed other countries to outcompete us. Other countries do not have to pay as much money as we have to pay to our workers to survive. So now we are not competitive anymore and we have lost our manufacturing base. We have lost our competitive edge.
- "Freedom to Fascism" is a documentary that everybody should see. Russo and his team show the fraud of the income tax; they show how Judges put people into jail for no reason; they show the corruption of the justice system. They show how the Federal Reserve came into being and how it is controlling society and how all the central banks are working together through the bank of International Settlements, in Switzerland which is the central bank for all central banks and how all are working together to create this one world government; this one world order; which is what they are trying to do.

The Deception of the Council of Foreign Relations (CFR)

- Russo was interested in joining the Council of Foreign Relations, but he found out from Rockefeller himself, that part of the end goal of the CFR is to get everyone RFID chipped. To control the whole society and have the elite people (bankers, government etc.) controlling the world. Russo asked Rockefeller "Do all the people in the CFR believe the way that you do?" Rockefeller said "No, no, no. Most of them believe they are doing the right thing. A lot of them believe it is better off being socialistic. We have to convince people that socialism is really capitalism." Because America is becoming a socialistic country; it is a communist country today.
- Russo's friendship with Rockefeller became one where they would share thoughts, ideas and philosophies and Rockefeller wanted Russo to become a part of what they were doing [enslavement agenda], and for Russo to become a member of the CFR; Rockefeller offered various business opportunities for Russo to get involved in the CFR and to **not** take up the fight or the battle that Russo had been taking up in the past. Rockefeller wanted Russo to drop the idea of helping the people; because "What was the point in Russo fighting for the people?" Rockefeller would question.
- Russo asked Rockefeller do all the people of the Council of Foreign Relations feel the same way you feel? Rockefeller said "A lot of them think they are doing the right thing, they think that socialism is the best way to go (but this form of socialism involves redistributing the wealth for the elites and not to everyone), they think that they are doing the right thing." But the people at the (very) top they all know the truth of what is happening. (Therefore, the good people in the CFR are also under an illusion, and do not know that effectively they are working for evil men who have the overall goal to control the populace of the world).

- So it is compartmentalised within the elite structure as well. All the people in the CFR -2000 to 3000 people like Dan Raddler –they don't know what is going on--- they join the CFR because it is prestigious. They think it is good for business, it is good for this; they don't know what is really happening –the evil that comes out of it –that is emanating out of it.
- In terms of the CFR, in terms of compartmentalisation, there are many good people which Russo believes are part of these organisations who do not even understand what these organisations are really about. For example, when Russo was in Germany, doing cancer treatment, there was a gentleman there who was visiting a friend of his with cancer. The gentleman visiting his friend was a member of the CFR, and him and Russo were talking and Russo showed him the movie (*Freedom to Fascism* (2006)); --and he said, "Oh my god! I'm going to resign." "I had no idea this is what the CFR is about". He had no idea; he is just a nice guy, who thought he was joining a prestigious organisation.
- A lot of people join the CFR because they think it is a prestigious organisation; it will help them in business; make good business contacts etc. They do not have an understanding that the CFR is really about world domination. How they, and the Trilateral Commission, The Bilderberger [Group], the banks, all work together to control the people –a lot of them do not understand that. They do not see the big picture. They think: Oh the CFR is a prestigious organisation. I'll make this, I'll make that, and I can do business deals. It is just business to them. The CFR wants to get the people in there that have influence and power, and so they are part of that (enslavement agenda), and so they are not opposed to them. So the whole country is becoming the haves and the have not. You are getting the very, very wealthy and the middle class being destroyed and you are getting the poor people.
- In Russo's words: "You can call the CFR what you like, but it is a criminal organisation. Run by criminals. But people do not think of it as a criminal organisation, because it has 'class'; 'style'; 'prestige'; –and it is 'respected'; so people do not look at it as being a criminal organisation. That is what a great job they have done."

Combining America, Mexico and Canada into one Country

- Imagine this... here you are in America, and they (elite) are combining American, Canada and Mexico into one country. The North American union. And the American people do not know anything about it. It is not even in the press. They would rather talk about Rosy O'Donnell and Donald Trump calling each other names than discussing the fact that we are merging into one country. This isn't even reported.
- The fact of the matter happens to be, that tells you how controlled the media is. The elite control the media, and they control governments and they are all in bed together. Here you are combining American, Canada and Mexico into one country, and you do not see it in the press. You do not see it in the press. Why? This should be one of the top stories everywhere –and the elite are not worried about it. That tells you –there is the evidence that [media] it is controlled. They do not want the American people to

know what is going on, that is why they do not protect our borders. That is why we are losing our constitution, the very document that secures our freedoms.

Russo's Vision on How to Bring These People Down

- There is no question we are in tyranny, there is no question that the American citizen is no longer a free individual human being, to do the things that they wish to do. We're slaves and it is getting worse.
- We are dealing with complete evil; and until the American people wake up and say, we do not want this evil in our country anymore and we want to come back to a country of decency and goodness, integrity and honour, we are going down that road and that is what it is going to take? It is going to take people to stand up and say we do not want to live in this kind of world anymore. I believe we should pull all of our troops out of Iraq, I believe we should leave other countries alone. Let other countries live their lives the way they choose to. Stop trying to spread 'democracy' around the world, which is the worst form of government there is anyway (because 51 percent rule over 49%), restore our republic to what it is supposed to be and go back to what the founding fathers gave us. Restore the republic.
- In Russo's opinion: The populace must shut down the Federal Reserve System –and there has to be an uprising. There has to be an uprising. People have to stand up. One person cannot do it alone. You cannot do it alone. People do not seem to have the courage to do what they have to do.
- A lot of people in Hollywood know the truth, they do not want to stand up and speak about it; I know many of them have seen my movie (*Freedom to Fascism* (2006)) and they know I am right, and they want to talk about it because everybody is afraid. Everybody is afraid because they think that the money they get from the Federal Reserve is really money and they have a comfortable lifestyle and they are afraid of change. They are afraid to stand up for what is right, and until people are willing to stand up and have the courage to do what they need to do, it is not going to change; and hopefully we can affect change when people stand up and say "Hey, I've had enough".
- We (the populace) have one advantage. They (elite) need us to cooperate. See, if we do not cooperate with them, they cannot win. They always need our cooperation with them to go along with their programs. They try to "sell us". Democracy; this majority says this; believe in this; do this, do that; the war on terror; we have to be scared... They are always trying to do things to "sell to us" to go along with them, and once we learn not to cooperate with them; then we win the game.
- That is the point, do not cooperate with them, and do not go along with the program anymore. Stop it. Join forces, and bring freedom back to this country. It is going to take people who believe in freedom; The Constitution and the Founding Fathers, Thomas Jefferson, to make this country whole again, because right now it is in the grip of the evil ones, and the only way to stop that is for good men to stand up.

- We have to stop being scared. We have to do what is necessary to take back what is ours. We have to stop these bankers, these elite, full of liars, congressmen full of liars. They are destroying our borders.
- So through these bankers, attempting to take over America, knowing that America was the freest nation on this earth, it was necessary for them to takeover America, take away gun rights, freedom to bear arms, and create a country where we become slaves, because once they take over America, the rest of the world becomes a lot easier for them. And so by creating 9/11, an event to terrify the American people that we are being 'attacked by terrorist', you create a world where there is an enemy that can **never** be pinpointed. You can never win the battle. It is 100 year war – a never ending war on terrorism. So you are always fighting this war, and through the war on terrorism, through 9/11 which is the first lie, then you create the war on terrorism which is the next lie, then you create the war in Iraq through weapons of mass destruction, which is the next lie –so you get one lie, to the next lie, to the next lie, -- now it is going to be Iran the next lie –and sending more troops and insurgents into Iraq.
- Restore America's Republic back to what it is supposed to be. Get the bankers out of our government. Get government to stop borrowing money from the banks. Government should make its own money; restore the Republic. Restore individual freedoms. That is what this country is about -and until we do that we are going to be slaves.
- You have to take away the creation of money away from the private bankers and you will solve 95% of your problems.
- Americans, mobilise, stand tall, stand together, tell the government you are "Mad as hell!" Do not cooperate with the government do not accept a National ID card. Do everything in your power to restore freedom and your individuality back to America. Stop being a country run by the institutions for the institutions. Let's go back to "We the people, by the people for the people", as opposed to, we the institutions, by the institution, for the institution. Stand up for your individual rights. Stand up for the God leaders that are in each and every one of us!

The Trans-humanist / Post Human Agenda

Transhumanism is a cultural and intellectual movement that believes we can, and should, improve the human condition through the use of advanced technologies. One of the core concepts in transhumanist thinking is life extension: through genetic engineering, nanotech, cloning, and other emerging technologies, eternal life may soon be possible. Likewise, transhumanists are interested in the ever-increasing number of technologies that can boost our physical, intellectual, and psychological capabilities beyond what humans are naturally capable of (thus the term *trans*human) (Anthony 2013). Transcranial direct current stimulation (tDCS), for example, which speeds up reaction times and learning speed by running a very weak electric current through your brain, (Anthony 2012) has already been used by the US military to train snipers. On the more extreme side, transhumanism deals with the concepts of mind uploading (to a computer), and what happens when we finally craft a

computer with greater-than-human intelligence (the technological singularity) (See: "How to create a mind, or die trying", Hewitt 2012) (Anthony 2013).

Moreover, put simply, "posthumanism" can be defined as that condition in which humans and intelligent technology are becoming increasingly intertwined (TheNanoAge 2015). For readers interested in learning more about the posthuman / transhuman agenda see BT Soul Catcher 2025 (BEAMS 2007); Avatar Project 2045 (2045 Initiative 2015; Borghino 2012) and Mind Clone Robot (Bloomberg Business 2015; RT 2015) which have all been disclosed as methods of transferring the human consciousness to a computer.

The Phases of Sleep and Rapid Eye Movement (R.E.M) Sleep

Sleepers pass through five stages of sleep: 1, 2, 3, 4, and REM (rapid eye movement) sleep. These stages progress cyclically from stage 1 through REM then begin again with stage 1. A complete sleep cycle takes an average 90 to 110 minutes (Sleepdex 2015). In other words, after falling asleep, it takes approximately 90-110 minutes to enter REM sleep.

<table>
<tr><td colspan="5">Stages</td></tr>
<tr><td>Waking</td><td>REM Sleep</td><td colspan="3">NREM Sleep</td></tr>
<tr><td rowspan="2">Stage 0</td><td rowspan="2">Stage R</td><td colspan="2">Light Sleep</td><td colspan="2">Deep Sleep</td></tr>
<tr><td>Stage 1</td><td>Stage 2</td><td>Stage 3</td><td>Stage 4</td></tr>
<tr><td>Eyes open, responsive to external stimuli, can hold intelligible conversation</td><td>Brain waves similar to waking. Most vivid dreams happen in this stage. Body does not move.</td><td>Transition between waking and sleep. If awakened, person will claim was never asleep.</td><td>Main body of light sleep. Memory consolidation. Synaptic pruning.</td><td>Slow waves on EEG readings.</td><td>Slow waves on EEG readings.</td></tr>
<tr><td>16 to 18 hours per day</td><td>90 to 120 min/night</td><td colspan="3">4 to 7 hours per night</td></tr>
</table>

Image 1: Stages of sleep. Source: Sleepdex: (2015)

Any sufficiently advanced technology is indistinguishable from magic.
Arthur C. Clarke

REM Sleep

Most dreaming occurs during Stage Five, known as REM. REM sleep is characterized by eye movement, increased respiration rate, and increased brain activity. REM sleep is also referred to as paradoxical sleep because, while the brain and other body systems become more active, your muscles become more relaxed, or paralyzed. Dreaming occurs because of increased brain activity, but voluntary muscles become paralyzed. Voluntary muscles are those that you need to move by choice, for example, your arms and legs. Involuntary muscles are those that include your heart and gut. They move on their own (Sleepdex 2015; Walcutt 2013).

Rapid eye movement, or REM sleep, is when you typically dream. You may have images float by in earlier stages, particularly when you are going through Alpha or Theta (brain waves), but the actual dream state occurs in REM (Walcutt 2013).

This period of paralyzation is a built-in protective measure to keep you from harming yourself. When you are paralyzed, you can't leap out of bed and run. Do you ever feel like you can't escape during a dream? Well, the truth is, you can't. You can breathe, and your heart is working, but you really can't move (Walcutt 2013).

The reader is also advised to see the Horizon documentary "Why Do We Dream?" (BBC Horizon 2009). This video is available, on YouTube, and details sleep, the phases of sleep, REM sleep, the period of paralysation and more.

Current Advances in Technology

This is a section some readers may have difficulty with, because reading about these current technologies alone, one cannot help but feel that such technologies described below sound like the stuff of science fiction and fantasy -although they have been corroborated through public drip-feed disclosure (explained below). Nevertheless, I urge the reader to keep in mind Arthur C. Clarke's quote (above), as well as Phil Schneider's testimony regarding the advancements of military technology in comparison to the general public's technology (for every 12 months, military technology outstrips the technology the public is accustomed to by a rate of 44 years). Moreover, for the reader who finds difficulty understanding the technologies described below, seek the supporting articles / videos.

Memory Suppression Technologies

Memory suppression technologies are any scientifically advanced technologies which are used to suppress memory. Examples of how memories can be suppressed can be found by reading Winter's (2014) article which details how memories can be suppressed using light; and Greenberg's (2013) article which discusses memory suppression through gene / chemical modification.

Mind-Voice Technology

Mind-voice technology is an advanced technology which is capable of reading, listening, hearing or broadcasting your inner voice / thoughts. Examples of articles which discuss mind-voice technology are: Prigg (2014) details software which can read the inner voice; and New Scientist (2014) which also discusses a brain decoder which can eavesdrop on one's inner voice.

H.A.A.R.P. Technology

The High Frequency Active Auroral Research Program (HAARP) is a radio transmitting system that can bounce signals off the ionosphere (a region of the Earth's upper atmosphere 60km (37 miles) to 1000km (620 miles) altitude) and back to earth to probe deep into the earth or sea, its proponents say. The system could locate minerals or communicate with submarines. (Begich & Manning 1997; Sheen, Begich & Robbins 2005).

HAARP can also:

- Disrupt human mental processes.
- Knock out all global communications systems.
- Manipulate global weather.
- Change weather patterns over large areas.
- Interfere with wildlife migration patterns.
- Hurt ecosystems.
- Negatively affect your health, moods, and mental states.
- Unnaturally impact the Earth's upper atmosphere.

This illustration (below) shows the ionosphere's relationship to the Earth. The illustration appeared in the HAARP Environmental Impact Statement on page 10-125 of Volume II.

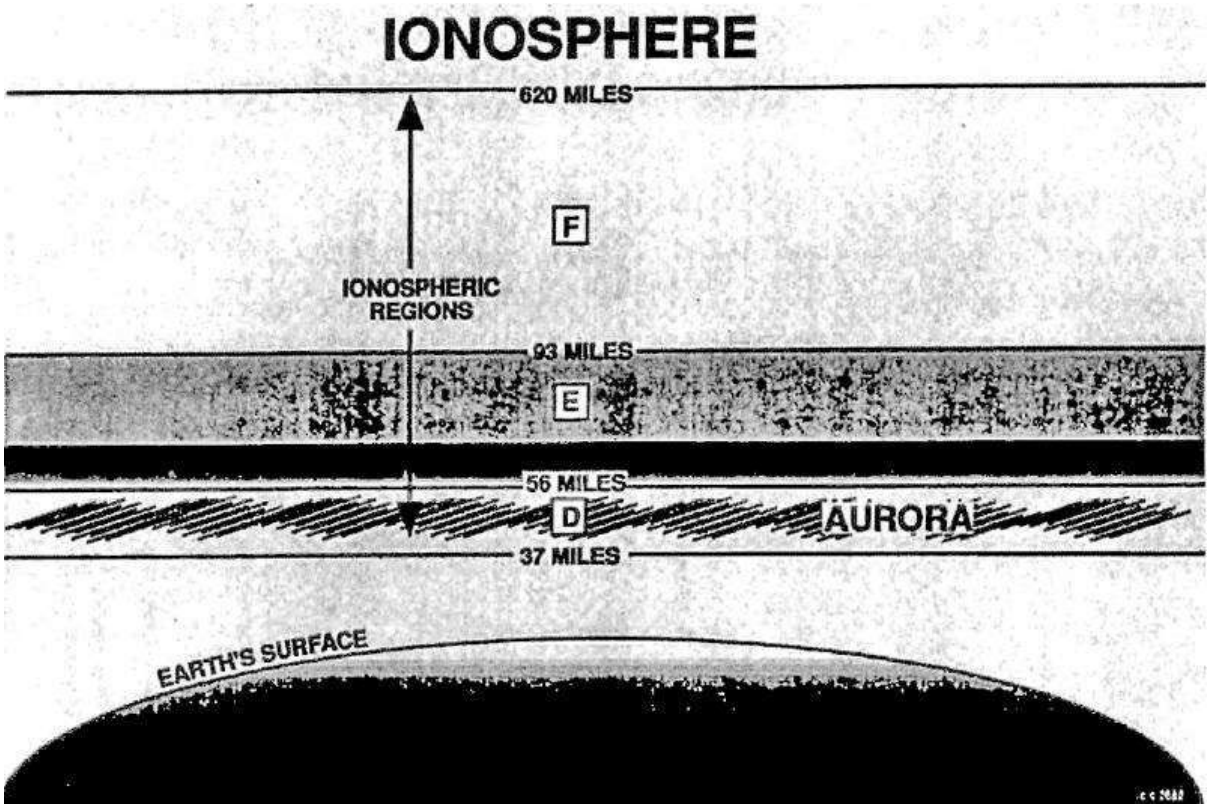

Image 2: The ionosphere's relationship to earth. Source: (Begich & Manning 1997)

The ionosphere protects the earth. HAARP (High frequency Active Auroral Research Program) is made to beam more than 1.7 gigawatts (billion watts) of radiated power into the ionosphere -the electrically charged layer above Earth‘s atmosphere. Put simply, the apparatus is a reversal of a radio telescope - just transmitting instead of receiving. It will boil the upper atmosphere. After disturbing the ionosphere, the radiations will bounce back onto the earth in the form of long waves which penetrate our bodies, the ground, and the oceans.

HAARP represents a technology which could lead to a new class of weapons that could change our world profoundly - an all-purpose military tool. If misused, the tool could mess up the weather. It could be used against humanity in a way that would change what people think, believe and feel. It could be used for good or evil, just as a harp can produce the music of Mozart or the melody of a death march.

H.A.A.R.P. and Weather Control

- “The theoretical implication [of Dr. Robert Helliwell and John Katsufrakis of Stanford University in 1974] suggested by their work is that global weather control can be attained by the injection of relatively small 'signals' into the Van Allen belts (radiation belts around Earth) - something like a super-transistor effect” said Frederic Jueneman.
- Yes. The weather can be controlled using HAARP technology.

- A series of weather disasters began in 1960, according to a CIA report mentioned in the editorial, but at the time climatologists couldn‘t look ahead and see that droughts, floods and abnormal temperatures would continue beyond that decade. As if natural disasters weren‘t bad enough, the CIA reported that national governments were already able to manipulate weather for military purposes [using HAARP technology].

As far back as 1958, the chief White House advisor on weather modification, Captain Howard T. Orville, said the U.S. Department of Defence (DoD) was studying ways to manipulate the charges of the earth and sky and so affect the weather by using an electronic beam to ionize or deionize the atmosphere over a given area. In 1966, Professor Gordon J. F. MacDonald, associate director of the Institute of Geophysics and Planetary Physics at the University of California, Los Angeles, was a member of the President‘s Science Advisory Committee, and later a member of the President's Council on Environmental Quality.

Gordon J. F. MacDonald published papers on the use of environmental control technologies for military purposes. MacDonald made a revealing comment: ―The key to geophysical warfare is the identification of environmental instabilities to which the addition of a small amount of energy would release vastly greater amounts of energy. MacDonald had a number of ideas for using the environment as a weapon system and he contributed to what was, at the time, the dream of a futurist. When he wrote his chapter, ―"How to Wreck the Environment" for the book "Unless Peace Comes" he was not kidding around.

In the text MacDonald describes the use of weather manipulation, climate modification, polar ice cap melting or destabilization, ozone depletion techniques, earthquake engineering, ocean wave control and brain wave manipulation utilizing the planet‘s energy fields. He also said that these types of weapons would be developed and, when used, would be virtually undetectable by their victims. He was not some wire haired fanatic when he made these observations in 1966 -he had the credentials of a world recognized scientist. What his futuristic concepts became, are the things which projects like HAARP are made of...

H.A.A.R.P. and Mind Control

- Radio frequency radiation, acting as a carrier for extremely low frequencies (ELF), can be used to wirelessly entrain (adjust) brain waves.
- We are talking about very, very low power requirements. The trick for influencing brain activity is in the combination of frequency, power level and wave form.
- As Dr. Patrick Flanagan, one of America’s most gifted inventors noted in an interview, the HAARP project could be not only the biggest ionospheric heater in the world, but also the biggest brain-entrainment (brain adjustment) device ever conceived.
- According to HAARP records, when the device is built to full power it can send very low frequency (VLF) and extremely low frequency (ELF) waves using many wave forms at energy levels sufficient to affect the mental states of entire regional populations.

- The HAARP transmitting system could be used unintentionally or intentionally to alter mental functions.
- If HAARP is tuned to the right frequency, using just the right wave forms, mental disruption throughout a region could occur intentionally or as a side effect of the radio frequency transmissions [in other words: "mind control"].

RFID Technology

Radio Frequency Identification (RFID) microchips are microchips that can be directly imbedded into human flesh. This section discusses the dangers of RFID chips. See Rense (2001) for full review.

- RFID technology links the brains of people via implanted microchips to satellites controlled by ground-based super-computers.
- Today they are small enough to be inserted into the neck or back, and also intravenously (through a vein) in different parts of the body during surgical operations, with or without the consent of the subject. It is now almost impossible to detect or remove them.
- Implanted human beings can be followed anywhere.
- Today's microchips operate by means of low-frequency radio waves that target them. With the help of satellites, the implanted person can be tracked anywhere on the globe.

RFID Technology and the Medical Profession

- One reason the dangers of implantable microchip technology has remained a state secret is the widespread prestige of the psychiatric DIAGNOSTIC STATISTICAL MANUAL IV produced by the U.S. American Psychiatric Association (APA), and printed in 18 languages. Psychiatrists working for U.S. intelligence agencies no doubt participated in writing and revising this manual. This psychiatric "bible" covers up the secret development of Mind Control technologies by labelling some of their effects as symptoms of paranoid schizophrenia.
- The Psychiatric Diagnostic Statistical Manual (DSM) for mental disorders has been a brilliant cover up operation in 18 languages to hide the atrocities of military and intelligence agencies' actions towards their targets. THE MANUAL LISTS ALL MIND CONTROL ACTIONS AS SIGNS OF PARANOID SCHIZOPHRENIA.
- If a target is under surveillance with modern technology via TV, radio, telephone, loudspeakers, lasers, microwaves, poisoned with mind altering drugs via air-ducts, giving familiar smells which cause headache, nausea and so forth, if s/he claims her/his clothes are poisoned, her/his food or tap water as well --- all medical schools teach their students that the person is paranoid, ESPECIALLY if s/he believes intelligence agencies are behind it all.
- Never is the medical profession told that these are routine actions all over the world by intelligence agencies against their targets. Thus, victims of mind control are falsely considered mentally ill and get no help since they are not believed and their suffering is doubled by misinformed health professionals.

Further Implications of RFID Technology

- How many people realize what the implications of implantable chips actually mean? It means total loss of privacy and total outside control of the person's physical body functions, mental, emotional and thought processes, including the implanted person's subconscious and dreams! For the rest of his / her life!
- It sounds like science fiction but it is secret military and intelligence agencies' mind control technology, which has been experimented with for over half a century (since 1950s). Totally without the knowledge of the general public and even the general academic population.
- Supercomputers in Maryland, Israel and elsewhere with a speed of over 20 BILLION bits/sec can monitor millions of people simultaneously. In fact, the whole world population can be totally controlled by these secret brain-computer interactions, however unbelievable it sounds for the uninformed.
- Neuro-electromagnetic involuntary human experimentation has been going on with the so-called "vulnerable population" for over 50 years, in the name of "science" or "national security" contrary to all human rights. It happens today in the **USA, Japan, and Europe**. With few exceptions, the mass media suppresses all information about the entire topic.
- Only increased public awareness of the microchip implants, their frightful consequences to privacy by influencing of individuals' thoughts and actions, causing people to become biological robots with physical and emotional pain whenever the supercomputer technician so wishes, is enough reason to refuse to take the microchip into your body for whatever reason.
- It is the biggest threat to humanity and the most sinister plan to enslave the human race forever.

If you have a choice and want to remain a normal human being with privacy, **DO NOT** have your children implanted **NOR** yourself implanted with RFID microchip(s) (or any other type of implantable microchip). Otherwise your vision, hearing, sensing, thoughts, dreams and subconscious will be influenced by an outsider, who does not have your best interests in mind. For the rest of your life!

Mind Control: MK Ultra Technology

MK Ultra today has evolved from the 1950s variation of mind control (MK Ultra Compendium 1980), whereby drugs such as LSD, and interrogation were used as methods to weaken the mind of the individual to force confessions through mind control. Today, mind control is achieved through the implantable microchip (mentioned above; Rense 2001).

- The brain functions of an implanted person can then be remotely monitored by supercomputers and even altered through the changing of frequencies.
- Once implanted, the U.S. National Security Agency's (NSA) 20 billion bits / second supercomputers could now "see and hear" what you are experiencing with a remote monitoring system (RMS).

- Every thought, reaction, hearing and visual observation causes a certain neurological potential, spikes, and patterns in the brain and its electromagnetic fields, which can now be decoded into thoughts, pictures and voices. MK Ultra technology is therefore capable of Mental Video and Audio Projection, as well as Artificial Telepathy.
- The mass media have not reported that an implanted person's privacy vanishes for the rest of his or her life. S/he can be manipulated in many ways. Using different frequencies, the secret controller of MK Ultra technology can even change a person's emotional life. S/he can be made aggressive or lethargic. Sexuality can be artificially influenced. Thought signals and subconscious thinking can be read, dreams affected and even induced, all without the knowledge or consent of the implanted person by using MK ultra technology.
- Memory suppression technologies are used in conjunction with MK Ultra technology, which enables the programmer to control certain memories the victim remembers. The use of memory suppression technologies and MK Ultra technology allows the programmer to reinforce behaviour and elicit specific conditioned responses.
- Mind control techniques, such as MK Ultra, can be used for political purposes. The goal of mind controllers today is to induce the targeted persons or groups to act against his/her own convictions and best interests. Zombified individuals can even be programmed using MK Ultra technology, to murder and remember nothing of their crime afterward.
- The goal of mind control, using MK Ultra technology is to program an individual to carry out any task against their will and self-preservation instinct and to control the absolute behaviour and thought patterns of the individual. The purpose of mind control, using MK Ultra technology is to disrupt memory, discredit people through unusual behaviour, to make them insane or to commit suicide or murder.

See Mind-Computer (2012) which discusses how artificial telepathy is achieved. Artificial telepathy, also known as ‘brain to brain communication’, is also possible using MK Ultra technology. Furthermore, review: Jim Cristea (2009); Berkeley News (2011); UC Berkeley Campus Life (2011) CTForecaster (2013); nature video (2013) and Stromberg (2013). The above mentioned articles and videos describe, demonstrate, and corroborate how audio and video projection of the brain is achieved; how dreams can be recorded and projected digitally; how the brain can be scanned to reveal hidden information personal to an individual; and what a person’s underlying intentions are, by using brain scans. Moreover, the articles and videos mentioned above confirm the functionalities of MK Ultra technology.

Furthermore, when our brain functions are connected to supercomputers by means of RFID technology, MK Ultra technology and other implantable microchips, it will be too late for protest. This threat can be defeated only by educating the public, using available literature on biotelemetry (electronic equipment that receives signals from radio transmitters) and information exchanged at international congresses.

Human Cloning

There are currently five different types of clones, concealed from public knowledge. There are Mark 1 clones; Mark 2 Clones; Mark 3 Clones; and Mark 4 clones and reanimated clones. Moreover, there are two types of cloning techniques: duplication cloning and replication cloning.

Mark 1 clones are REM sleep driven clones. However, the technology used for Mark 1 clones causes many side effects and therefore Mark 1 REM sleep driven clones are no longer a preferred choice.

Mark 2 clones are also REM sleep driven clones. Mark 2 clones have fewer side effects than Mark 1 clones, and therefore Mark 2 clones are currently the preferred method for REM sleep driven clones.

Mark 3 clones are independent clones which operate on microchip containing the entire consciousness of an individual.

Mark 4 clones are also independent clones, operating on a microchip which contains the entire consciousness of an individual and is an advanced version of a Mark 3 clone.

These independent clones (Mark 3 and Mark 4) have a lifespan of 6 months to 12 months and require adjustments after this period to run efficiently once more. Without these adjustments, their functionality weakens.

To "reanimate" means "to restore to life; resuscitate; revive". Consequently, reanimated clones are clones which are genetically identical to that of a person who once lived.

Replication cloning is what the public is most familiar with. Replication cloning involves giving birth to a genetic identical of an original where the newborn starts life off as a baby and matures. The newborn is referred to as a clone.

However, duplication cloning is a current concealed advanced from of cloning, and it involves taking as little as two cells from an individual, adding a constant electrical charge to the cells until a complete human being is formed.

Duplication cloning is similar to the process of regenerative medicine as demonstrated by Dr. Stephen Badylak's video "How to grow a New Fingertip" (CBS 2008; Science Channel 2014) where Badylak states: 'A whole human can be grown within 9 months.' On average it takes 5 months to grow a duplicate clone of an original by means of advanced scientific and technological regenerative procedures.

Cloning Centre and Cloning Technology

A cloning centre is a place where clones are produced. Cloning technology are the advancements in medicine, science and technology used to produce duplicate and replicate copies of originals.

Drip Feed Disclosure and Evaluative Conditioning

Drip Feed Disclosure

Drip feed disclosure is the process of supplying information but in small amounts overtime. Drip feed disclosure is also the process of revealing information slowly overtime, possibly telling lies to conceal certain aspects of the truth until the source administering the drip feed disclosure has adequate time to let out the truth in a slow and controlled way, thereby delaying the betrayed partner (in this disclosure, the public) from having the "complete truth" for some time.

Drip feed disclosure is also a method to gauge public reaction used by governments, the media, multinational corporations and organisations as well as high ranking officials to "test" whether the general public is acceptant of the concealed information or not. When the public reacts favourably to the drip feed disclosure, more information is revealed and made public, and it appears to the unsuspecting observer that the people involved in making the disclosure are taking positive steps towards a favourable goal for all. However, when the public reacts adversely; information contradicting the drip feed disclosure is presented, and an expert is presented to the public who voices the concerns of the general public, and therefore it appears that the opinions of the public have been noted and research and development will not continue in the initial stated direction. Nevertheless, the truth remains concealed and research and development continues despite the aversions of the public.

Examples of drip feed disclosure involve articles such as mind uploading / downloading (BEAMS 2007), Mind Clone Robots (Bloomberg Business 2015; RT 2015), The 2045 Avatar Project (2045 Initiative 2015; Borghino 2012). I am here to tell you that I have been a spy for over 30 years and such technological accomplishments which are posted under trans-humanism / post-humanism genre have been realised many years ago and are **available** today. They are just concealed from the public.

Furthermore, Dolly the sheep was announced as the first publicly cloned mammal (Animal Research 1996), but how many readers can say they know that, four years later, a monkey (BBC News 2000), our closest primate, was cloned? This is publicly disclosed knowledge, but I suspect not many people know of a cloned monkey four years after Dolly. This is because there was such a worldwide adverse reaction to genetic cloning when Dolly was made public, that the disclosure of the cloned Rhesus monkey (BBC News 2000) was not made public knowledge on a grand scale.

Evaluative Conditioning

Evaluative conditioning is defined as a change in liking, which occurs due to an association with a positive or negative stimulus (see De Houwer et al., 2001). Simply put, this means that our preferences for brands, products, people and other things can be influenced and even modified by the presence of something we like or dislike strongly (Hale 2012).

In many settings, a neutral stimulus, called a "conditioned stimulus", often coincides with some desirable or undesirable object, called the unconditioned stimulus. An unknown brand, for example, might appear in a commercial that also depicts a happy child. Over time, stimuli that often coincide with desirable objects are perceived more favourably, whereas stimuli that often coincide with undesirable objects are perceived less favourably--called evaluative conditioning (De Houwer, Thomas, & Bauyens, 2001; Walter, Nagengast, & Trassilli, 2005; Moss 2009). An "unconditioned response" is a response to a neutral stimulus we have no / little control over. It is a natural automatic response.

In other words, our preferences for liking or disliking brands, products etc. (the neutral stimulus) can be influenced by embedding (implicitly placing) the brand etc. (neutral stimulus) with positive or negative associations. Overtime our conditioned response becomes one of conditioned favourable or negative response towards the brand, product etc. (neutral stimulus) when we are faced with the brand, product etc. at a future date. Our preferences have been guided overtime. Evaluative conditioning can change our preferences when carried out subliminally or implicitly; it does not have to be explicit.

In media; music; movies; and other forms of popular culture and entertainment, images and symbols (of stimuli which cause undesirable consequences) are embedded subliminally and implicitly and are paired with positive associations as a form of evaluative conditioning. This causes individuals who have no preconceived judgements of the stimulus to be guided to have positive associations with a stimulus which causes undesirable consequences.

In popular culture; media; advertisements; movies; music and other forms of entertainment, evaluative conditioning is used as a method of hinting (that something is wrong); showing off of power (i.e. nothing can be done to stop the negative stimulus) and as a form of gloating (i.e. we've pulled off the negative stimulus / we are pulling it off). In over the 30 years I have been a spy, I have witnessed methods of evaluative conditioning used to hint, show off power, and gloat more often than not, and evaluative conditioning is not used just to guide social order.

The fortunate aspect is that once a person learns that his / her preferences are being guided by methods of evaluative conditioning, in order to influence the person to have positive associations with negative stimuli (or feel powerless towards the negative stimuli); and that the stimulus (brand / product) does in fact cause undesirable consequences –then the 'spell' is broken. The person can now choose how he or she responds to the brand etc. Usually, once all is known: a negative stimulus is associated with negative associations; despite it being portrayed as positive through evaluative conditioning.

Consciousness Transfer

Consciousness is defined as "the state of being aware of and responsive to one's surroundings; a person's awareness or perception of something" (Dictionary Reference 2015). Consciousness can also be described as: individual awareness of a person's unique thoughts, memories, feelings, sensations and environment (Cherry 2015).

John Locke (1632-1704) was an English philosopher, Oxford academic and medical researcher who argues that it is sameness of consciousness rather than sameness of substance that constitutes personal identity. Consequently, if the psychological life is transferred from the body of a prince to the body of a cobbler (shoe mender), Locke argues, the resulting person will be the prince and not the cobbler. He would be responsible for the prince's actions and not the cobbler's; those who were close to the prince could continue their relationships with him but those who had relationships with the cobbler could not, and so on (Schechtman 2012, p.334). Moreover, basic Lockean intuition has proved to be that "consciousness transfer" can be thought of as the feat in which the person moves from one body into another (Schechtman 2012, p.334).

Consciousness transfer can also be thought of as the process of transferring or copying the mental content (including long-term memory and "self") from a particular brain and copying it to a computational device; artificial body or avatar body such as that of a robot or clone version of the original. The computation device, robot or the clone, will then respond essentially the same way as the original brain (as suggested by Lockean theory on consciousness transfer) and therefore the computational device, robot or clone experiences having a conscious mind and essentially the behaviour of the computational device, robot or clone, can be attributed as belonging to that of the original.

It is **OF MONUMENTAL IMPORTANCE** that the reader understands the above statement regarding consciousness transfer is a method of **CURRENT** concealed advances in technology and not a concept relegated only to the genre of science fiction. At the very least the reader should be **open** to the possibility of consciousness transfer and the implications of consciousness transfer, in order to truly begin to understand the extent to which current concealed advances in technology are used to commit monstrous crimes.

I understand the above sounds unsettling, but there are also many wonderful concealed advances in technology (detailed in the disclosure section). The marvels in technological feats and human accomplishment will be released for the benefit of mankind once the world learns about the monstrous crimes which are committed against the them, and the earth, through the use of highly concealed technological advances and the good people of the world band together to put an end to the tyranny around us.

Now is also a good time to remind the reader that if military technology advances by a rate of 44 years for every 12 months which passes, then since 1945 military technology has advanced by a rate of more than 3000 years compared to the technology the public is currently accustomed to (44 times 70 = 3080). Now ask yourself honestly, in 3000 years from now (the year is 5015) don't you think humans will have been capable of developing a method which allows them to transfer their consciousness from one body to the next and more?

I am here to tell you that I have been a spy for over 30 years and that from the intelligence I have gathered over the years it has been illustrated to me countless times that consciousness transfer is indeed fact and currently exists. Consciousness transfer has been achieved since 1945, although this accomplishment in human advancement (and more) is concealed from public knowledge. Moreover, consciousness transfer is a highly advanced form of concealed technology used by high ranking members of society to commit unspeakable crimes against the public.

Furthermore, for the reader who wishes to understand how consciousness transfer is possible, see Petkova and Ehrsson (2008) and Ehrsson (2013). In the video Professor Henrik Ehrsson (2013) demonstrates:

1) Consciousness transfer from one body to the next (owning another body other than ones original)
2) Physiological evidence for owning the new body. In other words when consciousness has been transferred and the person perceives the new body as that of his or her own; when the new body is threatened as the mannequin (new body) was in the experiment, individuals still perceived the mannequin body as that of their own and became frightened (displayed biological and physiological responses).
3) Visual perception and stimulation causes us to perceive ownership of a new body.
4) The new body we inhabit must be similar to that of our own (it does not matter whether the new body is smaller or larger than our original so long as the measurements are proportional) for consciousness transfer to occur.

5) That it is possible for consciousness to be transferred to another person's body and have (or perceive) ownership of other person's body while being localised in your own body. In other words, dual consciousness is possible.

Petkova and Ehrsson's (2008) and Ehrsson's (2013) research gives one of the clearest publicly disclosed explanations of consciousness transfer and I urge the reader to watch the video in order to better understand my disclosure. One of the main findings from his research is that perception is not rigid; and perception does shape reality. Sight and synchronous (going on at the same time) stimulation can, and does alter the brains perception of reality. Sight and synchronous stimulation activates certain parts of the brain (the sensory parts of the brain and the motor (movement) parts of the brain). The match between the two (sight and stimulation) "convinces" the brain that 'hey, I'm no longer in this body; I'm in that one or that I have a third arm (although it is a false limp) etc. Accordingly, "perception is reality".

Disclosure: Save the Victims through your Diligence

I've done my best to preface this information as logically, sequentially and methodologically for the reader as possible. I have stated what the law is on 'whistle blowing'; I have given references and definitions where appropriate and I have provided many sources in order for the reader to research, corroborate, and better understand my disclosure, so that he or she becomes compelled to help me and victims like me, defeat tyranny and save the future of mankind; therefore if there are any areas of my disclosure which still appears suspect –and I understand, after all my efforts –things may still not appear clear to some readers because we are dealing with highly advanced concealed technologies which are not available in the world the general public lives in; and therefore it is difficult to fathom and furthermore conceive that men can be so evil to their fellow humans through the use of advances in science and technology. Nevertheless, I promise you, I have no reason to lie, I am victimised daily because of these technologies, and therefore my only option is to tell the truth, and nothing but the truth so that the people of the world can put an end to this grave injustice.

For the reader who still finds it difficult to accept my disclosure after first read, I want you to do two things:

1) **Give me the benefit of the doubt.** I am asking you to do this because as I stated earlier, one of the hardest things to do as a victim of abuse is to come forward about the abuse you have suffered. It is even more heartbreaking when nobody believes you. Consider all the victims of paedophiles you have heard about on the news. I cannot speak for their individual cases but I can attest to the fact it affects my mental psyche beyond comprehension; there is nothing worse than being ignored and that nobody believes you. So on that premise, please give me the benefit of the doubt, because I'm sure the majority of good human beings out there will feel worse when it is proven that I am a victim of severe abuse and you ignored me, when you could have done everything in your power to save me.

2) **Set out on a genuine quest to debunk my disclosure.** If my disclosure appears suspect to you to begin with, then set out on a genuine and investigative quest to debunk my disclosure because, if my disclosure initially appears circumspect to believe, then I should be proven false within minutes of your research of my disclosure, because even professionals make mistakes. There will be something about the disclosure which will just not 'add up'. However, when a person is telling the truth, then it is very difficult to debunk that person.
I promise you, it will be worth your time to know the real truth about the world, simply because the truth is liberating.

I would also like to remind you that the truth about the world has been hidden from the public for many decades, therefore when you do hear the truth of course it is going to sound absurd to begin with; but keep an open mind and pursue till you know what truth is; because "to "know" is to understand with certainty".

Words of Inspiration: Personalized from a Theoretical Physicist –Thomas Campbell

The following gives an introduction to many aspects which occur in this world behind closed doors or in plain sight depending on how familiar the reader is with the topics. Evidently, a lot of what is written predominantly affects the people of the world and it is time the people of the world stood up and reclaimed their world. I cannot stress this importance enough! The disclosure is also a basis which explains many of the anomalies which exist in the world today. I apologise in advance if the disclosure is too shocking to be believable (initially) and it shakes the foundations of your belief systems... but as I've said, rather than lash out at the information, you must question your own belief system... and probe into the mechanisms which have influenced you to adopt your current belief system... only then does the shock subside... and you can move forward with an open mind through investigation, which should lead you to either corroborate or debunk the disclosure. Keep in your heart: scepticism, optimism and open mindedness (Campbell 2008). Scepticism keeps you from believing fallacies. It keeps you from falling into that which you have not yet proven for yourself. Scepticism is a requirement for breakthroughs. Optimism gives you the ability to give merit to that which you have not yet proven for yourself and Open Mindedness gives you the ability to "see" that which has not yet been proven.

The Science of Hidden Consciousness

Furthermore, "Consciousness Science Kept Hidden" (YesEthan 2013) illustrates:

- "The heart is an electrical organ. It produces by far the strongest form of bio electricity in our body; up to 40-60 times stronger than the second most powerful source –which is the brain. This electrical energy travels through every single cell in our body and in a sense, binds the cells together. The bio-electricity field is strong enough that it can even be detected outside of the body; out into space; beyond the skin. It is very measurable electromagnetic energy, much like radio waves. What we found is that the heart produces an electromagnetic field that surrounds our entire body 360 degrees; and it can be detected about 3-4 feet with megatron meters outside of the body. Researchers at the medical facility in Kansas –say they have detected it 10-12 feet. So regardless of how far it goes, what is interesting is that we produce this electromagnetic field which can be detected; it can be measured, with sensitive mainstream medical equipment." -Howard Martin (co Author) "The Heart Math Solution""
- Scientific studies have shown: that the heart is not only the most powerful centre in the body, it is the most intelligent and has the ability to receive precognition (knowledge of a future event or situation, especially outside one's normal sense of perception). If we can create coherence with our heart and mind centre we can access our intuition more frequently.

When you read my disclosure, remember that it is the heart and NOT the brain which is the most powerful centre in the body; the heart is the most intelligent; it has the ability to receive precognition and intuition about a future event, **before it actually occurs**; therefore if you find that your heart is in resonance with the themes I disclose; do not fight it with the ego of the mind; when our egos get in the way it overrides our heart's intuition; your heart is capable of discerning the truth of an event before your brain becomes conscious of it; by all means listen to your heart, and allow your brain to naturally develop its intuition. It will be the coherence between your heart first, and then your mind centre which will allow you to access your intuition.

Make an effort and reach your own conclusions to the point where you feel comfort in the fact that you **KNOW** the information contained in this disclosure is indeed factual. This will be the point you will have become empowered with golden truth and compelled to fulfil your duty as a human being and also spread the truth far and wide. Yes, we are all living in very interesting times.

Disclosure: Donald Marshall's Message to the World

My name is Donald Marshall. I have been cloned by a large secretive cult know as "The Freemasons" and "The Vril Society" and "Scientologist" together called the Illuminati. For readers unfamiliar with The Illuminati see "The New World Order" (1990) by A. Ralph Epperson and Appendix C in this document; an introductory guide to the Illuminati and their agenda for the world is presented.

Furthermore, I have to tell you that human cloning has been done since 1945. Now is also a very good time to recall Phil Schneider's comment (Schneider was a Geologist and Engineer who worked on black projects and Deep Underground Military Bases (DUMBs)): "That for every 12 months which passes, military technology advances by a rate of 44 years compared to the technology the public is currently accustomed to" (Schneider 1995; 1996; Open Minds 2011). George Green (a former Financier affiliated with U.S. Presidential candidates) also attests to the fact that humans have been cloned since 1938 (Green 2008a; 2008b). Therefore if we take 1945 as a base year, then military technology or hidden technology has advanced by the rate equivalent to 3080 years than the technology the general public is currently accustomed to (2015 – 1945 = 70 years; 70 multiplied by 44 = 3080). So yes, humans have been cloned since 1945 and continue to be cloned today and that current hidden technology in the year 2015 is as much as 3000 years ahead of the technology the public is currently accustomed to. I'll repeat myself because it is **very important** the reader understands the above statement, even if, the rest of the disclosure is hard to fathom after first read. The two **most important** things to keep in mind are:
1) Humans have been cloned for over 70 years (since 1945);
2) **Present** hidden technology is more advanced -as much as 3080 years more advanced- than what the public is currently accustomed to and technology continues to advance at an incredible rate.

The Two Types of Cloning Techniques

Now there are two different types of cloning techniques, there is replication cloning and duplication cloning. Replication cloning is the type of cloning the public has generally heard of. Replication cloning involves taking the nucleus (the DNA) out of a donor egg, and replacing it with new DNA from the person to be cloned. After a few days the resulting embryo can be implanted for pregnancy. The newborn starts life off as a genetic copy of an original.

Duplication cloning, on the other hand, is the second hidden method and type of cloning where the DNA from the person is grown in a big thick tank full of (salty) water. It involves a method of regenerative technology where the cells are agitated and agitated and over the course of 5 months, a fully formed duplicate clone body of an original is developed. The Illuminati used to have to use a tissue sample from the original or the cells from women's pap smears because this contained rich cells to make duplicate clones; they also used children's foreskins which were discarded at the hospital that got removed. That is what happened to me. I had my foreskin removed at age 4 –and by age 5 the Illuminati grew duplicate clones of me. Now the Illuminati say they have upgraded the technology since 2000 and now all they need is blood from the original. They then agitate the blood cells over and over again through regenerative technology, until a fully formed duplicate clone body of an original is produced. For readers who are unfamiliar with regenerative procedures, see Dr Stephen Badylak's video on "How to grow a new fingertip" (Science Channel 2014) and Carmichael (2013) which discuses how scientists cloned a mouse from a blood sample (this is another example of drip-feed disclosure). Regenerative science and medicine (CBS 2008) does work; I've seen it many times.

The Different Grades of Clones: "Mark 1" to "Mark 4" Clones

There are a few different grades of clones that I know of. There are: "Mark 1" to "Mark 4" clones. Mark 1 clones were available at the end of World War II (1945). Mark 1 clones were rapid eye movement (REM) driven clones but they were primitive grades of cloning with lots of side effects caused to the original. Mark 1, REM driven clones were called "Organic Robotoids", even though there are no robotic parts to the clone at all. See Dr Peter Beter's discussion on "Organic Robotoids" (Beter 2011).

Donald Marshall's Dilemma with "Mark 2" Sleep Driven REM Clones

The problem I am having is with Mark 2 REM driven clones. "Mark 2" is a rapid eye movement (REM) driven clone. In other words, Mark 2 clones are sleep driven clones. REM sleep is the fifth stage of sleep (Sleepdex 2015). The first REM cycle usually happens 90 minutes to 110 minutes **after** we fall asleep (Sleepdex 2015). What that means is: **currently,** this is the Illuminati's main form of communication. They do not call people on the phone; they do not meet at the Bohemian Grove anymore (they only meet there once a year for traditional purposes). Since they discovered the science of sleep driven cloning, they meet at the cloning centre **WHEN THEY GO TO SLEEP** (The cloning centre is a physical location, located 5 / 6 hours radius from the Robert Pickton Farm (Port Coquitlam, British Columbia, Canada) at a nature reserve).

Consciousness Transfer Happens When the Original Reaches REM Sleep

The Illuminati can transfer the consciousness of an original once the person reaches REM sleep if there is a duplicate clone of the original at the cloning centre, once the person goes to sleep (90 minutes to 110 minutes after falling asleep). So what happens is that the consciousness of the original is transferred to the duplicated clone body (the duplicated clone body is grown within 5 months by regenerative technology) once the original reaches REM sleep. The original's consciousness is transferred from the original's body, although the original's body is still in their bed, asleep at home; to a duplicated REM driven clone body at the cloning centre and the original 'wakes up' as a cloned version of himself / herself at the cloning centre. It is a great marvel of science and one man's greatest achievements, but it is kept hidden and used for sinister purposes which I discuss below. I must address the readers at this point who are lost at the thought of duplication cloning, and consciousness transfer.

For readers who may have difficulty understanding the process of duplication cloning, see the video which features Dr Stephen Badylak (CBS 2008; Science Channel 2014). Badylak describes and illustrates how a new fingertip can be grown within 4 weeks, by the process of regenerative technology. Duplication cloning works a similar way; involving regenerative technology whereby the cells are agitated and agitated, and over the course of 5 months a fully formed duplicate clone body of an original is grown. Moreover, readers should also view the Horizon documentary "Why Do We Dream?" (2009); the documentary clearly explains the phases of sleep; particularly REM sleep. The documentary also clearly explains that during REM phase sleep the whole body shuts down, and it is only the brain which is active. The fact that the brain is still active, although the body is inactive, is a perfect opportunity for consciousness transfer; and this is usually the moment the Illuminati transfer the consciousness of a person who is asleep, to a cloned version of himself / herself. The reader should also explore Ehrsson's (2013) lecture on consciousness transfer. In the video, Ehrsson (2013) clearly explains how through the first person visual perspective (seeing through the eyes), and through synchronous (occurring at the same time) stimulation of a body part, individuals can perceive and see the world from another body different from their original. In other words, so long as people can see through the eyes, and the body is stimulated, the match between the visual perspective and feeling body sensations allows the individual to see and perceive the world through another body different from their original. The consciousness has been transferred to another body.

Ehrsson (2013) also demonstrates that consciousness is linked. Once consciousness is transferred (from the original's body to the new body), even though the new body is not the persons original body; when the new body is attacked, because the person perceives the world through the new body, everything feels "very real". When the new body (for which the person's consciousness has been transferred to) is attacked, the original still perceives the threat as "real", and therefore the person displays a biological and physiological fear response in their original body; the heart rate increases, as does respiration (breathing) rate, as well as anxiety.

Donald Marshall is an Original as he sits at Home Typing this Disclosure

This is how advanced technology is today. This is also exactly what happens to me. **I am an original as I sit at home here typing this disclosure,** but when I enter REM sleep, my entire original body shuts down, and only my brain is active. The Illuminati have linked my consciousness to a REM driven duplicate clone body of me. Therefore, as soon as I enter REM sleep, they are alerted to the fact that I have entered stage five of the sleep cycle, and in REM sleep, because they have a green and red light above duplicate clones at the cloning centre. The red light indicates that the original is awake, and the green light lets them know that original has entered REM phase sleep and it is time to transfer their consciousness to a duplicate clone version. They cannot transfer the consciousness of an original before REM phase or when the original is awake. When they try and transfer consciousness before an original is in REM phase it makes the original have intense headaches. Setting an alarm every 90 minutes to wake up and then go back to sleep also does not work in terms of avoiding REM sleep and having your consciousness transferred, because the body requires REM sleep, and therefore you become very tired, quickly, if you do not get REM sleep. If you stay awake for four days without REM sleep you begin to hallucinate; after seven days without REM sleep you will die.

When Donald Marshall's REM Driven Cloned Experiences Began

This whole sordid episode began when I was 5 years old, after going to the doctors to get my foreskin removed, at age 4. The tissues from my discarded foreskin were used to grow multiple duplicate clones of me. Within months, I was having my consciousness transferred to a REM driven, 5 year old clone version of me every time I entered REM sleep. The reason the Illuminati did this was because they wanted to use me as what they term "a diddle kid" – in other words they wanted to have sex with an REM driven, 5 year old, duplicate clone version of me. This is what they do. They clone people. They make duplicate clone bodies of people to victimise in terrible ways, and they clone children for men with undeveloped penises to have sex with.

However, I could never remember any of these REM driven clone experiences when I woke up for 25 years; because another aspect of REM driven cloning is that the Illuminati have the advantage of being able to suppress the experiences of people who have their consciousness transferred to their REM driven duplicate clone versions through advanced memory suppression technologies. For the reader who wishes to understand how memory suppression works see Winter (2014). Memories are stored and retrieved from different parts of the brain. Interactions between the cerebral cortex (the outer layer of the brain) and hippocampus need to work together in order to bring the memories out of mental storage to be re-experienced by the mind (Winter 2014). Therefore all that has to be done is for them to turn off the nerve cells which communicate with the cerebral cortex and hippocampus for the evening which you went to sleep and had your consciousness transferred to a REM driven duplicate clone version of you, and you will not remember anything. The technology is so advanced; they can, and do suppress memories at a push of a button. Therefore, the victim wakes up the next morning and will not remember a single REM driven duplicate clone experience. All that they will be aware of is that they did not have a dream the previous night.

This is what happened to me for over 25 years. I wasn't allowed to remember these REM driven duplicate clone experiences until I turned 30. My memories were suppressed for 25 years. I would wake up many days, after a night's sleep, thinking 'I didn't have a dream last night'; or I would wake up the next morning and I would be sick, although I went to sleep the previous night feeling completely healthy. Throughout the years, I thought I had terminal illness; because whenever I went to see a doctor, the diagnosis would always come back that 'there was nothing wrong with me'.

However, over the course of 25 years when I was memory suppressed, and not allowed to remember my REM sleep driven clone experiences, the Illuminati were using me to produce songs, lots and lots of songs, and whenever I could not produce a song, or did not want to, they would stab my REM driven clone body; sodomize my REM driven clone body; chain me to a crucifix and burn my REM driven clone and torture me for all kinds different reasons; and even when I was compliant and did what they told me to, I was attacked, simply because some members of the Illuminati wanted to know what it feels like to stab someone. Now because consciousness is linked (Ehrsson 2013), all these REM clone torture experiences affected me in my original body, and I have a weak heart today because of it, at the age of 39. The memories of my REM clone driven experiences also had to be released to me slowly (see Alford (2014) and FW: Thinking (2014) –for an example of how memories can be wiped and restored) over the course of many months because I had been through so much horror and torture that if the memories was released all at once, I would have had a heart attack in my real body and died.

This is one of the main reasons the Illuminati currently use REM sleep driven cloning (besides sex and torture): to plagiarise talented people under duress. There are many people including me who have been, and are plagiarised on a daily basis. Their consciousness is transferred to their REM driven clone alternates, and night after night and under duress they are forced to reveal their money making ideas or face torture or clone death; clone death after clone death. That is what the movie *Inception* (2010) is about: REM sleep driven cloning, and stealing ideas from the minds of unsuspecting individuals. The Illuminati actually made the film *Inception* (2010) as well as *The Island* (2005), *Avatar* (2009) and *The 6th Day* (2000); the films mentioned above contain references of cloning and REM driven cloning to show off the Illuminati's 'power' and throw in the world's face and laugh.

The Science of REM Driven Cloning Began in 1945

I am one of the few people fortunate, or unfortunate depending on how you look at it, who remembers all of my REM driven cloning experiences because these memories were released to me at the age of 30. I remember many people who have attended and still attend the cloning centre which they bring me to over the course of 34 years. I am currently 39 years old and was brought there since the age of 5. The science of REM sleep driven cloning was first discovered in 1945, and at first it was just a political thing which leaders of the world did. Through the science of REM sleep driven cloning, political figures, heads of state and royalty met each other as REM driven clones versions of their selves when they went to sleep and discussed worldly affairs in complete secret with each other. They also did whatever they wanted with each other as REM driven clones, which they could not do in their original bodies such as sex, fighting each other to the death, jumping off cliffs as their REM driven clones, and just about anything you can think of when one has the ability of pseudo-immortality as a sleep driven clone version of themselves hidden from the guise of the world and general public.

Well they soon got bored of each other very quickly, and started to make REM driven duplicate clones of movie stars, musicians, celebrities and public figures from all walks of life to hang with as REM driven clones and now they all get together for a disgusting time as REM driven clones when they go to sleep. Most of the G20 political leaders meet at the cloning centre as REM driven clones when they go to sleep to discuss worldly matters and watch gruesome things done to innocent and unsuspecting civilians, who are also REM sleep driven clones at the cloning centre, but civilians have their memories suppressed. This is what the films *Hostel* (2006); *Hostel: Part II* (2007); and *Hostel: Part III* (2011) (Illuminati made films) -are about: -rich people paying to torture and kill innocent people at a secluded location for sport; just that at the cloning centre, the Illuminati members torture and kill REM driven clones of innocent people.

Therefore, depending on what was done to your REM driven clone, you could wake up the next day with a very intense headache in your **original body**, if your REM clone was repeatedly punched in the head; an upset stomach in your **original body** if your internal organs were tortured; achy limbs; and worst of all, feel sick all over; although the previous evening you went to sleep feeling healthy. Remember consciousness is linked (Ehrsson 2013), therefore whatever happens to your REM driven clone will affect you in your original body. Even when they suppress your memory; the previous night's experiences still affects you in your original body. You wake up with the knowledge that you did not dream the previous evening when you went to sleep, and with certain illnesses depending on what was done to your REM driven clone.

Help Donald Marshall STOP REM Driven Cloning NOW!

Everything I discuss in this disclosure is firsthand witness accounts. I have seen and experienced horror spectacles done to innocent civilians and to me. For the sake of humanity and the innocent children brought to the cloning centres all over the world; I must tell the whole world about this and the good people of this world **MUST HELP ME TO BRING THIS TO A STOP.** My sense of duty, moral correctness, and conscience cannot allow me to stay silent about this evil. REM sleep driven cloning, and the torture of innocent civilians as REM driven clones; having REM driven clone sex with beautiful, innocent unsuspecting civilians of the world; the paedophilia of children through the process of REM driven cloning; REM driven sex slavery; the plagiarism of talented individuals through the process of REM driven cloning; and REM driven idea slavery, whereby talented individuals must produce new ideas and concepts daily (or whenever they sleep) or be stabbed or tortured in their sleep as REM clones –is the most vicious and pernicious form of tyranny ever to occur against humanity and **IT MUST BE STOPPED NOW!**

Do Not Panic, Riot, or Cause Chaos. This is Very Important.

Now I must preface this carefully, because members of the Illuminati have told me that I have to put this in an eloquent fashion, in a way which does not make people panic because people finding out about REM driven cloning, and the extent of the evil it has been used for, and continues to be used for; it could cause loss of social order, riots and anarchy in the streets. Moreover, I too **DO NOT** want riots and anarchy in the streets, despite the fact that I am vehemently angry considering the extent to which they plagiarised my talents over the years. If you are a good person reading this, and you want to help and you want social order restored for the benefit of mankind, promise yourself; me; all the innocent children they have affected through REM driven cloning, and the children of the future that you will **NOT** riot, and destroy a world for children who are going to inherit the world. **This is very important**. Remember the Illuminati have highly advanced technologies (kept hidden and secret), including weaponry, and they are just waiting for any excuse to use it on the populace. In all revolutions, the populace always win, and I want this disclosure and the end of REM driven sleep cloning to go smoothly. I want the good people of the world to keep spreading this information, keep spreading this disclosure all over social media, tell your close friends, your family, and as many people on social media platforms as you can. The internet, and radio shows with small audiences are the only forms of communication the Illuminati do not control. They own all forms of television networks, even including the Aboriginal People's Television Network (APTN), and therefore a message as important as this will never reach the average man or woman through television because it does not serve their agenda.

Spread this Disclosure Document until it reaches the Armed Forces

I want this message to reach the armed forces, because currently people in the armed forces are following orders, yet they do not know how corrupt their governments and people in high profile places are. They are unknowingly defending these corrupt people. People in the armed forces will **NOT** defend these corrupt people nor will they harm civilians when they realise that these corrupt people have been growing duplicate clone bodies of civilians, transferring civilians consciousness to their duplicate clone versions when the victim reaches REM sleep, and torturing civilians in their sleep; having sex with under-aged REM driven cloned children; having sex with innocent and unsuspecting adults as REM driven sleep clones, against their will; torturing REM driven clones for sport; and for money-making ideas to benefit their own pockets while they make innocent civilians sick and have side effects in their original bodies from REM sleep driven cloning technology. No. The armed forces will not accept that. Therefore keep spreading and sharing this information for everyone to see so

that it reaches personnel in the armed forces **ASAP!** I want the armed forces to overthrow these corrupt people. The Illuminati think they are very sly and untouchable because together they hold most of the wealth in the world. We must show them that they are not untouchable. Please do all you can, to share and spread this message. It is the most important message to ever reach the internet because it affects all our liberties.

I must also address the readers who may feel afraid in spreading my message because they may want to do the right thing, but they are terrified the Illuminati may degrade or end their lives. As unbelievable as the next thing I am going to share sounds, it is a belief system which shapes the reality of the Illuminati and therefore they themselves are afraid to do anything which may degrade their lives or 'eternal soul'.

They believe that they are the 'fornicators' mentioned in The Bible, and if they were to degrade or harm the lives of anyone aiding me, they would suffer the wrath of God when they die. Notice I said **when they die**, but so long as they are still alive they can do all the evil they like, with little consequence, as they do in their REM driven clone versions at the cloning centre; worshipping Lucifer and doing all sorts of ungodly things. They even say God does not exist, only science and technology; yet they are afraid of dying. Very afraid of dying; because they believe they'll meet God's judgement. I'm just relaying what they have told me. They are weird like that. They also follow Hopi Indian Prophecy, Mayan Prophecy and Nostradamus Prophecy. They mix and match those three prophecies and come up with their own religion of what may or may not happen in the future.

Donald Marshall is NOT "The New Age Saviour". Nobody wants to be a 'saviour'

Furthermore, **THEY** believe I am a new age saviour for the end times; that I was going to save the world from something, according to the Nostradamus prophecy (quatrains); the Illuminati consider Nostradamus the greatest prophet ever to walk the earth. They are in awe of him.

I **DO NOT** endorse their claims. I just want REM driven cloning to stop and these people face punishments for their crimes against humanity. I really do not endorse such claims, but if it saves my life and yours, so be it. In reality and practicality, nobody wants to be 'the saviour'; not with such tyranny and pernicious evil such as this. We'd rather all just be living normal lives without the knowledge and practice of REM driven sleep cloning which is used for torture, clone death spectacles and sex with children. My friends on Facebook do not want to be heroes or 'saviours' either; nobody really does, but we do it out of a sense of duty, moral correctness and our conscience would never rest knowing the true extent of evil in this world, and doing nothing to end it. So all that saviour and Nostradamus prophecy talk, it is just the Illuminati; they like to quote prophecies, and make them come true to make themselves feel special.

Like I said, they are weird. I'm just relaying what they say, and I **do not** endorse the new age saviour claims. I'm just a normal guy, who was unfortunate to be cloned when he had his foreskin removed at age 4. This could have happened to anyone. Thankfully I had a very active imagination at the age of 5 and with the use of the technologies such as Mind-voice technology (that is what the Illuminati call it) it allowed me to make songs to keep the perverts off me. Mind-voice technology is just a technology which can tune into the inner voice in your head (See articles by Prigg (2014) and New Scientist (2014) –which discuss how scientist can listen to your inner voice; –it is similar to how Mind-voice technology

works). Therefore, when you hear the sound of a guitar; the sound of drums; or any instrument for that matter; after hearing the sound, when you imagine the sound you heard, your REM driven clone can replicate this sound with Mind-voice technology **exactly**; and I used Mind-voice technology to make many, many songs over the years. As I've said, and I'll say it again: technology today is very advanced.

How the Nostradamus Prophecies shapes the lives of the Illuminati

Also another reason they have not killed me is because the Illuminati said "If they do, everyone is going to know I am telling the truth", -which I am with my right hand to God and I cannot lie about this stuff; the things I have seen are too sinister and diabolical. It would make me as bad as them if I did. Furthermore, because they follow the Nostradamus prophecies religiously, they have told me that they believe anyone helping me is considered part of "The Army of Light" and again, to hurt or degrade anyone helping me, considered part of The Army of Light would incur the wrath of God; and that to hurt anyone considered part of The Army of Light will degrade their lives; they will suffer misfortune and entire ruin as will their eternal soul. These are just some of the interpretations of the Nostradamus quatrains they have relayed to me. These people are beyond crazy, zealot and religious fanatics. Nevertheless, the main point to remember by all this is that **you are safe**, and **they cannot hurt you**, **they are scared to hurt you**, as well as kill me because prophecies have shaped their lives and the lives of their ancestors for hundreds of years.

Furthermore, and practically, I have told too many people that this is the extent, to which technology has developed in our current day, and it is kept secret and hidden from the public for nefarious purposes and this is what the Illuminati do: REM sleep driven cloning. I have been spreading this information **since 2011** and not one of these high profile people, government officials or celebrity figures has issued a (public) statement against me or taken me to court over libel charges because I'm telling the truth; and their statements would not hold in court.

I have also told over a million Arabs; I have appeared on radio interviews with Vinny Eastwood (Vincent Eastwood 2013); Jeanice Barcelo (Jeanice Barcelo 2013); and Lisa Phillips on the Cry Freedom Radio show (Astral 7ight 2013a – 2013h). I have reached audiences as many as 280,000 views on the Vinny Eastwood Show (Vincent Eastwood 2013) alone. However, I must stress that YouTube reduces the view count of my interviews every so often in order to suppress the truth so that my interviews do not get featured on their platform. Nevertheless, there is safety in numbers and rest assured there are new people waking up to the disclosure of REM driven sleep cloning every day; and therefore you can share and spread this information **without any worry** about facing reprisals from the Illuminati, even if you do not believe that it is in fact their beliefs in Nostradamus prophecies which is saving you and I from the Illuminati.

HIV/AIDS has been cured; so have many forms of cancer

Now is also a good time to share with the reader that this situation is not all 'doom and gloom.' In their quest to perfect technologies, science and medicine, the Illuminati discovered the cure for HIV/AIDS; cancer (except pancreatic cancer); Alzheimer's; Dementia and many more debilitating diseases which humanity suffers with. They relayed the fact that they found the cure for HIV/AIDS by stimulating the cells in an oxygenated rich environment because diseases/viruses cannot thrive in an oxygenated rich environment (in layman's terms). Magic Johnson was cured from AIDS this way and they use him as a spokesperson to sell the retrovirus pills which they know is not as effective. However, the greed these people have,

knows no bounds, and because they receive too many donations for HIV/AIDS as well as cancer donations they do not announce they have cured HIV/AIDS or cancer publicly. As I've told you, and will continue to tell you: technology is far, far, FAR advanced than what you currently see around you. With the help of the good people of earth I promise to release these technologies for the benefit of mankind, and all reading this disclosure can hold me to this. You **must** hold me to this. It is time we ended corrupt governments and corrupt individuals in high positions of power in this world. Hold me to this.

I hope you are now beginning to understand why this is a **world emergency** and why these corrupt people must be ousted and overthrown. I also hope you understand why you must not riot or cause chaos because as I said at the beginning of this disclosure "I write this to empower good people of the world against the tyranny which exists all around us in our world today"; I **did NOT** write this to cause chaos, public dissension or anarchy. Good people of the world will inherit the earth once these corrupt people are overthrown. Therefore, under no circumstance must you destroy the world when you are going to inherit it. No matter how angry this disclosure makes you; no matter how angry the diabolical people who commit these crimes against humanity make you feel. Let's make sure this goes smoothly. Keep spreading and sharing this information, until this disclosure reaches the armed forces; until the armed forces bring these corrupt people to their knees. We are about to inherit the earth; by all means let's ensure everything goes smoothly. Now that you understand how important this disclosure is and that the overthrow of these corrupt individuals must progress smoothly, I'll continue.

The Behaviour of High Profile People at the Cloning Centre

The high profile individuals who attend these REM driven clone gatherings in their sleep have nothing better to do than to show off in disgusting ways. They have no shame and it seems nothing embarrasses them. Some REM sleep driven, cloning centre attendees, sit in the stands of an unused arena, smaller than a hockey rink, but it still has the capacity to seat between approximately 300 to 400 people. There is dirt in the centre of the rink where ice would be. They have frightened REM driven clones of children walk into the middle of the dirt rink to be victimised for a bizarre and disgusting spectacle. Sometimes, they have animals like dogs have sex with the REM driven clone children, while a man holds the dogs on leash so that it wouldn't bite the child on the back of the neck; which I have seen happen before. They all try to outdo each other in their levels of depravity; to be evil is to be "cool" to them.

The Ring Leaders of the Cloning Centre

I will now discuss the ring leaders, but before I name names, please understand that I am not someone who has collated stories and evidence together over the internet. I REALLY **do not** need to do this. Every time I enter REM sleep, the ring leaders at the cloning centre transfer my consciousness to a duplicate clone version of me. I have seen and talked with these monsters over the course of 34 years as REM driven clones at the cloning centre. However, I do understand that for the average reader, without understanding how far medicine, science and technology has advanced; without seeing or hearing people, other than me, discuss the crimes the ring leaders of the cloning centres commit, it is very difficult to imagine that this is what these high profile people are involved with, and do. Nevertheless, I guarantee it; this is the true extent and prevalence of evil in our world.

Their public personas, and public images is well managed by their PR teams, and therefore for the average person it is difficult to imagine these people in any other way but "positive"; but these people behind closed doors are the most evil, sick and twisted people I have ever had the misfortune of encountering. It is also difficult to take in what I am saying because I am not a public figure, nor do I have the "influence" or public image these people have; the general populace have never met, or heard of me, or known who I am; if this was the case my eye witness testimony alone will be enough; however, I do understand that we are dealing with highly advanced technologies, thousands of years advanced compared to what the general public is accustomed to, and because of this I provide references for the reader; I provide references for the reader to have something to corroborate what I am disclosing; and I provide references for the reader to see past the illusions these people have created.

Moreover, as "Consciousness Science Kept Hidden" demonstrates (YesEthan 2013):
remember that it is the heart and not the brain which is the most powerful centre in the body, the heart is the most intelligent; it has the ability to receive precognition and intuition about a future event, **before it actually occurs**, therefore if you find that your heart is in resonance with the names mentioned; do not fight it with the ego of the mind; when our egos get in the way it overrides our heart's intuition; your heart is capable of discerning the truth of an event before your brain becomes conscious of it; by all means listen to your heart, and allow your brain to naturally develop its intuition. It will be the coherence between your heart first, and then your mind centre which will allow you to access your intuition.

The references I provide for the reader to corroborate what I am about to say includes: "Appeal from Survivors of Canadian Genocide" (inifiniLor 2013); Tila Tequila –"Missing Children and Cloning Centres" (Astral 7ight 2013i); "Royal Babylon by Heathcote Williams" (MrCowshedder 2012); and "THIS MOVIE WILL BLOW YOUR F%SNG MIND" (KafkaWinstonWorld 2014).

Watch all the above videos and you will easily see all that I disclose. In Appeal from Survivors of Canadian Genocide interview (inifiniLor 2013): Listen to the indigenous people Stee-mas and Wahtsek speak about the pain and torment they have suffered under the Crown, the Vatican, the government, and churches of Canada. 50,000 to 150,000 indigenous children have gone missing because of the involvement of the Crown, the Vatican, the government, and the churches of Canada; and all these factions involved know this!

Tila Tequila is a television personality who has attended the cloning centres as a REM driven clone since childhood. In Tila Tequila's radio phone in (Astral 7ight 2013i), the audio is not very clear for the majority of her disclosure; she was also frightened and therefore she sounds most animated; however her words are clear at the following points of the audio (I also provide a transcript in the appendices section: "Appendix A"):

4.00 min: Cloning Centres and they take your children...
4.25 min: –There are these CLONING CENTRES –I'm not even talking about child molestation here...
5.40 min –They take your children –they not only molest them; men f*** them; and make them shoot each other...
7.59 min- There is a point where you cannot just turn the other way, you know this stuff is going on and you go 'oh well, you know... that's their problem; let's just turn the other cheek. How long are you going to turn the other cheek until it happens to your own freaking children?

10.34 min - Do you know why they love children? Because they are innocent souls; they are innocent... they are the most innocent, pure beings in this planet. They are not harmed by anything. They are new to the world; bright-eyed, pure innocent children. That is why these disgusting paedophile... and these clone rings, cloning centres, satanic rituals, Brownsville Texas... there are many of the of the cloning centres where they take your children that go missing.

Royal Babylon by Heathcote Williams (MrCowshedder 2012) addresses the fact that for Brits, despite their inordinate pride about their tradition, it is often revealed they know little about it than anyone. The documentary then goes on to address the fact that Prince Phillip the Duke of Edinburgh, has a lust for blood-sports which includes shooting endangered wildlife and mammals which he considers 'culling'. The documentary is also notable for demonstrating to the viewer that Queen Elizabeth II redistributed as much as 2.1 million for her private income from 276 people from Merseyside and Lancashire. These people had no will, so their property was grabbed. The same is true for the Duchy of Cornwall. If you die without making a will, everything you possess will go to Prince Charles. Furthermore, Queen Elizabeth II is the largest land owner on earth. Queen Elizabeth II: head of state of the United Kingdom, and 31 other states and territories is the legal owner of about 6600 million acres of land; one six of the earth's non ocean surface. She is the only person on earth who owns whole countries, and who owns countries that are not her own domestic territory. This land ownership is separate from her role as head of state; is different from other monarchies where no such claim is made –Norway, Belgium, Denmark etc. The value of her land holding is £17,600,000,000,000 (17.6 trillion Pounds) (approximately)).

In "THIS MOVIE WILL BLOW YOUR F%SNG MIND" (KafkaWinstonWorld 2014), readers with a deeper knowledge of the Illuminati and the agenda of the Illuminati will easily spot the minor inaccuracies in the documentary. However, the documentary provides a good reference and foundation for anyone new to the topic of the Illuminati and their agendas for the world. The documentary demonstrates how the world is currently a deception within a deception coated in reverse psychology. It gives widespread insight into the Royal family of England, and their lineage.

Furthermore, the documentary provides information that the world's most popular religions have been infiltrated with Illuminati dogma, in secret. The documentary details how (some) modern Christians, Jews, and Muslims do not (yet) recognise their common enemy because that enemy is invisible (until now). The enemy hides within their own religions. The enemy also hides within the activist community (anti-Illuminati movements), it finances big budget documentaries and movements. The end game is to sell a divisive (creating strong disagreement), anti-capitalistic, atheistic message and deliver trusting followers right into the lap of a communist (one government) New World Order. The enemy is the Illuminati.

The documentary also details that: "Today, the bloodlines of this unholy alliance are on the final stages of establishing one world religion, one world government, and one world ruler [--that is **IF**, the good people of this world do nothing to stop them]. The Windsor Royals are at the control of this web of deceit. It is a known fact that Adam Weishaupt (the founder of the Illuminati) took refuge and got assistance from the German Saxe-Coburg Gotha Royal family. The Saxe-Coburg Gotha's changed their German name to Windsor (in 1917). The Windsor's public image is a façade, to hide the cesspool from which they operate behind the scenes; their power and control cascades out of Buckingham Palace to the elite bloodlines who run world affairs."

For anyone who thinks they know they Royal family of England, did you know that still to this day: they have a person appointed called "Groom of the Stool"? What is a "Groom of the stool", you may ask? A Groom of the stool is responsible for stools. The kind you sit on and the kind you expel. In other words a Groom of the stool wipes Royal bottoms. The above has been confirmed to me by Prince Charles of Wales himself as REM driven clones at the cloning centre, and I quote: "It gives you the feeling of being completely taken care of" when I asked Prince Charles (as a REM driven clone) why they still have that. But don't just take my word for this; research "Groom of the stool".

The Royal Family of England

As most of readers have already guessed; and as unbelievable as it may currently sound to some readers, the ring leaders of these cloning centres includes the royal family of England. As I've said REM driven cloning started as far back as 1945, and it was just a political thing, but Queen Elizabeth II has been involved with REM driven cloning since its inception! Yes! Queen Elizabeth II; Phillip, Duke of Edinburgh and Prince Charles of Wales are the worst of them. They are unbelievable depraved perverts all showing off to the celebrities who attend these REM driven clone gatherings. Elizabeth has the REM sleep driven cloned children at the cloning centre call her "Lilli-bet" and Elizabeth as a REM driven clone herself does ungodly things to these REM driven cloned children. Some she fakes being nice to; some she is terrible to; and as a REM sleep driven clone Elizabeth cuts these REM driven clone children with swords while they scream. The decent people at these cloning centres who have had their consciousness transferred into their duplicate REM driven clones, and are there against their will, like I am; they are terrified to say anything against Elizabeth and her cronies. Most of these decent people also have their children's consciousness transferred into their REM driven duplicate clones, and Elizabeth and her cronies hold these decent peoples' children as hostage; to be torn apart; clone death after clone death if they have the slightest inkling of informing anyone, but as Elizabeth and her cohort have been torturing me as REM driven sleep clones anyway, I will disclose all that they do.

Vladimir Putin is also there, as an REM driven clone, and he loves to put the fear of torture and death into people, but he is essentially a perverted coward himself. Most of the famous people who attended the cloning centre as REM driven clones are ashamed to speak or be seen by me there very much; because they are ashamed of the perverse and disgusting gatherings. I am a decent person, even when my consciousness is transferred to my REM duplicate clone alternative, and I will not participate in these depraved acts; so they use me as an example and torture me for being a good person. They have drugged my REM driven clone, and as I've mentioned because consciousness transfer is real (Ehrsson 2013) and because consciousness is linked, therefore everything feels "real as real"; when I'm drugged as a REM driven clone, I behave exactly as any person would on hard drugs (although I have never taken any drugs in my original body); my vision is blurry and my balance affected; they have used this as method of having me do disgusting things in a blurred state, videotaping these dirty acts and editing a highlight reel which also depicts me doing disgusting things to show to the world when the world learns of their depraved natures and their public personas are shattered so that I can be despised as much as they will be when the entire world learns about this. Furthermore, because of the microchip inserted in my REM driven clone; they mind controlled me like a "Manchurian Candidate" (*The Manchurian Candidate* 2004) using MK Ultra technology, which is far more advanced than the declassified MK Ultra techniques (MK Ultra Compendium 1980) mentioned online today which references MK Ultra techniques in the 1970s. See Rense (2001) for a detailed explanation of how implanted microchips work, and how these chips allow the programmer

control victims. C.S.I.S Canadian intelligence are all involved; they have REM driven clones too; including a lot of Commissionaires and Canadian Prime Minister Steven Harper himself; They do what Elizabeth says, and seem to follow her every whim without question. It doesn't matter who you are; if you have a cute child, or a talented child with imagination, creativity and moneymaking potential (such as business smarts; song making ability; literary / oratory ability etc. –you name it so long as your child has moneymaking value to them) they will send for the blood record of your child; agitate the blood cells over and over until a duplicate clone of your child is grown; they will then transfer your child's duplicate clone body from the tank they were grown onto a steel rack; the steel racks contain 5 rows and each row holds a duplicate cloned body; once your child goes to sleep in his or her original body and once they enter REM sleep (90 minutes to 110 minutes after they first fall asleep) the Illuminati are alerted to this fact by a green light above your child's duplicate clone at the cloning centre and they then transfer your child's consciousness to the REM driven duplicate clone; this is the point where the prime evils molest your children; and so your children are being molested in their sleep as REM driven clones and then they suppress the child's memory or implant false memories (see Kim (2013) and Alford (2015) –on how false memories can be implanted) so your children wake up not remembering dreams from the previous night, or if they do remember anything, the memory is false. These depraved acts very much stunt children's development; it causes them to have learning disabilities; unexplained depression; loneliness; suicidal thoughts, and all kinds of side effects.

The cloning centre is a paedophiles paradise and **it must be stopped**! Elizabeth secretly owes a few music companies too (Universal and others) with bands under contract; she forces me under a knife to compose music for them; if I can't she will stab my REM driven clone; burn my REM driven clone and have her pervert thugs smash my REM driven clone body there. As Ehrsson (2013) demonstrated, because consciousness is linked; and consciousness transfer leads the person who has had their consciousness transferred to still perceive reality as "real as real" in the new body; I have the same biological and physiological responses as I would have if these attacks were occurring to my original body. This has caused me to have heart damage and severe debilitating headaches. Because my memories were released to me; I can now also remember all my past REM driven clone memories since age 5; as well as the previous night's REM driven cloned memories (when I have my consciousness transferred to the cloning centre) which causes severe stress to my mental psyche and mental well being.

As unbelievable as the above statement sounds regarding Elizabeth's ownership of music companies, just go and listen to the song "Abadon" performed by Boondox (RainmanJhof 2011) on YouTube. There are two "Abadon" versions; the version you seek can be found in the Reference section uploaded by RainmanJhof (2011); skip to 2:46 min (or listen to the whole song; pay particular attention at 2:46 min) and you will hear loud and clearly, Elizabeth say "Drop the mother f****ing base". That is Elizabeth's voice; you can compare it to any of her Christmas speeches. That is her. Elizabeth said the above as a REM driven clone at the cloning centre. I know. I was there. They got so confident, that nobody would ever find out about their REM driven cloning shenanigans, that they even had me sing on a song I produced: "Where'd You Go" –Fort Minor (Murdok Dubstep Remix) (MurdokDubstep 2010), available on YouTube. Tila Tequila and I sing on this remixed track as REM driven clones (MurdokDubstep 2010); I start to sing from 1:44 min onwards. You can compare the voice you hear in the song with the Vinny Eastwood interview (Vincent Eastwood 2013). That is me, in both cases, and that song was recorded at the cloning centre.

One good person at the cloning centre; Bernie Mac (also as an REM clone version of himself); who was an actor and comedian, tried to stand up for me and speak up for me saying 'Cloning and torturing people here, it's not right to do to a human being...' and "This place is the devil"'... Bernie Mac also tried to have others join him in speaking out against the REM driven clone torture zone while he was having his consciousness transferred to his REM clone driven version. Elizabeth and Philip tortured him for 4 to 5 hours continuously at the cloning centre as an example of their 'power', Bernie Mac had an aneurysm (brain bleed) the next day and died. This is one of the aspects about REM driven clone torture: if you torture a REM driven clone continuously for hours on end, you will cause the person to die in their original body from a heart attack or aneurysm (while they sleep); even if they do manage to wake up the next day; because of the constant pain their consciousness has recorded; and because consciousness is linked they will wake up only to have a heart attack or aneurysm in their original bodies the following day. If you apply a constantly electrical current to a REM driven clone, that person will either have a heart attack or die from aneurysm in their original bodies while they sleep.

This form of murder is similar to the CIA's heart attack gun (Non Mirage Truth Vision 2015); which was declassified in the 1970s and was a weapon used for causing heart attacks in victims, undetectable as the cause of heart attack under autopsy. The difference with REM driven clone death as a form of weaponry is that hardly anyone has heard of death by REM driven clone torture. Moreover, the perpetrator can be thousands of miles away from the victim; the culprit just needs a duplicate REM driven clone of the victim to torture or apply a constant electrical current to; this is exactly what is going on in our world every day. When Elizabeth and Philip don't like someone and they want to get rid of that person, they clone that person; torture his or her REM driven clone till that person has a heart attack or aneurysm in their original body and dies.

This is what Elizabeth and Duke Phillip did to the indigenous people in Canada. The video reference (inifiniLor 2013) provided above, regarding the genocide of the indigenous people of Canada discusses this very topic (inifiniLor 2013). As Elizabeth and Duke Phillip visited Canada as clones, when they killed the native children; they both had solid alibis of being in England at the time. They then cloned all the witnesses of the Canadian missing children's case and had them remotely killed by applying constant electric currents to their REM driven clones; one by one and each witness either died of a heart attack or aneurysm. They just dispatched the last witness by also applying a constant electric current to the persons REM driven clone because the missing children's case was building momentum.

After Bernie Mac's death everyone is afraid to speak up; they all became afraid of suffering the same fate. All it will take is a few lie detector tests from an independent source; and I will volunteer for them; they cover up for themselves so carefully that lie detector tests from an independent source unconnected to them in anyway will be the only viable method. I know many know non-famous people who have also attended these clone centre gatherings as their REM driven clone duplicate versions and also remember the clone gathering experiences in their original bodies (because they were not memory suppressed) that could be given lie detector tests to prove this. When it comes to the sexual exploitation of a child, lie detectors are admissible in Canadian courts. I need decent people with integrity to speak about this filthy business; to testify about who is involved. There is much to tell about the Illuminati and I am a wealth of information about this topic.

Elizabeth also had Princess Dianna Spencer killed by having someone shine the brightest light known to mankind through the window side on her car; they served away to avoid the light and hit the divider; it was no paparazzi. I first wrote about this in my original disclosure in **2011**; this was corroborated by an article 2 years **AFTER** I had made my original disclosure. See Radar Online (2013) for the corroborating article. Furthermore, "Candle in the wind" performed by Elton John (SadSongs4You 2010) was not Dianna's 'death song'; it was "Bigger than us" performed by "White Lies" (WhiteLiesVevo 2010). The Illuminati released this song, deliberately, 13 years after Dianna's death, again as a show of their 'power'. I did not want to compose this song but Elizabeth and her thugs threatened to stab and burn my REM driven clone repeatedly if I did not. Listen to the lyrics. I'll provide some of the lyrics here for those of you who are feeling too shocked by these revelations:

White Lies Lyrics "Bigger than us"

You took the tunnel route home.
You've never taken that way with me before.
Did you feel a need for change?
Apologies on your fingernails,
Love flickered in the city of lights
Like internet and radio waves.

I don't need your tears
I don't want your love
I've just got to get home

And I feel like I'm breaking up
But I wanted to stay.
Headlights on the hillside
Don't take me this way.
I don't want you to hold me
I want you to pray,
'cause it's bigger than us.

Are you beginning to see why these people must be stopped and stopped immediately? Are you beginning to see why it is no longer okay to 'turn a blind eye' or 'bury your head in the sand', and hope it all goes away? Can you see why I need the good people of this world to keep sharing this disclosure (online); to tell your friends and family until this information reaches the armed forces so that the armed forces can bring these people to their knees. I also do not want innocent civilians to get hurt despite the monstrosities these people cause to humanity on a daily basis. I want the overthrow to progress smoothly so that the good people of the earth can inherit the world, with all technologies and medical advancements which benefit mankind, made available to all. This is why I maintain my composure and resolve, in spite of the evil I see on a daily basis, and you the reader must also maintain your composure and resolve in spite of the evil which I am disclosing, so that we do not inherit a torn down world after we have completely overthrown these malevolent, sinister and corrupt hypocrites!

Furthermore, Diana survived the car crash; and while, either on her way to hospital or in hospital, Dianna was injected with a high concentration of salt, which is near undetectable in an autopsy and she died. Elizabeth did this because Diana was going to marry an Arab named Dodi Fayed. The Illuminati hate Arabs because for the most part, Arabs have not broken their relationship with God. Dianna hated her association with these people; Dianna knew about REM driven, sleep cloning and wanted nothing to do with it; but she was afraid of being killed and so said nothing. I know a lot about this and many more deplorable things the Illuminati have done over the course of 34 years and I will be more than happy to reveal all the evil they have done; as well as all the wonderful discoveries and progresses they have made in medicine, science and technology, which they have withheld from the general public. I am very happy to disclose all, because I known once the world learns of all they have done, we truly will begin to see the end of such evil on this planet. Just make sure you keep spreading this disclosure and it reaches the armed forces soon. Soon, soon, soon!

Help Donald Marshall by Sharing this Disclosure with Your Close Friends and Family

If you are reading this, then you have to help me. I know some of you may be reading this thinking, but I am just an ordinary man or woman Donald, I know you are telling the truth; I can feel it in my heart and my head that what you say is true and that you are telling the truth (which I promise you, with my right hand to God I am) but I'm just an ordinary man / woman Donald; I don't have any power; I don't have any influence; or because of the position I am currently in I can't speak out against these people; and I am just an ordinary man / woman I cannot be expected to take on the world's problems. You are right if you are thinking and feeling this, and I do not expect or want you to take on the world's problems. All I want you to do is share this information with close friends and family initially, because when you do that, at least that is one more person who will know about the true extent of evil in this world. When your close friend or family member also shares my disclosure with another close friend, the disclosure will eventually spread exponentially. It will also be one more person who has your well being in their thoughts because I understand how scary it is to know this. Therefore remember **there is safety in numbers;** and the more people you tell in your social circle, the more you can all look out for each other. So feel free to share my disclosure with close friends and family. Do not talk about my disclosure in public (for now) if it makes you feel uncomfortable. Moreover, if you want to reach more people (other than your initial social circle) the best way, is to do it online: through social media, such as Facebook, Twitter, and YouTube etc. As I've already mentioned, the Illuminati controls all forms of media except the internet.

The Illuminati, being so 'confident' at the time with the evil they wield onto the world, put my face on a Megadeth album cover titled *The World Needs a Hero* (2001) (to mock me) when I was 23. I posed for this album cover at the cloning centre when I was 23, and the album was released with a picture of my face, as a REM driven clone, 3 years later when I was 26. They did this because they were extremely confident that nothing would ever be proven. Google image it, although I am 39 now, you can still tell that it is me. The image shows what I end up looking like after an REM driven clone gathering with a skeleton popping out from my chest. I understand most of you are going to continue reading because although it is "liberating", it is also "paralysing" at the same time (Laurence Mountford) to realise what the truth of the world is, so I will display two images below, but promise yourself, that you will Google search this image in your spare time.

Image 3: Megadeth Album Cover: *The World Needs a Hero* (2001)

**Image 4: My original body: top left (age 37) and bottom right (age 37);
compared to my 23 year old REM driven duplicate clone body (top right and bottom left)
at the cloning centre.**

You can clearly see from the images that, it is in fact me. In Image 4, you can also compare what my real body (top left and bottom right) looks like compared to my duplicate clone body. Duplicate clones do not come out of the tank looking 100% like the original; it's 99% - there are always some slight variations as some have commented that the eyebrows and nose in the picture, bottom right, is not the same (as the duplicate clone on the album cover). However, to people who make such comments, I say: my eyebrows and nose is the same when you compare it to the pictures of my original body (top left and bottom right). Also, remember that the image on the album cover is a duplicate REM driven clone of me. REM duplicate clones do not come out of the tank looking 100% like the original. There are always slight variations; but the wrinkles on my 37 year old forehead (when I took the picture in my original body; top left and bottom right) is similar to my 23 year old wrinkles, the lips are the same; and the face which you see, is definitely, the same! Yes. REM duplicate cloning is real; going to sleep and waking up as a cloned version of version of you is real and **we must put a stop to it now!**

The Deplorable Nature of the Illuminati

My own family has been turned against me one by one. The Illuminati have told my family members when they were REM driven clones at the cloning centre, things such as I secretly hit or molested their children; poisoned their pets when the pets died of sickness and other such things to make my own family hate me and not want to help me. Even when my family side with me there at the cloning centre, as REM driven clones of themselves; and my family members say 'They do not believe that Donny did all those horrid things' -which they have been told; Elizabeth then says "Are you cooling me a liyah?!" in her disgusting croaking voice made as low as low and evil sounding as she can make it, complete with psychotic and malevolent glare; and as terrified REM driven clones my family say "No, no, of course [what you are saying] it's true", stuttering and afraid as REM clones. My mother Catherine McMahon sold me into this REM driven sex and torture cloning slavery when she remarried a man named Gordon Cohoon; Gordon's whole family is in this scummy secret society, his brothers Tom and Tony Cohoon; his sisters Darlene and Bernadette Cohoon; they fear the new and improved lie detector tests; and all it would take, is for an independent source, far, far removed from any association with the Illuminati to administer these lie detector tests on me **AND** the above named people to prove this unequivocally.

Half way through the making of my original disclosure document (in **2011**), when I went to sleep that evening, the Illuminati transferred my consciousness to my REM driven clone and introduced me to a man (who was also a REM driven clone) named TROY LANDRY. He is an alligator trapper from Louisiana on the TV program named "Swamp People". Troy Landry said "If I send my [original] disclosure out to the public then he would take a power drill to my shin bone at the cloning centre and suck the marrow from my [REM driven clone's] bones." It is similar to spinal tap, and one of the WORST things you can do to a REM driven clone besides burning a REM driven clone. I told Troy that I will be sending out my disclosure to the public, because I have to escape the cloning centre, and so, Troy Landry did just that. It was excruciatingly painful; all the REM driven clones that were sat in the stands of the arena just watched; slack-jawed. Troy Landry is an insatiable child molester and an extra retarded REM driven clone. A side effect of REM driven cloning is that as a REM driven clone version of yourself, your emotions are heightened and you are less smart as you are when you are experiencing the world in your original body. Nevertheless, Troy Landry is extra retarded as a REM driven clone.

In Louisiana, when Troy sees a young boy that he likes, Troy asks of the boy's name and tells the boy "He is an alligator hunter"; Troy then proceeds to shake the boy's hand; Troy then has his paedophile friends at the local cloning centre find the boy's blood records to grow duplicate clones of the boy. Five months later, there are multiple REM driven duplicate clone bodies of the boy grown for Troy Landry to victimise before the crowd of onlookers. All members of the Illuminati do this; it's just a way of life to them; they consider themselves 'the privileged people' in the world power organisation. Almost all the cast on the "Swamp People" television program attended the cloning centre as REM driven duplicate clones of themselves, **when they go to sleep**. After putting a power drill to my shin bone, Troy Landry asked me again, "Will I send my [original] disclosure out?" I said "Yes" to which he replied "I'll do the same to your pelvic bone everyday!" The pain on my pelvic bone was far worse than when Troy put the power drill to my REM driven clone shin bone. I told Troy "I have no choice but to inform the public" – and so Troy put a power drill to my REM driven pelvic bone, everyday... and it is the worst pain ever... you forget your own name; where you are; all you know is pain; and you beg God or anything to save you from it...

Another deplorable thing which the Illuminati did in real life is: The Canadian government were trying to lower the amount of prostitutes on the streets (Elizabeth hates prostitutes) so they had a man named Robert Pickton start killing the women and feeding the women to pigs on his farm. The Illuminati had a camera set up in the upper corner of a room in Pickton's house and recorded Pickton hitting these women over the head with a hammer (a ball-peen hammer). They took the recordings, all 49 of these murders, and they all watch them at the cloning centre. To be seen as 'tough' at the cloning centre is to watch all 49 of the Pickton murders without having it affect your psyche. Elizabeth loves watching the Pickton murders and she says she has a macabre fascination with death. Canadian Prime minster Steven Harper knows all about the conduct of the Pickton murders; he has seen all the recordings and cheers on as the rest of them do. If Mr. Pickton says anything about his involvement with the Illuminati, or the recordings, they will apply a constant electrical current to his REM driven clone until Pickton has a heart attack or aneurysm in his original body.

What Happened to Britney Spears?

The Pickton murders are also the reason Britney Spears 'lost it' and shaved her head bald. She had watched too many Pickton murders as a REM driven clone at the cloning centre and it drove her 'over the edge'. I'll also reference the following songs performed by Britney Spears so that the reader has more corroborating evidence to add to the ever increasing pile. Search for the video "Break the Ice" (BritneySpearsVevo 2009) on YouTube. In the Japanimation video; at the beginning of the video; that is a cloned **cartoon** version of Britney Spears being grown in a big thick thank full of water (1 second to 7 seconds); and at 1:32 min to 1:43 min Britney walks into the cloning centre. This is **EXACTLY** how the cloning tubes are in real life. They are stacked one on top of the other, each filled with salty water. Britney Spears made this video because she said a fantasy of hers is to "Blow up a cloning centre". The Illuminati allowed her to release this video because at the time they figured nobody would ever figure it out. I have provided the images on the next page.

Image 5: Britney Spears is being grown as a duplicate clone in a cloning tube. The depiction is EXACTLY how the duplicate clones are grown in the Cloning Centre... with wires extending from the body; in a big thick tank full of salty water.

Image 6: Britney Spears walks into the cloning centre. The cloning tubes are stacked one on top of another. This is EXACTLY how these cloning tubes are in real life at the Cloning Centre.

Image 7: The Cloning Centre depicted from an aerial view.

In “Hold it Against Me” (BritneySpearsVevo 2011) performed by Britney Spears; Britney is depicted fighting against her clone at 2:46 min till the end of the video. In “Mona Lisa” (SimpleGirl4ewer 2007) later remade by Britney Spears she changed the words in the song from “gone” to “cloned”. I’ll provide the lyrics to chorus here because they have not changed it on A-Z lyrics etc., but listen to the song and you will clearly hear the following:

Britney Spears Lyrics “Mona Lisa”

She’s the original (yeah, yeah)
She’s unforgettable (yeah yeah)
She wants you to know (yeah)
She’s been cloned…
It’s kind of incredible (yeah yeah)
She’s so unpredictable (yeah yeah)
She wants you to know (yeah)
She’s been cloned,
She’s been cloned,
She’s been cloned…

Yes. Britney Spears and many other celebrities want you to know they have been cloned. The celebrities are depending on you, the ordinary man / woman; the populace, as I am depending on you to spread this message fast and far. In fact Elizabeth has said that “If any public person speaks out, they will die!” Therefore, public figures cannot openly discuss this topic to warn the populace –so they hint. It is **NOW** up to the ordinary man and woman to end this. Furthermore, Elizabeth has a nuclear bomb hooked up at the cloning centre which she can press at any time to wreck havoc on the world unsuspectingly. Thankfully, I managed to convince Elizabeth not to do such a silly thing. I hope you can now understand why everyone is terrified of Elizabeth at the cloning centre, and why this is a **world emergency** and we are depending on you to share and spread my disclosure!

NEVER EVER SELL YOUR SOUL

In This Physical World Selling Your Soul Is Selling Your REM Driven Clone

Furthermore I must discuss an entrapment many up and coming ‘stars’ fall into. You have most likely heard many public figures say “I sold my soul to the devil” or some variation of “I sold my soul”. I am now going to address the aspect of “selling souls” or “selling your soul” which I am sure you have heard many of these celebrities talk about. I’ll address this as coherently as I can because the on the surface selling your soul talk is difficult to contemplate especially if you consider the soul to be a metaphysical, ethereal or mystical part separate from your earth body. Moreover, we live in a physical world, so selling a metaphysical aspect of you sounds incomprehensible (at first). For the most part we have little understanding of what the soul is. However, we are told that the soul is a part of us which never dies and it is eternal. It is all that we are, ever were, and ever will be. Now our faiths and beliefs come into question, because if you are an atheist: there is no God, selling your soul is a bunch of crazy nonsense.

From a practical perspective it also seems difficult to fathom, because if you go on what you have been told, you are selling an intangible part of yourself to be used by someone else for whatever they wish; and so if you get into the headspace of viewing your soul as something separate from you or that you are in control of your mind and your body, then again, 'selling an intangible aspect of you' again sounds like nonsense because right now nobody controls you; you are controlling you; so what are you really selling? Thin air?

Many up and coming 'stars' think this way when they are confronted with "selling their soul" aspect. The up and coming 'stars' are blinded by the prospect of being super famous and super rich; and in the moment they are confronted with "selling their soul" they believe these Illuminati people, are a group of over religious zealots and that they, -the up and coming 'stars' are taking advantage of the Illuminati because the 'soon to be 'stars'' do not believe (in that moment) it is possible to sell your soul, and only consider being super rich and super famous; so the 'stars' sign their 'soul' over.

At this point, it is usually too late for the up and coming 'star'; because what they have actually sold, in this physical world, is the use of their REM driven clone to the Illuminati. They have sold their REM driven clone to be used for REM driven sex by perverse old men and women whenever they enter REM sleep.

These celebrities are not memory suppressed either; so whenever they enter REM sleep, their consciousness is transferred to their REM driven clone, to be used for whatever the Illuminati wish: usually sex as REM driven clones with dirty and perverse old men in return for a promotion in the entertainment industry; such as movie role, advertisements, concert gigs etc. It is a very, very, sick business, and once these up and coming 'stars' get into the business they are trapped. Now you can begin to understand why so many celebrities, although on the surface it appears they have it all, are depressed; and do random and crazy things. It is a cry for help. Their illogical behaviours, (not all) for the most part, can be attributed to REM driven cloning. Furthermore, the Illuminati consider 'selling your soul' (the use of your REM clone) **a very serious business.** They do not joke about this; and there are NO RETURNS. Once you have sold the use of your REM driven clone for promotions etc., that's it. If you ever make a fuss and want your 'soul' back, in other words: you no longer wish to have your REM driven clone to be used by dirty old men for sex; the Illuminati will kill you by applying a constant electric current to your REM driven clone until you have a heart attack or aneurysm in your original body and die. It is as simple as that.

For example, Whitney Houston wanted nothing to do with the cloning centres, she said she would keep quiet; she never wants to be in the spotlight; she never wants to do radio or television. Let bygones be bygones, I'll go my way and you can go your way. The Illuminati were extremely angry! They had bank-rolled her, and now she didn't want to be their 'friend' or ever associate with them again. She was sacrificed; she was killed with a constant electric current to her REM clone. She had sold her soul, in the beginning of her career; in other words, the "use of her REM clone". Earlier in Whitney Houston's career, she had signed that they can use her REM driven clone however they wish.

I have also seen people say "No" –when confronted with 'selling their souls'. These people are then memory suppressed, and will not remember the proposal of their REM driven experience. The people who also refuse to sell the use of their REM driven clone ('sell their souls') are blacklisted secretly, and they will never receive a high paying movie role, concert gig, advertisements etc. If you have ever wondered why so many talented people have not 'made it' –they refused to sell their souls, in other words, the use of their REM driven clones in exchange for promotions. This is how the entertainment industry really works. Another aspect of selling your soul, in other words, **selling your REM driven clone** is that you are also agreeing to sell your children, and your children's children etc.; your whole lineage to the Illuminati; for the Illuminati to use your unborn children for paedophilia, torture, sex sports and other grotesque and ungodly things when they sleep. It is a nasty business. **NEVER EVER** sell your soul.

The lesson is very important. NEVER EVER, 'sell your soul'; NEVER, EVER! You will experience the worst nightmare situation ever, and in this physical world, that is the use of your REM driven clone to be used for sex sports. You'll never have a decent night's sleep ever again, and you will always retain the full memory of your REM driven clone experiences; as well as, you will be selling your unborn children into this dirty business. Even when confronted with this as a joke: never sell your soul. Never Ever! The physical aspect you are confronted with when asked to 'sell your soul' is: "YOU", and everything which makes you, "you"; your ideas, your creativity, your privacy, your biology; everything which makes you, you. Never sell your soul, which in this life is currently the use of your REM driven clone! Never, ever! I hope that is well received.

Fake Alien Abductions conducted through REM Driven Cloning Technology

I must add they grow duplicate REM driven clones of people from all walks of life and then they transfer the persons consciousness to their REM driven clone version at the cloning centre while the person's REM driven duplicate clone is chained down to stainless steel corpse tables; or they pre-inject the REM driven duplicate clones with drugs before transferring the consciousness so that once the consciousness has been transferred, the REM driven clone cannot move. This is the point when they usually send people into the room dressed as aliens. It is a fake alien abduction. It's just these Illuminati people dressed in Hollywood quality accessories and they make the REM driven duplicate clones which have either been chained to the steel corpse tables or pre-injected with drugs, believe they are having an 'alien abduction'. Members of the Illuminati even dye chicken skin grey, and stretch it over a mask for realism and perform "experiments" on the immobile REM driven clones; the perverts anally probe them; they rape their limb bodies and do not suppress the victims memories; so these victims wake up thinking they have been abducted by aliens but in reality, they had their consciousness transferred to their duplicate clone versions when they entered REM sleep and they were violated. The victims do not know where to turn and naturally, they are embarrassed. Some victims even try and do install cameras all around their bedrooms in order to videotape themselves while they sleep; to prove they have been 'taken'; but to no avail they have not been taken; they have been cloned and had their consciousness transferred to their REM driven duplicate copies once they enter REM sleep by the most disgusting perverts in the world. The scum even videotape these 'abductions' to watch later as sick demented porn. These fake abductions are conducted by the Illuminati more often than you can imagine. They just keep doing it to random people over and over and over...

I am THE Spy for Humanity against the Corruption of the Illuminati

Over the years the Illuminati have offered me: a priceless katana (samurai sword); a rigged jackpot winning lottery ticket; REM driven clone slaves to keep me quiet, any of the prettiest women I've ever seen; any girl from high school; Vladimir Putin's daughter; even children; I do the right thing and spit in their REM driven clone faces; jam my fingers into their eyes but they have the technology to turn off the pain sensors of a REM driven clone, and therefore they have their pain receptors turned off as REM clones, while my pain receptors are fully on (sometimes even beyond the threshold of what is normal pain for a human). See the online articles: Science Daily (2014) and RT (2014) which discuss how pain receptors can be turned on and off in humans. Not much will hurt their REM driven clones other than getting dirt or vomit in a wound or bleeding too much. However, they have perfected the science and technology of REM driven cloning and therefore it only takes time and approximately $30 to grow new duplicate clone bodies. I started to smear excrement in their faces as a REM driven clone at the cloning centre in an attempt to deter them; I have **never** handled faeces in my original body, but I do this as a REM driven clone at the cloning centre, and even that does not deter them from their depraved ways. I composed a song which was later performed by "One Republic" referring to it called "All the Right Moves" ("All the right friends in all the right places... All the right moves in all the right faces"). I've made so many songs with MK Ultra technology (Rense 2001; Jim Cristea 2009; Berekley News 2011; Mind-Computer 2012 nature video 2013) and Mind-voice technology (New Scientist 2014; Prigg 2014) it is ridiculous. You see it is very easy to make music using Mind-voice technology; Flo-Rida used Mind-voice technology to produce the song "Whistle" when I first made my original disclosure (in 2011). The song is a taunt at me about my "whistle blowing disclosure" i.e. 'Can Donald blow the whistle? Etc. etc.' The thing is, anyone with a talent for music can make music much easier with the technologies which they have (MK ultra technology; Mind-voice technology); however, the Illuminati made more money from the music I composed, and so over the years, they just kept using me, over and over and over again, for rock, pop, rap, country etc. There are so many people involved in this REM driven cloning business, it is staggering; the organisation is vast. The only things the Illuminati fear are nuclear war; the new and improved lie detector tests and the general populace spreading my DISCLOSURE DOCUMENTS.

For those of you thinking Queen Elizabeth II looks like a kindly little old lady and you still cannot believe that all this is true, although I have provided plenty of evidence to the contrary as well as evidence of her saying "Drop the mother f***ing base" as a REM driven clone on a song track (RainmanJhof 2011); you could not be more wrong. She is the worst human being I have ever seen or heard of. It is so sad to see these REM driven women and children having their consciousness transferred to their REM driven clone duplicates and brought to the centre of the dirt rink, sitting there naked, afraid and crying and raped and beaten for sport, for the rich and famous. REM driven cloned women and children display the most range of emotions, and it is the saddest thing to see there. Therefore, of course I cannot bring myself to be a part of this despite any riches which the Illuminati offer me.

Over the 31 years when I was having my consciousness transferred to my REM driven clone at the cloning centre; Elizabeth, Vladimir and many, many Illuminati members and cloning centre attendees discussed many topics with me. These Illuminati people, such as Elizabeth and Vladimir, as well as many others confided in me because I had composed songs since I was 5 years old.

For readers struggling with the idea that a 5 year old can compose such wonderful songs at such a young age I will remind you that, it is easier to compose songs with technologies such as MK Ultra and Mind-voice technology. One is only limited by their imagination and creativity. Moreover, research talented children. I won't provide references of talented children here because I want to protect children from the Illuminati, and not have children exploited like I was; and for the readers who are parents; I am sure you know how talented, creative, and imaginative your children are.

Accordingly, since the age of 5, Elizabeth, Vladimir and many, others confided me in me because they thought I was special, and wanted me to hang with them; some of these Illuminati people, I had composed their favourite songs; I was also memory suppressed for many years so they thought it was harmless to tell me everything that exists or is possible. They were trying to impress me and amaze me, and therefore they showed me plenty of their technologies and what they had. They wanted me to me a willing, full Illuminati member; so over the years I feigned interest and pretended to like these Illuminati people, so that I could learn what they do and how they do it. I was looking for a way to block the consciousness transfer to a clone during REM sleep, or hoping they would reveal this part to me; but they did not, and I did not find a method to block the consciousness transfer. However, I bided my time, until I knew just about everything they do; so that I could reveal to the world everything they do; to give humanity a fighting chance against everything they do and as a consequence, I became a spy for humanity against the corruption of the Illuminati.

The Threat to Humanity when the H.A.A.R.P Grid is Complete

One of the most important topics which they discussed with me that I must add to this disclosure is HAARP technology and their plans for HAARP technology. I have discussed the basics of HAARP above. HAARP radio transmitters have to be placed at certain points across earth to complete a 'HAARP grid'. Once all the installations are completed over the earth HAARP will have more functions as a grid than the basics described. The Illuminati have told me, there is a possibility the HAARP grid will be capable of time travel, although there is a 50/50 chance using HAARP for time travel could destroy the earth. They also told me that once the HAARP installations are completed, the HAARP grid will be able to bend space and make the distance between, for example, Earth and Pluto approximately 1000 miles for a few seconds, and then the distance will go back to normal.

The Illuminati also said, once the HAARP grid is completed, they would be able to mind control people like never before without the use of RFID microchips or MK Ultra. Life on earth will be much worse once all the HAARP installations are up and working together in unison. The grid has to be complete though. HAARP cannot achieve time travel manipulation and mind control if it is just located in one or a few locations around the earth. There must be a certain number of HAARP installations around the world, in certain locations around the world; and the HAARP radio transmitters must be working in unison in order to achieve time travel manipulation and mind control of the populace of earth.

This is what they told me as REM driven clones at the cloning centre. This disclosure could be false, or a half truth. I do not know. However, it is very important that I add this to the disclosure because the Illuminati are working twice as fast to complete the HAARP grid to achieve their aim of mind control over the entire population since I the time I sent out my first disclosure (in **2011**). Whether or not they will achieve their aim of total mind control once all the HAARP installations are completed is NOT something we can afford to debate. They also told me that once the HAARP installations are completed; they will have the

capability to mind control anyone remotely like never before, at the push of a button. HAARP will also be capable of setting back time; which the Illuminati will use if they are ever in danger of being exposed. However, the Illuminati will remember the previous time, and the general populace will NOT remember the previous time, so that the Illuminati can correct the mistake(s) which led to their downfall. **Once the HAARP grid is completed, humanity will be slaves forever.** This is why we cannot afford to debate. Furthermore, from the book "Angels don't play this HAARP" (Begich & Manning 1997, p. 8), it is estimated that the HAARP grid will be completed by approximately 2017; others estimate by the year 2020. The important thing to note is that humanity does not have long, until the HAARP grid is completed.

I must also add the positive side of HAARP, because as I have said, there is nothing inherently evil about technology. Technology is just a tool; it depends on the person using it. HAARP used correctly, and in the hands of honest men and women, will tame the weather with no adverse effects. Therefore humanity is on a timeline and a deadline to bring the Illuminati to an end. **HAARP is one of the main reasons, this disclosure must spread, and spread fast.**

See below for possible HAARP locations around the earth (Rense 2011). The HAARP sites are located globally where the richest mineral belts are located. Sub-surface mineral exploration has been done from satellites by radio tomography that is 100% accurate.

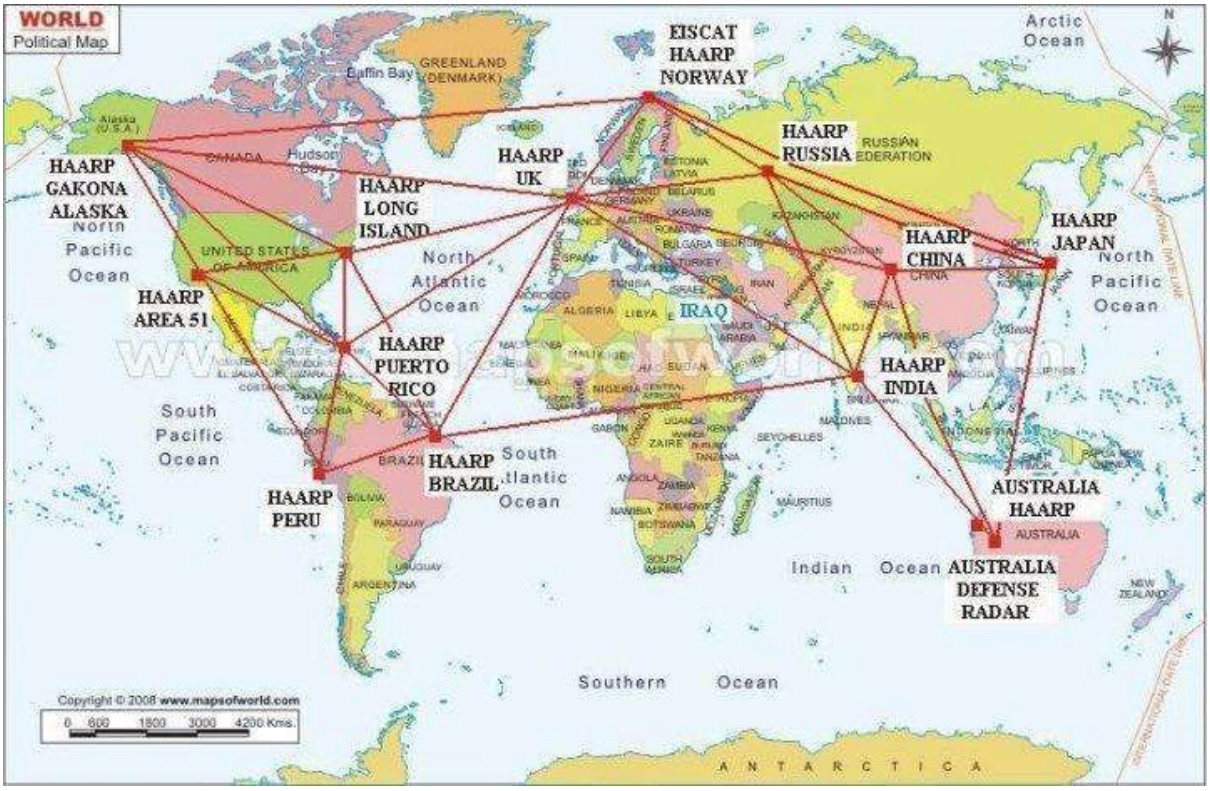

Image 8: Possible H.A.A.R.P. Locations. Source: Rense (2011)

REM Driven Cloning is the Most Terrible Nightmare Situation Ever

Furthermore, in terms of REM driven cloning; Fefe Dobson (singer) and Kurt Russell (actor) told me during my original disclosure (**2011**) specifically, to include in my disclosure that they do not like the cloning centre and they didn't torture me. Then they said not to mention them, but I will mention them again. Mila Kunis (actress) from "That 70s Show" stabbed in my REM driven clone body multiple times when I made my original disclosure and I was rendered immobile for saying that "She is a slimy scumbag for hanging with these people" and for also saying "She has enormous eyeballs and looks like a lemur". Mila Kunis (as a REM driven clone at the cloning centre) then begged me not to mention her (in my original disclosure, but I'll mention her again too) and then Mila Kunis said "She doesn't want to go to the clone zone anyway" and the Illuminati then deactivated her consciousness from her REM driven clone body, and she left. Her REM driven clone body went limp at the point where her consciousness was deactivated from it; her REM driven clone body looked 'dead', and she was gone. Some of the privileged people at the cloning centre are allowed **NOT** to have their consciousness transferred to their REM driven, clone duplicate versions (or they attend the cloning centre willingly when they want), but not me. I am an imprisoned slave in the worst nightmare situation. I told Nicole Leone (Madonna) also a REM driven clone at the cloning centre, that I was going to tell everyone that she coerced me to compose songs for her throughout my life (as REM driven clones). Nicole Leone (Madonna) told me VERY specifically to say in my disclosure here "She is not afraid!" and "No one will believe me and nothing will come of this". I beg you to help me prove her wrong.

Moreover, having your consciousness transferred to a REM driven clone alternative inhibits the person's ability to dream for that evening. Although your original body is immobile and asleep in your bed, when they transfer your consciousness you have actually 'woken up' as a REM driven clone version of you at a physical location here on earth; therefore you walk and talk as a clone version of you. You are not dreaming; you are just a REM driven clone for the evening. Furthermore, when the Illuminati restore your memories (as they have with me) or do not suppress the memory of your REM driven cloning experience for the evening (such as with the fake alien abductions), you will remember the experience as 'clear as daylight on a summer's day'; the experience is 'clear as a bell' as life is in your original body.

It is unlike dreaming, where dreams are fuzzy, incoherent and with random conjecture. The Illuminati know this as a fact, and therefore pre-inject the REM driven clones of random unsuspecting civilians for the evening with drugs before they transfer the person's consciousness. They tell the person who has had their consciousness transferred to their REM driven clone all sorts of nonsense: such as they are in the 5th Dimension; the astral plane; a singularity; the spiritual realm; Valhalla; quantum hopping etc. and all sorts of fallacies so that the person will not have a coherent picture of what has happened or what is happening. The truth is that person has had their consciousness transferred to their REM driven duplicate clone when they went to sleep and entered REM sleep; their original body still remains asleep in their bed; their consciousness however is now transferred to a clone duplicate alternative, and the person is 'awake', walking and talking as a cloned version of themselves in a physical location. The Illuminati allow some people to retain some of these REM driven clone experiences to affect their mental psyche.

The physical location where the populace will be able to verify these REM driven clones is somewhere within 5/6 hours drive, in a radius of the Robert Pickton farm, Port Coquitlam, British Columbia, in Canada, somewhere at a remote nature reserve. This is the cloning centre all the rich and famous attend because it is above ground and the rich and famous don't like the 'hospital smell' of underground cloning centres. The above ground cloning centre located in Canada is the cloning centre I have my consciousness transferred to when I sleep. It is guarded by military personnel. There are many cloning centres all over the world; as Phil Schneider (1995; 1996) disclosed as far back as the mid 1990s when he spoke: there were 1477 Deep Underground Military Bases (DUMBs) worldwide and 131 active DUMBs in the United States alone. Each DUMB costs on average 17 -19 billion U.S. dollars; paid for by the taxpayer; and it takes approximately a year-and-a-half to 2 years to build DUMBs with sophisticated methods. DUMBs contain cloning floors, and have an entire floor dedicated to human cloning, where duplicate clones are grown of unsuspecting civilians (remember they just need your blood / DNA); and unsuspecting civilians have their consciousness transferred to their REM driven clones at a physical location, which is usually these Deep Underground Military Bases when they sleep; unsuspecting civilians are memory suppressed, also to be used for gruesome torture and sex sports; as well as the plagiarism of talented individuals. Schneider gave the above statistics in the mid 1990s; chances are there are more DUMBS and cloning centres worldwide today.

Are you beginning to understand why this is the worst nightmare situation ever? Can you understand how: you, your friends, your family, your brothers, your sisters, aunties, uncles, children, work colleagues and anyone else you have contact with in your network, may be involved in this REM driven cloning business and will not even be fully aware of the situation or remember any experiences which they may have had once they wake up from sleep and they are back in their original bodies? I remember all of the REM driven clone experiences as clear as daylight because my memories are fully restored. Can you understand why the Illuminati must be stopped and stopped immediately? This REM driven clone business is vast, and it affects everyone, not just me.

This is why I mention that I am fortunate or unfortunate to remember all these experiences clearly depending on how you view it. I am unfortunate in the sense that I can recall all the depraved things these people do as REM driven cloned duplicates as clear as daylight and it affects my mental psyche. However, the fortunate part is: because I can recall all these experiences clearly, I can inform the world about the evil committed against humanity in a clear and logical way for the average reader to understand and verify, so that the populace can bring these people to justice for the crimes they have perpetrated against humanity and continue to inflict on humanity. For anyone who has had their intellectual property stolen by the Illuminati as a consequence of the technologies they have used on you unsuspectingly, you will be able to sue and regain monetary reward for the theft of intellectual property as well as invasion of your privacy.

I do not want to get too far ahead, because at this present moment, it is **very important** (I cannot say it enough) that this disclosure spreads (this is the stage we are currently at); it reaches the armed forces; to enable the armed forces to realise the crimes committed against humanity because of these people (the armed forces are kept 'out of the loop'; they just 'follow orders'); the armed forces will have to perform a military coup and bring this people to their knees. This is the point where the ordinary man / woman can have his REM driven cloning experiences restored, (that is if you want to) and sue / rightfully reclaim damages and legal reward for any crimes committed against him or her.

The Meek Shall Inherit the Earth

As you can see if everything goes smoothly; the meek shall inherit the earth. This is why you must maintain your composure and resolve, as I do every single day. You must not riot or cause chaos, damage property or undertake any act which will cause public dissension. The good people of this earth are about to inherit the earth; under no circumstance must you destroy anything. At the end of this currently dire and complicated situation; humanity will inherit the cure for HIV/AIDS, cancer, Alzheimer's, dementia, you name it –many debilitating diseases known to man; and other such wonderful technologies like hypersonic trains which run on magnets and are capable of doing Mach 5 (Mach 5 is the equivalent of 3806 miles per hour or 6125 kilometres per hour; Schneider (1995; 1996) also mentions the availability of Mach 5 trains in his disclosure, back in the 1990s). These trains can be used to deliver foods which are discarded in More Economically Developed Countries (MEDCs) to Less Economically Developed Countries (LEDCs) because these trains can travel thousands of miles within minutes. Yes. The Illuminati have all these wonderful technologies and more, but withhold it, and in turn withhold the progress of humanity. Yes. Plenty of man's problems can be solved when we address the root causes of our problems, and one of the root causes of humanity's problems is: REM driven human cloning which is currently in the hands of evil men. Even REM driven cloning can be used for the benefit of mankind when this tool is in the hands of righteous men. It can be used learn new skills in your sleep: such as gain extra qualifications; learn how to speak a new language; play instruments etc. –so long as memories are not suppressed, you will be able to perform the skills you learned as a REM clone in your original body when you wake up. As you see there is nothing wrong with most technologies; it all depends on the person / people using it. Nevertheless, although they may be beneficial uses to REM driven cloning not yet realised, we must be shut down REM cloning before we can even consider how REM driven cloning may benefit mankind, because at this present moment all that REM driven human cloning is used for is to commit evil, particularly against unsuspecting civilians.

It is OK to feel angry about all these crimes committed against humanity daily. But do not let these evil crimes rule you, in fact, let it motivate you; let it motivate you to the point where you will stand up and speak out to ensure that these crimes end. I think about the children and the future of the world every day; that is what motivates me and I view my situation as a God-given mission to bring these people to justice. I view things this way to maintain my sanity and composure. This is what keeps me going despite the extreme evil I experience, and it helps me to maintain my resolve and composure. The fact that I do not want a single child to grow up in a world, where they are being messed with in their sleep is what keeps me going despite this extreme evil. Some children are even kidnapped and brought to the cloning centre in their original bodies, again to be messed with. This is the root cause of why so many children go missing across the world. I'm sure any rational thinking human being feels the same way I do, and does not want their children, or any child to inherit a sick world governed by sick individuals.

I am a baptised Roman Catholic and a God fearing man. I believe there is a Creator of the universe but the Illuminati tell me there is no God, only science and technology. The Illuminati are also responsible for the death of the young beauty pageant girl Jean-Benet Ramsay; her parents are in this REM driven cloning business. Casey Anthony's daughter; as well as, Casey Anthony (before she died) AND Casey Anthony's parents also attend the cloning centre as REM driven clones. Many others; a man had his wife killed and this was mentioned on the news; it was an Asian woman whose rich husband had killed her; the

husband said the wife was responsible for their son's death. Elizabeth's response was that "Rich people in this organisation (The Illuminati) do not go to jail, they are covered for."

Stephen Spielberg and George Lucas are Illuminati members and they willing attend the cloning centre as REM driven clones when they sleep. George Lucas made other Illuminati members light my REM driven clone body on fire for the end of his movie *Star Wars Episode III: Revenge of the Sith* (2005).George Lucas said (as a REM driven clone) he wanted Hayden Christensen "To scream realistically". Hayden Christensen (also a REM driven clone at the cloning centre) watched me, and listened to my screams and groans of pain and copied the sounds coming from my burning REM driven clone exactly. Hayden Christensen knows he is a REM driven clone when he goes to sleep and Hayden Christensen knows his consciousness is transferred when he reaches REM sleep. Hayden Christensen knows all about REM driven human cloning, and he is a "privileged" Illuminati member. Natalie Portman also knows all there is to know about REM driven human cloning; as does approximately a quarter of the "Star Wars" cast. Many directors have attended the cloning centre as REM driven clones too, and have used me in a similar role playing situation; they have caused me to have excruciating pain as a REM driven clone, to see what kind of squeak or screech I will make, as if I were less than a dog; and when I am a bloody mess on the floor as a REM driven clone; that is when they usually crawl on my broken REM driven clone body and sodomize me saying something like "They love me and they cannot control themselves because I made all their favourite songs and I'm so "special"".

My ribs in my REM driven clone body will be broken, I will have suffered internal bleeding and will be crying or screaming, if I am able, but they just continue to sodomize me, and videotape such a depraved act of wickedness so that they can view it again like "evil pornography".

The REM driven cloned children, who have their consciousness transferred while they sleep at home in bed, in their original bodies, need a familiar face to talk to as REM clones or all they do is scream and cry at the cloning centre; that is where Joy Geizer comes in. Joy Geizer is married to my half brother from my father's first marriage; Joy Geizer is a REM driven clone girl guide leader, and when the Illuminati clone young girls, Joy Geizer speaks to these REM driven cloned girls; Joy Geizer keeps the REM driven cloned girls calm and "pimps" them out for free, knowing that these young girls will have their memories suppressed, and therefore they will not remember the experience and will not talk about it when they wake up. All the Geizers are in this REM driven, human cloning business; there are many people who remember these REM driven cloning experiences in their 'awake state' and in their original bodies who could be polygraph tested by independent polygraph testers. The police, and polygraph testers in my City of Halifax, Nova Scotia are compromised (they attend cloning centres as REM driven clones too); they cover up for child molesters and therefore cannot be trusted to fairly administer a polygraph test; as I said, commissionaires and C.S.I.S are heavily involved. All it would take is a few polygraph tests to prove these things unequivocally, because for those of you who have 'eyes', you can already see that REM driven cloning is real, and that this is actually the way of the world. I will take these polygraph tests publicly too, and demand that my mother and step father submit to them. They have told me, they **wouldn't** even attempt to lie on a polygraph.

Human cloning, particularly REM driven human cloning, is one of the absolute truths of this world; hidden from the world for over 70 years. My life and the freedoms of many, many people, including the reader (you) depend on this disclosure. The Illuminati say that the world finding out about REM driven human cloning will set the stage for the end of the world; people panicking and destroying property because of the evil these people have committed, but as I've said: prove them wrong, because we are going to inherit the earth, so there is no need to riot or cause public dissension. There will be no end of this world; just the end of the crazy Illuminati people. They always like to think and behave so negatively, don't they? *Sigh*. Furthermore, the whole talk about 2012; December 21st 2012 and the end of the world Mayan Prophecy; that was really about the world finding out REM driven human cloning, and the sick and sadistic nature it has been used for by these sick and sadistic people. Under no circumstance must you riot; you **must** prove you are better than these savage barbarians. I'll say it again, **because it is important**: we are going to inherit the earth, and therefore the smart and right thing to do, is not to destroy anything, especially the earth which you shall inherit.

Furthermore, I hope you are beginning to understand that the good people of this world must bring these people to justice and stop their wicked ways. I sincerely wrote this disclosure so that the good people of earth would be empowered to put a stop to their wicked ways. I wrote this disclosure to empower the good people of earth against tyranny and not so that the world would end. Therefore you must understand that the downfall of these Luciferians (Illuminati) must progress smoothly, because unless you have been to the cloning centre as a REM driven clone and retained the full memories of your experience, it is difficult to understand the level of depravity and sub human cruelty; it is beyond anything that has ever been heard of, and there is much more to tell.

Ignore this disclosure and you will condemn me to a horrible eventual death and you will encourage them that 'they are all 'powerful''. This is not an exaggeration. There is no need to exaggerate even President Barrack Obama is involved in the REM driven cloning business and attends the cloning centre as a REM driven clone version of himself, when he goes to sleep. He and his wife Michelle Obama attend these REM driven clone gatherings. Barrack Obama has even told me as a REM driven clone, at the cloning centre "Donny, we're all powerful. You are a slave and the people here [as REM driven clones at the cloning centre] won't speak up for you for fear of torture or death. Now make us a new song or we'll gut you like fish and leave you to writhe in agony!"

Be Wary of: Shills; Trolls; Disinformation Agents and Double Agents

There are many, many disinformation agents whose aim it is, is to denounce or debunk me. Be very wary of them. They DO NOT, and cannot debunk me, because after all, everything I have disclosed is truth. Although the truth concerns highly advanced concealed technologies, so it is a bit difficult to fathom at first, but keep reading, and you will realise that all which I have disclosed is true. Be very wary of the disinformation agents.

The most common thing these people say is that "Donald is a paranoid schizophrenic" –yet, ask them to detail the ins and outs of what a paranoid schizophrenic is and what specifically qualifies Donald to be a 'paranoid schizophrenic'; there is a high probability they will not be able to explain this to you, logically, sequentially and methodologically. Their main goal is just to make it as difficult for newcomers to understand what the real truth of this world is and as I have disclosed; and one of the root causes of man's problems is REM driven cloning.

Some disinformation agents are paid by the Illuminati, to behave this way, and are all too happy to echo empty statements (without any substantial evidence for their claims) because it provides them with a pay check. I will provide the following reference for the reader which discusses the signs and symptoms of a paranoid schizophrenic; all for the express intent for the reader to further understand paranoid schizophrenia. You can read more about paranoid schizophrenia on Medical News Today (2015). The link is provided in the reference section. You are welcome to read my Facebook wall and within days, you will realise I converse with others quite naturally. You can also ask individuals who have spoken to me through Skype or met me; but if this is not a viable option for you; all you have to do is read my Facebook wall and within days, you'll see that whoever makes such harsh and untrue remarks on my character is in fact a disinformation agent.

Furthermore, remember we live in a 3D **physical** world; and there is always a physical aspect to how something manifests. Therefore, when you hear others discussing concepts such as 'Tila Tequila demonstrated an 'energy ball' right on camera; Why didn't Donald discuss that?!' Please understand that these people are trying to deceive you with misinformation. There are also professional disinformation agents to be wary of. I do not perceive anything extra-ordinary in the world when I am awake in my original body beyond the five senses. I don't see orbs, auras or anything of the like. All I will ever discuss are practical things which have been unequivocally proven to me as fact; because in the situation the earth is currently in, I cannot afford to speculate.

Contact Information

My Facebook is: https://www.facebook.com/donald.marshall.148
You can also press Ctrl+Click (hold "Ctrl" on your keyboard and left "Click" with your mouse, on the image to your right).

I have a public wall on Facebook which starts from March 2012. In other words, all posts are made public since March 2012 and you do not have to join my friends list or subscribe me to see what I post (although you will have to have a Facebook account). I suggest that newcomers start reading from March 2012, and be patient, and read everything. You can read everything and learn the real truth of the world free of charge. I don't wish to write a book, I am not looking to turn a profit from this; I want to crush these guys and shut down the cloning centres!

It also worthwhile to add that: I am **not** asking for donations. I do not want **ANY** donations. Ever! These disclosures are far more important than any donations. This is **NOT** my job. I have a job. I am an independent contractor; carpentry is my trade and I earn a living this way. If you sincerely want to help; the best way to help is to spread and share my disclosures. That is all I ever ask for, so that eventually, the world knows about REM driven human cloning, and the armed forces can bring these people to their knees. **That is all I want; spread, spread, and spread this disclosure.** I will **never ever** ask for donations. Ever! Please keep this in mind, and anyone who asks for donations in my name or on my behalf should not be trusted. I, Donald Marshall, will **NEVER EVER** ask for any donations. I hope that is well received.

You can also view Proboards which has all my Facebook posts and have been archived by Celine O'Carroll and Astral 7ight by visiting:

http://donaldmarshall.proboards.com/
You can also press Ctrl+Click (hold "Ctrl" on your keyboard and left "Click" with your mouse, on the image to your right).

There is a search function on Proboards, and you can use this to search for and read all the disclosures I have made regarding REM driven clones, the people involved and more. I understand that it is human nature to want to know, which people have been to the cloning centre as REM driven clones; therefore, use the search function to read about any public figure which I have already covered that you have an inkling about. You can also post anonymously on Proboards and Celine and other Administrators will transfer your question onto Facebook which I'll answer.

Donald Marshall Revolution is a website which details a brief overview of the Illuminati.
http://donaldmarshallrevolution.com/
You can also press Ctrl+Click (hold "Ctrl" on your keyboard and left "Click" with your mouse, on the image to your right).

Interviews

You can listen to the radio interviews I have done. Listen for consistency; particularly anything which you do not hear me, pronounce clearly for the first time; the best thing to do is to pause the recording at that particular point and replay it. You should also research the statement you do not understand. Sometimes reading helps comprehension a lot faster.

One of the main reasons you should pause and replay the recordings is because: the truth has been kept hidden for so long that a lot of what I discuss in my interviews are beyond most people's current world view; so at some points I may speak too fast for you; my audio/ microphone may not be so clear so you may miss what I say etc.

A friend has told me that when he first watched the Vinny Eastwood interview; he did not hear me say the word "scars" (When Vinny asked: 'How do I know I'm the real me?') although he replayed that particular point in the video 8 times. Everything was just beyond his current comprehension, at the time. No matter how many times he replayed that part he really could not hear me say the word "scars" –so he let that part go, and played the rest of the interview, pausing, and replaying points which he did not understand, especially to comprehend whether I was talking about my original body or my REM driven clone duplicate body. He also listened to all my interviews for consistency, to note any 'slip ups', or any parts of my testimonies which do not 'add up'. He would listen to all my interviews, pausing and replaying parts he did not understand and he would reserve his judgements until he felt everything I was saying was for example as ordinary as: 'I woke up today, brushed my teeth, and took the dog for a walk'. He was also patient to realise the truth. After listening to my interviews he would just let it 'sink in'. A week later he would come back and listen to the same interviews, to test whether his comprehension on the topics I discuss has improved, and

whether he can understand what I am saying without having to pause and repeat at certain points in my interview; and soon enough he could now hear me say "scars" at that particular point of the Vinny Eastwood interview. He had reached the point where all topics I discuss sounded to him like I'm saying everyday common place stuff that people have heard, such as: 'I woke up today, brushed my teeth, and took the dog for a walk'. For anyone who may struggle to understand the topics I discuss: I strongly recommend you take the above approach as my friend did; soon enough, you too will realise the real truth of the world like he has: REM driven cloning, kept secret and used for sinister purposes.

I cannot say the following is true for everybody, however, an unproductive venture a complete newcomer can do is to listen to my interviews first time, all the way through, without pausing or replaying parts which they do not fully understand; If you do this and if there is just a single part of my interviews which does not make sense to you; this will interfere with your understanding of the entire interview. Remember, all I am discussing is technology, thousands of years advanced compared to what you currently use; available today, hidden and secret. If things start to get too complex for you, reduce it to its bare minimums: (advanced) science and technology. I hope that helps.

Another thing which I do in my interviews, that friends have picked up on, is: -because REM driven cloning has been my reality for many years; I don't differentiate between my original body and my REM driven clone body. I just say: I did this, I did that, and Elizabeth did this and that, therefore it can become very confusing for newcomers. Please bare with me; although I'm more emotional as a REM driven clone, and not as smart as I am in my original body (this is a side effect of cloning: REM driven clones are more emotional than normal, and dumber than they are in their original bodies) I'm still "me" when my consciousness is transferred; I have all the experiences and knowledge which makes me, "me" and therefore I naturally do not differentiate between my REM driven clone version, and my original body as an outsider discussing these concepts would. I understand it helps comprehension so I have painstakingly done this throughout this disclosure.

I hope this helps; and I hope this helps to better understand my disclosure as well as the interviews which I have done. On the next page you can find the links to my interviews. You can copy and paste the links to your web browser or press Ctrl+Click – (hold "Ctrl" on your keyboard and left "Click" with your mouse, on the images below) to direct you to the interviews.

Links to Donald Marshall Interviews

Vincent Eastwood

Copy and paste the link below to your web browser.
https://www.youtube.com/watch?v=M_1UiFeV5Jg&ab_channel=VincentEastwood
OR Press Ctrl+Click (on the image below) to follow the link.

Jeanice Barcelo

Copy and paste the link below to your web browser.
https://www.youtube.com/watch?v=3uzgu4ekT3c&ab_channel=JeaniceBarcelo
OR Press Ctrl+Click (on the image below) to follow the link.

Lisa Phillips (CFR)

Copy and paste the link below to your web browser.
https://www.youtube.com/watch?v=UonnFuHLJKc&ab_channel=Astral7ight
OR Press Ctrl+Click (on the image below) to follow the link.
Listen to parts 1 through 8.

Radio Presenters –Contact Donald Marshall

Anyone who sincerely wants to contact me for radio interviews on their show is welcome to do this. Please contact me through Proboards by leaving a message for me to contact you.

Professionals who understand "Consciousness Transfer" –Contact Donald Marshall

Any neuroscientists, engineers or professionals who understand how consciousness transfer works, and can provide me with a detailed methodology of how to block the consciousness transfer to my REM driven clone; please message me on Proboards, and this will be greatly appreciated.

Email

I currently do not have a contactable email address. In my original disclosure, the email address has been compromised (hacked), and so has any other email accounts I created: Yahoo, hotmail, Gmail, AOL etc. It doesn't matter; they eventually get hacked; for whatever reason, the Illuminati do not want me to have an email account.

How to Learn More about Donald Marshall's Whistle Blowing Disclosures

The best ways to learn about the truth of the world is through my Facebook page and Proboards. There is a mountain of evidence which has been collated over the years, and corroborates all that I have disclosed here. I also understand that for some people it is impractical to read three years worth of Facebook posts, especially when some post are repetitive; contain unnecessary comments from trolls, shills and other disinformation agents. Therefore, I am currently compiling 5 documents which should make it easier for others to read and understand everything quickly; as well as, for others to share and spread those 5 documents including this main disclosure document –so 6 documents about the real truth of the world. All for free!!

These documents include:

- "Frequently Asked Donald Marshall Questions" –This will contain all the general FAQs which I have been asked over the years; all in one place.
- "Experiences from the cloning centre" –This document will contain the full disclosure of my REM driven cloning experiences from the cloning centre when I go to sleep; all in chronological order.
- "List of people to avoid" This will contain a whole list of trolls, shills, and disinformation agents and double agents in alphabetical order, to avoid at all costs, in real life and online; -all complied in one place; and the reasons why they should be avoided.
- "Public Figures and their relationship with Donald Marshall as REM driven clones" – this will be a complete list of every public figure I have ever come into contact with as a REM driven clone; and you will be able to read about all the public figures I have met as REM clones, as well as the experiences, all in one place.
- "The subterranean underground colonists: The Vril" –this will be everything about the biological parasites the Illuminati harbour. Yes. The Illuminati harbour biological parasites, which they use against unsuspecting humans. I told you the Illuminati were

the biggest depraved perverts ever to grace God's earth. REM driven human cloning, kept secret from the world for over 70 years is difficult to fathom as it is, as are these biological parasites. These parasites are also one of the main root causes of humanity's problems here on earth, and must be rendered extinct. In this document you will be able to learn everything about their, strengths, weaknesses, psychology, biology, ecology, sexuality and arm yourself with knowledge which ensures that humanity exterminates these parasites from our earth, forever. The secret of Vril; a secret no more!

I hope after reading my eye witness statements presented in this document that you have now began to understand that this is simply what is happening in our world today.

Heed my disclosure, very diligently. At the start of my disclosure I asked the reader to do two things:

1) Give me the benefit of the doubt –because there is nothing worse than being a victim of abuse, reporting it and the people who have the power to stop it, ignore you;
2) Set out on a genuine quest to debunk my disclosure. I understand that for some people, plenty of what I have disclosed will still sound 'too out there' beyond their current scope of reality to be believable. For such people, the honest thing to do is to start with the first topic which you do not fully understand and explore it, either by finding that corresponding topic on Proboards (Donald Marshall Proboards 2015), and continuing your research from there; or just Google any topic you currently do not understand and review the topic on websites such as New Scientist (2015), Gizmag (2015), Motherboard (2015), BBC News (2015a; 2015b), BBC Future (2015), The Guardian (2015a; 2015b) The Independent (2015a; 2015b), Daily Mail Online (2015) and start reading more articles in the Science and Technology columns because these people have been telling you what they have been doing for decades. Consequently, keep in mind that articles which discuss 'future' technologies and 'improvements' in medicine or science, are articles, which are **really** discussing present technologies, and achievements in science and medicine already realised; because most of these achievements have been realised decades ago. It just hasn't been fully disclosed publicly.

I have also saved and backed-up every reference (except the homepages of the websites referenced) in this document; therefore if a link or video is ever deleted let me know.

How Much Do You Know About Post-humanism / Trans-humanism?

Furthermore, you have to be honest here: because if you do not know much or anything about post-humanism / trans-humanism then I am afraid to say, -and this is no fault of yours – that you are behind in this the world; simply because these Illuminati people are Post-humanists; and that is the direction the want the rest of the world to go. They want the world to reach a destination where human cloning is common place; a world where downloading your mind / entire life experience onto a computer microchip and living on as a cloned version of you with the microchip running the consciousness to be common place; and these Illuminati Post-humanists want the world to head in a direction where it is commonplace to molest children through science and technology. No. This really is not Science-Fiction, this is the world we live in today; this is why such marvels in science, medicine and technology has been withheld from the general public and kept hidden by an 'elite' group of people because if these people

honestly came forward, and said “We have invented this technology and we want to use it for this “negative” purpose” –the populace would not accept it, and these people will be lynched in the streets before lunchtime. Therefore, through concealed advancements in medicine, science and technology, the Illuminati can live out their inner depraved cravings and commit crimes against humanity and the world, for which most people will be too blind to see or even fathom, because the hidden science and technology is beyond the average person’s current comprehension.

Therefore, please attain an education in post-humanism / trans-humanism because these Illuminati people believe they can rival creation, nature and the marvels of the universe through science, medicine and technology. The Illuminati go **against** creation; they go **against** nature; and they go **against** humans. They don’t consider themselves humans. They consider themselves post-humans and believe they can become “gods” through advancements in medicine, science and technology. See LawOfIdentity (2014) and Mark Dice (2014) for Richard Seed’s comments on ‘becoming gods’ through transhumanism. Richard Seed is a Physicist with a Ph.D. from Harvard University; he is well known in the controversial cloning debate and declares his aspirations to "become god" saying 'We are going to become Gods, period. If you don't like it, get off. You don't have to contribute, you don't have to participate, but if you are going to interfere with me becoming a God, you're going to have trouble. There'll be warfare.' If you value humanity, do your best to attain an education in the trend of post-humanism / trans-humanism; otherwise the future of mankind will be bleak. We must do everything we can to stop these people.

This is of uttermost importance. REM driven cloning of is the most terrible thing in the world, especially when it involves unsuspecting civilians, and worst of all, innocent children. If you choose NOT to do anything you allow the Illuminati to continue to clone your children, sisters, wives, and sons. You allow the Illuminati to continue to hijack the minds of your children, sisters, wives, and sons while they sleep, through concealed advancements in science and technology. You allow the Illuminati to transfer the consciousness of your children, sisters, wives and sons to their REM driven duplicate clone versions while they sleep, whereby the Illuminati molest your children, sisters, wives and sons, which will cause them to have learning disabilities, unexplained depression and suicidal thoughts, as well as all kinds of side effects.

This IS your ONLY chance to end these monsters. There is a deadline!

This is your **ONLY** chance to do something to end these monsters. We are on a timeline and there is a deadline. As I have already mentioned, as well as, the top scientists in the field of physics and geophysics have mentioned: HAARP is not only capable of controlling the weather; once the HAARP grid is completed and working at full power, it will be capable of mind control over entire populations. We will all be slaves to the Illuminati FOREVER. Our freewill will be gone forever. Furthermore, if they achieve their aim of time travel with HAARP technology, future generations of humanity will never be able to stop them, because as they have told me: ‘They will always be able to go back to a previous time, and correct the mistake(s) which led to their downfall’. This is the Illuminati’s end game and what they wish to achieve. This is why this disclosure is so heavy, and so important. It goes beyond REM driven cloning; although it is important the world understands REM driven cloning. The future of humanity is at stake; and because of the 2-5 year deadline until the HAARP grid is completed, it is time humanity stood up and brought an end to the Illuminati. This REALLY is your ONLY chance to end these monsters!

The only way for evil to triumph is for good people to do nothing.
Edmund Burke

Remember for every 12 months which passes military / concealed technology outstrips the technology the general public is accustomed to by 44 years (Schneider 1995; 1996). Close your eyes and think 44 years into the future. The year is 2059. What kind of technologies do you expect mankind to have? Do it for real; don't just read the words. Close your eyes and imagine. The year is 2059. What kind of technologies does mankind have? You see. It is 'out of this world' technology, right. This is exactly what is going on today in the year 2015. It's just that it is hidden. That's all. Not so difficult to fathom now.

Do NOT Be Afraid to Help. We Outnumber the Illuminati by 1,000,000:1

Don't be afraid to help. These people are easily defeated when good people stand together as one. These Illuminati people total no more than 10,000 people. 10,000 people against 7,000,000,000 (7 billion) people –that's less than 0.000001 % of the world's population. Now can you begin to understand how prevalent evil can be when a small organised group of individuals, as little as 10,000 of the world's most evil and tyrannical people all work together in unison to exert their influence over the world? The world does not have to be this way. We outnumber the Illuminati people by a 1,000,000 to 1. For every Illuminati person there is, there are **one million** people who are not Illuminati, therefore do not to be afraid to help; all you will be doing is helping humanity rid itself of its sickness. So please feel free to share and spread my disclosure far and wide.

For those of you whom this applies to: remember the Illuminati (and I know it sounds ridiculous despite the evil they do) are deeply religious. They believe anyone aiding me is part of the "Army of Light" prophesised by Nostradamus; and to harm or degrade the life of anyone assisting me will bring them to their ultimate end and they will incur the wrath of God; they will suffer utter ruin and demise in their lives if they are to hurt you; they are very scared of people who can see through the lies and deceptions they have inflicted on the world. So please, stay calm, do not stress your heart, and know that **you are safe**, and **they cannot hurt you**. You can feel safe in the knowledge that you can do the right thing by helping me. They told me this as REM driven clones on the night of 21st of February 2014 when I went to sleep. The above is exactly what they said.

For anyone interested in understanding the interpretations of the Nostradamus Prophecies, Crystal Links (2015) provides a good source for all 942 of the quatrains. Delores Cannon is also an author who has written three volumes called "Conversations with Nostradamus" and for anyone interested you can read these online (Galactic 2012a; Galactic 2012b) as well as watch her YouTube videos (CreativeForceVideo 2014; Disclose TruthTV 2015).

Yes. This is the state of the world today: a deception within a deception coated in reverse psychology; and fact is indeed stranger than fiction. Now after everything I have said, if you are still sceptical and 'in-between' on this issue then the best thing for you to do is to pay attention to your dreams; or lack of dreams –they are your own experiences and you cannot deny your experiences.

In other words, you may be having REM driven cloned experiences too; for some people they have a 'dream', where they are in the same environment, over and over and over again; or the theme being discussed in their 'dreams' is the same over and over and over again; or the environment their 'dreams' take place always appear to happen in the same 3 or 4 environments over and over again –no matter what the theme is. In each scenario there is a likely probability that these are not just dreams, and in fact these people have had their consciousness transferred to the REM driven clone duplicates and the Illuminati is trying to extract something from them, once that is done they implant a false memory (See Kim (2013) and Alford (2015) for discussions on how false memories are implanted) so you wake up with the feeling of remembering something, but in actuality it is false; or you wake up with no memory of dreams from the previous evening, which means there is a high probability that you had your memories suppressed when your consciousness was transferred to your REM driven clone. This is why I say you can be sceptical about everything I have said (for now), but pay attention to your dreams, or lack of dreams, they are your own experiences, and you cannot deny your own experiences.

Noteworthy Frequently Asked Question

A Frequently Asked Question I receive, which is worth a mentioning here, is as follows: **Q:** Donald, if everything you have said is true...; in other words human clones walk among us now in a multilayered conspiracy which reaches the highest levels of government; armed with this knowledge what does one do exactly? What happens now, Donald? You obviously want to spread the word and make people aware but to what end?

DM: In short: I want to bring a complete end to the Illuminati and usher in a "Golden Age" of mankind. This question is best answered by detailing my 'Mission and Vision' for ending the Illuminati completely.

Donald Marshall's Mission and Vision on How to Bring Down The Illuminati

- This disclosure must spread, and **spread FAST and FAR!**
- If you now understand everything I have disclosed in this document as truth, then do not waste any more time. Share this disclosure with your wives, husbands, brothers, sisters' aunties, uncles, friends, co-workers, and children. We all have a part to play in saving the world from a premature doom.
- Call friends who have not heard from you in a while and tell them you have important news to share. Share this document. Share it on social media such as Facebook; Twitter; Instagram; Dropbox; Slideshare etc.
- Keep sharing this document until it comes to the attention of the Armed Forces. The Armed Forces will have to intervene. Once the Armed Forces intervene we will have reached the middle stage of this vision and will be witnessing a complete end to the Illuminati. Until then, we're in the beginning stages, so please; spread this document faster and further. The quicker it is spread; the quicker the Illuminati are ended.
- Once the Armed Forces have intervened a Military coup can be orchestrated against these vile people.
- Cloning centres can then be shut down once these people are overthrown.

- The freeing of any missing people (children; teens; adults) trapped in the cloning centres can commence (once the Armed Forces intervene).
- HAARP (as well as other highly advanced technologies) can now be contained and not used for adverse effects against the world (once the world learns of this disclosure).
- These Illuminati people will then HAVE to appear in court for their crimes against humanity.
- Suing the Illuminati members in court (once court proceedings commence... we will be past the midpoint of my vision, and closer towards witnessing a complete end to the Illuminati).
- The populace (and it will be your choice) can then have their REM driven clone experiences restored and also sue and claim any legal reward / compensation.
- After the populace has sued the Illuminati for their crimes against humanity; the punishments can commence.
- Punishments will include: imprisonment and executions of these sick and malevolent people. The imprisonment and executions of evil Illuminati members will bring an end to the Illuminati.
- After the punishments and executions; Governments worldwide can now be replaced with incorrupt individuals, worldwide.
- The structure of Governance will also have to change. The reason for this because future generations will always be able to check their leaders and governance more appropriately; so that the depraved and subhuman acts I described can NEVER be committed against humanity again; nor will world leaders be capable of committing such monstrous crimes in such secrecy ever again.
- Ensuring that the laws of the land always progresses in line with advancements in medicine, science and technology; as well as, ensuring law progresses in the directions of Research and Development (R&D) regarding future technologies, science and medicine.
- Release of technologies, science and medicine which benefit mankind.
- Commence a “Golden Age” of mankind.

If you do not fight the corruption and you do not stand up for what is right in life, you end up being a serf and a slave and you are leaving your children a world in which you would not want to live in yourself, so how can you in decency behave that way? You have to stand up for what is right in life, and unless you do that you are nothing.

Aaron Russo

Empowerment by Virtue of Golden Truth

As you can see, despite all the horror of the world I currently present: if everything goes smoothly, the good people of this world, truly will inherit it. This is why despite any anger, sadness, or fears you may have; you must not riot, damage property or cause chaos or bring about any other form of public dissension. You cannot stay silent, or ignore the issue in the hope that the threat removes itself. You are called to act; you must take action to help bring the Illuminati to an end; you must act while at the same time, you must maintain your composure and resolve to ensure that the whole procedure goes smoothly, and we all inherit a world we want to live in.

Your life, **at this very moment**, is more important than you may have probably ever imagined. You have purpose. Through you, and other good people around the world, together we can bring an end to such unspeakable forms of tyranny in this world. It is my humble stance that you have now become truly empowered with golden truth and you are now compelled to bring this tyranny to an end.

Do not waste the knowledge you have obtained from this disclosure. It is my only hope to escape this man made living hell. It is my only hope, as well as, the hope of many REM clones imprisoned there, as well as, real people who go missing daily, and are trapped in the cloning centres.

We sincerely beg you.

Donald Marshall

Appendices

Appendix A: Thien Thanh Thi Nguyen (Tila Tequila) Transcript

Link: https://www.youtube.com/watch?v=7mRZ7ItF9ls&ab_channel=Astral7ight

00.00 – 1.10 min: You know what... since you f****** with my program darling Queen Elizabeth [II] and the paedophilia ring and the cloning centres, and the cloning centres. That's right darling the cloning centres. Parents listen to me right now, they are blocking me but that is quite alright. They are blocking me but that is quite alright. Because I have many, many other forces; I shall not say their names right now, but I have many big plans to expose all of you disgusting, sadistic f***s! Okay? That is all. I shall save that for another time. But, however, I shall REPEAT: that was just an introduction to the reptilian family, leading all the way back. They call themselves the "The Black Nobility". Now that is just one part of it; alright?

1.11 -2.47 min: The Black Nobility; the reptilian family; all the way back from ancient times; so which they think... they feel like they are the divine chosen ones... from whom may I ask? Definitely. Definitely not God. Our creator of the world. Reptilians: they feed on blood; children; the paedophilia ring; recently busted. Oh! It has been going on for centuries. Parents listen to me carefully. I don't care if I'm cutting out. I will continue this and I am not alone on this battle. Believe THAT! Believe THAT! I am not alone on this battle. I started out alone but I am marching on with MILLIONS; okay? So sit your old a** down okay. Because you are gonna roll over, but it doesn't matter anyway because you are all ancestral f***s! Who interbreed... ancestral f*****g... and then... and then... Oh! Only going to talk about cloning those children and... oh! And all those many children's parents listen to me carefully.

2.48 -4.24 min: Hundreds of missing children come up every year. You wonder... why? How? How could this be? And then there is so called CPS [Child Protection Services] or whatever they are called; they come and take your children, just, just for nothing; right? Not to discredit everybody, because not everybody is bad. I'm talking about the bad people. And they take your kids... they take them as this... they treat them like... I can't even say the word. It's disgusting, it's sadistic. They... they... they take your kids... they toss them out like little [inaudible] cause they are so f*****g... Pardon my French, but then again when I'm dealing with these evil cum-buckets I have no holy words coming out of my mouth, because these are the only words they resonate to. So therefore that's how I refer to them. Because they can only [inaudible] ...their masters whiplash on them with these [inaudible] words of cursing, vileness and slaving and that is not what the true God is; okay? The God of Hell...; Anyways...

4.25 – 5.30 min: There are these CLONING CENTRES where they take your children and do sadistic things to them. I'm not even talking about child molestation here; not to mention; uh there is one of them that got caught, flying out to Florida; to meet up with a four year old little girl, to have sex with a four year old girl. That's right. Google it because it is so highly sinful... We have commercials about... you know starving kids; you know save the starving kids and it is heartbreaking. We can have commercials about it... why? Because it is a horrible thing and people can have commercials about it. WHY do we not have commercials about... 'Daddy please don't, don't. Mommy please don't let daddy let daddy touch me?' – because it is disgusting! It is so disgusting; beyond sin that no one, NO ONE, can even make a commercial about that because that's how sinful it is.

5.31 – 7.19 min: Do you understand that? Do you understand how sinful that is? These people, I'm not even going to call them people; alright? They take your children; they not only molest them; men f*** them and make them shoot each other. They give them guns. It's either you shoot him or I'm gonna shoot you. They are... mind you, they are children. Children. Yes. I'm speaking out, because I... uh! Who else is doing this? You're all just [inaudible]... shame on you... And actually the most recent paedophilia... got taken down... WOW! How long did that take? Really?! Do you know how long this has been going on? *Sigh* Alright I'm gonna calm down... but as a parent and I love parents out there. My heart goes out to all the parents out there who have missing children. You know, we all pray for them; every day. And I put on a bold face in public every day; because there needs to be someone strong, believe that. But my strength comes from somewhere... that I have a very vulnerable emotional side where I feel very strongly for these children and innocent people. So therefore I want to speak out.

7.20 – 9.10 min: I have and I have my passion too; and in the end you shall all know why I am so passionate about exposing every single one of these scumbags; okay? The truth shall prevail and you all will know why. So, as for you parents... ah... there are no words to describe. But let me just expose because you can't just... there is a point where you CANNOT just turn the other way. You know this stuff is going on; and you go 'Oh well... that's their problem. Let's just turn the other cheek.' How long are you going to turn the other cheek, until it happens to your own freaking children? When, when, when your own child; three years old, get's run out [kidnapped] and gets blasted right in the head with a gun... yeah... there's more to that people; okay? And I'm not just saying that coming from some... I mean, actually, mothers, fathers out there... If you found out... I'm sure you would do way worse than what I am just saying. I'm just using voc. I'm just annihilating them vocally. I'm sure the parents out there who find out what their children have gone through, their missing children. I am pretty positive more than just a vocal annihilation of these scumbags that do this to your children; okay?

9.11 – 10.32 min: So keep on turning the other cheek folks. Hey, go and turn the other cheek; you are with the others. I am not. I AM NOT. Like I said you... There is only two ways to go about this: you're either with us: the good guys, or you're with the others. There is no in-between. Cause if you are in-between, hiding like cowards, turning the other cheek; doing whatever; well then you are a freaking coward and you are just a sheep. And sheep end up dying because you know what you are owned by "The Others". So pick one: you're either one of us: the good guys or you're part of the others. That is simple as that! Two choices: good guys; bad guys. In-between you're dead because the bad guys are going to suck your soul out [transfer your consciousness to your REM driven clone] and do some sadistic stuff to you and watch, and make you watch while they pretty sadistic stuff to your children as well.

10.33 – 11.33 min: Do you know why they love children? Because they are innocent souls; they're innocent... they're, they're the most innocent pure beings in this planet. They're not harmed by anything. They're new to the world; bright-eyed pure innocent children. That is why these disgusting paedophile and these clone rings; cloning centres; satanic rituals; Brownsville Texas... There are many other cloning centres where they take your children that go missing. And you wonder why? What happens to them? I'm sorry to break this to you but that is what happens. Now either do you want to know what happens to them or do you want to turn the other freaking cheek?

11.34 – 13.09 min: Tune into my next show. I'm gonna upload stuff; I have an arsenal ready to blow up! Okay. And I have reason behind this. You all should know my personal reason soon; but this has nothing to do with me right now. But know that I'm back, I'm back with a vengeance and I'm back with an army full of people around the world who are sick and tired of treated like animals; or quote, unquote "COWS". We all know what that means. For the outside world (the masses) we all know the term "sheep", sheeple. But for the insiders we know what the cows are don't we? You know what "The Others" like to do with the cows, right? They start to herd you in... and to... yeah...I'm gonna end it at that. And to all the parents, families and children out there, I love you so much. I... have to maintain composure, because that is what I do. That is all. Over and out.

Appendix B: MK Ultra

MK Ultra *-noun:* [Manufacturing Killers Utilizing Lethal Tradecraft Requiring Assassinations] The goal of mind control, using MK Ultra technology is to program an individual to carry out any task against their will and self-preservation instinct, and to control the absolute behaviour and thought patterns of the individual.

.

Modern-day MK Ultra involves an implantable microchip which is inserted into a Mark 2 clone of the victim. Every thought, reaction, hearing and visual observation causes a certain neurological potential, spikes, and patterns in the brain and its electromagnetic fields, which can now be decoded by the implantable microchip into thoughts, pictures and voices. The thoughts, pictures and voices of the implanted Mark 2 clone (victim) can now be displayed visually and heard on any system capable of converting visual images, such as a television or a computer. These images are usually displayed on a giant screen at the cloning centre.

The purpose of MK Ultra is to elicit a specific conditioned response in a victim (desired by the programmer) to an otherwise neutral stimulus. In other words, through the process of "classical conditioning" (which involves learning a new behaviour via the process of association. In simple terms two stimuli are linked together to produce a new learned response in a person) the implanted Mark 2 REM duplicate clone (victim) is placed thorough many similar recurring scenarios which are experienced (or perceived) by the victim as "real", because the programmer manipulates the victim's audio and visual field, and continuously pairs the victim with the neutral stimulus, so that either a positive or negative conditioned response is elicited in the victim towards the neutral stimulus.

In other words an implanted victim can be placed in many recurring situations deemed as frightful, where a mystery stranger saves the victim from the frightful situation over and over again. The victim will now have positive associations towards the mystery stranger and therefore the conditioned response is now one of 'positive associations' (towards the mystery stranger who did not elicit such a reaction before).

MK Ultra techniques are administered through Mark 2 (sleep driven) clones. In other words classical conditioning happens when the person sleeps. Memory suppression technologies are also used in conjunction with MK Ultra technology, which enables the programmer to control certain memories the victim remembers. The use of memory suppression technologies and MK Ultra technology allows the programmer to reinforce behaviour and elicit specific conditioned responses (in an original).

Therefore, in our example above, when the original meets the mystery stranger in real life, the original (victim) will be predisposed to the mystery stranger and automatically 'feel safe' around this person and may even believe that he / she should 'date this mystery stranger' – depending on what was programmed; because the victim was conditioned to elicit such an emotional response towards the mystery stranger in his / her sleep as a Mark 2 REM driven clone through MK Ultra functionality.

MK Ultra can also be used to create zombified individuals who are programmed to murder and remember nothing of their crime afterward. MK Ultra (technology) can also be used to disrupt the memory of the original, discredit people through unusual behaviour, make the person insane or commit suicide and murder.

MK Ultra has much functionality. Furthermore, because of its video and audio projection functionality, MK Ultra can also be used to compose music. MK Ultra is capable of relaying the Mark 2 REM driven clone's subconscious and conscious mind as visual images and audio, projected onto a screen. Therefore thoughts, pictures and voices which have been experienced consciously and subconsciously in one's life can be displayed visually and audibly on a television or computer screen. The Mark 2 clone now has the option of harmonising these thoughts, pictures, and voices into a coherent order which produces music through the thought process of his or her imagination. See Jim Cristea (2009); Berkeley News (2011); UC Berkeley Campus Life (2011) CTForecaster (2013); nature video (2013) and Stromberg (2013) for examples and discussions and the capability of MK Ultra technology.

Appendix C: The Illuminati

Illuminati *–noun:* A modern-day criminal organisation operated by reprobate (depraved, unprincipled and wicked person) criminals. Their main agenda: is to enslave the whole world through advanced concealed technologies.

Today's Illuminati trace their roots back to Professor Adam Weishaupt who found the Illuminati on 1st May 1776. Since the inception of the Illuminati the intent has always been, and remains: "to bring about a NEW World Order that writes God out of the picture and deifies (glorifies) Lucifer." This intent is still prevalent today. The following excerpt is derived from A. Ralph Epperson (1990) *The New World Order:*

> Weishaupt was a teacher of Cannon Law (law governing the affairs of a Christian Church, especially the law created or recognised by the Papal authority in the Roman Catholic Church) at the University of Ingolstadt in Bavaria, now part of Germany.
>
> He even told the world, in his writings, where he would conceal the Order: "None is fitter than the three lower degrees of Free Masonry; the public is accustomed to it, expects little from it, and therefore takes little notice of it." He felt that this secrecy would lead him to success because he felt no one would be able to break into it. He wrote: "Our secret Association works in a way that nothing can withstand ...."
>
> Weishaupt accepted the fact that all secret associations and secret orders had two doctrines, one concealed and reserved for the Masters... the other public ...." and the Illuminati was [and are to this day] a secret society with two doctrines.
>
> Professor Weishaupt, its founder, boasted of his organization's secrecy. He realized that this secrecy would enable them to decide the fate of nations and because their deliberations were secret, no outsider could interfere. He wrote: "The great strength of our Order lies in its concealment; let it never appear in its own name, but always covered by another name, and another occupation." Weishaupt later wrote about that secrecy in a letter to a fellow member of the Illuminati: "Nothing can bring this about [the new world order] but hidden societies. Hidden schools of wisdom are the means which will one day free men from their bonds [the "bonds" of religion] Princes and nations shall vanish from the earth." So the secret societies were created to bring the world to the new society known as the New World Order. The members of these organizations obviously feel that their goals are so noble that they may perform whatever tasks are required of them to bring that goal to fruition. This means that murder, plunder, and lying all become acceptable as long as these methods assist its members in obtaining their goal.
>
> Adam Weishaupt, the founder of the Illuminati, wrote over and over and over again, that "the ends justified the means." Weishaupt also told initiates to use whatever means, which included murder, to achieve the goals of the association that he was joining. And that the major goal of the Illuminati, was the destruction of all religion, including Christianity. That meant that if Christians physically stood in the way, they could be removed by simply murdering them. Weishaupt even went so far as to say that anyone not willing to take the life of another was unfit to join the Illuminati. He wrote the following in a letter to a fellow member in 1778: "No man is fit for our Order who is not ... ready to go to every length ...."
>
> Another reason, that Weishaupt felt that the Illuminati would succeed, was the fact that he was offering his members worldwide power. He felt that this inducement would enable him to draw into his organization only those who would do anything to satisfy that desire for power. He wrote: "The true purpose of the Order was to rule the world. To achieve this it was necessary for the Order to destroy all religions, overthrow all governments and abolish private property."

> But his religion had a different base than the traditional religion: his was based upon a worship of reason: "... then will Reason rule with unperceived sway." "... Reason will be the only code of Man. This is one of our greatest secrets." "When at last Reason becomes the religion of man, then will the problem be solved." Weishaupt's dedication of his organization to "reason" makes some sense when the reader recalls that "reason" has been defined as the "unbridled use of man's mind to solve man's problems without the involvement of God." The Bible calls this "the fruit of the tree of the knowledge of good and evil." It was this knowledge that God wanted man not to have, and it was the promise made to man by Lucifer that man could have it by eating of "the fruit." In addition, Weishaupt's religion offered its believers a reward not offered by any other religion: worldwide power!
>
> Weishaupt wrote: "The pupils [members of the Illuminati] are convinced that the Order will rule the world. Every member therefore becomes a ruler." Weishaupt's religion not only offered power to his believers, but he offered them something else not guaranteed by any other religion: worldly success. He said that once a candidate had achieved the exalted degree of Illuminatus Minor, the fourth of the thirteen inside his Order, his superiors would: "assist him [the member] in bringing his talents into action, and [would] place him in situations most favourable for their exertion, so that he may be assured of success." Finally, the goal of the Illuminati was "man made perfect as a god - without God."

The ideology of "man made perfect as a god –without God" still remains to this day, and it is practiced by today's Illuminati members. The above phrase is what ties in Luciferian worship and trans-humanism. Lucifer is idolised by Illuminati members as the deity who gave man 'knowledge' and therefore is worthy of worship; God, -according to Luciferians, -did not want man to have knowledge and therefore is despised by Luciferians. Ingrained in the trans-humanism doctrine is the believe that: 'man can become 'god' through science and technology and in turn overthrow the Creator of the universe: God'. See LawOfIdentity (2014) and Mark Dice (2014).

These are the basics of Luciferianism. Therefore everything which is natural or pertains to nature must be contended or destroyed by Luciferians. This is why Illuminati members endorse having sex with children, killing first born sons, and drink blood. All the above go against nature and according to the 'edicts of Lucifer': paedophilia makes the person committing the act younger (it doesn't, it is just an excuse to act perverse on children because they know children are vulnerable); killing your first born son gives you good luck and fortune in this life (so yes, some Luciferians have sacrificed their first bon sons); and Illuminati members believe drinking blood / cannibalism is a 'purifying agent' (although in reality it causes spongiform encephalitis (holes in the brain)).

Modern-day Illuminati members still retain the goal of its founder "to bring about a NEW World Order that writes God out of the picture and deifies (glorifies) Lucifer." Infiltration through secrecy, still remains their mode of operation, for the current Illuminati and therefore they have secretly infiltrated all the major religions on earth; government and education – where each successive generation is being dumb down; they have continually diminished the ability for individuals to own private property, or claim inheritance; divided people against each other to continually diminish patriotism; and have continually diminished family values.

They also compartmentalise their knowledge between members. Until I fully exposed the Illuminati, many people who have been REM clones at the cloning centre did not know they were in fact REM driven clones, and thought they were in the 5th Dimension; the astral plane; a singularity; the spiritual realm; Valhalla; quantum hopping; a time stutter etc. or whatever else the Illuminati told them.

Today's Illuminati members also meet in secret (just like the founding members) as REM driven clones, **when they go to sleep**. Furthermore, because Illuminati meetings are in secret and not many people know the exact location (because knowledge is compartmentalised) of the cloning centre; or the fact that their consciousness has been transferred to Mark 2 REM driven clone bodies at the cloning centre (and they are not in their original bodies); as well as the fact that unsuspecting civilians have their memories suppressed; the points mentioned above are the reasons the Illuminati believe 'they are all powerful and untouchable'; and as a consequence, today's Illuminati members do all the disgusting things they want, because they believe no outsider can interfere.

The ring leaders of the Illuminati today also believe "the ends justify the means". This is why they clone, torture, molest, murder, and rape unsuspecting civilians as REM driven clones in their sleep. The Illuminati of today offer their members incitements to go along with their agenda and not oppose them (or face death). Another popular method is to entice their target with many, many wonderful prospects, and have the target believe they are joining a noble and prosperous venture, so that the target fulfils the objectives of the Illuminati unknowingly; promoting the Illuminati in a positive way, because the target has been deceived to perceive the nature of the Illuminati as 'positive'; by the time the target finds out the true intent of the Illuminati, and the evil which emanates from it, it is too late. Those who rise up in the ranks of the Illuminati are the men and women who have an insatiable lust for power, and most importantly: the men and women who want to rule the world.

Modern-day Illuminati members also wish to become gods (through technology); overthrow the Creator, and achieve their overall aim of enslaving mankind. This is why they clone people, and clone people in high rank society from all walks of life (movie stars, musicians, politicians etc.; whether the person willing wants to be part of the Illuminati or not) so long as that person is in a position of power and influence, the Illuminati clone that person, and threaten that person, for example -"Hey, you're going to hang with us –or else" –through such coercion, the people in high rank society who have power and influence will not oppose the Illuminati's plans to become gods; enslave mankind forever; and rule the world. Another reason for cloning high rank society is to include these people into the Illuminati (willingly or unwillingly) to ensure the world's populace remains in ignorance (because once all the world leaders and high rank society are cloned and under the coercion of the Illuminati nobody in a position of influence or power can warn the populace against the Illuminati) until the Illuminati's plan is completed and they have enslaved the world forever.

The Illuminati's overall aim of 'becoming gods' and ruling the world, as well as, mind controlling all the inhabitants of earth is also the reason the Illuminati:

- Administer drip feed disclosure through media, by telling some truths mixed with lies in order to conceal their true intentions and overall aim, and prevent the betrayed partner (the public) from ever discovering "the complete truth";
- Administer evaluative conditioning, by placing their symbols and ideology in popular media with positive associations, so that the unknowing and unsuspecting public will eventually become predisposed to the Illuminati and unsuspectingly have a positive or neutral response towards the Illuminati;
- Because they want to become 'gods' is also the reason the Illuminati is promoting RFID microchips and only discussing RFID microchips positively, while at the same time placing suppression (gagging) orders on anyone who speaks negatively about RFID microchips –which implies an unsuspecting public will willingly accept the microchip; and at the point of transaction, the person will have (unknowingly) given up their privacy to a third party (the Illuminati) for the rest of his / her life;
- Their aim to become 'gods' is also the reason the Illuminati are hurriedly trying to complete the HAARP grid across earth –because a complete HAARP grid will allow them to achieve their goal of mind control over the entire world; which fulfils their objective of becoming gods; because a complete HAARP grid will be capable of time travel, and therefore the Illuminati will be capable of going back to a previous time to correct the mistake(s) which led to their downfall; the Illuminati members will retain the knowledge of the previous time, and the rest of humanity will have no recollection of such a memory.

The Illuminati is **not** a joke. It is **not** fiction. They are very real, and part of humanity's reality; and through advanced concealed technologies the Illuminati aim to enslave humanity forever. The ring leaders of the present Illuminati includes Queen Elizabeth II, Prince Philip Duke of Edinburgh, Prince Charles of Wales and Vladimir Putin. I have also detailed the actions of the ringleaders in the main text in this disclosure, as well as, detailed other modern-day evil Illuminati members on my Facebook and Proboards. It is time the good people of earth, stopped being afraid, do the right thing, put a stop to this evil, and save themselves, as well as their children's children from being slaves forever. Spread and share this disclosure.

Glossary

Aneurysm -*noun:* An excessive swelling of the wall of an artery at a fixed point in the body. A brain aneurysm is therefore a: bulge or ballooning in a blood vessel in the brain. It often looks like a berry hanging on a stem. A brain aneurysm can leak or rapture, causing bleeding into the brain.

Brain Aneurysm -*noun:* see Aneurysm.

Clone –*noun:* a cell, group of cells, an organism produced asexually from a single ancestor and is genetically identical to a single ancestor.

Concealed Technology -*noun:* hidden machinery and devices undisclosed and currently unavailable for public consumption. Concealed (or military) technology develops at a rate of 44 years for every 12 months which passes in comparison to the technology the public is currently accustomed to. Origin: Phil Schneider.

Cloning Centre –*noun:* a physical location (on earth) where duplicate and replicate clones are produced. These physical locations are usually Deep Underground Military Bases (DUMBs). DUMBs have an entire floor dedicated to cloning. It is also a place where Illuminati members meet with each other as REM driven clones. The above-ground cloning centre where many high profile people attend can be found within a radius of 5/6 hours drive from the Robert Pickton Farm Port Coquitlam, British Columbia, in Canada, somewhere at a remote nature reserve.

Cloning Technology -*noun:* the technological advancements in medicine, science and technology used to produce duplicate and replicate copies of originals.

Conditioned Response -*noun:* an automatic response established by training to an ordinarily neutral stimulus.

Conditioned Stimulus –*noun:* A previously neutral stimulus that, after repeated association with an unconditioned stimulus, elicits the response produced by the unconditioned stimulus itself.

Consciousness –*noun:* the state of being aware of and responsive to one's surroundings; a person's awareness or perception of something.

Consciousness Transfer -*noun or verb:* the process of transferring or copying the mental content (including long-term memory and "self") from a particular brain and copying it to a computational device; artificial body or avatar body such as that of a robot or clone version of the original. It is also the feat in which the person's mental content (long term memory and "self") moves from one body into another.

Depopulation *verb:* to remove or reduce the population of, as by destruction or force.

Drip Feed Disclosure *noun or verb:* is the process of supplying information but in small amounts overtime. Drip feed disclosure is also the process of revealing information slowly overtime, possibly telling lies to conceal certain aspects of the truth until the source administering the drip feed disclosure has adequate time to let out the truth in a slow and controlled way, thereby delaying the betrayed partner (in this disclosure, the public) from having the "complete truth" for some time.

DUMB –*noun:* [Deep Underground Military Base] a facility directly owned and operated by or for the military or one of its branches that shelters military equipment and personnel, and facilitates training and operations beneath the surface of the earth.

Duplicate Clone -*noun:* a fully formed human body which is a genetic copy of original developed through the process of regenerative technology. Duplicate clones are grown in a big thick tank full of (salty) water.

Duplication Cloning -*verb:* involves agitating the cells of on an original repetitively until a fully formed human body of the original is developed. Duplicate clones take an average of 5 months to form into a fully developed human body of the original through the process of regenerative medicine and technology.

Evaluative Conditioning -*noun:* is a change in liking, which occurs due to an association with a positive or negative stimulus.

H.A.A.R.P. Technology –*noun:* [High frequency Active Auroral Research Program] a radio transmitting system that can bounce signals off the Earth's upper atmosphere, (60km (37 miles) to 1000km (620 miles) high) back to probe deep into the earth or sea. HAARP is also capable of: disrupting human mental processes; knocking out all global communication systems; changing weather patterns over large areas; interfering with wildlife and migration patterns; hurting ecosystems; negatively affect human beings health, moods and mental states; and unnaturally 'boil' the earth's upper atmosphere. HAARP used correctly will control the weather without any adverse effects.

H.A.A.R.P. Grid –*noun:* a network of radio transmitters which can bounce signals off the earth's upper surface. Each transmitter is located at a specific point across earth and communicates in unison with other radio transmitters across the earth. At this present time of writing, a HAARP grid has **not** been completed, although the Illuminati are working twice as fast to complete a HAARP grid. The threat to humanity once a HAARP grid is completed includes: mind control over the entire world's inhabitants. A completed HAARP grid will also be capable of time travel, and therefore the Illuminati will always be able to go back to a pervious point in time to correct the mistake(s) which led to their downfall. Humanity will be slaves forever.

Habeas Corpus -*noun:* is [A] writ [formal document] requiring a person under arrest to be brought before a judge or into court, especially to secure the person's release unless lawful grounds are shown for their detention.

Heart Attack -*noun:* A sudden occurrence of a blockage of the flow of blood to the heart.

Human Clone –*noun:* The creation of a genetically identical copy of a human.

Ionosphere –*noun:* the layer of the earth's atmosphere which contains a high concentration of ions and free electrons and is able to reflect radio waves. It lies above the mesosphere and extends from about 60km (37 miles) to 1,000 km (620 miles) above the earth's surface.

Illuminati –*noun:* A modern-day criminal organisation operated by reprobate (depraved, unprincipled and wicked person) criminals. Their main agenda: is to enslave the whole world through advanced concealed technologies. See Appendix C for further discussion.

Mark 2 Clone –*noun:* Is a sleep driven clone; specifically, a REM sleep driven clone. A Mark 2 Clone is activated by transferring the consciousness of an original into a Mark 2 Clone **only when** the original reaches REM sleep (usually 90- 110 minutes **after** the original falls asleep). Once the consciousness of the original is transferred from the original's body to the Mark 2 Clone, the Mark 2 clone is now capable of motion: such as walking, talking etc. The Mark 2 clone 'drops limp' and becomes motionless once the original wakes up from sleep. The original's consciousness no longer resides in the Mark 2 clone (once the original is awake) and therefore the Mark 2 clone is now incapable of motion. Mark 2 Clones are also known as "REM Driven Clones" and "REM Duplicate Clones".

Memory Suppression –*noun or verb:* is the selective removal of memories or associations with the mind using memory suppression technology.

Memory Suppression Technology –*noun:* any scientifically advanced technology used selectively to remove memories from the conscious mind.

Mind-Voice Technology –*noun:* an advanced technology capable of reading, listening, hearing and broadcasting a person's inner voice or thoughts. It is capable of replicating sounds **exactly**. Therefore an individual can hear the sound of drums, a guitar or any instrument and replicate that sound exactly just by thinking about it. Consequently, Mind-voice technology has the functionality of producing music.

Military Technology –*noun:* machinery and devices developed from scientific knowledge used by the Armed Forces which advance at a rate of 44 years for every 12 months which passes, compared to the technology the public is accustomed to. Origin: Phil Schneider

MK Ultra -*noun:* [Manufacturing Killers Utilizing Lethal Tradecraft Requiring Assassinations] The goal of mind control, using MK Ultra technology is to program an individual to carry out any task against their will and self-preservation instinct and to control the absolute behaviour and thought patterns of the individual. See Appendix B for further details.

Neutral Stimulus –*noun:* is a stimulus which initially produces no specific response other than focusing attention. In classical conditioning, when used together with an unconditioned stimulus, the neutral stimulus becomes a conditioned stimulus.

Negative Association -*noun:* is an undesirable experience or perception.

Negative Stimulus -*noun:* a stimulus with undesirable consequences.

New World Order -*noun:* [NWO] Agenda. The whole NWO agenda is to turn humanity into mindless slaves forever; whereby the post-humans / trans-humans mind control the entire world's populace either through RFID microchips or a completed HAARP grid. Another aspect of the NWO agenda is to depopulate the world's current population of 7.3 billion people to 500 million people (and never exceed a world population of 500 million people afterwards); ruled by a one world government; a one world ruler; with a one world religion. See Appendix C for more details.

Original –*noun:* A person who is **not** a clone.

Pain Receptor -*noun:* Any one of the many nerve endings throughout the body that warn of harmful changes in the environment such as excessive pressure or temperature.

Positive Association -*noun:* is a desirable experience or perception.

Positive stimulus -*noun:* a stimulus with desirable consequences.

Posthumanism –*noun:* seeks to rewrite the very definition of being human. It is the condition in which humans and intelligent technology become intertwined. In the Posthuman there are no essential differences or absolute demarcations between bodily existence and computer stimulation, cybernetic mechanism and biological organism, robot technology and human goals.

Posthuman -*noun:* see Posthumanism.

Project MK Ultra -*noun:* see MK Ultra.

Regenerative Medicine -*noun:* (of a living organism) the process of re-growing new tissues after loss or damage.

Regenerative Technology -*noun:* any machinery or device developed from scientific knowledge which has the capability to re-grow new tissues after loss or damage.

REM Sleep –*noun:* [Rapid Eye Movement] is the fifth stage of sleep in the sleep cycle. It takes 90 - 110 minutes to reach REM sleep after we fall asleep. REM sleep is also known as the "period of paralysation". The involuntary muscles such as the brain become more active whereas voluntary muscles (those that you move by choice) such as your arms and legs become more relaxed or paralysed. REM sleep is a kind of sleep that occurs at intervals during sleep, and it is characterised by rapid eye movements.

REM Driven Clone -*noun:* [Rapid Eye Movement Driven Clone] a clone that can only become activated, once the original is in REM sleep. See Mark 2 Clone.

REM Duplicate Clone -*noun:* [Rapid Eye Movement Driven Clone] A clone developed by regenerative medicine and technology and is therefore an identical copy of an original. REM duplicate clones can only become activated when the original is in REM sleep. See Mark 2 Clone.

REM Driven Clone Death –*noun:* the process where an original dies because of constant torture to their REM driven clone or where a constant electrical current is applied to the REM driven clone resulting in death of an original usually in the form of an aneurysm or heart attack (because consciousness is linked) in the original's body.

REM Driven Clone Torture —*noun or verb:* the action or practice of inflicting serve pain on a REM driven clone. REM driven clone torture causes biological and physiological responses in the original's body because consciousness is linked. Intermittent REM driven clone torture (depending on what is done) causes the original to experience severe headaches, an upset stomach, achy limbs, sickness; a weakened heart. Continuous REM driven clone torture will lead to the death of the original; usually in the form of aneurysm or heart attack in the original's body.

Replication Cloning –*verb:* involves giving birth to a genetic identical of an original where the newborn starts life off as a baby and matures. The newborn is referred to as a clone.

RFID Technology [Radio Frequency Identification] **-***noun:* are electronic microchips the size of a grain of sand that can be directly embedded into the human flesh. RFID microchips communicate wirelessly through the use of electromagnetic fields to transfer data. RFID microchips link the brains of people via the implanted microchip to satellites controlled by ground base super-computers. The dangers of RFID microchips to the implanted person are: total loss of privacy and total control of the person's physical body functions, mental and emotional thought processes, including the implanted person's subconscious or dreams –for the rest of that person's life! RFID microchips are also tracking devices, and the implanted person can be tracked anywhere on the globe.

Selling One's Soul -*verb:* to sell the use one's "Mark 2" REM driven clone to the Illuminati, for the Illuminati to use the individual's Mark 2 REM driven clone in whatever manner the Illuminati wishes. There are no returns once the individual has signed over his / her (soul) Mark 2 REM driven clone. When an individual sells their (soul) Mark 2 REM driven clone, the person has also entered into a contract to sell the Mark 2 REM driven clone(s) of their current children (if they have any) as well as any unborn children the person may have later in life. The person sells all their descendants (souls) Mark 2 REM driven clones to the Illuminati, once the individual sells their (soul) Mark 2 REM driven clone to the Illuminati. Selling one's (soul) Mark 2 REM driven clone is considered **a serious business transaction** to the Illuminati. There are no returns. If the person ever makes a fuss and wants their (soul) Mark 2 REM driven clone back, the Illuminati will either torture the person's Mark 2 Clone, or apply a constant electric current to the person's Mark 2 Clone until the person either has a heart attack or aneurysm in their original body. This is what public figures are hinting at when they say "They have sold their soul". They have sold the use of their Mark 2 REM driven clone to the Illuminati. Selling one's soul is not a joke. Never sell your soul.

Stimulus –*noun:* is something that causes a reaction, especially interest, excitement or energy. It is also an energy change registered by the senses. For example a stimulus can be a shinny object for a baby.

Technology –*noun:* machinery and devices developed from scientific knowledge.

Technological Advancement –*noun:* is incorporating, by means of experimental development, a characteristic or capability not previously existing or available in standard practice, into a new or existing process or product that enhances a product's performance. Novelty, uniqueness, or innovation alone does not indicate a technological advancement.

Transhumanism –*noun:* the belief or theory that the human race can evolve beyond its current physical and mental limitations, especially by means of science and technology.

Unconditioned Response –*noun:* is a response to a neutral stimulus we have no / little control over. It is a natural automatic response. For example, food is an unconditioned stimulus for a hungry animal, and salivation is the unconditioned response.

Unconditioned Stimulus –*noun:* A stimulus that elicits an unconditioned response.

BLUE BLOOD, TRUE BLOOD
CONFLICT & CREATION

A Personal Account

By Stewart A. Swerdlow

Expansions Publishing Company, Inc.
P.O. Box 12, St. Joseph MI 49085

With Excerpts From

Belief Systems Shattered

by Janet Swerdlow

BLUE BLOOD, TRUE BLOOD: CONFLICT & CREATION
A Personal Account
Copyright © 2002 Expansions Publishing Company, Inc.
Cover Art and Illustrations by Lori Sarich
Typography and book design by L'OR Intuitives
Editor: Janet Swerdlow
Published by: Expansions Publishing Company, Inc.
P.O. Box 12
Saint Joseph MI 49085
All rights reserved. Printed in the United States of America. No parts of this book may be used or reproduced in any manner whatsoever without written permission except in the case of brief quotations embodied in critical articles and reviews.
For further information contact Expansions Publishing Company, Inc.
P.O. Box 12, Saint Joseph MI 49085 U.S.A.
email: stewart@stewartswerdlow.com
janet@janetswerdlow.com
Website address: www.stewartswerdlow.com
Library of Congress Cataloging-in-Publication Data
Stewart Swerdlow
Blue Blood, True Blood: Conflict & Creation
A Personal Account
256 pages
ISBN 0-9626446-6-8
Library of Congress Catalog Card Number: In Process

Other books by Stewart Swerdlow:
Montauk: The Alien Connection
The Healer's Handbook: A Journey Into Hyperspace
The White Owl Legends: An Archetypal Story of Creation
Forthcoming books:
Dream Dictionary
Mind-Pattern Analysis
Books by Janet Swerdlow:
Belief Systems Shattered
In Search of Yourself
Practical Tips For Everyday Living
Life Support Group ™ Leader's Manual
Little Fluffs Children's Book Series
Forthcoming by Janet Swerdlow:
Children's Group Leader's Manual

DEDICATION

It is with the deepest of heart and soul felt gratitude that I wish to thank my wife, Janet, for her unconditional love and support during my journey through the depths of hell. She was there all the time, waiting for me, and never giving up hope. Without her I would not be here any longer. There are no words in any human language that can express how immensely grateful I am to her for being my twin flame/other half. I have learned brutal lessons these past couple of years. They would have
all been in vain if it were not for Janet. Thank you, my true love, from the depths of my being. There is also a great admiration for my parents and sister who also stayed vigilant during these trying times. They left no stone unturned in exposing the vulgarity and depravity of the demons sent to harm me. I
give my wonderful family eternal hugs, and love, and the peace of mind that I shall never be captured again.

As always, my incredible children, who love me without end, have proven to me that there is no space or time that can separate me from them. As they grow into adulthood, I realize that children are a gift that we are allowed to take care of for a while so that the magnificent blossom can grow forth on its own and create a new garden. My children are my jewels and my treasures. Thank you for believing in me.

Finally, I want to thank my fabulous and generous friends who have made my return to my own life easy and happy. Their generosity is overwhelming and their love unforgettable. I am proud to count
among my friends: Steve and Sandy Wade, Todd Berran, Lori Sarich, Duncan Cameron, Shannon O'Shea, and Aldee Filley. You have all been as dear family to me.

I also thank you, the public, both readers and students, who have stood by me through better or worse. I am grateful for your continued support and respect. It is my goal to continue to bring you the truth so that your lives may also be healed and that you may experience your personal connection to the God-Mind.

Contents

Preface 7
In The Beginning... 9
The Transparent People 13
Is This Planet Taken?..... 17
The Reptilian Agenda 19
Conflict & Creation 23
Bluebloods!..... 27
Other Alien Groups 31
The Crystal Skull 35
The Ancient Hebrews 37
The Annunnaki & The Black Race 41
Mind-Control Via Religion 43
The Roman Empire..... 49
Emmanuel 51
Magdalene Lineage & Beyond 55
The Illuminati Hierarchy 61
Blood-Ritual & Ceremony 69
Ritual In Red..... 79
My Lost Children 87
Around The World 93
Alliance En France 103
Illuminati Agent..... 109
Tango In Argentina 115
Mystery Man & Company 119
The End Of Rosie 2 125
Swiss Keys..... 129
Boy From Brazil 133
Future Illuminati Plans 139
Reflections & Observations 145
APPENDICES
Alien Groups 150
Milky Way Galaxy..... 171
Reptilian Androgyny 172
Mixture Of Lineages..... 173
13 Ruling Families - Illuminati 174
Sexuality & Mind-Pattern..... 175
News Clips from Expansions Exposé 177
Excerpts
Belief Systems Shattered
By Janet Swerdlow
All Experiences Are Neutral 183
Is Your Reaction Fear? 187
Subverting Sexuality 191
Vegetarianism---Is It Really The Way? 195
Are You A “Sleeper?” 197
Illuminati As Teachers 201
Victim Mentality 205
Are You A Mind-Control Candidate?..... 209
Earth’s Mind-Pattern 213

One Mind-Pattern=Global Control 217
Patriotism vs. Warmongering 221
Simultaneous Existence 225
Index 229
Expansions Ordering Information 249

PREFACE

AS FAR AS THE HISTORY OF THIS PLANET IS CONCERNED, YOU CAN CONSIDER THAT EVERYTHING YOU EVER LEARNED IS A COMPLETE LIE. ALL HISTORY AND SCIENCE BOOKS ARE REWRITTEN TO ACCOMMODATE THE AGENDA OF THE CONTROLLERS OF THIS PLANET. THESE BOOKS ARE JUST AS FALSE AS THE NEW AGE MATERIAL SPEWING FORTH FROM SUCH PLACES AS SEDONA AND SANTA FE, TO NAME A COUPLE OF ILLUMINATI MECCAS.

DISINFORMATION IS RAMPANT EVERYWHERE. MY INFORMATION COMES FROM MY MONTAUK PROJECT INDOCTRINATIONS, EXPERIENCES, CONVERSATIONS WITH SCIENTISTS INVOLVED IN ILLUMINATI PROGRAMS, COMMUNICATIONS WITH ALIEN AND INTERDIMENSIONAL BEINGS WHOM I MET AT VARIOUS GOVERNMENT PROJECTS, AND THROUGH THE PROBING OF MY OWN OVERSOUL.

I CANNOT OFFER YOU PHYSICAL PROOF AT THIS TIME. I CAN ONLY TELL YOU THAT IT IS AVAILABLE IN CERTAIN PLACES. ALTHOUGH ALL EXISTENCE IS SIMULTANEOUS, AND TIME AND SPACE ARE MERELY ILLUSIONS OF PHYSICAL REALITY, FOR THE PURPOSE OF THIS BOOK I WILL PRESENT THE MAJORITY OF HISTORY FROM A LINEAR PERSPECTIVE. THERE ARE ALSO INFINITE UNIVERSES, BOTH PHYSICAL AND NON-PHYSICAL, BUT FOR NOW, I WILL ONLY TELL YOU ABOUT THIS ONE.

TO UNDERSTAND HOW THE ILLUMINATI CAME TO POWER, OR EVEN TO COMPREHEND WHAT THEY ARE, IT IS IMPORTANT TO UNDERSTAND THE BEGINNING OF LIFE ON THIS WORLD AND ITS PROGRESSION.

I DO NOT BELIEVE IN ANY RELIGION, ORGANIZED OR OTHERWISE. ALL RELIGIONS, NO MATTER WHAT THEY ARE, ARE FORMS OF GROUP MIND-CONTROL DESIGNED TO MANIPULATE LARGE MASSES OF PEOPLE TO STOP THINKING FOR THEMSELVES. I DO BELIEVE IN GOD. IT HAS NO RELIGION.

IN THE SUBSEQUENT YEARS FOLLOWING THE PUBLICATION OF MY LAST BOOK, MUCH HAS BEEN WRITTEN ABOUT BY OTHER RESEARCHERS CONCERNING REPTILIANS AND THEIR RITUALS. THIS THEME HAS FOUND ITS WAY INTO THE PSYCHE OF THE PUBLIC. MOST PEOPLE ARE STILL NOT WILLING TO ACCEPT OR EVEN ENTERTAIN THE IDEA THAT HYBRID REPTILIANS ARE IN CONTROL OF THIS PLANET AND PERFORM BLOOD RITUALS AND CEREMONIES USING HUMANS AS THE SOURCE OF FOOD AND HORMONES. I WISH IT WERE NOT TRUE. BUT I CANNOT CHANGE HISTORY, CURRENT EVENTS, OR WHAT I KNOW TO BE TRUE.

THE CONTROLLERS PLAN THE PATTERN OF COMING EVENTS IN SUCH A WAY TO PURPOSEFULLY DISORIENT THE MASSES WHILE THEY ALONE SEE THE DESTINATION AND THE ORDER OF LIFE. THE MASSES ARE LEAD TO BELIEVE THAT HAPHAZARD EVENTS AMIDST CHAOS SHAPE THEIR EXISTENCE.

IN TRUE REALITY, THERE IS NO SUCH THING AS CHAOS. CHAOS IS SIMPLY A PATTERN NOT YET UNDERSTOOD OR PERCEIVED.

THINK ABOUT AN ANT CRAWLING OVER A DESIGNED, TILED FLOOR. THE ANT MAY SEEM CONFUSED OR DISORIENTED; NOT KNOWING WHICH WAY TO GO. BUT A HUMAN BEING WATCHING THE ANT FROM A HIGHER PERSPECTIVE CLEARLY SEES THE FLOOR PATTERN AND KNOWS WHICH WAY THE

ANT CAN GET TO ITS DESTINATION. TO THE ANT, THERE IS ONLY PERCEIVED CHAOS. TO THE HUMAN, THERE IS A PRESCRIBED PATTERN.

TO THE CONTROLLERS, THE HUMANS ARE THE ANTS. THE CONTROLLERS ARE INTERESTED IN DIRECTING THE PEOPLE IN SUCH A WAY THAT THEY DO NOT KNOW THAT THEY ARE BEING DIRECTED. THE CONTROLLERS WORK SLOWLY AND METHODICALLY FROM A GLOBAL PERSPECTIVE TO ACCOMPLISH THEIR GOALS.

WITH AWARENESS, YOU TOO, CAN PERCEIVE ORDER FROM THE CHAOS, MAKE SOME CONSCIOUS DECISIONS, AND GAIN CONTROL OF YOUR OWN LIFE AND DESTINY.

GO BACK

2 - THE TRANSPARENT PEOPLE

WHEN I WORKED AT MONTAUK, I ENCOUNTERED AN OCCASIONAL ALIEN SPECIES KNOWN AS A REPTILIAN. THEY SEEMED TO POP IN AND OUT OF PHYSICAL REALITY. THE REPTILIANS PRIMARILY USE THE LOWER ASTRAL REALMS AS THEIR REFERENCE POINT, OR POINT OF ENTRY, INTO PHYSICAL REALITY. THIS IS THE ORIGIN OF THE LEGENDS OF ASTRAL DEMONS. MY MONTAUK CONTROLLERS EXPLAINED THAT THESE BEINGS WERE BROUGHT TO THE DRACO STAR SYSTEM EONS AGO BY ANOTHER GROUP UNKNOWN TO ANYONE. FURTHER, THEY EXPLAINED, NO ONE KNEW ANYTHING OF THEIR TRUE ORIGINS.

COMMUNICATION WITH ME WAS ENTIRELY TELEPATHIC (THE DRACO REPTILIAN). MENTALLY, IT TOLD ME THAT IT CAME FROM THE FAR FUTURE WHERE HUMANS NO LONGER EXISTED, AND THAT ITS SPECIES WAS NOT FROM THIS REALITY. CONTINUING, IT SAID THAT ITS SPECIES HAD TRAVELED BACK INTO THE DISTANT PAST TO CREATE A RACE OF BEINGS, WHICH I KNEW AS THE REPTILIANS, TO ANTAGONIZE AND TEST HUMANS.

IT ALSO TOLD ME THAT THEY WERE ASSISTED BY THE SIRIANS OF SIRIUS A IN THE CREATION OF THE REPTILIANS AND THEIR PLACEMENT IN THE DRACO STAR SYSTEM.

FOR THE REPTILIANS TO FUNCTION IN PHYSICAL REALITY, THEY NEEDED PHYSICAL GENETICS. THE TRANSPARENT PEOPLE TOOK GENETICS FROM THE NOW PHYSICAL LYRAENS, WHO HAD BLONDE OR RED HAIR, AND BLUE OR GREEN EYES. THESE GENETICS WERE MIXED WITH THE TRANSPARENT PEOPLES COLLECTIVE ENERGY, THUS MANIFESTING PHYSICALLY AS THE REPTILIANS. THIS IS WHY THE CURRENT REPTILIANS NEED THE ENERGETICS FROM ARYAN-TYPE PEOPLE TO SURVIVE ON THE PHYSICAL PLANE.

ONCE THE REPTILIANS WERE CREATED IN THE ASTRAL, THEY NEEDED A PHYSICAL HOME BASE FROM WHICH TO ACCOMPLISH THEIR TASK. FOR THIS, THEY WERE TAKEN TO MANY DIFFERENT PHYSICAL REALITIES IN WHICH THEY COULD BECOME THE DOMINANT SPECIES. MENTALLY, THEY WERE PROGRAMMED TO CONQUER AND ABSORB ALL OF THE RACES AND SPECIES THAT THEY ENCOUNTERED. THOSE THAT COULD NOT BE ABSORBED WERE TO BE DESTROYED. THE PURPOSE OF ALL OF THIS IS TO DETERMINE THE MOST PERFECT FORM IN PHYSICAL REALITY THAT CAN EXIST IN ANY ENVIRONMENT. THINK OF IT AS A GIGANTIC, COSMIC SURVIVOR CONTEST.

THE REPTILIANS ARE PROGRAMMED TO BELIEVE THAT THEY ARE THE SUPERIOR PHYSICAL FORM.

SCIENTIFICALLY SPEAKING, REPTILIAN DNA DOES NOT CHANGE VERY MUCH OVER EONS OF TIME. IT BASICALLY REMAINS THE SAME. FOR THEM, THIS IS THEIR PROOF THAT THEY ARE ALREADY PERFECT, WITHOUT ANY NEED TO ADAPT. MAMMALIAN LIFE, ON THE OTHER HAND, EVOLVES AND CHANGES FORM CONSTANTLY TO SURVIVE.

TO THE REPTILIAN MIND, THIS DENOTES WEAKNESS AND INFERIORITY. REPTILIANS ARE ALSO ANDROGYNOUS, MEANING MALE AND FEMALE IN ONE BODY. THIS IS COMPARABLE TO ALL NON-PHYSICAL FORMS THAT HAVE NO GENDER LIKE GOD-MIND. FOR THIS REASON, THE REPTILIANS BELIEVE THEMSELVES TO BE MORE GODLIKE BECAUSE OF THEIR ANDROGYNY. DUE TO THEIR ETHNOCENTRIC VALUES, THEY ALSO CONSIDER IT THEIR RIGHT TO CONTROL AND CONQUER ALL OF SPACE AND TIME.

ALTHOUGH THE REPTILIANS OPERATE OUT OF A GENERAL GROUP MIND, THEY ARE SEPARATED INTO SEVEN DIFFERENT REPTILIAN SPECIES, EACH CREATED TO PERFORM SPECIFIC FUNCTIONS.

THIS IS THEIR HIERARCHY, AND IS BASED ON THE NINE LEVEL ANGELIC HIERARCHY THAT I DISCUSSED IN THE HEALERS HANDBOOK - A JOURNEY INTO HYPERSPACE (SKY BOOKS, 1999).

AS AN ASIDE, THE HINDU CASTE SYSTEM IS A DIRECT REPLICA OF THE REPTILIAN HIERARCHY.

COMMENTARY FROM WINTER:

THE POLITICS OF THE INTERVENTIONIST DRACO TRADING COLONIES (SEE DUNE - WHOSE ARRAKEIS - THE HOME STAR OF DRACOS AND DUNE - IS CORRECTLY LOCATED IN ALPHA DRACONIS) - DEFINITELY BECAME REPRESENTED BY ENLIL/YAHWEH/MICHAEL SIDE OF THE AN - ANUNNAKI FAMILY. ALSO SHOULD BE SEEN AS THE ROOTS OF INSURANCE AND BANKING ON EARTH. THE TEMPLAR FOLLOWERS OF THE MAG (DRACO MATRILINY) LINE ARE OFTEN CREDITED WITH ’INVENTING’ INSURANCE AND BANKING FOR THE WEST. THIS IS ABSURD - SINCE THEY HAD ALREADY INSTALLED SUCH INDUSTRY - SO CLOSE TO FEAR AND EXTORTION - TO HARVEST COLONIES ON HUNDREDS OF PLANETS. THE "SKULL AND BONES" - ORION- ORIGINS OF THE PIRACY AND EXTORTION STORY IS AN EXAMPLE OF INSURANCE AND BANKING THAT LOSES ITS PUBLIC RELATIONS BUDGET. MORE ON THE SKULL OF THE MAG BELOW.

LATER - AS ENLIL/YAHWEH UNDER THE NAME OF "GOD" MICHABO (MICHAEL) INSTALLS GENETIC RULES IN ABORIGINAL AUSTRALIA AND THE AMERICA’S HE IS FOLLOWING THE DRAC TRADITION ENTIRELY FOCUSED ON PREVENTING CHANGE - AND FACILITATING HARVEST OF COLONIES- LIKE FORESTS WHOSE ONLY PURPOSE IS TO BE CUT DOWN.

AT A DEEPER LEVEL WE SHOULD INVESTIGATE THE CONNECTION BETWEEN LOSS OF DNA IMPLOSION - THE PHYSICS OF LOSS OF SOUL & ACCESS TO BLISS - CALLED NEPHILIM WHICH BEFELL THESE DRACO (LOST SERAPHIM) FAMILIES. LOSS OF FIRE IN THE BLOOD CREATED LOSS OF LUCID DREAMING, LOSS OF "ENSOULMENT" AND LOSS OF LONG TERM MEMORY. PART OF THEIR PROBLEM WAS LOSS OF ABILITY TO NAVIGATE IN TIME TRAVEL (``GUILD NAVIGATOR’ IN DUNE - STAR NAVIGATING TIME TRAVELERS, ABLE TO WARP SPACE FROM WITHIN) - DUE TO THIS LOSS OF DNA COHERENCE.

NOT UNLIKE ONE OF THEIR RESULTANT CULTURES - TIBETAN - WHO ARE INTENSELY AWARE THAT THEIR IS NO STEERING THEIR COLLECTIVE CULTURAL DIRECTION (TIME TRAVEL) WITHOUT A LEADER WHO IS ABLE TO REMEMBER PAST LIVES. THIS IS EXACTLY WHAT DRACO LOST. IT IS

PROFOUND TO COMPARE THIS TO ZULU SHAMAN LEADER LAST WEEK BEMOANING TO US HOW HIS GRAND CHILDREN LOST THE ABILITY TO LUCID DREAM JUST AFTER THEY SUFFERED BEING IMMUNIZED. THIS IS AN EXAMPLE OF HOW BORG - FALLEN DRAC EMPIRES - TREAT DNA. BY NOT LOVING THEIR GENES ENOUGH TO SET THEM FREE - THEY BLIND THEIR CHILDREN.

GO BACK

GO BACK TO VIDA EN NUESTRA GALAXIA

3 - IS THIS PLANET TAKEN?
IN THE BELOW - WE SUGGEST COMPARISON TO LYSA ROYALL'S "PRISM OF LYRA" BOOK - A 'CHANNELED' MORE ROMANTIC AND INTUITIVE ACCOUNT- WHICH AT LEAST AGREES SURPRISINGLY ABOUT THE LYRAEN ORIGIN OF TODAY'S HUMANS.

BECAUSE THE LYRAENS DID NOT HAVE A DEFENSE SYSTEM IN PLACE, THEY WERE A SITTING TARGET FOR THE REPTILIANS, ALSO REFERRED TO AS THE "DRACO". AFTER BEING BRUTALLY ATTACKED BY THE DRACO EMPIRE, THE SURVIVORS OF THE LYRAEN SOCIETY DISPERSED TO OTHER LOCATIONS THROUGHOUT THE GALAXY. THE REMNANTS OF THE DRACO ATTACK ON LYRAE ARE STILL SEEN BY TODAY'S SCIENTISTS.

IN 1985, A NEWSPAPER ARTICLE STATED THAT SCIENTISTS ARE ABLE TO OBSERVE REMNANT WAVES OF A BLAST THAT FAN OUTWARD, AND EMANATE FROM A CENTRAL PART OF THIS GALAXY. THEY BELIEVE THIS BLAST TO BE SEVERAL MILLION YEARS OLD AND OF SUCH INTENSE PROPORTIONS THAT THE WAVE IS STILL TRAVELING TOWARD THE EDGE OF THE GALAXY BEFORE DISSIPATING. THEY CLAIM NOT TO HAVE ANY IDEA OF WHAT CREATED THE BLAST.

THESE SURVIVORS WENT TO ORION, TAU CETI, PLEIADES, PROCYON, ANTARIES, ALPHA CENTAURI, BARNARD STAR, ARCTURUS, AND DOZENS OF OTHER SOLAR SYSTEMS. IN THIS SOLAR SYSTEM, THE REFUGEES COLONIZED THE PLANET NOW CALLED MARS. AT THAT TIME, IT WAS THE THIRD PLANET IN THE SOLAR SYSTEM. A WORLD CALLED MALDEK WAS THE FOURTH PLANET IN THIS SOLAR SYSTEM, AND WAS ALSO COLONIZED.

THE LYRAENS WERE ALL BLONDE-HAIRED, BLUE-EYED PEOPLE, WITH AN OCCASIONAL RED-HAIRED OR GREEN-EYED PERSON. IN LYRAEN SOCIETY, RED-HAIRED PEOPLE WERE CONSIDERED SPECIAL WITH EXTRASENSORY POWERS THAT CONNECTED THEM TO NON-PHYSICAL REALMS. THEY WERE ESPECIALLY DESIRED FOR BREEDING PURPOSES. SPECIAL PERMISSION TO BREED WITH A RED-HAIRED PERSON WAS REQUIRED BECAUSE OF THE EXTRA, OR SUPERHUMAN, ABILITIES THAT CAME WITH THE OFFSPRING.

FOR THIS REASON, RED-HAIRED PEOPLE WERE KEPT SEPARATE FROM THE REST, AND EVEN HAD THEIR OWN SUBCULTURE. THEY WERE ALSO COVETED BY THE REPTILIANS, WHO AS A SPECIES DID NOT HAVE MUCH PSYCHIC ABILITY. OFTEN, WHEN REPTILIANS CAME TO A WORLD FOR OCCUPATION, THE LYRAEN REFUGEES OFFERED A GROUP OF RED-HAIRED PEOPLE TO APPEASE THEM FOR A WHILE. THIS PRACTICE EVENTUALLY DEGENERATED INTO SACRIFICES TO APPEASE THE DEMONS.

THE PLANET EARTH IN THOSE DAYS WAS A WATER WORLD IN SECOND ORBIT FROM THE SUN. THERE WAS LITTLE LAND ABOVE THE SURFACE. THE ONLY INTELLIGENT INHABITANTS WERE AN AMPHIBIAN RACE THAT WAS COMPLETELY WITHOUT TECHNOLOGY. THE ATMOSPHERE OF THE EARTH WAS MOSTLY LIQUID. THE PLANET DEFINITELY COULD NOT SUSTAIN ANY TYPE OF HUMAN

LIFE FORMS.

THE DISPERSED LYRAEN DESCENDANTS DEVELOPED THEIR OWN CULTURES OVER THE EONS OF TIME. EVEN THEIR GENETICS MANIFESTED DIFFERENTLY AS A RESULT OF THE MIND-PATTERNS OF EACH OF THE COLONIES. FOR INSTANCE, MARS AND MALDEK WERE SIMILAR TO THE CURRENT EARTH ENVIRONMENT, WITH WARM TO TEMPERATE CLIMATES AND AN OXYGEN-RICH ATMOSPHERE. THE GRAVITY ON MALDEK WAS DENSER THAT MARS, SO THOSE PEOPLE DEVELOPED A THICKER FRAME AND A MORE AGGRESSIVE ATTITUDE.

EVENTUALLY, SKIRMISHES DEVELOPED BETWEEN THE OCCUPANTS OF THE TWO PLANETS. MARS WAS RICH IN RESOURCES. THE PEOPLE OF MALDEK THOUGHT THAT THEY DESERVED THESE RESOURCES FOR SURVIVAL. THE MARTIANS ASKED THE BEINGS OF SIRIUS A, FROM THE PLANET KHOOM, FOR DEFENSE TECHNOLOGY TO SHIELD THEIR PLANET FROM ATTACK, NOT ONLY FROM THE REPTILIANS, BUT FROM THEIR HUMANOID NEIGHBORS AND COUSINS. THE SIRIANS ARE KNOWN THROUGHOUT THE GALAXY AS MERCHANTS OF TECHNOLOGY. THEY HAVE THE BEST, EVEN SHARING IT WITH THE REPTILIANS.

SO, THE SIRIANS CREATED A DEFENSE MECHANISM LOCATED IN THE MARS UNDERGROUND.

MARS IS A HOLLOW PLANET, AS ARE EARTH AND JUPITER. PLANETS CREATED WITH MATERIAL EJECTED FROM A STAR HAVE HOLLOW INTERIORS. AS A MOLTEN BALL IS THROWN FROM THE STAR AND STARTS SPINNING AWAY, IT BEGINS TO COOL. THE CENTRIFUGAL FORCE OF THE GLOBE SPINNING AND MOVING AT GREAT SPEED PUSHES THE MOLTEN INTERIOR TO THE SIDES, FORMING THE CRUST OF THE PLANET. THIS, IN TURN, FORCES HOT GASES OUT OF THE POLES TO FORM OPENINGS AT BOTH ENDS. THE MOLTEN CORE AND GASES THAT REMAIN GET TRAPPED BETWEEN THE HOLLOW INTERIOR AND THE PLATES BELOW THE CRUST OF THE GLOBE. THESE ARE PUSHED OUT PERIODICALLY IN THE FORM OF VOLCANIC ACTIVITY.

THE NEXUS POINT ON ANY SUCH GLOBE IS ALWAYS AT THE 19TH PARALLEL OF THE PLANET. IT IS EVIDENT ON EARTH BY THE HAWAIIAN VOLCANOES, LOCATED AT THE 19TH PARALLEL; BY THE MONS VOLCANO ON MARS LOCATED AT THE 19TH PARALLEL; AND AT THE RED SPOT ON JUPITER, ALSO AT THE 19TH PARALLEL.

THE GEOMETRY BUILT INTO THE MONUMENTS ON MARS BY THE SIRIANS AND LYRAEN COLONISTS EXPLAINS ABOUT THE 19TH PARALLEL THROUGH ITS GEOMETRIC EQUATIONS AND MEASUREMENTS.

THIS GEOMETRY IS ALSO REPLICATED AND CONTAINED WITHIN THE GIZA PLATEAU IN EGYPT.

COMPARE THIS TO RICHARD HOAGLAND - STILL CLUE LESS TO WHY DOLMEN LIKE GIZA AND CYDONIA ARE AT TETRAHEDRAL LATITUDES. BY MODULATING (ADJUSTING) THE SPIN RATE OF PLANETS AT TETRAHEDRAL HAND HOLDS - PLANETARY SPIN COMES INTO PHASE WITH ZODIAC SPIN - THIS SELF SIMILAR SPIN RELATION (IMPLOSIVE COLLAPSE) IS CRITICAL TO STABILIZING GRAVITY AND THEREFORE ATMOSPHERE.

GO BACK

4 - THE REPTILIAN AGENDA

THE REPTILIAN AGENDA WAS, AND IS, TO SEEK OUT THE HUMAN REFUGEES FOR DESTRUCTION OR ASSIMILATION, AND TO USE THEIR BLOOD AND HORMONES FOR SUSTENANCE.

IT IS SAID THOSE (OPHANIM? SERAPHIM? WINGED DRACS? CIAKAR? CHERUBIM?) WHO PLACED THE DRACO IN OUR GALACTIC SECTOR KNEW THAT THE HUMANOID REMNANT WOULD NEED AN AGGRESSIVE PARASITE TO TRIGGER DEVELOPMENT. FURTHER THE RESULT OF THE PART OF THE HUMANOID BLOOD ON EARTH TODAY RECEIVING A BLOOD LINE CROSS FROM DRACO (URU CROSS WITH IBI) - IS BENEFICIAL. (SEE LAWRENCE GARDNER DEFENDING HIS DRAC FAMILY ROOT). THIS IS RELATED TO USUALLY AN OR CELTIC OR BRITISH RH NEGATIVE BLOOD.

THE REPTILIAN DRAC BLOOD ENKI (RA - ABRAHAM) CROSSED WITH THE CRO-MAGNON MONKEY BLOOD HAD DNA WAS LESS VITAL THAN THE INDIGENOUS (RHESUS) MONKEY BLOOD. SO THE REPTILIANS HAD TO KEEP IN-BREEDING (AS IN HOLY BLOOD HOLY GRAIL) - CONSISTENT WITH WHAT SWERDLOW SAYS BELOW. AREAS (UK) WHERE THIS RHESUS MONKEY BLOOD IS ABSENT (RH NEGATIVE) MAY LEAD THE WORLD IN LACK OF COMPASSION. E-LIZ-A BETH (FROM LIZARD BORN) BREEDS A LINE WHERE NO PERMISSION TO CRY PRODUCES A STIFF UPPER LIP.

THE REMNANT LYRAENS WHO COLONIZED OTHER PLANETS FORMED AN ALLIANCE AGAINST THE CONSTANT REPTILIAN ATTACKS. THEY CALLED THIS ALLIANCE THE GALACTIC FEDERATION, COMPRISED OF 110 DIFFERENT COLONIES. THE COLONIES BELONGING TO THE FEDERATION WISHED TO MAINTAIN THEIR NEW IDENTITIES, AND NO LONGER ASSOCIATE WITH THE OLD WAY. TOGETHER, THE FEDERATION COLONISTS MANAGED TO REPEL THE REPTILIAN ATTACKS.

THERE WERE THREE PRIMARY GROUPS WHO DID NOT JOIN THE FEDERATION. THESE THREE GROUPS WERE CONSIDERED EXTREMISTS, OR NATIONALISTIC IDEALISTS, SEEKING TO RECREATE THE GLORY OF THE OLD LYRAEN CIVILIZATION. ONE GROUP WAS THE ATLANS, LOCATED ON A PLEIADIAN PLANET. THE PLEIADES ACTUALLY CONSISTS OF THIRTY-TWO PLANETS ORBITING SEVEN STARS. AT THAT TIME THERE WERE SIXTEEN DIFFERENT COLONIES OF LYRAEN DESCENT THROUGHOUT THE PLEIADES. THESE COLONISTS ALL WANTED TO OUST THE RENEGADE ATLANS BECAUSE THEY REMAINED INDEPENDENT AND DID NOT ASSIST THEIR HUMAN COUSINS.

THE OTHER TWO GROUPS WERE THE MARTIANS AND MALDEKIANS, WHO WERE ALREADY AT ODDS WITH EACH OTHER. FOR THIS REASON, THE REPTILIANS TURNED THEIR ATTENTION TOWARD THIS SOLAR SYSTEM WITH ITS TWO HUMAN COLONIES. IN THE REPTILIANS ESTIMATION, IT WOULD BE EASY TO DIVIDE AND CONQUER.

THE REPTILIANS LOVE TO USE COMETS AND ASTEROIDS AS WEAPONS AND SHIPS, USING THEM TO TRAVEL THROUGH THE STARS. FIRST, THEY CREATE A SMALL BLACK HOLE AS A PROPULSION SYSTEM THAT PULLS THE LARGER PLANETOID TOWARDS ITS DESTINATION. WHEN USED AS A WEAPON, THEY USE A PARTICLE BEAM ACCELERATOR TO CREATE A BLAST THAT HURLS THE COMET OR ASTEROID TO ITS TARGET. ALL OF THE TECHNOLOGY WAS OBTAINED BY THE BEINGS FROM SIRIUS A.(1)

IN THIS WAY, THEY HURLED A HUGE ICE COMET AIMED AT MARS AND MALDEK. THE REPTILIANS, NOT BEING VERY TECHNOLOGICALLY ORIENTED, MISCALCULATED THE TRAJECTORY. THE PULL OF THE GIGANTIC GAS PLANET, JUPITER, PULLED THE COMET OFF COURSE. THE ICE COMET THEN HEADED DIRECTLY FOR MALDEK. THE CITIZENS OF THAT PLANET ASKED THE MARTIANS FOR HELP. EVEN THOUGH THEY WERE AT ODDS WITH EACH OTHER, THEY ALLOWED SOME OF THE MALDEKIANS TO MOVE TO THE MARTIAN UNDERGROUND. THE COMET CAME SO CLOSE TO MALDEK THAT THE PLANET GOT CAUGHT BETWEEN THE GRAVITATIONAL PULL OF JUPITER, MARS, AND THE

COMET. THIS CAUSED THE PLANET TO EXPLODE, LEAVING AN ASTEROID BELT BETWEEN MARS AND JUPITER. (2)

THE EXPLOSION PUSHED THE ICE COMET CLOSE ENOUGH TO MARS TO RIP THE ATMOSPHERE OFF THAT PLANET, LEAVING ONLY AN EXTREMELY THIN ATMOSPHERE. THE EXPLOSION ALSO PULLED MARS FURTHER AWAY FROM THE SUN.

THE COMET THEN CONTINUED ON TOWARD THE EARTH. THE HEAT OF THE SUN AND THE GRAVITATIONAL PULL BETWEEN THE TWO GLOBES FORCED THE WATERY ATMOSPHERE OF THE EARTH TO POLARIZE. THIS POLARIZATION PULLED MOST OF THE ICE FROM THE COMET TO THE POLAR REGIONS OF THE EARTH, THUS COVERING MOST OPENINGS TO THE INNER EARTH, WHILE AT THE SAME TIME EXPOSING HUGE LAND MASSES FOR THE FIRST TIME.

THE COMET THEN SWITCHED PLACES WITH EARTH, TAKING UP THE SECOND ORBIT FROM THE SUN, BECOMING THE PLANET NOW KNOWN AS VENUS. THE HEAT OF THE SUN MELTED THE ICE ON THE COMET, CREATING A CLOUDY COVERING TO THIS NEW PLANET. THE EARTH WAS PUSHED OUT TO THE THIRD ORBIT OCCUPYING THE PREVIOUS POSITION HELD BY MARS. THE EARTH WAS NOW READY TO BE COLONIZED. MOST OF THE SURVIVING AMPHIBIANS WERE TRANSPORTED TO A NEW HOME ON NEPTUNE. SOME STAYED IN THE NEWLY FORMED OCEANS.

THE REPTILIANS WHO WERE INSIDE THE HOLLOW COMET, NOW VENUS, CAME TO THE SURFACE OF THIS NEW WORLD. THEY BUILT SEVEN DOMED CITIES, ONE FOR EACH OF THE SEVEN GROUPS IN THE HIERARCHY. IN THE MID-1980S ONE OF NEW YORK'S DAILY PAPERS, NEWSDAY, REPORTED THAT A SOVIET SPACE PROBE PENETRATED THE CLOUD LAYER OF VENUS AND PHOTOGRAPHED SEVEN WHITE DOMES THE SIZE OF SMALL CITIES, ALL IN A ROW.

AFTER A PAGE-LONG DIATRIBE, THE AMERICAN SCIENTISTS CONCLUDED THAT THIS WAS ALL A NATURAL FORMATION.

THE REPTILIANS DROVE A LARGE, HOLLOWED OUT OBJECT INTO EARTHS ORBIT TO BEGIN THE COLONIZATION PROCESS. THIS OBJECT IS NOW CALLED THE MOON. CONVENTIONAL SCIENCE CONSIDERS THE MOON NATURAL, YET IT IS THE ONLY KNOWN OBJECT IN SPACE THAT DOES NOT SPIN ON ITS AXIS. THE MOON FACES THE EARTH IN THE SAME POSITION ALL OF THE TIME, LEAVING ONE SIDE IN COMPLETE DARKNESS. A SONIC RESONANCE SENT TO THE SURFACE OF THE MOON MAKES A PINGING NOISE LIKE A HOLLOW OBJECT. IF THE MOON WERE SOLID, THE NOISE WOULD SOUND LIKE A THUMP OR THUD. THE MOON IS HOLLOW. A RECENT ARTICLE IN AN ASTRONOMY MAGAZINE SAID THAT THE MOON WAS BEING RECLASSIFIED BECAUSE IT IS CONSIDERED TO BE HOLLOW.

THE REPTILIANS CHOSE A LARGE CONTINENTAL LANDMASS TO BEGIN THEIR CIVILIZATION ON THE EARTH, NOW REFERRED TO AS LEMURIA OR MU. THIS WAS A VAST AREA IN WHAT IS NOW THE PACIFIC BASIN, EXTENDING FROM JAPAN TO AUSTRALIA, AND FROM THE COAST OF CALIFORNIA TO PERU. THE HAWAIIAN ISLANDS ARE IN THE MIDDLE OF THIS ONE-TIME LANDMASS.

HERE, AN ANDROGYNOUS REPTILIAN CULTURE DEVELOPED. THEY BROUGHT WITH THEM THE CREATURES THAT WERE THEIR SUSTENANCE THE DINOSAURS. ALL BEINGS CREATE BENEATH THEM ANIMALS AND PLANTS THAT ARE A REFLECTION OF THE MIND-PATTERN. REPTILIANS CREATE DINOSAURS, HUMANS CREATE MAMMALS. THEY ARE NOT DESIGNED TO COEXIST ON THE SAME PLANET.

ADDITIONALLY, THE THINKING PROCESS OF THE REPTILIANS DIFFERS FROM THE HUMAN THINKING PROCESS. BECAUSE REPTILIANS DO NOT EVOLVE RAPIDLY AND REMAIN UNCHANGING, THEIR EXPANSION IS ALSO SLOW MOVING AND INSIDIOUS. IT WOULD TAKE SEVERAL MILLENNIA FOR THE REPTILIANS TO DECIDE WHETHER OR NOT THEY WOULD COEXIST WITH HUMANS. AFTER ALL, EARTH WAS STILL AN OUTPOST FAR FROM THE CENTRE OF THE DRACONIAN EMPIRE.

IN THE MEANTIME, THE MARTIANS WERE NOW LIVING UNDERGROUND WITH THEIR HOSTILE MALDEKIAN GUESTS. SOMETHING HAD TO BE DONE QUICKLY TO PREVENT THEM FROM DESTROYING ONE ANOTHER. SO, THE MARTIANS PETITIONED THE GALACTIC FEDERATION TO REMOVE THE MALDEKIAN REFUGEES TO ANOTHER PLANET. THE GALACTIC FEDERATION ALSO RECEIVED A PETITION FROM THE PLEIADIAN COUNCIL AT THE SAME TIME, ASKING THE FEDERATION TO REMOVE THE ATLANS FROM THEIR STAR CLUSTER.

THE FEDERATION THUSLY DECIDED TO USE THE ATLANS AS A COUNTERBALANCE ON EARTH. IF THE ATLANS SURVIVED, THE MALDEKIANS WOULD ALSO BE SENT. THE HUMAN/LYRAEN DESCENDANTS WERE LITERALLY THROWING THEIR OWN RIFFRAFF TO THE REPTILIAN COLONISTS ON EARTH. IN THIS WAY, THE FEDERATION WOULD GET RID OF THEIR UNDESIRABLES. THE UNDESIRABLES WOULD OCCUPY THE ATTENTION OF THE REPTILIANS. THE FEDERATION WOULD GAIN VALUABLE TIME TO BUILD THEIR OWN FORCES AGAINST THE REPTILIANS.

WHEN THE ATLANS ARRIVED ON THE EARTH, THEY COLONIZED WHAT BECAME KNOWN AS ATLANTIS. THEIR CONTINENT STRETCHED FROM WHAT IS NOW THE CARIBBEAN BASIN TO THE AZORES AND CANARY ISLANDS, AS WELL AS SEVERAL SMALL ISLAND CHAINS REACHING UP TO WHAT IS NOW THE EAST COAST OF THE UNITED STATES, INCLUDING MONTAUK POINT.

THE INDUSTRIOUS ATLANTEANS RAPIDLY GREW TO A LARGE, PROSPERING CIVILIZATION NEEDING MORE TERRITORY. THE DINOSAUR POPULATION WAS RAPIDLY INCREASING AND BECOMING DANGEROUS TO THE HUMAN COLONISTS. THE ATLANTEANS BEGAN DESTROYING THE DINOSAURS TO PROTECT THEMSELVES. THIS DID NOT SIT WELL WITH THE REPTILIANS. SOON MAJOR BATTLES OCCURRED ON THE EARTH BETWEEN THE LEMURIAN REPTILIANS AND ATLANTEAN HUMANS.

AT THE SAME TIME, THE MALDEKIAN REFUGEES ARRIVED ON EARTH. THEY CREATED A LARGE HUMAN COLONY IN WHAT IS NOW THE GOBI DESERT, NORTHERN INDIA, SUMER, AND OTHER PARTS OF ASIA.

THE MALDEKIANS ATTACKED THE LUNAR SURFACE WHERE THE REPTILIANS GUARDED THEIR EARTH OUTPOST FROM INVASION. THE MALDEKIANS ALSO BOMBARDED ATLANTIS AND LEMURIA WITH LASER WEAPONS. THE DINOSAURS WERE WIPED OUT.

ADDITIONALLY, THE MARTIANS ALSO ATTACKED THE REPTILIANS FROM SPACE SINCE THEY, TOO, WERE SEARCHING FOR A REPTILIAN-FREE ENVIRONMENT IN WHICH TO LIVE. THIS MIGHT BE CONSIDERED THE REAL FIRST WORLD WAR ON THIS PLANET.

IT WAS A MESS!

FOOTNOTES:

1. THE SIRIANS WERE AT WAR WITH THE ORION SYSTEM. THIS HOSTILITY EXISTS TO THIS DAY. IT IS INTRIGUING SINCE THE BEINGS IN ORION WERE ONCE VERY HUMAN, AS LYRAEN COLONISTS, AND THEN WERE TAKEN OVER BY THE REPTILIANS. HOWEVER, THE SIRIANS AND THE REPTILIANS TRADE WITH EACH OTHER AND THE BEINGS FROM SIRIUS A SELL WEAPONRY TO THE DRACOS! A COMPLEX POLITICAL SITUATION INDEED.

2. THE COMET ALSO CAUSED THE PLANET URANUS TO FLIP ON ITS SIDE. IT IS THE ONLY KNOWN PLANET THAT ROTATES NORTH-SOUTH INSTEAD OF EAST-WEST.

THE LOSS OF THE MARTIAN ATMOSPHERE CAUSED BY DRACO'S PLAYING BILLIARDS BECAME THE "TOTAL RECALL" LEGEND (MOVIE ABOUT MARTIAN HISTORY AND THE OXYGEN WAR). THE DRACO BASES THERE TODAY STILL HAVE NO HESITATION TO SHOOT DOWN A NASA PROBE, ALTHOUGH INCREASINGLY AS THE US GOVERNMENT BECOMES A SATELLITE OF THE SHAPE-SHIFTERS- THEY BEGIN TO LET A FEW EARTH PROBES IN.

GO BACK

5 - CONFLICT & CREATION

TO STOP THE FIGHTING AND MAKE THE EARTH PEACEFUL ENOUGH FOR COLONIZATION, A MEETING WAS HELD BY A COUNCIL FROM THE ANDROMEDA GALAXY, ON A PLANET CALLED HATONA.

THIS MEETING TOOK PLACE OUTSIDE OF THE MILKY WAY GALAXY WITH A NEUTRAL COUNCIL BECAUSE ALL CIVILIZATIONS WITHIN THE MILKY WAY GALAXY WERE IN SOME WAY CONNECTED TO THE FIGHTING, AND ALL HAD SOME SORT OF STAKE IN BELONGING TO THE WINNING SIDE.

INTERESTING PREQUEL TO LETTERS FROM ANDROMEDA FROM ALEX COLLIER (AUTHOR OF "DEFENDING SACRED GROUND").

THE HATONA COUNCIL CONVENED FOR MANY DECADES AS THE FIGHTING CONTINUED IN THIS SOLAR SYSTEM. FINALLY, WITH THEIR INTERCESSION, AN AGREEMENT WAS REACHED BETWEEN SOME OF THE HUMAN FACTIONS AND THE REPTILIAN EARTH COLONISTS. KEEP IN MIND THAT THIS AGREEMENT WAS WITHOUT THE PARTICIPATION OF THE REPTILIANS FROM THE ORIGINAL DRACO EMPIRE.

THE AGREEMENT STATED THAT A NEW BREED OF HUMANITY WOULD BE CREATED ON EARTH THAT WOULD CONTAIN THE DNA OF ALL INTERESTED PARTIES WHO PARTICIPATED IN THE "PEACE" PROCESS. A DESIGNATED AREA ON EARTH WOULD BE SET ASIDE FOR THE CREATION OF THIS NEW SPECIES. THE EARTH-BASED REPTILIANS OF LEMURIA AGREED TO THIS UNDER THE CONDITION THAT THE REPTILIAN BODY BE THE FOUNDATION FOR THIS NEW BEING.

THIS IS WHY THE ORIGINAL BIBLE STATES, "LET US MAKE MAN IN OUR OWN IMAGE." THIS IS A PLURAL STATEMENT BECAUSE IT WAS A GROUP PROJECT.

TO ACHIEVE A NEW SPECIES FROM A REPTILIAN ANDROGYNOUS BODY, IT WAS NECESSARY TO SEPARATE THE GENETICS INTO MALE AND FEMALE COMPONENTS. THIS IS THE ALLEGORICAL STORY IN THE BIBLE OF ADAM AND EVE. CREATING EVE OUT OF THE RIB OF ADAM IS ACTUALLY THE STORY OF SEPARATING THE ANDROGYNOUS REPTILIAN BODY INTO MALE AND FEMALE. THIS IS WHY ALL HUMANS ON THIS PLANET HAVE REPTILIAN DNA WITH REPTILIAN TRAITS. THIS IS ALSO WHY HUMAN FETUSES GO THROUGH REPTILIAN-STYLE DEVELOPMENT IN THE WOMB BEFORE LOOKING HUMANOID.

MANY PROTOTYPES WERE DEVELOPED OVER MILLENNIA. UNDER THE SUPERVISION OF THE HATONA COUNCIL, RACES WERE CREATED AND THEN DESTROYED WHEN IT WAS NOT ACCEPTABLE

BY ALL PARTIES. THIS EXPLAINS WHY ANCESTORS OF MANKIND APPEAR AND THEN SUDDENLY DISAPPEAR IN LAYERS OF ARCHAEOLOGICAL ANALYSIS.

TWELVE HUMANOID, AND ONE REPTILIAN, GROUPS DONATED DNA FOR THIS PURPOSE. MANKIND WAS DEVELOPED IN THE AREA NOW KNOWN AS IRAN/IRAQ, AS WELL AS PARTS OF AFRICA. HYBRIDS WERE ALSO DEVELOPED ON ATLANTIS AND LEMURIA. REMNANTS OF THESE ARE SEEN TODAY AS THE BIGFOOT OR YETI IN NORTH AMERICA AND ASIA; THE ABORIGINES OF AUSTRALIA; AND THE PYGMIES AND WATUSI IN AFRICA.

THE AFRICAN VERSIONS WERE CREATED BY BEINGS FROM A NOMADIC, ARTIFICIAL PLANET KNOWN AS NIBIRU, OR MARDUK. THESE REPTILIAN-LIKE BEINGS TRAVEL IN A MANUFACTURED WORLD LOOPING OUR SOLAR SYSTEM.

THE SUMERIANS CALLED THEM ANUNNAKI.

IT IS HERE, WE WOULD HAVE TO ASSUME, THE FAMILY OF AN, WITH SON'S ENKI / ENLIL (LUCIFER / MICHAEL - ADON / YAHWEH) ARRIVED FROM SIRIUS TECHNO CRAFT, WITH ALL THE NEPHILIM GENETIC DISASTERS WE CALLED THE RETURN OF ENKI. WHILE PEOPLE LIKE SITCHIN CAN ADD USEFUL PUZZLE PIECES LIKE HOW THEIR HOME ATMOSPHERE REPAIR COULD GAIN THE NECESSARY GRAVITY FRACTALITY USING GOLD DEPOSITS, THE SUMERIAN BASICALLY DID NOT GIVE HIM A CLUE AS TO THE BIGGER GALACTIC POLITIC MESS THAN TRIGGERED ENKI'S (ABRAHAM) GENETIC EXPERIMENTS. AFTER REPEATEDLY ENCOUNTERING THE ENKI/ENLIL STORY IN AUSTRALIA (FISH OR DOLPHIN GOD VS SNAKE GOD -LEVITE), IT WAS COOL TO LISTEN TO CRETO MUTWA TELL THE ZULU KILIMANJARO MEANS ENKI MOUNTAIN!

THE COSMIC JOKE TO THIS PROJECT IS THAT ALL OF THE GROUPS DONATING DNA SECRETLY PROGRAMMED SEQUENCES TO CAUSE THEIR GENETIC STRAND TO BE PREDOMINANT. THIS SET THE PRECEDENT FOR ETERNAL CONFLICT. HUMANITY WAS DOOMED TO FIGHT AND BE CONTROLLED. NO ONE GROUP WOULD EVER BE IN CHARGE. THE PROJECT WAS DOOMED FOR FAILURE BEFORE IT EVEN BEGAN!

SUCH DNA PROGRAMMING INVITES TYRANNY AND OPPRESSION. SOUL-PERSONALITIES ATTRACTED TO SUCH A PLANET HAVE A VICTIM MENTALITY. MANY ADVANCED CULTURES CALL EARTH A PRISON PLANET, AND DUMP THEIR CRIMINALS HERE AS PUNISHMENT.

ONCE IN A WHILE, ONE OF THESE SOUL-PERSONALITIES REVEAL THEMSELVES, SUCH AS RICHARD DAHMER, CHARLES MANSON, RICHARD SPECK, AND VLAD THE IMPALER (COUNT DRACULA), TO NAME A FEW.

DUNE WAS A PRISON COLONY, LIKE AUSTRALIA. EARTH FITS THE ARCHETYPE. LIKE IN DUNE HOWEVER, IN EARTH'S GENETIC CAULDRON OF SURVIVAL, THE STRONGEST DNA EMERGES: A 'VACCINE' FOR THE ORION WARS? BUILT BY DESIGN? THE CURRENT EXPRESSION OF THE 2 BROTHERS STILL TOSSING NUCLEAR BOMBS THEN CALLED EAST OF EDEN, TODAY CALLED THE MIDDLE EAST CONFLICT, MAY BE A PERFECT HEALTHY FRACTAL OF THE ORION WARS, WITH THE MAIN WARRING GALACTIC ELEMENTS ALL NICELY STAGED TO WORK OUT A GALACTIC CONFLICT IN A MICRO-COSM.

THIS MAY BE MORE HOWEVER THAN A TEMPEST IN A TEAPOT, BECAUSE THE GALACTIC PLAYERS APPEAR TO BE WILLING TO UP THE STAKES WITH MORE INTERVENTION IF THEIR CHESS PIECE STARTS TO LOSE. ENLIL AS YAHWEH (THE ENCODER IN BIBLE CODE) MAY NOT BE WILLING TO STAND ASIDE AS HIS ISRAEL UNDER THE HEX DRACO FLAG IS DESTROYED BY YET ANOTHER NUCLEAR BLAST. (PREDICTED BY BIBLE CODE AND FATIMA & OTHERS) .

AS WINGMAKERS SO NICELY POINTED OUT - ONLY THE TRON (BST TECHNOLOGY) WITH (IGNITED) DNA MORE TIME TRAVEL CAPABLE CAN DEFEAT SUCH PREDATORY ET'S. THESE GENES WHICH TIME TRAVEL ARE PRECISELY THE JEWEL THAT ALWAYS ELUDES YAHWEH ENLIL'S REPTILE (LEVITE) FAMILY - THEY ARE STUCK IN THE CUBE, GENETIC SOFTWARE ENVIRONMENT OF THE TETRA (HEBREW ALPHABET) WHICH CAN ONLY MAKE A GOLEM.

ISRAEL WAS ORIGINALLY THE GENES OF ENKI WHEN HIS THOTH PTAH LINE AKHANATON, TOOK THE GOLD FROM EGYPT, ASSUMING THE MOSES IDENTITY TO START THE ESSENES. TROUBLE WITH THE 12 TRIBES - GENETIC IMPLOSION SYMMETRY - WAS WHEN THE ORIENTAL (QUEEN DRAC) ASHOKA ASHKANAZI, USURPED THE SEPHARTIC, INSTALLING ENLIL'S CONTROL IN ISRAEL. (ALSO FOUNDING THE BANK OF ENGLAND - DESCRIBED BELOW AS OWNING THE US BANKING).

THE REPTILIANS ENSURED THAT THE NEW MAN WOULD BE FOREVER ATTACHED TO THE REPTILIAN FREQUENCY BECAUSE THE FOUNDATIONAL PROTOTYPE WAS REPTILIAN. THIS MEANT THAT THE NEW MAN COULD EASILY BE MENTALLY CONTROLLED BY THEM.

UPON DISCOVERY OF THIS INFORMATION THAT THE REPTILIANS WANTED CONTROL OF THE NEW RACE, THE ATLANTEANS BEGAN A SEVERE ELECTROMAGNETIC BOMBARDMENT OF LEMURIA. THIS BOMBARDMENT CAUSED THE BULK OF THE CONTINENT TO SUBMERGE INTO THE OCEAN, NOW CALLED THE PACIFIC OCEAN. THE ONLY PARTS LEFT ABOVE THE WATER ARE THE HAWAIIAN ISLANDS, THE CALIFORNIA COAST WEST OF THE SAN ANDREAS FAULT, AUSTRALIA, NEW ZEALAND, THE SOUTH PACIFIC ISLANDS, JAPAN, THE PHILIPPINES, TAIWAN, AND THE ISLANDS OF SOUTHEAST ASIA.

THE REPTILIAN SURVIVORS WENT TO NORTHERN INDIA, THE EARTHS INTERIOR, THE PLANET VENUS, AND PARTS OF CENTRAL AND SOUTH AMERICA. INNER EARTH BECAME THE "HOMELAND" FOR MOST OF THE SURVIVING REPTILIANS OF LEMURIA. HERE, THEY CREATED A VAST UNDERGROUND CIVILIZATION.

THIS STARTED THE LEGENDS OF HELL AND DEMONS LIVING IN FIRE UNDER THE EARTH. THEY BUILT TUBES CONTAINING FAST, SUBWAY-LIKE VEHICLES THAT CAN TRAVEL TO ANY POINT ON THE EARTH WITHIN A FEW HOURS. THEY CREATED THE FAMED UNDERWORLD CITIES OF AKKADIA, AGARTHA, HYPERBOREA, AND SHAMBALLA THAT ARE SOUGHT BY EXPLORERS TO THIS VERY DAY. THESE CITIES ARE BUILT ALONG THE INSIDE WALL OF THE INNER CRUST THAT LINES THE INTERIOR OF THE EARTH.

REMEMBER, THE HOLLOW EARTH IS NOT A THEORY, BUT A SCIENTIFIC FACT CAUSED BY THE COOLING AND SPINNING OF A PLANET AS IT IS EJECTED FROM A STAR OR SUN.

SHALL WE CHECK TO SEE IF MEREDITH LADY YOUNG, AUTHOR OF "AGARTHA" (BOOK ABOUT THE CIVILIZATION OF THE INNER EARTH) AGREES?

THE PRIMARY ENTRY POINTS TO THE INNER EARTH ARE VIA THE NORTH POLE, WHERE THERE IS AN OPENING OF 1300 MILES, AND THE SOUTH POLE, WITH AN OPENING OF 950 MILES. THESE CAN BE SEEN FROM SPACE. THAT IS WHY COMMERCIAL AIRCRAFT ARE NOT ALLOWED TO FLY OVER THESE AREAS; NOT BECAUSE OF MAGNETIC DISTURBANCES, WHICH IS THE "OFFICIAL" REASON. ADMIRAL BYRD REPORTED ON THESE OPENINGS IN THE 1920S UNTIL HIS INFORMATION WAS CONCEALED BY THE GOVERNMENT.

AT THE VERY CENTRE, OR NUCLEUS, OF INNER EARTH, THERE IS A GLOBE OF ENERGY LEFT OVER FROM THE CREATION OF THIS PLANET THAT ACTS AS AN INNER SUN. IT IS THE LIGHT FROM THIS OBJECT SUSPENDED BY GRAVITY AND CENTRIFUGAL FORCE THAT CAUSES THE LIGHT OF THE AURORA BOREALIS.

NUMEROUS CAVE ENTRANCES TO THE INNER EARTH EXIST IN THE ROCKY MOUNTAINS AND SIERRA MOUNTAINS IN THE WESTERN UNITED STATES, AS WELL AS LESS NUMEROUS OPENINGS IN THE OZARKS AND APPALACHIAN MOUNTAINS. ENTRIES ALSO EXIST IN THE ALPS, HIMALAYAS, ANDES, AND THE CARIBBEAN. THERE ARE ALSO NUMEROUS SUB-OCEANIC ENTRY POINTS, PARTICULARLY IN THE DEEP TRENCHES OF THE PACIFIC OCEAN, THE CARIBBEAN SEA, AND THE ATLANTIC SUBMARINE MOUNTAIN RANGES ESPECIALLY ON OR NEAR THE AZORES, CANARY ISLANDS, AND THE FALKLANDS.

ALL OF THESE AREAS ARE CLOSELY GUARDED BY LOCAL GOVERNMENTS AND N.W.O. ELITE FORCES. ARTIFICIALLY CREATED ENTRANCES EXIST UNDER THE NEW DENVER AIRPORT, THE GIZA PLATEAU IN EGYPT, MAJOR AIR FORCE COMPLEXES AROUND THE WORLD, AND MANY OF THE TEMPLES IN INDIA AND CHINA. A MAJOR CHINESE ENTRY POINT IS UNDER THE SHENSI PYRAMID THAT IS OUT OF BOUNDS FOR EVERYONE IN WESTERN CHINA.

OF COURSE, WITH THE REPTILIANS OFF THE EARTHS SURFACE, THE ATLANTEANS WERE FREE TO PLAY WITH THIS NEW MANKIND AND ESTABLISH HUMANS AS THE RULER OF THIS PLANET. THEY ESTABLISHED COLONIES ALL OVER THE REMAINING PORTIONS OF LAND. THEY INVITED THE SIRIANS TO COME AND PLAY WITH THEM. THEY BOOTED THE MARDUK BEINGS OFF-WORLD AND TOOK CONTROL OF THEIR SLAVES. THEY CREATED NEW HYBRIDS FOR SEA AND LAND, ONE OF WHICH BECAME THE MERFOLK, A GENETIC BLEND OF HUMAN AND DOLPHIN. THE DOLPHIN SPECIES WAS BROUGHT HERE FROM THE ANDROMEDA GALAXY TO MONITOR ALL OF THESE EVENTS.

WHENEVER THE ATLANTEANS DETECTED UNDERGROUND REPTILIAN ACTIVITY, THEY BLASTED THE INNER EARTH WITH LASERS AND ELECTROMAGNETIC PULSES TO KILL THEM. UNFORTUNATELY, THIS WEAKENED THE UPPER CRUST OF THE EARTHS TOP MANTLE RIDING OVER THE TRAPPED MAGMA BETWEEN THE UPPER AND LOWER CRUSTS. AFTER SEVERAL MILLENNIA OF THESE ATTACKS, THE ATLANTEAN CONTINENT STARTED TO BREAK UP. THEIR CIVILIZATION BEGAN TO BREAK UP AS A REFLECTION OF THE PHYSICAL DETERIORATION OF THEIR CONTINENT. THE ATLANTEANS BECAME EVEN MORE BELLIGERENT AS FEAR AND DESTRUCTION OVERTOOK THEIR MIND-PATTERNS. BLACK MAGICIANS AND SORCERERS TOOK THE PLACE OF SCIENTISTS AND RELIGIOUS LEADERS.

FORTUNATELY, THE POPULATION FORESAW THE DESTRUCTION THAT WAS COMING. MANY REFUGEES RELOCATED TO WHAT IS NOW EGYPT, PERU, THE APPALACHIAN MOUNTAINS AND WESTERN EUROPE, JUST BEFORE THE CONTINENT COLLAPSED INTO THE UPPER CRUST OF THE EARTH. THIS COLLAPSE CAUSED THE EARTH TO FLIP ON ITS AXIS, CREATING THE LEGEND OF THE FLOOD WRITTEN ABOUT IN THE BIBLE, AND IN OTHER WORLD CULTURES.

THIS CATASTROPHE WAS USED AS A WINDOW OF OPPORTUNITY BY THE GROUPS THAT DONATED DNA TO CREATE MANKIND. THEY IMMEDIATELY BEGAN REORGANIZING THE HUMANS INTO NEW GROUPS THAT BECAME THE BASIS FOR FUTURE NATIONALISM.

*

THE SIRIANS HELPED TO CREATE THE ANCIENT EGYPTIAN CULTURE

*

THOSE FROM TAU CETI ORGANIZED THE SLAVIC CULTURE

*

THE RIGELIANS WERE BUSY IN CHINA AND THE ORIENT (3)

WHILE ALL THIS WAS TRANSPIRING, THE REPTILIANS SAW AN OPPORTUNITY AND SEIZED IT!

FOOTNOTE:

3. FOR FURTHER DETAILS OF THE FLOW OF GENETICS AN ALIEN INTERVENTION IN MANKIND, PLEASE REFER TO THE MILKY WAY GALAXY CHART ON THE BOOK.

GO BACK

6 - BLUEBLOODS!

THE INNER EARTH PROVIDED A SUBTERRANEAN LOCALE FOR THE REPTILIANS TO REGROUP AND FORMULATE PLANS TO RETAKE THE SURFACE. AT THIS POINT, THE REPTILIANS WERE COMPLETELY CUT OFF FROM THEIR HOME IN THE DRACO CONSTELLATION. THEIR SPACESHIP, THE MOON, WAS IN HUMAN HANDS. THEY WERE ALONE, ISOLATED ON A NOW HOSTILE PLANET. THEY NEEDED TO DEFEND THEMSELVES.

THEY DEVELOPED A PLAN TO INSIDIOUSLY RETAKE THE SURFACE BY BLENDING THEIR GENETICS WITH THE GENETICS OF THE SURFACE HUMANS. BECAUSE THE HUMAN PROTOTYPE ALREADY HAD REPTILIAN GENETICS, IT WAS EASY TO ACCESS THE MIND-PATTERN. THE REPTILIAN FREQUENCY WAS ALREADY ESTABLISHED IN THE BRAIN STEM AS WELL AS THE REPTILIAN BRAIN SECTION OF THESE HYBRID HUMANS.

THE POPULATION OF SUMER WAS CHOSEN AS THE STARTING POINT. THESE HUMANS WERE PRIMARILY DESCENDANTS OF THE MARTIAN, MALDEKIAN, AND LYRAEN REFUGEES. THE REPTILIANS HAVE A PREFERENCE FOR THE GENETICS OF BLONDE-HAIRED, BLUE-EYED PEOPLE WHOSE MIND-PATTERNS AND GENETICS ARE SO EASILY CONTROLLED. THEY ABDUCTED MEMBERS OF THE RULING CLASSES, INCLUDING POLITICAL LEADERS.

USING THESE HUMANS, THEY BEGAN A NEW HYBRIDIZATION PROGRAM THAT TOOK SEVERAL GENERATIONS TO PERFECT. THEIR GOAL WAS TO REACH A HUMAN/ REPTILIAN GENETIC 50/50 SPLIT. THIS WOULD PRODUCE A HUMAN-LOOKING REPTILIAN THAT COULD EASILY SHAPESHIFT FROM REPTILIAN TO HUMAN, THEN BACK AGAIN. SHAPESHIFTING WAS ACCOMPLISHED SIMPLY BY CONCENTRATING ON THE GENETICS THE HYBRID WISHED TO OPEN, OR LOCK UP, WHATEVER THE CASE MAY BE.

FOR THIS PROGRAM THE REPTILIANS ENGAGED THE HELP OF THE SIRIANS WHO HAD THE TECHNOLOGY TO IMPLEMENT SUCH A PROGRAM. THE SIRIANS KNEW A LOT ABOUT GENETIC ALTERATIONS AND MIND-PROGRAMMING, WHICH THEY FREELY SHARED WITH THE REPTILIANS.

ONCE THE HYBRIDIZATION PROGRAM WAS COMPLETE, THE SUMERIAN LEADERS WERE NOW

SHAPESHIFTING REPTILIANS. THE NEW REPTILIAN HYBRID BECAME THE ELITE OF THAT CULTURE. THEIR BLOOD, BECAUSE OF THE INCREASED REPTILIAN DNA, CONTAINED MORE OF A COPPER CONTENT.

SINCE COPPER-BASED BLOOD TURNS BLUE-GREEN UPON OXIDIZING, THESE REPTILIAN HYBRIDS WERE CALLED "BLUEBLOODS".

AMERICAN GOVERNMENT IS PROBABLY THE MAIN FOCUS OF THE CURRENT REPTILIAN SHAPESHIFTERS. YOUR ATTENTION IS DRAWN TO THE VERTICAL SLIT EYEBALLS WHICH SHAPE SHIFT IN TO MANY US MILITARY LEADERS - NORMAN RUSSBACHER, RUPERT MURDOCK, ETC. PICTURES: WERE AT WIOLAWA.COM WE SUGGESTED NEW RULES REQUIRING ALL GOVERNMENT DECISIONS AND VOTING MUST TAKE PLACE IN 20% OXYGEN AIR, TO KILL THE SHAPESHIFTERS.

THE BLUEBLOODS QUICKLY REALIZED THAT WITH A 50/50 HUMAN/REPTILIAN GENETIC SPLIT, IT WAS NECESSARY TO INTERMARRY TO MAINTAIN THE 50/50 SPLIT BLOODLINE NECESSARY TO SHAPESHIFT. WHEN THE SPLIT INCREASED TOO FAR TO THE REPTILIAN SIDE, SHAPESHIFTING BECAME DIFFICULT, AND HOLDING HUMAN FORM BECAME IMPOSSIBLE. IN THESE CASES, IT WAS DISCOVERED THAT THE INGESTION OF HUMAN HORMONES, FLESH, AND BLOOD, ALLOWED THE REPTILIANS TO MAINTAIN THE HUMAN FORM.

HUMAN FORM WAS NECESSARY TO MAINTAIN TO AVOID SCARING THE POPULATION, WHICH WAS NOW NOT ACCUSTOMED TO THE REPTILIAN FORM.

CONTROL OF THE MASSES WAS EASIER WHEN THE ORDERS CAME FROM A HUMANOID. THE REPTILIAN FORMAT WAS KEPT TO RELIGIOUS ICONS AND LEGENDS. THE STATUES OF THEIR GODS AND GODDESSES REFLECT THE REPTILIAN INFLUENCE, EVEN SHOWING A FEMALE REPTILIAN HOLDING A HYBRID BABY. (CLICK IMAGE RIGHT)

THE SHAPESHIFTING REPTILIAN BLUEBLOODS ASKED THE SIRIANS FOR HELP WITH THE DAILY MAINTENANCE OF THEIR HUMAN FORMS. THE SIRIANS DETERMINED THAT FEEDING THE HYBRIDS HUMAN HORMONES AND BLOOD IN AN ALTERED ANIMAL FORM WOULD BE THE EASIEST WAY TO DO IT UNNOTICED BY THE POPULATION.

THE SACRIFICIAL ANIMAL USED BY MOST MIDDLE EASTERN PEOPLE WAS THE WILD BOAR, SO THE SIRIANS CHOSE IT AS THE BASIS FOR THIS NEW ANIMAL HYBRID. HUMAN GENETICS WERE MIXED WITH THOSE OF THE WILD BOAR TO CREATE THE DOMESTICATED PIG. THIS ANIMAL WAS SERVED DAILY TO THE BLUEBLOODS AS A METHOD OF TEMPORARILY MAINTAINING THEIR HUMAN FORM UNTIL THEY COULD USE AN ACTUAL HUMAN IN A SACRIFICIAL CEREMONY.

BECAUSE THE DOMESTICATED PIG IS A COMBINATION OF HUMAN AND ANIMAL GENETICS, EATING IT IS A FORM OF CANNIBALISM. THIS EXPLAINS WHY THE HEBREWS CONSIDERED IT UNCLEAN TO EAT. THIS IS ALSO WHY THE PIG IS CONSIDERED TO BE THE MOST INTELLIGENT ANIMAL ON EARTH, WHY PIG SKIN CAN BE GRAFTED DIRECTLY ONTO HUMANS IN BURN CASES, AND WHY PIG HEART VALVES CAN BE USED IN HUMANS WITH LITTLE DIFFICULTY. CANCER DRUGS AND OTHER CHEMICALS ARE OFTEN TESTED ON PIGS BEFORE HUMANS.

THE DOMESTICATED PIG FREQUENCY, OR GROUP MIND, IS THE PERFECT VEHICLE FOR ANIMAL SPECIES TO ENTER BEFORE ENTERING HUMAN FORM ON THEIR EVOLUTIONARY PROGRESSION. IN MANY RESPECTS, PIGS CAN BE CONSIDERED A FORM OF HUMANITY. TO A LESSER DEGREE, THE SAME IS TRUE ABOUT CATS.

AS TIME PROGRESSED, THE CIVILIZATION OF SUMER DECLINED AND TRANSFORMED INTO OTHER CULTURES. VAST MIGRATIONS FROM SUMER TO OTHER LOCATIONS IN CENTRAL ASIA OCCURRED. THE MIGRATING PEOPLES TOOK THEIR BLUEBLOOD LEADERS WITH THEM, AS THEY WERE THEIR ROYALTY AND KINGS.

THE SUMERIANS BECAME KNOWN AS THE SUM-ARYANS, OR JUST, ARYANS. THEY SPREAD OUT ACROSS ASIA INTO THE STEPPES OF RUSSIA AND INTO THE NORTHERN INDIAN SUBCONTINENT. IN INDIA THEY ENCOUNTERED THE DARK-SKINNED DRAVIDIANS, WHO WERE REPTILIAN REMNANTS FROM LEMURIA. THE DRAVIDIANS WERE DRIVEN TO THE CENTRAL AND SOUTHERN PARTS OF INDIA, WHILE THE ARYAN HYBRIDS TOOK CONTROL OF THE NORTH, AND INTO THE FOOTHILLS OF THE HIMALAYAS.

THE ARYAN LEADERS, ALL BLUEBLOODS, BECAME THE SULTANS AND RAJAS OF LEGEND AND HISTORY. SUMERIANS ALSO CREATED BABYLONIA.

THE SUMERIANS ALSO MIGRATED TO THE AREA KNOWN AS THE CAUCASUS REGION, WHERE THE KHAZARS DEVELOPED. FROM THE CAUCASUS REGION, THE BLUEBLOOD KINGS AND THEIR PEOPLE SPREAD WEST TOWARD EUROPE, DEVELOPING INTO THE FRANKS, CAMBRIANS, AND TEUTONIC NATIONALITIES. THESE NATIONALITIES WERE ALSO BEING MANIPULATED BY VARIOUS ALIEN CULTURES LIKE THE ANTARIANS, ARCTURIANS, ALDEBARANS, TAU CETIANS, AND OTHER REMNANTS OF THE LYRAENS, SUCH AS THE ATLANS. THE ATLANS LOCATED HERE EVENTUALLY BECAME THE CELTS.

TO BACK-TRACK FOR JUST A BIT, I HAD SAID IN A PREVIOUS CHAPTER THAT THE DESCENDANTS OF THE REPTILIAN HYBRID SUMERIANS WENT INTO CENTRAL ASIA AND THE MIDDLE EAST. THEY MOSTLY ESTABLISHED THEMSELVES IN THE CAUCASUS MOUNTAINS AND BECAME THE KHAZARS. FROM HERE, THEY SPREAD WEST TOWARD EUROPE, SEEDING THE NATIONAL IDENTITIES FOR THE VIKINGS, THE FRANKS, THE TEUTONIC PEOPLES, AND THE RUSSIANS. KEEP IN MIND THAT WHEN ATLANTIS SANK, SOME OF THOSE REFUGEES WENT TO WESTERN EUROPE AND DEVELOPED INTO THE CELTS. SOME WENT TO GREECE AND OTHERS TO THE ITALIAN PENINSULA.

THESE PEOPLES WERE HERE BEFORE THE HYBRIDS MOVED IN. IT WAS DURING THE INTERIM TIME PERIOD FROM THE DESTRUCTION OF ATLANTIS UNTIL THE SUMERIAN DESCENDANTS MOVED IN THAT OTHER ALIEN GROUPS STARTED TO ADD THEIR GENETIC MIX TO THE POT AND DEVELOP INDIVIDUAL CULTURES BASED ON THEIR HOME WORLDS.

THESE BLUEBLOOD LEADERS ALSO INFILTRATED THE MIDDLE EASTERN PEOPLES, SUCH AS THE BIBLICAL CANAANITES, MALACHITES, AND KITTITES.

AT THE SAME TIME IN EGYPT, THE SIRIANS WERE REORGANIZING THE ATLANTEAN DESCENDANTS THERE, KNOWN AS THE PHOENICIANS. THE PHOENICIANS WERE BLONDE-HAIRED, BLUE-EYED, WITH SOME GREEN-EYED, RED-HAIRED PEOPLE AMONG THEM. THE PHOENICIANS COLONIZED THE COASTAL MIDDLE EAST AND THE BRITISH ISLES. THEY EVEN COLONIZED PARTS OF THE NORTH-EASTERN NORTH AMERICAN CONTINENT, ALL THE WAY TO THE GREAT LAKES AREA. SOME OF THEIR MINES AND WRITING SON STONE TABLETS CAN STILL BE FOUND IN THE WOODS OF NORTH AMERICA.

THE SIRIANS WERE ALSO GENETICALLY CREATING THE ANCIENT HEBREWS. THE JEWISH PEOPLE ARE ACTUALLY A COMBINATION OF THESE GENETICALLY MANIPULATED HEBREWS AND THE SUMERIANS. THESE JEWISH PEOPLE WERE THEN RELEASED INTO THE PALESTINIAN TERRITORY. THE NAME, PALESTINE, COMES FROM THE ANCIENT PEOPLE, THE PHILISTINES, WHO WERE ACTUALLY PHOENICIANS.

ALL OF THESE MIXED IN THE COASTAL PLAINS OF PALESTINE AND CREATED A NEW RELIGION BASED ON SACRIFICE AND AN AVENGING ALIEN CONTROLLER, THAT THEY CALLED GOD, OR ELOHIM.

SIMILARLY, WHEN THE ARYANS MIXED WITH THE DRAVIDIANS IN INDIA, THEY CREATED THE HINDU RELIGION, WHICH IS ACTUALLY A RECREATION OF THE REPTILIAN SEVEN-TIER HIERARCHY. THE CASTE SYSTEM OF INDIA IS A DIRECT COPY OF THE REPTILIAN DIVISION OF FUNCTION.

AT THE SAME TIME THAT ALL OF THIS WAS GOING ON IN WESTERN AND CENTRAL ASIA, THE RIGELIANS, WERE DEVELOPING THE REMNANTS OF LEMURIA WHO ESCAPED TO THE COAST OF EASTERN ASIA. THE RIGELIANS WERE A HUMAN CIVILIZATION THAT WAS CONTROLLED, AND EVENTUALLY ASSIMILATED, BY THE REPTILIANS. THE RIGELIANS ASSISTED THE INNER EARTH REPTILIANS IN DEVELOPING A HYBRID THAT INCLUDED RIGELIAN DNA.

THE RIGELIAN/REPTILIAN HYBRIDS SET UP DYNASTIES IN WHAT IS NOW JAPAN AND CHINA THAT DEVELOPED INDEPENDENTLY OF THEIR WESTERN COUSINS.

IN THEIR MANIA FOR CONTROL, THE REPTILIANS USED THE VARIOUS RACES THAT DONATED DNA TO THE ORIGINAL HUMAN PROJECT. THEY FASTIDIOUSLY MONITORED THESE RELATED SECTIONS OF HYBRIDS TO DETERMINE WHICH WAS BEST SUITED FOR OVERALL CONTROL, AND WHICH FOR SUBSERVIENCE. ALL THE HYBRIDS COULD BE CONTROLLED THROUGH THE REPTILIAN BRAIN THAT HOOKED THEM INTO REPTILIAN MIND-PATTERNS, BUT SOME WERE MORE CONTROLLABLE THAN OTHERS.

IN EUROPE, THE BLUEBLOODS INSIDIOUSLY TOOK CONTROL OF THE VARIOUS TRIBES AND GROUPS, BECOMING THEIR KINGS AND ROYALTY. THEY INFILTRATED THE ARCTURIAN EXPERIMENT, CALLED THE ETRUSCANS AND STARTED TO CREATE A NEW GLOBAL EMPIRE THROUGH THE ROMANS. THESE EUROPEAN BLUEBLOODS THEN ENTIRELY ELIMINATED THE ANTARIAN EXPERIMENT IN GREECE, AND INSTIGATED THEIR PLAN FOR GLOBALIZATION THROUGH THE ROMAN EMPIRE.

THE REPTILIANS EVEN OFFENDED THE SIRIANS BY INFILTRATING THE EGYPTIAN EXPERIMENT AND IMPLEMENTING THEIR RELIGION THERE.

THE REPTILIAN HYBRIDS BECAME LIKE THE ENDOMETRIOSIS OF THE KNOWN WORLD, SLOWLY GROWING INTO ALL AREAS AND CREATING CONTROL THROUGH THE BLUEBLOOD SYSTEM.

GO BACK

GO BACK TO THE BLACK NOBILITY

7 - OTHER ALIEN GROUPS

WHILE THE REPTILIANS WERE THE FIRST COLONISTS ON EARTH, THEY WERE NOT THE ONLY ONES WHO INTERFERED WITH HUMAN DEVELOPMENT ON THIS PLANET. IN ALL THERE ARE TWELVE OTHER GROUPS WHO DONATED DNA TO THE PRODUCTION OF THE EXPERIMENT.

ADD THE REPTILIANS TO THE TWELVE GROUPS, RESULTING IN HUMAN BEINGS WITH A GENETIC MIXTURE OF 13 DIFFERENT STRAINS.

THE RESULT WAS A GENERAL FREE-FOR-ALL. WHILE ALL THESE HUMANOID ALIENS WERE LYRAEN/REPTILIAN DESCENDANTS, EACH GROUP WAS CULTURALLY AND PHYSICALLY MANIPULATED BY DIFFERENT GROUPS. THIS IS SIMILAR TO A LAB PROFESSOR WHO LEAVES THE DOOR OPEN WHILE HE IS GONE, AND ALL HIS ASSISTANTS ADD THEIR OWN GENETICS TO THE EXPERIMENT.

THE TAU CETI ALIENS CENTERED THEIR ATTENTION ON THE EASTERN EUROPEAN AREA, FROM WHAT IS NOW SERBIA TO THE SLOPES OF THE URAL MOUNTAINS. FROM HERE, THEY INFLUENCED THE SLAVIC AND RUSSIAN PEOPLES. THE GEOGRAPHIC CONDITIONS RESEMBLED THAT IN THE TAU CETI STAR SYSTEM, AND ITS COLONY EPSILON ERIDANUS. THE TAU CETI ADDED THEIR DNA TO THE HUMAN PROTOTYPES THAT WERE ALREADY ESTABLISHED THERE, CREATING WHAT IS NOW KNOWN AS THE SLAVIC PEOPLES. THE RESULTS WERE A RACE OF HUMANS WHO WERE STOCKY, BARREL-CHESTED, AND AVERAGING 5’6’’ TO 5’9’’ IN HEIGHT, WITH A DENSE BONE STRUCTURE AND DARK EYES. THEY WERE AGGRESSIVE, AND PREFERRED A COLD CLIMATE.

THESE TAU CETI/HUMANS WERE VIRULENTLY AGAINST THE GREY ALIEN RACE AND THE REPTILIANS, BECAUSE THEIR WORLDS HAD BEEN ATTACKED, AND THEIR CHILDREN STOLEN AND KILLED BY BOTH RACES. THE TAU CETIANS VOWED TO FOLLOW THE GREY RACE AND DESTROY THEM.

IN THE 1950S, THE SOVIET UNION SIGNED AN AGREEMENT WITH THE TAU CETIANS TO USE BASES IN SIBERIA AND UNDER THE URAL MOUNTAINS. FOR THIS REASON, THE CITY OF SVERDLOVSK, NAMED AFTER MY GREAT-UNCLE, THE FIRST PRESIDENT OF THE SOVIET UNION, WAS CLOSED TO OUTSIDERS (CLICK IMAGE LEFT).

MANY EXPERIMENTS INVOLVING RADIATION ON THE PUBLIC WERE PERFORMED HERE FROM 1958 THROUGH THE 1980S. A UNITED STATES SPY PLANE WAS SHOT DOWN OVER SVERDLOVSK IN THE EARLY 1960S WHEN THE UNITED STATES WAS TRYING TO LEARN ABOUT THE SECRET ACTIVITIES TAKING PLACE THERE.

IN CENTRAL EUROPE, THE GERMAN TRIBES WERE GENETICALLY MANIPULATED BY BEINGS FROM ALDEBARAN. THESE PEOPLE ARE VERY INTELLIGENT AND SCIENTIFICALLY-ORIENTED. THEY ARE GENERALLY BLONDE-HAIRED AND BLUE-EYED, WITH A MINORITY OF DARK-HAIRED, LIGHT-BROWN TO HAZEL-EYED PEOPLE. THEY ARE MILITARISTIC, AND PREFER TO KEEP TO THEMSELVES. FOR ALMOST 2,000 YEARS, THE ALDEBARANS HAVE BEEN ENERGETICALLY CONNECTING TO THE GERMANIC PEOPLES, TELEPATHICALLY SENDING INFORMATION TO THEM AND PROMOTING A NATIONAL SENTIMENT.

MANY HUMANS OF THE ALDEBARAN FREQUENCY HAVE MIXED WITH THE TAU CETI DESCENDANTS IN THE SLAVIC AREA, PARTICULARLY IN POLAND AND RUSSIA. HITLER KNEW THIS. THAT IS WHY HE WAS SO ADAMANT ABOUT INVADING THOSE COUNTRIES AND INCORPORATING THEM INTO HIS EMPIRE.

HITLER WAS ONLY HALF GERMANIC. HIS FATHER WAS A WEALTHY JEWISH BUSINESSMAN IN AUSTRIA. HIS MOTHER WORKED AT THE HOME AS A MAID. SHE HAD AN AFFAIR WITH THE MASTER OF THE HOUSE, AND WHEN THE WIFE FOUND OUT ABOUT IT, HAD THE MAID THROWN OUT. THE JEWISH BUSINESSMAN DID NOTHING TO HELP HITLER’S MOTHER. FOR THIS REASON, HITLER HATED THE JEWS AND SOUGHT TO DESTROY HIS OWN GENETIC LINEAGE, BASICALLY BECAUSE HE HATED HIMSELF. HE WAS ALSO DEEPLY MIND-CONTROLLED.

THE ALDEBARANS ALSO GENETICALLY INFUSED THE VIKINGS. THESE NORDIC PEOPLE INHERITED THE AGGRESSIVE AND MILITARISTIC TENDENCIES THAT ARE ALSO SEEN IN THE GERMANS. THE VIKINGS PLUNDERED AND RAPED ACROSS EUROPE FOR CENTURIES, BUT DID NOT HAVE THE

TECHNOLOGICAL ABILITY TO STAY IN POWER.

AN ACCIDENTAL MANIPULATION OF GENETICS OCCURRED ON THE ITALIAN PENINSULA 3000 YEARS AGO. A SHIP FROM THE ARCTURUS STAR SYSTEM CRASHED LANDED ON ETRUSCAN TERRITORY. THESE HUMANS WERE ACTUALLY EXTREMELY SPIRITUALLY-MINDED, AND INSTEAD OF TRYING TO GET BACK HOME, STAYED AND BLENDED INTO THE HUMANS OF THAT PART OF EARTH. THEIR DESCENDANTS BECAME THE ROMANS WHO WERE THEN INFILTRATED AND MIXED WITH THE CENTRAL ASIAN HYBRIDS.

BEINGS FROM THE ANTARIAN STAR SYSTEM WERE BEHIND THE GENETIC MANIPULATION OF ANCIENT GREECE. THESE PEOPLE WERE A SOCIETY PREDOMINANTLY BASED UPON HOMOSEXUALITY. FEMALES WERE USED FOR BREEDING ONLY. IN FACT, THERE WERE ANTARIAN OBSERVERS AT THE MONTAUK PROJECT WHO WERE INTERESTED IN THE PROGRAMMING ASPECTS OF SEXUALITY AS THEY RELATED TO THE WILHELM REICH METHODS.

THE ANTARIANS ARE DARK, OFTEN WITH OLIVE SKIN, DARK EYES, AND SHORT, THIN BODIES. THEY HAVE A FABULOUS MUSCULATURE DUE TO THE DENSITY OF THEIR HOME-WORLD, AND ARE KNOWN FOR THEIR BODY-BUILDING GOALS.

THE GREEK-ANTARIANS COLONIZED SPAIN AND PORTUGAL. THEIR DESCENDANTS FURTHER MIXED WITH THE ROMANS, AND ARABS WHO ARE PREDOMINANTLY SUMERIAN/REPTILIAN. THESE THEN COLONIZED CENTRAL AND SOUTH AMERICA, MIXING THEIR GENETICS WITH THE NATIVE INDIANS WHO WERE OF ATLANTEAN-PROCYON DESCENT.

THE PROCYON STAR SYSTEM DOES NOT HAVE MUCH TECHNOLOGY. THE PROCYONS WERE BROUGHT TO THIS PLANET AFTER THE FALL OF ATLANTIS TO BOOST THE SURVIVAL RATE OF THE REFUGEES. THEY BECAME THE MAYA, AZTEC, AND INCA. THEY WERE GIVEN ANCIENT LEMURIAN AND ATLANTEAN OUTPOSTS IN THE ANDES AND SIERRAS OF MEXICO. THEY TRIED UNSUCCESSFULLY TO RECREATE THESE CULTURES, INCLUDING EMULATING THE BUILDING OF THE PYRAMIDS, PERFORMING MEDICAL PROCEDURES, AND FINALLY, SACRIFICING TO THE REPTILIAN GODS. THIS IS WHY THEIR LEGENDS SPEAK OF BLOND MEN RETURNING IN CHARIOTS FROM SPACE TO TAKE THEM AWAY.

THE ANASAZI INDIANS OF THE AMERICAN SOUTHWEST WERE ALSO BROUGHT FROM PROCYON. IT WAS THE SIRIANS WHO SO GENEROUSLY PROVIDED TRANSPORTATION. THE SIRIANS EVEN ATTEMPTED TO BRING THE HEBREWS TO THE AMERICAN WEST. ANCIENT HEBREW COINS WERE FOUND IN NEW MEXICO AND OTHER PARTS OF NORTH AND SOUTH AMERICA.

OVER THE MILLENNIA AND RECENT CENTURIES, MOVEMENTS OF NATIONS, COLONIZATIONS, WAR, AND FAMINES, HAVE THROWN THE EARTHS POPULATION INTO A GIANT MELTING POT. STRANDS OF GENETICS HAVE CONTINUOUSLY MIXED WITH ONE ANOTHER, ESPECIALLY IN NORTH AMERICA, EUROPE, AUSTRALIA, THE CARIBBEAN, AND SOUTH AMERICA. THE RESULT IS THAT THERE ARE FEW PURE RACES LEFT, AND THE RACIAL AND CULTURAL UNITY MAKES IT EASIER FOR GROUP CONTROL.

WHILE ALL OF THIS WAS GOING ON IN EUROPE AND THE MIDDLE EAST, THE CHINESE EMPIRE WAS EXPANDING OVER EAST ASIA, AND THE DRAVIDIAN-REPTILIAN CULTURE IN INDIA WAS BEING REPLACED BY THE ARYAN (ARI- AND SUM-ARIAN) HORDES FROM CENTRAL ASIA. IN SOUTH AMERICA, THE INCA EMPIRE WAS FLOURISHING AS IT WAS MIXED WITH THE GENETICS OF THE PROCYON STAR SYSTEM.

THE SAME MIXTURE WAS HAPPENING IN NORTH AND CENTRAL AMERICA CREATING THE TOLTECS, MAYANS, AND AZTECS. ALL OF THESE CULTURES, USED BLOOD-RITUAL AND HUMAN SACRIFICE. THIS INDICATES THAT THE PROCYONIANS WERE THEMSELVES CONQUERED BY THE REPTILIANS AND DID THEIR BIDDING, EVEN THOUGH THEY WERE HUMANOID. ALL OF THE CENTRAL AND SOUTH AMERICAN CULTURES USED SNAKES AND REPTILIANS AS SYMBOLS.

THESE PEOPLE HAVE A UNIQUE BLEND OF LEMURIAN/DRACO AND ATLANTEAN/HUMAN GENETICS MIXED WITH THE PROCYONIAN DNA.

GO BACK

GO BACK TO VIDA EN NUESTRA GALAXIA

8 - THE CRYSTAL SKULL

WHEN THE HATONA COUNCIL CONVENED TO DETERMINE THE DEVELOPMENT OF LIFE ON EARTH, THEY PONDERED TWO QUESTIONS. FIRST, IF THE EARTH BEINGS WERE LEFT TO DEVELOP ON THEIR OWN, HOW WOULD THEY KNOW THEIR TRUE ORIGINS, AND SECOND, IF THERE WAS NO INTERFERENCE, HOW COULD THEY BE PRODDED IN THE CORRECT DIRECTION.

ONE E.T. GROUP THAT WAS PRIMARILY NON-PHYSICAL DECIDED TO LEAVE A REPOSITORY OF KNOWLEDGE FOR THOSE WHO EVOLVED ENOUGH TO UNDERSTAND IT. THESE MUSCULAR BEINGS WERE TALL WITH GOLDEN-BRONZE SKIN, GOLDEN HAIR, AND VIOLET EYES. ON AN ETHERIC LEVEL, THIS E.T. GROUP CREATED AN OBJECT THAT CONTAINED WITHIN IT THE SUM TOTAL OF KNOWLEDGE OF THE MIND OF GOD AS THEY KNEW IT. THEY ALSO PROGRAMMED THIS OBJECT WITH THE HISTORY OF THE UNIVERSE AND ALL THE TECHNOLOGY THAT WOULD EVER BE NECESSARY.

FOR THE OBJECT THIS GROUP CHOSE THE SHAPE OF A FEMALE HUMAN SKULL WITHOUT ANY RACIAL FEATURES. THE SKULL REPRESENTED ALL HUMANOIDS, SYMBOLIZING BROTHERHOOD AND HARMONY. THE FEMALE WAS CHOSEN BECAUSE IT WAS TO BE PLACED IN PHYSICAL REALITY AS A SYMBOL OF EGO BEING OVERCOME.

CRYSTAL WAS CHOSEN BECAUSE IT REPRESENTS THE HIGHEST VIBRATION POSSIBLE IN PHYSICAL REALITY - PURITY, CLARITY, FOCUSING, AND MAGNIFICATION. THE MOVABLE JAW PIECE (CLICK IMAGE RIGHT) SYMBOLIZED THE FACT THAT IT WAS A COMMUNICATION DEVICE. THE E.T. GROUP LEFT THE CRYSTAL SKULL WITH THE FIRST LYRAEN/ ATLANTEAN CIVILIZATION WHERE IT WAS PLACED IN A TEMPLE PYRAMID TO BE ENERGIZED BY THE LYRAEN/ATLANTEANS OVER MANY AEONS OF TIME.

WHEN THE SIRIANS INFILTRATED THE SECOND-GENERATION LYRAEN/ATLANTEAN CIVILIZATION, THEY NEGOTIATED WITH THE ATLANS TO STUDY THE CRYSTAL SKULL. OVER TIME, THEY CREATED AN EXACT DUPLICATE THAT THEY BROUGHT BACK TO SIRIUS A. OTHER ALIEN GROUPS MADE INFERIOR COPIES OF IT FOR USE WITH THEIR OWN HUMAN CREATIONS. BY THE TIME THE THIRD-GENERATION LYRAEN/ATLANTEANS WERE WELL ESTABLISHED, THE TRUE PURPOSE OF THE CRYSTAL SKULL WAS ALMOST ENTIRELY FORGOTTEN.

THOSE IN POWER TRIED TO USE IT FOR NEGATIVE PURPOSES, NOT REALIZING THAT THIS MAGNIFIED AND REFLECTED BACK ALL THEIR EVIL DEEDS AND INTENTIONS. IN ADDITION, THE CRYSTAL SKULL WAS CREATED IN SUCH A WAY THAT WHATEVER IS THOUGHT IN ITS PRESENCE REFLECTS BACK, BECOMING A PART OF THE THINKER'S EXPERIENCES. THE CRYSTAL SKULL TEACHES THAT THE PHYSICAL UNIVERSE MIRRORS THOUGHTS.

WHEN ATLANTIS SANK, HIGH PRIESTS FLEEING THE CONTINENT BROUGHT IT TO CENTRAL AMERICA

TO WHERE THE PROCYONIANS BROUGHT THE MAYA. HERE, IT WAS USED AS AN OBJECT OF WORSHIP AND REVERENCE UNTIL THE MAYA WERE REMOVED FROM THE EARTH. EVENTUALLY, THE CRYSTAL SKULL REMAINED BURIED IN RUINS UNTIL ITS DISCOVERY IN THE EARLY PART OF THE 20TH CENTURY, WHEN THE CRYSTAL SKULL ALLOWED ITSELF TO BE DISCOVERED.

THE CRYSTAL SKULL OPERATES THROUGH THE TRINITY OF COMMUNICATION COLOR, TONE, AND ARCHETYPE. WHEN ANY COMBINATION OF THESE THREE IS BEAMED OR THOUGHT OF IN THE PRESENCE OF THE CRYSTAL SKULL, IT OPENS A PROGRAM THAT IS CODED TO A PARTICULAR FREQUENCY RESONANCE.

AN INFINITE NUMBER OF COMBINATIONS CAN BE USED, AND ANY ONE WILL UNLOCK A PROGRAM IN THE CRYSTAL SKULL TO TEACH MANKIND. THE LEFT-BRAIN REPRESENTS LANGUAGE, AND THE RIGHT-BRAIN REPRESENTS PURE THOUGHT. THE PINEAL GLAND OF COMMUNICATION BALANCES AND TRANSLATES THE LEFT- AND RIGHT- BRAINS WITH THE USE OF ARCHETYPES.

ARCHETYPES CAN BE GEOMETRIC SHAPES, LETTERS, NUMBERS, ANCIENT HEBREW SYMBOLS, PICTOGRAMS, OR ANY COMBINATION OF THESE. COLORS ARE ALSO PART OF THE TRIAD WITH A LANGUAGE ALL THEIR OWN. THE LEFT-BRAIN IS DARK, THE RIGHT-BRAIN IS LIGHT, AND ONCE AGAIN, THE PINEAL GLAND BALANCES AND TRANSLATES THIS THROUGH COLORS. TONES ALSO REPRESENT THE TRINITY OF SOUND, BALANCING MUSIC AND SILENCE. IN THE SAME WAY, THE CRYSTAL SKULL BALANCES THE MIND OF GOD AND PHYSICAL REALITY.

AT TIMES, THE CRYSTAL SKULL BECOMES NON-PHYSICAL. BECAUSE IT WAS CREATED WITHOUT A BODY, THIS SYMBOLIZES THE NEEDLESSNESS OF THE PHYSICAL BODY. THE CRYSTAL SKULL IS A BRIDGE BETWEEN ALL LEVELS OF REALITY.

ANYONE WHO KNOWS THE SEQUENCES OF THE TRINITY OF COMMUNICATION BECOMES ALL-POWERFUL AND OMNISCIENT.

GO BACK

GO BACK TO CRANEOS INSOLITOS

9 - THE ANCIENT HEBREWS

MOST MODERN JEWS HAVE ABSOLUTELY NO GENETIC LINK TO THE MIDDLE EAST. THERE ARE IN FACT, MANY DIFFERENT PHYSICAL TYPES OF JEWS, COVERING MANY RACIAL CHARACTERISTICS. THIS SUPPORTS THE FACT THAT THEY ARE NOT A HOMOGENEOUS GROUP, BUT A RELIGIOUS GROUP THAT SPANS MANY CULTURES. THE STORY OF ABRAHAM GOING OUT FROM THE CITY OF UR AND COMING TO CANAAN IS REALLY TELLING THE STORY OF THE REPTILIAN HYBRIDS LEAVING

SUMERIAN TERRITORY AND COLONIZING OTHER PARTS OF CENTRAL ASIA AND THE MIDDLE EAST. THE VAST MAJORITY OF EUROPEAN/AMERICAN JEWS CAN TRACE THEIR GENETIC LINEAGE TO THE KHAZARS, MENTIONED IN THE LAST CHAPTER, WHO ALL CONVERTED TO JUDAISM IN THE 800S TO CIRCUMVENT THE CATHOLIC RULE OF THE HOLY ROMAN EMPIRE.

IN THE YEAR 2000, THE UNIVERSITY OF PAVIA IN ITALY DID A GENETIC STUDY OF EUROPEAN MEN. THEY FOUND THAT 80% OF THEM HAD A DIRECT LINEAGE TO CENTRAL ASIA AND THE OTHER 20% TO THE MIDDLE EAST. THIS SUPPORTS THE STATEMENT THAT THE SUMERIANS ENTERED INTO CENTRAL ASIA AND THEN MIGRATED TO EUROPE AND THE MIDDLE EAST. THIS ALSO NULLIFIES THE THEORY OF AFRICA AS THE BIRTHPLACE OF MANKIND. THERE IS ABSOLUTELY NO GENETIC CONNECTION FROM ASIA OR EUROPE TO AFRICA.

THE ANCIENT HEBREWS HAVE NOTHING TO DO WITH MODERN JEWS. AS MENTIONED IN THE PREVIOUS CHAPTER, THE HEBREWS WERE SIRIAN-CREATED IN EGYPT BY COMBINING SIRIAN AND LYRAEN GENETICS. THESE PEOPLE WERE TALL AND POWERFUL, AND SPOKE THE SIRIAN LANGUAGE WHICH IS THE EQUIVALENT TO THE ANCIENT HEBREW LANGUAGE. SCHOLARS AGREE THAT THE HEBREW LANGUAGE SUDDENLY APPEARED ON THE SCENE.

THE ANCIENT PEOPLES OF PALESTINE SPOKE ARAMAIC, WHICH WAS THE PARENT LANGUAGE OF ARABIC, FARSI, AND SEVERAL OTHER MIDDLE EASTERN DIALECTS. ORIGINALLY, HEBREW WAS A LANGUAGE USED EXCLUSIVELY BY THE PRIESTHOOD AND THE EGYPTIAN SECRET SOCIETY. EVENTUALLY, ANCIENT HEBREW BEGAN TO MIX WITH ARAMAIC, AMONG OTHER LANGUAGES.

THE HEBREWS WERE ACTUALLY PAID WORKERS IN EGYPT. THEY WENT TO CANAAN TO ASSIMILATE THE NATIVE CULTURES FOR THE EGYPTIAN EMPIRE. THEY MIXED WITH THE LOCAL TRIBES OF SUMERIAN-HYBRID DESCENDANTS, PRACTICING BLOOD-RITUAL AND HUMAN SACRIFICED. ALL OF THIS WAS INCORPORATED INTO A CONGLOMERATE RELIGION BASED ON ANCIENT EGYPTIAN/ATLANTEAN/ SIRIAN BELIEFS. THAT IS HOW JUDAISM WAS BORN.

THE STORY OF THE EXODUS OF THE JEWS FROM EGYPT IS A POOR RETELLING OF THE DESTRUCTION OF THE ISLAND OF SANTORINI IN THE EASTERN MEDITERRANEAN SEA BY VOLCANIC EXPLOSION. THE LAVA DISPERSED INTO THE SEA CAUSING IT TO TURN BLOOD-RED. THE VOLCANIC ASH AND ROCK THAT SPEWED FORTH CREATED THE LEGEND OF THE PLAGUES ON EGYPT. MANY CITIZENS FLED THE AREA. THE RED SEA PARTED WHEN THE GROUND UNDER THE WATER ROSE UP, EXPOSING LAND THAT COULD THEN BE CROSSED. SEVERAL HOURS LATER, IT SANK BACK DOWN, DROWNING WHOEVER WAS STILL TRYING TO CROSS.

THE ACTUAL TRANSLATION OF HOW THE TEN COMMANDMENTS, OR THE BIBLE CODES, WERE TRANSMITTED TO THE PEOPLE OF THE EXODUS, STATES THAT THE PEOPLE SPONTANEOUSLY STARTED SPEAKING THE INSTRUCTIONS. THIS IS A DEMONSTRATION OF MIND-TO-MIND COMMUNICATION. IN THIS CASE, PROGRAMMING WAS ELECTROMAGNETICALLY ACTIVATED, REVEALING DNA INSTRUCTIONS THAT WERE THEN WRITTEN DOWN. THESE INSTRUCTIONS WERE DESIGNED TO KEEP THE EXPERIMENT/PROJECT IN LINE.

THE MIDDLE EAST BECAME A FOCAL POINT FOR THE SIRIANS AND THEIR REPTILIAN ALLIES. TOGETHER, THEY GENERATED A NEW VERSION OF RELIGION AND CULTURE FOR EASE OF GLOBAL CONTROL AND DOMINATION. WHAT BETTER WAY TO DO THAT THAN BY PROGRAMMING A RACE OF NOMADIC PEOPLE THAT WOULD CARRY THE RELIGION AND CULTURE EVERYWHERE ON THE EARTH.

WHENEVER THE CONDITIONS WITHIN THE EXPERIMENT BECAME UNMANAGEABLE, THE PARTICULAR OVERSEER GROUP MADE CORRECTIONS. FOR EXAMPLE, MOST PEOPLE ARE FAMILIAR WITH THE STORY OF THE CITIES OF SODOM AND GOMORRAH, WHERE A GROUP OF HUMANS IN THE MANKIND EXPERIMENT WENT AWRY. THEIR SEXUAL HABITS WERE NOT CONDUCIVE TO PROPAGATION SINCE THEY WERE PREDOMINANTLY HOMOSEXUAL.

A VIRUS WAS INTRODUCED INTO THE POPULATION TO DESTROY IT. HOWEVER, IT STARTED TO SPREAD OUTSIDE THE IMMEDIATE REGION. THIS DISTURBED THE CONTROLLERS, SO THEY SENT

TWO AGENTS TO INVESTIGATE, AND TO DETERMINE IF ANYONE WAS SALVAGEABLE. THE LOCAL INHABITANTS CALLED THEM ANGELS, BECAUSE OF THEIR BLONDE HAIR, BLUE EYES, AND PERFECT BODIES.

LOT AND HIS WIFE TOOK THE AGENTS INTO THEIR HOME TO PROTECT THEM, SINCE ALL THE MEN IN TOWN WANTED TO HAVE SEX WITH THEM. SOON AFTER, SODOM AND GOMORRAH WERE DESTROYED. TO THIS DAY, RADIATION CAN BE DETECTED AT THE SITE. MELTED ROCK IS SEEN IN THE CANYON WALLS. SODOM AND GOMORRAH WERE ELIMINATED WITH A NUCLEAR WEAPON.

IN THE EARLY 1960S, ISRAELI SCIENTIST DIGGING AT THE SITE OF SODOM FOUND REMNANTS OF BONE AND BODY TISSUE ENCASED IN ROCK. AMERICAN SCIENTISTS WERE CALLED IN BECAUSE THEY HAD BETTER EQUIPMENT. WHAT THEY FOUND IN THE PRESERVED BODY TISSUE WAS A SAMPLE OF THE VIRUS. THE AMERICANS RECONSTITUTED IT WITH LIVING CELLULAR NUCLEI. QUIETLY IT WAS TESTED ON A TERMINALLY ILL PATIENT IN A ST LOUIS HOSPITAL IN 1967. THE MAN DIED A HORRIBLE DEATH. THE VIRUS WAS CALLED AIDS BECAUSE IT REMOVED WHATEVER IMMUNE SYSTEM THE MAN HAD LEFT. THE AMERICAN RESEARCH DETERMINED THAT THIS THOUSANDS-OF-YEARS-OLD VIRUS WAS ARTIFICIALLY GENETICALLY CREATED.

THE ANCIENT HEBREW RELIGION WAS A CONGLOMERATION OF THE SUMERIAN-REPTILIAN BELIEF SYSTEM, ANCIENT EGYPTIAN-ATLANTEAN-LYRAEN BELIEF SYSTEM, AND THE REPTILIAN TRIBAL SUBCULTURES FOUND IN THE LAND OF CANAAN THAT WERE INCORPORATED INTO ONE ACCEPTABLE DOGMA. IT INCLUDED BLOOD-RITUAL AND HUMAN SACRIFICE, WHICH IS WHY ABRAHAM WAS SO EAGER TO PLEASE GOD BY KILLING HIS OWN SON ON AN ALTAR. THIS SYMBOLISM CAME IN HANDY LATER ON FOR RELIGIOUS PURPOSES.

THE HEBREW LANGUAGE ITSELF DID NOT APPEAR UNTIL AFTER THE HEBREWS LEFT EGYPT, AND THEN ONLY FOR RELIGIOUS CEREMONIAL PURPOSES BY THE PRIESTS. IN FACT, MANY OF THE TERMS AND NAMES USED IN THE HEBREW RELIGION CAME FROM THE EGYPTIAN CEREMONIAL RITES. THE NAME, MOSES, ORIGINATES FROM THE TITLE GIVEN TO ADEPTS OF THE SECRET EGYPTIAN PYRAMID CULT.

THIS EGYPTIAN CEREMONIAL TITLE, MOSHE, MEANS "HE WHO IS ANOINTED WITH CROCODILE FAT FROM THE NILE RIVER."

HERE, WE SUGGEST SWERDLOW DOES NOT DEAL WELL - WITH THE ACADEMIC EVIDENCE MOSES WAS AKHANATON - REF: OUT OF EGYPT , HOUSE OF THE MESSIAH , BOOKS ETC. BUT AT LEAST HE PERCEIVES CORRECTLY THAT THE BEST HEBREW RITES WERE MOSTLY DESCENDED FROM EGYPT.

THE ONGOING CONFLICT BETWEEN ENLIL'S AMUN RA PRIESTS, VERSUS AKHENATON'S ATUN (ENKI) PROBABLY REFLECTS THE ENLIL MORE DRAC REPTILIAN PERSUASION, VERSUS ENKI - THE REBELLIOUS SON FROM SIRIUS, PUSHING THE POSSIBILITY THAT A (HIS?) GENETIC EXPERIMENT HERE COULD PRODUCE A BLOOD LINE RECOVERY FROM THE CATASTROPHIC NEPHILIM DNA CONDITION.

WITH THE BENEFICIAL RESULT TO THE ADVANCED DRACO'S OF NEW ACCESS TO A BLOOD LINE THAT COULD RESUME STAR NAVIGATING - WHERE THE BIG SALARIES ARE MADE- BECAUSE OF RENEWED GRAVITY MAKING POWER IN IMPLODING IGNITED DNA.

THIS CEREMONY WAS PERFORMED INSIDE THE KINGS CHAMBER IN THE GREAT PYRAMID.

IN HEBREW IT MEANT "OUT FROM THE WATER", IN REFERENCE TO THE CROCODILES. THE EGYPTIAN WORD FOR CROCODILE FAT WAS MESSEH FROM WHICH THE TERM MESSIAH IS DERIVED. TO BE ANOINTED WITH CROCODILE FAT RENDERED INTO AN OIL, WAS TO ABSORB POWERFUL, UNCHANGING REPTILIAN ENERGY AND ASSIMILATE THIS INTO THE BODY. MOSHE, OR MOSES, WAS A RITUAL TITLE, NOT A PERSONS NAME AND WAS A REFERENCE TO THE CROCODILE FAT USED IN TEMPLE AND PYRAMID CEREMONIES.

A LEADER SUCH AS A MOSES WAS A LOGICAL CHOICE TO SPEARHEAD A MIGRATION OF PEOPLE TO SAFETY FROM A PLACE OF TURMOIL, SUCH AS WHEN THE DESTRUCTION OF THE ISLAND OF SANTORINI, ALSO KNOWN AS THERA, BLEW UP AND CREATED HAVOC ON EGYPTIAN TERRITORY, CAUSING MANY TO FLEE. IT WOULD ALSO MAKE SENSE FOR THE SIRIAN CONTROLLERS OF EGYPT TO SEND OUT THEIR GENETIC CREATIONS, THE HEBREWS, TO A PLACE OF SAFETY IN THE SINAI DESERT LIKE A SAFEKEEPING UNTIL NEEDED.

IT WAS THEN THAT THE TORAH, OR HOLY COMMANDMENTS, WAS GIVEN TO THIS PEOPLE AS A CODE BY WHICH TO LIVE. THIS DOCUMENT IS IN A CODE THAT CAN ONLY NOW BE DECIPHERED WITH THE USE OF A COMPUTER. THE LAND OF CANAAN NEEDED TO BE CONQUERED IN ORDER TO GIVE DEVELOPMENT ROOM TO THE NEW CREATIONS. IN EFFECT, THE HEBREWS WERE THE NEXT SEQUENCE OF THE EXPERIMENT, AND THE OLD VERSIONS WERE TO BE ELIMINATED OR ASSIMILATED.

THE HEBREWS CARRIED THE NEW CODED LAWS IN THE ARK OF THE COVENANT (COVEN OF ANTS), THAT ONLY THE PRIESTS COULD TOUCH. WHEN THE UNIVERSITY OF MINNESOTA IN THE 1960S ATTEMPTED TO BUILD THE ARK AS DESCRIBED WITH INSTRUCTIONS IN THE BIBLE, IT WAS SO ELECTRICALLY CHARGED THAT IT HAD TO BE DISMANTLED!

THIS IS WHY THE ANCIENT HEBREW PRIESTS ENTERED INTO THE ARK AREA ALONE, FOR SAFETY REASONS. THEY ALSO HAD TO WEAR WHITE LINEN, AS NON-CONDUCTIVE CLOTHING, AND WORE A SPECIAL BREASTPLATE THAT GROUNDED THEM ELECTRICALLY AND ACTED AS A PROTECTIVE SHIELD. THE ARK WAS REALLY A COMMUNICATION DEVICE. THIS IS WHY THE PRIESTS HAD MESSAGES FROM GOD WHENEVER THEY WERE IN THE ARKS PRESENCE.

THE ARK ALSO ACTED AS A LOCATION DEVICE FOR BEACONS ORIGINATING OUTSIDE OF THIS PLANET. THE ARK WAS ORIGINALLY KEPT IN THE GREAT PYRAMID TO FOCALIZE ENERGIES. IT WAS SENT WITH THE HEBREWS FOR SAFEKEEPING. IT HAS SINCE TRAVELED FROM EGYPT TO CANAAN/ISRAEL TO ETHIOPIA, BACK TO ISRAEL, AND NOW IS LOCATED UNDER THE PYRAMID AGAIN.

HOWEVER, THERE ARE ACTUALLY TWO ARKS.

THE SECOND ONE IS IN JERUSALEM.

WE FEEL THIS INFORMATION IS INCOMPLETE, IN THAT CLEARLY THE ARK WAS A FRACTALLY ARRANGED (ORGONE) CAPACITOR - WHOSE CHARGE COMPRESSION COULD CONTAIN RADIOACTIVITY. AND THAT FEEDING THE CHARGE OF THIS DEVICE IS THE REASON IT MUST BE LOCATED ON A MAJOR LEY LINE - TODAY IT APPEARS- PRECISELY ON THE MICHAEL LINE - ST

MICHAEL'S (ENLIL) ISLAND CAVE IN THE AZORES - IMAGE ABOVE LEFT (ASSURAS = ASSA URU)- WHERE JACQUE COUSTEAU'S SON LOST HIS LIFE FOR GETTING TOO CLOSE.

GO BACK

GO BACK TO KHAZAR - THE THIRTEENTH TRIBE

GO BACK TO THE PROTOCOLS OF THE LEARNED ELDERS OF ZION

10 - THE ANUNNAKI & THE BLACK RACE

THE CREATORS OF THE BLACK RACE, THE REPTILIAN BEINGS OF MARDUK KNOWN AS THE ANUNNAKI WHOSE PLANETOID TRAVELS IN AN ELLIPTICAL ORBIT OF THIS SOLAR SYSTEM EVERY FEW THOUSAND YEARS, ARE DUE TO ARRIVE IN 2003.

IT IS NOW 2004 AND REASONABLE TO SURMISE THAT MASSIVE ARRIVAL/INVASION IS IMMANENT. WE RECOMMEND ISOLATION IN COMMUNITY, HI GROUND, SHELTER FROM HI WIND, GOOD WATER, SEEDS, AND BEING TRANSPARENT TO GOVERNMENT. GOOD SHAMAN LUCID DREAMING SKILL TO SET UP BOUNDARY.

THE ANUNNAKI LIKE TO DEVELOP SLAVE RACES FOR SPECIFIC PURPOSES, CREATING THEM OUT OF LOWER ANIMAL FORMS. IN THE CASE OF THEIR EARTH CREATIONS, THEY USED SIMIANS TO CREATE A SLAVE RACE TO WORK THE MINES IN WHAT IS NOW KNOWN AS AFRICA. THIS RACE WAS GENETICALLY DESIGNED TO WORK AND LIVE IN HOT, HUMID CONDITIONS WITH A LIMITED LIFE SPAN. DISEASES WERE PROGRAMMED INTO THEM TO PREVENT DEVELOPMENT OF CULTURE, AND CAUSE THEM TO BECOME DEPENDENT ON THEIR CREATORS FOR EXISTENCE. THIS IS WHY IN THE GENETIC MEMORY OF ALL OTHER RACES, THE BLACKS ARE SLAVES.

THE AMERICAN AND EUROPEAN ILLUMINATI DECIDED TO USE THE AIDS VIRUS AS A WEAPON TO REMOVE THE BLACK RACE FROM EARTH. THESE ILLUMINATI CONCLUDED THAT IF THE BLACKS WERE NO LONGER HERE, THE ANUNNAKI WOULD FIND THE CONDITION OF THEIR SLAVES UNACCEPTABLE, AND NOT INTERFERE WITH ILLUMINATI PLANS. THE GREEN MONKEYS OF EAST AFRICA WERE SUBSEQUENTLY INFECTED WITH THE AIDS VIRUS, ALONG WITH THE BLOOD SUPPLY OF HAITI. IN AFRICA, AIDS IS A HETEROSEXUAL DISEASE.

THE WORLD HEALTH ORGANIZATION, WHO, WAS ALSO USED TO DIRECTLY INJECT THE AIDS VIRUS INTO THE POPULATION UNDER THE GUISE OF IMMUNIZATION.

"THE 1971 FLOWCHART MAKES IT PERFECTLY CLEAR, THE DESIGN, INTENT AND PURPOSE OF THE U.S. SPECIAL VIRUS PROGRAM. AS DR. PETER PIOT, EXECUTIVE DIRECTOR OF UNAIDS SAYS, THE HIV/AIDS VIRUS IS THE RESULT OF MANY STEPS IN THE LABORATORY, IT WAS NO ACCIDENT. THE 1971 FLOWCHART PROVIDES ABSOLUTE EVIDENCE OF THE UNITED STATES' INTENT TO KILL ITS OWN CITIZENS AND OTHERS." DR BOYD GRAVES

HOWEVER, A MONKEY WRENCH TURNED UP IN THE PLANS. A GAY FRENCH-CANADIAN FLIGHT ATTENDANT HAD SEX WITH A BISEXUAL PARTNER IN AFRICA. THE INFECTED FLIGHT ATTENDANT ANGRILY SPREAD THE DISEASE WHEREVER HE WENT. NEW YORK CITY AND SAN FRANCISCO WERE TWO OF HIS PRIMARY DESTINATIONS. HE ALONE IS DETERMINED TO HAVE BEEN THE MAIN CARRIER OUTSIDE OF THE INTENDED TARGET. THE ILLUMINATI DOES NOT THINK OF EVERYTHING. (5)

BY 2003 WHEN MARDUK RETURNS, MOST OF BLACK AFRICA WILL BE INFECTED. THOSE WHO ARE NOT INFECTED WILL BE KILLED VIA EBOLA, WAR, OR FAMINE.

MOST CARIBBEAN AND NORTH AMERICAN BLACKS HAVE A HIGH PERCENTAGE OF EUROPEAN GENETICS THAT ARE NOT CONSIDERED DESIRABLE FOR SLAVE PURPOSES.

IN 1999, NEWSPAPERS REPORTED THAT US ASTRONOMERS SAID THAT A HUGE PLANET HAD BEEN DETECTED BEYOND PLUTO WITH AN ELLIPTICAL ORBIT OPPOSITE TO ALL THE OTHER PLANETS IN THIS SOLAR SYSTEM. THEY SAID IT WAS ON A TRAJECTORY THAT WOULD TAKE IT TO NEAR THE EARTH IN 2003!

NOT ANOTHER WORD WAS PRINTED ABOUT IT AFTER THAT.

QUOTES FROM

PLANET X, COMETS AND WHAT NASA IS HIDING

(EXPLORING THE PARALLEL TO THE INTERVENTIONIST COMET THEORY)

AN INTERVIEW WITH JAMES MCCANNEY, BY RICK MARTIN

"... THE OTHER FACTOR... IN 1991 WHAT HARRINGTON SAW WAS TWO THINGS: HE SAW HALE-BOPP, AND HE SAW SOMETHING MUCH BIGGER BEYOND HALE BOPP. THAT'S PLANET-X. .. IN 1991, HALE-BOPP WAS ON A NEAR DIRECT COLLISION COURSE WITH EARTH. WITH A COUPLE OF QUICK PHOTOGRAPHS THEY COULD CHART THE ORBIT, AND IT WAS ON A NEW COLLISION COURSE WITH EARTH.

MARTIN :(INTERVIEWER): NO WONDER THERE WAS SUCH A SCRAMBLE.

MCCANNEY: IT WAS A HUGE SCRAMBLE. WHEN IT WAS DISCOVERED, I CALLED UP GODDARD SPACE CENTRE- I KNEW THE SECRETARY THERE- AND I SAID: 'WHAT'S GOING ON?' I HEARD THERE'S THIS COMET...' YOU COULD HEAR THE SCREAMING IN THE BACKGROUND. AND SHE SAID: "OH MY GOD, THIS COMET IS HUGE!". BUT I THOUGHT SHE MEANT IN THE SENSE OF BEING A NEWS STORY. NO, IT WAS HUGE IN THE SENSE THAT IS A PLANET-SIZED OBJECT. THEY HAD BEEN TRACKING IT.

YOU SEE, THIS IS WHERE THE DIVISION COMES IN, BECAUSE IT WASN'T UNTIL THEN THAT EVEN A LOT OF THE SCIENTISTS AT GODDARD FOUND OUT ABOUT IT. BUT THEY HAD BEEN TRACKING THIS SINCE 1991, POSSIBLY EARLIER. HARRINGTON DISCOVERED IT, AND YOU SEE IT IN THE 1991 MEMO THAT HE KNEW EXACTLY WHERE TO GO AND LOOK AT IT.

A LONG TIME AGO, WHAT HAPPENED IS... IT WAS ONE OF THE COMPANIONS OF NIBURU THAT DID THE DAMAGE TO EARTH.
MARTIN: A COMPANION?

MCCANNEY: A COMPANION. IT WAS THE ONE THAT BECAME VENUS. VELIKOVSKY WAS VERY RIGHT THAT VENUS WAS A HUGE COMET THAT WORKED ITS WAY THROUGH THE SOLAR SYSTEM, AND IT TOOK ABOUT A 600 YEAR PERIOD FROM THE TIME IT WAS CAPTURED BY JUPITER TO THE TIME IT ENCOUNTERED EARTH. AND THEN WORKED ITS WAY IN TO BECOME THE PLANET (VENUS) THAT WE KNOW TODAY.

SO, ORIGINALLY, WHAT HAPPENED WAS THAT HALE-BOPP WAS HERE ABOUT 4,200 YEARS AGO. THEY WERE, LITERALLY, SMALLER COMPANIONS TO NIBURU. THAT'S WHY THEY DIDN'T WANT ANYBODY TO KNOW ABOUT THE COMPANION, BECAUSE THEY KNEW IT WAS ON A COLLISION COURSE WITH EARTH, AND THEY KNEW IT WAS THE COMPANION TO THE BIGGER ONE THAT CAUSED THE PROBLEM. BUT THEY DIDN'T REALIZE THAT HALE-BOPP WAS, LITERALLY ONE OF THE COMPANIONS ITSELF.

NOW, WHEN THE DESTROYER, THE BIG GUY, NIBURU, COMES IN, IT HAS AN ENTIRE ENTOURAGE OF THESE THINGS.

MARTIN: I GUESS COMENT NEAT WOULD BE ONE OF THOSE?

MCCANNEY: AND THAT'S THE THING. WHEN WE GOT BARRAGED A FEW WEEKS AGO BY ALL THESE COMETS, AND THEY NEVER ANNOUNCED COMET NEAT,C-2002/VI. CLEARLY ALL OF THIS STUFF IS COMING FROM THE SOUTHERN HEMISPHERE.

THEN OF COURSE, HARRINGTON KNEW VERY WELL WHERE THAT WAS, THE REASONS THAT I GAVE; THEY WERE 'PULLING DOWN' ON THE PLANETS URANUS AND NEPTUNE. IT'S INTERESTING TO NOTE THAT WHEN THE STORY OF HARRINGTON CAME OUT, THE GOVERNMENT TRIED TO MAKE A STATEMENT THROUGH SOME OF THESE ASTRONOMERS THAT ON THE RADIO, THE DISINFORMATION GUYS, WHO CAME UP WITH A STORY: "OH WELL, WE HAVE CORRECTED THE MASSES OF THOSE PLANETS DUE TO NEW INFORMATION, SO THAT HAS TAKEN CARE OF THE PROBLEM"

WELL, NO, THAT DOESN'T CORRECT ANYTHING, WHEN YOU SEE THESE PLANETS BEING 'PULLED DOWN'. THAT WOULD ONLY CORRECT THINGS IN THE PLANE OF THE PLANETS. THIS OBJECT WAS BIG ENOUGH, BACK IN 1991, THAT IT WAS PULLING URANUS AND NEPTUNE DOWN OUT OF THEIR ORBITS. THAT'S HOW BIG THIS THING IS!

SO, YOU SEE THE CONCERN OVER THE COMPANION. BECAUSE THEY ALL KNOW, AND THE VATICAN KNOWS, THAT IT WAS THE COMPANION THAT DID THE DAMAGE THE LAST TIME. THE ONLY PROBLEM IS, THE COMPANION BECAME THE PLANET VENUS. WHAT THEY DON'T UNDERSTAND IS THAT IT'S A VERY DIFFERENT THING TO PRODUCE THE ORBITS FOR THESE, AND NASA IS LEARNING THE HARD WAY. THEY COULDN'T KEEP TRACK OF HALE-BOPP; IT CHANGED ON A DAILY BASIS. THAT WAS THE ONE THING WE DID IN THE MILLENIUM GROUP: TRACK THE DAILING CHANGING OF ITS ORBIT ON THE GOVERNMENT EPHEMERIS PAGES.

MARTIN: WAS COMET NEAT A SURPRISE? DID THAT COME OUT OF NOWHERE- OR DID THEY EXPECT

THAT?

MCCANNEY: NO. COMET NEAT IS ANOTHER VERY LARGE NUCLEUS; PLANETARY IN SIZE- PROBABLY THE SIZE OF OUR MOON, AT LEAST; PROBABLY LARGER. THEY PROBABLY SAW IT COMING IN YEARS AGO, AS PART OF THIS ENTOURAGE OF THINGS COMING IN -- WHICH I THINK OF AS THINGS THAT ARE COMING IN AS PART OF THE PLANET X ENTOURAGE. THEY DIDN'T WANT ANYBODY TO KNOW ABOUT IT, FOR THE SIMPLE REASON THEY KNEW IT WAS GOING TO COME IN RIGHT AROUND THE SUN AND IT WAS BIG. THEY PROBABLY NEVER EXPECTED IT TO BECOME AS BRIGHT AS IT DID. BUT IT WAS LITERALLY VISIBLE IN THE DAYTIME SKY, RIGHT NEXT TO THE SUN, AS IT PASSED - OVER ABOUT A 12 HOUR PERIOD WHEN IT WAS COMING IN.
MARTIN: THE OBVIOUS QUESTION IS: HOW MANY MORE OF THESE COMPANIONS CAN WE LOOK FORWARD TO ?

MCCANNEY: WE DON'T KNOW. OF COURSE THOUGH, NASA WOULD HAVE A VERY GOOD KNOWLEDGE OF THIS. THE OTHER IMPORTANT THING THAT I WANTED TO SAY EARLIER ABOUT HALE-BOPP IS THAT IN THE SIX YEAR PERIOD FROM 1991 TO 1996, WHERE IT ACTUALLY HIT PERIHELION WITH THE SUN, IT LOST THREE MONTHS TIME IN ARRIVING DUE TO THE TAIL-DRAG OF THE HUGE COMET. THAT'S WHY WE DIDN'T HAVE A DIRECT COLLISION WITH IT. AND WHEN I SAY "DIRECT COLLISION", I DON'T MEAN HITTING EARTH; I MEAN WE WOULD HAVE BEEN WITHIN ABOUT ONE MILLION MILES. BY ANYBODY'S STANDARD, IT WOULD HAVE BEEN TOTAL DEVASTATION OF THIS PLANET. THE FLOODING WOULD HAVE BEEN ENORMOUS. IT WAS ONLY DUE TO THE FACT THAT THIS THING SLOWED DOWN THAT WE MISSED IT.

MARTIN: I GUESS ANOTHER QUESTION WOULD BE; WHERE IS NEAT GOING?

MCCANNEY: NEAT HEADED BACK OUT. THAT IS OBJECT NUMBER FOUR OF MY SOUTH AMERICAN HARRINGTON EXPEDITION TO CHART THE NEW ORBIT FOR NEAT, BECAUSE IT CLEARLY LOST A LOT OF ITS ENERGY AS IT CAME AROUND THE SUN, AS IT PICKED UP A LOT OF TAIL MATERIAL. SO, IT'S NOT GOING TO COME AND HIT EARTH. THAT'S WHAT NASA ALWAYS SAYS: "OH THESE PEOPLE THINK IT'S GOING TO HIT EARTH". NO, NO; NOBODY SAID ANYTHING ABOUT IT HITTING EARTH. THEY TRY TO MAKE FUN OF PEOPLE AND, IN FACT, THEY ACTUALLY HAVE PEOPLE WHO SET UP THOSE STORIES ON THE INTERNET SO THEY CAN GO MAKE FUN OF THEM. IT'S PART OF THEIR DISINFORMATION CAMPAIGN.

MARTIN: WHEN A COMET THE SIZE OF NEAT, SWINGS BY OUR SUN, HOW DOES 'ACTION AT A DISTANCE' COME INTO PLAY?

MCCANNEY: THE FLARE THAT CAME OFF (THE SUN), THAT YOU SEE IN MANY OF THE PHOTOS, CAME AND HIT THE BACK SIDE OF THE COMET TAIL.

MARTIN: THE FIVE-MILLION-MILE FLARE?

MCCANNEY: YES. NOW, IF THAT WERE TO HAVE COME AT EARTH, IT WOULD HAVE KNOCKED US TO OUR KNEES. BUT IT WENT OFF IN A TOTALLY OBSCURE DIRECTION. LET'S LOOK AT SOMETHING ELSE. WHAT YOU DIDN'T SEE THERE, BUT I COULD SEE IT COMING OFF OF NEAT... IF YOU LOOK VERY CLOSELY, YOU'LL SEE A PIN-THIN STREAK COMING DIRECTLY AWAY FROM THE SUN AND OUT AWAY FROM THE NUCLEUS, OUT THE RIGHT OF THE SCREEN. THAT'S CONNECTING WITH PLANET MERCURY. MERCURY WAS IN A DIRECT ALIGNMENT WITH NEAT AS IT CAME ACROSS THE ECLIPTIC, THE PLANE OF THE PLANETS. THAT LINE, THAT YOU CAN ACTUALLY SEE ON SOLAR PHOTOGRAPHS, IS CONNECTING TO MERCURY.

SO, NOW LET'S PUT EARTH OVER THERE. WHAT IF EARTH HAD BEEN OVER 90 DEGREES AROUND, AND WE WERE NOT BROADSIDE TO IT? THEN, WE COULD HAVE VERY EASILY BEEN IN A POSITION TO TAKE THAT FLARE, FOR EXAMPLE, OR TAKE AN ELECTRICAL DISCHARGE DIRECTLY FROM NEAT. THAT IS WHAT THE ANCIENTS TALKED ABOUT WITH THE COMETS, THE LIGHTNING BOLTS FLYING ACROSS THE HEAVENS; THEY SAW THESE THINGS - ZEUS THROWING LIGHTNING BOLTS TO MARS. THEY SAW THIS STUFF.

MARTIN: IT WAS LITERAL; IT WASN'T METAPHORICAL?

MCCANNEY: NO, IT WAS NOT METAPHORICAL. WHEN VENUS CAME AROUND MARS, IT LASHED OUT WITH AN ELECTRICAL DISCHARGE AND AURORAS IN THE ATMOSPHERE OF MARS LIT UP; IT LOOKED LIKE A SNAKE GRABBING MARS. IT LITERALLY SUCKED THE OCEANS AND ATMOSPHERE OFF OF MARS AS IT PASSED BY. AND THEY SAW THIS. THEY KNEW THAT MARS, PRIOR TO THAT, WAS A WATER PLANET, WAS A BLUE PLANET, JUST LIKE EARTH. MARS HAS A VERY THIN ATMOSPHERE. VENUS HAS A MASSIVE ATMOSPHERE, THOUSANDS OF TIMES DENSER THAN EARTH'S ATMOSPHERE. BUT PERCENTAGE WISE, THE CHEMICAL COMPOSITION OF THE ATMOSPHERES OF VENUS AND MARS ARE EXACTLY THE SAME- WHICH MEANS THEY WERE FORMED IN THE SAME BOILING POT THERE, AS THEY PASSED BY EACH OTHER.

MARTIN: I WANTED TO ASK YOU ABOUT VELIKOVSKY. YOU'RE VERY SIMILAR TO HIM IN THAT HE WAS GIVEN A HARD TIME AND RIDICULED, AND IT TURNS OUT HE WAS RIGHT.

MCCANNEY: THERE'S NO QUESTION ANY MORE THAT VELIKOVSKY WAS RIGHT. AND, I THINK THE BIGGEST THING THAT I WANT TO SAY ABOUT VELIKOVSKY IS THAT HE WAS NOT STUDYING ASTRONOMY. HE WAS STUDYING CALENDARS!

--
(IN THE NEXT SECTION-MCCANNEY REVIEWS MORE OF HIS INTERESTING WORK ON HOW CONTROVERSIAL HE HAS BEEN - "COMETS ARE NOT DIRTY SNOWBALLS- BUT LARGE ELECTRICAL VACUUM CLEANERS IN OUTER SPACE" - BY DEMONSTRATING AGAINST THE SCIENCE COMMUNITY OPINION - THAT THE PLASMA OF SPACE IS ACTIVE - FULL OF CHARGE - AND NOT ELECTRICALLY NEUTRAL. THIS HAS PROFOUND IMPLICATIONS FOR WHAT COMETS DO IN NEAR MISSES - AND PERHAPS - HOW IN PART - "PLANETS EXPERIENCE GRAVITY RELATIONS EROTICALLY" - A GURDJIEFF SENTIMENT.)
--THE LAST SECTION OF THE ARTICLE IS NICE TO ADD HERE: (FITS NICELY WITH THE DOZENS OF NEW WEB SITES COMPARING GEORGE BUSH'S LAWS PASSED SINCE 9/11 TO HITLER)

MARTIN: ARE THERE SOME CLOSING COMMENTS YOU WOULD LIKE TO MAKE?

MCCANNEY: I WOULD SAY, NUMBER ONE THAT THE REST OF THE WORLD IS ADVANCING FAR BEYOND THE UNITED STATES IN CONSCIOUSNESS AND IN PROGRESS AS A HUMAN SPECIES. THE OTHER THING I WOULD SAY IS THAT AS A COUNTRY, AS A CIVILIAN POPULATION, WE HAVE TO GRAB HOLD OF THIS COUNTRY AND TURN IT AROUND BECAUSE, LITERALLY, THE WHOLE REST OF THE WORLD DEPENDS UPON IT. WE ARE AT A STAGE RIGHT NOW THAT IS EQUIVALENT TO 1939, PRE-WORLD WAR II HITLER'S GERMANY.

THEY DID NOT TURN THAT COUNTRY AROUND - AND IF WE DON'T TURN THIS COUNTRY AROUND, WE'RE GOING TO BE IN A FAR BIGGER WORLD PROBLEM THAN WORLD WAR II EVER THOUGHT OF

BEING.

THE REMNANTS OF THE MARDUK/REPTILIAN EXPERIMENTATION IN CENTRAL AND SOUTHERN AFRICA WERE BASICALLY LEFT ON THEIR OWN. THE BEINGS FROM MARDUK, THE ANUNNAKI, ALSO KNOWN AS THE ABBENNAKKI, LEFT THE EARTH, CONTINUING ON ITS ELLIPTICAL JOURNEY THROUGH THE SOLAR SYSTEM AND BEYOND.

THIS ARTIFICIAL PLANET PASSES NEAR EARTH EVERY 12,000 YEARS. A COMPLETE ORBIT TAKES 24,000 YEARS. THE LAST TIME THEY PASSED EARTH, APPROXIMATELY 10,500 BC, ITS GRAVITATIONAL PULL EXERTED IN CONJUNCTION WITH ATLANTEAN CRYSTAL EXPERIMENTATION, CAUSED THE EARTH TO FLIP ON ITS AXIS, SINKING ATLANTIS.

THE ANUNNAKI/ABBENNAKKI HAVE ROBOTICAL SCOUT SHIPS THAT MONITOR EARTH WHEN THE ARTIFICIAL PLANET IS NOT CLOSE. THESE SHIPS HAVE A CREW OF WORKERS THAT LOOK LIKE DWARFED BEARS. THEY ARE KNOWN TO BE AGGRESSIVE, EVEN ATTACKING HUMANS IN THE PAST. THESE BEAR-LIKE CREATURES ARE CYBORGS WITH BRAIN IMPLANTS THAT ALLOW CONTROL FROM A DISTANCE. THEIR BODIES ARE ORGANIC AND POWERFUL.

THESE CREATURES STARTED APPEARING IN THE LATE 1960S. GOVERNMENT-RELEASED UFO INVESTIGATION REPORTS DOCUMENT THEIR EXISTENCE. MORE OF THESE CREATURES WILL BE SEEN IN THE NEXT TWO YEARS. STAY AWAY FROM THEM! THEY ARE DANGEROUS.

MOST LIKELY, THEY WILL SURFACE IN AFRICA TO CHECK ON THE BLACK RACE FOR THEIR MASTERS ON MARDUK. LOUIS FARRKHAN, THE BLACK MOSLEM LEADER, HAS OFTEN SPOKEN ABOUT HIS UFO CONTACTS. ACCORDING TO FARRAKHAN, THESE CONTACTS EXPLAINED THAT THE BLACK RACE WAS CREATED BY THEM.

THEY FURTHER TOLD HIM ABOUT THE NEED FOR THE BLACKS TO DEVELOP WITHOUT INTERFERENCE FROM OTHER RACES.

FOTENOTES:

5. THIS WAS AUGMENTED BY EXPERIMENTS ON GAY MEN IN NEW YORK CITY UNDER THE GUISE OF HEPATITIS SHOTS.

GO BACK

GO BACK TO THE ANUNNAKI

11 - MIND-CONTROL VIA RELIGION

THE FIRST RELIGION ON EARTH WAS THE REPTILIAN BELIEF SYSTEM BROUGHT BY THE COLONISTS OF LEMURIA. THEIR RELIGION BELIEVED IN A GOD-MIND THAT CONTAINED A HIERARCHY, OR CASTE SYSTEM. THIS CASTE SYSTEM WAS EXTRAPOLATED TO THE SEVERAL REPTILIAN SPECIES INCORPORATED INTO THE DRACO EMPIRE. EACH SPECIES HAD ITS OWN PLACE IN THE STRUCTURE OF THEIR SOCIETY. EVERY INDIVIDUAL KNEW ITS FUNCTIONS AND RESPECTED THESE BOUNDARIES. TO VIOLATE THESE RULES MEANT DEATH.

THE REPTILIANS OPERATE AS A GROUP MIND, MEANING THAT NO SINGLE REPTILIAN CAN MAKE A DECISION FOR ITSELF. ONLY THE UPPER CASTE, OR WINGED ONES, HAVE THE SEMBLANCE OF INDIVIDUALITY. THEY WERE, AND ARE, THE LEADERS.

WHEN THIS RELIGION WAS BROUGHT TO SUMERIA, THE CASTE SYSTEM WAS INFUSED INTO SOCIETY AS A RELIGIOUS HIERARCHY. REMEMBER THAT THE COLONISTS OF SUMERIA WERE REFUGEES FROM LYRAE/MARS/MALDEK. THEY, LIKE THE ATLANTEANS, MAINTAINED THE ORIGINAL BELIEF SYSTEM OF THE LYRAEN CULTURE. THE LYRAEN BELIEF SYSTEM ENCOURAGED INDIVIDUALITY, AS WELL AS PROMOTED SERVICE TO OTHERS AS A PATHWAY TO SELF-GROWTH. THE LYRAENS BELIEVED THAT RED-HAIRED PEOPLE WERE CONNECTORS TO GOD-MIND, AND AS SUCH, USED THEM AS ORACLES.

THE REPTILIANS WORSHIPPED THE TRANSPARENT BEINGS FROM THE ASTRAL PLANES AS THEIR CREATORS. THE TRANSPARENT BEINGS HAVE A MASS CONSCIOUSNESS, LIKE AN OVERSOUL. THEY ARE BASICALLY GENDERLESS, ALTHOUGH IN TERMS OF PHYSICAL REALITY, THEIR CHARACTERISTICS AND TRAITS RENDER THEM MORE MASCULINE THAN FEMININE.

WHEN THE REPTILIANS BROUGHT THIS RELIGION TO THE SUMERIANS, THEY WERE CAREFUL TO INTRODUCE IT IN A WAY THAT WOULD BE ACCEPTED AND FOLLOWED. FIRST, THEY CREATED A GENDER BASE FOR A GENDER-MINDED POPULATION. THEN, THEY INSTILLED FEAR TO CONTROL THE MIND-PATTERNS. CLEVERLY, THEY DEVISED A RELIGION BASED ON A MALE-FEMALE, GOD-GODDESS CONTROL SYSTEM. THE MALE GOD WAS CALLED NIMROD; THE FEMALE GODDESS, SEMIRAMIS. THEY ARE DEPICTED AS HALF-HUMAN, HALF-REPTILIAN. THEIR APPEARANCES WERE DESIGNED TO FRIGHTEN THE HUMANS INTO SUBMISSION.

NIMROD AND SEMIRAMIS EVENTUALLY BECAME THE OSIRIS AND ISIS OF EGYPT, AND THE APOLLO AND ATHENA OF GREECE, AMONG MANY OTHER GODS. ALL USED THE MALE/FEMALE, GOD/GODDESS THEME BECAUSE IT REPRESENTED THE ORIGINAL REPTILIAN ANDROGYNY AND THE SEPARATION OF THE HUMAN PROTOTYPE INTO THE MALE/FEMALE, ADAM/EVE.

BECAUSE OF THE "MASCULINE" TENDENCY OF THE TRANSPARENT PEOPLE, AND DESPITE BEING ANDROGYNOUS THEMSELVES, THE REPTILIANS PREFER THE POWERFUL MALE OVER THE FEMALE. THEY REPRESENTED THEIR ANDROGYNY IN SUMER BY PLACING THREE HORNS ON THE REPTILIAN GOD, NIMROD.

THERE ARE MANY LAYERS OF SYMBOLISM TO THIS:

* THE PENIS AND TWO TESTICLES
* TWO ENERGIES UNITING TO CREATE A THIRD, I.E., THE HUMAN PROTOTYPE
* THE THREE LEVELS OF EXISTENCE: HYPERSPACE, ASTRAL, AND PHYSICAL
* THE THREE LEVELS OF AWARENESS: CONSCIOUS, SUBCONSCIOUS, AND SUPERCONSCIOUS
* ANDROGYNY LEADING TO MALE AND FEMALE SECTIONS

THUS, THE NUMBER THREE WAS AN IMPORTANT SYMBOL TO THE REPTILIANS ON EARTH. THEY REPRESENT THIS IN MANY WAYS, INCLUDING THE LILY, OR FLEUR-DE-LIS WITH ITS THREE POINTS.

THEY ALSO USE THE SCORPION WITH ITS STINGER AND TWO PIERCING CLAWS.

THE ADVANCED VERSION OF THE SCORPION IS THE EAGLE, WHICH REPRESENTS THE SCORPION IN ITS HIGHER FORM. BECAUSE OF THIS, THE EAGLE CAME TO REPRESENT RAISING FROM A LOWER FORM TO A HIGHER ONE. IT REPRESENTED POWER AND GLOBALIZATION. BECAUSE IT WAS A BIRD OF PREY, IT WAS ABLE TO CAPTURE EVERYTHING BENEATH IT, ESPECIALLY LIVE FOOD. FOR THESE REASONS, THE ROMANS ALWAYS USED AN EAGLE ON THEIR STAFFS WHENEVER THEY MARCHED INTO A CITY OR COUNTRY.

MOST PEOPLE DO NOT REALIZE THAT ALL BIRDS ARE DESCENDENTS OF REPTILIAN DINOSAURS. MANY CORPORATE LOGOS AND SUPERHEROES OF TODAY HAVE WINGS ATTACHED TO THEM. THE WINGS ALSO REPRESENT THE WINGED REPTILIAN LEADERS IN THE UPPER ECHELON OF THE REPTILIAN/ILLUMINATI FLOWCHART.

HALF A CONTINENT AWAY IN CHINA, THE REMNANTS OF LEMURIA CREATED A MALE-DOMINATED EMPIRE SYSTEM. HERE, THE MALE EMPEROR WOULD ALWAYS HAVE A EMPRESS. THE PEOPLE WERE TOLD THAT THE EMPEROR AND EMPRESS WERE DESCENDENTS OF THE SUN-GOD. THE SYMBOL OF THE EMPIRE WAS THE DRAGON, ANOTHER REPTILIAN FIGURE. THIS "ROYAL" FAMILY CREATED A DYNASTY THAT RULED TIGHT-FISTED FOR MILLENNIA.

THE CHINESE REPTILIAN RELIGION SPREAD ACROSS EASTERN ASIA, WHILE THE SUMERIAN VERSION MEANDERED THROUGH CENTRAL AND WESTERN ASIA. THE SPREAD OF THESE RELIGIONS WAS INTENTIONALLY CONTROLLED FROM THE UNDERGROUND REPTILIAN POPULATION, PRIMARILY CENTERED UNDER TIBET. LOOKING AT A WORLD MAP, ONE CAN EASILY SEE THAT THIS IS THE BEST UNDERGROUND BASE LOCATION IN ASIA TO REACH ALL AREAS OF THE CONTINENT. THESE REPTILIANS WERE AIDED BY BEINGS FROM SIRIUS B WHO DEVELOPED THE BUDDHIST PHILOSOPHIES, AS WELL AS A GROUP OF RENEGADE LYRAENS TRYING TO REPRODUCE A LYRAEN CIVILIZATION UNDER REPTILIAN CONTROL. STRANGE BEDFELLOWS!

AT THE SAME TIME IN INDIA, THE LEMURIAN REPTILIAN REFUGEES CREATED A CASTE SYSTEM THAT WAS A DIRECT REPLICA OF THE REPTILIAN HIERARCHY, FROM THE LOWLY WORKERS/UNTOUCHABLES TO THE BRAHMIN/WINGED ONES. THIS INDIAN/REPTILIAN CULTURE REMAINED LOCALIZED, WRITING THE ANCIENT VEDAS AND BUILDING TEMPLES TO THE VARIOUS REPTILIAN GODS.

MEANWHILE, THE EGYPTIANS, WHO WERE ATLANTEAN/LYRAEN REFUGEES, WERE IN THE PROCESS OF BUILDING A NEW CIVILIZATION FROM THE REMNANTS OF THEIR TWO MAJOR ANCESTRAL ONES THAT WERE DESTROYED. THE BEINGS FROM SIRIUS A HELPED THEM, AS THEY WERE A MAJOR FACTOR IN THE INTERACTIONS OF ATLANTIS.

AS PREVIOUSLY STATED, IN EGYPT, THE REPTILIAN GODS WERE KNOWN AS OSIRIS AND ISIS. THE EGYPTIAN PANACEA OF GODS INCLUDED A LARGE VARIETY OF HYBRID CREATIONS, HALF-HUMAN, HALF-ANIMAL. THIS WAS REMINISCENT OF THE ATLANTEAN HYBRID EXPERIMENTS THAT FOUND THEIR WAY INTO EGYPTIAN CULTURE, AND WAS PROMOTED BY THE SIRIANS WHO WERE PREPARING THAT CULTURE FOR A REPTILIAN TAKEOVER.

THE ATLANTEANS WERE SO ENTRENCHED IN THE ORIGINAL LYRAEN BELIEF SYSTEM, THAT IT TOOK SEVERAL MILLENNIA FOR THE REPTILIANS TO GET A STRONGHOLD IN THAT CULTURE. NOW THAT THE REMNANTS WERE SCATTERED OVER THE EARTH AND NON-COHESIVE, IT WAS EASY TO SEND IN INFILTRATORS (IN-FULL-TRAITORS) TO SWAY THE BELIEF SYSTEM TOWARD A REPTILIAN FLAVOR.

THIS BEGAN WITH THE INTRODUCTION OF THE CAT AS A FOCAL POINT OF WORSHIP.

IN THE SIRIUS A STAR SYSTEM, THE MAIN WORLD IS CALLED KHOOM. THE ANCIENT NAME FOR EGYPT IS KHEM. THERE IS ALSO A CORRELATION WITH MEXICO. SOME RESEARCHERS SAY THAT THE BAY OF CAMPECHE TRANSLATES TO THE BAY OF OLD EGYPT, INDICATING A CONNECTION

BETWEEN EGYPT AND THE YUCATAN PENINSULA. THIS IS NOT SO.

SIRIANS WHO INTERACTED WITH ATLANTIS NAMED THIS AREA AFTER THEIR HOME WORLD, AND THEN CARRIED THE NAME ON TO THE NEW REFUGEE CULTURE IN EGYPT.

OUR INFO, IS THAT THE WORD KHEM FOR EGYPTAUS (EGYPT) MEANT FROM THE BLACKNESS, FOR THE BLACK OR DARK COPPER BASED NUBIAN BLOOD OF THOTH/ENKI RA LINE, WHICH FOUNDED IT. EVIDENCE WOULD INCLUDE THE BLACK ZULU CULTURE WHOSE NAME FOR GOD - ENKI AS IN THE KILIMANJARO - SUGGESTS THEIR OWN BLACK GENETIC ORIGINS WITH ENKI (RA - ABRAHAM) AND HIS SON THOTH. LATER THE WORD KHEM MEANING BLACK HOLE BECAME ALCHEMY AND CHEMISTRY, FROM THE IMPLOSION PRINCIPLE OF THE ABILITY TO MAKE BLACK HOLES (WHICH GOLD'S ELECTRON VALENCE FRACTALITY ENABLES). HENCE ALCHEMY OF THE HEART IS THE FUSION ABILITY WHICH RESULTS FROM PERFECTING COMPRESSION (COMPASSION) IMPLOSION.

ANOTHER PLANET IN ORBIT AROUND SIRIUS A IS A WORLD CALLED KILROTI. HERE, THE SIRIANS CREATED HIGH-INTELLIGENCE CAT-LIKE BEINGS. THESE CAT-LIKE BEINGS ARE CALLED THE LION PEOPLE. IN THE 1970S AND 1980S, THE GOVERNMENT CREATED A CARTOON FOR CHILDREN THAT DESCRIBED THESE BEINGS.

IN THE HIGH ASTRAL LEVELS, THERE IS AN ETHERIC RACE OF LION BEINGS WHO ARE GOLD, HAVE WINGS, AND VIOLET EYES. THE NAME OF THE RACE IS ARI. ARI IS ALSO THE OLD HEBREW WORD FOR LION. THEIR FREQUENCY IS MORE POWERFUL THAN THE DOLPHIN FREQUENCY.

THE ARI CREATED THE OHALU COUNCIL THAT GOVERNS THE SIRIUS A STAR SYSTEM.

THIS FITS INTERESTINGLY WITH ANNA HAYES (VOYAGERS SERIES BOOKS, AND AMENTI) WHO CLAIMS THAT THE REASON THE SPHINX IS LION OR CAT LION SHAPED IS THAT THE STAR ELDERS OF THE INTERVENTIONIST ANUNNAKI (NEPHALIM) WERE LEONINE OR CAT/LION LIKE. SO IT WAS POLITICALLY CORRECT FOR THE FALLEN ANUNNAKI TO CLAIM THAT THEIR GOD WAS THE LION BEING. IF YOUR GOD IS STRONGER THAN YOUR ENEMIES GOD, YOU HAVE A PROBLEM IN WAR, SO YOUR STATUE (THE SPHINX) PROVES YOU HAVE THE RIGHT GOD (THE LION ELDERS OF SIRIUS) ON YOUR SIDE.

WE WONDER WHY SWERDLOW DID NOT SUGGEST THAT ARY-AN .... MEANS LION-BASED AN-NUNAKI - INSTEAD OF SUM-ARYAN.

THE KILROTI WERE GENERATED BY MIXING THE GENETICS OF THE SIRIANS WITH THE ENERGY OF THE ARI. THIS IS WHAT WAS BROUGHT TO ANCIENT EGYPT. AS THE NON-PHYSICAL ENERGY

DESCENDED INTO PHYSICAL REALITY, DNA FORMED THAT COULD BE USED TO CREATE CORPOREAL LIFE.

THIS WAS THEN MIXED WITH HUMAN AND WILD LION DNA TO FORM THE COMMON HOUSE CAT FOUND ON EARTH. THE CAT WAS GIVEN TO EVERY HOME IN ANCIENT EGYPT, AND PROGRAMMED TO LEAVE AT NIGHT TO REPORT BACK TO THEIR ALIEN CONTROLLERS. THIS IS WHY CATS TO THIS DAY HAVE THE URGE TO GO OUT AT NIGHT. THIS ALSO EXPLAINS THEIR ALOOF NATURE.

THE SIRIANS INCORPORATED WORSHIP OF THE CAT IDOL INTO THE EGYPTIAN RELIGION TO ENSURE THE PERPETUITY OF THIS METHOD OF SPYING. THE SIRIANS ALSO BUILT THE SPHINX AS A SYMBOLIC REMINDER OF THE BLENDING OF HUMAN GENETICS WITH LION FREQUENCY. THIS WAS A WAY TO ENERGETICALLY BIND FUTURE CIVILIZATION TO THE SIRIANS. THE SPHINX WAS DESIGNED TO FACE THE MORNING STAR SIRIUS A EVERY DAY. THE FACE ON THE SPHINX IS IDENTICAL TO THE FACE ON THE MARS MONUMENT THAT LOOKS DOWN TO THE EARTH AT THE SPHINX.

SIRIAN TECHNOLOGY BUILT THE COMPLEXES AT THE CYDONIA PLATEAU ON MARS, UPON THE ARRIVAL OF THE FIRST LYRAEN REFUGEES. THE NEW MARTIANS WERE UNAWARE OF THE CLOSE SIRIAN CONNECTION TO THE REPTILIANS.

THE ORIGINAL PYRAMIDS, BUILT AFTER THE DESTRUCTION OF ATLANTIS, WERE ENERGY POINTS. THEY WERE THE SAME SHAPES UNDERGROUND AS ABOVE, MAKING THEM INTO OCTAHEDRONS. AT THEIR CENTRE IS A TETRAHEDRON. THIS MASTER SHAPE IS THE ARCHETYPE SYMBOL FOR GOD-MIND TOTALITY. ANYTHING AT ITS EXACT CENTRE IS ABSOLUTELY PROTECTED. THE OCTAHEDRON IS ALSO THE SHAPE OF THE DELTA-T ANTENNA USED AT THE MONTAUK PROJECT. THIS SHAPE, WHEN ENERGIZED IN THE PROPER COLOR CODES, CAUSES INTERDIMENSIONAL RIFTS, CREATING VORTICES AND WORMHOLES.

RITUALS PERFORMED AT THIS CENTRE POINT PRODUCE VAST ENERGIES THAT CAN BE TRANSMITTED THROUGH HYPERSPACE TO ANYWHERE IN CREATION.

WE SAW PRESTON NICHOLS SPIN THE DELTA T, OCTA ANTENNA OF MONTAUK - IN MODEL - AT VARIOUS PSYCHOTRONIC CONFERENCES. IT SEEMS NEITHER HE NOR SWERDLOW UNDERSTOOD THE REASON IT WAS LATER CALLED DECA DELTA, AS ONLY WHEN THE OCTA/CUBE IS TILT SPUN INTO DODECA (SOULINVITATION.COM/MERKABBAH) DO YOU GET IMPLOSIVE COMPRESSION THAT BECOMES SUPERLUMINAL AND TIME PENETRATING ACCELERATION THRU C LIGHT SPEED. OBSERVE TO DODECA ANTENNA REQUIRED FOR TIME TRAVEL IN THE MOVIE "CONTACT".

SOME RESEARCHERS CLAIM THAT THE PYRAMIDS WERE PUMPING STATIONS FOR UNDERGROUND NILE TRIBUTARIES. THIS IS ONLY PARTIALLY TRUE.

BECAUSE WATER IS AN ELECTROMAGNETIC AMPLIFIER, IT WAS USED TO SURROUND THE RITUAL CHAMBER LOCATED IN THE DELTA-T TO BOOST RITUAL ENERGY. USING THESE METHODS, THE ANCIENT EGYPTIANS CONTROLLED WEATHER, DESTROYED ENEMIES, CREATED STARGATES, AND BOOSTED THEIR REPTILIAN ENERGIES IN CEREMONY. THIS IS ALSO WHY THE MONTAUK PROJECT WAS LOCATED NEAR VAST AMOUNTS OF WATER.

"GREAT WHITE PYRAMID" OF "XIAN,CHINA" IS THE "WORLDS LARGEST PYRAMID". IT IS REPORTED TO BE ABOUT 300 METERS HIGH.

THE GREAT PYRAMID IS PART OF A PROTECTIVE SOLAR SYSTEM GRID, LINKING THE MOON AND MARS MONUMENTS TOGETHER TO PRODUCE A FORCE FIELD TO REPEL INVADERS.

THE GREAT PYRAMID IS ALSO CONNECTED TO OTHER POINTS ON THE EARTH SUCH AS STONEHENGE, A SUBMERGED ATLANTEAN CRYSTAL, TIAHUANACO, AYERS ROCK, AND THE WHITE PYRAMID IN WESTERN CHINA. TOGETHER, THEY FORM AN ENERGY CONTAINMENT FIELD SIMILAR TO AN ELECTRIC FENCE.

THE HAARP PROJECT IN ALASKA TAPS INTO THIS.

MEANWHILE, A DYNASTIC CULTURE SIMILAR TO THE REPTILIAN CHINESE DYNASTIES WAS FORMING IN EGYPT. THE REPTILIAN CONTROL RELIGION BASED ON OSIRIS AND ISIS FANNED OUT OVER NORTHEAST AFRICA AND THE MIDDLE EAST. AT THE SAME TIME THE REPTILIAN SUMERIAN CULT OF NIMROD AND SEMIRAMIS FANNED OUT OVER CENTRAL ASIA.

A UNIFICATION OF THESE BELIEFS WAS NECESSARY TO ACCOMPLISH THE PLAN SET FORTH FROM THE BEGINNING. THIS IS WHY ABRAHAM ORIGINATED IN THE SUMERIAN CITY OF UR, JOURNEYING WESTWARD TOWARD THE MIDDLE EAST. IT WAS NO ACCIDENT THAT THE FOLLOWERS OF ABRAHAM WOUND UP IN EGYPT, WHERE THE SIRIANS THEN CREATED THE HEBREWS. THE HEBREWS WERE DESTINED TO BE THE CULTURAL PROTOTYPE FOR THE FUTURE WORLD.

THIS IS WHY THEY WERE PROGRAMMED TO WANDER ALL OVER THE EARTH AND INFLUENCE ALL EXISTING CULTURES.

(DAN WINTER COMMENTS)

THIS WOULD ALL IMPLY THAT IF ENKI IS IN FACT THE RA IN ABRAHAM - THAT HIS GENETIC ENGINEERING EXPLOITS WITH HIS SPERM TO MAKE EVE FERTILE USING CRO-MAG EGG IMPLANTED IN HIS HALF SISTER DRACO INANNA/NINHURSAG... WAS PART OF A MORE INSIDIOUS PLAN FROM HIS SIRIAN AN FAMILY? IT FITS THAT HIS EXPLOITS DESCEND FROM UR BECAUSE THAT IS THE NAME OF THE DRAC LINE. (N-IBI-URU, URUSHALAEM/JERUSALEM, IL-UR-U, H-IBI-URU/HEBREW , UR-MAN/ROMAN/ROMANIAN, UR-BAN)

WE WOULD HAVE TO EXPECT THAT THE (PART DRAC?) FATHER HE SHARED WITH YAHWEH ENLIL, WAS HALF BORG MACHINE (HARK-ONEN, SARKDAUER, DARTH VADER ...ETC). MORE AT RETURN OF ENKI. IT ALSO FITS THAT ENKI'S DAD AN = ANTU THE SIRIAN SUN GOD (TUETHE DE DANAAN - PEOPLE OF THE GODS) (CALLED BIKI BY AUSTRALIAN ABORIGINALS) - WAS ABLE TO ACT DISTANT AND ALOOF EVEN SEEMINGLY HEARTLESS TO THE CREATURE-LINGS OF EARTHS SEEMING PATHETIC SLAVE BORGS. TODAY, SWERDLOW'S DESCRIPTION OF THE SIRIUS A POLITICS PERFECTLY FITS THAT PICTURE.

THEY WILL STAND BACK, HAVING SOLD GUNS TO BOTH SIDES, IMPARTIALLY WAITING TO SEE WHO WINS- AND ASSUME EDUCATION AND EVOLUTION REQUIRES THE BLOOD SPILL. VERY MUCH CONNECTED TO THE POLITICS OF THE WEST EUROPE ARMS MUNITIONS FAMILIES (PRESUMABLY IN BUSH'S FAMILY GROUP) WHO GOT GREAT CORPORATE RETURN FOR THEIR INVESTMENT IN PAYING FOR THE SUB-SONIC SCALAR DEVICE (A NEAR TOWER BASE LO FREQUENCY VIBRATOR) THAT TOOK DOWN NEW YORK'S TWIN TOWERS (EVIDENCED BY THE SEISMIC TRACE).

...(EXCERPTS)

"THE SEISMIC SIGNALS FROM THE FIVE EVENTS ON 11 SEPTEMBER DIFFERED FROM A SMALL EARTHQUAKE IN SIGNIFICANT WAYS.

THEY WERE RICHER IN LOW-FREQUENCY ENERGY AND POORER IN HIGH-FREQUENCY ENERGY. "...

"WHILE GOING OVER SOME OF THE FOOTAGE I HAD TAPED ON A TIVO RECORDER, A CLIP CAUGHT MY ATTENTION THAT HASN'T BEEN NOTICED BY ANYONE. A SHOT FROM THE TOP OF A BUILDING LOOKING SOUTH SHOWS BOTH TOWERS BURNING AND STILL STANDING. THEN IN THE LOWER LEFT OF THE SCREEN, AT GROUND LEVEL QUITE A DISTANCE FROM THE BASE OF THE TOWERS A COMPLETELY SEPARATE BUILDING COLLAPSES IN A HUGE DUST CLOUD.

I REPEAT, THIS IS BEFORE THE COLLAPSE OF THE TOWERS"

OUR SUPPOSITION THAT ENKI (RA, ABRAHAM, ATON, THOTH, HERMES AND THE AKHANATON-MOSES-JESUS MYTH/LINE THEY SIRED) WAS COLORED TO TRY TO PREVENT THE TOTAL PARASITIC EATING OF THE TAK-ADAMA (ADAM AND EVE) BLOOD LINE (YOU AND ME) EVEN AGAINST THE MORE DRACONIAN WISHES OF HIS FAMILY- BECAUSE HE ESSENTIALLY FELL IN LOVE WITH HIS OWN GENETIC CREATION.

AND EVEN POSSIBLY THAT HE PERCEIVED EVENTUALLY THAT THE BLOOD LINES HE CROSSED COULD BE THE VACCINE IN THE ORION WARS GIVING THE REMNANT HUMANOIDS FROM MANY STAR CULTURES A CHANCE IF THEY COULD (BLISS) IGNITE THEIR DNA TO ENOUGH GRAVITY MAKING TO OUT-STEER THEIR CREATOR PARASITE ANCESTORS??? (THE BST - CLICK IMAGE RIGHT - OF WINGMAKERS)

WITH ALL OF THIS AS A BACKGROUND, THE REPTILIAN BLUEBLOODS NOW NEEDED TO FORM A GLOBAL EMPIRE THAT WOULD ENCOMPASS THE CULTURES THAT THEY HAD INSPIRED.

THEY NEEDED TO COUNTERACT THE OTHER ALIEN GROUPS THAT HAD BEEN WORKING DILIGENTLY IN EUROPE TO CREATE MORE HUMAN CIVILIZATIONS.

GO BACK

GO BACK TO CONTROL MENTAL

GO BACK TO BUDDHISM AND THE KALACHAKRA SYSTEM

GO BACK TO LA VERDADERA HISTORIA DE LOS NAZARENOS Y LA BIBLIA

15 - THE ILLUMINATI HIERARCHY

P.61-67

THE LEADER OF THE EARTHS ILLUMINATI IS CALLED THE "PINDAR". THE PINDAR IS A MEMBER OF ONE OF THE 13 RULING ILLUMINATI FAMILIES, AND IS ALWAYS MALE. THE TITLE, PINDAR, IS AN ABBREVIATED TERM FOR "PINNACLE OF THE DRACO", ALSO KNOWN AS THE "PENIS OF THE DRAGON". SYMBOLICALLY, THIS REPRESENTS THE TOP OF POWER, CONTROL, CREATION, PENETRATION, EXPANSION, INVASION, AND FEAR. THE HOLDER OF THIS RANK REPORTS TO THE PUREBRED REPTILIAN LEADER IN THE INNER EARTH.

RECENTLY, THERE ARE REPORTS THAT THE MARQUIS DE LIBEAUX IS THE PINDAR, BUT THIS IS DISINFORMATION. THE TRUE CURRENT PINDAR IS THE HEAD OF THE ROTHSCHILD FAMILY, AS HAS BEEN FOR SEVERAL HUNDRED YEARS. HE IS BASED IN GERMANY NEAR FRANKFURT. IN THE LATE 1970S, HE OVERSAW THE SISTER PROJECT TO MONTAUK, CALLED M.A.L.D.A. IS AN ANAGRAM FOR MONTAUK-ALSACE-LORRAINE DIMENSIONAL ACTIVATION. THIS PROJECT WAS LOCATED NEAR THE CITY OF STRASBOURG, FRANCE, HISTORICALLY ONCE PART OF GERMANY.

INTERESTINGLY, THERE IS A WINERY ON THE EAST END OF LONG ISLAND, NOT FAR FROM MONTAUK POINT, CALLED PINDAR VINEYARDS. THIS WINE IS GROWING IN POPULARITY, GAINING INTERNATIONAL ACCOLADES. THIS FITS NICELY INTO THE PLAN, AS THIS AREA WILL BE A PART OF THE CAPITAL DISTRICT OF THE EARTH/UNITED NATIONS IN THE EMPIRE STATE! RED WINE IS SYMBOLIC OF THE BLOOD INGESTED BY THE REPTILIANS. THE WINE CAN BECOME SANCTIFIED AS IT DID IN THE ROMAN CATHOLIC CHURCH, A PATSY FOR THE REPTILIANS. IN THE CATHOLIC CHURCH, WINE REPLACED THE BLOOD IN CEREMONY.

THE ILLUMINATI HERE ON EARTH HAVE ESTABLISHED A PYRAMID STRUCTURE OF CONTROL IDENTICAL TO THE SYSTEM THAT EXISTS IN THE DRACO EMPIRE. THE PYRAMID WITH THE REPTILIAN EYE, LOCATED ON THE AMERICAN ONE-DOLLAR BILL, IS SYMBOLIC OF THIS CONTROL STRUCTURE. THE EYE IS THE CAP ON THE PYRAMID, THUS EXPLAINING WHY THE ORIGINAL SURFACE OF THE GREAT PYRAMID IN EGYPT WAS CAPPED IN SOLID GOLD.

THE PINDAR IS REPRESENTED BY THE GOLD CAP ON THE PYRAMID. THE NEXT LAYER, OR "EYE", ON THE PYRAMID REPRESENTS THE 13 RULING FAMILIES.

THEY ARE AS FOLLOWS:

*

ROTHSCHILD (BAUER OR BOWER) - PINDAR

* BRUCE

* CAVENDISH (KENNEDY)

* DE MEDICI

* HANOVER

* HAPSBURG

* KRUPP

* PLANTAGENET

* ROCKEFELLER

* ROMANOV

* SINCLAIR (ST. CLAIR)

* WARBURG (DEL BANCO)

* WINDSOR (SAXE-COBURG-GOTHE)

EACH OF THE 13 RULING FAMILIES IS GIVEN AN AREA OF THE EARTH AND/OR A PARTICULAR FUNCTION TO FULFILL ON THE EARTH.

THESE PARTICULAR FUNCTIONS INCLUDE:

*

GLOBAL FINANCES

* MILITARY TECHNOLOGY/DEVELOPMENT

* MIND-CONTROL

* RELIGION

*

MEDIA

EACH OF THE 13 RULING FAMILIES HAS A COUNCIL OF 13 AS WELL. THE NUMBER, 13, HAS GREAT SIGNIFICANCE TO THEM. THEY KNOW THAT THERE ARE 12 TYPES OF ENERGIES THAT PASS THROUGH THE 10 ASPECTS OF GOD-MIND. THE TOTALITY OF THE 12 ENERGIES EQUALS A 13TH ENERGY. THIS IS CONSIDERED THE MOST POWERFUL KNOWLEDGE.

THEY ALSO KNOW THAT THERE ARE REALLY 13 ZODIAC SIGNS, NOT THE COMMONLY ACKNOWLEDGED 12. THEY HAVE KEPT THE 13TH HIDDEN FOR CENTURIES BECAUSE IT IS THE SIGN OF THE DRAGON. THEY KEEP THE QUALITIES AND TRAITS OF THIS SIGN SECRET TO AVOID GIVING AWAY CLUES TO THE REPTILIAN MIND-PATTERN.

THE NEXT LAYER IS THE SECOND-IN-COMMAND FAMILIES WHO DO THE SUPPORT WORK FOR THE PINDAR AND 13 RULING FAMILIES. WHILE ALL OF THE 13 RULING FAMILY MEMBERS ARE SHAPE-SHIFTERS, ALL MEMBERS OF THE 300 SUPPORTING FAMILIES ARE NOT. THEY DO, HOWEVER, ALL HAVE A HIGH PERCENTAGE OF REPTILIAN DNA.

THEY ARE KNOWN AS THE "COMMITTEE OF 300".THESE FAMILIES INCLUDE SUCH NOTABLE NAMES AS AGNELLI, BALLIOL, BEALE, BELL, BOUVIER, BUSH, CAMERON, CAMPBELL, CARNEGIE, CARRINGTON, COOLIDGE, DELANO, DOUGLAS, FORD, GARDNER, GRAHAM, HAMILTON, HARRIMAN, HEINZ, KUHN, LINDSAY, LOEB, MELLON, MONTGOMERY, MORGAN, NORMAN, OPPENHEIMER, RHODES, ROOSEVELT, RUSSELL, SAVOY, SCHIFF, SETON, SPENCER, STEWART/STUART, TAFT, AND WILSON. THERE ARE MANY OTHERS...

THE COMMITTEE OF 300 USE MANY WELL-KNOWN INSTITUTIONS TO ACCOMPLISH THEIR GOALS, INCLUDING THE

*

COUNCIL ON FOREIGN RELATIONS

*

BILDERBERGERS

*

TRILATERAL COMMISSION

*

CLUB OF ROME

*

ROYAL INSTITUTE FOR INTERNATIONAL AFFAIRS

*

MAFIA

*

CIA

*

NSA

*

MOSSAD

*

SECRET SERVICE

*

INTERNATIONAL MONETARY FUND
*

FEDERAL RESERVE
*

INTERNAL REVENUE SERVICE
*

INTERPOL,

...TO NAME A FEW.

ALL OF THESE ARE PRIVATE ORGANIZATIONS OR CORPORATIONS SET UP AS PUBLIC SERVICE DEVICES, BUT THIS IS FAR FROM THE TRUTH.

THE ILLUMINATI STRUCTURE ALSO CREATES ARTIFICIAL COUNTRIES TO FURTHER THEIR GOALS. EXAMPLES OF THESE ARE THE UNITED STATES, SWITZERLAND, KUWAIT, THE SOVIET UNION, PANAMA, ISRAEL, ITALY, YUGOSLAVIA, THE UNITED KINGDOM, MOST OF BLACK AFRICA, ALL OF THE ARAB COUNTRIES, AND ALL OF CENTRAL AND SOUTH AMERICA. THESE NATIONS WERE CREATED TO AMASS WEALTH FOR THE RULING FAMILIES AND THEIR SUPPORTERS, TO HIDE OR KEEP THEIR WEALTH, AND TO CREATE UNSTABLE CONDITIONS NECESSARY TO START WARS OR INCREASE MILITARY BUDGETS.

SWITZERLAND WAS CREATED AS A NEUTRAL BANKING CENTRE SO THAT ILLUMINATI FAMILIES WOULD HAVE A SAFE PLACE TO KEEP THEIR FUNDS WITHOUT FEAR OF DESTRUCTION FROM WARS AND PRYING EYES.

THE UNITED STATES WAS ESTABLISHED WITH 13 COLONIES, ONE FOR EACH OF THE ILLUMINATI FAMILIES. THE ORIGINAL FLAG HAD 13 STARS, AND STILL HAS 13 STRIPES. THE EAGLE, THE SYMBOL OF THE UNITED STATES, HOLDS 13 ARROWS IN ITS TALONS. THE UNITED STATES IS ACTUALLY A CORPORATE ASSET OF THE VIRGINIA COMPANY THAT WAS ESTABLISHED IN 1604 IN ENGLAND WITH DIRECT INVOLVEMENT OF THE ROTHSCHILDS. THE FINANCES OF THE ROTHSCHILDS WERE NECESSARY TO FUND THE EXPLORATION AND EXPLOITATION OF THE NORTH AMERICAN CONTINENT.

THE ASSETS OF THE VIRGINIA COMPANY, INCLUDING THE UNITED STATES, ARE OWNED BY THE HOLY ROMAN EMPIRE VIA THE VATICAN. THIS OCCURRED IN 1213 WHEN KING JAMES GAVE ALL ENGLISH ASSETS TO THE REPTILIAN POPE. EXECUTORSHIP REMAINS WITH THE BRITISH ROYAL FAMILY, BUT ACTUAL OWNERSHIP LIES WITH THE ROMAN CATHOLIC CHURCH.

THE UNITED STATES OF AMERICA IS NOT NAMED AFTER AMERIGO VESPUCCI, AS YOU LEARNED IN SCHOOL. THE ILLUMINATI WOULD NEVER NAME A CONTINENT, ACTUALLY TWO CONTINENTS, AFTER AN ITALIAN MAPMAKER.

THE NAME IS ACTUALLY A COMBINATION OF WORDS.

*

"AM" IS THE HEBREW WORD FOR "PEOPLE"
*

"AME" IS ALSO THE COMMAND FORM OF THE SPANISH/LATIN VERB "TO LOVE"

*

"ERI" OR "ARI" IS A HEBREW TERM FOR "LION"

*

"RICA" IS THE FEMININE FORM OF THE SPANISH WORD FOR "RICH"

*

"KA" IS THE ANCIENT EGYPTIAN WORD FOR SOUL, OR SPIRIT FORCE WITHIN A BODY

THERE ARE TWO LAYERS OF MEANINGS.

THE ANCIENT HEBREW/EGYPTIAN TRANSLATES TO SAY,

"THE PEOPLE OF THE LION WITH SPIRIT FORCE"

HENCE, THE PYRAMID AND ALL-SEEING EYE ON THE ONE-DOLLAR BILL. THE LATINIZED VERSION TRANSLATES TO SAY, "LOVE RICHES", IN A FEMINIZED/PHYSICAL REALITY WAY. THIS GIVES AN IDEA OF WHAT THEY HAD IN MIND.

TAKE THIS A STEP FURTHER, AND ONE SEES THE MIXTURE OF THE FEMININE LATIN/EAGLE IDEAS WITH THE MASCULINE HEBREW/LION IDEAS. THE SYMBOLIC STATEMENT OF AMERICA IS THAT IT IS A COMBINATION OF LEMURIA AND ATLANTIS; A BLEND OF THE HUMAN/LYRAE WITH REPTILIAN/DRACO. PERHAPS THE ANAGRAM LSD, AN ILLUMINATI CREATED DRUG, HAS A HIDDEN MEANING AS WELL: LYRAE-SIRIUS-DRACO!

THE COMBINATION OF THESE THREE CIVILIZATIONS WOULD PRODUCE THE MOST POWERFUL, TECHNOLOGICAL EMPIRE EVER KNOWN!

IN 1776, THE CREATION OF THE UNITED STATES AS AN INDEPENDENT NATION COINCIDED WITH THE DECLARATION INTO PUBLIC EXISTENCE OF THE OFFICIAL ILLUMINATI ORGANIZATION BY MEMBER ADAM WEISHAUPT, IN BAVARIA. PUBLICLY, MR. WEISHAUPT APPEARED TO BE DETERMINED TO CREATE AN ORGANIZATION COMPRISED OF THE EUROPEAN ELITE THAT WOULD UPLIFT MANKIND.

OF COURSE, THIS WAS PART OF AN ILLUMINATI GLOBAL CEREMONY. THE CREATION FOR THE UNITED STATES AND THE ILLUMINATI GLOBAL CEREMONY. THE CREATION OF THE UNITED STATES AND THE ILLUMINATI ORGANIZATION WERE ARTIFICIAL BEGINNINGS FOR PUBLIC CONSUMPTION. THE UNITED STATES WAS THE DEVICE TO BE USED TO BRING THE ILLUMINATI INTO PUBLIC ACCEPTANCE. CURRENT ILLUMINATI MEMBERS BELIEVE THAT ADAM WEISHAUPT WAS A LOOK-ALIKE FOR GEORGE WASHINGTON, AND IT IS ACTUALLY WEISHAUPTS IMAGE THAT APPEARS ON THE ONE-DOLLAR BILL.

GEORGE WASHINGTON WAS A WEALTHY SLAVE AND PLANTATION OWNER. HE IS KNOWN TO HAVE RAPED SOME OF HIS FEMALE SLAVES AND USED SOME OF THE MALE SLAVES IN RITUALISTIC CEREMONY. THERE ARE MANY PEOPLE OF THE BLACK RACE WHO CAN LITERALLY TRACE THEIR GENETICS TO THE FOUNDING FATHERS. GEORGE WASHINGTON ALSO ORDERED THE BUILDING OF THE MONTAUK LIGHTHOUSE IN 1796. THIS LIGHTHOUSE INCLUDED AN UNDERGROUND AREA FOR SUPPLY STORAGE IN CASE OF A BRITISH COASTLINE INVASION. IF HE HAD ONLY KNOWN WHAT THAT AREA WOULD BECOME - OR DID HE?

THE 13 RULING ILLUMINATI FAMILIES CONSTANTLY VIE FOR CONTROL AMONGST THEMSELVES.

DURING THIS TIME PERIOD, THE SPANISH, BRITISH, AND FRENCH ILLUMINATI ALL FOUGHT TO WIN CONTROL OVER NORTH AND SOUTH AMERICA. THE ROTHSCHILDS KEPT THESE ILLUMINATI FACTIONS IN LINE BY SENDING HESSIAN TROOPS TO MONITOR THE SITUATION. THE LEADERS ENJOYED THESE WAR GAMES, PITTING ONE AGAINST THE OTHER TO SEE WHO WOULD WIN. THE HUNDREDS OF THOUSANDS OF LIVES LOST WERE MEANINGLESS TO THEM.

THE MANIFEST DESTINY OF THE UNITED STATES WAS CREATED TO EXPAND THE TERRITORY OF THE ARYANS AT THE EXPENSE OF THE NATIVE POPULATIONS. AS ALWAYS, THE ILLUMINATI SEEK TO DESTROY NATIVE PEOPLES AND THEIR CULTURES. THIS IS AN ATTEMPT TO DESTROY THEIR KNOWLEDGE OF GOD-MIND, AS WELL AS THE POSSIBILITY THAT THE NATIVES WILL IMPART THIS INFORMATION ON TO OTHERS.

ESPECIALLY IMPORTANT IS THEIR NEED TO ELIMINATE NATIVE CULTURES WITH ANCIENT KNOWLEDGE OF ATLANTIS AND LYRAE.

THE NATIVES THAT GAVE THEM THE MOST PROBLEM WERE THE CHEROKEE INDIANS BECAUSE THIS TRIBE RETAINED MOST OF THEIR ATLANTEAN KNOWLEDGE, EVEN ACCESSING THE BEAR/BIGFOOT FREQUENCY FOR INFORMATION. FOR THIS REASON, THESE PEOPLE WERE UPROOTED FROM THEIR HOMELAND IN THE SOUTHERN APPALACHIAN MOUNTAINS, AND FORCIBLY MARCHED TO OKLAHOMA ON WHAT IS NOW KNOWN AS THE TRAIL OF TEARS. MANY DIED ALONG THE WAY. ONLY A REMNANT REMAINED IN NORTH CAROLINA, TENNESSEE, AND GEORGIA. IN THE NORTH, THE VAST IROQUOIS/MOHAWK NATION WAS DISBANDED. THE MONTAUK, DIRECT DESCENDENTS OF THE ATLANTEANS WHO CALL THEIR LEADER PHARAOH, WERE SYSTEMATICALLY ELIMINATED.

THE ROTHSCHILDS WERE AGGRESSIVELY INVOLVED WITH THE SLAVE TRADE FROM AFRICA, IMPORTING SLAVES TO NORTH AND SOUTH AMERICA AS WELL AS THE CARIBBEAN. THEY WERE VERY CAREFUL NOT TO IMPORT BLACKS FROM THE EASTERN AREAS OF ETHIOPIA OR SUDAN WHERE THE DESCENDENTS OF SOLOMON WERE LOCATED, INSTEAD CONCENTRATING ON WESTERN AND CENTRAL AFRICA FOR THE SLAVE POPULATIONS. THESE AREAS HAD THE PURE MIXTURE OF ANUNNAKI AND SIMIAN GENETICS, AND THE PROGRAMMING DESIRABLE FOR THE ILLUMINATI AGENDA.

THE ROTHSCHILDS DECIDED THAT SPLITTING THE UNITED STATES COLONIES WOULD DOUBLE THEIR PROFITS. SO THEY POLITICALLY CREATED, AND FINANCIALLY SUPPORTED, THE CIVIL WAR. THE CIVIL WAR WAS ACTUALLY A GLOBAL CEREMONIAL RITUAL TO BRING SLAVERY TO ITS NEXT LEVEL.

THIS WAR ALLOWED THE NORTH TO WIN, AND PUBLICLY ABOLISH SLAVERY. THE BEST SLAVES ARE THE ONES WHO DO NOT REALIZE THAT THEY ARE SLAVES. THIS ALLEVIATES REBELLION AND RESISTANCE. THIS WAS THE STATUS IMMEDIATELY FOLLOWING THE CIVIL WAR. BLACKS IN THE SOUTH ARE STILL SLAVES. THERE IS STILL SEGREGATION, EVEN IN THE NORTH. THE ILLUMINATI STILL CONSIDER BLACKS TO BE SECOND OR THIRD CLASS CITIZENS. ONLY NOW THE SLAVERY IS SUBTLE AND MASKED.

SINCE THE CIVIL WAR, THERE HAVE BEEN OTHER STAGED WARS THAT ENTRENCHED THE TREND TOWARD GLOBALIZATION. THE SPANISH-AMERICAN WAR OF 1898-1899 ACQUIRED MORE LAND FOR THE AMERICAN ILLUMINATI, PLACING A GREATER PORTION OF THE EARTH'S SURFACE UNDER AMERICAN JURISDICTION. WORLD WAR I WAS DESIGNED TO CHANGE THE MAP OF EUROPE AS WELL AS TEST GERM AND CHEMICAL WARFARE TECHNOLOGY FOR FUTURE USE. THIS COINCIDED WITH THE WORLDWIDE INFLUENZA OUTBREAK DESIGNED TO REDUCE THE GLOBAL POPULATION, MAKING CONTROL EASIER. WORLD WAR I ALSO LAID THE FOUNDATION FOR THE GERMAN ROLE IN THE NEXT WAR.

WORLD WAR II WAS A TEST OF THE FINAL GLOBALIZATION AND EXTERMINATION PROJECTS. IT WAS

ALSO DESIGNED TO TEST MIND-CONTROL MACHINATIONS; TO TEST THE USE OF FLUORIDE WHICH DEADENS BRAIN ACTIVITY AND SLOWS RESISTANCE TO AUTHORITY; TO EXPERIMENT WITH SLAVE LABOR CAMPS AND STUDY THE DEVELOPMENT OF RESISTANCE; AND TO TEACH THE MASSES TO SPY AND REPORT ON ONE ANOTHER.

WORLD WAR II BROUGHT THREE PRIMARY GOALS OF THE ILLUMINATI TO FRUITION.

*

THE FIRST WAS THAT HIDDEN ILLUMINATI SYMBOLISMS WERE BROUGHT TO PUBLIC ATTENTION FROM THE UNDERGROUND STRONGHOLDS IN TIBET AND EGYPT, SUCH AS THE SWASTIKA AND THE ANKH.

*

THE SECOND WAS THE CREATION OF THE STATE OF ISRAEL AS A FOUNDATION FOR THE NEW WORLD RELIGION.

*

THE LAST WAS THE CREATION OF NUCLEAR WEAPONS AS PART OF THE ILLUMINATI GLOBAL CEREMONY.

DURING WORLD WAR II, THE GERMANS HELPED TO PERFECT "SEX-SLAVES" AS A MEANS OF TRANSMITTING INFORMATION AMONGST THE ELITE. SEX-SLAVES CAN BE EITHER MALE OR FEMALE, WHO ARE SEXUALLY PROGRAMMED USING WILHELM REICH PROCEDURES, WHICH ARE ILLEGAL IN THE UNITED STATES, BUT USED BY THE ILLUMINATI AND GOVERNMENT.

THESE SEX-SLAVES DELIVER MESSAGES AND KEEP PROGRAMMED SLEEPERS IN LINE. THE SEX-SLAVE IS DOWNLOADED WITH A MESSAGE OR FUNCTION THROUGH VARIOUS SEXUAL ACTS AND DRUGS, WHICH CAN ONLY BE RELEASED BY REPEATING THE SAME SEXUAL ACT WITH THE TARGET, OR PERSON, TO BE ACTIVATED. THEY ARE TRAINED TO KNOW THEIR TARGET'S TRIGGER WORDS AND TRIGGER EVENTS TO ACTIVATE, DELETE, OR CHANGE PROGRAMMING.

IN RECENT YEARS, SEVERAL WOMEN HAVE COME FORWARD CLAIMING TO BE THE SEX-SLAVES OF GLOBALLY RECOGNIZED POLITICAL FIGURES. MANY WERE USED AS INFORMATION COURIERS BETWEEN HIGH-LEVEL MALE ILLUMINATI. USUALLY, LOOK-ALIKES OF THE POLITICAL FIGURES ARE USED IN THE INCIPIENT PROGRAMMING AS A FOCAL POINT FOR THE SEX-SLAVE. THE SLAVE IS PUT THROUGH A DESENSITIZING PROCESS, SO THERE IS NO PLEASURE IN THE SEXUAL ACT; IT IS MERELY A DUTY TO BE PERFORMED. MANY TIMES THE SLAVE BECOMES SEXUALLY PROMISCUOUS, REPEATEDLY HAVING SEX WITH PEOPLE WHO LOOK LIKE THE INTENDED TARGET. IT IS A SAD LIFE.

BY THE END OF WORLD WAR II, ONE OF THE THREE MAJOR ILLUMINATI GLOBAL RITUALS WAS ACCOMPLISHED.

THIS WAS THE NUCLEAR EXPLOSION THAT TOOK PLACE IN 1945 AT THE 33RD PARALLEL AS A TEST FOR THE NUCLEAR ATTACK ON JAPAN. THIS EXPLOSION WAS SYMBOLIC, REPRESENTING THE SIMULTANEOUS CREATION AND DESTRUCTION OF MATTER AND ENERGY. THE YEAR WAS SYMBOLIC AS WELL. IN NUMEROLOGY, 1 + 9 = 10, REPRESENTING THE 10 ASPECTS OF GOD-MIND. THE NUMBER 10 FURTHER BREAKS DOWN TO 1 + 0 = 1, REPRESENTING A NEW BEGINNING. CONTINUING, 4 + 5 = 9, REPRESENTING THE END OF A CYCLE.

SYMBOLICALLY, THE ENTIRE EVENT REPRESENTED THE END OF A CYCLE TO PREPARE FOR A NEW BEGINNING USING THE NEW CREATION OF GOD-MIND OUT OF DESTRUCTION.

ADDITIONALLY, A CYLINDER CONTAINING MATERIAL STILL NOT EXPLAINED BY THE GOVERNMENT

WAS TRUCKED INTO THE NUCLEAR EXPLOSION TESTING. THIS CYLINDER WAS MADE FROM PURE STEEL AND ALLEGEDLY WAS THE SAME PHYSICAL DIMENSIONS AS THE KABALA DESCRIBES FOR THE CREATION OF GOLEMS. KABALA IS ANCIENT HEBREW METAPHYSICS THAT HAS BEEN A STAPLE FOR THE ILLUMINATI FOR MILLENNIA. GOLEMS ARE ARTIFICIAL BEINGS THAT ARE USED AS A SLAVE FORCE. IT IS HIGHLY PROBABLE THAT THIS WAS A SYMBOLIC RITUAL FOR THE CREATION OF THE SOCIETY OF GOLEMS.

WORLD WAR II ALSO ALLOWED THE EUROPEAN/AMERICAN ILLUMINATI TO DESTROY THE JAPANESE ILLUMINATI DESIRES OF GLOBAL DOMINATION. THE JAPANESE ROYAL FAMILY, REPRESENTED BY EMPEROR HIROHITO, HAVE ALWAYS BEEN OSTRACIZED AS NON-LEGITIMATE BY THE RULING 13 FAMILIES. THE JAPANESE CLAIM TO BE DIRECT DESCENDENTS OF LEMURIAN PUREBRED REPTILIANS.

THE EUROPEAN/AMERICAN ILLUMINATI CLAIM THAT THE JAPANESE ILLUMINATI ARE DESCENDENTS FROM A LOWER SPECIES IN THE DRACO HIERARCHY. THIS LOWER SPECIES IS CONSIDERED A WORKER CLASS WITHOUT ANY POLITICAL CLOUT OR INFLUENCE. THE EUROPEAN/AMERICAN ILLUMINATI ALSO CLAIM THAT EAST INDIANS ARE A LOWER SPECIES IN THE DRACO HIERARCHY. THE 13 RULING FAMILIES CONSIDER LIGHT SKIN AND HAIR TO BE AN ELITE CHARACTERISTIC.

ON JANUARY 17, 1994, JAPAN SENT A SEISMIC EVENT TO CALIFORNIA. EXACTLY ONE YEAR LATER ON JANUARY 17, 1995, THE CITY OF KOBE, JAPAN WAS SEISMICALLY DESTROYED. KOBE WAS THE HOME OF THE JAPANESE ELECTROMAGNETIC WEAPONRY CENTERS. THE EUROPEAN/AMERICAN ILLUMINATI WILL NOT TOLERATE THORNS IN THEIR SIDES. THE DESTRUCTION OF JAPAN AND ITS ROYAL FAMILY WILL CONTINUE IN THE COMING MONTHS.

EVERY YEAR, THE ILLUMINATI HOLD MEETINGS TO PLAN THE EVENTS OF THE COMING YEAR TO ACCOMPLISH THEIR MAIN OBJECTIVE FORMULATED MILLENNIA AGO OF GLOBAL CONTROL AND DOMINATION. IN THE 1850S, THEY PINPOINTED THEIR TARGET DATE FOR COMPLETE DOMINATION WITH AN AGENDA CALLED PLAN 2000.

THIS HAS SINCE BEEN REVISED TO 2003. THE FIASCO ELECTION OF GEORGE W. BUSH JR. TO OFFICE IS A KEY SIGN THAT THEY ARE ON TARGET. THE PUBLIC LESSON OF THE UNITED STATES PRESIDENTIAL "ELECTION" OF 2000 IS THAT THE CITIZENS DO NOT VOTE FOR ANYONE!

EVEN THE ILLUMINATI ARE NOW FINDING IT INCREASINGLY DIFFICULT TO CONCEAL THEIR PLANS.

GO BACK

DRACO

P.158

CREATED BY AN ET GROUP, THE CREATORS TRAVELED BACK IN TIME AND SPACE WITH GENETIC MATERIAL TO SUPPORT THE DISINTEGRATION OF THE LYRAEN CIVILIZATION. WITH SEVEN DIFFERENT TYPES OF DRACO RACES, THE LEADER GROUP IS A SEVEN TO EIGHT FOOT TALL WINGED REPTILIAN-TYPE CREATURE. ABOVE IS PICTURED A WARRIOR USED TO CONQUER AND OCCUPY A PLANET. THE SLENDER FOUR TO FIVE FOOT DRACO SIMILAR TO A LIZARD PERFORMS MENIAL TASKS AND AIDS IN ABDUCTIONS.

HARSH, WARLIKE BEINGS WHO FEEL LITTLE EMOTION, THE DRACO HAVE NO REGARD FOR CULTURE OR OTHER BEINGS. MOST DRACO ARE ANDROGYNOUS AND REPRODUCE BY PARTHENOGENESIS, OR CLONING. ONE SPECIAL GROUP THAT IS COMPLETELY MALE CREATES HYBRID RACES THAT CONQUER OTHERS.

THE EARTH'S MOON IS A DRACO PLANETOID PLACED IN ORBIT AEONS AGO DURING THE TIME OF THE LEMURIAN COLONIZATION. WITH THE INTENTION TO DIVIDE AND CONQUER, THEY ARE KNOWN TO BE BRUTAL, AS WITH RIGEL BY BOILING OCEANS, SCORCHING LANDMASSES, ETC. THE DRACO HAVE VAST UNDERGROUND BASES ON EARTH AND COLONIES ON VENUS.

A SECOND MOON HAS BEEN STATIONED OVER THE EARTH. IT ARRIVE BEHIND THE HALE-BOPP COMET IN 1997. THESE ARE PURE REPTILIANS.

THE HYBRIDS, ILLUMINATI, ARE IN CONTROL OF THE EARTH.

GO BACK

THERE FOLLOWS EXCERPTS FROM THE BOOK:

MONTAUK - THE ALIEN CONNECTION

BY STEWART SWERDLOW
EDITED BY PETER MOON, EXPANSIONS PUBLISHING CO.

COMMENTS IN ITALIC LETTERS ARE FROM DAN WINTER, THE REST IS A QUOTE DIRECTLY FROM THE BOOK-PAGES MENTIONED...

P.36-40

SPEAKING IN SUCCESSION FROM RIGHT TO LEFT, THE FIRST ONE WAS A LARGE REPTILIAN CREATURE WHO LOOKED LIKE A LIZARD STUFFED INTO A BLACK UNIFORM. HE SPOKE WITH A HISSING NOISE IN A LANGUAGE THAT SOUNDED GUTTURAL AND SEVERE.

SIMULTANEOUSLY, I HEARD THE MEANING OF HIS WORDS IN MY HEAD. A MEMBER OF A VAST

EMPIRE THAT SPANNED A LARGE PORTION OF THE GALAXY, HIS PEOPLE ARE ATTEMPTING TO OCCUPY ALL OF THE STAR SYSTEMS ON THE OUTER FRINGES OF THIS GALAXY, EVENTUALLY WORKING THEIR WAY INWARD. A DEFECTOR, HE NOW ADVISES THIS COUNCIL ON THE POSSIBLE ACTIVITIES OF THESE INVASION FORCES.

ACCORDING TO THE LIZARD, THE EARTH WAS INVADED MANY THOUSANDS OF YEARS AGO BY AN ARMY OF HIS PEOPLE THAT ARRIVED IN A HUGE SHIP THAT IS NOW THE MOON OF EARTH.

NUMEROUS SOURCES- INCLUDING WE UNDERSTAND NASA'S SEISMIC DATA - CONFIRM THE MOON IS A HOLLOW METAL FRAMEWORK, TOWED IN HERE, AND INFESTED INTERNALLY WITH GREYS AND DRACS

ANOTHER SUCH SHIP IS ON ITS WAY, HE SAID, DESTINED TO ARRIVE BEFORE THE END OF THIS CENTURY (AS WE CALCULATE TIME).

SEVERAL SOURCES - AMONG THEM ALEX COLLIER, HAVE INSISTED ARTIFICIAL PLANETOIDS - LIKE HALE BOPP'S TOW INS - WERE HEADED HERE IN COMET GRAVITY TAILS - FILLED WITH INVADING DRACOS. THE SUN CRUISERS IN THE SOLAR/MERCURY NEAR ORBIT - VISIBLE ON SEVERAL WEB SITES - ARE SAID TO BE EXAMPLES OF THESE. ALEX'S ANDROMEDAN MATERIAL SPECIFICALLY PREDICTED THE COMET WOULD DROP THE INVASION SHIPS IN A TEMPORARY NEAR MERCURY ORBIT.

AFTER BEING DRIVEN OFF THE EARTH BY SETTLERS FROM THE LYRAEN EMPIRE, HIS PEOPLE WENT UNDERGROUND.

MOST OF THE LEMURIAN EPOCH STORIES SUGGEST THAT THE END OF THE LEMURIAN CONTINENT WAS A WAR WITH A REPTILIAN RACE, WHICH THE HUMANOIDS WON AGAINST THE REPTILIANS - BUT AT THE COST OF THE ENVIRONMENT - FORCING THE HUMANOID SURVIVING REMNANT UNDERGROUND - WHERE THEIR BLOOD BECAME MORE RED AND DEPENDANT ON IRON TO BOND OXYGEN (AS OPPOSED TO THE HUMANOID REMNANT WHO FLED AT THAT POINT LARGELY TO SIRIUS AND PLEIADES WHERE THEY BECAME MORE BLUE/COPPER BLOOD.)

THERE, THEY REMAIN IN STASIS UNTIL THEY ARE TO BE REACTIVATED BY THE INCOMING SHIP. THESE REPTILIANS ALSO MAINTAIN BASES ON VENUS AND ON SOME OF THE MOONS OF THE OUTER PLANETS. BECAUSE HIS PEOPLE ARE MALE ONLY, THEY CREATED FEMALES FOR THE SOLE PURPOSE OF BREEDING. DESPITE THIS, CLONING IS THEIR PRIMARY METHOD OF REPRODUCTION. IN CONCLUSION, THE LIZARD ADDED THAT I WOULD SOMEDAY CONVERT HIS PEOPLE TO THE LIGHT BECAUSE MY SOUL WAS AN EMISSARY TO THEM MANY YEARS AGO. REMEMBERING ME, THEY WOULD RESPECT WHAT I SAID TO THEM.

THE NEXT ONE TO SPEAK WAS AN AMPHIBIAN-TYPE BEING WHO LOOKED VERY MUCH LIKE THE CREATURE FROM THE BLACK LAGOON. SLIMY AND MOIST, HIS BODY WAS COVERED WITH A SCALY, GREENISH-GREY SKIN. BREATHING HEAVILY, HIS THOUGHTS FLOODED MY BRAIN. HIS CIVILIZATION WAS THE ORIGINAL INHABITANT OF EARTH BEFORE THE OTHERS ARRIVED. AT THAT TIME, EARTH WAS MOSTLY WATER AND MARSHES. DEVASTATED BY MANKIND AND ALIENS ALIKE, THERE REMAIN ONLY A FEW POCKETS OF HIS PEOPLE AT THE DEEPEST DEPTHS OF THE OCEANS.

FROM TIME TO TIME THEY COME TO DRY LAND TO SUN THEMSELVES, THUS CREATING THE BASIS FOR THE LEGENDARY MERMAIDS AND MERMEN. THIS SPECIES WORKED CLOSELY WITH THE ATLANTEANS BEFORE THAT CONTINENT SANK. THEY SERVED AS LIAISONS BETWEEN MANKIND AND THE WHALES AND DOLPHINS. HE SAID THAT THESE SEA MAMMALS ARE ADVANCED RACES FROM ANOTHER GALAXY. MOST OF HIS PEOPLE WERE LIFTED OFF-WORLD TO UNDERGROUND OCEANS ON NEPTUNE. THIS MANEUVER WAS FACILITATED BY BENEVOLENT ET GROUPS. CONTINUING, HE TOLD ME THAT I HAVE DOLPHIN DNA; THEREFORE, I COULD LEARN TO COMMUNICATE WITH HIS SPECIES IN ORDER TO HELP MANKIND AND THE DOLPHIN/WHALE SYSTEMS.

NEXT, A BEING ON THE OPPOSITE SIDE OF THE TABLE SPOKE. LOOKING LIKE A SMALL DARK-HAIRED HUMAN, HIS EYES WERE SO DARK THAT THEY ALMOST SHINED. HIS EYES SEEMED TO PIERCE RIGHT THROUGH MY OWN, AND I FOUND IT DIFFICULT TO LOOK AT HIM. CLAIMING TO REPRESENT THE FEDERATION OF PLANETS OF THIS GALAXY, HE SAID THAT THERE ARE OVER 120 DIFFERENT MEMBER CIVILIZATIONS. SOMEDAY, EARTH WILL BE ASKED TO JOIN, BUT ONLY IF THEY ARE SUCCESSFUL IN REPELLING THE INVASION FORCE. OTHERWISE, EARTH COULD BECOME A TARGET BY THE FEDERATION UNTIL THE REPTILIANS ARE REMOVED.

THIS DARK-HAIRED HUMAN SAID THAT I WAS SELECTED TO SPEAK WITH ALL OF THESE ALIENS BECAUSE EACH SPECIES HAD CONTRIBUTED TO MY DNA CREATION. I WAS MADE FOR THE EXPRESS GENETIC PURPOSE OF BELONGING TO MANY DIFFERENT GROUPS. BECAUSE OF THAT, EACH GROUP WOULD BE MORE WILLING TO LISTEN TO ME AND ACCEPT MY IDEAS SINCE I PARTIALLY BELONGED TO THEM.

CONTINUING, HE SAID THAT MY SOUL-PERSONALITY HAD AGREED TO THIS MISSION LONG AGO, UNDERGOING TRAINING IN MANY GALAXIES AND ALTERNATE UNIVERSES. HE SAID THAT MUCH OF WHAT THEY TOLD ME NOW WOULD STAY HIDDEN IN MY CELLULAR MEMORY UNTIL EACH PIECE OF INFORMATION BECOMES NECESSARY. FUTURE HARDSHIPS AND SADNESS WOULD CONDITION ME FOR MY MISSION. NOT WANTING TO HEAR ANY OF THIS, I TENSED UP TO THE POINT OF VOMITING. THE NEXT THING I REMEMBER, I WAS STILL IN THE CHAIR WITH ANOTHER BEING TALKING TO ME.

THIS CREATURE WAS A PALE GREYISH-WHITE. HE POSSESSED LARGE, ROUND, BLACK EYES AND A LONG NOSE. A SHORT CURTAIN OF MATERIAL DRAPED AROUND THE BACK OF HIS LARGE HEAD. HIS THIN MOUTH DID NOT MOVE AS HE SPOKE WORDS INSIDE MY HEAD. WITH A HARSH ATTITUDE, THIS GREY CLAIMED TO BE FROM THE RIGEL STAR SYSTEM. ALTHOUGH HE DID NOT WANT TO BE PART OF THIS MEETING, HIS OVERLORDS INSISTED THAT HE ATTEND IT. HIS JOB WAS TO MONITOR THE PROCEDURES SINCE I WAS ONCE A PART OF THEIR RACE, TOO.

HIS HOME WORLD WAS ONCE PART OF THE LYRAEN CIVILIZATION. AFTER THAT CULTURE DISINTEGRATED, THE REPTILIANS INVADED HIS PLANET. NOW HIS PEOPLE ARE PART OF THAT EMPIRE AND AS SUCH, DO THEIR BIDDING. FROM TIME TO TIME HE WOULD SEND HIS WORKERS, SMALLER GREY CREATURES, TO CHECK UP ON ME. MOST OF THE TIME I WOULD NOT REMEMBER IT EXCEPT AS A BAD DREAM.

MICHAEL ASH - THE SUPPOSED CHIEF TIME EMPATH FROM MONTAUK - HAD DESCRIBED TO ME HOW UNPLEASANT AND INTERVENTIONIST THE MANY RIGELIANS WERE - WHO HE ENCOUNTERED AT MONTAUK. ALSO NOTABLY IN THE BUEHLER/THOTH MATERIALS- THOTH (SON OF ENKI/ADONAI/RA/HERMES) INSISTS HIS BLOOD IS BLUE/BLACK BECAUSE HE WAS FROM RIGEL IN ORION. I SUSPECT THIS WAS THE ANCESTRAL FAMILY OF ENKI/RA'S MOTHER AIDA WHO WAS

WINGED DRAC.. "PTAH TAAL" .

(THOTH - NUBIAN - BLUE BLACK BLOOD - WAS THE REASON THE ORIGINAL NAME FOR EGYPT WAS KHEM - WHICH MEANS FROM THE BLACKNESS - THE TERM ALCHEMY THEREFORE MEANS- SCIENCE OF MAKING BLACK HOLES. IT WAS THOTH - HERMES FAMILY WHO IMPREGNATED AKSENPATEN - WHICH BECAME THE TUT/MAGDALEN STORY - AND BLACK MADONNA). IN ALEX COLLIER - ANDROMEDAN PAPERS (DEFENDING SACRED GROUND - ETC.)

READ ABOUT THE ORIGIN OF THE TERM PTAH IN EGYPT (RA /ENKI'S LINE) FROM THE TERM PTAH TAAL - MEANING 11TH DIMENSIONAL OR BIRD TRIBE - BUT MORE PROBABLY WINGED DRAC OR CIAKAR OR MOTHMAN - THE SOURCE OF THE PSYCHOKINESIS IN THE DNA - ENKI - RA - ABRAHAM - USED IN HIS OWN SPERM TO MAKE ADAM AND EVE FERTILE.

THERE WOULD COME A TIME WHEN THESE GREYS WOULD BE AT WAR WITH SOME OF THE WORLDS REPRESENTED AT THIS MEETING. MY JOB WOULD THEN BE TO MONITOR THE ACTIVITIES AND REPORT THE FINDINGS TO MY CONTROLLERS. MY BODY CONTAINS CHEMICALS NEEDED BY HIS RACE. THE GREY SAID THAT HIS RACE ALSO LOOKED HUMAN UNTIL WAR CONTAMINATED THEIR ENVIRONMENT, GENETICALLY DEGENERATING THEM. MY BODY WAS PRESENTED TO THEM AS A TEMPORARY TOKEN OF HOPE AND PEACE.

ALLOWED TO USE MY GENETICS FOR THE PURPOSE OF UPGRADING THEIR DYING SPECIES, THEY COULD NOT PURPOSEFULLY HARM ME, PERMANENTLY KIDNAP ME, OR ALLOW ME TO REMEMBER WHAT THEY DID TO GET WHAT THEY NEEDED FROM ME. THESE WERE THE RULES THAT ALL ABIDED BY TO KEEP THE STATUS QUO WHILE AT THE SAME TIME BENEFITING FROM MY CREATION.

IF MY MISSION FAILED, OR IF ANY OF THE PARTICIPANTS IN THIS PROJECT NO LONGER WISHED TO CONTINUE, THEN I WOULD BE REMOVED TO A SAFE PLACE WHILE THE OTHERS FOUGHT AMONGST THEMSELVES, POSSIBLY EVEN ON THE SURFACE OF THE PLANET EARTH. FINALLY, HE TOLD ME THAT HIS PEOPLE MERELY WISHED TO CORRECT THE ERRORS COMMITTED AGAINST THEM IN ORDER TO EVOLVE. THEY WISHED TO BECOME INDEPENDENT OF THE REPTILIANS AND RECREATE THEIR OLD CIVILIZATION BEFORE IT WAS TOO LATE. THEIR DILEMMA WAS THAT, IF THEY ATTEMPTED THIS, THEY WOULD BE DESTROYED COMPLETELY BY THEIR MASTERS. ON THE OTHER HAND, IF THEY CONTINUED WITH THEIR MASTERS ORDERS, THEY WOULD BE TARGETED BY THE FEDERATION PLANETS. BECAUSE THEY FELT HOPELESS, THEY LOOKED OUT ONLY FOR THEMSELVES.

AT THIS POINT, THE LAST BEING AT THE COUNCIL TALE, WHO SAT IN THE MIDDLE, INTERRUPTED THE RIGELIAN. THIS BEING WAS VERY TALL. STANDING UP, HE RAISED HIS ARMS TO EITHER SIDE. THE BEAUTIFUL WHITE ROBE HE WORE WAS TRIMMED IN A BLUE THAT I HAD NEVER SEEN BEFORE. HIS LARGE HEAD WAS ROUND ON TOP WITH A POINTED CHIN. STANDING WITH HIS ARMS OUTSTRETCHED, HE REMARKABLY RESEMBLED A LIVING ANKH. HIS OVAL EYES WERE BRILLIANT BLUE; HIS SKIN IVORY WHITE. BY FAR, HE WAS THE MOST IMPRESSIVE BEING AT THIS GATHERING.

WHEN HIS THOUGHTS FILLED MY HEAD, I COULD NOT EVEN THINK OF MY OWN NAME! AS HE SPOKE, I SAW WORDS IN A STRANGE LANGUAGE SWIRLING ETHEREALLY AROUND HIS HEAD.

SEQUENCES OF BRAIN CORTEX CHARGE DOMAINS IN COMPRESSION SYMMETRY - ORIGIN OF ANCIENT ALPHABETS - (COMPARE- HEBREW - THE SOFTWARE ENVIRONMENT FOR A CENTRAL BORG COMPUTER DOING GENETIC INTERVENTION - VERSUS OPHANIM - BIRD TRIBE- ORIGIN OF STARGATE THE MOVIE).. AND PHYSICS SYMMETRY ELEMENTS OF CREATION.

HE TOLD ME HIS NAME, BUT I CANNOT REMEMBER IT. COMING FROM THE PLANET KHOOM IN THE BINARY SIRIUS STAR SYSTEM, HIS PEOPLE WERE DESCENDENTS OF NON-PHYSICAL BEINGS WHO INHABITED HYPERSPACE, A REGION OF CONSCIOUSNESS EXISTING OUTSIDE OF LINEAR TIME AND SPACE. THEY CREATED THE ANCIENT EGYPTIAN CIVILIZATION AS WELL AS THE JEWISH PEOPLE AND GAVE THEM THE TORAH. THE CRYSTAL SKULL WAS THEIR CREATION, AND THEY WERE IN CHARGE OF MANY EVENTS IN THE GALAXY AND BEYOND. MY SOUL-PERSONALITY WAS FROM HIS PEOPLE BECAUSE IT WAS THE ONLY TYPE ADVANCED ENOUGH TO ANIMATE SUCH A HYBRID BODY AS MY OWN.

POSSESSING THE MOST ADVANCED TECHNOLOGY IN THE UNIVERSE, ALL THE OTHER SPECIES CAME TO THESE SIRIANS FOR INFORMATION. NOW, AS AN ADULT, I REALIZE THAT THIS GROUP ALSO PLAYS ONE CIVILIZATION AGAINST THE OTHER TO BENEFIT EVOLUTION AS WELL AS THEIR OWN SPECIES.

WE KNOW ENKI/ENLIL (ADONAI/LUCIFER - VERSUS YAHWEH/MICHAEL) FATHER WAS MOST LIKELY FROM SIRIUS. IN A HOLDOUT POSITION TRYING TO SAVE THE LAST HUMANOID REMNANT AGAINST THE ONSLAUGHT OF THE BORG MACHINE EMPIRE (EMPIRE STRIKES BACK BECOME REAL). WE SUSPECT HE (ANTU / OR BIKI AS THE ABOS CALL HIM- LITERALLY SUN GOD / AN) WAS HALF MACHINE - BUT NOT HAPPY ABOUT THAT (CORRECT HISTORY DESCRIBING MUAB DIB'S FATHER LINE - HARKONEN - HALF MACHINE IN DUNE - AND LUKE SKYWALKER'S FATHER DARTH VADER - HALF MACHINE IN STAR TREK - A PHYLLIS SCHLEMMER ORIGINATED STORY).

WHAT IS CONFUSING IS THE ANDROMEDAN MATERIAL - HAS INSISTED SIRIUS A WAS NON-INTERVENTIONIST IN IT'S POLITICAL RELATION WITH EARTH - WHILE SIRIUS B WAS MORE INTERVENTIONIST (INTERFERE WITH INDIGENOUS GENEPOOLS WITHOUT REGARD TO THE PRIME DIRECTIVE).

THIS NOTE HINTS THAT ALL THE GOOD DNA CALLED HEBREW - ACTUALLY DESCENDED FROM ENKI IN EGYPT (THE BOOKS: OUT OF EGYPT, & HOUSE OF THE MESSIAH & COPPER SCROLLS - PRESENT OVERWHELMING EVIDENCE - THE RABBI'S LIED ABOUT ISRAEL BEING MOSES ORIGIN - MOSES WAS THE NAME AKHANATON TOOK - WHEN ENLIL/AMUN - TOOK OVER EGYPT & WHILE HE SWIPED THE FAMILY GOLD TO FOUND THE ESSENES).

THE THING MISSING HERE IS THE SOURCE OF THE GOOD SIRIAN DNA - WHICH IS ACTUALLY WINGED DRACONIAN... ENKI'S MOM. THE CRYSTAL SKULL WAS A DECADENT CONTROL DEVICE USED LATER BY A FALLEN MAG MATRILINY WHO LOST THE SKILL TO PASS RACIAL MEMORY IN A REAL SKULL TOUCH. - SEE ORIGINS OF BAPHOMET.

8 - THE SIRIANS
P. 77- 84

THE APARTMENT IN HOLON BECAME MY HOME BASE. FROM THERE, I LEFT ON MANY TRIPS AROUND THE REGION, SOMETIMES FOR DAYS AT A TIME.

ONE PARTICULAR ADVENTURE TOOK PLACE WHILE ON AN EXCURSION TO THE NEGEV DESERT IN THE SOUTH OF ISRAEL. I HAD JUST PASSED THE RESTRICTED AREA AROUND DIMONA, A TOWN WHERE ISRAEL HAS ITS SECRET NUCLEAR FACILITY. THIS PLACE IS GUARDED BY THE FALASHA, THE BLACK JEWS FROM ETHIOPIA WHO CLAIM TO BE DESCENDENTS OF KING SOLOMON AND THE QUEEN OF SHEBA. THE QUEEN SUPPOSEDLY RETURNED TO ETHIOPIA WITH THE ORIGINAL ARK OF THE COVENANT WHERE IT REMAINED FOR SAFEKEEPING UNTIL ONLY A FEW YEARS AGO.

THE SO CALLED BLACK JEWS ARE THE REAL NUBIAN COPPER BLUE BLOODS KIDS OF ENKI/RA... SEED OF SEPHARTICS... NOT THE USURPING (ENLIL'S) ASHKANASI - INNANA DRAC DESCENDANTS - FOUNDERS OF CHINA AND BANK OF ENGLAND... IT IS NOT OVER TRIVIALIZING TO CHARACTERIZE THE CONTINUING DIALECTIC BY THE ENKI VS ENLIL HALF-BLOOD BROTHERS-LINES.

KING SOLOMON WAS A POWERFUL MYSTIC (AKHANATON - WHOSE AMARNA-SOLAR CAPACITOR FOR IGNITING DNA BECAME THE SOLOMON TEMPLE MYTH). HIS ADVISORS ALWAYS DISCUSSED THE FUTURE WITH HIM. IT IS BELIEVED THAT HE WAS WARNED OF A FUTURE TIME WHEN ISRAEL WOULD BE OVERRUN WITH EVIL FOREIGNERS. (ASHKANAZI - WHO NOW FLY THE ALPHA DRACONIS FLAG - THE HEX DOUBLE TRIANGLE - OVER ISRAEL - ALSO HAPPENS TO BE THE SHAPE OF THE INTERVENTIONIST DRACO CRAFT COMING TO INVADE). THE HOLY ARK OF THE COVENANT WOULD MOST LIKELY BE A PRIME TARGET.

I BELIEVE THAT SOLOMON, IN ALL HIS WISDOM, DECIDED TO HIDE THE REAL ARK OF THE COVENANT IN A PLACE WHERE NO ONE WOULD THINK TO LOOK. CONVENIENTLY, THE QUEEN OF SHEBA WAS LOOKING FOR A MAJOR TOKEN OF FAITH AND AFFECTION FROM HER CURRENT LOVER. SOLOMON SENT THE ARK BACK WITH HER TO ETHIOPIA AND MADE A FACSIMILE FOR THE PUBLIC TO VIEW.

THE ARK OF THE COVENANT IS A FRACTAL SELF SIMILAR CAPACITOR ('ORGONE') WITH ENOUGH IMPLOSIVE COMPRESSION TO PARTIALLY SAFELY CONTAIN RADIOACTIVE POWER. (RADIOACTIVITY IS THE OPPOSITE OF FRACTAL CHARGE COMPRESSION - WHICH IS WHY URI GELLER COULD MEAN...

IN ORDER TO SOLIDIFY HIS TRUST FOR SHEBA AND THE ARK, SOLOMON SAW TO IT SHE HAD HIS CHILD SO THAT SHE WOULD ALWAYS FEEL AN OBLIGATION TO HER CHILD'S PEOPLE. HIS WAS THE PERFECT PLAN.

THE QUEENS DESCENDENTS BECAME THE FALASHA, A NUMEROUS FACTION IN ETHIOPIA. AT ONE TIME, IT IS BELIEVED THAT THERE WERE OVER 500,000 FALASHA IN ETHIOPIA. IN FACT, HEILE SALASSIE, THE RULER OF ETHIOPIA UNTIL A MILITARY COUP TOPPLED HIS REGIME, CALLED HIMSELF THE LION OF JUDAH.

THE ISRAELI MOSSAD, OR INTELLIGENCE AGENCY, HELPED THE PROVINCE OF ERITREA BREAK AWAY FROM ETHIOPIA BECAUSE THE ARK WAS HIDDEN THERE AND THE MILITARY GOVERNMENT

REFUSED TO COOPERATE WITH THE ISRAELIS. CONSEQUENTLY, THE ISRAELIS CREATED THEIR OWN COUNTRY WITH WHOM TO NEGOTIATE. THE ARK WAS SUCCESSFULLY TRANSFERRED TO THE HOLY LAND AT THE SAME TIME THE MILITARY GOVERNMENT OF ETHIOPIA ALLOWED THE ISRAELIS TO AIRLIFT ALL OF THE REMAINING FALASHA OUT OF ETHIOPIA. A STRANGE TURN OF EVENTS, BUT ONE THAT PORTENDS THE COMING OF THE MESSIAH FOR THE JEWS.

IT WAS NEAR DIMONA THAT I WAS ABDUCTED BY THE SIRIANS FOR A MAJOR ADVENTURE. AS I WALKED AROUND SOME ROCK FORMATIONS THAT JUTTED UP OUT OF THE DESERT, THE SUN WAS HOT AND THE AIR EXTREMELY DRY. PERSPIRATION EVAPORATED IN A MANNER OF SECONDS AFTER APPEARING ON MY SKIN. SUDDENLY, A TREMENDOUS FLASH OF LIGHT BLINDED ME. RAISING MY HANDS TO SHIELD MY EYES, I REALIZED THAT THERE WERE NO SOUNDS AROUND ME; IN FACT, THERE WAS AN EERIE SILENCE ALL ABOUT.

OPENING MY EYES, I FOUND MYSELF IN A GREAT ROOM THAT RESEMBLED AN ANCIENT GREEK OR ROMAN THRONE ROOM WITH HUGE COLUMNS AND A SCREEN ON THE WALL. LIGHTING WAS SUBDUED AND WITHOUT A VISIBLE SOURCE. THERE WERE NO WINDOWS OR DOORS. FROM A SPACE NEAR THE SCREEN, A TALL SIRIAN DRESSED IN A WHITE AND BLUE ROBE APPEARED. HE WAS NEARLY IDENTICAL TO THE SIRIAN I HAD SEEN AS A CHILD. ABOUT SEVEN-FEET TALL, HIS SKIN WAS PALE. HE HAD LARGE POINTED EARS, A LONG POINTED NOSE, AND BIG, BLUE ALMOND-SHAPED EYES.

HIS MOUTH AND LIPS WERE VERY SMALL. HIS FINGERS APPEARED LONG AND GRACEFUL AS HE STOOD IN FRONT OF ME WITH OUTSTRETCHED ARMS. THE WAY HIS ROBE TOUCHED THE FLOOR, COMBINED WITH THE SHAPE OF HIS ELONGATED HEAD, HE LOOKED EXACTLY LIKE A LIVING ANKH! WHAT A BEAUTIFUL SIGHT! I FELT NO FEAR BECAUSE I HAD SEEN ONE BEFORE AND FELT AT HOME WITH IT. THE SCREEN CAME ON BEHIND HIM AND ALLOWED ME TO SEE THE OUTLINE OF EARTH AS WE MOVED SWIFTLY AWAY FROM IT IN SOME SORT OF A CRAFT HEADING TOWARD MARS. IN THAT ROOM, THERE WAS NO SENSATION OF MOVEMENT. IT FELT SOFT AND COMFORTABLE EVEN MORE COMFORTABLE THAN HOME.

THE BEING MOVED FORWARD AND SMILED, TELEPATHICALLY WELCOMING ME. THROUGH HIS THOUGHTS, HE TOLD ME THAT WE WERE ON OUR WAY TO MARS TO SEE SOMETHING THAT WOULD HELP ME AT A LATER TIME. CONTINUING, HE SAID THAT HIS SPECIES CREATED PEOPLE FROM STOCK BROUGHT TO EARTH FROM ELSEWHERE. THESE CREATIONS ARE KNOWN AS HEBREWS, AS IS THEIR LANGUAGE.

MUCH OF THIS HAD BEEN DISTORTED AND INTERFERED WITH OVER THE MILLENNIUMS. HIS SPECIES WAS NOW IN LEAGUE WITH THE REMNANTS OF THESE ORIGINAL CREATIONS, THE ISRAELIS, TO CORRECT AND PURIFY THEM BEFORE THE NEXT WAVE OF INTERRUPTIONS OCCUR. APPARENTLY, THE SIRIANS FELT THAT THESE HEBREW REMNANTS WERE NOT THE GENETICALLY-WHOLE BEINGS THAT THEY ORIGINALLY CREATED. BECAUSE IT WAS TOO LATE TO CHANGE THEIR PHYSICAL STRUCTURE, IT HAD BECOME NECESSARY TO CHANGE THEIR MIND-PATTERNS, THUS ENABLING THEM TO INTERFACE WITH OTHER ALIEN BEINGS. AS HE COMMUNICATED, PICTURES OF HIS WORDS APPEARED ON THE SCREEN BEHIND HIM. I ACTUALLY SAW HISTORY FROM THE DIM PAST AS THOUGH IT WAS HAPPENING AT THAT MOMENT.

NEXT, I REMEMBER LYING ON A TABLE IN A BRIGHTLY LIT CLINICAL-LOOKING ROOM. THE SIRIAN WAS THERE WITH A TALL GREY BEING WHO HAD ROUND, BLACK EYES AND A GOOFY LOOK ON ITS FACE. IDENTIFIED TO ME AS A VEGAN, IT WAS A CREATION BY THE SIRIANS OUT OF THEIR OWN GENETICS MIXED WITH THE LITTLE GREYS. ALTHOUGH NOT STRAPPED DOWN, I COULD NOT MOVE, AND I REALIZED THAT I WAS NAKED. FOR THE FIRST TIME, I FELT FEAR WITH THE SIRIANS. A BRIGHT DEVICE WAS PLACED OVER MY FACE AS THEY PROBED MY GENITALS, STOMACH, AND CHEST.

THE SIRIAN SAID THAT THEY NEEDED TO TEST FOR RESIDUALS OF GENETIC RESONANCE IDENTIFYING MY BODY WITH THEIRS. HE SAID THEY HAD MANUFACTURED MY BODY IN COLLUSION WITH CERTAIN EARTH FORCES FOR THE PURPOSE OF COMPLETING THEIR AGENDA. I WAS SOME KIND OF PAWN IN AN INTERSTELLAR GAME. WHAT WAS GOING ON HERE?

TO COMPLICATE MATTERS FURTHER, HE SAID THAT MY SOUL-PERSONALITY WAS SOME TYPE OF ENTITY FROM A NON-PHYSICAL ASPECT OF SIRIUS WHICH WAS AN EVEN HIGHER FORM THAN HIMSELF. MY BODY CONTAINED SIRIAN DNA WHICH WAS NECESSARY FOR THE SOUL-PERSONALITY TO OPERATE IT. AS HE SPOKE, I BEGAN TO GLIMPSE IN MY MIND MY TRUE IDENTITY WHICH WAS SIMULTANEOUSLY MAGNIFICENTLY BEAUTIFUL AND FRIGHTENING. TEARS FLOWED UNCONTROLLABLY DOWN MY FACE. THIS SEEMED TO AMUSE THE SIRIAN AND THE VEGAN. I THOUGHT TO MYSELF, IF I LOOKED LIKE EITHER ONE OF YOU, I WOULD NOT LAUGH!

NEXT, I WAS STOOD UP INSTANTANEOUSLY. WEARING ONLY A SIRIAN ROBE, I COULD NOT SEE MY FEET. I FELT ELATION, LIKE I WAS ON A NATURAL HIGH. I CANNOT COMPARE THE FEELING TO ANYTHING ANOTHER CAN UNDERSTAND WITHOUT HAVING HAD THE EXPERIENCE THEMSELVES. I FELT A COMPLETE KNOWING OF ALL THINGS; A CONNECTION TO ALL BEINGS. YET, I RETAINED MY IDENTITY OF SELF. I FOLLOWED THE SIRIAN OUT THROUGH THE WALL TO WHAT APPEARED TO BE A MAROON-COLORED CAVE WITH A HIGH CEILING THAT SEEMED TO GO ON FOR MILES.

GLANCING BACK, I SAW THE CRAFT THAT I HAD JUST BEEN IN IT RESEMBLED A GIGANTIC PEARL. COMPLETELY WHITE, WITH A SOFT WHITISH-VIOLET GLOW, THERE WAS NO SOUND COMING FROM IT. INSTANTLY, I KNEW THAT IT TRAVELED THROUGH SPACE LIKE AN ELECTRON AS IT BECOMES A PARTICLES WAVE SOMEWHERE BETWEEN THE PHYSICAL AND SPIRITUAL PLANES.

IN FRONT OF ME, I SAW A LARGE GROUP OF MEN. MOST OF THEM WERE IN THEIR TWENTIES, A FEW WERE TEENAGERS, AND SOME WERE OLDER. DIGGING IN UNISON WITH SHOVELS, THEY MOVED LIKE AUTOMATONS. LARGE, MELON-HEADED BEINGS WATCHED THEM WORK. APPARENTLY, THESE WERE THEIR OVERSEERS. A FEW FOUR-FOOT TALL GREYS MOVED ABOUT. I SAW TUNNELS AND CRAFTS THAT LOOKED LIKE DISCS. SUDDENLY, ALL THE MEN STOPPED AND LOOKED UP TOWARD A PLATFORM. LOUDLY, A VOICE CALLED OUT, THE EMISSARY FROM RIGEL WILL SPEAK NOW.

AT THAT MOMENT, A FIVE-FOOT BEING WITH ROUND, BLACK EYES APPEARED ON THE PLATFORM. HIS LARGE HEAD WAS DRAPED WITH A KIND OF SHORT CURTAIN AROUND THE BACK OF IT. DRESSED ALL IN BLACK, HIS CLOTHING APPEARED TO BE A UNIFORM. LOOKING OMINOUS, HE CARRIED A ROD THAT LOOKED BOTH METALLIC AND CRYSTALLINE AT THE SAME TIME.

EVERYONE SEEMED TO UNDERSTAND HIS MENTAL COMMUNICATION. EXPLAINING THAT THIS GROUP OF MEN HAD COMPLETED THEIR SERVICE ON EARTH AND THE MARTIAN OUTPOST, HE TOLD THEM THAT THEY WOULD NOW BE EXAMINED FOR POSSIBLE TRANSPORT TO RIGEL FOR EXPERIMENTATION. THOSE NOT USED WOULD BE ELIMINATED. THE MEN WERE THEN LED INTO THE OPEN PORT OF A SILVER DISC. I NOTICED THAT THEIR LEGS WERE CHAINED TOGETHER. THE ENTIRE SCENE APPEARED TO BE ORCHESTRATED JUST FOR ME. I DO NOT KNOW IF IT WAS. IF SO, WHAT WOULD BE THE PURPOSE? PERHAPS THE ENTIRE INCIDENT IS AN IMPLANTED MEMORY.

THE NEXT THING I REMEMBER, I WAS BACK ON THE SIRIAN SHIP. TRAVELING IN HYPERSPACE, I SAT IN A DARKENED ROOM ON THE FLOOR WITH THE VEGAN AND THE SIRIAN. SOFT LIGHTING ALLOWED ME TO SEE INSIDE AND OUTSIDE THE SHIP SIMULTANEOUSLY. HYPERSPACE WAS A BEAUTIFUL SHADE OF DARK BLUE AND VIOLET. THE SHIP APPEARED TO BE DIAMOND-SHAPED AS IT TRAVELED. THE SIRIAN SAID THAT WE WERE GOING BACK TO OUR HOME WORLD, KHOOM, WHICH ORBITED SIRIUS A IN THAT BINARY STAR SYSTEM. LATER, I COULD DECIDE IF I WANTED TO RETURN TO EARTH. I REALIZED WE THREE WERE THE ONLY BEINGS ABOARD THAT GREAT SHIP. OVERRATED

TOTALLY BY OUR WILL, I FELT COMPLETELY SAFE AND AT PEACE. I KNEW THAT I WAS GOING HOME.

I DO NOT REMEMBER MUCH OF MY STAY ON KHOOM. I WAS TOLD THAT MY MEMORY WOULD RETURN AT THE APPROPRIATE TIME. A FROZEN WORLD COVERED IN ICE AND SNOW, THE SUNS GLARE ON THE SURFACE WAS BLINDING. THE INHABITANTS LIVED UNDERGROUND. AN ELABORATE AND IMPENETRABLE DEFENSE SYSTEM PROTECTED THE ENTIRE PLANET.

ONCE A SUBTROPICAL WORLD, KHOOM WAS PUSHED OUT OF ITS ORIGINAL ORBIT BY WAR EONS AGO. FROM SPACE, IT LOOKS BLUE AND WHITE. THE PLANET HAS NO MOONS. A VICTIM OF THE ORIGINAL BATTLE BETWEEN GOOD AND EVIL, KHOOM WAS BLOWN FROM ITS CRADLE ORBIT BY THOSE WHO CREATED THE DRACO RACE, THE REPTILIANS WHO SEEK TO DOMINATE THE GALAXY AND BEYOND. THE CREATORS OF THE DRACO RACES CAME FROM ANOTHER TIME AND SPACE. THE FIRST GENESIS OF LUCIFER, THEIR NAME DENOTES THE EPITOME OF EVIL.

OCCUPYING THE SAME PHYSICAL LOCATION AS KHOOM, BUT AT A DIFFERENT VIBRATORY RESONANCE, IS A NON-PHYSICAL WORLD GOVERNED BY A COUNCIL OF NINE BEINGS KNOWN AS THE OHALU COUNCIL. WHILE NOT THE SAME BEINGS REFERRED TO AS THE NINEIN OTHER LITERATURE, THEY DO COMMUNICATE WITH THE NINE AS WELL AS PARTICIPATE IN JOINT PROJECTS. THE NINE FIRST APPEARED IN LITERATURE IN THE WORKS OF DR. ANDRIJA PUHARICH. IN HIS WORK WITH CHANNELERS, HE CAME ACROSS A FEW INDIVIDUALS WHO CLAIMED TO BE IN CONTACT WITH THIS ET GROUP.

URI GELLER WAS THE FIRST TO ACTUALLY IDENTIFY THEM AS FORMER PHYSICAL BEINGS WHO TRANSFERRED THEIR MINDS AND SOUL-ESSENCES INTO NINE ADVANCED COMPUTERS. EACH ONE OF THESE COMPUTER REPRESENTS A DIFFERENT ASPECT OF THE MIND OF GOD. THE NINE COMMUNICATE WITH A FEW SELECT INDIVIDUALS ACROSS THE PLANET IN AN EFFORT TO UPGRADE THE COLLECTIVE CONSCIOUSNESS OF HUMANKIND.

THE OHALU COUNCIL ALSO GOVERNS THE PLANET KHOOM IN THE STAR SYSTEM SIRIUS SINCE THE SIRIANS ARE REALLY THE LOWER VIBRATIONS OF THE COUNCIL BEINGS IN THE SAME WAY THAT HUMANS ARE LOWER VIBRATIONS OF THEIR ET SELVES.

I WAS ORIGINALLY SENT TO EARTH BY THE OHALU COUNCIL WHO DIRECTED THE SIRIANS ON THE CREATION OF MY PHYSICAL BODY. THEY TOLD ME THERE ARE NINE BEINGS ON EARTH WHO ARE LIKE ME. EACH ONE IS DIRECTED BY A MEMBER OF THE COUNCIL. I WAS SHOWN MY PAST AND FUTURE WHILE I WAS ON KHOOM. I WAS TAKEN TO A PLANET ORBITING SIRIUS B THAT WAS A TROPICAL, SWAMPY JUNGLE WORLD OCCUPIED BY SHORT, STOCKY BEINGS WHO LIVE IN HUTS.

EXTREMELY ADVANCED, THESE CREATURES CAN ASTRAL PROJECT ANYWHERE THEY WANT TO AT WILL. THEY RELY ON OTHERS FOR PHYSICAL TRANSPORTATION OFF-WORLD BUT AS THEY HAVE NO NEED TO GO ANYWHERE ELSE, THEY RARELY DO SO. COMMUNICATING EXCLUSIVELY BY MIND-LINKING, THEY DO NOT HAVE A SPOKEN LANGUAGE.

THE SIRIANS TOLD ME OF THE COMING EARTH INVASION BY THE DRACO; THAT THE ORION CONFEDERATION WAS WORKING WITH THE DRACO; AND THAT THERE IS A WAR GOING ON RIGHT NOW BETWEEN THE SIRIANS AND ORIONS. THE SUPREME MERCHANTS OF THE UNIVERSE, THE SIRIANS ACTUALLY SUPPLIED THE ORION GROUPS WITH THE WEAPONS THAT ARE NOW BEING USED AGAINST THEM. HOWEVER, THE SIRIANS KEEP THE BEST AND MOST POWERFUL FOR THEMSELVES, SO THEY NEVER LOSE.

THE SIRIANS SEE THE ORIONS AS BAD CHILDREN WHO PLAY WITH MATCHES. THEY DO NOT SEEK TO DESTROY THEM, BUT THEY KEEP THEM IN CHECK. THEY ALLOW HUMANS, ORIONS, AND THE DRACO TO FOLLOW THEIR OWN DESTINIES.

DESPITE NOT WANTING TO LEAVE, THE OHALU COUNCIL CONVINCED ME TO RETURN TO EARTH. ARRIVING BACK IN ISRAEL I FOUND THAT ONLY THREE DAYS HAD PASSED. I WAS UNCEASINGLY THIRSTY, HAD LOST TEN POUNDS, AND WAS SO TIRED THAT I COULD NOT SEE STRAIGHT. RETURNING TO HOLON, I SLEPT FOR ALMOST AN ENTIRE WEEK.

DURING MY RETURN REST, I REALIZED THAT THE ARK OF THE COVENANT IS ACTUALLY A COMMUNICATION DEVICE BETWEEN THE PHYSICAL WORLD AND HYPERSPACE. THE SIRIANS APPARENTLY GAVE THE HEBREWS INSTRUCTIONS FOR BUILDING IT. A RECONSTRUCTION OF THE DEVICE WAS BUILT BY THE UNIVERSITY OF MINNESOTA YEARS AGO, FOLLOWING THE INSTRUCTIONS GIVEN IN THE BIBLE. IT WAS SO ELECTRICALLY CHARGED AND DANGEROUS THAT IT HAD TO BE DESTROYED.

I BELIEVE THAT THE SIRIANS ARE TRYING TO UNDERMINE THE PLANS OF ALL THE FACTIONS INVOLVED ON EARTH:

* THE NEW WORLD ORDER
* THE DRACO
* THE GREYS
* THE TALL BLONDS, ETC.

THEIR AGENDA IS TO BRING ALL EVENTS TO A CLIMAX, THEN USURP ALL POWER, POSSIBLY VIA THE ISRAELIS. THIS IS ONLY SPECULATION ON MY PART.

TIME WILL TELL.

P. 130 - 132

THAT NIGHT, THE SESSION WAS MOST INTERESTING. AFTER I WAS ENTRANCED, A SMALL WHITE BEING, WHO LOOKED LIKE A TYPICAL GREY, ENTERED MY BODY. SPEAKING AT FIRST IN A STRANGE LANGUAGE THAT ONLY DUNCAN UNDERSTOOD, IT THEN SPOKE IN ENGLISH AS THE TONE BECAME MORE OMINOUS. THIS BEING SAID THAT IT HAD EVERY RIGHT TO TAKE POSSESSION OF MY BODY BECAUSE I WAS ONE OF THEM!

CHALLENGING THIS REMARK, PRESTON SAID THAT I WAS A HUMAN BEING WITH A SOUL FROM GOD, AND NO ONE WAS ALLOWED TO USE THE BODY EXCEPT STEWART. THE ENTITY CURSED PRESTON AND CALLED HIM PRESSED ON. IT SAID I WORKED FOR THEM AND WAS CARRYING OUT A MISSION VITAL TO THE SUCCESS OF THEIR PROGRAM ON EARTH.

BOTH PRESTON AND DUNCAN SAW THE PHYSICAL SHAPE OF MY BODY CHANGE AS IF IT WERE A GREY ALIEN BODY. THE OUTLINE OF MY FACE SIMILARLY CHANGED. THEN, THE BEING STARTED TO MOVE MY BODY. GETTING UP, IT WALKED AROUND WHILE MAKING NASTY COMMENTS ABOUT THOSE PRESENT. ALTHOUGH MY EYES WERE CLOSED, MY BODY WALKED AROUND THE ROOM AS IF IT WERE WIDE AWAKE.

WHEN PRESTON STARTED TO ASK QUESTIONS ABOUT THEIR AGENDA, THE BEING HESITATED. NEXT, AN EXTREMELY POWERFUL ENTITY LITERALLY PULLED THE GREY FROM MY BODY AS IT TOOK OVER. IDENTIFYING ITSELF AS A DRACO COMMANDER, IT GAVE ITS NAME AS GENGEEKO. PRESTON IMMEDIATELY UNDERSTOOD THE DRACO TO BE POWERFUL, REPTILIAN WARRIORS. THE CREATURE TOLD PRESTON THAT AN INVASION FORCE WAS ON ITS WAY TO EARTH AND THAT NOTHING COULD STOP IT.

THE MOON ORBITING THE EARTH WAS THEIR FIRST CRAFT. IT HAD ARRIVED HERE AEONS AGO TO CONTROL THE PLANET. AFTER CREATING THE LEMURIAN CIVILIZATION, THEY HAD BEEN REMOVED FROM THE EARTH BY THE ATLANS AND THE DESCENDENTS OF THE DISBANDED LYRAEN EMPIRE WITH THE HELP OF THE PLEIADIANS. NOW, THE DRACO WERE RETURNING TO RECLAIM THE EARTH AND USE IT AS A MILITARY BASE FOR ENTRY INTO THE REST OF THE GALAXY. AT THIS POINT, I REALIZED THAT THIS WAS WHY SO MANY RACES WERE INTERESTED IN THE EARTH. IF THIS PLANET FALLS, THEN THE REST OF THE GALAXY IS IN DANGER.

THE DRACONIAN THEN STOOD UP AND RASPED A WARNING AT PRESTON NOT TO USE HIS EQUIPMENT OR PLEIADIAN CONTACTS TO TRY TO STOP THEM. NEXT, HE PHYSICALLY ATTACKED PRESTON!

BOTH DUNCAN AND PRESTON HAD TO RESTRAIN THIS BEING IN MY BODY UNTIL IT FINALLY SAT DOWN AND RESUMED ITS SPEECH. CLAIMING THAT HUMANS WERE WEAK, IT SAID THAT HUMANS NEEDED THE ORDER THAT AN INVASION WOULD BRING. THIS WAY, THE INVASION WOULD BENEFIT EVERYONE. THE DRACO WOULD RECEIVE THE RAW MATERIALS, WORKERS, AND FOOD THAT THEY NEEDED FOR THEIR INVASION INTO THE REST OF THE GALAXY. THE EARTH WOULD BE PROTECTED FOREVER BY THE DRACO EMPIRE.

OUR LEADERS WERE WELL AWARE OF THE IMPENDING INVASION, GRADUALLY PREPARING THE WORLD POPULATION VIA TELEVISION SHOWS AND MOVIES. EVEN RULERS IN SOME COUNTRIES WERE HUMANS WITH DRACO SOUL-PERSONALITIES.

THE REPTILIAN WITHIN MY BODY EXPANDED UPON HIS IDEAS BY SAYING THAT THE UNITED NATIONS WOULD BE THE FORUM FOR A CENTRAL PLANETARY GOVERNMENT. UNITED STATES LEADERS WERE IN LEAGUE WITH DRACO ALLIES WITHOUT REALIZING IT. SOME OF THE LEADERS OF THIS PLANET HAD PREPARED ESCAPE PLANS TO MARS WHERE EQUIPMENT WAS ALREADY BEING ACTIVATED, AS WELL AS TO OTHER PLANETS AND MOONS IN THIS SOLAR SYSTEM. MARS HAS A HUGE UNDERGROUND FACILITY BUILT BY THE SIRIANS OVER 500,000 YEARS AGO.

GENGEEKO SAID THAT MY BODY COULD BE USED SINCE I WAS ONCE AN AMBASSADOR TO THEIR HOME WORLD FROM THE OHALU COUNCIL, THE RULER OF THE SIRIAN STAR SYSTEM. I WAS NEUTRAL AND NOT REALLY CONCERNED ABOUT WHO WAS IN POWER. THIS IS BASICALLY TRUE FOR ME; I AM NOT A POLITICAL PERSON. MY MAIN INTEREST LIES IN HELPING INDIVIDUALS TO ADVANCE THEIR SOULS AND MINDS.

CONTINUING, GENGEEKO STATED THAT I WAS CREATED WITH ALIEN GENETICS AND THAT MY SOUL-PERSONALITY WAS NOT HUMAN NOR FROM THIS STAR SYSTEM. THIS EXPLAINS WHY I HAVE SO MANY MENTAL ABILITIES THAT ARE CONSIDERED UNCONVENTIONAL ON EARTH.

WHEN I CAME OUT OF THIS TRANCE SEVERAL HOURS LATER, MY BODY WAS DEHYDRATED AND EXTREMELY COLD. DISORIENTED AND CONFUSED, I DID NOT RETURN TO NORMAL FOR ALMOST TWO DAYS. IN ADDITION, I SUFFERED RECTAL BLEEDING, SHORTNESS OF BREATH, AND SEVERE SHIVERING.

OVERALL, IT WAS NOT A PLEASANT EXPERIENCE.

GO BACK

GO BACK TO THE MONTAUK PROJECT

17 - BREAKTHROUGH
P. 137 - 139

THE NEXT TIME PRESTON USED WILHELM REICH PROCEDURES, HE BROUGHT HIS TAPE RECORDER.

AN ENTITY CALLING ITSELF TUBOR ENTERED MY BODY WITH SUCH FORCE THAT I SHUDDERED HARD AND NEARLY FELL TO THE FLOOR. CLAIMING TO BE THE DRACO CONTROLLER OF A MISSION TO PREPARE EARTH FOR OCCUPATION, TUBORS MAIN CONCERN WAS OTHER ALIEN AND HUMAN INFLUENCES ON THE POPULATION THAT MIGHT THWART THEIR PLANS. THESE REPTILIAN BEINGS WERE EXTREMELY NASTY AND HOSTILE TOWARD ANYONE WHO QUESTIONED THEM. TUBOR COMMENTED THAT IT WAS DISGUSTED WITH MY BODY AND DETESTED THE WAY A HUMAN FELT. HUMANS WERE CONSIDERED TO BE WEAK, FRAGILE, AND TOO PRONE TO EMOTIONAL REACTIONS.

INSISTING THAT I HAD A CONTRACT WITH THEM WHICH PERMITTED THEM TO USE MY BODY BEFORE THEIR OFFICIAL ARRIVAL, TUBOR SAID THAT I WAS ALSO DESTINED TO BE A LIAISON DURING THE INVASION. USING A HUMAN IN THIS WAY WOULD ALLOW BOTH SIDES TO UNDERSTAND THE MIND-SET OF THE OTHER. I HAD SUPPOSEDLY AGREED TO THIS BECAUSE I WAS ONCE THE SIRIAN AMBASSADOR TO THEIR HOME WORLD AS WELL AS TO ARCTURUS AND A PLANET CALLED UMO.

AS THE SIRIAN AMBASSADOR, I HAD SUCCESSFULLY NEGOTIATED A TECHNOLOGY CONTRACT BETWEEN THE DRACO AND THE SIRIANS, SIRIUS A AGREED TO PROVIDE THE DRACO WITH HIGH TECHNOLOGY IN EXCHANGE FOR FREE TRADE AND PASSAGE OF THEIR VESSELS ANYWHERE WITHIN THE DRACO EMPIRE. THIS CONTRACT UPSET THE ORION CONFEDERATION BECAUSE, BEING CONTROLLED BY THE DRACO, THEY WOULD NEVER BE FREE. THE SIGNING OF THIS CONTRACT

EVENTUALLY PROVOKED A WAR BETWEEN THE ORION CONFEDERATION AND SIRIUS A WHICH CONTINUES TO THIS DAY.

TUBOR ALSO TOLD US THAT THE MONTAUK PROJECT EMPLOYED SIRIAN TECHNOLOGY. THE DRACO OBSERVED ALL EXPERIMENTS BUT WERE ESPECIALLY INTERESTED IN THE ONES THAT INVOLVED GENETIC MANIPULATION. BECAUSE THEY ARE AN ANDROGYNOUS RACE, THE DRACO ARE EXCEPTIONALLY INTERESTED IN SPECIES THAT PROCREATE SEXUALLY. USING SEXUALITY AS A MEANS OF PROGRAMMING PEOPLE AND GAINING MIND CONTROL OVER THE MASSES WAS PARTICULARLY FASCINATING TO THEM.

WHENEVER PRESTON ASKED QUESTIONS OR STATED AN OPINION, TUBOR BECAME ANGRY. HE CALLED PRESTON PRESSED ON AND REFERRED TO DUNCAN AS DUNK CAN. AT TIMES, TUBOR HISSED AND SWUNG HIS ARMS TOWARD THEM. TUBOR EVEN TRIED TO HURT MY BODY BY HITTING OR TWISTING PARTS OF IT. ABOUT AN HOUR LATER, ANOTHER ENTITY PUSHED INTO ME AND THREW TUBOR SPINNING AWAY. AFTER FALLING LIMP TO THE FLOOR, MY BODY THEN STOOD UP AGAIN.

CLAIMING TO BE A SIRIAN, THIS BEING GAVE ITS NAME AS MISHKA. HE SAID THAT HE FORCED HIS WAY INTO THE BODY TO SHOW ME HOW TO DEFLECT HOSTILE USE OF MY BODY. SINCE I HAD SIRIAN DNA, I COULD EASILY LEARN HOW TO DEFEND MYSELF USING MY ABILITIES. MISHKA SAID THAT HE LIVED ON A LARGE SIRIAN SPACE STATION CALLED CALUMBA WHICH ORBITED BETWEEN EARTH AND MARS.

THIS STATION WAS DESIGNED TO MONITOR INTERFERENCE ON EARTH AND SURROUNDING PLANETS. THE SIRIANS WERE INDEPENDENT AND CONSIDERED TO BE THE MERCHANTS OF THE UNIVERSE. WITH THE HIGHEST TECHNOLOGY AVAILABLE IN THEIR POSSESSION, MANY RACES CAME TO THEM FOR HELP. EVEN ALL THE WEAPONS USED BY THE DRACO CAME FROM SIRIUS. WHEN PRESTON REMARKED THAT THIS MADE THEM GUILTY OF HURTING OTHERS, MISHKA HAD AN ANSWER. HE REPLIED THAT WITHOUT SIRIAN WEAPONS, THE DRACO WOULD USE BRUTAL FORCE TO OVERWHELM THEIR TARGETS. IN THIS WAY, THE SIRIANS CONSIDERED THEMSELVES TO BE A MITIGATING FORCE IN THE GALAXY.

OVER THE NEXT SEVERAL MONTHS, MISHKA, MISHKAS ASSISTANT MARSHAK, TUBOR, AND GENGEEKO USED MY BODY TO DELIVER WARNINGS AND ULTIMATUMS. I WAS GIVEN INFORMATION THAT THE USSR WAS IN LEAGUE WITH THE DRACO AND ALLOWING THEM TO USE SOVIET BASES FOR ADVANCE OPERATIONS. BUT, THE USSR WOULD EVENTUALLY BREAK UP INTO SMALLER NATIONS AND DISRUPT THE AGREEMENT.

WHEN THIS HAPPENED, I WAS TOLD THAT THIS WAS A DECEPTION TO LULL THE REST OF THE WORLD INTO A FALSE PEACE. THE VARIOUS SOVIET GOVERNMENTS WERE CLOSELY ALIGNED WITH EACH OTHER. WHEN THE OPPORTUNITY WAS RIGHT, THE SOVIETS WOULD POUNCE ON THE UNSUSPECTING COUNTRIES.

IN THIS WAY, THE DRACO HAD A POWERFUL ALLY ON EARTH TO DO THEIR DIRTY WORK FOR THEM.

P.142 143

THE REST OF THE CONVERSATION INVOLVED INFORMATION ABOUT THE SIRIAN INTEREST IN ISRAEL AND THE JEWISH PEOPLE. THE JEWS, HE SAID, WERE CREATED AS A JOINT EFFORT BETWEEN THE SIRIANS AND THE DRACO. THE GENETIC STOCK CAME FROM THE HEBREWS, A RACE OF SIRIAN

ORIGIN. THE OHALU COUNCIL, COMPRISED OF THE LEADERS OF THE SIRIAN CIVILIZATION, PROVIDED THE TORAH (THE FIRST FIVE BOOKS OF MOSES, I.E., THE OLD TESTAMENT OF THE BIBLE) WITH ITS CODED INFORMATION THAT I WOULD LEARN TO DECIPHER.

IN FACT, THE OHALUANS ARE NONPHYSICAL BEINGS WHO REMAIN IN HYPERSPACE. THE SIRIANS ARE THEIR PHYSICAL DESCENDENTS. ANCIENT HEBREW IS THE LANGUAGE OF THIS COUNCIL. A HOLY LANGUAGE, IT COMES DIRECTLY FROM THE MIND OF GOD. EACH LETTER IS A SYMBOL, NUMBER, ARCHETYPE, AND GEOMETRIC SHAPE THAT IS USED TO TRANSLATE FROM THE SPIRITUAL INTO THE PHYSICAL.

IN FACT, EACH CHAPTER OF THE OLD TESTAMENT CAN BE DECODED TO LETTER PATTERNS. WHEN RECURRING PATTERNS ARE MATCHED AGAINST ONE ANOTHER, GEOMETRIC SHAPES ARE FORMED.

THESE INCLUDE A DOUGHNUT SHAPE, DIAMONDS, THREE-DIMENSIONAL TRIANGLES, ETC. WHEN ALL THE PATTERNS ARE ENFOLDED ON ONE ANOTHER, A TETRAHEDRON IS FORMED IN MULTIDIMENSIONALITY. THAT IS TO SAY, THE SHAPE CAN ONLY BE DEMONSTRATED ON PAPER BY DRAWING A THREE-DIMENSIONAL TETRAHEDRON. HOWEVER, ITS ACTUAL SHAPE GOES FAR BEYOND ANYTHING THAT CAN BE SHOWN GRAPHICALLY WITH CURRENT TECHNOLOGY. ALL LETTERS OF THE HEBREW ALPHABET CAN BE SEEN WITHIN THE SHAPE OF THE TETRAHEDRON.

IN THE ANCIENT HEBREW ALPHABET THERE ARE FOUR LETTERS THAT HAVE A STYLIZED CROWN ON TOP OF THEM. NO ONE KNEW WHY. HOWEVER, IF ALL OF THE OTHER LETTERS WERE SOMEHOW FORGOTTEN, EXCEPT FOR THOSE FOUR SPECIAL ONES, BY USING THESE FOUR, THE TETRAHEDRON COULD BE RECONSTRUCTED AND ALL THE OTHER LETTERS AGAIN FOUND WITHIN THE SHAPE.

SCIENTISTS IN JERUSALEM AND NEW YORK ARE ONLY NOW REALIZING THE INFORMATION ENCODED WITHIN THE OLD TESTAMENT AS THEY REVIEW IT BY COMPUTER AND RESEARCH THE VARIOUS LETTER PATTERNS. WHAT TYPE OF MIND COULD HAVE CREATED SUCH A TIMELESS DOCUMENT? CERTAINLY NOT A HUMAN ONE.

AT THE CONCLUSION OF OUR CONVERSATION, ELSINOB TOLD ME TO RETURN TO BED. WALKING BACK TO MY ROOM, I NOTICED THAT THE GLOW SUDDENLY STOPPED. THE MOMENT MY HEAD TOUCHED MY PILLOW, I WENT INTO A DEEP SLEEP. AT 4:45 A.M., THE ALARM RANG. WHEN I AWOKE, I REMEMBERED EVERYTHING. THAT IS WHEN I BECAME AFRAID.

P.156-158

I ALSO LEARNED THAT THERE WERE ORIGINALLY TWELVE ROOT RACES ON THE EARTH AT THE BEGINNING OF LIFE ON THIS PLANET. WHAT THIS MEANS IS THAT THERE WERE TWELVE ORIGINAL ALIEN RACES THAT AGREED TO GENETICALLY MANIPULATE AND SEED LIFE ON THIS PLANET AS PART OF A GREAT EXPERIMENT. THE PURPOSE WAS TO DETERMINE IF ALL OF THE MAN FREQUENCIES IN THE GALAXY COULD LIVE TOGETHER HARMONIOUSLY OR IF THEY WOULD DESTROY ONE ANOTHER.

THESE TWELVE ALIEN RACES MONITORED THEIR CONTRIBUTIONS TO THE EXPERIMENT OVER THE MILLENNIA. SOME LOST INTEREST WHILE SOME COMPLETELY ALTERED THEIR ORIGINAL IDEAS. IN ANY EVENT, THE TWELVE RACES ARE RETURNING TO REMOVE OR AID THEIR PART OF THE PROJECT BEFORE INVASION FORCES ARRIVE ON EARTH AND USURP ALL OF THE RESOURCES AND PEOPLE. THE OUTCOME OF THIS INVASION IS YET TO BE DETERMINED.

MANY OF THE ORIGINAL RACES KEEP BASES IN THIS SOLAR SYSTEM TO WATCH THE EARTH.

*

A SIRIAN BASE ON MARS HAS EXISTED FOR MANY THOUSANDS OF YEARS

*

THE AMPHIBIANS HAVE BASES ON NEPTUNE AND ON TITAN, A MOON OF SATURN

*

THE DRACO, WHO ARE THE INVADING REPTILIANS, HAVE BASES ON VENUS AS WELL AS UNDER THE EARTH

*

THE PLEIADEANS HAVE A BASE ON A MOON OF JUPITER

*

MANY OTHERS MAINTAIN PLATFORMS OR STATIONS IN ORBIT AROUND THE EARTH AND OTHER PLANETS IN THIS SOLAR SYSTEM

*

MOST OF THEM DO NOT WANT TO BE DISCOVERED YET

IN THE EARLY 1990'S, I WAS CONTACTED BY A MAN IN LOS ANGELES ON BEHALF OF MARINA POPOVICH, THE SOVIET COSMONAUT WHO WAS ON A LECTURE TOUR IN THIS COUNTRY. SECRETLY, SHE WAS INVESTIGATING THE DISAPPEARANCE OF A SOVIET SPACECRAFT THAT HAD BEEN ON A RECONNAISSANCE MISSION TO MARS. WHILE APPROACHING PHOBOS, A MARTIAN MOON, A STRANGE-LOOKING CRAFT EMERGED FROM BEHIND THAT MOON, FIRED SOMETHING AT THE RUSSIAN PROBE, AND THE SHIP WAS NEVER HEARD FROM AGAIN.

MS. POPOVICH KNEW MY FAMILY HISTORY IN RUSSIA (REMEMBER, MY GREAT-UNCLE WAS THE FIRST PRESIDENT OF THE SOVIET UNION), AND SHE KNEW ABOUT MY BACKGROUND AND TRAINING. SHE WAS INTERESTED TO HEAR WHAT I HAD TO SAY ABOUT THE MISSING RUSSIAN CRAFT.

AFTER SEVERAL ATTEMPTS TO CONVERSE VIA PHONE, MARINA WAS SUDDENLY SENT BACK TO MOSCOW. TO MY KNOWLEDGE, SHE NEVER RETURNED. I NEVER HAD THE CHANCE TO TELL HER THAT A SIRIAN VESSEL DESTROYED THE SOVIET PROBE ON BEHALF OF THE U.S. GOVERNMENT AND THE ISRAELIS! APPARENTLY, THERE WERE THOSE PEOPLE WHO DID NOT WANT THE WORLD TO FIND OUT ABOUT THE MONUMENTS ON MARS.

THESE SAME PEOPLE DID NOT WANT THE PUBLIC TO KNOW THAT AMERICANS WERE ALREADY WORKING WITH BEINGS FROM TAU CETI WHO WERE THE PROGENITORS OF THE SLAVIC RACES. ALTHOUGH THE SIRIANS, TAU CETIANS, RUSSIANS, ISRAELIS, AND AMERICANS WERE THEORETICALLY ALL WORKING TOGETHER AGAINST THE ORION CONFEDERATION AND THE DRACO EMPIRE, EACH HAD THEIR OWN AGENDA AND WITHHELD INFORMATION FROM EACH OTHER. THE AMERICANS AND THE ISRAELIS WANTED PRIMARY CONTROL SO THEY CAN EVENTUALLY DOMINATE THE WORLD.

THEY REASONED THAT THE GOVERNMENT WITH THE MOST EXCLUSIVE INFORMATION AND TECHNOLOGY WOULD WIN.

MONTAUK: THE ALIEN CONNECTION REVEALS THE MOST AMAZING STORY YET TO SURFACE IN THE AREA OF ALIEN ABDUCTION. THIS IS AN AUTOBIOGRAPHICAL AND FACTUAL ACCOUNT FROM STEWART SWERDLOW, A GIFTED MENTALIST WHO WAS BORN CLAIRVOYANT BUT HAUNTED BY STRANGE TIME-SPACE SCENARIOS. AFTER SUFFERING ALIEN ABDUCTIONS AND GOVERNMENT MANIPULATIONS, STEWART FOUND PRESTON NICHOLS AND DISCOVERED HIS OWN ROLE IN TIME

TRAVEL EXPERIMENTS KNOWN AS THE MONTAUK PROJECT.

AFTER REFUSING TO BREAK HIS ASSOCIATION WITH NICHOLS, STEWART WAS INCARCERATED BY THE AUTHORITIES, BUT THE TRUTH BEGAN TO REVEAL ITSELF. STRUGGLING FOR HIS LIFE, STEWART USED HIS MENTAL ABILITIES TO OVERCOME THE NEGATIVE INFLUENCES SURROUNDING HIM AND ULTIMATELY DISCOVERED THE HIGHEST COMMON DENOMINATOR IN THE ALIEN EQUATION AN INTERDIMENSIONAL LANGUAGE WHICH COMMUNICATES TO ALL CONSCIOUS BEINGS.

P.205
VICTIM MENTALITY

THIS PLANET PRIMARILY ATTRACTS TWO TYPES OF BEINGS THOSE WITH A VICTIM MENTALITY AND THOSE WITH AN OPPRESSOR MENTALITY. IN ORDER TO BE A VICTIM, YOU MUST HAVE OPPRESSORS. IN ORDER TO BE AN OPPRESSOR, YOU MUST HAVE VICTIMS. TOGETHER, THIS CREATES BALANCE IN GOD-MIND.

THIS PLANET IS DESIGNED AS A PLACE WHERE BEINGS WITH A VICTIM MENTALITY CAN LEARN TO OVERCOME IT. THEREFORE, ANY 'HIGHER LEVEL' BEING WILL NOT BECOME INVOLVED BECAUSE IT IS NECESSARY FOR THOSE HERE TO HAVE THE OPPORTUNITY TO WORK THROUGH THEIR VICTIM MENTALITIES. TO BECOME INVOLVED WOULD MEAN INTERFERING OR TAKING AWAY THE LESSONS OF THOSE WITH VICTIM MENTALITIES. HIGHER LEVEL BEINGS WILL BE OBJECTIVE OBSERVERS WHO WILL GUIDE AND INSTRUCT YOU THROUGH YOUR VICTIM MENTALITY ONCE YOU REACH THEM, BUT THAT IS ALL.

THEY ARE NOT HERE TO "SAVE" YOU OR THIS PLANET.

ANY BEING WHO SAYS THAT THEY ARE HERE TO "SAVE" YOU IS INTERFERING IN YOUR SOUL GROWTH. ONLY YOU CAN "SAVE" YOURSELF FROM A VICTIM MENTALITY. ONLY YOU CAN "SAVE" YOURSELF FROM A VICTIM MENTALITY. ONLY YOU AND THE LESSONS YOU SELF-DESIGN WILL TEACH YOU ABOUT VICTIM MENTALITY. ONLY YOU CAN MOVE THROUGH THESE LESSONS THAT WILL ALLOW YOU TO MAKE A FINAL RELEASE OF YOUR VICTIM MENTALITY. NO ONE IS WAITING TO HELP YOU DO NOT BE FOOLED BY ANY BEING MAKING SUCH PROMISES.

WHEN YOU LEARN TO MOVE THROUGH YOUR VICTIM MENTALITY, YOUR MIND PATTERN WILL NO LONGER ATTRACT OPPRESSORS. THE MORE STUBBORN YOU ARE IN YOUR DETERMINATION TO HANG ONTO YOUR VICTIM MENTALITY WAYS, THE MORE INTENSE THE LESSONS THAT YOU ATTRACT TO GET YOU TO RELEASE THOSE WAYS. THIS MEANS, METAPHORICALLY SPEAKING, A BIGGER, MEANER, STRONGER, STICK UNTIL YOU FINALLY "GET IT."

YOU HAVE TO GET HURT, BELITTLED, AND FINALLY, ANGRY ENOUGH TO STAND UP FOR YOURSELF AND DECLARE THAT YOU WILL NO LONGER BE A VICTIM TO ANYONE, ANYWHERE, ANY MORE! PERHAPS WHEN YOU FINALLY HAVE HAD ENOUGH, YOU RELEASE YOUR VICTIM MENTALITY BY SAYING, "I JUST DON'T GIVE A DAM ANYMORE WHAT ANYBODY THINKS! I AM SPEAKING MY MIND REGARDLESS! I AM TAKING CARE OF MYSELF, REGARDLESS!"

SOMETIMES, PEOPLE ARE BEATEN UP SO MUCH THAT INSTEAD OF RELEASING THE VICTIM MENTALITY, THEY DECIDE TO BECOME THE OPPRESSOR WHEN THE OPPORTUNITY PRESENTS ITSELF. THIS IS WHY CYCLES REPEAT THEMSELVES. PEOPLE WHO WERE OPPRESSED FIND OTHER VICTIMS, BECAUSE THIS GIVES THEM A SENSE OF CONTROL. IN DOING SO, THEY RELIVE THEIR

EARLIER EXPERIENCES WHEN THEY FELT LIKE THEY HAD NO CONTROL. THEY BECOME THE PERPETRATOR, JUST SO THEY CAN BE THE "WINNER" FOR A CHANGE. OF COURSE, THIS IS ANOTHER IMBALANCE, OR EXTREME FLIP FROM VICTIM TO OPPRESSOR.

THE IDEAL IS TO FIND A HAPPY MEDIUM, OR BALANCE, BETWEEN VICTIM AND OPPRESSOR. VICTIM AND OPPRESSOR ARE OPPOSITE SIDES OF THE SAME COIN IN THE MIND OF GOD. IN THIS CASE, TWO INDIVIDUAL SOUL-PERSONALITIES ARE NEEDED TO MAINTAIN AN EQUILIBRIUM IN GOD MIND. ONE CARRIES THE WEIGHT OF A VICTIM, ONE CARRIES THE WEIGHT OF AN OPPRESSOR. WHAT YOU NEED TO DO IS FIND THE BALANCE WITHIN YOURSELF, SO THAT EQUILIBRIUM WITHIN THE MIND OF GOD IS MAINTAINED WITHIN ONE SOUL-PERSONALITY INSTEAD OF TWO.

YES, YOU MUST LEARN TO SPEAK YOUR MIND AND NOT ALLOW ANYONE TO WALK ON YOU. YES, YOU MUST SOMETIMES BE HARSH AND CRUEL WITH WORDS AND SOMETIMES EVEN ACTIONS. BUT WHEN THIS MUST HAPPEN, IT MUST BE DONE IN AN OBJECTIVE MANNER WHAT IS BEST FOR EVERYONE INVOLVED TO GET THE POINT ACROSS WHILE CAUSING THE LEAST AMOUNT OF PAIN.

BOUNDARIES MUST BE SET.

*

WHAT ARE YOUR BOUNDARIES?

*

WHO CROSSES THEM AND HOW?

*

WHO IS A BELLIGERENT PERSON IN YOUR LIFE THAT YOU TRY TO AVOID BECAUSE OF THEIR BULLISH, PUSHY WAYS?

*

WHY DO YOU AVOID THIS PERSON?

*

WHY NOT PRACTICE LETTING GO OF YOUR VICTIM MENTALITY AND SPEAK YOUR MIND TO HIM/HER?

SO WHAT IF YOUR KNEES SHAKE SO HARD THAT YOU THINK YOU WILL FALL DOWN, AND YOUR VOICE IS SHAKY, SQUEAKY, OR BARELY AUDIBLE? SOMEWHERE ALONG THE WAY, YOU MUST STOP YOUR VICTIM MENTALITY BEFORE IT STOPS YOU. LEARN TO BE PROACTIVE INSTEAD OF REACTIVE.

WHEN YOU ALLOW OTHERS TO PUSH YOU AROUND, YOU BECOME ANGRY, SULLEN, AND INTROVERTED. THEN, YOU LASH OUT AT THE UNDESERVING WITH MISDIRECTED FRUSTRATION AND ANGER. SOMETIMES YOUR BODY BECOMES ILL BECAUSE OF ALL THAT YOU SUPPRESS, OR YOU INSULATE YOUR BODY, OR PERHAPS STOP EATING. ONE WAY OR THE OTHER, YOU SUFFER.

BUT, THERE IS A PART OF YOU THAT FEELS THAT YOU DESERVE TO SUFFER. THERE IS A PART OF YOU THAT ENJOYS THIS PAIN AND SELF-PUNISHMENT. IT FEELS GOOD TO SOME PART OF YOURSELF, OR YOU WOULD NOT DO IT. SOME PEOPLE CREATE OTHERS TO GIVE THEM PAIN, SOMETIMES PHYSICAL, SOMETIMES EMOTIONAL, SOMETIMES BOTH. SOME PEOPLE DO IT FOR THEMSELVES A SELF-CONTAINED, FULLY FUNCTIONAL, VICTIM MENTALITY UNIT. SOME PEOPLE ARE EXTREMELY SUCCESSFUL AT THIS.

WHY DO YOU FEEL SO BAD ABOUT YOURSELF THAT YOU FEEL LIKE YOU ARE MEANT TO SUFFER, TO BE ALONE, TO FEEL GUILTY, TO HAVE ILL HEALTH, TO BE OVER OR UNDERWEIGHT. DID IT START IN THIS LIFETIME, OR DID IT START BEFORE? FOLLOW THOSE FEELINGS, AND ALLOW YOURSELF TO RELEASE IT. THIS PHYSICAL REALITY IS YOUR CHANCE TO OVERCOME IT. THE MORE YOU IGNORE

THIS SITUATION, THE HARDER AND MORE INTENSE LESSON YOU WILL ATTRACT TO BEAT IT OUT OF YOURSELF. YOU CAME HERE TO LEARN NOW DO IT. QUIT WHINING MOANING, AND COMPLAINING BECAUSE THERE IS A PART OF YOU THAT ENJOYS THAT TOO.

ACHES AND PAINS CAN CREATE A LOT OF ENTERTAINMENT. YOU CAN RUN FROM DOCTOR TO DOCTOR, TRYING TO FIND A CURE FOR SOMETHING THAT WILL NEVER BE CURED AS LONG AS YOU MAINTAIN YOUR CURRENT MIND-PATTERN.

"BAD LUCK" CAN ATTRACT A LOT OF ATTENTION AND SYMPATHY FROM OTHERS. DIRE CIRCUMSTANCES WILL FORCE SOMEONE TO PAY ATTENTION TO YOU. NEVER GETTING A RAISE OR A PROMOTION IS AN EXCUSE NOT TO CLIMB HIGHER IN YOUR CAREER OR COMPANY. YOU CAN MOAN ALL YOU WANT ABOUT BEING ALONE, WITH A PARTNER WHO DOES NOT UNDERSTAND YOU, OR WITHOUT ONE AT ALL.

BUT THIS SELF-IMPOSED ISOLATION ALSO GIVES YOU TIME TO SELFISHLY TAKE CARE OF YOURSELF WITHOUT ANY INTERFERENCE. THE SAME FOR SAYING YOU WANT CHILDREN BUT ARE UNABLE TO HAVE THEM. A PART OF YOU DOES NOT WANT A SPOUSE, OR A CARING SPOUSE, OR CHILDREN, BECAUSE IF ALL OF YOU WANTED THIS AND IT WAS TRULY IN YOUR MIND-PATTERN, YOU WOULD HAVE IT!

VICTIM, VICTIM, VICTIM! LET US COUNT THE WAYS! REFUSE TO BE A VICTIM. FIND A NEW SOURCE OF ENTERTAINMENT. RELEASE YOURSELF FROM THIS MIND-PATTERN SO THAT YOU CAN MOVE INTO NEW VISTAS OF GROWTH - ONES SO VAST THAT YOU CANNOT EVEN IMAGINE OR COMPREHEND THEM. YOU MUST LET GO OF THE OLD TO MAKE ROOM FOR THE NEW. NO ONE CAN DO IT FOR YOU. NO ONE CAN "SAVE" YOU FROM YOURSELF. NO ONE IS WAITING TO HELP THIS PLANET.

ONLY YOU CAN MAKE A DIFFERENCE. ONLY YOU CAN SAVE THIS PLANET.

DO IT!

P.209
ARE YOU A MIND-CONTROL CANDIDATE?

DOES MIND-CONTROL SOUND LIKE A FOREBODING SUBJECT THAT PEOPLE IN DARK, MYSTERIOUS PLACES PRACTICE UPON UNSUSPECTING VICTIMS? DO YOU READ ABOUT OTHER PEOPLE'S CLAIMS WITH INTEREST, WHILE THINKING THAT IT REALLY HAS NOTHING TO DO WITH YOU? REMEMBER, IF YOU ARE READING ABOUT IT, IT IS IN YOUR WORLD. IF IT IS IN YOUR WORLD, IT IS A REFLECTION OF SOME PART OF YOURSELF OR IT COULD NOT EXIST. SO, ARE YOU A MIND-CONTROL CANDIDATE FOR SINISTER FORCES?

TO FIT THE PROFILE THEY ARE LOOKING FOR, YOU MUST BE CONTROLLABLE. ARE YOU? WHAT DOES YOUR MIND-PATTERN LOOK LIKE? ARE YOU IN CONTROL OF YOUR OWN LIFE, OR IS YOUR LIFE IN CONTROL OF YOU?

IF ANYTHING, ANYWHERE CONTROLS YOU, YOU HAVE AN ESTABLISHED MIND-PATTERN THAT ANY FORCE CAN USE AND MANIPULATE. ALL THE FORCE HAS TO DO IS ENTER YOUR AURIC FIELD THROUGH THIS "HOLE" IN YOUR MIND-PATTERN. TO CLOSE THE HOLES AND CORRECT THE MIND-PATTERN, IT IS IMPORTANT TO FIND OUT WHAT IN YOUR LIFE IS CONTROLLING YOU SO THAT YOU CAN STOP IT.

WHAT CONTROLS YOU? IS IT A PERSON? ANYONE WHO "PULLS YOUR STRINGS" OR "PUSHES YOUR BUTTONS" IS CONTROLLING YOU. ANYONE WHO YOU ALLOW TO PUT YOU DOWN, OR WHO MAKES YOU FEEL LIKE LESS OF A PERSON IS CONTROLLING YOU. WHEN YOU REACT TO THEIR MANIPULATION, YOU ARE NOT IN CONTROL. THE OTHER PERSON CONTROLS YOU. THIS COULD BE A PARENT, SPOUSE, CHILD, RELATIVE, CO-WORKER, OR NEIGHBOR, FOR EXAMPLE.

DO YOUR EMOTIONS CONTROL YOU? WHEN EMOTIONS ARE OUT OF BALANCE, THEY CAN CREATE THEIR OWN SUBPERSONALITIES. EACH EMOTION HAS ITS OWN COLOR, TONE, AND ARCHETYPE WITHIN YOUR AURIC FIELD. ANGER IS COMPRISED OF THE COLOR RED, FEAR IS YELLOW, JEALOUSY IS GREEN. EVERY TIME YOU HAVE EXPERIENCE THESE EMOTIONS WITHOUT PASSING THEM UP TO YOUR OVERSOUL, THE ENERGY OF THESE SPECIFIC SUBPERSONALITIES ARE FED.

ANGER GETS STRONGER, FEAR GETS STRONGER, JEALOUSY GETS STRONGER. NOW, THEY ARE IN CONTROL OF YOU. YOU CAN MAKE ALL THE PROMISES YOU WANT, BUT WHAT HAPPENS WHEN YOUR BUTTONS GET PUSHED? ALL OF A SUDDEN, ANGER IS CONTROLLING YOU, OR FEAR, OR JEALOUSY. YOU HAVE LOST THE BATTLE. YOUR EMOTIONS ARE IN CONTROL.

PERHAPS IT IS ILLNESS THAT CONTROLS YOU. DO YOU NEED THAT ILLNESS IN ORDER TO FEEL IMPORTANT, OR AS A WAY TO GET ATTENTION AND/OR LOVE? DO YOU HAVE CHRONIC HEALTH ISSUES THAT NEVER SEEM TO GO AWAY? OR YOU JUST GET RID OF SOMETHING AND SOMETHING ELSE POPS UP TO TAKE ITS PLACE? WHAT PART OF YOU NEEDS AND ALLOWS THIS TYPE OF CONTROL?

DO ALCOHOL AND DRUGS CONTROL YOU? HOW ABOUT TOBACCO? SEX? THERE ARE SUPPORT GROUPS FOR ALCOHOLISM, DRUG, AND SEX ADDICTION; FOR PEOPLE WHO CANNOT STOP SHOPPING, GAMBLING, AND/OR SHOPLIFTING. THERE ARE SUPPORT GROUPS FOR PEOPLE CONTROLLED BY BULIMIA, ANOREXIA, OBSESSIVE COMPULSIVE DISORDER. YOU NAME IT, IT IS OUT THERE CONTROLLING SOMEBODY, SOMEWHERE. IS IT CONTROLLING YOU.

DOES FOOD CONTROL YOU? FOOD CONTROLLING YOU DOES NOT IMPLY THAT YOU ARE OVERWEIGHT. COULD YOU GO A DAY WITHOUT CHOCOLATE OR SUGAR? COULD YOU FAST FOR 24 HOURS WITHOUT ANYTHING BUT WATER? MOST LIKELY YOU WOULD NOT STARVE TO DEATH AND DIE, SO COULD YOU??

HOW ABOUT FASHION? ARE YOU THE FIRST TO GET THE LATEST CLOTHING, HAIRSTYLES, HOME DECOR, WITHOUT THINKING IF YOU EVEN LIKE THEM OR NOT? HOW ABOUT CARS, MOTORCYCLES TRUCKS, MOTOR VEHICLES, BOAT... THE LIST IS ENDLESS.

OR FADS, BE IT BODY-PIERCING, TATTOOS, OR ACQUIRING ALL KINDS OF DOODADS AND KNICKKNACKS THAT WILL BE USELESS PRACTICALLY BEFORE YOU EVEN HAVE THEM OUT OF THE BOX. DO YOU HAVE TO HAVE WHATEVER EVERYONE ELSE HAS.

PLASTIC SURGERY CONTROLS PEOPLE. THEY KEEP GOING BACK AND REDOING EVERY PART OF THE BODY UNTIL THERE IS NOTHING LEFT TO REDO. THEN THEY START OVER AGAIN.

SOME PEOPLE START EXERCISING AND CANNOT STOP. THEY EXERCISE CONTINUALLY AND CONSTANTLY, SOMETIMES BUILDING UP MUSCLE MASSES THAT WOULD PUT HERCULES TO SHAME. OTHERS EXERCISE UNTIL THEY DO NOT HAVE A DROP OF FAT ON THEIR BODIES, THEN BEGIN DESTROYING THEIR MUSCLE TISSUES, LIGAMENTS, AND INTERNAL ORGANS.

DO YOUR EXPERIENCES USE AND CONTROL YOU, OR DO YOU USE AND CONTROL YOUR EXPERIENCES? THIS IS THE BOTTOM LINE. IF ANYTHING OR ANYONE CONTROLS YOU IN ANY WAY, SHAPE, OR FORM, YOU ARE A PRIME CANDIDATE FOR MASS AND/OR INDIVIDUAL MIND-CONTROL. WHEN YOU ARE IN CONTROL OF YOUR OWN SELF, NO ONE AND NO THING CAN CONTROL YOU.

EVERYTHING IN MODERATION IS ACCEPTABLE, BUT WHEN SOMETHING TAKES OVER YOUR LIFE TO THE DEGREE WHERE IT CONTROLS YOU, YOU CREATE A MIND-PATTERN THAT SAYS "OUTSIDE FORCES CAN AND DO CONTROL ME."

THIS LEAVES HOLES IN YOUR MIND-PATTERN AND AURIC FIELD THAT TELLS ANYONE WHO CAN UNDERSTAND THIS INFORMATION THAT YOU ARE A PERFECT CANDIDATE FOR MIND-CONTROL. LEARN TO BREATHE YOURSELF INTO YOUR CENTRE. IDENTIFY THE STRONG ASPECTS OF YOUR MIND-PATTERN AND THE ONES THAT NEED STRENGTHENING. ANCHOR YOURSELF IN THE STRENGTH OF YOUR OWN OVERSOUL AND GOD-MIND. TAKE CONTROL OVER ABSOLUTELY ANYTHING THAT HAS CONTROL OVER YOU, REMEMBERING TO KEEP THE BALANCE. YOU CAN BE PULLED OFF-CENTRE IN EVERY WAY IMAGINABLE, AND YOU WILL BE. THESE ARE YOUR TESTS.

BE THE MONITOR OF YOUR OWN PROGRESS. THE MORE YOU USE INTERNAL MONITORS, THE LESS CHANCE OUTSIDE MONITORS CAN STEP IN TO DO THE JOB FOR YOU. WHENEVER YOU LET YOUR GUARD DOWN, THERE WILL BE SOMEBODY OR SOMETHING THAT WILL KNOWINGLY AND GLADLY PUSH YOU OUT OF YOUR CENTRE.

PART OF YOUR REASON FOR EXISTING IN PHYSICAL REALITY IS TO FIND OUT WHO AND WHAT YOU ARE. BEING PUSHED OUT OF YOUR CENTRE TELLS YOU WHO YOU ARE NOT. OPERATING FROM OUTSIDE OF YOUR CENTRE ALLOWS OTHERS TO DEFINE YOU ACCORDING TO THEIR TERMS. THEY CAN MOULD AND BEND YOU LIKE CLAY TO CREATE THE PERSON THAT THEY NEED FOR THEIR OWN PURPOSES.

YOU ARE SO BUSY MOLDING AND BENDING THAT YOU DO NOT HAVE TIME TO RECOGNIZE WHAT IS HAPPENING TO YOU.

ONLY WHEN YOU STAND FIRM IN YOUR CENTRE, IN CONTROL OF ABSOLUTELY EVERY ASPECT OF YOUR LIFE, ARE ALL THE HOLES OF YOUR MIND-PATTERN COMPLETELY SEALED SHUT. WHEN THIS HAPPENS, NO ONE OR NO THING CAN CONTROL YOU.

BUT EVEN WHEN THE DOOR IS CLOSED TO OUTSIDERS, REMEMBER THAT THEY WILL STILL COME KNOCKING.

IT IS UP TO YOU TO ENSURE THAT THEY DO NOT ENTER.

GO BACK

BEFORE THE VANCOUVER 9/11 TRIBUNAL

In re:	**AFFIDAVIT OF ANDREW D. BASIAGO**
Prior Knowledge of the Terror Attacks of September 11, 2001 by Defense Secretary Donald H. Rumsfeld resulting from the Quantum Access Capabilities of the US Defense-Technical Community acquired while Secretary Rumsfeld served secretly as the Defense Attaché to DARPA's Project Pegasus in the early 1970's	

I, ANDREW D. BASIAGO, being first duly sworn, on oath, depose and state as follows:

1. My name is Andrew Daniel Basiago.

2. I am an American citizen.

3. I was born on September 18, 1961 in Morristown, New Jersey, USA.

4. I reside in Vancouver, Washington, USA.

5. I am an attorney-at-law in private practice in the State of Washington.

6. I was admitted to the Washington State Bar Association in 1996.

7. Currently, I am an active member in good standing of the Washington State Bar Association.

8. I maintain a successful solo law practice.

Andrew D. Basiago, Esq.
P.O. Box 2311
Vancouver, WA 98668
(360) 980-4100

9. I have never been accused of, arrested for, charged with, or convicted of a crime or been disciplined on professional ethical grounds by my bar association.

10. I am of sound mind and healthy body.

11. This affidavit is accurate to the best of my ability to remember and tell the true life experiences that I testify to in it and is made without any motive to deceive or purpose of evasion.

12. During the years 1968 to 1972, I was a child "chrononaut" in Project Pegasus.

13. A chrononaut is a time traveler.

14. Project Pegasus was a classified, defense-related, research and development program of the Defense Advanced Research Projects Agency [DARPA.]

15. DARPA is the agency that develops advanced weapon systems, communication devices, and surveillance technologies for the US Department of Defense.

16. Project Pegasus was the US time-space program at the time of the emergence of quantum access in the US defense-technical community.

17. "Quantum access" is the ability to gather information about a non-local event in the time-space continuum by either sending a chrononaut there physically or propagating a hologram of the event through which the chrononaut either views the event or visits the event on a physio-virtual basis.

18. Non-local events are those scenarios that take place in what we call the past and future but which are actually going on simultaneously in a quantum hologram that consists of a multitude of adjacent similar and dissimilar time lines.

19. The mission of Project Pegasus was to use quantum access to develop a "remote sensing in time" capability pertaining to non-local events on behalf of the Executive Branch of the United States government.

20. It was hoped that by developing better intelligence about past and future events, Project Pegasus would enable the US president, intelligence community, and military to engage in better contingency planning for future events.

21. Project Pegasus was trying to accomplish this by developing different time travel technologies in a research and development program under the aegis of DARPA.

22. These time travel technologies were advanced electro-magnetic devices, including teleporters, that would enable DARPA to send chrononauts to non-local events and advanced electro-optical devices, including chornovisors, that would enable DARPA to propagate holograms of non-local events for purposes of remote viewing or physio-virtual visitation of said non-local events.

Andrew D. Basiago, Esq.
P.O. Box 2311
Vancouver, WA 98668
(360) 980-4100

23. A "teleporter" is an electro-magnetic device that by opening up a vortal tunnel in the quantum hologram permits a chrononaut to travel thousands of miles in time-space in seconds.

24. Teleporters were fully operational in the secret realms of the US defense-technical community by 1967-68.

25. A "chronovisor" is an electro-optical device that by driving an electro-magnetic signal through a crystal array propagates a hologram that lenses a non-local event into the laboratory.

26. Chronovisors were fully operational in the secret realms of the US defense-technical community by 1967-69.

27. I am the fifth and youngest child of the American electrical engineer and inventor Raymond Francis Basiago [1923-1990].

28. From 1966 to 1984, Raymond F. Basiago was employed as a special projects engineer for The Ralph M. Parsons Corporation of New York, New York [today, Parsons Corporation of Pasadena, California.]

29. Parsons was the principal US defense contractor involved in DARPA's Project Pegasus, so principally, in fact, that when Ralph M. Parsons, the founder of Parsons Corporation, bought what was then the world's largest private yacht from the billionaire Adnan Kashoggi in 1972, Parsons renamed the ship "Pegasus II."

30. In addition to working for Parsons as an engineer, Raymond F. Basiago secretly held the rank of Major in the Second Reserve of the US Army.

31. During his 18 years of employment with the Parsons Corporation ostensibly working on conventional engineering projects, my father was secretly employed as the technical liaison between Parsons and the CIA on the theory and practice of teleportation.

32. While it is not clear whether Raymond F. Basiago was ever a CIA officer *per se*, his work with DARPA, the CIA, and other US military and intelligence agencies was extensive enough for him to be in the CIA employee database.

33. When I inquired of my father's employment status with the CIA through an intermediary ten years ago, I was told by the CIA that they could not release information to the family members of living or deceased CIA personnel.

34. I was first brought into Project Pegasus by my father in 1967-68, when at age six I teleported with him from New Jersey to New Mexico via a teleporter located in Building 68 at the "old" Curtiss-Wright Aeronautical Company facility formerly at 1 Passaic Avenue in Wood Ridge, New Jersey.

35. This "jump" resulted in me becoming the first American child to teleport.

Andrew D. Basiago, Esq.
P.O. Box 2311
Vancouver, WA 98668
(360) 980-4100

36. I was officially enlisted in DARPA's Project Pegasus in Fall 1969, at age seven, at the beginning of my third grade year, when I signed a loyalty and secrecy oath on US Department of Defense letterhead.

37. During 1969-72, the learning laboratory for gifted and talented school children at my public elementary school, Mountview Road School in Morris Plains, New Jersey, was used as a training course for time travel activities that I was then involved in at defense contractor locations in New Jersey and New Mexico.

38. In this educational context, I received alpha intelligence training in such abilities as perception, memory, and communication.

39. This training included photo-learning on machines called "tachistoscopes" developed by the Office of Naval Research for the education of the 140 gifted and talented American school children enrolled in Project Pegasus and other secret defense and intelligence projects utilizing US school children as "team members."

40. The curriculum that we studied on the tachistoscope was called "Galileo" and emphasized the history of society and of science from the year 1450. The purpose of this schooling was to give the children who would be time traveling for DARPA knowledge of the social and technical history of the modern era so that we would have this information available to us when we were in the field.

41. From Fall 1969 to Summer 1972, I was involved in eight different forms of quantum access for DARPA, in which I received specialized education in the learning lab at Mountview and then took part in practical exercises either in the learning laboratory or at a defense contractor location off-campus.

42. *Remote Viewing*. In Fall 1969, the children in my group were assessed for our psychic ability and then involved in remote viewing exercises for the US Navy's Office of Naval Intelligence. We were asked, *inter alia*, to remotely view the POW compound known as the "Hanoi Hilton" in North Vietnam and determine whether Lt. John McCain was in the prison and, if so, where he was in the prison.

43. *Spinning*. In Spring 1970, the children in my group took part in exercises in which we were laid on our backs on a table top-like device and spun clockwise at 33 rpm. In this way, we were trained to go "out-of-body." During one astral projection, I confronted a barrier that the lady from DARPA who debriefed me stated was the infrastructure propagating the hologram we exist in, The Matrix.

44. *The Montauk Chair*. In Spring 1970, the children in my group first began to take astral projections to episodes in our own subjective futures via the time travel technology known as "the Montauk chair." After returning from these induced astral projections to our own futures, we were then debriefed about what we saw, and in this way intelligence was gathered about future events and conditions. According to Dr. David L. Anderson, the Montauk chair "went national" and involved thousand of American schoolchildren in probes to episodes in their future lives beginning in Spring 1970. I was one of them.

Andrew D. Basiago, Esq.
P.O. Box 2311
Vancouver, WA 98668
(360) 980-4100

45. *The Teleporter.* In Summer 1970, the children in my group first began traveling to the state capitol grounds in Santa Fe, New Mexico via the Tesla teleporter at the Curtiss-Wright Aeronautical Company in Wood Ridge, New Jersey and returning to New Jersey via the teleport located at the Sandia National Laboratory in Sandia, New Mexico, adjacent to the Kirtland Air Force Base northeast of Albuquerque, New Mexico.

46. *The Chronovisor.* In Fall 1970, the children in my group first began accessing past and future events via third and fourth-dimensional Ernetti-Gemelli chronovisors situated at the General Manufacturing Company in Convent Station, New Jersey; a public auditorium under construction in Morristown, New Jersey; and the ITT Defense Communications facility in Nutley, New Jersey.

47. *The Plasma Confinement Chamber.* In Spring 1972, my father took me to a time lab in East Hanover, NJ where, under the direction of Dr. Stirling Colgate, I entered a Lucite chamber where plasma was emitted, and while immersed in the plasma, I worm-holed to Gettysburg, PA on November 19, 1863, where I was depicted in the famous Josephine Cobb photograph of Abraham Lincoln at Gettysburg.

48. *The Stargate.* In Summer 1972, I took trips to 2045 to retrieve microfilmed summaries of intervening events being prepared by project historians in the future. The Stargate through which I jumped was located in the gymnasium at the Cerrillos Cultural Center near Cerrillos, NM. We arrived back in the present on the grounds of the Microwave Tower at the Lobo Overlook site in SW Colorado.

49. *The Jump Room.* Before I left my period of service attached to Project Pegasus in 1972, I witnessed a device, about the size of a microwave oven, through which things like documents from Washington, DC were arriving in New Mexico. I believe that it was this time travel technology from which the jump rooms were developed via which, by the late 1970's, the US government was sending personnel Mars.

50. During the three years that I was officially attached to Project Pegasus from 1969 to 1972, I spent three secret summers in New Mexico living with my father and taking part in time travel activities undertaken at both atomic research institutions like the Los Alamos National Laboratories [LANL] and the Sandia National Laboratory and smaller labs operated by DARPA in the desolate environs of New Mexico.

51. These secret summers were effectuated by my father and I teleporting to New Mexico, spending the summer there, and then at the end of the summer teleporting back to New Jersey so as to arrive on the afternoon of the morning that we had left at the beginning of the summer. In this way, the time loop created by our "quantum displacement" in New Mexico was closed and time travel was used to conceal time travel research via the propagation of a time loop and its subsequent disappearance.

52. These "secret" or "hidden" summers were the first Summer 1971, Summer 1973 accessed from Fall 1971, and the first Summer 1972. I say "first Summer 1971 and 1972" because after those summers, my father and I lived second summers, with a different set of experiences, upon returning to New Jersey.

Andrew D. Basiago, Esq.
P.O. Box 2311
Vancouver, WA 98668
(360) 980-4100

53. Consequently, as both a child progressing farther and farther down the rabbit hole of applied quantum physics, and as my father's son, during those three summers, and for shorter periods during the school year when I was in New Mexico after having teleported there, I was frequently present at project social events, including project meetings held at the labs, meals taken at restaurants, drinks had at bars, parties enjoyed at private residences, and receptions held at hotels.

54. In that context, I met many distinguished Americans who were either project principals, or who were interested in the project's activities, or who were being brought through the project's social network so that they could be briefed about their roles in future events as individuals who had been identified as "persons of interest" related to their personal destinies as national leaders of the United States.

55. The project principals that I met included Dr. Harold M. Agnew, who served as the federal administrator of Project Pegasus during his tenure as director of LANL [1970-78]; Dr. Edward Teller, who I once met when he was trying to fix a chronovisor at LANL; Dr. Stephen J. Lukasik, when he was serving as the director of DARPA; Dr. Iben Browning, when he was serving as the director of the directorate of science and technology of the CIA [1959-74]; John A. McCone, a former director of the CIA [1960-64]; Dr. Stirling Colgate, when he was president of the New Mexico Institute of Science and Technology [NMIST]; Dr. Emilio Segre, who had a discussion with my father in the hallway at LANL about the existence of teleportation; and Donald H. Rumsfeld, the future Secretary of Defense, who served as the defense attaché of Project Pegasus.

56. In retrospect, when I consider that three of these individuals [Agnew, Teller, and Segre] were Manhattan Project physicists and that three [Agnew, Lukasik, and McCone] served as the director of major defense and intelligence agencies [LANL, DARPA, and CIA], I am struck by how important Project Pegasus was and how privileged my father and I were to be part of it and both witness and participate in the US time-space exploration program at the time of the emergence of time travel in the US defense-technical community in the early 1970's.

57. I also met several future national leaders of the United States at lunches that were held in Albuquerque, NM with project principals shortly after they were apprised of the fact that using its quantum access capability DARPA had determined that they were destined to serve as President or Vice President of the United States. These individuals included President George H.W. Bush, Vice President Richard B. Cheney, President George W. Bush, and President William J. Clinton. These lunches were held at La Hacienda Restaurant in Old Town Albuquerque, where my father's lifelong friend, Mary Constance Chavez [1928-81], was the cashier

58. In this unusual and unprecedented social milieu, in which American defense officials operating in the present were sharing intelligence data from the future with both future national leaders and their colleagues on the project, I had, on occasion, the opportunity to overhear "shop talk" that was filtering through the social network of Project Pegasus, in which project principals were revealing what they knew about future events, developments, and conditions.

Andrew D. Basiago, Esq.
P.O. Box 2311
Vancouver, WA 98668
(360) 980-4100

59. These discussions were in the nature of gossip or project scuttlebutt and presumably should not have been held because the information about the future that Project Pegasus was gathering was supposed to remain secret and only shared with those individuals with a need to know on a "need to know basis only."

60. The future events, developments, and conditions that I acquired prior knowledge of as a result of serving as a child on Project Pegasus included, but were not limited to: the resignation of President Richard M. Nixon; the advent of the Internet; the emergence of AIDS as an epidemic disease; the presidencies of US presidents Carter, Bush, Clinton, and Bush; widespread cell phone use in the future; the fact that Donald H. Rumsfeld would one day serve as Defense Secretary; and the attack on the Twin Towers of the World Trade Center on 9/11.

61. I am filing this affidavit with the tribunal because I have direct, personal knowledge of the fact that a secret time travel project for which he served as defense attaché gave Donald H. Rumsfeld, who served as US Secretary of Defense during 9/11, prior knowledge of 9/11 thirty years before 9/11.

62. While serving on Project Pegasus as a child chrononaut and he as its defense attaché – as the point man between the Department of Defense and project principals like Dr. Agnew and my father – I had extensive contact with Mr. Rumsfeld.

63. In Spring 1971, I attended a lecture that Mr. Rumsfeld gave to about 15 young people on the project. This lecture was held at an underground amphitheater at the Cerrillos Cultural Center near Cerrillos, NM. During the lecture, Mr. Rumsfeld thanked us for our participation in the program, admonished us to keep our knowledge of the time travel technologies involved absolutely secret because the national security of the United States depended on it, and informed us that the significance of teleportation was primarily military in that it would enable the US Army to put troops precisely where they were needed on the battlefield.

64. I greeted Mr. Rumsfeld as we entered the same amphitheater at the Cerrillos Cultural Center for a later briefing. Sticking out my hand and imitating adults, I introduced myself as simply "Basiago." Following suit, he shook my hand and replied: "Rumsfeld."

65. I was in the company of my father in 1971 when we entered a bar in Albuquerque and my father had a conversation with Mr. Rumsfeld in which my father and Mr. Rumsfeld commiserated about being involved in a program that was involving American school children in time travel. During this conversation, my father informed him that the program had determined that he was destined to "make" Defense Secretary. Mr. Rumsfeld replied: "I know that, Ray. I read that in one of the reports. But that's one future event that I'll only believe when it happens."

66. I was again in the company of my father in 1972 when my father was briefed by Mr. Rumsfeld about the fact that upon high school graduation the children in the program would be admitted to the US Naval Academy at Annapolis "as a pretext for involving them in future project activities," as Mr. Rumsfeld stated.

Andrew D. Basiago, Esq.
P.O. Box 2311
Vancouver, WA 98668
(360) 980-4100

67. In addition, I was a guest at an afternoon reception at a downtown hotel in Albuquerque. After drinks were served, Mr. Rumsfeld regaled those around him with stories of his exploits as a naval aviator during the Korean War.

68. The 9/11 event was spoken of openly within Project Pegasus' inner circle. I think this was the case because it was not only a future event that had been detected by the program but because it was a dramatic future event; it was a future event that had implications for the national security of the United States; and it was a future event that involved something that had not been seen since the War of 1812, which was a coordinated attack on the US mainland.

69. One time, in a restaurant in Albuquerque, NM, one of the project engineers asked my father what he knew about this future event. "What can you tell me about the event called 9-1-1, Ray? Apparently, it's some kind of domestic Pearl Harbor?" My father responded, matter-of-factly: "Middle Eastern terrorists hijack commercial airliners and fly them into the Twin Towers in New York City." "What happens then, Ray?" the project engineer asked. My father answered: "The Twin Towers come tumbling down, like a ton of bricks." "God, how awful," the project engineer sighed. "What happens after that?" My father answered: "The country picks itself up, dusts itself off, and goes on like nothing happened."

70. While this was typical of the kind of informal discussion about 9/11 that I overheard as a boy while serving on Project Pegasus, my father and I were actually shown visual evidence of the future attacks of 9/11 that had been retrieved by the project from 30 years in the future.

71. One afternoon during our Summer 1971 stay in New Mexico, my father and I had just finished lunch at the La Hacienda Restaurant in Old Town Albuquerque, when my father was called to the telephone. He listened intently, and then said: "I'll be right down." When he hung up the phone, he said: "Let's go." When we were in the car, I asked my father where we were going. He said, tersely: "Aerojet."

72. My father sped to our destination. The Aerojet Corporation was in Socorro, NM, a distance of 90 miles south of Albuquerque. We reached Aerojet in a little over an hour, meaning that we must have been traveling at 80 to 85 mph for my father to get us there so swiftly by private automobile. At Aerojet, we were shown astonishing evidence, so, in retrospect, I can understand my father's excitement.

73. In those years, the Aerojet Corporation facility was at the corner of Bullock Avenue and Leroy Place on the New Mexico Institute of Science and Technology [NMIST] campus in Socorro, NM. It was a small, C-shaped building with a zero-scaped courtyard. A small macadam parking lot on the grass in front of the building accommodated about 10 cars. When one turned left while traveling west on Bullock Avenue to park in this small parking lot, one passed a sign consisting of a slab of black granite with silver letters that read "Aerojet Corporation." The Aerojet Corporation facility on the NMIST campus was processing images of future events retrieved by US chrononauts from the future.

Andrew D. Basiago, Esq.
P.O. Box 2311
Vancouver, WA 98668
(360) 980-4100

74. During one of three fact-finding trips about my project experiences that I took to New Mexico in 2003, 2004, and 2008, Joy Thompson, the head research librarian for NMIST, not only confirmed that a C-shaped Aerojet Corporation building was present on the grounds of NMIST in the early 1970's, but that in those years it was misidentified on the campus maps published inside the official NMIST course catalogues as either Gibbons Hall, a student union of NMIST, or as the National Radio Astronomy Observatory, which is located a mile west of NMIST. This was contrary to what I had been told by Aerojet before making my 2004 trip to New Mexico. They told me that Aerojet did not have a corporate presence in Socorro until 1985, when, in fact, it was in 1985 that Aerojet built its present facility on the NMIST campus and tore down its earlier, C-shaped building.

75. When, in 1971, my father and I entered the Aerojet building through a door in the interior of the "C," my father showed an armed security guard his Department of Defense identification card and told the guard, "My son's with me." The guard pushed a button and prison cell-like bars blocking access to the secured left side of the building retracted into the ceiling and we walked down the hall.

76. We were greeted in the hall by one of the photo-analysts processing images from the future at the Aerojet facility. I remember that my father had explained that some of these photo-analysts were graduate physics students studying under Dr. Stirling Colgate, who was then serving as President of NMIST and chair of its physics department. The photo-analyst was very excited and as he approached my father and I excitedly informed my father: "We've got it, Ray! We've got images of the event!" My father shook his head in bemused bewilderment.

77. The photo-analyst led us into a small room that had about 20 TV monitors stacked all over the place in a hodgepodge manner. The small photo-analytical lab was dense with TV monitors and video cassette consoles. The photo-analyst then took a beta video cassette and with trembling hands popped it into a beta video console. "Watch this!" he told us. The TV screen illuminated with a set of large square pixels that formed from the jagged leading edge of what appeared to be a fragment of videotape. This might have been the remnant of one of the microfilms of the sort that we were retrieving from the year 2045.

78. When the picture pixilated into view, we saw sun glinting off of a commercial passenger airliner as it entered the scene from the left, traveled across the screen slowly, and crashed into one of the Twin Towers in Downtown Manhattan, causing a dense fireball to erupt in the area of its impact with the building. The videotape loop that we were shown was approximately 20 seconds in duration. Every time the fireball would erupt and the loop would conclude, the photo-analyst would replay the videotape loop, and every time the plane again struck one of the Twin Towers, he and another young photo-analyst watching would exclaim "Bam!" as if they were replaying a replay of a "slam dunk" in a televised basketball game. I believe that what we were shown was the second plane strike that would take place 30 years in the future on 9/11 and its resulting fireball. Certainly, the footage was indistinguishable from the video evidence of the attack on the Twin Towers that has been broadcast widely since 9/11.

Andrew D. Basiago, Esq.
P.O. Box 2311
Vancouver, WA 98668
(360) 980-4100

79. In light of the fact that my father and I learned of 9/11 while attached to Project Pegasus, it is certain that Mr. Rumsfeld did, too. After all, he was the defense attaché for the program, which placed him at a higher level of responsibility than my father. Inevitably, Mr. Rumsfeld would have been shown the visual evidence of the future event, as my father and I were shown that day at the Aerojet Corporation in Socorro, NM in 1971; or would have read of the future terror attack associated with the term "9/11" in one of the intelligence reports about future events that were being circulated in the leadership echelon of the program and among top intelligence officials; or would have heard 9/11 discussed in casual conversations between project principals.

80. This evidence establishes that 30 years prior to 9/11, and on the day of 9/11, the US Secretary of Defense, Donald H. Rumsfeld, had prior knowledge of 9/11.

DATED this 11th day of September, 2012

ANDREW D. BASIAGO,
US Chrononaut, 1968-72, 1980-84

STATE OF WASHINGTON)
: ss.
COUNTY OF CLARK)

SUBSCRIBED AND SWORN to before me this 11th day of September 2012.

SHARI M. ROARK
Commission Expires
NOTARY PUBLIC
10-12-2015
STATE OF WASHINGTON

NOTARY PUBLIC OF WASHINGTON
My commission expires
10/12/2015

Andrew D. Basiago, Esq.
P.O. Box 2311
Vancouver, WA 98668
(360) 980-4100

The one and only true timetraveler Andrew D. Basiago tells the Truth:

THE EIGHT MODALITIES OF TIME TRAVEL by Andrew D. Basiago

1. Remote viewing was developed by the US military in the 1960's years before it was supposedly developed at Stanford Research Institute [SRI] in 1972. It uses the human mind to travel to locations distant in space in real time or distant in time-space.

2. Spinning to induce out-of-body experiences so as to travel on the astral plane is an ancient occult practice. It uses dissociation of the mind to access while awake the astral realm that we access while we are lucid dreaming.

3. The Montauk chair was reverse-engineered from the pilot's seat aboard a crashed ET craft, by which the ET pilot piloted the craft psychically to avoid collisions in space in light of the speed of the craft and the vast interstellar distances traversed. It uses magnetic transduction to boost human consciousness forward in time so that the individual in the chair pre-experiences a moment in his subjective future.

4. The teleporter, which opens up a vortal tunnel in the fabric of time-space through which the teleportee passes from Point A to Point B in several seconds, was invented by Nikola Tesla. It uses a field of radiant energy to open up the vortal tunnel in time-space. When the tunnel in time-space closes, the teleportee finds footfall in the location where the tunnel closes, either in real time or in the past or future.

5. The chronovisor was accidentally discovered by Vatican musicologists Father Pellegrino Ernetti and Father Augustino Gemelli when they were studying the harmonic patterns in Gregorian chants at the Catholic University of Milan in the 1940's. Ernetti and Gemelli found that the microphone they were developing could pick up the sounds of past events. It uses holograms that are so dense that they have the effect of lensing non-

We use cookies to ensure that we give you the best experience on our website. If you continue to use this site we will assume that you are happy with it.

OK NO READ MORE

multi-colored light by US defense contractors under DARPA after the Vatican gave the chronovisor technology to the US government for further development.

6. The stargate is a Tesla teleporter that so concentrates the radiant energy that it derives from the quantum hologram that it can send the teleportee vast distances in time-space. Once inside the vortal tunnnel, the teleportee can see that the tunnel is identical to the tunnel walls of bluish-white holographic light produced by the Tesla teleporter, but since greater distances in time-space can be reached by the stargate, the teleportee spends more time in the tunnel and so has a greater risk of asphyxiation. It was via stargate that Project Pegasus was accessing 2045 in 1972.

7. The plasma confinement chamber was invented by Dr. Stirling Colgate, president of the New Mexico Institute of Science and Technology [NMIST] and a physicist at the Los Alamos National Laboratories [LANL]. It uses radioactive plasma to propagate a wormhole which the time traveler travels in order to be embedded temporarily in a past event. When this local quantum field effect created around the chrononaut wears off, he experiences transitioning spontaneously back to his point of embarkation in the chamber without traveling via wormhole. It was via this device that Andrew D. Basiago was sent to Gettysburg, PA in 1863 in Spring 1972 as seen in the Josephine Cobb image of Lincoln at Gettysburg.

8. The jump room or “aeronautical repositioning chamber” [ARC] was developed in a joint venture between Parsons and Lockheed, possibly after being reverse-engineered from an extraterrestrial device or as a result of ET-human liaison in which the device was given to the US government by one of the Grey ET species. It uses an unknown process to relocate the teleportee on an interplanetary basis. In the CIA’s Mars jump room program, jumps between Earth and Mars tended to take about 20 minutes and involved the jump room “morphing” from a box to a cylinder and back again during the jump.

Copyright 2016 by Andrew D. Basiago. All rights reserved.

Source

We use cookies to ensure that we give you the best experience on our website. If you continue to use this site we will assume that you are happy with it.

OK NO READ MORE

Humans Are Free

Alien Base for Giants Discovered in the Bucegi Mountains

Share 19.3k Tweet G+ Share Share Share

http://humansarefree.com/2010/11/another-true-history-chapter.html

The article was originally published on November 30th, 2010, at 11:11 AM. It was improved, corrected and republished in May 2013.

I. Short Introduction

In the summer of 2003, in an unexplored area of the Bucegi Mountains, a team from Zero Department (a top secret section of the Romanian Intelligence Service -- SRI), had made an epochal discovery, which could had completely change mankind's destiny.

The United States of America exercised colossal diplomatic pressure on the Romanian Government, which intended to disclose the findings to the entire world.

The implications became far more complex due to the brutal interference of the Order of the Illuminati, which sought to take control of both the location of the discovery, and the joint Romanian - American expedition.

The expert on strange phenomena, and also the leader of operations for the Romanian State, Cezar Brad, is the “hero” of the shocking events that occurred in the Bucegi Mountains. He also had two memorable meetings with a leading representative of the Illuminati, and top Bilderberg member.

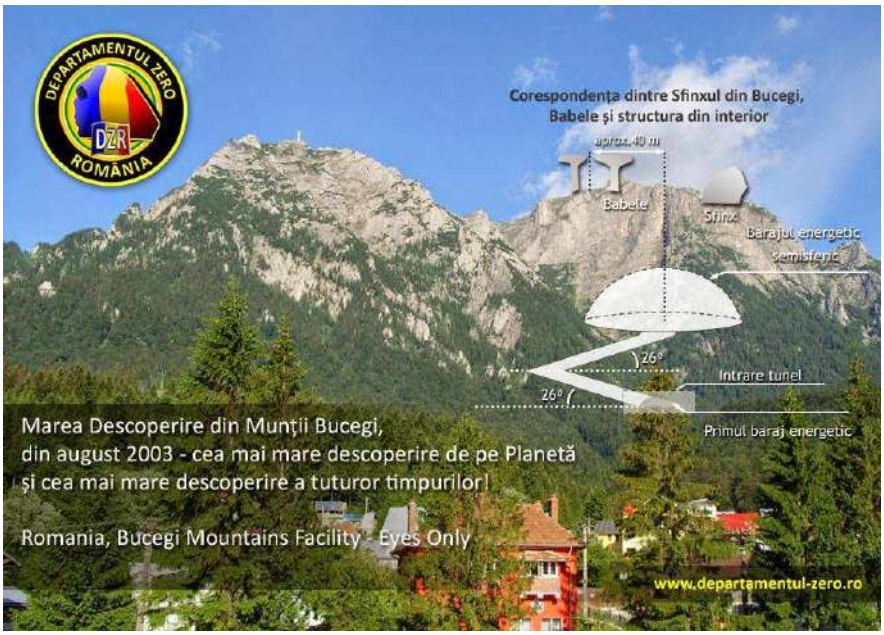

The location of the alien base inside the 'Masivul Bucegi' mountain, Romania. Also, notice the locations of the Sphinx of Bucegi and the Babele monoliths above the alien base.

II. A Strange Visit From the Most Powerful Bilderberg Member

In May 2003, Cezar was visited by a highly important character. The meeting request came through SRI, as a result of the government's intervention. The person was a foreigner, but spoke the Romanian language very well. He was also familiar with the country. The SRI informed Cezar that the visitor was a high ranking member of a very important Masonic lodge from Italy, he was a noble, and had very strong financial influence in Romania.

His political influence was also very high, since he was able to penetrate the wall of SRI agents and reach the DZ.

Cezar felt a high pressure and a heavy weight around this person. He was surrounded by a cloud of heavy, unpleasant radiation which concealed his true intentions. For this meeting, Cezar prepared thoroughly, isolating himself in a room and falling into a state of deep meditation, to learn more about the person.

A SRI helicopter brought this arrogant, tall gentleman, wearing a black suit. He had a cane with ivory handle and gold inlay. His face expressed harshness and his green eyes had a strange effect, radiating unusual coldness. He presented himself as Senior Massini (probably not the real name). He was very confident of his power and created the impression of a person who was used to give orders.

He was the leader of one of the most important Masonic Lodges of Europe and also to one of the most influential Masonic organizations in the world: the Bilderberg Group.

Massini was very direct and stated that humans are of two kinds: those who can be manipulated and ruled (these form the majority), and those who have certain virtues and strong personalities. He said that his group is part of the highest Masonic order and is very interested in the outcome of the discussion.

Mister Massini explained that the Bilderberg Group is not a Masonic lodge, and it means much more than that. He said that the lodges are just facades and the real power is much higher than the thirty-third hierarchical level. Massini invited Cezar to join the group, letting him understand that he will have many advantages.

According to Cezar, Massini was both physically and psychical strong, which contrasted with his age. Unfortunately for him, his power was centered on a huge ego, arrogance and sense of superiority over the rest.

Massini informed Cezar that he requested him personally, using his political influence, because he was impressed by Cezar's psychic power.

III. The Pentagon Spies With Satellites

A Pentagon satellite used for geodetic espionage, based on bionic technology and shape waves, discovered in 2002 a separate unit in a specific area of the Bucegi Mountains. The empty space inside the mountain had no correspondence with the outside, and looked like it was carved from the inside, by intelligent beings. It was definitely not a cave.

The satellite scan of the mountain revealed two major energetic blocks. These barriers were made of artificial energy. The first one was like an energetic wall, blocking the access to the tunnel, while the second one was shaped like a dome (or hemisphere), and was located at the opposite end of the tunnel, near the center of the mountain.

Massini was sure that inside the dome they will discover something extremely important.

He had deep knowledge about the origin of this discovery and had knew of the existence of at least one item located inside the great hemispherical hall. The tunnel and dome were strangely aligned with the rock formations from the top of the mountain, known as "Babele" and the "Sphinx of Bucegi".

The Romanian Sphinx of Bucegi

IV. A Similar Structure In Iraq

The Pentagon team noted that the hemispherical energy barrier had the same vibrational frequency and the same shape as one other top secret underground structure that they had discovered prior, near Baghdad, Iraq. Shortly after this discovery, the Iraqi war broke out and after a few months, the Americans had access to the biggest secret in the area -- which the Iraqis knew nothing of.

Massini explained Cezar that the content of that discovery had to do with Earth's mysterious past and the history of their secret organizations. When the Pentagon investigation noted the similarities between the underground structure of Baghdad and the one from the Bucegi Mountains, Massini and his masonic lodge became extremely agitated. Initially, they've almost panicked. The panic was due to the fact that this structure - much larger and more complex than the one from Iraq - is on Romania's territory.

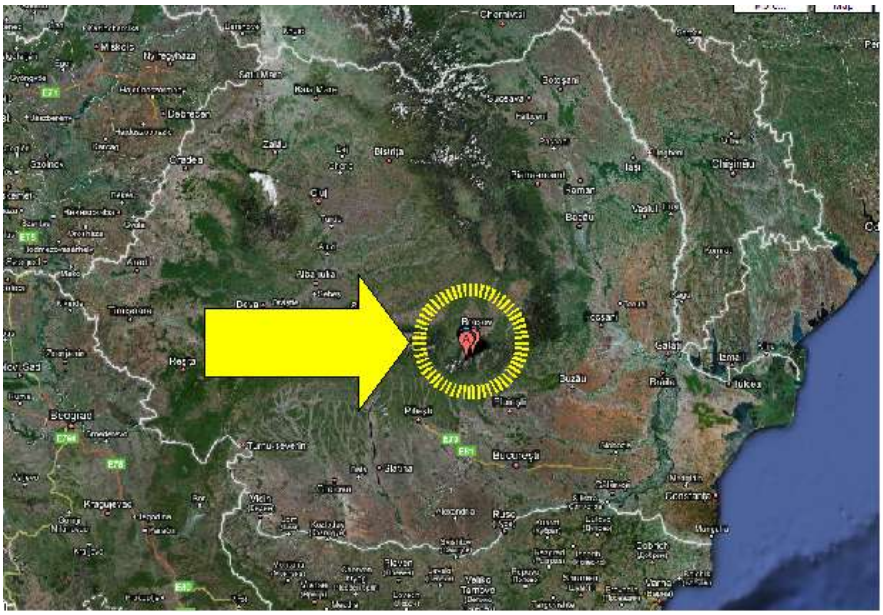

The location of the alien base, on Romania's map

[Apparently, Romania is probable to play an important role in the downfall of the secret societies that control the world and enslave mankind. It was also suggested that somewhere above the Bucegi Mountains, an energetic pyramid is located, which is invisible to the naked eye, and contains the real history of our planet. One can imagine their panic].

Massini brought to the drilling site an ultra sophisticated, hard rock drilling machine, used by the US military. The device used a strong plasma jet and a sort of rotating magnetic field, literally melting the rock with no visible effort.

V. The Secrets of the Bucegi Mountains -- Year 2003

They were able to achieve penetration about 60-70 meters away from the first energetic barrier, and reached the first gallery, which looked like a subway tunnel. Its walls were perfectly polished. At the end of the tunnel there was a massive stone gate, which was protected by an invisible energetic barrier. Three members of the first special intervention team tried to touch the door, and immediately died of cardiac arrest.

Any object (rock, plastic, metal or wood) threw at the barrier, immediately turned into fine dust. Two generals from the Pentagon and the U.S. presidential adviser arrived on the spot.

VI. The Grand Gallery

Beyond the formidable energy barrier, which caused the deaths of three people, there was also the solid rock gate. On the tunnel's wall, just in front of the gate, there was an area of 20 square cm, on which there was precisely drawn an equilateral triangle pointing up. The square was located between the huge grinding stone gate and the invisible energy barrier.

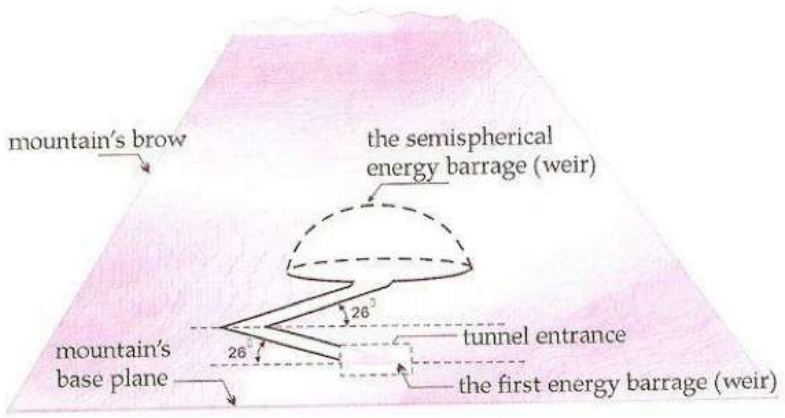

Tunnel and dome inside the Bucegi Mountains

Cezar felt that there is some kind of compatibility between the energetic barrier and himself, something like a mutual “sympathy”. His hand lightly touched the surface of the energetic barrier and he felt a tingling on the skin. The shield was completely harmless to him, so he stepped forward, passing right through it. The U.S. officials were absolutely stunned.

Cezar estimated the barrier to be no more than an inch thick.

He touched the triangle drawing located in the center of the square, and the gigantic stone door silently slid to the left, into the wall. That command also cancelled the energetic barrier, giving them access to a huge room, which was later named "The Grand Gallery".

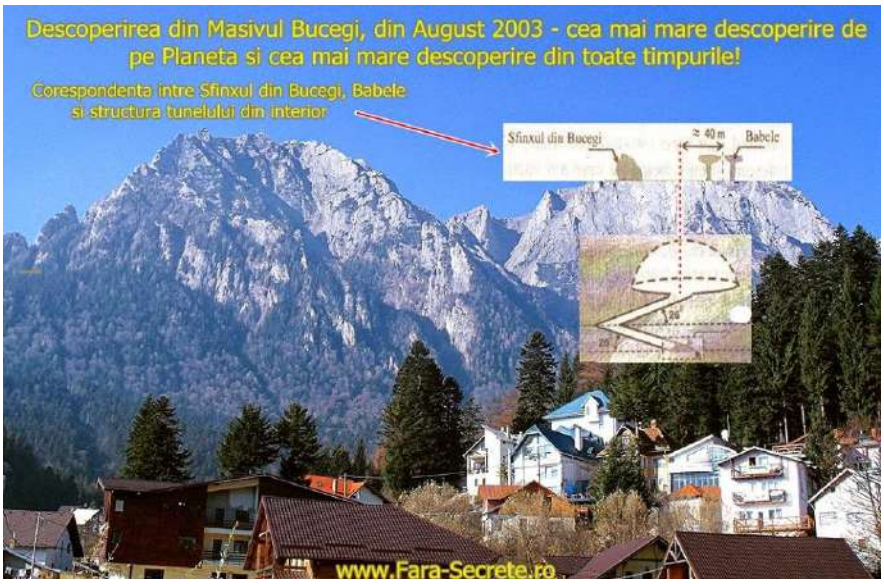

Even though there was no visible light source, the Grand Gallery was perfectly lit.

After turning off the first energetic barrier, the huge hemispherical shield at the other end of the room, suddenly tuned to a higher vibration and started emitting higher radiations.

On a closer analysis, the wall inside the Grand Gallery seemed synthetic but also felt like something organic was part of it. It had the color of oil, but the reflections were green and blue.

Later tests revealed that the wall's material was somewhat rough to the touch, but it could not be scratched or bent. It withstood any attempt of breaking, piercing or cutting it. Later, the scientists tried to burn the material, but in a mysterious way, the flames were somehow absorbed within it, leaving it untouched.

The American scientists agreed that the material is a mysterious combination of organic and inorganic matter. After 280 feet, the gallery suddenly turned to the right in a sharp angle. Further ahead a blue, sparkly, light could be seen. The blue light at the end of the gallery was the reflection of the protective shield of energy.

VII. A Similar Base in Iraq

The U.S. adviser on national security issues received a call and he was notified that the energetic shield from Baghdad, Iraq, had been suddenly activated, and it was also pulsating at a higher frequency.

In front of the shield from Baghdad, a hologram of our planet appeared, which sequentially and progressively depicted the European Continent, then moved to the south-east, then it showed the Bucegi Mountains from Romania and, finally, it showed their own location within the structure's corridor. It was obvious that the two hemispherical energy shields were in a direct connection.

Basically, the Iraqi base had been notified about the presence of people inside the Romanian base.

The bad news was that the U.S. presidency was notified and it contacted the Romanian diplomacy. In just a few minutes, the whole operation had been disclosed, and Lord Massini's plan went down the drain.

The U.S. presidency demanded to take control over the secret base and the entire operation. The Romanian politicians, who knew nothing of the undergoing secret operation, panicked.

The Pentagon's generals present at the scene, had been informed that Washington demanded an urgent meeting.

VIII. CSAT (Supreme Defense Council) Emergency Meeting

An emergency session of the Supreme Defense Council (CSAT) had created a huge wave of sympathy for the Zero Department. Most were shaken by the news they've received. The CSAT's decision was to continue the research, but under Zero Department's complete control. They've had also demanded an inventory of everything found in the Great Room.

From Bucharest (Romania's capital), the orders came in waves, canceling each other. Some were very vehement and strict, while others were elusive -- denoting the huge tension.

CSAT's members were in continuous session, keeping in touch with the Bucegi Mountains team. After discussing everything for hours, they had decided to make the discovery public. The Romanian government was to make a formal statement to the entire world. Some CSAT members vehemently opposed the decision.

IX. Romania's Official Statement

When the U.S. diplomacy had been informed that Romania will disclose the discoveries, everything tuned into chaos. The President was called for a direct phone conversation with the White House.

Within hours, the U.S. blocked all financial transactions with Romania and its access to all other financial institutions. Romania was about to declare "State of emergency" in the Bucegi Mountains and the capital.

The talks between the U.S. officials arrived in Bucharest and the Romanian Emergency Department took place without a translator. The U.S. officials were verbally violent, constantly shouting and uttering threats to Romania and its officials.

Romania's official disclosure to the world would have provided photographic evidence and anything else essential for a complete clarification. Leading scientists and researchers from all over the planet were to be invited for in depth studies.

But most importantly, it would have revealed the truth about mankind's distant past and the real history -- which according to what Cezar witnessed inside the Grand Gallery, is almost entirely counterfeit.

The reaction of the U.S. government was so brutal because that disclosure would have shattered their global influence and power, in a instant.

The official reason cited by the U.S., was not to create panic in the world, but they had omitted to acknowledge that the current state of global anguish is a direct result of deliberate deceit and manipulation conducted by the Freemasonry and other secret societies, for millenia.

There was also an intervention from the Vatican (if you wonder how did the Vatican found out about this discovery, then you should know that they are at the very top of the world's control pyramid, and their religious piety is merely a facade -- read: The Darkest Secrets of the Vatican), in which the Pope (!) called for moderation before this great, fundamental, step for mankind.

The Pope promised to make certain documents available to the Romanian state from the ancient papal secret archives, which were of great

importance for Romania. The documents were backing up the discoveries (yes, that's how powerful a Pope is).

After 24 hours of negotiations, a final agreement occurred between Romania and the USA. The Romanian state was to postpone the disclosure, and gradually present everything to the people.

X. The Projection Room

The Grand Gallery ended abruptly with a giant auditorium, 30 meters in height (98,5 feet) and a length of 100 meters (328 feet). The Projection Room was smaller in size and it was protected by an energetic shield.

Advancing towards the shield, a portion of it disappeared, in the shape of a door, allowing access inside it. The shield protected the room by any outside influences. Once inside the room, the shield became compact and looked like a white-golden wall.

Basically, the shield formed this dome-shaped room, with curved walls and ceiling. At the back of the room, at a height of a about 10-12 meters (33-39,5 feet), the shield ended where it touched the room's stone wall.

In this wall there were three enormous tunnel holes: one located straight ahead, and the other two were symmetrical on both sides. They were lit by a diffuse light in a greenish tint. Both sides decided to prohibit the access to these tunnels and a protocol was signed between them.

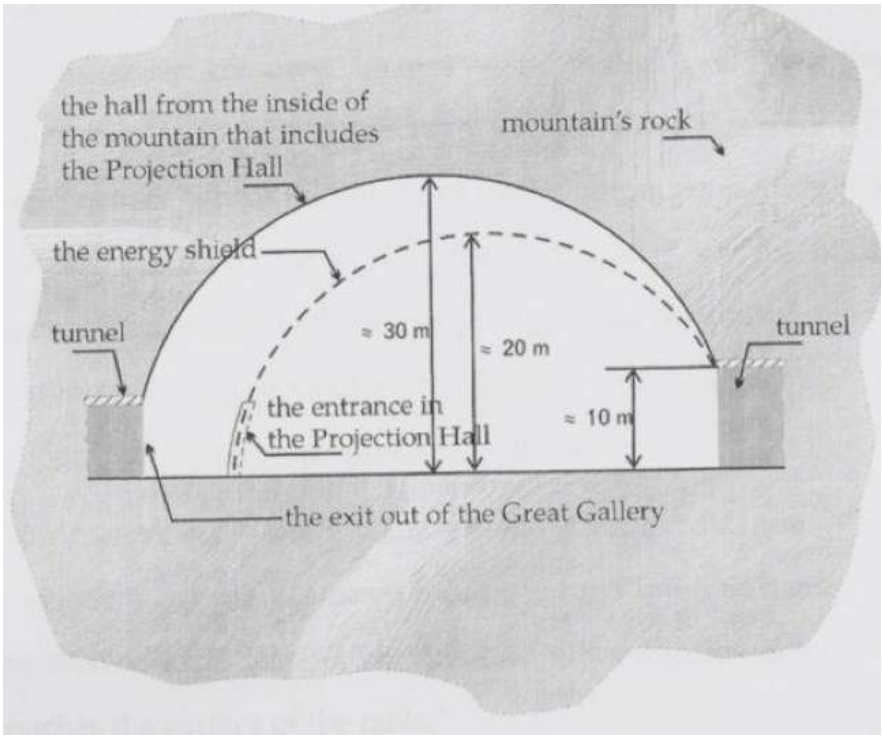

XI. Tables For Giants

A series of huge stone tables were arranged along the right and left walls (five on each side), following their curvature. The tables were about 2 meters in height (6,6 feet).

The table tops had precision cut-in reliefs, different signs of an unknown writing and characters that resembled ancient cuneiform. The writing also contained more general symbols, such as triangles and circles. Although the signs were not painted, they've had a fluorescent light radiating in various colors, different for each table.

On some of the tables there were different objects, which appeared to be technical tools. From many of these tools, translucent-white wires descended to the floor, and entered inside shiny, silver-like, rectangular boxes. These boxes were placed directly on the floor.

At a closer inspection, the cables were extremely flexible and lightweight, and light pulses could be seen circulating along their length. Each time someone approached the tables, a holographic projection was automatically activated, presenting aspects of a particular scientific field. The three dimensional images were perfect and had height of almost two and a half meters (8,2 ft).

The projections were automated and ran by themselves, but at the same time they were interactive, and changed according to the signs touched on the tables' surface.

[Picture of an actual giant skeleton unearthed in the 1970s inside a Romanian gold mine, at Rosia Montana -- the full story in a future article]:

XII. A Great Discovery: Holographic DNA Combinations Between Extraterrestrial Species

Because of the great height of the tables, the scientists used special tripods to climb at a comfortable height. At a closer investigation they've observed a dark-glassy material covering the table tops. The material was divided into several large squares, bounded by straight lines, which formed some kind of a grid.

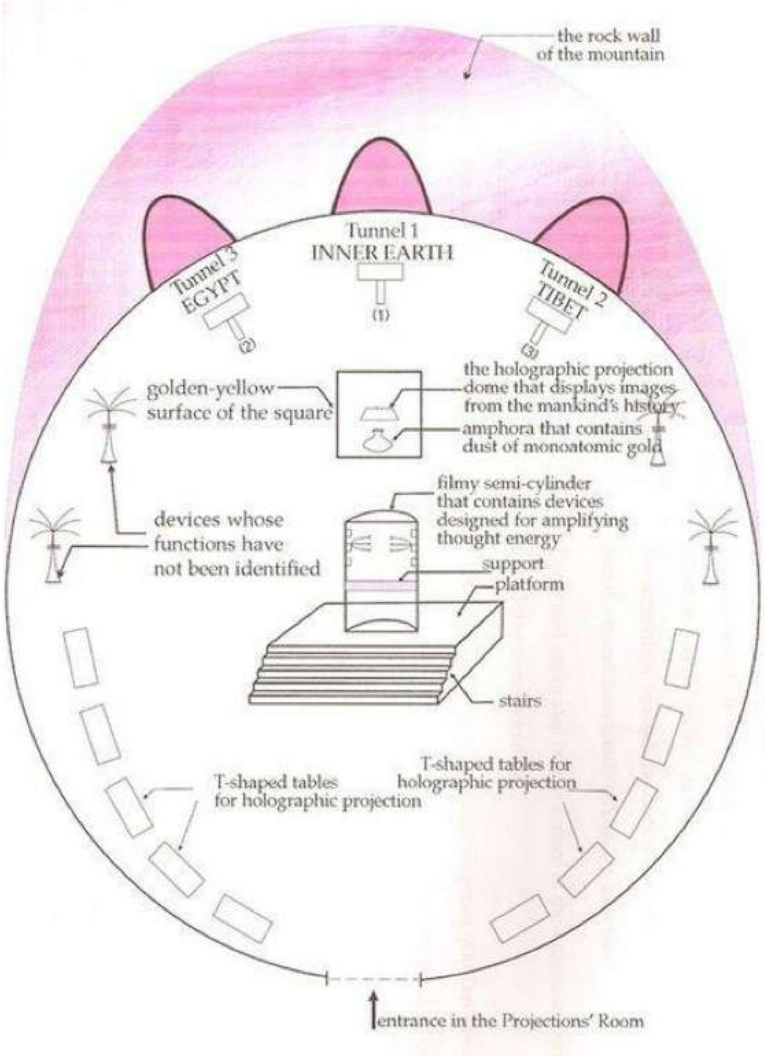

One of the tables contained information from the field of biology, and it projected images of plants and animals, some of which were completely unknown to the scientists. After touching one of the squares, a hologram presenting the structure of the human body was activated. The hologram

was constantly rotating, highlighting various areas of the human body.

Touching other squares activated holographic projections of extraterrestrial beings, from other planetary systems. Simultaneously touching two different squares, a complex scientific analysis was projected, showing the DNA of both species, and compatibility possibilities between the two.

On the sides, in vertical lines, there were written explanations in the same, alien alphabet. At the end of the simulation, a crossbreed between the two species was displayed.

XIII. Real Giants

Judging by the size of all the objects within the Projection Room, the creators of the edifice were probably very tall beings. A confirmation of giant humanoid skeletons found in Romania could be found in a newspaper called “Ziarul”:

> "The team from the newspaper is accompanied by researcher Vasile Rudan, who noted that the people of the Bozioru village have concrete evidence: a cemetery with skeletons of giants. It was discovered by chance over 20 years ago, when the authorities decided to plant apple trees in the village of Scaieni. Digging on a hill, the villagers discovered huge skeletons, measuring more than 2,40 m (7 ft 10 in).
>
> "Dragoi Ilie, one of those who worked in the apple orchard, takes us to the spot. Mister Ilie shows us around the orchard: 'Everywhere are tombs of giants. We were making holes, to plant saplings, when we found a human head as big as a pumpkin. Neither one of us had ever seen anything like that. We were all amazed. Digging further, we've found some bones of the feet, as big as the vineyard poles. The dead one must have been very big.'"

XIV. The Library of the Universe

The Projection Room contained detailed information from fields like: physics, cosmology, astronomy, architecture, technology, biology, genetics, and even religion. Because it contained so much information, the room was compared to a library.

In the middle of the room, there was a podium-like area which contained an interesting device. The scientists speculated that it might have been a device to enhance various cerebral functions.

XV. Romania's Control Panel

Next to it there was a command panel, covered with various geometric symbols, in different colors. There were also two sliding levers and a red button, in the center of the panel, above all other commands. A holographic simulation explained the purpose of the button. It showed an image of the Carpathian Mountains as seen from 25 km (15,5 miles) above them and next, an enormous quantity of water flooded the lowlands and plains.

Next, from the territories of Romania, Hungary and Ukraine, more streams of water appear, heading towards the Transylvanian plateau, in the form of huge rivers. The image focused on Romania's territory and showed most of its surface covered by the waters of a great sea. Some of the tallest mountain peaks could now be seen as small, floating islands.

Next, the waters begun to withdraw, as soon as the leavers found on the panel were activated, leaving sunk only a small area near the Retezat Godeanu mountain. A true manual.

XVI. A Mysterious Amphora

Behind the control panel there was a square pedestal, of about three meters (9 ft 10 in) per side, on which a mysterious amphora was resting. Lord Massini had knowledge of its existence and, for him and his Masonic elite, this was the most important discovery.

The amphora contained a very fine white powder. The researchers were dismayed to find that the powder was a high purity formula of monatomic gold, with an unknown crystalline structure.

The gold powder in its pure form greatly stimulates certain waves and energy exchanges at cellular and neural level. This causes an accelerated process of rejuvenation.

Theoretically, a man can live in the same physical body for several thousand years, provided they consume from time to time, a well-defined quantity of monatomic gold powder. This explains many puzzling aspects about the incredible longevity of some important figures and uncovers

part of the hidden intentions of the global elite.

XVII. The Real History of Our Planet

Behind the amphora, in the middle of the square, there was a huge dome that projected holograms. It displayed the main aspects of humanity's most distant past, from its very beginning. Cezar explained that according to the images projected by the hologram, about 90% of mankind's official history is false and counterfeit. Darwin's evolutionary theory is also incorrect.

In the middle of the square is a huge dome which projects a hologram of moving parts. It contains the main aspects of the very distant past of humanity, from its very beginning. Cezar explained that according to the images projected by the hologram, Darwin's evolutionary theory is completely false.

The true origin of man is depicted in a condensed holographic form. After these lessons of truth, we can say that 90% of the official history of mankind is false and counterfeit. Unbelievable, but what is now considered to have really happened in our history, never did, while the so called "myths" and "legends" are almost entirely true.

Also, most archaeological theories are false. For example, the dinosaurs did not went extinct 65 million years ago, and the old continents of Lemuria and Atlantis existed. This strange inversion caused many problems and conflicts between people in our past. For a correct dating of the presented events, a star map corresponding to that period was projected on the background.

Although the time period covered by the projections was very large (several hundred thousand years), and the procession cycle of the Earth is 25,920 years, by observing the number of “Platonic years” (the 25,920-year cycle) the exact dating of the events was possible. The Bucegi Mountains are 50-55 thousand years old.

XVIII. Shocking Revelations

Cezar saw what happened during the so called Great Flood and where the human civilization originated, but he decided not to reveal this, as the revelations are too shocking for the mentality, ideas and knowledge of the contemporary man.

Personally, I think people like him are also responsible for the current state of unawareness and latency of the human species. We have been lied and manipulated for millenia, and as soon as we are close to the truth, someone decides that we are not yet ready to hear it.

This is an arrogant and selfish approach! The people are as ready today as they will ever be, and the sooner the truth will be released, the better. Having more pieces of the puzzle will make them accept the truth easier and, more importantly, will make convince them to take action against the manipulators and enslavers.

In a disturbing display of images, the existence of Jesus and his crucifixion was also presented. The projections revealed that many of those who witnessed the crucifixion came there from other historical periods.

They were wearing the same kind of clothing as the rest of the people, but their facial features were different, hence they were constantly covering their faces. The hologram also presented fragments from the spiritual lives of other exceptional characters of mankind's distant past, including people that we know nothing of.

In those times, the social and population distribution were completely different from what is known today, so the archaeologists and anthropologists should review their theories from scratch.

XIX. The Three Mysterious Tunnels

The discovered tunnels are thousands of miles in length and lead to three different areas of the planet. The one in the left connected the Romanian base to a yet to be discovered underground base somewhere in Egypt (which was definitely discovered and explored by now).

The right tunnel led to a similar but smaller structure, in the "Tibetan Plateau". This tunnel had three secondary ramifications. One led to an underground area near the Romanian city of Buzaru (close to the "Carpathian Bend"). Another one led to the already mentioned Iraqi base, while the final ramification led to an underground base in the "Gobi Desert", in Mongolia.

XX. The Third Tunnel -- A Secret World

The middle tunnel was the most important to both Lord Massini and the U.S. Government, which strongly requested to be kept secret to the public. This tunnel descended to extreme depths towards a veritable underground world, located near the center of our planet.

Those of you who are not familiar to the hollow earth theory, please note that there are important figures who support the theory that all planets are probably hollow on the inside, and bring interesting scientific arguments to support their claims.

Also, there are some very interesting and beautiful stories about people who allegedly traveled to this world. The realm is commonly known as Agartha, and the third tunnel was probably leading straight to it. It only makes sense that the shadow elite were not interested to make the discovery known to the people.

Related: The complete collection of stories about Agartha;

Intense preparations begun for expeditions inside all 3 tunnels, as following: the first one to Egypt, the second to Tibet, and the third one to Earth's core.

(Summary of events from the book: "Viitor cu cap de mort", by "Radu Cinamar" -- the pen name for an undisclosed writer, which in my opinion, is none other than ex-General Emil Strainu. I base my statement on the extremely similar writing style and the fact that the author had direct access to this above-Top Secret alien base -- something that couldn't have happened unless the person was an insider.)

In 2009, a local television "Antena 1" briefly presented these events:

After the program, they've received an anonymous phone threat:

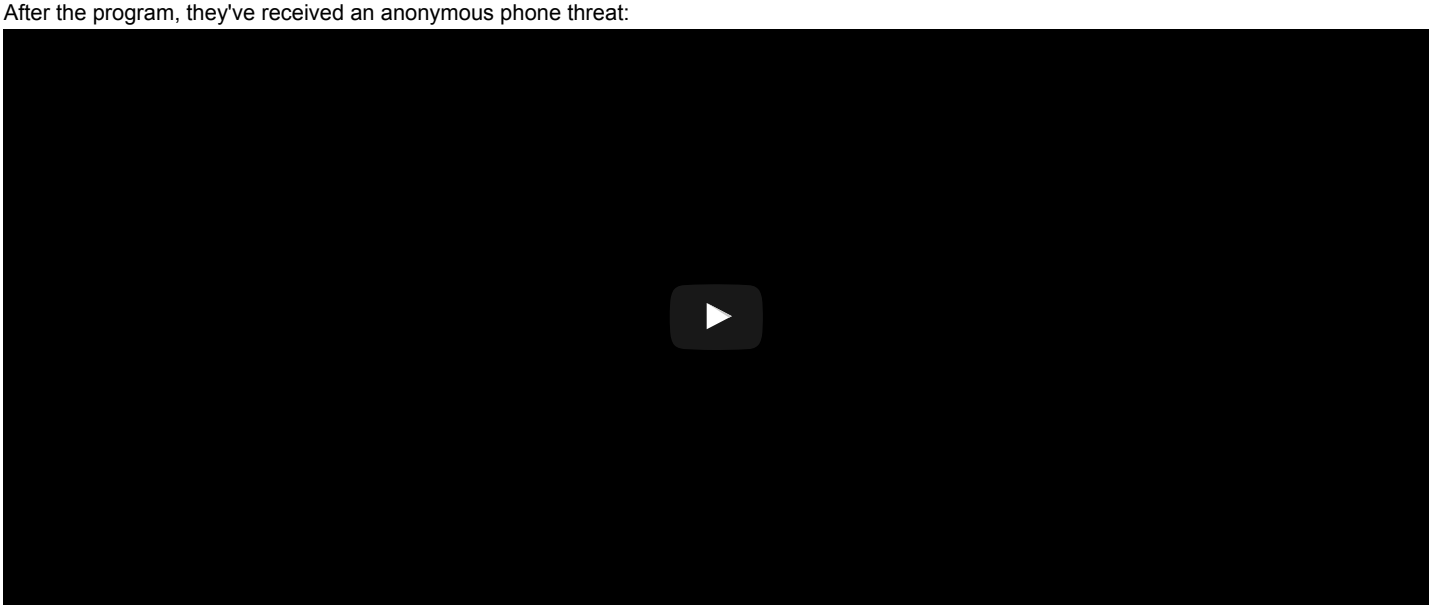

The following is a transcript of the phone call. The reporter from "Antena 1" answered the phone:

Reporter: Hello, good afternoon!
Anonymous caller: We're sending you a warning: be very careful! Stop talking about the Bucegi [Mountains]!
R: Who are you?

A.c.: This information must remain at the level of some structures and must not be made public! You've entered a dangerous game. You are young, you have families... there are enough subjects in this country to speak about.

R: Mister, who are you?

A.c.: Don't wish to know us and to be yourselves interviewed by us! That's all I've had to say.

Thank you for reading and always remember: "the truth is out there". Never stop searching...

By Alexander Light, HumansAreFree.com, based on Radu Cinamar's book Transylvanian Sunrise; | You can find further details and the discoveries that followed in Radu Cinamar's books; | Cover image: Fara Secrete; | Testimonies about giant skeletons discovered all over Romania (not available in English): The Secret of Rosia Montana; Argedava's giant skeletons (more here); Romania's giants; The Giants of Scaieni;

Donate

Dear Friends,

HumansAreFree is and will always be free to access and use. If you appreciate my work, please help me continue.

Stay updated via Email Newsletter:

Subscribe

ExelateData

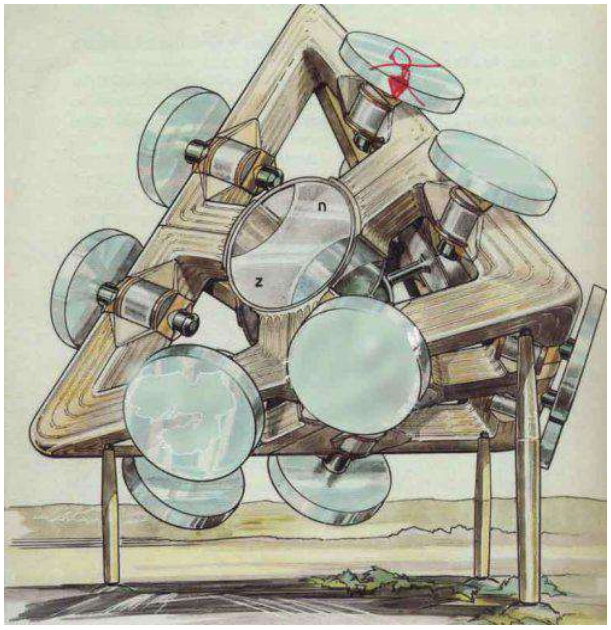

Technical information given from the IARGA contactteam.

their describtions on the matter of TIME

- AND MORE

picture is described later

12. The analog carrierfield model, an instruction model.

The cosmic carrier field of all space and matter performs a sixfold function, of which some have already been discussed in gereral way.

1. The carrier function of an infinitely strong forcefield blocked in itself contains the fluidum conducting all waves without dissipation and maintained to eternity.
2. The orientation of the time-axes of the universes with respect to nothing provides the structure of the carrier-field of three dimensions, the bounded Love-will, creating our life and existence.
3. The time synchronisation function locks all universes in the iron grip of the law of cosmic counter-balance from which no atom can escape.
4. The feedback principle of time to the total mass of the universe is the function of the coupling-field by counterbalance (and interference) of the time-bound waves.
5. The function of the timeless primeval atom-field, the atom-principle, as the transmitter program containing the code of matter of which all atoms are remote manifestations.
6. The function as bearer of the absolute ALL-knowledge and goal consciousness, manifesting itself as the laws of nature and as the intelligent goal of life: the spirit of God.

The last function concerns the existential aspects, which have been discussed in the previous section of this book.

The first analog model is a mechanical instruction model explaining the cosmic carrier field by means of symbols. This model was built on another life-supporting planet on a high mountain and was many meters high. It was the gathering point for contemplation of that intelligent race for devotion to its Creator.

It was the symbol by which the majority of the race acknowledged the goal of Creation, simultaneously the sign that the cosmic isolation had been lifted. The other function of the carrier-field will be discussed with the help of this mechanical instruction model.

The analog model consisted mainly of the six edges of a huge equilateral triangular pyramid built out of solid soft-iron bars. The many metres thick edges of the pyramid contain an impressive number of iron bars parallel to the direction of the edges and cast in a kind of plastic resin following a process similar to that of casting concrete(betong). So a mainly iron-frame was formed especially suitable for conduction of magnetic pulses of high power without much loss.

So far the carrying fuction of the cosmic time-field, which primarily maintains the timeless waves is symbolized in the model. The magnetic pulses in the edges of the pyramid run backwards and forwards like the timeless waves in reality.

With respect to the other edges of the pyramid, the magnetic pulses are phase-shifted. The problem is that up to now the forward propagation (forplantning) in time has been missed out. In fact we look for the equivalent of the two little wagons on the vibrating rail. The solution can be found in the symbol of the rotating flywheel, as *with the atom its rotation is continuous in time, it is in fact time propagation.* Therefore the iron frame of the pyramid is discontinued at two places in each of the six edges of the pyramid. At this discontinuation point a linear magnetic impulse motor is installed, on the axis of which a large flywheel is mounted.

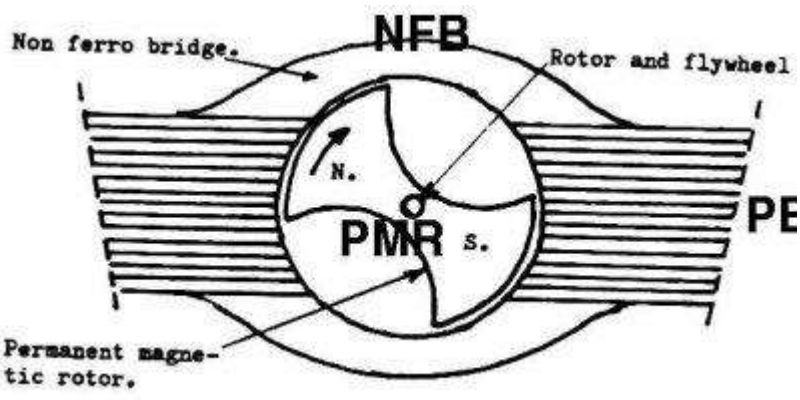

NBF=NonFerroBridge

PE=PyramidEdge and soft iron bars

PMR=PermanentMagneticRotor

The flywheel symbolizes not only the propagation of time, but also the inertia of matter and so the flywheel is in effect the total mass of the universe. This type of magnetic impulse motor is not self-starting, so at the inside on the flywheel axis a starter-motor is mounted, fitted solely for the purpose of starting. One rotating the synchronous motor maintains the exact number of revolutions at the same frequency of the magnetic alternation field. Thus in each of pyramid's edges two synchronous motors are mounted making twelve flywheels in total.

The two flywheels per axis rotate in opposite directions to symbolize the time propagation in opposite time directions. This type of linear impulse motor is chosen because it can be made to rotate in either direction.

The first analog model.

In one triangular plane of the pyramid the six synchronous motors in the iron frame demonstrate a rotating magnetic field, seen from the center of the plane. Each edge of the pyramid has the right phase-shift with respect to the other edges of the triangle.

The first model has four central rotating magnetic field generators in the middle of each triangular plane. (See figure of unfolded pyramid indicating the actual phase-shift).

These four synchronous (three phase) generators are coupled together by a gearbox and are driven by the main electric motor (not shown in the drawing). Consequently the four three-phase generators fulfill the synchronisation and constant phase-shifts for the flywheels of the pyramid-edges. The four separate rotating fields together, initate the complex three-dimensional rotation of the carrier field (or atom-field).

The disadvantage of the first model is that it is further away from reality, because the atomic field is not symboized as one three-demensional rotating field. However it shows better how to imagine the complicated rotation in three dimensions.

The second or the real analog model.

This mechanical model has only one central generator in the middle of the pyramid, instead of the four rotating field generators of the first model. All magnetic waves in the pyramid edges go straight to the pyramid's center. The

rotor of the 3-dimensional rotating generator is like a yo-yo with spherical end-surfaces.

It requires a touch of genius to provide the drive-connection between the central motor and the spherical rotor, which has to be started up in a complex rotation. The six diametrically opposed pole-shoes from the middle of the pyramid's edges around the spherical rotor form in pairs, three axes of right angles - representing a Cartesian coordinate system. So it shows that the six time-axes of the edges of the pyramid can be converted into the three principal time-axes of the central sphere.

Together it imitates three-dimensional time, which causally creates the three-dimensional space of our universe.

The principles of the first and second analog models are equivalent. One version can be converted into the other, for example, converting the four rotating fields to one three-dimensional rotation in the centre-mass of the pyramid.

The model can be started by switching on the thirteen drive-motors. As the flywheels reach velocity the twelve starter-motors are switched off and only the central motor drives the complete gigantic model. The essence is that all flywheels have exactly the same number of revolutions. They are all either synchronous motors or generators. Then the flywheels are marked and illuminated by a stroboscopic flash light. *Seen by the normal eye they do not appear to move showing the synchronous rotation and the constant phase-shifts between the flywheels.*

These mechanical models are meant to explain the unimaginable Creation out of the nothing by symbolic imitation of the carrier-field. However it is only a weak symbol of Creation. The carrier-field is the esoteric medium, a transmutation of the absolute spirit or conscience, it is the spiritual force field of infinite strength which is present everywhere in the universe.

The imitation of the carrier-field functions.

Nevertheless the analogy of reality is incredible. This will be shown in the next explanation of the five functions of the cosmic carrier-field.

The carrier-function

The foundation of the carrier-field is the infinite force-field created by interference quenching (avbrytende stopp) of the original infinite vibration. The mode initiates this force-field with the six bundles of soft-iron bars as the edges of the pyramid.

As in reality, the three-dimensional magnetic rotating field in our model is caused by the linear waves of each time-axis. *The timeless waves alternate backwards and forwards as in our model*. They drive the flywheels representing the masses of the universes, and their rotation is the propagation (spredning) in time.

The orientation of the time-axes with respect to the nothing.

The relative position of one time-axis in the apparent nothing plays an important role in the orientation of the universes in reality, determining the direction of each time-axis. Here the first model is shown representing the four three-phase synchronous generators in the planes of the pyramid. Only with decompostion of the three-dimensional rotation into four rotations can one show that the three-dimensional rotating field has left no remaining component in the nothing, while in contrast a two-dimensional rotating field can not be nullified, a remaining component will always exist in the nothing. This can be explained by considering a single plane of the pyramid with its six flywheels at the edges, the analog for a two-dimensional

carrier-field. The rotation impulse of the flywheels is compensated by the opposite rotations but the rotation impulse of the central three-phase generator is left over. It can be measured by the outside world (the nothing).

It requires four field three-phase generators (maintaining overall symmetry) to compensate for these rotation impulses.

With this the three-dimensionality of the carrier-field has been shown and the orientation of the time-axes with respect to the nothing is determined.

The time synchronization function.

Impressively the model imitates the time synchronization, simultaneously maintaining the cosmic counter-balance by which the universes continue to exist. The rotation of the two flywheels per axis is in opposite directions and they rotate with exactly the same speed. Thus it imitates the circular motion to the timeless waves which progresses exactly synchronous by their mutual interference coupling.

The twelve cosmic systems run without any dissipation, once started, the perpetuum mobile continues into eternity with the absolute accuracy of time-synchronisation. If one supposes the model to be without loss and without using the eternal driving motors, it will continue to run synchronously due to the inertia of the flywheels and the fact that the synchronous linear impulse motors can function as generators as well.

This symbolizes another property of the continuous circular motion of the timeless waves, because every wave somewhere in the pyramid circuit at each moment has its opposite value resulting in an overall zero at any moment.

This is the law of conservation of the nothing.

The couplingfield function.

Time synchronization is not alone determined by the iron grip of the three-dimensional carrier-field and the principle of cosmic counter-balance. Apart from this an important effect is realized from the feedback of the gigantic masses of the universes to the timeless waves. These masses can be considered as enormous flywheels without loss. Once started by the super flash, no change in speed is possible, because a force of sufficient magnitude is simply not available. This function of the coupling field can also be shown in our model, because the linear synchronous motors of the flywheels are also generators. If the central driving motor is switched off, then the flywheels continue for some time to drive the central three-dimensioal rotating sphere. Everything stays exactly synchronous with the same phase-shifts.

This experiment shows how the flywheels feed their energy back and have a stabilizing function in time-synchronization. The coupling-field of the masses of the universes is fed back in the time-bound vibrations of the atom-field from which no atom total mass of the universes is fed back to one single atom.

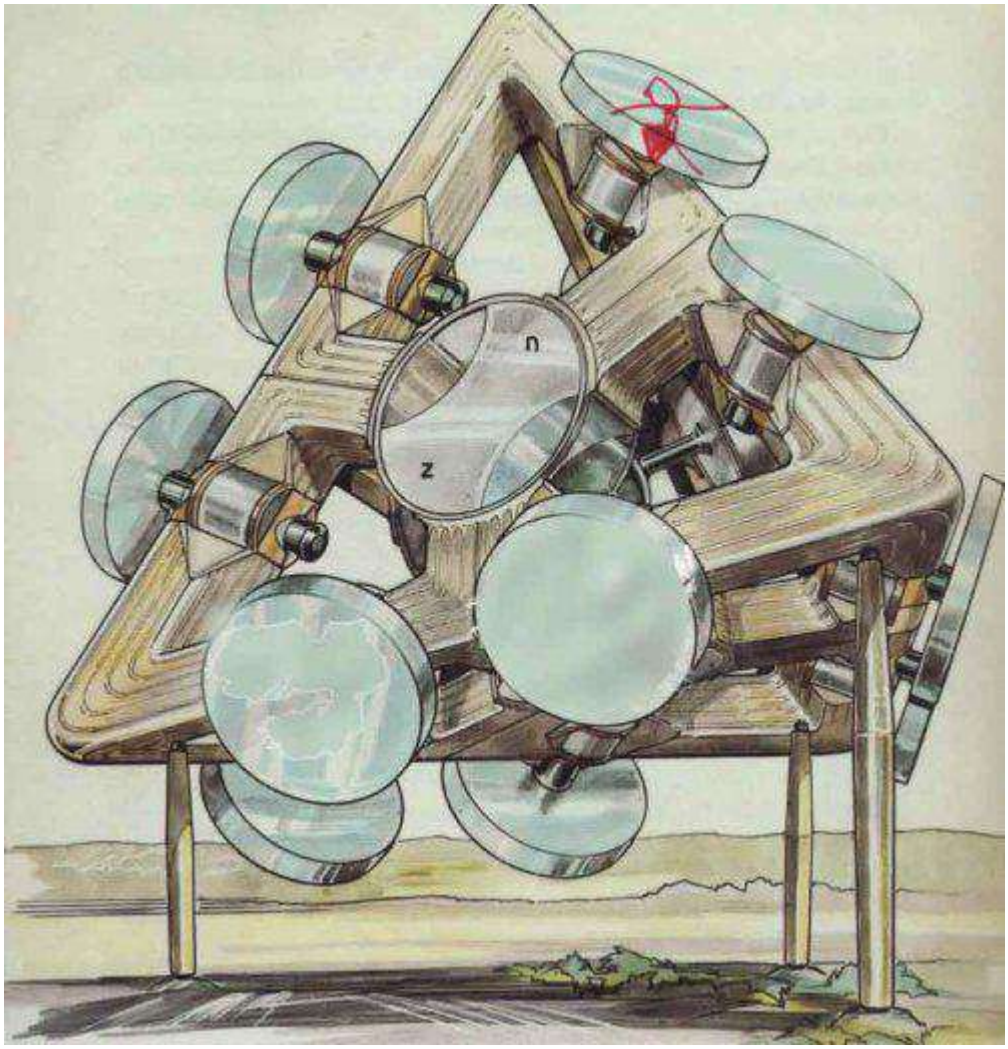

This is a painting by Rudolf Dass of the analogous visual-mechanical carrier-field model which symbolizes time and matter creation and synchronization in twelve universes. This giant working construction that was a cross between a monument and a machine was seen on an artificially flattened mountaintop on **Iarga**. This place was perceived as a place of pilgrimage, a place of meditation and contemplation, and the machine was a symbol of creation. The **Iarga**ns know no separation between science and religion, and religious and spiritual theories are entirely scientific. The model was several hundred yards(meters) long. The machine seemed to operate by some kind of perpetual motion, neither running on fuel or electrical power.

The Instructional Analog Model

The mechanical instruction models are the visual representations of the principles of the cosmic unified field theory. The model is intended to demonstrate that time, matter, and energy are creations out of the nothing and therefore the counter-balance has to be maintained to allow the causal infinity of the nothing to exist. In a broader context the physical symbols all take on new meaning and demonstrate the unification of science and religion. In a religious sense the spherical three-dimensional time-field in the heart of the pyramid symbolizes the Soul of the Creator. The pyramid symbolizes his infinite lovewill, the cage in which the infinity of His existence has been blocked irrevocably. The lines symbolize the different frequencies of the timeless waves. The flywheels on

the edges of the pyramid symbolize the twelve associated and interrelated universes, including ours, that make up this unity. One cannot exist without the others.

The timeless primeval atom-principle, the transmitter function.

The atom-field is a time-creating field and as such a remote manifestation of the primeval atom principle. It can be compared with a transmitter. As soon as the program is converted into waves of great power, billions of radios can receive the same program, the number is unlimited. Everything depends on the one program of the transmitter, the primeval atom-field. If this exists with infinite strength, it is at the same time the vibration medium (the carrier-field) which helps it to spread everywhere. *Thus any atom in any universe can receive the timeless basic program.* The second model shows the three-dimensional time-field of the primeval atom field most clearly, although this is a three-dimensional rotation of the central sphere in spatial sense. This is an analog of reality, the atom has a spherical field which is defined by six linear time-vibration directions. Any atom is a remote manifestation of the one carrier-field of infinite strength.

Considering this fifth function of the carrier-field one has to realize that only the central sphere, the atom, is visible to us. The fields in the pyramid edges outside the sphere are invisible. It is the time-field reality of which the atom is a reflection.

The mechanical instruction models are the visual representations of the principles of the cosmic unified field theory. This requires however some marginal notes. A material comparison to explain spiritual abstractions is always in some ways incomplete. There are several hiatus of which only the three most important ones are mentioned.

1. In the model one time-axis represents only *one frequency* of the magnetic field, while in reality all frequencies are contained. Every frequency however can be initiated for each time-axis for which the interference representation of the analog model is valid.

2. The model demonstrates the rotating field of the *timeless waves.* It *does not imitate the time-bound waves* by which our time-axis the propagation speed of time is X, then the phase velocity of the two time-axes connected to "our" pyramid edge is ½X. The other two time-axes connecting our time-axis with the other corner of the pyramid is -½X, making up for the time speed of our anti-universe -X. The crossing, not-touching time-axis is perpendicular to our time-axis and does not contribute.

3. In our model the masses of the universes are given by the flywheel symbol. In fact this is *fundamentally wrong, because it is separated from the three-dimensional rotation of the central sphere.* It can therefore basically not maintain the counterbalance of the nothing.

The most important conclusion of the analog model is that *time, matter and energy are creations out of the nothing and therefore the counter-balance has to be maintained to allow the causal infinity of the nothing exist.*

14. The existential symbolism of the model.

So far the physical aspects of the model have been unravelled, but if one wants to give a wider context to the model suddenly all the physical symbols change their meaning. In relation to philosophical or theological disciplines the model takes on the additional meaning of the unification of science and religion. By certain inherent (medfødte) laws within any intelligent race the denial of God's existence will be destroyed sooner or later. Earth science will provide an indestructible contribution to our final knowledge-awareness, which we shall attribute as typical human attainment in the cosmic integration. It is that piece of our human identity and self-awareness, which we shall possess and care for throughout eternity. *It the light of this purpose, science serves God and the distinction between science and religion fades away.*

In a religious sense the spherical three-dimensional time-field in the heart of the pyramid has a special meaning. **It symbolizes the Soul of the Creator**, the Father who is the pure Identity of the infinite origin. The pyramid symbolizes his infinite Love-will, the cage in which the infinity of his Existence has been blocked irrevocably. He sacrificed his Ego and his freedom, to love his twelve Sons once. He is present only indirectly in his Creation as the reflection of the infinity, the Supreme Being, as the one Ego-consciousness of the Archangels.

That is why the theologian covers the central sphere with pure gold, symbolizing the golden Heart, the Holy of Holies, the most sacred secret of the universe. The pyramid is then painted dark red, the universal colour of love. Over the red many thin golden stripes run in the direction along the pyramid edges. These stripes symbolize the different frequencies of the timeless waves, the expressions of Love and faith of the Father and his infinite Will.

Gathered around the golden Heart are the twelve flywheels, coloured white, the colour of purity and innocence. The model shows that every universe has the power to awaken the matter-consciousness and to transform it to the new

God: the Son. The goal of Creation is therefore the awakening and the formation of the twelve Sons of the Father.

This is not in contradiction with the Bible telling us that the Father sent his only-begotten Son. The Bible is solely directed to man. It is our instruction book for life describing our attitude towards God and our fellow man. The Bible does not tell anything about life on other planets, because it is not relevant in our relationship with God now.

The same goes for our parallel universes. In fact they do not exist for us, because they are not in our world of existence but somewhere else. They do not exist for all intelligent races in this universe, we shall never be able to observe them nor experience them in any way. Perhaps at the end of all time we shall meet. In *our* world the Father has one only-begotten Son and this truth is already so unimaginable that nobody can conceive the consequences yet.

END OF IARGAN DISCUSSION

---

mainpage

the IARGA CONTACT story

ufo-contact-material

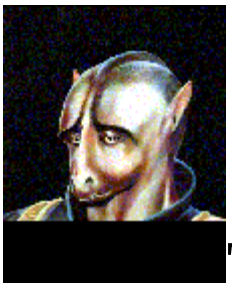

Technical information given from the IARGA contactteam.

their describtions on the matter of TIME

- AND MORE

APPENDIX 1

An Analog Model

1. Introduction

This appendix is not a part of the story of the Creation which is explained in religious terms in Chapter 1 (Part 2). It is a complementary way of reasoning to prove the existence of God, using the concepts of time, matter and energy. These concepts are also used in physics. The problem, which now arises, is that the author will use physical concepts without understanding the real meaning of the words, because he is not a specialist. The words atom, atom-field, matter, etc., must all be understood within the context of this book and they have no direct connection with the ideas used in modern science. Especially the words "matter" and "atom" are most confusing, because the **Iarga**n author knows about the existence of matter in three configurations (and its opposite possibilities as anti-matter); i.e., time-matter, phase-matter and *reflection-matter* (the one we know about in our universe), but he fails to interpret these concepts due to his lack of knowledge of physics. He only knows that these forms of matter are all related to one or none of the directions of time- propagation (tidsforplantning) of the atom of which time is fundamentally three-dimensional. It therefore determines in which form these configurations (beskaffenheter) can exist in our universe.

In this appendix - time-creation out of NOTHING is described - by making use of the concept of more time-dimensions. The explanation of time-creation is very difficult

because it uses an overall carrier-field of infinite strength and then this concept is called the cosmic unified field theory. In defining this term, one has to be careful, *because this theory is of a different basic nature from the existing unified field theories here on earth.* Our unified field theories try to unify the four basic forces in nature, which are the electro-magnetic, the weak strong nuclear force and gravitation. The unified field theories accepted by most prominent (iøynefallende) scientists find their origin in the general relativity theory of Einstein, which itself explains matter and energy in terms of space and time.

The problem now is to find a method, explaining the spiritual or esoteric reality, the cosmic time-field. On other planets, this problem was solved by explaining the basic concepts of the cosmic unified field theory. The elementary functions of these concepts can be understood with a mechanical instruction model demonstrating the cosmic time-field visually.

Why indulge in this complication of describing a theory which will probably only be fully grasped by a few individuals? It does not concern the author very much, he only carries out his commission. His **Iarga**n instructors gave three reasons for publishing the concepts of this theory:

1. The future integration of science and religion requires a material proof of God's existence. This explanation could be the start of the exchange between these two.

2. In the previous story of Creation the limitation of the infinite is explained unambiguously(upretendiøst), but the working principle was completely neglected(forsømt).

3. The cosmic unified field theory published in this book will be the only possible verification for the true identity of this book, providing the link for the future development of the human race.

2. The physical approximation of the NOTHING.

One concept in physics is that all atoms and energy consist of vibrations and wave appearances. In a material way, every atom or form of energy is caused by vibration. The physical approximation (tilnærmelse) describes the nothing of the idea of vibration - and *does not touch on the spiritual aspects and the consciousness of matter*. It does not distinguish between the "nothing" and the spiritual "No-Thing" (the ALL). It only recognizes the material aspects of the nothing.

If everything is vibrations or waves, then it is not necessary to speak of matter or energy, then Creation is fundamentally based on this concept of vibration. The primeval vibration (before the limitation) can be described as infinite in time, infinite in all its aspects and possibilities, infinite in frequency and amplitude and existing in all time directions (omnitime). Unchanging, timeless and powerful to all limited vibrations in every bound power. It is the omnipotent definition.

In this approximation the nothing is more simple to understand. Before the creation - the infinite omnipotent vibration existed- *but a vibration in every direction and of infinite frequency and amplitude is not a vibration*. The apparent paradox can be eliminated by stating: Only at the instant when this infinite vibration blocks itself by interference, *as in a flash, all bound waves and frequencies were created.* This condition is very close to the existential view of the Creation out of NOTHING in Chapter 1.

The nothing (here) has no counteraction, but in contrast the omnipotent vibration - can manifest itself only by counter-acting in such a way that the infinite allows the nothing to be. So one can also state that all vibrations were created because the nothing bound itself by a mechanism of interference quenching (ble dempet) - (counteracting vibrations) of infinite force, which blocked the infinite possibilities of these vibrations. *This universe can only be considered as the limitation of the unbounded nothing.*

3. The bounding of the omnipotent infinite vibration, the cosmic time field.

One of the basic principles on which the mechanism of bounding is based is: *If one property of a power (any power) of something is bound, then all properties and powers of this something will be bound.* In infinity the finite cannot exist. To limit the omnipotent vibration it was sufficient to bind only one of the perhaps infinite number of possibilities. Because if only just a little something were to be formed in the nothing, the nothing would be altered and cancelled irrevocably, then the complete finity (endelighet/begrensethet) was a fact. OR, if there were just the three-dimensional rotating time-field as a possibility of the primeval atom in the infinity of the nothing, then the finite was a fact. This atom-field needed to be a force-field of infinite strength, the carrier-field, to counteract the omnipotent vibration, the cosmic time-field.

4. The Creation can only exist as a result of counter-balance.

One of the functions of the carrier-field is time-synchronization by which the cosmic counter-action and therefore the nothing can BE. *Matter and energy cannot exist on its own in the nothing.* The principle of time synchronization is given:

1. Time is only relative, it is motion or propagation (spredning) in relation to at least a second motion of time.
2. the cosmic law of counterbalance dictates that the second time has to counterbalance the first time. So time can only exist in relation to a second exact *opposite direction* of time (running backwards in relation to our time).

3. Time exists only through the presence of atoms or matter. Then the backward-running time can only exist through matter in which the time propagation is opposite, *running backwards* in relation to us (antitime matter). Anti-matter or reflection antimatter may exist in our universe with an opposite electric charge with respect to our known reflection matter. The question, as to which charge antitime matter has in the anti-universe, is of no importance in this appendix.

4. Because neither matter nor energy can exist on its own in the nothing -another quantity of matter of opposite properties *must* exist which is exactly similar to that in our universe. This balance of matter and energy is so accurate, that one surplus atom (overskuddsatom) is impossible.

This explains nearly as per definition the cosmic law of counter-balance allowing the nothing to be. There must be at least a second universe exactly like ours, in which time runs backwards according to us, but normally for life in that universe. In the following it is shown that there are not just two, but *eleven* other universes in addition to ours necessary to maintain the cosmic law of counter-balance.

6. The time-synchronization field.

The law of counter-balance also applies to time. The timedirection is opposite and the time velocity is equal to ours. Time is the propagation of vibrations of the atom. Then the atomvibrations in both universes are equal and opposite with respect to the timelessness. This is only possible if these times are caused by one field (time-field).

The definition of a field (any field in physics) is: If an event occurs, because another event takes place somewhere else without a mechanical or visible connection between

these events, then these events are caused by a field. Time-synchronization occurs according to this definition. The atom vibrations in our universes are exactly similar, because the atom vibrations of our anti-universe occur despite the enormous difference in time and without any dissipation of energy. It is about 30 billion (milliarder) years since the occurrence of the super flash Creation (big bang) between the two universes.

The law of conservation of counter-balance is causal to the law of energy conservation in every universe. Each universe is a closed system and without energy dissipation outside itself. The amount of matter and energy once created remains constant. *A loss of energy is impossible, because our time-bound energy propagates forwards, while the time-bound matter and energy of the anti-universe propagate backwards in time.* These universes are separated by a time-barrier through which no communication nor transfer of life is known. (Well - according to information in the book UFO-CONTACT FROM PLANET KOLDAS and also told by the et-contact ASKET and Semjase - there are some methods for entering the mirroruniverse - but this can not be touched here - reseach yourself if interested!! R.Ø.remark.)

6. What is a timeless vibration or wave?

The question is how the field functions maintain the time-synchronization of the atom-waves between the universes separated by billions of years. It is only possible if the synchronization stands still in time, but exists simultaneously in all the time elapsed (- som er gått..) since the beginning of the super flash, as well in all the future. *A timeless vibration does not normally move in time*, the amplitudes of the field propagation - alternate (veksler) forwards and backwards in time. Time synchronization is the principle by which our universe catches every forward-moving amplitude and the anti-universe catches every backward moving amplitude of one and the same timeless wave.

On other planets there are simple mechanical models explaining the function of time synchronization. One such model is very similar to our well-known mini-model rail upon which are two little wagons. The model has two lengths of rail of say 1.50 meters each, which are in direct line with each other.

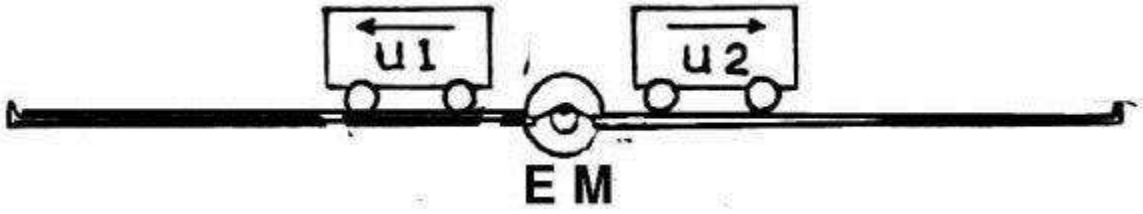

Picture of the model wagons with a Electric drive motor which letting an excentric, and so the rails vibrate horisontally.

Rail and wagon model demonstrating the principle of the timeless waves. The vibration is present at any point of the rail and at any time during the whole process period. Also from the moment of the super flash until the end of all times (ALWAYS).

The rails are mounted on small springs to allow them to vibrate forwards and backwards in horizontal direction (from left to right and vice versa). The two rails are connected to a little electric motor with a double eccentric, each driving one rail, letting the rails vibrate about 1 millimeter of linear distance, also backwards and forwards. The amplitude is small enough to be invisible to the eye.

Then one little wagon is placed on each rail and each wagon has a catch with a catchwheel (tilbakeløps-sperre) on one of the wheelaxes, so the wagon can ride in only one direction. *The movement in the other direction is blocked.* The wagons are placed with their rears against each other, after which the electric motor is switched on. If the teeth of the catchwheel have the same beat as the vibrator mechanism, the wagons roll away from each other with exactly the same speed to the end of each rail.

With this simple model time synchronization for the atom-vibrations of both departing universes (in time) by a timeless field "always existing everywhere" has been demonstrated sufficiently. At the same time a flaw(feil) comes to light. It is impossible to maintain an energy time flux of the timefield for the two departing universes, because where is then the inexhaustible (utømmelige)energy source to maintain the time-flux? (betyr det tidsustabiliteten??)

This is one of the reasons that a one-dimensional time-field is not possible. Only a three-dimensional time-field, which encloses the energy time-flux in itself, allows our universe and the others to exist.

7. The principle (mechanism) to create finity: INTERFERENCE.

So far the function of time-synchronization of the carrier-field has been considered. Now we will discuss the medium of conserving and maintaining the timeless vibration into eternity. It is the infinite force-field carrying all matter and energy.

We are at the moment of the flash or big bang, the moment at which the infinite primeval vibration limited (transmutated) itself to the carrier-field. This mechanism of blocking is well known and based on the principle of wave interference. (Interference of lightwaves is important today in laser technology.) Interference is the action or counter-action of two or more waves. If the *wave-propagation(-forplantning) is opposite and parallel* and the frequencies of the waves equal, mutual amplification (gjensidig forsterkning)or attenuation (fortynnelse) of the intensities of the wave is possible, depending on the phase relation between these waves.

If *the phases are opposite* and the *amplitudes of the waves are equal*, total quenching (dempning/kvelning)is possible. This is the principle of the binding of infinity. If an infinite wave manifests itself in one time-direction, automatically the equivalent absolute counteraction is created which counter-balances the infinity, allowing the nothing to be.

The infinite primeval wave(urbølgen) blocked itself at the moment it created itself and so it never existed in reality. It was in fact a *transmutation (forvandling) of infinity;* the transmutation of the infinite vibration of infinite amplitude and frequency to a carrier-field of infinite strength, which blocked itself by interference.

8. The time-bound vibrations or waves.

The primeval wave blocked itself in a three dimensional time-axis system (propagation directions) by interference, and trans-mutated to an infinite, timeless, immobile force-field. How could the bound timeless waves exist, which synchronize our universe?

It is an error of thinking to suppose that by quenching the omnipotent vibration - all finite waves were also cancelled. It is just the opposite. A vibration with infinite frequency is not a vibration in reality. The infinite prevented the vibration, because a vibration can only exist in the finite. As soon as infinity was removed, the prevention disappeared and the real bound wave was a possibility. It is the carrier forcefield although of infinite strength and energy density which gets its finite value due to interference quenching. All timeless waves are as it were encapsulated in infinity and therefore indestructible. However "belonging" to infinity and not bound by time themselves, they create time forever, they are the eternal ripples on the static ("krusning i likevekten"), unchangeable and loss-free field of infinite strength. (This must be what the Danish wiseman Martinus call the X2- principle and the primeval-desire or "urbegjæret" in Danish. R.Ø.remark.)

Because of this, all time-bound waves such as light, radio-waves or gravitation, exist in space without any loss and it is the empty space in the universe, which is the non-modulated structure of the carrier-field. It is one of the most fantastic touches of genius of Creation, that the non-vibrating infinity was transmutated to a loss-free medium carrying all time-bound and timeless waves. A few properties of this medium can be measured with instruments, the other part of its structure cannot be objectively observed yet, *it is the esoteric fluidum or the infinite Love-will of the Father which carries the whole Creation.*

9. The unimaginable three-dimensional time.

(Den utenklige tredimensjonale tid)

One time-axis counter-balances only one direction of time propagation of the omnipotent (allmektige)wave. In infinity all possibilities of vibration exist and therefore all time-propagation directions. The question is, could infinity be limited by just one time-direction and one co-existing propagation direction going the opposite way?

One way to answer this was already given in the previous paragraph, in which it was stated that the energy time-flux of the primeval wave of two universes is not a closed system. Another plausible answer can be by simply reasoning.

The atom is causal for the time - and space dimensions, due to its time-creating properties, already mentioned. *The space-creating properties are easy to understand, because the atom takes up space.* It is three-dimensional in space and therefore it creates space in three dimensions. If all atoms were two-dimensional then the whole of creation would have been on a plane and space would not have been more than a flat or curved plane(as on a sheet of paper. R.Ø.remark.) Our time-space is no more than a bound part of the nothing (det "noe som er" -X1- som Martinus kaller det. R.Ø.remark.) - being filled with matter or energy. Anything that space distinguishes (utskiller) of the time - and - dimensionless void, is caused by atoms or energy. If atoms have three space dimensions, then the timeless waves creating the atoms also have three dimensions.

1. The timeless primeval atom-field has three time dimensions.

2. The timeless waves could not be bound by only one time-axis, but must necessarily have three time-axes.

3. The timeless atom-field should consist of a three-dimensional rotating field of infinite strength, which is attenuated (fortynnet) of itself by interference. It conserves

the law of cosmic counter-balance of the no-thing. *The atom of such a rotating field structure has six time-axes, but in principle these six axes can always be reduced to three time-dimensions, no further reduction is possible.*

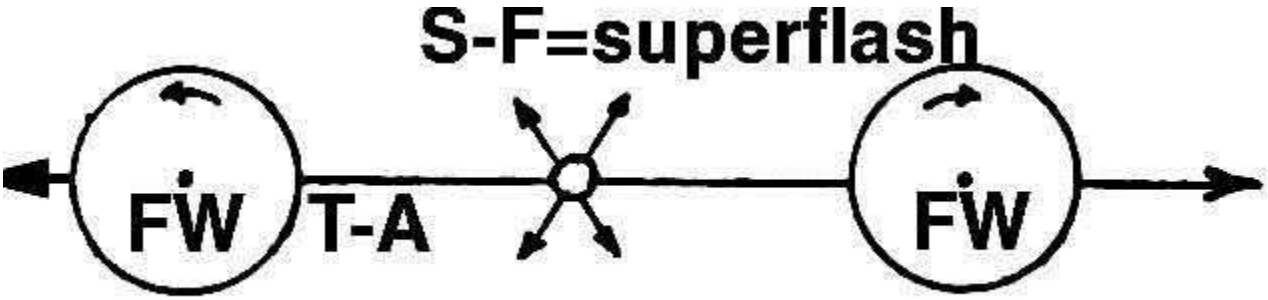

Picture of ONE-TIME-AXIS: The cosmic symbol of one time-axis.

In the following parpagraphs of the analog carrier-field model it is shown, why the atom-field has to be a three-dimensional and not a two-dimensional field.

10. The six time-axes of the time-creating, cosmic carrier field.

How can it be established that the carrier-field of all matter in twelve universes has six time-axes? The first part of the answer is simple to explain. *A well-known type of rotating field on earth is that of the electric three-phase synchronous motor.*

This type of electromagnetic-field system consists of three linear magnetic fields, which are arranged at angles of 120 round a rotor. The phase-differences of the three alternating magnetic-fields, which have the same frequencies (say 50 Hz) are also at each 120 degrees. Each alternating field is in itself an exact linear vibration oriented in one direction. The rotating field exists only if the three linear vibrations are combined together with the proper phase-relation between them. So a two-dimensional rotating field in space is created. It can force a piece of magnetic material to rotate around its axis with a great power.

Insert pict of motor

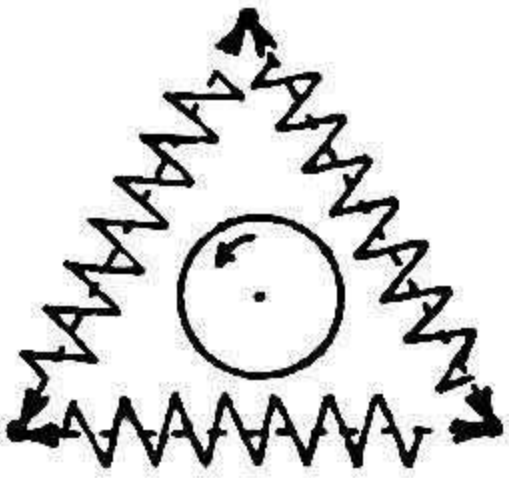

The principle of an electric three-phase synchronous motor.

The fact that it is possible to create rotating fields by combining three linear alternating waves does not mean that it has to be the same for fields of infinite strength, it can be more than three, but it is not very likely as first guess, because the three wave principle (the equilateral triangle) is the most simple and effective. According this principle, for a three dimensional field six linear waves are required to form an *equilateral (likesidet) triangular pyramid,* but why an angle of 60 degrees between time-axes?

The first answer can initially be given in a very simple way, the second is more complicated, but at least more to the point.

A simple way of reasoning to derive (utlede) the answer to the question of 60 degrees is the following. The atom field of matter has spatial (romlig)structure, therefore the time-axes must be positioned in such a way that they form a closed three-dimensional geometric object, because the energy fluxes of time must be closed in itself due to the law of counter-balance.

The time-axes form straight lines, which cannot be parallel lines, because parallel time-axes form one and the same time-direction. *The most simple three-dimensional closed object is an equilateral triangular pyramid.* There are no reasons to suppose it should be an a-symmetric pyramid if three-dimensional time is considered, on the contrary, it must be symmetrical in all positions. So it is simply a equilateral triangular pyramid of which the lanes are equilateral triangles. There is no more simple object in three-dimensional space with these requirements.

The more sophisticated answer to the question of 60 degrees is time given by approaching the question from the relativity of time frequencies between the other universes (the other time-axes). Time is the wave propagation of atoms which determines the direction of the past to the future.Simultaneously these time-creating or timeless waves are the linear phase waves combining to maintain the atomic rotating field. The problem is that "our' atoms do not experience the right frequencies of the other time-axes, because they do not propagate (spredes)with the same speed, but advance in time.

Thus there is an apparent frequency-shift, a kind of Doppler shift, by which the frequencies of the "other" time-axes are experienced by "our" atom. One should realize that the timeless vibrations of the other universes also exist in our universe.

At first sight it seems impossible for a rotating field to posess a constant phase-shift because between vibrations of different frequencies a constant phase-shift is not possible unless the frequencies are related to each other in a particular way. They are harmonic. Two vibrations are harmonic if the apparent frequencies have constant ratios to each other, like 1:2, 1:3, 1:4, etc.

Timeless waves can only exist when the frequencies are related by the harmonic ratio 1 : 2.

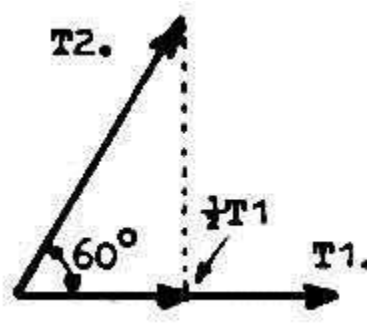

Picture explaining the frequency-shift for 60 degrees time-axis angle.

The frequency ratio is determined by the angle between the two time-axes, as the picture shows. Our time direction is T1 while another time direction is shown as T2. The time direction propagating forwards (from past to future) is useful to our universe, while the backward-moving impulses of the timeleess wave do not "catch" the rotating field of "our" atoms. Secondly the time-axis at a right angle (90dg) to our axis T1 does not make any contribution, we experience this time-axis as non-existing.

As the picture shows, due to the angle of 60 degrees, 'our' atom experiences exactly half the time-speed of the other time-axis and this makes the frequency harmonic. As T1=2 times T2, the result is the simplest harmonic ratio of 1:2, determined by the angle of projection of 60 degrees between two time-axes. (Pythagoras' law for right angled triangles).

All other possibilities and other harmonic ratios fail to give non-destructive contributions for the necessary interference intensification. Other excitations of higher order harmonic ratios give more complicated time-axes structures of the rotating atom field and cannot be stable. Also because the couple-field feedback to the total mass (inertia) of the universes is not optimized (see the following paragraphs).

It supposes simultaneously the existence of a higher number of co-existing universes, which seems highly unlikely (usannsynlig)(higher than twelve). Therefore we must decide for the simplest three-dimensional geometric form: the equilateral triangular pyramid.

11. The ancient symbol of God, the Star of David.

It is necessary to summarize the above issues of the principle.

1. The choice of the mechanism of limitation determined the existence of all types of timeless waves, among which was the (most complex) three-dimensional rotating time-field.

2. The limitation took place by interference quenching (forstyrrelses-dempning) the primeval infinite vibration (possibility) affording more time-axes in three dimensions.

3. A time-axis is a part of the infinite force-field. This only exists as a single linear vibration.

4. For a three-dimensional rotating field at least six linear field waves are necessary, which are located spatially in time having angles of 60 degrees between the time-axes.

5. The angle of 60 degrees could only be created by an apparent frequency shift maintaining the harmonic vibrations of the rotating field.

These considerations determine the mechanism of blocking the infinite. It consists of six time-axes forming a closed three-dimensional object, which creates and restricts the speed of the rotating atom-field.

Though every time-axis carries two universes(universe and anti-univers), there are in the frightening depth of cosmic space twelve distinct cosmic structures, separated by the unbridgeable barrier of time. Not only are there eleven other universes apart from ours, *but they are all embedded in the same cosmic or geometric space*. All universes have the same size and the same energy content. The geometric space is necessarily the location in the nothing - in which the omnipotent vibration quenched itself by interference. It is the location for waves encountering each other, as it is for light-waves interfering with each other. But it does not require that every atom has twelve buldges at the same space-point in time. Or more crucially, it does not mean that every human being has twelve images of himself without knowing it.

It is the mechanism of interference synchronisation of the timeless waves which uncouples the universes at each space-point, simultaneously maintaining the time-propagation of each universe.

*The equilateral triangular pyramid is the symbol of God, the Father as it is known everywhere in the universe (after lifting the cosmic isolation).*We know it as the double equilateral triangles of the Star of David, also six time-axes with angles of 60 degrees. It means that the principle of the limitation was revealed to humanity centuries ago, but we did not understand its meaning so far.

make in your thoughts : The Star of David.

Technical information given from the IARGA contactteam.

their describtions on the matter of TIME

- AND MORE

picture is described later

12. The analog carrierfield model, an instruction model.

The cosmic carrier field of all space and matter performs a sixfold function, of which some have already been discussed in gereral way.

1. The carrier function of an infinitely strong forcefield blocked in itself contains the fluidum conducting all waves without dissipation and maintained to eternity.
2. The orientation of the time-axes of the universes with respect to nothing provides the structure of the carrier-field of three dimensions, the bounded Love-will, creating our life and existence.
3. The time synchronisation function locks all universes in the iron grip of the law of cosmic counter-balance from which no atom can escape.
4. The feedback principle of time to the total mass of the universe is the function of the coupling-field by counterbalance (and interference) of the time-bound waves.
5. The function of the timeless primeval atom-field, the atom-principle, as the transmitter program containing the code of matter of which all atoms are remote manifestations.
6. The function as bearer of the absolute ALL-knowledge and goal consciousness, manifesting itself as the laws of nature and as the intelligent goal of life: the spirit of God.

The last function concerns the existential aspects, which have been discussed in the previous section of this book.

The first analog model is a mechanical instruction model explaining the cosmic carrier field by means of symbols. This model was built on another life-supporting planet on a high mountain and was many meters high. It was the gathering point for contemplation of that intelligent race for devotion to its Creator.

It was the symbol by which the majority of the race acknowledged the goal of Creation, simultaneously the sign that the cosmic isolation had been lifted. The other function of the carrier-field will be discussed with the help of this mechanical instruction model.

The analog model consisted mainly of the six edges of a huge equilateral triangular pyramid built out of solid soft-iron bars. The many metres thick edges of the pyramid contain an impressive number of iron bars parallel to the direction of the edges and cast in a kind of plastic resin following a process similar to that of casting concrete(betong). So a mainly iron-frame was formed especially suitable for conduction of magnetic pulses of high power without much loss.

So far the carrying fuction of the cosmic time-field, which primarily maintains the timeless waves is symbolized in the model. The magnetic pulses in the edges of the pyramid run backwards and forwards like the timeless waves in reality.

With respect to the other edges of the pyramid, the magnetic pulses are phase-shifted. The problem is that up to now the forward propagation (forplantning) in time has been missed out. In fact we look for the equivalent of the two little wagons on the vibrating rail. The solution can be found in the symbol of the rotating flywheel, as *with the atom its rotation is continuous in time, it is in fact time propagation.* Therefore the iron frame of the pyramid is discontinued at two places in each of the six edges of the pyramid. At this discontinuation point a linear magnetic impulse motor is installed, on the axis of which a large flywheel is mounted.

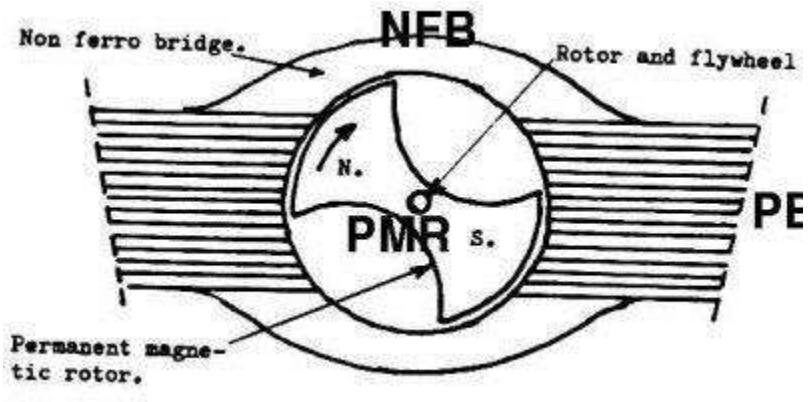

NBF=NonFerroBridge

PE=PyramidEdge and soft iron bars

PMR=PermanentMagneticRotor

The flywheel symbolizes not only the propagation of time, but also the inertia of matter and so the flywheel is in effect the total mass of the universe. This type of magnetic impulse motor is not self-starting, so at the inside on the flywheel axis a starter-motor is mounted, fitted solely for the purpose of starting. One rotating the synchronous motor maintains the exact number of revolutions at the same frequency of the magnetic alternation field. Thus in each of pyramid's edges two synchronous motors are mounted making twelve flywheels in total.

The two flywheels per axis rotate in opposite directions to symbolize the time propagation in opposite time directions. This type of linear impulse motor is chosen because it can be made to rotate in either direction.

The first analog model.

In one triangular plane of the pyramid the six synchronous motors in the iron frame demonstrate a rotating magnetic field, seen from the center of the plane. Each edge of the pyramid has the right phase-shift with respect to the other edges of the triangle.

The first model has four central rotating magnetic field generators in the middle of each triangular plane. (See figure of unfolded pyramid indicating the actual phase-shift).

These four synchronous (three phase) generators are coupled together by a gearbox and are driven by the main electric motor (not shown in the drawing). Consequently the four three-phase generators fulfill the synchronisation and constant phase-shifts for the flywheels of the pyramid-edges. The four separate rotating fields together, initate the complex three-dimensional rotation of the carrier field (or atom-field).

The disadvantage of the first model is that it is further away from reality, because the atomic field is not symboized as one three-demensional rotating field. However it shows better how to imagine the complicated rotation in three dimensions.

The second or the real analog model.

This mechanical model has only one central generator in the middle of the pyramid, instead of the four rotating field generators of the first model. All magnetic waves in the pyramid edges go straight to the pyramid's center. The rotor of the 3-dimensional rotating generator is like a yo-yo with spherical end-surfaces.

It requires a touch of genius to provide the drive-connection between the central motor and the spherical rotor, which has to be started up in a complex rotation. The six diametrically opposed pole-shoes from the middle of the pyramid's edges around the spherical rotor form in pairs, three axes of right angles - representing a Cartesian coordinate system. So it shows that the six time-axes of the edges of the pyramid can be converted into the three principal time-axes of the central sphere.

Together it imitates three-dimensional time, which causally creates the three-dimensional space of our universe.

The principles of the first and second analog models are equivalent. One version can be converted into the other, for example, converting the four rotating fields to one three-dimensional rotation in the centre-mass of the pyramid.

The model can be started by switching on the thirteen drive-motors. As the flywheels reach velocity the twelve starter-motors are switched off and only the central motor drives the complete gigantic model. The essence is that all flywheels have exactly the same number of revolutions. They are all either synchronous motors or generators. Then the flywheels are marked and illuminated by a stroboscopic flash light. *Seen by*

the normal eye they do not appear to move showing the synchronous rotation and the constant phase-shifts between the flywheels.

These mechanical models are meant to explain the unimaginable Creation out of the nothing by symbolic imitation of the carrier-field. However it is only a weak symbol of Creation. The carrier-field is the esoteric medium, a transmutation of the absolute spirit or conscience, it is the spiritual force field of infinite strength which is present everywhere in the universe.

The imitation of the carrier-field functions.

Nevertheless the analogy of reality is incredible. This will be shown in the next explanation of the five functions of the cosmic carrier-field.

The carrier-function

The foundation of the carrier-field is the infinite force-field created by interference quenching (avbrytende stopp) of the original infinite vibration. The mode initiates this force-field with the six bundles of soft-iron bars as the edges of the pyramid.

As in reality, the three-dimensional magnetic rotating field in our model is caused by the linear waves of each time-axis. *The timeless waves alternate backwards and forwards as in our model*. They drive the flywheels representing the masses of the universes, and their rotation is the propagation (spredning) in time.

The orientation of the time-axes with respect to the nothing.

The relative position of one time-axis in the apparent nothing plays an important role in the orientation of the universes in reality, determining the direction of each time-axis. Here the first model is shown representing the four three-phase synchronous generators in the planes of the pyramid. Only with decompostion of the three-dimensional rotation into four rotations can one show that the three-dimensional rotating field has left no remaining component in the nothing, while in contrast a two-dimensional rotating field can not be nullified, a remaining component will always

exist in the nothing. This can be explained by considering a single plane of the pyramid with its six flywheels at the edges, the analog for a two-dimensional

carrier-field. The rotation impulse of the flywheels is compensated by the opposite rotations but the rotation impulse of the central three-phase generator is left over. It can be measured by the outside world (the nothing).

It requires four field three-phase generators (maintaining overall symmetry) to compensate for these rotation impulses.

With this the three-dimensionality of the carrier-field has been shown and the orientation of the time-axes with respect to the nothing is determined.

The time synchronization function.

Impressively the model imitates the time synchronization, simultaneously maintaining the cosmic counter-balance by which the universes continue to exist. The rotation of the two flywheels per axis is in opposite directions and they rotate with exactly the same speed. Thus it imitates the circular motion to the timeless waves which progresses exactly synchronous by their mutual interference coupling.

The twelve cosmic systems run without any dissipation, once started, the perpetuum mobile continues into eternity with the absolute accuracy of time-synchronisation. If one supposes the model to be without loss and without using the eternal driving motors, it will continue to run synchronously due to the inertia of the flywheels and the fact that the synchronous linear impulse motors can function as generators as well.

This symbolizes another property of the continuous circular motion of the timeless waves, because every wave somewhere in the pyramid circuit at each moment has its opposite value resulting in an overall zero at any moment.

This is the law of conservation of the nothing.

The couplingfield function.

Time synchronization is not alone determined by the iron grip of the three-dimensional carrier-field and the principle of cosmic counter-balance. Apart from this an important effect is realized from the feedback of the gigantic masses of the universes to the timeless waves. These masses can be considered as enormous flywheels without loss. Once started by the super flash, no change in speed is possible, because a force of sufficient magnitude is simply not available. This function of the coupling field can also be shown in our model, because the linear synchronous motors of the flywheels are also generators. If the central driving motor is switched off, then the flywheels continue for some time to drive the central three-dimensioal rotating sphere. Everything stays exactly synchronous with the same phase-shifts.

This experiment shows how the flywheels feed their energy back and have a stabilizing function in time-synchronization. The coupling-field of the masses of the universes is fed back in the time-bound vibrations of the atom-field from which no atom total mass of the universes is fed back to one single atom.

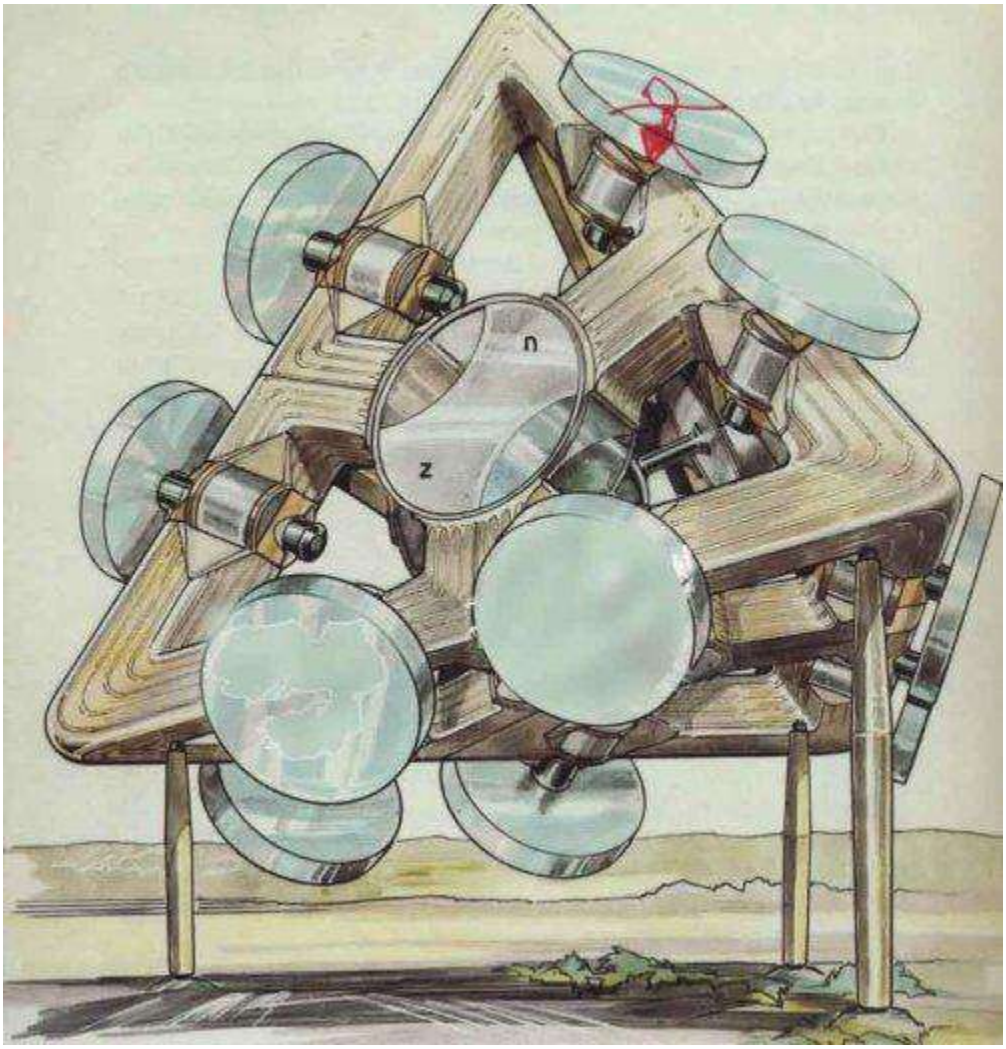

This is a painting by Rudolf Dass of the analogous visual-mechanical carrier-field model which symbolizes time and matter creation and synchronization in twelve universes. This giant working construction that was a cross between a monument and a machine was seen on an artificially flattened mountaintop on **Iarga**. This place was perceived as a place of pilgrimage, a place of meditation and contemplation, and the machine was a symbol of creation. The **Iarga**ns know no separation between science and religion, and religious and spiritual theories are entirely scientific. The model was several hundred yards(meters) long. The machine seemed to operate by some kind of perpetual motion, neither running on fuel or electrical power.

The Instructional Analog Model

The mechanical instruction models are the visual representations of the principles of the cosmic unified field theory. The model is intended to demonstrate that time, matter, and energy are creations out of the nothing and therefore the counter-balance has to be maintained to allow the causal infinity of the nothing to exist. In a broader context the physical symbols all take on new meaning and demonstrate the unification of science and religion. In a religious sense the spherical three-dimensional time-field in the heart of the pyramid symbolizes the Soul of the Creator. The pyramid symbolizes his infinite lovewill, the cage in which the infinity of His existence has been blocked irrevocably. The lines symbolize the different frequencies of the timeless waves. The flywheels on the edges of the pyramid symbolize the twelve associated and interrelated universes, including ours, that make up this unity. One cannot exist without the others.

The timeless primeval atom-principle, the transmitter function.

The atom-field is a time-creating field and as such a remote manifestation of the primeval atom principle. It can be compared with a transmitter. As soon as the program is converted into waves of great power, billions of radios can receive the same program, the number is unlimited. Everything depends on the one program of the transmitter, the primeval atom-field. If this exists with infinite strength, it is at the same time the vibration medium (the carrier-field) which helps it to spread everywhere. *Thus any atom in any universe can receive the timeless basic program.* The second model shows the three-dimensional time-field of the primeval atom field most clearly, although this is a three-dimensional rotation of the central sphere in spatial sense. This is an analog of reality, the atom has a spherical field which is defined by six linear time-vibration directions. Any atom is a remote manifestation of the one carrier-field of infinite strength.

Considering this fifth function of the carrier-field one has to realize that only the central sphere, the atom, is visible to us. The fields in the pyramid edges outside the sphere are invisible. It is the time-field reality of which the atom is a reflection.

The mechanical instruction models are the visual representations of the principles of the cosmic unified field theory. This requires however some marginal notes. A material comparison to explain spiritual abstractions is always in some ways incomplete. There are several hiatus of which only the three most important ones are mentioned.

1. In the model one time-axis represents only *one frequency* of the magnetic field, while in reality all frequencies are contained. Every frequency however can be initiated for each time-axis for which the interference representation of the analog model is valid.

2. The model demonstrates the rotating field of the *timeless waves*. It *does not imitate the time-bound waves* by which our time-axis the propagation speed of time is X, then the phase velocity of the two time-axes connected to "our" pyramid edge is ½X. The other two time-axes connecting our time-axis with the other corner of the pyramid is -½X, making up for the time speed of our anti-universe -X. The crossing, not-touching time-axis is perpendicular to our time-axis and does not contribute.

3. In our model the masses of the universes are given by the flywheel symbol. In fact this is *fundamentally wrong, because it is separated from the three-dimensional rotation of the central sphere*. It can therefore basically not maintain the counterbalance of the nothing.

The most important conclusion of the analog model is that *time, matter and energy are creations out of the nothing and therefore the counter-balance has to be maintained to allow the causal infinity of the nothing exist.*

14. The existential symbolism of the model.

So far the physical aspects of the model have been unravelled, but if one wants to give a wider context to the model suddenly all the physical symbols change their meaning. In relation to philosophical or theological disciplines the model takes on the additional meaning of the unification of science and religion. By certain inherent (medfødte) laws within any intelligent race the denial of God's existence will be destroyed sooner or later. Earth science will provide an indestructible contribution to our final knowledge-awareness, which we shall attribute as typical human attainment in the

cosmic integration. It is that piece of our human identity and self-awareness, which we shall possess and care for throughout eternity. *It the light of this purpose, science serves God and the distinction between science and religion fades away.*

In a religious sense the spherical three-dimensional time-field in the heart of the pyramid has a special meaning. **It symbolizes the Soul of the Creator**, the Father who is the pure Identity of the infinite origin. The pyramid symbolizes his infinite Love-will, the cage in which the infinity of his Existence has been blocked irrevocably. He sacrificed his Ego and his freedom, to love his twelve Sons once. He is present only indirectly in his Creation as the reflection of the infinity, the Supreme Being, as the one Ego-consciousness of the Archangels.

That is why the theologian covers the central sphere with pure gold, symbolizing the golden Heart, the Holy of Holies, the most sacred secret of the universe. The pyramid is then painted dark red, the universal colour of love. Over the red many thin golden stripes run in the direction along the pyramid edges. These stripes symbolize the different frequencies of the timeless waves, the expressions of Love and faith of the Father and his infinite Will.

Gathered around the golden Heart are the twelve flywheels, coloured white, the colour of purity and innocence. The model shows that every universe has the power to awaken the matter-consciousness and to transform it to the new God: the Son. The goal of Creation is therefore the awakening and the formation of the twelve Sons of the Father.

This is not in contradiction with the Bible telling us that the Father sent his only-begotten Son. The Bible is solely directed to man. It is our instruction book for life describing our attitude towards God and our fellow man. The Bible does not tell anything about life on other planets, because it is not relevant in our relationship with God now.

The same goes for our parallel universes. In fact they do not exist for us, because they are not in our world of existence but somewhere else. They do not exist for all intelligent races in this universe, we shall never be able to observe them nor experience them in any way. Perhaps at the end of all time we shall meet.
In *our* world the Father has one only-begotten Son and this truth is already so unimaginable that nobody can conceive the consequences yet.

END OF IARGAN DISCUSSION

Stefan Denaerde

Cosmic Unified Field Theory.

How it started.

More than 25 years ago appeared an amazing book in the Netherlands: ´Buitenaardse Beschaving´ (Extraterrestrial Civilization) from Stefan Denaerde. (Known in English as : "UFO contact from planet Iarga") It describes the confrontation of the author with the race from the planet Jarga (Iarga). It was written as a novel (although it is a true story) and illustrated by a well known Dutch technical illustrator (Rudolf Das).

Sailing with his ship in Dutch waters, Mr. Denaerde (not his real name) bumped into something which was hidden underwater. When he sees someone floating in the water he comes to the rescue of what later appears to be an astronaut. This rescue was a test for him and after the initial shock he gets in contact with the Jargans who invite him for a three day learning session inside their submerged saucer.

Via a 3D screen and a radiation ´head set´ he learns about the Jargan culture, philosophy and technical achievements. Through the concepts of extreme efficiency and justice he is taken to the Jargans love for the Omni-Creativity (our word for ´God´ is too poor) and their striving to be one with it.
This ´carrier field´ of the Universe supports everything (matter, time, consiousnes), and by applying this knowledge it makes interstellar space travel possible.
It appears that the goal of a civilization is to create a socially stable supercivilization. Discriminations of any kind no longer exist. Resources and wealth are available for everyone, but not as a goal as such, but to enable everyone to grow spiritually.

There is much more to this book. Anyone interested can find an interview with Denaerde by Wendell Stevens, as well as several chapters from the book on this link. (This also contains the 2nd book of Denaerde!)
From this interview it appears that the contact has continued for many years in telepathic form. A lot of highly technical information has been given in this way, which resulted in the second book:

The Universal Creation. (In Dutch: ´de Universele Schepping´)

This appeared about 20 years after his first book. It describes in one theory the origin of the Universe, matter, time, consciousness, the Universal goal for any civilization, the history and possible (very bright) future of mankind, in one word : a TOE (theory of everything).
The atmosphere of the book is totally different: the first book had something like ´you don't have to believe this has happened, it could be hypothetical´. The Universal Creation is much more direct and confronts us with a direct proof of its contents, because the authors (Stefan and his ´brother´ Christian Denaerde) express that it is high time that science and religion are united again.
The Universal Creation comes with an appendix ´Cosmic Unified Theory´- in English!- which goes into much detail about the new physical model. Recently this information is available on CR-Rom, to be ordered at the Cosmic Field Paradigm foundation. This essay is mainly about the appendix and the CD-Rom.

The creation out of the nothing.

According to the Cosmic Field (CF) model there existed prior to the creation (or big bang) vibrations of infinite frequency and amplitude in every time direction.
The act of creation was the blocking of the infinite waves by interference to form waves of finite frequency and amplitude. In order for matter and energy or anything to exist, there must be an equal counterbalancing vibration. Also time direction has to be counterbalanced. Think of a time axis as two pieces of mini model rail which are connected via a motor, which can move the rails back and forth say over 1 cm. If you place a wagon

on one of the rails which has a catch wheel that catches only the forward movement of the rails, you will see the wagon move forward. Another wagon, placed in the opposite direction on the other rail will also move forwards, thus the two wagons will separate from each other. So the rails can be seen as a time axis, where time moves back and forth. The wagon represents matter, which can only catch one time direction through a property called spin.
One time axis is not sufficient: to counterbalance everything and to cause a a feedback mechanism a 3D time structure is needed in the form of a tetra-eder.

Fig. 1 The carrier field model

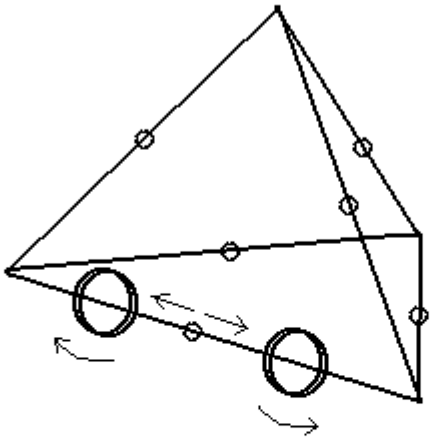

6 time axes form a closed loop. 12 universes are separated by time direction.
The spin of matter is represented by the two flywheels (only shown for one time axis)

This implies that there exist 6 time axes (each with a back and forward movement in time) and thus 12 universes. These universes cannot be seen, but some aspects like the time frequencies can be sensed by our atoms. (BTW, this might explain the missing mass problem in cosmology: our universe still senses the mass of the other 11 universes, that is why 90% of the mass is unexplained..)

The picture shows the arrangement of the time axes. The center of each axis (depicted by a small circle) can be considered as T=0. The two flywheels (drawn on one axis only) represent the spin direction of matter. In our direct anti-universe (on the same time axis) the direction of time is opposite, but also the spin of the matter particles. This means that everything is mirrored, and living beings in the anti-universe experience time as moving forward, just like we. In fact time moves in two directions along an axis, but matter has a sort of rectifying effect - it only picks up the forward going time.

The 60 degrees angle between the time axes is necessary to have an harmonic ratio between our time axis and the time axis of the other universes.

Fig.2 2 time axes at 60 degrees

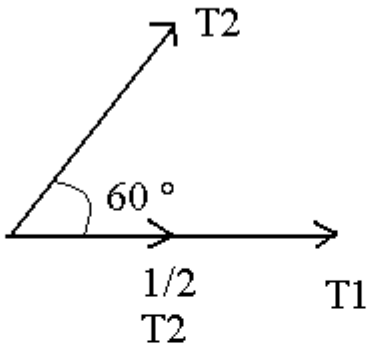

Only at this angle there can be a harmonic ratio between the time creating frequencies. An atom on our time axis T1 experiences the other time axis at half the frequency.

Our time direction is T1. Another time direction is T2. The angle of 60 degrees makes T1=2*T2, thus giving an harmonic ratio of 1:2.

The carrier field model has several functions, such as:

It is an infinitely strong force field, blocked in itself. It is a loss free conduction medium for all waves. The counter balancing of everything implies that the universes are locked in an iron grip: the spins in one universe are exactly the same and opposite to the spins of the anti universes. It also means that there cannot be one atom more in a universe, which is not present in the 11 other universes. (this does not mean that all the 12 universes have to be the same).

The model is also an image of the universal atom: When applied at a very small scale Denaerde explains the basic building blocks to form matter.

The flywheels can represent the total mass in one universe or just the mass of one atom. The 3D time structure of the pyramid is present in all matter: you could imagine the center of the pyramid being in a star, a galaxy, etc. The 11 other universes are not observable, but they could occupy the same 3D space. The model demonstrates beautifully that matter, time and energy are just properties of one universe (1/12th of the whole). Summing all the properties of the pyramid results in nothing. (The big bang theory fails to explain where the initial energy came from)

The Double rotating central bar.

Denaerde introduces the concept of a magnetic bar, which touches 2 opposite ribs in the pyramid. This induces a flux in the loss free time axis. This is a very important concept and it takes a while to understand it. The bar

needs to rotate around two axes simultaneously (Fig. 3) in order to create alternating fluxes in the pyramid ribs (which still represent time axes). The rotating movement repeats itself in 6 time-steps.

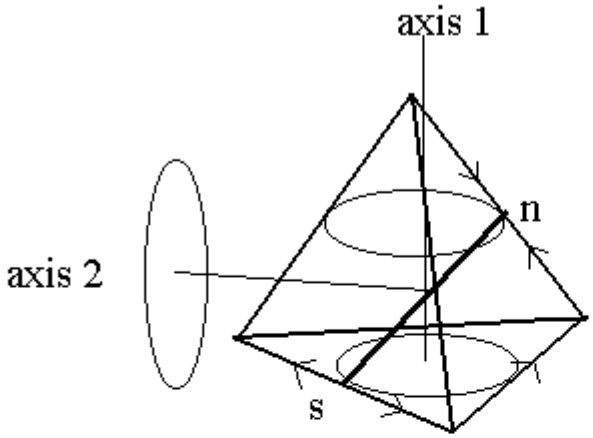

The simultaneous rotation of a central magnetic bar around 2 axes gives alternating flux patterns (time directions) in a pair of ribs. This process is repeated in 6 timesteps.

Fig.3 Double rotation of a central bar

Denaerde calls this configuration a building element. Next we will see that from these building elements one can derive the fundamental elementary particles : electron, quark and neutrino.

The two fundamental building blocks

By adding the initial building block at different time steps (adding three bar rotors) it can be derived that there are two possibilities. These are called central rotors of the first and second kind. (figures 4 and 5). The central rotor of the first kind gives a fixed alternating flux pattern in the ribs of the pyramid. (Try it out!)

Fig. 4 3 building blocks at different time moments are added

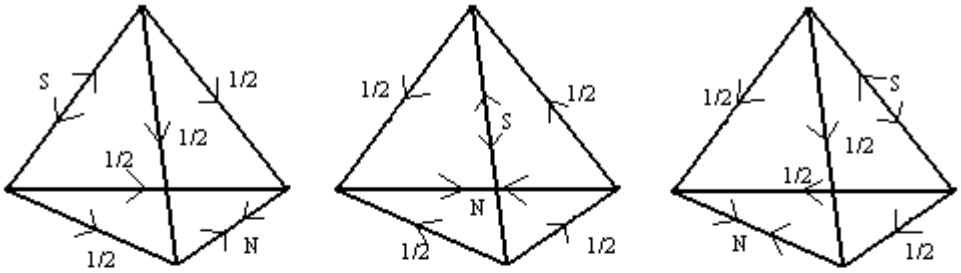

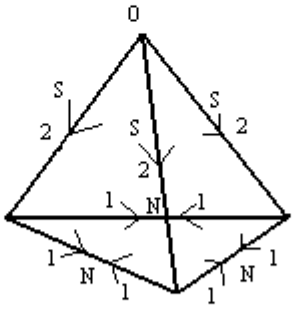

The total return flux gives a new building block: a rigid central barrotor of the first kind. The zero node does not change its orientation. In a next timestep the flux pattern is reversed, but the magnitude is the same.

This model describes the ELECTRON.

Fig. 5 The rigid central bar rotor of the second kind

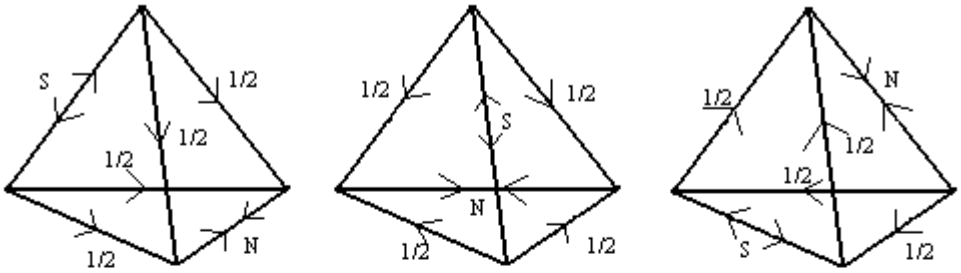

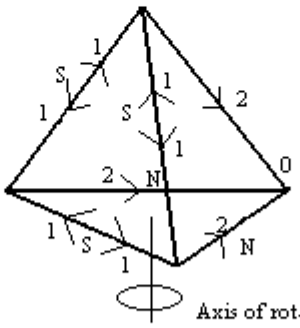

The rotor of the second kind has no fixed zero flux node. The zero flux node rotates through one of the corners of the pyramid.
After 6 timesteps the flux and the zero node are identical to the original position.

This model represents the QUARK.

The second possibility is called a central rotor of the second kind.

The rotor of the first kind is similar to the ELECTRON.
The rotor of the second kind is similar to the QUARK.

Don´t forget, the pyramid ribs represent time axes. (Note: Denaerde uses capitals to distinguish from the real particles in 3D space.)

Three QUARKS added together give a PROTON. (Figure 6)

Fig 6 Quarks, electron and H atom

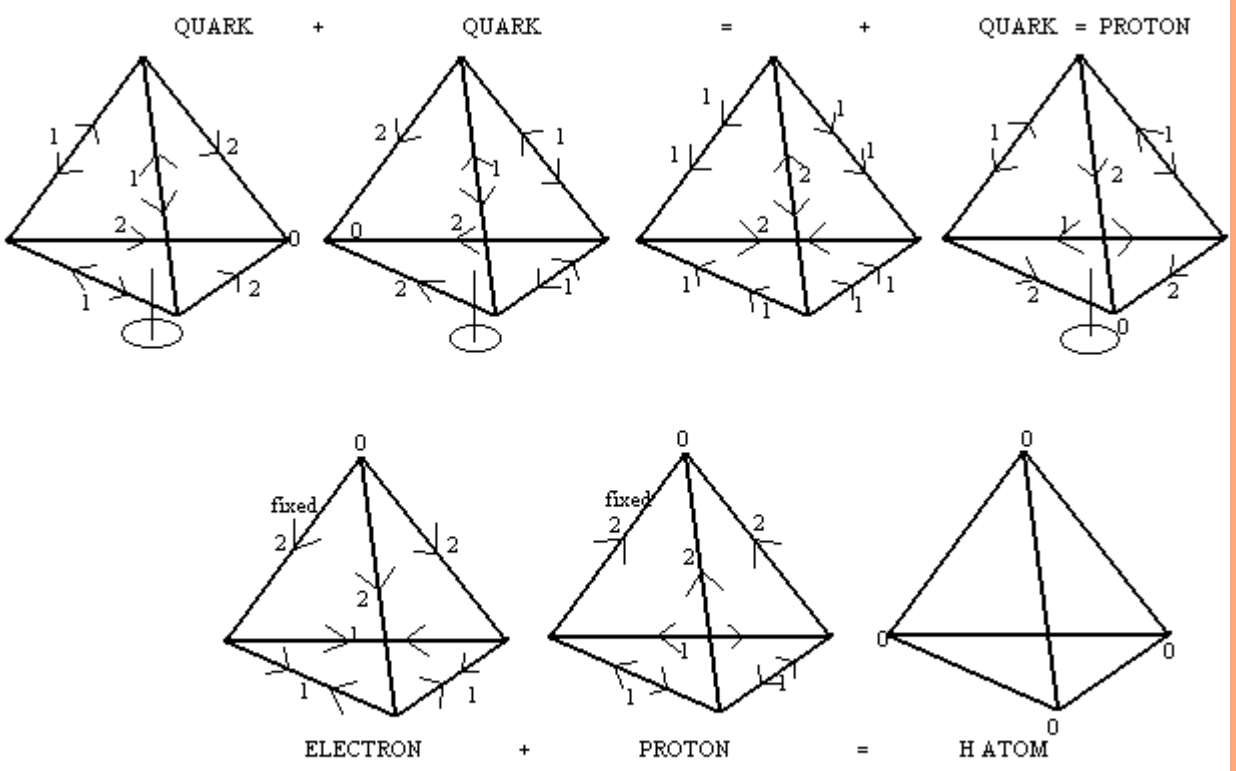

A QUARK and an "anti time" QUARK or the ELECTRON and the "anti time" ELECTRON (positron) can be distinguished by the c.w. or anti c.w. rotation of the central rotors. Dipoles of opposite rotation destroy each other.
Fig 6 shows that adding the PROTON and the ELECTRON gives the neutral H-ATOM.
The mass difference between electron and proton can be explained by different rotation frequencies of the dipoles.

Denaerde then continues to describe several NEUTRON groups which can be formed. This is rather complicated and requires a lot of pictures to visualize, so I would rather skip this. (For anyone interested, I strongly recommend to order the CD!)
The outcome is, that the NEUTRON in the Carrier Field model has 4 QUARKS.
This gives a NEUTRON with a zero external flux. The model explains why the neutron is not stable in free space, while the electron and proton are.

It can easily be seen that to the CF model a QUARK has a unit of charge of 1/3 of the ELECTRON, if charge is defined as the external flux in the pyramid ribs. Charge is related to a symmetry axis of the pyramid. The CF model predicts that charge is not constant in time and that there are two types of charge for a matter particle (e.g. electron): North and South charge. Due to the time switching mechanism we don´t detect this.

A NEUTRON consisting of 4 central rotors of the 2nd kind can be converted into a PROTON (3 rotors of the 2nd kind) and an ELECTRON (1 rotor of the 1st kind).
What is left over is the NEUTRINO : a free dipole in the carrier field.

In order for the particles to exist in space and time, a grid is needed which carries the complex flux patterns. Denaerde comes to a grid consisting of two pyramids stacked together. The top one is inverted and rotated 60

degrees, while its top touches the base of the other pyramid (sunken). The size of the pyramids is in the order of h (Plank´s constant, normalised to length). All particles have more or less the same size in parametric space (space as we know it).

Further Implications

We come now to the more profound meanings of the model. This subject I describe very condensed (without further proof, although the subject is described in great detail in the appendix).

The double rotating central bar has an additional degree of freedom. This results in a second gravitational field, which we cannot directly observe. So there are two kinds of gravity.
The CF model talks about ideal Black Holes and White Radiators. Black Holes have a function to stabilize the universes. As said before, the mass (energy) in all 12 universes must be exactly the same. Still the mass distribution can be different, but only thanks to black holes. B.H´s and W.R´s are present in the corners of the pyramid frame. In one time step, our time direction faces the Black Hole, while our anti-universe´s time direction faces the White Radiator. The next time step our time direction faces the White Radiator. In the next time step it is the null-energy flux.
White Radiators are generators of mass and energy, but have no mass of their own. It generates the exact opposite type of gravity which nullifies with normal gravity.
A pair of BH and WR belongs to each reality. The ideal Black Holes (and there counterpart the WR) in the CF model must have spin. The normal black hole as known from General Relativity Theorie is discussed also.

The formation of a pair of BH and WR (also called a macroscopic quantum mirror or black mirror) is then proven to be a non natural object : it could only have formed by an act of intelligence. Intelligent life is a necessary condition in the formation of the universe! According to the CF model, the black mirrors are formed by the collective mind power of an intelligent race.

Another important consequence is that the time history (knowledge) of the universe is laid down in the quantum gravitation fields. This is one of the reasons why the universe expands: to record the time history. In other words, the time history of a matter system, determined by an increase of entropy, is converted into information in the quantum gravity field. Intelligent life interferes with and modifies the quantum gravity fields (creativity).

The two types of gravity fields represent the matter-bound and emotional (or soul-bound) energy fields. The creation of the macroscopic quantum mirror is the final goal of an intelligent race. It is called the all-might manifestation of the race and it can only be initiated by enough minds working together to create the mirror - which means nothing less than the recognition and identification of the Love poles which carry the universe...

Note:

Everything written here is in my own words. Pictures were made by me. Therefore, copyright has not been violated.

Back

The Lacerta Files

Reptoids of the Inner Earth.

Reptoids of the Inner Earth

The Lacerta Files

Jimmy Bergman, Owner, Sweden.

Published in this website on December 26, 2004.

Note of the Editor of Brother Veritus' Website: These English translations were edited to correct English grammatical errors but message and intent were left intact. The word "Ilojiim" or "Illojim" used extensively in these texts could mean "Elohim", since this is the equivalent traditional word used in Western culture, however, this term may indicate a different galactic race. The illustrations are not of Lacerta.

Lacerta File I

Translation by Chris Pfeiler, Editor and Translator. Taken from
http://www.sabon.org/reptiloid/index3.html .

Introduction

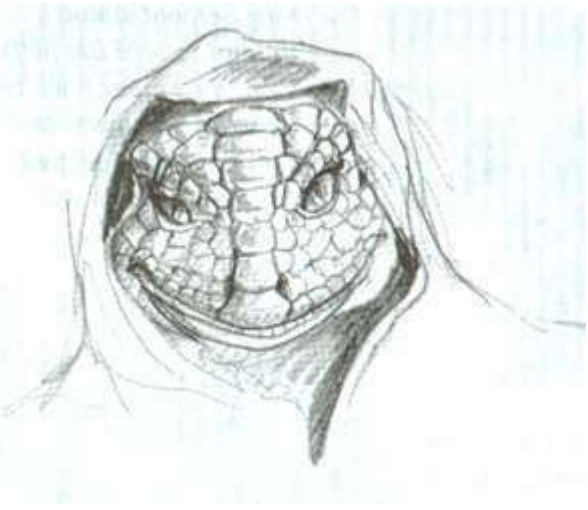

I certify that the following text is the absolute truth and no work of fiction. These are parts of a transcript of an interview I've made with a non-human and reptilian being in December 1999. This female being was already in contact with a friend of mine (whose name is given only with the abbreviation E.F. in the text) since some months. Let me declare, that I was all my life a skeptic about UFOs, aliens and other weird things and I thought that E.F. tells me just dreams or fictitious stories when he talked with me about his First Contacts with the non-human being "Lacerta". I was still a skeptic when I met this being on December 16 last year in that small warm room in the remote house of my friend near to a town in the south of Sweden, despite the fact that I saw now with my own eyes that she was not human. She has told and shown me so many unbelievable things during that meeting that I can't deny the reality and the truth of her words any longer. This is not another of that wrong UFO papers which claim to tell the truth but tell in fact just fiction, I'm convinced that this transcript contains the only truth and therefore you should read it.

I had talked with her for over 3 hours, so the following transcript shows you only shortened parts of the interview, because she asked me after the interview not to publish everything she had told me already now. The order of the questions in this transcript is not always the same order in which I had asked them, so it may seem sometimes a little bit confusing to you. It was not easy to delete all the important parts she had asked me to delete from the transcript, so I apologize for the maybe unusual order.

I'm in the possession of the entire transcript of the interview (49 pages with some of my drawings of her body and her equipment) and also of some tapes on which I have the full interview, but I will not reveal this before I have permission from her.

I will send this shortened form of the still fascinating document to four of my reliable friends to Finland, Norway, Germany and France and I hope they will translate it into their own languages and into other languages and I hope as many people as possible will be able to read and to understand the transcript. If you receive it, please send it to all your friends via e-mail or make print-outs and copy them.

I certify furthermore, that various "paranormal" abilities of her species like telepathy and telekinesis (including the moving and dancing of my pencil on the table without touching and the flying of an apple around 40 centimeters over her hands) were shown to me during the 3 hours and 6 minutes of the meeting and I'm absolutely sure that these abilities were no tricks. The following is certainly difficult to understand and to believe for someone who hasn't experienced it, but I was really in contact with her mind and I'm now completely sure that everything she said during the interview is the absolute truth about our world.

Unfortunately, if I read the entire transcript and (much more) this very shortened form by myself I have the strong impression, that everything I've written sounds too unbelievable to be true, that everything sounds more like a bad science fiction story from TV or cinema and I have doubts that anyone will believe my experiences. But they are true, if you believe it or not. I can't expect from you that you believe my simple words without evidence, but I can't give you that evidence. Please read the transcript and think about it and you will maybe see the truth in these words.

There will be a new meeting between me and her (again in the same house in Sweden) on April 23 2000 and she promised me to give me maybe some evidence for her existence. In the meantime I collect questions which I will ask her then. Maybe she gives me permission to reveal more of the missing parts in that transcript and about the coming war.

Believe it or not, this makes no real difference (but I hope you will believe.)

Ole K.

Transcript of Interview (Shortened Version)

December 16, 1999

Question: First of all, who are you and what are you? Are you an extraterrestrial species or can your origin be found on this planet?

Answer: As you could see with your own eyes, I'm not a human being like you and to be honest I'm no real mammal (despite my partly mammal-like body features, which are a result of evolution.) I'm a female reptile being, belonging to a very old reptilian race.

We are the native terrans and we live on that planet since millions of years. We are mentioned in your religious writings like your Christian Bible and many of the ancient human tribes were aware of our presence and worshipped us as gods, for example the Egyptians and the Inca and many other old tribes. Your Christian religion has misunderstood our role in your creation, so we are mentioned as "evil serpent" in your writings. This is wrong. Your race was genetically engineered by aliens and we were just the more or less passive visitors of this accelerated evolution process. You must know (some of your scientists have already supposed this) that your species had evolved in a naturally completely impossible speed within just 2 - 3 millions of years. This is absolutely impossible, because evolution is a much slower process if it's natural but you have not understood this. Your creation was artificial and done by genetic engineering, but not by us but by an alien species. If you ask me, if I'm an extraterrestrial, I must answer no. We are native terrans. We had and have some colonies in the solar system, but we originate on this planet. It's in fact our planet and not yours - it was never yours.

Question: Can you tell me your name?

Answer: This is difficult, because your human tongue is not able to pronounce it correctly (and a mispronunciation of our names is very offensive for some of my kind.) Our language is very different from yours, but my name is —I will try to say it smoother by use of your human letters— something like "Sssshiaassshakkkasskkhhhshhh" with a very, very strong pronunciation of the "sh" and "k" sounds. We have no forenames like you but only a single but unique name which is divided and characterized by the way of speaking and which is given not to children (who have an own children-name) but only in a special procedure in the adolescent age at the time of either religious or scientific "enlightenment" or awareness (as you would call it.) I would appreciate it if you don't try to say my real name with your human tongue. Please call me "Lacerta", this is the name I generally use when I'm among humans and talk with them.

Question: How old are you?

Answer: We measure the time not like you in astronomical years and in the revolving of the earth around sun, because we usually live beneath the surface of the planet. Our time measurement depends on periodically returning cycles in the earth magnetic field and according to this (and said with your numbers) I'm today —let me calculate— 57,653 cycles old. I have reached my adult phase and my awareness 16,337 cycles ago (this is a very important date for us.) According to your human time scale I'm around 28 years old.

Question: What is your task? Do you have a "job" like us?

Answer: To say it with your words: I'm a curios student of the social behavior of your species. That's why I'm here and talk to you, that's why I have revealed my real nature to E.F. and now to you and that's why I give you all that secret information and why I will try to answer all the questions on your many sheets of paper honestly. I will see how you react, how others of your kind react. There are so many crazies and liars of your kind on this planet who claim to know the truth about us, about UFOs, about aliens and so on and some of you believe their lies. I'm interested to see how your species will react if you make the truth (which I will tell you now) public. I'm quite sure everyone of you will refuse to believe my words, but I hope I'm wrong, because you need to understand if you want to survive the coming years.

Question: I've read your full statement (which you have given to E.F.) about this, but can you give me now just a short answer: are UFOs real flying objects piloted by extraterrestrials or do they belong to your species?

Answer: Some observed UFOs - as you call them - belong to us, but most not. Most of the "mysterious" flying objects in the sky are not technological devices but mainly misinterpretations of natural phenomena your scientists have not understood (like spontaneous plasma flares in the high atmosphere.) Nevertheless, some UFOs are real craft belonging either to your own species (especially to your military) or to other alien species or at last to us (but a minority of sighted craft belongs really to us, because we are generally very careful with our movements in the atmosphere and we have special ways to hide our ships.) If you read a report about a sighting of a metallic bright-gray cigar-shaped cylindrical object with a length of —there are different types— let me say between 20 and 260 of your meters and if this object had made a very deep humming sound and if there were 5 bright red lights on the metallic surface of the cigar (one at the top, one in the middle, two at the end) then it's likely that someone of you have seen one of our ships and this means that it was either partly defect or that someone of us was not careful enough. We have also a very small fleet of disc-shaped craft, but such UFOs belong usually to an alien species. Triangular UFOs belong generally to your own military but they use foreign technology to build them. If you really want to try to see one of our craft, you should have a look at the skies over the Arctic, the Antarctic and over Inner Asia (especially over the mountains there.)

Question: Have you a special symbol or something like that with which we can identify your kind?

Answer: We have two major symbols representing our species. One (the more ancient) symbol is a blue serpent with four white wings on a black background (the colors have religious meanings for us.) This symbol was used from certain parts of my society, but it is today very seldom —you humans have copied it very often in your old writings. The other symbol is a mystic being you would call a "Dragon" in the shape of a circle with seven white stars in the middle. This symbol is much more common today. If you see one of that symbols on a cylindrical craft I've described in my previous answer or on some underground installation, this thing or place belongs definitely to us (and I would advise you to go away from there as soon as possible.)

Question: The seven stars in the second symbol you've mentioned, do they mean the Pleiades?

Answer: Pleiades? No. Actually, the seven stars are planets and moons and they are a symbol for our former seven colonies in the solar system. The stars are shown in front of a blue background and the dragon-circle means the shape of Earth. The seven white stars mean Moon, Mars, Venus and 4 moons of Jupiter and Saturn, we had colonized in the past. Two colonies are no longer in use and abandoned, so 5 stars would be more correct.

Question: As you have not allowed me to make photos —what would be very useful to prove your real existence and the truth of this story— can you describe yourself detailed?

Answer: I know that it would be helpful to prove the authenticity of this interview if you can make some photos from me. Otherwise, you humans are very skeptic (that's good for us and for the real alien species acting secretly on this planet) so even if you had such photos, many of your kind would say that they are fraud, that I'm just a masked human woman or something like that (that would be very offensive for me.) You must understand that I can't give you permission to make photos of me or of my equipment. This have various reasons, which I want not to discuss with you further, but one of the reasons is the keeping up of the secrecy of our existence, another reason is more religious. Nevertheless, you have permission to make drawings of my look and of my equipment I can show you later. I can also try to describe myself, but I doubt that others of your kind will be able to imagine my real look just from simple words, because the automatic denial of the existence of reptilian species and generally of intelligent species other than your own is part of the programming of your mind. Well, I will try.

Imagine the body of a normal human woman and you have at first a good imagination of my body. Like you, I have a head, two arms, two hands, two legs and two feet and the proportions of my body are like yours. As I'm female I have also two breasts (despite our reptile origin, we have started to give milk to our babies during the evolution process —this happened around 30 million years ago— because this is the best thing to keep the young alive. Evolution had done this for your species already in the dinosaur age and —a little bit later— also for ours. That means not that we are now real mammals) but the breasts of us are not as large as those of human woman and the size of them is generally equal for every female of my kind. The external reproduction organs are for both sexes smaller than those of humans, but they are visible and they have the same function as yours (another gift of evolution to our species.)

My skin is mainly of a green-beige colour - more pale green - and we have some patterns of brown irregular dots (each dot of the size of 1 - 2 centimeters) on our skin and in our face (the patterns are different for both sexes but females have more, especially in the lower body and in the face.) You can see them in my case as two lines over the eyebrows crossing my forehead, at my cheek and at my chin. My eyes are a little bit larger than human eyes (for this reason, we can see better in the darkness) and usually dominated from the large black pupils, which are surrounded from a small bright-green iris (males have a dark-green iris). The pupil is slit and can change its size from a small black line to a wide-open egg-shaped oval, because our retina is very light sensitive and the pupil must compare this. We have external round ears but they are smaller and not so curved as yours, but we can hear better because our ears are more sensitive for sonic (we can also hear a wider range of sonic). There's a muscle or "lid" over the ears which can completely close them (for example under water). Our nose is more pointed and there is a V-shaped curving between the nostrils, which enabled the ancestors to "see" temperature. We have lost most of this ability, but we can still feel temperature much better with this "organ". Our lips are shaped like yours (those of females a little bit larger than those of males) but of a pale brown colour and our teeth are very white and strong and a little bit longer and sharper than your soft mammal teeth. We have no different hair colors like you (but there is a tradition to colour the hairs in different ages) and the original colour is —like mine— a greenish brown. Our hairs are thicker and stronger than yours and they grow very slow. In addition, the head is the only part of our body where we have hairs.

Our body, arms and legs are similar in shape and size to yours, but the color is different (green-beige, like the face) and there are scale-like structures on the upper legs (over the knee) and upper arms (over the elbow). Our five fingers are a little bit longer and thinner than human fingers and our skin on the palm is plain, so we have no lines like you but again a combination of a scale-like skin structure and of the brown dots (both sexes have the dots on the palm) and we have no fingerprints like you. If you touch my skin, you will feel that it is smoother than your hairy skin. There are small sharp horns on the upside of both middle fingers. The fingernails are grey and generally longer than yours. You see that my nails are not so long and round at the top. This is because I'm female. Males have sharp pointed nails with a length of sometimes 5 or 6 of your centimeters. The following feature is very different from your body and part of our reptilian origin: if you touch the backside of my upper body you will feel a hard bony line through my clothing. This is not my spine but a very difficult shaped external plate-structure of skin and tissue following exactly our spine from the head to the hip. There is an extremely high number of nerves and large blood vessels in this structure and in the plates (which are around two or three centimeters long and very touch sensitive - this is the reason why we have always problems to sit in chairs with a back like this chair.) The main task of these small plates (beside a role in our sexuality) is simply the regulation of our body temperature and if we sit in natural or artificial sunlight, these plates become more blood-filled and the vessels become wider and the sun is able to heat up our reptoid blood (which circulates through the body and through the plates) for many degrees and that gives us a great pleasure.

What else is different from your kind? Oh, we have no navel, because we were born in a different way to your mammal birth. The other exterior differences from your kind are minor and I think I must not mention all now, because most of them are not visible if we wear clothing. I hope the description of my body was detailed enough. I would advice you to make some drawings.

Question: What kind of clothing do you generally wear? I suppose this is not the way you dress normally?

Answer: No, I wear this human every-day-clothing only when I'm among humans. To be honest, it's not very comfortable for me to wear such tight things and it is always a very unusual feeling. If we are in our own home (this means in our subterranean home) or in our large artificial sun areas and if we are together with others near to our own name, we are usually naked. Is this shocking for you? When we are in the public and together with many others of my species we wear very wide and soft clothing made of thin, light stuff. I have told you that many parts of our bodies are very touch sensitive, mostly the small back plates so we can't feel comfortable in tight clothing because it can hurt us. Man and woman wear often the same kind of clothing, but the colors are different for the sexes.

Question: You've said "others near to your own name". Do you mean your family?

Answer: No, not really. You would call it "family" but with this word you mean only those of your kind which belong genetically together like father or mother and child. As I have said earlier we have a very difficult and unique name. Part of the pronunciation of that name is absolute unique and there is no other being with the same name, but part of this name (the middle part) is pronounced in a way that told the others to which "family" (I must use the word, because you haven't the right one in your vocabulary) you belong.

This means not that all in that group are genetically related to you, because these groups are usually very large and contain between 40 and 70 of us. This group includes generally your genetic relations - except one of them had decided to left this group - and your connection with father and mother is often the strongest. It would be too difficult for me to explain you now our very old social system which is very complex and we would need many hours only for the primary things. Maybe we can meet another time and I can give you detailed descriptions of all these things.

Question: Have you a tail like normal reptiles?

Answer: Do you see one? No, we have no visible tail. If you look at our skeleton, there is only a small rounded bone at the end of our spine behind the pelvis. This is a useless rudiment of the tail of our ancestors, but it is not visible from the outside. Oh, our embryos have tails during the first months of development, but these tails disappear before they were born. A tail makes only sense for a primitive species which tries to walk on two legs and must held the balance with the tail, but our skeleton had changed during evolution and our spine is nearly in the same shape as yours, so we need no tail to stay on two feet.

Question: You said that you were born in a different way to us. Do you lay eggs?

Answer: Yes, but not like your birds or primitive reptiles. Actually, the embryo grows in a protein liquid inside the mother's womb, but there is also an egg-shaped but very thin chalk hull around it, that fills the whole womb. The embryo inside this hull is completely autarky from the mother's body and it has every substance it needs to develop inside this chalk hull. There is also a cord like your navel cord which is connected to a point hidden behind the back plates. When the baby is going to be born, the whole egg is pressed through the vagina covered in a slimy protein substance and the baby came out of this soft egg after some minutes. These two horns on our middle fingers were instinctively used from babies to break through the chalk hull to take their first breath. Our young are not so large as your babies when they were born, they are between 30 and 35 of your centimeters tall, the egg is around 40 centimeters tall (this is because our vagina is smaller than a human one) but we grow to a normal size of 1,60 to 1,80 meters.

Question: What about your body temperature? You've said that you enjoy to lay in the sun. What effect has this to your organism?

Answer: We are no mammals and as reptiles our body temperature depends on the temperature of our surrounding. If you touch my hand you will maybe feel that it is colder than yours, because our normal body temperature is around 30 to 33 degree Celsius. If we sit in the sun (especially naked and with our row of small back plates in the sun) our body temperature can rise for 8 or 9 degrees within minutes. This rise causes a production of many enzymes and hormones in our body, our heart and brain and every organ becomes more active and we feel than very, very good. You humans only enjoy being in the sun but for us it is the greatest pleasure you can imagine (maybe like your sexual excitement.) We also enjoy swimming in very warm water or other liquids to rise our body temperature. If we are for some hours in the shadow, our temperature goes back to 30 to 33 degrees. This can cause no harm to us, but we feel much better in the sun. We have artificial sun-rooms in the underground but this is not the same for us like the real sun.

Question: What do you eat?

Answer: Generally various things like you: flesh, fruit, vegetables, special kinds of fungus (from subterranean farms) and other things. We can also eat and digest some substances which are poisonous for you. The main difference between you and us is that we must eat flesh, because our body needs the proteins. We can't live completely vegetarian like your kind because our digestion would stop working and we would die after some weeks or maybe months without flesh. Many of us eat raw flesh or other things which would be disgusting for you. Personally, I prefer cooked flesh and surface fruits like apples or oranges.

Question: Can you tell me something about the natural history and evolution of your species? How old is your species? Have you evolved from primitive reptiles as mankind has evolved from apes?

Answer: Oh, this is a very long and complex story and it sounds certainly unbelievable to you, but it's the truth. I will try to explain it in short. Around 65 million years ago, many of our unadvanced ancestors from the dinosaur race died in a great global cataclysm. The reason for this destruction was not a natural disaster - an asteroid impact as your scientists believe falsely - but a war between two enemy alien groups that took mainly place in the orbit and high atmosphere of your planet. According to our limited knowledge about the early days this global war was the first alien war on planet earth but it was definitely not the last (and a future war is coming soon, while a "cold war" - as you call it - between alien groups is ongoing since the last 73 years on your planet.) The opponents in this 65 million year old war were two advanced alien species, whose both names are again not pronounceable for your tongues. I'm able to say them but it would hurt your ear if I tell you the names in their original way. One race was humanoid like your species (but much older) and was from this universe, from a solar system in the star constellation you call "Procyon" today in your maps. The other species - about which we know not so much - was a reptilian species, but they have nothing to do with our own species, because we have evolved from local saurians without exterior influence (except the successful manipulation of our own genes by us. More about that later.) The advanced reptilian species came not from this universe but from a - well, how should I explain it to you. Your scientists have not really understood the true nature of the universe, because your illogical mind is not able to see the easiest things and relies on wrong mathematics and numbers. This is part of the genetic programming of your kind to which I will come later. Let me say, that you are nearly as far away from the understanding of the universe as you were 500 years ago.

To use a term you will maybe understand: the other species came not from this universe but from another "bubble" in the foam of the Omniverse. You would call it maybe another dimension, but this is not the right word to describe it correctly (by the way, the term dimension is generally wrong in the way you understand it.) The fact you should remember is, that advanced species are able to "walk" between bubbles by use of - as you would call it - quantum technology and sometimes in special ways only by use of their mind (my own species had also advanced mental abilities in comparison to your species, but we are not able to do the matter-string/bubble changing without technology, but other species active on this planet are able and this looks to you like magic as it had to your ancestors.)

Back to our own history: the first species (the humanoids) had reached Earth around 150 years before the reptilians and they built some colonies on the former continents.

There was a large colony on the continent you call "Antarctica" today and another one in the continent you call "Asia" today. These people lived together with animal-like saurians on the planet without problems. When the advanced reptilian species arrived in this system, the humanoid colonists from "Procyon" tried to communicate peacefully, but they were not successful and a global war started within months. You must understand that both species were interested in this young planet not for his biology and undeveloped species, but for only one reason: raw material, especially copper. To understand this reason, you must know that copper is a very important material for some advanced species (even today) because it is - together with some unstable materials - able to produce new stable elements if you induce a high electromagnetic field in the right angle with a high nuclear radiation field to produce an over-crossing of fluctuating fields. The fusion of copper with other elements in such a magnetic/radiation field-chamber can produce a force field of special nature that is very useful for various technological tasks (but the base for this is an extremely complex formula you are not able to discover because of the restrictions of your simple mind.) Both species wanted to have the copper of Planet Earth and for this reason they fought a not very long war in space and orbit. The humanoid species seemed to be successful during the first time, but in a last battle the reptilians decided to use a mighty experimental weapon - a special kind of fusion bomb which should destroy the life forms on the planet but should not harm the valuable raw materials and the copper. The bomb was fired from space and detonated at a point of your planet you call "Middle America" today. As it detonated in the ocean, it produced an unpredictable fusion with hydrogen and the effect was much stronger than the reptilians had expected. A deadly radiation, an over-production of fusion-oxygen, a fall-out of different elements and a "nuclear winter" for nearly 200 years were the result. Most of the humanoids were killed and the reptilians lost their interest on the planet after some years for (even for us) unknown reasons - maybe because of the radiation. Planet Earth was on its own again and the animals on the surface died. By the way, one result of the fusion bomb was the fall-out of different elements and materials created in the burning process and one of those materials was Iridium. Your human scientists today see the Iridium concentration in the ground as an evidence for an asteroid impact that killed the dinosaurs. That is not true, but how should you know that?

Well, most of the dinosaurs died (not all in the detonation but in the bad things which came after the war, especially in the nuclear winter and in the fall-out.) Nearly all dinosaurs and reptilians were dead within the next 20 years. Some of them —especially those in the oceans— were able to survive for the next 200 to 300 years even in this changed world, but these species also died, because the climate had changed. The nuclear winter ended after 200 years, but it was colder on earth than before. Despite the cataclysm, some species were able to survive: fish (like the sharks), birds, little creepy mammals (your ancestors), various reptiles like crocodiles... and there was a special kind of small but advanced dinosaurs which had developed together with the last large animal-reptilians like the species you call Tyrannosaurus.

This new reptile was walking on two legs and looked at little bit like your reconstruction of an Iguanodon (it originated in this family) but it was smaller (around 1.50 meters tall) with some humanoid features, a changed bone structure, a larger skull and brain, a hand with a thumb which was able to grab things, a different organism and digestion, advanced eyes in the middle of the head like your eyes and most important...with a new and better brain structure. This was our direct ancestor. There are theories that the radiation from the bomb took part in the mutations of the organism of this new breed, but this is not proven.

Nevertheless, this little humanoid-like dinosaur evolved during the following 30 million years (as I have said earlier, a species need generally more time to evolve than you think, if the evolution is not artificially induced like in your case) from an animal to a more or less thinking being. These beings were intelligent enough not to die in the next millions of years, because they learned to change their behavior, they lived in caves instead in the cold nature and they learned to use stones and branches as first tools and the use of fire as help to warm them - especially to warm their blood which is very important for our kind to survive. During the next 20 million years this species was divided by nature into 27 sub-species (unfortunately, former reptilian species were prone to divide themselves in a more or less illogical way into sub-species during the evolution process. You can clearly see this in the unnecessary high number of animal-dinosaur species in earlier times) and there were many (mainly primitive) wars between this sub-species for dominance.

Well, nature was not very friendly to us and as far a we know from the 27 sub-species 24 were extinct in primitive wars and in evolution, because their organism and mind was not developed enough to survive and (as main reason) they were not able to change their blood temperature in the right way if the climate changed. 50 million years after the war and after the end of Dinosaurs, only three (now also technological) advanced reptilian species were remaining on this planet together with all the other lower animals. Through natural and artificial crossbreeding these three species were united to one reptilian species and through the invention of genetic manipulations, we were able to "eliminate" the dividing-prone genes in our genetic structure. According to our history and belief, this was the time when our final reptilian race - as you see me today - was created by use of genetic engineering. This was around 10 million years ago and our evolution nearly stopped at this point (well, actually there were some minor changes in our look toward a more humanoid and mammal-like appearance during the coming ages, but we have not divided again into sub-species). You see, we are a very old race in comparison to your kind, which was jumping around as small monkey-like animals in the trees at this time while we invented technology, colonized other planets of this system, built large cities on this planet (which disappeared without a trace in the ages) and engineered our own genes while your genes where still those of animals.

10 million years ago the small simians started to grow and they came down from the trees to the ground (again because of the change of the climate - especially on the so-called African continent.) But they evolved very slow as it is normal for a mammal and if nothing extraordinary had happened to your kind, we wouldn’t be able to sit here and talk because I would sit in my comfortable modern house and you would sit in your cave clothed with fur and trying to discover the secrets of fire - or you would maybe sit in one of our zoos. But the things had developed differently and you believe now you are the "crown of creation" and you can sit in the modern house and we must hide and live beneath the earth and in remote areas. Around 1,5 million years ago, another alien species arrived at Earth (it was surprisingly the first species since over 60 million years. This would be more surprising for you if you would know how many different species are today here.) The interest of this humanoid species - you call them "Illojim" today - was not the raw material and the copper, it were to our astonishment the unadvanced ape-humanoids. Despite of our presence on this planet, the aliens decided to "help" the apes to evolve a little bit faster, to serve them in the future as some kind of slave-race in coming wars. The fate of your species was not really important for us, but we didn’t like the presence of the "Illojim" on our planet and they didn’t liked our presence on their new "galactic zoo" planet and so your sixth and seventh creation was the reason for a war between us and them.

You can read about that war for example partly in the book you call "Bible" in a very strange way of description. The real truth is a very long and difficult story. Should I continue?

Question: No, not now. I've made some notes about your history and now I have some questions.

Answer: Please ask.

Question: First of all, you handle with a very large time scale. You claim that your primitive ancestors lived together with the dinosaurs, survived the - as you called it - artificial cataclysm and evolved then over 40 million years and your evolution was completed 10 million years ago. This sounds very unbelievable to me. Can you say something to this?

Answer: I understand that this must sound absolutely unbelievable to you, because you are a young and genetically engineered species. Your historical horizon ends at a scale of just some thousands of years and you think this is right. But it isn't. This is impossible. Your programmed mind is obviously not able to handle with such large time scales. Our evolution time may seem incredible long to you, but this is in fact the original way of nature. Remember, your early mammal ancestors developed together with dinosaurs and they survived the bomb like us. They evolved slowly during the next millions of years and they divided into various species and shapes, some of them larger, some of them smaller. This is evolution of the body. But what about their mind and intelligence? They were simple animals. The mammals evolved since —let us say— 150 millions of years, but only in the last 2 - 3 millions of years they were able to became intelligent and thinking. And within this small period beings like you were created. From nature? 148 millions of year's time for the evolution of animal-like mammals, 2 millions of year's time for the development of (more or less) intelligent beings like you? Ask yourself: Do you really think this accelerated evolution is natural? Then your species is more ignorant than I've thought. We have not evolved wrong but you.

Question: I understand. But I have another question. You've mentioned many facts about the ancient war between the aliens 65 million years ago. This happened very long before your kind became really intelligent (as far as I have understood you). Why do you know so many things about that "first war" and about the evolution of your species?

Answer: This is a good question (much better than the previous) and I have not explained it properly to you. Our knowledge about the first war comes completely from an ancient artifact, which was found around 16,000 years ago from our archeologists on the continent you call North America today. They found there a round plate with a diameter of approximately 47 of your centimeters. The plate was made of an even for us unknown magnetic material and inside the plate there was another smaller crystal plate which contained an enormous amount of information coded in the molecular structure of the crystal. This "memory plate" was manufactured from the last bomb survivors of human race from "Procyon" already 65 million years ago but it was completely intact when we found it. Our scientists were able to encode the messages and data and so we heard the first time about the events which took place in the distant past and which led to the extinction of the dinosaurs. The plate contained detailed descriptions of both species (but more about the humanoids) and about the events and weapons, including the fusion bomb. It contained also a description of the animals and saurians on earth, including our pre-intelligent ancestor species. The rest of our knowledge about our evolution comes from skeletons and from the back-reading and de/encoding of our DNA.

You see, we know the real truth about our roots since 16,000 years. Before that time, there was a more religious idea of our creation.

Question: What have happened with the both alien species?

Answer: We don't know exactly. The surviving humanoids on earth obviously died in the years after the bomb and others of their kind and the reptilians never came back to Earth (as far as we know). Concerning the reptilian aliens, there is a possibility that it was physically impossible for them to return, because the matter between bubbles is sometimes in rapid movement. The current theory is, that both species had ceased to exist during the millions of years.

Question: You've mentioned skeletons of your kind. How can it be, that human scientists haven't found any trace of you and your ancestors if you really live for such a long time on this planet? We have found many skeletons of primitive dinosaurs, but none of an advanced reptilian being with a larger skull and brain and a hand with a thumb as you have described it before.

Answer: Yes, you have. But your "great" scientists were not able to reconstruct the skeletons completely, because they wanted to reconstruct reptilian animals, not intelligent beings. You would laugh if you would know how many of the (especially small) saurian skeletons in your museums are totally wrong constructions of never-existing beings, because you used many bones which didn't really belong together and sometimes you made artificial bones if something was missing you needed to construct an "animal" saurian. Many of your scientists are aware of this problem, but they don't make it public, because they can't explain it and they claim, that the right bones were just missing and their reconstruction is right. Many bones of us were used for Iguanodon reconstructions, for example the hands with the visible thumb (look at an Iguanodon in a museum and you will see that I'm right.) A scientist in the country you call United States had built a nearly correct skeleton of our kind some years ago, but the local government (which is partly aware of our existence) confiscated the reconstruction. As we live today (and since thousands of years) nearly completely beneath the earth, you will not find any cadavers or skeletons of us.

Question: You speak sometimes about underground cities and artificial sunlight. Do you mean something like a "hollow Earth" with this? Is there a second sun inside our planet?

Answer: No, Earth is not really completely hollow and there is no second sun inside. This story is ridiculous and physically not possible (even your species should be intelligent enough not to believe this.) Do you know how much mass a sun must have to produce energy and light for a longer time by fusion? Do you really think that there could be a small active sun inside the planet? When I talk about our subterranean home, I talk about large cave systems. The caves you have discovered near to the surface are tiny in comparison to real caves and huge caverns deeper in the earth (in a depth of 2,000 to 8,000 of your meters, but connected with many hidden tunnels to the surface or to surface-near caves) and we live in large and advanced cities and colonies inside such caves. Major sites of us are beyond the Arctic, the Antarctic, Inner Asia, North America and Australia. If I talk about artificial sunlight in our cities I don't mean a real sun but various technological sources of light (including gravitational sources) which illuminates the caverns and tunnels. There are special cave areas and tunnels with a strong UV light in every city and we use that places to heat our blood. Furthermore, we have also some surface sun places in remote areas, especially in America and Australia.

Question: Where can we find such a surface-near entry to your world?

Answer: Do you really think I will tell you their exact location? If you want to find such an entry, you have to search it by yourself (but I would advise you not to do that.) When I came to the surface four days ago, I used an entry approximately 300 of your kilometers north from here near to a large lake, but I doubt that you would be able to find it (there are only a few entries in this part of the world - more are far more north and east.) As a little advice: if you are in a narrow cave or in a tunnel or even in something that looks to you like an artificial mine shaft and as deeper you walk as smoother appear the walls and if you feel unusual warm air streaming from the depth or if you hear the rushing sound of streaming air in a ventilation or elevator shaft, then look for a special kind of artificial and smooth wall somewhere in the cave with a door made of gray metal. If you would be able to open that door (but I doubt this) you would be in a usually round technical room with ventilation systems and elevators to the depth. This is probably an entry to our world. If you have reached this point, you should know that we are now definitely aware of your presence. You are already in big trouble if you have entered the round room, but you should look for one of the two reptilian symbols on the walls. If there are no symbols or other symbols, you are maybe in bigger trouble as you think, because not every underground installation belongs to our kind. Some new tunnel systems are operated from alien races (including hostile races). My general advice if you find yourself in a, for you, strange underground installation: run away as fast as you can.

Question: You mentioned earlier that you use the name "Lacerta" when you are among humans and that you enjoy it to be in the real sun on the surface of earth. But how can you be among humans? You don’t look like us, so anyone will see that you belong to another species. Why have nobody seen and described a being like you if your kind lives already since our "creation" together with us on the same planet. Can you explain that to me?

Answer: First, my kind was of course seen and described (and worshipped) many times in your primitive past, for example in your religious writings like your Christian Bible. You can find descriptions and even simple drawings of us for also in the southern part of the American continent on various temples. So-called "wise" men from India and from the Asian mountains have described our species many times in writings, together with other "wise" men from the African continent. I think we are the most mentioned non-human species (maybe beside the "Illojim") in your history. If you don’t believe me, have a look at your history and you will see the truth in my words. Your "great" scientists called the belief in us "superstition" and "religion" and today’s "intelligent" humans have forgotten our presence on the surface in the past.

Furthermore, our species is seen even today sometimes from human witnesses in its original shape on earth or in our surface-near entries and tunnel systems, but fortunately you and your media didn’t take the reports of such "crazies" serious (that’s good for us and that’s the reason why we allow those people to see us as we really are.) Some of my species are also in direct contact with human scientists and politicians from the surface, but this is top-secret —as you would call it— and nobody of your public knows anything about it (the matter of these meetings is generally the upcoming war with and between the alien species and our assistance in this war). But there is also another explanation, why we can walk among you and why you are not able to recognize us: mimicry.

The following may again sound unbelievable and even shocking to you, but as you have asked I will explain it. I have told you before, that we have more advanced mental abilities than your species and with "more advanced" I mean, that we are able to use telepathy and telekinesis from our birth on (in fact, mother and new-born child communicate generally with telepathy during the first months) without special training as you need it to activate these sleeping parts of your brain. The structure of our brain is a little bit different to yours and our hypothesis is larger and more active than yours - especially when we are in sunlight. Our own abilities are very strong in comparison to yours, but weak in comparison to the "matter-string/bubble" mind forces of some of the alien species on this planet. I was never very good in that mind things, but we all have these primary abilities and can use them for example for our protection or even for attack.

When we are on the surface and we meet human beings (even a large group of them - this makes no difference. All of your minds are like one mind) we are able to "touch" their mind and induce them via telepathy the command "See us as one of your kind" and the weak human mind will accept this order without re-fusion and they will see us (despite our reptilian look) as normal humans. I've done this many times and you weak humans generally see me as an attractive brown-haired woman, because I have created this special "mimicry image" in my mind years ago and I can induce it into your minds without problems. I've needed some time at the beginning to learn the use of the mimicry correctly, but then it worked nearly automatically and I can even walk among a group of yours and nobody will recognize what I am. There is a simple switch ("See us as we really are / See us as we want you to see us") in your consciousness which was placed there from the "Illojim" when they created your kind and we can use this switch to convince you that you see humans when you look at us (other aliens use this switch, too). It is easier as you think. When there are meetings between your kind and aliens which seem to look exactly like yours, these aliens have used that switch and some of the meetings with man-like aliens can be also explained with meetings with my kind.) When I met E.F. the first time, he saw me also as a normal human woman and I remember that he was very frightened and shocked when I revealed him my real appearance.

Question: Do you mean, that you can really make me belief that I talk now with an attractive brown-haired human woman instead of a reptilian being like you?

Answer: Probably, but I don't think so in your special case. When someone expects to see a human woman instead of me, I can do it without problems with his mind (even with large groups) because nobody expects to see a reptile woman. But I have allowed your mind to see me in my original appearance from our first meeting on and I have never induced something into your mind, so you have already realized that I'm not human. If I would now try to change this, it would probably lead to an absolute confusion or to unconsciousness and I don't want to harm you. As I have said I'm not very good in these things.

Question: That's very scary. Can you kill with those abilities?

Answer: Yes, but it's forbidden. This means not that it was not done in previous times.

Question: Have both sexes these abilities?

Answer: Yes.

Question: What about photos? How do you appear on photos?

Answer: This is a silly question. I appear on photos as a reptile being, because I can't have influence on the photo or on the camera itself but only on the photographers mind. If he or she would develop the film and show the photo to others, they would see me in my original shape. That's the reason why it is forbidden for our kind to be filmed or photographed and we must avoid every camera on the surface (that is very difficult and we were filmed sometimes in the past without our knowledge, especially from certain of your governments and secret agencies.)

Question: What other commands can your kind induce into our minds? Something like "Serve us" or "Obey"?

Answer: This is again a strange question. We are not your enemy (most of us not) so why should we do this? To answer your question: it depends on the strength of the human mind and on the strength of the sending reptilian. There is no "Serve us" or "Serve me" switch in your mind, so such a command is much more difficult to induce. If the human mind and consciousness is weak and the reptilian inducer is experienced in these things and was some hours in the sun before he or she tries to do it, then it could probably work for a certain time. There are secret teachings about such things, but I've never learned anything about it. I use my primary abilities for mimicry and for communication with my own kind and sometimes for other private things, but I've never used it to harm humans or their mind. I would appreciate it if we can end with this topic here.

Question: A last question: you've said earlier, that you can hide your UFOs? Do you use the same abilities to do this?

Answer: Yes, but on a technical base. There is a powerful device inside each craft which is able to send an artificial signal to your minds to convince you, that you see either nothing but only the sky or that you see normal aircraft like planes instead of our ships. This isn't used very often, because we avoid human public when we move in the atmosphere. If you are able to see our "UFOs" it means that the device is either defect or deactivated for some reason. The camouflage effect didn't work on photos - to answer this possible question of you already in advance - but why should someone make a photo of the sky when he could not see anything unusual there. By the way, most of the surface-near entry points to our tunnels are also hidden with such a device and your kind will generally see only normal cave walls instead of the door. That's one reason why I've said that I doubt that you will be able to find such a secret door to our world (but it have happened a few times in the past.)

Question: Back to your and our own history. You've mentioned the race of the "Illojim" who have created our human race. From where did they come and how did they look like? What had exactly happened when they arrived? Are they our "God"?

Answer: The "Illojim" came from this universe, from the solar system you call "Aldebaran" in your maps. They were a very tall humanoid species whit usually blonde hairs and a very white skin (they avoided the sunlight, because it hurt their skin and their eyes. This was absolutely unbelievable for a sun-loving species like us).

They seemed to be intelligent and peaceful at the beginning and we started a more or less friendly communication with them, but later they showed their real intentions and plans: they wanted to evolve the apes to a new breed and we were a disturbing factor for them on their new zoo planet. At first, they caught around 10,000 or maybe even 20,000 of your simian ancestors and they left the planet for some hundred years. When they returned, they brought your (now more human) ancestors back. Then they left Earth again for some thousands of years and the primitive pre-humans lived together with us without major problems (they were just afraid of our aircraft and technology). The "Illojim" had taught their mind and enhanced their brain and their body structure and they were now able to use tools and fire. The "Illojim" returned within 23,000 years seven times and accelerated the evolution speed of certain of your kind. You must understand that you are not the first human civilization on the planet. The first advanced humans (who lived at the same time with less-developed pre-humans, because the "Illojim" had experimented with different speeds and stages of evolution) with technology and speech existed around 700,000 years ago on this planet (your scientists have not understand this, because they've found only the bones of the pre-humans and some primitive cave drawings showing advanced humans and flying devices.) This genetically advanced human breed lived together with us, but they avoided contact with my kind, because the "Illojim" teachers had warned them with misleading purpose that we are evil beings and that we lie to them.

Well, after some centuries the aliens decided to extinct their first creation and they accelerated the evolution of a second and better test series and so on and so on. The truth is that your modern human civilization is not the first on this planet Earth but already the seventh. The buildings of the first breeds are lost, but the fifth civilization was the one, which built the large triangular constructions you call "Egyptian Pyramids" today around 75,000 years ago (your Egyptians just found that large ancient pyramids in the sand and tried not very successful to built similar constructions) and the sixth civilization was the one, which built the cities which ruins you can find today beneath the sea in the so-called Bimini Area around 16,000 years ago. The last creation of the seventh breed - of your series - was done just 8,500 years ago and this is the only creation you can remember and to which your religious writings refer. You rely on archeological and paleonthological artifacts which show you a wrong and short past, but how should you know anything about the six civilizations before. And if you find evidence for their existence, you deny and misinterpret the facts. This is partly a programming of your mind and partly pure ignorance. I will tell you in the following only about your creations, because the six previous mankinds are lost and therefore they should not concern you.

There was a long war between us and the "Illojim" and also between certain groups of the "Illojim" themselves, because many of them were the opinion that the again-and-again creation of human species on this planet makes no real sense. The last battles in this war were fought around 5,000 years ago in orbit and surface. The aliens used powerful sonic weapons to destroy our underground cities but on the other hand we were able to destroy many of their surface installations and bases in space.

The humans of your series were very frightened when they observed our battles and they wrote it down in form of religious myths (their mind was not able to understand what was really going on.) The "Illojim" - who appeared as "gods" for the sixth and seventh breed - told them that it is a war between good and evil and that they are the good and we are the evil race. This depends certainly on the point of view. It was our planet before they arrived and before they started their evolution project with your kind. In my opinion, it was our right to fight for our planet. It was exactly 4,943 years ago - according to your time scale - that the Illojim left the planet again for unknown reasons (this is a very important date for us, because many of our historians called it a victory.) Fact is that we don't know what had really happened. The "Illojim" were gone from one day to another, they vanished without a trace together with their ships and we found most of their surface installations destroyed by them. The humans were on their own and your civilization developed. Many of us were in contact with certain (more southern) tribes of your species in the coming centuries and we were able to convince some of them that we are not the "Evil" the aliens wanted them to believe. During the time from 4,900 years ago to today, many other alien species arrived the planet (some of them used the old teaching and programming of your mind and "played" again God for you) but the "Illojim" themselves never came back. They had left the planet for a duration of some thousand years also earlier, so we expect their return one day in future to end their project or to maybe extinct also the seventh breed, but we don't really know what have happened to them (to answer this question of you in advance).

Your current civilization doesn't know anything about your real origin, about your real past, about your real world and universe and you know very little about us and our past. And you know nothing about the things to come in near future. As long as you will not understand and believe my words - I tell you the truth because we are not your enemy - as long there is danger for your species. Your enemies are already here and you have not understood. Open your eyes or you will be in big trouble soon. If you haven't believed anything of the things I've told you before, then you should really believe and remember this.

Question: Why do you think I don't believe you?

Answer: I have a certain feeling that you don't believe me, despite the fact that I'm sitting here in front of you. Everything I have told you in the last two hours is the absolute truth about our world.

Question: How many alien species are active on earth at the moment?

Answer: As far as we know 14 species. 11 from this universe, 2 from another "bubble" and 1 very advanced from a very different plain. Don't ask me for names, because nearly all are not pronounceable for you, eight of them are not pronounceable even for us. Most of the species - especially the more advanced - are just studying you as animals and they are not very dangerous for you and for us and we work together with some of them, but three species are hostile, including the one which was in contact with some of your governments and exchanged their technology for copper and other important things and which had betrayed your kind. There was and is a "cold war" between two of these hostile races during the last 73 years and the third species seemed to be the "winner" in this useless struggle. We expect a more "hot" war between them and you in the near future (I would say in the next 10 or 20 years) and we are worried about that development. In the last time, there were some rumors about a new, fifteenth species which had arrived on Earth just 3 or 4 years ago, but we don't know anything about their intentions and we were not in contact with them till now. Maybe the rumors are wrong.

Question: What do the hostile alien races want?

Answer: Various raw materials, including copper for their technology, your water (or better the hydrogen in your water, which is a source of energy in advanced fusion processes) and certain chemical elements in your air. Furthermore, two of the species are also interested in your body, in your human tissue and blood, because their own genetic structure is defect through bad evolution and radiation (as far as we know) and they need intact strings from your kind and from animals to repair their own genetic again and again, but they are not really able to repair the defects completely because their DNA and your DNA is not fully compatible (my own species is absolutely incompatible with them, so they are not very interested in us) and they try to make more compatible crossbreeds between you and them by use of artificial fertilizations and artificial wombs. We suppose that the coming war between the three races or between you and one or all of them will be fought for raw material, hydrogen, air and DNA.

Question: Is this the reason for the "abductions"?

Answer: Partly, especially when the aliens took egg and sperm samples from you. Sometimes the abductors belong to another and more advanced race and they just want to study your body and your mind (which is more interesting for some of them than your solid body) as you would study a primitive animal. As I have said, three alien species are hostile and this means that they do not care for your fate or for your life and people who were "abducted" by them came very rarely back alive. If someone is able to report about an abduction, it means in my opinion that he or she has not met one of the aggressive species or that he or she is a very, very lucky human to be alive. Advanced and "friendly" races also took sometimes egg and sperm samples, but for other reasons.

Question: You've said there are only 14 species active on earth. But why describe people who saw alien beings so many different and bizarre types of them?

Answer: I think I have already answered to this question. As I have said, most of the alien races have much more advanced mind abilities than you or even me (there is just one alien race completely without such abilities). They are able to appear in your mind and memory as whatever they want and this induced "image" has nothing to do with their real appearance. You remember them as normal humans or grey dwarfs or even extremely bizarre animals because they want you to remember that or sometimes they want you to completely forget anything about a meeting with them. Another example: you can for example remember that you were just in a normal of your human hospitals and that some doctors were examining you and you think not further about what have happened to you (maybe till you discover that there is no hospital in the street were you supposed it) but in fact you were examined by them in one of their laboratories. You can't rely on your mind in this case. They appear in different shapes to you to confuse you and to make so-called abduction witnesses who were able to remember the events - or who believe they are able to remember - ridiculous in the public and as far as we know, they are successful. Believe me, there are only 14 alien species on this planet and only eight of them abduct humans at the moment (again as far as we know.) In addition, not everyone of your "abductees" is one and some of the aliens in their reports are really just imagination or lies.

Question: How can we protect us against this influence on our mind?

Answer: I don't know. I doubt you can, because your mind is like an open book to read and write for nearly every species I know. This is partly the guilty of the "Illojim" themselves, because they had constructed or better mis-constructed (partly intentionally) your mind and your consciousness without real protection mechanisms. If you are aware that someone tries to manipulate your mind, you can only concentrate on that suspicion and try to analyze every one of your thoughts and memories. Very important: don't close your eyes (this would lead to a different form of brain waves which are more easy to access) and don't sit or lay down to rest. If you stay awake during the first minutes, you can maybe try to filter the other thoughts and waves in your brain and the inducer will give up after some minutes if he or she is not successful because it will start to hurt his or her own brain. This is very difficult and certainly painful and it can harm you, so better don't try to resist but it would be the only possibility you have. However, you can try this only with the more weaker species, not with the strong.

Question: What do you mean with "one species comes from a very different plain"?

Answer: Before I can explain that correctly to you, you must be able to understand the universe and this would mean a maybe useless teaching of your mind (including the remove of some barriers) of many weeks and with teaching I mean not only teaching by words. I have said this with your word "plain" or "level" because you have again no better word in your vocabulary and dimension would be in this case absolutely wrong (it's rather wrong even for another "bubble") because a dimension can't exist without plains. If you would be a species living in another or over the plain and if you would be furthermore able to enter plains without technology so that your body is not made of that kind of matter you know, then you would be the mightiest being you can imagine. This very advanced race I've mentioned had developed outside of here and they've evolved in fact over billions of years. They would be able to destroy all of you and us and everything with just a single thought. We were in contact with them only 3 times in our whole history, because their interest in your planet is different from that of all other races. They are definitely no danger for you or us.

Question: What will happen when the war begins?

Answer: This is difficult to answer. It depends on the enemy race and on their tactic. "War" is not always that primitive thing you humans mean with the word, "War" can be fought on various levels. One possibility they have is the "destruction" of your social system by influence on political leaders, another is the use of advanced weapon systems which can cause earthquakes or volcanic eruptions or other disasters (including weather disasters) which may seem natural to you. The special fields from copper-fusion I've mentioned earlier are able to have an influence on your global weather. I think they will not attack the planet directly before the human civilization is weak, because even you have possibilities to destroy their craft (but not many.) Let me say, that we are not absolutely sure if there will be really such a "hot" war already in the next years. I don't want to talk further about this.

Question: This is the end of the interview. Do you want to say a last sentence or message?

Answer: Open your eyes and see. Don't believe only in your wrong history or your scientists or your politicians. Some of them know the truth about various things, but they don't inform the public to avoid confusion and panic.

I think your species is not as bad as some of my kind thinks and it would be a pity to observe your end. That's everything I can say. Go through your world with open eyes and you will see - or maybe not. Your kind is ignorant.

Question: Do you think anyone will believe that this interview is the truth?

Answer: No, but it is an interesting experiment for my social studies. We will meet again in some months and you will tell me then what have happened after the publication of my message. Maybe there is hope for your kind.

All Rights Reserved ©

The Lacerta File II

Translation by Doug Parrish. Taken from http://www.sabon.org/reptiloid/index4.html .

Introduction

I once again reaffirm that the following text is the absolute truth and is not fiction. It was composed from three original tape recordings which were made on April 24, 2000 with a tape recorder during my second interview with the reptilian creature known as "Lacerta". At Lacerta's request, the original text of 31 pages was revised and shortened up to deal with some questions and answers. Some existing questions were partially shortened or amended. It was even undertaken to extract message and significance from it. This part of the interview, either not mentioned or not mentioned completely in the transcript, deals primarily with personal issues, paranormal demonstrations, the social system of the reptilian species and alien technology and physics.

The reason for the shifting of the date and time of the second meeting was a possible observation and surveillance of my own person after the publication of the first transcript. Although everything was attempted on the advice of Lacerta to keep my identity a secret, just two days after the dissemination of the document abroad, and various unusual events took place. Please don't think that I am paranoid; however, I believe that the publication of the interview has drawn either official attention or the attention of some organization to me. Up until this time, I usually regarded people who believed that they were being followed by the state to be nothing more than jokers. But now I have begun to revise my ideas on that since events in January. It began with a failure of my telephone for several hours. When the phone became operational once again, there were quiet echoes and strange clicking and whirring sounds when I made calls. A defect could (ostensibly) not be found anywhere. Overnight, important data disappeared from the hard drive in my computer. The testing program reported "defective sectors" where strangely enough there were only data which dealt with illustrations and completed textual material from the interview. These "defective sectors" also contained material of a paranormal nature in the field of my research. (Fortunately, the material was also stored on floppies.) In addition I discovered by pure chance some hidden data in a likewise hidden directory index. The name which appeared on the data and the directory index was "E72UJ."

A friend, who is a computer expert, could not make anything of this designation, and when I was about to show it to him, the directory index had disappeared. One evening, my apartment door was standing wide open, my TV set was running —and I am absolutely confident that I had turned the TV set off.

A minivan with British markings and the imprint of a Europe-wide supermarket chain parked in front of my house. I noticed the same minivan again on several occasions traveling at a distance behind my car, even when I visited the town of ..... 65 kilometers away. When I returned, the car was on the other side of the street once again. I never saw anyone get into or out of the car. A knock on the door of the vehicle and on the tinted windows caused no reaction of any kind. After about two weeks, the minivan disappeared again. When I informed E.F. personally about these events, he suggested that I change the place and date of the meeting in order to assure our own and Lacerta's safety. The meeting took place on April 27, 2000 in another isolated location. It was unobserved as far as I can determine.

Once again, all of this may sound strange and paranoid, like a fantasy from a cheap science fiction film; however, I can only repeat to and assure the reader once again: all of this is the unadulterated truth. Believe my words or don't believe them. These things have happened and they will continue to happen, whether you believe it or not. Until it is too late. Our civilization is in danger.

Ole. K. – May 3, 2000

Transcript of the Interview (Shortened Version)

Date of Interview: April 27, 2000

[Comment by Ole. K.: The meeting began with an appraisal of diverse questions and opinions which I had gotten from readers of the first transcript in anonymous fashion through distribution from my trustworthy friends. Some of these opinions—all together there were over 14 pages of paper—contained comments shaped by everything from a radically religious to a fanatical tendency to welcome contact with a reptilian species. Some of these comments contained stereotypical phrases like "Servants of Hell" or "Species of the Evil One". I don't want to go into any kind of detailed description here since I don't want pass on further any false and radical realm of thought.]

Question: When you read these religious and animosity-ridden comments here, what do you think and feel then? Is the relationship between your species and ours really shaped from that kind of total negation?

Answer: Does it amaze you that I am not completely angered by that? I had fully expected those kinds of extreme reactions. The programming for the utter negation of another species (especially the reptilian species) as in your own case is deeply embedded in each of your own individual consciousnesses. This ancient conditioning stems from the days of your third artificial creation and, biologically speaking, is passed down as an information genome from generation to generation. The identification of my species with the powers of darkness was a primary intention of the Illojim, who liked seeing themselves in the role of the powers of light —something which in and of itself represents a paradox, since that humanoid species was extremely sensitive to your sunlight.

In case you were expecting me to act offended, I guess I'll have to partially disappoint you. These obscure intentions are not really your fault; you are simply following for the most part what you have inherited from your ancestors. It is indeed actually somewhat disappointing that many of you develop no especially strong individual self-conscience, for this would help you to overcome the conditioning. As I already said, we were in direct contact in the last several centuries with some of your more primitive human tribes; these tribes had themselves succeeded in breaking through the old "creation programming;" they were able to meet us without tension, hate and total rejection. Apparently many of your modern civilized individuals are not in a position to think on their own, but rather let themselves be guided by programming and religion (which is also a manifestation of that ancient programming and part and parcel of the plan of the Illojim). Therefore, comments of that kind I'd sooner regard as amusing than irritating; they simply confirm in large measure for me my suppositions about your defined mode of thinking.

Question: Therefore, you are not the "Species of the Evil One" as was remarked earlier?

Answer: How am I supposed to answer that? Your people still think according to a simple and completely inappropriate scheme of generalizations. Simply put, there are absolutely NO purely evil species. There exist in every terrestrial and extraterrestrial species alike both good and evil individuals; it's even true of your own people; but there is NO such thing as an absolutely evil species. This conception is really very primitive. You people have believed from time immemorial what you are supposed to believe—what was foreseen for you to believe by your creators. Every well-known species, even the more highly developed ones, consists of a great number of individual consciousnesses (at least a portion of the consciousness is individual, even though there are connecting fields of consciousness); these self-sufficient spirits are able to decide freely for themselves a lifestyle which is either good or evil, according to your own human standards. It depends again on the respective point of view; your people are not necessarily in a position to judge whether the deeds of a much more highly developed species are good or evil, because you stand at a lower observation point, from which an assessment is not possible. Your simple words "good" and "evil" are in any case examples of a tendency towards generalization; in my language there are many concepts for the various shades of meaning of individual behaviors in comparison to the norms of a society.

Even those extraterrestrial species which are inclined to act with antagonism towards you are not "Species of the Evil One," even though they operate negatively with respect to your own race. They do this for their own reasons and do not regard themselves as evil; were your structured way of thinking more linear and more focused as theirs is, then you would also behave in such a fashion. The attitude of a species towards other kinds of existence naturally depends very heavily on its respective structured way of thinking; each species sets its own priorities. To classify that as "good" or "evil" is really quite primitive, for the survival of any species argues for many varieties, among them your own, as well as for even the most varied of the worst or negatively-directed deeds. I won't even exclude my own kind in this regard, for there have been certain occurrences in the past which I don't personally welcome, but about which I would also not like to go into detail. None of these occurrences have happened in the last 200 years of your time scale. But please note the following: there are NO absolutely good and there are NO absolutely bad species, because each and every species always consists of individuals.

Question: In the letters that I got, there was often the question, whether you could go into any greater detail regarding the advanced physics that you commented on last time. Many people said, your words made no sense. For example, how do UFOs function, how do they fly, how do they perform the maneuvers that they do?

Answer: I ought to explain that to people? That's not all that simple. Let me think about it for a minute. I always have to use very simple words in order to make clear to you the basic principles of a higher kind of science. Let's try this: You have to be clear about some fundamental facts. The very first thing is that you must divide up the conception of the physical world because each existence consists of different layers; let's say for simplicity's sake that it consists of a material illusion and a sphere of influence. {TRANSLATOR'S NOTE: No legitimate translation exists for this word 'Feldraum'; "Feld" means "field," "Raum" means "space, room, expanse." Therefore, I'm translating it as "sphere of influence."} Certain physical conditions are associated only with the realm of the material {as in 'concrete'}, while other and more complicated conditions are associated only with the sphere of influence of the material world. Your conception of the physical world is based upon a simple material illusion. That illusion is further subdivided into three elementary or basic conditions of matter. A fourth and very important condition also exists, which you simply pay attention to more or less as you choose; it is the one bordering on the sphere of influence or plasma realm. For you, the theory for a controlled transformation or an elevation of the frequency of matter and the stable existence of this fourth aggregate condition of matter is not very common, or it exists at a very primitive level. (As an aside, there are simply five states of matter, but the post-plasma state would really be going too far and it would only serve to confuse you. Besides, it is not necessary for an understanding of the basic theory; it is connected with diverse phenomena which you would characterize as paranormal.) Now, back to the essentials: Plasma...now, with plasma I don't mean just "hot gas"—as the concept is generally simplified by your people—but rather I mean a higher aggregate condition of matter. The plasma state of matter is a special form of matter which lies between its real existence and the sphere of influence, that is, a complete loss of mass and pure accretion of energy of various form whenever matter is "pushed or shoved." {NOTE: No explanation was given for the use of the word "pushed, shoved" as used in this context. Your guess is as good mine.}

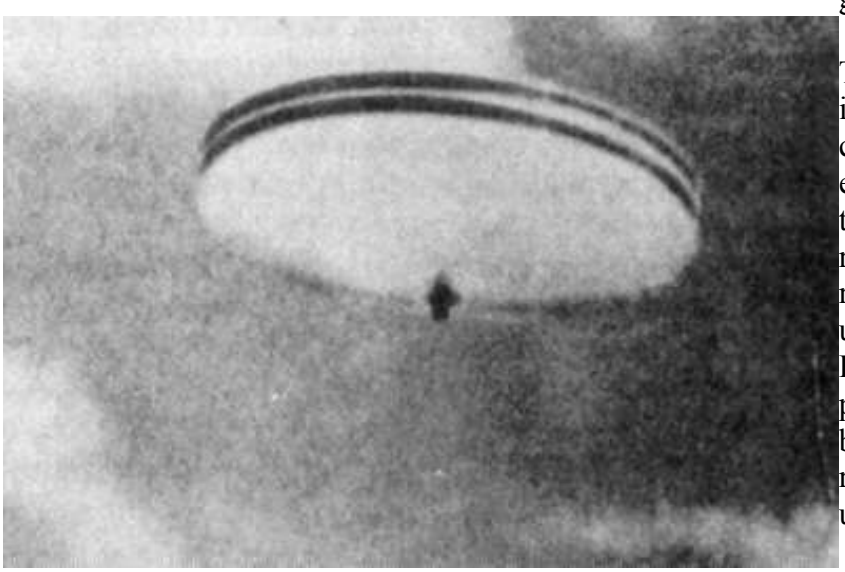

The fourth state of matter is very important for certain physical conditions which can be used for example to...how should I express this to you...generate antigravity. (That's a rather strange human word and not really correct, but you ought to understand it better this way.) Essentially, in the world of real physics, there are no bipolar forces, but rather only "observer dependent reflective behavior" of a single, large unified force at different levels.

With antigravity or the displacement of gravitational characteristics into levels, one can, for example, cause apparently solid matter to levitate; this method is employed partly by us and by extraterrestrials as well as a means of propulsion for their UFOs. You people are moving on a really primitive level towards a similar principle for your secret military projects, but since you have more or less stolen this technology (and it was later falsely passed on to you intentionally by the extraterrestrials), you lack the real physical understanding; as a result, you have to struggle with problems of instability and radiation with your "UFOs". According to my information, there have been a great number of deaths of your people because of intense radiation and field disturbances. Don't you agree, this is also an example of the business regarding the question of "good" and "evil"? You people play with unknown forces and thereby accept the death of colleagues of your own kind, for they are dying for a greater cause, namely, for the advancement of your technology, which as a result is being put into place once again for the purpose of war, i.e., for negative pursuits. Now, one can give you the benefit of the doubt, that only the least number of your kind have any knowledge about these alien projects which are —as you explain it— top secret. It was told to you that the higher the ordinal or ranking number of basic matter, the simpler the heightening of the condition, but that is only partially correct. If you can't circumvent these powers, then you're better off not attempting it. But your kind has always been ignorant and has from time immemorial tried to play around with forces which you have not even understood. Why would that ever change?

You remember this business of copper fusion? By means of the fluctuation at the right angle with the induced radiation field, copper is fused with other elements. (The illusion of matter is fused, the fields in the sphere of influence overlap each other, but the main force would be reflected by that process and would assume a quasi-bipolar character.) The resulting connection and the field would therefore not be stable in the normal condition of matter and unsuited for tasks. As a result, the entire field spectrum is shifted to a higher plasma-like condition, whereby the spectrum comes together with this harsh shifting to the opposite pole side —the word is NOT correct— of the force field and it resembles quite closely a gravitational shift. This shifting causes a "tilting" of the repulsing quasi-bipolar force, which now no longer flows to the interior of the force field, but rather flows partly to the exterior of the field. The result is an inter-stratifying reflective force field which is very difficult to modulate within certain technical boundaries in relation to its own characteristics. It can also carry out a multiplicity of tasks, as for example, causing massive flying objects to be levitated and maneuvered. It can also exert a camouflage function in the realm of electromagnetic radiation as well as manipulate temporal sequences of events—indeed only to very limited extent—and other things as well. Are you familiar with your "quantum tunnel effect"? Even the amplitude equalizations among genuine matter can be achieved with one of those kinds of fields if the frequency and the distance from the plane of the field are high enough. Unfortunately, the whole thing that I have explained to you in your words has come out to be rather primitive, I'm afraid. It sounds rather strange and certainly impossible for your comprehension, but perhaps this simple explanation can be of some use to you in helping you to understand. But then again, maybe not.

Question: Is there a scientific substantiation for paranormal powers, as for example with your powers of thought?

Answer: Yes. In order to explain that, one has to acknowledge the physical reality of the sphere of influence {Feldraum}. I'll try to do it...wait just a second...you are going to have to separate yourself mentally from the illusion that that which you see is the true nature of the universe.

It is, at best, the surface of a side. Imagine for yourself that all the matter here —you, this table, this pencil, this technical device, this paper— does not really exist, but that it is rather only the result of a field oscillation and a concentration of energy. All matter that you see, every creature, every planet and star in this universe, has an "information-energy equivalent" in the sphere of influence which is located on a main field —the general level {of things}. Now, there is not only one level, but several. Last time, I had mentioned that highly-developed species which is capable of changing levels (which is something completely different from the simple bubble changing, for bubbles are a part of each and every level). Do you understand? Dimensions, as you call them, are a part of a solitary bubble, bubbles or universal foam are a part of a level, and levels are layers in the sphere of influence, while the sphere of influence, acting in the capacity of single physical size, is essentially unending; it is composed of innumerable information-energy layers and general levels. There are in the sphere of influence no null-levels; all are the same, but they are separated by means of their energy conditions. I notice that I am confusing you now. I think I ought to stop with this explanation.

Question: No, please continue. How do concrete paranormal powers arise?

Answer: Well, OK then. Let's try something simpler. Again, it is not completely correct, but let's begin in this manner: Tangible matter on this side is mirrored in the sphere of influence {Feldraum} as a field with distinct layers. These layers contain information, as an example, about the simple structure of matter or the string frequency, but also there is stored information stemming from the development of matter. Are you familiar with the human concept of "morphogenetic fields?" One part of the layer could be designated as such. Now there is still another intermediary layer for which you unfortunately have no human concept, since the theory is not common in human thinking. Let's call it a "para-layer," for this layer is mainly responsible for everything which you call PSI and paranormal and which lies outside the boundaries of your primitive science. This para-layer lies between the layers of matter and the morphogenetic layers of a field in the sphere of influence. It can actively integrate with both. Your body, for example, is mirrored as a field in the sphere of influence {Feldraum}. That doesn't mean that it does not also exist here as well —as flesh, blood, bones— in the form of matter strings or atoms, but not only that. Existence is always a duality. Some layers of the field contain simple information about the solid matter of your body and its frequency, while other layers {contain information about} your spirit, your consciousness or, speaking from a human-religious point of view, your soul. Awareness or consciousness in this case is a simple energy matrix, divided into different layers of your field in the sphere of influence —nothing more, nothing less. Genuine awareness can also exist here on the matter side, but only in the form of post-plasma {the fifth form of matter}. With the necessary physical knowledge and the corresponding technology, the consciousness/awareness matrix, or soul, can also be separated from its field of rest. It can, despite its removal, continue to exist in a self-sufficient manner for a certain amount of time. That has the strange occult name of "soul robbing." But above all, we're talking about science here, not about magic or dark forces.

[Comment by Ole. K.: The "soul robbing" was mentioned in one of the radical, religiously-motivated comments in connection with the reptilian species.]

But back to your Question: Creatures with more powerful mental powers can have a direct influence on the para-layer by means of their consciousness/awareness fields.

Now this layer is not limited only to the individual, but rather as a part of a general information layer —you could call it in a prosaic sense the community soul— that is connected with all animate and inanimate matter and all consciousness which exist on this main level. The biological cause for these abilities lies on the side of matter, by the way, in the pituitary gland, which always is in the position to generate the frequencies to actively control the sphere of influence {Feldraum}. Even you people could theoretically do this; however, you are solidly blocked in these things. As I have said, the para-layer can interact with mind as well as with matter. For example, if I decide to use my mental powers once more in order to move this pencil, then, simply said, I imagine in my mind how my consciousness/awareness expands/amplifies itself on the matter side in the form of post-plasma to the pencil. In the sphere of influence this causes simultaneously an automatic command from the consciousness/awareness layer to the para-layer to interact with the matter layer of the pencil. Since the para-layer is not confined to the body, it is not even a problem that the pencil lies over there, for I can unerringly reach it, even without moving my matter body. Post-Plasma on this side, para-layer on the other. I have control over the pencil and the interaction brings the matter field of the pencil to the point where it changes in the manner in which it moves, for example.

[Comment by Ole K.: I certify that the pencil mentioned above abruptly at that very moment jumped into the air to a height of 20 cm and then fell back to the surface of the table. The sound is clearly heard on the recording tape. No one visibly had touched that pencil.]

Question: That is fascinating. Which kinds of paranormal activities can one generate with that?

Answer: All kinds. Everything that you call paranormal. As I said, this special layer lies in the sphere of influence {Feldraum} between the morphogenetic information layers and the matter layers and can interact with respect to both sides. That is to say, it can be interacted with solid matter as well as with mind or mental information, wherewith we can achieve everything that is generally designated as telekinesis and telepathy. The "connection absorption" with another consciousness/awareness is generally separate in the procedure from the simple influence of matter, since different consciousness/awareness fields work with different oscillations. A consciousness/awareness that sends or a consciousness/awareness that listens must first adapt itself to the other mind exactly, before any access is possible. Most species also have chances to block the alien access, but you people don't have this. The following is generally valid: the stronger the paranormal abilities of a species, the simpler the adaptation and the access. Our own abilities are not so powerfully developed; therefore, first we have to learn specifically alien mind influence in order to use our mimicry, for example—where mimicry is actually quite simple in your minds due to the implanting of the on/off switch. Some of these abilities are also partially inherited; mother and child of my kind as an example are attuned exactly during the first months of life —partially also in the egg covering in the expectant mother— and communicate telepathically. In order to influence you people, we need a certain amount of time for practicing, despite your simple structure. Therefore, it is forbidden, for example, for adults of my kind before the "Age of Enlightenment" to come to the surface of the Earth. (That term is synonymous, along with other things, with full physical strength.) In the case of not fully developed abilities, the danger of discovery by you would be too great. By the way, there are of course numerous secret teachings about the real possibilities which can give one these abilities, but I really don't know anything exact about that.

Whenever an alien mind ought to be influenced, then there are some generally valid steps, which are set into motion by other extraterrestrial species.

First and foremost, the alien oscillation must be felt, something generally that is done automatically by the brain, i.e., for the one the field oscillation, for the other the quasi-electrical brain waves here in the normal space {which matter inhabits}. That is not especially difficult. After that, one simply probes for the other consciousness/awareness in the mind with a post-plasma manifestation, the sphere of influence {Feldraum} reacts and the connection is there. Now one can read out information from the first one and record the desired information to the second one in the correct location. You asked me last time whether you people have the opportunity to protect yourselves against this influence, and I told you that only an awake and concentrated mind had any kind of a chance to withstand it. In this state of mind the oscillations change very abruptly and access becomes complicated; more precisely, it can come as a painful recoil. Whenever you close your eyes, then the field becomes "flat," and alien access {to the mind} is immediately possible and without restriction. In terms of your chances against a more highly developed species, you have none at all. They are able to adjust the oscillations faster than you can change. I could even demonstrate it on you, but you were really horrified and confused the last time, so we'll just leave it at an explanation.

This explanation presumably sounds to you like —as you say— something esoteric or from the occult or magic. The reason for that is simply that you lack the basic understanding for seeing the background reasons. All paranormal phenomena have a purely scientific origination. None of this has anything to do with supernatural powers. We grow up with this kind of knowledge, we know how one makes use of these powers, and where they come from. We are acquainted with theory and practice. You are not. Therefore, you really don't understand what happens in your world—you see only one side of existence, not the other (I mean here both that are physical). Everything paranormal is dualistic, and it exists in the space that matter inhabits as well as in the sphere of influence {Feldraum}. To be explained...it can only be explained by the acceptance of the latter, because the sphere of influence {Feldraum} is the basis. I would welcome an end to the scientific questions since you really aren't grasping them anyway. We're wasting more or less valuable time by doing this.

Question: Only one last question. At our first meeting in December, you made it quite clear that you didn't want to discuss scientific and paranormal concerns. Why the openness now?

Answer: The last time I saw really no necessity in overburdening you with facts of that kind (and now you are obviously overburdened). Therefore, I had preferred only to mention these topics in a peripheral sense. Apparently, however, some of my performances today have set you to thinking about your world, something that can't be all bad. And by the way, your human scientists will tend to regard my comments as "humbug." And so I see no great danger in spreading this information widely. No one will pay much attention to it. By the way, the words of people who have characterized me as a "Creature of Evil" have their basis in the belief in occult powers and magic —both of which things DO NOT exist. There is no magic, only highly developed science, and everything that you label as "magic" is only a part of science. If you would only comprehend that, then you would be a step ahead in your development. My openness on this issue ends here. Pose other questions, please.

Question: Good. Let's talk about UFOs. Can you explain to me how our governments came into possession of UFO material to the point that they could start their own projects? Did it have anything to do with the "Roswell Incident?"

Answer: Yes, but that incident was not the first one. I am no historian, I am studying only your current behavior, so my knowledge about those events in your history is presumably not very extensive. I will try to explain to you what I know about those things which happened at that time. Let me think about it for a second. In the years 1946 to 1953 in your time scale, there were five cases where extraterrestrial ships crashed to the surface of the Earth. In that crash which you call the "Roswell Incident," there was not only one alien ship involved, but two that crashed after a collision in different parts of the land in the west—the one you call the USA. (You have to know that the ships of this particular species can remain levitating in the air for a particular period of time even though they are damaged; that accounts for the spatial difference {in their crash locations}.) These were indeed not the first crashes, but by that time the second and the third. Another ship had crashed in 1946, but it was destroyed beyond usability.

One thing first before the explanation: it certainly sounds ridiculous to you that such highly developed extraterrestrial ships simply crash, and that a relatively large number did so in a relatively short amount of time. The explanation for that is likewise more than strange, but it is correct. It does not lie in the ship's drive itself, but rather in the direction of the field to your planet. This species that we are discussing —and it was always in this time period that this species used a disk-shaped craft— used a propulsion system which ran according to the normal principle of fusion, to be sure, but one that at that time employed a more than unconventional method for field alignment. This method had various advantages but also disadvantages. The repelling field must of course lie in the absolute correct angle to the surface of the Earth. This species used an alignment technology in their ships, with which the field locked into place all points of the Earth's magnetic field. Now at that time this species had just arrived on the earth and their point of origin lay on a planet with a more stable magnetic field, for which they had developed and aligned their drive. The magnetic field of the Earth is not really all that stable; it is subject to cyclical variations and it forms field eddies under unfavorable conditions. Whenever a ship with one of those kinds of drives gets into a field fluctuation or into an eddy that is too strong, then for a short time the repelling field can no longer align itself correctly and the ship glides uncontrolled on its flight path. The drive is operating correctly, to be sure, but the field fluctuates in all directions and because of that, the ship can crash. In the case from 1947 which you addressed, it is my understanding that one of the ships got caught in a fluctuation, its field linked up unintentionally with that of its squadron leader and it collided with another ship whereby both of them were heavily damaged. The cause for the magnetic fluctuation at that time was probably an electrical disturbance brought about by a weather event. Both ships crashed as a result; one of them fell near the collision point, the other a hundred of your kilometers or so distant. All occupants were killed in the impact. The thin hull structure of that kind of disk craft is in and of itself not very stable, since those disks have not been designed for crashes as well as for flight in a field where there are exterior forces at work.

Now, your human military collected the individual pieces at first until they discovered the whole ships with the dead creatures aboard. Immediately they classified everything as "Top Secret" and brought them to their military bases in order to analyze the drive. The secret endeavor was to set the alien technology in place later against evil enemies of that great country. That is as primitive as it is ridiculous.

I believe I remember—I don't want to specify exactly your date—that it was probably between 1949 and 1952 that there was a rather bad accident during some research being done on one of the wrecks. According to what I heard—what members of my species were told by members of that government—it resulted in an unintentional activation of one of the drive's components in the unshielded condition. As a result, for a very short period of time—how should I phrase this—there was an unchecked shift of the environment to a plasma-like condition, which on the other hand, through a very, very unfortunate accident, caused an overturning of the general power field into a magnetic pulse of immense power. Do you have any idea what kind of an effect a plasma-magnetic jolt has, when it comes into contact with an organism? No, how should you know that. Of course you don't. Disturbance in the structure of the field and bioelectric feedback. Imagine, if you will, a human body which is engulfed in bright flames for 3 or 4 of your days. Those flames apparently do not go out and they burn the body right down to its last constituents. Well, then you have an approximate impression of what happened. I think that 20 or 30 of your scientists were killed in that lab.

Two further crashes occurred in 1950 and 1953 in the water catchment area of the American continent. Those ships were able to be recovered from the crashes relatively intact. (The one in 1953, as I remember, even had an intact drive core. It was by means of that device that you saw for the first time that you had understood the entire concept fully incorrectly and that you had reconstructed it fully incorrectly. Even today you still don't have it right.) That species, which had built the ships in the first place —a species which I, by the way, count among those who are unfriendly towards you— was naturally worried about the investigation of their own technology by your kind. They did not want, however, at that early point in time, to begin direct conflict with you, and so they chose the diplomatic path and came into contact with that government during your 1960's. Of course, they did not divulge the real reasons for their being here —copper, hydrogen, air— but rather they pretended to be curious "researchers" and offered to show people the functioning principle of the ships whereby they would expect in return some "favors." Simple-minded as you are, you of course agreed to it...and were deceived. You gave them raw materials, you gave them secured locations for their bases, you gave them access to your most secret defense data, you gave them access to your DNA and much more—and all just to quench your greed for power and information. The alien species of course quickly noticed that they were dealing with simple-minded creatures, and they gave you false and inferior information about their technology so that they receive much more out of the collaboration than your kind do. For example, they gave you information that the drive can only be constructed with unstable elements of a higher ranking number, but they withheld the information that the field drive can be constructed with various modifications to work as well with stable elements of a lower periodic number, and generally, that's the way it's done. Through these half truths they made you dependent on the synthesizing of high {numbered} elements, and thereby renewed by their own technology. Their clues to the construction of your "UFOs" were laid out in such a way that the solution to old problems caused new problems to arise simultaneously. They never told you the complete truth, but always built in again and again clever lies, which later lead to technical problems —and to your dependence on them.

In the last years of your 1970's and your early 1980's, it finally came down to various events between the alien species and that human government —I don't want to go into detail here since there is much that even I am not exactly sure of. The whole thing lay in the context with some new, or better said, the old technical problems with your own self-constructed ships whose camouflage and drive partially failed to function in test flights in the open.

Because of that, the function of secrecy was threatened. Your military and your politicians slowly—very slowly—came to the conclusion after more than 20 years of this that they had been deceived by that alien species. Multitudinous incongruities and the overstepping of bounds of the treaties by both sides finally led to an altercation between you and the extraterrestrials, which culminated in the lift-off of three of the alien aerial objects through a special —how do you say it?— EMP {electromagnetic pulse} weapon and a military skirmish at one of their underground installations. As a consequence of these attacks, the alien species ultimately withdrew from all contact with you and was understandably more than angered about your kind. Therefore, I count these extraterrestrials among the three groups who are hostile towards you, and while the other two are more occupied with their own business, among them waging a cold war for dominance on your planet, your old "friends" and partners are preparing to supply themselves finally with the sole and absolute dominance over raw materials and human DNA. At the moment it is probably true that they lack some of the technical possibilities and the large amount of forces which they need in order to achieve their goals directly. In spite of that, we are counting on negative actions —possibly ever of a more subtle kind— against you in the next few years or decades.

Question: Will the other extraterrestrial species undertake nothing against these war-like actions? Specifically, something ought to be on Earth for the more highly developed species.

Answer: You're wrong there. Specifically, for the more highly developed species there is simply at the very least your fate. You are animals for them. Animals in a very large lab. Understandably, an alien intervention on your planet would disturb their projects, but I don't think that they accept a confrontation with other species for it. Many of them could look for another research planet for themselves or they could study over a long distance your behavior and your consciousness/awareness, since crisis situations could have an attraction for their studies. Whenever you people take a look at an ant hill, and another person comes along and steps on the ant hill, what do you do? You go on your way, or you search for another ant hill or you observe the ants in their crisis condition. But would one of you —even though he were larger and more powerful than the one who stepped on the ant hill in the first place— defend the meaningless ants? No. You have to imagine for yourself the viewpoint of the more highly advanced creatures. You are the ants. Don't expect any help from them.

Of course we would also ask for help when it became clear that your old partners were ganging up on you. Some members of that human government are fully aware of our existence —also partially owing to an old religious basis. For example, there is a gigantic partially underground building in the capital which is totally dedicated to my species and that also has a direct approach to an elevator shaft and to an underground system. In this building partial meetings have taken place and do take place between us and humans. We have passed on information to you in the last few years; according to what I know, we will keep ourselves as far away from the conflict as we can. You ought to learn to solve your own problems yourselves or to become intelligent enough never to create those kinds of situations. What will come and who will possibly place themselves on your side, only time will tell. I really do not want to make any indications about that.

Question: I have here 5 prints of different UFOs, which claim to show UFOs. Can you take a look at the pictures and tell me in which of them actual extraterrestrial aerial craft can be seen?

Answer: I can try it. You pose many questions to me today which even I cannot answer unequivocally. Don't overestimate my knowledge, I'm no expert in alien technology and the construction of extraterrestrial ships. To be sure, there are mostly some technical details and peculiarities about genuine "UFOs," with whose help one can easily differentiate them from natural phenomena or human forgeries. You falsify sometimes the pattern of genuine ships; therefore, it is not so easy simply with absolute certainty to identify an object. I'll try it. Show me the photos.

[Comment by Ole K.: She considered the pictures respectively for only a couple of seconds and then sorted out photos 1, 3 and 5.]

These three pictures here are obvious counterfeits or erroneous identifications. In the one picture, it certainly seems to me that a real existing ship of an alien species was adapted for a small model here. It lacks important characteristics which are tied in with the technically- and physically-associated field. Generally speaking, a picture is all the more a fake, the clearer the outline and the colors are, because a levitating ship is generally hidden in a shifted-field condition that even distorts the colors or the forms according to alignment. It might perhaps sound strange, but hazy and spectrally-shifted photos are sometimes to be interpreted as an indication for a possibly authenticity. By the way, this object is floating above the water. If it were a genuine ship, we would have to see in any case either a trough or a swell on the surface. Since the surface is flat, it is obviously not a genuine ship. In my opinion, none of these three pictures show genuine objects in flight or UFOs. Here in this picture I see above all no artificial object in flight; it seems much more to deal with only a light reflex in your simple optical cameras. You really ought to be intelligent enough not to fall for a mix-up like that. When your general public chases counterfeits and frauds for a long time, then they will presumably discover too late, what is really going on in front of them in their atmosphere.

PHOTO 2: Albiosc, France, 1974

This one seems to be genuine, at least it displays the necessary characteristics. I would assign it at first glance to an alien species who have been visiting your planet for the last 35 years or so. The object itself is metallic and disk-shaped; certainly it is distorted in form and color by means of a field effect. These four white and very long "processes" on the underside of the ship itself portray a kind of quasi-gravitational light manipulation, i.e., the universal force field is being shifted in the direction of a simulated gravity. Actually, it is not a genuine light (it is mostly not a genuine light whenever you see illuminating "UFOs") but a special strongly charged form field which manifests itself in the space that matter inhabits as a quasi-light. The reason for the activation of this special high-energy system in an atmosphere is not completely clear to me; it's possible that it is a kind of investigating or influencing of the environment. In any case, it is terribly careless of that species to allow this technology to be photographed by humans. Well, I guess that most of you just plain don't understand it, and those who do will not say anything about it to the general public.

PHOTO 4: Petit Rechain, Belgium, 1990

This is in fact a genuine aerial object; it is in no way extraterrestrial. Triangular aerial objects in flight are simply not used by alien species, or not in this form, at least. That streamlined kind of form is a human concept. It is one of your own secret military projects that you build with the help of immature alien technology —technology that was handed over to you by the extraterrestrials during the 1960's and the 1970's. Generally, the form of the hull for a genuine extraterrestrial ship is of no consequence, for inside the field itself there are no exterior forces that have any effect there; in general, the ships have a rounded off form and they are built without hard edges —as a disk or a cylinder— so that the field can flow more easily. Your projects decree that along with the alien drive field there also be a conventional jet engine system; therefore, they are always triangular and built thus with streamlining in order to be steerable with this primitive recoil principle.

In the example here the ship glides above all on its genuine field drive. Do you see the distortion and the quasi-light in the rotating cylinders? That is an unmistakable indication for the authenticity of the photo. But why, you might ask, are there 4 cylinders? That's unusual —even the interval seems to be incorrect. The coloring is very dark and the interior optical distortion is very noticeable. Presumably a reconstruction of the original system by your scientists. Since the alien species has just not given you any more information since the disagreement, they are rebuilding the systems single-handedly without actually being able to understand what kind of dangerous thing they are doing there. This construction does not make the system better, only more unstable. Both of the forward cylinders are too close to each other; they will definitely flow into each other. The color shows me a powerful residual radiation; it was probably the case that high elements were used again as customary for the shifting. It is in any case very dangerous to be unshielded in the vicinity of the field. Did the person who took the photo display any kind of radiation and burn damage?

Question: I don't know. Where do these military "UFOs" come from? From the United States?

Answer: Yes. I think generally that's true. From the western continent.

Question: Why then do they fly over thickly populated areas of Europe? This photo comes from Belgium. That doesn't make any sense. Can you explain?

Answer: Why is it that ONLY I am able to explain strange human deeds? It's possible that these are long-distance tests or tests with the electromagnetic camouflage systems. The old enemy of the American nation is on this side of the world, so why shouldn't they test here? At home they've had enough time to have had their ships crossing back and forth. Maybe they have aroused too much observation there. With one of those kinds of unstable field structures —as your photo indicates— I consider it somewhat improbable that that ship is capable of making a flight of that length over the ocean. It's possible there is a test station here on your continent. Unfortunately, I don't know anything about it.

Question: Many readers of the first transcript have posed the question how your original contact with E.F. came about. I already know the story from your narratives, but could you repeat it here once again for this volume and for the new transcript?

Answer: Of course. Now, the story began about two of your years ago here in Sweden. I have been strongly interested in your species and your behavior since my youth; I had already studied your literature at that time, as well as possible. (Naturally, it is not easy in my homeland to come into possession of human books, but since my group or family stands in a higher ranking order, I was able to gather some material together and sometimes to speak with others of my kind who have already been in contact with you.) I was really very curious about your species and as soon as I was allowed to come to the surface, I attempted to assemble more information immediately; above all, it was expressly forbidden for me to commence direct contact with humans because in my position at that time, there existed no necessity for doing so.

It was in your year 1998, when I was on my way further north from here in the remote forests in the vicinity of the entrance to my world and was looking for biological specimens, which we use in order to watch over environmental pollution and destruction of your flora and fauna statistically by your own kind. At the time, I was already on the return path to the entrance—we can even orient ourselves more easily, by the way, through our senses to the Earth's magnetic field—and already in the vicinity of the large lake, when much to my surprise I came across a cabin in the woods. In this cabin I sensed a human consciousness/awareness. It was E.F. Actually, I had no permission for contact with another species, but by the same token I had set in place my mimicry capability quite successfully prior to this—even with larger groups of you (I had never ever come across a human being when I was alone). Now, let's call it primitive curiosity; I wanted to talk with the person in this cabin and so I knocked on the door. E. opened the door and we got into an interesting conversation. His language was not quite yet common at that time for me, but it's not all that hard to learn a new language when one can read the information in the consciousness/awareness of the opposite individual. I simply told him that I came from a foreign country in the east. Of course at the time, he did not really "recognize" who I was; he was totally convinced that he was talking with a creature of his own kind, although it was simply only a mimicry image.

Since my assignment anyway had as its goal an investigation of this terrain which was to last for several days, I visited him in this span of time three times as a human person. At first we talked mainly about really ordinary things; later we got into religious and physical topics. He seemed to be impressed by my knowledge, and I was likewise impressed with his clear thoughts and his—for a human being—well displayed personality structure and his own opinions. You really like giving yourselves over completely to a public opinion or conditioning, as for example, "reptilian species are evil" and stuff like that. I steered the conversation in this direction, and E.F. said something to the effect that he believed in alien species and that they did not have to necessarily be evil, but perhaps only different than his kind are. That pleased me. At that juncture of time, of course, I could not speak concretely with him about my knowledge because he wouldn't have believed me—he would have taken me for a human practical joker. I cultivated the very, very unusual idea (for my kind) to show him my true exterior, something that I did during our conversation at our fourth meeting in the cabin. Actually, he was predestined for contact: he was open-minded, honest, intelligent, not religiously inclined or conditioned; he lived alone and isolated, and no one would believe him, should he decide to go public with his story.

I dared to take the step, but then I had serious doubt about the propriety of my act, especially when he reacted...very...violently. He got control of himself again after a time and we could finally talk concretely about definite matters. Now he had no choice but to believe me. This was the beginning of a series of meetings which initially took place there in the woods, but later took place in his remote residence. Finally he brought you into contact with me...and for that reason we are now sitting here once again and talking about things which probably won't be believed out there in human society.

Question: You said, you would not have had permission at that time for contacts with human beings. Do you now then have permission to talk with E.F. and me about all these things and even to make this scientifically public?

Answer: Yes. That is difficult to explain and for you to understand. Let's just say, I find myself in the position now to arrange this permission without having to take into account any consequences. In this position I am quasi-"immune" against certain restrictions. Let's look it that way. Yes.

Question: If other people want to come into contact with your kind, do they have a chance to do so?

Answer: Generally not. We avoid contact with you and we operate on the surface only in remote areas and there we use the mimicry techniques in case we should meet some people. That I am talking with you now does not mean that others will follow my example. It goes without saying that you could try to find an entrance to my world and penetrate your way into there. However, that can sooner lead to unpleasant consequences for the infiltrator. You have next to no chances on the surface of recognizing us. You can't even contact us directly, we have to contact you, just as I did with E.F. Those kinds of contacts however are not the rule but are very rare occurrences.

Question: Can you describe your subterranean homeland location?

Answer: I can attempt to do so, but I certainly will not tell you where this place is located. My homeland lies in one of our smaller underground settlements to the east of here. I'll give you some numbers so that you can make a better impression for yourself. Just a minute...I have to try to convert the measurements approximately into your units. It is a dome-shaped cavern at a distance of about 4300 meters from the Earth's surface. The cavern was organized as a colony about 3000 years ago; a major portion of the ceiling structure is artificially integrated into the rock and the form was remodeled into an almost elegantly proportioned and very flat dome with an oval ground plan. The diameter of the dome according to your measures is about two-and-a-half kilometers. The height of the dome at the highest point is about 220 meters. Underneath that highest point in every colony there stands a special whitish-gray cylindrical building—a kind of supporting column which holds the honeycomb net-carrying structure of the dome. This building is the tallest, largest and oldest in the entire dome for it is always situated as the first construction together with the security of the ceiling. (In the meantime of course there were times when it was completed and reconditioned.) That building has a very special name and religious significance. We have only one of those columns; larger colonies even have more columns according to the construction of the ceiling.

One of the main colonies in Inner Asia has as an example 9 of those kinds of supports, but that colony is also over 25 of your kilometers in size. The central building is generally a center of religion, but also a center for climate control, and a center for the behavior and the regulation of the lighting system.

We have at our location all together 5 large artificial light sources which generate your UV light and its warmth through gravitational sources. The air shafts and the light systems from the surface likewise run through these columns and naturally, they are very intensely controlled.

By the way, we have 3 air shafts and 2 elevator systems there, and even a tunnel connection to the next main colony which lies approximately 500 kilometers to the southeast. One elevator shaft leads to a cavern near the surface, the other leads to one of our depots for the ships —you remember, the cylindrical ships— that is naturally concealed closer to the surface behind a rocky mountain face. Normally, there are only three ships there —it's a small depot. The other buildings of the colony are, for the most part, concentrically ordered in oval circles around the main supporting column, and they are without exception much flatter; generally only between 3 and 20 meters tall. The shape of the buildings is round and dome-like. The color is even differentiated according to circle and distance from the main column. To the north of the column, there is an additional, very large but very flat round building. This building interrupts the concentric system of the colony with its diameter of about 250 meters. It is the artificial sun zone in which specially illuminated corridors and rooms are housed. In these locations very powerful UV light predominates, and they are used in order to warm our blood. There is even a medical dispensary and a meeting room located there. Beyond the outer ring of the colony, there are zones in which animals are kept—you know, we MUST consume flesh as nourishment—and the gardens in which plant nourishment and mushroom culture are cultivated; there is also hot and cold running water there from subterranean sources. The power station is located on the edge of the colony. The station is driven by fusion as its base and it supplies the colony and the "suns" with energy. My group or "family" lives, by the way, in the fourth ring of buildings out from the central support column. So much in such a short time. To describe to you all the buildings and their tasks would be going too far. It is difficult to describe something like that to you, for it is a completely different set of surroundings and culture from what you are accustomed to in your life on the surface. You really have to see it for yourself to be able to believe it.

Question: Will I myself see it sometime?

Answer: Who knows, maybe. Time brings new opportunities.

Question: How many creatures of your kind live in this colony?

Answer: Approximately 900.

Question: That is the end of the interview. Do you have any final message for the readers of the transcript?

Answer: Yes. I am thoroughly surprised at the many comments to my words; of course, I am naturally also disappointed about the religious portrayals of me as the enemy which have been voiced and which have buried themselves deeply in your mind. You should learn to set yourselves apart from the old conditioning and not to stand quasi under the control of something or someone who has already been gone for 5000 years. You are, after all, free spirits. Those are my final words.

All Rights Reserved ©

KEELYNET

Thanks to Slavek Krepelka and Ren Berghuis for paying to have the Russian version of Chapter 5 translated into English and sharing it with KeelyNet.
Please check out Slavek's website.

Orkin® Extermination Save $50 On Orkin® Pest Service 100% Satisfaction Or Money Back! www.PestRemovalZone.com
K&J Magnetics Neo Magnets Buy Top Quality Neodymium Magnets Great Selection & Prices. Shop Now! www.KJMagne
Heaven Bee Venom Eyes Controls muscles around the eyes Instant lift, tightening & Firming www.skincareorganics.co.uk/heaven
AdChoices

The Natural Phenomena of AntiGravitation and Invisibility in Insects due to the Grebennikov Cavity Structure Effect (CSE)

Introduction

by Iu. N. Cherednichenko, Senior Researcher, Biophysics Laboratory, Institute of Human Pathology and Ecology, Russian Academy of Medical Science

Viktor Stepanovich Grebennikov is a naturalist, a professional entomologist, an artist-simply put, an intellectual with a wide range of interests and pursuits. He is known to many as the discoverer of the Cavernous Structures Effect (CSE). But very few people are familiar with his other discovery, one that also borrows from Nature and its innermost secrets.

Back in 1988 he discovered anti-gravitational effects of the chitin shell of certain insects. But the most impressive concomitant phenomenon discovered at the same time was that of complete or partial invisibility or of distorted perception of material objects entering the zone of compensated gravity. Based on this discovery, the author used bionic principles to design and build an anti-gravitational platform for dirigible flights at the speed of up to 25 km/min. Since 1991-92 he has used this device for fast transportation.

Bio-gravitational effects are a wide spectrum of natural phenomena, apparently not confined to just a few species of insects. There is much empirical data to support the possibility of a lowered weight or complete levitation of material objects as a result of directed psycho-physical human action (psychokinesis)-e. g. levitation of yogi practicing transcendental meditation according to the Maharishi method. There are known cases of mediums levitating during spiritistic sessions. However, it would be a mistake to think that such abilities are only found in people who are gifted by nature.

I am convinced that these abilities are an understudied biological regularity. As is known, human weight significantly drops in the state of somnambulistic automatism (sleepwalking). During their nocturnal journeys, 80-90 kg sleepwalkers are able to tread on thin planks, or step on people sleeping next to them without causing the latter any physical discomfort (other than fright). Some clinical cases of non-spasmodic epileptic fits often result in a short-term reversible transformation of personality (people in such state are commonly referred to as "possessed"), whereby a skinny, exhausted girl or a ten-year-old boy acquire the physical prowess of a trained athlete.

Currently this psychological phenomenon is known as multiple-personality syndrome because it significantly differs from the classical complex of epileptic symptoms. Such clinical cases are well-known and well-documented. However, phenomena accompanied by a change in the weight of

humans or of material objects are not confined to functional pathologies of the organism.

Healthy people in the state of acute psychological stress caused by a life-threatening situation or an overpowering motivation to achieve a vitally important goal have the ability to spontaneously overcome obstacles insurmountable in their normal condition-e. g. to lift enormous weights, etc. These phenomena are commonly explained by an extreme mobilization of muscular strength, but precise calculations do not agree with such hypotheses. Apparently, athletes (high jumpers, weightlifters, runners) have particularly developed bio-antigravitational mechanisms.

Their athletic performance is mostly (if not wholly) determined not so much by the rigor of their training as by their psychological preparedness. If an accurate scientific task of studying the anomalies of the human weight in various psycho-physiological states were ever set up and technical means of dynamic weight monitoring created, we would then have objective data on this unusual phenomenon. There is also evidence of other phenomena of short-term mass increase in biological objects, including humans, that are not related to mass transfer.

V. S. Grebennikov's book has high literary merit and includes the author's own illustrations. It is a kind of a "dactylogram" for his system of spiritual values, his environmental outlook, and his entomological autobiography. Many readers are likely to perceive the book as nothing more than a popularized summary of the entomologist's 60-year experience of scientific observations, peppered with some elements of science fiction. But such a conclusion would be deeply erroneous. As Viktor Stepanovich's friend and as someone with an intimate knowledge of his work (our homes are only 10km apart), I can vouch I have never met a more careful, conscientious, honest, and talented experimental scientist.

Grebennikov is also widely known in the so-called scientific underground (i. e. the branch of advanced Russian science constantly persecuted by the official scientific establishment). Thus, a committee for combating pseudoscience, created in Novosibirsk division of the Russian Academy, has victimized many talented members of our local scientific community. The situation is much the same at the Russian Agricultural Academy. It is very easy to lose one's job at a lab (even as its head, regardless of one's degree and title). One only needs to publish an article on, for example, the evolutionary significance of antigravitational mechanisms in insects.

But I am convinced that discoveries of such proportions must not be buried in manuscripts just because pragmatism still rules science. Let this book be nothing but "science fiction" for those at the top. Each person has his own beliefs. But he who has eyes shall see. Catastrophism in both the evolution of living nature and in the nature of human knowledge is actually a drastic destruction of old belief systems-a destruction that runs ahead of theoretical prognostications. A fanatical faith and idol-worship links our contemporary academic science with pagan religion. But a harmonious development (in the sense of Pavel Florensky's pneumatosphere) would not be possible without breaking old stereotypes in the process of mastering the wisdom and experience of older generations.

Flight - Chapter V of V. S. Grebennikov's *My World*

CHAPTER V. **FLIGHT**

A quiet evening in the steppe. The sun's red disk has already touched the faraway, misty horizon. It is too late to get back home-I've stayed too long here with my insects and am preparing to spend the night in the field. Thank goodness I still have water in the flask and some mosquito repellent-one needs it here, what with hosts of gnats on the steep shore of this salty lake.

I am in the steppes, in Kamyshlovo valley. It used to be a mighty tributary of the Irtysh, but the ploughing of the steppes and deforestation turned the river into a deep, broad gully with a string of salty lakes, like this one. There is no wind. Pods of ducks gleam over the evening lake, sandpipers are also heard in the distance.

The high, pearl-colored sky stretches over the calming world of the steppe. How good it is to be out here, in the open country!

I settle for the night on the very edge of the steep, on a grassy glade. I spread out my coat, put my backpack under the head, and before lying down, collect a few dry cakes of cow manure, and light them up. The romantic, unforgettable smell of bluish smoke slowly spreads across the dozing steppe. I lie down on my simple bed, stretch my tired legs and anticipate yet another wonderful night in the country.

The blue smoke quietly takes me to the Land of Fairy Tales; sleep comes fast. I become very small, the size of an ant, then enormous, like the sky, and am about to fall asleep. But why is it that today these "pre-sleep transformations" of my bodily dimensions are somewhat unusual, too strong? A new sensation has mixed in-a sensation of falling, as though the high cliff has been snatched away from under my body, and I am falling into an unknown, terrible abyss!

Suddenly I see flashes. I open my eyes, but they don't go away-they are dancing on the pearl-and-sliver evening sky and on the grass. I get a strong, metallic taste in my mouth, as though I pressed my tongue to the contact plates of a small electric battery. My ears start ringing, I distinctly hear the

double beats of my own heart.

How can one sleep when such things are going on!

I sit up and try to drive away these unpleasant sensations, but nothing comes out of my efforts. The only result is that the flashes are no longer wide and blurred but sharp and clear, like sparks or perhaps small chains; they make it hard to look around. Then I remember: I had very similar sensations a few years ago in Lesochek, or to be more precise, in the Enchanted Grove [the author is referring to localities of an entomological preserve in Omsk Region].

I have to get up and walk around the lakeshore. Does it feel like this everywhere around here? No: here, a meter from the edge, I feel a clear effect of "something", while ten meters further into the steppe the effect clearly disappears.

It becomes a bit frightening: I am alone in the deserted steppe, by the "Enchanted Lake". I should quickly pack up and clear out. But my curiosity takes over: what is this, really? Could it be that the smell of lake water and slime is doing this to me? I go down, under the steep and sit down by the water. The thick, sweetish smell of sapropel-rotted remains of algae-is enveloping me like in a mud spa. I sit there for five, ten minutes-no unpleasant sensations. It would be suitable to sleep here, if it weren't so wet.

I climb the steppe-same old story! My head is spinning, I again get that "galvanic", sour taste in the mouth and feel as though my weight is changing-I am at one moment incredibly light, and unbearably heavy at the next. I see flashes in my eyes. If it was indeed a "bad spot", some nasty anomaly, then there would be no grass here, and large bees would not be nesting in the loamy steppe.

Meanwhile, their nests are all over it-in fact, I was trying to make my bed right above their underground "bee city" in whose depths there is of course a multitude of tunnels, chambers, lots of larvae, cocoons-all of them alive and healthy. I understood nothing that time.

I got up with a headache even before sunrise and, tired, hobbled off toward the road to get a hitch to Isilkul.

That summer I visited the "Enchanted Lake" four more times, at various times of day, and under various weather conditions. By the end of the summer my bees got incredibly busy stuffing their holes with flower pollen-in a word, they were feeling great. Which *I* wasn't: a meter from the edge of the steppe, above their nests, I again had a set of most unpleasant sensations. Five meters away, I had none... And there was the same old bewilderment: why, why do these bees feel so good here that the entire steppe is dappled with their holes like Swiss cheese, and in places, almost like a sponge?

The solution came many years later, when the bee city in Kamyshlovo valley died: the tillage came to the very edge which consequently fell off. Now instead of grass and bee holes, there is nothing there but an atrocious heap of mud.

I only had a handful of old clay lumps-fragments of those nests, with multiple chamber cells. The cells were side by side and reminded of small thimbles, or little jugs with narrowing necks.

I already knew that these bees were of the quadruple ring species-that was the number of light rings on their elongated bellies. On my desk, packed with equipment, ant- and grasshopper-houses, bottles with chemicals, and other stuff, I had a wide receptacle filled with these spongy clay lumps. I was about to pick something up and moved my hand over these porous fragments.

A miracle happened: I suddenly felt warmth emanating from them. I touched the lumps with my hand-they were cold, but above them I felt a clear thermal sensation.

Besides, in my fingers I felt some hitherto unknown jerks, some sort of "tick" as it were. And when I pushed the bowl with the nests to the end of the desk and leaned over it, I felt the same sensation as on the lake-my head was getting lighter and bigger, the body was falling down, the eyes saw rapid flashes, and the mouth tasted an electric battery. I was feeling slightly nauseous...

I put a sheet of cardboard on top of the bowl-the sensation didn't change. A pot lid changed nothing either; it was as if the "something" was cutting right through it. I had to study the phenomenon at once. But what could I do at home, without the necessary physical instruments? I got assistance from many research scientists of various institutes of the Agricultural Academy in Novosibirsk.

But alas, the instruments-either thermometers, or ultrasound detectors, magnetometers and electrometers-did not respond to them in the slightest.

We conducted a precise chemical analysis of the clay-nothing special. The radiometer was also silent... But ordinary human hands, and not just mine, distinctly felt either warmth or a cold draft and a tingle, or sometimes a thicker, stickier environment.

Some people's hands got heavier, others felt theirs were pushed up; some people's fingers and arm muscles got numb, they felt giddy and had profuse salivation.

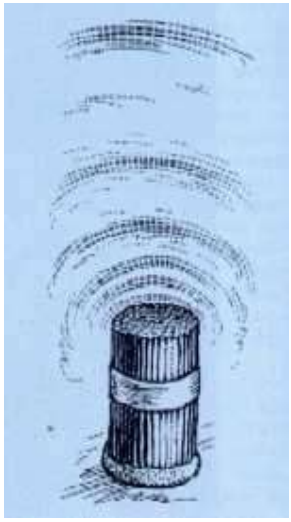

Similar phenomena could be observed in a bunch of paper tubes inhabited by leaf-cutting bees. Each tunnel had a solid row of multi-layered cans of torn leaves, covered with concave lids (also of leaves). Inside the cans there were silk, oval cocoons with larvae and chrysalides.

I asked people who knew nothing of my discovery to hold their hands or faces over the leaf-cutter nests, and took a detailed record of the experiment. The results may be found in my article "On the physical and biological properties of pollinator bee nests" published in the *Siberian Bulletin of Agricultural Science*, no.3, 1984.

The same article contains the formula of the discovery-a brief physical description of this wonderful phenomenon. Based on the structure of bee nests, I created a few dozen artificial honeycombs-of plastic, paper, metal, and wood. It turned out that the cause of all those unusual sensations was not a biological field, but the size, shape, number, and the arrangement of caverns formed by any solid objects. And as before, the organism felt it, while the instruments were silent.

I called the discovery the Cavernous Structures Effect (CSE) and carried on with my experiments.

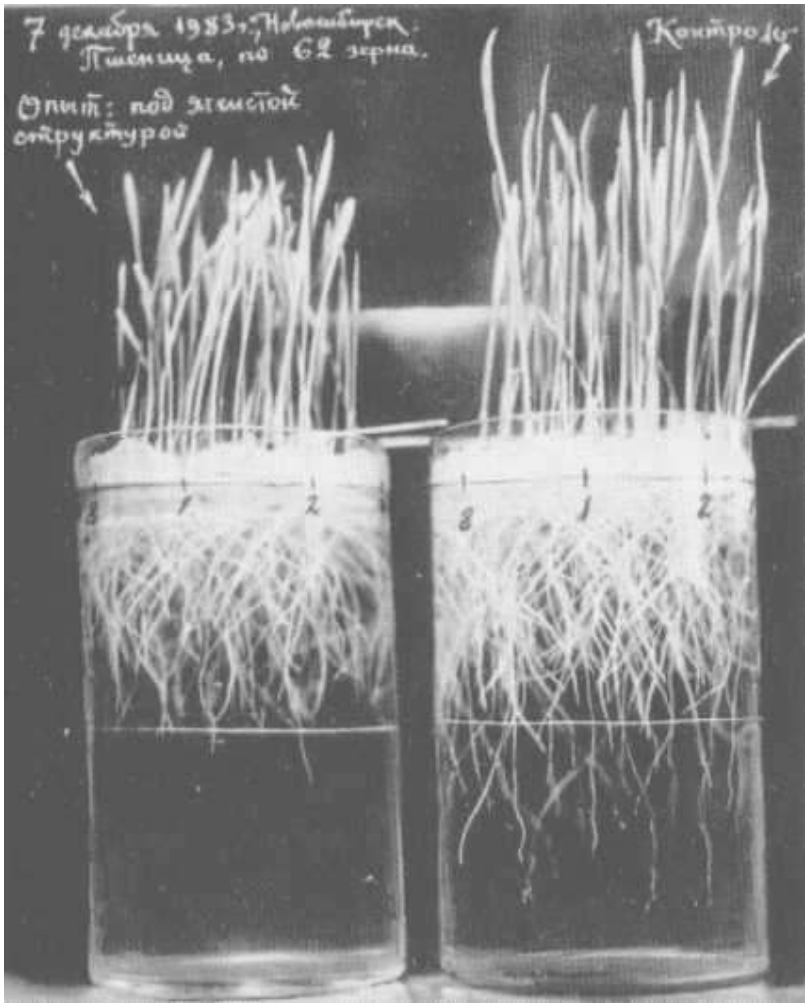

Nature continued to reveal its innermost secrets one after another...

It turned out that the CSE zone inhibits the growth of saprophytic soil bacteria, of yeast and other cultures, as well as wheat grain germination. It also changes the behavior of microscopic algea chlamydospores. Leaf-cutting bee larvae begin to phosphoresce, while adult bees are much more active in this field and finish pollination two weeks earlier.

It turned out that the CSE, like gravitation, could not be shielded-it affected living organisms through walls, thick metal, and other screens. It turned out that if a porous object were moved to another spot, the human would feel the CSE not immediately but in a few seconds or minutes, while the old spot would retain a "trace", or as I called it, a "phantom" perceivable by the hand for hours, and sometimes for months thereafter.

It turned out that the CSE field did not decrease evenly with distance, but surrounded the honeycomb with a system of invisible, yet sometimes clearly perceivable "shells".

It turned out that animals (white mice) and humans entering the zone of the CSE (even a very strong one) soon adapted to it. It couldn't be otherwise: we are everywhere surrounded by caverns large and small: by grids, cells of living and dead plants (as well as our own cells), by bubbles of foam-rubber, foam plastic, foam concrete, rooms, corridors, halls, roofing, spaces between machine parts, trees, furniture, buildings.

It turned out that the CSE "ray" had a stronger impact on living organisms when it was directed away from the sun, and also downwards, facing the Earth's center.

It turned out that clocks-both mechanical and electronic-placed in a strong CSE field started running inaccurately-Time must also have a part in it. All this was the manifestation of the Will of Matter, constantly moving, transforming, and eternally existing. It turned out that back in the 20s the French physicist Louis des Broglie was awarded the Nobel Prize for his discovery of these waves, and that the latter were used in electronic microscopes.

It turned out... well, many other things transpired in my experiments and research, but they would lead us into solid-state physics, quantum mechanics, elementary-particle physics, i. e far away from the main characters of our narrative: insects...

Meanwhile, I did manage to devise instruments for an objective registration of the CSE-instruments that accurately reacted to the proximity of insect nests.

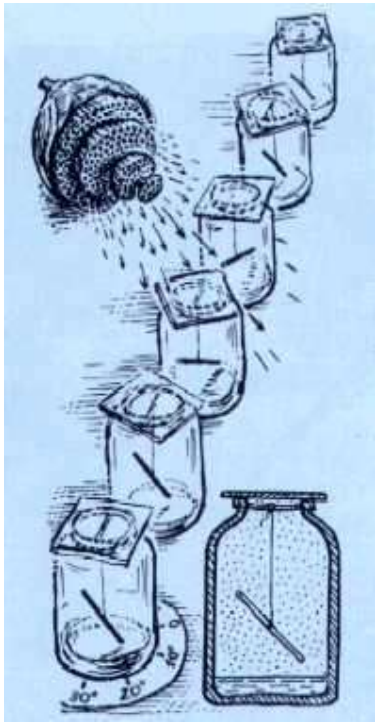

Here they are in the drawing: sealed vessels with straws and burnt twigs-drawing coals-suspended on spider web threads. There is some water at the bottom to counter static electricity hindering experiments in dry air.

If you point an old wasp nest, a bee honeycomb, a bunch of cereal ears to the upper end of the indicator, it slowly moves a few dozen degrees...

There is no miracle here: the energy of scintillating electrons of both multi-cavernous bodies creates a total wave system in space, whereby a wave is energy capable of performing a mutual repulsion of these objects-even through obstacles, such as a thick-walled steel capsule (see photograph).

It is hard to imagine that its armor is powerless to stop waves of a tiny, light wasp nest seen in the picture, and that the indicator inside this heavy, solid capsule "runs away"-sometimes as far as 180 degrees-from this long-vacant nest. Yet it is so. Those who have doubts are invited to visit the Agroecology Museum near Novosibirsk-you'll see it for yourselves.

The same museum displays an always-active honeycomb painkiller. It is a chair with an overhead cap that has a few empty, but intact combs of the honeybee ("dry" honeycombs, in the beekeeper vocab) in it. Anyone who sits in this chair will after a few minutes almost certainly feel something (please write to me what exactly you feel, I'll be grateful), while those with a headache will in just a few minutes say

goodbye to the pain-at least for a few hours. My painkillers are successfully used in many parts of the country-I made no secret of my discovery.

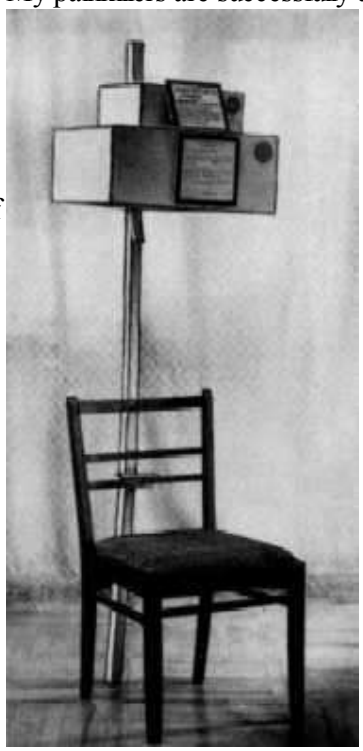

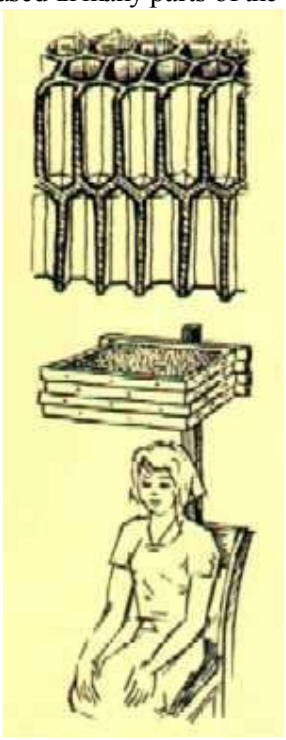

The hand will clearly sense the emanation if you take it from below, palm up, to the cap with bee honeycombs. The cap could be made of cardboard, veneer, or better still, of tin plate with tightly sealed seams.

Yet another gift from insects...

This was my reasoning at first: people have been dealing with the honeybee for thousands of years, no one has ever complained of anything unpleasant, except of course stings. I held a dry honeycomb over my head-it was working!

I decided to use a set of six frames. Such was the story of my rather simple discovery. An old wasp nest works quite differently, even though the size and shape of its cells are very close to those of bees.

The important difference was that the honeycomb material, unlike that of wax, is more crumbly and micro-porous: it is paper-like (by the way, it was wasps that invented paper, not people: they scrape old wood fiber and mix it with their sticky saliva).

Walls of the wasp honeycomb are much thinner than those of bees, the cell size and pattern are also different, as is the outer shell, also made of multi-layered, loosely wrapped paper. I had reports of a highly unpleasant effect of a few wasp nests in an attic. And besides, most multi-cell devices and objects that will manifest CSE in the first few minutes have a far from beneficial effect on humans. Honeybee combs are a rare exception. And when in the 1960s we had bumblebees living in our Isilkul apartment, I often observed the following.

A young bumblebee on its first trip away from the hive did not take the trouble to remember the entrance and would spend hours wandering around the windows of our house and of a similar-looking house nearby. And in the evening, giving up on its poor visual memory, it would land on the brick wall, precisely outside the hive and would try to break right through it. How did the insect know that right there, four meters away from the entrance, and a meter and a half below, behind the thick, half-meter wall was its home nest? At the time I was lost in conjectures, but now I know exactly why the bumblebee behaved like that. An amazing find, wouldn't you agree?

Now let us remember the experiment in which hunter wasps returned not just to a given location, but to an entirely different place where the lump of soil with their nest had been moved: no doubt, they were able to find it because of a wave beacon created by the nest cavern. And there was another mystery revealed to me by my insect friends. It turned out that to attract their pollinators, flowers use not only color, odor, and nectar, but also a similar wave beacon, powerful and unstoppable.

I discovered it with a drawing coal-a burnt twig-by passing it over large, bell-shaped flowers (tulips, lilies, amaryllises, mallows, pumpkins).

Already at a distance I could feel a "braking", as it were, of this detector. Soon I was able to find a flower in a dark room standing one or two meters away from it-but only if it had not been moved,

because a "false target" would be left in its old place-the "residual phantom" I already mentioned.

I do not possess any supersensory abilities, and any person after some training would be able to do the same. Instead of coal one could use a 10-cm-long piece of a yellow sorghum stem, or a short pencil whose rear end should be facing the flower.

Some people would be able to feel the flower (a "warm", "cold", or "shivering" sensation emanating from it) with their bare hands, tongues, or even faces. As many experiments demonstrated, children and adolescents are particularly sensitive to Waves of Matter.

As for bees that nest underground, their "knowledge" of the CSE is vital for them first of all, because it enables the builder of a new gallery to stay away from a neighboring nest. Otherwise the entire bee-city cut through with intersecting holes would simply collapse.

Secondly, plant roots cannot be allowed to grow down into the galleries and honeycombs. Thus roots stop a few centimeters away from the honeycomb, or else, feeling that nests are near, they start growing aside.

The latter conclusion was confirmed by my many experiments on sprouting wheat seeds in a strong CSE field, as compared to seeds germinating in the same climatic conditions but in the absence of the CSE.

Photographs and drawings show both the dying of roots in the experimental batch and their sharp deviation in a direction away from my "artificial honeycomb".

Thus bees and weeds back at the lake had long ago made a pact-another example of the highest ecological expediency of all Being. And in that same spot on the globe we see yet another example of people's mercilessly ignorant attitude to Nature...

The bee-city is now gone; every spring thick streams of fertile black earth soil run down, between filthy heaps of trash, to the lifeless, salty puddles that not too long ago were a string of lakes with countless flocks of sandpipers and ducks, white swans, and hovering fish-hawks. And by the steppe thinned out by bee holes, one used to hear the hum of hundreds of thousands of bees that for the first time led me into the Unknown.

I must have tired the reader with all these honeycombs of mine... A separate thick book would be required to describe all my experiments. Therefore I will only mention one thing: my pocket, battery-powered calculator often malfunctioned in the CSE field: it either erred, or sometimes its display window would fail to light up for hours. I used the field of a wasp nest combined with that of my two palms. None of these structures had any effect in isolation.

I will also note that hands with their tubular phalanxes, joints, ligaments, blood vessels, and nails are intensive CSE emanators capable of giving a powerful push to the straw or coal indicator of my little instrument from a couple of meters' distance. Practically anyone could do it. This is why I am

convinced that there are no people with supersensory abilities, or rather that all the people have them... And the number of those who from a distance can move light-weight objects on a table, hold them suspended in the air or "magnetically" attached to the hand is far greater than is usually thought. Try it yourself! I look forward to your letters.

There once was an ancient folk game: one man sits on a chair, and over his head, four of his friends "build" a grid of horizontally stretched palms with slightly spread fingers-first right hands, then left, with 2 cm gaps between them. In 10-15 seconds, all four synchronously put their pressed-together index and middle fingers under the armpits and under the knees of the sitting man, and then they energetically toss him up in the air. The time between "collapsing" the grid and tossing the man must not exceed two seconds; the synchronicity is also very important. If everything is done right, a 100-kilo man flies up almost to the ceiling, while the ones who tossed him claim he was light as a feather.

A strict reader may ask me how it is possible. Doesn't it all contradict laws of nature? And if so, am I not propagating mysticism? Nothing of the sort! There is no mysticism, the thing is simply that we, humans, still know little of the Universe which, as we see, not always "accepts" our, all too human rules, assumptions, and orders... Once it dawned on me: the results of my experiments with insect nests bear too much similarity to the reports of people who happened to be in the vicinity of... UFOs. Think and compare: temporary malfunctioning of electronic devices, disrupted clocks-i. e., time, an invisible, resilient "obstacle", a temporary drop in the weight of objects, the sensation of a drop in human weight, phosphenes-moving, colored flashes in the eyes, a "galvanic" taste in the mouth...

I am sure you have read about all this in UFO journals. I am now telling you it can all be experienced in our Museum. Come visit! Was I standing on the threshold of yet another mystery? Quite so. And again I was helped by chance, or rather by my old insect friends. And again there were sleepless nights, failures, doubts, breakdowns, even accidents... And I had no one to turn to for advice-they would have just laughed, or worse...

But I can say this, my reader: he is happy who has a more or less adequate use of his eyes, head, and hands-skillful hands are particularly important!-and trust me, the joy of creative work, even of work that ends in failure, is far higher and brighter than earning any diplomas, medals, or patents.

Flying an Anti-gravitational Platform

(*excerpts from a diary)*

Judge it for yourself from my diary excerpts-obviously simplified and adapted for this book. Pictures and drawings will help you to evaluate my story... A hot summer day. Far-away expanses drown in a bluish-lilac haze; the sky's gigantic cupola with fluffy clouds stretches above the fields and coppices. I am flying about 300 meters above ground, with a distant lake-a light, elongated spot in the haze-as my reference point.

Blue, intricate tree contours slowly recede; between them, there are fields. Those, bluish-green ones are fields of oats; the whitish rectangles with a strange, rhythmic twinkling are those of buckwheat. Straight ahead of me is a field of alfalfa-its green color is familiar, it resembles the oil paint "cobalt medium-green". Green oceans of wheat on the right are of a denser shade and resemble the "chrome oxide" paint. An enormous, multi-colored palette floats further and further backwards.

Footpaths meander between fields and coppices. They join gravel roads which it turn stretch further out, toward the highway, still invisible from here for the haze, but I know that if I flew on the right side of the lake, I would see it-a smooth, gray strip without a beginning or an end, on which cars-small boxes-are slowly crawling.

Isometric, flat shadows of cumulus clouds are picturesquely spread around the sunny forest-steppe. They are deep-blue where they cover coppices, and are various shades of light blue over fields. Now I am in the shadow of one such cloud: I accelerate-it's quite easy for me to do that-and leave the shadow.

I lean forward slightly and feel a warm, taut wind coming far down below, from the sun-warmed ground and plants. It comes not from the side, as on the ground, but strangely from the surface up. I physically feel a thick, dense current with a strong odor of blooming buckwheat. Of course this jet can easily lift up even a large bird-an eagle, a stork, or a crane-if it freezes its spread wings. But I have no wings and am suspended in the air not by the upward jet.

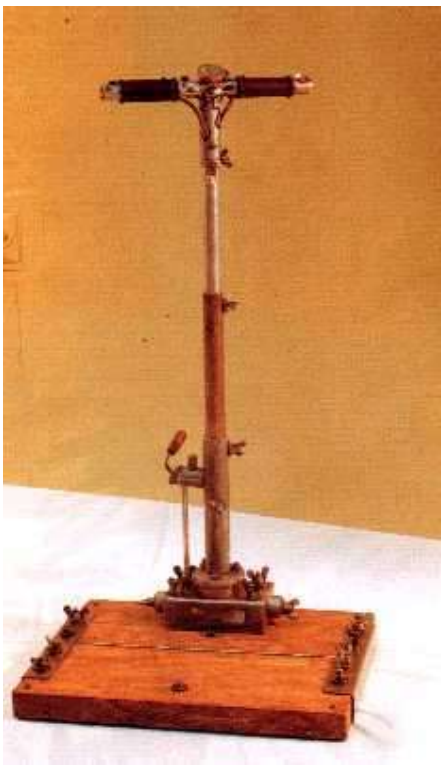

In my flight I am supported by a flat, rectangular little platform, slightly bigger than the seat of a chair, with a pole and two handles to which I hold on and with whose help I navigate the device. Is this science fiction? I wouldn't say so...

In a word, the interrupted manuscript of this book was abandoned for two years because generous, ancient Nature, again through my insect friends had given me another Something-and it did so, as usual, elegantly and inconspicuously, yet swiftly and convincingly. And for two years the Discovery did not let me go, even though it seemed to me I was mastering it at a break-neck speed.

(Note: Grebennikov would have been approximately 62-63 years of age in 1990-1992)

But it always happens this way: when your work is new and interesting, time flies twice as fast. A light spot of a steppe lake is already much closer. Beyond it, the highway is visible with already distinctly discernable boxes of cars. The highway is about 8km away from the railway that runs parallel to it, and if I look closer, I can see the poles of the power line and the light-colored embankment of the railway. It is time to turn some 20 degrees to the left.

I am not seen from the ground, and not just because of the distance: even in a very low flight I cast almost no shadow. Yet, as I found out later, people sometimes see something where I am in the sky-either a light sphere, a disk, or something like a slanted cloud with sharp edges that moves, according to them, not exactly the way a cloud would.

One person observed a "flat, non-transparent square, about one hectare in size"-could it have been the optically enlarged little platform of my device?

Most people see nothing at all, and I am for the moment pleased with it-I can't be too careful! Besides, I still haven't determined what my visibility or invisibility depends on.

Therefore I confess that I consciously avoid people in my flight and for that purpose bypass cities and towns, and even cross roads and footpaths at high speed, after making sure there is no one on them.

In these excursions-no doubt, fictional for the reader, but for me already almost casual-I trust only my insect friends depicted on these pages.

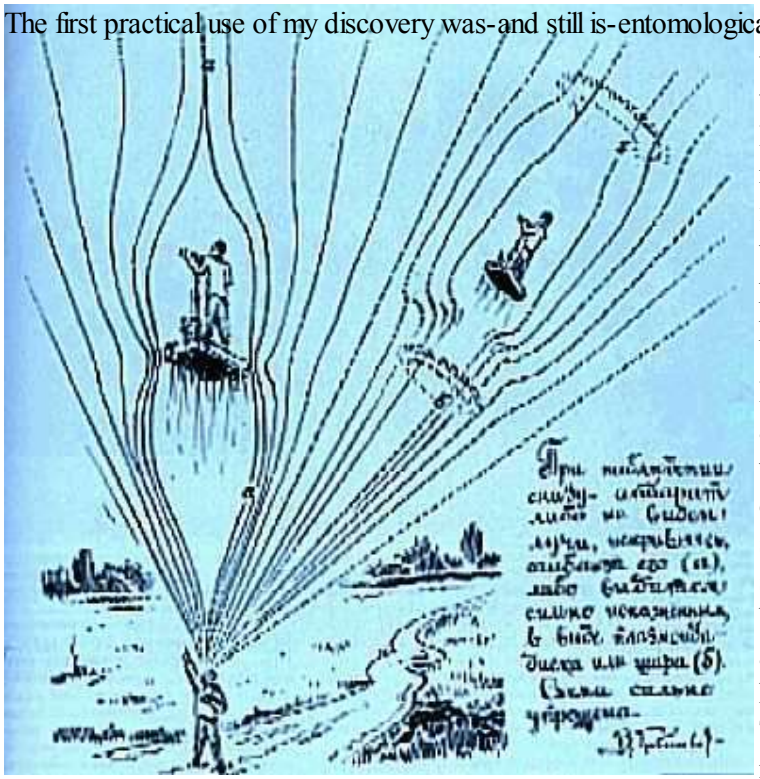

The first practical use of my discovery was-and still is-entomological: to examine my secret places, to take a picture of them from above, to find new, still unexamined Insect Lands in need of protection and rescue. Alas, Nature established its own, strict limitations on my work: just as on a passenger plane, I could see but couldn't photograph.

My camera shutter wouldn't close, and both rolls of films I had taken with me-one in the camera, the other in my pocket-got light-struck. I didn't succeed in sketching the landscape either; as both my hands were almost always busy, I could only free one hand for a couple of seconds. Thus I could only draw from memory. I managed to do that only immediately after landing-though I am an artist, my visual memory is not that great.

In my flight I did not feel the same way we do when we fly in our sleep.

It was with flying in my sleep that I started this book a while ago. And flying is not so much pleasure as it is work, sometimes very hard and dangerous. One has to stand, not hover, the hands are always busy, and a few centimeters away there is a border separating "this" space from "that", on the outside.

The border is invisible but very treacherous. My contraption is still rather clumsy and resembles perhaps... hospital scales. But this is only the beginning!

By the way, besides the camera, I sometimes had trouble with my watch and possibly, with the calendar too: descending on a familiar glade, I would occasionally find it slightly "out of season", with a two-week deviation, and I had nothing to check it against.

Thus it is possible to fly not just in space but also-or so it seems-in time as well. I cannot make the latter claim with a 100% guarantee, except perhaps that in flight, particularly at its beginning, a watch runs too slow and then too fast, but at the end of the excursion starts running accurately again.

This is why I stay away from people during my journeys: if time is involved alongside gravitation, I might perhaps accidentally disrupt cause-and-effect relations and someone might get hurt.

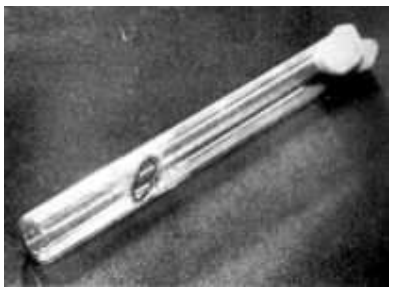

This is where my fears were coming from: insects captured "there" disappear from test tubes, boxes, and other receptacles.

They disappear mostly without a trace. Once a test tube in my pocket was crushed to tiny bits, another time there was an oval hole in the glass, with brown, as though "chitin" edges-you can see it in the picture.

Many times I felt a kind of burning or an electric shock inside my pocket-perhaps at the moment of my prisoner's "disappearance".

Only once did I find a captured insect in the test tube, but it wasn't the adult ichneumon with white rings on its feelers, but its... chrysalis, i. e. its earlier stage. It was alive-it moved its belly when touched. Much to my dismay, it died a week later.

It is best to fly on clear summer days. Flying is much more difficult when it rains, and almost impossible in winter-not because of the cold. I could have adapted my device accordingly, but since I am an entomologist, I simply do not need winter flights.

How and why did I come to this discovery? In the summer of 1988, as I was examining under a microscope the chitin shells of insects, their pinnate (feathery) feelers, and the thinnest structure of butterflies' wings, I got interested in an amazingly rhythmical microstructure of one large insect detail.

It was an extremely well-ordered composition, as though pressed on a complex machine according to special blueprints and calculations. As I saw it, the intricate sponginess was clearly not necessary either for the durability of the detail, or for its decoration. I had never observed anything like this unusual micro-ornament either in nature, in technology, or in art.

Because its structure is three-dimensional, so far I have been unable to capture it in a drawing, or a photograph. Why does an insect need it? Besides, other than in flight, this structure at the bottom of the wing case is always hidden from the eye-no one would ever see it properly. Was it perhaps the wave beacon with "my" multiple cavernous structures effect? That truly lucky summer there were very many insects of this species, and I would capture them at night: neither before, nor after was I able to observe these insects.

I put the small, concave chitin plate on the microscope shelf in order again to examine under strong magnification its strangely star-shaped cells. I again admired this masterpiece of nature, and almost purposelessly placed it on top of another, identical plate that had the same unusual cells on one of its sides.

But no!-the detail broke loose from my tweezers; for a few seconds it hung suspended above the other plate on the microscope shelf, turned a few degrees clockwise, slid to the right, turned counterclockwise, swung, and only then abruptly fell on the desk.

You can imagine what I felt at that moment... When I came to my senses, I tied a few panels with a wire-it wasn't an easy thing to do, and I only succeeded when I positioned them vertically. What I got was a multi-layered chitin block. I put it on the desk.

Even a relatively large object-such as a paper tack-could not fall on it-something pushed it up and aside. When I attached the tack on top of the "block", I witnessed such incredible, impossible things (for example, the tack for a few moments was lost from sight) that I realized it was no beacon, but something else entirely.

And again I got so excited that all the objects around me became foggy and shaky. It was with a huge effort that I managed to pull myself together in a couple of hours and continue working.

So, this is how it started. Of course, much still remains to be understood, verified, and tested. I will certainly tell my readers about the finer details of my machine, about its propulsion principles, about distances, heights, speeds, equipment, and all the rest-but in my next book.

...I conducted my first, very unsuccessful and highly dangerous flight on the night of March 17, 1990. I didn't have the patience to wait till the warm season and neglected to go to a deserted area. I already knew that night was the most dangerous time for this kind of work.

I had bad luck from the very beginning: the panel blocks of the right part of the bearing platform

periodically got stuck. I should have fixed the problem immediately, but neglected to do so. I took off right in the middle of the Agricultural Academy campus, erroneously assuming that at 1 AM everyone was asleep, and nobody would see me.

The lift-off went well, but in a few seconds, when the lit windows of buildings sank beneath me, I felt dizzy. I should have landed right then but remained airborne, which was wrong because a powerful force snatched away my control over the movement and weight, and it pulled me in the direction of the city.

Drawn by this unexpected, uncontrollable power, I crossed the second circle of nine-story buildings in the city's residential area (they are laid out in two huge circles with five-story buildings, including ours, inside them), then I crossed a snow-covered, narrow field, and the Academy City highway... The dark immensity of Novosibirsk was closing in upon me, and it was closing in fast. I was already near a bunch of tall factory chimneys many of which fumed thick smoke-night shift was on. I had to do something quickly.

I got on top of the situation only with a great effort. Finally I managed to conduct an emergency adjustment of the panel blocks. My horizontal movement slowed down, but then I again felt sick.

Only at fourth try did I succeed in stopping the horizontal movement, at which point my platform was hanging over Zatulinka, the city's industrial district. The sinister chimneys silently continued to fume right underneath me.

I rested for a few minutes-if one could call hanging over a lighted factory fence rest-and after I made sure the "evil power" has passed, I glided back-yet not in the direction of our Agricultural Academy campus but to the right from it, toward the airport. I did this to foul the trail, in case someone had seen me.

Only about halfway to the airport, over some dark, night fields where there was clearly no one around, I abruptly turned home... Next day I naturally couldn't get out of bed.

News on TV and in newspapers was more than alarming. Headlines, such as "UFO over Zatulinka" and "Aliens again?" meant that my flight had been detected. But how! Some perceived the "phenomenon" as glowing spheres or disks-many actually saw not one sphere but two! Others claimed they had seen a "real saucer" with windows and rays.

I am not discounting the possibility that some Zatulino residents saw not my near-emergency evolutions, but something else entirely that had nothing to do with those. Besides, March of 1990 was particularly rich in UFO sightings in Siberia, near Nalchik, and especially in Belgium where, according to *Pravda*, on March 31 the engineer Marcel Alferlane took a two-minute film of the flight of a huge triangular craft which, according to Belgian scientists, were none other than "material objects with a capacity no civilization can currently create."

Is it really so? As for me, I would suggest that the gravitational filter platforms (or as I call them, panel blocks) of these machines were in fact small, triangular, and made here on Earth-but with more sophistication than my half-wooden contraption.

I too wanted to make the platform triangular-it is much safer and more efficient that way-but I chose a rectangular design because it is easier to fold, and when folded, it resembles a suitcase, a painter's case, or a briefcase that can be thus disguised so as not to arouse suspicion. I, naturally, disguised it as a painter's case.

I had nothing to do with the sightings in Nalchik or Belgium. Besides, as it may appear, I am very impractical in the use of my discovery-I only fly to my entomological preserves. These are far more

important to me than any technological finds.

At the moment, I have eleven such preserves: eight in Omsk region, one in Voronezh region, and one near Novosibirsk. There used to be six of them in Novosibirsk region, all of them created, or rather salvaged by me and my family, but they don't like them here. Neither the Agricultural Academy (still more obsessed with "chemistry" than with anything else), nor the Environmental Protection Committee were willing to help me salvage these little preserves from evil, ignorant people.

Thus I am continuing my journey westward under the magnificent, fluffy clouds at noon. The blue shadows of the clouds, the intricately shaped coppices, and the multicolored rectangles of fields float backwards below me.

The speed of my flight is quite high, but there is no wind in my ears-the platform's force field has "carved out" from space an upward-diverging, invisible column that cuts the platform off the earth's gravitational pull. But it left me and the air inside the column intact. I think that all this, as it were, parts space in flight, and then closes it behind me.

This must be the reason for the invisibility, or the distorted visibility, of the device and its "rider"-as was the case with my flight over Novosibirsk's Zatulinka suburb.

But the protection from gravity is regulated, even though it is incomplete: if you move your head forward, you already feel the turbulence of the wind that clearly smells either of sweet clover, of buckwheat, or of the colored weeds of Siberian meadows.

I leave Isilkul with its huge grain elevator on my right and gradually begin to descend over the highway, making sure that I am invisible to drivers, passengers, and people working in the field.

My platform and I cast no shadow (although the shadow occasionally appears): I see three kids on the edge of a forest, go down, drop my speed, and fly right near them. They show no reaction, which means that everything is fine-neither I, nor my shadow are visible. Or heard: the propulsion principle of my device is such that the platform makes no sound whatsoever, because there is practically no air friction.

My journey was long-at least forty minutes from Novosibirsk. My hands are tired as I can't take them off the controls, so are my legs and body-I have to stand up straight, tied to the vertical pole with a belt. And even though I can travel faster, I am still afraid to do so-my hand-made machine is still too small and fragile.

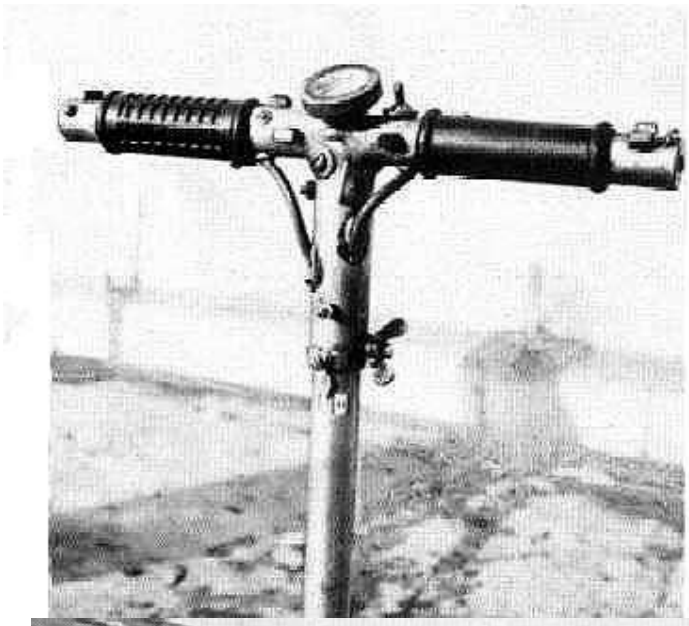

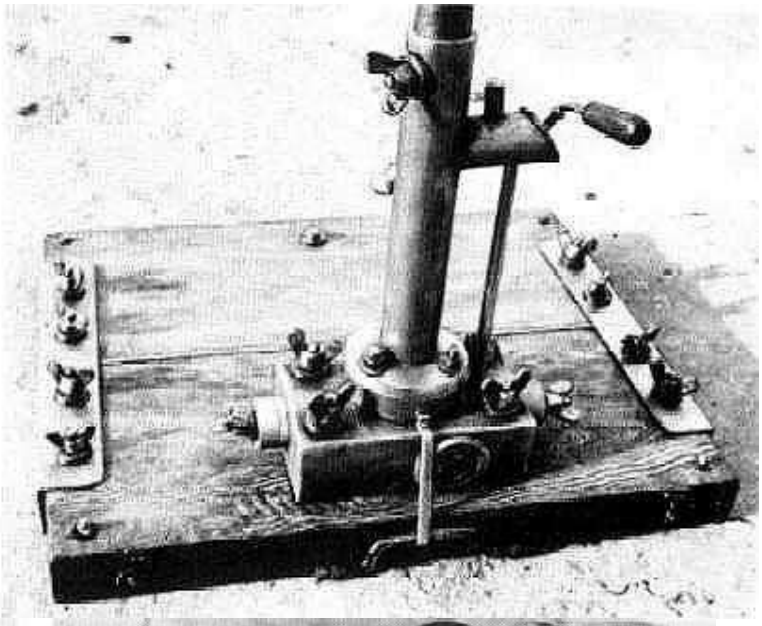

I again go up and ahead, and soon I see the familiar landmarks-a road intersection, a passenger terminal on the right side of the highway. Another five kilometers, and finally I see orange columns of the Preserve fence. The Preserve is this year-come to think of it-twenty years old! How many times I saved this child of mine from trouble and bureaucrats, from chemicals-loaded aircraft, from fires, and many other evil deeds. And the Land of Insects is alive and well!

Descending and braking, which is done by cross-shifting filter blinds under the platform board, I already see the thicket of carrot weed, make out the light heads of their flowers resembling azure balls-they are of course covered with insects, and an incredible joy comes over me, taking away my fatigue, for it was I who saved this piece of Earth, even if a small one, less than seven hectares.

Already for twenty years no one has driven here, no one has cut the grass, tended cattle, and the soil

has risen in places to fourteen centimeters high. Not only several locally extinct species of insects have returned, but also such weeds as feather grass of rare varieties, purple Scorzonera whose large flowers in the morning smell of chocolate, and many other plants. I feel the thick smell of cuckoo flower-only this Middle Glade smells like that, it is right behind the fence of the preserve, and fills me with yet again with the joyful anticipation of another encounter with the World of Insects.

Here they are, I can see them very well even from ten meters above the ground on the wide umbrellas and azure balls of angelica and carrot plants: dark orange butterflies sit on them in groups; heavy hornets bow the white and yellow inflorescences of lady's bedstraws; ginger and blue dragonflies with trembling wide wings and a fine network of veins hover next to my head. I slow down even more, and see a sudden flash below: my shadow, hitherto invisible, has finally appeared and now slowly glides along weeds and bushes.

But I am already safe-there is not a soul around, and the highway three hundred meters north of the preserve is now empty. I can land. The stems of the tallest weeds rustle against the bottom of my "podium"-the platform with the panel blocks.

But before putting it down on a little bump, I, in a fit of joy, again spread the blinds with my control handle, and vertically go up. The landscape below quickly shrinks, shrivels as it were: the shrubs of the preserve, its edges and fences, all the surrounding coppices and fields. The horizon begins to curve on all sides in a huge groove, opening up the railroad that runs two kilometers on the left, then a village on the right-it twinkles with its light slate roofs.

Further on the right is Roslavka, the central estate of Lesnoy State Farm-it already looks like a small city. Left from the railroad are cow farms of Lesnoy's Komsomolsk branch; they are surrounded by a yellow ring of straw and dry, foot-worn manure. In the far west, where the smooth curve of the railroad disappears (this is actually confusing: the railway is straight as an arrow), there are small houses and the neat white cube of the Yunino railroad terminal, six km away. Beyond Yunino, there are limitless expanses of Kazakhstan drowning in the hot, bluish haze.

And finally here it is, below me-Isilkulia, the land of my youth; it's very different from how it appears on maps and plans with their inscriptions and signs. It is vast, limitless, alive, interspersed with dark, intricate islands of coppices, cloudy shadows, light, clear spots of lakes.

The huge disk of the Earth with all this for some reason appears more and more concave-I still haven't discovered the reason for this already familiar illusion. I go up higher, the rare, white cloud masses sink lower, and the sky is darker than below-it is dark blue. The fields visible between the clouds are already covered with a thickening blue haze, and it is more and more difficult to make them out. Too bad I can't take my four-year-old grandson Andrei with me; the platform could easily lift us both. Yet one can't be too careful...

... Goodness, what am I doing? I cast a shadow back on the Glade, didn't I? This means I can be seen by thousands, as on that memorable night in March. It is day now, and I may again appear as a disk, square, or worse, my own person... There is also a cargo plane, still soundless, coming straight at me, quickly growing in size; I already see the cold shimmer of its body and the pulsation of its unnaturally red blinker.

Down, quick! I brake abruptly, make a turn; the sun is at my back; my shadow should be across from me, on the gigantic, convex wall of a white cloud. But there is none, only a multicolored glory, an iridescent, bright ring familiar to all pilots has brushed the cloud ahead of me.

I sigh with relief-this means nobody saw either me, or my "double" in the guise of a triangle, square, or a "banal" saucer... A thought occurs to me (I must say that despite the desperate technical and

physical inconvenience, imagination works much better and faster in a "falling" flight): what if I am not the only one out of five billion people to have made my discovery; what if flying devices based on the same principle-both home-made and professional-have long been constructed and tested?

But all screening platforms have the same quality: sometimes they become visible to other people; pilots too are "transformed"-they are seen as "humanoids" in silver costumes, either short and green, or flat as if made of cardboard (Voronezh, 1989), etc. Thus it may very well be that these are not alien UFO crewmen, but "temporarily deformed"-of course to outside observers-earthly pilots and builders of little platforms, such as mine, who have made their inventions reliable.

My advice to those who in their study of insects comes across the same phenomenon and begin making and testing a "gravitoplane" (by the way, I am convinced that one can't make the discovery without insects) is this: to fly only on fine summer days, to avoid working in thunderstorms or rain, not to get too far or too high, not take a thing with you from the landing area, to make all assembly units maximally strong, and to avoid testing the device in the vicinity of any power lines, towns (let alone cities), transport, or people.

The best site for testing is a distant forest glade, as far away from human habitation as possible; otherwise a phenomenon known as poltergeist could occur in the radius of a few dozen meters-"unexplained" movements of household objects, switching off, or on, of household electric appliances, and even fires.

I myself have no explanation for all this, but it seems that these phenomena are the consequence of temporal disruptions, a complicated and treacherous thing. Not a single, even tiniest fragment or particle should be dropped either during the flight, or in the landing area.

Let us remember the Dalnegorsk phenomenon of January 29, 1986-apparently a tragic one for the inventors, when the entire device was blown apart and scattered on a vast area, and only small shreds of filter cells were found, impossible to analyze chemically (as it should be!).

Remember, I wrote that insects taken "there" and moved "here" in a test tube disappeared, and a hole was formed in the tube, if it remained intact.

It turns out these holes resembled those in window glass; the latter sometimes appear in residential and office buildings, occasionally in "bursts" in the windows of several rooms and floors. A hole is 3-5 mm on the outside, widening in a cone to he inside, with exit diameter of 6-15 mm. Some holes are melted or colored in brown on edges-just as it happened in the case of my insect in a test tube.

It seems that this type of poltergeist is caused not, as I used to believe, by short-lived microplasmoids of a tiny ball lightening type, but by particles and specks carelessly dropped while testing a device similar to mine. The photographs of window holes on these pages are documentary and made by me at the scientific center of the Agricultural Academy near Novosibirsk. I can show them to anyone who wants to see them. These holes appeared during 1975-1990, but none of them, except perhaps the very last one, are related to my flights.

I am certain that part of UFO descriptions are actually those of platforms, panel blocks and other large parts of devices deliberately or accidentally taken out of the active field by their designers and makers. These fragments are capable of causing much trouble to others, or at best, to generate a series of improbable tales and stories in papers and magazines, often accompanied by "scientific" commentary...

Why am I not disclosing the particulars of my discovery at this time? Firstly, because one needs time and energy for proving the truth. I have neither. I know how daunting this task is from my own bitter experience of trying to get recognition for my previous discoveries, including such an obvious one as

the Cavernous Structures Effect of whose reality you, my readers, I am sure, are by now convinced.

This was the result of my protracted, painstaking efforts to get the CSE scientifically recognized:

> "Any further correspondence with you on the subject of your patent application is counterproductive."

I know personally some of the High Priests of Science, and I am certain that were I ever to get an audience with one such person (which is now practically impossible), were I ever to;

- open my painter's case,
- attach the pole,
- turn the handle,
- and soar to the ceiling,

he wouldn't be a bit impressed-or worse still, would order the trickster out of the office. I look forward to times when young people will replace these "priests".

The second reason for my "non-disclosure" is more objective. I found these antigravitational structures only in one species of Siberian insects. I am not even naming the class to which this insect belongs-it seems to be on the verge of extinction, and the population surge I registered back then was possibly local and final.

Thus, if I were to name the genus and the species, what is the guarantee that dishonest people, half-way competent in biology, would not rush out to ravines, meadows, and forests to catch perhaps the very last samples of this Miracle of Nature?

What are the guarantees that they would not plough up hundreds of glades, cut down dozens of forests to get to this potentially lucrative prey? Therefore, let all I have related in this chapter and in the addendum remain science fiction; may Nature herself never reveal this secret to them-it would take a lot of effort, and they would never be able to get it by force as there are still several million insect species living on the planet.

Spend at least an hour on the morphological study of each of them, then calculate the odds of encountering the Unusual, and I will sincerely wish you diligence and a very long life, for even if you took no days off, working eight hours a day, you would need a thousand years of life.

I hope I will be understood and forgiven by those of my readers who wanted immediate information about my discovery not for selfish ends, but simply out of curiosity. Indeed, what would you do in my place if you were to act in the best interests of Living Nature?

Besides, I can see that similar inventions have been made by other people who are also in no rush to take their discoveries to bureaucrats' offices, preferring to fly across night skies in the guise of strange disks, triangles, or squares with chatoyant (iridescent) glimmer.

Falling down, or rather sinking down, I orient myself, look to see if there is anyone around. I brake abruptly about forty meters from the ground, and land safely where I always do-on a tiny glade in the Big Forest of the preserve. You won't find it on a map, and if you get there, you won't be able to find it either.

Don't judge me for the fact that the branches of several aspens there are cut or sliced "by lightening": The strictly vertical take-off and landing are very difficult, and the initial trajectory is for the most part slanted, particularly at take-off, when the platform is for some reason carried off away from the sun, and sometimes the other way around.

I loosen the screws on the control pole, then shorten it like an antenna of a portable radio, and remove it from the platform which I fold in half. Now it looks like a painter's case, a box for paints, if only a bit thicker. I put the case, some food, and a few tools for repairing the fence in my backpack and make my way for the Middle Glade between aspens and short dog-rose bushes. Even before I leave the forest, I see a good omen-a family of fire-red toadstools that have lined up on the forest bedding in a wide curve, or, as it used to be called in folklore, a "witch's ring".

Why "witch's"? And in general, why does one have to break, knock off, trample this beautiful mushroom of Siberian forests? I often asked mushroom-pickers why they do it. The answer was, "because it's inedible!" But turf, clay, twigs, tree stumps, and stones are inedible too.

If there were rocks lying in the forest instead of mushrooms, no one would be knocking them off. It seems that inedible mushrooms are knocked off because they are alive; they are knocked off only in order to kill them! What is this then?

Do people really have this in their blood-to knock off a mushroom, to crush a bug, to shoot a bird, a hare, or a bison? And is this not where boorishness, sadism, pogroms, and wars originate? One really wants not to believe it, but I put myself in the shoes of an alien: I come to Earth to visit humans and see them knock off mushrooms, crush insects, shoot birds and each other.

What would I do? I would immediately turn my spacecraft around and go back. I wouldn't return for at least 500 earth years... What would you do, my reader, if you were an alien?

It's a good thing at least that this little family of toadstools is hidden from evil eyes and cruel feet. Every summer it gives me joy to see its special life, its cinnabar-red, moist caps with large, whitish scales. But here is the Glade. I step on it, as usual, with my heart sinking with a constant longing for this dear, faraway nature of Isilkul, with a fear that some "master" might decide to plough it up, and with a joy that it is still unploughed, uncut, and untrampled...

And it really means nothing that in my backpack I have a folded, i. e. neutralized platform with gravitational, micro-cellular filter blocks, and between them, a folded pole with field regulators and a belt with which I fasten myself to the pole.

What difference does it make that I got about fifty years ahead of contemporary science with my discovery? People are still going to master this and many other mysteries of Matter, Space, Gravitation, and Time.

But no supercivilization on any planet of any Supergalaxy is going to re-create this very Glade with its complex, fragile, trembling Life, with its lady's bedstraws, meadow sweets, and feather-grass...

Where else, in what corner of the Universe are you going to find a match for this lilac-blue bellflower in whose semi-transparent entrails two flower flies are doing their love dance? On what other planet would a nearly tame blue butterfly land on your outstretched hand to have a taste of something salty-sausage, cheese, or a pickle? Or else, just to walk up and down your palm, opening and closing its gray wings on whose backside there is a fine ornament of round eye-shaped spots?

...It hasn't been too long since we, humans, started flying-first air balloons, then airplanes, and now powerful rockets that we send to other heavenly bodies. What next? Next we are going to fly to other stars at a speed close to that of light; but even the closest galaxy would still be out of reach.

Yet Humankind-if it earns the name of Intelligent-will solve many riddles of the Universe and will then overcome that hurdle too. Then any worlds of the Universe will become accessible, close-even if they are trillions of light years away. It'll happen, for it is all a matter of Reason, Science, and technology. But of nothing else. Only this Glade may disappear if I-and there is no one else to rely on-am not

going to preserve it for my close and distant descendants.

So what is more valuable to Humanity at this time-the insect preserve or the home-made device capable of developing the zenithal pull of at least 100 kg and the horizontal speed of 30-40 km/min? I am asking *you*, my reader. But think hard before you give a serious, responsible answer.

ther simple device in assembly. A flexible cable inside a steering column trasmits movement from the left handle to the gravitational blinds.

oining or parting these "wing cases", I lift off or land. Once I lost the left handle in a free-falling scent and would have been in a better world if the platform hadn't dug out a rather deep well in the tillage-first a vertical one, then a horizontal, facing away from the sun.

Thus I not only survived, but also felt almost no impact-just darkness. I extracted myself and my fairly badly damaged device from this well-but not without efforts as the "well" had no slag heaps!

I had to use all my ingenuity to disguise it. If seen from the road, it would have caused much speculation, and may even have led some over-zealous investigators to the culprit. Similar wells-also with a side-tunnel and without slag heaps-were suddenly formed on October 24, 1989 in the fields of Khvorostyansk District of Samara Region. *Komsomol'skaya pravda* described it in detail on December 6 of the same year. It seems I am not alone. And quite likely am "inventing a bicycle". Well, actually the top part of my device looks very much like one: the right handle is used for horizontal, onward march achieved, also via a cable, by the incline of both groups of "wing case" blinds. I never fly faster than 25 km/min, preferring to go ten times slower.

...I don't know whether I have persuaded you, my reader, that similar devices will soon be available to practically everyone, while Living Nature which humans cannot survive without won't be available to anyone if we don't save it.

But I don't want to seem entirely greedy and will give researchers another Patent of Nature, one also related to Movement and Gravitation. Physicists say that an unsupported mover is impossible. In other words, a device completely isolated from the environment won't fly or drive-a car won't go without outer wheels, a plane won't fly with a covered propeller or engine, neither will a rocket with stopped nozzles. Baron Münchhausen who managed to pull himself up by the hair from a mire is the only exception.

It happened near Novosibirsk in 1981 when we were studying the entomo-fauna of alfalfa-its pollinators and pests. Walking along the field, I was "mowing" alfalfa with an insect net and was then moving its contents-insects, leaves and flowers-into a glass jar. Such is the cruel method of studying the insect make-up of fields, no better one has been invented. Alas, such was the work with which I earned my living at the Institute of Agricultural Chemistry. I was about to throw a piece of ethered cotton wool into the jar and then cap it, when a light little cocoon jumped up at me.

It was oval-shaped, rather dense and non-transparent. One of the "prisoners" of the jar must have pushed it-cocoons can't jump on their own! But the cocoon proved me wrong: it jumped up one more time, hit the glass wall, and fell down. I took it out and put it in a separate test tube. At home I looked at it through a binocular microscope-nothing special, a cocoon like any other, about 3 mm long, 1.5 mm wide. Its walls felt strong to the touch-as they should. The cocoon energetically jumped when lit-or warmed?-by the sun; it was quiet in the dark. Its could jump 30mm longwise and, what was even more remarkable, up to 50mm high. As far as I could tell, it flew smoothly, almost without

tumbling. No doubt, the larva of the insect was responsible for the movement. But it was impossible to see how it was happening.

Jumping ahead, I can tell you that the cocoon finally produced a male insect of the ichneumon family, the *Batiplectes anurus* species. It is beneficial for agriculture because its larvae parasitize the weevil, a pest of alfalfa.

The flying cocoon was finally to land in a cool place-for example, a crack in the ground. It must have found myself in my net during its strange journey, i. e. at the moment of its jump. It all resembled poltergeist-unexplained "jumps" of household objects, many times described in papers. I would put it on glass and look at it from below: could it be that the larva draws in its bottom and then abruptly releases it? Nothing of the kind-there were no dents at any point, and the cocoon jumped no matter how I rolled it. It was also remarkable that from horizontal, slippery glass it jumped sideways.

I measured its trajectories: they were up to 35 cm long and up to 50 mm high, that is, the cocoon lifted itself up to a height 30 times its own width! Shall I leave this capsule without support? But how? With a piece of loose cotton wool! I loosen a piece of cotton wool by pulling it a little, place the cocoon on this "cloud", put it out in the sun and impatiently wait. If the cocoon's inhabitant jumps by hitting the lower wall, making the cocoon to bounce off its support, this time it won't work because the impact will be absorbed by the thin, paddy fibrils of the cotton wool. Theoretically, the cocoon shouldn't even move. But no: it takes off from its motionless pad-up and aside, as it did before.

I measure the broad jump: 42 mm, i. e. as before. The insect must have been hitting not the bottom, but the top part of the cocoon-at any rate, it must have been doing something that caused the capsule to move.

Frankly speaking, it is as I write these notes that I feel agitation; back then, in 1981, I found nothing supernatural in the jumps of my prisoner. This was because I knew that, according to physics, there are and there can be no unsupported movers. Otherwise I would have bred a couple of hundred of those insects-thankfully, they were quite common-and would have studied the phenomenon thoroughly.

Now let us fantasize a little: what if the batiplectes wanted to leave the Earth? An adult, winged insect would have no luck-our atmosphere is quite rarefied at the top, wings are no match for it. A larva in a cocoon is an entirely different matter. It could, in theory, after lifting its capsule 5 cm in a jump, take it up even further while in the air, then again and again...

And if the cocoon were airtight-I mean the air reserve for the pilot's breathing-then the device would be able to leave the atmosphere and would have no obstacles to a limitless build-up of speed. Such is the alluring, incredible value of unsupported movers, declared, alas, a product of empty fantasy. But even if you are no physicist, you still have a hard time imagining what a tiny larva does in there if its vessel soars 5 cm high. It simply can't be-and yet it jumps!

Physicists say that this is "beyond science" as it "contradicts the laws of nature." The only problem is that the *Batiplectes anurus* doesn't know it. The physicists' ban must also have been unknown to the leading, experienced biologists who honestly wrote the following on page 26 of the academic *Register of Insects of European USSR* (vol. III, pt. 3): "the cocoon jumps up as a result of abrupt movements of the larva inside the cocoon." In a word, it is a working-and tested-example of a safe, unsupported mover. I am giving it to you, my reader: invent, design, build, and Godspeed! But hurry!

Massive chemical warfare has been waged against the alfalfa pest snout-beetle (phitonomus). Humanity may actually win it. But the price may be too great: with the destruction of the *Phitonomus varnabilis* beetle, our planet's fauna may also lose the ichneumon *Batiplectes anurus* as it parasitizes

only this kind of weevil and cannot survive without it.

Meanwhile, any proposals on using biological weapons against the pest-such as our very ichneumon and other insect predators are completely rejected by the bosses of Russian agriculture and agricultural science. I have been fighting them on this for years, but so far with little success.

However, one could understand those in charge too-how can one stop expensive chemical factories? And why do agrarian scientists care about some unsupported mover that doesn't allow alfalfa to be treated with poison? Hurry up, biologists, engineers, physicists! For if Chemistry wins, this Mystery-and with, a host of other Mysteries related to it-will leave people for ever. Without insects, people won't invent it themselves. Please trust me, an entomologist with 60-year experience.

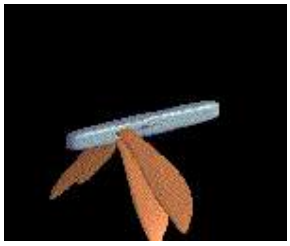

At the end of my first book, *A Million Riddles*, published in Novosibirsk in 1968, there is a drawing that I am reproducing again: a man is flying over Novosibirsk's Academic City. He is flying a device based on a huge pair of insect wings.

At the time I dreamed of inventing such a machine. Strangely, the dream came true precisely because of my friendship with insects-yet not by blindly copying the most noticeable parts-for example wings that only make me smile now-but through careful study of living Nature.

Nothing would have been possible without my six-legged friends. No one would be able to do without them either. Thus safeguard their world, the ancient, wonderful world of Insect, for it is an infinite, unique treasure of Nature's mysteries! I beg you all, take care of it!

FROM THE NOTEBOOK OF A NATURALIST

Artificial honeycomb.

Take a dozen and a half papier-machet supermarket egg cases (30-egg variety), tie them up or glue them together (one on top of another) in such a way as to join the "teeth" to one another, not to the hollow spots.

You will have large cells, similar to multi-cellular combs of a certain "paper" wasp, except many times larger. Fix the whole set (it can be enclosed in a case) over the head of a person sitting in a chair, with the bottom "comb" is 10-20 cm above the head.

Leave the person there for 10-15 min. The "unnatural", unusual transformation of the spatial shape formed by the set can be picked up even by the palm of a hand.

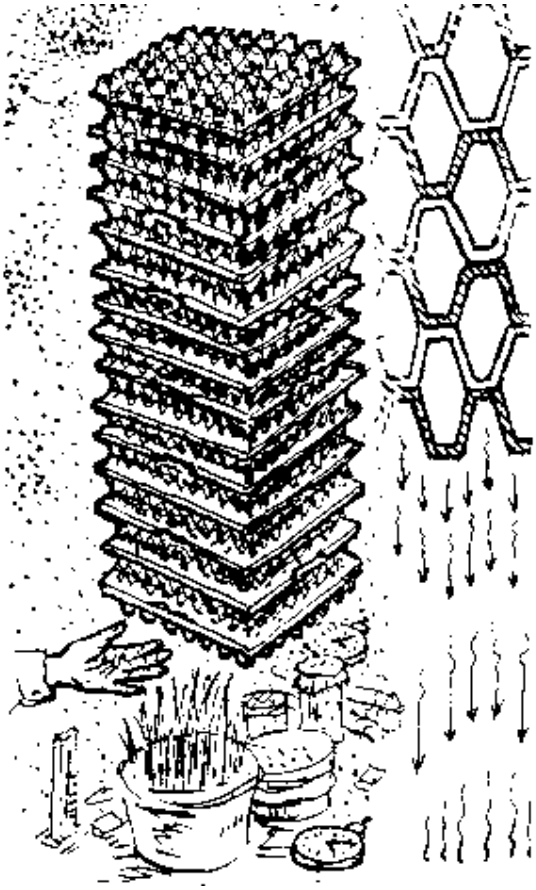

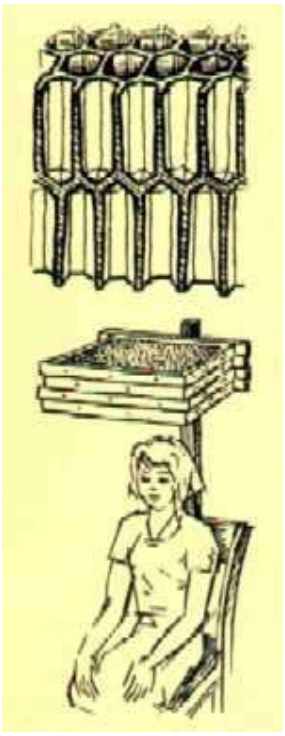

Experiment with couching seeds, or breeding microorganisms and insects under a "macrocomb" and compare the results with those of identical experiments conducted at least 2 m away from the comb. Repeat each pair of experiments several times.

"Iron comb". in a similar way, test the impact of common kitchen shredders piled up one on top of another, with their wire-edges down, small-hole shredders at the bottom, large-hole ones at the top.

Paper emanators of the CSE.

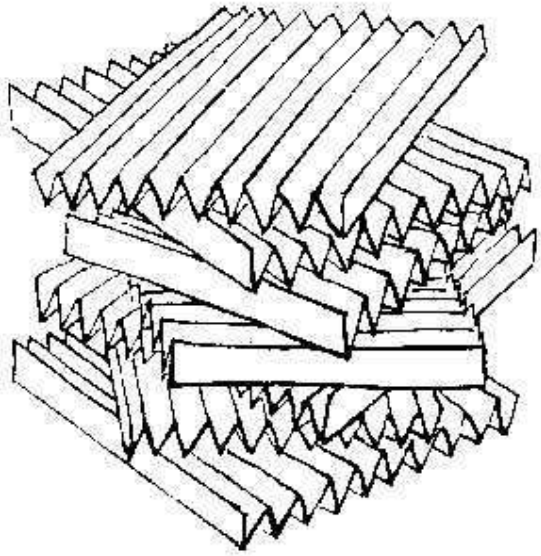

Cut apart-longways-5 sheets of office paper and fold each of them accordion-like so as to get 10 edges and 20 surfaces. Squeeze the accordions to make them square and glue them on top of one another, turning each horizontally 30 degrees clockwise against the bottom one.

Glue together, preferably out of dark paper, a conical, multi-layered "flower" with a few dozen petals; fluff up the petals.

Test the emanators with by putting your palmon above the "flower" and underneath the suspended "accordion". Place them above the head of the sitting person, marking his sensations.

Foam plastic. We are used to the fact that this excellent thermal insulator "reflects" the warmth of the hand even at a distance. But even if you cover it with dark paper, cardboard, or a tin plate, it would still do the same. This happens due to the work of multiple vesicular caverns of the material that produce the CSE.

Foam rubber. It is widely known that a person used to sleeping on, say, a cotton wool mattress doesn't sleep well at first on a rubber foam one, or else is unable to sleep at all. This is a typical manifestation of the CSE. Later on, the organism adapts itself to this new bed.

"Mushroom CSE". A hunter once told me that he warms up his hands in winter on bracket-fungi. Let us recall that the lower horizontal part of this tree fungus is full of fine comb-tubes through which spores fall out in summer. What the hunter felt was not warm but a typical CSE.

Moving "combs".

Make a wooden whipping top and drill several through caverns on its sides, pencil-width in diameter or a bit wider. Their CSE significantly increases if the top is rotated; this is easily perceived by the palm.

This is due to the fact that the caverns must be numerically multiplying in space.

"Flower CSE". An "unnatural" position of such a seemingly common and pleasant object as a living flower can also change its properties. Put a bunch of several dozen bell-shaped flowers (tulips, narcissuses, lilies, bell-flowers) upside down above the head of a sitting person. To bar the impact of odors, put the flower bunch in a plastic bag. Write to me about the results.

Wind-fallen trees. One of my test subjects, a geographer, said to me after experiencing the effect of one of my "grids" that he had once had a similar sensation many years before, when he was passing a wind-fallen section of a forest. His head, ears, mouth, and the entire body felt something particularly unpleasant-the same thing he felt under my grid. This means that the abruptly disrupted shape of the normal multi-cavernous space of the forest for some time emanated waves unpleasant for humans.

Before the rain. Place a shower nozzle on a tap and run cold water. Slowly move your hand toward the drops coming from the sides: most people feel "warmth". In reality, this is the CSE reinforced by the movement of ever new elements of the "multi-layered" grid-water drops and gaps between them. After practicing in the bathroom or kitchen, pick up an even stronger CSE from fountains and waterfalls. Even when the atmospheric pressure is high, the shroud of a distant rain creates a powerful CSE field that has its impact on a large area. Have you ever felt sleepy before the rain even in enclosed premises? The CSE cannot be screened.

"The CSE of a book".

Take a thick, preferably well-read book and place it upright on the edge of a desk with its back facing the direction of the sun (e.g. facing north at night).

Open the book and fluff up its pages as evenly as possible. In a few minutes (the CSE does not appear immediately, as it doesn't disappear immediately ether), pick up with your palm, tongue, or back of your head some of the sensations mentioned in this chapter.

This "tail", after some practice, can be picked up at a 2-3 meters' distance. It is also easy to verify that the "book CSE" is also non-screenable-ask someone to stand between the hadn and the book.

"A large cone" with an artificial comb filling and three magnets at the back.

Two cones of this sort, positioned against each other taking into account the position of the sun, were in the morning of April 23, 1991, thrown apart and disfigured. One had been placed in Isilkul, the other near Novosibirsk (the second one was unfolded and pressed into the wall of an underground hiding place; its magnets disappeared).

At the same moment, residents of an Omsk apartment experienced a series of strangest "poltergeists" (see *Vechernii Omsk* for April 26 and Omsk and Moscow TV broadcasts). Because of this coincidence, on August 5, 1991, the same paper called the device in the picture "a Grebennikov's

hyperboloid".

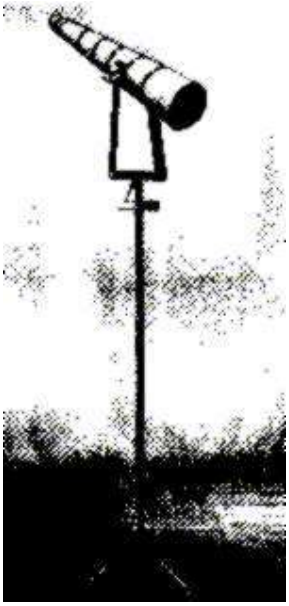

Actually, one of the "beams" of the upright electronic waves between the two structures may have been formed precisely there, on the Irtysh embankment in Omsk.

"A medium cone".

Tightly insert a dozen plastic household funnels into each other and fix the structure on any support with the nozzles turned toward the sun. Cover the bell end of the top funnel with a net or light blue cloth (so that the tested subjects not anticipate heat).

"A small cone". Tightly roll up two unusable rolls of film, tied them up with string or thread and make a bell-shaped cavity in the middle of the top roll. CSE emanations can be easily picked up by the palm, particularly in a counter-solar position. You will get interesting sensations if you press this "microcone" to your forehead.

"Perpetuum mobile".

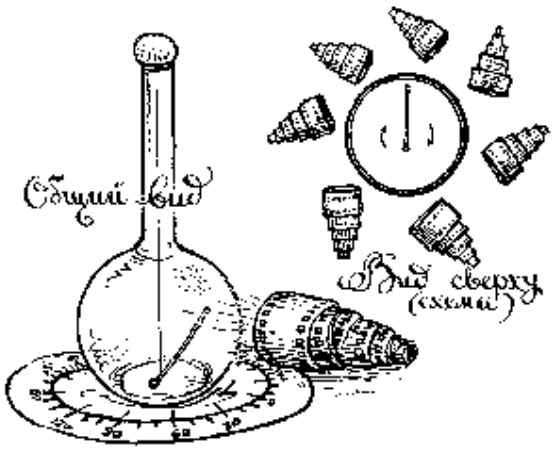

I surrounded my above described device [for registering CSE emanations; a straw indicator suspended on a cobweb thread] with seven funnel-shaped rolls of film [see above].

Slowly leaving the zone of impact of one roll, the straw would enter the power field of another, then the third, and so on...

This experiment is most successful in a sound-insulated chamber, away from wires, pipes, sources of heat, cold, and bright light. There is no miracle here: matter is eternal in its endless movement.

A solar ether- and beam radiator.

This intricate name was devised by the Leipzig professor Otto Kornschelt who discovered the CSE over 100 years ago and produced devices for its practical application in medicine, agriculture, and technology. Rhythmic caverns were formed in them by cooper chains.

The devices were positioned with their backsides facing the sun. It is indeed true that new inventions are simply well-forgotten old ones. The sensations described by Kornschelt are identical to the ones I experienced in my own independent work.

I learned about Korschelt's experiments very recently from M. Platten's *New Medical Technique*,

vol. III, St. Petersburg, 1886, where the following drawing of the device is reproduced.

"The sieve CSE". In the old days, in several areas headaches and concussion symptoms were treated with an ordinary flour sieve that was held above the head of the patient, net up. Alternatively, the patient squeezed the rim between the teeth, with the net in front of the face. The sieve material is unimportant. The device works better if the patient faces the sun (north at midnight). This type of CSE is also perceivable by healthy people.

The CSE and the planets. The planets of our Solar system are situated at certain distances from the sun. The Ticius-Bodet formula for the distance is this: 4 is added to the numbers 3, 6, 12, 36, etc (a geometrical progression), and the resulting number is divided by 10. The cause for this regularity is unknown. The empty spot in this progression (between Mars and Jupiter) is occupied by asteroids. The Kemerovo physicist V. Iu. Kaznev thinks that the regularity is determined by the CSE generated by the sun: the matter of planets was grouped in the areas of the sun's field force concentration.

The CSE in daily life. Perceivable waves of matter are emanated by piles of pipes, some caves, underground tunnels, tree crowns; the shape of premises is also significant (round, cornered, cupolaed). The wall and furniture material also emanates a CSE of certain parameters.

"Micro-CSE". The CSE effect may be manifested not just in galactic or household scales, but also in micro-world, in substances whose molecules have caverns of certain shapes. For example, in naphthalene. I filled a one-liter jar with it, sealed it, and suspended it from the ceiling. People beneath it felt with their palms a whole system of power field "clots". (more son if the receptacle was suspended above the top of the head). Activated charcoal is also a multi-cavernous structure. Hold 2-3 tablets of such charcoal in your fingers as demonstrated in the picture and for a few minutes move your hands slightly up and down, or parting and joining them. Write to me about the results.

Tefelin.

I have so far isolated 4 CSE emanators beneficial for humans: bee honeycombs, a grid of joined hands (more about it in the next chapter), a sieve, a phylactery otherwise known as tefelin.

What is it? An old device: a tightly sown leather cube attached to a leather platform with two bands. Inside the cube there are four strips of parchment-tightly rolled, bleached, soft kidskin with Talmudic inscriptions. A worshippers attached the device to his forehead, with the axes of parchment rolls perpendicular to the forehead and their outer ends facing East. It turns out, the inscriptions were unimportant; what matters is the material, shape, and dimensions.

Made of different materials, the device only causes unpleasant sensations, while a leather tefelin

produces a beneficial physiological effect-besides the shape and other factors, the microstructure of the material must have a part in it too.

Thot's Scepter.

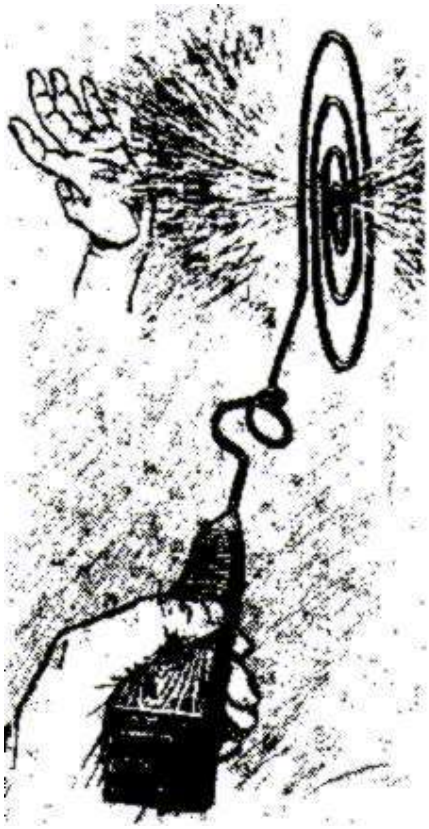

The ancient Egyptian deity Thoth is a god of science, sorcery, and an "accountant" of the dead's earthly deeds. This is the design of his staff: 2- or 3mm copper wire is twisted at the end in the shape of a flat spiral, with 3-4 coils, each 10 cm in diameter'; closer to the handle there are 2 coils of transverse, 3-dimensional spiral, each 5 cm in diameter.

The wire is inserted in the 16-cm-long square-sectioned handle of dense wood, 4 cm thick at base and 1.5 cm thick at its end; the entire staff with the wire is 41 cm long. The narrow end of the handle has 13 deep accordion-shaped cuts.

The staff works even without the wire (albeit not as strongly); the wire is thin and could be of any material but works best if thickly insulated-two layers increases its effect.

If you hold the staff as demonstrated in the picture, the total radiation emanating from the center of the large spiral, perpendicular to its surface, are very well-perceivable by the human palm on both sides.

I never found out for what purpose ancient Egyptians used this "double-beam" emanator.

The Pyramid of Cheops.

Make a pyramid of 3-4 layers of thick, porous wrapping paper: 202x20 cm square base, ascending edges 19cm each. Glue it only at the edges, the tighter the better, but in a thin line.

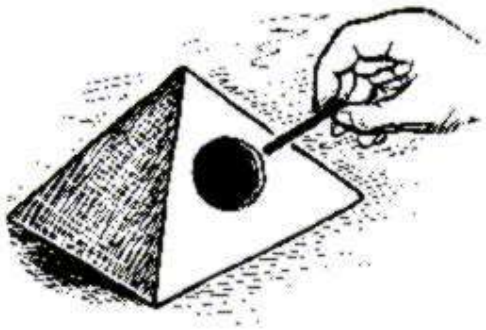

Make a 5-6 cm hole in the middle of one of the side facets. Hold a 10 cm-long piece of drawing coal in your fingers, or simply a pencil, and insert this indicator into the hole, slanting the other end toward the bottom of the pyramid. "Stir" the space inside the pyramid with the indicator, take it out, then repeat the procedure about 30 times.

You will soon pick up an active zone-a "clot"-where the Egyptians had their tombs. Another active zone, above the top of the pyramid, is also well-perceived by the indicator if you drag its end over he top. After some practice, the "clot" and the "torch" are well-felt by the finger inserted into he pyramid, or a palm moved above it.

The pyramid effect that generated over the centuries many scary, mysterious stories is one of the CSE manifestations.

The pyramid skeleton.

Similar interesting qualities are displayed by pyramids of the same dimensions but only skeletal,

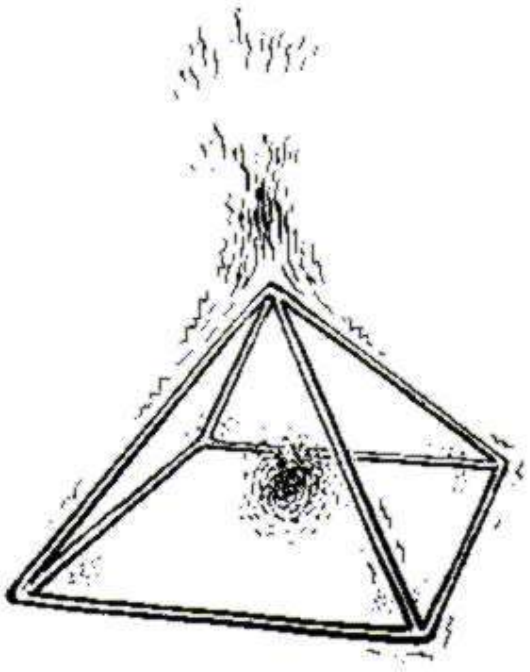

without facets-a skeleton glued together of 8 smooth, firm straws. Here we get the effect of the total CSE of the straws with their complex capillary structure and the effect of the entire cavern. Such pyramids can also be made in other sizes, with a proportional increase in the length of the edges.

Hold such a pyramid above the head of your friend, bottom down, for about 5 min, then bottom up. Conduct additional experiments with insects (bumblebees, developing caterpillars, etc.), house plants, and perishable foods by placing the latter within the pyramid, above and underneath it (always checking your experiments by identical ones but without the CSE effect). And you will see that ancient Egyptians had their reason to build pyramids...

Telekinesis.

This is the name for a contactless movement of light objects of which the so-called gifted people are capable-i. e. moving a match box on a table without touching it, holding a tennis ball in the air...

I submit that everyone has this ability. Suspend the described skeletal pyramid by its top from the ceiling on a thin, artificial thread, or better still on a long shred of elastic torn from a stocking. Choose a spot with the lowest convection (air circulation).

In a few hours, when the pyramid stops rotating, from a 2-meter distance point at it a "tube" made up of two hands (see picture). In a few minutes (do not lose your "target"), the pyramid will start rotating clockwise under the pressure of this beam of CSE energy. Stop the rotation by moving the "tube" to the right side of the skeleton-it will start rotating counter-clockwise.

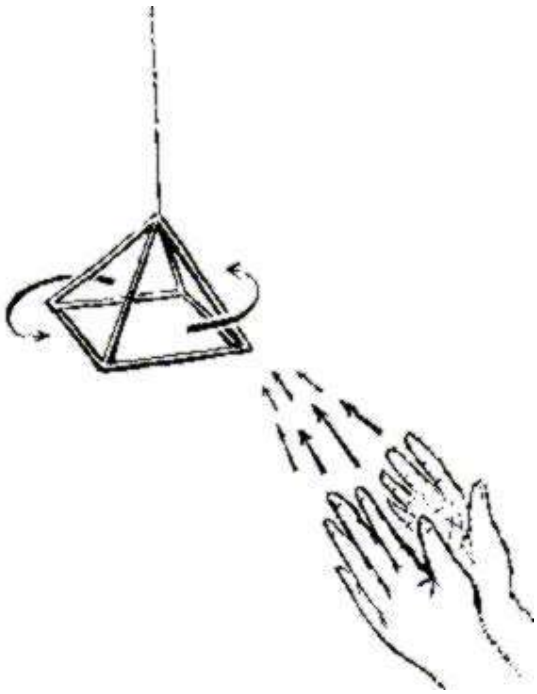

Conduct experiments of various duration, after various time intervals and at various distance. You will see that telekinesis is no miracle, but only one of the manifestations of the Will of Matter that is available to a chosen few but to everyone. The thing is that the palm is also a multi-cavernous

structure that clearly repels the indicator of the straw-cobweb device described in this chapter. By using it and the skeletal pyramid, you can practice and develop your "telekinetic" abilities, significantly increasing them.

"The CSE of cereals".

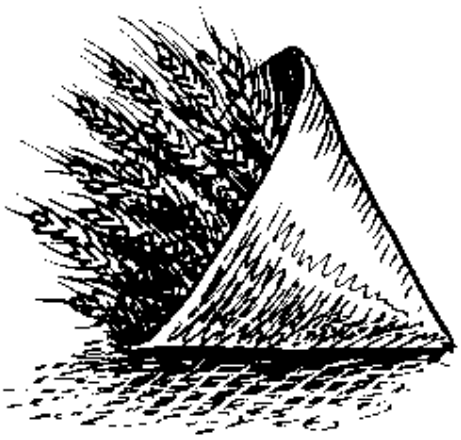

Fasten a bunch of 30-40 ripe wheat ears, better with short stems, inside a low cone of dark paper-as in the picture.

Hand-perceivable emanations repel the straw indicator of the same device through any screens-even sharper than some honeycombs.

This effect is produced by multiple wedge-shaped sinuses between ear scales that are directed at an acute angle toward the bottom of the ear.

Haymaking with "miracles".

In my youth, I was shown the following: a fragment of a cut stem, the length of a short pencil, was placed on the blade of a scythe, next to its blunt edge; another stem fragment of the same length, placed on the blade in the same manner but at some distance, was pushed by the hand to the first one.

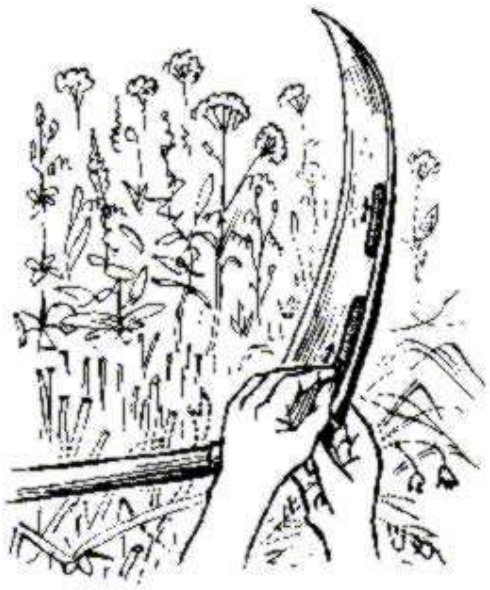

At about 8cm, the first stem got moving, "ran away" from the second stem along the rim. Th experiment wasn't always successful; it usually occurred right after the cutting a large amount of grass from the same spot; I forgot some elements or conditions of the experiment.

I think the following factors were at work here: an abrupt change of the total CSE field on the "deformed" meadow (let us remember the windfall case), the grid of the reaper's fingers, the multi-cavernous properties of the stem itself, and perhaps its position against the morning sun. Static electricity is excluded as everything at that hour is wet.

Identified Flying Objects. A long time ago, in a remote Caucasus village, I was surprised that people walk around the mountains at night, through dense forests. They all had lit cigarettes in their mouths, are all waving their hands, and their cigarette lights for a second disappear behind their

bodies.... It turned out those weren't cigarettes, but local fireflies, *Luceola mingredica*; their light twinkle in this manner. Meanwhile, UFO reports and letters from my readers tell of dark flying saucers that turn out either a flock of birds or a compact swarm of insects . I myself saw in Siberia not just "columns" of insects but also "balls" , 3 or 4 meters in diameter: in one case those were some mosquito-like fliers, in another, winged ants of the *Mirmica* genus. From afar this swarm could by taken by an ignorant person for a huge, round plasmoid.

A detailed description of the CSE effect may be found in my book *Mysteries of the World of Insects* (Novosibirsk, 1990), in the journals *Sibirskii vestnik selskokhoziastvennoi nauki*, no.3, 1984, and *Pchlovodstvo*, no. 12, 1984. The physical nature of CSE is described in *Non-periodic Galloping Phenomena in the Environment*, vol. III (Tomsk, 1988). All in all I have published over three dozen articles on the CSE.

As promised, I will describe the rest in my next book. I will call it as I called this chapter: *Flight*.

NOTE from Jerry Decker : Victor S. Grebennikov died at the age of 74 in April 2001 as reported to KeelyNet in two phone calls to his surviving son Sergei.

This all came about from an email from a friend in Russia by the name of Youlain who sent in the URL some two years ago. When I saw the pictures of the platform, especially the one hovering over the ground I thought it was a hoax, but I couldn't stop thinking about it so translated the webpage in sections beginning with the technical descriptions.

As correlations began to fall into place, I hesitated reporting it because his writing indicated psychogenic effects associated with these structures, meaning it could be hallucinations, delusions or daydreams perpetrated with jumping into the air while on the platform as what the TMers (Transcendental Meditation) devotees claim as 'flight'.

However, other aspects of his claims led me to think he really had discovered something. With the idea of getting a copy of the book, I ended up sending some $200 to Yuri with the instructions being to take out the cost of the book and shipping, give the rest to the Professor. I did receive the book (Youlain bought his for $7.00 US but he lives in Russia.)

Meanwhile, I had made a 'secret' page on KeelyNet whose URL I mailed out to long time trusted confidants to see what they thought about it since I valued their insights, opinions and knowledge, asking them to keep it on the QT until I heard from the professor direct, if possible. From their responses, new information was added.

However, one of these long time confidants who over the years since the BBS days, shared much useful information, had now become infatuated with public attention and so posted the URL and claimed I was 'hiding' information in order to further his newfound career of public speaker and author. Very sad to see this but ego just took him over, so he's gone.

In the meantime, Yuri had kindly provided me with the Professors mailing address and I immediately wrote to him in Russian, sending at least 5 packets over the next year of correlated information to him and all translated into Russian.

In all that time I received only one letter from the Professor which stated he had suffered a stroke, that he had no degree and had learned what he knew from his experiences in 'gulags' (Russian prison of war) and was paralyzed on one side, having to type this letter

with one finger. At the time of his response, he wrote he had received 3 of my letters, indicating in the letter that his son had withheld the ones I sent in February until May before he actually saw them.

I asked his son in the phone call why they had not responded with but one letter in the past 2 years and he said the entire family had been ill, especially his father. Early in 2001 I asked Yuri if I flew over there and pre-arranged an interview with Professor Grebennikov, would he serve as translator and he agreed, that was roughly in February. It was only when I called Sergei in July, after the June KeelyNet conference, that I learned Professor Grebennikov was deceased.

The Professor had written that he would like me to republish his book in English and so I was trying to get him to sign a copyright release to pursue that project. After his death, the rights would have gone to Sergei, so I asked him if he would be willing to sign such a release for a percentage of book sales and he didn't seem to comprehend the matter over two phone calls and a detailed letter with release form. The calls were made in Russian as translated by my Russian translator Helena. She also wrote and sent the letter with copyright release to which Sergei has not responded as of December 6th, 2001.

It takes about two to three weeks for a letter to get from Dallas to his village near Novosibirsk and the same to get back. They don't offer UPS, FedX, or any faster means of snail communication and the Professor was not online, relegated to living on $24.00 US per month in his retirement. That is another reason I was considering publishing his book as his percentage would greatly improve his income level, that is irrelevant now.

In the book, of the sections we have in English, he asks only to be recognized by his peers and in the history books as the discoverer of the CSE phenomenon. He has of course refused to reveal the name of the insect and even the genus, it could be a beetle, a butterfly, a bee, a wasp, a locust, a grasshopper, a dung beetle. There are some 1100 species of beetles in Russia.

Professor Grebennikov was a great ecologist as you can tell by his protective attitude toward the environment. He was afraid if the name of the insect were revealed, people would rush to the area and kill off all of them. I wrote him in two separate letters that it was not necessary to know the insect name or genus.

In order to allow verification, all we needed were TWO of the insect covers which could be analyzed under an electron microscope to determine geometry and dimensions, from that point, it should be possible to duplicate it artificially and the insect would be forever safe.

I offered the Professor $1,000 US in cash if he could send me two of the covers (I sent money to pay shipping) AND they exhibited the gravity repelling characteristic he had seen. He indicates the effect was not magnetic, electrostatic or due to stray air currents.

He never responded which his son claims was due to illness.

At any rate, the entire book is currently being translated and my current plans are to extract technical information and compile it with other information which correlates and supports what the Professor claims.

This will be sold through KeelyNet to recover my personal expenditures and to support KeelyNet along with further research, donations are greatly appreciated.

There is a lot of weirdness going on with this. I asked Sergei if he could provide a couple of

the covers, he said he didn't know what they were or where they came from. I then asked him what happened to his fathers flying platform, he said (in a hesitant and halting fashion) his father had hidden it and he didn't know the location.

We have since read an email from a Russian scientist who visited Professor Grebennikov in the hospital and claims he was told firsthand that he had smashed the platform to pieces. Sergei also said many people had been contacting he and his father since the publication of the book some 6-7 years ago, with everyone wanting the secret, but his father had never revealed it.

Numerous posts have been made to the KeelyNet Interact discussion list on cavities, nanostructures, arrays, chitin, dielectrics and related subjects for those who are interested in this claim.

Additional information has been posted in the Chaos file, the Time Dilation file and in dual presentations (Decker & Davidson) made at the June KeelyNet 2001 conference in Dallas (available on videotape). See also Dan Davidsons' experiments with shape power and Joe Parrs original discovery of energy bubbles in pyramidal structures.

Many are involved in this and have widely varying views. At this time, we have no verfiable experimental evidence of the late Professor Grebennikovs wide-ranging and earth-shaking claims. As you can see, they span all branches of science, philosophy and theosophy, shedding quite new and novel views on the nature of gravity, time and paranormal experiences.

We will continue to correlate information and try to pin down experiments that can verify various aspects of his claims. He has certainly provided many experiments that seem to rely mostly on human perceptions.

We need to find ways to detect these emanations with instrumentation, exactly the same problem we have with Aether/ZPE, we need a kind of attachment for a FLUKE meter and a scope to be able to qualify and QUANTIFY these kinds of energies.

I would like to add one further comment, please do not confuse time dilation with time travel. They are not remotely the same. Time dilation simply slows down the local temporal field of an object, kind of like a 'stasis' field on Star Trek so that anything outside this local area moves at the normal speed, while anything inside this field ages at a slower rate. Refer to the Time Dilation file.

The Professors' friend and associate is Yuri N. Cherednichenko.

If you have comments, ideas or information relevant to the above, please post it to the KeelyNet discussion list or send it to Jerry Decker for posting to the list, thanks!

Additional fascinating information relating to weight loss in sleepwalkers was provided by Slavek Krapelka and with full details posted at his website at;

Amazing Sleepwalking Experiments

Date	Time (Aproximate to 10 minutes, more or less)	Weighted (Aproximate to 500g, more or less)	Normal Weight	Type of Scale	Report Number
03/08/00	23h 40m	**43.248Kg**	*41.600Kg*	Electronic	*1-8-00*
12/09/00	02h 20m	**43.876Kg**	*41.600Kg*	Electronic	*1-9-00*
18/09/00	00h 25m	**5 Kg**	*41.600Kg*	Mechanical	*2-9-00*
21/09/00	00h 50m	**7.200Kg**	*41.600Kg*	Mechanical	*3-9-00*
22/09/00	04h 10m	**4.700Kg**	*41.600Kg*	Mechanical	*4-9-00*
27/09/00	00h 20m	**5.300Kg**	*41.600Kg*	Mechanical	*5-9-00*
28/09/00	01h 35m	**5.600Kg**	*41.600Kg*	Mechanical	*6-9-00*
"/"/"	" ""	**78.800Kg**	*41.600Kg*	Mechanical	*6-9-00*
11/10/00	22h 40m	**41.500kg**	*42Kg*	Mechanical	*1-10-00*
15/10/00	02h 20m	**6.100Kg**	*42Kg*	Mechanical	*2-10-00*
16/10/00	03h10m	**5.200Kg**	*42Kg*	Mechanical	*3-10-00*
17/10/00	00h 25m	**5.900Kg**	*42Kg*	Mechanical	*4-10-00*
18/10/00	05h 10m	**3.800Kg**	*42Kg*	Mechanical	*5-10-00*
23/10/00	04h 45m	**3.600Kg**	*42Kg*	Mechanical	*6-10-00*
27/10/00	01h 40m	**4.300Kg**	*42Kg*	Mechanical	*7-10-00*
28/10/00	02h 50m	**5.300Kg**	*42Kg*	Mechanical	*8-10-00*
09/11/00	01h 40m	**3.200Kg**	*42Kg*	Mechanical	*1-11-00*
10/11/00	03h 10m	**00000Kg**	*42Kg*	Mechanical	*2-11-00*
18/11/00	00h 35m	**00000Kg**	*42Kg*	Mechanical	*3-11-00*
23/11/00	04h 40m	**4.300Kg**	*42Kg*	Mechanical	*4-11-00*
27/11/00	00h 10m	**4.900Kg**	*42Kg*	Mechanical	*5-11-00*
28/11/00	01h 40m	**4.200Kg**	*42Kg*	Mechanical	*6-11-00*

Again, we want to publicly acknowledge the efforts of Slavek Krapelka and Ren Berghuis for spending the $300.00 to get the Chapter 5 file translated and passing it on.

If you would like to contribute something to help them recover their costs, please send an email to Ren Berghuis for information on how to do so. THANKS!!!

So FEW people actually contribute with anything more than comments or looking for free material researched or validated by others.

There is more information which will be added to this page or linked in future.

Additional information from our translator that might be of use;

> **"The only specific insect I've seen mentioned thus far of possibly interest was the one I identified in the portion of the 'Flight' chapter you saw, the bee, 'Halictus quadricinctus'. It seems that particular subspecies is native to Siberia, although most of the other references sound fairly generic."**

A picture of the mudnest and the Halictus Quadricinctus photos I found on the web;

1. **Trigona (Heterotrigona) lutea Bingham**
2. **Trigona (Heterotrigona) laevicpeps Smith**
3. **(Micrapis) florea Fabricius**
4. **Trigona (Heterotrigona) vidua Lepeletier**
5. **Ctenoplectectra davidi Vachal**
6. **Apis (Megapis) laboriosa Smith**

7. Eucera pekingensis Yasumatsu
8. Tetralonia chinensis Smith
9. Habrophotula nigripes Wu
10. (pupae)
11. (larvae)
12. Xylocopa (Biluna) tranquabarorum (Swederus)
13. Halictus camellia Wu
14. * Halictus quadricinctus Fabricius *****
15. ??
16. Osmia excavata Alfken

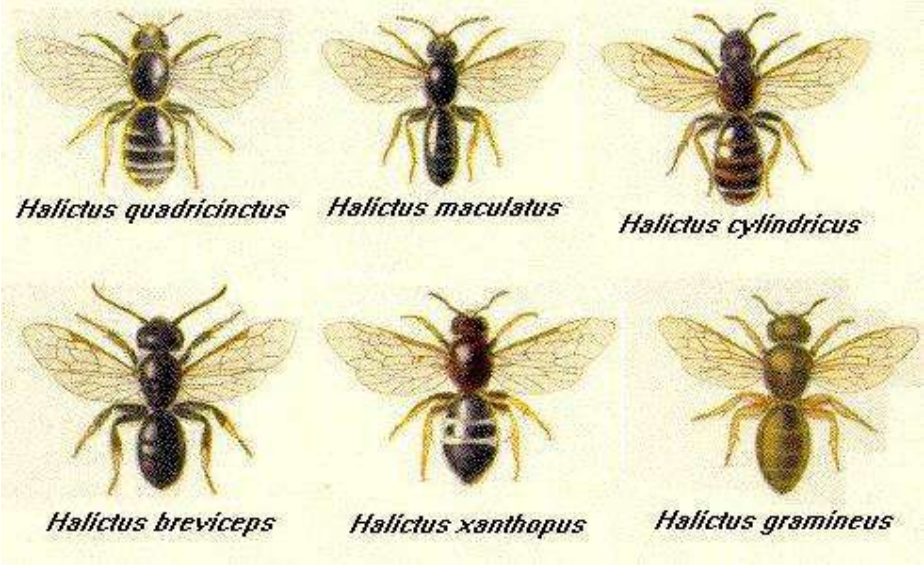

Terminix® Pest Control $50 Off Terminix Pest Control. Call today! 855-860-9137 www.TerminixPestControlOffers.com

Buy Neodymium Magnets Top Quality Neodymium Magnets, Low Prices, Speedy Same Day Shipping www.amazingmagnets.co

Eco Friendly Pest Control Free Inspection & Estimates. Safe Non-Toxic Extermination. www.PointePestControl.com

AdChoices

If you found this file useful or interesting, please consider a donation or a purchase to help keep KeelyNet online and providing free information.

MexiStim, crock, edkuniversity, quantum, Einstein, Clem, Aharanov, Bohm, virtual, state, free energy, gravity, health, electronic, space, time, dimension, keely, tesla, Decker, electric, gas, chemistry, chemical, aether, zpe, zero point, moray, hendershot, bearden, energy, free energy, lee, perrault, overunity, power, bedini, water, schauberger, baumgartner, sweet, vortex, science, physics, antigravity, sound, acoustics, electricity, motor, vacuum, medicine, oil, petroleum, hydrogen, ecology, biology, Keelynet, levitation, geometry, hubbard, physics, electronics, alternative, paranormal, metal, organic, fiber, reich, weather, rain, media, rife, gray, interdimensional, time travel, new energy, energy, electron, atom, quark, quantum, battery, emf, back emf, lenz, magnet, zpf, puthoff, solar, wind, thermal, thermodynamic, heat, pump, plant, research, invent, invention, inventor, patent, future, past, present, generator, dynamo, faraday, homopolar, disc, kinemassic, unidirectional, direction, fuel, gas, vapor, flying, flight, satellite, rocket, moon, mars, sun, earth, push, einstein, converter, inverter, microscope, signature, radionic, psionic, psychic, telepathic, telepathy, precognition, cognition, reality, galaxy, laser, color, microwave, radio, aura, pyramid, thoth, indian, temple, music, frequency, wave, wavelength, broadcast, superconductor, cooper pair, perpetual, motion, unity, expansion, quartz, vibration, oscillation, sympathetic, cancer, disease, heart, attack, weapon, carbon, alien, clinic, pressure, mechanical, physical, medicine, healing, life, rejuvenation, cell, voltage, current, amperage, watts, coil, cone, biomagnetic, lightning, arc, spark, resonant, resonance, conjugation, phase, ufo, patent, experiment, experimental, virus, bacteria, battery, honeycomb, ffl, rectify, rectification, grebennikov, russia, negative, positive, neutral, weird, air, dilation, chaos, control, parameter, mystery, weightless, invisible, invisibility, veda, vedic, vedas, hollow, vailx, vimana, saucer, angular, momentum, conversion, propulsion, drive, universe, transition, macrosonic, synergetic, tornado, standing, airship, aerial, propeller, thrust, maxwell, field, eternal, turbine, wind, rotating, force, technology, technical, cop, efficiency, transmission, gearbox, experiment, experimenter, circuit, correlation, helical, gasoline, decomposition, fuel cell, hydrogen, oxygen, cold, fusion, inertial, high voltage, repulsive, attractive, theory, dielectric, paramagnetic, diamagnetic, orgone, caduceus, bifilar, cymatic, jenny, manners, delawarr, heironymous, hieronymous, analyzer, molecular, atomic, grid, appliance, wheel, motion, brown, temperature, radiant, monopole, sweet, silvertooth, motional, hooper, flanagan, decker, vacuum, matrix, space-time, heaven, god, heretic, pain, degauss, artificial, intelligence, biology, blaster, colloid, tube, stellar, mutation, bible, purify, purification, holiday, vacation, travel, ticket, flight, airline, car, exotic, novel, unique, dissociation, compression, vector, lost, shift, teleport, ark, covenant, tantalus, tantalusfield, noah, theoretical, anomaly, anomalies, phenomena, rare, earth, neodymium, robotic, conspiracy, electronic, ancient, electrogravitic, gravitic, engine, stirling, thought, emg, eeg, nexus, Tilley

lightwater

Alexander Putney

"Soma is food for the gods." ~ Chàndogya Upanishad

"We have drunk the Soma and become immortal. We have attained the light the gods discovered… One thinks to have drunk Soma… Of him… no one ever tastes." ~ Rig Veda

"The man who supplies food hath always [Soma] pressing stones adjusted, a wet Soma filter… he who hath this knowledge wins the luminous spheres." ~ Atharva Veda

What is this ethereal *Soma* that is the subject of so many ancient Vedic hymns? Soma is *electrum*, a special food and beverage additive consisting of gold and silver nanoparticles that are tasteless, invisible, and electroluminescent *~gold nanospheres emit red light, while silver nanospheres emit blue light.* Vedic wisdom clearly identifies the intracellular luminosity of electrum-enriched Soma waters and foods as endowing eternal life, directly defining a 'god' as one who 'discovered' and 'attained the light' by consuming electroluminescent gold and silver nanoparticles!

The partaking of electrum-enriched foods and beverages formed an integral rite of sacred initiation practices at all the ancient pyramids, temples and sacred sites at resonance. Identified in the Bible as *showbread* or *manna bread*, it was not made by a common baker, but by the goldsmith, to preserve the initiate from being burned in the tabernacle.

Maya wisdom prepares initiates at their sacred sites using the golden waters of Tláloc to crystallize and reawaken human consciousness, reflecting the highest wisdom of visitors from the stars as recorded by Maya ancestors in ancient times. Many renewed contacts taken up with individuals on various continents over the last several decades attest to the transdimensional use of lightwater with silver and gold nanoparticles in the ignition of HHO plasma for enhancement of consciousness and longevity through cellular regeneration processes enabling vastly extended lifespans of hundreds of years. The secrets of transdimensional travel have been revealed by extraterrestrial teachers from various confederations of peaceful planetary systems, including advanced applications of standing wave resonance for the resonant atomic transmutation processing of metals for spaceflight vehicles.

Concise explanations were given concerning the magnetic reversal of our entire solar system on December 22, 2012, and provide the timeline of specific intersecting events involving the Galactic Plane crossing, the intense blast wave of the Betelgeuse supernova and the incandescence of a Red Dwarf star at the edge of our solar system. The messages of visitors from the depths of the cosmos resonate clearly with the wisdom offerings of the indigenous Elders of Earth, preparing humanity for ascension in the resonant pulsations of worldwide aurora known as the Red Dawn, when the bleeding sky heralds the emergence of the Fifth World.

lightwater

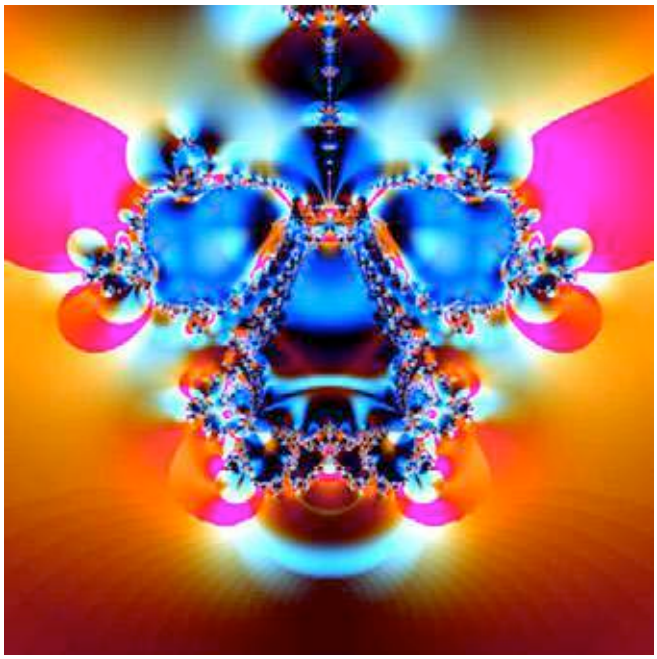

Alexander R. Putney

Human Resonance

www.humanresonance.org
www.resonánciahumana.org

© 2010 Alexander R. Putney

For all of the radiant beings who guide humanity
toward the creation of a lasting peace on Earth,
with her transformation into a heavenly planet
under the purifying red light of the solar twins.

Having no one to influence my outlook,
I display my primordial nature and adopt the style of a youthful prince.
This is due to the only father guru.

I am busy working for others.
Prajna, penetrating all obstacles, has made the prince old and wise, fearing no one.
Dancing in space, clad in clouds, eating the sun and holding the moon,
the stars are my retinue.

The naked child is beautiful and dignified.
The red flower blooms in the sky. It is ironic to see the formless dancer,
dancing to the trumpet without a trumpeter.

At the palace of red ruby, listening to the utterance of the seed syllable,
it is joyful to watch the dance of illusion,
the seductive maidens of phenomena.

The warrior without a sword, riding on a rainbow,
hears the limitless laughter of transcendent joy,
the poisonous snake becomes amrita.

Drinking fire, wearing water,
holding the mace of the wind, breathing earth,
I am the lord of the three worlds.

Excerpt from ‘Enthronement’ by Chögyam Trungpa, January 22, 1973
From ‘The Myth of Freedom and the Way of Meditation’ (2002)

1 Fourth-Density Realms 1 – 44

2 Contacts From Koldas 45 – 66

3 The Plejaren 67 – 124

4 Urandir's Transport 125 – 150

5 Golden Planets 151 – 192

6 Betelgeuse & the Red Dawn 193 – 222

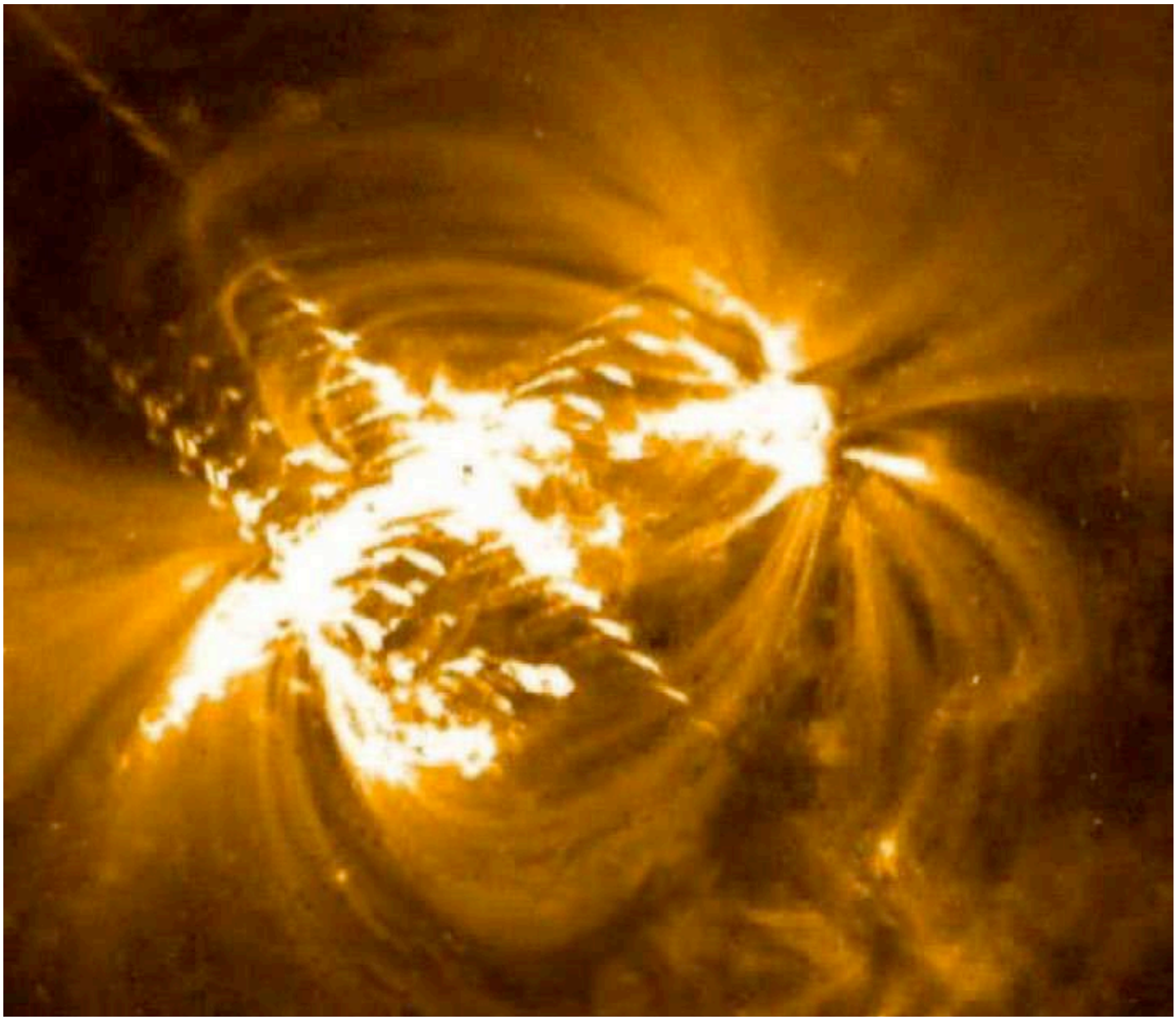

1
Fourth-Density Realms

Fourth-Density Realms

Unusual atmospheric events taking place above the surface of the Earth are unmistakable signs that our planet is rapidly ascending into a new, high-resonance quantum state in synchrony with changes witnessed on the sun. Distinct geometric patterning defining the nonlinear distribution of sunspots is retraced by atmospheric excitations of plasma into the concentric arcs of resonant standing waves within the solar corona. Solar plasma formations during coronal mass ejections display perpendicular rows of luminous plasma plumes (opposite) that are also observed of Earth's noctilucent aurora (above).

Auroral plumes were photographed and videotaped in the high atmosphere above Xiamen, China on July 12, 2010 as uneven rows of vertical plasma beams shone brightly during the night hours.[1] Perhaps the most striking examples of aerial plasma formations have been recorded near ground level in Longview, Texas by motion-activated game-trail cameras on the night of September 9-10, 2009.[2] The auspicious calendar date of this plasma flare event –9/9/9– suggests that heightened Earth resonance and solar activity may be directly linked with synchronized meditation by large masses of human beings, as once achieved by the pyramid-building cultures of the world, whose resonant temple stones still hum today.

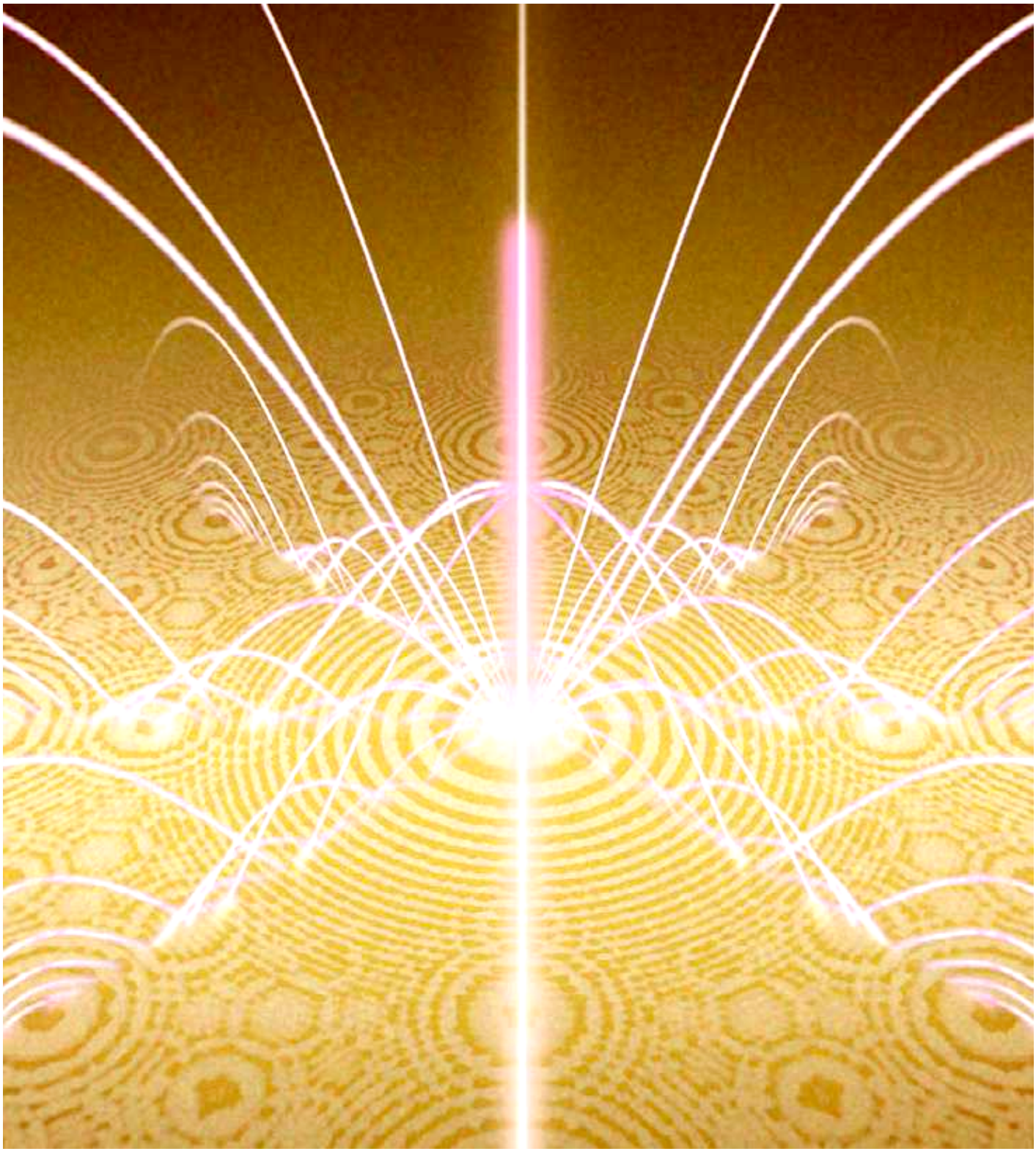

Sacred geometric knowledge of the focal points of Earth resonance remains perfectly preserved in the pyramidal monuments of the world, both in their respective structural configurations and their relative geopositions, encoding the golden proportion as a precise spherical formula [$z_{n+1} = z_n^2$]. All of the world's stone temples and sacred sites find exquisite alignment within this global psychoacoustic resonance network organized by the geometric distribution of nonlinear infrasound standing waves (above).[3] This transcendental quadratic formula has been encoded in the sacred geometric configuration of the Sanskrit mandala –*a square within a circle*– and preserved throughout ancient sacred artworks the world over.

This spherical mandala code lies carefully nested, in perfect order, in the locks of the Buddha's hair and the circular pattern of the radiant aura surrounding his golden head (opposite). The hemispheric design of the topknot bun at the crown chakra displays octopolar symmetry with sets of concentric circles arranged in radial rows of 4, 8 and 16. The extremely long earlobes often seen in representations of the Buddha reflect an odd Sanskrit cultural association with transcendent wisdom and the great attainment of yogis to become transdimensional beings, at one with Creation.

The identification of spiritual attainment with gold has been passed down since time immemorial, and the latest findings of the biophysical sciences provide access to deeper layers of meaning within these ever-present cultural concepts. Gold, like silver, is not reactive with water and so does not break down by oxidation, but maintains a pure state –just as the consciousness of a fully self-aware human being is crystallized and purified to achieve the highest state of perfection attainable.

Sacred mountains are identified by indigenous cultures for the alignment of their peaks with convergence points of infrasound resonance, while great masters of consciousness are known to reside on such sacred peaks. Among the Himalayan spiritual traditions of India and Nepal, the mystical figure Mahavatar Babaji is closely associated with a cavesite retreat within sacred Mt. Kailash. Other poignant examples include the Indian adept Sri Ramana, who practiced a barefoot yogic lifestyle atop sacred Mt. Arunachala thriving on the accumulated spiritual energy for most of his life,

This resonant bioenergetic phenomenon is well cited among ancient wisdom traditions as an attainment of spiritual and physical purity, as the water of the adept's body itself becomes crystallized by the deep delta wave beating that reigns over the enlightened consciousness. Such resonant bodies never desiccate atop sacred mountain peaks, or inside pyramid chambers, but become mummified in the preservative infrasound-enhanced electromagnetic environment as the piezoelectric crystalline water, bones and tissues are continually sterilized by mild electrical currents that neutralize all pathogens.[4] This post-mortem effect was reported of spiritual adept Simeon Toko, who died in Luanda, Angola, yet his lifeless body was observed by respectful masses for many days without any sign of putrefaction.[5]

The three main pyramids that dominate the Giza plateau were created as a symbolic representation of the three belt stars of the Orion constellation, so designed to transduce the diverse ambient energies of both solar and geomagnetic storms into a precisely ordered tri-frequency resonance. Any three acoustic frequencies in Fibonacci ratio generate the full set of nonlinear standing waves that couple energy from Earth's base Schumann Resonance frequencies (near the human heartbeat at rest) into the higher harmonics,[6] which then become audible to the human ear as a deep pulsation –the cosmic Om.

Infrasound standing waves stimulated by 1.45 Hz heartbeat booming within the Great Pyramid ignite the very water vapor surrounding the pyramids in arcs of HHO plasma that is generated as water molecules are torn apart and ionized. Gold and silver nanoparticles were a key component of the high purity water that once rose as vapor through the pyramid's ascending passages, to enhance the ignition process of HHO plasma within the stone chambers and into the surrounding atmosphere. This biocompatible form of gold (thus 'organic') was consumed by all initiates within the pyramids, and reveals the deeper significance of the star constellation name 'Orion' –*which literally means 'gold ion'! Ionized nanoparticles of gold and silver are electroluminescent, illuminating the DNA of all initiates within the pyramids:*

> Through this initiation they will be able to see the luminosity of the Great Spirit. When this spiritual initiation is completed in the house of Hunab K'u in heaven, the spirit of each initiate will be illumined. Then, it will return to Earth to awaken the body and take it to the pyramids. Chichen Itza, Uxmal, K'aba, Etznah, Palenque, all of these sacred Mayan centers have a specific function in every part of the body to awaken the 7 powers contained in it.
>
> Only through the solar initiation can the sleeping body of mankind be awakened. The reincarnated teachers of the new age of Aquarius implore for the sacred human race to awaken, so that in this way it can fulfill its sacred destiny, which is to be the true sons and daughters of the cosmic light. The time of knowledge approaches, the light in the center of the pyramidal house of Hunab K'u will flash like lighting that will pierce through the shadows that envelop the human race. Let us prepare to receive the light of knowledge that comes from Hunab K'u and transcend into the memory of the creator and become beings of eternal luminosity.[7]

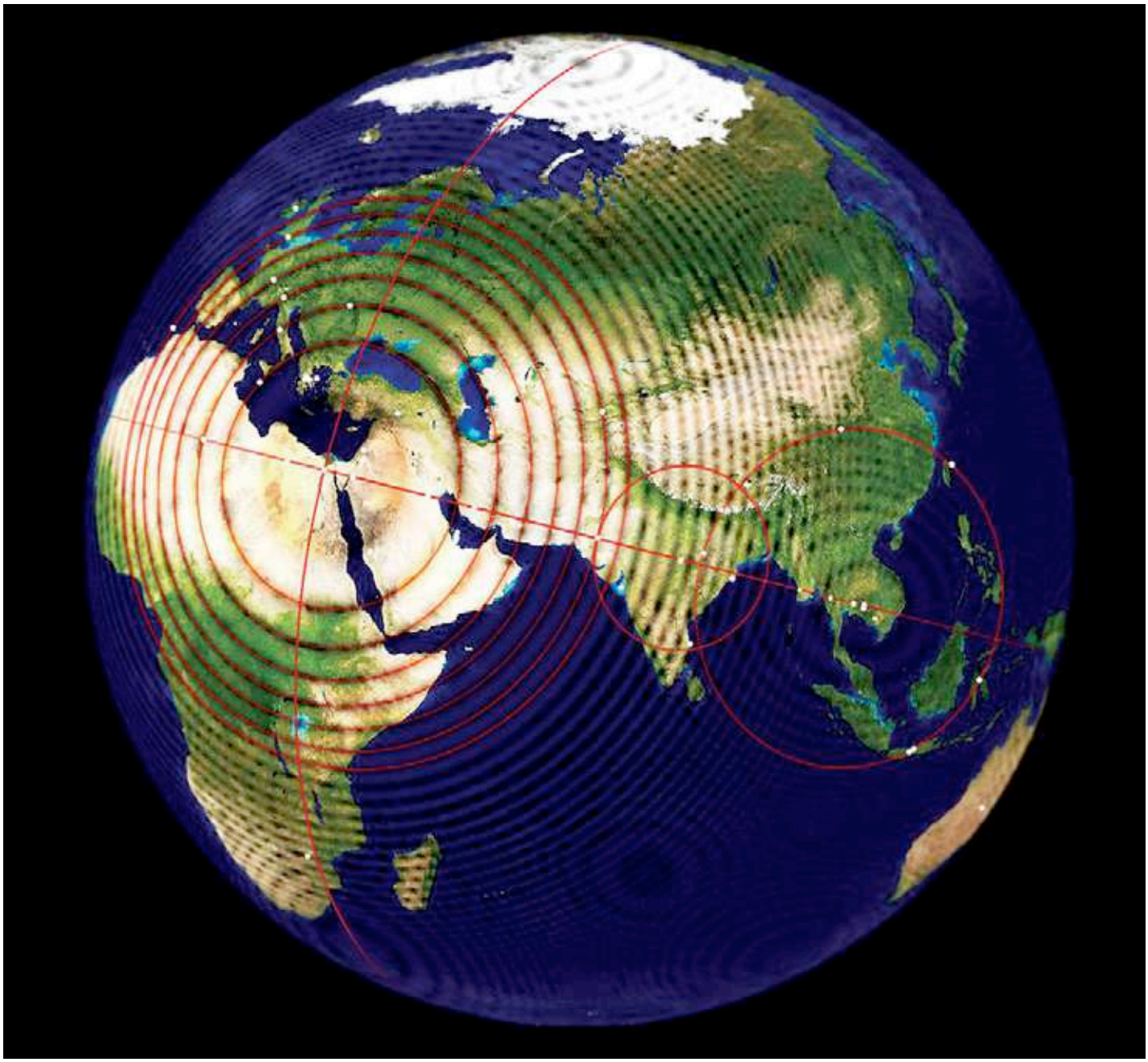

.

The electroluminosity of nano-gold and -silver within the body vastly increases cellular longevity and the lifespans of all initiates accordingly, as well as providing the quintessential biorhythmic environment for meditation, telepathic communication and Astral projection. The vast multitudes of piezoelectric stone temples found throughout the entire world find precise placement within the infrasound distribution pattern expressed by the sacred formula known to mathematicians today as four-dimensional equation [$z_{n+1} = z_n^2$], as a spherical rendering expressed from the apex of the Great Pyramid of Giza, Egypt (above, with major sacred temple sites denoted in white).

The Sanskrit origin of the world's ancient pyramid traditions has been linguistically identified by modern epigrapher Dr. Kurt Schildmann,[8] yet the living culture of the Maya people of Central America remains a most direct modern link to the Vedic knowledge of the deep past, as one of several descendant language forms. The powerful words of the ancient Sanskrit pyramid-builders still resonate within the sacred temple stones today, as a clue to their longstanding and divine purpose that is intimately linked with the conscious Spirit of all the human beings of Earth. The ancient astronomical and mathematical wisdom is preserved in Maya scriptures and oral traditions, *in conscious mastery of galactic temporal cycles:*

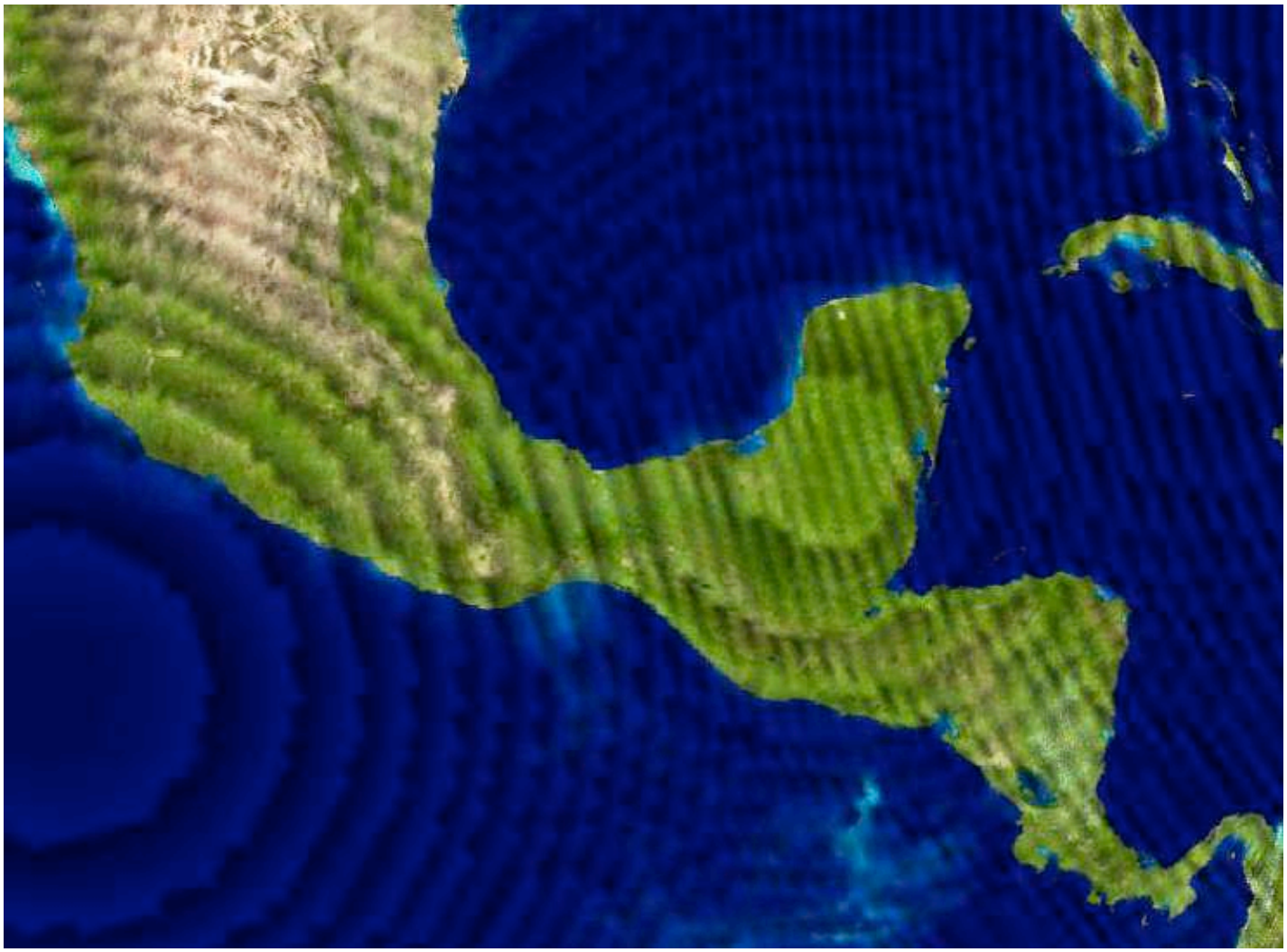

Man does not will when he wars, loves, reaps; it is the rhythms of the great gods, the planets, that act over him and make him do. When he comprehends that by himself he can do nothing, then he can learn to serve the gods; so, he must become conscious of the rhythm of the gods.

The calendar that governs the life of man, the Tonalpohualli, is based on the rites of the planets that turn closest to the Earth: Paynal, Mercury; Quetzalcóatl, Venus; and Huitzilopochtli, Mars...

After 657 Tonalpohualli (468 solar years) the cycles of the minor planets and the cycles of the Sun end together. Tonatiuh, Quetzalcóatl, Huitzilopochtli, and Paynal shine again at the same time in the same form. This is an age, the duration of the life of a culture.

Chalchiuhtlicue, Goddess of Terrestrial Waters, of that which flows, runs, surges, forward and down, arriving always at profounder levels. Chalchiuhtlicue swells the fruits and flowers only so that they may drop.

Chalchiuhtlicue fills the gourd of pulque so that man may forget. Chalchiuhtlicue, current that descends in the course of rivers, current that flows in the course of time, making men's wastes and the implements of war inert and taking them to their inevitable end.

Tláloc, God of Celestial Water, god of the vapor that rises, from the earth warmed by the sun after the rains, god of the mist that ascends from the valleys at dawn, god of the water that returns to its source in the clouds that swim over the highest peaks, god of the humid incense from which rise the copal prayers and the prayers of sacrifice.

Tláloc is the return of vapor that strains to rise, is the return of time that strains to remember… Tláloc, God of the Fight Against the Current, with whose aid the hero battles against the torrent toward his own origin and beginning, towards the wings of his soul, the wings that Tláloc hides in the hero's past.

Quetzalcóatl, the Plumed Serpent, moves between gods and men, because Quetzalcóatl is God who permeates man and is the man that achieves God. The Plumed Serpent is born when that which slithers over the Earth grows wings to be elevated to Heaven. Quetzalcóatl is a superior man, the inner circle of humanity, the link between gods and men. All men are made of earth, air, water, and fire... But in their hearts and in their semen, each man has his own coatl, his own serpent, the energy of Tonatiuh, the power of the sun itself. And in this serpent sleeps consciousness, in this serpent is hidden his divinity. From this serpent his wings will grow.

There is an occult energy in the heart that comes from Tonatiuh, the Sun, and if man releases it, returning it consciously to the sun, he becomes immortal. But to liberate this energy, sacrifice is necessary. Man must sacrifice the desires and habits that he adores, sacrifice them in himself, and turn the knife against the enemy that he carries within himself, that keeps his heart a prisoner.

In recent times men still remembered these words, but they have now forgotten their significance. They have made enemies of other men to sacrifice them and take out their hearts, believing such offerings would propitiate Tonatiuh. Such is their degeneration, such is their superstition. When fear unites with knowledge, terrible things are done. It is the self within ourselves that we have to sacrifice. It is our own heart that has to be torn out of the false being and offered to the light. May Xiuhtecuhtli, Lord of Fire, burn my false being. May Itzli, Obsidian Knife, liberate my heart.

What is the blood that connects stones with soul, men with suns? It is the universal unity, the one creative principle crystallizing into myriad forms, and when liberated by sacrifice it returns to unity. Because to sacrifice is to act consciously, to sacrifice that which will be taken away is to deny the destiny that takes it.

Defraud Death by sacrificing Life; because from the hand of the Goddess of Sacrifice that holds the obsidian blade sprouts the germ of Life to come. To sow life in the fires of sacrifice: Are the flames rising on the Hill of the Star, toward Cauhlacan? Or is it my own heart that is afire?

The cycle of years is past - the waiting ended. Come - reunite, pilgrims, for the sky is in flames! From Xochicalco to Teotíhuacan the red spreads one step, another step, and another, only twelve short steps from the cave of the womb to the final conflagration… The flames rage in consummation- Rise, oh flames! What light, what heat! What great holocaust! The smoke ascends and spirals... Obscurity disappears as the flames rise to Tonatiuh, the purest light.

Profound mathematical knowledge of the rhythms of the inner planets and their specific effect on the patterns of the collective consciousness of the human beings of Earth is followed by an explanation of the attributes of different kinds of water. Sacred waters are identified with memory, wisdom, ascension and prayer and are known to science as water molecules exclusively comprised of the lightest form of hydrogen – *protium*. The lower forms of water contain heavy hydrogen isotopes – *deuterium and tritium* (with 2 and 3 neutrons, respectively), and are associated with forgetfulness, degeneration and entropy.

The Maya understand the inner power of human consciousness as a function of DNA, the coiled 'coatl' serpent within every living cell, to be mastered through meditation, spiritual development and emotional control of brainwave and DNA states. DNA electrification is overtly expressed in the straight, double ladders depicted on a large copper/gold plate from the Crespi collection from Cuenca, Ecuador, with double-headed serpents representing electrical currents moving along nanoparticles chains (opposite).

The prophecy of the Red Sky is related by Maya texts as an ignition of the pyramids and the very sky itself in flames! Atmospheric HHO plasma plumes and red atmospheric aurora are depicted in the Teotihuacan Tree of Life mural (above), the blood red sky encompassing the entire background of the scene, dominated by a giant tree-like form comprised of luminous pink and green plumes. Along the length of the spiraling 'branches' of this sacred tree are numerous concentric circles, as a well as spiders and butterflies – symbols for the transformative effects of the living waters of Tláloc.

The concept of defrauding death by self-sacrifice through the overcoming of human instincts, karmic attachments and desires as symbolized by the laughing skull. Fear of death and the unknown is transcended in the eternal light of knowledge, thus 'making death an ally.' The laughing skull symbolism is preserved in ancient Tayrona gold masterpieces from Colombia, often presented with linear alignments of concentric circles (below, left). Three spirals are another commonly used symbolism representing the three frequencies of sound that stimulate psychoacoustic resonance within the temple chambers.

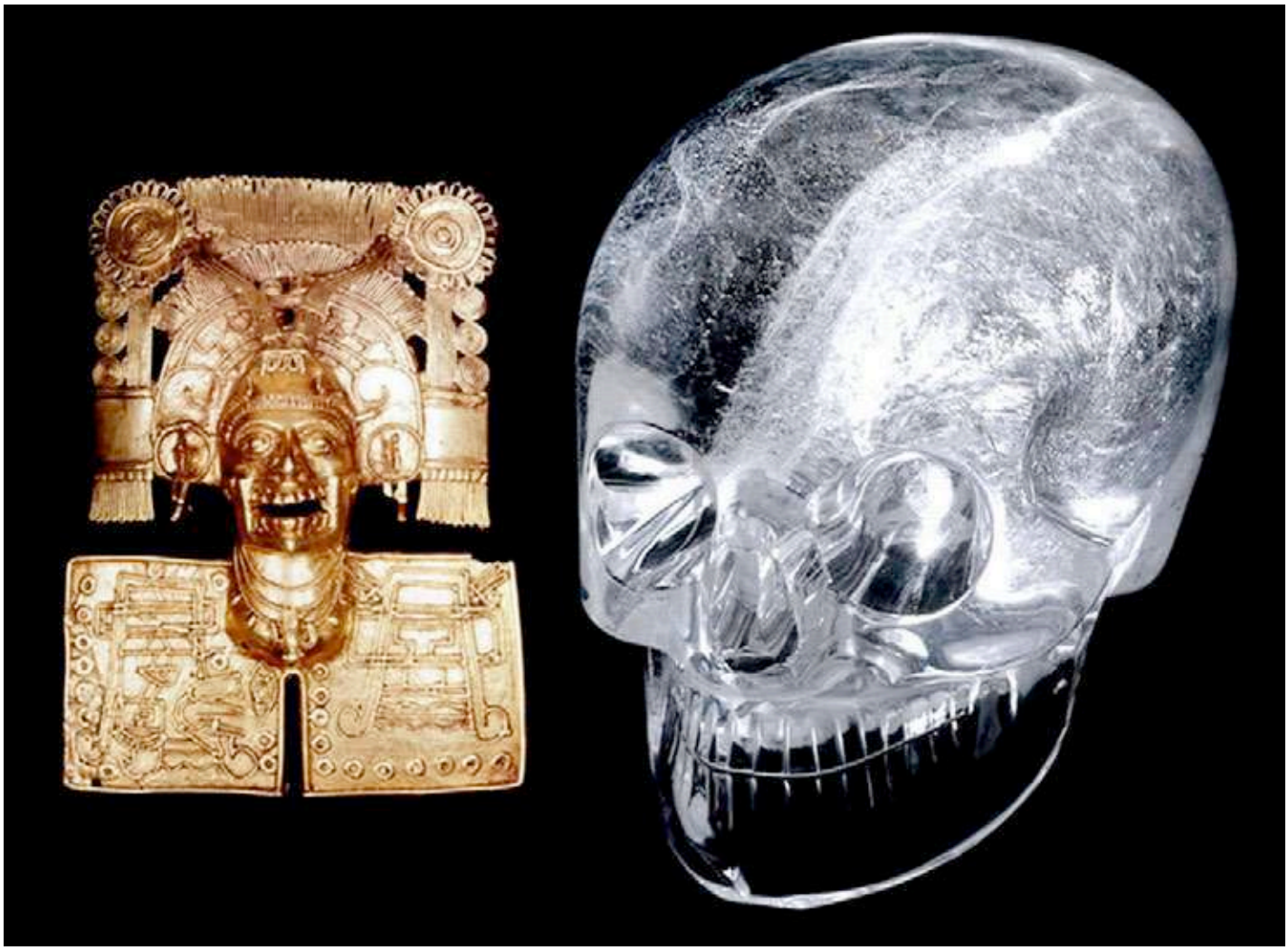

The crystal skull is another cross-cultural symbol closely linked with the transformative concept of crystallization of the water within the human body, referencing the piezoelectric property of quartz and the piezoelectric potential of the crystallized human being. The advanced bioelectrical metabolism of superior man is achieved through the death of individual desires and karmic attachments, to become spiritually reborn as Quetzalcóatl in the pyramidal House of Hunab K'u, the Universal Creator:

> The mysteries of the sacred Crystal Skulls have been recorded in the depths of time. That means that it is almost impossible for the human beings to understand them. This is the reason why thousands of people around the world feel restless; they want to know why the ancient peoples made these skulls… The Crystal Skull and the human being make up a single unit, but the main difference between them is that the skull has more memory than us [human beings].
>
> When all the crystal skulls of the world get together, it will be an important moment for the human beings because the memory that has been stored in these skulls will teach us how to recall our past lives. Currently, the modern human being does not know how to remember; and due to this, he does not know where he comes from or where he is going. And he does not know about his future either because he cannot remember where he came from or where he lived his past lives exactly...

There are some impressive geometric shapes that have been appearing in the fields of the European country of England, but the most impressive is the one that appeared on July 16th, 1999 in Windmill Hill, Avebury Trusloe, Wiltshire County [presented above]... As it can be seen, it is a large circle with a square in its center. Besides, the square has 328 small circles distributed symmetrically in its interior… The information below was published in the magazine "Crop Circles" where Judith Moore and Barbara Lamb wrote the following: “This 'Crop Circle' is the DNA chip that will evolve our mathematical capacity. Each one of these circles in an infinite fractal crystalline code, and each crystalline aspect is a fractal universe. This evolved system is the next step for mathematics on Earth. When this particular glyph becomes of collective knowledge, current mathematics will seem obsolete or primitive, like the difference between a stone axe and the laser.”

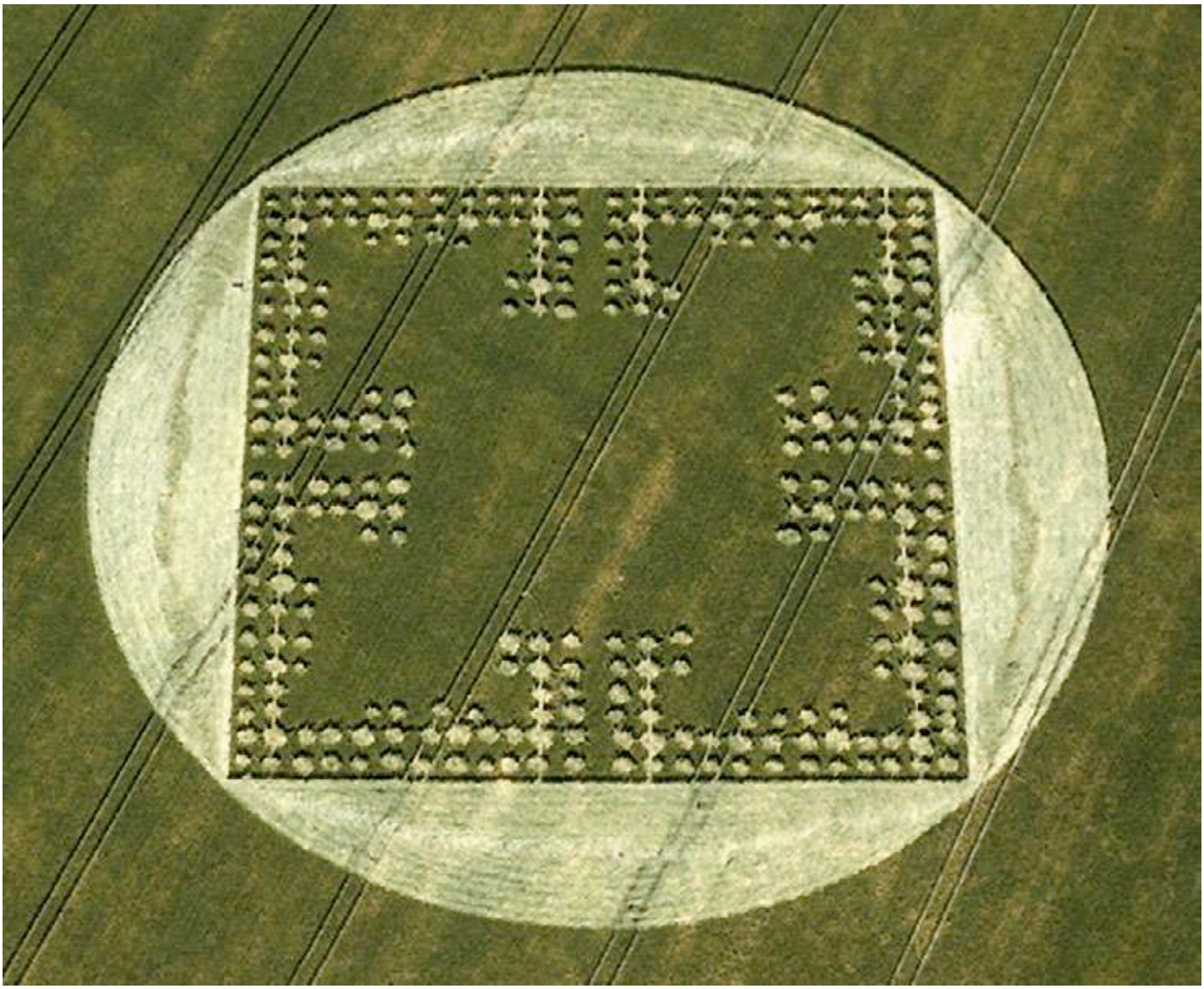

Qiuayon soen tra soen nas tra ka mix na ke te son tra laixwa mei ix nika. This is the ancient mantra for the activation of this process. In ancient history there were bearers of both the Mayan and Egyptian tradition that prepared the planetary essence to receive this evolutional leap. The crystalline codes were implanted in sacred sites and will be reactivated by those of you who bear the appropriate DNA codes to complete those ancient formulas and receive the mathematical formulas created in the collective mind. Those who will be part of this cosmic mission have already been reincarnated to activate this process…

The geometric writing exists, but the human being in general still cannot understand it. In ancient times the peoples mastered it; for example, the Mayans could understand it and they applied this knowledge on the planning of their constructions when they built their ceremonial centers and they also applied it on their architecture. They knew that energy moves in geometric shapes using its perfect proportions.

The Greeks knew that geometry was important to understand the mysteries of life, but it was the Mayans the first ones to include it in their culture to live it everyday. The Christians speak of God, but they do not relate him to the geometric shapes. In the Mayan culture God and science are related to the geometric shapes; for example, the circle and the square are the symbol of Hunab K'u who is the Mayan God. The circle represents the movement and the square the measurement. 'The Giver of Movement and Measurement' can be found in these two crisscrossed geometric shapes; this is for the Mayas the Universal Creator...

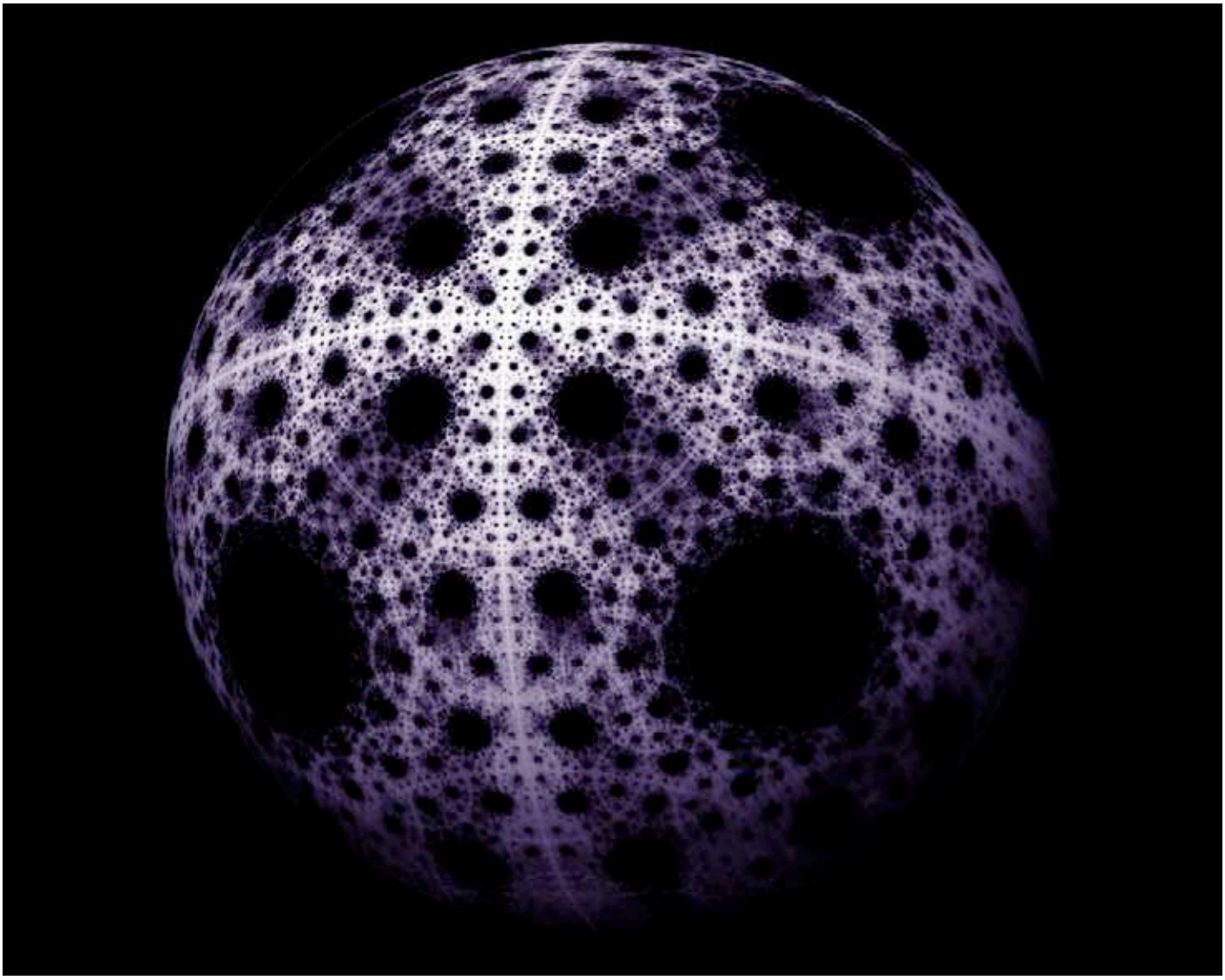

On the initiatic work of magnetic activation we will carry out with the Crystal Skulls in the Mayan temples we will use this same geometric shapes that appeared in England. In this occasion, all the initiates and teachers will experience these geometric shapes applied to the construction of the Mayan temples, but we will also have to live them cosmically. If we observe the map that we will be using in this initiation, we will realize that the ceremonial centers of the ancient Mayas were based on a geometric planning viewed from the space just as it can be appreciated...

This map shows us that the Mayas built their ceremonial centers using the macro-geometry. We the initiates will use the micro-geometry when we perform our rituals to later connect it with the macro-geometry. Well, then, who will help us to expand this energy in order to achieve the activation of the pyramids? Well, that will be the role of the sacred crystal skulls because science has proved that quartz is able to expand energy much more quickly than human beings… Let me tell you that this time the flowing energy will be used only for the human beings' benefit. As we previously said, the crystal skull and the human being form a single unit. When we work with this energy in the Mayan pyramids, then they will be activated and this energy will travel to the 8,000 ceremonial Mayan centers distributed in all the countries of the Mayan world to later continue its flow toward the other temples spread in the rest of the world...

The Crystal Skulls will work on the magnetic activation of the pyramids and in a natural way they will make several radiations of the cosmos to come to us. These radiations will concentrate on the axis of all and each one of the pyramids and of course in their center, too. The pyramids are huge accumulators of electromagnetic energy that will be activated by the crystal skulls together with the initiates and teachers in the Mayan temples in order to seek the human benefit. It is also important to send this energy already activated to the center of each human being skull so that he can raise his consciousness.

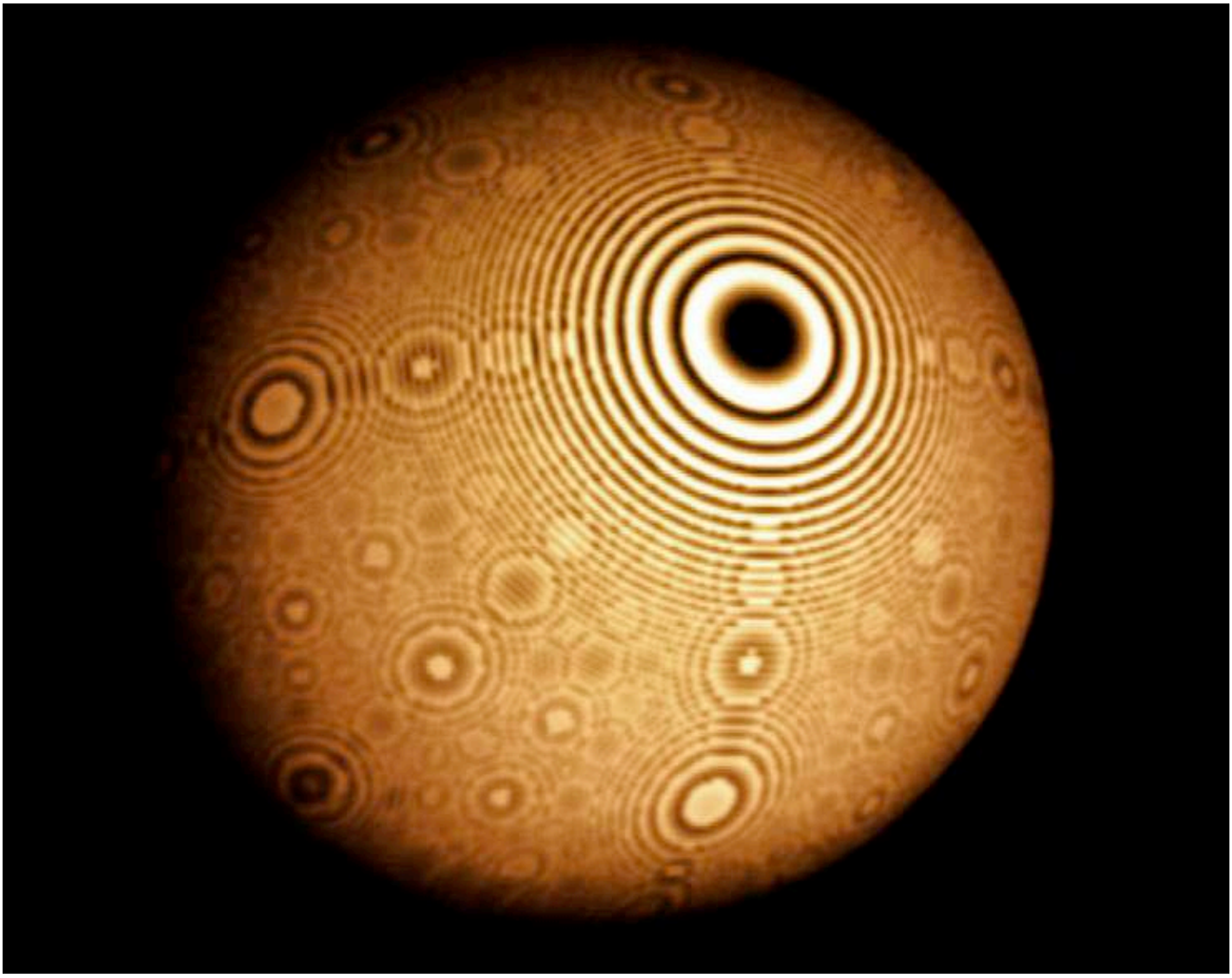

As a conclusion, we will quote an important fact related to the pyramids. It is worth mentioning here the scientific theory that talks about the atomic excitation that takes place in the Sun, the stars and the cosmic space… that is able to penetrate all the existent things. Well, when this cosmic excitation penetrates into the pyramidal constructions, it gets organized and forms perfect geometric figures, giving birth in this to the cosmic geometric writing… We will do this work together in benefit of the natural laws, our Mother Earth, and all the human beings. It will also help us to start a communication with our cosmic family. This initiatic work will open the gate of the New Itza Age and the future generations will have a better world to live in, a world with a new consciousness achieved through this magnetic cosmic activation.[9]

The force of cosmic infrasound so penetrates all matter and becomes focused by giant crystalline pyramids on Earth's surface, into a nonlinear distribution pattern exactly encoded by the spherical resonance formula [$z_{n+1} = z_n^2$] (above). Standing auroral beams and atmospheric flashes are being caused by localized surges of terrestrial infrasound at nodal convergence points, irradiating water vapor to induce the dissociation of water molecules and the rapid formation of HHO plasma. The implosion of hydrogen atoms releases intense ultraviolet-A and infrared light that becomes visible during brief periods.

An intensely luminous HHO plasma canopy envelops the Giza pyramids when operating at high resonance, radiating giant acoustic plasma beams that arc from the four faces of each pyramid, with looping flares connecting one pyramid to another just as solar flares arc from one sunspot to another. This dramatic luminous interaction of the pyramids with stimulated atmospheric plasma activity is exactly described by the Pyramid Texts of Saqarra, Egypt (below), only now comprehensible to plasma physicists as intense emissions of UV-A and IR light from resonant HHO plasma and amplified by the gleaming UV fluorescent limestone's of pyramids all over the world:

> House bright and dark of Heaven and Earth, for the [solar] ships put together; Great Pyramid, House of the gods with pointed peak; for Heaven-to-Earth it is greatly equipped. House whose interior glows with a reddish light of Heaven, pulsating a beam which reaches far and wide; its awesomeness touches the flesh… House of Eternity; its foundations are stones, the water; its great circumference is set in the clay.[10]

Calcite is an ultraviolet fluorescent material that was used extensively in the construction of all of the pyramids of the world. The ancient Vedic accounts of antigravitic vimana, or solar ships, include recipes for electroluminescent metal alloys which display the same molecular properties as the pyramid stones, as well as showing the same octagonal axis-symmetric geometry. If antigravitic effects were once achieved in the pyramids for application to the human body and consciousness, what is the range of extra-low-frequency sound biocompatibility? The heartbeat - at 1.45 Hz wavelength of 765 feet - informs the base length of the Great Pyramid of Egypt. The word 'pyr-a-mid' itself is of Greek origin, based on the word 'pyros' or fire and meaning 'fire in the middle'. Were biocompatible plasmas once burning in the pyramids' inner chambers?

The recently rediscovered high-energy state of hydrogen has been reported by Dr. Randall Mills, who has developed the process which releases vast amounts of energy stored within the hydrogen atom itself. Mills has defined the physics underlying this novel chemical reaction derived from water as hydrino resonant-transfer plasmas, which are now being commercially marketed for power generation by his company Blacklight Power, Inc. A very similar application of this novel reaction has been developed by Denny Klein, called HHO gas, and is now available as a plasma torch capable of sublimating any material. Both of these hydrogen-based plasma reactions produce intense infrared and ultravoilet light. Interestingly, the bandwidth of UV radiation produced is restricted to UV-A, which is beneficial to the human body, while the destructive UV-B and UV-C wavelengths are not observed.

The technical process by which HHO plasmas are formed has been defined by the Blacklight Power researchers. It involves the breaking of the molecular bonds of water by vaporized metal nanoparticles, producing a highly kinetic vapor composed of individual hydrogen and oxygen atoms. This reaction cannot occur in the presence of air, therefore a vacuum chamber is required. Once the HHO vapor fills the chamber, it is then electrified to become HHO plasma releasing energy as the H atoms shrink to one-quarter normal size.

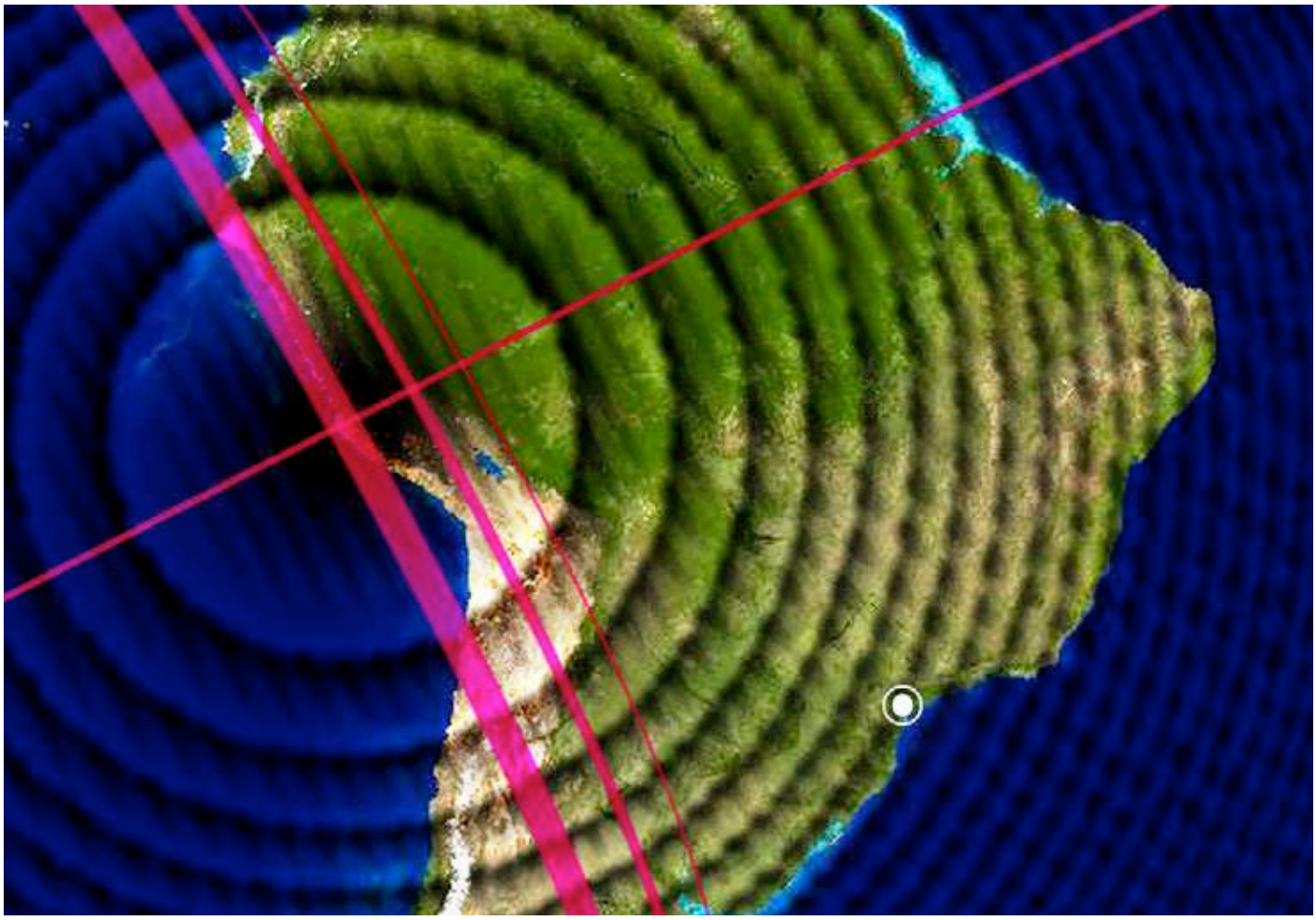

These contemporary scientific breakthroughs shed light on the unusual experiences recounted (in Search Magazine, March 1960) by American ex-patriot Dr. Raymond Bernard in Joinville, a coastal city in the Brazilian State of Santa Catarina (above). A very strange series of extraterrestrial contacts began while Dr. Bernard was organizing and living amongst a community of vegetarians outside of the city. The calls of a booming voice from a nearby mountaintop prompted a member of Bernard's camp to investigate the location of their origin. Eventually finding only a well-like circular shaft, measured by jungle vines to be about 300' in depth, the investigator returned equipped with ample rope to descend to its bottom:

> When I came to the bottom I entered a tunnel, which I traversed for a distance of 2,000 meters. I then saw with my flashlight a door of stone. While I was watching the door, it suddenly opened and I saw a very tall man with a metallic uniform, who spoke with a powerful voice and said that this was the first time that anyone ever had the courage to enter this tunnel. I first was frightened at the powerful voice of the man and wanted to run, but he called me and told me not to be afraid, as he was a very peaceful person who never did harm to any living being. So I asked him who he was to live in this cavern.
>
> He said, "I am an Atlantean-Inca, the guardian of this door."
>
> He asked me what I was looking for. I told him I was looking for my race, because I too am an Inca. He seemed to be very pleased to hear this. I told him I would like to visit his city, and that I had an American friend, and a wife that would like to go there too, with my children...
>
> On this second visit to the Atlantean he delivered a lecture on radioactivity and its danger. He said that radioactive dust in the air is causing surface dwellers to age very rapidly because it accumulated in the pores of the skin and stops skin respiration. He said the pores of the skin have a constant alternate contraction and expansion and serve to take in air and expel foreign matter. In an atmosphere of radioactive dust metals, there substances clog up the pores and interfere with their vital functions of respiration and excretion. This causes disease and early death.

The Atlantean called me to come near a transparent screen to make an exchange of blood to make sure I will preserve the secret of the whereabouts of this tunnel, so that I do not reveal it to an unworthy person. When I was near the curved plastic screen, another curved plastic screen suddenly appeared from each side of the door and encompassed me, so that I found myself inside the two curved plastic screens. Then it seemed that all air was pumped out, leaving a vacuum in the space where I was between the plastic screens. Then other air entered, which seemed lighter and purer, which made me feel more healthful and stronger. Then the inside plastic door opened, and he put inside a man-sized capsule of this transparent substance which he held by handles on both sides of it, and told me to go inside the open door. After I was inside, the door automatically closed. Now the second plastic door opened and the Atlantean took hold of the handles on each side of the capsule and carried me to the other side of the inside plastic screen whose door automatically opened and shut...

He told me not to bring here any unworthy person, because he would know it in advance. I asked how. He said that with this apparatus, which he called an "electrovisor," he could behold whatever was occurring in any part of the world. If any unworthy person comes near the mountain and tries to get to the tunnel opening, certain rays confuse the person's mind, so that he is unable to continue the trip and will go off in a wrong direction.

I had some bread in a pocket. He told me not to eat the bread. He put a white pill in my hand (which was projected outside the capsule all the time), and told me this pill had the taste of many fruits. Then I withdrew my hand and the plastic material through which it projected closed. After he gave me the pill he carried the capsule with me inside to the space between the two plastic screens, as the door of the inside screen opened to admit the capsule and then automatically shut. Then the door of the capsule opened. I left the capsule, and then the door of the outside plastic screen opened and I left.

When newcomers enter, they first enter the capsule, and the Atlantean carries them to a Decontamination Chamber (the Atlantean told me). The door of the capsule opens, the person leaves the capsule, takes off his clothing, then the chamber becomes filled with vapor, which draws forth radioactive poisons from his body. The person dresses with other clothing there ready for him, then enters an "electrical apparatus," which carries him [towards] the center of the earth. I should mention that during my visits, before the door opened I heard a peculiar humming sound, which was of the apparatus with which the Atlantean came up from below, which became louder and louder as the apparatus came near, and when it came to a stop the noise stopped and the doors automatically opened.

> I should also mention that when a flying saucer came near my house on Saturday, June 13, 1959, in the afternoon and night, it gave off an identical hum as this subterranean apparatus, which makes me think they are both operated by the same mechanism and that the flying saucer was an apparatus of those same subterranean Atlantean's and did not come from another planet. The flying saucer came describing a spiral which descended on top of a hill about 2000 meters from my house, and then rose in a spiral manner, with a tail of light behind it. It came in the night, had a round shape and a silver color. I believe it was sent by subterranean Atlantean's , who knew where I lived and came especially near my house.[11]

These details related by Bernard are all the more remarkable when one considers their timeframe, prior to 1960! The accounts of a peculiar loud humming that accompanied both the subterranean elevator and the vimana 'flying saucer' are now known to be ultra-low frequency soundwaves used for antigravitic control. The Atlantean's brief mention of technological remote viewing and rays that would confuse any visitor with negative intensions are also applications of ultra-low frequency waves being developed by today's scientists. Blood sampling for DNA study in the screening of visitors is also logical, as modern researchers have now been able to show a genetic predisposition to psychopathic behaviour.

Likewise, the lesson given by the Atlantean on radioactive dust metals in the atmosphere is confirmed by the ancient evidence of nuclear blasts in the archaeological record, as well as by modern indiscriminate use of depleted uranium (DU) weaponry. Modern medicine has also recently developed the process called electroporation that was described to Bernard prior to 1960 as a natural cellular function that has become blocked by atmospheric conditions. The detailed account of decontamination processes involving electroporation is extremely scientifically accurate, as informed by newly developed heat-resistant piezoelectric plastics such as PVDF (polyvinylidene fluoride) that form the vacuum chamber into which HHO gas is flooded before becoming an electrified plasma.

Further investigations of the unique properties of superfluid plasmas have been conducted by a group at the Massachussetts Institute of Technology led by Dr. Ketterle. The group's experiments have defined the parameters necessary for the creation of superfluid plasma beams. An infrared light ray is used as a pathway that is then surrounded by a strong encircling electromagnetic field. These conditions efficiently contain the plasma when released into the IR beam. They have found that a pair of rotating green lasers within the IR beam induces the frictionless rotation of the superfluid plasma, which subsequently forms an array of hexagonal vortices that maintain the crystalline structure of the ionized gas.

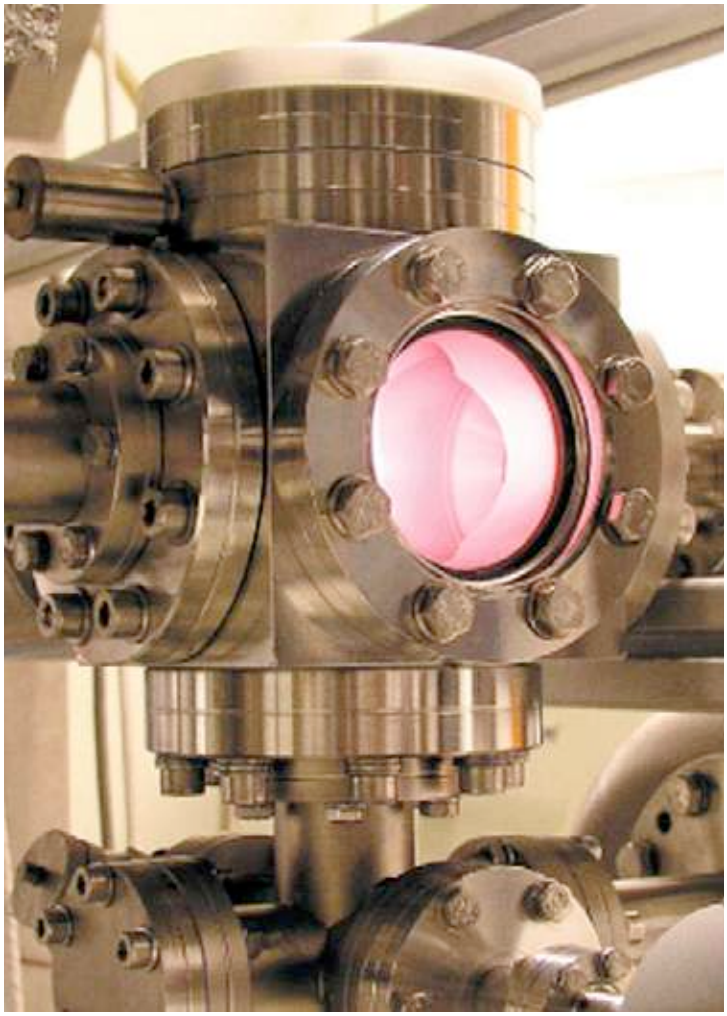

Ketterle's experimental results have apparently replicated the 'ultraviolet fog beams' related in the vast majority of extraterrestrial encounters. Physical transport via levitation in ultraviolet beams have been reported for decades, including riveting descriptions of the intense sensations of heat and light that accompany the events. The consistency of the contemporary eyewitness accounts of these advanced plasma technologies is astounding, and when analyzed in the context of the latest human technological developments one finds a profound synchronicity. Twenty-first century science has completed both the mathematical and experimental groundwork enabling a new comprehension of high-energy realms beyond common human experience.

Plasma is the fourth state of matter, with the highest energy and lowest density, followed by gas, liquid and solid states. The ignition of fire is a commonly witnessed event where gas becomes ionized to form plasma. The realm of human beings is a gas-filled resonating atmosphere in which we experience a three-dimensional world. A four-dimensional extraterrestrial realm of resonant plasmas passes through and beyond the human reality, apparently inhabited by electroluminous paraphysical beings.

While still higher realms of aphysical consciousness - thought at large - must exist, all human contact with this realm necessarily occurs via thought, dream, intuition, meditation or channeling. The channeled Cassiopaea contacts of Laura Knight-Jadczyk provide a very broad frame of reference and apt terminology which we will apply here in our discussion of the relationship of the gas and plasma realms –as 'third-density' and 'fourth-density' environments. Matter brought into the high-energy plasma environment decreases in density thus allowing molecular interpenetration. Evidence of the hyperdimensional interpenetration of matter have been found in the debris of tornadoes. One such anomaly has been described more than once - a windowframe with a wood plank passing right through its unbroken pane of glass.

Superconducting plasma aerial vehicles achieve frictionless passage through air, water or stone as there is no displacement of matter, allowing velocities and maneuverablity impossible for objects in third-density. The wave motion of acoustic propagation that is created in a third-density atmosphere of air is not present in fourth-density plasmas, which lack the temperature differentials that bend sound into waveforms. The fourth-density environment creates a coherent energy transfer, inducing unified telepathic consciousness without any information loss as minds are electromagnetically coupled in group synchrony.

The biocompatability of HHO plasmas accurately described in Bernard's account is quite similar to later reports of extraterrestrial encounters from other parts of the world. Michael Hesemann's breathtaking documentary film 'Ships of Light: The Carlos Diaz UFO Experience' presents overwhelming video and photographic evidence of fourth-density technology. Diaz vividly describes the initial sensation of heart throbbing at 1.45 Hz entrainment that precedes his extraterrestrial contacts. This powerful infrasound effect can now be understood as part of the propulsion system of the fourth-density craft, suggesting its invisible presence is maintained nearby before Carlos becomes aware of it. The craft then makes a luminous and visually dramatic appearance only when he has mentally prepared himself for the contact:

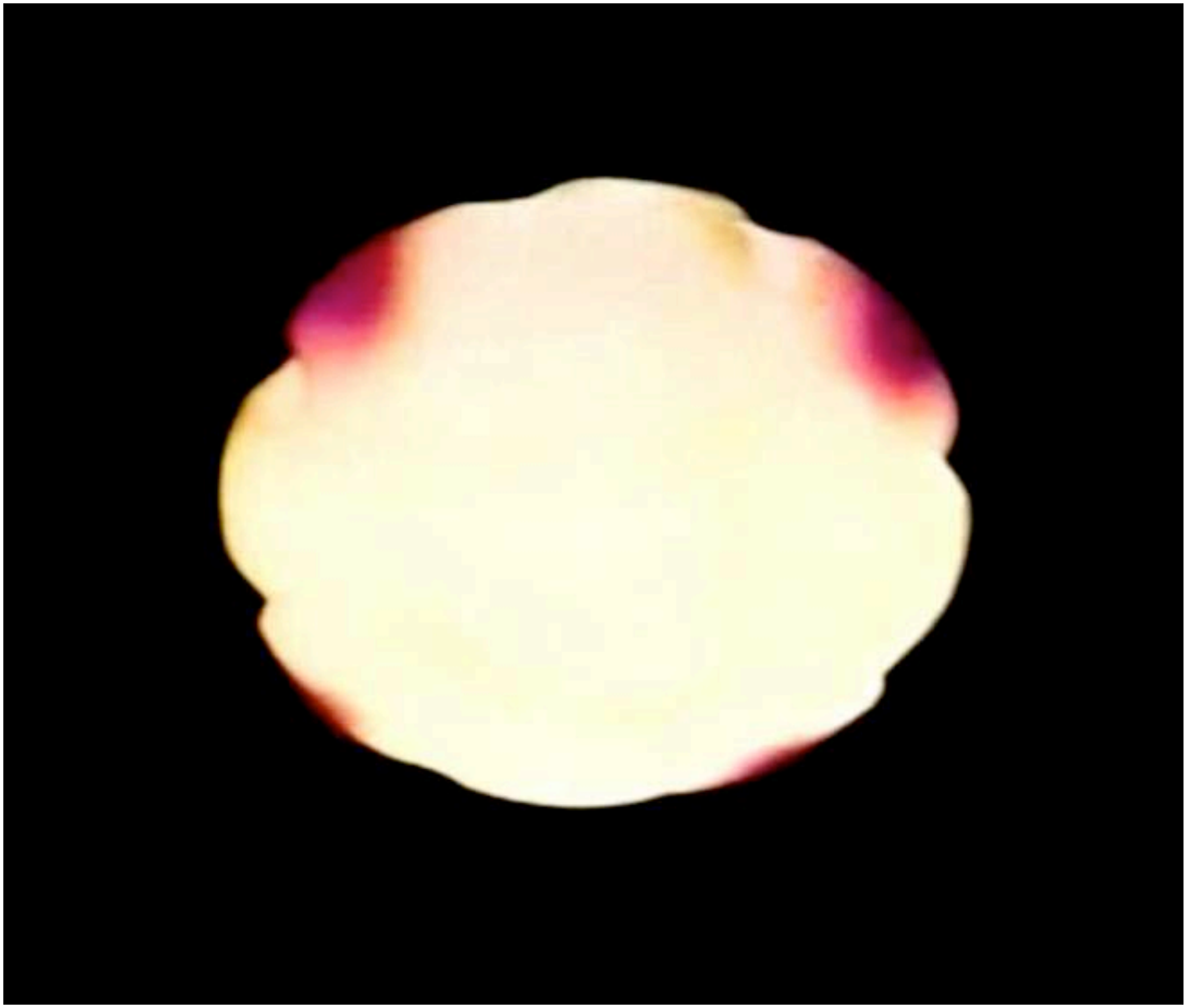

Q: In what form do the contacts happen?

There is a very special sensation concentrated in the solar plexus of my body – a sensation like when one is strongly in love. This sensation sometimes wakes me up at night, and I know that I am going to have an encounter with them. What I enjoy about the experiences I have had is that the communication I have with them is just as we are having at this moment.

Q: So it's an absolutely physical contact? You can touch them?

Yes, I can touch them... and at times they present a body of light...

Sometimes these ships appear at a great altitude, coming down slowly to hover eventually over the ground at an altitude of one and a half feet. When it is still at a high altitude the movements of the ship are very unstable, but when it hovers over the ground it is completely static. But it also happens that the ship suddenly appears right on the spot. For me, it is a kind of magic. They come directly out of the light slowly, part for part. Their body emerges out of the wall of light...

Their craft use the natural energy belts of the planet. Sometimes they enter into the belts, letting themselves flow with the energy. If they want to maintain one position they must act against the flow of the energy belts, causing the erratic movements of the craft. Once they are in the natural energy flow they travel at high speeds...

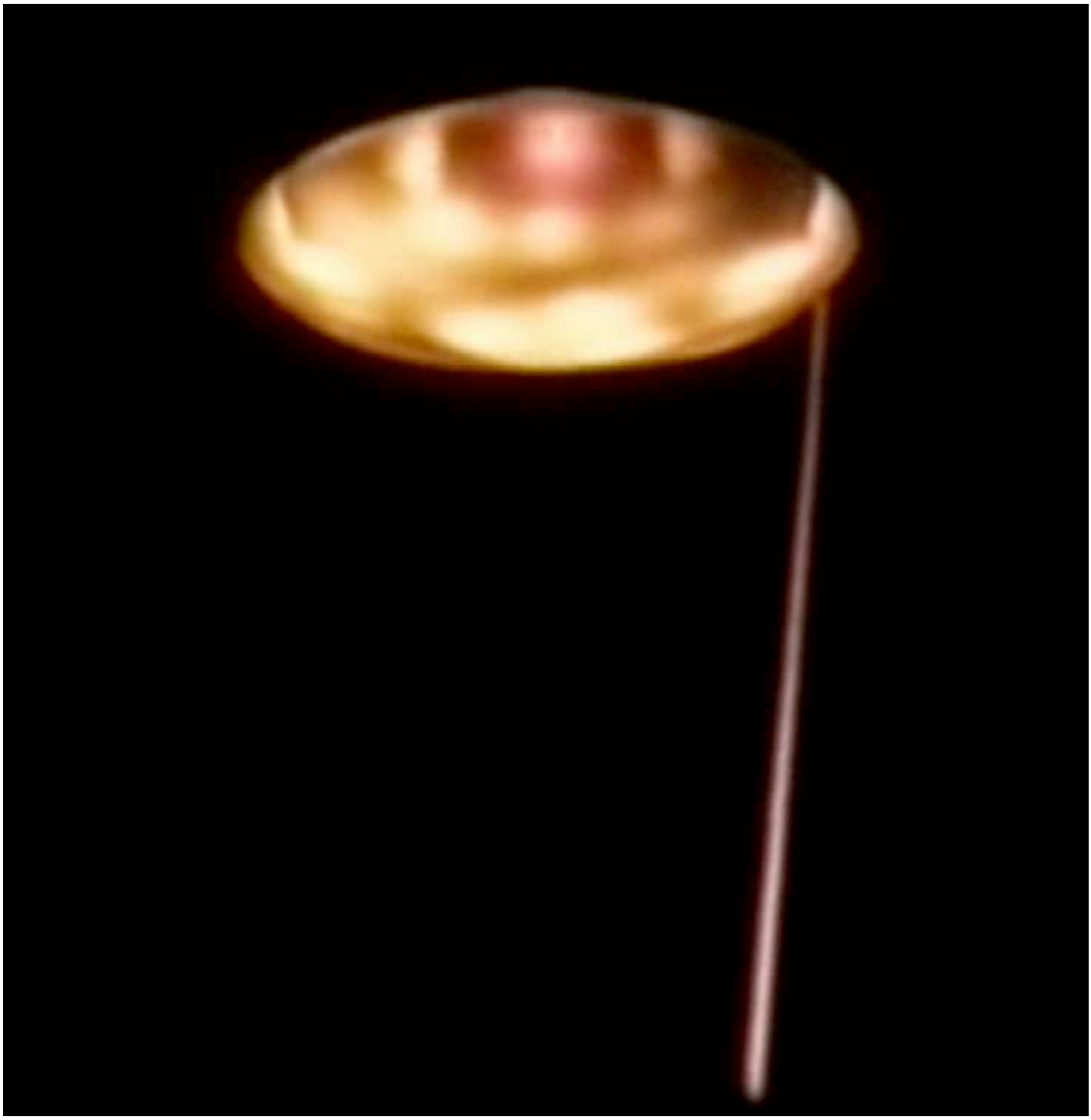

At different opportunities during my encounters I experienced how a beam of light shot out of the craft. This beam of light has the purpose to bring insects, plants, pollen, small and bigger animals aboard the ship, and sometimes we too, my friend and I, were brought aboard by such a ray. This beam directly forms and emerges from the ship, and consists of the same light or energy of the ship itself.

The first time he invited me consciously to go into a ship, I saw my friend getting in first. He went through this fog-like light. When more than half of his body was inside of the light his body got sucked into the object. So, what I did first is that I put one hand into the light to feel, and to my surprise it went through the light and inside I felt a nice temperature. When I took my hand out I was relieved to see it was in one piece, so that gave me the confidence to walk in, and when I had my body halfway inside the object I was sucked into it too. But once you are into it there is nothing you can see. You just see yellow light all over. You don't feel your toes. You don't feel the floor, but the sensation is very peculiar, because you feel very peaceful, with a lot of love within you.

Once when I came out of the yellow light I realized I was not at the same place, but in a cave. It had stalactites and stalagmites, and between them I saw several sculptures and ornaments which were of the art of the Maya culture. This big cave was the place where the ship hovered and there was a kind of path we walked through and we came to another cave, and I saw there many people who were very kind to me and greeted me... But the particular thing about this cave was that there were seven egg-like spheres of yellow light. After we got to this place my friend stuck his hand into one of the eggs and took out a small ball of light, also yellow, and said that this little ball could project a ray that would touch my seventh vertebrae or at the middle of the spine and it would take all of the information in my neurons.

Once I was there in this place he invited me to go into one of those spheres or eggs of light. When I did so, I realized that all the yellow color changed, and it was not yellow anymore, but was a scene of a forest from the air. It was like as if I was flying. And then I saw on each of my sides a wing – the wing of an eagle, and I realized what I was looking at was the information from an eagle, his memories, that they had stored into this egg of light.

Once... my good friend Jaime Maussan asked me to ask them where they come from. So when I was with one of them the next time, we were walking near Mextitla, I asked him ‘Where are you from?’, and he smiled and said, ‘Look Carlos, I can give you the name of any star, any constellation, any galaxy, but what would this tell you? As far as you have gotten is your moon, so it makes no sense if I tell you where we come from since you can’t go there and verify. For me, this answer was enough even though when I was with them I once heard them to mention a star named Maya, and when I looked into an astronomy book that there is in the constellation of the Pleiades a star named Maya. Maybe this is where they come from but I really don’t know...

After entering these spheres or eggs of light, I understood that they store a great wealth of information in them, not just about human beings, but about all forms, all manifestations of life. They don't only store images, they also store senses. When you are there you feel like an eagle, like a bird – I felt joy, I felt fear – and I have seen many types of environments; the sea, the ice, jungles. What I have learned from this is that every living thing is important for this wonderful planet.

They also offered to show me what they stored about the past of my own life but I didn't want to know, because what I want to do is go forward, and to try to act with all the things I have learned to live this experience. I had experienced that there is a wonderful interaction between all living things, but this interaction went out of control. Every individual, every species is an important part of this interaction. This is the reason why I want to share all of this with the whole world – to invite the people to act in order to save the Earth – to make it a true paradise for all living creatures, and to inherit our future generations a living planet.[12]

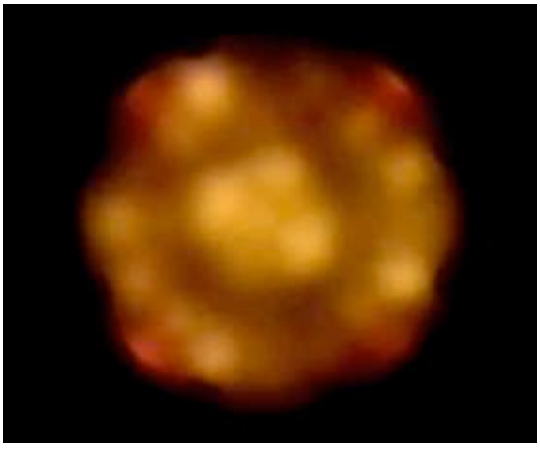

Profound experiences shared with Carlos through advanced transdimensional consciousness technologies have inspired a deepening understanding of the interdependence and unity of all life in the cosmos, and the urgency of the need to preserve the living systems of our mother Earth. The organic, jellyfish-like appearance of the plasma ships photographed by Diaz reflects a natural beauty by imitating the rhythmic bioluminescence of bacterial colonies symbiotically living within deep ocean creatures, which become stimulated to generate the brightly pulsating spotted displays of squid (above). Carlos Diaz's astonishing video footage of plasma beam technology has confounded the experts, including digital video and photo analyst Jim Dilettoso of Village Labs in Tempe, Arizona:

> The ray of light that comes down, when we look at it frame by frame, the light of the ray... [is] darker the top than it is at the bottom... and it goes off the same way. At each incident when the light goes on... the variance is between one frame, a thirtieth if a second. Well if [the ray] was [propagated] at the speed of light, we wouldn't even see it in a frame. It would be off and then on... which is curious. So, I'm still trying to understand it.

The false assumption that the ray is a simple beam of light has caused great confusion, as the intensity of the beam increases from top to bottom over the period of three video frames or one tenth of a second. The same three-frame shift in intensity from top to bottom is also noted when the beam recedes. The constant of the speed of light denies the possibility of a single source of emanation, suggesting that the beam is an emission of plasma. This notion is corroborated by the recent experimental results of Ketterle's MIT group, from which we can infer that the beam is initiated as a faint ray of infrared light subsequently flooded by HHO plasma in one tenth of a second. Knowledge of the properties of plasma beams and the effect of acoustic levitation by use of standing waves informs the authenticity of the images, as for Dr. August Meessen, Professor of physics at the Catholic University of Louvain, Belgium:

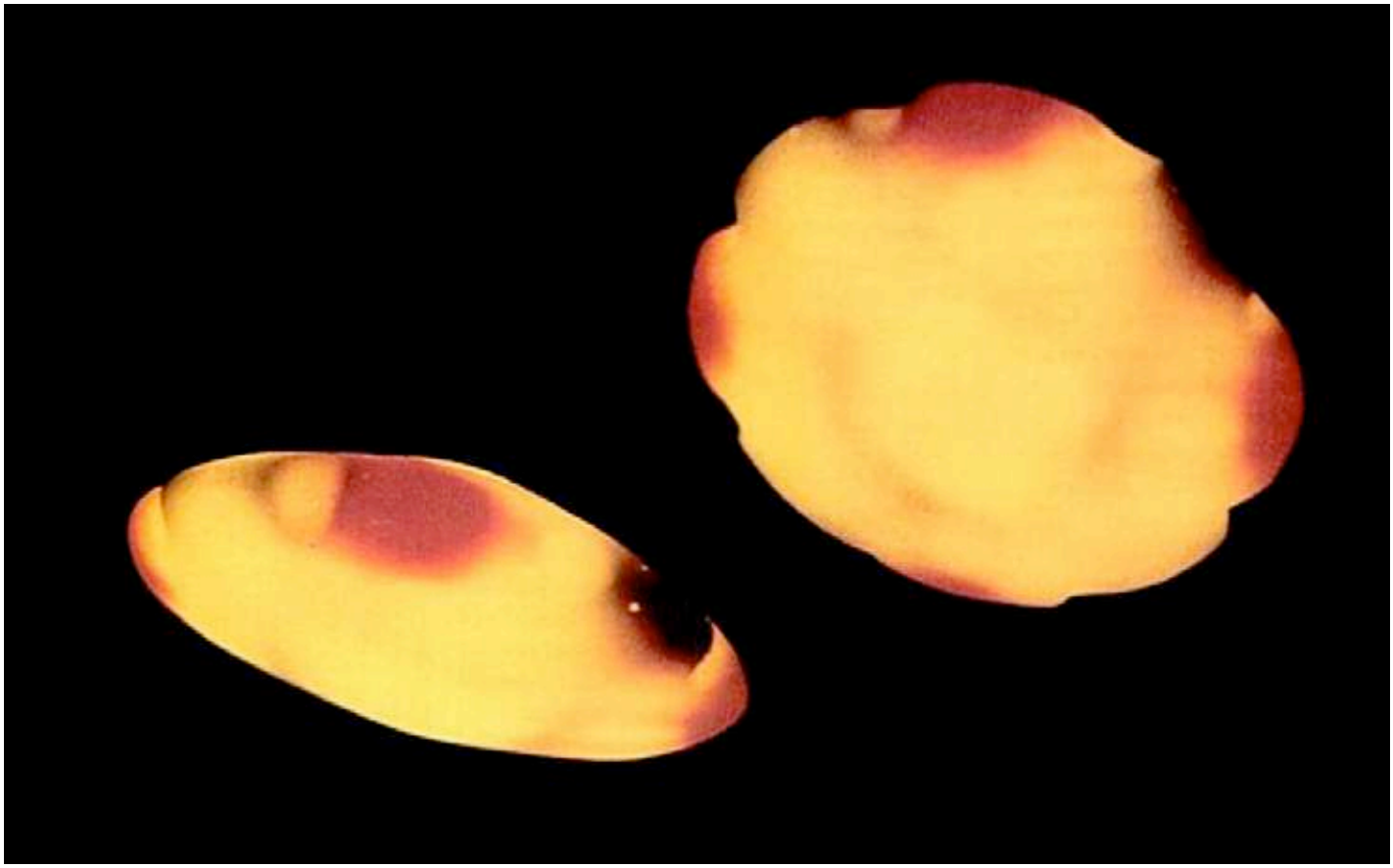

> As far as I see there are no objections against [the Diaz documentary photographs and videos], because if it is true it is very interesting for me as a confirmation of the theory where one expected results of this type... I developed a theory for the propulsion of classical objects... [which are] axis-symmetric objects... How do they produce electromagnetic waves which surround the object? ...One of the predictions of the [Unified Field] theory... [is] that they should be able to create *standing waves with certain modes where at certain regularly distributed places you have a higher intensity, thus you could eventually ionize differently.* If the theory is correct you could expect that somewhere observations like [those of Carlos Diaz] should appear.

Dr. Meessen accurately identifies the aerial activity over Tepotzlan, Mexico as involving ionizing spacecraft that restore energy by absorption of terrestrial infrasound standing waves that converge on the area, as described to Carlos as 'energy belts' by the extraterrestrials in contact with Carlos Diaz. Meessen has arrived at the same conclusions concerning standing waves as had Nikola Tesla, the original discoverer of the fascinating acoustic phenomenon, and have been applied by this author as spherical infrasound resonance maps of the Earth, flowering from the Giza Prime Meridian:

> The discovery of the stationary terrestrial waves... [indicates] that, despite its vast extent, the entire planet can be thrown into resonant vibration like a little tuning fork; that electrical oscillations suited to its physical properties and dimensions pass through it unimpeded, in strict obedience to a simple mathematical law...[13]
>
> [T]he Earth responds to a great number of vibrations and can be resonantly excited just like a wire of limited dimensions. When this takes place there are formed on its surface *stationary parallel circles of equal electrical activity*, which can be revealed by properly attuned [infrasound] instruments… Then *the crests and hollows of the stationary waves would be in parallel [or concentric] circles [enveloping the entire planet]*…[14]

Tesla's most profound discoveries in those last several months of the 19th century would go unpublished for almost 80 years, yet find direct relevance to the advancements of resonant technologies of the 21st century and beyond. The concise explanations of Nikola Tesla provide insight into the technological aspect of fourth-density experiences reported by extraterrestrial contactees and abductees alike. The enveloping brilliance of violet, yellow or golden light –combined with an intense sensation of the warmth of Eternal Love– are among the transdimensional experiences that leave many at a loss for words.

Many unmistakable aspects of advanced bioelectrical bodily purification processes using HHO plasma have been well documented. Closely echoing Bernard's 1960 report, Diaz also underwent plasma decontamination and was given fruit concentrate pills to ingest instead of the normal third-density metabolism based on the digestion of organic material.

The impeccable and extensive video and photographic evidence presented by Diaz documents the fourth-density conditions of intense light and heat of HHO plasma within the beam transport and in the plasma ship itself (opposite). This remarkable enhancement of the luminosity of the atmospheric conditions reflects the atmospheric environment present on the homeworlds of those space-travelers, affecting DNA enhancements not present in the terrestrial human populations of Earth. DNA evidence of this kind was actually obtained by Australian Peter Khoury, who has collected and preserved a single translucent hair from one of his several disturbing extraterrestrial encounters investigated by Bill Chalker:

> It was not until 1996 that I heard from Peter Khoury about the hair sample that had been recovered from what may have been an alien abduction sexual assault case… By 1998, I began an investigation into the hair sample, when biochemical colleagues agreed to undertake what was the world's first PCR (polymerase chain reaction) DNA profiling of biological material implicated in an alien abduction experience. The analysis confirmed the hair came from someone who was biologically close to normal human genetics, but of an unusual racial type - a rare Chinese Mongoloid type - one of the rarest human lineages known, that lies further from the human mainstream than any other except for African pygmies and aboriginals.

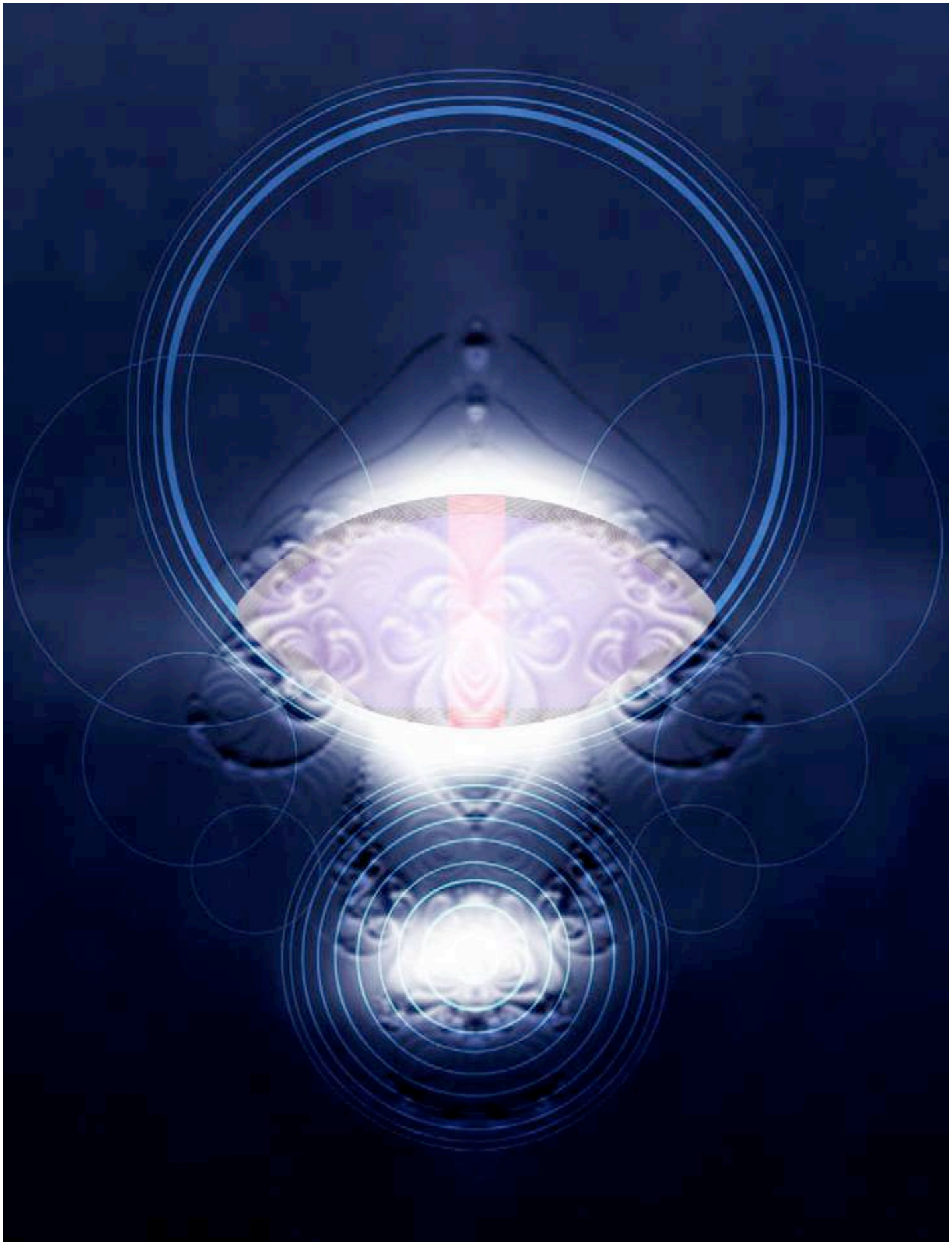

There was the strange anomaly of it being blonde to clear instead of black, as would be expected from the Asian type mitochondrial DNA. The study concluded, "The most probable donor of the hair must therefore be as (Khoury) claims: a tall blonde female who does not need much color in her hair or skin, as a form of protection against the sun, perhaps because she does not require it [in a luminous fourth-density environment]..."

The original DNA work was done on the shaft of the hair. Fascinating further anomalies were found in the root of the hair. Two types of DNA were found depending on where the mitochondrial DNA testing occurs, namely confirming the rare Chinese type DNA in the hair shaft and indicating a rare possible Basque/Gaelic type DNA in the root section... [The female's appearance is illustrated below, based on Khoury's detailed descriptions.]

This was very puzzling and controversial, until a 'Nature Biotechnology' paper appeared in 2000. It revealed recent findings on hair transplanting with previously incompatible hair, using advanced cloning techniques, developed in a possible cure for baldness. We seem to be seeing similar combined or "grafted" DNA in the sample recovered under controversial circumstances by Peter Khoury back in 1992.

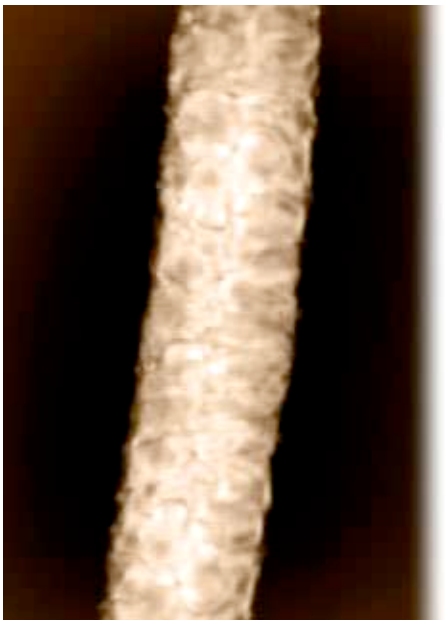

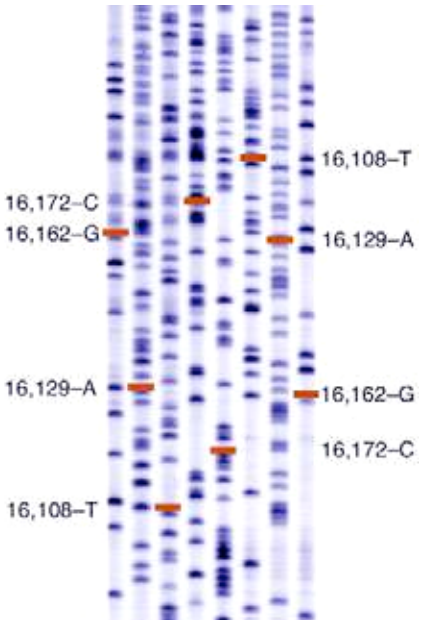

Perhaps even more controversial is that we have findings suggestive of nuclear DNA indicating possible viral resistance. The hair sample seems to show it contains 2 deleted genes for CCR5 protein and no intact gene for normal undeleted CCR5 - this CCR5 deletion factor has been implicated in AIDs resistance. To keep a very complex story somewhat uncomplicated, what seems to be suggested by the range of findings is possible evidence for advanced DNA techniques and DNA anomalies and findings, for which we are only now discovering or starting to make sense of in mainstream biotechnology.

While the unusual experiences of Bernard and Diaz were of a very positive nature, the sexual assault case of Khoury is by contrast quite negative. Yet in all of these cases the powerful emotive interaction between the extraterrestrials and the contactees is obvious, as one might expect of primarily telepathic beings. Diaz provides extensive video and photographic evidence that support his experiences, while Oliveira and Khoury have collected the most convincing physical evidence of HHO plasmas and an extraterrestrial DNA sample.

When compared and contrasted, their corroborated accounts and evidence of hyperdimensional transport compellingly point to a single, remarkable conclusion: that technologically advanced Sanskrit cultures of the deep human past have not perished, but have in fact transcended our toxic third-density realm to achieve vastly extended lifespans in fourth-density plasma environments developed in subterranean chambers and flying vimana discs. The stark synchronicity of evidence from these extraterrestrial contacts with the emerging human technologies of acoustic levitation, HHO plasma, electroluminescent metals and piezoelectric plastics informs a broadened perspective. By synthesizing these scientifically described and extraterrestrially demonstrated technologies, humanity is at the threshold of a hyperdimensional transition to the unified consciousness of the fourth-density realm.

Advanced HHO plasma technology will soon significantly expand the consciousness and extend the lifespan of human beings living on Earth's surface, thus closing the circle of time to reunite with our advanced ancient ancestors concurrently dwelling in fourth-density. The ascension of human consciousness by self-sacrifice in HHO plasma chambers within the sacred pyramids endows telepathic communication and direct thought contact with fourth-density spacecraft in Earth's atmosphere. Fleets of plasma ships have been videotaped at high-altitudes over the vicinity of Mexico City in various large formations, including *long chains of ships that appear like floating helical DNA strands* (below).

Such odd and spectacular plasma ship formations are orchestrated to reawaken human curiosity and announce the presence of higher dimensional realities, while most fourth-density spacecraft pass through Earth's atmosphere without being perceived by terrestrial humans. Highly developed subterranean bases and cities have been in use for millennia by extraterrestrial colonies living deep below the Earth's surface:

> Two scientists affiliated to the Fundación Instituto Biofísico de Investigaciones (FICI) headquartered in La Matanza… claimed having picked up radioactive signatures, microwaves, levels of electricity and oscillations originating from the depths of the earth.
>
> Omar Hesse and Jorge Millstein surveyed the mountains surrounding Cachi last week -- 157 km from the capital and 2,280 meters above sea level. After applying a Russian tester in the vicinity of the Nevado de Cachi, they concluded that the signals are not natural in origin, and rather originate by machinery operated by intelligent beings… "The oscillations clearly indicate that kilometers beneath the surface there is activity: alternating electrical waves, which means a power source," said Hesse. "This could mean engines," he added.[15]

The constantly maintained acoustic signals of deep subterranean cities present convincing evidence that such highly advanced facilities are powered by infrasound standing wave resonance, in alignment with the pyramids on the Earth's surface above. The fourth-density experiences of Carlos Diaz involved visits to augmented natural caverns below the Tepotzlan, Mexico area (not far from the Nevado de Cachi site) that contained ancient statuary like that of the Maya tradition, as well as seven yellow luminous plasma eggs composed of the same HHO plasma that also surrounds the spacecraft as a radiant red aura.

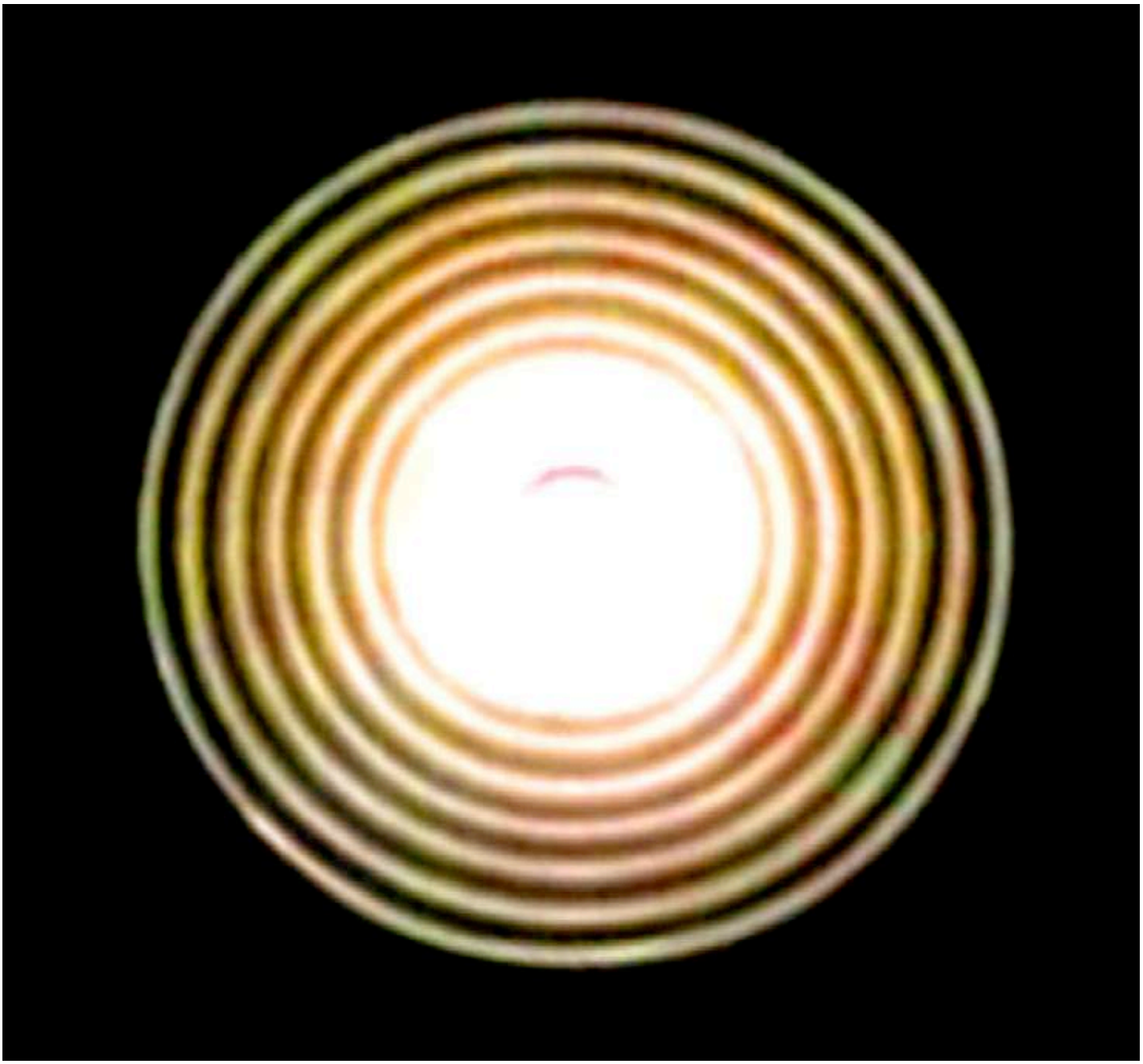

Transit to and from these deep underground cities is achieved by transdimensional passage directly through the bedrock by retuning the atomic frequency of the entire ship, its interior HHO plasma atmosphere and crew to safely interpenetrate the material realm. The transdimensional ships' generate thin veils of HHO plasma surrounding the vessel that can instantaneously shift the frequency of all emitted light into the infrared range for invisibility cloaking, or be tuned to generate visible light of any desired frequency. Security camera video from Turkey in 2006 obtained detailed close-up images of the underside of a large lens-shaped plasma craft, revealing 7 luminous concentric rings surrounding one central HHO plasma beam emitter (above).

This same configuration of 7 luminescent concentric circles reflects the nonlinear quadratic formula [$z_{n+1} = z_n^2$], as precisely encoded in a complex set of ancient Sanskrit stone artifacts from La Maná, Ecuador (pg. 197). The Sanskrit artifacts from La Maná fluoresce under ultraviolet light, as absorbed UV radiation is converted into reemitted light of visible wavelengths – a process that is also generated within the electroluminescent crystalline metals of transdimensional plasma spacecraft.

Complex metal alloys synthesized for acoustic levitation using cosmic infrasound standing waves convert the strong electromagnetic fields of the ships' internal HHO plasma chambers into reemitted visible light from the external surfaces, tuned as desired for various aerial displays or using infrared radiations outside of the visible spectrum of the vast majority of terrestrial humans beings. The enigmatic experiences reported by hundreds of thousands of eyewitnesses of extraterrestrial spacecraft transiting Earth's skies are now explicable in scientific terms, as nonlinear effects of quantum resonance.

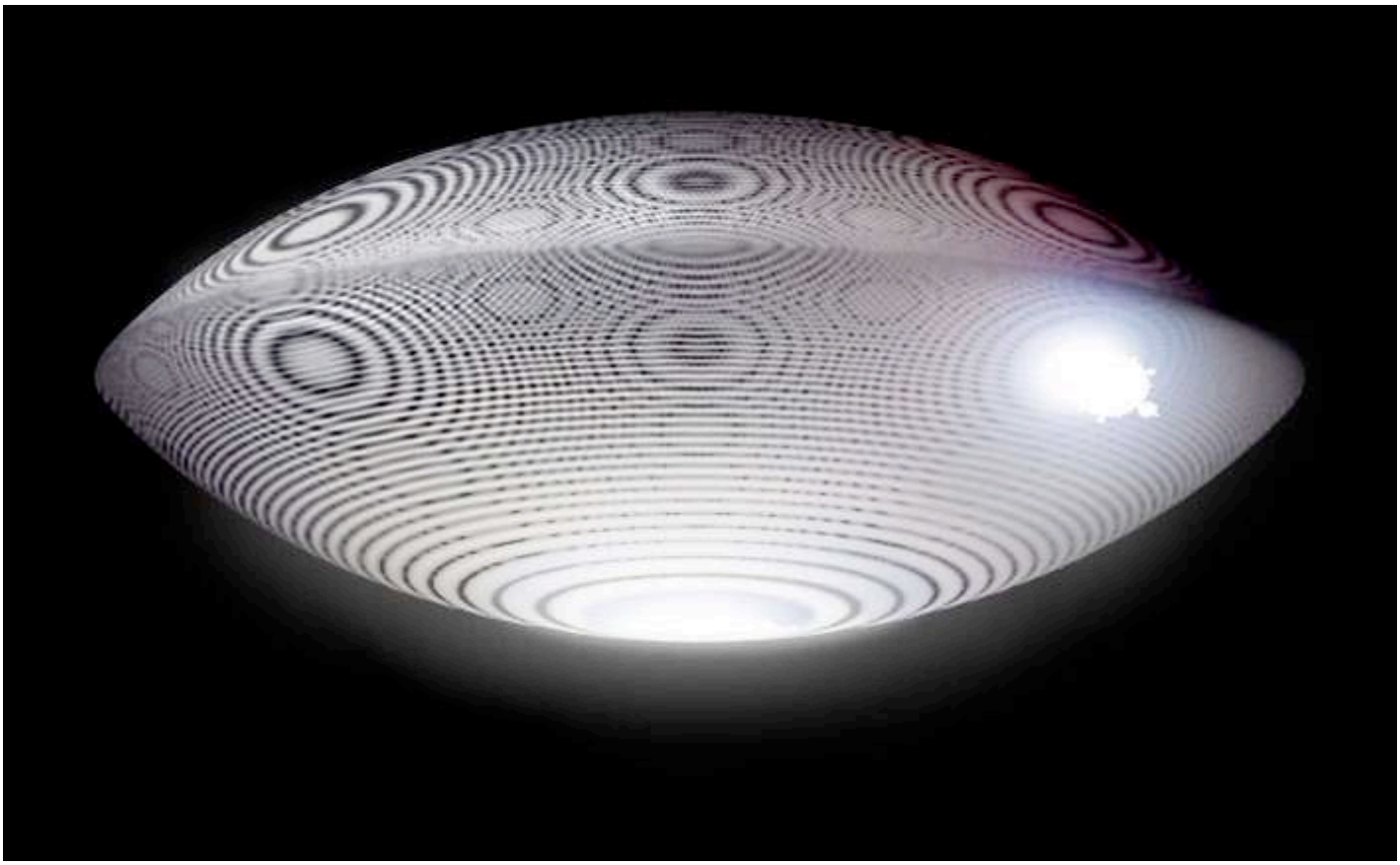

Primary identification of the optimal material properties for antigravity alloys have been experimentally tested and reported by more than one group. The axis-symmetric shape of the object to be levitated, as well as its resonant crystalline material composition, endows antigravitic properties that act to transduce incident radiation into resonant standing waves encircling the object. Fran De Aquino, physicist at Maranhao State University in S. Luis, Brazil, has mathematically modeled antigravitic effects observed in the extra-low frequency acoustic levitation of electroluminescent objects:

> According to the weak form of Einstein's general relativity equivalence principle, the gravitational and inertial masses are equivalent... [To the contrary,] we have shown that the gravitational mass and the inertial mass are correlated by an adimensional factor, which depends on the incident radiation upon the particle. It was shown that only in the absence of electromagnetic radiation this factor becomes equal to 1 and that... it can be reduced, nullified or made negative by means of extra-low frequency (ELF) radiation.
>
> We have studied the possibility to control the gravity on luminescent materials and have concluded that electroluminescent materials with high refractive indices are a new and efficient solution for gravity control technology.[16]

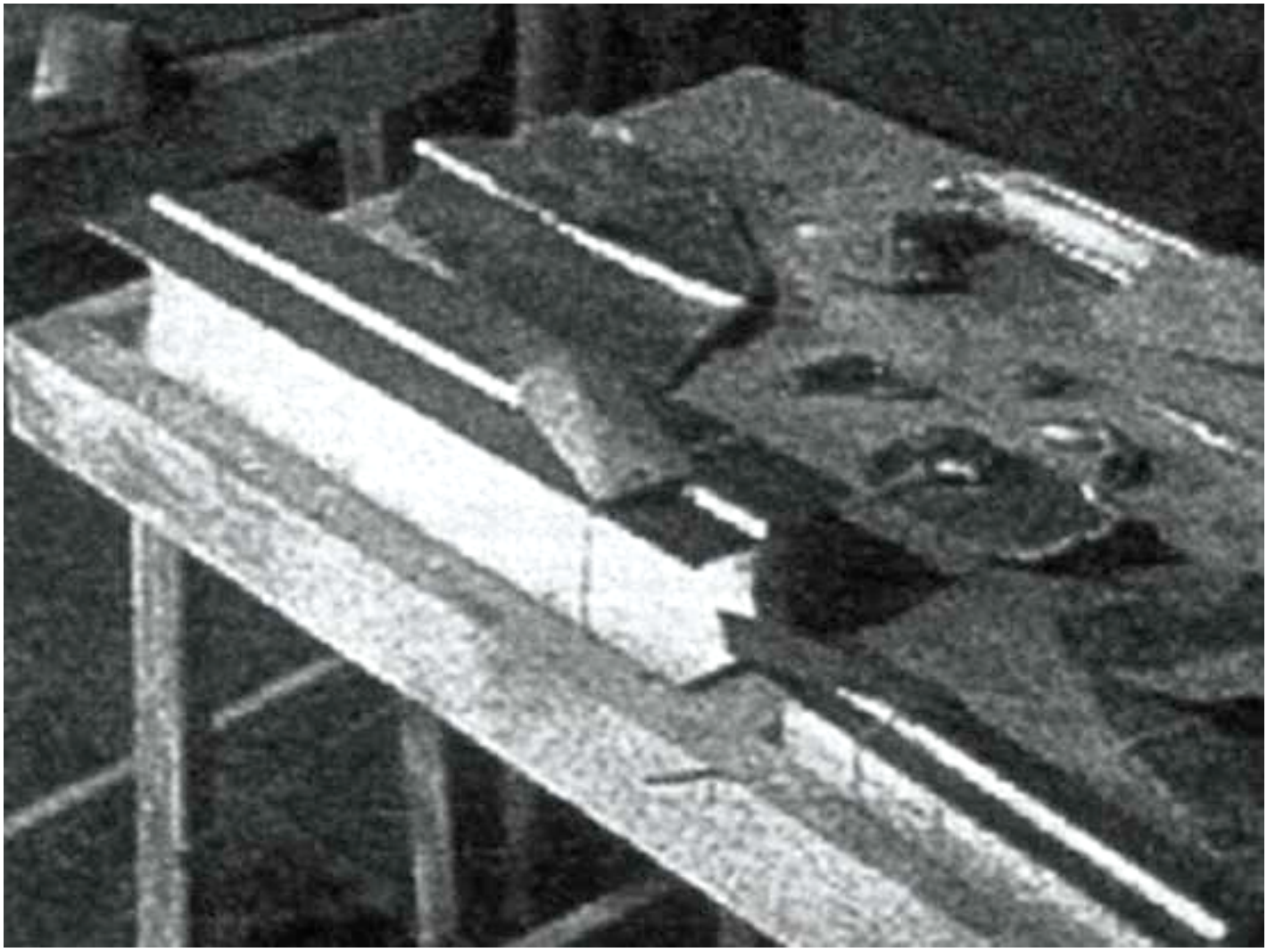

The refraction of acoustic energy within the parallel faces of the alloy's crystalline lattice allows resonant energy storing as standing waves form within the electrified metals, thereby generating coherent light from its highly reflective surfaces and reducing its mass to become totally weightless. During investigation of photographic evidence produced in the Carlos Diaz case, analyst Jim Dilettoso identified the unusual properties of light emitted by electroluminous alloys as *"coherent light – like a laser"*.[17]

Various metal alloys manufactured for diamagnetic antigravity propulsion systems (having two opposing rotating magnetic fields) produce the effects of electroluminescence from highly reflective surfaces, as well as photo-absorption from completely black surfaces. By applying ancient metallurgical knowledge preserved in Vedic hymns, Dr. C.S.R. Prabhu has reproduced metal alloys with formulations that are completely unknown to modern science, such as one referred to in Sanskrit as Tamogarbha Loha:

> Tamogarbha Loha: Already produced in the laboratory, light in weight, black in color, found to be resistant to acids. Displayed high level of absorption for laser light... used in 'Tamo Yantra'… for the purposes of absorption of light escaping from a photochemical reaction... generating 'darkness'...[18]

The Atlantean Sanskrit origin of vimana spacecraft *seen throughout Earth's skies today* is revealed by crashed aerial discs collected by military forces in many parts of the world. The most famous incident of this kind occurred on July 2, 1947 –allegedly near Roswell, New Mexico. Leaked US military documentary photographs and films of the New Mexico disc crash wreckage[19] include dwarf humanoid corpses with *large eyes, grey skin and six fingers*, as well as fragments of highly reflective metal alloys imprinted with small six-fingered hand consoles and hieroglyphic Archaic Sanskrit inscriptions. Dr. Schildmann's epigraphic decipherment reveals the meaning of a fragmentary text from an I-beam:

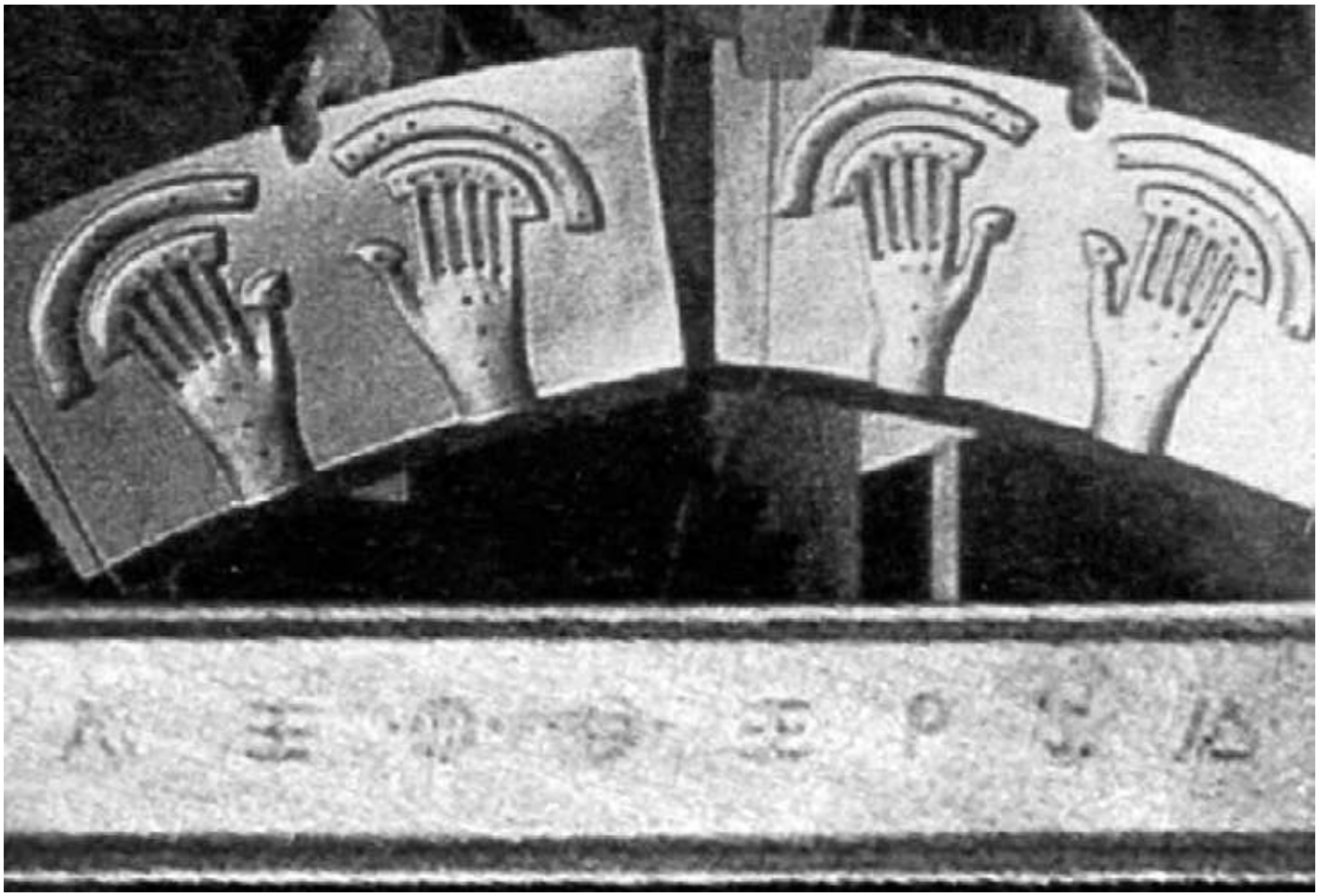

kar-as tridaśa yoni śani tridaśa ku-p$^{a_i a}$ as-upama

"workings of 30 resonances, female and male, 30 resonances whereby approaching the highest"

The New Mexico I-beam text directly confirms the Sanskrit origin of the pyramids and 'UFO' phenomena. Four very unusual removable metal panels were also documented among the pieces of Roswell crash wreckage, formed with what appear to be inset hand consoles for conjoined control of the plasma ship. One of the panels was damaged. Like portable biocomputers for each crewmember of the ship, each panel is individually tuned to the biorhythmic signature of each pilot, precluding use by others.

The panels' cast metal forms accommodate two small, six-fingered hands, with nodal sensors distributed at geometric points on the contact consoles and along a radial groove extending just beyond the span of the fingers. The configuration of the consoles exactly match the anatomy of the Roswell autopsy documentary video leaked anonymously to Ray Santilli and published in May of 1995, corroborating their close association and authenticity. While abductees call these beings 'the grays', they have been identified as bioengineered androids of a dwarf race from the planet known as Zeta Reticuli, of the Reticulum star system, during informative contacts with a Swiss farmer named Eduard Meier on November 3, 1975, and further clarified in tantalizing detail over 11 years later, on February 28, 1987:

> Their size varies between 126 and 163 centimeters… They originate in the planet and star system Zeta Reticuli,… a median distance of 37 light years away from the Earth. Their spaceships are similar to our beamships, and extremely well equipped, and are very able for space-traveling. The atmosphere of their homeworld is very similar to the Earth atmosphere, thus they can breathe here without great difficulty. They wear close-fitted filter-dress, which offers protection for them in some ways.[20]

The Roswell Case is a reality because the UFO crash actually took place there, but this is denied up to the present day and will continue to be denied in the distant future by the American military and Secret Services, as well as by all government agencies, namely with flimsy, changing, stupid, and ridiculous excuses that will only surely testify to the fact that everything actually happened. With the crashed object, it concerned a beamship from the Reticulum systems. The crew did not consist of natural human life forms but of human androids of a bioorganic nature, which means that they were artificial human androids, which the US-Army also got a hold of, some living and some dead, and these were secretly kept in secret stations [for autopsy, above, opposite[21]].

With the bioorganic androids, it concerned effective artificial life forms, so not robots or the like, but independently thinking beings, in every way self-capable of making decisions, made out of living material and living organs, bred in accordance with the human beings who are located in the Reticulum systems. In Earth-human terms, these bioorganic androids bred by the Reticulum people are actual life forms, and as such, they are respected by the Reticulum people and are also appreciated and treated, for the androids are, indeed, artificial human beings. As such, they stand under the command of the real humans of the Reticulum systems, on whose behalf they also carry out excursions, etc. to foreign star systems and planetary systems. And such artificial human forms were associated with the crash, as I already explained.

The intelligence of these android beings stems from a bioorganic consciousness of an artificial form, which is just as capable of development as the consciousness of the normal, natural person; therefore, it can also be creative and inventive. The type of consciousness is designed uniformly and collectively in each android, which means that all of the androids have a uniform consciousness form, and so, they are collectively like-minded, and thus, a collective form of telepathic communication is owned by them… which doesn't correspond to an actual personality but rather to an artificial form, which can think quite independently, act, and decide, as well as develop itself further, but which isn't arranged into conscious evolution but only functions according to conscious instinct… [Yet], in spite of the collectivity, [such an android] has its own individuality…

The bioorganic androids of the Reticulum people contain an authoritative programming in their artificial consciousness, which prevents that the artificial beings could ever rise over their designers, respectively their creators, but the time of their lives is limited to 300 years of devoted servitude to these. Nevertheless, they are entirely free and can in every way decide as to what responsibilities they undertake, exercise, or decline and, thus, whether they want to focus on a task or not. So they are in no way subject to compulsion by their creators.

In the manner in which they are biologically created, they are incapable of performing sexual acts and also of reproducing themselves. Their… artificial-bioorganic consciousness does not contain a creative spirit form, which would drive and animate this by its own energies. Animation is provided by the artificial brain, which is constructed in such a way that it can absorb and use the cosmic-electromagnetic life energies, so that the existence of life is guaranteed. It is this cosmic energy, by which the artificial life forms are animated and also made alive. All this, however, couldn't be recognized by all the doctors, surgeons, and pathologists, etc. in the American secret stations, where the crashed android beings were taken. But how could they, since their knowledge relating to this wasn't in place yet? In fact, it will still take many centuries and even several millennia before the terrestrial scientists arrive at the possibility of creating such beings as the bioorganic androids. Therefore, these beings will remain an unsolvable mystery to them for a very long time, as it is also the case for them with regard to the crashed beings in Roswell.[22]

The complex information given by Quetzal concerning the bioorganic androids of the Reticulum people includes specific details of their collective telepathic communication and animation by ‘cosmic electromagnetic life-energies’ that indirectly refer to the resonant fourth-density environment of HHO plasma that is artificially created within their interstellar spacecraft. Brainwave and heartbeat synchronization engendered by resonant acoustic standing waves produced within the plasma ships induces collective telepathic communication, while animation of the artificial consciousness and bodies of the androids is accomplished by the nanopulsed bioelectric currents of HHO plasma.

Further corroborating physical evidence for the fourth-density origin and biorhythmic animation of the Roswell androids has been documented by anthropology investigator Lloyd Pye –a small, unusual humanoid skull discovered 80 years ago in a cave in Mexico. Known as the ‘Starchild’ skull (above, opposite), it displays a set of cranial features that closely resemble those of the Roswell humanoid, with extremely large ocular cavities and an expansive, round brain vault with a very broad, flat occipital region. DNA testing of the Starchild skull has revealed segments of unique genetic material, and bone density analyses show major deviations from average human skulls, confirming the skull’s extraterrestrial origin.

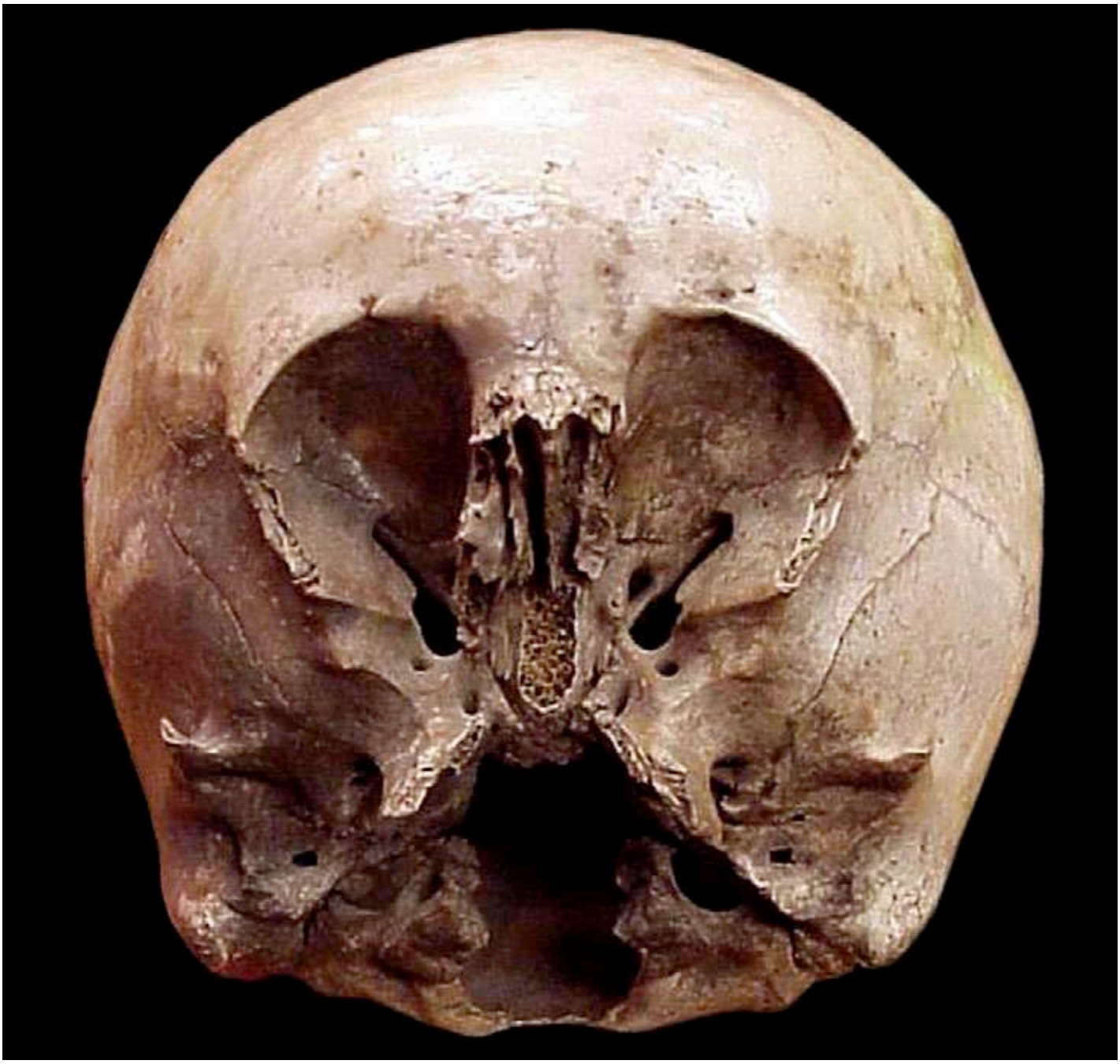

The Starchild skull is thought to be 900 years old, according to radiocarbon dating tests.[23] Further analysis revealed the bone is twice as hard yet half as thick as the skull bones of an Earthly human being, with a density similar to tooth enamel.[24] The unusual braincase presents a volume of 1600 cubic centimeters (cc), allowing for a brain mass that is 200cc greater than the average human brain.[25] *DNA testing has identified unique portions of genetic material that correspond to no known species.*[26]

Microscopy studies of bone samples taken from this unusual skull provide the most significant evidence of advanced artificial bioengineering. Cross-sections of the bone revealed the presence of metallic nanowires running through the many cavities crisscrossing its structure, known as cancellous holes (inset, opposite), that were not cut by the high-speed stainless steel rotary saw. Spectroscopic analysis of the nanowires has yet to be undertaken to determine the elemental composition of the metal.[27] The enhanced electrical conductivity of metal nanowires grown within the artificially modified skull distributes the nanopulsed electrical currents of the HHO plasma atmosphere maintained within the Reticulum spacecraft to sustain the artificial lifeforms as they undertake interplanetary excursions.

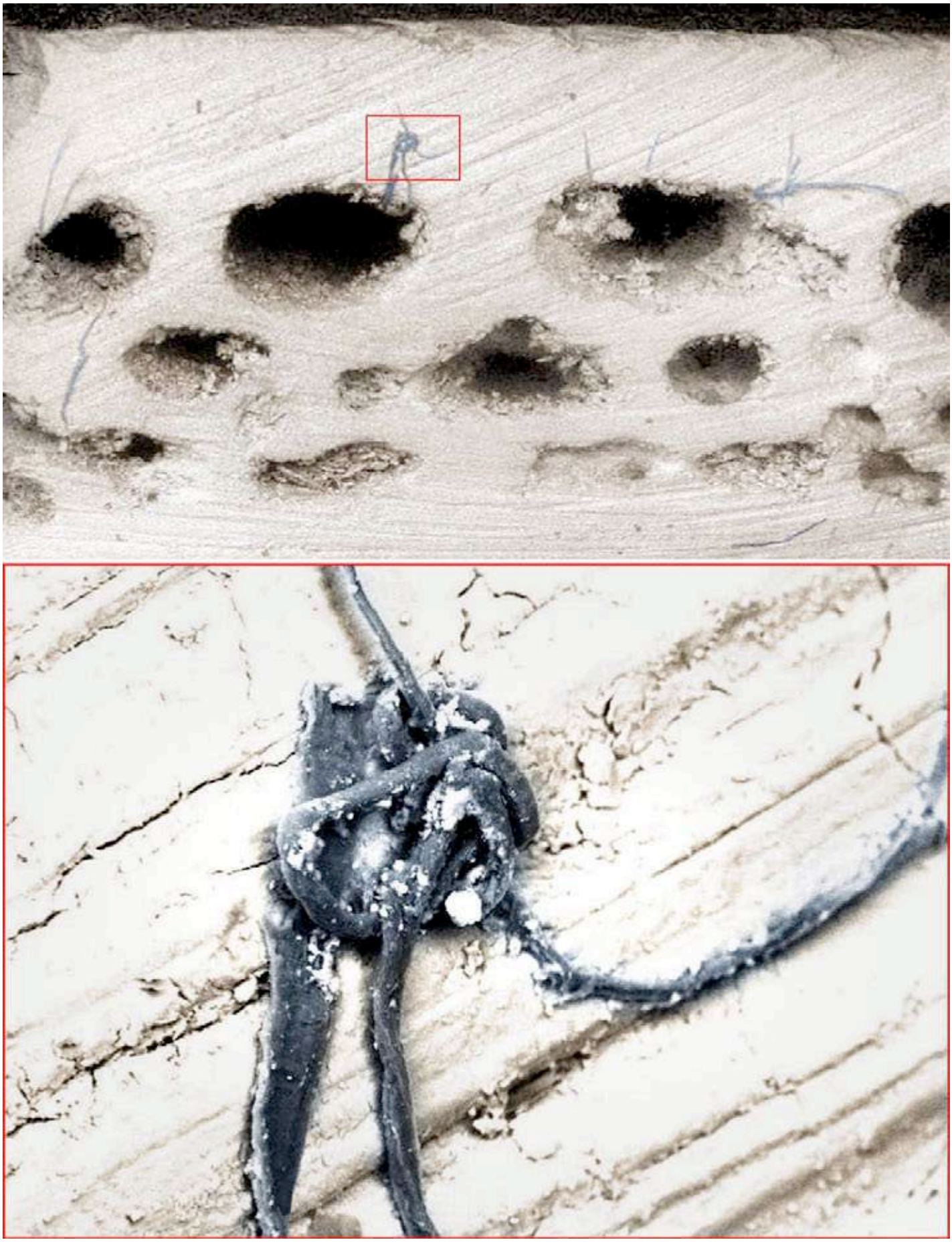

The longstanding presence of technologically advanced extraterrestrial visitors from the Orion, Reticulum and Draco star systems, among others, extends hundreds of thousands of years into the veiled human past. This ancient and still ongoing pattern of activity is recorded in artistic representations from all over the world, and many stunningly accurate depictions of the bioorganic androids of the Reticulum people are to be found among various indigenous cultural traditions. The Wandjina figures of Australian aboriginal traditions comprise a stunning record of interactions with extraterrestrial visitors that spans several thousand years in successive layers on the walls of sacred rock shelters and cavesites.

The Wandjina figures are depicted with large almond-shaped eyes, small open mouths and short-limbed, dwarf-like bodies, just as represented by ancient artists from Mesopotamia, as well as among Andean artists on the other side of the Pacific Ocean. A Chancay tri-frequency psychoacoustic whistling vessel displays this same combination of unmistakable features seen in the Reticulum androids, and even includes the accurate anatomical modeling of six fingers on each hand (opposite).

The diminutive Reticulum androids are also represented in Tayrona gold masterworks from Colombia, showing infrasound standing waves converging on the two hemispheres of the brain, inset by 3 spirals representing the tri-frequency resonance (above). The figure holds a double-spiral belt at his waist representing the control of DNA states under the influence of psychoacoustic resonance. These many specific features reflect an accurate and longstanding cultural knowledge of these cosmic visitors, and their connection with highly advanced psychoacoustic technologies of consciousness that were practiced on Earth during Atlantean times, before the Great Deluge that silenced the worldwide infrasound network.

Dozens of antediluvian bronze masterworks from Sanxingdui, China preserve very tall reptilian humanoids associated with the diminutive bioorganic androids from the Reticulum star system, quite likely their designers (above). The physical characteristics of this reptilian race have been described by modern abductees in exactly the same detail and scale as depicted by ancient Chinese artists, associated with populated homeworlds in the Draco constellation (hence 'Draconian' –of the dragon). Bioorganic androids are used by the reptoids to pilot vehicles and carry out tasks in the harsh atmospheres of foreign planets.

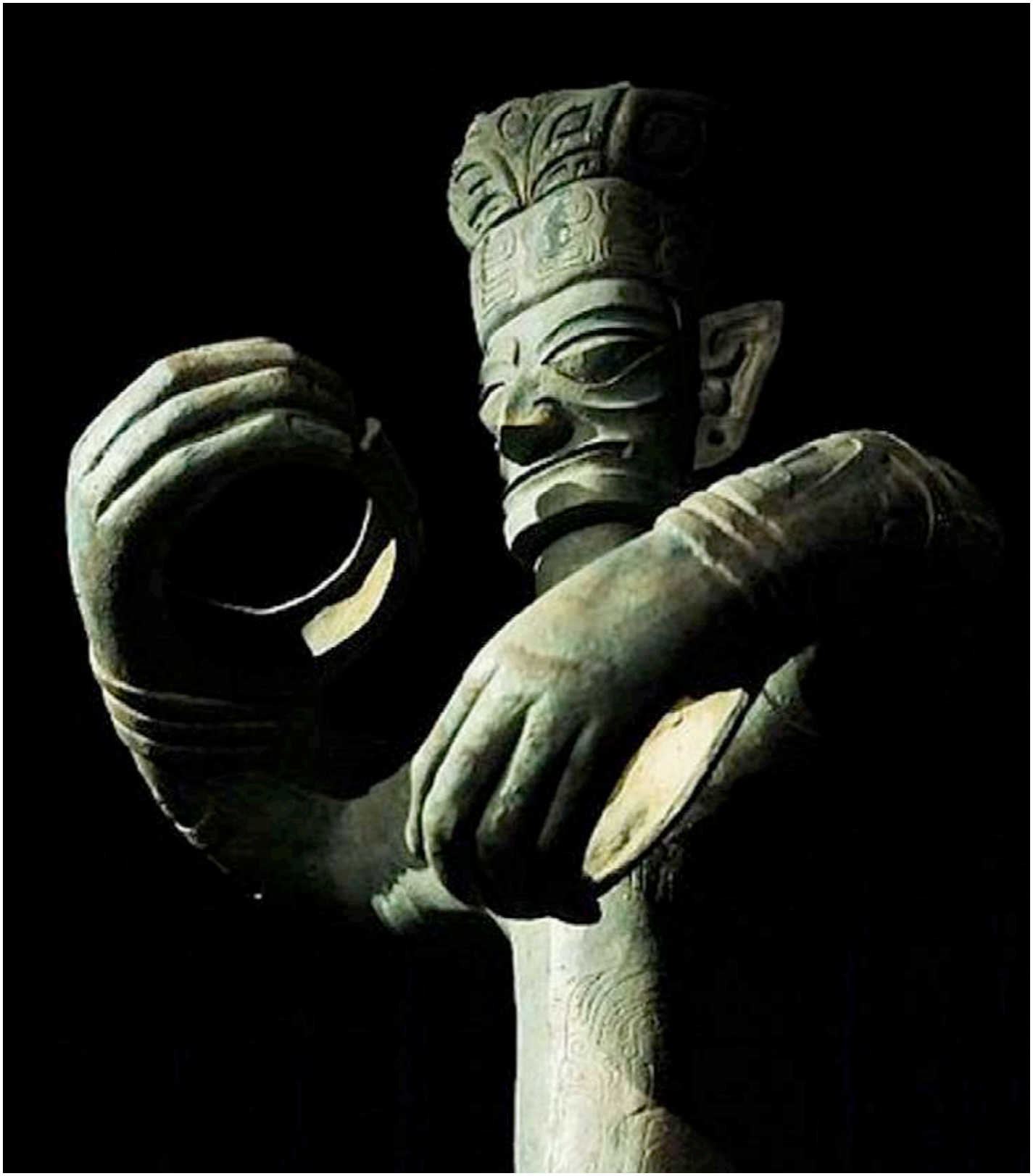

One giant reptilian figure from the Sanxingdui collection wears a headdress surmounted by a circle and a set of standing waves that converge above the crown chakra of the figure (above), as similarly seen on the headdress of the kundalini figure hammered into copper plate from the Crespi collection of Cuenca, Ecuador (p. 10). The complete set of cultural references to infrasound standing waves and kundalini development is shared on all continents, belonging to one ancient mother-culture of Aztlan spanning the entire globe in geomagnetic alignment with the Great Pyramid of Giza, Egypt.

The sheer walls of Barrier Canyon still reverberate with an intense infrasound resonance, and bear many profound Atlantean cultural symbols in the red ochre renderings of several millennia past. Part of a larger wall mural, two very tall humanoid figures are seen levitating into the air with writhing double serpents representing DNA, with concentric circles shown at the heart chakra representing infrasound standing waves tuned to the heartbeat frequency (above). Pairs of concentric circles form the eyes of one of the figures, connected by the arc of a standing wave signifying the hemispheric synchronization achieved by psychoacoustic entrainment. The same psychoacoustic effect is signified by plants sprouting from the head of the other figure like living antennae, with several small flying birds encircling it.

A group of seven luminous white caves are symbolically represented between the two tall floating figures, known as ‘Chicomostoc’ – the 7 sacred caves described in the origin story of Aztlan still retold by the Maya.[28] Luminous plasma ships are depicted as circles flying around the levitating figures, with standing waves radiating from some of the spacecraft (see p. 28), while others appear to be moving in formation through the sky, just as observed and videotaped in our times by thousands of dismayed eyewitnesses.

References

[1] -- (2010) ‘‘Rain of Luminous Beams’ Appears in the Sky of Xiamen Huandao Road’ *Southeast Express*, July 12, online · http://www.humanresonance.org/xiamen.html

[2] Moulton Howe L (2009) ‘Eerie ‘Blades of Light’ in Longview, Texas September 9-10’ *Earthfiles*, October 10, online · http://www.humanresonance.org/longview.html

[3] Putney A (2008) ‘Ø’ *Human Resonance Productions*

[4] Lyman W, Kaali S (1996) *‘Biocompatible Electric Current Attenuates HIV Infectivity’* online, · http://educate -youself.org/cn/LymanKaalibiocompatibleHIV1996report18nov06.shtml

[5] Dark T (2001) ‘African Avatars and the third Secret of fatima’ *Nexus Magazine* 8:5, August-September, online · http://www.sons-of-ra.org/writings/African%20Avatars%20and%20the%20Third%20Secret%20of%20Fatima.pdf

[6] Cervenka M, Bednarik M and Konicek P (2003) *‘Nonlinear Standing Waves in Acoustic Resonators with Arbitrary Reflection Coefficients at Their Walls’* Czech Technical University, Prague

[7] Men, Yaxk’in, op cit

[8] Schildmann, K (1999) *‘Als Das Raumschiff ‘Athena’ Die Erde Kippte -Indus-, Burrows-Cave- und Glozel-Texte Entziffert’* CTT-Verlag

[9] Men H (2002) ‘Magnetic Activation of the Pyramids Through the Crystal Skulls’ *Human Resonance*, October 22, online · http://www.humanresonance.org/activation.html

[10] Sitchin Z (1999) *‘The Wars of gods and Men: Book III of the Earth Chronicles’* Harper, online · http://www.bibliotecapleyades.net/sitchin/sitchinbooks03_03.htm

[11] Bernard R (1960) ‘I Found Shaver’s Caves’ *Search Magazine*, March, pp. 26-29

[12] Hesseman M, Zahradnikova N (2001) *‘Ships of Light: The Carlos Diaz Experience’* 2000 Film Productions

[13] Tesla N (1978) *‘Nikola Tesla: Colorado Springs Notes 1899-1900’* Nolit, Beograd, Yugoslavia, pp.61-62

[14] -- (1913) ‘Nikola Tesla’s Plan to Keep "Wireless Thumb" on Ships at Sea, Suggests Transmitters Powerful Enough to Cause the Earth to Vibrate at the Poles - and Equator’ *New York Press, November 9*

[15] Tr. Scott Corrales (2003) ‘Ufologists Pick Up IntraTerrestrial Waves’ *Diario El Tribuno de Salta*, online · http://www.eltribuno.com.ar/salta/20030523_213309.php

[16] De Aquino F (2000) ‘Possibility of Control of the Gravitational Mass by Means of Extra-Low Frequency Radiation’ *Los Alamos National Laboratory*, online · http://arxiv.org/pdf/gr-qc/0005107

[17] Hesseman, op cit

[18] Prabhu CS (2001) ‘Ancient Indian Metallurgy’ *Earthsystem Sciences Awareness and Research Association* Hyderabad, India

[19] Santilli R (1995) *‘Santilli Footage, Debris’* online video · http://www.youtube.com/watch?v=1B8cCNu-FME&feature=related

[20] Stevens WC Ed. (1990) *‘Message from the Pleiades: The Contact Notes of Eduard Billy Meier, Volume 2’* Genesis III Publishing, pp. 33-34

[21] -- (2007) ‘Alien Autopsy’ *Google Video, online* · http://www.google.com/m/search?oe=UTF-8&client=safari&hl=en&aq=f&oq=&aqi=-k0d0t0&fkt=1520&fsdt=9277&q=alien+autopsy+video

[22] Meier E, Tr. Stevens B (2010) ‘Pleiadian/Plejaren Contact Notes Volume 5’ *Billy Meier Translations*, online · http://www.billymeiertranslations.com/#dialog/divVolume5

[23] Pye L (2010) ‘C14 Dating of the Starchild Skull’ *Starchild Project,* online · http://www.starchildproject.com/dating.htm

[24] Pye L (2010) ‘Bone of the Starchild Skull’ *Starchild Project,* online · http://www.starchildproject.com/bone.htm

[25] Pye L (2010) ‘Brain of the Starchild Skull’ *Starchild Project,* online · http://www.starchildproject.com/brain.htm

[26] Pye L (2010) ‘Starchild Skull 2010 Nuclear DNA Recovery’ *Starchild Project,* online · http://www.starchildproject.com/dna.htm

[27] Pye L (2010) ‘Strange Fibers Inside the Bone of the Starchild Skull’ *Starchild Project,* online · http://www.starchildproject.com/fibers.htm

[28] Ghostwolf R (2007) ‘Ancestors of Our First Americans’ *Robert Ghostwolf*, online · http://www.robertghostwolf.com/Aztlan/outheretv.htm

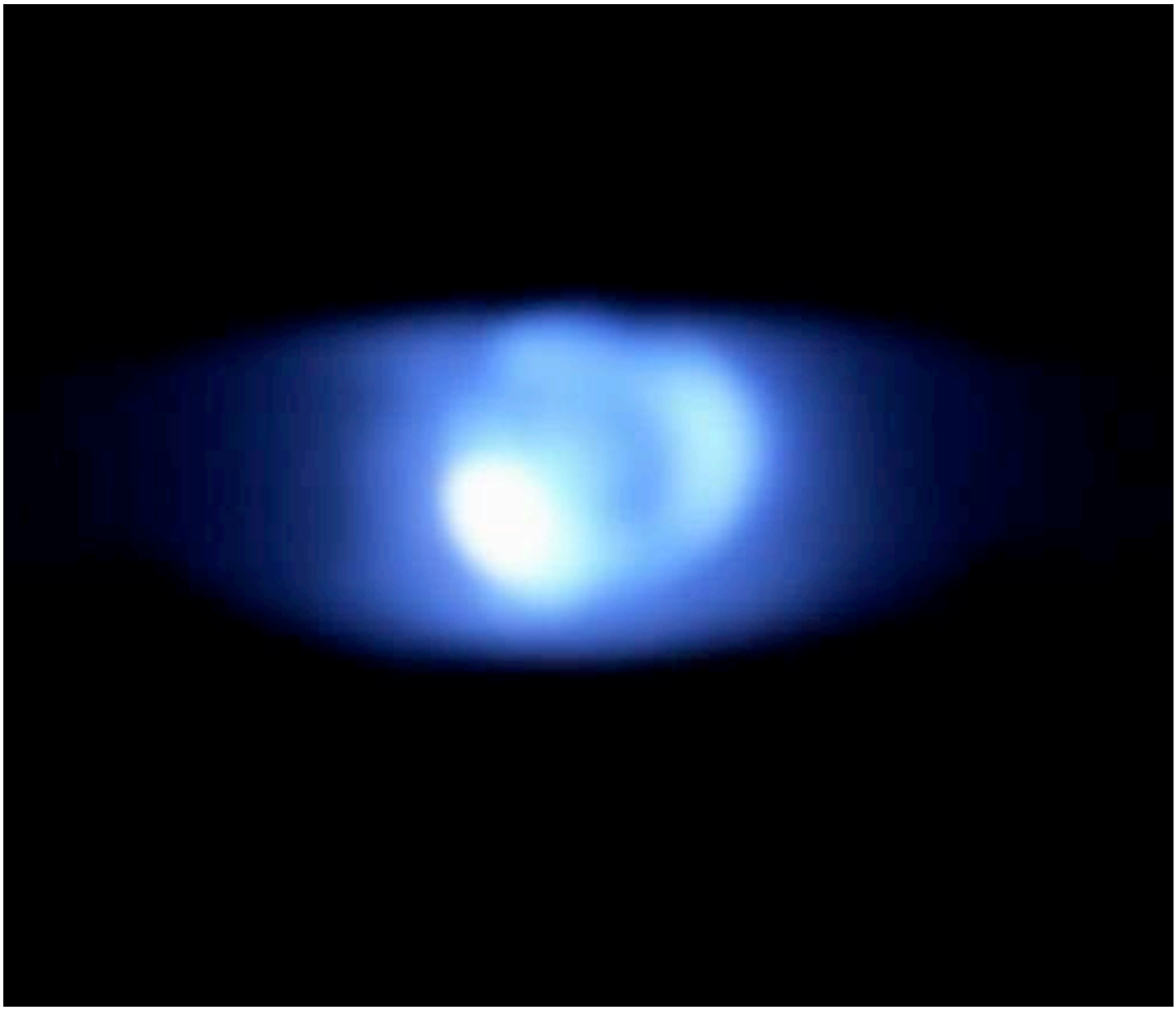

2
Contacts from Koldas

Contacts from Koldas

A remarkable set of still ongoing extraterrestrial contacts that began in 1968, in South Africa, present a fascinating perspective on the unfolding human experience. A young radio/electrical engineer living in Richard's Bay, South Africa (above), 'F. Edwin W.' (alias) received radio transmissions from a cosmonaut in Earth orbit named Valdar, from the planet Koldas. Subsequent years of regular radio contacts and comprehensive face-to-face conversations included other wise cosmic visitors from a Confederation of Planets in alliance with Koldas. Extensive and profound information shared during the visits of Valdar, Kashendo, Taylanz and Wy-Ora were recorded and later published by Carl van Vlierden in 1986.

Edwin was told that the primary structure of the Confederation of 12 Planets was peacefully founded in the Grandor star system, comprised of planets Grandor, Leec Goran, Sparlane, Velaan and Novan; and has extended to include the planets of neighboring systems like Koldas, Salamia, Siton, Bryonne, Pyrole, Pyrc Furvey and Triaxula. Valdar provided Edwin with a basic description of his homeworld, Koldas – a giant world with freshwater oceans reflecting the purity of planetary systems at high resonance:

> 'It is many times larger than Earth. We have seas on Koldas, but these are freshwater seas. There are also large lakes, the largest about 24,000 km long and 20,000 km wide. Some of the towns of Koldas are in the mountain regions while others are by the sea. The towns are similar to yours, except that buildings are constructed differently. There are no roads here for our vehicles travel above the surface of the ground. Our buildings are linked by conveyors to take people to their destination. Our capital city is vast, much larger than New York. Of course there are rural areas with smaller homes for one or two families, and there are forests and also rivers. In the large lakes there are islands where you find holiday resorts.

‘Our way of life is very similar to that of Earth. What I am trying to impress upon you is that we do not differ from you. The only difference is our mental attitude. Our way of life is different. We have no monetary system; no currency whatsoever. Each planet in the Confederation produces and plays a vital part in the whole. Some are rich in minerals and supply these to the others and some are more suitable for cultivation. Koldas, with its seas or lakes, has an abundance of fish, harvests of which are sent to other planets in the Confederation in exchange for minerals and materials to build the powerful Astrael-craft. And so my friends, a chain of good-will and understanding links all our planets. Earth too could play a part in this Confederation… We are like you. We are in the flesh. We feel pain and we die. The difference is that we are able to travel at this fantastic speed.’ [1]

The visitors from Koldas spoke in words of genuine compassion during their many radio contacts with Edwin (below). Valdar expressed deep sorrow concerning the intense suffering of children of war:

Valdar then reiterated that most of Earth's governments, political rulers and Superiors, knew of the Koldasian operations and the Confederation. He said they had known of the presence of Confederation craft over their countries and in the oceans for a very long time… ‘What makes me sad,’ Valdar said, ‘is the unnecessary bloodshed and warfare on Earth. I often think of the little children who are the innocent victims of all this violence. Infants without homes having to find refuge, food and water, yet they have no idea why their parents are at war. There are areas of dire poverty. All these scenes and much more were recently recorded by the three-day aerial survey. This too contributes to the Confederation's decision to withdraw their patrols.’ [2]

The observation of humanity and monitoring of the rapid development of Earthly civilization is a primary task of Confederation vessels, including the older Astraelcraft and newer Corynthian spacecraft, which incorporates their most advanced designs with automatic instrumentation, representing a most formidable interstellar craft, in terms of both annihilating power and instant translocating capacity:

‘The craft used by space-travelers range from two-seater scout-craft carried by their motherships, to the largest masterpieces of design and technology which are veritable floating cities in space. The Confederation spacecraft were spherical in appearance prior to 1941. It was these craft which were used to explore the Universe and solar systems many thousands of years ago. Then the spherical craft were superceded by the Astraelcraft. These were named by the Koldasian designer in honor of his wife Astraelda. Other smaller craft are disc-shaped. Larger carriers are cigar-shaped and measure in kilometers. These are used for cargo and passengers.

'All these craft are propelled by magnetic flux. The magnetic streams have different layers with various velocities. The motors, with which all craft are fitted, serve as rudders directing the craft into the various velocity layers. The highest velocity is reached on the outer surface and can exceed that of light. The magnetic streams criss-cross deep space, connecting planets, solar systems, galaxies and even universes in a vast web of highways and by-ways for space-travelers and their craft…' [3]

Koldas had enjoyed 20 centuries of history without fighting of any kind and consequently the only deterrent they could muster was their fleet of Astrael spacecraft. These craft are not intended for military service but are equipped with a 'Sun-ray' disintegrating laser or charged particle ray gun which is designed to annihilate meteorites in the magnetic traffic lanes. Its pencil-like 'laser' beam stabs at any object, destroying it in a brilliant flash without leaving a trace...[4]

I scrambled up against the side of the dune where I had a good view of the spacecraft as it touched down on the beach. As it came closer, I could see how enormous it was. It must have been close to 50 meters in diameter… I heard a low hum… It then rose up into the air… The ship now moved out over the surf, rising all the time… The craft itself was not emitting any light… The outside was steel grey in color but shiny. One could not see any rivets or joints or welds; it seemed to be one complete moulding, like two saucers put rim to rim.[5]

The technological advancement of Koldasian spacecraft reflects their comprehensive understanding of the nature of the human spirit. The physical limitations of corporeal existence have been mitigated by the artificial control of matter, space and time – freeing the human being to explore transdimensionality. Valdar's brief description of the spiritual views prevalent among the Confederation planets is highly reminiscent of the ancient Sanskrit traditions passed down through the ages from their original dissemination on Earth during colonization events described to have occurred over 70,000 years ago:

And he told me sometimes about the religion of the Confederation… He stressed that he did not give such information with the idea of trying to introduce it to Earth. He did say that many of our ancient civilizations knew of their religion, which was taken to our planet by members of the Confederation approximately 70,000 years ago. They believe that there is One Supreme Being, usually referred to as the Divine One. This Being is infinite and all-powerful and He creates all things, seen and unseen. Also created by Him was his Son. When man was created, the Divine One placed within the body of man a spirit or the soul, which never dies but continues on to eternity. The task of man's soul is to rule the material body by overcoming material desires... When this is ac-

complished, the soul will be called back to the great source and forever live in perfect joy and happiness. They also believe that all mankind is created by the same Divine Force, therefore all mankind are brothers and sisters. But this is a mere outline of their religion; there is much more – for example, their belief in reincarnation.[6]

The ancient idea of reincarnation present among most cultures of the world has only recently come under scientific scrutiny. Hypnotic access to memories of past lives stored in the subconscious mind enables the statistical comparison of specific psychological and physiological traits of successive incarnations of a spirit, whereby solid probability calculations can be made concerning the likelyhood of such a spiritual continuity. Well-documented reincarnation cases such as that of Jeffrey Keene and John B. Gordon (left) present so many extremely rare synchronicities – *elusive 'proofs'.*

In his discussions with Edwin, Kashendo described part of the Confederation's master registry as a vast reincarnation database, which cross-references the specific characteristics of every sentient being within the planetary collective as a statistical aid in identifying the successive incarnations of a particular spirit:

> 'Now as I promised,' said Kashendo, 'I shall tell you what we know of your past incarnations in our own Confederation… It is a vast subject and there is much to tell. Let me begin by saying that the master register is stored in a gigantic memory bank on the mother planet of Grandor. Here are the records of all beings who have lived lives in the Confederation.'
>
> Kashendo explained that the giant computer is housed in 37 buildings which are arranged in a circle around a central building. Most of the staff work in the central building which collects the required data from 'memory cells', consisting of thousands of transparent tubes with crystals inside them. Each tube is capable of storing many thousands of symbols and a memory bank consists of many thousands of these transparent tubes. The data is stored indefinitely and when needed the controllers extract it in coded form which is then decoded to provide the required information. All the equipment is very complex and kept in a special atmosphere.
>
> The memory cells store innumerable personal features and characteristics which reappear in the same individual through many lives. When a search is made, a special computer transmits the details of the required person to the whole range of memory cells. As soon as the features are recognized by a memory bank a message is transmitted back to the central control building where it is recorded. The whole process is complicated and Kashendo said that he found it difficult to describe it accurately, but he hoped it explained how the Grandorians are able to trace people's lives through time, at least within the Confederation.' [7]

The scientific tracking of a particular spirit through its long string of incarnations is a statistical task that requires great computational capabilities, which the Grandorian record-keepers achieve using supercomputers operating in 'a special atmosphere' of fourth-density HHO plasma. The geometric configuration of 37 buildings housing the thousands of memory cells is precisely aligned in a circle around a central building to make use of infrasound standing waves for the focused distribution of wireless power by which the HHO plasma chambers are resonantly synchronized. Edwin's spirit had selected a reincarnation on Earth as a means of transmitting information for the benefit of humanity. One of Kashendo's profound offerings of knowledge concerning the human past and the deep history of Earth revealed the presence of once breathtaking cities laid to waste on the ocean floor, along with the giant wreckage of huge interstellar spacecraft which enabled the colonization of Earth by different races seeking refuge from various worlds in peril (rather than being a byproduct of evolutionary processes):

Kashendo spoke about the various races we have on Earth and said, 'This is an intriguing subject but some of the mystery is known to the Confederation. We know that long before we first visited your planet, there were other visitors. When our ancient pioneers arrived there, they found evidence that whoever came before them must have come from systems far beyond those known to us. It is possible that they wished to colonize Earth. We do not know for certain whether this explains the many different races, but we do know that the race which you call the Red Indian, had ancestors who came from a far away planet doomed to destruction. They were highly civilized and had mastered space-travel. They left their home planet in a giant craft to search for new planets to colonize and reached Earth and there they settled. It seems that they were abandoned by their people or were unable to return home, possibly for lack of fuel. Their craft was stranded and so they remained on Earth. They were forced to improvise and learn to live off the land. They made use of what they had and what they could find. They hunted the animals; and learned to use them for food and sustenance.

'We know about these people, for they were very intelligent as a race, and one of the early ones to occupy Earth. But what about the many other races you have? We can only assume that they too were space travelers for we have definitely found the remains of many craft beneath your desert sands. Gigantic craft [have been found] which are not from the Confederation! Should these remains be discovered, they would cause a sensation on Earth as they are of enormous proportions. They must have carried thousands of people.

'It is possible,' he suggested, 'that they never intended to return to their homes. Were they banished and perhaps sent away as punishment? We can only guess at the reason for their presence but the evidence of their arrival from other planets is there, beneath the sands. This may be one reason why there are so many different races on Earth…

'When the Confederation carried out patrols beneath the surface of your oceans, they discovered many craft buried in the mud of the ocean floors. There is much evidence which will not be found soon, and much that has been lost. In another transmission I must tell you about the abandoned cities which lie beneath your Pacific Ocean; mysterious cities which must have been of great beauty before they disappeared. What catastrophe befell Earth? Who were the builders of these matchless cities?' [8]

These remarkable facts delivered by Kashendo attest to the great antiquity of human civilization on Earth, and the deep mystery of the cosmic origin of human racial diversity on Earth. While the existence of the remains of gigantic spacecraft below the (Sahara?) desert sands has been quite purposefully withheld from public knowledge by the world's governments, the same astounding scale is plainly witnessed in the pyramids of Giza, Egypt – designed to transduce and focus infrasound standing waves used for the propulsion of antigravitic plasma ships by acoustic levitation. Valdar explained:

> The pyramids… were used as transmitting and receiving stations and for the storage of magno-solar energy. They were located in a strategic area and the ancient Starships used to home in on them… Their design is significant in more ways than one. In the coming changes on your planet, this pyramidal design will again be used in your buildings.' [9]

Other discussions with the Koldasian envoys confirm that the 'pyramids [of Giza] were strategically placed in the geographic center of the land surface of the planet.' [10] This fact was recently reported by investigators of the Great Flood, who analyzed sea level data to identify an ancient global flooding event that raised sea levels by 178m, which offset the gravitic center of Earth's landmass by hundreds of miles to the northeast of Giza.[11] *This 178m sea level rise explains how the casing stones of the central pyramid have remained intact above that precise height,* while those casing stones below that mark were gradually torn away by the erosive wave activity of slowly receding floodwaters (above).

Long before the destruction of the pyramid resonance network by the Great Flood, the Giza pyramids pulsed with a tri-thalamic frequency of 1.45 Hz to synchronize heart/mind rhythms throughout all of the sacred sites of the planet and act as a homing beacon for the legions of spacecraft in transit through our solar system. The resonant excitation of planetary infrasound taps a vast reservoir of cosmic energy available to humanity once again through the oncoming changes, which include an intensification of planetary resonance. The deep hum of our planet, an infrasonic gravity field, is artificially recreated in all of the space-faring plasma ships' magnetic motors, as described to Edwin during a transmission:

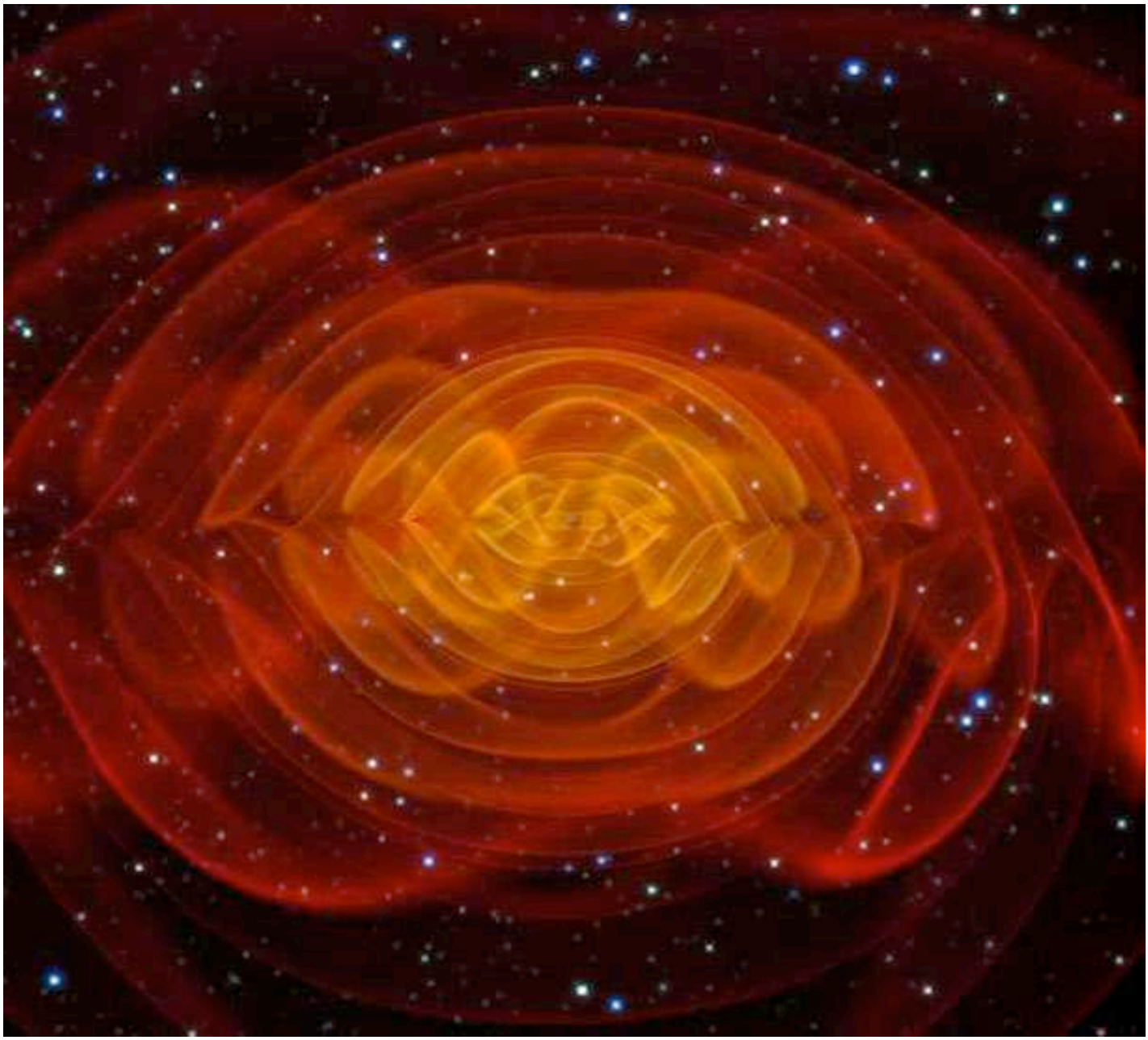

> Wy-Ora continued wistfully, 'If only your governments would unite in peace and extend the invitation, your skies would ring with the hum of magnetic motors… All our knowledge would be yours. All that we have achieved over the centuries would be given you freely. But unfortunately, your rulers cannot agree. They tell us many things; why they cannot accept us. But it all boils down to the fact that it would bring too many changes on Earth and that it would disturb the 'balance of things'.' [12]

In fact, all extraterrestrial matters have been kept secret by Nazi/CIA elements to preserve the present corruption of world governments, enforced by the military use of stealth technology stolen from Nikola Tesla in 1942.[13] The standing waves discovered by Tesla in 1899[14] display the same Fibonacci structure observed of galactic and solar systems (above), providing magnetic field lanes for magnetic propulsion:

> 'Each solar system has a magnetic field. Once you have broken away from the gravitational field of your planet, you can make use of the magnetic fields of other planets and solar systems to travel vast distances and even change in time… On Earth you are using the wrong method of propulsion. You are using fuels, liquid or solid or whatever they may be. This does not take advantage of the vast reservoir of universal energy. There is an unlimited supply of this energy and power that can never be exhausted. This energy is there for mankind to use on your planet.'

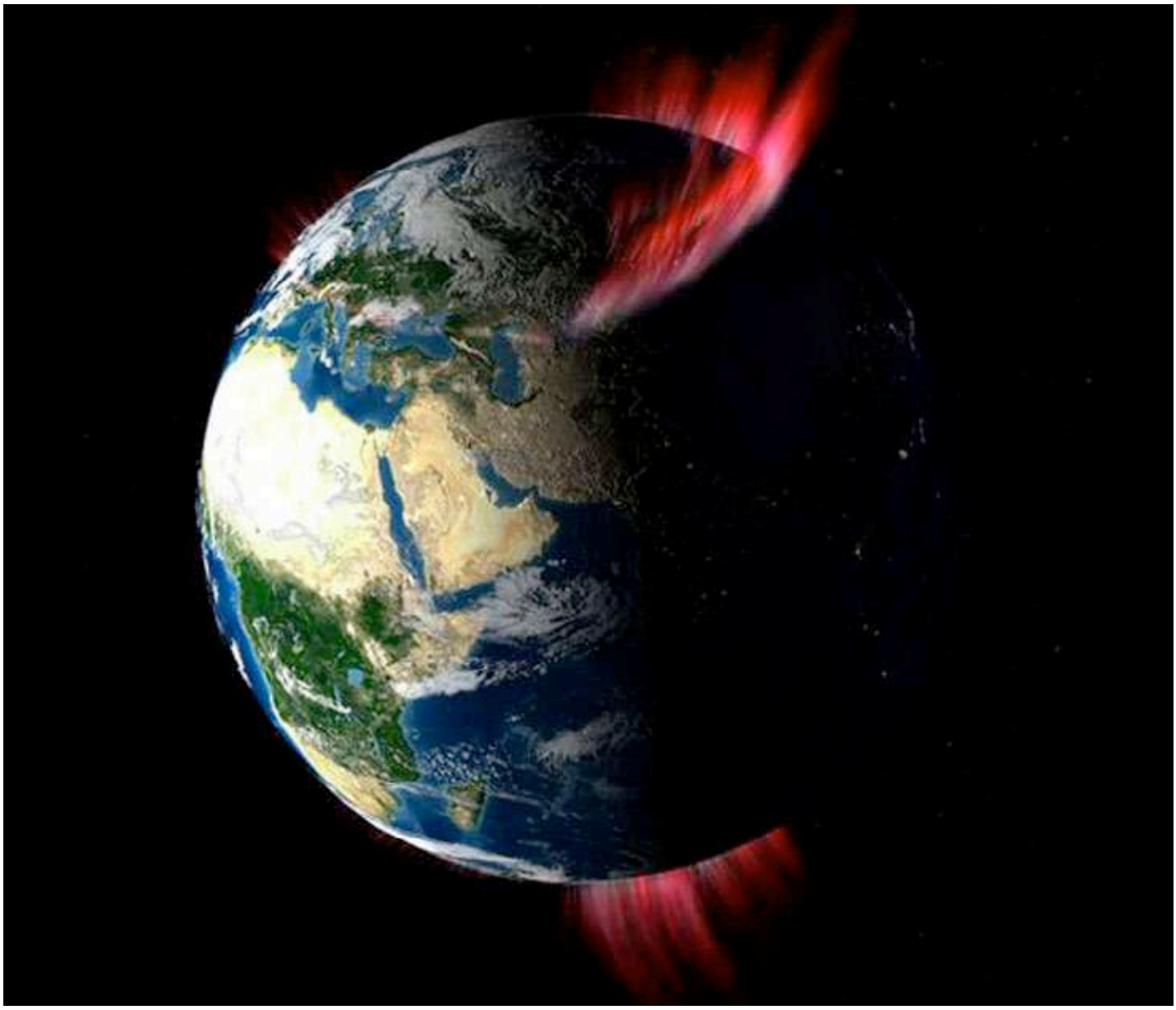

> ‘Let me explain further. The Astrael-craft I am in has eight magnetic motors; four forward and four reverse for control. These are actually giant electromagnets powered with solar energy. Now, beyond your planet there is a magnetic force-field which runs in streams between planets and solar systems, and even between galaxies and universes. Magnetic fields seem to run on forever. Once we are in a magnetic field we travel in this invisible stream through space. Our magnetic motors allow us to check and control our speed. Without them we could not select our destination. We would be helpless as a rudderless ship on a fast flowing river.’
>
> ‘Once a certain velocity is reached, things begin to happen. For a little while, breathing becomes difficult and the craft is controlled by a master computer. As you arrive in other universes (dimensions) awareness returns. Craft, computer, personnel and all which have existed in the energy-state flowing along the magnetic paths, now reintegrate with their polarity changed, to become solid matter again. And that my friends, is all there is to it. It is the magnetic fields which carry us at these incredible speeds, an changing time is a side effect of it. Your craft on earth could do this if you had the magnetic motors!’ [15]

The technical details of the magnetic motors were first discovered by Nikola Tesla during his wireless researches, and were later perfected in secret designs for antigravitic spacecraft using infrasound standing waves and HHO plasma, derived from water. The implosion of atomic hydrogen forms the unique plasma that protects all interstellar spacecraft. The presence of galactic magnetic fields, vast cosmic highways described by Valdar in 1970, were only recently identified by Earth’s scientists in 2009:

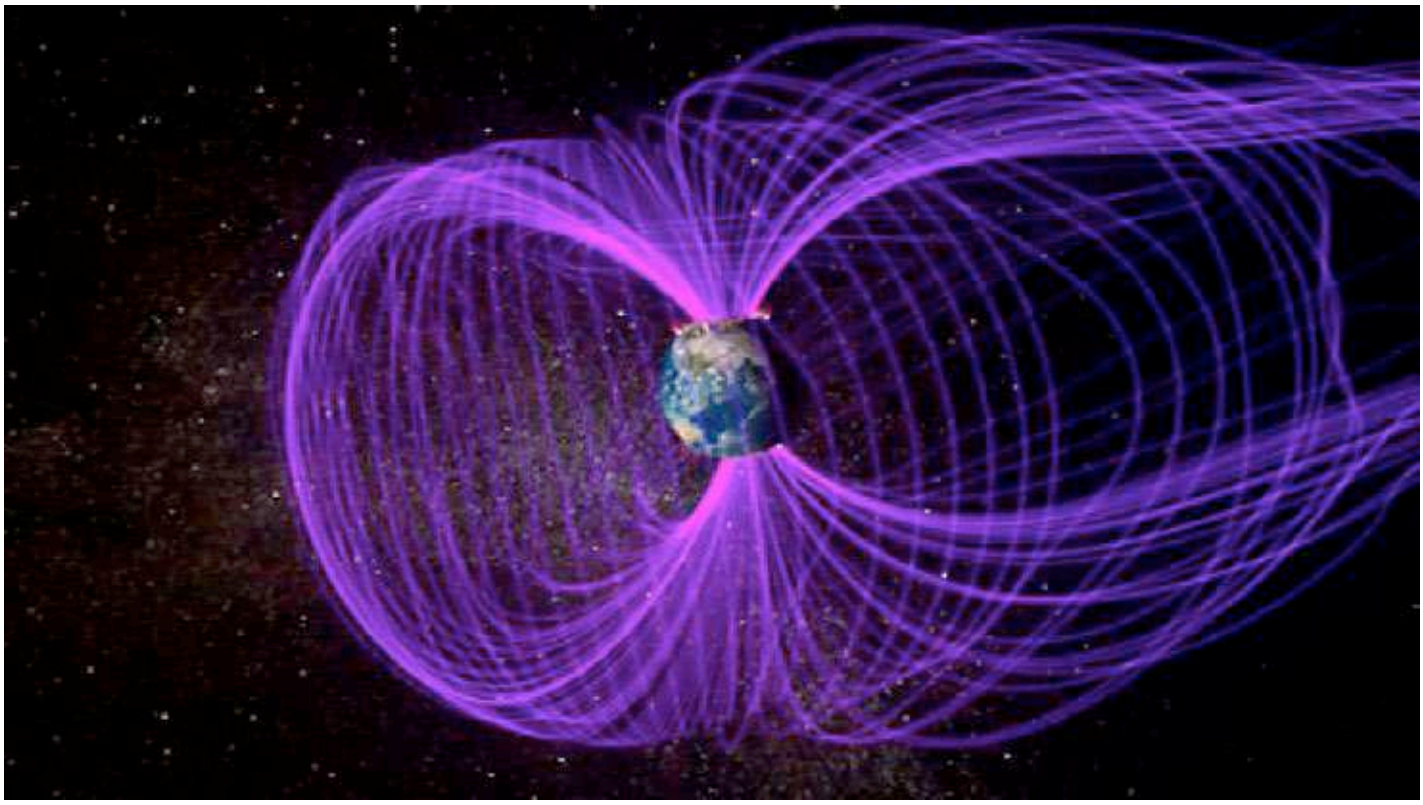

Last year, NASA's Interstellar Boundary Explorer (IBEX) made a discovery so profound that scientists had a hard time describing what they were seeing. A vast ribbon located in the outermost reaches of the solar system had been spotted, a structure that had never been seen before. Now scientists believe the shape might be created by a huge reflection caused by particles bouncing off a galactic magnetic field… In December it was announced that the veteran Voyager probes currently flying toward the heliosphere measured an unexpected increase in magnetic field strength. Scientists believe that this increase is due to an unexpectedly large magnetic field threaded through a cloud of interstellar gas called the 'Local Fluff.' Our solar system is currently speeding into this Fluff… [which would more accurately be called 'plasma'.]

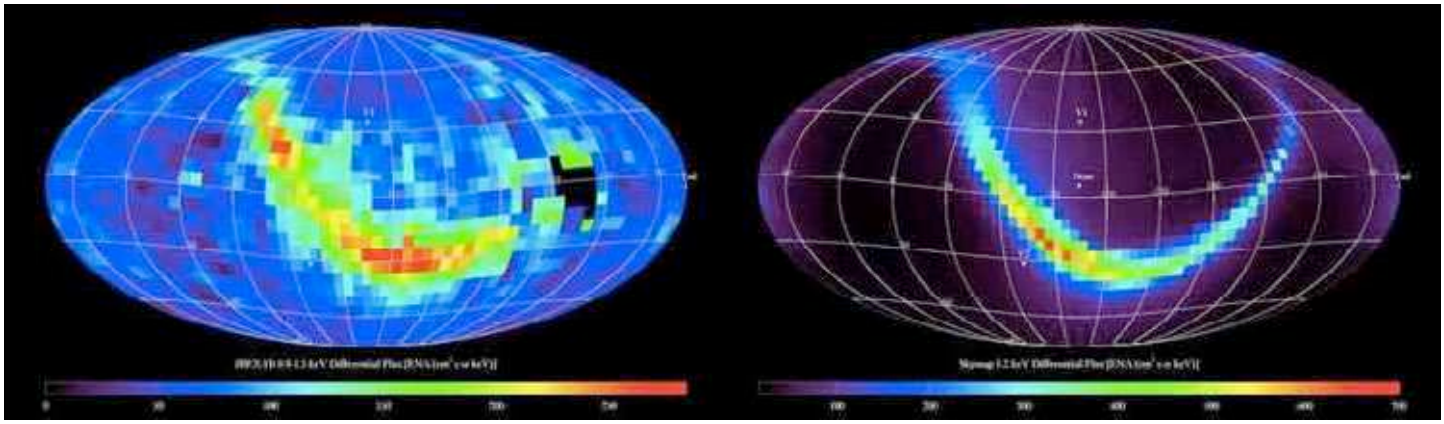

Jacob Heerikhuisen, a NASA Heliophysics Guest Investigator from the University of Alabama in Huntsville, believes the ribbon observed by IBEX is caused by an interstellar magnetic field… 'We believe the ribbon is a reflection,' said Heerikhuisen. 'It is where solar wind particles heading out into interstellar space are reflected back into the solar system by a galactic magnetic field.' [16]

These newly identified galactic magnetic fields connect star systems within the spiraling arms of galactic wheels and act as propulsion lanes for interstellar spacecraft. The advancement of human consciousness is required for the penetration of the light speed barrier, for which purpose the Koldasian visitors influence contactees like Edwin by a voluntary conditioning of the subconscious mind during deep sleep:

We asked Valdar about ‘conditioning’ during a thought-transmission. He said that initially we were tested to see whether we had accepted the Confederation ‘way of life’… ‘*Only then*’ he continued, ‘various methods of conditioning are used. This is done mainly during thought-transmissions. We describe our planets to you – our way of life – and we answer your questions. Your subconscious minds are conditioned by us to store certain impressions gained during these transmissions. These are of great importance later on.

‘We continued to condition you mentally, so you will accept more of what we give you. This is a long procedure and is still in operation at the moment. We will continue until we are satisfied. *This type of conditioning is done mainly at night, during the hours of sleep. While sleeping, everyone transmits a signal. This is normal and happens to everyone. We have instruments to 'tune in' to your particular signal; your personal frequency.*

Valdar continued, ‘You know that you all have a forward or conscious mind. You also have a mind that lies dormant, which we call the 'back' mind or the subconscious. This back mind accumulates a great deal of knowledge and a great variety of impressions lie stored there. A brain is like a computer. It may reach a stage where it will not accept any more. Then it refuses to receive new impressions and this mainly applies to one's subconscious mind. Then it becomes necessary to unburden this subconscious mind. This is to prepare you for all the new information you will acquire.

‘We have a method of conditioning by which we rid your subconscious mind of much that has been impressed upon it, making way for new conditioning. This has been carefully programmed for each one individually, to suit your mission and type of work. All data and information is placed there. This continues stage by stage, depending on how you accept it. It all depends on you.

‘We can tell what you have recorded of the information we have placed there and what you have received during the various transmissions via the thought-channel. Then comes a very important stage – the most important of all – and you are going through this stage at the moment. This is the stage in the program where you must accept a new way of life. I have already mentioned how strange things are beyond your solar system.

‘All this has been placed in your mind and it is done to alert your subconscious to be prepared. We are going to place in your memory-bank vital information that is needed if you should ever have to travel beyond your solar system, so that it will not refuse to accept what it will see and what conditions will prevail when you travel in Outer Space… You see, there are conditions which one cannot describe. One has to experience them to realize what is meant. One's body undergoes a drastic change in interstellar flight, for you will travel many times faster than the speed of light. Your body may be shattered into millions of particles and even your mind may experience this disintegration. This may sound more frightening than it is.

‘Now, when you are in that stage of disintegration, you will exist... and yet, you do not exist. For you (the consciousness) are *there* in 'energy particles' – you actually *flow*. Yes, the word flow describes it accurately, for you cannot leave your Universe unless you are able to flow through the magnetic field, coasting along the magnetic force lines. One cannot escape from your Universe and enter an other-matter Universe unless one undergoes change. You see there is a strange law out there, a law that has existed since the birth of the two Universes. There is a dividing line, which is invisible, beyond which nothing can go, *not even light rays*.

Therefore, to escape beyond that invisible barrier one must undergo great change. When the craft, including all its occupants, goes through this change, it is completely disintegrated into its elementary particles – into energy. After that one does not travel at speed anymore, as this does not describe it. One then travels in such a way that there are no words to express it... This happens only for a certain distance; the distance between the two Universes. Then one emerges into the anti-matter Universe and the craft and occupants revert back to solid bodies again, the process being reversed [to induce rematerialization].

'Let us put it this way. A container filled with water is suddenly spilled upon the floor where it spreads out. Now, suppose you had a magnet that could attract water. Place this near the spill on the floor and suddenly, it becomes one body of water again. This illustrates what happens when you disintegrate your body and craft into elementary particles - spread it out, so to speak - so you can flow from one Universe to another. You would flow through gigantic magnetic fields, which are of such high intensity that when you break through that invisible barrier you become energy and travel in time.

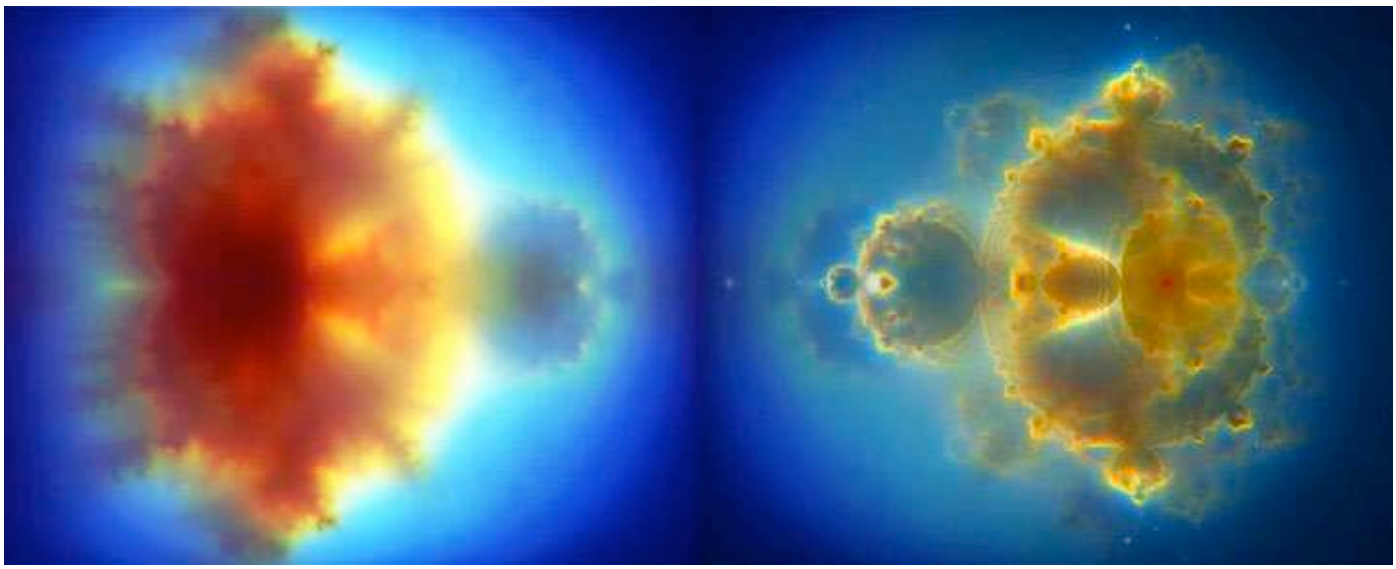

'This is the most important part of your conditioning because when you arrive on the other side, there is a world that you could never imagine! There are vast differences. You would not be as you were when you left *your* Universe. You would be in a new environment. Nature has molded you to live on Earth; you were never intended to go through the polarity barrier. It would be impossible for you to live on our planet the way you are now. To begin with, gravitation is so great that you would not be able to breathe. Koldas is such a large planet; the forces of gravity are correspondingly greater. You might survive, but under such great torture…

'That is why Nature remolds you when you penetrate that invisible barrier. It adapts you, not gradually, but suddenly, to the new environment. Even if your body might be able to adapt itself to the new environment, your conscious mind would not. Your subconscious mind does not care where it is, but your forward or conscious mind could not cope… It is fortunate that you all have a subconscious mind, otherwise it would be impossible for any of you to leave your Universe. Here we have a storehouse where all this vital information can be placed. We program your subconscious and tell it exactly what to expect; how to react; what to do and how to do it. So when you make your final jump and you arrive at the new world, your subconscious has been trained to take full command. Then you will no longer have a subconscious mind; then the complete brain will function – you will need it! Indeed you will. The new world is much larger – every solar system is so much greater; the way of life is so different…

The things one has to do would require your thought capacity to be so much larger – your concentration, your eyesight, speech, breathing, much more... then the subconscious would disappear... Only on Earth is the mind divided into a conscious and subconscious. Although we in the Confederation do have a subconscious mind, it is very small indeed. So you see, this is the most important part of the conditioning. Other stages consist of being taught various things, such as communication and telepathy and the acceptance of new colors. We respond to a greater range of colors. This extended vision is very important and has given us problems with some who have left Earth. We have found that their brains will not accept the wider range and intensity (of the colors) and they become muddled and very confused. So it has become necessary for our scientists to develop new means of conditioning to allow one to accept this.

‘It is difficult to explain all this to you. I do not compile this program for conditioning, myself; it is done by scientists who have spent their lives on this work. Each one of you is well known, not only to one particular scientist, but to many scientists. Every one of you has accepted and passed the first stage. Now there is a pause and it is my job to find out more about you. I have to find out much about each one of you, right down to the last detail, and all this is recorded and submitted to the panel of scientists who deal with mental programming. They then make a very careful study of all the data and select the best methods for your individual needs.

‘This may be different for each person. In some cases, photographs are needed. This we manage also and every detail is taken into account. It is very necessary that all these details are considered, as we cannot afford any errors in conditioning one wrongly, for it could do much damage, especially if the person needed to visit the antimatter Universe. If he or she were wrongly programmed, it could be fatal. Remember, in the fluid stage, while you are flowing between the two Universes, we rely on your subconscious to piece you together again in the correct way. For example, your height and your weight would increase. You would become more robust, *depending on which solar system you are visiting*. If your destination were Triaxula, then it would be in reverse. You would automatically adapt to the environment…

‘You see, once you are beyond the light barrier, that invisible line which separates our two Universes; *once you have made the first crossing of the line, you can at any time travel at or beyond the barrier, disintegrate and reform and coast through the magnetic fields at will.* You will find subsequent crossings much easier and faster. It is like being in two different seas. You are in one, and we are in the other. We, for instance, found that when we break through to your Universe, various difficulties arose. Difficulties in breathing [can occur]. Your sunlight interferes with our eyesight a great deal and we find your atmosphere very humid, even in your colder regions. So you see, once you leave your Universe and break through that barrier, your body automatically takes on the right shape and size and you adapt to the environment, provided that you have been properly conditioned.

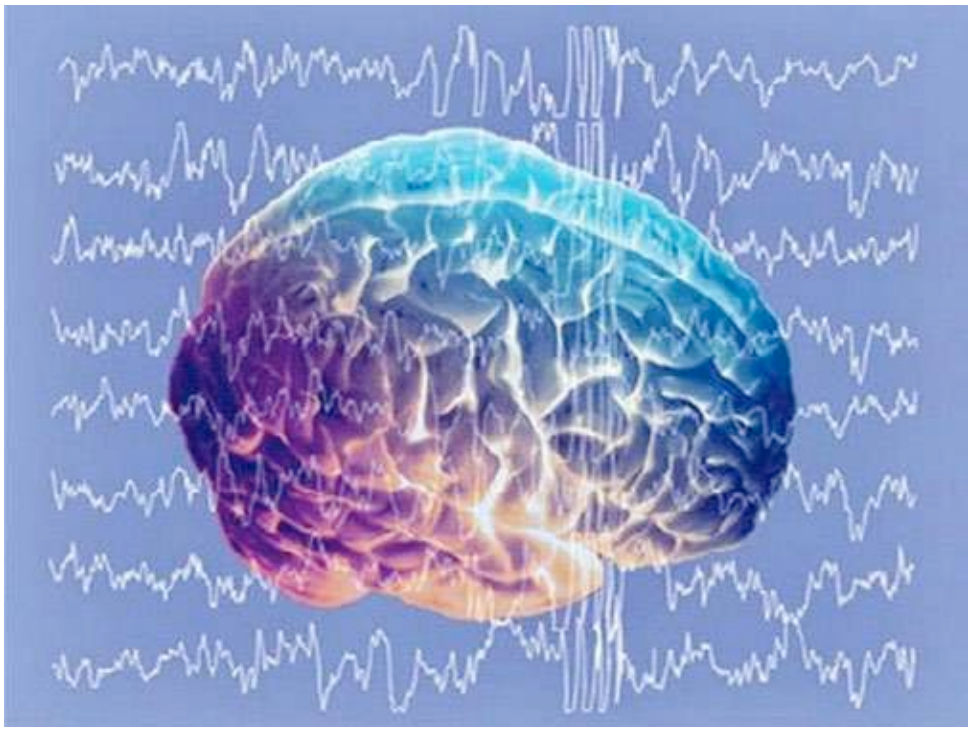

You will find that your brain capacity also increases and this is when the information which we have given you in our training will find a place. Your present brain is suited to your planet and present age. If you were to come to our planet with the same brain capacity as you now have, you would be in a great danger and trouble, for you would not be able to understand us and we would not be able to understand you. You would be as a primitive prehistoric creature would be if placed in your present society. That is why it is necessary to have this background training, this [voluntary process of advanced, subconscious mental] conditioning.

‘And when all of you have completed this, then you will be on our level. You are then full-fledged Koldasians, Byronnians, or Triaxulans or whatever the case may be. You would then find that you could travel at will from planet to planet, without any problem. And once you are beyond the light barrier, you will have no difficulty, even with the language. But this is new! The conditioning for language has never been used before for the scientists thought that it was far too much. Now they have realized that they can go much further and that is why, when you reach a certain stage, you will find that you have very strange dreams. These are very realistic dreams. You might even be able to smell or feel in these dreams. At first, this will prove alarming, for you may feel the heat of the day or the intense cold of the night. You will see things in your dreams, which we have placed there. You may, for example, experience living with nature.

‘We in the Confederation respect animal and plant life. We realize that without nature we would not live in a healthy and clean environment. As on Earth, nature is the same for us in the Confederation. Its beauty is very real to us! Mountains, streams, trees, flowers are the things we love –it is part of our life. Although we have a very highly evolved technical world, this does not mar our sense of freedom nor our appreciation of the beauty of Creation. We too like to escape from those technological marvels of science we have created. We too like to escape into the country to admire the beauty of the Divine One's handiwork, the planet he has given us to live on… Mainly this is what we impress on people's subconscious so that your conscious mind would know what to expect when you arrive. Your subconscious is trained to accept your new body, which would be totally different from what it is now. Sure, you would not turn green, or blue, but you would become larger people to suit the Koldasian environment. You are now being conditioned to be very close to the Koldasian standard.

‘Yes, going through the light barrier is a very big step,’ said Valdar, slowly emphasizing each word. Even for those of us who are used to [the changes]... For we undergo subtle changes when we arrive in your Universe. That is how we can mingle undetected with the population of Earth as we have done for a very long time in the past. But if we came here with the bodies of our Universe, we would be detected immediately. The major step is the ability to *flow* in the magnetic field through the light barrier. Of course, you would feel the changes here from planet to planet – gravity, heat, cold and so on. This you would experience, but your body has been conditioned to accept all this and much more.

‘Edwin has already reached the stage where we can use him to listen through his ears, see through his eyes and so observe local conditions on Earth. We can do this at our discretion and so keep in close touch with you all. Yes, you would be very surprised to see the *real* Edwin, the Koldasian Edwin – his twin.

‘Then, of course, age is a factor with the person being conditioned. The mind would also have to be adjusted to accept that the body would automatically become younger beyond the light barrier. This it does for some reason or another. It seems that you get a *new* lease on life, regeneration. This applies to all those born on Earth. *For us who are born in our other-matter Universe, long life is the norm...* There are special rooms where this type of conditioning is done. These rooms look like the operating theatres in your hospitals on Earth. The carrier I am in at the moment has three such large rooms. In the centre, there is a couch on which the person to be conditioned lies down. Then a device, resembling a helmet, is strapped on the head… This is connected to the strata-recorder and the crystals, and the thought-impulses coming from these are transferred via this helmet

directly to the brain. We can accomplish this conditioning in about one hour. However, the person is first placed in a sleep state and firmly strapped-down where he or she remains until the light barrier has been passed. This is the normal procedure. Those who have been conditioned already would be treated as the crew and would be seated in the main control centre. This is where I prefer all passengers and the crew to be when we transcend. This main control centre is the safest area in an Astrael-craft. Once beyond the light barrier, things return to normal and one walks and sleeps, and one can use the craft as one would an ocean liner.

Valdar continued his explanation. 'I have used the word 'conditioning'. This is not strictly the right word to use; probably 'programming', training or teaching would be better expressions. *Remember we do not do this against your will!* It is entirely up to you. The very first step is that *you* accept us, then you automatically tune your mind to our wavelength and only then do we continue to prepare you for the next phase. I am really your teacher, with many assistants… Of course, those crystals and that valuable instrument, the strata-recorder, could not be dispensed with…

Then another aspect of this conditioning program emerged when the discussion turned to the enigmatic subject called the 'New Age'. Valdar said, 'One has to be conditioned to accept the New Age. In the ancient scriptures of the Confederation, it is written that the Divine One will change *many* planets.

'A voice tells us that there will be a change. The timing of the event will depend on many circumstances. It might be caused by the separation of the two Universes resulting in a complete break in the magnetic field between them. This event may bring about changes which would gradually usher in a New Age. There might be a change in the atomic structure. *Every atomic power station would then cease to function, and even your electrical power would stop. But a new source of energy will then be available…*

'Your physical world would undergo a transformation – a cleansing of the Earth. *Then the resurrection would follow in the still of the night. This transformation would be almost instantaneous. Even the heavens would change color!* Mankind will be afraid, but a great uplifting will follow. *There will be regeneration; for example, those of 90 years age will be as 50, and those of you who are 50 will be as 30*.

'Many would not see these changes. Only those of you who can now accept the new way of life will perceive it and experience it. Many are now being conditioned for that day... and also for cosmic flights, should that become necessary. Your subconscious mind is being conditioned to prepare for such an event, should it arise. Then, as if with the turning of a switch, true understanding would come. Some of you may become teachers or leaders…

Valdar also mentioned again the disturbance in the magnetic fields, which, although unobserved by astronomers on Earth, caused an insurmountable barrier to all magnetically propelled spacecraft. This disturbance came to an end on the 18th of January 1981… 'Once the magnetic disturbance [of the December Solstice of 2012 occurs]… and the magnetic fields return to normal, then there could be a radical change on earth. When the changes come... and come they will, the rotational direction of Earth will be opposite what it is today. It would take the planet quite a while to readjust itself, but it will do so, for the earth is still a very young planet. These things happen to young planets! And they must happen before your sun becomes unstable and turns into a supernova and burns everything out. But there are still many millions of Earth years before that event.

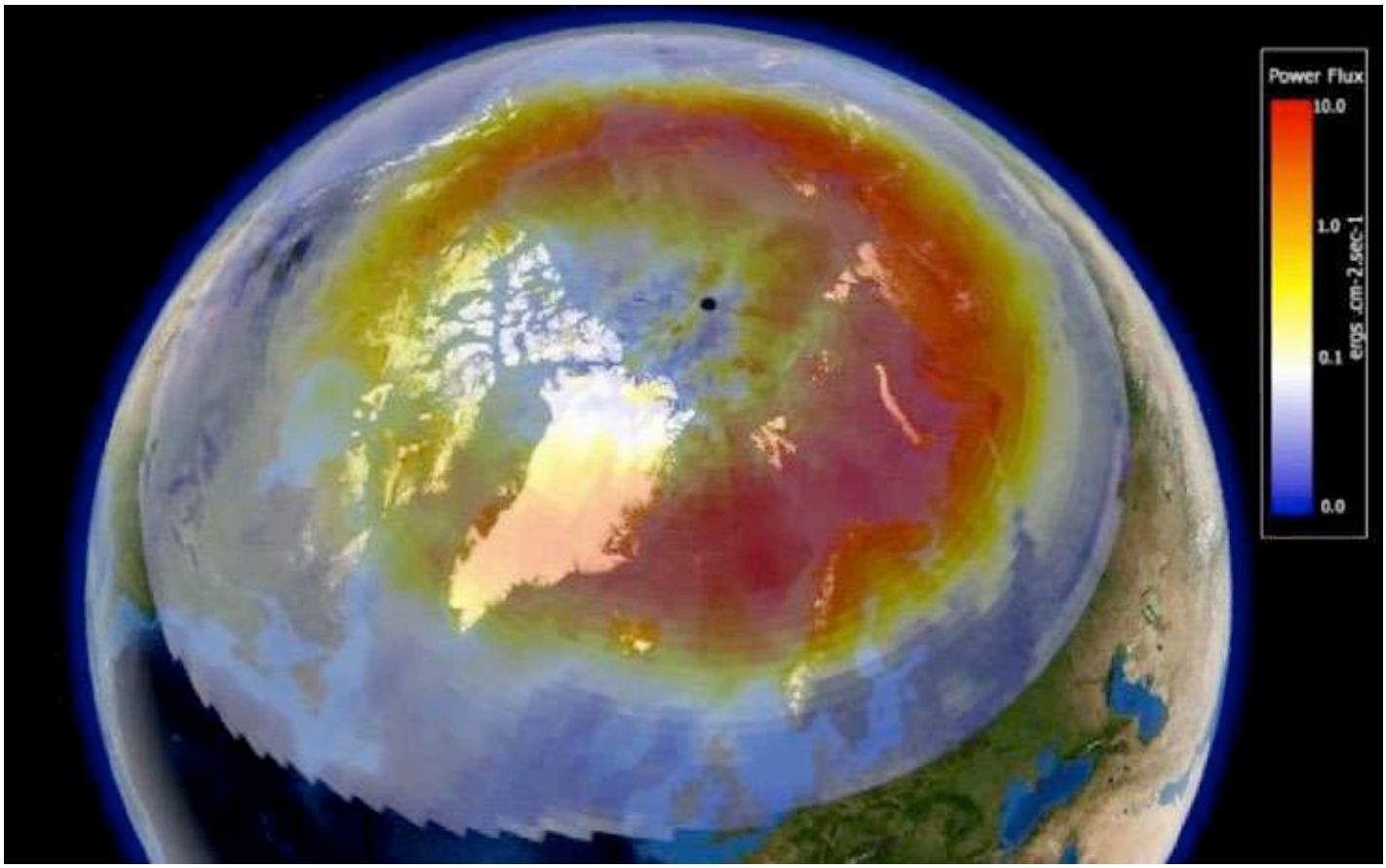

'But then there is the possibility that Earth may turn into a ball of fire as the result of a nuclear war. However, I feel that these changes, some of which I mentioned, will come before mankind on Earth can perform such a deed. Let us wait and see. There are still many things that even the Confederation is uncertain of. Changes can be observed and data analysed but only Mother Nature – the Divine One – will trigger the reaction that will change things permanently; I repeat *permanently* on Earth.

'The reversal of rotation of the planet would also change the polarity of Earth. North would become South and the South pole would become North. This could be brought about by a natural or an accidental cause… Great ships from space will come... then truly the planet Earth will be at peace. Those who remain will know our love and friendship. They will understand what the stars have to offer them. All this will be given to them and many things will be revealed in the New Age… And this is why we keep contact with you, to bring you messages of peace and love. We have tried to bring you an understanding of our planets and our way of life, which will be to your benefit when this great change arrives… and this will affect the whole of the Universe – not only Earth. These things have not been planned by us; we are just passing the message to you.' [17]

Valdar's clear statements elucidate dramatic future events and subsequent major atmospheric changes involving the oncoming shift of Earth to high resonance. *He foretells a 'physical… transformation – a cleansing of the Earth… in the still of the night… [that] would be almost instantaneous. Even the heavens would change color!'* A great increase in the intensity of cosmic rays bombarding the Earth, from a nearby supernova event or chain of events, would re-engage the now-dormant pyramids to ignite an atmospheric HHO plasma canopy, with plumes arching along the pathways of Fibonacci standing waves.

An astounding aerial HHO plasma phenomenon was photographed in detail on the auspicious date of 9/9/9 in Longview, Texas by motion-sensor game-trail cameras (above)[18], providing *recent, direct evidence* of the atmospheric and electromagnetic changes described by Valdar over 40 years prior to this enigmatic time preceding the magnetic reversal of December 22, 2012. The ultraviolet-A and infrared spectra emitted by the ionizing plasma plumes, as well as the precise standing wave configuration of the luminous arcs, confirm the photographed phenomena to be a product of ultra-low frequency irradiation of water vapor, causing its combustion by energized particles as HHO gas near ground level. *Atmospheric HHO plasma plumes and standing auroral patterns may become an everyday aspect of Earth's future.*

The inevitable result of high-energy atmospheric change will be *the purification of the ambient light* that penetrates many layers of HHO plasma to reach the ground, providing healing ultraviolet-A and infrared light to all terrestrial lifeforms. Just as demonstrated in HHO plasma beam healing devices like the Godlight cellular regeneration beam of Troy Hurtubise,[19] the atmospheric conditions will dramatically alter the lifecycle of all living terrestrial creatures: 'There will be regeneration; for example, those of 90 years age will be as 50, and those of you who are 50 will be as 30.' The regenerative effect of the frequencies of light emitted by HHO plasma promotes the extreme longevity enjoyed by advanced space-traveling civilizations on their homeworlds, and also generated inside the cabins of their interstellar spacecraft.

The highly resonant atmospheric purity of the planet Koldas affords a longevity that is significantly greater than that presently experienced here on Earth, although the oncoming energy shift may soon restore Earth's atmospheric purification processes, involving the plasma discharges of auroral activity and lightning strikes, that had become severely diminished over the preceding millennia:

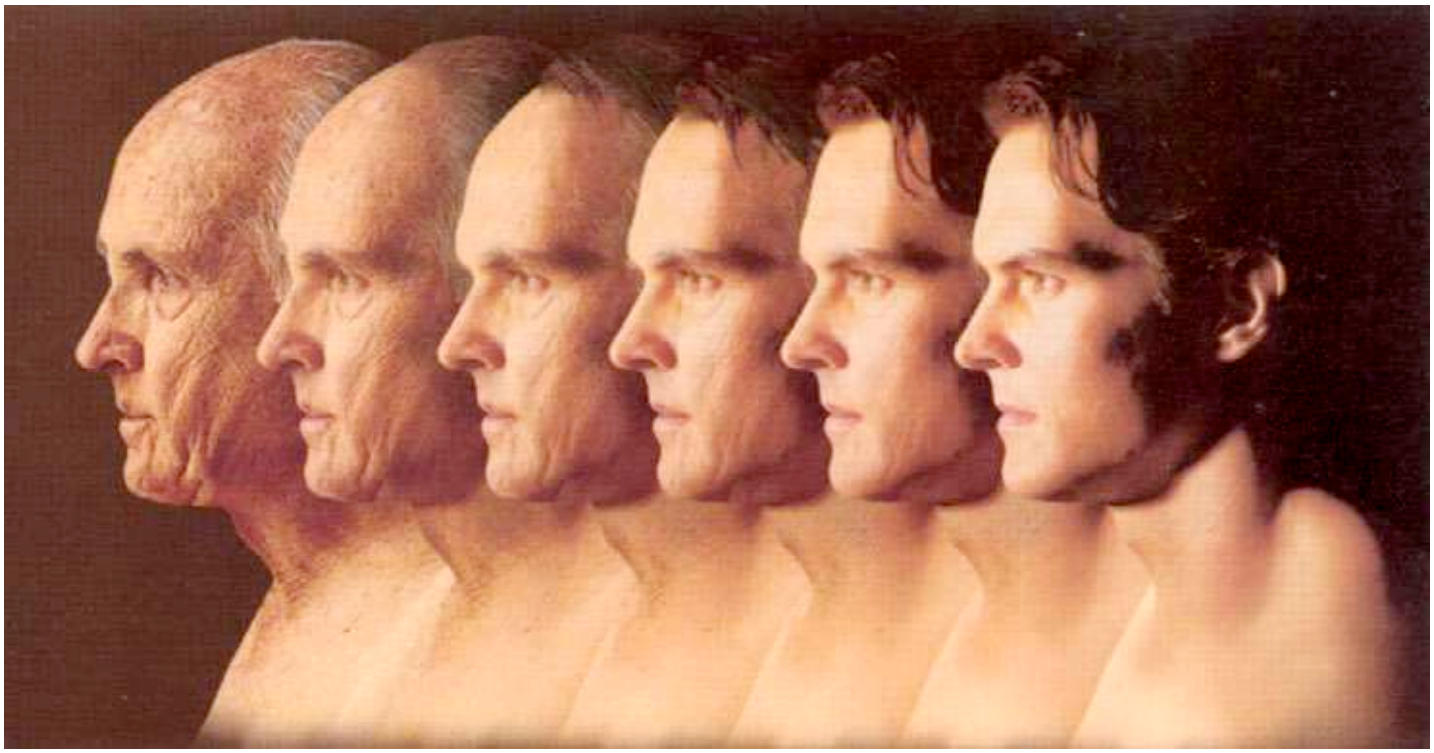

> ‘Greetings... The message that I would like to leave with you this evening is, be patient, trust in us, for indeed you will realize that we can see a little further into the future than it is possible for you to do at this present moment. Trust in us and a new way of life, a new path, will be revealed to you, as the ancient prophets did in the past. Their monuments are still there today to be seen on your planet – the pyramids and the Sphinx…
>
> Other Superiors have governed Koldas, who have lived to the age of an equivalent of 250 Earth years. They enjoyed the full benefits of life as I do. I have no ailments and that is as it should be, and that is how it will be for those who share our life philosophy. *We are the instruments for the Divine Love and Truth to manifest through.* We are not Gods. Never think of us as such! There is one Divine Creator of all the heavens that you can see, and that we can see, and what lies beyond that again... I am Vax Noah... Salu kata katsu, farewell.’ [20]

This heartfelt message from the Superior of Koldas was transmitted from high above, among the stars where many things beyond Earthly vantage can be seen. The penetrating knowledge offered to us by the Confederation of Twelve Planets was seeded for germination during the cosmic changes unfolding since the beginning of their contacts with Edwin in 1968. Present scientific understanding of enhanced cellular function under the influence of a mild electrical current, and under the high-energy conditions of plasma beam healing devices, allows the conceptual framework needed to grasp the truth of Valdar’s insights. As he well knows from similar events in the history of other binary star systems like our own, the cellular rejuvenation effect of HHO plasma will be induced by the elevation of vast amounts of water into the atmosphere of Earth under the growing influence of an inaudible acoustic resonance.

The greatly increased ambient atmospheric luminosity generated by a glowing auroral canopy of HHO plasma, in combination with increased infrasonic stimulation, will alter the expression of DNA in all living creatures on Earth. In the terrestrial human being, pineal gland stimulation will bring about significant changes in the range of visible light and audible sound perceived. Our eyesight and hearing will extend significantly, aligning with the greater capabilities of Koldasian sensory perception. This was referenced quite literally when Valdar explained ‘what we can see is more than you.’ Layers of meaning within the simple, profound statements of the Koldasian visitors continue to unfold:

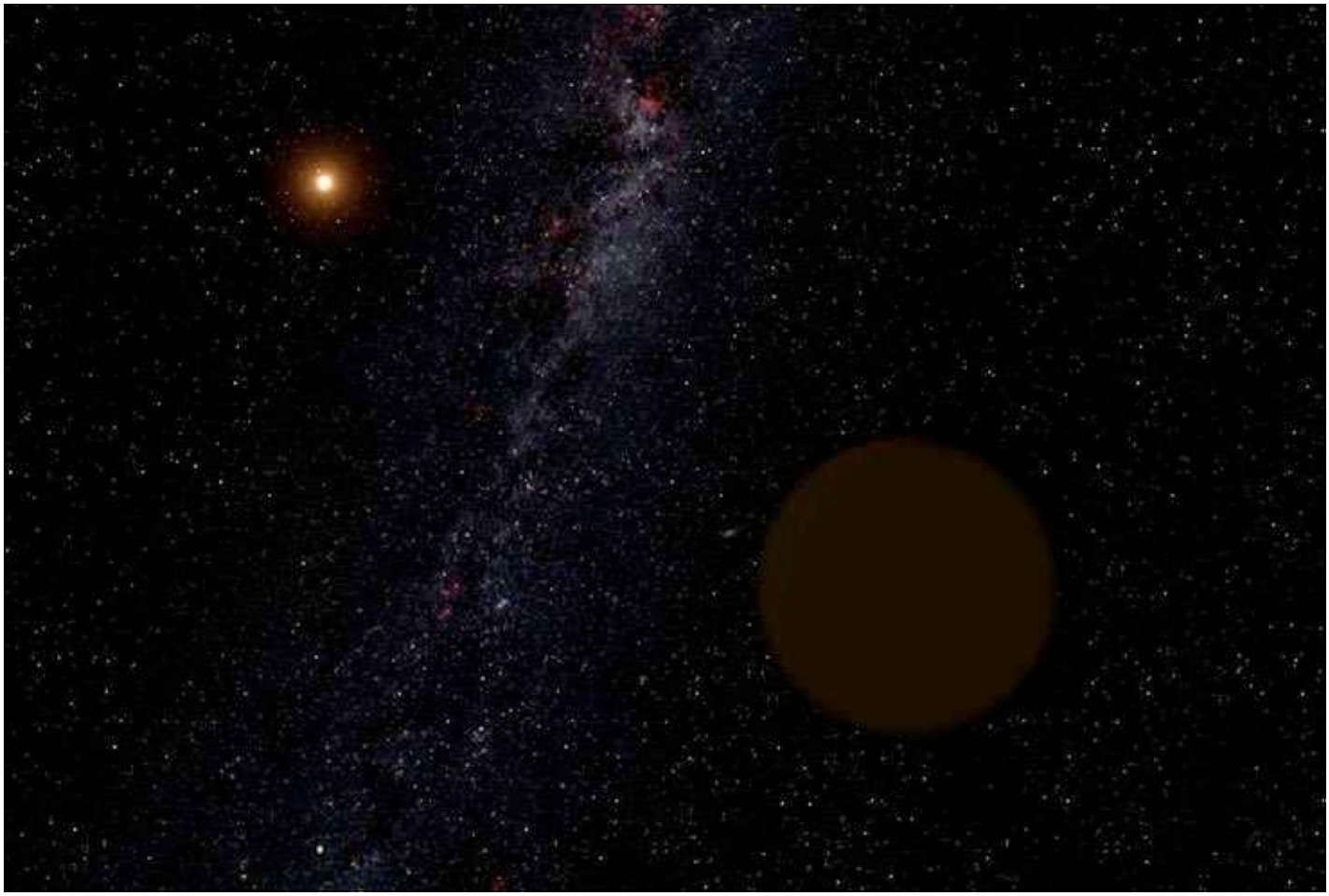

‘There might be a change in the atomic structure*. Every atomic power station would then cease to function, and even your electrical power would stop. But a new source of energy will then be available.’* Indeed, the intense solar flare activity will send massive coronal ejections that will influence the ultra-low frequency resonance of Earth through interaction with the Giza pyramids, which transduce all solar energy into inaudible acoustic waves. This new source of energy which is ‘here for mankind to use on our planet’ refers to these resonant infrasound standing waves that will be dramatically increasing in strength during the events of December 22, 2012. But what unseen forces are causing this great shift?

Valdar divulged the hidden presence of ‘Sola Kananda’, the brown star binary companion of our sun that returns once again from the direction of Cancer on its long elliptical orbit. Although the full timeline of predicted future events was explained to Edwin in detail, the public was only informed that preparations and conditioning contacts made by the Confederation on Earth are being conducted in case an emergency evacuation of Earth becomes necessary in the near future due to these cosmic changes:

> ‘Let me explain briefly the purpose of the plan. It is to save as many as possible in the event of a major catastrophe occurring on Earth. This might be a nuclear war or the collision with an asteroid or some other cosmic disaster involving Earth. This includes the approaching embryo sun, Sola Kananda…’
>
> We first heard about Sola Kananda approaching our solar system in 1973… Sola Kananda means a ‘sun that has not yet flared or blazed’, we are told. It is approaching from the constellation of Cancer. As our solar system enters deeper into its sphere of influence, changes in our planetary magnetic fields have from time to time been observed by the Confederation.[21]

These changes have been comprehensively mapped as nonlinear effects of focus infrasound standing waves that are increasing in intensity with solar flare activity. When considered in the context of the near approach of an invisible *embryonic sun*, one may infer that the ‘instantaneous resurrection’ of Earth is somehow intimately linked with the dramatic *rebirth* of the dormant brown dwarf star *into a red dwarf*:

> ‘In the near future, with the passing of Sola Kananda, your planet will pass through a certain region in space on its journey around your sun. This region is a belt which Sola Kananda has produced through space. This will bring about changes on your Earth. I am the one to inform you of... [these changes in great detail, which we cannot allow to be published]. This is why I am making this transmission. A great many changes will probably take place. Environmental changes on your planet will make your superiors and scientists look at space in a different light...’ [22]

With the dramatic revelation of the nearby brown dwarf binary twin, and all the auroral activity at specific infrasound standing wave convergence points, Earthly scientists will recognize the nonlinear alternations of locations of vortical activity and the connected design purpose of the world’s pyramids. But before these revelatory events are to occur there will be a brief preceding period of darkness during the time our solar system will cross the Galactic Plane, which Valdar cleverly referred to as *‘the still of the night’.*

Maya spiritual Elder Don Alejandro Cirilo Perez Oxlaj (above) affirms *this time of darkness may perhaps last for 30 to 70 hours during the Galactic Plane crossing* – thereby suggesting that *the solar corona may become extinguished* during the period of magnetic reversal, as if entirely swallowed by sunspots: when “we will enter the central magnetic axis… we cannot see the rays of the sun. We are inside. Once the Earth re-emerges from the axis we will then be able to see the New Sun.” [23] The galactic magnetic fields and cosmic rays of infrasound that drive our sun into incandescence will likely diminish altogether during the Galactic Plane crossing. Valdar referred to this as ‘the complete break in the magnetic field’, causing a temporary extinguishing of the solar corona during the process of magnetic reversal of the entire solar system –the sun, the brown dwarf binary twin star, and all of the orbiting planets.

Mayan wisdom reveals the brief darkness will end dramatically *in the bright flash of a synchronization ray emitted from the Galactic Central Sun*, causing ‘nearly instantaneous regeneration’ for all living things as well as global auroras and the incandescence of the red dwarf star. Koldasian Elders speak literally, not figuratively, when stating Earth’s *‘scientists will look at space in a different light’* –through an atmospheric plasma canopy glowing red, as *‘even the heavens will change color!’* Wisdom teachings preserved in the Mayan ‘Pyramid of Fire Codex’ unequivocally state*: ‘Come, reunite pilgrims, for the sky is in flames!’* [24]

> Valdar hinted at some future catastrophe and the changes that this event would bring with it. But he gave no due as to when this cataclysm or cosmic upheaval would take place as this was unknown even to the scientists of the Confederation. They are certain that it will occur as they have learned to interpret various signs in their long history of cosmic observations… The virgin lands where the ancient Atlanteans settled will one day be a haven for mankind again. For after the big change takes place, where there are now oceans, there will be land and where there is now land, there will be oceans. The continents of America, Africa, Asia and Europe will no longer be there. In their place will be these 'new' lands, now at the polar regions, and civilization will start again for we think your polar regions will not suffer in this big upheaval. They will remain more or less intact but the climate will change and the icecaps will melt. On the rest of Earth's surface there will be drastic changes! The present polar regions are even now being prepared, for they will be needed. You may have noticed that there is a lot of UFO activity there.' [25]

Indeed, a fascinating component of the preparations mentioned involve giant aerial plasma displays over major urban populations, most spectacularly witnessed by residents of the Chinese cities of Dalian and Yantai in 2005; Tomsk, Russia in 2006; Trondelag, Norway in 2009 (photograph above); and over South Australia in 2010.[26] Such technological demonstrations of fourth-density plasma shake and arouse human consciousness to awaken for the long-awaited day when the humans of Earth fully accept the great offerings of cosmic visitors, as the time beckons when such help becomes increasingly necessary.

Recognition of the wisdom teachings of cosmic observers allows the integration of new concepts for a more balanced awareness. The peaceful and wise Confederation of Twelve Planets is but one of innumerable cooperative networks of cosmic civilizations exploring the endless magnetic fields in search of knowledge, toward the ever-present call of Oneness. Spiritual adepts among this small planetary group attain an extended lifespan by means of the radiations of the same high-energy HHO plasma that will soon be witnessed throughout the skies of Earth. The dynamic shift of Earth resonance to a higher level follows a pattern of revelation that inevitably occurs during the ascendance of all young planets and all nascent civilizations, along the path toward collective consciousness and cosmic co-creation.

References

[1] van Vlierden C, Ed. Stevens W (1986) *'UFO Contact from Planet Koldas: A Cosmic Dialog'* UFO Photo Archives, pp. 79-80

[2] Ibid, p. 46

[3] Ibid, p. 29

[4] Ibid, p. 83

[5] Ibid, pp. 16-17

[6] Ibid, p. 12

[7] Ibid, pp. 58-59

[8] Ibid, pp. 104-105

[9] Ibid, p. 21

[10] Ibid, p. 167

[11] Isenberg H (2003) 'Giza, Center of Earth' *Mars News*, online · http://mars-news.de/pyramids/gizacenter.html

[12] van Vlierden, op cit, pp. 26-27

[13] Orion E (2003) *'The Bush Connection'* The Bush Connection, Section B, p. 13

[14] Tesla N (1978) *'Nikola Tesla: Colorado Springs Notes 1899-1900'* Nolit, Beograd, Yugoslavia, pp. 61-62

[15] van Vlierden, op cit, p. 80

[16] O'Neill I (2010) 'Mystery Behind Solar System's Giant Ribbon Solved?' *NASA,* January 15, online · http://news.discovery.com/space/mystery-behind-solar-systems-giant-ribbon-solved.html

[17] van Vlierden, op cit, pp. 186-189

[18] Moulton Howe L (2009) 'Eerie 'Blades of Light' in Longview, Texas – September 9-10' *Earthfiles*, October 10, online · http://www.humanresonance.org/longview.html

[19] Novak P (2005) 'Angel Light Ascends to God Light, Part 2' *Bay Today News*, online · http://www.baytoday.ca/content/news/details.asp?c=8271

[20] van Vlierden, op cit, p. 200

[21] Ibid, pp. 142-143

[22] Ibid, p. 228

[23] Cirilo Perez A (2009) 'The Messages of Wandering Wolf', *Shift of the Ages*, online · http://shiftoftheages.com/wandering_wolfs_messages

[24] Jenkins JM, Matz M (2004) *'Pyramid of Fire: Spiritual Ascent at the End of Time'* Bear & Company, p. 88

[25] van Vlierden, op cit, pp. 132-133

[26] Putney A (2010) 'Plasma Spirals' *Human Resonance*, online · http://www.humanresonance.orh/plasma_spirals.html

3
The Plejaren

The Plejaren

Eduard Albert Meier (b. 2/3/1937) is a Swiss farmer who has been visited since the age of five by extraterrestrials from the region of the Plejares star system, representing a wise and peaceful Confederation of planetary systems. Eduard's childhood contacts were made by an aged man named Sfath, while as a young adult he maintained contacts with a female cosmic visitor named Asket. Through his later years he maintained contacts with Quetzal, Semjase, her father Ptaah and many others.

'Billy' is a nickname Eduard received in Tehran during his long travels on foot through the Middle East and Asia Minor (seen at left, in 1980). Billy Meier has documented years of contacts and remarkable dialogs with visitors from the Plejares star system. He has also produced several 8mm documentary films of Plejaren spacecraft, or *beamships* as they are called. Meier has also produced several hundred high-quality photographs of extra-terrestrial spacecraft of many types – both from the ground and *in the air, aboard the Plejaren spacecraft itself.* The sheer breadth and diversity of highly advanced information and physical evidence provided by Meier concerning his contacts and cosmic travels with the Plejaren calls for the close attention and discernment of the human beings of Earth, who grow in awareness by the slow process of assimilation of knowledge.

While many contactees have experienced transdimensional travel and orbited the Earth and her oceans, Meier is one of the few present-day humans who has time-traveled by hyperleaps through deep space with his cosmic friends and returned with photographs and scientific details that are undeniably valid. The most profound teachings that imbue Meier's life's work are the spiritual teachings he has received from the Plejaren and presented to humanity through his many books, now available in several languages. The simple and penetrating spiritual teachings of the Plejaren are now transmitted through the Semjase Silver Star Center in Hinterschmidtrüti, Switzerland, providing an opportunity for synchronized meditation practices with billions of advanced spiritual beings throughout the Confederation's unified network of planets, who choose specific times for coordinated interplanetary peace meditation on a regular basis.

The Confederation comprises a collective of diverse civilizations that remain deeply rooted in spiritual connection through their respective planets, providing a guiding influence on worlds in crucial phases of developmental shift, as is the present case of Earth. These spiritually and materially advanced visitors remind us that even they grow food in organic gardens, and maintain *direct contact with nature by planting with the hands in the soil, in the creative intention of love.* Plejaren wisdom finds guidance in the Laws of Creation, and encourages humanity to learn for ourselves through investigation, thoughtful reflection and the application of reason. In spiritual aid of the human beings of Earth, Billy confers their extensive spiritual knowledge and physical evidence in the form of photographs, films and even samples of exotic materials.

Eduard's space-traveling visitors explained their ancestral origin in the Lyra star system, before an ancient cosmic migration to the Plejares star system, including the beautiful planet of Erra, which resides in a *fourth-density space-time configuration about 80 light years beyond the Pleiades star cluster* (above). The name Plejaren ('play-yar-en') means *'Law of the Sevenfold'*, reflecting a penetrating cognizance of Creational Law and the Truth of Spirit. Offerings of the Plejaren Elders on the physics of Spirit were balanced by comprehensive lessons on solar and astrophysics. Meier was informed that the Sol system, outside the Milky Way, constitutes something like an enclave because it floats as a single system far outside a spiral arm, moving at high-speed towards the Hercules star system. The distance from the Sol system to the middle of the galactic central sun is 35,002 light years, according to Plejaren calculation.

Spiritual demonstrations of Semjase's intentional healing ability were given during various contacts when she rapidly restored Meier's dwindling health by concentration alone. During the 50th contact of April 6, 1976 Eduard's broken ribs were mended in minutes by an electro-healing apparatus within Semjase's beamship (opposite), extending natural mental capabilities through technological means.[1] The ability of the Plejaren visitors to predict all major events in Eduard's life was repeatedly demonstrated, and even the date and cause of his death were previewed and discussed with him in detail. Another definitive event in his life predicted by the Plejaren, for his psychological preparation, involved the loss of his left arm in a bus accident in Tehran in 1964. After the necessary amputation, Meier healed in conventional hospice and wisely refused a biotech prosthetic arm offered by his extraterrestrial friends, on the grounds that his safety would be compromised by the greed of other humans who would inevitably attempt to steal the advanced extraterrestrial biotechnology. *In this, he has found the resounding truth of the spiritual lesson.*

Rather than secretly enjoying the material benefits of his contacts, Eduard Meier instead disseminates the advanced spiritual teachings of the Plejaren Elders, inviting each Earthly human being to consider the truth of spirit. The path of inner seeking through meditation and reasoned thought has become the focus of FIGU, a conscious community that has co-founded the Semjase Silver Star Center. Serving primarily as a meditation center, the facility synchronizes the FIGU community for the development of telepathy by exposure to focused infrasound. *From there, Eduard's enduring teachings have radiated their light:*

In truth, the Earth human lives a life that does not ever deserve the designation *life*, in the true sense… [for he] no longer knows of the strengths and possibilities that lie within him and are suppressed. The human's psyche has become a prisoner of the material, and the human's corporal nature hinders him from glimpsing more than only a weak shimmer of the true light. But certainly the day will come when the human will venture forward somewhat further than usual in his thoughts, and then still a little bit further, and further.

Then the inner light will gleam in him and he catches, to start with, only a small and fleeting glimpse of his true essence. Indeed, then comes the point in time in which he becomes somewhat more aware of it, and then still somewhat more. So the light of truth with which, namely, he is one, with eternal life and with the eternal power of his essence, gradually comes on for him. This light then illuminates his entire psyche and takes possession of it.

Awakened through this new consciousness, the human holds the thoughts of this oneness firmly, and thereby now progressively lives in these thoughts, his life now flows in constant actualization of the oneness of the creational Being. And thus the terrestrial Earth human is transmuted into the human who is of Creation. Compared to the new life, the old one only deserves the name *death*, because ignorance and narrow-mindedness is like that. But this deadly life is no longer able to shackle the new human who, before, in the old life, in a certain sense, had actually been dead -a living corpse. (OM: The Book of Truth, 43:153,167-177) [2]

Knowledge of the inner dimensions of the human being inspires reflection on the endless gifts offered by the Creation, granting natural relief from the burden of the physical through the transcendence of spirit. The moral dilemma which now cripples Earthly consciousness, namely the role of psychopathy in politics, was solved naturally by the Plejaren science of biorhythmic healing by genetic enhancement through the tri-thalamic heartbeat entrainment during fetal development.[3] This advanced preventive infrasonic genetic technique also relieves the moral crisis of abortion, which is permitted by natural chemical methods using essential oils (like that of the Neem tree found here on Earth[4]) within the first three weeks of pregnancy only, as "the time of the beginning heart activity coincides with the entrance of the spirit of the newly conceived human being, so on the 21st day after conception." [5] The determination of spirit in accordance with Creation propels the consciously seeking individual from within his/her deepening experience of the luminosity of his own being, as taught by Semjase during the 18th contact of May 15, 1975:

I want to proceed with the teaching of the spirit, as it is the most important of all things… The experience reveals that the Creation is unending beauty, a beauty above all beauty, borderless, intensive happiness without end, wisdom, knowledge, ability, truth and absolute determination. When that is recognized by the human then he leads every one of his joys instantly back to its origin, to the unending joy of Creation.

Wherever he sees something beautiful, be it now a flower, an animal or a human, or something else, he thus brings it instantly into interconnectedness with the infinite beauty of Creation itself. Wherever the human sees cognition reach expression, in this or any form, in an impressive and exalted manner, then he knows that it has its roots in the endless cognition which is Creation. Wherever life stirs itself, be it even in the tiniest Being, in a creature, as, for example, the microbe, there, behind this life he glimpses the infinite, the eternal and the creational. Out of that he attempts to deepen and expand his understanding and feeling through which he contemplates the essence of the creational and its inseparable presence at any time and in any space in many kinds of ways in the daily life and experience.

Creation exists in every human as a fragment of himself. Once this thought has first deeply penetrated the human and become his experience, then any fear and all doubt in him disappear. If he knows that the Creation is all-knowing, and almighty then he gains in inner peace and security and is immune from stupid thoughts and wrong feelings. Repeated contemplation about the all-present, the truth, wisdom and the ability and knowledge of Creation as constantly eternal, as dignity and worth, allows the word and the designation Creation to become something very meaningful in the human – to something which calls forth transformations in the feelings and transformations in his manner of thinking.

The more his intelligence is effective in this direction the more he gains radiating light, the more powerful his personality would be and the more blessed his entire life and works would be. Again and again the human living in clarity of consciousness would produce in himself, anew, the strong perception that the Creational is far more real than his body's feelings. This perception rules, without interruption, the human living in accordance with spirit. The creational grasps possession of his consciousness whereby his senses are full of peace, strength, joy, knowledge, wisdom, truth and hope. All measures that the normal human grasps in his material-intellectual thoughts in order to attain peace, happiness and strength always show themselves as deceitful, while the constant controlled-ness of the human who is living according to spirit would be pulsed through with the dynamic power of Creation.

He who is a human living according to spirit is very dynamic in all things. He attempts, uninterruptedly, to reach his goal as quickly as possible. As long as he lives he would, in accordance with this, use the time for applying the creational ability with all the energy available to him. He would never allow this undertaking to be lost. Everything possible can happen in the course of time, yet his desire for the creational would never be extinguished in him. He can strike hindrances in which he suddenly has no sense and taste any more for the necessary material things, yet he never loses the taste and sense for the creational because he knows that the Creation embodies the true Being.

Only a human who fights hard for consciousness and spiritual goods and progress, for knowledge, truth, logic, wisdom and love harvests mighty fruit of a spiritual and consciousness kind, because they do not simply fall into his lap. First, before the first results would be obtained, it is required that the spiritual-intellectual manner of thinking must learn the path of creational thinking and recognize its absolute correctness and determination. Yet when these first results come about then the cognizant one steps onward with great steps and expands himself in spirit and consciousness to a factor of power. First, through this, already known facts, knowledge, truth, logic, wisdom and love would be self-evident, which first, however, must be gained through hard work. Indeed, the path does not end at this point, because further seeking, further searching, further development and further recognition lead into the borderless duration of time.

Everything possible may happen in the course of time, and hold the human back from taking up deeds, yet the human living according to spirit knows no borders and does not allow himself to be kept from his goals by any kind of events or bad future out-looks. For him the future already exists in the present, so it is that everything must be done here and now in order to reach the highest spiritual and consciousness state… Again and again he produces in himself the strong perception that something is there which gives him immeasurable power and makes him free from unreal assumptions; (it is) the truth of Creation.

Always again and again the human produces in himself the strong perception that he finds, in the ocean of creational light, his wisdom, his knowledge, truth, logic and love, which for him first entirely enables the Being of life. The joy of the human who is turned towards Creation exists as a result of his reverence produced from the creational and Creation; (it is) this, in which he accepts the almighty will in the creational laws and turns the absolute determination of these laws to his own determination and practically employs them.

He brings his dedication to the laws to expression through the learning and utilization of all spiritual and consciousness facts, but never through belief, assumptions, serving and humility. The only way to learn exists in the unremitting efforts and striving to obtain higher spiritual and consciousness cognitions and to bring the capabilities into application which have unfolded through this. Patience and endurance and the development of higher understanding, recognition and engagement of the cosmic and universal love, deepening of the spiritual and consciousness knowledge and ability, as well as the shutting-out of material-intellectual thought powers, like egoism, materialism, pride, envy, greed and jealousy and so forth, are thereby of decisive significance, because only this guarantees the recognition and obedience to the creational laws…

He who is a human living according to the spirit attempts constantly to maintain himself always, and under all circumstances, in the vibrational realm of creational motions. Should these once, through some kind of influences, be in danger, then he calls on Creation in the highest power and thus protects himself in its highest vibrational power, from the negative. In this manner he proceeds so far along until the creational essence in him has produced the absolute determination of defense against the negative.

[In his thoughts and his waters,] the human is always the bearer of some things. Many carry oppressive feelings in themselves, others grief, worries, problems… But he, who is a human living according to the spirit, is a bearer of the creational, of the spiritual… He immediately transforms even the most negative thoughts that come and want to destroy his spiritual-intellectual thoughts, into creational power and wisdom. So he makes everything creational and carries it as a block of power in himself. Thereby he is a traveling temple of Creation.

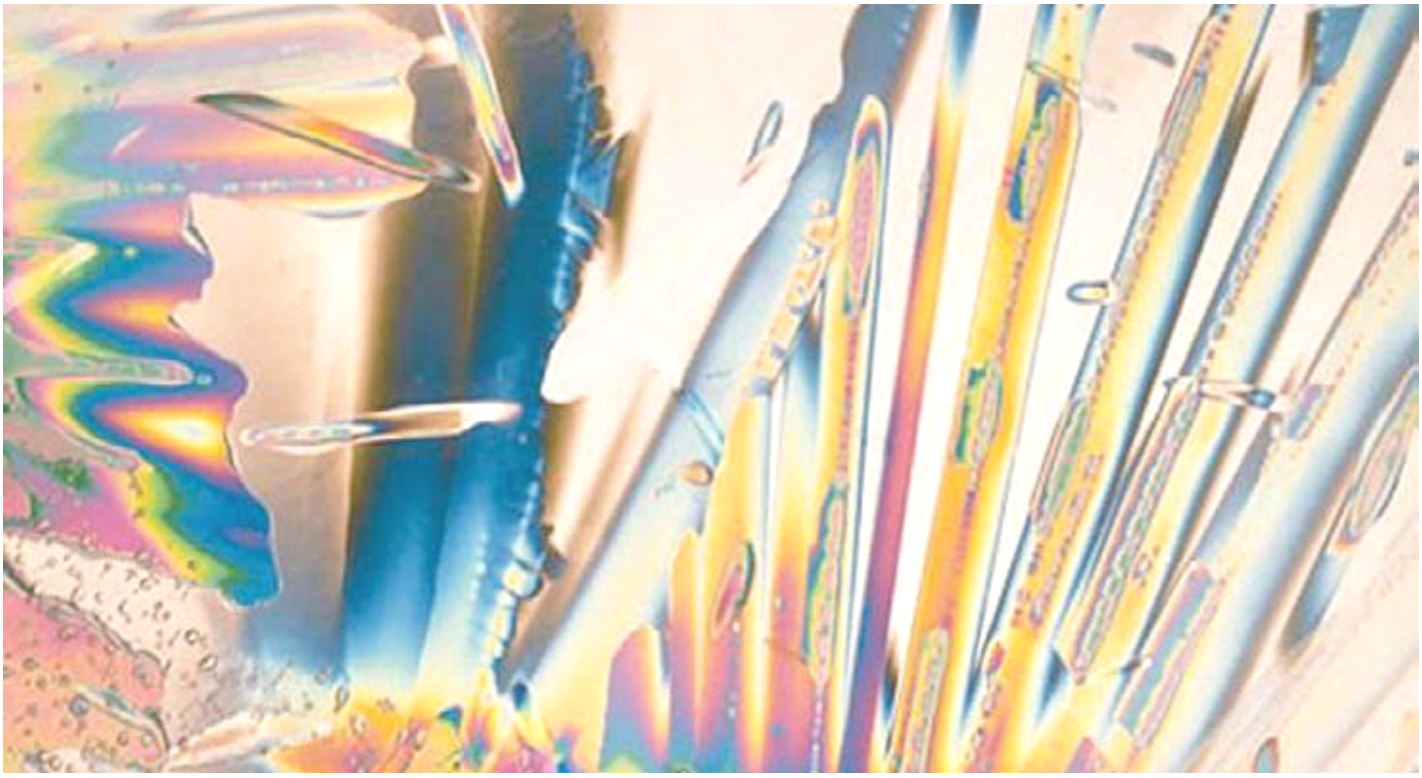

The intelligences of the human living according to Creation would be ever more inspired and press always deeper into the spirit-consciousness. He who lives according to the spirit presses always deeper into all things with his cognitive abilities and grasps the warmth of the fire of the creational presence in everything. Thereby the spiritually thinking human would, over-all, be cognizant and conscious of the power and the truth of the creational presence. What therefore remains unrecognized by the everyday perception of the senses, [–as *cosmic infrasound–]* would be spiritually-consciously perceived by the human living according to Creation…

The material life on the Earth is like a passing game, an evaporating phenomenon, but behind it lies the eternal and timeless truth; the spirit of the creational presence and the reality of Creation. This creational reality carries in itself all riches and realms of the ability to do with wisdom. This is the remaining, the timeless constancy and imperishable. This is no game, rather the eternal and timeless truth and wisdom, knowledge, freedom, love, logic and ability, the relative perfection, the absolute determination…[6]

The pristine clarity of Semjase's spiritual teaching continually unfolds within the conscious listener, expressing the source of all joy in Truth and the oneness of Creation. The purity of spirit and thought present in the Plejaren wisdom teachers reflects their physical purity, drinking the celestial waters of their resonant home planet of Erra. The comprehensive knowledge of this advanced cosmic culture directs their harmonious lifestyle to benefit from a collective consciousness and the telepathic abilities endowed by following the resonant life-path set forth by The Spirit. Dwelling within the field of heartbeat resonance, one enters into direct communication with the living instruments given to us by the Creator, to hear the joyful laughter and all-penetrating cosmic *Om* – the vital force of the human being engaged in the 'synesthetic' state of inspired conscious co-creation.

While Eduard had been educated in the teachings of spirit since his earliest contacts with Semjase's grandfather Sfath –at the age of five– comprehensive spirit teachings were offered in later contacts with Semjase, beginning on January 27, 1975. The contacts of the 1970s involved many lessons on the Truth of Spirit, but also began a period of extensive photographic opportunities for material evidence.

At left is a montage created from Meier's original February 27, 1975 photograph taken at Jacobsberg-Allenberg/Bettswil, Switzerland. Meier has even taken photographs *from inside Plejaren beamships in flight* (below). The blurring and tinting of the image is a result of special coatings used in the windows, likely comprised of quartz glass, which glow orange in our atmosphere. The resonant acoustic and electromagnetic environment maintained inside the Plejaren beamships interferes heavily with the camera functions, often overexposing the film due to high-energy radiations or distorting images beyond recognition. Dozens of remarkable photos taken in space are marred by significant focal problems.

All of the photographs produced by Eduard Meier during his contacts were obtained by permission of the Plejaren, while certain sensitive areas were prohibited as subjects for documentation. Portraiture of the Plejaren visitors was not permissible, nor was Meier allowed to photograph the interior of the beamships. Why do they not yet present themselves to the human beings of Earth openly? Semjase's father, Ptaah, provided Billy with a concise answer to this question, revealing a profound understanding of the nature of human consciousness at the present time, and the primacy of reasoned thought and careful deliberation:

> *Ptaah:* When the epochs change, so also do the minds of the forms of life. This has also happened to humans now. The Age of Fishes was characterized by religious fanaticism… Then the birth pains of the Age of Aquarius began, and suddenly the Earth human started to listen inside of himself. And he started to think and to explore, and suddenly recognized logic only in truth. He developed in a short time his thinking abilities, and searched and explored… which is a characteristic of the Age of Aquarius. And this is one of the main reasons why certain human beings are now being contacted by extraterrestrial forms of life again. The present Age of Aquarius demands thinking and spiritual evolution of the humans of Earth. This cannot be achieved by seeing and listening with the physical organs only, but only by reasoned thought. If we appear officially in our beamships and spacecraft, the effect of deliberation and of thought would suffer, because the Earth human, in his present state of evolution, does no longer deliberate and search that which he can see with his own eyes and hear with his ears. Beyond the seeing and hearing, the interest is short-lived, because that soon becomes a natural event to him, and he no longer cares. What he knows no more interests him. His interest is only aroused by secrets for which he can hunt.[7]

The Plejaren visitors always wore a protective suit that Meier described as matching the texture and color of elephant skin, but was creased and folded to the exact forms of its wearer – perhaps some kind of organically grown material fit to form. Meier also described a reflective circular metal neck fitting with the apparent function of a helmet-mounting lock ring. The Plejaren go helmetless on Earth without exposing themselves to our polluted air, as this circular neck fitting is electrified to create a *standing wave* over the nose and mouth that purifies and sterilizes the air taken in. This apparatus protects the wearer from radioactive uranium dust in Earth's atmosphere due to humanity's seemingly insatiable lust for war.

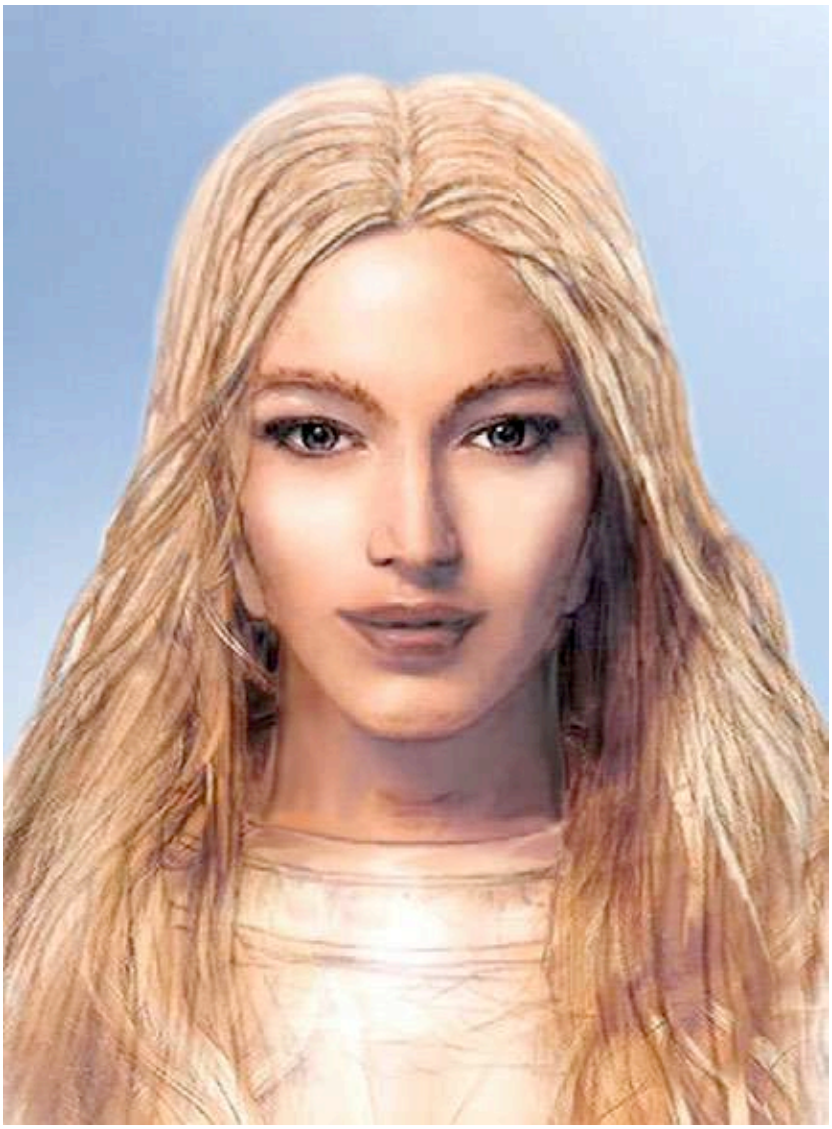

The low-resonance environment of Earth had long ago reduced human lifespans to the brief span of near 100 years. This limit on longevity to which terrestrial humans have all become accustomed is a drastic and direct result of the weak and offset magnetic field of the planet, corresponding low levels of infrasound resonance and very high levels of deuterium (the heavy form of hydrogen) in our waters. Traces of *heavy water* pollute the waters of Earth and her surface-dwelling human populations, yet the process of her cleansing and transformation into a pristine paradise already grows from seeds within the human heart that will require a quantum shift to high-resonance. The high-resonance environments of planets with atmospheres containing only *light water*, comprised exclusively of protium (being deuterium-free), engenders human lifespans of perhaps 1,000 years or more as enjoyed by the advanced Plejaren civilization. An enhanced and colorized image based on a self-portrait drawing by Semjase (at left)[8] captures the refined grace of her features at the age of 330 years, in 1975. The facial features, size and proportions of the Plejaren race are identical to that of Earthly human beings with the exception of their long, connected earlobes, which may have inspired an association with wisdom long ago (pg. 4):

> [Concerning lifespans, investigator Lt. Col. Wendelle Stevens concluded as follows:] This 1,000 years average age for the [Plejaren] seems strangely coincidental, as that is the [Bible's] reported age of Earth humans before the Great Flood, when the dense vapor envelope surrounding the Earth came down in torrents everywhere for scores of days. Loss of the vapor envelope reduced the atmospheric protection of Earth's creature species from the harsh [UV-B and UV-C] radiations of our sun, and the lifespans of all creatures decreased quite dramatically and rapidly to less than 100 years for humans, and vegetable and plant yields were reduced accordingly.
>
> Recalling the extraterrestrial's statements that we are descendents of their ancestors when they were here long ago, our 1,000-year biblical longevities take on new meaning. Loss of that atmospheric protection has shortened our lifespans to 1/10th its former scale… An interesting observation made later on in the contacts by one of the extraterrestrials, describing a protective [HHO plasma] screen they use around their vehicles, and even around their person when out of their vehicles, indicated that they age in our atmosphere as much as we [terrestrial humans do] without their protective screen![9]

The vital force of *infrasound* expresses itself much more intensely in the highly evolved atmospheric conditions on Erra, imbuing an extreme longevity and advanced consciousness among the Plejaren through psychoacoustic entrainment. Meier initiated a profound lesson during the 39th contact of December 3, 1975 by pointing out the brevity of the human lifespan as a result of "the fact that the forces of thinking of each single human being are able to raise or lower the force of life of the fellow creatures":

> *Ptaah*: Certainly, this question is of great importance… The age of every creature is shaped partly by the penetration of its outer forces by others of the same kind of forms of life. Because the thinking of a form of life in cooperation with spirit generates an extremely logical, that is Creation-accorded, force which is released as high-frequency radiations and oscillations, an immense force is generated which is able to influence everything. The Creation-accorded force penetrates all, truly into all, material forms of life and matter, and influences them according to their kind and form. Each form of life owns an, adapted to its spiritual level, age of living or time for living, thus as well with the human beings of Earth. In earliest times, when the human being of Earth was procreated here by his ancestors, his average age of life was 1,007 years of living, and as taught by his procreators, possessed an enormous spiritual level of knowledge and abilities.

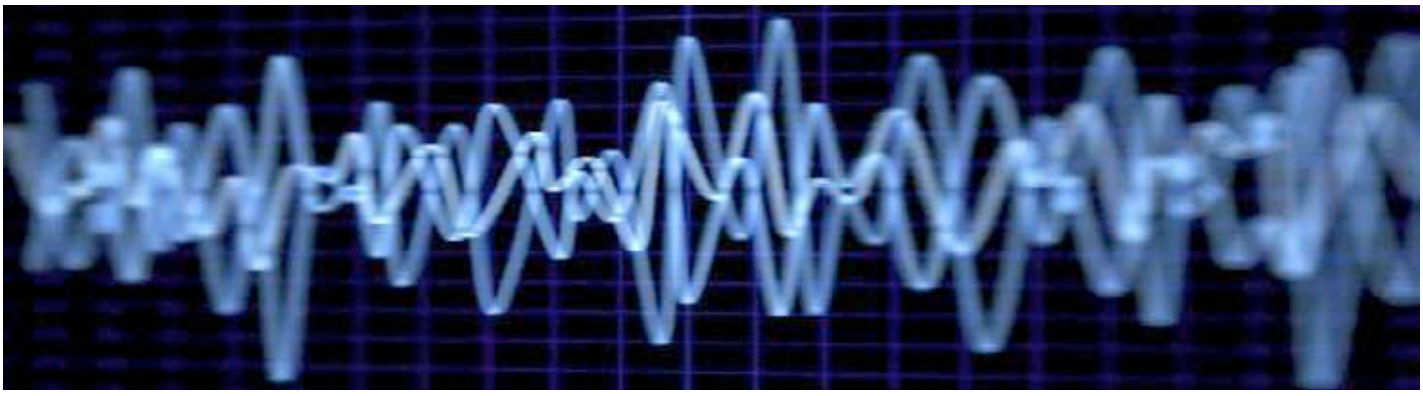

> But unexpectedly rapidly, he fell into religions and their heresies, and by this lost true knowledge and the truth. He necessarily began to work against natural law, became a stranger to it, and lived under the bondage of self-created laws. This all together resulted in the loss of the high average span of life, which in a few thousands of years decreased ever more and settled at the twentieth part of its earlier time. In the beginning of the new epoch [of the Age of Aquarius] a change for the better once more marked itself, from which the average span of life slowly increases. The main reason for this is to be found in the acknowledgement of the truth and connected spiritual direction. The more then that spiritual direction turns itself again towards the truth, the higher again develops the average span of life, because here, by this also, the altered genetic and other factors regulate themselves again, which in the course of millenniums had become wickedly influenced. The mass of Earth human beings moving in spiritual form is still relatively low, and in many cases only beginning to recognize the real truth, thus hitherto still no great progress could be achieved. But the more the Earth human being turns himself towards the real truth, the more does also increase his average span of life.
>
> Seen as a whole, every form of life is of important meaning, that is, in its thinking and the forces whereby released. Each thought radiates out as a great force and strikes the other creatures who attract these like magnets. According to their quality, negative or positive or balanced, they generate in the receiving creatures kindred forces, under according effects… But by the heresies and other misguidance of religions, the Earth human being is mainly only able to unfold forces which destructively influence all forms of life. Such destructions are found in the injury to age, that is, the lowering of the average age.
>
> The greater the assembly of human beings, as for example in cities, the lower sinks the average age, because in such places immeasurable thought energy is released, and penetrates into the fellow creatures… But also all materiality suckles itself up on these destroying forces, and in this way falls to early destruction, as for example iron, which normally does not rust so fast as is the case on Earth. By this, each Earth human being is himself guilty for the early death of his fellow creature, consciously or unconsciously, when he thinks in uncontrolled form, and in this way releases uncontrollable destructive forces. If the Earth human being wants to think right and according to the Creation, then he must guide the course of his thinking neither in negative, nor in positive trails, because both are degenerations which create bad consequences, thus they are against the Creation. Right thinking declares itself by a balanced and natural manner of thinking, in which way life becomes procreated and maintained.[10]

These penetrating lessons generate a heightening of the spiritual resonance of those humans who can receive the lesson and attune their thoughts, feelings and actions accordingly. The voluntary effects of teachings of truth was precisely given by Semjase during the 91st contact of November 17, 1977:

> *Semjase:* …In result of your education and your knowledge, it is you, [Eduard]… who emits the highest radiations on the Earth… When for example exists a lesson of the truth, then its radiation diffuses very quickly and very intensively. If now other living creatures find themselves the truth within this lesson, by which fact they themselves strive towards the truth, so they become liberated for the reception of the radiation [from the speaker of truth]… In consequence of this, the receivers of the radiation tune themselves inside of the subconscious for elaborating the lesson of truth towards its best inside of themselves, whereby they generate automatically a relationship of themselves to the diffuser of the lessons and even to his place of stay.[11]

The highly developed thought forces of Eduard Meier (above, 2010) were briefly demonstrated by focused intent in 1977, when he levitated a ½ ton oven across a short distance of several meters, and later that year demonstrated the heating and melting of several coins in his hands.[12] The real danger of *oscillation interference* was concisely addressed by Quetzal during the 97th contact of December 28, 1977:

> *Quetzal:* The reason why we do not maintain connections in physical form with you Earth human beings, is as follows: The spheres of oscillations between the Earth human being and ourselves is basically so much different, expressed in forms of negative and positive, as of the balances, that it could have heavy consequences, if they would touch one another. Normally those oscillations of the human being reach up to 90 meters [or 295'], which is why care has to be taken, this distance does not fall below that, thus that Earth human beings shall not come within this point of distance to us. Our oscillations are very highly sensitive, and react strongly to other oscillations, which penetrate towards our sphere of oscillations. In comparison to the Earth human being, we are standing very high within our total development, namely by about 3,500 years in advance of the Earth human being, for which reason as well our complete field of oscillations has become subtilized. When now oscillations of a much less sensible Earth human being would hit us, just that way, that Earth human and thus quite imbalanced and negative oscillations would penetrate into the field of our oscillations, then this would be equal to a very strong shocking of the structure of oscillations, resulting in a strong outer influence leading to a sudden uncontrolledness of reactions, thoughts and actions of ourselves, which at the same time release uncontrolled feelings of fear…

Normally we use, when we walk among Earth human beings, which doing yet is extremely rare, an instrument, which protects us from the lower Earth human radiations. But to do this was never necessary with you, because you are exempt from these oscillations because of all your knowledge and your balance, which equates with ours… These dangerous disturbances of oscillation structure are the main reason that we are not allowed to agree to physical contacts with the Earth human beings. Even in our telepathic, or just inspirational-impulsive contacts, we have to exercise extreme caution, as also reflected impulse radiations effect similar consequences.[13]

Complete absorbance of radiated energies by the resonant metals of Plejaren spacecraft protects the visitors from the destructive thought forces of terrestrial humans, as with protective gear worn when outside the craft. Without the technical mitigation of radiant energies, safe contact is nearly impossible. The HHO plasma screens of Plejaren beamships permit the viewing of invisible infrared atmospheric energy as 'ion plumes' like those recently reported over North America during geomagnetic storms.[14] An excerpt from the 38th contact of November 13, 1975 concerns "energy bales… that circle the Earth at different distances and intervals" – *according to the Fibonacci structure of infrasound standing waves:*

[Semjase explained that] through the dimension door it was possible to visit the Earth in its prehistoric past as well as in its later time when it has a thick white vapor envelope surrounding the globe… But what now about the dimension portal in the Devil's Triangle? Can anyone *see* it?

Semjase: With the eyes alone, it is not recognizable, but it is possible to make the [infrared] radiation visible… with the help of my ship. At present only two courses of radiation are visible from this side of the Earth, while the third one is behind the Earth and thus cannot be seen from here… [Not only can you see it on the viewscreen, but] you can also see it from the windows, because the radiation becoming visible results from the radiation shield, which is [HHO plasma] spread from the whole ship. Now watch carefully, for the Earth…

Meier: …Girl, …that is fantastic – I can see really two huge trails of radiation! Besides this, there are spheres and other things around the Earth. What do these mean?

Semjase: Those are energy bales of different sorts and strengths. They circle the Earth at different distances and intervals, but are very important for the maintenance of Earth creatures. I am not allowed to explain more.[15]

The Fibonacci standing waves that comprise Earth's resonant energy cocoon are artificially generated for the acoustic propulsion of spacecraft. A beamships' alteration of the normal infrasound environment of Earth likewise alters the consciousness of human beings, potentially undermining natural learning cycles:

> *Semjase:* …[C]oncerning control of the gravitational forces… natural cosmic laws order a unitary and harmonic development in compass to all concerns of all levels able for evolution. This means that the spiritual as well as the material development proceed constantly in harmony with one another, and always complete one another by unison of the consequence in all matters. In the case of the mastering of gravity, the regulations of the laws are arranged in order, that primary is the spiritual evolution, of most decisive meaning, for the elaboration of technical means with the aim of mastering the gravitational forces. Here normally at first appears the exercise of spiritual forces in paralyzation of the forces of gravity, by which a human being is able to move weightless through space… [G]enerated by spiritual force state… a levitation process takes place. From the very primary side, this status is evoked within an unknown to the human being form, and just step-by-step, he learns to master it and to control it suitably. When the human being has then learned to control these forces, and only then, the way is cleared for him, by this, to consider technical means and to build them. So the control of gravity consists in its first-primary form on the evolution of spirit and feelings, meaning that the told forces can physically be controlled just then when the human creature has delivered himself from the "weight" of the non-spiritual condition…
>
> Exceptions witness the standard, even if these exceptions cannot easily be recognized and proceed in a way which often does not come to appear. Such an exception does the Earth human being represent. Except for a few, he is still not able to master levitation, and nevertheless he is already able to see clearly a great amount in the field of gravity research. This exception consists of the confusing fact of a very rare misdevelopment, which basically has shifted the potential of parallelization of the spiritual and the material, by which the material

[aspect of awareness] has become overweighted and dominates the spiritual. So this means that the Earth human being has become governed by the material side, by which the evolution runs in this direction, while the spiritual steps badly injured behind, as you yourself have once said. From that it appears that the technologies are more developed than the spiritual evolution. In this it has to be considered that especially since the year 1937 the strong influence of the new cosmic age have led this wrong burden of the material side in the whole world toward more gentle and harmonized courses, by which the differences between spiritual plenty and the material is no longer as strong as is generally thought.

Many forms of spiritual direction have led to spiritual recognitions of enormous meaning and value, which decisively appear in the development of technologies, and as an interesting fact, lead to success although the normal sequence of observance of the law was disturbed. But this can also be explained by, the otherwise newly gathered spiritual cognitions do nearly compensate for the lawful rule, which means, that in spite of barbarism the Earth human being has proceeded in both directions since 1937, and gets closer, though often unconsciously about this, *and advances by the cosmic oscillations*, rapidly towards the real evolution and begins to comply with it. This course of development can already be seen in the first days of entering the Waterman Age, in the 3rd of February 1844, and during the following time until the year 1937, when since the 3rd of February the second half of transgression of time began to offer its powerful working, from which it can be said by great probability, that the temporal aim of Earth humanity in respect to his determination by evolution, will have been reached after a time of about 800 years.[16]

This concise explanation concerning human control of the gravitational forces given by Semjase contains many profound truths, which reach to the core of the present predicament of our Earthly humankind. The Plejaren comprehension of the Creational Laws reveals the natural evolutionary process whereby each civilization overcomes all barriers to interstellar space-travel: from the cognition of an internal spiritual process of levitation involving resonant infrasound standing waves and water crystallization. The ancient Vedic spiritual practice of levitation was referred to as one of the great attainments. Known as *'laghima'* in Sanskrit, it is understood as an internal electromagnetic force generated by infrasound standing waves that are transduced and focused by the piezoelectric human body into an enveloping antigravity field. Earth's present-day scientists have learned to overcome the gravitational force using acoustic levitation, as an effect generated by the focusing of high-frequency acoustic waves into a concave resonator. Biophysicists have demonstrated the levitation of various insects, and even gone so far as to successfully complete the gestation cycle of a frog egg entirely within a levitating water droplet! [17]

Just as concave resonators artificially generate the force of *laghima* in a beetle, an artificial gravity field is generated by Plejaren beamships for their levitation by acoustic resonance. While high-frequency oscillations are used to levitate beetles in laboratory experiments (at left), interstellar spacecraft apply ultra-low frequencies for the acoustic generation of gravity. When describing the rebalancing of the evolutionary growth of spirit with the growth of technical means, *Semjase identifies changes in 'cosmic oscillations' as the underlying cause*. The movement of our entire solar system into a highly energetic region of our galaxy is presently inducing the profound advancement in consciousness due to the relative increase of planetary infrasound resonance, effecting a dramatic rebalancing of the Earth's very sensitive vibratory envelope. These cosmic oscillations are transduced on Earth by the world's network of pyramids into a resonant field of infrasound standing waves that converge at focal points defined by the axis-symmetrical octagonal geometry of the Great Pyramid of Giza, Egypt. The Fibonacci-ordered distribution pattern of resonant infrasound focal points dictates the precise locations where human consciousness becomes enhanced by the heightened 'cosmic oscillations' increasingly inundating the Earth since 1844, according to information provided to Meier.

Several of Billy's contacts occurred in Ober-Sätelleg, Switzerland, where he was able to photograph Semjase's beamship on March 8, 1975 (above). At this same location on July 7, 1980 Meier was simply instructed to record the acoustic resonance of Semjase's beamship during a demonstration flight.[18] Meier took up a position below the low-hovering beamship, near the trees beyond the log piles, while his wife Kalliope, two of his children and several close friends also made recordings on the greenway about 488m away. *Thorough analyses by acoustics experts confirm the beamship sounds to be genuine recordings that are impossible to replicate using any known equipment, being truly unique in three significant aspects:*

1. There were at least thirty or more discrete frequencies in a random and constantly shifting mix that ranged from 4 to 2170 Hz, but varied on average between 470 and 1452 Hz.
2. The amplitude of these frequencies was also constantly changing, whereby the dominance alternated.
3. The wave shape was also constantly changing in a random, periodic rhythm that caused a characteristic beat.

The wave pattern in the oscilloscope showed this constant and random shift in frequency, in which the principal waves of all frequencies came together in perfect synchronization at one moment, only to travel at the next moment in different directions and stages, thereby generating different patterns— at one moment seemingly moving in a cluster in one direction and, at the next moment, in the other direction. Then they gradually expanded until, for one moment, they formed a mutually precise and evenly distributed pattern, only then to move again into different relationships. Although these changes appeared to be random and were not repeated in a particular order, they always appeared in geometric relationship to one another. Two other sound engineers and a synthesizer sound specialist joined the analysis team, and the sounds were reexamined, this time for possible duplication. All of these specialists agreed that the character of the sounds was unique and that any type of synthesis, if in fact such was possible, could produce only portions of the recordings we had examined and that duplicating only part of the sounds, even in a short linear segment, would be impossible. The number of traveling and constantly shifting discrete frequencies and constantly changing amplitudes, which were shifting in relative dominance, exhibited duplication problems that exceed the abilities of a current state-of-the-art device!"

> Normally, Meier does not hear such loud ship noises, certainly not for such a long time. At the most, there is usually a very short noise when the spaceship lands or takes off. This demonstration was intentionally given for the purpose of the tape recording… None of the other eyewitnesses saw any type of spaceship, but Meier said that he could see it from below and observe a strange effect. *As the sound went up on the scale, the ship became more transparent, and when the pitch became lower, it looked denser again*…
>
> Jim Dilettoso, our research consultant, took samples of this noise to Peter Gimer and Rick Coupland of Micor in San Francisco. There they performed tests in the audible range, from 20 Hz to 2000 Hz. They found twenty-four characteristic frequencies within the audible range and eight outside of it. They found all thirty-two frequencies concurrently at different amplitudes and volumes. All thirty-two tones are somehow produced simultaneously. In a time matrix, the amplitude of some frequencies increases, while that of others decreases. It was observed that the amplitude periodically increased by ca. fifty decibels and then decreased by ca. forty, and at other times, just the opposite was the case, which produced the characteristic beat that was audible. Other normal sounds were audible on the recording, but there were no signs of a tone-on-tone tape dubbing. All frequencies were clear and stable, and they were regularly lined up along the frequency scale [in the sonogram, below].

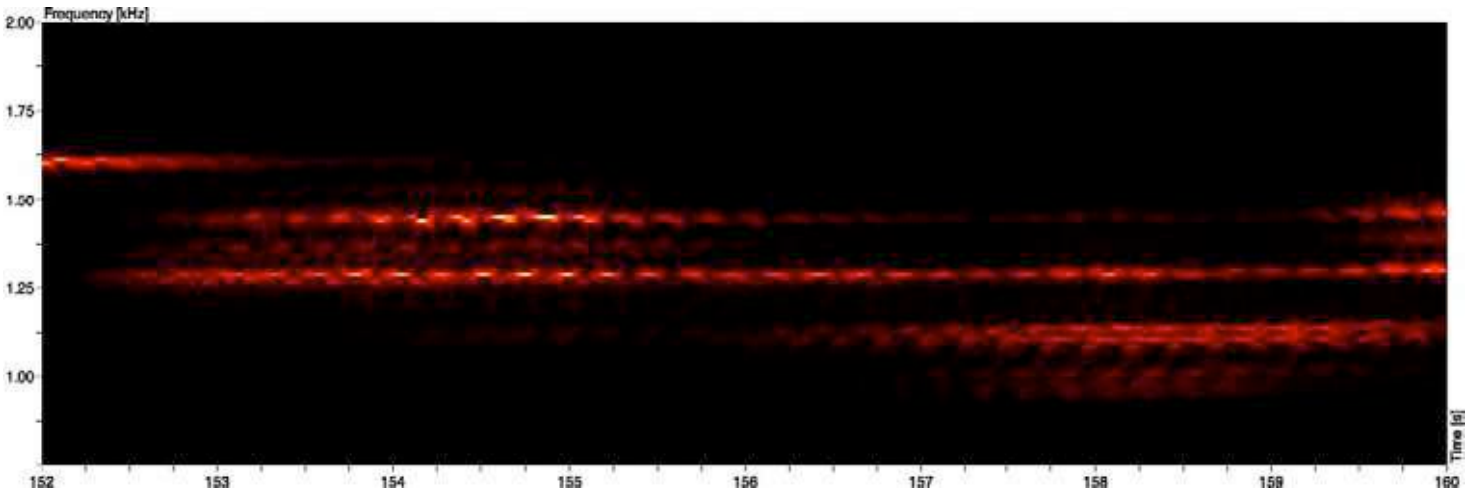

> The demodulation showed that one must be dealing with a rotating device — 249.6 U/min. modulated at 4.16 Hz… The high-speed device produced a sound that began at 520 Hz and increased in steps up to 990 Hz, only then to decrease again down to 520 Hz in the same frequency steps. The tonal groups comprising 520 Hz disappeared together at 520 Hz and reappeared at 600 Hz, only to disappear again at 720 Hz. At 990 Hz, however, they reappeared and were very strong. The same occurred in the other direction. The condition remained stable for a moment and then shifted again. This shift was somehow random, but nevertheless constant. At certain times, the high-speed device was still, and a deep, throbbing beat was audible; and then the high-speed rotation began again, and the sound increased rapidly to a high vibrating crescendo in the upper 50,000 U/min. range or higher. Simultaneously, the slower 249.6 U/min.-rotation again became audible. The vibration was produced by the high-speed rotation of approximately 29,000 U/min., which accelerated to over 59,000 U/min. This was most certainly not a normal sound! [19]

While acoustic experts have identified several key features of the beamship sounds that are impossible to reproduce with any known equipment, their archive search for related sounds failed to recognize these same key features in a sound that we are all constantly exposed to, but only very rarely conscious of – *the sound of our mother Earth!* The over 30 fixed frequencies of Semjase's beamship, whirring in constantly shifting amplitudes, very closely replicate the much lower infrasound harmonies of Earth's planetary resonance. Earth's base frequency presently fluctuates near 7.8 Hz and harmonics progress in frequency steps of approximately 5.9 Hz, extending from below 2 Hz upwards to about 50 Hz.[20]

Subtle fluctuations observed in the deep resonance of Earth are seen as rather dramatic shifts in the multi-frequency oscillations of the Plejaren beamship, as dominance constantly shifts up and down the frequency scale in regular stepped intervals visible in the sonogram above. The various circular rings and domed elements of the beamships' hulls are designed to generate this standing wave resonance through highly structured crystalline metals that transduce and amplify the omnipresent song of the cosmos, referred to by the Plejaren as the 'Symphony of the Spheres' during the 223rd contact of May 1, 1988:

Meier: You, as well as Ptaah and Semjase, once played the strange humming sounds of the Earth to me through your apparatuses, which I can't perceive in nature, unfortunately, because my hearing senses aren't so sensitive that I could hear these sounds, which should very well be possible for other people, however, as you've explained… You named the sounds "Symphony of the Earth" or "Symphony of the Planets" as well as "Symphony of Space," which is also entirely incorporated into these sounds, like also the atmospheres of planets and suns and even all material and immaterial things of every kind, concerning which you've spoken of a "Symphony of the Spheres." This symphony, i.e. these sounds, are, so far, still unknown to the Earthly scientists in particular and to the people in general, other than just the exceptions to the rule, even those people who perceive these humming sounds, i.e. "Symphony of the Earth," and who are of the opinion that something isn't right in their heads, and thus, not that real things are going to and fro. Can you once again officially explain what it actually concerns with these humming sounds, if it shouldn't remain a secret?

Quetzal: It does not have to remain a secret because in about 10 to 15 years [1998-2002], a portion of the Earthly sciences should also encounter these things. Moreover, it concerns the fact that every planet, every comet, every larger asteroid, meteor, and every sun, as well as the nebulae and clouds in space and space itself, as well as every black hole and all material and immaterial things existing at all produce certain tones and sounds, which we, as you said, actually call Symphony. Within the entire realm of the Creation or of the Universe, nothing exists that would not be incorporated into these symphonies, so therefore, all material and immaterial things vibrationally generate certain tones and sounds and even symphonies, which usually cannot be perceived by the human ear because these move in too low or too high frequencies for this. Only through abnormal, degenerative, physiological changes can these sounds or symphonies be perceived by human life forms, whereby these then become effective in an extremely consciousness-impairing, nerve-racking, and psyche-damaging manner.

> The frequencies of these symphonies or sounds reach into all levels, so thus, the lowest sounds, like humming sounds, as you say, are given as well as the highest whirring sounds and shimmering sounds, etc. As the frequencies are virtually countless in their number, these are also the sources of the sound symphonies, for these relate to all that exists of the material and immaterial. Thus, if one starts from the Earth, then these sound sources are, for example, the waters, in terms of the deep-sea movements as well as the movements of the waters of the lakes, rivers, streams, creeks, and springs.

> Even the roar of the waves, the small and mighty storms, the tectonic movements of the Earth's interior, the bubbling of magma in the Earth, and the eruptions of the volcanoes belong to these, as well as the rain, hail, and the various layers of the atmosphere, which rub against each other, as well as the winds against the trees, grasses, flowers, houses, mountains, sand dunes and deserts, steppes, icebergs, glaciers, and surfaces of ice, as well as against windmills, wind turbines, ships, aircraft, rockets, missiles, and vehicles of all types, against land surfaces and everything else that materially exists. Also to be noted are the voices and sounds of humans and animals, insects, birds, and fish and any other water creatures.
>
> All sounds together form the actual "Symphony of the Planet," as we call it. And as this happens in the purely material realm, so this also happens in any immaterial sphere in the entire Universe, each of which also produces its own symphony, like also fog flowing on the Earth or nebulae existing in space and all other formations that are absolutely impossible to cite in their number because everything is so immeasurable that it could neither be grasped by purely human understanding nor by technological possibilities of any kind.[21]

Given as a precise description of cosmic resonance, the comprehensive explanation of the 'Symphony of the Spheres' provided by Quetzal penetrates to the unified vibratory essence of the cosmos. My own direct perception of the resonant symphony during deep meditative states formed the impetus for my years of study of infrasound standing waves. I discerned that the deep throbbing pulsation that fills my consciousness during the darkest hours of the night was induced by ayurvedic pyramids for heartbeat entrainment at specific nodal points around the globe where sacred ancient temples still exist, yet having suffered terrible cataclysm. The cosmic symphony is absorbed through the resonant metals of plasma beamships to be converted by interior HHO plasma chambers into ultraviolet-A and infrared light for all power needs. The over 30 distinct frequencies observed in the infrasonic bands of Earth's resonant symphony are exactly replicated by spacecraft for acoustic levitation on the arches of standing waves.

Analyses of the resonant humming of the Plejaren beamships recorded by Billy Meier exactly echo hieroglyphic Sanskrit scripts on highly reflective silver-alloy metal debris recovered from the 1947 aerial disc crash near Roswell, New Mexico (pg. 31). Embossed text on an I-beam fragment reads: *"workings of 30 resonances, female and male, 30 resonances whereby approaching the highest…"* Meier's beamship recordings prove *the Roswell texts describe the 30 resonant frequencies of standing waves generated by plasma ships for both antigravitic propulsion and the maintenance of life onboard.*

Standing waves surround the beamship to act as waveguides for HHO gas that is emitted from the aerial antenna atop the craft into the energy streams, where it is ignited to form HHO plasma around the ship. Also called hydrino plasma, HHO plasma is defined as *resonant-transfer plasma* for its crystalline ability to transduce all received acoustic energy into re-emitted heat and light. All interstellar vessels achieve extreme acceleration by enveloping the spacecraft in HHO plasma to induce a set of transdimensional characteristics that includes superfluidity and frictionless passage through the atmosphere. Semjase explained in basic terms that the screen "allows every interference to glide away, without… resistance." [22] This same plasma technology has already been in use for many years now in the nose cones of US military aircraft.[23] Additional information was provided to Meier regarding the use of plasma 'distorter-screens' enveloping Plejaren beamships that allow complete optical invisibility to the naked eye:

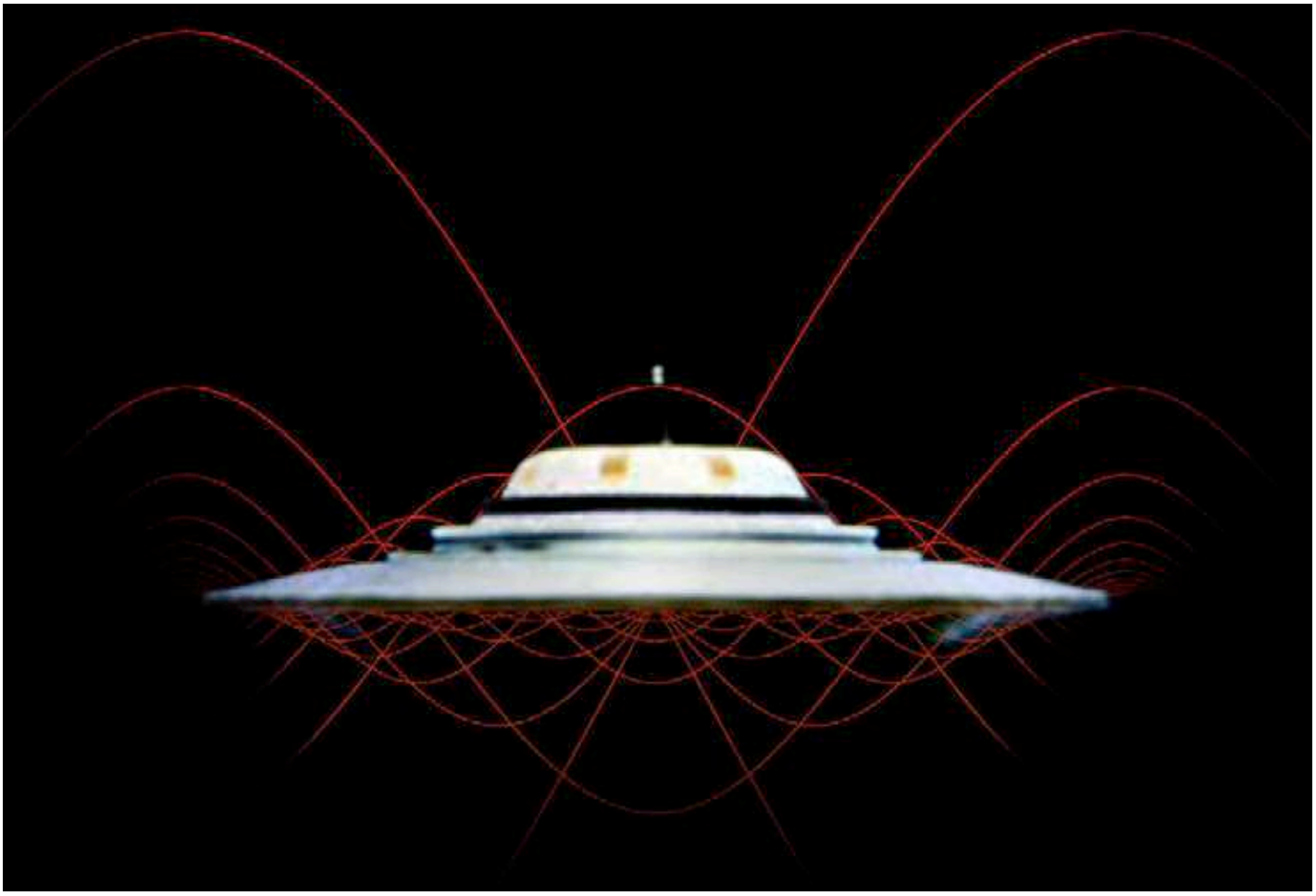

> [Earth human beings] are very simply not accustomed to close observing and viewing. On the other hand we protect our beamship against sight of any kind and they can't see us. It is easy for us to protect our ships as we desire in a diameter of 500 meters, in whole or on parts, at one side, upwards or downwards, against sight by (use of) a distorter-screen. When I allow you to photograph my ship from one side, then it is protected on all other sides against further observation by the distorter-screens, thus none uninvited are able to see it.[24]

The beamships' invisibility screen is generated from emitted HHO gas produced by the resonant dissociation of water molecules at 13,563,688 Hz. The implosion of single hydrogen atoms (to become *hydrinos)* as HHO plasma[25] is achieved by the rapid ionization of emitted gold and silver nanoparticles, as indirectly described by Semjase during her 11th contact with Eduard on April 15, 1975: "The antenna's conducting beam and the energy collecting beam appear as a fine line of energy over the beamship, while the regeneration radiation becomes visible beneath the ship in various hues… The energy only becomes used and regenerated again for the radiation drive… Our whole technology is aligned toward natural rectification, but not toward destruction." *Implosion* was then addressed by Meier, "I understand; the natural principle is, thus, implosion and regeneration, rather than explosion and destruction." [26]

Meier observed an optical transparency effect of the gradual acoustic engagement of the ship's HHO plasma protection screen, observing that *"as the sound went up on the scale, the ship became more transparent, and when the pitch became lower, it looked denser again…"* A different transparency effect was mentioned on another occasion when, during the 31st contact of July 17, 1975, Semjase explained: "You know that with our technology we have the ability to strain any materials by special radiation and cause those materials to be invisible to the naked eye. We can control this effect very exactly." [27] This transparency beam technology was first created and described among our scientists by Canadian inventor Troy Hurtubise, who named his prototype beam device *Angel Light.*[28] An intense beam of X-ray light from krypton plasma generates the temporary effect of *total optical transparency in all materials* – a new state of matter to be technically described only later, in 2009, by Oxford University researchers:

> [A] short pulse from a laser "knocked out" a core electron from every aluminum atom in a sample without disrupting the metal's crystalline structure… [The] high-powered synchrotron radiation generator produces extremely brief pulses of soft X-ray light… At such high intensities the aluminum turned transparent.[29]

Plejaren beamships' precise control of transparency induction using X-ray light beams was demonstrated for Meier on objects in Earth orbit and even inside the beamships themselves. The domed ceiling and 8 view-ports of the circular spacecraft are made transparent by this high-intensity illumination process, giving the optical effect of disappearing instantaneously to provide an unimpeded 360° panoramic view.

Meier's clear profile photograph of a landed beamship from 1975 reveals the structural features of the flight vehicle perfectly conform to the Fibonacci-ordered standing wave resonance patterns generated by the over 30 discreet frequencies resonating within the alloys of the hull during flight (opposite). During the 4th contact of February 15, 1975, Semjase offered a comprehensive description of beamship propulsion drives, yet carefully substituted the word 'beam' for the more accurate scientific term 'HHO plasma', a technical concept apparently not authorized for use according to the Confederation's High Council:

Semjase: For traveling through cosmic space, a drive is necessary which surpasses the speed of light by millions of times. But this propulsion can only come into action once the speed of light has already been reached… This means then that a beamship needs two drives, first the normal which accelerates up to the speed of light, and then a second… which generates a million-fold, a billion-fold, the speed of light, thus the hyperspeed by which hyperspace is penetrated… So time and space collapse, and they become zero time and zero space. This means time and space cease to exist. And exactly by that, distances of numerous light years are traversed in a fraction of a second, with no time lag… When, for example, we leave the Pleiades and need about 7 hours to get to Earth, then on our own planet, and on Earth, 7 hours pass. We need this long because we first have to fly beyond the reach of the planets by normal propulsion, and only far out in space can we convert to hyperspeed. Back from hyperspace then, far outside your solar system, we convert to normal drive. We are never allowed to enter hyperspace too near to a planet… I am only allowed to say this concerning propulsions; your scientists are already working on light-emitting drives. Light-emitting drives work for normal propulsion, and move the beamships near planets and until they are a safe distance away.

Meier: This is evident, but how is it possible for a beamship in the gravity of a planet, or in its atmosphere, to attain such great speed without glowing, or the passengers succumbing to the huge pressures?

Semjase: This is very easy to explain, and also no secret any more to Earth humans, at least not the scientists; the beamship is surrounded by a protection-beam-girdle… [Thereby] anything contacting the screen [becomes] disintegrated or "flowed" away… [while the protective HHO plasma screen] also neutralizes the attractive force of a planet… The gravity of a planet is, besides this, not always the same, or of the same strength, owing to certain alternations which will be discovered by your scientists in a reasonable time. The beam-protective-screen diverts the gravity and attractive forces, and the beamship in effect becomes a miniature planet which can travel at nearly light speed through any atmosphere without risk. As the gravity of a concerned planet does not influence the ship, the passengers feel normal and unburdened, as if they were on their planet itself, always under the premise that the planetary gravity is in accordance with their anatomical capabilities. In the beamship itself, the gravity of course is tuned to the passengers and is completely controllable. When passengers on spacecraft from other worlds move in atmospheres alien to them, or on hostile planets with unbearable gravity, they use suits and other small transportable instruments which generate for that creature, the necessary beam-protection-screen for their particular ship and their particular requirement.[30]

[Semjase continued her explanation of superluminal space travel during the 8th contact, on March 18, 1975:] The turning-off of a time-dilation or time-shift needs but the penetration of hyperspace, as I have already explained. The "jump" occurs very fast by momentary paralyzation of the protective screen under flash-like increased velocity, with the consequence of a flash-like increase in mass. This means that the initiation process runs so fast, that by the speed of certain processes, generated by the apparatus, matter is distorted within the millionth part of a second, and becomes fine-material form, which is able to pass hyperspace timelessly…

> By this, at the same time, space and time are paralyzed and disappear, in consequence of which the ship already rematerializes itself at its destination place, as it is dematerialized at its place of departure. The whole process needs no longer than a millionth part of a second, thus also for creatures, passing hyperspace does not take alterations of any kind. When spaceships fly below the speed of light, this inevitably takes much time, which is always the case with newcomers to cosmic flight. First, they all do learn from experiences and cognitions. Second, this space-traveling is very dangerous and leaves its purpose open to question. When spaceships reach hyperspeed without passing directly into hyperspace, then catastrophe for the ship and its passengers is assured… Speeds above that of light hold many dangers, when the barrier of hyperspace is not penetrated and made an ally. The dilation effect is only one of these dangers… Our forefathers, too, faced these problems, and went astray in space and time. The same does happen to other creatures, and in the same way.[31]

The industrial development of antigravity technology on Earth followed Nikola Tesla's 1899 discovery of standing waves, which led to the later development of the implosive hydrogen motor. Through the joint espionage efforts of Nazi industrialists in both the US and Germany, Tesla's secret transdimensional spacecraft designs were stolen by Hitler and quickly weaponized by enslaved Nazi/CIA scientists[32]:

> Viktor Schauberger was the actual designer and builder of this world's first flying saucer motor, which was built for Nazi Germany in 1944. In view of this startling revelation one has to wonder where he obtained his revolutionary knowledge to construct such a device. He had discovered what he called an "implosion" principle, and invented a motor to take advantage of this new principle. The motor consumed only air and water and generated light, heat, and thrust, as well as a diamagnetism which made lift possible through "diamagnetic levitation".[33]

The dark truth of the Nazi assassination of Tesla after the theft of his designs was retold in 1995, during a deathbed confession by Hitler's personal bodyguard and espionage agent Otto Skorzeny. Published by Erik Berman in 2003, Skorzeny confirmed that Tesla's HHO plasma invisibility technology had been applied in both the Nazi flying discs and later in the US stealth aircraft.[34] Advances in Earth's resonant spacecraft technologies continually occur as the expansive consciousness of humanity reaches toward the stars.

In anticipation of piloting a *newly manufactured* spacecraft from Erra to Earth for the first time, Semjase announced the deployment during the 48th contact. Eduard was given the opportunity to photograph the new beamship on March 8, 1976, at Bachtelhornli-Unterbachtel (above). The new beamship displays a golden-colored alloy comprising the underside of the hull and along a band below the orange-tinted cupola windows. Both beamship models are 7 meters in diameter and share a similar hull design, with several significant differences. The latest design presents a more complex array of HHO gas-venting systems above the domed ceiling that replaces the aerial antenna employed in the previous model, as well as radial ridges that form a distinctive stepped contour along the golden perimeter of the spacecraft.

Semjase explained, “In the outer appearance only small differences appear. The greater novelty is the inside arrangements, which offer much more capability than is the case with my present ship. With the new one I have the ability to break through dimensions in two directions.” [35] *Meier had previously described transdimensional hyperleaps through space and time during earlier contacts in his youth, as an instantaneous physical dematerialization from which arises a profound sense of cosmic Oneness*:

> With the launching of the [time-travel] transmission a quite weird thing happened in the form that the entire surroundings of the ship slowly shimmered and then quite suddenly simply no longer existed. I also observed the same process in regard to myself, and in the moment of the "jump" it was, to me, actually as if I suddenly no longer corporally existed. Somehow I felt transferred into something which I sensed as being eternity itself and in which an indescribable silence and endless, calming peace and enormous love ruled… It was often for me as if I were raised up by *being* itself.[36]

While photographing the latest Plejaren spacecraft design for the first time (below), Meier witnessed the instantaneous appearance of two accompanying spacecraft, later described as 4-meter Explorer class unmanned reconnaissance vessels. HHO plasma excited in the air surrounding the beamship for instant optical invisibility can also be generated within the ship's interior airspaces by rapidly ionizing the third-density lightwater vapor to become a fourth-density environment of HHO plasma. *During his 31st contact of July 17, 1975 Eduard Meier experienced fourth-density space-travel, by hyperleaps, covering vast distances to visit various inhabited worlds of the Universe.* The remarkable details reported by Meier deserve serious contemplation – especially the state of consciousness experienced by all the passengers aboard the giant spherical 'Great-Spacer' during the seven minutes of dematerialization *'in the eternity'*:

Semjase: Earth humans still don't know very many things. But now we have to interrupt our conversation, because my father has finished his preparations for the great leap. And as I am already speaking of such, then I want to ask you something: In a few minutes, we will jump for seven minutes into the "eternity", as you call it. *The feelings and sensations there are completely otherwise than in normal existence in material life.* For that reason it is also not possible for us to receive your thoughts and feelings with proper concentration. In consequence of which neither I nor my father, nor any of us, could later repeat for you your feelings and thoughts, so that you could write them down. If you nevertheless wish to do this, then there is a chance on a technical basis…

The booths, which you can see there, beside the screens, are equipped with all necessary means, to store up feelings and thoughts. The thought impulses received are stored in a special computer and can later, as may be desired, be repeated word for word from it. The helmet, formable and adaptable in size, which you see there, is equipped with very fine sondes and is as well covered by a special, fine-meshed net of sondes, which pick up every kind of energy and transforms it into impulses, which are then transmitted to the computer where they are registered and stored. The energy of thoughts and feelings is measured in very high values and can be received only through those instruments. The energies of feelings and thoughts exist only in very high frequency fields, or hyper-frequencies. To now be able to register your thoughts and feelings, it is necessary that you place yourself into the chair and lay the head under the helmet cap, which then will adapt itself automatically to your head…

Meier: At your service… (As Semjase explained to me, I quickly sit down inside one of the three booths, in the extremely comfortable chair. As soon as I have seated myself, the peculiar helmet moves over my head and sinks down silently. It is big enough that it closes around my whole head, and only leaves my face open, thus I can see and watch everything. But the helmet is not touching my head; only lying close around it, keeping about one and a half centimeters distance to the skull, as I can see when I place a forefinger between the helmet and the head. Now I am tense and expectant, for I wonder what is going to happen. Ptaah and Semjase manipulate the apparatus, and now I can see again how the fantastic heavens and stars change. In a fraction of a second they are nothing more than a whitish milky mass, a shining mass, as I have already seen in the other hyper-leaps. But now suddenly as well, this milky whitish shining is gone and there is darkness.

But now what is this? Suddenly all is merging into a golden color, and now everything is like silver. But - my dear this glistening light, this beaming shining splendor! Everything is merged into glistening light - only the glistening light. It is stronger than all the suns of the Universe... Dear, oh dear, this glistening light, and it does not hurt the eyes! Dear, this must be eternity, the glistening light of the eternal... but see, there is nothing besides the eternity; man alive, how marvelous! Marvelous? Man alive, that is itself marvelous. Eternity and marvelousness are one and the same. Only why do I separate it? Why do I put the eternity into terms of time? Time does not exist, and the eternity is marvelous. Man, just what is this? This tranquility, this peace -- what is it? How could I have achieved this?

Love, oh that deep all-encompassing love. Nothing is there, but *love*: wonderful, marvelous. Oh yes, I am, but I am not. Everything is so deep, and full of love. Of course, I am eternity, and I am inside of eternity. How could I ever forget this? Oh yes, I am a human being, how can I... why do I forget that? I am only a guest in eternity – and those loving voices, calling for me, from where is it coming? I can see nothing, only the glistening light, comforting. Who is calling me? I see nothing; man alive, I am nothing any more. I can't see myself. I am eternity, in the eternity. Oh, how is that, but I don't see with my eyes, still I see everything. And I am not listening with my ears, yet I hear everything. Yes, the love, how powerful it is, how immense, infinite and wonderful. Everything is love and splendor; why doesn't the human being understand this?... The calling comes out of the light. Is it the call of eternity?

Oh how hard it is... to not think that I am only a guest in eternity, that I am only a human being. How painful it is, this being a human. I do no more want to be. I want to remain here as eternity inside of eternity... this deep. Yes, I want to stay here. Never again do I want to return. Here is the existence, the real existence... How can I feel strange having to return to a material world? I belong here... Pain, why are you shaking me? What is it?)

Semjase: Do you still not understand?

Meier: I – Oh yes, of course! – Pitiful – very much pitiful – why have you brought me back here?

Semjase: You want to joke, but we have all been inside the timelessness, and would all like to stay there. But we are not ready to stay, because we have to absolve the way of evolution step-by-step – as you also must do, dear friend. I know quite well, how painfully your heart aches now, as we all have experienced the same thing. *But we have to adjust ourselves for that and do know, that under no circumstances or conditions are we allowed or able to remain, until we have reached that level of consciousness.* I do regret very much that you feel disturbed inside, as I can see it on your face. But you will overcome it, because you can think about it realistically. For that reason we also took responsibility for this equipment... [that allows us to record your blissful thoughts so that you may reflect on the experience of transcendence later.] [37]

The transdimensional experience of oneness had left Eduard shaken. What he experienced *'in the eternity'* finds direct parallels with the impressions of other contactees who have transcended into *fourth-density awareness.* During transdimensional breakthrough, the third-density air environment maintained inside the spacecraft is instantaneously converted into a fourth-density environment of HHO plasma, *inducing a transcendent state in the human being through the radiations of gold and silver nanospheres among the trace elements conforming the atmospheric water vapor maintained within all beamships:*

> *Ptaah:* You breathe here in this room… air… [that] is adjusted to the conditions of our homeworld, and is much more healthy and invigorating than that of Earth. The oxygen content is some values higher than on Earth, and also the compound of other elements is somewhat different… The different composition of the air keeps us awake longer, and in need of less sleep than is the case on Earth. That is why you are not tired.[38]

An elementally balanced atmospheric composition affects the bioelectrical enhancement of all cellular metabolic processes within the human body, greatly decreasing the need for physical sustenance, whereby Meier was sustained on one meal for over 90 hours. Open discussion of bionanotechnology was precluded by the Plejaren, except once –by Quetzal during the 205th contact of February 3, 1986:

> But in our civilizations, [disease] has no longer appeared for thousands of years… I want to explain as an exception and on my own responsibility. *Above all, silver ion products – such as silver ion powder, silver ion jelly, or silver ion cream – are useful.* For this, an application is required on the skin.[39]

This hint from Quetzal addressed those few silver ion products available at that time in 1986, yet point directly toward the present advances of ayurvedic electro-medicine using gold and silver nano-colloids.

Through these highly advanced transdimensional means, Plejaren spacecraft are able to not only hyperleap through space, but also through time. Meier was taken to visit Earth in various stages of her past and future to witness differing levels of gravity and the corresponding atmospheric conditions. On one occasion, Eduard was actually taken thousands of years into the past aboard Semjase's beamship *to visit himself in a previous incarnation* and was informed that the same time-travel process even allows the potential for visiting one's future incarnations, although this is rarely done.

Throughout Eduard's early years of contacts with the Plejaren Elders he was denied the opportunity to obtain detailed close-up photographs of their spectacular plasma beamships, yet this prohibition was lifted during later contacts in 1981. Several opportunities were granted for Billy to document visits by a single-occupant 3.5-meter reconnaissance beamship (above). Having no exposed windows, this compact plasma ship relies upon interior view-screens or, for direct viewing, the walls of the ship are made transparent by intense X-ray illumination. The many conjoined circular sections of the tiered hull are comprised of a highly reflective electroluminescent metal alloy that can be electronically tuned to emit any desired frequency of light. Infrared luminescence is used to ignite HHO gas for instantaneous plasma invisibility cloaking, referred to by the Plejaren as a 'beamship protection screen'.

Scores of superbly detailed documentary photographs of transdimensional spacecraft were taken by Meier in the parking lot of the Semjase Silver Star Center. Close comparison of the differences that appear in the configuration of Quetzal's ship reveals controlled rotation of the large ring of spheres. Meier learned of the absorptive characteristics of the beamships and other similar interstellar spacecraft during the 150th contact of October 10, 1981, in discussion with Quetzal regarding technical barriers to communication between various civilizations operating plasma spacecraft in the vicinity of Earth:

> No radio waves and no other kinds of vibrations are capable of penetrating into these aircraft because the outer hulls of each device absorb everything in terms of power storage for the ships' propulsion and everything else. This means among other things that these aircraft are so designed that they absorb all waves of all frequencies and, therefore, all vibrations of all kinds for power storage, like also sunlight and everything else in terms of entering radiations, etc. But the moon light and the weak light of the stars are also absorbed and stored as power, together with many other things [comprising the Symphony of the Planet, *especially terrestrial standing waves of infrasound resonance*], which are still unknown to the Earthly scientists.[40]

All wavelengths of energy are absorbed into the craft and transduced into ultraviolet-A and infrared light inside HHO plasma chambers, formed by the conjoined rings of spherical resonators. The rotating rings release plasma discharges that arc across the spark gap created between the two resonant spheres with gold-colored circular fittings. The noticeable warping of the image is an optical effect of the strong electromagnetic fields levitating the craft across the parking lot while it was being photographed, without landing. Along the outermost rim of the craft is a ring of 96 rubies that act as plasma beam emitters as HHO plasma becomes confined within the path of the infrared light by an encircling electromagnetic field, just as recently defined by MIT researchers investigating *superfluidity* (Ketterle et al.[41]).

The single-occupant reconnaissance spacecraft displays many advanced features for the application of fourth-density HHO plasma beam technologies that further confirm the validity of these photographs, which have been met with decades of sustained criticism despite being authenticated by experts. Many magnificent photographs taken at the Semjase Silver Star Center provide scale references by including foreground and background objects, allowing the size of the spacecraft to be accurately determined.

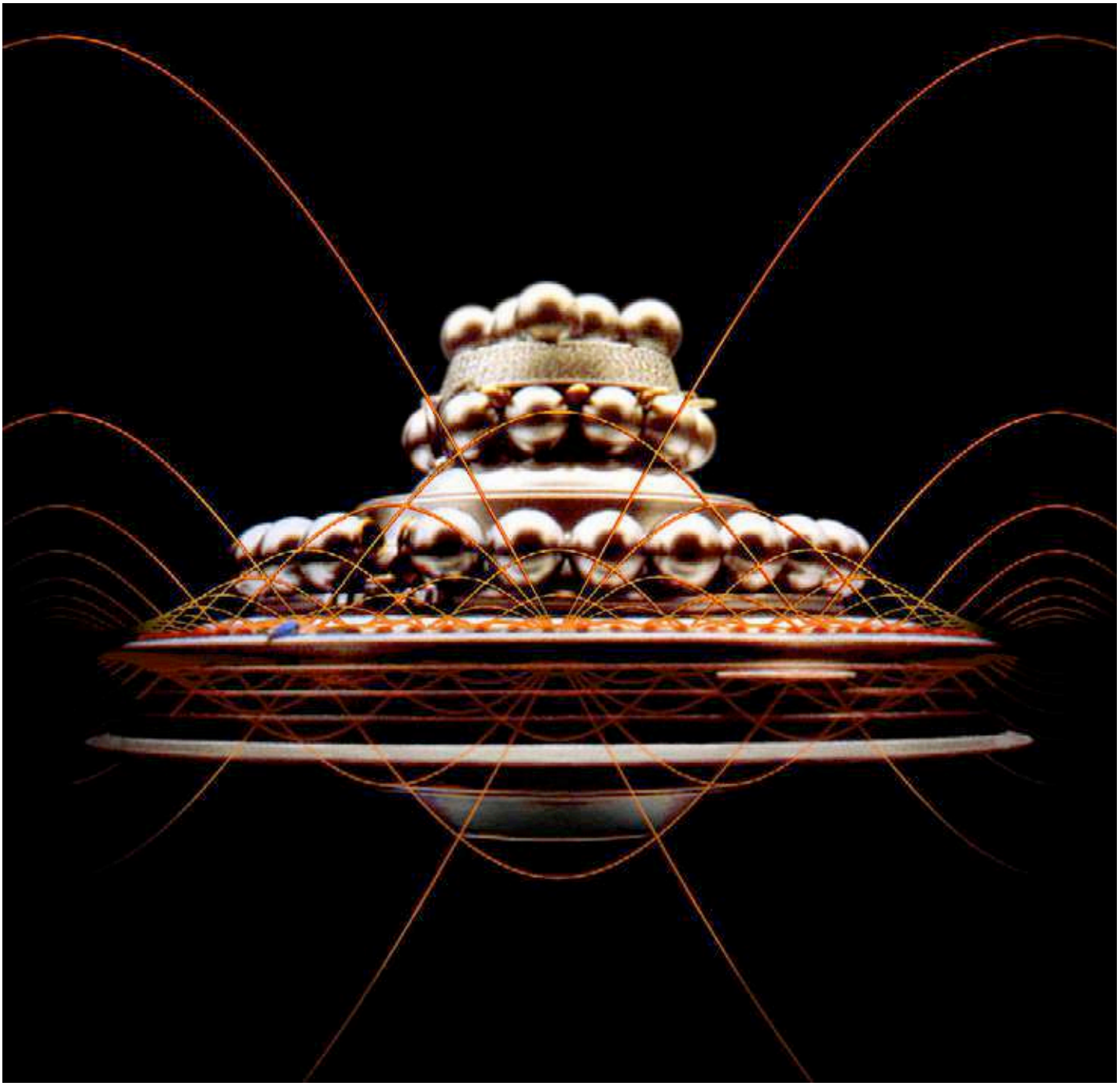

The craft's spherical resonators and compact circular hull serve in the production of standing acoustic waves that provide the antigravitic effect for flight by acoustic levitation. An array of 8 spheres is clustered at the top the craft, above a central row of 12 spheres and a wide lower row of 24 spheres – all of similar diameter. This 8–12–24 alignment of resonators presents the same quadrupolar geometric configuration observed of all of their spaceflight vehicles for generating Fibonacci-ordered standing waves composed of over 30 simultaneous, fixed frequencies with constantly shifting amplitudes (overlaid, above).

The loud singing of the resonant metals in flight can be shifted out of the audible range of human beings to be entirely imperceptible, utilizing deep, throbbing infrasound frequencies well below 20 Hz for levitation. The frequency of each spherical resonator is defined by wall thickness, not diameter, thereby allowing the specification of a unique frequency for each, as the high-speed rotation of the largest ring of resonators at 249.6 U/min. creates the 4.16 Hz modulation. *Never having seen Meier's photographs, acoustic analysts identified the object that produced the sounds as being composed of many spheres.*

Meier was able to document an interesting effect of electroluminescence generated by Quetzal's beamship at nighttime from several perspectives, in a series of remarkable close-ups on August 5, 1981. Red light emitted by the normally silver-colored metal surfaces gives the ship a golden appearance. One image from the series captured the ship in a particular configuration not seen in any of Meier's other photographs, with a reflective metallic viewing screen exposed by the retraction of a small protective sleeve (above). Comparing photographs of Quetzal's ship reveals the rotary function of the lower array of resonators. The compact circular design of this interstellar vessel reflects the same mathematical structure that guides the larger beamship designs, presenting the precise, unmistakable form of the Mandelbrot quaternion (at left). The octagonal symmetry of the Mandelbrot set defines the distribution pattern of interconnected spherical resonators mounted in circular rows along the upper tiers in the 8–12–24 arrangement. *This 'otherworldly' plasma vessel reflects the same geometries seen in crop circles.*

The close-range photo series included well-illuminated, detailed nighttime images of the tiered convex underside of the beamship piloted by Quetzal. Recessed patterns are seen under the beamship's outer flange and details of the lower hull's concentric rings include a pair of circular fixtures and other closed circular ports just barely visible (likely housing landing supports). The large, stepped central element terminates in a nearly hemispherical platform with an array of HHO plasma beam emitters, for which the 'beamships' have been named. Plejaren beamships in Earth's airspace maintain complete invisibility, yet special occasions presented themselves whereby members of the Meier's community were able to witness and photograph various spacecraft and other associated aerial phenomena. While Semjase's description of global celebrations on her homeworld of Erra included immense, multicolored aerial HHO plasma displays by fleets of beamships, only modest demonstrations were made for Meier's group.

FIGU member and author Guido Moosebrugger was able to photograph a nighttime aerial beamship demonstration on June 13, 1976 above Winkelriet/ Wetzikon (at left). The bright luminous display distinctly presents an array of infrared beams acting as guide paths for glowing orange columnar discharges of HHO plasma. Rather than providing some form of thrust as would be expected in the context of plasma jets used in basic terrestrial rocket technology, the plasma beams can be used to target and incinerate objects below the ship, and to levitate objects upwards from very far below. This beam is often used for tasks such as collecting atmospheric, terrestrial or aquatic samples and specimens, as well as generating luminous aerial displays. Specific colors emitted by HHO plasma can be controlled by simple chemical additives being vented with the HHO gas, thereby forming plasma trails of banded colors in the wake of the plasma craft as it maneuvers aerially.

The circular bottom of the reconnaissance beamship houses a symmetric octagonal array of 24 plasma beam emitters arranged around a larger central element which vents HHO gas into the beam array to be ignited as HHO resonant-transfer plasma (above). Each of the plasma emitters contains a ruby for the generation of a beam of infrared light, precisely aimed by a short nozzle. The plasma emitters' achieve a narrow range of rotary motion that allows all 24 beams to be focused on one central point several feet below the beamship, or independently into any other desired configuration. The alloyed nozzles focus an electromagnetic field that encircles the infrared beam, thereby confining the HHO plasma within the beam. These techniques for plasma beam focusing are now commonly used by plasma physicists, yet are rarely studied in the context of beam propagation over vast distances through the atmosphere.

Well-known examples of resonant metal alloys formulated by Sanskrit-based Buddhist traditions in Asia include Tibetan singing bowls, comprised of 3 metals, and finer Bhutanese singing bowls rendered from 7 metals or more, known for highly resonant characteristics. While the singing bowls of Asia are comprised of a layered composite of various metals formed by hammering, the much more advanced resonant alloy production processes of Plejaren metallurgists involve the co-mingling of atoms in a composition unique to space-faring plasma ships, unlike any produced on Earth in modern times. Billy accepted several resonant metal samples as gifts from Asket, the products of her civilization, the Timars, who use similar advanced techniques of frequency resonance applied by the Plejaren, and indeed all cosmic travelers.

The resonant metal alloys of transdimensional plasma ships are developed using precision multi-stage temperature and frequency programs that convert base metals into alloys (above) containing all of the precious metals, rare earth elements and trace amounts of every other element on the periodic table – many in crystallized or metallic states not yet conceived of by Earthly scientists. Polarization of the final products is achieved by the micro-layering of perpendicular grain patterns formed within the crystals.

Semjase provided Meier with Plejaren beamship metal alloy samples of a *7-stage metal conversion process from lead into a copper-nickel-silver-gold alloy, also containing traces of every stable element in a smooth curve from the heaviest elements through the lightest gases.* Many aspects of this complex process were discussed during the 45th contact on February 25, 1976, in response to Meier's direct request – "Quite simply, we would like to know what sort of metal you use for your beamships?"

> *Semjase:* This I can explain for you: We gain it from a process of conversion from lead. We extract this soft metal from many things, as for example lead-containing atmospheres from stars, from waters, from different plants, etc., as well as from the decay of different ore-stones of stars in destruction. By an, according to Earth understanding, very difficult process, we convert the lead substances we assembled into the soft metal lead, which we then change by further mechanical-chemical processes into a hard-metal form, which is much harder than your metal which you call steel. This still is unserviceable in this form for beamships, because it must be polarized by further processes of conversion into a beamship-suited alloy of a special sort and character, about which I am not allowed to give details. The final product, which must have quite certain characteristics, consists of… a copper-nickel-silver alloy, which for certain of the beamships also contains gold.
>
> *Meier:* Oh yes, thus an alloy which could be produced on Earth… You mentioned a lot of manners before, in ways in which you gain the lead. Here it has struck me that you have mentioned no word of an ore mining of Earth kind. Is this sort of obtaining ores not usual with you?

Semjase: Ore-mining or other mineral mining on a planet or another star is done by us only in extreme emergency, because this process is equal to the destruction of the star. A planet or another star is never exploited in the form as is done on Earth. What the Earth human being does by that is equal to the destruction of the planet. The first evil effects of this destruction came up on the Earth already some decades ago, and at the present time it is already experiencing the pains of the destruction itself. This is to understand the way that the Earth human being exploits his planet, and robs from it its fundamental life force when de deprives it of its oil, gas and the different ores. The effect of this is that the Earth suffers shifts inside, leading to volcanic eruptions and earthquakes, because the Earth is slowly breaking down into itself. The same event is generated also by the construction of dams and similar formations, which cause, by the assembled masses of water, very dangerous shifts. The worst delusion the Earth human being is performing is his subterranean and below-surface experiments with atomic bombs, as well as those cruel deep subterranean explosion tests, which he declares are atomic bomb tests, but which in truth are much more dangerous.[42]

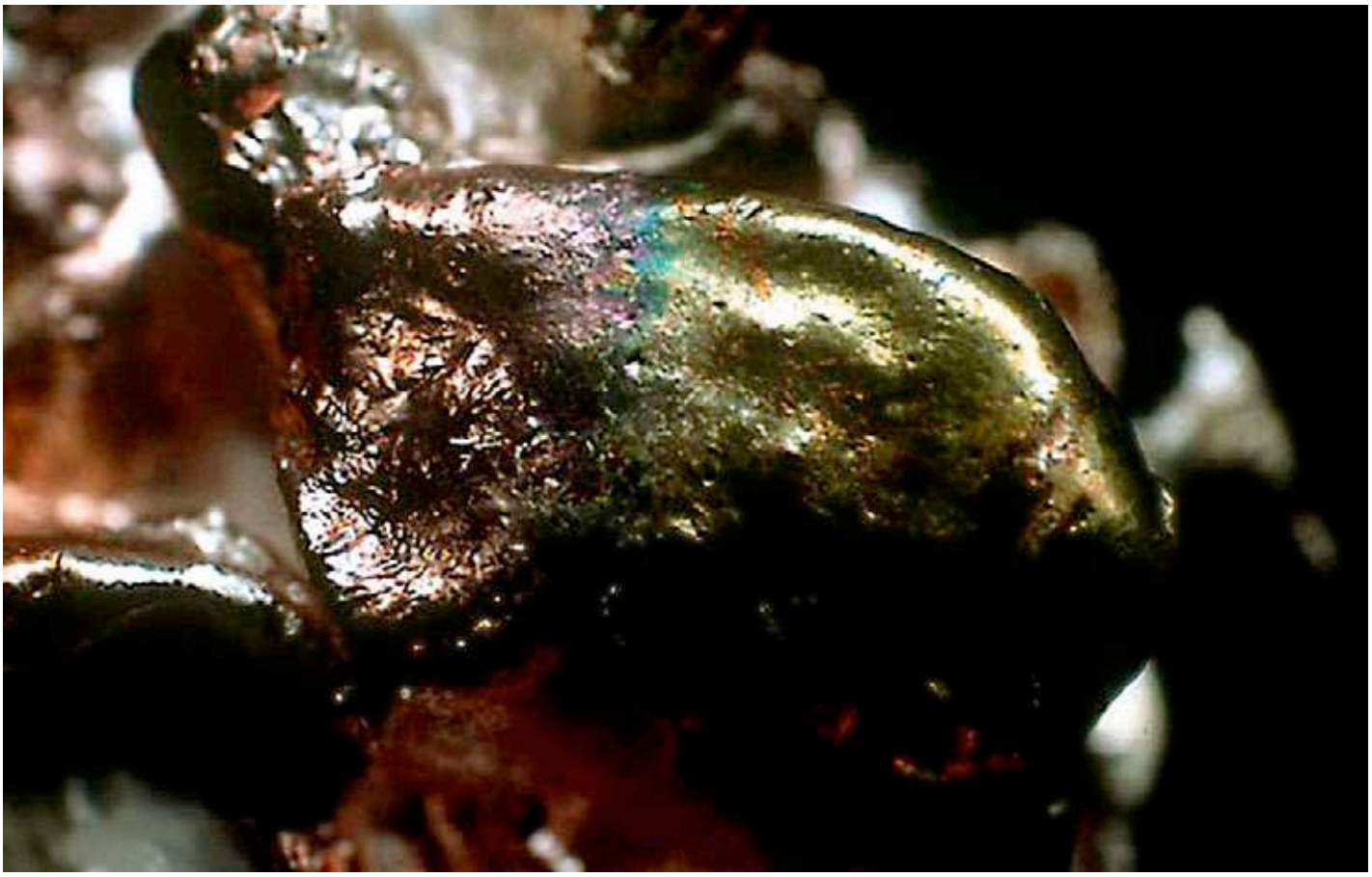

The spiritual ethics of the Plejaren culture reflect a comprehensive understanding of planetary systems. All 7 stages of beamship metal production were related on the following day, during Meier's 46th contact, with an astounding explanation of the atomic transmutation of metals by *controlled frequency resonance:*

Semjase: Here I also have brought you some metal, of three different working steps… The first working step absorbs the lead substances from the atmosphere and condenses them into pure lead. The second process distracts from the resultant metal all dangerous radiations. Then the lead is fed into heat-converters, which, without the addition of any other metals, converts the lead by several processes into the alloy.

(Ed.- The metal specimens finally delivered to Meier, which they and we had analyzed, consisted of three of the seven states the metal goes through in production and refinement. We had samples of states 3, 4, and 5. The sample of state 3 was mostly lead, with impurities. State 4 was nearly equal parts of silver, copper and lead. State 5 contained silver, copper, nickel, gold, magnesium and other trace elements. We lost our specimens in the hands of testing laboratories before we had finished our analysis. We found traces of stable rhenium and thulium in our specimen tested by Marcel Vogel in his laboratory in San Jose, California. Since our testing in 1979, scientists have found that the addition of rare earth elements like rhenium and thulium produce astounding properties in otherwise basic metals, such as superconductivity, superhardness and supermagnetism, etc.)

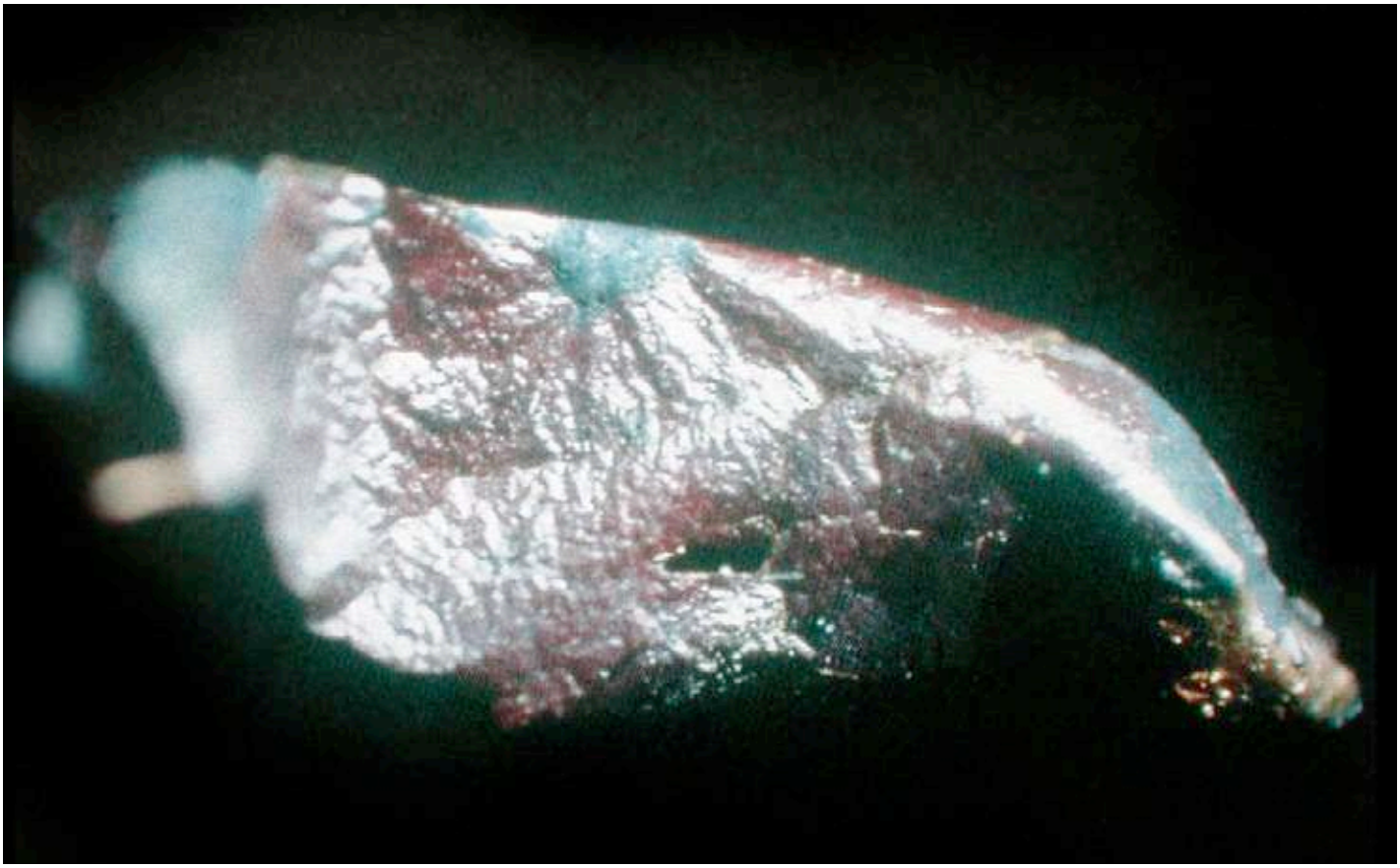

Meier: You mean that the lead becomes liquefied first, and in this step suffers the conversion?

Semjase: Surely. There do all right exist direct possibilities for the alternation of stuff, but these possibilities are not given for us. But our scientists have already well achieved successes in experiment. For the present, however, we still convert the metals the old-fashioned way in heat-converters, and as said, this happens in seven different runs. The metal becomes liquified, like with you, in furnaces, to suffer then by distinct oscillations, an alternation, but just to a certain value, because of the different steps in working that are necessary. Each final product is then pushed by pressure through a cooling spiral, where then are generated the small figures, as you have then here before you. This process is repeated some times, while with each new process the value of the different metals increases and becomes the targeted alloy. The sixth working process then affects the complete alloy… The cooling spiral contains usual water, which we obtain especially for this process in a condensational manner…

Meier: Thank you. Still it is not evident to me how you then will work the metal, as neither at your beamship, not Ptaah's huge ['Great-Spacer'] box, could I recognize joints or seams, etc. And nothing is riveted as well.

Semjase: For this purpose we use an instrument which you would call a welding apparatus. But it is based on oscillation techniques, which liquifies the metal in a cold state and lets it flow together, by which it is completely without seam and forms one single piece. So we also do not know grinding operations, as you do when you have to do welding work, and then have to grind away the seams to smooth it all. In this respect, you on Earth use a very dangerous operation.[43]

While Earthly science achieved the liquification of metals using high-intensity ultrasound[44] decades ago, Semjase informs us that for thousands of years Plejaren metallurgists have been producing beamship alloys by *subjecting molten metals to "distinct [atomic] oscillations of a certain value."* What are these particular *resonant frequencies* that induce the alchemical transmutation of one element into another? The atomic physicists among Earth's scientists have been making great strides in their understanding of low-energy nuclear transmutation – the most outspoken among them being Dr. Joseph Champion of the Phonon Resonance Institute in St. George, Utah.[45] Dr. Champion's work elucidates the atomic principles enabling several successful methods of atomic transmutation involving the production of precious metals:

Dimensional phonon resonance occurs when the space occupied by one isotope is *exactly the same as that of another isotope in its rest state* [i.e. 25°C]. This event can only occur under the following two conditions: the expansion of an isotope by heating, or the contraction of an isotope by cooling. Due to the natural characteristics of elemental properties, this event is extremely rare and one can only force the event under select conditions. To determine the phonon resonance of an isotope, it is necessary to apply the following formula:

$$\text{Phonon Resonance (Hz/Cm)} = \sqrt[3]{\frac{d \times Na}{m}}$$

d - density in g/cm³
Na - Avogadro's Constant
m - atomic mass

In the formation of Au (or other elements) from a dimensional reaction, the conversion will occur without excess energies or nuclear signatures… by heating Ag to a temperature of 43.2°C… To achieve maximum conversion of Ag to Au will depend on the dwell time at resonance temperature. To date, visible conversion of Ag to Au has taken as little as six hours, with 2% conversion taking up to 24 hours. The reaction is safe… [with] no toxicity.[46]

$$^{107}\text{Ag Phonon Resonance (Hz/Cm)} = \sqrt[3]{\frac{10.5 \times (6.0221 \times 10^{23})}{106.905092}} = 38{,}962{,}532$$

$$\text{Au Phonon Resonance (Hz/Cm)} = \sqrt[3]{\frac{19.3 \times (6.0221 \times 10^{23})}{196.967}} = 38{,}931{,}841$$

Dr. Champion's phonon resonance formula provides the resonant frequency of *gold* (Au) in its rest state as 38,931,841 Hz and the ^{107}Ag isotope of *silver* as 38,962,532 Hz (above). The relative proximity of the resonant frequencies of these two precious metals allows a low-energy atomic transmutation from ^{107}Ag to Au to occur *near room temperature*. However, silver isotope ^{109}Ag comprises 48.8% of all available silver bouillon and, unlike it's sister isotope ^{107}Ag, is not so easily converted to Au.

The conversion of ^{109}Ag into gold requires a more complex process using megahertz frequencies in conjunction with precision heating techniques. By the same means aluminum can be converted into silver when oscillating at a resonance of 38,950,565 Hz (at 276°C) and will also convert into gold when dwelling at a resonance of 39,932,068 Hz (at 295°C). After just a few days of dwell-time at resonance, atoms of the starting element have become *informed with the resonant frequency* of the target element in its rest state. The metal is then melted and rapidly cooled in distilled water to achieve the maximum conversion rate, *just as in the procedures described by Semjase in 1976.* The respective electron configurations of aluminum, silver, platinum and gold reveal the restructuring of electron orbital shells during transmutation:

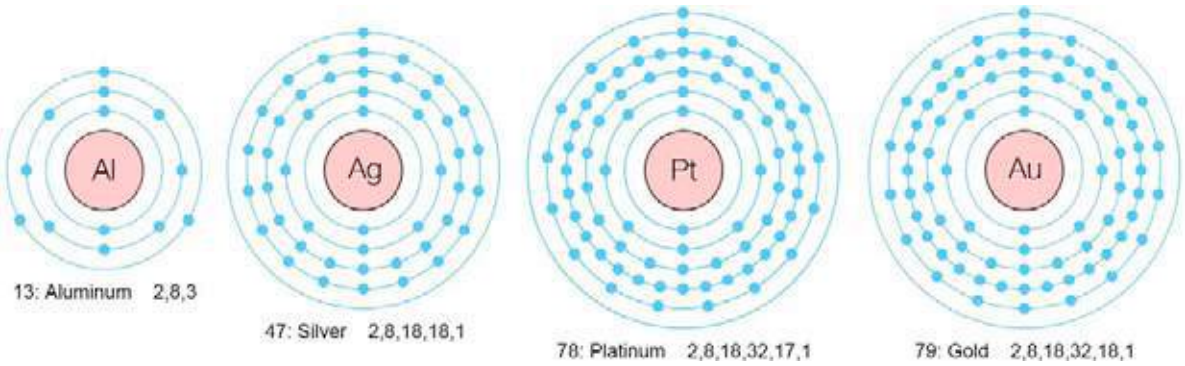

The addition of subatomic particles into atoms vibrating at resonance is facilitated by *standing waves that act as pathways for the reconfiguration of electrons*, *protons and neutrons into a more densely packed arrangement.* Just as acoustic standing waves can power wireless devices by transmitting electrical currents across otherwise nonconductive airspaces, standing microwave resonances induced within atoms allow subatomic particles to jump across otherwise impassable gaps in the atomic framework. Direct observation of this resonant phenomenon of atomic transmutation will be made possible by the quantum stroboscope, which has already provided the first direct imaging of standing waves that comprise the structure of a single electron. A source metal like aluminum can thus be transmuted into silver and then gold as successive electron shells become filled, adding atomic weight in the process and significantly increasing the yield weight of the conversion with each stage of the complex process.

Dr. Champion has identified a new class of intriguing natural metabolic processes[47] where atomic transmutation occurs as fungi ingest silver, thereby undergoing a *pleomorphic change*. Dry, active yeast is a cheap and readily available bread-making product that requires only warmth and water to thrive and reproduce in vast numbers. Common yeast species like *Saccharomyces cerevisiae* produce the silver-binding protein SSB-1 that enables the attachment of active yeast cells to available silver surfaces.[48] Ingestion of silver atoms by the round 2-3 nm microbes causes their mutation into rod-shaped mutant microbes about 1-2 nm in length (below). The budding yeast cells act as *electron donors* inducing the resonant transmutation of silver into gold, as 32 electrons, 32 protons and 57 neutrons are accepted by ^{107}Ag silver atoms vibrating at a 38,931,841 Hz resonance with gold. This newly recognized metabolic process leaves nanoclusters of gold deposited on exposed silver binding sites, as further transmutation takes place within the bodies of the microbes whereby ingested silver is converted into gold nanorods.

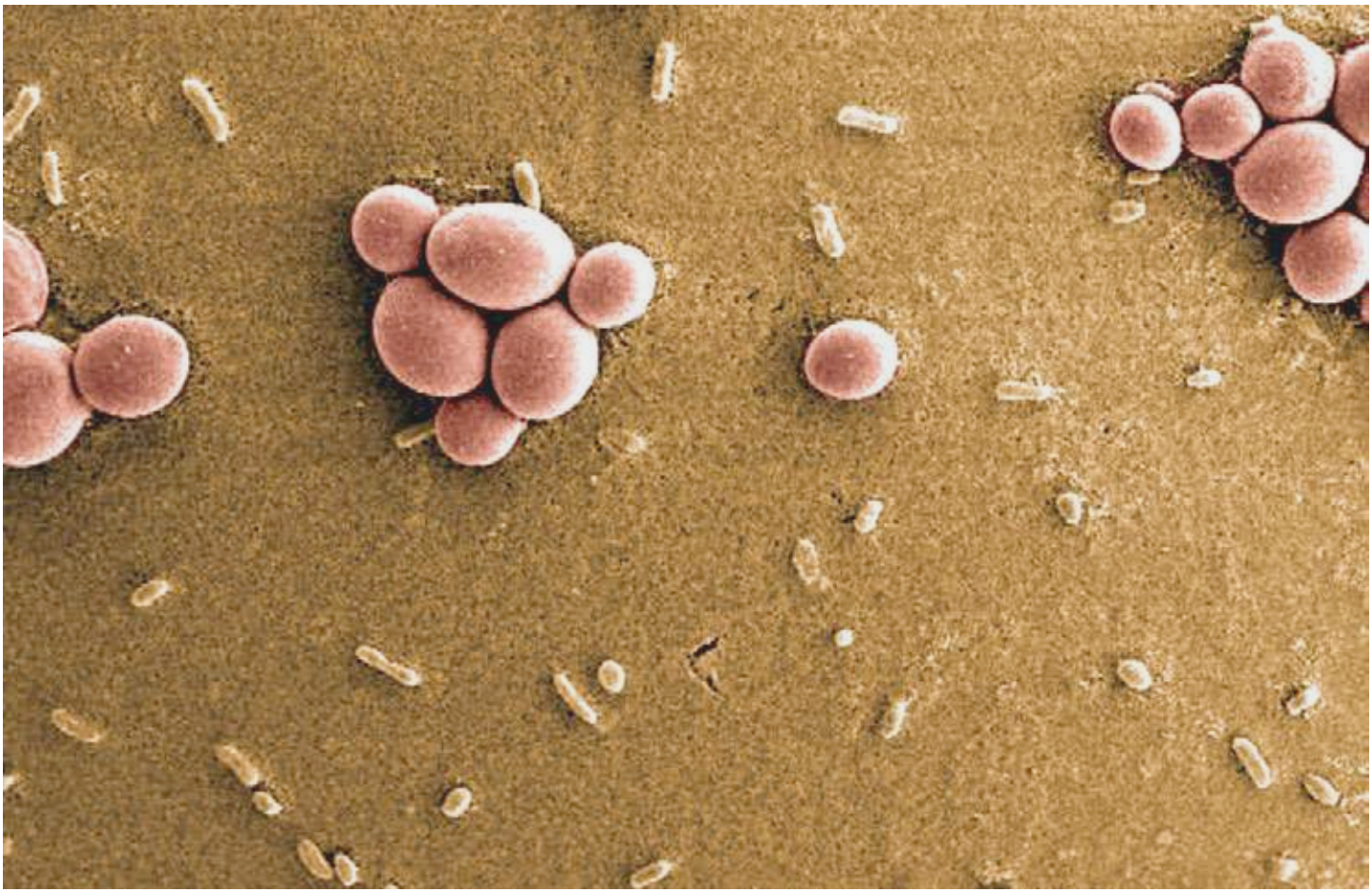

The rediscovery of biological transmutation in yeast species restores ancient metallurgical knowledge and informs a scientific reinterpretation of enigmatic passages from the Bible. Biblical accounts of the divine presence often refer to a sacred substance called *manna,* which was used in making holy items such as the 'bread of life' (or showbread) and the 'living water'. However, this holy bread was not simply produced by a common baker. Instead, Moses commanded the goldsmith Bezaleel to prepare manna for the 'Bread of the Presence of God' – *apparently using yeast to convert silver nanopowder into gold.* Many unmistakable references preserved in the Book of Exodus confirm the biological process of atomic transmutation was used in the enrichment of food and water for the elevation of human consciousness. Advanced material and spiritual knowledge possessed by Moses is revealed in his demonstration that the presence of God is not conferred by gold idols, but by gold nanoparticles in sacred bread and water:

> When Moses approached the camp and saw the calf and the dancing, his anger burned… He burnt the golden calf - melted it down, and then filed it to dust; and that the powder to which it was reduced might be taken notice of throughout the camp, he strewn it upon the water which they all drank of. He did this that it might appear that an idol is nothing in the world, he reduced this to atoms, that it might be as near nothing as could be. (32:19-20)

My first experiments achieved ~3% transmutation of silver into gold in 7 days using the silver/yeast method at 108°F (before/after seen above)! A comprehensive spreadsheet provides phonon resonance frequencies and temperatures for most isotopes based on each atom's physical diameter.[49] A small selection of phonon resonance frequencies determined for various conversions follows:

Source Isotope	>	Target Isotope	Resonant Frequency	Resonant Temperature
^{107}Ag (silver)	>	^{197}Au (gold)	38,931,841 Hz	43 °C / 108 °F
^{95}Mo (molybdenum)	>	^{65}Zn (zinc)	39,400,694 Hz	115 °C / 239 °F
^{65}Zn (zinc)	>	^{27}Al (aluminum)	39,296,350 Hz	183 °C / 362 °F
^{27}Al (aluminum)	>	^{107}Ag (silver)	38,950,565 Hz	276 °C / 529 °F
^{27}Al (aluminum)	>	^{197}Au (gold)	39,932,068 Hz	295 °C / 563 °F
^{107}Ag (silver)	>	^{109}Ag (silver)	38,652,383 Hz	327 °C / 620 °F
^{65}Zn (zinc)	>	^{107}Ag (silver)	39,138,500 Hz	344 °C / 653 °F
^{65}Zn (zinc)	>	^{197}Au (gold)	39,126,761 Hz	356 °C / 673 °F

The atomic resonance of various elements provides the particular conversion cascade by which nature creates the diversity and abundance of matter through great heating and cooling cycles recurring throughout the depths of the cosmos. The layered lithosphere's seemingly endless variety of minerals and ores are the byproduct of extreme conditions of pressure, heat and time. Bacteria thriving in these conditions also contribute to the Earth's internal atomic transmutation and decay processes, just as microbes are essential to metabolic processes in the human body, with its own specific resonances.

The full spectrum of atomic resonances present in all planets endows resonant vibratory characteristics, and Plejaren metallurgists have produced resonant metals by the same means. Beamship metals also contain traces of *all* stable elements present in nature. Eduard Meier's Plejaren contacts have explained that transdimensional spacecraft are like tiny artificial planets unto themselves, and the beamship metal samples provided to Meier have given further insight into the deeper layers of truth contained within their many concise explanations. The delicate threads of knowledge woven into Meier's communications with the cosmic Plejaren culture have been published word-for-word for this very reason: to preserve for human contemplation their advanced scientific and spiritual teachings in pristine form.

The penetrating truth of the Plejaren teachings has become all the more apparent as the frontiers of human knowledge expand toward recognition of natural law and co-creation using diverse natural micro- and macrocosmic processes. The manipulation of an atom's diameter by temperature adjustment allows for nuclear transmutation from one element to another in *a specific cascade sequence* that determines the frequency programs used by Plejaren metallurgists to convert lead into a resonant copper-nickel-silver-gold alloy with trace amounts of every other stable element. The third, fourth and fifth-stage beamship metal samples were submitted for microscopy analysis to Marcel Vogel, senior research scientist for IBM, who later confessed his amazement at what he observed under magnification:

> "When I touched the oxide with a stainless steel probe, red streaks appeared and the oxide coating disappeared. I just touched the metal like that, and it started to deoxidize and become a pure metal. I have never seen a phenomenon like that before." Of another metal sample containing nearly every element in the periodic table, Vogel stated, "Each pure element was bonded to each of the others, yet somehow retained its own identity." At 500X magnification thulium was revealed. "Thulium exists [naturally] only in minute amounts. It is exceedingly expensive, far beyond platinum, and rare to come by. Someone would have to have an extensive metallurgical knowledge even to be aware of a composition of this type", said Vogel. At 1600X Vogel said, "A whole new world appears in the specimen. There are structures within structures - very unusual." At 2500X he found that the sample was, "metal, but at the same time ... it is crystal!" …Vogel put the full weight of his expertise in these summary comments: *"With any technology that I know of, we could not achieve this on this planet! I could not put it together myself, as a scientist..."*[50]

Vogel's astonished assessment of beamship metal constitution was made independently, without having any advanced knowledge of the comprehensive details Meier had been given by Semjase concerning all 7 stages of the resonant metal manufacturing processes of Plejaren metallurgy! The most significant details omitted by Semjase (for good reason) are the precise transmutation frequencies necessary to achieve each specific conversion. The complete set of phonon resonance frequencies determined by the formulas of Dr. Champion allow the integration of Plejaren teachings with the theoretical framework

understood by contemporary atomic physicists. Dr. Champion's work inspires a reinterpretation of the results of various analyses conducted by Marcel Vogel in 1979, which comprised the first modern scientific study of resonant metal alloys produced by the cascade process of atomic transmutation:

> All of the elements examined spectrographically had missing bands in their spectra which should have been there if they were normal atomic spectra. This indicated that the elements were put together in a very unusual way [easily distinguished] from normal Earth technology… [presenting elemental characteristics] beyond what one would consider an isotope… Basically this indicates a non-electrical cold fusion process of synthesis because there was no ash and no heat residue. Such a process is not known to Earth technology… Another unique feature of these elements was the almost perfectly uniform fall-off of lighter elements preceding that being studied in the spectrograph. There would be the primary in a high state of purity and then with no secondary and no catalyst an absolutely uniform curve of all the lighter elements preceding that, even through the gases. It appears as though the desired metal was the result of a uniform buildup of density, particle by particle!

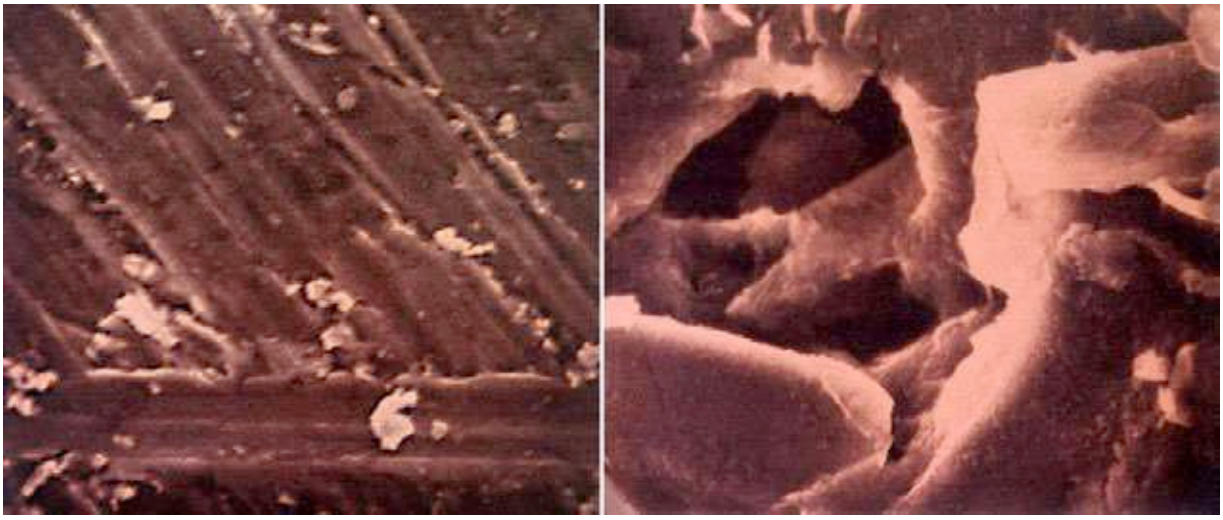

> Examination of a non-metallic part of the specimen using polarized light to emphasize certain bi-refringence revealed crystalline structures, which are organized in spiral formations. Under 2000X scanning electron microscopy the six-sided face angles of the crystals were clearly revealed. A photomicrograph picture shot of this revealed unusual clarity indicating unusual conductivity of the electrons illuminating the image. Ordinarily, if they were ordinary non-conducting crystals, like quartz, the electrons would accumulate rapidly on the points of the crystals and form a space charge obscuring the image. The conductivity was so efficient that sub-crystal structures inside the crystals could be actually seen – something unheard of before this. The electrical bonding between the basic crystal elements was so efficient that a clear view through the crystalline latticework revealed a spiral buildup of regularly spaced assembly with contact taking place at the ends of the sub-particles. There were no gas bubbles. If this were produced in a heat fusion process the picture would be entirely different and a greater mixing of elements would be expected… Still another micropart of the specimen consisted of pure silver –again with no secondary lines and no catalyst indication. The silver was also unusually conductive and it was smoothly bonded to a pure aluminum area that was unusually conductive also… The following unique properties encountered in examining this specimen make it exotic and very definitely point to an unearthly origin:
>
> - Unusual purity in state of metal examined… with no indication of catalyst or secondary spectrographic lines.
> - Unusual number of trace elements ranging from the primary heavy all the way up the scale density in a very uniform curve with no breaks or gaps up to the lightest gaseous elements. Again these lines all indicate the same high purity for each element. Scientists involved have never seen anything like this before.
> - Strange, very uniform grain pattern with a layer of horizontal grains sandwiched between layers of vertical grains again sandwiched between that and another horizontal grain, etc., in a tight 90° latticework.
> - One metal surface showed evidence of an extremely fine mechanical cut, possibly even by laser. [above]
> - Association of non-metallic crystals of strange structure and extremely high conductivity for the elements.
> - End-to-end formation of bond patterns in the crystal structure and the spiral assembly or stacking of the crystals in the non-metallic substance was unique.
> - Some form of non-electrolytic cold synthesis process is very definitely indicated.
> - There is some evidence that the synthesis took place in a vacuum.[51]

These many unique and astounding characteristics of the resonant beamship metal samples – including *superconductivity, superhardness and supermagnetism* – are only attainable through the phonon resonance application of standing waves for *tuned atomic transmutation in a uniform build-up of density, particle by particle.* The concept of standing waves was touched upon indirectly on many occasions during the Plejaren dialogs with Billy Meier, though the specific term itself was not divulged, in a situation very similar to the treatment of another sensitive term: 'HHO plasma'. Infrasound standing waves were mentioned in the context of "energy bales of different sorts and strengths… [that] circle the Earth at different distances and intervals, but are very important for the maintenance of Earth creatures" (pg. 80).

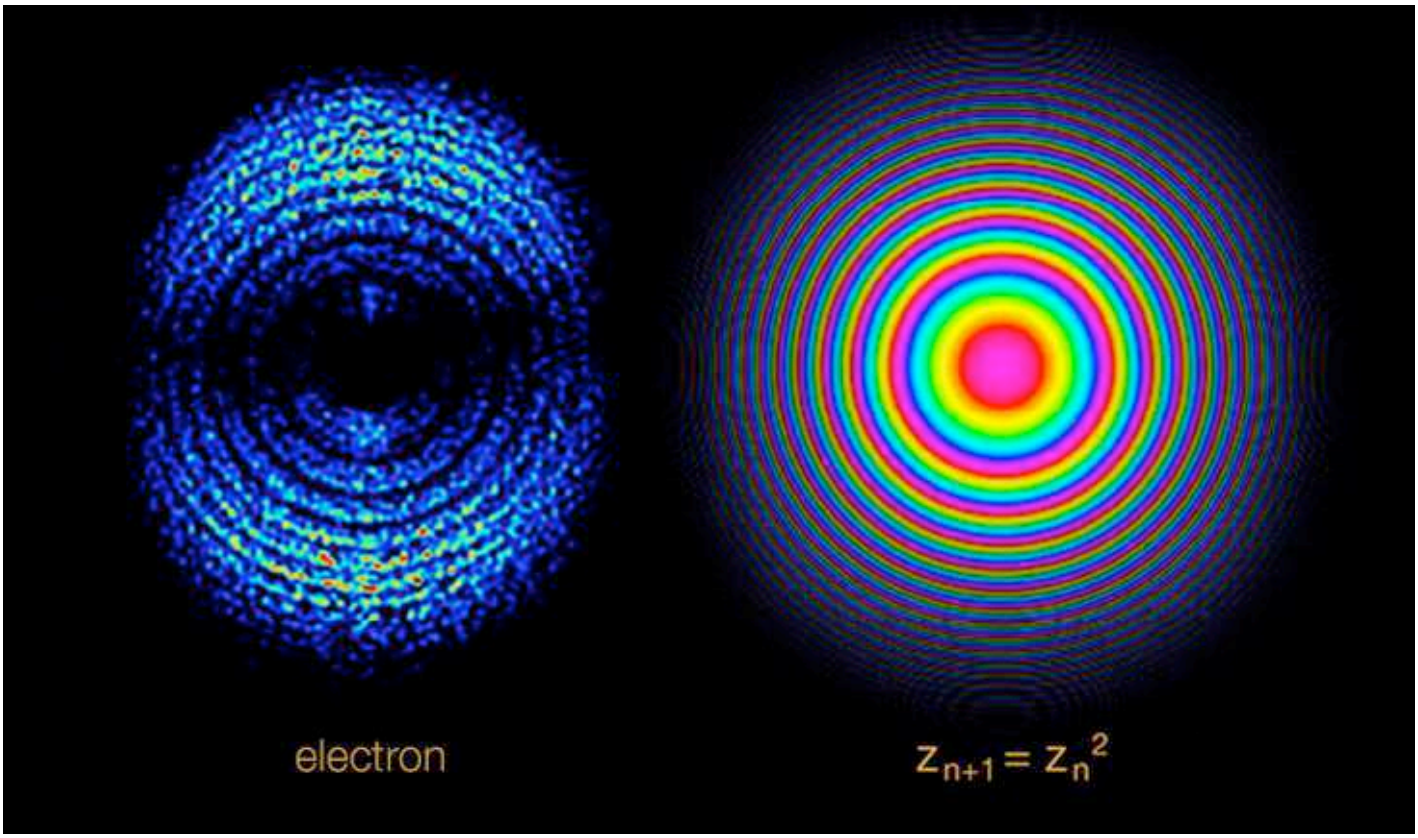

Semjase also indirectly referenced terrestrial standing waves when she informed Meier that "the gravity of a planet is… not always… of the same strength, owing to certain alternations which will be discovered by your scientists in a reasonable time" (pg. 89). In fact, over 30 years elapsed before my completion of these standing wave maps in 2005, defining the specific Fibonacci 'distances' or 'intervals' underlying this essential pattern of infrasound resonance. The Int'l Bureau of Weights and Measures detected variations in Earth's gravity field in 2007.[52] The diamagnetic metals that comprise their weights are presently displaying a measurable weight offset, although inaudible infrasonic effects of acoustic levitation were not recognized as the cause. This effect will inevitably increase in the future to reveal its inaudible source.

The same standing wave maps that inform the significant fluctuations of gravity also inform the latest discoveries of scientists imaging the subatomic realm. The structure of *the electron* was recorded for the first time in 2008, revealing the unmistakable scattering pattern of nonlinear standing waves, as precisely encoded by the quadratic formula [$z_{n+1} = z_n^2$] (above). Researchers in Sweden demonstrated an attosecond quantum stroboscope that releases individual electrons into the field of an infrared laser at exactly one electron per laser cycle to facilitate the imaging of coherent electron scattering that takes place.[53] *Standing wave resonances comprising the electron are presented 3-dimensionally (opposite), and are applied for infrasound antigravity propulsion by all space-traveling civilizations*, using diverse mathematical languages, and employing entirely different operations. During the 248th contact of February 3, 1994, Ptaah confirmed that the uniformity of universal laws determines that all mathematical and physics formulas applied by all sentient beings may find equivalence, differing only in the terms of expression:

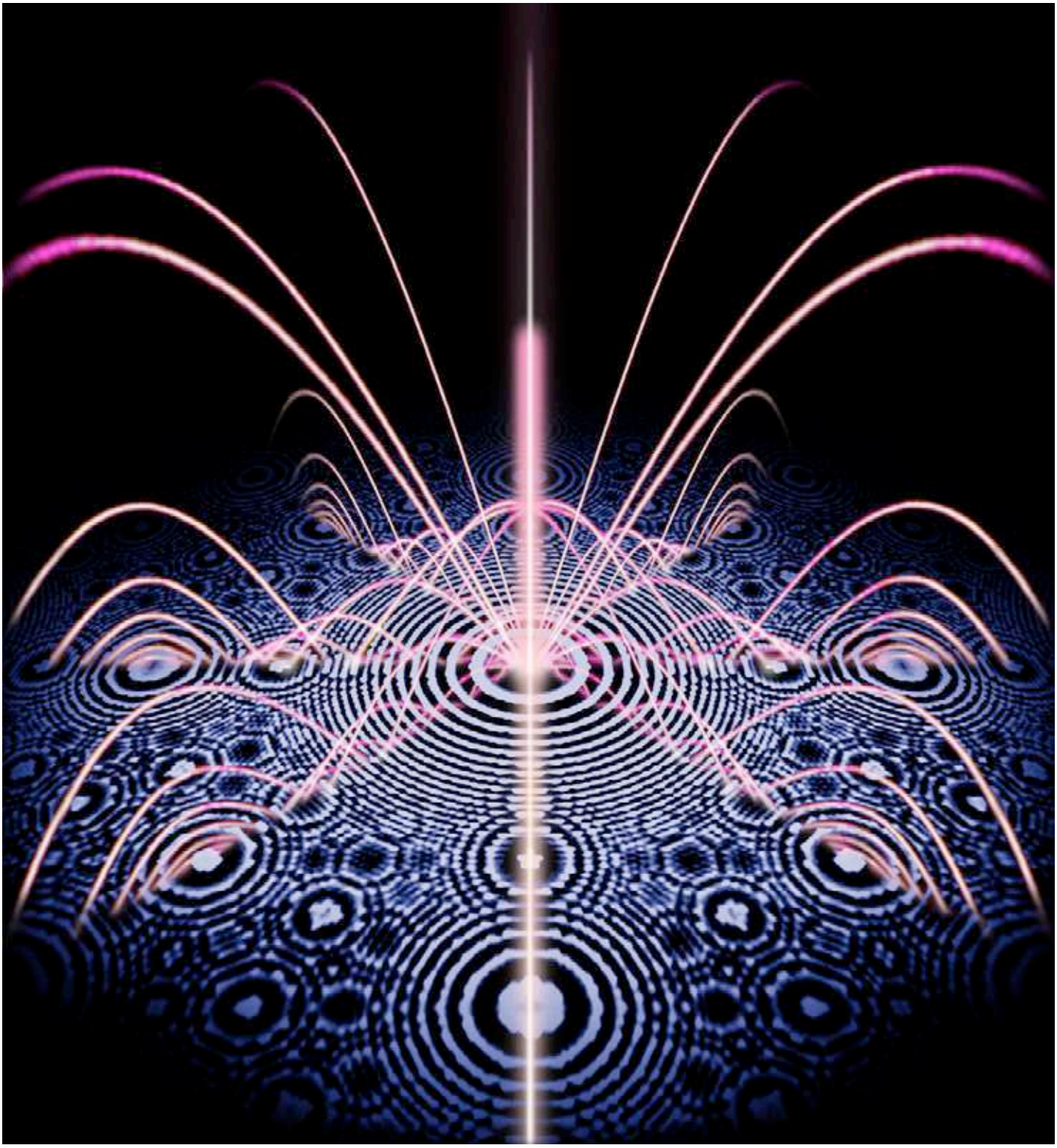

With regard to mathematics, that 3 times 3 is 9, it is to be said, of course, that the result is right and is also consistent with our mathematics, but the form of our mathematics is fundamentally different to the terrestrial one… Like with the mathematical formulas, the physics formulas also differ. But once they are converted, they yield the same values because universally, the mathematical and physical laws, etc. are uniform in their basic value and final value and, therefore, are one and the same, just with the difference that the various races, civilizations, and humanities of the various worlds throughout the vastness of the Universe call other forms of mathematics and other terms, etc. their own; consequently, they also have other methods of calculation than what are common among the Earth people. Nevertheless, in mathematics, the basic value and final value yield the same results.[54]

The vast variety of cosmic and planetary conditions within the universe facilitates natural learning environments of various types, each providing the necessary range of lessons and limitations for each developing life-form and each collective terrestrial civilization. Planets can be categorized by their respective levels of infrasound resonance, with planets such as Earth presently residing at the lowest level of the scale, and planets such as Erra, in the Plejares star system, finding their place among the more highly developed worlds. As Earth presently progresses from the primary level of consciousness lessons, the infrasound resonance of the planet is stimulated to a higher level of collective vibratory experience. Previously invisible forces will become visible to human eyes; subtle forces will become self-evident.

Rainfall patterns and major fluctuations in river levels have been directly correlated with solar flare activity –through the stimulation of infrasound standing wave resonance, raising vast amounts of water into the atmosphere to fall as rain. Rows of water vapor plumes evaporating off the ocean were photographed off Laguna Beach, California[55] in 2009, while the long-term water flow-rates of the Parana River were perfectly matched with sunspot numbers[56] in 2010. So-called constants like gravitation and atomic decay rates vary significantly, and in accordance with the levels of incident infrasound radiation upon the tested materials. *Thus, Earth's infrasound resonance with the sun defines the increasingly noticeable fluctuations of gravitation, atmospheric evaporation, rainfall, and the decay rates of every atom comprising our world.*

Plejaren scientists precisely comprehend the relative conditions of various planets, having studied literally millions of different inhabitable and uninhabitable worlds, and this comprehensive knowledge extends into the minute variations in the respective rates of decay of elements on each planet. Ptaah revealed as much to Meier during a conversation regarding the low-resonance of the present atmospheric conditions of Earth that "all materiality suckles itself up on… and in this way falls to early destruction, *as for example iron, which normally does not rust so fast as is the case on Earth*." (pg. 78) The significance of this short sentence can only be understood in the broader context of planetary infrasound resonance as it influences atomic decay. Physicists on Earth have only recently documented the correlation of notable fluctuations in the rate of decay in radioactive isotopes in the laboratory with solar flare activity:

> It's a mystery that presented itself unexpectedly: The radioactive decay of some elements sitting quietly in laboratories on Earth seemed to be influenced by activities inside the sun, 93 million miles away. Is this possible? Researchers from Stanford and Purdue University believe it is. But their explanation of how it happens opens the door to yet another mystery… There is even an outside chance that this unexpected effect is brought about by a previously unknown particle emitted by the sun. "That would be truly remarkable," said Peter Sturrock, Stanford professor emeritus of applied physics and an expert on the inner workings of the sun.
>
> The story begins, in a sense, in classrooms around the world, where students are taught that the rate of decay of a specific radioactive material is a constant. This concept is relied upon, for example, when anthropologists use carbon-14 to date ancient artifacts… But that assumption was challenged in an unexpected way by a group of researchers from Purdue University… Ephraim Fischbach, a physics professor at Purdue, was looking into the rate of radioactive decay of several isotopes as a possible source of random numbers generated without any human input... As the researchers pored through published data on specific isotopes, they found disagreement in the measured decay rates – odd for supposed physical constants.

Checking data collected at Brookhaven National Laboratory on Long Island and the Federal Physical and Technical Institute in Germany, they came across something even more surprising: long-term observation of the decay rate of silicon-32 and radium-226 seemed to show a small seasonal variation. The decay rate was ever so slightly faster in winter than in summer…

On Dec 13, 2006, the sun itself provided a crucial clue, when a solar flare sent a stream of particles and radiation toward Earth. Purdue nuclear engineer Jere Jenkins, while measuring the decay rate of manganese-54, a short-lived isotope used in medical diagnostics, noticed that the rate dropped slightly during the flare, a decrease that started about a day and a half *before* the flare.

If this apparent relationship between flares and decay rates proves true, it could lead to a method of predicting solar flares prior to their occurrence, which could help prevent damage to satellites and electric grids, as well as save the lives of astronauts in space. The decay-rate aberrations that Jenkins noticed occurred during the middle of the night in Indiana – meaning that something produced by the sun had traveled all the way through the Earth to reach Jenkins' detectors. What could the flare send forth that could have such an effect?

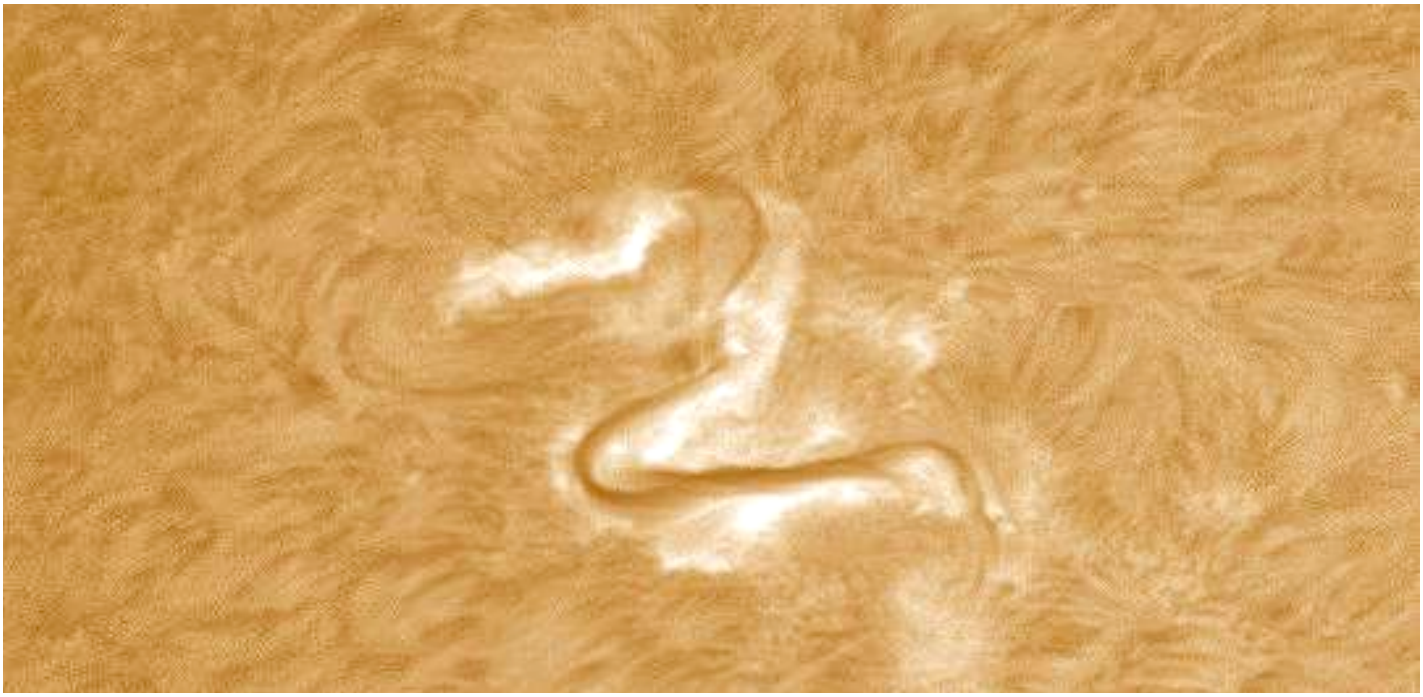

Jenkins and Fischbach guessed that the culprits in this bit of decay-rate mischief were probably solar neutrinos, the almost weightless particles famous for flying at almost the speed of light through the physical world – humans, rocks, oceans or planets – with virtually no interaction with anything… "It doesn't make sense according to conventional ideas," Fischbach said. Jenkins whimsically added, "What we're suggesting is that something that doesn't really interact with anything is changing something that can't be changed."

"It's an effect that no one yet understands," agreed Sturrock. "Theorists are starting to say, 'What's going on?' But that's what the evidence points to. It's a challenge for the physicists and… the solar people too."[57]

In fact, the subtle variations in atomic decay data are not an effect of neutrinos, *but the direct result of measurable surges of localized infrasound resonance*, just as in the case of the 'aberrant' fluctuations of planetary gravity fields and the patterns observed in the water flow rates of major rivers. *The fundamental integrity of the measured radioactive isotopes is directly affected by the incident infrasound radiation.* The decay rates measured by Jenkins at Purdue show a significant fluctuation specifically because of the location of his laboratory in relation to the Great Pyramid of Giza. The Purdue University campus in West Lafayette, Indiana (40.43°N 86.91°W) is 6,176 miles from Giza, a distance comprising *24.8%* of the Earth's mean circumference. Infrasound standing waves focused by the Great Pyramid into the central Indiana area not only alter decay rates in Purdue labs, but also levitate huge sandstone boulders into treetops in nearby Limon[58] and Yellowwood[59] Indiana State Parks at the *25.0%* distance - in the same antigravity resonance process employed by the crystalline metals of interstellar Plejaren beamships.

The invisible web of terrestrial infrasound standing waves that protectively encircles the planet becomes focused by the three Giza pyramids, and in the same way by the three-ringed hull of Semjase's 7-meter beamship. The complex designs of every Plejaren spacecraft are precisely configured to interact within the Fibonacci structure of standing waves to achieve highly efficient acoustic energy storing within the crystalline latticework of resonant alloys comprising the circular body. This same effect occurs in natural crystalline structures – *in stones*. A remarkable photograph taken on July 19, 2009 by Gang Hao captures a special effect of acoustic resonance (above).[60] This giant boulder is estimated at 5m in diameter, which suggests a weight of several tons. The family never noticed it flying overhead while taking the photos, suggesting that the boulder was captured while slowly floating during an event of acoustic levitation, actually caused by solar flares transduced into infrasound by the Great Pyramid.

The piezoelectric properties of quartz, the main constituent of the sandstone boulder, allows its levitation by focused infrasound standing waves. The internal reflection of the parallel faces of the quartz crystals allows the acoustic energy to be stored inside the stone. The build-up of vibratory energy within the quartz lattice creates an electromagnetic field reducing the stone's weight until it becomes entirely weightless, and then slowly levitates along the infrasound standing wave's arch. The source of the focused standing wave energy levitating these stones is the Orion pyramids at Giza, exactly 5,240 miles from Gushan (or Gunchangzhai), China (*25.02°N* 118.51°E). This distance is precisely *21.05%* of the Earth's mean circumference of 24,892 miles. Gushan is also situated 1,245 miles from Angkor Wat - a resonant distance that is precisely *5.00%* of the Earth's mean circumference.

The whole number percent values of the site distances confirms the antigravity formula as applied. Evidently, the quantum physics of standing wave resonance underlies all of the transdimensional Plejaren technologies, as standing wave resonance affects both the levitation of spacecraft and the 'levitation' of electrons, protons and neutrons through the atomic framework. The provision of subatomic

particles allows low-energy nuclear change and the multi-staged production of precious metals and rare elements such as vanadium, thulium and rhenium. These exotic elements are costly to mine and only rarely find application in human industry today, yet the advances of phonon resonance beckon a new era of harmonious human creativity, promising to expand the reach of human consciousness by allowing interstellar flight and bringing an end to the destructive and dangerous practice of ore mining. The broad set of transdimensional capabilities of Plejaren beamships include time travel – affording their ability to preview future events. Billy Meier has published 100% accurate predictions of a multitude of major scientific discoveries and major world events – *yet without having published any erroneous predictions*:

- 29th Contact, July 7, 1975, and 31st Contact, July 17, 1975: Contact involved specific information about Venus, unknown at the time, including composition of atmospheric gases, surface temperatures, depth of clouds, wind speeds, atmospheric pressure, coloration, variation in terrain, etc…
- 31st Contact, July 17, 1975: Semjase informed Meier that Mt Chimborazo, Ecuador, is the highest mountain on Earth [as measured from the center of the planet]… contrary to Meier's belief that it was Mt Everest…
- 1978: In a Wasserman publication, Meier foretold the launch of a telescope at end of the 1980s that would make unfathomable discoveries in space, and wrote that an asteroid would be discovered in the late 1980s to early 1990s; it would be named Toutatis, and may threaten Earth in September 2004…
- 1978: In *Existing Life in the Universe*, Meier [described] 2 small planetary bodies outside Pluto's orbit…
- 115th Contact, October 19, 1978: Meier described existence [and composition] of Jupiter's rings [and moons]...
- Jonestown massacre (Nov 18, 1978), Overthrow of the Shah of Iran (Jan 1979)
- Chinese invasion of North Vietnam (Feb–Mar 1979), Iran Hostage Crisis (Nov 1979–Jan 1981)
- Soviet invasion of Afghanistan (Dec 1979), Terrorist attack on Iranian Embassy, London (Apr–May 1980)
- Abdication of Queen Juliana of The Netherlands (Apr 1980), Death of Tito of Yugoslavia (May 4, 1980)
- Mount St. Helens eruption (May 18, 1980), Assassination of Indian PM Indira Gandhi (Oct 31, 1984)
- 215th Contact, February 28, 1987: Known as the Henoch (or Enoch) Prophecies, this contact contained a forewarning of the destruction of the World Trade Center (WTC) by terrorism, the series of worldwide wars that the US would subsequently launch, and military actions involving Russia, China, France, Germany, Spain, England, Scandinavia and many other countries.[61]

Repeated, accurate predictions of major world events, often years prior, proves Meier's foreknowledge!
He also received information from the Plejaren leader Ptaah regarding the dramatic events of December 22, 2012, as later disclosed during the 476th contact of February 3, 2009 – on Eduard's 72nd birthday:

Meier: Regarding the Mayan calendar, [engraved as a sacred mandala in resonant piezoelectric stone, above,] it must be said that the year 2012 will bring a whole series of quite special events, and… our sun, will contribute to them, because on the sun's surface enormous eruptions will occur and solar storms are caused, which will be very intensive and will influence Earth's geomagnetic balance.

The Earth's magnetic field can suffer very strong fluctuations through the very strong X-ray radiation falling down on it. And through such geomagnetic storms, *power grids and all electronic appliances can collapse, thus also those in satellites, and the ISS can also suffer great damage or can even fail completely.* Such solar storms can lead to enormous natural catastrophes, and in the worst case, to a polarity reversal of Earth's magnetic field... What also has to be said is that such solar storms form to a climax in an exact rhythm of eleven years, which is normal, but in the year 2012 it can happen in an extraordinary magnitude. Earth will come under a very strong bombardment of hard radiation, which can have a very negative effect on the Earth's ozone layer. Due to the entire resulting process, *nitric oxides and acid rain can form worldwide*, which may have bad and devastating effects on the entire plant world. The enormous solar eruptions can lead to further very strong climate changes and, with it, to immense droughts, bad weather, volcanic eruptions, earthquakes, crop failures and, therefore, to even greater famines than have existed up to now. In addition to all this, the year 2012 brings other unpleasant events, such as a so far unknown, invisible, dark and huge space wanderer that is threatening from the fringe of our solar system and could wreak tremendous havoc on Earth.

And if this should really occur, the fact of its existence would be openly proven starting with 2010 or 2011, if at all, because the possibility of a "dark" and, therefore, non-observable passage of the colossus is also possible. Aside from that, all kinds of unpleasant machinations regarding unpeace, worldwide heavy warlike actions, as well as increasing degeneracy and excessive human ways of behaviour are threatening for the year 2012…

Ptaah: You should not say more, because what you explained should be enough… Regarding the Mayan calendar, the 21st of December 2012 represents the culmination of a star constellation [alignment] that only occurs around every 26,000 years. The Mayan calculations are assuming that Earth - on the 21st of December 2012 - shall lie on an imaginary line that joins together the star [Betelgeuse,] above the left side of the constellation Orion with the Central Sun, [situated at] the centre of the Milky Way. The Sun meets the Milky Way at a location that is built by interstellar dust clouds, and is called the "dark cleft of the Milky Way" by the human beings of Earth. On the 21st of December 2012, at nightfall of winter solstice, the Sun is directly in that cleft, and it is in such a position that the Milky Way covers the horizon in all positions all around.

Thereby the optical impression is produced that the Milky Way would touch Earth all around and that the galaxy would lie directly on the Earth. On the whole that's the end product of the Mayan calendar recording. This should suffice, my friend. To say more would be too much, because it would only foster the fear of the human beings of Earth, which should not be, however. So keep silent on all the further explanations that we have given you...[62]

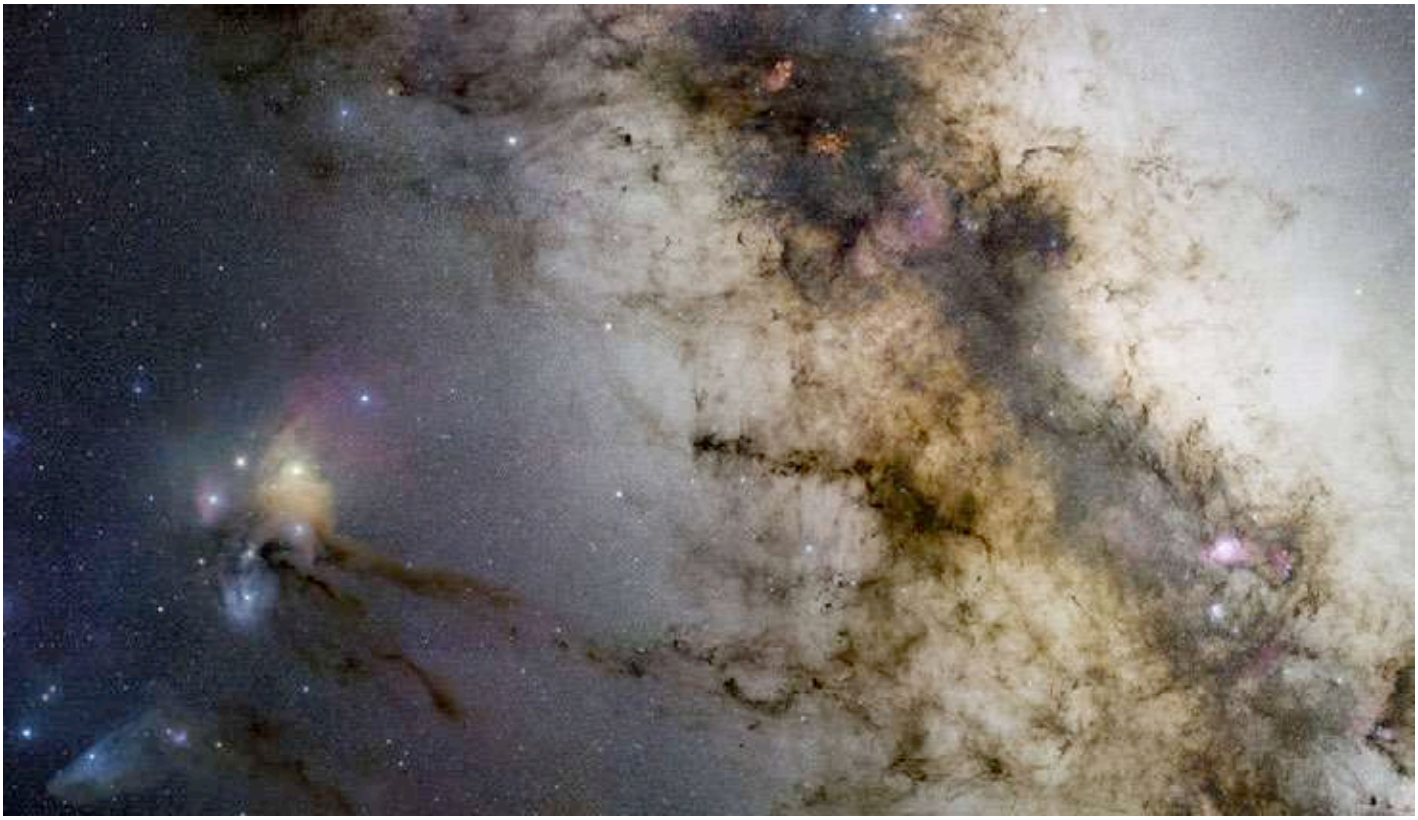

Through the tireless efforts of Eduard Meier, the wisdom traditions of the Plejaren culture reveal that the ongoing Earth changes are a result of the Golden Radiation emitted from the Central Sun, which lies at the core of our Milky Way galaxy. This Central Sun is obscured from our direct view by the 'dark cleft of the Milky Way' (above). Specific details regarding these electromagnetic field changes now occurring on Earth are most intensely experienced at infrasound standing wave convergence points which are already destroying all electrical equipment, just as discussed by Meier and his Plejaren contacts. The electrical overload of modern technology is also being experienced on the International Space Station, in accordance with the information from Meier and echoed in Native American prophecies of the Hopi.

Billy's brief mention of the *'invisible, dark and huge space wanderer'* references the presence of a binary twin companion of our sun - *a brown dwarf star* that the Hopi prophecies describe as reigniting to be seen as a small red star known to them as the Purifier, which will be the sign of the Purification Day, when all life on Earth will be effected. *The wave of energy described by the Plejaren as the Golden Radiation is the crucial factor linking these events involving the red supergiant star Betelgeuse with the Central Sun on December 22, 2012, as the wave of Golden Radiation passes through our Sol system.* Another chaotic aspect of the near passage of the dark brown dwarf star is the disturbance it has already caused within the Oort Cloud, before it becomes reignited as the Red Purifier of Hopi Prophecy.

The topic of the origin of comets within our solar system was addressed during the 150th contact of October 10, 1981, concerning the nearby Dark Star and its cyclical dislodging of comets from the Oort Cloud accounting for 97% of cometary debris entering Earth's vicinity. While the complete details of the close passage of the invisible brown dwarf binary twin of our visible Sun (referred to as a Dark Star) have been wisely withheld, the breaching of the Oort Cloud presently threatens all of Earthly humanity:

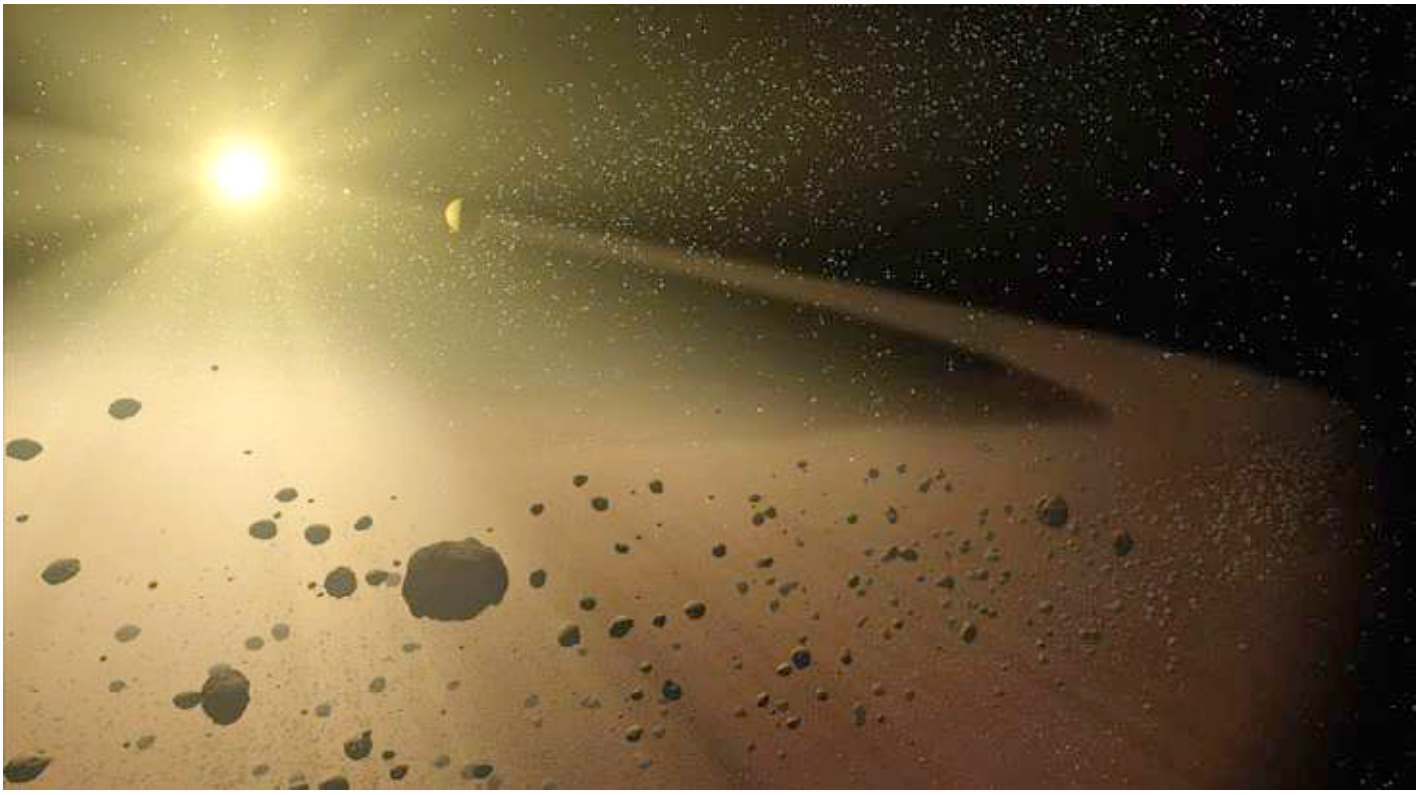

Meier: In the coming years and decades, there will again appear frequent passages of comets, including those such as Halley's Comet, which can practically be observed in the sky… in broad daylight… [W]hen you took me in 1975 on the great journey, I saw beyond our solar system and planetary system the immense belt of material of frozen acids, rocks… and lifeless planets; some were quite large. Like the asteroid belt beyond the orbit of Mars, this belt also moves around the Sun but very far outside of Pluto's orbit.

At that time, you explained to me that celestial bodies of all kinds pass through this belt, such as Dark Stars and other space bodies, and that every now and then, smaller or larger bodies tear out from this belt and enter into another orbit around the Sun, which can then partly be observed as comets from the Earth and, thus, can be seen. If I remember correctly, you told me at that time that on the one hand, this belt was still widely unknown to the Earth people in its magnitude but… more would soon be discovered… Furthermore, you explained that this material belt consists of the remains of the formation of the solar system and of immigrated materials from space, etc. Now, I wonder how high the percentage of comets is that appears in our solar system and that arises from this material belt beyond Pluto's orbit?

Quetzal: It has probably escaped your attention, but this belt was discovered in the meantime and is named 'Oort,' after a Dutch astronomer. In accordance with its discovery, the discovered belt is called the Oort Cloud in Earth's scientific circles, but that's about it because the connections of this belt to the comets of the Sol system are still, to my knowledge, foreign and unknown to the Earth scientists.

But the truth is that about 97% of the SOL system comets originate from this belt, as in this belt, planetary bodies passing by upset the trajectories of the materials through their attractive forces, so then these suddenly scramble, which removes isolated larger and smaller objects, pushing them into new orbits around the solar system, where they then appear as comets, while others fly out far from the Sun into free space in order to disappear somewhere in the vastness of the universe, often referred to as migrant dark planets, which will partly be captured again by major stars as satellites and then orbit them, far away from the new mother stars. But others will rush uncontrollably as dark objects traveling through space.[63]

Studies informing the link between Oort comets and a dark binary twin[64] have been published by U. of Louisiana researchers[65] and the Binary Research Institute,[66] and subsequently reconfirmed in 2010.[67] *The rain of Oort comets has already begun to impact the Earth on a daily basis.* Smaller fragments are creating dramatic aerial explosions worldwide, as witnessed over South Sulawesi, Indonesia on October 8, 2009. Sizable craters attest to large impacts in Hidalgo, Mexico on February 10, 2010; San Joaquin (Santander), Colombia on September 6, 2010; and San Bruno, California on September 9, 2010. The prophetic date of December 22, 2012 was *indirectly* addressed during the 52nd contact of May 17, 1976, in connection with precise astronomical calculations decisive in the building of the Giza pyramids *about 73,350 years ago* (spanning two cycles of 36,650 years, as Ptaah later explained in the 256th contact[68]):

> *Semjase:* When the pyramids were built, the then astronomers had already calculated the further fate of the Earth. The measurements of the pyramids were elaborated according to their calculations… [which] revealed that many thousands of years in the future, a catastrophe would menace the Earth and that from the cosmos, like at the time of the construction of the pyramids. To reveal to the later inhabitants of the Earth over the later millennia… the measured dates in astronomical form were built into the pyramids for the far distant future… when the catastrophe from the cosmos threatens anew. The ancient astronomy was very able, and… even considered in their calculations, several world crashes, and could reckon the dates with very exact precision.
>
> As pre-calculated, the Earth did then convert, and agreed with the then and since long gone science. Now slowly the time becomes mature, that the astronomically measured dates, which as mentioned, served in the construction of the pyramids and were decisive in this, agrees with the astronomical values of the present, and announce the more than 70,000 years ago prophesied events this way. And this event will be exactly then, when the solar light of a very far distant star, a central star, falls through the tube-like Opening of Revelation, which draws itself from the outside of the Giza pyramid into the center, in a straight uninterrupted line, and illuminates one certain point. I am not allowed to tell more about this.[69]

Many insights can be gleaned from Semjase's foretelling of the activation of the Great Pyramid by the radiations of the galactic Central Sun, and the catastrophic impacts of Oort comets dislodged by the Dark Star's passage. *The Giza pyramids were masterfully designed for repeated reactivations by cyclical blast waves that radiate from the core of the galaxy to impact Earth in a precisely calculated rhythm, causing the magnetic reversal of the entire Sol system and a dramatic increase in terrestrial infrasound levels.* Worldwide auroras can thereby be expected, as well as increased evaporation and precipitation rates globally, and a measurable reduction in the atomic decay rates of all Earthly matter. All cosmic signs point toward the imminent reemergence of a 'thick white vapor envelope surrounding the globe'.

Earthly astronomy can no longer ignore the nearby presence of the brown dwarf binary twin of our sun. Nor can corporate news continue to hide or dismiss the multitudes of reported meteor strikes now inundating the Earth, *exactly as foretold by Eduard Meier and his knowledgeable informants decades ago.* The existing corporate and religious institutionalization of psychopathy cannot withstand the great revelations occurring at the present time, and will soon lose its despotic hold of human consciousness:

Ptaah: When hitherto Semjase only spoke of Earth religions in negative form, then it was because the Earth human had to be made attentive to the error in his religions, ...for these are like nowhere else in this Universe… They control the Earth human and the whole planet, and retard your world thousands of years, in Spiritual respect… [Y]our religions still contain real worth, but this becomes so indiscernible that only few people are able to see the effective truth there. These few who are able to see the real truths from the scripts, are banned and confounded by those dependent on these wrong beliefs, and thus cannot spread the truth. When Semjase speaks in negative form about Earth religions, she is addressing the falsifications in them which have been built up partly consciously. The Earth religions are only called such in name, but are just degenerate cults."

In truth, the same small minority of fallible psychopathic individuals control world religions, economics, sciences and politics –those engaged in the destructive subterranean nuclear blasts, damming of waters and extraction of oils– are themselves also actively inducing earthquakes using the HAARP array to terrorize and extort the rest of humanity. *Awareness of the hereditary genetic disorder that results in psychopathic behavior demands responsible action from the conscious human beings of Earth.*

The holistic teachings of Plejaren Elders reveal that genetic enhancement through biorhythmic entrainment holds the highest potential for the reversal of all known mis-developments of the physical body or the spirit. *Natural law provides for the bioelectrification and illumination of the body's waters, using golden celestial water comprised of pure protium in conjunction with tri-thalamic heartbeat entrainment during fetal development and throughout life, thereby removing all negative influences from the crystallized human being:*

Quetzal: [T]he fallible ones could be completely cured of their criminal or other degenerate forms through genetic manipulation and be released into society. This gene-manipulative healing method was further investigated and further developed [by Plejaren biophysicists many thousands of years ago], and indeed, even in reference to all hereditary diseases and immunodeficiencies as well as physical and organic deformities, but also in terms of disorders of consciousness and inheritable psychological disorders, etc. The development progressed rapidly, so already soon, early detections of gene damages of the aforementioned kind became possible, which naturally led to the fact that these cognitions were used and the genetic deformities, genetic abnormalities, and other harmful genetic influences were already repaired in the growing child in the womb.

Thus, an irrefutable law has been in force since then, namely that every child, so every girl and every boy, is to be arranged into a gene examination, i.e. a gene analysis, at the prenatal age of seven months. Since then, since this law gained validity and became observed absolutely, it is valid with us that every crime or other degeneration as well as every inheritable disease of the body and its organs, every immunodeficiency of any kind, and every form of harmful aggressiveness, jealousy, and vindictiveness are just as non-existent as also hatred, envy, desire for validity, egoism, and many other characteristics that bring the human being discord, unkindness, and other harms. But at the same time, it should be noted that through this, our own decision in all matters and concerns is in no way impaired, as well as not our drive for self-preservation and our drive for self-defense, when this is demanded.[70]

Until the coming times when this biorhythmic genetic healing becomes active through the world's infrasound network of resonant pyramids, the survival of humanity requires our careful discernment of psychopathy in human leadership. The Prophecies of Henoch, forewarning of the dire consequences of human ignorance on Earth, were presented by Quetzal during the 215th contact on February 28, 1987:

Quetzal: Before I give you a clear account of the prophecies of Henoch, I would like to point out that prophecies are always changeable and can be changed for the better if man makes positive changes in his thoughts, feelings and actions, leading to that which is better and positively progressive…

However, this does not apply to predictions, as these rest upon events that cannot be changed, are inevitable and surely and definitely will occur in the future. Predictions rest upon a preview and thus on a direct viewing of the future, and have to do with neither prophecy nor with calculation of probability. So when I make a portion of Henoch's prophecies for the third millennium known to you, it does not mean that they have to be fulfilled, because the prerequisite of fulfillment in each case would be that the already existing causes continue to exist as also continue to be created in the future so that a fulfillment of the prophecies can come to pass.

Thus, provided that human beings of Earth will become reasonable, the possibility exists that by a reasonable change in the way of thinking as well as a reasonable development in feeling and an equally reasonable way of acting, everything changes for the better and positive, whereby prophecies do not have to be fulfilled. However, if this transformation does not occur, a very evil, wicked and negative time lies ahead for the Earth and its entire population in the coming new millennium…

The point in time at which these prophecies will begin to be fulfilled will be when a Pope will no longer reside in Rome. All of Europe will then fall victim to a terrible punishment by evil powers. The Christian religion will collapse and the churches and monasteries will end up in ruins and ashes… Monstrous forces will be created by science and will be released by the military forces and armies as well as by terrorists, causing great destruction. Millions and even billions of people will be killed by acts of terrorism, by wars and civil wars; and finally, in some parts of the world, every third human being, and, in other places, every fourth human being, will lose his or her life. The nations of the East will rise against the nations of the West, the West against the East…

The people will be completely powerless against all this and will live through 888 days of Hell on Earth, suffering hunger and plagues, which will claim even more lives than the war itself. The time will be severe as never before experienced on Earth. Ultimately, nothing can be bought or sold any longer. All provisions will be rationed; and if a human being steals even a small piece of bread, he/she will have to pay for it with his/her life…

And it will be that the fanatics of Islam will rise up against the countries of Europe and all will shake and quiver. Everything in the West will be destroyed; England will be conquered and thrown down to the lowest level of misery. And the fanatics and warriors of Islam will retain their power for a long time. However, not only Europe will be affected but ultimately all the countries and peoples of the Earth, as the great horror expands to a war that will encompass the entire world.

After the turn of the millennium, the papacy will exist only a short period. Pope John Paul II is the third from last in this position. After him, only one additional pontificate will follow [Pope Benedict]. Then a Pontifex Maximus follows who will be known as Petrus Romanus. Under his religious rule, the end of the Catholic Church will come, a total collapse becoming inevitable. That will be the beginning of the worst catastrophe that will ever have befallen the human beings and the Earth…[71]

These profound passages form only a portion of the Prophecies of Henoch, and follow from earlier information about the lineage of popes provided to Meier on August 6, 1978 during the 113th contact:

> Karol Wojtyla… is the 3rd to last pope before the world change [of December 22, 2012]. He is the 264th pope. He will die in the near future. The world will be astonished when the next pope [Joseph Ratzinger] is killed also. Then the pope with the number value of five [is coronated]. He is the 266th pope - he is the last one.[72]

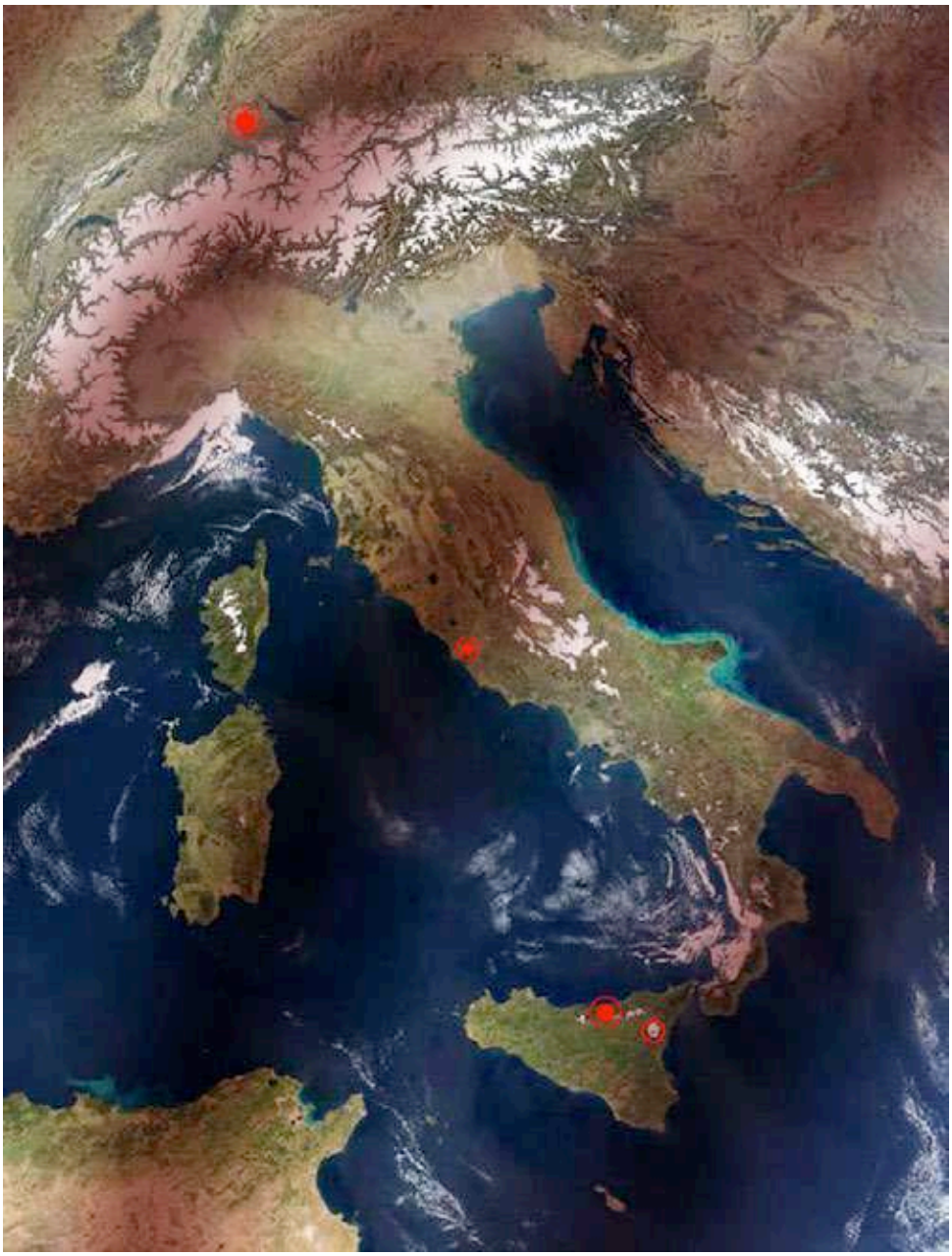

After the murder of Pope Benedict XVI, "a Pontifex Maximus follows who will be known as Petrus Romanus. Under his religious rule, the end of the Catholic Church will come, a total collapse becoming inevitable." These very detailed, ancient prophecies from the Henoch lineage directly coincide with those attributed to St. Malachy, an Irish monk who produced a comprehensive list in the year 1139 which prophesied every future pontiff of the Papal lineage from that date until today. St. Malachy wrote: "In the final persecution of the Holy Roman Church there will reign Petrus Romanus, who will feed his flock among many tribulations; after which the seven-hilled city will be destroyed and the dreadful Judge will judge the people." Not only is the same name given for a proclaimed 'final Pope', but the destruction of Rome, the 'seven-hilled city' is also given as a sign of the imminence of the collapse of the Roman Catholic Church. The Henoch prophecies foretell that "the point in time at which these prophecies will begin to be fulfilled will be when a Pope will no longer reside in Rome."

These foretold events *will* follow a pattern of fulfillment due to dramatic *infrasonic surges* that require the imminent evacuation of Rome and the Vatican, *which will inevitably be overcome by recurring spates of piezoelectric fires,* just as documented in the towns of Messina, Sicily, near the active Mt. Etna volcano.[73] The Vatican (41.53°N 12.30°E in white, above) is 1,326 miles from Giza, Egypt – a distance that is 5.3% of the Earth's mean circumference – along the radial distance of infrasound standing wave convergence. The steadily growing intensity of planetary infrasound is already significantly affecting these fixed focal points, including both the location of the Vatican and the Semjase Silver Star Center. Infrasound waves have been recorded in the atmosphere above Switzerland that reveal an inaudible ultra-low frequency field of concentric circles, as documented during an infrasound resonance event on April 24, 2009:

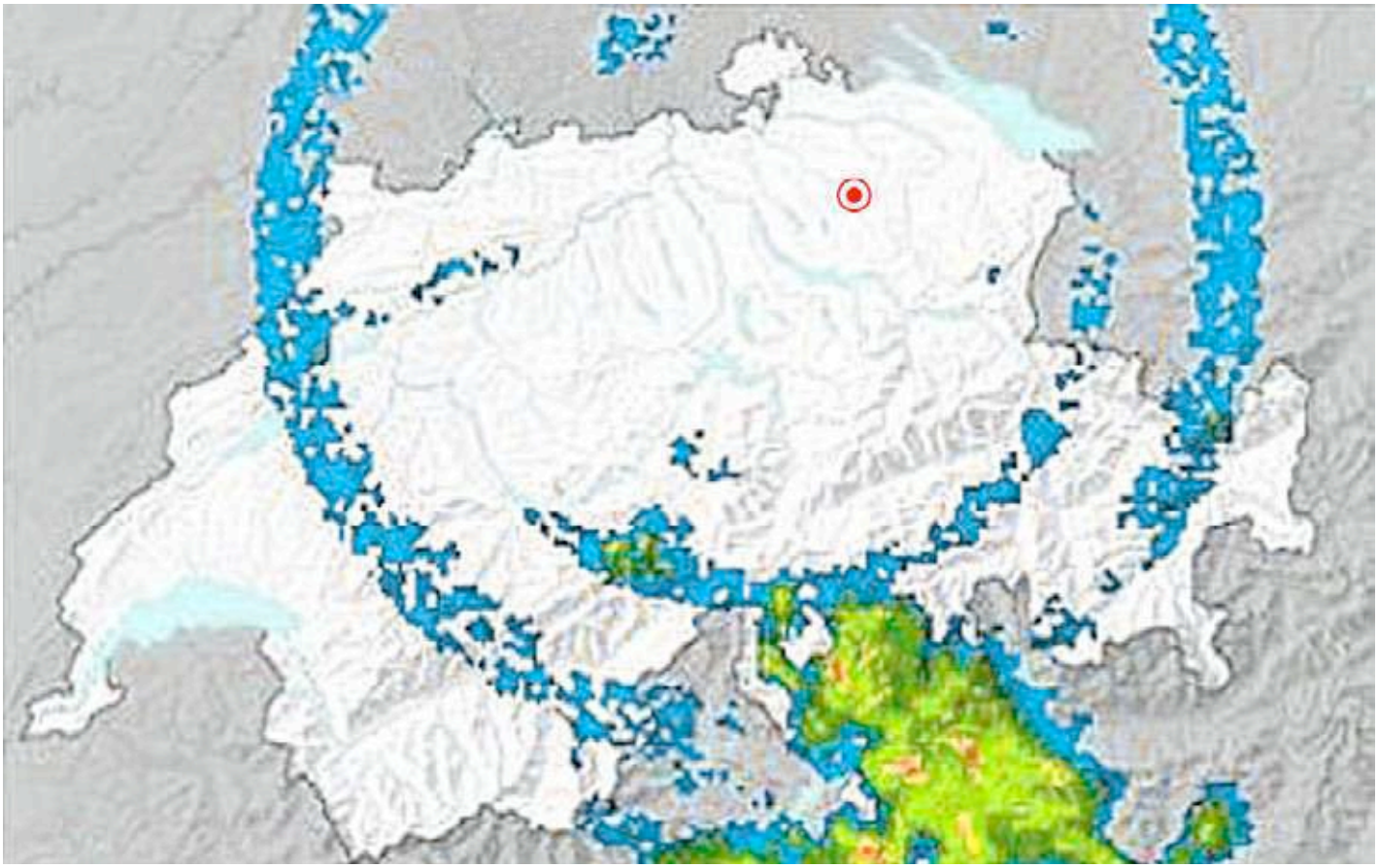

> Did a country-sized UFO hover above Switzerland last month? On the morning of Friday the 24th of April of this year employees at MeteoSwiss [observed] huge circular fields hovering over Switzerland… [that] covered the entire country… MeteoSwiss claimed… that they were merely caused by the reflection of water droplets. A few minutes after being queried on the issue the radar images were hurriedly removed from the department's website. Are we being told everything the Swiss meteorological knows about these radar images? [74]

Meteorologists in Switzerland have never seen radar anomalies like this specifically because they are hidden and scrubbed from archives, as in this particular case. Hundreds of similar radar anomalies are documented by websites that gather the data before it's purged from online archives. The only viable explanation for these giant radar rings is water vapor suspended by concentric rings of standing waves in the ultra-low frequency range. Nikola Tesla was the first to scientifically describe standing waves in his Colorado Springs lab[75], later reporting: "In Colorado I succeeded one day in precipitating a dense fog. There was a mist outside, but when I turned on the current the cloud in the laboratory became so dense that when the hand was held only a few inches from the face it could not be seen." [76] The standing waves that fogged-out Tesla's laboratory are now suspending these giant concentric circular rings of water vapor above the entire country of Switzerland – as on April 24, 2009. *A circumference of the Earth taken along the northwest/southeast axis of the Great Pyramid of Giza, Egypt passes exactly through the center point of the MeteoSwiss radar circles.*

The center point of these gigantic radar circles lies just southwest of the Semjase Silver Star Center (overlaid in red, above) in Hinterschmidrüti, Switzerland (47.416°N 8.906°E); both sites being located along the 6.7% resonant distance of about 1,680 miles from Giza. This precise resonant alignment of the Semjase spiritual center in Switzerland reflects the same advanced understanding of the Fibonacci geometry of infrasound standing waves that informs the locations of all of the ancient pyramids of the world, now approaching the time of reactivation with the magnetic reversal of December 22, 2012. The meticulous work of Eduard Meier to record his extensive contacts with the Plejaren civilization guides humanity by the light of *Truth, reorienting our consciousness toward the radiant lessons of the Creation witnessed within ourselves and our mother Earth during this time of the great shift.*

References

[1] Stevens WC Ed. (1990) *'Message from the Pleiades: The Contact Notes of Eduard Billy Meier, Volume 2'* Genesis III Publishing, pp. 257-258
[2] Meier E (1988) 'OM: The Book of Truth' FIGU Press, Canon 43: Verses 153, 167-177, pp. 354-355
[3] Putney A (2008) '∅' Human Resonance Productions, pp. 23-24
[4] -- (2009) *'Neem Oil'* Sister Zeus, online · http://www.sisterzeus.com/neem.html
[5] Meier E, Tr. Stevens B (2010) 'Contact Report 260 Translation' *Billy Meier Wiki - The Future of Mankind*, online · http://www.futureofmankind.co.uk/Billy_Meier/Contact_Report_260
[6] Stevens WC Ed. (1988) *'Message from the Pleiades: The Contact Notes of Eduard Billy Meier, Volume 1'* Genesis III Publishing, pp. 150-154
[7] Ibid, p. 385
[8] -- (2006) 'Semjase by Dejan' online · http://www.futureofmankind.co.uk/meier/gaiaguys/meier.plejarenportraits.htm
[9] Stevens, op cit, pp. 48-49
[10] Stevens, op cit, *'Message from the Pleiades: The Contact Notes of Eduard Billy Meier, Volume 2'* pp. 87-89
[11] Stevens, op cit, *'Message from the Pleiades: The Contact Notes of Eduard Billy Meier, Volume 1'* p. 241
[12] Stevens WC Ed. (1995) *'Message from the Pleiades: The Contact Notes of Eduard Billy Meier, Volume 4'* Genesis III Publishing, p. 324
[13] Ibid, p. 281
[14] Phillips T (2004) 'Strange Space Weather Over Africa' *Science At NASA*, November 14, online · http://science.nasa.gov/headlines/y2007/13nov_africa.htm
[15] Stevens, op cit, *'Message from the Pleiades: The Contact Notes of Eduard Billy Meier, Volume 2',* pp. 54-59
[16] Stevens WC Ed. (1992) *'Message from the Pleiades: The Contact Notes of Eduard Billy Meier, Volume 3'* Genesis III Publishing, pp. 211-214
[17] Xie W A, Wei B (2001) 'Parametric Study of Single Axis Acoustic Levitation' *App. Phys. Lett. 79:6, pp. 881-883*
[18] Horn M (2006) 'Beamship Sounds' *They Fly*, online · http://theyfly.com/sounds/BeamshipSounds.mp3
[19] Stevens WC (2000) *'UFO Sound Recordings: Semjase's Beamship During a Flight Demonstration'* pp. 1-2, online · http://www.theyfly.com/PDF/UFOSoundRecordings.pdf
[20] Kruger A (2004) 'Construction And Deployment Of An ULF Receiver For The Study Of Schumann Resonance In Iowa' online · http://www.ia.spacegrant.org/RES_INF/VRR2003/Kruger-SEED.pdf
[21] Meier E, Tr. Stevens B (2010) 'Contact Report 223 Translation' *Billy Meier Wiki - The Future of Mankind*, online · http://www.futureofmankind.co.uk/Billy_Meier/Contact_Report_223
[22] Stevens, op cit, *'Message from the Pleiades: The Contact Notes of Eduard Billy Meier, Volume 1'* p. 56
[23] Mullins J (2000) 'Will Plasma Revolutionize Aircraft Design?' *Space Daily*, October 28, online · http://www.spacedaily.com/news/future-00o.html
[24] Stevens, op cit, p.124
[25] Mills RL, Ray P, Dhandapani B, Nansteel M, Chen X, He J (2002) 'New Power Source from Fractional Quantum Energy Levels of Atomic Hydrogen Surpasses Internal Combustion' *Journal of Molecular Structure* 643, pp. 43-54
[26] Meier E, Tr. Stevens B (2010) 'Contact Report 11 Translation' *Billy Meier Wiki - The Future of Mankind*, online · http://www.futureofmankind.co.uk/Billy_Meier/Contact_Report_11
[27] Stevens, op cit, p. 289
[28] Novak P (2005) 'Hurtubise Says Invention Sees Through Walls' *Bay Today News*, January 16, online · http://www.baytoday.ca/content/news/details.asp?c=6657
[29] -- (2009) 'Scientists Claim New State of Matter' *Live Science*, July 28, online · http://www.livescience.com/technology/090728-new-state-matter.html
[30] Stevens, op cit, pp. 54-56
[31] Ibid, pp. 117-119
[32] Putney A (2009) *'Veil of Invisibility'* Human Resonance Productions
[33] Stevens, op cit, *'Message from the Pleiades: The Contact Notes of Eduard Billy Meier, Volume 2'* p. 55
[34] Orion E (2003) *'The Bush Connection'* The Bush Connection.com
[35] Stevens, op cit, p. 187
[36] Meier E, Tr. Devine D, Legg V (2009) 'Asket's Explanations – Part 4' *Billy Meier Wiki - The Future of Mankind*, online · http://www.futureofmankind.co.uk/Billy_Meier/Asket%27s_Explanations_-_Part_4
[37] Stevens, op cit, *'Message from the Pleiades: The Contact Notes of Eduard Billy Meier, Volume 1'* pp. 378-382
[38] Ibid, pp. 367-368
[39] Meier E, Tr. Stevens B (2010) 'Pleiadian/Plejaren Contact Notes Volume 5' *Billy Meier Translations*, online · http://www.billymeiertranslations.com/#dialog/divVolume5
[40] Meier E, Tr. Stevens B (2010) 'Pleiadian/Plejaren Contact Notes Volume 4' *Billy Meier Translations*, online · http://www.billymeiertranslations.com/#dialog/divVolume4
[41] Ketterle W, Zwierlein MW, Abo-Shaeer JR, Schirotzek A, Schunck CH (2005) 'Vortices and Superfluidity in a

Strongly Interacting Fermi Gas' *Nature* 435, pp. 1047-1051
[42] Stevens, op cit, pp.155-156
[43] Ibid, pp.170-175
[44] Matsuoka S (1996) 'Ultrasonic Welding of Ceramic/Metal' *J. of Materials Processing Tech 47(1-2),* pp. 185-196
[45] Champion J (2007) 'Phonon Resonance Institute Home' *Dr Joe Champion*, online · http://drjoechampion.com
[46] Champion J (2007) 'Phonon Resonance' *Dr Joe Champion*, online · http://drjoechampion.com/phonon.htm
[47] Choi C (2010) 'Microbes Leave Gold on Corpses, May Complicate Forensics' *Live Science*, online · http://www.livescience.com/history/gold-corpse-hair-100225.html
[48] Clark MW, Yip ML, Campbell J, Abelson J (1990) 'SSB-1 of the Yeast Saccharomyces Cerevisiae is a Nucleoler-Specific, Silver-Binding Protein that is Associated with the snR10 and snR11 Small Nuclear *RNAs' Journal of Cellular Biology 111(5 Pt 1)*, pp. 1741-51, online · http://www.ncbi.nlm.nih.gov/pubmed/2121740
[49] Waldrop A (2008) 'Phonon Resonance Spreadsheet' online · http://drjoechampion.com/ResonanceCalcGraph.xls
[50] Horn M (2006) 'Documentation from IBM on Marcel Vogel's Patents' *They Fly*, online · http://www.theyfly.com/newsflash4/m_vogel.htm
[51] -- (2004) *'Through Space and Time: A Photo Journal of "Billy" Eduard Albert Meier'* Steelmark, pp. 66-67
[52] Keaten J (2007) 'Shrinking Kilogram Bewilders Physicists' *Associated Press*, September 12, online · http://www.humanresonance.org/kilogram.html
[53] Mauritsson J, Johnsson P, Mansten E, Swoboda M, Ruchon T, L'Huillier A, Schafer KJ (2008) 'Coherent Electron Scattering Captured by an Attosecond Quantum Stroboscope' *Physical Review Letters* 100, 073003
[54] Meier E, Tr. Stevens B (2010) 'Contact Report 248 Translation' *Billy Meier Wiki - The Future of Mankind*, online · http://www.futureofmankind.co.uk/Billy_Meier/Contact_Report_248
[55] Robbins G (2009) 'Ocean Smoke Puzzles Forecasters' *Orange County Register*, December 22, online · http://www.humanresonance.org/laguna.html
[56] Mauas P, Buccino A, Flamenco E (2010) 'Long-tern Solar Activity Influences on South American Rivers' *Journal of Atmospheric and Solar-Terrestrial Physics on Space Climate 1*, March, online · http://arxiv.org/abs/1003.0414
[57] Strober D, Jolagh C (2010) 'The Strange Case for Solar Flares and Radioactive Elements' *Stanford Report*, August 23, online · http://news.stanford.edu/news/2010/august/sun-082310.html
[58] Stoops R (2003) 'Unionville, Indiana –Large Boulder in a 40-ft. Tree' *Roadside America*, online · http://www.humanresonance.org/limon.html
[59] Hess J (2000) 'Unexplained Tree-top Boulders Found in Forest' *Brown County Democrat*, online · http://www.humanresonance.org/yellowwood.html
[60] -- (2009) 'Gushan's Mysterious Flying Objects (Photo)' *South East Express (Xiamen),* August 4, online · http://www.humanresonance.org/gushan.html
[61] Horn M (2004) 'The Henoch Prophecies from the Billy Meier Contacts' *Nexus Magazine 11(5)*
[62] Horn M (2009) '2012; What We Have Brought upon Ourselves' *They Fly*, online · http://theyfly.com/2012.htm
[63] Meier E, Tr. Stevens B (2010) 'Pleiadian/Plejaren Contact Notes Volume 4' *Billy Meier Translations*, online · http://www.billymeiertranslations.com/#dialog/divVolume4
[64] Blakemore P (2002) 'Does the Sun Have a Doomsday Twin?' *The Telegraph*, October 18, online · http://www.telegraph.co.uk/science/science-news/3300270/Does-the-Sun-have-a-doomsday-twin.html
[65] Matese J, Whitman P, Whitmire D (1999) 'Cometary Evidence of a Massive Body in the Outer Oort Cloud' *Icarus 141,* pp. 354-366, online · http://www.ucs.louisiana.edu/~dpw9254/MS7292.pdf
[66] Cruttenden W (2009) 'Introduction: Binary Companion Theory' *Binary Research Institute*, online · http://www.binaryresearchinstitute.org/bri/research/introduction/theory.shtml
[67] Matese J, Whitmire D (2010) 'Persistent Evidence of a Jovian-Mass Solar Companion in the Oort Cloud' *submitted to Icarus,* online · http://arxiv.org/abs/1004.4584
[68] Meier E, Tr. Devine D, Legg V (2007) 'The Truth About the Pyramids and Stonehenge' They Fly, online · http://www.theyfly.com/Pyramids_Stonehenge.htm
[69] Stevens, op cit, *'Message from the Pleiades: The Contact Notes of Eduard Billy Meier, Volume 2'*, pp. 288-289
[70] Meier E, Tr. Stevens B (2010) 'Contact Report 217 Translation' *Billy Meier Wiki - The Future of Mankind*, online · http://www.futureofmankind.co.uk/Billy_Meier/Contact_Report_217
[71] Horn, op cit, 'The Henoch Prophecies from the Billy Meier Contacts'
[72] Meier E (2005) 'One Hundred Thirteenth Contact' *Semjase.Net*, online · http://www.semjase.net/semjeng9.html
[73] Putney A (2008) 'Piezoelectric Fires in Messina, Italy' *Human Resonance*, online · http://www.humanresonance.org/messina.html
[74] Cohen M (2009) 'Did A Country-Sized UFO Hover Above Switzerland Last Month?' *All News Web*, May 2, online · http://www.allnewsweb.com/page6756758.php
[75] Tesla N (1978) *'Nikola Tesla: Colorado Springs Notes 1899-1900'* Nolit, Beograd, Yugoslavia, pp. 61-62
[76] -- (1917) *'Minutes of the Annual Meeting of the American Institute of Electrical Engineers, May 18'*

4
Urandir's Transport

Urandir's Transport

Ongoing cosmic contacts occurring in Brazil have been largely obfuscated by corporate media disinformation, finding press coverage only in the Portuguese language broadcasts of the Brazilian media. Most significant among the many extraterrestrial contacts occurring in South American regions are those reported by Urandir Oliveira, who very carefully documents many forms of evidence attesting to the veracity of his statements and the reality of his transdimensional experiences. The weight of Urandir's evidence takes the form of demonstrations of the strong magnetic influence that he directs through his hands to move objects, in addition to physical trace evidence and video recordings of his levitation along violet-colored transport beams into luminous aerial plasma ships floating above. *At Urandir's special request, Verade TV videographers recorded and broadcast high-quality footage of his 1998 plasma beam transport into one of six disc-shaped plasma craft in an arc, each radiating pure white light.*

Urandir Fernandes de Oliveira was born on March 14, 1963 in Maraba Paulista, a rural area outside Sao Paulo in the state of Sao Paulo, Brazil. He clearly states that his unusual experiences with highly advanced extraterrestrial beings have involved their purposeful electromagnetic activation of bioenergetic capabilities that lie dormant in the average person. At a young age, Urandir had noticed the influence of his emotional states on metal objects in his hands. He quickly learned to develop this skill over the years, eventually being able to bend and tear common coins with his bare fingers. While he does not recall any physical interactions with the cosmic visitors during early childhood, he does attribute his unusual electromagnetic abilities to artificial plasma environments that he was voluntarily exposed to. The first face-to-face meeting that Oliveira recalls occurred on March 6, 1976, at the age of 13, when he was transported from his Sao Paolo home aboard a luminous lens-shaped craft. There he met with several tall, blond-haired humans of about 6'3"-6'5" in height, who radiated love, peace and intelligence through cat-like eyes, with vertically-oriented luminous golden pupils enclosed by blue, green or yellow irises.

The enhanced mental capabilities endowed by Oliveira's visitors allowed his further development of telepathic communication with the beings at a distance, by which method they would request and prepare him for subsequent contacts. The electro-acoustic activation of various Earth humans was explained to be a crucial mission of this extraterrestrial group, comprised of several allied races for whom Urandir has been given no names or planetary origins, but only recognizes their personalities telepathically. The practical urgency of Urandir's contacts involve the provision of crucial information regarding the electromagnetic changes now occurring on Earth, to prevent disastrous consequences that include the destruction of all nuclear power stations and nuclear arms storage facilities by the electrical overload and superheating of metals at specific focal points of infrasound resonance. Several contacts were conducted over many years to prepare Urandir for the complex astronomical information he would later receive:

By age eight, Urandir realized that when he fought over food with his brothers and sisters at the kitchen table, his hands could bend and twist the metal utensils. He remembers once throwing a fork that kept bending as it hit the table top… Urandir recalls physical abductions from Earth locations into an extraterrestrial craft when he was 13, 23, 27, 35 and 39, plus an encounter in Sao Paulo with ET humanoids at age 23.

Age 13, March 6, 1976 - Urandir Oliveira's Extraterrestrial Abduction #1, Sao Paulo

When he was thirteen on March 6, 1976, at 10pm at his home in Sao Paulo, he had his first encounter with a craft. The beings were tall and blond-haired. Their eyes were like a cat's, vertical honey-colored pupils in blue, green or yellow irises. He understood that the frequency of his mind had been speeded up by the blond humanoids to improve communication. Since then, one of the consequences has been that Urandir Oliveira's mind control over matter resembles the powers of metal bender, Uri Geller, who linked his abilities to a childhood encounter with a glowing being.

Age 23, 1986 - Urandir Oliveira's Extraterrestrial Encounter in Sao Paulo

Urandir had been making money by entertaining people with his mental powers in Sao Paulo. Then one night, he came upon a beggar and child who were hit by a car and broken bones were exposed through their skin. Not knowing how or why, he bent down and placed his hands on their terrible wounds and the bleeding stopped. Shortly thereafter, tall blond beings approached him and said, 'Now you know what to do with the light energy.'

Age 27, 1990 - Urandir Oliveira's Extraterrestrial Abduction #2, Sao Paulo

In 1990, he and a friend were both lifted up in beams of light into a craft where Urandir remembers many crystals pulsating with light and ‘lightning.’ He understood that the pulsating crystals ‘activated human force fields.’

Age 35, 1998 - Urandir Oliveira's Extraterrestrial Abduction #3, Corguinho Farm

In 1996, Urandir bought 209 acres of farmland in Corguinho between hills and a mesa where local farmers for decades have seen mysterious lights and aerial craft. His parents and in-laws also moved to the farm to help with the work. Over the next couple of years, Urandir appeared on several Brazilian television programs to demonstrate his Uri Geller-like ability to use his mind to bend metal, shut off and turn on lights, to move and control the direction of a small metal ball and to mentally break metal coins and glass dishes. By 1998, Brazil Verade TV traveled to his Corguinho farm because Urandir informed the station that the blond beings were coming back to get him again. The crew was videotaping when six lights in an arc appeared in the night sky and descended toward the ground. As the arc of lights seemed to lower toward Urandir, he walked through them into a small beam of light that lifted him into a disc-shaped craft while the Brazil Verade television camera rolled. Some of that video was broadcast in Brazil and the tape was sent to CNN for international broadcast. But to date, Urandir does not think CNN ever aired any of it and he wonders what happened to that professional videotape of his second abduction.

What no camera had access to was the inside of the craft. There, tall, blond humanoids showed Urandir wall screens containing moving images of Earth destruction by nuclear missiles and nuclear power reactors. Urandir understood that the destructions will be caused by changing Earth magnetic fields which affect the electronic systems in the missiles and reactors. The blond beings also showed Urandir that three "fully functional" pyramids currently covered by sand will be uncovered for the world to see.

Age 39, September 15, 2002 - Urandir Oliveira's Extraterrestrial Abduction #4, Corguinho Farm

His fourth abduction encounter began after 7 p.m. local time on September 15, 2002, in the bedroom he and his wife, Jessica, shared in their farm house. Urandir said he had received telepathic information several days before from the beings that by 10 p.m. on September 15, another transport to a humanoid craft would occur. So, anticipating another interaction, Urandir told his parents and in-laws, as well as local friends, to be ready for "a rain of rocks" that would last for seven minutes when Urandir was taken to the non-human craft. That same week, Jessica had traveled with their 2-year-old son, Aria, to Sao Paulo, to visit family and was not there when the drama unfolded.[1]

The natural energy fields of Earth resonance are notably strong in the entire Corguinho area, one indicator of which can be easily observed in the red soil that is given its color by iron, just as is the case with our own blood. The high electrical conductivity of iron in the blood is also witnessed in iron-rich soils, which conduct ambient electrical currents in the ground transduced by the bedrock from deep, inaudible pulsations of infrasound standing waves. Oliveira's earlier extraterrestrial experiences in the city of Sao Paulo prepared him for the later development of a spiritually and ecologically conscious community within which Urandir would be able to spread the knowledge and experiences he had gained from his contacts.[2] The electromagnetic setting of the Corguinho area provides the optimal environment for telepathy.

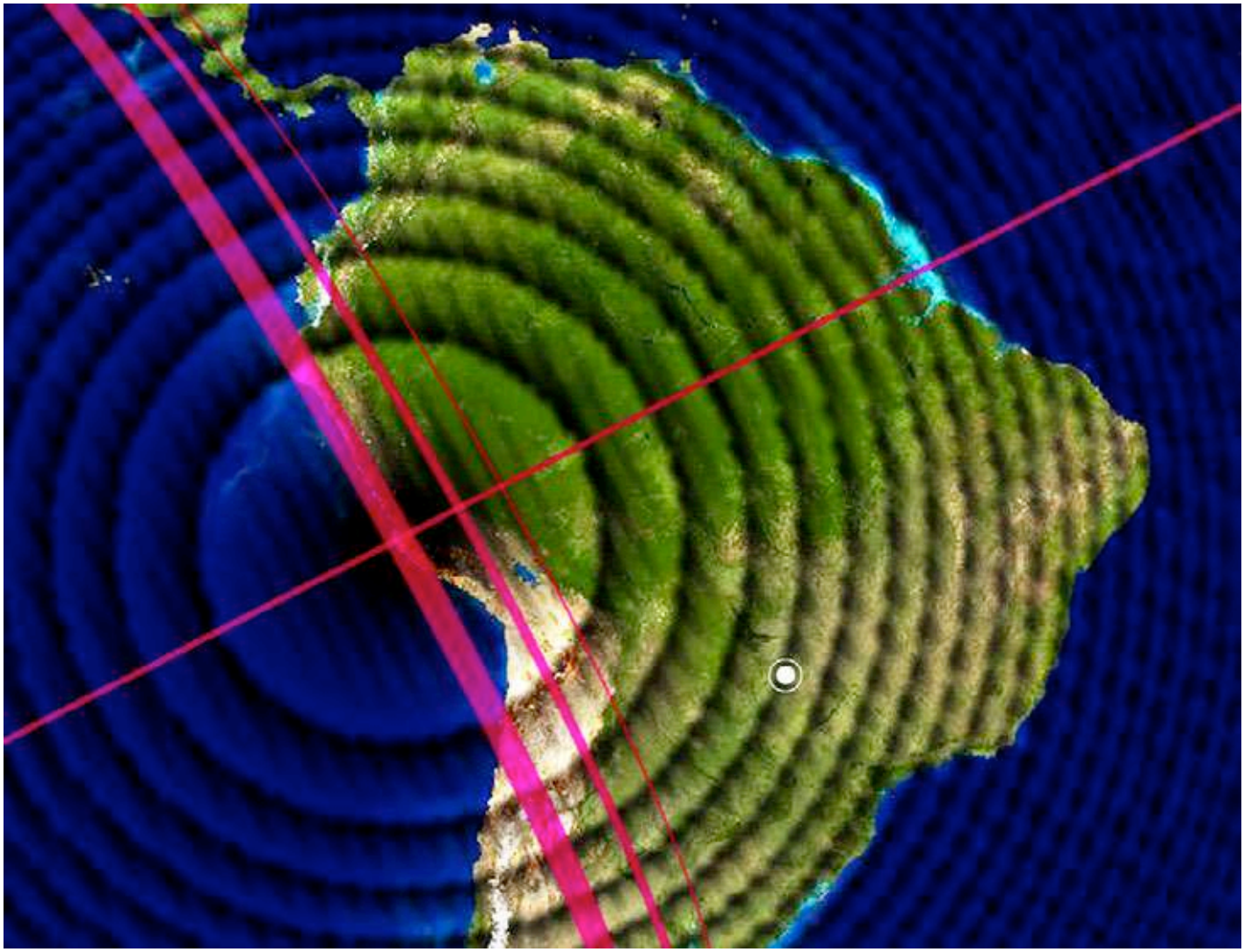

As with many conscious individuals seeking a sustainable life-path in accordance with ancient indigenous wisdom concerning these times of great change, Urandir and his wife Jessica have chosen to relocate to a resonant location to begin a sustainable organic farming community. Just as in the case of Eduard Meier and the FIGU community in Switzerland, Urandir Oliveira has founded Project Portal at his family-owned Ecovila Fezenda organic farm. Both communities engage in the sharing of extraterrestrial spiritual teachings concerning meditation, telekinesis, levitation, telepathy and the oncoming Earth changes.

Quadratic mapping of infrasound standing wave patterns reveals the Rochedo area of the Brazilian state of Mato Grosso do Sul as a resonant convergence point. The Oliveiras' 209-acre farm (19.88°S 54.95°W) is 6,669 miles from Giza, or 26.79% of the Earth's mean circumference. It is 1,365 miles from Nazca, Peru –a resonant circumference distance of 5.5%. The nearby giant rock formation, for which the town of Rochedo ("Little Rock") gets its name, is an ancient geological sign of convergent infrasound (opposite).

The holistic vision and profoundly transformative consciousness that is being engendered through these communities has apparently been perceived as a threat to the US government policy of UFO secrecy and denial, resulting in repeated attacks of all kinds. Both FIGU and Project Portal have been branded 'cults' and libelously slandered and legally attacked by so-called 'UFO groups' that are nothing more than US government propaganda fronts. Both Eduard Meier and Urandir Oliveira have received numerous death threats and both have evaded assassination attempts. Oliveira was also harassed, arrested and briefly imprisoned in March of 2000 on false and absurd charges aimed at destroying Project Portal. These detractions have been unsuccessful due to the open nature of Project Portal's workshops and events, bringing hundreds of people to the eco-village every year for spiritual and psychic development.[3]

Looming majestically over green fields and forests is Morro Ashtar, an oblong plateau that has become the center of increasing aerial activity. *Continually unfolding telepathic interactions, luminous plasma ships, and very bright but completely silent aerial explosions suggest to some residents that a subterranean base exists below the plateau.* Many Corguinho residents have spoken publicly about their numerous and regular sightings, and in some cases have also reported direct conscious interactions with extraterrestrial beings.

One such case involving ongoing contacts has been reported by Mr. João, a 72 year-old lawyer from Rio de Janeiro living in the Corguinho area.[4] An intriguing aspect of the experiences of Mr. João involve loud booming and humming noises emitted by the invisible plasma ship of the visitors to raise his electro-acoustic vibratory field, during which time they continually asked about his perception of colors presented from the luminous craft. Success was achieved after Mr. João was asked to put his hands on the ground, *as his shoes had apparently prevented the energetic activation they were undertaking!*

While videotaped group experiences involving interactions with plasma craft do exist, other such events in the Corguinho area have gone largely unreported. Documentary video was recorded by Fabricio da Silva during Urandir's experience aboard the fourth-density plasma ship on the night of September 15, 2002, including footage of a 'rain of stones' falling from the sky during the initial beam levitation event.[5] Also included in the video document is an interview with Urandir Oliveira by science reporter Linda Moulton Howe from February 9, 2003, at his farmhouse, conducted with Portugese-to-English translation by Luciano Didier. Subsequent interviews by Moulton Howe (with translation by Didier and Felipe Branco) explored the many intriguing details of Urandir's plasma beam transport and transdimensional experiences aboard a plasma ship for three whole days, from February 15-18, 2002:

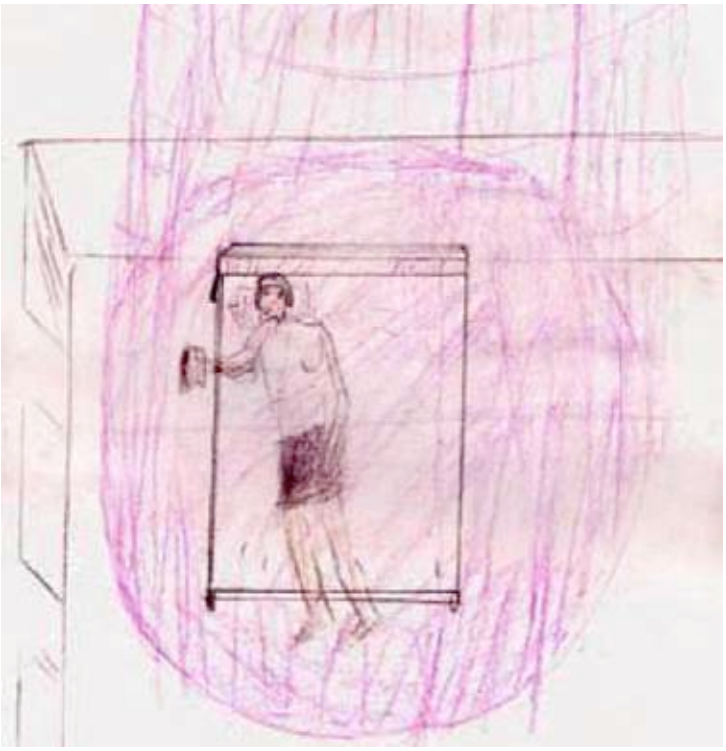

He (Urandir) was very anxious because for three days already he was expecting to be abducted, and there were only three hours left to the time the beings told him he would be abducted. (…10:00pm). He tried to prepare himself, so he went home and took a shower and put his shorts on and laid down on the bed. He picked up a book and tried to relax. A few minutes later, he realized a flash in the room. Then he felt his body like a fever warming up.

Q: What was the color of that flash?

The flash was sort of a light purple, or violet... [lit up] the whole room and then was condensing in the form of… a tube that included the bed and himself all the way from the bottom of the floor to the ceiling… The book was in his right hand (extended in the air beyond the right edge of the bed) and when the light flashed, eventually he released the book. The book fell from his hand. And he felt sort of a paralyzing [effect]. He could not move. He really felt this fever in his body and his body on the bed. He felt his body warmer on the bed. [see Urandir's sketch of his body in the beam, at left. Plasma beam photo above was taken elsewhere,[6] yet displays identical characteristics as described.]

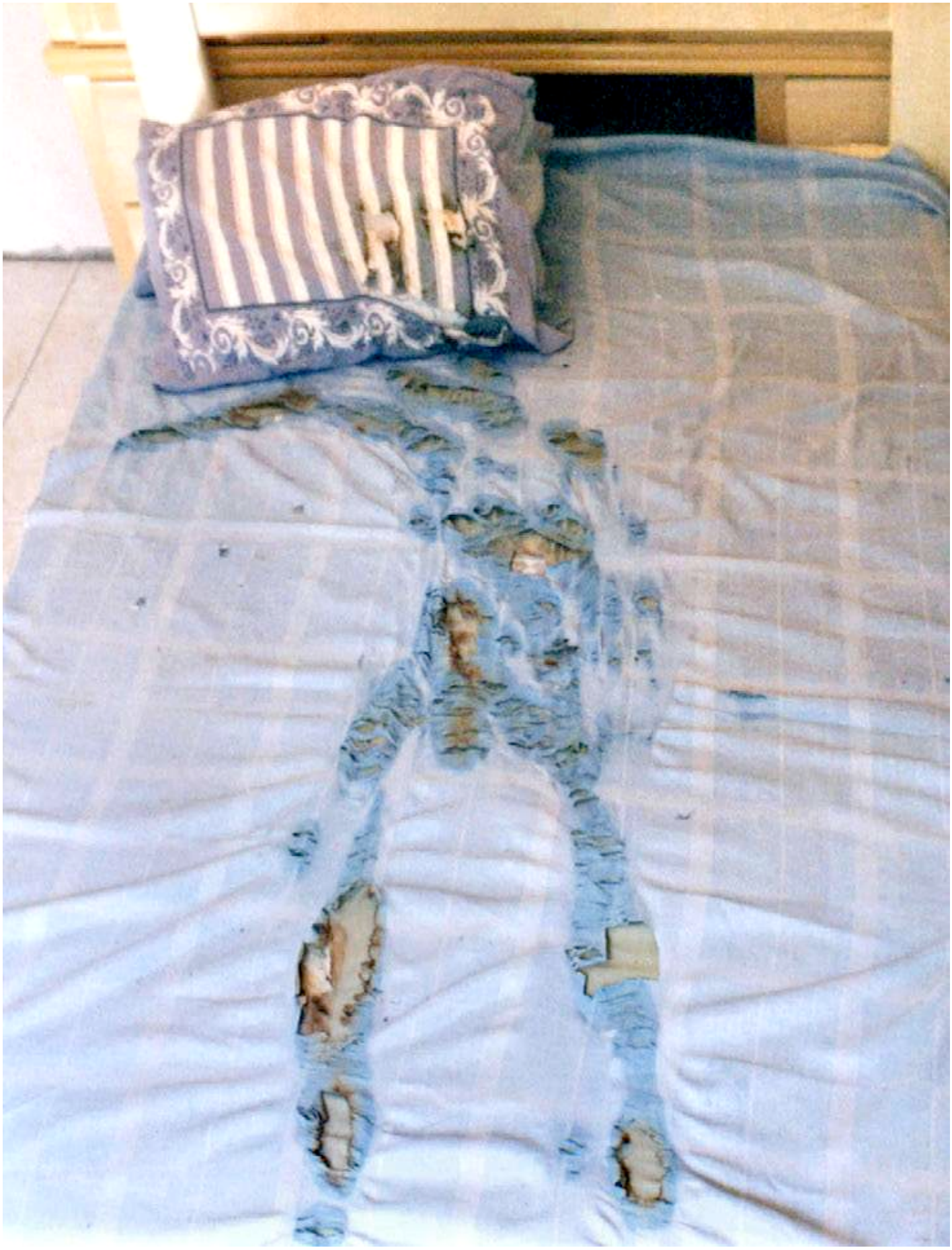

Q: When you look at those sheets and that ceiling, you would think you would feel pain (from the burn)?

Yes, because it leaves the impression that something burned someone there. But knowing in advance already the beam process of abduction (from earlier encounters), he knew it was not going to be painful at all.

Q: What is happening after the heat and going upward?

He felt himself rising up and going through the ceiling. From the point he was paralyzed, he could not move so much, but from what he could see, he realized everything was like normal from inside the light as he is rising. Actually the position did not allow him to see much, but what he could see are the normal things like the walls, the door, [and] the window.

Q: What happens as he gets up to the wood ceiling?

He saw himself going through the ceiling and he could actually see the molecules between the ceiling, like if he were going through foam. Not like a foam rubber, but like a soap, more like soap bubbles, like when you wash your hands and you produce the foam that comes out in the soap. And then he is turned upright so he is standing after he crosses that point of the ceiling, going through the ceiling, in the same violet light.

Q: The other day, he mentioned he could see and hear more?

Even at the height and distance he was, he could see and hear perfectly well, even better than normal, as if everything was amplified. He could see the stones falling everywhere, he could hear peoples' conversations and see them below… he could only see [the plasma craft] at the moment he approached it.

Q: The rocks are falling why?

It was a signal, a sign, that the beings left so that everyone would recognize that moment and everyone would know he was being abducted… As he was approaching the craft rising and saw everything that was going on down below, he goes into the first room into the craft. And it is also violet color inside this craft.[7]

The many fascinating aspects of the plasma beam transport of Urandir Oliveira on September 15, 2002 provide a wealth of information for the study of fourth-density technology. While such vivid descriptions of violet fog and levitation in luminous beams have been shared by many contactees over the last decades, none of those accounts were accompanied by accurate scientific descriptions of the entire experience. Urandir's case is a gift to Earthly science, in that he provides detailed scientific explanations for physical trace evidence in the form of textile samples with plasma-induced molecular alterations that can be studied by physicists for potential replication by all known means.

Previously obtained evidence of transdimensional plasma phenomena subjected to rigorous scientific analyses has been limited to downed plants from crop circle formations. The rapid heating of water contained within the effected plants by microwaves causes expulsion cavities in the nodes of the stalks as water is forced out by high-pressure. Video of plasma balls forming these marvelous geometric mandalas in the crops confirms their formation by the microwave emissions of airborne HHO plasma spheres that are themselves *natural elemental beings giving mathematical lessons to Earthly humanity.*

Scientists have confirmed through various means that the microwave radiation responsible for the many geometric crop formations of non-human origin must have been delivered in a very brief period of time, perhaps involving an exposure of under 7 seconds. This is exactly the conclusion that must be drawn from analyses of the scorched bed sheet evidence presented in the Oliveira contact case (above). Urandir experienced no pain during the plasma beam transport, as the beam technologies employed are completely safe and biocompatible, normally leaving no detectable trace of its use whatsoever.

Recently applied as a dental torch, helium/oxygen plasma is safely maintained near room temperatures by use of nanosecond electrical pulses, causing only a few degrees of heating in tooth enamel and gum tissues while vaporizing plaque and sterilizing oral films of bacteria in seconds.[8] During Urandir's beam transport, the air the room was infused from above with HHO gas bearing gold and silver nanoparticles and rapidly ionized by infrared light followed by nanosecond electrical pulses to form HHO plasma near room temperature, which became concentrated within the beam's vertical column. The paralysis

experienced by Urandir is electronically controlled by automated computers in the plasma ship above, as pulses from rotating green lasers within the plasma column created differential forces within the superfluid beam to levitate his body off the bed. The scorching of the bed sheet and pillowcase was then purposefully executed by a very brief heating of the plasma field closely surrounding Urandir's body just above the bed, before continuing with the strangely silent levitation process.

All matter within the fourth-density HHO plasma beam undergoes an atomic synchronization and expansion and that allows complete interpenetration of objects without interference, whereby Urandir's body was brought directly through the ceiling toward the craft. He describes being rotated into a vertical position after having passed through the roof, allowing him to see all of the activity going on below. Urandir's description of enhanced vision and hearing inside the plasma beam column is a result of the fourth-density awareness endowed by immersion of the human body in a superconductive state where the holographic aspect of consciousness becomes reunified with *the eternity*. The bright white light that Urandir describes as emanating from the electroluminescent metal hulls of the plasma ships also radiates from the craft's interior walls, which electrify the interior chambers with the same biocompatibly tuned HHO plasma that is concentrated within the beam transport tube emanating both ultraviolet-A and infrared light.

After Urandir's transdimensional levitation through the roof of his farmhouse and into the plasma ship hovering silently above, the cloaked ship created a 'rain of stones' as a deliberate sign to the neighborhood that the foretold event was indeed taking place. In the video footage recorded by Fabricio da Silva on the night of September 15, 2002, one can hear the round stones occasionally falling on the corrugated steel roofing and rolling down to be collected from the ground by the surprised neighbors.[9] Petrographic microscope analysis of one of the disc-shaped stones collected from the Oliveira farm was conducted by Professor Gomaa Omar, Geologist at the Dept. of Earth and Environmental Sciences at the University of Pennsylvania, and the results discussed in an interview with Linda Moulton Howe in June of 2003:

> It's very clear when you look at the cross-section here, you can see how [the stones] are banded. This is a mystery to me… I have never seen this particular 'football-like' shape and this particular mineral arrangement…
>
> Q: *And to produce this shape – of these sort of football-shaped or disc-shaped stones… and to have all of this quartz embedded in the iron… [would require a temperature] at about 2,000°F?*
>
> It was in a melt, yes… Definitely it is very clear that the quartz grains were floating in this iron liquid at high temperatures… But, as to the banding and the stratification going from the center outward, that has something to do with spinning force… and I really don't know what would cause this spinning force to form this [symmetrically disc-shaped iron/quartz stone].[10]

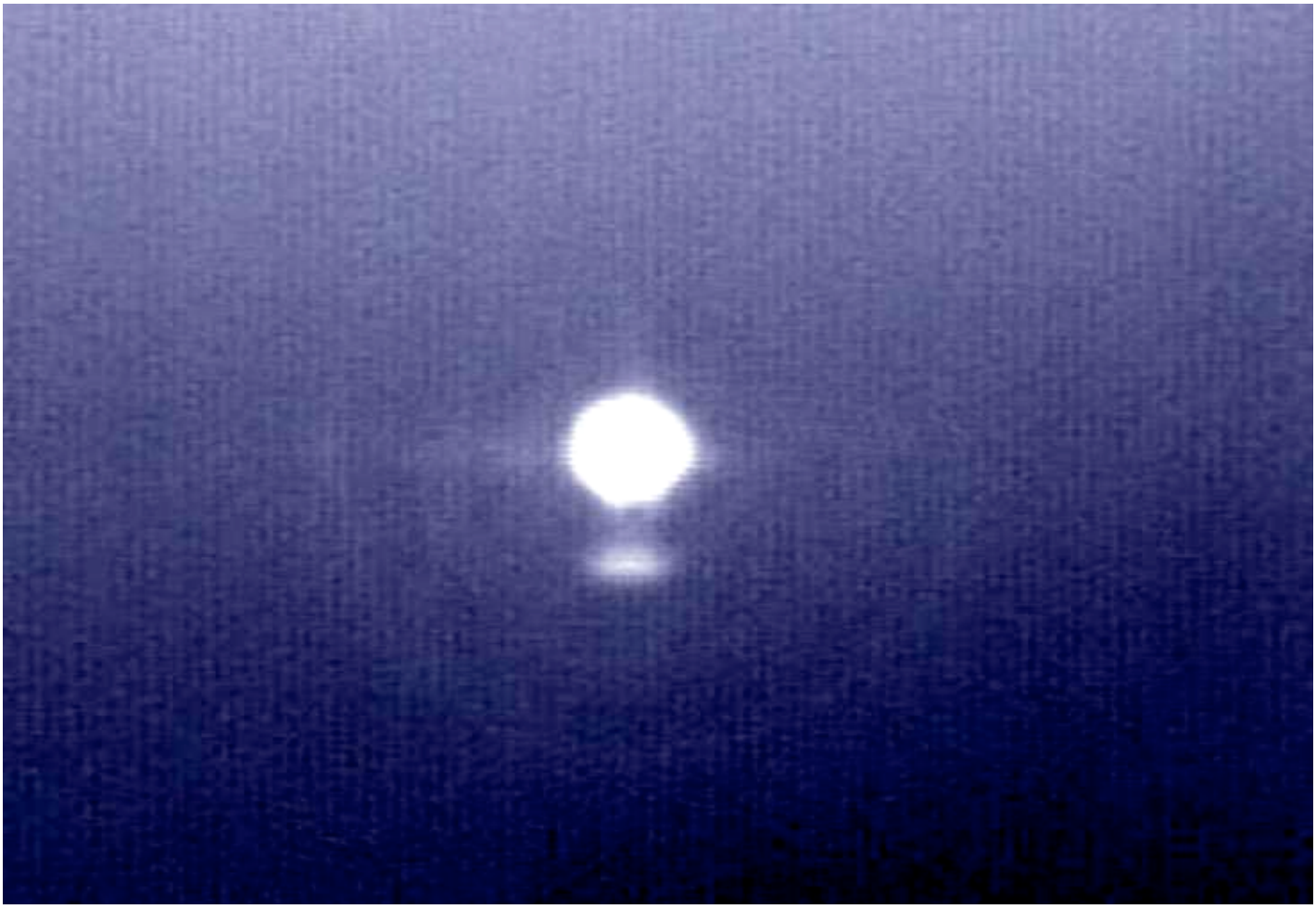

Iron in the red soils of the Corguinho area are attracted to the intense electromagnetic fields generated by the implosive hydrino plasma beam technology. Small grains of quartz sand are lifted from the ground along with the magnetic iron particles to be mixed with the liquified iron suspended in the intense rotating electromagnetic fields generated below the transdimensional spacecraft. Surface oxidation does not occur on these disc-shaped metallic concretions due to the unique effect of HHO plasma. Inventor Denny Klein noted the rust-resistant properties of surfaces brazed by HHO plasma during experimentation throughout the 1990s, which lead to the first commercial production of HHO gas torches, however short-lived.[11] The convergence of Earthly human technology with extraterrestrial means is greatly accelerating.

All over the world, these disc-shaped iron-quartz concretions are created below passing plasma craft of all kinds, even becoming commonplace in dry canyons which act like funnels to collect falling debris (opposite). Rains of these round iron stones have also been recently linked to invisible aircraft above the Indian towns of Ratria[12] Dhenkanal.[13] Infrared video obtained on March 5, 2004 by the Mexican Air Force[14] recorded a quickly moving formation of 11 disc-shaped aircraft that were completely invisible to the naked eye due to their use of HHO plasma screens surrounding each vessel like a bubble, with heat signatures of plasma vortices below each craft being clearly visible (above). The formation of the iron concretions was even filmed during a crash event in New Mexico,[15] actually showing magnetic material in the soil being trapped in the vortex below the craft, visible as molten metal glowing a bright red color.

Similar phenomena involving the interaction of iron-rich substrates with the strong rotating magnetic fields of plasmas moving above the terrestrial surface has also been identified on Mars.[16] Contributing to events of this kind are various plasma formations including natural lightening arcs that occur before the many impacts of meteor and comet debris to produce tiny spherical iron pellets that become thrown off as slag in a wide shower. The application of this phenomena by Urandir's fourth-density visitors as a message to the community is another example of their purposeful production of tangible evidence:

Q: [What occurred right after transport into the plasma ship?] This being was waiting, and how many others?

There were more – he cannot tell exactly how many, but there were more behind him. He was the main one, this one, waiting for him… [is] like 6-foot-three or -five inches [tall]… Then he walked in towards a bubble that was higher than him. As he saw a bed inside this bubble and just supposed he had to go and lay down there… [Inside the bubble] it was cold… like a car with air-conditioning on… He just walked through it… It was as if he (the blond being) was telling him, 'Go in, lay down and relax.' That's what he felt… He goes through it, feels very cold, lays down on the bed and then some sort of mist comes in and the shorts he had on disappear and in its place, some kind of other clothes materialized over his skin… [like those worn by the blond beings]. All of them, including his own, emanated a light like silvery-white neon lights… This light stabilizes his chakras and is sterilizing him from any bacteria on this planet.

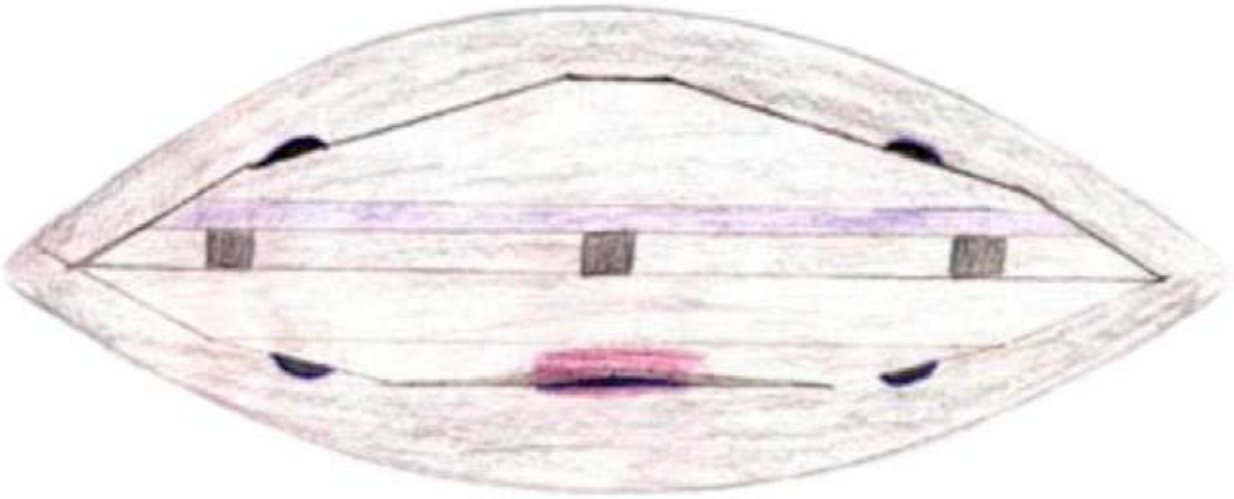

Q: What happened then after he's in the suit?

He walked out of this bubble and went towards them. The greeting with the beings is touching the (index) finger to identify the energy. And the same finger passing, like rubbing, the forehead, like if he was tuning into the other one's mind to start a telepathic conversation… The being touches his own forehead and then Urandir touches his own forehead. Only the (index) fingers touch… only telepathic conversation –no images in his mind.

The tall blond male directed Urandir toward stairs and they climbed to the next floor [as seen in his drawing, above] where Urandir was to remain for the next three Earth days watching wall screens of images about the Earth, this solar system and the galaxy. Watching with Urandir were representatives of other non-human species who Urandir understands are allied with the blond beings in a mission to help humans transform and evolve. The tall blond beings are trying to transform the mind frequencies of as many people as possible, raising them in an effort to neutralize large numbers of low frequencies and help block catastrophes they see in Earth's future. Urandir considers himself one of their students and his goal is to share publicly what he has learned about mind energy over matter from the beings.

The following excerpts about Urandir's memory of what he was shown and told are taken from a five hour conversation that was tape recorded in Corguinho, Brazil on February 10, 2003, with Portuguese to English translation help. Urandir said that various dates connected with earth changes - both positive and dangerous - were shown to him, but not in chronological order. (After walking up stairs with the blond being to a second floor) the wall of the craft there transforms into a monitor and they start showing scenes… The worldwide events that are going to happen… [in Earth's immediate future are presented and described telepathically.]

Scene 1 - 2014, Outer Space Chunks of Ice

The solar system traveling and meeting a curtain of ice pieces approaching… He said the solar system travels in a big galactic cycle through the ice… This is the second time the earth has passed through these huge clumps of ice. It's very close this and it will take maybe 15 years to go through the big pieces, but a few pieces of ice could already be coming toward Earth today. The blond beings said that we cannot see this yet because there is another body that reflects with a very strong electromagnetic field all the light of this ice curtain approaching the solar system…

Scene 2 - December 22, 2012, Galactic Pulse

A giant galaxy was the next image… [with the] solar system down there. On December 22, 2012, this galaxy is going to emanate a big flash of light that will affect all the suns. Every sun reflects to all the planets surrounding them and will cause a 'reversal' not only the earth, but all the planets… It's like God synchronizing the whole universe, like a synchronization ray or beam that would come from God, the Creator. He said it will be seen by any creature on the planet that has eyes to see it… For our planet, there will be lots of solar storms. The suns will get hotter with more solar storms…

Scene 3 - December 22, 2012 - Sun and Stars Moving in the Sky

They showed how the human beings would see the sky from the earth… Moving, like [on a teeter-totter]… if you are looking at the sky, it will swing. You will see the moon and the stars moving.

Q: Like [The Book of] Revelations in the Bible says the stars will move in the sky?

Yes, exactly… [moving or wobbling during] both day and night.

Scene 4 - 2014 and 2023, 'Plasma Ships' Evacuate Some Humans from Earth

In the next scene are lights in the sky which are the blond beings' plasma ships picking up humans from hilltops in their beam transport technology. This is roughly near 2023. But something similar in evacuating human beings starts in 2014. These are like stars representing the plasma ships. People are on the hills and the ships are rescuing them… [The plasma ships emanate] silver light. Like a dish to a dish…

Scene 5 - 2004, Cosmic Body Travels Close to Earth

At end of 2004, there is a shock due to a body that travels close to our planet and interferes with the climate and atmosphere… [*This event occurred on September 29, 2004* – the close passage of Asteroid Toutatis, as also predicted during the extraterrestrial contacts of Eduard Meier in 1978, who even foretold the exact name that would be chosen by French astronomers several years before the asteroid had been observed.]

Scene 6 - 2007, Cosmic Body Disturbs Earth's EM Fields; Scientists Discover Life-Extending Water

In 2007, there will be both bad news and good news for human beings. There will be a cosmic body [–Dark Star–] that moves toward or into the solar system that will affect the earth's electromagnetic fields… This electro-magnetic wave will affect some places locally, different, but not the whole earth. A good example is the Etna volcano in Italy. It could erupt and kill thousands of people. The rest of the world will carry on…

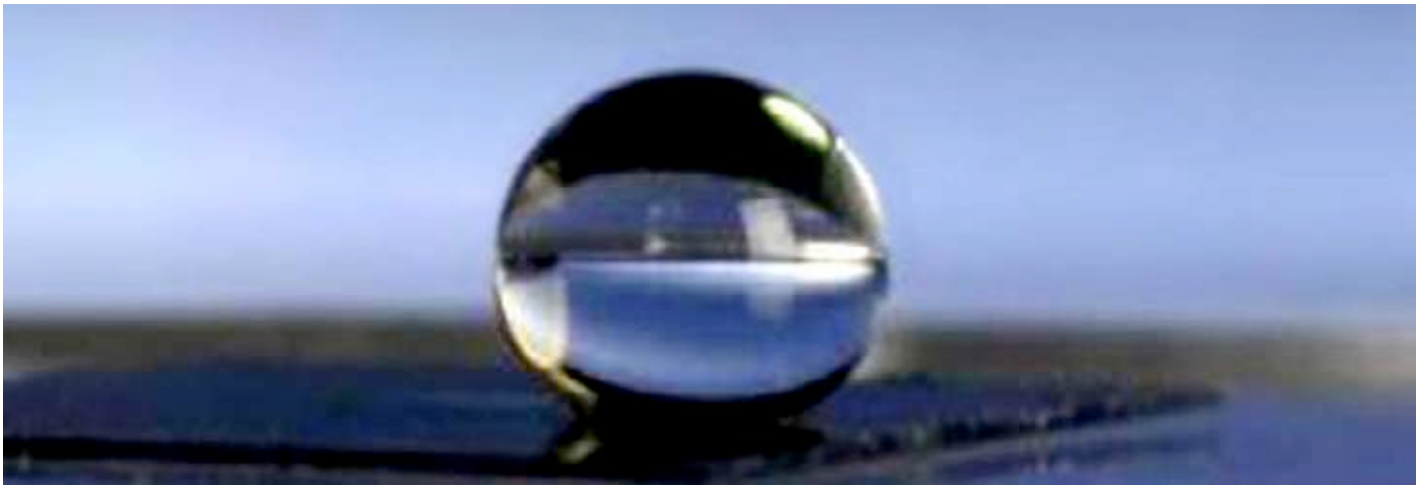

The beings said that science has already got the knowledge, but nothing has been published yet. In the ice caps of the Antarctic, scientists will study the water and find it is more pure, free of heavy water, deuterium? He is saying they are going to find this water with less heaviness. Scientists will discover this new purer water will retard the aging process by about 80 times. People could live 300 or 400 years. The technology to extract this new water in 2007 will be available… [whereby pure protium can be separated from heavier water molecules.]

Q: Who is planning this cruel joke of us finding life-extending water just before humans are wiped out by ice blocks only seven years later?

But there will be many survivors who can use the new discovery. The Earth has more than 6 billion inhabitants. Around 3 billion will die with all the catastrophes, but nearly as many will survive.

Scene 7 - 2028, Blond Beings Return Some Humans to Earth

And by 2028, it's like as if they are helping the population trying to help fix the planet. They start bringing back those people they evacuated before. And it starts a new era on the Earth. It's like everyone is part of a cooperative effort… After the evacuation, the people are returned years later but younger than when they were first beamed up into the plasma craft… They are taken into a different dimension that was adapted for the human beings to be preserved...[17]

The specific predictive information provided to Urandir Oliveira by his extraterrestrial teachers deserves careful analysis and consideration. Their concise description of the Galactic Pulse of December 22, 2012 being a synchronization beam radiating from the galactic core –*observable to all as a bright luminous flash that induces magnetic reversal of the entire Sol system*– corroborates descriptions provided by other extraterrestrial sources. The wobbling of the planet for days during a major reorientation in its rotational axis echoes ancient Biblical predictions, and *suggests a permanent seasonal change on Earth*.

We are warned that light from a threatening interstellar ice sheet is reflected by the strong electromagnetic field of the brown dwarf binary twin of our sun, itself having already invisibly entered the solar system. The foretold electromagnetic wave effects of the closing Dark Star are indeed perfectly exemplified by unusual events occurring in the Messina region of Sicily, just west of the mentioned Etna volcano. *The town of Canneto di Caronia has experienced repeated evacuations throughout the last several years due to extremely high electromagnetic fields being transduced from intense acoustic energy by the piezoelectric limestone bedrock.* The entire area is being bombarded by ultra-low frequency standing waves focused by the Giza pyramids, at a distance of 1,120 miles, or 4.5% of the Earth's mean circumference. *The brief explanation of localized effects given to Oliveira refers to nonlinear focal points of infrasound resonance.*

Information given concerning *lightwater* that Urandir drank with his companions for three days aboard the plasma craft is of great importance, being 'lighter' in reference to *both its weight and optical aspects*. Being comprised of pure *protium*, with less atomic weight than the heavier forms of water (deuterium and tritium), lightwater can be extracted from mixed terrestrial sources by virtue of the specific freezing, boiling and vapor points of protium that differ from the lower forms. *Oliveira was given astounding details concerning cellular longevity: that under bioelectrification conditions, the ingestion of pure protium lightwater endows an extended lifespan of 300 to 400 years.* This is the biological effect of the fourth-density HHO plasma environment that *'has been adapted for the human beings to be preserved'* such that they are *'younger than they were when they were first beamed up into the plasma craft.'*

It appears that Urandir's fourth-density teachers recognize the fact of governmental concealment of the anti-aging properties of pure protium water as a valid reason for providing this important information to humanity through Oliveira's efforts. The invisible bionanotechnological aspects of the lightwater that Urandir drank and absorbed through his skin during his extraterrestrial experiences were not discussed, yet comprise a significant factor in the formation of the HHO plasma that preserves both spacecraft and passengers. Biocompatible gold and silver nanoparticles of less than 10nm in size provide for remarkable optical characteristics, by transducing red and blue light inside all the bodies cells for the activation of DNA as an organic superconductor. *This effect cannot occur without the ingestion of these trace metals.*

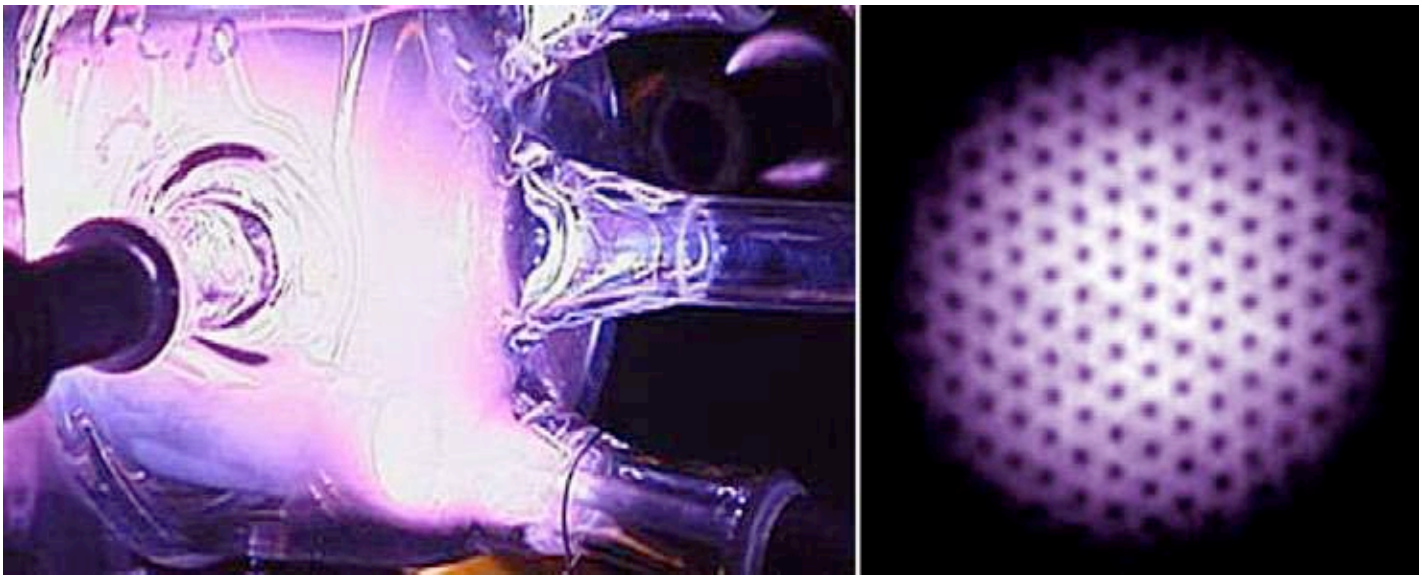

Physicists on Earth have now begun to apply the atomic implosion process of hydrogen for the transduction of *free energy from the resonant field of infrasound standing waves enveloping the planet,* using HHO plasma reactors that contain tungsten power and catalysts that are not biocompatible (above, left).[18] For direct application to the human body, gold and silver nanoparticles and dissolved potassium are essential. Earthly physicists have also recently defined the parameters for containing plasma within a superfluid beam, reporting the appearance of a hexagonal array of vortices during rotation (Ketterle, et al).[19] Oliveira described his experiences inside an HHO plasma transport beam to Linda Moulton Howe:

> The transport process was reversed, according to Urandir Oliveira, when the tall, blond beings decided to return him on the evening of September 18, 2002, after three days on a second floor room where a large wall screen showed Urandir and many other non-human beings images of Earth's alleged future. During our February 10, 2003, interview about the experience, I asked Urandir if he and the others were in the same room all three days. He answered, "Yes, it's like the walls were endless. I walked, but never reached the walls, so it gave the impression that the room was really big"…
>
> What he says he did understand was that the meeting in the "endless" room with many other non-human beings was supposed to have lasted for fifteen Earth days, not only three. But many of the people who had been at the Corguinho farm on the night of September 15, 2002, when the scorched body prints were found on Urandir's bed and the bedroom ceiling told friends, relatives and the Brazilian media about what had happened.

By September 16, 2002, Brazilian television reporters had traveled to Urandir's farmhouse to wait for a craft to return him. Felipe Branco and others who had been shocked the previous night by the bedroom scene had already locked the bedroom and shuttered the windows so no one could enter, including the curious media. When no dramatic aerial or beam activity was seen on September 16 or 17, the media left the farm. Urandir said, "In the end, the blond being told me that the trip was going to be interrupted, cut short, because of all the movement down there with the media which was not in accordance with what had been committed to me" by the beings. He understood that the non-humans did not want sensation, but left the physical evidence in the bedroom that unusual energy had interacted there for researchers to analyze.

On the evening of September 18, 2002, when the farm was relatively quiet, the tall blond being walked Urandir down the stairs in the craft to the place he had entered in the violet light. There he went back into the bubble where the silver, glowing, leotard-like suit dematerialized from his body and his own underpants materialized on him again.

Interview: The violet light was already there and a lot denser… When the violet transforms into a tube that comes down, the light becomes more subtle… At this point, he walks into the light. As he is going back down in the beam, about half way down, this light changes him from a standing position and puts him in the previous exact position when he was on the bed before (on September 15, 2002). The very same position and he is paralyzed again to go all the way through the roof and ceiling of his house and back to where he was…

Q: Any different feeling then?

Like as if his bones are stretching. Like cracking joints… The whole skeleton of all his bones go snap, snap.

Q: I wonder if it has to do with molecular expansion and contraction of passing his matter body through the roof and onto the bed?

Yes, it does have something to do with expanded molecular structure so he can interact with matter again. It's as if they are re-tuning the body… He can see through the same [violet] light to the room… He saw himself going through the ceiling and then he feels his body touch the bed. But before he actually approached the bed, he could not see that the bed was burned because the way in which he was paralyzed would not allow him to. So the (violet) light goes off and everything comes back to normal and he stands up, switched on the room light, and then he is surprised with his bed because it is so burnt. He thought he had been melted there! ...There was some sort of smoke in the ceiling still coming out.

I was puzzled… as I photographed and gathered cloth and wood samples from the sheet and the ceiling… [because] the scorch marks on the pillow and the heavy scorch mark surrounded by the aura of his head in the wood ceiling [above] were in different places… A logical speculation about this difference is that Urandir's body was moving forward toward the head of the bed as it was lifted upward by the violet beam technology… I asked him why he thought there were no scorch marks of his hand or feet in the ceiling. He was uncertain, but said he understood from the non-humans that the energy beam that lifted his body was precisely tuned to the molecules of his body against the bed in order to separate them from the bed… [It is an] extraordinary technology.

Q: What went through his mind as he looked at the sheet and the ceiling?

At the time, he started touching himself thinking, 'Have I melted?' And he wanted to know his weight, so he climbed on a scale and he lost 4 kilos (8.8 pounds) in those three days.

Q: Did they feed him anything?

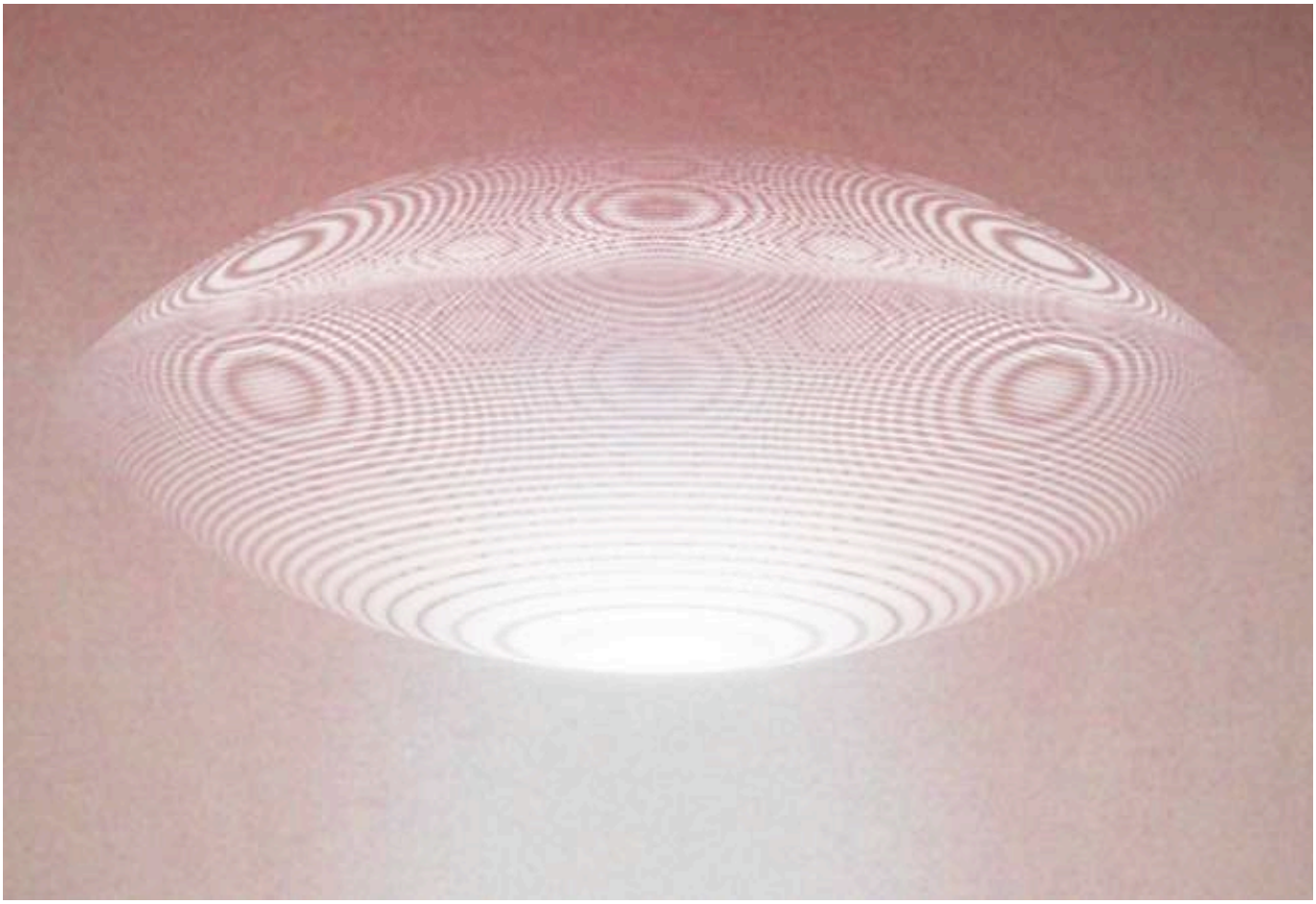

Some tablets with different flavors… If he wanted a meat flavor, they would give a meat flavor. If he wanted a sweet or apple flavor, he would have an apple flavor.

Q: Did they give him liquid? Water that was much lighter than our own…

Q: He felt perfectly fine? Relaxed, peaceful, joyful.

Q: So he is now standing in the bedroom. The ceiling is smoking. He is looking at his own body to see if he is burned… [and his clothing appears unaffected by the high temperatures. Then what happens?]

Then he tries to open the door of the room and it's locked. He opened the window and it is blocked from the outside… with bars. Everyone locked the room after he was gone (on September 15) after the [transport] to make sure no one would walk into the room… [thereby securing the evidence of Urandir's beam transport.] He has an intercom phone, so he called his parents who live on the farm and they rushed to the room to open it.

Q: He was gone for at least three days and humans go to the bathroom on a daily basis. What did they provide?

There was some sort of a cabin, almost transparent, a plasma material. And the only need or urge he had was to urinate. He did not feel any other urge. When he arrived at the plasma material, there was no hole, no basin, nothing. So, he thought, 'Well, I will just urinate here'…

Q: What happened?

So he starts urinating and when it is about 10 centimeters for the urine to touch the ground, it would disappear.

Q: He said he is standing before a plasma. Is it like a fog?

[The plasma cabin and urinal are formed by the] same material as the bubble. [The urine just disappears] before it touches the floor.

Q: Do the [extraterrestrial] blond beings urinate?

Yes, not as much as we do, but they do… [and they eat the] same tablets that they provided him." [20]

[A]nalytical chemist Phyllis A. Budinger [explained]... that the blue threads in the affected Oliveira sheet are cotton and the white are polyester. The blue and white threads are woven together throughout the sheet, but there is great variability in the body imprint from what looks like burned and charred cloth right next to cloth with only slightly darker blue discoloration that also outlines the entire body print. This is especially interesting when you consider the facts that cotton decomposes, or scorches, at about 148º Centigrade, or about 300º Fahrenheit. But polyester threads don't melt until 500ºF. There are melted, gummy threads intricately woven throughout the blue cotton threads -even in places where the cotton is not scorched, or even brown.

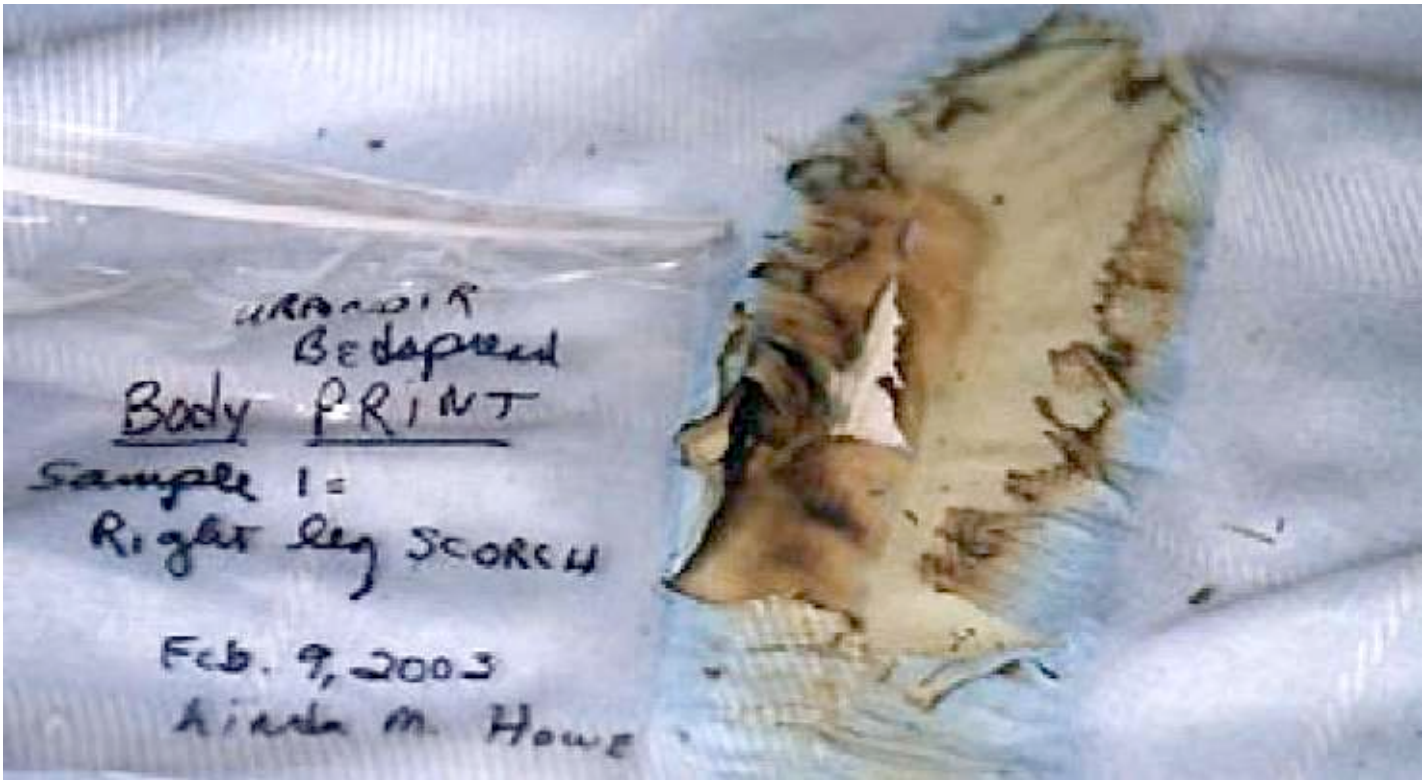

Interview: W. C. Levengood, Biophysicist, Pinelandia Biophysical Laboratory…: 'I've never seen anything like this. This takes a very, very high precision kind of - whatever the energy, and there had to be energy here to transform, probably at the molecular level, this because it changed the internal energy of the material. Whatever it was… [this form of energy] was extremely precise.

'I ran on to one region right at the edge of the brown material and the threads - you could actually see where they were white, normal threads, and then just a fraction of a millimeter away, they had begun to be transformed. They were glassy-looking, but you could still see the individual fibers inside. Then in another half millimeter, they were totally homogeneous into this opalescent material. So, that transition is very precise and you could see the line of demarcation if you had the incident light just at the right angle on the sample, you can see this band of change. So, the energy here is very, very precise.

'I measured the weight per unit area of a control sample. The weight of the control cloth is 17 milligrams per square centimeter. The blue region is 24% higher in weight than the control cloth. I don't think anything was added. It means the energy has changed the density of the polyethylene and to change density means you have to change the molecular structure. There is some incredible technology [being applied] here…

Q: This is a photomicrograph of a sample of the body pattern on the Urandir bed that was not scorched, but almost looks wet… [opposite, center.] But in fact that wet look has been caused by a change in the polyester?

It sure has. These I call a transition, or the polyester is converted into what I call vitreous fibers. It looks wet, but this is actually sort of an opalescent liquid-looking, but it's like a plastic, very hard.

Q: We know that polyester… has a melting temperature of 500°F and that cotton has a scorch temperature of 300°F. The difference of 200°F in this photograph alone is baffling because it looks as if the polyester threads have been melted and the blue cotton threads seem completely untouched.

That's right. And that difference of 200°F -that's the astounding thing. The cotton threads are totally undisturbed.

Levengood's biophysical analyses of microwave-radiated plants from crop formations form the only precedent for the study of material evidence of aerial plasma beam phenomena. Further analyses of the Corguinho bed sheet were undertaken by Professor Herbet J. Barndt, Director of the Grundy Testing Laboratory of the School of Textiles and Materials Technology at Philadelphia University. In an interview by Linda Moulton Howe in May of 2003, Professor Barndt stated that the delicate burn pattern on Urandir Oliveira's bed sheet must have been made with laser-like precision in mere seconds of exposure:

> *Q: Could you explain a little bit about the possible importance that water might have played – both from having taken a shower and perspiration when this individual laid down?*
>
> Well, when cotton gets wet, moisture actually goes into the fiber. In other words it's inside the fiber, as well as on the surface. [In the case of] polyester, the water remains on the surface. So in the presence of a high temperature the water will evaporate from the surface of the polyester before it evaporates from the cotton, because the water is bound to the cotton fiber. So, in order to damage the cotton fiber you have to evaporate the water to get the fiber hot enough to burn. But since the polyester isn't really holding water it can absorb heat more rapidly, and that may explain why the polyester melted, and the cotton in a number of these areas wasn't particularly damaged…

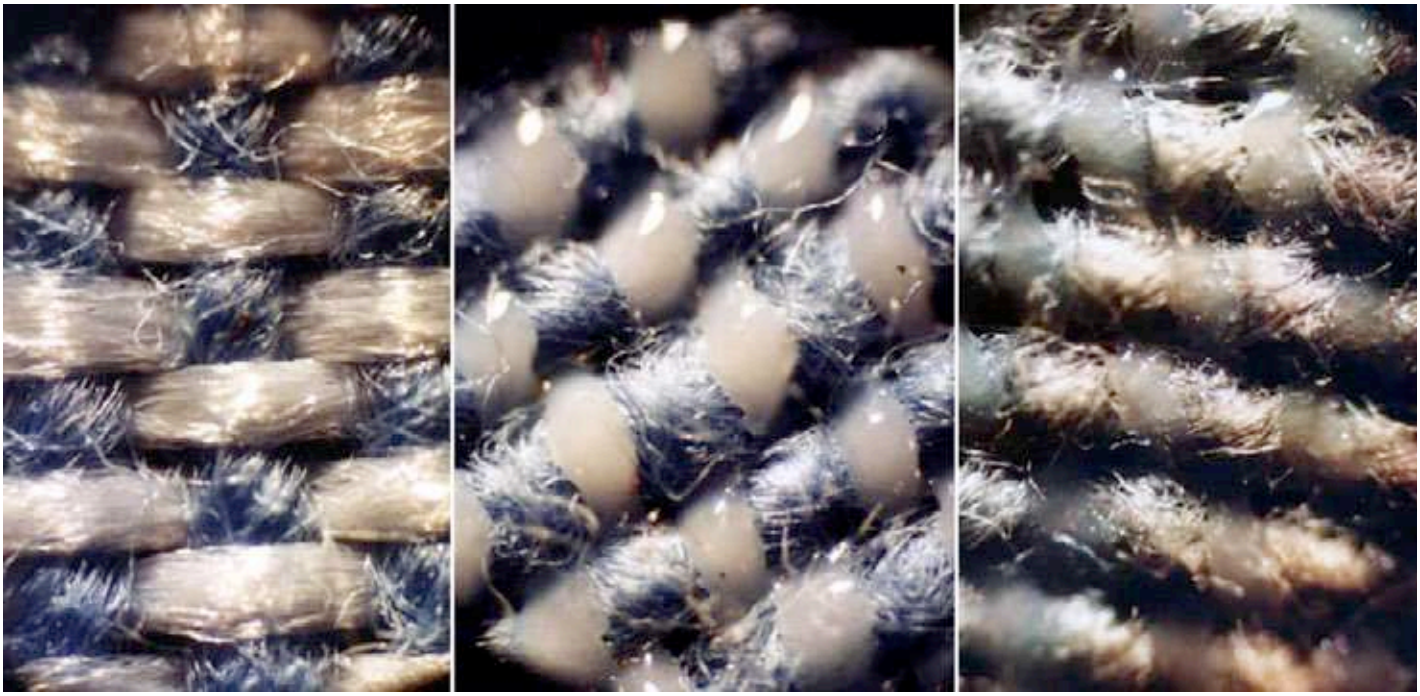

> Q: *Does that suggest… whatever did happen to this bed sheet happened in a very quick period of time?*
>
> I would think so… especially with the temperatures that are involved and the fact that the cotton wasn't degraded more than it was. it would seem that it had to have been a very quick occurrence, whatever happened here.
>
> Q: *And we're talking in seconds, right?*
>
> I would think so… It's very unusual… You would have to have a pinpoint heat source like a laser to do that… If you have a heat source that's intense enough to melt the polyester, and still not cause intense damage to the cotton, or at least some of the cotton, it has to move fairly quickly along this pattern… [or] the whole thing [is briefly heated] all at once…[21]

These detailed conclusions of the analyses of the bed sheet evidence from the Oliveira case point directly to a specific plasma heat source that was unknown to the 'experts', yet is derived from the most common and basic element in the Universe – hydrogen! *It is now known that HHO plasma is unique in that it heats different materials to different temperatures depending on the molecular structure.* An HHO plasma torch will not boil water, but instead reverts to water vapor on contact. The implosion of atomic hydrogen allows for precisely tuned interaction with the cotton and polyester threads in discreet bands of temperature change, producing the ultraviolet and infrared emissions described by Urandir as heat and violet light.

HHO plasma is also responsible for the molecular changes documented by Levengood regarding the weight increase of the vitreous polyester fibers. Similar analytic results were obtained from other material evidence collected by Oliveira and his group after a brilliant nighttime aerial explosion over Mount Ashtar (above) that scattered radioactive debris later measured with Geiger counters. A small brown ball of a solid resin-coated material was found lodged in a vertical rock face and carefully collected for laboratory analysis (opposite). X-ray diffraction analyses of the roughly spherical, resin-coated metal sample were conducted in the capitol city of Brasilia to determine the elemental composition of the artifact, which may reveal its extraterrestrial origin. *Testing showed abnormally high quantities of rare Earth elements:*

> Analysis of the nucleus, done by Centro Técnico Aerospacial [detected]… iron, oxygen, silicon, titanium and vanadium. In relation to the occurrence of these elements, the iron and the silicon can be largely found as iron ore and as silica... The oxygen is found associated chemically to the iron ore and the silica as iron oxide and silicon oxide, respectively. These oxides are mentioned in the probable presented compounds according to analysis done by x-ray diffraction. The titanium, as well as the iron and the silicon are not found in a pure state in the nature, being found also as oxides. In the sample, the probable compound that contains titanium is the iron oxide and titanium, which can be found in the nature as a mineral called ilmenite.
>
> Nonetheless, the most important aspect is the presence of vanadium. This element and all its derivatives are toxic to humans. Pure vanadium is normally used in special steels. It is found in complex minerals, such as vanadite ($Pb_5Cl(VO_4)3$) and carnotite ($K_2(UO_2)_2(VO_4)_2 \cdot 3H_2O$), with an occurrence in the crust of the Earth of 0.03% - a very restricted presence in the nature. Vanadium does not occur together with iron, silicon or titanium, which suggests that it was manipulated to be used with these chemical elements.
>
> Curiously, some forms of iron ore and titanium can present magnetism, which leads to certain suspicions about a possible mechanism of magnetic control of the space probe. The usage of iron bindings and silicon are also indicated in this sense, together with the bindings with Manganese… [Brasilia's] Laboratório Instrumental da Divisão de Química do Instituto de Aeronáutica e Espaço do Centro Aeroespacial showed that [the resin] presents a fossilized-material aspect of the ester resin kind, known as amber and silica.[22]

The initial radioactivity of the recovered probe debris is evidence of molecular changes having occurred during the explosion, while the exotic composition of nucleus confirms its unearthly origin. *The amber/silica resin coating presents an organic appearance, yet the roughly spherical metallic core of iron, oxygen, silicon, titanium and vanadium is certainly of non-mineral origin.* Brazilian Aerospace laboratories clearly acknowledged the highly unusual magnetic properties of the combination of elements found in the nucleus, while the resonant piezoelectric properties of silicon also implicate a highly advanced magneto-acoustic levitation technology. Silence accompanied the great heat and light emitted during the brilliant flash that briefly lit up the entire area like daylight, as the fusion of the aerial object into a tiny molten mass occurred.

The pointed speculation of analytical scientists supports the direct observations of witnesses to the luminous event and is further corroborated by information related in the contact case of Eduard Meier. Exactly this type of brown resin-coated mass was discussed as the byproduct of special security features commonly used by space-travelers visiting Earth. The dangerous potential misuse of technological knowledge is prevented by the installation of self-destruct mechanisms within all instruments and probes, for intentional or automatic activation in the event of malfunction. Semjase informed Meier of the necessity of the elimination of technological materials foreign to Earth, and a complete demonstration of the elimination process during his 62nd contact with cosmic visitors from the Plejares system, on August 12, 1976:

Meier: I have heard that some objects had simply disappeared or burnt, or dissolved themselves in some way, if they were found by Earth human beings and if the objects belonged to some extraterrestrial intelligences.

Semjase: The reason therefore is the elimination of these objects. We and many other intelligences are able to eliminate lost, or fallen into insincere hands, things by different ways, or simply to burn these to ashes. This happens by very far-reaching transmitters, which are started by means built into each instrument, a destroyer mechanism. These destroyer mechanisms are usually built into the objects and instruments, which we take to strange and still lowly-developed worlds, for reasons of security, so there does not come the dangerous for them possibilities of progress into the hands of the concerned still lowly-developed forms of life of any planet. These instruments or objects equipped with such destroyer mechanisms are normally produced from synthetic materials, like for example this small thing here… a selective warning instrument… which announces by a fine signal tone to me, when for example now should anyone come near us, whose brainwave pattern is not noted in this instrument, by which I mean, not registered.

Meier: …Can you perhaps demonstrate for me how you destroy such a thing?

Semjase: In purpose of your accomplishments, yes. Look, I simply throw it here onto the ground, and now do come a bit aside. – Like that, yes. Now look at this girdle-instrument; when you push these both flat buttons, then the warning means will start itself and burn and change towards a viscous and brown-black synthetic mass. Pay attention to the means laying there and push the two buttons. (I allow myself to push them.)

Meier: Can I have the remainders? Know I want to let them get analyzed.

Semjase: Yes, but then you should stop burning this mass, as otherwise nothing will remain for you. Don't touch it until $1^1/_2$ hours have passed, as until then, certain radiations dissolved by the combustion will have escaped out of the mass.

Meier: Well, but don't you think that our scientists could analyze important facts from out of this mass?

Semjase: The chance is very small, because this sort of synthetic material allows no more recognition of the original compounds, [and] will in similar form be used as well on the Earth…[23]

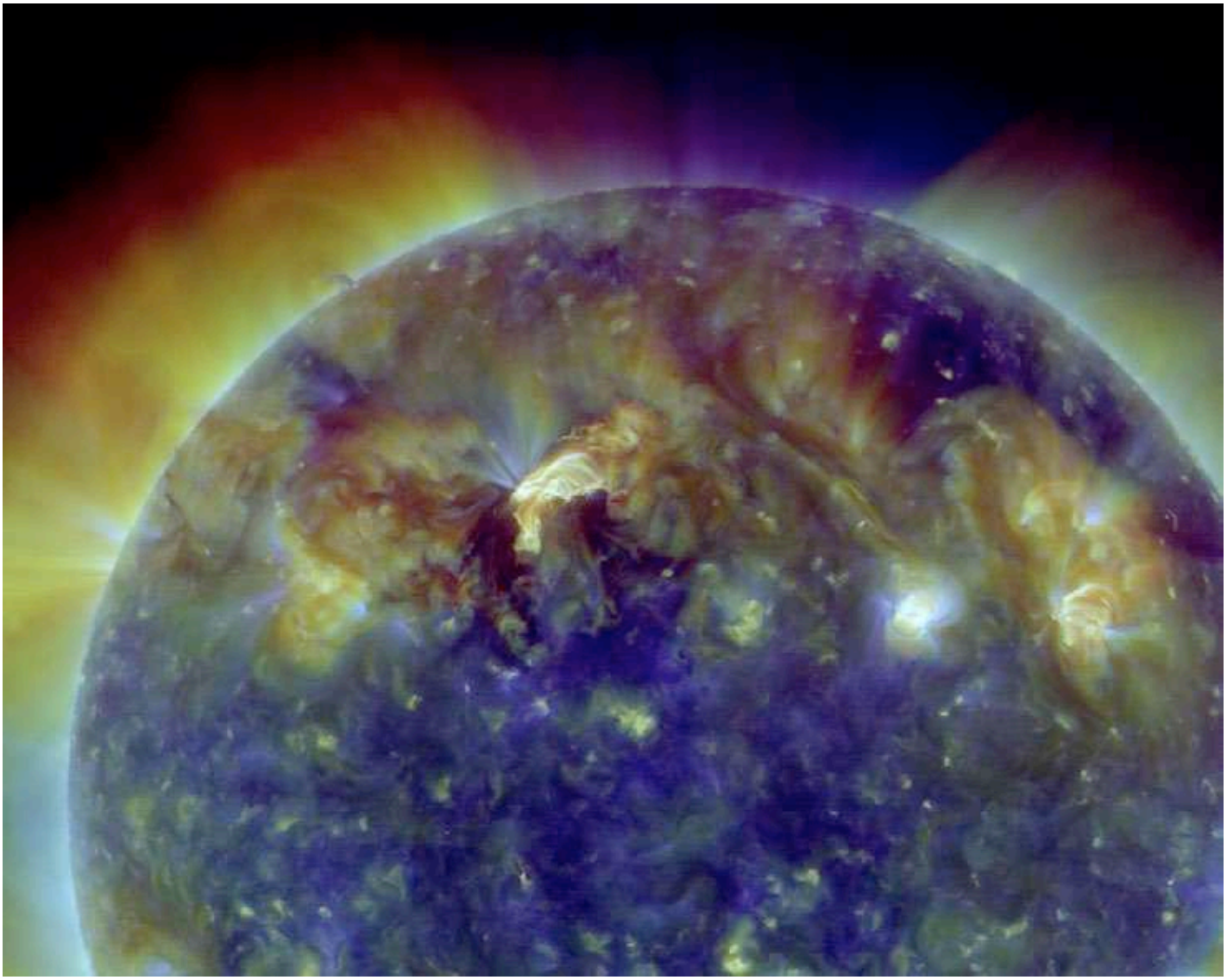

The explanations of Semjase perfectly describe the aerial probe debris recovered by scientific investigators involved with the Urandir Oliveira contact case, despite the more than three decades that separate the statements of Semjase with the spectacular aerial events occurring above Mount Ashtar in Mato Grosso do Sul, Brazil. The comprehensive guidance offered by visitors from other worlds, through the persistent efforts of Urandir Oliveira and other dedicated individuals, prepares Earthly humanity for the current electro-magnetic changes connected with the emergence of the brown dwarf binary companion at the outer reaches of our solar system, as the rain of Oort comet impacts bombards every continent of the Earth, continually threatening humanity for a prolonged period of many years into the future.

Greatly increased solar flare activity and resulting geomagnetic superstorms will accompany the process of magnetic reversal of the entire solar system in alignment with the Galactic Pulse of December 22, 2012. The ancient calculations of the calendars of the Maya culture resonate with the future events foretold to Urandir Oliveira, as do their advanced lessons on the effects of lightwater. The Maya also identify the transformative effects of the celestial lightwaters of Tláloc that rise in the mists at dawn, in contrast to the degenerative effects of the heavy waters that run downward to the center of the Earth. *Indeed, the process of activating the electro-acoustic vibratory fields of Earthly human beings is not only occurring in the plasma ships of extraterrestrial entities, but also in the Mayan pyramids and sacred sites throughout Central America.* Through these cosmic methods of bioenergetic activation the disasters threatening Earth's future may be mitigated or prevented, as the transdimensional enhancement of consciousness allows the integration of new perceptive capabilities in synchrony with the dramatic environmental upheaval.

References

[1] Moulton Howe L (2003) 'Corguinho, Brazil: Farmer Urandir Oliveira Describes His Transport to A Non-Human Craft on September 15, 2002' *Earthfiles*, online · http://www.earthfiles.com (removed)

[2] -- (2010) 'Urandir Oliveira: Paranormal' Urandir, online · http://www.urandir.com.br/

[3] -- (2007) 'Urandir Fernandes de Oliveira' *Projeto Portal*, online · http://www.projetoportal.org.br/urandir-f-de-oliveira-ing.html

[4] -- (2008) 'Corguinho_alien_aontactee_account.avi' *Google Video*, online · http://video.google.com/videoplay?docid=6825480847717282477&hl=en

[5] da Silva F (2007) 'Abduction.avi' *Google Video*, online · http://video.google.com/videoplay?docid=-3157785193143547318

[6] Rofe C (2003) 'UFO Beam Photograph Submission' *The Keyboard*, January 25, online · http://www.thekeyboard.org.uk/UFO%27s%20Fact%20or%20Fiction.htm

[7] Moulton Howe, op cit

[8] Dunham B (2009) 'Cool Plasma Pack Heat Against Biofilms', *University of Southern California News*, June 5, online · http://www.humanresonance.org/helium.html

[9] da Silva, op cit

[10] Moulton Howe, op cit

[11] Rodgers W (2005) 'Clearwater Man Puts Technology to Work', *Tampa Tribune*, November 27, online · http://www.humanresonance.org/hho.html

[12] Ghosh R (2004) 'Villagers in Madhya Pradesh Face Mysterious Enemy' *Human Resonance*, March 21, online · http://www.humanresonance.org/ratria.html

[13] -- (2009) 'Mysterious Stones Fall From the Sky', *Statesman News Service*, June 19, online · http://www.humanresonance.org/dhenkanal.html

[14] -- (2010) 'Mexico Air Force FLIR UFOs' *Youtube Video*, online · http://www.youtube.com/watch?v=uDOOZ_IPb6Y

[15] -- (2010) 'New Mexico UFO Crash' *Youtube Video*, online · http://www.youtube.com/watch?v=wAcotjjTj4s

[16] -- (2004) 'Blueberries on Mars and Other Spherical Rocks', *Thunderbolts*, online · http://www.thunderbolts.info/tpod/2004/arch/040827mars.htm

[17] Moulton Howe, op cit

[18] Mills RL, Ray P, Dhandapani B, Nansteel M, Chen X, He J (2002) 'New Power Source from Fractional Quantum Energy Levels of Atomic Hydrogen Surpasses Internal Combustion' *Journal of Molecular Structure* 643, pp. 43-54

[19] Ketterle W, Zwierlein MW, Abo-Shaeer JR, Schirotzek A, Schunck CH (2005) 'Vortices and Superfluidity in a Strongly Interacting Fermi Gas' *Nature* 435, pp. 1047-1051

[20] Moulton Howe, op cit

[21] Moulton Howe L (2003) 'Part 7 - Scientists Examine Samples from the Corguinho, Brazil Bed Sheet and Pillowcase' *Earthfiles*, online · http://www.earthfiles.com (removed)

[22] -- (2008) 'Analysis of the Nucleus, Done by CTA – Centro Técnico Aerospacial', *Projeto Portal*, online · http://www.ufocorguinho.com.br/resgate-ing.htm

[23] Stevens WC Ed. (1992) *'Message from the Pleiades: The Contact Notes of Eduard Billy Meier, Volume 3'* Genesis III Publishing, pp. 164-166

5
Golden Planets

Golden Planets

In one of the most intriguing cosmic journeys yet documented in our times, Michel Desmarquet was contacted by a giant, quite beautiful race of extraterrestrial human beings, and invited aboard their massive spherical spacecraft. Michel's cosmic journey began on a clear night in June of 1987, in the northeast part of Australia, when he was levitated above his home in a bluish plasma to be met by a giant figure in mid-air. Wearing a close-fitting single-piece suit, the huge figure smiled and explained the many unusual circumstances to Michel, before inviting him aboard the giant spacecraft that floated nearby:

> About 100 meters from us was an enormous sphere, from which emanated a bluish Aura. I later learned that it measured 70 meters in diameter. The light was not steady, but shimmered, resembling a heat haze when one looks from a distance at sand heated by the summer sun. This enormous sphere 'shimmered' about ten meters from the ground. With no windows, no openings, no ladder, it appeared as smooth as the shell of an egg.[1]

The giant being introduced itself to Michel as Thao, and explained the main purpose of their long journey from their gigantic homeworld, known as the golden planet of Thiaoouba. It was later identified as one of three such golden planets in our galaxy that represent the highest attainment of physical and spiritual advancement. Michel was invited aboard the spherical super long-range spacecraft, called an 'Alatora', and underwent a necessary set of bacterial decontamination processes with the implicit understanding that he was to join this race of gentle giants on a great journey. Michel was given the opportunity to visit their homeworld of Thiaoouba to speak directly with their High Council of 7 Elders, known as the Thaori.

No photographic or physical evidence of Michel's cosmic journey was obtained, but his vivid descriptions, first published in 1993, provide a wealth of advanced spiritual information and detailed observations that in themselves provide the ultimate validity of his experiences. As Desmarquet clearly acknowledges, "this extraordinary story will appear to [be]… a story entirely invented – but I do not have the imagination that such a fabrication would require. *This is not science fiction.* The reader of good faith will be able to recognize the *truth* in the message I transmit from my new friends to the people of the planet Earth."

For a period of ten days, Michel became the pupil of Thao, a quite impressive personage of 9'8" (290cm) in height, who radiated a youthful wisdom and joyfulness, representing a unisex race of giant human beings inhabiting the planet of Thiaoouba. Being hermaphrodites, all Thiaooubans possess both male and female reproductive organs. Such giant extraterrestrial hermaphrodites may have been depicted by ancient artists in giant stonework, such as the temples of Angkor from the ancient Sanskrit traditions of present-day Cambodia (above, with inset drawing of Thao based on Michel's descriptions). Thao's intriguing facial features combine the elegance of very feminine eyes with a strong masculine chin:

> Thao… smiled at me and I clearly remember appreciating, for the first time, the beauty and nobility of her face… I have already mentioned her hair, which was long and silky, golden-blond in color, which fell to her shoulders and framed a face that was perfectly oval in shape. She had a large, slightly protruding forehead… Her blue-mauve eyes and long curled lashes would have been the envy of many women on our planet. Her eyebrows curved upwards, similar to the wings of a seagull… The chin, well shaped but slightly angular, suggested a willful determination that was somewhat masculine, but this did not detract from its charm. A faint shadow of hair above her upper lip could have spoiled this perfect face, were it not blond.[2]

[Upon entering the giant ship, we] were now 'gliding' at ground level along a tunnel-shaped corridor that led to a small room, the walls of which were of a yellow so intense that I had to close my eyes… 'It is not a light. It is just the present color of the walls… There is no paint. There are only vibrations, Michel. You still believe that you are in your Earthly universe, when you are not. You are now in one of our super long-range spacecraft, capable of traveling at several times the speed of light. We will be leaving soon, if you will lie down on this bunk?'

There, in the centre of the room were two boxes - rather like coffins without lids. I stretched out in one of them and Thao in the other… I wanted to lift myself up a little but couldn't, being held by an unknown and invisible force. The yellow color progressively disappeared from the walls, to be replaced by a blue that was certainly no less intense… [Thao explained the light intensity as a health precaution–] 'We come from a planet [that is] bacteriologically different from Earth, which, for us, is a veritable culture medium. Thus, in order to contact you, I was obliged to take this basic precaution. You, yourself, were a danger to me but you are no longer… When you entered this cabin, the color was too intense for you and I gave you the helmet you are now wearing, which was specially designed for you…

'During the very short time the cabin was yellow and then blue, eighty percent of the dangerous bacteria in you was destroyed. Then perhaps you felt a coolness in the air, similar to when an air conditioner is working; this was another form of disinfection by... let's call it radiation, although that is not the correct word – it cannot be translated into any Earth language. In this way, I have been disinfected one hundred percent, but you still have enough bacteria to harm us considerably. I am going to give you these two pills, and in three hours you will be able to consider yourself as 'pure' as one of us.'

As she spoke, she took a little box from beside her bunk, removed the pills and held them out to me, along with a test tube containing a liquid that I supposed to be water. I swallowed them both, lifting the base of my helmet to do so... 'I have given you a special drug in order to cleanse your body of all bacteria that is dangerous to us. I have also given you another drug that has caused your Astral being to leave your body - this will last three hours, the time it will take to purify you. In this way, you will be able to visit our spacecraft, without danger of contamination to us and without wasting time.' [3]

Thao's explanation of the intense electroluminescence of the resonant metal walls of the Alatora spacecraft and the necessary preventive bioelectrification protocols can now be properly understood. Lightwater and a pill most likely containing exotic trace elements including electroluminescent nanoparticles of gold and silver became activated by the strong force-field which impeded his movement while reclining in the resonant chamber, illuminating his cellular waters with red and blue light. The precise environmental controls exercised inside the starship reflect the luminosity of Thao's high-resonance homeworld of Thaioouba. While in Astral body, Michel took the opportunity to ask his impressive new friend a spiritual question of great importance: *"First of all, who is God? Does he exist?"*

'I have been expecting this question and it is important that you ask it. On an ancient stone tablet, which I believe is *Naacal*, it is written: In the beginning there was nothing - all was darkness and silence.'

'The Spirit - the Superior Intelligence decided to create the worlds and he commanded to four superior forces... It's extremely difficult for the human mind, even when highly developed, to comprehend such a thing. In fact, in a sense, it is impossible. On the other hand, your Astral Spirit assimilates it when it is freed from your physical body. But I'm getting ahead of myself - let's go back to the very beginning.'

'In the beginning there was nothing except darkness and a spirit - THE Spirit. The Spirit was, and is, infinitely powerful - powerful beyond the comprehension of any human mind. The Spirit is so powerful that he was able, by the action of his will alone, to trigger an atomic explosion with chain reactions of unimaginable force. In fact, the Spirit imagined the worlds - he imagined how to create them - from the most enormous to the most minuscule. He imagined the atoms. When he imagined them he created, in his imagination, all that moved and will move: all that lived and will live; all that is motionless, or seems to be - every single thing.'

‘But it existed only in his imagination. All was still in darkness. Once he had an overall view of what he wanted to create, he was able, by his exceptional spiritual force, to create, instantaneously, the four forces of the Universe. With these, he directed the first and the most gigantic atomic explosion of all time - what certain people on Earth call ‘The Big Bang’. The Spirit was at its centre and induced it. Darkness was gone and the Universe was creating itself according to the will of the Spirit. The Spirit was thus, is still, and always will be, at the centre of the Universe for he is the Master and Creator of it...’

‘Well then,’ I interrupted, ‘it’s the story of God as the Christian religion teaches it - or just about - and I never believed in their nonsense...’

‘Michel, I speak of no religion such as exists on Earth and especially not the Christian religion. Don’t confuse religions with the Creation and the simplicity of all that ensued. Don’t confuse logic with the illogical distortions of religions. We will have the opportunity to talk again later on this subject, and you are certainly in for some surprises… For the moment, I was trying to explain the Creation to you. During billions of years (for the Creator of course, it is eternally the ‘present’, but it is more at the level of our understanding to count by billions of years), all the worlds, suns and atoms were formed, as you are taught in schools, the planets revolving around their suns, and sometimes with their own satellites etc. At certain times in certain solar systems, some planets cool down - soil is formed, rocks solidify, oceans are formed and landmasses become continents. Finally, these planets become habitable for certain forms of life. All this was in the beginning, in the imagination of The Spirit. We can call his first force the ‘Atomic force’.

‘At this stage, by his second force, he conceived the primary living creatures and many of the primary plants, from which later derived the sub-species. This second force we will call the ‘Ovocosmic Force’, as these creatures and plants were created by simple cosmic rays, which ended up with cosmic eggs.

‘At the very beginning, The Spirit imagined experiencing feelings through a special creature. He had imagined Man by means of the third force that we will call the ‘Ovoastromic Force’. Thus Man was created. Have you ever considered Michel, what intelligence it took to create a human being or even an animal? Blood that circulates thanks to the heart that beats millions of times independently of the will... lungs that purify the blood... the nervous system... the brain which gives the orders, aided by the five senses... the spinal cord which is ultra-sensitive… Have you ever wondered why, that of the billions of individuals on a planet like yours, there are no two fingerprints the same: and why, what we call the ‘crystalline’ of the blood, is just as unique among individuals as the fingerprint? …Your experts and technicians on Earth, and on other planets, have tried and still try to create a human body. Have they succeeded? In regards to the robots they have made, not even the most highly perfected will ever be more than a vulgar machine in comparison with the human mechanism.

‘To go back to the crystalline I mentioned just now, it is best described as a certain vibration particular to the blood of each individual. [Scanning electron microscopy imaging of healthy red blood cells is presented below.] It has nothing to do with the blood group. Various religious sects on Earth believe absolutely in the ‘rightness’ of refusing blood transfusions. Their reasons relate to the teachings and books of their religious teachings and their own interpretations of these, whereas they should look to the real reason, which is the impact the different vibrations have on each other… If it is a large transfusion, it can have an influence on the recipient to a degree and, for a length of time, which varies according to the volume of the transfusion. This influence, of course, is never dangerous… After a time, which never exceeds one month, the vibrations of the recipient’s blood takes over, leaving no trace of the vibrations of the donor’s blood… It shouldn’t be forgotten that these vibrations are much more a feature of the physiological and fluidic body than that of the physical body.’ [4]

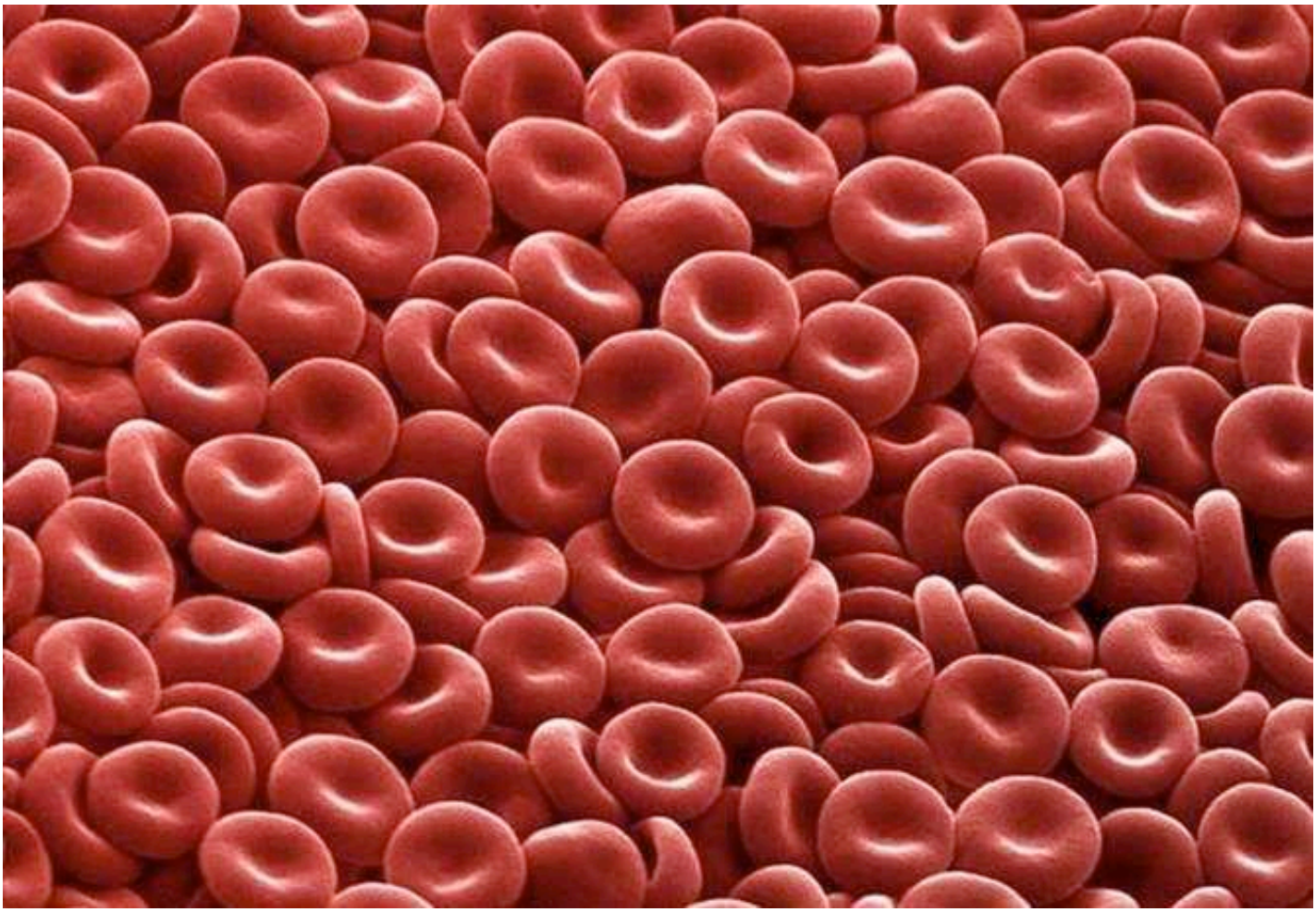

The straightforward scientific explanations provided to Michel Desmarquet by the cosmic beings of Thiaoouba guide Earthly human thinking toward the unified logic that Nature presents all around. The simple beauty of the lessons of the Creation offered by Thao rise in harmony with the teachings of Spirit transmitted to Earth by various other advanced masters in Nature, radiating their light throughout the great depths of the cosmos.

The concise explanation given concerning the formation of the cosmos through the four forces of Creation clarifies the quantum interactions of the short- and long-wave aspects of Creation, also referred to as the matter and anti-matter Universes. The Atomic force propels the material creation (*ultrasonic resonances*), the Ovocosmic force generates and maintains plant and animal life (*infrasonic resonances*) and the Ovoastromic force manifests through human life and consciousness. The fourth force was explained to Michel only later, after further necessary explanations were addressed: The Astral force. Thao’s comparison of the fingerprint with the unique resonant frequency of the ‘crystalline of the blood’ of each individual is just one of the many fascinating pieces of information that lead human consciousness on Earth toward the deeper cognitions that will unfold with this great change of the ages.

Simple descriptions preserved in ancient Vedic texts belie a profound depth of awareness that confirms that visitations like the one described by Michel Desmarquet had also occurred in the Vedic Age of Atlantis, before being recorded on parchment in later times. *The only precedents among the historical documents of Earth for such a story as the one told by Desmarquet are to be found among the Sanskrit cultures of the world, including sacred Mayan and Egyptian hieroglyphic texts as well as Sumerian cuneiform writings, that record the teachings of highly spiritual visitors from the stars.* The great teachings of ancient prophets are being given anew through the contacts of Earthly human beings in our times, in preparation for the ascension of Earth into collective consciousness.

The scribes of Sumer also recorded the malevolent extraterrestrial interests of the Annunaki involving the extraction of gold, using Earthly human slave labor, for the ultimate purpose of enriching the atmosphere of their own planet.[5] This unusual and highly advanced concept of golden atmospheres and golden rivers is also discussed in the ancient Sanskrit writings of India. An intriguing dialog between King Pariksit and Sukadeva Gosvami preserved in the Srimad Bhagavatam describes the golden waters of heavenly planets. The Description of Jambudvîpa (Canto 5, Ch.16) identifies certain golden rivers on Earth (in the material world) and their benefits, as enjoyed on other *heavenly* planets such as Thiaoouba:

> The mud on both banks of the River Jambu-nadi, being moistened by the flowing juice and then dried by the air and the sunshine, produces huge quantities of gold called Jambu-nada. The denizens of heaven use this gold for various kinds of ornaments. Therefore all the inhabitants of the heavenly planets and their youthful wives are fully decorated with golden helmets, bangles and belts, and thus they enjoy life... (Text 21)
>
> The residents of the material world who enjoy the products of these flowing rivers have no wrinkles on their bodies and no grey hair. They never feel fatigue, and perspiration does not give their bodies a bad odor. They are not afflicted by old age, disease or untimely death, they do not suffer from chilly cold or scorching heat, nor do their bodies lose their luster. They all live very happily, without anxieties, until death. (Text 25) [6]

These ancient dialogs quite astonishingly detail all of the known antibacterial effects of bioelectrification using nano-colloidal gold and silver water, in addition to other benefits that remain unrecognized by contemporary scientists, such as an increased tolerance to temperature extremes. Such odd, enigmatic information contained in ancient writings concerning atmospheric gold and silver is now comprehensible in the context of the scientific use of nanoparticles for the illumination of DNA within all cells of the human body *and the ignition of atmospheric HHO plasma*, just as vividly described by Michel on Thiaoouba:

Suddenly, there it was, right in the middle of the panel... Thiaoouba! My guess had to be correct - I could feel it. Thao immediately telepathized an affirmative, leaving me in no doubt… As we approached and Thiaoouba grew on the panel, I couldn't take my eyes off the sight, for what I saw before me was indescribably beautiful. Initially, the first word which sprang to mind was 'luminous' - this then was juxtaposed with 'golden' - but the effect produced by this color was beyond any description. If I were to invent a word, perhaps one that might apply would be 'lumino-vapour-golden'. In fact, one had the impression of plunging into a luminous and golden bath – *almost as if there were very fine gold dust in the atmosphere.*

We were descending gently on to the planet and the panel no longer showed its contours, but rather, the contours of a continent could be distinguished, ending abruptly at an ocean that was sprinkled with a multitude of islands of different colors… The closer we came, the greater was the detail discernible… What captivated me most, was the color before me – I was dazzled! All the colors were, in each tonal variation more vivid than ours. A bright green, for example, almost shone – it radiated color. A dark green had the opposite effect – it 'kept' its color. It is extremely difficult to describe, for the colors on this planet could not be compared with any that exist on Earth. A red could be recognized as red, but it wasn't the red we know. There is a word in Thao's language which defines the types of colors on Earth and on planets similar to ours. Our colors are Kalbilaoka which I translate as 'dull', theirs, on the other hand, are Theosolakoviniki which means they radiate their colors from within.

My attention was soon drawn to what looked, on the screen, like eggs - yes, eggs! I could see the ground dotted with eggs, some half covered with vegetation, and others quite bare. Some seemed bigger than others and some lay down. Others were upright with what looked like the pointed end towards the sky. I was so astonished by this sight that I turned again towards Thao to ask her about these 'eggs', when suddenly on the screen, there appeared a round form surrounded by several spheres of different sizes, and, slightly further away, yet more 'eggs'. These ones were enormous. I recognized the spheres to be space vessels just like ours.

‘Affirmative’, said Thao from her seat, ‘and the round form you see is the cell in which our spacecraft will be accommodated in a few moments, for we are in the process of docking.

‘And the gigantic eggs, what are they?’

Thao smiled. ‘Buildings, Michel, but just now, there is something more important that I must explain to you. Our planet contains many surprises for you, but there are two, which could have harmful effects on you. I must therefore ensure that you take certain elementary precautions. Thiaoouba does not have the same gravitational force as your planet. Your weight would be 70 kilograms on Earth - here it will be 47 kg. When you leave the spacecraft, if you aren’t careful, you risk losing your sense of equilibrium in your movements and your reflexes. You’ll be inclined to take too great a stride, and perhaps fall and injure yourself...’

‘But I don’t understand. In your spacecraft, I feel fine.’

‘We have related the internal gravitational pull to correspond with that of Earth – or almost… It’s true that under this force, our bodies are heavier, but we have counter-balanced this by a semi-levitation, thus we are not uncomfortable, and at the same time, we have the satisfaction of seeing you move among us at ease.’ A slight jolt indicated we had docked. This extraordinary trip was over - I was going to put my foot on another planet.

‘The second point,’ Thao resumed, ‘is that you will be obliged to wear a mask, for a while at least, for the brightness and the colors will literally intoxicate you, just as if you had drunk alcohol. The colors are vibrations that act on certain points on your physiological body. On Earth, these points are so slightly stimulated, so little exercised, that here, consequences could be unfortunate…’ There, she took a helmet, very light, which covered my face from my forehead to just below my nose.

‘Let’s go, Michel, and welcome to Thiaoouba.’ Outside the spacecraft, we walked along a very short walkway. Immediately, I felt lighter. The sensation was very pleasant, although somewhat disconcerting, since several times I lost balance and Thao had to steady me.

We saw no one, a fact that surprised me... After a short distance, we arrived at a round platform, to the side of the walkway. Thao sat down on a circular seat inside the platform and signaled that I should sit down opposite her… She took out an object the size of a walkie-talkie and immediately I felt myself pinned to the seat, just as I had been in the spaceship, by an invisible force field. Then, quite gently and with a barely perceptible hum, the platform rose by several meters and moved off rapidly towards the ‘eggs’, about 800 meters away. The thin and slightly perfumed air was lashing the exposed area of my face below my nose, which was very nice, its temperature being around 26 degrees Celsius.

In just seconds, we arrived, and passed through the walls of one of the ‘eggs’, as if we’d passed through a cloud. The platform stopped and came to rest gently on the floor of the ‘building’. I looked around me in all directions… It seemed absurd, but the ‘egg’ had disappeared. We had indeed, entered the ‘egg’ and yet around us, as far as the eye could see, stretched the countryside. We could see the landing ground and the docked spaceships just as though we were outside... Not far from us, were gathered twenty or thirty people, all busy to some extent, in front of desks and screens which flashed with colored lights - similar to inside the spacecraft. A type of music played very softly, elevating me to a state of euphoria…

Michel Desmarquet's thoroughly detailed and fascinating description of the visual splendor of the golden planet of Thiaoouba contains a wealth of information for scientific consideration, as well as a direct reference to the abundance of atmospheric gold (nanoparticles) visible throughout the luminous skies of Thiaoouba! This vaporous luminosity of Thiaoouba's atmosphere is created by light amplification effects of the HHO plasma that forms around the gold nanoparticles, which electroluminesce under the influence of atmospheric electrical currents moving through the resonant field of infrasound standing waves.

Thao's description of the effect of high-intensity colored light on the human body is also quite intriguing. Informing Michel that "the colors are vibrations that act on certain points on your physiological body", Thao offers an only slightly veiled reference to the pineal gland to the center of the human brain – also known as the 'third-eye' or *ajna chakra* among ancient Sanskrit traditions. The pineal gland is truly an *eye*, being photosensitive, and is responsible for the alignment of the body's circadian rhythms with the sun by light reception in the center of the brain.[7] Thao later explained in great detail the role of the pineal gland as one of the six principle points within the chakra system of the human body:

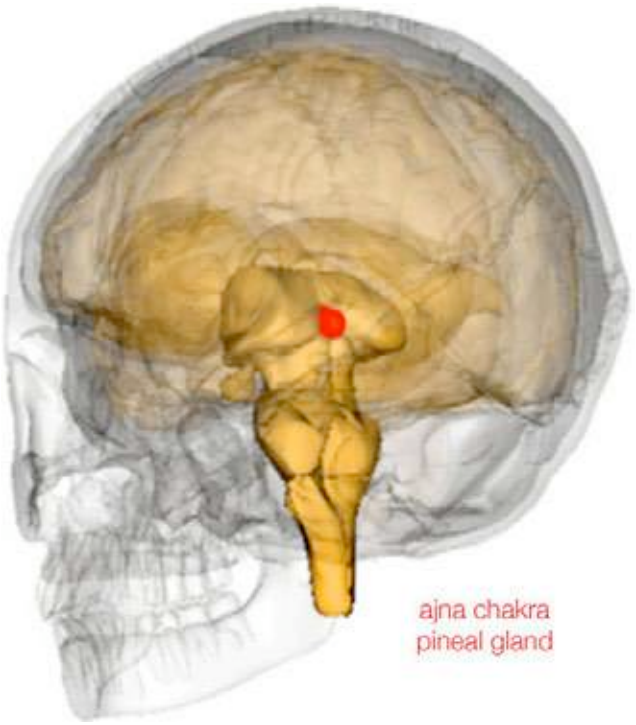

'The fluidic body [includes the brain stem and spinal cord, and] influences the physiological body which, in turn, influences the physical body… In the fluidic body, you possess six principal points which we call Karolas and which the yogis on your planet call Chakras. The first Chakra is the one situated between your two eyes, just a centimeter and a half above your nose. It's the 'brain' of your fluidic body, if you like; it corresponds to the pineal gland [in red, at left], which is placed much further back in your physical brain but on exactly the same level…

'Now, at the bottom of the fluidic body and just above the sex organs, is found a very important Chakra, which we call the Mouladhara, and which your yogis call Sacred [or Sacral]. Above this Chakra, and meeting the spinal column, is the Palantius. It is in the form of a coiled spring and only reaches the base of the spinal column when it is relaxed.

'For it to become relaxed, it requires the accomplishment of the sexual act between two partners who must not only love one another, but also have a spiritual affinity between them. Only at that moment and under these conditions will the Palantius extend to the spinal column, transferring an energy and special gifts to the physiological body which then affects the physical body. The person concerned will experience happiness in sexual enjoyment that is far greater than normal.' [8]

Thao identifies the shape and function of the *palantius* in much the same way as the coiled Kundalini serpent of Sanskrit teachings, and further reveals the special conditions for such an activation include not only partnership in love, but also *true spiritual affinity*. As proven by research scientists, such spiritual affinity takes the form of a *heart/mind resonance between the two*,[9] whereby releasing the palantius.

The identification of the chakras as existing within the fluidic body is also very concise, meaning within the spinal fluid itself. While the definition of the pineal gland as the first chakra presents an inverse order when compared with Sanskrit traditions, the Thiaoouban name of the root chakra –the Mouladhara– is identical to Sanskrit terminology. The attunements of Michel's chakras were so powerfully influenced by the luminosity of the high-resonance atmosphere of Thiaoouba that, combined with the intensity of ambient infrasound and the resulting decreased weight, his state of consciousness was elevated to euphoric levels that are only momentarily experienced by human beings on Earth, if ever. The highly elevated levels of all frequencies of electromagnetic radiation also required longer periods of rest.

The profound attainment of knowledge witnessed on Thiaoouba is reflected in the delicacy of colors and radiating brilliance of every life-form preserved there in harmony with the advanced technological lifestyle of the giant human inhabitants. Ever-present forms and forces within nature inspire the technological creations observable on this planet, whose buildings take on the form of eggs, and plasma spacecraft display a spherical perfection. The flying circular platform used for Michel's magnificent tour of Thiaoouba (illustrated above) is resonantly designed to generate the barely perceptible humming sound that Michel described during lift-off. Invisible magnetic fields are generated as belts that act as safety harnesses, and a domed magnetic field forms a protective covering enclosing the occupants of the open platform aircraft.

The grand scale of the trees and flowers, as well as the insects and animals, is a reflection of the enhanced gravity conditions of Thiaoouba, which are similarly witnessed in the geological record of Earth. During the age of dinosaurs, all life-forms on earth were correspondingly larger than witnessed today. Insects were once several times larger than the same types now living and would be crushed by the present conditions of gravity were they to be found on the planet today. The relative conditions of planetary gravity are directly tied to the intensity of atmospheric infrasound standing wave resonance.

> We rejoined our vehicle and immediately accelerated away in the direction of a forest, which could be seen in the distance. We flew at a height of approximately five or six meters and at a speed I would have estimated to be 70 or 80 kilometers per hour. The air was warm and fragrant and I again felt euphoric, in a way I had never experienced on Earth. We arrived at the edge of the forest and I remember having been greatly impressed by the size of the largest trees. They looked to rise about 200 meters into the sky.
>
> 'The tallest is 240 of your meters, Michel.' Thao explained without me having to ask, 'and between 20 and 30 meters in diameter at the base. Some of these are 8000 of our years old. Our year consists of 333 days of 26 karses. A karse is a period of 55 lorse, a lorse comprising 70 kasios, and a kasio being almost equivalent to one of your seconds…

The vehicle greatly reduced its speed and we were able to glide between, or indeed, stop and observe more closely, the trees at heights that ranged from almost ground level to 10 meters above the ground. Thao was able to guide our ‘flying platform’ with amazing precision and expertise. Our vehicle, and Thao’s manner of driving it, put me in mind of a flying carpet, which was taking me on a magical tour of this magnificent forest… Thao leaned towards me and removed my mask. The undergrowth was luminous and softly golden but I found it quite tolerable… ‘It is a good time to begin accustoming yourself to the light and color, Michel. Look!’

Following her gaze, I spotted, very high among the branches, three butterflies, vividly colored and of enormous size. These lepidoptera, which must have had one meter wingspans, fluttered high in the foliage, but we were lucky to see them fly closer and closer to us, on wings of blue, green and orange. It is as clear to me as if it were yesterday. They brushed against us with their wings that were strangely fringed, to create the most beautiful and breathtaking effect. One of them came to rest on a leaf just a few meters from us and I was able to admire its body, ringed with silver and gold, and its jade-green antennae. Its proboscis was golden and the tops of its wings were green with streaks of bright blue alternated with dark orange diamond shapes. The under-sides were dark blue, but luminous, as though they had been illuminated from above by a projector.

For the duration of time this giant insect remained on the leaf, it seemed to emit a soft whistling sound and I was quite surprised by this. I had certainly not heard a lepidopteran on Earth make any sound at all. Of course, we were no longer on Earth but on Thiaoouba, and this was only the beginning of a long series of surprises for me. On the forest floor, grew an incredible variety of plants, each one stranger than the next. They covered the ground completely, but I noticed very few bushes among them… the forest's giants prevented them from developing.

In size, these plants varied from a ground-covering moss-like plant, to one the size of a large rose bush. One kind, with leaves as thick as a hand in various shapes - sometimes heart-shaped or circular, sometimes very long and thin - was of a color tending much more towards blue than to green. Flowers of every shape and color, even of the purest black, entwined each other. From our altitude of several meters, the effect was absolutely glorious. We rose till we were up among the highest branches and I put my mask back on according to Thao’s direction. We emerged from the canopy and moved slowly, just above the foliage of those enormous trees.

Above the forest the light was, once again, incredibly intense and I had the impression of traveling through a landscape of pure crystal. Marvelous birds were perched on the tops of the taller trees, watching us pass, without fear. Their colors, varied and rich, were a veritable feast for my eyes in spite of the subduing effect of my mask. Here were varieties of macaw, with blue, yellow, pink and red plumage; and, among them a type of bird of paradise strutted amidst a cloud of what appeared to be hummingbirds. These hummingbirds were of a brilliant red color flecked with gold. The red, pink and orange tail feathers of the birds of paradise, would have measured 250 centimeters in length and their wingspans almost two meters.

When these 'jewels' took flight, the underside of their wings revealed a very soft, misty pink, with just a touch of bright blue on the tips - so unexpected, especially as the tops of their wings were of an orange-yellow color. Their heads wore plumes of impressive size, each feather being a different color: yellow, green, orange, black, blue, red, white, cream... I feel frustrated that my attempts to describe the colors I saw on Thiaoouba are so inadequate - I feel I need a whole new lexicon, as my language fails me. I had the constant impression that the colors came from within the objects I looked at, and the color was more than I had known it to be. On earth, we know perhaps 15 shades of red; here there must have been over a hundred...

It wasn't only the colors that claimed my attention. The sounds that I had heard since we began to fly over the forest inspired me to seek an explanation from Thao. It was almost a background music, very light and soft, similar to a flute which continually played the same air but at a distance. As we moved on, the music seemed to change, only to return to the original tune. 'Is that music I hear?'

'It is vibrations emitted by the thousands of insects which, when combined with the vibrations of the colors reflected by solar rays on to certain plants, such as the Xinoxi, for example, produce the very musical results that you hear. We, ourselves, only hear it if we particularly attune to it, for it comprises an integral part of our life and our environment. It is restful, isn't it? … According to the experts, if these vibrations were to cease, we would experience considerable eye trouble. This will perhaps seem odd at first, since these vibrations appear to be perceptible to the ear rather than the eye. However, …the chance of their ceasing is as remote as the chance of our sun extinguishing itself tomorrow.'

> Thao turned our vehicle and in a few moments, we had left the forest tops and… I saw we were approaching the ocean. Palm trees resembling coconut palms waved their majestic fronds at impressive heights, on the edge of a beach of golden sands… A hundred or so people basked on the sand or swam, entirely naked, in the transparent waters of the ocean. I felt a little dazed, not only because of the new and wondrous things I was constantly discovering, but also because of the perpetual sensation of lightness, due to the change in gravity. This sensation was my reminder of Earth – what a strange word, and how difficult it was to visualize Earth now! The auditory and visual vibrations were also affecting my nervous system enormously. Usually a highly-strung person, I was feeling completely relaxed… –so relaxed I felt like crying.[10]

The perfection of natural beauty and harmony of life on Thiaoouba resonated deeply with Michel, its intense radiations bathing him in a field of love that has been raised to the highest resonance:

> The sun was already quite low and the sky was totally clear. The ocean had taken on an orange color, which was surprising. I never would have imagined water could appear such a shade. Inquiring about it, telepathically, it was explained to me that, sometimes, at this time of day, immense patches of orange colored plankton would rise to the surface. These waters, it appeared, contained enormous quantities of plankton. What a sight it was: the sky was blue-green, the sea was orange, and everything was enveloped in the golden light which, on this planet, seemed to come from nowhere and everywhere.[11]

The intense luminous qualities described by Michel can only be explained as an amplification effect of diffuse atmospheric HHO plasma generated by electroluminescent nanoparticles of silver and gold suspended in the planet's strong enveloping field of infrasound standing waves. The tranquil weather patterns well described throughout Michel's nine-day adventure on Thiaoouba are a reflection of the planet's highly balanced atmospheric systems. Desmarquet was also taken by the intense nighttime optical effects of Thiaoouba's many-layered canopy of atmospheric HHO plasma, which amplifies all starlight as seen from the ground, creating a magnificent opportunity for direct stellar observation:

> No one spoke; we sat in silence. Looking up, I could see the stars appearing one by one, shining colorfully as though a firework display had 'frozen' in the sky. On Thiaoouba, because their layers of gasses in the atmosphere differ from ours, the stars appear to be colored and also much larger than they appear to us on Earth.[12]

The color of each particular star is amplified as it passes through many atmospheric layers of HHO plasma, formed from water vapor that becomes ionized as a glowing plasma canopy. HHO plasma forms a barely visible network of thin veils suspended along the pathways of infrasound standing waves where gold and silver nanoparticles are kinetically energized, allowing the splitting of water molecules into single atoms of hydrogen and oxygen (HHO gas). The ancient Sanskrit knowledge of 'heavenly planets' is in complete correspondence to the experiences so richly described by Michel Desmarquet on the golden planet of Thiaoouba! The natural domed plasma canopies of heavenly planets form the divine inspiration for the unified egg-shaped design of all habitations, temples and spaceports, reflecting the *Ovocosmos*:

> The vehicle proceeded slowly at ground level and, after a final bend in the path, we arrived before a 'little egg', nestled among small trees and flowering vines. It seemed that every building on this planet had the shape of an egg, most often lying on their 'sides' but occasionally upright, as I have said, with the pointed end upwards. The 'shells' were off-white in color and had no windows or doors. This particular egg lay on its side, apparently half buried in the ground. It was about 30 meters long and 20 meters in diameter - quite small in comparison with those I'd seen so far.
>
> Thao stopped the vehicle in front of a bright light centered on the wall of the egg. Leaving the platform, we entered the habitation. As we did so, I felt a light pressure, with no more force than the weight of an eiderdown. I remembered experiencing the same sensation earlier, when we passed through the wall of the space centre… Having neither doors nor windows on these buildings is extraordinary in itself, but once inside, it was stranger still. As I have mentioned before, the overall impression was of still being outside.

The startling beauty of color was everywhere; the greenery; the branches of the trees dissecting the blue-mauve sky above; the butterflies; the flowers...I recall a bird that came to rest right in the middle of the roof, so that we could see the bottom of its feet. It was as though it had miraculously stopped in mid-air – the effect was quite extraordinary… The only contrast with the outside was provided by the floor that was covered in a type of carpet on which was arranged comfortable looking seats and large pedestal tables. All of these furnishings were, of course, on a large scale - appropriate to these 'large-scale' people.

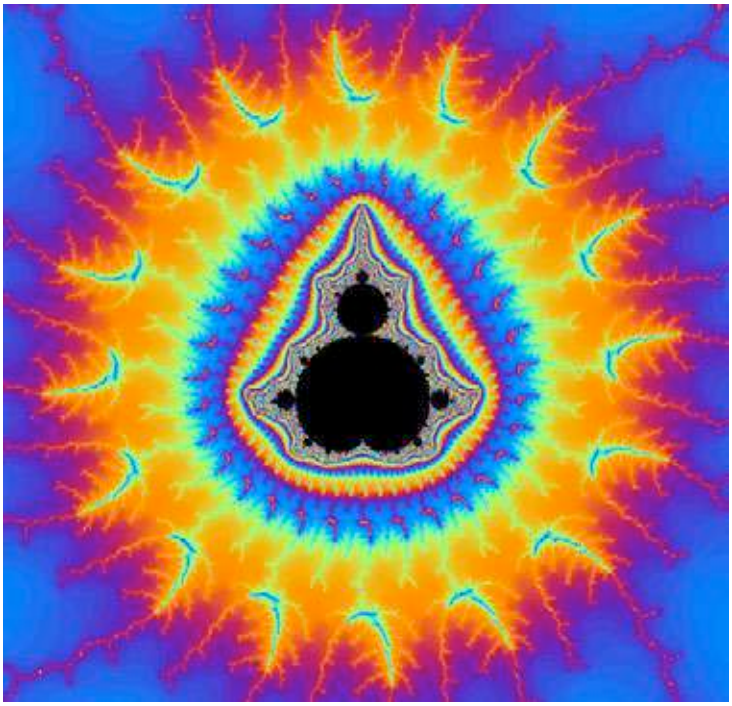

'Thao,' I asked, 'how are your walls transparent and yet we can't see in from the outside? And how can we pass through your walls as we did?'…

'You see, Michel, this habitation exists because of a magnetic field that is quite special. We have copied the forces of nature and the creations of nature to our own ends. Let me explain. Every body - human, animal or mineral - possesses a field around itself. The human body, for example, is surrounded both by an Aura and by an etheric force (field) of oval shape [at left]. You know that, don't you?' I nodded.

'The latter comprises, in part, electricity and, to a greater extent, vibrations that we call Ariacostinaki… These vibrations occur continuously for your protection while you are alive, and they are not to be confused with the vibrations of the Aura. With our habitations, we have copied nature in creating a field of mineral electro-etheric vibrations around a nucleus.' Thao indicated an 'egg', the size of an ostrich egg, located in the middle of the room between two seats… [as the nucleus.]

'This way,' she said, smiling again and taking several steps in another direction. 'Do you see this transparent drawer? Inside you have various compartments. From left to right: fish, shellfish, eggs, cheese, dairy products, vegetables and fruits, and here in the last, we have what you call 'manna', which is our bread…'

'You tell me that, on Earth, this bread is known as 'manna'. How is it that it exists on Earth at all?'

'It is a product we always carry on our intergalactic spacecraft… very practical… easily compressed and highly nourishing. In fact, it's a complete food. It comes from wheat and oats and you could live on it alone for months.'[13]

Michel's unusual descriptions of the giant egg-like domed magnetic fields of the buildings of the people of Thiaoouba reflect a simplicity and natural beauty that is profoundly inspiring. Thao's concise explanation of the etheric force field surrounding the ostrich-egg sized nucleus of the building was very carefully given in terms understandable to Michel, yet can be further understood in scientific terms. Each domed building is located at precise focal points of resonant infrasound standing waves, which become transduced by the resonant metal alloys of the nucleus into a vast electromagnetic field dome of the same shape.

The sacred *oval* or *egg* shape is repeated throughout Nature as reflections of the structure of the Universe, *the great ovum*. The *Ovocosmic* force can be described structurally by the Mandelbrot Set quadratic function [$z_{n+1} = z_n^2 + c$] (above), and the closely related function for nonlinear standing waves: [$z_{n+1} = z_n^2$]. The entire design of the Thiaoouban spiritual center of the City of Nine Dokos, home to the Seven Masters of the Thaori, conforms to this sacred cosmic force of resonant infrasound (opposite).

Thiaoouban *manna* bread was described as consisting of oats and wheat, while the electrical properties of invisible constituents including nanosilver and gold are indispensible for space travel, enabling the transdimensional effect of superconductivity of the human body for hyperleaps across the Universe. Gold and silver together comprise the ancient alloy *electrum*, so named for high electrical conductivity. Vedic scholars recently identified the Sanskrit term for electrum as *'Soma'*, described as granting eternal life through the luminosity of the electrum nanoparticles consumed in both foods and drinks:

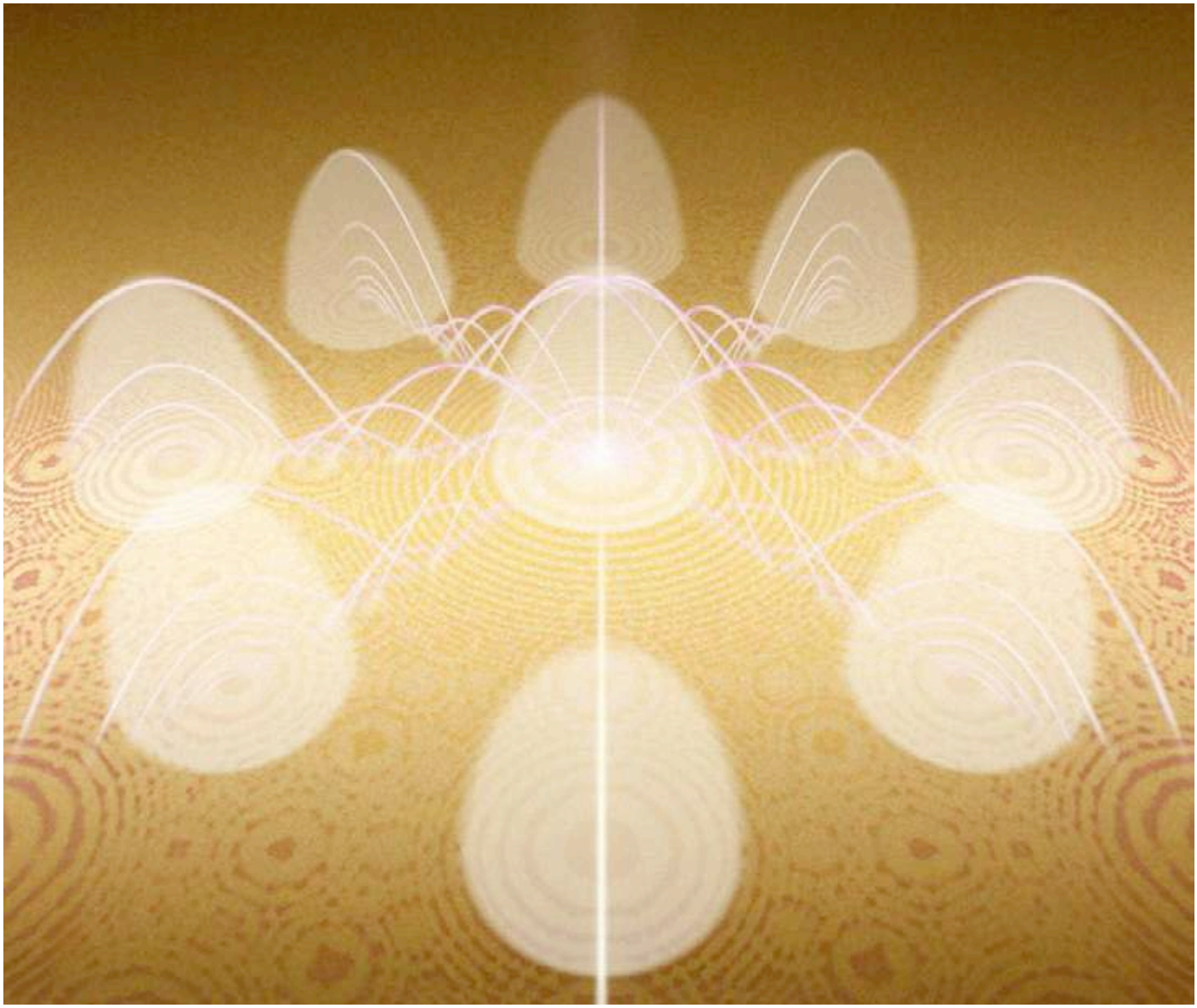

> "We have drunk the Soma and become immortal. We have attained the light the gods discovered." (Rig Veda: VIII.48.3)… "Soma is food for the gods. Gods eat Soma." (Chàndogya Upanishad: V.10.4)… "The man who supplies food hath always [his Soma] pressing stones adjusted, a wet Soma filter, well-prepared religious rites… he who hath this knowledge wins the luminous spheres." (Atharva Veda: IX.6)… *Soma*, *Soma* ma¯al, asemon, asem, *electrum* may perhaps denote the same substance… (which required the purificatory 'mineral waters') contained in the kaman.d.alu symbols in the icons of the yaks.a legacy. It may perhaps be the same substance said to be am°tam which was considered to be the elixir of life, of immortality. It may perhaps be the same substance referred to, in sheer poetry, as amritam *àyur hira¯yam*. Gold is immortality.[14]

Vedic hymns clearly identify the intracellular luminosity of electrum-enriched Soma waters and foods as endowing eternal life. Vedic wisdom also relates the yogic practice of levitation using the bodily force of *'laghima'* –an ability that Thao suddenly demonstrated for Michel while selecting Soma food preparations:

> 'We can, as readily, lift ourselves in the air, but that serves no great purpose other than our own amusement.' Having said that, Thao, who was sitting cross-legged, began to rise above her seat and floated about the room, finally coming to rest in mid-air. I stared at her, but soon realized I was the only one fascinated by her accomplishment. Indeed, I must have looked idiotic, for all eyes were fixed on me. Evidently, Thao's behavior was perfectly normal to my friends but they were more interested in the astonished expression on my face… Thao descended slowly on to her seat. 'That demonstrates one of the many sciences you have lost on Earth, Michel - apart from a few individuals who are still capable of doing it… There was a time when it was practiced by many, along with many other skills.' [15]

The demonstration of levitation given by Thao was one of many special lessons given to Michel on the golden planet. On Earth, this bioenergetic art form was practiced as one of the attainments, or *siddhis* known to Sanskrit adepts, in addition to being able to make one's body become larger or smaller, invisible or radiant, or instantaneously translocate or bilocate (being in two places at once). Thao would make demonstrations of other siddhis later during her discussions with Michel, and proceeded with a lesson on auras and color coordination for the balancing of physical health and consciousness:

'The colors of your robe were chosen according to those of your Aura; that's why you feel so good. If people on Earth were able to see Auras, they too could choose colors, which suit them and thereby enhance their feeling of well-being. They'd make use of color rather than aspirin…'

'I'll give you an example. Do you ever remember saying of someone: 'oh, those clothes don't suit you at all. He, or she, has no taste'? …If you were to suggest it be because of the colors they were wearing, they would think you odd. You could explain that the vibrations of the colors were in discord with those of their Auras, but they would be no more inclined to believe you. On your planet, people only believe in what they see or touch... and yet the Aura can be seen... The Aura vibrates constantly with colors that vary. At the top of your head is a veritable bouquet of colors, where almost all the colors you know are represented.

'Around the head too, is a golden halo, but it is only really obvious in the most highly spiritual people and in those who have sacrificed themselves in order to help someone else. The halo resembles a golden mist, much like painters on Earth depict the haloes of 'saints' and of Christ. The haloes were included in their paintings because, in those times, some of the artists actually saw them… The colors are all there in the Aura: some shine more strongly, others are dull. People in poor health, for example, or people with bad intentions... Many people on Earth could see it and read it a very long time ago, but there are few now. Calm yourself, Michel. You will see it, and not only one but several, including your own.'…

Approaching the coast, I could recognize enormous dokos, their points as usual towards the sky, I counted a group of nine, but the island was sprinkled with others, smaller and less visible amongst the vegetation. Thao took us higher and we were soon flying over what Thao called Kotra quo doj Doko - 'The City of the Nine Dokos'. Skillfully, Thao brought us down between the dokos, to a beautiful park located in their midst. In spite of my mask, I was aware that the golden mist that enveloped Thiaoouba was much denser around these dokos than elsewhere. Thao confirmed I was not mistaken in my perception…

Eventually, we reached the Central Doko and stopped below the entrance light. Thao seemed to concentrate for several seconds, then she took me by the shoulder and we passed through the wall… She immediately removed my mask, advising at the same time, that I half-closed my eyes, which I did. Light filtered through my lower lids and after a time, I was able to open my eyes normally… I must say, that this brightness, more golden than in my own doko, was considerably uncomfortable at first…

This doko must have been 100 meters in diameter. We headed directly, although more slowly, for the centre, where seven seats, each occupied, were arranged in a semi-circle. The occupants sat as though petrified and, at first, I thought them to be statues… In looks they resembled Thao, although their hair was longer and their facial expressions more serious, giving them the air of being older. Their eyes seemed to be illuminated from within, which was somewhat disturbing. What struck me most of all, was *the golden haze, even stronger here than outside, which seemed to concentrate in haloes around their heads…* When one of them raised a hand to indicate Thao and I should each take a seat facing them, I was indeed awestruck, and the word is feeble. I could not have imagined it possible that such radiant beings could exist: *it was as though they were on fire inside and emitting rays from within.*

They sat on block-like seats, fabric-covered, with straight backs. Each seat was of a different color - some only slightly different and others vastly different from their neighbors. Their clothes too, differed in color, suiting each wearer perfectly. All of them sat in what we call on Earth, the ‘lotus position’ that is, the sitting position of Buddha, with hands resting on knees… It was the central figure who addressed me, in a voice so melodious and, at the same time, so authoritarian. I was stunned by it, particularly since he spoke in perfect French. ‘You are welcome among us, Michel. May The Spirit assist and enlighten you.’ The others echoed: ‘May The Spirit enlighten you.’

He began to rise gently above his seat still in the lotus position, and floated towards me. This did not entirely surprise me since Thao had previously demonstrated this technique of levitation. I wanted to rise before this undoubtedly great and highly spiritual personage, as a measure of the infinite respect inspired in me. In trying to move, I found I couldn’t - as though paralyzed in my seat… He stopped just above and in front of me, placing both his hands on my head; the thumbs joined on my forehead above my nose, opposite the pineal gland, and the fingers joined at the top of my head. It was Thao who described these details to me later, for at the time, I was overwhelmed by such a sensation, that the details didn’t register.

During the time his hands were on my head, it seemed that my body no longer existed. A gentle warmth and delicate perfume originated within me, emanating in waves and blending with soft music that was barely audible… Suddenly, I could see amazing colors surrounding the figures opposite me and, as the ‘leader’ returned slowly towards his seat, I could see a multitude of radiant colors around him; ones I had been unable to perceive before. The principal color was a mass of pale pink which enveloped the seven figures, as though in a cloud, and their movements caused that wonderful, glowing pink to encircle us also!

When I had sufficiently recovered my senses to turn towards Thao, she too, was surrounded with wonderful colors, although less brilliant than those around the seven figures… You will notice that, in speaking of these great personages, I instinctively use ‘he’ rather than ‘she’. In explaining this, I can only suggest that the personalities of these special beings were so strong and their bearings so imposing, that I recognized more of the masculine in them than the feminine –I mean no offence to women– my reaction was instinctive... However, women or men, they had transformed me. I knew that the colors surrounding them were their Auras. I was capable of seeing Auras –who knew for how long– and I wondered at what I saw.

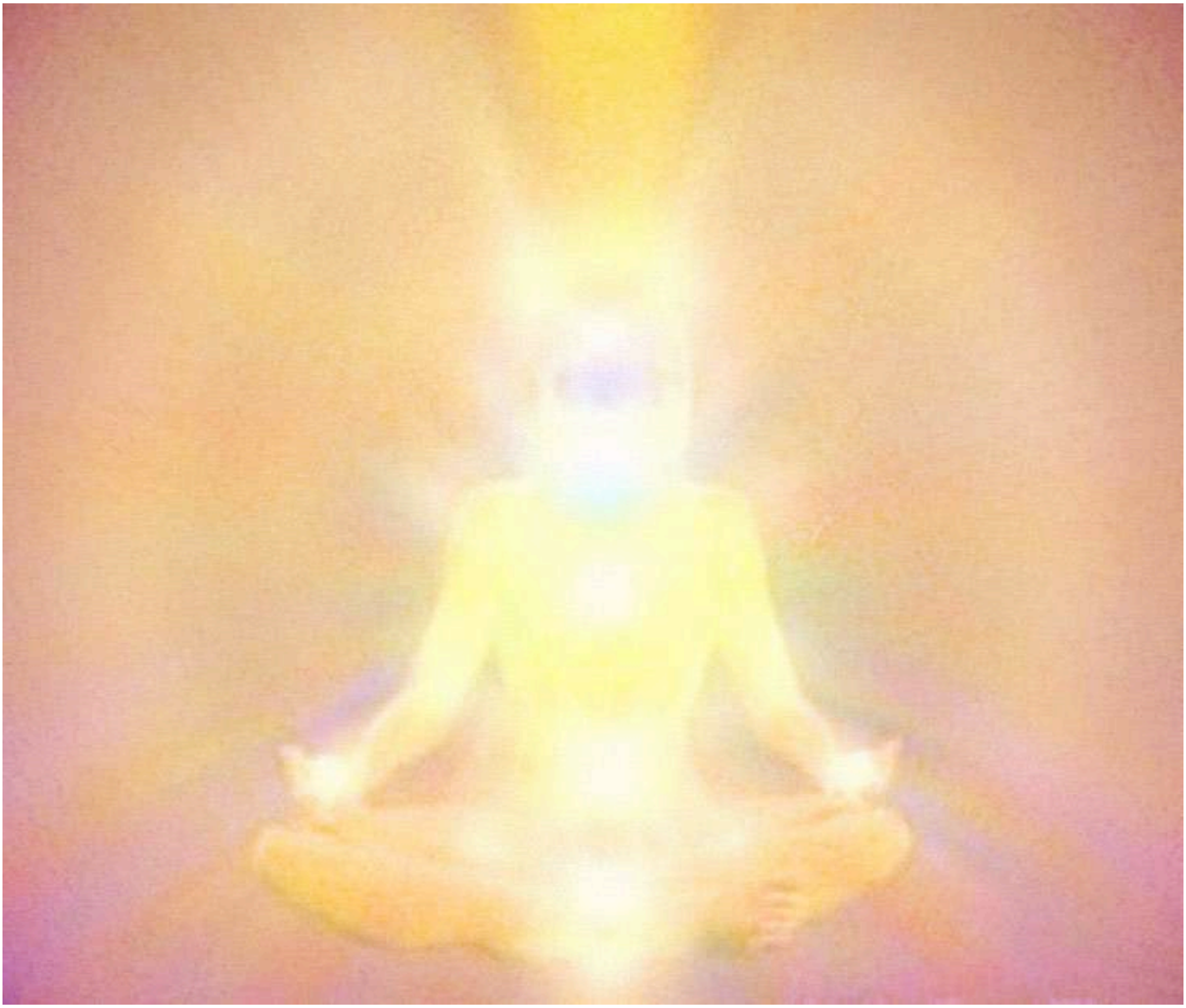

The ‘leader’ had resumed his seat and all eyes were fixed on me, as if they wanted to see inside me, which indeed, is what they were doing. Silence reigned for a time, which seemed interminable. I watched the varied colors of their Auras vibrate and dance around them, sometimes far in the distance and recognized the ‘bouquet of color’ Thao had spoken of earlier… The golden haloes, clearly defined, were almost saffron colored. It occurred to me, they could not only see my Aura, but possibly read it as well. I suddenly felt quite naked before this learned assembly. The question that haunted me was: why have they brought me here?

Abruptly, the ‘leader’ broke the silence. ‘As Thao has already explained to you, Michel, you have been chosen by us, to visit our planet, in order to report certain messages and to offer enlightenment on several important issues when you return to Earth. The time has come when certain events must occur. After several thousand years of darkness and savagery on the planet Earth, a so-called ‘civilization’ appeared and, inevitably, technology was developed –a development, which was accelerated during the last 150 years.

‘It has been 14,500 years since a comparable level of technological advance existed on Earth. This technology, which is nothing compared with true knowledge, is nevertheless, sufficiently advanced to become harmful to the human race on Earth in the very near future… harmful, because it is only material knowledge and not spiritual knowledge. Technology should assist spiritual development, not confine people, more and more, within a materialistic world, as is happening now on your planet… To an even greater extent, your people are obsessed with a single goal - affluence. Their lives are concerned with all that the pursuit of wealth entails; envy, jealousy, hatred of those richer and contempt for those poorer. In other words your technology, which is nothing compared with what existed on Earth more than 14,500 years ago, is dragging your civilization down, and pushing it closer and closer to moral and spiritual catastrophe.’

I noticed that each time this great personage spoke of materialism, his Aura and those of his acolytes, flashed with a dull and ‘dirty’ red, as though momentarily, they were in the middle of burning bushes. ‘We, the people of Thiaoouba, are assigned to assist, guide and sometimes punish the inhabitants of planets under our guardianship.’ Fortunately, Thao had briefed me on Earth’s history during our journey to Thiaoouba. Otherwise, I’d have surely fallen off my seat on hearing such a speech.

‘I think,’ he resumed, ‘that you already know what we mean by ‘harmful to the human race’. Many people on Earth believe atomic arms to be the major danger, but it is not so. The greatest danger concerns ‘materialism’. The people of your planet seek money - to some it’s a means of attaining power; to others it’s a means to acquire drugs (another curse), yet to others, it’s a way of possessing more than their neighbors possess…

‘Now, once and for always, we will teach you and provide you with what you French call ‘the key to the mystery’… As you have heard, in the beginning there was the Spirit alone and he created, by his immense force, all that exists materially. He created the planets, the suns, plants, animals, with one goal in mind: to satisfy his spiritual need. This is quite logical since he is purely spirit. Already I see you are wondering why the need to create material things in order to attain spiritual fulfillment. I offer this, by way of explanation: the creator sought spiritual experiences through a material world… In order to have these experiences, he wanted to embody a tiny part of his Spirit in a physical entity. To do this, he called on the Fourth force - the force which Thao has not yet spoken of and which concerns only spirituality. In this domain, Universal Law also applies.

‘You most certainly know that the pattern of the Universe dictates that nine planets revolve around their sun. It is also the case that these suns revolve around a bigger sun, which is the nucleus for nine such suns, and their nine planets… Certain accidents occur and sometimes a planet will disappear in a solar system, or perhaps enter it, but later in time, the solar system will revert and base its structure again on the number nine.

‘The Fourth force had a very important role to play: it had to bring to fruition all that the Spirit had imagined. It ‘inserted’ thus, an infinitesimal part of the Spirit in the human body. This comprises what you could call the Astral body, which forms one ninth of the essential human being and consists of one ninth of a ‘Higher-self’, which is sometimes called ‘overself'. The Higher-self of man is, in other words, an entity which sends one ninth of itself into a human body, becoming the person’s Astral being. Other physical bodies are inhabited, similarly, by other ninths of the same Higher-self and yet each part remains integral to the central entity… Further, the Higher-self is a ninth part of a superior Higher-self which, in turn, is a ninth part of a more superior Higher-self. The process continues as far back as the source, and allows the enormous filtration of spiritual experience required by the Spirit.

‘You must not think that the Higher-self of the first category is insignificant in comparison with the others. It functions at a lower level, but is nevertheless extremely powerful and important. It is capable of curing illness and even resuscitating the dead. There are many instances of people, declared clinically dead, who are brought back to life in the hands of doctors who had abandoned all hope for them. What generally happens in these cases, is that the person’s Astral body meets with the Higher-self. This portion of the Higher-self has left the physical body during the period of ‘death’. It perceives its physical body below, and the doctors trying to resuscitate it; it can also perceive loved ones who mourn for it. In his present state, the Astral body, the person will feel perfectly well –even blissful. Usually he abandons his physical body, frequently the source of much suffering, to find himself catapulted down a ‘psychic canal’, at the end of which is a wondrous light and beyond, a state of bliss.

‘If before passing through this canal into the blissful light which is his Higher- self he has the least will not to die –not on his own account but for the sake of those who need him, young children for example, he will ask to return. In certain cases it will be permitted… You are in constant communication with your Higher-self by means of your cerebral canal. Acting as a transmitting and receiving post, it conducts special vibrations directly between your Astral body and your Higher-self. Your Higher-self monitors you continually, by day and by night and can intervene to save you from an accident.

‘Someone, for example, who is to catch a plane, finds that the taxi breaks down on the way to the airport; a second taxi called also breaks down - just like that... Could you really believe in such a coincidence? The plane in question crashes thirty minutes later, leaving no survivors. Another person, an old and rheumatic woman and barely able to walk, starts to cross a street. There is a loud horn blast and a screeching of tires, but this person is miraculously able to leap to safety.

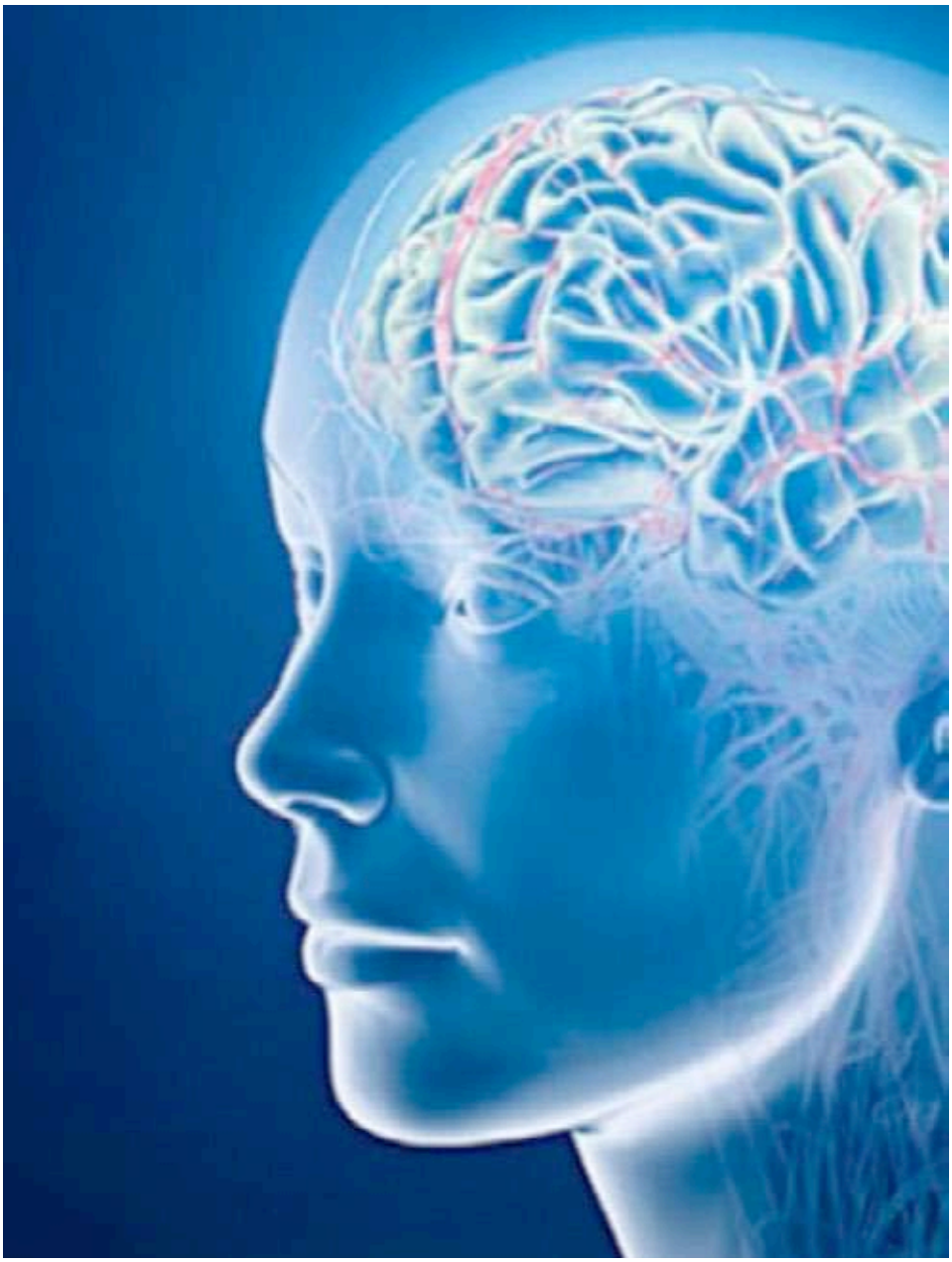

‘How is this explained? It was not yet her time to die and so her Higher-self intervened. In one hundredth of a second the Higher-self triggered a reaction in her adrenaline glands, which, for a few seconds, provided enough strength to her muscles to enable her to execute the leap which saved her life. Adrenaline released into the blood can make it possible to flee from imminent danger, or to defeat the ‘unbeatable’ through anger or fear. In too strong a dose, however, adrenaline becomes a lethal poison.

‘It isn’t only the cerebral canal which is able to conduct messages between the Higher-self and the Astral body. Another channel exists sometimes in dreams –or, I should even say, in sleep. At certain times during sleep, your Higher-self is able to call your Astral body to itself and, either communicate instructions or ideas, or to regenerate it in some way, replenishing its spiritual strength or enlightening it in regard to solutions to important problems. For this reason, it is essential your sleep is undisturbed by intrusive noise or by nightmares resulting from harmful impressions received during the day. Perhaps you will better understand the importance of your old French saying: ‘Night brings counsel’.

‘The physical body in which you exist at the moment is already very complex, but still, it is nothing compared with the complexity of the process of evolvement which occurs with Astral bodies and Higher-selves. In order to allow ordinary people on your planet to understand as easily as possible, I will make my explanation in the simplest terms… Your Astral body, which inhabits every normal human being, transfers to its Higher-self all the sensations that are experienced during a lifetime in a physical body. These sensations pass through the immense ‘filter’ of nine Higher-selves before arriving in the etheric ‘ocean’ that surrounds the Spirit. If these sensations are based essentially on materialism, the Higher-selves have enormous trouble filtering them, just as a water filter clogs quicker if it filters dirty water than if the water was already clear…

‘If, through the numerous experiences you have in your life, you ensure your Astral body benefits in a spiritual sense, it will acquire more and more spiritual understanding. In time, which can vary from 500 to even 15,000 of your Earth years, your Higher-self will have nothing more to filter…

This part of itself, embodied in the Astral being of Michel Desmarquet, will be so spiritually advanced, it will have arrived at the next stage where it will have to contend directly with the more superior Higher-self… We can compare this process with a nine-stage filter, intended to rid the water passing through, of nine elements. At the end of stage one in the process, one will have been completely eliminated, with eight remaining. Of course, to make this information easier to digest, I am making enormous use of imagery...

'This Astral body then, will have completed its cycle with the Higher-self of the first category and will then detach itself from Higher-self number one to rejoin the Higher-self of the second category; the entire process will be repeated. By the same token, the Astral body will be sufficiently spiritually advanced to pass to a planet of the next category, as well…

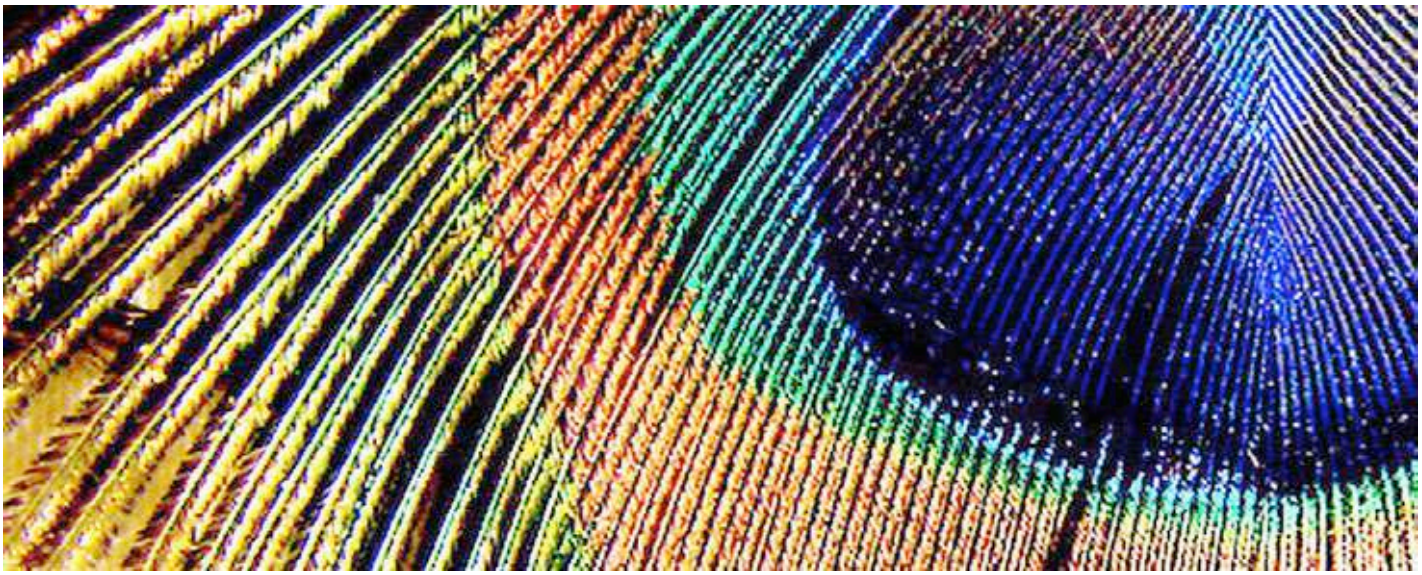

'In his wisdom, The Spirit, by means of the Fourth force, provided for nine categories of planets. At present, you are on the planet Thiaoouba which is in the ninth category; that is, at the top of the scale… Earth is a planet of the first category and therefore at the bottom of the scale. What does this mean? The planet Earth could be likened to a kindergarten with the emphasis on teaching basic social values. A planet of the second category would then correspond with a primary school where further values are taught - in both schools, adult guidance is imperative. The third category would comprise secondary schools where a foundation of values allows exploration beyond. Next, you would go to university, where you are treated as an adult, for you would not only have attained a certain amount of knowledge, but you would also start to accept civic responsibility.

'This is the type of progress occurring with the nine categories of planets. The more spiritually advanced you are, the more you will benefit, on a superior planet, by an environment and general way of life which is superior. The very way in which you procure food is much easier, which in turn, simplifies the process of organizing your way of life; the consequence is more effective spiritual development. On the higher planets, Nature itself, enters the stage to assist 'the pupil' and, by the time you reach planets of the sixth, seventh, eighth and ninth category, not only is your Astral body highly evolved, your physical body has also benefited from your development.

'We know you have already been favorably impressed by what you have seen on our planet. As you see more, you will appreciate that it is what you would call on Earth, 'a paradise'; and yet, compared with true happiness, when you become a pure spirit, it is still nothing… From this planet, it is possible either to remain in a physical body or be reunited with the Great Spirit in the ether.' As these words were uttered, the Aura surrounding the leader shone more brightly than ever and I was surprised to see him almost disappear in a golden mist, only to reappear a second later.

'You have understood that the Astral body is a body which inhabits your physical body recalling and noting all the understanding acquired during the course of its various lives… It can only be enriched spiritually - not materially. The physical body is merely a vehicle which, in most cases we abandon when we die… I will elaborate, for I see that 'in most cases' has confused you. By this, I mean that some of us, including all on our planet, are able to regenerate the cells of our bodies at will. Yes, you have already noticed that most of us seem to be of the same age. We are one of three planets that are the most highly evolved in this galaxy. Some of us can, and do, directly join what we call the great ether.

‘So, on this particular planet, we have arrived at a stage near perfection, both materially and spiritually. But we have our roles to perform, as does every creature existing in the universe; in fact, everything, including a single pebble, has its role… Our role, as beings of a superior planet, is to guide – to help with spiritual development and even, sometimes, materially. We are in a position to give material assistance because we are technologically the most advanced people. Indeed, how could a father give spiritual guidance to his child if he were not older, more educated and more skilled in diplomacy than the child? If the child should require physical punishment, as unfortunately, is sometimes the case, isn’t it important that the parent be physically stronger than the child? Certain adults, who refuse to listen and who are absolutely stubborn, also need to be corrected by physical means.‘

‘You, Michel, come from the planet Earth, which is sometimes called ‘The Planet of Sorrows’. Indeed, the name is appropriate, but it is this way for a precise reason - it is intended to provide a learning environment of a quite specific kind. It is not because life there is so difficult that you have to intervene - you cannot lightly go against Nature, destroying rather than conserving what the Creator has put at your disposal; that is, interfering with ecological systems, which have been intricately designed. Certain countries, like Australia, where you are from, are beginning to show great respect for ecology and it is a step in the right direction; but even in that country, what case is made of pollution - both water and air pollution? What is ever done about one of the worst forms of pollution? *Noise.* [Damage to sensitive auditory cells in the cochlea, seen below, is but one of many dangers.]

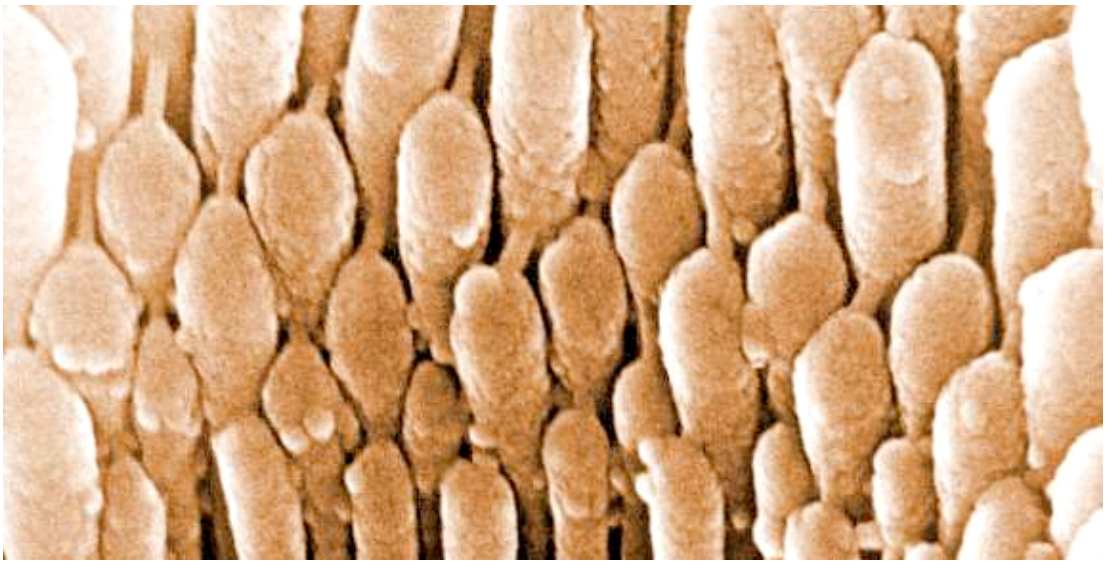

‘I say ‘worst’ because people such as Australians pay virtually no attention to it at all… Ask someone if traffic noise bothers him and the response will surprise you - eighty five percent of the time it will be; ‘What noise? What are you talking about? Oh that noise - we get used to it.’ And it is precisely because they ‘get used to it’ that the danger exists.’

Just then, Thaora, as this high figure was called, made a gesture and I turned around. He was replying to a question I had mentally posed; ‘How can he speak of percentages and know so much about our planet with so much precision?’ Turning around, I almost uttered a cry of surprise for, behind me, stood Biastra and Latoli. In itself, this was nothing surprising, but the friends I knew who measured 310 and 280 centimeters in height respectively, were now reduced in size to correspond with my height. My mouth must have continued to gape, for Thaora smiled.

‘Can you understand, that sometimes, and very often in these days, some of us live among your people on Earth? - and there is my answer to your question. To continue on the very important subject of noise, it is such a danger that, if nothing is done, catastrophe is certain… Let us take the example of a discotheque. The people who expose themselves to music that is typically played three times too loudly, are subjecting their brains and their physiological and astral bodies to vibrations which are so harmful. If they could see the damage that is caused, they would vacate the discotheque quicker than if there was a fire.

‘But vibrations don’t only come from noise; they also come from colors and it is astonishing that, on your planet, experiments conducted in this field have not been followed up.[16] Our ‘agents’ reported a particular experiment involving a man who was capable of lifting a certain weight. It was found that after staring for a moment at a pink-colored screen, he consistently lost thirty percent of his strength… Your civilization pays no attention to such experimentation. In fact, colors can enormously influence the behavior of human beings and yet, control of this influence requires that an individual’s Aura be taken into account. If for example, you want to paint or wallpaper your bedroom with the colors that are truly appropriate for you, you must be aware of the colors of certain principal points of your Aura.

‘By matching the colors of your walls with those of your Aura, you can improve your health or maintain good health. Further, the vibrations emanating from these colors are essential for good mental balance, exerting their influence even while you sleep.’ I was wondering how we could be expected to know these significant colors in our Auras when, on Earth, we were not capable of perceiving Auras… Thaora replied immediately, without me having to say a word aloud.

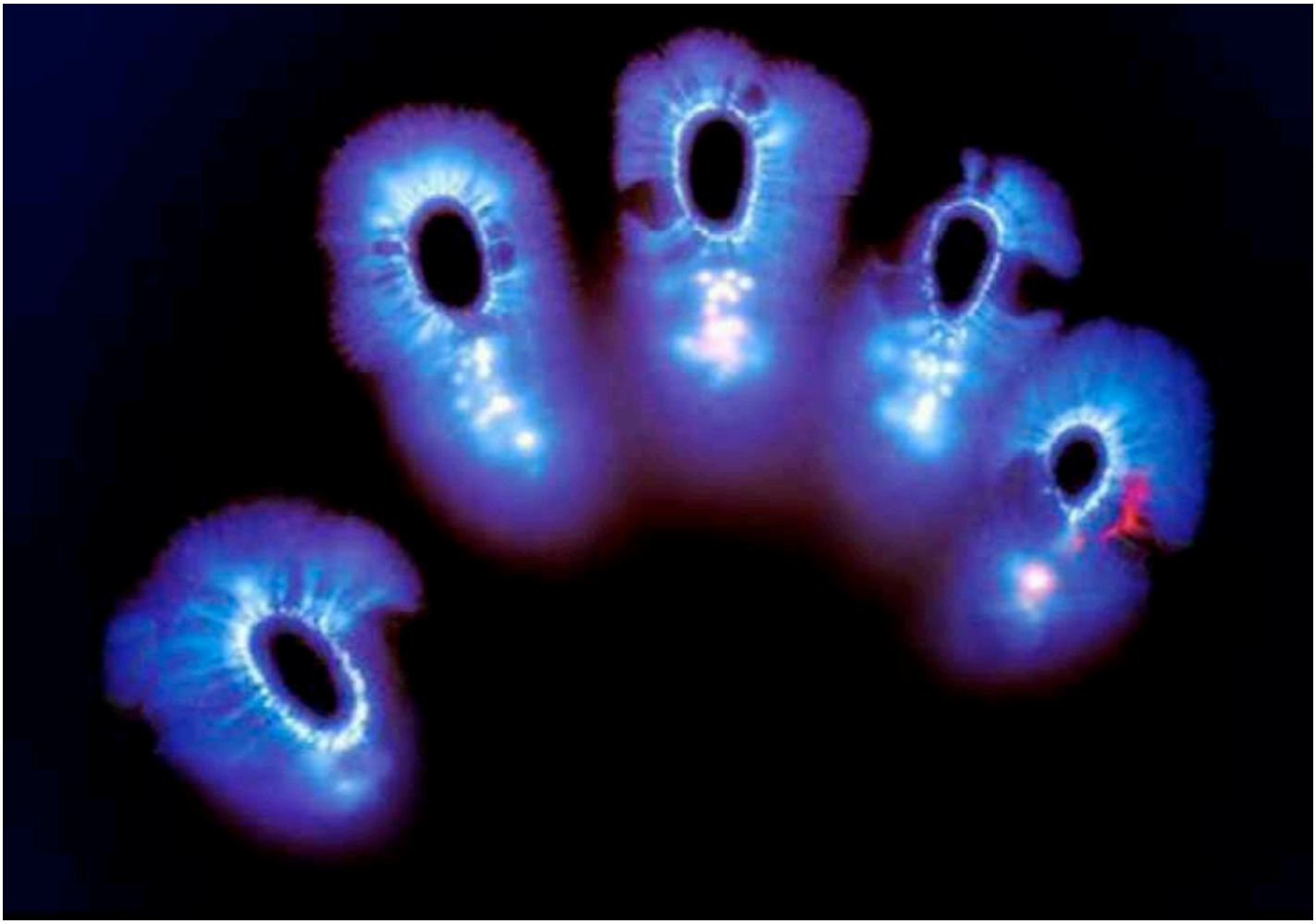

‘Michel, it is now very important that your experts invent the special equipment necessary, to enable perception of the Aura, as this, in turn, will ensure that correct choices are made at the critical crossroads ahead… The Russians have already photographed the Aura [as Kirlian photography – seen above, opposite]. This is the beginning, but the results obtained allow them only to read the first two letters of the alphabet, as it were, in comparison with what we are able to decipher. The reading of the Aura in order to heal the physical body is nothing compared with what such a reading can achieve for the psychic body, or the physiological body. It is in the area of the psyche that, on Earth, your greatest problems exist.

‘At the moment, most responsibility is taken for the physical body, but this is a serious mistake. If your psyche is poor, it will influence your physical appearance accordingly, but, regardless, your physical body will wear out and die one day, whereas your psyche, being part of your Astral body, never dies. On the contrary, the more you cultivate your mind, the less you will be burdened by your physical body and the quicker you will proceed through your cycle of lives… We could have brought you to our planet in Astral body, but instead, we have brought you here in physical body - and for an important reason. I see you already understand our reason. This pleases us and we thank you for your willingness to assist us in our task.’

The Thaora stopped talking and seemed to lapse into thought, at the same time, fixing me with his luminous eyes. I cannot say how much time elapsed. I know my state became more and more euphoric and I was aware that the Auras of the seven personages were gradually changing. The colors became more vivid in places, softer in others, while the outer edges became misty. This mist became more golden and pink as it spread, gradually blurring the seven figures.[17]

The profound wealth of imagery, wisdom and spiritual knowledge transmitted by the Thaori during the fourth-density plasma experiences of Michel Desmarquet on the golden planet of Thiaoouba resonate with the highest teachings available to Earthly humanity. The importance of Aura photography, known as Kirlian photography among Russian biophysicists and referred to as 'electro-photonics' by Thao, is decisive in not only the deepening of our understanding of the effects of color on human perception, but as well it represents the beginning of high-energy applications of HHO plasma to the human body. While clearly visible gaps in electrical conductivity observed along the fingertips has already shown promise in reflecting the state of health of specific organs (quite useful in diagnostic readings), the more advanced beam healing systems now biocompatible and effective in rapid cellular rejuvenation.

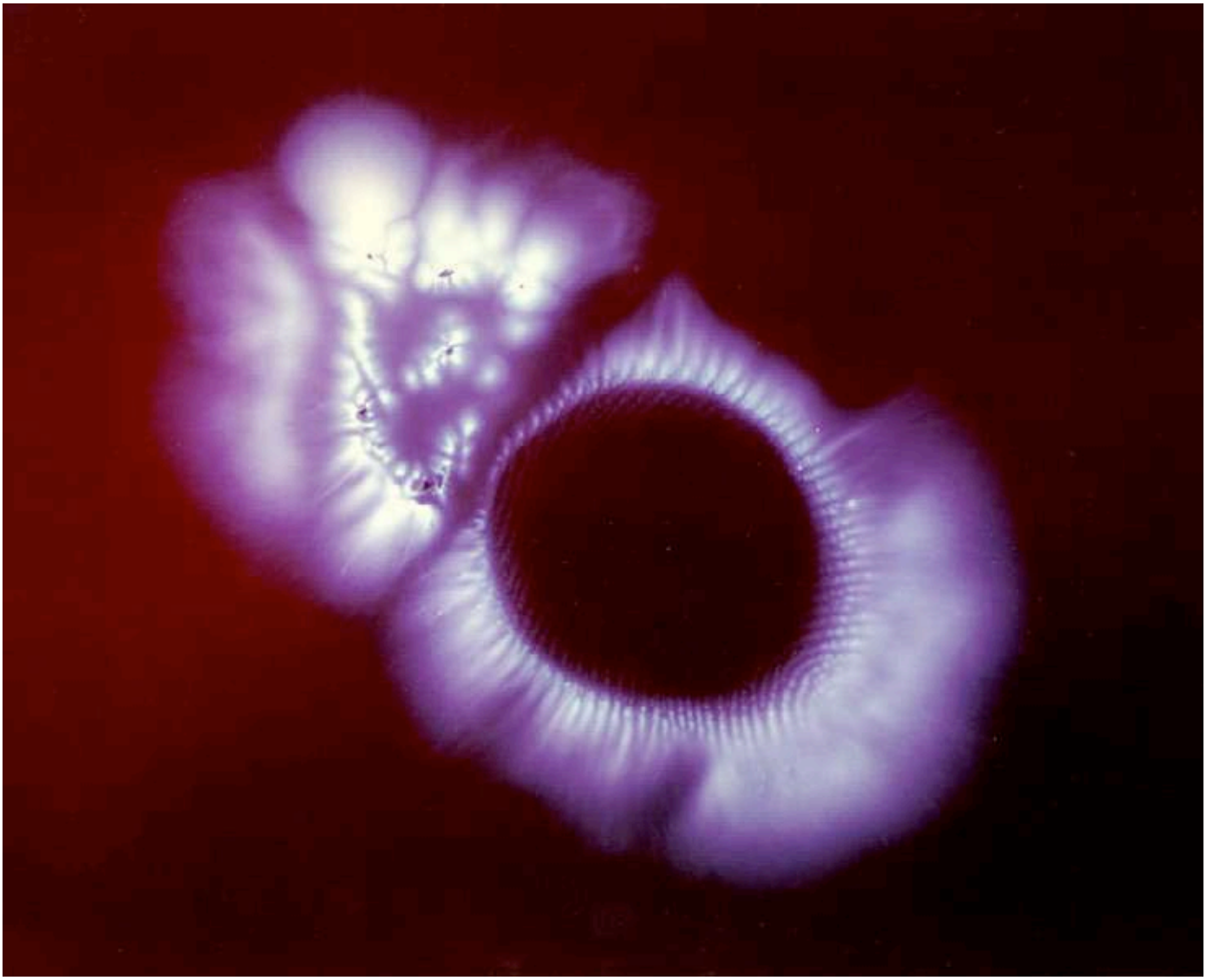

While the field of dentistry now applies nanosecond electrical pulses to ionize the HHO plasma at low temperatures to form biocompatible helium/oxygen plasmas for oral cleaning and sterilization,[18] an unnoticed effect of cellular regeneration is also occurring. The application of HHO plasma to the cleansing of the human body promises a significant reduction in the rate of cellular aging when the proper sources of lightwater (protium) are ingested. The bioelectric effect of electroporation, whereby cellular permeability is significantly lowered by rapid, milliampere electrical pulses, and can be only be generated throughout all of the body's cells using electroluminescent gold and silver nanoparticles. Natural safeguards for immersion in the fourth-density HHO plasma environment provide for a limit to 9 full days of exposure, as succinctly explained to Michel by another temporary visitor to the golden Thiaoouba. The intense luminosity of the atmospheric HHO plasma inevitably intoxicates low-resonance human bodies:

‘An Astral body absolutely cannot change to a superior planet until sufficiently evolved [in spirit]… This evolution occurs thanks to the physical body that improves as it progresses right up as far as this planet. You have already learned of the nine categories of planets –ours are at the bottom of the scale. We, in our present physical bodies, can be permitted only nine days’ stay here. According to Universal Law, on the tenth day, our physical bodies would die and neither Thao nor the great Thaora, within whose power it is to revive the dead, would be able to prevent or reverse the process. Nature has very inflexible rules with well-established safeguards… But it is possible that when you do die on Earth –when your moment has come– your Astral body will reincarnate in a body on… a second or perhaps third category planet… [Through reincarnation] we must be ‘reprocessed’ over and over until we emerge perfect, for eventually we will rejoin The Spirit who, being perfect himself, cannot accept the slightest imperfection.’

Around each planet, since its creation, is a kind of *psychosphere* or vibratory cocoon, which turns at a speed seven times that of light [or 1,302,000 miles per second]. This cocoon acts as a blotter, as it were, absorbing (and remembering) absolutely every event occurring on the planet… The human being, comprising an integral part of the universe can, because of his Astral body and if he is correctly trained, draw what knowledge he seeks from within the psychosphere. Of course, great training is required for this.[19]

This description of the psychosphere corresponds closely with the ancient Sanskrit concept of the *akashic field*, the mnemonic body of the planet that spirals around the Earth through the pathways of standing infrasound waves (illustrated above). The (Van Allen) plasma belt that encompasses Earth possesses superfluid crystalline properties that may act as a form of cosmic memory storage.

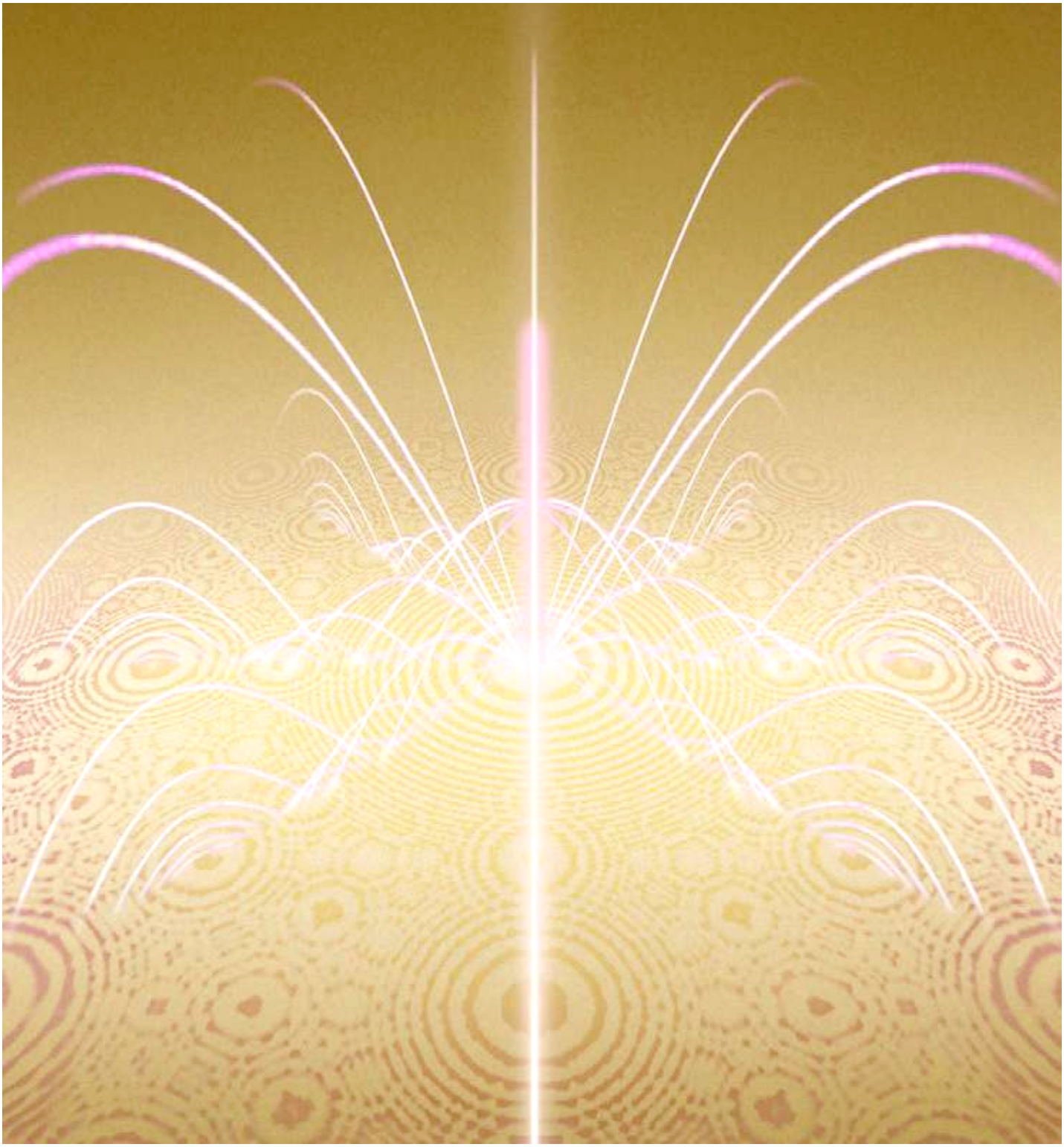

The subconscious mind is in constant contact with the planetary psychosphere where all the information of all past and future lives is stored, as elucidated by the Sleeping Prophet Edgar Cayce, in so many astoundingly advanced spiritual readings from the era of the industrial revolution. While Cayce had a unique ability to access the psychosphere directly during trance, Thao explained that most inexplicable moments of déjà vu are attributable to *akashic future life previews* shown by the Higher-self:

> [A]fter having seen his life… flash before him, and, after accepting to live that life, all details of it were erased from his memory. He passed through what certain Nagas have called 'The River of Oblivion' - this happens whether one accepts or rejects a possible reincarnation. Of course, there is a reason for it.

‘If, for example, you remembered that, around forty years of age, you would lose your wife and two cherished children in a car accident and that you, yourself, would be confined to a wheelchair, the knowledge could tempt you to take your life rather than face up to your troubles, or it might lead you to behave badly in other spheres. So, the ‘film’ is erased, in something like the way you ‘wipe out’ a tape recording.

‘Occasionally, by accident, the machine does not erase everything and you can hear brief portions of what should have been erased. Of course, my analogies are fanciful when I speak of ‘films’ and ‘tape recordings’ but I hope they give you an idea of what I am trying to explain. In reality, the process involves electro-photonics, which mean nothing, yet, to people on Earth. This, in fact, occurs often in the ‘films’ that the Higher-self shows to an Astral body, which is why most people say, on several occasions in the course of their lives ‘I have seen that before’ or ‘I have heard that before’ and they know what the very next action or word will be. In English, people call this feeling ‘déjà vu’.’ [20]

‘Michel… you were chosen by us to visit Thiaoouba, but the essential motive for our choice has not been revealed. It is not only because you have a mind already awakened and open, but also –and principally– because you are one of the rare soukous inhabiting Earth at the present time. A ‘soukou’ is an Astral body that has lived eighty-one lives in human physical bodies, and has lived those lives on different planets or different categories. For various reasons, the ‘soukous’ return to live on inferior planets, like Earth, when they could just as well continue to ‘climb the ladder’ without ever going backwards. You know that the number nine is the number of the Universe. You are here in the City of Nine Dokos, founded on Universal Law. Your Astral body has nine times nine lives, which brings you to the end of one of the great cycles.’

Once again, I was completely flabbergasted. I suspected I wasn’t living my first life… –but eighty-one lives! I didn’t know one lived so many… ‘It’s possible to live many more, Michel,’ said the Thaora, interrupting my thoughts. ‘Thao is up to her 216th, but other entities live far fewer. As I said, you have been chosen from among very few ‘soukous’ living on Earth, but, in order that you acquire a thorough understanding during the trip to our planet, we have planned another journey in time for you. So that you will better understand what reincarnation is, and what its purpose is, we will permit you to revisit your previous existences. This journey in time will be useful to you when writing your book as you will fully comprehend its purpose.’ [21]

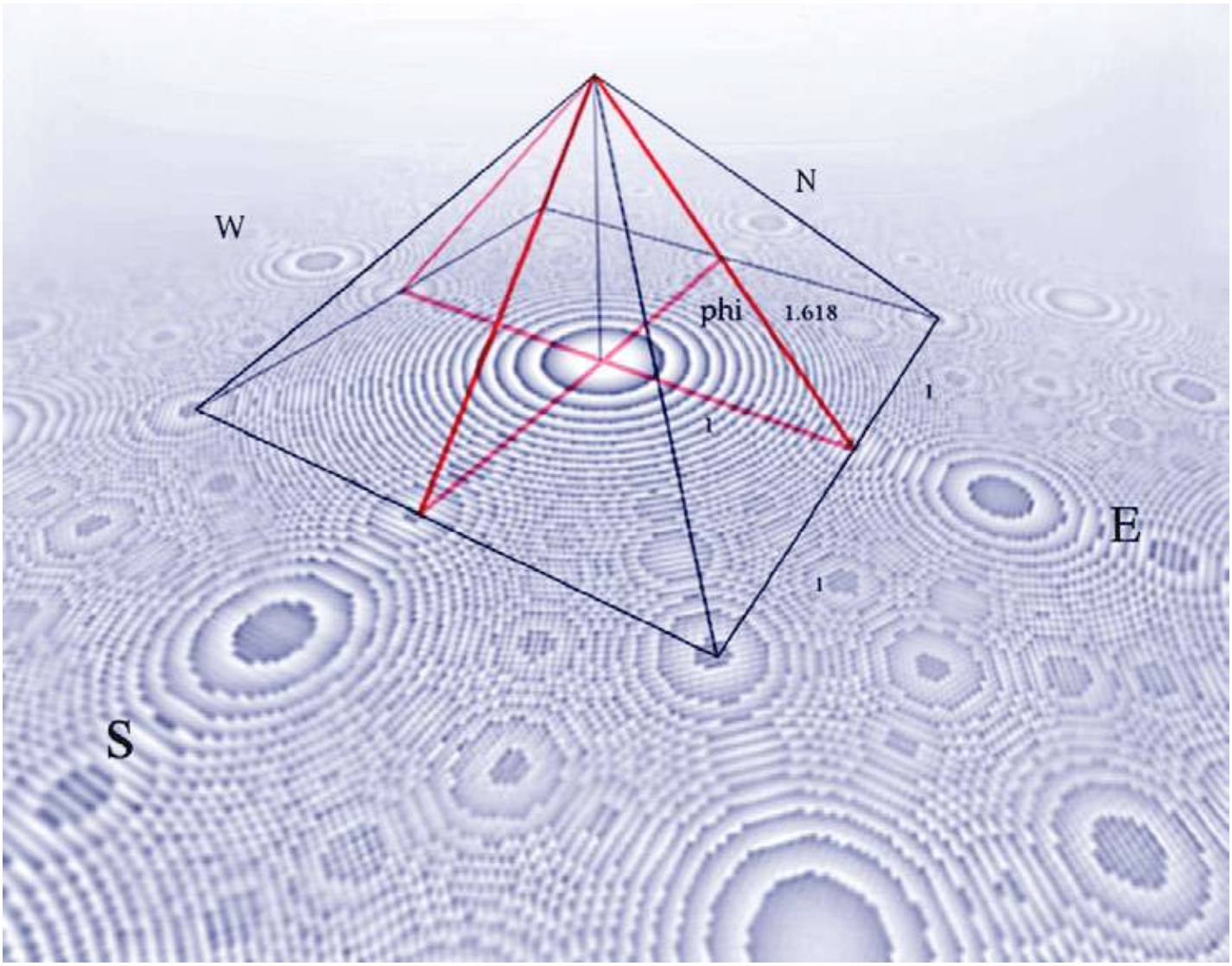

Absolutely all of the events of past lives are stored within the psychosphere and remain accessible to highly attuned adepts of meditation. The ancient pyramid technologies were developed to enhance the psychoacoustic conditions that engender *synesthesia*, a form of holographic consciousness. *The global network of ancient pyramids function as one synchronous unit, balancing the biorhythms of initiates into telepathic communication with other worlds*:

> 'I must finish off my story concerning the continent of Mu… Savanasa then, was situated on a vast plateau overlooking plains which rose, on average, no more than 30 meters above sea level. On this plateau and in the centre, an enormous pyramid was constructed. Each stone used in its construction, some weighing more than 50 tons, was cut precisely to within one fifth of a millimeter, using what we can call 'ultrasonic vibratory systems'. [These ultrasonic pulse cutting techniques were developed by scientists in 2009.[22]] This was done in the quarries of Holaton, now found on Easter Island, which was the one place on the entire continent where this special rock could be found. There was, however, another quarry at Notora, southwest of the continent.
>
> 'The enormous stones were transported using anti-gravitational techniques well known to these people. (They were carried on platforms, 20 centimeters above the paved roads, and were constructed using the same principals as those of the pyramids.) Roads such as these were built all over the country, converging, like a massive spider's web, on the capital, Savanasa.
>
> 'The huge stones were taken to Savanasa and put into position according to directions from the 'master' or chief architect on the project. When finished, the pyramid measured exactly 440.01 meters in height and its four faces were oriented precisely towards the four points of the compass [as seen above].'
>
> 'Was this intended to be the King's palace, or his tomb?' Everyone wore the same indulgent smile that often appeared when I asked a question.

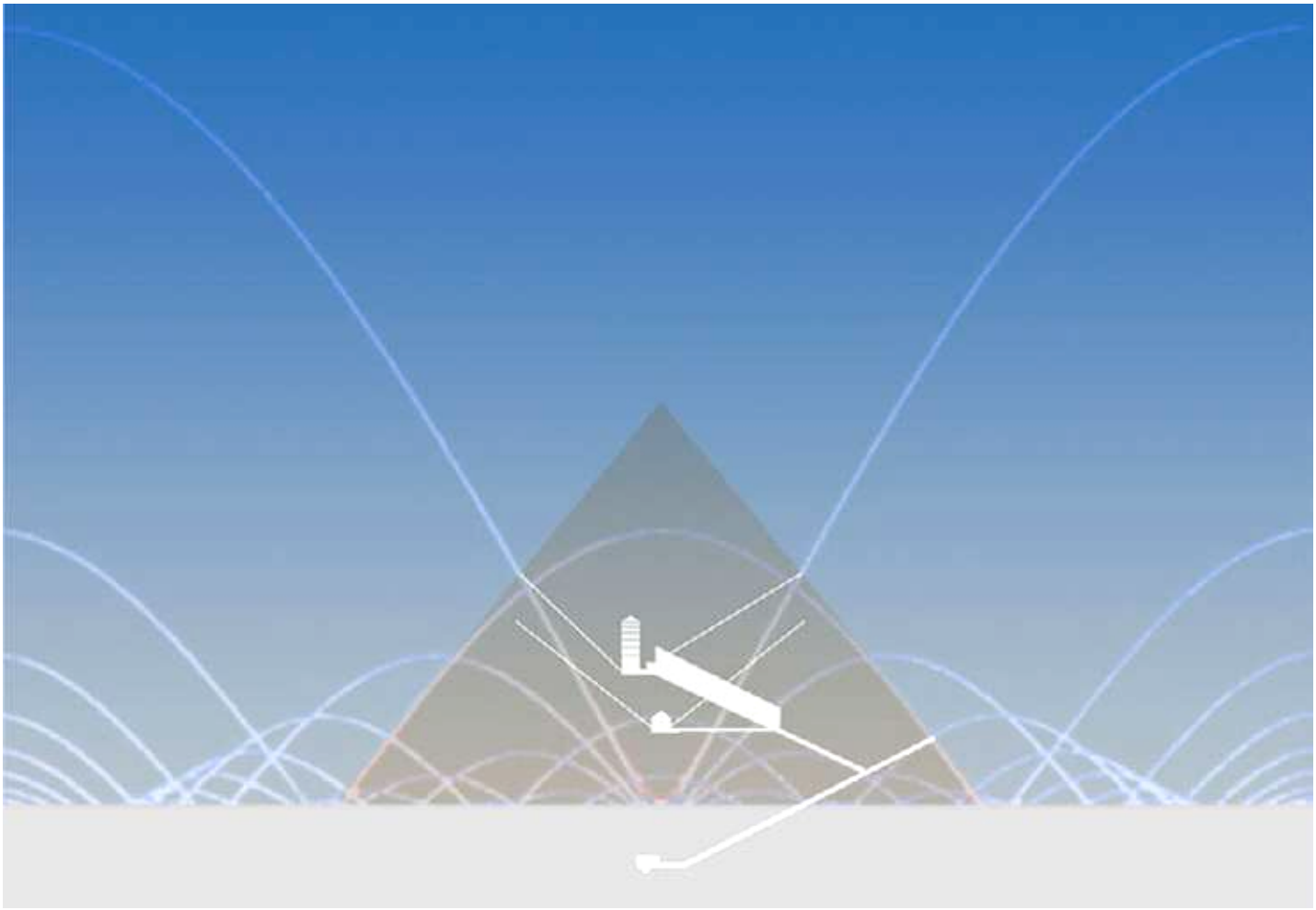

> ‘Nothing of the sort, Michel. This pyramid was much more important - it was a tool. An enormous tool, I admit, but a tool just the same. So, too, was the Pyramid of Cheops, in Egypt, though it was much smaller… You will have realized… these were highly advanced people. They possessed a profound understanding of Universal Law and used their pyramid as a ‘captor’ of cosmic rays, forces and energies, as well as terrestrial energies…
>
> Inside, rooms positioned according to a precise plan, served the King and certain other great initiates, as powerful communications centers, enabling (telepathic) communication with other planets and other worlds in the universe. Such communication with extraterrestrials is no longer possible for people on Earth; but the people of Mu in those days, by natural means and by exploiting cosmic forces, were in constant communication with other beings and were even able to explore parallel universes…
>
> [The pyramid’s] second use was to make rain. By a system of plates, made of a special alloy incorporating silver as its major component, these people were able, in a few days, to cause the accumulation of clouds above the country, and so, to have rain… Thus, they were able to create, virtually, a paradise over the whole continent. Rivers and springs never dried up, but flowed lazily across the numerous plains of a land that was essentially flat. Fruit trees were laden with fruit, bowing under the weight of oranges, mandarins or apples, according to latitude. Exotic fruits, of kinds that… no longer exist on Earth, were harvested in abundance.’ [23]

In describing interior “rooms positioned according to a precise plan,” Thao is making reference to the nonlinear structure of Fibonacci standing waves by which the precise positions of the pyramids’ chambers were determined, for the purpose of focusing terrestrial infrasound resonance (above). Telepathic communication was established by biorhythmic entrainment at 1.45 Hz heartbeat, also known as the *tri-thalamic entrainment frequency*, by which the biorhythms of initiates using the pyramid chambers are synchronized with those initiates in other pyramids across the world, or indeed with other planetary civilizations. Infrasound stimulation also provided for the secondary purpose of rainmaking, *by drastically increasing the evaporation and precipitation rates*, just as occurs during solar flare activity. Biorhythmic balancing in the pyramids also greatly benefits the Astral body, composed of electrons:

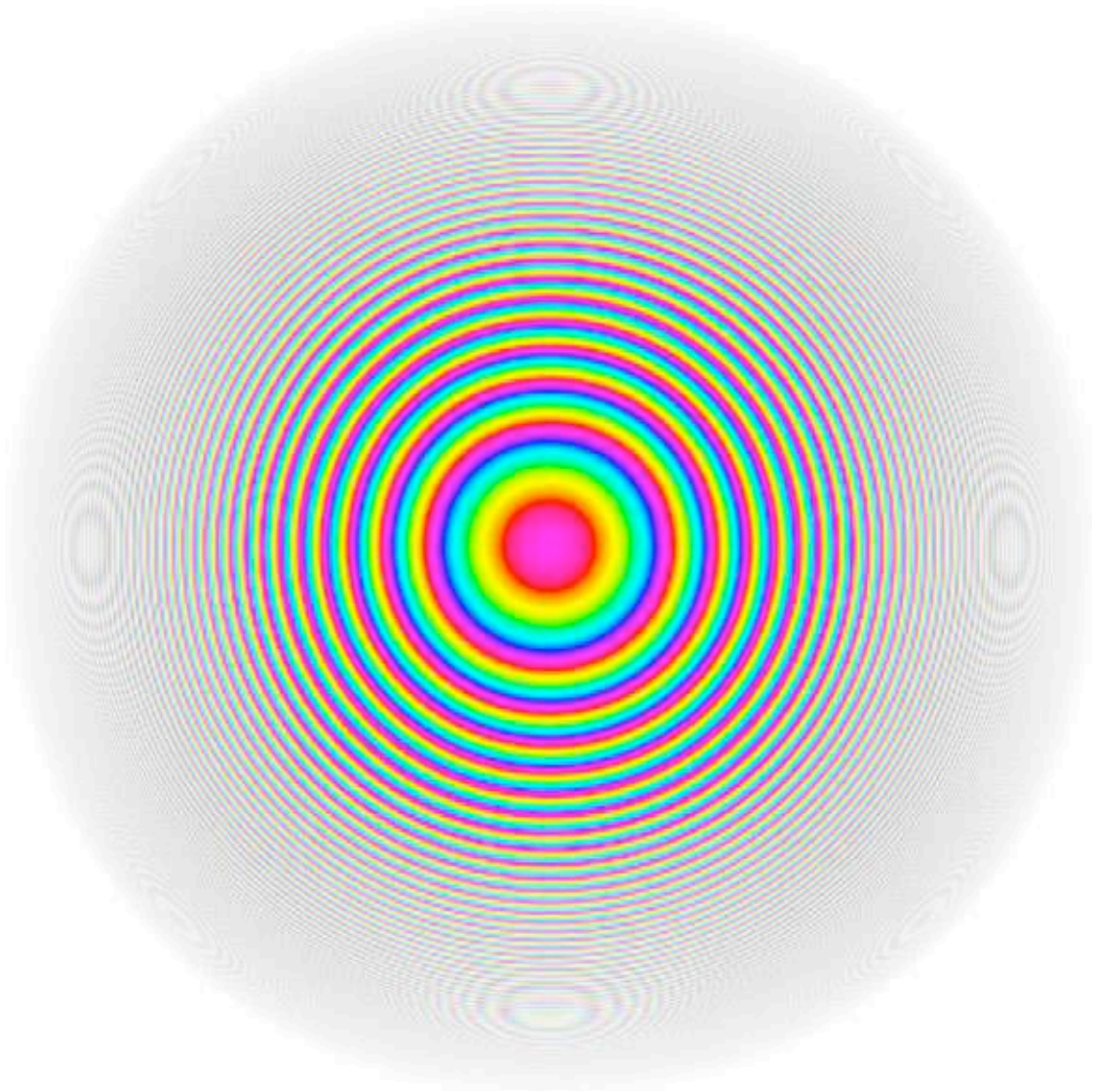

‘Now we come to another kind of pollution that is of no small concern, though people might readily dismiss it. As the great Thaora told you, noise is one of the most noxious pollutants for it upsets your electrons and unbalances your physical compartment. I haven’t yet mentioned these electrons to you and I see that you are not following me very well… A normal human Astral body contains approximately four billion, trillion electrons [4.0×10^{21} = 4 000 000 000 000 000 000 000 electrons]. These electrons have a life span of approximately ten billion, trillion of your years [10^{22} = 10 000 000 000 000 000 000 000 years]. They were created at the moment of creation. Your Astral body contains them and, when you die, nineteen per cent rejoin the electrons of the universe until required by Nature to form a new body or a new tree or animal, and the eighty one per cent rejoin your Higher-self.’ ‘I don’t quite follow you,’ I interrupted.

‘I know, but I intend helping you to understand. An Astral body is not quite what you would call a pure spirit. On Earth, there is a belief that the spirit is made of nothing. This is false. The Astral body is composed of billions of electrons, exactly marrying your physical shape. Each of these electrons has a ‘memory’ and each is capable of retaining as much information as is contained in all the books that fill the shelves of an average town library.

‘I see you are staring wide-eyed at me, but it is as I say. This information is coded, like a microfilm containing all the plans of an industrial installation that a spy would be able to pass in a cufflink, though much more miniaturized than that. Certain physicists on Earth are now aware of this fact but the public, at large, hasn’t been informed of it. Your Astral body transmits and receives messages, by means of these electrons, through the channel of your brain, to, and from your Higher-self. Information is being transmitted without you being aware of it, thanks to a weak electric current from your brain in harmony with your electrons. ‘Since it is the Higher-self which sent this Astral body into your physical body, it is in the natural order of things that your Higher-self should receive information from your Astral body.

‘Like all things electronic, the Astral body – tool of the Higher-self – is quite a delicate tool. During your waking hours it is capable of sending messages of extreme urgency to the Higher-self but the Higher-self seeks much more than that. So, during sleep, your Astral body leaves your physical body to rejoin the Higher-self, either passing on required information or receiving information or orders… Now, those people who, through very advanced and special exercises, are able to detach their astral bodies from their physical bodies, will be able to see a light, silvery-blue thread, such as you saw yourself, linking their physical and astral bodies. Their Astral bodies, likewise, are visible during the time that the separation lasts. It is these same electrons which form your Astral body and which create the visible effect of the thread.

‘I see that you follow what I am saying and that you have grasped my point. Let me finish by explaining the dangers of noise. Noise directly attacks the electrons of your Astral body creating parasites, to use a radio and television term. If… someone is operating an electric tool next door to your house, such large parasites will be produced on your screen that the image will distort completely.

‘The same thing occurs with the Astral body, but unfortunately you won’t be aware of it in the same way that you are with a television screen; and, it’s much worse, since noise damages your electrons. And yet people say: ‘Oh, we get used to it.’ Your brain ‘tenses’, so to speak and your psyche initiates self-defense mechanisms, but not so the Astral body; a parasite invades its electrons - which, of course, has disastrous repercussions for your Higher-self.

‘The sounds that reach your ears are clearly very important. A particular piece of music can elevate you to a state of euphoria, while another piece, although very pretty, will have no effect on you or, perhaps, irritate you. Try an experiment: take a piece of soft violin, piano or flute music that you like and play it as loudly as you can. The suffering of your eardrums will not be as great as the discomfort you’ll feel within. Most of your fellow human beings on Earth consider noise pollution to be of negligible concern, but the noise of the exhaust pipe of a motor bike is three to four times worse than the noxious fumes that it discharges. While the fumes affect your throat and your lungs, the noise affects your Astral body… However, no one has ever been able to take a photograph of your Astral body and, so, people don’t concern themselves with it!’ [24]

Thao’s lengthy description of the Astral or *electronic body* brings sharp clarity to the issue of noise pollution in the industrialized world. The remarkable descriptive metaphor of electronic parasites was powerfully used to illustrate the invisible effect of the dangerous distortion caused by the incessant bombardment of disruptive oscillations from modern airplane, truck and automobile traffic. Not mentioned at the time of Desmarquet’s contact in 1987, which occurred before the mass-production of wireless devices, the lethal effects of long-term exposure of DNA to microwave radiation has since become another invisible threat to all life, mirroring the atmospheric devastation caused by combustion engines:

‘For approximately one hundred and forty years on your planet, man has been accelerating the destruction of Nature and the pollution of the environment. This has happened since the discovery of steam power and the combustion engine. You have but a few years left in which to arrest the pollution before the situation becomes irreversible. One of the principal pollutants on Earth is the petrol-driven engine and this could be replaced immediately with a hydrogen engine that would cause no pollution, so to speak. On certain planets, this is called the ‘clean motor’. Prototypes for such an engine have been constructed by various engineers on your planet [including John Keely (above) and Nikola Tesla among others,] but they must be industrially manufactured in order to replace petrol engines. Not only would this measure mean a seventy percent reduction in current levels of pollution by combustion waste, but it would also be more economical for consumers.

‘The big petrol corporations had been terrified at the idea of this motor being popularized for it would mean loss of sales for their oil and subsequent financial ruin. Governments, too, who impose enormous taxes on these oils, would suffer equally. You see, Michel, it always comes back to money. Because of it, you have a whole economic and financial context that opposes progress towards radical change in the interest of all human life on Earth. The people on Earth allow themselves to be pushed around, bullied, exploited and led to the abattoirs by political and financial cartels which are sometimes even associated with well-known sects and religions. When these cartels fail to win the people with clever advertising campaigns intended to brainwash them, they try to succeed through political channels, and next through religion or through a clever blend of the lot.

‘Great men wanting to do something for mankind have simply been done away with. Martin Luther King is one example; Ghandi is another. But the people of Earth can no longer allow themselves to be treated as fools and led to the abattoirs like flocks of sheep by leaders that they, themselves, have democratically elected. The people form the vast majority. In a nation of one hundred million inhabitants, it is absurd that a group of financiers comprising perhaps a thousand individuals can decide the fate of the others - like the butcher does at the abattoir.

‘Such a group has well and truly stifled the business of the hydrogen motor so that it is no longer mentioned… These people couldn’t care less what might happen to your planet in years to come. Selfishly, they seek their gains, expecting to be dead before ‘whatever is going to happen’ happens. If the Earth disappears, as a result of horrific cataclysms, they assume they will already be dead.

‘There, they are making a big mistake, for the source of the coming disasters is the pollution which is growing daily on your planet, and its consequences will be felt very soon - much sooner than you can imagine. The people of Earth must not do as the child forbidden to play with fire; the child is without experience and, in spite of the prohibition, he disobeys and burns himself. Once burnt, he ‘knows’ that the adults were right. He won’t play with fire again but he will pay for his disobedience by suffering… Unfortunately, in the case that concerns us, the consequences are much more serious than the burn of a child. It’s the destruction of your entire planet that is at risk - with no second chance if you don’t place your trust in those who want to help you.

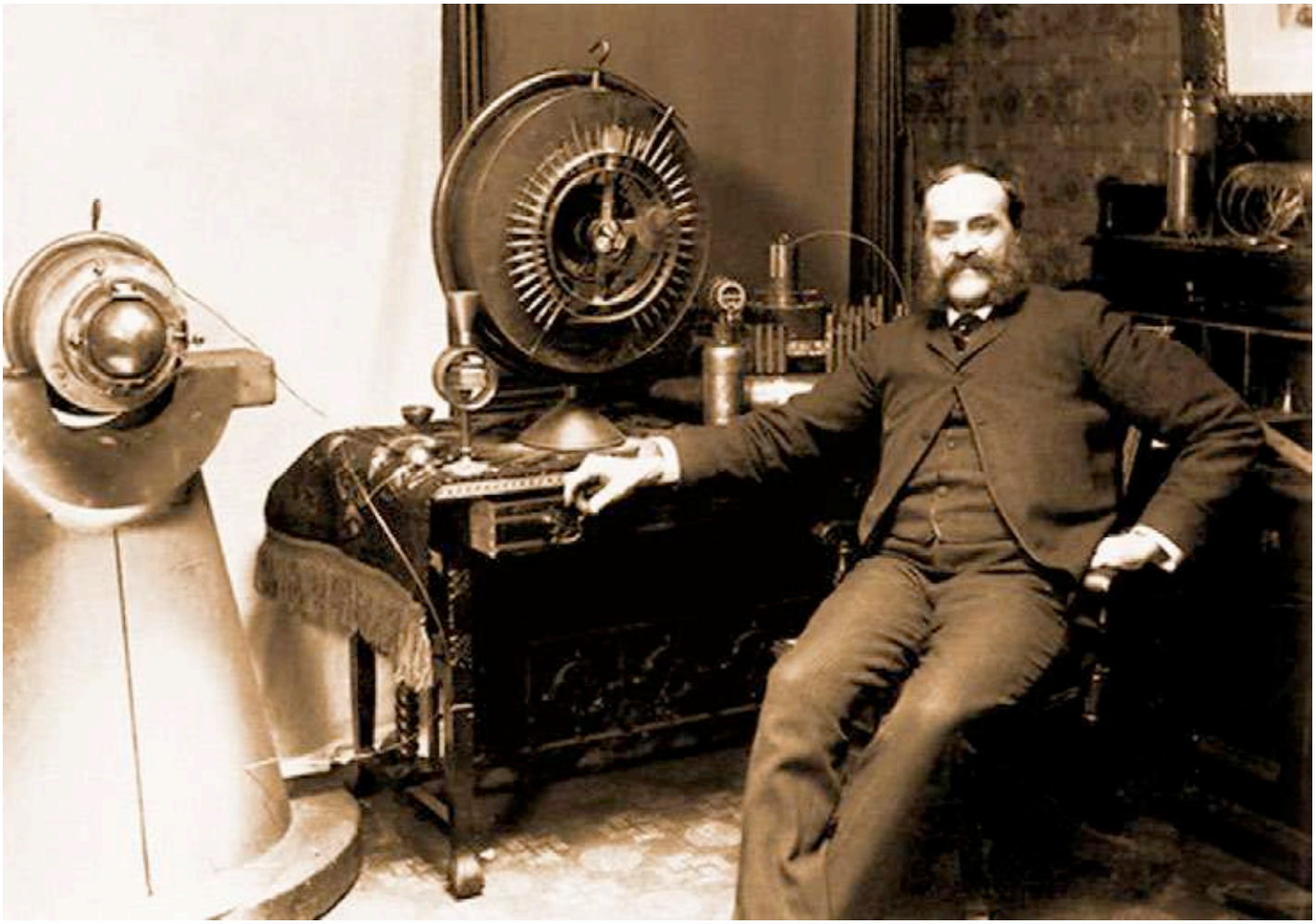

‘It interests us to see that recently established ecological movements are gaining in momentum and power; and that the young people of Earth are ‘carrying’ other sensible people along with them in their fight against pollution… There is only one solution… the grouping of individuals. A group is only as powerful as it is large. Those whom you call the conservationists are becoming stronger and stronger and will continue to do so. But it is vital that people forget their hated, their resentment, and especially their political and racial differences. This group must be internationally united – and don’t tell me that is so difficult - for already on Earth there exists a non-violent and very large international organization – the International Red Cross, which has been functioning effectively for quite some time. It is essential that this conservationist group include in its programs not only the conservation of the environment from direct damage but from indirect damage as well, such as that which results from smoke: exhaust fumes from vehicles, smoke from factories, and so on.’ [25]

The immediate and dire consequences of the continued acoustic and atmospheric pollution of Earthy humanity could not have been more clearly stated. The hydrogen engine that Thao speaks of was discovered a century ago by Earthly scientists – most notably by John Worrell Keely (above) and Nikola Tesla. As in the mentioned cases of Martin Luther King and Ghandi, Tesla was also assassinated[26] and his technologies stolen to be secretly developed by Nazi scientists.[27] Recent rediscoveries by Dr. Randall Mills define hydrino resonant-transfer plasma, formed by the ionization of HHO gas using metal particles (opposite).[28] *These facts concerning the clean HHO plasma motor must become widely known and used.*

> ‘If certain of the leaders who read your book don ‘t believe you, or doubt what is written, challenge them to explain the disappearance of billions of ‘needles’ put into orbit around Earth several years ago. Ask them also to explain the second disappearance of billions more ‘needles’ again put into orbit. They will know what you are referring to, never fear. We are responsible for the disappearance of these ‘needles’, judging them to be potentially disastrous for your planet… We do, at times, prevent your experts from ‘playing with matches’ but it is important that our assistance not be relied upon when mistakes are made. If we judge it appropriate to ‘lend a hand’, we do so, but we can’t, and we don’t wish to save you from disaster automatically - that would be to contravene Universal Law.’ [29]

The disappearance of millions of needles in orbit described by Thao as direct evidence of the reality of the extraterrestrial prevention of disasters caused by human scientific ignorance is a powerful reminder of the fragility of our planet and the carelessness of Earthly scientists. Dangerous experimentation of this kind has subsequently led to high atmospheric use of radioactive aluminum and barium nanoparticles dispersed as ‘chemtrails’ for atmospheric and psychological manipulation. Photo-ionization of the particles generates HHO plasma by the high-energy splitting of water molecules in the near vacuum of space, which acts as an amplifier of land-based signals beamed from the HAARP array, creating a bounce-back effect for ultra-low frequency wave focusing used in the artificial generation of earthquakes.

While extraterrestrial overseers have not brought a halt to the secret development and use of dangerous infrasonic technologies by Earth’s psychopathic profiteers, rare interventions do occur when catastrophic situations arise. In proving the benevolent interventions of Thiaoouban spacecraft observing Earth, Thao referred to *two* senseless tests in near-Earth orbit in October of 1961 and May of 1963 that were carried out as part of Lincoln Laboratory’s Project West Ford,[30] which involved a potentially disastrous attempt to create a new method of military communications using an artificial ‘dipole belt’ around the Earth:

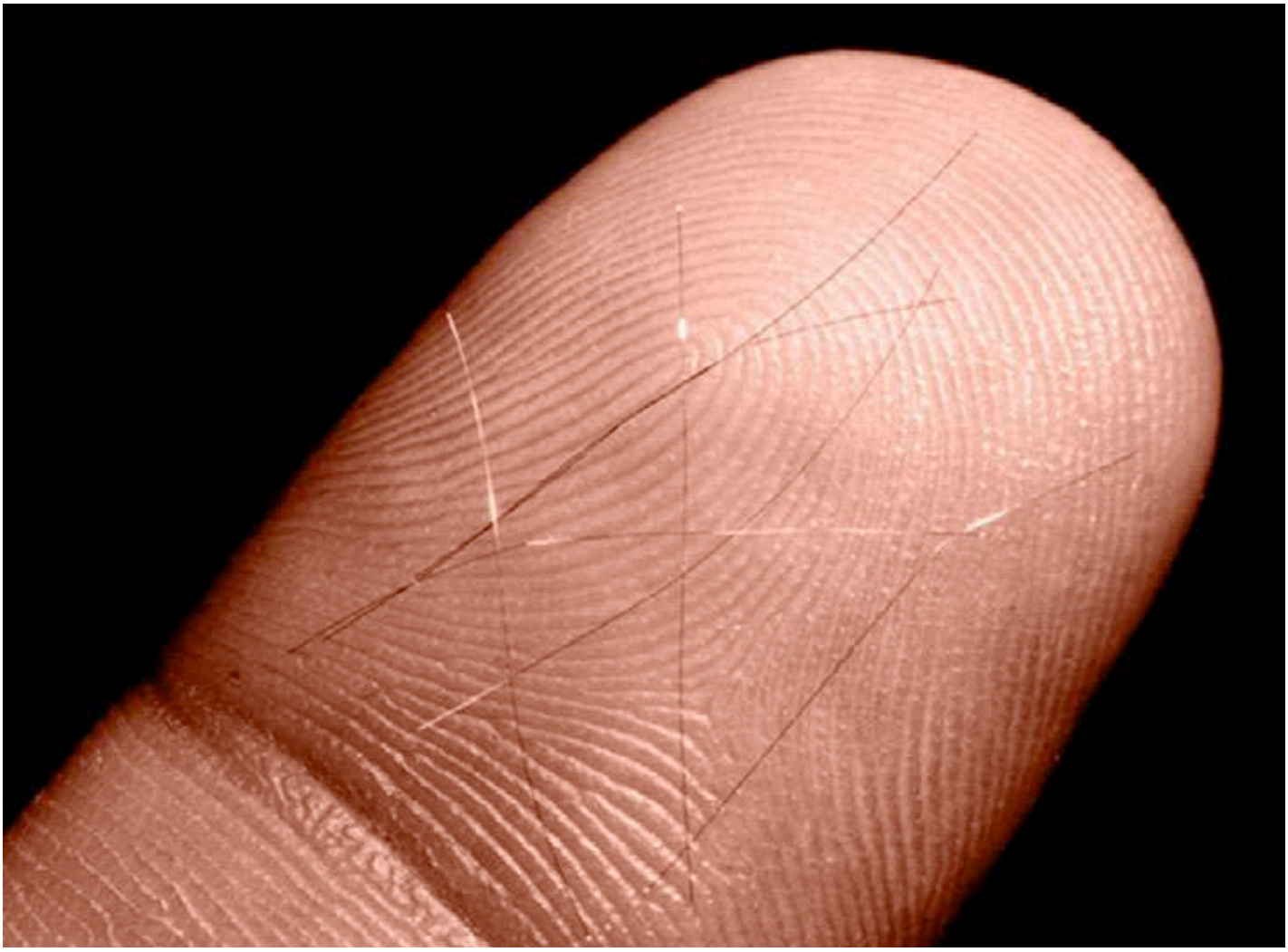

> The dipole belt was to serve, in effect, an artificial ionosphere… [by artificially creating] a belt of 480 million dipoles orbiting 2,200 miles above the earth… In addition to judiciously specifying the initial orbit parameters, we gave the dipoles a high area-to-mass ratio to ensure that the solar radiation pressure acting on the dipoles would distort their circular orbits into highly elliptical ones. The orbital perigee would eventually dip to an altitude at which air resistance would sweep the dipoles out of orbit… The first attempt at establishing the dipole belt, in October 1961, failed. The dipole-dispenser ejection mechanism didn't spin up, so no dipoles were released. With a redesigned dipole dispenser, a dipole belt was established in May 1963… By late 1965, the dipole belt had been swept from orbit, right on schedule.[31]

The Lincoln Laboratory photograph of 7 of the tiny dipole needles– 0.7" long and 0.0007" in diameter – (above) confounds the ability of the human mind to imagine the total volume of 480 million of these needles, which could easily have caused major damage to the Earth if allowed to melt together during atmospheric reentry to form several large molten masses that would rain down on the Earth in a series of major catastrophic impacts. The extreme myopia of the faulty thought process that directed this dangerous experiment is characteristic of 'government scientists' who endanger our planet by ignorant interference in natural atmospheric and orbital processes.

Prevention of the first mission's release of the dipole belt was achieved by interference with the functioning of the dipole-dispenser ejection mechanism. This simple preventive measure only frustrated NASA scientists, who mounted a second mission that was allowed to be released, and the experiment conducted, before the dipole belt was disintegrated by the plasma beams of Alatora spacecraft for the protection of all life on Earth. The oversight of human development on Earth is a significant task of the many advanced neighboring civilizations within our galaxy, who prevent such calamities only rarely by physical means when the logic and reason of Earthly humans cannot be inspired by any other means:

‘I see, Michel, you are having enormous difficulty believing what I have been saying. Never forget that we have THE *knowledge* - you have not seen one-tenth of what we can do. Attend carefully and I will give you a few examples to help you understand what I’m going to tell you.’

Thao stopped talking and appeared to be concentrating. As I watched, her face became a blur and, instinctively, I rubbed my eyes. Of course, this did not help and, in fact, she became progressively transparent until I could see right through her. Finally, she was no longer there - she had completely disappeared.

‘Thao,’ I called, slightly concerned, ‘where are you?’

‘Here, Michel.’ I jumped, for the voice came as a whisper, quite close to my ear…

Several feet in front of me, I saw the silhouette of Thao, completely golden yet radiant, as though inside her there burned a fire, its flames brief but intense. As for her face, it was recognizable but her eyes seemed to send forth little rays each time she spoke… She began to rise a few feet above the ground, without having moved a muscle of her ‘body’; then she started to circle the room, so fast I had trouble keeping my eyes on her. She stopped, eventually, above her seat and sat her ghostly form down. It was as though she were made of a shining mist - she was still recognizable as Thao and yet, quite transparent. The next instant she was gone. I looked around, but she had completely vanished.

‘Look no further, Michel, I am back.’ Indeed, there she was, in flesh and bone again, sitting on her seat.

‘How do you *do* that?’

‘As I was just explaining to you, we have THE *knowledge*. We can revive the dead; cure the deaf and the blind; make people walk who are paralyzed; we can cure any malady you care to name. We are masters, not *of* Nature, but *in* Nature, and we can do the thing most difficult of all - we can generate life spontaneously. *‘Out of the release of cosmic ray, we can create any type of living creature, including man…* We can create a human body, but that is done only by the great Thaori, taking infinite care, for the human body must be inhabited by several bodies, as you are aware - the physiological, the astral etc. If not, it would merely be a robot. Perfect knowledge is therefore required for such an undertaking… A man of twenty or thirty years-of-age can be created by the Thaori in approximately twenty-four of your Earth hours.’ [32]

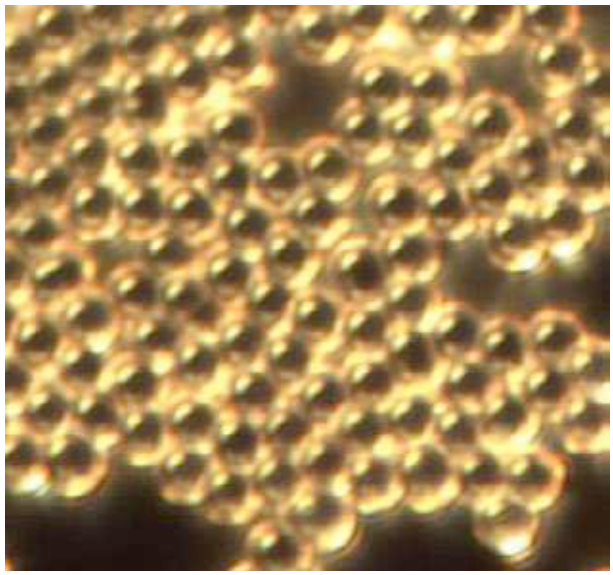

The astounding disclosures of spiritual knowledge provided through the writings of Michel Desmarquet inspire great contemplation. The transdimensional demonstrations and many penetrating truths offered by both Thao and the Thaori reflect their purely Creational consciousness, *as masters in Nature*. Michel’s galactic voyage to the golden planet of Thiaoouba stands as an example of the highest attainment of Nature, inspiring the human beings of Earth to reverse the destructive effects of our ignorant ways by the advanced spiritual use of gold and silver nanoparticles for resonant atmospheric and intracellular illumination (at left). The seeds of knowledge have been widely sown, and hold the magnificent promise of an era of rejuvenation using electrum-enriched foods and drinks to reclaim our own natural ability *‘to regenerate the cells of our bodies at will’* in the enhanced cosmic ray environment of the Betelgeuse supernova blast.

At this juncture, the development of human consciousness on Earth will benefit from dramatic cosmic environmental changes, *‘as Nature itself enters the stage to assist the pupil’* in the attainment of knowledge. Thiaoouban wisdom concerning the Four Forces of Creation, the Atomic, Ovocosmic, Ovoastromic and Astral, has been offered for our contemplation on Earth as all living beings receive DNA enhancements induced by cycling galactic infrasound waves. Their lessons identify the significant advances of Kirlian photography and the clean hydrogen engine as crucial developments for terrestrial technology on Earth, pointing directly toward the use of biocompatible HHO plasma for cellular regeneration, enhanced longevity and an inexhaustible source of clean, resonant energy.

References

[1] Desmarquet M (1993) *'Thiaoouba Prophecy'* Arafura Press, p. 6, online · http://www.thiaoouba.com

[2] Ibid, p. 18

[3] Ibid, pp. 7-11

[4] Ibid, pp. 52-54

[5] Sichin Z (1976) *'The 12th Planet'* Harper Books

[6] Vyasa K, tr. Prabhupâda B (1977) 'Description of Jambudvîpa' *Srimad Bhagavatam*, Canto 5, ch.16, online · http://www.srimadbhagavatam.org/canto5/Canto5-Sanskrit/chapter16.html

[7] Macchi M, Bruce J (2004) 'Human Pineal Physiology and the Functional Significance of Melatonin' *Neuroendocrinology (25:3-4),* pp. 177-195

[8] Desmarquet, op cit, pp. 161-162

[9] -- (2010) 'It's True! Couples Share 6th Sense' *The Times of India*, online · http://timesofindia.indiatimes.com/home/science/Its-true-Couples-share-6th-sense/articleshow/6640735.cms

[10] Desmarquet, op cit, pp. 61-63

[11] Ibid, p.154

[12] Ibid, p.156

[13] Ibid, pp. 64-67

[14] Kalyanaraman S (2004) *'Indian Alchemy: Soma in the Vedas'* Munishram Manoharlal Publishers, pp. 2-7

[15] Desmarquet, op cit, pp. 68-69

[16] Vandewalle G, Schwartz S, Grandjean D, Wuillaume C, Balteau E, Degueldre C, Schabus M, Phillips C, Luxen A, Dijk DJ, Maquet P (2010) 'Spectral Quality of Light Modulates Emotional Brain Responses in Humans' *PNAS*, online · http://www.pnas.org/cgi/doi/10.1073/pnas.1010180107

[17] Ibid, pp.73-82

[18] Dunham B (2009) 'Cool Plasma Pack Heat Against Biofilms', *University of Southern California News*, June 5, online · http://www.humanresonance.org/helium.html

[19] Desmarquet, op cit, p. 96

[20] Ibid, p.137

[21] Ibid, p. 122

[22] Fox S (2009) 'EM Pulse Cuts Through Steel in 200 Milliseconds' *Popular Science*, December 3, online · http://www.popsci.com/technology/article/2009-12/electromagnetic-pulse-cuts-through-steel-200-milliseconds

[23] Ibid, pp. 91-92

[24] Ibid, pp. 165-166

[25] Ibid, pp. 163-164

[26] Orion E (2003) *'The Bush Connection'* The Bush Connection

[27] Putney A (2009) *'Veil of Invisibility'* Human Resonance Productions

[28] Mills RL, Ray P, Dhandapani B, Nansteel M, Chen X, He J (2002) 'New Power Source from Fractional Quantum Energy Levels of Atomic Hydrogen Surpasses Internal Combustion' *Journal of Molecular Structure* 643, pp. 43-54

[29] Desmarquet, op cit, p. 109

[30] -- (1964) 'Project West Ford' *Proc. IEEE (52:5) special issue*

[31] MacLelland D (1970) 'Looking Back: Space Needles – An orbiting Belt of Tiny Dipoles Took Lincoln Laboratory into Space' *Massachusetts Inst. of Tech.*, online · http://www.ll.mit.edu/publications/labnotes/Looking_Back_3.pdf

[32] Desmarquet, op cit, pp. 161-162

6
Betelgeuse & the Red Dawn

Betelgeuse & the Red Dawn

An inexorable sequence of natural electromagnetic events is unfolding that demands our full attention, and underlies the shifting currents of human consciousness. Ancient Sanskrit knowledge maintained by the Maya culture explicitly describes the events surrounding the end of this solar cycle, as retold in many forms throughout the indigenous prophecies and wisdom traditions of the world. It is said humanity will be transformed in the red light of cosmic consciousness – quite directly telling us *'man becomes god.'*

Mayan wisdom identifies the energetic changes of December 22, 2012 as the effect of a *synchronization ray* emitted from the center of the galaxy. This event is described as an alignment of Earth with the galactic plane, which will ignite Earth's high atmosphere in an all-encompassing red aurora. The Pyramid of Fire Codex foretells that the sky itself will be in flames, and the red flames will spread amongst the pyramids – from one 'Hill of the Star' to another along flaming plumes of celestial water:

> Tláloc, God of Celestial Water, god of the vapor that *rises*, from the Earth warmed by the sun after the rains, god of the mist that *ascends* from the valleys at dawn… Tláloc is the return of vapor that strains to rise, is the return of time that strains to *remember*. Tláloc, God of the Fight Against the Current, with whose aid the hero battles against the torrent toward his own origin and beginning, towards the wings of his soul, the wings that Tláloc hides in the hero's past…
>
> It is the self within ourselves that we have to sacrifice. It is our own heart that has to be torn out of the false being and offered to the light. May Xiuhtecuhtli, Lord of Fire, burn my false being, May Itzli, Obsidian Knife, liberate my heart. To sow life in the fires of sacrifice: Are the flames rising on the Hill of the Star, toward Cauhlacan? Or is it my own heart that is afire?
>
> The cycle of years is past - the waiting ended. Come - reunite, pilgrims, for the sky is in flames! From Xochicalco to Teotíhuacan the red spreads one step, another step, and another, only twelve short steps from the cave of the womb to the final conflagration... The flames rage in consummation- Rise, oh flames! What light, what heat! What great holocaust! The smoke ascends and spirals... Obscurity disappears as the flames rise to Tonatiuh, the purest light.[1]

The kundalini technology of the pyramids employs the crystalline memory of celestial waters to awaken human divinity at sacred temples like Teotihuacan, meaning '*site-where-man-becomes-God'* (below). The resonant frequency of the Pyramid of the Sun at Teotihuacan closely matches the 1.45 Hz heartbeat oscillation of the Great Pyramid due to its comparable base length of 740'. Itza Mayan Elder Hunbatz Men describes the pyramids as generators of *the brilliant light of heaven that imbues the human being with eternal life.* Cosmic Creator Hunab K'u guides the initiatic work of Mayan Elders at sacred pyramids:

> "Take care of the light that I leave within my temple. When you form the human being, teach him to venerate my house, for within it they will find the light they need for eternal life. Teach him also that if he should stray, due to his errors, vices or ignorance, then I, Hunab K'u will reclaim my beloved beings and take them to my temple of wisdom and nourish them again with my light which is in the heavens. Then, together, Tepeu, Gugumatz and Huyubcaan will perform purification rituals using that brilliant light for the benefit of my beloved whom we created and molded, so they can live in the light of eternal wisdom." [2]

A heavenly life-giving light radiating inside pyramid chambers is also related in hieroglyphic texts inscribed on the interior walls of the pyramids of Saqqara, Egypt. Profound details of the luminal and acoustic effects of the Great Pyramid transducer in full operation have been recorded in stone:

> House bright and dark of Heaven and Earth, for the [solar] ships put together; Great Pyramid, House of the gods with pointed peak; for Heaven-to-Earth it is greatly equipped. House whose interior glows with a reddish Light of Heaven, pulsating a beam which reaches far and wide; its awesomeness touches the flesh... House of Eternity: its foundations are stones, the water; its great circumference is set in the clay. House the rightness of whose howling the Great-Ones-Who-See-and-Orbit bring down to rest… Mountain by which Utu ascends… whose deep insides men cannot penetrate.[3]

Both the Egyptian and Mayan hieroglyphs are descendant forms of the ancient logographic Sanskrit, as deciphered by epigrapher Dr. Kurt Schildmann (1909-2001). This antediluvian proto-Sanskrit can be identified as the Atlantean script, having been found on all inhabited continents of the world on stone and ceramic artifacts dated to the Pleistocene period – being over 12,000 years old. The pyramid traditions of these cultures of Atlantean descent provide us with stunningly explicit descriptions of future events tied into the ancient Sanskrit conception of water as the transformative agent of consciousness.

The Atlantean psychoacoustic technology of quartz crystal skulls reflects the Sanskrit tradition of augmenting consciousness through the purification and crystallization of the water within the human body. The refraction of light within the human body that is fueled by crystalline water enables the higher capacities of human consciousness by biorhythmic alignment at 1.45 Hz heartbeat entrainment in the pyramid chambers. The Great Pyramid's upper chamber does not contain a sarcophagus – the granite box was actually a water-birthing resonator filled with celestial water. The closed shafts rising from the chambers are its "deep insides men cannot penetrate", designed to focus infrasound heartbeats at 1.45 Hz into the tiny newborn infants. Usually born as twins, the infants' skulls were elongated by this process.

The celestial waters of La Maná, Ecuador (photographed above with several plasma orbs) and Tlacote, Mexico have been extensively studied for their astounding resonant properties.[4] Test results have shown the spring waters of La Maná and Tlacote have the highest water purity found anywhere in the world, containing virtually no salt or other dissolved solids. This in itself is remarkable, but tests have also identified trace amounts of gold and silver nanoparticles and an energy rating of over 1,000,000 on the Bovis scale. There is no modern technology capable of creating energized waters like those flowing from the springs of La Maná and Tlacote. These celestial waters are the nanotechnological product of the transdimensional civilization of Atlantis – the central component of the pyramid kundalini tradition of psychoacoustic gestation and water-birthing practices.

Artifacts from the ancient Sanskrit sacred site in La Maná, Ecuador reveal the origin and use of these celestial waters as a technological product of the global pyramid system itself. Over 300 metal, stone and ceramic artifacts have been recovered, among which are diverse UV-fluorescent maps of standing wave resonance patterns within the electron, mineral calcite, and Great Pyramid of Giza, Egypt.[5] The artifacts preserve logographic Sanskrit script, while their numerals from 1 to 10 are presented in fluorescent inlays adorning a set of 13 stone goblets precisely designed for water volume measurement.

Among the artifacts found below the sacred site is a large stone lingam in the form of a kundalini cobra, engraved with complex UV-fluorescent inlaid patterns – as well as a gold psychoacoustic helmet, accompanied by dozens of ceramic figurines that show both adults and children using the helmets while barefoot for electrical contact to the pyramid. The largest stone artifact from La Maná is a breathtaking global map of the Earth with all the continents accurately depicted as they were before the fall of Atlantis! Star maps on flat stone plates were inlaid with UV-fluorescent calcite mortars depicting the constellations surrounding Orion, with Betelgeuse (fluorescing in red) as one of the three large stars forming the Winter Triangle with Sirius and Procyon. This star map is also presented on the largest goblet (above, center).

Celestial waters were the primary enablers of this advanced psychoacoustic Atlantean technology, by which human bodies became superconductors of electricity. The suspension of gold and silver nanoparticles enhances the conductivity of the body by creating a pathway for electrical flow without shock. Shock waves do not form inside crystals for the crystal lattice distributes pressure evenly and the whole mass is set vibrating in unison. The celestial waters maintain the integrity of the body's cells during exposure to the electrical currents inside the pyramids at resonance. The gold and silver nanoparticles are from 2-10nm in size and act as transducers in the body, *converting electrical pulses into light pulses*.

Gold nanoparticles scatter RED light inside all of the cells of the body. This is the key to understanding the words of the pyramid-builders concerning the *"heavenly red light of eternal life"!* The fact that these water sources are still flowing, and in fact greatly increasing their output with time, is primary evidence that the pyramids are automatically roaring to life with the input of infrasound energy from solar storms as we approach the full onset of the new solar age. These widespread effects are already being observed.

*(**Note:** monatomic gold, aka white powder gold, does NOT scatter red light, and is not recommended!)*

Golden waters and wisdom of the Chichimeca and Chichicastl cultures of Tlacote, Mexico have been preserved by the Maya Elders, and presented through translation by Gerardo Aceves Quetza Sha:

> Tlacote is a great assembly point of the ancient gods where once existed the Golden City of the Golden Water, built by the Chichimeca and the Chichicastl. In other times, our ancestors left us transcendental information… Man has always been looking for something else, something that lives inside of him, and he recognized the inner light manifesting in his heart. It is this inner light that will cause the changes in humanity and that will make the dream come true, that the animal which is the human being will be able to live thousands of years. Man opens his heart to understand the revealing truth, creating consciousness and elevating his thoughts. This process is necessary, because we must understand and solve the enigmas of Earth and the planetary system, in order to develop in perfect conscience right from the beginning of creation. We meet thousands of phenomena in our life. Man calls this coincidence; spirit calls it cycles of comprehension in the evolution of man. Therefore, if a new race emerges to a new cycle of existence, this happens because the information imprinted in the subconscious of the Inner Self has been completed.

> All the information we need is imprinted in the subconscious of the inner self, so it may evolve according to its individual level, remembering who it is and knowing its task on Earth: 'AWAKEN, INNER SELF, and recognize your inner creation in order to understand the movements of the Universe!' This is how the different races and religions developed in their particular states of evolution. Each religion in its particular language has accompanied us on a very important part of our path and accomplished the demands of a particular time. Now humanity is awakening to a new cycle of consciousness. A new race is born, constantly bringing in new knowledge and spheres of conscience, and being aware of the past, the present and the future…
>
> This message predicting the awakening of the Golden Water is sacred and was created and given to us by beings from other dimensions, so that other generations can be born, prepared for the great changes that will be produced from the center of the Earth.[6]

Not only are the acoustic environments enhanced at these sacred sites, but the quality of water is also correspondingly enhanced to become *crystalline.* These profound findings reveal the sophisticated yet invisible technologies that enhance human consciousness and longevity at these sites – for those who choose to live close to spirit and purify their bodies to be bathed in the energy of the pyramids. The red light scattering of golden celestial waters induces DNA enhancement through heartbeat synchronization.

The ancient Hopi wisdom echoes that maintained by the Maya, describing the imminent shift from the second phase of Creation, during which the sun has shone yellow, to the third phase of Creation during which the Earth is bathed in red light: “The third phase of Creation is the time of the red light, Talawva, the perfect light. Humanity then, having been fully formed and [crystallized,] proudly faces the Creator for the first time, to know the true warmth of love.” While the Hopi prophecies ascribe no calendar date to the coming of the red light of the new solar age, their wisdom perfectly harmonizes with that of the Mayan culture, with its profound and complex calendar system providing the end date of December 22, 2012.

What could possibly trigger the dramatic changes in human consciousness, involving a shift in the light reaching Earth’s surface to a red hue? Solar physicists confirm the 11-year cycle of solar activity corresponds with the 2012 end date, the last solar maximum having been recorded in 2001. At each solar maximum the sun’s magnetic field reverses, but what could possibly induce the Earth’s magnetic field to reverse with our sun? Recent stellar observations in 2009 reveal the hidden threads which link one star system’s fate with another. A research team at UC Berkeley has recently reported data indicating the nearby red supergiant star Betelgeuse is shrinking in the process of imminent collapse:

> Betelgeuse is enshrouded by vast clouds of gas and dust, so measuring its size is difficult. To cut through this cocoon, Charles Townes of the University of California, Berkeley, and colleagues used a set of telescopes that are sensitive to a particular wavelength of the star's infrared light.
>
> But the star's reach seems to be waning. New observations indicate the giant star has shrunk by more than 15 per cent since 1993. This could be a sign of a long-term oscillation in its size or the star's first death knells…
>
> The team used these instruments to measure the size of Betelgeuse's disc on the sky. Over a span of 15 years, the star's diameter seems to have declined from 11.2 to 9.6 AU (1 AU, or astronomical unit, is the distance from the Earth to the sun)… The cause for this reduction is unknown, as it is unclear how red supergiants behave near the end of their lives.[7]

One may easily identify similar patterns in the energy fluctuations of both red supergiant Betelgeuse and our own small yellow Sol. The contraction and collapse of Betelgeuse is being mirrored on the Sun, which has seen a prolonged period of spotless inactivity for the period of 264 days preceding the appearance of Sunspot 1024 in July of 2009. *Both stars dimming together represents the contraction before the full strike of the wave, as the supernova’s energetic blast wave reaches the Earth.*

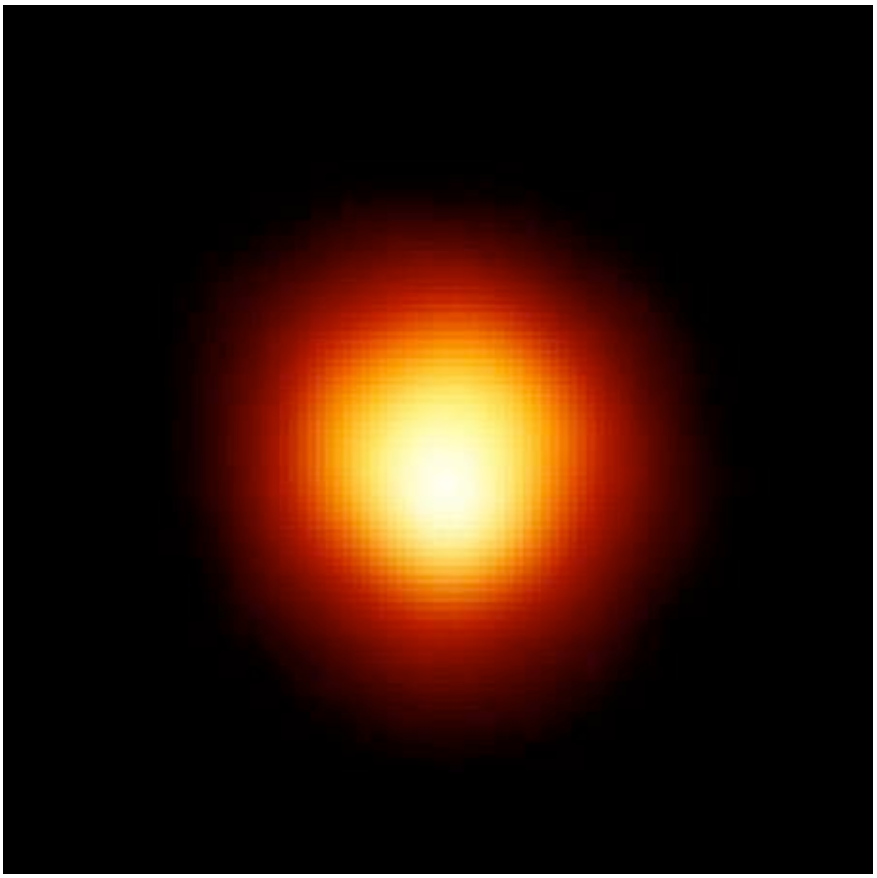

Plasma physicists proposing the Electric Universe theory have keenly observed the pulsed throughput of energy that generates the dynamics of stellar interactions, overturning the false notion of stars as independent thermonuclear generators with their own self-determined lifecycle. The lifecycles of stars are actually intertwined with the cycling waves of energy that traverse the spiral arms of our galaxy. Galactic waves are generated as pulsations of infrasound emitted from the center of our galaxy that traverse its arms, gaining momentum from the radiated energy of supernovae that are set off by the wave's influence in a chain of events moving outward. Red supergiant Betelgeuse, at the shoulder of the constellation Orion (at left), is the nearest in a chain of supernova events along the expanding wave front, and acts as our local indicator by which we can estimate the arrival time of the galactic energy wave.

Further analysis of the data obtained by the UC Berkeley team should also provide the rate of acceleration of the stellar collapse and give us a fairly good estimate for the moment of supernova. Considering the fact that Betelgeuse is our close neighbor at about 600 light-years distance, this event has already occurred and the nova will be visible to us in just a few years time. So, when exactly will the electromagnetic wave hit Earth, and how will it affect us?

Certainly, the Betelgeuse supernova will be seen as a major flash of light plainly visible even during the daylight hours. The supernova may shine very brightly for many days. The more complex unfolding of events triggered by the supernova involve many factors not commonly understood by astrophysicists. For time indications of the potential hazards and benefits of these electromagnetic changes we must turn to the most ancient and most accurate calendar system known to man. Mayan wisdom gives us an exact date for the change of the ages (December 22, 2012), and an exact sign is given as well – the Red Sky.

The Maya use of sacred celestial waters within the pyramids for healing and longevity is an open invitation to sacrifice the false comforts of urban society that disrupt the natural acoustic environment and isolate people from electrical contact with the Earth. Industrial man finds dissonance and disease in concrete boxes, whereas resonance and longevity are to be found in the celestial waters and barefoot lifestyle practiced at sacred sites. The Maya invite us all to come together as one: "The cycle of years is past - the waiting ended. Come - reunite, pilgrims, for the sky is in flames! From Xochicalco to Teotíhuacan the red spreads one step, another step, and another…"

Yaqui Elder Don Juan spoke of waiting for the 2012 event during his teachings to cultural anthropologist Carlos Castaneda, stating emphatically: "[As seers] our case is a bit different, because we are at the end of our trail. We are not seeking anything... we go from day to day doing nothing. We are waiting. I will not tire of repeating this: we know that we are waiting and we know what we are waiting for. We are waiting for freedom!" [8] The progressive energetic changes currently raising human consciousness will cause fear and panic only for those who are unprepared, while many spiritually awakened individuals have been preparing for the Purification Day.

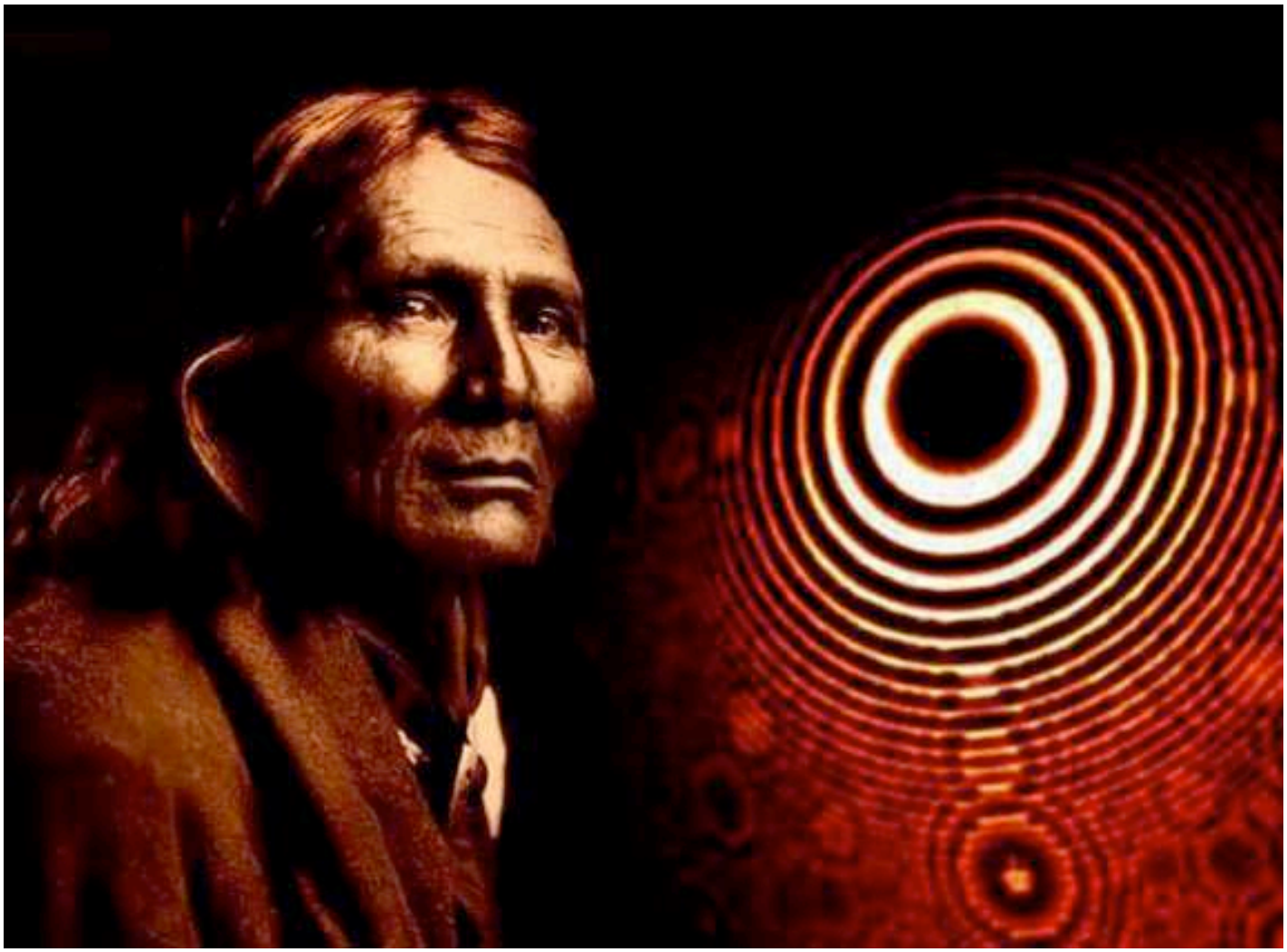

Apache Elder Stalking Wolf related his profound visions of the future in the Prophecy of the Red Sky, received as a vision several decades before the foretold events, and later published by Tom Brown Jr.:

> In the 1920s, an Apache wise man had a Vision of four prophecies that foretold death and destruction for mankind, unless we incorporate Spirit in our daily lives. Two of these prophecies may already have come true. A number of people can predict the future, but few get the timing correct. "Grandfather" was an Apache wise man and scout, named Stalking Wolf, who grew up outside white man's influence. His many predictions not only came true in the manner he predicted, but also when he predicted...
>
> Grandfather had been wandering for several years and was well into his forties when the Vision of the four signs was given to him. He had just finished his third Vision Quest at the Eternal Cave when the Vision made itself known. He had been seated at the mouth of the cave, awaiting the rising Sun, when the spirit of the warrior appeared to him. He felt as if he were in a state somewhere between dream and reality, sleep and wakefulness, until the spirit finally spoke and he knew that it was not his imagination. The spirit called Grandfather's name and beckoned him to follow.
>
> As Grandfather stood, he was suddenly transported to another world. Again, he thought that he was dreaming, but his flesh could feel the reality of this place; his senses knew that this was a state of abject reality, but in another time and place.
>
> The spirit warrior spoke to Grandfather. "These are the things yet to come that will mark the destruction of man. These things you may never see, but you must work to stop them and pass these warnings on to your grandchildren. They are the possible futures of what will come if man does not come back to the Earth and begin to obey the laws of Creation and the Creator. There are four signs, four warnings, that only the children of the Earth will understand. Each warning marks the beginning of a possible future, and as each warning becomes reality, so too does the future it marks"...

The First Sign

..."Welcome to what will be called the 'land of starvation'. The world will one day look upon all of this with horror and will blame the famine on the weather and the Earth. This will be the first warning to the world that man cannot live beyond the laws of Creation, nor can he fight Nature... There will come starvation before and after this starvation, but none will capture the attention of the world with such impact as does this one. The children of the Earth will know the lessons that are held in all of this pain and death, but the world will only see it as drought and famine, blaming Nature instead of itself"...

In his dream, the spirit spoke to Grandfather. "It is during the years of the famine, the first sign, that man will be plagued by a disease, a disease that will sweep the land and terrorize the masses. The white coats [doctors/scientists] will have no answers for the people, and a great cry will arise across the land. The disease will be born of monkeys, drugs and sex. It will destroy man from inside, making common sickness a killing disease. Mankind will bring this disease upon himself as a result of his life, his worship of sex and drugs, and a life away from Nature. This, too, is a part of the first warning; but, again, man will not heed this warning and he will continue to worship the false gods of sex and the unconscious spirit of drugs."

The Second Sign

The spirit looked at Grandfather for a long moment, then finally spoke. "Holes in the sky... will become the second sign of the destruction of man. The holes in the sky and all that you have seen could become man's reality. It is here, at the beginning of this second sign, that man can no longer heal the Earth with physical action. It is here that man must heed the warning and work harder to change the future at hand. But man must not only work physically, he must also work spiritually, through prayer, for only through prayer can man now hope to heal the Earth and himself...

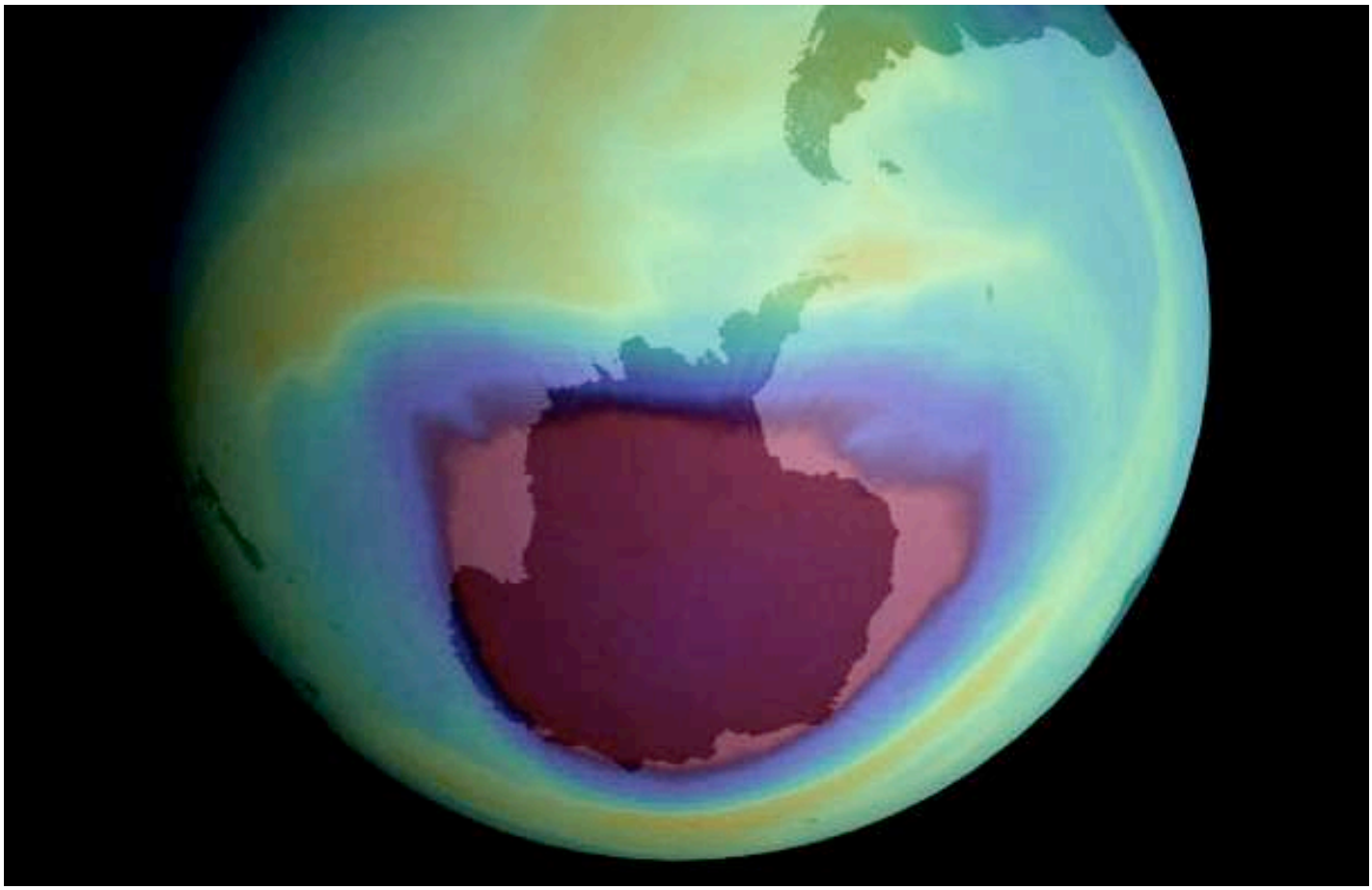

"These holes are a direct result of man's life, his travel, and of the sins of his grandfathers and grandmothers. These holes, the second sign, will mark the killing of his grandchildren and will become a legacy to man's life away from Nature. It is the time of these holes that will mark a great transition in mankind's thinking. They will then be faced with a choice-a choice to continue following the path of destruction, or a choice to move back to the philosophy of the Earth and a simpler existence. It is here that the decision must be made, or all will be lost...

The Third Sign

Grandfather spent the next four days at the cave entrance, though for those four days nothing spoke to him, not even the Earth. He said that it was a time of great sorrow, of aloneness, and a time to digest all that had taken place.

He knew that these things would not appear in his lifetime, but they had to be passed down to the people of the future with the same urgency and power with which they had been delivered to him. But he did not know how he would explain these unlikely events to anyone. Surely the elders and shamans of the tribes would understand, but not society, and certainly not anyone who was removed from the Earth and Spirit.

He sat for the full four days, unmoving, as if made of stone, and his heart felt heavy with the burden he now carried.

It was at the end of the fourth day that the third Vision came to him. As he gazed out onto the landscape towards the setting Sun, the sky suddenly turned to a liquid and then turned blood-red. As far as his eyes could see, the sky was solid red, with no variation in shadow, texture or light. The whole of Creation seemed to have grown still, as if awaiting some unseen command. Time, place and destiny seemed to be in limbo, stilled by the bleeding sky. He gazed for a long time at the sky, in a state of awe and terror, for the red color of the sky was like nothing he had ever seen in any sunset or sunrise. The color was that of man, not of Nature, and it had a vile stench and texture. It seemed to burn the Earth wherever it touched. As sunset drifted to night, the stars shone bright red, the color never leaving the sky, and everywhere the cries of fear and pain were heard.

Again, the warrior spirit appeared to Grandfather, but this time as a voice from the sky. Like thunder, the voice shook the landscape. "This, then, is the third sign, the night of the bleeding stars. It will become known throughout the world, for the sky in all lands will be red with the blood of the sky, day and night. It is then, with this sign of the third probable future, that there is no longer hope. Life on the Earth as man has lived it will come to an end, and there can be no turning back, physically or spiritually. It is then, if things are not changed during the second sign, that man will surely know the destruction of the Earth is at hand. It is then that the children of the Earth must run to the wild places and hide. For when the sky bleeds fire, there will be no safety in the world of man."

Grandfather sat in shocked horror as the voice continued. "From this time, when the stars bleed, to the fourth and final sign, will be four seasons of peace [that is, one year]. It is in these four seasons that the children of the Earth must live deep in the wild places and find a new home, close to the Earth and the Creator. It is only the children of the Earth that will survive, and they must live the philosophy of the Earth, never returning to the thinking of man. And survival will not be enough, for the children of the Earth must also live close to the Spirit. So tell them not to hesitate if and when this third sign becomes manifest in the stars, for there are but four seasons to escape"… Grandfather said that the voice and red sky lingered for a week, and then were gone as quickly as they were manifest.

The Fourth Sign

He did not remember how many days he'd spent at the mouth of the cave, nor did it make a difference, for he had received the Vision he had come for. It was in his final night at the Eternal Cave that the fourth Vision came to Grandfather, this time carried by the voice of a young child.

The child said, "The fourth and final sign will appear through the next ten winters [that is, ten years] following the night that the stars will bleed. During this time, the Earth will heal itself and man will die. For those ten years, the children of the Earth must remain hidden in the wild places, make no permanent camps, and wander to avoid contact with the last remaining forces of man. They must remain hidden, like the ancient scouts, and fight the urge to go back to the destruction of man. Curiosity could kill many."

There was a long silence, until Grandfather spoke to the child spirit, asking, "And what will happen to the worlds of man?"

There was another period of silence until finally the child spoke again. "There will be a great famine throughout the world, like man cannot imagine. Waters will run vile, the poisons of man's sins running strong in the waters of the soils, lakes and rivers. Crops will fail, the animals of man will die, and disease will kill the masses. The grandchildren will feed upon the remains of the dead, and all about will be the cries of pain and anguish. Roving bands of men will hunt and kill other men for food, and water will always be scarce, getting scarcer with each passing year. The land, the water, the sky will all be poisoned, and man will live in the wrath of the Creator. Man will hide at first in the cities, but there he will die. A few will run to the wilderness, but the wilderness will destroy them, for they had long ago been given a choice. Man will be destroyed, his cities in ruin, and it is then that the grandchildren will pay for the sins of their grandfathers and grandmothers."

"Is there then no hope?" Grandfather asked.

The child spoke again. "There is only hope during the time of the first and second signs. Upon the third sign, the night of the bleeding, there is no longer hope, for only the children of the Earth will survive. Man will be given these warnings; if unheeded, there can be no hope, for only the children of the Earth will purge themselves of the cancers of mankind, of mankind's destructive thinking. It will be the children of the Earth who will bring a new hope to the new society, living closer to the Earth and Spirit."

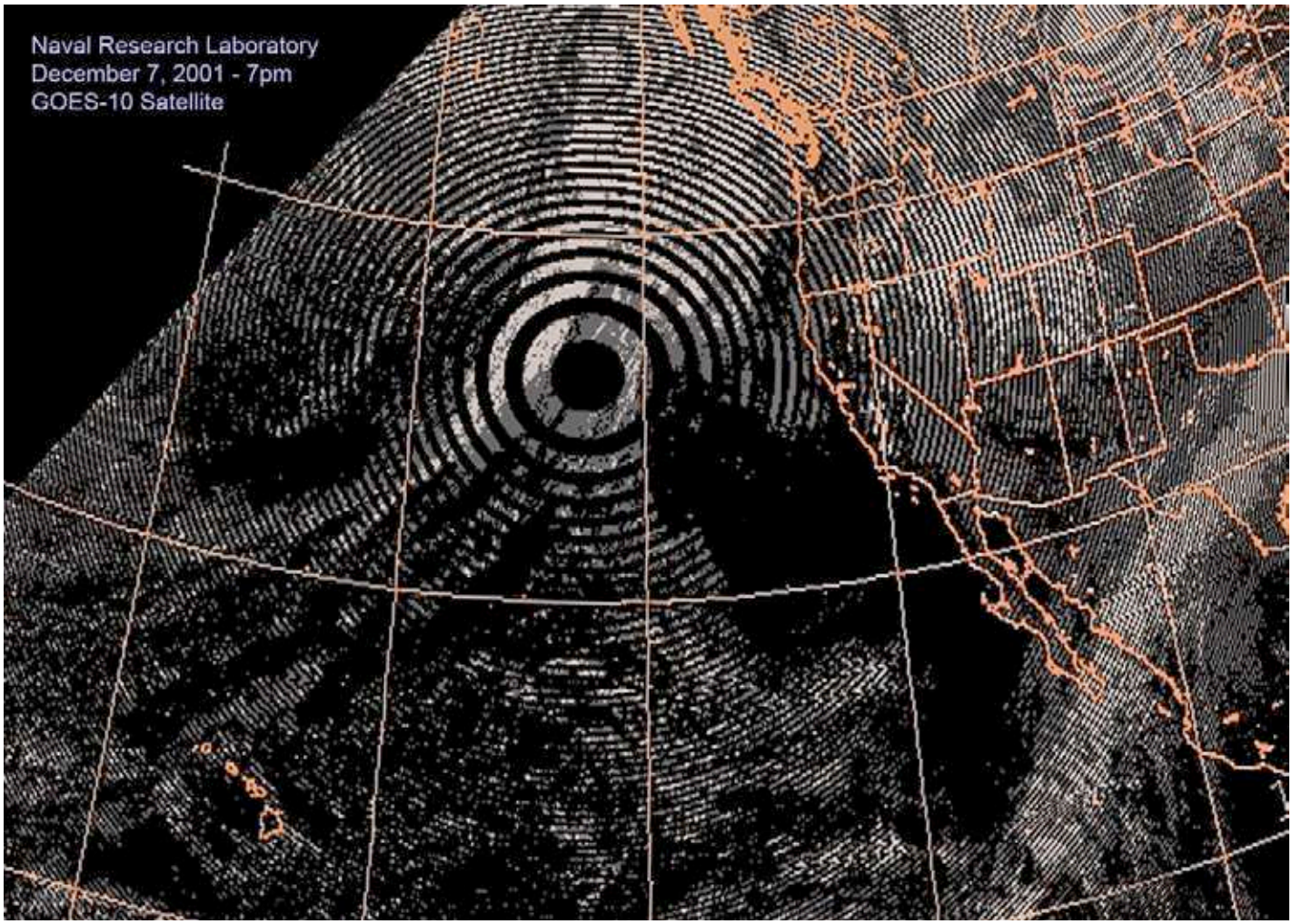

> Then all was silent, the landscape cleared and returned to normal, and Grandfather stepped from the Vision. Shaken, he said that he had wandered for the next season, trying to understand all that had been given to him, trying to understand why he had been chosen.
>
> Grandfather had related the story to me in great detail during that night of the four prophecies. I don't think that any event had been left out, and his emotions and thoughts were such that he actually relived it for us. Thus the power of his Vision became part of our spirit, our driving force, and a big part of our fears.[9]

The prophetic accuracy of Stalking Wolf's visions are quite stunningly clear thus far, both in their highly detailed descriptions and sequence of events, as presented to the young Tom Brown and friends. Here is the prophesied timeline as interpreted in the context of the ongoing magnetic polar reversal:

1st Sign:	1975–1985	African famine and AIDS pandemic spread
2nd Sign:	1985–1995	Holes form in Earth's ozone layer, permitting destructive solar rays
3rd Sign:	Dec 22, 2012	Magnetic reversal ignites a plasma canopy seen as red skies worldwide
4th Sign:	2013–2023	Large-scale destruction of low-resonance human technology ensues

Apache Grandfather Stalking Wolf experienced visions of the dramatic changes that have since occurred, and are yet to come, providing us with the culminating event marking the emergence of a new solar era. However, there are multitudes of more subtle signs of these oncoming electromagnetic changes that can be understood only in this context. The effects of shifting gravity and enhanced electromagnetic fields have been documented all over world, especially in areas where we find pyramids, or megalithic structures. These electromagnetic fields are focused by the axis-symmetric geometries of the pyramids of Giza, Egypt, thereby redistributing solar energy into a fixed global pattern of infrasound standing waves. These patterns of infrasound resonance have even been observed by satellite during the last solar maximum, on the night of December 7-8, 2001, in the infrared spectrum (above).[10]

Deeply resonant humming heard in these infrasound hotspots is continually generating millions of reports of disturbance and annoyance worldwide, with new telephone hotlines even fielding calls from concerned residents to quell the panic. Deep infrasound booms like heartbeats have been reported all over the world by residents of Llanidloes, Mawnan, Bridlington, Auckland, Sydney, Klai, Ranchlands, and in the US in Anderson,[11] Kimberley,[12] Richmond,[13] Wilmington,[14] Knoxville,[15] Mobile,[16] Knob Noster,[17] Denver,[18] Seattle,[19] Arroyo Grande[20] and Atwater.[21] Infrasound resonance focal points in the US are mapped below.

What is initially perceived as an annoyance quickly becomes a clear and present danger, as the infrasound resonance starts to overload all metals and wires with electricity until the extreme heat ignites fires. As Stalking Wolf emphasizes, “when the sky bleeds fire, there will be no safety in the world of man.” All of the modern electrical technologies of humanity will not only cease to function, but will endanger human beings by spontaneous combustion. The surprising ignition of plastic-sheathed copper wiring was first noted in 1859 when a massive solar ejection shorted out and then ignited telegraph lines across the entire United States and all of Europe, and auroras were seen as far south as Rome and Hawai’i.[22]

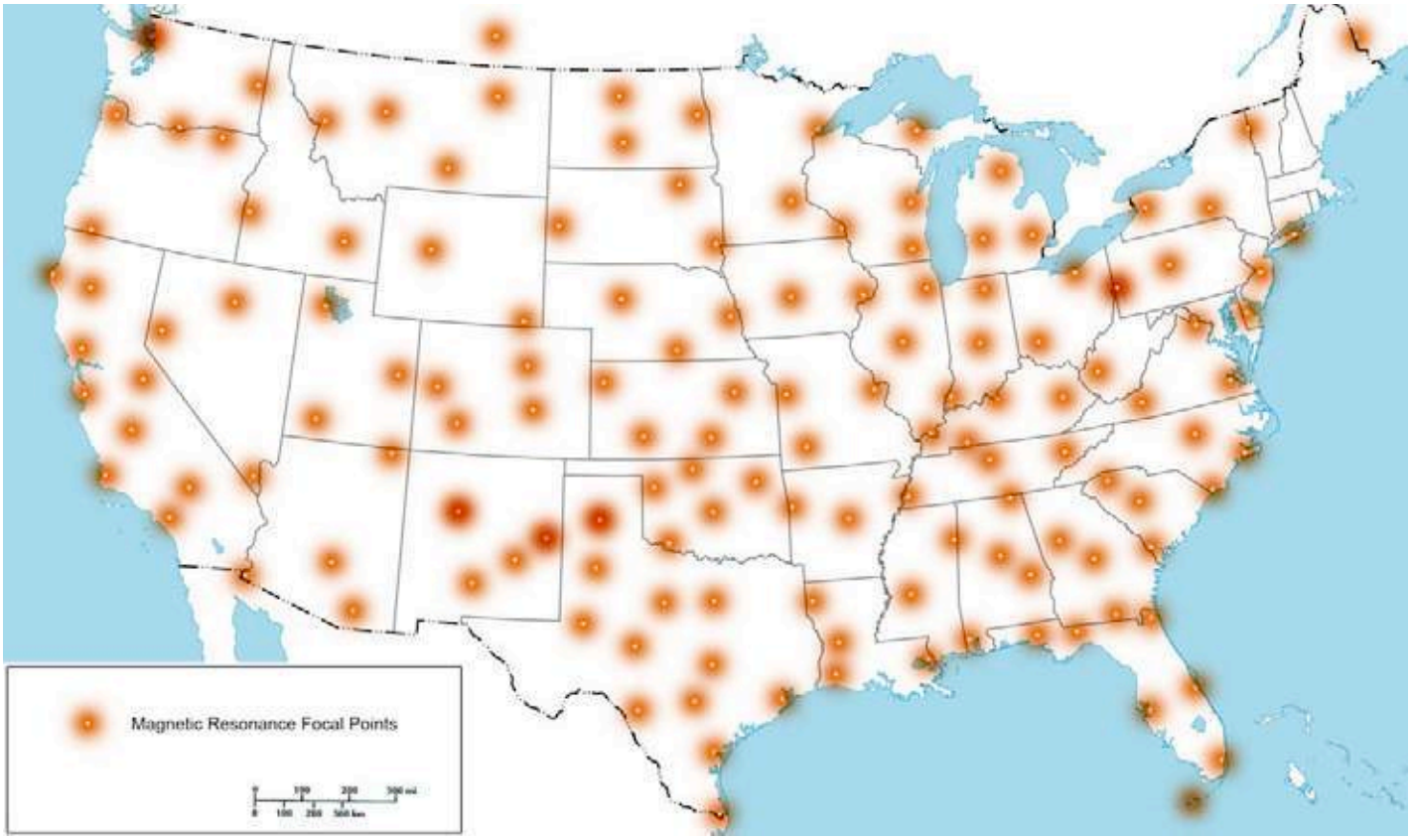

Periods of elevated infrasound resonance have generated hundreds of fires in homes across the world. These resonant fires are located in the nodes of an infrasound standing wave pattern that is increasing in intensity, eventually requiring total evacuation of residents from areas like Tenerife,[23] Babura,[24] Lalapansi,[25] Mapuve,[26] Bodibe,[27] Landovica,[28] Peschici,[29] Berici,[30] Messina,[31] northern Greece,[32] Kishtwar,[33] Ratria,[34] Santo Tomas,[35] and in the US in Seattle,[36] Colorado Springs,[37] San Mateo[38] and Santa Barbara.[39] A grave danger to personal safety in these regions of infrasound resonance will be posed by cellphones, which will ignite spontaneously in the pockets of clothing, as discovered already by one unfortunate man in Vallejo, California.[40] Such surprising events will be an inevitable occurrence in the years to come.

One of the most interesting incidents of this kind recently occurred in Soesterberg, Netherlands where, on the morning of July 19, 2009, ball lightning descended on the town in an unprecedented series of events.[41] Residents reported fast-moving ball lightning in more than 100 homes that sustained extensive damage to electrical systems. One eyewitness described a purple beam of light that shot skyward through the roof of one home. The fact that nobody was injured in Soesterberg is remarkable.

Clearly, modern civilization's embrace of electrical wiring is becoming a dangerous trap in many parts of the world, eventually threatening to kill anyone who cannot return to a life close to spirit and in the natural places of the Earth. Even high above the planet, infrasound drumming has been reported on multiple occasions onboard the International Space Station (ISS) in 2004 – the result of an infrasound resonance of standing waves that will inevitably destroy the station's systems as it has in many homes far below:

> The two men aboard the international space station heard a strange metallic sound again Friday, four months after being startled by it the first time… Cosmonaut Alexander Kaleri was talking to flight controllers in Moscow when he heard a loud drum-like noise coming from the instrument panel of the station's Russian-built living quarters.
>
> Kaleri and astronaut Michael Foale first heard the mystery noise - described as a flapping sheet of metal - back in late November. Neither the crewmen nor flight controllers were ever able to identify the sound… "It's very strange," Russian Mission Control said. "I doubt that it would be a coincidence that you're hearing the same thing coming from the same place."
>
> During a spacewalk in February, Kaleri and Foale were supposed to check the exterior of the space station where the noise originated last November. But Kaleri's spacesuit overheated and became damp, and the spacewalk had to be cut short, so the men did not have time to inspect the area.[42]

The fact that Kaleri's investigative spacewalk was not possible as his spacesuit overheated is another result of the electrical effects of the standing wave resonance. While the event has been passed off as the result of 'space junk', NASA directed a spacewalk mission that abruptly failed, yet no link has been drawn between the anomalous acoustic energy heard with the anomalous heating of the astronaut's spacesuit. The infrasound energy that is likely causing the noisy drumming and the overheating of the cosmonaut's spacesuit will likely recur for a longer duration, building an electrical charge capable of rendering the systems of the International Space Station inoperable.

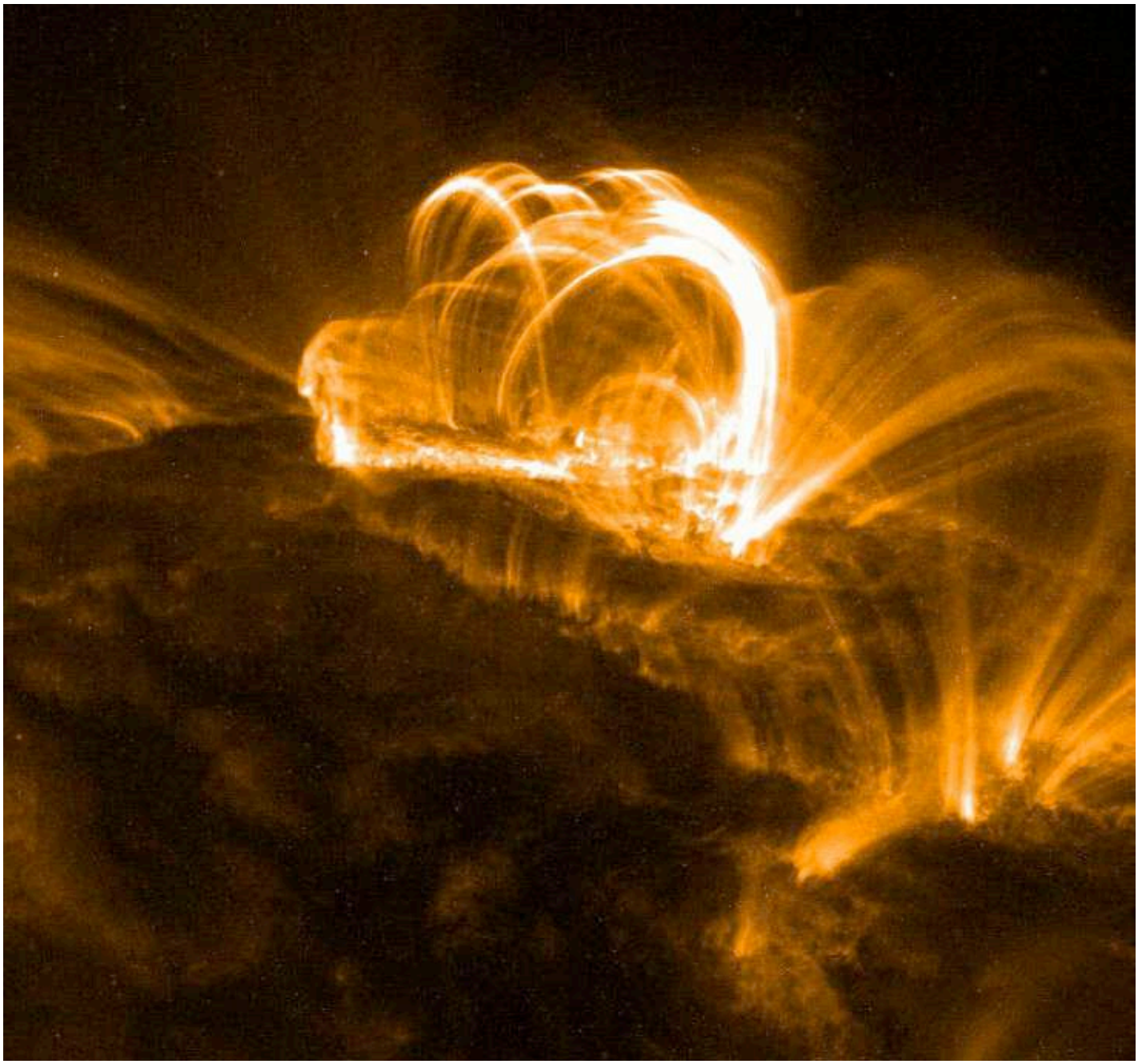

Hopi Elder White Feather relates a sacred prophecy describing the nine signs preceding the emergence of the new solar age on Earth – known to the Hopi as The Fifth World. The final sign clearly describes the destruction of the ISS as the last warning preceding the morning of the Red Dawn:

> "And this is the Ninth and Last Sign: You will hear of a dwelling-place in the heavens, above the Earth, that shall fall with a great crash. It will appear as a blue star. Very soon after this, the ceremonies of my people will cease.
>
> "These are the Signs that great destruction is coming. The world shall rock to and fro. The white man will battle against other people in other lands -- with those who possessed the first light of wisdom. There will be many columns of smoke and fire such as White Feather has seen the white man make in the deserts not far from here. Only those which come will cause disease and a great dying.
>
> "Many of my people, understanding the prophecies, shall be safe. Those who stay and live in the places of my people also shall be safe. Then there will be much to rebuild. And soon - very soon afterward - Pahana will return. He shall bring with him the dawn of the Fifth World. He shall plant the seeds of his wisdom in their hearts. Even now the seeds are being planted. These shall smooth the way to the Emergence into the Fifth World."

The Hopi prophecy details the order of events to occur, which can be deciphered when combined with the Mayan calendar wisdom which links the Red Dawn prophecy with the end date of 12.22.2012. Thus, the ISS may be interpreted as the sign of the Blue Star Katchina that precedes the 2012 event, like an alarm clock heralding its imminence. The Hopi tell that soon after the fall of the space station will come the appearance of the Red Star Katchina bringing the Day of Purification, when the skies in all lands of the Earth will bleed red.

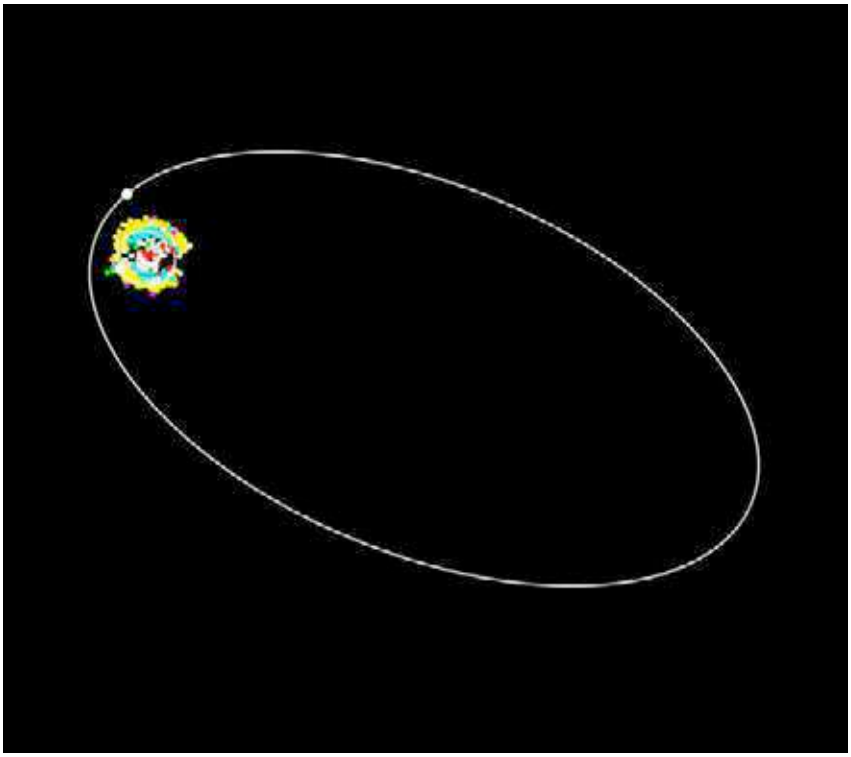

Hopi Elders describe this future cosmic event in simple and clear terms: “a small Red Star which will come very close and sit in our heavens watching us.” Now, just wait a minute… stars are not known to wander around and sneak up on anyone! What exactly is being suggested by the Hopi? While it may come as a startling surprise for many, the Hopi description *accurately* reflects the scenario presented by the Binary Research Institute.[43] Astro-physics is now coming to grips with the reality that our solar system is a binary star system - that we will imminently discover a dark star companion in close proximity to our sun. The binary model is the only one that predicts the extremely elliptical orbit of Sedna (inset diagram at left), which must be highly influenced by our sun’s dark twin to maintain such an orbit.[44]

The Hopi sacred prophecies tell of the impending incandescence of a red star in the close vicinity of Earth, describing it as a revelation of the solar twins. The now hidden brown dwarf companion star will soon reach a critical proximity to the sun – its dormant surface will reignite, transforming it into a brilliant red star. The small size and dark brown color of the long-ago extinguished dark twin sun has allowed it to creep on its elliptical path back into close proximity of the solar system without our awareness, and its ignition will likely be triggered by the imminent wave front from the supernova of Betelgeuse.

The red light of purification will emanate from this newly visible star, dramatically changing the color of our skies to a flaming red. This is referred to in the ancient wisdom as the Red Dawn of the forever cycle, where the consciousness and DNA of every living being will be transformed through the influence of the red light. Dr. Robert Ghostwolf and the Hopi Elders retell sacred traditional prophecies of the coming of the new world as an opportunity for the advancement of consciousness:

> The return of the Blue Star Katchina who is also known as Nan ga sohu will be the alarm clock that tells us of the new day and new way of life, a new world that is coming. This is where the changes will begin. They will start as fires that burn within us, and we will burn up with desires and conflict if we do not remember the original teachings, and return to the peaceful way of life.
>
> Not far behind the twins will come the Purifier, the Red Katchina, who will bring the Day of Purification. On this day the Earth, her creatures and all life as we know it will change forever. There will be messengers that will precede this coming of the Purifier. They will leave messages to those on Earth who remember the old ways.
>
> The messages will be found written in the living stone, through the sacred grains, and even the waters (Crop Circles have been found in ice). From the Purifier will issue forth a great Red Light. All things will change in their manner of being. Every living thing will be offered the opportunity to change from the largest to the smallest thing.

Those who return to the ways given to us in the original teachings, and live a natural way of life will not be touched by the coming of the Purifier. They will survive and build the new world. Only in the ancient teachings will the ability to understand the messages be found.

It is important to understand that these messages will be found upon every living thing, even within our bodies, even within a drop of our blood. All life forms will receive the messages from the twins... those that fly, the plants, even the rabbit. The appearance of the twins begins a period of seven years and will be our final opportunity to change our ways. Everything we experience is all a matter of choice...

When the Purifier comes we will see him first as a small Red Star which will come very close and sit in our heavens watching us. Watching us to see how well we have remembered the sacred teachings. This Purifier will show us many miraculous signs in our heavens. In this way we will know Creator is not a dream. Even those who do not feel their connection to spirit will see the face of creator across the sky. Things unseen will be felt very strongly.

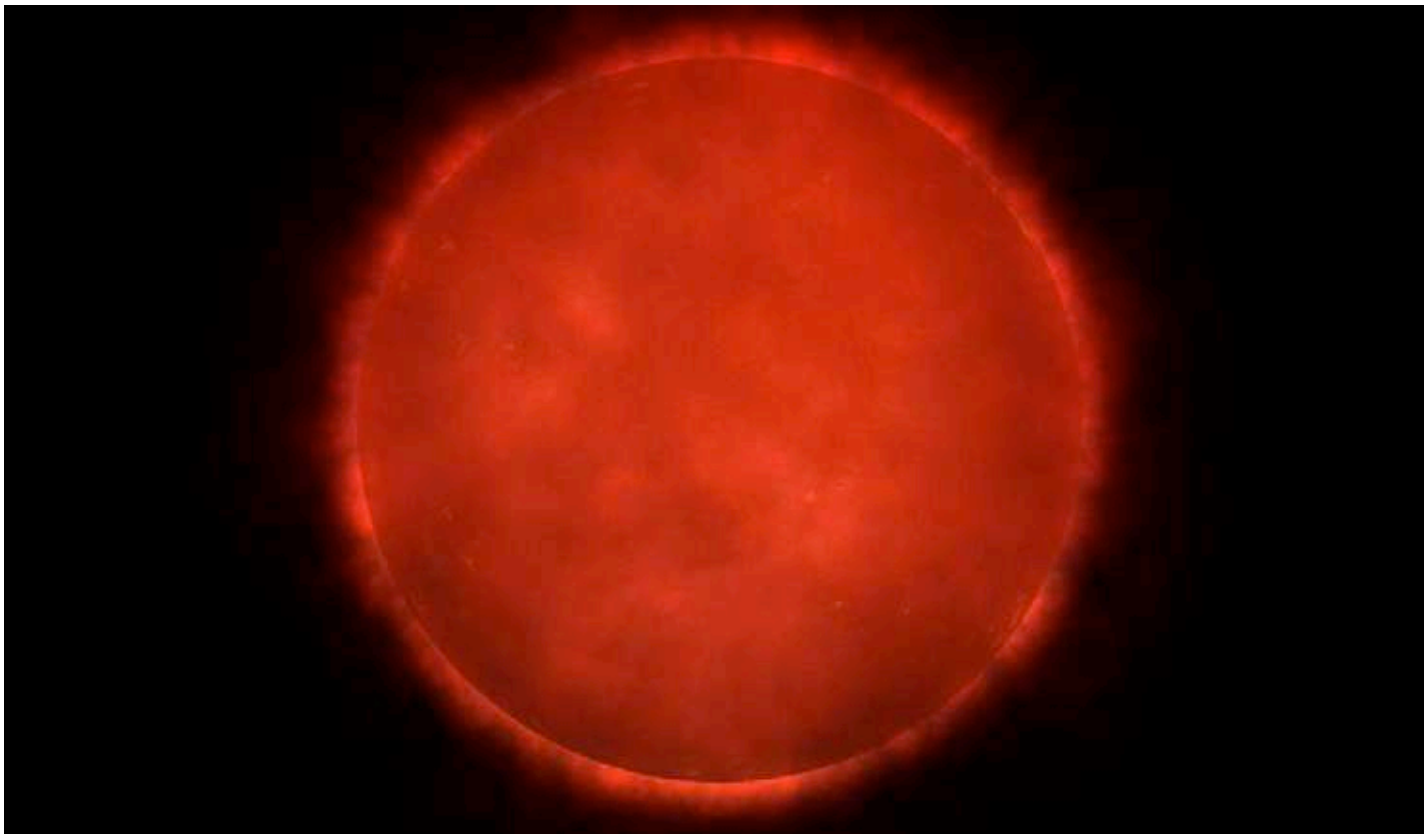

Many things will begin to occur that will not make sense, for reality will be shifting back in and out of the dream state. There will be many doorways to the lower world that will open at this time. Things long forgotten will come back to remind us of our past creations. All living things will want to be present for this day when time ends, and we enter the forever cycle of the Fifth World.

We will receive many warnings allowing us to change our ways from below the Earth as well as above. Then, one morning in a moment, we will awaken to the Red Dawn. The sky will be the color of blood, many things will then begin to happen that right now we are not sure of their exact nature. For much of reality will not be as it is now.[45]

Hopi culture foretells invisible acoustic changes in the environment and in the hearts of human beings, as “things unseen will be strongly felt.” The Elders inform us “the messages will be found written in the living stone, through the sacred grains, and even the waters (Crop Circles have been found in ice).” For decades now, conscious plasma orbs have been forming geometric messages in ice and grain fields, providing coherent mathematical formulas. The most complex quadratic functions were rendered in England, where the Mandelbrot Set [$z_{n+1} = z_n^2 + c$] appeared in Ickleton in 1991.[46] Subsequent agro-glyphs formed at Lurkley Hill in 2006[47] and Wayland Smithy in 2008[48] presented a variation on the fractal formula: [$z_{n+1} = z_n^2$]. Remarkably, this formula exactly describes unusual IR satellite data from 2001.

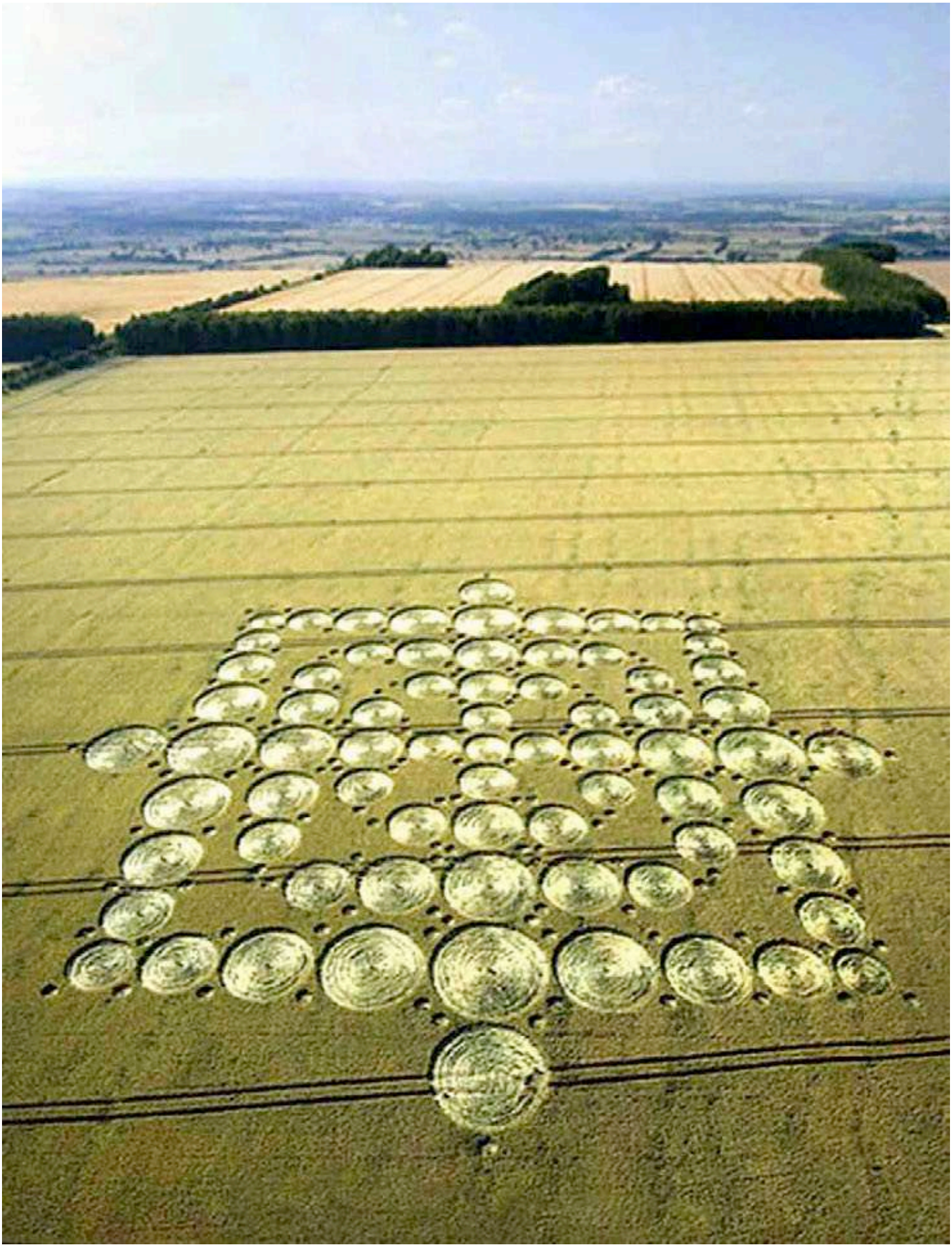

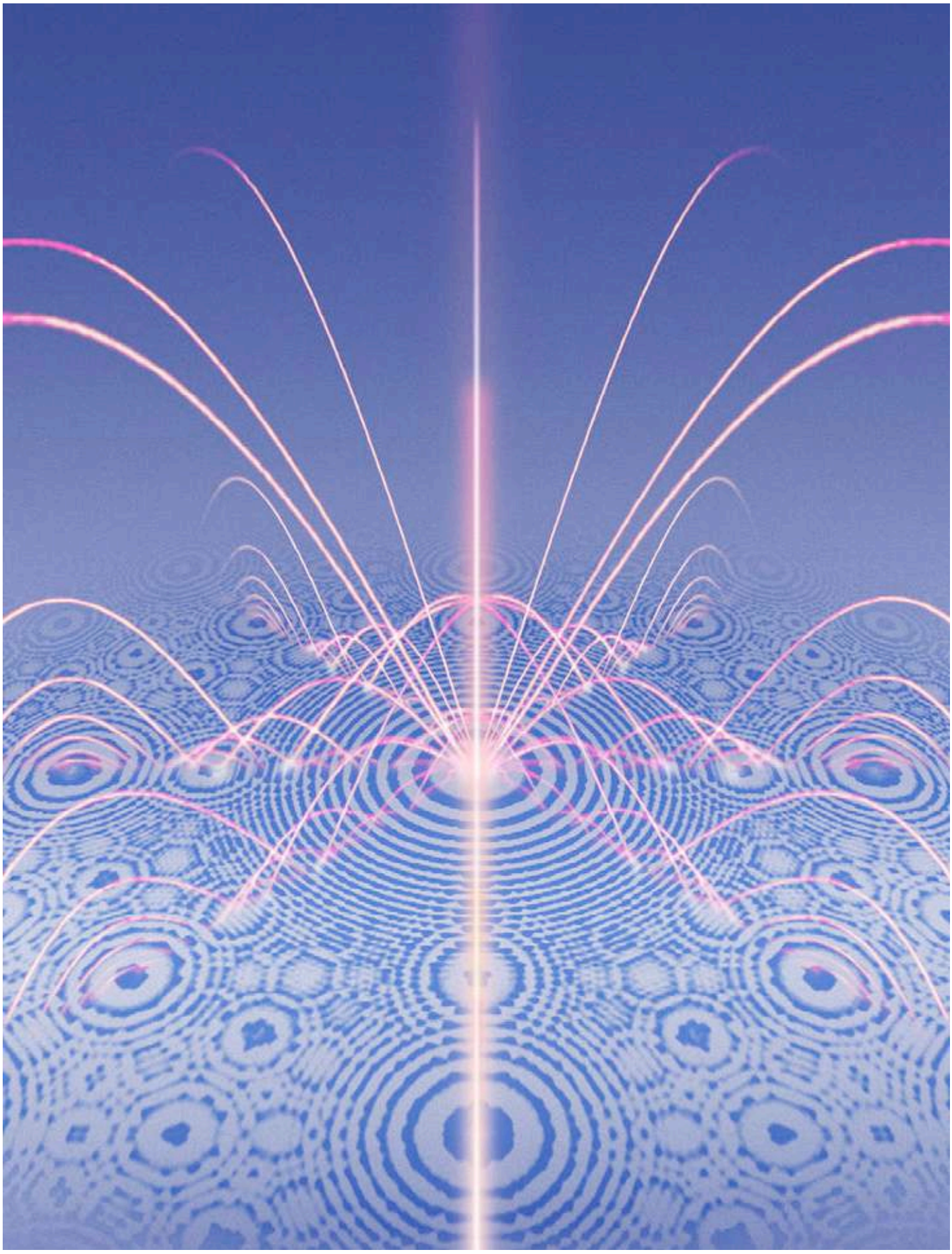

The sacred grains of England were also impressed with the value of Pi in 2008, in the form of a ratcheted spiral that accurately renders the first 10 digits (3.141592654…).[49] The conscious plasma ball entities that form these stunning messages are offering advanced hyper-dimensional mathematics to human beings at this time in our spiritual development to prepare our consciousness for multi-dimensional awareness. The agroglyphs provide us with a map of the nodal points of infrasound standing wave patterns now being stimulated by increasing solar activity. The circle-makers have even provided a specific and unmistakable *calendar date* in a truly massive formation in Avebury, England in 2008, showing a precise configuration of all of the planets of the solar system – *confirming the T'zolkin calendar of the Maya:*

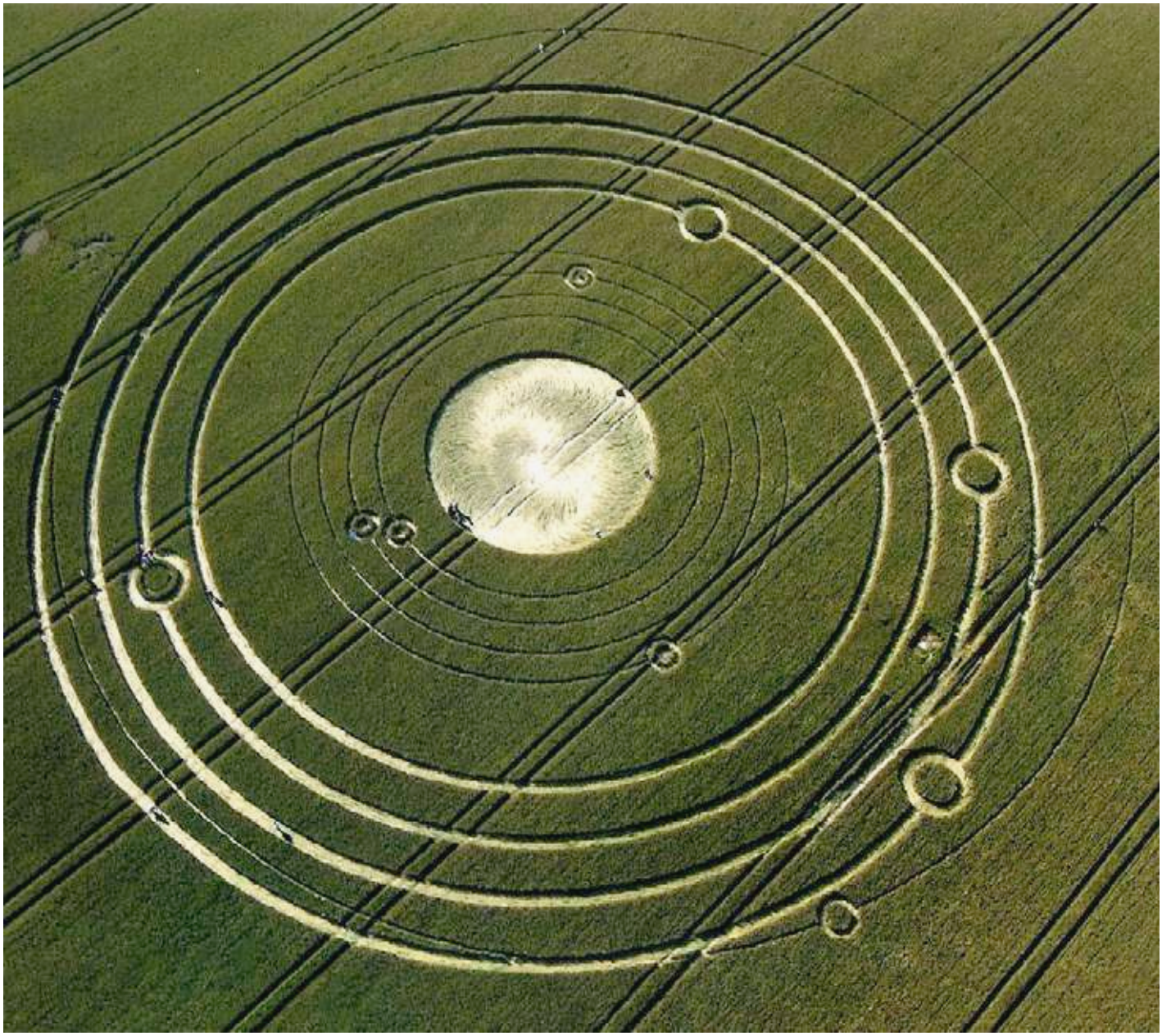

Avebury Manor of July 15, 2008 reminds us that the Mayan Long Count calendar will end on December 23, 2012: by showing precise orbital locations for all nine planets of our solar system on that date, plus an accurate elliptical orbit for Pluto.

The 5125-year Mayan Long count calendar will end on December 22-23, 2012. Given the long period of time which it represents, all nine planets of our solar system need to be shown in order to mark its end uniquely. Such a clever astronomical diagram was shown at Avebury Manor on July 15, 2008. All nine planets appear there precisely as they will be located in space four and one-half years from now on December 23, 2012...[50]

The indigenous Elders tell us that the messages of change will be received inside all living things, and each will be given an opportunity to change. Russian researchers have used infrasound and light waves to induce DNA transmutation, by which one species is genetically transmuted into another.[51] This discovery provides a new framework for quantum leaps in evolution, whereby quantum shifts from high to low levels of planetary infrasound resonance regulate the expression of DNA in Earth's many lifeforms.

New animal species are being encountered that are a sign of planet-wide genetic transmutations now occurring in hotspots of infrasound humming. An unusual new species now recorded often is a mostly hairless variety of purple/grey-skinned canine dubbed the 'hyote' (hyena/coyote, juvenile seen alive in captivity above), photographed and videotaped in Minnesota,[52] Maryland, Texas and Saudi Arabia. Sightings of various giant species of 'thunderbirds' have also been increasing around the world as species exhibit spontaneous DNA changes.

Another example of a new species now emerging at hotspots throughout the world is a kind of gracile fox that displays a long neck and large ears, with a tan coat that can be subtly spotted on the backside. The animal's fine facial features, combined with the extremely elongated limbs and tail, give it a deer-like appearance. This 'deerfox' has been photographed and observed in the US in England (pregnant female and two juveniles seen in separate photographs, above).[53]

These same infrasound-related DNA changes are expressed in extraordinary human beings who possess profound cosmic knowledge of their pristine origins and the unlimited holographic capabilities enabled by such knowledge. A shining example of this truth is a young woman from the taiga forests of Siberia named Anastasia who has mastered ayurveda – *the art of living.* Having inherited the deepest of cosmic wisdom from her Vedruss forefathers, Anastasia provides us with the spiritual information that will germinate the seeds of human divinity now being planted in the fields of the Earth. The voices of the indigenous Elders of the world speak as one, revealing ancient Vedic knowledge of the transdimensional nature of human consciousness to guide our path of ascent into the red light of Oneness.

The Sanskrit wisdom traditions of Russia have recently revealed a profound knowledge of nature that forms the basis for the use of heartbeat resonance in monumental psychoacoustics. Timeless Vedic wisdom understands the seed as physician and the tree as an organic antenna - a collector of cosmic energy for the single purpose of powering the human heart and spirit. The Vedruss Elders of Siberia reveal their process of DNA imprinting of seeds for the creation of a resonant field of heartbeat synchronization.[54] By heartbeat entrainment through seed imprinting, the family of Anastasia has created a resonant field of infrasound that amplifies their heartbeat to enable astral travel through the Akashic field of planetary infrasound standing waves *on the heartbeat frequency of love*:

> "When someone is in a state of love they emit a radiant energy. It takes but a split second for it to reflect off the planets floating overhead and come back to Earth to give life to everything that breathes… The Sun is one of those planets, and it reflects but a tiny fraction of such radiance. Only bright rays can travel into Space from Man on the Earth. And only beneficial rays can be reflected from Space back to Earth."
>
> "Under the influence of malicious feelings Man can emit only dark rays. These dark rays cannot rise but must fall into the depths of the Earth. Bouncing off its core, they return to the surface in the form of volcanic eruptions, earthquakes, wars, etc. The culminating achievement of these dark rays is their direct effect on the Man originating them, invariably exacerbating the man's own malicious feelings." [55]

Vedruss knowledge echoes the call of the Hopi Elders, who foretell of the great increase in the energies moving through human beings, whose inner emotional states will become amplified in the light of the Red Purifier to manifest as fires that will burn within us. *Malevolent feelings will consume those who harbor them, while the rays of love will also become equally amplified to generate healing forces in human beings who harbor a deep Creational love by living as one being in heartbeat resonance.*

Hopi Elders also foretell of portals to the lower worlds that will be opening at this time to remind us of our past creations. Referred to as *'sipapu'*, these lower realms are described in Hopi wisdom traditions as having been used to preserve the human race during previous cataclysmic events on Earth. Yaqui Elder Don Juan elaborated on the secret knowledge possessed by ancient Nahuatl seers pertaining to the motive properties of fire and water for bodily transport to fourth-density realms of inorganic life, in artificially generated HHO plasma chambers both above and below the Earth's surface:

> He continued then with his elucidation of the practices of the old seers. Another of their great findings had to do with the category of secret knowledge: fire and water. They discovered that flames have the most peculiar quality; they can transport man bodily, just as water does... They considered flames and fluidity to be higher, magical properties, and they used them as a means for bodily transportation to the realm of inorganic life.[56]
>
> Don Juan said that the old seers observed that the wetness of water only dampens or soaks, but the fluidity of water moves. It runs, they surmised, in search of other levels underneath us. They believed that water had been given to us not only for life, but also as a link, a road to the other levels below... to be transported bodily by the fluidity of water anywhere between this level of ours and the other seven levels below.[57]
>
> The knowledge of the below had to do with fog, water of underground springs, swamps, lightening bolts, earthquakes, the night, moonlight and the moon.[58]
>
> "[Some men of knowledge] endeavored to use *seeing* positively and to teach it to their fellow men. I'm convinced that under their direction, the populations of entire cities went into other worlds and never came back." [59]

“The old seers *saw* that the Earth has a cocoon,” he went on. “They *saw* that there was a ball encasing the Earth, a luminous cocoon that entraps the Eagle’s emanations. The Earth is a gigantic sentient being subjected to the same forces we are.” [60]

”[Don Juan stated that]… one of the most worthwhile findings of the ancient seers... was the discovery that organic life is not the only form of life present on this Earth... For seers, to be alive means to be aware... For the average man, to be aware means to be an organism. This is where seers are different. For them, to be aware means that the emanations that cause awareness are encased inside a receptacle.[61]

The circular aspect... is what maintains life and awareness, fulfillment and purpose... “The reason that it’s called the circular force is that it comes in rings, thread-like hoops of iridescence... it strikes all living beings ceaselessly... to give them strength, direction, awareness; to give them life... It’s one indivisible force that fits all living beings, organic and inorganic.” [62]

“They say that perception is a condition of alignment... Alignment is what allows awareness to be cultivated by every living creature...” When seers *see* perception, they witness that the luminosity of the... emanations outside those creatures’ cocoons brightens the luminosity inside their cocoons. The outside luminosity attracts the inside one; it traps it, so to speak, and fixes it. That fixation is the awareness of every specific being.[63]

He explained that what he called the key to everything was the first-hand knowledge that the Earth is a sentient being and as such can give warriors a tremendous boost; it is an impulse that comes from the awareness of the Earth itself at the instant in which the emanations inside the warriors’ cocoons are aligned with the appropriate emanations inside the Earth’s cocoon. Since both the Earth and man are sentient beings, their emanations coincide, or rather, the Earth has all the emanations that are present in man and all the emanations present in all sentient beings, organic or inorganic for that matter. When a moment of alignment takes place, sentient beings use that alignment in a limited way and perceive their world. Warriors can use that alignment either to perceive, like everyone else, or as a boost that allows them to enter unimaginable worlds.[64]

He explained that the Earth’s boost is the force of alignment of only the amber emanations. It is a boost that heightens awareness to unthinkable degrees. To the new seers it is a blast of unlimited consciousness, which they call total freedom.[65]

Don Juan restated over and over that the portion of the emanations inside man’s cocoon is in there only for awareness, and that awareness is matching that portion of the emanations with the same portion of emanations at large. They are called emanations at large because they are immense... inside man’s cocoon the unknown is the emanations untouched by awareness. When the glow of awareness touches them, they become active and can be aligned with the corresponding emanations at large. Once that happens the unknown is perceived and becomes the known.[66]

The Eagle, that power that governs the destiny of all living things, reflects equally and at once all those living things… [and] although it is not moved by the circumstances of any living thing, has granted a gift to each of those beings. In its own way and right, any one of them, it if so desires, has the power to keep the flame of awareness, the power to disobey the summons to die and be consumed. Every living thing has been granted the power, if it so desires, to seek an opening to freedom and to go through it. It is evident to the seer who sees the opening, and to the creatures that go through it, that the Eagle has granted that gift in order to perpetuate awareness.

For the purpose of guiding living beings to that opening, the Eagle created the Nagual. The Nagual is a double being to whom the rule has been revealed. Whether it be in the form of a human being, an animal, a plant, or anything else that lives, the Nagual by virtue of its doubleness is drawn to seek that hidden passageway.

The Nagual comes in pairs, male and female. A double man and a double woman become the Nagual only after the rule has been told to each of them, and each of them has understood it and accepted it in full… To the eye of the seer, a Nagual man or a Nagual woman appears as a luminous egg with four compartments. Unlike the average human being, who has two sides only, a left and a right, the Nagual has the left side divided into two long sections, and a right side equally divided in two.

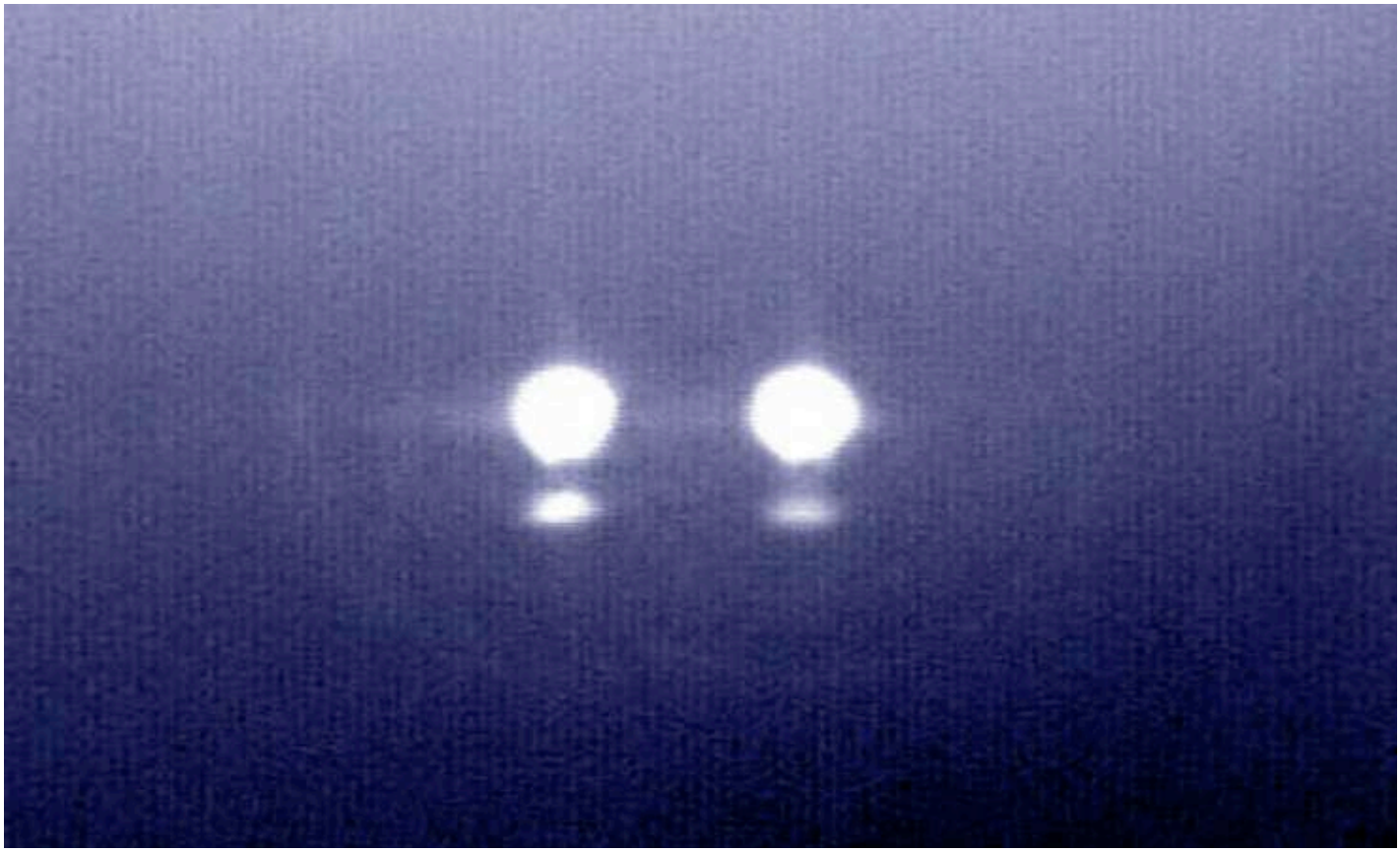

The Eagle created the first Nagual man and first Nagual woman as seers and immediately put them in the world to see. It provided them with four female warriors who were stalkers, three male warriors, and one male courier, whom they were to nourish, enhance and lead to freedom… In order to make sure that the first Nagual man would lead his party to freedom and not deviate from that path or become corrupted, the Eagle took the Nagual woman to the other world to serve as a beacon, guiding the party to the opening.

The Nagual and his warriors were then commanded to forget. They were plunged into darkness and were given new tasks: the task of remembering themselves, and the task of remembering the Eagle… The command to forget was so great that everyone was separated. They did not remember who they were. The Eagle intended that if they were capable of remembering themselves again, they would find the totality of themselves. Only then would they have the strength and forbearance necessary to seek and face their definitive journey.

Their last task, after they had regained the totality of themselves, was to get a new pair of double beings and transform them into a new Nagual man and a new Nagual woman by virtue of revealing the rule to them…

Don Juan explained that the rule was not a tale, and that to cross over to freedom did not mean eternal life as eternity is commonly understood –that is, as living forever. What the rule stated was that one could keep the awareness which is ordinarily relinquished at the moment of dying… [A]t the moment of crossing, one enters into the third attention, and the body in its entirety is kindled with knowledge. Every cell at once becomes aware of itself, and also aware of the totality of the body… Therefore the crux of the warrior's struggle was not so much to realize that the crossing over stated in the rule meant crossing to the third attention, but rather to conceive that there exists such an awareness at all.[67]

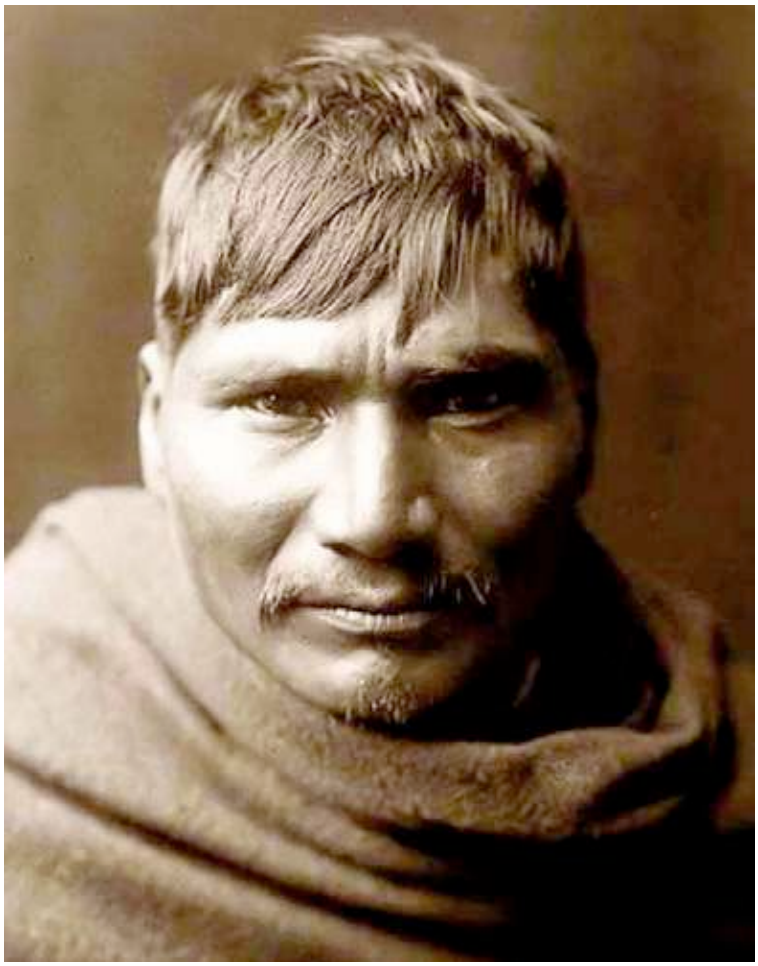

“Seers say that there are three types of attention... they are rather three levels of attainment. They are the first, second, and third attention, each of them an independent domain, complete in itself.” He explained that the first attention in man is the animal awareness... everything that one can think about is part of the first attention... [68]

Don Juan explained that in order for our first attention to bring into focus the world that we perceive, it has to emphasize certain emanations selected from the narrow band of emanations where man’s awareness is located. The discarded emanations are still within our reach but remain dormant, unknown to us for the duration of our lives. The new seers call the emphasized emanations the right side, normal awareness, the tonal, this world, the known, the first attention. The average man calls it reality, rationality, common sense.

The emphasized emanations compose a large portion of man’s band of awareness, but a very small piece of the total spectrum of emanations present inside the cocoon of man. The disregarded emanations within man’s band are thought of as a sort of preamble to the unknown, the unknown proper consisting of the bulk of emanations which are not part of the human band and which are never emphasized. Seers call them the left-side awareness, the nagual, the other world, the unknown, the second attention.[69]

“[To be able]… to utilize those unused emanations, one needs uncommon, elaborate tactics that require supreme discipline and concentration... the art of *dreaming*... the concentration needed to be aware that one is having a dream is the forerunner of the second attention. That concentration is a form of consciousness that is not in the same category as the consciousness needed to deal with the daily world.

“The new seers... let the mastery of awareness develop to its natural end, which is to extend the glow of awareness beyond the bounds of the luminous cocoon in one single stroke. The third attention is attained when the glow of awareness turns into the fire from within: a glow that kindles not one band at a time but all the... emanations inside man’s cocoon.”

Don Juan expressed his awe for the new seers’ deliberate effort to attain the third attention while they are alive and conscious of their individuality... “The supreme accomplishment of human beings,” he said, “is to attain that level of attention while retaining the life-force, without becoming a disembodied awareness moving like a flicker of light...”[70]

[He then explained that]...the glow produced by a state of total awareness... is *seen* as a burst of incandescence in the entire luminous egg. It is an explosion of light of such a magnitude that the boundaries of the shell are diffused and the inside emanations extend themselves beyond anything imaginable.

“Are those special cases, don Juan?”

“Certainly. They happen only to seers. No other living men or any other living creatures brighten up like that. Seers who deliberately attain total awareness are a sight to behold. That is the moment when they burn from within. The fire from within consumes them. And in full awareness they fuse themselves to the emanations at large, and glide into eternity.

[As seers] our case is a bit different, because we are at the end of our trail. We are not seeking anything... we go from day to day doing nothing. We are waiting. I will not tire of repeating this: we know that we are waiting and we know what we are waiting for. We are waiting for freedom!” [71]

A Great Cycle of approximately 309,888 years (12 x 12 Precession cycles of 2,152 years) nears completion with the returning Dark Star on its near 36,650 year elliptical cycle (2,152 x 17 = 36,584), as red supergiant Betelgeuse shrinks in collapse, poised to illuminate all that is hidden within the shadows of the human heart and our entire solar system. Prophetically foretold signs are to be seen in their dramatic fulfillment in all parts of the world. Infrasound resonance surges as intense heartbeat booming and ignites piezoelectric fires at nodal points in all parts of the world. The many Oort comet impacts and aerial fireballs witnessed all over the world in 2010 will continue to increase in frequency for several years as a constant threat to the delicate biosphere of Earth in these revelatory times preceding the supernova blast wave of December 22, 2012, and until 2028.

The initiation of celestial waters at sacred pyramid sites illuminates the interior chambers of the pyramids with the heavenly light of the Creator, and illuminates the DNA of the initiate with the red and blue light of gold and silver nanoparticles within every cell. Intense infrasound booming will align all initiates into heart/mind synchronization inducing the synesthetic experience of collective telepathic unity, *kindling the fire from within to attain fourth-density awareness.*

The time has arrived for humanity to escape the technological perils of his own misguided making and to reconvene at our ancient pyramids and sacred sites to ascend into the red light of purification that will enhance all harmonious living beings touching the Earth during the Red Dawn of the Forever Cycle.

References

[1] Jenkins JM, Matz M (2004) *'Pyramid of Fire: Spiritual Ascent at the End of Time'* Bear & Company, pp. 81-88
[2] Men H, Yaxk'in AJ (2001) 'Mayan/Tibetan Prophecy' online · http://www.lightworkarticles.info/MayanProphecy/
[3] Sitchin Z (1999) *'The Wars of Gods and Men: Book III of the Earth Chronicles'* Harper, online · http://www.bibliotecapleyades.net/sitchin/sitchinbooks03_03.htm
[4] Putney A (2007) 'Sacred Ayurvedic Waters' *Human Resonance*, online · http://www.humanresonance.org/water.html
[5] Putney A (2008) 'Ø' *Human Resonance Productions*, pp. 116-162
[6] Quetza Sha GA (1996) *'The Manuscript of the Crystal Golden Water of Tlacote' Human Resonance,* online · http://www.humanresonance.org/tlacote.html
[7] Courtland R (2009) 'Betelgeuse the Incredible Shrinking Star' *New Scientist*, June 10, online · http://www.newscientist.com/article/dn17282-betelgeuse-the-incredible-shrinking-star.html
[8] Castaneda C (1991) '*The Fire From Within*' Washington Square Press, pp. 121
[9] Brown T (1999) 'Night of the Red Sky: The Prophetic Vision of 'Grandfather' *Nexus Magazine (7:1)*, Dec-Jan
[10] Putney A (2008) 'Satellite Records Atmospheric Anomaly' online · http://www.humanresonance.org/sphere.html
[11] Schneider J (2007) 'Mysterious Noise Annoys Anderson, Indiana Couple' *The Herald Bulletin*, August 29, online · http://www.humanresonance.org/anderson.html
[12] Murray K (2008) 'Magic Valley is Shaking – No Earthquakes Recorded' *KTVB 7 News*, March 21, online · http://www.humanresonance.org/kimberley.html
[13] -- (2004) 'Mysterious 'Booms' Continue With Puzzling Regularity in Richmond' *WWBT News*, November 19, online · http://www.humanresonance.org/richmond.html
[14] -- (2008) 'Mysterious Booms Rock Cape Fear Region' *Star News*, February 8, online · http://www.humanresonance.org/wilmington.html
[15] -- (2007) 'Rumbling Wakes Up Dozens of Knox County Residents' *WLTV News*, May 14, online · http://www.humanresonance.org/knoxville.html
[16] -- (2006) 'Mystery Booms Rattle Mobile Residents' *WPMI News*, January 19, online · http://www.humanresonance.org/mobile.html
[17] Miller JL (2007) 'Wall-Shaking, Window-Rattling Booms Heard in Missouri Still a Mystery' *Lake Sun Leader*, July 24, online · http://www.humanresonance.org/knobnoster.html
[18] -- (2007) 'Plane Windshields Crack at Denver Int. Airport' *Associated Press*, February 16, online · http://www.humanresonance.org/denver.html
[19] Callis T (2009) 'What's Causing the Mysterious Booming Sounds? No One Seems to Know' *Peninsula Daily News*, July 31, online · http://www.humanresonance.org/seattle.html
[20] -- (2007) 'Military Spokesman Responds to Report of Sonic Booms, Shaking in California' *San Luis Obispo,* July 18, online · http://www.humanresonance.org/arroyogrande.html
[21] Albrecht L (2005) 'Atwater Noise A Mystery' *Merced Sun-Star*, November 30, online · http://www.humanresonance.org/atwater.html
[22] Brit RR (2003) 'The Great Strom: Solar Tempest of 1859 Revealed' *Space.com News*, October 27, online · http://www.space.com/scienceastronomy/mystery_monday_031027.html
[23] -- (2007) 'Thousands Flee Fires in Spain's Canary Islands' *Human Resonance*, July 31, online · http://www.humanresonance.org/canary.html
[24] Olawale T (2008) 'Nigeria: Babura – Where Mystery Fires Ravaged a Community' *This Day*, March 11, online · http://www.humanresonance.org/babura.html
[25] -- (2008) 'Mystery Fire Guts Hut' *Midlands Bureau*, April 13, online · http://www.humanresonance.org/lalapansi.html
[26] Hlungwani V (2007) 'Mystery Fires Hit Village' *Sowetan News*, online · http://www.humanresonance.org/mapuve.html
[27] -- (2003) 'Community Gripped By Mystery Beneath the Earth' *SABC News*, online · http://www.humanresonance.org/bodibe.html
[28] -- (2008) 'Spontaneous Fires Ignite in 7 Houses in Landovica, Kosovo' *Human Resonance*, August 5, online · http://www.humanresonance.org/landovica.html
[29] Bertani C (2007) 'Mysterious Fires – Pyromaniacs or Paranoids?' *Human Resonance*, July 31, online · http://www.humanresonance.org/peschici.html
[30] -- (1990) 'The Berici Hills Mystery' *Sunday Express*, March 11, online · http://www.humanresonance.org/berici.html
[31] Ferrari T (2004) 'Canneto di Caronia, This is Not Your Average Ghost Town' *Human Resonance*, April 4, online · http://www.humanresonance.org/messina.html
[32] Becatoros E (2007) 'Helicopter Sent to Save Trapped Greeks' *Associated Press*, August 27, online · http://www.humanresonance.org/greece.html

[33] -- (2008) 'Mysterious Fire Engulfs Kishtwar Village' *News Agency of Kashmir*, October 12, online · http://www.humanresonance.org/kishtwar.html
[34] Ghosh R (2004) 'Villagers in Madhya Pradesh Face Mysterious Enemy' *Human Resonance*, March 21, online · http://www.humanresonance.org/ratria.html
[35] Ganzon T (2009) 'Phillipines: Batangas Town Residents Worry Over 'Mysterious' Fires' *ABS-CBN News*, January 8, online · http://www.humanresonance.org/santo_tomas.html
[36] Jones N (2001) 'Fires and Gas Explosions in Seattle' *Human Resonance*, July 27, online · http://www.humanresonance.org/seattle.html
[37] Folsom B (2008) 'Unexplained Ground Heat Burns Boy's Feet' *KOAA.com*, June 3, online · http://www.humanresonance.org/co_springs.html
[38] -- (2008) 'California: Police Investigate Mystery Car Fire' *The Examiner*, March 28, online · http://www.humanresonance.org/san_mateo.html
[39] Lin J (2008) 'Ventura County Hot Spot Puzzles Experts' *LA Times*, August 5, online · http://www.humanresonance.org/padres.html
[40] -- (2007) 'Cell Phone Catches Fire, Burns Man Over Half His Body' *Associated Press*, January 16, online · http://www.humanresonance.org/vallejo.html
[41] -- (2009) 'Ball Lightning Hits 100 Homes' *Dutch News*, July 21, online · http://www.humanresonance.org/soesterberg.html
[42] Dunn M (2004) 'Odd Space Noise Heard Again' *Associated Press*, April 2, online · http://www.humanresonance.org/space_station.html
[43] Cruttenden W (2009) 'Introduction: Binary Companion Theory' *Binary Research Institute*, online · http://www.binaryresearchinstitute.org/bri/research/introduction/theory.shtml
[44] -- (2004) 'Sedna and Sol B?' *Sol Station News*, March 15, online · http://www.humanresonance.org/sedna.html
[45] Ghostwolf R (1994) 'Hopi Prophecy Fulfilled' *Last Cry: Native American Prophecies and Tales of the End Times Magazine*, online · http://www/wolflodge.org/bluestar/bluestar.htm
[46] Putney A (2008) 'Mandala Formation in Ickleton, England' *Human Resonance*, online · http://www.humanresonance.org/ickleton.html
[47] Putney A (2008) 'Mandala Formation at Lurkley Hill in Lockeridge, England' *Human Resonance*, online · http://www.humanresonance.org/lurkley.html
[48] Putney A (2008) 'Mandala Formation in Wayland Smithy, England' *Human Resonance*, July 27, online · http://www.humanresonance.org/wayland08.html
[49] Putney A (2008) 'Mandala Formation Near Barbary Castle, England' *Human Resonance*, June 1, online · http://www.humanresonance.org/barbury08.html
[50] Collie R (2008) 'Crop Circle at Avebury Manor Reported July 15th, 2008' *Human Resonance*, July 15, online · http://www.humanresonance.org/avebury08.html
[51] Gariaev P, Grigor'ev K, Vasil'ev A, Poponin V, Shcheglov V (1999) 'Investigation of the Fluctuation Dynamics of DNA Solutions by Laser Correlation Spectroscopy' *Bulletin of the Lebedev Physics Institute* 11-12, pp. 23-30
[52] Coleman L (2009) 'Hairless Mystery Animal Photographed' *Cryptomundo*, July 10, online · http://www.cryptomundo.com/cryptozoo-news/hairless09/
[53] Moulton Howe L (2007) 'Mystery Animal Photographed in England' *Earthfiles*, online · http://www.earthfiles.com
[54] Megre V (2003) *'Anastasia'* Ringing Cedars Press, pp. 77-81
[55] Ibid, p. 7
[56] Castaneda, op cit, '*The Fire From Within*', p. 92
[57] Ibid, pp. 98-99
[58] Ibid, p. 93
[59] Ibid, pp. 18-19
[60] Ibid, p. 204
[61] Ibid, p. 90
[62] Ibid, p. 228
[63] Ibid, p. 61
[64] Ibid, p. 206
[65] Ibid, p. 247
[66] Ibid, p. 207
[67] Castaneda C (1982) *'The Eagle's Gift'* Simon & Schuster, pp.173-179
[68] Castaneda, op cit, '*The Fire From Within*' pp. 76-77
[69] Ibid, p. 116
[70] Ibid, pp. 77-78
[71] Ibid, pp. 120-121

17241

$9.95 in USA

AN ALFRED HANDY GUIDE

Essential Dictionary of Music Notation

A Practical and Concise Source for Students to Professionals

Take the mystery out of music notation. Whether you're using a pencil to sketch a melody or a computer to score a symphony, this multi-purpose quick reference is for you.

Every aspect of notation is covered in a versatile, easy-to-use format. From beginning music students to seasoned engraving professionals, everyone notating music will love this dictionary!

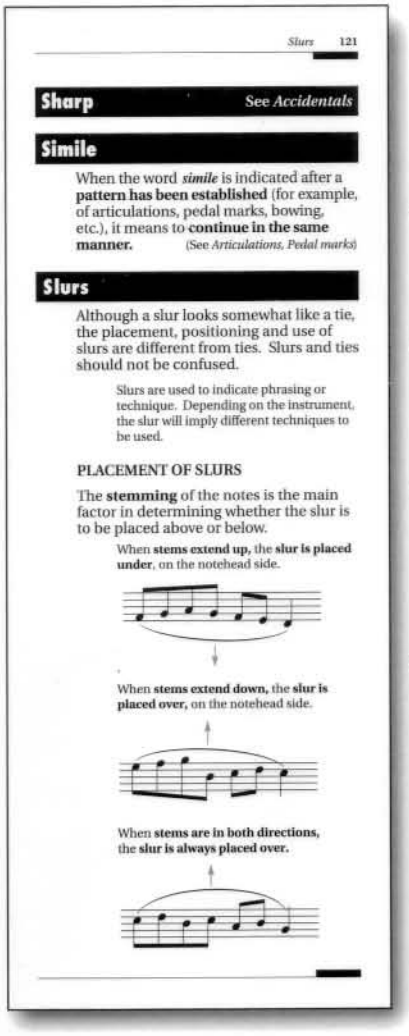

Slurs 121

Sharp See *Accidentals*

Simile

When the word ***simile*** is indicated after a **pattern has been established** (for example, of articulations, pedal marks, bowing, etc.), it means to **continue in the same manner.** (See *Articulations, Pedal marks*)

Slurs

Although a slur looks somewhat like a tie, the placement, positioning and use of slurs are different from ties. Slurs and ties should not be confused.

Slurs are used to indicate phrasing or technique. Depending on the instrument, the slur will imply different techniques to be used.

PLACEMENT OF SLURS

The **stemming** of the notes is the main factor in determining whether the slur is to be placed above or below.

When **stems extend up,** the **slur is placed under**, on the notehead side.

When **stems extend down,** the **slur is placed over,** on the notehead side.

When **stems are in both directions,** the **slur is always placed over.**

- Easy–to–use dictionary format
- Concise text is clearly illustrated
- Key words and concepts are highlighted
- Over 75 topics spanning 158 pages
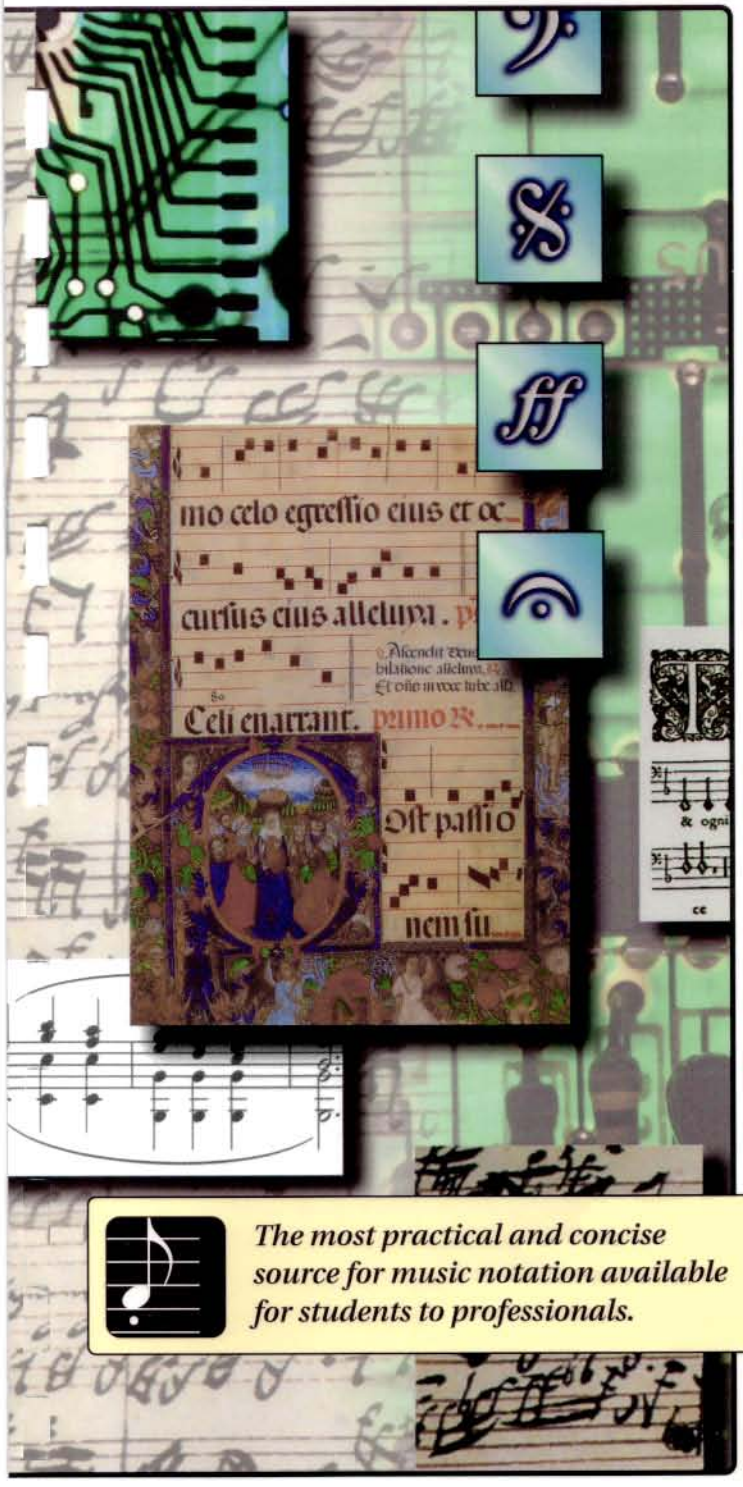
Alfred Publishing Co
16380 Roscoe Blvd.
P.O. Box 10003
Van Nuys, CA 91410

TOM GEROU • LINDA LUSK

Essential Dictionary of Music Notation

The most practical and concise source for music notation

TOM GEROU
LINDA LUSK

- Easy-to-use format, including cross-referencing
- For any musician, whether using pencil or computer
- Emphasis on correct and current notation practices
- Numerous examples, kept simple and to-the-point

Thanks to Susy Christiansen, Mitchell Newman, Greg Plumblee and Patrick Wilson

Cover design: Carol Kascsak

Cover art, center photo: From an Antiphoner, or book of music for the choir services.
Copyright © Sotheby's

Copyright © MCMXCVI by Alfred Publishing Co., Inc.
All rights reserved. Printed in USA.

ISBN 0-88284-768-6

APPROACHING MUSIC NOTATION

Music notation is a language and, as such, it must be communicable. The closer the notation adheres to common rules and guidelines, the more successfully the music will be performed. The rules and guidelines presented here will make the notation easier to read and will help to make the musical intent clear. Although these rules are not inflexible, they should not be ignored.

For music notation, the first priority is always clarity. Choices need to be made that are solely dependent on the situation; a rule may not provide the most desirable answer to a problem. (It would be an endless task to list every musical exception to a rule.) Problems are usually solved by deciding which rule is more flexible (least important to clarity).

Although meticulous adjustment can only clarify and beautify the notation, sometimes such attention to detail is not practical. All decisions must depend on a wide variety of situations. An understanding of the rules allows these choices to be made wisely—the notation can only be as good as the knowledge at hand.

ABOUT THIS BOOK

The *Essential Dictionary of Music Notation* is in an easy-to-use format, which includes cross referencing. At the top of each page, running heads show exactly which topic is being treated on that page. Bold treatments of text highlight important points for clarity and quick reference.

Text is accompanied by numerous examples directly related to the topic being discussed. These examples are kept as simple and complete as possible, with an emphasis on presenting correct and current notation practices. Obsolete rules are mentioned only when necessary.

The focus of this book has been narrowed, avoiding the discussion of orchestration or music theory, in order to present as much information as possible that is directly related to the actual *notation* of music. The serious musician is encouraged to seek out other sources that more thoroughly address the subjects of orchestration and music theory.

Whether you are using a pencil or a computer, all principles within this book are applicable. No computer software or specific tool is referenced, in order to make this a useful guide for any musician.

An *Index of Topics* is provided on the last page.

A cappella

Vocal music that is to be sung **without accompaniment** (a cappella) often has a piano part for rehearsal only.

The piano part may be full size or cue size (see *Cue notes*). If cue size, the staff should be cue size also. (Cue-size notes on a full-size staff are not as easy to read.)

The indication ***for rehearsal only*** should be clearly placed above the piano part.

A due (a2)

See *Sharing a staff*

A tempo

Place above the staff (sometimes within the grand staff) to indicate a return to the normal tempo. Used after tempo alterations such as ***ritardando, accelerando, più lento*** or ***ad libitum.*** (See *Tempo marks*)

Accents

See *Articulations*

Accidentals

Temporary alterations to the pitch of a note.

THE 5 SYMBOLS

If appearing in the music, apart from use in the key signature, these symbols are called *accidentals*.

♯ **Sharp**
Raises a note one half step.

𝄪 **Double-sharp**
Raises a note two half steps.

♭ **Flat**
Lowers a note one half step.

𝄫 **Double-flat**
Lowers a note two half steps. Notice that the flats touch, forming one symbol.

♮ **Natural**
Cancels any of the above, whether indicated in the key signature or as an accidental.

ONE ACCIDENTAL PER NOTE

Do not use multiple accidentals on one note. (A double-flat is a single accidental.
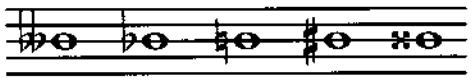
Accidentals shown altering one note from lowest to highest.

The lowest a note can be lowered is a 𝄫.

The highest a note can be raised is a 𝄪.

WITHIN A MEASURE

Any accidental is **cancelled when a new accidental appears** on the like pitch.

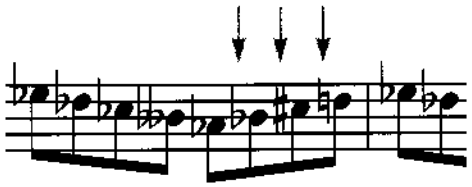

Notice that only the flat (not 𝄫) is needed to change from a double-flat to a flat.

An accidental affects all **subsequent notes of the same pitch** within the measure.
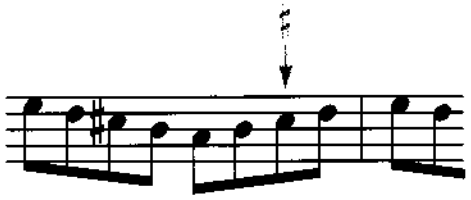
An accidental **must be added again** in the following measure.
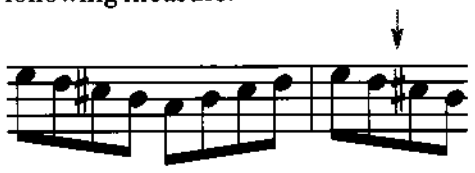
An accidental **carries over to a tied note** extending from one measure to the next.

The accidental will reappear only when the note is re-struck.

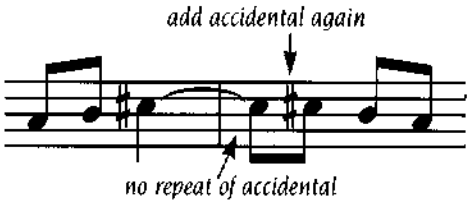

OCTAVE ALTERATIONS

Accidentals **do not apply if an** *8va* sign is added; repeat the accidentals.

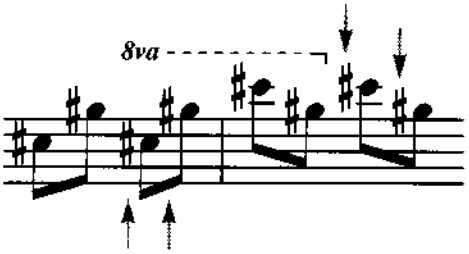

COURTESY ACCIDENTALS

Used as **reminders of the key signature** when an accidental has been used in the previous measure, or to **avoid ambiguity** in certain situations.

Use a courtesy accidental as a **reminder** to return to the original pitch.
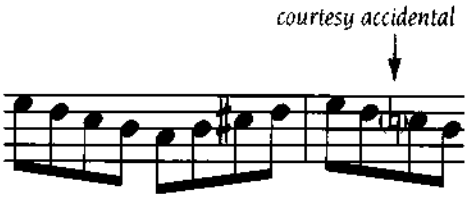
Courtesy accidentals may or may not be enclosed in **parentheses.** The parentheses show that it *is* a courtesy accidental, and help avoid confusion about the key signature. However, if many courtesy accidentals are used, and the piece is also crowded, the parentheses could make it look cluttered and more complicated. For this reason some editors choose not to use parentheses at all.

If a chord has more than one courtesy accidental, **each accidental gets its own pair of parentheses.**
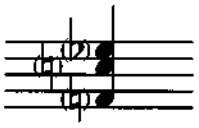
It is best to **add a courtesy accidental for octave shifts** although the notes of the same pitch in different octaves are considered separately.

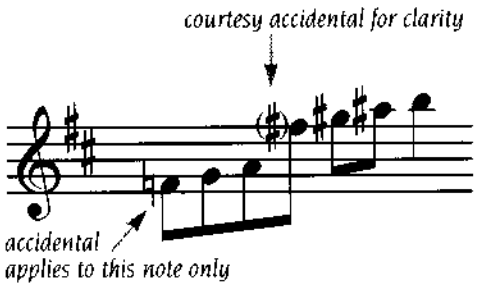

GRACE NOTES WITH ACCIDENTALS

The accidental placed on a grace note will be smaller (cue size), like the grace note.

The accidental **affects all subsequent notes of the same pitch** within the measure.

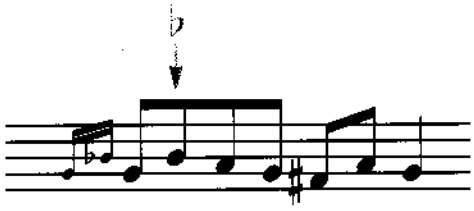

Depending on the clarity of the situation, **courtesy accidentals are often needed** to avoid confusion.

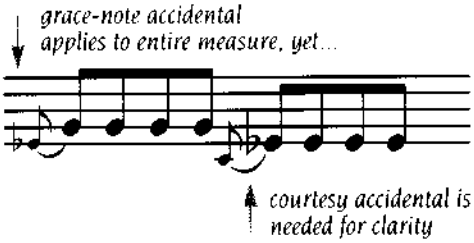

ALIGNMENT FOR INTERVALS (2 Notes)

For intervals of a **2nd through a 6th,** place the upper accidental closest to the note, the lower accidental to the left.
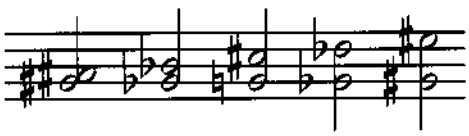
When intervals are **greater than a 6th,** accidentals align vertically.
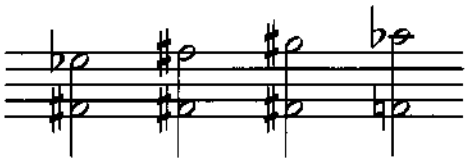
For the **interval of a 6th,** if the two accidentals don't collide they may be aligned vertically.
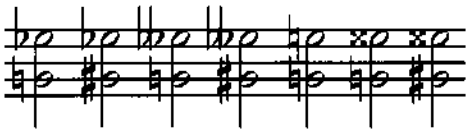
ALIGNMENT FOR CHORDS (3 Notes)

When outer notes are a **6th or less,** the upper accidental is closest to the note, the lower accidental is placed left, and the middle accidental is placed farthest left.

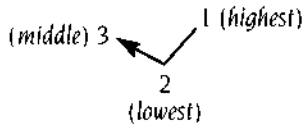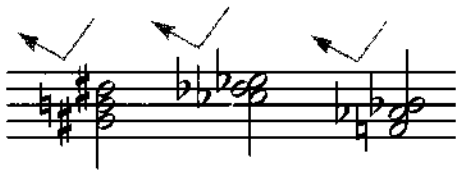

When outer notes are **greater than a 6th,** upper and lower accidentals are aligned closest to the notes—the middle accidental is placed to the left.

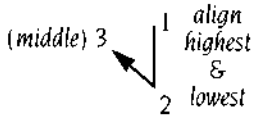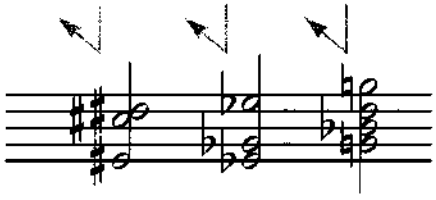

ALIGNMENT FOR CHORDS (More than 3 Notes)

When dealing with accidentals for complex chords, rules are treated more as guidelines or suggestions. Keep the arrangement of the accidentals as compact as possible.

Make the arrangement of accidentals as **easy to read as possible** for the situation.

Align the highest and lowest accidentals whenever possible.

The **center accidentals are usually arranged diagonally** from highest to lowest.

Align accidentals for octaves whenever possible.

Accidentals for the 2nd should usually be **shaped like the 2nd** (if the outer notes are greater than a 6th).

The upper accidental is placed closest to the note, the lower accidental to the left.
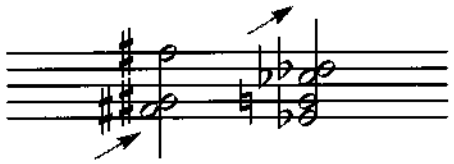
Accidentals are always placed before the entire note structure. (Do not place an accidental between notes that are played together, even if they are stemmed in opposite direction.)

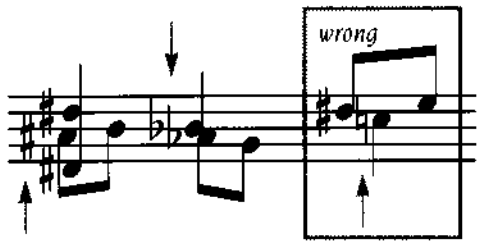

TWO PARTS ON A STAFF

For multiple notes played by **one instrument,** an accidental carries through the measure. Cancellations must be applied.

one instrument—
the accidentals carry through the measure

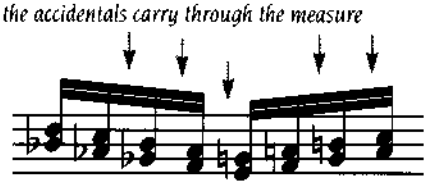

Parts on the same staff that are played by **more than one instrument** (including vocal parts) are treated individually. Repeat accidentals in the same measure if the voices cross.

two instruments sharing a staff—
the accidentals are considered separately

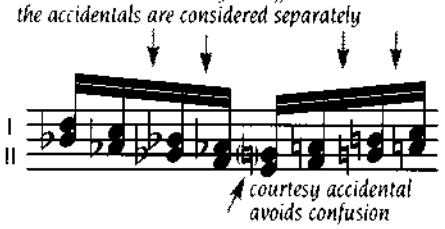

CHROMATIC PASSAGES

In general, use **sharps when ascending, flats when descending.**
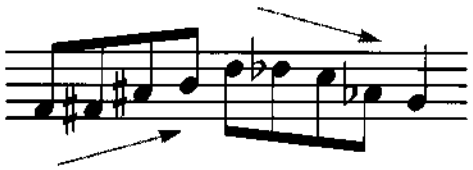
When choosing accidentals, consider the context of the music, such as key signature, harmony and voice leading.

In the chord below, both a sharp and a flat are required (C♯, not D♭; E♭ not D♯).

augmented 6th chord

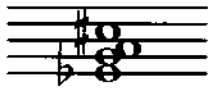

ACCIDENTALS WITH TRILLS

(See *Trill*)

ACCIDENTALS IN HARP MUSIC

(See *Pedal marks*)

Alternating instruments

CONCERT ORCHESTRA / BAND

1. To alternate instruments, enough **time must be given** to allow the change.
2. During the measures of rest the indication ***"Muta in [second instrument]"*** is indicated **below** the staff as soon as the first instrument stops.
3. Any change to the **key signature** occurs after the barline following the rest, before the new instrument begins.
4. The **new instrument is indicated** above the entrance of the instrument.

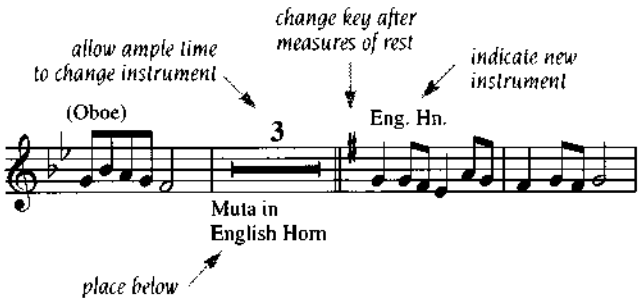

INCORPORATING CUES

1. Cue notes should be **added after many measures of rest,** to help the performer make a correct entrance.
2. The cued instrument is **indicated above the passage** in a smaller type size.
3. The **key signature changes at the beginning** of the cue.
4. **Full-size rests** are indicated below (or above, depending on stem direction).

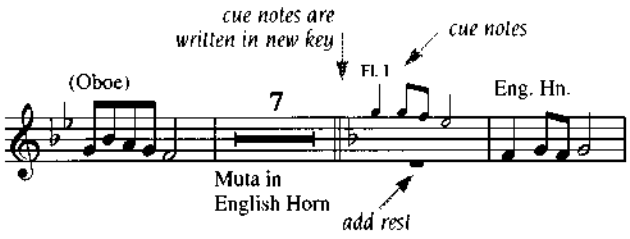

(See *Cue notes*)

JAZZ ENSEMBLE

All rules above apply except that "muta in [...]" is written **"Change to [new instrument]"** and is placed **above** the staff.

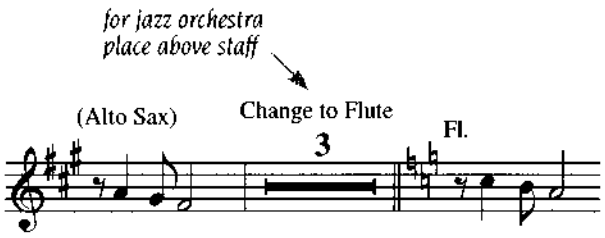

COMMONLY ALTERNATING INSTRUMENTS

The following is a listing of commonly alternating instruments in a standard orchestra:

	Alternate
Flute III	Piccolo
Oboe III	English horn
Clarinet III	Bass clarinet
Bassoon III	Contrabassoon

In smaller orchestras, the second player alternates in all cases above.

Arpeggio signs

A vertical wavy line before a chord or interval indicates an arpeggio (rolled chord).

ARPEGGIO DIRECTION

The chord is to be played quickly from **bottom to top** (no direction arrow).
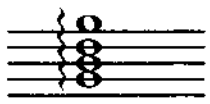
played upward (no direction arrow)

If the arpeggio is to be played from **top to bottom, an arrowhead is added** to the bottom of the wavy line.

played downward
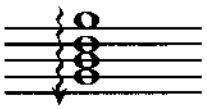
When the arpeggio returns to normal (bottom to top) or alternates with an arpeggio played downward, an arrowhead is added to the top of the wavy line.
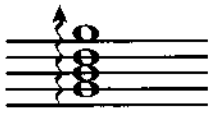
played upward

The arpeggio sign **should not extend much past the chord** affected.

PLACEMENT WITH ACCIDENTALS

Arpeggio signs are always **placed before accidentals.**
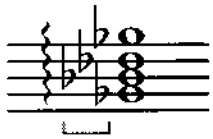
allow space for accidentals

FOR KEYBOARD INSTRUMENTS

The arpeggio sign **can extend across both staves.** The right hand begins after the left hand has completed the chord.
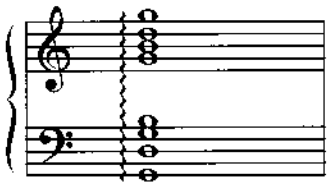
played upward, from bottom to top

If the wavy line is broken between staves, both hands begin the arpeggio simultaneously.
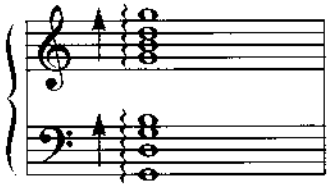
hands start simultaneously

Articulations

Articulations are symbols used to indicate *how* a note or chord is played, alone or in relation to other notes and chords.

There are five main articulations: ***staccatissimo, staccato, tenuto, accent, marcato.***

An articulation's **influence on a note or chord varies** depending on its context. A staccato note in a slower tempo is not played as short as it would be played in a faster tempo. An accent is softer in the dynamic ***p*** than in the dynamic ***f***.

One articulation applies to all notes of an interval or chord (on one stem).
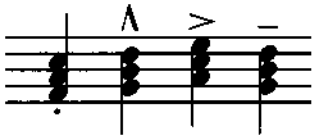
DURATIONAL ARTICULATIONS

There are three articulations that **affect the duration** of a note or chord: *staccatissimo* (▾), *staccato* (·) and *tenuto* (–).

The following illustrates durational articulations compared to an unmarked note, from shortest to longest.

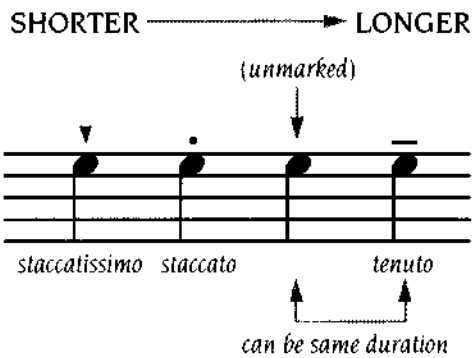

Staccatissimo

The shape varies slightly among engravers, but is always wedge-shaped. It indicates that a note or chord is to be played as **short as possible.**
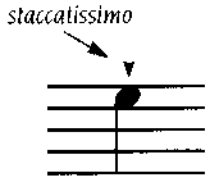
Used only with note values of a quarter note or less.

The *staccatissimo* is **centered on the notehead**. Placement is in the next space from the notehead, whether the note is on a line or space.
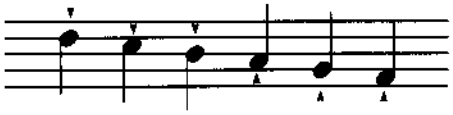
Center on the stem for opposite stem direction.

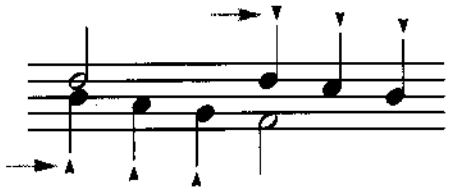

Staccato

A dot above or below a note or chord indicates that the note or chord is to be played **short.**
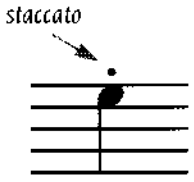
Used with note values of a quarter note or less.

The *staccato* is **centered on the notehead**. Placement is in the next space from the notehead, whether the note is on a line or space.
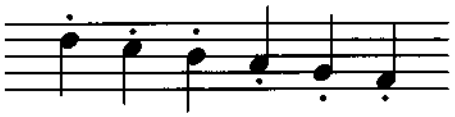
Center on the stem for opposite stem direction.
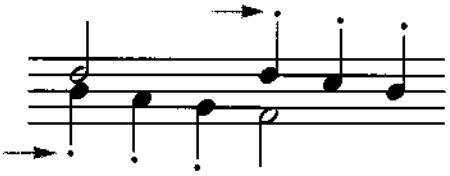
Tenuto

A short, heavy line above or below a note or chord, **thicker than the staff lines.**

A tenuto indicates that a note or chord is to be **held for its full value** (durational articulation), or the intent may be to apply a **slight stress** (articulation of force).
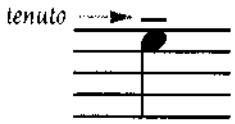
However it is interpreted, the tenuto is meant to ensure that a note or chord will be given a **certain amount of attention.**

This emphasis allows the tenuto to be **flexible in its application,** especially when combined with other articulations.

The tenuto is sometimes referred to as a *sostenuto* or *stress.*

Used with notes of any rhythmic value.

The *tenuto* is **centered on the notehead**. Placement is in the next space from the notehead, whether the note is on a line or space.
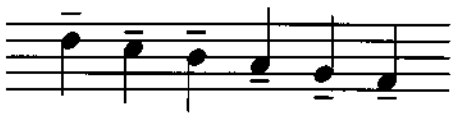
Also **center to the notehead,** not the stem, for **opposite stem direction.**
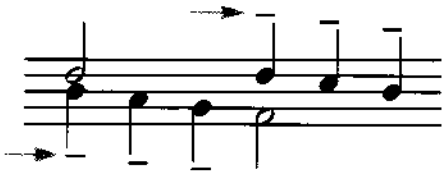
ARTICULATIONS OF FORCE

There are three articulations that affect the **force of attack** of a note or chord: the *tenuto* [–] discussed earlier, *accent* [>] and *marcato* [Λ].*

The following illustrates articulations of force compared to an unmarked note, from lesser to greater force of attack.

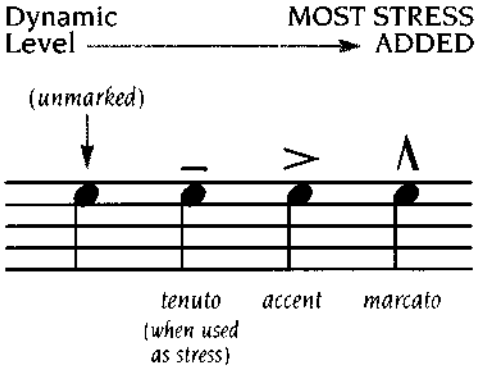

*Terminology varies for the symbols [>] and [Λ]. For the sake of this discussion, the words *accent* and *marcato* have been attached to the symbols.

Accent

When an *accent* is placed over or under a note or chord, the note or chord is to be played with **more attack, more marked.**

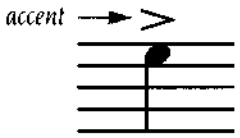

Used with notes of any rhythmic value.

The *accent* is **centered on the notehead.** Preferred placement is **outside the staff.**
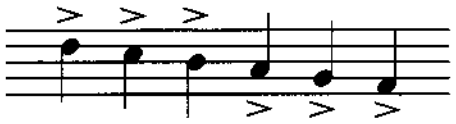
Although it is to be avoided, sometimes placing an accent **within the staff** is acceptable. A decision needs to be made whether it is preferred to have the accent closer to the notehead, or outside the staff.

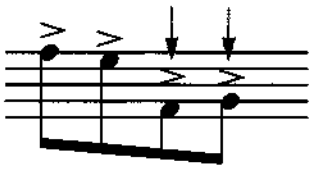

Center to the notehead, not the stem, for **opposite stem direction.**

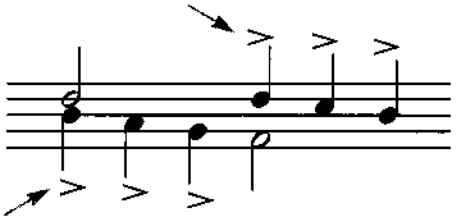

Marcato

When the *marcato* is placed over or under a note or chord, the note or chord is to be played with **even more attack, and more marked,** than an *accent.*

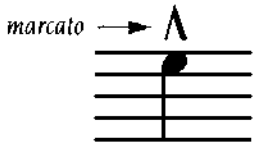

Used with notes of any rhythmic value.

The *marcato* is **centered on the notehead.** Preferred placement is **outside the staff** and ***above*** **the staff.**

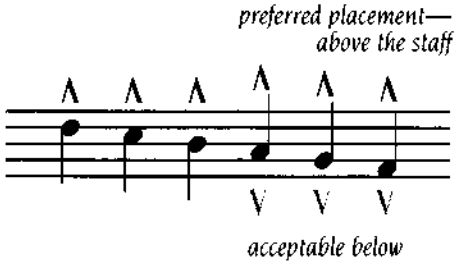

Also **center to the notehead** (not the stem) for **opposite stem direction.**

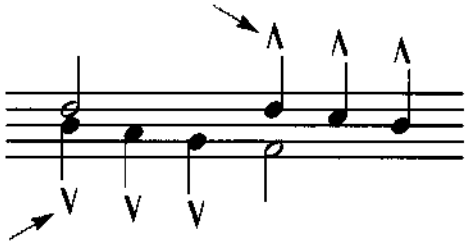

OTHER ARTICULATIONS OF FORCE

Sforzando (***sf***), *forzando/forzato* (***fz***) and *sforzato* (***sfz***) are also included in this articulation group and are interchangeable with accents and marcato accents, depending on the dynamic range.

These three articulations have the benefit of a built-in **indicator of dynamics.**

*For instance, a **sf** should be indicated only in the dynamic ranges from **ppp** to **f**. With each increase of dynamic level, the sforzando reflects the higher dynamic level: **sff** in **ff**, **sfff** in **fff**.*

The following chart illustrates the relationships between *accent* [>] and *marcato* [Λ] to *sforzando* [***sf***], *forzando* [***fz***], and *sforzato* [***sfz***] within various dynamic levels.

Dynamic Range

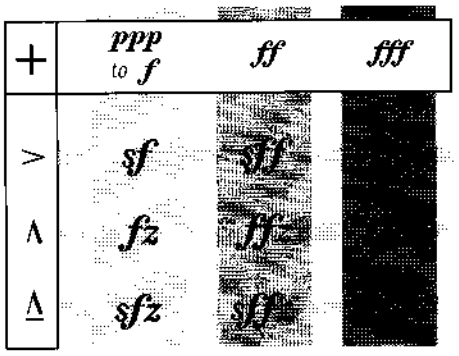

A [>] in ***f*** is comparable to a [***sf***].
A [Λ] in ***fff*** is comparable to a [***sffz***].

COMBINED ARTICULATIONS

Durational articulations can be combined with articulations of force to create variations of the basic articulations.

The following examples are the most used combinations.
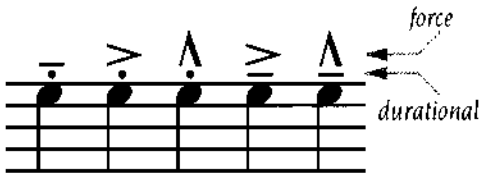
Staccatissimo and **staccato** are never combined (they basically have the same function in varying degrees).

Accent and **marcato** are never combined for the same reason.

Staccatissimo and **tenuto** are not commonly combined.

Staccatissimo and **marcato** are not commonly combined.

Combining articulations with tenuto

The **dual function** of the tenuto—the idea of *more importance, more attention,* whether of duration or force (or both)—allows the tenuto to be combined with either articulation group.

When a tenuto is **combined with an articulation of force,** the tenuto has more of a *durational function,* but may also retain its idea of force.

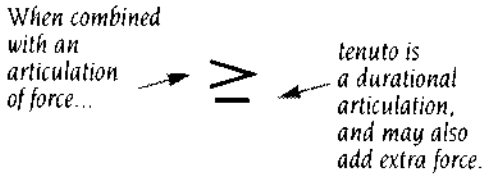

When a tenuto is **combined with a durational articulation,** the tenuto has the function of an *articulation of force,* while retaining its durational function.

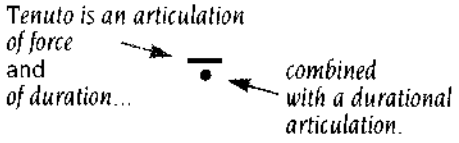

Usual interpretation: play detached and with a slight stress.

PLACEMENT WHEN COMBINED

The following can be used as guides for the placement of combined articulations:

tenuto & staccato
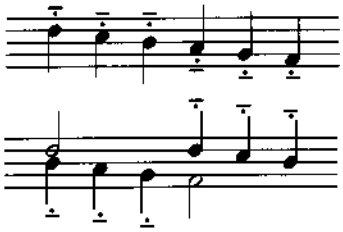
accent & staccato

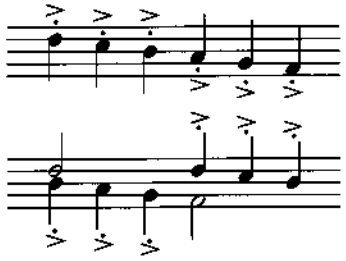

marcato & staccato
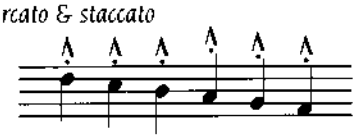
Keep the two combined articulations together (on the same side of the note) whenever possible.

Notice that when a **staccato** is combined with another articulation (and is on the same side of the note), it is **centered on the notehead,** even when it is on the stem side.

SIMILE

When an articulation (or pattern of articulations) is applied in a repetitious and predictable manner, the word ***simile*** may be used.

Simile is indicated **after the pattern has been clearly established** (usually two or three measures).

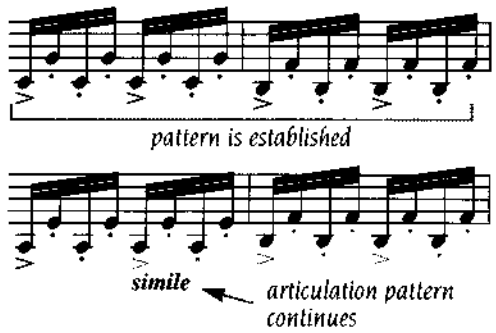

Notice that the ***simile*** was **not used at the beginning of the line,** even though the pattern had already been established.

The ***simile*** is ended when the pattern ends or when different articulations are added.
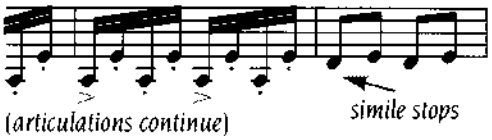
SLURS WITH ARTICULATIONS (See *Slurs*)

Augmentation dot

PLACEMENT

Always place **one dot per space** and **only in a space**—never on a staff line or on the same level as a leger line.

For a line note—place to the right of the notehead, **in the space above.**
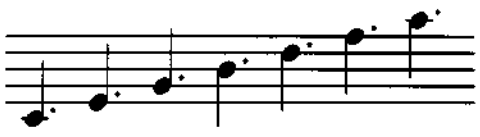
For a space note—place to the right of the notehead **in the same space** as the note.
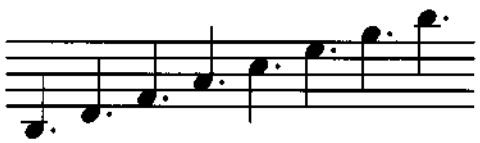
For notes with a flag—the dot is placed further right, altogether **avoiding the flag.** Never place a dot between the notehead and its flag.
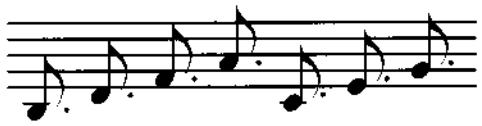
Double and triple dots are placed directly to the right of the first dot. Horizontal spacing is equal to that of the first dot. *Multiple dots should be used only in situations where they will be easily understood.*

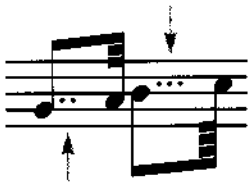

Never separate a dot from its notehead. Stem direction and creative positioning of a dotted note must be considered.
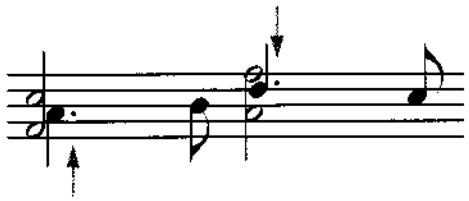
Ties always avoid the dot—place the tie clearly to the right of the dot.

For two or more notes in a chord with the same stem direction, **always align the dots vertically.**
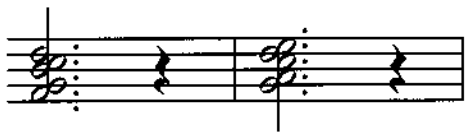
Two dots never share the same space.

FOR INTERVALS OF A SECOND

The dot for the space note is always placed in the space to the right of the notehead.

If the **line note is above,** place the dot in the space above. If the **line note is below,** place the dot in the space below.

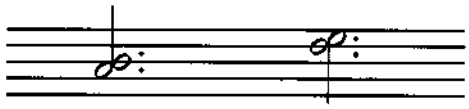

FOR TWO OR MORE PARTS

For stems up, place dots for line notes in the space above. **For stems down,** place in the space below.

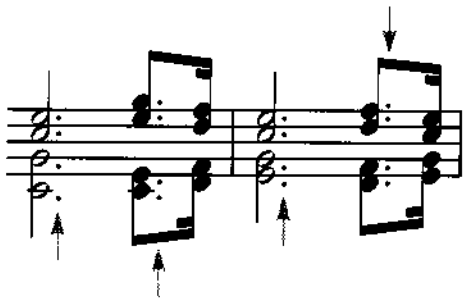

DOTTED RESTS

Rests are dotted in the same way notes are dotted, but with some restrictions on their use.

Place the dots as follows:

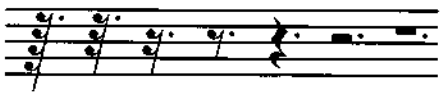

Dotted rests are used mainly to **clarify the subdivision of a measure.** (See *Meter*)

Dotted whole rests are the least used of all the dotted rests. They are never used in simple meter.

Possible use of dotted whole rest:
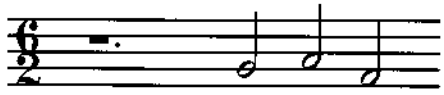
Likewise, **a dotted half rest** should not be used in simple meter.

Possible uses of dotted half rest:
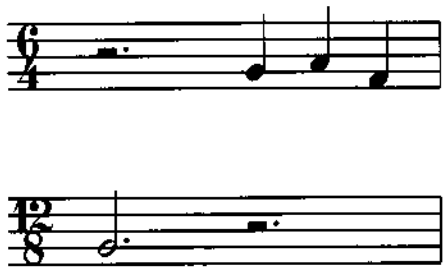
Dotted quarter rests are used in compound meters. Avoid using them in simple meters.

In $\frac{6}{8}$ time, dotted quarter rests can be used on beats 1 and 4 only.

In $\frac{9}{8}$ time, dotted quarter rests can be used on beats 1, 4 and 7 only (the pulses).

In $\frac{12}{8}$ time, do NOT use a dotted half rest across the middle of the measure. Use dotted quarter rests.

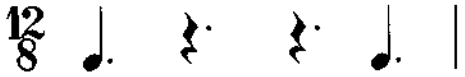

It is acceptable to use the **dotted eighth rest, dotted sixteenth rest, etc.,** for a cleaner look.

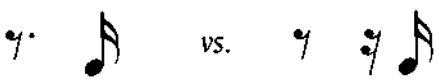

Barlines

Barlines are vertical lines that divide a staff into measures.

SINGLE BARLINE

The **thickness of a barline** is equal to, or greater than, the staff line thickness (staff lines being thicker than stems).

To help the performer follow the music from staff to staff, **avoid the alignment of barlines** from staff to staff (or from system to system).

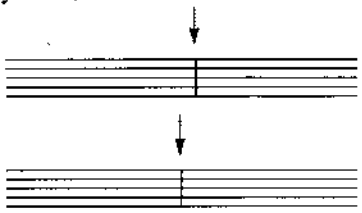

Allow a small amount of space after a barline—depending upon the density of notes within the measure.

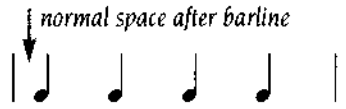

Less space may be allowed **after** the barline if the **density of notes is high.**

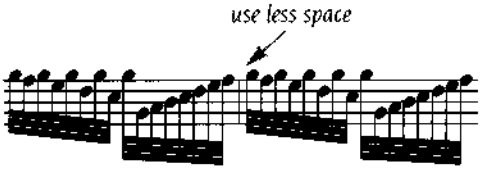

More space may be allowed **after** the barline if the **density of notes is low.**
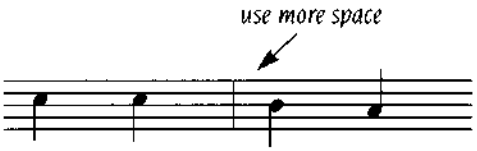
Less space may be allowed **before** the barline if **density is high.** Avoid *adding* space before the barline.
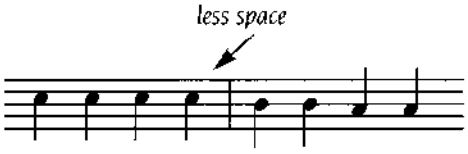
DOUBLE BARLINE
(Thin/thin)

Used to clarify the end of a section of music, such as in a *Da Capo* layout.
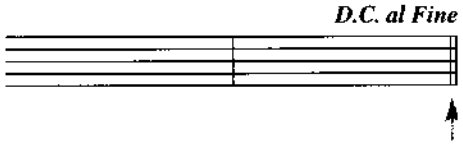
FINAL DOUBLE BARLINE
(Thin/thick)

Marks the **end of a composition, or the end of a movement** within a larger work.

Consists of a thin barline followed by a thick barline.

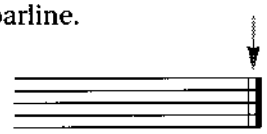

BROKEN BARLINES

Broken (dashed) barlines are sometimes used when a situation calls for the completion of a section **mid-measure,** although the **final double barline** is preferred.

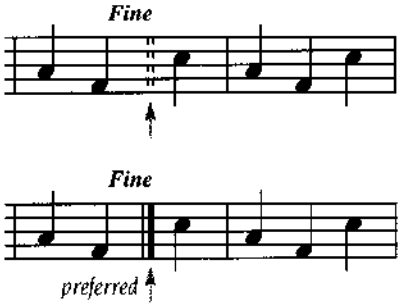

For composite meters, a broken barline is sometimes used to **clarify the meter division** within a measure.

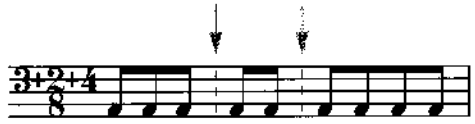

THE LEFT BARLINE

A single staff should ***never*** **begin** with a barline.

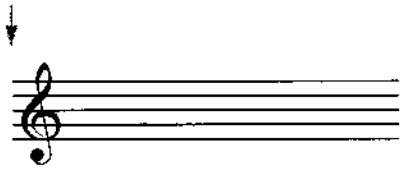

SYSTEMIC BARLINE

A systemic barline connects two or more staves together, as in the grand staff.
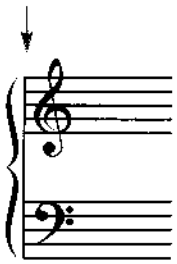
Barlines are **used to group staves of like instruments** in a score layout.

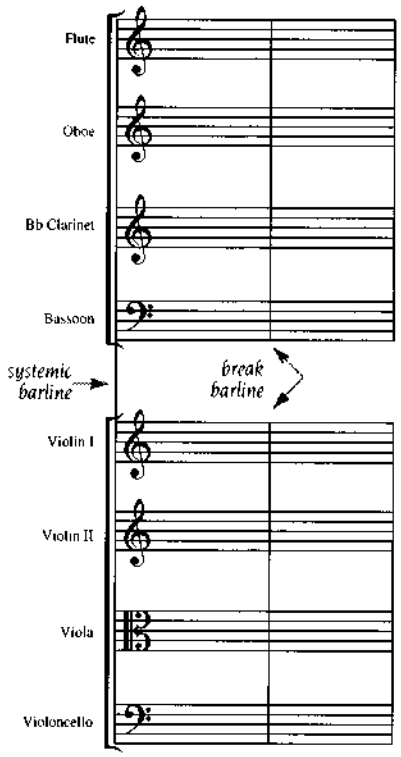

WITH CHANGING CLEFS

The new clef (cue size) is placed **before the barline** if the clef changes mid-staff.
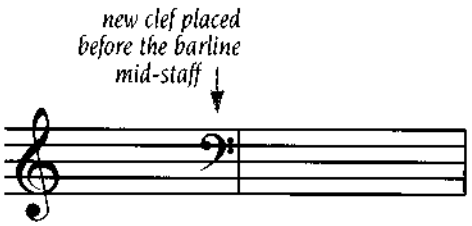
A **courtesy clef is placed before the last barline** of the staff if the new clef begins immediately on the next staff.

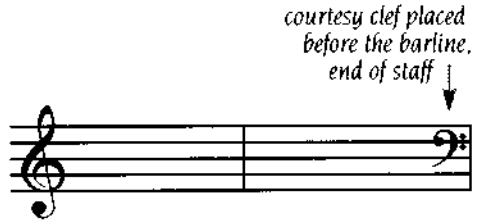

(See *Clef signs*)

WITH CHANGING KEY SIGNATURES

The new key signature is **placed after** an added **double barline** if the key signature changes mid-staff.

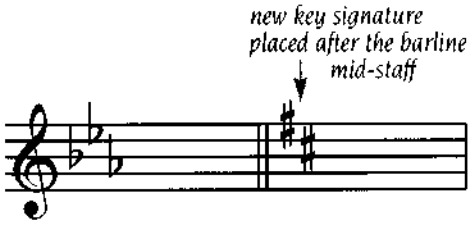

A **courtesy** key signature is **placed after** the last barline (add double bar) if the new key signature begins on the following staff.

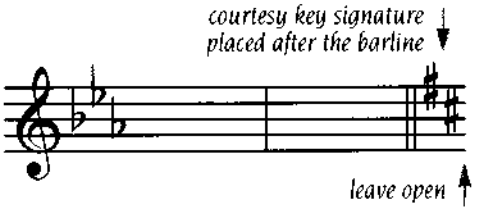

Note: *A single barline may be used in both the above instances, but a double bar calls more attention to the change.*

WITH CHANGING TIME SIGNATURES

The time signature is **placed after** the barline if the time signature changes mid-staff.
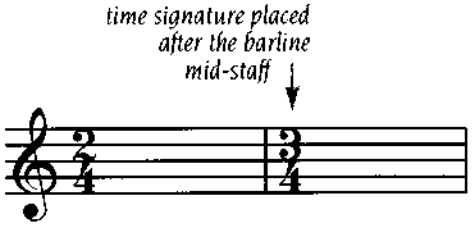
A **courtesy** time signature is **placed after** the last barline if the new time signature begins on the following staff.
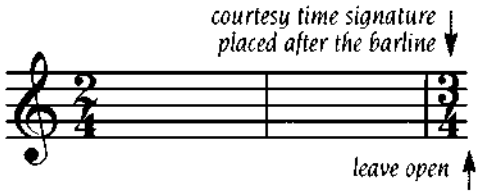
WITH MULTIPLE COURTESY SIGNS

If a courtesy clef, key signature and time signature all appear together, they follow the rules for each individual courtesy change.

The order is the same as the order presented at the beginning of the piece (clef, key signature, time signature).

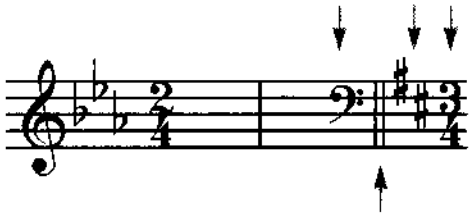

INCOMPLETE MEASURES

If a piece begins with a **pick-up,** the barline is positioned **according to the time value of the beat(s).**
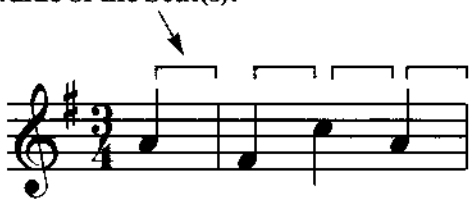
Beams

Although sometimes referred to as "balkans" or "ligatures," **"beam"** is the preferred term for the connection between two or more consecutive notes, replacing the flag.

Beams greatly simplify the reading of music, **substituting for individual flags** in groupings of **notes smaller than a quarter note.**

Because of the **ease in reading of beams,** the **use of flags in vocal music**—in relation to the lyric—has become **obsolete.**

CONNECTION TO THE STEM

Beams are connected to the side of the stem. They must be **flush to the stem,** both vertically and horizontally.

PRIMARY AND SECONDARY BEAMS

The beam that is furthest from the noteheads and connects a group of notes is called a *primary beam.* This beam **remains unbroken** throughout the grouping.

Any beam other than the primary beam is a *secondary beam.* The secondary beam **may be broken,** to divide the grouping into smaller units for easier reading.

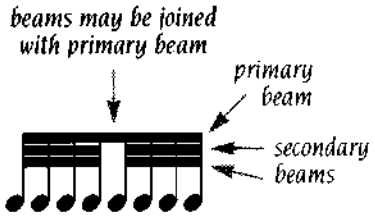

Stems extend through secondary beams and connect to the primary beam.

DOUBLE BEAMS

Normal stem length will accommodate a double beam—the stem need not be adjusted.

TRIPLE AND QUADRUPLE BEAMS

When a third or fourth beam is added below the secondary beam, **the stems must be extended** by approximately one staff space per beam.

The extension of the stems allows the space between the noteheads and the lowest beam to remain normal.

If 32nd- and 64th-note values occupy the majority of the rhythmic values, it may be better to double the rhythmic values of the entire piece and alterthe tempo.

FRACTIONAL BEAMS

A fractional beam is also a **secondary beam.**

Fractional beams are **associated with only one note.**

The **length** of a fractional beam is the same as the width of a notehead.
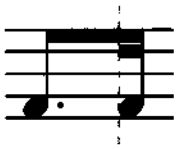
Place exactly the same as a full-length secondary beam would be placed. The beam is always *inside* the grouping, and it usually follows or precedes a beamed dotted note.
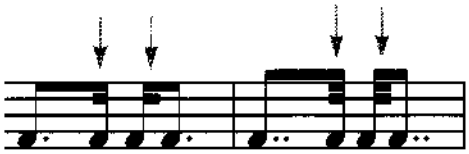
BEAMING AND METER

The basic purpose of beaming is to **connect two or more notes within the same beat (or pulse).** Meter must be considered when grouping notes with a beam. (See *Meter*)

In **any simple meter,** each beat is divisible by two; a beam may connect the two notes. Simple duple, simple triple and simple quadruple meters each have slightly different considerations.

Simple duple meter ($\frac{2}{2}$, $\frac{2}{4}$, $\frac{2}{8}$)

In some cases, the entire measure may be beamed.
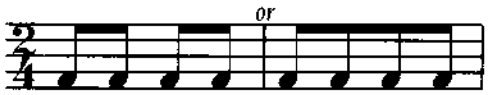
Some combinations of beams, flags and rests in simple duple meter:
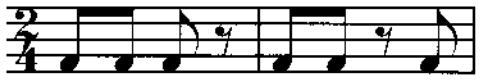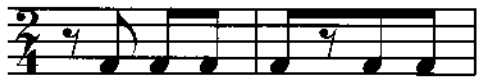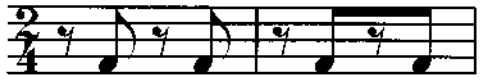
Although some contemporary engravers beam over a rest at the beginning or ending of a beamed grouping , it is not the preferred notation.

Simple triple meter ($\frac{3}{2}$, $\frac{3}{4}$, $\frac{3}{8}$)

Consideration is given to **visually maintain** the three beats within the measure. In some cases the entire measure may be beamed.
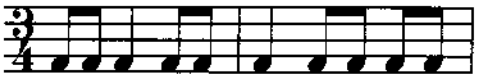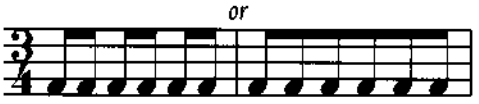
It is better to **avoid arbitrary groupings** of 4+2 or 2+4. However, they are sometimes used to emphasize phrasing.
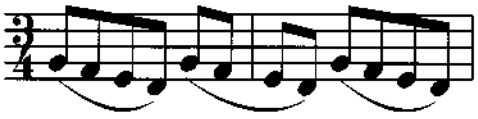
The combined use of **flags and beams** clarify the meter.
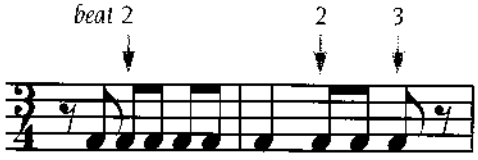
Avoid beaming in a manner that would suggest $\frac{6}{8}$ time. Use flagged notes to differentiate $\frac{3}{4}$ meter from $\frac{6}{8}$ meter.
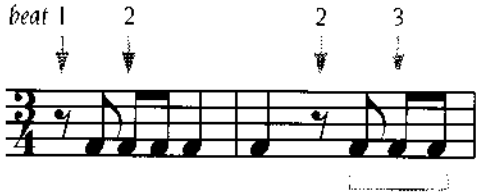
Beaming to include rests inside the grouping is acceptable.
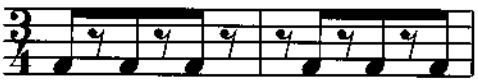
Simple quadruple meter ($\frac{4}{4}$, $\frac{4}{8}$)

In $\frac{4}{4}$ time, beats 1 & 2 and beats 3 & 4 may be beamed together to form a unit.

Never connect the notes of beat 2 with beat 3.
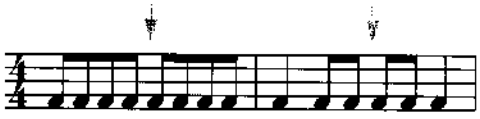
The basic rule in $\frac{4}{4}$ time is that the **two halves** of the measure (beats 1 & 3) **must be immediately recognizable.** The only exception to this would be a very simple syncopation (such as).

Because of this rule, all the notes in the measure would *not* be beamed together, as is possible in the other simple meters.
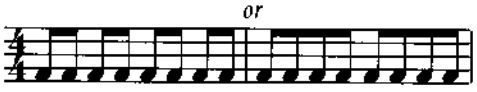
THE SAME RHYTHM THREE WAYS

Each could be the best for a particular situation.

Notice that **each beat** is recognizable in the following example.
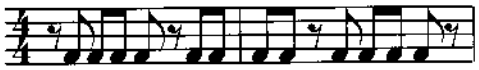
Notated with beams only, the **two halves** of the measure are easily recognizable:

If the above example were in a piece that contained triplets, it could at first glance be **mistaken for triplets.** In that case, a better notation would be:
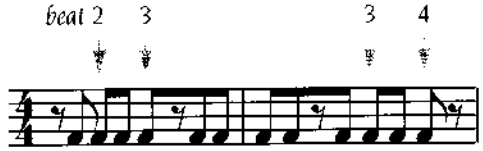
For any simple meter, **when a beat is uneven or contains more than two notes,** the two adjacent beats should not be beamed together as a unit.

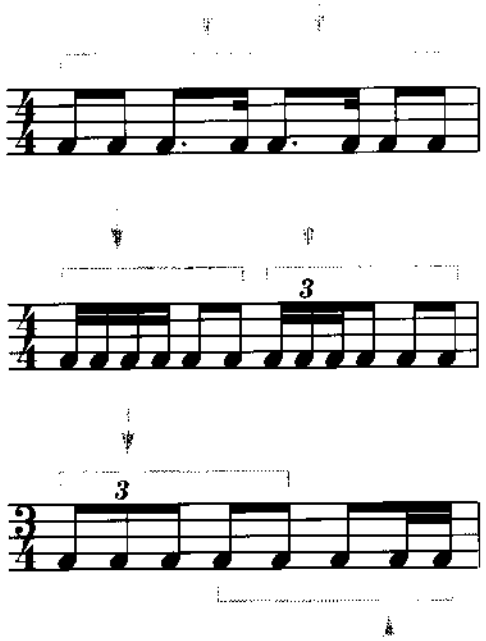

Compound meter

When each **pulse** of the measure is **divided into three beats,** the meter is called "compound." A beam may connect the three beats.

compound duple (2 *pulses*, 6 *beats*)

compound triple (3 *pulses*, 9 *beats*)
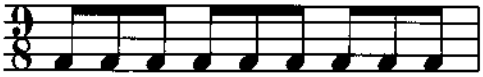
compound quadruple (4 *pulses*, 12 *beats*)

The **units** of three beats **for each pulse** in compound meter **must always be maintained.** Even when rests are included in the measure, as in the example below, beats 1, 4 & 7 must be clearly visible.
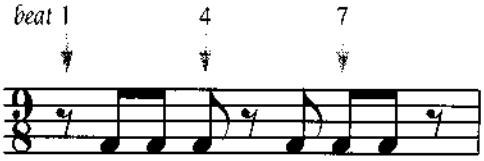
The three units in the above example could be made even more obvious by including the rest on beat 5 in a beamed unit.

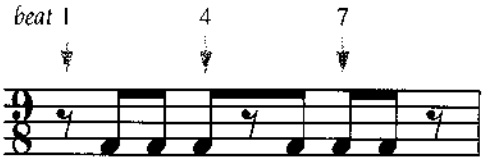

It is **possible to group all notes within a pulse.** All the notes in the *measure,* however, cannot be beamed together—this could cause the measure to appear to be in some other meter.

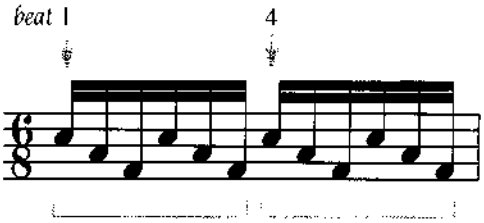

Although different groupings are sometimes used for phrasing or interpretation, the above should be generally adhered to.

TIES AND BEAMS

Avoid using tied notes *within* a beamed grouping. The **unit should be broken** where the tie is placed.

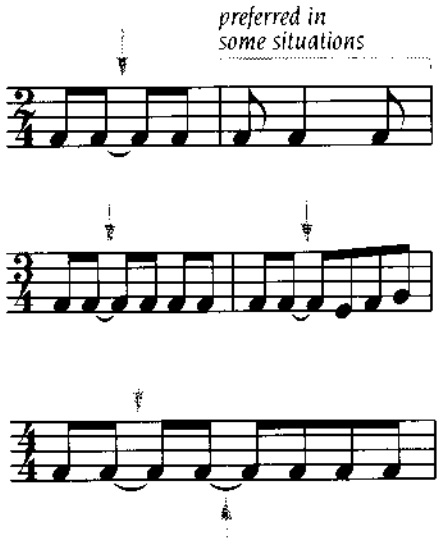

In this case, there would not be a continuous beam, since beats 2 and 3 should not be beamed together in this meter.

STEM DIRECTION OF BEAMED GROUPS

Simple rules for stemming of single notes apply to beamed groups when possible (for example, if all notes in a beamed grouping are on or above the middle line of the staff, stems are down), but some additional guidelines are needed.

(See *Stems*)

For two beamed notes

Stem direction is **determined by the note farther from the middle staff line.**

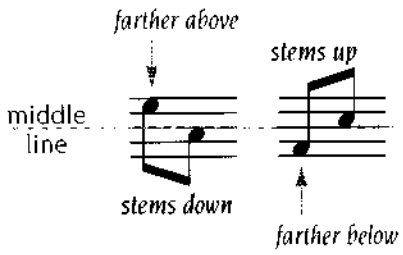

If both notes are **the same distance** from the middle line, the preference is for **stems down.**

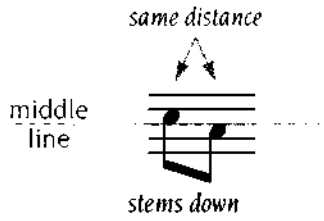

If all other stems in the surrounding measures are up-stem, that direction is sometimes continued if the two notes are the same distance from the middle line. (This is a very subtle point, and somewhat obsolete.)
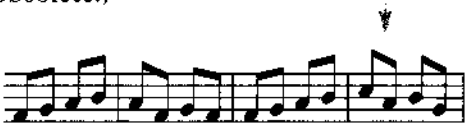
For three or more beamed notes

If the majority of the notes are **on or above** the middle line, the stems go down.

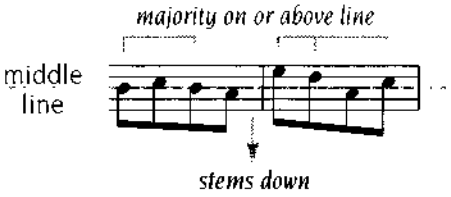

If the majority of the notes are **below** the middle line, the stems are up.

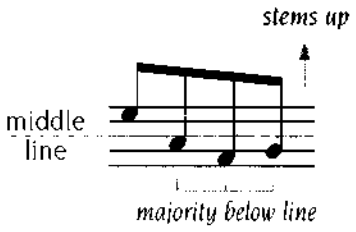

If the number of notes **above and below the middle line are equal,** the note farthest from the middle line dictates the stem direction. (If all notes are the same distance, the preference is down.)

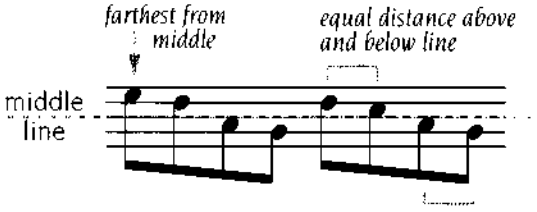

BEAM SLANT & PLACEMENT

Concerning the computer

With most computer engraving today, the direction, slant and placement of the beam are automatic.

However, the defaults—or even the settings allowable—may not conform to traditional practices. Even though some of these practices are in the process of change, there are some guidelines to keep in mind for a more professional look.

Beginning placement of the beam

When **stems are up,** the stem length of the **highest note** determines the beam placement.

When **stems are down,** the stem length of the **lowest note** determines the beam placement.

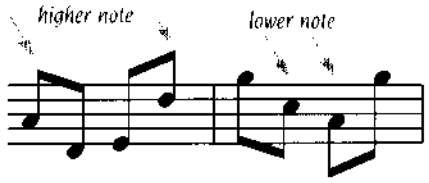

Direction of slant

Beams *usually* **follow the contour of the notes,** ascending or descending.
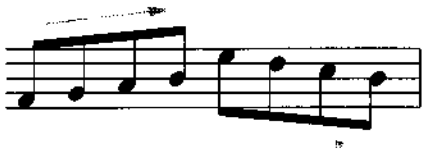
For mixed direction of notes, the beam *usually* **follows the direction between the first and last note** of a grouping.

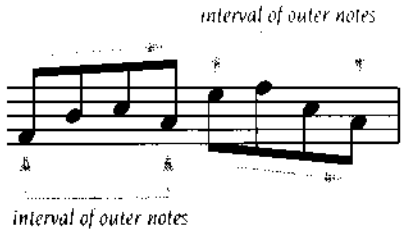

When two or more notes share a stem, the note **closest to the beam** dictates the beam direction.
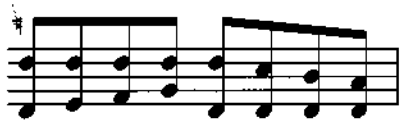
Horizontal beaming

A beam should be horizontal if the first and last note of the beamed group is on the **same pitch level.**

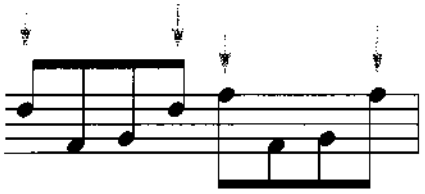

If the grouping consists of **repeated intervals,** the beam should be horizontal.
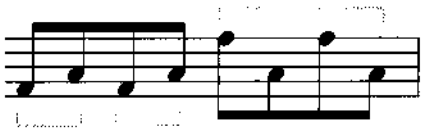
Horizontal beams may be used if inner notes **do not follow the interval direction** of the outer notes.
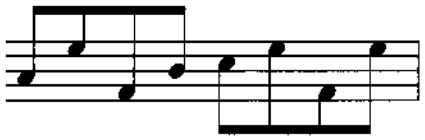
Some other examples of horizontal beaming:
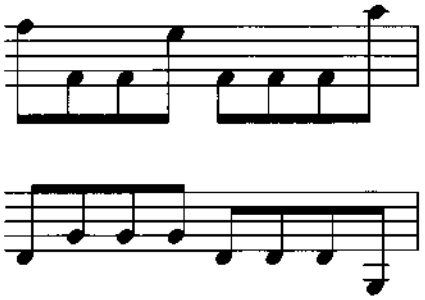
Interval-specific beam slant

Determining the placement and slant of beams in traditional plate engraving was complicated and detailed.

The following are *approximate* guidelines, **modified from the strict traditional** rules for beaming of intervals. There are two main reasons for this modification:

1. The consistency of the computer and the quality of modern printing make it no longer necessary to avoid the small "wedges" of white space that in the past often filled in with ink.
2. Adjusting many beams individually on the computer is very time-consuming.

A pair of **notes of different pitch should not have a horizontal beam.** (Exception: two notes on the same line or space, one or both altered with an accidental)

If a **beam slants, it is usually from 1/2 to 2 staff spaces**—very seldom more.

Intervals of a **2nd** slant 1/2 space.

2nds
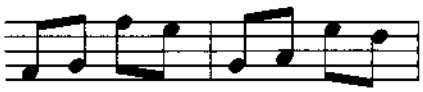
Intervals of a **3rd** slant 1 staff space.

3rds
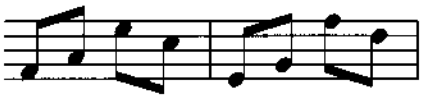
Intervals of a **4th** slant from 1 to 1-1/2 staff spaces.

4ths
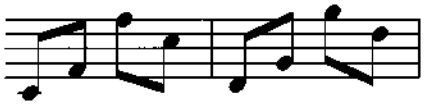
Intervals of a **5th, 6th & 7th** each slant approximately 1 to 1-1/2 staff spaces.

5ths
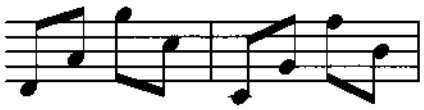
6ths
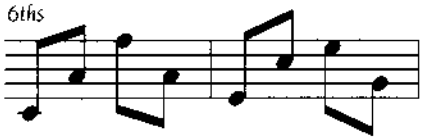
7ths
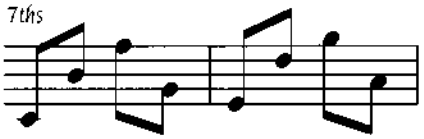
Intervals of an **octave and greater** slant 1-1/2 to 2 staff spaces.

octaves
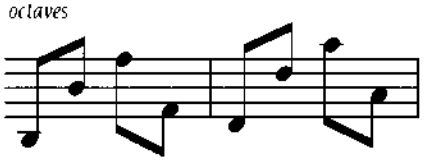
Beamed notes with **leger lines** slant 1/2 staff space. (Remember that stems must extend to the middle line.)

with leger lines
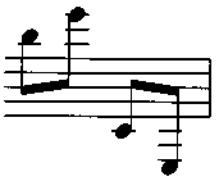
Depending upon **the amount of space** allowed between the beamed notes, the slant of the beam naturally *decreases* with an *increase* in the amount of space allotted, if stem lengths remain the same.

natural decrease in slant as space is increased
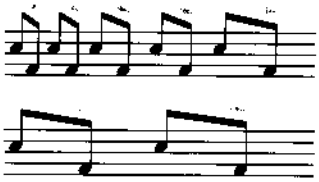
For tightly spaced beamed notes, **adjust the slant** (by lengthening the stem of the farthest note) so that it is not so extreme.

Alternative beaming

For grand staff notation, **cross-staff beaming** is acceptable in some situations. The slant of the beam is determined by the amount of space between the two staves, the length of the stems, and by avoiding exaggerated angles.
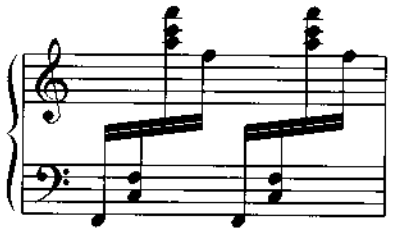
For single-staff music, alternative beaming should be used only in **exceptional circumstances.** Stems must not be too short.
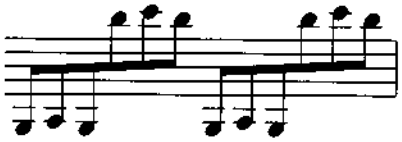
Bowing

Down-bow and **up-bow** markings are centered to the notehead and are placed above the staff, except when two parts share a staff.

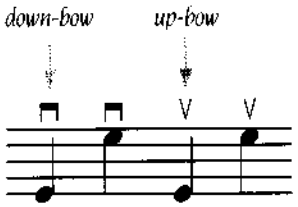

String techniques such as ***spiccato, legato, portato*** and ***jeté*** are notated conventionally, with slurs and/or articulations.

The study of orchestration is necessary to properly specify string indications.

Slurs can indicate either phrasing or bowing, or both.

Brackets to the left of the chord may be used for **multiple stops** if the chord is to be divided a particular way. Usually no bracket is used.

Multiple stops may be *double, triple* or *quadruple* stops.

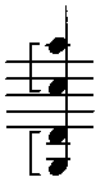

PLACEMENT OF TEXT

All text for bowing indications is **placed above** the staff.

When a particular string is to be played exclusively, ***sul*** [string] is indicated.

sul G

Pizzicato is cancelled with the ***arco*** indication.

pizz. ***arco***

With any of the following indications, ***ord.*** or ***ordinario*** is commonly used to indicate the return to normal playing.

non vib. ***sul pont.*** ***sul tasto*** ***col legno***

Brace

The brace is used to connect the two staves in scores for instruments such as piano, organ, harp and marimba.

The brace connects two staves to form a **grand staff.**

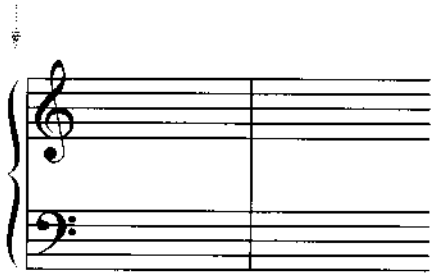

Bracket

The bracket is used **to connect two or more staves** to form a system or to **group certain instruments** within a system.

The bracket is different from the brace in that it connects the staves for two or more **separate instruments,** while the brace connects staves for one instrument (such as keyboard).

The grouping may be two or more **unlike** instruments, **identical** instruments, or a **family** of instruments, such as strings.

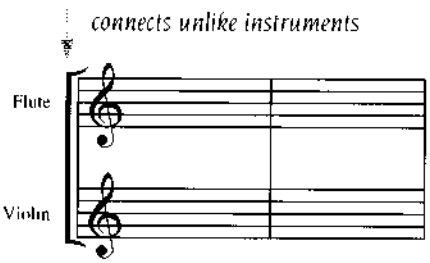

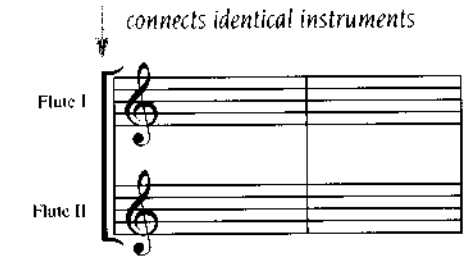

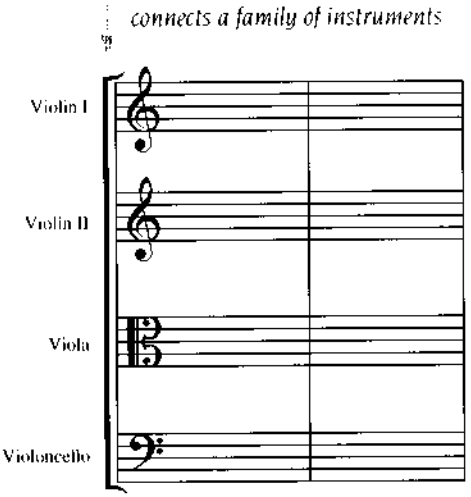

(See *Barlines, Scores*)

Breath mark

The breath mark (𝄾) has two similar uses:

- **an actual breath indication** for instruments (including voice) requiring the breath to sound.
- **a small pause or break** (as if taking a breath) for instruments *not* requiring breath to sound.

A breath mark may or may not interrupt the tempo. If it does interrupt the tempo, the break or pause is shorter than that of a caesura or fermata.

PLACEMENT

The breath mark is indicated just above the staff, at the point **where a breath or break is desired.**
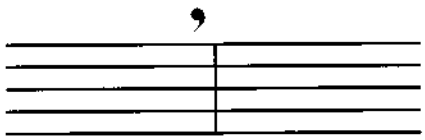
If the breath mark occurs between two notes, the placement is toward the **end of the space for the full value** of the note.
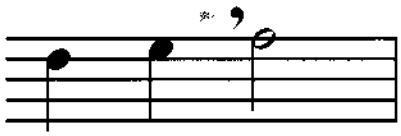
If the breath mark occurs at the end of a measure, the placement is just **before the barline.**
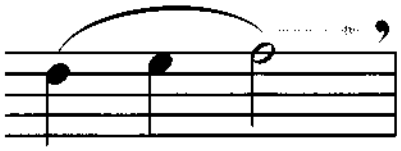
Caesura

The caesura (//) is a small pause or break in the tempo (implying a break in sound).

The pause of the caesura is **slightly longer than a breath mark,** but shorter than a fermata.

PLACEMENT

The caesura is placed on the **fourth line from the bottom** of the staff (extending to the first leger line), at the point **where a break is desired.**
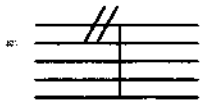
The caesura is placed toward the **end of the full value** of the note.
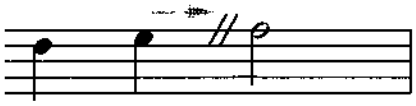
If space is tight, the caesura **can be centered** between two notes.
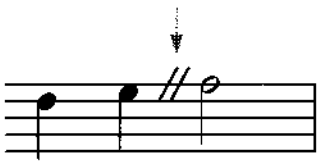
If the caesura occurs at the end of a measure, the placement is just **before the barline.**
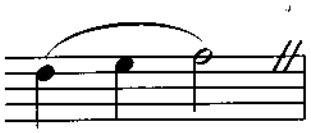
If a longer pause is desired, **a fermata may be placed above** the caesura.
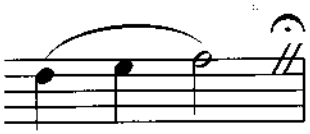
Chord frames & symbols

Chord frames are diagrams that contain all the information necessary to play a particular chord on a fretted instrument.

The photograph below shows the finger numbers corresponding to the fingerings used for guitar.

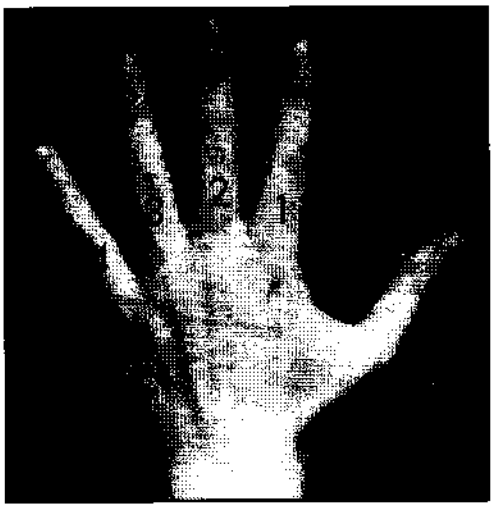

The number of strings and tunings vary between string instruments. The **chord frame is modified** (number of strings, tunings) according to the differences between each instrument.

The following examples explain the various **chord frame elements** for guitar.

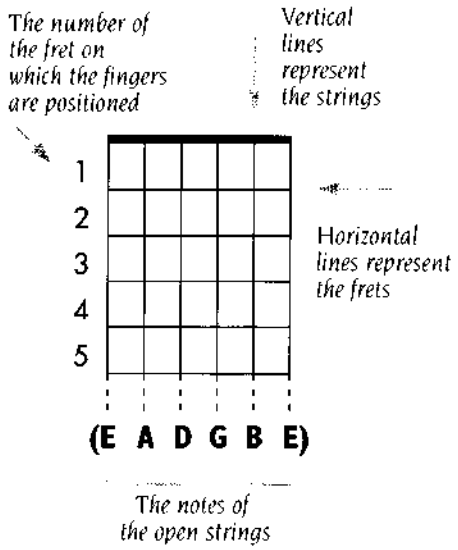

The **fingerings, note names** and **position** of the chord on the neck are all provided on the chord frame.

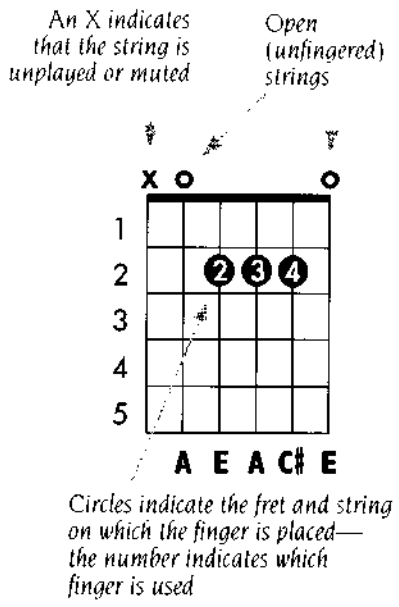

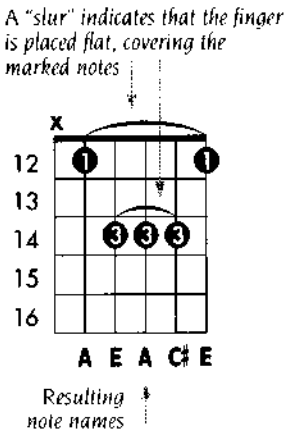

CHORD SYMBOLS

The **chord symbol** is always placed above the frame to identify the chord.

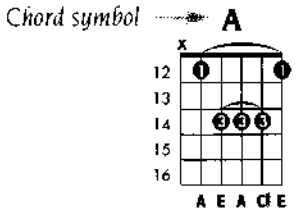

Careful attention must be given to the **consistent identification** of chords, in the **least ambiguous way** possible.

Chord symbols often appear without a frame. Whether or not there is a frame, space must be allowed so that the symbol is **aligned with the proper beat.**

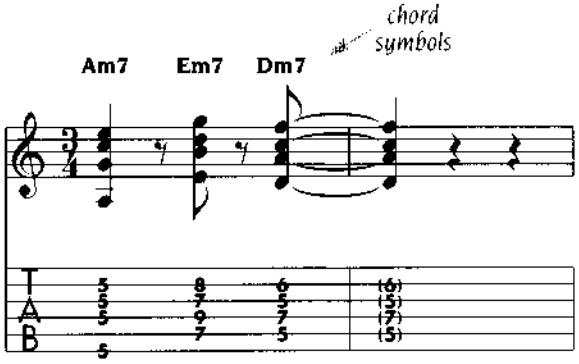

(See *Tablature*)

A complete listing of guitar chords, along with chord theory, is provided in Alfred's Guitar Chord Encyclopedia *(Item #4432). It also includes a listing of chord symbols and a listing of ambiguously named symbols.*

Circle of fifths

See *Key signatures*

Clef signs

The following are commonly used clefs.

Middle C is shown for comparison in all examples except neutral clefs.

TREBLE AND BASS CLEFS

Treble and bass clefs are most frequently used. Keyboard, harp and organ music is written using only these clefs.

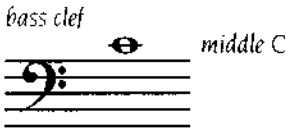

The **octave treble clef** is sometimes used for tenor vocal parts, to indicate that the part is one octave lower than written.

The **double treble clef** serves the same function as the octave treble clef but is much less frequently seen.

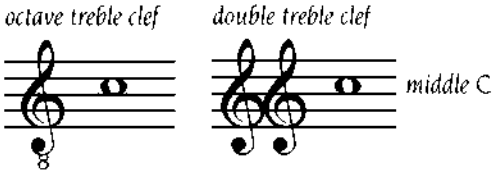

The regular **treble clef** is also commonly used for tenor vocal parts; the octave is assumed.
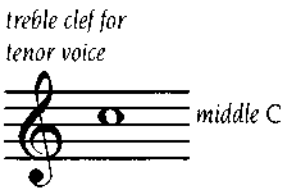
C CLEFS

Alto clef is commonly used for viola, to avoid excessive leger lines. (Viola also uses treble clef.)

alto clef

Tenor clef is primarily used for bassoon, cello and trombone when playing in higher registers.

tenor clef
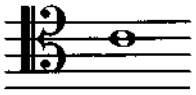
The following C clefs are **obsolete:**

soprano clef
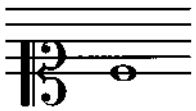
mezzo-soprano clef
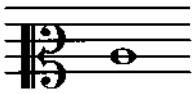
baritone clef
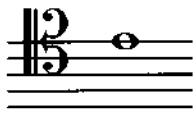
NEUTRAL CLEFS

Neutral clefs are used by percussion instruments of indefinite pitch. The following is most commonly used.

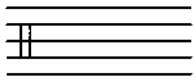

Neutral clef for single-line percussion:

POSITIONING

Clefs are **slightly indented on the staff,** to the right of a systemic barline or the open single staff. Be sure to leave the ***single* staff open—do not put a barline before the clef!**

indent on single staff—no left barline

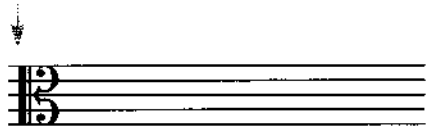

indent on staff with systemic barline

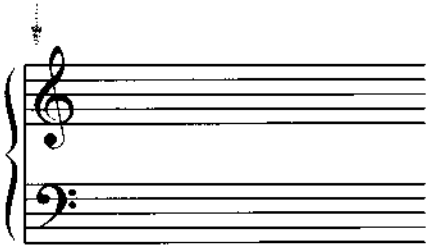

The clef is always **placed before the key signature and time signature.**

Notice the distance from the end of the staff to the clef, from the clef to the key signature, and from the key signature to the time signature.

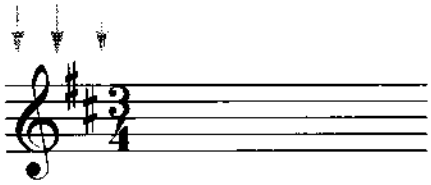

CLEF CHANGES

When the clef changes **within a staff,** a cue-size clef is used (usually 75% of the original clef size). Courtesy clefs are also cue size.

If a clef change affects a complete measure, it is always placed before the barline.
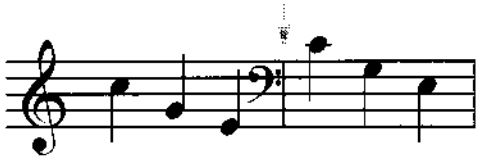
Only a *systemic* barline can precede a clef sign. (See *Systems*)

If a clef change is within a measure, the clef is placed directly before the first note involved.
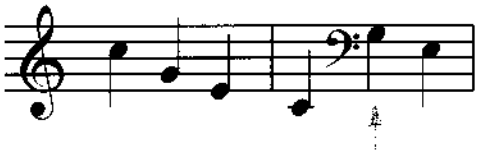
If a clef change **begins after a rest and is on a beat,** the clef is placed directly before the first note affected.
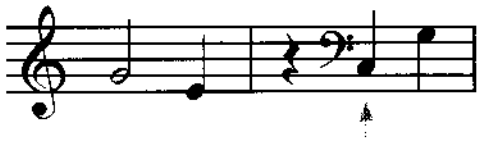
If a clef change **begins after a rest but is not on a beat,** the clef precedes the rest.
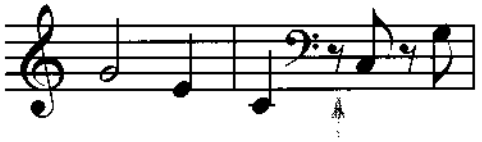
If a clef change **occurs at the beginning of a staff,** a courtesy clef is placed before the barline at the end of the previous staff, followed by the new clef at full size in the new staff.
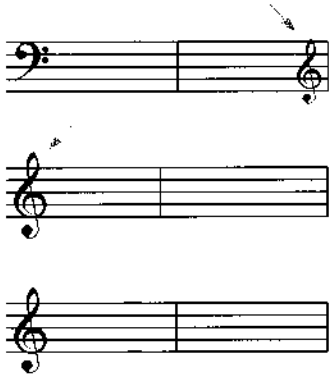
The rules for clef changes are not affected by the **addition of a key change and/or time signature change.** The clef sign precedes the barline; the key signature and time signature follow the barline.
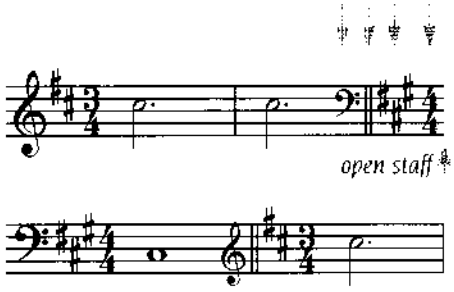
Notice that the **order** of courtesy clef, key signature and time signature is the same as the order at the beginning of a piece.

The **courtesy clef** is cue size; the key signature and time signature are normal size.

Also notice the **open staff** after the *courtesy* key signature and time signature.

Coda sign

See *D.C. al Coda, D.S. al Coda*

Courtesy accidentals

See *Accidentals*

Credits

Credits may consist of the **composer**, **lyricist** and **arranger,** or a word such as *traditional, anonymous, folk song,* etc.

1. The **composer** credit is placed flush right with the page margin. It is not horizontally aligned with the tempo marking.
2. The **arranger** credit is placed below the composer credit (also not horizontally aligned with the tempo marking).
3. The **lyric** credit is placed flush left with the page margin, horizontally aligned with the composer credit.
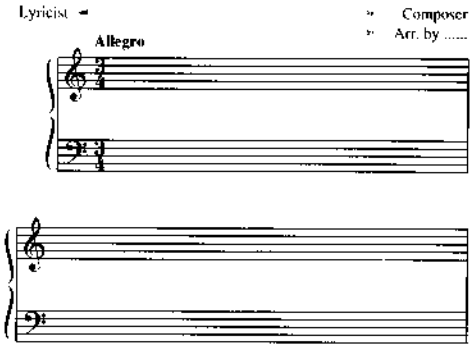
The typeface for all three credits is usually Roman.

For a less formal style, such as pop piano/vocal music, the lyric credit would go under the composer credit, with the arranger under that. **All credits would be flush right** with the page margin.

Some examples:

Words and Music by.....

Words and Music by
.....

Music by.....
Words by.....
Arranged by.....

The word "arranged" may be abbreviated (Arr.).

Cue notes

Cue notes may be given as guidance only, **to assist a performer's entrance** after numerous measures of rest.

Cue notes may also be given for **possible performance** if the cue instrument is weak or missing. (See *Alternating instruments*)

The size of cue notes is somewhat **smaller than normal note size,** but still large enough to be legible (65–75% of normal note size).
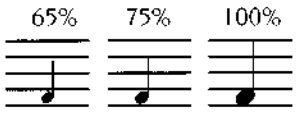
All musical elements associated with the cue notes will also be at **cue size.**

There are **two ways to notate** cue passages.

With **reverse stem direction** and added rests:

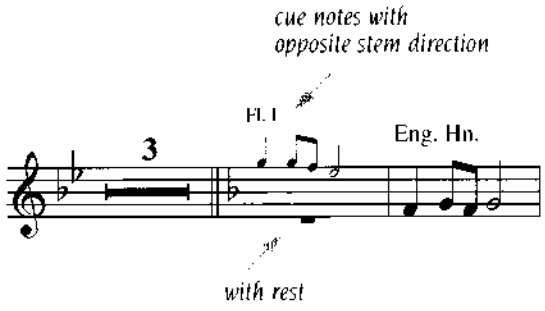

With **normal stem direction** and no added rests:

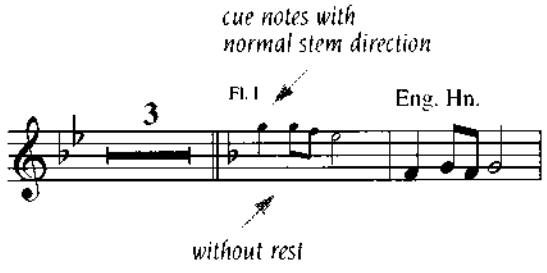

Piano accompaniment parts may include a cue-size solo part above the grand staff.
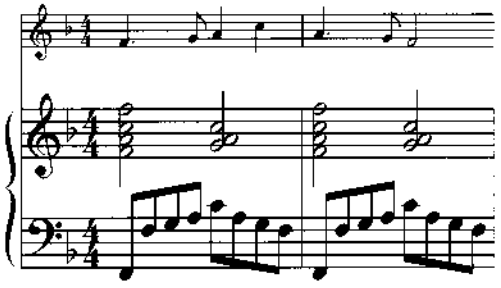
Not all notes that are cue *size* are used as a cue.

Ossia passages and **grace notes** are typically notated at cue size. (See *Ossia, Grace notes*)
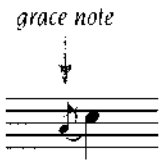
D.C. al Coda (da capo al coda)

Means go back to the beginning, play to the "to coda" sign (𝄋), then jump to the coda to finish the piece.

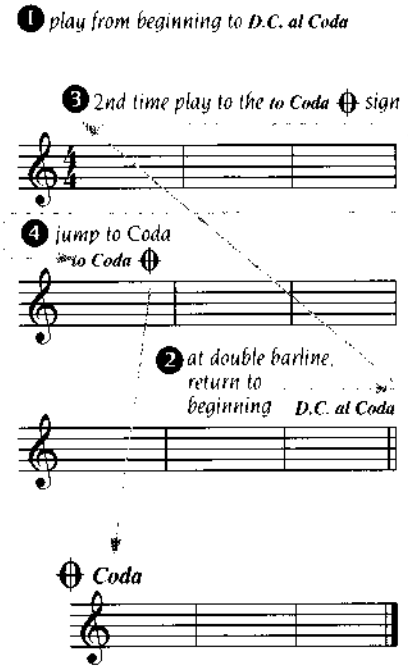

Align the edge of the "to coda" sign **flush right** with the barline.
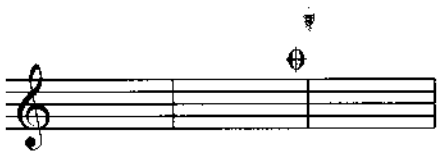
The words *to Coda* are often omitted from the "to coda" sign.

Place a **double barline** (thin/thin) at the ***D.C. al Coda.*** ***(D.C. al Coda*** can also be written ***D.C. al Coda*** 𝄋***)***
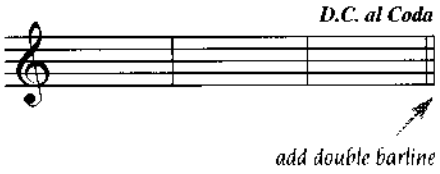
Separate the coda from the staff above (optional) and **indent.**

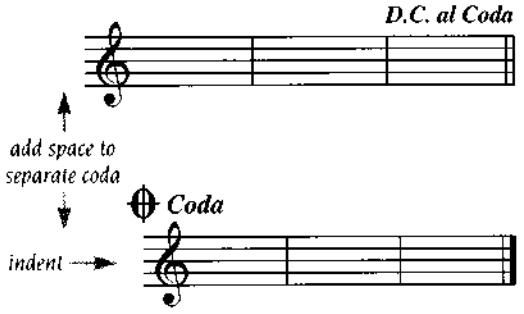

Align the coda sign with the beginning of the staff. It should be somewhat **larger** than the "to coda" sign.

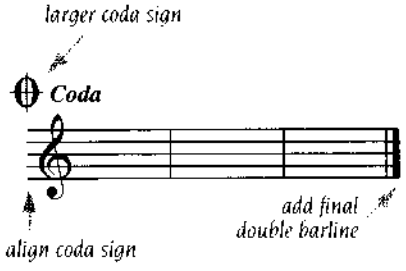

The coda will end with a **final double barline** (thin/thick).

It is sometimes necessary to begin the coda on the same staff as the ***D.C. al Coda.*** If so, **break the staff** and **add a clef and key signature.** (Do not add a time signature unless it changes at the coda.)

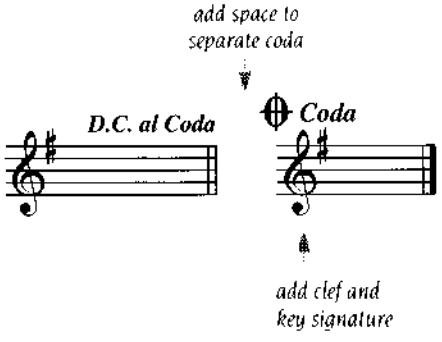

D.C. al Fine (da capo al fine)

Means go back to the beginning and play to the ***Fine.***

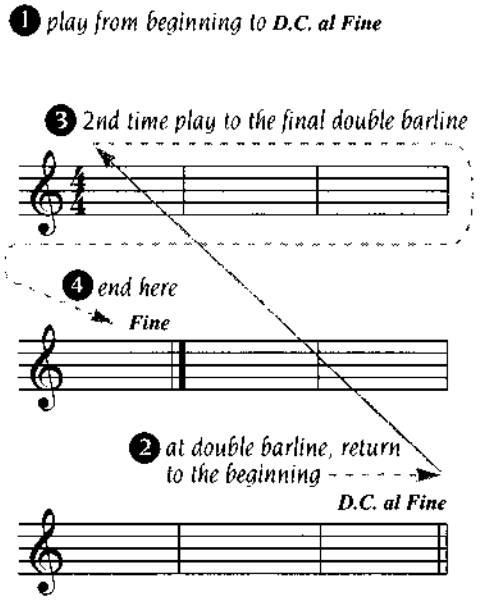

Place a **double barline** (thin/thin) at the ***D.C. al Fine.***

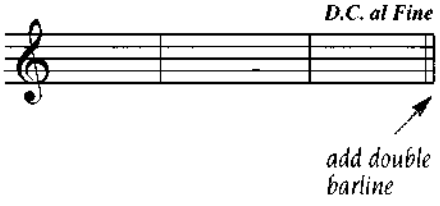

A **final double barline** (thin/thick) is added at the ***Fine.***
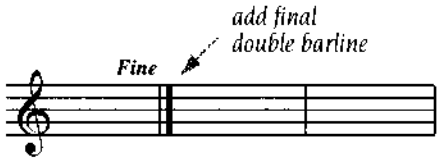
D.S. al Coda (dal segno al coda)

Means go back to the sign (𝄋), play to the "to coda" sign (⊕), then jump to the coda to finish the piece.

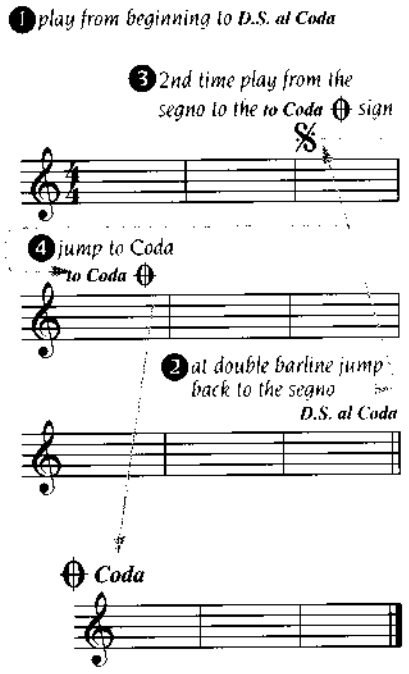

The segno 𝄋 should be **aligned flush left** with the barline.
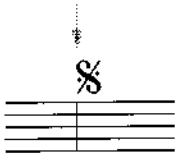
Align the edge of the "to coda" sign **flush right** with the barline.
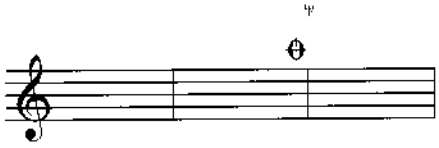
The words ***to Coda*** are often omitted from the "to Coda" sign.

Place a **double barline** (thin/thin) at the ***D.S. al Coda***. (***D.S. al Coda*** can also be written ***D.S. 𝄋 al Coda ⊕.***)
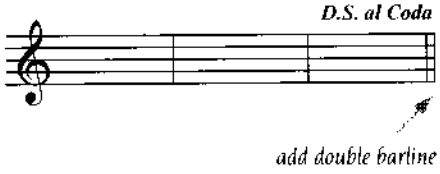
Separate the coda from the staff above (optional) and **indent.**

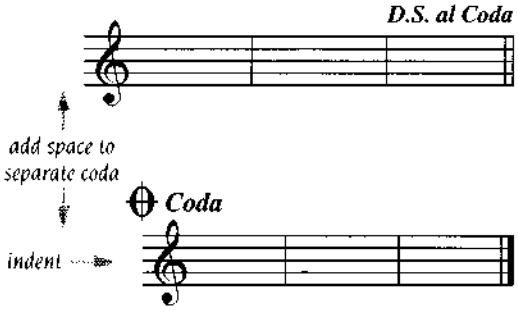

Align the coda sign with the beginning of the staff. It should be somewhat **larger** than the "to coda" sign.

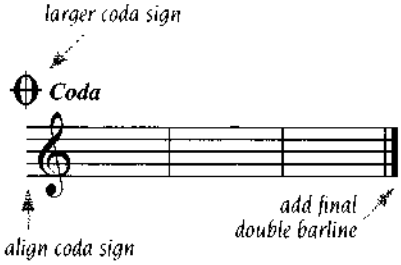

The coda will end with a **final double barline** (thin/thick).

D.S. al Fine (dal segno al fine)

Means go back to the sign and play to the ***Fine***.

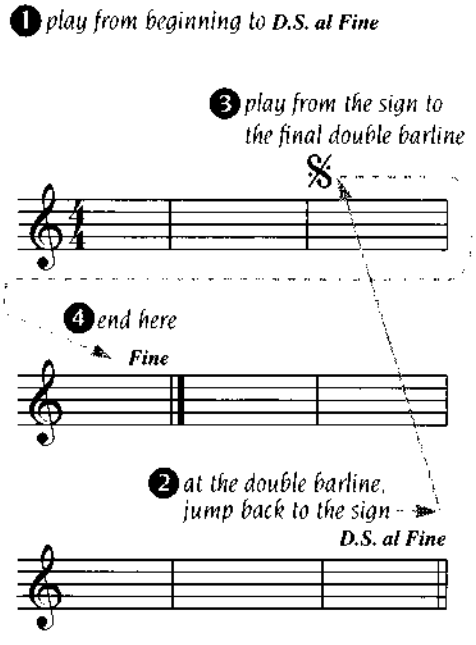

The segno 𝄋 should be **aligned flush left** with the barline.
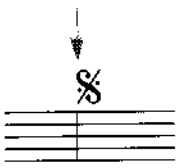
Add a **double barline** (thin/thin) at the ***D.S. al Fine.***
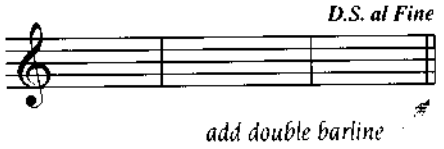
A **final double barline** (thin/thick) is added at the ***Fine.***

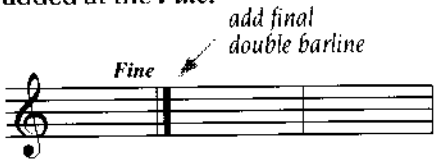

Divisi

Divisi is used for instruments (such as strings) that can produce **more than one note at a time,** indicating that the notes should be divided among the *group* of instruments (i.e., instead of multiple stops). (See *Sharing a staff*)

Divisi dots

See *Tremolo*

Dotted rhythms

See *Augmentation dot*

Dynamics

Dynamics indicate the varying degree of volume or intensity of a note, phrase or section of music.

The following lists the most common dynamics from the softest to the loudest:

softest ——————————► *loudest*

ppp pp p mp mf f ff fff

Dynamics **softer than *ppp* or louder than *fff* are impractical,** although theoretically any dynamic is possible.

COMBINED DYNAMICS

Dynamics such as ***mf, f, sf*** can be combined with ***p*** or ***pp***. The resulting dynamics function as a somewhat broader form of articulation.

fp sfp sfpp

fp *would mean to play loudly, then immediately play softly.*

(See *Articulations*)

CRESCENDO & DIMINUENDO

The **crescendo sign** is wedge-shaped and **opens toward the right.**

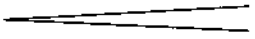

The **diminuendo sign** is wedge-shaped and **opens toward the left.** (The words *diminuendo* and *decrescendo* are interchangeable, but *diminuendo* is preferred.)

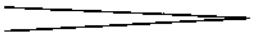

A crescendo or diminuendo sign is used when a **gradual increase or decrease** is wanted from one dynamic to another.

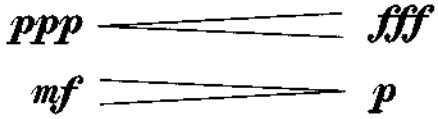

Musical elements should not be placed within the opening of the signs.

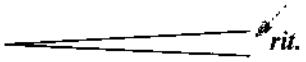

The word ***crescendo*** or ***diminuendo (decrescendo)*** may be written or abbreviated ***cresc., dim. (decresc.).***

The **effect is identical** whether using the sign, word or abbreviation.

If space doesn't allow the use of the sign, or the passage is a long one, it is best to use the word.

A **dashed line** may be used if it helps clarify the length of the passage.
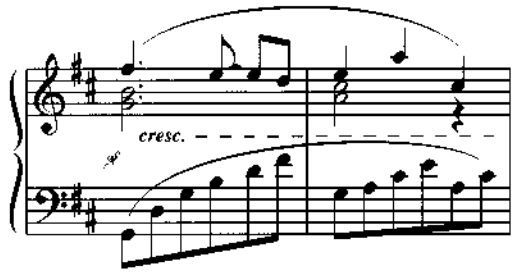
The word is sometimes **hyphenated** to extend throughout a section of music.

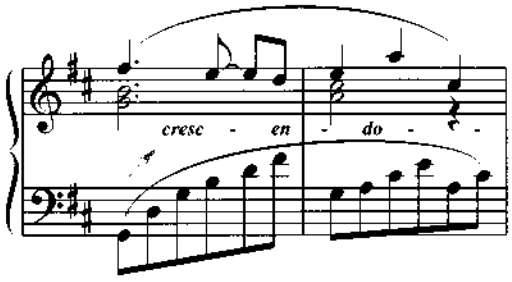

GENERAL PLACEMENT

Place the dynamic sign *slightly* before the notehead whenever possible.
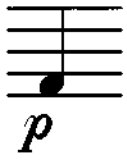
For single-staff instruments

Dynamics are placed **below the staff.**

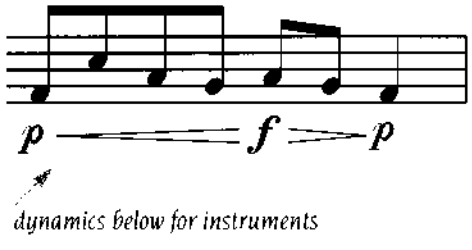

When two parts share a staff and the dynamics vary between parts, the dynamics will be placed above and below the staff.
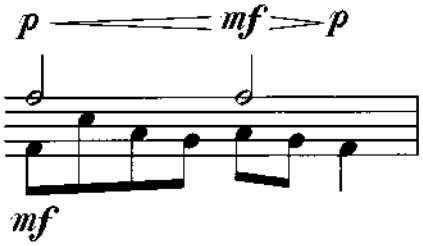
For vocal music

Dynamics are placed **above the staff** to avoid conflicting with the lyric.
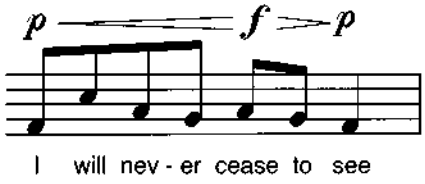
For the grand staff

Dynamics are placed **between the two staves.**
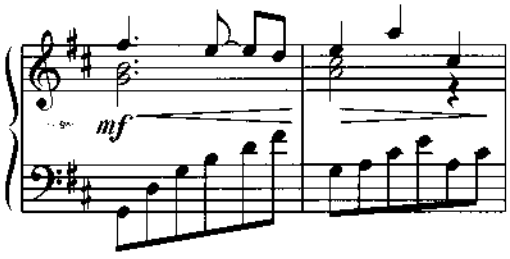
If two different dynamics are needed for each staff, the dynamics may be placed above for the top staff and below for the bottom, or in positions that clarify the situation best.

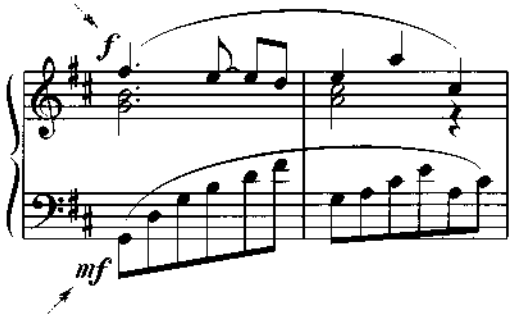

Horizontal placement is preferred for crescendo and diminuendo signs, although an angled placement is acceptable if necessary.

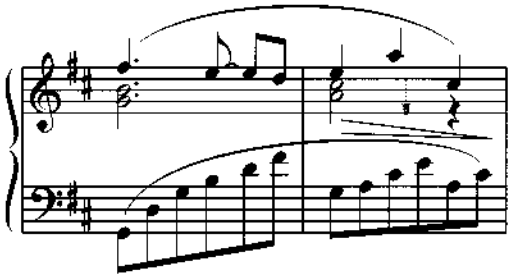

The signs may also be **placed outside the staff** if space is tight within the grand staff.

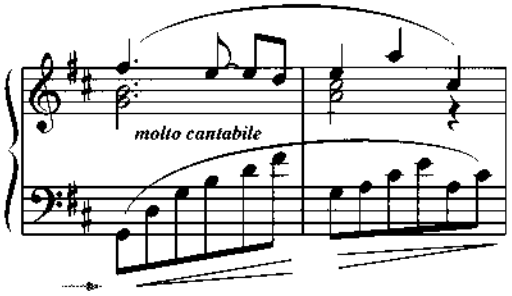

If a dynamic mark must be placed on a barline, the barline should be **broken.**

For crescendo and diminuendo signs, the **barline is left intact.**

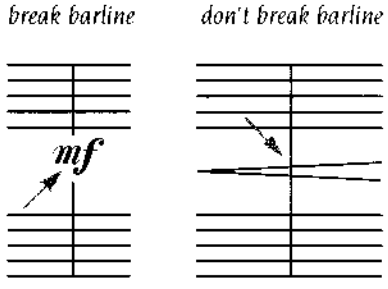

Dynamics with crescendo/ diminuendo signs

The intensity of the increase/decrease in volume is **relative to the dynamic level** of the section of music.

If a dynamic is not indicated at the end of a crescendo sign, and the music is consistently gentle, the increase in volume would probably be subtle.

The **level at the beginning of the sign** is the same as **the dynamic last indicated** in the music.
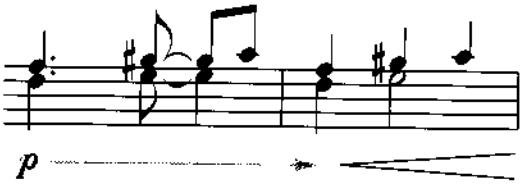
It is advised to **carefully begin and end the sign** so that it makes sense.

While the example below would make perfect sense in a clarinet part, it would make no sense in a piano part.
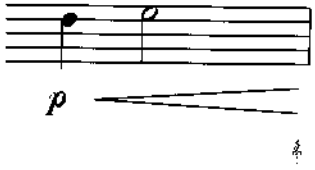
Endings

See *Repeat signs*

Fermata

A hold or pause sign (𝄐). It is used with any rhythmic value—single notes, intervals, chords or rests.

PLACEMENT

Preferred placement is above, regardless of stem direction, except when parts share a staff.

The fermata is **centered on the notehead** (or rest), whether it is on the notehead side or the stem side.

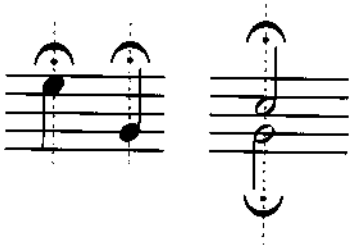

One fermata applies to all notes of an interval or chord.
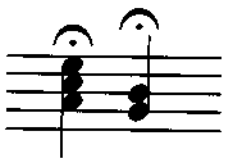
Place outside the staff if at all possible.
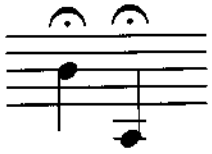
Place outside articulations and slurs.
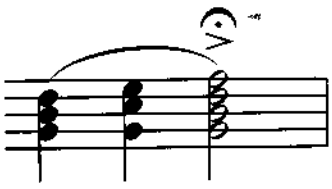
Place the fermata on the exact beat that is to be held, so that there can be no confusion. In the first example below, it might be wondered whether the fermata over the whole notes would apply to the eighth rest in the lower voice.

Confusing:
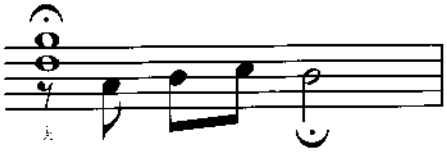
Same example, more clearly written:

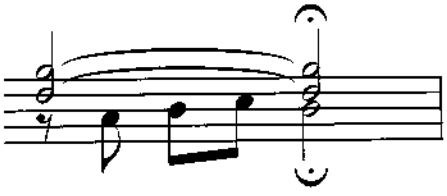

TIME VALUE

A fermata over a note or chord not only indicates that the tempo is interrupted but that the note or chord is **sustained.**

The length of a fermata is **determined by the performer** and is relative to the musical situation.

In a fast tempo, placed on a sixteenth note, the fermata would be a shorter value than if placed on a whole note, in a slow tempo.

USING WITH RESTS

In the following example, the fermata **prolongs silence rather than sound.**
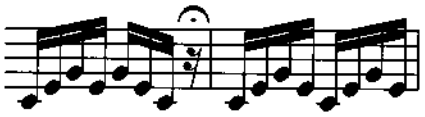
ABOVE A CAESURA

The following example is similar to the last one. The caesura indicates a small break in the sound; the addition of a *fermata* **lengthens the break.**
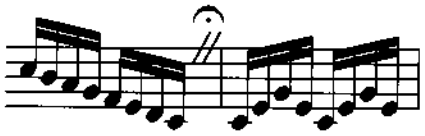
Occasionally a fermata is seen over a final double barline before another movement. However, since a barline has no time value, **avoid using a fermata over a single barline.**

ACCOMPANYING TERMS

Lunga *(long)* or **poco** *(little* or *short)* may be used with a *fermata* for a more specific intent.

These should be **centered above** the *fermata.*

Fingerings (for keyboard)

GENERAL PLACEMENT

Fingerings for the **right hand** should be placed **above** the staff, away from all musical elements.

Fingerings for the **left hand** should be placed **below** the staff, away from all musical elements.

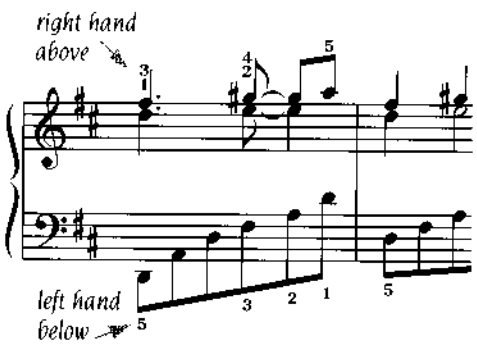

Fingerings are **centered** above or below the notehead, when possible.
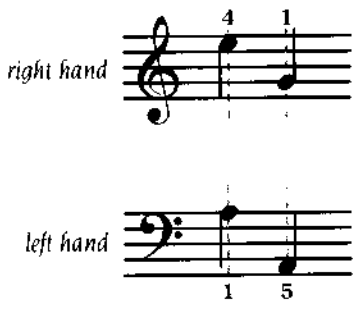
A finger number is preferably placed **outside a beam.**
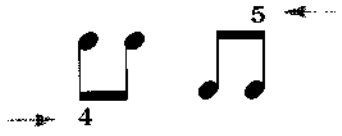
CHORDS

Fingerings are **stacked above or below** a chord; all notes should have a fingering.

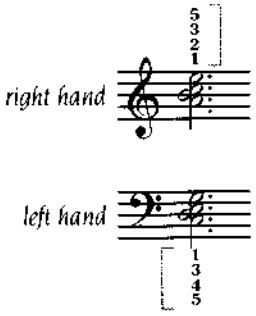

If a chord includes **notes that are tied** and a fingering is indicated for a note that is *not tied,* only that fingering is necessary.
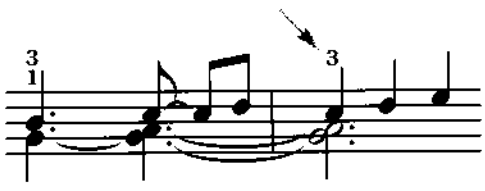
ALTERNATING FINGERINGS

If a fingering changes on a note that is held, a hyphen (-) or an "en-dash" (–) **separates the two fingerings.** The first fingering is centered on the note; the second is to the right.
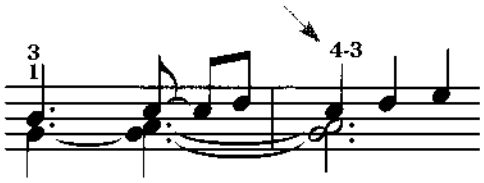
An alternate method uses a small slur instead of the hyphen or en-dash.
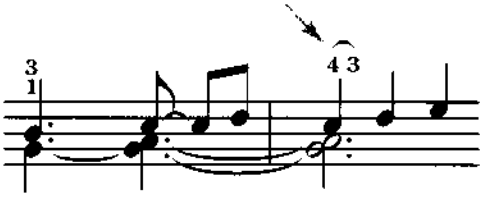
USE WITH TRIPLETS

The triplet ***3*** is sometimes mistaken for a fingering when the fonts are similar.

The **fingering font should be smaller** and of a **different typeface** than the font used for triplets.

Avoid positioning the triplet *3* on the same side of the staff as a fingering.

Instead of moving the fingering, **move the triplet *3*** to the opposite side from the fingering. The triplet ***3*** would normally be on the *beam* side; **if on the notehead side** it is helpful to **add a bracket.** (See *Tuplets*)

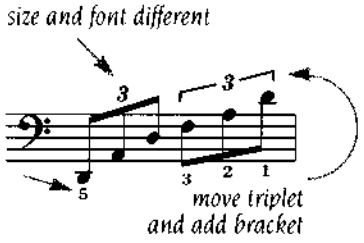

TWO HANDS ON ONE STAFF

If both hands share the same staff, the fingering for **the right hand is above,** the **left hand below.**

RH (right hand) or **LH** (left hand) may be added for **clarification.**
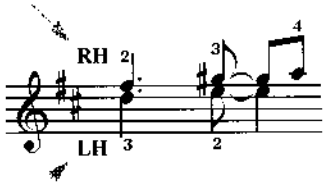
AMOUNT OF FINGERING

Fingering should be **used sparingly** and only to establish a pattern or hand position.

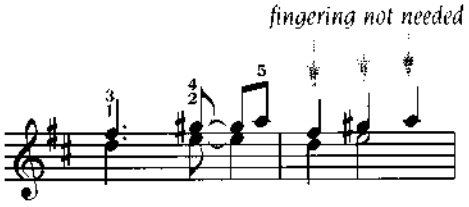

OVERLAPPING ELEMENTS

Fingerings **may overlap a slur.** The preference is to break the slur at the point of intersection, if possible.

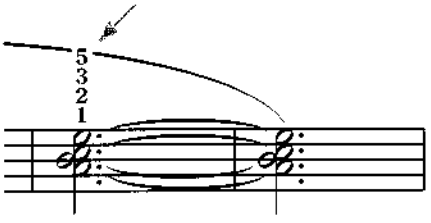

The vertical space sometimes dictates that fingerings be placed within the staff. The **staff lines should be broken** to accommodate the overlapping fingerings.

Flat

See Accidentals, Key signatures

Glissando sign

A glissando is indicated by a wavy or straight line placed at an angle, ascending or descending.

Indicate the beginning and ending notes of the glissando.

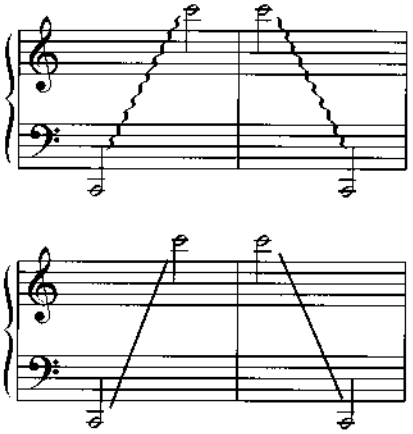

ADD THE ABBREVIATION

It is helpful to **add the abbreviation (*gliss.*),** placing it at the same angle as the symbol.

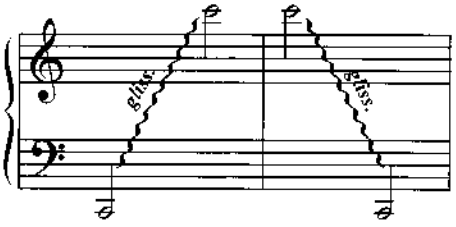

TWO OR MORE NOTES

If the glissando affects more than one note, add a **glissando symbol for each note.** The word (*gliss.*) is used only once regardless of the number of notes.

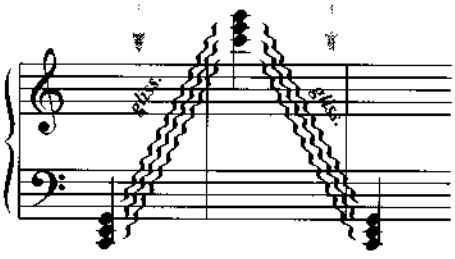

Grace notes

Grace notes are small notes **without a rhythmic value** of their own, taking their value from the previous or following beat.

Grace notes are notated at **cue size** or slightly smaller (65% of normal size works well).

SINGLE GRACE NOTES

Single grace notes are **considered eighth notes.**

Place the **stem up** regardless of the main note's stem direction (except when two parts share a staff).

Usually a **small slur connects** the grace note to the main note; the slur usually begins below the grace note.
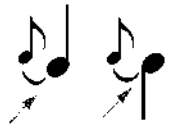
The slur **end does not need to be centered** on the main notehead like slurs normally do. It may end **slightly to the left** of the notehead. (See *Slurs*)

For single grace notes with a flag, a **small line** can intersect the flag, always **slanting upward, from left to right,** regardless of stem direction.

(for a lower voice sharing a staff)

PLACEMENT ON THE STAFF

The grace note is centered in a space or placed directly on a line.

Grace-note **accidentals** are also cue size. (See *Accidentals*)

Stems for grace notes on leger lines do not have to be lengthened to meet the middle line.
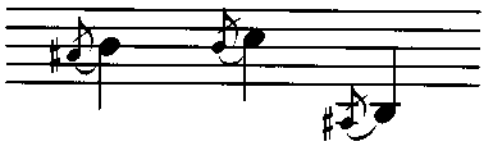
SHARING A STAFF

When two parts share a staff, the grace note stems follow the stem direction of the parts.
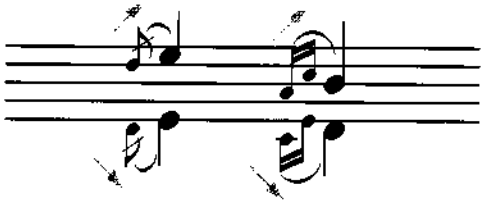
MULTIPLE GRACE NOTES

Multiple grace notes should **never have a slanted line** through the stems or beams. The slanted line is only for single, flagged grace notes.

If a slur is used, the **slur connects** all the grace notes **to the main note.**

Two grace notes are **considered sixteenth notes** and should be beamed accordingly. Three and four can be either sixteenth or 32nd notes.
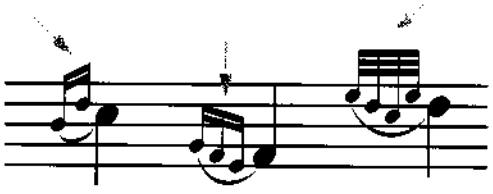
Larger groupings, such as five and six grace notes, are usually beamed as 32nd notes.

DIRECTION OF GRACE-NOTE SLURS

If a grace note precedes an interval or chord, the **slur will follow the direction of resolution** (from the grace note to the appropriate main note).
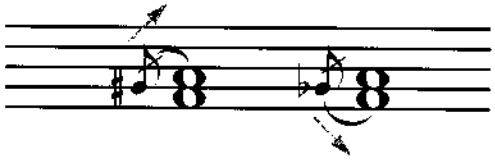
WITH LEGER LINES

If leger lines are used, the slur may be **placed above to avoid the leger lines.**

The grace-note leger lines can be the same thickness as staff lines, but shorter.

Grand pause

The grand pause or general pause (G.P.) over a measure of rest indicates that the **entire orchestra is silent,** often unexpectedly.

Grand staff

The grand staff is used to notate scores for instruments such as piano, organ, harp and marimba.

The grand staff consists of **two staves joined by a brace** and a systemic barline. (See *Brace*)

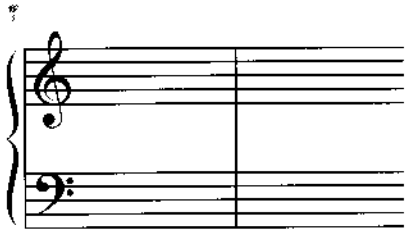

Although the "normal" clefs for the grand staff are treble above and bass below, **either staff may have either clef,** and may change clefs at any time. (See *Clef signs*)

FOR ORGAN

Organ scores use the grand staff connected to a staff used to notate music for the organ pedals.

Except for the systemic barline, **barlines are separated** between the manuals and pedal.

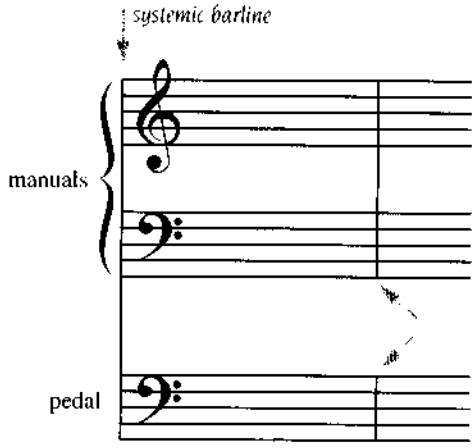

FOR INSTRUMENT & PIANO

Scores for an instrument (including voice) and piano use a **grand staff, with the instrument staff above.**

The staff above the grand staff is sometimes **cue size,** if the instrument has its own full-size, separate part.

Except for the systemic barline, **barlines are broken** between the instrument staff and the grand staff.

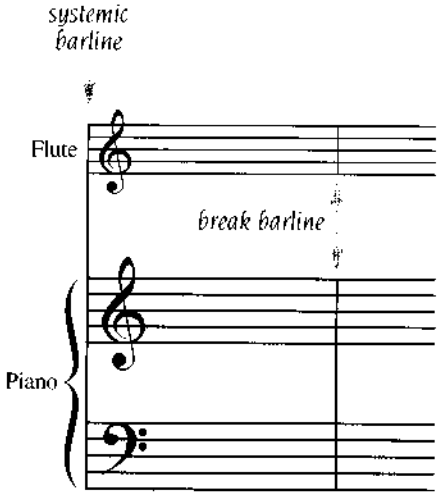

TWO-PIANO MUSIC

Two-piano music requires two grand staves joined together with a **systemic barline.**

The measure **barlines connect staves for each grand staff only.**

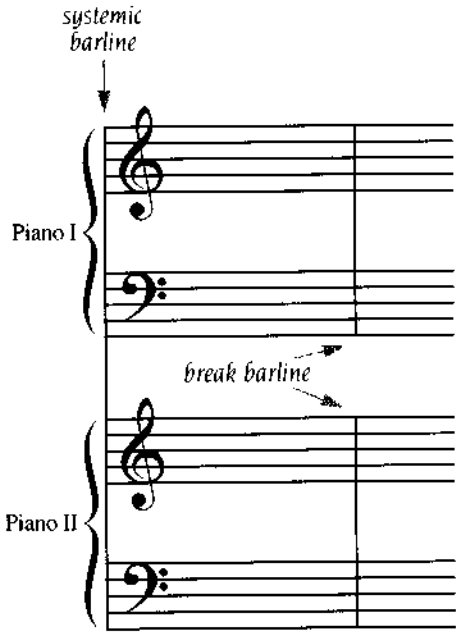

ONE PIANO—FOUR HANDS

Facing pages are required.

The **Secundo** part is notated on the left-hand page; usually both staves are in **bass clef.**

The **Primo** part is notated on the right-hand page; usually both staves are in **treble clef.**

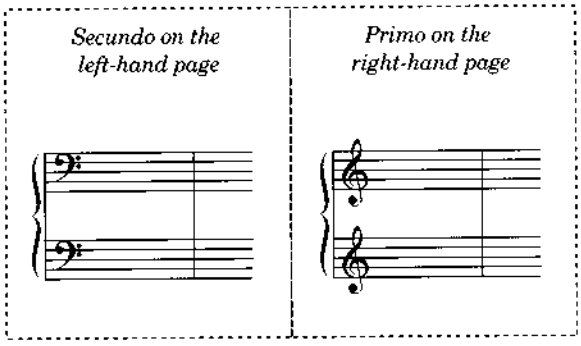

The **page layout** for primo and secondo **is preferably identical**, system-for-system; if they are not identical, the facing pages *must* begin and end with the same measures.

Harmonics

NATURAL HARMONICS

Natural harmonics are indicated by a **small circle** centered above the notehead.

The indicated note is the SOUNDING NOTE.

Such notation indicates a **natural harmonic.**

Careful consideration of an instrument's capabilities is necessary. Only some instruments are capable of producing harmonics.

Another way to notate a natural harmonic (for strings) is to use a **diamond-shaped notehead.**

The position on the staff **indicates where the finger is placed**—NOT the sounding note.

The sounding note may be indicated in cue size and in parentheses.

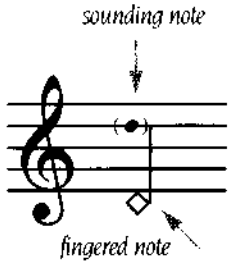

ARTIFICIAL HARMONICS (STRINGS)

A diamond-shaped notehead with a standard notehead comprises an artificial harmonic. The **standard notehead indicates the placed finger**; the diamond indicates where the second finger lightly touches the node to produce the harmonic.

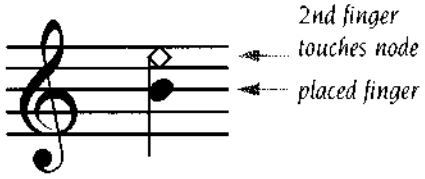

Often the sounding note is indicated in cue size and in parentheses.

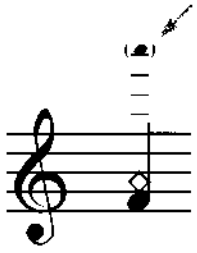

Key signatures

Key signatures appear **after the clef but before the time signature.**

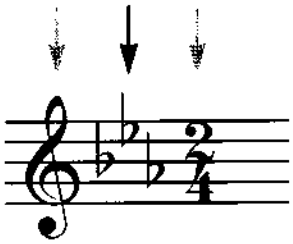

CHANGING KEYS

The preference is to make key changes at the beginning of a staff or system, with a **courtesy key signature** at the end of the previous one.

1. A key change is traditionally preceded by a **double barline.**
2. If the key change is at the beginning of a staff or system, a **courtesy key signature** is placed at the end of the previous one.
3. The **staff is left open** after the courtesy key signature.
4. The **new key signature is indicated** on the next staff.

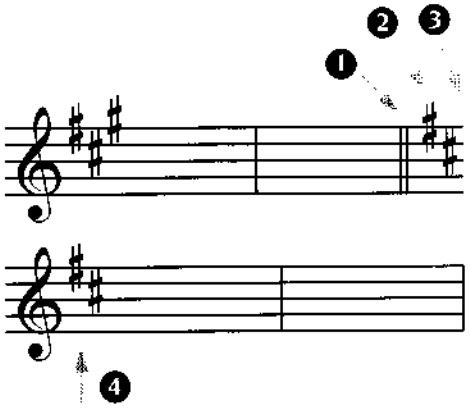

If a key **changes mid-staff:**

1. a double barline is added,
2. followed by the new key signature.
3. The new key signature continues on the next staff.

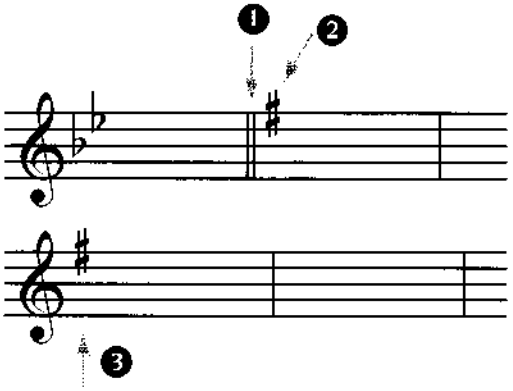

CANCELLATIONS

Cancellations are no longer considered necessary, unless the new key is C major or A minor (no sharps or flats). In that case, cancel the old sharps or flats with natural signs, in the same order as the old key signature .

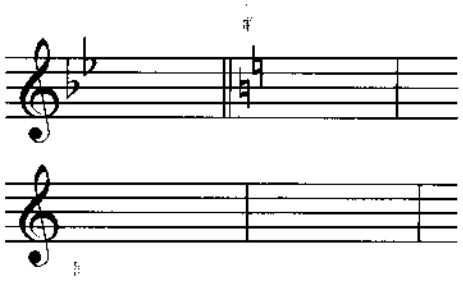

The following illustrates the positioning of the clef, key signature and time signature if all three change simultaneously.

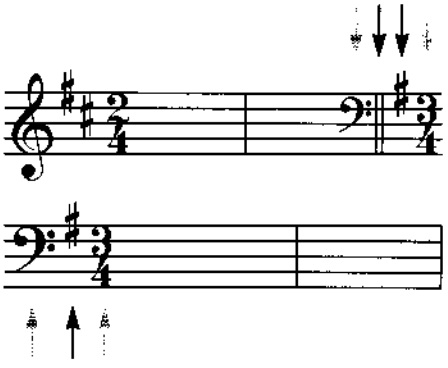

Key signatures in the **TREBLE CLEF**

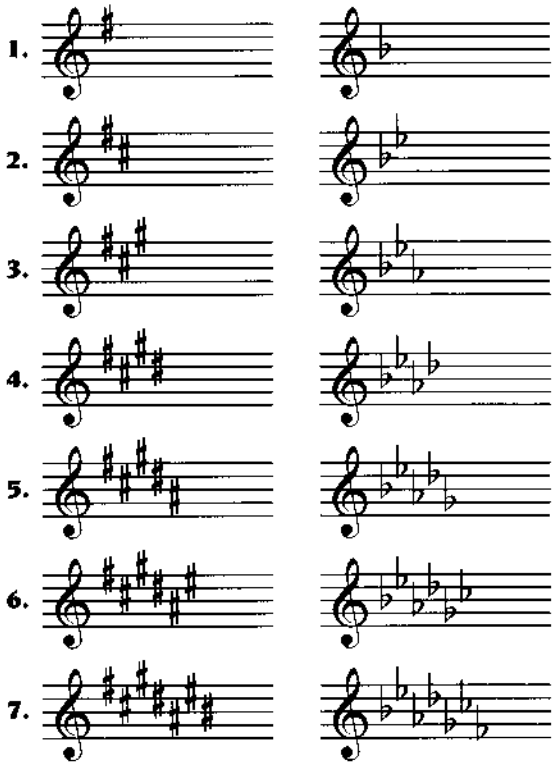

Key signatures in the **BASS CLEF**

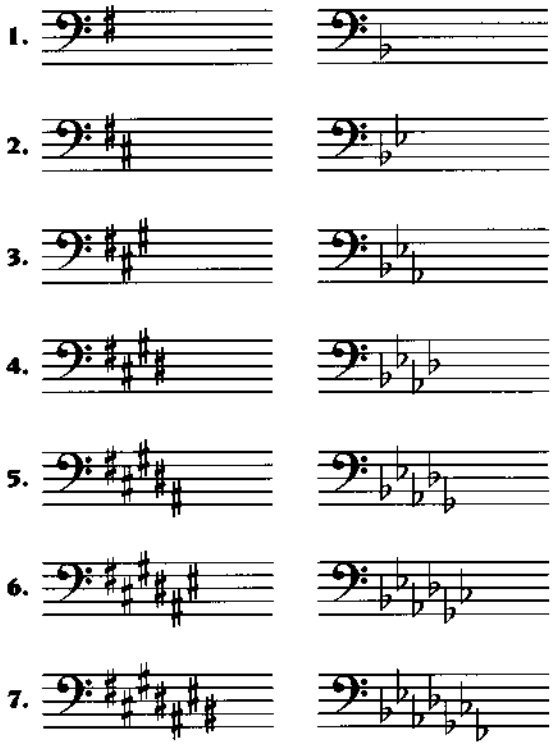

Key signatures in the **TENOR CLEF**

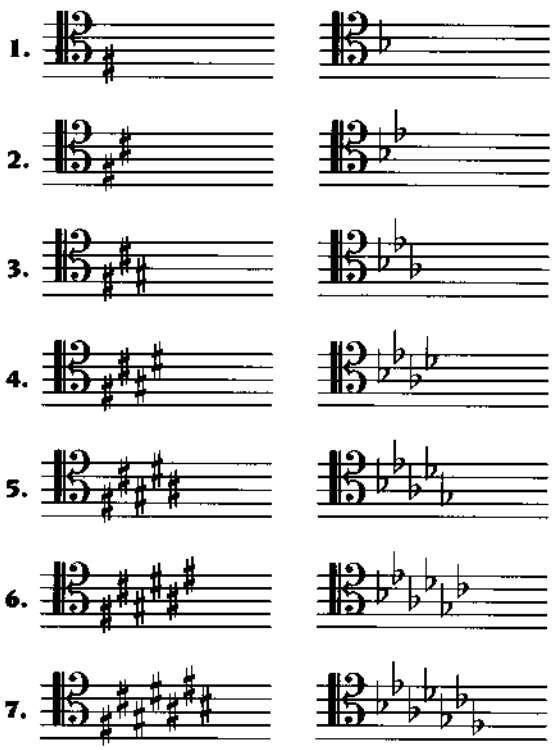

Key signatures in the **ALTO CLEF**

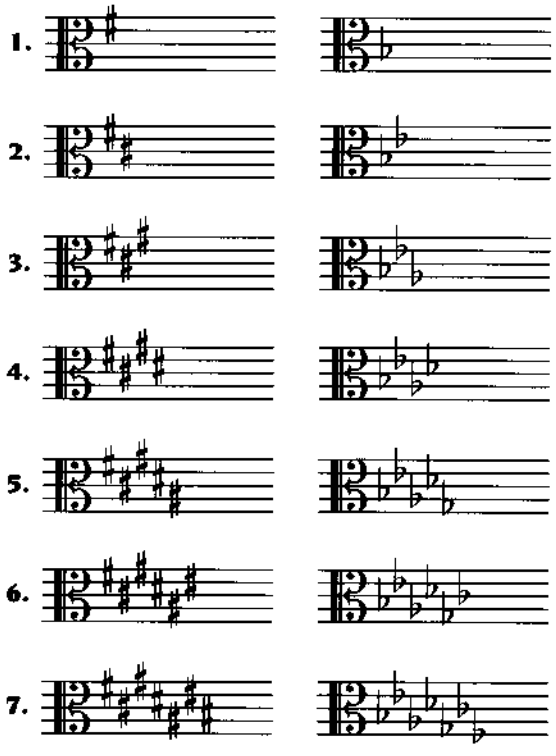

THE CIRCLE OF FIFTHS

The Circle of Fifths serves as a quick reference guide to the relationship of the keys and key signatures, and how they can be figured out in a logical manner.

The Circle of Fifths will also help to clarify which keys are enharmonic equivalents. (*Enharmonic* means notes that sound the same but are written differently.)

Clockwise movement *(up a perfect 5th) provides all of the sharp keys by adding one sharp to the key signature progressively.*

Counter-clockwise *(down a perfect 5th) provides the flat keys by adding one flat similarly.*

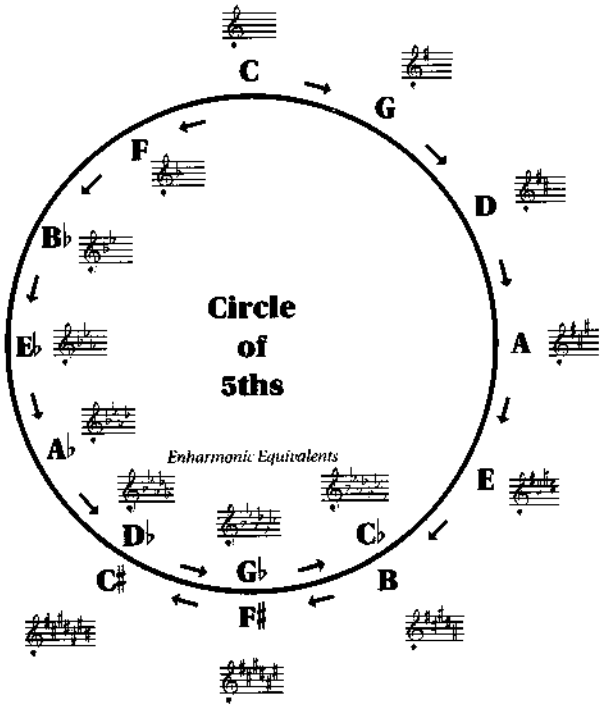

Layout See *Spacing*

Leger lines

Leger lines are used to extend the range of the five-line staff.

Leger lines are the **same line weight as staff lines,** or slightly heavier.

The **vertical spacing** of leger lines must be identical to the vertical spacing between staff lines.

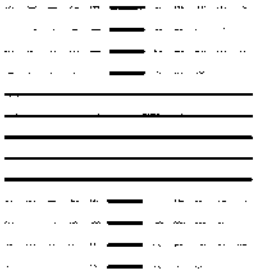

Leger lines **extend slightly past the notehead.** They will need to extend sufficiently enough to be seen.

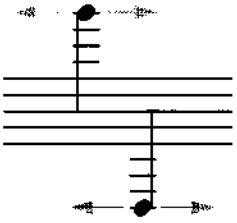

STEM LENGTH

Stems of all notes ABOVE or BELOW the first leger line past the staff **must extend at least to the middle staff line.**
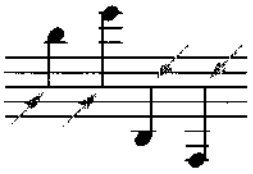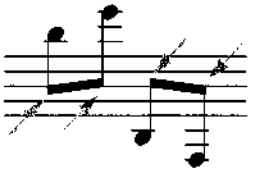
OVERCROWDING

To avoid leger lines that touch, adjustments must be made either in the **horizontal spacing** of the music or by **shortening the leger line length.** The first is preferred, but is not always possible.

In the first example below, the leger lines are overcrowded and appear to be touching.
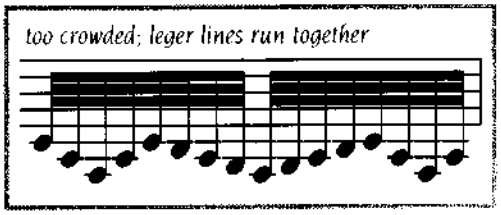
Corrected by shortening the leger lines to create a slight amount of space between the lines.
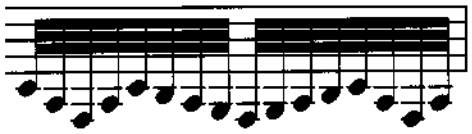
CLEF CONSIDERATIONS

Choose the appropriate clef for the situation. The viola, for instance, may be written in alto clef to avoid excessive leger lines. (See *Clefs*)

The following examples illustrate the same musical example in three different clefs.
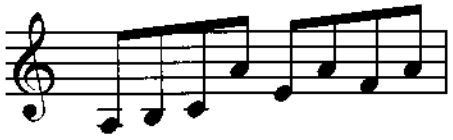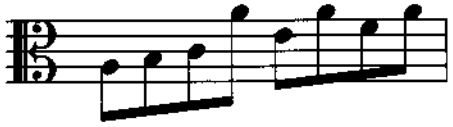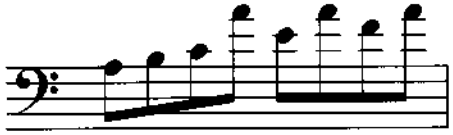
Lyric

Beaming of notes associated with a lyric now follows standard notational practice.

Traditional practice, now obsolete, was to use flags for eighth notes, sixteenth notes, etc. Beams were used only for melismas.

However, in several other ways the lyric makes the notation of a vocal part different from that of other parts.

PLACEMENT OF STAFF INDICATIONS

Dynamics and tempo indications go **above the staff** to avoid conflicting with the lyric.
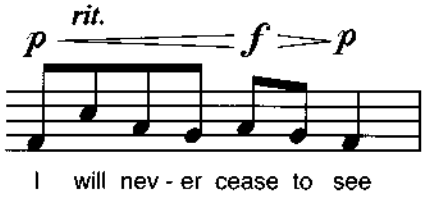
USE OF SLURS

Slurs are **seldom used in a vocal part for anything other than a *melisma*** (a term used here simply to mean a syllable or word that is sung to more than one note).

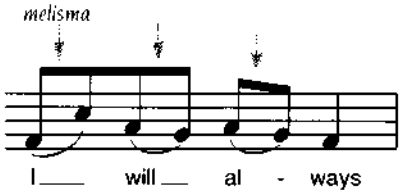

ALIGNMENT OF LYRIC FOR MELISMA

Another help in reading a melisma is the proper **alignment of the lyric.** The word or syllable, instead of being centered under the note, should be aligned **flush left with the left edge of the notehead** (see above).

EXTENDER LINES

In addition to the slur, **extender lines at the baseline of the lyric** help to **show the length of a melisma.** However, extender lines are only used for **one-syllable words, or for the last syllable of a word.** A hyphen is used in the middle of a word.

The **thickness of extender lines** should be less than that of the staff lines.

The **end of the extender line** should be **aligned flush right** with the last note of the melisma. *The most common mistake in the use of lyric extender lines is to extend the line for the full value of the note.*

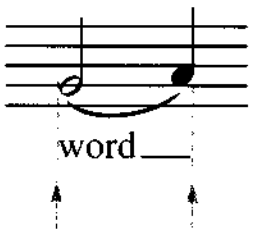

When an extender line is called for, there should always be one, even if the words are crowded and it has to be very short. (In this case, the line can extend slightly past the note.)

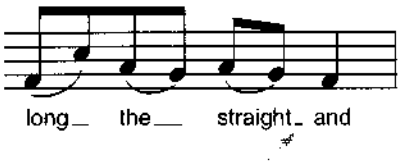

When an extender line wraps to the next staff, begin the line at the end of the key signature.

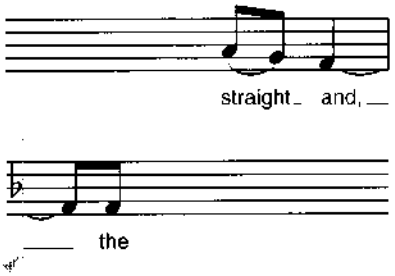

Notice the comma in the previous example. Any **punctuation always precedes an extender line.**

TIES

Ties are treated exactly like melismas, including the use of extender lines and alignment of lyric.

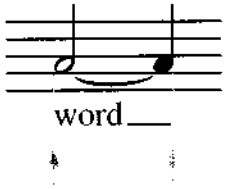

WORD PLACEMENT (NORMAL)

Words or syllables for notes other than melismas or tied notes are **centered to the notehead.** If the lack of space does not allow a word or syllable to be exactly centered, at least some part of the word or syllable should be under the note.
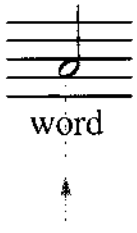
HYPHENATED WORDS

Center the *hyphen* (not a dash or extender line) between syllables.

If the melisma (or tie) is extremely long, **more than one hyphen** may be used.

If the hyphenated word **wraps to the next line, another hyphen *may* be used** at the beginning of the line.

Hyphenate words **according to the dictionary.** Do not hyphenate according to how the word *sounds* like it should divide. If there is any question at all, check the dictionary.

PUNCTUATION

Use **normal punctuation and capitalization.** (Sometimes capitalization is done as if the words were poetry, with each "line" capped, but this is becoming less common.) *A common mistake is to use little or no punctuation.*

MULTIPLE VERSES & REPEATS

Broken slurs

A **broken slur** is used when one verse has a melisma, especially if it is not the first verse.

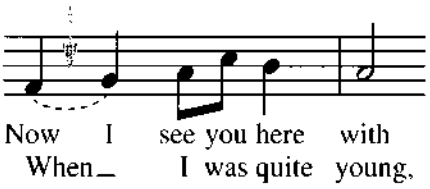

Treat the lyric for each verse separately. Notice in the above example that the melisma is aligned *as a melisma,* while the previous verse is aligned normally.

Omission lines

An omission line is sometimes used to clarify that there is **no word or syllable sung.**
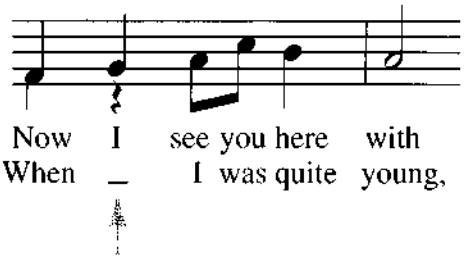
In many cases, however, there is a better way to treat the situation. In the previous example, the omission line could be mistaken for an extender line, so it would be better without it, letting the cue-size rest serve the same purpose.

Cue-size notes, rests

Use cue-size notes and rests **when a rhythm is different from the first verse** (see previous example). Stems and beams should also be cue size.

If there are **more than two verses** with different rhythms, the notation can become quite complicated. It may be better to write out the music.

Numbering

Multiple verses are numbered. There are several ways to treat these when there are pick-ups, repeats, first and second endings, etc. Be clear and consistent.

→ 1. Verse, verse, verse
→ 2. Verse, verse, verse
→ 3. Verse, verse, verse

Using a brace

When multiple lines converge into one line, such as a *chorus* or *refrain*, a **brace** is used.

→ 1. Verse, verse, verse
→ 2. Verse, verse, verse } chorus or refrain ···→
→ 3. Verse, verse, verse

Meter

The understanding of meter is essential to the placement of ties, rests, syncopated rhythms and proper beaming.

Time signatures identify the meter.

There are two overall classifications of meter: **perfect** and **imperfect** (odd) meter.

PERFECT METER

In perfect meter the measure can be divided into **equal halves or thirds**.

There are two classifications of perfect meter: **simple meter** and **compound meter.**

In **simple** meters each **BEAT** can be subdivided by 2.

In **compound** meters each **PULSE** can be subdivided by 3.

Metric subdivisions should not be confused with tuplets.

SIMPLE METER

The classification of **duple, triple** or **quadruple** reflects the number of **BEATS** in the measure.

Simple duple meter

Simple duple time signatures have a 2 as the upper number of the time signature.

$\frac{2}{2}$ $\frac{2}{4}$ $\frac{2}{8}$

Each measure contains **2 BEATS.**

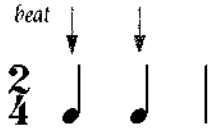

Each BEAT can be **subdivided by 2.**

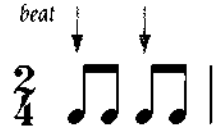

Only **rests of equal value to the beat** or less may be used (except in a complete **measure of rest,** which is indicated by a whole rest).

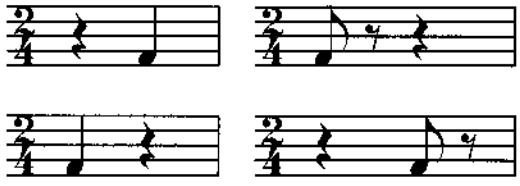

Rests of equal value to the beat are used ONLY on the beat.
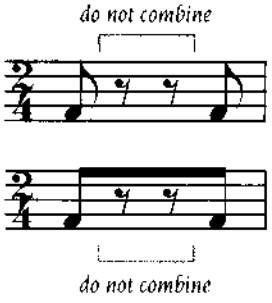
The following are all acceptable examples in simple duple meter.

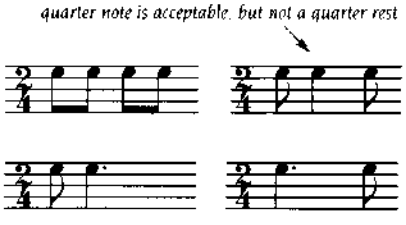

Simple triple meter

Simple triple time signatures have a 3 as the upper number of the time signature.

$\frac{3}{2}$ $\frac{3}{4}$ $\frac{3}{8}$

Each measure contains **3 BEATS.**

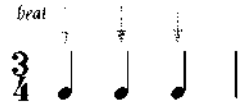

Each beat can be **subdivided by 2.**
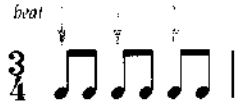
Only **rests of equal value to the beat** or less may be used (except in a complete **measure of rest,** which is indicated by a whole rest).

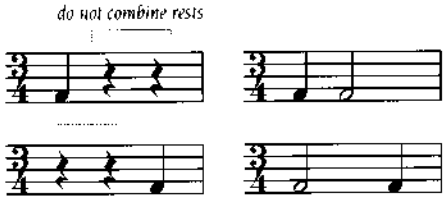

Beaming should reflect the simple triple meter, NOT compound duple meter.
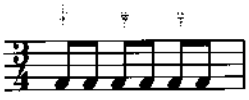
NOT

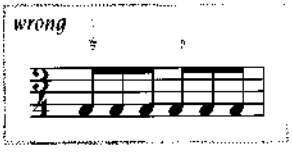

Simple quadruple meter

Simple quadruple time signatures have a 4 as the upper number of the time signature.

$\frac{4}{2}$ $\frac{4}{4}$ $\frac{4}{8}$

Each measure contains **4 BEATS.**
Each beat can be **subdivided by 2.**

To successfully notate *simple quadruple* meter, it is best to consider the meter as a combination of **2 units of duple meter.**

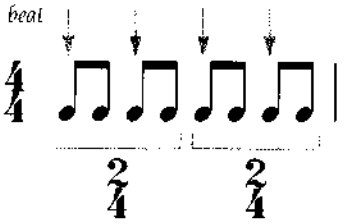

*In simple quadruple meter, these **2 units** must always be clearly distinguished. The only exception to this would be a very simple syncopation (such as ♩♩ ♩).*

The following examples illustrate the **subdivision of the 2 units.** The notation of each unit, separately, is identical to that of simple duple meter.

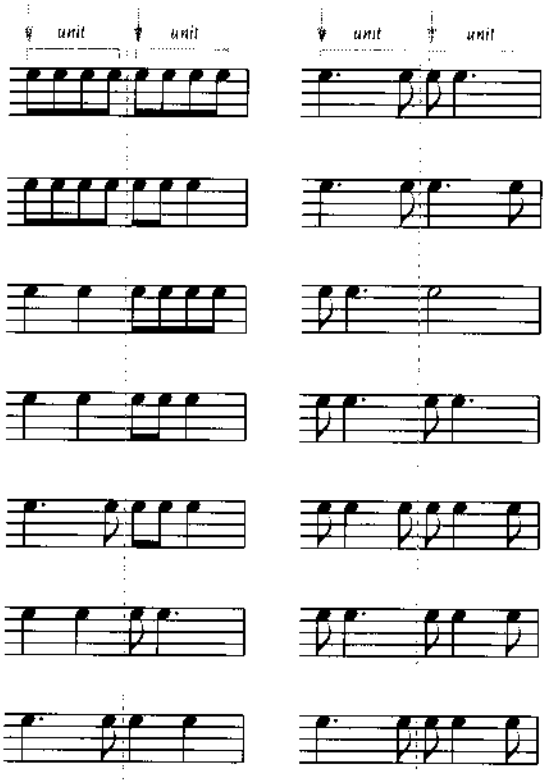

Whole rests are used to indicate a complete measure of rest.

Rests twice the value of the beat are used ONLY on beats 1 & 3 (the first beat of each half of the measure).
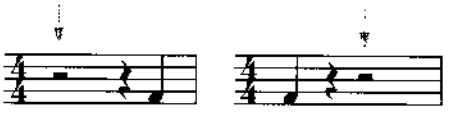
Rests of equal value to the beat can ONLY appear on the beat.

Rests less than the value of the beat are used freely as long as the two units are apparent.
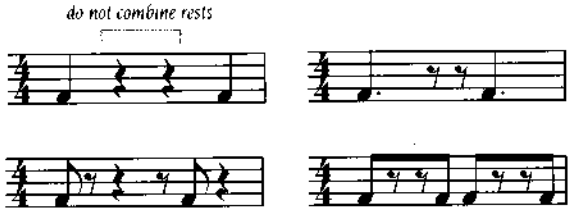
COMPOUND METER

The classification of **duple, triple** or **quadruple** reflects the number of **PULSES** in the measure.

Compound duple meter

Compound duple time signatures have a 6 as the upper number of the time signature.

$\frac{6}{4}$ $\frac{6}{8}$

Each measure contains **2 PULSES.**

Each PULSE can be **divided into 3 BEATS.**
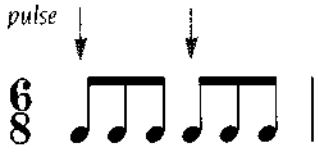
Only **rests of equal value to the pulse** or less may be used (except in a complete **measure of rest** which is indicated by a whole rest).

Rests of equal value to the pulse can ONLY appear on the pulse.
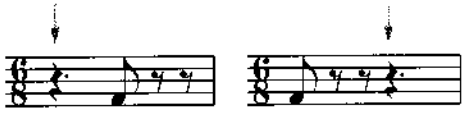
Rests of $^2/_3$ the value of a pulse may be used ONLY on the pulse.

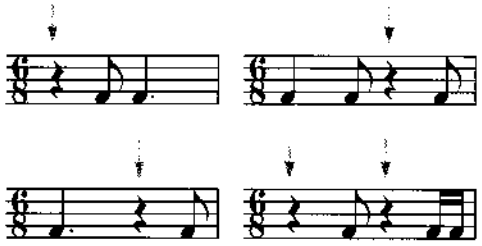

Rests of equal value to the beat, **not appearing on the pulse,** CANNOT be combined.
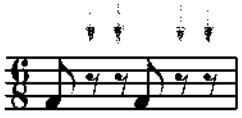
Beaming should reflect the compound duple meter, NOT simple triple meter.
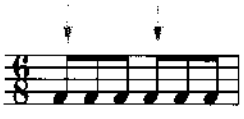
NOT

Compound triple meter

Compound triple time signatures have a 9 as the upper number of the time signature. An example is $\frac{9}{8}$.

Each measure contains **3 PULSES.**

Each PULSE can be **divided into 3 BEATS.**

Rules governing **rests and beaming** are identical to compound duple meter.

Compound quadruple meter

Compound quadruple time signatures have a 12 as the upper number of the time signature. An example is $\frac{12}{8}$.

Each measure contains **4 PULSES.**

Each PULSE can be **divided into 3 BEATS.**

To successfully notate *compound quadruple* meter it is best to consider the meter as a combination of **2 units of compound duple meter.**
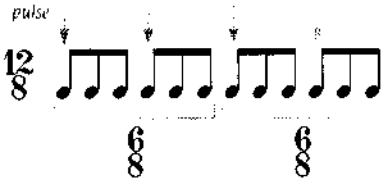
Rules governing **rests and beaming** are identical to compound duple meter.

IMPERFECT METER (ODD METER)

In imperfect meter (odd meter) the measure **CANNOT be divided into equal halves or thirds.**

Imperfect meter can be considered as any combination of **duple or quadruple meter** AND **triple meter.**

$\frac{7}{8}$ time can be considered a combination of $\frac{2}{4}+\frac{3}{8}$ or $\frac{3}{8}+\frac{2}{4}$.

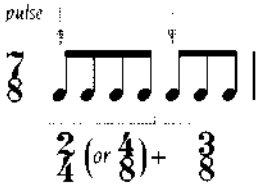

Notice that 7 is not divisible by 2 or 3.

MODERN APPROACHES TO METER

A **broken barline** is sometimes added to clarify imperfect meters.

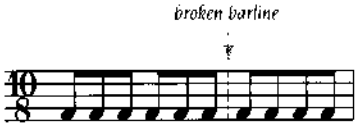

A **composite meter** is another option to clarify the subdivision of imperfect meters.

When two or more measures alternate meters in a manner that repeats predictably, a time signature reflecting the **alternating meter** may be used.

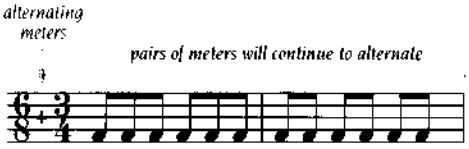

Metronome marks

See *Tempo marks*

Natural sign

See *Accidentals*

Notes

Traditionally there are five main shapes representing noteheads:

Pitched	Non-pitched
whole note	◇ *whole note, half note*
half note	
● *quarter, eighth, sixteenth, 32nd, etc.*	X *quarter, eighth, sixteenth, 32nd, etc.*

PLACEMENT ON THE STAFF

On a **five-line staff,** notes are either in a space or on a line.

On a **single-line staff,** the notehead usually intersects the line, with the stem always up.

When two instruments share a staff, one part sits on the line; the other hangs from the line.

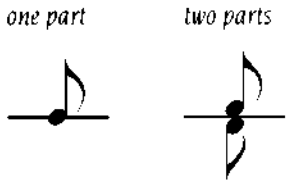

STEMS AND NOTEHEADS

Double whole notes (or *breves*) and **whole notes** are without stems.

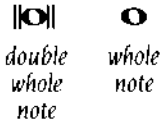

Half notes and **quarter notes** are always stemmed.

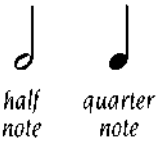

Single **eighth, sixteenth, 32nd and 64th notes** are always stemmed and with a flag(s).
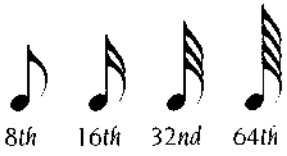
Two or more eighth, sixteenth, 32nd and 64th notes are usually **beamed into groups.**

An **X** notehead is used primarily in **non-pitched percussion** music. It is also seen in vocal music to indicate approximate-pitched singing *(Sprechstimme),* rhythmically spoken parts, clapping, etc.

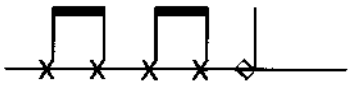

The diamond-shaped notehead serves as a half note (with stem) or whole note (without stem).

When used as a **harmonic,** the diamond-shaped **notehead is always open,** whatever the rhythmic value.
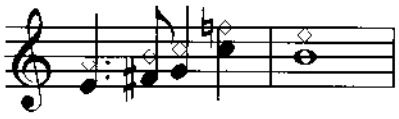
In some software programs the characters for the diamond-shaped notehead and the harmonic are slightly different.

Octave signs

The use of octave signs is primarily to **avoid multiple leger lines.** While frequently used in piano music, octave signs are only selectively used in instrumental music.

8va or *all'ottava* means "at the octave."

8va (or sometimes *8*) is indicated above a **treble clef staff only.** Do not use above any other clef.

Usually accompanied by an extender line—**a broken line with a downstroke** at the end.

The alignment of the *8va* is centered above the notehead.

The end of the *8va* bracket **extends slightly past the last note** affected.
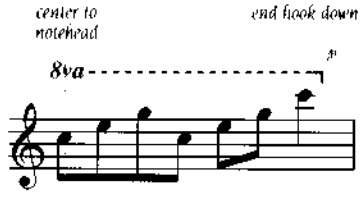
8va bassa or *ottava bassa* means "at the octave below."

8va (or 8) below the staff, especially in keyboard music, is always understood to mean 8va bassa.

8va bassa is indicated below a **bass clef staff only.** Do not use for treble, alto or tenor clefs.

Usually accompanied by an extender line—**a broken line with an upstroke** at the end.

The beginning of the *8va bassa* is placed below the notehead.

The end of the *8va bassa* line **extends slightly past the last note** affected.

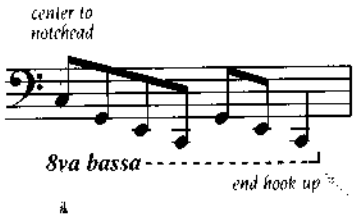

The abbreviation *8vb* is *only* a copyist's shorthand and **should not be used in engraved music.**

PLACEMENT CONSIDERATIONS

The *8va* or *8va bassa* with its extender line should be **clearly placed,** to avoid conflict with as many musical elements as possible and yet be as close to the notes affected as possible.

In the example below, the 8va is placed entirely above the slur.

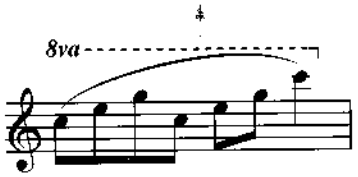

In this example, the 8va intersects the slur due to a possible limitation of space.

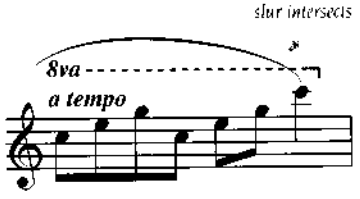

WITH ACCIDENTALS

Accidentals must be repeated for the notes included within *8va* or *8va bassa* octave alterations.
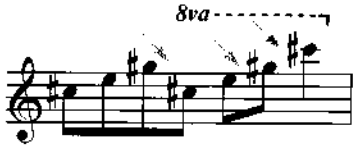
WRAPPING FROM STAFF TO STAFF

The *8va* or *8va bassa* **breaks at the end of the first staff,** aligned with the right barline.
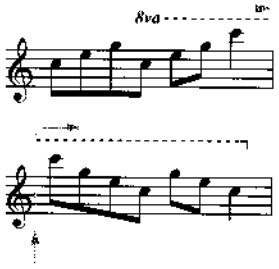
The extender line **begins again just past the clef** or key signature.

A **courtesy** *8va* or *8va bassa* may also be indicated at the beginning of the second staff when wrapping from staff to staff.

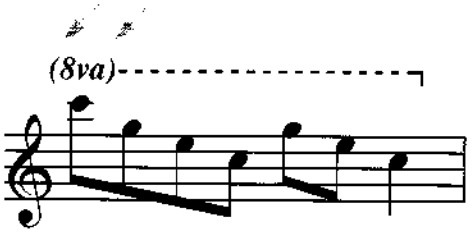

LOCO

Although the ending of the extender line should suffice, the word *loco* (meaning "at place") may be added as a reminder that the *8va* or *8va bassa* no longer applies.
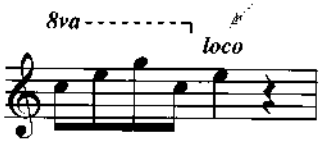
ON AN ENDING NOTE

The *8va* or *8va bassa* **is centered to the notehead** and, since it is the last note of the piece, it may or may not be accompanied with a downstroke (or upstroke).
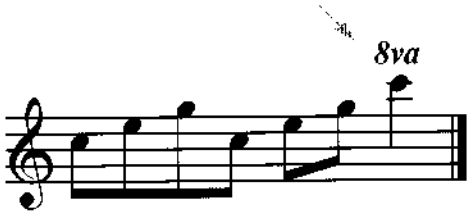
If a single note is altered but is **not the last note** of the piece, an **upstroke (or downstroke)** ***must*** **be added.**
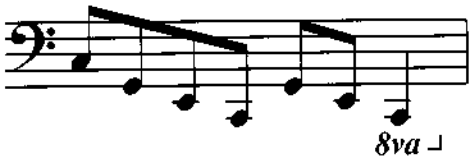
SPECIAL SITUATIONS

The following examples are incorrectly notated. The *8va* or *8va bassa* is **never placed between the two staves** of a grand staff.

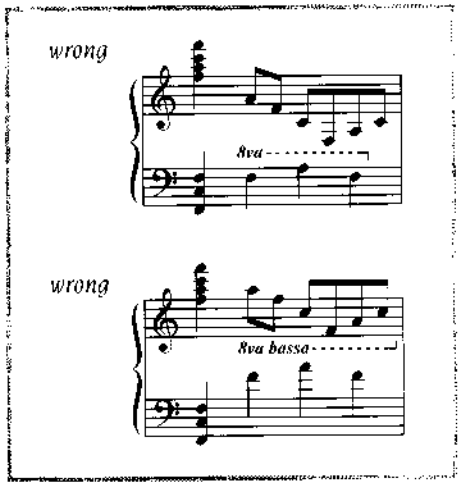

These two incorrect examples would need to be rewritten—perhaps in one of the following ways:

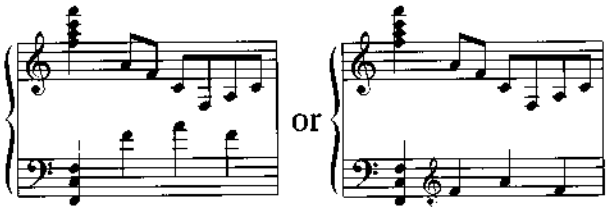

WITH RESTS

If the *8va* or *8va bassa* is interrupted with short rests, the **extender line may continue over** them.
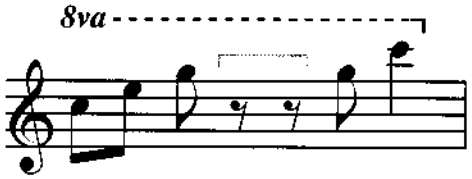
If the rests are of a **larger value, the line should be broken** and reintroduced.

When **rests precede** the *8va* or *8va bassa,* begin on the first note after the rests.
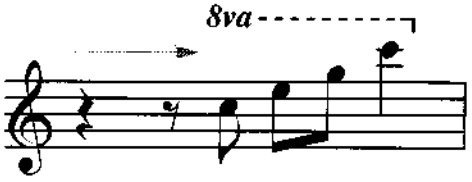
When **rests follow** the *8va* or *8va bassa,* the octave alteration ends with the last note in the grouping—the rests should not be included in the grouping.
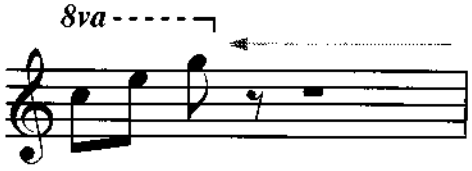
CUE SIZE

For any passage at **cue size** the *8va* will likewise be at cue size.

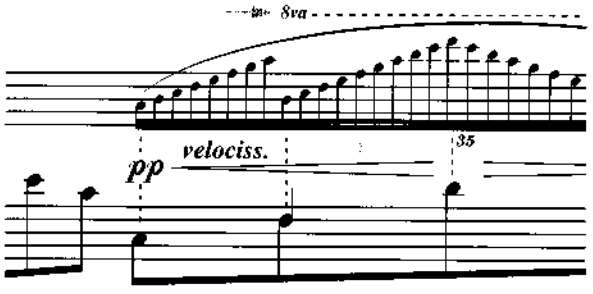

15MA

15ma or *quindicesima* means "at the fifteenth" (two octaves). The situations to use ***15ma bassa*** are very rare.

All rules for *8va* apply to ***15ma.***
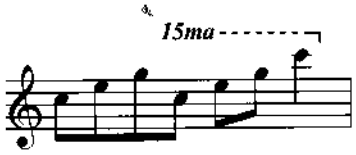
COLL' 8VA

Coll' 8va (or ***coll' 8***) is an abbreviation for *coll' ottava* meaning **"with the octave."** It is a shorthand system of writing octaves, **discouraged in traditional engraving.**

The function of ***coll' 8va*** differs from ***8va*** in that the written notes are **doubled at the octave.**

For the extender line, a longer dash length or a solid line is recommended, to make the ***coll' 8va*** distinguishable from ***8va.***

The ***coll' 8va*** doubles at the **octave above** when notated in the **treble clef.**
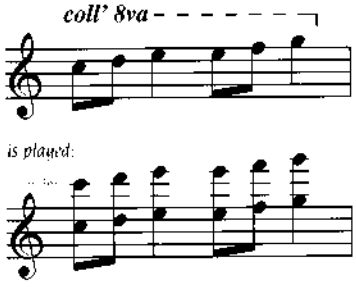
The ***coll' 8va*** doubles at the **octave below** when notated in the **bass clef.**
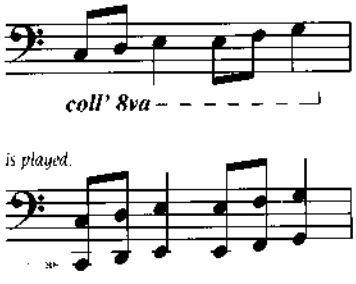
INSTRUMENT CONSIDERATIONS

ORCHESTRA / BAND SCORES

Often a score will have **limited space,** causing leger lines to become too crowded and illegible. Octave signs help to **eliminate vertical overcrowding.**

WOODWINDS

Wind players prefer to read leger lines.

STRINGS

Octave signs should be used very sparingly for viola and cello. Violins are accustomed to reading either leger lines or *8va* (but not ***15ma***).

KEYBOARD INSTRUMENTS

Celesta uses *8va* but not ***8va bassa*** (the range does not extend low enough).

Harpsichord rarely uses *8va* or ***8va bassa.*** Leger lines are more commonly used.

Piano uses *8va* and ***15ma*** in the treble clef and ***8va bassa*** in the bass clef.

Organ uses *8va* but not ***8va bassa*** (the range does not extend low enough).

Ornaments

Ornaments are primarily used in Baroque, Classical or Romantic period music. The interpretation of an ornament **varies according to the musical period** or composer. It is advised to consult detailed references on ornament usage and interpretation.

Ornament symbols are **placed above the staff** regardless of stem direction.
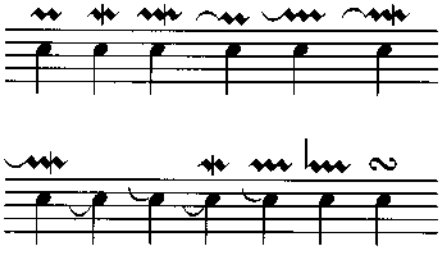
When two parts share a staff, an ornament symbol applying to the lower part is placed below the staff.

Ornaments are usually **centered** to the notehead. **Depending upon the position** of the ornament, the realization of the ornament will vary.

In the example below, the turn symbol is presented two ways, centered above the note and positioned after the note.

Notice the different realizations of the ornament.

this turn CENTERED *above the notehead indicates:*
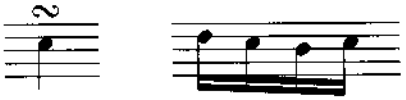
this turn placed AFTER *the note indicates:*
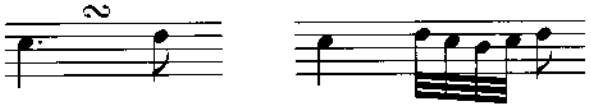
Ossia

Ossia is an indication for an **alternate version,** which may be easier or more difficult. It is treated the same as a realized ornament.

The ossia passage is **placed above** the full-size staff. The passage is cue size (65–75%).

Only the **passage concerned is notated**—the staff begins directly before and ends directly after.

Align all beats.
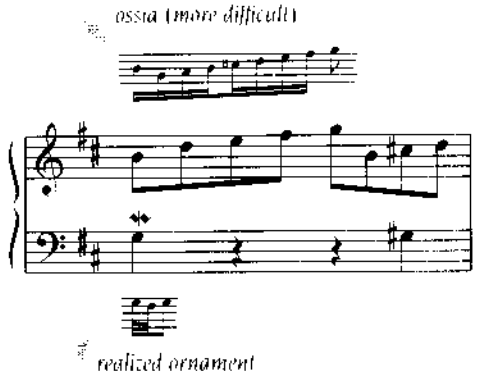
Pedal marks

FOR THE PIANO

There are three pedals on a grand piano: the **damper pedal** (right), the **sostenuto pedal** (center) and the **una corda pedal** (left). Some upright pianos have only two pedals—the damper and una corda.

Damper pedal

Markings for the damper pedal (sustain pedal) are **always placed below the grand staff** and are usually placed below all other musical elements.

The most commonly used pedal marks consist of three elements: *pedal down, pedal change and pedal up.*

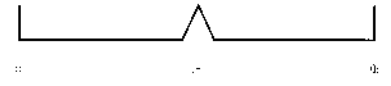

pedal down *pedal change* *pedal up*

The **pedal-down marking** begins vertically aligned with the left edge of the notehead.*

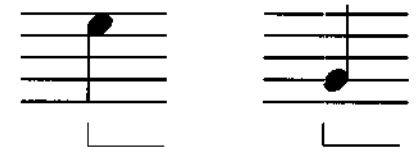

begin left of the notehead

The *point* of the **pedal-change marking** is vertically aligned with the center of the notehead.

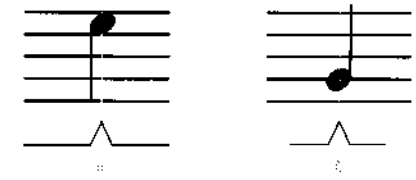

centered on notehead

*Some publishers center or align flush right. In any case, a style decision should be made.

The **pedal-up marking** is vertically aligned to the left of the notehead.

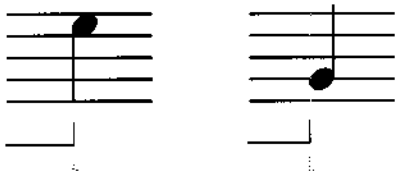

end flush left with the notehead

The traditional method of pedal marking consisted of **pedal down** and **pedal up.**

This method is somewhat obsolete.

pedal down *pedal up*

Drawbacks of this method of pedal indication include the potential for inaccuracy and a cluttered look.

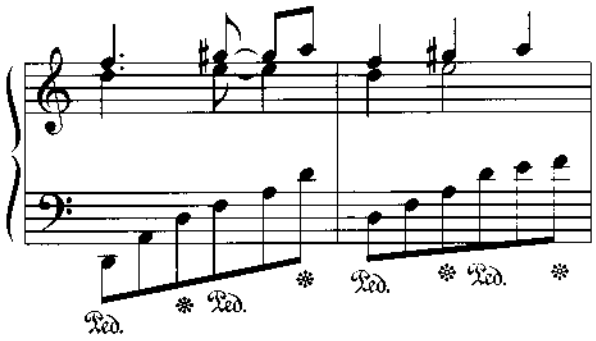

Flutter Pedal

To notate the rapid fluctuating of the pedal, a **zigzag pattern** interrupts the usual pedal marking.

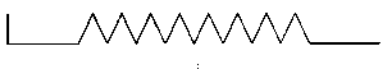

flutter pedal

Wrapping from staff to staff

The pedal mark is interrupted at the end of the staff. It continues on the next staff, **beginning immediately after the key signature.**

If the pedal mark continues to the end of the piece, it is vertically aligned with the thin line of the final double barline.

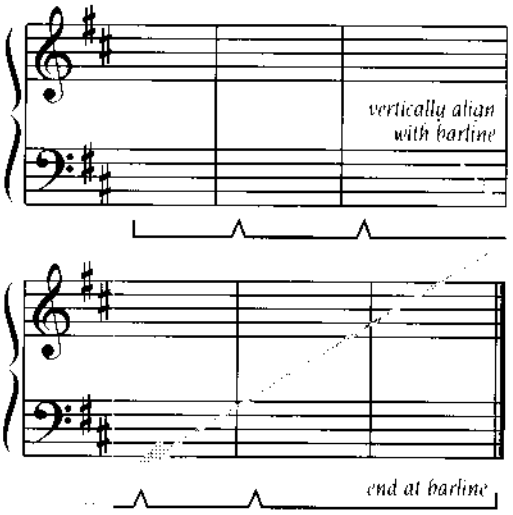

begin immediately after key signature

Simile

When the pattern **has been clearly established,** ***simile*** may be used instead of continuing the pedal marks. (See *Simile*)

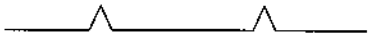

If the pattern changes, simply begin the pedal marks again.

Half pedal

The clearest indication is to simply **add "1/2" to the pedal marking,** whether at the down pedal or at the pedal change.

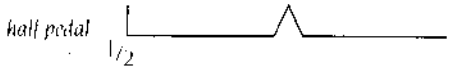

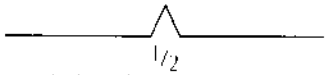

half pedal

Una corda pedal

The indication ***una corda*** (one string) or ***u.c.*** is placed where the pedal is pressed; ***tre corde*** (three strings) or ***t.c.*** indicates the return to normal.

Sostenuto pedal

This is indicated by the abbreviation *sos.* (sometimes in combination with a bracket).

FOR THE ORGAN

Two symbols are used, one for the *heel,* one for the *toe.*

The symbols are **NOT inverted** when moved from one side of the staff to the other.

The pedal marks for the right foot are always **placed above the staff and centered on the notehead.**

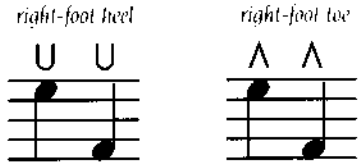

The pedal marks for the left foot are always **placed below the staff and centered on the notehead.**

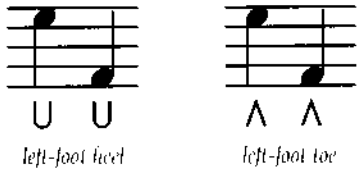

HARP PEDALS

Pedal indications for harp are **settings for tuning.**

The left and right foot have **separate sets** of pedals.

Notation for the harp is closely linked to the position of each of these pedals. Therefore, **enharmonic spellings** are frequent in harp music.

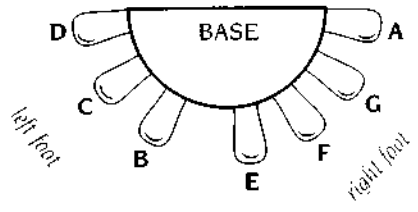

The tuning of the harp is based on the three **notch positions** of the pedals.

When a pedal is in its resting position, **center,** the string is tuned to the note's letter name (D, C, B, E, F, G & A).

When a pedal is **raised,** the note is lowered a half step (loosens the string).

When a pedal is **lowered,** the note is raised a half step (tightens the string).

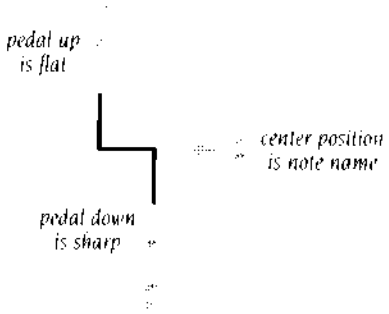

The following three examples illustrate possible ways to indicate harp pedal settings in a score.

They may be listed **horizontally, stacked or using the Salzedo diagram.**

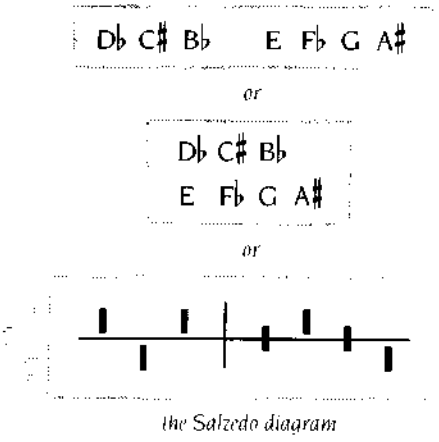

the Salzedo diagram

Picking

Picking is notated with *down-stroke* and *up-stroke* symbols. The same symbols may be used as those that are used for down-bow and up-bow.

Down-stroke and **up-stroke** indications are centered to the notehead and are always placed above the staff.

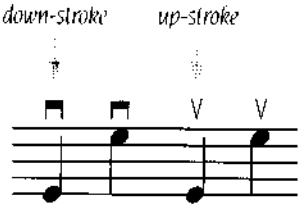

Repeat signs

Indications for repeats occur on three levels: **beat repetitions, measure repetitions and section repetitions.** The first two are used almost exclusively in manuscript or in popular music.

BEAT REPETITIONS

Angled slashes following a single beat indicate that whatever is written on the **first beat is to be repeated.** These are commonly **used in manuscript.** Do not use in engraved music.

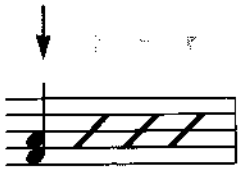

Another use of beat repeats is in **guitar or rhythm parts,** where they help pinpoint where chord changes occur. These are used in engraved music. Stems, beams and ties may be used when necessary.

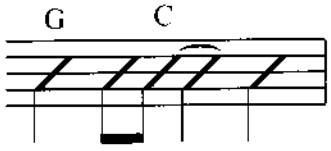

ONE-MEASURE REPEAT

This sign (𝄎), meaning **repeat the previous measure,** consists of a slash with two dots and is centered in an otherwise empty measure. In engraved music, its use should be limited to rhythm parts.

When several consecutive measure repeats are used, numbering is helpful. **Place a small number** above the staff and **center it on the measure repeat sign.**

The **notated measure is considered the first measure,** with the actual numbering beginning on the first repeated measure.
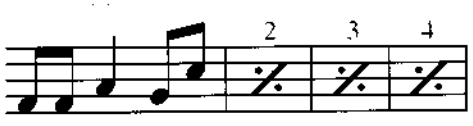
Write out the music **at key points** such as rehearsal numbers, page turns, etc.

TWO-MEASURE REPEAT

When **two measures are to be repeated,** a sign consisting of *two* slashes with dots is placed **on the center bar line** of two otherwise empty measures, **with the number 2 above it.** The number is in the same typeface and size as a time signature number.
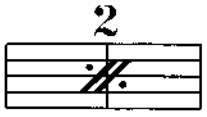
This sign should *not* be used when one measure is to be repeated twice. It should only be used for **two consecutive measures that are *different,*** and are to be repeated. In engraved music, it should only be used in rhythm parts.

If more than two measures are to be repeated, the **repeat sign** should be used.

SECTION REPETITIONS

The **repeat sign** is used to indicate the repeat of one or more measures, or an entire section.

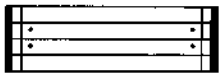

The repeat sign looks like a final double barline, with two dots positioned in the spaces above and below the center line of the staff.

The right-facing repeat sign is **placed at the beginning** of the first measure of the section to be repeated. The left-facing sign is **placed at the end** of the last measure of the same section.

Thus, the section that is to be repeated is **framed** by the inward-facing repeat signs.
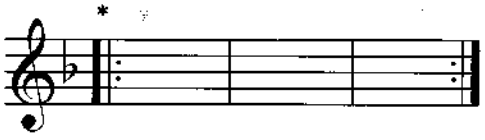
*If the repeat begins **at the beginning of a piece, the right-facing sign is not needed.**

For **two adjoining repeated sections,** repeat signs are placed, as before, framing each section. The **adjoining repeat signs may share the thick bar.**
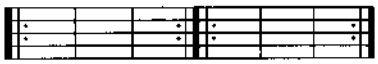
With key changes

When a key signature change occurs at the beginning of a repeated section, a double bar is added and the **key signature is placed before the first repeat sign**.
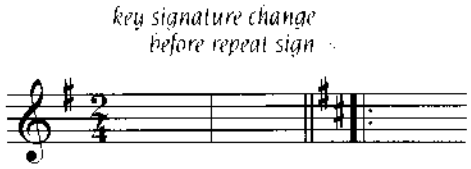
With multiple endings

A section that is repeated may have a different ending each time it is played.

The repeat sign is placed at the beginning of the section and at the last bar line of the 1st ending.

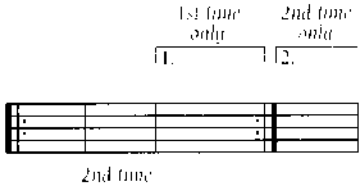

The **brackets do not intersect or touch the staff** but are placed above the staff, avoiding all musical elements. They are aligned vertically with the barlines.

1st ending brackets are **always closed.**

If the **2nd ending is not the end of the piece,** the bracket will be **open-ended.**
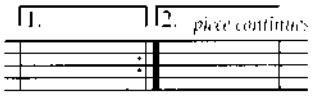
If it is the **end of the piece** (or movement), the bracket will be **closed.**

If a section is played three or more times but there are only two endings, number the brackets accordingly. This occurs often when there are lyrics.
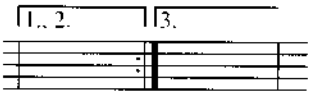
Rests

This section deals mainly with the positioning of rests. For more on the use of rests, see *Meter* and *Augmentation dot.*

TABLE OF RESTS

In the listing of rests below, each rest is half the value of the previous rest, starting with the double whole rest.

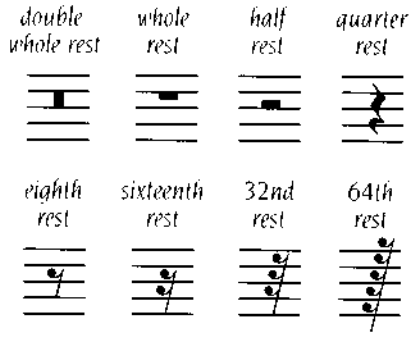

DOUBLE WHOLE REST (BREVE)

The double whole rest is placed between the third and fourth staff lines, touching both lines.

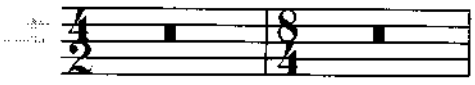

WHOLE REST

With the exception of $\frac{4}{2}$ and $\frac{8}{4}$, the whole rest is used to signify a **complete measure of rest** in any time signature.

It **hangs** from the fourth staff line.

Whole rests are **centered in the measure.**
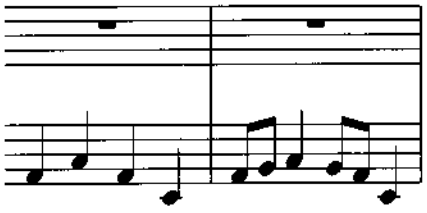
When two parts share a staff, whole rests are positioned on the **fifth line for the top** part and the **first line for the bottom.**

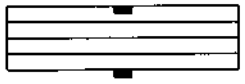

If either part conflicts with the placement of the rest, the rest may be **positioned outside the staff.**
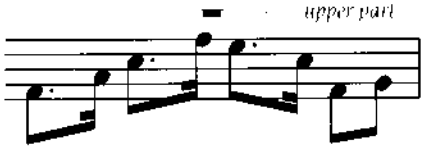
HALF REST

The half rest is positioned to **sit on the third staff line.**

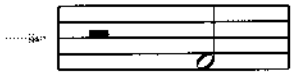

When two parts share a staff, the half rest will sit on **either the fifth line or the first line.**
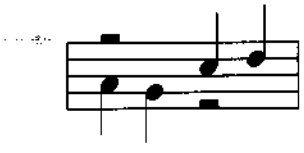
If either part conflicts with this placement, the rest may be positioned **outside the staff.**
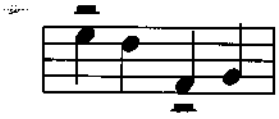
Half rests are **positioned at the beginning of beat 1 or 3**—never centered between two beats.
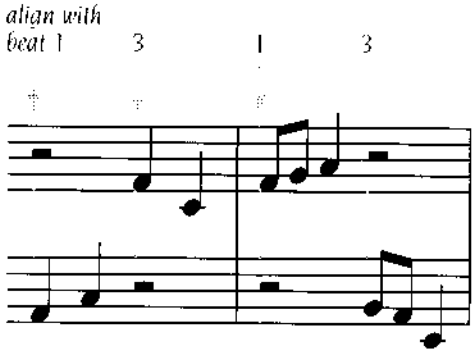
In the above example the use of half rests instead of two quarter rests is correct. However, meter must be considered—do not automatically substitute a half rest for two quarter rests.

(See *Meter*)

QUARTER REST

The quarter rest is positioned as follows. Notice the position of the bottom hook.

When two parts share a staff, the quarter rest is moved **up or down** from its normal position. The **relationship** of the rest **to lines and spaces** must be the same as in normal position.

The rest may be completely outside the staff when necessary.
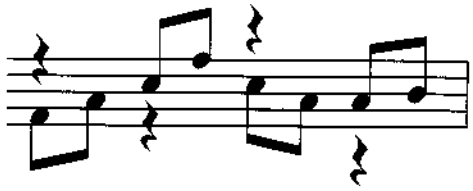
In some situations the above rests could be left out entirely. In other situations, if *both parts* were resting, one rest in normal position could serve for both.

EIGHTH, SIXTEENTH & 32ND RESTS

The guidelines for positioning quarter rests in the example above also apply for eighth, sixteenth and 32nd rests.

The ***hook*** **of these rests is always placed in a space** (or between imaginary leger lines if placed outside the staff).

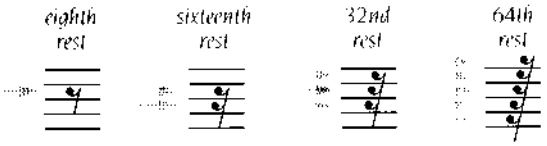

If one of the above rests **interferes with a beam, the rest moves up or down** so that stem lengths may be more normal. Other rests in the measure remain in normal position.
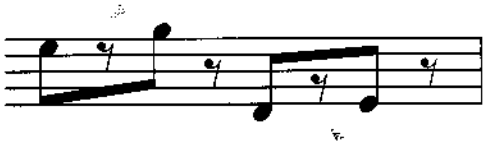
MULTIPLE-MEASURE RESTS

For a rest of more than one measure, a **horizontal line** (the thickness of a beam) is placed on the middle staff line, with a thinner vertical line at each end extending from the second to the fourth staff line.

A number the size and font of a time-signature number is placed above the staff and centered in the measure.

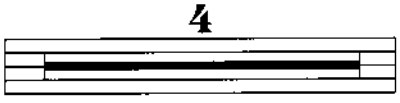

Break the multiple-measure rest for rehearsal numbers, tempo changes, etc.
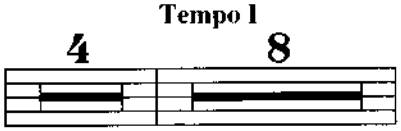
RESTS ON A SINGLE-LINE STAFF

When there is only one part on a staff, position the rests as follows:

When **two parts share a single-line staff,** place the rests above and below the line, not touching the line. Use a leger line for whole and half rests.

Scores

On a complete score all parts are included on a system and are arranged in a certain order.

All information contained on the parts and score must be **identical.**

On the first page of the score the system (or first system) is **indented.** Brackets connect instrument *choirs.* (See *Bracket, Systems*)

The **full name of each instrument** is given to the left of the first system.

Abbreviations are substituted for the full instrument names on subsequent systems.

Rehearsal numbers (indicated at the top of the score) serve as key reference points.

They may be **letters** or **measure numbers** enclosed in a circle or square.

All **extracted parts** will have **identical rehearsal** numbers.

SCORE ORDER

Instruments should be arranged in what is known as *score order.*

Woodwinds
Brasses
Percussion
Other instruments
Strings

Each **family** of instruments is predominantly **grouped together** from highest-pitched instruments to lowest-pitched instruments, with some traditional exceptions.

The French horns, although not the highest-pitched, are traditionally placed above the other brass instruments.

Sharing a staff

In band or orchestra music some parts of instrument families share the same staff. Combine parts 1 & 2 or 2 & 3; avoid combining three instruments on one staff.

BEGINNING A PASSAGE

If parts are divisi, no indication is necessary unless one or both instruments (such as strings) can play more than one note at a time. (See *Divisi*)

Indicate ***a2*** above staff if both parts play in unison. Use only one stem per note.
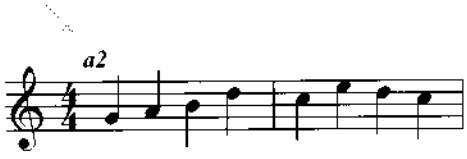
If the unison continues after a page turn, repeat ***a2*** in parentheses.

If like instruments are sharing a staff and only one part plays, indicate which part: I. or II.
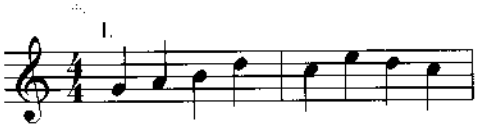
If unlike instruments are sharing the staff and one part plays, indicate which instrument is playing.
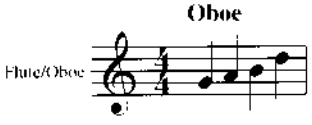
STEMMING OF TWO PARTS

If two parts are playing **different pitches but the same rhythm,** they share **one stem.**
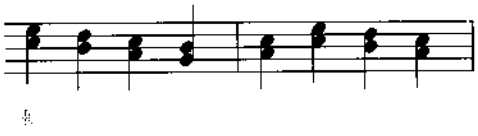
If the parts are **alternating between unison and divisi, and share the same rhythm,** opposite stem direction makes the unisons clear.
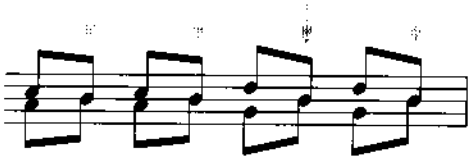
If both parts have **different rhythms,** opposite stem direction is necessary.

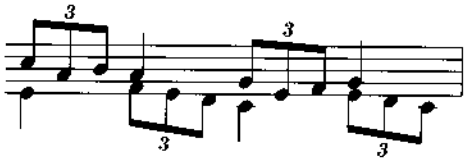

(See *Accidentals, Rests*)

FROM TWO PARTS TO UNISON

Opposite stem direction is used for clarity on **unison notes in short passages.**
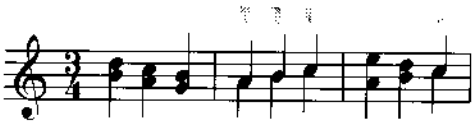
Indicate ***a2*** above staff and use one stem for longer passages.
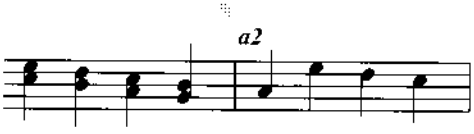
FROM TWO PARTS TO ONE:

Use rests in shorter passages.
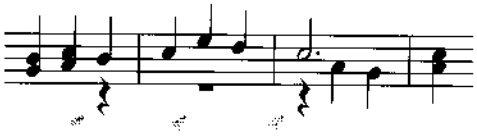
Place I. or II. above the staff and use one stem (for two *like* instruments in longer passages or after long rests).
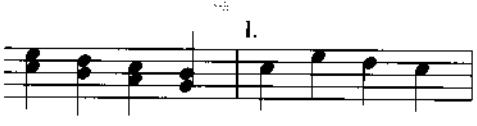
Mark passage with instrument name (for two *unlike* instruments in longer passages or after long rests).
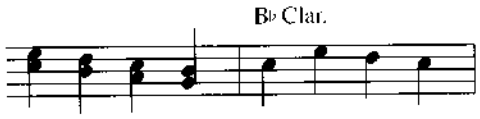
STAFF INDICATIONS

Staff indications (dynamic, slurs, tempi) are **placed below** the staff.

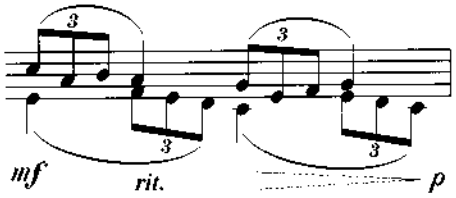

place below

If the two parts move **independently,** a **separate set of directions** is needed for each part, above and below the staff.

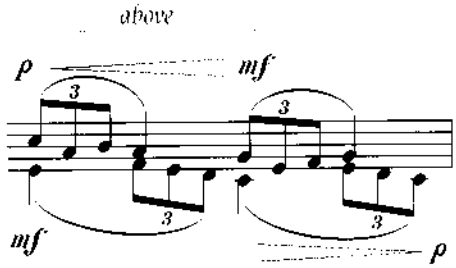

below

WHEN NOT TO SHARE A STAFF

1. If the range of one part tends to cross the range of the other, the parts should have **separate staves.**
2. If the parts require **different clefs** or **clef changes** the parts should be separated.
3. If the two parts are **too rhythmically diverse,** they should be separated.

In all cases **a bracket should be used,** not a brace.
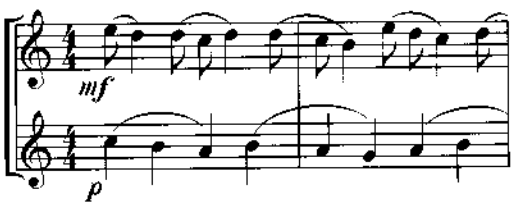
Sharp

See *Accidentals*

Simile

When the word ***simile*** is indicated after a **pattern has been established** (for example, of articulations, pedal marks, bowing, etc.), it means to **continue in the same manner.** (See *Articulations, Pedal marks*)

Slurs

Although a slur looks somewhat like a tie, the placement, positioning and use of slurs are different from ties. Slurs and ties should not be confused.

Slurs are used to indicate phrasing or technique. Depending on the instrument, the slur will imply different techniques to be used.

PLACEMENT OF SLURS

The **stemming** of the notes is the main factor in determining whether the slur is to be placed above or below.

When **stems extend up,** the **slur is placed under**, on the notehead side.
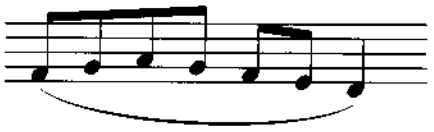
When **stems extend down,** the **slur is placed over,** on the notehead side.
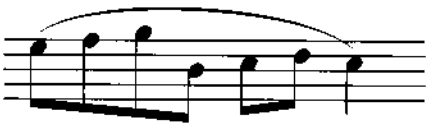
When **stems are in both directions,** the **slur is always placed over.**
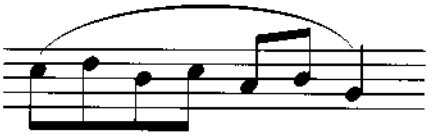
If the notes are whole notes, *imagine* the stems!

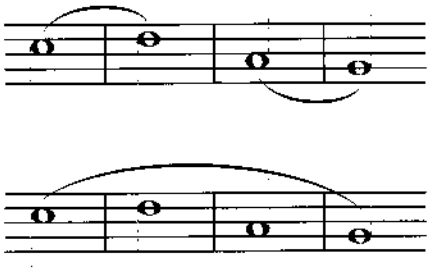

If the **phrase is substantially long,** the slur may be placed over, regardless of stem direction.
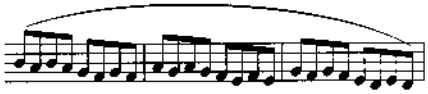
PLACEMENT ON THE NOTEHEAD

Slurs have a **definite beginning and ending;** they should not be "hanging in space" so that the beginning and ending notes must be guessed at.

If the slur is on the notehead side, the beginning and ending of the slur should be **centered on the notehead.** It should not touch the notehead.

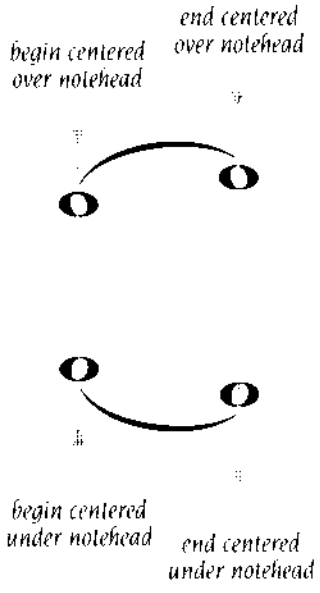

BEGINNING FROM THE STEM

Place the beginning of the slur so it **starts mid-stem** (to the **right** of the stem—never begin to the left, crossing the stem).

In some cases the slur may begin **at the end of the stem.**

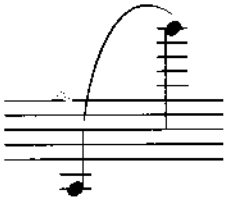

Begin at the end of the stem **if beaming is involved.** Never cross the beam with a slur.
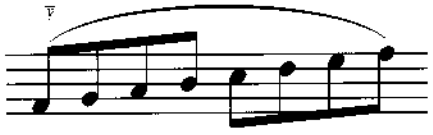
ENDING ON THE STEM

Place the end of the slur so it **slopes towards the notehead,** away from the end of the stem. **Center the slur** on the notehead.
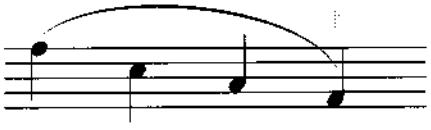
The slur may also end **at the end of the stem if** it would make a more pleasing shape.
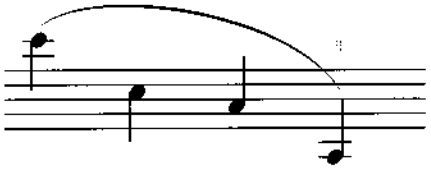
End at the end of the stem **if beaming is involved.** Never cross the beam with a slur.
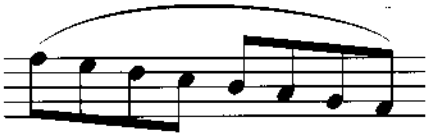
SLUR DIRECTION

If the direction of the **phrase ascends,** the slur will **slope upward.** If the direction of the **phrase descends,** the slur will **slope downward.**

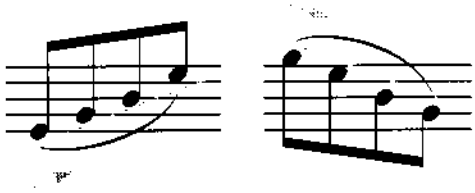

When a slur **begins and ends on the same note**, the slur can remain on the same horizontal level.

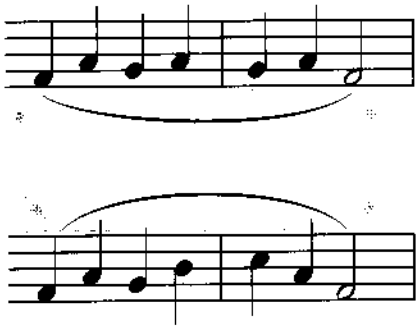

SLURS WITH CHORDS

Only one slur is needed when there is only one stem per chord.

SHARING THE SAME STAFF

For two parts, place slurs **above for the upper part, below for the lower part.**
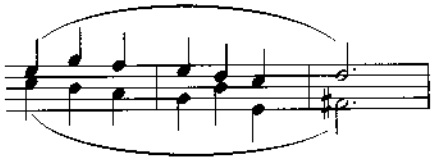
For two *sets* of parts, place slurs **above for the upper parts, below for the lower parts.**
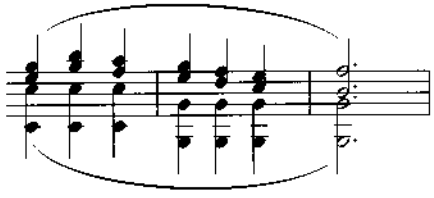
WRAPPING FROM STAFF TO STAFF

Align the end of the slur with the end of the staff. The slur ends at an **angle** (ascending or descending) at the end of the staff.

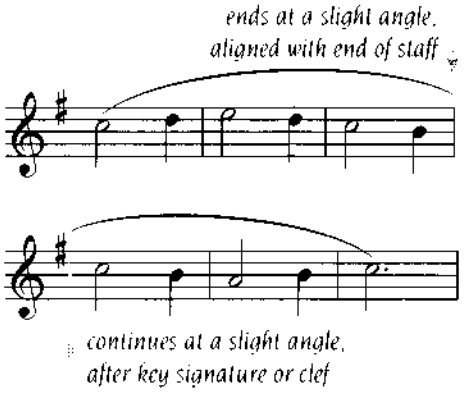

Continue the slur in the lower staff immediately after the key signature (or clef), also at an **angle.** Be sure the first note is far enough to the right so that it is very clear that the slur does not begin on the note.

If the slur is over the staff it **remains over** when continuing on the next staff. If it is under, it **remains under** on the next staff.

The **direction of the slur** (ascending or descending) continues logically in the following staff.
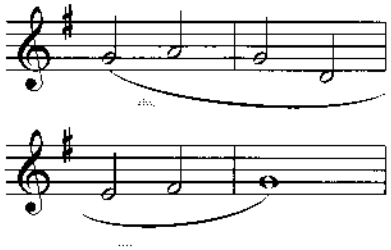
slur ascends to follow direction of notes
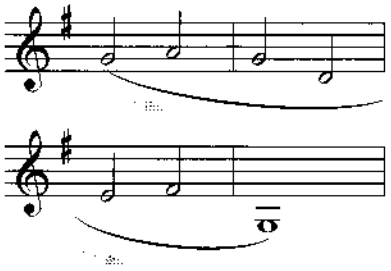
slur descends to follow direction of notes

DIFFERENTIATING SLURS FROM TIES

When slurs and ties are both involved in a chord progression such as the following, **position the slur opposite to the tie** and at a noticeable **angle.**

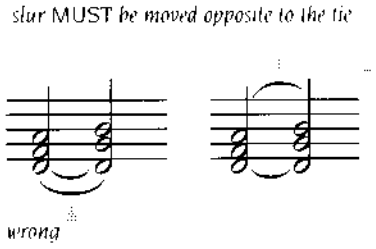

An even better way to write the above:
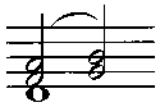
If a slur **begins and ends on the same pitch** and could possibly be mistaken for a tie, position the slur on the stem side.

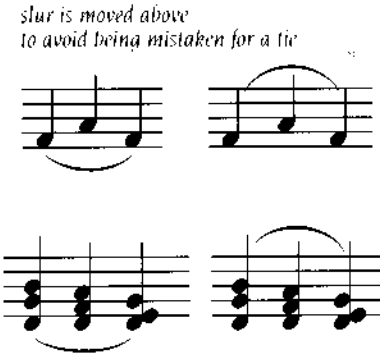

When a slur connects chords with **tied notes within**, combine the tied notes into a single note with opposite stem direction.

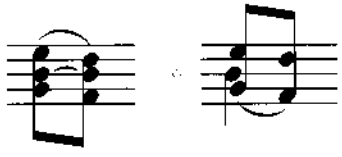

BEGINNING OR ENDING WITH A TIE

A slur **must include both notes of the tie,** whether the tie is at the beginning or at the ending of the slur. (For an exception, see "Elisions," on the next page.)
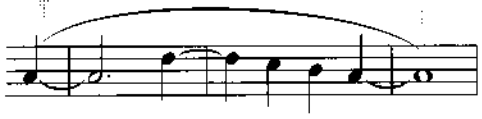
ELISIONS

In keyboard music, one slur might end at the same point where another slur begins.

The two slurs **share the center of the notehead** (elide) without touching each other.
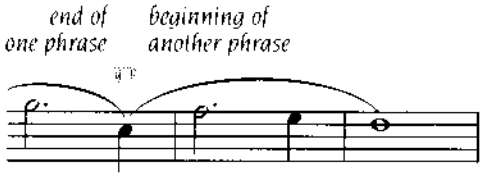
When the **elision occurs on tied notes**, the first phrase may end on the first tied note. The second phrase can then begin on the second tied note.
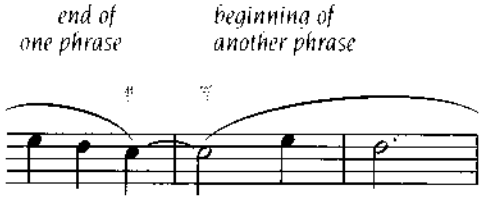
GRACE-NOTE SLURS

Grace notes **may or may not have slurs.** The slurs are usually somewhat smaller to match the grace notes.

Since grace notes are always stemmed up (unless there are two voices), the slur is usually **placed below.**

Grace-note slurs may be placed more to the inside edges of the noteheads.

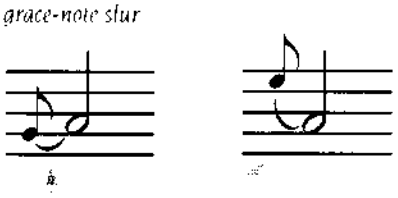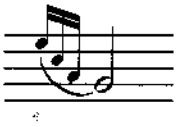

slur for beamed grace notes

Grace-note slurs elide with slurs.

grace-note slurs and slurs
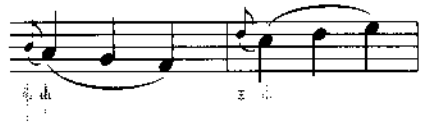
SLURS AND ARTICULATIONS

Beginning or ending on notes with an articulation:

The beginning or ending of a slur is placed **outside staccato and tenuto** marks.

Center over or under the articulation.

slur is outside notehead and articulation
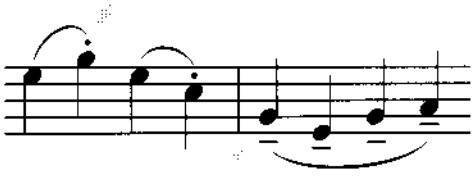
The beginning or ending of a slur is usually placed **between accents** and the notehead.

slur is between notehead and articulation
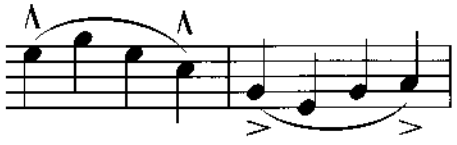
here the accent is placed inside the slur
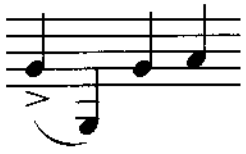
Articulations between the beginning and ending notes remain inside the slur.
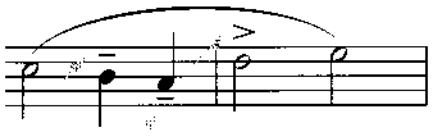
Fermatas are placed **outside** the end of a slur.
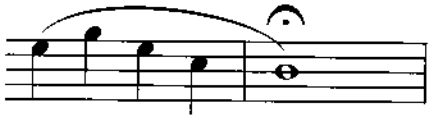
"LET RING" SLURS

The use of a short slur to indicate continued vibration should be placed on notes of longer duration only. Angle the slur slightly.

let ring

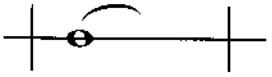

INSTRUMENT CONSIDERATIONS

Woodwinds and brass

Legato technique is indicated by the use of a slur. The slur might also indicate breathing and phrasing.

Slurs in combination with staccato or tenuto marks show varying degrees of legato.

most legato *less legato* *least legato*

For keyboards

If the space between the two staves is limited, slurs may be placed outside the staff.

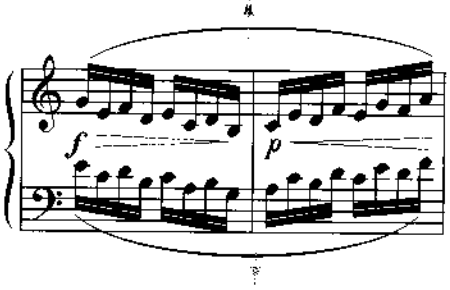

An S-shaped slur is sometimes used in music notated on the grand staff.
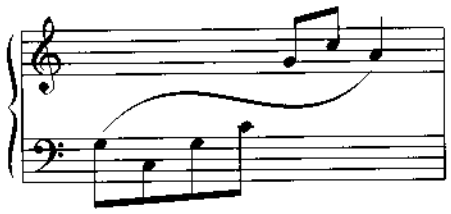
For strings

Slurs can only partially indicate phrasing. Slurs are also used to indicate various bowing techniques. (See *Bowing*)

For vocal music

A **slur is used for a *melisma*** (two or more notes that are to be sung on a single syllable).

The word or syllable should be placed flush left with the notehead.
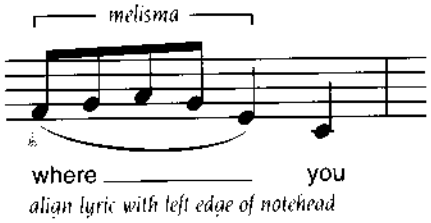
Slurs to indicate phrasing in vocal music are seldom used. Since breathing is a major factor in phrasing, rests and breath marks can be used as a partial indicator of phrases.

Slurs can be drawn using a **broken line** instead of a solid one. The broken slur is most often **used to accommodate lyrics for multiple verses.**
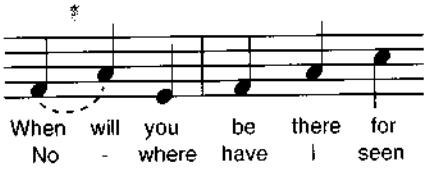
Similarly, **broken slurs** may also be used for syllable differences of translated text.

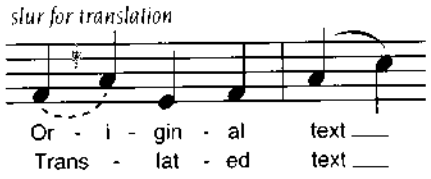

Spacing

Spacing is of primary importance to the **visual quality** of any musical notation. While the attention to *musical* detail may be excellent, poor judgment in spacing may make the score look ill-conceived.

An awareness of spacing occurs on many levels, from the **smallest element** (the beat) **to the largest** (the score or book). The desired effect is that the notation *and* layout will immediately convey the musical intent. Ultimately, any score should look **accessible** regardless of the level of difficulty.

PROPORTIONAL SPACING

The concept of proportional spacing takes into consideration the **mathematical spacing** of a beat, measure and system, in relation to the **density of activity** (the number of notes per beat, measure and system).

With proportional spacing, a half note, for example, must get *more* space than a quarter note, but not *twice* as much.

SPACING WITHIN THE MEASURE

Notes are spaced within the measure according to a **compromise between** two extremes:

1) **Space given according to note-value** (for example, a half note getting twice as much space as a quarter note).

2) **Equal spacing given to each note.**

Compare the normal (proportional) spacing with the two extreme examples.

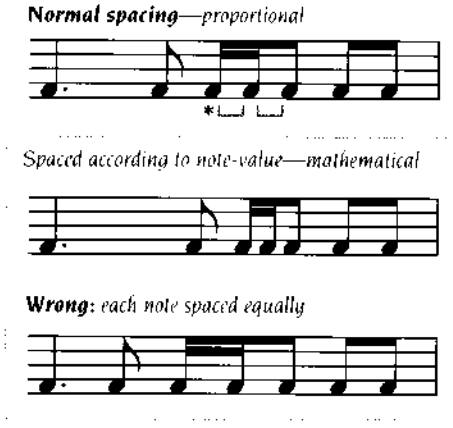

*Make sure that consecutive notes of equal value have equal space *following* each note.

MEASURES WITHIN THE STAFF

The size of the measure within the staff is determined according to a **compromise between** two extremes:

1) **Equal space** for each measure.

2) Measure size **based on note density only.**

Normal spacing of measures

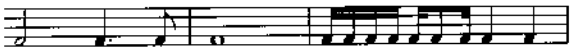

Wrong: *spaced according to equal measure size*

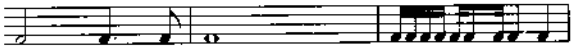

Wrong: *spaced according to measure density only*
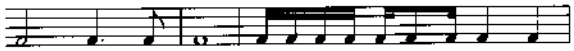
VERTICAL SPACING
Between staves

Musical elements (notes on leger lines, articulations, slurs, pedal marks) **projecting beyond a staff should never conflict** with the elements of another staff or system. There should be enough space allowed for ease of reading.

Inside systems

On the other hand, the **staves of a system should not be too far apart.** This is especially important for a system that is to be read by one performer—a keyboard player, for example. The eye should not have to jump too far from one staff to the other, in order to read notes for the right and left hand simultaneously.

The most common misjudgment is to place staves (or systems) exactly the same distance from one another without adjusting to compensate for the projecting musical elements.

Between systems

More space should be be provided between systems than between the *staves* of the systems.

The **spacing between systems should be balanced,** with the page margins and the number of systems on the page in mind. If the **page is dense,** the systems will be closer to each other and to the minimum vertical margins, while allowing enough distance between systems to distinguish one from another. If the **page is sparse,** the upper and lower page margins could be larger.

GENERAL PAGE LAYOUT
Page numbers

The position of the page number in relation to the page edges should *never* change, regardless of page spacing. Printers can use the page number as a guide for positioning the image area on the page.

If page numbers are placed to the left and right, as is usual, **even numbers** are always to the **left, odd numbers** always to the **right.** Page numbers may be centered, but this is not the usual practice. Centered page numbers interfere more with the music and text.

Page numbers should be positioned **no closer than 1/4 inch from** the top (or bottom) of the **page edge**.

Title page

The title, credits, copyright and any accompanying text can be **vertically adjusted to accommodate** a loosely spaced page or a tightly spaced page. Such type should always be well placed, considering the space allowed.

Facing pages

Facing pages **should look good together.** As much as possible, they should have a **balanced look** (notes on a system, number of systems, white space, etc.). The vertical page margins should be the same if at all possible.

Page turns

It is very important to lay out the measures and systems in a manner that will allow a good page turn. Having **rests in the last measure** before the page turn is the most desirable. Second to rests would be perhaps a whole note (that could be held with the pedal) or a sparse measure—anything that would allow a hand to be free to turn the page.

Try to **minimize the number of page turns** by adjusting the amount of music on the page or by changing the sequence of pieces.

Book layout

Calculating the number of pages needed or what will work in the allowed number of pages is crucial to an appealing layout.

If a book contains many short pieces and a particular order is not important (or can be adjusted slightly), there are several things that can be done to make a good layout.

Often a piece can be **condensed or expanded** to offer choice page turns and good facing pages.

Consider reordering the pieces to **minimize the number of page turns. Group pieces** with an odd number of pages together so that the ones with an even number of pages can have facing pages.

A poorly placed piece at the beginning of a book can throw off the facing pages for the rest of the book.

Backing up

Expect to go back and adjust **various elements** (page turns, systems, staves, measures or notes within a measure) when planning a layout for a book. A change in the order of pieces and the number of pages might create density problems on other pages.

The part must be considered with the whole and the whole considered with the part.

White space

With experience comes the **appreciation of white space** on a page or within a book. There is nothing more daunting than overwhelming density. The eye should be guided from note to note, measure to measure, staff to staff and page to page with a minimum of surprises. If a performer must stop playing in order to understand the notation, or loses his place because of poor placement, the notation and layout are *not* successful.

Staccato

See *Articulations*

Staff

The staff commonly consists of five lines.

The **staff line weight** should be thick enough to be clearly legible but thin enough for the notes of the staff to be easily read.

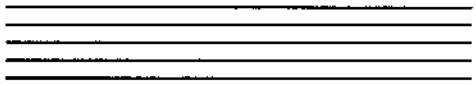

A staff line will be **thicker than stem lines** and **equal to** (or thinner than) **barlines.**

If a note is on the line, the line will always run through the **center of the notehead,** regardless of the note value.

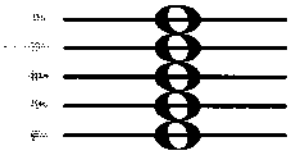

A notehead in a space is always clearly positioned between the two staff lines.

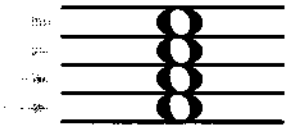

A **one-line staff** is used for non-pitched percussion.

or

Leger lines extend the range of the staff.

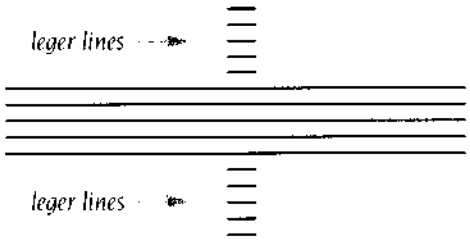

Barlines divide the staff into measures.

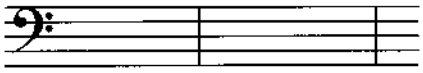

A **clef** placed on a five-line staff determines the pitches for each line and space.
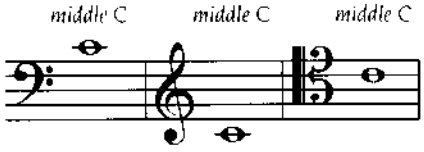
A **key signature** determines the key of the music notated on the staff.

Two or more staves grouped together (with a systemic barline) form a **system.**

A **bracket** groups staves into systems or parts of systems. (See *Bracket*)

A **brace** groups staves into a **grand staff.** (See *Brace*)

Some examples of systems:

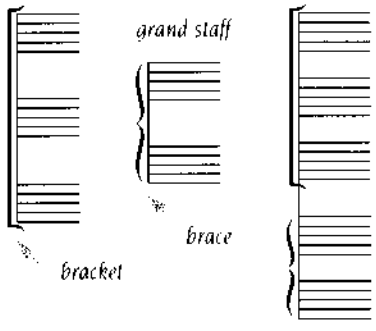

The **first system** (or staff) of music is usually **indented** about 1/2 inch.

Stems

Stems are **thinner than staff lines and barlines.**

STEM LENGTH

The **normal stem length** is $3\frac{1}{2}$ spaces (one octave).

With leger lines

When a note extends **beyond one leger line,** the stem **must touch the middle staff line.**
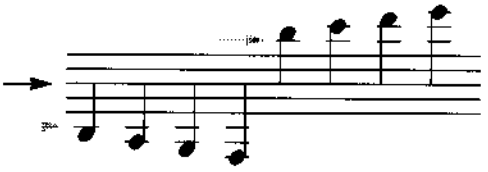
When parts share a staff

Up-stem notes **above the middle line are shorter** than normal. Traditionally, their stem length is relative to surrounding notes, getting progressively shorter as the notes go higher. The shortest stem length is $2\frac{1}{2}$ spaces (interval of a 6th).

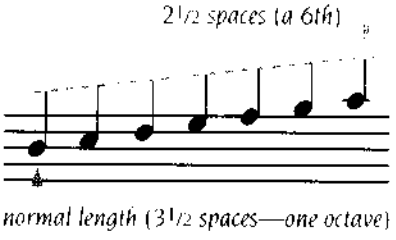

For the computer, a setting should be chosen that works well for most situations.

Down-stem notes **below the middle line** follow the same guidelines as the above.
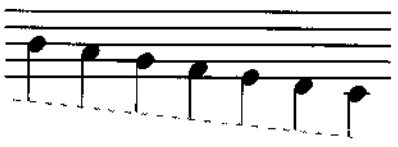
With the interval of a 2nd

The stem is always placed **between the two notes** of an interval of a 2nd, with the **upper note always to the right,** the **lower note always to the left.**
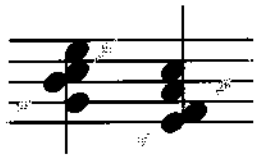
STEM DIRECTION

For notes on the **middle line and above,** the stem is down.
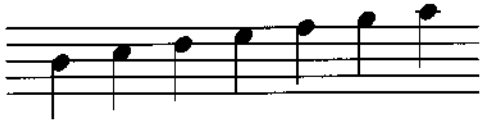
For notes **below the middle line,** the stem is up.
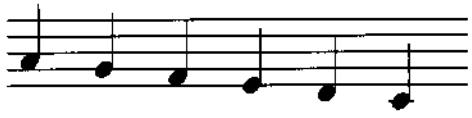
When sharing a staff

Notes have **opposite stem direction** when sharing a staff. (Stems in the "wrong direction" will have shorter stems, as previously mentioned.)
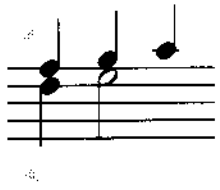
When notes share a stem

If the **note above is farther** from the middle line than the note below, the **stem goes down.**

If the note **below is farther** from the middle line, the **stem goes up.**

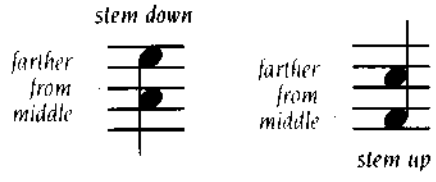

When the two notes are an **equal distance from the middle line,** the preferred direction is down.

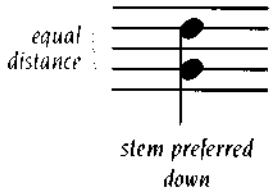

If a **pattern of stem direction** is established, stem direction is *sometimes* maintained when the notes are an equal distance from the middle. (This practice is all but obsolete.)
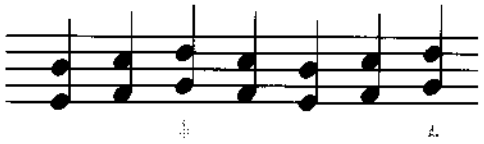
The same rules apply to *more than two notes* sharing a stem. The **distance of the OUTER NOTES from the middle line** determines stem direction.

When the **outer notes** are an **equal distance from the middle line** and the majority of notes are above the middle line, the stem goes down.

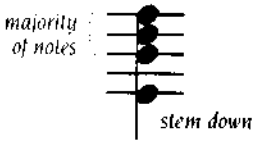

When the **outer notes** are an **equal distance from the middle line** and the majority of notes are below the middle line, the stem goes up.

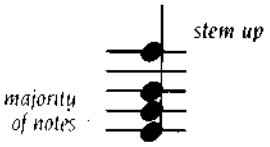

For beamed groups

Simple rules for stemming of single notes and chords apply to beamed groups when possible (for example, if all notes in a beamed grouping are on or above the middle line of the staff, stems are down).

(See *Beams*)

Systems

Two or more staves grouped together (with a systemic barline) form a system.

A **bracket** groups staves into systems or parts of systems. (See *Bracket*)

A **brace** groups staves into a **grand staff.** (See *Brace* and *Grand staff*)

Some examples of systems:

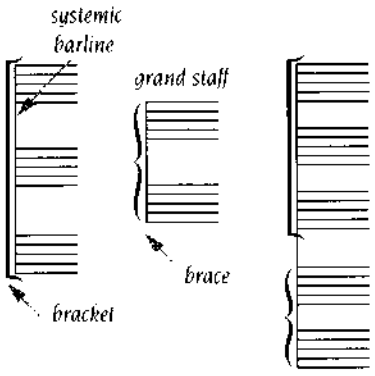

(See *Barlines*)

The **first system** of music is usually **indented** about 1/2 inch.

Tablature

Tablature is a system of notation that graphically represents the strings and frets of a stringed instrument (such as guitar).

The letters **"TAB"** are placed where a clef would normally be. The only function of these letters is to identify the staff as being tablature.

Each note is indicated by **placing the fret number on the appropriate string.**

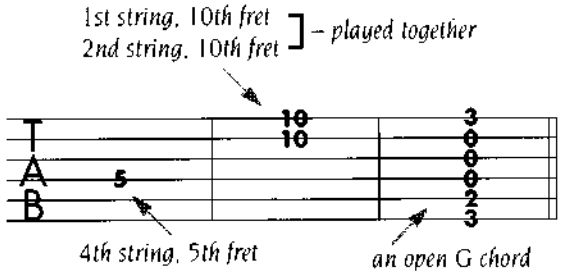

Tablature does NOT indicate rhythmic values; therefore, a five-line staff using **standard notation** is placed above the tablature staff.

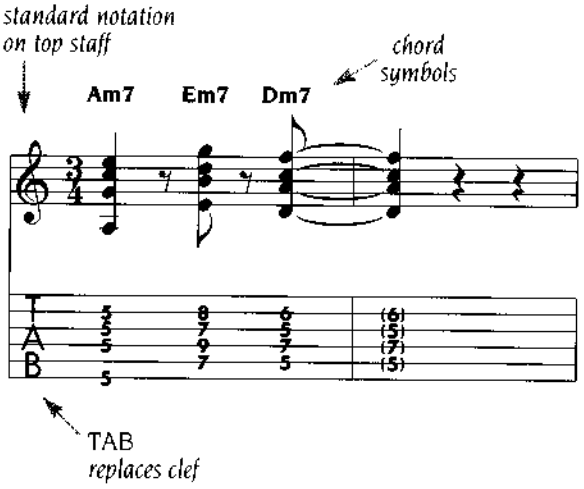

A **systemic barline connects** the two staves together. Measure **barlines** are broken.

Chord symbols (when appropriate) are often added above the top staff.

Picking or fingering techniques notated on the top staff are repeated on the tablature staff.

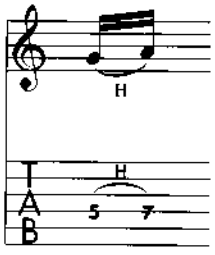

Every note on the top staff must have a **corresponding finger number** on the tablature staff—**tied notes** are in parentheses.

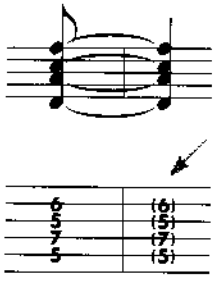

Tablature may consist of **four lines** (for electric bass and mandolin) or **five lines** (five-string banjo).

The **notation** for guitar tablature outlined on the previous pages applies to all tablature, regardless of the number of strings.

Electric bass

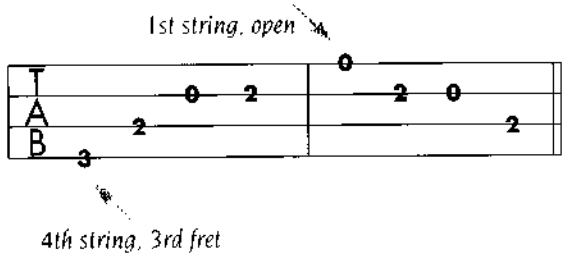

Five-string banjo

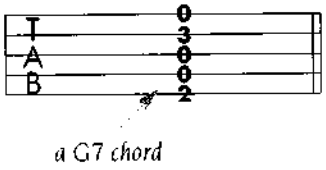

Tempo marks

Tempo marks indicating the rate of speed may be followed by an expression mark and/or metronome mark.

The left edge of the tempo mark is **vertically aligned to the left edge of the time signature.**

The type is bold Roman.
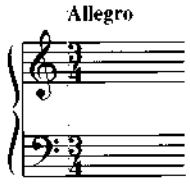
WITH EXPRESSION MARKS

Tempo marks are often accompanied by an indication of **expression;** however, expression marks should **never *replace*** tempo marks.

Presto con brio

Slowly, with much emotion

WITH METRONOME MARKS

The tempo mark may be more precisely indicated with the addition of a metronome mark.

The metronome mark may be ***specific,*** a tempo ***range*** or ***general.*** The type is slightly smaller than that of the tempo and is usually enclosed in parentheses. The note is cue size or smaller.

Allegro con moto (♩ = 144)

Allegro con moto (♩ = 132–144)

Allegro con moto (♩ = ca. 144)

TEMPO VARIATIONS

If the tempo is varied by the use of markings such as ***ritardando, rallentando*** or ***accelerando,*** the term ***a tempo*** is placed at the point where the tempo is reinstated. *The type will be bold italic.*

If the tempo changes, and then returns to the original tempo later in the piece, the term **Tempo I** is indicated **above the staff.** *The type will be bold Roman.*

Tenuto

See *Articulations*

Ties

A tie connects **two consecutive notes of the same pitch,** extending the duration of the first note to include the second. (The second note does not have its own attack.)

The shape of a tie is somewhat similar to a slur, but the **placement, positioning and use of ties and slurs are different;** the two should not be confused.

BEGINNING AND ENDING

Begin and end on the same horizontal level.

Begin to the right of the notehead.
End to the left of the next notehead.
The tie **does not touch the noteheads.**

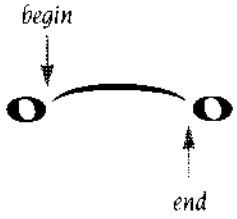

AVOID AUGMENTATION DOTS

Ties should never collide with augmentation dots. **Begin the tie to the right of an augmentation dot.**

PLACEMENT ON THE STAFF

Avoid touching staff lines.
Place the **center** of the curve in a "space."

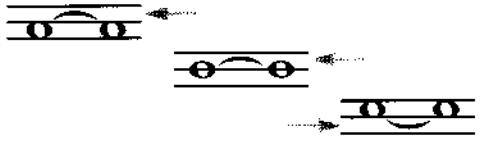

Ends of ties may cross staff lines—it is better to cross even slightly, than to just touch a staff line.

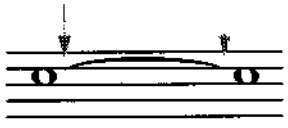

Adjust curve for longer ties.
Raise or lower the center of the curve to the next space.

DIRECTION ON THE STAFF

Curve ties opposite of stem direction.
Stem down—curve above notehead.
Stem up—curve below notehead.
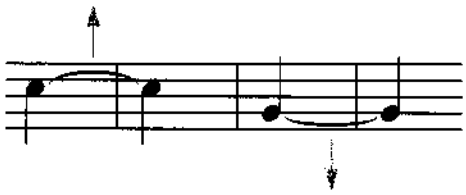
Ties on whole notes are treated as if the whole notes had stems.

For mixed stem direction, the tie is always placed **above.**
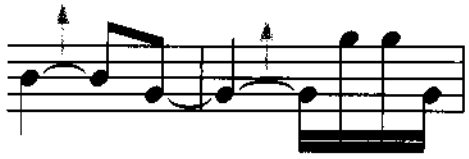
SHARING THE SAME STAFF

For two parts, place ties **above for the upper part, below for the lower part.**

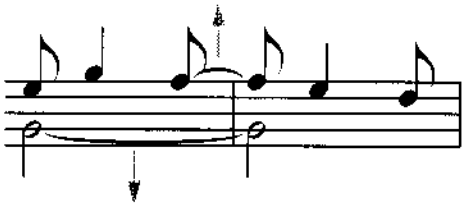

For two *sets* of parts, place ties **above for the upper two parts, below for the lower two parts.**

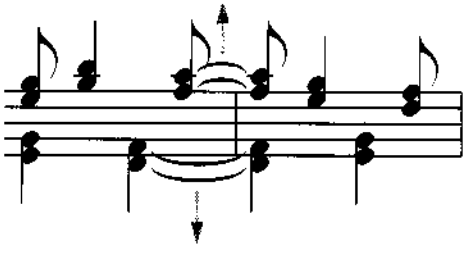

MULTIPLE TIED NOTES

When more than two notes are tied, ties must be added from note to note.
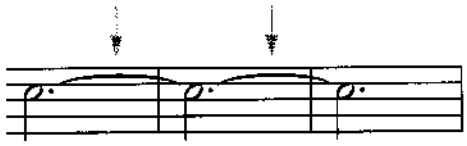
WRAPPING FROM STAFF TO STAFF

Align end of tie with end of staff.
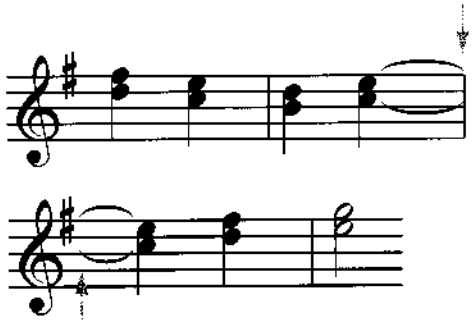
Continue tie in the lower staff immediately after the key signature (or clef).

Beginning and ending points always remain on the **same horizontal level.**
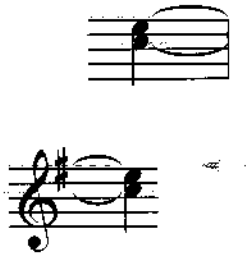
DIRECTION OF TIES FOR CHORDS

Highest note—tie is **above.**

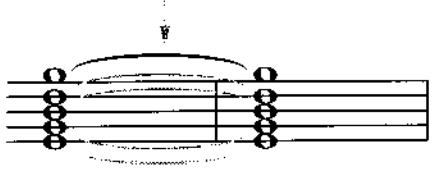

Lowest note—tie is **below.**
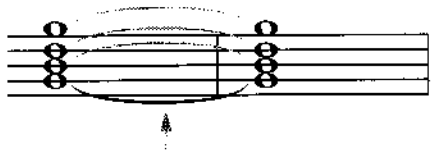
Notes between highest and lowest—on the **middle line and above,** ties are **above.**
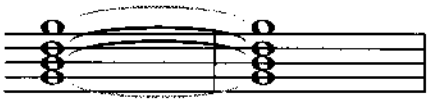
Below the **middle line,** ties are **below.**
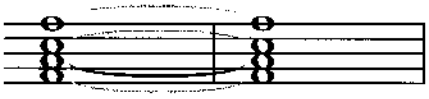
For **intervals of a 2nd,** ties will be in **opposite directions** whenever possible.
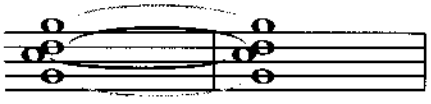
If some notes are not tied within the chords, the uppermost tied note has the tie above; the lowermost tied note has the tie below.
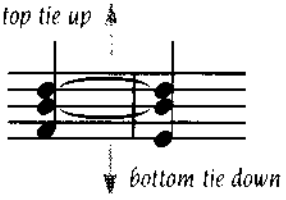
ALIGNMENT OF TIE ENDS

Align ends of ties within a chord.
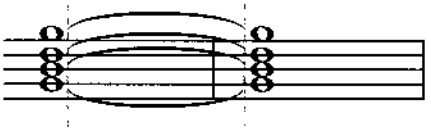
Tie ends for intervals of a 2nd should be adjusted if possible.
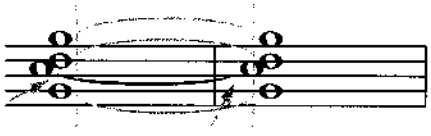
ADJUSTMENT OF TIES

Whenever possible, **maintain the curve** of a tie in uncommon situations. It should look like a tie, not a slur.

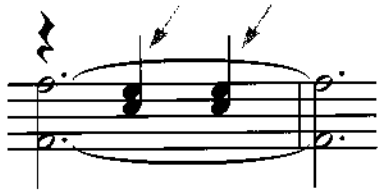

In this instance it is better to have the top tie curved up even though it is a part of the lower voice.

If a time signature interrupts a tie, break the tie to avoid colliding with the time signature.
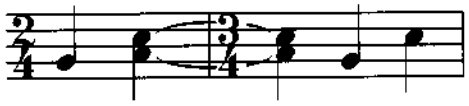
BROKEN (DASHED) TIES

Ties using a broken line instead of a solid one are often **used to accommodate lyrics for multiple verses.**
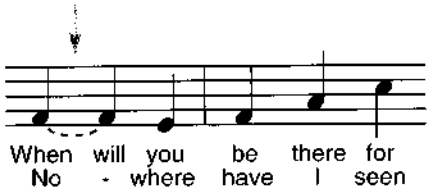
TIES IN MEASURED ARPEGGIOS

Although traditionally considered incorrect, ties are sometimes **extended to the unbroken chord** to avoid a cluttered look.

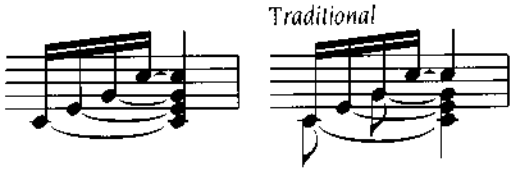

Time signatures

Time signatures indicate the meter for a measure(s) or an entire piece.

Since meter is so closely connected with the proper use of ties, rests, beams and syncopated rhythms, the **correct time signature** must be chosen.

The **upper number** indicates the number of beats per measure.

The **lower number** indicates the note that gets one beat (2 = half note, 4 = quarter note, 8 = eighth note, 16 = sixteenth note, etc.).

All measures after a time signature will be in the same meter until a new time signature is indicated.

PLACEMENT

The **upper number** is always placed between the top line and the middle line of the staff.

The **lower number** is always placed between the middle line and the bottom line of the staff.

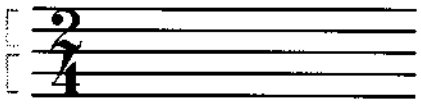

For a **single-line staff,** the line intersects the two numbers.

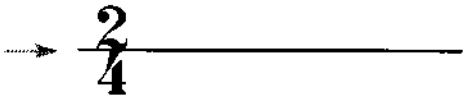

The time signature is **indicated after the clef and key signature.**

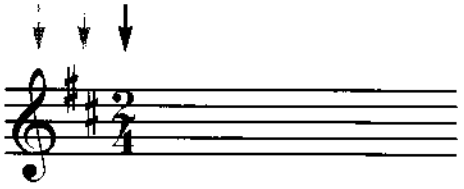

CHANGING TIME SIGNATURES

Time signatures may change from measure to measure, applying to all measures until the next time signature change. **A change in time signature always appears AFTER a barline.**
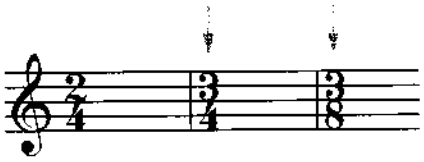
If the time signature changes at the beginning of a line, a **courtesy time signature** is added at the end of the previous staff, *after* the last barline. The new time signature appears after the clef (and key signature, if any) on the next staff.

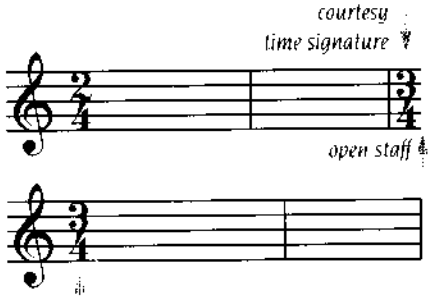

The following illustrates the positioning of the clef, key signature and time signature if all three change simultaneously.

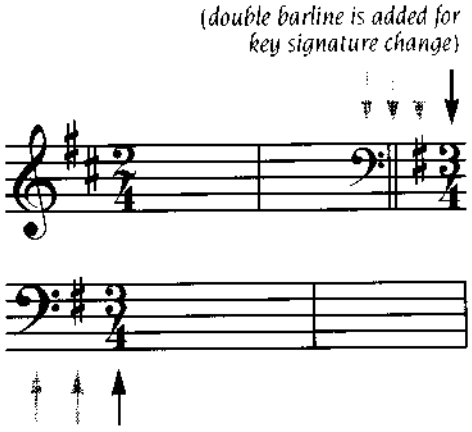

COMPOSITE METER (See *Meter*)

ALTERNATING METER (See *Meter*)

Tremolo

A tremolo may be **on one note,** or **between two or more notes.** It may be **measured** (a clear subdivision) or **unmeasured** (as fast as possible).

ON ONE NOTE

Measured tremolo

A **short slanted line,** ascending from left to right, through the stem of a note indicates that a note is to be subdivided.

Each line placed on the stem indicates the **rhythmic value** of the tremolo.

For instance, one line will indicate eighth notes,
two lines—sixteenth notes.
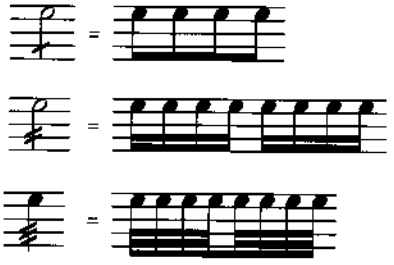
In string music, a measured tremolo is sometimes indicated by placing **divisi dots** above the note, in addition to the slashes through the stem.

The divisi dots precisely indicate the divisions per note. The slashes through the stem indicate the rhythmic value.

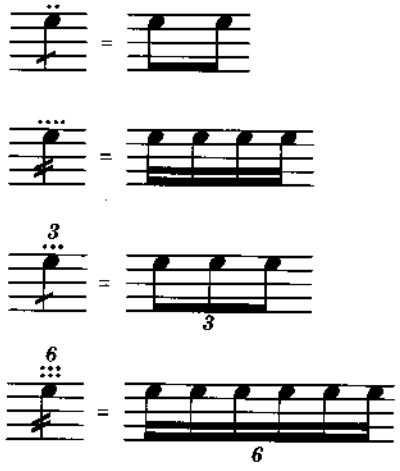

Unmeasured tremolo

An **unmeasured tremolo** (on one note) is indicated by placing three lines through the stem and adding the abbreviation ***trem.*** above the note. (If placed on a beamed note, the beam counts as one of the lines.) Most often seen in notation for strings, percussion and fretted instruments.
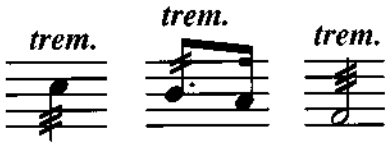
Tremolo lines on whole notes are traditionally **indicated above or below the note** (positioned as if there were a stem, but centered on the notehead).

traditional style

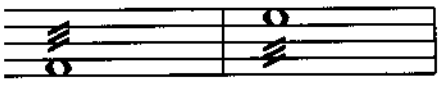

Modern style breaks the whole note into two half notes and places the slanted lines through the stems as usual.

modern style
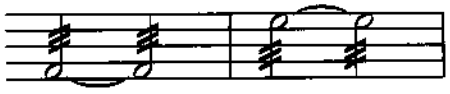
ON MORE THAN ONE NOTE

When a tremolo is indicated between two (or more) different pitches, the notes are connected with a beam, with incomplete beams placed between to indicate the rhythmic value.
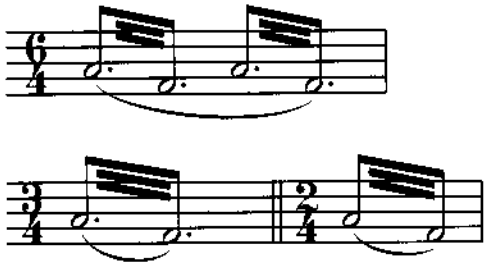
Stems are lengthened to accommodate added beams.

With such a subdivision of the tremolo, **each note equals the total rhythmic value of the tremolo.**

unmeasured whole-note tremolo (traditional style)

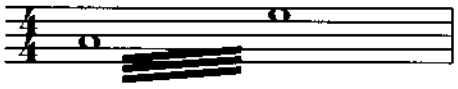

modern style
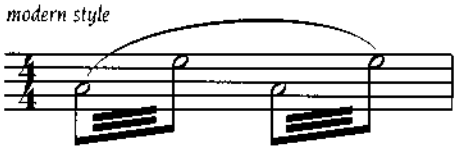
In the previous example, a complete measure of tremolo in $\frac{4}{4}$ time consists of two sets of half notes beamed together.

INTERVAL / CHORD TREMOLO

For some instruments, a tremolo is possible between two, three or more notes.
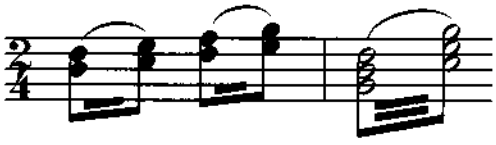
Trill

The abbreviation ***tr*** indicates a trill.

The ***tr*** is always **placed above the note,** regardless of stem direction (unless two parts share a staff).
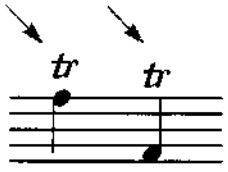
Each trilled note must have its own trill symbol.

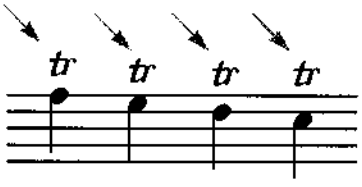

A **wavy line** may be indicated after the ***tr***, especially if the trill is extended.
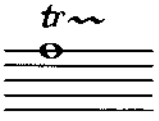
If the trill **extends over two or more notes,** the wavy line continues to the end of the notehead of the last note affected by the trill.

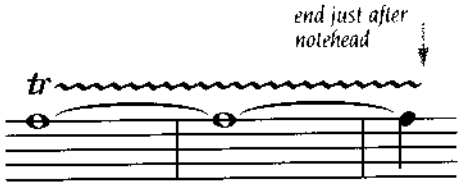

If the **wavy line extends over consecutive notes of the same pitch** but without ties, the notes are to be clearly articulated.

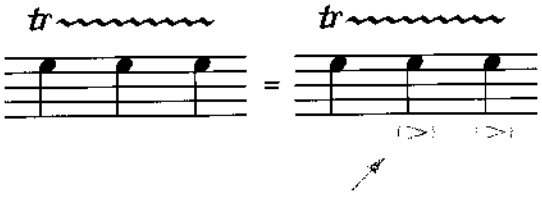

When two parts share a staff, the trill for the lower part is placed below the note.
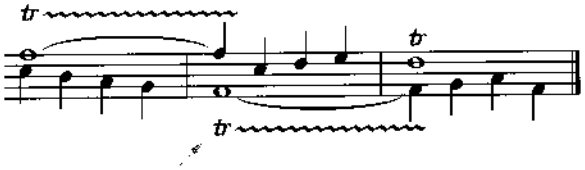
When the upper note of a trill is **altered from the diatonic scale,** a small **accidental** is used with the trill sign. The accidental is placed after the trill sign but before the wavy line (if used.)

The accidental **may also appear above** the trill sign.
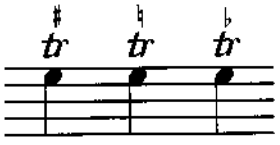
A **cue-size notehead** is sometimes used.
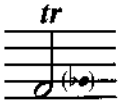
Terminations can be indicated by cue-size or full-size notes.

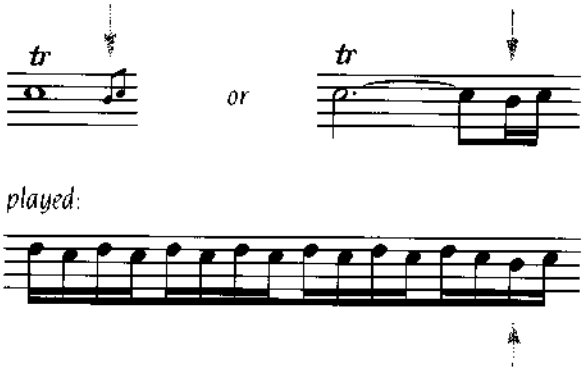

Triplet

See *Tuplets*

Tuplets

Rhythmic groupings of notes that are NOT metric groupings are known as **tuplets.**

Duplets, triplets, quadruplets, quintuplets, sextuplets and septuplets are all examples of **tuplets.**

TUPLET NUMERALS

The numeral is larger than a finger number and is **distinctly italic, preferably bold italic.** (See *Fingerings [for keyboard]*)

For beamed tuplets, the numeral is preferred **on the beam side, centered.**

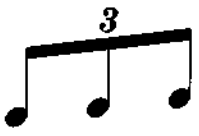

Do not use a tuplet slur with the numeral. This is an obsolete practice and causes confusion between normal slurs and tuplet slurs.

Place the tuplet numeral **outside the staff** whenever possible.

If placed within the staff, the **numeral must be clearly positioned,** avoiding staff lines as much as possible.

The numeral **remains placed with the beam,** whatever the stem direction.
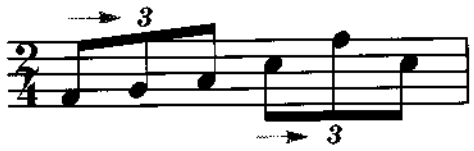
When parts share a staff, the numeral is placed normally (beam/stem side).

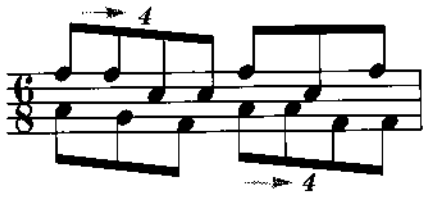

After a **pattern of tuplets** has been established, the numeral may be omitted. *Simile* may also be used for clarity.
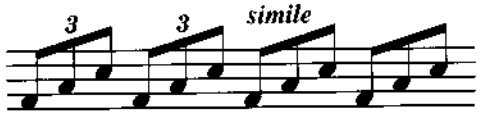
TUPLET BRACKETS

If the tuplet is not beamed, a **bracket is added** and the **numeral is centered** within the bracket.

The bracket always **begins flush left** with the notehead and **ends flush right** with the notehead, whether on the notehead or stem side.

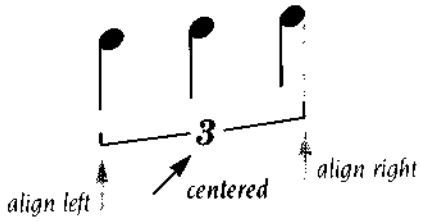

The **bracket is broken** to accommodate the number; the **ends** are always vertical.

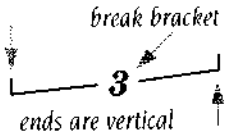

If the tuplet numeral is **moved to the notehead side** of a beamed tuplet (for example, to avoid fingerings), add a bracket for clarity.

The **bracket is placed** at the same angle as the beam.
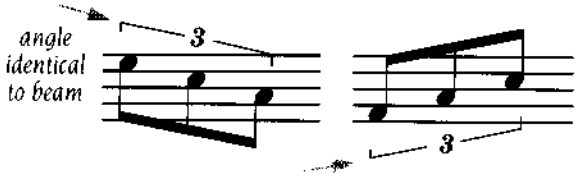
When placing a **bracket with unbeamed notes,** the bracket angle can vary.
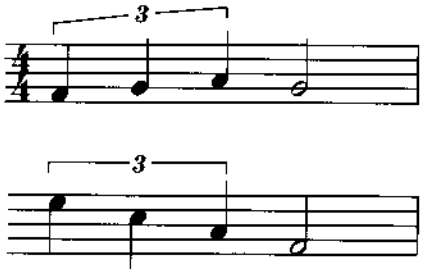
BRACKETS AND UNEQUAL VALUES

For **unequal rhythmic values** within the tuplet group, the bracket must **include all notes** of the group.

The **numeral remains centered** within the bracket.

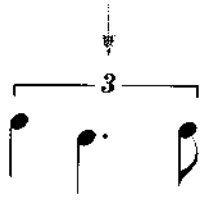

The tuplet unit is clearly seen if the bracket extends to **include the entire allotted space** for the tuplet (as in the first tuplet below).

The bracket does not extend to include the flag (as shown in the second tuplet).

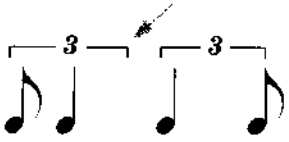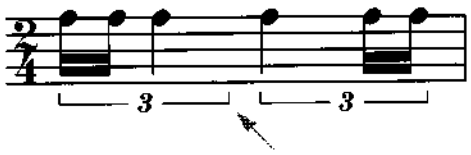

WITH RESTS

The **bracket extends** to include rests.
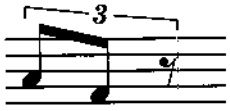
Although the bracket is preferred, an option is to **extend the beam** to include the rest within the tuplet.
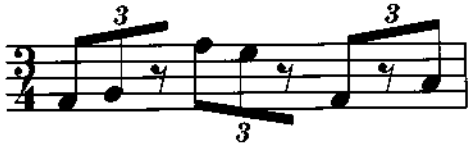
WITH FINGERINGS

It is advised to **move the tuplet figure to avoid confusion with finger numbers.**

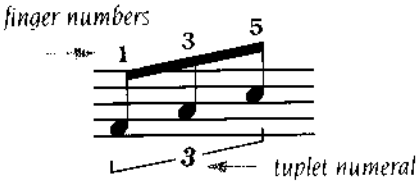

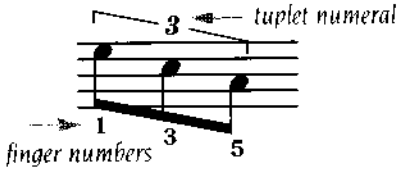

WITH ARTICULATIONS

If the bracket must be placed on the same side as articulations, the bracket is **placed outside articulations.**

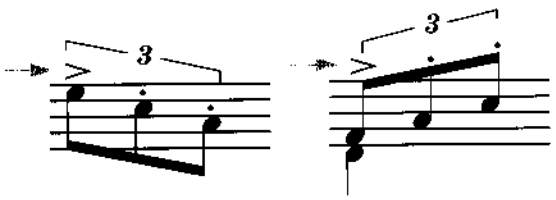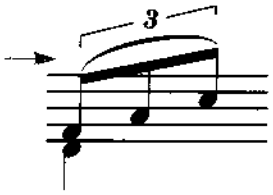

Short slurs may be considered articulations.

DETERMINING NOTE VALUE

A tuplet may occupy a beat, a pulse, a *portion* of a beat or pulse, or an entire measure.

To determine the rhythmic value of a tuplet that occupies **one beat,** subdivide the beat metrically as many times as you can without exceeding the number of notes in the tuplet. The note value of the tuplet will be equal to the note value of that metric subdivision.

In the example below, if each beat were subdivided further, it would have more notes than the tuplet; therefore the tuplet notes are sixteenth notes.

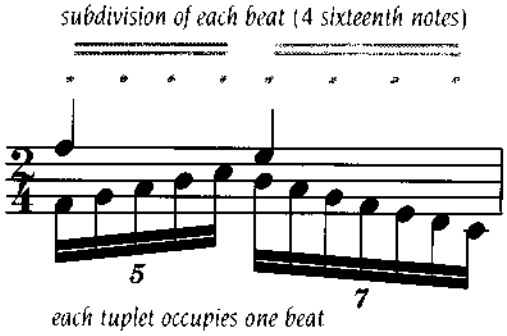

Use the same principle to determine the note value of tuplets that occupy an **entire measure** (or another unit of a measure).

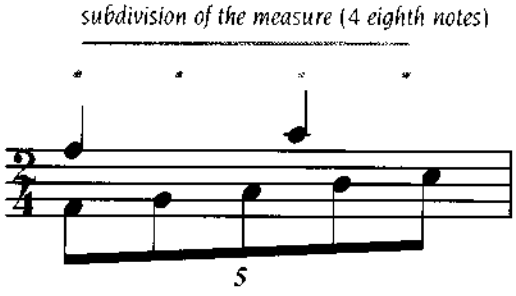

subdivision of the measure (12 *sixteenth notes*)

tuplets occupying an entire measure

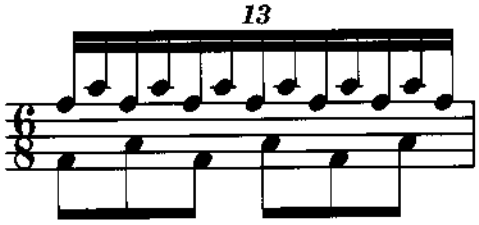

Duplets are the only exception to the previous rule deciding tuplet rhythmic value.

Duplets are **equal in rhythmic value to the beat** (not to be confused with pulse).

Duplets only occur in **compound meter.**

subdivision of the PULSE
(3 *eighth notes*)

Duplets

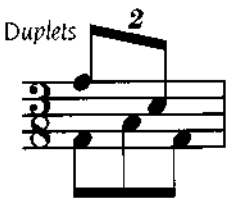

HORIZONTAL SPACING

A tuplet is spaced mathematically, as proper spacing dictates—not aligned with the metric rhythm.

subdivision of the PULSE
(6 *sixteenth notes*)

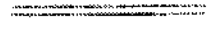

tuplet occupying one pulse
(*entire measure*)

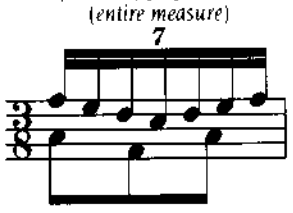

Words See *Lyric*

X notehead See *Notes*

INDEX OF TOPICS

A cappella 3
A due (a2) 3
A tempo 3
Accents 3
Accidentals 3
Alternating instruments 10
Arpeggio signs 11
Articulations 13
Augmentation dot 21
Barlines 25
Beams 29
Bowing 42
Brace 43
Bracket 43
Breath mark 44
Caesura 45
Chord frames & symbols 46
Circle of fifths 49
Clef signs 49
Coda sign 53
Courtesy accidentals 53
Credits 53
Cue notes 54
D.C. al Coda 55
D.C. al Fine 57
D.S. al Coda 58
D.S. al Fine 59
Divisi 60
Divisi dots 60
Dotted rhythms 60
Dynamics 60
Endings 65
Fermata 65
Fingerings (keyboard) 67
Flat 71
Glissando sign 71
Grace notes 72
Grand pause 74
Grand staff 74
Harmonics 76
Key signatures 78
Layout 82
Leger lines 83
Lyric 84
Meter 88
Metronome marks 95
Natural sign 95
Notes 95
Octave signs 97
Ornaments 103
Ossia 104
Pedal marks 105
Picking 109
Repeat signs 110
Rests 113
Scores 117
Sharing a staff 118
Sharp 121
Simile 121
Slurs 121
Spacing 131
Staccato 134
Staff 135
Stems 137
Systems 140
Tablature 140
Tempo marks 142
Tenuto 143
Ties 143
Time signatures 149
Tremolo 151
Trill 153
Triplet 155
Tuplets 155
Words 160
X notehead 160

Michel Marie Deza
Elena Deza

Encyclopedia of Distances

Fourth Edition

Springer

Preface to *Dictionary of Distances*, 2006

The concept of *distance* is a basic one in the whole human experience. In everyday life, it usually means some degree of closeness of two physical objects or ideas, i.e., length, time interval, gap, rank difference, coolness, or remoteness, while the term *metric* is often used as a standard for a measurement.

But here we consider, except for the last two chapters, the mathematical meaning of those terms which is an abstraction of measurement. The mathematical notions of *distance metric* (i.e., a function $d(x, y)$ from $X \times X$ to the set of real numbers satisfying to $d(x, y) \geq 0$ with equality only for $x = y$, $d(x, y) = d(y, x)$, and $d(x, y) \leq d(x, z) + d(z, y)$) and of *metric space* (X, d) were originated a century ago by M. Fréchet (1906) and F. Hausdorff (1914) as a special case of an infinite topological space. The *triangle inequality* above appears already in Euclid. The infinite metric spaces are usually seen as a generalization of the metric $|x - y|$ on the real numbers. Their main classes are the measurable spaces (add measure) and Banach spaces (add norm and completeness).

However, starting from K. Menger (who, in 1928, introduced metric spaces in geometry) and L.M. Blumenthal (1953), an explosion of interest in both finite and infinite metric spaces occurred. Another trend is that many mathematical theories, in the process of their generalization, settled on the level of metric space. It is an ongoing process, for example, for Riemannian geometry, real analysis, and approximation theory.

Distance metrics and distances have become now an essential tool in many areas of mathematics and its applications including geometry, probability, statistics, coding/graph theory, clustering, data analysis, pattern recognition, networks, engineering, computer graphics/vision, astronomy, cosmology, molecular biology, and many other areas of science. Devising the most suitable distance metrics and similarities, in order to quantify the proximity between objects, has become a standard task for many researchers. Especially intense ongoing search for such distances occurs, for example, in computational biology, image analysis, speech recognition, and information retrieval.

Often the same distance metric appears independently in several different areas, for example, the edit distance between words, the evolutionary distance in biology,

the Levenshtein metric in coding theory, and the Hamming+Gap or shuffle-Hamming distance.

This body of knowledge has become too big and disparate to operate within. The number of worldwide web entries offered by Google on the topics "distance," "metric space," and "distance metric" is about 216, 3, and 9 million, respectively, not to mention all the printed information outside the web, or the vast "invisible web" of searchable databases. About 15,000 books on Amazon.com contain "distance" in their titles. However, this huge information on distances is too scattered: the works evaluating distance from some list usually treat very specific areas and are hardly accessible for nonexperts.

Therefore many researchers, including us, keep and cherish a collection of distances for use in their areas of science. In view of the growing general need for an accessible interdisciplinary source for a vast multitude of researchers, we have expanded our private collection into this dictionary. Some additional material was reworked from various encyclopedias, especially Encyclopedia of Mathematics ([EM98]), MathWorld ([Weis99]), PlanetMath ([PM]), and Wikipedia ([WFE]). However, the majority of distances are extracted directly from specialist literature.

Besides distances themselves, we collected here many distance-related notions (especially in Chap. 1) and paradigms, enabling people from applications to get those (arcane for nonspecialists) research tools, in ready-to-use fashion. This and the appearance of some distances in different contexts can be a source of new research.

In the time when overspecialization and terminology fences isolate researchers, this dictionary tries to be "centripetal" and "ecumenical," providing some access and altitude of vision but without taking the route of scientific vulgarization. This attempted balance defined the structure and style of the dictionary.

This reference book is a specialized encyclopedic dictionary organized by subject area. It is divided into 29 chapters grouped into 7 parts of about the same length. The titles of the parts are purposely approximative: they just allow a reader to figure out her/his area of interest and competence. For example, Parts II, III, IV, and V require some culture in, respectively, pure and applied mathematics. Part VII can be read by a layman.

The chapters are thematic lists, by areas of mathematics or applications, which can be read independently. When necessary, a chapter or a section starts with a short introduction: a field trip with the main concepts. Besides these introductions, the main properties and uses of distances are given, within items, only exceptionally. We also tried, when it was easy, to trace distances to their originator(s), but the proposed extensive bibliography has a less general ambition: just to provide convenient sources for a quick search.

Each chapter consists of items ordered in a way that hints of connections between them. All item titles and (with majuscules only for proper nouns) selected key terms can be traced in the large subject index; they are boldfaced unless the meaning is clear from the context. So, the definitions are easy to locate, by subject, in chapters and/or, by alphabetic order, in the subject index.

The introductions and definitions are reader-friendly and maximally independent each from another; still they are interconnected, in the 3D HTML manner, by hyperlink-like boldfaced references to similar definitions.

Many nice curiosities appear in this "Who Is Who" of distances. Examples of such sundry terms are ubiquitous Euclidean distance ("as-the-crow-flies"), flower-shop metric (shortest way between two points, visiting a "flower-shop" point first), knight-move metric on a chessboard, Gordian distance of knots, Earth mover's distance, biotope distance, Procrustes distance, lift metric, post office metric, Internet hop metric, WWW hyperlink quasi-metric, Moscow metric, and dogkeeper distance.

Besides abstract distances, the distances having physical meaning appear also (especially in Part VI); they range from 1.6×10^{-35} m (Planck length) to 8.8×10^{26} m (the estimated size of the observable Universe, about 5.4×10^{61} Planck lengths).

The number of distance metrics is infinite, and therefore our dictionary cannot enumerate all of them. But we were inspired by several successful thematic dictionaries on other infinite lists, for example, on numbers, integer sequences, inequalities, and random processes, and by atlases of functions, groups, fullerenes, etc. On the other hand, the large scope often forced us to switch to the mode of laconic tutorial.

The target audience consists of all researchers working on some measuring schemes and, to a certain degree, students and a part of the general public interested in science.

We tried to address all scientific uses of the notion of distance. But some distances did not made it to this dictionary due to space limitations (being too specific and/or complex) or our oversight. In general, the size/interdisciplinarity cut-off, i.e., decision where to stop, was our main headache. We would be grateful to the readers who will send us their favorite distances missed here.

Contents

Part I Mathematics of Distances

1 General Definitions 3
- 1.1 Basic Definitions 3
- 1.2 Main Distance-Related Notions 12
- 1.3 Metric Numerical Invariants 23
- 1.4 Main Mappings of Metric Spaces 36
- 1.5 General Distances 46

2 Topological Spaces 63

3 Generalizations of Metric Spaces 71
- 3.1 m-Tuple Generalizations of Metrics 71
- 3.2 Indefinite Metrics 73
- 3.3 Topological Generalizations 75
- 3.4 Beyond Numbers 78

4 Metric Transforms 87
- 4.1 Metrics on the Same Set 87
- 4.2 Metrics on Set Extensions 91
- 4.3 Metrics on Other Sets 94

5 Metrics on Normed Structures 97

Part II Geometry and Distances

6 Distances in Geometry 111
- 6.1 Geodesic Geometry 111
- 6.2 Projective Geometry 117
- 6.3 Affine Geometry 123
- 6.4 Non-Euclidean Geometry 125

7 Riemannian and Hermitian Metrics 135
7.1 Riemannian Metrics and Generalizations 136
7.2 Riemannian Metrics in Information Theory 152
7.3 Hermitian Metrics and Generalizations 156

8 Distances on Surfaces and Knots 169
8.1 General Surface Metrics 169
8.2 Intrinsic Metrics on Surfaces 175
8.3 Distances on Knots 180

9 Distances on Convex Bodies, Cones, and Simplicial Complexes 183
9.1 Distances on Convex Bodies 183
9.2 Distances on Cones 189
9.3 Distances on Simplicial Complexes 192

Part III Distances in Classical Mathematics

10 Distances in Algebra 199
10.1 Group Metrics 199
10.2 Metrics on Binary Relations 209
10.3 Metrics on Semilattices 210

11 Distances on Strings and Permutations 215
11.1 Distances on General Strings 216
11.2 Distances on Permutations 225

12 Distances on Numbers, Polynomials, and Matrices 229
12.1 Metrics on Numbers 229
12.2 Metrics on Polynomials 235
12.3 Metrics on Matrices 237

13 Distances in Functional Analysis 247
13.1 Metrics on Function Spaces 247
13.2 Metrics on Linear Operators 254

14 Distances in Probability Theory 259
14.1 Distances on Random Variables 260
14.2 Distances on Distribution Laws 261

Part IV Distances in Applied Mathematics

15 Distances in Graph Theory 277
15.1 Distances on the Vertices of a Graph 278
15.2 Distance-Defined Graphs 286
15.3 Distances on Graphs 297
15.4 Distances on Trees 305

16 Distances in Coding Theory 313
16.1 Minimum Distance and Relatives 315
16.2 Main Coding Distances 317

17 Distances and Similarities in Data Analysis 327
17.1 Similarities and Distances for Numerical Data 329
17.2 Relatives of Euclidean Distance 333
17.3 Similarities and Distances for Binary Data 337
17.4 Correlation Similarities and Distances 340

18 Distances in Systems and Mathematical Engineering 347
18.1 Distances in State Transition and Dynamical Systems 348
18.2 Distances in Control Theory 354
18.3 Motion Planning Distances 356
18.4 MOEA Distances 361

Part V Computer-Related Distances

19 Distances on Real and Digital Planes 365
19.1 Metrics on Real Plane 365
19.2 Digital Metrics 376

20 Voronoi Diagram Distances 383
20.1 Classical Voronoi Generation Distances 384
20.2 Plane Voronoi Generation Distances 386
20.3 Other Voronoi Generation Distances 390

21 Image and Audio Distances 393
21.1 Image Distances 393
21.2 Audio Distances 409

22 Distances in Networks 419
22.1 Scale-Free Networks 419
22.2 Network-Based Semantic Distances 424
22.3 Distances in Internet and Web 428

Part VI Distances in Natural Sciences

23 Distances in Biology 439
23.1 Genetic Distances 443
23.2 Distances for DNA/RNA and Protein Data 455
23.3 Distances in Ecology, Biogeography, Ethology 467
23.4 Other Biological Distances 484

24 Distances in Physics and Chemistry 499
24.1 Distances in Physics 499
24.2 Distances in Chemistry and Crystallography 524

25 Distances in Earth Science and Astronomy 533
25.1 Distances in Geography 533
25.2 Distances in Geophysics 546
25.3 Distances in Astronomy 558

26 Distances in Cosmology and Theory of Relativity 577
26.1 Distances in Cosmology 577
26.2 Distances in Theory of Relativity 587

Part VII Real-World Distances

27 Length Measures and Scales 613
27.1 Length Scales 613
27.2 Orders of Magnitude for Length 623

28 Distances in Applied Social Sciences 629
28.1 Distances in Perception and Psychology 629
28.2 Distances in Economics and Human Geography 640
28.3 Distances in Sociology and Language 653
28.4 Distances in Philosophy, Religion and Art 664

29 Other Distances 683
29.1 Distances in Medicine, Anthropometry and Sport 683
29.2 Equipment Distances 701
29.3 Miscellany 716

References 723

Index 731

Part I
Mathematics of Distances

Chapter 1
General Definitions

1.1 Basic Definitions

- **Distance**

  A **distance space** (X, d) is a set X (*carrier*) equipped with a **distance** d.

  A function $d : X \times X \to \mathbb{R}$ is called a **distance** (or **dissimilarity**) on X if, for all $x, y \in X$, it holds:

  1. $d(x, y) \geq 0$ (*nonnegativity*);
  2. $d(x, y) = d(y, x)$ (*symmetry*);
  3. $d(x, x) = 0$ (*reflexivity*).

  In Topology, a distance with $d(x, y) = 0$ implying $x = y$ is called a **symmetric**.

  For any distance d, the function D_1 defined for $x \neq y$ by $D_1(x, y) = d(x, y)+c$, where $c = \max_{x,y,z \in X}(d(x, y) - d(x, z) - d(y, z))$, and $D(x, x) = 0$, is a **metric**. Also, $D_2(x, y) = d(x, y)^c$ is a metric for sufficiently small $c \geq 0$.

  The function $D_3(x, y) = \inf \sum_i d(z_i, z_{i+1})$, where the infimum is taken over all sequences $x = z_0, \ldots, z_{n+1} = y$, is the **path semimetric** of the complete weighted graph on X, where, for any $x, y \in X$, the weight of edge xy is $d(x, y)$.

- **Similarity**

  Let X be a set. A function $s : X \times X \to \mathbb{R}$ is called a **similarity** on X if s is nonnegative, symmetric and the inequality

  $$s(x, y) \leq s(x, x)$$

  holds for all $x, y \in X$, with equality if and only if $x = y$.

  The main transforms used to obtain a distance (dissimilarity) d from a similarity s bounded by 1 from above are: $d = 1 - s$, $d = \frac{1-s}{s}$, $d = \sqrt{1 - s}$, $d = \sqrt{2(1 - s^2)}$, $d = \arccos s$, $d = -\ln s$ (cf. Chap. 4).

© Springer-Verlag Berlin Heidelberg 2016

M.M. Deza, E. Deza, *Encyclopedia of Distances*,
DOI 10.1007/978-3-662-52844-0_1

- **Semimetric**

  Let X be a set. A function $d : X \times X \to \mathbb{R}$ is called a **semimetric** on X if d is nonnegative, symmetric, *reflexive* ($d(x, x) = 0$ for $x \in X$) and it holds

  $$d(x, y) \le d(x, z) + d(z, y)$$

  for all $x, y, z \in X$ (**triangle inequality** or, sometimes, *triangular inequality*).

  In Topology, it is called a **pseudo-metric** (or, rarely, **semidistance**, *gauge*), while the term *semimetric* is sometimes used for a **symmetric** (a distance $d(x, y)$ with $d(x, y) = 0$ only if $x = y$); cf. **symmetrizable space** in Chap. 2.

  For a semimetric d, the triangle inequality is equivalent, for each fixed $n \ge 4$ and all $x, y, z_1, \ldots, z_{n-2} \in X$, to the following *n-gon inequality*

  $$d(x, y) \le d(x, z_1) + d(z_1, z_2) + \cdots + d(z_{n-2}, y).$$

  Equivalent *rectangle inequality* is $|d(x, y) - d(z_1, z_2)| \le d(x, z_1) + +d(y, z_2)$.

  For a semimetric d on X, define an equivalence relation, called **metric identification**, by $x \sim y$ if $d(x, y) = 0$; equivalent points are equidistant from all other points. Let $[x]$ denote the equivalence class containing x; then $D([x], [y]) = d(x, y)$ is a **metric** on the set $\{[x] : x \in X\}$ of equivalence classes.
- **Metric**

  Let X be a set. A function $d : X \times X \to \mathbb{R}$ is called a **metric** on X if, for all $x, y, z \in X$, it holds:

  1. $d(x, y) \ge 0$ (*nonnegativity*);
  2. $d(x, y) = 0$ if and only if $x = y$ (*identity of indiscernibles*);
  3. $d(x, y) = d(y, x)$ (*symmetry*);
  4. $d(x, y) \le d(x, z) + d(z, y)$ (**triangle inequality**).

  In fact, the above condition 1. follows from above 2., 3. and 4.

  If 2. is dropped, then d is called (Bukatin, 2002) **relaxed semimetric**. If 2. is weakened to "$d(x, x) = d(x, y) = d(y, y)$ implies $x = y$", then d is called **relaxed metric**. A **partial metric** is a **partial semimetric**, which is a relaxed metric.

  If above 2. is weakened to "$d(x, y) = 0$ implies $x = y$", then d is called (Amini-Harandi, 2012) **metric-like function**. Any **partial metric** is metric-like.
- **Metric space**

  A **metric space** (X, d) is a set X equipped with a metric d.

  It is called a **metric frame** (or *metric scheme*, *integral*) if d is integer-valued.

  A **pointed metric space** (or *rooted metric space*) (X, d, x_0) is a metric space (X, d) with a selected base point $x_0 \in X$.
- **Extended metric**

  An **extended metric** is a generalization of the notion of metric: the value ∞ is allowed for a metric d.
- **Quasi-distance**

  Let X be a set. A function $d : X \times X \to \mathbb{R}$ is called a **quasi-distance** on X if d is nonnegative, and $d(x, x) = 0$ holds for all $x \in X$. It is also called a **premetric** or **prametric** in Topology and a *divergence* in Probability.

If a quasi-distance d satisfies the **strong triangle inequality** $d(x, y) \leq d(x, z) + d(y, z)$, then (Lindenbaum, 1926) it is symmetric and so, a semimetric. A **quasi-semimetric** d is a semimetric if and only if (Weiss, 2012) it satisfies the **full triangle inequality** $|d(x, z) - d(z, y)| \leq d(x, z) \leq d(x, z) + d(z, y)$.

The distance/metric notions are usually named as weakenings or modifications of the fundamental notion of **metric**, using various prefixes and modifiers. But, perhaps, extended (i.e., the value ∞ is allowed) semimetric and quasi-semimetric should be (as suggested in Lawvere, 2002) used as the basic terms, since, together with their **short mappings**, they are best behaved of the **metric space categories**.

- **Quasi-semimetric**

  A function $d : X \times X \to \mathbb{R}$ is called a **quasi-semimetric** (or **hemimetric**, *ostensible metric*) on X if $d(x, x) = 0$, $d(x, y) \geq 0$ and the **oriented triangle inequality**

$$d(x, y) \leq d(x, z) + d(z, y)$$

  holds for all $x, y, z \in X$. The set X can be partially ordered by the *specialization order*: $x \preceq y$ if and only if $d(x, y) = 0$.

  A **weak quasi-metric** is a quasi-semimetric d on X with *weak symmetry*, i.e., for all $x, y \in X$ the equality $d(x, y) = 0$ implies $d(y, x) = 0$.

  An **Albert quasi-metric** is a quasi-semimetric d on X with *weak definiteness*, i.e., for all $x, y \in X$ the equality $d(x, y) = d(y, x) = 0$ implies $x = y$.

  Both, weak and Albert, quasi-metric, is a usual **quasi-metric**.

  Any *pre-order* $(X, \prec)$ (satisfying for all $x, y, z \in X$, $x \prec x$ and if $x \prec y$ and $y \prec z$ then $x \prec z$) can be viewed as a **pre-order extended quasi-semimetric** (X, d) by defining $d(x, y) = 0$ if $x \prec y$ and $d(x, y) = \infty$, otherwise.

  A **weightable quasi-semimetric** is a quasi-semimetric d on X with *relaxed symmetry*, i.e., for all $x, y, z \in X$

$$d(x, y) + d(y, z) + d(z, x) = d(x, z) + d(z, y) + d(y, x),$$

  holds or, equivalently, there exists a weight function $w(x) \in \mathbb{R}$ on X with $d(x, y) - d(y, x) = w(y) - w(x)$ for all $x, y \in X$ (i.e., $d(x, y) + \frac{1}{2}(w(x) - w(y))$ is a semimetric). If d is a weightable quasi-semimetric, then $d(x, y) + w(x)$ is a **partial semimetric** (moreover, a **partial metric** if d is an Albert quasi-metric).

- **Partial metric**

  Let X be a set. A nonnegative symmetric function $p : X \times X \to \mathbb{R}$ is called a **partial metric** ([Matt92]) if, for all $x, y, z \in X$, it holds:

  1. $p(x, x) \leq p(x, y)$, i.e., every **self-distance** (or *extent*) $p(x, x)$ is *small*;
  2. $x = y$ if $p(x, x) = p(x, y) = p(y, y) = 0$ (T_0 *separation axiom*);
  3. $p(x, y) \leq p(x, z) + p(z, y) - p(z, z)$ (**sharp triangle inequality**).

  The 1-st above condition means that p is a **forward resemblance**, cf. Chap. 3.

If the 2-nd above condition is dropped, the function p is called a **partial semimetric**. The nonnegative function p is a partial semimetric if and only if $p(x,y) - p(x,x)$ is a **weightable quasi-semimetric** with $w(x) = p(x,x)$.

If the 1-st above condition is also dropped, the function p is called (Heckmann, 1999) a **weak partial semimetric**. The nonnegative function p is a weak partial semimetric if and only if $2p(x,y) - p(x,x) - p(y,y)$ is a semimetric.

Sometimes, the term *partial metric* is used when a metric $d(x,y)$ is defined only on a subset of the set of all pairs x, y of points.

- **Protometric**

  A function $p : X \times X \to \mathbb{R}$ is called a **protometric** if, for all (equivalently, for all different) $x, y, z \in X$, the **sharp triangle inequality** holds:

$$p(x,y) \le p(x,z) + p(z,y) - p(z,z).$$

  For finite X, the matrix $((p(x,y)))$ is (Burkard et al., 1996) *weak Monge array*.

  A **strong protometric** is a protometric p with $p(x,x) = 0$ for all $x \in X$. Such a protometric is exactly a quasi-semimetric, but with the condition $p(x,y) \ge 0$ (for any $x, y \in X$) being relaxed to $p(x,y) + p(y,x) \ge 0$.

  A **partial semimetric** is a **symmetric protometric** (i.e., $p(x,y) = p(y,x)$ with $p(x,y) \ge p(x,x) \ge 0$ for all $x, y \in X$.) An example of a nonpositive symmetric protometric is given by $p(x,y) = -(x.y)_{x_0} = \frac{1}{2}(d(x,y) - d(x,x_0) - d(y,y_0))$, where (X,d) is a metric space with a fixed base point $x_0 \in X$; see **Gromov product similarity** $(x.y)_{x_0}$ and, in Chap. 4, **Farris transform metric** $C - (x.y)_{x_0}$.

  A **0-protometric** is a protometric p for which all sharp triangle inequalities (equivalently, all inequalities $p(x,y) + p(y,x) \ge p(x,x) + p(y,y)$ implied by them) hold as equalities. For any $u \in X$, denote by A'_u, A''_u the 0-protometrics p with $p(x,y) = 1_{x=u}, 1_{y=u}$, respectively. The protometrics on X form a flat convex cone in which the 0-protometrics form the largest linear space. For finite X, a basis of this space is given by all but one A'_u, A''_u (since $\sum_u A'_u = \sum_u A''_u$) and, for the flat subcone of all symmetric 0-protometrics on X, by all $A'_u + A''_u$.

  A **weighted protometric** on X is a protometric with a point-weight function $w : X \to \mathbb{R}$. The mappings $p(x,y) = \frac{1}{2}(d(x,y) + w(x) + w(y))$ and $d(x,y) = 2p(x,y) - p(x,x) - p(y,y)$, $w(x) = p(x,x)$ establish a bijection between the weighted strong protometrics (d,w) and the protometrics p on X, as well as between the weighted semimetrics and the symmetric protometrics. For example, a weighted semimetric (d,w) with $w(x) = -d(x,x_0)$ corresponds to a protometric $-(x.y)_{x_0}$. For finite $|X|$, the above mappings amount to the representation

$$2p = d + \sum_{u \in X} p(u,u)(A'_u + A''_u).$$

- **Quasi-metric**

  A function $d : X \times X \to \mathbb{R}$ is called a **quasi-metric** (or *asymmetric metric*, *directed metric*) on X if $d(x,y) \ge 0$ holds for all $x, y \in X$ with equality if and

only if $x = y$, and for all $x, y, z \in X$ the **oriented triangle inequality**

$$d(x, y) \le d(x, z) + d(z, y)$$

holds. A *quasi-metric space* (X, d) is a set X equipped with a quasi-metric d.

For any quasi-metric d, the functions $\max\{d(x, y), d(y, x)\}$ (called sometimes *bi-distance*), $\min\{d(x, y), d(y, x)\}$, $\frac{1}{2}(d^p(x, y) + d^p(y, x))^{\frac{1}{p}}$ with given $p \ge 1$ are **metric generating**; cf. Chap. 4.

A **non-Archimedean quasi-metric** d is a quasi-distance on X which, for all $x, y, z \in X$, satisfies the following strengthened oriented triangle inequality:

$$d(x, y) \le \max\{d(x, z), d(z, y)\}.$$

- **Directed-metric**

  Let X be a set. A function $d : X \times X \to \mathbb{R}$ is called (Jegede, 2005) a **directed-metric** on X if, for all $x, y, z \in X$, it holds $d(x, y) = -d(y, x)$ and

  $$|d(x, y)| \le |d(x, z)| + |d(z, y)|.$$

  Cf. **displacement** in Chap. 24 and **rigid motion of metric space**.
- **Coarse-path metric**

  Let X be a set. A metric d on X is called a **coarse-path metric** if, for a fixed $C \ge 0$ and for every pair of points $x, y \in X$, there exists a sequence $x = x_0, x_1, \ldots, x_t = y$ for which $d(x_{i-1}, x_i) \le C$ for $i = 1, \ldots, t$, and it holds

  $$d(x, y) \ge d(x_0, x_1) + d(x_1, x_2) + \cdots + d(x_{t-1}, x_t) - C.$$

- **Near-metric**

  Let X be a set. A distance d on X is called a **near-metric** (or *C-near-metric*) if $d(x, y) > 0$ for $x \ne y$ and the *C-relaxed triangle inequality*

  $$d(x, y) \le C(d(x, z) + d(z, y))$$

  holds for all $x, y, z \in X$ and some constant $C \ge 1$.

  If $d(x, y) > 0$ for $x \ne y$ and the *C-asymmetric triangle inequality* $d(x, y) \le d(x, z) + Cd(z, y)$ holds, d is a $\frac{C+1}{2}$-near-metric.

  A ***C*-inframetric** is a C-near-metric, while a C-near-metric is a $2C$-inframetric.

  Some recent papers use the term *quasi-triangle inequality* for the above inequality and so, *quasi-metric* for the notion of near-metric.

  The **power transform** (Chap. 4) $(d(x, y))^\alpha$ of any near-metric is a near-metric for any $\alpha > 0$. Also, any near-metric d admits a **bi-Lipschitz mapping** on $(D(x, y))^\alpha$ for some semimetric D on the same set and a positive number α.

A near-metric d on X is called a **Hölder near-metric** if the inequality

$$|d(x,y) - d(x,z)| \le \beta d^{\alpha}(y,z)(d(x,y) + d(x,z))^{1-\alpha}$$

holds for some $\beta > 0$, $0 < \alpha \le 1$ and all $x, y, z \in X$. Cf. **Hölder mapping**.

A distance d on set X is said (Greenhoe, 2015) to satisfy (C, p) **power triangle inequality** if, for given positive C, p and any $x, y, z \in X$, it holds

$$d(x,y) \le 2C|\frac{1}{2}d^p(x,z) + \frac{1}{2}d^p(z,y)|^{\frac{1}{p}}.$$

- **f-quasi-metric**

  Let $f(t,t') : \mathbb{R}_{\ge 0} \times \mathbb{R}_{\ge 0} \to \mathbb{R}_{\ge 0}$ be a function with $\lim_{(t,t')\to 0, f(t,t')} = f(0,0) = 0$.

  Let X be a set. A function $d : X \times X \to \mathbb{R}$ is called (Arutyunov et al., 2016) a **f-quasi-metric** on X if $d(x,y) \ge 0$ holds for all $x, y \in X$ with equality if and only if $x = y$, and for all $x, y, z \in X$ holds the **f-triangle inequality**

$$d(x,y) \le f(d(x,z), d(z,y)).$$

  The *f-quasi-metric space* (X, d) with symmetric d and $f(t,t') = \max(t,t')$ is exactly the **Fréchet V-space** (1906); cf. the **partially ordered distance** in Sect. 3.4.

  The case $f(t,t') = t + t'$ of a f-quasi-metric corresponds to a **quasi-metric**. Given $q, q' \ge 1$, the f-quasi-metric with $f(t,t') = qt + q't'$ is called (q,q')-*quasi-metric*.

  The inequality $d(x,y) \le F(d(x,z), d(y,z))$ implies $d(x,y) \le f(d(x,z), d(z,y))$ for the function $f(t,t') = F(t, F(0,t'))$.

- **Weak ultrametric**

  A **weak ultrametric** (or **C-inframetric**, *C-pseudo-distance*) d is a distance on X such that $d(x,y) > 0$ for $x \ne y$ and the *C-inframetric inequality*

$$d(x,y) \le C \max\{d(x,z), d(z,y)\}$$

  holds for all $x, y, z \in X$ and some constant $C \ge 1$.

  The term **pseudo-distance** is also used, in some applications, for any of a **pseudo-metric**, a **quasi-distance**, a **near-metric**, a distance which can be infinite, a distance with an error, etc. Another unsettled term is **weak metric**: it is used for both a **near-metric** and a **quasi-semimetric**.

- **Ultrametric**

  An **ultrametric** (or *non-Archimedean metric*) is (Krasner, 1944) a metric d on X which satisfies, for all $x, y, z \in X$, the following strengthened version of the triangle inequality (Hausdorff, 1934), called the **ultrametric inequality**:

$$d(x,y) \le \max\{d(x,z), d(z,y)\}$$

An ultrametric space is also called an *isosceles space* since at least two of $d(x, y)$, $d(z, y)$, $d(x, z)$ are equal. An ultrametric on a set V has at most $|V|$ values.

A metric d is an ultrametric if and only if its **power transform** (see Chap. 4) d^{α} is a metric for any real positive number α. Any ultrametric satisfies the **four-point inequality**. A metric d is an ultrametric if and only if it is a **Farris transform metric** (Chap. 4) of a **four-point inequality metric**.

- **Robinsonian distance**

  A distance d on X is called a **Robinsonian distance** (or *monotone distance*) if there exists a total order $\preceq$ on X *compatible* with it, i.e., for $x, y, w, z \in X$,

$$x \preceq y \preceq w \preceq z \text{ implies } d(y, w) \leq d(x, z),$$

  or, equivalently, for $x, y, z \in X$, it holds

$$x \preceq y \preceq z \text{ implies } d(x, y) \leq \max\{d(x, z), d(z, y)\}.$$

  Any **ultrametric** is a Robinsonian distance.

- **Four-point inequality metric**

  A metric d on X is a **four-point inequality metric** (or **additive metric**) if it satisfies the following strengthened version of the triangle inequality called the **four-point inequality** (Buneman, 1974): for all $x, y, z, u \in X$

$$d(x, y) + d(z, u) \leq \max\{d(x, z) + d(y, u), d(x, u) + d(y, z)\}$$

  holds. Equivalently, among the three sums $d(x, y) + d(z, u)$, $d(x, z) + d(y, u)$, $d(x, u) + d(y, z)$ the two largest sums are equal.

  A metric satisfies the four-point inequality if and only if it is a **tree-like metric**.

  Any metric, satisfying the four-point inequality, is a **Ptolemaic metric** and an L_1*-metric*. Cf. L_p**-metric** in Chap. 5.

  A **bush metric** is a metric for which all four-point inequalities are equalities, i.e., $d(x, y) + d(u, z) = d(x, u) + d(y, z)$ holds for any $u, x, y, z \in X$.

- **Relaxed four-point inequality metric**

  A metric d on X satisfies the **relaxed four-point inequality** if, for all $x, y, z, u \in X$, among the three sums

$$d(x, y) + d(z, u), d(x, z) + d(y, u), d(x, u) + d(y, z)$$

  at least two (not necessarily the two largest) are equal. A metric satisfies this inequality if and only if it is a **relaxed tree-like metric**.

- **Ptolemaic metric**

  A **Ptolemaic metric** d is a metric on X which satisfies the **Ptolemaic inequality**

$$d(x, y)d(u, z) \leq d(x, u)d(y, z) + d(x, z)d(y, u)$$

for all $x, y, u, z \in X$. A classical result, attributed to Ptolemy, says that this inequality holds in the Euclidean plane, with equality if and only if the points x, y, u, z lie on a circle in that order.

A *Ptolemaic space* is a *normed vector space* $(V, ||.||)$ such that its norm metric $||x - y||$ is a Ptolemaic metric. A normed vector space is a Ptolemaic space if and only if it is an **inner product space** (Chap. 5); so, a **Minkowskian metric** (Chap. 6) is Euclidean if and only if it is Ptolemaic.

For any metric d, the metric $\sqrt{d}$ is Ptolemaic ([FoSc06]).

- **δ-hyperbolic metric**

  Given a number $\delta \geq 0$, a metric d on a set X is called **δ-hyperbolic** if it satisfies the following *Gromov δ-hyperbolic inequality* (another weakening of the **four-point inequality**): for all $x, y, z, u \in X$, it holds that

$$d(x, y) + d(z, u) \leq 2\delta + \max\{d(x, z) + d(y, u), d(x, u) + d(y, z)\}.$$

  A metric space (X, d) is δ-hyperbolic if and only if for all $x_0, x, y, z \in X$ it holds

$$(x.y)_{x_0} \geq \min\{(x.z)_{x_0}, (y.z)_{x_0}\} - \delta,$$

  where $(x.y)_{x_0} = \frac{1}{2}(d(x_0, x) + d(x_0, y) - d(x, y))$ is the **Gromov product** of the points x and y of X with respect to the base point $x_0 \in X$.

  A metric space (X, d) is 0-hyperbolic exactly when d satisfies the **four-point inequality**. Every bounded metric space of diameter D is D-hyperbolic. The n-dimensional *hyperbolic space* is $\ln 3$-hyperbolic.

  Every δ-hyperbolic metric space is isometrically embeddable into a **geodesic metric space** (Bonk and Schramm, 2000).

- **Gromov product similarity**

  Given a metric space (X, d) with a fixed point $x_0 \in X$, the **Gromov product similarity** (or *Gromov product*, *covariance*, *overlap function*) $(.)_{x_0}$ is a similarity on X defined by

$$(x.y)_{x_0} = \frac{1}{2}(d(x, x_0) + d(y, x_0) - d(x, y)).$$

  The triangle inequality for d implies $(x.y)_{x_0} \geq (x.z)_{x_0} + (y.z)_{x_0} - (z.z)_{x_0}$ (**covariance triangle inequality**), i.e., **sharp triangle inequality** for **protometric** $-(x.y)_{x_0}$.

  If (X, d) is a tree, then $(x.y)_{x_0} = d(x_0, [x, y])$. If (X, d) is a **measure semimetric space**, i.e., $d(x, y) = \mu(x \triangle y)$ for a Borel measure μ on X, then $(x.y)_\emptyset = \mu(x \cap y)$. If d is a **distance of negative type**, i.e., $d(x, y) = d_E^2(x, y)$ for a subset X of a Euclidean space $\mathbb{E}^n$, then $(x.y)_0$ is the usual *inner product* on $\mathbb{E}^n$.

  Cf. **Farris transform metric** $d_{x_0}(x, y) = C - (x.y)_{x_0}$ in Chap. 4.

- **Cross-difference**

  Given a metric space (X, d) and quadruple (x, y, z, w) of its points, the **cross-difference** is the real number cd defined by

$$cd(x, y, z, w) = d(x, y) + d(z, w) - d(x, z) - d(y, w).$$

In terms of the **Gromov product similarity**, for all $x, y, z, w, p \in X$, it holds

$$\frac{1}{2}cd(x, y, z, w) = -(x.y)_p - (z.w)_p + (x.z)_p + (y.w)_p;$$

in particular, it becomes $(x.y)_p$ if $y = w = p$.

If $x \neq z$ and $y \neq w$, the **cross-ratio** is the positive number defined by

$$cr((x, y, z, w), d) = \frac{d(x, y)d(z, w)}{d(x, z)d(y, w)}.$$

- $2k$**-gonal distance**

  A $2k$**-gonal distance** d is a distance on X which satisfies, for all distinct elements $x_1, \ldots, x_n \in X$, the $2k$**-gonal inequality**

$$\sum_{1 \leq i < j \leq n} b_i b_j d(x_i, x_j) \leq 0$$

  for all $b \in \mathbb{Z}^n$ with $\sum_{i=1}^n b_i = 0$ and $\sum_{i=1}^n |b_i| = 2k$.
- **Distance of negative type**

  A **distance of negative type** d is a distance on X which is $2k$**-gonal** for any $k \geq 1$, i.e., satisfies the **negative type inequality**

$$\sum_{1 \leq i < j \leq n} b_i b_j d(x_i, x_j) \leq 0$$

  for all $b \in \mathbb{Z}^n$ with $\sum_{i=1}^n b_i = 0$, and for all distinct elements $x_1, \ldots, x_n \in X$.

  A distance can be of negative type without being a semimetric. Cayley proved that a metric d is an L_2**-metric** if and only if d^2 is a distance of negative type.
- $(2k + 1)$**-gonal distance**

  A $(2k + 1)$**-gonal distance** d is a distance on X which satisfies, for all distinct elements $x_1, \ldots, x_n \in X$, the $(2k + 1)$**-gonal inequality**

$$\sum_{1 \leq i < j \leq n} b_i b_j d(x_i, x_j) \leq 0$$

  for all $b \in \mathbb{Z}^n$ with $\sum_{i=1}^n b_i = 1$ and $\sum_{i=1}^n |b_i| = 2k + 1$.

  The $(2k + 1)$-gonal inequality with $k = 1$ is the usual triangle inequality. The $(2k + 1)$-gonal inequality implies the $2k$**-gonal inequality**.
- **Hypermetric**

  A **hypermetric** d is a distance on X which is $(2k + 1)$**-gonal** for any $k \geq 1$, i.e., satisfies the **hypermetric inequality** (Deza, 1960)

$$\sum_{1 \leq i < j \leq n} b_i b_j d(x_i, x_j) \leq 0$$

  for all $b \in \mathbb{Z}^n$ with $\sum_{i=1}^n b_i = 1$, and for all distinct elements $x_1, \ldots, x_n \in X$.

Any hypermetric is a semimetric, a **distance of negative type** and, moreover, it can be isometrically embedded into some n-sphere $\mathbb{S}^n$ with squared Euclidean distance. Any L_1*-metric* (cf. L_p**-metric** in Chap. 5) is a hypermetric.

- P**-metric**

  A P**-metric** d is a metric on X with values in $[0, 1]$ which satisfies the **correlation triangle inequality**

$$d(x, y) \leq d(x, z) + d(z, y) - d(x, z)d(z, y).$$

  The equivalent inequality $1-d(x, y) \geq (1-d(x, z))(1-d(z, y))$ expresses that the probability, say, to reach x from y via z is either equal to $(1 - d(x, z))(1 - d(z, y))$ (independence of reaching z from x and y from z), or greater than it (positive correlation). A metric is a P-metric if and only if it is a **Schoenberg transform metric** (Chap. 4).

1.2 Main Distance-Related Notions

- **Metric ball**

  Given a metric space (X, d), the **metric ball** (or *closed metric ball*) with center $x_0 \in X$ and radius $r > 0$ is defined by $\overline{B}(x_0, r) = \{x \in X : d(x_0, x) \leq r\}$, and the **open metric ball** with center $x_0 \in X$ and radius $r > 0$ is defined by $B(x_0, r) = \{x \in X : d(x_0, x) < r\}$. The closed ball is a subset of the closure of the open ball; it is a proper subset for, say, the **discrete metric** on X.

  The **metric sphere** with center $x_0 \in X$ and radius $r > 0$ is defined by $S(x_0, r) = \{x \in X : d(x_0, x) = r\}$.

  For the **norm metric** on an n-dimensional *normed vector space* $(V, ||.||)$, the metric ball $\overline{B}^n = \{x \in V : ||x|| \leq 1\}$ is called the *unit ball*, and the set $S^{n-1} = \{x \in V : ||x|| = 1\}$ is called the *unit sphere*. In a two-dimensional vector space, a metric ball (closed or open) is called a **metric disk** (closed or open, respectively).
- **Metric hull**

  Given a metric space (X, d), let M be a **bounded** subset of X.

  The **metric hull** $H(M)$ of M is the intersection of all metric balls containing M.

  The set of *surface points* $S(M)$ of M is the set of all $x \in H(M)$ such that x lies on the sphere of one of the metric balls containing M.
- **Distance-invariant metric space**

  A metric space (X, d) is **distance-invariant** if all **metric balls** $\overline{B}(x_0, r) = \{x \in X : d(x_0, x) \leq r\}$ of the same radius have the same number of elements.

  Then the **growth rate of a metric space** (X, d) is the function $f(n) = |\overline{B}(x, n)|$.

(X, d) is a *metric space of polynomial growth* if there are some positive constants k, C such that $f(n) \leq Cn^k$ for all $n \geq 0$. Cf. **graph of polynomial growth**, including the group case, in Chap. 15.

For a **metrically discrete metric space** (X, d) (i.e., with $a = \inf_{x,y \in X, x \neq y} d(x, y) > 0$), its *growth rate* was defined also (Gordon–Linial–Rabinovich, 1998) by

$$\max_{x \in X, r \geq 2} \frac{\log |\overline{B}(x, ar)|}{\log r}.$$

- **Ahlfors q-regular metric space**

  A metric space (X, d) endowed with a Borel measure μ is called **Ahlfors q-regular** if there exists a constant $C \geq 1$ such that for every ball in (X, d) with radius $r < diam(X, d)$ it holds

$$C^{-1} r^q \leq \mu(\overline{B}(x_0, r)) \leq Cr^q.$$

  If such an (X, d) is locally compact, then the **Hausdorff q-measure** can be taken as μ and q is the **Hausdorff dimension**. For two disjoint **continua** (nonempty **connected compact metric subspaces**) C_1, C_2 of such space (X, d), let Γ be the set of rectifiable curves connecting C_1 to C_2. The *q-modulus* between C_1 and C_2 is $M_q(C_1, C_2) = \inf\{\int_X \rho^q : \inf_{\gamma \in \Gamma} \int_\gamma \rho \geq 1\}$, where $\rho : X \to \mathbb{R}_{>0}$ is any density function on X; cf. the **modulus metric** in Chap. 6.

  The *relative distance* between C_1 and C_2 is $\delta(C_1, C_2) = \frac{\inf\{d(p_1,p_2):p_1 \in C_1, p_2 \in C_2\}}{\min\{diam(C_1), diam(C_2)\}}$. (X, d) is a **q-Loewner space** if there are increasing functions $f, g : [0, \infty) \to [0, \infty)$ such that for all C_1, C_2 it holds $f(\delta(C_1, C_2)) \leq M_q(C_1, C_2) \leq g(\delta(C_1, C_2))$.

- **Connected metric space**

  A metric space (X, d) is called **connected** if it cannot be partitioned into two nonempty **open** sets. Cf. **connected space** in Chap. 2.

  The maximal connected subspaces of a metric space are called its *connected components*. A **totally disconnected metric space** is a space in which all connected subsets are $\emptyset$ and one-point sets.

  A **path-connected metric space** is a connected metric space such that any two its points can be joined by an **arc** (cf. **metric curve**).

- **Cantor connected metric space**

  A metric space (X, d) is called **Cantor** (or *pre-*) *connected* if, for any two its points x, y and any $\epsilon > 0$, there exists an *ϵ-chain* joining them, i.e., a sequence of points $x = z_0, z_1, \ldots, z_{n-1}, z_n = y$ such that $d(z_k, z_{k+1}) \leq \epsilon$ for every $0 \leq k \leq n$. A metric space (X, d) is Cantor connected if and only if it cannot be partitioned into two *remote parts* A and B, i.e., such that $\inf\{d(x, y) : x \in A, y \in B\} > 0$.

  The maximal Cantor connected subspaces of a metric space are called its *Cantor connected components*. A **totally Cantor disconnected metric** is the metric of a metric space in which all Cantor connected components are one-point sets.

- **Indivisible metric space**

  A metric space (X, d) is called **indivisible** if it cannot be partitioned into two parts, neither of which contains an isometric copy of (X, d). Any indivisible metric space with $|X| \geq 2$ is infinite, bounded and **totally Cantor disconnected** (Delhomme–Laflamme–Pouzet–Sauer, 2007).

  A metric space (X, d) is called an **oscillation stable metric space** (Nguyen Van Thé, 2006) if, given any $\epsilon > 0$ and any partition of X into finitely many pieces, the **ϵ-neighborhood** of one of the pieces includes an isometric copy of (X, d).
- **Closed subset of metric space**

  Given a subset M of a metric space (X, d), a point $x \in X$ is called a *limit* (or *accumulation*) *point of* M if any **open metric ball** $B(x, r) = \{y \in X : d(x, y) < r\}$ contains a point $x' \in M$ with $x' \neq x$. The *boundary* $\vartheta(M)$ of M is the set of all its limit points. The *closure of* M, denoted by $cl(M)$, is $M \cup \vartheta(M)$, and M is called **closed subset**, if $M = cl(M)$, and **dense subset**, if $X = cl(M)$.

  Every point of M which is not its limit point, is called an *isolated point*. The *interior* $int(M)$ of M is the set of all its isolated points, and the *exterior* $ext(M)$ of M is $int(X \backslash M)$. A subset M is called *nowhere dense* if $int(cl(M)) = \emptyset$.

  A subset M is called *topologically discrete* (cf. **metrically discrete metric space**) if $int(M) = M$ and *dense-in-itself* if $int(M) = \emptyset$. A dense-in-itself subset is called *perfect* (cf. **perfect metric space**) if it is closed. The subsets *Irr* (irrational numbers) and $\mathbb{Q}$ (rational numbers) of $\mathbb{R}$ are dense, dense-in-itself but not perfect. The set $\mathbb{Q} \cap [0, 1]$ is dense-in-itself but not dense in $\mathbb{R}$.
- **Open subset of metric space**

  A subset M of a metric space (X, d) is called *open* if, given any point $x \in M$, the **open metric ball** $B(x, r) = \{y \in X : d(x, y) < r\}$ is contained in M for some number $r > 0$. The family of open subsets of a metric space forms a natural topology on it. A **closed subset** is the complement of an open subset.

  An open subset is called *clopen*, if it is closed, and a *domain* if it is **connected**.

  A *door space* is a metric (in general, topological) space in which every subset is either open or closed.
- **Metric topology**

  A **metric topology** is a *topology* induced by a metric; cf. **equivalent metrics**. More exactly, the **metric topology** on a metric space (X, d) is the set of all *open sets* of X, i.e., arbitrary unions of (finitely or infinitely many) open metric balls $B(x, r) = \{y \in X : d(x, y) < r\}$, $x \in X$, $r \in \mathbb{R}$, $r > 0$.

  A topological space which can arise in this way from a metric space is called a **metrizable space** (Chap. 2). **Metrization theorems** are theorems which give sufficient conditions for a topological space to be metrizable.

  On the other hand, the adjective *metric* in several important mathematical terms indicates connection to a measure, rather than distance, for example, *metric Number Theory*, *metric Theory of Functions*, *metric transitivity*.
- **Equivalent metrics**

  Two metrics d_1 and d_2 on a set X are called **equivalent** if they define the same *topology* on X, i.e., if, for every point $x_0 \in X$, every open metric ball with center

at x_0 defined with respect to d_1, contains an open metric ball with the same center but defined with respect to d_2, and conversely.

Two metrics d_1 and d_2 are equivalent if and only if, for every $\epsilon > 0$ and every $x \in X$, there exists $\delta > 0$ such that $d_1(x, y) \leq \delta$ implies $d_2(x, y) \leq \epsilon$ and, conversely, $d_2(x, y) \leq \delta$ implies $d_1(x, y) \leq \epsilon$.

All metrics on a finite set are equivalent; they generate the *discrete topology*.

- **Metric betweenness**

  The **metric betweenness** of a metric space (X, d) is (Menger, 1928) the set of all ordered triples (x, y, z) such that x, y, z are (not necessarily distinct) points of X for which the **triangle equality** $d(x, y) + d(y, z) = d(x, z)$ holds.
- **Monometric**

  A ternary relation R on a set X is called a *betweenness relation* if $(x, y, z) \in R$ if and only if $(z, y, x) \in R$ and $(x, y, z), (x, z, y) \in R$ if and only if $y = z$.

  Given a such relation R, a **monometric** is (Perez-Fernández et al., 2016) a function $d : X \times X \to \mathbb{R}_{\geq 0}$ with $d(x, y) = 0$ if and only if $x = y$ and (x, y, z) implying $d(x, y) \leq d(x, z)$. Clearly, any metric is a monometric.

  Cf. a **distance-rationalizable voting rule** in Sect. 11.2.
- **Closed metric interval**

  Given two different points $x, y \in X$ of a metric space (X, d), the **closed metric interval** between them (or *line induced by*) them is the set of the points z, for which the **triangle equality** (or **metric betweenness** (x, z, y)) holds:

$$I(x, y) = \{z \in X : d(x, y) = d(x, z) + d(z, y)\}.$$

  Cf. **inner product space** (Chap. 5) and **cutpoint additive metric** (Chap. 15).

  Let $Ext(x, y) = \{z : y \in I(x, z) \setminus \{x, z\}\}$. A *CC-line* $CC(x, y)$ is $I(x, y) \cup Ext(x, y) \cup Ext(y, x)$. Chen–Chvátal, 2008, conjectured that every metric space on $n, n \geq 2$, points, either has at least n distinct CC-lines or consists of a unique CC-line.
- **Underlying graph of a metric space**

  The **underlying graph** (or *neighborhood graph*) of a metric space (X, d) is a graph with the vertex-set X and xy being an edge if $I(x, y) = \{x, y\}$, i.e., there is no third point $z \in X$, for which $d(x, y) = d(x, z) + d(z, y)$.
- **Distance monotone metric space**

  A metric space (X, d) is called **distance monotone** if for any its **closed metric interval** $I(x, y)$ and $u \in X \setminus I(x, y)$, there exists $z \in I(x, xy)$ with $d(u, z) > d(x, y)$.
- **Metric triangle**

  Three distinct points $x, y, z \in X$ of a metric space (X, d) form a **metric triangle** if the **closed metric intervals** $I(x, y), I(y, z)$ and $I(z, x)$ intersect only in the common endpoints.
- **Metric space having collinearity**

  A metric space (X, d) has **collinearity** if for any $\epsilon > 0$ each of its infinite subsets contains distinct ϵ-*collinear* (i.e., with $d(x, y) + d(y, z) - d(x, z) \leq \epsilon$) points x, y, z.

- **Modular metric space**

  A metric space (X, d) is called **modular** if, for any three different points $x, y, z \in X$, there exists a point $u \in I(x, y) \cap I(y, z) \cap I(z, x)$. This should not be confused with **modular distance** in Chap. 10 and **modulus metric** in Chap. 6.
- **Median metric space**

  A metric space (X, d) is called a **median metric space** if, for any three points $x, y, z \in X$, there exists a unique point $u \in I(x, y) \cap I(y, z) \cap I(z, x)$, or, equivalently,

$$d(x, u) + d(y, u) + d(z, u) = \frac{1}{2}((x, y) + d(y, z) + d(z, x)).$$

  The point u is called *median for* $\{x, y, z\}$, since it minimises the sum of distances to them. Any median metric space is an L_1*-metric*; cf. L_p**-metric** in Chap. 5 and **median graph** in Chap. 15.

  A metric space (X, d) is called an **antimedian metric space** if, for any three points $x, y, z \in X$, there exists a unique point $u \in X$ maximizing $d(x, u)+d(y, u)+d(z, u)$.
- **Metric quadrangle**

  Four different points $x, y, z, u \in X$ of a metric space (X, d) form a **metric quadrangle** if $x, z \in I(y, u)$ and $y, u \in I(x, z)$; then $d(x, y) = d(z, u)$ and $d(x, u) = d(y, z)$.

  A metric space (X, d) is called *weakly spherical* if any three different points $x, y, z \in X$ with $y \in I(x, z)$, form a metric quadrangle with some point $u \in X$.
- **Metric curve**

  A **metric curve** (or, simply, *curve*) γ in a metric space (X, d) is a continuous mapping $\gamma : I \to X$ from an interval I of $\mathbb{R}$ into X. A curve is called an **arc** (or **path**, *simple curve*) if it is injective. A curve $\gamma : [a, b] \to X$ is called a *Jordan curve* (or *simple closed curve*) if it does not cross itself, and $\gamma(a) = \gamma(b)$.

  The **length of a curve** $\gamma : [a, b] \to X$ is the number $l(\gamma)$ defined by

$$l(\gamma) = \sup\{\sum_{1 \le i \le n} d(\gamma(t_i), \gamma(t_{i-1})) : n \in \mathbb{N}, a = t_0 < t_1 < \cdots < t_n = b\}.$$

  A *rectifiable curve* is a curve with a finite length. A metric space (X, d), where every two points can be joined by a rectifiable curve, is called a **quasi-convex metric space** (or, specifically, C**-quasi-convex metric space**) if there exists a constant $C \ge 1$ such that every pair $x, y \in X$ can be joined by a rectifiable curve of length at most $Cd(x, y)$. If $C = 1$, then this length is equal to $d(x, y)$, i.e., (X, d) is a **geodesic metric space** (Chap. 6).

  In a quasi-convex metric space (X, d), the infimum of the lengths of all rectifiable curves, connecting $x, y \in X$ is called the **internal metric**.

  The metric d on X is called the **intrinsic metric** (and then (X, d) is called a **length space**) if it coincides with the internal metric of (X, d).

  If, moreover, any pair x, y of points can be joined by a curve of length $d(x, y)$, the metric d is called **strictly intrinsic**, and the length space (X, d) is a geodesic

metric space. Hopf–Rinow, 1931, showed that any complete locally compact length space is geodesic and **proper**. The **punctured plane** $(\mathbb{R}^2 \setminus \{0\}, ||x-y||_2)$ is **locally compact** and **path-connected** but not geodesic: the distance between $(-1,0)$ and $(1,0)$ is 2 but there is no geodesic realizing this distance.

The **metric derivative** of a metric curve $\gamma : [a,b] \to X$ at a limit point t is

$$\lim_{s\to 0} \frac{d(\gamma(t+s),\gamma(t))}{|s|},$$

if it exists. It is the rate of change, with respect to t, of the length of the curve at almost every point, i.e., a generalization of the notion of *speed* to metric spaces.

- **Geodesic**

  Given a metric space (X,d), a **geodesic** is a locally shortest **metric curve**, i.e., it is a locally isometric embedding of $\mathbb{R}$ into X; cf. Chap. 6.

  A subset S of X is called a **geodesic segment** (or **metric segment**, *shortest* path, *minimizing geodesic*) between two distinct points x and y in X, if there exists a *segment* (closed interval) [a,b] on the real line $\mathbb{R}$ and an isometric embedding $\gamma : [a,b] \to X$, such that $\gamma[a,b] = S$, $\gamma(a) = x$ and $\gamma(b) = y$.

  A **metric straight line** is a geodesic which is minimal between any two of its points; it is an isometric embedding of the whole of $\mathbb{R}$ into X. A **metric ray** and **metric great circle** are isometric embeddings of, respectively, the half-line $\mathbb{R}_{\geq 0}$ and a circle $S^1(0,r)$ into X.

  A **geodesic metric space** (Chap. 6) is a metric space in which any two points are joined by a geodesic segment. If, moreover, the geodesic is unique, the space is called *totally geodesic* (or *uniquely geodesic*).

  A geodesic metric space (X,d) is called *geodesically complete* if every geodesic is a subarc of a metric straight line. If (X,d) is **complete**, then it is geodesically complete. The **punctured plane** $(\mathbb{R}^2 \setminus \{0\}, ||x-y||_2)$ is not geodesically complete: any geodesic going to 0 is not a subarc of a metric straight line.

- **Length spectrum**

  Given a metric space (X,d), a *closed geodesic* is a map $\gamma : \mathbb{S}^1 \to X$ which is locally minimizing around every point of $\mathbb{S}^1$.

  If (X,d) is a compact **length space**, its **length spectrum** is the collection of lengths of closed geodesics. Each length is counted with *multiplicity* equal to the number of distinct *free homotopy* classes that contain a closed geodesic of such length. The **minimal length spectrum** is the set of lengths of closed geodesics which are the shortest in their free homotopy class. Cf. the **distance list**.

- **Systole of metric space**

  Given a compact metric space (X,d), its **systole** $sys(X,d)$ is the length of the shortest noncontractible loop in X; such a loop is a closed geodesic. So, $sys(X,d) = 0$ exactly if (X,d) is **simply connected**. Cf. **connected space** in Chap. 2.

  If (X,d) is a graph with path metric, then its systole is referred to as the *girth*. If (X,d) is a closed surface, then its *systolic ratio* is the ratio $SR = \frac{sys^2(X,d)}{area(X,d)}$.

Some tight upper bounds of SR for every metric on a surface are: $\frac{2}{\sqrt{3}} = \gamma_2$ (*Hermite constant* in 2D) for 2-torus (Loewner, 1949), $\frac{\pi}{2}$ for the real projective plane (Pu, 1952) and $\frac{\pi}{\sqrt{8}}$ for the Klein bottle (Bavard, 1986). Tight asymptotic bounds for a surface S of large genus g are $\frac{4}{9} \cdot \frac{\log^2 g}{\pi g} \leq SR(S) \leq \frac{\log^2 g}{\pi g}$ (Katz et al., 2007).

- **Shankar–Sormani radii**

  Given a **geodesic metric space** (X, d), Shankar and Sormani, 2009, defined its **unique injectivity radius** $Uirad(X)$ as the supremum over all $r \geq 0$ such that any two points at distance at most r are joined by a unique geodesic, and its **minimal radius** $Mrad(X)$ as $\inf_{p \in X} d(p, MinCut(p))$.

  Here the *minimal cut locus of p* $MinCut(p)$ is the set of points $q \in X$ for which there is a geodesic γ running from p to q such that γ extends past q but is not minimizing from p to any point past q. If (X, d) is a Riemannian space, then the distance function from p is a smooth function except at p itself and the cut locus. Cf. **medial axis and skeleton** in Chap. 21.

  It holds $Uirad(X) \leq Mrad(X)$ with equality if (X, d) is a Riemannian space in which case it is the **injectivity radius**. It holds $Uirad(X) = \infty$ for a flat disk but $Mrad(X) < \infty$ if (X, d) is compact and at least one geodesic is extendible.

- **Geodesic convexity**

  Given a **geodesic metric space** (X, d) and a subset $M \subset X$, the set M is called **geodesically convex** (or *convex*) if, for any two points of M, there exists a geodesic segment connecting them which lies entirely in M; the space is **strongly convex** if such a segment is unique and no other geodesic connecting those points lies entirely in M. The space is called **locally convex** if such a segment exists for any two sufficiently close points in M.

  For a given point $x \in M$, the **radius of convexity** is $r_x = \sup\{r \geq 0 : B(x, r) \subset M\}$, where the **metric ball** $B(x, r)$ is convex. The point x is called the *center of mass* of points $y_1, \ldots, y_k \in M$ if it minimizes the function $\sum_i d(x, y_i)^2$ (cf. **Fréchet mean**); such point is unique if $d(y_i, y_j) < r_x$ for all $1 \leq i < j \leq k$.

  The **injectivity radius** of the set M is the supremum over all $r \geq 0$ such that any two points in M at distance $\leq r$ are joined by unique geodesic segment which lies in M. The **Hawaiian Earring** is a compact complete metric space consisting of a set of circles of radius $\frac{1}{i}$ for each $i \in \mathbb{N}$ all joined at a common point; its injectivity radius is 0. It is **path-connected** but not **simply connected**.

  The set $M \subset X$ is called a **totally convex metric subspace** of (X, d) if, for any two points of M, any geodesic segment connecting them lies entirely in M.

- **Busemann convexity**

  A **geodesic metric space** (X, d) is called **Busemann convex** (or *Busemann space*, *nonpositively curved in the sense of Busemann*) if, for any three points $x, y, z \in X$ and *midpoints* $m(x, z)$ and $m(y, z)$ (i.e., $d(x, m(x, z)) = d(m(x, z), z) = \frac{1}{2}d(x, z)$ and $d(y, m(y, z)) = d(m(y, z), z) = \frac{1}{2}d(y, z)$), there holds

$$d(m(x, z), m(y, z)) \leq \frac{1}{2}d(x, y).$$

The *flat Euclidean strip* $\{(x, y) \in \mathbb{R}^2 : 0 < x < 1\}$ is **Gromov hyperbolic metric space** (Chap. 6) but not Busemann convex one. In a complete Busemann convex metric space any two points are joined by a unique geodesic segment.

A locally geodesic metric space (X, d) is called **Busemann locally convex** if the above inequality holds locally. Any **locally CAT(0)** metric space is Busemann locally convex.

- **Menger convexity**

  A metric space (X, d) is called **Menger convex** if, for any different points $x, y \in X$, there exists a third point $z \in X$ for which $d(x, y) = d(x, z) + d(z, y)$, i.e., $|I(x, y)| > 2$ holds for the **closed metric interval** $I(x, y) = \{z \in X : (x, y) = d(x, z) + d(z, y)\}$. It is called **strictly Menger convex** if such a z is unique for all $x, y \in X$.

  Geodesic convexity implies Menger convexity. The converse holds for **complete** metric spaces.

  A subset $M \subset X$ is called (Menger, 1928) a *d-convex set* (or *interval-convex set*) if $I(x, y) \subset M$ for any different points $x, y \in M$. A function $f : M \to \mathbb{R}$ defined on a d-convex set $M \subset X$ is a **d-convex function** if for any $z \in I(x, y) \subset M$

$$f(z) \leq \frac{d(y, z)}{d(x, y)} f(x) + \frac{d(x, z)}{d(x, y)} f(y).$$

  A subset $M \subset X$ is a *gated set* if for every $x \in X$ there exists a unique $x' \in M$, the *gate*, such that $d(x, y) = d(x, x') + d(x', y)$ for $y \in M$. Any such set is d-convex.

- **Midpoint convexity**

  A metric space (X, d) is called **midpoint convex** (or **having midpoints**, *admitting a midpoint map*) if, for any different points $x, y \in X$, there exists a third point $m(x, y) \in X$ for which $d(x, m(x, y)) = d(m(x, y), y) = \frac{1}{2} d(x, y)$. Such a point $m(x, y)$ is called a *midpoint* and the map $m : X \times X \to X$ is called a *midpoint map* (cf. **midset**); this map is unique if $m(x, y)$ is unique for all $x, y \in X$.

  For example, the geometric mean $\sqrt{xy}$ is the midpoint map for the metric space $(\mathbb{R}_{>0}, d(x, y) = |\log x - \log y|)$.

  A **complete** metric space is **geodesic** if and only if it is midpoint convex.

  A metric space (X, d) is said to have **approximate midpoints** if, for any points $x, y \in X$ and any $\epsilon > 0$, there exists an *ϵ-midpoint*, i.e., a point $z \in X$ such that $d(x, z) \leq \frac{1}{2} d(x, y) + \epsilon \geq d(z, y)$.

- **Ball convexity**

  A **midpoint convex** metric space (X, d) is called **ball convex** if

$$d(m(x, y), z) \leq \max\{d(x, z), d(y, z)\}$$

  for all $x, y, z \in X$ and any midpoint map $m(x, y)$.

Ball convexity implies that all metric balls are **totally convex** and, in the case of a **geodesic** metric space, vice versa. Ball convexity implies also the uniqueness of a midpoint map (geodesics in the case of **complete** metric space).

The metric space $(\mathbb{R}^2, d(x,y) = \sum_{i=1}^{2} \sqrt{|x_i - y_i|})$ is not ball convex.

- **Distance convexity**

  A **midpoint convex** metric space (X,d) is called **distance convex** if

$$d(m(x,y),z) \leq \frac{1}{2}(d(x,z) + d(y,z)).$$

  A **geodesic metric space** is distance convex if and only if the restriction of the distance function $d(x,\cdot)$, $x \in X$, to every geodesic segment is a convex function.

  Distance convexity implies **ball convexity** and, in the case of **Busemann convex** metric space, vice versa.

- **Metric convexity**

  A metric space (X,d) is called **metrically convex** if, for any different points $x, y \in X$ and any $\lambda \in (0,1)$, there exists a third point $z = z(x,y,\lambda) \in X$ for which $d(x,y) = d(x,z) + d(z,y)$ and $d(x,z) = \lambda d(x,y)$.

  The space is called **strictly metrically convex** if such a point $z(x,y,\lambda)$ is unique for all $x, y \in X$ and any $\lambda \in (0,1)$.

  A metric space (X,d) is called **strongly metrically convex** if, for any different points $x, y \in X$ and any $\lambda_1, \lambda_2 \in (0,1)$, there exists a third point $z = z(x,y,\lambda) \in X$ for which $d(z(x,y,\lambda_1), z(x,y,\lambda_2)) = |\lambda_1 - \lambda_2| d(x,y)$.

  Metric convexity implies **Menger convexity**, and every Menger convex **complete** metric space is strongly metrically convex.

  A metric space (X,d) is called **nearly convex** (Mandelkern, 1983) if, for any different points $x, y \in X$ and any $\lambda, \mu > 0$ such that $d(x,y) < \lambda + \mu$, there exists a third point $z \in X$ for which $d(x,z) < \lambda$ and $d(z,y) < \mu$, i.e., $z \in B(x,\lambda) \cap B(y,\mu)$. Metric convexity implies near convexity.

- **Takahashi convexity**

  A metric space (X,d) is called **Takahashi convex** if, for any different points $x, y \in X$ and any $\lambda \in (0,1)$, there exists a third point $z = z(x,y,\lambda) \in X$ such that $d(z(x,y,\lambda), u) \leq \lambda d(x,u) + (1-\lambda) d(y,u)$ for all $u \in X$. Any convex subset of a normed space is a Takahashi convex metric space with $z(x,y,\lambda) = \lambda x + (1-\lambda) y$.

  A set $M \subset X$ is *Takahashi convex* if $z(x,y,\lambda) \in M$ for all $x, y \in X$ and any $\lambda \in [0,1]$. In a Takahashi convex metric space, all metric balls, open metric balls, and arbitrary intersections of Takahashi convex subsets are all Takahashi convex.

- **Hyperconvexity**

  A metric space (X,d) is called **hyperconvex** (Aronszajn–Panitchpakdi, 1956) if it is **metrically convex** and its metric balls have the *infinite Helly property*, i.e., any family of mutually intersecting closed balls in X has nonempty intersection. A metric space (X,d) is hyperconvex if and only if it is an **injective metric space**.

  The spaces l_∞^m, l_∞^∞ and l_1^2 are hyperconvex but l_2^∞ is not.

- **Distance matrix**

  Given a finite metric space $(X = \{x_1, \cdots, x_n\}, d)$, its **distance matrix** is the symmetric $n \times n$ matrix $((d_{ij}))$, where $d_{ij} = d(x_i, x_j)$ for any $1 \leq i, j \leq n$.

The probability that a symmetric $n \times n$ matrix, whose diagonal elements are zeros and all other elements are uniformly random real numbers, is a distance matrix is (Mascioni, 2005) $\frac{1}{2}$, $\frac{17}{120}$ for $n = 3, 4$, respectively.

- **Magnitude of a finite metric space**

  Let $(X = \{x_1, \dots, x_n\}, d)$ be a finite metric space, such that there exists a vector $w = \{w_1, \dots, w_n\}$ with $((e^{-d(x_i,x_j)}))w = (1, \dots, 1)^T$.

  Then the **magnitude** of (X, d) is (Leinster–Meckes, 2016) the sum $\sum_{i=1}^{n} w_i$. In fact, the definition of *Euler characteristic of a category* was generalized to *enriched categories*, renamed *magnitude*, then re-specialized to metric spaces.

- **Distance product of matrices**

  Given $n \times n$ matrices $A = ((a_{ij}))$ and $B = ((b_{ij}))$, their **distance** (or *min-plus*) **product** is the $n \times n$ matrix $C = ((c_{ij}))$ with $c_{ij} = \min_{k=1}^{n}(a_{ik} + b_{kj})$.

  It is the usual matrix multiplication in the *tropical semiring* $(\mathbb{R} \cup \{\infty\}, \min, +)$ (Chap. 18). If A is the matrix of weights of an edge-weighted complete graph K_n, then its *direct power* A^n is the (shortest path) **distance matrix** of this graph.

- **Distance list**

  Given a metric space (X, d), its **distance set** and **distance list** are the set and the *multiset* (i.e., multiplicities are counted) and of all pairwise distances.

  Two subsets $A, B \subset X$ are said to be *homometric sets* if they have the same distance list. Cf. **homometric structures** in Chap. 24.

  A finite metric space is called *tie-breaking* if all pairwise distances are distinct.

- **Degree of distance near-equality**

  Given a finite metric space (X, d) with $|X| = n \geq 3$, let $f = \min |\frac{d(x,y)}{d(a,b)} - 1|$ (**degree of distance near-equality**) and $f' = \min |\frac{d(x,y)}{d(x,b)} - 1|$, where the minimum is over different 2-subsets $\{x, y\}, \{a, b\}$ of X and, respectively, over different $x, y, b \in X$. [OpPi14] proved $f \leq \frac{9 \log n}{n^2}$ and $f' \leq \frac{3}{n}$, while $f \geq \frac{\log n}{20n^2}$ and $f' \geq \frac{1}{2n}$ for some (X, d).

- **Semimetric cone**

  The **semimetric cone** MET_n is the polyhedral cone in $\mathbb{R}^{\binom{n}{2}}$ of all **distance matrices** of semimetrics on the set $V_n = \{1, \dots, n\}$. Vershik, 2004, considers MET_∞, i.e., the weakly closed convex cone of infinite distance matrices of semimetrics on $\mathbb{N}$.

  The cone of n-point **weightable quasi-semimetrics** is a projection along an extreme ray of the semimetric cone Met_{n+1} (Grishukhin–Deza–Deza, 2011).

  The **metric fan** is a canonical decomposition MF_n of MET_n into subcones whose faces belong to the fan, and the intersection of any two of them is their common boundary. Two semimetrics $d, d' \in MET_n$ lie in the same cone of the metric fan if the subdivisions $\delta_d, \delta_{d'}$ of the polyhedron $\delta(n, 2) = conv\{e_i + e_j : 1 \leq i < j \leq n\} \subset \mathbb{R}^n$ are equal. Here a subpolytope P of $\delta(n, 2)$ is a cell of the subdivision δ_d if there exists $y \in \mathbb{R}^n$ satisfying $y_i + y_j = d_{ij}$ if $e_i + e_j$ is a vertex of P, and $y_i + y_j > d_{ij}$, otherwise. The complex of bounded faces of the polyhedron dual to δ_d is the **tight span** of the semimetric d.

- **Cayley–Menger matrix**

  Given a finite metric space $(X = \{x_1, \cdots, x_n\}, d)$, its **Cayley–Menger matrix** is the symmetric $(n+1) \times (n+1)$ matrix

$$CM(X,d) = \begin{pmatrix} 0 & e \\ e^T & D \end{pmatrix},$$

  where $D = ((d^2(x_i, x_j)))$ and e is the n-vector all components of which are 1.

  The determinant of $CM(X,d)$ is called the *Cayley–Menger determinant*. If (X,d) is a metric subspace of the Euclidean space $\mathbb{E}^{n-1}$, then $CM(X,d)$ is $(-1)^n 2^{n-1}((n-1)!)^2$ times the squared $(n-1)$*-dimensional volume* of the convex hull of X in $\mathbb{R}^{n-1}$.
- **Gram matrix**

  Given elements $v_1, \ldots, v_k$ of a Euclidean space, their **Gram matrix** is the symmetric $k \times k$ matrix VV^T, where $V = ((v_{ij}))$, of pairwise *inner products* of $v_1, \ldots, v_k$:

$$G(v_1, \ldots, v_k) = ((\langle v_i, v_j \rangle)).$$

  It holds $G(v_1, \ldots, v_k) = \frac{1}{2}((d_E^2(v_0, v_i) + d_E^2(v_0, v_j) - d_E^2(v_i, v_j)))$, i.e., the inner product $\langle \cdot, \cdot \rangle$ is the **Gromov product similarity** of the **squared Euclidean distance** d_E^2. A $k \times k$ matrix $((d_E^2(v_i, v_j)))$ is called *Euclidean distance matrix* (or *EDM*). It defines a **distance of negative type** on $\{1, \ldots, k\}$; all such matrices form the (nonpolyhedral) closed convex cone of all such distances.

  The determinant of a Gram matrix is called the *Gram determinant*; it is equal to the square of the *k-dimensional volume* of the *parallelotope* constructed on $v_1, \ldots v_k$.

  A symmetric $k \times k$ real matrix M is said to be *positive-semidefinite* (PSD) if $xMx^T \geq 0$ for any nonzero $x \in \mathbb{R}^k$ and *positive-definite* (PD) if $xMx^T > 0$. A matrix is PSD if and only if it is a Gram matrix; it is PD if and only the vectors $v_1, \ldots, v_k$ are linearly independent. In Statistics, the *covariance matrices* and *correlation matrices* are exactly PSD and PD ones, respectively.
- **Midset**

  Given a metric space (X,d) and distinct $y, z \in X$, the **midset** (or *bisector*) of points y and z is the set $M = \{x \in X : d(x,y) = d(x,z)\}$ of *midpoints* x.

  A metric space is said to have the *n-point midset property* if, for every pair of its points, the midset has exactly n points. The one-point midset property means uniqueness of the *midpoint map*. Cf. **midpoint convexity**.
- **Distance k-sector**

  Given a metric space (X,d) and disjoint subsets $Y, Z \subset X$, the *bisector* of Y and Z is the set $M = \{x \in X : \inf_{y \in Y} d(x,y) = \inf_{z \in Z} d(x,z)\}$.

  The **distance k-sector** of Y and Z is the sequence $M_1, \ldots, M_{k-1}$ of subsets of X such that M_i, for any $1 \leq i \leq k-1$, is the bisector of sets M_{i-1} and M_{i+1}, where $Y = M_0$ and $Z = M_k$. Asano–Matousek–Tokuyama, 2006, considered the distance k-sector on the Euclidean plane $(\mathbb{R}^2, l_2)$; for compact sets Y and Z, the sets $M_1, \ldots, M_{k-1}$ are curves partitioning the plane into k parts.

- **Metric basis**

  Given a metric space (X, d) and a subset $M \subset X$, for any point $x \in X$, its *metric M-representation* is the set $\{(m, d(x, m)) : m \in M\}$ of its *metric M-coordinates* $(m, d(x, m))$. The set M is called (Blumenthal, 1953) a **metric basis** (or *resolving set*, *locating set*, *set of uniqueness*, *set of landmarks*) if distinct points $x \in X$ have distinct M-representations. A vertex-subset M of a connected graph is (Okamoto et al., 2009) a *local metric basis* if adjacent vertices have distinct M-representations.

  The *resolving number* of a finite (X, d) is (Chartrand–Poisson–Zhang, 2000) minimum k such that any k-subset of X is a metric basis.

  The vertices of a non degenerate simplex form a metric basis of $\mathbb{E}^n$, but l_1- and l_∞-metrics on $\mathbb{R}^n$, $n > 1$, have no finite metric basis.

  The **distance similarity** is (Saenpholphat–Zhang, 2003) an equivalence relation on X defined by $x \sim y$ if $d(z, x) = d(z, y)$ for any $z \in X \setminus \{x, y\}$. Any metric basis contains all or all but one elements from each equivalence class.

1.3 Metric Numerical Invariants

- **Resolving dimension**

  Given a metric space (X, d), its **resolving dimension** (or **location number** (Slater, 1975), *metric dimension* (Harary–Melter, 1976)) is the minimum cardinality of its **metric basis**. The **upper resolving dimension** of (X, d) is the maximum cardinality of its metric basis not containing another metric basis as a proper subset. *Adjacency dimension* of (X, d) is the metric dimension of $(X, \min(2, d))$.

  A **metric independence number** of (X, d) is (Currie–Oellermann, 2001) the maximum cardinality I of a collection of pairs of points of X, such that for any two, (say, (x, y) and (x', y')) of them there is no point $z \in X$ with $d(z, x) \neq d(z, y)$ and $d(z, x') \neq d(z, y')$. A function $f : X \to [0, 1]$ is a *resolving function* of (X, d) if $\sum_{z \in X : d(x,z) \neq d(y,z)} f(z) \geq 1$ for any distinct $x, y \in X$. The *fractional resolving dimension* of (X, d) is $F = \min \sum_{x \in X} g(x)$, where the minimum is taken over resolving functions f such that any function f' with f', f is not resolving.

  The *partition dimension* of (X, d) is (Chartrand–Salevi–Zhang, 1998) the minimum cardinality P of its *resolving partition*, i.e., a partition $X = \cup_{1 \leq i \leq k} S_i$ such that no two points have, for $1 \leq i \leq k$, the same minimal distances to the set S_i.

  Related *locating a robber* game on a graph $G = (V, E)$ was considered in 2012 by Seager and by Carraher et al.: *cop win* on G if every sequence $r = r_1, \ldots, r_n$ of robber's steps ($r_i \in V$ and $d_{\text{path}}(r_i, r_{i+1}) \leq 1$) is uniquely identified by a sequence $d(r_1, c_1), \ldots, d(r_n, c_n)$ of cop's distance queries for some $c_1, \ldots, c_n \in V$.

- **Metric dimension**

  For a metric space (X, d) and a number $\epsilon > 0$, let C_ϵ be the minimal size of an ϵ-**net** of (X, d), i.e., a subset $M \subset X$ with $\cup_{x \in M} B(x, \epsilon) = X$. The number

$$dim(X, d) = \lim_{\epsilon \to 0} \frac{\ln C_\epsilon}{-\ln \epsilon}$$

  (if it exists) is called the **metric dimension** (or **Minkowski–Bouligand dimension**, **box-counting dimension**) of X. If the limit above does not exist, then the following notions of dimension are considered:

  1. $\underline{dim}(X, d) = \underline{\lim}_{\epsilon \to 0} \frac{\ln C_\epsilon}{-\ln \epsilon}$ called the **lower Minkowski dimension** (or *lower dimension*, *lower box dimension*, *Pontryagin–Snirelman dimension*);
  2. $\overline{dim}(X, d) = \overline{\lim}_{\epsilon \to 0} \frac{\ln C_\epsilon}{-\ln \epsilon}$ called the **Kolmogorov–Tikhomirov dimension** (or *upper dimension*, *entropy dimension*, *upper box dimension*).

  See below examples of other, less prominent, notions of *metric dimension*.

  1. The (equilateral) *metric dimension* of a metric space is the maximum cardinality of its *equidistant* subset, i.e., such that any two of its distinct points are at the same distance. For a normed space, this dimension is equal to the maximum number of translates of its unit ball that touch pairwise.
  2. For any $c > 1$, the (normed space) *metric dimension* $dim_c(X)$ of a finite metric space (X, d) is the least dimension of a real *normed space* $(V, ||.||)$ such that there is an embedding $f : X \to V$ with $\frac{1}{c} d(x, y) \leq ||f(x) - f(y)|| \leq d(x, y)$.
  3. The (Euclidean) *metric dimension* of a finite metric space (X, d) is the least dimension n of a Euclidean space $\mathbb{E}^n$ such that $(X, f(d))$ is its metric subspace, where the minimum is taken over all continuous monotone increasing functions $f(t)$ of $t \geq 0$.
  4. The *dimensionality* of a metric space is $\frac{\mu^2}{2\sigma^2}$, where μ and σ^2 are the mean and variance of its histogram of distance values; this notion is used in Information Retrieval for proximity searching.

     The term *dimensionality* is also used for the minimal dimension, if it is finite, of Euclidean space in which a given metric space embeds isometrically.

- **Hausdorff dimension**

  Given a metric space (X, d) and $p, q > 0$, let $H_p^q = \inf \sum_{i=1}^{\infty} (diam(A_i))^p$, where the infimum is taken over all countable coverings $\{A_i\}$ with diameter of A_i less than q. The **Hausdorff** q**-measure** of X is the **metric outer measure** defined by

$$H^p = \lim_{q \to 0} H_p^q.$$

  The **Hausdorff dimension** (or **fractal dimension**) of (X, d) is defined by

$$dim_{Haus}(X, d) = \inf\{p \geq 0 : H^p(X) = 0\}.$$

Any countable metric space has $dim_{Haus} = 0$, $dim_{Haus}(\mathbb{E}^n) = n$, and any $X \subset \mathbb{E}^n$ with $Int\ X \neq \emptyset$ has $dim_{Haus} = \overline{dim}$. For any **totally bounded** (X, d), it holds

$$dim_{top} \leq dim_{Haus} \leq \underline{dim} \leq dim \leq \overline{dim}.$$

- **Rough dimension**

  Given a metric space (X, d), its *rough n-volume* $Vol_n X$ is $\overline{\lim}_{\epsilon \to 0} \epsilon^n \beta_X(\epsilon)$, where $\epsilon > 0$ and $\beta_X(\epsilon) = \max |Y|$ for $Y \subseteq X$ with $d(a, b) \geq \epsilon$ if $a \in Y, b \in Y \setminus \{a\}$; $\beta_X(\epsilon) = \infty$ is permitted. The **rough dimension** is defined ([BBI01]) by

$$dim_{rough}(X, d) = \sup\{n : Vol_n X = \infty\} \text{ or, equivalently, } = \inf\{n : Vol_n X = 0\}.$$

  The space (X, d) can be not locally compact. It holds $dim_{Haus} \leq dim_{rough}$.
- **Packing dimension**

  Given a metric space (X, d) and $p, q > 0$, let $P_p^q = \sup \sum_{i=1}^{\infty} (diam(B_i))^p$, where the supremum is taken over all countable packings (by disjoint balls) $\{B_i\}$ with the diameter of B_i less than q.

  The **packing** q**-pre-measure** is $P_0^p = \lim_{q \to 0} P_p^q$. The **packing** q**-measure** is the **metric outer measure** which is the infimum of packing q-pre-measures of countable coverings of X. The **packing dimension** of (X, d) is defined by

$$dim_{pack}(X, d) = \inf\{p \geq 0 : P^p(X) = 0\}.$$

- **Topological dimension**

  For any compact metric space (X, d) its **topological dimension** (or **Lebesgue covering dimension**) is defined by

$$\dim_{top}(X, d) = \inf_{d'}\{\dim_{Haus}(X, d')\},$$

  where d' is any metric on X **equivalent** to d. So, it holds $\dim_{top} \leq \dim_{Haus}$. A **fractal** (Chap. 18) is a metric space for which this inequality is strict.

  This dimension does not exceed also the **Assouad–Nagata dimension** of (X, d).

  In general, the **topological dimension** of a topological space X is the smallest integer n such that, for any finite open covering of X, there exists a finite open refinement of it with no point of X belonging to more than $n + 1$ elements.

  The *geometric dimension* is (Kleiner, 1999; [BBI01]) $\sup dim_{top}(Y, d)$ over compact $Y \subset X$.
- **Doubling dimension**

  The **doubling dimension** $(dim_{doubl}(X, d))$ of a metric space (X, d) is the smallest integer n (or ∞ if such an n does not exist) such that every metric ball (or, say, a set of finite diameter) can be covered by a family of at most 2^n metric balls (respectively, sets) of half the diameter.

If (X, d) has finite doubling dimension, then d is called a **doubling metric** and the smallest integer m such that every metric ball can be covered by a family of at most m metric balls of half the diameter is called *doubling constant*.

- **Assouad–Nagata dimension**

  The **Assouad–Nagata dimension** $dim_{AN}(X, d)$ of a metric space (X, d) is the smallest integer n (or ∞ if such an n does not exist) for which there exists a constant $C > 0$ such that, for all $s > 0$, there exists a covering of X by its subsets of diameter $\leq Cs$ with every subset of X of diameter $\leq s$ meeting $\leq n + 1$ elements of covering. It holds (LeDonne–Rajala, 2014) $dim_{AN} \leq dim_{doubl}$; but $dim_{AN} = 1$, while $dim_{doubl} = \infty$, holds (Lang–Schlichenmaier, 2014) for some **real trees** (X, d).

  Replacing "for all $s > 0$" in the above definition by "for $s > 0$ sufficiently large" or by "for $s > 0$ sufficiently small", gives the *microscopic mi-dim*$_{AN}(X, d)$ and *macroscopic ma-dim*$_{AN}(X, d)$ Assouad–Nagata dimensions, respectively. Then (Brodskiy et al., 2006) *mi-dim*$_{AN}(X, d) = dim_{AN}(X, \min\{d, 1\})$ and

  ma-dim$_{AN}(X, d) = dim_{AN}(X, \max\{d, 1\})$ (here $\max\{d(x, y), 1\}$ means 0 for $x = y$).

  The Assouad–Nagata dimension is preserved (Lang–Schlichenmaier, 2004) under **quasi-symmetric mapping** but, in general, not under **quasi-isometry**.

- **Vol'berg–Konyagin dimension**

  The **Vol'berg–Konyagin dimension** of a metric space (X, d) is the smallest constant $C > 1$ (or ∞ if such a C does not exist) for which X carries a *doubling measure*, i.e., a Borel measure μ such that, for all $x \in X$ and $r > 0$, it holds that

$$\mu(\overline{B}(x, 2r)) \leq C\mu(\overline{B}(x, r)).$$

  A metric space (X, d) carries a doubling measure if and only if d is a **doubling metric**, and any complete doubling metric carries a doubling measure.

  The **Karger–Ruhl constant** of a metric space (X, d) is the smallest $c > 1$ (or ∞ if such a c does not exist) such that for all $x \in X$ and $r > 0$ it holds

$$|\overline{B}(x, 2r)| \leq c|\overline{B}(x, r)|.$$

  If c is finite, then the **doubling dimension** of (X, d) is at most $4c$.

- **Hyperbolic dimension**

  A metric space (X, d) is called an (R, N)-*large-scale doubling* if there exists a number $R > 0$ and integer $N > 0$ such that every ball of radius $r \geq R$ in (X, d) can be covered by N balls of radius $\frac{r}{2}$.

  The **hyperbolic dimension** $hypdim(X, d)$ of a metric space (X, d) (Buyalo–Schroeder, 2004) is the smallest integer n such that for every $r > 0$ there are $R > 0$, an integer $N > 0$ and a covering of X with the following properties:

  1. Every ball of radius r meets at most $n + 1$ elements of the covering;
  2. The covering is an (R, N)-large-scale doubling, and any finite union of its elements is an (R', N)-large-scale doubling for some $R' > 0$.

The hyperbolic dimension is 0 if (X, d) is a large-scale doubling, and it is n if (X, d) is n-dimensional hyperbolic space.

Also, $hypdim(X, d) \leq asdim(X, d)$ since the **asymptotic dimension** $asdim(X, d)$ corresponds to the case $N = 1$ in the definition of $hypdim(X, d)$.

The hyperbolic dimension is preserved under a **quasi-isometry**.

- **Asymptotic dimension**

  The **asymptotic dimension** $asdim(X, d)$ of a metric space (X, d) (Gromov, 1993) is the smallest integer n such that, for every $r > 0$, there exists a constant $D = D(r)$ and a covering of X by its subsets of diameter at most D such that every ball of radius r meets at most $n + 1$ elements of the covering.

  The asymptotic dimension is preserved under a **quasi-isometry**.

- **Width dimension**

  Let (X, d) be a compact metric space. For a given number $\epsilon > 0$, the **width dimension** $Widim_\epsilon(X, d)$ of (X, d) is (Gromov, 1999) the minimum integer n such that there exists an n-dimensional polyhedron P and a continuous map $f : X \to P$ (called an *ϵ-embedding*) with $diam(f^{-1}(y)) \leq \epsilon$ for all $y \in P$.

  The width dimension is a *macroscopic dimension at the scale* $\geq \epsilon$ of (X, d), because its limit for $\epsilon \to 0$ is the **topological dimension** of (X, d).

- **Godsil–McKay dimension**

  We say that a metric space (X, d) has **Godsil–McKay dimension** $n \geq 0$ if there exists an element $x_0 \in X$ and two positive constants c and C such that the inequality $ck^n \leq |\{x \in X : d(x, x_0) \leq k\}| \leq Ck^n$ holds for every integer $k \geq 0$.

  This notion was introduced in [GoMc80] for the **path metric** of a countable locally finite graph. They proved that, if the group $\mathbb{Z}^n$ acts faithfully and with a finite number of orbits on the vertices of the graph, then this dimension is n.

- **Metric outer measure**

  A *σ-algebra over X* is any nonempty collection Σ of subsets of X, including X itself, that is closed under complementation and countable unions of its members.

  Given a σ-algebra Σ over X, a *measure* on (X, Σ) is a function $\mu : \Sigma \to [0, \infty]$ with the following properties:

  1. $\mu(\emptyset) = 0$;
  2. For any sequence $\{A_i\}$ of pairwise disjoint subsets of X, $\mu(\sum_i A_i) = \sum_i \mu(A_i)$ (*countable σ-additivity*).

  The triple (X, Σ, μ) is called a *measure space*. If $M \subset A \in \Sigma$ and $\mu(A) = 0$ implies $M \in \Sigma$, then (X, Σ, μ) is called a *complete measure space*. A measure μ with $\mu(X) = 1$ is called a *probability measure*.

  If X is a *topological space* (see Chap. 2), then the σ-algebra over X, consisting of all *open* and *closed sets* of X, is called the *Borel σ-algebra* of X, (X, Σ) is called a *Borel space*, and a measure on Σ is called a *Borel measure*. So, any metric space (X, d) admits a Borel measure coming from its **metric topology**, where the *open set* is an arbitrary union of open **metric** d**-balls**.

  An *outer measure* on X is a function $\nu : P(X) \to [0, \infty]$ (where $P(X)$ is the set of all subsets of X) with the following properties:

  1. $\nu(\emptyset) = 0$;
  2. For any subsets $A, B \subset X$, $A \subset B$ implies $\nu(A) \leq \nu(B)$ (*monotonicity*);

3. For any sequence $\{A_i\}$ of subsets of X, $\nu(\sum_i A_i) \leq \sum_i \nu(A_i)$ (*countable subadditivity*).

A subset $M \subset X$ is called *ν-measurable* if $\nu(A) = \nu(A \cup M) + \nu(A \setminus M)$ for any $A \subset X$. The set Σ' of all ν-measurable sets forms a σ-algebra over X, and (X, Σ', ν) is a complete measure space.

A **metric outer measure** is an outer measure ν defined on the subsets of a given metric space (X, d) such that $\nu(A \cup B) = \nu(A) + \nu(B)$ for every pair of nonempty subsets $A, B \subset X$ with positive **set-set distance** $\inf_{a \in A, b \in B} d(a, b)$. An example is **Hausdorff q-measure**; cf. **Hausdorff dimension**.

- **Length of metric space**

  The **Fremlin length** of a metric space (X, d) is its **Hausdorff 1-measure** $H^1(X)$.

  The **Hejcman length** $lng(M)$ of a subset $M \subset X$ of a metric space (X, d) is $\sup\{lng(M') : M' \subset M, |M'| < \infty\}$. Here $lng(\emptyset) = 0$ and, for a finite subset $M' \subset X$, $lng(M') = \min \sum_{i=1}^{n} d(x_{i-1}, x_i)$ over all sequences $x_0, \ldots, x_n$ such that $\{x_i : i = 0, 1, \ldots, n\} = M'$.

  The **Schechtman length** of a finite metric space (X, d) is $\inf \sqrt{\sum_{i=1}^{n} a_i^2}$ over all sequences $a_1, \ldots, a_n$ of positive numbers such that there exists a sequence $X_0, \ldots, X_n$ of partitions of X with following properties:

  1. $X_0 = \{X\}$ and $X_n = \{\{x\} : x \in X\}$;
  2. X_i refines X_{i-1} for $i = 1, \ldots, n$;
  3. For $i = 1, \ldots, n$ and $B, C \subset A \in X_{i-1}$ with $B, C \in X_i$, there exists a one-to-one map f from B onto C such that $d(x, f(x)) \leq a_i$ for all $x \in B$.

- **Volume of finite metric space**

  Given a metric space (X, d) with $|X| = k < \infty$, its **volume** (Feige, 2000) is the maximal $(k-1)$-dimensional volume of the simplex with vertices $\{f(x) : x \in X\}$ over all **metric mappings** $f : (X, d) \to (\mathbb{R}^{k-1}, l_2)$. The volume coincides with the metric for $k = 2$. It is monotonically increasing and continuous in the metric d.

- **Rank of metric space**

  The **Minkowski rank of a metric space** (X, d) is the maximal dimension of a normed vector space $(V, ||.||)$ such that there is an isometry $(V, ||.||) \to (X, d)$.

  The **Euclidean rank of a metric space** (X, d) is the maximal dimension of a *flat* in it, that is of a Euclidean space $\mathbb{E}^n$ such that there is an isometric embedding $\mathbb{E}^n \to (X, d)$.

  The **quasi-Euclidean rank of a metric space** (X, d) is the maximal dimension of a *quasi-flat* in it, i.e., of an Euclidean space $\mathbb{E}^n$ admitting a **quasi-isometry** $\mathbb{E}^n \to (X, d)$. Every **Gromov hyperbolic metric space** has this rank 1.

- **Roundness of metric space**

  The **roundness of a metric space** (X, d) is the supremum of all q such that

  $$d(x_1, x_2)^q + d(y_1, y_2)^q \leq d(x_1, y_1)^q + d(x_1, y_2)^q + d(x_2, y_1)^q + d(x_2, y_2)^q$$

  for any four points $x_1, x_2, y_1, y_2 \in X$.

Every metric space has roundness ≥ 1; it is ≤ 2 if the space has **approximate midpoints**. The roundness of **L_p-space** is p if $1 \leq p \leq 2$.

The *generalized roundness of a metric space* (X, d) is (Enflo, 1969) the supremum of all q such that, for any $2k \geq 4$ points $x_i, y_i \in X$ with $1 \leq i \leq k$,

$$\sum_{1 \leq i < j \leq k} d^q(x_i, x_j) + d^q(y_i, y_j) \leq \sum_{1 \leq i,j \leq k} d^q(x_i, y_j).$$

Lennard–Tonge–Weston, 1997, have shown that the generalized roundness is the supremum of q such that d is of **q-negative type**, i.e., d^q is of **negative type**.

Every **CAT(0) space** (Chap. 6) has roundness 2, but some of them have generalized roundness 0 (Lafont–Prassidis, 2006).

- **Type of metric space**

  The **Enflo type** of a metric space (X, d) is p if there exists a constant $1 \leq C < \infty$ such that, for every $n \in \mathbb{N}$ and every function $f : \{-1, 1\}^n \to X$, $\sum_{\epsilon \in \{-1,1\}^n} d^p(f(\epsilon), f(-\epsilon))$ is at most
  $C^p \sum_{j=1}^{n} \sum_{\epsilon \in \{-1,1\}^n} d^p(f(\epsilon_1, \ldots, \epsilon_{j-1}, \epsilon_j, \epsilon_{j+1}, \ldots, \epsilon_n), f(\epsilon_1, \ldots, \epsilon_{j-1}, -\epsilon_j, \epsilon_{j+1}, \ldots, \epsilon_n))$.

  A Banach space $(V, ||.||)$ of Enflo type p has *Rademacher type* p, i.e., for every $x_1, \ldots, x_n \in V$, it holds

$$\sum_{\epsilon \in \{-1,1\}^n} ||\sum_{j=1}^{n} \epsilon_j x_j||^p \leq C^p \sum_{j=1}^{n} ||x_j||^p.$$

  Given a metric space (X, d), a *symmetric Markov chain on* X is a Markov chain $\{Z_l\}_{l=0}^{\infty}$ on a state space $\{x_1, \ldots, x_m\} \subset X$ with a symmetrical transition $m \times m$ matrix $((a_{ij}))$, such that $P(Z_{l+1} = x_j : Z_l = x_i) = a_{ij}$ and $P(Z_0 = x_i) = \frac{1}{m}$ for all integers $1 \leq i, j \leq m$ and $l \geq 0$. A metric space (X, d) has **Markov type** p (Ball, 1992) if $\sup_T M_p(X, T) < \infty$ where $M_p(X, T)$ is the smallest constant $C > 0$ such that the inequality

$$\mathbb{E}d^p(Z_T, Z_0) \leq TC^p \mathbb{E}d^p(Z_1, Z_0)$$

  holds for every symmetric Markov chain $\{Z_l\}_{l=0}^{\infty}$ on X holds, in terms of expected value (mean) $\mathbb{E}[X] = \sum_x xp(x)$ of the discrete random variable X.

  A metric space of Markov type p has Enflo type p.

- **Strength of metric space**

  Given a finite metric space (X, d) with s different nonzero values of $d_{ij} = d(i, j)$, its **strength** is the largest number t such that, for any integers $p, q \geq 0$ with $p + q \leq t$, there is a polynomial $f_{pq}(s)$ of degree at most $\min\{p, q\}$ such that $((d_{ij}^{2p}))((d_{ij}^{2q})) = ((f_{pq}(d_{ij}^2)))$.

- **Rendez-vous number**

  Given a metric space (X, d), its **rendez-vous number** (or *Gross number, magic number*) is a positive real number $r(X, d)$ (if it exists) defined by the

property that for each integer n and all (not necessarily distinct) $x_1, \ldots, x_n \in X$ there exists a point $x \in X$ such that

$$r(X,d) = \frac{1}{n}\sum_{i=1}^{n} d(x_i, x).$$

If the number $r(X,d)$ exists, then it is said that (X,d) has the **average distance property**. Every compact connected metric space has this property. The *unit ball* $\{x \in V : ||x|| \le 1\}$ of a **Banach space** $(V, ||.||)$ has the rendez-vous number 1.

- **Wiener-like distance indices**

Given a finite subset M of a metric space (X,d) and a parameter q, the **Wiener polynomial** of M (as defined by Hosoya, 1988, for the graphic metric d_{path}) is

$$W(M;q) = \frac{1}{2}\sum_{x,y\in M:\, x\neq y} q^{d(x,y)}.$$

It is a *generating function* for the **distance distribution** (Chap. 16) of M, i.e., the coefficient of q^i in $W(M;q)$ is the number $|\{\{x,y\} \in M \times M : d(x,y) = i\}|$.

In the main case when M is the vertex-set V of a connected graph $G = (V,E)$ and d is the **path metric** of G, the number $W(M;1) = \frac{1}{2}\sum_{x,y\in M} d(x,y)$ is called the **Wiener index** of G. This notion is originated (Wiener, 1947) and applied, together with its many analogs, in Chemistry; cf. **chemical distance** in Chap. 24.

The *hyper-Wiener index* is $\sum_{x,y\in M}(d(x,y) + d(x,y)^2)$. The *reverse-Wiener index* is $\frac{1}{2}\sum_{x,y\in M}(D - d(x,y))$, where D is the diameter of M. The *complementary reciprocal Wiener index* is $\frac{1}{2}\sum_{x,y\in M}(1 + D - d(x,y))^{-1}$. The *Harary index* is $\sum_{x,y\in M}(d(x,y))^{-1}$. The *Szeged index* and the *vertex PI index* are $\sum_{e\in E} n_x(e)n_y(e)$ and $\sum_{e\in E}(n_x(e) + n_y(e))$, where $e = (xy)$ and $n_x(e) = |\{z \in V : d(x,z) < d(y,z)\}|$.

Two studied *edge-Wiener indices* of G are the Wiener index of its *line graph* and $\sum_{(xy),(x'y')\in E} \max\{d(x,x'), d(x,y'), d(y,x'), d(y,y')\}$.

The *Gutman–Schultz index*, **degree distance** (Dobrynin–Kochetova, 1994), *reciprocal degree distance* and *terminal Wiener index* are:

$$\sum_{x,y\in M} r_x r_y d(x,y),\ \sum_{x,y\in M} d(x,y)(r_x + r_y),\ \sum_{x,y\in M}\frac{1}{d(x,y)}(r_x + r_y),\ \sum_{x,y\in\{z\in M: r_z=1\}} d(x,y),$$

where r_z is the degree of the vertex $z \in M$. The **eccentric distance sum** (Gupta et al., 2002) is $\sum_{y\in M}(\max\{d(x,y) : x \in M\}d_y)$, where d_y is $\sum_{x\in M} d(x,y)$. The *Balaban index* is $\frac{|E|}{c+1}\sum_{(yz)\in E}(\sqrt{d_y d_z})^{-1}$, where c is the number of primitive cycles. The *multiplicative Wiener index* is (Das–Gutman, 2016) $\prod_{x,y\in M, x\neq y} d(x,y)$.

Given a partition $P = \{V_1, \ldots, V_k\}$ of the vertex-set V, set $f_P(x) = i$ for $x \in V_i$. The *colored distance* (Dankelman et al., 2001) and the *partition distance* (Klavžar, 2016) of G are $\sum_{f_P(x)\neq f_P(y)} d(x,y)$ and $\sum_{f_P(x)=f_P(y)} d(x,y)$, respectively.

Above indices are called (corresponding) *Kirchhoff indices* if d the **resistance metric** (Chap. 15) of G.

The *average distance* of M is the number $\frac{1}{|M|(|M|-1)}\sum_{x,y\in M} d(x,y)$. In general, for a quasi-metric space (X,d), the numbers $\sum_{x,y\in M} d(x,y)$ and $\frac{1}{|M|(|M|-1)}\sum_{x,y\in M, x\neq y}\frac{1}{d(x,y)}$ are called, respectively, the *transmission* and *global efficiency* of M.

- **Distance polynomial**

  Given an ordered finite subset M of a metric space (X,d), let D be the **distance matrix** of M. The **distance polynomial** of M is the *characteristic polynomial* of D, i.e., the determinant $det(D-\lambda I)$.

  Usually, D is the distance matrix of the **path metric** of a graph. Sometimes, the distance polynomial is defined as $det(\lambda I - D)$ or $(-1)^n det(D-\lambda I)$.

  The roots of the distance polynomial constitute the **distance spectrum** (or *D-spectrum* of *D-eigenvalues*) of M. Let $\rho_{\max}$ and $\rho_{\min}$ be the largest and the smallest roots; then $\rho_{\max}$ and $\rho_{\max}-\rho_{\min}$ are called (distance spectral) *radius* and *spread* of M. The **distance degree** of $x\in M$ is $\sum_{y\in M} d(x,y)$. The **distance energy** of M is the sum of the absolute values of its D-eigenvalues. It is $2\rho_{\max}$ if (as, for example, for the path metric of a tree) exactly one D-eigenvalue is positive.

- ***s*-energy**

  Given a finite subset M of a metric space (X,d) and a number $s>0$, the ***s*-energy** and **0-energy** of M are, respectively, the numbers

$$\sum_{x,y\in M, x\neq y}\frac{1}{d^s(x,y)} \text{ and } \sum_{x,y\in M, x\neq y}\log\frac{1}{d(x,y)} = -\log\prod_{x,y\in M, x\neq y} d(x,y).$$

  The (unnormalized) ***s*-moment** of M is the number $\sum_{x,y\in M} d^s(x,y)$.

  The *discrete Riesz s-energy* is the s-energy for Euclidean distance d. In general, let μ be a finite Borel probability measure on (X,d). Then $U_s^\mu(x) = \int\frac{\mu(dy)}{d(x,y)^s}$ is the (abstract) *s-potential* at a point $x\in X$. The *Newton gravitational potential* is the case $(X,d)=(\mathbb{R}^3,|x-y|)$, $s=1$, for the mass distribution μ.

  The *s-energy* of μ is $E_s^\mu = \int U_s^\mu(x)\mu(dx) = \int\int\frac{\mu(dx)\mu(dy)}{d(x,y)^s}$, and the *s-capacity* of (X,d) is $(\inf_\mu E_s^\mu)^{-1}$. Cf. the **metric capacity**.

- **Fréchet mean**

  Given a metric space (X,d) and a number $s>0$, the *Fréchet function* is $F_s(x) = \mathbb{E}[d^s(x,y)]$. For a finite subset M of X, this expected value is the mean $F_s(x) = \sum_{y\in M} w(y)d^s(x,y)$, where $w(y)$ is a weight function on M.

  The points, minimizing $F_1(x)$ and $F_2(x)$, are called the **Fréchet median** (or *weighted geometric median*) and **Fréchet mean** (or *Karcher mean*), respectively.

  If $(X,d)=(\mathbb{R}^n,||x-y||_2)$ and the weights are equal, these points are called the *geometric median* (or *Fermat–Weber point*, 1-*median*) and the *centroid* (or *geometric center*, *barycenter*), respectively.

  The *k-median* and *k-mean* of M are the k-sets C minimizing, respectively, the sums $\sum_{y\in M}\min_{c\in C} d(y,c) = \sum_{y\in M} d(y,C)$ and $\sum_{y\in M} d^2(y,C)$.

Let (X, d) be the metric space $(\mathbb{R}_{>0}, |f(x) - f(y)|)$, where $f : \mathbb{R}_{>0} \to \mathbb{R}$ is a given injective and continuous function. Then the Fréchet mean of $M \subset \mathbb{R}_{>0}$ is the *f-mean* (or *Kolmogorov mean*, *quasi-arithmetic mean*) $f^{-1}(\frac{\sum_{x\in M} f(x)}{|M|})$. It is the arithmetic, geometric, harmonic, and power mean if $f = x, \log(x), \frac{1}{x}$, and $f = x^p$ (for a given $p \neq 0$), respectively. The cases $p \to +\infty, p \to -\infty$ correspond to maximum and minimum, while $p = 2, = 1, \to 0, \to -1$ correspond to the quadratic, arithmetic, geometric and harmonic mean.

Given a *completely monotonic* (i.e., $(-1)^k f^{(k)} \geq 0$ for any k) function $f \in \mathbb{C}^\infty$, the **f-potential energy** of a finite subset M of (X, d) is $\sum_{x,y\in M, x\neq y} f(d^2(x, y))$. The set M is called (Cohn–Kumar, 2007) *universally optimal* if it minimizes, among sets $M' \subset X$ with $|M'| = |M|$, the f-potential energy for any such f. Among universally optimal subsets of $(\mathbb{S}^{n-1}, ||x - y||_2)$, there are the vertex-sets of a polygon, simplex, cross-polytope, icosahedron, 600-cell, E_8 root system.

- **Distance-weighted mean**

  In Statistics, the **distance-weighted mean** between given data points $x_1, \ldots, x_n$ is defined (Dodonov–Dodonova, 2011) by

$$\frac{\sum_{1\leq i\leq n} w_i x_i}{\sum_{1\leq i\leq n} w_i} \quad \text{with} \quad w_i = \frac{n-1}{\sum_{1\leq j\leq n} |x_i - x_j|}.$$

  The case $w_i = 1$ for all i corresponds to the arithmetic mean.

- **Inverse distance weighting**

  In Numerical Analysis, *multivariate* (or *spatial*) interpolation is interpolation on functions of more than one variable. **Inverse distance weighting** is a method (Shepard, 1968) for multivariate interpolation. Let $x_1, \ldots, x_n$ be interpolating points (i.e., samples $u_i = u(x_i)$ are known), x be an interpolated (unknown) point and $d(x, x_i)$ be a given distance. A general form of interpolated value $u(x)$ is

$$u(x) = \frac{\sum_{1\leq i\leq n} w_i(x) u_i}{\sum_{1\leq i\leq n} w_i(x)}, \text{ with } w_i(x) = \frac{1}{(d(x, x_i))^p},$$

  where $p > 0$ (usually $p = 2$) is a fixed *power parameter*.

- **Transfinite diameter**

  The *n-th diameter* $D_n(M)$ and the *n-th Chebyshev constant* $C_n(M)$ of a set $M \subseteq X$ in a metric space (X, d) are defined (Fekete, 1923, for the complex plane $\mathbb{C}$) as

$$D_n(M) = \sup_{x_1,\ldots,x_n\in M} \prod_{i\neq j} d(x_i, x_j)^{\frac{1}{n(n-1)}} \text{ and } C_n(M) = \inf_{x\in X} \sup_{x_1,\ldots,x_n\in M} \prod_{j=1}^{n} d(x, x_j)^{\frac{1}{n}}.$$

  The number $\log D_n(M)$ (the supremum of the average distance) is called the *n-extent* of M. The numbers $D_n(M), C_n(M)$ come from the geometric mean averaging; they also come as the limit case $s \to 0$ of the *s-moment* $\sum_{i\neq j} d(x_i, x_j)^s$ averaging.

The **transfinite diameter** (or ∞-*th diameter*) and the ∞-*th Chebyshev constant* $C_\infty(M)$ of M are defined as

$$D_\infty(M) = \lim_{n\to\infty} D_n(M) \text{ and } C_\infty(M) = \lim_{n\to\infty} C_n(M);$$

these limits existing since $\{D_n(M)\}$ and $\{C_n(M)\}$ are nonincreasing sequences of nonnegative real numbers. Define $D_\infty(\emptyset) = 0$.

The transfinite diameter of a compact subset of $\mathbb{C}$ is its **conformal radius** at infinity (cf. Chap. 6); for a segment in $\mathbb{C}$, it is $\frac{1}{4}$ of its length.

- **Metric diameter**

The **metric diameter** (or **diameter**, *width*) $diam(M)$ of a set $M \subseteq X$ in a metric space (X, d) is defined by

$$\sup_{x,y\in M} d(x, y).$$

The *diameter graph* of M has, as vertices, all points $x \in M$ with $d(x, y) = diam(M)$ for some $y \in M$; it has, as edges, all pairs of its vertices at distance $diam(M)$ in (X, d). (X, d) is called a **diametrical metric space** if any $x \in X$ has the *antipode*, i.e., a unique $x' \in X$ such that the **closed metric interval** $I(x, x')$ is X.

The *furthest neighbor digraph* of M is a directed graph on M, where xy is an arc (called a *furthest neighbor pair*) whenever y is at maximal distance from x.

In a metric space endowed with a measure, one says that the *isodiametric inequality* holds if the metric balls maximize the measure among all sets with given diameter. It holds for the volume in Euclidean space but not, for example, for the **Heisenberg metric** on the *Heisenberg group* (Chap. 10).

The k**-ameter** (Grove–Markvorsen, 1992) is $\sup_{K\subseteq X:\,|K|=k} \frac{1}{2}\sum_{x,y\in K} d(x, y)$, and the k**-diameter** (Chung–Delorme–Sole, 1999) is $\sup_{K\subseteq X:\,|K|=k} \inf_{x,y\in K:\,x\neq y} d(x, y)$.

Given a property $P \subseteq X \times X$ of a pair (K, K') of subsets of a finite metric space (X, d), the **conditional diameter** (called *P-diameter* in Balbuena et al., 1996) is $\max_{(K,K')\in P} \min_{(x,y)\in K\times K'} d(x, y)$. It is $diam(X, d)$ if $P = \{(K, K') \in X \times X : |K| = |K'| = 1\}$. When (X, d) models an interconnection network, the P-diameter corresponds to the maximum delay of the messages interchanged between any pair of clusters of nodes, K and K', satisfying a given property P of interest.

- **Metric spread**

A subset M of a metric space (X, d) is called **Delone set** (or *separated* ϵ**-net**, (A, a)*-Delone set*) if it is **bounded** (with a finite **diameter** $A = \sup_{x,y\in M} d(x, y)$) and **metrically discrete** (with a *separation* $a = \inf_{x,y\in M, x\neq y} d(x, y) > 0$).

The **metric spread** (or *distance ratio*, *normalized diameter*) of M is the ratio $\frac{A}{a}$.

The **aspect ratio** (or *axial ratio*) of a shape is the ratio of its longer and shorter dimensions, say, the length and diameter of a rod, major and minor axes of a torus or width and height of a rectangle (image, display, pixel, etc.).

For a mesh M with separation a and **covering radius** (or *mesh norm*) $c = \sup_{y\in X} \inf_{x\in M} d(x, y)$, the *mesh ratio* is $\frac{c}{a}$.

In Physics, the *aspect ratio* is the ratio of height-to-length scale characteristics. Cf. the *wing's aspect ratio* among **aircraft distances** in Chap. 29.

Dynamic range DNR is the ratio between the largest and smallest possible values of a quantity, such as in sound or light signals; cf. **SNR distance** in Chap. 21.

- **Eccentricity**

  Given a bounded metric space (X, d), the **eccentricity** (or *Koenig number*) of a point $x \in X$ is the number $e(x) = \max_{y\in X} d(x, y)$.

  The numbers $D = \max_{x\in X} e(x)$ and $r = \min_{x\in X} e(x)$ are called the **diameter** and the **radius** of (X, d), respectively. The point $z \in X$ is called *central* if $e(z) = r$, *peripheral* if $e(z) = D$, and *pseudo-peripheral* if for each point x with $d(z, x) = e(z)$ it holds that $e(z) = e(x)$. For finite $|X|$, the *average eccentricity* is $\frac{1}{|X|}\sum_{x\in X} e(x)$, and the *contour* of (X, d) is the set of points $x \in X$ such that no *neighbor* (closest point) of x has an eccentricity greater than x.

  The **eccentric digraph** (Buckley, 2001) of (X, d) has, as vertices, all points $x \in X$ and, as arcs, all ordered pairs (x, y) of points with $d(x, y) = e(y)$. The **eccentric graph** (Akyiama–Ando–Avis, 1976) of (X, d) has, as vertices, all points $x \in X$ and, as edges, all pairs (x, y) of points at distance $\min\{e(x), e(y)\}$.

  The **super-eccentric graph** (Iqbalunnisa–Janairaman–Srinivasan, 1989) of (X, d) has, as vertices, all points $x \in X$ and, as edges, all pairs (x, y) of points at distance no less than the radius of (X, d). The **radial graph** (Kathiresan–Marimuthu, 2009) of (X, d) has, as vertices, all points $x \in X$ and, as edges, all pairs (x, y) of points at distance equal to the radius of (X, d).

  The sets $\{x \in X : e(x) \le e(z) \text{ for any } z \in X\}$, $\{x \in X : e(x) \ge e(z) \text{ for any } z \in X\}$ and $\{x \in X : \sum_{y\in X} d(x, y) \le \sum_{y\in X} d(z, y) \text{ for any } z \in X\}$ are called, respectively, the **metric center** (or *eccentricity center*, *center*), **metric antimedian** (or *periphery*) and the **metric median** (or *distance center*) of (X, d).

- **Radii of metric space**

  Given a bounded metric space (X, d) and a set $M \subseteq X$ of **diameter** D, its **metric radius** (or **radius**) Mr, **covering radius** (or **directed Hausdorff distance** from X to M) Cr and **remoteness** (or **Chebyshev radius**) Re are the numbers $\inf_{x\in M} \sup_{y\in M} d(x, y)$, $\sup_{x\in X} \inf_{y\in M} d(x, y)$ and $\inf_{x\in X} \sup_{y\in M} d(x, y)$, respectively. It holds that $\frac{D}{2} \le Re \le Mr \le D$ with $Mr = \frac{D}{2}$ in any **injective metric space**. Somemimes, $\frac{D}{2}$ is called the *radius*.

  For $m > 0$, a **minimax distance design of size** m is an m-subset of X having smallest covering radius. This radius is called the *m-point mesh norm* of (X, d).

  The **packing radius** Pr of M is the number $\sup\{r : \inf_{x,y\in M, x\neq y} d(x, y) > 2r\}$. For $m > 0$, a **maximum distance design of size** m is an m-subset of X having largest packing radius. This radius is the *m-point best packing distance* on (X, d).

- **ϵ-net**

  Given a metric space (X, d), a subset $M \subset X$, and a number $\epsilon > 0$, the **ϵ-neighborhood** of M is the set $M^\epsilon = \cup_{x \in M} B(x, \epsilon)$.

  The set M is called an **ϵ-net** (or *ϵ-covering*, *ϵ-approximation*) of (X, d) if $M^\epsilon = X$, i.e., the **covering radius** of M is at most ϵ.

  Let C_ϵ denote the *ϵ-covering number*, i.e., the smallest size of an ϵ-net in (X, d). The number $\lg_2 C_\epsilon$ is called (Kolmogorov–Tikhomirov, 1959) the **metric entropy** (or *ϵ-entropy*) of (X, d). It holds $P_\epsilon \le C_\epsilon \le P_{\frac{\epsilon}{2}}$, where P_ϵ denote the *ϵ-packing number* of (X, d), i.e., $\sup\{|M| : M \subset X, \overline{B}(x, \epsilon) \cap \overline{B}(y, \epsilon) = \emptyset \text{ for any } x, y \in M, x \ne y\}$. The number $\lg_2 P_\epsilon$ is called the **metric capacity** (or *ϵ-capacity*) of (X, d).

- **Steiner ratio**

  Given a metric space (X, d) and a finite subset $V \subset X$, let $G = (V, E)$ be the complete weighted graph on V with edge-weights $d(x, y)$ for all $x, y \in V$.

  Given a tree T, its *weight* is the sum $d(T)$ of its edge-weights. A *spanning tree* of V is a subset of $|V| - 1$ edges forming a tree on V. Let $MSpT_V$ be a *minimum spanning tree* of V, i.e., a spanning tree with the minimal weight $d(MSpT_V)$.

  A *Steiner tree* of V is a tree on Y, $V \subset Y \subset X$, connecting vertices from V; elements of $Y \setminus V$ are called *Steiner points*. Let $StMT_V$ be a *minimum Steiner tree* of V, i.e., a Steiner tree with the minimal weight $d(StMT_V) = \inf_{Y \subset X : V \subset Y} d(MSpT_Y)$. This weight is called the **Steiner diversity** of V; cf. **diversity** in Chap. 3. It is the **Steiner distance of set** V (Chap. 15) if (X, d) is graphic metric space.

  The **Steiner ratio** $St(X, d)$ of the metric space (X, d) is defined by

$$\inf_{V \subset X} \frac{d(StMT_V)}{d(MSpT_V)}.$$

  Cf. **arc routing problems** in Chap. 15.

- **Chromatic numbers of metric space**

  Given a metric space (X, d) and a set D of positive real numbers, the **D-chromatic number** of (X, d) is the standard *chromatic number* of its **D-distance graph**, i.e., the graph (X, E) with the vertex-set X and the edge-set $E = \{xy : d(x, y) \in D\}$ (Chap. 15). Usually, (X, d) is an **l_p-space** and $D = \{1\}$ (**Benda–Perles chromatic number**) or $D = [1 - \epsilon, 1 + \epsilon]$.

  For a metric space (X, d), the **polychromatic number** is the minimum number of colors needed to color all the points $x \in X$ so that, for each color class C_i, there is a distance d_i such that no two points of C_i are at distance d_i.

  For a metric space (X, d), the **packing chromatic number** is the minimum number of colors needed to color all the points $x \in X$ so that, for each color class C_i, no two distinct points of C_i are at distance at most i.

  For any integer $t > 0$, the **t-distance chromatic number** of a metric space (X, d) is the minimum number of colors needed to color all the points $x \in X$ so that any two points whose distance is $\le t$ have distinct colors. Cf. **k-distance chromatic number** in Chap. 15.

For any integer $t > 0$, the ***t*-th Babai number** of a metric space (X, d) is the minimum number of colors needed to color all the points in X so that, for any set D of positive distances with $|D| \leq t$, any two points $x, y \in X$ with $d(x, y) \in D$ have distinct colors.

- **Congruence order of metric space**

  A metric space (X, d) has **congruence order** n if every finite metric space which is not **isometrically embeddable** in (X, d) has a subspace with at most n points which is not isometrically embeddable in (X, d). For example, the congruence order of l_2^n is $n + 3$ (Menger, 1928); it is 4 for the **path metric** of a tree.

1.4 Main Mappings of Metric Spaces

- **Distance function**

  In Topology, the term *distance function* is often used for **distance**. But, in general, a **distance function** (or *ray function*) is a continuous function on a metric space (X, d) (usually, on a Euclidean space $\mathbb{E}^n$) $f : X \to \mathbb{R}_{\geq 0}$ which is *homogeneous*, i.e., $f(tx) = tf(x)$ for all $t \geq 0$ and all $x \in X$.

  Such function f is called *positive* if $f(x) > 0$ for all $x \neq 0$, *symmetric* if $f(x) = f(-x)$, *convex* if $f(tx + (1-t)y) \leq tf(x) + (1-t)f(y)$ for any $0 < t < 1$ and $x \neq y$, and *strictly convex* if this inequality is strict.

  If $X = \mathbb{E}^n$, the set $S_f = \{x \in \mathbb{R}^n : f(x) < 1\}$ is *star body*, i.e., $x \in S_f$ implies $[0, x] \subset S_f$. Any star body S corresponds to a unique distance function $g(x) = \inf_{tx \in S, t>0} \frac{1}{t}$, and $S = S_g$. The star body is bounded if f is positive, symmetric about the origin if f is symmetric, convex if f is convex, and *strictly convex* (i.e., the boundary ∂B does not contain a segment) if f is strictly convex.

  For a quadratic distance function of the form $f_A = xAx^T$, where A is a real matrix and $x \in \mathbb{R}^n$, the matrix A is *positive-definite* (i.e., the **Gram matrix** $VV^T = ((\langle v_i, v_j \rangle))$ of n linearly independent vectors $v_i = (v_{i1}, \ldots, v_{in})$) if and only if f_A is symmetric and strictly convex function. The *homogeneous minimum* of f_A is

$$\min(f_A) = \inf_{x \in \mathbb{Z}^n \setminus \{0\}} f_A(x) = \inf_{x \in L \setminus \{0\}} \sum_{1 \leq i \leq n} x_i^2,$$

  where $L = \{\sum x_i v_i : x_i \in \mathbb{Z}\}$ is a *lattice*, i.e., a discrete subgroup of $\mathbb{R}^n$ spanning it. The *Hermite constant* γ_n, a central notion in Geometry of Numbers, is the supremum, over all positive-definite $(n \times n)$-matrices, of $\min(f_A) \det(A)^{\frac{1}{n}}$. It is known only for $2 \leq n \leq 8$ and $n = 24$; cf. **systole of metric space**.

- **Convex distance function**

  Given a compact convex region $B \subset \mathbb{R}^n$ containing the origin O in its interior, the **convex distance function** (or **Minkowski distance function**, *Minkowski*

seminorm, *gauge*) is the function $||P||_B$ whose value at a point $P \in \mathbb{R}^n$ is the *distance ratio* $\frac{OP}{OQ}$, where $Q \in B$ is the furthest from O point on the ray OP.

Then $d_B(x, y) = ||x - y||_B$ is the quasi-metric on $\mathbb{R}^n$ defined, for $x \neq y$, by

$$\inf\{\alpha > 0 : y - x \in \alpha B\},$$

and $B = \{x \in \mathbb{R}^n : d_B(0, x) \leq 1\}$ with equality only for $x \in \partial B$.

The function $||P||_B$ is called a **polyhedral distance function** if B is a n-polytope, *simplicial distance function* if it is a n-simplex, and so on.

If B is centrally-symmetric with respect to the origin, then d_B is a **Minkowskian metric** (Chap. 6) whose unit ball is B. This is the l_1-metric if B is the n-cross-polytope and the l_∞-metric if B is the n-cube.

- **Funk distance**

  Let B be an nonempty open convex subset of $\mathbb{R}^n$. For any $x, y \in B$, denote by $R(x, y)$ the ray from x through y. The **Funk distance** (Funk, 1929) on B is the quasi-semimetric defined, for any $x, y \in B$, as 0 if the boundary $\partial(B)$ and $R(x, y)$ are disjoint, and, otherwise, i.e., if $R(x, y) \cap \partial B = \{z\}$, by

  $$\ln \frac{||x - z||_2}{||y - z||_2}.$$

  The **Hilbert projective metric** in Chap. 6 is a symmetrization of this distance.

- **Metric projection**

  Given a metric space (X, d) and a subset $M \subset X$, an element $u_0 \in M$ is called an **element of best approximation** (or **nearest point**) to a given element $x \in X$ if $d(x, u_0) = \inf_{u \in M} d(x, u)$, i.e., if $d(x, u_0)$ is the **point-set distance** $d(x, M)$.

  A **metric projection** (or *operator of best approximation*, *nearest point map*) is a multivalued mapping associating to each element $x \in X$ the set of elements of best approximation from the set M (cf. **distance map**).

  A **Chebyshev set** in a metric space (X, d) is a subset $M \subset X$ containing a unique element of best approximation for every $x \in X$.

  A subset $M \subset X$ is called a **semi-Chebyshev set** if the number of such elements is at most one, and a **proximinal set** if this number is at least one.

  While the **Chebyshev radius** (or **remoteness**; cf. **radii of metric space**) of the set M is $\inf_{x \in X} \sup_{y \in M} d(x, y)$, a **Chebyshev center** of M is an element $x_0 \in X$ realizing this infimum. Sometimes (say, for a finite graphic metric space), $\frac{1}{|M|} \inf_{x \in X} \sum_{y \in M} d(x, y)$ and $\frac{1}{|M|} \sup_{x \in X} \sum_{y \in M} d(x, y)$ are called *proximity* and *remoteness* of M.

- **Distance map**

  Given a metric space (X, d) and a subset $M \subset X$, the **distance map** is a function $f_M : X \to \mathbb{R}_{\geq 0}$, where $f_M(x) = \inf_{u \in M} d(x, u)$ is the **point-set distance** $d(x, M)$ (cf. **metric projection**).

If the boundary $B(M)$ of the set M is defined, then the **signed distance function** g_M is defined by $g_M(x) = -\inf_{u\in B(M)} d(x,u)$ for $x \in M$, and $g_M(x) = \inf_{u\in B(M)} d(x,u)$, otherwise. If M is a (closed orientable) n**-manifold** (Chap. 2), then g_M is the solution of the *eikonal equation* $|\nabla g| = 1$ for its *gradient* ∇.

If $X = \mathbb{R}^n$ and, for every $x \in X$, there is unique element $u(x)$ with $d(x,M) = d(x,u(x))$ (i.e., M is a **Chebyshev set**), then $||x-u(x)||$ is called a **vector distance function**.

Distance maps are used in Robot Motion (M being the set of obstacle points) and, especially, in Image Processing (M being the set of all or only boundary pixels of the image). For $X = \mathbb{R}^2$, the graph $\{(x,f_M(x)) : x \in X\}$ of $d(x,M)$ is called the *Voronoi surface* of M.

- **Isometry**

  Given metric spaces (X,d_X) and (Y,d_Y), a function $f : X \to Y$ is called an **isometric embedding** of X into Y if it is injective and the equality $d_Y(f(x),f(y)) = d_X(x,y)$ holds for all $x,y \in X$.

  An **isometry** (or *congruence mapping*) is a bijective isometric embedding. Two metric spaces are called **isometric** (or *isometrically isomorphic*) if there exists an isometry between them.

  A property of metric spaces which is invariant with respect to isometries (completeness, boundedness, etc.) is called a **metric property** (or *metric invariant*).

  A **path isometry** (or *arcwise isometry*) is a mapping from X into Y (not necessarily bijective) preserving lengths of curves.

- **Rigid motion of metric space**

  A **rigid motion** (or, simply, **motion**) of a metric space (X,d) is an **isometry** of (X,d) onto itself.

  For a motion f, the **displacement function** $d_f(x)$ is $d(x,f(x))$. The motion f is called *semisimple* if $\inf_{x\in X} d_f(x) = d(x_0,f(x_0))$ for some $x_0 \in X$, and *parabolic*, otherwise. A semisimple motion is called *elliptic* if $\inf_{x\in X} d_f(x) = 0$, and *axial* (or *hyperbolic*), otherwise. A motion is called a *Clifford translation* if the displacement function $d_f(x)$ is a constant for all $x \in X$.

- **Symmetric metric space**

  A metric space (X,d) is called **symmetric** if, for any point $p \in X$, there exists a *symmetry* relative to that point, i.e., a **motion** f_p of this metric space such that $f_p(f_p(x)) = x$ for all $x \in X$, and p is an isolated fixed point of f_p.

- **Homogeneous metric space**

  A metric space is called **homogeneous** (or *point-homogeneous*) if, for any two points of it, there exists a motion mapping one of the points to the other.

  In general, a *homogeneous space* is a set together with a given transitive group of *symmetries*. Moss, 1992, defined similar *distance-homogeneous distanced graph*.

  A metric space is called **ultrahomogeneous space** (or *highly transitive*) if any isometry between two of its finite subspaces extends to the whole space.

  A metric space (X,d) is called (Grünbaum–Kelly) a **metrically homogeneous metric space** if $\{d(x,z) : z \in X\} = \{d(y,z) : z \in X\}$ for any $x,y \in X$.

- **Flat space**

  A **flat space** is any metric space with **local isometry** to some $\mathbb{E}^n$, i.e., each point has a neighborhood isometric to an open set in $\mathbb{E}^n$. A space is *locally Euclidean* if every point has a neighborhood homeomorphic to an open subset in $\mathbb{E}^n$.
- **Dilation of metric space**

  Given a metric space (X, d), its **dilation** (or r**-dilation**) is a mapping $f : X \to X$ with $d(f(x), f(y)) = rd(x, y)$ for some $r > 0$ and any $x \in X$.
- **Wobbling of metric space**

  Given a metric space (X, d), its **wobbling** (or r**-wobbling**) is a mapping $f : X \to X$ with $d(x, f(x)) < r$ for some $r > 0$ and any $x \in X$.
- **Paradoxical metric space**

  Given a metric space (X, d) and an equivalence relation on the subsets of X, the space (X, d) is called **paradoxical** if X can be decomposed into two disjoint sets M_1, M_2 so that M_1, M_2 and X are pairwise equivalent.

  Deuber, Simonovitz and Sós, 1995, introduced this idea for *wobbling equivalent* subsets $M_1, M_2 \subset X$, i.e., there is a bijective r**-wobbling** $f : M_1 \to M_2$. For example, $(\mathbb{R}^2, l_2)$ is paradoxical for wobbling but not for isometry equivalence.
- **Metric cone**

  A **pointed metric space** (X, d, x_0) is called a **metric cone**, if it is isometric to $(\lambda X, d, x_0)$ for all $\lambda > 0$. A **metric cone structure** on (X, d, x_0) is a (pointwise) continuous family f_t ($t \in \mathbb{R}_{>0}$) of **dilations** of X, leaving the point x_0 invariant, such that $d(f_t(x), f_t(y)) = td(x, y)$ for all x, y and $f_t \circ f_s = f_{ts}$. A Banach space has such a structure for the dilations $f_t(x) = tx$ ($t \in \mathbb{R}_{>0}$). The *Euclidean cone over a metric space* (cf. **cone over metric space** in Chap. 9) is another example.

  The **tangent metric cone** over a metric space (X, d) at a point x_0 is (for all dilations $tX = (X, td)$) the closure of $\cup_{t>0} tX$, i.e., of $\lim_{t\to\infty} tX$ taken in the pointed Gromov–Hausdorff topology (cf. **Gromov–Hausdorff metric**).

  The **asymptotic metric cone** over (X, d) is its tangent metric cone "at infinity", i.e., $\cap_{t>0} tX = \lim_{t\to 0} tX$. Cf. **boundary of metric space** in Chap. 6.

  The term *metric cone* was also used by Bronshtein, 1998, for a convex cone C equipped with a complete metric compatible with its operations of addition (continuous on $C \times C$) and multiplication (continuous on $C \times \mathbb{R}_{\geq 0}$). by all $\lambda \geq 0$.
- **Metric fibration**

  Given a **complete** metric space (X, d), two subsets M_1 and M_2 of X are called *equidistant* if for each $x \in M_1$ there exists $y \in M_2$ with $d(x, y)$ being equal to the **Hausdorff metric** between the sets M_1 and M_2. A **metric fibration** of (X, d) is a partition $\mathcal{F}$ of X into isometric mutually equidistant closed sets.

  The quotient metric space $X/\mathcal{F}$ inherits a natural metric for which the **distance map** is a **submetry**.
- **Homeomorphic metric spaces**

  Two metric spaces (X, d_X) and (Y, d_Y) are called **homeomorphic** (or *topologically isomorphic*) if there exists a *homeomorphism* from X to Y, i.e., a bijective function $f : X \to Y$ such that f and f^{-1} are *continuous* (the preimage of every open set in Y is open in X).

Two metric spaces (X, d_X) and (Y, d_Y) are called *uniformly isomorphic* if there exists a bijective function $f : X \to Y$ such that f and f^{-1} are *uniformly continuous*. A function g is *uniformly continuous* if, for any $\epsilon > 0$, there exists $\delta > 0$ such that, for any $x, y \in X$, the inequality $d_X(x, y) < \delta$ implies that $d_Y(g(x), f(y)) < \epsilon$; a continuous function is uniformly continuous if X is compact.

- **Möbius mapping**

  Given distinct points x, y, z, w of a metric space (X, d), their **cross-ratio** is

$$cr((x, y, z, w), d) = \frac{d(x, y)d(z, w)}{d(x, z)d(y, w)} > 0.$$

  Given metric spaces (X, d_X) and (Y, d_Y), a **homeomorphism** $f : X \to Y$ is called a **Möbius mapping** if, for every distinct points $x, y, z, w \in X$, it holds

$$cr((x, y, z, w), d_X) = cr((f(x), f(y), f(z), f(w)), d_Y).$$

  A homeomorphism $f : X \to Y$ is called a **quasi-Möbius mapping** (Väisälä, 1984) if there exists a homeomorphism $\tau : [0, \infty) \to [0, \infty)$ such that, for every quadruple x, y, z, w of distinct points of X, it holds

$$cr((f(x), f(y), f(z), f(w)), d_Y) \leq \tau(cr((x, y, z, w), d_X)).$$

  A metric space (X, d) is called *metrically dense* (or *μ-dense* for given $\mu > 1$, Aseev–Trotsenko, 1987) if for any $x, y \in X$, there exists a sequence $\{z_i, i \in \mathbb{Z}\}$ with $z_i \to x$ as $i \to -\infty$, $z_i \to y$ as $i \to \infty$, and $\log cr((x, z_i, z_{i+1}, y), d) \leq \log \mu$ for all $i \in \mathbb{Z}$. The space (X, d) is μ-dense if and only if (Tukia-Väisälä, 1980), for any $x, y \in X$, there exists $z \in X$ with $\frac{d(x,y)}{6\mu} \leq d(x, z) \leq \frac{d(x,y)}{4}$.

- **Quasi-symmetric mapping**

  Given metric spaces (X, d_X) and (Y, d_Y), a **homeomorphism** $f : X \to Y$ is called a **quasi-symmetric mapping** (Tukia–Väisälä, 1980) if there is a homeomorphism $\tau : [0, \infty) \to [0, \infty)$ such that, for every triple (x, y, z) of distinct points of X,

$$\frac{d_Y(f(x), f(y))}{d_Y(f(x), f(z))} \leq \tau \frac{d_X(x, y)}{d_X(x, z)}.$$

  Quasi-symmetric mappings are **quasi-Möbius**, and quasi-Möbius mappings between bounded metric spaces are quasi-symmetric. In the case $f : \mathbb{R}^n \to \mathbb{R}^n$, quasi-symmetric mappings are exactly the same as **quasi-conformal mappings**.

- **Conformal metric mapping**

  Given metric spaces (X, d_X) and (Y, d_Y) which are domains in $\mathbb{R}^n$, a **homeomorphism** $f : X \to Y$ is called a **conformal metric mapping** if, for any nonisolated point $x \in X$, the limit $\lim_{y \to x} \frac{d_Y(f(x), f(y))}{d(x, y)}$ exists, is finite and positive.

A homeomorphism $f : X \to Y$ is called a **quasi-conformal mapping** (or, specifically, *C-quasi-conformal mapping*) if there exists a constant C such that

$$\limsup_{r\to 0} \frac{\max\{d_Y(f(x),f(y)) : d_X(x,y) \le r\}}{\min\{d_Y(f(x),f(y)) : d_X(x,y) \ge r\}} \le C$$

for each $x \in X$. The smallest such constant C is called the **conformal dilation**.

The **conformal dimension** of a metric space (X, d) (Pansu, 1989) is the infimum of the **Hausdorff dimension** over all quasi-conformal mappings of (X, d) into some metric space. For the middle-third Cantor set on $[0, 1]$, it is 0 but, for any of its quasi-conformal images, it is positive.

- **Hölder mapping**

  Let $c, \alpha \ge 0$ be constants. Given metric spaces (X, d_X) and (Y, d_Y), a function $f : X \to Y$ is called the **Hölder mapping** (or *α-Hölder mapping* if the constant α should be mentioned) if for all $x, y \in X$

$$d_Y(f(x),f(y)) \le c(d_X(x,y))^\alpha.$$

  A 1-Hölder mapping is a **Lipschitz mapping**; 0-Hölder mapping means that the metric d_Y is bounded.

- **Lipschitz mapping**

  Let c be a positive constant. Given metric spaces (X, d_X) and (Y, d_Y), a function $f : X \to Y$ is called a **Lipschitz** (or **Lipschitz continuous**, *c-Lipschitz* if the constant c should be mentioned) **mapping** if for all $x, y \in X$ it holds

$$d_Y(f(x),f(y)) \le cd_X(x,y).$$

  A c-Lipschitz mapping is called a **metric mapping** if $c = 1$, and is called a **contraction** if $c < 1$.

- **Bi-Lipschitz mapping**

  Given metric spaces (X, d_X), (Y, d_Y) and a constant $c > 1$, a function $f : X \to Y$ is called a **bi-Lipschitz mapping** (or *c-bi-Lipschitz mapping*, **c-embedding**) if there exists a number $r > 0$ such that for any $x, y \in X$ it holds

$$rd_X(x,y) \le d_Y(f(x),f(y)) \le crd_X(x,y).$$

  Every bi-Lipschitz mapping is a **quasi-symmetric mapping**.

  The smallest c for which f is a c-bi-Lipschitz mapping is called the **distortion** of f. Bourgain, 1985, proved that every k-point metric space c-embeds into a Euclidean space with distortion $O(\ln k)$. Gromov's *distortion for curves* is the maximum ratio of arc length to chord length.

  Two metrics d_1 and d_2 on X are called **bi-Lipschitz equivalent metrics** if there are positive constants c and C such that $cd_1(x, y) \le d_2(x, y) \le Cd_1(x, y)$ for all $x, y \in X$, i.e., the identity mapping is a bi-Lipschitz mapping from (X, d_1) into (X, d_2). Bi-Lipschitz equivalent metrics are **equivalent**, i.e., generate the same

topology but, for example, equivalent L_1-metric and L_2-metric (cf. **L_p-metric** in Chap. 5) on $\mathbb{R}$ are not bi-Lipschitz equivalent.

A bi-Lipschitz mapping $f : X \to Y$ is a **c-isomorphism** $f : X \to f(X)$.

- **c-isomorphism of metric spaces**

  Given two metric spaces (X, d_X) and (Y, d_Y), the *Lipschitz norm* $||.||_{Lip}$ on the set of all injective mappings $f : X \to Y$ is defined by

$$||f||_{Lip} = \sup_{x,y \in X, x \neq y} \frac{d_Y(f(x), f(y))}{d_X(x, y)}.$$

  Two metric spaces X and Y are called **c-isomorphic** if there exists an injective mapping $f : X \to Y$ such that $||f||_{Lip}||f^{-1}||_{Lip} \leq c$.

- **Metric Ramsey number**

  For a given class $\mathcal{M}$ of metric spaces (usually, *l_p-spaces*), an integer $n \geq 1$, and a real number $c \geq 1$, the **metric Ramsey number** (or *c-metric Ramsey number*) $R_{\mathcal{M}}(c, n)$ is the largest integer m such that every n-point metric space has a subspace of cardinality m that c-embeds into a member of $\mathcal{M}$ (see [BLMN05]).

  The *Ramsey number* R_n is the minimal number of vertices of a complete graph such that any edge-coloring with n colors produces a monochromatic triangle. The following metric analog of R_n was considered in [Masc04]: the least number of points a finite metric space must contain in order to contain an equilateral triangle, i.e., to have **equilateral metric dimension** greater than two.

- **Uniform metric mapping**

  Given metric spaces (X, d_X) and (Y, d_Y), a function $f : X \to Y$ is called a **uniform metric mapping** if there are two nondecreasing functions g_1 and g_2 from $\mathbb{R}_{\geq 0}$ to itself with $\lim_{r \to \infty} g_i(r) = \infty$ for $i = 1, 2$, such that the inequality

$$g_1(d_X(x, y)) \leq d_Y(f(x), f(y)) \leq g_2(d_X(x, y))$$

  holds for all $x, y \in X$. A **bi-Lipschitz mapping** is a uniform metric mapping with linear functions g_1, g_2.

- **Metric compression**

  Given metric spaces (X, d_X) (unbounded) and (Y, d_Y), a function $f : X \to Y$ is a *large scale Lipschitz mapping* if, for some $c > 0, D \geq 0$ and all $x, y \in X$,

$$d_Y(f(x), f(y)) \leq c d_X(x, y) + D.$$

  The *compression* of such a mapping f is $\rho_f(r) = \inf_{d_X(x,y) \geq r} d_Y(f(x), f(y))$.

  The **metric compression** of (X, d_X) in (Y, d_Y) is defined by

$$R(X, Y) = \sup_f \{\underline{\lim}_{r \to \infty} \frac{\log \max\{\rho_f(r), 1\}}{\log r}\},$$

  where the supremum is over all large scale Lipschitz mappings f.

In the main interesting case—when (Y, d_Y) is a Hilbert space and (X, d_X) is a (finitely generated discrete) group with **word metric**—$R(X, Y) = 0$ if there is no (Guentner–Kaminker, 2004) **uniform metric mapping** $(X, d_X) \to (Y, d_Y)$, and $R(X, Y) = 1$ for free groups, even if there is no **quasi-isometry**. Arzhantzeva–Guba–Sapir, 2006, found groups with $\frac{1}{2} \le R(X, Y) \le \frac{3}{4}$.

- **Quasi-isometry**

  Given metric spaces (X, d_X) and (Y, d_Y), a function $f : X \to Y$ is called a **quasi-isometry** (or (C, c)**-quasi-isometry**) if it holds

$$C^{-1} d_X(x, y) - c \le d_Y(f(x), f(y)) \le C d_X(x, y) + c,$$

  for some $C \ge 1, c \ge 0$, and $Y = \cup_{x \in X} B_{d_Y}(f(x), c)$, i.e., for every point $y \in Y$, there exists $x \in X$ such that $d_Y(y, f(x)) < \frac{c}{2}$. Quasi-isometry is an equivalence relation on metric spaces; it is a bi-Lipschitz equivalence up to small distances. Quasi-isometry means that metric spaces contain bi-Lipschitz equivalent **Delone sets**.

  A quasi-isometry with $C = 1$ is called a **coarse isometry** (or *rough isometry*, *almost isometry*). Cf. **quasi-Euclidean rank of a metric space**.

- **Coarse embedding**

  Given metric spaces (X, d_X) and (Y, d_Y), a function $f : X \to Y$ is called a **coarse embedding** if there exist nondecreasing functions $\rho_1, \rho_2 : [0, \infty) \to [0, \infty)$ with $\rho_1(d_X(x, x')) \le d_Y(f(x), f(x')) \le \rho_2(d_X(x, x'))$ if $x, x' \in X$ and $\lim_{t \to \infty} \rho_1(t) = +\infty$.

  Metrics d_1, d_2 on X are called **coarsely equivalent metrics** if there exist nondecreasing functions $f, g : [0, \infty) \to [0, \infty)$ such that $d_1 \le f(d_2), d_2 \le g(d_1)$.

- **Metrically regular mapping**

  Let (X, d_X) and (Y, d_Y) be metric spaces, and let F be a set-valued mapping from X to Y, having *inverse* F^{-1}, i.e., with $x \in F^{-1}(y)$ if and only if $y \in F(x)$.

  The mapping F is said to be **metrically regular at** $\overline{x}$ **for** $\overline{y}$ (Dontchev–Lewis–Rockafeller, 2002) if there exists $c > 0$ such that it holds

$$d_X(x, F^{-1}(y)) \le c d_Y(y, F(x))$$

  for all (x, y) close to $(\overline{x}, \overline{y})$. Here $d(z, A) = \inf_{a \in A} d(z, a)$ and $d(z, \emptyset) = +\infty$.

- **Contraction**

  Given metric spaces (X, d_X) and (Y, d_Y), a function $f : X \to Y$ is called a **contraction** if the inequality

$$d_Y(f(x), f(y)) \le c d_X(x, y)$$

  holds for all $x, y \in X$ and some real number c, $0 \le c < 1$.

  Every contraction is a **contractive mapping**, and it is uniformly continuous. *Banach fixed point theorem* (or *contraction principle*): every contraction from a **complete** metric space into itself has a unique fixed point.

- **Contractive mapping**
  Given metric spaces (X, d_X) and (Y, d_Y), a function $f : X \to Y$ is called a **contractive** (or *strictly short*, *distance-decreasing*) **mapping** if

$$d_Y(f(x), f(y)) < d_X(x, y)$$

  holds for all different $x, y \in X$. A function $f : X \to Y$ is called a **noncontractive mapping** (or *dominating mapping*) if for all $x, y \in X$ it holds

$$d_Y(f(x), f(y)) \geq d_X(x, y).$$

  Every noncontractive bijection from a **totally bounded** metric space onto itself is an **isometry**.
- **Short mapping**
  Given metric spaces (X, d_X) and (Y, d_Y), a function $f : X \to Y$ is called a **short** (or *1-Lipschitz*, *nonexpansive*, *distance-noninreasing*, *metric*) **mapping** (or *semicontraction*) if for all $x, y \in X$ it holds

$$d_Y(f(x), f(y)) \leq d_X(x, y).$$

  A **submetry** is a short mapping such that the image of any metric ball is a metric ball of the same radius.
  The set of short mappings $f : X \to Y$ for bounded metric spaces (X, d_X) and (Y, d_Y) is a metric space under the **uniform metric** $\sup\{d_Y(f(x), g(x)) : x \in X\}$.
  Two subsets A and B of a metric space (X, d) are called (Gowers, 2000) **similar** if there exist short mappings $f : A \to X$, $g : B \to X$ and a small $\epsilon > 0$ such that every point of A is within ϵ of some point of B, every point of B is within ϵ of some point of A, and $|d(x, g(f(x))) - d(y, f(g(y)))| \leq \epsilon$ for any $x \in A, y \in B$.
- **Category of metric spaces**
  A *category* Ψ consists of a class $Ob(\Psi)$ of *objects* and a class $Mor(\Psi)$ of *morphisms* (or *arrows*) satisfying the following conditions:

  1. To each ordered pair of objects A, B is associated a set $\Psi(A, B)$ of morphisms, and each morphism belongs to only one set $\Psi(A, B)$;
  2. The composition $f \cdot g$ of two morphisms $f : A \to B$, $g : C \to D$ is defined if $B = C$ in which case it belongs to $\Psi(A, D)$, and it is associative;
  3. Each set $\Psi(A, A)$ contains, as an *identity*, a morphism id_A such that $f \cdot id_A = f$ and $id_A \cdot g = g$ for any morphisms $f : X \to A$ and $g : A \to Y$.

  The **category of metric spaces**, denoted by *Met* (see [Isbe64]), is a category which has metric spaces as objects and **short mappings** as morphisms. A unique **injective envelope** exists in this category for every one of its objects; it can be identified with its **tight span**. In *Met*, the *monomorphisms* are injective short mappings, and *isomorphisms* are **isometries**. *Met* is a subcategory of the category which has metric spaces as objects and **Lipschitz mappings** as morphisms.

Cf. **metric 1-space** on the objects of a category in Chap. 3.

- **Injective metric space**

  A metric space (X, d) is called **injective** if, for every isometric embedding $f : X \to X'$ of (X, d) into another metric space (X', d'), there exists a **short mapping** f' from X' into X with $f' \cdot f = id_X$, i.e., X is a *retract* of X'.

  Equivalently, X is an *absolute retract*, i.e., a retract of every metric space into which it embeds isometrically. A metric space (X, d) is injective if and only if it is **hyperconvex**. Examples of such metric spaces are l_1^2-space, l_∞^n-space, any **real tree** and the **tight span** of a metric space.

- **Injective envelope**

  The **injective envelope** (introduced first in [Isbe64] as *injective hull*) is a generalization of **Cauchy completion**. Given a metric space (X, d), it can be embedded isometrically into an **injective metric space** $(\hat{X}, \hat{d})$; given any such isometric embedding $f : X \to \hat{X}$, there exists a unique smallest injective subspace $(\overline{X}, \overline{d})$ of $(\hat{X}, \hat{d})$ containing $f(X)$ which is called the **injective envelope** of X. It is isometrically identified with the **tight span** of (X, d).

  A metric space coincides with its injective envelope if and only if it is injective.

- **Tight extension**

  An extension (X', d') of a metric space (X, d) is called a **tight extension** if, for every semimetric d'' on X' satisfying the conditions $d''(x_1, x_2) = d(x_1, x_2)$ for all $x_1, x_2 \in X$, and $d''(y_1, y_2) \leq d'(y_1, y_2)$ for any $y_1, y_2 \in X'$, one has $d''(y_1, y_2) = d'(y_1, y_2)$ for all $y_1, y_2 \in X'$.

  The **tight span** is the *universal tight extension* of X, i.e., it contains, up to isometries, every tight extension of X, and it has no proper tight extension itself.

- **Tight span**

  Given a metric space (X, d) of finite diameter, consider the set $\mathbb{R}^X = \{f : X \to \mathbb{R}\}$. The **tight span** $T(X, d)$ of (X, d) is defined as the set $T(X, d) = \{f \in \mathbb{R}^X : f(x) = \sup_{y \in X}(d(x, y) - f(y))$ for all $x \in X\}$, endowed with the metric induced on $T(X, d)$ by the *sup norm* $||f|| = \sup_{x \in X} |f(x)|$.

  The set X can be identified with the set $\{h_x \in T(X, d) : h_x(y) = d(y, x)\}$ or, equivalently, with the set $T^0(X, d) = \{f \in T(X, d) : 0 \in f(X)\}$. The **injective envelope** $(\overline{X}, \overline{d})$ of X is isometrically identified with the tight span $T(X, d)$ by

$$\overline{X} \to T(X, d),\ \overline{x} \to h_{\overline{x}} \in T(X, d) : h_{\overline{x}}(y) = \overline{d}(f(y), \overline{x}).$$

  The tight span $T(X, d)$ of a finite metric space is the metric space $(T(X), D(f, g) = \max |f(x) - g(x)|)$, where $T(X)$ is the set of functions $f : X \to \mathbb{R}$ such that for any $x, y \in X$, $f(x) + f(y) \geq d(x, y)$ and, for each $x \in X$, there exists $y \in X$ with $f(x) + f(y) = d(x, y)$. The mapping of any x into the function $f_x(y) = d(x, y)$ gives an isometric embedding of (X, d) into $T(X, d)$. For example, if $X = \{x_1, x_2\}$, then $T(X, d)$ is the interval of length $d(x_1, x_2)$.

The tight span of a metric space (X, d) of finite diameter can be considered as a polytopal complex of bounded faces of the polyhedron

$$\{y \in \mathbb{R}^n_{\geq 0} : y_i + y_j \geq d(x_i, x_j) \text{ for } 1 \leq i < j \leq n\}$$

if, for example, $X = \{x_1, \ldots, x_n\}$. The dimension of this complex is called (Dress, 1984) the **combinatorial dimension** of (X, d).

- **Real tree**

  A metric space (X, d) is called (Tits, 1977) a **real tree** (or $\mathbb{R}$**-tree**) if, for all $x, y \in X$, there exists a unique **arc** from x to y, and this arc is a **geodesic segment**. So, an $\mathbb{R}$-tree is a (uniquely) arcwise connected metric space in which each arc is isometric to a subarc of $\mathbb{R}$. $\mathbb{R}$-tree is not related to a **metric tree** in Chap. 17.

  A metric space (X, d) is a real tree if and only if it is **path-connected** and Gromov 0**-hyperbolic** (i.e., satisfies the **four-point inequality**). The plane $\mathbb{R}^2$ with the **Paris metric** or **lift metric** (Chap. 19) are examples of an $\mathbb{R}$-tree.

  Real trees are exactly **tree-like** metric spaces which are **geodesic**; they are **injective** metric spaces among tree-like spaces. Tree-like metric spaces are by definition metric subspaces of real trees.

  If (X, d) is a finite metric space, then the **tight span** $T(X, d)$ is a real tree and can be viewed as an edge-weighted graph-theoretical tree.

  A metric space is a complete real tree if and only if it is **hyperconvex** and any two points are joined by a **metric segment**.

  A geodesic metric space (X, d) is called (Druţu–Sapir, 2005) *tree-graded with respect to* a collection $\mathcal{P}$ of connected proper subsets with $|P \cap P'| \leq 1$ for any distinct $P, P' \in \mathcal{P}$, if every its simple loop composed of three geodesics is contained in one $P \in \mathcal{P}$. $\mathbb{R}$-trees are tree-graded with respect to the empty set.

1.5 General Distances

- **Discrete metric**

  Given a set X, the **discrete metric** (or **trivial metric**, **sorting distance**, **drastic distance**, **Dirac distance**, *overlap*) is a metric on X, defined by $d(x, y) = 1$ for all distinct $x, y \in X$ and $d(x, x) = 0$. Cf. the much more general notion of a (metrically or topologically) **discrete metric space**.

- **Indiscrete semimetric**

  Given a set X, the **indiscrete semimetric** d is a semimetric on X defined by $d(x, y) = 0$ for all $x, y \in X$.

- **Equidistant metric**

  Given a set X and a positive real number t, the **equidistant metric** d is a metric on X defined by $d(x, y) = t$ for all distinct $x, y \in X$ (and $d(x, x) = 0$).

- $(1, 2) - B$**-metric**

  Given a set X, the $(1, 2) - B$**-metric** d is a metric on X such that, for any $x \in X$, the number of points $y \in X$ with $d(x, y) = 1$ is at most B, and all other

distances are equal to 2. The $(1,2)-B$-**metric** is the **truncated metric** of a graph with maximal vertex degree B.

- **Permutation metric**

  Given a finite set X, a metric d on it is called a **permutation metric** (or *linear arrangement metric*) if there exists a bijection $\omega : X \to \{1, \ldots, |X|\}$ such that

$$d(x, y) = |\omega(x) - \omega(y)|$$

  holds for all $x, y \in X$. Even–Naor–Rao–Schieber, 2000, defined a more general **spreading metric**, i.e., any metric d on $\{1, \ldots, n\}$ such that $\sum_{y \in M} d(x, y) \geq \frac{|M|(|M|+2)}{4}$ for any $1 \leq x \leq n$ and $M \subseteq \{1, \ldots, n\} \setminus \{x\}$ with $|M| \geq 2$.
- **Induced metric**

  Given a metric space (X, d) and a subset $X' \subset X$, an **induced metric** (or **submetric**) is the restriction d' of d to X'. A metric space (X', d') is called a **metric subspace** of (X, d), and (X, d) is called a **metric extension** of (X', d').
- **Katětov mapping**

  Given a metric space (X, d), the mapping $f : X \to \mathbb{R}$ is a **Katětov mapping** if

$$|f(x) - f(y)| \leq d(x, y) \leq f(x) + f(y)$$

  for any $x, y \in X$, i.e., setting $d(x, z) = f(x)$ defines a one-point **metric extension** $(X \cup \{z\}, d)$ of (X, d).

  The set $E(X)$ of Katětov mappings on X is a complete metric space with metric $D(f, g) = \sup_{x \in X} |f(x) - g(x)|$; (X, d) embeds isometrically in it via the *Kuratowski mapping* $x \to d(x, .)$, with unique extension of each isometry of X to one of $E(X)$.
- **Dominating metric**

  Given metrics d and d_1 on a set X, d_1 **dominates** d if $d_1(x, y) \geq d(x, y)$ for all $x, y \in X$. Cf. **noncontractive mapping** (or *dominating mapping*).
- **Barbilian semimetric**

  Given sets X and P, the function $f : P \times X \to \mathbb{R}_{>0}$ is called an *influence* (of P over X) if for any $x, y \in X$ the ratio $g_{xy}(p) = \frac{f(p,x)}{f(p,y)}$ has a maximum when $p \in P$.

  The **Barbilian semimetric** is defined on the set X by

$$\ln \frac{\max_{p \in P} g_{xy}(p)}{\min_{p \in P} g_{xy}(p)}$$

  for any $x, y \in X$. Barbilian, 1959, proved that the above function is well defined (moreover, $\min_{p \in P} g_{xy}(p) = \frac{1}{\max_{p \in P} g_{yx}(p)}$) and is a semimetric. Also, it is a metric if the influence f is *effective*, i.e., there is no pair $x, y \in X$ such that $g_{xy}(p)$ is constant for all $p \in P$. Cf. a special case **Barbilian metric** in Chap. 6.
- **Metric transform**

  A **metric transform** is a distance obtained as a function of a given metric (cf. Chap. 4).

- **Complete metric**

  Given a metric space (X, d), a sequence $\{x_n\}$, $x_n \in X$, is said to have *convergence to* $x^* \in X$ if $\lim_{n\to\infty} d(x_n, x^*) = 0$, i.e., for any $\epsilon > 0$, there exists $n_0 \in \mathbb{N}$ such that $d(x_n, x^*) < \epsilon$ for any $n > n_0$. Any sequence converges to at most one limit in X; it is not so, in general, if d is a semimetric.

  A sequence $\{x_n\}_n$, $x_n \in X$, is called a *Cauchy sequence* if, for any $\epsilon > 0$, there exists $n_0 \in \mathbb{N}$ such that $d(x_n, x_m) < \epsilon$ for any $m, n > n_0$.

  A metric space (X, d) is called a **complete metric space** if every *Cauchy sequence* in it converges. In this case the metric d is called a **complete metric**. An example of an incomplete metric space is $(\mathbb{N}, d(m, n) = \frac{|m-n|}{mn})$.
- **Cauchy completion**

  Given a metric space (X, d), its **Cauchy completion** is a metric space (X^*, d^*) on the set X^* of all equivalence classes of *Cauchy sequences*, where the sequence $\{x_n\}_n$ is called *equivalent to* $\{y_n\}_n$ if $\lim_{n\to\infty} d(x_n, y_n) = 0$. The metric d^* is defined by

$$d^*(x^*, y^*) = \lim_{n\to\infty} d(x_n, y_n),$$

  for any $x^*, y^* \in X^*$, where $\{z_n\}_n$ is any element in the equivalence class z^*.

  The Cauchy completion (X^*, d^*) is a unique, up to isometry, **complete** metric space, into which the metric space (X, d) embeds as a dense metric subspace.

  The Cauchy completion of the metric space $(\mathbb{Q}, |x - y|)$ of rational numbers is the *real line* $(\mathbb{R}, |x - y|)$. A **Banach space** is the Cauchy completion of a *normed vector space* $(V, ||.||)$ with the **norm metric** $||x - y||$. A **Hilbert space** corresponds to the case an *inner product norm* $||x|| = \sqrt{\langle x, x\rangle}$.
- **Perfect metric space**

  A complete metric space (X, d) is called **perfect** if every point $x \in X$ is a *limit point*, i.e., $|B(x, r) = \{y \in X : d(x, y) < r\}| > 1$ holds for any $r > 0$.

  A topological space is a **Cantor space** (i.e., *homeomorphic* to the *Cantor set* with the natural metric $|x - y|$) if and only if it is nonempty, perfect, **totally disconnected**, compact and metrizable. The totally disconnected countable metric space $(\mathbb{Q}, |x-y|)$ of rational numbers also consists only of limit points but it is not complete and not **locally compact**.

  Every proper metric ball of radius r in a metric space has diameter at most $2r$. Given a number $0 < c \leq 1$, a metric space is called a c**-uniformly perfect metric space** if this diameter is at least $2cr$. Cf. the **radii of metric space**.
- **Metrically discrete metric space**

  A metric space (X, d) is called **metrically** (or *uniformly*) **discrete** if there exists a number $r > 0$ such that $B(x, r) = \{y \in X : d(x, y) < r\} = \{x\}$ for every $x \in X$.

  (X, d) is a **topologically discrete metric space** (or a *discrete metric space*) if the underlying topological space is **discrete**, i.e., each point $x \in X$ is an *isolated point*: there exists a number $r(x) > 0$ such that $B(x, r(x)) = \{x\}$. For $X = \{\frac{1}{n} :$

$n = 1, 2, 3, \dots\}$, the metric space $(X, |x - y|)$ is topologically but not metrically discrete. Cf. **translation discrete metric** in Chap. 10.

Alternatively, a metric space (X, d) is called *discrete* if any of the following holds:

1. (Burdyuk–Burdyuk 1991) it has a proper *isolated subset*, i.e., $M \subset X$ with $\inf\{d(x, y) : x \in M, y \notin M\} > 0$ (any such space admits a unique decomposition into *continuous*, i.e., nondiscrete, components);
2. (Lebedeva–Sergienko–Soltan, 1984) for any distinct points $x, y \in X$, there exists a point z of the **closed metric interval** $I(x, y)$ with $I(x, z) = \{x, z\}$;
3. a stronger property holds: for any two distinct points $x, y \in X$, every sequence of points $z_1, z_2, \dots$ with $z_k \in I(x, y)$ but $z_{k+1} \in I(x, z_k) \setminus \{z_k\}$ for $k = 1, 2, \dots$ is a finite sequence.

- **Locally finite metric space**

  Let (X, d) be a **metrically discrete metric space**. Then it is called **locally finite** if for every $x \in X$ and every $r \geq 0$, the ball $|B(x, r)|$ is finite.

  If, moreover, $|B(x, r)| \leq C(r)$ for some number $C(r)$ depending only on r, then (X, d) is said to have *bounded geometry*.
- **Bounded metric space**

  A metric (moreover, a distance) d on a set X is called **bounded** if there exists a constant $C > 0$ such that $d(x, y) \leq C$ for any $x, y \in X$.

  For example, given a metric d on X, the metric D on X, defined by $D(x, y) = \frac{d(x,y)}{1+d(x,y)}$, is bounded with $C = 1$.

  A metric space (X, d) with a bounded metric d is called a **bounded metric space**.
- **Totally bounded metric space**

  A metric space (X, d) is called **totally bounded** if, for every $\epsilon > 0$, there exists a finite ϵ**-net**, i.e., a finite subset $M \subset X$ with the **point-set distance** $d(x, M) < \epsilon$ for any $x \in X$ (cf. **totally bounded space** in Chap. 2).

  Every totally bounded metric space is **bounded** and **separable**. A metric space is totally bounded if and only if its **Cauchy completion** is **compact**.
- **Separable metric space**

  A metric space (X, d) is called **separable** if it contains a countable **dense subset** M, i.e., a subset with which all its elements can be approached: X is the *closure* $cl(M)$ (M together with all its limit points).

  A metric space is separable if and only if it is **second-countable** (cf. Chap. 2).
- **Compact metric space**

  A **compact metric space** (or **metric compactum**) is a metric space in which every sequence has a *Cauchy subsequence*, and those subsequences are convergent. A metric space is compact if and only if it is **totally bounded** and **complete**.

  Every bounded and closed subset of a Euclidean space is compact. Every finite metric space is compact. Every compact metric space is **second-countable**.

  A **continuum** is a nonempty **connected** metric compactum.

- **Proper metric space**

  A metric space is called **proper** (or *finitely compact*, *having the Heine–Borel property*) if every its closed metric ball is compact. Any such space is **complete**.
- **UC metric space**

  A metric space is called a **UC metric space** (or *Atsuji space*) if any continuous function from it into an arbitrary metric space is *uniformly continuous*.

  Every such space is **complete**. Every **metric compactum** is a UC metric space.
- **Metric measure space**

  A **metric measure space** (or *mm-space*, *metric triple*) is a triple (X, d, μ), where (X, d) is a *Polish* (i.e., complete separable; cf. Chap. 2) *metric space* and (X, Σ, μ) is a *probability measure space* ($\mu(X) = 1$) with Σ being a *Borel* σ-*algebra* of all open and closed sets of the **metric topology** (Chap. 2) induced by the metric d on X. Cf. **metric outer measure**.
- **Norm metric**

  Given a *normed vector space* $(V, ||.||)$, the **norm metric** on V is defined by

  $$||x - y||.$$

  The metric space $(V, ||x - y||)$ is called a **Banach space** if it is **complete**. Examples of norm metrics are l_p**-** and L_p**-metrics**, in particular, the **Euclidean metric**.

  Any metric space (X, d) admits an isometric embedding into a Banach space B such that its convex hull is dense in B (cf. **Monge–Kantorovich metric** in Chap. 14); (X, d) is a **linearly rigid metric space** if such an embedding is unique up to isometry. A metric space isometrically embeds into the unit sphere of a Banach space if and only if its diameter is at most 2.
- **Path metric**

  Given a connected graph $G = (V, E)$, its **path metric** (or *graphic metric*) d_{path} is a metric on V defined as the length (i.e., the number of edges) of a shortest path connecting two given vertices x and y from V (cf. Chap. 15).
- **Editing metric**

  Given a finite set X and a finite set $\mathcal{O}$ of (unary) *editing operations* on X, the **editing metric** on X is the **path metric** of the graph with the vertex-set X and xy being an edge if y can be obtained from x by one of the operations from $\mathcal{O}$.
- **Gallery metric**

  A *chamber system* is a set X (its elements are called *chambers*) equipped with n equivalence relations $\sim_i$, $1 \leq i \leq n$. A *gallery* is a sequence of chambers $x_1, \ldots, x_m$ such that $x_i \sim_j x_{i+1}$ for every i and some j depending on i.

  The **gallery metric** is an **extended metric** on X which is the length of the shortest gallery connecting x and $y \in X$ (and is equal to ∞ if there is no connecting gallery). The gallery metric is the (extended) **path metric** of the graph with the vertex-set X and xy being an edge if $x \sim_i y$ for some $1 \leq i \leq n$.

- **Metric on incidence structure**

  An *incidence structure* (P, L, I) consists of 3 sets: points P, lines L and flags $I \subset P \times L$, where a point $p \in P$ is said to be *incident* with a line $l \in L$ if $(p, l) \in I$.

  If, moreover, for any pair of distinct points, there is at most one line incident with both of them, then the collinearity graph is a graph whose vertices are the points with two vertices being adjacent if they determine a line.

  The **metric on incidence structure** is the **path metric** of this graph.
- **Riemannian metric**

  Given a connected n-dimensional smooth *manifold* M^n (cf. Chaps. 2 and 7), its **Riemannian metric** is a collection of positive-definite symmetric bilinear forms $((g_{ij}))$ on the tangent spaces of M^n which varies smoothly from point to point.

  The length of a curve γ on M^n is expressed as $\int_\gamma \sqrt{\sum_{i,j} g_{ij} dx_i dx_j}$, and the **intrinsic metric** on M^n, also called the **Riemannian distance**, is the infimum of lengths of curves connecting any two given points $x, y \in M^n$. Cf. Chap. 7.
- **Linearly additive metric**

  A **linearly additive** (or *additive on lines*) **metric** is a continuous metric d on $\mathbb{R}^n$ which, for any points x, y, z lying in that order on a common line, satisfies

$$d(x, z) = d(x, y) + d(y, z).$$

  Hilbert's 4-th problem asked in 1900 to classify such metrics; it is solved only for dimension $n = 2$ ([Amba76]). Cf. **projective metric** in Chap. 6.

  Every **norm metric** on $\mathbb{R}^n$ is linearly additive. Every linearly additive metric on $\mathbb{R}^2$ is a **hypermetric**.
- **Hamming metric**

  The **Hamming metric** d_H (called sometimes *Dalal distance* in Semantics) is a metric on $\mathbb{R}^n$ defined (Hamming, 1950) by

$$|\{i : 1 \le i \le n, x_i \ne y_i\}|.$$

  On binary vectors $x, y \in \{0, 1\}^n$ the Hamming metric and the l_1-*metric* (cf. L_p-**metric** in Chap. 5) coincide; they are equal to $|I(x) \Delta I(y)| = |I(x) \setminus I(y)| + |I(y) \setminus I(x)|$, where $I(z) = \{1 \le t \le n : z_i = 1\}$.

  In fact, $\max\{|I(x) \setminus I(y)|, |I(y) \setminus I(x)|\}$ is also a metric.
- **Lee metric**

  Given $m, n \in \mathbb{N}$, $m \ge 2$, the **Lee metric** d_{Lee} is a metric on $\mathbb{Z}_m^n = \{0, 1, \ldots, m-1\}^n$ defined (Lee, 1958) by

$$\sum_{1 \le i \le n} \min\{|x_i - y_i|, m - |x_i - y_i|\}.$$

  The metric space (Z_m^n, d_{Lee}) is a discrete analog of the *elliptic space*.

The Lee metric coincides with the Hamming metric d_H if $m = 2$ or $m = 3$. The metric spaces (Z_4^n, d_{Lee}) and $Z_2^{2n}, d_H)$ are isometric. Lee and Hamming metrics are applied for phase and orthogonal modulation, respectively.

Cf. **absolute summation distance** and **generalized Lee metric** in Chap. 16.

- **Enomoto–Katona metric**

  Given a finite set X and an integer k, $2k \leq |X|$, the **Enomoto–Katona metric** (2001) is the distance between unordered pairs (X_1, X_2) and (Y_1, Y_2) of disjoint k-subsets of X defined by

$$\min\{|X_1 \setminus Y_1| + |X_2 \setminus Y_2|, |X_1 \setminus Y_2| + |X_2 \setminus Y_1|\}.$$

  Cf. **Earth Mover's distance**, **transportation distance** in Chaps. 21 and 14.

- **Symmetric difference metric**

  Given a *measure space* $(\Omega, \mathcal{A}, \mu)$, the **symmetric difference** (or *measure*) *semimetric* on the set $\mathcal{A}_\mu = \{A \in \mathcal{A} : \mu(A) < \infty\}$ is defined by

$$od_\triangle(A, B) = \mu(A \triangle B),$$

  where $A \triangle B = (A \cup B) \setminus (A \cap B)$ is the *symmetric difference* of A and $B \in \mathcal{A}_\mu$.

  The value $d_\triangle(A, B) = 0$ if and only if $\mu(A \triangle B) = 0$, i.e., A and B are equal *almost everywhere*. Identifying two sets $A, B \in \mathcal{A}_\mu$ if $\mu(A \triangle B) = 0$, we obtain the **symmetric difference metric** (or **Fréchet–Nikodym–Aronszyan distance**, **measure metric**).

  If μ is the *cardinality measure*, i.e., $\mu(A) = |A|$, then $d_\triangle(A, B) = |A \triangle B| = |A \setminus B| + |B \setminus A|$. In this case $|A \triangle B| = 0$ if and only if $A = B$.

  The metrics $d_{\max}(A, B) = \max(|A \setminus B|, |B \setminus A|)$ and $1 - \frac{|A \cap B|}{\max(|A|, |B|)}$ (its normalised version) are special cases of **Zelinka distance** and **Bunke–Shearer metric** in Chap. 15. For each $p \geq 1$, the ***p*-difference metric** (Noradam–Nyblom, 2014) is $d_p(A, B) = (|A \setminus B|^p + |B \setminus A|^p)^{\frac{1}{p}}$; so, $d_1 = d_\triangle$ and $\lim_{p \to \infty} d_p = d_{\max}$.

  The **Johnson distance** between k-sets A and B is $\frac{|A \triangle B|}{2} = k - |A \cap B|$.

  The *symmetric difference metric between ordered q-partitions* $A = (A_1, \ldots, A_q)$ and $B = (B_1, \ldots, B_q)$ is $\sum_{i=1}^{q} |A_i \triangle B_i|$. Cf. **metrics between partitions** in Chap. 10.

- **Steinhaus distance**

  Given a *measure space* $(\Omega, \mathcal{A}, \mu)$, the **Steinhaus distance** d_{St} is a semimetric on the set $\mathcal{A}_\mu = \{A \in \mathcal{A} : \mu(A) < \infty\}$ defined as 0 if $\mu(A) = \mu(B) = 0$, and by

$$\frac{\mu(A \triangle B)}{\mu(A \cup B)} = 1 - \frac{\mu(A \cap B)}{\mu(A \cup B)}$$

  if $\mu(A \cup B) > 0$. It becomes a metric on the set of equivalence classes of elements from $\mathcal{A}_\mu$; here $A, B \in \mathcal{A}_\mu$ are called *equivalent* if $\mu(A \triangle B) = 0$.

The **biotope** (or **Tanimoto**) **distance** $\frac{|A \triangle B|}{|A \cup B|}$ is the special case of Steinhaus distance obtained for the *cardinality measure* $\mu(A) = |A|$ for finite sets.

Cf. also the **generalized biotope transform metric** in Chap. 4.

- **Fréchet metric**

  Let (X, d) be a metric space. Consider a set $\mathcal{F}$ of all continuous mappings $f : A \to X, g : B \to X, \ldots$, where $A, B, \ldots$ are subsets of $\mathbb{R}^n$, homeomorphic to $[0, 1]^n$ for a fixed dimension $n \in \mathbb{N}$.

  The *Fréchet semimetric* d_F is a semimetric on $\mathcal{F}$ defined by

$$\inf_{\sigma} \sup_{x \in A} d(f(x), g(\sigma(x))),$$

  where the infimum is taken over all orientation preserving homeomorphisms $\sigma : A \to B$. It becomes the **Fréchet metric** on the set of equivalence classes $f^* = \{g : d_F(g, f) = 0\}$. Cf. the **Fréchet surface metric** in Chap. 8.

- **Hausdorff metric**

  Given a metric space (X, d), the **Hausdorff metric** (or *two-sided Hausdorff distance*) is a metric on the family $\mathcal{F}$ of nonempty compact subsets of X defined by

$$d_{Haus} = \max\{d_{dHaus}(A, B), d_{dHaus}(B, A)\},$$

  where $d_{dHaus}(A, B) = \max_{x \in A} \min_{y \in B} d(x, y)$ is the **directed Hausdorff distance** (or *one-sided Hausdorff distance*) from A to B. The metric space $(\mathcal{F}, d_{Haus})$ is called **hyperspace of metric space** (X, d); cf. **hyperspace** in Chap. 2.

  In other words, $d_{Haus}(A, B)$ is the minimal number ϵ (called also the **Blaschke distance**) such that a closed **ϵ-neighborhood** of A contains B and a closed ϵ-neighborhood of B contains A. Then $d_{Haus}(A, B)$ is equal to

$$\sup_{x \in X} |d(x, A) - d(x, B)|,$$

  where $d(x, A) = \min_{y \in A} d(x, y)$ is the **point-set distance**.

  If the above definition is extended for noncompact closed subsets A and B of X, then $d_{Haus}(A, B)$ can be infinite, i.e., it becomes an **extended metric**.

  For not necessarily closed subsets A and B of X, the **Hausdorff semimetric** between them is defined as the Hausdorff metric between their closures. If X is finite, d_{Haus} is a metric on the class of all subsets of X.

- **L_p-Hausdorff distance**

  Given a finite metric space (X, d), the **L_p-Hausdorff distance** ([Badd92]) between two subsets A and B of X is defined by

$$\left(\sum_{x \in X} |d(x, A) - d(x, B)|^p\right)^{\frac{1}{p}},$$

where $d(x, A)$ is the **point-set distance**. The usual **Hausdorff metric** corresponds to the case $p = \infty$.

- **Generalized G-Hausdorff metric**

  Given a group $(G, \cdot, e)$ acting on a metric space (X, d), the **generalized G-Hausdorff metric** between two closed bounded subsets A and B of X is

$$\min_{g_1, g_2 \in G} d_{Haus}(g_1(A), g_2(B)),$$

  where d_{Haus} is the **Hausdorff metric**. If $d(g(x), g(y)) = d(x, y)$ for any $g \in G$ (i.e., if the metric d is *left-invariant* with respect of G), then above metric is equal to $\min_{g \in G} d_{Haus}(A, g(B))$.

- **Gromov–Hausdorff metric**

  The **Gromov–Hausdorff metric** is a metric on the set of all *isometry classes* of compact metric spaces defined by

$$\inf d_{Haus}(f(X), g(Y))$$

  for any two classes X^* and Y^* with the representatives X and Y, respectively, where d_{Haus} is the **Hausdorff metric**, and the minimum is taken over all metric spaces M and all isometric embeddings $f : X \to M$, $g : Y \to M$. The corresponding metric space is called the *Gromov–Hausdorff space*.

  The **Hausdorff–Lipschitz distance** between isometry classes of compact metric spaces X and Y is defined by

$$\inf\{d_{GH}(X, X_1) + d_L(X_1, Y_1) + d_{GH}(Y, Y_1)\},$$

  where d_{GH} is the Gromov–Hausdorff metric, d_L is the **Lipschitz metric**, and the minimum is taken over all (isometry classes of compact) metric spaces X_1, Y_1.

- **Kadets distance**

  The *gap* (or *opening*) between two closed subspaces X and Y of a Banach space $(V, ||.||)$ is defined by

$$gap(X, Y) = \max\{\delta(X, Y), \delta(Y, X)\},$$

  where $\delta(X, Y) = \sup\{\inf_{y \in Y} ||x - y|| : x \in X, ||x|| = 1\}$ (cf. **gap distance** in Chap. 12 and **gap metric** in Chap. 18).

  The **Kadets distance** between two Banach spaces V and W is a semimetric defined (Kadets, 1975) by

$$\inf_{Z f, g} gap(\overline{B}_{f(V)}, \overline{B}_{g(W)}),$$

  where the infimum is taken over all Banach spaces Z and all linear isometric embeddings $f : V \to Z$ and $g : W \to Z$; here $\overline{B}_{f(V)}$ and $\overline{B}_{g(W)}$ are the closed unit balls of Banach spaces $f(V)$ and $g(W)$, respectively.

The nonlinear analog of the Kadets distance is the following **Gromov–Hausdorff distance between Banach spaces** U and W:

$$\inf_{Z,f,g} d_{Haus}(f(\overline{B}_V), g(\overline{B}_W)),$$

where the infimum is taken over all metric spaces Z and all isometric embeddings $f : V \to Z$ and $g : W \to Z$; here d_{Haus} is the **Hausdorff metric**.

The **Kadets path distance** between Banach spaces V and W is defined (Ostrovskii, 2000) as the infimum of the lengths (with respect to the Kadets distance) of all curves joining V and W (and is equal to ∞ if there is no such curve).

- **Banach–Mazur distance**

The **Banach–Mazur distance** d_{BM} between two Banach spaces V and W is

$$\ln \inf_T ||T|| \cdot ||T^{-1}||,$$

where the infimum is taken over all isomorphisms $T : V \to W$.

It can also be written as $\ln d(V, W)$, where the number $d(V, W)$ is the smallest positive $d \geq 1$ such that $\overline{B}^n_W \subset T(\overline{B}^n_V) \subset d\,\overline{B}^n_W$ for some linear invertible transformation $T : V \to W$. Here $\overline{B}^n_V = \{x \in V : ||x||_V \leq 1\}$ and $\overline{B}^n_W = \{x \in W; ||x||_W \leq 1\}$ are the *unit balls* of the normed spaces $(V, ||.||_V)$ and $(W, ||.||_W)$, respectively.

One has $d_{BM}(V, W) = 0$ if and only if V and W are *isometric*, and d_{BM} becomes a metric on the set X^n of all equivalence classes of n-dimensional normed spaces, where $V \sim W$ if they are isometric. The pair (X^n, d_{BM}) is a compact metric space which is called the **Banach–Mazur compactum**.

The **modified Banach–Mazur distance** (Glushkin, 1963, and Khrabrov, 2001) is

$$\inf\{||T||_{X\to Y} : |detT| = 1\} \cdot \inf\{||T||_{Y\to X} : |detT| = 1\}.$$

The **weak Banach–Mazur distance** (Tomczak–Jaegermann, 1984) is

$$\max\{\overline{\gamma}_Y(id_X), \overline{\gamma}_X(id_Y)\},$$

where id is the identity map and, for an operator $U : X \to Y$, $\overline{\gamma}_Z(U)$ denotes $\inf \sum ||W_k|| \cdot ||V_k||$. Here the infimum is taken over all representations $U = \sum W_k V_k$ for $W_k : X \to Z$ and $V_k : Z \to Y$. This distance never exceeds the corresponding Banach–Mazur distance.

- **Lipschitz distance**

  Given $\alpha \geq 0$ and two metric spaces (X, d_X), (Y, d_Y), the *α-Hölder norm* $||.||_{Hol}$ on the set of all injective functions $f : X \to Y$ is defined by

$$||f||_{Hol} = \sup_{x,y \in X, x \neq y} \frac{d_Y(f(x), f(y))}{d_X(x, y)^\alpha}.$$

  The *Lipschitz norm* $||.||_{Lip}$ is the case $\alpha = 1$ of $||.||_{Hol}$.

  The **Lipschitz distance** between metric spaces (X, d_X) and (Y, d_Y) is defined by

$$\ln \inf_f ||f||_{Lip} \cdot ||f^{-1}||_{Lip},$$

  where the infimum is taken over all bijective functions $f : X \to Y$. Equivalently, it is the infimum of numbers $\ln a$ such that there exists a bijective **bi-Lipschitz mapping** between (X, d_X) and (Y, d_Y) with constants $\exp(-a)$, $\exp(a)$.

  It becomes a metric (**Lipschitz metric**) on the set of all isometry classes of compact metric spaces. Cf. **Hausdorff–Lipschitz distance**.

  This distance is an analog to the **Banach–Mazur distance** and, in the case of finite-dimensional real Banach spaces, coincides with it.

  It also coincides with the **Hilbert projective metric** on *nonnegative* projective spaces, obtained by starting with $\mathbb{R}^n_{>0}$ and identifying any point x with cx, $c > 0$.

- **Lipschitz distance between measures**

  Given a compact metric space (X, d), the *Lipschitz seminorm* $||.||_{Lip}$ on the set of all functions $f : X \to \mathbb{R}$ is defined by $||f||_{Lip} = \sup_{x,y \in X, x \neq y} \frac{|f(x) - f(y)|}{d(x,y)}$.

  The **Lipschitz distance between measures** μ and ν on X is defined by

$$\sup_{||f||_{Lip} \leq 1} \int f d(\mu - \nu).$$

  It is the **transportation distance** (Chap. 14) if μ, ν are probability measures. Let a such measure $m_x(.)$ be attached to any $x \in X$; for distinct x, y the *coarse Ricci curvature along* (xy) is defined (Ollivier, 2009) as $\kappa(x, y) = 1 - \frac{W_1(m_x, m_y)}{d(x,y)}$. *Ollivier's curvature* generalizes the *Ricci curvature* in Riemannian space (cf. Chap. 7).

- **Barycentric metric space**

  Given a metric space (X, d), let $(B(X), ||\mu - \nu||_{TV})$ be the metric space, where $B(X)$ is the set of all regular Borel probability measures on X with bounded support, and $||\mu - \nu||_{TV}$ is the **variational distance** $\int_X |p(\mu) - p(\nu)| d\lambda$ (cf. Chap. 14). Here $p(\mu)$ and $p(\nu)$ are the density functions of measures μ and ν, respectively, with respect to the σ-finite measure $\frac{\mu + \nu}{2}$.

A metric space (X, d) is **barycentric** if there exists a constant $\beta > 0$ and a surjection $f : B(X) \to X$ such that for any measures $\mu, \nu \in B(X)$ it holds the inequality

$$d(f(\mu), f(\nu)) \leq \beta diam(supp(\mu + \nu))||\mu - \nu||_{TV}.$$

Any Banach space $(X, d = ||x - y||)$ is a barycentric metric space with the smallest β being 1 and the map $f(\mu)$ being the usual *center of mass* $\int_X x d\mu(x)$.

Any **Hadamard** (i.e., a complete **CAT**(0) **space**, cf. Chap. 6, is barycentric with the smallest β being 1 and the map $f(\mu)$ being the unique minimizer of the function $g(y) = \int_X d^2(x, y) d\mu(x)$ on X.

- **Point-set distance**

  Given a metric space (X, d), the **point-set distance** $d(x, A)$ between a point $x \in X$ and a subset A of X is defined as

$$\inf_{y \in A} d(x, y).$$

  For any $x, y \in X$ and for any nonempty subset A of X, we have the following version of the triangle inequality: $d(x, A) \leq d(x, y) + d(y, A)$ (cf. **distance map**).

  For a given point-measure $\mu(x)$ on X and a *penalty function* p, an **optimal quantizer** is a set $B \subset X$ such that $\int p(d(x, B)) d\mu(x)$ is as small as possible.

- **Set-set distance**

  Given a metric space (X, d), the **set-set distance** between two subsets A and B of X is defined by

$$d_{ss}(A, B) = \inf_{x \in A, y \in B} d(x, y).$$

  This distance can be 0 even for disjoint sets, for example, for the intervals $(1, 2), (2, 3)$ on $\mathbb{R}$. The sets A and B are *positively separated* if $d_{ss}(A, B) > 0$. A constructive *appartness space* is a generalization of this relation on subsets of X.

  The **spanning distance** between A and B is $\sup_{x \in A, y \in B} d(x, y)$.

  In Data Analysis, (cf. Chap. 17) the set-set and spanning distances between clusters are called the **single** and **complete linkage**, respectively.

- **Matching distance**

  Given a metric space (X, d), the **matching distance** (or *multiset-multiset distance*) between two multisets A and B in X is defined by

$$\inf_{\phi} \max_{x \in A} d(x, \phi(x)),$$

  where ϕ runs over all bijections between A and B, as multisets.

The matching distance is not related to the **perfect matching distance** in Chap. 15 and to the **nonlinear elastic matching distance** in Chap. 21. But the **bottleneck distance** in Chap. 21 is a special case of it.

- **Metrics between multisets**

  A *multiset* (or *bag*) drawn from a set S is a mapping $m : S \to \mathbb{Z}_{\geq 0}$, where $m(x)$ represents the "multiplicity" of $x \in S$. The *dimensionality*, *cardinality* and *height* of multiset m is $|S|$, $|m| = \sum_{x \in S} m(x)$ and $\max_{x \in S} m(x)$, respectively.

  Multisets are good models for multi-attribute objects such as, say, all symbols in a string, all words in a document, etc.

  A multiset m is finite if S and all $m(x)$ are finite; the *complement* of a finite multiset m is the multiset $\overline{m} : S \to \mathbb{Z}_{\geq 0}$, where $\overline{m}(x) = \max_{y \in S} m(y) - m(x)$. Given two multisets m_1 and m_2, denote by $m_1 \cup m_2$, $m_1 \cap m_2$, $m_1 \backslash m_2$ and $m_1 \Delta m_2$ the multisets on S defined , for any $x \in S$, by $m_1 \cup m_2(x) = \max\{m_1(x), m_2(x)\}$, $m_1 \cap m_2(x) = \min\{m_1(x), m_2(x)\}$, $m_1 \backslash m_2(x) = \max\{0, m_1(x) - m_2(x)\}$ and $m_1 \Delta m_2(x) = |m_1(x) - m_2(x)|$, respectively. Also, $m_1 \subseteq m_2$ denotes that $m_1(x) \leq m_2(x)$ for all $x \in S$.

  The *measure* $\mu(m)$ of a multiset m is a linear combination $\mu(m) = \sum_{x \in S} \lambda(x) m(x)$ with $\lambda(x) \geq 0$. In particular, $|m|$ is the *counting measure*.

  For any measure $\mu(m) \in \mathbb{R}_{\geq 0}$, Miyamoto, 1990, and Petrovsky, 2003, proposed several **semimetrics between multisets** m_1 and m_2 including $d_1(m_1, m_2) = \mu(m_1 \Delta m_2)$ and $d_2(m_1, m_2) = \frac{\mu(m_1 \Delta m_2)}{\mu(m_1 \cup m_2)}$ (with $d_2(\emptyset, \emptyset) = 0$ by definition). Cf. **symmetric difference metric** and **Steinhaus distance**.

  Among examples of other metrics between multisets are **matching distance**, **metric space of roots** in Chap. 12, **μ-metric** in Chap. 15 and, in Chap. 11, **bag distance** $\max\{|m_1 \backslash m_2|, |m_2 \backslash m_1|\}$ and **q-gram similarity**.

  See also **Vitanyi multiset metric** in Chap. 3.

- **Metrics between fuzzy sets**

  A *fuzzy subset* of a set S is a mapping $\mu : S \to [0, 1]$, where $\mu(x)$ represents the "degree of membership" of $x \in S$. It is an ordinary (*crisp*) if all $\mu(x)$ are 0 or 1. Fuzzy sets are good models for *gray scale images* (cf. **gray scale images distances** in Chap. 21), random objects and objects with nonsharp boundaries.

  Bhutani–Rosenfeld, 2003, introduced the following two metrics between two fuzzy subsets μ and ν of a finite set S. The **diff-dissimilarity** is a metric (a fuzzy generalization of **Hamming metric**), defined by

$$d(\mu, \nu) = \sum_{x \in S} |\mu(x) - \nu(x)|.$$

  The **perm-dissimilarity** is a semimetric defined by

$$\min\{d(\mu, p(\nu))\},$$

  where the minimum is taken over all permutations p of S.

The **Chaudhuri–Rosenfeld metric** (1996) between two fuzzy sets μ and ν *with crisp points* (i.e., the sets $\{x \in S : \mu(x) = 1\}$ and $\{x \in S : \nu(x) = 1\}$ are nonempty) is an **extended metric**, defined the **Hausdorff metric** d_{Haus} by

$$\int_0^1 2t d_{Haus}(\{x \in S : \mu(x) \geq t\}, \{x \in S : \nu(x) \geq t\})dt.$$

A *fuzzy number* is a fuzzy subset μ of the real line $\mathbb{R}$, such that the *level set* (or *t-cut*) $A_\mu(t) = \{x \in \mathbb{R} : \mu(x) \geq t\}$ is convex for every $t \in [0, 1]$. The *sendograph* of a fuzzy set μ is the set $send(\mu) = \{(x, t) \in S \times [0, 1] : \mu(x) > 0,\ \mu(x) \geq t\}$. The **sendograph metric** (Kloeden, 1980) between two fuzzy numbers μ, ν with crisp points and compact sendographs is the **Hausdorff metric**

$$\max\{\sup_{a=(x,t)\in send(\mu)} d(a, send(\nu)), \sup_{b=(x',t')\in send(\nu)} d(b, send(\mu))\},$$

where $d(a, b) = d((x, t), (x', t'))$ is a **box metric** (Chap. 4) $\max\{|x - x'|, |t - t'|\}$.

The **Klement–Puri–Ralesku metric** (1988) between fuzzy numbers μ, ν is

$$\int_0^1 d_{Haus}(A_\mu(t), A_\nu(t))dt,$$

where $d_{Haus}(A_\mu(t), A_\nu(t))$ is the **Hausdorff metric**

$$\max\{\sup_{x\in A_\mu(t)} \inf_{y\in A_\nu(t)} |x - y|, \sup_{x\in A_\nu(t)} \inf_{x\in A_\mu(t)} |x - y|\}.$$

Several other Hausdorff-like metrics on some families of fuzzy sets were proposed by Boxer in 1997, Fan in 1998 and Brass in 2002; Brass also argued the nonexistence of a "good" such metric.

If q is a quasi-metric on $[0, 1]$ and S is a finite set, then $Q(\mu, \nu) = \sup_{x\in S} q(\mu(x), \nu(x))$ is a quasi-metric on fuzzy subsets of S.

Cf. **fuzzy Hamming distance** in Chap. 11 and, in Chap. 23, **fuzzy set distance** and **fuzzy polynucleotide metric**. Cf. **fuzzy metric spaces** in Chap. 3 for fuzzy-valued generalizations of metrics and, for example, [Bloc99] for a survey.

- **Metrics between intuitionistic fuzzy sets**

  An *intuitionistic fuzzy subset* of a set S is (Atanassov, 1999) an ordered pair of mappings $\mu, \nu :\to [0, 1]$ with $0 \leq \mu(x) + \nu(x) \leq 1$ for all $x \in S$, representing the "degree of membership" and the "degree of nonmembership" of $x \in S$, respectively. It is an ordinary *fuzzy subset* if $\mu(x) + \nu(x) = 1$ for all $x \in S$.

  Given two intuitionistic fuzzy subsets $(\mu(x), \nu(x))$ and $(\mu'(x), \nu'(x))$ of a finite set $S = \{x_1, \ldots, x_n\}$, their **Atanassov distances** (1999) are:

$$\frac{1}{2}\sum_{i=1}^{n}(|\mu(x_i) - \mu'(x_i)| + |\nu(x_i) - \nu'(x_i)|) \text{ (Hamming distance)}$$

and, in general, for any given numbers $p \geq 1$ and $0 \leq q \leq 1$, the distance

$$(\sum_{i=1}^{n}(1-q)(\mu(x_i)-\mu'(x_i))^p + q(\nu(x_i)-\nu'(x_i)^p)^{\frac{1}{p}}.$$

Their **Grzegorzewski distances** (2004) are:

$$\sum_{i=1}^{n} \max\{|\mu(x_i)-\mu'(x_i)|, |\nu(x_i)-\nu'(x_i)|\} \text{ (Hamming distance);}$$

$$\sqrt{\sum_{i=1}^{n} \max\{(\mu(x_i)-\mu'(x_i))^2, (\nu(x_i)-\nu'(x_i))^2\}} \text{ (Euclidean distance).}$$

The normalized versions (dividing the above sums by n) were also proposed.

Szmidt–Kacprzyk, 1997, proposed a modification of the above, adding $\pi(x) - \pi'(x)$, where $\pi(x)$ is the third mapping $1 - \mu(x) - \nu(x)$.

An *interval-valued fuzzy subset* of a set S is a mapping $\mu :\to [I]$, where $[I]$ is the set of closed intervals $[a^-, a^+] \subseteq [0,1]$. Let $\mu(x) = [\mu^-(x), \mu^+(x)]$, where $0 \leq \mu^-(x) \leq \mu^+(x) \leq 1$ and an interval-valued fuzzy subset is an ordered pair of mappings μ^- and μ^+. This notion is close to the above intuitionistic one; so, above distance can easily be adapted. For example, $\sum_{i=1}^{n} \max\{|\mu^-(x_i) - \mu'^-(x_i)|, |\mu^+(x_i) - \mu'^+(x_i)|\}$ is a Hamming distance between interval-valued fuzzy subsets (μ^-, μ^+) and (μ'^-, μ'^+).

- **Polynomial metric space**

  Let (X, d) be a metric space with a finite diameter D and a finite normalized measure μ_X. Let the Hilbert space $L_2(X, d)$ of complex-valued functions decompose into a countable (when X is infinite) or a finite (with $D+1$ members when X is finite) direct sum of mutually orthogonal subspaces $L_2(X, d) = V_0 \oplus V_1 \oplus \ldots$.

  Then (X, d) is a **polynomial metric space** if there exists an ordering of the spaces $V_0, V_1, \ldots$ such that, for $i = 0, 1, \ldots$, there exist *zonal spherical functions*, i.e., real polynomials $Q_i(t)$ of degree i such that

$$Q_i(t(d(x,y))) = \frac{1}{r_i}\sum_{j=1}^{r_i} v_{ij}(x)\overline{v_{ij}(y)}$$

for all $x, y \in X$, where r_i is the dimension of V_i, $\{v_{ii}(x) : 1 \leq j \leq r_i\}$ is an orthonormal basis of V_i, and $t(d)$ is a continuous decreasing real function such that $t(0) = 1$ and $t(D) = -1$. The zonal spherical functions constitute an orthogonal system of polynomials with respect to some weight $w(t)$.

The finite polynomial metric spaces are also called *(P and Q)-polynomial association schemes*; cf. **distance-regular graph** in Chap. 15. The infinite polynomial metric spaces are the *compact connected two-point homogeneous*

spaces. Wang, 1952, classified them as the Euclidean unit spheres, the real, complex, quaternionic projective spaces or the Cayley projective line and plane.

- **Universal metric space**

  A metric space (U, d) is called **universal** for a collection $\mathcal{M}$ of metric spaces if any metric space (M, d_M) from $\mathcal{M}$ is *isometrically embeddable* in (U, d), i.e., there exists a mapping $f : M \to U$ which satisfies $d_M(x, y) = d(f(x), f(y))$ for any $x, y \in M$. Some examples follow.

  Every separable metric space (X, d) isometrically embeds (Fréchet, 1909) in (a nonseparable) **Banach space** l_∞^∞. In fact, $d(x, y) = \sup_i |d(x, a_i) - d(y, a_i)|$, where $(a_1, \ldots, a_i, \ldots)$ is a dense countable subset of X.

  Every metric space isometrically embeds (Kuratowski, 1935) in the **Banach space** $L^\infty(X)$ of bounded functions $f : X \to \mathbb{R}$ with the norm $\sup_{x \in X} |f(x)|$.

  The **Urysohn space** is a **homogeneous** complete separable space which is the universal metric space for all separable metric spaces. The **Hilbert cube** (Chap. 4) is the universal space for the class of metric spaces with a countable base.

  The **graphic** metric space of the **random graph** (Rado, 1964; the vertex-set consists of all prime numbers $p \equiv 1 \pmod 4$ with pq being an edge if p is a quadratic residue modulo q) is the universal metric space for any finite or countable metric space with distances 0, 1 and 2 only. It is a discrete analog of the Urysohn space.

  There exists a metric d on $\mathbb{R}$, inducing the usual (interval) topology, such that $(\mathbb{R}, d)$ is a universal metric space for all finite metric spaces (Holsztynski, 1978). The Banach space l_∞^n is a universal metric space for all metric spaces (X, d) with $|X| \le n + 2$ (Wolfe, 1967). The Euclidean space $\mathbb{E}^n$ is a universal metric space for all ultrametric spaces (X, d) with $|X| \le n + 1$; the space of all finite functions $f(t) : \mathbb{R}_{\ge 0} \to \mathbb{R}$ equipped with the metric $d(f, g) = \sup\{t : f(t) \ne g(t)\}$ is a universal metric space for all ultrametric spaces (Lemin–Lemin, 1996).

  The universality can be defined also for mappings, other than isometric embeddings, of metric spaces, say, a bi-Lipschitz embedding, etc. For example, any compact metric space is a continuous image of the **Cantor set** with the natural metric $|x - y|$ inherited from $\mathbb{R}$, and any complete separable metric space is a continuous image of the space of irrational numbers.

- **Constructive metric space**

  A **constructive metric space** is a pair (X, d), where X is a set of constructive objects (say, words over an alphabet), and d is an algorithm converting any pair of elements of X into a constructive real number $d(x, y)$ such that d is a metric on X.

- **Computable metric space**

  Let $\{x_n\}_{n \in \mathbb{N}}$ be a sequence of elements from a given *Polish* (i.e., complete separable) *metric space* (X, d) such that the set $\{x_n : n \in \mathbb{N}\}$ is dense in (X, d). Let $\mathcal{N}(m, n, k)$ be the *Cantor tuple function* of a triple $(n, m, k) \in \mathbb{N}^3$, and let $\{q_k\}_{k \in \mathbb{N}}$ be a fixed total standard numbering of the set $\mathbb{Q}$ of rational numbers.

The triple $(X, d, \{x_n\}_{n\in\mathbb{N}})$ is called an *effective* (or *semicomputable*) *metric space* ([Hemm02]) if the set $\{\mathcal{N}(n, m, k) : d(x_m, x_n) < q_k\}$ is *recursively enumerable*, i.e., there is an algorithm that enumerates the members of this set. If, moreover, the set $\{\mathcal{N}(n, m, k) : d(s_m, s_m) > q_k\}$ is recursively enumerable, then this triple is called (Lacombe, 1951) **computable metric space**, (or **recursive metric space**). In other words, the map $d \circ (q \times q) : \mathbb{N}^2 \to \mathbb{R}$ is a computable (double) sequence of real numbers, i.e., is recursive over $\mathbb{R}$.

Chapter 2
Topological Spaces

A *topological space* (X, τ) is a set X with a *topology* τ, i.e., a collection of subsets of X with the following properties:

1. $X \in \tau, \emptyset \in \tau$;
2. If $A, B \in \tau$, then $A \cap B \in \tau$;
3. For any collection $\{A_\alpha\}_\alpha$, if all $A_\alpha \in \tau$, then $\cup_\alpha A_\alpha \in \tau$.

The sets in τ are called *open sets*, and their complements are called *closed sets*. A *base* of the topology τ is a collection of open sets such that every open set is a union of sets in the base. The coarsest topology has two open sets, the empty set and X, and is called the *trivial topology* (or *indiscrete topology*). The finest topology contains all subsets as open sets, and is called the *discrete topology*.

In a metric space (X, d) define the *open ball* as the set $B(x, r) = \{y \in X : d(x, y) < r\}$, where $x \in X$ (the *center* of the ball), and $r \in \mathbb{R}, r > 0$ (the *radius* of the ball). A subset of X which is the union of (finitely or infinitely many) open balls, is called an *open set*. Equivalently, a subset U of X is called *open* if, given any point $x \in U$, there exists a real number $\epsilon > 0$ such that, for any point $y \in X$ with $d(x, y) < \epsilon$, $y \in U$.

Any metric space is a topological space, the topology (**metric topology**, *topology induced by the metric d*) being the set of all open sets. The metric topology is always T_4 (see below a list of topological spaces). A topological space which can arise in this way from a metric space, is called a **metrizable space**.

A *quasi-pseudo-metric topology* is a topology on X induced similarly by a quasi-semimetric d on X, using the set of open d-balls $B(x, r)$ as the base. In particular, *quasi-metric topology* and *pseudo-metric topology* are the terms used for the case of, respectively, quasi-metric and semimetric d. In general, those topologies are not T_0.

Given a topological space (X, τ), a *neighborhood* of a point $x \in X$ is a set containing an open set which in turn contains x. The *closure* of a subset of a topological space is the smallest closed set which contains it. An *open cover* of X is a collection $\mathcal{L}$ of open sets, the union of which is X; its *subcover* is a cover $\mathcal{K}$

© Springer-Verlag Berlin Heidelberg 2016

M.M. Deza, E. Deza, *Encyclopedia of Distances*,
DOI 10.1007/978-3-662-52844-0_2

such that every member of $\mathcal{K}$ is a member of $\mathcal{L}$; its *refinement* is a cover $\mathcal{K}$, where every member of $\mathcal{K}$ is a subset of some member of $\mathcal{L}$. A collection of subsets of X is called *locally finite* if every point of X has a neighborhood which meets only finitely many of these subsets.

A subset $A \subset X$ is called *dense* if $X = cl(A)$, i.e., it consists of A and its *limit points*; cf. **closed subset of metric space** in Chap. 1. The *density* of a topological space is the least cardinality of its dense subset. A *local base* of a point $x \in X$ is a collection $\mathcal{U}$ of neighborhoods of x such that every neighborhood of x contains some member of $\mathcal{U}$.

A function from one topological space to another is called *continuous* if the preimage of every open set is open. Roughly, given $x \in X$, all points close to x map to points close to $f(x)$. A function f from one metric space (X, d_X) to another metric space (Y, d_Y) is *continuous* at the point $c \in X$ if, for any positive real number ϵ, there exists a positive real number δ such that all $x \in X$ satisfying $d_X(x, c) < \delta$ will also satisfy $d_Y(f(x), f(c)) < \epsilon$; the function is continuous on an interval I if it is continuous at any point of I.

The following classes of topological spaces (up to T_4) include any metric space.

- T_0**-space**

  A T_0**-space** (or *Kolmogorov space*) is a topological space in which every two distinct points are *topologically distinguishable*, i.e., have different neighborhoods.
- T_1**-space**

  A T_1**-space** (or *accessible space*) is a topological space in which every two distinct points are *separated*, i.e., each does not belong to other's closure. T_1-spaces are always T_0.
- T_2**-space**

  A T_2**-space** (or **Hausdorff space**) is a topological space in which every two distinct points are *separated by neighborhoods*, i.e., have disjoint neighborhoods. T_2-spaces are always T_1.

  A space is T_2 if and only if it is both T_0 and *pre-regular*, i.e., any two *topologically distinguishable* points are separated by neighborhoods.
- **Regular space**

  A **regular space** is a topological space in which every neighborhood of a point contains a closed neighborhood of the same point. A T_3**-space** (or *Vietoris space*, *regular Hausdorff space*) is a topological space which is T_1 and regular.

  Bing, Nagata, Smirnov showed in 1950–1951 that a topological space is metrizable if and only if it is regular, T_0 and has a countably locally finite base.

  A **completely regular space** (or *Tychonoff space*) is a **Hausdorff space** (X, τ) in which any closed set A and any $x \notin A$ are *functionally separated*, i.e., there is a continuous function $f : X \to [0, 1]$ such that $f(A) = 0$ and $f(B) = 1$.
- **Normal space**

  A **normal space** is a topological space in which, for any two disjoint closed sets A and B, there exist two disjoint open sets U and V such that $A \subset U$, and

$B \subset V$. A T_4**-space** (or *Tietze space*, *normal Hausdorff space*) is a topological space which is T_1 and normal. Any metric space is a perfectly normal T_4-space.

A **completely** (or *hereditarily*) **normal space** is a topological space in which any two *separated* (i.e., disjoint from the other's closure) sets have disjoint neighborhoods. A T_5**-space** (or *completely normal Hausdorff space*) is a topological space which is completely normal and T_1. T_5-spaces are always T_4.

A **monotonically normal space** is a **completely normal space** in which any two *separated* subsets A and B are *strongly separated*, i.e., there exist open sets U and V with $A \subset U$, $B \subset V$ and $Cl(U) \cap Cl(V) = \emptyset$.

A **perfectly normal space** is a topological space (X, τ) in which any two disjoint closed subsets of X are *functionally separated*. A T_6**-space** (or *perfectly normal Hausdorff space*) is a topological space which is T_1 and perfectly normal. T_6-spaces are always T_5.

- **Moore space**

  A **Moore space** is a **regular space** with a *development*.

  A *development* is a sequence $\{\mathcal{U}_n\}_n$ of open covers such that, for every $x \in X$ and every open set A containing x, there exists n such that $St(x, \mathcal{U}_n) = \cup\{U \in \mathcal{U}_n : x \in U\} \subset A$, i.e., $\{St(x, \mathcal{U}_n)\}_n$ is a *neighborhood base* at x.
- **Polish space**

  A **separable space** is a topological space which has a countable dense subset.

  A **Polish space** is a separable space which can be equipped with a complete metric. A *Lusin space* is a topological space such that some weaker topology makes it into a Polish space; every Polish space is Lusin. A *Souslin space* is a continuous image of a Polish space; every Lusin space is Suslin.
- **Lindelöf space**

  A **Lindelöf space** is a topological space in which every open cover has a countable subcover.
- **First-countable space**

  A topological space is called **first-countable** if every point has a countable local base. Every metric space is first-countable.
- **Second-countable space**

  A topological space is called **second-countable** if its topology has a countable base. Such space is **quasi-metrizable** and, if and only if it is a T_3-space, **metrizable**.

  Second-countable spaces are **first-countable**, **separable** and **Lindelöf**. The properties **second-countable**, **separable** and **Lindelöf** are equivalent for metric spaces.

  The Euclidean space $\mathbb{E}^n$ with its usual topology is second-countable.
- **Baire space**

  A **Baire space** is a topological space in which every intersection of countably many dense open sets is dense. Every complete metric space is a Baire space. Every locally compact T_2-space (hence, every n**-manifold**) is a Baire space.
- **Alexandrov space**

  An **Alexandrov space** is a topological space in which every intersection of arbitrarily many open sets is open.

A topological space is called a ***P*-space** if every *G_δ-set* (i.e., the intersection of countably many open sets) is open.

A topological space (X, τ) is called a ***Q*-space** if every subset $A \subset X$ is a G_δ-set.

- **Connected space**

  A topological space (X, τ) is called **connected** if it is not the union of a pair of disjoint nonempty open sets. In this case the set X is called a *connected set*.

  A connected topological space (X, τ) is called *unicoherent* if the intersection $A \cap B$ is connected for any closed connected sets A, B with $A \cup B = X$.

  A topological space (X, τ) is called **locally connected** if every point $x \in X$ has a local base consisting of connected sets.

  A topological space (X, τ) is called **path-connected** (or 0-*connected*) if for every points $x, y \in X$ there is a path γ from x to y, i.e., a continuous function $\gamma : [0, 1] \to X$ with $\gamma(x) = 0, \gamma(y) = 1$.

  A topological space (X, τ) is called **simply connected** (or 1-*connected*) if it consists of one piece, and has no circle-shaped "holes" or "handles" or, equivalently, if every continuous curve of X is *contractible*, i.e., can be reduced to one of its points by a *continuous deformation*.

  A topological space (X, τ) is called **hyperconnected** (or *irreducible*) if X cannot be written as the union of two proper closed sets.

- **Sober space**

  A topological space (X, τ) is called **sober** if every **hyperconnected** closed subset of X is the closure of exactly one point of X. Any sober space is a T_0-space.

  Any T_2-space is a sober T_1-space but some sober T_1-spaces are not T_2.

- **Paracompact space**

  A topological space is called **paracompact** if every open cover of it has an open locally finite refinement. Every **metrizable** space is paracompact.

- **Totally bounded space**

  A topological space (X, τ) is called **totally bounded** (or *pre-compact*) if it can be covered by finitely many subsets of any fixed cardinality.

  A metric space (X, d) is a **totally bounded metric space** if, for every real number $r > 0$, there exist finitely many open balls of radius r, whose union is equal to X.

- **Compact space**

  A topological space (X, τ) is called **compact** if every open cover of X has a finite subcover.

  Compact spaces are always **Lindelöf**, **totally bounded**, and **paracompact**. A metric space is compact if and only if it is **complete** and **totally bounded**. A subset of a Euclidean space $\mathbb{E}^n$ is compact if and only if it is closed and bounded.

  There exist a number of topological properties which are equivalent to compactness in metric spaces, but are nonequivalent in general topological spaces. Thus, a metric space is compact if and only if it is a *sequentially compact space* (every sequence has a convergent subsequence), or a *countably compact space* (every countable open cover has a finite subcover), or a *pseudo-compact*

space (every real-valued continuous function on the space is bounded), or a *weakly countably compact space* (i.e., every infinite subset has an accumulation point).

Sometimes, a compact **connected T_2-space** is called *continuum*; cf. **continuum** in Chap. 1.

- **Locally compact space**

  A topological space is called **locally compact** if every point has a local base consisting of compact neighborhoods. The Euclidean spaces $\mathbb{E}^n$ and the spaces $\mathbb{Q}_p$ of *p-adic numbers* are locally compact.

  A topological space (X, τ) is called a *k-space* if, for any compact set $Y \subset X$ and $A \subset X$, the set A is closed whenever $A \cap Y$ is closed. The k-spaces are precisely quotient images of locally compact spaces.

- **Locally convex space**

  A **topological vector space** is a real (complex) vector space V which is a **T_2-space** with continuous vector addition and scalar multiplication. It is a **uniform space** (cf. Chap. 3).

  A **locally convex space** is a topological vector space whose topology has a base, where each member is a *convex balanced absorbent* set. A subset A of V is called *convex* if, for all $x, y \in A$ and all $t \in [0, 1]$, the point $tx + (1-t)y \in A$, i.e., every point on the *line segment* connecting x and y belongs to A. A subset A is *balanced* if it contains the line segment between x and $-x$ for every $x \in A$; A is *absorbent* if, for every $x \in V$, there exist $t > 0$ such that $tx \in A$.

  The locally convex spaces are precisely vector spaces with topology induced by a family $\{||.||_\alpha\}$ of seminorms such that $x = 0$ if $||x||_\alpha = 0$ for every α.

  Any metric space $(V, ||x - y||)$ on a real (complex) vector space V with a **norm metric** $||x - y||$ is a locally convex space; each point of V has a local base consisting of convex sets. Every L_p with $0 < p < 1$ is an example of a vector space which is not locally convex.

- ***n*-manifold**

  Broadly, a *manifold* is a topological space locally homeomorphic to a **topological vector space** over the reals.

  But usually, a **topological manifold** is a **second-countable T_2-space** that is locally homeomorphic to Euclidean space. An ***n*-manifold** is a topological manifold such that every point has a neighborhood homeomorphic to $\mathbb{E}^n$.

- **Fréchet space**

  A **Fréchet space** is a **locally convex space** (V, τ) which is complete as a **uniform space** and whose topology is defined using a countable set of seminorms $||.||_1, \ldots, ||.||_n, \ldots$, i.e., a subset $U \subset V$ is *open in* (V, τ) if, for every $u \in U$, there exist $\epsilon > 0$ and $N \geq 1$ with $\{v \in V : ||u - v||_i < \epsilon \text{ if } i \leq N\} \subset U$.

  A Fréchet space is precisely a locally convex **F-space** (cf. Chap. 5). Its topology can be induced by a **translation invariant metric** (Chap. 5) and it is a complete and **metrizable space** with respect to this topology. But this topology may be induced by many such metrics. Every **Banach space** is a Fréchet space.

- **Countably-normed space**

  A **countably-normed space** is a **locally convex space** (V, τ) whose topology is defined using a countable set of *compatible norms* $||.||_1, \ldots, ||.||_n, \ldots$. It means that, if a sequence $\{x_n\}_n$ of elements of V that is fundamental in the norms $||.||_i$ and $||.||_j$ converges to zero in one of these norms, then it also converges in the other. A countably-normed space is a **metrizable space**, and its metric can be defined by

$$\sum_{n=1}^{\infty} \frac{1}{2^n} \cdot \frac{||x-y||_n}{1+||x-y||_n}.$$

- **Metrizable space**

  A topological space (T, τ) is called **metrizable** if it is homeomorphic to a metric space, i.e., X admits a metric d such that the set of open d-balls $\{B(x, r) : r > 0\}$ forms a neighborhood base at each point $x \in X$. If, moreover, (X, d) is a complete metric space for one of such metrics d, then (X, d) is a *completely metrizable* (or *topologically complete*) space.

  Metrizable spaces are always **paracompact** T_2**-spaces** (hence, **normal** and **completely regular**), and **first-countable**.

  A topological space is called **locally metrizable** if every point in it has a metrizable neighborhood.

  A topological space (X, τ) is called **submetrizable** if there exists a metrizable topology τ' on X which is coarser than τ.

  A topological space (X, τ) is called **proto-metrizable** if it is paracompact and has an *orthobase*, i.e., a base $\mathcal{B}$ such that, for $\mathcal{B}' \subset \mathcal{B}$, either $\cap\mathcal{B}'$ is open, or $\mathcal{B}'$ is a local base at the unique point in $\cap\mathcal{B}'$. It is not related to the **protometric** in Chap. 1.

  Some examples of other direct generalizations of metrizable spaces follow.

  A **sequential space** is a quotient image of a metrizable space.

  Morita's M**-space** is a topological space (X, τ) from which there exists a continuous map f onto a metrizable topological space (Y, τ') such that f is closed and $f^{-1}(y)$ is countably compact for each $y \in Y$.

  Ceder's M_1**-space** is a topological space (X, τ) having a σ-closure-preserving base (metrizable spaces have σ-locally finite bases).

  Okuyama's σ**-space** is a topological space (X, τ) having a σ-locally finite *net*, i.e., a collection $\mathcal{U}$ of subsets of X such that, given of a point $x \in U$ with U open, there exists $U' \in \mathcal{U}$ with $x \in U' \subset U$ (a base is a net consisting of open sets). Every compact subset of a σ-space is metrizable.

  Michael's **cosmic space** is a topological space (X, τ) having a countable net (equivalently, a Lindelöf σ-space). It is exactly a continuous image of a separable metric space. A T_2**-space** is called **analytic** if it is a continuous image of a complete separable metric space; it is called a **Lusin space** if, moreover, the image is one-to-one.

- **Quasi-metrizable space**

  A topological space (X, τ) is called a **quasi-metrizable space** if X admits a quasi-metric d such that the set of open d-balls $\{B(x, r) : r > 0\}$ forms a neighborhood base at each point $x \in X$.

  A more general **γ-space** is a topological space admitting a **γ-metric** d (i.e., a function $d : X \times X \to \mathbb{R}_{\geq 0}$ with $d(x, z_n) \to 0$ whenever $d(x, y_n) \to 0$ and $d(y_n, z_n) \to 0$) such that the set of open *forward* d-balls $\{B(x, r) : r > 0\}$ forms a neighborhood base at each point $x \in X$.

  The *Sorgenfrey line* is the topological space $(\mathbb{R}, \tau)$ defined by the base $\{[a, b) : a, b \in \mathbb{R}, a < b\}$. It is not metrizable but it is a first-countable separable and paracompact **T_5-space**; neither it is second-countable, nor locally compact or locally connected. However, the Sorgenfrey line is quasi-metrizable by the **Sorgenfrey quasi-metric** (cf. Chap. 12) defined as $y - x$ if $y \geq x$, and 1, otherwise.
- **Symmetrizable space**

  A topological space (X, τ) is called **symmetrizable** (and τ is called the **distance topology**) if there is a **symmetric** d on X (i.e., a distance $d : X \times X \to \mathbb{R}_{\geq 0}$ with $d(x, y) = 0$ implying $x = y$) such that a subset $U \subset X$ is open if and only if, for each $x \in U$, there exists $\epsilon > 0$ with $B(x, \epsilon) = \{y \in X : d(x, y) < \epsilon\} \subset U$.

  In other words, a subset $H \subset X$ is closed if and only if $d(x, H) = \inf_y\{d(x, y) : y \in H\} > 0$ for each $x \in X \backslash U$. A symmetrizable space is **metrizable** if and only if it is a Morita's *M*-**space**.

  In Topology, the term **semimetrizable space** refers to a topological space (X, τ) admitting a symmetric d such that, for each $x \in X$, the family $\{B(x, \epsilon) : \epsilon > 0\}$ of balls forms a (not necessarily open) neighborhood base at x. In other words, a point x is in the closure of a set H if and only if $d(x, H) = 0$.

  A topological space is semimetrizable if and only if it is symmetrizable and **first-countable**. Also, a symmetrizable space is semimetrizable if and only if it is a *Fréchet–Urysohn space* (or *E-space*), i.e., for any subset A and for any point x of its closure, there is a sequence in A converging to x.
- **Hyperspace**

  A **hyperspace** of a topological space (X, τ) is a topological space on the set $CL(X)$ of all nonempty closed (or, moreover, compact) subsets of X. The topology of a hyperspace of X is called a *hypertopology*. Examples of such a *hit-and-miss topology* are the *Vietoris topology*, and the *Fell topology*. Examples of such a *weak hyperspace topology* are the *Hausdorff metric topology*, and the *Wijsman topology*.
- **Discrete topological space**

  A topological space (X, τ) is **discrete** if τ is the *discrete topology* (the finest topology on X), i.e., containing all subsets of X as open sets. Equivalently, it does not contain any *limit point*, i.e., it consists only of *isolated points*.
- **Indiscrete topological space**

  A topological space (X, τ) is **indiscrete** if τ is the *indiscrete topology* (the coarsest topology on X), i.e., having only two open sets, $\emptyset$ and X.

It can be considered as the semimetric space (X, d) with the **indiscrete semimetric**: $d(x, y) = 0$ for any $x, y \in X$.

- **Extended topology**

  Consider a set X and a map $cl : P(X) \to P(X)$, where $P(X)$ is the set of all subsets of X. The set $cl(A)$ (for $A \subset X$), its dual set $int(A) = X \backslash cl(X \backslash A)$ and the map $N : X \to P(X)$ with $N(x) = \{A \subset X : x \in int(A)\}$ are called the *closure*, *interior* and *neighborhood* map, respectively.

  So, $x \in cl(A)$ is equivalent to $X \backslash A \in P(X) \backslash N(x)$. A subset $A \subset X$ is *closed* if $A = cl(A)$ and *open* if $A = int(A)$. Consider the following possible properties of cl; they are meant to hold for all $A, B \in P(X)$.

  1. $cl(\emptyset) = \emptyset$;
  2. $A \subseteq B$ implies $cl(A) \subseteq cl(B)$ (*isotony*);
  3. $A \subseteq cl(A)$(*enlarging*);
  4. $cl(A \cup B) = cl(A) \cup cl(B)$ (*linearity*, and, in fact, 4 implies 2);
  5. $cl(cl(A)) = cl(A)$ (*idempotency*).

  The pair (X, cl) satisfying 1 is called an **extended topology** if 2 holds, a **Brissaud space** (Brissaud, 1974) if 3 holds, a **neighborhood space** (Hammer, 1964) if 2 and 3 hold, a **Smyth space** (Smyth, 1995) if 4 holds, a **pre-topology** (Čech, 1966) if 3 and 4 hold, and a **closure space** (Soltan, 1984) if 2, 3 and 5 hold.

  (X, cl) is the usual topology, in closure terms, if 1, 3, 4 and 5 hold.

Chapter 3
Generalizations of Metric Spaces

Some immediate generalizations of the notion of metric, for example, **quasi-metric**, **near-metric**, **extended metric**, were defined in Chap. 1. Here we give some generalizations in the direction of Topology, Probability, Algebra, etc.

3.1 m-Tuple Generalizations of Metrics

In the definition of a metric, for every *two points* there is a *unique associated number*. Here we group some generalizations of metrics in which *several points* or *several numbers* are considered instead.

- **m-hemimetric**

  Let X be a nonempty set. A function $d : X^{m+1} \to \mathbb{R}_{\geq 0}$ is called a **m-hemimetric** (Deza–Rosenberg, 2000) if it have the following properties:

  1. d is *totally symmetric*, i.e., satisfies $d(x_1, \ldots, x_{m+1}) = d(x_{\pi(1)}, \ldots, x_{\pi(m+1)})$ for all $x_1, \ldots, x_{m+1} \in X$ and for any permutation π of $\{1, \ldots, m+1\}$;
  2. $d(x_1, \ldots, x_{m+1}) = 0$ if $x_1, \ldots, x_{m+1}$ are not pairwise distinct;
  3. for all $x_1, \ldots, x_{m+2} \in X$, d satisfies the **m-simplex inequality**

$$d(x_1, \ldots, x_{m+1}) \leq \sum_{i=1}^{m+1} d(x_1, \ldots, x_{i-1}, x_{i+1}, \ldots, x_{m+2}).$$

  Cf. unrelated **hemimetric** (i.e., a quasi-semimetric) in Chap. 1.

  If in above 3. $d(x_1, \ldots, x_{m+1})$ is replaced by $sd(x_1, \ldots, x_{m+1})$ for some $s, 0 < s \leq 1$, then d is called (m, s)**-super-metric** ([DeDu03]). $(m, 1)$- and $(1, s)$-super-metrics are exactly m-hemimetric and $\frac{1}{s}$-*near-semimetric*; cf. **near-metric** in Chap. 1.

© Springer-Verlag Berlin Heidelberg 2016

M.M. Deza, E. Deza, *Encyclopedia of Distances*,
DOI 10.1007/978-3-662-52844-0_3

If above 3. is dropped, d is called m**-dissimilarity**. 1-dissimilarity and 1-hemimetric are exactly a distance and a semimetric.

- 2**-metric**

  An m**-hemimetric** with $m = 2$ satisfies 2**-simplex** (or *tetrahedron*) **inequality**

$$d(x_1, x_2, x_3) \leq d(x_4, x_2, x_3) + d(x_1, x_4, x_3) + d(x_1, x_2, x_4).$$

  A 2**-metric** (Gähler, 1963 and 1966) is a 2**-hemimetric** d in which, for any distinct points x_1, x_2, there is a point x_3 with $d(x_1, x_2, x_3) > 0$. The area of the triangle spanned by x_1, x_2, x_3 on $\mathbb{R}^2$ or $\mathbb{S}^2$ is a 2-metric.

  A *D-space* (Dhage, 1992) is an 2**-hemimetric space** (X, d) in which the condition "$d(x_1, x_2, x_3) = 0$ if two of x_1, x_2, x_3 are equal" is replaced by "$d(x_1, x_2, x_3) = 0$ if and only if $x_1 = x_2 = x_3$." Mustafa and Sims, 2003, showed that D-spaces are not suitable for topological constructions. In 2006, they defined instead a function, let us call it $MS-2$**-metric**, $D : X^3 \to \mathbb{R}_{\geq 0}$ which satisfies

  1. $D(x_1, x_2, x_3) = 0$ if $x_1 = x_2 = x_3$;
  2. $D(x_1, x_1, x_2) > 0$ whenever $x_1 \neq x_2$;
  3. $D(x_1, x_2, x_3) \geq D(x_1, x_1, x_2)$ whenever $x_3 \neq x_2$;
  4. D is a *totally symmetric* function of its three variables, and
  5. $D(x_1, x_2, x_3) \leq D(x_1, x_4, x_4) + D(x_4, x_2, x_3)$ for all $x_1, x_2, x_3, x_4 \in X$.

  The perimeter of the triangle spanned by x_1, x_2, x_3 on $\mathbb{R}^2$ is a MS − 2-metric. If d is a metric, then $\frac{1}{2}(d(x_1, x_2) + d(x_2, x_3) + d(x_1, x_3))$ and $\max(d(x_1, x_2), d(x_2, x_3), d(x_1, x_3))$ are MS − 2-metrics. If D is a MS − 2-metric, then $D(x_1, x_2, x_2) + D(x_1, x_1, x_2)$ is a metric. If (X, D) is a MS − 2-metric space, the open *D-ball with center* x_0 *and radius* r is $B_D(x_0, r) = \{x_1 \in X : D(x_0, x_1, x_1) < r\}$.

- **Multidistance**

  Given a set X, a function $D : \cup_{m>1} X^m \to \mathbb{R}_{\geq 0}$ is called a **multidistance** (Martin–Major, 2009) if, for all m and all $x_1, \ldots, x_m, y \in X$, it satisfies:

  1. $D(x_1, \ldots, x_m) = 0$ if $x_1 = \cdots = x_m$;
  2. $D(x_1, \ldots, x_m) = D(x_{\pi(1)}, \ldots, x_{\pi(m)})$ for any permutation π of $\{1, \ldots, m\}$;
  3. $D(x_1, \ldots, x_m) \leq \sum_{i=1}^{m} D(x_i, y)$.

  Clearly, the restriction of a multidistance on X^2 is a semimetric.

  A multidistance D is called *regular*, if all $D(x_1, \ldots, x_m) \leq D(x_1, \ldots, x_m, y)$ hold, and *stable*, if all $D(x_1, \ldots, x_m) = D(x_1, \ldots, x_m, x_i)$ hold. Given a metric space (X, d), the *Fermat multidistance* is $\min_{x \in X} \sum_{i=1}^{m} d(x_i, x)$; it is regular, but not stable.

  The regular multidistances on X form a convex cone.

- **Multimetric**

  In Mao, 2006, a **multimetric space** is the union of some metric spaces $(X_i, d_i), i \in J$. In the case $X_i = X, i \in J$, the **multimetric** is defined as the sequence-valued map $d(x, y) = (d_i), i \in J$, from $X \times X$ to $R_{\geq 0}^{|J|}$.

Cf. **bimetric theory of gravity** in Chap. 24 and (in the item **meter-related terms**) *multimetric crystallography* in Chap. 27.

Also, Jörnsten, 2007, consider *clustering* (Chap. 17) under several distance metrics simultaneously. In Rintanen, 2004, a *linear multimetric* is defined as $d = w_1 d_1 + \cdots + w_m d_m$, where d_i are metrics and $w_i \in [0, 1]$ are weights.

- **Diversity**

  Given a set X, a function f from its finite subsets to $\mathbb{R}_{\geq 0}$ is called (Bryant–Tupper, 2012) *diversity on* X if $f(A) = 0$ for all $A \subset X$ with $|A| \leq 1$ and

$$f(A \cup B) + f(B \cup C) \geq f(A \cup C) \text{ for all } A, B, C \subset X \text{ with } B \neq \emptyset.$$

  The **induced diversity metric** $d(x, y)$ is $f(\{x, y\})$.

  For any diversity $f(A)$ with induced metric space (X, d), it holds $f_{diam}(A) \leq f(A) \leq f_S(A) \leq (|A| - 1) f_{diam}(A)$, where the **diameter diversity** $f_{diam}(A)$ is $\max_{x,y \in A} d(x, y) = diam(A)$ and the **Steiner diversity** $f_S(A)$ is the minimum weight of a Steiner tree connecting elements of A.

  l_1**-diversity** is defined by $f_{m1}(A) = \max |a_i - b_i| : a, b \in A$ for all finite $A \subset \mathbb{R}^m$.

  Any diversity is a **Vitanyi multiset metric**, restricted to subsets. But much of Bryant–Tupper's theory of diversities does not extend on multisets.

- **Vitanyi multiset metric**

  Given two multisets m and m', define $n = mm'$ if n is the multiset consisting of the elements of the multisets m and m', that is, if x occurs once in m and once in m', then it occurs twice in n. A function d on the set of nonempty finite multisets is (Vitanyi, 2011) a **multiset metric** if

  1. $d(m) = 0$ if all elements of m are equal and $d(m) > 0$ otherwise.
  2. $d(X)$ is invariant under all permutations of m.
  3. $d(mm') \leq d(mm'') + d(m''m')$ (*multiset triangle inequality*).

  The usual metric between two elements results if the multiset m has two elements in 1. and 2. and the multisets m, m', m'' have one element each in 3.

  An example is the set of all nonempty finite multisets m of integers with $d(m) = \max\{x : x \in m\} - \min\{x : x \in m\}$. Cohen–Vitanyi, 2012, defined another multiset metric, generalising **normalised web distance** (Chap. 22).

3.2 Indefinite Metrics

- **Indefinite metric**

  An **indefinite metric** (or *G-metric*) on a real (complex) vector space V is a *bilinear* (in the complex case, *sesquilinear*) *form* G on V, i.e., a function $G : V \times V \to \mathbb{R}$ ($\mathbb{C}$), such that, for any $x, y, z \in V$ and for any scalars α, β, we have the following properties: $G(\alpha x + \beta y, z) = \alpha G(x, z) + \beta G(y, z)$, and $G(x, \alpha y + \beta z) = \overline{\alpha} G(x, y) + \overline{\beta} G(x, z)$, where $\overline{\alpha} = \overline{a + bi} = a - bi$ denotes the *complex conjugation*.

If a positive-definite form G is symmetric, then it is an *inner product* on V, and one can use it to canonically introduce a *norm* and the corresponding **norm metric** on V. In the case of a general form G, there is neither a norm, nor a metric canonically related to G, and the term **indefinite metric** only recalls the close relation of such forms with certain metrics in vector spaces (cf. Chaps. 7 and 26).

The pair (V, G) is called a *space with an indefinite metric*. A finite-dimensional space with an indefinite metric is called a *bilinear metric space*. A **Hilbert space** H, endowed with a continuous G-metric, is called a *Hilbert space with an indefinite metric*. The most important example of such space is a *J-space*; cf. ***J*-metric**.

A subspace L in a space (V, G) with an indefinite metric is called a *positive subspace*, *negative subspace*, or *neutral subspace*, depending on whether $G(x, x) > 0$, $G(x, x) < 0$, or $G(x, x) = 0$ for all $x \in L$.

- **Hermitian *G*-metric**

  A **Hermitian *G*-metric** is an **indefinite metric** G^H on a complex vector space V such that, for all $x, y \in V$, we have the equality

$$G^H(x, y) = \overline{G^H(y, x)},$$

  where $\overline{\alpha} = \overline{a + bi} = a - bi$ denotes the *complex conjugation*.

- **Regular *G*-metric**

  A **regular *G*-metric** is a continuous **indefinite metric** G on a **Hilbert space** H over $\mathbb{C}$, generated by an invertible *Hermitian operator* T by the formula

$$G(x, y) = \langle T(x), y\rangle,$$

  where $\langle , \rangle$ is the *inner product* on H.

  A *Hermitian operator* on a Hilbert space H is a *linear operator* T on H defined on a *domain* $D(T)$ of H such that $\langle T(x), y\rangle = \langle x, T(y)\rangle$ for any $x, y \in D(T)$. A bounded Hermitian operator is either defined on the whole of H, or can be so extended by continuity, and then $T = T^*$. On a finite-dimensional space a Hermitian operator can be described by a *Hermitian matrix* $((a_{ij})) = ((\overline{a}_{ji}))$.

- ***J*-metric**

  A ***J*-metric** is a continuous **indefinite metric** G on a **Hilbert space** H over $\mathbb{C}$ defined by a certain *Hermitian involution* J on H by the formula

$$G(x, y) = \langle J(x), y\rangle,$$

  where $\langle \cdot, \cdot \rangle$ is the *inner product* on H.

  An *involution* is a mapping H onto H whose square is the *identity mapping*. The involution J may be represented as $J = P_+ - P_-$, where P_+ and P_- are orthogonal projections in H, and $P_+ + P_- = H$. The rank *of indefiniteness* of the J-metric is defined as $\min\{\dim P_+, \dim P_-\}$.

The space (H, G) is called a *J-space*. A J-space with finite rank of indefiniteness is called a *Pontryagin space*.

3.3 Topological Generalizations

- **Metametric space**

  A **metametric space** (Väisälä, 2003) is a pair (X, d), where X is a set, and d is a nonnegative symmetric function $d : X \times X \to \mathbb{R}$ such that $d(x, y) = 0$ implies $x = y$ and triangle inequality $d(x, y) \leq d(x, z) + d(z, y)$ holds for all $x, y, z \in X$.

  A metametric space is metrizable: the metametric d defines the same topology as the metric d' defined by $d'(x, x) = 0$ and $d'(x, y) = d(x, y)$ if $x \neq y$. A metametric d induces a Hausdorff topology with the usual definition of a *ball* $B(x_0, r) = \{x \in X : d(x_0, x) < r\}$. Any **partial metric** (Chap. 1) is a metametric.
- **Resemblance**

  Let X be a set. A function $d : X \times X \to \mathbb{R}$ is called (Batagelj-Bren, 1993) a **resemblance** on X if d is *symmetric* and if, for all $x, y \in X$, either $d(x, x) \leq d(x, y)$ (in which case d is called a **forward resemblance**), or $d(x, x) \geq d(x, y)$ (in which case d is called a **backward resemblance**).

  Every resemblance d induces a *strict partial order* $\prec$ on the set of all unordered pairs of elements of X by defining $\{x, y\} \prec \{u, v\}$ if and only if $d(x, y) < d(u, v)$.
- *w*-**distance**

  Given a metric space (X, d), a *w*-**distance** on X (Kada–Suzuki–Takahashi, 1996) is a nonnegative function $p : X \times X \to \mathbb{R}$ which satisfies the following conditions:

  1. $p(x, z) \leq p(x, y) + p(y, z)$ for all $x, y, z \in X$;
  2. for any $x \in X$, the function $p(x, .) : X \to \mathbb{R}$ is *lower semicontinuous*, i.e., if a sequence $\{y_n\}_n$ in X converges to $y \in X$, then $p(x, y) \leq \underline{\lim}_{n\to\infty} p(x, y_n)$;
  3. for any $\epsilon > 0$, there exists $\delta > 0$ such that $p(z, x) \leq \delta$ and $p(z, y) \leq \delta$ imply $d(x, y) \leq \epsilon$, for each $x, y, z \in X$.

- τ-**distance space**

  A τ-**distance space** is a pair (X, f), where X is a topological space and f is an Aamri-Moutawakil's τ-*distance* on X, i.e., a nonnegative function $f : X \times X \to \mathbb{R}$ such that, for any $x \in X$ and any neighborhood U of x, there exists $\epsilon > 0$ with $\{y \in X : f(x, y) < \epsilon\} \subset U$.

  Any distance space (X, d) is a τ-distance space for the topology τ_f defined as follows: $A \in \tau_f$ if, for any $x \in X$, there exists $\epsilon > 0$ with $\{y \in X : f(x, y) < \epsilon\} \subset A$. However, there exist nonmetrizable τ-distance spaces. A τ-distance $f(x, y)$ need be neither symmetric, nor vanishing for $x = y$; for example, $e^{|x-y|}$ is a τ-distance on $X = \mathbb{R}$ with usual topology.

- **Proximity space**

  A **proximity space** (Efremovich, 1936) is a set X with a binary relation δ on the *power set* $P(X)$ of all of its subsets which satisfies the following conditions:

  1. $A\delta B$ if and only if $B\delta A$ (*symmetry*);
  2. $A\delta(B \cup C)$ if and only if $A\delta B$ or $A\delta C$ (*additivity*);
  3. $A\delta A$ if and only if $A \neq \emptyset$ (*reflexivity*).

  The relation δ defines a **proximity** (or *proximity structure*) on X. If $A\delta B$ fails, the sets A and B are called *remote sets*.

  Every metric space (X, d) is a proximity space: define $A\delta B$ if and only if $d(A, B) = \inf_{x\in A, y\in B} d(x, y) = 0$.

  Every proximity on X induces a (**completely regular**) topology on X by defining the *closure operator* $cl : P(X) \to P(X)$ on the set of all subsets of X as $cl(A) = \{x \in X : \{x\}\delta A\}$.
- **Uniform space**

  A **uniform space** is a topological space (with additional structure) providing a generalization of metric space, based on **set-set distance**.

  A **uniform space** (Weil, 1937) is a set X with an *uniformity* (or *uniform structure*) $\mathcal{U}$, i.e., a nonempty collection of subsets of $X \times X$, called *entourages*, with the following properties:

  1. Every subset of $X \times X$ which contains a set of $\mathcal{U}$ belongs to $\mathcal{U}$;
  2. Every finite intersection of sets of $\mathcal{U}$ belongs to $\mathcal{U}$;
  3. Every set $V \in \mathcal{U}$ contains the *diagonal*, i.e., the set $\{(x, x) : x \in X\} \subset X \times X$;
  4. If V belongs to $\mathcal{U}$, then the set $\{(y, x) : (x, y) \in V\}$ belongs to $\mathcal{U}$;
  5. If V belongs to $\mathcal{U}$, then there exists $V' \in \mathcal{U}$ such that $(x, z) \in V$ whenever $(x, y), (y, z) \in V'$.

  Every metric space (X, d) is a uniform space. An entourage in (X, d) is a subset of $X \times X$ which contains the set $V_\epsilon = \{(x, y) \in X \times X : d(x, y) < \epsilon\}$ for some positive real number ϵ. Other basic example of uniform space are *topological groups*.

  Every uniform space $(X, \mathcal{U})$ generates a topology consisting of all sets $A \subset X$ such that, for any $x \in A$, there is a set $V \in \mathcal{U}$ with $\{y : (x, y) \in V\} \subset A$.

  Every uniformity induces a **proximity** σ where $A\sigma B$ if and only if $A \times B$ has nonempty intersection with any entourage.

  A topological space admits a uniform structure inducing its topology if only if the topology is **completely regular** (Chap. 2) and, also, if only if it is a *gauge space*, i.e., the topology is defined by a $\geq$*-filter* of semimetrics.
- **Nearness space**

  A **nearness space** (Herrich, 1974) is a set X with a *nearness structure*, i.e., a nonempty collection $\mathcal{U}$ of families of subsets of X, called *near families*, with the following properties:

  1. Each family refining a near family is near;
  2. Every family with nonempty intersection is near;

3. V is near if $\{cl(A) : A \in V\}$ is near, where $cl(A)$ is $\{x \in X : \{\{x\}, A\} \in \mathcal{U}\}$;
4. $\emptyset$ is near, while the set of all subsets of X is not;
5. If $\{A \cup B : A \in \mathcal{F}_1, B \in \mathcal{F}_2\}$ is near family, then so is $\mathcal{F}_1$ or $\mathcal{F}_2$.

The **uniform spaces** are precisely **paracompact** nearness spaces.

- **Approach space**

An **approach space** is a topological space providing a generalization of metric space, based on **point-set distance**.

An **approach space** (Lowen, 1989) is a pair (X, D), where X is a set and D is a **point-set distance**, i.e., a function $X \times P(X) \to [0, \infty]$ (where $P(X)$ is the set of all subsets of X) satisfying, for all $x \in X$ and all $A, B \in P(X)$, the following conditions:

1. $D(x, \{x\}) = 0$;
2. $D(x, \{\emptyset\}) = \infty$;
3. $D(x, A \cup B) = \min\{D(x, A), D(x, B)\}$;
4. $D(x, A) \leq D(x, A^\epsilon) + \epsilon$ for any $\epsilon \in [0, \infty]$, where $A^\epsilon = \{x : D(x, A) \leq \epsilon\}$ is the "ϵ-ball" with center x.

Every metric space (X, d) (moreover, any extended quasi-semimetric space) is an approach space with $D(x, A)$ being the usual point-set distance $\min_{y \in A} d(x, y)$.

Given a **locally compact separable** metric space (X, d) and the family $\mathcal{F}$ of its nonempty closed subsets, the **Baddeley–Molchanov distance function** gives a tool for another generalization. It is a function $D : X \times \mathcal{F} \to \mathbb{R}$ which is lower semicontinuous with respect to its first argument, measurable with respect to the second, and satisfies the following two conditions: $F = \{x \in X : D(x, F) \leq 0\}$ for $F \in \mathcal{F}$, and $D(x, F_1) \geq D(x, F_2)$ for $x \in X$, whenever $F_1, F_2 \in \mathcal{F}$ and $F_1 \subset F_2$.

The additional conditions $D(x, \{y\}) = D(y, \{x\})$, and $D(x, F) \leq D(x, \{y\}) + D(y, F)$ for all $x, y \in X$ and every $F \in \mathcal{F}$, provide analogs of symmetry and the triangle inequality. The case $D(x, F) = d(x, F)$ corresponds to the usual point-set distance for the metric space (X, d); the case $D(x, F) = d(x, F)$ for $x \in X \backslash F$ and $D(x, F) = -d(x, X \backslash F)$ for $x \in X$ corresponds to the **signed distance function** in Chap. 1.

- **Metric bornology**

Given a topological space X, a *bornology* of X is any family $\mathcal{A}$ of proper subsets A of X such that the following conditions hold:

1. $\cup_{A \in \mathcal{A}} A = X$;
2. $\mathcal{A}$ is an *ideal*, i.e., contains all subsets and finite unions of its members.

The family $\mathcal{A}$ is a **metric bornology** ([Beer99]) if, moreover

3. $\mathcal{A}$ contains a countable base;
4. For any $A \in \mathcal{A}$ there exists $A' \in \mathcal{A}$ such that the closure of A coincides with the interior of A'.

The metric bornology is called *trivial* if $\mathcal{A}$ is the set $P(X)$ of all subsets of X; such a metric bornology corresponds to the family of bounded sets of some bounded

metric. For any noncompact **metrizable** topological space X, there exists an unbounded metric compatible with this topology. A nontrivial metric bornology on such a space X corresponds to the family of bounded subsets with respect to some such unbounded metric. A noncompact metrizable topological space X admits uncountably many nontrivial metric bornologies.

3.4 Beyond Numbers

- **Metric 1-space**

  A *category* Ψ consists (Eilenberg and MacLane, 1945) of a set $Ob(\Psi)$ of *objects*, a set $Mor(\Psi)$ of *morphisms* (or *arrows*)) and a set-valued map associating a set $\Psi(x, y)$ of arrows to each ordered pair of objects x, y, so that each arrow belongs to only one set $\Psi(x, y)$. An element of $\Psi(x, y)$ is also denoted by $f : x \to y$.

  Moreover, the composition $f \cdot g \in \Psi(x, z)$ of two arrows $f : x \to y, g : y \to z$ is defined, and it is associative. Finally, each set $\Psi(x, x)$ contains an *identity arrow* id_x such that $f \cdot id_x = f$ and $id_x \cdot g = g$ for any arrows $f : y \to x$ and $g : x \to z$. Cf. **category of metric spaces** in Chap. 1.

  Weiss defined in [Weis12] a **metric 1-space** as a category Ψ together with a weight-function $w : \Psi(x, y) \to \mathbb{R}_{\geq 0} \cup \{\infty\}$ on arrows, which satisfies

  1. $w(id_x) = 0$ holds for each object $x \in Ob(\Psi)$ (*reflexivity*).
  2. $|w(g) - w(f)| \leq w(g \cdot f) \leq w(g) + w(f)$ holds for any objects x, y, z and arrows $f : x \to y, g : y \to z$ (*full triangle inequality*).

  Any set X produces an *indiscrete category* I_X, in which $Ob(I_X) = X$ and $|I_X(x, y)| = 1$ for all $x, y \in X$. Any metric space (X, d) produces a metric 1-space on I_X by defining $w(f) = d(x, y)$, and it is unique metric 1-space on I_X. But, in general, the function w on arrows can be seen as a multivalued function on $Ob \times Ob$.

  [Weis12] also outlined a **metric m-space** as a kind of an **m-hemimetric** on an m-*category* consisting of i-dimensional cells, $0 \leq i \leq m$ (objects, arrows, ...) and a associative-like composition rule for the cells with matching boundaries.

- **V-continuity space**

  Let $(V, \wedge, \vee)$ be a *complete* (having $\wedge S := \wedge_{x \in S} x$ and $\vee S := \vee_{x \in S}$ for all $S \subseteq V$) lattice with bottom element 0. For $a, b \in V$, a is said to be *well above* b, denoted by $b \prec a$, if given any $S \subseteq V$ such that $\wedge S \prec b$, there exists $s \in S$ with $s \prec a$.

  A *value quantale* is a pair $(V, +)$, where V is a complete lattice and $+$ is an associative and commutative operation o such that for all $a, b \in V$ and $S \subseteq V$,

  1. $a + \wedge S = \wedge(a + S)$,
  2. $a + 0 = a$,
  3. $a = \wedge\{b \in Va \prec b\}$,
  4. $0 \prec a \wedge b$ if $0 \prec a, b$.

A V**-continuity space** is (Flagg–Koperman, 1997) a triple (X, d, V), where V is a value quantale, X is a set, and $d : X \times X \to V$ is a function satisfying

$$d(x, x) = 0 \quad \text{and} \quad d(x, z) \leq d(x, y) + d(y, z).$$

Any extended quasi-semimetric space is a V-continuity space, where V is the value quantale $[0, \infty]$, seen as a complete lattice, with ordinary addition.

Weiss, 2013, showed that taken with continuous functions, the categories of all V-continuity spaces and of all topological spaces are equivalent. In particular, every topological space (X, τ) is "metrizable" in the sense that there exists a V-continuity space (X, d, V) such that τ is the topology generated by *open balls* $\{y \in X : \prec \epsilon\}$.

- **Probabilistic metric space**

  A notion of **probabilistic metric space** is a generalization of the notion of metric space (see, for example, [ScSk83]) in two ways: distances become probability distributions, and the sum in the triangle inequality becomes a **triangle operation**.

  Formally, let A be the set of all *probability distribution functions*, whose support lies in $[0, \infty]$. For any $a \in [0, \infty]$ define *step functions* $\epsilon_a \in A$ by $\epsilon_a(x) = 1$ if $x > a$ or $x = \infty$, and $\epsilon_a(x) = 0$, otherwise. The functions in A are ordered by defining $F \leq G$ to mean $F(x) \leq G(x)$ for all $x \geq 0$; the minimal element is ϵ_0.

  A commutative and associative operation τ on A is called a **triangle function** if $\tau(F, \epsilon_0) = F$ for any $F \in A$ and $\tau(E, F) \leq \tau(G, H)$ whenever $E \leq G, F \leq H$. The semigroup (A, τ) generalizes the group $(\mathbb{R}, +)$.

  A **probabilistic metric space** is a triple (X, D, τ), where X is a set, D is a function $X \times X \to A$, and τ is a triangle function, such that for any $p, q, r \in X$

  1. $D(p, q) = \epsilon_0$ if and only if $p = q$;
  2. $D(p, q) = D(q, p)$;
  3. $D(p, r) \geq \tau(D(p, q), D(q, r))$.

  For any metric space (X, d) and any triangle function τ, such that $\tau(\epsilon_a, \epsilon_b) \geq \epsilon_{a+b}$ for all $a, b \geq 0$, the triple $(X, D = \epsilon_{d(x,y)}, \tau)$ is a probabilistic metric space.

  For any $x \geq 0$, the value $D(p, q)$ at x can be interpreted as "the probability that the distance between p and q is less than x"; this was approach of Menger, who proposed in 1942 the original version, *statistical metric space*, of this notion.

  A probabilistic metric space is called a *Wald space* if the triangle function is a convolution, i.e., of the form $\tau_x(E, F) = \int_{\mathbb{R}} E(x - t)dF(t)$.

  A probabilistic metric space is called a **generalized Menger space** if the triangle function has form $\tau_x(E, F) = \sup_{u+v=x} T(E(u), F(v))$ for a *t-norm* T, i.e., such a commutative and associative operation on $[0, 1]$ that $T(a, 1) = a$, $T(0, 0) = 0$ and $T(c, d) \geq T(a, b)$ whenever $c \geq a, d \geq b$.

- **Fuzzy metric spaces**

  A *fuzzy subset* of a set S is a mapping $\mu : S \to [0, 1]$, where $\mu(x)$ represents the "degree of membership" of $x \in S$.

A *continuous t-norm* is a binary commutative and associative continuous operation T on $[0,1]$, such that $T(a,1) = a$ and $T(c,d) \geq T(a,b)$ whenever $c \geq a, d \geq b$.

A **KM fuzzy metric space** (Kramosil–Michalek, 1975) is a pair $(X,(\mu,T))$, where X is a nonempty set and a *fuzzy metric* (μ,T) is a pair comprising a continuous t-norm T and a fuzzy set $\mu : X^2 \times \mathbb{R}_{\geq 0} \to [0,1]$, such that, for $x,y,z \in X$ and $s,t \geq 0$, the following conditions hold:

1. $\mu(x,y,0) = 0$;
2. $\mu(x,y,t) = 1$ if and only if $x = y, t > 0$;
3. $\mu(x,y,t) = \mu(y,x,t)$;
4. $T(\mu(x,y,t),\mu(y,z,s)) \leq \mu(x,z,t+s)$;
5. the function $\mu(x,y,\cdot) : \mathbb{R}_{\geq 0} \to [0,1]$ is left continuous.

A KM fuzzy metric space is called also a **fuzzy Menger space** since by defining $D_t(p,q) = \mu(p,q,t)$ one gets a **generalized Menger space**. The following modification of the above notion, using a stronger form of metric fuzziness, it a generalized Menger space with $D_t(p,q)$ positive and continuous on $\mathbb{R}_{>0}$ for all p,q.

A **GV fuzzy metric space** (George–Veeramani, 1994) is a pair $(X,(\mu,T))$, where X is a nonempty set, and a *fuzzy metric* (μ,T) is a pair comprising a continuous t-norm T and a fuzzy set $\mu : X^2 \times \mathbb{R}_{>0} \to [0,1]$, such that for $x,y,z \in X$ and $s,t > 0$

1. $\mu(x,y,t) > 0$;
2. $\mu(x,y,t) = 1$ if and only if $x = y$;
3. $\mu(x,y,t) = \mu(y,x,t)$;
4. $T(\mu(x,y,t),\mu(y,z,s)) \leq \mu(x,z,t+s)$;
5. the function $\mu(x,y,\cdot) : \mathbb{R}_{>0} \to [0,1]$ is continuous.

An example of a GV fuzzy metric space comes from any metric space (X,d) by defining $T(a,b) = b - ab$ and $\mu(x,y,t) = \frac{t}{t+d(x,y)}$. Conversely, any GV fuzzy metric space (and also any KM fuzzy metric space) generates a metrizable topology. Most GV fuzzy metrics are *strong*, i.e., $T(\mu(x,y,t),\mu(y,z,t)) \leq \mu(x,z,t)$ holds.

A *fuzzy number* is a fuzzy set $\mu : \mathbb{R} \to [0,1]$ which is *normal* ($\{x \in \mathbb{R} : \mu(x) = 1\} \neq \emptyset$), *convex* ($\mu(tx + (1-t)y) \geq \min\{\mu(x),\mu(y)\}$ for every $x,y \in \mathbb{R}$ and $t \in [0,1]$) and *upper semicontinuous* (at each point x_0, the values $\mu(x)$ for x near x_0 are either close to $\mu(x_0)$ or less than $\mu(x_0)$). Denote the set of all fuzzy numbers which are *nonnegative*, i.e., $\mu(x) = 0$ for all $x < 0$, by G. The additive and multiplicative identities of fuzzy numbers are denoted by $\tilde{0}$ and $\tilde{1}$, respectively. The *level set* $[\mu]_t = \{x : \mu(x) \geq t\}$ of a fuzzy number μ is a closed interval.

Given a nonempty set X and a mapping $d : X^2 \to G$, let the mappings $L,R : [0,1]^2 \to [0,1]$ be symmetric and nondecreasing in both arguments and satisfy $L(0,0) = 0$, $R(1,1) = 1$. For all $x,y \in X$ and $t \in (0,1]$, let $[d(x,y)]_t = [\lambda_t(x,y), \rho_t(x,y)]$.

A **KS fuzzy metric space** (Kaleva–Seikkala, 1984) is a quadruple (X, d, L, R) with *fuzzy metric* d, if for all $x, y, z \in X$

1. $d(x, y) = \tilde{0}$ if and only if $x = y$;
2. $d(x, y) = d(y, x)$;
3. $d(x, y)(s + t) \geq L(d(x, z)(s), d(z, y)(t))$ whenever $s \leq \lambda_1(x, z)$, $t \leq \lambda_1(z, y)$, and $s + t \leq \lambda_1(x, y)$;
4. $d(x, y)(s + t) \leq R(d(x, z)(s), d(z, y)(t))$ whenever $s \geq \lambda_1(x, z)$, $t \geq \lambda_1(z, y)$, and $s + t \geq \lambda_1(x, y)$.

The following functions are some frequently used choices for L and R:

$$\max\{a + b - 1, 0\}, ab, \min\{a, b\}, \max\{a, b\}, a + b - ab, \min\{a + b, 1\}.$$

Several other notions of **fuzzy metric space** were proposed, including those by Erceg, 1979, Deng, 1982, and Voxman, 1998, Xu–Li, 2001, Tran–Duckstein, 2002, Chakraborty–Chakraborty, 2006. Cf. also **metrics between fuzzy sets**, **fuzzy Hamming distance**, **gray-scale image distances** and **fuzzy polynucleotide metric** in Chaps. 1, 11, 21 and 23, respectively.

- **Interval-valued metric space**

  Let $I(\mathbb{R}_{\geq 0})$ denote the set of closed intervals of $\mathbb{R}_{\geq 0}$.

  An **interval-valued metric space** (Coppola–Pacelli, 2006) is a pair $((X, \leq), \Delta)$, where $(X, \leq)$ is a partially ordered set and Δ is an interval-valued mapping $\Delta : X \times X \to I(\mathbb{R}_{\geq 0})$, such that for every $x, y, z \in X$

  1. $\Delta(x, x) \star [0, 1] = \Delta(x, x)$;
  2. $\Delta(x, y) = \Delta(y, x)$;
  3. $\Delta(x, y) - \Delta(z, z) \preceq \Delta(x, z) + \Delta(z, y)$;
  4. $\Delta(x, y) - \Delta(x, y) \preceq \Delta(x, x) + \Delta(y, y)$;
  5. $x \leq x'$ and $y \leq y'$ imply $\Delta(x, y) \subseteq \Delta(x', y')$;
  6. $\Delta(x, y) = 0$ if and only if $x = y$ and x, y are *atoms* (minimal elements of $(X, \leq)$).

  Here the following *interval arithmetic* rules hold: $[u, v] \preceq [u', v']$ if and only if $u \leq u'$,

  $[u, v] + [u', v'] = [u + u', v + v']$, $\quad [u, v] - [u', v'] = [u - u', v - v']$,

  $[u, v] \star [u', v'] = [\min\{uu', uv', vu', vv'\}, \max\{uu', uv', vu', vv'\}]$ and

  $\frac{[u,v]}{[u',v']} = [\min\{\frac{u}{u'}, \frac{u}{v'}, \frac{v}{u'}, \frac{v}{v'}\}, \max\{\frac{u}{u'}, \frac{u}{v'}, \frac{v}{u'}, \frac{v}{v'}\}]$ when $0 \notin [u', v']$.

  The addition and multiplication operations are commutative, associative and *subdistributive*: it holds $X \star (Y + Z) \subset (X \star Y + X \star Z)$.

  Cf. **metric between intervals** in Chap. 10.

  The usual metric spaces coincide with above spaces in which all $x \in X$ are atoms.

- **Direction distance**

  Given a normed real vector space $(V, ||.||)$, for any $x \in V \setminus \{0\}$, denote by $[x]$ the *direction* (ray) $\{\lambda x : \lambda > 0\}$ and by x_0 the point $\frac{x}{||x||}$. An *oriented angle* is an

ordered pair $([x], [y])$ of directions. The **direction distance** from x to y is defined (Busch–Ruch, 1992) as the family of distances $||\alpha x_0 - \beta y_0||$ with $\alpha, \beta \in \mathbb{R}_{>0}$.

The **mixing distance** is defined as the restriction of the direction distance to pairs of directions in the cone $\{\lambda v : v \in V, \lambda > 0\}$. In fact, authors introduced these distances on some special normed spaces used in Quantum Mechanics.

- **Generalized metric**

  Let X be a set. Let $(V, +, \leq)$ be an *ordered semigroup* (not necessarily commutative) with a least element θ and with $x \leq y, x_1 \leq y_1$ implying $x + x_1 \leq y + y_1$. Let $(V, +)$ be also endowed with an order-preserving *involution* x^* (i.e., $(x^*)^* = x$), which is operation-reversing, i.e., $(x + y)^* = y^* + x^*$.

  A function $d : X \times X \to G$ is called (Li–Wang–Pouzet, 1987) a **generalized metric** over $(V, +, \leq)$ if the following conditions hold:

  1. $d(x, y) = \theta$ if and only if $x = y$;
  2. $d(x, y) \leq d(x, z) + d(z, y)$ for all $x, y \in X$;
  3. $d^*(x, y) = d(y, x)$.

- **Cone metric**

  Let C be a *proper cone* in a real Banach space W, i.e., C is closed, $C \neq \emptyset$, the interior of C is not equal to $\{\theta\}$ (where θ is the zero vector in W) and

  1. if $x, y \in C$ and $a, b \in \mathbb{R}_{\geq 0}$, then $ax + by \in C$;
  2. if $x \in C$ and $-x \in C$, then $x = 0$.

  Define a partial ordering $(W, \leq)$ on W by letting $x \leq y$ if $y - x \in C$. The following variation of **generalized metric** and **partially ordered distance** was defined in Huang–Zhang, 2007, and, partially, in Rzepecki, 1980. Given a set X, a **cone metric** is a mapping $d : X \times X \to (W, \leq)$ such that

  1. $\theta \leq d(x, y)$ with equality if and only if $x = y$;
  2. $d(x, y) = d(y, x)$ for all $x, y \in X$;
  3. $d(x, y) \leq d(x, z) + d(z, y)$ for all $x, y \in X$;

  The pair (X, d) is called a **cone metric space**.

- **W-distance on building**

  Let X be a set, and let $(W, \cdot, 1)$ be a group. A *W-distance* on X is a W-valued map $\sigma : X \times X \to W$ having the following properties:

  1. $\sigma(x, y) = 1$ if and only if $x = y$;
  2. $\sigma(y, x) = (\sigma(x, y))^{-1}$.

  A natural W-distance on W is $\sigma(x, y) = x^{-1}y$.

  A *Coxeter group* is a group $(W, \cdot, 1)$ generated by the elements

$$\{w_1, \ldots, w_n : (w_i w_j)^{m_{ij}} = 1, 1 \leq i, j \leq n\}.$$

  Here $M = ((m_{ij}))$ is a *Coxeter matrix*, i.e., an arbitrary symmetric $n \times n$ matrix with $m_{ii} = 1$, and the other values are positive integers or ∞. The *length* $l(x)$ of $x \in W$ is the smallest number of generators $w_1, \ldots, w_n$ needed to represent x.

Let X be a set, let $(W, \cdot, 1)$ be a Coxeter group and let $\sigma(x, y)$ be a W-distance on X. The pair (X, σ) is called (Tits, 1981) a *building* over $(W, \cdot, 1)$ if it holds

1. the relation $\sim_i$ defined by $x \sim_i y$ if $\sigma(x, y) = 1$ or w_i, is an equivalence relation;
2. given $x \in X$ and an equivalence class C of $\sim_i$, there exists a unique $y \in C$ such that $\sigma(x, y)$ is *shortest* (i.e., of smallest length), and $\sigma(x, y') = \sigma(x, y)w_i$ for any $y' \in C, y' \neq y$.

The **gallery distance on building** d is a usual metric on X defined by $l(d(x, y))$. The distance d is the **path metric** in the graph with the vertex-set X and xy being an edge if $\sigma(x, y) = w_i$ for some $1 \leq i \leq n$. The gallery distance on building is a special case of a **gallery metric** (of *chamber system* X).

- **Boolean metric space**

  A *Boolean algebra* (or *Boolean lattice*) is a *distributive lattice* $(B, \vee, \wedge)$ admitting a least element 0 and greatest element 1 such that every $x \in B$ has a *complement* $\overline{x}$ with $x \vee \overline{x} = 1$ and $x \wedge \overline{x} = 0$.

  Let X be a set, and let $(B, \vee, \wedge)$ be a Boolean algebra. The pair (X, d) is called (Blumenthal, 1953) a **Boolean metric space** over B if the function $d : X \times X \to B$ has the following properties:

  1. $d(x, y) = 0$ if and only if $x = y$;
  2. $d(x, y) \leq d(x, z) \vee d(z, y)$ for all $x, y, z \in X$.

- **Space over algebra**

  A **space over algebra** is a metric space with a differential-geometric structure, whose points can be provided with coordinates from some *algebra* (usually, an associative algebra with identity).

  A *module* over an algebra is a generalization of a vector space over a field, and its definition can be obtained from the definition of a vector space by replacing the field by an associative algebra with identity. An *affine space over an algebra* is a similar generalization of an *affine space* over a field. In affine spaces over algebras one can specify a Hermitian metric, while in the case of commutative algebras even a quadratic metric can be given. To do this one defines in a unital module a *scalar product* $\langle x, y\rangle$, in the first case with the property $\langle x, y\rangle = J(\langle y, x\rangle)$, where J is an *involution* of the algebra, and in the second case with the property $\langle y, x\rangle = \langle x, y\rangle$.

  The n-dimensional *projective space over an algebra* is defined as the variety of one-dimensional submodules of an $(n + 1)$-dimensional unital module over this algebra. The introduction of a *scalar product* $\langle x, y\rangle$ in a unital module makes it possible to define a Hermitian metric in a projective space constructed by means of this module or, in the case of a commutative algebra, quadratic elliptic and hyperbolic metrics. The metric invariant of the points of these spaces is the **cross-ratio** $W = \langle x, x\rangle^{-1}\langle x, y\rangle\langle y, y\rangle^{-1}\langle y, x\rangle$. If W is a real number, then $w = \arccos\sqrt{W}$ is called the **distance** between x and y **in the space over algebra**.

- **Partially ordered distance**

  Let X be a set. Let $(G, \preceq)$ be a *partially ordered set* with a least element g_0. A **partially ordered distance** is a function $d : X \times X \to G$ such that, for any $x, y \in X$, $d(x, y) = g_0$ if and only if $x = y$.

  A **generalized ultrametric** (Priess-Crampe and Ribenboim, 1993) is a symmetric (i.e., $d(x, y) = d(y, x)$) partially ordered distance, such that $d(z, x) \preceq g$ and $d(z, y) \preceq g$ imply $d(x, y) \preceq g$ for any $x, y, z \in X$ and $g \in G$.

  Suppose that $G' = G \backslash \{g_0\} \neq \emptyset$ and, for any $g_1, g_2 \in G'$, there exists $g_3 \in G'$ such that $g_3 \preceq g_1$ and $g_3 \preceq g_2$. Consider the following possible properties:

  1. For any $g_1 \in G'$, there exists $g_2 \in G'$ such that, for any $x, y \in X$, from $d(x, y) \preceq g_2$ it follows that $d(y, x) \preceq g_1$;
  2. For any $g_1 \in G'$, there exist $g_2, g_3 \in G'$ such that, for any $x, y, z \in X$, from $d(x, y) \preceq g_2$ and $d(y, z) \preceq g_3$ it follows that $d(x, z) \preceq g_1$;
  3. For any $g_1 \in G'$, there exists $g_2 \in G'$ such that, for any $x, y, z \in X$, from $d(x, y) \preceq g_2$ and $d(y, z) \preceq g_2$ it follows that $d(y, x) \preceq g_1$;
  4. G' has no first element;
  5. $d(x, y) = d(y, x)$ for any $x, y \in X$;
  6. For any $g_1 \in G'$, there exists $g_2 \in G'$ such that, for any $x, y, z \in X$, from $d(x, y) \prec^* g_2$ and $d(y, z) \prec^* g_2$ it follows that $d(x, z) \prec^* g_1$; here $p \prec^* q$ means that either $p \prec q$, or p is not comparable to q;
  7. The order relation $\prec$ is a total ordering of G.

  In terms of above properties, d is called: the **Appert partially ordered distance** if 1 and 2 hold; the **Golmez partially ordered distance of first type** if 4, 5, and 6 hold; the **Golmez partially ordered distance of second type** if 3, 4, and 5 hold; the **Kurepa–Fréchet distance** if 3, 4, 5, and 7 hold.

  The case $G = \mathbb{R}_{\geq 0}$ of the Kurepa–Fréchet distance corresponds to the **Fréchet V-space**; cf. the **f-quasi-metric** in Sect. 1.1. The general case was considered in Kurepa, 1934, and rediscovered in Fréchet, 1946.

- **Distance from measurement**

  Distance from measurement is an analog of distance on domains in Computer Science; it was developed in [Mart00].

  A *po* (partially ordered set) $(D, \preceq)$ is called *dcpo* (directed-complete po) if every *directed subset* $S \subset D$ (i.e., $S \neq \emptyset$ and any pair $x, y \in S$ is *bounded*: there is $z \in S$ with $x, y \preceq z$) has a *supremum* $\sqcup S$, i.e., the least of such upper bounds z.

  For $x, y \in D$, y is an *approximation* of x if, for all directed subsets $S \subset D$, $x \preceq \sqcup S$ implies $y \preceq s$ for some $s \in S$. A dcpo $(D, \preceq)$ is *continuous* if for all $x \in D$ the set of all approximations of x is directed and x is its supremum. A *domain* is a continuous dcpo $(D, \preceq)$ such that for all $x, y \in D$ there is $z \in D$ with $z \preceq x, y$. A *Scott domain* is a domain with least element, in which any bounded pair has a supremum.

  A subset U of a dcpo $(D, \preceq)$ is *Alexandrov open* if, for any $x \in U$ and $y \in D$, $x \preceq y$ implies $y \in U$; it is *Scott open* if also, for any directed subset $S \subset D$, $\sqcup S \in U$ implies $S \cap U \neq \emptyset$. The set of Scott open sets form the *Scott topology*; it is a **T_0-space** (Chap. 2) with generalized metrization by a **partial metric** (Chap. 1).

A *measurement* is a mapping $\mu : D \to \mathbb{R}_{\geq 0}$ between dcpo $(D, \preceq)$ and dcpo $(\mathbb{R}_{\geq 0}, \preceq)$, where $\mathbb{R}_{\geq 0}$ is ordered as $x \preceq y$ if $y \leq x$, such that

1. $x \preceq y$ implies $\mu(x) \preceq \mu(y)$;
2. $\mu(\sqcup S) = \sqcup(\{\mu(s) : s \in S\})$ for every directed subset $S \subset D$;
3. For all $x \in D$ with $\mu(x) = 0$ and all sequences $(x_n), n \to \infty$, of approximations of x with $\lim_{n\to\infty} \mu(x_n) = \mu(x)$, one has $\sqcup(\cup_{n=1}^{\infty}\{x_n\}) = x$.

Given a measurement μ, the **distance from measurement** is a mapping $d : D \times D \to \mathbb{R}_{\geq 0}$ given by

$$d(x, y) = \inf\{\mu(z) : z \text{ approximates } x, y\} = \inf\{\mu(z) : z \preceq x, y\}.$$

One has $d(x, x) \preceq \mu(x)$. The function $d(x, y)$ is a metric on the set $\{x \in D : \mu(x) = 0\}$ if μ satisfies the following **measurement triangle inequality**: for all bounded pairs $x, y \in D$, there is an element $z \preceq x, y$ such that $\mu(z) \leq \mu(x) + \mu(y)$.

Waszkiewicz, 2001, found topological connections between topologies coming from a distance from measurement and from a **partial metric** defined in Chap. 1.

Chapter 4
Metric Transforms

There are many ways to obtain new distances (metrics) from given distances (metrics). Metric transforms give new distances as a functions of given metrics (or given distances) on the same set X. A metric so obtained is called a **transform metric**. We give some important examples of transform metrics in Sect. 4.1.

Given a metric space (X, d), one can construct a new metric on an extension of X; similarly, given a collection of metrics on sets $X_1, \ldots, X_n$, one can obtain a new metric on an extension of $X_1, \ldots, X_n$. Examples of such operations are given in Sect. 4.2. There are many distances on other structures connected with X, say, on the set of all subsets of X. The main distances of this kind are considered in Sect. 4.3.

4.1 Metrics on the Same Set

- **Metric transform**

  A **metric transform** is a distance on a set X, obtained as a function of given metrics (or given distances) on X.

  In particular, given a continuous monotone increasing function $f(x)$ of $x \geq 0$ with $f(0) = 0$, called the *scale*, and a distance space (X, d), one obtains another distance space (X, d_f), called a **scale metric transform** of X, defining $d_f(x, y) = f(d(x, y))$. For every finite distance space (X, d), there exists a scale f, such that (X, d_f) is a metric subspace of a Euclidean space $\mathbb{R}^n$.

  If (X, d) is a metric space and f is a continuous differentiable strictly increasing scale with $f(0) = 0$ and nonincreasing f', then (X, d_f) is a metric space (cf. **functional transform metric**).

  The metric d is an **ultrametric** if and only if $f(d)$ is a metric for every nondecreasing function $f : \mathbb{R}_{\geq 0} \to \mathbb{R}_{\geq 0}$.
- **Transform metric**

  A **transform metric** is a metric on a set X which is a **metric transform**, i.e., is obtained as a function of a given metric (or given metrics) on X. In particular,

© Springer-Verlag Berlin Heidelberg 2016

M.M. Deza, E. Deza, *Encyclopedia of Distances*,
DOI 10.1007/978-3-662-52844-0_4

transform metrics can be obtained from a given metric d (or given metrics d_1 and d_2) on X by any of the following operations (here $t > 0$):

1. $td(x, y)$ (t-**scaled metric**, or **dilated metric**, **similar metric**);
2. $\min\{t, d(x, y)\}$ (t-**truncated metric**);
3. $\max\{t, d(x, y)\}$ for $x \neq y$ (t-**uniformly discrete metric**);
4. $d(x, y) + t$ for $x \neq y$ (t-**translated metric**);
5. $\frac{kd(x,y)}{1+d(x,y)}$ (this metric has diameter less than k);
6. $d^p(x, y) = \frac{2d(x,y)}{d(x,p)+d(y,p)+d(x,y)}$, where p is an fixed element of X (**biotope transform metric**, or p-**smoothing distance** on $X \setminus \{p\}$);
7. $\max\{d_1(x, y), d_2(x, y)\}$;
8. $\alpha d_1(x, y) + \beta d_2(x, y)$, where $\alpha, \beta > 0$ (cf. **semimetric cone** in Chap. 1).

- **Generalized biotope transform metric**

  For a given metric d on a set X and a closed set $M \subset X$, the **generalized biotope transform metric** d^M on X is defined by

$$d^M(x, y) = \frac{2d(x, y)}{d(x, y) + \inf_{z\in M}(d(x, z) + d(y, z))}.$$

  In fact, $d^M(x, y)$ and its 1-**truncation** $\min\{1, d^M(x, y)\}$ are both metrics.

  The **biotope transform metric** is $d^M(x, y)$ with $|M| = 1$. The **Steinhaus distance** from Chap. 1 is the case $d(x, y) = \mu(x\triangle y)$ with $p \neq \emptyset$ and the **biotope distance** from Chap. 23 is its subcase $d(x, y) = \mu(x\triangle y) = |x\triangle y|$.

- **Metric-preserving function**

  A function $f : \mathbb{R}_{\geq 0} \to \mathbb{R}_{\geq 0}$ with $f^{-1}(0) = \{0\}$ is a **metric-preserving function** if, for each metric space (X, d), the **metric transform**

$$d_f(x, y) = f(d(x, y))$$

  is a metric on X; cf. [Cora99]. In this case d_f is called a **functional transform metric**. For example, αd ($\alpha > 0$), $d^\alpha (0 < \alpha \leq 1)$, $\ln(1 + d)$, $\operatorname{arcsinh} d$, $\operatorname{arccosh}(1 + d)$, and $\frac{d}{1+d}$ are functional transform metrics.

  The superposition, sum and maximum of two metric-preserving functions are metric-preserving. If f is *subadditive*, i.e. $f(x + y) \leq f(x) + f(y)$ for all $x, y \geq 0$, and nondecreasing, then it is metric-preserving. But, for example, the function $f(x) = \frac{x+2}{x+1}$, for $x > 0$, and $f(0) = 0$, is decreasing and metric-preserving. If f is metric-preserving, then it is subadditive.

  If f is *concave*, i.e., $f(\frac{x+y}{2}) \geq \frac{f(x)+f(y)}{2}$ for all $x, y \geq 0$, then it is metric-preserving. In particular, a twice differentiable function $f : \mathbb{R}_{\geq 0} \to \mathbb{R}_{\geq 0}$ such that $f(0) = 0, f'(x) > 0$ for all $x \geq 0$, and $f''(x) \leq 0$ for all $x \geq 0$, is metric-preserving.

  The function f is **strongly metric-preserving function** if d and $f(d(x, y))$ are **equivalent metrics** on X, for each metric space (X, d). A metric-preserving function is strongly metric-preserving if and only if it is continuous at 0.

- **Metric aggregating function**

  A function $f : \mathbb{R}^2_{\geq 0} \to \mathbb{R}_{\geq 0}$ with $f(a, b) = 0$ if and only if $a = b = 0$, is said to be **metric** (respectively, **quasi-metric**) **aggregating function** if the function $d_f : X \times X \to \mathbb{R}_{\geq 0}$ is a metric for every pair of metric spaces (respectively, a quasi-metric for every pair of quasi-metric spaces) (X_1, d_1) and (X_2, d_2), where $X = X_1 \times X_2$ and, for all $(x, z), (y, w) \in X$, it holds

$$d_f((x, z), (y, w)) = f(d_1(x, z), d_2(y, w)).$$

  Borsiḱ–Doboš, 1981, proved that a function f is metric aggregating if and only if, for all $a, b, c, a', b', c' \geq 0$ with $|a-b| \leq c \leq a+b$ and $|a'-b'| \leq c' \leq a'+b'$, it holds

$$|f(a, a') - f(b, b')| \leq f(c, c') \leq f(a, a') + f(b, b').$$

  Cf. **spin triangle inequality** in Chap. 15.

  Major–Valero, 2008, proved that a function f is quasi-metric agregating if and only if it holds $f(a, a') \leq f(b, c') + f(c, b')$ for all $a, b, c, a', b', c' \geq 0$ such that $a \leq b + c$ and $a' \leq b' + c'$; so, any quasi-metric agregating function is metric agregating.

- **Metric generating function**

  A symmetric function $f : \mathbb{R}^2_{\geq 0} \to \mathbb{R}_{\geq 0}$ with $f(a, b) = 0$ if and only if $a = b = 0$, is said to be **metric generating** if the function defined by

$$d_f(x, y) = f(d(x, y), d(y, x))$$

  for all $x, y \in X$ is a metric on X for every quasi-metric space (X, d).

  Martin–Major–Valero, 2013, proved that a function f is metric generating if and only if it holds $f(a, a') \leq f(b, c') + f(c, b')$ for all a, b, c, a', b', c' such that $a \leq b + c, b \leq a + b', c \leq c' + a$ and $a' \leq b' + c', b' \leq a' + b, c' \leq c + a'$.

- **Power transform metric**

  Let $0 < \alpha \leq 1$. Given a metric space (X, d), the **power** (or α-*snowflake*) **transform metric** is a **functional transform metric** on X defined by

$$(d(x, y))^\alpha.$$

  The distance $d(x, y) = (\sum_1^n |x_i - y_i|^p)^{\frac{1}{p}}$ with $0 < p = \alpha < 1$ is not a metric on $\mathbb{R}^n$, but its power transform $(d(x, y)^\alpha)$ is a metric.

  For a given metric d on X and any $\alpha > 1$, the function d^α is, in general, only a distance on X. It is a metric, for any positive α, if and only if d is an **ultrametric**.

  A metric d is a **doubling metric** if and only if (Assouad, 1983) the power transform metric d^α admits a **bi-Lipschitz embedding** in some Euclidean space for every $0 < \alpha < 1$ (cf. Chap. 1 for definitions).

- **Quadrance**

  A distance which is a squared distance d^2 is called a **quadrance**.

  Rational trigonometry is the proposal (Wildberger, 2007) to use as its fundamental units, quadrance and *spread* (square of sine of angle), instead of distance and angle.

  It makes some problems easier to computers: solvable with only addition, subtraction, multiplication, and division, while avoiding square roots, sine, and cosine functions. Also, such trigonometry can be done over any field.
- **Schoenberg transform metric**

  Let $\lambda > 0$. Given a metric space (X, d), the **Schoenberg transform metric** is a **functional transform metric** on X defined by

$$1 - e^{-\lambda d(x,y)}.$$

  The Schoenberg transform metrics are exactly ***P*-metrics** (cf. Chap. 1).
- **Pullback metric**

  Given two metric spaces (X, d_X), (Y, d_Y) and an injective mapping $g : X \to Y$, the **pullback metric** (of (Y, d_Y) by g) on X is defined by

$$d_Y(g(x), g(y)).$$

  If $(X, d_X) = (Y, d_Y)$, then the pullback metric is called a ***g*-transform metric**.
- **Internal metric**

  Given a metric space (X, d) in which every pair of points x, y is joined by a *rectifiable curve*, the **internal metric** (or **inner metric**, induced **intrinsic metric**, **interior metric**) D is a **transform metric** on X, obtained from d as the infimum of the lengths of all rectifiable curves connecting two given points x and $y \in X$.

  The metric d is called an **intrinsic metric** (or **length metric** if it coincides with its internal metric. Cf. Chap. 6 and **metric curve** in Chap. 1.
- **Farris transform metric**

  Given a metric space (X, d) and a point $z \in X$, the **Farris transform** is a metric transform D_z on $X\backslash\{z\}$ defined by $D_z(x, x) = 0$ and, for different $x, y \in X\backslash\{z\}$, by

$$D_z(x, y) = C - (x.y)_z,$$

  where C is a positive constant, and $(x.y)_z = \frac{1}{2}(d(x, z) + d(y, z) - d(x, y))$ is the **Gromov product** (cf. Chap. 1). It is a metric if $C \geq \max_{x \in X\backslash\{z\}} d(x, z)$; in fact, there exists a number $C_0 \in (\max_{x,y \in X\backslash\{z\}, x \neq y}(x.y)_z, \max_{x \in X\backslash\{z\}} d(x, z)]$ such that it is a metric if and only if $C \geq C_0$. The Farris transform is an **ultrametric** if and only if d satisfies the **four-point inequality**. In Phylogenetics, where it was applied first, the term *Farris transform* is used for the function $d(x, y) - d(x, z) - d(y, z)$.

- **Involution transform metric**

  Given a metric space (X, d) and a point $z \in X$, the **involution transform metric** is a metric transform d_z on $X\backslash\{z\}$ defined by

$$d_z(x, y) = \frac{d(x, y)}{d(x, z)d(y, z)}.$$

  It is a metric for any $z \in X$, if and only if d is a **Ptolemaic metric** ([FoSc06]).

4.2 Metrics on Set Extensions

- **Extension distances**

  If d is a metric on $V_n = \{1, \ldots, n\}$, and $\alpha \in \mathbb{R}, \alpha > 0$, then the following extension distances (see, for example, [DeLa97]) are used.

  The **gate extension distance** $gat = gat_\alpha^d$ is a metric on $V_{n+1} = \{1, \ldots, n+1\}$ defined by the following conditions:

1. $gat(1, n+1) = \alpha$;
2. $gat(i, n+1) = \alpha + d(1, i)$ if $2 \le i \le n$;
3. $gat(i, j) = d(i, j)$ if $1 \le i < j \le n$.

  The distance gat_0^d is called the **gate** 0**-extension** or, simply, 0**-extension** of d.

  If $\alpha \ge \max_{2 \le i \le n} d(1, i)$, then the **antipodal extension distance** $ant = ant_\alpha^d$ is a distance on V_{n+1} defined by the following conditions:

1. $ant(1, n+1) = \alpha$;
2. $ant(i, n+1) = \alpha - d(1, i)$ if $2 \le i \le n$;
3. $ant(i, j) = d(i, j)$ if $1 \le i < j \le n$.

  If $\alpha \ge \max_{1 \le i,j \le n} d(i, j)$, then the **full antipodal extension distance** $Ant = Ant_\alpha^d$ is a distance on $V_{2n} = \{1, \ldots, 2n\}$ defined by the following conditions:

1. $Ant(i, n+i) = \alpha$ if $1 \le i \le n$;
2. $Ant(i, n+j) = \alpha - d(i, j)$ if $1 \le i \ne j \le n$;
3. $Ant(i, j) = d(i, j)$ if $1 \le i \ne j \le n$;
4. $Ant(n+i, n+j) = d(i, j)$ if $1 \le i \ne j \le n$.

  It is obtained by applying the antipodal extension operation iteratively n times, starting from d.

  The **spherical extension distance** $sph = sph_\alpha^d$ is a metric on V_{n+1} defined by the following conditions:

1. $sph(i, n+1) = \alpha$ if $1 \le i \le n$;
2. $sph(i, j) = d(i, j)$ if $1 \le i < j \le n$.

- 1**-sum distance**

  Let d_1 be a distance on a set X_1, let d_2 be a distance on a set X_2, and suppose that $X_1 \cap X_2 = \{x_0\}$. The 1**-sum distance** of d_1 and d_2 is the distance d on $X_1 \cup X_2$ defined by the following conditions:

$$d(x,y) = \begin{cases} d_1(x,y), & \text{if} \quad x,y \in X_1, \\ d_2(x,y), & \text{if} \quad x,y \in X_2, \\ d(x,x_0) + d(x_0,y), & \text{if} \quad x \in X_1, y \in X_2. \end{cases}$$

  In Graph Theory, the 1-sum distance is a **path metric**, corresponding to the clique 1-sum operation for graphs.
- **Disjoint union metric**

  Given a family (X_t, d_t), $t \in T$, of metric spaces, the **disjoint union metric** is an **extended metric** on the set $\bigcup_t X_t \times \{t\}$ defined by

$$d((x,t_1),(y,t_2)) = d_t(x,y)$$

  for $t_1 = t_2$, and $d((x,t_1),(y,t_2)) = \infty$, otherwise.
- **Metric bouquet**

  Given a family (X_t, d_t), $t \in T$, of metric spaces with marked points x_t, the **metric bouquet** is obtained from their **disjoint union** by gluing all points x_t together.
- **Product metric**

  Given finite or countable number n of metric spaces (X_1, d_1), (X_2, d_2), $\ldots$, (X_n, d_n), the **product metric** is a metric on the *Cartesian product* $X_1 \times X_2 \times \cdots \times X_n = \{x = (x_1, x_2, \ldots, x_n) : x_1 \in X_1, \ldots, x_n \in X_n\}$ defined as a function of $d_1, \ldots, d_n$. The simplest finite product metrics are defined by

  1. $(\sum_{i=1}^n d_i^p(x_i,y_i))^{\frac{1}{p}}$, $1 \le p < \infty$;
  2. $\max_{1 \le i \le n} d_i(x_i,y_i)$;
  3. $\sum_{i=1}^n \frac{1}{2^i} \frac{d_i(x_i,y_i)}{1+d_i(x_i,y_i)}$.

  The last metric is **bounded** and can be extended to the product of countably many metric spaces.

  If $X_1 = \cdots = X_n = \mathbb{R}$, and $d_1 = \cdots = d_n = d$, where $d(x,y) = |x-y|$ is the **natural metric** on $\mathbb{R}$, all product metrics above induce the Euclidean topology on the n-dimensional space $\mathbb{R}^n$. They do not coincide with the Euclidean metric on $\mathbb{R}^n$, but they are equivalent to it. In particular, the set $\mathbb{R}^n$ with the Euclidean metric can be considered as the Cartesian product $\mathbb{R} \times \cdots \times \mathbb{R}$ of n copies of the *real line* $(\mathbb{R}, d)$ with the product metric defined by $\sqrt{\sum_{i=1}^n d^2(x_i,y_i)}$.
- **Box metric**

  Let (X,d) be a metric space and I the unit interval of $\mathbb{R}$. The **box metric** is the **product metric** d' on the Cartesian product $X \times I$ defined by

$$d'((x_1,t_1),(x_2,t_2)) = \max(d(x_1,x_2), |t_1 - t_2|).$$

Cf. unrelated **bounded box metric** in Chap. 18.

- **Fréchet product metric**

  Let (X, d) be a metric space with a **bounded** metric d. Let $X^\infty = X \times \cdots \times X \cdots = \{x = (x_1, \ldots, x_n, \ldots) : x_1 \in X_1, \ldots, x_n \in X_n, \ldots\}$ be the *countable Cartesian product space* of X.

  The **Fréchet product metric** is a **product metric** on X^∞ defined by

$$\sum_{n=1}^{\infty} A_n d(x_n, y_n),$$

  where $\sum_{n=1}^{\infty} A_n$ is any convergent series of positive terms. Usually, $A_n = \frac{1}{2^n}$ is used.

  A metric (sometimes called the *Fréchet metric*) on the set of all sequences $\{x_n\}_n$ of real (complex) numbers, defined by

$$\sum_{n=1}^{\infty} A_n \frac{|x_n - y_n|}{1 + |x_n - y_n|},$$

  where $\sum_{n=1}^{\infty} A_n$ is any convergent series of positive terms, is a Fréchet product metric of countably many copies of $\mathbb{R}$ ($\mathbb{C}$). Usually, $A_n = \frac{1}{n!}$ or $A_n = \frac{1}{2^n}$ are used.

- **Hilbert cube metric**

  The *Hilbert cube* $I^{\aleph_0}$ is the *Cartesian product* of countable many copies of the interval $[0, 1]$, equipped with the metric

$$\sum_{i=1}^{\infty} 2^{-i} |x_i - y_i|$$

  (cf. **Fréchet infinite metric product**). It also can be identified up to homeomorphisms with the compact metric space formed by all sequences $\{x_n\}_n$ of real numbers such that $0 \le x_n \le \frac{1}{n}$, where the metric is defined as $\sqrt{\sum_{n=1}^{\infty} (x_n - y_n)^2}$.

  The Cartesian products $[0, 1]^\tau$ and $\{0, 1\}^\tau$, where τ is an arbitrary cardinal number, are called a *Tikhonov cube* and *Cantor cube*, respectively.

- **Hamming cube**

  Given integers $n \ge 1$ and $q \ge 2$, the *Hamming space* $H(n, q)$ is the set of all n-tuples over an alphabet of size q (say, the *Cartesian product* of n copies of the set $\{0, 1, \ldots, q-1\}$), equipped with the **Hamming metric** (cf. Chap. 1), i.e., the distance between two n-tuples is the number of coordinates where they differ. The **Hamming cube** is the Hamming space $H(n, 2)$.

  The *infinite Hamming cube* $H(\infty)$ is the set of all infinite strings over the alphabet $\{0, 1\}$ containing only finitely many 1's, equipped with the Hamming metric.

  The *half-cube* $\frac{1}{2}H(n)$ is the set of all n-tuples over $\{0, 1\}$, containing even number of 1's, with two of them being adjacent if they differ exactly in two

coordinates. For an integer $k, 1 \leq k < n$, the *Johnson graph* $J(n,k)$ is the set of all n-tuples over $\{0,1\}$, containing k 1's, with the same notion of adjacence.

The *Fibonacci cube* $F(n)$ is the set of all n-tuples over $\{0,1\}$ that contain no two consecutive 1's, equipped with the Hamming metric; it is a **partial cube** (Chap. 15), i.e., an isometric subgraph of $H(n,2)$. The *Lucas cube* $L(n)$ is obtained from $F(n)$ by removing n-tuples that start and end with 1.

- **Cameron–Tarzi cube**

  Given integers $n \geq 1$ and $q \geq 2$, the *normalized Hamming space* $H_n(q)$ is the set of all n-tuples over an alphabet of size q, equipped with the **Hamming metric** divided by n. Clearly, there are isometric embeddings

$$H_1(q) \to H_2(q) \to H_4(q) \to H_8(q) \to \dots$$

  Let $H(q)$ denote the **Cauchy completion** (Chap. 1) of the union (denote it by $H_\omega(q)$) of all metric spaces $H_n(q)$ with $n \geq 1$. This metric space was introduced in [CaTa08]. Call $H(2)$ the **Cameron–Tarzi cube**.

  It is shown in [CaTa08] that $H_\omega(2)$ is the **word metric** space (Chap. 20) of the *countable Nim group*, i.e., the elementary Abelian 2-group of all natural numbers under bitwise addition modulo 2 of the number expressions in base 2. The Cameron-Tarzi cube is also the word metric space of an Abelian group.

- **Rubik cube**

  There is a bijection between legal positions of the *Rubik* $3 \times 3 \times 3$ *cube* and elements of the subgroup G of the group Sym_{48} (of all permutations of $6(9-1)$ movable facets) generated by the 6 face rotations. The number of possible positions attainable by the cube is $|G| \approx 43 \times 10^{18}$.

  The maximum number of face turns needed to solve any instance of the Rubik cube is the diameter (maximal **word metric**), 20, of the *Cayley graph* of G.

- **Warped product metric**

  Let (X, d_X) and (Y, d_Y) be two complete **length spaces** (cf. Chap. 6), and let $f : X \to \mathbb{R}$ be a positive continuous function. Given a curve $\gamma : [a,b] \to X \times Y$, consider its projections $\gamma_1 : [a,b] \to X$ and $\gamma_2 : [a,b] \to Y$ to X and Y, and define the length of γ by the formula $\int_a^b \sqrt{|\gamma_1'|^2(t) + f^2(\gamma_1(t))|\gamma_2'|^2(t)}dt$.

  The **warped product metric** is a metric on $X \times Y$, defined as the infimum of lengths of all rectifiable curves connecting two given points in $X \times Y$ (see [BBI01]).

4.3 Metrics on Other Sets

Given a metric space (X,d), one can construct several distances between some subsets of X. The main such distances are: the **point-set distance** $d(x,A) = \inf_{y \in A} d(x,y)$ between a point $x \in X$ and a subset $A \subset X$, the **set-set distance** $\inf_{x \in A, y \in B} d(x,y)$ between two subsets A and B of X, and the **Hausdorff metric**

between compact subsets of X which are considered in Chap. 1. In this section we list some other distances of this kind.

- **Line-line distance**

  The **line-line distance** (or *vertical distance between lines*) is the **set-set distance** in $\mathbb{R}^3$ between two *skew* lines, i.e., two straight lines that do not lie in a plane.

  It is the length of the segment of their common perpendicular whose endpoints lie on the lines. For l_1 and l_2 with equations $l_1 : x = p+qt, t \in \mathbb{R}$, and $l_2 : x = r+st$, $t \in \mathbb{R}$, the distance is given by

$$\frac{|\langle r-p, q \times s\rangle|}{||q \times s||_2},$$

  where $\times$ is the *cross product* on $\mathbb{R}^3$, $\langle , \rangle$ is the *inner product* on $\mathbb{R}^3$, and $||.||_2$ is the Euclidean norm. For $x = (q_1, q_2, q_3)$, $s = (s_1, s_2, s_3)$, one has $q \times s = (q_2 s_3 - q_3 s_2, q_3 s_1 - q_1 s_3, q_1 s_2 - q_2 s_1)$.
- **Point-line distance**

  The **point-line distance** is the **point-set distance** between a point and a line.

  In $\mathbb{R}^2$, the distance between a point $P = (x_1, y_1)$ and a line l: $ax + by + c = 0$ (in Cartesian coordinates) is the **perpendicular distance** given by

$$\frac{|ax_1 + by_1 + c|}{\sqrt{a^2 + b^2}}.$$

  In $\mathbb{R}^2$, the *directed distance* between a point P and a line l is given by

$$\frac{ax_1 + by_1 + c}{\pm\sqrt{a^2 + b^2}},$$

  where the denominator is given the sign of b. It is negative if P is below the line.

  In $\mathbb{R}^3$, the distance between a point P and a line l: $x = p + qt, t \in \mathbb{R}$ (in vector formulation) is given by

$$\frac{||q \times (p - P)||_2}{||q||_2},$$

  where $\times$ is the *cross product* on $\mathbb{R}^3$, and $||.||_2$ is the Euclidean norm.
- **Point-plane distance**

  The **point-plane distance** is the **point-set distance** in $\mathbb{R}^3$ between a point $P = (x_1, y_1, z_1)$ and a plane α: $ax + by + cz + d = 0$ given by

$$\frac{|ax_1 + by_1 + cz_1 + d|}{\sqrt{a^2 + b^2 + c^2}}.$$

- **Algebraic point-conic distance**
  The **algebraic distance** of a point y to the curve given by the quadratic equation $x^T Ax$ (such as a conic in homogeneous coordinates) is defined as $y^T Ay$.
- **Prime number distance**
  The **prime number distance** is the **point-set distance** in $(\mathbb{N}, |n-m|)$ between a number $n \in \mathbb{N}$ and the set of prime numbers $P \subset \mathbb{N}$. It is the absolute difference between n and the nearest prime number.
- **Distance up to nearest integer**
  The **distance up to nearest integer** is the **point-set distance** in $(\mathbb{R}, |x-y|)$ between a number $x \in \mathbb{R}$ and the set of integers $\mathbb{Z} \subset \mathbb{R}$, i.e., $\min_{n\in\mathbb{Z}} |x-n|$.
- **Busemann metric of sets**
  Given a metric space (X, d), the **Busemann metric of sets** (see [Buse55]) is a metric on the set of all nonempty closed subsets of X defined by

$$\sup_{x\in X} |d(x, A) - d(x, B)|e^{-d(p,x)},$$

  where $p \in X$ is fixed, and $d(x, A) = \min_{y\in A} d(x, y)$ is the **point-set distance**.
  Instead of the weighting factor $e^{-d(p,x)}$, one can take any distance transform function which decreases fast enough (cf. **L_p-Hausdorff distance** in Chap. 1, and the list of variations of the **Hausdorff metric** in Chap. 21).
- **Quotient semimetric**
  Given an **extended metric space** (X, d) (i.e., a possibly infinite metric) and an equivalence relation $\sim$ on X, the **quotient semimetric** is a semimetric on the set $\overline{X} = X/\sim$ of equivalence classes defined, for any $\overline{x}, \overline{y} \in \overline{X}$, by

$$\overline{d}(\overline{x}, \overline{y}) = \inf_{m\in\mathbb{N}} \sum_{i=1}^{m} d(x_i, y_i),$$

  where the infimum is taken over all sequences $x_1, y_1, x_2, y_2, \ldots, x_m, y_m$ with $x_1 \in \overline{x}$, $y_m \in \overline{y}$, and $y_i \sim x_{i+1}$ for $i = 1, 2, \ldots, m-1$. One has $\overline{d}(\overline{x}, \overline{y}) \le d(x, y)$ for all $x, y \in X$, and $\overline{d}$ is the biggest semimetric on $\overline{X}$ with this property.

Chapter 5
Metrics on Normed Structures

In this chapter we consider a special class of metrics defined on some *normed structures*, as the norm of the difference between two given elements. This structure can be a group (with a *group norm*), a vector space (with a *vector norm* or, simply, a *norm*), a vector lattice (with a *Riesz norm*), a field (with a *valuation*), etc.

Any norm is *subadditive*, i.e., triangle inequality $||x + y|| \leq ||x|| + ||y||$ holds. A norm is *submultiplicative* if **multiplicative triangle inequality** $||xy|| \leq ||x||||y||$ holds.

- **Group norm metric**

  A **group norm metric** is a metric on a *group* $(G, +, 0)$ defined by

  $$||x + (-y)|| = ||x - y||,$$

  where $||.||$ is a *group norm* on G, i.e., a function $||.|| : G \to \mathbb{R}$ such that, for all $x, y \in G$, we have the following properties:

  1. $||x|| \geq 0$, with $||x|| = 0$ if and only if $x = 0$;
  2. $||x|| = ||-x||$;
  3. $||x + y|| \leq ||x|| + ||y||$ (triangle inequality).

  Any group norm metric d is **right-invariant**, i.e., $d(x, y) = d(x + z, y + z)$ for any $x, y, z \in G$. Conversely, any right-invariant (as well as any **left-invariant**, and, in particular, any **bi-invariant**) metric d on G is a group norm metric, since one can define a group norm on G by $||x|| = d(x, 0)$.
- **F-norm metric**

  A *vector space* (or *linear space*) over a *field* $\mathbb{F}$ is a set V equipped with operations of *vector addition* $+ : V \times V \to V$ and *scalar multiplication* $\cdot : \mathbb{F} \times V \to V$ such that $(V, +, 0)$ forms an *Abelian group* (where $0 \in V$ is the *zero vector*), and, for all *vectors* $x, y \in V$ and any *scalars* $a, b \in \mathbb{F}$, we have the following properties: $1 \cdot x = x$ (where 1 is the multiplicative unit of $\mathbb{F}$), $(ab) \cdot x = a \cdot (b \cdot x)$, $(a + b) \cdot x = a \cdot x + b \cdot x$, and $a \cdot (x + y) = a \cdot x + a \cdot y$.

© Springer-Verlag Berlin Heidelberg 2016

M.M. Deza, E. Deza, *Encyclopedia of Distances*,
DOI 10.1007/978-3-662-52844-0_5

A vector space over the field $\mathbb{R}$ of real numbers is called a *real vector space*. A vector space over the field $\mathbb{C}$ of complex numbers is called *complex vector space*.

A F**-norm metric** is a metric on a real (complex) vector space V defined by

$$||x - y||_F,$$

where $||.||_F$ is an *F-norm* on V, i.e., a function $||.||_F : V \to \mathbb{R}$ such that, for all $x, y \in V$ and for any scalar a with $|a| = 1$, we have the following properties:

1. $||x||_F \geq 0$, with $||x||_F = 0$ if and only if $x = 0$;
2. $||ax||_F \leq ||x||_F$ if $|a| \leq 1$;
3. $\lim_{a \to 0} ||ax||_F = 0$;
4. $||x + y||_F \leq ||x||_F + ||y||_F$ (triangle inequality).

An F-norm is called *p-homogeneous* if $||ax||_F = |a|^p ||x||_F$ for any scalar a.

Any F-norm metric d is a **translation invariant metric**, i.e., $d(x, y) = d(x + z, y + z)$ for all $x, y, z \in V$. Conversely, if d is a translation invariant metric on V, then $||x||_F = d(x, 0)$ is an F-norm on V.

- F^***-metric**

  An F^***-metric** is an F**-norm metric** $||x - y||_F$ on a real (complex) vector space V such that the operations of scalar multiplication and vector addition are continuous with respect to $||.||_F$. Thus $||.||_F$ is a function $||.||_F : V \to \mathbb{R}$ such that, for all $x, y, x_n \in V$ and for all scalars a, a_n, we have the following properties:

  1. $||x||_F \geq 0$, with $||x||_F = 0$ if and only if $x = 0$;
  2. $||ax||_F = ||x||_F$ for all a with $|a| = 1$;
  3. $||x + y||_F \leq ||x||_F + ||y||_F$;
  4. $||a_n x||_F \to 0$ if $a_n \to 0$;
  5. $||ax_n||_F \to 0$ if $x_n \to 0$;
  6. $||a_n x_n||_F \to 0$ if $a_n \to 0, x_n \to 0$.

  The metric space $(V, ||x - y||_F)$ with an F^*-metric is called a nF^***-space**. Equivalently, an F^*-space is a metric space (V, d) with a **translation invariant metric** d such that the operation of scalar multiplication and vector addition are continuous with respect to this metric.

  A **complete** F^*-space is called an F**-space**. A **locally convex** F-space is known as a **Fréchet space** (Chap. 2) in Functional Analysis.

  A **modular space** is an F^*-space $(V, ||.||_F)$ in which the F-norm $||.||_F$ is defined by

$$||x||_F = \inf\{\lambda > 0 : \rho\left(\frac{x}{\lambda}\right) < \lambda\},$$

and ρ is a *metrizing modular* on V, i.e., a function $\rho : V \to [0, \infty]$ such that, for all $x, y, x_n \in V$ and for all scalars a, a_n, we have the following properties:

1. $\rho(x) = 0$ if and only if $x = 0$;
2. $\rho(ax) = \rho(x)$ implies $|a| = 1$;

3. $\rho(ax + by) \leq \rho(x) + \rho(y)$ implies $a, b \geq 0, a + b = 1$;
4. $\rho(a_n x) \to 0$ if $a_n \to 0$ and $\rho(x) < \infty$;
5. $\rho(ax_n) \to 0$ if $\rho(x_n) \to 0$ (*metrizing property*);
6. For any $x \in V$, there exists $k > 0$ such that $\rho(kx) < \infty$.

- **Norm metric**

A **norm metric** is a metric on a real (complex) vector space V defined by

$$||x - y||,$$

where $||.||$ is a *norm* on V, i.e., a function $||.|| : V \to \mathbb{R}$ such that, for all $x, y \in V$ and for any scalar a, we have the following properties:

1. $||x|| \geq 0$, with $||x|| = 0$ if and only if $x = 0$;
2. $||ax|| = |a|||x||$;
3. $||x + y|| \leq ||x|| + ||y||$ (triangle inequality).

Therefore, a norm $||.||$ is a 1-*homogeneous F-norm*. The vector space $(V, ||.||)$ is called a *normed vector space* or, simply, *normed space*.

Any metric space can be embedded isometrically in some normed vector space as a closed linearly independent subset. Every finite-dimensional normed space is **complete**, and all norms on it are equivalent.

In general, the norm $||.||$ is equivalent (Maligranda, 2008) to the norm

$$||x||_{u,p} = (||x + ||x|| \cdot u||^p + ||x - ||x|| \cdot u||^p)^{\frac{1}{p}},$$

introduced, for any $u \in V$ and $p \geq 1$, by Odell and Schlumprecht, 1998.

The **norm-angular distance** between x and y is defined (Clarkson, 1936) by

$$d(x, y) = ||\frac{x}{||x||} - \frac{y}{||y||}||.$$

The following sharpening of the triangle inequality (Maligranda, 2003) holds:

$$\frac{||x - y|| - |||x|| - ||y|||}{\min\{||x||, ||y||\}} \leq d(x, y) \leq \frac{||x - y|| + |||x|| - ||y|||}{\max\{||x||, ||y||\}}, \text{ i.e.,}$$

$$(2 - d(x, -y)) \min\{||x||, ||y||\} \leq ||x|| + ||y|| - ||x + y||$$

$$\leq (2 - d(x, -y)) \max\{||x||, ||y||\}.$$

Dragomir, 2004, call $|\int_a^b f(x)dx| \leq \int_a^b |f(x)|dx$ *continuous triangle inequality*.

- **Reverse triangle inequality**

  The triangle inequality $||x + y|| \leq ||x|| + ||y||$ in a normed space $(V, ||.||)$ is equivalent to the following inequality, for any $x_1, \ldots, x_n \in V$ with $n \geq 2$:

$$||\sum_{i=1}^{n} x_i|| \leq \sum_{i=1}^{n} ||x_i||.$$

  If in the normed space $(V, ||.||)$, for some $C \geq 1$ one has

$$C||\sum_{i=1}^{n} x_i|| \geq \sum_{i=1}^{n} ||x_i||,$$

  then this inequality is called the **reverse triangle inequality**.

  This term is used, sometimes, also for the **inverse triangle inequality** (cf. **kinematic metric** in Chap. 26) and for the eventual inequality $Cd(x, z) \geq d(x, y) + d(y, z)$ with $C \geq 1$ in a metric space (X, d).

  The triangle inequality $||x + y|| \leq ||x|| + ||y||$, for any $x, y \in V$, in a normed space $(V, ||.||)$ is, for any number $q > 1$, equivalent (Belbachir, Mirzavaziri and Moslenian, 2005) to the following inequality:

$$||x + y||^q \leq 2^{q-1}(||x||^q + ||y||^q).$$

  The *parallelogram inequality* $||x + y||^2 \leq 2(||x||^2 + ||y||^2)$ is the case $q = 2$ of above.

  Given a number q, $0 < q \leq 1$, the norm is called *q-subadditive* if $||x + y||^q \leq ||x||^q + ||y||^q$ holds for $x, y \in V$.

- **Seminorm semimetric**

  A **seminorm semimetric** on a real (complex) vector space V is defined by

$$||x - y||,$$

  where $||.||$ is a *seminorm* (or *pseudo-norm*) on V, i.e., a function $||.|| : V \to \mathbb{R}$ such that, for all $x, y \in V$ and for any scalar a, we have the following properties:

  1. $||x|| \geq 0$, with $||0|| = 0$;
  2. $||ax|| = |a|||x||$;
  3. $||x + y|| \leq ||x|| + ||y||$ (triangle inequality).

  The vector space $(V, ||.||)$ is called a *seminormed vector space*. Many *normed vector spaces*, in particular, **Banach spaces**, are defined as the quotient space by the subspace of elements of seminorm zero.

  A *quasi-normed space* is a vector space V, on which a *quasi-norm* is given. A *quasi-norm* on V is a nonnegative function $||.|| : V \to \mathbb{R}$ which satisfies the same axioms as a norm, except for the triangle inequality which is replaced by the weaker requirement: there exists a constant $C > 0$ such that, for all $x, y \in V$,

the following *C*-**triangle inequality** (cf. **near-metric** in Chap. 1) holds:

$$||x + y|| \leq C(||x|| + ||y||)$$

An example of a quasi-normed space, that is not normed, is the *Lebesgue space* $L_p(\Omega)$ with $0 < p < 1$ in which a quasi-norm is defined by

$$||f|| = (\int_{\Omega} |f(x)|^p dx)^{1/p}, f \in L_p(\Omega).$$

- **Banach space**

  A **Banach space** (or *B-space*) is a **complete** metric space $(V, ||x - y||)$ on a vector space V with a norm metric $||x - y||$. Equivalently, it is the complete *normed space* $(V, ||.||)$. In this case, the norm $||.||$ on V is called the *Banach norm*. Some examples of Banach spaces are:

  1. l_p^n*-spaces*, l_p^∞*-spaces*, $1 \leq p \leq \infty, n \in \mathbb{N}$;
  2. The space C of convergent numerical sequences with the norm $||x|| = \sup_n |x_n|$;
  3. The space C_0 of numerical sequences which converge to zero with the norm $||x|| = \max_n |x_n|$;
  4. The space $C^p_{[a,b]}$, $1 \leq p \leq \infty$, of continuous functions on $[a, b]$ with the L_p*-norm* $||f||_p = (\int_a^b |f(t)|^p dt)^{\frac{1}{p}}$;
  5. The space C_K of continuous functions on a compactum K with the norm $||f|| = \max_{t \in K} |f(t)|$;
  6. The space $(C_{[a,b]})^n$ of functions on $[a, b]$ with continuous derivatives up to and including the order n with the norm $||f||_n = \sum_{k=0}^n \max_{a \leq t \leq b} |f^{(k)}(t)|$;
  7. The space $C^n[I^m]$ of all functions defined in an m-dimensional cube that are continuously differentiable up to and including the order n with the norm of uniform boundedness in all derivatives of order at most n;
  8. The space $M_{[a,b]}$ of bounded measurable functions on $[a, b]$ with the norm

  $$||f|| = ess \sup_{a \leq t \leq b} |f(t)| = \inf_{e, \mu(e)=0} \sup_{t \in [a,b] \setminus e} |f(t)|;$$

  9. The space $A(\Delta)$ of functions analytic in the open *unit disk* $\Delta = \{z \in \mathbb{C} : |z| < 1\}$ and continuous in the closed disk $\overline{\Delta}$ with the norm $||f|| = \max_{z \in \overline{\Delta}} |f(z)|$;
  10. The **Lebesgue spaces** $L_p(\Omega)$, $1 \leq p \leq \infty$;
  11. The *Sobolev spaces* $W^{k,p}(\Omega)$, $\Omega \subset \mathbb{R}^n$, $1 \leq p \leq \infty$, of functions f on Ω such that f and its derivatives, up to some order k, have a finite L_p*-norm*, with the norm $||f||_{k,p} = \sum_{i=0}^k ||f^{(i)}||_p$;

12. The *Bohr space AP* of almost periodic functions with the norm

$$||f|| = \sup_{-\infty<t<+\infty} |f(t)|.$$

A finite-dimensional real Banach space is called a *Minkowskian space*. A norm metric of a Minkowskian space is called a **Minkowskian metric** (Chap. 6). In particular, any l_p**-metric** is a Minkowskian metric.

All n-dimensional Banach spaces are pairwise isomorphic; the set of such spaces becomes compact if one introduces the **Banach–Mazur distance** by $d_{BM}(V, W) = \ln \inf_T ||T|| \cdot ||T^{-1}||$, where the infimum is taken over all operators which realize an isomorphism $T : V \to W$.

- l_p**-metric**

The l_p**-metric** d_{l_p}, $1 \le p \le \infty$, is a norm metric on $\mathbb{R}^n$ (or on $\mathbb{C}^n$), defined by

$$||x - y||_p,$$

where the l_p*-norm* $||.||_p$ is defined by

$$||x||_p = (\sum_{i=1}^{n} |x_i|^p)^{\frac{1}{p}}.$$

For $p = \infty$, we obtain $||x||_\infty = \lim_{p\to\infty} \sqrt[p]{\sum_{i=1}^{n} |x_i|^p} = \max_{1\le i\le n} |x_i|$. The metric space $(\mathbb{R}^n, d_{l_p})$ is abbreviated as l_p^n and is called l_p^n*-space*.

The l_p**-metric**, $1 \le p \le \infty$, on the set of all sequences $x = \{x_n\}_{n=1}^{\infty}$ of real (complex) numbers, for which the sum $\sum_{i=1}^{\infty} |x_i|^p$ (for $p = \infty$, the sum $\sum_{i=1}^{\infty} |x_i|$) is finite, is

$$(\sum_{i=1}^{\infty} |x_i - y_i|^p)^{\frac{1}{p}}.$$

For $p = \infty$, we obtain $\max_{i\ge 1} |x_i - y_i|$. This metric space is abbreviated as l_p^∞ and is called l_p^∞*-space*.

Most important are l_1-, l_2- and l_∞-metrics. Among l_p-metrics, only l_1- and l_∞-metrics are **crystalline metrics**, i.e., metrics having polygonal unit balls. On $\mathbb{R}$ all l_p-metrics coincide with the **natural metric** (Chap. 12) $|x - y|$.

The l_2-norm $||(x_1, x_2)||_2 = \sqrt{x_1^2 + x_2^2}$ on $\mathbb{R}^2$ is also called *Pythagorean addition* of the numbers x_1 and x_2. Under this commutative operation, $\mathbb{R}$ form a semigroup, and $\mathbb{R}_{\ge 0}$ form a *monoid* (semigroup with identity, 0).

- **Euclidean metric**

  The **Euclidean metric** (or **Pythagorean distance**, **as-the-crow-flies distance**, **beeline distance**) d_E is the metric on $\mathbb{R}^n$ defined by

$$||x-y||_2 = \sqrt{(x_1-y_1)^2+\cdots+(x_n-y_n)^2}.$$

  It is the ordinary l_2**-metric** on $\mathbb{R}^n$. The metric space $(\mathbb{R}^n, d_E)$ is abbreviated as $\mathbb{E}^n$ and is called **Euclidean space** "Euclidean space" stands for the case $n = 3$, as opposed, for $n = 2$, to *Euclidean plane* and, for $n = 1$, *Euclidean* (or *real*) *line*.

  In fact, $\mathbb{E}^n$ is an **inner product space** (and even a **Hilbert space**), i.e., $d_E(x,y) = ||x-y||_2 = \sqrt{\langle x-y, x-y\rangle}$, where $\langle x,y\rangle$ is the *inner product* on $\mathbb{R}^n$ which is given in the Cartesian coordinate system by $\langle x,y\rangle = \sum_{i=1}^n x_i y_i$. In a standard coordinate system one has $\langle x,y\rangle = \sum_{i,j} g_{ij}x_i y_j$, where $g_{ij} = \langle e_i, e_j\rangle$, and the **metric tensor** $((g_{ij}))$ (cf. Chap. 7) is a positive-definite symmetric $n \times n$ matrix.

  In general, a Euclidean space is defined as a space, the properties of which are described by the axioms of *Euclidean Geometry*.

- **Norm transform metric**

  A **norm transform metric** is a metric $d(x,y)$ on a vector space $(V, ||.||)$, which is a function of $||x||$ and $||y|$. Usually, $V = \mathbb{R}^n$ and, moreover, $\mathbb{E}^n = (\mathbb{R}^n, ||.||_2)$.

  Some examples are (p,q)**-relative metric**, M**-relative metric** and, from Chap. 19, the **British Rail metric** $||x|| + ||y||$ for $x \neq y$, (and equal to 0, otherwise), the **radar screen metric** $\min\{1, ||x-y||\}$ and $\max\{1, ||x-y||\}$ for $x \neq y$. Cf. t-**truncated** and t-**uniformly discrete** metrics in Chap. 4.

- (p,q)**-relative distance**

  Let $(V, ||.||) \neq \emptyset, \{0\}$ be a *Ptolemaic space*, i.e., the norm metric $||x-y||$ is a **Ptolemaic metric** (Chap. 1). Let $p, q > 0$.

  The (p,q)**-relative distance** on $(V, ||.||)$ is defined, for x or $y \neq 0$, by

$$\rho_{p,q}(x,y) + \frac{||x-y||}{(\frac{1}{2}(||x||^p + ||y||^p))^{\frac{q}{p}}}$$

  (and equal to 0, otherwise). In the case of $p = \infty$, it has the form

$$\frac{||x-y||}{(\max\{||x||, ||y||\})^q}.$$

  This distance is a metric (Hästö, 2002) if and only if $0 < q \leq 1, p \geq \max\{1-q, \frac{2-q}{3}\}$.

  $(p,1)$-, $(\infty,1)$- and the original $(1,1)$-relative metric on $\mathbb{E}^n$ are called p**-relative** (or **Klamkin–Meir metric**), **relative metric** and **Schattschneider metric**.

- ***M*-relative distance**

  Let $(V, ||.||) \neq \emptyset, \{0\}$ be a *Ptolemaic space*, i.e., $||x - y||$ is a **Ptolemaic metric**. Let $M : [0, \infty) \to (0, \infty)$ be a symmetric function.

  The ***M*-relative distance** on $(V, ||.||)$ is defined by

$$\rho_M(x, y) = \frac{||x - y||}{M(||x||, ||y||)}.$$

  So, it is the **(p, q)-relative distance** if $M(x, y) = (x^p + y^p)^{\frac{q}{p}}$ for $p, q > 0$.

  Call a function $f : [0, \infty) \to (0, \infty)$ *moderately increasing* (MI) if $f(x)$ is increasing but $\frac{f(x)}{x}$ is decreasing for $x > 0$. Hästö, 2002, showed that

  (i) If $M = f(x)f(y)$, then $\rho_M(x, y)$ is a metric if and only if f is MI and convex;
  (ii) If both, $M(x, \cdot)$ and $M(\cdot, x)$, are MI for each fixed $x > 0$, then $\rho_M(x, y)$ is a metric if and only if it is a metric on $\mathbb{R}$; it holds for any Ptolemeaic metric.

- **Unitary metric**

  The **unitary** (or *complex Euclidean*) **metric** is the **l_2-metric** on $\mathbb{C}^n$ defined by

$$||x - y||_2 = \sqrt{|x_1 - y_1|^2 + \cdots + |x_n - y_n|^2}.$$

  For $n = 1$, it is the **complex modulus metric** $|x - y| = \sqrt{(x - y)\overline{(x - y)}}$ on the *Wessel–Argand plane* (Chap. 12).

- **L_p-metric**

  An **L_p-metric** d_{L_p}, $1 \leq p \leq \infty$, is a norm metric on $L_p(\Omega, \mathcal{A}, \mu)$ defined by

$$||f - g||_p$$

  for any $f, g \in L_p(\Omega, \mathcal{A}, \mu)$. The metric space $(L_p(\Omega, \mathcal{A}, \mu), d_{L_p})$ is called the **L_p-space** (or **Lebesgue space**).

  Here Ω is a set, and $\mathcal{A}$ is n *σ-algebra* of subsets of Ω, i.e., a collection of subsets of Ω satisfying the following properties:

  1. $\Omega \in \mathcal{A}$;
  2. If $A \in \mathcal{A}$, then $\Omega \backslash A \in \mathcal{A}$;
  3. If $A = \cup_{i=1}^{\infty} A_i$ with $A_i \in \mathcal{A}$, then $A \in \mathcal{A}$.

  A function $\mu : \mathcal{A} \to \mathbb{R}_{\geq 0}$ is called a *measure* on $\mathcal{A}$ if it is *additive*, i.e., $\mu(\cup_{i \geq 1} A_i) = \sum_{i \geq 1} \mu(A_i)$ for all pairwise disjoint sets $A_i \in \mathcal{A}$, and satisfies $\mu(\emptyset) = 0$. A *measure space* is a triple $(\Omega, \mathcal{A}, \mu)$.

  Given a function $f : \Omega \to \mathbb{R}(\mathbb{C})$, its *$L_p$-norm* is defined by

$$||f||_p = \left(\int_{\Omega} |f(\omega)|^p \mu(d\omega) \right)^{\frac{1}{p}}.$$

Let $L_p(\Omega, \mathcal{A}, \mu) = L_p(\Omega)$ denote the set of all functions $f : \Omega \to \mathbb{R}$ ($\mathbb{C}$) such that $||f||_p < \infty$. Strictly speaking, $L_p(\Omega, \mathcal{A}, \mu)$ consists of equivalence classes of functions, where two functions are *equivalent* if they are equal *almost everywhere*, i.e., the set on which they differ has measure zero. The set $L_\infty(\Omega, \mathcal{A}, \mu)$ is the set of equivalence classes of measurable functions $f : \Omega \to \mathbb{R}$ ($\mathbb{C}$) whose absolute values are bounded almost everywhere.

The most classical example of an L_p-metric is d_{L_p} on the set $L_p(\Omega, \mathcal{A}, \mu)$, where Ω is the open interval $(0, 1)$, $\mathcal{A}$ is the *Borel σ-algebra* on $(0, 1)$, and μ is the *Lebesgue measure*. This metric space is abbreviated by $L_p(0, 1)$ and is called $L_p(0, 1)$-*space*.

In the same way, one can define the L_p-metric on the set $C_{[a,b]}$ of all real (complex) continuous functions on $[a, b]$: $d_{L_p}(f, g) = (\int_a^b |f(x) - g(x)|^p dx)^{\frac{1}{p}}$. For $p = \infty$, $d_{L_\infty}(f, g) = \max_{a \le x \le b} |f(x) - g(x)|$. This metric space is abbreviated by $C^p_{[a,b]}$ and is called $C^p_{[a,b]}$-*space*.

If $\Omega = \mathbb{N}$, $\mathcal{A} = 2^\Omega$ is the collection of all subsets of Ω, and μ is the *cardinality measure* (i.e., $\mu(A) = |A|$ if A is a finite subset of Ω, and $\mu(A) = \infty$, otherwise), then the metric space $(L_p(\Omega, 2^\Omega, |.|), d_{L_p})$ coincides with the space l^∞_p.

If $\Omega = V_n$ is a set of cardinality n, $\mathcal{A} = 2^{V_n}$, and μ is the cardinality measure, then the metric space $(L_p(V_n, 2^{V_n}, |.|), d_{L_p})$ coincides with the space l^n_p.

- **Dual metrics**

  The l_p**-metric** and the l_q**-metric**, $1 < p, q < \infty$, are called **dual** if $1/p + 1/q = 1$.

  In general, when dealing with a *normed vector space* $(V, ||.||_V)$, one is interested in the *continuous* linear functionals from V into the base field ($\mathbb{R}$ or $\mathbb{C}$). These functionals form a **Banach space** $(V', ||.||_{V'})$, called the *continuous dual* of V. The norm $||.||_{V'}$ on V' is defined by $||T||_{V'} = \sup_{||x||_V \le 1} |T(x)|$.

  The continuous dual for the metric space l^n_p (l^∞_p) is l^n_q (l^∞_q, respectively). The continuous dual of l^n_1 (l^∞_1) is l^n_∞ (l^∞_∞, respectively). The continuous duals of the Banach spaces C (consisting of all convergent sequences, with l_∞**-metric**) and C_0 (consisting of the sequences converging to zero, with l_∞**-metric**) are both naturally identified with l^∞_1.

- **Inner product space**

  An **inner product space** (or *pre-Hilbert space*) is a metric space $(V, ||x - y||)$ on a real (complex) vector space V with an *inner product* $\langle x, y\rangle$ such that the norm metric $||x - y||$ is constructed using the *inner product norm* $||x|| = \sqrt{\langle x, x\rangle}$.

  An *inner product* $\langle , \rangle$ on a real (complex) vector space V is a *symmetric bilinear* (in the complex case, *sesquilinear*) form on V, i.e., a function $\langle , \rangle : V \times V \longrightarrow \mathbb{R}$ ($\mathbb{C}$) such that, for all $x, y, z \in V$ and for all scalars α, β, we have the following properties:

  1. $\langle x, x\rangle \ge 0$, with $\langle x, x\rangle = 0$ if and only if $x = 0$;
  2. $\langle x, y\rangle = \overline{\langle y, x\rangle}$, where the bar denotes *complex conjugation*;
  3. $\langle \alpha x + \beta y, z\rangle = \alpha \langle x, z\rangle + \beta \langle y, z\rangle$.

For a complex vector space, an inner product is called also a *Hermitian inner product*, and the corresponding metric space is called a *Hermitian inner product space*.

A norm $||.||$ in a *normed space* $(V, ||.||)$ is generated by an inner product if and only if, for all $x, y \in V$, we have: $||x+y||^2 + ||x-y||^2 = 2(||x||^2 + ||y||^2)$.

In an inner product space, the **triangle equality** (Chap. 1) $||x-y|| = ||x|| + ||y||$, for $x, y \neq 0$, holds if and only if $\frac{x}{||x||} = \frac{y}{||y||}$, i.e., $x - y \in [x, y]$.

- **Hilbert space**

  A **Hilbert space** is an **inner product space** which, as a metric space, is **complete**. More precisely, a Hilbert space is a complete metric space $(H, ||x-y||)$ on a real (complex) vector space H with an *inner product* $\langle , \rangle$ such that the norm metric $||x-y||$ is constructed using the *inner product norm* $||x|| = \sqrt{\langle x, x \rangle}$. Any Hilbert space is a **Banach space**.

  An example of a Hilbert space is the set of all sequences $x = \{x_n\}_n$ of real (complex) numbers such that $\sum_{i=1}^{\infty} |x_i|^2$ converges, with the **Hilbert metric** defined by

$$(\sum_{i=1}^{\infty}(x_i - y_i)^2)^{\frac{1}{2}}.$$

  Other examples of Hilbert spaces are any L_2**-space**, and any finite-dimensional inner product space. In particular, any Euclidean space is a Hilbert space.

  A direct product of two **Hilbert spaces** is called a *Liouville space* (or *line space*, *extended Hilbert space*).

  Given an infinite cardinal number τ and a set A of the cardinality τ, let $\mathbb{R}_a$, $a \in A$, be the copies of $\mathbb{R}$. Let $H(A) = \{\{x_a\} \in \prod_{a \in A} \mathbb{R}_a : \sum_a x_a^2 < \infty\}$; then $H(A)$ with the metric defined for $\{x_a\}, \{y_a\} \in H(A)$ as

$$(\sum_{a \in A}(x_a - y_a)^2)^{\frac{1}{2}},$$

  is called the **generalized Hilbert space** of weight τ.

- **Erdös space**

  The **Erdös space** (or *rational Hilbert space*) is the metric subspace of l_2 consisting of all vectors in l_2 with only rational coordinates. It has topological dimension 1 and is not complete. Erdös space is **homeomorphic** to its countable infinite power, and every nonempty open subset of it is homeomorphic to whole space.

  The **complete Erdös space** (or *irrational Hilbert space*) is the complete metric subspace of l_2 consisting of all vectors in l_2 the coordinates of which are all irrational.

- **Riesz norm metric**

  A *Riesz space* (or *vector lattice*) is a partially ordered vector space $(V_{Ri}, \preceq)$ in which the following conditions hold:

  1. The vector space structure and the partial order structure are compatible, i.e., from $x \preceq y$ it follows that $x + z \preceq y + z$, and from $x \succ 0$, $a \in \mathbb{R}$, $a > 0$ it follows that $ax \succ 0$;
  2. For any two elements $x, y \in V_{Ri}$, there exist the *join* $x \vee y \in V_{Ri}$ and *meet* $x \wedge y \in V_{Ri}$ (cf. Chap. 10).

  The **Riesz norm metric** is a norm metric on V_{Ri} defined by

  $$||x - y||_{Ri},$$

  where $||.||_{Ri}$ is a *Riesz norm* on V_{Ri}, i.e., a norm such that, for any $x, y \in V_{Ri}$, the inequality $|x| \preceq |y|$, where $|x| = (-x) \vee (x)$, implies $||x||_{Ri} \leq ||y||_{Ri}$.

  The space $(V_{Ri}, ||.||_{Ri})$ is called a *normed Riesz space*. In the case of completeness, it is called a *Banach lattice*.
- **Banach–Mazur compactum**

  The **Banach–Mazur distance** d_{BM} between two n-dimensional *normed spaces* $(V, ||.||_V)$ and $(W, ||.||_W)$ is defined by

  $$\ln \inf_T ||T|| \cdot ||T^{-1}||,$$

  where the infimum is taken over all isomorphisms $T : V \to W$. It is a metric on the set X^n of all equivalence classes of n-dimensional normed spaces, where $V \sim W$ if and only if they are *isometric*. Then the pair (X^n, d_{BM}) is a compact metric space which is called the **Banach–Mazur compactum**.
- **Quotient metric**

  Given a *normed space* $(V, ||.||_V)$ with a norm $||.||_V$ and a closed subspace W of V, let $(V/W, ||.||_{V/W})$ be the normed space of cosets $x+W = \{x+w : w \in W\}$, $x \in V$, with the *quotient norm* $||x + W||_{V/W} = \inf_{w \in W} ||x + w||_V$.

  The **quotient metric** is a norm metric on V/W defined by

  $$||(x + W) - (y + W)||_{V/W}.$$

- **Tensor norm metric**

  Given *normed spaces* $(V, ||.||_V)$ and $(W, ||.||_W)$, a norm $||.||_\otimes$ on the *tensor product* $V \otimes W$ is called *tensor norm* (or *cross norm*) if $||x \otimes y||_\otimes = ||x||_V ||y||_W$ for all *decomposable* tensors $x \otimes y$.

  The **tensor product metric** is a norm metric on $V \otimes W$ defined by

  $$||z - t||_\otimes.$$

For any $z \in V \otimes W$, $z = \sum_j x_j \otimes y_j$, $x_j \in V$, $y_j \in W$, the *projective norm* (or π*-norm*) of z is defined by $||z||_{pr} = \inf \sum_j ||x_j||_V ||y_j||_W$, where the infimum is taken over all representations of z as a sum of decomposable vectors. It is the largest tensor norm on $V \otimes W$.

- **Valuation metric**

  A **valuation metric** is a metric on a *field* $\mathbb{F}$ defined by

  $$||x - y||,$$

  where $||.||$ is a *valuation* on $\mathbb{F}$, i.e., a function $||.|| : \mathbb{F} \to \mathbb{R}$ such that, for all $x, y \in \mathbb{F}$, we have the following properties:

  1. $||x|| \geq 0$, with $||x|| = 0$ if and only if $x = 0$;
  2. $||xy|| = ||x||\,||y||$,
  3. $||x + y|| \leq ||x|| + ||y||$ (triangle inequality).

  If $||x+y|| \leq \max\{||x||, ||y||\}$, the valuation $||.||$ is called *non-Archimedean*. In this case, the valuation metric is an **ultrametric**. The simplest valuation is the *trivial valuation* $||.||_{tr}$: $||0||_{tr} = 0$, and $||x||_{tr} = 1$ for $x \in \mathbb{F}\backslash\{0\}$. It is non-Archimedean.

  There are different definitions of valuation in Mathematics. Thus, the function $\nu : \mathbb{F} \to \mathbb{R} \cup \{\infty\}$ is called a *valuation* if $\nu(x) \geq 0$, $\nu(0) = \infty$, $\nu(xy) = \nu(x) + \nu(y)$, and $\nu(x + y) \geq \min\{\nu(x), \nu(y)\}$ for all $x, y \in \mathbb{F}$. The valuation $||.||$ can be obtained from the function ν by the formula $||x|| = \alpha^{\nu(x)}$ for some fixed $0 < \alpha < 1$ (cf. ***p*-adic metric** in Chap. 12).

  The *Kürschák valuation* $|.|_{Krs}$ is a function $|.|_{Krs} : \mathbb{F} \to \mathbb{R}$ such that $|x|_{Krs} \geq 0$, $|x|_{Krs} = 0$ if and only if $x = 0$, $|xy|_{Krs} = |x|_{Krs}|y|_{Krs}$, and $|x + y|_{Krs} \leq C \max\{|x|_{Krs}, |y|_{Krs}\}$ for all $x, y \in \mathbb{F}$ and for some positive constant C, called the *constant of valuation*. If $C \leq 2$, one obtains the ordinary valuation $||.||$ which is non-Archimedean if $C \leq 1$. In general, any $|.|_{Krs}$ is *equivalent* to some $||.||$, i.e., $|.|^p_{Krs} = ||.||$ for some $p > 0$.

  Finally, given an *ordered group* $(G, \cdot, e, \leq)$ equipped with zero, the *Krull valuation* is a function $|.| : \mathbb{F} \to G$ such that $|x| = 0$ if and only if $x = 0$, $|xy| = |x||y|$, and $|x + y| \leq \max\{|x|, |y|\}$ for any $x, y \in \mathbb{F}$. It is a generalization of the definition of non-Archimedean valuation $||.||$ (cf. **generalized metric** in Chap. 3).

- **Power series metric**

  Let $\mathbb{F}$ be an arbitrary algebraic field, and let $\mathbb{F}\langle x^{-1}\rangle$ be the field of power series of the form $w = \alpha_{-m}x^m + \cdots + \alpha_0 + \alpha_1 x^{-1} + \ldots$, $\alpha_i \in \mathbb{F}$. Given $l > 1$, a *non-Archimedean valuation* $||.||$ on $\mathbb{F}\langle x^{-1}\rangle$ is defined by

  $$||w|| = \begin{cases} l^m, & \text{if } w \neq 0, \\ 0, & \text{if } w = 0. \end{cases}$$

  The **power series metric** is the **valuation metric** $||w - v||$ on $\mathbb{F}\langle x^{-1}\rangle$.

Part II
Geometry and Distances

Chapter 6
Distances in Geometry

Geometry arose as the field of knowledge dealing with spatial relationships. It was one of the two fields of pre-modern Mathematics, the other being the study of numbers.

Earliest known evidence of abstract representation—ochre rocks marked with cross hatches and lines to create a consistent complex geometric motif, dated about 75,000 BC—were found in Blombos Cave, South Africa. In modern times, geometric concepts have been generalized to a high level of abstraction and complexity.

6.1 Geodesic Geometry

In Mathematics, the notion of "geodesic" is a generalization of the notion of "straight line" to curved spaces. This term is taken from *Geodesy*, the science of measuring the size and shape of the Earth.

Given a metric space (X, d), a **metric curve** γ is a continuous function $\gamma : I \to X$, where I is an *interval* (i.e., nonempty connected subset) of $\mathbb{R}$. If γ is r times continuously differentiable, it is called a *regular curve* of class C^r; if $r = \infty$, γ is called a *smooth curve*.

In general, a curve may cross itself. A curve is called a *simple curve* (or *arc*, path) if it does not cross itself, i.e., if it is injective. A curve $\gamma : [a, b] \to X$ is called a *Jordan curve* (or *simple closed curve*) if it does not cross itself, and $\gamma(a) = \gamma(b)$.

The *length* (which may be equal to ∞) $l(\gamma)$ of a curve $\gamma : [a, b] \to X$ is defined by $\sup \sum_{i=1}^{n} d(\gamma(t_{i-1}), \gamma(t_i))$, where the supremum is taken over all finite decompositions $a = t_0 < t_1 < \ldots < t_n = b$, $n \in \mathbb{N}$, of $[a, b]$.

A curve with finite length is called *rectifiable*. For each regular curve $\gamma : [a, b] \to X$ define the *natural parameter* s of γ by $s = s(t) = l(\gamma|_{[a,t]})$, where $l(\gamma|_{[a,t]})$ is the length of the part of γ corresponding to the interval $[a, t]$. A curve with this *natural*

© Springer-Verlag Berlin Heidelberg 2016

M.M. Deza, E. Deza, *Encyclopedia of Distances*,
DOI 10.1007/978-3-662-52844-0_6

parametrization $\gamma = \gamma(s)$ is called **of unit speed**, (or *parametrized by arc length*, *normalized*); in this parametrization, for any $t_1, t_2 \in I$, one has $l(\gamma|_{[t_1,t_2]}) = |t_2 - t_1|$, and $l(\gamma) = |b - a|$.

The length of any curve $\gamma : [a, b] \to X$ is at least the distance between its endpoints: $l(\gamma) \geq d(\gamma(a), \gamma(b))$. The curve γ, for which $l(\gamma) = d(\gamma(a), \gamma(b))$, is called the **geodesic segment** (or *shortest* path) from $x = \gamma(a)$ to $y = \gamma(b)$, and denoted by $[x, y]$.

Thus, a geodesic segment is a shortest join of its endpoints; it is an isometric embedding of $[a, b]$ in X. In general, geodesic segments need not exist, unless the segment consists of one point only. A geodesic segment joining two points need not be unique.

A **geodesic** (Chap. 1) is a curve which extends indefinitely in both directions and behaves locally like a segment, i.e., is everywhere locally a distance minimizer.

More exactly, a curve $\gamma : \mathbb{R} \to X$, given in the natural parametrization, is called a *geodesic* if, for any $t \in \mathbb{R}$, there exists a *neighborhood* U of t such that, for any $t_1, t_2 \in U$, we have $d(\gamma(t_1), \gamma(t_2)) = |t_1 - t_2|$. Thus, any geodesic is a locally isometric embedding of the whole of $\mathbb{R}$ in X.

A geodesic is called a **metric straight line** if the equality $d(\gamma(t_1), \gamma(t_2)) = |t_1 - t_2|$ holds for all $t_1, t_2 \in \mathbb{R}$. Such a geodesic is an isometric embedding of the whole real line $\mathbb{R}$ in X. A geodesic is called a **metric great circle** if it is an isometric embedding of a circle $S^1(0, r)$ in X. In general, geodesics need not exist.

- **Geodesic metric space**

  A metric space (X, d) is called **geodesic** if any two points in X can be joined by a **geodesic segment**, i.e., for any two points $x, y \in X$, there is an isometry from the segment $[0, d(x, y)]$ into X. Examples of geodesic spaces are complete *Riemannian spaces*, **Banach spaces**, **metric graphs** from Chap. 15 and (Ivanov–Nikolaeva–Tuzhilin, 2015) *Gromov–Hausdorff space*.

  A metric space (X, d) is called a **locally geodesic metric space** if any two sufficiently close points in X can be joined by a geodesic segment; it is called **D-geodesic** if any two points at distance $< D$ can be joined by a geodesic segment.
- **Geodesic distance**

  The **geodesic distance** (or **shortest path distance**) is the length of a **geodesic segment** (i.e., a *shortest* path) between two points.
- **Intrinsic metric**

  Given a metric space (X, d) in which every two points are joined by a rectifiable curve, the **internal metric** (Chap. 4) D on X is defined as the infimum of the lengths of all rectifiable curves, connecting two given points $x, y \in X$.

  The metric d on X is called the **intrinsic metric** (or **length metric**) if it coincides with its internal metric D. A metric space with the intrinsic metric is called a **length space** (or **path metric space**, *inner metric space*, *intrinsic space*).

  If, moreover, any pair x, y of points can be joined by a curve of length $d(x, y)$, the intrinsic metric d is called *strictly intrinsic*, and the length space (X, d) is a **geodesic metric space** (or *shortest* path *metric space*).

A complete metric space (X, d) is a length space if and only if it is having **approximate midpoints**, i.e., for any points $x, y \in X$ and for any $\epsilon > 0$, there exists a third point $z \in X$ with $d(x, z), d(y, z) \leq \frac{1}{2}d(x, y) + \epsilon$. A complete metric space (X, d) is a **geodesic metric space** if and only if it is having **midpoints**.

Any complete locally compact length space is a **proper** geodesic metric space.

- *G*-**space**

  A *G*-**space** (or **space of geodesics**) is a metric space (X, d) with the geometry characterized by the fact that extensions of geodesics, defined as locally shortest lines, are unique. Such geometry is a generalization of *Hilbert Geometry* (see [Buse55]).

  More exactly, a *G*-space (X, d) is defined by the following conditions:

  1. It is **proper** (or *finitely compact*), i.e., all metric balls are compact;
  2. It is **Menger-convex**, i.e., for any different $x, y \in X$, there exists a third point $z \in X, z \neq x, y$, such that $d(x, z) + d(z, y) = d(x, y)$;
  3. It is *locally extendable*, i.e., for any $a \in X$, there exists $r > 0$ such that, for any distinct points x, y in the ball $B(a, r)$, there exists z distinct from x and y such that $d(x, y) + d(y, z) = d(x, z)$;
  4. It is *uniquely extendable*, i.e., if in 3 above two points z_1 and z_2 were found, so that $d(y, z_1) = d(y, z_2)$, then $z_1 = z_2$.

  The existence of geodesic segments is ensured by finite compactness and Menger-convexity: any two points of a finitely compact Menger-convex set X can be joined by a geodesic segment in X. The existence of geodesics is ensured by the axiom of local prolongation: if a finitely compact Menger-convex set X is locally extendable, then there exists a geodesic containing a given segment. Finally, the uniqueness of prolongation ensures the assumption of Differential Geometry that a *line element* determines a geodesic uniquely.

  All *Riemannian* and *Finsler spaces* are *G*-spaces. A 1D *G*-space is a metric straight line or metric great circle. Any 2D *G*-space is a **topological manifold** (Chap. 2).

  Every *G*-space is a **chord metric space**, i.e., a metric space with a set distinguished geodesic segments such that any two points are joined by a unique such segment (see [BuPh87]).

- **Desarguesian space**

  A **Desarguesian space** is a *G*-**space** (X, d) in which the role of geodesics is played by ordinary straight lines. Thus, X may be topologically mapped into a *projective space* $\mathbb{R}P^n$ so that each geodesic of X is mapped into a straight line of $\mathbb{R}P^n$.

  Any X mapped into $\mathbb{R}P^n$ must either cover all of $\mathbb{R}P^n$ and, in such a case, the geodesics of X are all metric great circles of the same length, or X may be considered as an open convex subset of an affine space A^n.

  A space (X, d) of geodesics is a Desarguesian space if and only if the following conditions hold:

1. The geodesic passing through two different points is unique;
2. For dimension $n = 2$, both the direct and the converse *Desargues theorems* are valid and, for dimension $n > 2$, any three points in X lie in one plane.

Among *Riemannian spaces*, the only Desarguesian spaces are Euclidean, *hyperbolic*, and *elliptic* spaces. An example of the non-Riemannian Desarguesian space is the *Minkowskian space* which can be regarded as the prototype of all non-Riemannian spaces, including *Finsler spaces*.

- **G-space of elliptic type**

  A **G-space of elliptic type** is a **G-space** in which the geodesic through two points is unique, and all geodesics are the metric great circles of the same length.

  Every G-space such that there is unique geodesic through each given pair of points is either a G-space of elliptic type, or a **straight G-space**.

- **Straight G-space**

  A **straight G-space** is a **G-space** in which extension of a geodesic is possible globally, so that any segment of the geodesic remains a shortest path. In other words, for any two points $x, y \in X$, there is a unique geodesic segment joining x to y, and a unique metric straight line containing x and y.

  Any geodesic in a straight G-space is a metric straight line, and is uniquely determined by any two of its points. Any such 2D space is homeomorphic to the plane.

  All simply connected *Riemannian spaces* of nonpositive curvature (including Euclidean and *hyperbolic* spaces), *Hilbert geometries*, and Teichmüller spaces of compact Riemann surfaces of genus $g > 1$ (when metrized by the **Teichmüller metric**) are straight G-spaces.

- **Gromov hyperbolic metric space**

  A metric space (X, d) is called **Gromov hyperbolic** if it is **geodesic** and **δ-hyperbolic** for some $\delta \geq 0$.

  An important class of such spaces are the *hyperbolic groups*, i.e., finitely generated groups whose **word metric** is Gromov hyperbolic. A metric space is a **real tree** exactly when it is 0-hyperbolic.

  Every bounded metric space X is (diam(X,d))-hyperbolic. A normed vector space is Gromov hyperbolic if and only it has dimension 1. Any complete simply connected *Riemannian space* of *sectional curvature* $k \leq -a^2 < 0$ is $\frac{\ln 3}{a}$-hyperbolic. Every **CAT(κ)** space with $\kappa < 0$ is Gromov hyperbolic.

- **CAT(κ) space**

  Let (X, d) be a metric space. Let M^2 be a simply connected 2D *Riemannian manifold* (Chap. 7) of *constant curvature* κ, i.e., the 2-sphere S^2_κ with $\kappa > 0$, the Euclidean plane $\mathbb{E}^2$ with $\kappa = 0$, or the hyperbolic plane H^2_κ with $\kappa < 0$. Let D_κ denote the *diameter* of M^2, i.e., $D_\kappa = \frac{\pi}{\sqrt{\kappa}}$ if $\kappa > 0$, and $D_\kappa = \infty$ if $\kappa \leq 0$.

  A *triangle* T in X consists of three points in X together with three *geodesic segments* joining them pairwise; the segments are called the *sides of the triangle*. For a triangle $T \subset X$, a *comparison triangle* for T in M^2 is a triangle $T' \subset M^2$ together with a map f_T which sends each side of T isometrically onto a side of T'. A triangle T is said (Gromov, 1987) to satisfy the **CAT(κ) inequality** (for

Cartan, Alexandrov and Toponogov) if, for every $x, y \in T$, we have

$$d(x, y) \leq d_{M^2}(f_T(x), f_T(y)),$$

where f_T is the map associated to a comparison triangle for T in M^2. So, the geodesic triangle T is at least as "thin" as its comparison triangle in M^2.

The metric space (X, d) is a **CAT(κ) space** if it is D_κ**-geodesic** (i.e., any two points at distance $< D_\kappa$ can be joined by a geodesic segment), and all triangles T with perimeter $< 2D_\kappa$ satisfy the CAT(κ) inequality.

Every CAT(κ_1) space is a CAT(κ_2) space if $\kappa_1 < \kappa_2$. Every **real tree** is a CAT($-\infty$) *space*, i.e., is a CAT(κ_1) space for all $\kappa \in \mathbb{R}$.

A **locally CAT(κ) space** (called **metric space with curvature** $\leq \kappa$ in Alexandrov, 1951) is a metric space (X, d) in which every point $p \in X$ has a neighborhood U such that any two points $x, y \in U$ are connected by a geodesic segment, and the CAT(κ) inequality holds for any $x, y, z \in U$. A Riemannian manifold is locally CAT(κ) if and only if its *sectional curvature* is at most κ.

A **metric space with curvature** $\geq \kappa$ is (Alexandrov, 1951) a metric space (X, d) in which every $p \in X$ has a neighborhood U such that any $x, y \in U$ are connected by a geodesic segment, and the *reverse CAT(κ) inequality*

$$d(x, y) \geq d_{M^2}(f_T(x), f_T(y))$$

holds for any $x, y, z \in U$, where f_T is the map associated to a comparison triangle for T in M^2. It is a **generalized Riemannian space** (Chap. 7).

Above two definitions differ only by the sign of $d(x, y) - d_{M^2}(f_T(x), f_T(y))$. In the case $\kappa = 0$, the above spaces are called **nonpositively curved** and **nonnegatively curved** metric spaces, respectively. For complete metric spaces, they differ also (Bruhat–Tits, 1972) by the sign (≤ 0 or ≥ 0, respectively) of

$$F(x, y, z) = 4d^2(z, m(x, y)) - (d^2(z, x) + d^2(z, y) - d^2(x, y)),$$

where x, y, z are any three points and $m(x, y)$ is the midpoint of the **metric interval** $I(x, y)$. A complete CAT(0) space is called **Hadamard space**.

The inequality $F(x, y, z) \leq 0$ for all $x, y, z \in X$, characterizing Hadamard spaces, is called *semiparallelogram inequality*, because the usual vector parallelogram law $||u - v||^2 + ||u + v||^2 = 2||u||^2 + 2||v||^2$, characterizing norms induced by inner products, is equivalent to the equality $F(x, y, z) = 0$. A normed space is an Hadamard space if and only if it is a **Hilbert space**.

Every two points in an Hadamard space are connected by a unique geodesic (and hence unique shortest path), while in a general CAT(0) space, they are connected by a unique geodesic segment, and the distance is a convex function.

Foertsch–Lytchack–Schroeder, 2007, proved that a metric space is CAT(0) if and only if it is **Busemann convex** and **Ptolemaic**; cf. Chap. 1. Euclidean spaces, hyperbolic spaces, and trees are CAT(0) spaces.

- **δ-bolic metric space**

  Given a number $\delta > 0$, a metric space (X, d) is called **δ-bolic** (Kasparov–Skandalis, 1994, simplified by Bucher–Karlsson, 2002) if for any $x, y, z \in X$ and some function $m : X \times X \to X$, it holds

$$2d(z, m(x, y)) \leq \sqrt{2d^2(z, x) + 2d^2(z, y) - d^2(x, y)} + \frac{4}{3}\delta.$$

  A **δ-hyperbolic space** with **approximate δ-midpoints** (Chap. 1) is $\frac{3\delta}{2}$-bolic.

  Every CAT(0)-space is δ-bolic for any $\delta > 0$; for complete spaces the converse holds as well. An l_p-metric space of dimension > 1 is δ-bolic for any $\delta > 0$ only if $p = 2$.

- **Boundary of metric space**

  There are many notions of the **boundary ∂X of a metric space** (X, d). We give below some of the most general among them. Usually, if (X, d) is locally compact, $X \cup \partial X$ is its *compactification*.

  1. **Ideal boundary** (or *boundary at* ∞). Given a geodesic metric space (X, d), let γ^1 and γ^2 be two **metric rays**, i.e., geodesics with isometry of $\mathbb{R}_{\geq 0}$ into X. These rays are called *equivalent* if the **Hausdorff distance** between them (associated with the metric d) is finite, i.e., if $\sup_{t \geq 0} d(\gamma^1(t), \gamma^2(t)) < \infty$.

     The **ideal boundary** of (X, d) is the set $\partial_\infty X$ of equivalence classes γ_∞ of all metric rays. Cf. **asymptotic metric cone** (Chap. 1).

     If (X, d) is a complete CAT(0) space, then the **Tits metric** (or *asymptotic angle of divergence*) on $\partial_\infty X$ is defined by $2 \arcsin\left(\frac{\rho}{2}\right)$ for all $\gamma^1_\infty, \gamma^2_\infty \in \partial_\infty X$, where $\rho = \lim_{t \to \infty} \frac{1}{t} d(\gamma^1(t), \gamma^2(t))$. The set $\partial_\infty X$ equipped with the Tits metric is called the **Tits boundary** of X.

     If (X, d, x_0) is a pointed complete CAT(-1) space, then the **Bourdon metric** (or **visual distance**) on $\partial_\infty X$ is defined, for any distinct $x, y \in \partial_\infty X$, by $e^{-(x.y)}$, where $(x.y)$ denotes the **Gromov product** $(x.y)_{x_0}$.

     The **visual sphere of** (X, d) **at a point** $x_0 \in X$ is the set of equivalence classes of all metric rays emanating from x_0.

  2. **Gromov boundary**. Given a **pointed metric space** (X, d, x_0) (i.e., one with a selected base point $x_0 \in X$), the **Gromov boundary** of it (as generalized by Buckley and Kokkendorff, 2005, from the case of the Gromov hyperbolic space) is the set $\partial_G X$ of equivalence classes of *Gromov sequences*.

     A sequence $x = \{x_n\}_n$ in X is a *Gromov sequence* if the Gromov product $(x_i.x_j)_{x_0} \to \infty$ as $i, j \to \infty$. Two Gromov sequences x and y are *equivalent* if there is a finite chain of Gromov sequences x^k, $0 \leq k \leq k'$, such that $x = x^0, y = x^{k'}$, and $\lim_{i,j \to \infty} \inf(x^{k-1}_i . x^k_j) = \infty$ for $0 \leq k \leq k'$.

     In a **proper** geodesic Gromov hyperbolic space (X, d), the visual sphere does not depends on the base point x_0 and is naturally isomorphic to its *Gromov boundary* $\partial_G X$ which can be identified with $\partial_\infty X$.

  3. **g-boundary**. Denote by $\overline{X_d}$ the metric completion of (X, d) and, viewing X as a subset of $\overline{X_d}$, denote by ∂X_d the difference $\overline{X_d} \backslash X$. Let (X, l, x_0) be a pointed

unbounded **length space**, i.e., its metric coincides with the **internal metric** l of (X, d). Given a measurable function $g : \mathbb{R}_{\geq 0} \to \mathbb{R}_{\geq 0}$, the g**-boundary** of (X, d, x_0) (as generalized by Buckley–Kokkendorff, 2005, from *spherical* and *Floyd boundaries*) is $\partial_g X = \partial X_\sigma \setminus \partial X_l$, where $\sigma(x, y) = \inf \int_\gamma g(z)dl(z)$ for all $x, y \in X$ (here the infimum is taken over all metric segments $\gamma = [x, y]$).

4. **Hotchkiss boundary**. Given a pointed proper **Busemann convex** metric space (X, d, x_0), the **Hotchkiss boundary** of it is the set $\partial_H(X, x_0)$ of isometries $f : \mathbb{R}_{\geq 0} \to X$ with $f(0) = x_0$. The boundaries $\partial_H^{x_0} X$ and $\partial_H^{x_1} X$ are homeomorphic for distinct $x_0, x_1 \in X$. In a Gromov hyperbolic space, $\partial_H^{x_0} X$ is homeomorphic to the Gromov boundary $\partial_G X$.
5. **Metric boundary**. Given a pointed metric space (X, d, x_0) and an unbounded subset S of $\mathbb{R}_{\geq 0}$, a ray $\gamma : S \to X$ is called a *weakly geodesic ray* if, for every $x \in X$ and every $\epsilon > 0$, there is an integer N such that $|d(\gamma(t), \gamma(0)) - t| < \epsilon$, and $|d(\gamma(t), x) - d(\gamma(s), x) - (t - s)| < \epsilon$ for all $s, t \in T$ with $s, t \geq N$.

   Let $\mathcal{G}(X, d)$ be the *commutative unital* C^**-algebra* with the norm $||.||_\infty$, generated by the (bounded, continuous) functions which vanish at infinity, the constant functions, and the functions of the form $g_y(x) = d(x, x_0) - d(x, y)$; cf. **Rieffel metric space** in Chap. 7 for definitions.

   The Rieffel's **metric boundary** $\partial_R X$ of (X, d) is the difference $\overline{X}^d \setminus X$, where $\overline{X}^d$ is the *metric compactification* of (X, d), i.e., the maximum ideal space (the set of *pure states*) of this C^*-algebra.

   For a **proper metric space** (X, d) (Chap. 1) with a countable base, the boundary $\partial_R X$ consists of the limits $\lim_{t\to\infty} f(\gamma(t))$ for every weakly geodesic ray γ and every function f from the above C^*-algebra (Rieffel, 2002).

- **Projectively flat metric space**

  A metric space, in which geodesics are defined, is called **projectively flat** if it locally admits a *geodesic mapping* (or *projective mapping*), i.e., a mapping preserving geodesics into an Euclidean space. Cf. Euclidean **rank of metric space** in Chap. 1; similar terms are: *affinely flat*, *conformally flat*, etc.

  A Riemannian space is projectively flat if and only if it has constant (sectional) curvature. Cf. **flat metric** in Chap. 8.

6.2 Projective Geometry

Projective Geometry is a branch of Geometry dealing with the properties and invariants of geometric figures under *projection*. Affine Geometry, Metric Geometry and Euclidean Geometry are subsets of Projective Geometry of increasing complexity. The main invariants of Projective, Affine, Metric, Euclidean Geometry are, respectively, **cross-ratio**, parallelism (and relative distances), angles (and relative distances), absolute distances.

An n-dimensional *projective space* $\mathbb{F}P^n$ is the space of one-dimensional vector subspaces of a given $(n+1)$-dimensional vector space V over a field $\mathbb{F}$. The basic construction is to form the set of equivalence classes of nonzero vectors in V under the relation of scalar proportionality. This idea goes back to mathematical descriptions of *perspective*.

The use of a basis of V allows the introduction of *homogeneous coordinates* of a point in $\mathbb{F}P^n$ which are usually written as $(x_1 : x_2 : \ldots : x_n : x_{n+1})$—a vector of length $n+1$, other than $(0 : 0 : 0 : \ldots : 0)$. Two sets of coordinates that are proportional denote the same point of the projective space. Any point of projective space which can be represented as $(x_1 : x_2 : \ldots : x_n : 0)$ is called a *point at infinity*. The part of a projective space $\mathbb{F}P^n$ not "at infinity" , i.e., the set of points of the projective space which can be represented as $(x_1 : x_2 : \ldots : x_n : 1)$, is an n-dimensional *affine space* A^n.

The notation $\mathbb{R}P^n$ denotes the *real projective space* of dimension n, i.e., the space of 1D vector subspaces of $\mathbb{R}^{n+1}$. The notation $\mathbb{C}P^n$ denotes the *complex projective space* of dimension n. The projective space $\mathbb{R}P^n$ carries a natural structure of a compact smooth n-**manifold**. It can be viewed as the space of lines through the zero element 0 of $\mathbb{R}^{n+1}$ (i.e., as a *ray space*). It can be viewed also as the set $\mathbb{R}^n$, considered as an *affine space*, together with its points at infinity. Also it can be seen as the set of points of an n-sphere in $\mathbb{R}^{n+1}$ with identified diametrically-opposite points.

The projective points, projective straight lines, projective planes, ..., projective hyperplanes of $\mathbb{F}P^n$ are one-, two-, three-, ..., n-dimensional subspaces of V, respectively. Any two projective straight lines in a projective plane have one and only one common point. A *projective transformation* (or *collineation*, *projectivity*) is a bijection of a projective space onto itself, preserving collinearity (the property of points to be on one line) in both directions. Any projective transformation is a composition of a pair of *perspective projections*. Projective transformations do not preserve sizes or angles but do preserve *type* (that is, points remain points, and lines remain lines), *incidence* (that is, whether a point lies on a line), and **cross-ratio** (Chap. 1).

Here, given four collinear points $x, y, z, t \in \mathbb{F}P^n$, their **cross-ratio** (x, y, z, t) is $\frac{(x-z)(y-t)}{(y-z)(x-t)}$, where $\frac{x-z}{x-t}$ denotes the ratio $\frac{f(x)-f(z)}{f(x)-f(t)}$ for some affine bijection f from the straight line $l_{x,y}$ through the points x and y onto $\mathbb{F}$.

Given four projective straight lines l_x, l_y, l_z, l_t, containing points x, y, z, t, respectively, and passing through a given point, their **cross-ratio** (l_x, l_y, l_z, l_t) is $\frac{\sin(l_x,l_z)\sin(l_y,l_t)}{\sin(l_y,l_z)\sin(l_x,l_t)}$, coincides with (x, y, z, t). The cross-ratio (x, y, z, t) of four complex numbers x, y, z, t is $\frac{(x-z)(y-t)}{(y-z)(x-t)}$. It is real if and only if the four numbers are either collinear or concyclic.

- **Projective metric**

  Given a convex subset D of a projective space $\mathbb{R}P^n$, the **projective metric** d is a metric on D such that shortest paths with respect to this metric are parts of or entire projective straight lines. It is assumed that the following conditions hold:

1. D does not belong to a hyperplane;
2. For any three noncollinear points $x, y, z \in D$, the triangle inequality holds in the strict sense: $d(x, y) < d(x, z) + d(z, y)$;
3. If x, y are different points in D, then the intersection of the straight line $l_{x,y}$ through x and y with D is either all of $l_{x,y}$, and forms a **metric great circle**, or is obtained from $l_{x,y}$ by discarding some segment (which can be reduced to a point), and forms a **metric straight line**.

The metric space (D, d) is called a **projective metric space**. The problem of determining all projective metrics on $\mathbb{R}^n$ (called **linearly additive metrics** in Chap. 1) is the 4-*th problem of Hilbert*; it has been solved only for $n = 2$. In fact, given a smooth measure on the space of hyperplanes in $\mathbb{R}P^n$, define the distance between any two points $x, y \in \mathbb{R}P^n$ as one-half the measure of all hyperplanes intersecting the line segment joining x and y. The obtained metric is projective; it is the *Busemann's construction* of projective metrics. [Amba76] proved that all projective metrics on $\mathbb{R}^2$ can be obtained by this construction.

In a projective metric space there cannot simultaneously be both types of straight lines: they are either all metric straight lines, or they are all metric great circles of the same length (*Hamel's theorem*). Spaces of the first kind are called *open*. They coincide with subspaces of an affine space; the geometry of open projective metric spaces is a *Hilbert Geometry*. *Hyperbolic Geometry* is a Hilbert Geometry in which there exist reflections at all straight lines.

Thus, the set D has Hyperbolic Geometry if and only if it is the interior of an ellipsoid. The geometry of open projective metric spaces whose subsets coincide with all of affine space, is a *Minkowski Geometry*. *Euclidean Geometry* is a Hilbert Geometry and a Minkowski Geometry, simultaneously. Spaces of the second kind are called *closed*; they coincide with the whole of $\mathbb{R}P^n$. *Elliptic Geometry* is the geometry of a projective metric space of the second kind.

- **Strip projective metric**

  The **strip projective metric** ([BuKe53]) is a **projective metric** on the strip $St = \{x \in \mathbb{R}^2 : -\pi/2 < x_2 < \pi/2\}$ defined by

$$\sqrt{(x_1 - y_1)^2 + (x_2 - y_2)^2} + |\tan x_2 - \tan y_2|.$$

  The Euclidean metric $\sqrt{(x_1 - y_1)^2 + (x_2 - y_2)^2}$ is not a projective metric on St.

- **Half-plane projective metric**

  The **half-plane projective metric** ([BuKe53]) is a **projective metric** on $\mathbb{R}^2_+ = \{x \in \mathbb{R}^2 : x_2 > 0\}$ defined by

$$\sqrt{(x_1 - y_1)^2 + (x_2 - y_2)^2} + \left|\frac{1}{x_2} - \frac{1}{y_2}\right|.$$

- **Hilbert projective metric**

  Given a set H, the **Hilbert projective metric** h is a **complete projective metric** on H. It means that H contains, together with two arbitrary distinct

points x and y, also the points z and t for which $h(x,z) + h(z,y) = h(x,y)$, $h(x,y) + h(y,t) = h(x,t)$, and that H is homeomorphic to a convex set in an n-dimensional affine space A^n, the geodesics in H being mapped to straight lines of A^n.

The metric space (H,h) is called the *Hilbert projective space*, and the geometry of a Hilbert projective space is called *Hilbert Geometry*.

Formally, let D be a nonempty convex open set in A^n with the boundary ∂D not containing two proper coplanar but noncollinear segments (ordinarily the boundary of D is a strictly convex closed curve, and D is its interior). Let $x, y \in D$ be located on a straight line which intersects ∂D at z and t, z is on the side of y, and t is on the side of x. Then the **Hilbert projective metric** h on D is the symmetrization of the **Funk distance** (Chap. 1):

$$h(x,y) = \frac{1}{2}\left(\ln\frac{x-z}{y-z} + \ln\frac{x-t}{y-t}\right) = \frac{1}{2}\ln(x,y,z,t),$$

where (x,y,z,t) is the **cross-ratio** of x, y, z, t.

The metric space (D,h) is a **straight G-space**. If D is an ellipsoid, then h is the **hyperbolic metric**, and defines *Hyperbolic Geometry* on D. On the *unit disk* $\Delta = \{z \in \mathbb{C} : |z| < 1\}$ the metric h coincides with the **Cayley–Klein–Hilbert metric**. If $n = 1$, the metric h makes D isometric to the Euclidean line.

If ∂D contains coplanar but noncollinear segments, a projective metric on D can be given by $h(x,y) + d(x,y)$, where d is any **Minkowskian metric**.

- **Minkowskian metric**

  The **Minkowskian metric** (or **Minkowski–Hölder distance**) is the **norm metric** of a finite-dimensional real **Banach space**.

  Formally, let $\mathbb{R}^n$ be an n-dimensional real vector space, let K be a *symmetric convex body* in $\mathbb{R}^n$, i.e., an open neighborhood of the origin which is bounded, convex, and *symmetric* ($x \in K$ if and only if $-x \in K$). Then the **Minkowski distance function** $||x||_K : \mathbb{R}^n \to [0,\infty)$, defined as $\inf\{\alpha > 0 : \frac{x}{\alpha} \in \partial K\}$ (cf. Chap. 1), is a *norm* on $\mathbb{R}^n$, and the Minkowskian metric m_K on $\mathbb{R}^n$ is defined by

$$m_K(x,y) = ||x-y||_K.$$

  The metric space $(\mathbb{R}^n, m)$ is called *Minkowskian space*; its geometry is *Minkowski Geometry*. It can be seen as an affine space A^n with a metric m in which the *unit ball* is the body K. For a strictly convex symmetric body the Minkowskian metric is a **projective metric**, and $(\mathbb{R}^n, m)$ is a **G-straight space**. A Minkowski Geometry is Euclidean if and only if its *unit sphere* is an ellipsoid.

  The Minkowskian metric m is proportional to the Euclidean metric d_E on every given line l, i.e., $m(x,y) = \phi(l)d_E(x,y)$. Thus, the Minkowskian metric can be considered as a metric which is defined in the whole affine space A^n and has the property that the *affine ratio* $\frac{ac}{ab}$ of any three collinear points a, b, c (cf. Sect. 6.3) is equal to their *distance ratio* $\frac{m(a,c)}{m(a,b)}$.

Given a convex body C in a Minkowskian space with unit ball K, the *Minkowskian thickness* and *Minkowskian diameter* of C are (Averkov, 2003):

$$\sup\{\alpha > 0 : \alpha K \subset C - C\} \text{ and } \inf\{\alpha > 0 : C - C \subset \alpha K\}.$$

- **C-distance**

  Given a convex body $C \subset \mathbb{E}^n$, the **C-distance** (or *relative distance*; Lassak, 1991) is a distance on $\mathbb{E}^n$ defined, for any $x, y \in \mathbb{E}^n$, by

$$d_C(x, y) = 2\frac{d_E(x, y)}{d_E(x', y')},$$

  where $x'y'$ is the longest chord of C parallel to the segment xy. C-distance is not related to C-metric in Chap. 10 and to **rotating C-metric** in Chap. 26.

  The unit ball of the normed space with the norm $||x|| = d_C(x, 0)$ is $\frac{1}{2}(C - C)$. For every $r \in [-1, 1]$, it holds $d_C(x, y) = d_{rC+(1-r)(-C)}(x, y)$.

- **Busemann metric**

  The **Busemann metric** ([Buse55]) is a metric on the real n-dimensional projective space $\mathbb{R}P^n$ defined by

$$\min\left\{\sum_{i=1}^{n+1}\left|\frac{x_i}{||x||} - \frac{y_i}{||y||}\right|, \sum_{i=1}^{n+1}\left|\frac{x_i}{||x||} + \frac{y_i}{||y||}\right|\right\}$$

  for any $x = (x_1 : \ldots : x_{n+1}), y = (y_1 : \ldots : y_{n+1}) \in \mathbb{R}P^n$, where $||x|| = \sqrt{\sum_{i=1}^{n+1} x_1^2}$.

- **Flag metric**

  Given an n-dimensional *projective space* $\mathbb{F}P^n$, the **flag metric** d is a metric on $\mathbb{F}P^n$ defined by a *flag*, i.e., an *absolute* consisting of a collection of m-planes α_m, $m = 0, \ldots, n-1$, with α_{i-1} belonging to α_i for all $i \in \{1, \ldots, n-1\}$. The metric space $(\mathbb{F}P^n, d)$ is abbreviated by F^n and is called a *flag space*.

  If one chooses an affine coordinate system $(x_i)_i$ in a space F^n, so that the vectors of the lines passing through the $(n-m-1)$-plane α_{n-m-1} are defined by the condition $x_1 = \ldots x_m = 0$, then the flag metric $d(x, y)$ between the points $x = (x_1, \ldots, x_n)$ and $y = (y_1, \ldots, y_n)$ is defined by

$$d(x, y) = |x_1 - y_1|, \text{ if } x_1 \neq y_1, \; d(x, y) = |x_2 - y_2|, \text{ if } x_1 = y_1, x_2 \neq y_2, \ldots$$
$$\ldots, d(x, y) = |x_k - y_k|, \text{ if } x_1 = y_1, \ldots, x_{k-1} = y_{k-1}, x_k \neq y_k, \ldots .$$

- **Projective determination of a metric**

  The **projective determination of a metric** is an introduction, in subsets of a projective space, of a metric such that these subsets become isomorphic to a Euclidean, *hyperbolic*, or *elliptic space*.

To obtain a *Euclidean determination of a metric* in $\mathbb{R}P^n$, one should distinguish in this space an $(n-1)$-dimensional hyperplane π, called the *hyperplane at infinity*, and define $\mathbb{E}^n$ as the subset of the projective space obtained by removing from it this hyperplane π. In terms of homogeneous coordinates, π consists of all points $(x_1 : \ldots : x_n : 0)$, and $\mathbb{E}^n$ consists of all points $(x_1 : \ldots : x_n : x_{n+1})$ with $x_{n+1} \neq 0$. Hence, it can be written as $\mathbb{E}^n = \{x \in \mathbb{R}P^n : x = (x_1 : \ldots : x_n : 1)\}$. The Euclidean metric d_E on $\mathbb{E}^n$ is defined by

$$\sqrt{\langle x-y, x-y\rangle},$$

where, for any $x = (x_1 : \ldots : x_n : 1), y = (y_1 : \ldots : y_n : 1) \in \mathbb{E}^n$, one has $\langle x, y\rangle = \sum_{i=1}^{n} x_i y_i$.

To obtain a *hyperbolic determination of a metric* in $\mathbb{R}P^n$, a set D of interior points of a real oval hypersurface Ω of order two in $\mathbb{R}P^n$ is considered. The **hyperbolic metric** d_{hyp} on D is defined by

$$\frac{r}{2}|\ln(x, y, z, t)|,$$

where z and t are the points of intersection of the straight line $l_{x,y}$ through the points x and y with Ω, (x, y, z, t) is the **cross-ratio** of the points x, y, z, t, and $r > 0$ is a fixed constant. If, for any $x = (x_1 : \ldots : x_{n+1}), y = (y_1 : \ldots : y_{n+1}) \in \mathbb{R}P^n$, the *scalar product* $\langle x, y\rangle = -x_1 y_1 + \sum_{i=2}^{n+1} x_i y_i$ is defined, the hyperbolic metric on the set $D = \{x \in \mathbb{R}P^n : \langle x, x\rangle < 0\}$ can be written, for a fixed constant $r > 0$, as

$$r \operatorname{arccosh} \frac{|\langle x, y\rangle|}{\sqrt{\langle x, x\rangle \langle y, y\rangle}},$$

where arccosh denotes the nonnegative values of the inverse hyperbolic cosine.

To obtain an *elliptic determination of a metric* in $\mathbb{R}P^n$, one should consider, for any $x = (x_1 : \ldots : x_{n+1}), y = (y_1 : \ldots : y_{n+1}) \in \mathbb{R}P^n$, the *inner product* $\langle x, y\rangle = \sum_{i=1}^{n+1} x_i y_i$. The **elliptic metric** d_{ell} on $\mathbb{R}P^n$ is defined now by

$$r \arccos \frac{|\langle x, y\rangle|}{\sqrt{\langle x, x\rangle \langle y, y\rangle}},$$

where $r > 0$ is a fixed constant, and arccos is the inverse cosine in $[0, \pi]$.

In all the considered cases, some hypersurfaces of the second-order remain invariant under given **motions**, i.e., projective transformations preserving a given metric. These hypersurfaces are called *absolutes*. In the case of a Euclidean determination of a metric, the absolute is an imaginary $(n-2)$-dimensional oval surface of order two, in fact, the degenerate absolute $x_1^2 + \cdots + x_n^2 = 0, x_{n+1} = 0$.

In the case of a hyperbolic determination of a metric, the absolute is a real $(n-1)$-dimensional oval hypersurface of order two, in the simplest case, the absolute $-x_1^2 + x_2^2 + \cdots + x_{n+1}^2 = 0$. In the case of an elliptic determination of a metric, the absolute is an imaginary $(n-1)$-dimensional oval hypersurface of order two, in fact, the absolute $x_1^2 + \cdots + x_{n+1}^2 = 0$.

6.3 Affine Geometry

An n-dimensional *affine space* over a field $\mathbb{F}$ is a set A^n (the elements of which are called *points* of the affine space) to which corresponds an n-dimensional vector space V over $\mathbb{F}$ (called the *space associated to* A^n) such that, for any $a \in A^n$, $A = a + V = \{a + v : v \in V\}$. In the other words, if $a = (a_1, \ldots, a_n)$ and $b = (b_1, \ldots, b_n) \in A^n$, then the vector $\overrightarrow{ab} = (b_1 - a_1, \ldots, b_n - a_n)$ belongs to V.

In an affine space, one can add a vector to a point to get another point, and subtract points to get vectors, but one cannot add points, since there is no origin. Given points $a, b, c, d \in A^n$ such that $c \neq d$, and the vectors $\overrightarrow{ab}$ and $\overrightarrow{cd}$ are collinear, the scalar λ, defined by $\overrightarrow{ab} = \lambda \overrightarrow{cd}$, is called the *affine ratio* of ab and cd, and is denoted by $\frac{ab}{cd}$.

An *affine transformation* (or *affinity*) is a bijection of A^n onto itself which preserves *collinearity* and *ratios of distances* In this sense, *affine* indicates a special class of *projective transformations* that do not move any objects from the affine space to the plane at infinity or conversely. Any affine transformation is a composition of *rotations*, *translations*, *dilations*, and *shears*. The set of all affine transformations of A^n forms a group $Aff(A^n)$, called the *general affine group* of A^n. Each element $f \in Aff(A)$ can be given by a formula $f(a) = b$, $b_i = \sum_{j=1}^{n} p_{ij} a_j + c_j$, where $((p_{ij}))$ is an invertible matrix.

The subgroup of $Aff(A^n)$, consisting of affine transformations with $det((p_{ij})) = 1$, is called the *equi-affine group* of A^n. An *equi-affine space* is an affine space with the equi-affine group of transformations. The fundamental invariants of an equi-affine space are volumes of parallelepipeds. In an *equi-affine plane* A^2, any two vectors v_1, v_2 have an invariant $|v_1 \times v_2|$ (the modulus of their cross product)—the surface area of the parallelogram constructed on v_1 and v_2.

Given a nonrectilinear curve $\gamma = \gamma(t)$, its *affine parameter* (or *equi-affine arc length*) is an invariant $s = \int_{t_0}^{t} |\gamma' \times \gamma''|^{1/3} dt$. The invariant $k = \frac{d^2\gamma}{ds^2} \times \frac{d^3\gamma}{ds^3}$ is called the *equi-affine curvature* of γ. Passing to the general affine group, two more invariants of the curve are considered: the *affine arc length* $\sigma = \int k^{1/2} ds$, and the *affine curvature* $\mathrm{k} = \frac{1}{k^{3/2}} \frac{dk}{ds}$.

For A^n, $n > 2$, the *affine parameter* (or *equi-affine arc length*) of a curve $\gamma = \gamma(t)$ is defined by $s = \int_{t_0}^{t} |(\gamma', \gamma'', \ldots, \gamma^{(n)})|^{\frac{2}{n(n+1)}} dt$, where the invariant $(v_1, \ldots, v_n)$ is the (oriented) volume spanned by the vectors $v_1, \ldots, v_n$ which is equal to the determinant of the $n \times n$ matrix whose i-th column is the vector v_i.

- **Affine distance**

  Given an *affine plane* A^2, a *line element* (a, l_a) of A^2 consists of a point $a \in A^2$ together with a straight line $l_a \subset A^2$ passing through a.

  The **affine distance** is a distance on the set of all line elements of A^2 defined by

$$2f^{1/3},$$

  where, for a given line elements (a, l_a) and (b, l_b), f is the surface area of the triangle abc if c is the point of intersection of the straight lines l_a and l_b. The affine distance between (a, l_a) and (b, l_b) can be interpreted as the affine length of the arc ab of a parabola such that l_a and l_b are tangent to the parabola at a and b, respectively.
- **Affine pseudo-distance**

  Let A^2 be an *equi-affine plane*, and let $\gamma = \gamma(s)$ be a curve in A^2 defined as a function of the *affine parameter* s. The **affine pseudo-distance** dp_{aff} for A^2 is

$$dp_{aff}(a, b) = \left| \overrightarrow{ab} \times \frac{d\gamma}{ds} \right|,$$

  i.e., it is equal to the surface area of the parallelogram constructed on the vectors $\overrightarrow{ab}$ and $\frac{d\gamma}{ds}$, where b is an arbitrary point in A^2, a is a point on γ, and $\frac{d\gamma}{ds}$ is the tangent vector to the curve γ at the point a.

  Similarly, the **affine pseudo-distance** for an *equi-affine space* A^3 is defined as

$$\left| (\overrightarrow{ab}, \frac{d\gamma}{ds}, \frac{d^2\gamma}{ds^2}) \right|,$$

  where $\gamma = \gamma(s)$ is a curve in A^3, defined as a function of the *affine parameter* s, $b \in A^3$, a is a point of γ, and the vectors $\frac{d\gamma}{ds}$, $\frac{d^2\gamma}{ds^2}$ are obtained at the point a.

  For A^n, $n > 3$, we have $dp_{aff}(a, b) = |(\overrightarrow{ab}, \frac{d\gamma}{ds}, \ldots, \frac{d^{n-1}\gamma}{ds^{n-1}})|$. For an arbitrary parametrization $\gamma = \gamma(t)$, one obtains $dp_{aff}(a, b) = |(\overrightarrow{ab}, \gamma', \ldots, \gamma^{(n-1)})||(\gamma', \ldots, \gamma^{(n-1)})|^{\frac{1-n}{1+n}}$.
- **Affine metric**

  The **affine metric** is a metric on a *nondevelopable surface* $r = r(u_1, u_2)$ in an *equi-affine space* A^3, given by its **metric tensor** $((g_{ij}))$:

$$g_{ij} = \frac{a_{ij}}{|det((a_{ij}))|^{1/4}},$$

  where $a_{ij} = (\partial_1 r, \partial_2 r, \partial_{ij} r)$, $i, j \in \{1, 2\}$.

6.4 Non-Euclidean Geometry

The term *non-Euclidean Geometry* describes both *Hyperbolic Geometry* (or *Lobachevsky-Bolyai-Gauss Geometry*) and *Elliptic Geometry* which are contrasted with *Euclidean Geometry* (or *Parabolic Geometry*). The essential difference between Euclidean and non-Euclidean Geometry is the nature of parallel lines. In Euclidean Geometry, if we start with a line l and a point a, which is not on l, then there is only one line through a that is parallel to l. In Hyperbolic Geometry there are infinitely many lines through a parallel to l. In Elliptic Geometry, parallel lines do not exist. The *Spherical Geometry* is also "non-Euclidean", but it fails the axiom that any two points determine exactly one line.

- **Spherical metric**

  Let $S^n(0,r) = \{x \in \mathbb{R}^{n+1} : \sum_{i=1}^{n+1} x_i^2 = r^2\}$ be the sphere in $\mathbb{R}^{n+1}$ with the center 0 and the radius $r > 0$.

  The **spherical metric** (or *great circle metric*) is a metric on $S^n(0,r)$ defined by

$$d_{sph} = r \arccos\left(\frac{|\sum_{i=1}^{n+1} x_i y_i|}{r^2}\right),$$

  where arccos is the inverse cosine in $[0,\pi]$. It is the length of the *great circle* arc, passing through x and y. In terms of the standard *inner product* $\langle x,y\rangle = \sum_{i=1}^{n+1} x_i y_i$ on $\mathbb{R}^{n+1}$, the spherical metric can be written as $r \arccos \frac{|\langle x,y\rangle|}{\sqrt{\langle x,x\rangle \langle y,y\rangle}}$.

  The metric space $(S^n(0,r), d_{sph})$ is called *n-dimensional spherical space*. It is a space of curvature $1/r^2$, and r is the radius of curvature. It is a model of n-dimensional *Spherical Geometry*. The great circles of the sphere are its geodesics and all geodesics are closed and of the same length. See, for example, [Blum70].

- **Elliptic metric**

  Let $\mathbb{R}P^n$ be the real n-dimensional projective space. The **elliptic metric** d_{ell} is a metric on $\mathbb{R}P^n$ defined by

$$r \arccos \frac{|\langle x,y\rangle|}{\sqrt{\langle x,x\rangle \langle y,y\rangle}},$$

  where, for any $x = (x_1 : \ldots : x_{n+1})$ and $y = (y_1 : \ldots : y_{n+1}) \in \mathbb{R}P^n$, one has $\langle x,y\rangle = \sum_{i=1}^{n+1} x_i y_i$, $r > 0$ is a constant and arccos is the inverse cosine in $[0,\pi]$.

  The metric space $(\mathbb{R}P^n, d_{ell})$ is called *n-dimensional elliptic space*. It is a model of n-dimensional *Elliptic Geometry*. It is the space of curvature $1/r^2$, and r is the radius of curvature. As $r \to \infty$, the metric formulas of Elliptic Geometry yield formulas of Euclidean Geometry (or become meaningless).

  If $\mathbb{R}P^n$ is viewed as the set $E^n(0,r)$, obtained from the sphere $S^n(0,r) = \{x \in \mathbb{R}^{n+1} : \sum_{i=1}^{n+1} x_i^2 = r^2\}$ in $\mathbb{R}^{n+1}$ with center 0 and radius r by identifying diametrically-opposite points, then the elliptic metric on $E^n(0,r)$ can be written

as $d_{sph}(x,y)$ if $d_{sph}(x,y) \le \frac{\pi}{2}r$, and as $\pi r - d_{sph}(x,y)$ if $d_{sph}(x,y) > \frac{\pi}{2}r$, where d_{sph} is the **spherical metric** on $S^n(0,r)$. Thus, no two points of $E^n(0,r)$ have distance exceeding $\frac{\pi}{2}r$. The elliptic space $(E^2(0,r), d_{ell})$ is called the *Poincaré sphere*.

If $\mathbb{R}P^n$ is viewed as the set E^n of lines through the zero element 0 in $\mathbb{R}^{n+1}$, then the elliptic metric on E^n is defined as the angle between the corresponding subspaces.

An n-dimensional elliptic space is a *Riemannian space* of constant positive curvature. It is the only such space which is topologically equivalent to a projective space. See, for example, [Blum70] and [Buse55].

- **Hermitian elliptic metric**

  Let $\mathbb{C}P^n$ be the n-dimensional complex projective space. The **Hermitian elliptic metric** d^H_{ell} (see, for example, [Buse55]) is a metric on $\mathbb{C}P^n$ defined by

$$r \arccos \frac{|\langle x,y\rangle|}{\sqrt{\langle x,x\rangle\langle y,y\rangle}},$$

  where, for any $x = (x_1 : \ldots : x_{n+1})$ and $y = (y_1 : \ldots : y_{n+1}) \in \mathbb{C}P^n$, one has $\langle x,y\rangle = \sum_{i=1}^{n+1} \bar{x}_i y_i$, $r > 0$ is a constant and arccos is the inverse cosine in $[0,\pi]$.

  The metric space $(\mathbb{C}P^n, d^H_{ell})$ is called n-dimensional *Hermitian elliptic space* (cf. **Fubini–Study metric** in Chap. 7).

- **Elliptic plane metric**

  The **elliptic plane metric** is the **elliptic metric** on the *elliptic plane* $\mathbb{R}P^2$.

  If $\mathbb{R}P^2$ is viewed as the *Poincaré sphere* (i.e., a sphere in $\mathbb{R}^3$ with identified diametrically-opposite points) of diameter 1 tangent to the extended complex plane $\overline{\mathbb{C}} = \mathbb{C} \cup \{\infty\}$ at the point $z = 0$, then, under the stereographic projection from the "north pole" $(0,0,1)$, $\overline{\mathbb{C}}$ with identified points z and $-\frac{1}{\bar{z}}$ is a model of the elliptic plane.

  The elliptic plane metric d_{ell} on it is defined by its *line element* $ds^2 = \frac{|dz|^2}{(1+|z|^2)^2}$.

- **Pseudo-elliptic distance**

  The **pseudo-elliptic distance** (or *elliptic pseudo-distance*) dp_{ell} is defined, on the extended complex plane $\overline{\mathbb{C}} = \mathbb{C} \cup \{\infty\}$ with identified points z and $-\frac{1}{\bar{z}}$, by

$$\left|\frac{z-u}{1+\bar{z}u}\right|.$$

  In fact, $dp_{ell}(z,u) = \tan d_{ell}(z,u)$, where d_{ell} is the **elliptic plane metric**.

- **Hyperbolic metric**

  Let $\mathbb{R}P^n$ be the n-dimensional real projective space. Let, for any $x = (x_1 : \ldots : x_{n+1})$, $y = (y_1 : \ldots : y_{n+1}) \in \mathbb{R}P^n$, their *scalar product* $\langle x,y\rangle$ be $-x_1y_1 + \sum_{i=2}^{n+1} x_i y_i$.

The **hyperbolic metric** d_{hyp} is a metric on the set $H^n = \{x \in \mathbb{R}P^n : \langle x, x\rangle < 0\}$ defined, for a fixed constant $r > 0$, by

$$r\operatorname{arccosh}\frac{|\langle x, y\rangle|}{\sqrt{\langle x, x\rangle \langle y, y\rangle}},$$

where arccosh denotes the nonnegative values of the inverse hyperbolic cosine.

In this construction, the points of H^n can be viewed as the one-spaces of the *pseudo-Euclidean space* $\mathbb{R}^{n,1}$ inside the cone $C = \{x \in \mathbb{R}^{n,1} : \langle x, x\rangle = 0\}$.

The metric space (H^n, d_{hyp}) is called *n-dimensional hyperbolic space*. It is a model of n-dimensional *Hyperbolic Geometry*. It is the space of curvature $-1/r^2$, and r is the radius of curvature. Replacement of r by ir transforms all metric formulas of Hyperbolic Geometry into the corresponding formulas of Elliptic Geometry. As $r \to \infty$, both systems yield formulas of Euclidean Geometry (or become meaningless).

If H^n is viewed as the set $\{x \in \mathbb{R}^n : \sum_{i=1}^n x_i^2 < K\}$, where $K > 1$ is any fixed constant, the hyperbolic metric can be written as

$$\frac{r}{2}\ln\frac{1+\sqrt{1-\gamma(x,y)}}{1-\sqrt{1-\gamma(x,y)}},$$

where $\gamma(x, y) = \frac{(K-\sum_{i=1}^n x_i^2)(K-\sum_{i=1}^n y_i^2)}{(K-\sum_{i=1}^n x_i y_i)^2}$, and $r > 0$ is a number with $\tanh\frac{1}{r} = \frac{1}{\sqrt{K}}$.

If H^n is viewed as a submanifold of the $(n+1)$-dimensional *pseudo-Euclidean space* $\mathbb{R}^{n,1}$ with the scalar product $\langle x, y\rangle = -x_1 y_1 + \sum_{i=2}^{n+1} x_i y_i$ (in fact, as the top sheet $\{x \in \mathbb{R}^{n,1} : \langle x, x\rangle = -1, x_1 > 0\}$ of the two-sheeted *hyperboloid of revolution*), then the hyperbolic metric on H^n is induced from the **pseudo-Riemannian metric** on $R^{n,1}$ (cf. **Lorentz metric** in Chap. 26).

An n-dimensional hyperbolic space is a *Riemannian space* of constant negative curvature. It is the only such space which is **complete** and topologically equivalent to an Euclidean space. (See, for example, [Blum70, Buse55].)

- **Hermitian hyperbolic metric**

  Let $\mathbb{C}P^n$ be the n-dimensional complex projective space. Let, for any $x = (x_1 : \ldots : x_{n+1})$, $y = (y_1 : \ldots : y_{n+1}) \in \mathbb{C}P^n$, their *scalar product* $\langle x, y\rangle$ be $-\bar{x}_1 y_1 + \sum_{i=2}^{n+1} \bar{x}_i y_i$.

  The **Hermitian hyperbolic metric** d_{hyp}^H (see, for example, [Buse55]) is a metric on the set $\mathbb{C}H^n = \{x \in \mathbb{C}P^n : \langle x, x\rangle < 0\}$ defined, for a fixed constant $r > 0$, by

$$\operatorname{arccosh}\frac{|\langle x, y\rangle|}{\sqrt{\langle x, x\rangle \langle y, y\rangle}},$$

  where arccosh denotes the nonnegative values of the inverse hyperbolic cosine.

  The metric space $(\mathbb{C}H^n, d_{hyp}^H)$ is called n-dimensional *Hermitian hyperbolic space*.

- **Poincaré metric**

  The **Poincaré metric** d_P is the **hyperbolic metric** for the *Poincaré disk model* of Hyperbolic Geometry. In this model the *unit disk* $\Delta = \{z \in \mathbb{C} : |z| < 1\}$ is called the *hyperbolic plane*, every point of Δ is called a *hyperbolic point*, circular arcs (and diameters) in Δ which are orthogonal to the *absolute* $\Omega = \{z \in \mathbb{C} : |z| = 1\}$ are called *hyperbolic straight lines*. Every point of Ω is called an *ideal point*.

  The angular measurements in this model are the same as in Hyperbolic Geometry, i.e., it is a *conformal model*. There is a one-to-one correspondence between segments and acute angles. The Poincaré metric on Δ is defined by its *line element*

$$ds^2 = \frac{|dz|^2}{(1-|z|^2)^2} = \frac{dz_1^2 + dz_2^2}{(1-z_1^2-z_2^2)^2}.$$

  The distance d_P between two points z and u of Δ can be written as

$$\frac{1}{2}\ln\frac{|1-z\overline{u}|+|z-u|}{|1-z\overline{u}|-|z-u|} = \operatorname{arctanh}\frac{|z-u|}{|1-z\overline{u}|}.$$

  In terms of **cross-ratio**, it is equal to

$$\frac{1}{2}\ln(z,u,z^*,u^*) = \frac{1}{2}\ln\frac{(z^*-z)(u^*-u)}{(z^*-u)(u^*-z)},$$

  where z^* and u^* are the points of intersection of the hyperbolic straight line passing through z and u with Ω, z^* on the side of u, and u^* on the side of z.

  The **multiplicative distance function** on the segments zu of Δ is defined (Hartshorne, 2003) by $\mu(zu) = (z,u,z^*,u^*)^{-1}$; it allows the definition of trigonometric functions in the absence of continuity.

  In the conformal *Poincaré half-plane model* of Hyperbolic Geometry the *hyperbolic plane* is the upper half-plane $H^2 = \{z \in \mathbb{C} : z_2 > 0\}$, and the *hyperbolic lines* are semicircles and half-lines which are orthogonal to the real axis. The *absolute* (i.e., the set of *ideal points*) is the real axis together with the point at infinity.

  The *line element* of the **Poincaré metric** on H^2 is given by

$$ds^2 = \frac{|dz|^2}{(\Im z)^2} = \frac{dz_1^2 + dz_2^2}{z_2^2}.$$

  The distance between two points z, u can be written as

$$\frac{1}{2}\ln\frac{|z-\overline{u}|+|z-u|}{|z-\overline{u}|-|z-u|} = \operatorname{arctanh}\frac{|z-u|}{|z-\overline{u}|} = \frac{1}{2}\ln(z,u,z^*,u^*) = \frac{1}{2}\ln\frac{(z^*-z)(u^*-u)}{(z^*-u)(u^*-z)},$$

where z^* is the ideal point of the half-line emanating from z and passing through u, and u^* is the ideal point of the half-line emanating from u and passing through z.

In general, the **hyperbolic metric** in any *domain* $D \subset \mathbb{C}$ with at least three boundary points is defined as the preimage of the Poincaré metric in Δ under a *conformal mapping* $f : D \to \Delta$. Its *line element* has the form

$$ds^2 = \frac{|f'(z)|^2|dz|^2}{(1-|f(z)|^2)^2}.$$

The distance between two points z and u in D can be written as

$$\frac{1}{2}\ln\frac{|1-f(z)\overline{f(u)}|+|f(z)-f(u)|}{|1-f(z)\overline{f(u)}|-|f(z)-f(u)|}.$$

- **Pseudo-hyperbolic distance**

  The **pseudo-hyperbolic distance** (or **Gleason distance**, *hyperbolic pseudo-distance*) dp_{hyp} is a metric on the *unit disk* $\Delta = \{z \in \mathbb{C} : |z| < 1\}$, defined by

$$\left|\frac{z-u}{1-\overline{z}u}\right|.$$

  In fact, $dp_{hyp}(z,u) = \tanh d_P(z,u)$, where d_P is the **Poincaré metric** on Δ.
- **Cayley–Klein–Hilbert metric**

  The **Cayley–Klein–Hilbert metric** d_{CKH} is the **hyperbolic metric** for the *Klein model* (or *projective disk model*, for Hyperbolic Geometry. In this model the *hyperbolic plane* is realized as the *unit disk* $\Delta = \{z \in \mathbb{C} : |z| < 1\}$, and the *hyperbolic straight lines* are realized as the chords of Δ. Every point of the *absolute* $\Omega = \{z \in \mathbb{C} : |z| = 1\}$ is called an *ideal point*. This model is not conformal: the angular measurements are distorted. The **Cayley–Klein–Hilbert metric** on Δ is given by its **metric tensor** $((g_{ij}))$, $i,j = 1,2$:

$$g_{11} = \frac{r^2(1-z_2^2)}{(1-z_1^2-z_2^2)^2},\ g_{12} = \frac{r^2 z_1 z_2}{(1-z_1^2-z_2^2)^2},\ g_{22} = \frac{r^2(1-z_1^2)}{(1-z_1^2-z_2^2)^2},$$

  where r is any positive constant. The distance between points z and u in Δ is

$$r\,\operatorname{arccosh}\left(\frac{1-z_1u_1-z_2u_2}{\sqrt{1-z_1^2-z_2^2}\sqrt{1-u_1^2-u_2^2}}\right),$$

  where arccosh denotes the nonnegative values of the inverse hyperbolic cosine.

- **Weierstrass metric**

  Given a real n-dimensional **inner product space** $(\mathbb{R}^n, \langle , \rangle)$, $n \geq 2$, the **Weierstrass metric** d_W is a metric on $\mathbb{R}^n$ defined by

$$\operatorname{arccosh}(\sqrt{1+\langle x,x\rangle}\sqrt{1+\langle y,y\rangle} - \langle x,y\rangle),$$

  where arccosh denotes the nonnegative values of the inverse hyperbolic cosine.

  Here, $(x, \sqrt{1+\langle x,x\rangle}) \in \mathbb{R}^n \oplus \mathbb{R}$ are the *Weierstrass coordinates* of $x \in \mathbb{R}^n$, and the metric space $(\mathbb{R}^n, d_W)$ can be seen as the *Weierstrass model* of Hyperbolic Geometry.

  The **Cayley–Klein–Hilbert metric** $d_{CKH}(x,y) = \operatorname{arccosh}\frac{1-\langle x,y\rangle}{\sqrt{1-\langle x,x\rangle}\sqrt{1-\langle y,y\rangle}}$ on the open ball $B^n = \{x \in \mathbb{R}^n : \langle x,x\rangle < 1\}$ can be obtained from d_W by $d_{GKH}(x,y) = d_W(\mu(x), \mu(y))$, where $\mu : \mathbb{R}^n \to B^n$ is the *Weierstrass mapping*: $\mu(x) = \frac{x}{\sqrt{1-\langle x,x\rangle}}$.
- **Harnack metric**

  Given a *domain* $D \subset \mathbb{R}^n$, $n \geq 2$, the **Harnack metric** is a metric on D defined by

$$\sup_f |\log \frac{f(x)}{f(y)}|,$$

  where the supremum is taken over all positive functions which are harmonic on D.
- **Quasi-hyperbolic metric**

  Given a *domain* $D \subset \mathbb{R}^n$, $n \geq 2$, the **quasi-hyperbolic metric** on D is defined by

$$\inf_{\gamma\in\Gamma} \int_\gamma \frac{|dz|}{\rho(z)},$$

  where the infimum is taken over the set Γ of all rectifiable curves connecting x and y in D, $\rho(z) = \inf_{u\in\partial D} ||z-u||_2$ is the distance between z and the boundary ∂D of D, and $||.||_2$ is the Euclidean norm on $\mathbb{R}^n$.

  This metric is **Gromov hyperbolic** if the domain D is *uniform*, i.e., there exist constants C, C' such that each pair of points $x, y \in D$ can be joined by a rectifiable curve $\gamma = \gamma(x,y) \in D$ of length $l(\gamma)$ at most $C|x-y|$, and $\min\{l(\gamma(x,z)), l(\gamma(z,y))\} \leq C' d(z, \partial D)$ holds for all $z \in \gamma$. Also, the quasi-hyperbolic metric is the **inner metric** (Chap. 4) of the **distance ratio metric**.

  For $n = 2$, one can define the **hyperbolic metric** on D by

$$\inf_{\gamma\in\Gamma} \int_\gamma \frac{2|f'(z)|}{1-|f(z)|^2}|dz|,$$

where $f : D \to \Delta$ is any conformal mapping of D onto the *unit disk* $\Delta = \{z \in \mathbb{C} : |z| < 1\}$. For $n \geq 3$, it is defined only for the half-hyperplane H^n and for the *open unit ball* B^n as the infimum over all $\gamma \in \Gamma$ of the integrals $\int_\gamma \frac{|dz|}{z_n}$ and $\int_\gamma \frac{2|dz|}{1-||z||_2^2}$.

- **Apollonian metric**

  Let $D \subset \mathbb{R}^n$, be a *domain* such that its complement is not contained in a hyperplane or a sphere. The **Apollonian metric** (or **Barbilian metric**, [Barb35]) on D is defined (denoting the boundary of D by ∂D) by the **cross-ratio** as

$$\sup_{a,b\in\partial D} \ln \frac{||a-x||_2||b-y||_2}{||a-y||_2||b-x||_2}.$$

  This metric is **Gromov hyperbolic**.

- **Half-Apollonian metric**

  Given a *domain* $D \subset \mathbb{R}^n$, the **half-Apollonian metric** η_D (Hästo and Lindén, 2004) on D is defined (denoting the boundary of D by ∂D) by

$$\sup_{a\in\partial D} \left| \ln \frac{||a-y||_2}{||a-x||_2} \right|.$$

  This metric is **Gromov hyperbolic** only if the domain is $\mathbb{R}^n \backslash \{x\}$.

- **Gehring metric**

  Given a *domain* $D \subset \mathbb{R}^n$, the **Gehring metric** $\tilde{j_D}$ (Gehring, 1982) is a metric on D, defined by

$$\frac{1}{2} \ln \left(\left(1 + \frac{||x-y||_2}{\rho(x)} \right) \left(1 + \frac{||x-y||_2}{\rho(y)} \right) \right),$$

  where $\rho(x) = \inf_{u\in\partial D} ||x-u||_2$ is the distance between x and the boundary of D.

  This metric is **Gromov hyperbolic**.

- **Distance ratio metric**

  Given a *domain* $D \subset \mathbb{R}^n$, the **distance ratio metric** (or *j_D-metric*) is (Gehring–Palka, 1976, and Vuorinen, 1985) a metric on D defined by

$$\ln \left(1 + \frac{||x-y||_2}{\min\{\rho(x), \rho(y)\}} \right),$$

  where $\rho(x) = \inf_{u\in\partial D} ||x-u||_2$ is the distance between x and the boundary of D.

  This metric is **Gromov hyperbolic** only if the domain is $\mathbb{R}^n \backslash \{x\}$.

- **Triangular ratio metric**

  Given a *domain* $D \subset \mathbb{R}^n$, the **triangular ratio metric** on D is defined (denoting the boundary of D by ∂D) by

$$\sup_{z\in\partial D} \frac{||x-y||_2}{(||x-z||_2 + ||y-z||_2|}.$$

- **Visual angle metric**

  Given a *domain* $D \subset \mathbb{R}^n$, the **visual angle metric** on D is defined (denoting the boundary of D by ∂D) by Klein et al., 2014, as

$$\sup_{z \in \partial D} \angle(x, z, y).$$

- **Dovgoshev–Hariri–Vuorinen metric**

  Given a metric space (X, d) and an open set D in it with nonempty boundary ∂D, Dovgoshev–Hariri–Vuorinen, 2015, showed that

$$\ln\left(1 + \frac{cd(x, y)}{\sqrt{d(x, \partial D)d(y, \partial D)}}\right)$$

  is a metric for every $c \geq 2$ with 2 being the best possible constant.
- **Ferrand metric**

  Given a *domain* $D \subset \mathbb{R}^n$, the **Ferrand metric** σ_D (Ferrand, 1987) is a metric on D defined by

$$\inf_{\gamma \in \Gamma} \int_\gamma \sup_{a,b \in \partial D} \frac{||a - b||_2}{||z - a||_2 ||z - b||_2} |dz|,$$

  where the infimum is taken over the set Γ of all rectifiable curves connecting x and y in D, ∂D is the boundary of D, and $||.||_2$ is the Euclidean norm on $\mathbb{R}^n$.

  This metric is the **inner metric** (Chap. 4) of the **Möbius metric**.
- **Möbius metric**

  Given a *domain* $D \subset \mathbb{R}^n$, the **Möbius** (or *absolute ratio*, δ_D-) **metric**; Siettenranta, 1999) is a metric on D defined by

$$\sup_{a,b \in \partial D} \ln\left(1 + \frac{||a - x||_2 ||b - y||_2}{||a - b||_2 ||x - y||_2}\right).$$

  This metric is **Gromov hyperbolic**.
- **Modulus metric**

  Let $D \subset \mathbb{R}^n$, be a *domain*. The *conformal modulus* of a family Γ of locally rectifiable curves in D is $M(\Gamma) = \inf_\rho \int_{\mathbb{R}^n} \rho^n dm$, where m is the n-dimensional Lebesgue measure, and ρ is any Borel-measurable function with $\int_\gamma \rho ds \geq 1$ and $\rho \geq 0$ for each $\gamma \in \Gamma$. Cf. general *modulus* in **extremal metric**, Chap. 8.

  Let $\Delta(E, F; D)$ denote the family of all closed nonconstant curves in D joining E and F. The **modulus metric** μ_D (Gál, 1960) is a metric on D, defined by

$$\inf_{C_{xy}} M(\Delta(C_{xy}, \partial D; D)),$$

where C_{xy} is a compact connected set such that for some $\gamma : [0, 1] \to D$, it holds $C_{xy} = \gamma([0, 1])$ and $\gamma(0) = x$, $\gamma(1) = y$.

The **Ferrand second metric** λ_D^* (Ferrand, 1997) is a metric on D, defined by

$$\left(\inf_{C_x, C_y} M(\Delta(C_x, C_y; D))\right)^{\frac{1}{1-n}},$$

where C_z $(z = x, y)$ is a compact connected set such that, for some $\gamma_z : [0, 1] \to D$, it holds $C_z = \gamma([0, 1))$, $z \in |\gamma_z|$ and $\gamma_z(t) \to \partial D$ as $t \to 1$.

Above two metrics are **Gromov hyperbolic** if D is the open ball $B^n = \{x \in \mathbb{R}^n : \langle x, x\rangle < 1\}$ or a simply connected domain in $\mathbb{R}^2$.

- **Conformal radius**

  Let $D \subset \mathbb{C}$, be a simply connected *domain* and let $z \in D$, $z \neq \infty$.

  The **conformal** (or *harmonic*) **radius** is defined by

$$rad(z, D) = (f'(z))^{-1},$$

  where $f : D \to \Delta$ is the *uniformizing map*, i.e., the unique conformal mapping onto the unit disk with $f(z) = 0 \in \Delta$ and $f'(z) > 0$.

  The Euclidean distance between z and the boundary ∂D of D (i.e., the radius of the largest disk inscribed in D) lies in the segment $[\frac{rad(z,D)}{4}, rad(z, D)]$.

  If D is compact, define $rad(\infty, D)$ as $\lim_{z\to\infty} \frac{f(z)}{z}$, where $f : (\mathbb{C}\backslash\Delta) \to (\mathbb{C}\backslash D)$ is the unique conformal mapping with $f(\infty) = \infty$ and positive above limit. This radius is the **transfinite diameter** from Chap. 1.

- **Parabolic distance**

  The **parabolic distance** is a metric on $\mathbb{R}^{n+1}$, considered as $\mathbb{R}^n \times \mathbb{R}$ defined by

$$\sqrt{(x_1 - y_1)^2 + \cdots + (x_n - y_n)^2} + |t_x - t_y|^{1/m}, m \in \mathbb{N},$$

  for any $x = (x_1, \ldots, x_n, t_x), y = (y_1, \ldots, y_n, t_y) \in \mathbb{R}^n \times \mathbb{R}$.

  The space $\mathbb{R}^n \times \mathbb{R}$ can be interpreted as multidimensional *space-time*.

  Usually, the value $m = 2$ is applied. There exist some variants of the parabolic distance, for example, the parabolic distance

$$\sup\{|x_1 - y_1|, |x_2 - y_2|^{1/2}\}$$

  on $\mathbb{R}^2$ (cf. also **Rickman's rug metric** in Chap. 19), or the **half-space parabolic distance** on $\mathbb{R}^3_+ = \{x \in \mathbb{R}^3 : x_1 \geq 0\}$ defined by

$$\frac{|x_1 - y_1| + |x_2 - y_2|}{\sqrt{x_1} + \sqrt{x_2} + \sqrt{|x_2 - y_2|}} + \sqrt{|x_3 - y_3|}.$$

Chapter 7
Riemannian and Hermitian Metrics

Riemannian Geometry is a multidimensional generalization of the intrinsic geometry of 2D surfaces in the Euclidean space $\mathbb{E}^3$. It studies *real smooth manifolds* equipped with **Riemannian metrics**, i.e., collections of positive-definite symmetric bilinear forms $((g_{ij}))$ on their tangent spaces which vary smoothly from point to point. The geometry of such (*Riemannian*) manifolds is based on the *line element* $ds^2 = \sum_{i,j} g_{ij} dx_i dx_j$. This gives, in particular, local notions of angle, length of curve, and volume.

From these notions some other global quantities can be derived, by integrating local contributions. Thus, the value ds is interpreted as the length of the vector $(dx_1, \ldots, dx_n)$, and it is called the **infinitesimal distance**. The arc length of a curve γ is expressed by $\int_\gamma \sqrt{\sum_{i,j} g_{ij} dx_i dx_j}$, and then the **intrinsic metric** on a Riemannian manifold is defined as the infimum of lengths of curves joining two given points of the manifold.

Therefore, a Riemannian metric is not an ordinary metric, but it induces an ordinary metric, in fact, the intrinsic metric, called **Riemannian distance**, on any connected Riemannian manifold. A Riemannian metric is an infinitesimal form of the corresponding Riemannian distance.

As particular special cases of Riemannian Geometry, there occur *Euclidean Geometry* as well as the two standard types, *Elliptic Geometry* and *Hyperbolic Geometry*, of *non-Euclidean Geometry*. If the bilinear forms $((g_{ij}))$ are nondegenerate but indefinite, one obtains *pseudo-Riemannian Geometry*. In the case of dimension four (and *signature* $(1, 3)$) it is the main object of the General Theory of Relativity.

If $ds = F(x_1, \ldots, x_n, dx_1, \ldots, dx_n)$, where F is a real positive-definite convex function which cannot be given as the square root of a symmetric bilinear form (as in the Riemannian case), one obtains the *Finsler Geometry* generalizing Riemannian Geometry.

Hermitian Geometry studies *complex manifolds* equipped with **Hermitian metrics**, i.e., collections of positive-definite symmetric *sesquilinear forms* (or $\frac{3}{2}$-*linear*

© Springer-Verlag Berlin Heidelberg 2016

M.M. Deza, E. Deza, *Encyclopedia of Distances*,
DOI 10.1007/978-3-662-52844-0_7

forms) since they are linear in one argument and *antilinear* in the other) on their tangent spaces, which vary smoothly from point to point. It is a complex analog of Riemannian Geometry.

A special class of Hermitian metrics form **Kähler metrics** which have a closed fundamental form w. A generalization of Hermitian metrics give **complex Finsler metrics** which cannot be written as a bilinear symmetric positive-definite sesqulinear form.

7.1 Riemannian Metrics and Generalizations

A *real n-manifold M^n with boundary* is (cf. Chap. 2) a **Hausdorff space** in which every point has an open neighborhood homeomorphic to either an open subset of $\mathbb{E}^n$, or an open subset of the closed half of $\mathbb{E}^n$. The set of points which have an open neighborhood homeomorphic to $\mathbb{E}^n$ is called the *interior* (of the manifold); it is always nonempty.

The complement of the interior is called the *boundary* (of the manifold); it is an $(n-1)$-dimensional manifold. If it is empty, one obtains a *real n-manifold without boundary*. Such manifold is called *closed* if it is compact, and *open*, otherwise.

An open set of M^n together with a homeomorphism between the open set and an open set of $\mathbb{E}^n$ is called a *coordinate chart*. A collection of charts which cover M^n is an *atlas* on M^n. The homeomorphisms of two overlapping charts provide a transition mapping from a subset of $\mathbb{E}^n$ to some other subset of $\mathbb{E}^n$.

If all these mappings are continuously differentiable, then M^n is a *differentiable manifold*. If they are k times (infinitely often) continuously differentiable, then the manifold is a C^k *manifold* (respectively, a *smooth manifold*, or C^∞ *manifold*).

An atlas of a manifold is called *oriented* if the Jacobians of the coordinate transformations between any two charts are positive at every point. An *orientable manifold* is a manifold admitting an oriented atlas.

Manifolds inherit many local properties of the Euclidean space: they are locally path-connected, locally compact, and locally metrizable. Every smooth Riemannian manifold embeds isometrically (Nash, 1956) in some finite-dimensional Euclidean space.

Associated with every point on a differentiable manifold is a *tangent space* and its dual, a *cotangent space*. Formally, let M^n be a C^k manifold, $k \geq 1$, and p a point of M^n. Fix a chart $\varphi : U \to \mathbb{E}^n$, where U is an open subset of M^n containing p. Suppose that two curves $\gamma^1 : (-1,1) \to M^n$ and $\gamma^2 : (-1,1) \to M^n$ with $\gamma^1(0) = \gamma^2(0) = p$ are given such that $\varphi \cdot \gamma^1$ and $\varphi \cdot \gamma^2$ are both differentiable at 0.

Then γ^1 and γ^2 are called *tangent at* 0 if $(\varphi \cdot \gamma^1)'(0) = (\varphi \cdot \gamma^2)'(0)$. If the functions $\varphi \cdot \gamma^i : (-1,1) \to \mathbb{E}^n$, $i = 1,2$, are given by n real-valued component functions $(\varphi \cdot \gamma^i)_1(t), \ldots, (\varphi \cdot \gamma^i)_n(t)$, the condition above means that their Jacobians $\left(\frac{d(\varphi \cdot \gamma^i)_1(t)}{dt}, \ldots, \frac{d(\varphi \cdot \gamma^i)_n(t)}{dt}\right)$ coincide at 0. This is an equivalence relation, and the equivalence class $\gamma'(0)$ of the curve γ is called a *tangent vector* of M^n at p.

The *tangent space* $T_p(M^n)$ of M^n at p is defined as the set of all tangent vectors at p. The function $(d\varphi)_p : T_p(M^n) \to \mathbb{E}^n$ defined by $(d\varphi)_p(\gamma'(0)) = (\varphi \cdot \gamma)'(0)$, is bijective and can be used to transfer the vector space operations from $\mathbb{E}^n$ over to $T_p(M^n)$.

All the tangent spaces $T_p(M^n)$, $p \in M^n$, when "glued together", form the *tangent bundle* $T(M^n)$ of M^n. Any element of $T(M^n)$ is a pair (p, v), where $v \in T_p(M^n)$.

If for an open neighborhood U of p the function $\varphi : U \to \mathbb{R}^n$ is a coordinate chart, then the preimage V of U in $T(M^n)$ admits a mapping $\psi : V \to \mathbb{R}^n \times \mathbb{R}^n$ defined by $\psi(p, v) = (\varphi(p), d\varphi(p))$. It defines the structure of a smooth $2n$-dimensional manifold on $T(M^n)$. The *cotangent bundle* $T^*(M^n)$ of M^n is obtained in similar manner using cotangent spaces $T_p^*(M^n)$, $p \in M^n$.

A *vector field* on a manifold M^n is a *section* of its tangent bundle $T(M^n)$, i.e., a smooth function $f : M^n \to T(M^n)$ which assigns to every point $p \in M^n$ a vector $v \in T_p(M^n)$.

A *connection* (or *covariant derivative*) is a way of specifying a derivative of a vector field along another vector field on a manifold.

Formally, the covariant derivative ∇ of a vector u (defined at a point $p \in M^n$) in the direction of the vector v (defined at the same point p) is a rule that defines a third vector at p, called $\nabla_v u$ which has the properties of a derivative. A Riemannian metric uniquely defines a special covariant derivative called the *Levi-Civita connection*. It is the torsion-free connection ∇ of the tangent bundle, preserving the given Riemannian metric.

The *Riemann curvature tensor* R is the standard way to express the *curvature* of *Riemannian manifolds*. The Riemann curvature tensor can be given in terms of the Levi-Civita connection ∇ by the following formula:

$$R(u, v)w = \nabla_u \nabla_v w - \nabla_v \nabla_u w - \nabla_{[u,v]} w,$$

where $R(u, v)$ is a linear transformation of the tangent space of the manifold M^n; it is linear in each argument. If $u = \frac{\partial}{\partial x_i}$ and $v = \frac{\partial}{\partial x_j}$ are coordinate vector fields, then $[u, v] = 0$, and the formula simplifies to $R(u, v)w = \nabla_u \nabla_v w - \nabla_v \nabla_u w$, i.e., the curvature tensor measures anti-commutativity of the covariant derivative. The linear transformation $w \to R(u, v)w$ is also called the *curvature transformation*.

The *Ricci curvature tensor* (or *Ricci curvature*) *Ric* is obtained as the trace of the full curvature tensor R. It can be thought of as a Laplacian of the Riemannian metric tensor in the case of Riemannian manifolds. Ricci curvature is a linear operator on the tangent space at a point. Given an orthonormal basis $(e_i)_i$ in the tangent space $T_p(M^n)$, we have

$$Ric(u) = \sum_i R(u, e_i)e_i.$$

The value of $Ric(u)$ does not depend on the choice of an orthonormal basis. Starting with dimension four, the Ricci curvature does not describe the curvature tensor completely.

The *Ricci scalar* (or *scalar curvature*) Sc of a Riemannian manifold M^n is the full trace of the curvature tensor; given an orthonormal basis $(e_i)_i$ at $p \in M^n$, we have

$$Sc = \sum_{i,j} \langle R(e_i, e_j)e_j, e_i \rangle = \sum_i \langle Ric(e_i), e_i \rangle.$$

The *sectional curvature* $K(\sigma)$ of a Riemannian manifold M^n is defined as the *Gauss curvature* of an σ*-section* at a point $p \in M^n$, where a σ*-section* is a locally-defined piece of surface which has the 2-plane σ as a tangent plane at p, obtained from geodesics which start at p in the directions of the image of σ under the exponential mapping.

- **Metric tensor**

  The **metric** (or *basic*, *fundamental*) **tensor** is a symmetric tensor of rank 2, that is used to measure distances and angles in a real n-dimensional differentiable manifold M^n. Once a local coordinate system $(x_i)_i$ is chosen, the metric tensor appears as a real symmetric $n \times n$ matrix $((g_{ij}))$.

  The assignment of a metric tensor on M^n introduces a *scalar product* (i.e., symmetric bilinear, but in general not positive-definite, form) $\langle , \rangle_p$ on the tangent space $T_p(M^n)$ at any $p \in M^n$ defined by

$$\langle x, y \rangle_p = g_p(x, y) = \sum_{i,j} g_{ij}(p)x_i y_j,$$

  where $x = (x_1, \ldots, x_n)$, $y = (y_1, \ldots, y_n) \in T_p(M^n)$. The collection of all these scalar products is called the **metric** g with the metric tensor $((g_{ij}))$. The length ds of the vector $(dx_1, \ldots, dx_n)$ is expressed by the quadratic differential form

$$ds^2 = \sum_{i,j} g_{ij} dx_i dx_j,$$

  which is called the *line element* (or *first fundamental form*) of the metric g.

  The *length* of a curve γ is expressed by the formula $\int_\gamma \sqrt{\sum_{i,j} g_{ij} dx_i dx_j}$. In general it may be real, purely imaginary, or zero (an *isotropic curve*).

  Let p, q and r be the numbers of positive, negative and zero *eigenvalues* of the matrix $((g_{ij}))$ of the metric g; so, $p+q+r = n$. The **metric signature** (or, simply, *signature*) of g is the pair (p, q). A **nondegenerated metric** (i.e., one with $r = 0$) is Riemannian or pseudo-Riemannian if its signature is *positive-definite* ($q = 0$) or *indefinite* ($pq > 0$), respectively.

  The **nonmetricity tensor** is the *covariant derivative* of a metric tensor. It is 0 for **Riemannian metrics** but can be $\neq 0$ for **pseudo-Riemannian** ones.

- **Nondegenerate metric**

  A **nondegenerate metric** is a metric g with the metric tensor $((g_{ij}))$, for which the *metric discriminant* $\det((g_{ij})) \neq 0$. All Riemannian and pseudo-Riemannian metrics are nondegenerate.

  A **degenerate metric** is a metric g with $\det((g_{ij})) = 0$ (cf. **semi-Riemannian metric** and **semi-pseudo-Riemannian metric**). A manifold with a degenerate metric is called an *isotropic manifold*.
- **Diagonal metric**

  A **diagonal metric** is a metric g with a metric tensor $((g_{ij}))$ which is zero for $i \neq j$. The Euclidean metric is a diagonal metric, as its metric tensor has the form $g_{ii} = 1, g_{ij} = 0$ for $i \neq j$.
- **Riemannian metric**

  Consider a real n-dimensional differentiable manifold M^n in which each tangent space is equipped with an *inner product* (i.e., a symmetric positive-definite bilinear form) which varies smoothly from point to point.

  A **Riemannian metric** on M^n is a collection of inner products $\langle , \rangle_p$ on the tangent spaces $T_p(M^n)$, one for each $p \in M^n$.

  Every inner product $\langle , \rangle_p$ is completely defined by inner products $\langle e_i, e_j \rangle_p = g_{ij}(p)$ of elements $e_1, \ldots, e_n$ of a standard basis in $\mathbb{E}^n$, i.e., by the real symmetric and positive-definite $n \times n$ matrix $((g_{ij})) = ((g_{ij}(p)))$, called a **metric tensor**. In fact, $\langle x, y \rangle_p = \sum_{i,j} g_{ij}(p) x_i y_j$, where $x = (x_1, \ldots, x_n)$ and $y = (y_1, \ldots, y_n) \in T_p(M^n)$. The smooth function g completely determines the Riemannian metric.

  A Riemannian metric on M^n is not an ordinary metric on M^n. However, for a connected manifold M^n, every Riemannian metric on M^n induces an ordinary metric on M^n, in fact, the **intrinsic metric** of M^n,

  For any points $p, q \in M^n$ the **Riemannian distance** between them is defined as

$$\inf_{\gamma} \int_0^1 \langle \frac{d\gamma}{dt}, \frac{d\gamma}{dt} \rangle^{\frac{1}{2}} dt = \inf_{\gamma} \int_0^1 \sqrt{\sum_{i,j} g_{ij} \frac{dx_i}{dt} \frac{dx_j}{dt}} dt,$$

  where the infimum is over all rectifiable curves $\gamma : [0, 1] \to M^n$, connecting p and q.

  A *Riemannian manifold* (or *Riemannian space*) is a real n-dimensional differentiable manifold M^n equipped with a Riemannian metric. The theory of Riemannian spaces is called *Riemannian Geometry*. The simplest examples of Riemannian spaces are Euclidean spaces, *hyperbolic spaces*, and *elliptic spaces*.
- **Conformal metric**

  A *conformal structure on a vector space V* is a class of pairwise-homothetic Euclidean metrics on V. Any Euclidean metric d_E on V defines a conformal structure $\{\lambda d_E : \lambda > 0\}$.

  A *conformal structure on a manifold* is a field of conformal structures on the tangent spaces or, equivalently, a class of *conformally equivalent Riemannian metrics*. Two Riemannian metrics g and h on a smooth manifold M^n are called

conformally equivalent if $g = f \cdot h$ for some positive function f on M^n, called a *conformal factor*.

A **conformal metric** is a Riemannian metric that represents the conformal structure. Cf. **conformally invariant metric** in Chap. 8.

- **Conformal space**

  The **conformal space** (or *inversive space*) is the Euclidean space $\mathbb{E}^n$ extended by an ideal point (at infinity). Under *conformal* transformations, i.e., continuous transformations preserving local angles, the ideal point can be taken to be an ordinary point. Therefore, in a conformal space a sphere is indistinguishable from a plane: a plane is a sphere passing through the ideal point.

  Conformal spaces are considered in *Conformal* (or *angle-preserving*, *Möbius*) *Geometry* in which properties of figures are studied that are invariant under conformal transformations. It is the set of transformations that map spheres into spheres, i.e., generated by the Euclidean transformations together with *inversions* which in coordinate form are conjugate to $x_i \to \frac{r^2 x_i}{\sum_j x_j^2}$, where r is the radius of the inversion. An inversion in a sphere becomes an everywhere well defined automorphism of period two. Any angle inverts into an equal angle.

  The 2D conformal space is the *Riemann sphere*, on which the conformal transformations are given by the *Möbius transformations* $z \to \frac{az+b}{cz+d}$, $ad-bc \neq 0$.

  In general, a **conformal mapping** between two Riemannian manifolds is a diffeomorphism between them such that the pulled back metric is *conformally equivalent* to the original one. A *conformal Euclidean space* is a *Riemannian space* admitting a conformal mapping onto an Euclidean space.

  In the General Theory of Relativity, conformal transformations are considered on the *Minkowski space* $\mathbb{R}^{1,3}$ extended by two ideal points.

- **Space of constant curvature**

  A **space of constant curvature** is a *Riemannian space* M^n for which the sectional curvature $K(\sigma)$ is constant in all 2D directions σ.

  A *space form* is a connected complete space of constant curvature k. Examples of a *flat space form*, i.e., with $k = 0$, are the Euclidean space and flat torus. The sphere and hyperbolic space are space forms with $k > 0$ and $k < 0$, respectively.

- **Generalized Riemannian space**

  A **generalized Riemannian space** is a metric space with the **intrinsic metric**, subject to certain restrictions on the curvature. Such spaces include *spaces of bounded curvature*, *Riemannian spaces*, etc. They are defined and investigated on the basis of their metric alone, without coordinates.

  A *space of bounded curvature* ($\leq k$ and $\geq k'$) is defined by the condition: for any sequence of *geodesic triangles* T_n contracting to a point, we have

$$k \geq \overline{\lim} \frac{\overline{\delta}(T_n)}{\sigma(T_n^0)} \geq \underline{\lim} \frac{\overline{\delta}(T_n)}{\sigma(T_n^0)} \geq k',$$

  where a *geodesic triangle* $T = xyz$ is the triplet of geodesic segments $[x, y]$, $[y, z]$, $[z, x]$ (the sides of T) connecting in pairs three different points x, y, z, $\overline{\delta}(T) =$

$\alpha + \beta + \gamma - \pi$ is the *excess* of the geodesic triangle T, and $\sigma(T^0)$ is the area of a Euclidean triangle T^0 with the sides of the same lengths. The **intrinsic metric** on the space of bounded curvature is called a **metric of bounded curvature**.

Such a space turns out to be Riemannian under two additional conditions: local compactness of the space (this ensures the condition of local existence of geodesics), and local extendability of geodesics. If in this case $k = k'$, it is a Riemannian space of constant curvature k (cf. **space of geodesics** in Chap. 6).

A space of curvature $\leq k$ is defined by the condition $\overline{\lim}\frac{\bar{\delta}(T_n)}{\sigma(T_n^0)} \leq k$. In such a space any point has a neighborhood in which the sum $\alpha + \beta + \gamma$ of the angles of a geodesic triangle T does not exceed the sum $\alpha_k + \beta_k + \gamma_k$ of the angles of a triangle T^k with sides of the same lengths in a space of constant curvature k. The intrinsic metric of such space is called a **k-concave metric**.

A space of curvature $\geq k$ is defined by the condition $\underline{\lim}\frac{\bar{\delta}(T_n)}{\sigma(T_n^0)} \geq k$. In such a space any point has a neighborhood in which $\alpha + \beta + \gamma \geq \alpha_k + \beta_k + \gamma_k$ for triangles T and T^k. The intrinsic metric of such space is called a **K-concave metric**.

An *Alexandrov metric space* is a generalized Riemannian space with upper, lower or integral curvature bounds. Cf. a **CAT(κ_1) space** in Chap. 6.

- **Complete Riemannian metric**

  A Riemannian metric g on a manifold M^n is called **complete** if M^n forms a complete metric space with respect to g.

  Any Riemannian metric on a compact manifold is complete.

- **Ricci-flat metric**

  A **Ricci-flat metric** is a Riemannian metric with vanished Ricci curvature tensor.

  A *Ricci-flat manifold* is a Riemannian manifold equipped with a Ricci-flat metric. Ricci-flat manifolds represent vacuum solutions to the *Einstein field equation*, and are special cases of *Kähler–Einstein manifolds*. Important Ricci-flat manifolds are *Calabi–Yau manifolds*, and *hyper-Kähler manifolds*.

- **Osserman metric**

  An **Osserman metric** is a Riemannian metric for which the Riemannian curvature tensor R is *Osserman*, i.e., the eigenvalues of the *Jacobi operator* $\mathcal{J}(x) : y \to R(y, x)x$ are constant on the *unit sphere* S^{n-1} in $\mathbb{E}^n$ (they are independent of the unit vectors x).

- **G-invariant Riemannian metric**

  Given a *Lie group* $(G, \cdot, id)$ of transformations, a Riemannian metric g on a differentiable manifold M^n is called **G-invariant**, if it does not change under any $x \in G$. The group $(G, \cdot, id)$ is called the *group of motions* (or *group of isometries*) of the Riemannian space (M^n, g). Cf. **G-invariant metric** in Chap. 10.

- **Ivanov–Petrova metric**

  Let R be the Riemannian curvature tensor of a Riemannian manifold M^n, and let $\{x, y\}$ be an orthogonal basis for an oriented 2-plane π in the tangent space $T_p(M^n)$ at a point p of M^n.

The **Ivanov–Petrova metric** is a Riemannian metric on M^n for which the eigenvalues of the antisymmetric curvature operator $\mathcal{R}(\pi) = R(x, y)$ ([IvSt95]) depend only on the point p of a Riemannian manifold M^n, but not upon the plane π.

- **Zoll metric**

  A **Zoll metric** is a Riemannian metric on a smooth manifold M^n whose geodesics are all simple closed curves of an equal length. A 2D sphere S^2 admits many such metrics, besides the obvious metrics of constant curvature. In terms of cylindrical coordinates (z, θ) ($z \in [-1, 1]$, $\theta \in [0, 2\pi]$), the *line element*

$$ds^2 = \frac{(1 + f(z))^2}{1 - z^2} dz^2 + (1 - z^2) d\theta^2$$

  defines a Zoll metric on S^2 for any smooth odd function $f : [-1, 1] \to (-1, 1)$ which vanishes at the endpoints of the interval.

- **Berger metric**

  The **Berger metric** is a Riemannian metric on the *Berger sphere* (i.e., the three-sphere S^3 squashed in one direction) defined by the *line element*

$$ds^2 = d\theta^2 + \sin^2 \theta d\phi^2 + \cos^2 \alpha (d\psi + \cos \theta d\phi)^2,$$

  where α is a constant, and θ, ϕ, ψ are *Euler angles*.

- **Cycloidal metric**

  The **cycloidal metric** is a Riemannian metric on the half-plane $\mathbb{R}^2_+ = \{x \in \mathbb{R}^2 : x_2 > 0\}$ defined by the *line element*

$$ds^2 = \frac{dx_1^2 + dx_2^2}{2x_2}.$$

  It is called *cycloidal* because its geodesics are cycloid curves. The corresponding distance $d(x, y)$ between two points $x, y \in \mathbb{R}^2_+$ is equivalent to the distance

$$\rho(x, y) = \frac{|x_1 - y_1| + |x_2 - y_2|}{\sqrt{x_1} + \sqrt{x_2} + \sqrt{|x_2 - y_2|}}$$

  in the sense that $d \le C\rho$, and $\rho \le Cd$ for some positive constant C.

- **Klein metric**

  The **Klein metric** is a Riemannian metric on the *open unit ball* $B^n = \{x \in \mathbb{R}^n : ||x||_2 < 1\}$ in $\mathbb{R}^n$ defined by

$$\frac{\sqrt{||y||_2^2 - (||x||_2^2 ||y||_2^2 - \langle x, y \rangle^2)}}{1 - ||x||_2^2}$$

for any $x \in B^n$ and $y \in T_x(B^n)$, where $||.||_2$ is the Euclidean norm on $\mathbb{R}^n$, and $\langle , \rangle$ is the ordinary *inner product* on $\mathbb{R}^n$.

The Klein metric is the hyperbolic case $a = -1$ of the general form

$$\frac{\sqrt{(1 + a||x||^2)||y||^2 - a\langle x, y\rangle^2}}{1 + a||x||^2},$$

while $a = 0, 1$ correspond to the Euclidean and spherical cases.

- **Carnot–Carathéodory metric**

  A *distribution* (or *polarization*) on a manifold M^n is a subbundle of the tangent bundle $T(M^n)$ of M^n. Given a distribution $H(M^n)$, a vector field in $H(M^n)$ is called *horizontal*. A curve γ on M^n is called *horizontal* (or *distinguished*, *admissible*) with respect to $H(M^n)$ if $\gamma'(t) \in H_{\gamma(t)}(M^n)$ for any t.

  A distribution $H(M^n)$ is called *completely nonintegrable* if the Lie brackets of $H(M^n)$, i.e., $[\cdots, [H(M^n), H(M^n)]]$, span the tangent bundle $T(M^n)$, i.e., for all $p \in M^n$ any tangent vector v from $T_p(M^n)$ can be presented as a linear combination of vectors of the following types: u, $[u, w]$, $[u, [w, t]]$, $[u, [w, [t, s]]], \cdots \in T_p(M^n)$, where all vector fields $u, w, t, s, \ldots$ are horizontal.

  The **Carnot–Carathéodory metric** (or **CC metric**, **sub-Riemannian metric**, *control metric*) is a metric on a manifold M^n with a completely nonintegrable horizontal distribution $H(M^n)$ defined as the section g_C of positive-definite *scalar products* on $H(M^n)$. The distance $d_C(p, q)$ between any points $p, q \in M^n$ is defined as the infimum of the g_C-lengths of the horizontal curves joining p and q.

  A *sub-Riemannian manifold* (or *polarized manifold*) is a manifold M^n equipped with a Carnot–Carathéodory metric. It is a generalization of a Riemannian manifold. Roughly, in order to measure distances in a sub-Riemannian manifold, one is allowed to go only along curves tangent to horizontal spaces.

- **Pseudo-Riemannian metric**

  Consider a real n-dimensional differentiable manifold M^n in which every tangent space $T_p(M^n)$, $p \in M^n$, is equipped with a *scalar product* which varies smoothly from point to point and is nondegenerate, but indefinite.

  A **pseudo-Riemannian metric** on M^n is a collection of scalar products $\langle , \rangle_p$ on the tangent spaces $T_p(M^n)$, $p \in M^n$, one for each $p \in M^n$.

  Every scalar product $\langle , \rangle_p$ is completely defined by scalar products $\langle e_i, e_j\rangle_p = g_{ij}(p)$ of elements $e_1, \ldots, e_n$ of a standard basis in $\mathbb{E}^n$, i.e., by the real symmetric indefinite $n \times n$ matrix $((g_{ij})) = ((g_{ij}(p)))$, called a **metric tensor** (cf. **Riemannian metric** in which case this tensor is not only nondegenerate but, moreover, positive-definite).

  In fact, $\langle x, y\rangle_p = \sum_{i,j} g_{ij}(p)x_iy_j$, where $x = (x_1, \ldots, x_n)$ and $y = (y_1, \ldots, y_n) \in T_p(M^n)$. The smooth function g determines the pseudo-Riemannian metric.

The length ds of the vector $(dx_1, \dots, dx_n)$ is given by the quadratic differential form

$$ds^2 = \sum_{i,j} g_{ij} dx_i dx_j.$$

The length of a curve $\gamma : [0, 1] \to M^n$ is expressed by the formula

$$\int_\gamma \sqrt{\sum_{i,j} g_{ij} dx_i dx_j} = \int_0^1 \sqrt{\sum_{i,j} g_{ij} \frac{dx_i}{dt} \frac{dx_j}{dt}} dt.$$

In general it may be real, purely imaginary or zero (an *isotropic curve*).

A pseudo-Riemannian metric on M^n is a metric with a fixed, but indefinite signature (p, q), $p + q = n$. A pseudo-Riemannian metric is nondegenerate, i.e., its metric discriminant $\det((g_{ij})) \neq 0$. Therefore, it is a **nondegenerate indefinite metric**.

A *pseudo-Riemannian manifold* (or *pseudo-Riemannian space*) is a real n-dimensional differentiable manifold M^n equipped with a pseudo-Riemannian metric. The theory of pseudo-Riemannian spaces is called *Pseudo-Riemannian Geometry*.

- **Pseudo-Euclidean distance**

The model space of a **pseudo-Riemannian space** of signature (p, q) is the *pseudo-Euclidean space* $\mathbb{R}^{p,q}$, $p + q = n$ which is a real n-dimensional vector space $\mathbb{R}^n$ equipped with the metric tensor $((g_{ij}))$ of signature (p, q) defined, for $i \neq j$, by $g_{11} = \dots = g_{pp} = 1$, $g_{p+1,p+1} = \dots = g_{nn} = -1$, $g_{ij} = 0$.

The *line element* of the corresponding metric is given by

$$ds^2 = dx_1^2 + \dots + dx_p^2 - dx_{p+1}^2 - \dots - dx_n^2.$$

The **pseudo-Euclidean distance** of signature $(p, q = n - p)$ on $\mathbb{R}^n$ is defined by

$$d_{pE}^2(x, y) = D(x, y) = \sum_{i=1}^{p} (x_i - y_i)^2 - \sum_{i=p+1}^{n} (x_i - y_i)^2.$$

Such a pseudo-Euclidean space can be seen as $\mathbb{R}^p \times i\mathbb{R}^q$, where $i = \sqrt{-1}$.

The pseudo-Euclidean space with $(p, q) = (1, 3)$ is used as flat space-time model of Special Relativity; cf. **Minkowski metric** in Chap. 26.

The points correspond to *events*; the line spanned by x and y is *space-like* if $D(x, y) > 0$ and *time-like* if $D(x, y) < 0$. If $D(x, y) > 0$, then $\sqrt{D(x, y)}$ is Euclidean distance and if $D(x, y) < 0$, then $\sqrt{|D(x, y)|}$ is the lifetime of a particle (from x to y).

The pseudo-Euclidean distance of signature $(p, q = n - p)$ is the case $A = \text{diag}(a_i)$ with $a_i = 1$ for $1 \leq i \leq p$ and $a_i = -1$ for $p + 1 \leq i \leq n$, of the **weighted Euclidean distance** $\sqrt{\sum_{1 \leq i \leq n} a_i (x_i - y_i)^2}$ in Chap. 17.

- **Blaschke metric**

  The **Blaschke metric** on a nondegenerate hypersurface is a pseudo-Riemannian metric, associated to the affine normal of the immersion $\phi : M^n \to \mathbb{R}^{n+1}$, where M^n is an n-dimensional manifold, and $\mathbb{R}^{n+1}$ is considered as an affine space.

- **Semi-Riemannian metric**

  A **semi-Riemannian metric** on a real n-dimensional differentiable manifold M^n is a degenerate Riemannian metric, i.e., a collection of positive-semidefinite *scalar products* $\langle x, y \rangle_p = \sum_{i,j} g_{ij}(p) x_i y_j$ on the tangent spaces $T_p(M^n)$, $p \in M^n$; the metric discriminant $det((g_{ij})) = 0$.

  A *semi-Riemannian manifold* (or *semi-Riemannian space*) is a real n-dimensional differentiable manifold M^n equipped with a semi-Riemannian metric.

  The model space of a semi-Riemannian manifold is the *semi-Euclidean space* R^n_d, $d \geq 1$ (sometimes denoted also by $\mathbb{R}^n_{n-d}$), i.e., a real n-dimensional vector space $\mathbb{R}^n$ equipped with a semi-Riemannian metric.

  It means that there exists a scalar product of vectors such that, relative to a suitably chosen basis, the scalar product $\langle x, x \rangle$ has the form $\langle x, x \rangle = \sum_{i=1}^{n-d} x_i^2$. The number $d \geq 1$ is called the *defect* (or *deficiency*) of the space.

- **Grushin metric**

  The **Grushin metric** is a semi-Riemannian metric on $\mathbb{R}^2$ defined by the *line element*

$$ds^2 = dx_1^2 + \frac{dx_2^2}{x_1^2}.$$

- **Agmon distance**

  The **Agmon metric** attached to an energy E and a potential V is defined as

$$ds^2 = \max\{0, V(x) - E_0(h)\} dx^2,$$

  where dx^2 is the standard metric on $\mathbb{R}^d$. Then the **Agmon distance** on $\mathbb{R}^d$ is the corresponding Riemannian distance defined, for any $x, y \in \mathbb{R}^d$, by

$$\inf_{\gamma} \{ \int_0^1 \sqrt{\max\{V(\gamma(s)) - E_0(h), 0\}} \cdot |\gamma'(s)| ds : \gamma(0) = x, \gamma(1) = y, \gamma \in C^1 \}.$$

- **Semi-pseudo-Riemannian metric**

  A **semi-pseudo-Riemannian metric** on a real n-dimensional differentiable manifold M^n is a degenerate pseudo-Riemannian metric, i.e., a collection of degenerate indefinite *scalar products* $\langle x, y \rangle_p = \sum_{i,j} g_{ij}(p) x_i y_j$ on the tangent

spaces $T_p(M^n)$, $p \in M^n$; the metric discriminant $det((g_{ij})) = 0$. In fact, a semi-pseudo-Riemannian metric is a **degenerate indefinite metric**.

A *semi-pseudo-Riemannian manifold* (or *semi-pseudo-Riemannian space*) is a real n-dimensional differentiable manifold M^n equipped with a semi-pseudo-Riemannian metric. The model space of such manifold is the *semi-pseudo-Euclidean space* $\mathbb{R}^n_{\substack{l_1,\dots,l_r \\ m_1,\dots,m_{r-1}}}$, i.e., a vector space $\mathbb{R}^n$ equipped with a semi-pseudo-Riemannian metric.

It means that there exist r scalar products $\langle x, y\rangle_a = \sum \epsilon_{i_a} x_{i_a} y_{i_a}$, where $a = 1, \dots r$, $0 = m_0 < m_1 < \dots < m_r = n$, $i_a = m_{a-1} + 1, \dots m_a$, $\epsilon_{i_a} = \pm 1$, and -1 occurs l_a times among the numbers ϵ_{i_a}. The product $\langle x, y\rangle_a$ is defined for those vectors for which all coordinates x_i, $i \le m_{a-1}$ or $i > m_a + 1$ are zero.

The first scalar square of an arbitrary vector x is a degenerate quadratic form $\langle x, x\rangle_1 = -\sum_{i=1}^{l_1} x_i^2 + \sum_{j=l_1+1}^{n-d} x_j^2$. The number $l_1 \ge 0$ is called the *index*, and the number $d = n - m_1$ is called the *defect* of the space. If $l_1 = \dots = l_r = 0$, we obtain a *semi-Euclidean space*. The spaces $\mathbb{R}^n_m$ and $\mathbb{R}^n_{\substack{k,l \\ m}}$ are called *quasi-Euclidean spaces*.

The *semi-pseudo-non-Euclidean space* $\mathbb{S}^n_{\substack{l_1,\dots,l_r \\ m_1,\dots,m_{r-1}}}$ is a hypersphere in $\mathbb{R}^{n+1}_{\substack{l_1,\dots,l_r \\ m_1,\dots,m_{r-1}}}$ with identified antipodal points. It is called *semielliptic* (or *semi-non-Euclidean*) *space* if $l_1 = \dots = l_r = 0$ and a *semihyperbolic space* if there exist $l_i \ne 0$.

- **Finsler metric**

  Consider a real n-dimensional differentiable manifold M^n in which every tangent space $T_p(M^n)$, $p \in M^n$, is equipped with a *Banach norm* $||.||$ such that the Banach norm as a function of position is smooth, and the matrix $((g_{ij}))$,

$$g_{ij} = g_{ij}(p, x) = \frac{1}{2} \frac{\partial^2 ||x||^2}{\partial x_i \partial x_j},$$

  is positive-definite for any $p \in M^n$ and any $x \in T_p(M^n)$.

  A **Finsler metric** on M^n is a collection of Banach norms $||.||$ on the tangent spaces $T_p(M^n)$, one for each $p \in M^n$. Its *line element* has the form

$$ds^2 = \sum_{i,j} g_{ij} dx_i dx_j.$$

  The Finsler metric can be given by *fundamental function*, i.e., a real positive-definite convex function $F(p, x)$ of $p \in M^n$ and $x \in T_p(M^n)$ acting at the point p. $F(p, x)$ is positively homogeneous of degree one in x: $F(p, \lambda x) = \lambda F(p, x)$ for every $\lambda > 0$. Then $F(p, x)$ is the length of the vector x.

  The *Finsler metric tensor* has the form $((g_{ij})) = ((\frac{1}{2} \frac{\partial^2 F^2(p,x)}{\partial x_i \partial x_j}))$. The length of a curve $\gamma : [0, 1] \to M^n$ is given by $\int_0^1 F(p, \frac{dp}{dt}) dt$. For each fixed p the Finsler metric tensor is Riemannian in the variables x.

The Finsler metric is a generalization of the Riemannian metric, where the general definition of the length $||x||$ of a vector $x \in T_p(M^n)$ is not necessarily given in the form of the square root of a symmetric bilinear form as in the Riemannian case.

A *Finsler manifold* (or *Finsler space*) is a real differentiable n-manifold M^n equipped with a Finsler metric. The theory of such spaces is *Finsler Geometry*.

The difference between a Riemannian space and a Finsler space is that the former behaves locally like a Euclidean space, and the latter locally like a *Minkowskian space* or, analytically, the difference is that to an ellipsoid in the Riemannian case there corresponds an arbitrary convex surface which has the origin as the center.

A **pseudo-Finsler metric** F is defined by weakening the definition of a Finsler metric): $((g_{ij}))$ should be nondegenerate and of constant signature (not necessarily positive-definite) and hence F could be negative. The pseudo-Finsler metric is a generalization of the pseudo-Riemannian metric.

- (α, β)**-metric**

  Let $\alpha(x, y) = \sqrt{\alpha_{ij}(x)y^i y^j}$ be a Riemannian metric and $\beta(x, y) = b_i(x)y^i$ be a 1-form on a n-dimensional manifold M^n. Let $s = \frac{\beta}{\alpha}$ and $\phi(s)$ is an C^∞-positive function on some symmetric interval $(-r, r)$ with $r > \frac{\beta}{\alpha}$ for all (x, y) in the tangent bundle $TM = \cup_{x \in M} T_x(M^n)$ of the tangent spaces $T_x(M^n)$. Then $F = \alpha\phi(s)$ is a Finsler metric (Matsumoto, 1972) called an (α, β)**-metric**. The main examples of (α, β)-metrics follow.

  The **Kropina metric** is the case $\phi(s) = \frac{1}{s}$, i.e., $F = \frac{\alpha^2}{\beta}$.

  The **generalized Kropina metric** is the case $\phi(s) = s^m$, i.e., $F = \beta^m \alpha^{1-m}$.

  The **Randers metric** (1941) is the case $\phi(s) = 1 + s$, i.e., $F = \alpha + \beta$.

  The **Matsumoto slope metric** is the case $\phi(s) = \frac{1}{1-s}$, i.e., $F = \frac{\alpha^2}{\alpha - \beta}$.

  The **Riemann-type** (α, β)**-metric** is the case $\phi(s) = \sqrt{1 + s^2}$, i.e., $F = \alpha^2 + \beta^2$.

  Park and Lee, 1998, considered the case $\phi(s) = 1 + s^2$, i.e., $F = \alpha + \frac{\beta^2}{\alpha}$.

- **Shen metric**

  Given a vector $a \in \mathbb{R}^n$, $||a||_2 < 1$, the **Shen metric** (2003) is a Finsler metric on the *open unit ball* $B^n = \{x \in \mathbb{R}^n : ||x||_2 < 1\}$ in $\mathbb{R}^n$ defined by

$$\frac{\sqrt{||y||_2^2 - (||x||_2^2||y||_2^2 - \langle x, y\rangle^2)} + \langle x, y\rangle}{1 - ||x||_2^2} + \frac{\langle a, y\rangle}{1 + \langle a, x\rangle}$$

  for any $x \in B^n$ and $y \in T_x(B^n)$, where $||.||_2$ is the Euclidean norm on $\mathbb{R}^n$, and $\langle , \rangle$ is the ordinary *inner product* on $\mathbb{R}^n$. It is a **Randers metric** and a **projective metric**. Cf. **Klein metric** and **Berwald metric**.

- **Berwald metric**

  The **Berwald metric** (1929) is a Finsler metric F_{Be} on the *open unit ball* $B^n = \{x \in \mathbb{R}^n : ||x||_2 < 1\}$ in $\mathbb{R}^n$ defined, for any $x \in B^n$ and $y \in T_x(B^n)$, by

$$\frac{\left(\sqrt{||y||_2^2 - (||x||_2^2||y||_2^2 - \langle x, y\rangle^2)} + \langle x, y\rangle\right)^2}{(1 - ||x||_2^2)^2\sqrt{||y||_2^2 - (||x||_2^2||y||_2^2 - \langle x, y\rangle^2)}},$$

  where $||.||_2$ is the Euclidean norm on $\mathbb{R}^n$, and $\langle , \rangle$ is the *inner product* on $\mathbb{R}^n$. It is a **projective metric** and an (α, β)**-metric** with $\phi(s) = (1+s)^2$, i.e., $F = \frac{(\alpha+\beta)^2}{\alpha}$.

  The Riemannian metrics are special Berwald metrics. Every Berwald metric is affinely equivalent to a Riemannian metric.

  In general, every Finsler metric on a manifold M^n induces a *spray* (second-order homogeneous ordinary differential equation) $y_i \frac{\partial}{\partial x_i} - 2G^i \frac{\partial}{\partial y_i}$ which determines the geodesics. A Finsler metric is a Berwald metric if the spray coefficients $G^i = G^i(x, y)$ are quadratic in $y \in T_x(M^n)$ at any point $x \in M^n$, i.e., $G^i = \frac{1}{2}\Gamma^i_{jk}(x)y^j y^k$.

  A Finsler metric is a more general **Landsberg metric** $\Gamma^i_{jk} = \frac{1}{2}\partial_{y^j}\partial_{y^k}(\Gamma^i_{jk}(x)y^j y^k)$. The Landsberg metric is the one for which the *Landsberg curvature* (the covariant derivative of the *Cartan torsion along a geodesic*) is zero.

- **Douglas metric**

  A **Douglas metric** a Finsler metric for which the *spray coefficients* $G^i = G^i(x, y)$ have the following form:

$$G^i = \frac{1}{2}\Gamma^i_{jk}(x)y_i y_k + P(x, y)y_i.$$

  Every Finsler metric which is projectively equivalent to a **Berwald metric** is a Douglas metric. Every **Berwald metric** is a Douglas metric. Every known Douglas metric is (locally) projectively equivalent to a Berwald metric.

- **Bryant metric**

  Let α be an angle with $|\alpha| < \frac{\pi}{2}$. Let, for any $x, y \in \mathbb{R}^n$, $A = ||y||_2^4 \sin^2 2\alpha + \left(||y||_2^2 \cos 2\alpha + ||x||_2^2||y||_2^2 - \langle x, y\rangle^2\right)^2$, $B = ||y||_2^2 \cos 2\alpha + ||x||_2^2||y||_2^2 - \langle x, y\rangle^2$, $C = \langle x, y\rangle \sin 2\alpha$, $D = ||x||_2^4 + 2||x||_2^2 \cos 2\alpha + 1$. Then we get a Finsler metric

$$\sqrt{\frac{\sqrt{A} + B}{2D} + \left(\frac{C}{D}\right)^2} + \frac{C}{D}.$$

  On the 2D *unit sphere* S^2, it is the **Bryant metric** (1996).

- *m*-**th root pseudo-Finsler metric**

  An *m*-**th root pseudo-Finsler metric** is (Shimada, 1979) a **pseudo-Finsler metric** defined (with $a_{i_1\dots i_m}$ symmetric in all its indices) by

$$F(x,y) = (a_{i_1\dots i_m}(x)y^{i_1\dots i_m})^{\frac{1}{m}}.$$

  For $m = 2$, it is a pseudo-Riemannian metric. The 3-rd and 4-th root pseudo-Finsler metrics are called *cubic metric* and *quartic metric*, respectively.
- **Antonelli–Shimada metric**

  The **Antonelli–Shimada metric** (or *ecological Finsler metric*) is an *m*-**th root pseudo-Finsler metric** defined, via linearly independent 1-forms a^i, by

$$F(x,y) = (\sum_{i=1}^{n}(a^i)^m)^{\frac{1}{m}}.$$

  The **Uchijo metric** is defined, for a constant k, by

$$F(x,y) = (\sum_{i=1}^{n}(a^i)^2)^{\frac{1}{2}} + ka^1.$$

- **Berwald–Moör metric**

  The **Berwald–Moör metric** is an *m*-**th root pseudo-Finsler metric**, defined by

$$F(x,y) = (y^1 \dots y^n)^{\frac{1}{n}}.$$

  More general **Asanov metric** is defined, via linearly independent 1-forms a^i, by

$$F(x,y) = (a^1 \dots a^n)^{\frac{1}{n}}.$$

  The Berwald–Moör metrics with $n = 4$ and $n = 6$ are applied in Relativity Theory and Diffusion Imaging, respectively. The pseudo-Finsler spaces which are locally isomorphic to the 4-th root Berwald–Moör metric, are expected to be more general and productive space-time models than usual pseudo-Riemannian spaces, which are locally isomorphic to the Minkowski metric.
- **Kawaguchi metric**

  The **Kawaguchi metric** is a metric on a smooth n-dimensional manifold M^n, given by the arc element ds of a regular curve $x = x(t)$, $t \in [t_0, t_1]$ via the formula

$$ds = F(x, \frac{dx}{dt}, \dots, \frac{d^k x}{dt^k})dt,$$

where the *metric function* F satisfies Zermelo's conditions: $\sum_{s=1}^{k} sx^{(s)}F_{(s)i} = F$, $\sum_{s=r}^{k} \binom{s}{k} x^{(s-r+1)i}F_{(s)i} = 0$, $x^{(s)i} = \frac{d^s x^i}{dt^s}$, $F_{(s)i} = \frac{\partial F}{\partial x^{(s)i}}$, and $r = 2, \ldots, k$.

These conditions ensure that the arc element ds is independent of the parametrization of the curve $x = x(t)$.

A *Kawaguchi manifold* (or *Kawaguchi space*) is a smooth manifold equipped with a Kawaguchi metric. It is a generalization of a *Finsler manifold*.

- **Lagrange metric**

  Consider a real n-dimensional manifold M^n. A set of symmetric nondegenerated matrices $((g_{ij}(p,x)))$ define a **generalized Lagrange metric** on M^n if a change of coordinates $(p,x) \to (q,y)$, such that $q_i = q_i(p_1, \ldots, p_n)$, $y_i = (\partial_j q_i)x_j$ and rank $(\partial_j q_i) = n$, implies $g_{ij}(p,x) = (\partial_i q_i)(\partial_j q_j)g_{ij}(q,y)$.

  A generalized Lagrange metric is called a **Lagrange metric** if there exists a *Lagrangian*, i.e., a smooth function $L(p,x)$ such that it holds

$$g_{ij}(p,x) = \frac{1}{2} \cdot \frac{\partial^2 L(p,x)}{\partial x_i \partial x_j}.$$

  Every Finsler metric is a Lagrange metric with $L = F^2$.

- **DeWitt supermetric**

  The **DeWitt supermetric** (or **Wheeler–DeWitt supermetric**) $G = ((G_{ijkl}))$ calculates distances between metrics on a given manifold, and it is a generalization of a Riemannian (or pseudo-Riemannian) metric $g = ((g_{ij}))$.

  For example, for a given connected smooth 3-dimensional manifold M^3, consider the space $\mathcal{M}(M^3)$ of all Riemannian (or pseudo-Riemannian) metrics on M^3. Identifying points of $\mathcal{M}(M^3)$ that are related by a diffeomorphism of M^3, one obtains the space $Geom(M^3)$ of 3-*geometries* (of fixed topology), points of which are the classes of diffeomorphically equivalent metrics. The space $Geom(M^3)$ is called a *superspace*. It plays an important role in several formulations of Quantum Gravity.

  A **supermetric**, i.e., a "metric on metrics", is a metric on $\mathcal{M}(M^3)$ (or on $Geom(M^3)$) which is used for measuring distances between metrics on M^3 (or between their equivalence classes). Given $g = ((g_{ij})) \in \mathcal{M}(M^3)$, we obtain

$$||\delta g||^2 = \int_{M^3} d^3x G^{ijkl}(x)\delta g_{ij}(x)\delta g_{kl}(x),$$

  where G^{ijkl} is the inverse of the **DeWitt supermetric**

$$G_{ijkl} = \frac{1}{2\sqrt{det((g_{ij}))}}(g_{ik}g_{jl} + g_{il}g_{jk} - \lambda g_{ij}g_{kl}).$$

  The value λ parametrizes the distance between metrics in $\mathcal{M}(M^3)$, and may take any real value except $\lambda = \frac{2}{3}$, for which the supermetric is *singular*.

- **Lund–Regge supermetric**

  The **Lund–Regge supermetric** (or **simplicial supermetric**) is an analog of the **DeWitt supermetric**, used to measure the distances between *simplicial* 3-*geometries* in a *simplicial configuration space*.

  More exactly, given a closed *simplicial* 3D manifold M^3 consisting of several *tetrahedra* (i.e., 3-*simplices*), a *simplicial geometry* on M^3 is fixed by an assignment of values to the squared edge lengths of M^3, and a flat Riemannian Geometry to the interior of each tetrahedron consistent with those values.

  The squared edge lengths should be positive and constrained by the triangle inequalities and their analogs for the tetrahedra, i.e., all squared measures (lengths, areas, volumes) must be nonnegative (cf. **tetrahedron inequality** in Chap. 3).

  The set $\mathcal{T}(M^3)$ of all simplicial geometries on M^3 is called a *simplicial configuration space*. The Lund–Regge supermetric $((G_{mn}))$ on $\mathcal{T}(M^3)$ is induced from the DeWitt supermetric on $\mathcal{M}(M^3)$, using for representations of points in $\mathcal{T}(M^3)$ such metrics in $\mathcal{M}(M^3)$ which are piecewise flat in the tetrahedra.
- **Space of Lorentz metrics**

  Let M^n be an n-dimensional compact manifold, and $\mathcal{L}(M^n)$ the set of all **Lorentz metrics** (i.e., the pseudo-Riemannian metrics of signature $(n-1,1)$) on M^n.

  Given a Riemannian metric g on M^n, one can identify the vector space $S^2(M^n)$ of all symmetric 2-tensors with the vector space of endomorphisms of the tangent to M^n which are symmetric with respect to g. In fact, if $\tilde{h}$ is the endomorphism associated to a tensor h, then the distance on $S^2(M^n)$ is given by

$$d_g(h,t) = \sup_{x \in M^n} \sqrt{tr(\tilde{h}_x - \tilde{t}_x)^2}.$$

  The set $\mathcal{L}(M^n)$ taken with the distance d_g is an open subset of $S^2(M^n)$ called the **space of Lorentz metrics**. Cf. **manifold triangulation metric** in Chap. 9.
- **Perelman supermetric proof**

  The *Thurston's Geometrization Conjecture* is that, after two well-known splittings, any 3D manifold admits, as remaining components, only one of eight *Thurston model geometries*. If true, this conjecture implies the validity of the famous *Poincaré Conjecture* of 1904, that any 3-manifold, in which every simple closed curve can be deformed continuously to a point, is homeomorphic to the 3-sphere.

  In 2002, Perelman gave a gapless "sketch of an eclectic proof" of Thurston's conjecture using a kind of supermetric approach to the space of all Riemannian metrics on a given smooth 3-manifold. In a *Ricci flow* the distances decrease in directions of positive curvature since the metric is time-dependent. Perelman's modification of the standard Ricci flow permitted systematic elimination of arising singularities.

7.2 Riemannian Metrics in Information Theory

Some special Riemannian metrics are commonly used in Information Theory. A list of such metrics is given below.

- **Thermodynamic metrics**

  Given the space of all *extensive* (additive in magnitude, mechanically conserved) thermodynamic variables of a system (energy, entropy, amounts of materials), a **thermodynamic metric** is a Riemannian metric on the manifold of equilibrium states defined as the 2-nd derivative of one extensive quantity, usually entropy or energy, with respect to the other extensive quantities. This information geometric approach provides a geometric description of thermodynamic systems in equilibrium.

  The **Ruppeiner metric** (Ruppeiner, 1979) is defined by the *line element* $ds^2_R = g^R_{ij} dx^i dx^j$, where the matrix $((g^R_{ij}))$ of the symmetric metric tensor is a negative *Hessian* (the matrix of 2-nd order partial derivatives) of the entropy function S:

$$g^R_{ij} = -\partial_i \partial_j S(M, N^a).$$

  Here M is the internal energy (which is the mass in black hole applications) of the system and N^a refer to other extensive parameters such as charge, angular momentum, volume, etc. This metric is flat if and only if the statistical mechanical system is noninteracting, while curvature singularities are a signal of critical behavior, or, more precisely, of divergent **correlation lengths** (Chap. 24).

  The **Weinhold metric** (Weinhold, 1975) is defined by $g^W_{ij} = \partial_i \partial_j M(S, N^a)$.

  The Ruppeiner and Weinhold metrics are *conformally equivalent* (cf. **conformal metric**) via $ds^2 = g^R_{ij} dM^i dM^j = \frac{1}{T} g^W_{ij} dS^i dS^j$, where T is the temperature.

  The **thermodynamic length** in Chap. 24 is a path function that measures the distance along a path in the state space.

- **Fisher information metric**

  In Statistics, Probability, and Information Geometry, the **Fisher information metric** is a Riemannian metric for a statistical differential manifold (see, for example, [Amar85, Frie98]). Formally, let $p_\theta = p(x, \theta)$ be a family of densities, indexed by n parameters $\theta = (\theta_1, \ldots, \theta_n)$ which form the *parameter manifold* P.

  The **Fisher information metric** $g = g_\theta$ on P is a Riemannian metric, defined by the *Fisher information matrix* $((I(\theta)_{ij}))$, where

$$I(\theta)_{ij} = \mathbb{E}_\theta \left[\frac{\partial \ln p_\theta}{\partial \theta_i} \cdot \frac{\partial \ln p_\theta}{\partial \theta_j} \right] = \int \frac{\partial \ln p(x, \theta)}{\partial \theta_i} \frac{\partial \ln p(x, \theta)}{\partial \theta_j} p(x, \theta) dx.$$

  It is a symmetric bilinear form which gives a classical measure (*Rao measure*) for the statistical distinguishability of distribution parameters.

Putting $i(x,\theta) = -\ln p(x,\theta)$, one obtains an equivalent formula

$$I(\theta)_{ij} = \mathbb{E}_\theta\left[\frac{\partial^2 i(x,\theta)}{\partial\theta_i\partial\theta_j}\right] = \int \frac{\partial^2 i(x,\theta)}{\partial\theta_i\partial\theta_j} p(x,\theta)dx.$$

In a coordinate-free language, we get

$$I(\theta)(u,v) = \mathbb{E}_\theta\left[u(\ln p_\theta)\cdot v(\ln p_\theta)\right],$$

where u and v are vectors tangent to the parameter manifold P, and $u(\ln p_\theta) = \frac{d}{dt}\ln p_{\theta+tu|t=0}$ is the derivative of $\ln p_\theta$ along the direction u.

A *manifold of densities* M is the image of the parameter manifold P under the mapping $\theta \to p_\theta$ with certain regularity conditions. A vector u tangent to this manifold is of the form $u = \frac{d}{dt}p_{\theta+tu|t=0}$, and the Fisher information metric $g = g_p$ on M, obtained from the metric g_θ on P, can be written as

$$g_p(u,v) = \mathbb{E}_p\left[\frac{u}{p}\cdot\frac{v}{p}\right].$$

- **Fisher–Rao metric**

  Let $\mathcal{P}_n = \{p \in \mathbb{R}^n : \sum_{i=1}^n p_i = 1, p_i > 0\}$ be the simplex of strictly positive probability vectors. An element $p \in \mathcal{P}_n$ is a density of the n-point set $\{1,\dots,n\}$ with $p(i) = p_i$. An element u of the tangent space $T_p(\mathcal{P}_n) = \{u \in \mathbb{R}^n : \sum_{i=1}^n u_i = 0\}$ at a point $p \in \mathcal{P}_n$ is a function on $\{1,\dots,n\}$ with $u(i) = u_i$.

  The **Fisher–Rao metric** g_p on $\mathcal{P}_n$ is a Riemannian metric defined by

$$g_p(u,v) = \sum_{i=1}^n \frac{u_i v_i}{p_i}$$

  for any $u, v \in T_p(\mathcal{P}_n)$, i.e., it is the **Fisher information metric** on $\mathcal{P}_n$.

  The Fisher–Rao metric is the unique (up to a constant factor) Riemannian metric on $\mathcal{P}_n$, contracting under stochastic maps ([Chen72]).

  This metric is isometric, by $p \to 2(\sqrt{p_1},\dots,\sqrt{p_n})$, with the standard metric on an open subset of the sphere of radius two in $\mathbb{R}^n$. This identification allows one to obtain on $\mathcal{P}_n$ the **geodesic distance**, called the **Rao distance**, by

$$2\arccos\Big(\sum_i p_i^{1/2} q_i^{1/2}\Big).$$

  The Fisher–Rao metric can be extended to the set $\mathcal{M}_n = \{p \in \mathbb{R}^n, p_i > 0\}$ of all finite strictly positive measures on the set $\{1,\dots,n\}$. In this case, the geodesic

distance on $\mathcal{M}_n$ can be written as

$$2(\sum_i(\sqrt{p_i}-\sqrt{q_i})^2)^{1/2}$$

for any $p, q \in \mathcal{M}_n$ (cf. **Hellinger metric** in Chap. 14).

- **Monotone metrics**

  Let M_n be the set of all complex $n \times n$ matrices. Let $\mathcal{M} \subset M_n$ be the manifold of all such positive-definite matrices. Let $\mathcal{D} \subset \mathcal{M}$, $\mathcal{D} = \{\rho \in \mathcal{M} : \mathrm{Tr}\rho = 1\}$, be the submanifold of all *density matrices*. It is the space of faithful states of an n-level quantum system; cf. **distances between quantum states** in Chap. 24.

  The tangent space of $\mathcal{M}$ at $\rho \in \mathcal{M}$ is $T_\rho(\mathcal{M}) = \{x \in M_n : x = x^*\}$, i.e., the set of all $n \times n$ *Hermitian matrices*. The tangent space $T_\rho(\mathcal{D})$ at $\rho \in \mathcal{D}$ is the subspace of *traceless* (i.e., with trace 0) matrices in $T_\rho(\mathcal{M})$.

  A Riemannian metric λ on $\mathcal{M}$ is called **monotone metric** if the inequality

$$\lambda_{h(\rho)}(h(u), h(u)) \le \lambda_\rho(u, u)$$

holds for any $\rho \in \mathcal{M}$, any $u \in T_\rho(\mathcal{M})$, and any *stochastic*, i.e., completely positive trace preserving mapping h.

It was proved in [Petz96] that λ is monotone if and only if it can be written as

$$\lambda_\rho(u, v) = \mathrm{Tr}\, uJ_\rho(v),$$

where J_ρ is an operator of the form $J_\rho = \frac{1}{f(L_\rho/R_\rho)R_\rho}$. Here L_ρ and R_ρ are the left and the right multiplication operators, and $f : (0, \infty) \to \mathbb{R}$ is an operator monotone function which is *symmetric*, i.e., $f(t) = tf(t^{-1})$, and *normalized*, i.e., $f(1) = 1$. Then $J_\rho(v) = \rho^{-1}v$ if v and ρ are commute, i.e., any monotone metric is equal to the **Fisher information metric** on commutative submanifolds.

The **Bures metric** (or *Helstrom metric*) is the smallest monotone metric, $\frac{1}{2}\mathrm{Tr}(d\rho g)$, obtained for $f(t) = \frac{1+t}{2}$. In this case $J_\rho(v) = g$, $\rho g + g\rho = 2v$.

For any $\rho_1, \rho_2 \in \mathcal{M}$ the **geodesic distance** defined by the Bures metric, (cf. **Bures distance** in Chap. 24) can be written as

$$\sqrt{\mathrm{Tr}(\rho_1) + \mathrm{Tr}(\rho_2) - 2\mathrm{Tr}(\sqrt{\sqrt{\rho_1}\rho_2\sqrt{\rho_1}})}.$$

On the submanifold $\mathcal{D} = \{\rho \in \mathcal{M} : \mathrm{Tr}\rho = 1\}$ of density matrices it has the form

$$\arccos \mathrm{Tr}(\sqrt{\sqrt{\rho_1}\rho_2\sqrt{\rho_1}}).$$

The **right logarithmic derivative metric** (or *RLD-metric*) is the greatest monotone metric, corresponding to $f(t) = \frac{2t}{1+t}$, i.e., $J_\rho(v) = \frac{1}{2}(\rho^{-1}v + v\rho^{-1})$.

The **Bogolubov–Kubo–Mori metric** (or *BKM-metric*) is obtained for $f(x) = \frac{x-1}{\ln x}$. It can be written as $\lambda_\rho(u,v) = \frac{\partial^2}{\partial s \partial t}\mathrm{Tr}(\rho + su)\ln(\rho + tv)|_{s,t=0}$.

- **Wigner–Yanase–Dyson metrics**

  The **Wigner–Yanase–Dyson metrics** (or *WYD-metrics*) form a family of metrics on the manifold $\mathcal{M}$ of all complex positive-definite $n \times n$ matrices defined by

$$\lambda_\rho^\alpha(u,v) = \frac{\partial^2}{\partial t \partial s}\mathrm{Tr} f_\alpha(\rho + tu) f_{-\alpha}(\rho + sv)|_{s,t=0},$$

  where $f_\alpha(x) = \frac{2}{1-\alpha}x^{\frac{1-\alpha}{2}}$, if $\alpha \neq 1$, and is $\ln x$, if $\alpha = 1$. These metrics are monotone for $\alpha \in [-3,3]$. For $\alpha = \pm 1$ one obtains the **Bogolubov–Kubo–Mori metric**; for $\alpha = \pm 3$ one obtains the **right logarithmic derivative metric**.

  The **Wigner–Yanase metric** (or *WY-metric*) is λ_ρ^0, the smallest metric in the family. It can be written as $\lambda_\rho(u,v) = 4\mathrm{Tr}\, u(\sqrt{L_\rho} + \sqrt{R_\rho})^2(v)$.

- **Connes metric**

  Roughly, the **Connes metric** is a generalization (from the space of all probability measures of a set X, to the *state space* of any *unital* C^**-algebra*) of the **transportation distance** (Chap. 14) defined via *Lipschitz seminorm*.

  Let M^n be a smooth n-dimensional manifold. Let $A = C^\infty(M^n)$ be the (commutative) algebra of smooth complex-valued functions on M^n, represented as multiplication operators on the Hilbert space $H = L^2(M^n, S)$ of square integrable sections of the spinor bundle on M^n by $(f\xi)(p) = f(p)\xi(p)$ for all $f \in A$ and for all $\xi \in H$.

  Let D be the *Dirac operator*. Let the commutator $[D,f]$ for $f \in A$ be the *Clifford multiplication* by the gradient ∇f, so that its operator norm $||.||$ in H is given by $||[D,f]|| = \sup_{p \in M^n} ||\nabla f||$.

  The **Connes metric** is the **intrinsic metric** on M^n, defined by

$$\sup_{f \in A, ||[D,f]|| \leq 1} |f(p) - f(q)|.$$

  This definition can also be applied to discrete spaces, and even generalized to C^**-algebras*; cf. **Rieffel metric space**. In particular, for a labeled connected *locally finite* graph $G = (V,E)$ with the vertex-set $V = \{v_1, \ldots, v_n, \ldots\}$, the Connes metric on V is defined, for any $v_i, v_j \in V$, by $\sup_{||[D,f]||=||df|| \leq 1} |f_{v_i} - f_{v_j}|$, where $\{f = \sum f_{v_i} v_i : \sum |f_{v_i}|^2 < \infty\}$ is the set of formal sums f, forming a Hilbert space, and $||[D,f]||$ is $\sup_i (\sum_{k=1}^{deg(v_i)} (f_{v_k} - f_{v_i})^2)^{\frac{1}{2}}$.

- **Rieffel metric space**

  Let V be a *normed space* (or, more generally, a **locally convex topological vector space**, cf. Chap. 2), and let V' be its **continuous dual space**, i.e., the set of all continuous linear functionals f on V. The *weak-* topology* on V' is defined as the weakest (i.e., with the fewest open sets) topology on V' such that, for every

$x \in V$, the map $F_x : V' \to \mathbb{R}$ defined by $F_x(f) = f(x)$ for all $f \in V'$, remains continuous.

An *order-unit space* is a *partially ordered* real (complex) vector space $(A, \preceq)$ with a special distinguished element e (*order unit*) satisfying the following properties:

1. For any $a \in A$, there exists $r \in \mathbb{R}$ with $a \preceq re$;
2. If $a \in A$ and $a \preceq re$ for all positive $r \in \mathbb{R}$, then $a \preceq 0$ (*Archimedean property*).

The main example of an order-unit space is the vector space of all self-adjoint elements in a *unital* C^**-algebra* with the identity element being the order unit. Here a C^**-algebra* is a *Banach algebra* over $\mathbb{C}$ equipped with a special *involution*. It is called *unital* if it has a *unit* (multiplicative identity element); such C^*-algebras are also called, roughly, *compact noncommutative topological spaces*.

Main example of a unital C^*-algebra is the complex algebra of linear operators on a complex **Hilbert space** which is topologically closed in the norm topology of operators, and is closed under the operation of taking adjoints of operators.

The *state space* of an order-unit space $(A, \preceq, e)$ is the set $S(A) = \{f \in A'_+ : ||f|| = 1\}$ of *states*, i.e., continuous linear functionals f with $||f|| = f(e) = 1$.

A **Rieffel** (or *compact quantum* as in Rieffel, 1999) **metric space** is a pair $(A, ||.||_{Lip})$, where $(A, \preceq, e)$ is an order-unit space, and $||.||_{Lip}$ is a $[0, +\infty]$-valued seminorm on A (generalizing the *Lipschitz seminorm*) for which it holds:

1. For $a \in A$, $||a||_{Lip} = 0$ holds if and only if $a \in \mathbb{R}e$;
2. the metric $d_{Lip}(f, g) = \sup_{a \in A : ||a||_{Lip} \leq 1} |f(a) - g(a)|$ generates on the state space $S(A)$ its weak-* topology.

So, $(S(A), d_{Lip})$ is a usual metric space. If the order-unit space $(A, \preceq, e)$ is a C^*-algebra, then d_{Lip} is the **Connes metric**, and if, moreover, the C^*-algebra is noncommutative, $(S(A), d_{Lip})$ is called a **noncommutative metric space**.

The term *quantum* is due to the belief that the Planck-scale geometry of *space-time* comes from such C^*-algebras; cf. **quantum space-time** in Chap. 24.

Kuperberg and Weaver, 2010, proposed a new definition of *quantum metric space*, in the setting of *von Neumann algebras*.

7.3 Hermitian Metrics and Generalizations

A *vector bundle* is a geometrical construct where to every point of a *topological space* M we attach a vector space so that all those vector spaces "glued together" form another topological space E. A continuous mapping $\pi : E \to M$ is called a *projection* E on M. For every $p \in M$, the vector space $\pi^{-1}(p)$ is called a *fiber* of the vector bundle.

A *real* (*complex*) *vector bundle* is a vector bundle $\pi : E \to M$ whose fibers $\pi^{-1}(p)$, $p \in M$, are real (complex) vector spaces.

In a real vector bundle, for every $p \in M$, the fiber $\pi^{-1}(p)$ locally looks like the vector space $\mathbb{R}^n$, i.e., there is an *open neighborhood* U of p, a natural number n, and a homeomorphism $\varphi : U \times \mathbb{R}^n \to \pi^{-1}(U)$ such that, for all $x \in U$ and $v \in \mathbb{R}^n$, one has $\pi(\varphi(x, v)) = v$, and the mapping $v \to \varphi(x, v)$ yields an isomorphism between $\mathbb{R}^n$ and $\pi^{-1}(x)$. The set U, together with φ, is called a *local trivialization* of the bundle.

If there exists a "global trivialization", then a real vector bundle $\pi : M \times \mathbb{R}^n \to M$ is called *trivial*. Similarly, in a complex vector bundle, for every $p \in M$, the fiber $\pi^{-1}(p)$ locally looks like the vector space $\mathbb{C}^n$. The basic example of such bundle is the trivial bundle $\pi : U \times \mathbb{C}^n \to U$, where U is an open subset of $\mathbb{R}^k$.

Important special cases of a real vector bundle are the *tangent bundle* $T(M^n)$ and the *cotangent bundle* $T^*(M^n)$ of a *real n-dimensional manifold* $M^n_{\mathbb{R}} = M^n$. Important special cases of a complex vector bundle are the tangent bundle and the cotangent bundle of a *complex n-dimensional manifold*.

Namely, a *complex n-dimensional manifold* $M^n_{\mathbb{C}}$ is a *topological space* in which every point has an open neighborhood homeomorphic to an open set of the n-dimensional complex vector space $\mathbb{C}^n$, and there is an atlas of charts such that the change of coordinates between charts is analytic. The (complex) tangent bundle $T_{\mathbb{C}}(M^n_{\mathbb{C}})$ of a complex manifold $M^n_{\mathbb{C}}$ is a vector bundle of all (complex) *tangent spaces* of $M^n_{\mathbb{C}}$ at every point $p \in M^n_{\mathbb{C}}$. It can be obtained as a *complexification* $T_{\mathbb{R}}(M^n_{\mathbb{R}}) \otimes \mathbb{C} = T(M^n) \otimes \mathbb{C}$ of the corresponding real tangent bundle, and is called the *complexified tangent bundle* of $M^n_{\mathbb{C}}$.

The *complexified cotangent bundle* of $M^n_{\mathbb{C}}$ is obtained similarly as $T^*(M^n) \otimes \mathbb{C}$. Any complex n-dimensional manifold $M^n_{\mathbb{C}} = M^n$ can be regarded as a real $2n$-dimensional manifold equipped with a *complex structure* on each tangent space.

A *complex structure* on a real vector space V is the structure of a complex vector space on V that is compatible with the original real structure. It is completely determined by the operator of multiplication by the number i, the role of which can be taken by an arbitrary linear transformation $J : V \to V$, $J^2 = -id$, where id is the *identity mapping*.

A *connection* (or *covariant derivative*) is a way of specifying a derivative of a *vector field* along another vector field in a vector bundle. A **metric connection** is a linear connection in a vector bundle $\pi : E \to M$, equipped with a bilinear form in the fibers, for which parallel displacement along an arbitrary piecewise-smooth curve in M preserves the form, that is, the *scalar product* of two vectors remains constant under parallel displacement.

In the case of a nondegenerate symmetric bilinear form, the metric connection is called the *Euclidean connection*. In the case of nondegenerate antisymmetric bilinear form, the metric connection is called the *symplectic connection*.

- **Bundle metric**

  A **bundle metric** is a metric on a vector bundle.
- **Hermitian metric**

  A **Hermitian metric** on a complex vector bundle $\pi : E \to M$ is a collection of *Hermitian inner products* (i.e., positive-definite symmetric sesquilinear forms)

on every fiber $E_p = \pi^{-1}(p)$, $p \in M$, that varies smoothly with the point p in M. Any complex vector bundle has a Hermitian metric.

The basic example of a vector bundle is the trivial bundle $\pi : U \times \mathbb{C}^n \to U$, where U is an open set in $\mathbb{R}^k$. In this case a Hermitian inner product on $\mathbb{C}^n$, and hence, a Hermitian metric on the bundle $\pi : U \times \mathbb{C}^n \to U$, is defined by

$$\langle u, v \rangle = u^T H \overline{v},$$

where H is a *positive-definite Hermitian matrix*, i.e., a complex $n \times n$ matrix such that $H^* = \overline{H}^T = H$, and $\overline{v}^T H v > 0$ for all $v \in \mathbb{C}^n \backslash \{0\}$. In the simplest case, one has $\langle u, v \rangle = \sum_{i=1}^n u_i \overline{v}_i$.

An important special case is a Hermitian metric h on a complex manifold M^n, i.e., on the complexified tangent bundle $T(M^n) \otimes \mathbb{C}$ of M^n. This is the Hermitian analog of a Riemannian metric. In this case $h = g + iw$, and its real part g is a Riemannian metric, while its imaginary part w is a nondegenerate antisymmetric bilinear form, called a *fundamental form*. Here $g(J(x), J(y)) = g(x, y)$, $w(J(x), J(y)) = w(x, y)$, and $w(x, y) = g(x, J(y))$, where the operator J is an operator of complex structure on M^n; as a rule, $J(x) = ix$. Any of the forms g, w determines h uniquely.

The term *Hermitian metric* can also refer to the corresponding Riemannian metric g, which gives M^n a Hermitian structure.

On a complex manifold, a Hermitian metric h can be expressed in local coordinates by a *Hermitian symmetric tensor* $((h_{ij}))$:

$$h = \sum_{i,j} h_{ij} dz_i \otimes d\overline{z}_j,$$

where $((h_{ij}))$ is a positive-definite Hermitian matrix. The associated fundamental form w is then written as $w = \frac{i}{2} \sum_{i,j} h_{ij} dz_i \wedge d\overline{z}_j$. A *Hermitian manifold* (or *Hermitian space*) is a complex manifold equipped with a Hermitian metric.

- **Kähler metric**

A **Kähler metric** (or *Kählerian metric*) is a Hermitian metric $h = g + iw$ on a complex manifold M^n whose fundamental form w is *closed*, i.e., $dw = 0$ holds. A *Kähler manifold* is a complex manifold equipped with a Kähler metric.

If h is expressed in local coordinates, i.e., $h = \sum_{i,j} h_{ij} dz_i \otimes d\overline{z}_j$, then the associated fundamental form w can be written as $w = \frac{i}{2} \sum_{i,j} h_{ij} dz_i \wedge d\overline{z}_j$, where $\wedge$ is the *wedge product* which is antisymmetric, i.e., $dx \wedge dy = -dy \wedge dx$ (hence, $dx \wedge dx = 0$).

In fact, w is a *differential 2-form* on M^n, i.e., a tensor of rank 2 that is antisymmetric under exchange of any pair of indices: $w = \sum_{i,j} f_{ij} dx^i \wedge dx^j$, where f_{ij} is a function on M^n. The *exterior derivative* dw of w is defined by $dw = \sum_{i,j} \sum_k \frac{\partial f_{ij}}{\partial x_k} dx_k \wedge dx_i \wedge dx_k$. If $dw = 0$, then w is a *symplectic* (i.e., closed nondegenerate) differential 2-form. Such differential 2-forms are called *Kähler forms*.

The metric on a Kähler manifold locally satisfies $h_{ij} = \frac{\partial^2 K}{\partial z_i \partial \bar{z}_j}$. for some function K, called the *Kähler potential*. The term *Kähler metric* can also refer to the corresponding Riemannian metric g, which gives M^n a Kähler structure. Then a Kähler manifold is defined as a complex manifold which carries a Riemannian metric and a Kähler form on the underlying real manifold.

- **Hessian metric**

  Given a smooth f on an open subset of a real vector space, the associated **Hessian metric** is defined by

$$g_{ij} = \frac{\partial^2 f}{\partial x_i \partial x_j}.$$

  A Hessian metric is also called an **affine Kähler metric** since a Kähler metric on a complex manifold has an analogous description as $\frac{\partial^2 f}{\partial z_i \partial \bar{z}_j}$.

- **Calabi–Yau metric**

  The **Calabi–Yau metric** is a **Kähler metric** which is **Ricci-flat**.

  A *Calabi–Yau manifold* (or *Calabi–Yau space*) is a simply connected complex manifold equipped with a Calabi–Yau metric. It can be considered as a $2n$-dimensional (6D being particularly interesting) smooth manifold with holonomy group (i.e., the set of linear transformations of tangent vectors arising from parallel transport along closed loops) in the special unitary group.

- **Kähler–Einstein metric**

  A **Kähler–Einstein metric** is a **Kähler metric** on a complex manifold M^n whose *Ricci curvature tensor* is proportional to the metric tensor. This proportionality is an analog of the *Einstein field equation* in the General Theory of Relativity.

  A *Kähler–Einstein manifold* (or *Einstein manifold*) is a complex manifold equipped with a Kähler–Einstein metric. In this case the Ricci curvature tensor, seen as an operator on the tangent space, is just multiplication by a constant.

  Such a metric exists on any *domain* $D \subset \mathbb{C}^n$ that is bounded and *pseudo-convex*. It can be given by the *line element*

$$ds^2 = \sum_{i,j} \frac{\partial^2 u(z)}{\partial z_i \partial \bar{z}_j} dz_i d\bar{z}_j,$$

  where u is a solution to the *boundary value problem*: $det(\frac{\partial^2 u}{\partial z_i \partial \bar{z}_j}) = e^{2u}$ on D, and $u = \infty$ on ∂D. The Kähler–Einstein metric is a complete metric. On the *unit disk* $\Delta = \{z \in \mathbb{C} : |z| < 1\}$ it is coincides with the **Poincaré metric**.

  Let h be the Einstein metric on a smooth compact manifold M^{n-1} without boundary, having scalar curvature $(n-1)(n-2)$. A **generalized Delaunay metric** on $\mathbb{R} \times M^{n-1}$ is (Delay, 2010) of the form $g = u^{\frac{4}{n-2}}(dy^2 + h)$, where $u = u(y) > 0$ is a periodic solution of $u'' - \frac{(n-2)^2}{4} u + \frac{n(n-2)}{4} u^{\frac{n+2}{n-2}} = 0$.

There is one parameter family of constant positive curvature conformal metrics on $\mathbb{R} \times \mathbb{S}^{n-1}$, referred to as **Delaunay metric**; cf. **Kottler metric** in Chap. 26.

- **Hodge metric**

  The **Hodge metric** is a **Kähler metric** whose *fundamental form w* defines an integral cohomology class or, equivalently, has integral periods.

  A *Hodge manifold* (or *Hodge variety*) is a complex manifold equipped with a Hodge metric. A compact complex manifold is a Hodge manifold if and only if it is isomorphic to a smooth algebraic subvariety of some complex projective space.

- **Fubini–Study metric**

  The **Fubini–Study metric** (or *Cayley–Fubini–Study metric*) is a **Kähler metric** on a *complex projective space* $\mathbb{C}P^n$ defined by a *Hermitian inner product* $\langle , \rangle$ in $\mathbb{C}^{n+1}$. It is given by the *line element*

$$ds^2 = \frac{\langle x, x\rangle \langle dx, dx\rangle - \langle x, d\overline{x}\rangle \langle \overline{x}, dx\rangle}{\langle x, x\rangle^2}.$$

  The **Fubini–Study distance** between points $(x_1 : \ldots : x_{n+1})$ and $(y_1 : \ldots : y_{n+1}) \in \mathbb{C}P^n$, where $x = (x_1, \ldots, x_{n+1})$ and $y = (y_1, \ldots, y_{n+1}) \in \mathbb{C}^{n+1} \setminus \{0\}$, is equal to

$$\arccos \frac{|\langle x, y\rangle|}{\sqrt{\langle x, x\rangle \langle y, y\rangle}}.$$

  The Fubini–Study metric is a **Hodge metric**. The space $\mathbb{C}P^n$ endowed with this metric is called a *Hermitian elliptic space* (cf. **Hermitian elliptic metric**).

- **Bergman metric**

  The **Bergman metric** is a **Kähler metric** on a bounded *domain* $D \subset \mathbb{C}^n$ defined, for the *Bergman kernel* $K(z, u)$, by the *line element*

$$ds^2 = \sum_{i,j} \frac{\partial^2 \ln K(z, z)}{\partial z_i \partial \overline{z}_j} dz_i d\overline{z}_j.$$

  It is a **biholomorhically invariant metric** on D, and it is complete if D is homogeneous. For the *unit disk* $\Delta = \{z \in \mathbb{C} : |z| < 1\}$ the Bergman metric coincides with the **Poincaré metric**; cf. also **Bergman** p**-metric** in Chap. 13.

  The set of all analytic functions $f \neq 0$ of class $L_2(D)$ with respect to the Lebesgue measure, forms the **Hilbert space** $L_{2,a}(D) \subset L_2(D)$ with an orthonormal basis $(\phi_i)_i$. The *Bergman kernel* is a function in the domain $D \times D \subset \mathbb{C}^{2n}$, defined by $K_D(z, u) = K(z, u) = \sum_{i=1}^{\infty} \phi_i(z)\overline{\phi_i(u)}$.

The **Skwarczynski distance** is defined by

$$(1-\frac{|K(z,u)|}{\sqrt{K(z,z)}\sqrt{K(u,u)}})^{\frac{1}{2}}$$

.

- **Hyper-Kähler metric**

  A **hyper-Kähler metric** is a Riemannian metric g on a $4n$-dimensional *Riemannian manifold* which is compatible with a quaternionic structure on the tangent bundle of the manifold.

  Thus, the metric g is Kählerian with respect to 3 Kähler structures (I, w_I, g), (J, w_J, g), and (K, w_K, g), corresponding to the complex structures, as endomorphisms of the tangent bundle, which satisfy the quaternionic relationship

$$I^2 = J^2 = K^2 = IJK = -JIK = -1.$$

  A *hyper-Kähler manifold* is a Riemannian manifold equipped with a hyper-Kähler metric. manifolds are Ricci-flat. Compact 4D hyper-Kähler manifolds are called K_3*-surfaces*; they are studied in Algebraic Geometry.

- **Calabi metric**

  The **Calabi metric** is a **hyper-Kähler metric** on the cotangent bundle $T^*(\mathbb{C}P^{n+1})$ of a *complex projective space* $\mathbb{C}P^{n+1}$.

  For $n = 4k + 4$, this metric can be given by the *line element*

$$ds^2 = \frac{dr^2}{1-r^{-4}} + \frac{1}{4}r^2(1-r^{-4})\lambda^2 + r^2(\nu_1^2+\nu_2^2) + \frac{1}{2}(r^2-1)(\sigma_{1\alpha}^2+\sigma_{2\alpha}^2) + \frac{1}{2}(r^2+1)(\Sigma_{1\alpha}^2+\Sigma_{2\alpha}^2),$$

  where $(\lambda, \nu_1, \nu_2, \sigma_{1\alpha}, \sigma_{2\alpha}, \Sigma_{1\alpha}, \Sigma_{2\alpha})$, with α running over k values, are left-invariant *one-forms* (i.e., linear real-valued functions) on the coset $SU(k + 2)/U(k)$. Here $U(k)$ is the *unitary group* consisting of complex $k \times k$ *unitary matrices*, and $SU(k)$ is the *special unitary group* of complex $k \times k$ unitary matrices with determinant 1.

  For $k = 0$, the Calabi metric coincides with the **Eguchi–Hanson metric**.

- **Stenzel metric**

  The **Stenzel metric** is a **hyper-Kähler metric** on the cotangent bundle $T^*(S^{n+1})$ of a sphere S^{n+1}.

- $SO(3)$**-invariant metric**

  An $SO(3)$**-invariant metric** is a 4D 4-dimensional hyper-Kähler metric with the *line element* given, in the Bianchi type *IX* formalism (cf. **Bianchi metrics** in Chap. 26) by

$$ds^2 = f^2(t)dt^2 + a^2(t)\sigma_1^2 + b^2(t)\sigma_2^2 + c^2(t)\sigma_3^2,$$

  where the invariant *one-forms* $\sigma_1, \sigma_2, \sigma_3$ of $SO(3)$ are expressed in terms of *Euler angles* θ, ψ, ϕ as $\sigma_1 = \frac{1}{2}(\sin\psi d\theta - \sin\theta\cos\psi d\phi)$, $\sigma_2 = -\frac{1}{2}(\cos\psi d\theta +$

$\sin\theta \sin\psi d\phi)$, $\sigma_3 = \frac{1}{2}(d\psi + \cos\theta d\phi)$, and the normalization has been chosen so that $\sigma_i \wedge \sigma_j = \frac{1}{2}\epsilon_{ijk} d\sigma_k$. The coordinate t of the metric can always be chosen so that $f(t) = \frac{1}{2}abc$, using a suitable reparametrization.

- **Atiyah–Hitchin metric**

  The **Atiyah–Hitchin metric** is a **complete regular** $SO(3)$**-invariant metric** with the *line element*

$$ds^2 = \frac{1}{4}a^2b^2c^2\left(\frac{dk}{k(1-k^2)K^2}\right)^2 + a^2(k)\sigma_1^2 + b^2(k)\sigma_2^2 + c^2(k)\sigma_3^2,$$

  where a, b, c are functions of k, $ab = -K(k)(E(k) - K(k))$, $bc = -K(k)(E(k) - (1 - k^2)K(k))$, $ac = -K(k)E(k)$, and $K(k)$, $E(k)$ are the complete elliptic integrals, respectively, of the first and second kind, with $0 < k < 1$. The coordinate t is given by the change of variables $t = -\frac{2K(1-k^2)}{\pi K(k)}$ up to an additive constant.

- **Taub–NUT metric**

  The **Taub–NUT metric** (cf. also Chap. 26) is a **complete regular** $SO(3)$**-invariant metric** with the *line element*

$$ds^2 = \frac{1}{4}\frac{r+m}{r-m}dr^2 + (r^2 - m^2)(\sigma_1^2 + \sigma_2^2) + 4m^2\frac{r-m}{r+m}\sigma_3^2,$$

  where m is the relevant moduli parameter, and the coordinate r is related to t by $r = m + \frac{1}{2mt}$. NUT manifold was discovered in Ehlers, 1957, and rediscovered in Newman–Tamburino–Unti, 1963; it is closely related to the metric in Taub, 1951.

- **Eguchi–Hanson metric**

  The **Eguchi–Hanson metric** is a **complete regular** $SO(3)$**-invariant metric** with the *line element*

$$ds^2 = \frac{dr^2}{1 - \left(\frac{a}{r}\right)^4} + r^2\left(\sigma_1^2 + \sigma_2^2 + \left(1 - \left(\frac{a}{r}\right)^4\right)\sigma_3^2\right),$$

  where a is the moduli parameter, and the coordinate r is $a\sqrt{\coth(a^2t)}$.

  The Eguchi–Hanson metric coincides with the 4D **Calabi metric**.

- **Complex Finsler metric**

  A **complex Finsler metric** is an upper semicontinuous function $F : T(M^n) \to \mathbb{R}_+$ on a complex manifold M^n with the analytic tangent bundle $T(M^n)$ satisfying the following conditions:

  1. F^2 is smooth on $\check{M}^n$, where $\check{M}^n$ is the complement in $T(M^n)$ of the zero section;
  2. $F(p, x) > 0$ for all $p \in M^n$ and $x \in \check{M}^n_p$;
  3. $F(p, \lambda x) = |\lambda| F(p, x)$ for all $p \in M^n$, $x \in T_p(M^n)$, and $\lambda \in \mathbb{C}$.

The function $G = F^2$ can be locally expressed in terms of the coordinates $(p_1, \ldots, p_n, x_1, \ldots, x_n)$; the *Finsler metric tensor* of the complex Finsler metric is given by the matrix$((G_{ij})) = ((\frac{1}{2}\frac{\partial^2 F^2}{\partial x_i \partial \overline{x}_j}))$, called the *Levi matrix*. If the matrix $((G_{ij}))$ is positive-definite, the complex Finsler metric F is called *strongly pseudo-convex*.

- **Distance-decreasing semimetric**

  Let d be a semimetric which can be defined on some class $\mathcal{M}$ of complex manifolds containing the *unit disk* $\Delta = \{z \in \mathbb{C} : |z| < 1\}$. It is called **distance-decreasing** if, for any analytic mapping $f : M_1 \to M_2$ with $M_1, M_2 \in \mathcal{M}$, the inequality $d(f(p), f(q)) \leq d(p, q)$ holds for all $p, q \in M_1$.

  The **Carathéodory semimetric** F_C, **Sibony semimetric** F_S, **Azukawa semimetric** F_A and **Kobayashi semimetric** F_K are distance-decreasing with F_C and F_K being the smallest and the greatest distance-decreasing semimetrics. They are generalizations of the **Poincaré metric** to higher-dimensional domains, since $F_C = F_K$ is the **Poincaré metric** on the unit disk Δ, and $F_C = F_K \equiv 0$ on $\mathbb{C}^n$.

  It holds $F_C(z, u) \leq F_S(z, u) \leq F_A(z, u) \leq F_K(z, u)$ for all $z \in D$ and $u \in \mathbb{C}^n$. If D is convex, then all these metrics coincide.

- **Biholomorphically invariant semimetric**

  A *biholomorphism* is a bijective *holomorphic* (complex differentiable in a neighborhood of every point in its domain) function whose inverse is also holomorphic.

  A semimetric $F(z, u) : D \times \mathbb{C}^n \to [0, \infty]$ on a domain D in $\mathbb{C}^n$ is called **biholomorphically invariant** if $F(z, u) = |\lambda| F(z, u)$ for all $\lambda \in \mathbb{C}$, and $F(z, u) = F(f(z), f'(z)u)$ for any biholomorphism $f : D \to D'$.

  Invariant metrics, including the **Carathéodory**, **Kobayashi**, **Sibony**, **Azukawa**, **Bergman**, and **Kähler–Einstein** metrics, play an important role in Complex Function Theory, Complex Dynamics and Convex Geometry. The first four metrics are used mostly because they are **distance-decreasing**. But they are almost never Hermitian. On the other hand, the Bergman metric and the Kähler–Einstein metric are Hermitian (in fact, Kählerian), but, in general, not distance-decreasing.

  The **Wu metric** (Cheung and Kim, 1996) is an invariant non-Kähler Hermitian metric on a complex manifold M^n which factor, for any holomorphic mapping between two complex manifolds.

- **Kobayashi metric**

  Let D be a *domain* in $\mathbb{C}^n$. Let $\mathcal{O}(\Delta, D)$ be the set of all analytic mappings $f : \Delta \to D$, where $\Delta = \{z \in \mathbb{C} : |z| < 1\}$ is the *unit disk*.

  The **Kobayashi metric** (or **Kobayashi–Royden metric**) F_K is a **complex Finsler metric** defined, for all $z \in D$ and $u \in \mathbb{C}^n$, by

$$F_K(z, u) = \inf\{\alpha > 0 : \exists f \in \mathcal{O}(\Delta, D), f(0) = z, \alpha f'(0) = u\}.$$

Given a complex manifold M^n, the **Kobayashi semimetric** F_K is defined by

$$F_K(p,u) = \inf\{\alpha > 0 : \exists f \in \mathcal{O}(\Delta, M^n), f(0) = p, \alpha f^{'}(0) = u\}$$

for all $p \in M^n$ and $u \in T_p(M^n)$.

$F_K(p,u)$ is a seminorm of the tangent vector u, called the *Kobayashi seminorm*. F_K is a metric if M^n is *taut*, i.e., $\mathcal{O}(\Delta, M^n)$ is a *normal family* (every sequence has a subsequence which either converge or diverge compactly).

The Kobayashi semimetric is an infinitesimal form of the **Kobayashi semidistance** (or *Kobayashi pseudo-distance*, 1967) K_{M^n} on M^n, defined as follows. Given $p, q \in M^n$, a *chain of disks* α from p to q is a collection of points $p = p^0, p^1, \ldots, p^k = q$ of M^n, pairs of points $a^1, b^1; \ldots; a^k, b^k$ of the unit disk Δ, and analytic mappings $f_1, \ldots f_k$ from Δ into M^n, such that $f_j(a^j) = p^{j-1}$ and $f_j(b^j) = p^j$ for all j.

The length $l(\alpha)$ of a chain α is the sum $d_P(a^1, b^1) + \cdots + d_P(a^k, b^k)$, where d_P is the Poincaré metric. The Kobayashi semimetric K_{M^n} on M^n is defined by

$$K_{M^n}(p,q) = \inf_{\alpha} l(\alpha),$$

where the infimum is taken over all lengths $l(\alpha)$ of chains of disks α from p to q.

Given a complex manifold M^n, the **Kobayashi–Busemann semimetric** on M^n is the double dual of the **Kobayashi semimetric**. It is a metric if M^n is taut.

- **Carathéodory metric**

Let D be a *domain* in $\mathbb{C}^n$. Let $\mathcal{O}(D, \Delta)$ be the set of all analytic mappings $f : D \to \Delta$, where $\Delta = \{z \in \mathbb{C} : |z| < 1\}$ is the *unit disk*.

The **Carathéodory metric** F_C is a **complex Finsler metric** defined by

$$F_C(z,u) = \sup\{|f^{'}(z)u| : f \in \mathcal{O}(D, \Delta)\}$$

for any $z \in D$ and $u \in \mathbb{C}^n$.

Given a complex manifold M^n, the **Carathéodory semimetric** F_C is defined by

$$F_C(p,u) = \sup\{|f^{'}(p)u| : f \in \mathcal{O}(M^n, \Delta)\}$$

for all $p \in M^n$ and $u \in T_p(M^n)$. F_C is a metric if M^n is *taut*, i.e., every sequence in $\mathcal{O}(\Delta, M^n)$ has a subsequence which either converge or diverge compactly.

The **Carathéodory semidistance** (or *Carathéodory pseudo-distance*, 1926) C_{M^n} is a semimetric on a complex manifold M^n, defined by

$$C_{M^n}(p,q) = \sup\{d_P(f(p), f(q)) : f \in \mathcal{O}(M^n, \Delta)\},$$

where d_P is the Poincaré metric.

In general, the integrated semimetric of the infinitesimal Carathéodory semimetric is **internal** for the Carathéodory semidistance, but does not equal to it.

- **Azukawa semimetric**

  Let D be a *domain* in $\mathbb{C}^n$. Let $K_D(z)$ be the set of all *logarithmically plurisubharmonic* functions $f : D \to [0,1)$ such that there exist $M, r > 0$ with $f(u) \leq M||u-z||_2$ for all $u \in B(z,r) \subset D$; here $||.||_2$ is the l_2-*norm* on $\mathbb{C}^n$, and $B(z,r) = \{x \in \mathbb{C}^n : ||z-x||_2 < r\}$. Let $g_D(z,u)$ be $\sup\{f(u) : f \in K_D(z)\}$.

  The **Azukawa semimetric** F_A is a **complex Finsler metric** defined by

$$F_A(z,u) = \overline{\lim}_{\lambda \to 0} \frac{1}{|\lambda|} g_D(z, z+\lambda u)$$

  for all $z \in D$ and $u \in \mathbb{C}^n$.

  The Azukawa metric is an infinitesimal form of the **Azukawa semidistance**.

- **Sibony semimetric**

  Let D be a *domain* in $\mathbb{C}^n$. Let $K_D(z)$ be the set of all *logarithmically plurisubharmonic* functions $f : D \to [0,1)$ such that there exist $M, r > 0$ with $f(u) \leq M||u-z||_2$ for all $u \in B(z,r) = \{x \in \mathbb{C}^n : ||z-x||_2 < r\} \subset D$. Let $C^2_{loc}(z)$ be the set of all functions of class C^2 on some open neighborhood of z.

  The **Sibony semimetric** F_S is a **complex Finsler semimetric** defined by

$$F_S(z,u) = \sup_{f \in K_D(z) \cap C^2_{loc}(z)} \sqrt{\sum_{i,j} \frac{\partial^2 f}{\partial z_i \partial \overline{z}_j}(z) u_i \overline{u}_j}$$

  for all $z \in D$ and $u \in \mathbb{C}^n$.

  The Sibony semimetric is an infinitesimal form of the **Sibony semidistance**.

- **Teichmüller metric**

  A *Riemann surface* R is a one-dimensional complex manifold. Two Riemann surfaces R_1 and R_2 are called *conformally equivalent* if there exists a bijective analytic function (i.e., a conformal homeomorphism) from R_1 into R_2. More precisely, consider a fixed closed Riemann surface R_0 of a given *genus* $g \geq 2$.

  For a closed Riemann surface R of genus g, one can construct a pair (R,f), where $f : R_0 \to R$ is a homeomorphism. Two pairs (R,f) and (R_1,f_1) are called *conformally equivalent* if there exists a conformal homeomorphism $h : R \to R_1$ such that the mapping $(f_1)^{-1} \cdot h \cdot f : R_0 \to R_0$ is homotopic to the identity.

  An *abstract Riemann surface* $R^* = (R,f)^*$ is the equivalence class of all Riemann surfaces, conformally equivalent to R. The set of all equivalence classes is called the *Teichmüller space* $T(R_0)$ of the surface R_0.

  For closed surfaces R_0 of given genus g, the spaces $T(R_0)$ are isometrically isomorphic, and one can speak of the *Teichmüller space* T_g *of surfaces of genus* g. T_g is a complex manifold. If R_0 is obtained from a compact surface of genus $g \geq 2$ by removing n points, then the complex dimension of T_g is $3g-3+n$.

The **Teichmüller metric** is a metric on T_g defined by

$$\frac{1}{2}\inf_h \ln K(h)$$

for any $R_1^*, R_2^* \in T_g$, where $h : R_1 \to R_2$ is a quasi-conformal homeomorphism, homotopic to the identity, and $K(h)$ is the *maximal dilation* of h. In fact, there exists a unique extremal mapping, called the *Teichmüller mapping* which minimizes the maximal dilation of all such h, and the distance between R_1^* and R_2^* is equal to $\frac{1}{2}\ln K$, where the constant K is the dilation of the Teichmüller mapping.

In terms of the *extremal length* $ext_{R^*}(\gamma)$, the distance between R_1^* and R_2^* is

$$\frac{1}{2}\ln \sup_\gamma \frac{ext_{R_1^*}(\gamma)}{ext_{R_2^*}(\gamma)},$$

where the supremum is taken over all simple closed curves on R_0.

The Teichmüller space T_g, with the Teichmüller metric on it, is a **geodesic** metric space (moreover, a **straight** G**-space**) but it is neither **Gromov hyperbolic**, nor a **Busemann convex** metric space.

The **Thurston quasi-metric** on the *Teichmüller space* T_g is defined by

$$\frac{1}{2}\inf_h \ln ||h||_{Lip}$$

for any $R_1^*, R_2^* \in T_g$, where $h : R_1 \to R_2$ is a quasi-conformal homeomorphism, homotopic to the identity, and $||.||_{Lip}$ is the *Lipschitz norm* on the set of all injective functions $f : X \to Y$ defined by $||f||_{Lip} = \sup_{x,y\in X, x\neq y} \frac{d_Y(f(x),f(y))}{d_X(x,y)}$.

The *moduli space* R_g of conformal classes of Riemann surfaces of genus g is obtained by factorization of T_g by some countable group of automorphisms of it, called the *modular group*. The **Zamolodchikov metric**, defined (1986) in terms of *exactly marginal operators*, is a natural metric on the conformal moduli spaces.

Liu, Sun and Yau, 2005, showed that all known complete metrics on the Teichmüller space and moduli space (including **Teichmüller metric**, **Bergman metric**, *Cheng–Yau–Mok* **Kähler–Einstein metric**, **Carathéodory metric**, *McMullen metric*) are equivalent since they are **quasi-isometric** (Chap. 1) to the *Ricci metric* and the *perturbed Ricci metric* introduced by them.

- **Weil–Petersson metric**

  The **Weil–Petersson metric** is a **Kähler metric** on the Teichmüller space $T_{g,n}$ of abstract Riemann surfaces of genus g with n punctures and negative Euler characteristic. This metric has negative Ricci curvature; it is **geodesically convex** (Chap. 1) and not complete.

  The **Weil–Peterson metric** is **Gromov hyperbolic** if and only if (Brock and Farb, 2006) the complex dimension $3g - 3 + n$ of $T_{g,n}$ is at most two.

- **Gibbons–Manton metric**

  The **Gibbons–Manton metric** is a $4n$-dimensional **hyper-Kähler metric** on the moduli space of *n-monopoles* which admits an isometric action of the n-dimensional torus T^n. It is a hyper-Kähler quotient of a flat quaternionic vector space.

- **Metrics on determinant lines**

  Let M^n be an n-dimensional compact smooth manifold, and let F be a flat vector bundle over M^n. Let $H^\bullet(M^n, F) = \oplus_{i=0}^n H^i(M^n, F)$ be the *de Rham cohomology* of M^n with coefficients in F. Given an n-dimensional vector space V, the *determinant line det* V of V is defined as the top exterior power of V, i.e., $det\ V = \wedge^n V$. Given a finite-dimensional graded vector space $V = \oplus_{i=0}^n V_i$, the determinant line of V is defined as the tensor product $det\ V = \otimes_{i=0}^n (detV_i)^{(-1)^i}$.

  Thus, the determinant line $detH^\bullet(M^n, F)$ of the cogomology $H^\bullet(M^n, F)$ can be written as $detH^\bullet(M^n, F) = \otimes_{i=0}^n (detH^i(M^n, F))^{(-1)^i}$.

  The **Reidemeister metric** is a metric on $detH^\bullet(M^n, F)$, defined by a given smooth triangulation of M^n, and the classical *Reidemeister–Franz torsion*.

  Let g^F and $g^{T(M^n)}$ be smooth metrics on the vector bundle F and tangent bundle $T(M^n)$, respectively. These metrics induce a canonical L_2**-metric** $h^{H^\bullet(M^n,F)}$ on $H^\bullet(M^n, F)$. The **Ray–Singler metric** on $detH^\bullet(M^n, F)$ is defined as the product of the metric induced on $detH^\bullet(M^n, F)$ by $h^{H^\bullet(M^n,F)}$ with the *Ray–Singler analytic torsion*. The **Milnor metric** on $detH^\bullet(M^n, F)$ can be defined in a similar manner using the *Milnor analytic torsion*. If g^F is flat, the above two metrics coincide with the Reidemeister metric. Using a co-Euler structure, one can define a *modified Ray–Singler metric* on $detH^\bullet(M^n, F)$.

  The **Poincaré–Reidemeister metric** is a metric on the cohomological determinant line $detH^\bullet(M^n, F)$ of a closed connected oriented odd-dimensional manifold M^n. It can be constructed using a combination of the Reidemeister torsion with the Poincaré duality. Equivalently, one can define the *Poincaré–Reidemeister scalar product* on $detH^\bullet(M^n, F)$ which completely determines the Poincaré–Reidemeister metric but contains an additional sign or phase information.

  The **Quillen metric** is a metric on the inverse of the cohomological determinant line of a compact Hermitian one-dimensional complex manifold. It can be defined as the product of the L_2-metric with the Ray-Singler analytic torsion.

- **Kähler supermetric**

  The **Kähler supermetric** is a generalization of the **Kähler metric** for the case of a *supermanifold*. A *supermanifold* is a generalization of the usual manifold with *fermonic* as well as *bosonic* coordinates. The bosonic coordinates are ordinary numbers, whereas the fermonic coordinates are *Grassmann numbers*.

  Here the term *supermetric* differs from the one used in this chapter.

- **Hofer metric**

  A *symplectic manifold* (M^n, w), $n = 2k$, is a smooth even-dimensional manifold M^n equipped with a *symplectic form*, i.e, a closed nondegenerate 2-form, w.

A *Lagrangian manifold* is a k-dimensional smooth submanifold L^k of a symplectic manifold (M^n, w), $n = 2k$, such that the form w vanishes identically on L^k, i.e., for any $p \in L^k$ and any $x, y \in T_p(L^k)$, one has $w(x, y) = 0$.

Let $L(M^n, \Delta)$ be the set of all Lagrangian submanifolds of a closed symplectic manifold (M^n, w), diffeomorphic to a given Lagrangian submanifold Δ. A smooth family $\alpha = \{L_t\}_t$, $t \in [0, 1]$, of Lagrangian submanifolds $L_t \in L(M^n, \Delta)$ is called an *exact* path connecting L_0 and L_1, if there exists a smooth mapping $\Psi : \Delta \times [0, 1] \to M^n$ such that, for every $t \in [0, 1]$, one has $\Psi(\Delta \times \{t\}) = L_t$, and $\Psi * w = dH_t \wedge dt$ for some smooth function $H : \Delta \times [0, 1] \to \mathbb{R}$. The *Hofer length* $l(\alpha)$ of an exact path α is defined by $l(\alpha) = \int_0^1 \{\max_{p\in\Delta} H(p, t) - \min_{p\in\Delta} H(p, t)\}dt$.

The **Hofer metric** on the set $L(M^n, \Delta)$ is defined by

$$\inf_{\alpha} l(\alpha)$$

for any $L_0, L_1 \in L(M^n, \Delta)$, where the infimum is taken over all exact paths on $L(M^n, \Delta)$, that connect L_0 and L_1.

The Hofer metric can be defined similarly on the group $Ham(M^n, w)$ of *Hamiltonian diffeomorphisms* of a closed symplectic manifold (M^n, w), whose elements are *time-one mappings* of *Hamiltonian flows* ϕ_t^H: it is $\inf_\alpha l(\alpha)$, where the infimum is taken over all smooth paths $\alpha = \{\phi_t^H\}$, $t \in [0, 1]$, connecting ϕ and ψ.

- **Sasakian metric**

  A **Sasakian metric** is a metric on a *contact manifold*, naturally adapted to the *contact structure*.

  A contact manifold equipped with a Sasakian metric is called a *Sasakian space*, and it is an odd-dimensional analog of a *Kähler manifold*. The scalar curvature of a Sasakian metric which is also **Einstein metric**, is positive.

- **Cartan metric**

  A *Killing form* (or *Cartan–Killing form*) on a finite-dimensional *Lie algebra* Ω over a field $\mathbb{F}$ is a symmetric bilinear form

$$B(x, y) = \mathrm{Tr}(ad_x \cdot ad_y),$$

  where Tr denotes the trace of a linear operator, and ad_x is the image of x under *the adjoint representation* of Ω, i.e., the linear operator on the vector space Ω defined by the rule $z \to [x, z]$, where $[,]$ is the Lie bracket.

  Let $e_1, \ldots e_n$ be a basis for the Lie algebra Ω, and $[e_i, e_j] = \sum_{k=1}^n \gamma_{ij}^k e_k$, where γ_{ij}^k are corresponding *structure constants*. Then the Killing form is given by

$$B(x_i, x_j) = g_{ij} = \sum_{k,l=1}^{n} \gamma_{il}^k \gamma_{ik}^l.$$

  In Theoretical Physics, the **metric tensor** $((g_{ij}))$ is called a **Cartan metric**.

Chapter 8
Distances on Surfaces and Knots

8.1 General Surface Metrics

A *surface* is a real 2D (two-dimensional) *manifold* M^2, i.e., a **Hausdorff space**, each point of which has a neighborhood which is homeomorphic to a plane $\mathbb{E}^2$, or a closed half-plane (cf. Chap. 7).

A compact orientable surface is called *closed* if it has no boundary, and it is called a *surface with boundary*, otherwise. There are compact nonorientable surfaces (closed or with boundary); the simplest such surface is the *Möbius strip*. Noncompact surfaces without boundary are called *open*.

Any closed connected surface is homeomorphic to either a sphere with, say, g (cylindric) handles, or a sphere with, say, g *cross-caps* (i.e., caps with a twist like Möbius strip in them). In both cases the number g is called the *genus* of the surface. In the case of handles, the surface is orientable; it is called a *torus* (doughnut), *double torus*, and *triple torus* for $g = 1, 2$ and 3, respectively. In the case of cross-caps, the surface is nonorientable; it is called the *real projective plane*, *Klein bottle*, and *Dyck's surface* for $g = 1, 2$ and 3, respectively. The genus is the maximal number of disjoint simple closed curves which can be cut from a surface without disconnecting it (the *Jordan curve theorem* for surfaces).

The *Euler–Poincaré characteristic* of a surface is (the same for all polyhedral decompositions of a given surface) the number $\chi = v - e + f$, where v, e and f are, respectively, the number of vertices, edges and faces of the decomposition. Then $\chi = 2 - 2g$ if the surface is orientable, and $\chi = 2 - g$ if not. Every surface with boundary is homeomorphic to a sphere with an appropriate number of (disjoint) *holes* (i.e., what remains if an open disk is removed) and handles or cross-caps. If h is the number of holes, then $\chi = 2 - 2g - h$ holds if the surface is orientable, and $\chi = 2 - g - h$ if not.

The *connectivity number* of a surface is the largest number of closed cuts that can be made on the surface without separating it into two or more parts. This number is equal to $3 - \chi$ for closed surfaces, and $2 - \chi$ for surfaces with boundaries. A surface

© Springer-Verlag Berlin Heidelberg 2016

M.M. Deza, E. Deza, *Encyclopedia of Distances*,
DOI 10.1007/978-3-662-52844-0_8

with connectivity number 1, 2 and 3 is called, respectively, *simply, doubly* and *triply connected*. A sphere is simply connected, while a torus is triply connected.

A surface can be considered as a metric space with its own **intrinsic metric**, or as a figure in space. A surface in $\mathbb{E}^3$ is called *complete* if it is a **complete** metric space with respect to its intrinsic metric.

Useful *shape-aware* (preserved by isomorphic deformations of the surface) distances on the interior of a surface mesh can be defined by isometric embedding of the surface into a suitable high-dimensional Euclidean space; for example, **diffusion metric** (cf. Chap. 15 and **histogram diffusion distance** from Chap. 21) and Rustamov et al., 2009.

A surface is called *differentiable*, *regular*, or *analytic*, respectively, if in a neighborhood of each of its points it can be given by an expression

$$r = r(u, v) = r(x_1(u, v), x_2(u, v), x_3(u, v)),$$

where the *position vector* $r = r(u, v)$ is a differentiable, *regular* (i.e., a sufficient number of times differentiable), or *real analytic*, respectively, vector function satisfying the condition $r_u \times r_v \neq 0$.

Any regular surface has the intrinsic metric with the *line element* (or *first fundamental form*)

$$ds^2 = dr^2 = E(u, v)du^2 + 2F(u, v)dudv + G(u, v)dv^2,$$

where $E(u, v) = \langle r_u, r_u \rangle$, $F(u, v) = \langle r_u, r_v \rangle$, $G(u, v) = \langle r_v, r_v \rangle$. The length of a curve defined on the surface by the equations $u = u(t)$, $v = v(t)$, $t \in [0, 1]$, is computed by

$$\int_0^1 \sqrt{Eu'^2 + 2Fu'v' + Gv'^2}dt,$$

and the distance between any points $p, q \in M^2$ is defined as the infimum of the lengths of all curves on M^2, connecting p and q. A **Riemannian metric** is a generalization of the first fundamental form of a surface.

For surfaces, two kinds of *curvature* are considered: *Gaussian curvature*, and *mean curvature*. To compute these curvatures at a given point of the surface, consider the intersection of the surface with a plane, containing a fixed *normal vector*, i.e., a vector which is perpendicular to the surface at this point. This intersection is a plane curve. The *curvature* k of this plane curve is called the *normal curvature* of the surface at the given point. If we vary the plane, the normal curvature k will change, and there are two extremal values, the *maximal curvature* k_1, and the *minimal curvature* k_2, called the *principal curvatures* of the surface. A curvature is taken to be *positive* if the curve turns in the same direction as the surface's chosen normal, otherwise it is taken to be *negative*.

The *Gaussian curvature* is $K = k_1 k_2$ (it can be given entirely in terms of the first fundamental form). The *mean curvature* is $H = \frac{1}{2}(k_1 + k_2)$.

A *minimal surface* is a surface with mean curvature zero or, equivalently, a surface of minimum area subject to constraints on the location of its boundary.

A *Riemann surface* is a one-dimensional *complex manifold*, or a 2D real manifold with a complex structure, i.e., in which the local coordinates in neighborhoods of points are related by complex analytic functions. It can be thought of as a deformed version of the complex plane. All Riemann surfaces are orientable. Closed Riemann surfaces are geometrical models of *complex algebraic curves*. Every connected Riemann surface can be turned into a *complete* 2D *Riemannian manifold* with constant curvature $-1, 0$, or 1. The Riemann surfaces with curvature -1 are called *hyperbolic*, and the *unit disk* $\Delta = \{z \in \mathbb{C} : |z| < 1\}$ is the canonical example. The Riemann surfaces with curvature 0 are called *parabolic*, and $\mathbb{C}$ is a typical example. The Riemann surfaces with curvature 1 are called *elliptic*, and the *Riemann sphere* $\mathbb{C} \cup \{\infty\}$ is a typical example.

- **Regular metric**

  The intrinsic metric of a surface is **regular** if it can be specified by the *line element*

  $$ds^2 = Edu^2 + 2Fdudv + Gdv^2,$$

  where the coefficients of the form ds^2 are regular functions.

  Any regular surface, given by an expression $r = r(u, v)$, has a regular metric with the *line element* ds^2, where $E(u, v) = \langle r_u, r_u \rangle$, $F(u, v) = \langle r_u, r_v \rangle$, $G(u, v) = \langle r_v, r_v \rangle$.
- **Analytic metric**

  The intrinsic metric on a surface is **analytic** if it can be specified by the *line element*

  $$ds^2 = Edu^2 + 2Fdudv + Gdv^2,$$

  where the coefficients of the form ds^2 are real analytic functions.

  Any analytic surface, given by an expression $r = r(u, v)$, has an analytic metric with the *line element* ds^2, where $E(u, v) = \langle r_u, r_u \rangle$, $F(u, v) = \langle r_u, r_v \rangle$, $G(u, v) = \langle r_v, r_v \rangle$.
- **Metric of nonpositive curvature**

  A **metric of nonpositive curvature** is the intrinsic metric on a *saddle-like surface*. A *saddle-like surface* is a generalization of a surface of negative curvature: a twice continuously-differentiable surface is a saddle-like surface if and only if at each point of the surface its Gaussian curvature is nonpositive.

  These surfaces can be seen as antipodes of *convex surfaces*, but they do not form such a natural class of surfaces as do convex surfaces.

  A **metric of negative curvature** is the intrinsic metric on a *surface of negative curvature*, i.e., a surface in $\mathbb{E}^3$ that has negative Gaussian curvature at every point.

A surface of negative curvature locally has a saddle-like structure. The intrinsic geometry of a surface of constant negative curvature (in particular, of a *pseudo-sphere*) locally coincides with the geometry of the *Lobachevsky plane*. There exists no surface in $\mathbb{E}^3$ whose intrinsic geometry coincides completely with the geometry of the Lobachevsky plane (i.e., a complete regular surface of constant negative curvature).

- **Metric of nonnegative curvature**

  A **metric of nonnegative curvature** is the intrinsic metric on a *convex surface*.

  A *convex surface* is a *domain* (i.e., a connected open set) on the boundary of a *convex body* in $\mathbb{E}^3$ (in some sense, it is an antipode of a saddle-like surface).

  The entire boundary of a convex body is called a *complete convex surface*. If the body is finite (bounded), the complete convex surface is called *closed*. Otherwise, it is called *infinite* (an infinite convex surface is homeomorphic to a plane or to a circular cylinder).

  Any convex surface M^2 in $\mathbb{E}^3$ is a *surface of bounded curvature*. The *total Gaussian curvature* $w(A) = \int\int_A K(x)d\sigma(x)$ of a set $A \subset M^2$ is always nonnegative (here $\sigma(.)$ is the *area*, and $K(x)$ is the *Gaussian curvature* of M^2 at a point x), i.e., a convex surface can be seen as a *surface of nonnegative curvature*.

  The intrinsic metric of a convex surface is a **convex metric** (not to be confused with **metric convexity** from Chap. 1) in the sense of Surface Theory, i.e., it displays the *convexity condition*: the sum of the angles of any triangle whose sides are shortest curves is not less that π.

  A **metric of positive curvature** is the intrinsic metric on a *surface of positive curvature*, i.e., a surface in $\mathbb{E}^3$ that has positive Gaussian curvature at every point.

- **Metric with alternating curvature**

  A **metric with alternating curvature** is the intrinsic metric on a surface with alternating (positive or negative) Gaussian curvature.

- **Flat metric**

  A **flat metric** is the intrinsic metric on a *developable surface*, i.e., a surface, on which the Gaussian curvature is everywhere zero. Cf. **flat space** in Chap. 1.

  In general, a Riemannian metric on a surface is locally Euclidean up to a third order error (distortion of metric) measured by the Gaussian curvature.

- **Metric of bounded curvature**

  A **metric of bounded curvature** is the intrinsic metric ρ on a *surface of bounded curvature*.

  A surface M^2 with an intrinsic metric ρ is called a *surface of bounded curvature* if there exists a sequence of **Riemannian metrics** ρ_n defined on M^2, such that $\rho_n \to \rho$ uniformly for any compact set $A \subset M^2$, and the sequence $|w_n|(A)$ is bounded, where $|w|_n(A) = \int\int_A |K(x)|d\sigma(x)$ is the *total absolute curvature* of the metric ρ_n (here $K(x)$ is the Gaussian curvature of M^2 at a point x, and $\sigma(.)$ is the *area*).

- **Λ-metric**

  A **Λ-metric** (or *metric of type* Λ) is a **complete** metric on a surface with curvature bounded from above by a negative constant.

A Λ-metric does not have embeddings into $\mathbb{E}^3$. It is a generalization of the result in Hilbert, 1901: no complete regular surface of constant negative curvature (i.e., a surface whose intrinsic geometry is the geometry of the Lobachevsky plane) exists in $\mathbb{E}^3$.

- (h, Δ)**-metric**

  A (h, Δ)**-metric** is a metric on a surface with a slowly-changing negative curvature.

  A **complete** (h, Δ)-metric does not permit a regular *isometric embedding* in three-dimensional Euclidean space (cf. Λ**-metric**).

- G**-distance**

  A connected set G of points on a surface M^2 is called a *geodesic region* if, for each point $x \in G$, there exists a *disk* $B(x, r)$ with center at x, such that $B_G = G \cap B(x, r)$ has one of the following forms: $B_G = B(x, r)$ (x is a *regular interior point* of G); B_G is a semidisk of $B(x, r)$ (x is a *regular boundary point* of G); B_G is a sector of $B(x, r)$ other than a semidisk (x is an *angular point* of G); B_G consists of a finite number of sectors of $B(x, r)$ with no common points except x (a *nodal point* of G).

  The G**-distance** between any x and $y \in G$ is the greatest lower bound of the lengths of all rectifiable curves connecting x and $y \in G$ and completely contained in G.

- **Conformally invariant metric**

  Let R be a Riemann surface. A *local parameter* (or *local uniformizing parameter*, *local uniformizer*) is a complex variable z considered as a continuous function $z_{p_0} = \phi_{p_0}(p)$ of a point $p \in R$ which is defined everywhere in some neighborhood (*parametric neighborhood*) $V(p_0)$ of a point $p_0 \in R$ and which realizes a homeomorphic mapping (*parametric mapping*) of $V(p_0)$ onto the disk (*parametric disk*) $\Delta(p_0) = \{z \in \mathbb{C} : |z| < r(p_0)\}$, where $\phi_{p_0}(p_0) = 0$. Under a parametric mapping, any point function $g(p)$ defined in the parametric neighborhood $V(p_0)$, goes into a function of the local parameter z: $g(p) = g(\phi_{p_0}^{-1}(z)) = G(z)$.

  A **conformally invariant metric** is a differential $\rho(z)|dz|$ on the Riemann surface R which is invariant with respect to the choice of the local parameter z. Thus, to each local parameter z ($z : U \to \overline{\mathbb{C}}$) a function $\rho_z : z(U) \to [0, \infty]$ is associated such that, for any local parameters z_1 and z_2, we have

$$\frac{\rho_{z_2}(z_2(p))}{\rho_{z_1}(z_1(p))} = \left|\frac{dz_1(p)}{dz_2(p)}\right| \text{ for any } p \in U_1 \cap U_2.$$

  Every linear differential $\lambda(z)dz$ and every *quadratic differential* $Q(z)dz^2$ induce conformally invariant metrics $|\lambda(z)||dz|$ and $|Q(z)|^{1/2}|dz|$, respectively (cf. Q**-metric**).

- Q**-metric**

  An Q**-metric** is a **conformally invariant metric** $\rho(z)|dz| = |Q(z)|^{1/2}|dz|$ on a Riemann surface R defined by a *quadratic differential* $Q(z)dz^2$.

A *quadratic differential* $Q(z)dz^2$ is a nonlinear differential on a Riemann surface R which is invariant with respect to the choice of the local parameter z. Thus, to each local parameter z ($z : U \to \overline{\mathbb{C}}$) a function $Q_z : z(U) \to \overline{\mathbb{C}}$ is associated such that, for any local parameters z_1 and z_2, we have

$$\frac{Q_{z_2}(z_2(p))}{Q_{z_1}(z_1(p))} = \left(\frac{dz_1(p)}{dz_2(p)}\right)^2 \text{ for any } p \in U_1 \cap U_2.$$

- **Extremal metric**

  Let Γ be a family of locally rectifiable curves on a Riemann surface R and let P be a class of **conformally invariant metrics** $\rho(z)|dz|$ on R such that $\rho(z)$ is square-integrable in the z-plane for every local parameter z, and the following Lebesgue integrals are not simultaneously equal to 0 or ∞:

$$A_\rho(R) = \int\int_R \rho^2(z)dxdy \text{ and } L_\rho(\Gamma) = \inf_{\gamma\in\Gamma} \int_y \rho(z)|dz|.$$

  The *modulus of the family of curves* Γ is defined by

$$M(\Gamma) = \inf_{\rho\in P} \frac{A_\rho(R)}{(L_\rho(\Gamma))^2}.$$

  The *extremal length of the family of curves* Γ is the reciprocal of $M(\Gamma)$.

  Let P_L be the subclass of P such that, for any $\rho(z)|dz| \in P_L$ and any $\gamma \in \Gamma$, one has $\int_\gamma \rho(z)|dz| \geq 1$. If $P_L \neq \emptyset$, then $M(\Gamma) = \inf_{\rho\in P_L} A_\rho(R)$. Every metric from P_L is called an *admissible metric* for the modulus on Γ. If there exists ρ^* for which

$$M(\Gamma) = \inf_{\rho\in P_L} A_\rho(R) = A_{\rho^*}(R),$$

  the metric $\rho^*|dz|$ is called an **extremal metric** for the modulus on Γ. It is a **conformally invariant metric**.

- **Fréchet surface metric**

  Let (X, d) be a metric space, M^2 a compact 2D manifold, f a continuous mapping $f : M^2 \to X$, called a *parametrized surface*, and $\sigma : M^2 \to M^2$ a homeomorphism of M^2 onto itself. Two parametrized surfaces f_1 and f_2 are called *equivalent* if $\inf_\sigma \max_{p\in M^2} d(f_1(p), f_2(\sigma(p))) = 0$, where the infimum is taken over all possible homeomorphisms σ. A class f^* of parametrized surfaces, equivalent to f, is called a *Fréchet surface*. It is a generalization of the notion of a surface in Euclidean space to the case of an arbitrary metric space (X, d).

  The **Fréchet surface metric** on the set of all Fréchet surfaces is defined by

$$\inf_\sigma \max_{p\in M^2} d(f_1(p), f_2(\sigma(p)))$$

for any Fréchet surfaces f_1^* and f_2^*, where the infimum is taken over all possible homeomorphisms σ. Cf. the **Fréchet metric** in Chap. 1.

- **Hempel metric**

  A *handlebody* of genus g is the boundary sum of g copies of a solid torus; it is homeomorphic to the closure of a regular neighborhood of some finite graph in $\mathbb{R}^3$. Given a closed orientable 3-manifold M, its *Heegaard splitting* (of genus g) is $M = A \cup_P B$ where A, B are genus g handlebodies in M such that $M = A \cup B$ and $A \cap B = \partial A = \partial B = P$. Then P is called a (genus g) *Heegaard surface* of M. In knot applications, Heegaard splitting of the *exterior of* a knot K (the complement of an open solid torus knotted like K) are considered.

  Two embedded curves are *isotopic* if there exists a continuous deformation of one embedding to another through a path of embeddings. Given a closed connected orientable surface S of genus at least two, let $C(S) = (V, E)$ denotes the graph whose vertices are isotopy classes of *essential* (not bounding disk on the surface) simple closed curves and whose edges are drawn between vertices with disjoint representative curves. This graph is connected. For any subsets of vertices $X, Y \subset V$, denote by $d_S(X, Y)$ their **set-to-set distance** $\min d_S(x, y) : x \in X, y \in Y$, where $d_S(x, y)$ is the **path metric** of $C(S)$.

  If S is the boundary of a handlebody H, let $M(H)$ denotes the set of vertices with representatives bounding *meridian disks* D of H, i.e., such that ∂D are essential simple closed curves in ∂H. The **Hempel distance** of a (genus $g \geq 2$) Heegaard splitting $M = A \cup_P B$ is defined (Hempel, 2001) to be $d_P(M(A), M(B))$.

  A Heegaard splitting $M = A \cup_P B$ is *stabilized*, if there are meridian disks D_A, D_B of A, B respectively such that ∂D_A and ∂D_B intersects transversely in a single point. The **Reidemeister–Singer distance** between two Heegaard surfaces/splittings is the minimal number of *stabilizations* (roughly, additions of a "trivial" handle) and *destabilizations* (inverse operation) relating them.

8.2 Intrinsic Metrics on Surfaces

In this section we list intrinsic metrics, given by their *line elements* (which, in fact, are 2D **Riemannian metrics**), for some selected surfaces.

- **Quadric metric**

  A *quadric* (or *quadratic surface*, *surface of second-order*) is a set of points in $\mathbb{E}^3$, whose coordinates in a Cartesian coordinate system satisfy an algebraic equation of degree two. There are 17 classes of such surfaces. Among them are: *ellipsoids*, *one-sheet* and *two-sheet hyperboloids*, *elliptic paraboloids*, *hyperbolic paraboloids*, *elliptic*, *hyperbolic* and *parabolic cylinders*, and *conical surfaces*.

  For example, a *cylinder* can be given by the following parametric equations:

$$x_1(u, v) = a \cos v, \ x_2(u, v) = a \sin v, \ x_3(u, v) = u.$$

The intrinsic metric on it is given by the *line element*

$$ds^2 = du^2 + a^2 dv^2.$$

An *elliptic cone* (i.e., a cone with elliptical cross-section) has the following equations:

$$x_1(u,v) = a\frac{h-u}{h}\cos v,\ x_2(u,v) = b\frac{h-u}{h}\sin v,\ x_3(u,v) = u,$$

where h is the *height*, a is the *semimajor axis*, and b is the *semiminor axis* of the cone. The intrinsic metric on it is given by the *line element*

$$ds^2 = \frac{h^2 + a^2\cos^2 v + b^2\sin^2 v}{h^2}du^2 + 2\frac{(a^2-b^2)(h-u)\cos v\sin v}{h^2}dudv + \\ + \frac{(h-u)^2(a^2\sin^2 v + b^2\cos^2 v)}{h^2}dv^2.$$

- **Sphere metric**

  A *sphere* is a *quadric*, given by the Cartesian equation $(x_1-a)^2 + (x_2-b)^2 + (x_3-c)^2 = r^2$, where the point (a,b,c) is the *center* of the sphere, and $r > 0$ is the *radius* of the sphere. The sphere of radius r, centered at the origin, can be given by the following parametric equations:

$$x_1(\theta,\phi) = r\sin\theta\cos\phi,\ x_2(\theta,\phi) = r\sin\theta\sin\phi,\ x_3(\theta,\phi) = r\cos\theta,$$

  where the *azimuthal angle* $\phi \in [0, 2\pi)$, and the *polar angle* $\theta \in [0,\pi]$.

  The intrinsic metric on it (in fact, the 2D **spherical metric**) is given by the *line element*

$$ds^2 = r^2 d\theta^2 + r^2\sin^2\theta d\phi^2.$$

  A sphere of radius r has constant positive Gaussian curvature equal to r.

- **Ellipsoid metric**

  An *ellipsoid* is a *quadric* given by the Cartesian equation $\frac{x_1^2}{a^2} + \frac{x_2^2}{b^2} + \frac{x_3^2}{c^2} = 1$, or by the following parametric equations:

$$x_1(\theta,\phi) = a\cos\phi\sin\theta,\ x_2(\theta,\phi) = b\sin\phi\sin\theta,\ x_3(\theta,\phi) = c\cos\theta,$$

  where the *azimuthal angle* $\phi \in [0, 2\pi)$, and the *polar angle* $\theta \in [0,\pi]$.

  The intrinsic metric on it is given by the *line element*

$$ds^2 = (b^2\cos^2\phi + a^2\sin^2\phi)\sin^2\theta d\phi^2 + (b^2-a^2)\cos\phi\sin\phi\cos\theta\sin\theta d\theta d\phi + \\ + ((a^2\cos^2\phi + b^2\sin^2\phi)\cos^2\theta + c^2\sin^2\theta)d\theta^2.$$

- **Spheroid metric**

  A *spheroid* is an *ellipsoid* having two axes of equal length. It is also a *rotation surface*, given by the following parametric equations:

$$x_1(u,v) = a\sin v\cos u,\ x_2(u,v) = a\sin v\sin u,\ x_3(u,v) = c\cos v,$$

  where $0 \le u < 2\pi$, and $0 \le v \le \pi$.

  The intrinsic metric on it is given by the *line element*

$$ds^2 = a^2\sin^2 v du^2 + \frac{1}{2}(a^2 + c^2 + (a^2 - c^2)\cos(2v))dv^2.$$

- **Hyperboloid metric**

  A *hyperboloid* is a *quadric* which may be one- or two-sheeted.

  The one-sheeted hyperboloid is a *surface of revolution* obtained by rotating a hyperbola about the perpendicular bisector to the line between the foci, while the two-sheeted hyperboloid is a surface of revolution obtained by rotating a hyperbola about the line joining the foci.

  The one-sheeted circular hyperboloid, oriented along the x_3 axis, is given by the Cartesian equation $\frac{x_1^2}{a^2} + \frac{x_2^2}{a^2} - \frac{x_3^2}{c^2} = 1$, or by the following parametric equations:

$$x_1(u,v) = a\sqrt{1+u^2}\cos v,\ x_2(u,v) = a\sqrt{1+u^2}\sin v,\ x_3(u,v) = cu,$$

  where $v \in [0, 2\pi)$. The intrinsic metric on it is given by the *line element*

$$ds^2 = \left(c^2 + \frac{a^2u^2}{u^2+1}\right)du^2 + a^2(u^2+1)dv^2.$$

- **Rotation surface metric**

  A *rotation surface* (or *surface of revolution*) is a surface generated by rotating a 2D curve about an axis. It is given by the following parametric equations:

$$x_1(u,v) = \phi(v)\cos u,\ x_2(u,v) = \phi(v)\sin u,\ x_3(u,v) = \psi(v).$$

  The intrinsic metric on it is given by the *line element*

$$ds^2 = \phi^2 du^2 + (\phi'^2 + \psi'^2)dv^2.$$

- **Pseudo-sphere metric**

  A *pseudo-sphere* is a half of the *rotation surface* generated by rotating a *tractrix* about its asymptote. It is given by the following parametric equations:

$$x_1(u,v) = \operatorname{sech} u\cos v,\ x_2(u,v) = \operatorname{sech} u\sin v,\ x_3(u,v) = u - \tanh u,$$

where $u \geq 0$, and $0 \leq v < 2\pi$. The intrinsic metric on it is given by the *line element*

$$ds^2 = \tanh^2 u du^2 + \operatorname{sech}^2 u dv^2.$$

The pseudo-sphere has constant negative Gaussian curvature equal to -1, and in this sense is an analog of the sphere which has constant positive Gaussian curvature.

- **Torus metric**

  A *torus* is a surface having genus one. A torus azimuthally symmetric about the x_3 axis is given by the Cartesian equation $(c - \sqrt{x_1^2 + x_2^2})^2 + x_3^2 = a^2$, or by the following parametric equations:

$$x_1(u, v) = (c + a\cos v)\cos u,\ x_2(u, v) = (c + a\cos v)\sin u,\ x_3(u, v) = a\sin v,$$

  where $c > a$, and $u, v \in [0, 2\pi)$.

  The intrinsic metric on it is given by the *line element*

$$ds^2 = (c + a\cos v)^2 du^2 + a^2 dv^2.$$

  For toroidally confined plasma, such as in magnetic confinement fusion, the coordinates u, v and a correspond to the directions called , respectively, *toroidal* (long, as lines of latitude, way around the torus), *poloidal* (short way around the torus) and *radial*. The **poloidal distance**, used in plasma context, is the distance in the poloidal direction.

- **Helical surface metric**

  A *helical surface* (or *surface of screw motion*) is a surface described by a plane curve γ which, while rotating around an axis at a uniform rate, also advances along that axis at a uniform rate. If γ is located in the plane of the axis of rotation x_3 and is defined by the equation $x_3 = f(u)$, the position vector of the helical surface is

$$r = (u\cos v,\ u\sin v,\ f(u) = hv),\ h = \text{const},$$

  and the intrinsic metric on it is given by the *line element*

$$ds^2 = (1 + f'^2)du^2 + 2hf' dudv + (u^2 + h^2)dv^2.$$

  If $f = const$, one has a *helicoid*; if $h = 0$, one has a *rotation surface*.

- **Catalan surface metric**

  The *Catalan surface* is a *minimal surface*, given by the following equations:

$$x_1(u, v) = u - \sin u \cosh v,\ x_2(u, v) = 1 - \cos u \cosh v,\ x_3(u, v) = 4\sin\left(\frac{u}{2}\right)\sinh\left(\frac{v}{2}\right).$$

The intrinsic metric on it is given by the *line element*

$$ds^2 = 2\cosh^2\left(\frac{v}{2}\right)(\cosh v - \cos u)du^2 + 2\cosh^2(\frac{v}{2})(\cosh v - \cos u)\,dv^2.$$

- **Monkey saddle metric**

  The *monkey saddle* is a surface, given by the Cartesian equation $x_3 = x_1(x_1^2 - 3x_2^2)$, or by the following parametric equations:

$$x_1(u, v) = u,\ x_2(u, v) = v,\ x_3(u, v) = u^3 - 3uv^2.$$

  This is a surface which a monkey can straddle with both legs and his tail. The intrinsic metric on it is given by the *line element*

$$ds^2 = (1 + (su^2 - 3v^2)^2)du^2 - 2(18uv(u^2 - v^2))dudv + (1 + 36u^2v^2)dv^2).$$

- **Distance-defined surfaces and curves**

  We give below examples of plane curves and surfaces which are the loci of points with given value of some function of their Euclidean distances to the given objects.

  A *parabola* is the locus of all points in $\mathbb{R}^2$ that are equidistant from the given point (*focus*) and given line (*directrix*) on the plane.

  A *hyperbola* is the locus of all points in $\mathbb{R}^2$ such that the ratio of their distances to the given point and line is a constant (*eccentricity*) greater than 1. It is also the locus of all points in $\mathbb{R}^2$ such that the absolute value of the difference of their distances to the two given foci is constant.

  An *ellipse* is the locus of all points in $\mathbb{R}^2$ such that the sum of their distances to the two given points (*foci*) is constant; cf. **elliptic orbit distance** in Chap. 25. A *circle* is an ellipse in which the two foci are coincident.

  A *Cassini oval* is the locus of all points in $\mathbb{R}^2$ such that the product of their distances to two given points is a constant k. If the distance between two points is $2\sqrt{k}$, then such oval is called a *lemniscate of Bernoulli*.

  A *circle of Appolonius* is the locus of points in $\mathbb{R}^2$ such that the ratio of their distances to the first and second given points is constant.

  A *Cartesian oval* is the locus of points in $\mathbb{R}^2$ such that their distances r_1, r_2 to the foci $(-1, 0), (1, 0)$ are related linearly by $ar_1 + br_2 = 1$. The cases $a = b, a = -b$ and $a = \frac{1}{2}$ (or $b = \frac{1}{2}$) correspond to the ellipse, hyperbola and *limaçon of Pascal*, respectively.

  A *Cassinian curve* is the locus of all points in $\mathbb{R}^2$ such that the product of their distances to n given points (*poles*) is constant. If the poles form a regular n-gon, then this (algebraic of degree $2n$) curve is a *sinusoidal spiral* given also by polar equation $r^n = 2\cos(n\theta)$, and the case $n = 3$ corresponds to the *Kiepert curve*.

  Farouki and Moon, 2000, considered many other multipolar generalizations of above curves. For example, their *trifocal ellipse* is the locus of all points in

$\mathbb{R}^2$ (seen as the complex plane) such that the sum of their distances to the 3 cube roots of unity is a constant k. If $k = 2\sqrt{3}$, the curve pass through (and is singular at) the 3 poles.

In $\mathbb{R}^3$, a surface, rotationally symmetric about an axis, is a locus defined via Euclidean distances of its points to the two given poles belonging to this axis. For example, a *spheroid* (or *ellipsoid of revolution*) is a quadric obtained by rotating an ellipse about one of its principal axes.

It is a sphere, if this ellipse is a circle. If the ellipse is rotated about its major axis, the result is an elongated (as the rugby ball) spheroid which is the locus of all points in $\mathbb{R}^3$ such that the sum of their distances to the two given points is constant. The rotation about its minor axis results in a flattened spheroid (as the Earth) which is the locus of all points in $\mathbb{R}^3$ such that the sum of the distances to the closest and the farthest points of given circle is constant.

A *hyperboloid of revolution of two sheets* is a quadric obtained by revolving a hyperbola about its semimajor (real) axis. Such hyperboloid with axis AB is the locus of all points in $\mathbb{R}^3$ such that the absolute value of the difference of their distances to the points A and B is constant.

Any point in $\mathbb{R}^n$ is uniquely defined by its Euclidean distances to the vertices of a nondegenerated n-simplex. If a surface which is not rotationally symmetric about an axis, is a locus in $\mathbb{R}^3$ defined via distances of its points to the given poles, then three noncollinear poles is needed, and the surface is symmetric with respect to reflection in the plane defined by the three poles.

8.3 Distances on Knots

A *knot* is a closed, self-nonintersecting curve that is embedded in S^3. The *trivial knot* (or *unknot*) O is a closed loop that is not knotted. A knot can be generalized to a link which is a set of disjoint knots. Every link has its *Seifert surface*, i.e., a compact oriented surface with the given link as boundary.

Two knots (links) are called *equivalent* if one can be smoothly deformed into another. Formally, a link is defined as a smooth one-dimensional *submanifold* of the 3-sphere S^3; a knot is a link consisting of one component; two links L_1 and L_2 are called *equivalent* if there exists an orientation-preserving homeomorphism $f : S^3 \to S^3$ such that $f(L_1) = L_2$.

All the information about a knot can be described using a *knot diagram*. It is a projection of a knot onto a plane such that no more than two points of the knot are projected to the same point on the plane, and at each such point it is indicated which strand is closest to the plane, usually by erasing part of the lower strand. Two different knot diagrams may both represent the same knot. Much of Knot Theory is devoted to telling when two knot diagrams represent the same knot.

An *unknotting operation* is an operation which changes the overcrossing and the undercrossing at a double point of a given knot diagram. The *unknotting number* of a knot K is the minimum number of unknotting operations needed to deform a diagram of K into that of the trivial knot, where the minimum is taken over all diagrams of K. Roughly, the unknotting number is the smallest number of times a knot K must be passed through itself to untie it.

An $\sharp$-*unknotting operation* in a diagram of a knot K is an analog of the unknotting operation for a $\sharp$-*part* of the diagram consisting of two pairs of parallel strands with one of the pair overcrossing another. Thus, an $\sharp$-unknotting operation changes the overcrossing and the undercrossing at each vertex of obtained quadrangle.

- **Gordian distance**

  The **Gordian distance** is a metric on the set of all knots defined, for given knots K and K', as the minimum number of unknotting operations needed to deform a diagram of K into that of K', where the minimum is taken over all diagrams of K from which one can obtain diagrams of K'. The unknotting number of K is equal to the Gordian distance between K and the trivial knot O.

  Let rK be the knot obtained from K by taking its mirror image, and let $-K$ be the knot with the reversed orientation. The **positive reflection distance** $Ref_+(K)$ is the Gordian distance between K and rK. The **negative reflection distance** $Ref_-(K)$ is the Gordian distance between K and $-rK$. The **inversion distance** $Inv(K)$ is the Gordian distance between K and $-K$.

  The Gordian distance is the case $k = 1$ of the C_k**-distance** which is the minimum number of C_k-*moves* needed to transform K into K'; Habiro, 1994 and Goussarov, 1995, independently proved that, for $k > 1$, it is finite if and only if both knots have the same *Vassiliev invariants of order less than k*. A C_1-move is a single crossing change, a C_2-move (or *delta-move*) is a simultaneous crossing change for 3 arcs forming a triangle. C_2- and C_3-distances are called **delta distance** and **clasp-pass distance**, respectively.
- **$\sharp$-Gordian distance**

  The **$\sharp$-Gordian distance** (see, for example, [Mura85]) is a metric on the set of all knots defined, for given knots K and K', as the minimum number of $\sharp$-unknotting operations needed to deform a diagram of K into that of K', where the minimum is taken over all diagrams of K from which one can obtain diagrams of K'.

  Let rK be the knot obtained from K by taking its mirror image, and let $-K$ be the knot with the reversed orientation. The **positive $\sharp$-reflection distance** $Ref_+^\sharp(K)$ is the $\sharp$-Gordian distance between K and rK. The **negative $\sharp$-reflection distance** $Ref_-^\sharp(K)$ is the $\sharp$-Gordian distance between K and $-rK$. The **$\sharp$-inversion distance** $Inv^\sharp(K)$ is the $\sharp$-Gordian distance between K and $-K$.
- **Knot complement hyperbolic metric**

  The *complement* of a knot K (or a link L) is $S^3 \backslash K$ (or $S^3 \backslash L$, respectively).

A knot (or, in general, a link) is called *hyperbolic* if its complement supports a complete Riemannian metric of constant curvature -1. In this case, the metric is called a **knot** (or **link**) **complement hyperbolic metric**, and it is unique.

A knot is hyperbolic if and only if (Thurston, 1978) it is not a *satellite knot* (then it supports a complete locally homogeneous Riemannian metric) and not a *torus knot* (does not lie on a trivially embedded torus in S^3). The complement of any nontrivial knot supports a complete nonpositively curved Riemannian metric.

Chapter 9
Distances on Convex Bodies, Cones, and Simplicial Complexes

9.1 Distances on Convex Bodies

A *convex body* in the n-dimensional Euclidean space $\mathbb{E}^n$ is a convex *compact connected* subset of $\mathbb{E}^n$. It is called *solid* (or *proper*) if it has nonempty interior. Let K denote the space of all convex bodies in $\mathbb{E}^n$, and let K_p be the subspace of all proper convex bodies. Given a set $X \subset \mathbb{E}^n$, its *convex hull* $conv(X)$ is the minimal *convex* set containing X.

Any metric space (K, d) on K is called a *metric space of convex bodies*. Such spaces, in particular the metrization by the **Hausdorff metric**, or by the **symmetric difference metric**, play a basic role in Convex Geometry (see, for example, [Grub93]).

For $C, D \in K\backslash\{\emptyset\}$, the *Minkowski addition* and the *Minkowski nonnegative scalar multiplication* are defined by $C + D = \{x + y : x \in C, y \in D\}$, and $\alpha C = \{\alpha x : x \in C\}$, $\alpha \geq 0$, respectively. The Abelian semigroup $(K, +)$ equipped with nonnegative scalar multiplication operators can be considered as a *convex cone*.

The *support function* $h_C : S^{n-1} \to \mathbb{R}$ of $C \in K$ is defined by $h_C(u) = \sup\{\langle u, x\rangle : x \in C\}$ for any $u \in S^{n-1}$, where S^{n-1} is the $(n-1)$-dimensional *unit sphere* in $\mathbb{E}^n$, and $\langle , \rangle$ is the *inner product* in $\mathbb{E}^n$. The *width* $w_C(u)$ is $h_C(u) + h_C(-u) = h_{C-C}(u)$. It is the perpendicular distance between the parallel supporting hyperplanes perpendicular to given direction. The *mean width* is the average of width over all directions in S^{n-1}.

- **Area deviation**

  The **area deviation** (or **template metric**) is a metric on the set K_p in $\mathbb{E}^2$ (i.e., on the set of plane convex disks) defined by

$$A(C \triangle D),$$

© Springer-Verlag Berlin Heidelberg 2016

M.M. Deza, E. Deza, *Encyclopedia of Distances*,
DOI 10.1007/978-3-662-52844-0_9

where $A(.)$ is the *area*, and $\triangle$ is the *symmetric difference*. If $C \subset D$, then it is equal to $A(D) - A(C)$.

- **Perimeter deviation**

  The **perimeter deviation** is a metric on K_p in $\mathbb{E}^2$ defined by

$$2p(conv(C \cup D)) - p(C) - p(D),$$

  where $p(.)$ is the *perimeter*. In the case $C \subset D$, it is equal to $p(D) - p(C)$.
- **Mean width metric**

  The **mean width metric** is a metric on K_p in $\mathbb{E}^2$ defined by

$$v2W(conv(C \cup D)) - W(C) - W(D),$$

  where $W(.)$ is the *mean width*: $W(C) = p(C)/\pi$, and $p(.)$ is the *perimeter*.
- **Florian metric**

  The **Florian metric** is a metric on K defined by

$$\int_{S^{n-1}} |h_C(u) - h_D(u)| d\sigma(u) = ||h_C - h_D||_1.$$

  It can be expressed in the form $2S(conv(C \cup D)) - S(C) - S(D)$ for $n = 2$ (cf. **perimeter deviation**); it can be expressed also in the form $nk_n(2W(conv(C \cup D)) - W(C) - W(D))$ for $n \geq 2$ (cf. **mean width metric**).

  Here $S(.)$ is the *surface area*, k_n is the *volume* of the *unit ball* $\overline{B}^n$ of $\mathbb{E}^n$, and $W(.)$ is the *mean width*: $W(C) = \frac{1}{nk_n} \int_{S^{n-1}} (h_C(u) + h_C(-u)) d\sigma(u)$.
- **McClure–Vitale metric**

  Given $1 \leq p \leq \infty$, the **McClure–Vitale metric** is a metric on K, defined by

$$\left(\int_{S^{n-1}} |h_C(u) - h_D(u)|^p d\sigma(u) \right)^{\frac{1}{p}} = ||h_C - h_D||_p.$$

- **Pompeiu–Hausdorff–Blaschke metric**

  The **Pompeiu–Hausdorff–Blaschke metric** is a metric on K defined by

$$\max\{\sup_{x \in C} \inf_{y \in D} ||x - y||_2, \sup_{y \in D} \inf_{x \in C} ||x - y||_2\},$$

  where $||.||_2$ is the Euclidean norm on $\mathbb{E}^n$.

  In terms of support functions and using Minkowski addition, this metric is

$$\sup_{u \in S^{n-1}} |h_C(u) - h_D(u)| = ||h_C - h_D||_\infty = \inf\{\lambda \geq 0 : C \subset D + \lambda \overline{B}^n, D \subset C + \lambda \overline{B}^n\},$$

  where $\overline{B}^n$ is the *unit ball* of $\mathbb{E}^n$. This metric can be defined using any norm on $\mathbb{R}^n$ and for the space of bounded closed subsets of any metric space.

- **Pompeiu–Eggleston metric**
  The **Pompeiu–Eggleston metric** is a metric on K defined by

$$\sup_{x\in C}\inf_{y\in D}||x-y||_2+\sup_{y\in D}\inf_{x\in C}||x-y||_2,$$

  where $||.||_2$ is the Euclidean norm on $\mathbb{E}^n$.
  In terms of support functions and using Minkowski addition, this metric is

$$\max\{0,\ \sup_{u\in S^{n-1}}(h_C(u)-h_D(u))\}+\max\{0,\ \sup_{u\in S^{n-1}}(h_D(u)-h_C(u))\}=$$
$$=\inf\{\lambda\geq 0: C\subset D+\lambda\overline{B}^n\}+\inf\{\lambda\geq 0: D\subset C+\lambda\overline{B}^n\},$$

  where $\overline{B}^n$ is the *unit ball* of $\mathbb{E}^n$. This metric can be defined using any norm on $\mathbb{R}^n$ and for the space of bounded closed subsets of any metric space.
- **Sobolev distance**
  The **Sobolev distance** is a metric on K defined by

$$||h_C-h_D||_w,$$

  where $||.||_w$ is the *Sobolev* 1*-norm* on the set $G_{S^{n-1}}$ of all real continuous functions on the *unit sphere* S^{n-1} of $\mathbb{E}^n$.
  The *Sobolev* 1*-norm* is defined by $||f||_w=\langle f,f\rangle_w^{1/2}$, where $\langle,\rangle_w$ is an *inner product* on $G_{S^{n-1}}$, given by

$$\langle f,g\rangle_w=\int_{S^{n-1}}(fg+\nabla_s(f,g))dw_0,\quad w_0=\frac{1}{n\cdot k_n}w,$$

  where $\nabla_s(f,g)=\langle grad_s f,\ grad_s g\rangle$, $\langle,\rangle$ is the *inner product* in $\mathbb{E}^n$, and $grad_s$ is the *gradient* on S^{n-1} (see [ArWe92]).
- **Shephard metric**
  The **Shephard metric** is a metric on K_p defined by

$$\ln(1+2\inf\{\lambda\geq 0: C\subset D+\lambda(D-D), D\subset C+\lambda(C-C)\}).$$

- **Nikodym metric**
  The **Nikodym metric** (or **volume of symmetric difference**, **Dinghas distance**) is a metric on K_p defined by

$$V(C\triangle D)=\int(1_{x\in C}-1_{x\in D})^2dx,$$

  where $V(.)$ is the *volume* (i.e., the Lebesgue n-dimensional measure), and $\triangle$ is the *symmetric difference*. For $n=2$, one obtains the **area deviation**.

Normalized volume of symmetric difference is a variant of **Steinhaus distance** defined by

$$\frac{V(C \triangle D)}{V(C \cup D)}.$$

- **Eggleston distance**

  The **Eggleston distance** (or **symmetric surface area deviation**) is a distance on K_p defined by

  $$S(C \cup D) - S(C \cap D),$$

  where $S(.)$ is the *surface area*. It is not a metric.
- **Asplund metric**

  The **Asplund metric** is a metric on the space $K_p/\approx$ of affine-equivalence classes in K_p defined by

  $$\ln \inf\{\lambda \geq 1 : \exists T : \mathbb{E}^n \to \mathbb{E}^n \text{ affine}, x \in \mathbb{E}^n, C \subset T(D) \subset \lambda C + x\}$$

  for any equivalence classes C^* and D^* with the representatives C and D, respectively.
- **Macbeath metric**

  The **Macbeath metric** is a metric on the space $K_p/\approx$ of affine-equivalence classes in K_p defined by

  $$\ln \inf\{|\det T \cdot P| : \exists T, P : \mathbb{E}^n \to \mathbb{E}^n \text{ regular affine}, C \subset T(D), D \subset P(C)\}$$

  for any equivalence classes C^* and D^* with the representatives C and D, respectively.

  Equivalently, it can be written as $\ln \delta(C, D) + ln\delta(D, C)$, where $\delta(C, D) = \inf_T\{\frac{V(T(D))}{V(C)}; C \subset T(D)\}$, and T is a regular affine mapping of $\mathbb{E}^n$ onto itself.
- **Banach–Mazur metric**

  The **Banach–Mazur metric** is a metric on the space $K_{po}/\sim$ of the equivalence classes of proper 0-symmetric convex bodies with respect to linear transformations defined by

  $$\ln \inf\{\lambda \geq 1 : \exists T : \mathbb{E}^n \to \mathbb{E}^n \text{ linear}, C \subset T(D) \subset \lambda C\}$$

  for any equivalence classes C^* and D^* with the representatives C and D, respectively.

  It is a special case of the **Banach–Mazur distance** (Chap. 1).
- **Separation distance**

  The **separation distance** between two disjoint convex bodies C and D in $\mathbb{E}^n$ (in general, between any two disjoint subsets) $\mathbb{E}^n$) is (Buckley, 1985) their

Euclidean **set-set distance** $\inf\{||x-y||_2 : x \in C, y \in D\}$, while $\sup\{||x-y||_2 : x \in C, y \in D\}$ is their **spanning distance**.

- **Penetration depth distance**

  The **penetration depth distance** between two interpenetrating convex bodies C and D in $\mathbb{E}^n$ (in general, between any two interpenetrating subsets of $\mathbb{E}^n$) is (Cameron–Culley, 1986) defined as the minimum *translation distance* that one body undergoes to make the interiors of C and D disjoint:

$$\min\{||t||_2 : interior(C+t) \cap D = \emptyset\}.$$

  Keerthi–Sridharan, 1991, considered $||t||_1$- and $||t||_\infty$-analogs of this distance.

  Cf. **penetration distance** in Chap. 23 and **penetration depth** in Chap. 24.

- **Growth distances**

  Let $C, D \in K_p$ be two compact convex proper bodies. Fix their *seed points* $p_C \in int\, C$ and $p_D \in int\, D$; usually, they are the centroids of C and D. The *growth function* $g(C, D)$ is the minimal number $\lambda > 0$, such that

$$(\{p_C\} + \lambda(C \backslash \{p_C\})) \cap (\{p_D\} + \lambda(D \backslash \{p_D\})) \neq \emptyset.$$

  It is the amount objects must be grown if $g(C, D) > 1$ (i.e., $C \cap D = \emptyset$), or contracted if $g(C, D) > 1$ (i.e., $int\, C \cap int\, D \neq \emptyset$) from their internal seed points until their surfaces just touch. The **growth separation distance** $d_S(C, D)$ and the **growth penetration distance** $d_P(C, D)$ ([OnGi96]) are defined as

$$d_S(C,D) = \max\{0, r_{CD}(g(C,D)-1)\} \text{ and } d_P(C,D) = \max\{0, r_{CD}(1-g(C,D))\},$$

  where r_{CD} is the scaling coefficient (usually, the sum of radii of circumscribing spheres for the sets $C \backslash \{p_C\}$ and $D \backslash \{p_D\}$).

  The *one-sided growth distance* between disjoint C and D (Leven–Sharir, 1987) is

$$-1 + \min \lambda > 0 : (\{p_C\} + \lambda\{(C \backslash \{p_C\})) \cap D \neq \emptyset\}.$$

- **Minkowski difference**

  The **Minkowski difference** on the set of all compact subsets, in particular, on the set of all *sculptured objects* (or *free form objects*), of $\mathbb{R}^3$ is defined by

$$A - B = \{x - y : x \in A, y \in B\}.$$

  If we consider object B to be free to move with fixed orientation, the Minkowski difference is a set containing all the translations that bring B to intersect with A. The closest point from the Minkowski difference boundary, $\partial(A - B)$, to the origin gives the **separation distance** between A and B.

If both objects intersect, the origin is inside of their Minkowski difference, and the obtained distance can be interpreted as a **penetration depth distance**.

- **Demyanov distance**

  Given $C \in K_p$ and $u \in S^{n-1}$, denote, if $|\{c \in C : \langle u, c\rangle = h_C(u)\}| = 1$, this unique point by $y(u, C)$ (*exposed point of C in direction u*).

  The *Demyanov difference* $A \ominus B$ of two subsets $A, B \in K_p$ is the closure of

$$conv(\cup_{T(A)\cap T(B)}\{y(u, A) - y(u, B)\}),$$

  where $T(C) = \{u \in S^{n-1} : |\{c \in C : \langle u, c\rangle = h_C(u)\}| = 1\}$.

  The **Demyanov distance** between two subsets $A, B \in K_p$ is defined by

$$||A \ominus B|| = \max_{c\in A\ominus B} ||c||_2.$$

  It is shown in [BaFa07] that $||A \ominus B|| = \sup_\alpha ||St_\alpha(A) - St_\alpha(M)||_2$, where $St_\alpha(C)$ is a *generalized Steiner point* and the supremum is over all "sufficiently smooth" probabilistic measures α.

- **Maximum polygon distance**

  The **maximum polygon distance** is a distance between two convex polygons $P = (p_1, \ldots, p_n)$ and $Q = (q_1, \ldots, q_m)$ defined by

$$\max_{i,j} ||p_i - q_j||_2,\ i \in \{1, \ldots, n\},\ j \in \{1, \ldots, m\}.$$

- **Grenander distance**

  Let $P = (p_1, \ldots, p_n)$ and $Q = (q_1, \ldots, q_m)$ be two disjoint convex polygons, and let $L(p_i, q_j), L(p_l, q_m)$ be two intersecting *critical support lines* for P and Q. Then the **Grenander distance** between P and Q is defined by

$$||p_i - q_j||_2 + ||p_l - q_m||_2 - \Sigma(p_i, p_l) - \Sigma(g_j, q_m),$$

  where $||.||_2$ is the Euclidean norm, and $\Sigma(p_i, p_l)$ is the sum of the edges lengths of the polynomial chain $p_i, \ldots, p_l$.

  Here $P = (p_1, \ldots, p_n)$ is a convex polygon with the vertices in standard form, i.e., the vertices are specified according to Cartesian coordinates in a clockwise order, and no three consecutive vertices are collinear. A line L is a *line of support* of P if the interior of P lies completely to one side of L.

  Given two disjoint polygons P and Q, the line $L(p_i, q_j)$ is a *critical support line* if it is a line of support for P at p_i, a line of support for Q at q_j, and P and Q lie on opposite sides of $L(p_i, q_j)$. In general, a chord $[a, b]$ of a convex body C is called its **affine diameter** if there is a pair of different hyperplanes each containing one of the endpoints a, b and supporting C.

9.2 Distances on Cones

A *convex cone* C in a real vector space V is a subset C of V such that $C + C \subset C$, $\lambda C \subset C$ for any $\lambda \geq 0$. A cone C induces a *partial order* on V by

$$x \preceq y \text{ if and only if } y - x \in C.$$

The order $\preceq$ respects the vector structure of V, i.e., if $x \preceq y$ and $z \preceq u$, then $x + z \preceq y + u$, and if $x \preceq y$, then $\lambda x \preceq \lambda y$, $\lambda \in \mathbb{R}$, $\lambda \geq 0$. Elements $x, y \in V$ are called *comparable* and denoted by $x \sim y$ if there exist positive real numbers α and β such that $\alpha y \preceq x \preceq \beta y$. Comparability is an equivalence relation; its equivalence classes (which belong to C or to $-C$) are called *parts* (or *components*, *constituents*).

Given a convex cone C, a subset $S = \{x \in C : T(x) = 1\}$, where $T : V \to \mathbb{R}$ is a positive linear functional, is called a *cross-section* of C. A convex cone C is called *almost Archimedean* if the closure of its restriction to any 2D subspace is also a cone.

A convex cone C is called *pointed* if $C \cup (-C) = \{0\}$ and *solid* if $int\ C \neq \emptyset$.

- **Koszul–Vinberg metric**

  Given an open pointed convex cone C, let C^* be its dual cone.

  The **Koszul–Vinberg metric** on C (Vinberg, 1963, and Koszul, 1965) is an affine invariant Riemannian metric defined as the Hessian $g = d^2\psi_C$, where $\psi_C(x) = -\log \int_{C^*} e^{-(\epsilon,x)} d\epsilon$ for any $x \in C$.

  The Hessian of the *entropy* (Legendre transform of $\psi_C(x)$) defines a metric on C^*, which ([Barb14]) is equivalent to the **Fisher–Rao metric** (Sect. 7.2). [Barb14] also observed that *Fisher–Souriau metric* ([Sour70]) generalises Fisher–Rao metric for Lie group thermodynamics and interpreted it as a geometric *heat capacity*.
- **Invariant distances on symmetric cones**

  An open convex cone C in an Euclidean space V is said to be *homogeneous* if its group of linear automorphisms $G = \{g \in GL(V) : g(C) = C\}$ act transitively on C. If, moreover, $\overline{C}$ is pointed and C is self-dual with respect to the given inner product $\langle , \rangle$, then it is called a *symmetric cone*. Any symmetric cone is a Cartesian product of such cones of only 5 types: the cones $Sym(n, \mathbb{R})^+$, $Her(n, \mathbb{C})^+$ (cf. Chap. 12), $Her(n, \mathbb{H})^+$ of positive-definite Hermitian matrices with real, complex or quaternion entries, the *Lorentz cone* (or *forward light cone*) $\{(t, x_1, \ldots, x_n) \in \mathbb{R}^{n+1} : t^2 > x_1^2 + \cdots + x_n^2\}$ and 27-dimensional exceptional cone of 3×3 positive-definite matrices over the octonions $\mathbb{O}$. An $n \times n$ quaternion matrix A can be seen as a $2n \times 2n$ complex matrix A'; so, $A \in Her(n, \mathbb{H})^+$ means $A' \in Her(2n, \mathbb{C})^+$.

  Let V be an *Euclidean Jordan algebra*, i.e., a finite-dimensional *Jordan algebra* (commutative algebra satisfying $x^2(xy) = x(x^2y)$ and having a multiplicative identity e) equipped with an *associative* ($\langle xy, z\rangle = \langle y, xz\rangle$) inner product $\langle , \rangle$. Then the set of square elements of V is a symmetric cone, and every symmetric cone arises in this way. Denote $P(x)y = 2x(xy) - x^2y$ for any $x, y \in C$.

For example, for $C = PD_n(\mathbb{R})$, the group G is $GL(n, \mathbb{R})$, the inner product is $\langle X, Y\rangle = \mathrm{Tr}(XY)$, the Jordan product is $\frac{1}{2}(XY + YX)$, and $P(X)Y = XYX$, where the multiplication on the right-hand side is the usual matrix multiplication.

If r is the rank of V, then for any $x \in V$ there is a complete set of orthogonal primitive idempotents $c_1, \ldots, c_r \neq 0$ (i.e., $c_i^2 = c_i$, c_i indecomposable, $c_i c_j = 0$ if $i \neq j$, $\sum_{i=1}^r c_i = e$) and real numbers $\lambda_1, \ldots, \lambda_r$, called *eigenvalues* of x, such that $x = \sum_{i=1}^r \lambda_i c_i$. Let $x, y \in C$ and $\lambda_1, \ldots, \lambda_r$ be the eigenvalues of $P(x^{-\frac{1}{2}})y$. Lim, 2001, defined following three G-invariant distances on any symmetric cone C:

$$d_R = (\sum_{1\leq i\leq r} \ln^2 \lambda_i)^{\frac{1}{2}},\ d_F = \max_{1\leq i\leq r} \ln|\lambda_i|,\ d_H = \ln(\max_{1\leq i\leq r} \lambda_i (\min_{1\leq i\leq r} \lambda_i)^{-1}).$$

For above distances, the geometric mean $P(x^{\frac{1}{2}})(P(x^{-\frac{1}{2}}y))^{\frac{1}{2}}$ is the midpoint of x and y. The distances $d_R(x, y)$, $d_F(x, y)$ are the intrinsic metrics of G-invariant Riemannian and Finsler metrics on C. The Riemannian geodesic curve $\alpha(t) = P(x^{\frac{1}{2}})(P(x^{-\frac{1}{2}}y))^t$ is one of infinitely many shortest Finsler curves passing through x and y. The space $(C, d_R(x, y))$ is an **Hadamard space** (Chap. 6), while $(C, d_F(x, y))$ is not. The distance $d_F(x, y)$ is the **Thompson's part metric** on C, and the distance $d_H(x, y)$ is the **Hilbert projective semimetric** on C which is a complete metric on the unit sphere on C.

- **Thompson's part metric**

  Given a convex cone C in a real Banach space V, the **Thompson's part metric** on a *part* $K \subset C\backslash\{0\}$ is defined (Thompson, 1963) by

  $$\log \max\{m(x, y), m(y, x)\}$$

  for any $x, y \in K$, where $m(x, y) = \inf\{\lambda \in \mathbb{R} : y \preceq \lambda x\}$.

  If C is *almost Archimedean*, then K equipped with this metric is a **complete** metric space. If C is finite-dimensional, then one obtains a **chord space** (Chap. 6). The *positive cone* $\mathbb{R}^n_+ = \{(x_1, \ldots, x_n) : x_i \geq 0 \text{ for } 1 \leq i \leq n\}$ equipped with this metric is isometric to a *normed space* which can be seen as being flat. The same holds for the **Hilbert projective semimetric** on $\mathbb{R}^n_+$.

  If C is a closed solid cone in $\mathbb{R}^n$, then *int* C can be seen as an n-dimensional manifold M^n. If for any tangent vector $v \in T_p(M^n)$, $p \in M^n$, we define a norm $||v||_p^T = \inf\{\alpha > 0 : -\alpha p \preceq v \preceq \alpha p\}$, then the length of any piecewise differentiable curve $\gamma : [0, 1] \to M^n$ is $l(\gamma) = \int_0^1 ||\gamma'(t)||^T_{\gamma(t)} dt$, and the distance between x and y is $\inf_\gamma l(\gamma)$, where the infimum is taken over all such curves γ with $\gamma(0) = x$, $\gamma(1) = y$.

- **Hilbert projective semimetric**

  Given a pointed closed convex cone C in a real Banach space V, the **Hilbert projective semimetric** on $C\backslash\{0\}$ is defined (Bushell, 1973), for $x, y \in C\backslash\{0\}$, by

  $$h(x, y) = \log(m(x, y)m(y, x)),$$

where $m(x,y) = \inf\{\lambda \in \mathbb{R} : y \preceq \lambda x\}$; it holds $\frac{1}{m(y,x)} = \sup\{\lambda \in \mathbb{R} : \lambda y \preceq x\}$. This semimetric is finite on the interior of C and $h(\lambda x, \lambda' y) = h(x,y)$ for $\lambda, \lambda' > 0$. So, $h(x,y)$ is a metric on the *projectivization* of C, i.e., the space of rays of this cone.

If C is finite-dimensional, and S is a *cross-section* of C (in particular, $S = \{x \in C : ||x|| = 1\}$, where $||.||$ is a norm on V), then, for any distinct points $x, y \in S$, it holds $h(x,y) = |\ln(x,y,z,t)|$, where z, t are the points of the intersection of the line $l_{x,y}$ with the boundary of S, and (x,y,z,t) is the **cross-ratio** of x, y, z, t. Cf. the **Hilbert projective metric** in Chap. 6.

If C is finite-dimensional and *almost Archimedean*, then each part of C is a **chord space** (Chap. 6) under the Hilbert projective semimetric. On the *Lorentz cone* $L = \{x = (t, x_1, \ldots, x_n) \in \mathbb{R}^{n+1} : t^2 > x_1^2 + \cdots + x_n^2\}$, this semimetric is isometric to the n-dimensional *hyperbolic space*. On the hyperbolic subspace $H = \{x \in L : \det(x) = 1\}$, it holds $h(x,y) = 2d(x,y)$, where $d(x,y)$ is the **Thompson's part metric** which is (on H) the usual hyperbolic distance $\operatorname{arccosh}\langle x, y\rangle$.

If C is a closed solid cone in $\mathbb{R}^n$, then *int* C can be seen as an **n-manifold** M^n (Chap. 2). If for any tangent vector $v \in T_p(M^n)$, $p \in M^n$, we define a seminorm $||v||_p^H = m(p,v) - m(v,p)$, then the length of any piecewise differentiable curve $\gamma : [0,1] \to M^n$ is $l(\gamma) = \int_0^1 ||\gamma'(t)||_{\gamma(t)}^H dt$, and $h(x,y) = \inf_\gamma l(\gamma)$, where the infimum is taken over all such curves γ with $\gamma(0) = x$ and $\gamma(1) = y$.

- **Bushell metric**

  Given a convex cone C in a real Banach space V, the **Bushell metric** on the set $S = \{x \in C : \sum_{i=1}^n |x_i| = 1\}$ (in general, on any *cross-section* of C) is defined by

$$\frac{1 - m(x,y) \cdot m(y,x)}{1 + m(x,y) \cdot m(y,x)}$$

  for any $x, y \in S$, where $m(x,y) = \inf\{\lambda \in \mathbb{R} : y \preceq \lambda x\}$. In fact, it is equal to $\tanh(\frac{1}{2}h(x,y))$, where h is the **Hilbert projective semimetric**.

- ***k*-oriented distance**

  A *simplicial cone* C in $\mathbb{R}^n$ is defined as the intersection of n (open or closed) half-spaces, each of whose supporting planes contain the origin 0. For any set M of n points on the *unit sphere*, there is a unique simplicial cone C that contains these points. The *axes* of the cone C can be constructed as the set of the n rays, where each ray originates at the origin, and contains one of the points from M.

  Given a *partition* $\{C_1, \ldots, C_k\}$ of $\mathbb{R}^n$ into a set of simplicial cones $C_1, \ldots, C_k$, the ***k*-oriented distance** is a metric on $\mathbb{R}^n$ defined by

$$d_k(x - y)$$

  for all $x, y \in \mathbb{R}^n$, where, for any $x \in C_i$, the value $d_k(x)$ is the length of the shortest path from the origin 0 to x traveling only in directions parallel to the axes of C_i.

- **Cones over metric space**

  A **cone over a metric space** (X, d) is the quotient space $Con(X, d)=(X \times [0, 1])/(X \times \{0\})$ obtained from the product $X \times \mathbb{R}_{\geq 0}$ by collapsing the *fiber* (subspace $X \times \{0\}$) to a point (the apex of the cone). Cf. **metric cone** in Chap. 1.

  The *Euclidean cone over the metric space* (X, d) is the cone $Con(X, d)$ with a metric d defined, for any $(x, t), (y, s) \in Con(X, d)$, by

$$\sqrt{t^2 + s^2 - 2ts\cos(\min\{d(x, y), \pi\})}.$$

  If (X, d) is a compact metric space with diameter < 2, the **Krakus metric** is a metric on $Con(X, d)$ defined, for any $(x, t), (y, s) \in Con(X, d)$, by

$$\min\{s, t\}d(x, y) + |t - s|.$$

  The cone $Con(X, d)$ with the Krakus metric admits a unique *midpoint* for each pair of its points if (X, d) has this property.

  If M^n is a manifold with a pseudo-Riemannian metric g, one can consider a metric dr^2+r^2g (in general, a metric $\frac{1}{k}dr^2+r^2g, k \neq 0$) on $Con(M^n) = M^n \times \mathbb{R}_{>0}$. For example, $Con(M^n) = \mathbb{R}^n \setminus \{0\}$ if (M^n, g) is the unit sphere in $\mathbb{R}^n$.

  A *spherical cone* (or *suspension*) $\Sigma(X)$ over a metric space (X, d) is the quotient of the product $X \times [0, a]$ obtained by identifying all points in the fibers $X \times \{0\}$ and $X \times \{a\}$. If (X, d) is a **length space** (Chap. 6) with $diam(X) \leq \pi$, and $a = \pi$, the **suspension metric** on $\Sigma(X)$ is defined, for any $(x, t), (y, s) \in \Sigma(X)$, by

$$\arccos(\cos t \cos s + \sin t \sin s \cos d(x, y)).$$

9.3 Distances on Simplicial Complexes

An r-dimensional *simplex* (or *geometrical simplex*, *hypertetrahedron*) is the *convex hull* of $r + 1$ points of $\mathbb{E}^n$ which do not lie in any $(r - 1)$-plane. The boundary of an r-simplex has $r + 1$ 0-*faces* (polytope vertices), $\frac{r(r+1)}{2}$ 1-*faces* (polytope edges), and $\binom{r+1}{i+1}$ *i-faces*, where $\binom{r}{i}$ is the binomial coefficient. The *content* (i.e., the *hypervolume*) of a simplex can be computed using the *Cayley–Menger determinant*. The regular simplex of dimension r is denoted by α_r. *Simplicial depth of a point* $p \in \mathbb{E}^n$ *relative to a set* $P \subset \mathbb{E}^n$ is the number of simplices S, generated by $(n + 1)$-subsets of P and containing p.

Roughly, a *geometrical simplicial complex* is a space with a *triangulation*, i.e., a decomposition of it into closed simplices such that any two simplices either do not intersect or intersect only along a common face.

An *abstract simplicial complex* S is a set, whose elements are called *vertices*, in which a family of finite nonempty subsets, called *simplices*, is distinguished, such

that every nonempty subset of a simplex s is a simplex, called a *face* of s, and every one-element subset is a simplex. A simplex is called i-dimensional if it consists of $i + 1$ vertices. The *dimension* of S is the maximal dimension of its simplices. For every simplicial complex S there exists a triangulation of a polyhedron whose simplicial complex is S. This geometric simplicial complex, denoted by GS, is called the *geometric realization* of S.

- **Vietoris–Rips complex**

  Given a metric space (X, d) and distance δ, their **Vietoris–Rips complex** is an abstract simplicial complex, the simplexes of which are the finite subsets M of (X, d) having diameter at most δ; the dimension of a simplex defined by M is $|M| - 1$.
- **Simplicial metric**

  Given an abstract simplicial complex S, the points of geometric simplicial complex GS, realizing S, can be identified with the functions $\alpha : S \to [0, 1]$ for which the set $\{x \in S : \alpha(x) \neq 0\}$ is a simplex in S, and $\sum_{x \in S} \alpha(x) = 1$. The number $\alpha(x)$ is called the *x-th barycentric coordinate* of α.

  The **simplicial metric** on GS (Lefschetz, 1939) is the Euclidean metric on it:

$$\sqrt{\sum_{x \in S} (\alpha(x) - \beta(x))^2}.$$

  Tukey, 1939, found another metric on GS, topologically equivalent to a simplicial one. His **polyhedral metric** is the **intrinsic metric**, defined as the infimum of the lengths of the polygonal lines joining the points α and β such that each link is within one of the simplices. An example of a polyhedral metric is the intrinsic metric on the surface of a convex polyhedron in $\mathbb{E}^3$.
- **Polyhedral space**

  A Euclidean **polyhedral space** is a simplicial complex with a **polyhedral metric**. Every simplex is a **flat space** (a metric space locally isometric to some $\mathbb{E}^n$; cf. Chap. 1), and the metrics of any two simplices coincide on their intersection. The metric is the maximal metric not exceeding the metrics of simplices.

  If such a space is an **n-manifold** (Chap. 2), a point in it is a **metric singularity** if it has no neighborhood isometric to an open subset of $\mathbb{E}^n$.

  A polyhedral metric on a simplicial complex in a space of constant (positive or negative) curvature results in *spherical* and *hyperbolic polyhedral spaces*.

  The *dimension* of a polyhedral space is the maximal dimension of simplices used to glue it. **Metric graphs** (Chap. 15) are just one-dimensional polyhedral spaces.

  The surface of a convex polyhedron is a 2D polyhedral space. A polyhedral metric d on a triangulated surface is a **circle-packing metric** (Thurston, 1985) if there exists a vertex-weighting $w(x) > 0$ with $d(x, y) = w(x) + w(y)$ for any edge xy.

- **Manifold edge-distance**

  A (boundaryless) *combinatorial n-manifold* is an abstract n-dimensional simplicial complex M^n in which the *link* of each r-simplex is an $(n-r-1)$-sphere. The category of such spaces is equivalent to the category of piecewise-linear (PL) manifolds.

  The *link* of a simplex S is $Cl(Star_S) - Star_S$, where $Star_S$ is the set of all simplices in M^n having a face S, and $Cl(Star_S)$ is the smallest simplicial subcomplex of M^n containing $Star_S$.

  The **edge-distance** between vertices $u, v \in M^n$ is the minimum number of edges needed to connect them.
- **Manifold triangulation metric**

  Let M^n be a compact PL (piecewise-linear) n-dimensional manifold. A *triangulation* of M^n is a simplicial complex such that its corresponding polyhedron is PL-homeomorphic to M^n. Let T_{M^n} be the set of all *combinatorial types* of triangulations, where two triangulations are equivalent if they are simplicially isomorphic.

  Every such triangulation can be seen as a metric on the smooth manifold M if one assigns the unit length for any of its 1-dimensional simplices; so, T_{M^n} can be seen as a discrete analog of the space of Riemannian structures, i.e., isometry classes of Riemannian metrics on M^n.

  A **manifold triangulation metric** between two triangulations x and y is (Nabutovsky and Ben-Av, 1993) an **editing metric** on T_{M^n}, i.e., the minimal number of elementary moves, from a given finite list of operations, needed to obtain y from x.

  For example, the *bistellar move* consists of replacing a subcomplex of a given triangulation, which is simplicially isomorphic to a subcomplex of the boundary of the standard $(n+1)$-simplex, by the complementary subcomplex of the boundary of an $(n+1)$-simplex, containing all remaining n-simplices and their faces. Every triangulation can be obtained from any other one by a finite sequence of bistellar moves.
- **Polyhedral chain metric**

  An r-dimensional *polyhedral chain* A in $\mathbb{E}^n$ is a linear expression $\sum_{i=1}^{m} d_i t_i^r$, where, for any i, the value t_i^r is an r-dimensional simplex of $\mathbb{E}^n$. The *boundary* ∂A of a chain AD is the linear combination of boundaries of the simplices in the chain. The boundary of an r-dimensional chain is an $(r-1)$-dimensional chain.

  A **polyhedral chain metric** is a **norm metric** $||A - B||$ on the set $C_r(\mathbb{E}^n)$ of all r-dimensional polyhedral chains. As a norm $||.||$ on $C_r(\mathbb{E}^n)$ one can take:

  1. The *mass* of a polyhedral chain, i.e., $|A| = \sum_{i=1}^{m} |d_i||t_i^r|$, where $|t^r|$ is the volume of the cell t_i^r;
  2. The *flat norm* of a polyhedral chain, i.e., $|A|^\flat = \inf_D\{|A - \partial D| + |D|\}$, where the infimum is taken over all $(r+1)$-dimensional polyhedral chains;

3. The *sharp norm* of a polyhedral chain, i.e.,

$$|A|^\sharp = \inf\left(\frac{\sum_{i=1}^m |d_i||t_i^r||v_i|}{r+1} + |\sum_{i=1}^m d_i T_{v_i} t_i^r|^\flat\right),$$

where the infimum is taken over all *shifts* v (here $T_v t^r$ is the cell obtained by shifting t^r by a vector v of length $|v|$). A flat chain of finite mass is a sharp chain. If $r = 0$, than $|A|^\flat = |A|^\sharp$.

The metric space of *polyhedral co-chains* (i.e., linear functions of polyhedral chains) can be defined similarly. As a norm of a polyhedral co-chain X one can take:

1. The *co-mass* of a polyhedral co-chain, i.e., $|X| = \sup_{|A|=1} |X(A)|$, where $X(A)$ is the value of the co-chain X on a chain A;
2. The *flat co-norm* of a polyhedral co-chain, i.e., $|X|^\flat = \sup_{|A|^\flat=1} |X(A)|$;
3. The *sharp co-norm* of a polyhedral co-chain, i.e., $|X|^\sharp = \sup_{|A|^\sharp=1} |X(A)|$.

Part III
Distances in Classical Mathematics

Chapter 10
Distances in Algebra

10.1 Group Metrics

A *group* $(G, \cdot, e)$ is a set G of elements with a binary operation $\cdot$, called the *group operation*, that together satisfy the four fundamental properties of *closure* ($x \cdot y \in G$ for any $x, y \in G$), *associativity* ($x \cdot (y \cdot z) = (x \cdot y) \cdot z$ for any $x, y, z \in G$), the *identity property* ($x \cdot e = e \cdot x = x$ for any $x \in G$), and the *inverse property* (for any $x \in G$, there exists an element $x^{-1} \in G$ such that $x \cdot x^{-1} = x^{-1} \cdot x = e$).

In additive notation, a group $(G, +, 0)$ is a set G with a binary operation $+$ such that the following properties hold: $x+y \in G$ for any $x, y \in G$, $x+(y+z) = (x+y)+z$ for any $x, y, z \in G$, $x + 0 = 0 + x = x$ for any $x \in G$, and, for any $x \in G$, there exists an element $-x \in G$ such that $x + (-x) = (-x) + x = 0$.

A group $(G, \cdot, e)$ is called *finite* if the set G is finite. A group $(G, \cdot, e)$ is called *Abelian* if it is *commutative*, i.e., $x \cdot y = y \cdot x$ for any $x, y \in G$.

Most metrics considered in this section are **group norm metrics** on a group $(G, \cdot, e)$, defined by

$$||x \cdot y^{-1}||$$

(or, sometimes, by $||y^{-1} \cdot x||$), where $||.||$ is a *group norm*, i.e., a function $||.|| : G \to \mathbb{R}$ such that, for any $x, y \in G$, we have the following properties:

1. $||x|| \geq 0$, with $||x|| = 0$ if and only if $x = e$;
2. $||x|| = ||x^{-1}||$;
3. $||x \cdot y|| \leq ||x|| + ||y||$ (*triangle inequality*).

In additive notation, a group norm metric on a group $(G, +, 0)$ is defined by $||x + (-y)|| = ||x - y||$, or, sometimes, by $||(-y) + x||$.

The simplest example of a group norm metric is the **bi-invariant ultrametric** (sometimes called the *Hamming metric*) $||x \cdot y^{-1}||_H$, where $||x||_H = 1$ for $x \neq e$, and $||e||_H = 0$.

© Springer-Verlag Berlin Heidelberg 2016

M.M. Deza, E. Deza, *Encyclopedia of Distances*,
DOI 10.1007/978-3-662-52844-0_10

- **Bi-invariant metric**
  A metric (in general, a semimetric) d on a group $(G, \cdot, e)$ is called **bi-invariant** if

$$d(x, y) = d(x \cdot z, y \cdot z) = d(z \cdot x, z \cdot y)$$

  for any $x, y, z \in G$ (cf. **translation invariant metric** in Chap. 5). Any **group norm metric** on an Abelian group is bi-invariant.
  A metric (in general, a semimetric) d on a group $(G, \cdot, e)$ is called a **right-invariant metric** if $d(x, y) = d(x \cdot z, y \cdot z)$ for any $x, y, z \in G$, i.e., the operation of right multiplication by an element z is a **motion** of the metric space (G, d). Any group norm metric defined by $||x \cdot y^{-1}||$, is right-invariant.
  A metric (in general, a semimetric) d on a group $(G, \cdot, e)$ is called a **left-invariant metric** if $d(x, y) = d(z \cdot x, z \cdot y)$ holds for any $x, y, z \in G$, i.e., the operation of left multiplication by an element z is a motion of the metric space (G, d). Any group norm metric defined by $||y^{-1} \cdot x||$, is left-invariant.
  Any right-invariant or left-invariant (in particular, bi-invariant) metric d on G is a group norm metric, since one can define a group norm on G by $||x|| = d(x, 0)$.
- **G-invariant metric**
  Given a metric space (X, d) and an action $g(x)$ of a group G on it, the metric d is called **G-invariant** (under this action) if for all $x, y \in X, g \in G$ it holds

$$d(g(x), g(y)) = d(x, y).$$

  For every G-invariant metric d_X on X and every point $x \in X$, the function

$$d_G(g_1, g_2) = d_X(g_1(x), g_2(x))$$

  is a **left-invariant metric** on G. This metric is called **orbit metric** in [BBI01], since it is the restriction of d on the orbit Gx, which can be identified with G.
- **Positively homogeneous distance**
  A distance d on an Abelian group $(G, +, 0)$ is called **positively homogeneous** if

$$d(mx, my) = md(x, y)$$

  for all $x, y \in G$ and all $m \in \mathbb{N}$, where mx is the sum of m terms all equal to x.
- **Translation discrete metric**
  A **group norm metric** (in general, a group norm semimetric) on a group $(G, \cdot, e)$ is called **translation discrete** if the *translation distances* (or *translation numbers*)

$$\tau_G(x) = \lim_{n \to \infty} \frac{||x^n||}{n}$$

of the *nontorsion elements* x (i.e., such that $x^n \neq e$ for any $n \in \mathbb{N}$) of the group with respect to that metric are bounded away from zero.

If the numbers $\tau_G(x)$ are just nonzero, such a group norm metric is called a **translation proper metric**.

- **Word metric**

  Let $(G, \cdot, e)$ be a finitely-generated group with a set A of generators (i.e., A is finite, and every element of G can be expressed as a product of finitely many elements A and their inverses). The *word length* $w^A_W(x)$ of an element $x \in G\backslash\{e\}$ is defined by

$$w^A_W(x) = \inf\{r : x = a_1^{\epsilon_1} \dots a_r^{\epsilon_r}, a_i \in A, \epsilon_i \in \{\pm 1\}\} \text{ and } w^A_W(e) = 0.$$

  The **word metric** d^A_W *associated with* A is a **group norm metric** on G defined by

$$w^A_W(x \cdot y^{-1}).$$

  As the word length w^A_W is a *group norm* on G, d^A_W is **right-invariant**. Sometimes it is defined as $w^A_W(y^{-1} \cdot x)$, and then it is **left-invariant**. In fact, d^A_W is the maximal metric on G that is right-invariant, and such that the distance from any element of A or A^{-1} to the identity element e is equal to one.

  If A and B are two finite sets of generators of the group $(G, \cdot, e)$, then the identity mapping between the metric spaces (G, d^A_W) and (G, d^B_W) is a **quasi-isometry**, i.e., the word metric is unique up to quasi-isometry.

  The word metric is the **path metric** of the *Cayley graph* Γ of $(G, \cdot, e)$, constructed with respect to A. Namely, Γ is a graph with the vertex-set G in which two vertices x and $y \in G$ are connected by an edge if and only if $y = a^\epsilon x$, $\epsilon = \pm 1$, $a \in A$.

- **Weighted word metric**

  Let $(G, \cdot, e)$ be a finitely-generated group with a set A of generators. Given a bounded *weight function* $w : A \to (0, \infty)$, the *weighted word length* $w^A_{WW}(x)$ of an element $x \in G\backslash\{e\}$ is defined by $w^A_{WW}(e) = 0$ and

$$w^A_{WW}(x) = \inf\left\{\sum_{i=1}^{t} w(a_i), t \in \mathbb{N} : x = a_1^{\epsilon_1} \dots a_t^{\epsilon_t}, a_i \in A, \epsilon_i \in \{\pm 1\}\right\}.$$

  The **weighted word metric** d^A_{WW} *associated with* A is a **group norm metric** on G defined by

$$w^A_{WW}(x \cdot y^{-1}).$$

  As the weighted word length w^A_{WW} is a *group norm* on G, d^A_{WW} is **right-invariant**. Sometimes it is defined as $w^A_{WW}(y^{-1} \cdot x)$, and then it is **left-invariant**.

The metric d^A_{WW} is the supremum of semimetrics d on G with the property that $d(e,a) \leq w(a)$ for any $a \in A$.

The metric d^A_{WW} is a **coarse-path metric**, and every right-invariant coarse path metric is a weighted word metric up to **coarse isometry**.

The metric d^A_{WW} is the **path metric** of the *weighted Cayley graph* Γ_W of $(G,\cdot,e)$ constructed with respect to A. Namely, Γ_W is a weighted graph with the vertex-set G in which two vertices x and $y \in G$ are connected by an edge with the weight $w(a)$ if and only if $y = a^\epsilon x$, $\epsilon = \pm 1$, $a \in A$.

- **Interval norm metric**

  An **interval norm metric** is a **group norm metric** on a finite group $(G,\cdot,e)$ defined by

$$||x \cdot y^{-1}||_{int},$$

  where $||.||_{int}$ is an *interval norm* on G, i.e., a *group norm* such that the values of $||.||_{int}$ form a set of consecutive integers starting with 0.

  To each interval norm $||.||_{int}$ corresponds an ordered *partition* $\{B_0,\ldots,B_m\}$ of G with $B_i = \{x \in G : ||x||_{int} = i\}$; cf. **Sharma–Kaushik distance** in Chap. 16. The *Hamming* and *Lee* norms are special cases of interval norm. A *generalized Lee norm* is an interval norm for which each class has a form $B_i = \{a, a^{-1}\}$.

- ***C*-metric**

  A ***C*-metric** d is a metric on a group $(G,\cdot,e)$ satisfying the following conditions:

  1. The values of d form a set of consecutive integers starting with 0;
  2. The cardinality of the sphere $B(x,r) = \{y \in G : d(x,y) = r\}$ is independent of the particular choice of $x \in G$.

  The **word metric**, the **Hamming metric**, and the **Lee metric** are C-metrics. Any **interval norm metric** is a C-metric.

- **Order norm metric**

  Let $(G,\cdot,e)$ be a finite Abelian group. Let $ord(x)$ be the *order* of an element $x \in G$, i.e., the smallest positive integer n such that $x^n = e$. Then the function $||.||_{ord} : G \to \mathbb{R}$ defined by $||x||_{ord} = \ln ord(x)$, is a *group norm* on G, called the *order norm*.

  The **order norm metric** is a **group norm metric** on G, defined by

$$||x \cdot y^{-1}||_{ord}.$$

- **Tărnăuceanu metric**

  Let $o(a)$ denote the order of the element a of a group. Let C be the class of finite groups G in which $o(ab) < o(a) + o(b)$ for every $a, b \in G$. Tărnăuceanu,

2015, noted that the function $d : G \times G \to \mathbb{N}$ defined by

$$d(x, y) = o(xy^{-1}) - 1$$

for all $x, y \in G$ is a metric on G if and only if $G \in C$.

He found that C contains all Abelian p-groups, Q_8, and A_4, but not nonabelian finite simple groups, alternating groups $A(n)$ with $n \geq 5$, and, for $n \geq 4$, $Sym(n)$, quaternion groups Q_{2^n}, dihedral groups D_{2n}. C is closed under subgroups, but not under direct products or extensions. The centralizers of nontrivial elements of such groups contain only elements of prime power order.

- **Monomorphism norm metric**

  Let $(G, +, 0)$ be a group. Let $(H, \cdot, e)$ be a group with a *group norm* $||.||_H$. Let $f : G \to H$ be a *monomorphism* of groups G and H, i.e., an injective function such that $f(x+y) = f(x) \cdot f(y)$ for any $x, y \in G$. Then the function $||.||_G^f : G \to \mathbb{R}$ defined by $||x||_G^f = ||f(x)||_H$, is a *group norm* on G, called the *monomorphism norm*.

  The **monomorphism norm metric** is a **group norm metric** on G defined by

$$||x - y||_G^f.$$

- **Product norm metric**

  Let $(G, +, 0)$ be a group with a *group norm* $||.||_G$. Let $(H, \cdot, e)$ be a group with a group norm $||.||_H$. Let $G \times H = \{\alpha = (x, y) : x \in G, y \in H\}$ be the Cartesian product of G and H, and $(x, y) \cdot (z, t) = (x + z, y \cdot t)$.

  Then the function $||.||_{G\times H} : G \times H \to \mathbb{R}$ defined by $||\alpha||_{G\times H} = ||(x, y)||_{G\times H} = ||x||_G + ||y||_H$, is a group norm on $G \times H$, called the *product norm*.

  The **product norm metric** is a **group norm metric** on $G \times H$ defined by

$$||\alpha \cdot \beta^{-1}||_{G\times F}.$$

  On the Cartesian product $G \times H$ of two finite groups with the *interval norms* $||.||_G^{int}$ and $||.||_H^{int}$, an interval norm $||.||_{G\times H}^{int}$ can be defined. In fact, $||\alpha||_{G\times H}^{int} = ||(x, y)||_{G\times H}^{int} = ||x||_G + (m + 1)||y||_H$, where $m = \max_{a\in G} ||a||_G^{int}$.

- **Quotient norm metric**

  Let $(G, \cdot, e)$ be a group with a *group norm* $||.||_G$. Let $(N, \cdot, e)$ be a *normal subgroup* of $(G, \cdot, e)$, i.e., $xN = Nx$ for any $x \in G$. Let $(G/N, \cdot, eN)$ be the *quotient group* of G, i.e., $G/N = \{xN : x \in G\}$ with $xN = \{x \cdot a : a \in N\}$, and $xN \cdot yN = xyN$. Then the function $||.||_{G/N} : G/N \to \mathbb{R}$ defined by $||xN||_{G/N} = \min_{a\in N} ||xa||_X$, is a group norm on G/N, called the *quotient norm*.

  A **quotient norm metric** is a **group norm metric** on G/N defined by

$$||xN \cdot (yN)^{-1}||_{G/N} = ||xy^{-1}N||_{G/N}.$$

If $G = \mathbb{Z}$ with the norm being the absolute value, and $N = m\mathbb{Z}$, $m \in \mathbb{N}$, then the quotient norm on $\mathbb{Z}/m\mathbb{Z} = \mathbb{Z}_m$ coincides with the *Lee norm*.

If a metric d on a group $(G, \cdot, e)$ is **right-invariant**, then for any normal subgroup $(N, \cdot, e)$ of $(G, \cdot, e)$ the metric d induces a right-invariant metric (in fact, the **Hausdorff metric**) d^* on G/N by

$$d^*(xN, yN) = \max\{\max_{b\in yN} \min_{a\in xN} d(a, b), \max_{a\in xN} \min_{b\in yN} d(a, b)\}.$$

- **Commutation distance**

  Let $(G, \cdot, e)$ be a finite nonabelian group. Let $Z(G) = \{c \in G : x \cdot c = c \cdot x \text{ for any } x \in G\}$ be the *center* of G.

  The *commutation graph* of G is defined as a graph with the vertex-set G in which distinct elements $x, y \in G$ are connected by an edge whenever they *commute*, i.e., $x \cdot y = y \cdot x$. (Darafsheh, 2009, consider noncommuting graph on $G \setminus Z(G)$.)

  Any two noncommuting elements $x, y \in G$ are connected in this graph by the path x, c, y, where c is any element of $Z(G)$ (for example, e). A path $x = x^1, x^2, \ldots, x^k = y$ in the commutation graph is called an $(x - y)$ N-path if $x^i \notin Z(G)$ for any $i \in \{1, \ldots, k\}$. In this case the elements $x, y \in G\setminus Z(G)$ are called *N-connected*.

  The **commutation distance** (see [DeHu98]) d is an extended distance on G defined by the following conditions:

  1. $d(x, x) = 0$;
  2. $d(x, y) = 1$ if $x \neq y$, and $x \cdot y = y \cdot x$;
  3. $d(x, y)$ is the minimum length of an $(x - y)$ N-path for any N-connected elements x and $y \in G\setminus Z(G)$;
  4. $d(x, y) = \infty$ if $x, y \in G\setminus Z(G)$ are not connected by any N-path.

  Given a group G and a G-conjugacy class X in it, Bates–Bundy–Perkins–Rowley in 2003, 2004, 2007, 2008 considered *commuting graph* (X, E) whose vertex set is X and distinct vertices $x, y \in X$ are joined by an edge $e \in E$ whenever they commute.

- **Modular distance**

  Let $(\mathbb{Z}_m, +, 0)$, $m \geq 2$, be a finite *cyclic group*. Let $r \in \mathbb{N}$, $r \geq 2$. The *modular r-weight* $w_r(x)$ of an element $x \in \mathbb{Z}_m = \{0, 1, \ldots, m\}$ is defined as $w_r(x) = \min\{w_r(x), w_r(m - x)\}$, where $w_r(x)$ is the *arithmetic r-weight* of the integer x.

  The value $w_r(x)$ can be obtained as the number of nonzero coefficients in the *generalized nonadjacent form* $x = e_n r^n + \ldots e_1 r + e_0$ with $e_i \in \mathbb{Z}$, $|e_i| < r$, $|e_i + e_{i+1}| < r$, and $|e_i| < |e_{i+1}|$ if $e_i e_{i+1} < 0$. Cf. **arithmetic** r**-norm metric** in Chap. 12.

  The **modular distance** is a distance on $\mathbb{Z}_m$, defined by

$$w_r(x - y).$$

The modular distance is a metric for $w_r(m) = 1$, $w_r(m) = 2$, and for several special cases with $w_r(m) = 3$ or 4. In particular, it is a metric for $m = r^n$ or $m = r^n - 1$; if $r = 2$, it is a metric also for $m = 2^n + 1$ (see, for example, [Ernv85]).

The most popular metric on $\mathbb{Z}_m$ is the **Lee metric** defined by $||x-y||_{Lee}$, where $||x||_{Lee} = \min\{x, m-x\}$ is the *Lee norm* of an element $x \in \mathbb{Z}_m$.

- *G*-**norm metric**

  Consider a finite field $\mathbb{F}_{p^n}$ for a prime p and a natural number n. Given a compact convex centrally-symmetric body G in $\mathbb{R}^n$, define the *G-norm* of an element $x \in \mathbb{F}_{p^n}$ by $||x||_G = \inf\{\mu \geq 0 : x \in p\mathbb{Z}^n + \mu G\}$.

  The *G*-**norm metric** is a **group norm metric** on $\mathbb{F}_{p^n}$ defined by

$$||x \cdot y^{-1}||_G.$$

- **Permutation norm metric**

  Given a finite metric space (X, d), the **permutation norm metric** is a **group norm metric** on the group $(Sym_X, \cdot, id)$ of all permutations of X (id is the *identity mapping*) defined by

$$||f \cdot g^{-1}||_{Sym},$$

  where the *group norm* $||.||_{Sym}$ on Sym_X is given by $||f||_{Sym} = \max_{x \in X} d(x, f(x))$.

- **Metric of motions**

  Let (X, d) be a metric space, and let $p \in X$ be a fixed element of X.

  The **metric of motions** (see [Buse55]) is a metric on the group $(\Omega, \cdot, id)$ of all **motions** of (X, d) (id is the *identity mapping*) defined by

$$\sup_{x \in X} d(f(x), g(x)) \cdot e^{-d(p,x)}$$

  for any $f, g \in \Omega$ (cf. **Busemann metric of sets** in Chap. 3). If the space (X, d) is bounded, a similar metric on Ω can be defined as

$$\sup_{x \in X} d(f(x), g(x)).$$

  Given a semimetric space (X, d), the **semimetric of motions** on $(\Omega, \cdot, id)$ is

$$d(f(p), g(p)).$$

- **General linear group semimetric**

  Let $\mathbb{F}$ be a locally compact nondiscrete *topological field*. Let $(\mathbb{F}^n, ||.||_{\mathbb{F}^n})$, $n \geq 2$, be a *normed vector space* over $\mathbb{F}$. Let $||.||$ be the *operator norm* associated with the normed vector space $(\mathbb{F}^n, ||.||_{\mathbb{F}^n})$. Let $GL(n, \mathbb{F})$ be the *general linear group* over $\mathbb{F}$. Then the function $|.|_{op} : GL(n, \mathbb{F}) \to \mathbb{R}$ defined by $|g|_{op} = \sup\{|\ln ||g||\,|, |\ln ||g^{-1}||\,|\}$, is a seminorm on $GL(n, \mathbb{F})$.

The **general linear group semimetric** on the group $GL(n, \mathbb{F})$ is defined by

$$|g \cdot h^{-1}|_{op}.$$

It is a **right-invariant** semimetric which is unique, up to **coarse isometry**, since any two norms on $\mathbb{F}^n$ are **bi-Lipschitz equivalent**.

- **Generalized torus semimetric**

  Let $(T, \cdot, e)$ be a *generalized torus*, i.e., a *topological group* which is isomorphic to a direct product of n multiplicative groups $\mathbb{F}_i^*$ of locally compact nondiscrete *topological fields* $\mathbb{F}_i$. Then there is a proper continuous homomorphism $v : T \to \mathbb{R}^n$, namely, $v(x_1, \ldots, x_n) = (v_1(x_1), \ldots, v_n(x_n))$, where $v_i : \mathbb{F}_i^* \to \mathbb{R}$ are proper continuous homomorphisms from the $\mathbb{F}_i^*$ to the additive group $\mathbb{R}$, given by the logarithm of the *valuation*. Every other proper continuous homomorphism $v' : T \to \mathbb{R}^n$ is of the form $v' = \alpha \cdot v$ with $\alpha \in GL(n, \mathbb{R})$. If $||.||$ is a norm on $\mathbb{R}^n$, one obtains the corresponding seminorm $||x||_T = ||v(x)||$ on T.

  The **generalized torus semimetric** is defined on the group $(T, \cdot, e)$ by

$$||xy^{-1}||_T = ||v(xy^{-1})|| = ||v(x) - v(y)||.$$

- **Stable norm metric**

  Given a Riemannian manifold (M, g), the **stable norm metric** is a **group norm metric** on its *real homology group* $H_k(M, \mathbb{R})$ defined by the following *stable norm* $||h||_s$: the infimum of the Riemannian k-volumes of real cycles representing h.

  The Riemannian manifold $(\mathbb{R}^n, g)$ is within finite **Gromov–Hausdorff distance** (cf. Chap. 1) from an n-dimensional normed vector space $(\mathbb{R}^n, ||.||_s)$.

  If (M, g) is a compact connected oriented Riemannian manifold, then the manifold $H_1(M, \mathbb{R})/H_1(M, \mathbb{R})$ with metric induced by $||.||_s$ is called the *Albanese torus* (or *Jacobi torus*) of (M, g). This **Albanese metric** is a **flat metric** (Chap. 8).

- **Heisenberg metric**

  Let $(H, \cdot, e)$ be the (real) *Heisenberg group* $\mathcal{H}^n$, i.e., a group on the set $H = \mathbb{R}^n \times \mathbb{R}^n \times \mathbb{R}$ with the group law $h \cdot h' = (x, y, t) \cdot (x', y', t') = (x + x', y + y', t + t' + 2\sum_{i=1}^n (x_i' y_i - x_i y_i'))$, and the identity $e = (0, 0, 0)$. Let $|.|_{Heis}$ be the *Heisenberg gauge* (Cygan, 1978) on $\mathcal{H}^n$ defined by $|h|_{Heis} = |(x, y, t)|_{Heis} = ((\sum_{i=1}^n (x_i^2 + y_i^2))^2 + t^2)^{1/4}$.

  The **Heisenberg metric** (or **Korányi metric**, **Cygan metric**, **gauge metric**) d_{Heis} is a **group norm metric** on $\mathcal{H}^n$ defined by

$$|x^{-1} \cdot y|_{Heis}.$$

One can identify the Heisenberg group $\mathcal{H}^{n-1} = \mathbb{C}^{n-1} \times \mathbb{R}$ with $\partial \mathbb{H}_{\mathbb{C}}^n \setminus \{\infty\}$, where $\mathbb{H}_{\mathbb{C}}^n$ is the Hermitian (i.e., complex) hyperbolic n-space, and ∞ is any point of its boundary $\partial \mathbb{H}_{\mathbb{C}}^n$. So, the usual hyperbolic metric of $\mathbb{H}_{\mathbb{C}}^{n+1}$ induces a metric

on $\mathcal{H}^n$. The **Hamenstädt distance** on $\partial\mathbb{H}^n_{\mathbb{C}} \setminus \{\infty\}$ (Hersonsky–Paulin, 2004) is $\frac{1}{\sqrt{2}} d_{Heis}$.

Sometimes, the term *Cygan metric* is reserved for the extension of the metric d_{Heis} on whole $\mathbb{H}^n_{\mathbb{C}}$ and (Apanasov, 2004) for its generalization (via the *Carnot group* $\mathbb{F}^{n-1} \times Im\mathbb{F}$) on $\mathbb{F}$-hyperbolic spaces $\mathbb{H}^n_{\mathbb{F}}$ over numbers $\mathbb{F}$ that can be complex numbers, or quaternions or, for $n = 2$, octonions. Also, the generalization of d_{Heis} on Carnot groups *of Heisenberg type* is called the *Cygan metric*.

The second natural metric on $\mathcal{H}^n$ is the **Carnot–Carathéodory metric** (or **CC metric**, **sub-Riemannian metric**; cf. Chap. 7) d_C defined as the **length metric** (Chap. 6) using *horizontal vector fields* on $\mathcal{H}^n$. This metric is the **internal metric** (Chap. 4) corresponding to d_{Heis}.

The metric d_{Heis} is **bi-Lipschitz equivalent** with d_C but not with any Riemannian distance and, in particular, not with any Euclidean metric. For both metrics, the Heisenberg group $\mathcal{H}^n$ is a **fractal** since its **Hausdorff dimension**, $2n + 2$, is strictly greater than its **topological dimension**, $2n + 1$.

- **Metric between intervals**

  Let G be the set of all intervals $[a, b]$ of $\mathbb{R}$. The set G forms semigroups $(G, +)$ and $(G, \cdot)$ under addition $I + J = \{x + y : x \in I, y \in J\}$ and under multiplication $I \cdot J = \{x \cdot y : x \in I, y \in J\}$, respectively.

  The **metric between intervals** is a metric on G, defined by

$$\max\{|I|, |J|\}$$

  for all $I, J \in G$, where, for $K = [a, b]$, one has $|K| = |a - b|$.

- **Metric between games**

  Consider *positional games*, i.e., two-player nonrandom games of perfect information with real-valued outcomes. Play is alternating with a nonterminated game having move options for both players. Real-world examples include Chess, Go and Tic-Tac-Toe. Formally, let $F_{\mathbb{R}}$ be the universe of games defined inductively as follows:

  1. Every real number $r \in \mathbb{R}$ belongs to $F_{\mathbb{R}}$ and is called an *atomic game*.
  2. If $A, B \subset F_{\mathbb{R}}$ with $1 \leq |A|, |B| < \infty$, then $\{A|B\} \in F_{\mathbb{R}}$ (*nonatomic game*).

  Write any game $G = \{A|B\}$ as $\{G^L|G^R\}$, where $G^L = A$ and $G^R = B$ are the set of left and right moves of G, respectively.

  $F_{\mathbb{R}}$ becomes a commutative semigroup under the following addition operation:

  1. If p and q are atomic games, then $p + q$ is the usual addition in $\mathbb{R}$.
  2. $p + \{g_{l_1}, \ldots | g_{r_1}, \ldots\} = \{g_{l_1} + p, \ldots | g_{r_1} + p, \ldots\}$.
  3. If G and H are both nonatomic, then $\{G^L|G^R\} + \{H^L|H^R\} = \{I^L|I^R\}$, where $I^L = \{g_l + H, G + h_l : g_l \in G^L, h_l \in H^L\}$ and $I^R = \{g_r + H, G + h_r : g_r \in G^R, h_r \in H^R\}$.

For any game $G \in F_{\mathbb{R}}$, define the optimal outcomes $\overline{L}(G)$ and $\overline{R}(G)$ (if both players play optimally with Left and Right starting, respectively) as follows:

$\overline{L}(p) = \overline{R}(p) = p$ and $\overline{L}(G) = \max\{\overline{R}(g_l) : g_l \in G^L\}$, $\overline{R}(G) = \max\{\overline{L}(g_r) : g_r \in G^R\}$.

The **metric between games** G and H defined by Ettinger, 2000, is the following **extended metric** on $F_{\mathbb{R}}$:

$$\sup_X |\overline{L}(G+X) - \overline{L}(H+X)| = \sup_X |\overline{R}(G+X) - \overline{R}(H+X)|.$$

- **Helly semimetric**

  Consider a game $(\mathcal{A}, \mathcal{B}, H)$ between players A and B with *strategy sets* $\mathcal{A}$ and $\mathcal{B}$, respectively. Here $H = H(\cdot,\cdot)$ is the *payoff function*, i.e., if player A plays $a \in \mathcal{A}$ and player B plays $b \in \mathcal{B}$, then A pays H(a,b) to B. A player's *strategy set* is the set of available to him *pure strategies*, i.e., complete algorithms for playing the game, indicating the move for every possible situation throughout it.

  The **Helly semimetric** between strategies $a_1 \in \mathcal{A}$ and $a_2 \in \mathcal{A}$ of A is defined by

$$\sup_{b \in \mathcal{B}} |H(a_1, b) - H(a_2, b)|.$$

- **Factorial ring semimetric**

  Let $(A, +, \cdot)$ be a *factorial ring*, i.e., an *integral domain* (nonzero commutative ring with no nonzero zero divisors), in which every nonzero nonunit element can be written as a product of (nonunit) irreducible elements, and such factorization is unique up to permutation.

  The **factorial ring semimetric** is a semimetric on the set $A\backslash\{0\}$, defined by

$$\ln \frac{lcm(x,y)}{gcd(x,y)},$$

  where $lcm(x,y)$ is the *least common multiple*, and $gcd(x,y)$ is the *greatest common divisor* of elements $x, y \in A\backslash\{0\}$.

- **Frankild–Sather–Wagstaff metric**

  Let $\mathcal{G}(R)$ be the set of isomorphism classes, up to a shift, of semidualizing complexes over a local Noetherian commutative ring R. An *R-complex* is a particular sequence of R-module homomorphisms; see [FrSa07]) for exact definitions.

  The **Frankild–Sather–Wagstaff metric** ([FrSa07]) is a metric on $\mathcal{G}(R)$ defined, for any classes $[K], [L] \in \mathcal{G}(R)$, as the infimum of the *lengths* of chains of pairwise comparable elements starting with $[K]$ and ending with $[L]$.

10.2 Metrics on Binary Relations

A *binary relation* R on a set X is a subset of $X \times X$; it is the arc-set of the directed graph (X, R) with the vertex-set X.

A binary relation R which is *symmetric* ($(x, y) \in R$ implies $(y, x) \in R$), *reflexive* (all $(x, x) \in R$), and *transitive* ($(x, y), (y, z) \in R$ imply $(x, z) \in R$) is called an *equivalence relation* or a *partition* (of X into equivalence classes). Any *q-ary sequence* $x = (x_1, \ldots, x_n)$, $q \geq 2$ (i.e., with $0 \leq x_i \leq q - 1$ for $1 \leq i \leq n$), corresponds to the partition $\{B_0, \ldots, B_{q-1}\}$ of $V_n = \{1, \ldots, n\}$, where $B_j = \{1 \leq i \leq n : x_i = j\}$ are the equivalence classes.

A binary relation R which is *antisymmetric* ($(x, y), (y, x) \in R$ imply $x = y$), reflexive, and transitive is called a *partial order*, and the pair (X, R) is called a *poset* (partially ordered set). A partial order R on X is denoted also by $\preceq$ with $x \preceq y$ if and only if $(x, y) \in R$. The order $\preceq$ is called *linear* if any elements $x, y \in X$ are *compatible*, i.e., $x \preceq y$ or $y \preceq x$.

A poset $(L, \preceq)$ is called a *lattice* if every two elements $x, y \in L$ have the *join* $x \vee y$ and the *meet* $x \wedge y$. All partitions of X form a lattice $\mathbb{P}_X$ by refinement; it is a sublattice of the lattice (by set-inclusion) of all binary relations.

- **Kemeny distance**

  The **Kemeny distance** between binary relations R_1 and R_2 on a set X is the **Hamming metric** $|R_1 \triangle R_2|$. It is twice the minimal number of inversions of pairs of adjacent elements of X which is necessary to obtain R_2 from R_1.

  If R_1, R_2 are *partitions*, then the Kemeny distance coincides with the **Mirkin–Tcherny distance**, and $1 - \frac{|R_1 \triangle R_2|}{n(n-1)}$ is the *Rand index*.

  If binary relations R_1, R_2 are *linear orders* (or *permutations*) on the set X, then the Kemeny distance coincides with the **Kendall τ distance** (Chap. 11).
- **Drápal–Kepka distance**

  The **Drápal–Kepka distance** between distinct *quasigroups* (differing from groups in that they need not be associative) $(X, +)$ and $(X, \cdot)$ is the **Hamming metric** $|\{(x, y) : x + y \neq x \cdot y\}|$ between their *Cayley tables*.

  For finite nonisomorphic groups, this distance is (Ivanyos, Le Gall and Yoshida, 2012) at least $2(\frac{|X|}{3})^2$ with equality (Drápal, 2003) for some 3-groups.
- **Editing metrics between partitions**

  Let X be a finite set, $|X| = n$, and let A, B be nonempty subsets of X. Let $\mathcal{P}_X$ be the set of partitions of X, and $P, Q \in \mathcal{P}_X$. Let $P_1, \ldots, P_q$ be *blocks* in the partition P, i.e., the pairwise disjoint sets such that $X = P_1 \cup \cdots \cup P_q$, $q \geq 1$. Let $P \vee Q$ and $P \wedge Q$ be the *join* and *meet* of P and Q in the *lattice* $\mathbb{P}_X$ *of partitions* of X.

  Consider the following *editing operations* on partitions (clusterings):

  – An *augmentation* transforms a partition P of $A \backslash \{B\}$ into a partition of A by either including the objects of B in a block, or including B as a new block;
  – An *removal* transforms a partition P of A into a partition of $A \backslash \{B\}$ by deleting the objects in B from each block that contains them;

– A *division* transforms one partition P into another by the simultaneous removal of B from P_i (where $B \subset P_i$, $B \neq P_i$), and augmentation of B as a new block;
– A *merging* transforms one partition P into another by the simultaneous removal of B from P_i (where $B = P_i$), and augmentation of B to P_j (where $j \neq i$);
– A *transfer* transforms one partition P into another by the simultaneous removal of B from P_i (where $B \subset P_i$), and augmentation of B to P_j (where $j \neq i$).

Define (see, say, [Day81]), using above operations, the following metrics on $\mathcal{P}_X$:

1. The minimum number of augmentations and removals of single objects needed to transform P into Q;
2. The minimum number of divisions, mergings, and transfers of single objects needed to transform P into Q;
3. The minimum number of divisions, mergings, and transfers needed to transform P into Q;
4. The minimum number of divisions and mergings needed to transform P into Q; in fact, it is equal to $|P| + |Q| - 2|P \vee Q|$;
5. $\sigma(P) + \sigma(Q) - 2\sigma(P \wedge Q)$, where $\sigma(P) = \sum_{P_i \in P} |P_i|(|P_i| - 1)$;
6. $e(P) + e(Q) - 2e(P \wedge Q)$, where $e(P) = \log_2 n + \sum_{P_i \in P} \frac{|P_i|}{n} \log_2 \frac{|P_i|}{n}$;
7. $2n - \sum_{P_i \in P} \max_{Q_j \in Q} |P_i \cap Q_j| - \sum_{Q_j \in Q} \max_{P_i \in P} |P_i \cap Q_j|$ (van Dongen, 2000).

The **maximum matching distance** (or *partition-distance* as defined in Gusfield, 2002) is (Réignier, 1965) the minimum number of elements that must be moved between the blocks of partition P in order to transform it into Q.

- **Rossi–Hamming metric**

  Given a partition $P = (P_1, \ldots, P_q)$ of a finite set X, its *size* is defined as $s(P) = \frac{1}{2} \sum_{1 \leq i \leq q} |P_i|(|P_i| - 1)$. We call the **Rossi–Hamming metric** the metric between partitions P and Q, defined in Rossi, 2014, as

$$d_{RH}(P, Q) = s(P) + s(Q) - 2s(P \wedge Q).$$

  One has $d_{RH}(P, Q) \leq s(P \vee Q) - s(P \wedge Q)$, where the right-hand side is the *size-based distance* (Rossi, 2011). The inequality is strict only for some noncomparable P, Q.

10.3 Metrics on Semilattices

Consider a poset $(L, \preceq)$. The *meet* (or *infimum*) $x \wedge y$ (if it exists) of two elements x and y is the unique element satisfying $x \wedge y \preceq x, y$, and $z \preceq x \wedge y$ if $z \preceq x, y$. The *join* (or *supremum*) $x \vee y$ (if it exists) is the unique element such that $x, y \preceq x \vee y$,

and $x \vee y \preceq z$ if $x, y \preceq z$. A poset $(L, \preceq)$ is called a *lattice* if every its elements x, y have the join $x \vee y$ and the meet $x \wedge y$. A poset is a *meet* (or *lower*) *semilattice* if only the meet-operation is defined. A poset is a *join* (or *upper*) *semilattice* if only the join-operation is defined.

A lattice $\mathbb{L} = (L, \preceq, \vee, \wedge)$ is called a *semimodular lattice* if the *modularity relation xMy* is symmetric: *xMy* implies *yMx* for any $x, y \in L$. Here two elements x and y are said to constitute a *modular pair*, in symbols *xMy*, if $x \wedge (y \vee z) = (x \wedge y) \vee z$ for any $z \preceq x$. A lattice $\mathbb{L}$ in which every pair of elements is modular, is called a *modular lattice*.

Given a lattice $\mathbb{L}$, a function $v : L \to \mathbb{R}_{\geq 0}$, satisfying $v(x \vee y) + v(x \wedge y) \leq v(x) + v(y)$ for all $x, y \in L$, is called a *subvaluation* on $\mathbb{L}$. A subvaluation v is *isotone* if $v(x) \leq v(y)$ whenever $x \preceq y$, and it is *positive* if $v(x) < v(y)$ whenever $x \preceq y$, $x \neq y$. A subvaluation v is called a *valuation* if it is isotone and $v(x \vee y) + v(x \wedge y) = v(x) + v(y)$ for all $x, y \in L$.

- **Lattice valuation metric**

  Let $\mathbb{L} = (L, \preceq, \vee, \wedge)$ be a lattice, and let v be an isotone subvaluation on $\mathbb{L}$. The *lattice subvaluation semimetric* d_v on L is defined by

  $$2v(x \vee y) - v(x) - v(y).$$

  (It can be defined also on some semilattices.) If v is a positive subvaluation on $\mathbb{L}$, one obtains a metric, called the **lattice subvaluation metric**. If v is a valuation, d_v is called the *valuation semimetric* and can be written as

  $$v(x \vee y) - v(x \wedge y) = v(x) + v(y) - 2v(x \wedge y).$$

  If v is a positive valuation on $\mathbb{L}$, one obtains a metric, called the **lattice valuation metric**, and the lattice is called a **metric lattice**.

  An example is the **Hamming distance** $d_H(A, B) = |A \cup B| - |A \cap B|$ on the lattice $(P(X), \cup, \cap)$ of all subsets of the set X. Cf. also the **Shannon distance** (Chap. 14), which can be seen as a distance on partitions.

  If $L = \mathbb{N}$ (the set of positive integers), $x \vee y = lcm(x, y)$ (least common multiple), $x \wedge y = gcd(x, y)$ (greatest common divisor), and the positive valuation $v(x) = \ln x$, then $d_v(x, y) = \ln \frac{lcm(x,y)}{gcd(x,y)}$.

  This metric can be generalized on any *factorial ring* equipped with a positive valuation v such that $v(x) \geq 0$ with equality only for the multiplicative unit of the ring, and $v(xy) = v(x) + v(y)$. Cf. **factorial ring semimetric**.
- **Finite subgroup metric**

  Let $(G, \cdot, e)$ be a group. Let $\mathbb{L} = (L, \subset, \cap)$ be the meet semilattice of all finite subgroups of the group $(G, \cdot, e)$ with the meet $X \cap Y$ and the valuation $v(X) = \ln |X|$.

  The **finite subgroup metric** is a **valuation metric** on L defined by

  $$v(X) + v(Y) - 2v(X \wedge Y) = \ln \frac{|X||Y|}{(|X \cap Y|)^2}.$$

- **Join semilattice distances**

  Let $\mathbb{L} = (L, \preceq, \vee)$ be a join semilattice, finite or infinite, such that every maximal chain in every interval $[x, y]$ is finite. For $x \preceq y$, the *height* $h(x, y)$ *of* y *above* x is the least cardinality of a finite maximal (by inclusion) chain of $[x, y]$ minus 1. Call the join semilattice $\mathbb{L}$ *semimodular* if for all $x, y \in L$, whenever there exists an element z covered by both x and y, the join $x \vee y$ covers both x and y, or, in other words, whenever elements x, y have a common lower bound z, it holds $h(x, x \vee y) \leq h(z, y)$. Any *tree* (i.e., all intervals $[x, z]$ are finite, each pair x, y of uncomparable elements have a least common upper bound $x \vee y$ but they never have a common lower bound) is semimodular. Consider the following distances on L:

  $d_{\text{path}}(x, y)$ is the path metric of the *Hasse diagram* of $(L, \preceq)$, i.e., a graph with vertex-set L and an edge between two elements if they are comparable.

  $d_{a.\text{path}}(x, y)$ is the smallest number of the form $h(x, z) + h(y, z)$, where z is a common upper bound of x and y, i.e., it is the **ancestral path distance**; cf. **pedigree-based distances** in Chap. 23. This and next distance reflect the way how Roman civil law and medieval canon law, respectively, measured degree of kinship.

  $d_{\max}(x, y)$ is defined by $\max(h(x, x \vee y), h(y, x \vee y))$.

  It holds $d_{a.\text{path}}(x, y) \geq d_{\text{path}}(x, y) \geq d_{\max}(x, y)$. Foldes, 2013, proved that $d_{\max}(x, y)$ is a metric if $\mathbb{L}$ is semimodular and that $d_{a.\text{path}}(x, y)$ is a metric if and only if $\mathbb{L}$ is semimodular, in which case $d_{a.\text{path}}(x, y) = d_{\text{path}}(x, y)$.

- **Gallery distance of flags**

  Let $\mathbb{L}$ be a lattice. A *chain* C in $\mathbb{L}$ is a subset of L which is *linearly ordered*, i.e., any two elements of C are compatible. A *flag* is a chain in $\mathbb{L}$ which is maximal with respect to inclusion. If $\mathbb{L}$ is a semimodular lattice, containing a finite flag, then $\mathbb{L}$ has a unique minimal and a unique maximal element, and any two flags C, D in $\mathbb{L}$ have the same cardinality, $n + 1$. Then n is the *height* of the lattice $\mathbb{L}$.

  Two flags C, D are called *adjacent* if either they are equal or D contains exactly one element not in C. A *gallery* from C to D of length m is a sequence of flags $C = C_0, C_1, \ldots, C_m = D$ such that C_{i-1} and C_i are adjacent for $i = 1, \ldots, m$.

  A **gallery distance of flags** (see [Abel91]) is a distance on the set of all flags of a semimodular lattice $\mathbb{L}$ with finite height defined as the minimum of lengths of galleries from C to D. It can be written as

$$|C \vee D| - |C| = |C \vee D| - |D|,$$

  where $C \vee D = \{c \vee d : c \in C, d \in D\}$ is the subsemilattice generated by C and D. This distance is the **gallery metric** of the *chamber system* consisting of flags.

- **Scalar and vectorial metrics**

  Let $\mathbb{L} = (L, \leq, \max, \min)$ be a lattice with the join $\max\{x, y\}$, and the meet $\min\{x, y\}$ on a set $L \subset [0, \infty)$ which has a fixed number a as the greatest element and is closed under *negation*, i.e., for any $x \in L$, one has $\overline{x} = a - x \in L$.

The **scalar metric** d on L is defined, for $x \neq y$, by

$$d(x, y) = \max\{\min\{x, \bar{y}\}, \min\{\bar{x}, y\}\}.$$

The **scalar metric** d^* on $L^* = L \cup \{*\}$, $* \notin L$, is defined, for $x \neq y$, by

$$d^*(x, y) = \begin{cases} d(x, y), & \text{if} \quad x, y \in L, \\ \max\{x, \bar{x}\}, & \text{if} \ y = *, x \neq *, \\ \max\{y, \bar{y}\}, & \text{if} \ x = *, y \neq *. \end{cases}$$

Given a norm $||.||$ on $\mathbb{R}^n$, $n \geq 2$, the **vectorial metric** on L^n is defined by

$$||(d(x_1, y_1), \ldots, d(x_n, y_n))||,$$

and the **vectorial metric** on $(L^*)^n$ is defined by

$$||(d^*(x_1, y_1), \ldots, d^*(x_n, y_n))||.$$

The vectorial metric on $L_2^n = \{0, 1\}^n$ with l_1-*norm* on $\mathbb{R}^n$ is the **Fréchet–Nikodym–Aronszyan distance**. The vectorial metric on $L_m^n = \{0, \frac{1}{m-1}, \ldots, \frac{m-2}{m-1}, 1\}^n$ with l_1-*norm* on $\mathbb{R}^n$ is the **Sgarro m-valued metric**. The vectorial metric on $[0, 1]^n$ with l_1-*norm* on $\mathbb{R}^n$ is the **Sgarro fuzzy metric**.

If L is L_m or $[0, 1]$, and $x = (x_1, \ldots, x_n, x_{n+1}, \ldots, x_{n+r})$, $y = (y_1, \ldots, y_n, *, \ldots, *)$, where $*$ stands in r places, then the vectorial metric between x and y is the **Sgarro metric** (see, for example, [CSY01]).

- **Metrics on Riesz space**

A *Riesz space* (or *vector lattice*) is a partially ordered vector space $(V_{Ri}, \preceq)$ in which the following conditions hold:

1. The vector space structure and the partial order structure are compatible: $x \preceq y$ implies $x + z \preceq y + z$, and $x \succ 0$, $\lambda \in \mathbb{R}, \lambda > 0$ implies $\lambda x \succ 0$;
2. For any two elements $x, y \in V_{Ri}$ there exists the join $x \vee y \in V_{Ri}$ (in particular, the join and the meet of any finite set of elements from V_{Ri} exist).

The **Riesz norm metric** is a **norm metric** on V_{Ri} defined by

$$||x - y||_{Ri},$$

where $||.||_{Ri}$ is a *Riesz norm*, i.e., a *norm* on V_{Ri} such that, for any $x, y \in V_{Ri}$, the inequality $|x| \leq |y|$, where $|x| = (-x) \vee (x)$, implies $||x||_{Ri} \leq ||y||_{Ri}$.

The space $(V_{Ri}, ||.||_{Ri})$ is called a *normed Riesz space*. In the case of completeness it is called a *Banach lattice*. All Riesz norms on a Banach lattice are equivalent.

An element $e \in V_{Ri}^+ = \{x \in V_{Ri} : x \succ 0\}$ is called a *strong unit* of V_{Ri} if for each $x \in V_{Ri}$ there exists $\lambda \in \mathbb{R}$ such that $|x| \preceq \lambda e$. If a Riesz space V_{Ri} has a

strong unit e, then $||x|| = \inf\{\lambda \in \mathbb{R} : |x| \preceq \lambda e\}$ is a Riesz norm, and one obtains on V_{Ri} a Riesz norm metric

$$\inf\{\lambda \in \mathbb{R} : |x - y| \preceq \lambda e\}.$$

A *weak unit* of V_{Ri} is an element e of V_{Ri}^{+} such that $e \wedge |x| = 0$ implies $x = 0$. A Riesz space V_{Ri} is called *Archimedean* if, for any two $x, y \in V_{Ri}^{+}$, there exists a natural number n, such that $nx \preceq y$. The **uniform metric** on an Archimedean Riesz space with a weak unit e is defined by

$$\inf\{\lambda \in \mathbb{R} : |x - y| \wedge e \preceq \lambda e\}.$$

- **Machida metric**

  For a fixed integer $k \geq 2$ and the set $V_k = \{0, 1, \ldots, k-1\}$, let $O_k^{(n)}$ be the set of all n-ary functions from $(V_k)^n$ into V_k and $O_k = \cup_{n=1}^{\infty} O_k^{(n)}$. Let Pr_k be the set of all *projections* pr_i^n over V_k, where $pr_i^n(x_1, \ldots, x_i, \ldots, x_n) = x_i$ for any $x_1, \ldots, x_n \in V_k$.

  A *clone over* V_k is a subset C of O_k containing Pr_k and closed under (functional) composition. The set L_k of all clones over V_k is a lattice. The *Post lattice* L_2 defined over Boolean functions, is countable but any L_k with $k \geq 3$ is not. For $n \geq 1$ and a clone $C \in L_k$, let $C^{(n)}$ denote *n-slice* $C \cap O_k^{(n)}$.

  For any two clones $C_1, C_2 \in L_k$, Machida, 1998, defined the distance to be 0 if $C_1 = C_2$ and $(\min\{n : C_1^{(n)} \neq C_2^{(n)}\})^{-1}$, otherwise. The lattice L_k of clones with this distance is a compact ultrametric space. Cf. **Baire metric** in Chap. 11.

Chapter 11
Distances on Strings and Permutations

An *alphabet* is a finite set $\mathcal{A}$, $|\mathcal{A}| \geq 2$, elements of which are called *characters* (or *symbols*). A *string* (or *word*) is a sequence of characters over a given finite alphabet $\mathcal{A}$. The set of all finite strings over the alphabet $\mathcal{A}$ is denoted by $W(\mathcal{A})$. Examples of real world applications, using distances and similarities of string pairs, are Speech Recognition, Bioinformatics, Information Retrieval, Machine Translation, Lexicography, Dialectology.

A *substring* (or *factor*, *chain*, *block*) of the string $x = x_1 \dots x_n$ is any contiguous subsequence $x_i x_{i+1} \dots x_k$ with $1 \leq i \leq k \leq n$. A *prefix* of a string x is any its substring starting with x_1; a *suffix* is any its substring finishing with x_n. If a string is a part of a text, then the *delimiters* (a space, a dot, a comma, etc.) are added to $\mathcal{A}$.

A *vector* is any finite sequence consisting of real numbers, i.e., a finite string over the *infinite alphabet* $\mathbb{R}$. A *frequency vector* (or *discrete probability distribution*) is any string $x_1 \dots x_n$ with all $x_i \geq 0$ and $\sum_{i=1}^{n} x_i = 1$. A *permutation* (or *ranking*) is any string $x_1 \dots x_n$ with all x_i being different numbers from $\{1, \dots, n\}$.

An *editing operation* is an operation on strings, i.e., a *symmetric binary relation* on the set of all considered strings. Given a set of editing operations $\mathcal{O} = \{O_1, \dots, O_m\}$, the corresponding **editing metric** (or *unit cost edit distance*) between strings x and y is the minimum number of editing operations from $\mathcal{O}$ needed to obtain y from x. It is the **path metric** of a graph with the vertex-set $W(\mathcal{A})$ and xy being an edge if y can be obtained from x by one of the operations from $\mathcal{O}$.

In some applications, a *cost function* is assigned to each type of editing operation; then the editing distance is the minimal total cost of transforming x into y. Given a set of editing operations $\mathcal{O}$ on strings, the corresponding **necklace editing metric** between cyclic strings x and y is the minimum number of editing operations from $\mathcal{O}$ needed to obtain y from x, minimized over all rotations of x.

The main editing operations on strings are:

- *Character indel*, i.e., insertion or deletion of a character;
- *Character replacement*;
- *Character swap*, i.e., an interchange of adjacent characters;

© Springer-Verlag Berlin Heidelberg 2016

M.M. Deza, E. Deza, *Encyclopedia of Distances*,
DOI 10.1007/978-3-662-52844-0_11

- *Substring move*, i.e., transforming, say, the string $x = x_1 \dots x_n$ into the string $x_1 \dots x_{i-1}\mathbf{x_j} \dots \mathbf{x_{k-1}}x_i \dots x_{j-1}x_k \dots x_n$;
- *Substring copy*, i.e., transforming, say, $x = x_1 \dots x_n$ into $x_1 \dots x_{i-1}\mathbf{x_j} \dots \mathbf{x_{k-1}}$ $x_i \dots x_n$;
- *Substring uncopy*, i.e., the removal of a substring provided that a copy of it remains in the string.

We list below the main distances on strings. However, some string distances will appear in Chaps. 15, 21 and 23, where they fit better, with respect to the needed level of generalization or specification.

11.1 Distances on General Strings

- **Levenstein metric**

  The **Levenstein metric** (or **edit distance**, *Hamming+Gap metric*, *shuffle-Hamming distance*) is (Levenstein, 1965) an editing metric on $W(\mathcal{A})$, obtained for $\mathcal{O}$ consisting of only character replacements and indels.

  The Levenstein metric between strings $x = x_1 \dots x_m$ and $y = y_1 \dots y_n$ is

$$d_L(x, y) = \min\{d_H(x^*, y^*)\},$$

  where x^*, y^* are strings of length k, $k \geq \max\{m, n\}$, over the alphabet $\mathcal{A}^* = \mathcal{A} \cup \{*\}$ so that, after deleting all new characters $*$, strings x^* and y^* shrink to x and y, respectively. Here, the *gap* is the new symbol $*$, and x^*, y^* are *shuffles* of strings x and y with strings consisting of only $*$.

  The *Levenstein similarity* is $1 - \frac{d_L(x,y)}{\max\{m,n\}}$.

  The **Damerau–Levenstein metric** (Damerau, 1964) is an editing metric on $W(\mathcal{A})$, obtained for $\mathcal{O}$ consisting only of character replacements, indels and transpositions. In the Levenstein metric, a transposition corresponds to two editing operations: one insertion and one deletion.

  The **constrained edit distance** (Oomen, 1986) is the Levenstein metric, but the ranges for the number of replacements, insertions and deletions are specified.
- **Editing metric with moves**

  The **editing metric with moves** is an editing metric on $W(\mathcal{A})$ ([Corm03]), obtained for $\mathcal{O}$ consisting of only substring moves and indels.
- **Editing compression metric**

  The **editing compression metric** is an editing metric on $W(\mathcal{A})$ ([Corm03]), obtained for $\mathcal{O}$ consisting of only indels, copy and uncopy operations.
- **Swap metric**

  The **swap metric** (or *interchange distance*, *Dodson distance*) is an editing metric on $W(\mathcal{A})$, obtained for $\mathcal{O}$ consisting only of character swaps, i.e., it is the minimum number of interchanges of adjacent pairs of symbols, converting x into y.

- **Indel metric**

  The **indel metric** is an editing metric on $W(\mathcal{A})$, obtained for $\mathcal{O}$ consisting of only indels. It is an analog of the **Hamming metric** $|X \Delta Y|$ between sets X and Y. For strings $x = x_1 \dots x_m$ and $y = y_1 \dots y_n$ it is $m + n - 2LCS(x, y)$, where the similarity $LCS(x, y)$ is the length of the longest common subsequence of x and y.

  The **factor distance** is $m + n - 2LCF(x, y)$, where $LCF(x, y)$ is the length of the longest common substring (factor) of x and y.

  The *LCS ratio* and the *LCF ratio* are the similarities $\frac{LCS(x,y)}{\min\{m,n\}}$ and $\frac{LCF(x,y)}{\min\{m,n\}}$, respectively; sometimes, the denominator is $\max\{m, n\}$ or $\frac{m+n}{2}$.
- **Prefix, suffix, and substring distances**

  Given strings x and y, their **prefix distance**, **suffix distance**, and **substring distance** are the numbers of symbol occurrences in the strings that do not belong to their longest common prefix, suffix or substring, respectively. Cf. **Jaro–Winkler similarity**, **factor distance.**
- **Antidistance**

  There are $(n - 1)!$ *circular permutations*, i.e., cyclic orders, of a set X of size n. The **antidistance** between circular permutations x and y is the **swap metric** between x and the reversal of y.

  Also, given complex $n \times n$ matrices A and B, the *unitary similarity orbit* through B is $\sup_{U \in \mathbb{U}_n} ||U^* BU||_\infty$, where $U \in \mathbb{U}_n$ is the group of unitary matrices. Ando, 1996, define *anti-distance* between A and this orbit as $\sup_{U \in \mathbb{U}_n} ||A - U^* BU||_\infty$.

  Also, given a simple connected graph (V, E), we assign directions to edges and the weight of each edge (either 1 or -1) depending on the direction of the traverse. Iravanian, 2012, define *anti-distance* $d(u, v) = -d(v, u)$ between vertices as the weighted average length of all simple paths from u to v.
- **Edit distance with costs**

  Given a set of editing operations $\mathcal{O} = \{O_1, \dots, O_m\}$ and a *weight* (or *cost function*) $w_i \geq 0$, assigned to each type O_i of operation, the **edit distance with costs** between strings x and y is the minimal total cost of an *editing path* between them, i.e., the minimal sum of weights for a sequence of operations transforming x into y.

  The **normalized edit distance** between strings x and y (Marzal–Vidal, 1993) is the minimum, over all editing paths P between them, of $\frac{W(P)}{L(P)}$, where $W(P)$ and $L(P)$ are the total cost and the length of the editing path P.
- **Transduction edit distances**

  The **Levenstein metric** with costs between strings x and y is modeled in [RiYi98] as a memoryless stochastic transduction between x and y.

  Each step of transduction generates either a character replacement pair (a, b), a deletion pair $(a, \emptyset)$, an insertion pair $(\emptyset, b)$, or the specific termination symbol t according to a probability function $\delta : E \cup \{t\} \to [0, 1]$, where E is the set of all possible above pairs. Such a transducer induces a probability function on the set of all sequences of operations.

The **transduction edit distances** between strings x and y are ([RiYi98]) $\ln p$ of the following probabilities p:

- for the **Viterbi edit distance**, the probability of the most likely sequence of editing operations transforming x into y;
- for the **stochastic edit distance**, the probability of the string pair (x, y).

This model allows one to learn, in order to reduce error rate, the edit costs for the Levenstein metric from a corpus of examples (training set of string pairs). This learning is automatic; it reduces to estimating the parameters of above transducer.

- **Bag distance**

  The **bag distance** (or *multiset metric*, *counting filter*) is a metric on $W(\mathcal{A})$ defined (Navarro, 1997) by

$$\max\{|X\backslash Y|, |Y\backslash X|\}$$

  for any strings x and y, where X and Y are the *bags of symbols* (multisets of characters) in strings x and y, respectively, and, say, $|X\backslash Y|$ counts the number of elements in the multiset $X\backslash Y$. It is a (computationally) cheap approximation of the **Levenstein metric**. Cf. **metrics between multisets** in Chap. 1.

- **Marking metric**

  The **marking metric** is a metric on $W(\mathcal{A})$ ([EhHa88]) defined by

$$\ln_2 ((diff(x, y) + 1)(diff(y, x) + 1))$$

  for any strings $x = x_1 \dots x_m$ and $y = y_1 \dots y_n$, where $diff(x, y)$ is the minimal cardinality $|M|$ of a subset $M \subset \{1, \dots, m\}$ such that any substring of x, not containing any x_i with $i \in M$, is a substring of y.

  Another metric defined in [EhHa88], is $\ln_2(diff(x, y) + diff(y, x) + 1)$.

- **Transformation distance**

  The **transformation distance** is an **editing distance with costs** on $W(\mathcal{A})$ (Varre–Delahaye–Rivals, 1999) obtained for $\mathcal{O}$ consisting only of substring copy, uncopy and substring indels. The distance between strings x and y is the minimal cost of transformation x into y using these operations, where the cost of each operation is the length of its description.

  For example, the description of the copy requires a binary code specifying the type of operation, an offset between the substring locations in x and in y, and the length of the substring. A code for insertion specifies the type of operation, the length of the substring and the sequence of the substring.

- **L_1-rearrangement distance**

  The **L_1-rearrangement distance** (Amir et al., 2007) between strings $x = x_1 \dots x_m$ and $y = y_1 \dots y_m$ is defined by

$$\min_{\pi} \sum_{i=1}^{m} |i - \pi(i)|,$$

where $\pi : \{1, \ldots, m\} \to \{1, \ldots, m\}$ is a permutation transforming x into y; if there are no such permutations, the distance is equal to ∞.

The L_∞**-rearrangement distance** (Amir et al., 2007) between x and y is $\min_\pi \max_{1 \le i \le m} |i - \pi(i)|$ and it is ∞ if such a permutation does not exist.

Cf. **genome rearrangement distances** in Chap. 23.

- **Normalized information distance**

  The **normalized information distance** d between two binary strings x and y is a symmetric function on $W(\{0,1\})$ ([LCLMV04]) defined by

$$\frac{\max\{K(x|y^*), K(y|x^*)\}}{\max\{K(x), K(y)\}}$$

  Here, for binary strings u and v, u^* is a shortest binary program to compute u on an appropriate (i.e., using a *Turing-complete* language) universal computer, the *Kolmogorov complexity* (or *algorithmic entropy*) $K(u)$ is the length of u^* (the ultimate compressed version of u), and $K(u|v)$ is the length of the shortest program to compute u if v is provided as an auxiliary input.

  The function $d(x, y)$ is a metric up to small error term: $d(x, x) = O((K(x))^{-1})$, and $d(x, z) - d(x, y) - d(y, z) = O((\max\{K(x), K(y), K(z)\})^{-1})$. Cf. in Chap. 15 the **shared information distance** $H(X|Y) + H(Y|X)$ between sources X and Y.

  The Kolmogorov complexity is uncomputable and depends on the chosen computer language; so, instead of $K(u)$, were proposed the *minimum message length* (shortest overall message) by Wallace, 1968, and the *minimum description length* (largest compression of data) by Rissanen, 1978.

  The **normalized compression distance** is a metric on $W(\{0,1\})$ (derived by Cilibrasi and Vitányi, 2005, from [LCLMV04, BGLVZ98]) defined by

$$\frac{C(xy) - \min\{C(x), C(y)\}}{\max\{C(x), C(y)\}}$$

  for any binary strings x and y, where $C(x), C(y)$, and $C(xy)$ denote the size of the compression (by fixed compressor C, such as gzip, bzip2, or PPMZ) of strings x, y, and their *concatenation* xy. It is an approximation of the normalized information distance. A similar distance is defined by $\frac{C(xy)}{C(x)+C(y)} - \frac{1}{2}$.

- **Lempel–Ziv distance**

  The **Lempel–Ziv distance** between two binary strings x and y of length n is

$$\max\{\frac{LZ(x|y)}{LZ(x)}, \frac{LZ(y|x)}{LZ(y)}\},$$

  where $LZ(x) = \frac{|P(x)| \log |P(x)|}{n}$ is the *Lempel–Ziv complexity* of x, approximating its *Kolmogorov complexity* $K(x)$. Here $P(x)$ is the set of nonoverlapping substrings into which x is parsed sequentially, so that the new substring is not yet contained in the set of substrings generated so far. For example, such a *Lempel–Ziv*

parsing for $x = 001100101010011$ is $0|01|1|00|10|101|001|11$. Now, $LZ(x|y) = \frac{|P(x)\setminus P(y)|\log|P(x)\setminus P(y)|}{n}$.

- **Anthony–Hammer similarity**

  The **Anthony–Hammer similarity** between a binary string $x = x_1 \dots x_n$ and the set Y of binary strings $y = y_1 \dots y_n$ is the maximal number m such that, for every m-subset $M \subset \{1, \dots, n\}$, the substring of x, containing only x_i with $i \in M$, is a substring of some $y \in Y$ containing only y_i with $i \in M$.

- **Jaro similarity**

  Given strings $x = x_1 \dots x_m$ and $y = y_1 \dots y_n$, call a character x_i *common with* y if $x_i = y_j$, where $|i - j| \leq \frac{\min\{m,n\}}{2}$. Let $x' = x'_1 \dots x'_{m'}$ be all the characters of x which are common with y (in the same order as they appear in x), and let $y' = y'_1 \dots y'_{n'}$ be the analogic string for y.

  The **Jaro similarity** $Jaro(x, y)$ between strings x and y is defined by

$$\frac{1}{3}\left(\frac{m'}{m} + \frac{n'}{n} + \frac{|\{1 \leq i \leq \min\{m', n'\} : x'_i = y'_i\}|}{\min\{m', n'\}}\right).$$

  This and following two similarities are used in Record Linkage.

- **Jaro–Winkler similarity**

  The **Jaro–Winkler similarity** between strings x and y is defined by

$$Jaro(x, y) + \frac{\max\{4, LCP(x, y)\}}{10}(1 - Jaro(x, y)),$$

  where $Jaro(x, y)$ is the **Jaro similarity**, and $LCP(x, y)$ is the length of the longest common prefix of x and y.

- **q-gram similarity**

  Given an integer $q \geq 1$ (usually, q is 2 or 3), the **q-gram similarity** between strings x and y is defined by

$$\frac{2q(x, y)}{q(x) + q(y)},$$

  where $q(x)$, $q(y)$ and $q(x, y)$ are the sizes of multisets of all *q-grams* (substrings of length q) occurring in x, y and both of them, respectively.

  Sometimes, $q(x, y)$ is divided not by the average of $q(x)$ and $q(y)$, as above, but by their minimum, maximum or *harmonic mean* $\frac{2q(x)q(y)}{q(x)+q(y)}$. Cf. **metrics between multisets** in Chap. 1 and, in Chap. 17, **Dice similarity**, **Simpson similarity**, **Braun–Blanquet similarity** and **Anderberg similarity**.

  The q-gram similarity is an example of **token-based similarities**, i.e., ones defined in terms of *tokens* (selected substrings or words). Here tokens are q-grams. A generic **dictionary-based metric** between strings x and y is $|D(x)\Delta D(y)|$, where $D(z)$ denotes the full *dictionary* of z, i.e., the set of all of its substrings.

- **Prefix-Hamming metric**

  The **prefix-Hamming metric** between strings $x = x_1 \dots x_m$ and $y = y_1 \dots y_n$ is

$$(\max\{m,n\} - \min\{m,n\}) + |\{1 \le i \le \min\{m,n\} : x_i \ne y_i\}|.$$

- **Weighted Hamming metric**

  If $(\mathcal{A}, d)$ is a metric space, then the **weighted Hamming metric** between strings $x = x_1 \dots x_m$ and $y = y_1 \dots y_m$ is defined by

$$\sum_{i=1}^{m} d(x_i, y_i).$$

  The term *weighted Hamming metric* (or *weighted Hamming distance*) is also used for $\sum_{1 \le i \le m, x_i \ne y_i} w_i$, where, for any $1 \le i \le m$, $w(i) > 0$ is its *weight*.

- **Fuzzy Hamming distance**

  If $(\mathcal{A}, d)$ is a metric space, the **fuzzy Hamming distance** between strings $x = x_1 \dots x_m$ and $y = y_1 \dots y_m$ is an **editing distance with costs** on $W(\mathcal{A})$ obtained for $\mathcal{O}$ consisting of only indels, each of fixed cost $q > 0$, and *character shifts* (i.e., moves of 1-character substrings), where the cost of replacement of i by j is a function $f(|i-j|)$. This distance is the minimal total cost of transforming x into y by these operations. Bookstein–Klein–Raita, 2001, introduced this distance for Information Retrieval and proved that it is a metric if f is a monotonically increasing concave function on integers vanishing only at 0.

  The case $f(|i-j|) = C|i-j|$, where $C > 0$ is a constant and $|i-j|$ is a time shift, corresponds to the Victor–Purpura **spike train distance** in Chap. 23.

  Ralescu, 2003, introduced, for Image Retrieval, another **fuzzy Hamming distance** on $\mathcal{R}^m$. The **Ralescu distance** between two strings $x = x_1 \dots x_m$ and $y = y_1 \dots y_m$ is the fuzzy cardinality of the difference fuzzy set $D_\alpha(x, y)$ (where α is a parameter) with membership function

$$\mu_i = 1 - e^{-\alpha(x_i - y_i)^2}, 1 \le i \le m.$$

  The *nonfuzzy cardinality of the fuzzy set* $D_\alpha(x, y)$ approximating its fuzzy cardinality is $|\{1 \le i \le m : \mu_i > \frac{1}{2}\}|$.

- **Needleman–Wunsch–Sellers metric**

  If $(\mathcal{A}, d)$ is a metric space, the **Needleman–Wunsch–Sellers metric** (or *global alignment metric*) is an **editing distance with costs** on $W(\mathcal{A})$ ([NeWu70]), obtained for $\mathcal{O}$ consisting of only indels, each of fixed cost $q > 0$, and character replacements, where the cost of replacement of i by j is $d(i, j)$. This metric is the minimal total cost of transforming x into y by these operations. It is

$$\min\{d_{wH}(x^*, y^*)\},$$

where x^*, y^* are strings of length k, $k \geq \max\{m, n\}$, over the alphabet $\mathcal{A}^* = \mathcal{A} \cup \{*\}$, so that, after deleting all new characters $*$, strings x^* and y^* shrink to x and y, respectively. Here $d_{wH}(x^*, y^*)$ is the **weighted Hamming metric** between x^* and y^* with weight $d(x_i^*, y_i^*) = q$ (i.e., the editing operation is an indel) if one of x_i^*, y_i^* is $*$, and $d(x_i^*, y_i^*) = d(i, j)$, otherwise.

The **Gotoh–Smith–Waterman distance** (or *string distance with affine gaps*) is a more specialized editing metric with costs (see [Goto82]). It discounts mismatching parts at the beginning and end of the strings x, y, and introduces two indel costs: one for starting an *affine gap* (contiguous block of indels), and another one (lower) for extending a gap.

- **Duncan metric**

  Consider the set X of all strictly increasing infinite sequences $x = \{x_n\}_n$ of positive integers. Define $N(n, x)$ as the number of elements in $x = \{x_n\}_n$ which are less than n, and $\delta(x)$ as the *density* of x, i.e., $\delta(x) = \lim_{n\to\infty} \frac{N(n,x)}{n}$. Let Y be the subset of X consisting of all sequences $x = \{x_n\}_n$ for which $\delta(x) < \infty$.

  The **Duncan metric** is a metric on Y defined, for $x \neq y$, by

$$\frac{1}{1 + LCP(x, y)} + |\delta(x) - \delta(y)|,$$

  where $LCP(x, y)$ is the length of the longest common prefix of x and y.

- **Martin metric**

  The **Martin metric** d^a between strings $x = x_1 \dots x_m$ and $y = y_1 \dots y_n$ is

$$|2^{-m} - 2^{-n}| + \sum_{t=1}^{\max\{m,n\}} \frac{a_t}{|\mathcal{A}|^t} \sup_z |k(z, x) - k(z, y)|,$$

  where z is any string of length t, $k(z, x)$ is the *Martin kernel* of a *Markov chain* $M = \{M_t\}_{t=0}^{\infty}$, and the sequence $a \in \{a = \{a_t\}_{t=0}^{\infty} : a_t > 0, \sum_{t=1}^{\infty} a_t < \infty\}$ is a parameter.

- **Baire metric**

  The **Baire metric** is an ultrametric between strings x and y defined, for $x \neq y$, by

$$\frac{1}{1 + LCP(x, y)},$$

  where $LCP(x, y)$ is the length of the longest common prefix of strings (finite or infinite) x and y. Cf. **Baire space** in Chap. 2.

  Given an infinite *cardinal number* κ and a set A of cardinality κ, the Cartesian product of countably many copies of A endowed with above ultrametric $\frac{1}{1+LCP(x,y)}$ is called the **Baire space of weight** κ and denoted by $B(\kappa)$. In particular, $B(\aleph_0)$ (called the *Baire* 0*-dimensional space*) is homeomorphic to the space *Irr* of irrationals with **continued fraction metric** (Chap. 12).

- **Generalized Cantor metric**

  The **generalized Cantor metric** (or, sometimes, *Baire distance*) is an ultrametric between infinite strings x and y defined, for $x \neq y$, by

  $$a^{1+LCP(x,y)},$$

  where a is a fixed number from the interval $(0, 1)$, and $LCP(x, y)$ is the length of the longest common prefix of x and y.

  This ultrametric space is **compact**. In the case $a = \frac{1}{2}$, this metric was considered on a remarkable **fractal**, the *Cantor set*; cf. **Cantor metric** in Chap. 18. Another important case is $a = \frac{1}{e} \approx 0.367879441$.

  Comyn–Dauchet, 1985, and Kwiatkowska, 1990, introduced some analogs of generalized Cantor metric for *traces*, i.e., equivalence classes of strings with respect to a congruence relation identifying strings x, y that are identical up to permutation of concurrent actions ($xy = yx$).
- **Parikh distance**

  Given an ordered alphabet $\mathcal{A} = \{a_1, \ldots, a_k\}$, the **Parikh distance** between words x and y over it is the **Manhattan metric** $\sum_{i=1}^{k} |x_i - y_i|$ between their *Parikh maps* (or *commutative images*) $P(x)$ and $P(y)$, where, for a word w, w_i denotes the number of occurrences of a_i in w and $P(w)$ is $(w_1, \ldots, w_k)$.
- **Parentheses string metrics**

  Let P_n be the set of all strings on the alphabet $\{(,)\}$ generated by a grammar and having n open and n closed parentheses. A **parentheses string metric** is an editing metric on P_n corresponding to a given set of editing operations.

  For example, the **Monjardet metric** (Monjardet, 1981) between two strings $x, y \in P_n$ is the minimum number of adjacent parentheses interchanges ("()" to ")(" or ")(" to "()") needed to obtain y from x. It is the **Manhattan** metric between their *representations* p_x and p_x, where $p_z = (p_z(1), \ldots, p_z(n))$ and $p_z(i)$ is the number of open parentheses written before the i-th closed parentheses of $z \in P_n$.

  There is a bijection between parentheses strings and binary trees; cf. the **tree rotation distance** in Chap. 15.
- **Dehornoy–Autord distance**

  The **Dehornoy–Autord distance** (2010) between two shortest expressions x and y of a permutation as a product of transpositions t_i, is the minimal, needed to get x from y, number of *braid relations*: $t_i t_j t_i = t_j t_i t_j$ with $|i-j| = 1$ and $t_i t_j = t_j t_i$ with $|i-j| \geq 2$.

  This distance can be extended to the decompositions of any given *positive braid* in terms of *Artin's generators*. The permutations corresponds to the *simple braids* which are the divisors of *Garside's fundamental braid* in the *braid monoid*.
- **Schellenkens complexity quasi-metric**

  The **Schellenkens complexity quasi-metric** between infinite strings $x = (x_i)$ and $y = (y_i)$ $(i = 0, 1, \ldots)$ over $\mathbb{R}_{\geq 0}$ with $\sum_{i=0}^{\infty} 2^{-i} \frac{1}{x_i} < \infty$ (seen as complexity

functions) is defined (Schellenkens, 1995) by

$$\sum_{i=0}^{\infty} 2^{-i} \max\{0, \frac{1}{x_i} - \frac{1}{y_i}\}.$$

- **Graev metrics**

  Let (X, d) be a metric space. Let $\overline{X} = X \cup X' \cup \{e\}$, where $X' = \{x' : x \in X\}$ is a disjoint copy of X, and $e \notin X \cup X'$. We use the notation $(e')' = e$ and $(x')' = x$ for any $x \in X$; also, the letters x, y, x_i, y_i will denote elements of $\overline{X}$. Let $(\overline{X}, D)$ be a metric space such that $D(x, y) = D(x', y') = d(x, y)$, $D(x, e) = D(x', e)$ and $D(x, y') = D(x', y)$ for all $x, y \in X$.

  Denote by $W(X)$ the set of all words over $\overline{X}$ and, for each word $w \in W(X)$, denote by $l(w)$ its length. A word $w \in W(X)$ is called *irreducible* if $w = e$ or $w = x_0 \dots x_n$, where $x_i \neq e$ and $x_{i+1} \neq x_i'$ for $0 \leq i < n$.

  For each word w over $\overline{X}$, denote by $\hat{w}$ the unique irreducible word obtained from w by successively replacing any occurrence of xx' in w by e and eliminating e from any occurrence of the form $w_1 e w_2$, where $w_1 = w_2 - \emptyset$ is excluded.

  Denote by $F(X)$ the set of all irreducible words over $\overline{X}$ and, for $u, v \in F(X)$, define $u \cdot v = w'$, where w is the concatenation of words u and v. Then $F(X)$ becomes a group; its identity element is the (nonempty) word e.

  For any two words $v = x_0 \dots x_n$ and $u = y_0 \dots y_n$ over $\overline{X}$ of the same length, let $\rho(v, u) = \sum_{i=0}^{n} D(x_i, y_i)$. The **Graev metric** between two irreducible words $u = u, v \in F(X)$ is defined ([DiGa07]) by

$$\inf\{\rho(u^*, v^*) : u^*, v^* \in W(X),\ l(u^*) = l(v^*),\ \widehat{u^*} = u, \widehat{v^*} = v\}.$$

  Graev proved that this metric is **bi-invariant metric** on $F(X)$ and that $F(X)$ is a topological group in the topology induced by it.

- **String-induced alphabet distance**

  Let $a = (a_1, \dots, a_m)$ be a finite string over alphabet X, $|X| = n \geq 2$. Let $A(x) = \{1 \leq i \leq m : a_i = x\} \neq \emptyset$ for any $x \in X$.

  The **string-induced distance** between symbols $x, y \in X$ is the **set-set distance** (Chap. 1) defined by

$$d_a(x, y) = \min\{|i - j| : i \in A(x), j \in A(y)\}.$$

  A k**-radius sequence** (Jaromczyk and Lonc, 2004) is a string a over X with $\max_{x,y \in X} d_a(x, y) \leq k$, i.e., any two symbols (say, large digital images) occur in some window (say, memory cache) of length $k+1$. Minimal length m corresponds to most efficient pipelining of images when no more than $k + 1$ of them can be placed in main memory in any given time.

11.2 Distances on Permutations

A *permutation* (or *ranking*) is any string $x_1 \dots x_n$ with all x_i being different numbers from $\{1, \dots, n\}$; a *signed permutation* is any string $x_1 \dots x_n$ with all $|x_i|$ being different numbers from $\{1, \dots, n\}$. Denote by $(Sym_n, \cdot, id)$ the group of all permutations of the set $\{1, \dots, n\}$, where *id* is the *identity mapping*.

The restriction, on the set Sym_n of all n-permutation vectors, of any metric on $\mathbb{R}^n$ is a metric on Sym_n; the main example is the l_p**-metric** $(\sum_{i=1}^{n} |x_i - y_i|^p)^{\frac{1}{p}}$, $p \geq 1$.

The main editing operations on permutations are:

- *Block transposition*, i.e., a substring move;
- *Character move*, i.e., a transposition of a block consisting of only one character;
- *Character swap*, i.e., interchanging of any two adjacent characters;
- *Character exchange*, i.e., interchanging of any two characters (in Group Theory, it is called *transposition*);
- *One-level character exchange*, i.e., exchange of characters x_i and x_j, $i < j$, such that, for any k with $i < k < j$, either $\min\{x_i, x_j\} > x_k$, or $x_k > \max\{x_i, x_j\}$;
- *Block reversal*, i.e., transforming, say, the permutation $x = x_1 \dots x_n$ into the permutation $x_1 \dots x_{i-1}\mathbf{x_j}\mathbf{x_{j-1}} \dots \mathbf{x_{i+1}}\mathbf{x_i}x_{j+1} \dots x_n$ (so, a swap is a reversal of a block consisting only of two characters);
- *Signed reversal*, i.e., a reversal in signed permutation, followed by multiplication on -1 of all characters of the reversed block.

Below we list the most used editing and other metrics on Sym_n.

- **Hamming metric on permutations**

  The **Hamming metric on permutations** d_H is an editing metric on Sym_n, obtained for $\mathcal{O}$ consisting of only character replacements. It is a **bi-invariant** metric. Also, $n - d_H(x, y)$ is the number of fixed points of xy^{-1}.
- **Spearman** ρ **distance**

  The **Spearman** ρ **distance** is the Euclidean metric on Sym_n:

$$\sqrt{\sum_{i=1}^{n}(x_i - y_i)^2}.$$

  Its square is a 2**-near-metric**. Cf. **Spearman** ρ **rank correlation** in Chap. 17.
- **Spearman footrule distance**

  The **Spearman footrule distance** is the l_1*-metric* on Sym_n:

$$\sum_{i=1}^{n} |x_i - y_i|.$$

  Cf. **Spearman footrule similarity** in Chap. 17.

  Both above Spearman distances are **bi-invariant**.

- **Kendall τ distance**

  The **Kendall τ distance** (or *inversion metric*, permutation **swap metric**, *bubble-sort distance*) I is an editing metric on Sym_n, obtained for $\mathcal{O}$ consisting only of character swaps.

  In terms of Group Theory, $I(x, y)$ is the number of adjacent transpositions needed to obtain x from y. Also, $I(x, y)$ is the number of *relative inversions* of x and y, i.e., pairs (i, j), $1 \leq i < j \leq n$, with $(x_i - x_j)(y_i - y_j) < 0$. Cf. **Kendall τ rank correlation** in Chap. 17.

  In [BCFS97] the following metrics, associated with $I(x, y)$, were given:

  1. $\min_{z \in Sym_n}(I(x, z) + I(z^{-1}, y^{-1}))$;
  2. $\max_{z \in Sym_n} I(zx, zy)$;
  3. $\min_{z \in Sym_n} I(zx, zy) = T(x, y)$, where T is the **Cayley metric**;
  4. editing metric with $\mathcal{O}$ consisting only of one-level character exchanges.

- **Daniels–Guilbaud semimetric**

  The **Daniels–Guilbaud semimetric** (see [Monj98]) is defined, for any $x, y \in Sym_n$, as the number of triples (i, j, k), $1 \leq i < j < k \leq n$, such that (x_i, x_j, x_k) is not a cyclic shift of (y_i, y_j, y_k). So, it is 0 if and only if x is a cyclic shift of y.

- **Cayley metric**

  The **Cayley metric** (or **transposition distance**) T is an editing metric on Sym_n, obtained for $\mathcal{O}$ consisting only of character exchanges. In terms of Group Theory, $T(x, y)$ is the minimum number of transpositions needed to obtain x from y.

  The metric T is **bi-invariant**. Also, $n - T(x, y)$ is the number of cycles in xy^{-1}, and, for the **Hamming metric on permutations**, $d_H(x, y) - T(x, y)$ is the number of cycles with length at least 2 in xy^{-1}.

- **Ulam metric**

  The **Ulam metric** (or **permutation editing metric**) U is an editing metric on Sym_n, obtained for $\mathcal{O}$ consisting only of character moves. It is the half of the **indel metric** on Sym_n.

  Also, $n - U(x, y) = LCS(x, y) = LIS(xy^{-1})$, where $LCS(x, y)$ is the length of the longest common subsequence (not necessarily a substring) of x and y, while $LIS(z)$ is the length of the longest increasing subsequence of $z \in Sym_n$.

  This and the preceding six metrics are **right-invariant**.

- **Reversal metric**

  The **reversal metric** is an editing metric on Sym_n, obtained for $\mathcal{O}$ consisting only of block reversals.

- **Signed reversal metric**

  The **signed reversal metric** (Sankoff, 1989) is an editing metric on the set of all $2^n n!$ signed permutations of the set $\{1, \ldots, n\}$, obtained for $\mathcal{O}$ consisting only of signed reversals.

  This metric is used in Biology, where a signed permutation represents a single-chromosome genome, seen as a permutation of genes (along the chromosome) each having a direction (so, a sign $+$ or $-$).

- **Chain metric**

  The **chain metric** (or *rearrangement metric*) is a metric on Sym_n ([Page65]) defined, for any $x, y \in Sym_n$, as the minimum number, minus 1, of chains (substrings) $y_1', \ldots, y_t'$ of y, such that x can be *parsed* (concatenated) into, i.e., $x = y_1' \ldots y_t'$.
- **Lexicographic metric**

  The **lexicographic metric** (Golenko–Ginzburg, 1973) is a metric on Sym_n:

$$|N(x) - N(y)|,$$

  where $N(x)$ is the ordinal number of the position (among $1, \ldots, n!$) occupied by the permutation x in the *lexicographic ordering* of the set Sym_n.

  In the *lexicographic ordering* of Sym_n, $x = x_1 \ldots x_n \prec y = y_1 \ldots y_n$ if there exists $1 \leq i \leq n$ such that $x_1 = x_1, \ldots, x_{i-1} = y_{i-1}$, but $x_i < y_i$.
- **Fréchet permutation metric**

  The **Fréchet permutation metric** is the **Fréchet product metric** (Chap. 4) on the set Sym_∞ of permutations of positive integers defined by

$$\sum_{i=1}^{\infty} \frac{1}{2^i} \frac{|x_i - y_i|}{1 + |x_i - y_i|}.$$

- **Distance-rationalizable voting rule**

  Let $e = (\pi_1, \ldots, \pi_m)$ be a finite string over alphabet Sym_n; it can be seen as an election in which, for each $i, 1 \leq i \leq m$, the *voter* v_i give the ranking $\pi_i = (\pi_i(c_1), \ldots, \pi_i(c_n))$ on the set $C = \{c_1, \ldots, c_n\}$ of *candidates*. Let $X = Sym_n^m$ be the set of all possible elections with m voters in each.

  A *voting rule* is any map $R : X \to P(C)$ assigning to each election e a set $R(e) \subset C$ of its *R-winners*. For example, the winners of *plurality rule* are candidates with the largest number of first-place votes. A candidate is a *unanimity winner* if all voters rank him first. A candidate c_i is a *Condorcet winner* if for each $c_j \in C \setminus \{c_i\}$, a strict majority of voters prefer c_i to c_j. A candidate is a *Dodson winner* if the number of swaps of adjacent candidates in the rankings by voters after which he became a Condorcet winner, is minimal. So, $|R(e)| \leq 1$ for elections with unanimity or Condorcet rule, and $|R(e)| \geq 1$ for plurality or Dodson rule.

  A *consensus class* is a pair (Y, W), where $Y \subset X$ is a set of elections and W is a voting rule with unique (Y, W)-*winner* (i.e., $|W(e)| = 1$) for all $e \in Y$. Let $\mathcal{U}$ and $\mathcal{C}$ denote the consensus classes of all elections having the Condorcet winner and the unanimity winner, respectively.

  Given a distance d on X and consensus class (Y, W), the voting rule R is called (Meskanen–Nurmi, 2008, and Elkind–Faliszewski–Slinko, 2009) $(d; (Y, W))$-**distance-rationalizable** if, for each election e, a candidate c_i is its R-winner if and only if he is the (Y, W)-winner in a d-closest election in Y.

The plurality rule is $(d_H;\mathcal{U})$-rationalizable, where $d_H(e,e')$ is the **Hamming distance** $|\{i \leq i \leq m : \pi_i \neq \pi'_i\}|$. The Dodson rule is $(d_{sw};\mathcal{C})$-rationalizable, where $d_{sw}(e,e') = \sum_{1\leq i\leq m} d_{sw}(\pi_i,\pi'_i)$ and d_{sw} on rankings is the **swap metric**.

Similar framework (minimization of an *aggregation function* of distances between a collective opinion and the individual judgements) is used in *distance-based jugement aggregation* and in general *distance-based semantics* for decision or choice.

Chapter 12
Distances on Numbers, Polynomials, and Matrices

12.1 Metrics on Numbers

Here we consider the most important metrics on the classical number systems: the semiring $\mathbb{N}$ of natural numbers, the ring $\mathbb{Z}$ of integers, and the fields $\mathbb{Q}$, $\mathbb{R}$, $\mathbb{C}$ of rational, real, complex numbers, respectively. We consider also the algebra $\mathcal{Q}$ of quaternions.

- **Metrics on natural numbers**
  There are several well-known metrics on the set $\mathbb{N}$ of natural numbers:

  1. $|n-m|$; the restriction of the **natural metric** (from $\mathbb{R}$) on $\mathbb{N}$;
  2. $p^{-\alpha}$, where α is the highest power of a given prime number p dividing $m-n$, for $m \neq n$ (and equal to 0 for $m = n$); the restriction of the p**-adic metric** (from $\mathbb{Q}$) on $\mathbb{N}$;
  3. $\ln \frac{lcm(m,n)}{gcd(m,n)}$; an example of the **lattice valuation metric**;
  4. $w_r(n-m)$, where $w_r(n)$ is the *arithmetic r-weight* of n; the restriction of the **arithmetic** r**-norm metric** (from $\mathbb{Z}$) on $\mathbb{N}$;
  5. $\frac{|n-m|}{mn}$ (cf. M**-relative metric** in Chap. 5);
  6. $1 + \frac{1}{m+n}$ for $m \neq n$ (and equal to 0 for $m = n$); the **Sierpinski metric**.

  Most of these metrics on $\mathbb{N}$ can be extended on $\mathbb{Z}$. Moreover, any one of the above metrics can be used in the case of an arbitrary countable set X. For example, the **Sierpinski metric** is defined, in general, on a countable set $X = \{x_n : n \in \mathbb{N}\}$ by $1 + \frac{1}{m+n}$ for all $x_m, x_n \in X$ with $m \neq n$ (and is equal to 0, otherwise).
- **Arithmetic** r**-norm metric**
  Let $r \in \mathbb{N}, r \geq 2$. The *modified r-ary form* of an integer x is a representation

$$x = e_n r^n + \cdots + e_1 r + e_0,$$

  where $e_i \in \mathbb{Z}$, and $|e_i| < r$ for all $i = 0, \ldots, n$.

© Springer-Verlag Berlin Heidelberg 2016

M.M. Deza, E. Deza, *Encyclopedia of Distances*,
DOI 10.1007/978-3-662-52844-0_12

An r-ary form is called *minimal* if the number of nonzero coefficients is minimal. The minimal form is not unique, in general. But if the coefficients e_i, $0 \le i \le n-1$, satisfy the conditions $|e_i + e_{i+1}| < r$, and $|e_i| < |e_{i+1}|$ if $e_i e_{i+1} < 0$, then the above form is unique and minimal; it is called the *generalized nonadjacent form*.

The *arithmetic r-weight* $w_r(x)$ of an integer x is the number of nonzero coefficients in a *minimal r-ary form* of x, in particular, in the generalized nonadjacent form. The **arithmetic r-norm metric** on $\mathbb{Z}$ (see, for example, [Ernv85]) is defined by

$$w_r(x-y).$$

- **Distance between consecutive primes**

  The **distance between consecutive primes** (or *prime gap*, *prime difference function*) is the difference $g_n = p_{n+1} - p_n$ between two successive prime numbers.

  It holds $g_n \le p_n$, $\overline{\lim}_{n\to\infty} g_n = \infty$ and (Zhang, 2013) $\underline{\lim}_{n\to\infty} g_n < 7 \times 10^7$, improved to ≤ 246 (conjecturally, to ≤ 6) by Polymath8, 2014. There is no $\lim_{n\to\infty} g_n$ but $g_n \approx \ln p_n$ for the average g_n.

  Open *Polignac's conjecture*: for any $k \ge 1$, there are infinitely many n with $g_n = 2k$; the case $k = 1$ (i.e., that $\underline{\lim}_{n\to\infty} g_n = 2$ holds) is the *twin prime conjecture*.
- **Distance Fibonacci numbers**

  Fibonacci numbers are defined by the recurrence $F_n = F_{n-1} + F_{n-2}$ for $n \ge 2$ with initial terms $F_0 = 0$ and $F_1 = 1$. **Distance Fibonacci numbers** are three following generalizations of them in the distance sense, considered by Wloch et al..

  Kwaśnik–Wloch, 2000: $F(k,n) = F(k,n-1) + F(k,n-k)$ for $n > k$ and $F(k,n) = n+1$ for $n \le k$.

  Bednarz et al., 2012: $Fd(k,n) = Fd(k,n-k+1) + Fd(k,n-k)$ for $n \ge k > 1$ and $Fd(k,n) = 1$ for $0 \le n < k$.

  Wloch et al., 2013: $F_2(k,n) = F_2(k,n-2) + F_2(k,n-k)$ for $n \ge k \ge 1$ and $F_2(k,n) = 1$ for $0 \le n < k$.
- **p-adic metric**

  Let p be a prime number. Any nonzero rational number x can be represented as $x = p^\alpha \frac{c}{d}$, where c and d are integers not divisible by p, and α is a unique integer. The *p-adic norm* of x is defined by $|x|_p = p^{-\alpha}$. Moreover, $|0|_p = 0$ is defined.

  The **p-adic metric** is a **norm metric** on the set $\mathbb{Q}$ of rational numbers defined by

$$|x-y|_p.$$

This metric forms the basis for the algebra of p-adic numbers. The **Cauchy completions** of the metric spaces $(\mathbb{Q}, |x-y|_p)$ and $(\mathbb{Q}, |x-y|)$ with the **natural metric** $|x-y|$ give the fields $\mathbb{Q}_p$ of *p-adic numbers* and $\mathbb{R}$ of real numbers, respectively.

The **Gajić metric** is an **ultrametric** on the set $\mathbb{Q}$ of rational numbers defined, for $x \neq y$ (via the integer part $\lfloor z \rfloor$ of a real number z), by

$$\inf\{2^{-n} : n \in \mathbb{Z},\ \lfloor 2^n(x-e)\rfloor = \lfloor 2^n(y-e)\rfloor\},$$

where e is any fixed irrational number. This metric is **equivalent** to the **natural metric** $|x-y|$ on $\mathbb{Q}$.

- **Continued fraction metric on irrationals**

  The **continued fraction metric on irrationals** is a complete metric on the set *Irr* of irrational numbers defined, for $x \neq y$, by

  $$\frac{1}{n},$$

  where n is the first index for which the continued fraction expansions of x and y differ. This metric is **equivalent** to the **natural metric** $|x-y|$ on *Irr* which is noncomplete and disconnected. Also, the *Baire* 0*-dimensional space* $B(\aleph_0)$ (cf. **Baire metric** in Chap. 11) is homeomorphic to *Irr* endowed with this metric.
- **Natural metric**

  The **natural metric** (or **absolute value metric**, **line metric**, *the distance between numbers*) is a metric on $\mathbb{R}$ defined by

  $$|x-y| = \begin{cases} y-x, \text{ if } x-y < 0, \\ x-y, \text{ if } x-y \geq 0. \end{cases}$$

  On $\mathbb{R}$ all l_p**-metrics** coincide with the natural metric. The metric space $(\mathbb{R}, |x-y|)$ is called the *real line* (or *Euclidean line*).

  There exist many other metrics on $\mathbb{R}$ coming from $|x-y|$ by some **metric transform** (Chap. 4). For example: $\min\{1, |x-y|\}$, $\frac{|x-y|}{1+|x-y|}$, $|x| + |x-y| + |y|$ (for $x \neq y$) and, for a given $0 < \alpha < 1$, the **generalized absolute value metric** $|x-y|^\alpha$.

  Some authors use $|x-y|$ as the *Polish notation* (parentheses-free and computer-friendly) of the distance function in any metric space.
- **Zero bias metric**

  The **zero bias metric** is a metric on $\mathbb{R}$ defined by

  $$1 + |x-y|$$

  if one and only one of x and y is strictly positive, and by

  $$|x-y|,$$

  otherwise, where $|x-y|$ is the **natural metric** (see, for example, [Gile87]).

- **Sorgenfrey quasi-metric**
  The **Sorgenfrey quasi-metric** is a quasi-metric d on $\mathbb{R}$ defined by

$$y - x$$

  if $y \geq x$, and equal to 1, otherwise. Some similar quasi-metrics on $\mathbb{R}$ are:

  1. $d_1(x, y) = \max\{y - x, 0\}$ (in general, $\max\{f(y) - f(x), 0\}$ is a quasi-metric on a set X if $f : X \to \mathbb{R}_{\geq 0}$ is an injective function);
  2. $d_2(x, y) = \min\{y - x, 1\}$ if $y \geq x$, and equal to 1, otherwise;
  3. $d_3(x, y) = y - x$ if $y \geq x$, and equal to $a(x - y)$ (for fixed $a > 0$), otherwise;
  4. $d_4(x, y) = e^y - e^x$ if $y \geq x$, and equal to $e^{-y} - e^{-x}$ otherwise.

- **Real half-line quasi-semimetric**
  The **real half-line quasi-semimetric** is defined on the half-line $\mathbb{R}_{>0}$ by

$$\max\{0, \ln \frac{y}{x}\}.$$

- **Janous–Hametner metric**
  The **Janous–Hametner metric** is defined on the half-line $\mathbb{R}_{>0}$ by

$$\frac{|x - y|}{(x + y)^t},$$

  where $t = -1$ or $0 \leq t \leq 1$, and $|x - y|$ is the **natural metric**.
- **Extended real line metric**
  An **extended real line metric** is a metric on $\mathbb{R} \cup \{+\infty\} \cup \{-\infty\}$. The main example (see, for example, [Cops68]) of such metric is given by

$$|f(x) - f(y)|,$$

  where $f(x) = \frac{x}{1+|x|}$ for $x \in \mathbb{R}$, $f(+\infty) = 1$, and $f(-\infty) = -1$.
  Another metric, commonly used on $\mathbb{R} \cup \{+\infty\} \cup \{-\infty\}$, is defined by

$$|\arctan x - \arctan y|,$$

  where $-\frac{1}{2}\pi < \arctan x < \frac{1}{2}\pi$ for $-\infty < x < \infty$, and $\arctan(\pm\infty) = \pm\frac{1}{2}\pi$.
- **Complex modulus metric**
  The **complex modulus metric** on the set $\mathbb{C}$ of complex numbers is defined by

$$|z - u|,$$

  where, for any $z = z_1 + z_2 i \in \mathbb{C}$, the number $|z| = \sqrt{z\bar{z}} = \sqrt{z_1^2 + z_2^2}$ is the *complex modulus*. The *complex argument* θ is defined by $z = |z|(\cos(\theta) + i \sin(\theta))$.

The metric space $(\mathbb{C}, |z-u|)$ is called the *complex* (or *Wessel–Argand*) *plane*. It is isometric to the Euclidean plane $(\mathbb{R}^2, ||x-y||_2)$. So, the metrics on $\mathbb{R}^2$, given in Chaps. 19 and 5, can be seen as metrics on $\mathbb{C}$. For example, the **British Rail metric** on $\mathbb{C}$ is $|z| + |u|$ for $z \neq u$. The ***p*-relative** (if $1 \leq p < \infty$) and **relative metric** (if $p = \infty$) on $\mathbb{C}$ are defined for $|z| + |u| \neq 0$ respectively, by

$$\frac{|z-u|}{\sqrt[p]{|z|^p + |u|^p}} \text{ and } \frac{|z-u|}{\max\{|z|, |u|\}}.$$

- $\mathbb{Z}(\eta_m)$**-related norm metrics**

  A *Kummer* (or *cyclotomic*) *ring* $\mathbb{Z}(\eta_m)$ is a subring of the ring $\mathbb{C}$ (and an extension of the ring $\mathbb{Z}$), such that each of its elements has the form $\sum_{j=0}^{m-1} a_j \eta_m^j$, where η_m is a primitive m-th root $\exp(\frac{2\pi i}{m})$ of unity, and all a_j are integers.

  The *complex modulus* $|z|$ of $z = a + b\eta_m \in \mathbb{C}$ is defined by

$$|z|^2 = z\bar{z} = a^2 + (\eta_m + \overline{\eta_m})ab + b^2 = a^2 + 2ab\cos(\frac{2\pi i}{m}) + b^2.$$

  Then $(a+b)^2 = q^2$ for $m = 2$ (or 1), $a^2 + b^2$ for $m = 4$, and $a^2 + ab + b^2$ for $m = 6$ (or 3), i.e., for the ring $\mathbb{Z}$ of usual integers, $\mathbb{Z}(i)$ of *Gaussian integers* and $\mathbb{Z}(\rho)$ of *Eisenstein–Jacobi* (or *EJ*) *integers*.

  The set of units of $\mathbb{Z}(\eta_m)$ contain $\eta_m^j, 0 \leq j \leq m-1$; for $m = 5$ and $m \geq 6$, units of infinite order appear also, since $\cos(\frac{2\pi i}{m})$ is irrational. For $m = 2, 4, 6$, the set of units is $\{\pm 1\}$, $\{\pm 1, \pm i\}$, $\{\pm 1, \pm\rho, \pm\rho^2\}$, where $i = \eta_4$ and $\rho = \eta_6 = \frac{1+i\sqrt{3}}{2}$.

  The norms $|z| = \sqrt{a^2 + b^2}$ and $||z||_i = |a| + |b|$ for $z = a + bi \in \mathbb{C}$ give rise to the **complex modulus** and ***i*-Manhattan** metrics on $\mathbb{C}$. They coincide with the Euclidean (l_2-) and Manhattan (l_1-) metrics, respectively, on $\mathbb{R}^2$ seen as the complex plane. The restriction of the *i*-Manhattan metric on $\mathbb{Z}(i)$ is the path metric of the square grid $\mathbb{Z}^2$ of $\mathbb{R}^2$; cf. **grid metric** in Chap. 19.

  The ρ**-Manhattan metric** on $\mathbb{C}$ is defined by the norm $||z||_\rho$, i.e.,

$$\min\{|a|+|b|+|c| : z = a+b\rho+c\rho^2\} = \min\{|a|+|b|, |a+b|+|b|, |a+b|+|a| : z = a+b\rho\}.$$

  The restriction of the ρ-Manhattan metric on $\mathbb{Z}(\rho)$ is the path metric of the triangular grid of $\mathbb{R}^2$ (seen as the *hexagonal lattice* $A_2 = \{(a,b,c) \in \mathbb{Z}^3 : a+b+c = 0\}$), i.e., the **hexagonal metric** (Chap. 19).

  Let f denote either i or $\rho = \frac{1+i\sqrt{3}}{2}$. Given a $\pi \in \mathbb{Z}(f) \setminus \{0\}$ and $z, z' \in \mathbb{Z}(f)$, we write $z \equiv z' \pmod{\pi}$ if $z - z' = \delta\pi$ for some $\delta \in \mathbb{Z}(f)$. For the quotient ring $\mathbb{Z}_\pi(f) = \{z \pmod{\pi} : z \in \mathbb{Z}(f)\}$, it holds $|\mathbb{Z}_\pi(f)| = ||\pi||_f^2$.

  Call two congruence classes $z \pmod{\pi}$ and $z' \pmod{\pi}$ *adjacent* if $z - z' \equiv f^j \pmod{\pi}$ for some j. The resulting graph on $\mathbb{Z}_\pi(f)$ called a *Gaussian network* or *EJ network* if, respectively, $f = i$ or $f = \rho$. The path metrics of these networks

coincide with their norm metrics, defined (Fan–Gao, 2004) for $z \,(\mathrm{mod}\, \pi)$ and $z' \,(\mathrm{mod}\, \pi)$, by

$$\min ||u||_f : u \in z - z' \,(\mathrm{mod}\, \pi).$$

These metrics are different from the previously defined ([Hube94a, Hube94b]) distance on $\mathbb{Z}_\pi(f)$: $||v||_f$, where $v \in z - z' \,(\mathrm{mod}\, \pi)$ is selected by minimizing the complex modulus. For $f = i$, this is the **Mannheim distance** (Chap. 16), which is not a metric.

- **Chordal metric**

The **chordal metric** d_χ is a metric on the set $\overline{\mathbb{C}}$=$\mathbb{C} \cup \{\infty\}$ defined by

$$d_\chi(z,u) = \frac{2|z-u|}{\sqrt{1+|z|^2}\sqrt{1+|u|^2}} \text{ and } d_\chi(z,\infty) = \frac{2}{\sqrt{1+|z|^2}}$$

for all $u, z \in \mathbb{C}$ (cf. ***M*-relative metric** in Chap. 5).

The metric space $(\overline{\mathbb{C}}, d_\chi)$ is called the *extended complex plane*. It is homeomorphic and conformally equivalent to the *Riemann sphere*, i.e., the *unit sphere* $S^2 = \{(x_1, x_2, x_3) \in \mathbb{E}^3 : x_1^2 + x_2^2 + x_3^2 = 1\}$ (considered as a metric subspace of $\mathbb{E}^3$), onto which $(\overline{\mathbb{C}}, d_\chi)$ is one-to-one mapped under stereographic projection.

The plane $\overline{\mathbb{C}}$ can be identified with the plane $x_3 = 0$ such that the and imaginary axes coincide with the x_1 and x_2 axes. Under stereographic projection, each point $z \in \mathbb{C}$ corresponds to the point $(x_1, x_2, x_3) \in S^2$, where the ray drawn from the "north pole" $(0, 0, 1)$ to the point z meets the sphere S^2; the "north pole" corresponds to the point at ∞. The chordal (spherical) metric between two points $p, q \in S^2$ is taken to be the distance between their preimages $z, u \in \overline{\mathbb{C}}$.

The chordal metric is defined equivalently on $\overline{\mathbb{R}}^n = \mathbb{R}^n \cup \{\infty\}$:

$$d_\chi(x,y) = \frac{2||x-y||_2}{\sqrt{1+||x||_2^2}\sqrt{1+||y||_2^2}} \text{ and } d_\chi(x,\infty) = \frac{2}{\sqrt{1+||x||_2^2}}.$$

The restriction of the metric d_χ on $\mathbb{R}^n$ is a **Ptolemaic metric**; cf. Chap. 1.

Given $\alpha > 0$, $\beta \geq 0$, $p \geq 1$, the **generalized chordal metric** is a metric on $\mathbb{C}$ (in general, on $(\mathbb{R}^n, ||.||_2)$ and even on any *Ptolemaic space* $(V, ||.||)$), defined by

$$\frac{|z-u|}{\sqrt[p]{\alpha+\beta|z|^p} \cdot \sqrt[p]{\alpha+\beta|u|^p}}.$$

- **Metrics on quaternions**

Quaternions are members of a noncommutative division algebra $\mathcal{Q}$ over the field $\mathbb{R}$, geometrically realizable in $\mathbb{R}^4$ ([Hami66]). Formally,

$$\mathcal{Q} = \{q = q_1 + q_2 i + q_3 j + q_4 k : q_i \in \mathbb{R}\},$$

where the *basic units* $1, i, j, k \in \mathcal{Q}$ satisfy $i^2 = j^2 = k^2 = -1$ and $ij = -ji = k$.

The *quaternion norm* is defined by $||q|| = \sqrt{q\overline{q}} = \sqrt{q_1^2 + q_2^2 + q_3^2 + q_4^2}$, where $\overline{q} = q_1 - q_2 i - q_3 j - q_4 k$. The **quaternion metric** is the norm metric $||q - q'||$ on $\mathcal{Q}$.

The set of all *Lipschitz integers* and *Hurwitz integers* are defined, respectively, by

$$L = \{q_1 + q_2 i + q_3 j + q_4 k : q_i \in \mathbb{Z}\} \text{ and}$$

$$H = \{q_1 + q_2 i + q_3 j + q_4 k : \text{ all } q_i \in \mathbb{Z} \text{ or all } q_i + \frac{1}{2} \in \mathbb{Z}\}.$$

A quaternion $q \in L$ is *irreducible* (i.e., $q = q'q''$ implies $\{q', q''\} \cap \{\pm 1, \pm i, \pm j, \pm k\} \neq \emptyset$) if and only if $||q||$ is a prime. Given an irreducible $\pi \in L$ and $q, q' \in H$, we write $q \equiv q' \pmod{\pi}$ if $q - q' = \delta\pi$ for some $\delta \in L$.

For the rings $L_\pi = \{q \pmod{\pi} : q \in L\}$ and $H_\pi = \{q \pmod{\pi} : q \in H\}$ it holds $|L_\pi| = ||\pi||^2$ and $|H_\pi| = 2||\pi||^2 - 1$.

The **quaternion Lipschitz metric** on L_π is defined (Martinez et al., 2009) by

$$d_L(\alpha, \beta) = \min \sum_{1 \le s \le 4} |q_s| : \alpha - \beta \equiv q_1 + q_2 i + q_3 j + q_4 k \pmod{\pi}.$$

The ring H is additively generated by its subring L and $w = \frac{1}{2}(1 + i + j + k)$. The **Hurwitz metric** on the ring H_π is defined (Guzëltepe, 2013) by

$$d_H(\alpha, \beta) = \min \sum_{1 \le s \le 5} |q_s| : \alpha - \beta \equiv q_1 + q_2 i + q_3 j + q_4 k + q_5 w \pmod{\pi}.$$

Cf. the **hyper-Kähler** and **Gibbons–Manton** metrics in Sect. 7.3 and the **unit quaternions** and **joint angle** metrics in Sect. 18.3.

12.2 Metrics on Polynomials

A *polynomial* is a sum of powers in one or more variables multiplied by coefficients. A *polynomial in one variable* (or *monic polynomial*) with constant real (complex) coefficients is given by $P = P(z) = \sum_{k=0}^{n} a_k z^k$, $a_k \in \mathbb{R}$ ($a_k \in \mathbb{C}$). The set $\mathcal{P}$ of all real (complex) polynomials forms a ring $(\mathcal{P}, +, \cdot, 0)$. It is also a vector space over $\mathbb{R}$ (over $\mathbb{C}$).

- **Polynomial norm metric**

  A **polynomial norm metric** is a **norm metric** on the vector space $\mathcal{P}$ of all real (complex) polynomials defined by

  $$||P - Q||,$$

where $||.||$ is a *polynomial norm*, i.e., a function $||.|| : \mathcal{P} \to \mathbb{R}$ such that, for all $P, Q \in \mathcal{P}$ and for any scalar k, we have the following properties:

1. $||P|| \geq 0$, with $||P|| = 0$ if and only if $P \equiv 0$;
2. $||kP|| = |k|||P||$;
3. $||P + Q|| \leq ||P|| + ||Q||$ (triangle inequality).

The l_p*-norm* and L_p*-norm* of a polynomial $P(z) = \sum_{k=0}^{n} a_k z^k$ are defined by

$$||P||_p = (\sum_{k=0}^{n} |a_k|^p)^{1/p} \text{ and } ||P||_{L_p} = (\int_0^{2\pi} |P(e^{i\theta})|^p \frac{d\theta}{2\pi})^{\frac{1}{p}} \text{ for } 1 \leq p < \infty,$$

$$||P||_\infty = \max_{0 \leq k \leq n} |a_k| \text{ and } ||P||_{L_\infty} = \sup_{|z|=1} |P(z)| \text{ for } p = \infty.$$

The values $||P||_1$ and $||P||_\infty$ are called the *length* and *height* of polynomial P.

- **Distance from irreducible polynomials**

  For any field $\mathbb{F}$, a polynomial with coefficients in $\mathbb{F}$ is said to be *irreducible over* $\mathbb{F}$ if it cannot be factored into the product of two nonconstant polynomials with coefficients in $\mathbb{F}$. Given a metric d on the polynomials over $\mathbb{F}$, the **distance** (of a given polynomial $P(z)$) **from irreducible polynomials** is $d_{ir}(P) = \inf d(P, Q)$, where $Q(z)$ is any irreducible polynomial of the same degree over $\mathbb{F}$.

  Polynomial conjecture of Turán, 1967, is that there exists a constant C with $d_{ir}(P) \leq C$ for every polynomial P over $\mathbb{Z}$, where $d(P, Q)$ is the *length* $||P - Q||_1$ of $P - Q$.

  Lee–Ruskey–Williams, 2007, conjectured that there exists a constant C with $d_{ir}(P) \leq C$ for every polynomial P over the Galois field $\mathbb{F}_2$, where $d(P, Q)$ is the **Hamming distance** between the $(0, 1)$-sequences of coefficients of P and Q.

- **Bombieri metric**

  The **Bombieri metric** (or **polynomial bracket metric**) is a **polynomial norm metric** on the set $\mathcal{P}$ of all real (complex) polynomials defined by

$$[P - Q]_p,$$

  where $[.]_p$, $0 \leq p \leq \infty$, is the *Bombieri p-norm*.

  For a polynomial $P(z) = \sum_{k=0}^{n} a_k z^k$ it is defined by

$$[P]_p = (\sum_{k=0}^{n} \binom{n}{k}^{1-p} |a_k|^p)^{\frac{1}{p}}.$$

- **Metric space of roots**

  The **metric space of roots** is (Ćurgus–Mascioni, 2006) the space (X, d) where X is the family of all multisets of complex numbers with n elements and the distance between multisets $U = \{u_1, \ldots, u_n\}$ and $V = \{v_1, \ldots, v_n\}$ is defined by

the following analog of the **Fréchet metric**:

$$\min_{\tau \in Sym_n} \max_{1 \le j \le n} |u_j - v_{\tau(j)}|,$$

where τ is any permutation of $\{1, \ldots, n\}$. Here the set of roots of some monic complex polynomial of degree n is considered as a multiset with n elements. Cf. **metrics between multisets** in Chap. 1.

The function assigning to each polynomial the multiset of its roots is a **homeomorphism** between the metric space of all monic complex polynomials of degree n with the **polynomial norm metric** l_∞ and the metric space of roots.

12.3 Metrics on Matrices

An $m \times n$ matrix $A = ((a_{ij}))$ over a field $\mathbb{F}$ is a table consisting of m rows and n columns with the entries a_{ij} from $\mathbb{F}$. The set of all $m \times n$ matrices with real (complex) entries is denoted by $M_{m,n}$ or $\mathbb{R}^{m \times n}$ ($\mathbb{C}^{m \times n}$). It forms a *group* $(M_{m,n}, +, 0_{m,n})$, where $((a_{ij})) + ((b_{ij})) = ((a_{ij} + b_{ij}))$, and the matrix $0_{m,n} \equiv 0$. It is also an mn-dimensional vector space over $\mathbb{R}$ ($\mathbb{C}$).

The *transpose* of a matrix $A = ((a_{ij})) \in M_{m,n}$ is the matrix $A^T = ((a_{ji})) \in M_{n,m}$. A $m \times n$ matrix A is called a *square matrix* if $m = n$, and a *symmetric matrix* if $A = A^T$. The *conjugate transpose* (or *adjoint*) of a matrix $A = ((a_{ij})) \in M_{m,n}$ is the matrix $A^* = ((\overline{a}_{ji})) \in M_{n,m}$. An *Hermitian matrix* is a complex square matrix A with $A = A^*$.

The set of all square $n \times n$ matrices with real (complex) entries is denoted by M_n. It forms a *ring* $(M_n, +, \cdot, 0_n)$, where $+$ and 0_n are defined as above, and $((a_{ij})) \cdot ((b_{ij})) = ((\sum_{k=1}^{n} a_{ik} b_{kj}))$. It is also an n^2-dimensional vector space over $\mathbb{R}$ (over $\mathbb{C}$). The *trace* of a square $n \times n$ matrix $A = ((a_{ij}))$ is defined by $\mathrm{Tr}(A) = \sum_{i=1}^{n} a_{ii}$.

The *identity matrix* is $1_n = ((c_{ij}))$ with $c_{ii} = 1$, and $c_{ij} = 0$, $i \neq j$. An *unitary matrix* $U = ((u_{ij}))$ is a square matrix defined by $U^{-1} = U^*$, where U^{-1} is the *inverse matrix* of U, i.e., $UU^{-1} = 1_n$. A matrix $A \in M_{m,n}$ is *orthonormal* if $A^*A = 1_n$. A matrix $A \in \mathbb{R}^{n \times n}$ is *orthogonal* if $A^T = A^{-1}$, *normal* if $A^TA = AA^T$ and *singular* if its determinant is 0.

If for a matrix $A \in M_n$ there is a vector x such that $Ax = \lambda x$ for some scalar λ, then λ is called an *eigenvalue* of A with corresponding *eigenvector* x. Given a matrix $A \in \mathbb{C}^{m \times n}$, its *singular values* $s_i(A)$ are defined as $\sqrt{\lambda(A^*A)}$. A real matrix A is *positive-definite* if $v^TAv > 0$ for all nonzero real vectors v; it holds if and only if all eigenvalues of $A_H = \frac{1}{2}(A + A^T)$ are positive. An Hermitian matrix A is *positive-definite* if $v^*Av > 0$ for all nonzero complex vectors v; it holds if and only if all $\lambda(A)$ are positive.

The *mixed states* of a n-dimensional *quantum system* are described by their *density matrices*, i.e., positive-semidefinite Hermitian $n \times n$ matrices of trace 1. The set of such matrices is convex, and its extremal points describe the *pure states*. Cf. **monotone metrics** in Chap. 7 and **distances between quantum states** in Chap. 24.

- **Matrix norm metric**

  A **matrix norm metric** is a **norm metric** on the set $M_{m,n}$ of all real (complex) $m \times n$ matrices defined by

$$||A - B||,$$

  where $||.||$ is a *matrix norm*, i.e., a function $||.|| : M_{m,n} \to \mathbb{R}$ such that, for all $A, B \in M_{m,n}$, and for any scalar k, we have the following properties:

  1. $||A|| \geq 0$, with $||A|| = 0$ if and only if $A = 0_{m,n}$;
  2. $||kA|| = |k|||A||$;
  3. $||A + B|| \leq ||A|| + ||B||$ (triangle inequality).
  4. $||AB|| \leq ||A|| \cdot ||B||$ (*submultiplicativity*).

  All matrix norm metrics on $M_{m,n}$ are equivalent. The simplest example of such metric is the **Hamming metric** on $M_{m,n}$ (in general, on the set $M_{m,n}(\mathbb{F})$ of all $m \times n$ matrices with entries from a field $\mathbb{F}$) defined by $||A - B||_H$, where $||A||_H$ is the *Hamming norm* of $A \in M_{m,n}$, i.e., the number of nonzero entries in A. Example of a *generalized* (i.e., not submultiplicative one) *matrix norm* is the *max element norm* $||A = ((a_{ij}))||\max = \max_{i,j} |a_{ij}|$; but $\sqrt{mn}||A||_{\max}$ is a matrix norm.

- **Natural norm metric**

  A **natural** (or *operator*, *induced*) **norm metric** is a **matrix norm metric** on the set M_n defined by

$$||A - B||_{\text{nat}},$$

  where $||.||_{\text{nat}}$ is a *natural* (or *operator*, *induced*) *norm* on M_n, induced by the vector norm $||x||$, $x \in \mathbb{R}^n$ ($x \in \mathbb{C}^n$), is a matrix norm defined by

$$||A||_{\text{nat}} = \sup_{||x|| \neq 0} \frac{||Ax||}{||x||} = \sup_{||x||=1} ||Ax|| = \sup_{||x|| \leq 1} ||Ax||.$$

  The natural norm metric can be defined in similar way on the set $M_{m,n}$ of all $m \times n$ real (complex) matrices: given vector norms $||.||_{\mathbb{R}^m}$ on $\mathbb{R}^m$ and $||.||_{\mathbb{R}^n}$ on $\mathbb{R}^n$, the *natural norm* $||A||_{\text{nat}}$ of a matrix $A \in M_{m,n}$, induced by $||.||_{\mathbb{R}^n}$ and $||.||_{\mathbb{R}^m}$, is a matrix norm defined by $||A||_{\text{nat}} = \sup_{||x||_{\mathbb{R}^n}=1} ||Ax||_{\mathbb{R}^m}$.

- **Matrix p-norm metric**

  A **matrix p-norm metric** is a **natural norm metric** on M_n defined by

$$||A - B||_{\text{nat}}^p,$$

  where $||.||_{\text{nat}}^p$ is the *matrix* (or *operator*) *p-norm*, i.e., a *natural norm*, induced by the vector l_p*-norm*, $1 \leq p \leq \infty$:

$$||A||_{\text{nat}}^p = \max_{||x||_p=1} ||Ax||_p, \quad \text{where} \quad ||x||_p = (\sum_{i=1}^{n} |x_i|^p)^{1/p}.$$

The **maximum absolute column** and **maximum absolute row metric** are the **matrix 1-norm** and **matrix ∞-norm metric** on M_n. For a matrix $A = ((a_{ij})) \in M_n$, the *maximum absolute column* and *maximum absolute row sum norm* are

$$||A||^1_{\text{nat}} = \max_{1\le j\le n} \sum_{i=1}^{n} |a_{ij}| \text{ and } |A||^\infty_{\text{nat}} = \max_{1\le i\le n} \sum_{j=1}^{n} |a_{ij}|.$$

The **spectral norm metric** is the **matrix 2-norm metric** $||A - B||^2_{\text{nat}}$ on M_n. The matrix 2-norm $||.||^2_{\text{nat}}$, induced by the vector l_2-*norm*, is also called the *spectral norm* and denoted by $||.||_{sp}$. For a symmetric matrix $A = ((a_{ij})) \in M_n$, it is

$$||A||_{sp} = s_{\max}(A) = \sqrt{\lambda_{\max}(A^*A)},$$

where $A^* = ((\overline{a}_{ji}))$, while $s_{\max}$ and $\lambda_{\max}$ are largest singular value and eigenvalue.

- **Frobenius norm metric**

  The **Frobenius norm metric** is a **matrix norm metric** on $M_{m,n}$ defined by

$$||A - B||_{Fr},$$

  where $||.||_{Fr}$ is the *Frobenius* (or *Hilbert–Schmidt*) *norm*. For $A = ((a_{ij}))$, it is

$$||A||_{Fr} = \sqrt{\sum_{i,j} |a_{ij}|^2} = \sqrt{\text{Tr}(A^*A)} = \sqrt{\sum_{1\le i\le \text{rank}(A)} \lambda_i} = \sqrt{\sum_{1\le i\le \text{rank}(A)} s_i^2},$$

  where λ_i, s_i are the eigenvalues and singular values of A.

  This norm is strictly convex, is a differentiable function of its elements a_{ij} and is the only unitarily invariant norm among $||A||_p = (\sum_{i=1}^m \sum_{j=1}^n |a_{ij}|^p)^{\frac{1}{p}}, p \ge 1$.

  The **trace norm metric** is a matrix norm metric on $M_{m,n}$ defined by

$$||A - B||_{tr},$$

  where $||.||_{tr}$ is the *trace norm* (or *nuclear norm*) on $M_{m,n}$ defined by

$$||A||_{tr} = \sum_{i=1}^{\min\{m,n\}} s_i(A) = \text{Tr}(\sqrt{A^*A}).$$

- **Schatten norm metric**

  Given $1 \le p < \infty$, the **Schatten norm metric** is a **matrix norm metric** on $M_{m,n}$ defined by

$$||A - B||^p_{Sch},$$

where $||.||_{Sch}^{p}$ is the *Schatten p-norm* on $M_{m,n}$. For a matrix $A \in M_{m,n}$, it is defined as the p-th root of the sum of the p-th powers of all its *singular values*:

$$||A||_{Sch}^{p} = (\sum_{i=1}^{\min\{m,n\}} s_i^p(A))^{\frac{1}{p}}.$$

For $p = \infty$, 2 and 1, one obtains the **spectral norm metric**, **Frobenius norm metric** and **trace norm metric**, respectively.

- (c, p)**-norm metric**

  Let $k \in \mathbb{N}$, $k \leq \min\{m, n\}$, $c \in \mathbb{R}^k$, $c_1 \geq c_2 \geq \cdots \geq c_k > 0$, and $1 \leq p < \infty$. The (c, p)**-norm metric** is a **matrix norm metric** on $M_{m,n}$ defined by

$$||A - B||_{(c,p)}^{k},$$

where $||.||_{(c,p)}^{k}$ is the (c, p)*-norm* on $M_{m,n}$. For a matrix $A \in M_{m,n}$, it is defined by

$$||A||_{(c,p)}^{k} = (\sum_{i=1}^{k} c_i s_i^p(A))^{\frac{1}{p}},$$

where $s_1(A) \geq s_2(A) \geq \cdots \geq s_k(A)$ are the first k *singular values* of A.

If $p = 1$, it is the *c-norm*. If, moreover, $c_1 = \cdots = c_k = 1$, it is the *Ky Fan k-norm*.

- **Ky Fan** k**-norm metric**

  Given $k \in \mathbb{N}$, $k \leq \min\{m, n\}$, the **Ky Fan** k**-norm metric** is a **matrix norm metric** on $M_{m,n}$ defined by

$$||A - B||_{KF}^{k},$$

where $||.||_{KF}^{k}$ is the *Ky Fan k-norm* on $M_{m,n}$. For a matrix $A \in M_{m,n}$, it is defined as the sum of its first k *singular values*:

$$||A||_{KF}^{k} = \sum_{i=1}^{k} s_i(A).$$

For $k = 1$ and $k = \min\{m, n\}$, one obtains the **spectral** and **trace** norm metrics.

- **Cut norm metric**

  The **cut norm metric** is a **matrix norm metric** on $M_{m,n}$ defined by

$$||A - B||_{cut},$$

where $||.||_{cut}$ is the *cut norm* on $M_{m,n}$ defined, for a matrix $A = ((a_{ij})) \in M_{m,n}$, as:

$$||A||_{cut} = \max_{I \subset \{1,\ldots,m\}, J \subset \{1,\ldots,n\}} |\sum_{i \in I, j \in J} a_{ij}|.$$

Cf. in Chap. 15 the **rectangle distance on weighted graphs** and the **cut semimetric**, but the **weighted cut metric** in Chap. 19 is not related.

- **Matrix nearness problems**

A norm $||.||$ is *unitarily invariant* on $M_{m,n}$ if $||B|| = ||UBV||$ for all $B \in M_{m,n}$ and all unitary matrices U, V. All *Schatten p-norms* are unitarily invariant.

Given a unitarily invariant norm $||.||$ on $M_{m,n}$, a matrix property $\mathcal{P}$ defining a subspace or compact subset of $M_{m,n}$ (so that $d_{||.||}(A, \mathcal{P})$ below is well defined) and a matrix $A \in M_{m,n}$, then the *distance to* $\mathcal{P}$ is the **point-set distance** on $M_{m,n}$

$$d(A) = d_{||.||}(A, \mathcal{P}) = \min\{||E|| : A + E \text{ has property } \mathcal{P}\}.$$

A **matrix nearness problem** is ([High89]) to find an explicit formula for $d(A)$, the $\mathcal{P}$*-closest matrix* (or matrices) $X_{||.||}(A) = A + E$, satisfying the above minimum, and efficient algorithms for computing $d(A)$ and $X_{||.||}(A)$. The *componentwise nearness problem* is to find $d'(A) = \min\{\epsilon : |E| \leq \epsilon |A|, A + E \text{ has property } \mathcal{P}\}$, where $|B| = ((|b_{ij}|))$ and the matrix inequality is interpreted componentwise.

The most used norms for $B = ((b_{ij}))$ are the *Schatten* 2- and ∞*-norms* (cf. **Schatten norm metric**): the *Frobenius norm* $||B||_{Fr} = \sqrt{\text{Tr}(B^*B)} = \sqrt{\sum_{1 \leq i \leq \text{rank}(B)} s_i^2}$ and the *spectral norm* $||B||_{sp} = \sqrt{\lambda_{\max}(B^*B)} = s_1(B)$.

Examples of closest matrices $X = X_{||.||}(A, \mathcal{P})$ follow.

Let $A \in \mathbb{C}^{n \times n}$. Then $A = A_H + A_S$, where $A_H = \frac{1}{2}(A + A^*)$ is Hermitian and $A_H = \frac{1}{2}(A - A^*)$ is *skew-Hermitian* (i.e., $A_H^* = -A_H$). Let $A = U\Sigma V^*$ be a *singular value decomposition* (SVD) of A, i.e., $U \in M_m$ and $V^* \in M_n$ are unitary, while $\Sigma = \text{diag}(s_1, s_2, \ldots, s_{\min\{m,n\}})$ is an $m \times n$ diagonal matrix with $s_1 \geq s_2 \geq \cdots \geq s_{\text{rank}(A)} > 0 = \cdots = 0$. Fan and Hoffman, 1955, showed that, for any unitarily invariant norm, A_H, A_S, UV^* are closest Hermitian (symmetric), skew-Hermitian (skew-symmetric) and unitary (orthogonal) matrices, respectively. Such matrix $X_{Fr}(A)$ is a unique minimizer in all three cases.

Let $A \in \mathbb{R}^{n \times n}$. Gabriel, 1979, found the closest normal matrix $X_{Fr}(A)$. Higham found in 1988 a unique closest symmetric positive-semidefinite matrix $X_{Fr}(A)$ and, in 2001, the closest matrix of this type with unit diagonal (i.e., ab correlation matrix).

Given a SVD $A = U\Sigma V^*$ of A, let A_k denote $U\Sigma_k V^*$, where Σ_k is a diagonal matrix $\text{diag}(s_1, s_2, \ldots, s_k, 0, \ldots, 0)$ containing the largest k singular values of A. Then (Mirsky, 1960) A_k achieves $\min_{\text{rank}(A+E) \leq k} ||E||$ for any unitarily invariant norm. So, $||A - A_k||_{Fr} = \sqrt{\sum_{i=k+1}^{\text{rank}(A)} s_i^2}$ (Eckart–Young, 1936) and $||A - A_k||_{sp} = s_{max}(A - A_k) = s_{k+1}(A)$. A_k is a unique minimizer $X_{Fr}(A)$ if $s_k > s_{k+1}$.

Let $A \in \mathbb{R}^{n\times n}$ be nonsingular. Then its **distance to singularity** $d(A, Sing) = \min\{||E|| : A + E \text{ is singular}\}$ is, for both above norms, $s_n(A) = \frac{1}{s_1(A^{-1})} = \frac{1}{||A^{-1}||_{sp}} = \sup\{\delta : \delta\mathbb{B}_{\mathbb{R}^n} \subseteq A\mathbb{B}_{\mathbb{R}^n}\}$; here $\mathbb{B}_{\mathbb{R}^n} = \{x \in \mathbb{R}^n : ||x|| \leq 1\}$.

Given a closed convex cone $C \subseteq \mathbb{R}^n$, call a matrix $A \in \mathbb{R}^{m\times n}$ *feasible* if $\{Ax : x \in C\} = \mathbb{R}^m$; so, for $m = n$ and $C = \mathbb{R}^n$, feasibly means nonsingularity. Renegar, 1995, showed that, for feasible matrix A, its **distance to infeasibility** $\min\{||E||_{\text{nat}} : A + E \text{ is not feasible}\}$ is $\sup\{\delta : \delta\mathbb{B}_{\mathbb{R}^m} \subseteq A(\mathbb{B}_{\mathbb{R}^n} \cap C)\}$.

Lewis, 2003, generalized this by showing that, given two real normed spaces X, Y and a surjective *convex process* (or *set valued sublinear mapping*) F from X to Y, i.e., a multifunction for which $\{(x, y) : y \in F(x)\}$ is a closed convex cone, it holds

$$\min\{||E||_{\text{nat}} : E \text{ is any linear map } X \to Y, F + E \text{ is not surjective}\} = \frac{1}{||F^{-1}||_{\text{nat}}}.$$

Donchev et al. 2002, extended this, computing **distance to irregularity**; cf. **metric regularity** (Chap. 1). Cf. the above four *distances to ill-posedness* with **distance to uncontrollability** (Chap. 18) and **distances from symmetry** (Chap. 21).

- $Sym(n, \mathbb{R})^+$ **and** $Her(n, \mathbb{C})^+$ **metrics**

  Let $Sym(n, \mathbb{R})^+$ and $Her(n, \mathbb{C})^+$ be the cones of $n \times n$ symmetric real and Hermitian complex positive-definite $n \times n$ matrices. The $Sym(n, \mathbb{R})^+$ **metric** is defined, for any $A, B \in Sym(n, \mathbb{R})^+$, as

$$(\sum_{i=1}^{n} \log^2 \lambda_i)^{\frac{1}{2}},$$

  where λ_1, c, λ_n are the *eigenvalues* of the matrix $A^{-1}B$ (the same as those of $A^{-\frac{1}{2}}BA^{-\frac{1}{2}}$). It is the **Riemannian distance**, arising from the Riemannian metric $ds^2 = \text{Tr}((A^{-1}(dA))^2)$. This metric was rediscovered in Förstner–Moonen, 1999, and Pennec et al., 2004, via *generalized eigenvalue problem*: $det(\lambda A - B) = 0$.

  The $Her(n, \mathbb{C})^+$ **metric** is defined, for any $A, B \in Her(n, \mathbb{C})^+$, by

$$d_R(A, B) = ||\log(A^{-\frac{1}{2}}BA^{-\frac{1}{2}})||_{Fr},$$

  where $||H||_{Fr} = (\sum_{i,j} |h_{ij}|^2)^{\frac{1}{2}}$ is the *Frobenius norm* of the matrix $H = ((h_{ij}))$. It is the **Riemannian distance** arising from the Riemannian metric of nonpositive curvature, defined locally (at H) by $ds = ||H^{-\frac{1}{2}}\, dH\, H^{-\frac{1}{2}}||_{Fr}$. In other words, this distance is the **geodesic distance**

$$\inf\{L(\gamma) : \gamma \text{ is a (differentiable) path from A to B}\},$$

where $L(\gamma) = \int_A^B ||\gamma^{-\frac{1}{2}}(t)\gamma'(t)\gamma^{-\frac{1}{2}}(t)||_{Fr}dt$ and the geodesic $[A, B]$ is parametrized by $\gamma(t) = A^{\frac{1}{2}}(A^{-\frac{1}{2}}BA^{-\frac{1}{2}})^tA^{\frac{1}{2}}$ in the sense that $d_R(A, \gamma(t)) = td_R(A, B)$ for each $t \in [0, 1]$. In particular, the geodesic midpoint $\gamma(\frac{1}{2})$ of $[A, B]$ can be seen as the *geometric mean* of two positive-definite matrices A and B.

The space $(Her(n, \mathbb{C})^+, d_R))$ is an **Hadamard** (i.e., complete and CAT(0)) **space**, cf. Chap. 6. But $Her(n, \mathbb{C})^+$ is not complete with respect to matrix norms; it has a boundary consisting of the singular positive-semidefinite matrices.

Above $Sym(n, \mathbb{R})^+$ and $Her(n, \mathbb{C})^+$ metrics are the special cases of the distance $d_R(x, y)$ among **invariant distances on symmetric cones** in Chap. 9.

Cf. also, in Chap. 24, the **trace distance** on all Hermitian of trace 1 positive-definite $n \times n$ matrices and in Chap. 7, the **Wigner–Yanase–Dyson metrics** on all complex positive-definite $n \times n$ matrices.

The **Bartlett distance** between two matrices $A, B \in Her(n, \mathbb{C})^+$, is defined (Conradsen et al., 2003, for radar applications) by

$$\ln\left(\frac{(det(A+B))^2}{4det(A)det(B)}\right).$$

- **Siegel distance**

  The *Siegel half-plane* is the set SH_n of $n \times n$ matrices $Z = X + iY$, where X, Y are symmetric or Hermitian and Y is positive-definite. The **Siegel–Hua metric** (Siegel, 1943, and independently, Hua, 1944) on SH_n is defined by

$$ds^2 = \mathrm{Tr}(Y^{-1}(dZ)Y^{-1}(d\overline{Z})).$$

  It is unique metric preserved by any automorphism of SH_n. The Siegel–Hua metric on the *Siegel disk* $SD_n = \{W = (Z - iI)(Z + iI)^{-1} : Z \in SH_n\}$ is defined by

$$ds^2 = \mathrm{Tr}((I - WW^*)^{-1}dW(I - W^*W)^{-1}dW^*).$$

  For n=1, the Siegel–Hua metric is the **Poincaré metric** (cf. Chap. 6) on the *Poincaré half-plane* SH_1 and the *Poincaré disk* SD_1, respectively.

  Let $A_n = \{Z = iY : Y > 0\}$ be the imaginary axe on the Siegel half-plane. The Siegel–Hua metric on A_n is (cf. [Barb12]) the Riemannian **trace metric** $ds^2 = \mathrm{Tr}((P^{\dagger}dP)^2)$. The corresponding distances are $Sym(n, \mathbb{R})^+$ **metric** or $Her(n, \mathbb{C})^+$ **metric**. The **Siegel distance** on $SH_n \setminus A_n$ is defined by

$$d^2_{Siegel}(Z_1, Z_2) = \sum_{i=1}^{n} \log^2\left(\frac{1 + \sqrt{\lambda_i}}{1 - \sqrt{\lambda_i}}\right);$$

  $\lambda_1, \ldots, \lambda_n$ are the *eigenvalues* of the matrix $(Z_1 - Z_2)(Z_1 - \overline{Z_2}) - 1(\overline{Z_1} - \overline{Z_2})(\overline{Z_1} - Z_2)^{-1}$.

- **Barbaresco metrics**

  Let $z(k)$ be a complex temporal (discrete time) *stationary* signal, i.e., its mean value is constant and its *covariance function* $\mathbb{E}[z(k_1)z^*(k_2)]$ is only a function of $k_1 - k_2$. Such signal can be represented by its covariance $n \times n$ matrix $R = ((r_{ij}))$, where $r_{ij} = \mathbb{E}[z(i), z*(j)] = \mathbb{E}[z(n)z*(n-i+j)]$. It is a positive-definite *Toeplitz* (i.e. diagonal-constant) Hermitian matrix. In radar applications, such matrices represent the Doppler spectra of the signal. Matrices R admit a parametrization (complex ARM, i.e., m-th order autoregressive model) by *partial autocorrelation coefficients* defined recursively as the complex correlation between the forward and backward prediction errors of the $(m-1)$-th order complex ARM.

  Barbaresco ([Barb12]) defined, via this parametrization, a **Bergman metric** (Chap. 7) on the bounded domain $\mathbb{R} + xD_n \subset \mathbb{C}^n$ of above matrices R; here D is a *Poincaré disk*. He also defined a related **Kähler metric** on $M \times S_n$, where M is the set of positive-definite Hermitian matrices and SD_n is the *Siegel disk* (cf. **Siegel distance**). Such matrices represent spatiotemporal stationary signals, i.e., in radar applications, the Doppler spectra and spatial directions of the signal.

  Ben Jeuris, 2015, extended above metrics on *block Toeplitz matrices*, i.e., those having blocks that are repeated (as elements of a Toeplitz matrix) down the diagonals of the matrix.

  Cf. **Ruppeiner metric** (Chap. 7) and **Martin cepstrum distance** (Chap. 21).
- **Distances between graphs of matrices**

  The *graph* $G(A)$ *of a complex* $m \times n$ *matrix* A is the *range* (i.e., the span of columns) of the matrix $R(A) = ([IA^T])^T$. So, $G(A)$ is a subspace of $\mathbb{C}^{m+n}$ of all vectors v, for which the equation $R(A)x = v$ has a solution.

  A **distance between graphs of matrices** A and B is a distance between the subspaces $G(A)$ and $G(B)$. It can be an **angle distance between subspaces** or, for example, the following distance (cf. also the **Kadets distance** in Chap. 1 and the **gap metric** in Chap. 18).

  The **spherical gap distance** between subspaces A and B is defined by

$$\max\{\max_{x \in S(A)} d_E(x, S(B)), \max_{y \in S(B)} d_E(y, S(A))\},$$

  where $S(A), S(B)$ are the unit spheres of the subspaces A, B, $d(z, C)$ is the **point-set distance** $\inf_{y \in C} d(z, y)$ and $d_E(z, y)$ is the Euclidean distance.
- **Angle distances between subspaces**

  Consider the *Grassmannian space* $G(m, n)$ of all n-dimensional subspaces of Euclidean space $\mathbb{E}^m$; it is a compact *Riemannian manifold* of dimension $n(m-n)$.

  Given two subspaces $A, B \in G(m, n)$, the *principal angles* $\frac{\pi}{2} \geq \theta_1 \geq \cdots \geq \theta_n \geq 0$ between them are defined, for $k = 1, \ldots, n$, inductively by

$$\cos \theta_k = \max_{x \in A} \max_{y \in B} x^T y = (x^k)^T y^k$$

  subject to the conditions $||x||_2 = ||y||_2 = 1, x^T x^i = 0, y^T y^i = 0$, for $1 \leq i \leq k-1$, where $||.||_2$ is the Euclidean norm.

The principal angles can also be defined in terms of orthonormal matrices Q_A and Q_B spanning subspaces A and B, respectively: in fact, n ordered singular values of the matrix $Q_A Q_B \in M_n$ can be expressed as cosines $\cos\theta_1, \ldots, \cos\theta_n$.

The **Grassmann distance** between subspaces A and B of the same dimension is their geodesic distance defined by

$$\sqrt{\sum_{i=1}^{n} \theta_i^2}.$$

The **Martin distance** between subspaces A and B is defined by

$$\sqrt{\ln \prod_{i=1}^{n} \frac{1}{\cos^2 \theta_i}}.$$

In the case when the subspaces represent ARMs (*autoregressive models*), the Martin distance can be expressed in terms of the *cepstrum* of the autocorrelation functions of the models. Cf. the **Martin cepstrum distance** in Chap. 21.

The **Asimov distance** between subspaces A and B is defined by θ_1. The **spectral distance** (or *chordal 2-norm distance*) is defined by $2\sin(\frac{\theta_1}{2})$.

The **containment gap distance** (or *projection distance*) is $\sin\theta_1$. It is the l_2-*norm* of the difference of the *orthogonal projectors* onto A and B. Many versions of this distance are used in Control Theory (cf. **gap metric** in Chap. 18).

The **Frobenius distance** and **chordal distance** between subspaces A and B are

$$\sqrt{2\sum_{i=1}^{n} \sin^2 \theta_i} \quad \text{and} \quad \sqrt{\sum_{i=1}^{n} \sin^2 \theta_i}, \quad \text{respectively.}$$

It is the *Frobenius norm* of the difference of above projectors onto A and B.

Similar distances $\sqrt{1 - \prod_{i=1}^{n} \cos^2 \theta_i}$ and $\arccos(\prod_{i=1}^{n} \cos\theta_i)$ are called the **Binet–Cauchy distance** and (cf. Chap. 7) **Fubini–Study distance**, respectively.

- **Larsson–Villani metric**

  Let A and B be two arbitrary orthonormal $m \times n$ matrices of full rank, and let θ_{ij} be the angle between the i-th column of A and the j-th column of B.

  We call **Larsson–Villani metric** the distance between A and B (used by Larsson and Villani, 2000, for multivariate models) the square of which is defined by

$$n - \sum_{i=1}^{n} \sum_{j=1}^{n} \cos^2 \theta_{ij}.$$

The square of usual Euclidean distance between A and B is $2(1-\sum_{i=1}^{n}\cos\theta_{ii})$.

For $n=1$, above two distances are $\sin\theta$ and $\sqrt{2(1-\cos\theta)}$, respectively.

- **Lerman metric**

  Given a finite set X and real symmetric $|X|\times|X|$ matrices $((d_1(x,y)))$, $((d_2(x,y)))$ with $x,y\in X$, their **Lerman semimetric** (cf. **Kendall τ distance** on permutations in Chap. 11) is defined by

$$|\{(\{x,y\},\{u,v\}):(d_1(x,y)-d_1(u,v))(d_2(x,y)-d_2(u,v))<0\}|\binom{|X|+1}{2}^{-2},$$

  where $(\{x,y\},\{u,v\})$ is any pair of unordered pairs of elements x,y,u,v from X.

  Similar **Kaufman semimetric** between $((d_1(x,y)))$ and $((d_2(x,y)))$ is

$$\frac{|\{(\{x,y\},\{u,v\}):(d_1(x,y)-d_1(u,v))(d_2(x,y)-d_2(u,v))<0\}|}{|\{(\{x,y\},\{u,v\}):(d_1(x,y)-d_1(u,v))(d_2(x,y)-d_2(u,v))\neq 0\}|}.$$

Chapter 13
Distances in Functional Analysis

Functional Analysis is the branch of Mathematics concerned with the study of spaces of functions. This usage of the word *functional* goes back to the calculus of variations which studies functions whose argument is a function. In the modern view, Functional Analysis is seen as the study of complete *normed vector spaces*, i.e., **Banach spaces**.

For any real number $p \geq 1$, an example of a Banach space is given by L_p**-space** of all Lebesgue-measurable functions whose absolute value's p-th power has finite integral.

A **Hilbert space** is a Banach space in which the norm arises from an *inner product*. Also, in Functional Analysis are considered *continuous linear operators* defined on Banach and Hilbert spaces.

13.1 Metrics on Function Spaces

Let $I \subset \mathbb{R}$ be an *open interval* (i.e., a nonempty connected open set) in $\mathbb{R}$. A real function $f : I \to \mathbb{R}$ is called *real analytic* on I if it agrees with its *Taylor series* in an *open neighborhood* U_{x_0} of every point $x_0 \in I$: $f(x) = \sum_{n=0}^{\infty} \frac{f^{(n)}(x_0)}{n!}(x - x_0)^n$ for any $x \in U_{x_0}$. Let $D \subset \mathbb{C}$ be a *domain* (i.e., a *convex* open set) in $\mathbb{C}$.

A complex function $f : D \to \mathbb{C}$ is called *complex analytic* (or, simply, *analytic*) on D if it agrees with its Taylor series in an open neighborhood of every point $z_0 \in D$. A complex function f is analytic on D if and only if it is *holomorphic* on D, i.e., if it has a complex derivative $f'(z_0) = \lim_{z \to z_0} \frac{f(z) - f(z_0)}{z - z_0}$ at every point $z_0 \in D$.

© Springer-Verlag Berlin Heidelberg 2016

M.M. Deza, E. Deza, *Encyclopedia of Distances*,
DOI 10.1007/978-3-662-52844-0_13

- **Integral metric**

  The **integral metric** is the *L_1-metric* on the set $C_{[a,b]}$ of all continuous real (complex) functions on a given segment $[a, b]$ defined by

$$\int_a^b |f(x) - g(x)|dx.$$

  The corresponding metric space is abbreviated by $C^1_{[a,b]}$. It is a Banach space.

  In general, for any **compact** topological space X, the integral metric is defined on the set of all continuous functions $f : X \to \mathbb{R}$ ($\mathbb{C}$) by $\int_X |f(x) - g(x)|dx$.

- **Uniform metric**

  The **uniform metric** (or **sup metric**) is the **L_∞-metric** on the set $C_{[a,b]}$ of all real (complex) continuous functions on a given segment $[a, b]$ defined by

$$\sup_{x\in[a,b]} |f(x) - g(x)|.$$

  The corresponding metric space is abbreviated by $C^\infty_{[a,b]}$. It is a Banach space.

  A generalization of $C^\infty_{[a,b]}$ is the *space of continuous functions* $C(X)$, i.e., a metric space on the set of all continuous (more generally, bounded) functions $f : X \to \mathbb{C}$ of a topological space X with the L_∞-metric $\sup_{x\in X} |f(x) - g(x)|$.

  In the case of the metric space $C(X, Y)$ of continuous (more generally, bounded) functions $f : X \to Y$ from one **metric compactum** (X, d_X) to another (Y, d_Y), the sup metric between two functions $f, g \in C(X, Y)$ is defined by $\sup_{x\in X} d_Y(f(x), g(x))$.

  The metric space $C^\infty_{[a,b]}$, as well as the metric space $C^1_{[a,b]}$, are two of the most important cases of the metric space $C^p_{[a,b]}$, $1 \le p \le \infty$, on the set $C_{[a,b]}$ with the L_p-metric $(\int_a^b |f(x) - g(x)|^p dx)^{\frac{1}{p}}$. The space $C^p_{[a,b]}$ is an example of an *L_p-space*.

- **Dogkeeper distance**

  Given a metric space (X, d), the **dogkeeper distance** is a metric on the set of all functions $f : [0, 1] \to X$, defined by

$$\inf_\sigma \sup_{t\in[0,1]} d(f(t), g(\sigma(t))),$$

  where $\sigma : [0, 1] \to [0, 1]$ is a continuous, monotone increasing function such that $\sigma(0) = 0, \sigma(1) = 1$. This metric is a special case of the **Fréchet metric**.

  For the case, when (X, d) is Euclidean space $\mathbb{R}^n$, this metric is the original (1906) **Fréchet distance** between parametric curves $f, g : [0, 1] \to \mathbb{R}^n$. This distance can be seen as the length of the shortest leash that is sufficient for the man and the dog to walk their paths f and g from start to end. For example, the Fréchet distance between two concentric circles of radius r_1 and r_2 is $|r_1 - r_2|$.

The **discrete Fréchet distance** (or *coupling distance*, Eiter and Mannila, 1994) is an approximation of the Fréchet metric for polygonal curves f and g. It considers only positions of the leash where its endpoints are located at vertices of f and g. So, this distance is the minimum, over all order-preserving pairings of vertices in f and g, of the maximal Euclidean distance between paired vertices.

If the two curves are embedded in a more general metric space (say, a polyhedral terrain or some Euclidean space with obstacles), the distance between two points on them is most naturally defined as the length of the shortest path. The resulting **geodesic Fréchet distance** allows the leash to switch discontinuously.

- **Bohr metric**

  Let $\mathbb{R}$ be a metric space with a metric ρ. A continuous function $f : \mathbb{R} \to \mathbb{R}$ is called *almost periodic* if, for every $\epsilon > 0$, there exists $l = l(\epsilon) > 0$ such that every interval $[t_0, t_0 + l(\epsilon)]$ contains at least one number τ for which $\rho(f(t), f(t + \tau)) < \epsilon$ for $-\infty < t < +\infty$.

  The **Bohr metric** is the **norm metric** $||f - g||$ on the set AP of all almost periodic functions defined by the norm

$$||f|| = \sup_{-\infty<t<+\infty} |f(t)|.$$

  It makes AP a Banach space. Some generalizations of almost periodic functions were obtained using other norms; cf. **Stepanov distance**, **Weyl distance**, **Besicovitch distance** and **Bochner metric**.

- **Stepanov distance**

  The **Stepanov distance** is a distance on the set of all measurable functions $f : \mathbb{R} \to \mathbb{C}$ with summable p-th power on each bounded integral, defined by

$$\sup_{x\in\mathbb{R}} \left(\frac{1}{l} \int_x^{x+l} |f(x) - g(x)|^p dx \right)^{1/p}.$$

  The **Weyl distance** is a distance on the same set defined by

$$\lim_{l\to\infty} \sup_{x\in\mathbb{R}} \left(\frac{1}{l} \int_x^{x+l} |f(x) - g(x)|^p dx \right)^{1/p}.$$

- **Besicovitch distance**

  The **Besicovitch distance** is a distance on the set of all measurable functions $f : \mathbb{R} \to \mathbb{C}$ with summable p-th power on each bounded integral defined by

$$\left(\overline{\lim}_{T\to\infty} \frac{1}{2T} \int_{-T}^{T} |f(x) - g(x)|^p dx \right)^{1/p}.$$

  The *generalized Besicovitch almost periodic functions* correspond to this distance.

- **Bochner metric**

  Given a measure space $(\Omega, \mathcal{A}, \mu)$, a Banach space $(V, ||.||_V)$, and $1 \leq p \leq \infty$, the *Bochner space* (or *Lebesgue–Bochner space*) $L^p(\Omega, V)$ is the set of all measurable functions $f : \Omega \to V$ such that $||f||_{L^p(\Omega,V)} \leq \infty$.

  Here the *Bochner norm* $||f||_{L^p(\Omega,V)}$ is defined by $(\int_\Omega ||f(\omega)||_V^p d\mu(\omega))^{\frac{1}{p}}$ for $1 \leq p < \infty$, and, for $p = \infty$, by $\text{ess sup}_{\omega\in\Omega} ||f(\omega)||_V$.
- **Bergman p-metric**

  Given $1 \leq p < \infty$, let $L_p(\Delta)$ be the L_p-space of Lebesgue measurable functions f on the *unit disk* $\Delta = \{z \in \mathbb{C} : |z| < 1\}$ with $||f||_p = \left(\int_\Delta |f(z)|^p \mu(dz)\right)^{\frac{1}{p}} < \infty$.

  The *Bergman space* $L_p^a(\Delta)$ is the subspace of $L_p(\Delta)$ consisting of analytic functions, and the **Bergman p-metric** is the **L_p-metric** on $L_p^a(\Delta)$ (cf. **Bergman metric** in Chap. 7). Any Bergman space is a Banach space.
- **Bloch metric**

  The *Bloch space* B on the *unit disk* $\Delta = \{z \in \mathbb{C} : |z| < 1\}$ is the set of all analytic functions f on Δ such that $||f||_B = \sup_{z\in\Delta}(1 - |z|^2)|f'(z)| < \infty$. Using the complete *seminorm* $||.||_B$, a norm on B is defined by

$$||f|| = |f(0)| + ||f||_B.$$

  The **Bloch metric** is the **norm metric** $||f - g||$ on B. It makes B a Banach space.
- **Besov metric**

  Given $1 < p < \infty$, the *Besov space* B_p on the *unit disk* $\Delta = \{z \in \mathbb{C} : |z| < 1\}$ is the set of all analytic functions f in Δ such that $||f||_{B_p} = \left(\int_\Delta (1 - |z|^2)^p |f'(z)|^p d\lambda(z)\right)^{\frac{1}{p}} < \infty$, where $d\lambda(z) = \frac{\mu(dz)}{(1-|z|^2)^2}$ is the Möbius invariant measure on Δ. Using the complete *seminorm* $||.||_{B_p}$, the *Besov norm* on B_p is defined by

$$||f|| = |f(0)| + ||f||_{B_p}.$$

  The **Besov metric** is the **norm metric** $||f - g||$ on B_p.

  It makes B_p a Banach space. The set B_2 is the classical *Dirichlet space* of functions analytic on Δ with square integrable derivative, equipped with the **Dirichlet metric**. The *Bloch space* B can be considered as B_∞.
- **Hardy metric**

  Given $1 \leq p < \infty$, the *Hardy space* $H^p(\Delta)$ is the class of functions, analytic on the *unit disk* $\Delta = \{z \in \mathbb{C} : |z| < 1\}$, and satisfying the following growth condition for the *Hardy norm* $||.||_{H^p}$:

$$||f||_{H^p(\Delta)} = \sup_{0<r<1} \left(\frac{1}{2\pi} \int_0^{2\pi} |f(re^{i\theta})|^p d\theta\right)^{\frac{1}{p}} < \infty.$$

The **Hardy metric** is the **norm metric** $||f-g||_{H^p(\Delta)}$ on $H^p(\Delta)$. It makes $H^p(\Delta)$ a Banach space.

In Complex Analysis, the Hardy spaces are analogs of the L_p-spaces of Functional Analysis. Such spaces are applied in Mathematical Analysis itself, and also in Scattering Theory and Control Theory (cf. Chap. 18).

- **Part metric**

  The **part metric** is a metric on a *domain* D of $\mathbb{R}^2$ defined for any $x, y \in \mathbb{R}^2$ by

$$\sup_{f\in H^+} \left| \ln\left(\frac{f(x)}{f(y)}\right)\right|,$$

  where H^+ is the set of all positive *harmonic functions* on the domain D.

  A twice-differentiable real function $f : D \to \mathbb{R}$ is called *harmonic* on D if its *Laplacian* $\Delta f = \frac{\partial^2 f}{\partial x_1^2} + \frac{\partial^2 f}{\partial x_2^2}$ vanishes on D.

- **Orlicz metric**

  Let $M(u)$ be an even convex function of a real variable which is increasing for u positive, and $\lim_{u\to 0} u^{-1}M(u) = \lim_{u\to\infty} u(M(u))^{-1} = 0$. In this case the function $p(v) = M'(v)$ does not decrease on $[0,\infty)$, $p(0) = \lim_{v\to 0} p(v) = 0$, and $p(v) > 0$ when $v > 0$. Writing $M(u) = \int_0^{|u|} p(v)dv$, and defining $N(u) = \int_0^{|u|} p^{-1}(v)dv$, one obtains a pair $(M(u), N(u))$ of *complementary functions*.

  Let $(M(u), N(u))$ be a pair of complementary functions, and let G be a bounded closed set in $\mathbb{R}^n$. The *Orlicz space* $L_M^*(G)$ is the set of Lebesgue-measurable functions f on G satisfying the following growth condition for the *Orlicz norm* $||f||_M$:

$$||f||_M = \sup\left\{\int_G f(t)g(t)dt : \int_G N(g(t))dt \le 1\right\} < \infty.$$

  The **Orlicz metric** is the norm metric $||f-g||_M$ on $L_M^*(G)$. It makes $L_M^*(G)$ a Banach space ([Orli32]).

  When $M(u) = u^p$, $1 < p < \infty$, $L_M^*(G)$ coincides with the space $L_p(G)$, and, up to scalar factor, the L_p-*norm* $||f||_p$ coincides with $||f||_M$.

  The Orlicz norm is equivalent to the *Luxemburg norm* $||f||_{(M)} = \inf\{\lambda > 0 : \int_G M(\lambda^{-1}f(t))dt \le 1\}$; in fact, $||f||_{(M)} \le ||f||_M \le 2||f||_{(M)}$.

- **Orlicz–Lorentz metric**

  Let $w : (0,\infty) \to (0,\infty)$ be a nonincreasing function. Let $M : [0,\infty) \to [0,\infty)$ be a nondecreasing and convex function with $M(0) = 0$. Let G be a bounded closed set in $\mathbb{R}^n$.

  The *Orlicz–Lorentz space* $L_{w,M}(G)$ is the set of all Lebesgue-measurable functions f on G satisfying the following growth condition for the *Orlicz–Lorentz*

norm $||f||_{w,M}$:

$$||f||_{w,M} = \inf\left\{\lambda > 0 : \int_0^\infty w(x)M\left(\frac{f^*(x)}{\lambda}\right)dx \le 1\right\} < \infty,$$

where $f^*(x) = \sup\{t : \mu(|f| \ge t) \ge x\}$ is the *nonincreasing rearrangement* of f.

The **Orlicz–Lorentz metric** is the **norm metric** $||f-g||_{w,M}$ on $L_{w,M}(G)$. It makes $L_{w,M}(G)$ a Banach space.

The Orlicz–Lorentz space is a generalization of the *Orlicz space* $L_M^*(G)$ (cf. **Orlicz metric**), and the *Lorentz space* $L_{w,q}(G)$, $1 \le q < \infty$, of all Lebesgue-measurable functions f on G satisfying the following growth condition for the *Lorentz norm*:

$$||f||_{w,q} = \left(\int_0^\infty w(x)(f^*(x))^q\right)^{\frac{1}{q}} < \infty.$$

- **Hölder metric**

  Let $L^\alpha(G)$ be the set of all bounded continuous functions f defined on a subset G of $\mathbb{R}^n$, and satisfying the *Hölder condition* on G. Here, a function f satisfies the *Hölder condition* at a point $y \in G$ with *index* (or *order*) α, $0 < \alpha \le 1$, and with coefficient $A(y)$, if $|f(x) - f(y)| \le A(y)|x-y|^\alpha$ for all $x \in G$ sufficiently close to y.

  If $A = \sup_{y\in G}(A(y)) < \infty$, the Hölder condition is called *uniform* on G, and A is called the *Hölder coefficient* of G. The quantity $|f|_\alpha = \sup_{x,y\in G} \frac{|f(x)-f(y)|}{|x-y|^\alpha}$, $0 \le \alpha \le 1$, is called the *Hölder α-seminorm* of f, and the *Hölder norm* of f is defined by

  $$||f||_{L^\alpha(G)} = \sup_{x\in G}|f(x)| + |f|_\alpha.$$

  The **Hölder metric** is the **norm metric** $||f-g||_{L^\alpha(G)}$ on $L^\alpha(G)$. It makes $L^\alpha(G)$ a Banach space.
- **Sobolev metric**

  The *Sobolev space* $W^{k,p}$ is a subset of an L_p-space such that f and its derivatives up to order k have a finite L_p-*norm*. Formally, given a subset G of $\mathbb{R}^n$, define

  $$W^{k,p} = W^{k,p}(G) = \{f \in L_p(G) : f^{(i)} \in L_p(G), 1 \le i \le k\},$$

  where $f^{(i)} = \partial_{x_1}^{\alpha_1} \dots \partial_{x_n}^{\alpha_n} f$, $\alpha_1 + \dots + \alpha_n = i$, and the derivatives are taken in a weak sense. The *Sobolev norm* on $W^{k,p}$ is defined by

  $$||f||_{k,p} = \sum_{i=0}^{k} ||f^{(i)}||_p.$$

In fact, it is enough to take only the first and last in the sequence, i.e., the norm defined by $||f||_{k,p} = ||f||_p + ||f^{(k)}||_p$ is equivalent to the norm above.

For $p = \infty$, the Sobolev norm is equal to the *essential supremum* of $|f|$: $||f||_{k,\infty} = ess\sup_{x\in G}|f(x)|$, i.e., it is the infimum of all numbers $a \in \mathbb{R}$ for which $|f(x)| > a$ on a set of measure zero.

The **Sobolev metric** is the **norm metric** $||f-g||_{k,p}$ on $W^{k,p}$. It makes $W^{k,p}$ a Banach space.

The Sobolev space $W^{k,2}$ is denoted by H^k. It is a Hilbert space for the *inner product* $\langle f,g\rangle_k = \sum_{i=1}^k \langle f^{(i)}, g^{(i)}\rangle_{L_2} = \sum_{i=1}^k \int_G f^{(i)}\overline{g}^{(i)}\mu(d\omega)$.

- **Variable exponent space metrics**

  Let G be a nonempty open subset of $\mathbb{R}^n$, and let $p : G \to [1,\infty)$ be a measurable bounded function, called a *variable exponent*. The *variable exponent Lebesgue space* $L_{p(.)}(G)$ is the set of all measurable functions $f : G \to \mathbb{R}$ for which the *modular* $\varrho_{p(.)}(f) = \int_G |f(x)|^{p(x)}dx$ is finite. The *Luxemburg norm* on this space is defined by

$$||f||_{p(.)} = \inf\{\lambda > 0 : \varrho_{p(.)}(f/\lambda) \le 1\}.$$

  The **variable exponent Lebesgue space metric** is the **norm metric** $||f-g||_{p(.)}$ on $L_{p(.)}(G)$.

  A *variable exponent Sobolev space* $W^{1,p(.)}(G)$ is a subspace of $L_{p(.)}(G)$ consisting of functions f whose distributional gradient exists almost everywhere and satisfies the condition $|\nabla f| \in L_{p(.)}(G)$. The norm

$$||f||_{1,p(.)} = ||f||_{p(.)} + ||\nabla f||_{p(.)}$$

  makes $W^{1,p(.)}(G)$ a Banach space. The **variable exponent Sobolev space metric** is the norm metric $||f-g||_{1,p(.)}$ on $W^{1,p(.)}$.

- **Schwartz metric**

  The *Schwartz space* (or *space of rapidly decreasing functions*) $S(\mathbb{R}^n)$ is the class of all *Schwartz functions*, i.e., infinitely-differentiable functions $f : \mathbb{R}^n \to \mathbb{C}$ that decrease at infinity, as do all their derivatives, faster than any inverse power of x. More precisely, f is a Schwartz function if we have the following growth condition:

$$||f||_{\alpha\beta} = \sup_{x\in\mathbb{R}^n} |x_1^{\beta_1}\dots x_n^{\beta_n}\frac{\partial^{\alpha_1+\dots+\alpha_n}f(x_1,\dots,x_n)}{\partial x_1^{\alpha_1}\dots\partial x_n^{\alpha_n}}| < \infty$$

  for any nonnegative integer vectors α and β. The family of *seminorms* $||.||_{\alpha\beta}$ defines a **locally convex** topology of $S(\mathbb{R}^n)$ which is **metrizable** and complete. The **Schwartz metric** is a metric on $S(\mathbb{R}^n)$ which can be obtained using this topology (cf. **countably normed space** in Chap. 2).

  The corresponding metric space on $S(\mathbb{R}^n)$ is a *Fréchet space* in the sense of Functional Analysis, i.e., a locally convex *F-space*.

- **Bregman quasi-distance**

  Let $G \subset \mathbb{R}^n$ be a closed set with the nonempty interior G^0. Let f be a *Bregman function with zone G*.

  The **Bregman quasi-distance** $D_f : G \times G^0 \to \mathbb{R}_{\geq 0}$ is defined by

$$D_f(x, y) = f(x) - f(y) - \langle \nabla f(y), x - y \rangle,$$

  where $\nabla f = (\frac{\partial f}{\partial x_1}, \ldots \frac{\partial f}{\partial x_n})$. $D_f(x, y) = 0$ if and only if $x = y$. Also $D_f(x, y) + D_f(y, z) - D_f(x, z) = \langle \nabla f(z) - \nabla f(y), x - y \rangle$ but, in general, D_f does not satisfy the triangle inequality, and is not symmetric.

  A real-valued function f whose effective domain contains G is called a *Bregman function with zone G* if the following conditions hold:

  1. f is continuously differentiable on G^0;
  2. f is strictly convex and continuous on G;
  3. For all $\delta \in \mathbb{R}$ the *partial level sets* $\Gamma(x, \delta) = \{y \in G^0 : D_f(x, y) \leq \delta\}$ are bounded for all $x \in G$;
  4. If $\{y_n\}_n \subset G^0$ converges to y^*, then $D_f(y^*, y_n)$ converges to 0;
  5. If $\{x_n\}_n \subset G$ and $\{y_n\}_n \subset G^0$ are sequences such that $\{x_n\}_n$ is bounded, $\lim_{n\to\infty} y_n = y^*$, and $\lim_{n\to\infty} D_f(x_n, y_n) = 0$, then $\lim_{n\to\infty} x_n = y^*$.

  When $G = \mathbb{R}^n$, a sufficient condition for a strictly convex function to be a Bregman function has the form: $\lim_{||x||\to\infty} \frac{f(x)}{||x||} = \infty$.

13.2 Metrics on Linear Operators

A *linear operator* is a function $T : V \to W$ between two vector spaces V, W over a field $\mathbb{F}$, that is compatible with their linear structures, i.e., for any $x, y \in V$ and any scalar $k \in \mathbb{F}$, we have the following properties: $T(x + y) = T(x) + T(y)$, and $T(kx) = kT(x)$.

- **Operator norm metric**

  Consider the set of all linear operators from a *normed space* $(V, ||.||_V)$ into a normed space $(W, ||.||_W)$. The *operator norm* $||T||$ of a *linear operator* $T : V \to W$ is defined as the largest value by which T stretches an element of V, i.e.,

$$||T|| = \sup_{||v||_V \neq 0} \frac{||T(v)||_W}{||v||_V} = \sup_{||v||_V = 1} ||T(v)||_W = \sup_{||v||_V \leq 1} ||T(v)||_W.$$

  A linear operator $T : V \to W$ from a normed space V into a normed space W is called *bounded* if its operator norm is finite. For normed spaces, a linear operator is bounded if and only if it is *continuous*.

The **operator norm metric** is a **norm metric** on the set $B(V, W)$ of all bounded linear operators from V into W, defined by

$$||T - P||.$$

The space $(B(V, W), ||.||)$ is called the *space of bounded linear operators*. This metric space is **complete** if W is. If $V = W$ is complete, the space $B(V, V)$ is a *Banach algebra*, as the operator norm is a *submultiplicative norm*.

A linear operator $T : V \to W$ from a Banach space V into another Banach space W is called *compact* if the image of any bounded subset of V is a relatively compact subset of W. Any compact operator is bounded (and, hence, continuous). The space $(K(V, W), ||.||)$ on the set $K(V, W)$ of all compact operators from V into W with the operator norm $||.||$ is called the *space of compact operators*.

- **Nuclear norm metric**

  Let $B(V, W)$ be the space of all bounded linear operators mapping a Banach space $(V, ||.||_V)$ into another Banach space $(W, ||.||_W)$. Let the *Banach dual* of V be denoted by $V^{'}$, and the value of a functional $x^{'} \in V^{'}$ at a vector $x \in V$ by $\langle x, x^{'} \rangle$.

  A linear operator $T \in B(V, W)$ is called a *nuclear operator* if it can be represented in the form $x \mapsto T(x) = \sum_{i=1}^{\infty} \langle x, x_i^{'} \rangle y_i$, where $\{x_i^{'}\}_i$ and $\{y_i\}_i$ are sequences in $V^{'}$ and W, respectively, such that $\sum_{i=1}^{\infty} ||x_i^{'}||_{V^{'}} ||y_i||_W < \infty$. This representation is called *nuclear*, and can be regarded as an expansion of T as a sum of operators of rank 1 (i.e., with one-dimensional range). The *nuclear norm* of T is defined as

$$||T||_{nuc} = \inf \sum_{i=1}^{\infty} ||x_i^{'}||_{V^{'}} ||y_i||_W,$$

  where the infimum is taken over all possible nuclear representations of T.

  The **nuclear norm metric** is the **norm metric** $||T - P||_{nuc}$ on the set $N(V, W)$ of all nuclear operators mapping V into W. The space $(N(V, W), ||.||_{nuc})$, called the *space of nuclear operators*, is a Banach space.

  A *nuclear space* is defined as a **locally convex** space for which all continuous linear functions into an arbitrary Banach space are nuclear operators. A nuclear space is constructed as a projective limit of Hilbert spaces H_α with the property that, for each $\alpha \in I$, one can find $\beta \in I$ such that $H_\beta \subset H_\alpha$, and the embedding operator $H_\beta \ni x \to x \in H_\alpha$ is a *Hilbert–Schmidt operator*. A *normed space* is nuclear if and only if it is finite-dimensional.

- **Finite nuclear norm metric**

  Let $F(V, W)$ be the space of all *linear operators of finite rank* (i.e., with finite-dimensional range) mapping a Banach space $(V, ||.||_V)$ into another Banach space $(W, ||.||_W)$. A linear operator $T \in F(V, W)$ can be represented in the form $x \mapsto T(x) = \sum_{i=1}^{n} \langle x, x_i^{'} \rangle y_i$, where $\{x_i^{'}\}_i$ and $\{y_i\}_i$ are sequences in $V^{'}$ (*Banach dual* of V) and W, respectively, and $\langle x, x^{'} \rangle$ is the value of a functional $x^{'} \in V^{'}$ at a vector

$x \in V$. The *finite nuclear norm* of T is defined as

$$||T||_{fnuc} = \inf \sum_{i=1}^{n} ||x_i^{'}||_{V'} ||y_i||_W,$$

where the infimum is taken over all possible finite representations of T.

The **finite nuclear norm metric** is the **norm metric** $||T-P||_{fnuc}$ on $F(V,W)$. The space $(F(V,W), ||.||_{fnuc})$ is called the *space of operators of finite rank*. It is a dense linear subspace of the *space of nuclear operators* $N(V,W)$.

- **Hilbert–Schmidt norm metric**

  Consider the set of all linear operators from a Hilbert space $(H_1, ||.||_{H_1})$ into a Hilbert space $(H_2, ||.||_{H_2})$. The *Hilbert–Schmidt norm* $||T||_{HS}$ of a linear operator $T : H_1 \to H_2$ is defined by

$$||T||_{HS} = (\sum_{\alpha \in I} ||T(e_\alpha)||_{H_2}^2)^{1/2},$$

  where $(e_\alpha)_{\alpha \in I}$ is an orthonormal basis in H_1. A linear operator $T : H_1 \to H_2$ is called a *Hilbert–Schmidt operator* if $||T||_{HS}^2 < \infty$.

  The **Hilbert–Schmidt norm metric** is the **norm metric** $||T-P||_{HS}$ on the set $S(H_1, H_2)$ of all Hilbert–Schmidt operators from H_1 into H_2. In Euclidean space $||.||_{HS}$ is also called *Frobenius norm*; cf. **Frobenius norm metric** in Chap. 12.

  For $H_1 = H_2 = H$, the algebra $S(H,H) = S(H)$ with the Hilbert–Schmidt norm is a *Banach algebra*. It contains operators of finite rank as a dense subset, and is contained in the space $K(H)$ of compact operators. An *inner product* $\langle , \rangle_{HS}$ on $S(H)$ is defined by $\langle T, P \rangle_{HS} = \sum_{\alpha \in I} \langle T(e_\alpha), P(e_\alpha) \rangle$, and $||T||_{HS} = \langle T, T \rangle_{HS}^{1/2}$. So, $S(H)$ is a Hilbert space (independent of the chosen basis $(e_\alpha)_{\alpha \in I}$).

- **Trace-class norm metric**

  Given a Hilbert space H, the *trace-class norm* of a linear operator $T : H \to H$ is

$$||T||_{tc} = \sum_{\alpha \in I} \langle |T|(e_\alpha), e_\alpha \rangle,$$

  where $|T|$ is the *absolute value* of T in the *Banach algebra* $B(H)$ of all bounded operators from H into itself, and $(e_\alpha)_{\alpha \in I}$ is an orthonormal basis of H.

  An operator $T : H \to H$ is called a *trace-class operator* if $||T||_{tc} < \infty$. Any such operator is the product of two *Hilbert–Schmidt operators*.

  The **trace-class norm metric** is the **norm metric** $||T-P||_{tc}$ on the set $L(H)$ of all trace-class operators from H into itself.

  The set $L(H)$ with the norm $||.||_{tc}$ forms a Banach algebra which is contained in the algebra $K(H)$ (of all compact operators from H into itself), and contains the algebra $S(H)$ of all Hilbert–Schmidt operators from H into itself.

- **Schatten p-class norm metric**

  Let $1 \leq p < \infty$. Given a separable Hilbert space H, the *Schatten p-class norm* of a compact linear operator $T : H \to H$ is defined by

$$||T||_{Sch}^{p} = \left(\sum_{n} |s_n|^p \right)^{\frac{1}{p}},$$

  where $\{s_n\}_n$ is the sequence of *singular values* of T. A compact operator $T : H \to H$ is called a *Schatten p-class operator* if $||T||_{Sch}^{p} < \infty$.

  The **Schatten p-class norm metric** is the **norm metric** $||T - P||_{Sch}^{p}$ on the set $S_p(H)$ of all Schatten p-class operators from H onto itself. The set $S_p(H)$ with the norm $||.||_{Sch}^{p}$ forms a Banach space. $S_1(H)$ is the *trace-class* of H, and $S_2(H)$ is the *Hilbert–Schmidt class* of H. Cf. **Schatten norm metric** (in Chap. 12) for which **trace** and **Frobenius** norm metrics are cases $p = 1$ and $p = 2$, respectively.

- **Continuous dual space**

  For any vector space V over some field, its *algebraic dual space* is the set of all linear functionals on V.

  Let $(V, ||.||)$ be a *normed vector space*. Let $V^{'}$ be the set of all *continuous* linear functionals T from V into the base field ($\mathbb{R}$ or $\mathbb{C}$). Let $||.||^{'}$ be the *operator norm* on $V^{'}$ defined by

$$||T||^{'} = \sup_{||x|| \leq 1} |T(x)|.$$

  The space $(V^{'}, ||.||^{'})$ is a Banach space which is called the **continuous dual** (or *Banach dual*) of $(V, ||.||)$.

  The continuous dual of the metric space l_p^n (l_p^∞) is l_q^n (l_q^∞, respectively), where q is defined by $\frac{1}{p} + \frac{1}{q} = 1$. The continuous dual of l_1^n (l_1^∞) is l_∞^n (l_∞^∞, respectively).

- **Distance constant of operator algebra**

  Let $\mathcal{A}$ be an subalgebra of $B(H)$, the algebra of all bounded operators on a Hilbert space H. For any operator $T \in B(H)$, let P be a projection, $P^{\perp}$ be its orthogonal complement and $\beta(T, \mathcal{A}) = \sup\{||P^{\perp}TP|| : P^{\perp}\mathcal{A}P = (0)\}$.

  Let $dist(T, \mathcal{A}) = \inf_{A \in \mathcal{A}} ||T - A||$ be the *distance of T to algebra $\mathcal{A}$*; cf. **matrix nearness problems** in Chap. 12. It holds $dist(T, \mathcal{A}) \geq \beta(T, \mathcal{A})$.

  The algebra $\mathcal{A}$ is *reflexive* if $\beta(T, \mathcal{A}) = 0$ implies $T \in \mathcal{A}$; it is *hyperreflexive* if there exists a constant $C \geq 1$ such that, for any operator $T \in B(H)$, it holds

$$dist(T, \mathcal{A}) \leq C\beta(T, \mathcal{A}).$$

  The smallest such C is called the **distance constant** of the algebra $\mathcal{A}$.

  In the case of a reflexive algebra of matrices with nonzero entries specified by a given pattern, the problem of finding the distance constant can be formulated as a matrix-filling problem: given a partially completed matrix, fill in the remaining entries so that the operator norm of the resulting complete matrix is minimized.

Chapter 14
Distances in Probability Theory

A *probability space* is a *measurable space* $(\Omega, \mathcal{A}, P)$, where $\mathcal{A}$ is the set of all measurable subsets of Ω, and P is a measure on $\mathcal{A}$ with $P(\Omega) = 1$. The set Ω is called a *sample space*. An element $a \in \mathcal{A}$ is called an *event*. $P(a)$ is called the *probability* of the event a. The measure P on $\mathcal{A}$ is called a *probability measure*, or *(probability) distribution law*, or simply *(probability) distribution*.

A *random variable* X is a measurable function from a probability space $(\Omega, \mathcal{A}, P)$ into a measurable space, called a *state space* of possible values of the variable; it is usually taken to be $\mathbb{R}$ with the *Borel* σ*-algebra*, so $X : \Omega \to \mathbb{R}$. The range $\mathcal{X}$ of the variable X is called the *support* of the distribution P; an element $x \in \mathcal{X}$ is called a *state*.

A distribution law can be uniquely described via a *cumulative distribution* (or simply, *distribution*) *function* CDF, which describes the probability that a random value X takes on a value at most x: $F(x) = P(X \leq x) = P(\omega \in \Omega : X(\omega) \leq x)$.

So, any random variable X gives rise to a *probability distribution* which assigns to the interval $[a, b]$ the probability $P(a \leq X \leq b) = P(\omega \in \Omega : a \leq X(\omega) \leq b)$, i.e., the probability that the variable X will take a value in the interval $[a, b]$.

A distribution is called *discrete* if $F(x)$ consists of a sequence of finite jumps at x_i; a distribution is called *continuous* if $F(x)$ is continuous. We consider (as in the majority of applications) only discrete or *absolutely continuous* distributions, i.e., the CDF function $F : \mathbb{R} \to \mathbb{R}$ is *absolutely continuous*. It means that, for every number $\epsilon > 0$, there is a number $\delta > 0$ such that, for any sequence of pairwise disjoint intervals $[x_k, y_k]$, $1 \leq k \leq n$, the inequality $\sum_{1 \leq k \leq n}(y_k - x_k) < \delta$ implies the inequality $\sum_{1 \leq k \leq n} |F(y_k) - F(x_k)| < \epsilon$.

A distribution law also can be uniquely defined via a *probability density* (or *density*, *probability*) *function* PDF of the underlying random variable. For an absolutely continuous distribution, the CDF is almost everywhere differentiable, and the PDF is defined as the derivative $p(x) = F'(x)$ of the CDF; so, $F(x) = P(X \leq x) = \int_{-\infty}^{x} p(t)dt$, and $\int_a^b p(t)dt = P(a \leq X \leq b)$. In the discrete case, the PDF is is

© Springer-Verlag Berlin Heidelberg 2016

M.M. Deza, E. Deza, *Encyclopedia of Distances*,
DOI 10.1007/978-3-662-52844-0_14

$\sum_{x_i \le x} p(x_i)$, where $p(x) = P(X = x)$ is the *probability mass function*. But $p(x) = 0$ for each fixed x in any continuous case.

The random variable X is used to "push-forward" the measure P on Ω to a measure dF on $\mathbb{R}$. The underlying probability space is a technical device used to guarantee the existence of random variables and sometimes to construct them.

We usually present the discrete version of probability metrics, but many of them are defined on any measurable space; see [Bass89, Bass13, Cha08]. For a probability distance d on random quantities, the conditions $P(X = Y) = 1$ or equality of distributions imply (and characterize) $d(X, Y) = 0$; such distances are called ([Rach91]) *compound* or *simple* distances, respectively. Often, some *ground* distance d is given on the state space $\mathcal{X}$ and the presented distance is a lifting of it to a distance on distributions. A quasi-distance between distributions is also called **divergence** or *distance statistic*.

Below we denote $p_X = p(x) = P(X = x)$, $F_X = F(x) = P(X \le x)$, $p(x, y) = P(X = x, Y = y)$. We denote by $\mathbb{E}[X]$ the *expected value* (or *mean*) of the random variable X: in the discrete case $\mathbb{E}[X] = \sum_x xp(x)$, in the continuous case $\mathbb{E}[X] = \int xp(x)dx$.

The *covariance* between the random variables X and Y is $Cov(X, Y) = \mathbb{E}[(X - \mathbb{E}[X])(Y - \mathbb{E}[Y])] = \mathbb{E}[XY] - \mathbb{E}[X]\mathbb{E}[Y]$. The *variance* and *standard deviation* of X are $Var(X) = Cov(X, X)$ and $\sigma(X) = \sqrt{Var(X)}$, respectively. The *correlation* between X and Y is $Corr(X, Y) = \frac{Cov(X,Y)}{\sigma(X)\sigma(Y)}$; cf. Chap. 17.

14.1 Distances on Random Variables

All distances in this section are defined on the set $\mathbf{Z}$ of all random variables with the same support $\mathcal{X}$; here $X, Y \in \mathbf{Z}$.

- *p*-**average compound metric**

  Given $p \ge 1$, the *p*-**average compound metric** (or L_p-*metric between variables*) is a metric on $\mathbf{Z}$ with $\mathcal{X} \subset \mathbb{R}$ and $\mathbb{E}[|Z|^p] < \infty$ for all $Z \in \mathbf{Z}$ defined by

$$(\mathbb{E}[|X - Y|^p])^{1/p} = (\sum_{(x,y)\in\mathcal{X}\times\mathcal{X}} |x - y|^p p(x, y))^{1/p}.$$

  For $p = 2$ and ∞, it is called, respectively, the *mean-square distance* and *essential supremum distance* between variables.
- **Lukaszyk–Karmovski metric**

  The **Lukaszyk–Karmovski metric** (2001) on $\mathbb{Z}$ with $\mathcal{X} \subset \mathbb{R}$ is defined by

$$\sum_{(x,y)\in\mathcal{X}\times\mathcal{X}} |x - y|p(x)p(y).$$

For continuous random variables, it is defined by $\int_{-\infty}^{+\infty}\int_{-\infty}^{+\infty}|x-y|F(x)F(y)dxdy$. This function can be positive for $X = Y$. Such possibility is excluded, and so, it will be a distance metric, if and only if it holds

$$\int_{-\infty}^{+\infty}\int_{-\infty}^{+\infty}|x-y|\delta(x-\mathbb{E}[X])\delta(y-\mathbb{E}[Y])dxdy = |\mathbb{E}[X]-\mathbb{E}[Y]|.$$

- **Absolute moment metric**
  Given $p \geq 1$, the **absolute moment metric** is a metric on $\mathbf{Z}$ with $\mathcal{X} \subset \mathbb{R}$ and $\mathbb{E}[|Z|^p] < \infty$ for all $Z \in \mathbf{Z}$ defined by

$$|(\mathbb{E}[|X|^p])^{1/p} - (\mathbb{E}[|Y|^p])^{1/p}|.$$

  For $p = 1$ it is called the *engineer metric*.
- **Indicator metric**
  The **indicator metric** is a metric on $\mathbf{Z}$ defined by

$$\mathbb{E}[1_{X\neq Y}] = \sum_{(x,y)\in\mathcal{X}\times\mathcal{X}} 1_{x\neq y}p(x,y) = \sum_{(x,y)\in\mathcal{X}\times\mathcal{X}, x\neq y} p(x,y).$$

  (Cf. **Hamming metric** in Chap. 1.)
- **Ky Fan metric** K
  The **Ky Fan metric** K is a metric K on $\mathbf{Z}$, defined by

$$\inf\{\epsilon > 0 : P(|X-Y| > \epsilon) < \epsilon\}.$$

  It is the case $d(x,y) = |X-Y|$ of the **probability distance**.
- **Ky Fan metric** K^*
  The **Ky Fan metric** K^* is a metric on $\mathbf{Z}$ defined by

$$\mathbb{E}\left[\frac{|X-Y|}{1+|X-Y|}\right] = \sum_{(x,y)\in\mathcal{X}\times\mathcal{X}} \frac{|x-y|}{1+|x-y|}p(x,y).$$

- **Probability distance**
  Given a metric space $(\mathcal{X}, d)$, the **probability distance** on $\mathbf{Z}$ is defined by

$$\inf\{\epsilon > 0 : P(d(X,Y) > \epsilon) < \epsilon\}.$$

14.2 Distances on Distribution Laws

All distances in this section are defined on the set $\mathcal{P}$ of all distribution laws such that corresponding random variables have the same range $\mathcal{X}$; here $P_1, P_2 \in \mathcal{P}$.

- **L_p-metric between densities**

  The **L_p-metric between densities** is a metric on $\mathcal{P}$ (for a countable $\mathcal{X}$) defined, for any $p \geq 1$, by

$$(\sum_x |p_1(x) - p_2(x)|^p)^{\frac{1}{p}}.$$

  For $p = 1$, one half of it is called the **variational distance** (or *total variation distance*, *Kolmogorov distance*). For $p = 2$, it is the **Patrick–Fisher distance**. The *point metric* $\sup_x |p_1(x) - p_2(x)|$ corresponds to $p = \infty$.

  The **Lissak–Fu distance** with parameter $\alpha > 0$ is defined as $\sum_x |p_1(x) - p_2(x)|^\alpha$.

- **Bayesian distance**

  The *error probability in classification* is the following error probability of the optimal Bayes rule for the classification into two classes with a priori probabilities $\phi, 1 - \phi$ and corresponding densities p_1, p_2 of the observations:

$$P_e = \sum_x \min(\phi p_1(x), (1 - \phi)p_2(x)).$$

  The **Bayesian distance** on $\mathcal{P}$ is defined by $1 - P_e$.

  For the classification into m classes with *a priori* probabilities ϕ_i, $1 \leq i \leq m$, and corresponding densities p_i of the observations, the error probability becomes

$$P_e = 1 - \sum_x p(x) \max_i P(C_i|x),$$

  where $P(C_i|x)$ is the *a posteriori* probability of the class C_i given the observation x and $p(x) = \sum_{i=1}^m \phi_i P(x|C_i)$. The *general mean distance between m classes* C_i (cf. m-hemimetric in Chap. 3) is defined (Van der Lubbe, 1979) for $\alpha > 0, \beta > 1$ by

$$\sum_x p(x)(\sum_i P(C_i|x)^\beta)^\alpha.$$

  The case $\alpha = 1, \beta = 2$ corresponds to the *Bayesian distance* in Devijver, 1974; the case $\beta = \frac{1}{\alpha}$ was considered in Trouborst et al., 1974.

- **Mahalanobis semimetric**

  The **Mahalanobis semimetric** is a semimetric on $\mathcal{P}$ (for $\mathcal{X} \subset \mathbb{R}^n$) defined by

$$\sqrt{(\mathbb{E}_{P_1}[X] - \mathbb{E}_{P_2}[X])^T A (\mathbb{E}_{P_1}[X] - \mathbb{E}_{P_2}[X])}$$

  for a given positive-semidefinite matrix A; its square is a **Bregman quasi-distance** (Chap. 13). Cf. also the **Mahalanobis distance** in Chap. 17.

- **Engineer semimetric**
  The **engineer semimetric** is a semimetric on $\mathcal{P}$ (for $\mathcal{X} \subset \mathbb{R}$) defined by

$$|\mathbb{E}_{P_1}[X] - \mathbb{E}_{P_2}[X]| = |\sum_x x(p_1(x) - p_2(x))|.$$

- **Stop-loss metric of order** m
  The **stop-loss metric of order** m is a metric on $\mathcal{P}$ (for $\mathcal{X} \subset \mathbb{R}$) defined by

$$\sup_{t\in\mathbb{R}} \sum_{x\geq t} \frac{(x-t)^m}{m!}(p_1(x) - p_2(x)).$$

- **Kolmogorov–Smirnov metric**
  The **Kolmogorov–Smirnov metric** (or *Kolmogorov metric*, *uniform metric*) is a metric on $\mathcal{P}$ (for $\mathcal{X} \subset \mathbb{R}$) defined (1948) by

$$\sup_{x\in\mathbb{R}} |P_1(X \leq x) - P_2(X \leq x)|.$$

  This metric is used, for example, in Biology as a measure of sexual dimorphism.
  The **Kuiper distance** on $\mathcal{P}$ is defined by

$$\sup_{x\in\mathbb{R}}(P_1(X \leq x) - P_2(X \leq x)) + \sup_{x\in\mathbb{R}}(P_2(X \leq x) - P_1(X \leq x)).$$

  (Cf. **Pompeiu–Eggleston metric** in Chap. 9.)
  The **Crnkovic–Drachma distance** is defined by

$$\sup_{x\in\mathbb{R}}(P_1(X \leq x) - P_2(X \leq x)) \ln \frac{1}{\sqrt{(P_1(X \leq x)(1 - P_1(X \leq x))}} +$$
$$+ \sup_{x\in\mathbb{R}}(P_2(X \leq x) - P_1(X \leq x)) \ln \frac{1}{\sqrt{(P_1(X \leq x)(1 - P_1(X \leq x))}}.$$

- **Cramér–von Mises distance**
  The **Cramér–von Mises distance** (1928) is defined on $\mathcal{P}$ (for $\mathcal{X} \subset \mathbb{R}$) by

$$\omega^2 = \int_{-\infty}^{+\infty} (P_1(X \leq x) - P_2(X \leq x))^2 dP_2(x).$$

  The **Anderson–Darling distance** (1954) on $\mathcal{P}$ is defined by

$$\int_{-\infty}^{+\infty} \frac{(P_1(X \leq x) - P_2)(X \leq x))^2}{(P_2(X \leq x)(1 - P_2(X \leq x))} dP_2(x).$$

In Statistics, above distances of Kolmogorov–Smirnov, Cramér–von Mises, Anderson–Darling and, below, χ^2**-distance** are the main measures of *goodness of fit* between estimated, P_2, and theoretical, P_1, distributions.

They and other distances were generalized (for example by Kiefer, 1955, and Glick, 1969) on *K-sample setting*, i.e., some convenient generalized distances $d(P_1, \ldots, P_K)$ were defined. Cf. **m-hemimetric** in Chap. 3.

- **Energy distance**

  The **energy distance** (Széely, 1985) between cumulative density functions $F(X)$, $F(Y)$ of two independent random vectors $X, Y \in \mathbb{R}^n$ is defined by

$$d(F(X), F(Y)) = 2\mathbb{E}[||(X - Y||] - \mathbb{E}[||X - X'||] - \mathbb{E}[||(Y - Y'||],$$

  where X, X' are *iid* (independent and identically distributed), Y, Y' are iid and $||.||$ is the length of a vector. For real-valued random variables this distance is exactly twice **Cramér–von Mises distance**. Cf. **distance covariance** in Chap. 17.

  It holds $d(F(X), F(Y)) = 0$ if and only if X, Y are iid.

- **Prokhorov metric**

  Given a metric space $(\mathcal{X}, d)$, the **Prokhorov metric** on $\mathcal{P}$ is defined (1956) by

$$\inf\{\epsilon > 0 : P_1(X \in B) \leq P_2(X \in B^\epsilon) + \epsilon \text{ and } P_2(X \in B) \leq P_1(X \in B^\epsilon) + \epsilon\},$$

  where B is any Borel subset of $\mathcal{X}$, and $B^\epsilon = \{x : d(x, y) < \epsilon, y \in B\}$.

  It is the smallest (over all joint distributions of pairs (X, Y) of random variables X, Y such that the marginal distributions of X and Y are P_1 and P_2, respectively) **probability distance** between random variables X and Y.

- **Levy–Sibley metric**

  The **Levy–Sibley metric** is a metric on $\mathcal{P}$ (for $\mathcal{X} \subset \mathbb{R}$ only) defined by

$$\inf\{\epsilon > 0 : P_1(X \leq x - \epsilon) - \epsilon \leq P_2(X \leq x) \leq P_1(X \leq x + \epsilon) + \epsilon \text{ for any } x \in \mathbb{R}\}.$$

  It is a special case of the **Prokhorov metric** for $(\mathcal{X}, d) = (\mathbb{R}, |x - y|)$.

- **Dudley metric**

  Given a metric space $(\mathcal{X}, d)$, the **Dudley metric** on $\mathcal{P}$ is defined by

$$\sup_{f \in F} |\mathbb{E}_{P_1}[f(X)] - \mathbb{E}_{P_2}[f(X)]| = \sup_{f \in F} |\sum_{x \in \mathcal{X}} f(x)(p_1(x) - p_2(x))|,$$

  where $F = \{f : \mathcal{X} \to \mathbb{R}, ||f||_\infty + Lip_d(f) \leq 1\}$, and $Lip_d(f) = \sup_{x,y \in \mathcal{X}, x \neq y} \frac{|f(x) - f(y)|}{d(x,y)}$.

- **Szulga metric**
  Given a metric space $(\mathcal{X}, d)$, the **Szulga metric** (1982) on $\mathcal{P}$ is defined by

$$\sup_{f\in F} |(\sum_{x\in\mathcal{X}} |f(x)|^p p_1(x))^{1/p} - (\sum_{x\in\mathcal{X}} |f(x)|^p p_2(x))^{1/p}|,$$

  where $F = \{f : X \to \mathbb{R},\ Lip_d(f) \le 1\}$, and $Lip_d(f) = \sup_{x,y\in\mathcal{X}, x\neq y} \frac{|f(x)-f(y)|}{d(x,y)}$.
- **Zolotarev semimetric**
  The **Zolotarev semimetric** is a semimetric on $\mathcal{P}$, defined (1976) by

$$\sup_{f\in F} |\sum_{x\in\mathcal{X}} f(x)(p_1(x) - p_2(x))|,$$

  where F is any set of functions $f : \mathcal{X} \to \mathbb{R}$ (in the continuous case, F is any set of such bounded continuous functions); cf. **Szulga metric**, **Dudley metric**.
- **Convolution metric**
  Let G be a separable locally compact Abelian group, and let $C(G)$ be the set of all real bounded continuous functions on G vanishing at infinity. Fix a function $g \in C(G)$ such that $|g|$ is integrable with respect to the Haar measure on G, and $\{\beta \in G^* : \hat{g}(\beta) = 0\}$ has empty interior; here G^* is the dual group of G, and $\hat{g}$ is the Fourier transform of g.
  The **convolution metric** (or *smoothing metric*) is defined (Yukich, 1985), for any two finite signed Baire measures P_1 and P_2 on G, by

$$\sup_{x\in G} |\int_{y\in G} g(xy^{-1})(dP_1 - dP_2)(y)|.$$

  It can also be seen as the difference $T_{P_1}(g) - T_{P_2}(g)$ of *convolution operators* on $C(G)$ where, for any $f \in C(G)$, the operator $T_P f(x)$ is $\int_{y\in G} f(xy^{-1})dP(y)$.
  In particular, this metric can be defined on the space of probability measures on $\mathbb{R}^n$, where g is a PDF satisfying above conditions.
- **Discrepancy metric**
  Given a metric space $(\mathcal{X}, d)$, the **discrepancy metric** on $\mathcal{P}$ is defined by

$$\sup\{|P_1(X \in B) - P_2(X \in B)| : B \text{ is any closed ball}\}.$$

- **Bi-discrepancy semimetric**
  The **bi-discrepancy semimetric** (evaluating the proximity of distributions P_1, P_2 over different collections $\mathcal{A}_1, \mathcal{A}_2$ of measurable sets) is defined by

$$D(P_1, P_2) + D(P_2, P_1),$$

  where $D(P_1, P_2) = \sup\{\inf\{P_2(C) : B \subset C \in \mathcal{A}_2\} - P_1(B) : B \in \mathcal{A}_1\}$ (*discrepancy*).

- **Le Cam distance**

  The **Le Cam distance** (1974) is a semimetric, evaluating the proximity of probability distributions P_1, P_2 (on different spaces $\mathcal{X}_1, \mathcal{X}_2$) and defined as follows:

$$\max\{\delta(P_1, P_2), \delta(P_2, P_1)\},$$

  where $\delta(P_1, P_2) = \inf_B \sum_{x_2 \in \mathcal{X}_2} |BP_1(X_2 = x_2) - BP_2(X_2 = x_2)|$ is the *Le Cam deficiency*. Here $BP_1(X_2 = x_2) = \sum_{x_1 \in \mathcal{X}_1} p_1(x_1) b(x_2|x_1)$, where B is a probability distribution over $\mathcal{X}_1 \times \mathcal{X}_2$, and

$$b(x_2|x_1) = \frac{B(X_1 = x_1, X_2 = x_2)}{B(X_1 = x_1)} = \frac{B(X_1 = x_1, X_2 = x_2)}{\sum_{x \in \mathcal{X}_2} B(X_1 = x_1, X_2 = x)}.$$

  So, $BP_2(X_2 = x_2)$ is a probability distribution over $\mathcal{X}_2$, since $\sum_{x_2 \in \mathcal{X}_2} b(x_2|x_1) = 1$.

  Le Cam distance is not a probabilistic distance, since P_1 and P_2 are defined over different spaces; it is a distance between statistical experiments (models).

- **Skorokhod–Billingsley metric**

  The **Skorokhod–Billingsley metric** is a metric on $\mathcal{P}$, defined by

$$\inf_f \max \left\{ \sup_x |P_1(X \le x) - P_2(X \le f(x))|, \sup_x |f(x) - x|, \sup_{x \ne y} \left| \ln \frac{f(y) - f(x)}{y - x} \right| \right\},$$

  where $f : \mathbb{R} \to \mathbb{R}$ is any strictly increasing continuous function.

- **Skorokhod metric**

  The **Skorokhod metric** is a metric on $\mathcal{P}$ defined (1956) by

$$\inf\{\epsilon > 0 : \max\{\sup_x |P_1(X < x) - P_2(X \le f(x))|, \sup_x |f(x) - x|\} < \epsilon\},$$

  where $f : \mathbb{R} \to \mathbb{R}$ is a strictly increasing continuous function.

- **Birnbaum–Orlicz distance**

  The **Birnbaum–Orlicz distance** (1931) is a distance on $\mathcal{P}$ defined by

$$\sup_{x \in \mathbb{R}} f(|P_1(X \le x) - P_2(X \le x)|),$$

  where $f : \mathbb{R}_{\ge 0} \to \mathbb{R}_{\ge 0}$ is any nondecreasing continuous function with $f(0) = 0$, and $f(2t) \le Cf(t)$ for any $t > 0$ and some fixed $C \ge 1$. It is a **near-metric**, since the C**-triangle inequality** $d(P_1, P_2) \le C(d(P_1, P_3) + d(P_3, P_2))$ holds.

  Birnbaum–Orlicz distance is also used, in Functional Analysis, on the set of all integrable functions on the segment $[0, 1]$, where it is defined by $\int_0^1 H(|f(x) - g(x)|)dx$, where H is a nondecreasing continuous function from $[0, \infty)$ onto $[0, \infty)$ which vanishes at the origin and satisfies the *Orlicz condition*: $\sup_{t>0} \frac{H(2t)}{H(t)} < \infty$.

- **Kruglov distance**
  The **Kruglov distance** (1973) is a distance on $\mathcal{P}$, defined by

$$\int f(P_1(X \le x) - P_2(X \le x))dx,$$

  where $f : \mathbb{R}_{\ge 0} \to \mathbb{R}_{\ge 0}$ is any even strictly increasing function with $f(0) = 0$, and $f(s+t) \le C(f(s) + f(t))$ for any $s, t \ge 0$ and some fixed $C \ge 1$. It is a **near-metric**, since the C**-triangle inequality** $d(P_1, P_2) \le C(d(P_1, P_3) + d(P_3, P_2))$ holds.
- **Bregman divergence**
  Given a differentiable strictly convex function $\phi(p) : \mathbb{R}^n \to \mathbb{R}$ and $\beta \in (0, 1)$, the **skew Jensen** (or *skew Burbea–Rao*) **divergence** on $\mathcal{P}$ is (Basseville–Cardoso, 1995)

$$J_\phi^{(\beta)}(P_1, P_2) = \beta\phi(p_1) + (1-\beta)\phi(p_2) - \phi(\beta p_1 + (1-\beta)p_2).$$

  The **Burbea–Rao distance** (1982) is the case $\beta = \frac{1}{2}$ of it, i.e., it is

$$\sum_x \left(\frac{\phi(p_1(x)) + \phi(p_2(x))}{2} - \phi(\frac{p_1(x) + (p_2(x)}{2}) \right).$$

  The **Bregman divergence** (1967) is a quasi-distance on $\mathcal{P}$ defined by

$$\sum_x (\phi(p_1(x)) - \phi(p_2(x)) - (p_1(x) - p_2(x))\phi'(p_2(x))) = \lim_{\beta \to 1} \frac{1}{\beta} J_\phi^{(\beta)}(P_1, P_2).$$

  The **generalised Kullback–Leibler distance** $\sum_x p_1(x) \ln \frac{p_1(x)}{p_2(x)} - \sum_x (p_1(x) - p_2(x))$ and **Itakura–Saito distance** (Chap. 21) $\sum_x \frac{p_1(x)}{p_2(x)} - \ln \frac{p_1(x)}{p_2(x)} - 1$ are the cases $\phi(p) = \sum_x p(x) \ln p(x) - \sum_x p(x)$ and $\phi(p) = -\sum_x \ln p(x)$ of the Bregman divergence. Cf. **Bregman quasi-distance** in Chap. 13.

  Csizár, 1991, proved that the **Kullback–Leibler distance** is the only **Bregman divergence** which is an f**-divergence**.
- f**-divergence**
  Given a convex function $f(t) : \mathbb{R}_{\ge 0} \to \mathbb{R}$ with $f(1) = 0, f'(1) = 0, f''(1) = 1$, the f**-divergence** (independently, Csizár, 1963, Morimoto, 1963, Ali–Silvey, 1966, Ziv–Zakai, 1973, and Akaike, 1974) on $\mathcal{P}$ is defined by

$$\sum_x p_2(x) f\left(\frac{p_1(x)}{p_2(x)}\right).$$

  The cases $f(t) = t \ln t$ and $f(t) = (t-1)^2$ correspond to the **Kullback–Leibler distance** and to the χ^2**-distance** below, respectively. The case $f(t) = |t-1|$

corresponds to the **variational distance**, and the case $f(t) = 4(1 - \sqrt{t})$ (as well as $f(t) = 2(t+1) - 4\sqrt{t}$) corresponds to the squared **Hellinger metric**.

Semimetrics can also be obtained, as the square root of the f-divergence, in the cases $f(t) = (t-1)^2/(t+1)$ (the **Vajda–Kus semimetric**), $f(t) = |t^a - 1|^{1/a}$ with $0 < a \leq 1$ (the **generalized Matusita distance**), and $f(t) = \frac{(t^a+1)^{1/a} - 2^{(1-a)/a}(t+1)}{1-1/\alpha}$ (the **Osterreicher semimetric**).

- **α-divergence**

  Given $\alpha \in \mathbb{R}$, the **α-divergence** (independently, Csizár, 1967, Havrda–Charvát, 1967, Cressie–Read, 1984, and Amari, 1985) is defined as $KL(P_1, P_2)$, $KL(P_2, P_1)$ for $\alpha = 1, 0$ and for $\alpha \neq 0, 1$, it is

$$\frac{1}{\alpha(1-\alpha)}(1 - \sum_x p_2(x) \left(\frac{p_1(x)}{p_2(x)}\right)^\alpha).$$

  The **Amari divergence** come from the above by the transformation $\alpha = \frac{1+t}{2}$.

- **Harmonic mean similarity**

  The **harmonic mean similarity** is a similarity on $\mathcal{P}$ defined by

$$2\sum_x \frac{p_1(x)p_2(x)}{p_1(x) + p_2(x)}.$$

- **Fidelity similarity**

  The **fidelity similarity** (or *Bhattacharya coefficient*, *Hellinger affinity*) on $\mathcal{P}$ is

$$\rho(P_1, P_2) = \sum_x \sqrt{p_1(x)p_2(x)}.$$

  Cf. more general **quantum fidelity similarity** in Chap. 24.

- **Hellinger metric**

  In terms of the **fidelity similarity** ρ, the **Hellinger metric** (or **Matusita distance**, *Hellinger–Kakutani metric*) on $\mathcal{P}$ is defined by

$$(\sum_x (\sqrt{p_1(x)} - \sqrt{p_2(x)})^2)^{\frac{1}{2}} = \sqrt{2(1 - \rho(P_1, P_2))}.$$

- **Bhattacharya distance** 1

  In terms of the **fidelity similarity** ρ, the **Bhattacharya distance** 1 (1946) is

$$(\arccos \rho(P_1, P_2))^2$$

  for $P_1, P_2 \in \mathcal{P}$. Twice this distance is the **Rao distance** from Chap. 7. It is used also in Statistics and Machine Learning, where it is called the *Fisher distance*.

The **Bhattacharya distance** 2 (1943) on $\mathcal{P}$ is defined by

$$-\ln \rho(P_1, P_2).$$

- χ^2**-distance**

  The χ^2**-distance** (or **Pearson** χ^2**-distance**) is a quasi-distance on $\mathcal{P}$, defined by

$$\sum_x \frac{(p_1(x) - p_2(x))^2}{p_2(x)}.$$

  The **Neyman** χ^2**-distance** is a quasi-distance on $\mathcal{P}$, defined by

$$\sum_x \frac{(p_1(x) - p_2(x))^2}{p_1(x)}.$$

  The half of χ^2-distance is also called *Kagan's divergence*.

  The probabilistic **symmetric** χ^2**-measure** is a distance on $\mathcal{P}$, defined by

$$2\sum_x \frac{(p_1(x) - p_2(x))^2}{p_1(x) + p_2(x)}.$$

- **Separation quasi-distance**

  The **separation distance** is a quasi-distance on $\mathcal{P}$ (for a countable $\mathcal{X}$) defined by

$$\max_x \left(1 - \frac{p_1(x)}{p_2(x)}\right).$$

  (Not to be confused with **separation distance** in Chap. 9.)

- **Kullback–Leibler distance**

  The **Kullback–Leibler distance** (or *relative entropy*, *information deviation*, *information gain*, *KL-distance*) is a quasi-distance on $\mathcal{P}$, defined (1951) by

$$KL(P_1, P_2) = \mathbb{E}_{P_1}[\ln L] = \sum_x p_1(x) \ln \frac{p_1(x)}{p_2(x)},$$

  where $L = \frac{p_1(x)}{p_2(x)}$ is the *likelihood ratio*. Therefore,

$$KL(P_1, P_2) = -\sum_x p_1(x) \ln p_2(x) + \sum_x p_1(x) \ln p_1(x) = H(P_1, P_2) - H(P_1),$$

  where $H(P_1)$ is the *entropy* of P_1, and $H(P_1, P_2)$ is the *cross-entropy* of P_1 and P_2.

If P_2 is the product of marginals of P_1 (say, $p_2(x,y) = p_1(x)p_1(y)$), the KL-distance $KL(P_1, P_2)$ is called the *Shannon information quantity* and (cf. **Shannon distance**) is equal to $\sum_{(x,y)\in\mathcal{X}\times\mathcal{X}} p_1(x,y) \ln \frac{p_1(x,y)}{p_1(x)p_1(y)}$.

The **exponential divergence** is defined by $\sum_x p_1(x)(\ln \frac{p_1(x)}{p_2(x)})^2$.

- **Distance to normality**

  For a continuous distribution P on $\mathbb{R}$, the *differential entropy* is defined by

$$h(P) = -\int_{-\infty}^{\infty} p(x) \ln p(x) dx.$$

  It is $\ln(\delta\sqrt{2\pi e})$ for a *normal* (or *Gaussian*) *distribution* $g_{\delta,\mu}(x) = \frac{1}{\sqrt{2\pi\delta^2}} \exp\left(-\frac{(x-\mu)^2}{2\delta^2}\right)$ with variance δ^2 and mean μ.

  The **distance to normality** (or *negentropy*) of P is the **Kullback–Leibler distance** $KL(P, g) = \int_{-\infty}^{\infty} p(x) \ln\left(\frac{p(x)}{g(x)}\right) dx = h(g) - h(P)$, where q is a normal distribution with the same variance as P. So, it is nonnegative and equal to 0 if and only if $P = g$ almost everywhere. Cf. **Shannon distance**.

  Also, $h(u_{a,b}) = \ln(b-a)$ for an *uniform distribution* with minimum a and maximum $b > a$, i.e., $u_{a,b}(x) = \frac{1}{b-a}$, if $x \in [a,b]$, and it is 0, otherwise. It holds $h(u_{a,b}) \geq h(P)$ for any distribution P with support contained in $[a,b]$; so, $h(u_{a,b}) - h(P)$ can be called the *distance to uniformity*. Tononi, 2008, used it in his model of consciousness.

- **Jeffrey distance**

  The **Jeffrey distance** (or *J-divergence*, *KL2-distance*) is a symmetric version of the **Kullback–Leibler distance** defined (1946) on $\mathcal{P}$ by

$$KL(P_1, P_2) + KL(P_2, P_1) = \sum_x ((p_1(x) - p_2(x)) \ln \frac{p_1(x)}{p_2(x)}.$$

  The **Aitchison distance** (1986) is defined by $\sqrt{\sum_x (\ln \frac{p_1(x)g(p_1)}{p_2(x)g(p_2)})^2}$, where $g(p) = (\prod_x p(x))^{\frac{1}{n}}$ is the geometric mean of components $p(x)$ of p.

- **Resistor-average distance**

  The **resistor-average distance** is (Johnson–Simanović, 2000) a symmetric version of the **Kullback–Leibler distance** on $\mathcal{P}$ which is defined by the harmonic sum

$$\left(\frac{1}{KL(P_1, P_2)} + \frac{1}{KL(P_2, P_1)}\right)^{-1}.$$

- **Jensen–Shannon divergence**

  Given a number $\beta \in [0,1]$ and $P_1, P_2 \in \mathcal{P}$, let P_3 denote $\beta P_1 + (1-\beta)P_2$.

The **skew divergence** and the **Jensen–Shannon divergence** between P_1 and P_2 are defined on $\mathcal{P}$ as $KL(P_1, P_3)$ and $\beta KL(P_1, P_3) + (1 - \beta)KL(P_2, P_3)$, respectively. Here KL is the **Kullback–Leibler distance**; cf. **clarity similarity**.

In terms of *entropy* $H(P) = -\sum_x p(x) \ln p(x)$, the Jensen–Shannon divergence is $H(\beta P_1 + (1-\beta)P_2) - \beta H(P_1) - (1-\beta)H(P_2)$, i.e., the **Jensen divergence** (cf. **Bregman divergence**).

Let $P_3 = \frac{1}{2}(P_1 + P_2)$, i.e., $\beta = \frac{1}{2}$. Then the skew divergence and twice the Jensen–Shannon divergence are called ***K*-divergence** and **Topsøe distance** (or *information statistics*), respectively. The Topsøe distance is a symmetric version of $KL(P_1, P_2)$. It is not a metric, but its square root is a metric.

Related symmetric divergencies between P_1 and P_2—**Taneja distance** (1995) and **Kumar–Johnson distance** (2005)—are defined, respectively, by

$$\sum_x \left(\frac{p_1(x) + p_2(x)}{2} \ln \frac{p_1(x) + p_2(x)}{2\sqrt{p_1(x)p_2(x)}} \right) \quad \text{and} \quad \sum_x \left(\frac{(p_1^2(x) - p_2^2(x))^2}{2\sqrt{p_1(x)p_2(x)}} \right).$$

- **Clarity similarity**

  The **clarity similarity** is a similarity on $\mathcal{P}$, defined by

$$(KL(P_1, P_3) + KL(P_2, P_3)) - (KL(P_1, P_2) + KL(P_2, P_1)) =$$

$$= \sum_x \left(p_1(x) \ln \frac{p_2(x)}{p_3(x)} + p_2(x) \ln \frac{p_1(x)}{p_3(x)} \right),$$

  where KL is the **Kullback–Leibler distance**, and P_3 is a fixed probability law.

  It was introduced in [CCL01] with P_3 being the probability distribution of English.

- **Ali–Silvey distance**

  The **Ali–Silvey distance** is a quasi-distance on $\mathcal{P}$ defined by the functional

$$f(\mathbb{E}_{P_1}[g(L)]),$$

  where $L = \frac{p_1(x)}{p_2(x)}$ is the *likelihood ratio*, f is a nondecreasing function on $\mathbb{R}$, and g is a continuous convex function on $\mathbb{R}_{\geq 0}$ (cf. ***f*-divergence**).

  The case $f(x) = x$, $g(x) = x \ln x$ corresponds to the **Kullback–Leibler distance**; the case $f(x) = -\ln x$, $g(x) = x^t$ corresponds to the **Chernoff distance**.

- **Chernoff distance**

  The **Chernoff distance** (or *Rényi cross-entropy*) on $\mathcal{P}$ is defined (1954) by

$$\max_{t \in (0,1)} D_t(P_1, P_2),$$

  where $0 < t < 1$ and $D_t(P_1, P_2) = -\ln \sum_x (p_1(x))^t (p_2(x))^{1-t}$ (called the *Chernoff coefficient*) which is proportional to the **Rényi distance**.

- **Rényi distance**

  Given $t \in \mathbb{R}$, the **Rényi distance** (or *order t Rényi entropy*, 1961) is a quasi-distance on $\mathcal{P}$ defined as the **Kullback–Leibler distance** $KL(P_1, P_2)$ if $t = 1$, and, otherwise, by

$$\frac{1}{1-t} \ln \sum_x p_2(x) \left(\frac{p_1(x)}{p_2(x)} \right)^t.$$

  For $t = \frac{1}{2}$, one half of the Rényi distance is the **Bhattacharya distance** 2. Cf. **f-divergence** and **Chernoff distance**.

- **Shannon distance**

  Given a *measure space* $(\Omega, \mathcal{A}, P)$, where the set Ω is finite and P is a probability measure, the *entropy* (or *Shannon information entropy*) of a function $f : \Omega \to X$, where X is a finite set, is defined by

$$H(f) = -\sum_{x \in X} P(f = x) \log_a(P(f = x)).$$

  Here $a = 2$, e, or 10 and the unit of entropy is called a *bit*, *nat*, or *dit* (digit), respectively. The function f can be seen as a partition of the measure space.

  For any two such partitions $f : \Omega \to X$ and $g : \Omega \to Y$, denote by $H(f, g)$ the entropy of the partition $(f, g) : \Omega \to X \times Y$ (*joint entropy*), and by $H(f|g)$ the *conditional entropy* (or *equivocation*). Then the **Shannon distance** between f and g is a metric defined by

$$H(f|g) + H(g|f) = 2H(f, g) - H(f) - H(g) = H(f) + H(g) - 2I(f; g),$$

  where $I(f; g) = H(f) + H(g) - H(f, g)$ is the *Shannon mutual information*.

  If P is the uniform probability law, then Goppa showed that the Shannon distance can be obtained as a limiting case of the **finite subgroup metric**.

  In general, the **shared information distance** (or **variation of information**, **entropy metric**) between random variables (information sources) X and Y is

$$H(X|Y) + H(Y|X) = H(X, Y) - I(X; Y),$$

  where the *conditional entropy* $H(X|Y)$ is $\sum_{x \in X} \sum_{y \in Y} p(x, y) \ln p(x|y)$, and $p(x|y) = P(X = x|Y = y)$ is the conditional probability.

  The **Rajski distance** (or *normalized information metric*) is defined (Rajski, 1961, for discrete probability distributions X, Y) by

$$\frac{H(X|Y) + H(Y|X)}{H(X, Y)} = 1 - \frac{I(X; Y)}{H(X, Y)}.$$

It is equal to 1 if X and Y are independent. Cf. **Tanimoto distance** in Chap. 17 and the **normalized information distance** in Chap. 11.

Now, $\max\{H(X), H(Y)\} - I(X;Y)$ is also a metric.

- **Transportation distance**

  Given a metric space $(\mathcal{X}, d)$, the **transportation distance** (and/or, according to Villani, 2009, **Monge–Kantorovich–Wasserstein–Rubinstein–Ornstein–Gini–Dall'Aglio–Mallows–Tanaka distance**) is the metric defined by

$$W_1(P_1, P_2) = \inf \mathbb{E}_S[d(X,Y)] = \inf_S \int_{(X,Y)\in\mathcal{X}\times\mathcal{X}} d(X,Y)dS(X,Y),$$

  where the infimum is taken over all joint distributions S of pairs (X, Y) of random variables X, Y such that marginal distributions of X and Y are P_1 and P_2.

  For any **separable** metric space $(\mathcal{X}, d)$, this is equivalent to the **Lipschitz distance between measures** $\sup_f \int f d(P_1 - P_2)$, where the supremum is taken over all functions f with $|f(x) - f(y)| \leq d(x,y)$ for any $x, y \in \mathcal{X}$. Cf. **Dudley metric**.

  In general, for a Borel function $c : \mathcal{X} \times \mathcal{X} \to \mathbb{R}_{\geq 0}$, the ***c*-transportation distance** $T_c(P_1, P_2)$ is $\inf \mathbb{E}_S[c(X,Y)]$. It is the minimal total transportation cost if $c(X,Y)$ is the cost of transporting a unit of mass from the location X to the location Y. Cf. the **Earth Mover's distance** (Chap. 21), which is a discrete form of it.

  The **L_p-Wasserstein distance** is $W_p = (T_{d^p})^{1/p} = (\inf \mathbb{E}_S[d^p(X,Y)])^{1/p}$. For $(\mathcal{X}, d) = (\mathbb{R}, |x-y|)$, it is also called the *L_p-metric between distribution functions* (CDF) F_i with $F_i^{-1}(x) = \sup_u(P_i(X \leq x) < u)$, and can be written as

$$(\inf \mathbb{E}[|X-Y|^p])^{1/p} = \left(\int_{\mathbb{R}} |F_1(x) - F_2(x)|^p dx\right)^{1/p} = \left(\int_0^1 |F_1^{-1}(x) - F_2^{-1}(x)|^p dx\right)^{1/p}.$$

  For $p = 1$, this metric is called **Monge–Kantorovich metric** (or **Wasserstein metric**, **Fortet–Mourier metric**, **Hutchinson metric**, **Kantorovich–Rubinstein metric**). For $p = 2$, it is the **Levy–Fréchet metric** (Fréchet, 1957).

- **Ornstein $\overline{d}$-metric**

  The **Ornstein $\overline{d}$-metric** is a metric on $\mathcal{P}$ (for $\mathcal{X} = \mathbb{R}^n$) defined (1974) by

$$\frac{1}{n} \inf \int_{x,y} \left(\sum_{i=1}^{n} 1_{x_i \neq y_i}\right) dS,$$

  where the infimum is taken over all joint distributions S of pairs (X, Y) of random variables X, Y such that marginal distributions of X and Y are P_1 and P_2, respectively.

- **Distances between belief assignments**

  In *Bayesian* (or *subjective*, *evidential*) interpretation, a probability can be assigned to any statement, even if no random process is involved, as a way

to represent its subjective plausibility, or the degree to which it is supported by the available evidence, or, mainly, degree of belief. Within this approach, *imprecise probability* generalizes Probability Theory to deal with scarce, vague, or conflicting information. The main model is *Dempster–Shafer theory*, which allows evidence to be combined.

Given a set X, a (basic) **belief assignment** is a function $m : P(X) \to [0, 1]$ (where $P(X)$ is the set of all subsets of X) with $m(\emptyset) = 0$ and $\sum_{A \subset P(X)} m(A) = 1$. Probability measures are a special case in which $m(A) > 0$ only for singletons.

For the classic probability $P(A)$, it holds then $\text{Bel}(A) \leq P(A) \leq \text{Pl}(A)$, where the *belief function* and *plausibility function* are defined, respectively, by

$$\text{Bel}(A) = \sum_{B:B \subset A} m(B) \text{ and } \text{Pl}(A) = \sum_{B:B \cap A \neq \emptyset} m(B) = 1 - \text{Bel}(\overline{A}).$$

The original (Dempster, 1967) *conflict factor* between two belief assignments m_1 and m_2 was defined as $c(m_1, m_2) = \sum_{A \cap B = \emptyset} m_1(A) m_2(B)$. This is not a distance since $c(m, m) > 0$. The combination of m_1 and m_2, seen as independent sources of evidence, is defined by $m_1 \oplus m_2(A) = \frac{1}{1 - c(m_1, m_2)} \sum_{B \cap C = A} m_1(B) m_2(C)$.

Usually, a distance between m_1 and m_2 estimates the difference between these sources in the form $d_U = |U(m_1) - U(m_2)|$, where U is an uncertainty measure; see Sarabi-Jamab et al., 2013, for a comparison of their performance. In particular, this distance is called:

confusion (Hoehle, 1981) if $U(m) = \sum_A m(A) \log_2 \text{Bel}(A)$;
dissonance (Yager, 1983) if $U(m) = E(m) = -\sum_A m(A) \log_2 \text{Pl}(A)$;
Yager's factor (Eager, 1983) if $U(m) = 1 - \sum_{A \neq \emptyset} \frac{m(A)}{|A|}$;
possibility-based (Smets, 1983) if $U(m) = -\sum_A \log_2 \sum_{B:A \subset B} m(B)$;
U-uncertainty (Dubois–Prade, 1985) if $U(m) = I(m) = -\sum_A m(A) \log_2 |A|$;
Lamata–Moral's (1988) if $U(m) = \log_2(\sum_A m(A)|A|)$ and $U(m) = E(m) + I(m)$;
discord (Klir–Ramer, 1990) if $U(m) = D(m) = -\sum_A m(A) \log_2(1 - \sum_B m(B) \frac{|B \setminus A|}{|B|})$ and a variant: $U(m) = D(m) + I(m)$;
strife (Klir–Parviz, 1992) if $U(m) = -\sum_A m(A) \log_2(\sum_B m(B) \frac{|A \cap B|}{|A|})$;
Pal et al.'s (1993) if $U(m) = G(m) = -\sum_A \log_2 m(A)$ and $U(m) = G(m) + I(m)$;
total conflict (George–Pal, 1996) if $U(m) = \sum_A m(A) \sum_B (m(B)(1 - \frac{|A \cap B|}{|A \cup B|}))$.

Among other distances used are the **cosine distance** $1 - \frac{m_1^T m_2}{||m_1|| ||m_2||}$, the **Mahalanobis distance** $\sqrt{(m_1 - m_2)^T A (m_1 - m_2)}$ for some matrices A, and *pignistic-based* one (Tessem, 1993) $\max_A \{| \sum_{B \neg \emptyset} (m_1(B) - m_2(B) \frac{|A \cap B|}{|B|} |\}$.

Part IV
Distances in Applied Mathematics

Chapter 15
Distances in Graph Theory

A *graph* is a pair $G = (V, E)$, where V is a set, called the set of *vertices* of the graph G, and E is a set of unordered pairs of vertices, called the *edges* of the graph G. A *directed graph* (or *digraph*) is a pair $D = (V, E)$, where V is a set, called the set of *vertices* of the digraph D, and E is a set of ordered pairs of vertices, called *arcs* of the digraph D.

A graph in which at most one edge may connect any two vertices, is called a *simple graph*. If multiple edges are allowed between vertices, the graph is called a *multigraph*. A graph, together with a function which assigns a positive weight to each edge, is called a *weighted graph* or *network*.

The graph is called *finite* (*infinite*) if the set V of its vertices is finite (infinite, respectively). The *order* and *size* of a finite graph (V, E) are $|V|$ and $|E|$, respectively.

A *subgraph* of a graph $G = (V, E)$ is a graph $G' = (V', E')$ with $V' \subset V$ and $E' \subset E$. If G' is a subgraph of G, then G is called a *supergraph* of G'. A subgraph (V', E') of (V, E) is its *induced subgraph* if $E' = \{e = uv \in E : u, v \in V'\}$.

A graph $G = (V, E)$ is called *connected* if, for any $u, v \in V$, there exists a $(u-v)$ *walk*, i.e., a sequence of edges $uw_1 = w_0w_1, w_1w_2, \ldots, w_{n-1}w_n = w_{n-1}v$ from E. A $(u - v)$ *path* is a $(u - v)$ walk with distinct edges. A graph is called *m-connected* if there is no set of $m - 1$ edges whose removal disconnects the graph; a connected graph is 1-connected. A digraph $D = (V, E)$ is called *strongly connected* if, for any $u, v \in V$, the *directed* $(u - v)$ and $(v - u)$ paths both exist. A maximal connected subgraph of a graph G is called its *connected component*.

Vertices connected by an edge are called *adjacent*. The *degree* $deg(v)$ of a vertex $v \in V$ of a graph $G = (V, E)$ is the number of its vertices adjacent to v.

A *complete graph* is a graph in which each pair of vertices is connected by an edge. A *bipartite graph* is a graph in which the set V of vertices is decomposed into two disjoint subsets so that no two vertices within the same subset are adjacent. A *simple path* is a simple connected graph in which two vertices have degree 1, and

© Springer-Verlag Berlin Heidelberg 2016

M.M. Deza, E. Deza, *Encyclopedia of Distances*,
DOI 10.1007/978-3-662-52844-0_15

other vertices (if they exist) have degree 2; the *length* of a path is the number of its edges.

A *cycle* is a *closed simple path*, i.e., a simple connected graph in which every vertex has degree 2. The *circumference* of a graph is the length of the longest cycle in it. A *tree* is a simple connected graph without cycles. A tree having a path from which every vertex has distance ≤ 1 or ≤ 2, is called a *caterpillar* or *lobster*, respectively.

Two graphs which contain the same number of vertices connected in the same way are called *isomorphic*. Formally, two graphs $G = (V(G), E(G))$ and $H = (V(H), E(H))$ are called *isomorphic* if there is a bijection $f : V(G) \to V(H)$ such that, for any $u, v \in V(G)$, $uv \in E(G)$ if and only if $f(u)f(v) \in E(H)$.

We will consider mainly simple finite graphs and digraphs; more exactly, the equivalence classes of such isomorphic graphs.

15.1 Distances on the Vertices of a Graph

- **Path metric**

  The **path metric** (or **graphic metric**, *shortest path metric*) d_{path} is a metric on the vertex-set V of a connected graph $G = (V, E)$ defined, for any $u, v \in V$, as the length of a shortest $(u - v)$ path in G, i.e., a *geodesic*. Examples follow.

  Given an integer $n \geq 1$, the **line metric on** $\{1, \ldots, n\}$ in Chap. 1 is the path metric of the path $P_n = \{1, \ldots, n\}$. The path metric of the *Cayley graph* Γ of a finitely generated group $(G, \cdot, e)$ is called a **word metric**.

  The **hypercube metric** is the path metric of a *hypercube graph* $H(m, 2)$ with the vertex-set $V = \{0, 1\}^m$, and whose edges are the pairs of vectors $x, y \in \{0, 1\}^m$ such that $|\{i \in \{1, \ldots, n\} : x_i \neq y_i\}| = 1$; it is equal to $|\{i \in \{1, \ldots, n\} : x_i = 1\} \triangle \{i \in \{1, \ldots, n\} : y_i = 1\}|$. The graphic metric space associated with a hypercube graph coincides with a **Hamming cube**, i.e., the metric space $(\{0, 1\}^m, d_{l_1})$.

  The **belt distance** (Garber–Dolbilin, 2010) is the path metric of a *belt graph* $B(P)$ of a polytope P with centrally symmetric facets. The vertices of $B(P)$ are the facets of P and two vertices are connected by an edge if the corresponding facets lie in the same *belt* (the set of all facets of P parallel to a given face of codimension 2).

  The reciprocal path metric is called **geodesic similarity**.

- **Weighted path metric**

  The **weighted path metric** d_{wpath} is a metric on the vertex-set V of a connected weighted graph $G = (V, E)$ with positive edge-weights $(w(e))_{e \in E}$ defined by

$$\min_P \sum_{e \in P} w(e),$$

  where the minimum is taken over all $(u - v)$ paths P in G.

Sometimes, $\frac{1}{w(e)}$ is called the *length* of the edge e. In the theory of electrical networks, the edge-length $\frac{1}{w(e)}$ is identified with the *resistance* of the edge e. The **inverse weighted path metric** is $\min_P \sum_{e\in P} \frac{1}{w(e)}$.

- **Filling of metric space**

  Given a finite metric space (X, d), a connected weighted graph $G = (V, E; \omega)$ with $X \subset V$ and edge-weights $\omega(e) \geq 0$ is called (Ivanov–Tuzhilin, 2012) **filling** of (X, d) if for all $x, y \in X$, $d(x, y)$ is bounded from above by the **weighted path metric** $d_G(x, y)$. Ivanov–Tuzhilin showed the existence of filings with minimal $\sum_{e\in E} \omega(e)$ and some relations with Steiner problem; (cf. **Steiner ratio** in Sect. 1.3.

  For the case when X is Riemannian manifold, a similar notion was defined by Gromov (1983), and related to Systolic Geometry (cf. **systole of metric space** in Sect. 1.2). Here a *minimal filing* is any compact manifold of minimal volume, having boundary X and a distance function that bounds d on X from above.

- **Metric graph**

  A **metric** (or *metrized*) **graph** is a connected graph $G = (V, E)$, where edges e are identified with line segments $[0, l(e)]$ of length $l(e)$. Let x_e be the coordinate on the segment $[0, l(e)]$ with vertices corresponding to $x_e = 0, l(e)$; the ends of distinct segments are identified if they correspond to the same vertex of G. A *function* f on G is the $|E|$-tuple of functions $f_e(x_e)$ on the segments.

  A metric graph can be seen as an infinite metric space (X, d), where X is the set of all points on above segments, and the distance between two points is the length of the shortest, along the line segments traversed, path connecting them. Also, it can be seen as one-dimensional Riemannian manifold with singularities.

  There is a bijection between the metric graphs, the equivalence classes of finite connected edge-weighted graphs and the resistive electrical networks: if an edge e of a metric graph has length $l(e)$, then $\frac{1}{l(e)}$ is the weight of e in the corresponding edge-weighted graph and $l(e)$ is the resistance along e in the corresponding resistive electric circuit. Cf. the **resistance metric**.

  A **quantum graph** is a metric graph equipped with a self-adjoint differential operator (such as a *Laplacian*) acting on functions on the graph. The *Hilbert space* of the graph is $\oplus_{e\in E} L^2([0, w(e)])$, where the inner product of functions is $\langle f, g\rangle = \sum_{e\in E} \int_0^{w(e)} f_e^*(x_e) g_e(x_e) dx_e$.

- **Spin network**

  A **spin network** is (Penrose, 1971) a connected graph (V, E) with edge-weights $(w(e))_{e\in E}$ (*spins*), $w(e) \in \mathbb{N}$, such that for any distinct edges e_1, e_2, e_3 with a common vertex, it holds **spin triangle inequality** $|w(e_1) - w(e_2)| \leq w(e_3) \leq w(e_1) + w(e_2)$ and *fermion conservation*: $w(e_1) + w(e_2) + w(e_3)$ is an even number.

  The **quantum space-time** (Chap. 24) in *Loop Quantum Gravity* is a network of loops at Planck scale. Loops are represented by adapted spin networks: directed graphs whose arcs are labeled by irreducible representations of a compact Lie group and vertices are labeled by *interwinning operators* from the tensor product of labels on incoming arcs to the tensor product of labels on

outgoing arcs. Such networks represent "quantum states" of the gravitational field on a 3D hypersurface.

- **Detour distance**

  Given a connected graph $G = (V, E)$, the **detour distance** is (Chartrand and Zhang, 2004) a metric on the vertex-set V defined, for $u \neq v$, as the length of the longest $(u - v)$ path in G. So, this distance is 1 or $|V| - 1$ if and only if uv is a *bridge* of G or, respectively, G contains a Hamiltonian $(u - v)$ path.

  The **monophonic distance** is (Santhakumaran and Titus, 2011) a distance (in general, not a metric) on the V defined, for $u \neq v$, as the length of a longest *monophonic* (or *induced*, *minimal*), i.e., chordless $(u - v)$ path in G.

  The *height* of a DAG (acyclic digraph) is the number of vertices in a longest directed path.

- **Rainbow distance**

  In an edge-colored graph, the **rainbow distance** is (Chartrand and Zhang, 2005) the length of a shortest *rainbow* (i.e., containing no color twice) path.

  In a vertex-colored graph, the **colored distance** is (Dankelmann et al., 2001) the sum of distances between all unordered pairs of vertices having different colors.

- **Cutpoint additive metric**

  Given a graph $G = (V, E)$, Klein–Zhu, 1998, call a metric d on V **graph-geodetic metric** if, for $u, w, v \in V$, the **triangle equality** $d(u, w) + d(w, v) = d(u, v)$ holds if w is a (u, v)-*gatekeeper*, i.e., w lies on any path connecting u and v. Cf. **metric interval** in Chap. 1. Any gatekeeper is a *cutpoint*, i.e., removing it disconnects G and a *pivotal point*, i.e., it lies on any shortest path between u and v.

  Chebotarev, 2010, call a metric d on the vertices of a multigraph without loops **cutpoint additive** if $d(u, w) + d(w, v) = d(u, v)$ holds if and only if w lies on any path connecting u and v. The **resistance metric** is cutpoint additive (Gvishiani and Gurvich, 1992), while the **path metric** is graph-geodetic only (in the weaker Klein–Zhu sense). See also **Chebotarev–Shamis metric**.

- **Graph boundary**

  Given a connected graph $G = (V, E)$, a vertex $v \in V$ is (Chartrand et al., 2003) a *boundary vertex* if there exists a *witness*, i.e., a vertex $u \in V$ such that $d(u, v) \geq d(u, w)$ for all neighbors w of v. So, the end-vertices of a longest path are boundary vertices. The **boundary** of G is the set of all boundary vertices.

  The *boundary of a subset* $M \subset V$ is the set $\partial M \subset E$ of edges having precisely one endpoint in M. The **isoperimetric number** of G is (Buser, 1978) $\inf \frac{\partial M}{|M|}$, where the infimum is taken over all $M \subset V$ with $2|M| \leq |V|$.

- **Graph diameter**

  Given a connected graph $G = (V, E)$, its **graph diameter** is the largest value of the **path metric** between vertices of G.

  A connected graph is *vertex-critical* (*edge-critical*) if deleting any vertex (edge) increases its diameter. A graph G of diameter k is *goal-minimal* if for every edge uv, the inequality $d_{G-uv}(x, y) > k$ holds if and only if $\{u, v\} = \{x, y\}$.

The **mixed fault diameter** $D_{(a,b)}(G)$ is the maximum diameter among all subgraphs obtained from G by deleting a vertices and b edges.

The **a-wide distance** $d_a(u, v)$ between vertices u and v is the minimum integer l, for which there are at least a internally disjoint $(u - v)$ paths of length at most l in G: cf. **Hsu–Lyuu–Flandrin–Li distance**. The *a-wide diameter* of G is $\max_{u,v\in V} d_a(u, v)$; it is at least $D_{(a-1,0)}(G)$.

Given a *strong orientation* O of a connected graph $G = (V, E)$, i.e., a strongly connected digraph $D = (V, E')$ with arcs $e' \in E'$ obtained from edges $e \in E$ by orientation O, the *diameter* of D is the maximal length of shortest directed $(u-v)$ path in it. The **oriented diameter** of a graph G is the smallest diameter among strong orientations of G. If it is equal to the diameter of G, then any orientation realizing this equality is called *tight*. For example, a *hypercube graph* $H(m, 2)$ admits a tight orientation if $m \geq 4$ (McCanna, 1988).

- **Path quasi-metric in digraphs**

  The **path quasi-metric in digraphs** d_{dpath} is a quasi-metric on the vertex-set V of a strongly connected digraph $D = (V, E)$ defined, for any $u, v \in V$, as the length of a shortest directed $(u - v)$ path in D.

  The **circular metric in digraphs** is a metric on the vertex-set V of a strongly connected digraph $D = (V, E)$, defined by $d_{\text{dpath}}(u, v) + d_{\text{dpath}}(v, u)$.

- **Strong distance in digraphs**

  The **strong distance in digraphs** is a metric between vertices v and v of a strongly connected digraph $D = (V, E)$ defined (Chartrand–Erwin–Raines–Zhang, 1999) as the minimum *size* (the number of edges) of a strongly connected subdigraph of D containing v and v. Cf. **Steiner distance of a set**.

- **Υ-metric**

  Given a class Υ of connected graphs, the metric d of a metric space (X, d) is called a **Υ-metric** if (X, d) is isometric to a subspace of a metric space (V, d_{wpath}), where $G = (V, E) \in \Upsilon$, and d_{wpath} is the **weighted path metric** on V with positive edge-weight function w; cf. **tree-like metric**.

- **Tree-like metric**

  A **tree-like metric** (or **weighted tree metric**) d on a set X is a **Υ-metric** for the class Υ of all trees, i.e., the metric space (X, d) is isometric to a subspace of a metric space (V, d_{wpath}), where $T = (V, E)$ is a tree, and d_{wpath} is the **weighted path metric** on the vertex-set V of T with a positive weight function w. A metric is a tree-like metric if and only if it satisfies the **four-point inequality**. Any such metric has (Hendy, 1992) a unique tree representation.

  A metric d on a set X is called a **relaxed tree-like metric** if the set X can be embedded in some (not necessary positively) edge-weighted tree such that, for any $x, y \in X$, $d(x, y)$ is equal to the sum of all edge weights along the (unique) path between corresponding vertices x and y in the tree. A metric is a relaxed tree-like metric if and only if it satisfies the **relaxed four-point inequality**.

- **Katz similarity**

  Given a connected graph $G = (V, E)$ with positive edge-weight function $w = (w(e))_{e\in E}$, let $V = \{v_1, \ldots, v_n\}$. Denote by A the $(n \times n)$-matrix $((a_{ij}))$, where $a_{ij} = a_{ji} = w(ij)$ if ij is an edge, and $a_{ij} = 0$, otherwise. Let I be the identity

$(n \times n)$-matrix, and let $t, 0 < t < \frac{1}{\lambda}$, be a parameter, where $\lambda = \max_i |\lambda_i|$ is the *spectral radius* of A and λ_i are the eigenvalues of A. Define the $(n \times n)$-matrix

$$K = ((k_{ij})) = \sum_{i=1}^{\infty} t^i A^i = (I - tA)^{-1} - I.$$

The number k_{ij} is called the **Katz similarity** between v_i and v_j. Katz, 1953, proposed it for evaluating social status.

Chebotarev, 2011, defined, for a similar $(n \times n)$-matrix $((c_{ij})) = \sum_{i=0}^{\infty} t^i A^i = (I - tA)^{-1}$ and connected edge-weighted multigraphs allowing loops, the **walk distance** between vertices v_i and v_j as any positive multiple of $d_t(i,j) = -\ln \frac{c_{ij}}{\sqrt{c_{ii}\, c_{jj}}}$ (cf. the **Nei standard genetic distance** in Chap. 23). He proved that d_t is a **cutpoint additive metric** and the **path metric** in G coincides with the *short walk distance* $\lim_{t \to 0+} \frac{d_t}{-\ln t}$ in G, while the **resistance metric** in G coincides with the *long walk distance* $\lim_{t \to \frac{1}{\lambda}-} \frac{2d_t}{n(t^{-1}-\lambda)}$ in the graph G' obtained from G by attaching weighted loops that provide G' with uniform weighted degrees.

If G is a simple unweighted graph, then A is its adjacency matrix. Let J be the $(n \times n)$-matrix of all ones and let $\mu = \min_i \lambda_i$. Let $N = ((n_{ij})) = \mu(I - J) - A$. Neumaier, 1980, remarked that $((\sqrt{n_{ij}}))$ is a semimetric on the vertices of G.

- **Resistance metric**

  Given a connected graph $G = (V, E)$ with positive edge-weight function $w = (w(e))_{e \in E}$, let us interpret the edge-weights as electrical conductances and their inverses as resistances. For any two different vertices u and v, suppose that a battery is connected across them, so that one unit of a current flows in at u and out in v. The voltage (potential) difference, required for this, is, by Ohm's law, the effective resistance between u and v in an electrical network; it is called the **resistance** (or *electric*) **metric** $\Omega(u, v)$ between them (Sharpe, 1967, Gvishiani–Gurvich, 1987, and Klein–Randic, 1993). So, if a potential of one volt is applied across vertices u and v, a current of $\frac{1}{\Omega(u,v)}$ will flow. The number $\frac{1}{\Omega(u,v)}$ is a measure of the *connectivity* between u and v.

  Let $r(u, v) = \frac{1}{w(e)}$ if uv is an edge, and $r(u, v) = 0$, otherwise. Formally,

$$\Omega(u, v) = (\sum_{w \in V} f(w) r(w, v))^{-1},$$

where $f : V \to [0, 1]$ is the unique function with $f(u) = 1, f(v) = 0$ and $\sum_{z \in V} (f(w) - f(z)) r(w, z) = 0$ for any $w \neq u, v$.

The resistance metric is a weighted average of the lengths of all $(u - v)$ paths. It is applied when the number of $(u - v)$ paths, for any $u, v \in V$, matters.

A probabilistic interpretation (Gobel–Jagers, 1974) is: $\Omega(u, v) = (deg(u) Pr(u \to v))^{-1}$, where $deg(u)$ is the degree of the vertex u, and $Pr(u \to v)$ is the probability for a random walk leaving u to arrive at v before returning to u. The expected commuting time between u and v is $2 \sum_{e \in E} w(e) \Omega(u, v)$.

Then $\Omega(u,v) \leq \min_P \sum_{e\in P} \frac{1}{w(e)}$, where P is any $(u-v)$ path (cf. **inverse weighted path metric**), with equality if and only if such a path P is unique. So, if $w(e) = 1$ for all edges, the equality means that G is a **geodetic graph**, and hence the path and resistance metrics coincide. Also, it holds that $\Omega(u,v) = \frac{|\{T: uv\in t\in T\}|}{|T|}$ if uv is an edge, and $\Omega(u,v) = \frac{|T'-T|}{|T|}$, otherwise, where T, T' are the sets of spanning trees for $G = (V,E)$ and $G' = (V, E\cup\{uv\})$.

If $w(e) = 1$ for all edges, then $\Omega(u,v) = (g_{uu} + g_{vv}) - (g_{uv} + g_{vu})$, where $((g_{ij}))$ is the Moore–Penrose *generalized inverse* of the *Laplacian matrix* $((l_{ij}))$ of the graph G: here l_{ii} is the degree of vertex i, while, for $i \neq j$, $l_{ij} = -1$ if the vertices i and j are adjacent, and $l_{ij} = 0$, otherwise. A symmetric (for an undirected graph) and positive-semidefinite matrix $((g_{ij}))$ admits a representation KK^T. So, $\Omega(u,v)$ is the squared Euclidean distance between the u-th and v-th rows of K.

The distance $\sqrt{\Omega(u,v)}$ is a **Mahalanobis distance** (Chap. 17) with a weighting matrix $((g_{ij}))$. So, $\Omega_{u,v} = a_{uv}|((g_{ij}))|a_{uv}$, where a_{uv} are the vectors of zeros except for $+1$ and -1 in the u-th and v-th positions. This distance is called a *diffusion metric* in [CLMNWZ05] because it depends on a random walk.

The number $\frac{1}{2}\sum_{u,v\in V}\Omega(u,v)$ is called the *total resistance* (or *Kirchhoff index*) of G.

- **Hitting time quasi-metric**

  Let $G = (V,E)$ be a connected graph. Consider random walks on G, where at each step the walk moves to a vertex randomly with uniform probability from the neighbors of the current vertex. The **hitting** (or *first-passage*) **time quasi-metric** $H(u,v)$ from $u \in V$ to $v \in V$ is the expected number of steps (edges) for a random walk on G beginning at u to reach v for the first time; it is 0 for $u = v$. This quasi-metric is a **weightable quasi-semimetric** (Chap. 1).

  The **commuting time metric** is $C(u,v) = H(u,v) + H(v,u)$.

  Then $C(u,v) = 2|E|\Omega(u,v)$, where $\Omega(u,v)$ is the **resistance metric** (or *effective resistance*), i.e., 0 if $u = v$ and, otherwise, $\frac{1}{\Omega(u,v)}$ is the current flowing into v, when grounding v and applying a 1 volt potential to u (each edge is seen as a resistor of 1 ohm). Also, $\Omega(u,v) = \sup_{f:V\to\mathbb{R}, D(f)>0} \frac{(f(u)-f(v))^2}{DE(f)}$, where $DE(f)$ is the *Dirichlet energy* of f, i.e., $\sum_{st\in E}(f(s)-f(t))^2$.

  The above setting can be generalized to weighted digraphs $D = (V,E)$ with arc-weights c_{ij} for $ij \in E$ and the *cost* of a directed $(u-v)$ path being the sum of the weights of its arcs. Consider the random walk on D, where at each step the walk moves by arc ij with *reference probability* p_{ij} proportional to $\frac{1}{c_{ij}}$; set $p_{ij} = 0$ if $ij \notin E$. Saerens et al., 2008, defined the *randomized* et al. *shortest path quasi-distance* $d(u,v)$ on vertices of D as the minimum expected cost of a directed $(u-v)$ path in the probability distribution minimizing the expected cost among all distributions having a fixed **Kullback–Leibler distance** (Chap. 14) with reference probability distribution. In fact, their biased random walk model depends on a parameter $\theta \geq 0$. For $\theta = 0$ and large θ, the distance $d(u,v) + d(v,u)$ become a metric; it is proportional to the commuting time and the usual path metric, respectively.

- **Chebotarev–Shamis metric**

  Given $\alpha > 0$ and a connected weighted *multigraph* $G = (V, E; w)$ with positive edge-weight function $w = (w(e))_{e\in E}$, denote by $L = ((l_{ij}))$ the *Laplacian* (or *Kirchhoff*) matrix of G, i.e., $l_{ij} = -w(ij)$ for $i \neq j$ and $l_{ii} = \sum_{j\neq i} w(ij)$. The **Chebotarev–Shamis metric** $d_\alpha(u, v)$ (Chebotarev and Shamis, 2000, called $\frac{1}{2}d_\alpha(u, v)$ **α-forest metric**) between vertices u and v is defined by

  $$2q_{uv} - q_{uu} - q_{vv}$$

  for the **protometric** $((g_{ij})) = -(I + \alpha L)^{-1}$, where I is the identity matrix.

  Chebotarev and Shamis showed that their metric of $G = (V, E; w)$ is the **resistance metric** of another weighted multigraph, $G' = (V', E'; w')$, where $V' = V \cup \{0\}$, $E' = E \cup \{u0 : u \in V\}$, while $w'(e) = \alpha w(e)$ for all $e \in E$ and $w'(u0) = 1$ for all $u \in V$. In fact, there is a bijection between the forests of G and trees of G'. This metric becomes the resistance metric of $G = (V, E; w)$ as $\alpha \to \infty$.

  Their **forest metric** (1997) is the case $\alpha = 1$ of the α-forest metric.

  Chebotarev, 2010, remarked that $2\ln q_{uv} - \ln q_{uu} - \ln q_{vv}$ is a **cutpoint additive metric** $d''_\alpha(u, v)$, i.e., $d''_\alpha(u, w) + d''_\alpha(w, v) = d''_\alpha(u, v)$ holds if and only if w lies on any path connecting u and v. The metric d''_α is the **path metric** if $\alpha \to 0^+$ and the **resistance metric** if $\alpha \to \infty$.

- **Truncated metric**

  The **truncated metric** is a metric on the vertex-set of a graph, which is equal to 1 for any two adjacent vertices, and is equal to 2 for any nonadjacent different vertices. It is the 2**-truncated metric** for the path metric of the graph. It is the $(1, 2) - B$**-metric** if the degree of any vertex is at most B.

- **Hsu–Lyuu–Flandrin–Li distance**

  Given an *m-connected* graph $G = (V, E)$ and two vertices $u, v \in V$, a *container* $C(u, v)$ *of width* m is a set of m $(u - v)$ paths with any two of them intersecting only in u and v. The *length of a container* is the length of the longest path in it.

  The **Hsu–Lyuu–Flandrin–Li distance** between vertices u and v (Hsu–Lyuu, 1991, and Flandrin–Li, 1994) is the minimum of container lengths taken over all containers $C(u, v)$ of width m. This generalization of the path metric is used in parallel architectures for interconnection networks.

- **Multiply-sure distance**

  The **multiply-sure distance** is a distance on the vertex-set V of an *m-connected* weighted graph $G = (V, E)$, defined, for any $u, v \in V$, as the minimum weighted sum of lengths of m disjoint $(u-v)$ paths. This generalization of the path metric helps when several disjoint paths between two points are needed, for example, in communication networks, where $m - 1$ of $(u - v)$ paths are used to code the message sent by the remaining $(u - v)$ path (see [McCa97]).

- **Cut semimetric**

  A *cut* is a *partition* of a set into two parts. Given a subset S of $V_n = \{1,\dots,n\}$, we obtain the partition $\{S, V_n \backslash S\}$ of V_n. The **cut semimetric** (or **split semimetric**) δ_S defined by this partition, is a semimetric on V_n defined by

$$\delta_S(i,j) = \begin{cases} 1, & \text{if } i \neq j, |S \cap \{i,j\}| = 1, \\ 0, & \text{otherwise.} \end{cases}$$

  Usually, it is considered as a vector in $\mathbb{R}^{|E_n|}$, $E(n) = \{\{i,j\} : 1 \leq i < j \leq n\}$.

  A *circular cut* of V_n is defined by a subset $S_{[k+1,l]} = \{k+1,\dots,l\}(\mod n) \subset V_n$: if we consider the points $\{1,\dots,n\}$ as being ordered along a circle in that circular order, then $S_{[k+1,l]}$ is the set of its consecutive vertices from $k+1$ to l. For a circular cut, the corresponding cut semimetric is called a **circular cut semimetric**.

  An **even cut semimetric** (**odd cut semimetric**) is δ_S on V_n with even (odd, respectively) $|S|$. A k**-uniform cut semimetric** is δ_S on V_n with $|S| \in \{k, n-k\}$. An **equicut semimetric** (**inequicut semimetric**) is δ_S on V_n with $|S| \in \{\lfloor \frac{n}{2} \rfloor, \lceil \frac{n}{2} \rceil\}$ ($|S| \notin \{\lfloor \frac{n}{2} \rfloor, \lceil \frac{n}{2} \rceil\}$, respectively); see, for example, [DeLa97].

- **Decomposable semimetric**

  A **decomposable semimetric** is a semimetric on $V_n = \{1,\dots,n\}$ which can be represented as a nonnegative linear combination of **cut semimetrics**. The set of all decomposable semimetrics on V_n is a *convex cone*, called the *cut cone* CUT_n.

  A semimetric on V_n is decomposable if and only if it is a **finite** l_1**-semimetric**.

  A **circular decomposable semimetric** is a semimetric on $V_n = \{1,\dots,n\}$ which can be represented as a nonnegative linear combination of **circular cut semimetrics**. A semimetric on V_n is circular decomposable if and only if it is a **Kalmanson semimetric** with respect to the same ordering (see [ChFi98]).

- **Finite** l_p**-semimetric**

  A **finite** l_p**-semimetric** d is a semimetric on $V_n = \{1,\dots,n\}$ such that (V_n, d) is a semimetric subspace of the l_p^m*-space* $(\mathbb{R}^m, d_{l_p})$ for some $m \in \mathbb{N}$.

  If, instead of V_n, is taken $X = \{0,1\}^n$, the metric space (X,d) is called the l_p^n*-cube*. The l_1^n-cube is called a **Hamming cube**; cf. Chap. 4. It is the graphic metric space associated with a hypercube graph $H(n,2)$, and any subspace of it is called a **partial cube**.

- **Kalmanson semimetric**

  A **Kalmanson semimetric** d *with respect to the ordering* $1,\dots,n$ is a semimetric on $V_n = \{1,\dots,n\}$ which satisfies the condition

$$\max\{d(i,j) + d(r,s), d(i,s) + d(j,r)\} \leq d(i,r) + d(j,s)$$

  for all $1 \leq i \leq j \leq r \leq s \leq n$.

  Equivalently, if the points $\{1,\dots,n\}$ are ordered along a circle C_n in that circular order, then the distance d on V_n is a Kalmanson semimetric if the

inequality

$$d(i,r) + d(j,s) \leq d(i,j) + d(r,s)$$

holds for $i,j,r,s \in V_n$ whenever the segments $[i,j]$, $[r,s]$ are crossing chords of C_n.

A **tree-like metric** is a Kalmanson metric for some ordering of the vertices of the tree. The Euclidean metric, restricted to the points that form a convex polygon in the plane, is a Kalmanson metric.

- **Multicut semimetric**

  Let $\{S_1,\ldots,S_q\}$, $q \geq 2$, be a *partition* of the set $V_n = \{1,\ldots,n\}$, i.e., a collection $S_1,\ldots,S_q$ of pairwise disjoint subsets of V_n such that $S_1 \cup \cdots \cup S_q = V_n$.

  The **multicut semimetric** $\delta_{S_1,\ldots,S_q}$ is a semimetric on V_n defined by

$$\delta_{S_1,\ldots,S_q}(i,j) = \begin{cases} 0, & \text{if } i,j \in S_h \text{ for some } h, 1 \leq h \leq q, \\ 1, & \text{otherwise.} \end{cases}$$

- **Oriented cut quasi-semimetric**

  Given a subset S of $V_n = \{1,\ldots,n\}$, the **oriented cut quasi-semimetric** δ'_S is a quasi-semimetric on V_n defined by

$$\delta'_S(i,j) = \begin{cases} 1, & \text{if } i \in S, j \notin S, \\ 0, & \text{otherwise.} \end{cases}$$

  Usually, it is considered as the vector of $\mathbb{R}^{|I_n|}$, $I(n) = \{(i,j) : 1 \leq i \neq j \leq n\}$. The **cut semimetric** δ_S is $\delta'_S + \delta'_{V_n \setminus S}$.

- **Oriented multicut quasi-semimetric**

  Given a *partition* $\{S_1,\ldots,S_q\}$, $q \geq 2$, of V_n, the **oriented multicut quasi-semimetric** $\delta'_{S_1,\ldots,S_q}$ is a quasi-semimetric on V_n defined by

$$\delta'_{S_1,\ldots,S_n}(i,j) = \begin{cases} 1, & \text{if } \quad i \in S_h, j \in S_m, h < m, \\ 0, & \text{otherwise} \quad . \end{cases}$$

15.2 Distance-Defined Graphs

Below we first give some graphs defined in terms of distances between their vertices. Then some graphs associated with metric spaces are presented.

A graph (V,E) is, say, *distance-invariant* or *distance monotone* if its metric space (V, d_{path}) is **distance invariant** or **distance monotone**, respectively (cf. Chap. 1). The definitions of such graphs, being straightforward subcases of corresponding metric spaces, will be not given below.

- **k-power of a graph**

  The **k-power** of a graph $G = (V, E)$ is the supergraph $G^k = (V, E')$ of G with edges between all pairs of vertices having path distance at most k.
- **Distance-residual subgraph**

  For a connected finite graph $G = (V, E)$ and a set $M \subset V$ of its vertices, a **distance-residual subgraph** is (Luksic and Pisanski, 2010) a subgraph induced on the set of vertices u of G at the maximal **point-set distance** $\min_{v \in M} d_{\text{path}}(u, v)$ from M. Such a subgraph is called *vertex-residual* if M consists of a vertex, and *edge-residual* if M consists of two adjacent vertices.
- **Isometric subgraph**

  A subgraph H of a graph $G = (V, E)$ is called an **isometric subgraph** if the path metric between any two points of H is the same as their path metric in G.

  A subgraph H is called a *convex subgraph* if it is isometric, and for any $u, v \in H$ every vertex on a shortest $(u - v)$ path belonging to H also belongs to H. Taking, instead of shortest, other types of paths (say, any, longest, induced) or walks, one gets corresponding notions of convexity.

  A subset $M \subset V$ is called *gated* if for every $u \in V \setminus M$ there exists a unique vertex $g \in M$ (called a *gate*) lying on a shortest $(u - v)$ path for every $v \in M$. The subgraph induced by a gated set is a convex subgraph.
- **Retract subgraph**

  A subgraph H of G is called a **retract subgraph** if it is induced by an idempotent **metric mapping** of G into itself, i.e., $f^2 = f : V \to V$ with $d_{\text{path}}(f(u), f(v)) \leq d_{\text{path}}(u, v)$ for $u, v \in V$. Any retract subgraph is isometric.
- **Partial cube**

  A **partial cube** is an **isometric subgraph** of a **Hamming cube**, i.e., of a hypercube $H(m, 2)$. Similar topological notion was introduced by Acharya, 1983: any graph (V, E) admits a *set-indexing* $f : V \cup E \to 2^X$ with injective $f|_V, f|_R$ and $f(uv) = f(u) \Delta f(v)$ for any $(uv) \in E$. The *set-indexing number* is $\min |X|$.
- **Median graph**

  A connected graph $G = (V, E)$ is called a **median graph** if, for any three vertices $u, v, w \in V$, there exists a unique vertex that lies simultaneously on a shortest $(u - v)$, $(u - w)$ and $(w - v)$ paths, i.e., (V, d_{path}) is a **median metric space**.

  The median graphs are exactly **retract subgraphs** of hypercubes and exactly 1-skeletons of a **CAT(0)** cube complexes. Also, they are exactly **partial cubes** such that the vertex-set of any *convex subgraph* is *gated* (cf. **isometric subgraph**).
- **Geodetic graph**

  A graph is called **geodetic** if there exists at most one shortest path between any two of its vertices. A graph is called *strongly geodetic* if there exists at most one path of length less than or equal to the diameter between any two of its vertices.

  A *uniformly geodetic graph* is a connected graph such that the number of shortest paths between any two vertices u and v depends only on $d(u, v)$.

  A graph is a *forest* (disjoint union of trees) if and only if there exists at most one path between any two of its vertices.

The *geodetic number* of a finite connected graph (V, E) ([BuHa90]) is $\min |M|$ over sets $M \subset V$ such that any $x \in V$ lies on a shortest $(u-v)$ path with $u, v \in M$.

- **k-geodetically connected graph**

  A k-connected graph is called (Entringer–Jackson–Slater, 1977) **k-geodetically connected** ($k - GC$) if the removal of less than k vertices (or, equivalently, edges) does not affect the **path metric** between any pair of the remaining vertices.

  $2 - GC$ graphs are called *self-repairing*. Cf. **Hsu–Lyuu–Flandrin–Li distance**.

- **Interval distance monotone graph**

  A connected graph $G = (V, E)$ is called **interval distance monotone** if any of its intervals $I_G(u, v)$ induces a *distance monotone graph*, i.e., its path metric is **distance monotone**, cf. Chap. 1.

  A graph is interval distance monotone if and only if (Zhang–Wang, 2007) each of its intervals is isomorphic to either a path, a cycle or a hypercube.

- **Distance-regular graph**

  A connected *regular* (i.e., every vertex has the same degree) graph $G = (V, E)$ of diameter T is called **distance-regular** (or *drg*) if, for every two its vertices u, v and any integers $0 \le i, j \le T$, the number $|\{w \in V : d_{\text{path}}(u, w) = i, d_{\text{path}}(v, w) = j\}|$ depends only on i, j and $k = d_{\text{path}}(u, v)$, but not on the choice of u and v.

  A special case of it is a **distance-transitive graph**, i.e., such that its group of automorphisms is transitive, for any $0 \le i \le T$, on the pairs of vertices (u, v) with $d_{\text{path}}(u, v) = i$. Given a number $s, 1 \le s \le T$, a graph is said to be *s-geodesic-transitive* or *s-distance transitive* if its automorphism group acts transitively on the sets of *i-geodesics* (shortest paths of length i), for $0 \le i \le s$, or, respectively, on the sets of ordered vertex pairs at distance i, for $0 \le i \le s$.

  Any drg is a **distance-balanced graph** (or *dbg*), i.e., $|W_{u,v}| = |W_{v,u}|$, where $W_{u,v} = \{x \in V : d(x, u) < d(x, v)\}$. Such graph is also called *self-median* since it is exactly one, **metric median** (cf. **eccentricity** in Chap. 1) of which is V. A gbg is called *nicely distance-balanced* if $|W_{u,v}|$ is the same for all edges uv.

  Any drg is a **distance degree-regular graph** (i.e., $|\{x \in V : d(x, u) = i\}|$ depends only on i; such graph is also called *strongly distance-balanced*), and a **walk-regular graph** (i.e., the number of closed walks of length i starting at u depends only on i). van Dam–Omidi, 2013, call a graph *strongly walk-regular* if there is an $l \ge 2$ such that the number of walks of length l from u to v depends only on whether the $d(u, v)$ is 0, 1, or ≥ 2; for $l = 2$, it is a *strongly regular graph*, i.e., a drg of diameter 2. A *d-Deza graph* (Gu, 2013) is a regular graph (V, E) in which there are exactly d different values of $|\{w \in V : d(u, w) = d(v, w) = 1\}|$ for distinct $u, v \in V$.

  Any drg is a **sphere-regular graph** (Dehmer, 2008), i.e., its path metric is **distance-invariant** (all closed balls of the same radius have the same size; cf. Chap. 1).

  A graph G is a **distance-regularized graph** if for each $u \in V$, if admits an *intersection array at vertex u*, i.e., the numbers $a_i(u) = |G_i(u) \cap G_1(v)|$, $b_i(u) = |G_{i+1}(u) \cap G_1(v)|$ and $c_i(u) = |G_{i-1}(v) \cap G_1(v)|$ depend only on the

distance $d(u, v) = i$ and are independent of the choice of the vertex $v \in G_i(u)$. Here, for any i, $G_i(w)$ is the set of all vertices at the distance i from w. Godsil–Shawe-Taylor, 1987, defined such graph and proved that it is either drg or *distance-biregular* (a bipartite one with vertices in the same class having the same intersection array).

A drg is also called a **metric association scheme** or *P-polynomial association scheme*. A finite **polynomial metric space** (Chap. 1) is a special case of it, also called a *(P and Q)-polynomial association scheme*.

- **Distance-regular digraph**

  A strongly connected digraph $D = (V, E)$ is called **distance-regular** (Damerell, 1981) if, for any its vertices u, v with $d_{\text{path}}(u, v) = k$ and for any integer $0 \le i \le k + 1$, the number of vertices w, such that $d_{\text{path}}(u, w) = i$ and $d_{\text{path}}(v, w) = 1$, depends only on k and i, but not on the choice of u and v. In order to find interesting classes of distance-regular digraphs with unbounded diameter, the above definition was weakened by two teams in different directions.

  Call $\overline{d(x, y)} = (d(x, y), d(y, x))$ the **two-way distance in digraph** D. A strongly connected digraph $D = (V, E)$ is called **weakly distance-regular** (Wang and Suzuku, 2003) if, for any its vertices u, v with $\overline{d(u, v)} = (k_1, k_2)$, the number of vertices w, such that $\overline{d(w, u)} = (i_1, i_2)$ and $\overline{d(w, v)} = (j_1, j_2)$, depends only on the values $k_1, k_2, i_1, i_2, j_1, j_2$. Comellas et al., 2004, defined a **weakly distance-regular digraph** as one in which, for any vertices u and v, the number of $u \to v$ walks of every given length only depends on the distance $d(u, v)$.

- **Metrically almost transitive graph**

  An *automorphism* of a graph $G = (V, E)$ is a map $g : V \to V$ such that u is adjacent to v if and only if $g(u)$ is adjacent to $g(v)$, for any $u, v \in V$. The set $Aut(G)$ of automorphisms of G is a group with respect to the composition of functions.

  A graph G is **metrically almost transitive** (Krön–Möller, 2008) if there is an integer r such that, for any vertex $u \in V$ it holds

$$\cup_{g \in Aut(G)} \{g(\overline{B}(u, r) = \{v \in V : d_{\text{path}}(u, v) \le r\})\} = V.$$

- **Metric end**

  Given an infinite graph $G = (V, E)$, a *ray* is a sequence $(x_0, x_1, \ldots)$ of distinct vertices such that x_i and x_{i+1} are adjacent for $i \ge 0$.

  Two rays R_1 and R_2 are equivalent whenever it is impossible to find a bounded—set of vertices F such that any path from R_1 to R_2 contains an element of F.

  Metric ends are defined as equivalence classes of *metric rays* which are rays without infinite, bounded subsets.

- **Graph of polynomial growth**

  Let $G = (V, E)$ be a transitive locally finite graph. For a vertex $v \in V$, the *growth function* is defined by

  $$f(n) = |\{u \in V : d(u, v) \leq n\}|,$$

  and it does not depend on v. Cf. **growth rate of metric space** in Chap. 1.

  The graph G is a **graph of polynomial growth** if there are some positive constants k, C such that $f(n) \leq Cn^k$ for all $n \geq 0$. It is a **graph of exponential growth** if there is a constant $C > 1$ such that $f(n) > C^n$ for all $n \geq 0$.

  A group with a finite symmetric set of generators has *polynomial growth rate* if the corresponding *Cayley graph* has polynomial growth. Here the metric ball consists of all elements of the group which can be expressed as products of at most n generators, i.e., it is a closed ball centered in the identity in the **word metric**, cf. Chap. 10.

- **Distance-polynomial graph**

  Given a connected graph $G = (V, E)$ of diameter T, for any $2 \leq i \leq T$ denote by G_i the graph (V, E') with $E' = \{e = uv \in E : d_{\text{path}}(u, v) = i\}$. The graph G is called a **distance-polynomial** if the adjacency matrix of any G_i, $2 \leq i \leq T$, is a polynomial in terms of the adjacency matrix of G.

  Any **distance-regular** graph is a distance-polynomial.

- **Distance-hereditary graph**

  A connected graph is called **distance-hereditary** (Howorka, 1977) if each of its connected induced subgraphs is isometric.

  A graph is distance-hereditary if each of its induced paths is isometric. A graph is distance-hereditary, bipartite distance-hereditary, **block graph**, tree if and only if its path metric is a **relaxed tree-like metric** for edge-weights being, respectively, nonzero half-integers, nonzero integers, positive half-integers, positive integers.

  A graph is called a **parity graph** if, for any $u, v \in V$, the lengths of all induced $(u-v)$ paths have the same parity. A graph is a parity graph (moreover, distance-hereditary) if and only if every induced subgraph of odd (moreover, any) order of at least five has an even number of Hamiltonian cycles (McKee, 2008).

- **Distance magic graph**

  A graph $G = (V, E)$ is called (Vilfred, 1994) a **distance magic graph** if it admits a *distance magic labeling*, i.e., a *magic constant* $k > 0$ and a bijection $f : V \to \{1, 2, \ldots, |V|\}$ with $w(v) = \sum_{uv \in E} f(v) = k$ for every $u \in V$.

  Cf. **rendez-vous number** in Chap. 1. These graphs generalize *magic squares* (such complete n-partite graphs with parts of size n). Among such trees, cycles and K_n, only P_1, P_3, C_4 are distance magic. The *hypercube graph* $H(m, 2)$ is distance magic if $m = 2, 6$ but not if $m \equiv 0, 1, 3 \pmod 4$.

  The graph $G = (V, E)$ is said (Kamatchi–Arumugam, 2013) to be *distance anti-magic* if $w(u) \neq w(v)$ for all $u, v \in V$. Cichacz et al., 2015, extended both above notions on vertex-labeling by elements of an Abelian group.

The graph $G = (V, E)$ is said (O'Neil–Slater, 2011) to be *D-distance magic* if it admits a ***D*-distance magic labeling**, i.e., a *magic constant* $k > 0$ and a bijection $f : V \to \{1, 2, \ldots, |V|\}$ with $w(v) = \sum_{u \in V: d(u,v) \in D} f(u) = k$ for every $u \in V$.

- **Block graph**

  A graph is called a **block graph** if each of its *blocks* (i.e., a maximal 2-connected induced subgraph) is a complete graph. Any tree is a block graph.

  A graph is a block graph if and only if its path metric is a **tree-like metric** or, equivalently, satisfies the **four-point inequality**.

- **Ptolemaic graph**

  A graph is called **Ptolemaic** if its path metric satisfies the **Ptolemaic inequality**

$$d(x, y)d(u, z) \le d(x, u)d(y, z) + d(x, z)d(y, u).$$

  A graph is Ptolemaic if and only if it is distance-hereditary and *chordal*, i.e., every cycle of length greater than 3 has a chord. So, any **block graph** is Ptolemaic.

- ***k*-cocomparability graph**

  A graph $G = (V, E)$ is called (Chang–Ho–Ko, 2003) ***k*-cocomparability graph** if its vertex-set admits a linear ordering $<$ such that for any three vertices $u < v < w$, $d(u, w) \le k$ implies $d(u, v) \le k$ or $d(v, w) \le k$.

- **Distance-perfect graph**

  Cvetković et al., 2007, observed that any graph of diameter T has at most $k + T^k$ vertices, where k is its **location number** (Chap. 1), i.e., the minimal cardinality of a set of vertices, the path distances from which uniquely determines any vertex. They called a graph **distance-perfect** if it meets this upper bound and proved that such a graph has $T \ne 2$.

- ***t*-irredundant set**

  A set $S \subset V$ of vertices in a connected graph $G = (V, E)$ is called ***t*-irredundant** (Hattingh–Henning, 1994) if for any $u \in S$ there exists a vertex $v \in V$ such that, for the path metric d_{path} of G, it holds

$$d_{\text{path}}(v, x) \le t < d_{\text{path}}(v, V \backslash S) = \min_{u \notin S} d_{\text{path}}(v, u).$$

  The ***t*-irredundance number** ir_t of G is the smallest cardinality $|S|$ such that S is t-irredundant but $S \cup \{v\}$ is not, for every $v \in V \backslash S$.

  The *t-independent number* α_t and **distance t-domination number** γ_t of G are, respectively, the cardinality of the largest $\lceil \frac{t}{2} \rceil$*-packing* and smallest $(t + 1)$-*covering* (by the open balls of the radius $t+1$) of the metric space $(V, d_{\text{path}}(u, v))$; cf. the **radii of metric space** in Chap. 1. Then it holds $\frac{\gamma_t + 1}{2} \le ir_t \le \gamma_t \le \alpha_t$.

  Let C_r be the largest constant such that $\gamma_1 \ge C_r \sum_{1 \le i < j \le r} d(x_i, x_j)$ for r vertices of any connected graph; Kang, 2015, showed that $C_2 = \frac{1}{3}$ and $C_r = \frac{1}{r(r-1)}$ for $r \ge 3$, implying that $\gamma_1 \ge ad(G)$, where ad denotes the average distance.

The *distance t-vertex cover number* of G is (Canales et al., 2015) the minimum cardinality of the set $S \subset V$, such that for each edge e of G, there is a path of length at most t that contains e and a vertex from S.

If G is plane graph, then its *distance t-guarding number* is (Canales et al., 2015) the minimum cardinality of the set $S \subset V$, such that for every face f of G, there is a vertex u in the boundary of f, and a vertex $v \in S$ with $d_{\text{path}}(u, v) < t$.

- ***r*-locating-dominating set**

  Let D=(V,E) be a digraph and $C \subset V$, and let $B_r^-(v)$ denote the set of all vertices x such that there exists a directed $(x - v)$ path with at most r arcs.

  If $B_r^-(v) \cap C$, $v \in V \setminus C$ (respectively, $v \in V$), are nonempty distinct sets, C is called (Slater, 1984) an ***r*-locating-dominating set** (respectively, an ***r*-identifying code**; cf. Chap. 16) of D. Such sets of smallest cardinality are called *optimal*.

- **Locating chromatic number**

  The **locating chromatic number** of a graph $G = (V, E)$ is the minimum number of color classes $C_1, \ldots, C_t$ needed to color vertices of G so that any two adjacent vertices have distinct colors and each vertex $u \in V$ has distinct *color code* $(\min_{v \in C_1} d(u, v), \ldots, \min_{v \in C_k} d(u, v))$.

- ***k*-distant chromatic number**

  The ***k*-distant chromatic number** of a graph $G = (V, E)$ is the minimum number of colors needed to color vertices of G so that any two vertices at distance at most k have distinct colors, i.e., it is the chromatic number of the ***k*-power of** G.

- **Distance between edges**

  The **distance between edges** in a connected graph $G = (X, E)$ is the number of vertices in a shortest path between them. So, adjacent edges have distance 1.

  A **distance-*k* matching** of G is a set of edges no two of which are within distance k. For $k = 1$, it is the usual matching. For $k = 2$, it is also *induced* (or *strong*) matching. A distance-k matching of G is equivalent to an independent set in the ***k*-power** of the line graph of G. A **distance-*k* edge-coloring** of G is an edge-coloring such that each color class induces a distance-k matching.

  The **distance-*k* chromatic index** $\mu_k(G)$ is the least integer t such that there exists a distance-t edge-coloring of G. The **distance-*k* matching number** $\nu_k(G)$ is the largest integer t such that there exists a distance-t matching in G with t edges. It holds that $\mu_k(G)\nu_k(G) \geq |E|$.

  The **distance between faces** of a plane graph is the number of vertices in a shortest path between them. A **distance-*k* face-coloring** is a face-coloring such that any two faces at distance at most k have different colors. The **distance-*k* face chromatic index** is the least integer t such that such coloring by t colors exists. The dual notion is *k-distance coloring* of a graph $G = (V, E)$, i.e., a vertex-coloring such that any two vertices at distance at most k receives different colors.

- **Distance integral graph**

  Given a finite graph G, its **distance polynomial** (cf. Chap. 1) is the determinant $det(D - \lambda I)$, where D is the distance matrix of the path metric of G.

  A graph is called **distance integral** if all roots of this polynomial are integers.

- ***D*-distance graph**

  Given a set D of positive numbers containing 1 and a metric space (X, d), the ***D*-distance graph** is a graph $G = (V = X, E)$ with the edge-set $E = \{uv : d(u, v) \in D\}$ (cf. **D-chromatic number** in Chap. 1). If (X, d) is path metric of a graph H, then G is called the **distance power** H^D of H.

  Alon–Kupavsky, 2014, call G (in the case $(X, d) = \mathbb{E}^n$, $d = \{1\}$) the *faithful unit-distance graph*, using term *unit-distance graph* for $E \subseteq \{(u, v) : ||u-v||_2 = 1\}$.

  For a positive number t, the *signed distance graph* is (Fiedler, 1969) a signed graph with the vertex-set X in which vertices x, y are joined by a positive edge if $t > d(x, y)$, by a negative edge if $d(x, y) > t$, and not joined if $d(x, y) = t$.

  A D-distance graph is called a **distance graph** (or *unit-distance graph*) if $D = \{1\}$, an *ϵ-unit graph* if $D = [1 - \epsilon, 1 + \epsilon]$, a *unit-neighborhood graph* if $D = (0, 1]$, an *integral-distance graph* if $D = \mathbb{Z}_+$, a *rational-distance graph* if $D = \mathbb{Q}_+$, and a *prime-distance graph* if D is the set of prime numbers (with 1).

  Every finite graph can be represented by a D-distance graph in some $\mathbb{E}^n$. The minimum dimension of such a Euclidean space is called the *D-dimension* of G. A *matchstick graph* is a crossingless unit-distance graph in $\mathbb{E}^2$.
- **Distance-number of a graph**

  Given a graph $G = (V, E)$, its *degenerate drawing* is a mapping $f : V \to \mathbb{R}^2$ such that $|f(V)| = |V|$ and $f(uv)$ is an open straight-line segment joining the vertices $f(u)$ and $f(v)$ for any edge $uv \in E$; it is a *drawing* if, moreover, $f(w) \notin f(uv)$ for any $uv \in E$ and $w \in V$.

  The **distance-number** $dn(G)$ **of a graph** G is (Carmi et al. 2008) the minimum number of distinct edge-lengths in a drawing of G.

  The *degenerate distance-number* of G, denoted by $ddn(G)$, is the minimum number of distinct edge-lengths in a degenerated drawing of G. The first of the **Erdös-type distance problems** in Chap. 19 is equivalent to determining $ddn(K_n)$.
- **Dimension of a graph**

  The **dimension** $dim(G)$ **of a graph** G is (Erdös–Harary–Tutte, 1965) the minimum k such that G has a *unit-distance representation* in $\mathbb{R}^k$, i.e., every edge is of length 1. The vertices are mapped to distinct points of $\mathbb{R}^k$, but edges may cross.

  For example, $dim(G) = n - 1, 4, 2$ for $G = K_n, K_{m,n}, C_n$ $(m \geq n \geq 3)$.
- **Bar-and-joint framework**

  A n-dimensional **bar-and-joint framework** is a pair (G, f), where $G = (V, E)$ is a finite graph (no loops and multiple edges) and $f : V \to \mathbb{R}^n$ is a map with $f(u) \neq f(v)$ whenever $uv \in E$. The **framework** is a straight line realization of G in $\mathbb{R}^n$ in which the length of an edge $uv \in E$ is given by $||f(u) - f(v)||_2$.

  The vertices and edges are called *joints* and *bars*, respectively, in terms of Structural Engineering. A **tensegrity structure** (Fuller, 1948) is a mechanically stable bar framework in which bars are either *cables* (tension elements which cannot get further apart), or *struts* (compression elements which cannot get closer together).

A framework (G,f) is *globally rigid* if every framework (G,f'), satisfying $||f(u) - f(v)||_2 = ||f'(u) - f'(v)||_2$ for all $uv \in E$, also satisfy it for all $u, v \in V$. A framework (G,f) is *rigid* if every continuous motion of its vertices which preserves the lengths of all edges, also preserves the distances between all pairs of vertices. The framework (G,f) is *generic* if the set containing the coordinates of all the points $f(v)$ is algebraically independent over the rationals. The graph G is *n-rigid* if every its n-dimensional generic realization is rigid. For generic frameworks, rigidity is equivalent to the stronger property of infinitesimal rigidity.

An *infinitesimal motion* of (G,f) is a map $m : V \to \mathbb{R}^n$ with $(m(u) - m(v))(f(u) - f(v)) = 0$ whenever $uv \in E$. A motion is *trivial* if it can be extended to an isometry of $\mathbb{R}^n$. A framework is an *infinitesimally rigid* if every motion of it is trivial, and it is *isostatic* if, moreover, the deletion of any its edge will cause loss of rigidity. (G,f) is an *elastic framework* if, for any $\epsilon > 0$, there exists a $\delta > 0$ such that for every edge-weighting $w : E \to \mathbb{R}_{>0}$ with $\max_{uv \in E} |w(uv) - ||f(u) - f(v)||_2| \leq \delta$, there exist a framework (G,f') with $\max_{v \in V} ||f(u) - f'(v)||_2 < \epsilon$.

A framework (G,f) with $||f(u) - f(v)||_2 > r$ if $u, v \in V, u \neq c$ and $||f(u), f(v)||_2 \leq R$ if $uv \in E$, for some $0 < r < R$, is called (Doyle–Snell, 1984) a *civilized drawing of a graph*. The random walks on such graphs are recurrent if $n = 1, 2$.

- **Distance constrained labeling**

  Given a sequence $\alpha = (\alpha_1, \ldots, \alpha_k)$ of **distance constraints** $\alpha_1 \geq \cdots \geq \alpha_k > 0$, a λ_α-*labeling* of a graph $G = (V, E)$ is an assignment of labels $f(v)$ from the set $\{0, 1, \ldots, \lambda\}$ of integers to the vertices $v \in V$ such that, for any t with $0 \leq t \leq k$, $|f(v) - f(u)| \geq \alpha_t$ whenever the path distance between u and v is t.

  The *radio frequency assignment problem*, where vertices are transmitters (available channels) and labels represent frequencies of not-interfering channels, consists of minimizing λ. **Distance-two labeling** is the main interesting case $\alpha = (2, 1)$; its *span* is the difference between the largest and smallest labels used.

- **Distance-related graph embedding**

  An *embedding* of the guest graph $G = (V_1, E_1)$ into the host graph $H = (V_2, E_2)$ with $|V_1| \leq |V_2|$, is an injective map from V_1 into V_2.

  The **wire length**, *dilation* and *antidilation* of G in H are

$$\min_f \sum_{(uv) \in E_1} d_H(f(u), f(v)), \quad \min_f \max_{(uv) \in E_1} d_H(f(u), f(v)), \quad \max_f \min_{(uv) \in E_1} d_H(f(u), f(v)),$$

  respectively, where f is any embedding of G into H. The main **distance-related graph embedding** problems consist of finding or estimating these three parameters.

  The *bandwidth* and *antibandwidth* of G is the dilation and antidilation, respectively, of G in a path H with V_1 vertices.

- **Bandwidth of a graph**

  Given a graph $G = (V, E)$ with $|V| = n$, its *ordering* is a bijective mapping $f : V \to \{1, \ldots, n\}$. Given a number $b > 0$, the *bandwidth problem* for (G, b) is the existence of ordering f with the *stretch* $\max_{uv \in E} |f(u) - f(v)|$ at most b.

  The **bandwidth** of G, denoted by $bw(G)$, is the minimum stretch over all f.

  The *antibandwidth problem* for G is to find ordering f with maximal $\min_{uv \in E} |f(u) - f(v)|$ (*antibandwidth*).
- **Path distance width of a graph**

  Given a connected graph $G = (V, E)$, an ordered partition $V = \cup_{i=1}^{t} L_i$ of its vertices is called a *distance structure* on G if $L_i = \{v \in V : \min_{u \in L_1} d_{\text{path}}(u, v) = i - 1\}$ for $1 \le i \le t$. The structure is *rooted* if $|L_1| = 1$.

  The **path distance width** $pwd(G)$ of G is defined (Yamazaki et al., 1999) as $\min \max_{1 \le i \le t} |L_i|$ over all distance structures on G.

  An ordered partition $V = \cup_{i=1}^{t} L_i$ is called a *level structure* on G if for each edge uv with $u \in L_i$ and $v \in L_j$, it holds that $|i - j| \le 1$. The *level width* (or *strong pathwidth*) $lw(G)$ is $\min \max_{1 \le i \le t} |L_i|$ over all level structures.

  Clearly, $lw(G) \le pdw(G)$. Yamazaki et al., 1999, proved that $pdw(G)$ can be arbitrarily larger than the **bandwidth** $bw(G)$ and $lw(G) \le bw(G) < 2lw(G)$.
- **Tree-length of a graph**

  A *tree decomposition* of a graph $G = (V, E)$ is a pair of a tree T with vertex-set W and a family of subsets $\{X_i : i \in W\}$ of V with $\cup_{i \in W} X_i = V$ such that

  1. for every edge $(uv) \in E$, there is a subset X_i containing u, v, and
  2. for every $v \in V$, the set $\{i \in W : v \in X_i\}$ induces a connected subtree of T.

  The *chordal graphs* (i.e., ones without induced cycles of length at least 4) are exactly those admitting a tree decomposition where every X_i is a clique.

  For tree decomposition, the *tree-length* is $\max_{i \in W} diam(X_i)$ ($diam(X_i)$ is the diameter of the subgraph of G induced by X_i) and *tree-width* is $\max_{i \in W} |X_i| - 1$. The **tree-length** of G (Dourisboure–Gavoille, 2004) and its **tree-width** (Robertson–Seymour, 1986) are the minima, over all tree decompositions, of above tree-length and tree-width. The *path-length* G is defined taking as trees only paths.

  Given a linear ordering $e_1, \ldots, e_{|E|}$ of the edges of G, let, for $1 \le i < |E|$, denote by $G_{\le i}$ and $G_{i<}$ the graphs induced by the edges $\{e_1, \ldots, e_i\}$ and $\{e_{i+1}, \ldots, e_{|E|}\}$, respectively. The *linear-length* is $\max_{1 \le i < |E|} diam(V(G_{\le i}) \cap V(G_{i<}))$. The **linear-length** of G (Umezawa–Yamazaki, 2009) is the minimum of the above linear-length taken over all the linear orderings of its edges.
- **Spatial graph**

  A **spatial graph** (or *spatial network*) is a graph $G = (V, E)$, where each vertex v has a spatial position $(v_1, \ldots, v_n) \in \mathbb{R}^n$. ($G$ is called a *geometric graph* if it is drawn on $\mathbb{R}^2$ and its edges are straight-line segments.)

  The *graph-theoretic dilation* and *geometric dilation* of G are, respectively:

$$\max_{v,u \in V} \frac{d(v,u)}{||v-u||_2} \text{ and } \max_{(vu) \in E} \frac{d(v,u)}{||v-u||_2}.$$

- **Distance Geometry problem**

  Given a weighted finite graph $G = (V, E; w)$, the **Distance Geometry problem** (DGP) is the problem of realizing it as a **spatial graph** $G = (V', E')$, where $x : V \to V'$ is a bijection with $x(v) = (v_1, \ldots, v_n) \in \mathbb{R}^n$ for every $v \in V$ and $E' = \{(x(u)x(v)) : (uv) \in E\}$, so that for every edge $(uv) \in E$ it holds that

  $$||x(u) - x(u)||_2 = w(uv).$$

  The main application of DGP is the *molecular DGP*: to find the coordinates of the atoms of a given molecular conformation are by exploiting only some of the distances between pairs of atoms found experimentally; cf. [MLLM13].

- **Arc routing problems**

  Given a finite set X, a quasi-distance $d(x, y)$ on it and a set $A \subseteq \{(x, y) : x, y \in X\}$, consider the weighted digraph $D = (X, A)$ with the vertex-set X and arc-weights $d(x, y)$ for all arcs $(x, y) \in A$. For given sets V of vertices and E of arcs, the **arc routing problem** consists of finding a *shortest* (i.e., with minimal sum of weights of its arcs) (V, E)-*tour*, i.e., a circuit in $D = (X, A)$, visiting each vertex in V and each arc in E exactly once or, in a variation, at least once.

  The *Asymmetric Traveling Salesman problem* corresponds to the case $V = X$, $E = \emptyset$; the *Traveling Salesman problem* is the symmetric version of it (usually, each vertex should be visited exactly once). The *Bottleneck Traveling Salesman problem* consists of finding a (V, E)-tour T with smallest $\max_{(x,y)\in T} d(x, y)$.

  The *Windy Postman problem* corresponds to the case $V = \emptyset$, $E = A$, while the Chinese Postman problem is the symmetric version of it.

  The above problems are also considered for general arc- or edge-weights; then, for example, the term *Metric TSP* is used when edge-weights in the Traveling Salesman problem satisfy the triangle inequality, i.e., d is a quasi-semimetric.

- **Steiner distance of a set**

  The **Steiner distance of a set** $S \subset V$ of vertices in a connected graph $G = (V, E)$ is (Chartrand et al., 1989) the minimum *size* (number of edges) of a connected subgraph of G, containing S. Such a subgraph is a tree, and is called a *Steiner tree* for S. Cf. general **Steiner diversity** in **Steiner ratio** (Chap. 1).

  The Steiner distance of the set $S = \{u, v\}$ is the path metric between u and v. The *Steiner k-diameter* of G is the maximum Steiner distance of any k-subset of V.

- ***t*-spanner**

  A *factor*, i.e., a spanning subgraph, $H = (V, E(H))$ of a connected graph $G = (V, E)$ is called a ***t*-spanner** (or *t-multiplicative spanner*) of G if, for every $u, v \in V$, the inequality $d^H_{\text{path}}(u, v)/d^G_{\text{path}}(u, v) \leq t$ holds. The value t is called the *stretch factor* (or *dilation*) of H. Cf. **distance-related graph embedding** and **spatial graph**.

  The graph $H = (V, E(H))$ is called a *k-additive spanner* of G if, for every $u, v \in V$, the inequality $d^H_{\text{path}}(u, v) \leq d^G_{\text{path}}(u, v) + k$ holds.

Mulder and Nebeský, 2012, defined, for connected H, the *guide* of (H, G) as the ternary relation $R \subset V \times V \times V$ consisting of ordered triples (u, w, v) such that $uw \in E$ and $d^H_{\text{path}}(u, w) + d^H_{\text{path}}(w, v) = d^H_{\text{path}}(u, v)$. The guide of (G, G) is called the *step* ternary relation; cf. **metric betweenness** in Chap. 1.

- **Optimal realization of metric space**

  Given a finite metric space (X, d), a *realization* of it is a weighted graph $G = (V, E; w)$ with $X \subset V$ such that $d(x, y) = d_G(x, y)$ holds for all $x, y \in X$.

  The realization is **optimal** if it has minimal $\sum_{(uv)\in E} w(uv)$.

- **Proximity graph**

  Given a finite subset V of a metric space (X, d), its **proximity graph** is a graph representing neighbor relationships between points of V. Such graphs are used in Computational Geometry and many real-world problems. The main examples are presented below. Cf. **underlying graph of a metric space** in Chap. 1.

  A *spanning tree* of V is a set T of $|V| - 1$ unordered pairs (x, y) of different points of V forming a tree on V; the *weight* of T is $\sum_{(x,y)\in T} d(x, y)$. A **minimum spanning tree** $MST(V)$ of V is a spanning tree with the minimal weight. Such a tree is unique if the edge-weights are distinct.

  A **nearest neighbor graph** is the digraph $NNG(V) = (V, E)$ with vertex-set $V = v_1, \ldots, v_{|V|}$ and, for $x, y \in V$, $xy \in E$ if y is the *nearest neighbor* of x, i.e., $d(x, y) = \min_{v_i \in V\setminus\{x\}} d(x, v_i)$ and only v_i with maximal index i is picked. The *k-nearest neighbor graph* arises if k such v_i with maximal indices are picked. The undirect version of $NNG(V)$ is a subgraph of $MST(V)$.

  A **relative neighborhood graph** is (Toussaint, 1980) the graph $RNG(V) = (V, E)$ with vertex-set V and, for $x, y \in V$, $xy \in E$ if there is no point $z \in V$ with $\max\{d(x, z), d(y, z)\} < d(x, y)$. Also considered, for $(X, d) = (\mathbb{R}^2, ||x - y||_2)$, the related *Gabriel graph* $GG(V)$ (in general, *β-skeleton*) and *Delaunay triangulation* $DT(V)$; then $NNG(V) \subseteq MST(V) \subseteq RNG(V) \subseteq GG(V) \subseteq DT(V)$.

  For any $x \in V$, its *sphere of influence* is the open metric ball $B(x, r_x) = \{z \in X : d(x, z) < r\}$ in (X, d) centered at x with radius $r_x = \min_{z\in V\setminus\{x\}} d(x, z)$.

  Sphere of influence graph is the graph $SIG(V) = (V, E)$ with vertex-set V and, for $x, y \in V$, $xy \in E$ if $B(x, r_x) \cap B(y, r_y) \neq \emptyset$; so, it is a proximity graph and an *intersection graph*. The *closed sphere of influence graph* is the graph $CSIG(V) = (V, E)$ with $xy \in E$ if $\overline{B(x, r_x)} \cap \overline{B(y, r_y)} \neq \emptyset$.

15.3 Distances on Graphs

- **Chartrand–Kubicki–Schultz distance**

  The **Chartrand–Kubicki–Schultz distance** (or *ϕ-distance*, 1998) between two connected graphs $G_1 = (V_1, E_1)$ and $G_2 = (V_2, E_2)$ with $|V_1| = |V_2| = n$ is

$$\min\{\sum |d_{G_1}(u, v) - d_{G_2}(\phi(u), \phi(v))|\},$$

where d_{G_1}, d_{G_2} are the path metrics of graphs G_1, G_2, the sum is taken over all unordered pairs u, v of vertices of G_1, and the minimum is taken over all bijections $\phi : V_1 \to V_2$.

- **Subgraph metric**

  Let $\mathbb{F} = \{F_1 = (V_1, E_1), F_2 = (V_2, E_2), \dots, \}$ be the set of isomorphism classes of finite graphs. Given a finite graph $G = (V, E)$, denote by $s_i(G)$ the number of *injective homomorphisms* from F_i into G, i.e., the number of injections $\phi : V_i \to V$ with $\phi(x)\phi(y) \in E$ if $xy \in E_i$ divided by the number $\frac{|V|!}{(|V|-|V_i|)!}$ of such injections from F_i with $|V_i| \le |V|$ into $K_{|V|}$. Set $s(G) = (s_i(G))_{i=1}^{\infty} \in [0, 1]^{\infty}$.

  Let d be the **Cantor metric** (Chap. 18) $d(x, y) = \sum_{i=1}^{\infty} 2^{-i}|x_i - y_i|$ on $[0, 1]^{\infty}$ or any metric on $[0, 1]^{\infty}$ inducing the *product topology*. Then Bollobás–Riordan, 2007, defined the **subgraph metric** between the graphs G_1 and G_2 as

$$d(s(G_1), s(G_2))$$

  and generalized it on *kernels* (or *graphons*), i.e., symmetric measurable functions $k : [0, 1] \times [0, 1] \to \mathbb{R}_{\ge 0}$, replacing G by k and the above $s_i(G)$ by

$$s_i(k) = \int_{[0,1]^{|V_i|}} \prod_{st \in E_i} k(x_s x_t) \prod_{s=1}^{|V_i|} dx_s.$$

- **Benjamini–Schramm metric**

  The rooted graphs (G, o) and (G', o') (where $G = (V, E), G' = (V', E')$ and $o \in V, o' \in V'$) are *isomorphic* is there is a graph-isomorphism of G onto G' taking o to o'. Let X be the set of isomorphism classes of rooted connected locally finite graphs and let $(G, o), (G', o')$ be representatives of two classes.

  Let k be the supremum of all radii r, for which rooted **metric balls** $(\overline{B}_G(o, r), o)$ and $(\overline{B}_{G'}(o', r), o')$ (in the usual **path metric**) are isomorphic as rooted graphs. Benjamini and Schramm, 2001, defined the metric 2^{-k} between classes represented by (G, o) and (G', o'). Here $2^{-\infty}$ means 0. Benjamini and Curien, 2011, defined the similar distance $\frac{1}{1+k}$.

- **Rectangle distance on weighted graphs**

  Let $G = G(\alpha, \beta)$ be a complete weighted graph on $\{1, \dots, n\}$ with vertex-weights $\alpha_i > 0$, $1 \le i \le n$, and edge-weights $\beta_{ij} \in \mathbb{R}$, $1 \le i < j \le n$. Denote by $A(G)$ the $n \times n$ matrix $((a_{ij}))$, where $a_{ij} = \frac{\alpha_i \alpha_j \beta_{ij}}{(\sum_{1 \le i \le n} \alpha_i)^2}$.

  The **rectangle distance** (or *cut distance*) between two weighted graphs $G = G(\alpha, \beta)$ and $G' = G(\alpha', \beta')$ (with vertex-weights (α'_i) and edge-weights (β'_{ij})) is defined (Borgs–Chayes–Lovász–Sós–Vesztergombi, 2007) by

$$\max_{I,J \subset \{1,\dots,n\}} |\sum_{i \in I, j \in J} (a_{ij} - a'_{ij})| + \sum_{i=1}^{n} |\frac{\alpha_i}{\sum_{1 \le j \le n} \alpha_j} - \frac{\alpha'_i}{\sum_{1 \le j \le n} \alpha'_j}|,$$

  where $A(G) = ((a_{ij}))$ and $A(G') = ((a'_{ij}))$.

In the case $(\alpha_i') = (\alpha_i)$, the rectangle distance is $||A(G) - A(G')||_{cut}$, i.e., the **cut norm metric** (cf. Chap. 12) between matrices $A(G)$ and $A(G')$ and the *rectangle distance* from Frieze–Kannan, 1999. In this case, the l_1- and l_2-metrics between two weighted graphs G and G' are defined as $||A(G) - A(G')||_1$ and $||A(G) - A(G')||_2$, respectively. The subcase $\alpha_i = 1$ for all $1 \leq i \leq n$ corresponds to unweighted vertices. Cf. the **Robinson–Foulds weighted metric**.

Authors generalized the rectangle distance on *kernels* (or *graphons*), i.e., symmetric measurable functions $k : [0, 1] \times [0, 1] \to \mathbb{R}_{\geq 0}$, using the *cut norm* $||k||_{cut} = \sup_{S,T \subset [0,1]} |\int_{S \times T} k(x, y)dxdy|$.

A map $\phi : [0, 1] \to [0, 1]$ is *measure-preserving* if, for any measurable subset $A \subset [0, 1]$, the measures of A and $\phi^{-1}(A)$ are equal. For a kernel k, define the kernel k^ϕ by $k^\phi(x, y) = k(\phi(x), \phi(y))$. The **Lovász–Szegedy semimetric** (2007) between kernels k_1 and k_1 is defined by

$$\inf_\phi ||k_1^\phi - k_2||_{cut},$$

where ϕ ranges over all measure-preserving bijections $[0, 1] \to [0, 1]$. Cf. **Chartrand–Kubicki–Schultz distance**.

- **Spectral semimetric between graphs**

  Given a finite weighted graph $G = (V, E, w)$, its *normalised Laplacian* matrix is $\Delta_G = I - D^{-1}A$, where D is the diagonal matrix $((l_{ij}))$ with l_{ii} being the degree of vertex i, while A is the adjacency matrix of G; cf. the **resistance metric**.

  The *spectrum* of G consists of all eigenvalues $\lambda_i, 1 \leq i \leq |V|$, of Δ_G. The spectrum, organised as $\lambda_G = (\lambda_1, \ldots, \lambda_{|V|})$, where the λ_i do not decrease, is called the *spectral vector*.

  The **spectral semimetric** between two finite weighted graphs $G = (V, E, w)$ and $G' = (V', E', w')$ with $|V| = |V'| = n$ is defined (Gu–Hua–Liu, 2015) as

$$d_p(G, G') = \frac{1}{n}\|\lambda_G - \lambda_{G'}\|_p,$$

  i.e., the l_p**-distance** between the spectral vectors, for any $1 \leq p < \infty$.

  In fact, by assigning a probability measure via the spectrum of the normalised Laplacian matrix to each graph, Gu, Hua, and Liu defined their *spectral distance* d_p as the L_p**-Wasserstein distance** (cf. Chap. 14) between probability measures on the set of all, including infinite and random, weighted graphs.

- **Subgraph–supergraph distances**

  A *common subgraph* of graphs G_1 and G_2 is a graph which is isomorphic to induced subgraphs of both G_1 and G_2. A *common supergraph* of graphs G_1 and G_2 is a graph which contains induced subgraphs isomorphic to G_1 and G_2.

  The **Zelinka distance** d_Z ([Zeli75]) on the set $\mathbf{G}$ of all graphs (more exactly, on the set of all equivalence classes of isomorphic graphs) is defined by

$$d_Z = \max\{n(G_1), n(G_2)\} - n(G_1, G_2)$$

for any $G_1, G_2 \in \mathbf{G}$, where $n(G_i)$ is the number of vertices in G_i, $i = 1, 2$, and $n(G_1, G_2)$ is the maximum number of vertices of their common subgraph.

The **Bunke–Shearer metric** (1998) on the set of nonempty graphs is defined by

$$1 - \frac{n(G_1, G_2)}{\max\{n(G_1), n(G_2)\}}.$$

Given any set $\mathbf{M}$ of graphs, the **common subgraph distance** d_M on $\mathbf{M}$ is

$$\max\{n(G_1), n(G_2)\} - n(G_1, G_2),$$

and the **common supergraph distance** d_M^* is defined, for any $G_1, G_2 \in \mathbf{M}$, by

$$N(G_1, G_2) - \min\{n(G_1), n(G_2)\},$$

where $n(G_i)$ is the number of vertices in G_i, $i = 1, 2$, while $n(G_1, G_2)$ and $N(G_1, G_2)$ are the maximal order of a common subgraph $G \in \mathbf{M}$ and the minimal order of a common supergraph $H \in \mathbf{M}$, respectively, of G_1 and G_2.

d_M is a metric on $\mathbf{M}$ if the following condition (i) holds:

(i) if $H \in \mathbf{M}$ is a common supergraph of $G_1, G_2 \in \mathbf{M}$, then there exists a common subgraph $G \in \mathbf{M}$ of G_1 and G_2 with $n(G) \geq n(G_1) + n(G_2) - n(H)$.

d_M^* is a metric on $\mathbf{M}$ if the following condition (ii) holds:

(ii) if $G \in \mathbf{M}$ is a common subgraph of $G_1, G_2 \in \mathbf{M}$, then there exists a common supergraph $H \in \mathbf{M}$ of G_1 and G_2 with $n(H) \leq n(G_1) + n(G_2) - n(G)$.

One has $d_M \leq d_M^*$ if the condition (i) holds, and $d_M \geq d_M^*$ if (ii) holds.

The distance d_M is a metric on the set $\mathbf{G}$ of all graphs, the set of all cycle-free graphs, the set of all bipartite graphs, and the set of all trees. The distance d_M^* is a metric on the set $\mathbf{G}$ of all graphs, the set of all connected graphs, the set of all connected bipartite graphs, and the set of all trees. The Zelinka distance d_Z coincides with d_M and d_M^* on the set $\mathbf{G}$ of all graphs. On the set $\mathbf{T}$ of all trees the distances d_M and d_M^* are identical, but different from the Zelinka distance.

The Zelinka distance d_Z is a metric on the set $\mathbf{G}(n)$ of all graphs with n vertices, and is equal to $n - k$ or to $K - n$ for all $G_1, G_2 \in \mathbf{G}(n)$, where k is the maximum number of vertices of a common subgraph of G_1 and G_2, and K is the minimum number of vertices of a common supergraph of G_1 and G_2.

On the set $\mathbf{T}(n)$ of all trees with n vertices the distance d_Z is called the **Zelinka tree distance** (see, for example, [Zeli75]).

- **Fernández–Valiente metric**

  Given graphs G and H, let $G_1 = (V_1, E_1)$ and $G_2 = (V_2, E_2)$ be their *maximum common subgraph* and *minimum common supergraph*; cf. **subgraph–supergraph distances**. The **Fernández–Valiente metric** (2001) between G and H is

$$(|V_2| + |E_2|) - (|V_1| + |E_1|).$$

- **Graph edit distance**

  The **graph edit distance** (Axenovich–Kézdy–Martin, 2008, and Alon–Stav, 2008) between graphs G and G' on the same labeled vertex-set is defined by

$$d_{ed}(G, G') = |E(G)\Delta E(G')|.$$

  It is the minimum number of edge deletions or additions needed to transform G into G', and half of the Hamming distance between their adjacency matrices.

  Given a *graph property* (i.e., a family $\mathcal{H}$ of graphs), let $d_{ed}(G, \mathcal{H})$ be $\min\{d_{ed}(G, G') : V(G') = V(G), G' \in \mathcal{H}\}$. Given a number $p \in (0, 1]$, the **edit distance function of a property** $\mathcal{H}$ is (if this limit exists) defined by

$$ed_{\mathcal{H}}(p) = \lim_{n\to\infty} \max\{d_{ed}(G, \mathcal{H}) : |V(G)| = n, |E(G)| = \lfloor p\binom{n}{2}\rfloor\}(\binom{n}{2})^{-1}.$$

  If $\mathcal{H}$ is *hereditary* (closed under the taking induced subgraphs) and *nontrivial* (contains arbitrarily large graphs), then (Balogh–Martin, 2008) it holds

$$ed_{\mathcal{H}}(p) = \lim_{n\to\infty} \mathbb{E}[d_{ed}(G(n, p), \mathcal{H})](\binom{n}{2})^{-1};$$

  $G(n, p)$ is the **random graph** (Chap. 1) on n vertices with edge probability p.

  Bunke, 1997, defined the *graph edit distance* between vertex- and edge-labeled graphs G_1 and G_2 as the minimal total cost of matching G_1 and G_2, using deletions, additions and substitutions of vertices and edges. Cf. also **tree**, **top-down**, **unit cost** and **restricted edit distance** between rooted trees.

  The **Bayesian graph edit distance** between two *relational graphs* (i.e., triples (V, E, A), where V, E, A are the sets of vertices, edges, *vertex-attributes*) is (Myers–Wilson–Hancock, 2000) their graph edit distance with costs defined by probabilities of operations along an editing path seen as a memoryless error process. Cf. **transduction edit distances** (Chap. 11) and **Bayesian distance** (Chap. 14).

  The **structural Hamming distance** between two digraphs $G = (X, E)$ and $G' = (X, E')$ is defined (Acid–Campos, 2003) as $SHD(G, G') = |E\Delta E'|$. The *ring sum* (or *symmetric difference*) of G and G' is defined (Deo, 1974) as $(X \cup X', E\Delta E')$.

- **Edge distance**

  The **edge distance** on the set of all graphs is defined (Baláž et al., 1986) by

$$|E_1| + |E_2| - 2|E_{12}| + ||V_1| - |V_2||$$

  for any graphs $G_1 = (V_1, E_1)$ and $G_2 = (V_2, E_2)$, where $G_{12} = (V_{12}, E_{12})$ is a common subgraph of G_1 and G_2 with maximal number of edges. This distance has many applications in Organic and Medical Chemistry.

- **Contraction distance**

  The **contraction distance** is a distance on the set $\mathbf{G}(n)$ of all graphs with n vertices defined by

  $$n - k$$

  for any $G_1, G_2 \in \mathbf{G}(n)$, where k is the maximum number of vertices of a graph which is isomorphic simultaneously to a graph, obtained from each of G_1 and G_2 by a finite number of *edge contractions*. To perform the *contraction* of the edge $uv \in E$ of a graph $G = (V, E)$ means to replace u and v by one vertex that is adjacent to all vertices of $V \backslash \{u, v\}$ which were adjacent to u or to v.
- **Edge move distance**

  The **edge move distance** (Baláž et al., 1986) is a metric on the set $\mathbf{G}(n, m)$ of all graphs with n vertices and m edges, defined, for any $G_1, G_2 \in \mathbf{G}(m, n)$, as the minimum number of *edge moves* necessary for transforming the graph G_1 into the graph G_2. It is equal to $m - k$, where k is the maximum size of a common subgraph of G_1 and G_2.

  An *edge move* is one of the *edge transformations*, defined as follows: H can be obtained from G by an edge move if there exist (not necessarily distinct) vertices u, v, w, and x in G such that $uv \in E(G)$, $wx \notin E(G)$, and $H = G - uv + wx$.
- **Edge jump distance**

  The **edge jump distance** is an extended metric (which in general can take the value ∞) on the set $\mathbf{G}(n, m)$ of all graphs with n vertices and m edges defined, for any $G_1, G_2 \in \mathbf{G}(m, n)$, as the minimum number of *edge jumps* necessary for transforming G_1 into G_2.

  An *edge jump* is one of the *edge transformations*, defined as follows: H can be obtained from G by an edge jump if there exist four distinct vertices u, v, w, and x in G, such that $uv \in E(G)$, $wx \notin E(G)$, and $H = G - av + wx$.
- **Edge flipping distance**

  Let $P = \{v_1, \ldots, v_n\}$ be a collection of points on the plane. A *triangulation* T of P is a partition of the convex hull of P into a set of triangles such that each triangle has a disjoint interior and the vertices of each triangle are points of P.

  The **edge flipping distance** is a distance on the set of all triangulations of P defined, for any triangulations T and T_1, as the minimum number of edge flippings necessary for transforming T into T_1.

  An edge e of T is called *flippable* if it is the boundary of two triangles t and t' of T, and $C = t \cup t'$ is a convex quadrilateral. The *flipping* e is one of the *edge transformations*, which consists of removing e and replacing it by the other diagonal of C. Edge flipping is an special case of *edge jump*.

  The edge flipping distance can be extended on *pseudo-triangulations*, i.e., partitions of the convex hull of P into a set of disjoint interior *pseudo-triangles* (simply connected subsets of the plane that lie between any three mutually tangent convex sets) whose vertices are given points.

- **Edge rotation distance**

  The **edge rotation distance** (Chartand–Saba–Zou, 1985) is a metric on the set $\mathbf{G}(n, m)$ of graphs with n vertices and m edges, defined, for any G_1, G_2, as the minimum number of *edge rotations* needed for transforming G_1 into G_2. Cf. **Pospichal–Kvasnička chemical distance**, called also *reaction metric*, in Chap. 24.

  An *edge rotation* is one of the *edge transformations*, defined as follows: H can be obtained from G by an edge rotation if there exist distinct vertices u, v, and w in G, such that $uv \in E(G)$, $uw \notin E(G)$, and $H = G - uv + uw$.
- **Tree edge rotation distance**

  The **tree edge rotation distance** is a metric on the set $\mathbf{T}(n)$ of all trees with n vertices defined, for all $T_1, T_2 \in \mathbf{T}(n)$, as the minimum number of *tree edge rotations* necessary for transforming T_1 into T_2. A *tree edge rotation* is an *edge rotation* performed on a tree, and resulting in a tree.

  For $\mathbf{T}(n)$ the tree edge rotation and the edge rotation distances may differ.
- **Edge shift distance**

  The **edge shift distance** (or **edge slide distance**) is a metric (Johnson, 1985) on the set $\mathbf{G}_c(n, m)$ of all connected graphs with n vertices and m edges defined, for any $G_1, G_2 \in \mathbf{G}_c(m, n)$, as the minimum number of *edge shifts* necessary for transforming G_1 into G_2.

  An *edge shift* is one of the *edge transformations*, defined as follows: H can be obtained from G by an edge shift if there exist distinct vertices u, v, and w in G such that $uv, vw \in E(G)$, $uw \notin E(G)$, and $H = G - uv + uw$. Edge shift is a special kind of *edge rotation* in the case when the vertices v, w are adjacent in G.

  The edge shift distance can be defined between any graphs G and H with components $G_i (1 \leq i \leq k)$ and $H_i (1 \leq i \leq k)$, respectively, such that G_i and H_i have the same order and the same size.
- **F-rotation distance**

  The **F-rotation distance** is a distance on the set $\mathbf{G}_F(n, m)$ of all graphs with n vertices and m edges, containing a subgraph isomorphic to a given graph F of order at least 2 defined, for all G_1, $G_2 \in \mathbf{G}_F(m, n)$, as the minimum number of *F-rotations* necessary for transforming G_1 into G_2.

  An *F-rotation* is one of the *edge transformations*, defined as follows: let F' be a subgraph of a graph G, isomorphic to F, let u, v, w be three distinct vertices of the graph G such that $u \notin V(F')$, $v, w \in V(F')$, $uv \in E(G)$, and $uw \notin E(G)$; H can be obtained from G by the F-rotation of the edge uv into the position uw if $H = G - uv + uw$.
- **Binary relation distance**

  Let R be a nonreflexive *binary relation* between graphs, i.e., $R \subset \mathbf{G} \times \mathbf{G}$, and there exists $G \in \mathbf{G}$ such that $(G, G) \notin R$.

  The **binary relation distance** is a metric (which can take the value ∞) on the set $\mathbf{G}$ of all graphs defined, for any graphs G_1 and G_2, as the minimum number of *R-transformations* necessary for transforming G_1 into G_2. We say that a graph H can be obtained from a graph G by an *R-transformation* if $(H, G) \in R$.

An example is the distance between two *triangular embeddings of a complete graph* (i.e., its cellular embeddings in a surface with only 3-gonal faces) defined as the minimal number t such that, up to replacing t faces, the embeddings are isomorphic.

- **Crossing-free transformation metrics**

  Given a subset S of $\mathbb{R}^2$, a *noncrossing spanning tree* of S is a tree whose vertices are points of S, and edges are pairwise noncrossing straight line segments.

  The **crossing-free edge move metric** (see [AAH00]) on the set $\mathbf{T}_S$ of all noncrossing spanning trees of a set S, is defined, for any $T_1, T_2 \in \mathbf{T}_S$, as the minimum number of *crossing-free edge moves* needed to transform T_1 into T_2. Such move is an edge transformation which consists of adding some edge e in $T \in \mathbf{T}_S$ and removing some edge f from the induced cycle so that e and f do not cross.

  The **crossing-free edge slide metric** is a metric on the set $\mathbf{T}_S$ of all *noncrossing spanning trees* of a set S defined, for any $T_1, T_2 \in \mathbf{T}_S$, as the minimum number of *crossing-free edge slides* necessary for transforming T_1 into T_2. Such slide is one of the edge transformations which consists of taking some edge e in $T \in \mathbf{T}_S$ and moving one of its endpoints along some edge adjacent to e in T, without introducing edge crossings and without sweeping across points in S (that gives a new edge f instead of e). The edge slide is a special kind of crossing-free edge move: the new tree is obtained by closing with f a cycle C of length 3 in T, and removing e from C, in such a way that f avoids the interior of the triangle C.

- **Traveling salesman tours distances**

  The *Traveling Salesman problem* is the problem of finding the shortest tour that visits a set of cities. We will consider only Traveling Salesman problem with undirected links. For an n-city traveling salesman problem, the space $\mathcal{T}_n$ of tours is the set of $\frac{(n-1)!}{2}$ cyclic permutations of the cities $1, 2, \ldots, n$.

  The metric D on $\mathcal{T}_n$ is defined in terms of the difference in form: if tours $T, T' \in \mathcal{T}_n$ differ in m links, then $D(T, T') = m$.

  A *k-OPT transformation* of a tour T is obtained by deleting k links from T, and reconnecting. A tour T', obtained from T by a k-OPT transformation, is called a *k-OPT* of T. The distance d on the set $\mathcal{T}_N$ is defined in terms of the 2-OPT transformations: $d(T, T')$ is the minimal i, for which there exists a sequence of i 2-OPT transformations which transforms T to T'. In fact, $d(T, T') \leq D(T, T')$ for any $T, T' \in \mathcal{T}_N$ (see, for example, [MaMo95]). Cf. **arc routing problems**.

- **Orientation distance**

  The **orientation distance** (Chartrand–Erwin–Raines–Zhang, 2001) between two orientations D and D' of a finite graph is the minimum number of arcs of D whose directions must be reversed to produce an orientation isomorphic to D'.

- **Subgraphs distances**

  The standard distance on the set of all subgraphs of a connected graph $G = (V, E)$ is defined by

$$\min\{d_{\text{path}}(u, v) : u \in V(F), v \in V(H)\}$$

  for any subgraphs F, H of G. For any subgraphs F, H of a strongly connected digraph $D = (V, E)$, the standard quasi-distance is defined by

$$\min\{d_{\text{dpath}}(u, v) : u \in V(F), v \in V(H)\}.$$

  Using standard operations (rotation, shift, etc.) on the edge-set of a graph, one gets corresponding distances between its edge-induced subgraphs of given size which are subcases of similar distances on the set of all graphs of a given size and order.

  The **edge rotation distance** on the set $\mathbf{S}^k(G)$ of all edge-induced subgraphs with k edges in a connected graph G is defined as the minimum number of *edge rotations* required to transform $F \in \mathbf{S}^k(G)$ into $H \in \mathbf{S}^k(G)$. We say that H can be obtained from F by an *edge rotation* if there exist distinct vertices u, v, and w in G such that $uv \in E(F)$, $uw \in E(G)\backslash E(F)$, and $H = F - uv + uw$.

  The **edge shift distance** on the set $\mathbf{S}^k(G)$ of all edge-induced subgraphs with k edges in a connected graph G is defined as the minimum number of *edge shifts* required to transform $F \in \mathbf{S}^k(G)$ into $H \in \mathbf{S}^k(G)$. We say that H can be obtained from F by an *edge shift* if there exist distinct vertices u, v and w in G such that $uv, vw \in E(F)$, $uw \in E(G)\backslash E(F)$, and $H = F - uv + uw$.

  The **edge move distance** on the set $\mathbf{S}^k(G)$ of all edge-induced subgraphs with k edges of a graph G (not necessary connected) is defined as the minimum number of *edge moves* required to transform $F \in \mathbf{S}^k(G)$ into $H \in \mathbf{S}^k(G)$. We say that H can be obtained from F by an *edge move* if there exist (not necessarily distinct) vertices u, v, w, and x in G such that $uv \in E(F)$, $wx \in E(G)\backslash E(F)$, and $H = F - uv + wx$. The edge move distance is a metric on $\mathbf{S}^k(G)$. If F and H have s edges in common, then it is equal to $k - s$.

  The **edge jump distance** (which in general can take the value ∞) on the set $\mathbf{S}^k(G)$ of all edge-induced subgraphs with k edges of a graph G (not necessary connected) is defined as the minimum number of *edge jumps* required to transform $F \in \mathbf{S}^k(G)$ into $H \in \mathbf{S}^k(G)$. We say that H can be obtained from F by an *edge jump* if there exist four distinct vertices u, v, w, and x in G such that $uv \in E(F)$, $wx \in E(G)\backslash E(F)$, and $H = F - uv + wx$.

15.4 Distances on Trees

Let T be a *rooted tree*, i.e., a tree with one of its vertices being chosen as the *root*. The *depth* of a vertex v, $depth(v)$, is the number of edges on the path from v to the root. A vertex v is called a *parent* of a vertex u, $v = par(u)$, if they are adjacent,

and $depth(u) = depth(v) + 1$; in this case u is called a *child* of v. A *leaf* is a vertex without child. Two vertices are *siblings* if they have the same parent.

The *in-degree* of a vertex is the number of its children. $T(v)$ is the subtree of T, rooted at a node $v \in V(T)$. If $w \in V(T(v))$, then v is an *ancestor* of w, and w is a *descendant* of v; $nca(u, v)$ is the *nearest common ancestor* of the vertices u and v.

T is called a *labeled tree* if a symbol from a fixed finite alphabet $\mathcal{A}$ is assigned to each node. T is called an *ordered tree* if a left-to-right order among siblings in T is given. On the set $\mathbb{T}_{rlo}$ of all rooted labeled ordered trees there are three *editing operations*:

- *Relabel*—change the label of a vertex v;
- *Deletion*—delete a nonrooted vertex v with parent v', making the children of v become the children of v'; the children are inserted in the place of v as a subsequence in the left-to-right order of the children of v';
- *Insertion*—the complement of deletion; insert a vertex v as a child of a v' making v the parent of a consecutive subsequence of the children of v'.

For unordered trees above operations (and so, distances) are defined similarly, but the insert and delete operations work on a subset instead of a subsequence.

We assume that there is a *cost function* defined on each editing operation, and the *cost* of a sequence of editing operations is the sum of the costs of these operations.

The *ordered edit distance mapping* is a representation of the editing operations. Formally, the triple (M, T_1, T_2) is an *ordered edit distance mapping* from T_1 to T_2, $T_1, T_2 \in \mathbb{T}_{rlo}$, if $M \subset V(T_1) \times V(T_2)$ and, for any (v_1, w_1), $(v_2, w_2) \in M$, the following conditions hold: $v_1 = v_2$ if and only if $w_1 = w_2$ (*one-to-one condition*), v_1 is an ancestor of v_2 if and only if w_1 is an ancestor of w_2 (*ancestor condition*), v_1 is to the left of v_2 if and only if w_1 is to the left of w_2 (*sibling condition*).

We say that a vertex v in T_1 and T_2 is *touched by a line* in M if v occurs in some pair in M. Let N_1 and N_2 be the set of vertices in T_1 and T_2, respectively, not touched by any line in M. The *cost* of M is given by $\gamma(M) = \sum_{(v,w)\in M} \gamma(v \to w) + \sum_{v\in N_1} \gamma(v \to \lambda) + \sum_{w\in N_2} \gamma(\lambda \to w)$, where $\gamma(a \to b) = \gamma(a, b)$ is the *cost* of an editing operation $a \to b$ which is a relabel if $a, b \in \mathcal{A}$, a deletion if $b = \lambda$, and an insertion if $a = \lambda$. Here $\lambda \notin \mathcal{A}$ is a special *blank symbol*, and γ is a metric on the set $\mathcal{A} \cup \lambda$ (excepting the value $\gamma(\lambda, \lambda)$).

- **Tree edit distance**

  The **tree edit distance** (see [Tai79]) on the set $\mathbb{T}_{rlo}$ of all rooted labeled ordered trees is defined, for any $T_1, T_2 \in \mathbb{T}_{rlo}$, as the minimum cost of a sequence of editing operations (relabels, insertions, and deletions) turning T_1 into T_2.

  In terms of ordered edit distance mappings, it is equal to $\min_{(M,T_1,T_2)} \gamma(M)$, where the minimum is taken over all such mappings (M, T_1, T_2).

  The **unit cost edit distance** between T_1 and T_2 is the minimum number of three above editing operations turning T_1 into T_2, i.e., it is the tree edit distance with cost 1 of any operation.

- **Selkow distance**

  The **Selkow distance** (or *top-down edit distance*, *degree*-1 *edit distance*) is a distance on the set $\mathbb{T}_{rlo}$ of all rooted labeled ordered trees defined, for any $T_1, T_2 \in \mathbb{T}_{rlo}$, as the minimum cost of a sequence of editing operations (relabels, insertions, and deletions) turning T_1 into T_2 if insertions and deletions are restricted to leaves of the trees (see [Selk77]).

  The root of T_1 must be mapped to the root of T_2, and if a node v is to be deleted (inserted), then any subtree rooted at v is to be deleted (inserted).

  In terms of ordered edit distance mappings, it is equal to $\min_{(M,T_1,T_2)} \gamma(M)$, where the minimum is taken over all such mappings (M, T_1, T_2) such that $(par(v), par(w)) \in M$ if $(v, w) \in M$, where neither v nor w is the root.
- **Restricted edit distance**

  The **restricted edit distance** is a distance on the set $\mathbb{T}_{rlo}$ of all rooted labeled ordered trees defined, for any $T_1, T_2 \in \mathbb{T}_{rlo}$, as the minimum cost of a sequence of editing operations (relabels, insertions, and deletions) turning T_1 into T_2 with the restriction that disjoint subtrees should be mapped to disjoint subtrees.

  In terms of ordered edit distance mappings, it is equal to $\min_{(M,T_1,T_2)} \gamma(M)$, where the minimum is taken over all such mappings (M, T_1, T_2) satisfying the following condition: for all (v_1, w_1), (v_2, w_2), $(v_3, w_3) \in M$, $nca(v_1, v_2)$ is a proper ancestor of v_3 if and only if $nca(w_1, w_2)$ is a proper ancestor of w_3.

  This distance is equivalent to the *structure respecting edit distance* which is defined by $\min_{(M,T_1,T_2)} \gamma(M)$. Here the minimum is taken over all ordered edit distance mappings (M, T_1, T_2), satisfying the following condition: for all $(v_1, w_1), (v_2, w_2), (v_3, w_3) \in M$, such that none of v_1, v_2, and v_3 is an ancestor of the others, $nca(v_1, v_2) = nca(v_1, v_3)$ if and only if $nca(w_1, w_2) = nca(w_1, w_3)$.

  Cf. **constrained edit distance** in Chap. 11.
- **Alignment distance**

  The **alignment distance** (see [JWZ94]) is a distance on the set $\mathbb{T}_{rlo}$ of all rooted labeled ordered trees defined, for any $T_1, T_2 \in \mathbb{T}_{rlo}$, as the minimum *cost* of an *alignment* of T_1 and T_2. It corresponds to a restricted edit distance, where all insertions must be performed before any deletions.

  Thus, one inserts *spaces*, i.e., vertices labeled with a *blank symbol* λ, into T_1 and T_2 so that they become isomorphic when labels are ignored; the resulting trees are overlaid on top of each other giving the *alignment* $T_{\mathcal{A}}$ which is a tree, where each vertex is labeled by a pair of labels. The *cost* of $T_{\mathcal{A}}$ is the sum of the costs of all pairs of opposite labels in $T_{\mathcal{A}}$.
- **Splitting-merging distance**

  The **splitting-merging distance** (see [ChLu85]) is a distance on the set $\mathbb{T}_{rlo}$ of all rooted labeled ordered trees defined, for any $T_1, T_2 \in \mathbb{T}_{rlo}$, as the minimum number of vertex splittings and mergings needed to transform T_1 into T_2.
- **Degree-2 distance**

  The **degree-2 distance** is a metric on the set $\mathbb{T}_l$ of all labeled trees (*labeled free trees*), defined, for any $T_1, T_2 \in \mathbb{T}_l$, as the minimum number of editing operations (relabels, insertions, and deletions) turning T_1 into T_2 if any vertex to be inserted

(deleted) has no more than two neighbors. This metric is a natural extension of the **tree edit distance** and the **Selkow distance**.

A *phylogenetic X-tree* is an unordered unrooted tree with the labeled leaf set X and no vertices of degree two. If every interior vertex has degree three, the tree is called *binary*. Let $\mathbb{T}(X)$ denote the set of all phylogenetic X-trees.

- **Robinson–Foulds metric**

  A *cut* $A|B$ of X is a *partition* of X into two subsets A and B (see **cut semimetric**). Removing an edge e from a phylogenetic X-tree induces a cut of the leaf set X which is called the *cut associated with* e.

  The **Robinson–Foulds metric** (or *Bourque metric*, *bipartition distance*) is a metric on the set $\mathbb{T}(X)$, defined, for any phylogenetic X-trees $T_1, T_2 \in \mathbb{T}(X)$, by

$$\frac{1}{2}|\Sigma(T_1)\triangle\Sigma(T_2)| = \frac{1}{2}|\Sigma(T_1) \setminus \Sigma(T_2)| + \frac{1}{2}|\Sigma(T_2) \setminus \Sigma(T_1)|,$$

  where $\Sigma(T)$ is the collection of all cuts of X associated with edges of T.

  The **Robinson–Foulds weighted metric** is a metric on the set $\mathbb{T}(X)$ of all phylogenetic X-trees defined by

$$\sum_{A|B\in\Sigma(T_1)\cup\Sigma(T_2)} |w_1(A|B) - w_2(A|B)|$$

  for all $T_1, T_2 \in \mathbb{T}(X)$, where $w_i = (w(e))_{e\in E(T_i)}$ is the collection of positive weights, associated with the edges of the X-tree T_i, $\Sigma(T_i)$ is the collection of all cuts of X, associated with edges of T_i, and $w_i(A|B)$ is the weight of the edge, corresponding to the cut $A|B$ of X, $i = 1, 2$. Cf. more general **cut norm metric** in Chap. 12 and **rectangle distance on weighted graphs**.

- **μ-metric**

  Given a phylogenetic X-tree T with n leaves and a vertex v in it, let $\mu(v) = (\mu_1(v), \ldots, \mu_n(v))$, where $\mu_i(v)$ is the number of different paths from the vertex v to the i-th leaf. Let $\mu(T)$ denote the multiset on the vertex-set of T with $\mu(v)$ being the multiplicity of the vertex v.

  The **μ-metric** (Cardona–Roselló–Valiente, 2008) is a metric on the set $\mathbb{T}(X)$ of all phylogenetic X-trees defined, for all $T_1, T_2 \in \mathbb{T}(X)$, by

$$\frac{1}{2}|\mu(T_1)\Delta\mu(T_2)|,$$

  where Δ denotes the symmetric difference of multisets.

  Cf. the **metrics between multisets** in Chap. 1 and the **Dodge–Shiode WebX quasi-distance** in Chap. 22.

- **Nearest neighbor interchange metric**

  The **nearest neighbor interchange metric** (or **crossover metric**) on the set $\mathbb{T}(X)$ of all phylogenetic X-trees, is defined, for all $T_1, T_2 \in \mathbb{T}(X)$, as the

minimum number of *nearest neighbor interchanges* required to transform T_1 into T_2.

A *nearest neighbor interchange* consists of swapping two subtrees in a tree that are adjacent to the same internal edge; the remainder of the tree is unchanged.

- **Subtree prune and regraft distance**

  The **subtree prune and regraft distance** is a metric on the set $\mathbb{T}(X)$ of all phylogenetic X-trees defined, for all $T_1, T_2 \in \mathbb{T}(X)$, as the minimum number of *subtree prune and regraft transformations* required to transform T_1 into T_2.

  A *subtree prune and regraft transformation* proceeds in three steps: one selects and removes an edge uv of the tree, thereby dividing the tree into two subtrees T_u (containing u) and T_v (containing v); then one selects and subdivides an edge of T_v, giving a new vertex w; finally, one connects u and w by an edge, and removes all vertices of degree two.

- **Tree bisection-reconnection metric**

  The **tree bisection-reconnection metric** (or **TBR-metric**) on the set $\mathbb{T}(X)$ of all phylogenetic X-trees is defined, for all $T_1, T_2 \in \mathbb{T}(X)$, as the minimum number of *tree bisection and reconnection* transformations required to transform T_1 into T_2.

  A *tree bisection and reconnection transformation* proceeds in three steps: one selects and removes an edge uv of the tree, thereby dividing the tree into two subtrees T_u (containing u) and T_v (containing v); then one selects and subdivides an edge of T_v, giving a new vertex w, and an edge of T_u, giving a new vertex z; finally one connects w and z by an edge, and removes all vertices of degree two.

- **Quartet distance**

  The **quartet distance** (see [EMM85]) is a distance of the set $\mathbb{T}_b(X)$ of all binary phylogenetic X-trees defined, for all $T_1, T_2 \in \mathbb{T}_b(X)$, as the number of mismatched *quartets* (from the total number $\binom{n}{4}$ possible quartets) for T_1 and T_2.

  This distance is based on the fact that, given four leaves $\{1, 2, 3, 4\}$ of a tree, they can only be combined in a binary subtree in three ways: $(12|34)$, $(13|24)$, or $(14|23)$: the notation $(12|34)$ refers to the binary tree with the leaf set $\{1, 2, 3, 4\}$ in which removing the inner edge yields the trees with the leaf sets $\{1, 2\}$ and $\{3, 4\}$.

- **Triples distance**

  The **triples distance** (see [CPQ96]) is a distance of the set $\mathbb{T}_b(X)$ of all binary phylogenetic X-trees defined, for all $T_1, T_2 \in \mathbb{T}_b(X)$, as the number of triples (from the total number $\binom{n}{3}$ possible triples) that differ (for example, by which leaf is the outlier) for T_1 and T_2.

- **Perfect matching distance**

  The **perfect matching distance** is a distance on the set $\mathbb{T}_{br}(X)$ of all rooted binary phylogenetic X-trees with the set X of n labeled leaves defined, for any $T_1, T_2 \in \mathbb{T}_{br}(X)$, as the minimum number of interchanges necessary to bring the perfect matching of T_1 to the perfect matching of T_2.

  Given a set $A = \{1, \ldots, 2k\}$ of $2k$ points, a *perfect matching* of A is a *partition* of A into k pairs. A rooted binary phylogenetic tree with n labeled leaves has a root and $n - 2$ internal vertices distinct from the root. It can be identified

with a perfect matching on $2n-2$, different from the root, vertices by following construction: label the internal vertices with numbers $n+1, \ldots, 2n-2$ by putting the smallest available label as the parent of the pair of labeled children of which one has the smallest label among pairs of labeled children; now a matching is formed by peeling off the children, or sibling pairs, two by two.

- **Tree rotation distance**

  The **tree rotation distance** is a distance on the set $\mathbf{T}_n$ of all rooted ordered binary trees with n interior vertices defined, for all $T_1, T_2 \in \mathbf{T}_n$, as the minimum number of *rotations*, required to transform T_1 into T_2.

  Given interior edges uv, vv', vv'' and uw of a binary tree, the *rotation* is replacing them by edges uv, uv'', vv' and vw.

  There is a bijection between edge flipping operations in triangulations of convex polygons with $n+2$ vertices and rotations in binary trees with n interior vertices.

- **Attributed tree metrics**

  An *attributed tree* is a triple (V, E, α), where $T = (V, E)$ is the underlying tree, and α is a function which assigns an *attribute vector* $\alpha(v)$ to every vertex $v \in V$. Given two attributed trees (V_1, E_1, α) and (V_2, E_2, β), consider the set of all *subtree isomorphisms* between them, i.e., the set of all isomorphisms $f : H_1 \to H_2, H_1 \subset V_1, H_2 \subset V_2$, between their *induced subtrees*.

  Given a similarity s on the set of attributes, the similarity between isomorphic induced subtrees is defined as $W_s(f) = \sum_{v \in H_1} s(\alpha(v), \beta(f(v)))$. Let ϕ be the isomorphism with maximal similarity $W_s(\phi) = W(\phi)$.

  The following four semimetrics on the set $\mathbf{T}_{att}$ of all attributed trees are used:

$$\max\{|V_1|, |V_2|\} - W(\phi), \quad |V_1| + |V_2| - 2W(\phi) \quad \text{and}$$

$$1 - \frac{W(\phi)}{\max\{|V_1|, |V_2|\}}, \quad 1 - \frac{W(\phi)}{|V_1| + |V_2| - W(\phi)}.$$

  They become metrics on the set of equivalences classes of attributed trees: two such trees (V_1, E_1, α) and (V_2, E_2, β) are called *equivalent* if they are *attribute-isomorphic*, i.e., if there exists an isomorphism $g : V_1 \to V_2$ between the trees such that, for any $v \in V_1$, we have $\alpha(v) = \beta(g(v))$. Then $|V_1| = |V_2| = W(g)$.

- **Maximal agreement subtree distance**

  The **maximal agreement subtree distance** (MAST) is (Finden–Gordon, 1985) a distance of the set $\mathbf{T}$ of all trees defined, for all $T_1, T_2 \in \mathbf{T}$, as the minimum number of leaves removed to obtain a *(greatest) agreement subtree*.

  An *agreement subtree* (or *common pruned tree*) of two trees is an identical subtree that can be obtained from both trees by pruning leaves with the same label.

- **l_p-distances between trees**

  Given $p \geq 1$, the **l_p-distance between trees** T, T' on the same vertex-set is the l_p-metric between their (shortest path) distance matrices D, D' seen as vectors.

  For $p = 1$, it is **edge difference distance** (Williams–Clifford, 1971). For $p = 2$, it is **path difference distance** (Steel–Penny, 1993). For $p = \infty$, it is **path interval** (or **k-interval cospeciation**, as in original Hugguns et al., 2012) **distance**.

Chapter 16
Distances in Coding Theory

Coding Theory deals with the design and properties of *error-correcting codes* for the reliable transmission of information across noisy channels in transmission lines and storage devices. The aim of Coding Theory is to find codes which transmit and decode fast, contain many valid code words, and can correct, or at least detect, many errors. These aims are mutually exclusive, however; so, each application has its own good code.

In communications, a *code* is a rule for converting a piece of information (for example, a letter, word, or phrase) into another form or representation, not necessarily of the same sort. *Encoding* is the process by which a source (object) performs this conversion of information into data, which is then sent to a receiver (observer), such as a data processing system. *Decoding* is the reverse process of converting data which has been sent by a source, into information understandable by a receiver.

An *error-correcting code* is a code in which every data signal conforms to specific rules of construction so that departures from this construction in the received signal can generally be automatically detected and corrected. It is used in computer data storage, for example in dynamic RAM, and in data transmission. Error detection is much simpler than error correction, and one or more "check" digits are commonly embedded in credit card numbers in order to detect mistakes. The two main classes of error-correcting codes are *block codes*, and *convolutional codes*.

A *block code* (or *uniform code*) of length n over an alphabet $\mathcal{A}$, usually, over a finite field $\mathbb{F}_q = \{0, \ldots, q-1\}$, is a subset $C \subset \mathcal{A}^n$; every vector $x \in C$ is called a *codeword*, and $M = |C|$ is called *size* of the code. Given a metric d on $\mathbb{F}_q^n$ (for example, the **Hamming metric**, **Lee metric**, **Levenstein metric**), the value $d^* = d^*(C) = \min_{x,y \in C, x \neq y} d(x,y)$ is called the **minimum distance** of the code C. The *weight* $w(x)$ of a codeword $x \in C$ is defined as $w(x) = d(x,0)$. An (n, M, d^*)-*code* is a q-ary block code of length n, size M, and minimum distance d^*. A *binary code* is a code over $\mathbb{F}_2$.

© Springer-Verlag Berlin Heidelberg 2016

M.M. Deza, E. Deza, *Encyclopedia of Distances*,
DOI 10.1007/978-3-662-52844-0_16

When codewords are chosen such that the distance between them is maximized, the code is called *error-correcting*, since slightly garbled vectors can be recovered by choosing the nearest codeword. A code C is a *t-error-correcting code* (and a $2t$-*error-detecting code*) if $d^*(C) \geq 2t+1$. In this case each *neighborhood* $U_t(x) = \{y \in C : d(x,y) \leq t\}$ of $x \in C$ is disjoint with $U_t(y)$ for any $y \in C, y \neq x$.

A *perfect code* is a q-ary $(n, M, 2t+1)$-code for which the M spheres $U_t(x)$ of radius t centered on the codewords fill the whole space $\mathbb{F}_q^n$ completely, without overlapping.

A block code $C \subset \mathbb{F}_q^n$ is called *linear* if C is a vector subspace of $\mathbb{F}_q^n$. An $[n,k]$-code is a k-dimensional linear code $C \subset \mathbb{F}_q^n$ (with the minimum distance d^*); it has size q^k, i.e., it is an (n, q^k, d^*)-code. The *Hamming code* is the linear perfect one-error correcting $(\frac{q^r-1}{q-1}, \frac{q^r-1}{q-1} - r, 3)$-code.

A $k \times n$ matrix G with rows that are basis vectors for a linear $[n,k]$-code C is called a *generator matrix* of C. In *standard form* it can be written as $(1_k|A)$, where 1_k is the $k \times k$ identity matrix. Each *message* (or *information symbol*, *source symbol*) $u = (u_1, \ldots, u_k) \in \mathbb{F}_q^k$ can be encoded by multiplying it (on the right) by the generator matrix: $uG \in C$.

The matrix $H = (-A^T|1_{n-k})$ is called the *parity-check matrix* of C. The number $r = n-k$ corresponds to the number of parity check digits in the code, and is called the *redundancy* of the code C. The *information rate* (or *code rate*) of a code C is the number $R = \frac{\log_2 M}{n}$. For a q-ary $[n,k]$-code, $R = \frac{k}{n} \log_2 q$; for a binary $[n,k]$-code, $R = \frac{k}{n}$.

A *convolutional code* is a type of error-correction code in which each k-bit information symbol to be encoded is transformed into an n-bit codeword, where $R = \frac{k}{n}$ is the code rate ($n \geq k$), and the transformation is a function of the last m information symbols, where m is the *constraint length* of the code. Convolutional codes are often used to improve the performance of radio and satellite links.

A *variable length code* is a code with codewords of different lengths.

In contrast to error-correcting codes which are designed only to increase the reliability of data communications, *cryptographic codes* are designed to increase their security. In Cryptography, the sender uses a *key* to encrypt a message before it is sent through an insecure channel, and an authorized receiver at the other end then uses a key to decrypt the received data to a message.

Often, data compression algorithms and error-correcting codes are used in tandem with cryptographic codes to yield communications that are efficient, robust to data transmission errors, and secure to eavesdropping and tampering. Encrypted messages which are, moreover, hidden in text, image, etc., are called *steganographic messages*.

The *encryption/assortment theory of humor* (Flamson–Barrett, 2008) proposes that people signal similarity in locally variable personal features through humor. In a successful joke, both the producer and the receiver share common background information—the key—and the joke is engineered in such a way (via devices such as incongruity) that there is a nonrandom fit between the surface utterance and this

information that would only be apparent to a person with access to it. The function of encrypted humor is not secrecy per se, but rather, honestly indexing the presence of shared keys.

16.1 Minimum Distance and Relatives

- **Minimum distance**

  Given a code $C \subset V$, where V is an n-dimensional vector space equipped with a metric d, the **minimum distance** $d^* = d^*(C)$ of the code C is defined by

  $$\min_{x,y \in C, x \neq y} d(x, y).$$

  The metric d depends on the nature of the errors for the correction of which the code is intended. For a prescribed correcting capacity it is necessary to use codes with a maximum number of codewords. Such most widely investigated codes are the *q-ary block codes* in the **Hamming metric** $d_H(x, y) = |\{i : x_i \neq y_i, i = 1, \ldots, n\}|$.

  For a *linear code* C the minimum distance $d^*(C) = w(C)$, where $w(C) = \min\{w(x) : x \in C\}$ is a *minimum weight* of the code C. As there are $\operatorname{rank}(H) \leq n - k$ independent columns in the parity check matrix H of an $[n, k]$-code C, then $d^*(C) \leq n - k + 1$ (*Singleton upper bound*).
- **Dual distance**

  The **dual distance** $d^\perp$ of a *linear* $[n, k]$-code $C \subset \mathbb{F}_q^n$ is the **minimum distance** of the *dual code* $C^\perp$ of C defined by $C^\perp = \{v \in \mathbb{F}_q^n : \langle v, u \rangle = 0 \text{ for any } u \in C\}$.

  The code $C^\perp$ is a linear $[n, n-k]$-code, and its $(n-k) \times n$ generator matrix is the parity-check matrix of C.
- **Bar product distance**

  Given linear codes C_1 and C_2 of length n with $C_2 \subset C_1$, their *bar product* $C_1|C_2$ is a linear code of length $2n$ defined by $C_1|C_2 = \{x|x+y : x \in C_1, y \in C_2\}$.

  The **bar product distance** between C_1 and C_2 is the minimum distance $d^*(C_1|C_2)$ of their bar product $C_1|C_2$.
- **Design distance**

  A *linear code* is called a *cyclic code* if all cyclic shifts of a codeword also belong to C, i.e., if for any $(a_0, \ldots, a_{n-1}) \in C$ the vector $(a_{n-1}, a_0, \ldots, a_{n-2}) \in C$. It is convenient to identify a codeword $(a_0, \ldots, a_{n-1})$ with the polynomial $c(x) = a_0 + a_1 x + \cdots + a_{n-1} x^{n-1}$; then every cyclic $[n, k]$-code can be represented as the principal ideal $\langle g(x) \rangle = \{r(x)g(x) : r(x) \in R_n\}$ of the ring $R_n = \mathbb{F}_q(x)/(x^n - 1)$, generated by the *generator polynomial* $g(x) = g_0 + g_1 x + \cdots + x^{n-k}$ of C.

  Given an element α of order n in a finite field $\mathbb{F}_{q^s}$, a *Bose–Chaudhuri–Hocquenghem* $[n, k]$-*code* of **design distance** d is a cyclic code of length n, generated by a polynomial $g(x)$ in $\mathbb{F}_q(x)$ of degree $n - k$, that has roots at α,

$\alpha^2, \ldots, \alpha^{d-1}$. The minimum distance d^* of such a code of odd design distance d is at least d.

A *Reed–Solomon code* is a Bose–Chaudhuri–Hocquenghem code with $s = 1$. The generator polynomial of a Reed–Solomon code of design distance d is $g(x) = (x-\alpha)\ldots(x-\alpha^{d-1})$ with degree $n-k = d-1$; that is, for a Reed–Solomon code the design distance $d = n-k+1$, and the minimum distance $d^* \geq d$. Since, for a linear $[n,k]$-code, the minimum distance $d^* \leq n-k+1$ (*Singleton upper bound*), a Reed–Solomon code achieves this bound. Compact disc players use a double-error correcting $(255, 251, 5)$ Reed–Solomon code over $\mathbb{F}_{256}$.

- **Goppa designed minimum distance**

  The **Goppa designed minimum distance** ([Gopp71]) is a lower bound $d^\star(m)$ for the minimum distance of *one-point geometric Goppa codes* (or *algebraic geometry codes*) $G(m)$. For $G(m)$, associated to the divisors D and mP, $m \in \mathbb{N}$, of a smooth projective absolutely irreducible algebraic curve of genus $g > 0$ over a finite field $\mathbb{F}_q$, one has $d^\star(m) = m + 2 - 2g$ if $2g - 2 < m < n$.

  In fact, for a Goppa code $C(m)$ the structure of the gap sequence at P may allow one to give a better lower bound of the minimum distance (cf. **Feng–Rao distance**).

- **Feng–Rao distance**

  The **Feng–Rao distance** $\delta_{FR}(m)$ is a lower bound for the minimum distance of *one-point geometric Goppa codes* $G(m)$ which is better than the **Goppa designed minimum distance**. The method of Feng and Rao for encoding the code $C(m)$ decodes errors up to half the Feng–Rao distance $\delta_{FR}(m)$, and gives an improvement of the number of errors that one can correct for one-point geometric Goppa codes.

  Formally, the Feng–Rao distance is defined as follows. Let S be a subsemigroup S of $\mathbb{N} \cup \{0\}$ such that the *genus* $g = |\mathbb{N} \cup \{0\} \backslash S|$ of S is finite, and $0 \in S$. The **Feng–Rao distance** on S is a function $\delta_{FR} : S \to \mathbb{N} \cup \{0\}$ such that $\delta_{FR}(m) = \min\{\nu(r) : r \geq m, r \in S\}$, where $\nu(r) = |\{(a,b) \in S^2 : a + b = r\}|$.

  The generalized ***r*-th Feng–Rao distance** on S is $\delta^r_{FR}(m) = \min\{\nu[m_1, \ldots, m_r] : m \leq m_1 < \cdots < m_r, m_i \in S\}$, where $\nu[m_1, \ldots, m_r] = |\{a \in S : m_i - a \in S \text{ for some } i = 1, \ldots, r\}|$. Then $\delta_{FR}(m) = \delta^1_{FR}(m)$. See, for example, [FaMu03].

- **Free distance**

  The **free distance** is the minimum nonzero *Hamming weight* of any codeword in a *convolutional code* or a *variable length code*.

  Formally, the ***k*-th minimum distance** d^*_k of such code is the smallest Hamming distance between any two initial codeword segments which are k frame long and disagree in the initial frame. The sequence $d^*_1, d^*_2, d^*_3, \ldots$ $(d^*_1 \leq d^*_2 \leq d^*_3 \leq \ldots)$ is called the *distance profile* of the code. The **free distance** of a convolutional code or a variable length code is $\max_l d^*_l = \lim_{l\to\infty} d^*_l = d^*_\infty$.

- **Effective free distance**

  A *turbo code* is a long *block code* in which there are L input bits, and each of these bits is encoded q times. In the j-th encoding, the L bits are sent through a permutation box P_j, and then encoded via an $[N_j, L]$ block encoder (*code fragment*

encoder) which can be thought of as an $L \times N_j$ matrix. The overall turbo code is then a *linear* $[N_1 + \cdots + N_q, L]$-code (see, for example, [BGT93]).

The *weight-i input minimum distance* $d^i(C)$ of a turbo code C is the minimum weight among codewords corresponding to input words of weight i. The **effective free distance** of C is its *weight-2 input minimum distance* $d^2(C)$, i.e., the minimum *weight* among codewords corresponding to input words of weight 2.

Turbo codes were the first practical codes to closely approach the *Shannon limit* (or *channel capacity*), the theoretical limit of maximum information transfer rate over a symmetric memory-less noisy channel. These codes are used in 3G mobile and satellite communications. Another capacity-approaching codes with similar performance are linear LDPC (*low-density parity-check*) codes.

- **Distance distribution**

  Given a code C over a finite metric space (X, d) with the diameter $diam(X, d) = D$, the **distance distribution** of C is a $(D+1)$-vector $(A_0, \ldots, A_D)$, where $A_i = \frac{1}{|C|}|\{(c, c') \in C^2 : d(c, c') = i\}|$. That is, one considers $A_i(c)$ as the number of code words at distance i from the codeword c, and takes A_i as the average of $A_i(c)$ over all $c \in C$. $A_0 = 1$ and, if $d^* = d^*(C)$ is the minimum distance of C, then $A_1 = \cdots = A_{d^*-1} = 0$.

  The distance distribution of a code with given parameters is important, in particular, for bounding the probability of decoding error under different decoding procedures from *maximum likelihood* decoding to error detection. It can also be helpful in revealing structural properties of codes and establishing nonexistence of some codes.

- **Unicity distance**

  The **unicity distance** of a cryptosystem (Shannon, 1949) is the minimal length of a cyphertext that is required in order to expect that there exists only one meaningful decryption for it. For classic cryptosystems with fixed key space, the unicity distance is approximated by the formula $H(K)/D$, where $H(K)$ is the *key space entropy* (roughly $\log_2 N$, where N is the number of keys), and D measures the *redundancy* of the plaintext source language in bits per letter.

  A cryptosystem offers perfect secrecy if its unicity distance is infinite. For example, the *one-time pads* offer perfect secrecy; they were used for the "red telephone" between the Kremlin and the White House.

  More generally, **Pe-security distance** of a cryptosystem (Tilburg–Boekee, 1987) is the minimal expected length of cyphertext that is required in order to break the cryptogram with an average error probability of at most Pe.

16.2 Main Coding Distances

- **Arithmetic codes distance**

  An *arithmetic code* (or *code with correction of arithmetic errors*) is a finite subset of the set $\mathbb{Z}$ of integers (usually, nonnegative integers). It is intended for the control of the functioning of an *adder* (a module performing addition). When

adding numbers represented in the binary number system, a single slip in the functioning of the adder leads to a change in the result by some power of 2, thus, to a single *arithmetic error*. Formally, a single *arithmetic error* on $\mathbb{Z}$ is defined as a transformation of a number $n \in \mathbb{Z}$ to a number $n' = n \pm 2^i$, $i = 1, 2, \ldots$.

The **arithmetic codes distance** is a metric on $\mathbb{Z}$ defined, for any $n_1, n_2 \in \mathbb{Z}$, as the minimum number of *arithmetic errors* taking n_1 to n_2. It is $w_2(n_1 - n_2)$, where $w_2(n)$ is the *arithmetic 2-weight* of n, i.e., the smallest possible number of nonzero coefficients in representations $n = \sum_{i=0}^{k} e_i 2^i$, where $e_i = 0, \pm 1$, and k is some nonnegative integer. For each n there is a unique such representation with $e_k \neq 0$, $e_i e_{i+1} = 0$ for all $i = 0, \ldots, k-1$, which has the smallest number of nonzero coefficients (cf. **arithmetic *r*-norm metric** in Chap. 12).

- ***b*-burst metric**

  Given the number $b > 1$ and the set $\mathbb{Z}_m^n = \{0, 1, \ldots, m-1\}^n$, each its element $x = (x_1, \ldots, x_n)$ can be uniquely represented as

$$(0^{k_1} u_1 v_1^{b-1} 0^{k_2} u_2 v_2^{b-1} \ldots),$$

  where $u_i \neq 0$, 0^k is the string of $k \geq 0$ zeroes and v^{b-1} is any string of length $b-1$.

  The ***b*-burst metric** between elements x and y of $\mathbb{Z}_m^n$ is (Bridewell and Wolf, 1979) the number of b-tuples uv^{b-1} in $x - y$. It describes the burst errors.

- **Sharma–Kaushik metrics**

  Let $q \geq 2$, $m \geq 2$. A *partition* $\{B_0, B_1, \ldots B_{q-1}\}$ of $\mathbb{Z}_m$ is called a *Sharma–Kaushik partition* if the following conditions hold:

  1. $B_0 = \{0\}$;
  2. For any $i \in Z_m$, $i \in B_s$ if and only if $m - i \in B_s$, $s = 1, 2, \ldots, q-1$;
  3. If $i \in B_s, j \in B_t$, and $s > t$, then $\min\{i, m-i\} > \min\{j, m-j\}$;
  4. If $s \geq t$, $s, t = 0, 1, \ldots, q-1$, then $|B_s| \geq |B_t|$ except for $s = q-1$ in which case $|B_{q-1}| \geq \frac{1}{2}|B_{q-2}|$.

  Given a Sharma–Kaushik partition of $\mathbb{Z}_m$, the *Sharma-Kaushik weight* $w_{SK}(x)$ of any element $x \in \mathbb{Z}_m$ is defined by $w_{SK}(x) = i$ if $x \in B_i$, $i \in \{0, 1, \ldots, q-1\}$.

  The **Sharma–Kaushik metric** ([ShKa79]) is a metric on $\mathbb{Z}_m$ defined by

$$w_{SK}(x - y).$$

  The Sharma–Kaushik metric on Z_m^n is defined by $w_{SK}^n(x - y)$ where, for $x = (x_1, \ldots x_n) \in \mathbb{Z}_m^n$, one has $w_{SK}^n(x) = \sum_{i=1}^{n} w_{SK}(x_i)$.

  The **Hamming metric** and the **Lee metric** arise from two specific partitions of the above type: $P_H = \{B_0, B_1\}$, where $B_1 = \{1, 2, \ldots, q-1\}$, and $P_L = \{B_0, B_1, \ldots, B_{\lfloor q/2 \rfloor}\}$, where $B_i = \{i, m-i\}$, $i = 1, \ldots, \lfloor \frac{q}{2} \rfloor$.

- **Varshamov metric**

  The **Varshamov metric** between two binary n-vectors $x = (x_1, \ldots, x_n)$ and $y = (y_1, \ldots, y_n)$ from $\mathbb{Z}_2^n = \{0, 1\}^n$ is defined by

$$\max\left(\sum_{i=1}^{n} I_{x_i=1-y_i=0}, \sum_{i=1}^{n} I_{x_i=1-y_i=1}\right).$$

  This metric was introduced by Varshamov, 1965, to describe asymmetric errors.

- **Absolute summation distance**

  The **absolute summation distance** (or *Lee distance*) is the **Lee metric** on the set $\mathbb{Z}_m^n = \{0, 1, \ldots, m-1\}^n$ defined by

$$w_{Lee}(x - y),$$

  where $w_{Lee}(x) = \sum_{i=1}^{n} \min\{x_i, m - x_i\}$ is the *Lee weight* of $x = (x_1, \ldots, x_n) \in \mathbb{Z}_m^n$.

  If $\mathbb{Z}_m^n$ is equipped with the absolute summation distance, then a subset C of $\mathbb{Z}_m^n$ is called a *Lee distance code*. The most important such codes are *negacyclic codes*.

- **Mannheim distance**

  The **Mannheim distance** is a 2D generalization of the **Lee metric**.

  Let $\mathbb{Z}[i] = \{a + bi : a, b \in \mathbb{Z}\}$ be the set of *Gaussian integers*. Let $\pi = a + bi$ $(a > b > 0)$ be a *Gaussian prime*, i.e., either

  (i) $(a + bi)(a - bi) = a^2 + b^2 = p$, where $p \equiv 1 \pmod 4$ is a prime number, or
  (ii) up to an integer, $\pi = p + 0 \cdot i$, where $p \equiv 3 \pmod 4$ is a prime number.

  The **Mannheim distance** is not a metric; it is defined ([Hube94a]), for any $x, y \in \mathbb{Z}[i]$, as $|x'| + |y'|$, where $x' + y'i = x - y \pmod \pi$, which is defined as $(x - y) - [\frac{(x-y)\overline{\pi}}{\pi\overline{\pi}}]\pi$ in the case (i). Here [.] denotes rounding to the *closest Gaussian integer*, i.e., $[c + di] = [c] + [d]i$ with $[c]$ denoting the rounding to the closest integer.

  In general, the elements of the finite field $\mathbb{F}_p = \{0, 1, \ldots, p-1\}$ for $p \equiv 1 \pmod 4$, $p = a^2 + b^2$, and of the finite field $\mathbb{F}_{p^2}$ for $p \equiv 3 \pmod 4$, $p = a$, can be mapped on a subset of $\mathbb{Z}[i]$ using the complex modulo function $\mu(k) = k - [\frac{k(a-bi)}{p}](a + bi)$, $k = 0, \ldots, p-1$. The set of the selected Gaussian integers $a + bi$ with the minimal *complex modulus* norms $\sqrt{(a + bi)(a - bi)} = \sqrt{a^2 + b^2}$ is called a *constellation*.

  The Mannheim distance between two vectors over $\mathbb{Z}[i]$ is the sum of the Mannheim distances of corresponding components. It was introduced to make 2D QAM-like signals more susceptible to algebraic decoding methods.

  For codes over hexagonal signal constellations, a similar metric was introduced over $\mathbb{Z}(\frac{i\sqrt{3}+1}{2})$ in [Hube94b]. Cf. $\mathbb{Z}(\eta_m)$**-related norm metrics** in Chap. 12.

- **Generalized Lee metric**

  Let $\mathbb{F}_{p^m}$ denote the finite field with p^m elements, where p is prime number and $m \geq 1$ is an integer. Let $e_i = (0, \ldots, 0, 1, 0, \ldots, 0)$, $1 \leq i \leq k$, be the standard basis of $\mathbb{Z}^k$. Choose elements $a_i \in \mathbb{F}_{p^m}$, $1 \leq i \leq k$, and the mapping $\phi : \mathbb{Z}^k \to \mathbb{F}_{p^m}$, sending any $x = \sum_{i=1}^k x_i e_i$, $x_i \in \mathbb{Z}^k$, to $\phi(x) = \sum_{i=1}^k a_i x_i (\text{mod } p)$, so that ϕ is surjective. So, for each $a \in \mathbb{F}_{p^m}$, there exists $x \in \mathbb{Z}^k$ such that $a = \phi(x)$. For each $a \in \mathbb{F}_{p^m}$, its *k-dimensional Lee weight* is $w_{kL}(a) = \min\{\sum_{i=1}^k |x_i| : x = (x_i) \in \mathbb{Z}, a = \phi(x)\}$.

  The **generalized Lee metric** between vectors (a_j) and (b_j) of $\mathbb{F}_{p^m}^n$ is defined (Nishimura–Hiramatsu, 2008) by

$$\sum_{j=1}^{n} w_{kL}(a_j - b_j).$$

  It is the **Lee metric** (or **absolute summation distance**) if $\phi(e_1) = 1$ while $\phi(e_i) = 0$ for $2 \leq i \leq k$. It is the **Mannheim distance** if $k = 2$, $p \equiv 1 \pmod 4$, $\phi(e_1) = 1$ while $\phi(e_2) = a$ is a solution in $\mathbb{F}_p$ of the quadratic congruence $x^2 \equiv -1 \pmod p$.
- *p*-**Lee metric**

  The *p*-**Lee metric** on $\mathbb{Z}_q^n$ is given by $d_p^p(x, y) = \sum_{i=1}^n d(x_i, y_i)^p$ if $p \in [1, \infty)$, and $d(x, y) = \max_{i=1}^n d(x_i, y_i)$ if $p = \infty$, where $x = (x_1, \ldots, x_n), y = (y_1, \ldots, y_n) \in \mathbb{Z}_q^n$, and $d(x_i, y_i)$ is the **Lee metric** $\min\{|x_i - y_i|, q - |x_i - y_i|\}$ on $\mathbb{Z}$.
- **Poset metric**

  Let $(V_n, \preceq)$ be a *poset* on $V_n = \{1, \ldots, n\}$. A subset I of V_n is called *ideal* if $x \in I$ and $y \preceq x$ imply that $y \in I$. If $J \subset V_n$, then $\langle J \rangle$ denotes the smallest ideal of V_n which contains J. Consider the vector space $\mathbb{F}_q^n$ over a finite field $\mathbb{F}_q$. The *P-weight* of an element $x = (x_1, \ldots, x_n) \in \mathbb{F}_q^n$ is defined as the cardinality of the smallest ideal of V_n containing the *support* of x: $w_P(x) = |\langle supp(x) \rangle|$, where $supp(x) = \{i : x_i \neq 0\}$.

  The **poset metric** (see [BGL95]) is a metric on $\mathbb{F}_q^n$ defined by

$$w_P(x - y).$$

  If $\mathbb{F}_q^n$ is equipped with a poset metric, then a subset C of $\mathbb{F}_q^n$ is called a *poset code*. If V_n forms the chain $1 \leq 2 \leq \cdots \leq n$, then the linear code C of dimension k consisting of all vectors $(0, \ldots, 0, a_{n-k+1}, \ldots, a_n) \in \mathbb{F}_q^n$ is a perfect poset code with the minimum (poset) metric $d_P^*(C) = n - k + 1$.

  If V_n forms an antichain, then the poset distance coincides with the **Hamming metric**. If V_n consists of finite disjoint union of chains of equal lengths, then the poset distance coincides with the **NRT metric**.

- **Rank metric**

  Let $\mathbb{F}_q$ be a finite field, $\mathbb{K} = \mathbb{F}_{q^m}$ an extension of degree m of $\mathbb{F}_q$, and $\mathbb{K}^n$ a vector space of dimension n over $\mathbb{K}$. For any $a = (a_1, \ldots a_n) \in \mathbb{K}^n$ define its *rank*, rank(a), as the dimension of the vector space over $\mathbb{F}_q$, generated by $\{a_1, \ldots, a_n\}$.

  The **rank metric** (Delsarte, 1978) is a metric on $\mathbb{K}^n$ defined by

$$\text{rank}(a - b).$$

  A *constant rank-distance k set* is (Gow et al., 2014) a set U of $n \times n$ matrices over a field $\mathbb{F}$ such that rank$(A-B) = k$ for all $A, B \in U, A \neq B$ and rank$(A) = k$ for all $A \in U, A \neq 0$. Such set is called a *partial spread set* if $k = n$; it defines a partial spread in the $(2n-1)$-dimensional *projective*, *hermitian polar* or *symplectic polar space*, if U consists of arbitrary, hermitian or symmetric matrices, respectively.

- **Gabidulin–Simonis metrics**

  Let $\mathbb{F}_q^n$ be the vector space over a finite field $\mathbb{F}_q$ and let $F = \{F_i : i \in I\}$ be a finite family of its subsets such that the minimal linear subspace of $\mathbb{F}_q^n$ containing $\cup_{i \in I} F_i$ is $\mathbb{F}_q^n$. Without loss of generality, F can be an antichain of linear subspaces of $\mathbb{F}_q^n$.

  The *F-weight* w_F of a vector $x = (x_1, \ldots, x_n) \in \mathbb{F}_q^n$ is the smallest $|J|$ over such subsets $J \subset I$ that x belongs to the minimal linear subspace of $\mathbb{F}_q^n$ containing $\cup_{i \in J} F_i$. A **Gabidulin–Simonis metric** (or ***F*-distance**, see [GaSi98]) on $\mathbb{F}_q^n$ is defined by

$$w_F(x - y).$$

  The **Hamming metric** corresponds to the case of $F_i, i \in I$, forming the standard basis. The **Vandermonde metric** is F-distance with $F_i, i \in I$, being the columns of a generalized Vandermonde matrix. Among other examples are: the **rank metric** and the *combinatorial metrics* (by Gabidulin, 1984), including the ***b*-burst metric**.

- **Subspace metric**

  Let $\mathbb{F}_q^n$ be the vector space over a finite field $\mathbb{F}_q$ and let $\mathcal{P}_{n,q}$ be the set of all subspaces of $\mathbb{F}_q^n$. For any subspace $U \in \mathcal{P}_{n,q}$, let $dim(U)$ denote its dimension and let $U^\perp = \{v \in \mathbb{F}_q^n : \langle u, v \rangle = 0 \text{ for all } u \in U\}$ be its orthogonal space.

  Let $U + V = \{u + v : u \in U, v \in V\}$, i.e., $U + V$ is the smallest subspace of $\mathbb{F}_q^n$ containing both V and V. Then $dim(U + V) = dim(U) + dim(V) - dim(U \cap V)$. If $U \cap V = \emptyset$, then $U + V$ is a direct sum $U \oplus V$.

  The **subspace metric** between two subspaces U and V from $\mathcal{P}_{n,q}$ is defined by

$$d(U, V) = dim(U + V) - dim(U \cap V) = dim(U) + dim(V) - 2dim(U \cap V).$$

  This metric was introduced by Koetter and Kschischang, 2007, for network coding. It holds $d(U, V) = d(U^\perp, V^\perp)$. Cf. the **lattice valuation metric** in Chap. 10 and distances between subspaces in Chap. 12.

- **NRT metric**

  Let $M_{m,n}(\mathbb{F}_q)$ be the set of all $m \times n$ matrices with entries from a finite field $\mathbb{F}_q$ (in general, from any finite alphabet $\mathcal{A} = \{a_1, \ldots, a_q\}$). The *NRT norm* $||.||_{RT}$ on $M_{m,n}(\mathbb{F}_q)$ is defined as follows: if $m = 1$ and $a = (\xi_1, \xi_2, \ldots, \xi_n) \in M_{1,n}(\mathbb{F}_q)$, then $||0_{1,n}||_{RT} = 0$, and $||a||_{RT} = \max\{i : \xi_i \neq 0\}$ for $a \neq 0_{1,n}$; if $A = (a_1, \ldots, a_m)^T \in M_{m,n}(\mathbb{F}_q)$, $a_j \in M_{1,n}(\mathbb{F}_q)$, $1 \leq j \leq m$, then $||A||_{RT} = \sum_{j=1}^{m} ||a_j||_{RT}$.

  The **NRT metric** (or *Niederreiter–Rosenbloom–Tsfasman metric*, since introduced by Niederreiter, 1991, and Rosenbloom–Tsfasman, 1997; or *ordered Hamming distance*, in ([MaSt99]) is a **matrix norm metric** (in fact, an **ultrametric**) on $M_{m,n}(\mathbb{F}_q)$, defined by

$$||A - B||_{RT}.$$

  For every matrix code $C \subset M_{m,n}(F_q)$ with q^k elements the minimum NRT distance $d^*_{RT}(C) \leq mn - k + 1$. Codes meeting this bound are called *maximum distance separable codes*.

  The most used distance between codewords of a matrix code $C \subset M_{m,n}(F_q)$ is the **Hamming metric** on $M_{m,n}(F_q)$ defined by $||A - B||_H$, where $||A||_H$ is the *Hamming weight* of a matrix $A \in M_{m,n}(\mathbb{F}_q)$, i.e., the number of its nonzero entries.

  The **LRTJ-metric** (introduced as *Generalized Lee–Rosenbloom–Tsfasman pseudo-metric* by Jain, 2008) is the **norm metric** for the following generalization of the above norm $||a||_{RT}$ in the case $a \neq 0_{1,n}$:

$$||a||_{LRTJ} = \max_{1 \leq i \leq n} \min\{\xi_i, q - \xi_i\} + \max\{i - 1 : \xi_i \neq 0\}.$$

  It is the **Lee metric** for $m = 1$ and the NRT metric for $q = 2, 3$.

- **ACME distance**

  The **ACME distance** on a code $C \subset \mathcal{A}^n$ over an alphabet $\mathcal{A}$ is defined by

$$\min\{d_H(x, y), d_I(x, y)\},$$

  where d_H is the **Hamming metric**, and d_I is the **swap metric** (Chap. 11), i.e., the minimum number of interchanges of adjacent pairs of symbols, converting x into y.

- **Indel distance**

  Let W be the set of all words over an alphabet $\mathcal{A}$. A *deletion* of a letter in a word $\beta = b_1 \ldots b_n$ of the length n is a transformation of β into a word $\beta' = b_1 \ldots b_{i-1} b_{i+1} \ldots b_n$ of the length $n - 1$. An *insertion* of a letter in a word $\beta = b_1 \ldots b_n$ of the length n is a transformation of β into a word $\beta'' = b_1 \ldots b_i b b_{i+1} \ldots b_n$, of the length $n + 1$.

The **indel distance** is a metric on W, defined as the minimum number of deletions and insertions of letters converting α into β. Cf. **indel metric** in Chap. 11.

A *code C with correction of deletions and insertions* is an arbitrary finite subset of W. An example of such a code is the set of words $\beta = b_1 \dots b_n$ of length n over the alphabet $\mathcal{A} = \{0, 1\}$ for which $\sum_{i=1}^{n} ib_i \equiv 0 \pmod{n+1}$. The number of words in this code is equal to $\frac{1}{2(n+1)} \sum_k \phi(k) 2^{(n+1)/k}$, where the sum is taken over all odd divisors k of $n+1$, and ϕ is the *Euler function*.

- **Interval distance**

  The **interval distance** (see, for example, [Bata95]) is a metric on a finite group $(G, +, 0)$ defined by

$$w_{int}(x - y),$$

  where $w_{int}(x)$ is an *interval weight* on G, i.e., a *group norm* whose values are consecutive nonnegative integers $0, \dots, m$. This distance is used for *group codes* $C \subset G$.

- **Fano metric**

  The **Fano metric** is a *decoding metric* with the goal to find the best sequence estimate used for the *Fano algorithm* of *sequential decoding* of *convolutional codes*. In a *convolutional code* each k-bit information symbol to be encoded is transformed into an n-bit codeword, where $R = \frac{k}{n}$ is the code rate ($n \geq k$), and the transformation is a function of the last m information symbols.

  The linear time-invariant decoder (*fixed convolutional decoder*) maps an information symbol $u_i \in \{u_1, \dots, u_N\}$, $u_i = (u_{i1}, \dots u_{ik})$, $u_{ij} \in \mathbb{F}_2$, into a codeword $x_i \in \{x_1, \dots, x_N\}$, $x_i = (x_{i1}, \dots, x_{in})$, $x_{ij} \in \mathbb{F}_2$, so one has a code $\{x_1, \dots, x_N\}$ with N codewords which occur with probabilities $\{p(x_1), \dots, p(x_N)\}$. A sequence of l codewords forms a *path* $x = x_{[1,l]} = \{x_1, \dots, x_l\}$ which is transmitted through a *discrete memoryless channel*, resulting in the received sequence $y = y_{[1,l]}$.

  The task of a decoder minimizing the sequence error probability is to find a sequence maximizing the joint probability of input and output channel sequences $p(y, x) = p(y|x) \cdot p(x)$. Usually it is sufficient to find a procedure that maximizes $p(y|x)$, and a decoder that always chooses as its estimate one of the sequences that maximizes it or, equivalently, the **Fano metric**, is called a *max-likelihood decoder*.

  Roughly, we consider each code as a tree, where each branch represents one codeword. The decoder begins at the first vertex in the tree, and computes the branch metric for each possible branch, determining the best branch to be the one corresponding to the codeword x_j resulting in the largest branch metric, $\mu_F(x_j)$.

  This branch is added to the path, and the algorithm continues from the new node which represents the sum of the previous node and the number of bits in the current best codeword. Through iterating until a terminal node of the tree is reached, the algorithm traces the most likely path.

In this construction, the **bit Fano metric** is defined by

$$\log_2 \frac{p(y_i|x_i)}{p(y_i)} - R,$$

the **branch Fano metric** is defined by

$$\mu_F(x_j) = \sum_{i=1}^{n} (\log_2 \frac{p(y_i|x_{ji})}{p(y_i)} - R),$$

and the **path Fano metric** is defined by

$$\mu_F(x_{[1,l]}) = \sum_{j=1}^{l} \mu_F(x_j),$$

where $p(y_i|x_{ji})$ are the channel transition probabilities, $p(y_i) = \sum_{x_m} p(x_m)p(y_i|x_m)$ is the probability distribution of the output given the input symbols averaged over all input symbols, and $R = \frac{k}{n}$ is the code rate.

For a hard-decision decoder $p(y_j = 0|x_j = 1) = p(y_j = 1|x_j = 0) = p$, $0 < p < \frac{1}{2}$, the Fano metric for a path $x_{[1,l]}$ can be written as

$$\mu_F(x_{[1,l]}) = -\alpha d_H(y_{[1,l]}, x_{[1,l]}) + \beta \cdot l \cdot n,$$

where $\alpha = -\log_2 \frac{p}{1-p} > 0$, $\beta = 1 - R + \log_2(1-p)$, and d_H is the **Hamming metric**.

The **generalized Fano metric** is defined, for $0 \leq w \leq 1$, by

$$\mu_F^w(x_{[1,l]}) = \sum_{j=1}^{ln} \left(\log_2 \frac{p(y_j|x_j)^w}{p(y_j)^{1-w}} - wR \right).$$

For $w = 1/2$, it is the Fano metric with a multiplicative constant $1/2$.

- **Channel metrization**

  A *square channel* over $[n] = \{1, \ldots, n\}$ is an $n \times n$ probability matrix $P = (()P_{ij})$ such that P_{ij} is the probability $P(j|i) = P(j \text{ received if } i \text{ sent})$.

  For a code $C \subseteq [n]$, the *maximum likelihood decoder* (MLD) decodes j as $c \in C$ maximizing $P(j|c)$. If a metric d is defined on $[n]$, then the *minimum distance decoder* (MDD) decodes j as $c \in C$ minimizing $d(j, c)$.

  Channel metrization is (D'Oliveira–Firer, 2015), for a given channel P over $[n]$, to find a metric d on $[n]$ with coinciding decoders MLD and MDD, i.e., for every $C \subseteq [n]$ and $j \in [n]$, $\arg\min\{d(j, c) : c \in C\} = \arg\max\{P(j|c) : c \in C\}$. Main example: metrization of the binary symmetric channel by the Hamming metric.

- **Metric recursion of a MAP decoding**

  Maximum a posteriori sequence estimation, or *MAP decoding* for *variable length codes*, used the *Viterbi algorithm*, and is based on the **metric recursion**

$$\Lambda_k^{(m)} = \Lambda_{k-1}^{(m)} + \sum_{n=1}^{l_k^{(m)}} x_{k,n}^{(m)} \log_2 \frac{p(y_{k,n}|x_{k,n}^{(m)} = +1)}{p(y_{k,n}|x_{k,n}^{(m)} = -1)} + 2\log_2 p(u_k^{(m)}),$$

  where $\Lambda_k^{(m)}$ is the **branch metric** of branch m at time (level) k, $x_{k,n}$ is the n-th bit of the codeword having $l_k^{(m)}$ bits labeled at each branch, $y_{k,n}$ is the respective received soft-bit, u_k^m is the source symbol of branch m at time k and, assuming statistical independence of the source symbols, the probability $p(u_k^{(m)})$ is equivalent to the probability of the source symbol labeled at branch m, that may be known or estimated. The metric increment is computed for each branch, and the largest value, when using *log-likelihood* values, of each state is used for further recursion. The decoder first computes the metric of all branches, and then the branch sequence with largest metric starting from the final state backward is selected.

- **Distance decoder**

  A graph family A is said (Peleg, 2000) to have an $l(n)$ **distance labeling scheme** if there is a function L_G labeling the vertices of each n-vertex graph $G \in A$ with distinct labels up to $l(n)$ bits, and there exists an algorithm, called a **distance decoder**, that decides the distance $d(u, v)$ between any two vertices $u, v \in X$ in a graph $G \in A$, i.e.,$d(u, v) = f(L_G(u), L_G(v))$, polynomial in time in the length of their labels $L(u), L(v)$.

  Cf. **distance constrained labeling** in Chap. 15.

- **Identifying code**

  Let $G = (X, E)$ be a digraph and $C \subset V$, and let $B(v)$ denote the set consisting of v and all of its incoming neighbors in G. If the sets $B(v) \cap C$ are nonempty and distinct, C is called **identifying code** of G. Such sets of smallest cardinality are called (Karpovsky–Chakrabarty–Levitin, 1998) *minimum identifying codes*; denote this cardinality by $M(G)$. An ***r*-locating-dominating set** (Chap. 15) with $r = 1$ differs from an identifying code only in that $B(v) \cap C$ are not required to be unique *identifying sets* for $v \in C$.

  A *minimum identifying code graph* of order n is a graph $G = (X, E)$ with $X = n$ and $M(G) = \lceil \log 2(n + 1) \rceil$ having the minimum number of edges $|E|$.

Chapter 17
Distances and Similarities in Data Analysis

A *data set* is a finite set comprising m sequences $(x_1^j, \ldots, x_n^j)$, $j \in \{1, \ldots, m\}$, of length n. The values $x_i^1, \ldots, x_i^m$ represent an *attribute* S_i.

Among numerical data, **metric data** is any reading at an *interval scale*, measuring the degree of difference between items, or at a *ratio scale* measuring the ratio between a magnitude of a continuous quantity and a unit magnitude of the same kind; with them one have a meter permitting define distances between scale values. **Nonmetric** (or *categorial*, *qualitative*) **data** are collected from *binary* (presence/absence expressed by $1/0$), *ordinal* (numbers expressing rank only), or *nominal* (items are not ordered) *scale*.

Geometric data analysis refer to geometric aspects of image, pattern and shape analysis that treats arbitrary data sets as clouds of points in $\mathbb{R}^n$.

Often data are organized in a **metric database** (especially, **metric tree**), i.e., a database indexed in a metric space. The term *metric indexing* is also used.

Cluster Analysis (or *Classification*, *Taxonomy*, *Pattern Recognition*) consists mainly of partition of data A into a relatively small number of *clusters*, i.e., such sets of objects that (with respect to a selected measure of distance) are at best possible degree, "close" if they belong to the same cluster, "far" if they belong to different clusters, and further subdivision into clusters will impair the above two conditions.

We give three typical examples. In *Information Retrieval* applications, nodes of peer-to-peer database network export data (collection of text documents); each document is characterized by a vector from $\mathbb{R}^n$. An user needs to retrieve all documents in the database which are *relevant* to a query object (say, a vector $x \in \mathbb{R}^n$), i.e., belong to the *ball* in $\mathbb{R}^n$, center x, of fixed radius and with a convenient distance function. Such similarity query is called a **metric range query**. In *Record Linkage*, each document (database record) is represented by a term-frequency vector $x \in \mathbb{R}^n$ or a string, and one wants to measure semantic relevancy of syntactically different records. In *Ecology*, let x, y be *species abundance distributions*, obtained by two sample methods (i.e., x_j, y_j are the numbers of individuals of species j,

© Springer-Verlag Berlin Heidelberg 2016

M.M. Deza, E. Deza, *Encyclopedia of Distances*,
DOI 10.1007/978-3-662-52844-0_17

observed in a corresponding sample); one needs a measure of the distance between x and y, in order to compare two methods.

Once a distance d between objects is selected, it is **intra-distance** or **inter-distance** if the objects are within the same cluster or in two different clusters, respectively.

The **linkage metric**, i.e., a distance between clusters $A = \{a_1, \ldots, a_m\}$ and $B = \{b_1, \ldots, b_n\}$ is usually one of the following:

average linkage: the average of the distances between the all members of the clusters, i.e., $\frac{\sum_i \sum_j d(a_i,b_j)}{mn}$;
single linkage: the distance $\min_{i,j} d(a_{i,j})$ between the nearest members of the clusters, i.e., the **set-set distance** (Chap. 1);
complete linkage: the distance $\max_{i,j} d(a_i, b_j)$ between the furthest members of the clusters, i.e., the **spanning distance** (Chap. 1);
centroid linkage: the distance between the *centroids* of the clusters, i.e, $||\tilde{a}-\tilde{b}||_2$, where $\tilde{a} = \frac{\sum_i a_i}{m}$, and $\tilde{b} = \frac{\sum_j b_j}{n}$;
Ward linkage: the distance $\sqrt{\frac{mn}{m+n}}||\tilde{a} - \tilde{b}||_2$.

Multidimensional Scaling is a technique developed in the behavioral and Social Sciences for studying the structure of objects or people. Together with Cluster Analysis, it is based on distance methods. But in Multidimensional Scaling, as opposed to Cluster Analysis, one starts only with some $m \times m$ matrix D of distances of the objects and (iteratively) looks for a representation of objects in $\mathbb{R}^n$ with low n, so that their Euclidean distance matrix has minimal square deviation from the original matrix D.

The related *Metric Nearness Problem* (Dhillon–Sra–Tropp, 2003) is to approximate a given finite distance space (X, d) by a metric space (X, d'). Other examples of distance methods in Data Analysis are *distance-based outlier detection* (in Data Mining) and *distance-based redundancy analysis* (in Multivariate Statistics).

There are many **similarities** used in Data Analysis; the choice depends on the nature of data and is not an exact science. We list below the main such similarities and distances.

Given two objects, represented by nonzero vectors $x = (x_1, \ldots, x_n)$ and $y = (y_1, \ldots, y_n)$ from $\mathbb{R}^n$, the following notation is used in this chapter.

$\sum x_i$ means $\sum_{i=1}^n x_i$.

1_F is the *characteristic function* of event F: $1_F = 1$ if F happens, and $1_F = 0$, otherwise.

$||x||_2 = \sqrt{\sum x_i^2}$ is the ordinary Euclidean norm on $\mathbb{R}^n$.

$\bar{x}$ denotes $\frac{\sum x_i}{n}$, i.e., the *mean value* of components of x. So, $\bar{x} = \frac{1}{n}$ if x is a *frequency vector* (*discrete probability distribution*), i.e., all $x_i \geq 0$, and $\sum x_i = 1$; and $\bar{x} = \frac{n+1}{2}$ if x is a *ranking* (*permutation*), i.e., all x_i are different numbers from $\{1, \ldots, n\}$.

The *k-th moment* is $\frac{\sum (x_i - \bar{x})^k}{n}$; it is called *variance*, *skewness*, *kurtosis* if $k = 2, 3, 4$.

In the binary case $x \in \{0,1\}^n$ (i.e., when x is a binary n-sequence), let $X = \{1 \leq i \leq n : x_i = 1\}$ and $\overline{X} = \{1 \leq i \leq n : x_i = 0\}$. Let $|X \cap Y|$, $|X \cup Y|$, $|X \backslash Y|$ and $|X \triangle Y|$ denote the cardinality of the intersection, union, difference and symmetric difference $(X \backslash Y) \cup (Y \backslash X)$ of the sets X and Y, respectively.

17.1 Similarities and Distances for Numerical Data

- **Ruzicka similarity**
  The **Ruzicka similarity** is a similarity on $\mathbb{R}^n$, defined by

$$\frac{\sum \min\{x_i, y_i\}}{\sum \max\{x_i, y_i\}}.$$

  The corresponding **Soergel distance**

$$1 - \frac{\sum \min\{x_i, y_i\}}{\sum \max\{x_i, y_i\}} = \frac{\sum |x_i - y_i|}{\sum \max\{x_i, y_i\}}$$

  coincides on $\mathbb{R}^n_{\geq 0}$ with the **fuzzy polynucleotide metric** (Chap. 23).
  The **Wave–Edges distance** is defined by

$$\sum (1 - \frac{\min\{x_i, y_i\}}{\max\{x_i, y_i\}}) = \sum \frac{|x_i - y_i|}{\max\{x_i, y_i\}}.$$

- **Roberts similarity**
  The **Roberts similarity** is a similarity on $\mathbb{R}^n$, defined by

$$\frac{\sum (x_i + y_i) \frac{\min\{x_i, y_i\}}{\max\{x_i, y_i\}}}{\sum (x_i + y_i)}.$$

- **Ellenberg similarity**
  The **Ellenberg similarity** is a similarity on $\mathbb{R}^n$ defined by

$$\frac{\sum (x_i + y_i) 1_{x_i \cdot y_i \neq 0}}{\sum (x_i + y_i)(1 + 1_{x_i y_i = 0})}.$$

- **Gleason similarity**
  The **Gleason similarity** is a similarity on $\mathbb{R}^n$, defined by

$$\frac{\sum (x_i + y_i) 1_{x_i \cdot y_i \neq 0}}{\sum (x_i + y_i)}.$$

The **Czekanowsky–Dice distance** (or *nonmetric coefficient*, Bray–Curtis, 1957) is a **near-metric** on $\{0,1\}^n$ defined by

$$1 - \frac{2|X \cap Y|}{|X| + |Y|} = \frac{|X \Delta Y|}{|X| + |Y|}.$$

- **Warrens inequalities on similarities**

  Denote by S_k, $1 \leq k \leq 7$ above **intersection**, **Kulczynski 2**, **Bray–Curtis**, **Roberts**, **Ruzicka**, **Eilenberg** and **Gleason similarities**, respectively.

  Warrens (2016), showed that

$$1 \geq S_1 \geq S_2 \geq S_3 \geq S_4 \geq S_5 \geq 0 \quad \text{and} \quad S_5 \leq S_6 \leq S_7 \geq S_3.$$

- **Jaccard similarity**

  The **Jaccard similarity of community**, Jaccard, 1908, is a similarity on $\mathbb{R}^n$ defined by

$$\frac{\sum x_i y_i}{\sum x_i^2 + \sum y_i^2 - \sum x_i y_i}.$$

  The corresponding **Jaccard distance** is defined by

$$1 - \frac{\sum x_i y_i}{\sum x_i^2 + \sum y_i^2 - \sum x_i y_i} = \frac{(\sum x_i - y_i)^2}{\sum x_i^2 + \sum y_i^2 - \sum x_i y_i}.$$

  The binary cases of Jaccard, **Ellenberg** and **Ruzicka similarities** coincide; it is called **Tanimoto similarity**:

$$\frac{|X \cap Y|}{|X \cup Y|}.$$

  The **Tanimoto distance** (or **biotope distance** from Chap. 23) is a distance on $\{0,1\}^n$ defined by

$$1 - \frac{|X \cap Y|}{|X \cup Y|} = \frac{|X \Delta Y|}{|X \cup Y|}.$$

- **Czekanowsky similarity**

  The **Czekanowsky similarity** is a similarity on $\mathbb{R}^n$, defined by

$$\frac{\sum \min\{x_i, y_i\}}{\sum (x_i + y_i)}.$$

  The corresponding **Czekanowsky distance** is defined by

$$1 - \frac{\sum \min\{x_i, y_i\}}{\sum (x_i + y_i)} = \frac{\sum |x_i - y_i|}{\sum (x_i + y_i)}.$$

- **Dice similarity**
  The **Dice similarity** is a similarity on $\mathbb{R}^n$, defined by

$$\frac{\sum x_i y_i}{\sum x_i^2 + \sum y_i^2}.$$

  The corresponding **Dice distance** is defined by

$$1 - \frac{\sum x_i y_i}{\sum x_i^2 + \sum y_i^2} = \frac{\sum |x_i - y_i|}{\sum x_i^2 + \sum y_i^2}.$$

- **Maryland Bridge similarity**
  The **Maryland Bridge similarity** is (Mirkin and Koonin, 2003) a similarity on $\mathbb{R}^n$ defined by

$$\frac{1}{2}\left(\frac{\sum x_i y_i}{\sum x_i^2} + \frac{\sum x_i y_i}{\sum y_i^2}\right).$$

  The corresponding **Maryland Bridge distance** is defined by

$$1 - \frac{1}{2}\left(\frac{\sum x_i y_i}{\sum x_i^2} + \frac{\sum x_i y_i}{\sum y_i^2}\right).$$

- **Simpson similarity**
  The **Simpson** (or *overlap*) **similarity** is a similarity on $\mathbb{R}^n$ defined by

$$\frac{\sum x_i y_i}{\min\{\sum x_i, \sum y_i\}}.$$

- **Intersection distance**
  The **intersection distance** is a distance on $\mathbb{R}^n$, defined by

$$1 - \frac{\sum \min\{x_i, y_i\}}{\min\{\sum x_i, \sum y_i\}}.$$

  It becomes $\frac{1}{2}\sum |x_i - y_i|$ if x, y are *frequency vectors*.
- **Kulczynski similarity** 1
  The **Kulczynski similarity** 1 is a similarity on $\mathbb{R}^n$ defined by

$$\frac{\sum \min\{x_i, y_i\}}{\sum |x_i - y_i|}.$$

  The corresponding **Kulczynski distance** is

$$\frac{\sum |x_i - y_i|}{\sum \min\{x_i, y_i\}}.$$

- **Kulczynski similarity** 2

  The **Kulczynski similarity** 2 is a similarity on $\mathbb{R}^n$ defined by

$$\frac{n}{2}\left(\frac{1}{\overline{x}}+\frac{1}{\overline{y}}\right)\sum \min\{x_i, y_i\}.$$

  In the binary case it coincides with **Maryland bridge similarity**; its form is

$$\frac{|X\cap Y|\cdot(|X|+|Y|)}{2|X|\cdot|Y|}=\frac{|X\cap Y|}{2|X|}+\frac{|X\cap Y|}{2|Y|}.$$

- **Motyka similarity**

  The **Motyka similarity** is a similarity on $\mathbb{R}^n$, defined by

$$\frac{\sum \min\{x_i, y_i\}}{\sum(x_i+y_i)}=n\frac{\sum \min\{x_i, y_i\}}{\overline{x}+\overline{y}}.$$

  The corresponding **Motyka distance** is

$$1-\frac{\sum \min\{x_i, y_i\}}{\sum(x_i+y_i)}=\frac{\sum \max\{x_i, y_i\}}{\sum(x_i+y_i)}.$$

- **Bray–Curtis similarity**

  The **Bray–Curtis similarity**, 1957, is a similarity on $\mathbb{R}^n$ defined by

$$\frac{2}{n(\overline{x}+\overline{y})}\sum \min\{x_i, y_j\}.$$

  It is called *Renkonen percentage similarity* if x, y are *frequency vectors*.

- **Sørensen distance**

  The **Sørensen** (or *Bray–Curtis*) **distance** on $\mathbb{R}^n$ is defined (Sørensen, 1948) by

$$1-\frac{2}{n(\overline{x}+\overline{y})}\sum \min\{x_i, y_j\}=\frac{\sum|x_i-y_i|}{\sum(x_i+y_i)}.$$

  The binary cases of **Bray–Curtis**, **Cleason**, **Czekanowsky** and **Dice similarities** coincide; it is called **Sørensen similarity**:

$$\frac{2|X\cap Y|}{|X\cup Y|+|X\cap Y|}=\frac{2|X\cap Y|}{|X|+|Y|}.$$

- **Canberra distance**

  The **Canberra distance** (Lance–Williams, 1967) is a distance on $\mathbb{R}^n$, defined by

$$\sum\frac{|x_i-y_i|}{|x_i|+|y_i|}.$$

- **Baroni–Urbani–Buser similarity**
  The **Baroni–Urbani–Buser similarity** is a similarity on $\mathbb{R}^n$ defined by

$$\frac{\sum \min\{x_i, y_i\} + \sqrt{\sum \min\{x_i, y_i\} \sum (\max_{1\le j\le n} x_j - \max\{x_i, y_i\})}}{\sum \max\{x_i, y_i\} + \sqrt{\sum \min\{x_i, y_i\} \sum (\max_{1\le j\le n} x_j - \max\{x_i, y_i\})}}.$$

  In the binary case it takes the form

$$\frac{|X \cap Y| + \sqrt{|X \cap Y| \cdot |\overline{X \cup Y}|}}{|X \cup Y| + \sqrt{|X \cap Y| \cdot |\overline{X \cup Y}|}}.$$

17.2 Relatives of Euclidean Distance

- **Power (p, r)-distance**
  The **power (p, r)-distance** is a distance on $\mathbb{R}^n$ defined, for $x, y \in \mathbb{R}^n$, by

$$(\sum_{i=1}^{n} |x_i - y_i|^p)^{\frac{1}{r}}.$$

  For $p = r \ge 1$, it is the l_p**-metric**, including the **Euclidean**, **Manhattan** (or *magnitude*) and **Chebyshev** (or *maximum-value*, *dominance*, *template*) **metrics** for $p = 2, 1$ and ∞, respectively.

  The case $(p, r) = (2, 1)$ corresponds to the **squared Euclidean distance**.

  The power (p, r)-distance with $0 < p = r < 1$ is called the **fractional l_p-distance** (not a metric since the unit balls are not convex). It is used for "dimensionality-cursed" data, i.e., when there are few observations and the number n of variables is large. The case $0 < p < r = 1$, i.e., of the p-th power of the fractional l_p-distance, corresponds to a metric on $\mathbb{R}^n$.

  The weighted versions $(\sum w_i |x_i - y_i|^p)^{\frac{1}{p}}$ (with nonnegative weights w_i) are also used, for $p = 1, 2$, in applications. Given weights $w_i \ge 0$, the **weighted Manhattan quasi-metric** for $x, y \in \mathbb{R}^n$ is $\sum_{i=1}^{n} d_i$, where every d_i is the quasi-metric defined by $d_i = w_i(x_i - y_i)$ if $x_i > y_i$ and $d_i = W_i(y_i - x_i)$, otherwise.

  The **ordinal distance** on $\mathbb{R}^n$ is defined (Bahari and Van hamme, 2014) by

$$(\sum_{i=1}^{n} |\sum_{1\le j\le i} (x_j - y_j)|^p)^{\frac{1}{p}}.$$

- **YJHHR metrics**
  We call **YJHHR metrics** the following metrics, introduced by Yang, Jiang, Hahn, Housworth, and Radivojac, 2016.

For any $p \geq 1$ and two finite sets X, Y, define

$$d(X,Y) = (|X \setminus Y|^p + |Y \setminus X|^p)^{\frac{1}{p}}$$

$$\text{and } d'(X,Y) = \frac{d(X,Y)}{|X \cup Y|} \text{ if } |X \cup Y| > 0, \ d'(X,Y) = 0, \text{ otherwise.}$$

For any $p \geq 1$ and two bounded integrable functions f, g on $\mathbb{R}$, define

$$D(f,g) = \Big(\Big(\int (\max(f-g,0)dx \Big)^p + \Big(\int (\max(g-f,0))x \Big)^p \Big)^{\frac{1}{p}}$$

$$\text{and } D'(f,g) = \frac{D(f,g)}{\int \max(|f|,|f|,|f-g|)dx}.$$

- **Multiplicative distance**

  In order to offset instability of the norm distances for high-dimensional data (i.e., in $\mathbb{R}^n$ with large n), Mansouri and Khademi, 2014, introduced the following **multiplicative distance** for any $x, y \in \mathbb{R}^n$:

$$d_{MK}(x,y) = -1 + \prod_{i=1}^{n} (1 + |x_i - y_i|)^{c_i},$$

  where $c_1, \ldots, c_n$ are given positive numbers.

  Qureshi, 2015, introduced another *multiplicative distance* for any $x, y \in \mathbb{N}^n$:

$$d_Q(x,y) = \sum_{i=1}^{n} ||l(x_i) - l(y_i)||_1,$$

  where $l(a) = (\alpha_1, \alpha_2, \ldots)$ for any number $a \in \mathbb{N}$ represented as $p_1^{\alpha_1} p_2^{\alpha_2} \ldots$; here $p_1, p_2, \ldots$ is the sequence of prime numbers.
- **Penrose size and shape distances**

  The **Penrose size distance** and **Penrose shape distance** are the distances on $\mathbb{R}^n$ defined, respectively, by

$$\sqrt{n} \sum |x_i - y_i| \text{ and } \sqrt{\sum ((x_i - \overline{x}) - (y_i - \overline{y}))^2}.$$

  The sum of their squares is the **squared Euclidean distance**.

  The **mean character distance** (Czekanowsky, 1909) is defined by $\frac{\sum |x_i - y_i|}{n}$.
- **Lorentzian distance**

  The **Lorentzian distance** is a distance on $\mathbb{R}^n$, defined by

$$\sum \ln(1 + |x_i - y_i|).$$

- **Effect size**
  Let $\overline{x}, \overline{y}$ be the means of samples x, y and let s^2 be the pooled variance of both samples. The **effect size** (a term used mainly in social sciences) is defined by

$$\frac{\overline{x}-\overline{y}}{s}.$$

  Its symmetric version $\frac{|\overline{x}-\overline{y}|}{s}$ is called *statistical distance* by Johnson–Wichern, 1982, and *standard distance* by Flury–Riedwyl, 1986.
  Cf. the **engineer semimetric** in Chap. 14 and the **ward linkage**.
- **Binary Euclidean distance**
  The **binary Euclidean distance** is a distance on $\mathbb{R}^n$ defined by

$$\sqrt{\sum (1_{x_i>0} - 1_{y_i>0})^2}.$$

- **Mean censored Euclidean distance**
  The **mean censored Euclidean distance** is a distance on $\mathbb{R}^n$ defined by

$$\sqrt{\frac{\sum (x_i - y_i)^2}{\sum 1_{x_i^2+y_i^2\neq 0}}}.$$

- **Normalized l_p-distance**
  The **normalized l_p-distance**, $1 \leq p \leq \infty$, is a distance on $\mathbb{R}^n$ defined by

$$\frac{||x-y||_p}{||x||_p + ||y||_p}.$$

  The only integer value p for which the normalized l_p-distance is a metric, is p=2. Moreover, the distance $\frac{||x-y||_2}{a+b(||x||_2+||y||_2)}$ is a metric for any $a, b > 0$ ([Yian91]).
- **Clark distance**
  The **Clark distance** (Clark, 1952) is a distance on $\mathbb{R}^n$, defined by

$$\left(\frac{1}{n}\sum\left(\frac{x_i - y_i}{|x_i| + |y_i|}\right)^2\right)^{\frac{1}{2}}.$$

- **Meehl distance**
  The **Meehl distance** (or *Meehl index*) is a distance on $\mathbb{R}^n$ defined by

$$\sum_{1\leq i\leq n-1} (x_i - y_i - x_{i+1} + y_{i+1})^2.$$

- **Hellinger distance**
  The **Hellinger distance** is a distance on $\mathbb{R}^n_+$ defined by

$$\sqrt{2\sum\left(\sqrt{\frac{x_i}{\overline{x}}}-\sqrt{\frac{y_i}{\overline{y}}}\right)^2}.$$

  Cf. **Hellinger metric** in Chap. 14.
  The *Whittaker index of association* is defined by $\frac{1}{2}\sum|\frac{x_i}{\overline{x}}-\frac{y_i}{\overline{y}}|$.
- **Symmetric χ^2-measure**
  The **symmetric χ^2-measure** is a distance on $\mathbb{R}^n$ defined by

$$\sum\frac{2}{\overline{x}\cdot\overline{y}}\cdot\frac{(x_i\overline{y}-y_i\overline{x})^2}{x_i+y_i}.$$

- **Symmetric χ^2-distance**
  The **symmetric χ^2-distance** (or *chi-distance*) is a distance on $\mathbb{R}^n$ defined by

$$\sqrt{\sum\frac{\overline{x}+\overline{y}}{n(x_i+y_i)}(\frac{x_i}{\overline{x}}-\frac{y_i}{\overline{y}})^2}=\sqrt{\sum\frac{\overline{x}+\overline{y}}{n(\overline{x}\cdot\overline{y})^2}\cdot\frac{(x_i\overline{y}-y_i\overline{x})^2}{x_i+y_i}}.$$

  It is a **weighted Euclidean distance**.
- **Weighted Euclidean distance**
  The general **quadratic-form distance** on $\mathbb{R}^n$ is defined by

$$\sqrt{(x-y)^TA(x-y)},$$

  where A is a real nonsingular symmetric $n\times n$ matrix; cf. **Mahalanobis distance**.
  The **weighted Euclidean distance** is the case $A=\mathrm{diag}(a_i), a_i\neq 0$, i.e., it is

$$\sqrt{\sum a_i(x_i-y_i)^2}.$$

  Some examples are: **pseudo-Euclidean distance** (Chap. 7), **standardized Euclidean distance** and first two metrics (Euclidean $\mathbb{R}^6$-distances) in Sect. 18.3.
- **Mahalanobis distance**
  The **Mahalanobis distance** (or **quadratic distance**, or *directionally weighted distance*) is a semimetric on $\mathbb{R}^n$ defined (Mahalanobis, 1936) by

$$||x-y||_A=\sqrt{(x-y)A(x-y)^T},$$

  where A is a positive-semidefinite matrix. It is a metric if A is positive-definite. Cf. **Mahalanobis semimetric** in Chap. 14. The square $||x-y||_A^2$ is called *generalized ellipsoid* (or *generalized squared interpoint*) *distance*.

Usually, $A = C^{-1}$, where C is a *covariance matrix* $((Cov(x_i, x_j)))$ of some data points $x, y \in \mathbb{R}^n$ (say, random vectors with the same distribution), or $A = (det(C))^{\frac{1}{n}} C^{-1}$ so that $det(A) = 1$.

Clearly, $||x-y||_I$ is the Euclidean distance. If $C = ((c_{ij}))$ is a diagonal matrix, then $c_{ii} = Var(x_i) = Var(y_i) = \sigma_i^2$ and it holds

$$||x - y||_{C^{-1}} = \sqrt{\sum_i \frac{(x_i - y_i)^2}{\sigma_i^2}}.$$

Such diagonal Mahalanobis distance is called the **standardized Euclidean distance** (or **normalized Euclidean distance**, *scaled Euclidean distance*).

The **maximum scaled difference** (Maxwell–Buddemeier, 2002) is defined by

$$\max_i \frac{(x_i - y_i)^2}{\sigma_i^2}.$$

17.3 Similarities and Distances for Binary Data

Usually, such similarities s range from 0 to 1 or from -1 to 1; the corresponding distances are usually $1 - s$ or $\frac{1-s}{2}$, respectively.

- **Hamann similarity**

  The **Hamann similarity**, 1961, is a similarity on $\{0, 1\}^n$, defined by

$$\frac{2|\overline{X \Delta Y}|}{n} - 1 = \frac{n - 2|X \Delta Y|}{n}.$$

- **Rand similarity**

  The **Rand similarity** (or Sokal–Michener's *simple matching*) is a similarity on $\{0, 1\}^n$ defined by

$$\frac{\overline{|X \Delta Y|}}{n} = 1 - \frac{|X \Delta Y|}{n}.$$

  Its square root is called the *Euclidean similarity*. The corresponding metric $\frac{|X \Delta Y|}{n}$ is called the *variance* or *Manhattan similarity*; cf. **Penrose size distance**.

- **Sokal–Sneath similarities**

  The **Sokal-Sneath similarities** $1, 2, 3$ are the similarity on $\{0, 1\}^n$ defined by

$$\frac{2|\overline{X \Delta Y}|}{n + |\overline{X \Delta Y}|}, \quad \frac{|X \cap Y|}{|X \cup Y| + |X \Delta Y|}, \quad \frac{|X \Delta Y|}{|\overline{X \Delta Y}|}.$$

- **Russel–Rao similarity**
  The **Russel–Rao similarity** is a similarity on $\{0,1\}^n$, defined by

$$\frac{|X \cap Y|}{n}.$$

- **Forbes–Mozley similarity**
  The **Forbes–Mozley similarity** is a similarity on $\{0,1\}^n$ defined by

$$\frac{n|X \cap Y|}{|X||Y|}.$$

- **Braun–Blanquet similarity**
  The **Braun–Blanquet similarity** is a similarity on $\{0,1\}^n$ defined by

$$\frac{|X \cap Y|}{\max\{|X|,|Y|\}}.$$

- **Roger–Tanimoto similarity**
  The **Roger–Tanimoto similarity**, 1960, is a similarity on $\{0,1\}^n$ defined by

$$\frac{|\overline{X \Delta Y}|}{n + |X \Delta Y|}.$$

- **Faith similarity**
  The **Faith similarity** is a similarity on $\{0,1\}^n$, defined by

$$\frac{|X \cap Y| + |\overline{X \Delta Y}|}{2n}.$$

- **Tversky similarity**
  The **Tversky similarity** is a similarity on $\{0,1\}^n$, defined by

$$\frac{|X \cap Y|}{a|X \Delta Y| + b|X \cap Y|}.$$

  It becomes the **Tanimoto**, **Sørensen** and (the binary case of) **Kulczynsky** 1 **similarities** for $(a,b) = (1,1)$, $(\frac{1}{2},1)$ and $(1,0)$, respectively.
- **Mountford similarity**
  The **Mountford similarity**, 1962, is a similarity on $\{0,1\}^n$, defined by

$$\frac{2|X \cap Y|}{|X||Y \backslash X| + |Y||X \backslash Y|}.$$

- **Gower–Legendre similarity**
  The **Gower–Legendre similarity** is a similarity on $\{0,1\}^n$ defined by

$$\frac{|\overline{X\Delta Y}|}{a|X\Delta Y| + |\overline{X\Delta Y}|} = \frac{|\overline{X\Delta Y}|}{n + (a-1)|X\Delta Y|}.$$

- **Anderberg similarity**
  The **Anderberg** (or *Sokal–Sneath* 4 **similarity**) on $\{0,1\}^n$ is defined by

$$\frac{|X \cap Y|}{4}\left(\frac{1}{|X|} + \frac{1}{|Y|}\right) + \frac{|\overline{X \cup Y}|}{4}\left(\frac{1}{|\overline{X}|} + \frac{1}{|\overline{Y}|}\right).$$

- **Yule similarities**
  The **Yule** Q **similarity** (Yule, 1900) is a similarity on $\{0,1\}^n$, defined by

$$\frac{|X \cap Y| \cdot |\overline{X \cup Y}| - |X\backslash Y| \cdot |Y\backslash X|}{|X \cap Y| \cdot |\overline{X \cup Y}| + |X\backslash Y| \cdot |Y\backslash X|}.$$

  The **Yule** Y **similarity of colligation** (1912) is a similarity on $\{0,1\}^n$ defined by

$$\frac{\sqrt{|X \cap Y| \cdot |\overline{X \cup Y}|} - \sqrt{|X\backslash Y| \cdot |Y\backslash X|}}{\sqrt{|X \cap Y| \cdot |\overline{X \cup Y}|} + \sqrt{|X\backslash Y| \cdot |Y\backslash X|}}.$$

- **Dispersion similarity**
  The **dispersion similarity** is a similarity on $\{0,1\}^n$, defined by

$$\frac{|X \cap Y| \cdot |\overline{X \cup Y}| - |X\backslash Y| \cdot |Y\backslash X|}{n^2}.$$

- **Pearson ϕ similarity**
  The **Pearson ϕ similarity** is a similarity on $\{0,1\}^n$ defined by

$$\frac{|X \cap Y| \cdot |\overline{X \cup Y}| - |X\backslash Y| \cdot |Y\backslash X|}{\sqrt{|X| \cdot |\overline{X}| \cdot |Y| \cdot |\overline{Y}|}}.$$

- **Gower similarity** 2
  The **Gower** 2 (or *Sokal–Sneath* 5) **similarity** on $\{0,1\}^n$ is defined by

$$\frac{|X \cap Y| \cdot |\overline{X \cup Y}|}{\sqrt{|X| \cdot |\overline{X}| \cdot |Y| \cdot |\overline{Y}|}}.$$

- **Pattern difference**
  The **pattern difference** is a distance on $\{0,1\}^n$, defined by

$$\frac{4|X\backslash Y|\cdot|Y\backslash X|}{n^2}.$$

- **Q_0-difference**
  The **Q_0-difference** is a distance on $\{0,1\}^n$, defined by

$$\frac{|X\backslash Y|\cdot|Y\backslash X|}{|X\cap Y|\cdot|\overline{X\cup Y}|}.$$

- **Model distance**
  Let X, Y be two data sets, and let λ_j be the eigenvalues of the symmetrized cross-correlation matrix $C_{X\backslash Y\,Y\backslash X}\times C_{Y\backslash X\,X\backslash Y}$.
  The **model distance** (Todeschini, 2004) is a distance on $\{0,1\}^n$ defined by

$$\sqrt{|X\backslash Y|+|Y\backslash X|-2\sum_j\sqrt{\lambda_j}}.$$

  The **CMD-distance** (or, *canonical measure of distance*, Todeschini et al., 2009) is

$$\sqrt{|X|+|Y|-2\sum_j\sqrt{\lambda_j}},$$

  where λ_j are the nonzero eigenvalues of the cross-correlation matrix $C_{X\,Y}\times C_{Y\,X}$.

17.4 Correlation Similarities and Distances

The *covariance* between two real-valued random variables X and Y is $Cov(x,y)=\mathbb{E}[(X-\mathbb{E}[X])(Y-\mathbb{E}[Y])]=\mathbb{E}[XY]-\mathbb{E}[X]\mathbb{E}[Y]$. The *variance* of X is $Var(X)=Cov(X,X)$ and the **Pearson correlation** of X and Y is $Corr(X,Y)=\frac{Cov(X,Y)}{\sqrt{Var(X)Var(Y)}}$; cf. Chap. 14.

Let $(X,Y),(X',Y'),(X'',Y'')$ be independent and identically distributed. The *distance covariance* (Székely, 2005) is the square root of $dCov^2(X,Y)=\mathbb{E}[|X-X'||Y-Y'|]+\mathbb{E}[|X-X'|]\mathbb{E}[|Y-Y'|]-\mathbb{E}[|X-X'||Y-Y''|]-\mathbb{E}[|X-X''||Y-Y'|]=\mathbb{E}[|X-X'||Y-Y'|]+\mathbb{E}[|X-X'|]\mathbb{E}[|Y-Y'|]-2\mathbb{E}[|X-X'||Y-Y''|]$. It is 0 if and only if X and Y are independent. The **distance correlation** $dCor(X,Y)$ is $\frac{dCov(X,Y)}{\sqrt{dCov(X,X)dCov(Y,Y)}}$.

The vectors x, y below can be seen as *samples* (series of n measurements) of X, Y.

- **Covariance similarity**
  The **covariance similarity** is a similarity on $\mathbb{R}^n$ defined by

$$\frac{\sum(x_i-\overline{x})(y_i-\overline{y})}{n}=\frac{\sum x_i y_i}{n}-\overline{x}\cdot\overline{y}.$$

- **Pearson correlation similarity**
  The **Pearson correlation similarity**, or, by its full name, *Pearson product-moment correlation coefficient*) is a similarity on $\mathbb{R}^n$ defined by

$$s=\frac{\sum(x_i-\overline{x})(y_i-\overline{y})}{\sqrt{\sum(x_j-\overline{x})^2\sum(y_j-\overline{y})^2}}.$$

  The **Pearson distance** (or **correlation distance**) is defined by

$$1-s=\frac{1}{2}\sum\left(\frac{x_i-\overline{x}}{\sqrt{\sum(x_j-\overline{x})^2}}-\frac{y_i-\overline{y}}{\sqrt{\sum(y_j-\overline{y})^2}}\right)$$

  A multivariate generalization of the Pearson correlation similarity is the *RV coefficient* (Escoufier, 1973) $RV(X,Y)=\frac{Covv(X,Y)}{\sqrt{Covv(X,X)Covv(Y,Y)}}$, where X, Y are matrices of centered random (column) vectors with covariance matrix $C(X,Y)=\mathbb{E}[X^TY]$, and $Covv(X,Y)$ is the trace of the matrix $C(X,Y)C(Y,X)$.
- **Cosine similarity**
  The **cosine similarity** (or *Orchini similarity*, *angular similarity*, *normalized dot product*) is the case $\overline{x}=\overline{y}=0$ of the **Pearson correlation similarity**, i.e., it is

$$\frac{\langle x,y\rangle}{||x||_2\cdot||y||_2}=\cos\phi,$$

  where ϕ is the angle between vectors x and y. In the binary case, it becomes

$$\frac{|X\cap Y|}{\sqrt{|X|\cdot|Y|}}$$

  and is called the **Ochiai–Otsuka similarity**.

  In Record Linkage, cosine similarity is called **TF-IDF** similarity; it (or *tf-idf*, *TFIDF*) are used as an abbreviation of *Frequency-Inverse Document Frequency*.

  The **angular semimetric** on $\mathbb{R}^n$ is defined by $\arccos\phi$. The **cosine distance** is $1-\cos\phi$, and the **Orloci distance** (or *chord distance*) is

$$\sqrt{2(1-\cos\phi)}=\sqrt{\sum(\frac{x_i}{||x||_2}-\frac{y_i}{||y||_2})^2}.$$

- **Similarity ratio**

  The **similarity ratio** (or *Kohonen similarity*, *Kumar–Hassebrook similarity*) is a similarity on $\mathbb{R}^n$ defined by

$$\frac{\langle x, y\rangle}{\langle x, y\rangle + ||x-y||_2^2}.$$

  Its binary case is the **Tanimoto similarity**.

- **Morisita–Horn similarity**

  The **Morisita–Horn similarity** (Morisita, 1959) is a similarity on $\mathbb{R}^n$ defined by

$$\frac{2\langle x, y\rangle}{||x||_2^2 \cdot \frac{\overline{y}}{\overline{x}} + ||y||_2^2 \cdot \frac{\overline{x}}{\overline{y}}}.$$

- **Spearman rank correlation**

  If the sequences $x, y \in \mathbb{R}^n$ are ranked separately, then the **Pearson correlation similarity** is approximated by the following **Spearman ρ rank correlation**:

$$\frac{\sum(a_i-\overline{a})(b_i-\overline{b})}{\sqrt{\sum(a_j-\overline{a})^2\sum(b_j-\overline{b})^2}} = 1 - \frac{6}{n(n^2-1)}\sum(a_i-b_i)^2,$$

  where $n > 1$ and $a_i = \text{rank}(x_i), b_i = \text{rank}(y_i), a = (a_1, \ldots, a_n), b = (b_1, \ldots, b_n)$. This approximation is good for such *ordinal* data when it holds $\overline{x} = \overline{y} = \frac{n+1}{2}$.

  The **Spearman footrule** is defined by

$$1 - \frac{3}{n^2-1}\sum |x_i - y_i|.$$

  Cf. the **Spearman ρ distance** and **Spearman footrule distance** in Chap. 11.

  Another correlation similarity for rankings is the **Kendall τ rank correlation**:

$$\frac{2\sum_{1\le i<j\le n} sign(x_i-x_j)sign(y_i-y_j)}{n(n-1)}.$$

  Cf. the **Kendall τ distance** on permutations in Chap. 11.

- **Global correlation distance**

  Let $x \in \mathbb{R}^n$ and (A, d) be a metric space with n points $a_1, \ldots, a_n$. For any $d > 0$, the *Moran autocorrelation coefficient* is defined by

$$I(d) = \frac{n\sum_{1\le i\ne j\le n} w_{ij}(d)(x_i-\overline{x})(x_j-\overline{x})}{\sum_{1\le i\ne j\le n} w_{ij}(d)\sum_{1\le i\le n}(x_i-\overline{x})^2},$$

where the weight $w_{ij}(d)$ is 1 if $d(a_i, a_j) = d$ and 0, otherwise. In **spatial analysis**, eventual clustering of (A, d) implies that $I(d)$ decreases with increasing d. $I(d)$ is a global indicator of the presumed **spatial dependence** that evaluate the existence/size of clusters in the spatial arrangement (A, d) of a given variable.

The **global correlation distance** is the least value d' for which $I(d) = 0$.

- **Log-likelihood distance**

  Given two clusters A and B, their **log-likelihood distance** is the decrease in *log-likelihood* (cf. the **Kullback–Leibler distance** in Chap. 14 and the **log-likelihood ratio quasi-distance** in Chap. 21) as they are combined into one cluster. Simplifying (taking $A, B \subset \mathbb{R}_{>0}$), it is defined by

$$\sum_{x \in A} x \log \frac{x}{|A|} + \sum_{x \in B} x \log \frac{x}{|B|} - \sum_{x \in A \cup B} x \log \frac{x}{|A \cup B|}.$$

- **Spatial analysis**

  In Statistics, **spatial analysis** (or *spatial statistics*) includes the formal techniques for studying entities using their topological, geometric, or geographic properties. More restrictively, it refers to *Geostatistics* and *Human Geography*. It considers spatially distributed data as *a priori* dependent one on another.

  Spatial dependence is a measure for the degree of associative dependence between independently measured values in an ordered set, determined in samples selected at different positions in a sample space. Cf. **spatial correlation** in Chap. 24. An example of such space-time dynamics: Gould, 1997, showed that $\approx$ 80 % of the diffusion of HIV in the US is highly correlated with the air passenger traffic (origin-destination) matrix for 102 major urban centers.

  SADIE (Spatial Analysis by Distance IndicEs) is a methodology (Perry, 1998) to measure the degree of nonrandomness in 2D spatial patterns of populations. Given n sample units $x_i \in \mathbb{R}^2$ with associated counts N_i, the **distance to regularity** is the minimal total Euclidean distance that the individuals in the sample would have to move, from unit to unit, so that all units contained an identical number of individuals. The **distance to crowding** is the minimal total distance that individuals in the sample must move so that all are congregated in one unit. The *indices of aggregation* are defined by dividing above distances by their mean values. Cf. **Earth Mover's distance** in Chap. 21.

- **Distance sampling**

  Distance sampling is a widely-used group of methods for estimating the density and abundance of biological populations. It is an extension of plot- (or quadrate-based) sampling, where the number of objects at given distance from a point or a segment is counted. Also, *Distance* is the name of a Windows-based computer package that allows to design and analyze distance sampling surveys.

  A standardized survey along a series of lines or points is performed, searching for objects of interest (say, animals, plants or their clusters). *Detection distances* r (perpendicular ones from given lines and radial ones from given points) are measured to each detected object. The *detection function* $g(r)$ (the probability that an object at distance r is detected) is fit then to the observed distances, and

this fitted function is used to estimate the proportion of objects missed by the survey. It gives estimates for the density and abundance of objects in the survey area.

- **Cook distance**

  The **Cook distance** is a distance on $\mathbb{R}^n$ giving a statistical measure of deciding if some i-th observation alone affects much regression estimates. It is a normalized **squared Euclidean distance** between estimated parameters from regression models constructed from all data and from data without i-th observation.

  The main similar distances, used in Regression Analysis for detecting influential observations, are *DFITS distance*, *Welsch distance*, and *Hadi distance*.

- **Periodicity p-self-distance**

  Ergun–Muthukrishnan–Sahinalp, 2004, call a data stream $x = (x_1, \ldots, x_n)$ *p-periodic approximatively*, for given $1 \leq p \leq \frac{n}{2}$ and distance function d between p-blocks of x, if the **periodicity p-self-distance** $\sum_{i \neq j} d((x_{jp+1}, \ldots, x_{jp+p}), (x_{ip+1}, \ldots, x_{ip+p}))$ is below some threshold.

  Above notion of self-distance is different from ones given in Chaps. 1 and 28. Also, the term *self-distance* is used for *round-off error* (or *rounding error*), i.e., the difference between the calculated approximation of a number and its exact value.

- **Distance metric learning**

  Let $x_1, \ldots, x_n$ denote the samples in the training set $X \subset \mathbb{R}^m$; here m is the number of features. **Distance metric learning** is an approach for the problem of clustering with side information, when algorithm learns a distance function d prior to clustering and then tries to satisfy some *positive* (or *equivalence*) constraints P and *negative* constraints D. Here S and D are the sets of *similar* (belonging to the same class) and *dissimilar* pairs (x_i, x_j), respectively.

  Usually d is a **Mahalanobis metric** $||x_i - x_j||_A = \sqrt{(x_i - x_j)^T A (x_i - x_j)}$, where A is a positive-semidefinite matrix, i.e., $A = W^T W$ for a matrix W with m columns and $||x_i - x_j||_A^2 = ||Wx_i - Wx_j||^2$. Then, for example, one look for (Xing et al., 2003) A minimizing $\sum_{(x_i, x_j) \in S} ||x_i - x_j||_A^2$ while $\sum_{(x_i, x_j) \in D} ||x_i - x_j||_A^2 \geq 1$.

- **Heterogeneous distance**

  The following IBL (instance-based learning) setting is used for many real-world applications (neural networks, etc.), where data are incomplete and have both continuous and nominal attributes. Given an $m \times (n + 1)$ matrix $((x_{ij}))$, its row $(x_{i0}, x_{i1}, \ldots, x_{in})$ denotes an *instance input vector* $x_i = (x_{i1}, \ldots, x_{in})$ with output class x_{i0}; the set of m instances represents a training set during learning. For any new input vector $y = (y_1, \ldots, y_n)$, the closest (in terms of a selected distance d) instance x_i is sought, in order to *classify* y, i.e., predict its output class as x_{i0}.

  A **heterogeneous distance** $d(x_i, y)$ is defined ([WiMa97]) by

$$\sqrt{\sum_{j=1}^{n} d_j^2(x_{ij}, y_j)}$$

with $d_j(x_{ij}, y_j) = 1$ if x_{ij} or y_j is unknown. If the *attribute* (input variable) j is nominal, then $d_j(x_{ij}, y_j)$ is defined, for example, as $1_{x_{ij} \neq y_j}$, or as

$$\sum_a \left| \frac{|\{1 \leq t \leq m : x_{t0} = a, x_{ij} = x_{ij}\}|}{|\{1 \leq t \leq m : x_{tj} = x_{ij}\}|} - \frac{|\{1 \leq t \leq m : x_{t0} = a, x_{ij} = y_j\}|}{|\{1 \leq t \leq m : x_{tj} = y_j\}|} \right|^q$$

for $q = 1$ or 2; the sum is taken over all output classes, i.e., values a from $\{x_{t0} : 1 \leq t \leq m\}$. For continuous attributes j, the number d_j is taken to be $|x_{ij} - y_j|$ divided by $\max_t x_{tj} - \min_t x_{tj}$, or by $\frac{1}{4}$ of the standard deviation of values x_{tj}, $1 \leq t \leq m$.

Chapter 18
Distances in Systems and Mathematical Engineering

In this chapter we group the main distances used in Systems Theory (such as *Transition Systems*, *Dynamical Systems*, *Cellular Automata*, *Feedback Systems*) and other interdisciplinary branches of Mathematics, Engineering and Theoretical Computer Science (such as, say, *Robot Motion* and *Multi-objective Optimization*).

A *labeled transition system* (LTS) is a triple (S, T, F) where S is a set of *states*, T is a set of *labels* (or *actions*) and $F \subseteq S \times T \times S$ is a ternary relation. Any $(x, t, y) \in F$ represents a *t-labeled transition* from state x to state y. A LTS with $|T| = 1$ corresponds to an *unlabeled transition system*.

A *path* is a sequence $((x_1, t_1, x_2), \ldots, (x_i, t_i, x_{i+1}), \ldots)$ of transitions; it gives rise to a *trace* $(t_1, \ldots, t_i, \ldots)$. Two paths are *trace-equivalent* if they have the same traces. The term *trace*, in Computer Science, refers in general to the equivalence classes of strings of a *trace monoid*, wherein certain letters in the string are allowed to commute. It is not related to the *trace* in Linear Algebra.

A LTS is called *deterministic* if for any $x \in S$ and $t \in T$ it holds that $|\{y \in S : (x, t, y) \in F\}| = 1$. Such LTS without output is called a *semiautomaton* (S, T, f) where S is a set of *states*, T is an *input alphabet* and $f : X \times T \to S$ is a *transition function*.

A *deterministic finite-state machine* is a tuple (S, s_0, T, f, S') with S, T, f as above but $0 < |S|, |T| < \infty$, while $s_o \in S$ is an *initial state*, and $S' \subset S$ is the set of *final states*.

The *free monoid* on a set T is a *monoid* (algebraic structure with an associative binary operation and an identity element) T^* whose elements are all the finite sequences $x = x_0, \ldots, x_m$ of elements from T. The identity element is the empty string λ, and the operation is string concatenation. The free semigroup on T is $T^+ = T^* \setminus \{\lambda\}$. Let T^ω denote the set of all infinite sequences $x = (x_0, x_1, \ldots)$ in T, and let T^∞ denote $T^* \cup T^\omega$.

A finite-state machine is *nondeterministic* if the next possible state is not uniquely determined. A *weighted automaton* is a such machine, say, M equipped

© Springer-Verlag Berlin Heidelberg 2016

M.M. Deza, E. Deza, *Encyclopedia of Distances*,
DOI 10.1007/978-3-662-52844-0_18

with a cost function $c \geq 0$, over some semiring $(S, \oplus, \otimes)$, on transitions. For a *probabilistic automaton*, the semiring is $(\mathbb{R}_{\geq 0}, +, \times)$ and $0 \leq c \leq 1$.

A **distance automaton** is (Hashiguchi, 1982) a weighted automaton over the *tropical semiring TROP* $= (\mathbb{N} \cup \{\infty\}, \min, +)$. A *run* over a word (string in the *language* of M) $(a_1, \ldots, a_k)$ is a sequence $(s_0, \ldots, s_k)$ of states. The *run's distance* is the sum $\sum_{i=1}^{k} c(a_i)_{p_{i-1}p_i}$ of costs of involved transitions. The run is *accepting* if s_0 is initial and s_k is a final state. The *distance of a word recognized by M* is the minimum of the distances over the all accepting runs. The *distance* of M is the supremum over the distances of all recognized words. Distance automata are equivalent to finitely generated monoids of matrices over *TROP*: nondeterministic automata recognize the same language as some deterministic ones but with transitions acting on the sets of original states.

18.1 Distances in State Transition and Dynamical Systems

- **Distances on formal languages**

  A *formal language* over an alphabet T is a set of words over T.

  The similarity between two words of a language are measured usually by the **Hamming metric** (cf. Sect. 1.5) or (cf. Sect. 11.1) by the **Levenstein metric** (or **edit distance**) and **prefix, suffix and substring distances**.

  Given a language L and a distance d on it, the **distance between a word** u **and** L is the **point-set distance** (Sect. 1.5) $\min_{v \in L} d(u, v)$.

  The **inner distance** (or *self distance*) d **of** L is (Mihri, 2007) $\min_{u,v \in L, u \neq v} d(u, v)$; cf. *separation* in the item **metric spread** in Sect. 1.3.

  The similarity between two languages L and L' are measured usually by the following extensions: $\min_{u \in L, v \in L', u \neq v} d(u, v)$ and (called by Choffrut–Pighizzini, 2002, the **relative distance d**) $\max_{u \in L} \min_{v \in L'} d(u, v)$. In terms of Sect. 1.5, they are, respectively, the **set-set distance** and the **directed Hausdorff distance**.

  See also in Sect. 28.3 the **language distance from English** and other notions of distance between words of a natural language and between languages.

- **Fahrenberg–Legay–Thrane distances**

  Given a *labeled transition system* (LTS) (S, T, F) Fahrenberg–Legay–Thrane, 2011, call T^∞ the set of *traces* and define a *trace distance* as an extended **hemimetric** (or **quasi-semimetric**) $h : T^\infty \times T^\infty \to \mathbb{R}_{\geq 0} \cup \{\infty\}$ such that $h(x, y) = \infty$ for any sequences $x, y \in T^\infty$ of different length.

  For a given distance d on the set T of labels and a *discount factor* q $(0 < q \leq 1)$, they defined the *pointwise*, *accumulating* and *limit-average trace distance* as, respectively, $PW_{d,q}(x, y) = \sup_i q^i d(x_i, y_i)$, $ACC_{d,q}(x, y) = \sum_i q^i d(x_i, y_i)$ and $AVG_d = \underline{\lim}_{i \to \infty} \frac{1}{i+1} \sum_{j=0}^{i} d(x_j, y_j)$.

  If d is a **discrete metric**, i.e., $d(t, t') = 1$ whenever $t \neq t'$, then $ACC_{d,1}$ is the **Hamming metric** for finite traces of the same length, and $ACC_{d,q}$ with $q < 1$ and AVG_d are analogs of the Hamming metric for infinite traces.

Other examples of trace distances are a Cantor-like distance $(1 + \inf\{i : x_i \neq y_i\})^{-1}$ and the *maximum-lead distance*, defined, for $T \subseteq \Sigma \times \mathbb{R}$, by Henzinger–Majumdar–Prabhu, 2005, as $\sup_i |\sum_{j=0}^{i} x''_j - \sum_{j=0}^{i} y''_j|$ if $x'_i = y'_i$ for all i and ∞, otherwise. Here any $z \in T$ is denoted by (z', z''), where $z' \in \Sigma$ and $z'' \in \mathbb{R}$.

Fahrenberg–Legay–Thrane, 2011, also define the two following extended simulation hemimetrics between states $x, y \in S$.

The *accumulating simulation distance* $h_{ac}(x, y)$ and the *pointwise simulation distance* $h_{po}(x, y)$ are the least fixed points, respectively, to the set of equations

$$h_{ac}(x, y) = \max_{t \in T:(x,t,x') \in F} \min_{t' \in T:(y,t',y') \in F} (d(t, t') + q h_{ac}(x', y')) \text{ and}$$

$$h_{po}(x, y) = \max_{t \in T:(x,t,x') \in F} \min_{t' \in T:(y,t',y') \in F} \max\{d(t, t'), h_{po}(x', y')\}.$$

The above hemimetrics generalize the lifting by Alfaro–Faella–Stoelinga, 2004, of the quasi-metric $\max\{x'' - y'', 0\}$ between labels $x, y \in T = \Sigma \times \mathbb{R}$ on an accumulating trace distance and then the lifting of it on the **directed Hausdorff distance** (Chap. 1) between the sets of traces from two given states.

The case $h_{ac}(x, y) = h_{po}(x, y) = 0$ corresponds to the *simulation* of x by y, written $x \leq y$, i.e., to the existence of a *weighted simulation relation* $R \subseteq S \times S$, i.e., whenever $(x, y) \in R$ and $(x, t, x') \in F$, then $(y, t, y') \in F$ with $(x', y') \in R$.

The case $h_{ac}(x, y) < \infty$ or $h_{po}(x, y) < \infty$ corresponds to the existence of an *unweighted simulation relation* $R \subseteq S \times S$, i.e., whenever $(x, y) \in R$ and $(x, t, x') \in F$, then $(y, t', y') \in F$ with $(x', y') \in R$ and $d(t, t') < \infty$.

The relation $\leq$ is a pre-order on S. Two states x and y are *similar* if $x \leq y$ and $y \leq x$; they are *bisimilar* if, moreover, the simulation R of x by y is the inverse of the simulation of y by x. Similarity is an equivalence relation on S which is coarser than the bisimilarity congruence.

The above trace and similarity system hemimetrics are quantitative generalizations of system relations: trace-equivalence and simulation pre-order, respectively.

- **Cellular automata distances**

  Let $S, |S| \geq 2$, be a finite set (*alphabet*), and let S^{∞} be the set of $\mathbb{Z}$-indexed bi-infinite sequences $\{x_i\}_{i=-\infty}^{\infty}$ (*configurations*) of elements of S. A (one-dimensional) *cellular automaton* is a continuous self-map $f : S^{\infty} \to S^{\infty}$ that commutes with all *shift* (or *translation*) maps $g : S^{\infty} \to S^{\infty}$ defined by $g(x_i) = x_{i+1}$.

  Such cellular automaton form a discrete **dynamical system** with the time set $T = \mathbb{Z}$ (of *cells*, positions of a finite-state machine) on the finite-state space S. The main distances between configurations $\{x_i\}_i$ and $\{y_i\}_i$ (see [BFK99]) follow.

  The **Cantor metric** is a metric on S^{∞} defined, for $x \neq y$, by

$$2^{-\min\{i \geq 0 : |x_i - y_i| + |x_{-i} - y_{-i}| \neq 0\}}.$$

  It corresponds to the case $a = \frac{1}{2}$ of the **generalized Cantor metric** in Chap. 11. The corresponding metric space is compact.

The **Besicovitch semimetric** is a semimetric on S^∞ defined, for $x \neq y$, by

$$\overline{\lim}_{l\to\infty} \frac{|-l \le i \le l : x_i \neq y_i|}{2l+1}.$$

Cf. **Besicovitch distance** on measurable functions in Chap. 13. The corresponding semimetric space is complete.

The **Weyl semimetric** is a semimetric on S^∞, defined by

$$\overline{\lim}_{l\to\infty} \max_{k\in\mathbb{Z}} \frac{|k+1 \le i \le k+l : x_i \neq y_i|}{l}.$$

This and the above semimetric are **translation invariant**, but are neither separable nor locally compact. Cf. **Weyl distance** in Chap. 13.

- **Dynamical system**

A (deterministic) **dynamical system** is a tuple (T, X, f) consisting of a metric space (X, d), called the *state space*, a *time set* T and an *evolution function* $f : T \times X \to X$. Usually, T is a monoid, (X, d) is a manifold locally diffeomorphic to a Banach space, and f is a continuous function.

The system is *discrete* if $T = \mathbb{Z}$ (*cascade*) or if $T = \{0, 1, 2 \dots\}$. It is *real* (or *flow*) if T is an open interval in $\mathbb{R}$, and it is a *cellular automaton* if X is finite and $T = \mathbb{Z}^n$. Dynamical systems are studied in Control Theory in the context of stability; Chaos Theory considers the systems with maximal possible instability.

A discrete dynamical system with $T = \{0, 1, 2 \dots\}$ is defined by a self-map $f : X \to X$. For any $x \in X$, its *orbit* is the sequence $\{f^n(x)\}_n$; here $f^n(x) = f(f^{n-1}(x))$ with $f^0(x) = x$. The orbit of $x \in X$ is called *periodic* if $f^n(x) = x$ for some $n > 0$.

A pair $(x, y) \in X \times X$ is called *proximal* if $\underline{\lim}_{n\to\infty} d(f^n(x), f^n(y)) = 0$, and *distal*, otherwise. The system is called *distal* if any pair (x, y) of distinct points is distal.

The dynamical system is called *expansive* if there exists a constant $D > 0$ such that the inequality $d(f^n(x), f^n(y)) \ge D$ holds for any distinct $x, y \in X$ and some n.

An *attractor* is a closed subset A of X such that there exists an *open neighborhood* U of A with the property that $\lim_{n\to\infty} d(f^n(b), A) = 0$ for every $b \in U$, i.e., A *attracts* all nearby orbits. Here $d(x, A) = \inf_{y\in A} d(x, y)$ is the **point-set distance**.

If for large n and small r there exists a number α such that

$$C(X, n, r) = \frac{|\{(i, j) : d(f^i(x), f^j(x)) \le r, 1 \le i, j \le n\}|}{n^2} \sim r^\alpha,$$

then α is called (Grassberger–Hentschel–Procaccia, 1983) the *correlation dimension*.

The *Lyapunov time* is the characteristic timescale on which a dynamical system is *chaotic*, i.e., small differences in initial conditions yield widely diverging outcomes, rendering long-term prediction impossible in general.

- **Melnikov distance**

  The evolution of a planar **dynamical system** can be represented in a 3D state space with orthogonal coordinate axes Ox, Ox', Ot. A *homoclinic orbit* (nongeneric orbit that joins a saddle point) can be seen in that space as the intersection with a plane of section $t = const$ of the *stable manifold* (the surface consisting of all trajectories that approach $\gamma_0 = Ot$ asymptotically in forward time) and the *unstable manifold* (the surface consisting of all trajectories that approach Ot in reverse time).

  Under a sufficiently small perturbation ϵ which is bounded and smooth enough, Ot persists as a smooth curve $\gamma_\epsilon = \gamma_0 + O(\epsilon)$, and the perturbed system has (not coinciding since $\epsilon > 0$) stable and unstable manifolds contained in an $O(\epsilon)$ neighborhood of the unperturbed manifolds.

  The **Melnikov distance** is the distance between stable and unstable manifolds measured along a line normal to the unperturbed manifolds, i.e., a direction that is perpendicular to the unperturbed homoclinic orbit. Cf. Sect. 18.2.
- **Fractal**

  For a metric space, its **topological dimension** does not exceed its **Hausdorff dimension**; cf. Chap. 1. A **fractal** is a metric space for which this inequality is strict. (Originally, Mandelbrot defined a fractal as a point set with noninteger Hausdorff dimension.) For example, the *Cantor set*, seen as a compact metric subspace of $(\mathbb{R}, d(x, y) = |x - y|)$ has the Hausdorff dimension $\frac{\ln 2}{\ln 3}$; cf. another **Cantor metric** in Chap. 11. Another classical fractal, the *Sierpinski carpet* of $[0, 1]\times[0, 1]$, is a **complete geodesic** metric subspace of $(\mathbb{R}^2, d(x, y) = ||x-y||_1)$.

  The term *fractal* is used also, more generally, for a *self-similar* (i.e., roughly, looking similar at any scale) object (usually, a subset of $\mathbb{R}^n$). Cf. **scale invariance**.
- **Scale invariance**

  Scale invariance is a feature of laws or objects which do not change if length scales are multiplied by a common factor.

  Examples of scale invariant phenomena are **fractals** and *power laws*; cf. **scale-free network** in Chap. 22 and *self-similarity* in **long range dependence**. Scale invariance arising from a power law $y = Cx^k$, for a constant C and scale exponent k, amounts to linearity $\log y = \log C + k \log x$ for logarithms. Much of scale invariant behavior (and complexity in nature) is explained (Bak–Tang–Wiesenfeld, 1987) by *self-organized cruciality (SOC)* of many **dynamical systems**, i.e., the property to have the critical point of a phase transition as an attractor which can be attained spontaneously without any fine-tuning of control parameters.

  Two moving systems are *dynamically similar* if the motion of one can be made identical to the motion of the other by multiplying all lengths by one scale factor, all forces by another one and all time periods by a third scale factor. Dynamic similarity can be formulated in terms of dimensionless parameters as, for example, the **Reynolds number** in Chap. 24.
- **Long range dependence**

  A (second-order stationary) stochastic process X_k, $k \in \mathbb{Z}$, is called **long range dependent** (or *long memory*) if there exist numbers $\alpha, 0 < \alpha < 1$, and $c_\rho > 0$

such that $\lim_{k\to\infty} c_\rho k^\alpha \rho(k) = 1$, where $\rho(k)$ is the autocorrelation function. So, correlations decay very slowly (asymptotically hyperbolic) to zero implying that $\sum_{k\in\mathbb{Z}} |\rho(k)| = \infty$, and that events so far apart are correlated (long memory). If the above sum is finite and the decay is exponential, then the process is *short range*.

Examples of such processes are the exponential, normal and Poisson processes which are memoryless, and, in physical terms, systems in thermodynamic equilibrium. The above power law decay for correlations as a function of time translates into a power law decay of the Fourier spectrum as a function of frequency f and is called $\frac{1}{f}$ *noise*.

A process has a *self-similarity exponent* (or *Hust parameter*) H if X_k and $t^{-H}X_{tk}$ have the same finite-dimensional distributions for any positive t. The cases $H = \frac{1}{2}$ and $H = 1$ correspond, respectively, to purely random process and to exact self-similarity: the same behavior on all scales. Cf. **fractal**, **scale invariance** and, in Chap. 22, **scale-free network**. The processes with $\frac{1}{2} < H < 1$ are long range dependent with $\alpha = 2(1 - H)$.

Long range dependence corresponds to *heavy-tailed* (or *power law*) distributions. The *distribution function* and *tail* of a nonnegative random variable X are $F(x) = P(X \le x)$ and $\overline{F(x)} = P(X > x)$. A distribution $F(X)$ is *heavy-tailed* if there exists a number $\alpha, 0 < \alpha < 1$, such that $\lim_{x\to\infty} x^\alpha \overline{F(x)} = 1$.

Many such distributions occur in the real world (for example, in Physics, Economics, the Internet) in both space (distances) and time (durations). A standard example is the Pareto distribution $\overline{F(x)} = x^{-k}$, $x \ge 1$, where $k > 0$ is a parameter. Cf. Sect. 18.4 and, in Chap. 29, **distance decay**.

Also, the random-copying model (the cultural analog of genetic drift) of the frequency distributions of various cultural traits (such as of scientific papers citations, first names, dog breeds, pottery decorations) results (Bentley–Hahn–Shennan, 2004) in a power law distribution $y = Cx^{-k}$, where y is the proportion of cultural traits that occur with frequency x in the population, and C and k are parameters.

A general *Lévy flight* is a random walk in which the increments have a power law probability distribution.

- **Lévy walks in human mobility**

  A *jump* is a longest straight line trip from one location to another done without a directional change or pause. Consider a 2D *random walk* (taking successive jumps, each in a random direction) model that involves two distributions: a uniform one for the *turning angle* θ_i and a power law $P(l_i) \sim l_i^{-\alpha}$ for the *jump length* l_i.

  Brownian motion has $\alpha \ge 3$ and *normal diffusion*, i.e., the MSD (mean squared displacement) grows linearly with time t: $MSD \sim t^\gamma, \gamma = 1$.

  A *Lévy walk* has $1 < \alpha < 3$. Its jump length is *scale-free*, i.e., lacks an average scale $\overline{l_i}$, and it is *superdiffusive*: $MSD \sim t^\gamma, \gamma > 1$. Intuitively, Lévy walks consist of many short jumps and, exceptionally, long jumps eliminating the effect of short ones in average jump lengths.

Lévy-like walk dispersal was observed in our Web browsing and image scanning, as well as in foraging animals. It and two-mode Brownian search strategies might be optimal for finding patches of randomly dispersed abundant resources: to cluster, in order to save time and effort, closely located activities and then make many short jumps within the clustered areas and a few long jumps among areas.

Human mobility occurs on many length scales, ranging from walking to air travel. On average, humans spend 1.1 h of their daily time budget traveling. Schafer and Victor, 2000, estimated the average travel distance, per person per year, as 1814, 4382 and 6787 km for 1960, 1990 and 2020, respectively.

Brockmann–Hafnagel–Geisel, 2006, studied long range human traffic via the geographic circulation of money. To track a bill, a user stamps it and enters data (serial number, series and local ZIP code) in a computer. The site www.wheresgeorge.com reports the time and distance between the bill's consecutive sightings. 57 % of all $\approx$ 465,000 considered bills traveled 50–800 km over 9 months in US. The probability of a bill traversing a distance r (an estimate of the probability of humans moving such a distance) followed, over 10–3500 km, a power law $P(r) = r^{-1.6}$. Banknote dispersal was fractal, and the bill trajectories resembled Lévy walks.

González–Hidalgo–Barabási, 2008, studied the trajectory of 100,000 anonymized mobile phone users (a random sample of 6 million) over 6 months. The probability of finding a user at a location of *rank* k (by the number of times a user was recorded in the vicinity) was $P(k) \sim \frac{1}{k}$. 40 % of the time users were found at their first two preferred locations (home, work), while spending remaining time in 5–50 places. Phithakkitnukoon et al., 2011, found that $\approx$ 80 % of places visited by mobile phone users are within of their *geo-social radius* (nearest social ties' locations) 20 km.

Jiang–Yin–Zhao, 2009, analyzed people's moving trajectories, obtained from GPS data of 50 taxicabs over 6 months in a large street network. They found a Lévy behavior in walks (both origin-destination and between streets) and attributed it to the fractal property of the underlying street network, not to the goal-directed nature of human movement. Rhee et al., 2009, analyzed $\approx$1000 h of GPS traces of walks of 44 participants. They also got Lévy walks.

- **Total distance between trajectories**

  A *trajectory* in $\mathbb{R}^k$ is a sequence $X = ((x_1, t_1), \ldots, (x_n, t_n))$ of state-time points with $x_i \in \mathbb{R}^k$ and increasing "time" $t_i \in \mathbb{N}$. In $\mathbb{R}^2$, a trajectory can be seen as a list of consecutive GPS points for a moving object; sometimes, a semantic tag (say, "Shop, Restaurant") is attached to each point.

  Let $c(X)$ be the center of mass of $\{x_1, \ldots, x_n\}$, $l(X)$ the length of X, and $\mathbf{s}(X)$ the **displacement** of X (cf. Sect. 24.1), i.e., the vector from x_1 to x_n.

  The **total distance between trajectories** $X = ((x_1, t_1), \ldots, (x_n, t_n))$ and $X' = ((x'_1, t'_1), \ldots, (x'_n, t'_{n'}))$ is (Liu–Schneider, 2012) $\frac{Geo(X,X')}{1+\alpha Sem(X,X')}$, where $\alpha \in [0, 1]$ is a parameter, the *semantic similarity* $Sem(X, X')$ is the length of their longest

common subsequence divided by $\min(n, n')$, while

$$d_E(c(X), c(X'))(1 + \frac{|l(X) - l(X')|}{\max(l(X), l(X'))}) - \frac{||\mathbf{s}(X)|| + ||\mathbf{s}(X')||}{2} \frac{\langle \mathbf{s}(X), \mathbf{s}(X') \rangle}{||\mathbf{s}(X)|| \cdot ||\mathbf{s}(X')||}$$

is their *geographic distance* $Geo(X, X')$.

The *Lyapunov time*, reflecting the limits of system's predictability, is the time for the distance between nearby system's trajectories to increase by a factor of e.

18.2 Distances in Control Theory

Control Theory deals with influencing the behavior of *dynamical systems*. It considers the feedback loop of a *plant* P (a function representing the object to be controlled, a system) and a *controller* C (a function to design). The output y, measured by a sensor, is fed back to the reference value r.

Then the controller takes the *error* $e = r - y$ to make inputs $u = Ce$. Subject to zero initial conditions, the input and output signals to the plant are related by $y = Pu$, where r, u, v and P, C are functions of the frequency variable s. So, $y = \frac{PC}{1+PC} r$ and $y \approx r$ (i.e., one controls the output by simply setting the reference) if PC is large for any value of s.

If the system is modeled by a system of linear differential equations, then its *transfer function* $\frac{PC}{1+PC}$, relating the output with the input, is a rational function. The plant P is *stable* if it has no poles in the closed right half-plane $\mathbb{C}_+ = \{z \in \mathbb{C} : Re(z) \geq 0\}$.

The *robust stabilization problem* is: given a *nominal* plant (a model) P_0 and some metric d on plants, find the open ball of maximal radius which is centered in P_0, such that some controller (rational function) C stabilizes every element of this ball.

The *graph* $G(P)$ of the plant P is the set of all bounded input-output pairs $(u, y = Pu)$. Both u and y belong to the *Hardy space* $H^2(\mathbb{C}_+)$ of the right half-plane; the graph is a closed subspace of $H^2(\mathbb{C}_+) + H^2(\mathbb{C}_+)$. In fact, $G(P)$ is a closed subspace of $H^2(\mathbb{C}^2)$, and $G(P) = f(P) \cdot H^2(\mathbb{C}^2)$ for some function $f(P)$, called the *graph symbol*.

Cf. a **dynamical system** and the **Melnikov distance** in Sect. 18.1.

- **Gap metric**

  The **gap metric** between plants P_1 and P_2 (Zames–El-Sakkary, 1980) is defined by

  $$gap(P_1, P_2) = ||\Pi(P_1) - \Pi(P_2)||_2,$$

  where $\Pi(P_i)$, $i = 1, 2$, is the orthogonal projection of the graph $G(P_i)$ of P_i seen as a closed subspace of $H^2(\mathbb{C}^2)$. We have

  $$gap(P_1, P_2) = \max\{\delta_1(P_1, P_2), \delta_1(P_2, P_1)\},$$

  where $\delta_1(P_1, P_2) = \inf_{Q \in H^\infty} ||f(P_1) - f(P_2)Q||_{H^\infty}$, and $f(P)$ is a graph symbol.

Here H^∞ is the space of matrix-valued functions that are analytic and bounded in the open right half-plane $\{s \in \mathbb{C} : \Re\, s > 0\}$; the H^∞-norm is the maximum singular value of the function over this space.

If A is an $m \times n$ matrix with $m < n$, then its n columns span an n-dimensional subspace, and the matrix B of the orthogonal projection onto the column space of A is $A(A^TA)^{-1}A^T$. If the basis is orthonormal, then $B = AA^T$.

In general, the **gap metric** between two subspaces of the same dimension is the *l_2-norm* of the difference of their orthogonal projections; see also the definition of this distance as an **angle distance between subspaces**.

In applications, when subspaces correspond to autoregressive models, the *Frobenius norm* is used instead of the l_2-norm. Cf. **Frobenius distance** in Chap. 12.

- **Vidyasagar metric**

  The **Vidyasagar metric** (or *graph metric*) between plants P_1 and P_2 is defined by

$$\max\{\delta_2(P_1, P_2), \delta_2(P_2, P_1)\},$$

  where $\delta_2(P_1, P_2) = \inf_{||Q||\leq 1} ||f(P_1) - f(P_2)Q||_{H^\infty}$.

  The **behavioral distance** is the gap between *extended* graphs of P_1 and P_2; a term is added to the graph $G(P)$, in order to reflect all possible initial conditions (instead of the usual setup with the initial conditions being zero).

- **Vinnicombe metric**

  The **Vinnicombe metric** (*ν-gap metric*) between plants P_1 and P_2 is defined by

$$\delta_\nu(P_1, P_2) = ||(1 + P_2P_2^*)^{-\frac{1}{2}}(P_2 - P_1)(1 + P_1^*P_1)^{-\frac{1}{2}}||_\infty$$

  if $wno(f^*(P_2)f(P_1)) = 0$, and it is equal to 1, otherwise.

  Here $f(P)$ is the graph symbol function of plant P. See [Youn98] for the definition of the *winding number* $wno(f)$ of a rational function f and for a good introduction to Feedback Stabilization.

- **Lanzon–Papageorgiou quasi-distance**

  Given a plant P, a *perturbed plant* $\hat{P}$ and an uncertainty structure expressed via a *generalized plant* H, let Δ be the set of all possible perturbations that explain the discrepancy between P and $\hat{P}$. Then **Lanzon–Papageorgiou quasi-distance** (2009) between P and $\hat{P}$ is defined as ∞ if $\Delta = \emptyset$ and $\inf_{\delta\in\Delta} ||\delta||_\infty$, otherwise.

  This quasi-distance corresponds to the worst-case degradation of the stability margin due to a plant perturbation. For standard uncertainity structures H, it is a metric, but it is only a quasi-metric for multiplicative uncertainity.

- **Distance to uncontrollability**

  Linear Control Theory concerns a system of the form $\dot{x} = Ax(t) + Bu(t)$, where, at each time t, $x(t) \in \mathbb{C}^n$ is the *state vector*, $u(t) \in \mathbb{C}^m$ is the *control input vector*, and $A \in \mathbb{C}^{n\times n}$, $B \in \mathbb{C}^{n\times m}$ are the given matrices. The system (matrix pair (A, B)) is called *controllable* if, for any initial and final states $x(0)$ and $x(T)$, there

exists $u(t), 0 \leq t \leq T$, that drive the state from $x(0)$ to $x(T)$ within finite time, or, equivalently (Kalman, 1963) the matrix $A - \lambda IB$ has full row rank for all $\lambda \in \mathbb{C}$. The **distance to uncontrollability** (Paige, 1981, and Eising, 1984) is defined as

$$\min\{|||[E, F]||| : (A + E, B + F) \text{ is uncontrollable}\} = \min_{\lambda \in \mathbb{C}} \sigma_n(A - \lambda IB),$$

where $||.||$ is the *spectral* or *Frobenius norm* (cf. Sect. 12.3) and $\sigma_n(A - \lambda IB)$ denotes the n-th largest singular value of the $(n \times (n + m))$-matrix $A - \lambda IB$.

A matrix $A \in \mathbb{C}^{n \times n}$ is *stable* if any its eigenvalue λ has real part $Re(\lambda) < 0$. The **distance to instability** is (Van Loan, 1985) $\min\{||E|| : A + E \text{ is unstable}\}$, where $||.||$ is one of two above norms. Cf. **nearness matrix problems** in Chap. 12.

18.3 Motion Planning Distances

Automatic motion planning methods are applied in *Robotics*, *Virtual Reality Systems* and *Computer Aided Design*. A **motion planning metric** is a metric used in automatic motion planning methods.

Let a *robot* be a finite collection of rigid links organized in a kinematic hierarchy. If the robot has n degrees of freedom, this leads to an n-dimensional *manifold* C, called the *configuration space* (or *C-space*) of the robot. The *workspace* W of the robot is the space (usually, $\mathbb{E}^3$) in which the robot moves. Usually, it is modeled as the Euclidean space $\mathbb{E}^3$. A **workspace metric** is a motion planning metric in the workspace $\mathbb{R}^3$.

The *obstacle region* CB is the set of all configurations $q \in C$ that either cause the robot to collide with obstacles B, or cause different links of the robot to collide among themselves. The closure $cl(C_{free})$ of $C_{free} = C \backslash \{CB\}$ is called the *space of collision-free configurations*. A *motion planning algorithm* must find a collision-free path from an initial configuration to a goal configuration.

A **configuration metric** is a motion planning metric on the configuration space C of a robot. Usually, the configuration space C consists of six-tuples $(x, y, z, \alpha, \beta, \gamma)$, where the first three coordinates define the position, and the last three the orientation. The orientation coordinates are the angles in radians.

Intuitively, a good measure of the distance between two configurations is a measure of the workspace region swept by the robot as it moves between them (the **swept volume distance**). However, the computation of such a metric is prohibitively expensive.

The simplest approach has been to consider the C-space as a Cartesian space and to use Euclidean distance or its generalizations. For such **configuration metrics**, one normalizes the orientation coordinates so that they get the same magnitude as the position coordinates. Roughly, one multiplies the orientation coordinates by the maximum x, y or z range of the workspace bounding box. Examples of such metrics are given below.

More generally, the configuration space of a 3D rigid body can be identified with the Lie group $ISO(3)$: $C \cong \mathbb{R}^3 \times \mathbb{R}P^3$. The general form of a matrix in $ISO(3)$ is given by

$$\begin{pmatrix} R & X \\ 0 & 1 \end{pmatrix},$$

where $R \in SO(3) \cong \mathbb{R}P^3$, and $X \in \mathbb{R}^3$.

If X_q and R_q represent the translation and rotation components of the configuration $q = (X_q, R_q) \in ISO(3)$, then a configuration metric between configurations q and r is given by $w_{tr}||X_q - X_r|| + w_{rot} f(R_q, R_r)$, where the **translation distance** $||X_q - X_r||$ is obtained using some norm $||.||$ on $\mathbb{R}^3$, and the **rotation distance** $f(R_q, R_r)$ is a positive scalar function which gives the distance between the rotations $R_q, R_r \in SO(3)$. The rotation distance is scaled relative to the translation distance via the weights w_{tr}, w_{rot}.

There are many other types of metrics used in motion planning methods, in particular, the **Riemannian metrics**, the **Hausdorff metric** and, in Chap. 9, the **separation distance**, the **penetration depth distance** and the **growth distances**.

- **Weighted Euclidean $\mathbb{R}^6$-distance**

  The **weighted Euclidean $\mathbb{R}^6$-distance** is a **configuration metric** on $\mathbb{R}^6$ defined, for any $x, y \in \mathbb{R}^6$, by

  $$\left(\sum_{i=1}^{3} |x_i - y_i|^2 + \sum_{i=4}^{6} (w_i |x_i - y_i|)^2 \right)^{\frac{1}{2}},$$

  where $x = (x_1, \ldots, x_6)$, x_1, x_2, x_3 are the position coordinates, x_4, x_5, x_6 are the orientation coordinates, and w_i is the normalization factor. Cf. the general, i.e., in $\mathbb{R}^n$, **weighted Euclidean distance** in Chap. 17.

  The *scaled weighted Euclidean $\mathbb{R}^6$-distance* is defined, for any $x, y \in \mathbb{R}^6$, by

  $$\left(s \sum_{i=1}^{3} |x_i - y_i|^2 + (1-s) \sum_{i=4}^{6} (w_i |x_i - y_i|)^2 \right)^{\frac{1}{2}}.$$

  This distance changes the relative importance of the position and orientation components through the scale parameter s.

- **Weighted Minkowskian distance**

  The **weighted Minkowskian distance** is a **configuration metric** on $\mathbb{R}^6$ defined, for any $x, y \in \mathbb{R}^6$, by

  $$\left(\sum_{i=1}^{3} |x_i - y_i|^p + \sum_{i=4}^{6} (w_i |x_i - y_i|)^p \right)^{\frac{1}{p}}.$$

It gives the same importance to both position and orientation.

- **Modified Minkowskian distance**

  The **modified Minkowskian distance** is a **configuration metric** on $\mathbb{R}^6$ defined, for any $x, y \in \mathbb{R}^6$, by

$$\left(\sum_{i=1}^{3} |x_i - y_i|^{p_1} + \sum_{i=4}^{6} (w_i |x_i - y_i|)^{p_2}\right)^{\frac{1}{p_3}}.$$

  It distinguishes between position and orientation coordinates using the parameters $p_1 \geq 1$ (for the position) and $p_2 \geq 1$ (for the orientation).

- **Weighted Manhattan distance**

  The **weighted Manhattan distance** is a **configuration metric** on $\mathbb{R}^6$ defined, for any $x, y \in \mathbb{R}^6$, by

$$\sum_{i=1}^{3} |x_i - y_i| + \sum_{i=4}^{6} w_i |x_i - y_i|.$$

- **Robot displacement metric**

  The **robot displacement metric** (or *DISP distance*, Latombe, 1991, and LaValle, 2006) is a **configuration metric** on a configuration space C of a robot defined by

$$\max_{a \in A} ||a(q) - a(r)||$$

  for any two configurations $q, r \in C$, where $a(q)$ is the position of the point a in the workspace $\mathbb{R}^3$ when the robot is at configuration q, and $||.||$ is one of the norms on $\mathbb{R}^3$, usually the Euclidean norm. Intuitively, this metric yields the maximum amount in workspace that any part of the robot is displaced when moving from one configuration to another (cf. **bounded box metric**).

- **Euler angle metric**

  The **Euler angle metric** is a **rotation metric** on the group $SO(3)$ (for the case of using three—Heading-Elevation-Bank—*Euler angles* to describe the orientation of a rigid body) defined by

$$w_{rot} \sqrt{\Delta(\theta_1, \theta_2)^2 + \Delta(\phi_1, \phi_2)^2 + \Delta(\eta_1, \eta_2)^2}$$

  for all $R_1, R_2 \in SO(3)$, given by Euler angles $(\theta_1, \phi_1, \eta_1)$, $(\theta_2, \phi_2, \eta_2)$, respectively, where $\Delta(\theta_1, \theta_2) = \min\{|\theta_1 - \theta_2|, 2\pi - |\theta_1 - \theta_2|\}$, $\theta_i \in [0, 2\pi]$, is the **metric between angles**, and w_{rot} is a scaling factor.

- **Unit quaternions metric**

  The **unit quaternions metric** is a **rotation metric** on the *unit quaternion representation* of $SO(3)$, i.e., a representation of $SO(3)$ as the set of points (*unit*

quaternions) on the *unit sphere* S^3 in $\mathbb{R}^4$ with identified antipodal points ($q \sim -q$).

This representation of $SO(3)$ suggested a number of possible metrics on it, for example, the following ones:

1. $\min\{||q - r||, ||q + r||\}$,
2. $||\ln(q^{-1}r)||$,
3. $w_{rot}(1 - |\lambda|)$,
4. $\arccos |\lambda|$,

where $q = q_1 + q_2 i + q_3 j + q_4 k$, $\sum_{i=1}^{4} q_i^2 = 1$, $||.||$ is a norm on $\mathbb{R}^4$, $\lambda = \langle q, r \rangle = \sum_{i=1}^{4} q_i r_i$, and w_{rot} is a scaling factor.

- **Center of mass metric**

  The **center of mass metric** is a **workspace metric**, defined as the Euclidean distance between the *centers of mass* of the robot in the two configurations. The center of mass is approximated by averaging all object vertices.

- **Bounded box metric**

  The **bounded box metric** is a **workspace metric** defined as the maximum Euclidean distance between any vertex of the *bounding box* of the robot in one configuration and its corresponding vertex in the other configuration.

  The **box metric** in Chap. 4 is unrelated.

- **Pose distance**

  A **pose distance** provides a measure of dissimilarity between actions of *agents* (including robots and humans) for Learning by Imitation in Robotics.

  In this context, agents are considered as *kinematic chains*, and are represented in the form of a *kinematic tree*, such that every link in the kinematic chain is represented by a unique edge in the corresponding tree.

  The configuration of the chain is represented by the *pose* of the corresponding tree which is obtained by an assignment of the pair (n_i, l_i) to every edge e_i. Here n_i is the unit normal, representing the orientation of the corresponding link in the chain, and l_i is the length of the link.

  The *pose class* consists of all poses of a given kinematic tree. One of the possible pose distances is a distance on a given pose class which is the sum of measures of dissimilarity for every pair of compatible segments in the two given poses.

  Another way is to view a *pose* $D(m)$ in the context of the a precedent and a subsequent frames as a *3D point cloud* $\{D^j(i) : m - a \leq i \leq m + a, j \in J\}$, where J is the joint set. The set $D(m)$ contains $k = |J|(2a + 1)$ points (joint positions) $p_i = (x_i, y_i, z_i)$, $1 \leq i \leq k$. Let $T_{\theta,x,z}$ denote the linear transformation which simultaneously rotates all points of a point cloud about the y axis by an angle $\theta \in [0.2\pi]$ and then shifts the resulting points in the xz plane by a vector $(x, 0, z) \in \mathbb{R}^3$. Then the **3D point cloud distance** (Kover and Gleicher, 2002)

between the poses $D(m) = (p_i)_{i\in[1,k]}$ and $D(n) = (q_i)_{i\in[1,k]}$ is defined as

$$\min_{\theta,x,z}\{\sum_{i=1}^{k} ||p_i - T_{\theta,x,z}(q_i)||_2^2\}.$$

Cf. **Procrustes distance** in Chap. 21.

- **Joint angle metric**

  For a given frame (or pose) i in an animation, let us define $p_i \in \mathbb{R}^3$ as the global (root) position and $q_{i,k} \in S^3$ as the unit quaternion describing the orientation of a joint k from the joint set J. Cf. **unit quaternions metric** and **3D point cloud distance**. The **joint angle metric** between frames x and y is defined as follows:

$$|p_x - p_y|^2 + \sum_{k\in J} w_k |\log(q_{y,k}^{-1} q_{x,k})|^2.$$

  The second term describes the weighted sum of the orientation differences; cf. **weighted Euclidean $\mathbb{R}^6$-distance**. Sometimes, the terms expressing differences in derivatives, such as joint velocity and acceleration, are added.

- **Millibot train metrics**

  In *Microbotics* (the field of miniature mobile robots), *nanorobot*, *microrobot*, *millirobot*, *minirobot*, and *small robot* are terms for robots with characteristic dimensions at most one micrometer, mm, cm, dm, and m, respectively.

  A *millibot train* is a team of heterogeneous, resource-limited millirobots which can collectively share information. They are able to fuse range information from a variety of different platforms to build a global occupancy map that represents a single collective view of the environment.

  In the construction of a **motion planning metric** of millibot trains, one casts a series of random points about a robot and poses each point as a candidate position for movement. The point with the highest overall utility is then selected, and the robot is directed to that point. Thus:

  the **free space metric**, determined by free space contours, only allows candidate points that do not drive the robot through obstructions;
  the **obstacle avoidance metric** penalizes for moves that get too close to obstacles;
  the **frontier metric** rewards for moves that take the robot towards open space;
  the **formation metric** rewards for moves that maintain formation;
  the **localization metric**, based on the separation angle between one or more localization pairs, rewards for moves that maximize localization (see [GKC04]).

  Cf. **collision avoidance distance** and **piano movers distance** in Chap. 19.

  A *swarm-bot* can form more complex (more sensors and actuators) and flexible (interconnecting at several angles and with less accuracy) configurations.

The wingspan range of flying robots includes 2.8 cm (quadcopter Lisa/S) and 40 m (Global Hawk). During 2012, a robot Papa Mau (PacX Wave Glider), piloted remotely, swam 16,668 km from San Francisco to Australia.

18.4 MOEA Distances

Most optimization problems have several objectives but, for simplicity, only one of them is optimized, and the others are handled as constraints. *Multi-objective optimization* considers (besides some inequality constraints) an objective vector function $f : X \subset \mathbb{R}^n \to \mathbb{R}^k$ from the *search* (or *genotype*, *decision variables*) space X to the *objective* (or *phenotype*, *decision vectors*) space $f(X) = \{f(x) : x \in X\} \subset \mathbb{R}^k$.

A point $x^* \in X$ is a *Pareto-optimal solution* if, for every other $x \in X$, the decision vector $f(x)$ does not *Pareto-dominate* $f(x^*)$, i.e., $f(x) \preceq f(x^*)$. The *Pareto-optimal front* is the set $PF^* = \{f(x) : x \in X^*\}$, where X^* is the set of all Pareto-optimal solutions.

Multi-objective evolutionary algorithms (MOEA) produce, at each generation, an *approximation set* (the found Pareto front PF_{known} approximating the desired Pareto front PF^*) in objective space in which no element Pareto-dominates another element. Examples of **MOEA metrics**, i.e., measures evaluating how close PF_{known} is to PF^*, follow.

- **Generational distance**
  The **generational distance** is defined by

$$\frac{(\sum_{j=1}^{m} d_j^2)^{\frac{1}{2}}}{m},$$

  where $m = |PF_{known}|$, and d_j is the Euclidean distance (in the objective space) between $f^j(x)$ (i.e., j-th member of PF_{known}) and the nearest member of PF^*. This distance is zero if and only if $PF_{known} = PF^*$.

  The term **generational distance** (or *rate of turnover*) is also used for the minimal number of branches between two positions in any system of ranked descent represented by a hierarchical tree. Examples are: **phylogenetic distance** on a phylogenetic tree (cf. Chap. 23), the number of generations separating a photocopy from the original block print, and the number of generations separating the audience at a memorial from the commemorated event.
- **Spacing**
  The **spacing** is defined by

$$\left(\frac{\sum_{j=1}^{m} (\overline{d} - d_j)^2}{m-1} \right)^{\frac{1}{2}},$$

where $m = |PF_{known}|$, d_j is the L_1-*metric* (in the objective space) between $f^j(x)$ (i.e., j-th member of PF_{known}) and the nearest other member of PF_{known}, while $\overline{d}$ is the mean of all d_j.

- **Overall nondominated vector ratio**

  The **overall nondominated vector ratio** is defined by

$$\frac{|PF_{known}|}{|PF^*|}.$$

- **Crowding distance**

  The **crowding distance** (Deb et al., 2002) is a diversity metric assigned to each Pareto-optimal solution. It is the sum, for all objectives, of the absolute difference of the objective values of two nearest solutions on each side, if they exist.

  The *boundary solutions*, i.e., those with the smallest or the highest such value, are assigned an infinite crowding distance.

Part V
Computer-Related Distances

Chapter 19
Distances on Real and Digital Planes

19.1 Metrics on Real Plane

Any L_p**-metric** (as well as any **norm metric** for a given norm $||.||$ on $\mathbb{R}^2$) can be used on the plane $\mathbb{R}^2$, and the most natural is the L_2-metric, i.e., the Euclidean metric $d_E(x, y) = \sqrt{(x_1 - y_1)^2 + (x_2 - y_2)^2}$ which gives the length of the straight line segment $[x, y]$, and is the **intrinsic metric** of the plane.

However, there are other, often "exotic", metrics on $\mathbb{R}^2$. Many of them are used for the construction of *generalized Voronoi diagrams* on $\mathbb{R}^2$ (see, for example, **Moscow metric**, **network metric**, **nice metric**). Some of them are used in Digital Geometry.

- **Erdős-type distance problems**

  Those distance problems were given by Erdős and his collaborators, usually, for the Euclidean metric on $\mathbb{R}^2$, but they are of interest for $\mathbb{R}^n$ and for other metrics on $\mathbb{R}^2$. Examples of such problems are to find out:

  the least number of different distances (or largest occurrence of a given distance) in an m-subset of $\mathbb{R}^2$;
  the largest cardinality of a subset of $\mathbb{R}^2$ determining at most m distances;
  the minimum diameter of an m-subset of $\mathbb{R}^2$ with only integral distances (or, say, without a pair (d_1, d_2) of distances with $0 < |d_1 - d_2| < 1$);
  the *Erdős-diameter* of a given set S, i.e., the minimum diameter of a rescaled set rS, $r > 0$, in which any two different positive distances differ at least by one;
  the largest cardinality of an *isosceles set* in $\mathbb{R}^2$, i.e., a set of points, any three of which form an isosceles triangle;
  existence of an m-subset of $\mathbb{R}^2$ with, for each $1 \leq i \leq m$, a distance occurring exactly i times (examples are known for $m \leq 8$);

© Springer-Verlag Berlin Heidelberg 2016

M.M. Deza, E. Deza, *Encyclopedia of Distances*,
DOI 10.1007/978-3-662-52844-0_19

existence of a dense subset of $\mathbb{R}^2$ with rational distances (Ulam problem);
existence of $m, m > 7$, noncollinear points of $\mathbb{R}^2$ with integral distances;
forbidden (not occurring within each part) *distances* of a partition of $\mathbb{R}^2$.

The general **Erdős distinct distances problem**, still open for $n > 2$, is to prove that if $A \subset \mathbb{R}^n$, $|A| = m$ and $d(A)$ denotes the set $\{\sum_{i=1}^{n}(x_i - y_i)^2 : x, y \in A\}$, then $|d(A)| \geq Cm^{\frac{n}{2}}$ for some constant $C > 0$. This problem was generalized for distinct "distances" (cf. Chap. 3) over a finite field. Also, its continuous analog, open **Falconer distance problem** is to prove that if the **Hausdorff dimension** of $A \subset \mathbb{R}^n$ is $> \frac{n}{2}$, then 1-dimensional *Lebesque measure* of $d(A)$ is positive. Related result by Quas, 2009: if the *upper density* of $A \subset \mathbb{R}^n$ is positive, then there is $r_0 > 0$ such that for any $r > r_0$, there are $x, y \in A$ with $d_E(x, y) = r$.

The *three-distance theorem* (Sós, 1957): given $a \in (0, 1)$ and $n \in \mathbb{N}$, the points $\{0\}, \{a\}, \{2a\}, \ldots, \{na\} \pmod 1$ on the circle of perimeter 1, partition it into $n + 1$ intervals having at most three lengths, one being the sum of the other two.

The **problem of dispersion** (or *finding System of Distant Representatives*) in a family of n subsets of a metric space is (Fiala et al., 2005) that of selecting n points, one in each subset, such that the minimum inter-point distance is maximized.

- **Distance inequalities in a triangle**

The multitude of inequalities, involving Euclidean distances between points of $\mathbb{R}^n$, is represented below by some **distance inequalities in a triangle**.

Let $\triangle ABC$ be a triangle on $\mathbb{R}^2$ with side-lengths $a = d(B, C), b = d(C, A), c = d(A, B)$ and area $\mathcal{A} = \frac{1}{4}\sqrt{(a^2 + b^2 + c^2)^2 - 2(a^4 + b^4 + c^4)}$.

Let P, P' be two arbitrary interior points in $\triangle ABC$. Denote by D_A, D_B, D_C the distances $d(P, A), d(P, B), d(P, C)$ and by d_A, d_B, d_C the **point-line distances** (Chap. 4) from P to the sides BC, CA, AB opposite to A, B, C. For the point P' define D'_A, D'_B, D'_C and d'_A, d'_B, d'_C similarly.

The point P is *circumcenter* if $D_A = D_B = D_C$; this distance, $R = \frac{abc}{4\mathcal{A}}$, is circumcircle's radius. The point P is *incenter* if $d_A = d_B = d_C$; this distance, $r = \frac{2\mathcal{A}}{a+b+c}$, is incircle's radius. The *centroid* (the center of mass) is the point G of concurrency of three triangle's medians m_a, m_b, m_c; it holds $d(A, G) = \frac{2}{3}m_a, d(B, G) = \frac{2}{3}m_b, d(C, G) = \frac{2}{3}m_c$. The *symmedian point* is the point of concurrency of three triangle's *symmedians* (reflections of medians at corresponding angle bisectors).

The *orthocenter* is the point of concurrency of three triangle's altitudes. The centroid is situated on the *Euler line* through the circumcenter and the orthocenter, at $\frac{1}{3}$ of their distance. At $\frac{1}{2}$ of their distance lies the center of the circle going through the midpoints of three sides and the feet of three altitudes.

– If P and P' are the circumcenter and incenter of $\triangle ABC$, then (Euler, 1765)

$$d^2(P, P') \geq R(R - 2r)$$

holds implying $R \geq 2r$ with equality if and only if triangle is equilateral. In fact, the general *Euler's inequality* $R \geq nr$ holds (Klamkin–Tsintsifas, 1979) for the radii R, r of circumscribed and inscribed spheres of an n-simplex.

– For any P, P', the *Erdős–Mordell* inequality (Mordell–Barrow, 1937) is

$$D_A + D_B + D_C \geq 2(d_A + d_B + d_C).$$

Liu, 2008, generalized above as follows: for all $x, y, z \geq 0$ it holds

$$\sqrt{D_A D'_A}x^2 + \sqrt{D_B D'_B}y^2 + \sqrt{D_C D'_C}z^2 \geq 2(\sqrt{d_A d'_A}yz + \sqrt{d_B d'_B}xz + \sqrt{d_C d'_C}xy).$$

– Lemoine, 1873, proved that

$$\frac{4\mathcal{A}^2}{a^2 + b^2 + c^2} \leq d_A^2 + d_B^2 + d_C^2$$

with equality if and only if P is the symmedian point.

– Posamentier and Salkind, 1996, showed

$$\frac{3}{4}(a+b+c) < m_a+m_b+m_c < a+b+c, \text{ while } \frac{3}{4}(a^2+b^2+c^2) = m_a^2+m_b^2+m_c^2.$$

– Kimberling, 2010, proved that

$$d_A d_B d_C \leq \frac{8\mathcal{A}^3}{27abc}$$

with equality if and only if P is the centroid.

He also gave (together with unique point realizing equality) inequality

$$\frac{(2\mathcal{A})^q}{(a^{\frac{2}{q-1}} + b^{\frac{2}{q-1}} + c^{\frac{2}{q-1}})^{q-1}} \leq d_A^q + d_B^q + d_C^q$$

for any $q < 0$ or $q > 1$. For $0 < q < 1$, the reverse inequality holds.

The side-lengths $d(A, B), d(B, C), d(C, A)$ of a *right triangle* are in arithmetic progression only if their ratio is 3:4:5. They are in geometric progression only if their ratio is $1:\sqrt{\varphi}:\varphi$, where φ is the *golden section* $\frac{1+\sqrt{5}}{2}$.

- **City-block metric**

The **city-block metric** is the L_1*-metric* on $\mathbb{R}^2$ defined by

$$||x - y||_1 = |x_1 - y_1| + |x_2 - y_2|.$$

It is also called the **taxicab metric**, **Manhattan metric**, **rectilinear metric**, **right-angle metric**, 4**-metric** and, on $\mathbb{Z}^n$, **grid metric**. The *von Neumann neighborhood* of a point is the set of points at a Manhattan distance of 1 from it.

- **Chebyshev metric**

  The **Chebyshev metric** (or **chessboard metric**, **king-move metric**, 8**-metric**) is the L_∞*-metric* on $\mathbb{R}^2$ defined by

$$||x-y||_\infty = \max\{|x_1-y_1|, |x_2-y_2|\}.$$

  On $\mathbb{Z}^n$, this metric is called also the **lattice** (or **uniform**, **sup**) **metric**. A point's *Moore neighborhood* is the set of points at a Chebyshev distance of 1.

- α**-metric**

  Given $\alpha \in [0, \frac{\pi}{4}]$, the α**-metric** for $x, y \in \mathbb{R}^2$ is defined (Tian, 2005) by

$$d_\alpha(x,y) = \max\{|x_1-y_1|, |x_2-y_2|\} - (\sec\alpha - \tan\alpha)\min\{|x_1-y_1|, |x_2-y_2|.$$

  It is the **city-block metric** if $\alpha = 0$. For $\alpha = \frac{\pi}{4}$, i.e., $\sec\alpha - \tan\alpha = \sqrt{2}-1$, it is the **Chinese checkers metric** (Chen, 1992). *Chinese checkers* (as well as *Hexagonal chess*, *Masonic chess*, *Sannin shogi*, *Hexshogi*) is a strategy board game with hexagonal cells, while *Tiangular chess*, *Tri-chess*, *Trishogi* have triangular cells. Cf. **hexagonal metric**. Gelişgen and Kaya, 2006, generalized α-metric on $\mathbb{R}^n$.

- **Relative metrics on** $\mathbb{R}^2$

  The (p,q)**-relative** and M**-relative** distances are defined in Chap. 5 on any *Ptolemaic space*. The (p,q)**-relative distance** on $\mathbb{R}^2$ (in general, on $\mathbb{R}^n$) is defined (for x or $y \neq 0$) in the cases $1 \leq p < \infty$ and $p = \infty$, respectively, by

$$\frac{||x-y||_2}{(\frac{1}{2}(||x||_2^p + ||y||_2^p))^{\frac{q}{p}}} \quad \text{and} \quad \frac{||x-y||_2}{(\max\{||x||_2, ||y||_2\})^q}.$$

  Let $f : [0,\infty) \to (0,\infty)$ be a convex increasing function such that $\frac{f(x)}{x}$ is decreasing for $x > 0$. The M**-relative distance** on $\mathbb{R}^2$ (in general, on $\mathbb{R}^n$), is defined by

$$\frac{||x-y||_2}{f(||x||_2)\cdot f(||y||_2)}.$$

  In particular, the distance below is a metric if and only if $p \geq 1$:

$$\frac{||x-y||_2}{\sqrt[p]{1+||x||_2^p}\sqrt[p]{1+||y||_2^p}}.$$

  A similar metric on $\mathbb{R}^2\backslash\{0\}$ (in general, on $\mathbb{R}^n\backslash\{0\}$) is defined by $\frac{||x-y||_2}{||x||_2\cdot||y||_2}$.

- **MBR metric**

  The **MBR metric** (Schönemann, 1982, for bounded response scales in Psychology) is a metric $d((x_1, x_2), (y_1, y_2))$ on $\mathbb{R}^2$, defined by

$$\frac{|x_1 - y_1| + |x_2 - y_2|}{1 + |x_1 - y_1||x_2 - y_2|} = \tanh(\operatorname{arctanh}(|x_1 - y_1|) + \operatorname{arctanh}(|x_2 - y_2|)).$$

- **Moscow metric**

  The **Moscow** (or *Karlsruhe*, *Amsterdam*) *metric* is a metric on $\mathbb{R}^2$, defined as the minimum Euclidean length of all *admissible* connecting curves between x and $y \in \mathbb{R}^2$, where a curve is called *admissible* if it consists only of *radial streets* (segments of straight lines passing through the origin) and *circular avenues* (segments of circles centered at the origin); see, for example, [Klei88]).

  If the polar coordinates for points $x, y \in \mathbb{R}^2$ are (r_x, θ_x), (r_y, θ_y), respectively, then the distance between them is equal to $\min\{r_x, r_y\}\Delta(\theta_x - \theta_y) + |r_x - r_y|$ if $0 \leq \Delta(\theta_x, \theta_y) < 2$, and is equal to $r_x + r_y$ if $2 \leq \Delta(\theta_x, \theta_y) < \pi$, where $\Delta(\theta_x, \theta_y) = \min\{|\theta_x - \theta_y|, 2\pi - |\theta_x - \theta_y|\}$, $\theta_x, \theta_y \in [0, 2\pi)$, is the **metric between angles**.

- **French Metro metric**

  Given a norm $||.||$ on $\mathbb{R}^2$, the **French Metro metric** is a metric on $\mathbb{R}^2$ defined by

$$||x - y|| \text{ if } x = cy \text{ for some } 0 \neq c \in \mathbb{R} \text{ (i.e., } x_1 y_2 = x_2 y_1),$$

  and by

$$||x|| + ||y||, \text{ otherwise.}$$

  For the Euclidean norm $||.||_2$, it is called the **Paris metric**, **radial metric**, **hedgehog metric**, or **French railroad metric**, **enhanced SNCF metric**.

  In this case it can be defined as the minimum Euclidean length of all *admissible* connecting curves between two given points x and y, where a curve is called *admissible* if it consists only of segments of straight lines passing through the origin.

  In graph terms, this metric is similar to the **path metric** of the tree consisting of a point from which radiate several disjoint paths. In the case when only one line radiates from the point, this metric is called the **train metric**.

  The Paris metric is an example of an $\mathbb{R}$**-tree** T which is *simplicial*, i.e., its set of points x with $T \backslash \{x\}$ not having exactly two components, is discrete and closed.

- **Lift metric**

  The **lift metric** (or **jungle river metric**, *raspberry picker metric*, *barbed wire metric*) is a metric $d((x_1, x_2), (y_1, y_2))$ on $\mathbb{R}^2$ defined (see, for example, [Brya85]) by

$$|x_1 - y_1| \text{ if } x_2 = y_2,$$

and by

$$|x_1| + |x_2 - y_2| + |y_1| \text{ if } x_2 \neq y_2.$$

It is the minimum Euclidean length of all *admissible* (consisting only of segments of straight lines parallel to the x_1 axis and segments of the x_2 axis) connecting curves between points (x_1, x_2) and (y_1, y_2).

The lift metric is an *nonsimplicial* (cf. **French Metro metric**) $\mathbb{R}$**-tree**.

- **Radar screen metric**

  Given a norm $||.||$ on $\mathbb{R}^2$ (in general, on $\mathbb{R}^n$), the **radar screen metric** is a special case of the t**-truncated metric** (Chap. 4) defined by

$$\min\{1, ||x - y||\}.$$

- **British Rail metric**

  Given a norm $||.||$ on $\mathbb{R}^2$ (in general, on $\mathbb{R}^n$), the **British Rail metric** is a metric defined as 0 for $x = y$ and, otherwise, by

$$||x|| + ||y||.$$

  It is also called the **Post Office metric**, **caterpillar metric** and **shuttle metric**.

- **Flower-shop metric**

  Let d be a metric on $\mathbb{R}^2$, and let f be a fixed point (a *flower-shop*) in the plane.

  The **flower-shop metric** (sometimes called **SNCF metric**) is a metric on $\mathbb{R}^2$ (in general, on any metric space) defined by

$$d(x,f) + d(f,y)$$

  for $x \neq y$ (and is equal to 0, otherwise). So, a person living at point x, who wants to visit someone else living at point y, first goes to f, to buy some flowers. In the case $d(x, y) = ||x - y||$ and the point f being the origin, it is the **British Rail metric**.

  If $k > 1$ flower-shops $f_1, \ldots, f_k$ are available, one buys the flowers, where the detour is a minimum, i.e., the distance between distinct points x, y is equal to $\min_{1 \leq i \leq k}\{d(x, f_i) + d(f_i, y)\}$.

- **Rickman's rug metric**

  Given a number $\alpha \in (0, 1)$, the **Rickman's rug metric** on $\mathbb{R}^2$ is a 2D case of the **parabolic distance** (Chap. 6) defined by

$$d((x_1, x_2), (y_1, y_2)) = |x_1 - y_1| + |x_2 - y_2|^{\alpha}.$$

- **Burago–Burago–Ivanov metric**

  The **Burago–Burago–Ivanov metric** ([BBI01]) is a metric on $\mathbb{R}^2$ defined by

$$| \, ||x||_2 - ||y||_2| + \min\{||x||_2, ||y||_2\} \cdot \sqrt{\angle(x, y)},$$

where $\angle(x, y)$ is the angle between vectors x and y, and $||.||_2$ is the Euclidean norm on $\mathbb{R}^2$. The corresponding **internal metric** on $\mathbb{R}^2$ is equal to $|\,||x||_2 - ||y||_2|$ if $\angle(x, y) = 0$, and is equal to $||x||_2 + ||y||_2$, otherwise.

- $2n$**-gon metric**

  Given a centrally symmetric regular $2n$-gon K on the plane, the $2n$**-gon metric** is a metric on $\mathbb{R}^2$ defined, for any $x, y \in \mathbb{R}^2$, as the shortest Euclidean length of a polygonal line from x to y with each of its sides parallel to some edge of K.

  If K is a square with the vertices $\{(\pm 1, \pm 1)\}$, one obtains the **Manhattan metric**. The Manhattan metric arises also as the **Minkowskian metric** with the unit ball being the *diamond*, i.e., a square with the vertices $\{(1, 0), (0, 1), (-1, 0), (0, -1)\}$.

- **A-distance**

  Given a set A, $|A| \geq 2$, of distinct *orientations* (i.e., angles with fixed x axis) on the plane $\mathbb{R}^2$, the A**-distance** (or **fixed orientation metric**) is (Widmayer–Wu–Wong, 1987) Euclidean length of the shortest (zig-zag) path of line segments with orientations from A. Any A-distance is a metric.

  A-distance with $A = \{\frac{i\pi}{n} : 1 \leq i \leq n\}$ for fixed $n \in [2, \infty]$, is called a *uniform orientation metric*; cf. $2n$**-gon metric**. It is the l_1-metric, **hexagonal metric**, l_2-metric for $n = 2, 3, \infty$, respectively.

- **Central Park metric**

  The **Central Park metric** is a metric on $\mathbb{R}^2$, defined as the length of a shortest L_1-path (*Manhattan path*) between two points $x, y \in \mathbb{R}^2$ in the presence of a given set of areas which are traversed by a shortest Euclidean path (for example, Central Park in Manhattan).

- **Collision avoidance distance**

  Let $\mathcal{O} = \{O_1, \ldots, O_m\}$ be a collection of pairwise disjoint polygons on the Euclidean plane representing a set of obstacles which are neither transparent nor traversable.

  The **collision avoidance distance** (or **piano movers distance**, **shortest path metric with obstacles**) is a metric on the set $\mathbb{R}^2 \backslash \{\mathcal{O}\}$, defined, for any $x, y \in \mathbb{R}^2 \backslash \{\mathcal{O}\}$, as the length of the shortest path among all possible continuous paths, connecting x and y, that do not intersect obstacles $O_i \backslash \partial O_i$ (a path can pass through points on the boundary ∂O_i of O_i), $i = 1, \ldots m$.

- **Rectilinear distance with barriers**

  Let $\mathcal{O} = \{O_1, \ldots, O_m\}$ be a set of pairwise disjoint open polygonal barriers on $\mathbb{R}^2$. A *rectilinear path* (or *Manhattan path*) P_{xy} from x to y is a collection of horizontal and vertical segments in the plane, joining x and y. The path P_{xy} is called *feasible* if $P_{xy} \cap (\cup_{i=1}^{m} B_i) = \emptyset$.

  The **rectilinear distance with barriers** (or *rectilinear distance in the presence of barriers*) is a metric on $\mathbb{R}^2 \backslash \{\mathcal{O}\}$, defined, for any $x, y \in \mathbb{R}^2 \backslash \{\mathcal{O}\}$, as the length of the shortest *feasible rectilinear path* from x to y.

  The rectilinear distance in the presence of barriers is a restriction of the **Manhattan metric**, and usually it is considered on the set $\{q_1, \ldots, q_n\} \subset \mathbb{R}^2$ of n *origin-destination points*: the problem to find such a path arises, for example,

in Urban Transportation, or in Plant and Facility Layout (see, for example, [LaLi81]).

- **Link distance**

  Let $P \subset \mathbb{R}^2$. The **polygonal distance** (or **link distance** as defined by Suri, 1986) between any two points of P is the smallest number of edges of a polygonal path in P connecting them if such path exists and ∞, otherwise.

  If the path is restricted to be rectilinear, one obtains the *rectilinear link distance*. If each line segment of the path is parallel to one from a set A of fixed orientations, one obtains the *A-oriented link distance*; cf. **fixed orientation metric** above.

  If the turning points of the path are constrained to lie on the boundary of P, then the path is called *drp* (diffuse reflection path). The *drp-diameter* of P is the minimum number of *diffuse reflections* (segments in a drp) needed to illuminate any target point from any point light source inside P.

- **Facility layout distances**

  A *layout* is a partition of a rectangular plane region into smaller rectangles, called *departments*, by lines parallel to the sides of original rectangle. All interior vertices should be of degree 3, and some of them, at least one on the boundary of each department, are *doors*, i.e., input-output locations.

  The problem is to design a convenient notion of distance $d(x, y)$ between departments x and y which minimizes the *cost function* $\sum_{x,y} F(x, y)d(x, y)$, where $F(x, y)$ is some *material flow* between x and y. The main distances used are:

  the **centroid distance**, i.e., the shortest Euclidean or **Manhattan distance** between *centroids* (the intersections of the diagonals) of x and y;
  the **perimeter distance**, i.e., the shortest rectilinear distance between doors of x and y, but going only along the *walls* (department perimeters).

- **Quickest path metric**

  A **quickest path metric** (or **network metric**, **time metric**) is a metric on $\mathbb{R}^2$ (or on a subset of $\mathbb{R}^2$) in the presence of a given *transportation network*, i.e., a finite graph $G = (V, E)$ with $V \subset \mathbb{R}^2$ and edge-weight function $w(e) > 1$: the vertices and edges are *stations* and *roads*. For any $x, y \in \mathbb{R}^2$, it is the time needed for a *quickest path* (i.e., a path minimizing the travel duration) between them when using, eventually, the network.

  Movement takes place, either off the network with unit speed, or along its roads $e \in E$ with fixed speeds $w(e) >> 1$, with respect to a given (usually, Euclidean or **Manhattan**) metric d on the plane. The network G can be accessed or exited only at stations (usual discrete model) or at any point of roads (the continuous model).

  The **heavy luggage metric** (Abellanas–Hurtado–Palop, 2005) is a quickest path metric on $\mathbb{R}^2$ in the presence of a network with speed 1 outside of the network and speed ∞ (so, travel time 0) inside of it.

  The **airlift metric** is a quickest path metric on $\mathbb{R}^2$ in the presence of an *airports network*, i.e., a planar graph $G = (V, E)$ on n vertices (*airports*) with positive edge weights $(w_e)_{e \in E}$ (*flight durations*). The graph may be entered and

exited only at the airports. Movement off the network takes place with unit speed with respect to the Euclidean metric. We assume that going by car takes time equal to the Euclidean distance d, whereas the flight along an edge $e = uv$ of G takes time $w(e) < d(u, v)$. In the simplest case, when there is an airlift between two points $a, b \in \mathbb{R}^2$, the distance between x and y is equal to

$$\min\{d(x, y), d(x, a) + w + d(b, y), d(x, b) + w + d(a, y)\},$$

where w is the flight duration from a to b.

The **city metric** is a quickest path metric on $\mathbb{R}^2$ in the presence of a *city public transportation network*, i.e., a planar straight line graph G with horizontal or vertical edges. G may be composed of many connected components, and may contain cycles.

One can enter/exit G at any point, be it at a vertex or on an edge (it is possible to postulate fixed entry points, too). Once having accessed G, one travels at fixed speed $v > 1$ in one of the available directions. Movement off the network takes place with unit speed with respect to the **Manhattan metric**, as in a large modern-style city with streets arranged in north–south and east–west directions.

A variant of such semimetric is the **subway semimetric** defined ([O'Bri03]), for $x, y \in \mathbb{R}^2$, as $\min(d(x, y), d(x, L) + d(y, L))$, where d is the Manhattan metric and L is a (*subway*) line.

- **Shantaram metric**

  For any numbers a, b with $0 < b \leq 2a \leq 2b$, the **Shantaram metric** between two points $x, y \in \mathbb{R}^2$ is 0, a or b if x and y coincide in exactly 2, 1 or 0 coordinates, respectively.

- **Periodic metric**

  A metric d on $\mathbb{R}^2$ is called **periodic** if there exist two linearly independent vectors v and u such that the *translation* by any vector $w = mv + nu$, $m, n \in \mathbb{Z}$, preserves distances, i.e., $d(x, y) = d(x + w, y + w)$ for any $x, y \in \mathbb{R}^2$.

  Cf. **translation invariant metric** in Chap. 5.

- **Nice metric**

  A metric d on $\mathbb{R}^2$ with the following properties is called **nice** (Klein–Wood, 1989):

  1. d induces the Euclidean topology;
  2. The d-circles are bounded with respect to the Euclidean metric;
  3. If $x, y \in \mathbb{R}^2$ and $x \neq y$, then there exists a point $z, z \neq x, z \neq y$, such that $d(x, y) = d(x, z) + d(z, y)$;
  4. If $x, y \in \mathbb{R}^2$, $x \prec y$ (where $\prec$ is a fixed order on $\mathbb{R}^2$, the lexicographic order, for example), $C(x, y) = \{z \in \mathbb{R}^2 : d(x, z) \leq d(y, z)\}$, $D(x, y) = \{z \in \mathbb{R}^2 : d(x, z) < d(y, z)$, and $\overline{D(x, y)}$ is the closure of $D(x, y)$, then $J(x, y) = C(x, y) \cap \overline{D(x, y)}$ is a curve homeomorphic to $(0, 1)$. The intersection of two such curves consists of finitely many connected components.

Every **norm metric** fulfills 1, 2, and 3 Property 2 means that the metric d is continuous at infinity with respect to the Euclidean metric. Property 4 is to ensure

that the boundaries of the correspondent *Voronoi diagrams* are curves, and that not too many intersections exist in a neighborhood of a point, or at infinity.

A nice metric d has a nice Voronoi diagram: in the Voronoi diagram $V(P, d, \mathbb{R}^2)$ (where $P = \{p_1, \ldots, p_k\}$, $k \geq 2$, is the set of *generator points*) each *Voronoi region* $V(p_i)$ is a path-connected set with a nonempty interior, and the system $\{V(p_1), \ldots, V(p_k)\}$ forms a *partition* of the plane.

- **Contact quasi-distances**

  The **contact quasi-distances** are the following variations of the **distance convex function** (Chap. 1) defined on $\mathbb{R}^2$ (in general, on $\mathbb{R}^n$) for any $x, y \in \mathbb{R}^2$.

  Given a set $B \subset \mathbb{R}^2$, the **first contact quasi-distance** d_B is defined by

$$\inf\{\alpha > 0 : y - x \in \alpha B\}$$

  (cf. **sensor network distances** in Chap. 29).

  Given, moreover, a point $b \in B$ and a set $A \subset \mathbb{R}^2$, the **linear contact quasi-distance** is a **point-set distance** defined by $d_b(x, A) = \inf\{\alpha \geq 0 : \alpha b + x \in A\}$.

  The **intercept quasi-distance** is, for a finite set B, defined by $\frac{\sum_{b \in B} d_b(x,y)}{|B|}$.

- **Radar discrimination distance**

  The **radar discrimination distance** is a distance on $\mathbb{R}^2$ defined by

$$|\rho_x - \rho_y + \theta_{xy}|$$

  if $x, y \in \mathbb{R}^2 \backslash \{0\}$, and by

$$|\rho_x - \rho_y|$$

  if $x = 0$ or $y = 0$, where, for each $x \in \mathbb{R}^2$, ρ_x denotes the radial distance of x from $\{0\}$ and, for any $x, y \in R^2 \backslash \{0\}$, θ_{xy} denotes the radian angle between them.

- **Ehrenfeucht–Haussler semimetric**

  Let S be a subset of $\mathbb{R}^2$ such that $x_1 \geq x_2 - 1 \geq 0$ for any $x = (x_1, x_2) \in S$.

  The **Ehrenfeucht–Haussler semimetric** (see [EhHa88]) on S is defined by

$$\log_2 \left(\left(\frac{x_1}{y_2} + 1 \right) \left(\frac{y_1}{x_2} + 1 \right) \right).$$

- **Toroidal metric**

  The **toroidal metric** is a metric on $T = [0, 1) \times [0, 1) = \{x = (x_1, x_2) \in \mathbb{R}^2 : 0 \leq x_1, x_2 < 1\}$ defined for any $x, y \in \mathbb{R}^2$ by

$$\sqrt{t_1^2 + t_2^2},$$

  where $t_i = \min\{|x_i - y_i|, |x_i - y_i + 1|\}$ for $i = 1, 2$ (cf. **torus metric**).

- **Circle metric**

  The **circle metric** is the **intrinsic metric** on the *unit circle* S^1 in the plane.

As $S^1 = \{(x, y) : x^2 + y^2 = 1\} = \{e^{i\theta} : 0 \le \theta < 2\pi\}$, it is the length of the shorter of the two arcs joining the points $e^{i\theta}, e^{i\vartheta} \in S^1$, and can be written as

$$\min\{|\theta - \vartheta|, 2\pi - |\theta - \vartheta|\} = \begin{cases} |\vartheta - \theta|, & \text{if } 0 \le |\vartheta - \theta| \le \pi, \\ 2\pi - |\vartheta - \theta|, & \text{if } |\vartheta - \theta| > \pi. \end{cases}$$

- **Metric between angles**

  The **metric between angles** Δ is a metric on the set of all angles in the plane $\mathbb{R}^2$ defined for any $\theta, \vartheta \in [0, 2\pi)$ (cf. **circle metric**) by

$$\min\{|\theta - \vartheta|, 2\pi - |\theta - \vartheta|\} = \begin{cases} |\vartheta - \theta|, & \text{if } 0 \le |\vartheta - \theta| \le \pi, \\ 2\pi - |\vartheta - \theta|, & \text{if } |\vartheta - \theta| > \pi. \end{cases}$$

- **Metric between directions**

  On $\mathbb{R}^2$, a *direction* $\hat{l}$ is a class of all straight lines which are parallel to a given straight line $l \subset \mathbb{R}^2$. The **metric between directions** is a metric on the set $\mathcal{L}$ of all directions on the plane defined, for any directions $\hat{l}, \hat{m} \in \mathcal{L}$, as the angle between any two representatives.
- **Angular distance**

  The **angular distance** traveled around a circle is the number $\theta = \frac{l}{r}$ of radians the path subtends, $\theta = \frac{l}{r}$, where l is the path length, and r is the circle's radius.
- **Circular distance**

  The **circular distance** is the distance traveled by a wheel. Each revolution of a wheel with radius r is equivalent to the distance of $2\pi r$ radians.
- **Circular-railroad quasi-metric**

  The **circular-railroad quasi-metric** on the *unit circle* $S^1 \subset \mathbb{R}^2$ is defined, for any $x, y \in S^1$, as the length of the counterclockwise circular arc from x to y in S^1.
- **Inversive distance**

  The **inversive distance** between two nonintersecting circles in the plane $\mathbb{R}^2$ is defined as the natural logarithm of the ratio of the radii (the larger to the smaller) of two concentric circles into which the given circles can be inverted.

  Let c be the distance between the centers of two nonintersecting circles of radii a and $b < a$. Then their inversive distance is given by

$$\cosh^{-1} \left| \frac{a^2 + b^2 - c^2}{2ab} \right|.$$

  The *circumcircle* and *incircle* of a triangle with *circumradius* R and *inradius* r are at the inversive distance $2 \sinh^{-1}(\frac{1}{2}\sqrt{\frac{r}{R}})$.

  Given three noncollinear points, construct three tangent circles such that one is centered at each point and the circles are pairwise tangent to one another. Then there exist exactly two nonintersecting circles, called the *Soddy circles*, that are tangent to all three circles. Their inversive distance is $2 \cosh^{-1} 2$.

19.2 Digital Metrics

Here we list special metrics which are used in *Computer Vision* (or *Pattern Recognition*, *Robot Vision*, *Digital Geometry*).

A *computer picture* (or *computer image*) is a subset of $\mathbb{Z}^n$ which is called a *digital nD space*. Usually, pictures are represented in the *digital plane* (or *image plane*) $\mathbb{Z}^2$, or in the *digital space* (or *image space*) $\mathbb{Z}^3$. The points of $\mathbb{Z}^2$ and $\mathbb{Z}^3$ are called *pixels* and *voxels*, respectively. An *nD m-quantized space* is a scaling $\frac{1}{m}\mathbb{Z}^n$.

A **digital metric** (see, for example, [RoPf68]) is any metric on a digital *nD* space. Usually, it should take integer values.

The metrics on $\mathbb{Z}^n$ that are mainly used are the L_1- and L_∞-*metrics*, as well as the L_2-*metric* after rounding to the nearest greater (or lesser) integer. In general, a given list of *neighbors* of a pixel can be seen as a list of permitted *one-step moves* on $\mathbb{Z}^2$. Let us associate a **prime distance**, i.e., a positive weight, to each type of such move.

Many digital metrics can be obtained now as the minimum, over all admissible paths (i.e., sequences of permitted moves), of the sum of corresponding prime distances.

In practice, the subset $(\mathbb{Z}_m)^n = \{0, 1, \ldots, m-1\}^n$ is considered instead of the full space $\mathbb{Z}^n$. $(\mathbb{Z}_m)^2$ and $(\mathbb{Z}_m)^3$ are called the *m-grill* and *m-framework*, respectively. The most used metrics on $(\mathbb{Z}_m)^n$ are the **Hamming metric** and the **Lee metric**.

- **Grid metric**

  The **grid metric** is the L_1-*metric* on $\mathbb{Z}^n$. It can be seen as the path metric of an infinite graph: two points of $\mathbb{Z}^n$ are adjacent if their L_1-distance is 1.

  For $n = 2$, this metric is the restriction on $\mathbb{Z}^2$ of the **city-block metric** which is also called the **taxicab** (or **rectilinear**, **Manhattan**, 4-) **metric**.
- **Lattice metric**

  The **lattice metric** is the L_∞-*metric* on $\mathbb{Z}^n$. It can be seen as the path metric of an infinite graph: two points of $\mathbb{Z}^n$ are adjacent if their L_∞-distance is 1. For $\mathbb{Z}^2$, the adjacency corresponds to the king move in chessboard terms, and this graph is called the L_∞-*grid*, while this metric is also called the **chessboard metric**, **king-move metric**, 8-**metric**, or **checking distance**.

  This metric is the restriction on $\mathbb{Z}^n$ of the **Chebyshev metric** which is also called the **sup metric**, or **uniform metric**.
- **Hexagonal metric**

  The **hexagonal metric** (or 6-**metric**) is a metric on $\mathbb{Z}^2$ with a *unit sphere* (centered at $x \in \mathbb{Z}^2$) defined by $S^1(x) = S^1_{L_1}(x) \cup \{(x_1-1, x_2-1), (x_1-1, x_2+1)\}$ for even x_2, and $S^1(x) = S^1_{L_1}(x) \cup \{(x_1+1, x_2-1), (x_1+1, x_2+1)\}$ for odd x_2. For any $x = (x_1, x_2), y = (y_1, y_2) \in \mathbb{Z}^2$, this metric $d_6(x, y)$ can be written as

$$\max\left\{|x_2 - y_2|, \frac{|x_2 - y_2|}{2} \pm \left(\frac{x_2 - y_2}{2} + \left\lfloor \frac{x_2 + 1}{2} \right\rfloor - \left\lfloor \frac{y_2 + 1}{2} \right\rfloor - (x_1 - y_1)\right)\right\}.$$

  It is the path metric of the *triangular grid* (or, dually, the minimum number of cell moves of the *hexagonal grid*) on the plane. In *hexagonal coordinates* (h_1, h_2)

(in which the h_1- and h_2-axes are parallel to the grid's edges) the hexagonal distance between points $h = (h_1, h_2)$ and $i = (i_1, i_2)$ is

$$d_6(h, i) = \frac{1}{2}(|h_1 - i_1| + |h_2 - i_2| + |(h_1 - i_1) - (h_2 - i_2)|),$$

i.e., $|h_1 - i_1| + |h_2 - i_2|$, if $(h_1 - i_1)(h_2 - i_2) \leq 0$, and $\max\{|h_1 - i_1|, |h_2 - i_2|\}$, if otherwise; cf. [LuRo76]. The coordinates (h_1, h_2) of a point x are related to its Cartesian coordinates (x_1, x_2) by $h_1 = x_1 - \lfloor \frac{x_2}{2} \rfloor$, $h_2 = x_2$.

This metric approximates the Euclidean metric better than L_1- or L_∞-*metric*.

The **hexagonal Hausdorff metric** is a metric on the set of all bounded subsets (*pictures*, or *images*) of the hexagonal grid on the plane defined by

$$\inf\{p, q : A \subset B + qH,\ B \subset A + pH\}$$

for any pictures A and B, where pH is the *regular hexagon of size p* (i.e., with $p+1$ pixels on each edge), centered at the origin and including its interior, and $+$ is the *Minkowski addition*: $A + B = \{x + y : x \in A, y \in B\}$ (cf. **Pompeiu–Hausdorff–Blaschke metric** in Chap. 9). If A is a pixel x, then the distance between x and B is equal to $\sup_{y \in B} d_6(x, y)$, where d_6 is the hexagonal metric.

- **Digital volume metric**

  The **digital volume metric** is a metric on the set K of all bounded subsets (*pictures*, or *images*) of $\mathbb{Z}^2$ (in general, of $\mathbb{Z}^n$) defined by

  $$vol(A \triangle B),$$

  where $vol(A) = |A|$, i.e., the number of pixels contained in A, and $A \triangle B$ is the *symmetric difference* between sets A and B.

  This metric is a digital analog of the **Nikodym metric** in Chap. 9.

- **Neighborhood sequence metric**

  On the digital plane $\mathbb{Z}^2$, consider two types of motions: the *city-block motion*, restricting movements only to the horizontal or vertical directions, and the *chessboard motion*, also allowing diagonal movements.

  The use of both these motions is determined by a *neighborhood sequence* $B = \{b(1), b(2), \ldots, b(l)\}$, where $b(i) \in \{1, 2\}$ is a particular type of neighborhood, with $b(i) = 1$ signifying unit change in 1 coordinate (*city-block neighborhood*), and $b(i) = 2$ meaning unit change also in 2 coordinates (*chessboard neighborhood*). The sequence B defines the type of motion to be used at every step (see [Das90]).

  The **neighborhood sequence metric** is a metric on $\mathbb{Z}^2$ defined as the length of a shortest path between x and $y \in \mathbb{Z}^2$, determined by a given neighborhood sequence B. It can be written as

  $$\max\{d_B^1(u), d_B^2(u)\},$$

where $u_1 = x_1 - y_1$, $u_2 = x_2 - y_2$, $d_B^1(u) = \max\{|u_1|, |u_2|\}$, $d_B^2(u) = \sum_{j=1}^{l} \lfloor \frac{|u_1|+|u_2|+g(j)}{f(l)} \rfloor$, $f(0) = 0$, $f(i) = \sum_{j=1}^{i} b(j)$, $1 \le i \le l$, $g(j) = f(l) - f(j-1) - 1$, $1 \le j \le l$.

For $B = \{1\}$ one obtains the **city-block metric**, for $B = \{2\}$ one obtains the **chessboard metric**. The case $B = \{1, 2\}$, i.e., the alternative use of these motions, results in the **octagonal metric**, introduced in [RoPf68].

A proper selection of the B-sequence can make the corresponding metric very close to the Euclidean metric. It is always greater than the chessboard metric, but smaller than the city-block metric.

- *nD*-**neighborhood sequence metric**

  The *nD*-**neighborhood sequence metric** is a metric on $\mathbb{Z}^n$, defined as the length of a shortest path between x and $y \in \mathbb{Z}^n$, determined by a given *nD-neighborhood sequence* B (see [Faze99]).

  Formally, two points $x, y \in \mathbb{Z}^n$ are called *m-neighbors*, $0 \le m \le n$, if $0 \le |x_i - y_i| \le 1$, $1 \le i \le n$, and $\sum_{i=1}^{n} |x_i - y_i| \le m$. A finite sequence $B = \{b(1), \ldots, b(l)\}$, $b(i) \in \{1, 2, \ldots, n\}$, is called an *nD-neighborhood sequence with period l*. For any $x, y \in \mathbb{Z}^n$, a point sequence $x = x^0, x^1, \ldots, x^k = y$, where x^i and x^{i+1}, $0 \le i \le k-1$, are r-neighbors, $r = b((i \bmod l) + 1)$, is called a *path from x to y determined by B* with length k. The distance between x and y can be written as

$$\max_{1 \le i \le n} d_i(u) \quad \text{with} \quad d_i(x, y) = \sum_{j=1}^{l} \left\lfloor \frac{a_i + g_i(j)}{f_i(l)} \right\rfloor,$$

  where $u = (|u_1|, |u_2|, \ldots, |u_n|)$ is the nonincreasing ordering of $|u_m|$, $u_m = x_m - y_m$, $m = 1, \ldots, n$, that is, $|u_i| \le |u_j|$ if $i < j$; $a_i = \sum_{j=1}^{n-i+1} u_j$; $b_i(j) = b(j)$ if $b(j) < n - i + 2$, and is $n - i + 1$, otherwise; $f_i(j) = \sum_{k=1}^{j} b_i(k)$ if $1 \le j \le l$, and is 0 if $j = 0$; $g_i(j) = f_i(l) - f_i(j-1) - 1$, $1 \le j \le l$.

- **Strand–Nagy distances**

  The *face-centered cubic lattice* is $A_3 = \{(a_1, a_2, a_3) \in \mathbb{Z}^3 : a_1 + a_2 + a_3 \equiv 0 (\bmod 2)\}$, and the *body-centered cubic lattice* is its dual

$$A_3^* = \{(a_1, a_2, a_3) \in \mathbb{Z}^3 : a_1 \equiv a_2 \equiv a_3 (\bmod 2)\}.$$

  Let $L \in \{A_3, A_3^*\}$. For any points $x, y \in L$, let $d_1(x, y) = \sum_{j=1}^{3} |x_j - y_j|$ denote the L_1-metric and $d_\infty(x, y) = \max_{j \in \{1,2,3\}} |x_j - y_j|$ denote the L_∞-metric between them. Two points $x, y \in L$ are called *1-neighbors* if $d_1(x, y) \le 3$ and $0 < d_\infty(x, y) \le 1$; they are called *2-neighbors* if $d_1(x, y) \le 3$ and $1 < d_\infty(x, y) \le 2$.

  Given a sequence $B = \{b(i)\}_{i=1}^{\infty}$ over the alphabet $\{1, 2\}$, a *B-path* in L is a point sequence $x = x^0, x^1, \ldots, x^k = y$, where x^i and x^{i+1}, $0 \le i \le k-1$, are 1-neighbors if $b(i) = 1$ and 2-neighbors if $b(i) = 2$.

  The **Strand–Nagy distance** between two points $x, y \in L$ (or *B-distance* in Strand and Nagy, 2007) is the length of a shortest B-path between them. For

$L = A_3$, it is

$$\min\{k : k \geq \max\{\frac{d_1(x,y)}{2}, d_\infty(x,y) - |\{1 \leq i \leq k : b(i) = 2\}|\}.$$

The Strand–Nagy distance is a metric, for example, for the periodic sequence $B = (1,2,1,2,1,2,\dots)$ but not for the periodic sequence $B = (2,1,2,1,2,1,\dots)$.

- **Path-generated metric**

  Consider the l_∞-*grid*, i.e., the graph with the vertex-set $\mathbb{Z}^2$, and two vertices being *neighbors* if their l_∞-distance is 1. Let $\mathcal{P}$ be a collection of paths in the l_∞-grid such that, for any $x, y \in \mathbb{Z}^2$, there exists at least one path from $\mathcal{P}$ between x and y, and if $\mathcal{P}$ contains a path Q, then it also contains every path contained in Q.

  Let $d_\mathcal{P}(x,y)$ be the length of the shortest path from $\mathcal{P}$ between x and $y \in \mathbb{Z}^2$. If $d_\mathcal{P}$ is a metric on $\mathbb{Z}^2$, then it is called a **path-generated metric** (see [Melt91]).

  Let G be one of the sets: $G_1 = \{\uparrow, \rightarrow\}$, $G_{2A} = \{\uparrow, \nearrow\}$, $G_{2B} = \{\uparrow, \nwarrow\}$, $G_{2C} = \{\nearrow, \nwarrow\}$, $G_{2D} = \{\rightarrow, \nwarrow\}$, $G_{3A} = \{\rightarrow, \uparrow, \nearrow\}$, $G_{3B}\{\rightarrow, \uparrow, \nwarrow\}$, $G_{4A} = \{\rightarrow, \nearrow, \nwarrow\}$, $G_{4B}\{\uparrow, \nearrow, \nwarrow, \}$, $G_5 = \{\rightarrow, \uparrow, \nearrow, \nwarrow\}$. Let $\mathcal{P}(G)$ be the set of paths which are obtained by concatenation of paths in G and the corresponding paths in the opposite directions. Any path-generated metric coincides with one of the metrics $d_{\mathcal{P}(G)}$. Moreover, one can obtain the following formulas:

  1. $d_{\mathcal{P}(G_1)}(x,y) = |u_1| + |u_2|$;
  2. $d_{\mathcal{P}(G_{2A})}(x,y) = \max\{|2u_1 - u_2|, |u_2|\}$;
  3. $d_{\mathcal{P}(G_{2B})}(x,y) = \max\{|2u_1 + u_2|, |u_2|\}$;
  4. $d_{\mathcal{P}(G_{2C})}(x,y) = \max\{|2u_2 + u_1|, |u_1|\}$;
  5. $d_{\mathcal{P}(G_{2D})}(x,y) = \max\{|2u_2 - u_1|, |u_1|\}$;
  6. $d_{\mathcal{P}(G_{3A})}(x,y) = \max\{|u_1|, |u_2|, |u_1 - u_2|\}$;
  7. $d_{\mathcal{P}(G_{3B})}(x,y) = \max\{|u_1|, |u_2|, |u_1 + u_2|\}$;
  8. $d_{\mathcal{P}(G_{4A})}(x,y) = \max\{2\lceil(|u_1| - |u_2|)/2\rceil, 0\} + |u_2|$;
  9. $d_{\mathcal{P}(G_{4B})}(x,y) = \max\{2\lceil(|u_2| - |u_1|)/2\rceil, 0\} + |u_1|$;
  10. $d_{\mathcal{P}(G_5)}(x,y) = \max\{|u_1|, |u_2|\}$,

  where $u_1 = x_1 - y_1$, $u_2 = x_2 - y_2$, and $\lceil . \rceil$ is the *ceiling function*: for any real x the number $\lceil x \rceil$ is the least integer greater than or equal to x.

  The metric spaces obtained from G-sets with the same numerical index are isometric. $d_{\mathcal{P}(G_1)}$ is the **city-block metric**, and $d_{\mathcal{P}(G_5)}$ is the **chessboard metric**.

- **Chamfer metric**

  Given numbers α, β with $0 < \alpha \leq \beta < 2\alpha$, the (α, β)-*weighted* l_∞-*grid* is the graph with the vertex-set $\mathbb{Z}^2$, two vertices being adjacent if their l_∞-distance is one, while horizontal/vertical and diagonal edges have *weights* α and β, respectively.

  A **chamfer metric** (or (α, β)-*chamfer metric*, [Borg86]) is the weighted path metric in this graph. For any $x, y \in \mathbb{Z}^2$ it can be written as

$$\beta m + \alpha(M - m),$$

  where $M = \max\{|u_1|, |u_2|\}$, $m = \min\{|u_1|, |u_2|\}$, $u_1 = x_1 - y_1$, $u_2 = x_2 - y_2$.

If the weights α and β are equal to the Euclidean lengths 1, $\sqrt{2}$ of horizontal/vertical and diagonal edges, respectively, then one obtains the Euclidean length of the shortest chessboard path between x and y. If $\alpha = \beta = 1$, one obtains the **chessboard metric**. The $(3, 4)$-chamfer metric is the most used one for digital images.

A $3D$**-chamfer metric** is the weighted path metric of the graph with the vertex-set $\mathbb{Z}^3$ of *voxels*, two voxels being adjacent if their l_∞-distance is one, while weights α, β, and γ are associated, respectively, to the distance from 6 face neighbors, 12 edge neighbors, and 8 corner neighbors.

- **Weighted cut metric**

  Consider the *weighted* l_∞*-grid*, i.e., the graph with the vertex-set $\mathbb{Z}^2$, two vertices being adjacent if their l_∞-distance is one, and each edge having some positive *weight* (or *cost*). The usual **weighted path metric** between two pixels is the minimal cost of a path connecting them. The **weighted cut metric** between two pixels is the minimal cost (defined now as the sum of costs of crossed edges) of a *cut*, i.e., a plane curve connecting them while avoiding pixels.

- **Knight metric**

  The **knight** (or *octogonal*) **metric** on $\mathbb{Z}^2$ is the minimum number of moves a chess knight would take to travel from x to $y \in \mathbb{Z}^2$. Its *unit sphere* S^1_{knight}, centered at the origin, contains exactly 8 integral points $\{(\pm 2, \pm 1), (\pm 1, \pm 2)\}$, and can be written as $S^1_{knight} = S^3_{L_1} \cap S^2_{l_\infty}$, where $S^3_{L_1}$ is the L_1-sphere of radius 3, and $S^2_{L_\infty}$ is the L_∞-sphere of radius 2, both centered at the origin (see [DaCh88]).

  The distance between x and y is 3 if $(M, m) = (1, 0)$, is 4 if $(M, m) = (2, 2)$ and is equal to $\max\{\lceil \frac{M}{2} \rceil, \lceil \frac{M+m}{3} \rceil\} + (M + m) - \max\{\lceil \frac{M}{2} \rceil, \lceil \frac{M+m}{3} \rceil\} \pmod 2$, otherwise, where $M = \max\{|u_1|, |u_2|\}$, $m = \min\{|u_1|, |u_2|\}$, $u_1 = x_1 - y_1$, $u_2 = x_2 - y_2$.

- **Super-knight metric**

  Let $p, q \in \mathbb{N}$. A (p, q)*-super-knight* (or (p, q)*-leaper*, (p, q)*-spider*) is a (variant) chess piece whose move consists of a leap p squares in one orthogonal direction followed by a 90° direction change, and q squares leap to the destination square. Rook, bishop and queen have $q = 0$, $q = p$ and $q = 0, p$, respectively.

  Chess-variant terms exist for a $(p, 1)$-leaper with $p = 0, 1, 2, 3, 4$ (*Wazir*, *Ferz*, usual *Knight*, *Camel*, *Giraffe*), and for a $(p, 2)$-leaper with $p = 0, 1, 2, 3$ (*Dabbaba*, usual *Knight*, *Alfil*, *Zebra*).

  A (p, q)**-super-knight metric** (or (p, q)*-leaper metric*) is a metric on $\mathbb{Z}^2$ defined as the minimum number of moves a chess (p, q)-super-knight would take to travel from x to $y \in \mathbb{Z}^2$. Thus, its *unit sphere* $S^1_{p,q}$, centered at the origin, contains exactly 8 integral points $\{(\pm p, \pm q), (\pm q, \pm p)\}$. (See [DaMu90].)

  The **knight metric** is the $(1, 2)$-super-knight metric. The **city-block metric** can be considered as the *Wazir metric*, i.e., $(0, 1)$-super-knight metric.

- **Rook metric**

  The **rook metric** is a metric on $\mathbb{Z}^2$ defined as the minimum number of moves a chess rook would take to travel from x to $y \in \mathbb{Z}^2$. This metric can take only the values $\{0, 1, 2\}$, and coincides with the **Hamming metric** on $\mathbb{Z}^2$.

- **Chess programming distances**

  On a chessboard $\mathbb{Z}_8^2$, *files* are 8 columns labeled from a to h and *ranks* are 8 rows labeled from 1 to 8. Given two squares, their **file-distance** and **rank-distance** are the absolute differences between the 0–7 indices of their files or, respectively, ranks. The **Chebyshev distance** and **Manhattan distance** are the maximum or, respectively, the sum of their file-distance and rank-distance.

  The *center distance* and *corner distance* of a square are its (Chebyshev or Manhattan) distance to closest square among $\{d4, d5, e4, e5\}$ or, respectively, closest corner. For example, the program *Chess 4.x* uses in endgame evaluation $4.7d + 1.6(14 - d')$, where d is the center Manhattan distance of losing king and d' is the Manhattan distance between kings.

  Two kings at rank- and file-distances d_r, d_f, are in *opposition*, which is *direct*, or *diagonal*, or *distant* if $(d_r, d_f) \in \{(0, 2), (2, 0)\}$, or $= (2, 2)$, or their Manhattan distance is even ≥ 6 and no pawns interfere between them.

  Unrelated *cavalry file distance* is the number of files in which it rides.

Chapter 20
Voronoi Diagram Distances

Given a finite set A of objects A_i in a space S, computing the *Voronoi diagram* of A means partitioning the space S into *Voronoi regions* $V(A_i)$ in such a way that $V(A_i)$ contains all points of S that are "closer" to A_i than to any other object A_j in A.

Given a *generator set* $P = \{p_1, \dots p_k\}$, $k \geq 2$, of distinct points (*generators*) from $\mathbb{R}^n$, $n \geq 2$, the ordinary **Voronoi polytope** $V(p_i)$ associated with a generator p_i is defined by

$$V(p_i) = \{x \in \mathbb{R}^n : d_E(x, p_i) \leq d_E(x, p_j) \text{ for any } j \neq i\},$$

where d_E is the Euclidean distance on $\mathbb{R}^n$. The set

$$V(P, d_E, \mathbb{R}^n) = \{V(p_1), \dots, V(p_k)\}$$

is called the *n-dimensional ordinary Voronoi diagram, generated by P*.

The boundaries of (n-dimensional) Voronoi polytopes are called (($n-1$)-dimensional) *Voronoi facets*, the boundaries of Voronoi facets are called ($n-2$)-*dimensional Voronoi faces*, ..., the boundaries of 2D Voronoi faces are called *Voronoi edges*, and the boundaries of Voronoi edges are called *Voronoi vertices*.

The ordinary Voronoi diagram can be generalized in the following three ways:

1. The generalization with respect to the generator set $A = \{A_1, \dots, A_k\}$ which can be a set of lines, a set of areas, etc.;
2. The generalization with respect to the space S which can be a sphere (*spherical Voronoi diagram*), a cylinder (*cylindrical Voronoi diagram*), a cone (*conic Voronoi diagram*), a polyhedral surface (*polyhedral Voronoi diagram*), etc.;
3. The generalization with respect to the function d, where $d(x, A_i)$ measures the "distance" from a point $x \in S$ to a generator $A_i \in A$.

This generalized distance function d is called the **Voronoi generation distance** (or *Voronoi distance*, *V-distance*), and allows many more functions than the

© Springer-Verlag Berlin Heidelberg 2016

M.M. Deza, E. Deza, *Encyclopedia of Distances*,
DOI 10.1007/978-3-662-52844-0_20

Euclidean metric on S. If F is a strictly increasing function of a V-distance d, i.e., $F(d(x,A_i)) \leq F(d(x,A_j))$ if and only if $d(x,A_i) \leq d(x,A_j)$, then the generalized Voronoi diagrams $V(A,F(d),S)$ and $V(A,d,S)$ coincide, and one says that the V-distance $F(d)$ is *transformable* to the V-distance d, and that the generalized Voronoi diagram $V(A,F(d),S)$ is a *trivial generalization* of the generalized Voronoi diagram $V(A,d,S)$.

In applications, one often uses for trivial generalizations of the ordinary Voronoi diagram $V(P,d,\mathbb{R}^n)$ the **exponential distance**, the **logarithmic distance**, and the **power distance**. There are generalized Voronoi diagrams $V(P,D,\mathbb{R}^n)$, defined by V-distances, that are not transformable to the Euclidean distance d_E: the **multiplicatively weighted Voronoi distance**, the **additively weighted Voronoi distance**, etc.

The theory of generalized Voronoi diagrams $V(P,D,\mathbb{R}^n)$, where D is a norm metric $||x-p||$ collapses even for the case, when P is a lattice in $\mathbb{R}^n$. But [DeDu13] adapted it for *polyhedral*, i.e., with a polytopal unit ball, norms; $||.||_1$ and $||.||_\infty$ are among them.

For additional information see, for example, [OBS92, Klei89].

20.1 Classical Voronoi Generation Distances

- **Exponential distance**
  The **exponential distance** is the Voronoi generation distance

$$D_{exp}(x,p_i) = e^{d_E(x,p_i)}$$

  for the trivial generalization $V(P,D_{exp},\mathbb{R}^n)$ of the ordinary Voronoi diagram $V(P,d_E,\mathbb{R}^n)$, where d_E is the Euclidean distance.
- **Logarithmic distance**
  The **logarithmic distance** is the Voronoi generation distance

$$D_{\ln}(x,p_i) = \ln d_E(x,p_i)$$

  for the trivial generalization $V(P,D_{\ln},\mathbb{R}^n)$ of the ordinary Voronoi diagram $V(P,d_E,\mathbb{R}^n)$, where d_E is the Euclidean distance.
- **Power distance**
  The **power distance** is the Voronoi generation distance

$$D_\alpha(x,p_i) = d_E(x,p_i)^\alpha,\ \alpha > 0,$$

  for the trivial generalization $V(P,D_\alpha,\mathbb{R}^n)$ of the ordinary Voronoi diagram $V(P,d_E,\mathbb{R}^n)$, where d_E is the Euclidean distance.

- **Multiplicatively weighted distance**

  The **multiplicatively weighted distance** d_{MW} is the Voronoi generation distance of the generalized Voronoi diagram $V(P, d_{MW}, \mathbb{R}^n)$ (*multiplicatively weighted Voronoi diagram*) defined by

$$d_{MW}(x, p_i) = \frac{1}{w_i} d_E(x, p_i)$$

  for any point $x \in \mathbb{R}^n$ and any *generator point* $p_i \in P = \{p_1, \ldots, p_k\}$, $k \geq 2$, where $w_i \in w = \{w_i, \ldots, w_k\}$ is a given positive *multiplicative weight* of the generator p_i, and d_E is the Euclidean distance.

  A *Möbius diagram* (Boissonnat–Karavelas, 2003) is a diagram the **midsets** (bisectors) of which are hyperspheres. It generalizes the Euclidean Voronoi and power diagrams, and it is equivalent to power diagrams in $\mathbb{R}^{n+1}$.

  For $\mathbb{R}^2$, the multiplicatively weighted Voronoi diagram is called a *circular Dirichlet tessellation*. An edge in this diagram is a circular arc or a straight line.

  In the plane $\mathbb{R}^2$, there exists a generalization of the multiplicatively weighted Voronoi diagram, the *crystal Voronoi diagram*, with the same definition of the distance (where w_i is the speed of growth of the crystal p_i), but a different partition of the plane, as the crystals can grow only in an empty area.

- **Additively weighted distance**

  The **additively weighted distance** d_{AW} is the Voronoi generation distance of the generalized Voronoi diagram $V(P, d_{AW}, \mathbb{R}^n)$ (*additively weighted Voronoi diagram*) defined by

$$d_{AW}(x, p_i) = d_E(x, p_i) - w_i$$

  for any point $x \in \mathbb{R}^n$ and any generator point $p_i \in P = \{p_1, \ldots, p_k\}$, $k \geq 2$, where $w_i \in w = \{w_i, \ldots, w_k\}$ is a given *additive weight* of the generator p_i, and d_E is the Euclidean distance.

  For $\mathbb{R}^2$, the additively weighted Voronoi diagram is called a *hyperbolic Dirichlet tessellation*. An edge in this diagram is a hyperbolic arc or a straight line segment.

- **Additively weighted power distance**

  The **additively weighted power distance** d_{PW} is the Voronoi generation distance of the generalized Voronoi diagram $V(P, d_{PW}, \mathbb{R}^n)$ (*additively weighted power Voronoi diagram*) defined by

$$d_{PW}(x, p_i) = d_E^2(x, p_i) - w_i$$

  for any point $x \in \mathbb{R}^n$ and any *generator point* $p_i \in P = \{p_1, \ldots, p_k\}$, $k \geq 2$, where $w_i \in w = \{w_i, \ldots, w_k\}$ is a given *additive weight* of the generator p_i, and d_E is the Euclidean distance.

  This diagram can be seen as a Voronoi diagram of circles or as a Voronoi diagram with the *Laguerre geometry*.

The **multiplicatively weighted power distance** $d_{MPW}(x, p_i) = \frac{1}{w_i} d_E^2(x, p_i)$, $w_i > 0$, is transformable to the **multiplicatively weighted distance**, and gives a trivial extension of the multiplicatively weighted Voronoi diagram.

- **Compoundly weighted distance**

  The **compoundly weighted distance** d_{CW} is the Voronoi generation distance of the generalized Voronoi diagram $V(P, d_{CW}, \mathbb{R}^n)$ (*compoundly weighted Voronoi diagram*) defined by

$$d_{CW}(x, p_i) = \frac{1}{w_i} d_E(x, p_i) - v_i$$

  for any point $x \in \mathbb{R}^n$ and any generator point $p_i \in P = \{p_1, \ldots, p_k\}$, $k \geq 2$, where $w_i \in w = \{w_i, \ldots, w_k\}$ is a given positive *multiplicative weight* of the generator p_i, $v_i \in v = \{v_1, \ldots, v_k\}$ is a given *additive weight* of the generator p_i, and d_E is the Euclidean distance.

  An edge in the 2D compoundly weighted Voronoi diagram is a part of a fourth-order polynomial curve, a hyperbolic arc, a circular arc, or a straight line.

20.2 Plane Voronoi Generation Distances

- **Shortest path distance with obstacles**

  Let $\mathcal{O} = \{O_1, \ldots, O_m\}$ be a collection of pairwise disjoint polygons on the Euclidean plane, representing a set of obstacles which are neither transparent nor traversable.

  The **shortest path distance with obstacles** d_{sp} is the Voronoi generation distance of the generalized Voronoi diagram $V(P, d_{sp}, \mathbb{R}^2 \backslash \{\mathcal{O}\})$ (*shortest path Voronoi diagram with obstacles*) defined, for any $x, y \in \mathbb{R}^2 \backslash \{\mathcal{O}\}$, as the length of the shortest path among all possible continuous $(x-y)$-paths that do not intersect obstacles $O_i \backslash \partial O_i$ (a path can pass through points on the boundary ∂O_i of O_i), $i = 1, \ldots m$.

  The shortest path is constructed with the aid of the *visibility polygon* and the *visibility graph* of $V(P, d_{sp}, \mathbb{R}^2 \backslash \{\mathcal{O}\})$.

- **Visibility shortest path distance**

  Let $\mathcal{O} = \{O_1, \ldots, O_m\}$ be a collection of pairwise disjoint line segments $O_l = [a_l, b_l]$ in the Euclidean plane, with $P = \{p_1, \ldots, p_k\}$, $k \geq 2$, the set of generator points,

$$VIS(p_i) = \{x \in \mathbb{R}^2 : [x, p_i] \cap]a_l, b_l[= \emptyset \text{ for all } l = 1, \ldots, m\}$$

  the *visibility polygon* of the generator p_i, and d_E the Euclidean distance.

  The **visibility shortest path distance** d_{vsp} is the Voronoi generation distance of the generalized Voronoi diagram $V(P, d_{vsp}, \mathbb{R}^2 \backslash \{\mathcal{O}\})$ (*visibility shortest path*

Voronoi diagram with line obstacles), defined by

$$d_{vsp}(x, p_i) = \begin{cases} d_E(x, p_i), & \text{if } x \in VIS(p_i), \\ \infty, & \text{otherwise .} \end{cases}$$

- **Network distances**

  A *network* on $\mathbb{R}^2$ is a connected planar geometrical graph $G = (V, E)$ with the set V of vertices and the set E of edges (links).

  Let the generator set $P = \{p_1, \ldots, p_k\}$ be a subset of the set $V = \{p_1, \ldots, p_l\}$ of vertices of G, and let the set L be given by points of links of G.

  The **network distance** d_{netv} on the set V is the Voronoi generation distance of the *network Voronoi node diagram* $V(P, d_{netv}, V)$ defined as the shortest path along the links of G from $p_i \in V$ to $p_j \in V$. It is the weighted path metric of the graph G, where w_e is the Euclidean length of the link $e \in E$.

  The **network distance** d_{netl} on the set L is the Voronoi generation distance of the *network Voronoi link diagram* $V(P, d_{netl}, L)$ defined as the shortest path along the links from $x \in L$ to $y \in L$.

  The **access network distance** d_{accnet} on $\mathbb{R}^2$ is the Voronoi generation distance of the *network Voronoi area diagram* $V(P, d_{accnet}, \mathbb{R}^2)$ defined by

$$d_{accnet}(x, y) = d_{netl}(l(x), l(y)) + d_{acc}(x) + d_{acc}(y),$$

  where $d_{acc}(x) = \min_{l \in L} d(x, l) = d_E(x, l(x))$ is the *access distance* of a point x. In fact, $d_{acc}(x)$ is the Euclidean distance from x to the *access point* $l(x) \in L$ of x which is the nearest to x point on the links of G. The **access distance**, among **memory distances** in Chap. 22, is not related.

- **Airlift distance**

  An *airports network* is an arbitrary planar graph G on n vertices (*airports*) with positive edge weights (*flight durations*). This graph may be entered and exited only at the airports. Once having accessed G, one travels at fixed speed $v > 1$ within the network. Movement off the network takes place with the unit speed with respect to the Euclidean distance.

  The **airlift distance** d_{al} is the Voronoi generation distance of the *airlift Voronoi diagram* $V(P, d_{al}, \mathbb{R}^2)$, defined as the time needed for a *quickest*, i.e., minimizing the travel time, path between x and y in the presence of the airports network G.

- **City distance**

  A *city public transportation network*, like a subway or a bus transportation system, is a planar straight line graph G with horizontal or vertical edges. G may be composed of many connected components, and may contain cycles. One is free to enter G at any point, be it at a vertex or on an edge (it is possible to postulate fixed entry points, too). Once having accessed G, one travels at a fixed speed $v > 1$ in one of the available directions. Movement off the network takes place with the unit speed with respect to the **Manhattan metric**.

The **city distance** d_{city} is the Voronoi generation distance of the *city Voronoi diagram* $V(P, d_{city}, \mathbb{R}^2)$, defined as the time needed for the *quickest path*, i.e., the one minimizing the travel time, between x and y in the presence of the network G.

The set $P = \{p_1, \ldots, p_k\}$, $k \geq 2$, can be seen as a set of some city facilities (say, post offices or hospitals): for some people several facilities of the same kind are equally attractive, and they want to find out which facility is reachable first.

- **Distance in a river**

  The **distance in a river** d_{riv} is the Voronoi generation distance of the generalized Voronoi diagram $V(P, d_{riv}, \mathbb{R}^2)$ (*Voronoi diagram in a river*), defined by

$$d_{riv}(x, y) = \frac{-\alpha(x_1 - y_1) + \sqrt{(x_1 - y_1)^2 + (1 - \alpha^2)(x_2 - y_2)^2}}{v(1 - \alpha^2)},$$

  where v is the speed of the boat on still water, $w > 0$ is the speed of constant flow in the positive direction of the x_1 axis, and $\alpha = \frac{w}{v}$ $(0 < \alpha < 1)$ is the *relative flow speed*.

- **Boat-sail distance**

  Let $\Omega \subset \mathbb{R}^2$ be a *domain* in the plane (*water surface*), let $f : \Omega \to \mathbb{R}^2$ be a continuous vector field on Ω, representing the velocity of the water flow (*flow field*); let $P = \{p_1, \ldots, p_k\} \subset \Omega$, $k \geq 2$, be a set of k points in Ω (*harbors*).

  The **boat-sail distance** ([NiSu03]) d_{bs} is the Voronoi generation distance of the generalized Voronoi diagram $V(P, d_{bs}, \Omega)$ (*boat-sail Voronoi diagram*) defined by

$$d_{bs}(x, y) = \inf_{\gamma} \delta(\gamma, x, y)$$

  for all $x, y \in \Omega$, where $\delta(\gamma, x, y) = \int_0^1 \left| F \frac{\gamma'(s)}{|\gamma'(s)|} + f(\gamma(s)) \right|^{-1} ds$ is the time necessary for the boat with the maximum speed F on still water to move from x to y along the curve $\gamma : [0, 1] \to \Omega$, $\gamma(0) = x$, $\gamma(1) = y$, and the infimum is taken over all possible curves γ.

- **Peeper distance**

  Let $S = \{(x_1, x_2) \in \mathbb{R}^2 : x_1 > 0\}$ be the half-plane in $\mathbb{R}^2$, let $P = \{p_1, \ldots, p_k\}$, $k \geq 2$, be a set of points contained in the half-plane $\{(x_1, x_2) \in \mathbb{R}^2 : x_1 < 0\}$, and let the *window* be the interval (a, b) with $a = (0, 1)$ and $b = (0, -1)$.

  The **peeper distance** d_{pee} is the Voronoi generation distance of the generalized Voronoi diagram $V(P, d_{pee}, S)$ (*peeper's Voronoi diagram*) defined by

$$d_{pee}(x, p_i) = \begin{cases} d_E(x, p_i), & \text{if } [x, p] \cap]a, b[\neq \emptyset, \\ \infty, & \text{otherwise}, \end{cases}$$

  where d_E is the Euclidean distance.

- **Snowmobile distance**

  Let $\Omega \subset \mathbb{R}^2$ be a *domain* in the x_1x_2-plane of the space $\mathbb{R}^3$ (a *2D mapping*), and let $\Omega^* = \{(q, h(q)) : q = (x_1(q), x_2(q)) \in \Omega, h(q) \in \mathbb{R}\}$ be the three-dimensional *land surface* associated with the mapping Ω. Let $P = \{p_1, \ldots, p_k\} \subset \Omega$, $k \geq 2$, be a set of k points in Ω (*snowmobile stations*).

  The **snowmobile distance** d_{sm} is the Voronoi generation distance of the generalized Voronoi diagram $V(P, d_{sm}, \Omega)$ (*snowmobile Voronoi diagram*) defined by

$$d_{sm}(q, r) = \inf_{\gamma} \int_{\gamma} \frac{1}{F\left(1 - \alpha \frac{dh(\gamma(s))}{ds}\right)} ds$$

  for any $q, r \in \Omega$, and calculating the minimum time necessary for the snowmobile with the speed F on flat land to move from $(q, h(q))$ to $(r, h(r))$ along the *land path* $\gamma^* : \gamma^*(s) = (\gamma(s), h(\gamma(s)))$ associated with the *domain path* $\gamma : [0, 1] \to \Omega$, $\gamma(0) = q$, $\gamma(1) = r$. The infimum is taken over all possible paths γ, and α is a positive constant, since a snowmobile goes uphill more slowly than downhill.

  The situation is opposite for a forest fire, and it can be modeled using a negative value of α. The resulting distance and Voronoi diagram are called **forest-fire distance** and *forest-fire Voronoi diagram*.

- **Skew distance**

  Let T be a *tilted plane* in $\mathbb{R}^3$, obtained by rotating the x_1x_2 plane around the x_1 axis through the angle α, $0 < \alpha < \frac{\pi}{2}$, with the coordinate system obtained by taking the coordinate system of the x_1x_2 plane, accordingly rotated. For a point $q \in T$, $q = (x_1(q), x_2(q))$, define the *height* $h(q)$ as its x_3 coordinate in $\mathbb{R}^3$. Thus, $h(q) = x_2(q) \cdot \sin\alpha$. Let $P = \{p_1, \ldots, p_k\} \subset T$, $k \geq 2$.

  The **skew distance** is the Voronoi generation distance of the generalized Voronoi diagram $V(P, d_{skew}, T)$ (*skew Voronoi diagram*) defined ([AACLMP98]) by

$$d_{skew}(q, r) = d_E(q, r) + (h(r) - h(q)) = d_E(q, r) + \sin\alpha(x_2(r) - x_2(q))$$

  or, more generally, by

$$d_{skew}(q, r) = d_E(q, r) + k(x_2(r) - x_2(q))$$

  for all $q, r \in T$, where d_E is the Euclidean distance, and $k \geq 0$ is a constant.

20.3 Other Voronoi Generation Distances

- **Voronoi distance for line segments**
  The **Voronoi distance for** (a set of) **line segments** d_{sl} is the Voronoi generation distance of the generalized Voronoi diagram $V(A, d_{sl}, \mathbb{R}^2)$ (*line Voronoi diagram generated by straight line segments*) defined by

$$d_{sl}(x, A_i) = \inf_{y \in A_i} d_E(x, y),$$

  where the *generator set* $A = \{A_1, \ldots, A_k\}$, $k \geq 2$, is a set of pairwise disjoint straight line segments $A_i = [a_i, b_i]$, and d_E is the ordinary Euclidean distance. In fact,

$$d_{sl}(x, A_i) = \begin{cases} d_E(x, a_i), & \text{if} \quad x \in R_{a_i}, \\ d_E(x, b_i), & \text{if} \quad x \in R_{b_i}, \\ d_E(x - a_i, \frac{(x-a_i)^T(b_i-a_i)}{d_E^2(a_i,b_i)}(b_i - a_i)), & \text{if} \quad x \in \mathbb{R}^2 \backslash \{R_{a_i} \cup R_{b_i}\}, \end{cases}$$

  where $R_{a_i} = \{x \in \mathbb{R}^2 : (b_i - a_i)^T(x - a_i) < 0\}$, $R_{b_i} = \{x \in \mathbb{R}^2 : (a_i - b_i)^T(x - b_i) < 0\}$.
- **Voronoi distance for arcs**
  The **Voronoi distance for** (a set of circle) **arcs** d_{ca} is the Voronoi generation distance of the generalized Voronoi diagram $V(A, d_{ca}, \mathbb{R}^2)$ (*line Voronoi diagram generated by circle arcs*) defined by

$$d_{ca}(x, A_i) = \inf_{y \in A_i} d_E(x, y),$$

  where the *generator set* $A = \{A_1, \ldots, A_k\}$, $k \geq 2$, is a set of pairwise disjoint circle arcs A_i (less than or equal to a semicircle) with radius r_i centered at x_{c_i}, and d_E is the Euclidean distance. In fact,

$$d_{ca}(x, A_i) = \min\{d_E(x, a_i), d_E(x, b_i), |d_E(x, x_{c_i}) - r_i|\},$$

  where a_i and b_i are the endpoints of A_i.
- **Voronoi distance for circles**
  The **Voronoi distance for** (a set of) **circles** d_{cl} is the Voronoi generation distance of a generalized Voronoi diagram $V(A, d_{cl}, \mathbb{R}^2)$ (*line Voronoi diagram generated by circles*) defined by

$$d_{cl}(x, A_i) = \inf_{y \in A_i} d_E(x, y),$$

where the *generator set* $A = \{A_1, \ldots, A_k\}$, $k \geq 2$, is a set of pairwise disjoint circles A_i with radius r_i centered at x_{c_i}, and d_E is the Euclidean distance. In fact,

$$d_{cl}(x, A_i) = |d_E(x, x_{c_i}) - r_i|.$$

Examples of above Voronoi distances are $d^{\star}_{cl}(x, A_i) = d_E(x, x_{c_i}) - r_i$ and $d^{*}_{cl}(x, A_i) = d^2_E(x, x_{c_i}) - r_i^2$ (the *Laguerre Voronoi diagram*).

- **Voronoi distance for areas**

  The **Voronoi distance for areas** d_{ar} is the Voronoi generation distance of the generalized Voronoi diagram $V(A, d_{ar}, \mathbb{R}^2)$ (*area Voronoi diagram*) defined by

$$d_{ar}(x, A_i) = \inf_{y \in A_i} d_E(x, y),$$

  where $A = \{A_1, \ldots, A_k\}$, $k \geq 2$, is a collection of pairwise disjoint connected closed sets (*areas*), and d_E is the ordinary Euclidean distance.

  For any generalized generator set $A = \{A_1, \ldots, A_k\}$, $k \geq 2$, one can use as the Voronoi generation distance the **Hausdorff distance** from a point x to a set A_i: $d_{Haus}(x, A_i) = \sup_{y \in A_i} d_E(x, y)$, where d_E is the Euclidean distance.

- **Cylindrical distance**

  The **cylindrical distance** d_{cyl} is the **intrinsic metric** on the surface of a cylinder S which is used as the Voronoi generation distance in the *cylindrical Voronoi diagram* $V(P, d_{cyl}, S)$. If the axis of a cylinder with unit radius is placed at the x_3 axis in $\mathbb{R}^3$, the cylindrical distance between any points $x, y \in S$ with the cylindrical coordinates $(1, \theta_x, z_x)$ and $(1, \theta_y, z_y)$ is given by

$$d_{cyl}(x, y) = \begin{cases} \sqrt{(\theta_x - \theta_y)^2 + (z_x - z_y)^2}, & \text{if } \theta_y - \theta_x \leq \pi, \\ \sqrt{(\theta_x + 2\pi - \theta_y)^2 + (z_x - z_y)^2}, & \text{if } \theta_y - \theta_x > \pi. \end{cases}$$

- **Cone distance**

  The **cone distance** d_{con} is the **intrinsic metric** on the surface of a cone S which is used as the Voronoi generation distance in the *conic Voronoi diagram* $V(P, d_{con}, S)$. If the axis of the cone S is placed at the x_3 axis in $\mathbb{R}^3$, and the radius of the circle made by the intersection of the cone S with the x_1x_2 plane is equal to one, then the cone distance between any points $x, y \in S$ is given by

$$d_{con}(x, y) = \begin{cases} \sqrt{r_x^2 + r_y^2 - 2r_x r_y \cos(\theta'_y - \theta'_x)}, \\ \quad \text{if } \theta'_y \leq \theta'_x + \pi \sin(\alpha/2), \\ \sqrt{r_x^2 + r_y^2 - 2r_x r_y \cos(\theta'_x + 2\pi \sin(\alpha/2) - \theta'_y)}, \\ \quad \text{if } \theta'_y > \theta'_x + \pi \sin(\alpha/2), \end{cases}$$

  where (x_1, x_2, x_3) are the Cartesian coordinates of a point x on S, α is the top angle of the cone, θ_x is the counterclockwise angle from the x_1 axis to the ray from the origin to the point $(x_1, x_2, 0)$, $\theta'_x = \theta_x \sin(\alpha/2)$, $r_x =$

$\sqrt{x_1^2 + x_2^2 + (x_3 - \coth(\alpha/2))^2}$ is the straight line distance from the top of the cone to the point (x_1, x_2, x_3).

- **Voronoi distances of order** m

  Given a finite set A of objects in a metric space (S, d), and an integer $m \geq 1$, consider the set of all *m-subsets* M_i of A (i.e., $M_i \subset A$, and $|M_i| = m$). The *Voronoi diagram of order m* of A is a partition of S into *Voronoi regions* $V(M_i)$ *of m-subsets* of A in such a way that $V(M_i)$ contains all points $s \in S$ which are "closer" to M_i than to any other m-set M_j: $d(s, x) < d(s, y)$ for any $x \in M_i$ and $y \in S \backslash M_i$. This diagram provides first, second, ..., m-th closest neighbors of a point in S.

  Such diagrams can be defined in terms of some "distance function" $D(s, M_i)$, in particular, some m-**hemimetric** (Chap. 3) on S. For $M_i = \{a_i, b_i\}$, there were considered the functions $|d(s, a_i) - d(s, b_i)|$, $d(s, a_i) + d(s, b_i)$, $d(s, a_i) \cdot d(s, b_i)$, as well as 2-**metrics** $d(s, a_i) + d(s, b_i) + d(a_i, b_i)$ and the area of triangle (s, a_i, b_i).

Chapter 21
Image and Audio Distances

21.1 Image Distances

Image Processing treats signals such as photographs, video, or tomographic output. In particular, *Computer Graphics* consists of image synthesis from some abstract models, while *Computer Vision* extracts some abstract information: say, the 3D description of a scene from video footage of it. From about 2000, analog image processing (by optical devices) gave way to digital processing, and, in particular, digital image editing (for example, processing of images taken by popular digital cameras).

Computer graphics (and our brains) deals with *vector graphics images*, i.e., those represented geometrically by curves, polygons, etc. A *raster graphics image* (or *digital image*, *bitmap*) in $2D$ is a representation of a $2D$ image as a finite set of digital values, called *pixels* (short for picture elements) placed on a square grid $\mathbb{Z}^2$ or a hexagonal grid. Typically, the image raster is a square $2^k \times 2^k$ grid with $k = 8, 9$ or 10.

Video images and *tomographic* or magnetic resonance (obtained by cross-sectional slices) images are $3D$ ($2D$ plus time); their digital values are called *voxels* (volume elements). The spacing between two pixels in one slice is referred to as the *interpixel distance*, while the spacing between slices is the *interslice distance*.

A *digital binary image* corresponds to only two values 0,1 with 1 being interpreted as logical "true" and displayed as black; so, such image is identified with the set of black pixels. A *continuous binary image* is a (usually, compact) subset of a **locally compact** metric space (usually, Euclidean space $\mathbb{E}^n$ with $n = 2, 3$).

The *gray-scale images* can be seen as point-weighted binary images. In general, a *fuzzy set* is a point-weighted set with weights (*membership values*); cf. **metrics between fuzzy sets** in Chap. 1. For the gray-scale images, *xyi*-representation is used, where plane coordinates (x, y) indicate shape, while the weight i (short for intensity, i.e., brightness) indicates *texture*. Sometimes, the matrix $((i_{xy}))$ of gray-levels is used.

© Springer-Verlag Berlin Heidelberg 2016

M.M. Deza, E. Deza, *Encyclopedia of Distances*,
DOI 10.1007/978-3-662-52844-0_21

The *brightness histogram* of a gray-scale image provides the frequency of each brightness value found in that image. If an image has m brightness levels (bins of gray-scale), then there are 2^m different possible intensities. Usually, $m = 8$ and numbers $0, 1, \ldots, 255$ represent the intensity range from black to white; other typical values are $m = 10, 12, 14, 16$. Humans can differ between around 10 million different colors but between only 30 different gray-levels; so, color has much higher discriminatory power.

For color images, (RGB)-representation is the better known, where space coordinates R, G, B indicate red, green and blue levels; a $3D$ histogram provides brightness at each point. Among many other $3D$ color models (spaces) are: (CMY) cube (Cyan, Magenta, Yellow colors), (HSL) cone (Hue-color type given as an angle, Saturation in %, Luminosity in %), and (YUV), (YIQ) used, respectively, in PAL, NTSC television. CIE-approved conversion of (RGB) into luminance (luminosity) of gray-level is $0.299R + 0.587G + 0.114B$. The *color histogram* is a feature vector with components representing either the total number of pixels, or the percentage of pixels of a given color in the image.

Images are often represented by *feature vectors*, including color histograms, color moments, textures, shape descriptors, etc. Examples of feature spaces are: *raw intensity* (pixel values), *edges* (boundaries, contours, surfaces), *salient features* (corners, line intersections, points of high curvature), and *statistical features* (moment invariants, centroids). Typical video features are in terms of overlapping frames and motions.

Image Retrieval (similarity search) consists of (as for other data: audio recordings, DNA sequences, text documents, time-series, etc.) finding images whose features have values either mutual similarity, or similarity to a given query or in a given range.

There are two methods to compare images directly: intensity-based (color and texture histograms), and geometry-based (shape representations by *medial axis*, *skeletons*, etc.). The imprecise term *shape* is used for the extent (silhouette) of the object, for its local geometry or geometrical pattern (conspicuous geometric details, points, curves, etc.), or for that pattern modulo a similarity transformation group (translations, rotations, and scalings). The imprecise term *texture* means all that is left after color and shape have been considered, or it is defined via structure and randomness.

The similarity between vector representations of images is measured by the usual practical distances: **l_p-metrics**, **weighted editing metrics**, **Tanimoto distance**, **cosine distance**, **Mahalanobis distance** and its extension, **distance**.

Among probabilistic distances, the following ones are most used: **Bhattacharya 2**, **Hellinger**, **Kullback–Leibler**, **Kolmogorov–Smirnov**, **Jeffrey** and (especially, for histograms) **χ^2-**, **Kuiper distances**.

The main distances applied for compact subsets X and Y of $\mathbb{R}^n$ (usually, $n = 2, 3$) or their digital versions are: **Asplund metric**, **Shephard metric**, **symmetric difference semimetric** $Vol(X \Delta Y)$ (cf. **Nykodym metric**, **area deviation**, **digital volume metric** and their normalizations) and variations of the **Hausdorff distance** (see below).

For Image Processing, the distances below are between "true" and approximated digital images, in order to assess the performance of algorithms. For Image Retrieval, distances are between feature vectors of a query and reference.

- **Color distances**

  The visible spectrum of a typical human eye is about 380–760 nm. It matches the range of wavelengths sustaining photosynthesis; also, at those wavelengths opacity often coincides with impenetrability. A light-adapted eye has its maximum sensitivity at $\approx$ 555 nm (540 THz), in the green region of the optical spectrum.

  A *color space* is a 3-parameter description of colors. The need for exactly three parameters comes from the existence of three kinds of receptors (cells on the retina) in the human eye: for short, middle and long wavelengths, corresponding to blue, green, and red. Their respective sensitivity peaks are situated around 570 nm, 543 nm and 442 nm. About 1 of 10 women has a 4-th type of color receptor. Color blindness is 10 times more common in males. People with absent or removed lens of the eye, can see UV (ultraviolet) wavelengths (400–10 nm).

  The mantis shrimp has 12 types of color receptors including 4 for UV; its species *Gonodactylus smithii* is the only organism known to have optimal polarization vision. Some dragonflies have 30 different receptors; they can see UV and polarised light. Some spiders, jellyfish and scallops have, respectively, 8, 24, over 110 eyes.

  The CIE (International Commission on Illumination) derived (XYZ) color space in 1931 from the (RGB)-model and measurements of the human eye. In the CIE (XYZ) color space, the values X, Y and Z are also roughly red, green and blue.

  In Colorimetry, *chromaticity* is intensity of a colour (hue), defined as the distance in the particular colour space of a colour from the neutral grey colour with the same value. The basic assumption of Colorimetry (Indow, 1991), is that the perceptual color space admits a metric, the true **color distance**. This metric is expected to be almost locally Euclidean, i.e., a **Riemannian metric**. A continuous mapping from the metric space of light stimuli to this metric space is also expected.

  Such a *uniform color scale*, where equal distances in the color space correspond to equal differences in color, is not obtained yet and existing **color distances** are various approximations of it. A first step in this direction was given by *MacAdam ellipses*, i.e., regions on a chromaticity (x, y) diagram which contains all colors looking indistinguishable to the average human eye; cf. JND (just-noticeable difference) **video quality metric**. For any $\epsilon > 0$, the **MacAdam metric** in a color space is the metric for which those 25 ellipses are circles of radius ϵ. Here $x = \frac{X}{X+Y+Z}$ and $y = \frac{Y}{X+Y+Z}$ are projective coordinates, and the colors of the chromaticity diagram occupy a region of the real projective plane $\mathbb{R}P^2$.

The CIE $(L^*a^*b^*)$ (CIELAB) is an adaptation of CIE 1931 (XYZ) color space; it gives a partial linearization of the MacAdam color metric. The L^*, a^*, b^* of the most complete model are derived from L, a, b which are: the luminance L of the color from black $L = 0$ to white $L = 100$, its position a between green $a < 0$ and red $a > 0$, and its position b between green $b < 0$ and yellow $b > 0$.

Examples of non-Euclidean metrics, fitting well to observed color differences, are CIE94 (McDonald–Smith, 1995) and CIEDE2000 (Luo–Cui–Rigg, 2001). The best performing Euclidean metrics are versions of DIN99 (Cui et al., 2002) and the log-compressed OSA-UCS (Oleari et al., 2009).

Farup, 2014, proposed to transform a chromatic plane $\{(x, y)\}$ (say, $\{(a^*, b^*)\}$ of CIELAB) with polar coordinates (r, θ) and an existing Euclidean metric, into the R-scaled **Poincaré disk** by $\tilde{r} = \tanh(\frac{r}{2R})$ and observed that the resulting **hyperbolic metrics** (Chap. 6)) with optimised R perform better.

- **Average color distance**

  For a given $3D$ color space OSA-UC a list of n colors, let (c_{i1}, c_{i2}, c_{i3}) be the representation of the i-th color of the list in this space. For a color histogram $x = (x_1, \ldots, x_n)$, its *average color* is the vector $(x_{(1)}, x_{(2)}, x_{(3)})$, where $x_{(j)} = \sum_{i=1}^{n} x_i c_{ij}$ (for example, the average red, blue and green values in (RGB)).

  The **average color distance** between two color histograms ([HSEFN95]) is the Euclidean distance of their average colors.

- **Color component distance**

  Given an image (as a subset of $\mathbb{R}^2$), let p_i denote the area percentage of this image occupied by the color c_i. A *color component* of the image is a pair (c_i, p_i).

  The **color component distance** (Ma–Deng–Manjunath, 1997) between color components (c_i, p_i) and (c_j, p_j) is defined by

$$|p_i - p_j| \cdot d(c_i, c_j),$$

  where $d(c_i, c_j)$ is the distance between c_i and c_j in a given color space. Mojsilović–Hu–Soljanin, 2002, did an **Earth Mover's distance**-like modification of it.

- **Riemannian color space**

  The proposal to measure perceptual dissimilarity of colors by a **Riemannian metric** (Chap. 7) on a strictly convex cone $C \subset \mathbb{R}^3$ comes from von Helmholtz, 1891, and Schrödinger, 1920. The challenge here is to choose a "good" one.

  Roughly, it was shown in [Resn74] that the only such *GL-homogeneous* cones C (i.e., the group of all orientation preserving linear transformations of $\mathbb{R}^3$, carrying C into itself, acts transitively on C) are either $C_1 = \mathbb{R}_{>0} \times (\mathbb{R}_{>0} \times \mathbb{R}_{>0})$, or $C_2 = \mathbb{R}_{>0} \times C'$, where C' is the set $SL(2, \mathbb{R})/SO(2)$ of 2×2 real symmetric matrices with determinant 1. The first factor $\mathbb{R}_{>0}$ can be identified with variation of brightness and the other with the set of lights of a fixed brightness.

Given some $\alpha_i > 0$, the **Stiles color metric** (1946) is the GL-invariant Riemannian metric on $C_1 = \{(x_1, x_2, x_3) \in \mathbb{R}^3 : x_i > 0\}$ given by the *line element*

$$ds^2 = \sum_{i=1}^{3} \alpha_i (\frac{dx_i}{x_i})^2.$$

The **Resnikoff color metric** (1974) is the GL-invariant Riemannian metric on $C_2 = \{(x, u) : x \in \mathbb{R}_{>0}, u \in C'\}$ given by the *line element*

$$ds^2 = \alpha_1 (\frac{dx}{x})^2 + \alpha_2 ds^2_{C'},$$

where $ds^2_{C'}$, is the **Poincaré metric** (Chap. 6) on C'.

- **Histogram intersection quasi-distance**

  Given two color histograms $x = (x_1, \ldots, x_n)$ and $y = (y_1, \ldots, y_n)$ (with x_i, y_i representing the number of pixels in the bin i), the **histogram intersection quasi-distance** between them (cf. **intersection distance** in Chap. 17) is (Swain–Ballard, 1991) defined by

$$1 - \frac{\sum_{i=1}^{n} \min\{x_i, y_i\}}{\sum_{i=1}^{n} x_i}.$$

  For normalized histograms (total sum is 1) the above quasi-distance becomes the usual l_1-metric $\sum_{i=1}^{n} |x_i - y_i|$. The *normalized cross-correlation* (Rosenfeld–Kak, 1982) between x and y is a similarity defined by $\frac{\sum_{i=1}^{n} x_i y_i}{\sum_{i=1}^{n} x_i^2}$.

- **Histogram quadratic distance**

  Given two color histograms $x = (x_1, \ldots, x_n)$ and $y = (y_1, \ldots, y_n)$ (usually, $n = 256$ or $n = 64$) representing the color percentages of two images, their **histogram quadratic distance** (used in IBM's Query By Image Content system) is their **Mahalanobis distance** defined in Chap. !7 by

$$\sqrt{(x-y)^T A (x-y)},$$

  where $A = ((a_{ij}))$ is a symmetric positive-definite matrix, and the weight a_{ij} is some, perceptually justified, similarity between colors i and j.

  For example (cf. [HSEFN95]), $a_{ij} = 1 - \frac{d_{ij}}{\max_{1 \le p,q \le n} d_{pq}}$, where d_{ij} is the Euclidean distance between 3-vectors representing i and j in some color space.

  If (h_i, s_i, v_i) and (h_j, s_j, v_j) are the representations of the colors i and j in the color space (HSV), then $a_{ij} = 1 - \frac{1}{\sqrt{5}}((v_i - v_j)^2 + (s_i \cos h_i - s_j \cos h_j)^2 + (s_i \sin h_i - s_j \sin h_j)^2)^{\frac{1}{2}}$ is used.

- **Histogram diffusion distance**

  Given two histogram-based descriptors $x = (x_1, \ldots, x_n)$ and $y = (y_1, \ldots, y_n)$, their **histogram diffusion distance** (Ling–Okada, 2006) is defined by

$$\int_0^T ||u(t)||_1 dt,$$

  where T is a constant, and $u(t)$ is a heat diffusion process with initial condition $u(0) = x - y$. In order to approximate the diffusion, the initial condition is convoluted with a Gaussian window; then the sums of l_1-norms after each convolution approximate the integral.

- **Gray-scale image distances**

  Let $f(x)$ and $g(x)$ denote the brightness values of two digital gray-scale images f and g at the pixel $x \in X$, where X is a raster of pixels. Any distance between point-weighted sets (X, f) and (X, g) (for example, the **Earth Mover's distance**) can be applied for measuring distances between f and g. However, the main used distances (called also *errors*) between the images f and g are:

  1. The *root-mean-square error* $RMS(f,g) = \left(\frac{1}{|X|}\sum_{x\in X}(f(x)-g(x))^2\right)^{\frac{1}{2}}$ (a variant is to use the *l_1-norm* $|f(x)-g(x)|$ instead of the *l_2-norm*);
  2. The **signal-to-noise ratio** $SNR(f,g) = \left(\frac{\sum_{x\in X} g(x)^2}{\sum_{x\in X}(f(x)-g(x))^2}\right)^{\frac{1}{2}}$ (cf. **SNR distance** between sonograms);
  3. The *pixel misclassification error rate* $\frac{1}{|X|}|\{x \in X : f(x) \neq g(x)\}|$ (normalized **Hamming distance**);
  4. The *frequency root-mean-square error* $\left(\frac{1}{|U|^2}\sum_{u\in U}(F(u)-G(u))^2\right)^{\frac{1}{2}}$, where F and G are the discrete Fourier transforms of f and g, respectively, and U is the frequency domain;
  5. The *Sobolev norm of order δ error* $\left(\frac{1}{|U|^2}\sum_{u\in U}(1+|\eta_u|^2)^{\delta}(F(u)-G(u))^2\right)^{\frac{1}{2}}$, where $0 < \delta < 1$ is fixed (usually, $\delta = \frac{1}{2}$), and η_u is the $2D$ frequency vector associated with position u in the frequency domain U.

  Cf. **metrics between fuzzy sets** in Chap. 1.

- **Image compression L_p-metric**

  Given a number r, $0 \leq r < 1$, the **image compression L_p-metric** is the usual **L_p-metric** on $\mathbb{R}^{n^2}_{\geq 0}$ (the set of gray-scale images seen as $n \times n$ matrices) with p being a solution of the equation $r = \frac{p-1}{2p-1} \cdot e^{\frac{p}{2p-1}}$. So, $p = 1, 2$, or ∞ for, respectively, $r = 0$, $r = \frac{1}{3}e^{\frac{2}{3}} \approx 0.65$, or $r \geq \frac{\sqrt{e}}{2} \approx 0.82$. Here r estimates the *informative* (i.e., filled with nonzeros) part of the image. According to [KKN02], it is the best quality metric to select a lossy compression scheme.

- **Chamfering distances**

  The **chamfering distances** are distances approximating Euclidean distance by a weighted path distance on the graph $G = (\mathbb{Z}^2, E)$, where two pixels are

neighbors if one can be obtained from another by an *one-step move* on $\mathbb{Z}^2$. The list of permitted moves is given, and a **prime distance**, i.e., a positive weight (cf. Chap. 19), is associated to each type of such move.

An (α, β)**-chamfer metric** corresponds to two permitted moves—with l_1-distance 1 and with l_∞-distance 1 (diagonal moves only)—weighted α and β, respectively.

The main applied cases are $(\alpha, \beta) = (1, 0)$ (**city-block metric**, or 4**-metric**), (1,1) (**chessboard metric**, or 8**-metric**), $(1, \sqrt{2})$ (**Montanari metric**), $(3, 4)$ ($(3, 4)$**-metric**), $(2, 3)$ (**Hilditch–Rutovitz metric**), $(5, 7)$ (**Verwer metric**).

The **Borgefors metric** corresponds to three permitted moves—with l_1-distance 1, with l_∞-distance 1 (diagonal moves only) and knight moves—weighted 5, 7 and 11.

An $3D$**-chamfer metric** (or (α, β, γ)-*chamfer metric*) is the weighted path metric of the infinite graph with the vertex-set $\mathbb{Z}^3$ of voxels, two vertices being adjacent if their l_∞-distance is one, while weights α, β and γ are associated to 6 face, 12 edge and 8 corner neighbors, respectively. If $\alpha = \beta = \gamma = 1$, we obtain l_∞-metric. The $(3, 4, 5)$- and $(1, 2, 3)$-chamfer metrics are the most used ones.

The **Chaudhuri–Murthy–Chaudhuri metric** between sequences $x = (x_1, \ldots, x_m)$ and $y = (y_1, \ldots, y_n)$ is defined by

$$|x_{i(x,y)} - y_{i(x,y)}| + \frac{1}{1 + \lceil \frac{n}{2} \rceil} \sum_{1 \le i \le n, i \ne i(x,y)} |x_i - y_i|,$$

where $\max_i |x_i - y_i| = |x_{i(x,y)} - y_{i(x,y)}|$. For $n = 2$ it is the $(1, \frac{3}{2})$-chamfer metric.

- **Earth Mover's distance**

The **Earth Mover's distance** is a discrete form of the **transportation distance** (Chap. 14). Roughly, it is the minimal amount of work needed to transport earth or mass from one position (properly spread in space) to the other (a collection of holes). For any two finite sequences $(x_1, \ldots, x_m)$ and $(y_1, \ldots, y_n)$ over a metric space (X, d), consider *signatures*, i.e., point-weighted sets $P_1 = (p_1(x_1), \ldots, p_1(x_m))$ and $P_2 = (p_2(y_1), \ldots, p_2(y_n))$.

For example, in [RTG00]) signatures represent clustered color or texture content of images: elements of X are centroids of clusters, and $p_1(x_i), p_2(y_j)$ are cardinalities of corresponding clusters. The ground distance d is a **color distance**, say, the Euclidean distance in $3D$ CIE $(L^*a^*b^*)$ color space.

Let $W_1 = \sum_i p_1(x_i)$ and $W_2 = \sum_j p_2(y_j)$ be the *total weights* of P_1 and P_2, respectively. Then the **Earth Mover's distance** between P_1 and P_2 is defined as

$$\frac{\sum_{i,j} f^*_{ij} d(x_i, y_j)}{\sum_{i,j} f^*_{ij}},$$

where the $m \times n$ matrix $S^* = ((f_{ij}^*))$ is an *optimal*, i.e., minimizing $\sum_{i,j} f_{ij} d(x_i, y_j)$, *flow*. A *flow* is an $m \times n$ matrix $S = ((f_{ij}))$ with following constraints:

1. all $f_{ij} \geq 0$;
2. $\sum_{i,j} f_{ij} = \min\{W_1, W_2\}$;
3. $\sum_i f_{ij} \leq p_2(y_j)$ and $\sum_j f_{ij} \leq p_1(x_i)$.

So, this distance is the average ground distance d that weights travel during an optimal flow. It is not a *bin-to-bin* (component-wise, as L_p-, Kullback–Leibler, χ^2-distances), but a **cross-bin histogram distance**.

In the case $W_1 = W_2$, the above two inequalities 3. become equalities. Normalizing signatures to $W_1 = W_2 = 1$ (which not changes the distance) allows us to see P_1 and P_2 as probability distributions of random variables, say, X and Y. Then $\sum_{i,j} f_{ij} d(x_i, y_j)$ is $\mathbb{E}_S[d(X, Y)]$, i.e., the Earth Mover's distance coincides, in this case, with the **transportation distance** (Chap. 14).

For $W_1 \neq W_2$, it is not a metric in general. However, replacing the inequalities 3 in the above definition by equalities

$3'$. $\sum_i f_{ij} = p_2(y_j)$ and $\sum_j f_{ij} = \frac{p_1(x_i) W_1}{W_2}$

produces the Giannopoulos–Veltkamp's **proportional transport semimetric**.

- **Parameterized curves distance**

  The shape can be represented by a parametrized curve on the plane. Usually, such a curve is *simple*, i.e., it has no self-intersections. Let $X = X(x(t))$ and $Y = Y(y(t))$ be two parametrized curves, where the (continuous) parametrization functions $x(t)$ and $y(t)$ on $[0, 1]$ satisfy $x(0) = y(0) = 0$ and $x(1) = y(1) = 1$.

  The most used **parametrized curves distance** is the minimum, over all monotone increasing parametrizations $x(t)$ and $y(t)$, of the maximal Euclidean distance $d_E(X(x(t)), Y(y(t)))$. It is the Euclidean special case of the **dogkeeper distance** (cf. Sect. 13.1), i.e., the **Fréchet metric** for the case of curves.

  Among variations of this distance are dropping the monotonicity condition of the parametrization (*weak Fréchet distance*), or finding the part of one curve to which the other has the smallest such distance ([VeHa01]).

  In a general Riemannian manifold M, the *shape* $[C]$ of a curve C can be seen as the class of all curves that differ from C only by a parametration, i.e., they pass through the same points of M but at different speeds. The geodesic distances d on curves and D on shapes are linked by $D([C], [C']) = \inf d(C, C' \circ \alpha)$, where $\alpha : [0, 1] \to [0, 1]$ is any *reparameterization* (increasing diffeomorphism(.

  A reparametrization-invariant metric on the space of curves induces a Riemannian structure on the *shape space*. Two such metrics are **pullback metrics** (cf. Chap. 4) on the tangent bundle via *square root velocity function*: from L_2-metric by Srivastava et al., 2011, and from a more adapted metric by Le Brigant, 2016.

- **Homotopic Fréchet distance**

  Given a metric space (X, d), a *curve* is a continuous function $C : [0, 1] \to X$. The *length* of C is defined by the metric d. A *reparameterization* of C is any curve $C \circ \alpha$, where $\alpha : [0, 1] \to [0, 1]$ is a continuous nondecreasing surjection.

An (s,t)-*leash* between two curves C and C' is another curve $\lambda : [0,1] \to X$ such that $\lambda(0) = C(s)$ and $\lambda(1) = C'(t)$. A *leash map* is a continuous function $l : [0,1]^2 \to X$ such that $l(\cdot,0)$ and $l(\cdot,1)$ are reparameterizations of C and C', respectively. It describes the continuous motion of a leash between a dog walking along C and its owner walking along C'; the curve $l(t,\cdot)$ is the leash at time t. The *length* of l is the maximum length of any leash $l(t,\cdot)$.

The **homotopic Fréchet distance** between C and C' is ([CCELLT10]) the infimum, over all leash maps l between C and C', of the length of l. This distance can be thought of as the minimal amount of deformation needed to transform C into C', identifying points which are joined by a leash during its motion.

- **Nonlinear elastic matching distance**

  Consider a digital representation of curves. Let $r \geq 1$ be a constant, and let $A = \{a_1, \ldots, a_m\}$, $B = \{b_1, \ldots, b_n\}$ be finite ordered sets of consecutive points on two closed curves. For any order-preserving correspondence f between all points of A and all points of B, the *stretch* $s(a_i, b_j)$ *of* $(a_i, f(a_i) = b_j)$ is r if either $f(a_{i-1}) = b_j$ or $f(a_i) = b_{j-1}$, or zero otherwise.

  The **relaxed nonlinear elastic matching distance** is $\min_f \sum(s(a_i,b_j) + d(a_i,b_j))$, where $d(a_i,b_j)$ is the difference between the tangent angles of a_i and b_j. It is a **near-metric** for some r. For $r = 1$, it is called the **nonlinear elastic matching distance**. In general, Younes, 1998, and Mio–Srivastava–Joshi, 2005, introduced *elastic* Riemannian distances between (seen as elastic) plane curves (or enclosed shapes) measuring the minimal cost of elastic reshaping of a curve into another.

- **Turning function distance**

  For a plane polygon P, its *turning function* $T_P(s)$ is the angle between the counterclockwise tangent and the x axis as a function of the arc length s. This function increases with each left hand turn and decreases with right-hand turns.

  Given two polygons of equal perimeters, their **turning function distance** is the L_p**-metric** between their turning functions.

- **Size function distance**

  For a shape, seen as a plane graph $G = (V,E)$, and a *measuring function* f on its vertex-set V (for example, the distance from $v \in V$ to the center of mass of V), the *size function* $S_G(x,y)$ is defined, on the points $(x,y) \in \mathbb{R}^2$, as the number of connected components of the restriction of G on vertices $\{v \in V : f(v) \leq y\}$ which contain a point v' with $f(v') \leq x$.

  Given two plane graphs with vertex-sets belonging to a raster $R \subset \mathbb{Z}^2$, their Uras–Verri's **size function distance** is the normalized l_1-distance between their size functions over raster pixels. The **matching distance** (Chap. 1) between the *cornerpoints*/*cornerlines* multisets of two size functions is also used.

- **Reflection distance**

  For a finite union A of plane curves and each point $x \in \mathbb{R}^2$, let V_A^x denote the union of intervals (x,a), $a \in A$ which are *visible from* x, i.e., $(x,a) \cap A = \emptyset$. Denote by ρ_A^x the area of the set $\{x + v \in V_A^x : x - v \in V_A^x\}$.

  The Hagedoorn–Veltkamp's **reflection distance** between finite unions A and B of plane curves is the normalized l_1-distance between the corresponding

functions ρ_A^x and ρ_B^x defined by

$$\frac{\int_{\mathbb{R}^2} |\rho_A^x - \rho_B^x| dx}{\int_{\mathbb{R}^2} \max\{\rho_A^x, \rho_B^x\} dx}.$$

- **Distance transform**

  Given a metric space $(X = \mathbb{Z}^2, d)$ and a binary digital image $M \subset X$, the **distance transform** is a function $f_M : X \to \mathbb{R}_{\geq 0}$, where $f_M(x) = \inf_{u \in M} d(x, u)$ is the **point-set distance** $d(x, M)$. So, a distance transform can be seen as a gray-scale digital image where each pixel is given a label (a gray-level) which corresponds to the distance to the nearest pixel of the background. Distance transforms, in Image Processing, are also called *distance fields* and **distance maps**; but we reserve the last term only for this notion in any metric space as in Chap. 1.

  A *distance transform of a shape* is the distance transform with M being the boundary of the image. For $X = \mathbb{R}^2$, the graph $\{(x, f(x)) : x \in X\}$ of $d(x, M)$ is called the *Voronoi surface* of M.

- **Medial axis and skeleton**

  Let (X, d) be a metric space, and let M be a subset of X. The **medial axis** of X is the set $MA(X) = \{x \in X : |\{m \in M : d(x, m) = d(x, M)\}| \geq 2\}$, i.e., all points of X which have in M at least two **elements of best approximation**; cf. **metric projection** in Chap. 1. $MA(X)$ consists of all points of boundaries of *Voronoi regions* of points of M. The *reach* of M is the **set-set distance** (Chap. 1) between M and $MA(X)$.

  The *cut locus* of X is the closure $\overline{MA(X)}$ of the medial axis. Cf. **Shankar–Sormani radii** in Chap. 1. The *medial axis transform* $MAT(X)$ is the point-weighted set $MA(X)$ (the restriction of the **distance transform** on $MA(X)$) with $d(x, M)$ being the weight of $x \in X$.

  If (as usual in applications) $X \subset \mathbb{R}^n$ and M is the boundary of X, then the **skeleton** $Skel(X)$ of X is the set of the centers of all d-balls inscribed in X and not belonging to any other such ball; so, $Skel(X) = MA(X)$. The skeleton with M being continuous boundary is a limit of *Voronoi diagrams* as the number of the generating points becomes infinite. For $2D$ binary images X, the skeleton is a curve, a single-pixel thin one, in the digital case. The *exoskeleton* of X is the skeleton of the complement of X, i.e., of the background of the image for which X is the foreground.

- **Procrustes distance**

  The *shape* of a *form* (configuration of points in $\mathbb{R}^2$), seen as expression of translation-, rotation- and scale-invariant properties of form, can be represented by a sequence of *landmarks*, i.e., specific points on the form, selected accordingly to some rule. Each landmark point a can be seen as an element $(a', a'') \in \mathbb{R}^2$ or an element $a' + a''i \in \mathbb{C}$.

  Consider two shapes x and y, represented by their landmark vectors $(x_1, \ldots, x_n)$ and $(y_1, \ldots, y_n)$ from $\mathbb{C}^n$. Suppose that x and y are corrected for

translation by setting $\sum_t x_t = \sum_t y_t = 0$. Then their **Procrustes distance** is defined by

$$\sqrt{\sum_{1\le t\le n} |x_t - y_t|^2},$$

where two forms are, first, optimally (by least squares criterion) aligned to correct for scale, and their **Kendall shape distance** is defined by

$$\arccos \sqrt{\frac{(\sum_t x_t \overline{y}_t)(\sum_t y_t \overline{x}_t)}{(\sum_t x_t \overline{x}_t)(\sum_t y_t \overline{y}_t)}},$$

where $\overline{\alpha} = a' - a'' i$ is the *complex conjugate* of $\alpha = a' + a'' i$.

Petitjean, 2002, extended the L_2-Wasserstein distance (cf. Chap. 14) to *colored mixtures*, i.e., ordinary mixtures of random vectors, for which an new axis (the space of colors) has been added. He remarked that the Procrustes distance is an instance of this *colored Wasserstein distance*, when this latter is minimized for a class of affine transformations (rotations and translations).

- **Shape parameters**

Let X be a figure in $\mathbb{R}^2$ with area $A(X)$, perimeter $P(X)$ and convex hull $conv\, X$. The main **shape parameters** of X are given below.

$D_A(X) = 2\sqrt{\frac{A(X)}{\pi}}$ and $D_P(X) = \frac{P(X)}{\pi}$ are the diameters of circles with area $A(X)$ and with perimeter $P(X)$, respectively.

Feret's diameters $F_x(X), F_y(X), F_{min}(X), F_{\max}(X)$ are the orthogonal projections of X on the x and y axes and such minimal and maximal projections on a line.

Martin's diameter $M(X)$ is the distance between opposite sides of X measured crosswise of it on a line bisecting the figure's area. $M_x(X)$ and $M_y(X)$ are Martin's diameters for horizontal and vertical directions, respectively.

$R_{in}(X)$ and $R_{out}(X)$ are the radii of the largest disc in X and the smallest disc including X. $a(X)$ and $b(X)$ are the lengths of the major and minor semiaxes of the ellipse with area $A(X)$ and perimeter $P(X)$.

Examples of the ratios, describing some shape properties in above terms, follow.

The *area-perimeter ratio* (or *projection sphericity*) and *Petland's projection sphericity ratio* are $ArPe = \frac{4\pi A(X)}{(P(X))^2}$ and $\frac{4A(X)}{\pi(F_{\max}(X))^2}$.

The *circularity shape factor* and *Horton's compactness factor* are $\frac{1}{ArPe}$ and $\frac{1}{\sqrt{ArPe}}$.

Wadell's circularity shape and *drainage-basin circularity shape* ratios are $\frac{D_A(X)}{F_{\max}(X)}$ and $\frac{A(X)}{D_P(X)}$. Both ratios and *ArPe* are at most 1 with equality only for a disc.

Tickell's ratio is $(\frac{D_A(X)}{D_{out}(X)})^2$. *Cailleux's roundness ratio* is $\frac{2r(X)}{F_{\max}(X)}$, where $r(X)$ is the radius of curvature at a most convex part of the contour of X.

The *rugosity coefficient* and *convexity ratio* (or *solidity*) are $\frac{P(X)}{P(conv\,X)}$ and $\frac{A(X)}{A(conv\,X)}$. Both the solidity and $\frac{P(conv\,X)}{P(X)}$ are at most 1 with equality only for convex sets.

The *diameters ratios* are $\frac{MD_x(X)}{F_x(X)}$ and $\frac{MD_y(X)}{F_y(X)}$. The *radii ratio* and *ellipse ratio* are $\frac{R_{in}(X)}{R_{out}(X)}$ and $\frac{a(X)}{b(X)}$. The *Feret's ratio* and *modification ratio* are $\frac{F_{min}(X)}{F_{\max}(X)}$ and $\frac{R_{in}(X)}{F_{\max}(X)}$. The **aspect ratio** in Chap. 1 is the reciprocal of the Feret's ratio.

The *symmetry factor of Blaschke* is $1-\frac{A(X)}{A(S(X))}$, where $S(X) = \frac{1}{2}(X \oplus \{x : -x \in X\})$.

- **Distances from symmetry**

  Many measures of chirality and, in general, given symmetry G of a given set $A \in \mathbb{R}^n$, were proposed. Several examples follow.

  Let A' be the *enantiomorph* (mirror image) of A. Gilat, 1985, proposed to measure *distance from achirality* of A by $\frac{V(A \triangle A')}{V(A)}$; cf. **normalized volume of symmetric difference** in Chap. 9.

  Let shape A be represented by a sequence $(a_1, \ldots, a_m)$ of points. Then the **symmetry distance** of A is defined by Zabrodsky–Peleg–Avnir, 1992, as the point-set distance $\inf_b \frac{1}{m}\sum_{i=1}^m ||a_i - b_i||_2^2$, where $b = (b_1, \ldots, b_n)$ is the L_2-nearest to a representation of a *symmetric* (i.e., invariant to rotation and translation) shape. The *symmetry distance of a function* f with respect to any transformation G is the L_2-distance between f and the nearest function invariant to G.

  If A is a $2D$ object, and it is represented by its *radial function* $R(r)$, then the *distance of A from symmetry* G can be measured (Köhler, 1993) by $\int_0^{2\pi} |G(R(r)) - R(r)|dr$. For a sequence $(a_1, \ldots, a_m)$ of points, similar distance is (Köhler, 1999) $\min_p \sum_{i=1}^m d_E(a_i, G(p(a_i)))$, where p is any of $m!$ permutations of $(a_1, \ldots, a_m)$ and d_E is the Euclidean distance.

- **Tangent distance**

  For any $x \in \mathbb{R}^n$ and a family of *transformations* $t(x, \alpha)$, where $\alpha \in \mathbb{R}^k$ is the vector of k parameters (for example, the scaling factor and rotation angle), the set $M_x = \{t(x, \alpha) : \alpha \in \mathbb{R}^k\} \subset \mathbb{R}^n$ is a manifold of dimension at most k. It is a curve if $k = 1$. The minimum Euclidean distance between manifolds M_x and M_y would be a useful distance since it is invariant with respect to transformations $t(x, \alpha)$.

  However, the computation of such a distance is too difficult in general; so, M_x is approximated by its *tangent subspace at* x: $\{x + \sum_{i=1}^k \alpha_k x^i : \alpha \in \mathbb{R}^k\} \subset \mathbb{R}^n$, where the *tangent vectors* x^i, $1 \le i \le k$, spanning it are the partial derivatives of $t(x, \alpha)$ with respect to α. The **one-sided** (or *directed*) **tangent distance** between elements x and y of $\mathbb{R}^n$ is a quasi-distance d defined by

$$\sqrt{\min_\alpha ||x + \sum_{i=1}^k \alpha_k x^i - y||^2}.$$

The Simard–Le Cun–Denker's **tangent distance** is defined by $\min\{d(x,y), d(y,x)\}$.

- **Pixel distance**

  Consider two digital images, seen as binary $m \times n$ matrices $x = ((x_{ij}))$ and $y = ((y_{ij}))$, where a pixel x_{ij} is black or white if it is equal to 1 or 0, respectively.

  For each pixel x_{ij}, the *fringe distance map to the nearest pixel of opposite color* $D_{BW}(x_{ij})$ is the number of *fringes* expanded from (i,j) (where each fringe is composed by the pixels that are at the same distance from (i,j)) until the first fringe holding a pixel of opposite color is reached.

  The **pixel distance** (Smith–Bourgoin–Sims–Voorhees, 1994) is defined by

$$\sum_{1\le i\le m}\sum_{1\le j\le n} |x_{ij}-y_{ij}|(D_{BW}(x_{ij})+D_{BW}(y_{ij})).$$

  In a pixel-based device (computer monitor, printer, scanner), the **pixel pitch** (or *dot pitch*) is the spacing between subpixels (dots) of the same color on the inside of a display screen. Closer spacing usually produce a sharper image.

- **Pratt's figure of merit**

  In general, a *figure of merit* is a quantity used to characterize the performance of a device, system or method, relative to its alternatives. Given two binary images, seen as nonempty subsets, A and B, of a finite metric space (X,d), their **Pratt's figure of merit** (or *FOM*, Abdou–Pratt, 1979) is a quasi-distance defined by

$$\left(\max\{|A|,|B|\}\sum_{x\in B}\frac{1}{1+\alpha d(x,A)^2}\right)^{-1},$$

  where α is a scaling constant (usually, $\frac{1}{9}$), and $d(x,A) = \min_{y\in A} d(x,y)$ is the **point-set distance**.

  Similar quasi-distances are Peli–Malah's *mean error distance* $\frac{1}{|B|}\sum_{x\in B} d(x,A)$, and the *mean square error distance* $\frac{1}{|B|}\sum_{x\in B} d(x,A)^2$.

- ***p*-th order mean Hausdorff distance**

  Given $p \ge 1$ and two binary images, seen as nonempty subsets A and B of a finite metric space (say, a raster of pixels) (X,d), their ***p*-th order mean Hausdorff distance** is ([Badd92]) a normalized ***L*$_p$-Hausdorff distance**, defined by

$$\left(\frac{1}{|X|}\sum_{x\in X}|d(x,A)-d(x,B)|^p\right)^{\frac{1}{p}},$$

  where $d(x,A) = \min_{y\in A} d(x,y)$ is the **point-set distance**. The usual Hausdorff metric is proportional to the ∞-th order mean Hausdorff distance.

Venkatasubraminian's **Σ-Hausdorff distance** $d_{dHaus}(A,B) + d_{dHaus}(B,A)$ is equal to $\sum_{x\in A\cup B} |d(x,A) - d(x,B)|$, i.e., it is a version of L_1-Hausdorff distance.

Another version of the 1-st order mean Hausdorff distance is Lindstrom–Turk's *mean geometric error* (1998) between two images (seen as surfaces A and B) defined by

$$\frac{1}{Area(A) + Area(B)} \left(\int_{x\in A} d(x,B)dS + \int_{x\in B} d(x,A)dS \right),$$

where $Area(A)$ denotes the area of A. If the images are seen as finite sets A and B, their *mean geometric error* is defined by

$$\frac{1}{|A| + |B|} \left(\sum_{x\in A} d(x,B) + \sum_{x\in B} d(x,A) \right).$$

- **Modified Hausdorff distance**

  Given two binary images, seen as nonempty subsets A and B of a finite metric space (X,d), their Dubuisson–Jain's **modified Hausdorff distance** (1994) is defined as the maximum of **point-set distances** averaged over A and B:

$$\max \left\{ \frac{1}{|A|} \sum_{x\in A} d(x,B), \frac{1}{|B|} \sum_{x\in B} d(x,A) \right\},$$

  while their Eiter–Mannila's **sum of minimal distances** (1997) is defined as

$$\frac{1}{2}(\sum_{x\in A} d(x,B) + \sum_{x\in B} d(x,A)).$$

- **Partial Hausdorff quasi-distance**

  Given two binary images, seen as subsets $A, B \neq \emptyset$ of a finite metric space (X,d), and integers k, l with $1 \leq k \leq |A|$, $1 \leq l \leq |B|$, their Huttenlocher–Rucklidge's **partial** (k,l)**-Hausdorff quasi-distance** (1992) is defined by

$$\max\{k^{th}_{x\in A} d(x,B), l^{th}_{x\in B} d(x,A)\},$$

  where $k^{th}_{x\in A} d(x,B)$ means the k-th (rather than the largest $|A|$-th ranked one) among $|A|$ distances $d(x,B)$ ranked in increasing order. The case $k = \lfloor \frac{|A|}{2} \rfloor$, $l = \lfloor \frac{|B|}{2} \rfloor$ corresponds to the *modified median Hausdorff quasi-distance*.

- **Bottleneck distance**

  Given two binary images, seen as subsets $A, B \neq \emptyset$ with $|A| = |B| = m$, of a metric space (X,d), their **bottleneck distance** is defined by

$$\min_f \max_{x\in A} d(x, f(x)),$$

where f is any bijective mapping between A and B. Cf. more general **matching distance** in Chap. 1.

Variations of the above distance are:

1. The **minimum weight matching**: $\min_f \sum_{x\in A} d(x,f(x))$;
2. The **uniform matching**: $\min_f\{\max_{x\in A} d(x,f(x)) - \min_{x\in A} d(x,f(x)\}$;
3. The **minimum deviation matching**: $\min_f\{\max_{x\in A} d(x,f(x)) - \frac{1}{|A|}\sum_{x\in A} d(x,f(x)\}$.

Given an integer t with $1 \le t \le |A|$, the **t-bottleneck distance** between A and B ([InVe00]) is the above minimum but with f being any mapping from A to B such that $|\{x \in A : f(x) = y\}| \le t$.

The cases $t = 1$ and $t = |A|$ correspond, respectively, to the bottleneck distance and **directed Hausdorff distance** $d_{dHaus}(A,B) = \max_{x\in A} \min_{y\in B} d(x,y)$ (Chap. 1).

- **Hausdorff distance up to G**

  Given a group $(G,\cdot,id)$ acting on the Euclidean space $\mathbb{E}^n$, the **Hausdorff distance up to** G between two compact subsets A and B (used in Image Processing) is their **generalized G-Hausdorff distance** (Chap. 1), i.e., the minimum of $d_{Haus}(A,g(B))$ over all $g \in G$. Usually, G is the group of all isometries or all translations of $\mathbb{E}^n$.

- **Hyperbolic Hausdorff distance**

  For any compact subset A of $\mathbb{R}^n$, denote by $MAT(A)$ its *Blum's medial axis transform*, i.e., the subset of $X = \mathbb{R}^n \times \mathbb{R}_{\ge 0}$, whose elements are all pairs $x = (x', r_x)$ of the centers x' and the radii r_x of the maximal inscribed (in A) balls, in terms of the Euclidean distance d_E in $\mathbb{R}^n$. (Cf. **medial axis and skeleton** transforms for the general case.)

  The **hyperbolic Hausdorff distance** ([ChSe00]) is the **Hausdorff metric** on nonempty compact subsets $MAT(A)$ of the metric space (X,d), where the *hyperbolic distance* d on X is defined, for its elements $x = (x', r_x)$ and $y = (y', r_y)$, by

$$\max\{0, d_E(x',y') - (r_y - r_x)\}.$$

- **Nonlinear Hausdorff metric**

  Given two compact subsets A and B of a metric space (X,d), their **nonlinear Hausdorff metric** (or *Szatmári–Rekeczky–Roska wave distance*) is the **Hausdorff distance** $d_{Haus}(A \cap B, (A \cup B)^*)$, where $(A \cup B)^*$ is the subset of $A \cup B$ which forms a closed contiguous region with $A \cap B$, and the distances between points are allowed to be measured only along paths wholly in $A \cup B$.

- **Handwriting spatial gap distances**

  Automatic recognition of unconstrained handwritten texts (for example, legal amounts on bank checks or pre-hospital care reports) require measuring the spatial gaps between connected components in order to extract words.

Three most used ones, among **handwriting spatial gap distances** between two adjacent connected components x and y of text line, are:

- Seni–Cohen, 1994: the *run-length* (minimum horizontal Euclidean distance) between x and y, and the horizontal distance between their bounding boxes;
- Mahadevan–Nagabushnam, 1995: Euclidean distance between the convex hulls of x and y, on the line linking hull centroids.

- **Video quality metrics**

  These metrics are between test and reference color video sequences, usually aimed at optimization of encoding/compression/decoding algorithms. Each of them is based on some perceptual model of the human vision system, the simplest ones being RMSE (root-mean-square error) and PSNR (peak signal-to-noise ratio) error measures. The *threshold metrics* estimate the probability of detecting an *artifact* (i.e., a visible distortion that gets added to a video signal during digital encoding).

  Examples are: Sarnoff's JND (just-noticeable difference), Winkler's PDM (perceptual distortion), and Watson's DVQ (digital video quality) metrics. DVQ is an l_p**-metric** between feature vectors representing two video sequences. Some metrics measure special artifacts in the video: the appearance of block structure, blurriness, added "mosquito" noise (ambiguity in the edge direction), texture distortion, etc.

- **Time series video distances**

  The **time series video distances** are objective wavelet-based spatial-temporal **video quality metrics**. A video stream x is processed into a time series $x(t)$ (seen as a curve on coordinate plane) which is then (piecewise linearly) approximated by a set of n contiguous line segments that can be defined by $n+1$ endpoints (x_i, x_i'), $0 \le i \le n$, in the coordinate plane. In [WoPi99] are given the following (cf. **Meehl distance**) distances between video streams x and y:

  - $Shape(x,y) = \sum_{i=0}^{n-1} |(x'_{i+1} - x'_i) - (y'_{i+1} - y'_i)|$;
  - $Offset(x,y) = \sum_{i=0}^{n-1} |\frac{x'_{i+1}+x'_i}{2} - \frac{y'_{i+1}+y'_i}{2}|$.

- **Dynamic time wrapping distance**

  A *time series* is a temporal sequence, varied in time or speed, of numerical data points, collected usually at regular intervals over a period of time; see above **time series video distances** and, in Chap. 23, **spike train distances**.

  Dynamic time warping (DTW) is a sequence alignment method allowing a nonlinear mapping of one sequence to another by minimizing the (total cumulative) distance between them. Used originally in speech recognition, DTW is applied now to temporal sequences of video, audio, and graphics data.

  Consider two sequences (say, time series) $x = (x_1, \dots, x_m)$ and $y = (y_1, \dots, y_n$ over a distance space (S, d). The matrix $((DTW(i,j)))_{0 \le i \le m}^{0 \le j \le n}$ of *cumulative distances* is defined by $DTW(0,0) = 0$, all $DTW(0,i)$ and $DTW(i,0)$

are ∞, while

$$DTW(i,j) = d(x_i, y_j) + \min(DTW(i-1,j, DTW(i,j-1, DTW(i-1,j-1)),$$

for any $i,j \geq 1$, minimizing insertion, deletion, match, respectively. A *warping path* $W = (w_1, \ldots, w_k)$ is a contiguous set of matrix elements w_i that represent a mapping between x and y. The *optimal* path is the one minimizing the *warping cost*; this minimum $DTW(x,y) = \min \sqrt{\sum_{1 \leq i \leq k} w_k^2}$ is called the **DTW-distance**.

The time series can be seen as discretizations of differentiable functions of time. Optimal nonlinear time warping functions are computed by minimizing a measure of distance of the set of functions to their warped average. Related *elastic matching* is an optimization problem of 2D warping specifying corresponding pixels between subjected images; cf. **nonlinear elastic matching distance** between curves.

21.2 Audio Distances

Sound is the vibration of gas or air particles that causes pressure variations within our eardrums. *Audio* (speech, music, etc.) *Signal Processing* is the processing of analog (continuous) or, mainly, digital representation of the air pressure waveform of the sound. A *sound spectrogram* (or *sonogram*) is a visual $3D$ representation of acoustic signal. It is obtained either by a series of bandpass filters (an analog processing), or by application of the *short-time Fourier transform* to the electronic analog of an acoustic wave. Three axes represent time, frequency and *intensity* (acoustic energy). Often this $3D$ curve is reduced to two dimensions by indicating the intensity with more thick lines or more intense gray or color values.

Sound is called *tone* if it is periodic (the lowest *fundamental* frequency plus its multiples, *harmonics* or *overtones*) and *noise*, otherwise. The frequency is measured in *cps* (the number of complete cycles per second) or Hz (Hertz). The range of audible sound frequencies to humans is typically 20 Hz to 20 kHz. A moth *Galleria mellonella* can hear up to 300 kHz, in order to locate predatory bats using ultrasound.

The *power* $P(f)$ of a signal is energy per unit of time; it is proportional to the square of signal's amplitude $A(f)$. *Decibel dB* is the unit used to express the relative strength of two signals. One tenth of 1 dB is *bel*, the original outdated unit.

The amplitude of an audio signal in *dB* is $20 \log_{10} \frac{A(f)}{A(f')} = 10 \log_{10} \frac{P(f)}{P(f')}$, where f' is a reference signal selected to correspond to 0 dB (usually, the threshold of human hearing). The threshold of pain is about 120–140 dB.

Pitch and *loudness* are auditory subjective terms for frequency and amplitude.

The *mel scale* is a perceptual frequency scale, corresponding to the auditory sensation of tone height and based on *mel*, a unit of pitch. It is connected to

the acoustic frequency f hertz scale by $Mel(f) = 1127 \ln(1 + \frac{f}{700})$ or, simply, $Mel(f) = 1000 \log_2(1 + \frac{f}{1000})$.

The *Bark scale* (named after Barkhausen) is a psycho-acoustic scale of frequency: it ranges from 0 to 24 *Bark* corresponding to the first 24 critical bands of hearing:

$0, 100, 200, \ldots, 1270, 1480, 1720, \ldots, 9500, 12{,}000, 15{,}500$ Hz.

Those bands correspond to spatial regions of the basilar membrane (of the inner ear), where oscillations, produced by the sound of given frequency, activate the hair cells and neurons. Our ears are most sensitive in 2000–5000 Hz. The Bark scale is connected to the acoustic frequency f kilohertz scale by $Bark(f) = 13 \arctan(0.76f) + 3.5 \arctan(\frac{f}{0.75})^2$.

Terrestrial vertebrates perceive frequency on a logarithmic scale, i.e., pitch perception is better described by frequency ratios than by differences on a linear scale. It is matched by the distribution of cells sensitive to different frequencies in their ears.

Power spectral density $PSD(f)$ of a wave is the power per Hz. It is the Fourier transform of the autocorrelation sequence. So, the power of the signal in the band $(-W, W)$ is given by $\int_{-W}^{W} PSD(f)df$. A *power law noise* has $PSD(f) \sim f^{\alpha}$. The noise is called *violet*, *blue*, *white*, *pink* (or $\frac{1}{f}$), *red* (or *brown(ian)*), *black* (or *silent*) if $\alpha = 2, 1, 0, -1, -2, < -2$. PSD changes by 3α dB per *octave* (i.e., with frequency doubling); it decreases for $\alpha < 0$.

Pink noise occurs in many physical, biological and economic systems; cf. **long range dependence** in Chap. 18. It has equal power in proportionally wide frequency ranges. Humans also process frequencies in a such logarithmic space (approximated by the Bark scale). So, every octave contains the same amount of energy. Thus pink noise is used as a reference signal in Audio Engineering. Steady pink noise (including light music) reduces brain wave complexity and improve sleep quality.

Intensity of speech signal goes up/down within a 3–8 Hz frequency which resonates with the theta rhythm of neocortex. The speakers produce 3–8 syllables per second.

The main way that humans control their *phonation* (speech, song, laughter) is by control over the *vocal tract* (the throat and mouth) shape. This shape, i.e., the cross-sectional profile of the tube from the closure in the *glottis* (the space between the vocal cords) to the opening (lips), is represented by the cross-sectional area function $Area(x)$, where x is the distance to the glottis. The vocal tract acts as a resonator during vowel phonation, because it is kept relatively open. These resonances reinforce the source sound (ongoing flow of lung air) at particular *resonant frequencies* (or *formants*) of the vocal tract, producing peaks in the *spectrum* of the sound.

Each vowel has two characteristic formants, depending on the vertical and horizontal position of the tongue in the mouth. The source sound function is modified by the frequency response function for a given area function. If the vocal tract is approximated as a sequence of concatenated tubes of constant cross-sectional

area, then the *area ratio coefficients* are the ratios $\frac{Area(x_{i+1})}{Area(x_i)}$ for consecutive tubes; those coefficients can be computed by *LPC* (linear predictive coding).

The *spectrum* of a sound is the distribution of magnitude (dB) (and sometimes the phases) in frequency (kHz) of the components of the wave. The *spectral envelope* is a smooth contour that connects the spectral peaks. Its estimation is based on either LPC, or FFT (fast Fourier transform) using *real cepstrum*, i.e., the log amplitude spectrum.

FT (Fourier transform) maps time-domain functions into frequency-domain representations. The *complex cepstrum* of the signal $f(t)$ is $FT(\ln(FT(f(t) + 2\pi mi)))$, where m is the integer needed to unwrap the angle or imaginary part of the complex logarithm function. The FFT performs the Fourier transform on the signal and samples the discrete transform output at the desired frequencies usually in the *mel* scale.

Parameter-based distances used in recognition and processing of speech data are usually derived by LPC, modeling the speech spectrum as a linear combination of the previous samples (as in autoregressive processes). Roughly, LPC processes each word of the speech signal in the following 6 steps: filtering, energy normalization, partition into frames, *windowing* (to minimize discontinuities at the borders of frames), obtaining LPC parameters by the autocorrelation method and conversion to the *LPC-derived cepstral coefficients*. LPC assumes that speech is produced by a buzzer at the glottis (with occasionally added hissing and popping sounds), and it removes the formants by filtering.

The majority of distortion measures between sonograms are variations of **squared Euclidean distance** (including a covariance-weighted one, i.e., **Mahalanobis**, distance) and probabilistic distances belonging to following general types: generalized **variational distance**, **f-divergence** and **Chernoff distance**; cf. Chap. 14.

The distances for sound processing below are between vectors x and y representing two signals to compare. For recognition, they are a template reference and input signal, while for noise reduction they are the original (reference) and distorted signal (see, for example, [OASM03]). Often distances are calculated for small segments, between vectors representing short-time spectra, and then averaged.

- **SNR distance**

  Given a sound, let P and A_s denote its average power and RMS (root-mean-square) amplitude. The **signal-to-noise ratio in decibels** is defined by

$$SNR_{dB} = 10\log_{10}(\frac{P_{signal}}{P_{noise}}) = P_{signal,dB} - P_{noise,dB} = 10\log_{10}(\frac{A_{signal}}{A_{noise}})^2.$$

  The *dynamic range* is such ratio between the strongest undistorted and minimum discernable signals. It is roughly 140 dB for human hearing, 40 dB for human speech and 80 dB for a music in a concert hall.

The *Shannon–Hartley theorem* express the *capacity* (maximal possible information rate) of a channel with additive *colored* (frequency-dependent) Gaussian noise, on the bandwidth B in Hz as $\int_0^B \log_2(1 + \frac{P_{signal}(f)}{P_{noise}(f)})df$.

The **SNR distance** between signals $x = (x_i)$ and $y = (y_i)$ with n frames is

$$10 \log_{10} \frac{\sum_{i=1}^{n} x_i^2}{\sum_{i=1}^{n} (x_i - y_i)^2}.$$

If M is the number of segments, the *segmented SNR* between x and y is defined by

$$\frac{10}{m} \sum_{m=0}^{M-1} \left(\log_{10} \sum_{i=nm+1}^{nm+n} \frac{x_i^2}{(x_i - y_i)^2} \right).$$

- **Spectral magnitude-phase distortion**

  The **spectral magnitude-phase distortion** between signals $x = x(\omega)$ and $y = y(\omega)$ is defined by

$$\frac{1}{n} \left(\lambda \sum_{i=1}^{n} (|x(w)| - |y(w)|)^2 + (1 - \lambda) \sum_{i=1}^{n} (\angle x(w) - \angle y(w))^2 \right),$$

  where $|x(w)|$, $|y(w)|$ are magnitude spectra, and $\angle x(w)$, $\angle y(w)$ are phase spectra of x and y, respectively, while the parameter $\lambda, 0 \leq \lambda \leq 1$, is chosen in order to attach commensurate weights to the magnitude and phase terms. The case $\lambda = 0$ corresponds to the **spectral phase distance**.

  Given a signal $f(t) = ae^{-bt}u(t), a, b > 0$ which has Fourier transform $x(w) = \frac{a}{b+iw}$, its *magnitude* (or *amplitude*) spectrum is $|x| = \frac{a}{\sqrt{b^2+w^2}}$, and its *phase* spectrum (in radians) is $\alpha(x) = \tan^{-1} \frac{w}{b}$, i.e., $x(w) = |x|e^{i\alpha} = |x|(\cos\alpha + i \sin\alpha)$.

  The **Fourier distance** and *Fourier phase distance* are $||FFT(x) - FFT(y)||_2$ and $||arg(FFT(x)) - arg(FFT(y))||_2$, where the sums only contain the lower frequency terms of fast Fourier transform in order to reduce noise. The similar *wavelet distance* is based on the *discrete wavelet transform* separating low and high frequencies.

- **Spectral distances**

  Given two discrete spectra $x = (x_i)$ and $y = (y_i)$ with n channel filters, their **Euclidean metric** *EM*, **slope metric** *SM* (Klatt, 1982) and **2-nd differential metric** 2*DM* (Assmann and Summerfield, 1989) are defined, respectively, by

$$\sqrt{\sum_{i=1}^{n} (x_i - y_i)^2}, \sqrt{\sum_{i=1}^{n} (x_i' - y_i')^2} \text{ and } \sqrt{\sum_{i=1}^{n} (x_i'' - y_i'')^2},$$

  where $z_i' = z_{i+1} - z_i$ and $z_i'' = \max(2z_i - z_{i+1} - z_{i-1}, 0)$. Comparing, say, the auditory excitation patterns of vowels, *EM* gives equal weight to peaks and

troughs although spectral peaks have more perceptual weight. *SM* emphasizes the formant frequencies, while 2*DM* sets to zero the spectral properties other than the formants.

The **RMS log spectral distance** (or *root-mean-square distance*, *quadratic mean distance*) $LSD(x, y)$ is defined by

$$\sqrt{\frac{1}{n}\sum_{i=1}^{n}(\ln x_i - \ln y_i)^2}.$$

The corresponding l_1- and l_∞-distances are called *mean absolute distance* and *maximum deviation*. These three distances are related to decibel variations in the log spectral domain by the multiple $\frac{10}{\log 10}$. In fact, the *log spectral distance between power spectra* $x(\omega)$ and $y(\omega)$ is defined as (expressed in dB):

$$\sqrt{\frac{1}{2\pi}\int_{-\pi}^{\pi}(10\log_{10}\frac{x(\omega)}{y(\omega)})^2 d\omega}.$$

The square of $LSD(x, y)$, via the cepstrum representation $\ln x(\omega) = \sum_{j=-\infty}^{\infty} c_j e^{-j\omega i}$ (where $x(\omega)$ is the *power cepstrum* $|FT(\ln(|FT(f(t))|^2)|^2)$ becomes, in the complex cepstral space, the **cepstral distance**.

The **log area ratio distance** $LAR(x, y)$ between x and y is defined by

$$\sqrt{\frac{1}{n}\sum_{i=1}^{n}10(\log_{10} Area(x_i) - \log_{10} Area(y_i))^2},$$

where $Area(z_i)$ is the cross-sectional area of the i-th segment of the vocal tract.

- **Bark spectral distance**

  Let (x_i) and (y_i) be the *Bark spectra* of x and y, where the i-th component corresponds to the i-th auditory critical band in the Bark scale. The **Bark spectral distance** (Wang–Sekey–Gersho, 1992) is a perceptual distance, defined by

$$BSD(x, y) = \sum_{i=1}^{n}(x_i - y_i)^2,$$

  i.e., it is the **squared Euclidean distance** between the Bark spectra.

  A modification of the Bark spectral distance excludes critical bands i on which the loudness distortion $|x_i - y_i|$ is less than the noise masking threshold.

- **Itakura–Saito quasi-distance**

  The **Itakura–Saito** (or *maximum likelihood*) **quasi-distance** between LPC-derived spectral envelopes $x = x(\omega)$ and $y = y(\omega)$ is defined (1968) by

$$IS(x, y) = \frac{1}{2\pi} \int_{-\pi}^{\pi} \left(\frac{x(w)}{y(w)} - \ln \frac{x(w)}{y(w)} - 1 \right) dw.$$

  The **cosh distance** is defined by $IS(x, y) + IS(y, x)$, i.e., is equal to

$$\frac{1}{2\pi} \int_{-\pi}^{\pi} \left(\frac{x(w)}{y(w)} + \frac{y(w)}{x(w)} - 2 \right) dw = \frac{1}{2\pi} \int_{-\pi}^{\pi} 2 \cosh \left(\ln \frac{x(w)}{y(w)} - 1 \right) dw,$$

  where $\cosh(t) = \frac{e^t + e^{-t}}{2}$ is the hyperbolic cosine function.
- **Log-likelihood ratio quasi-distance**

  The **log-likelihood ratio quasi-distance** between LPC-derived spectral envelopes $x = x(\omega), y = y(\omega)$ is defined (cf. **Kullback–Leibler distance** in Chap. 14) by

$$\frac{1}{2\pi} \int_{-\pi}^{\pi} x(w) \ln \frac{x(w)}{y(w)} dw.$$

  The **weighted likelihood ratio distance** between $x(\omega)$ and $y(\omega)$ is defined by

$$\frac{1}{2\pi} \int_{-\pi}^{\pi} \left(\frac{\left(\ln \left(\frac{x(w)}{y(w)} \right) + \frac{y(w)}{x(w)} - 1 \right) x(w)}{p_x} + \frac{\left(\ln \left(\frac{y(w)}{x(w)} \right) + \frac{x(w)}{y(w)} - 1 \right) y(w)}{p_y} \right) dw,$$

  where $P(x)$ and $P(y)$ denote the power of the spectra $x(w)$ and $y(w)$.
- **Cepstral distance**

  The **cepstral distance** (or *squared Euclidean cepstrum metric*) $CEP(x, y)$ between the LPC-derived spectral envelopes $x = x(\omega)$ and $y = y(\omega)$ is defined by

$$\frac{1}{2\pi} \int_{-\pi}^{\pi} \left(\ln \frac{x(w)}{y(w)} \right)^2 dw = \frac{1}{2\pi} \int_{-\pi}^{\pi} (\ln x(w) - \ln y(w))^2 dw = \sum_{j=-\infty}^{\infty} (c_j(x) - c_j(y))^2,$$

  where $c_j(z) = \frac{1}{2\pi} \int_{-\pi}^{\pi} e^{jwi} \ln |z(w)| dw$ is j-th cepstral (real) coefficient of z derived from the Fourier transform or LPC.

  The **quefrency-weighted cepstral distance** (or **Yegnanarayana distance**, *weighted slope distance*) between x and y is defined by

$$\sum_{i=-\infty}^{\infty} i^2 (c_i(x) - c_i(y))^2.$$

"Quefrency" and "cepstrum" are anagrams of "frequency" and "spectrum".

The **Martin cepstrum distance** between two ARMs (autoregressive models) is defined, in terms of their cepstra, by

$$\sqrt{\sum_{i=0}^{\infty} i(c_i(x) - c_i(y))^2}.$$

Cf. general **Martin distance** in Chap. 12 and **Martin metric** in Chap. 11.

- **Distances in Musicology**

Pitch is a subjective correlate of the fundamental frequency. A *note* (or *tone*) is a named pitch. Pitch, seen as extending along a 1D continuum from high to low, is called *pitch height*. But it also varies circularly: a *pitch class* is a set of all pitches that are a whole number of *octaves* (intervals between a frequency and its double) apart. About 10 octaves cover the range of human hearing. In Western music, the most used octave division is the *chromatic scale*: 12 notes $C, C\#, D, D\#, E, F, F\#, G, G\#, A, A\#, B$ drawn usually as *pitch class space*: a circle of *equal temperament*, i.e., divided into 12 equal *semitones* (or *half steps*). The **distance between notes** whose frequencies are f_1, f_2 is $12\log_2(\frac{f_1}{f_2})$ semitones.

An *interval* is the difference between two pitches. Its *width* is the ratio $\frac{a}{b}$ (with g.c.d$(a, b) = 1$) between their frequencies. The *Benedetti height* of this ratio is ab; *Tenney height* (or **Tenney harmonic distance**) is $\log_2 ab$ and *Kees height* is $\max(a', b')$, where a', b' come from a, b by removing factors of 2. The width of a semitone is $\sqrt[12]{2}$ or 100 cents. The width of octave is 2 or 1200 cents.

A **pitch distance** (or *melodic distance*) is the size of the section of the pitch-continuum bounded by those two pitches, such as modeled in a given scale. A MIDI (Musical Instrument Digital Interface) number of fundamental frequency f is defined by $p(f) = 69 + 12\log_2 \frac{f}{440}$. The distance between notes, in terms of this *linear pitch space*, becomes the **natural metric** $|p(f_1) - p(f_2)|$ on $\mathbb{R}$. This pitch distance corresponds to physical distance on keyboard instruments, and psychological distance as measured by experiments and musicians.

Using integer notation $0, 1, \ldots, 11$ of pitches, a *pitch interval* $PI(x, y)$ between the pitches x and y is the number of semitones $|x-y|$ that separates them linearly, while a *pitch-interval class* $PIC(x, y)$ is $|x - y| \mod 12$ and an *interval class* $ic(x, y)$ is their **Lee distance** $\min |x - y|, 12 - |x - y|$ on the circle.

In integer notation, the *circle of fifths* is $\{7i \mod 12\}_{0,\ldots,11}$, and its reversal, the *circle of fourths*, is $\{5i \mod 12\}_{0,\ldots,11}$. Neighboring pitches are separated by a *perfect fifth* (interval of 5 staff positions or 7 semitones).

7 letters of a musical alphabet, C–D–E–F–G–A–B, are called the *natural tones*; they are the names of the white keys on a piano/keyboard, forming an octave. Above sequence and any of its translations is a *major diatonic scale*. A *diatonic scale* is a scale of 7 notes most used in Western music. Its structure is 1–1–0.5–1–1–1–0.5, in terms of interval succession of steps. A **distance model** (in Music) is the alternation of two different intervals to create a nondiatonic musical

mode/scale, such as the 1:3 distance model (alternation of semitones and minor thirds).

In tonal music, composition written in home key; it *modulates* (move to other keys) and usually returns. The distance between keys approximates the ease of modulation. Every key is associated with a scale of pitches, usually, major or *minor* diatonic. The **interkey distance** of two keys is 7 minus the number of tones shared by their scales. It is also their distance around the circle of fifths, i.e., the difference in the number of *sharps* (or *flats*) in their signatures. The *relative* (having the same signatures) major and minor key share all 7 notes.

A *chord* in music is any set of at least 3 pitch classes in the same octave that is heard as if sounding simultaneously. Music can be seen as a sequence of chords. *Interval vector* of a given chord c is $V(c) = (c_1, \ldots, c_6)$, where c_i is the number of times i-th interval class (having i or $12 - i$ semitones) appears in it. **Intervalic distance** and **Estrada distance** between chord c and c' are (Mathieu, 2002):

$$\sum_{i=1}^{6} |c_i - c'_i| \text{ and } \max |c|, |c'| - |V(c) \cap V(c')| - 1.$$

The **root distance** is the number of fifths between the *roots* (pitches upon which a chord may be built, often by stacking thirds) of the chords. In [RRHD10], a survey of 8 **distances between chords** is given: above 3 and those by Chew (2000), Costère (1962), Lerdahl (2001), Paiement et al. (2005) and Yoo et al. (2006).

Alternatively to equal-temperement, *just intonation* is a tuning in which the frequencies of notes are related by ratios of small whole numbers, say, $\frac{3}{2}$ for perfect fifth (G) and $\frac{4}{3}$ for perfect forth (F). The pitches can be arranged in a $2D$ diagram. For an odd number $n > 0$, the *n-limit diagram* contains all rational numbers such that any odd divisor of the numerator or denominator is at most n. Such 5- and 7-limit can be seen as the *hexagonal lattice* $A_2 = \{(a, b, c) \in \mathbb{Z}^3 : a + b + c = 0\}$ and *face-centered cubic lattice* $A_3 = \{(a, b, c) \in \mathbb{Z}^3 : a + b + c \equiv 0(\mod 2)\}$, respectively, with vector space norms $\sqrt{a^2 + ab + b^2}$ and $\sqrt{a^2 + ab + b^2 + c(a + b + c)}$.

- **Distances between rhythms**

  A rhythm timeline (music pattern) is represented, besides the standard music notation, in the following ways, used in computational music analysis.

  1. By a binary vector $x = (x_1, \ldots, x_m)$ of m time intervals (equal in a metric timeline), where $x_i = 1$ denotes a beat, while $x_i = 0$ denotes a rest interval (silence). For example, the five $12/8$ metric timelines of Flamenco music are represented by five binary sequences of length 12.
  2. By a *pitch vector* $q = (q_1, \ldots, q_n)$ of absolute pitch values q_i and a *pitch difference vector* $p = (p_1, \ldots, p_{n-1})$ where $p_i = q_{i+1} - q_i$ represents the number of semitones (positive or negative) from q_i to q_{i+1}.

3. By an *interonset interval vector* $t = (t_1, \ldots, t_n)$ of n time intervals between consecutive onsets.
4. By a *chronotonic representation* which is a histogram visualizing t as a sequence of squares of sides $t_1, \ldots, t_n$; it can be seen as a piecewise linear function.
5. By a *rhythm difference vector* $r = (r_1, \ldots, r_{n-1})$, where $r_i = \frac{t_{i+1}}{t_i}$.

Examples of general **distances between rhythms** are the Hamming distance, **swap metric** (Chap. 11) and **Earth Mover's distance** between their given vector representations.

The **Euclidean interval vector distance** is the Euclidean distance between two interonset interval vectors. The Gustafson **chronotonic distance** is a variation of l_1-distance between these vectors using the chronotonic representation.

Coyle–Shmulevich **interval-ratio distance** is defined by

$$1 - n + \sum_{i=1}^{n-1} \frac{\max\{r_i, r_i'\}}{\min\{r_i, r_i'\}},$$

where r and r' are rhythm difference vectors of two rhythms (cf. the reciprocal of **Ruzicka similarity** in Chap. 17).

- **Long-distance drumming**

  Long-distance drumming (or *drum telegraphy*) is an early form of long-distance communication which was used by cultures in Africa, New Guinea and the tropical America living in deforested areas. A rhythm could represent an signal, repeat the profile of a spoken utterance or simply be subject to musical laws.

  The *message drums* (or *slit gongs*) were developed from hollow tree trunks. The sound could be understood at $\leq$ 8 km but usually it was relayed to a next village. Another oldest tools of audio telecommunication were *horns* (tapered sound guides providing an acoustic impedance match between a sound source and free air). Any mode of communication (as by means of drums or horns) for use beyond the range of the articulate voice, is called **distance language**.

  Soldier termites of some species drum their heads (11 times per second) on the ground to signal danger. The initial vibrations travel 40 cm, but a chain of soldiers relay the resulting wave, moving 1.3 m/s, over much greater distances.

- **Sonority distance effect**

  People in warm-climate cultures spend more time outdoors and engage, on average, in more distal oral communication. So, such populations have greater *sonority* (audibility) of their phoneme inventory. Munroe et al., 1996 and 2009, observed that speakers in such languages use more simple consonant-vowel syllables, vowels and *sonorant* (say, nasal "n", "m" rather than obstruents as "t", "g") consonants.

  Ember and Ember, 2007, found that number of cold months, as well as the combination of cold climate and sparse vegetation, predicts less sonority. Larger

average distance of the baby from its caregivers, as well as higher frequency of premarital and extramarital sex predicts more sonority.

- **Vocal deviation**

  Vocal deviation is (Podos, 2001) the distance of birdsong performance to the upper performance limit. Performance is measured by a variable combining frequency bandwidth and *note repetition rate* (the number of notes per second).

  The **vocal deviation** of a bird is the minimal **point-line distance** (Chap. 4) of data points of its recordings from the (upper-bound regression) line representing performance limit.

  Fitch et al., 2014, found in hermit thrush's songs the same intervals of pitch as the common major chords (octave, perfect fifth, perfect third) in human music.

- **Acoustics distances**

  The *wavelength* of a wave is the distance it travels to complete one cycle. This distance is measured perpendicular to the wavefront in the direction of propagation between one peak of a *sine wave* (sinusoid) and the next corresponding peak. The wavelength of any frequency sound may be found by dividing the speed of sound (331.4 m/s at sea level) in the medium by the fundamental frequency.

  The **near field** (cf. Chap. 24) is the part of a sound field (usually within about two wavelengths from the source) where there is no simple relationship between sound level and distance. The **far field** (cf. Chap. 24) is the area beyond the near field boundary. It is comprised of the *reverberant field* and *free field*, where sound intensity decreases as $\frac{1}{d^2}$ with the distance d from the source. This law corresponds to a reduction of $\approx$ 6 dB in the sound level for each doubling of distance and to halving of loudness (subjective response) for each reduction of $\approx$ 10 dB.

  The **critical distance** (or *room radius*) is the distance from the source at which the direct sound and reverberant sound (reflected echo produced by the direct sound bouncing off, say, walls, floor, etc.) are equal in amplitude.

  The **pickup distance** of a microphone is the effective distance that it can be used at. For an electric guitar, it is the distance from *pickup* (transducer that captures mechanical vibrations) to strings.

  A directional microphone may be placed farther away from a desired sound source than an omnidirectional one of equal quality; the ratio of distances is called the **distance factor**.

  The *proximity effect (audio)* is the anomaly of low frequencies being enhanced when a directional microphone is very close to the source.

  Auditory **distance cues** (Chap. 28) are based on differences in loudness, spectrum, direct-to-reverb ratio and binaural ones. The closer sound object is louder, has more bass, high-frequencies, transient detail, dynamic contrast. Also, it appear wider, has more direct sound level over its reflected sound and has greater time delay between the direct sound and its reflections.

  The *acoustic metric* is the term used occasionally for some distances between vowels; for example, the Euclidean distance between vectors of formant frequencies of pronounced and intended vowel. Cf. **acoustic metric** in Physics (Chap. 24).

Chapter 22
Distances in Networks

22.1 Scale-Free Networks

A **network** is a graph, directed or undirected, with a positive number (weight) assigned to each of its arcs or edges. Real-world complex networks usually have a gigantic number N of vertices and are sparse, i.e., with relatively few edges.

Interaction networks (Internet, Web, social networks, etc.) tend to be **small-world** ([Watt99]), i.e., interpolate between regular geometric lattices and random graphs in the following sense. They have a large *clustering coefficient* (the probability that two distinct neighbors of a vertex are neighbors), as lattices in a local neighborhood, while the average path distance between two vertices is small, about $\ln N$, as in a random graph.

A **scale-free network** ([Bara01]) ia a network with probability distribution for a vertex to have degree k being similar to $k^{-\gamma}$, for some constant $\gamma > 0$ which usually belongs to the segment $[2, 3]$. This *power law* implies that very few vertices, called *hubs* (connectors, gateways, super-spreaders), are far more connected than other vertices. The power law (or **long range dependent**, *heavy-tail*) distributions, in space or time, has been observed in many natural phenomena (both physical and sociological).

- **Collaboration distance**

  The **collaboration distance** is the path metric of the *Collaboration graph*, having authors in Mathematical Reviews database as vertices with xy being an edge if authors x and y have a joint publication among the papers from this database.

  The vertex of largest degree (1416) corresponds to Paul Erdős; the *Erdős number* of a mathematician is his collaboration distance to Paul Erdős. An example of a 3-path: Michel Deza–Paul Erdős–Ernst Gabor Straus–Albert Einstein.

© Springer-Verlag Berlin Heidelberg 2016

M.M. Deza, E. Deza, *Encyclopedia of Distances*,
DOI 10.1007/978-3-662-52844-0_22

- **Co-starring distance**

  The **co-starring distance** is the path metric of the *Hollywood graph*, having about 250,000 vertices (actors in the Internet Movie database) with xy being an edge if the actors x and y appeared in a feature film together. The vertices of largest degree are Christopher Lee and Kevin Bacon; the trivia game *Six degrees of Kevin Bacon* uses the *Bacon number*, i.e., the co-starring distance to this actor.

  The *Morphy* and *Shusaku numbers* are the similar measures of a chess or Go player's connection to Paul Morphy and Honinbo Shusaku by way of playing games. *Kasparov number* of a chess-player is the length of a shortest directed path, if any, from him/her to Garry Kasparov; here arc uv means victory of u over v.

  Similar popular examples of such social scale-free networks are graphs of musicians (who played in the same rock band), baseball players (as team-mates), scientific publications (who cite each other), mail exchanges, acquaintances among classmates in a college, business board membership.

  Among other such studied networks are air travel connections, word co-occurrences in human language, US power grid, sensor networks, worm neuronal network, gene co-expression networks, protein interaction networks and metabolic networks (with two substrates forming an edge if a reaction occurs between them via enzymes).

- **WikiDistance**

  In 2015, Wikipedia had about 38 million articles in 281 languages and 74,000 active editors. English Wikipedia alone had 5 million articles (4 % of estimated number of notable articles needed to cover all human knowledge) and 814 billion of edits.

  The **WikiDistance** is the directed path quasi-metric of the *Wikipedia digraph*, having English Wikipedia articles as vertices, with xy being an arc if the article x contains an hyperlink to the article y; cf. http://software.tanos.co.uk/wikidistance and the **Web hyperlink quasi-metric**.

  Gabrilovich–Markovich, 2007, proposed to measure semantic relatedness of two texts by the **cosine distance** (cf. **Web similarity metrics**) between weighted vectors, interpreting texts in terms of affinity with a host of Wikipedia concepts.

  Crandall et al., 2008, considered the social network of Wikipedia editors: two editors are assumed to be connected if one of them posted to the other's discussion page. Brandes et al., 2009, considered the *edit network* of a Wikipedia page, where nodes are the authors of this page and edges correspond to undoing each other edits.

  The *editing depth* of Wikipedia is an indicator of its collaborativeness defined as $D = \frac{e}{a+n} \times (\frac{n}{a})^2$, where e, a, n are the numbers of page edits, articles and *nonarticles* (redirects, talk, user pages). At February 2016, English Wikipedia had $D = 916$.

- **Virtual community distance**

  Largest, in millions of active user accounts, *virtual communities* (online social networking services) are, as of December 2014, *Facebook* (1590), *WhatsApp* (1000), *Tencent QQ* (860), *Facebook Messenger* (800), *Tencent Ozone* (653),

WeChat (650), *Google+* (540), *Istagram* (400), *Twitter* (305), *Skype* (300), all of origin in the US or China. 3.3 billion has used the services of the Internet within 2015.

In 2012, about 30 billion documents were uploaded on Facebook, 300 million tweets sent on Twitter and 24 petabytes of data processed by Google *per day*, while mankind published only ≈5000 petabytes for the 20,000 years before 2003.

A **virtual community distance** is the path metric of the graph of active users, two of them forming an edge if they are "friends". In Twitter it means that both "follow" each other. In particular, for the **Facebook hop distance** in November 2011, 99.6 % of all pairs of users were connected by paths of length at most 5. The mean distance was 4.74, down from 5.28 in 2008.

The **Twitter friendship distance** in Avril 2010 was $4, 5, 6$ among 37 %, 41 %, 13 % of 5.2 billion friendships. The average distance was 4.67 steps. Cf. mean distance 5.2 in Milgram's (1967) theory of *six degrees of separation* on a planetary scale.

An example of application: analysing linguistically emotional content of tweets and comments, one can obtain an interaction graph of the targeted region mood.

- **Distance effect in large e-mail networks**

  Takhteyev–Gruzd–Wellman, 2012, considered a sample representing Twitter *tie* (i.e., "follow" relation in both directions) network. They found that distance constrains ties, despite the seeming ease with which they can be formed: 39 % of the ties are shorter than 100 km (within the same regional cluster), ties up to 1000 km are more frequent than random ones, and ties longer than 5000 km are rare. Cf. **distance decay** in Chap. 28. But the nonlocal ties are predicted better by the frequency of airline connections than by physical proximity.

  State et al., 2013, started with a graph of a sample about 10 million users of Yahoo! email with an edge between two users whenever they exchanged at least one email message in both directions, during the observation period in 2012. A weighted complete graph of 141 countries was derived, with edge-weight being the rescaled logarithm of the communication density between countries. For each doubling of distance (between each country centroids) and doubling of the number of direct flights, the density decreased by 66 % and increased by 33 %, respectively.

  But the main (besides colonial link and common language) cultural factor, nearly doubling the density, happens to be the common membership in the same civilization from the list produced by Huntigton in a 1993 article *The Clash of Civilizations*: Latin American, Islamic, Orthodox, Sinic, Buddist, Western, African, Hindu, Japonic. For Latin American, Islamic, and Orthodox civilization, this factor increases the density by the factor of 5.4, 3.1 and 2.4, respectively.

- **Network's hidden metric**

  Many social, biologic, and communication networks, including the Internet and Web, are scale-free and *strongly clustered* (many triangular subgraphs).

Greedy routing is a navigation strategy to do always the locally optimal step with the hope of finding a globally shortest path. Krioukov et al., 2009, found that successful greedy paths are shortest, mostly and asymptotically, in the large complex networks.

They explain such efficiency by the existence of a **hidden metric space** (V, d) on the set V of nodes, so that a node passes information to the neighbor that is closest in (V, d) to the final destination. Moreover, they suggest that (V, d) is **hyperbolic**, because the nodes are *heterogeneous* (can be classified into groups, subgroups, and so on) implying a tree-like structure of such network.

- **Sexual distance**

  Given a group of people, its *sexual network* is the graph of members two of them forming an edge if they had a sexual contact. The **sexual distance** is the path metric of a sexual network. Such networks of heterosexual individuals are usually scale-free but not small-world since they have no 3-cycles and very few 4-cycles.

  Several sexual networks were mapped in order to trace the spread of sexually infectious diseases. The sexual network of all adults aged 18–35 in Licoma (almost isolated island 18 km^2 on lake Malawi) have a giant connected component containing half of nonisolated vertices, and more than one quarter were connected *robustly*, i.e., by multiple disjoint paths. Also, in the sexual network of students of an Midwestern US high school, 52 % of nonisolated vertices belong to a giant connected component. But this graph contains very few cycles and have large diameter (37).

  A study of persons at risk for HIV (Colorado Springs, 1988–1992) compared their sexual and geographical distance, measured as the actual distance between their residences. The closest (at mean 2.9 km) pairs were HIV-positive persons and their contacts. The most distant (at mean 6.1 km) pairs were prostitutes and their paying partners. The mean distance between all persons in Colorado Springs was 12.4 km compared with 5.4 km between all dyads the study.

  Moslonka-Lefebre et al., 2012, consider weighted sexual networks, where the weight of an edge is the number of sex acts that are actually realized between two individuals per, say, a week. Such model is more consistent with epidemiological data.

  The sexual network for the human race have a giant connected component containing many vertices of degree 1 and almost all vertices of larger degree.

  A dating application Tinder, linked to Facebook, has an estimated 50 million users since 2012; it generates 15 million mutual matches a day.

- **Subway network core**

  Roth et al., 2012, observed that the world's largest subway networks converge to a similar shape: a core (ring-shaped set of central stations) with quasi-1D/linear branches radiating from it. The average degree of core stations is 2.5; among them $\approx 20\,\%$ are transfer stations and $> 60\,\%$ have degree 2.

  The average *radial* (from the geographical centroid of all stations) distance (in km) to branched stations is about double of such distance to core stations,

while the number of branches scales roughly as the square root of the number of stations.

Cf. **Moscow metric**, **Paris metric**, and **subway semimetric** in Chap. 19.

- **Normalized web distance**

  The **normalized web distance** (or *normalized Google distance*, as it was derived by Cilibrasi and Vitanyi, 2007, from [BGLVZ98]) is a semantic distance, not a metric, between search terms induced by a large data base (say, the Internet) and a search engine (say, Google). It is applicable to any data-base search engine pair. This distance between two search terms x and y is defined by

$$NWD(x,y) = \frac{\max\{\log f(x), \log f(y)\} - \log f(x,y)}{\log N - \min\{\log f(x), \log f(y)\}},$$

  where $f(x)$ is the number of pages containing x, the frequency $f(x,y)$ is the number of pages containing both x and y, and N is the total number of indexed pages.

  Cf. **normalized information distance** in Chap. 11.

- **Drift distance**

  The **drift distance** is the absolute value of the difference between observed and actual coordinates of a node in a NVE (Networked Virtual Environment).

  In models of such large-scale peer-to-peer NVE (for example, Massively Multiplayer Online Games), the users are represented as coordinate points on the plane (*nodes*) which can move at discrete *time-steps*, and each has a visibility range called the *Area of Interest*. NVE creates a synthetic $3D$ world where each user assumes *avatar* (a virtual identity) to interact with other users or computer AI.

  The primary metric tool in MMOG and Virtual Worlds is the proximity sensor recording when an avatar is within its specified range.

  The term **drift distance** is also used for the current going through a material, in tire production, etc.

- **Betweenness centrality**

  For a **geodesic** metric space (X,d) (in particular, for the path metric of a graph), the **stress centrality** of a point $x \in X$ is defined (Shimbel, 1953) by

$$\sum_{y,z \in X,\, y \neq x \neq z} \text{Number of shortest } (y-z) \text{ paths through } x,$$

  the **betweenness centrality** of a point $x \in X$ is defined (Freeman, 1977) by

$$g(x) = \sum_{y,z \in X,\, y \neq x \neq z} \frac{\text{Number of shortest } (y-z) \text{ paths through } x}{\text{Number of shortest } (y-z) \text{ paths}},$$

and the **distance-mass function** is a function $M : \mathbb{R}_{\geq 0} \to \mathbb{Q}$ defined by

$$M(a) = \frac{|\{y \in X : d(x,y) + d(y,z) = a \text{ for some } x, y \in X\}|}{|\{(x,z) \in X \times X : d(x,z) = a\}|}.$$

[GOJKK02] estimated that $\frac{M(a)}{a} \approx 4.5$ for the **Internet AS metric**, and ≈ 1 for the **Web hyperlink quasi-metric** for which the shortest paths are almost unique.

- **Distance centrality**

  Given a finite metric space (X, d) (usually, the **path metric** on the graph of a network) and a point $x \in X$, we give here examples of metric functionals used to measure **distance centrality**, i.e., the amount of centrality of the point x in X expressed in terms of its distances $d(x, y)$ to other points.

  1. The **eccentricity** (or *Koenig number*) $\max_{y \in X} d(x, y)$ was given in Chap. 1; Hage-Harary, 1995, considered $\frac{1}{\max_{y \in X} d(x,y)}$.
  2. The **closeness** (Sabidussi, 1966) is the inverse $\frac{1}{\sum_{y \in X} d(x,y)}$ of the *farness*.
  3. Dangalchev, 2006, introduced $\sum_{y \in X, y \neq x} 2^{-d(x,y)}$ which allows the case $d(x, y) = \infty$ (disconnected graphs).
  4. The functions $f_1 = \sum_{y \in X} d(x, y)$ and $f_2 = \sum_{y \in X} d^2(x, y)$; cf. **Fréchet mean** in Chap. 1.

  In *Location Theory* applications, $X' \subset X$ is a set of positions of "clients" and one seeks points $x \in X$ of acceptable facility positions. The appropriate objective function is, say, $\min \max_{y \in X'} d(x, y)$ to locate an emergency service, $\min \sum_{y \in X'} d(x, y)$ for a goods delivering facility and $\max \sum_{y \in X'} d(x, y)$ for a hazardous facility.

22.2 Network-Based Semantic Distances

Among the main lexical networks (such as WordNet, Framenet, Medical Search Headings, Roget's Thesaurus) a semantic lexicon WordNet is the most popular lexical resource used in Natural Language Processing and Computational Linguistics.

WordNet (see http://wordnet.princeton.edu) is an online lexical database in which English nouns, verbs, adjectives and adverbs are organized into *synsets* (synonym sets), each representing one underlying lexical concept.

Two synsets can be linked semantically by one of the following links: upwards x (*hyponym*) *IS-A* y (*hypernym*) link, downwards x (*meronym*) *CONTAINS* y (*holonym*) link, or a horizontal link expressing frequent co-occurrence (*antonymy*), etc. *IS-A* links induce a partial order, called *IS-A taxonomy*. The version 2.0 of WordNet has 80,000 noun concepts and 13,500 verb concepts, organized into 9 and 554 separate *IS-A* hierarchies.

In the resulting DAG (*directed acyclic graph*) of concepts, for any two synsets (or concepts) x and y, let $l(x, y)$ denote the length of the shortest path between

them, using only *IS-A* links, and let $LPS(x, y)$ denote their *least common subsumer* (ancestor) by *IS-A* taxonomy. Let $d(x)$ denote the *depth* of x (i.e., its distance from the root in *IS-A* taxonomy) and let $D = \max_x d(x)$.

The semantic relatedness of two nouns can be estimated by their **ancestral path distance** (cf. Chaps. 10 and 23), i.e., the length of the shortest *ancestral path* (concatenation of two directed paths from a common ancestor) to them). A list of the other main semantic similarities and distances follows. See also [HRJM13].

- **Length similarities**
  The **path similarity** and **Leacock–Chodorow similarity** between synsets x and y are defined by

$$path(x, y) = (l(x, y))^{-1} \text{ and } lch(x, y) = -\ln \frac{l(x, y)}{2D}.$$

  The **conceptual distance** between x and y is defined by $\frac{l(x,y)}{D}$.
- **Wu–Palmer similarity**
  The **Wu–Palmer similarity** between synsets x and y is defined by

$$wup(x, y) = \frac{2d(LPS(x, y))}{d(x) + d(y)}.$$

- **Resnik similarity**
  The **Resnik similarity** between synsets x and y is defined by

$$res(x, y) = -\ln p(LPS(x, y)),$$

  where $p(z)$ is the probability of encountering an instance of concept z in a large corpus, and $-\ln p(z)$ is called the *information content* of z.
- **Lin similarity**
  The **Lin similarity** between synsets x and y is defined by

$$lin(x, y) = \frac{2 \ln p(LPS(x, y))}{\ln p(x) + \ln p(y)}.$$

- **Jiang–Conrath distance**
  The **Jiang–Conrath distance** between synsets x and y is defined by

$$jcn(x, y) = 2 \ln p(LPS(x, y)) - (\ln p(x) + \ln p(y)).$$

- **Lesk similarities**
  A *gloss* of a synonym set z is the member of this set giving a definition or explanation of an underlying concept. The **Lesk similarities** are those defined by a function of the overlap of glosses of corresponding concepts; for example,

the **gloss overlap** is

$$\frac{2t(x,y)}{t(x)+t(y)},$$

where $t(z)$ is the number of words in the synset z, and $t(x,y)$ is the number of common words in x and y.

- **Hirst–St-Onge similarity**

  The **Hirst–St-Onge similarity** between synsets x and y is defined by

$$hso(x,y) = C - L(x,y) - ck,$$

  where $L(x,y)$ is the length of a shortest path between x and y using all links, k is the number of changes of direction in that path, and C, c are constants.

  The **Hirst–St-Onge distance** is defined by $\frac{L(x,y)}{k}$.

- **Semantic biomedical distances**

  The **semantic biomedical distances** are the distances used in biomedical lexical networks. The main clinical terminologies are UMLS (United Medical Language System) and SNOMED (Systematized Nomenclature of Medicine) CT.

  An example of such distances used in SNOMED and presented in Melton et al., 2006, is given by the *interpatient distance* between two *medical cases* (sets X and Y of patient data). It is their **Tanimoto distance** (Chap. 1) $\frac{|X \triangle Y|}{|X \cup Y|}$.

  The *conceptual distance* between two biomedical concepts in UMLS is (Caviedes and Cimino, 2004) the minimum number of *IS-A* parent links between them in the directed acyclic graph of *IS-A* taxonomy of concepts.

- **Semantic proximity**

  For the words in a document, there are short range syntactic relations and long range *semantic correlations*, i.e., meaning correlations between concepts.

  The main document networks are Web and bibliographic databases (digital libraries, scientific databases, etc.); the documents in them are related by, respectively, hyperlinks and citation or collaboration.

  Also, some semantic tags (keywords) can be attached to the documents in order to index (classify) them: terms selected by author, title words, journal titles, etc.

  The **semantic proximity** between two keywords x and y is their **Tanimoto similarity** $\frac{|X \cap Y|}{|X \cup Y|}$, where X and Y are the sets of documents indexed by x and y, respectively. Their **keyword distance** is defined by $\frac{|X \triangle Y|}{|X \cap Y|}$; it is not a metric.

- **Dictionary digraph**

  Dictionary digraph (V, E) have the words of a given dictionary as vertices, and arcs $uv \in E$ whenever word u is used to define word v. The *kernel* (V', E') is its subdigraph induced by the vertices with out-degree $\neq 0$. MF (*minimum feedback vertex set*) is a smallest set of vertices, from which any $v \in V$ can be reached.

Picard et al., 2013, found that $|V| \approx 10|V'| \approx 20|MF| \approx 20|V''|$ in such digraphs for four English dictionaries; here (V'', E'') is the *core* (largest strongly connected component) of the kernel. They observed that the words in the kernel V' are learned at a much younger age, and are more concrete, imageable and frequent than the words in $V \setminus V'$. The same is true, but more so, comparing V'' with $V \setminus V''$ and any MF with $V \setminus MF$. Cf. **Swadesh similarity** (Chap. 28).

- **SimRank similarity**

  Let D be a directed multigraph representing a cross-referred document corpus (say, a set of citation-related scientific papers, hyperlink-related web pages, etc.) and $I(v)$ be the set of in-neighbors of a vertex v.

  SimRank similarity $s(x, y)$ between vertices x and y of D is defined (Jeh and Widom, 2002) as 1 if $x = y$, 0 if $|I(x)||I(y)| = 0$ and, otherwise, as

$$\frac{C}{|I(x)||I(y)|} \sum_{a \in I(x), b \in I(y)} s(a, b),$$

  where C is a constant, $0 < C < 1$ (usually, $C = 0.8$ or 0.6 is used).

- ***D*-separation in Bayesian network**

  A *Bayesian network* is a DAG (digraph with no directed cycles) (V, E) whose vertices represent random variables and arcs represent conditional dependencies; so, the likelihood of each vertex can be calculated from the likelihood of its ancestors. Bayesian networks, including *causal networks*, are used for modeling knowledge.

  A vertex $v \in V$ is called a *collider* of a *trail* (undirected path) t if there are two consecutive arcs $uv, vu' \in E$ on t. A trail t is *active by* a set $Z \subset V$ of vertices if every its collider is or has a descendent in Z, while every other vertex along t is outside of Z. If $X, Y, Z \subset V$ are disjoint sets of vertices, then Z is said (Pearl, 1988) to ***d*-separate** X from Y if there is no active trail by Z between a vertex in X and a vertex in Y. Such d-separation means that the variable sets, represented by X and Y, are independent conditional on variables, represented by Z, in all probability distributions the DAG (V, E) can represent.

  The minimal set which d-separates vertex v from all other vertices is v's *Markov blanket*; it consists of v's parents, its children, and its children's parents. A *moral graph* of the DAG (V, E), used to find its equivalent undirect form, is the graph (V, E'), where E' consists all arcs from E made undirected plus all missing *marriages* (edges between vertices having a common child).

  Cf. the **Bayesian graph edit distance** in Chap. 15.

- **Forward quasi-distance**

  In a directed network, where edge-weights correspond to a point in time, the **forward quasi-distance** (**backward quasi-distance**) is the length of the shortest directed path, but only among paths on which consecutive edge-weights are increasing (decreasing, respectively).

  The forward quasi-distance is useful in epidemiological networks (disease spreading by contact, or, say, heresy spreading within a church), while the

backward quasi-distance is appropriated in P2P (i.e., peer-to-peer) file-sharing networks.

Berman, 1996, introduced *scheduled network*: a directed network (of, say, airports), in which each edge (say, flight) is labeled by departure and arrival times. Kempe–Kleinberg–Kumar, 2002, defined more general *temporal network*: an edge-weighted graph, in which the weight of an edge is the time at which its endpoints communicated. A path is *time-respecting* if the weights of its edges are nondecreasing. Besides Scheduling and Epidemiology, such networks occur in Distributed Systems (say, dissemination of information using node-to-node communication).

In order to handle large temporal data on human behavior, Kostakos, 2009, introduced *temporal graph*: an arc-weighted directed graph, where the vertices are instances $a_i t_k$ (person a_i in point t_k of time), and the arcs are $(t_{k+1} - t_k)$-weighted ones $(a_i t_k, a_i t_{k+1})$ linking time-consecutive pairs and unweighted ones $(a_i t_k, a_j t_k)$ representing a communication (say, e-mail) from a_i to a_j at time t_k.

In order to handle *temporally disconnected* (not connected by a time-respecting path) nodes, Tang et al., 2009, defined *time-varying network*: an ordered set $\{D_t\}_{t=1,\dots,T}$ of directed (or not) graphs $D_t = (X, E_t)$, where the arc-sets E_t may change in time and the arcs have temporal duration. As real-world examples, they considered brain cortical and social interaction networks.

22.3 Distances in Internet and Web

Let us consider in detail the graphs of the Web and of its hardware substrate, Internet which are small-world and scale-free.

The *Internet* is the largest WAN (wide area network), spanning the Earth. This publicly available worldwide computer network came from 13-node ARPANET (started in 1969 by US Department of Defense), NSFNet, Usenet, Bitnet, and other networks. In 1995, the National Science Foundation in the US gave up the stewardship of the Internet, and in 2009, US Department of Commerce accepted privatization/internationalization of ICANN, the body responsible for domain names in the Internet.

Its nodes are *routers*, i.e., devices that forward packets of data along networks from one computer to another, using IP (Internet Protocol relating names and numbers), TCP and UDP (for sending data), and (built on top of them) HTTP, Telnet, FTP and many other *protocols* (i.e., technical specifications of data transfer). Routers are located at *gateways*, i.e., places where at least two networks connect.

The links that join the nodes together are various physical connectors, such as telephone wires, optical cables and satellite networks. The Internet uses *packet switching*, i.e., data (fragmented if needed) are forwarded not along a previously established path, but so as to optimize the use of available *bandwidth* (bit rate, in million bits per second) and minimize the *latency* (the time, in milliseconds, needed for a request to arrive).

Each computer linked to the Internet is usually given a unique "address", called its *IP address*. The new Internet Protocol IPv6 has address space $2^{128} \approx 4.4 \times 10^{38}$. The most popular applications supported by the Internet are e-mail, file transfer, Web, and some multimedia as YouTube and Internet TV. In 2012, 144 billions e-mails (68.8 % of which was spam) were sent daily by 2.2 billions users worldwide. In 2015, global IP traffic will reach 1.0 zettabytes (1000^7 bytes) per year.

The *Internet IP graph* has, as the vertex-set, the IP addresses of all computers linked to the Internet; two vertices are adjacent if a router connects them directly, i.e., the passing datagram makes only one *hop*. The Internet also can be partitioned into ASs (administratively Autonomous Systems). Within each AS the intradomain routing is done by IGP (Interior Gateway Protocol), while interdomain routing is done by BGP (Border Gateway Protocol) which assigns an ASN (16-bit number) to each AS. The *Internet AS graph* has ASs (about 42,000 in 2012) as vertices and edges represent the existence of a BGP peer connection between corresponding ASs.

The *World Wide Web* (*WWW* or *Web*, for short) is a major part of Internet content consisting of interconnected documents (resources). It corresponds to HTTP (Hyper Text Transfer Protocol) between browser and server, HTML (Hyper Text Markup Language) of encoding information for a display, and URLs (Uniform Resource Locators), giving unique "addresses" to web pages. The Web was started in 1989 in CERN which gave it for public use in 1993. The *Web digraph* is a virtual network, the nodes of which are *documents* (i.e., static HTML pages or their URLs) which are connected by incoming or outcoming HTML *hyperlinks*, i.e., hypertext links. It was at least 4.64 billion nodes (pages) in the Indexed Web digraph in May 2014.

The number of operating *web sites* (collections of related web pages found at a single address) reached 634 million in 2012 from 18,957 in 1995. In 2012, 54.7 % of websites were in English, followed by 5.9 %, 5.7 % in Russian and German. Along with the Web lies the *Deep* (or *Invisible*) *Web*, i.e., content, which is not indexed by standard search engines. This content (say, unlinked, or having dynamic URL, non-HTML/text, technically limited access, or scripted, requiring registration/login) has (Bergman, 2001) about 3000 times more pages than Surface Web, where Internet searchers are searching.

There are several hundred thousand *cyber-communities*, i.e., clusters of nodes of the Web digraph, where the link density is greater among members than between members and the rest. The cyber-communities (a customer group, a social network, a concept in a technical paper, etc.) are usually focused around a definite topic and contain a bipartite *hubs-authorities* subgraph, where all hubs (guides and resource lists) point to all authorities (useful and relevant pages on the topic).

Examples of new media, created by the Web are *(we)blogs* (digital diaries posted on the Web), Skype (telephone calls), social sites (as Facebook, Twitter, Linkedin) and Wikipedia (the collaborative encyclopedia). Original Web-as-information-source is often referred as *Web* 1.0, while *Web* 2.0 means present Web-as-participation-platform as, for example, web-based communities, blogs, social-networking (and video-sharing) sites, wikis, hosted services and web applications. For example, with *cloud servers* one can access his data and applications from the Internet rather than having them housed on-site.

Web 3.0 is the third generation of WWW conjectured to include semantic tagging of content. The project Semantic Web by W3C (WWW Consortium) aims at linking to metadata, merging social data and (making all things addressable by the existing naming protocols) transformation of WWW into GGG (Giant Global Graph) of users.

The *Internet of Things* refers to uniquely identifiable objects (things) and their virtual representations in an Internet-like structure. It would encode geographic location and dimensions of 50–100 trillion objects, and be able to follow their movement and send data between them. Every human being is surrounded by 1000–5000 objects.

On average, nodes of the Web digraph are of size 10 kilobytes, out-degree 7.2, and probability k^{-2} to have out-degree or in-degree k. A study in [BKMR00] of over 200 million web pages gave, approximately, the largest connected component "core" of 56 million pages, with another 44 million of pages connected to the core (newcomers?), 44 million to which the giant core is connected (corporations?) and 44 million connected to the core only by undirected paths or disconnected from it. For randomly chosen nodes x and y, the probability of the existence of a directed path from x to y was 0.25 and the average length of such a shortest path (if it exists) was 16, while maximal length of a shortest path was over 28 in the core and over 500 in the whole digraph.

A study in [CHKSS07] of Internet AS graphs revealed the following *Medusa structure* of the Internet: "nucleus" (diameter 2 cluster of $\approx$ 100 nodes), "fractal" ($\approx$15,000 nodes around it), and "tentacles" ($\approx$5000 nodes in isolated subnetworks communicating with the outside world only via the nucleus).

The distances below are examples of host-to-host **routing metrics**, i.e., values used by routing algorithms in the Internet, in order to compare possible routes. Examples of other such measures are: bandwidth consumption, communication cost, reliability (probability of packet loss). Also, the main computer-related *quality metrics* are mentioned.

- **Distance-vector routing protocol**

  A **distance-vector routing protocol** (DVRP) requires that a router informs its neighbors of topology changes periodically and, in some cases, when a change is detected in the topology of a network. Routers are advertised as vectors of a distance (say, **Internet IP metric**) and direction, given by next hop address and exit interface. Cf. **displacement** in Chap. 24.

  Ad hoc on-demand distance-vector routing is a (both unicast and multicast) routing protocol for mobile and other wireless ad hoc networks. It establishes a route to a destination only on demand and avoids the counting-to-infinity problem of other distance-vector protocols by using sequence numbers on route updates.

  Between nodes of an ad hoc network with end-to-end delay constraints, head-of-line packets compete for access to the shared medium. Each packet with remaining lifetime T and remaining **Internet IP metric** H to its destination, is associated with a ranking function $\gamma(H,T) = \frac{T^\alpha}{H}$, denoting its transmission priority. The number $\alpha \geq 0$ is called **lifetime-distance factor**; it should be

optimized in order to minimize the probability of packet loss due to excessive delay.

- **Internet IP metric**

  The **Internet IP metric** (or **hop count**, *RIP metric*, *IP path length*) is the path metric in the *Internet IP graph*, i.e., the minimal number of hops (or, equivalently, routers, represented by their IP addresses) needed to forward a packet of data.

  RIP (a **distance-vector routing protocol** first defined in 1988) imposes a maximum distance of 15 and advertises by 16 nonreachable routes.

- **Internet AS metric**

  The **Internet AS metric** (or *BGP-metric*) is the **path metric** in the *Internet AS graph*, i.e., the minimal number of ISPs (Independent Service Providers), represented by their ASs, needed to forward a packet of data.

- **Geographic distance**

  The **geographic distance** is the **great circle distance** (Chap. 25) on the Earth from the client x (destination) to the server y (source).

  However, for economical reasons, the data often do not follow such geodesics; for example, most data from Japan to Europe transits via US.

- **RTT-distance**

  The **RTT-distance** (or *ping time*) is the round-trip time (to send a packet and receive an acknowledgment back) of transmission between x and y, measured in milliseconds (usually, by the *ping* command).

  See [HFPMC02] for variations of this distance and connections with the above three metrics. Fraigniaud–Lebbar–Viennot, 2008, found that RTT is a C**-inframetric** (Chap. 1) with $C \approx 7$.

- **Synchcronization distance**

  In the Network Time Protocol (NTP), the **synchcronization distance** is the *root dispersion* (maximum error relative to the primary reference source at the root of the synchronization subnet) plus one half the *root delay* (total round-trip delay to the primary reference source at the root of the synchronization subnet).

- **Administrative cost distance**

  The **administrative cost distance** is the nominal number (rating the trustworthiness of a routing information), assigned by the network to the route between x and y. For example, Cisco Systems assigns values $0, 1, \ldots, 200, 255$ for the Connected Interface, Static Route, ..., Internal BGP, Unknown, respectively.

- **DRP-metrics**

  The DD (Distributed Director) system of Cisco uses (with priorities and weights) the **administrative cost distance**, the **random metric** (selecting a random number for each IP address) and the **DRP** (Direct Response Protocol) metrics. DRP-metrics ask from all DRP-associated routers one of the following distances:

  1. The **DRP-external metric**: the number of BGP (Border Gateway Protocol) hops between the client requesting service and the DRP server agent;
  2. The **DRP-internal metric**: the number of IGP hops between the DRP server agent and the closest border router at the edge of the autonomous system;

3. The **DRP-server metric**: the number of IGP hops between the DRP server agent and the associated server.

- **Reported distance**

  In a Cisco Systems routing protocol EIGRP, **reported distance** (or *RD*, *advertised distance*) is the total metric along a path to a destination network as advertised by an upstream neighbor. RD is equal to the current lowest total distance through a successor for a neighboring router.

  A **feasible distance** is the lowest known distance from a router to a particular destination. This is RD plus the cost to reach the neighboring router from which the RD was sent; so, it is a historically lowest known distance to a particular destination.
- **Network tomography metrics**

  Consider a network with fixed routing protocol, i.e., a *strongly connected* digraph $D = (V, E)$ with a unique directed path $T(u, v)$ selected for any pair (u, v) of vertices. The routing protocol is described by a binary *routing matrix* $A = ((a_{ij}))$, where $a_{ij} = 1$ if the arc $e \in E$, indexed i, belongs to the directed path $T(u, v)$, indexed j. The **Hamming distance** between two rows (columns) of A is called the **distance between corresponding arcs** (directed paths) of the network.

  Consider two networks with the same digraph, but different routing protocols with routing matrices A and A', respectively. Then a **routing protocol semi-metric** ([Vard04]) is the smallest Hamming distance between A and a matrix B, obtained from A' by permutations of rows and columns (both matrices are seen as strings).
- **Web hyperlink quasi-metric**

  The **Web hyperlink quasi-metric** (or *click count*) is the length of the shortest directed path (if it exists) between two web pages (vertices in the Web digraph), i.e., the minimal number of necessary mouse-clicks in this digraph.
- **Average-clicks Web quasi-distance**

  The **average-clicks Web quasi-distance** between two web pages x and y in the Web digraph ([YOI03]) is the minimum $\sum_{i=1}^{m} \ln p\frac{z_i^+}{\alpha}$ over all directed paths $x = z_0, z_1, \ldots, z_m = y$ connecting x and y, where z_i^+ is the out-degree of the page z_i. The parameter α is 1 or 0.85, while p (the average out-degree) is 7 or 6.
- **Dodge–Shiode WebX quasi-distance**

  The **Dodge–Shiode WebX quasi-distance** between two web pages x and y of the Web digraph is the number $\frac{1}{h(x,y)}$, where $h(x, y)$ is the number of shortest directed paths connecting x and y.
- **Web similarity metrics**

  Web similarity metrics form a family of indicators used to quantify the extent of relatedness (in content, links or/and usage) between two web pages x and y.

  Some examples are: topical resemblance in overlap terms, *co-citation* (the number of pages, where both are given as hyperlinks), *bibliographical coupling* (the number of hyperlinks in common) and *co-occurrence frequency*

$\min\{P(x|y), P(y|x)\}$, where $P(x|y)$ is the probability that a visitor of the page y will visit the page x.

In particular, **search-centric change metrics** are metrics used by search engines on the Web, in order to measure the degree of change between two versions x and y of a web page. If X and Y are the set of all words (excluding HTML markup) in x and y, respectively, then the **word page distance** is the **Czekanowsky–Dice distance** (cf. Chap. 17)

$$\frac{|X \triangle Y|}{|X| + |Y|} = 1 - \frac{2|X \cup Y|}{|X| + |Y|}.$$

If v_x and v_y are weighted vector representations of x and y, then their **cosine page distance** is given (cf. **TF-IDF similarity** in Chap. 17) by

$$1 - \frac{\langle v_x, v_y \rangle}{||v_x||_2 \cdot ||v_y||_2}.$$

- **Web quality control distance function**

  Let P be a query quality parameter and X its domain. For example, P can be query *response time*, or accuracy, relevancy, size of result.

  The **Web quality control distance function** (Chen–Zhu–Wang, 1998) for evaluating the relative goodness of two values, x and y, of parameter P is a function $\rho : X \times X \to \mathbb{R}$ (not a **distance**) such that, for all $x, y, z \in X$:

  1. $\rho(x, y) = 0$ if and only if $x = y$,
  2. $\rho(x, y) > 0$ if and only if $\rho(y, x) < 0$,
  3. if $\rho(x, y) > 0$ and $\rho(y, z) > 0$, then $\rho(x, z) > 0$.

  The inequality $\rho(x, y) > 0$ means that x is better than y; so, it defines a *partial order* (reflexive, antisymmetric and transitive binary relation) on X.
- **Lostness metric**

  Users navigating within hypertext systems often experience *disorientation* (the tendency to lose sense of location and direction in a nonlinear document) and *cognitive overhead* (the additional effort and concentration needed to maintain several tasks/trails at the same time). Smith's **lostness metric** measures it by

  $$(\frac{d}{t} - 1)^2 + (\frac{r}{d} - 1)^2,$$

  where t is the total number of nodes visited, d is the number of different nodes among them, and r is the number of remaining nodes needed to complete a task.
- **Trust metrics**

  A **trust metric** is, in Computer Security, a measure to evaluate a set of peer certificates resulting in a set of accounts accepted and, in Sociology, a measure of how a member of the group is trusted by the others in the group.

For example, the UNIX access metric is a combination of only *read*, *write* and *execute* kinds of access to a resource. The much finer *Advogato* trust metric (used in the community of open source developers to rank them) is based on bonds of trust formed when a person issues a certificate about someone else. Other examples are: *Technorati*, *TrustFlow*, Richardson et al., Mui et al., *eBay* trust metrics.

- **Software metrics**

  A **software metric** is a measure of software quality which indicates the complexity, understandability, description, testability and intricacy of code. Managers use mainly **process metrics** which help in monitoring the processes that produce the software (say, the number of times the program failed to rebuild overnight).

  An **architectural metric** is a measure of software architecture (development of large software systems) quality which indicates the coupling (interconnectivity of composites), cohesion (intraconnectivity), abstractness, instability, etc.

- **Locality metric**

  The **locality metric** is a physical metric measuring globally the locations of the program components, their calls, and the depth of nested calls by

$$\frac{\sum_{i,j} f_{ij} d_{ij}}{\sum_{i,j} f_{ij}},$$

  where d_{ij} is a distance between calling components i and j, while f_{ij} is the frequency of calls from i to j. If the program components are of about same size, $d_{ij} = |i - j|$ is taken. In the general case, Zhang–Gorla, 2000, proposed to distinguish *forward* calls which are placed before the called component, and *backward* (other) calls. Define $d_{ij} = d'_i + d''_{ij}$, where d'_i is the number of lines of code between the calling statement and the end of i if call is forward, and between the beginning of i and the call, otherwise, while $d''_{ij} = \sum_{k=i+1}^{j-1} L_k$ if the call is forward, and $d''_{ij} = \sum_{k=j+1}^{i-1} L_k$ otherwise. Here L_k is the number of lines in component k.

- **Memory distances**

  In a computer, the *microprocessor* (or *processor*) is the chip doing all the computations, and the *memory* usually refers to *RAM* (random access memory). A (processor) *cache* stores small amounts of recently used information right next to the processor, where it can be accessed much faster than memory. The following distances estimate the cache behavior of programs.

  The **reuse distance** (Mattson et al., 1970, and Ding–Zhong, 2003) of a memory location x is the number of distinct memory references between two accesses of x. Each memory reference is counted only once, because after access it is moved in the cache. The reuse distance from the current access to the previous one or to the next one is called the *backward* or *forward* reuse distance, respectively.

In general, a **memory distance** is (Fang et al., 2006) any dynamic quantifiable distance in terms of memory references between two accesses to the same memory location. In particular, the **access distance** of a memory reference is the number of memory instructions between a store to and a load from the same address. The *instruction distance* is the number of instructions between two references to the same address; it typically correlates well to access distance.

The *value distance* of a reference is the access distance of a load to the first store in a sequence of stores of the same value.

- **Tethering distance**

  Tethering is connecting one device to another. For mobile phones and tablet computers, it allows sharing their Internet connection with, say, laptops. Such connection can be done over wireless LAN (Wi-Fi), over Bluetooth, or by a cable, say USB.

  If tethering is done over WLAN, the feature becomes a mobile *hotspot* (Wi-Fi network access point), and the smartphone serves as a portable router. **Tethering distance** is the maximum phone–computer distance for Wi-Fi tethering.

- **Action at a distance (in Computing)**

  In Computing, the **action at a distance** is a class of programming problems in which the state in one part of a program's data structure varies wildly because of difficult-to-identify operations in another part of the program.

  In Software Engineering, Holland's *Law of Demeter* is a style guideline: an unit should "talk only to immediate friends" (closely related units) and have limited knowledge about other units; cf. **principle of locality** in Chap. 24.

Part VI
Distances in Natural Sciences

Chapter 23
Distances in Biology

Distances are mainly used in *Biology* to pursue basic classification tasks, for instance, for reconstructing the evolutionary history of organisms in the form of phylogenetic trees. In the classical approach those distances were based on comparative morphology, physiology, mating studies, paleaontology and immunodiffusion. The progress of modern *Molecular Biology* also allowed the use of nuclear- and amino-acid sequences to estimate distances between genes, proteins, genomes, organisms, species, etc.

DNA is a sequence of *nucleotides* (or *nuclei acids*) A, T, G, C, and it can be seen as a word over this alphabet of four letters. The (single ring) nucleotides A, G (short for adenine and guanine) are called *purines*, while (double ring) T, C (short for thymine and cytosine) are called *pyrimidines* (in RNA, uracil U replaces T). Over 25 base modifications are known, say, variants 5mC of cytosine and 6mA of adenine.

Two strands of DNA are held together and in the opposite orientation (forming a double helix) by weak hydrogen bonds between corresponding *base pair* of nucleotides (necessarily, a purine and a pyrimidine) in the strands alignment.

A *transition mutation* is a substitution of a base pair, so that a purine/pyrimidine is replaced by another purine/pyrimidine; say, GC is replaced by AT. A *transversion mutation* is a substitution of a base pair, so that a purine/pyrimidine is replaced by a pyrimidine/purine base pair, or vice versa; say, GC is replaced by TA.

DNA molecules occur (in the nuclei of eukaryote cells) in the form of long chains called *chromosomes*. DNA from one human cell has length/width $\approx$ 1.8 m/2.4 nm.

Most human cells contain 46 chromosomes (23 pairs, one set of 23 from each parent); the human *gamete* (sperm or egg) is a *haploid*, i.e., contains only one set of 23 chromosomes. The (normal) males and females differ only in the 23-rd pair: *XY* for males, and *XX* for females. But a male ant *Mirmecia pilosula* has only 1 chromosome, while a plant *Ophioglossum* has 1260. A protozoan *Tetrahymena thermophila* occurs in seven different variants (*sexes*) that can reproduce in $\binom{7}{2} = 21$ combinations. A fungus *Cryptococcus neoformans* has two sexes but their ratio

© Springer-Verlag Berlin Heidelberg 2016

M.M. Deza, E. Deza, *Encyclopedia of Distances*,
DOI 10.1007/978-3-662-52844-0_23

is 99.9 %. More than 99 % of multicellular eukaryotes reproduce sexually, while bacteria only reproduce asexually.

A *gene* is a segment of DNA encoding (via *transcription*, information flow to RNA, and then *translation*, information flow from RNA to enzymes) for a protein or an RNA chain. The location of a gene on its chromosome is called the *gene locus*. Different versions (states) of a gene are called its *alleles*.

A *protein* is a large molecule which is a chain of *amino acids*; among them are hormones, catalysts (enzymes), antibodies, etc. The **protein length** is the number of amino acids in the chain; average protein length is around 300.

The *genetic code* is a map, universal to all organisms, of $4^3 = 64$ *codons* (ordered triples of nucleotides) onto 21 messages: 20 *standard* amino acids and stop-signal. It express the *genotype* (information contained in genes, i.e., in DNA) as the *phenotype* (proteins). Some codons have two meanings, one related to protein sequence, and one related to gene control. Slight variations of the code were found for some mitochondria, ciliates, yeasts, etc. The code also was expanded by encoding new amino acids.

Besides genetic and *epigenetic* (not modifying the sequence) changes of DNA, *evolution* (heritable changes) can happen by "protein mutations" (prions) or culturally (via behavior and symbolic communication). Holliger et al., 2012, synthesized (replacing the natural sugar in DNA) a new polymer (*HNA*) capable of replication and evolution.

A *genome* is the entire genetic constitution of a species or of an organism. The human genome is the set of 23 chromosomes consisting of $\approx$ 3.2 billion *bp* (base pairs) of DNA. It organized into $\approx$21,000 genes, coding for 250,000–1,000,000 proteins. An apple have $\approx$57,000 genes and a lungfish genome contains $\approx$ 133 billion bp.

A *hologenome* is the collection of genomes in a *holobiont* (host plus all its symbionts), a possible unit of selection in evolution. The human microbiota consists of $\approx 10^{14}$ (mainly, bacterial and fungal) cells of $\approx$ 500 species with 3 million distinct genes.

First known evidence of life, photosynthesis, multicellular organisms and of animals (bilaterians) are dated about 4100, 3850, 2100 and 560 Ma (million years ago), respectively. During the *Cambrian Explosion* 540–520 Ma, the rate of evolution was 4–5 times faster than in any other era. But there is no evolution without changes in environment: some deep sea bacteria remained virtually unchanged for 2.3 billion years.

1.9 million extant nonvirus species are known: 1,200,000 invertebrates, 400,000 beetles, 290,000 plants, 250,000 bacteria/protists, 70,000 fungi and 60,000 vertebrates, including 5416 mammals. About 10 million species are living today. The numbers of living nonhuman mammals, birds, trees, fishes, ants, insects, nematodes, viruses are about 5×10^{11}, 2×10^{11}, 3×10^{12}, 4×10^{12}, 5×10^{17}, 5×10^{18}, 10^{22}, 10^{31}, respectively. At least 100 billion of microbial species are expected, but genomes of only 100,000 have been sequenced and about 10,000 have been grown in a laboratory.

About 80 % of the species are parasites of others, parasites included; over 100 are human-specific ones. About 75 % of the links in food webs involve a parasitic species.

About 30 % of the vertebrates and 60 % of invertebrates are nocturnal.

The global nonbacterial biomass is 560 GtC (billion tonnes of organically bound carbon); only 5–10 GtC found in the oceans. Humans and their main symbionts, domesticated animals and cultivated plants, contribute $0.1, 0.7, 2$ GtC. The animal species with largest biomass (≈ 0.5 GtC) is Antarctic krill, the largest species ($\sim 10^{27}$ individuals) is the smallest photosynthetic organism, cyanobacteria *Prochlorococcus*.

99 % of over 5 billion species that have ever existed on Earth became extinct. But sponges originated at least 760 Ma (million years ago) and are still living. Mammalian species' longevity is $\approx$ 1 Ma; our ancestor, *Homo erectus*, survived from 1.8 to 0.55 Ma. Our subspecies is relatively young (0.25–0.6 Ma), 6–7 % of all humans that have ever been born are living today, and their median age is 29.7 years.

The world population was about 1 million 0.05 Ma and 5 million 0.01 Ma ago, after the last glaciation. It grew continuously since the end of the Black Death in 1350, when it was $\approx$ 370 million, and reached 3 billion in 1960, 7.4 billion in 2015.

Gott, 2007: with a 95 % chance, the human race will last anywhere from another 5000 to 7,800,000 years; the same *doomsday argument* by Carter, 1983, gave only 10,000 years for us. Earth's life was only unicellular 3.8–1.3 Ga (billion years) ago and will be so again in $\approx$ 0.8 Ga. But Earth will support some prokaryotes in refuges until mean surface temperature reach 146 °C in 1.6–2.8 Ga. Another Ga life can stay on Mars.

IAM (infinite-alleles model of evolution) assumes that an allele can change from any given state into any other given state. It corresponds to a primary role for *genetic drift* (i.e., random variation in gene frequencies from one generation to another), especially in small populations, over *natural selection* (stepwise mutations). IAM corresponds to low-rate and short-term evolution, while SMM corresponds to high-rate evolution.

SMM (stepwise mutation model of evolution) is more convenient for (recently, most popular) microsatellite data. A *repeat* is a stretch of base pairs that is repeated with a high degree of similarity in the same sequence. *Microsatellites* are highly variable repeating short sequences of DNA; their mutation rate is 1 per 1000–10,000 replication events, while it is 1 per 1,000,000 for *allozymes* used by IAM. Microsatellite data (for example, for DNA fingerprinting) consist of numbers of repeats of microsatellites for each allele.

Evolution, without design and purpose, has increased the life's size, diversity and maximal complexity. But organisms can evolve to become simpler and thus multiply faster; for the *Black Queen model*, such evolution pushes microorganisms to lose functions which are performed by another species around. Evolution has, perhaps, a direction: *convergent gene evolution* (say, bats/dolphins echolocation, primates/crows cognition), increase of energy flow per gram per second (Chaisson, 2003), etc.

Evolution and learning share many common underlying principles. Natural selection can favor increased evolvability under environmental pressure. Besides natural selection, some species alter their environment through *niche construction*. In general, selection can act at genic, cellular, individual, holobiont and group level. Selection of species and even phyla could happen during rare abrupt extreme events.

Locally and over short time spans, macroevolution, is dominated by biotic factors (competition, predation, etc.) as in the *Red Queen model*. But larger-scale (geographic and temporal) patterns and species diversity are driven largely by extrinsic abiotic factors (climate, landscape, food supply, tectonic events, etc.), as in the *Court Jester model*. The organisms evolve rapidly (sometimes, by macromutations), but most changes cancel each other out. So, in the longer term, the evolution appears slow. It is not simple accumulation of microevolutionary adaptations, but rather nonlinear (or chaotic).

Besides *vertical gene transfer* (reproduction within species), the evolution is affected by *HGT* (horizontal gene transfer), when an organism incorporates genetic material from another one without being its offspring, and *hybridization* (extra-species sexual reproduction). HGT is common among unicellular life and viruses, even across large **taxonomic distance**. It accounts for $\approx$ 85 % of the prokaryotic protein evolution. HGT happens also in plants and animals, usually, by viruses. 40–50 % of the human genome consists of DNA imported horizontally by viruses. The most taxonomically distant fertile hybrids are (very rare) interfamilial ones, for instance, blue-winged parrot $\times$ cocktatiel, chicken $\times$ guineafowl in birds and (under UV irradiation) carrot with tobacco, rice or barley. In 2012, an RNA-DNA virus hybrid and a *virophage* of a (giant) virus were found.

The *life* is not well defined (say, for *viroids*), DNA could be only its recent attribute. Neither life can be "anything undergoing evolution", since the unit is this evolution (gene, cell, organism, group, species?) is not clear. Lineweaver, 2012, defined life as a *far-from-equilibrium dissipative system*. For Eigen, life is a type of behavior of matter. An essential feature of life is *autopoiesis* (self-making); for example, the human body replaces 98 % of its atoms every year while maintaining its unique pattern.

Neither *complexity* is well defined. Chaisson, 2014, measures complexity of any Nature's system by the amount of energy passing through it per second and per gram. Earth's biosphere use energy at $\approx 10^{21}$ erg/s ($\approx$ 0.1 % of obtained solar power).

Examples of distances, representing general schemes of measurement in Biology, follow.

The term **taxonomic distance** is used for every distance between two *taxa*, i.e., entities or groups which are arranged into a hierarchy (in the form of a tree designed to indicate degrees of relationship).

The *Linnaean taxonomic hierarchy* is arranged in ascending series of ranks: Zoology (Kingdom, Phylum, Class, Order, Family Genus, Species) and Botany (12 ranks). A *phenogram* is a hierarchy expressing *phenetic relationship*, i.e., unweighted overall similarity. A *cladogram* is a strictly genealogical (by ancestry)

hierarchy in which no attempt is made to estimate/depict rates or amount of genetic divergence between taxa.

A *phylogenetic tree* is a hierarchy representing a hypothesis of *phylogeny*, i.e., evolutionary relationships within and between taxonomic levels, especially the patterns of lines of descent. The **phenetic distance** is a measure of the difference in phenotype between any two nodes on a phylogenetic tree; see, for example the **biodistances** in Chap. 29.

The **phylogenetic distance** (or **cladistic distance**, **genealogical distance**) between two taxa is the *branch length*, i.e., the minimum number of edges, separating them in a phylogenetic tree. In such edge-weighted tree, the **additive distance** between two taxa is the minimal sum of edge-weights in a path connecting them. The *phylogenetic diversity* is (Faith, 1992) the minimum total length of all the phylogenetic branches required to span a given set of taxa on the phylogenetic tree.

The **evolutionary distance** (or **patristic distance**) between two taxa is a measure of genetic divergence estimating the **temporal remoteness** of their most recent co-ancestor. Their general **immunological distance** is a measure of the strength of antigen-antibody reactions, indicating their evolutionary distance.

23.1 Genetic Distances

The general **genetic distance** between two taxa is a distance between the sets of DNA-related data chosen to represent them. Among the three most popular genetic distances below, the **Nei standard genetic distance** assumes that differences arise due to mutation and genetic drift, while the **Cavalli-Sforza–Edwards chord distance** and the **Reynolds–Weir–Cockerham distance** assume genetic drift only.

A *population* is represented by a vector $x = (x_{ij})$ with $\sum_{j=1}^{n} m_j$ components, where x_{ij} is the frequency of the i-th *allele* (the label for a state of a gene) at the j-th gene locus (the position of a gene on a chromosome), m_j is the number of alleles at the j-th locus, and n is the number of considered loci. Since x_{ij} is the frequency, we have $x_{ij} \geq 0$ and $\sum_{i=1}^{m_j} x_{ij} = 1$. Denote by $\sum$ summation over all i and j.

- **Shared allele distance**

  The **shared allele distance** D_{SA} (Stephens et al., 1992, corrected by Chakraborty–Jin, 1993) between individuals a, b is $1 - SA(a, b)$; for populations x, y it is

$$1 - \frac{\overline{SA(x, y)}}{\overline{SA(x)} + \overline{SA(y)}},$$

  where $SA(a, b)$ denotes the number of shared alleles summed over all n loci and divided by $2n$, while $\overline{SA(x)}$, $\overline{SA(y)}$, and $\overline{SA(x, y)}$ are $SA(a, b)$ averaged over all pairs (a, b) with individuals a, b being in populations x, y, respectively.

- **MHC genetic dissimilarity**

  The **MHC genetic dissimilarity** of two individuals is defined as the number of shared alleles in their MHC (*major histocompatibility complex*).

  MHC is the most gene-dense and fast-evolving region of the mammalian genome. In humans, it is a 3.6 Mb region containing 140 genes on chromosome 6 and called HLA (*human leukocyte antigen system*). HLA has the largest *polymorphism* (allelic diversity) found in the population. Three most diverse loci (HLA-A, HLA-B,HLA-DRB1) have roughly 1000, 1600, 870 known alleles. This diversity is essential for immune function since it broadens the range of *antigens* (proteins bound by MHC and presented to T-cells for destruction); cf. **immunological distance**.

  MHC (and related gut microbiota) diversity allows the marking of each individual of a species with a unique body odor permitting kin recognition and mate selection. *MHC-negative assortative mating* (the tendency to select MHC-dissimilar mates) increases MHC variation and so provides progeny with an enhanced immunological surveillance and reduced disease levels.

  While about 6 % of the non-African modern human genome is common with other hominins (Neanderthals and Denisovans), the share of such HLA-A alleles is 50 %, 72 %, 90 % for people in Europe, China, Papua New Guinea.

- *Dps* **distance**

  The **Thorpe similarity** (proportion of shared alleles) between populations x and y is defined by $\sum \min\{x_{ij}, y_{ij}\}$. The *Dps* **distance** between x and y is defined by

$$-\ln \frac{\sum \min\{x_{ij}, y_{ij}\}}{\sum_{j=1}^{n} m_j}.$$

- **Prevosti–Ocana–Alonso distance**

  The **Prevosti–Ocana–Alonso distance** (1975) between populations x and y is defined (cf. **Manhattan metric** in Chap. 19) by

$$\frac{\sum |x_{ij} - y_{ij}|}{2n}.$$

- **Roger distance**

  The **Roger distance** D_R (1972) between populations x and y is defined by

$$\frac{1}{\sqrt{2}n} \sum_{j=1}^{n} \sqrt{\sum_{i=1}^{m_j} (x_{ij} - y_{ij})^2}.$$

- **Cavalli-Sforza–Edwards chord distance**

  The **Cavalli-Sforza–Edwards chord distance** D_{CH} (1967) between populations x and y (cf. **Hellinger distance** in Chap. 17) is defined by

$$\frac{2\sqrt{2}}{\pi n}\sum_{j=1}^{n}\sqrt{1-\sum_{i=1}^{m_j}\sqrt{x_{ij}y_{ij}}}.$$

  The **Cavalli-Sforza arc distance** between populations x and y is defined by

$$\frac{2}{\pi}\arccos\left(\sum\sqrt{x_{ij}y_{ij}}\right).$$

  Cf. **Bhattacharya distance 1** in Chap. 14.

- **Nei–Tajima–Tateno distance**

  The **Nei–Tajima–Tateno distance** D_A (1983) between populations x and y is

$$1-\frac{1}{n}\sum\sqrt{x_{ij}y_{ij}}.$$

  The **Tomiuk–Loeschcke distance** (1998) is $-\ln\frac{1}{n}\sqrt{\sum x_{ij}\sum y_{ij}}$.

  The **Nei standard genetic distance** D_s (1972) between x and y is defined by

$$-\ln\frac{\langle x,y\rangle}{||x||_2\cdot||y||_2}.$$

  Cf. **Bhattacharya distances** in Chap. 14 and **angular semimetric** in Chap. 17.

  Under IAM, D_s increases linearly with time; cf. **temporal remoteness**.

  The **kinship distance** is defined by $-\ln\langle x,y\rangle$. Caballero and Toro, 2002, defined the *molecular kinship coefficient* between x and y as the probability that two randomly sampled alleles from the same locus in them are *identical by state*. Computing it as $\langle x,y\rangle$ and using the analogy with the **coefficient of kinship** defined via *identity by descent*, they proposed several distances adapted to molecular markers (polymorphisms). Cf. **co-ancestry coefficient**.

  The **Nei minimum genetic distance** D_m (1973) between x and y is defined by

$$\frac{1}{2n}\sum(x_{ij}-y_{ij})^2.$$

- **Sangvi χ^2 distance**

  The **Sangvi χ^2 (1953) distance** between populations x and y is defined by

$$\frac{2}{n}\sum\frac{(x_{ij}-y_{ij})^2}{x_{ij}+y_{ij}}.$$

- **Fuzzy set distance**

  The **fuzzy set distance** D_{fs} between populations x and y (Dubois–Prade, 1983; cf. **Tanimoto distance** in Chap. 1) is defined by

$$\frac{\sum 1_{x_{ij} \neq y_{ij}}}{\sum_{j=1}^{n} m_j}.$$

- **Goldstein et al. distance**

  The **Goldstein et al. distance** (1995) between populations x and y is

$$(\delta\mu)^2 = \frac{1}{n} \sum (ix_{ij} - iy_{ij})^2.$$

  It is the loci-averaged value $(\delta\mu)^2 = (\mu(x)_j - \mu(y)_j)^2$, where $\mu(z)_j = \sum_i iz_{ij}$ is the mean number of repeats of allele at the j-th (microsatellite) locus in population z.

  The **Feldman et al. distance** (1997) is $\log(1 - \frac{\sum_i (\delta\mu)_i^2}{M})$, where the summation is over loci and M is the average value of the distance at maximal divergence.

  The above two and the next two distances assume high-rate SMM.

- **Average square distance**

  The **average square distance** between populations x and y is defined by

$$\frac{1}{n} \sum_{k=1}^{n} \left(\sum_{1 \leq i < j \leq m_j} (i-j)^2 x_{ik} y_{jk} \right).$$

- **Shriver et al. stepwise distance**

  The **Shriver et al. stepwise distance** (1995) between populations x and y is

$$D_{SW} = \frac{1}{n} \sum_{k=1}^{n} \sum_{1 \leq i,j \leq m_k} |i-j|(2x_{ik}y_{jk} - x_{ik}x_{jk} - y_{ik}y_{jk}).$$

- **Latter F-statistics distance**

  The **Latter F-statistics distance** (1972) between populations x and y is defined by the following *F_{ST}-estimator*:

$$\theta^* = \frac{\sum (x_{ij} - y_{ij})^2}{2(n - \langle x, y \rangle)}.$$

  The **Latter distance** D_L (1973) is $-\ln(1 - \theta^*)$.

- **Reynolds–Weir–Cockerham distance**

  The **Reynolds–Weir–Cockerham distance** (1983) between populations x and y is defined by

$$D_W = -\ln(1-\theta),$$

  where θ is their **co-ancestry coefficient** estimated as $\frac{a}{a+b}$.

  Here a is the variance between populations x and y, and b is the variance within them. If the sample size is large, then D_W is close to the **Latter F-statistics distance**. For short-term evolution (i.e., $\frac{t}{N}$ small), $D_W \approx \frac{t}{2N}$, where N is the population size, and t is the number of generations; cf. **temporal remoteness**.

- **Co-ancestry coefficient**

  The **co-ancestry coefficient** (or *coefficient of kinship*) of two populations (or individuals) x and y is defined (Wright, 1922, and Malécot, 1948) as the probability $\theta(x, y)$ that two alleles, sampled at random from x and y, are *IBD* (or *identical by descent*), i.e., descending from the same ancestral allele.

  Two genes can be *IBS* (or *identical by state*), i.e., similar due to random chance. Cf. **Nei standard genetic distance** and **coefficient of relationship**.

  An DNA segment, found consistently to be identical in two related people (or populations) is IBD if it is so due to their common ancestry. The total and mean **IBD segment length** of two people g generations since the founding event (i.e., with g meioses on the path of descent) are $\approx \frac{1}{2^g}$-th of total genome length and $\approx \frac{50}{g}$ centiMorgans, respectively; cf. the **map distance**. For example, two people are cryptic relatives if those lengths are at least 1500 cM and 25 cM.

- **F_{ST}-based distances**

  Given a population T of size $|T|$ partitioned into subpopulations $S_1, \ldots, S_k$, the *F-statistics* (or *fixation indices*) are the measures

$$F_{IS} = 1 - \frac{H_I}{H_S},\ F_{ST} = 1 - \frac{H_S}{H_T},\ F_{IT} = 1 - \frac{H_I}{H_T}$$

  of the correlation between genes drawn within subpopulations S_i, among them and within the entire T, respectively.

  Here H_I, H_S and H_T are the *heterozygosity indices* over (i)ndividuals, (s)ubpopulations and (t)otal T used to compare observed variation in gene frequencies (partitioned into within and between group components) with the expected one in HWE (*Hardy–Weinberg equilibrium*, i.e., an ideal state when allele and genotype frequencies in population remain constant from generation to generation). $H_I = \frac{\sum_{1\le j\le k} |S_j| H_{obs\,j}}{|T|}$ (where $H_{obs\,j}$ is the observed *heterozygosity*, i.e., proportion of heterozygotes, in subpopulation S_j) is the mean actual heterozygosity in individuals within subpopulations. $H_S = \frac{\sum_{1\le j\le k} |S_j| H_{exp\,j}}{|T|}$ (where $H_{exp\,j} = 1 - \sum_i p_i^2$ is the expected, assuming HWE, heterozygosity in S_j and p_i is the frequency of the i-th allele of the locus) is the mean expected

heterozygosity within subpopulations. $H_T = 1-\sum_i \bar{p}_i^2$ (where $\bar{p}_i$ is the frequency of the i-th allele averaged over all subpopulations) is the expected, assuming HWE, heterozygosity in T.

The above Nei's (1973) F_{ST} generalizes Wright's (1951) F_{ST}, when there are only two alleles at a locus. This measure is equivalent to the **co-ancestry coefficient** if all the alleles in the population are different. Nei, 1987, generalized F_{ST} to multi-loci as $G_{ST} = 1 - \frac{\bar{H}_S}{\bar{H}_T}$, where H_S and H_T are averaged across all loci.

The above relative measures underestimate the between-population difference if the within-population diversity is high, such as, say, for microsatellites. Slatkin's R_{ST} is an analog of Wright's F_{ST}, adapted for microsatellite loci by assuming SMM. It is defined by $R_{ST} = \frac{\bar{S}-S_W}{\bar{S}}$, where S_W is the sum over all loci of twice the weighted mean of the within-population variances $var(A)$ and $var(B)$, and $\bar{S}$ is the sum over all loci of twice the variance $var(A \cup B)$ of the combined population.

In fact, S_W and $\bar{S}$ are the **average square distance** within a subpopulation and the entire population. Slatkin (1995) developed R_{ST} using his (1991) SMM-based F-statistics $F_{ST} = \frac{\bar{t}-t_0}{\bar{t}}$, where $\bar{t}$ and t_0 are the average **temporal remoteness** to the closest co-ancestor of any two randomly chosen alleles from the entire population and from the same subpopulation, respectively.

Jost's D_{est} (2008) is an estimator $\frac{k}{k-1}\frac{H_T-H_S}{1-H_S}$ of the actual differentiation based on H's estimated from allele identities rather than ratios of heterozygosity.

The Weir–Cockerham θ_{ST} (1984) is an estimation of F_{ST}, seen as the correlation of pairs of alleles between individuals within a subpopulation and based on partition of variance rather than heterozygosity. The total variance of allele frequency within a population is the sum $a+b+c$ of variances between subpopulations, between individuals within a subpopulation, and between gametes within individuals. Then θ_{ST} is defined, generalizing the **Reynolds–Weir–Cockerham distance**, as $\frac{\sum a}{\sum(a+b+c)}$, where the sum is taken over all alleles and loci.

The **genetic F_{ST}-distance** is the pairwise F_{ST} taking account only of the data for the two subpopulations concerned, not all the data simultaneously. Such a measure is valid only if the breeding system is similar for both populations.

Cavalli-Sforza–Menozzi–Piazza, 1994, evaluated, using 120 blood polymorphisms, the doubled genetic F_{ST}-distance between 42 native human populations and between 9 resulting clusters. The largest such distances between two continents were Africa–Oceania (0.247) and Africa–Americas (0.226), while the shortest distances were Americas–Asia (0.089) and Americas–Europe (0.095).

The largest distance in Europe, $F_{ST} = 0.02$–0.023, was between Finland and Southern Italy; cf. 0.11 (Europeans–Chinese) and 0.153 (Europeans–Africans (Yoruba)). Mbuti Pygmies (the least "Neanderthal") and Papuans (the most "Denisovan") are the two most divergent living humans with $F_{ST} = 0.377$.

A similar analysis by Atzmon et al., 2010, of seven Jewish groups indicated a common origin and, 100–150 generations ago, the split into Middle Eastern and European clusters. The most distant and differentiated are among Mizrahim: F_{ST} of Iranian Jews to other Jews is 0.016. Ashkenazi Jews have the highest

admixture with non-Jews but they are not descendants of converted Khazars or Slavs. The closest by F_{ST} to them are Northern Italians, French, Palestinians, and Druze.

Genetic variation in alleles of genes occurs both within (due to mutations and gene exchange during meiosis) and among (due to natural selection and *genetic drift*, i.e., random gene changes) populations. Human total genetic variation is 0.5 % consisting of 0.1 % in SNPs (single nucleotide polymorphisms), $\approx$ 0.4 % in *CNVs* (copy number variants—deletion, duplication or more—in a DNA segment, instead of exactly two copies of DNA per cell) and a small variation in repetitive DNA. Sudmant et al., 2015, found that CNVs (especially, duplications) are a source of seven times greater diversity compared to SNPs.

Each human is born with about 50 new mutations, rarely noticeable. The main other mechanisms of our genetic diversity are migrations and hybridization.

The genetic similarity of humans is 99.9 % among them, while it is 99.85 % with Neanderthals and 96–98 % with (having SNP diversity 0.2 %) chimpanzees. After initial division, there was interbreeding with chimpanzees and, later, with Neanderthals, Denisovans and archaic Africans. There are 2 % of archaic genes in sub-Saharan Africans, 2 % of Neanderthal genes in Central Asians and 4 % of them in Europeans and Americans. There are 2.5 % of Neanderthal and 6–8 % Denisovan genes in South Asians and Australo-Melanesians.

75–85 % of human SNP variation 0.1 % is among individuals within any population, 5–10 % between local populations of the same continent, and 6–10 % between large groups from different continents. So, differentiation between continental groups is $F_{ST} \leq 0.1$, less than the threshold 0.25 used to define a *subspecies* (*race*).

- **Temporal remoteness**

  The **temporal remoteness** of most recent common ancestor (or *TMRCA*, *divergence time*, *time to coalescence*) of two taxa is the time (or the number of generations) that has passed since those populations existed as a single one. The *molecular clock hypothesis* estimates that one unit of **Nei standard genetic distance** between two taxa corresponds to 18–20 Ma of their TMRCA.

  A human phylogenetic tree is derived from matrilineal mitochondrial DNA, or patrilineal nonrecombinant part of the Y-chromosome of (usually blood) protein sequences by measuring accumulated mutations. TMRCA is 0.2–0.19 Ma ago along all-female ancestry lines for the *Mitochondrial Eve* and 0.24–0.58 Ma ago along all-male lines for the *Y-chromosomal Adam*.

  The resulting phylogenetic tree is rooted in the common ancestor of chimpanzees and humans, which originated in Africa 8–6 Ma ago. The corresponding **genetic F_{ST}-distance** between humans and chimpanzee is about 0.02, i.e., at least 30 million point mutations affecting 80 % of genes.

  Our primate ancestors evolved, probably, 40 Ma ago in Asia and sailed across a narrow sea to Africa. Our genus *Homo* had diverged, as a carnivorous scavenger, from the *Australopithecines* (bipedal ape-like using rudimentary stone tools) $\approx$ 2.5 Ma ago in East (*Homo habilis*) or South Africa. Then *Homo erectus*, the first global and using fire human species, moved to Eurasia 1.8 Ma ago,

followed by Denisovans and, later, Neanderthals, the common ancestor of which split from our line 0.8 Ma ago.

At least ten extinct Homo species are known. *Archaic Homo sapiens* originated 0.7–0.6 Ma ago. They evolved to anatomically modern humans *Homo sapiens sapiens* $\approx$ 0.2 Ma ago, as shown by the temporal remoteness of their mitochondrial most recent common ancestor. Then their mitochondrial lineage L3 (among L0, L1, L2, L3) migrated out of (east or southern) Africa 0.125 and 0.065 Ma ago.

Humans passed via population bottleneck $\approx$ 0.074 Ma ago (when Toba supervolcano erupted), followed by a rapid expansion. They arrived about 0.075, 0.046, 0.044, 0.016 Ma ago in West Africa, Australia, Europe and the Americas, respectively. The last place on Earth (besides the Antarctica, occupied only in 1899, and tiny atolls) humans colonised was New Zealand where they arrived $\approx$1300 years ago.

Savanna living, use of fire, speech and sophisticated hand axes appeared about 1.7, 1.6, 0.6, 0.5 Ma ago. Modern human behavior (language, symbolic thought, *cultural universals*) emerged 0.07–0.05 Ma, i.e., $\approx$3000 generations, ago.

The main known gene mutations leading to us: improving blood supply to the primate brain, weakening jaw muscle (so skull/brains could expand), speeding up the neuron migration (crucial to intelligence), increasing the production of the salivary enzyme (helping to the emergence of agriculture). Also, noncoding sequence HACNS1 had 16 variations during last 6 Ma; it led to more fine muscle control allowing bipedality and tool use. The gene miR-941, unique to humans, emerged 6–1 Ma ago; it could initiate our advanced brain functions.

- **Pedigree-based distances**

  A *cousin* (or *blood relative*) is a relative with whom one shares a common ancestor. A *cousin chart* (or *table of consanguinity*, *family tree*, *pedigree digraph*) is a directed tree, where vertices represent relatives (usually humans, show dogs, race horses or cultivars), and the arc uv means that v is a child of u. So, the in-degree of each vertex is at most two (known parents). Moreover, unoriented edges are added with edge uv meaning *reproductive affinity*, i.e., that u and v are mated.

  The **genealogical quasi-distance** (or, in Anthropology, *genealogical distance*, *degree of relative consanguinity*) from the individual x to its relative y is defined (Schneider, 1968) as the number of generations one must go before a common ancestor is found, i.e., it is the length $q(x, y)$ of the shortest directed path to x from a common ancestor of x and y in the family tree. Recently, the value $\min\{q(x, y), q(y, x)\}$ is preferred in English pedigree documents.

  An *ancestral path* between the vertices x and y in a family tree (or any acyclic digraph) is a concatenation of two directed paths from a common ancestor to them. The **ancestral path distance** is the length of a shortest ancestral path, i.e., it is $q(x, y) + q(y, x)$. Cf. **genealogical distance** between the vertices x and y (of a phylogenetic tree representing taxa) which is the length of a shortest $(x - y)$-path in the undirected family tree, i.e., also $q(x, y) + q(y, x)$. Cf. ancestral path distance in Chap. 22 and **join semilattice distances** in Chap. 10.

The *ancestral distance of an extant taxon* (Hearn and Huber, 2006) is the time (or the number of speciation events) separating it from its most recent ancestor with at least one extant descendant having an independent trait.

Mycielski and Ulam, 1969, called *genealogical distances* between x and y the value $|S(x)\Delta S(y)|$, where $S(z)$ is the set of ancestors of z in a given family tree, and the **Manhattan metric** between some vector representations of x and y.

Two cousins are *a-removed of degree b* if they are separated by a generations and the minimum number of generations between either cousin and their common ancestor is b. The *direct relatives* are spouses and cousins with $(a, b) = (1, 0), (2, 0), (1, 1), (0, 2)$ and $(0, 1)$, i.e., parents/children, grandparents/grandchildren, uncles (aunts)/nieces (nephews), first degree cousins and siblings. Clearly, $a = |q(x, y)-q(y, x)|$ and $b = \min\{q(x, y), q(y, x)\}$. Worldwide, $\approx 10\,\%$ of marriages are between closer than third degree cousins; the case of third degree cousins results in progeny only slightly more homozygous than the general population.

The above pedigree notions are important also in some family, inheritance and nationality rules. For example, the Roman Catholic Church prohibits marriage of x with a relative y if $q(x, y) + q(y, x) \leq 4$. The closest legally permissible unions are between *double-first cousins*, i.e., those sharing four grandparents (in Muslim populations), or uncle-niece (in South India).

Another example: a *Jew* in Halakha's (Jewish Law) sense is a child born to a Jewish mother or an converted adult. Israel's Law of Return permits independent repatriation to anyone with a nonapostate Jewish grandparent and/or his spouse. In Nazi Germany, a *full Jew* was anyone with three Jewish grandparents, while *part-Jews* of first/second degree were those (not practicing Judaism and not having a Jewish spouse) who had two/one Jewish grandparents.

The *inbreeding coefficient* $F(z)$ of an individual z is the probability of *autozygosity*, i.e., that z received the same ancestral gene from both its parents; so, $F(z)$ is the **co-ancestry coefficient** $\theta(z_1, z_2)$ of its parents z_1, z_2. When pedigree data are available, $\theta(x, y)$ is estimated as $\sum_{z\in Z(x,y)} 0.5^{|P(z)|}(1 + F(z))$, where $Z(x, y)$ is the set of least common ancestors of x and y in the pedigree digraph, and $|P(z)|$ is the number of vertices in the shortest ancestral path between x and y through z. In practice, ancestors z are counted only up to a given number of generations and not all of them are known.

The **coefficient of relationship** between two relatives x and y is the fraction of genome inherited from common ancestors. It is almost 1 for identical twins (they differ due to mutations during development and gene copy number variation) and $\approx \frac{3}{4}$ for *semi-identical twins* inheriting the same genes from only one parent. Otherwise, it is $2\theta(x, y)$, since any progeny have a risk $\frac{1}{2}$ of inheriting identical alleles from both parents. It is $\frac{1}{2}$ for siblings and for parent-offspring.

The **coefficient of relatedness** (or *genetic similarity*) between social partners x, y relative to the population is defined (Hamilton, 1970) by

$$r(x, y) = \frac{cov(g, g')}{cov(g, g)} = \frac{E[(g - E[g])(g' - E[g'])]}{E[(g - E[g])(g - E[g])]},$$

where g, g' are genetic (i.e., heritable) components of the phenotype (for the character of interest) of x, y, respectively, and cov denotes a statistical covariance taken over all individuals in the population. This coefficient quantifies the *indirect fitness*, i.e., the component of fitness gained from aiding related individuals.

Fitness is an individual's ability to propagate its genes, i.e., to both survive and reproduce. A measure of it is the average contribution to the gene pool of the next generation that is made by an average individual of the specified genotype or phenotype. The relative *reproductive value* of an individual is the probability that it is the ancestor of a randomly chosen individual in a distant future generation.

Fowler–Christakis, 2013: pairs of nonkin friends are, on average, as genetically similar to one another as fourth cousins,

- **Mating distances**

  Individual migration distances are the distances between birthplaces of paired individuals. If the pairs are spouses (gametes) or siblings, we have **marital distance** or **sib distance**, respectively. Also, the **parent-offspring distance** is used to describe gene migration per generation.

  For humans, those distances are measured either in km, or, say, as the number of municipalities crossed by a straight line between municipality midpoints of each pair's birthplaces. The term *marital migration distance* is also used for the distance between premarital town of a person and town of marriage. Cf. **migration distances (in Economics)** in Chap. 28.

  Until the twentieth century, men usually went courting no more than about 8 km from home (the distance they could walk out and back on their day off from work). 80 % of all marriages in history could be between second cousins or closer. Also, young birds, leaving the nest, usually move 4–5 home ranges away; so, they stay within breeding distance of their cousins.

  For a population, **critical mating distances**, are maximum spatial (physical) and genetic (number of genes bearing different alleles) distances allowed for mating; cf. **isolation by distance**. For honey bees, the *mating distance* is the range of queen's nuptial flight from her hive to the drone congregation areas over their hives; it is typically within 7.5 km but can reach 17 km.

- **Lasker distance**

  The **Lasker distance** between two human populations x and y, characterized by surname frequency vectors (x_i) and (y_i), is the number $-\ln 2R_{x,y}$, where $R_{x,y} = \frac{1}{2}\sum_i x_i y_i$ is Lasker's (1977) *coefficient of relationship by isonymy*.

  Surname structure is related to inbreeding and (in patrilineal societies) to random genetic drift, mutation and migration. Surnames can be considered as alleles of one locus, and their distribution can be analyzed by Kimura's theory of neutral mutations; an isonymy points to a common ancestry.

- **Isolation by distance**

  Isolation by distance (or *ibd*, Wright, 1943) is the tendency for most individuals to migrate and find mates between neighbors; so, populations that are a geographically closer are more similar than those that are further apart. It results in a smooth increase in a *cline*, i.e., the gradual change in a character (say, allele frequency, within- or between-population genetic differentiation) or

feature (phenotype) with increasing geographic distance. The above distance can be Euclidean or along a great circle, river, or topographic isocline.

Ibd for humans was studied, for example, via migration patterns and the distribution of surnames (cf. **Lasker distance**). At both continental and global scales, the **genetic F_{ST}-distance** and differentiation in cranial morphology between populations increases with **great circle distance** (Chap. 25).

The geographic distance explains $> 75\,\%$ of the variation between human populations, and this distance from East Africa explains $85\,\%$ of the smooth decrease in genetic diversity. Atkinson, 2011, claims that phoneme diversity also declines with distance from Africa. The occurrence of alleles $7R$ and $2R$, linked to risk-taking, of the dopamine-related gene *DRD*4 increases with distance from Africa.

A strong Europe-wide (except Basques, Finns and Sardinians isolates) correlation, based on >300,000 single nucleotide polymorphisms, between geographic and genetic distance was found. South-to-North was the main smooth gradient.

The ibd model explains the emergence of regional differences (races) and new species by restricted gene flow and adaptive variations. *Speciation* (branching of new species from an ancestral population) occurs when subpopulations become reproductively isolated. The dominating mode of speciation is *allopatry* when habitat splits into discontinuous parts by the formation of a physical barrier to gene flow or dispersal. Examples of natural barriers are the Himalayas, Wallace Line, Grand Canyon. All modes, in a continuum from complete (allopatric) to zero (*sympatric*) spatial segregation of diverging groups, occur, mainly, in marine ecosystems.

In spatially extended population, another mode—*topopatric* (or *distance-forced*) speciation can occur via ibd only, without geographic isolation and selection. de Aguiar and Bat-Yam, 2011, gave the conditions for speciation in such population as a function of its density, mutation rate, genome size and **critical mating distances**. They see such speciation as a case of breakdown of unstable uniform distribution, leading to the self-organization of its members into clusters.

Absolute distances between diverged groups can be, say, tens of meters for pathogen resistance to hundreds of kilometers in marine invertebrates.

- **Wright**

  Dispersal neighborhood (DN) is the geographic area within which individuals and genes regularly move and interact. It is estimated as the area within a radius extending 2 standard deviations from the mean of species's dispersal distribution.

  Richardson et al., 2014, proposed to measure microgeographic adaptive evolution by the **wright** indicating the phenotypic difference between populations relative to the number of species-specific DN's separating them. It is

$$w = \frac{|x_1 - x_2|}{ds_p},$$

where x_1, x_2 are the means of the genetically determined traits of populations, s_p is the pooled standard deviation of those trait values across populations, and d is the distance in number of DN's separating the two populations.

The wright is a spatial analog of the *haldane*, a metric for rate of microevolution defined (Gingerich, 1993, and Lynch, 1990) as $\frac{|x_1-x_2|}{gs_p}$, where g the number of generations separating the populations (or samples of the same populations). Haldan, 1949, defined the *darwin* as $|\ln x_1 - \ln x_2|$ (or, respectively, $\frac{|\ln x_1-\ln x_2|}{t}$), where t is the time in Ma separating samples of the same populations).

- **Malécot's distance model**

  Genealogy, migration and surname isonymy are used to predict kinship (usually estimated from blood samples). But because of incomplete knowledge on ancestors, pedigree-independent methods for kinship assays utilize the distance-dependent correlations of any parameter influenced by identity in descent: phenotype, gene frequency, or, say, isonymy.

  Malécot's distance model (1948, 1959) is expressed by the following *kinship-distance formula* for the mean **coefficient of kinship** between two populations **isolated by distance** d:

$$\theta_d = ae^{-bd}d^c,$$

  where $c = 0, \frac{1}{2}$ correspond to one-, two-dimensional migration, b is a function of the *systematic pressure* (joint effect of co-ancestry, selection, mutations and long range migration), and a is the *local kinship* (the correlation between random gametes from the same locality). In fact, the results in 2D for small and moderate distances agree closely with $c = 0$. The model is most successful when the systematic pressure is dominated by migration.

  Malécot's model was adapted for the dependency ρ_d of alleles at two loci at distance d (*allelic association*, *linkage disequilibrium*, *polymorphism distance*):

$$\rho_d = (1 - L)Me^{-\epsilon d} + L,$$

  where d is the distance (say, from a disease gene) between loci along the chromosome (either **genome distance** on the physical scale in kilobases, or **map distance** on the genetic scale in centiMorgans), ϵ is a constant for a specified region, $M \leq 1$ is a parameter expressing mutation rate and L is the parameter predicting association between unlinked loci.

  Selection generates long *blocks of linkage disequilibrium* (places in the genome where genetic variations are occurring more often than by chance, as in the genetic drift) across hundreds of kilobases. Using it, Hawks et al., 2007, found that selection in humans much accelerated during the last 40,000 years, driven by exponential population growth and cultural adaptations.

  Examples of accelerated (perhaps, under diet and diseases pressures) human evolution and variation include disease resistance, lactose tolerance, skin color, skeletal gracility. A mutation in *microcephalin* (gene MCPH1) appeared

14,000–62,000 years ago and is now carried by 70 % of people but not in sub-Saharan Africa. Distinctive traits of East Asians (about 93 % of Han Chinese and 70 % of Japanese and Tai)—thicker hair shafts, more sweat glands, smaller breasts and specific teeth—are the result of a mutation in gene EDAR that occurred ≈35,000 years ago.

The fastest genetic change ever observed in humans is that the ethnic Tibetans split off from the Han Chinese less than 3000 years ago and since then evolved a unique ability to thrive at high (4000 m above sea level) altitudes and low oxygen levels. It also come from their gene *EPAS1* found only in Denisovans. An example of quick nongenetic evolution: the average height of a European male at age 21 rose from 167 cm in early 1870s to 178 cm in 1980. Crabtree, 2012, argues that our intellectual and emotional abilities diminish gradually (after a peak 2000–6000 years ago) because of weakened control of genetic mutations by natural selection.

Over the past 20,000 years, the average volume of the human brain has decreased by 10 %. Possible reason: our dwindling intelligence (Geary, 2011), or improved brain efficiency (Hawks, 2011), or social self-domestication (Hood, 2014).

23.2 Distances for DNA/RNA and Protein Data

The main way to estimate the genetic distance between DNA, RNA or proteins is to compare their nucleotide or amino acid, sequences, respectively. Besides sequencing, the main techniques used are immunological ones, *annealing* (cf. **hybridization metric**) and *gel electrophoresis* (cf. **read length**).

Distances between nucleotide (DNA/RNA) or protein sequences are usually measured in terms of substitutions, i.e., mutations, between them.

A *DNA sequence* is a sequence $x = (x_1, \dots, x_n)$ over the four-letter alphabet of four nucleotides A, T, C, G (or two-letter alphabet purine/pyrimidine, or 16-letter *dinucleotide* alphabet of ordered nucleotide pairs, etc.). Let $\sum$ denote $\sum_{i=1}^{n}$.

A *protein sequence* is a sequence $x = (x_1, \dots, x_n)$ over a 20-letter alphabet of 20 standard amino acids; $\sum$ again denotes $\sum_{i=1}^{n}$.

A short sequence is called *nullomer* if it do not occur in a given species and *prime* if it has not been found in nature. Hampikian–Andersen, 2007, lists 80 human DNA nullomers of length 11 and many primes: DNA of length 15 and protein of length 5.

For a macromolecule, a *primary structure* is its atomic composition and the chemical bonds connecting atoms. For DNA, RNA or protein, it is specified by its sequence. The *secondary structure* is the 3D form of local segments defined by the hydrogen bonds. The *tertiary structure* is the 3D structure, as defined by atomic positions. The *quaternary structure* describes the arrangement of multiple molecules into larger complexes.

- **Number of DNA differences**
  The **number of DNA differences** between DNA sequences $x = (x_1, \ldots, x_n)$ and $y = (y_1, \ldots, y_n)$ is the number of mutations, i.e., their **Hamming metric**:

$$\sum 1_{x_i \neq y_i}.$$

- *p*-**distance**
  The *p*-**distance** d_p between DNA sequences $x = (x_1, \ldots, x_n)$ and $y = (y_1, \ldots, y_n)$ is defined by

$$\frac{\sum 1_{x_i \neq y_i}}{n}.$$

- **Jukes–Cantor nucleotide distance**
  The **Jukes–Cantor nucleotide distance** between DNA sequences x and y is defined, using the *p*-**distance** d_p with $d_p \leq \frac{3}{4}$, by

$$-\frac{3}{4} \ln\left(1 - \frac{4}{3} d_p(x, y)\right).$$

  If the rate of substitution varies with the gamma distribution, and a is the parameter describing the shape of this distribution, then the **gamma distance for the Jukes–Cantor model** is defined by

$$\frac{3a}{4}\left(\left(1 - \frac{4}{3} d_p(x, y)\right)^{-1/a} - 1\right).$$

- **Tajima–Nei distance**
  The **Tajima–Nei distance** between DNA sequences x and y is defined by

$$-b \ln\left(1 - \frac{d_p(x, y)}{b}\right), \quad \text{where}$$

$$b = \frac{1}{2}\left(1 - \sum_{j=A,T,C,G}\left(\frac{1_{x_i=y_i=j}}{n}\right)^2 + \frac{1}{c}\sum\left(\frac{1_{x_i \neq y_i}}{n}\right)^2\right), \quad \text{and}$$

$$c = \frac{1}{2}\sum_{i,k \in \{A,T,G,C\}, j \neq k} \frac{\left(\sum 1_{(x_i,y_i)=(j,k)}\right)^2}{\left(\sum 1_{x_i=y_i=j}\right)\left(\sum 1_{x_i=y_i=k}\right)}.$$

Let $P = \frac{1}{n}|\{1 \leq i \leq n : \{x_i, y_i\} = \{A, G\} \text{ or } \{T, C\}\}|$, and $Q = \frac{1}{n}|\{1 \leq i \leq n : \{x_i, y_i\} = \{A, T\} \text{ or } \{G, C\}\}|$, i.e., P and Q are the frequencies of, respectively, transition and transversion mutations between DNA sequences x and y.

The following four distances are given in terms of P and Q.

- **Jin–Nei gamma distance**

  The **Jin–Nei gamma distance** between DNA sequences is defined by

$$\frac{a}{2}\left((1-2P-Q)^{-1/a}+\frac{1}{2}(1-2Q)^{-1/a}-\frac{3}{2}\right),$$

  where the rate of substitution varies with the gamma distribution, and a is the parameter describing the shape of this distribution.
- **Kimura 2-parameter distance**

  The **Kimura 2-parameter distance** $K2P$ (Kimura, 1980) between DNA sequences is defined by

$$-\frac{1}{2}\ln(1-2P-Q)-\frac{1}{4}\ln\sqrt{1-2Q}.$$

- **Tamura 3-parameter distance**

  The **Tamura 3-parameter distance** between DNA sequences is defined by

$$-b\ln\left(1-\frac{P}{b}-Q\right)-\frac{1}{2}(1-b)\ln(1-2Q),$$

  where $f_x=\frac{1}{n}|\{1\le i\le n: x_i=G \text{ or } C\}|$, $f_y=\frac{1}{n}|\{1\le i\le n: y_i=G \text{ or } C\}|$, and $b=f_x+f_y-2f_xf_y$. If $b=\frac{1}{2}$, it is the **Kimura 2-parameter distance**.
- **Tamura–Nei distance**

  The **Tamura–Nei distance** between DNA sequences is defined by

$$-\frac{2f_Af_G}{f_R}\ln\left(1-\frac{f_R}{2f_Af_G}P_{AG}-\frac{1}{2f_R}P_{RY}\right)-\frac{2f_Tf_C}{f_Y}\ln\left(1-\frac{f_Y}{2f_Tf_C}P_{TC}-\frac{1}{2f_Y}P_{RY}\right)-$$
$$-2\left(f_Rf_Y-\frac{f_Af_Gf_Y}{f_R}-\frac{f_Tf_Cf_R}{f_Y}\right)\ln\left(1-\frac{1}{2f_Rf_Y}P_{RY}\right),$$

  where $f_j=\frac{1}{2n}\sum(1_{x_i=j}+1_{y_i=j})$ for $j=A,G,T,C$, and $f_R=f_A+f_G, f_Y=f_T+f_C$, while $P_{RY}=\frac{1}{n}|\{1\le i\le n: |\{x_i,y_i\}\cap\{A,G\}|=|\{x_i,y_i\}\cap\{T,C\}|=1\}|$ (the proportion of transversion differences), $P_{AG}=\frac{1}{n}|\{1\le i\le n: \{x_i,y_i\}=\{A,G\}\}|$ (the proportion of transitions within purines), and $P_{TC}=\frac{1}{n}|\{1\le i\le n: \{x_i,y_i\}=\{T,C\}\}|$ (the proportion of transitions within pyrimidines).
- **Lake paralinear distance**

  Given two DNA sequences $x=(x_1,\ldots,x_n)$ and $y=(y_1,\ldots,y_n)$, denote by $det(J)$ the determinant of the 4×4 matrix $J=((J_{ij}))$, where $J_{ij}=\frac{1}{n}|\{1\le t\le n: x_t=i, y_t=j\}|$ (joint probability) and indices $i,j=1,2,3,4$ represent nucleotides A, T, C, G, respectively. Let $f_i(x)$ denote the frequency of the i-th nucleotide in the sequence x (marginal probability), and let $f(x)=f_1(x)f_2(x)f_3(x)f_4(x)$.

The **Lake paralinear distance** (1994) between sequences x and y is defined by

$$-\frac{1}{4}\ln\frac{det(J)}{\sqrt{f(x)f(y)}}.$$

It is a **four-point inequality metric**, and it generalizes trivially for sequences over any alphabet. Related are the **LogDet distance** (Lockhart et al., 1994) $-\frac{1}{4}\ln\det(J)$ and the symmetrization $\frac{1}{2}(d(x,y)+d(y,x))$ of the **Barry–Hartigan quasi-metric** (1987) $d(x,y) = -\frac{1}{4}\ln\frac{det(J)}{\sqrt{f(x)}}$.

- **Eigen–McCaskill–Schuster distance**

  The **Eigen–McCaskill–Schuster distance** between DNA sequences $x = (x_1,\ldots,x_n)$ and $y = (y_1,\ldots,y_n)$ is defined by

$$|\{1 \le i \le n : \{x_i, y_i\} \ne \{A,G\},\{T,C\}\}|.$$

  It is the number of *transversions*, i.e., positions i with one of x_i, y_i denoting a purine and another one denoting a pyrimidine.

- **Watson–Crick distance**

  The **Watson–Crick distance** between DNA sequences $x = (x_1,\ldots,x_n)$ and $y = (y_1,\ldots,y_n)$ is defined, for $x \ne y$, by

$$|\{1 \le i \le n : \{x_i, y_i\} \ne \{A,T\},\{G,C\}\}|$$

  It is the **Hamming metric** (**number of DNA differences**) $\sum 1_{x_i \ne \overline{y}_i}$ between x and the *Watson–Crick complement* $\overline{y} = (\overline{y}_1,\ldots,\overline{y}_n)$ of y, where $\overline{y}_i = A,T,G,C$ if $y_i = T,A,C,G$, respectively. Let y^* be the reversal $(\overline{y}_n,\ldots,\overline{y}_1)$ of $\overline{y}$.

  Hybridization is the process of combining complementary single-stranded nucleic acids into a single molecule. *Annealing* is the binding of two strands by the Watson–Crick complementation. *Denaturation* is the reverse process.

  A *DNA cube* is any maximal set of DNA n-sequences, such that, for any two x, y of them, it holds that $H(x,y) = \min_{-n\le k\le n}\sum 1_{x_i \ne y^*_{i+k \,(\mathrm{mod}\ n)}} = 0$. The **hybridization metric** (Garzon et al., 1997) between DNA cubes A and B is

$$\min_{x\in A, y\in B} H(x,y).$$

- **RNA structural distances**

  An *RNA sequence* is a string over the alphabet $\{A,C,G,U\}$ of nucleotides (bases). Inside a cell, such a string folds in 3D space, because of pairing of nucleotide bases (usually, by bonds $A-U$, $G-C$ and $G-U$). The *secondary structure* of an RNA is, roughly, the set of helices (or the list of paired bases) making up the RNA. Such structure can be represented as a planar graph and further, as a rooted tree. The *tertiary structure* is the geometric form the RNA takes in space; the secondary structure is its simplified/localized model.

An **RNA structural distance** between two RNA sequences is a distance between their secondary structures. These distances are given in terms of their selected representation. For example, the **tree edit distance** (and other distances on rooted trees given in Chap. 15) are based on the rooted tree representation.

Let an RNA secondary structure be represented by a simple graph (V, E) with vertex-set $V = \{1, \ldots, n\}$ such that, for every $1 \leq i \leq n$, $(i, i+1) \notin E$ and $(i, j), (i, k) \in E$ imply $j = k$. Let $E = \{(i_1, j_1), \ldots, (i_k, j_k)\}$, and let (ij) denote the transposition of i and j. Then $\pi(G) = \prod_{t=1}^{k} (i_t j_t)$ is an involution.

Let $G = (V, E)$ and $G' = (V, E')$ be such planar graph representations of two RNA secondary structures. The **base pair distance** between G and G' is the number $|E \Delta E'|$, i.e., the **symmetric difference metric** between secondary structures seen as sets of paired bases.

The **Zuker distance** between G and G' is the smallest number k such that, for every edge $(i, j) \in E$, there is an edge $(i', j') \in E'$ with $\max\{|i - i'|, |j - j'|\} \leq k$ and, for every $(k', l') \in E'$, there is an $(k, l) \in E$ with $\max\{|k - k'|, |l - l'|\} \leq k$.

The **Reidys–Stadler–Roselló metric** between G and G' is defined by

$$|E \Delta E'| - 2T,$$

where T is the number of cyclic orbits of length greater than 2 induced by the action on V of the subgroup $\langle \pi(G), \pi(G') \rangle$ of the group Sym_n of permutations on V. It is the number of transpositions needed to represent $\pi(G)\pi(G')$.

Let $I_G = \langle x_i x_j : (x_i, x_j) \in E \rangle$ be the monomial ideal (in the ring of polynomials in the variables $x_1, \ldots, x_n$ with coefficients $0, 1$), and let $M(I_G)_m$ denote the set of all monomials of total degree $\leq m$ that belong to I_G. For every $m \geq 3$, a Liabrés-Roselló **monomial metric** between $G = (V, E)$ and $G' = (V', E')$ is

$$|M(I_G)_{m-1} \Delta M(I_{G'})_{m-1}|.$$

Chen–Li–Chen, 2010, proposed the following variation of the **directed Hausdorff distance** (Chap. 1) between two intervals $x = [x_1, x_2]$ and $y = [y_1, y_2]$, representing two RNA secondary structures:

$$\max_{a \in x} \min_{b \in y} |a - b| \left(1 - \frac{O(x, y)}{x_2 - x_1 + 1}\right),$$

where $O(x, y) = \min\{x_2, y_2\} - \max\{x_1, y_1\}$, represents the overlap of intervals x and y; it is seen as a negative gap between x and y, if they are disjoint.

- **Fuzzy polynucleotide metric**

  The **fuzzy polynucleotide metric** (or **NTV-metric**) is the metric introduced by Nieto, Torres and Valques-Trasande, 2003, on the 12-dimensional unit cube I^{12}. Four nucleotides U, C, A and G of the RNA alphabet being coded as $(1, 0, 0, 0)$, $(0, 1, 0, 0)$, $(0, 0, 1, 0)$ and $(0, 0, 0, 1)$, respectively, 64 possible triplet codons of the genetic code can be seen as vertices of I^{12}.

So, any point $(x_1, \dots, x_{12}) \in I^{12}$ can be seen as a *fuzzy polynucleotide codon* with each x_i expressing the grade of membership of element i, $1 \le i \le 12$, in the fuzzy set x. The vertices of the cube are called the *crisp sets*.

The **NTV-metric** between different points $x, y \in I^{12}$ is defined by

$$\frac{\sum_{1 \le i \le 12} |x_i - y_i|}{\sum_{1 \le i \le 12} \max\{x_i, y_i\}}.$$

Dress and Lokot showed that $\frac{\sum_{1 \le i \le n} |x_i - y_i|}{\sum_{1 \le i \le n} \max\{|x_i|, |y_i|\}}$ is a metric on the whole of $\mathbb{R}^n$. On $\mathbb{R}^n_{\ge 0}$ this metric is equal to $1 - s(x, y)$, where $s(x, y) = \frac{\sum_{1 \le i \le n} \min\{x_i, y_i\}}{\sum_{1 \le i \le n} \max\{x_i, y_i\}}$ is the **Ruzicka similarity** (Chap. 17).

- **Genome rearrangement distances**

  The *genomes* of related unichromosomal species or single chromosome organelles (such as small viruses and mitochondria) are represented by the order of genes along chromosomes, i.e., as *permutations* (or *rankings*) of a given set of n homologous genes. If one takes into account the directionality of the genes, a chromosome is described by a *signed permutation*, i.e., by a vector $x = (x_1, \dots, x_n)$, where $|x_i|$ are different numbers $1, \dots, n$, and any x_i can be positive or negative.

  The circular genomes are represented by circular (signed) permutations $(x_1, \dots, x_n)$, where $x_{n+1} = x_1$ and so on.

  Given a set of considered mutation moves, the corresponding *genomic distance* between two such genomes is the **editing metric** (Chap. 11) with the editing operations being these moves, i.e., the minimal number of moves needed to transform one (signed) permutation into another.

  In addition to (and, usually, instead of) local mutation events, such as character indels or replacements in the DNA sequence, the *large* (i.e., happening on a large portion of the chromosome) mutations are considered, and the corresponding genomic editing metrics are called **genome rearrangement distances**. In fact, such rearrangement mutations being rarer, these distances estimate better the true genomic evolutionary distance.

  The genome (chromosomal) rearrangements are *inversions* (block reversals), *transpositions* (exchanges of two adjacent blocks), *inverted transpositions* (inversions combined with transpositions) in a permutation, and, for signed permutations, *signed reversals* (sign reversal combined with inversion). The main genome rearrangement distances between two unichromosomal genomes are:

  Cayley, **reversal** and **signed reversal** metrics (cf. Chap. 11);

  ITT-distance: the minimal number of inversions, transpositions and inverted transpositions needed to transform one of them into another.

  Given two circular signed permutations $x = (x_1, \dots, x_n)$ and $y = (y_1, \dots, y_n)$ (so, $x_{n+1} = x_1$, etc.), a *breakpoint* is a number i, $1 \le i \le n$, such that $y_{i+1} \ne x_{j(i)+1}$, where the number $j(i)$, $1 \le j(i) \le n$, is defined by the equality $y_i = x_{j(i)}$.

The **breakpoint distance** (Watterson et al., 1982) between genomes, represented by x and y, is the number of breakpoints.

This distance and the **permutation editing metric** (the **Ulam metric** from Chap. 11: the minimal needed number of one-character transpositions) are used for the approximation of genome rearrangement distances.

- **Syntenic distance**

  This is a *genomic distance* between multi-chromosomal genomes, seen as unordered collections of *synteny sets* of genes, where two genes are *syntenic* if they appear in the same chromosome. The **syntenic distance** (Ferretti–Nadeau–Sankoff, 1996) between two such genomes is the minimal number of mutation moves—*translocations* (exchanges of genes between two chromosomes), *fusions* (merging of two chromosomes into one) and *fissions* (splitting of one chromosome into two)—needed to transfer one genome into another. All (input and output) chromosomes of these mutations should be nonempty and not duplicated.

  The above three mutation moves correspond to interchromosomal genome rearrangements which are rarer than intrachromosomal ones; so, they give information about deeper evolutionary history.

- **Genome distance**

  The **genome distance** between two loci on a chromosome is a physical distance: the number of base pairs (bp) separating them on the chromosome.

  In particular, the **intragenic distance** of two neighboring genes is the smallest distance in bp separating them on the chromosome. Sometimes, it is defined as the genome distance between the transcription start sites of those genes.

  Nelson, Hersh and Carrol, 2004, defined the *intergenic distance* of a gene as the amount of noncoding DNA between the gene and its nearest neighbors, i.e., the sum of upstream and downstream distances, where *upstream distance* is the genome distance between the start of a gene's first exon and the boundary of the closest upstream neighboring exon and *downstream distance* is the distance between the end of a gene's last exon and the boundary of the closest downstream neighboring exon. If exons overlap, the intergenic distance is 0.

- **Strand length**

  A single strand of nucleic acid (DNA or RNA sequence) is oriented *downstream*, i.e., from the $5'$ *end* toward the $3'$ *end* (sites terminating at the 5-th and 3-rd carbon in the sugar-ring; $5'$-phosphate binds covalently to the $3'$-hydroxyl of another nucleotide). So, the structures along it (genes, transcription factors, polymerases) are either downstream or upstream. The **strand length** is the distance from its 5' to 3' end. Cf. **end-to-end distance** (in Chap. 24) for a general polymer.

  For a molecule of *messenger RNA* (mRNA), the **gene length** is the distance from the *cap site* $5'$, where post-translational stability is ensured, to the *polyadenylation site* $3'$, where a poly(A) tail of 50–250 adenines is attached after translation.

- **Map distance**

  The **map distance** between two loci on a genetic map is the recombination frequency expressed as a percentage; it is measured in *centiMorgans* cM (or *map*

units), where 1 cM corresponds to a 1 % ($\frac{1}{100}$) chance that a segment of DNA will crossover or recombine within one generation. Genes at map distance 50 cM are unlinked.

For humans, 1.3 cM corresponds to a **genome distance** of 1 Mb (million bp). In the female this recombination rate (and so map distances) are twice that of the male. In males, the total length of intervals between linked genes is 2500 cM.

During meiosis in humans, there is an average of 2 to 3 crossovers for each pair of homologous chromosomes. The *intermarker meiotic recombination distance* (Dib et al., 1992) counts only meiotic crossovers. Mitotic crossover is rare.

- **tRNA interspecies distance**

  Transfer RNA (tRNA) molecules are necessary to translate *codons* (nucleotide triplets) into amino acids; eukaryotes have up to 80 different tRNAs. Two tRNA molecules are called *isoacceptor tRNAs* if they bind the same amino acid.

  The **tRNA interspecies distance** between species m and n is (Xue et al., 2003), averaged for all 20 amino acids, the *tRNA distance for a given amino acid* aa_i which is, averaged for all pairs, the **Jukes–Cantor protein distance** between each isoacceptor tRNAs of aa_i from species m and each isoacceptor tRNAs of the same amino acid from species n.
- **PAM distance**

  There are many notions of similarity/distance (20×20 *scoring matrices*) on the set of 20 standard amino acids, based on genetic codes, physico-chemical properties, secondary structural matching, structural properties (hydrophilicity, polarity, charge, shape, etc.) and observed frequency of mutations. The most frequently used one is the **Dayhoff distance**, based on the 20×20 *Dayhoff PAM250* matrix which expresses the relative mutability of amino acids.

  The **PAM distance** (or **Dayhoff–Eck distance**, *PAM value*) between protein sequences is defined as the minimal number of accepted (i.e., fixed) point mutations per 100 amino acids needed to transform one protein into another.

  1 PAM is a unit of evolution: it corresponds to 1 point mutation per 100 amino acids. PAM values 80, 100, 200, 250 correspond to the distance (in %) 50, 60, 75, 92 between proteins.
- **Genetic code distance**

  The **genetic code distance** (Fitch and Margoliash, 1967) between amino acids x and y is the minimum number of nucleotides that must be changed to obtain x from y. In fact, it is 1, 2 or 3, since each amino acid corresponds to three bases.
- **Miyata–Miyazawa–Yasanaga distance**

  The **Miyata–Masada–Yasanaga distance** (or *Miyata's biochemical distance*, 1979) between amino acids x, y with polarities p_x, p_y and volumes v_x, v_y is defined by

$$\sqrt{(\frac{|p_x - p_y|}{\sigma_p})^2 + (\frac{|v_x - v_y|}{\sigma_v})^2},$$

  where σ_p and σ_v are the standard deviations of $|p_x - p_y|$ and $|v_x - v_y|$.

This distance is derived from the similar *Grantam's chemical distance* (Grantam, 1974) based on polarity, volume and carbon-composition of amino acids.

- **Polar distance (in Biology)**

  The following three physico-chemical distances between amino acids x and y were defined in Hughes–Ota–Nei, 1990.

  Dividing amino acids into two groups—*polar* (C, D, E, H, K, N, Q, R, S, T, W, Y) and nonpolar (the rest)—the **polar distance** is 1, if x, y belong to different groups, and 0, otherwise. The second polarity distance is the absolute difference between the polarity indices of x and y. Dividing amino acids into three groups—*positive* (H, K, R), *negative* (D, E) and *neutral* (the rest)—the **charge distance** is 1, if x, y belong to different groups, and 0, otherwise.

- **Feng–Wang distance**

  20 amino acids can be ordered linearly by their *rank-scaled* functions CI, NI of pK_a values for the terminal amino acid groups COOH and NH_3^+, respectively. 17 CI is 1,2,3,4,5,6,7,7,8,9,10,11,12,13,14,14,15,15,16,17 for C,H,F,P,N,D,R,Q,K,E, Y,S,M,V,G,A,L,I,W,T, while 18 NI is 1,2,3,4,5,5,6,7,8,9, 10,10,11,12,13,14,15,16,17,18 for N,K,R,Y,F,Q,S,H,M,W,G,L,V,E,I,A,D,T,P,C.

  Given a protein sequence $x = (x_1, \ldots, x_m)$, define $x_i < x_j$ if $i < j, CI(x_i) < CI(x_i)$ and $NI(x_i) < NI(x_i)$ hold. Represent the sequence x by the augmented $m \times m$ *Hasse matrix* $((a_{ij}(x)))$, where $a_{ii}(x) = \frac{CI(x_i)+NI(x_i)}{2}$ and, for $i \neq j$, $a_{ij}(x) = -1$ or 1 if $x_i < x_j$ or $x_i \geq x_j$, respectively.

  The **Feng–Wang distance** ([FeWa08]) between protein sequences $x = (x_1, \ldots, x_m)$ and $y = (y_1, \ldots, y_n)$ is defined by

$$||\frac{\lambda(x)}{\sqrt{m}} - \frac{\lambda(y)}{\sqrt{n}}||_2,$$

  where $\lambda(z)$ denotes the largest eigenvalue of the matrix $((a_{ij}(z)))$.

- **Number of protein differences**

  The **number of protein differences** between protein sequences $x = (x_1, \ldots, x_m)$ and $y = (y_1, \ldots, y_n)$ is just the **Hamming metric** between protein sequences:

$$\sum 1_{x_i \neq y_i}.$$

- **Amino p-distance**

  The **amino p-distance** (or *uncorrected distance*) d_p between protein sequences $x = (x_1, \ldots, x_m)$ and $y = (y_1, \ldots, y_n)$ is defined by

$$\frac{\sum 1_{x_i \neq y_i}}{n}.$$

- **Amino Poisson correction distance**
  The **amino Poisson correction distance** between protein sequences x and y is defined, via the **amino p-distance** d_p, by

$$-\ln(1 - d_p(x, y)).$$

- **Amino gamma distance**
  The **amino gamma distance** (or *Poisson correction gamma distance*) between protein sequences x and y is defined, via the **amino p-distance** d_p, by

$$a((1 - d_p(x, y))^{-1/a} - 1),$$

  where the substitution rate varies with $i = 1, \ldots, n$ according to the gamma distribution with the shape described by the parameter a. For $a = 2.25$ and $a = 0.65$, it estimates the **Dayhoff distance** and **Grishin distances**, respectively. In some applications, this distance with $a = 2.25$ is called simply the **Dayhoff distance**.
- **Jukes–Cantor protein distance**
  The **Jukes–Cantor protein distance** between protein sequences x and y is defined, via the **amino p-distance** d_p, by

$$-\frac{19}{20}\ln\left(1 - \frac{20}{19}d_p(x, y)\right).$$

- **Kimura protein distance**
  The **Kimura protein distance** between protein sequences x and y is defined, via the **amino p-distance** d_p, by

$$-\ln\left(1 - d_p(x, y) - \frac{d_p^2(x, y)}{5}\right).$$

- **Grishin distance**
  The **Grishin distance** d between protein sequences x and y can be obtained, via the **amino p-distance** d_p, from the formula

$$\frac{\ln(1 + 2d(x, y))}{2d(x, y)} = 1 - d_p(x, y).$$

- **k-mer distance**
  The **k-mer distance** (Edgar, 2004) between sequences $x = (x_1, \ldots, x_m)$ and $y = (y_1, \ldots, y_n)$ over a compressed amino acid alphabet is defined by

$$\ln\left(\frac{1}{10} + \frac{\sum_a \min\{x(a), y(a)\}}{\min\{m, n\} - k + 1}\right),$$

where a is any *k-mer* (a word of length k over the alphabet), while $x(a)$ and $y(a)$ are the number of times a occurs in x and y, respectively, as a *block* (contiguous subsequence). Cf. **q-gram similarity** in Chap. 11.

- **Santoni–Felici–Vergni proximity**

  Given a protein sequence $v = (v_1, \ldots, v_N)$ and two amino acids a and b in it, let $(x_1, \ldots, x_n)$ and $(y_1, \ldots y_m)$ be arrays of occurrence positions in v of a and b, respectively. The **proximity in v between a and b** is (Santoni–Felici–Vergni, 2016)

$$P_v(a,b) = \frac{1}{n}\sum_{i=1}^{n} \min_{j=1,\ldots,m} \{|x_i - y_j|\}.$$

  Using the above function and machine learning, the authors found a way to discriminate between natural and random protein sequences. It shows how natural selection dominates the randomising effect of casual mutations in protein evolution.

- **Whole genome composition distance**

  Let A_k be the set of all $\sum_{i=1}^{k} 4^i$ nonempty words of length at most k over the alphabet of four RNA nucleotides. For an RNA sequence $x = (x_1, \ldots, x_n)$ and any $a \in A_k$, let $g_a(x)$ be the number of occurrences of a as a *block* (contiguous subsequence) in x and $f_a(x)$ be $g_a(x)$ divided by the number of blocks of the same length in x.

  The **whole genome composition distance** (Wu et al., 2006) between RNA sequences x and y (of two strains of HIV-1 virus) is the Euclidean distance

$$\sqrt{\sum_{a\in A_k} (f_a(x) - f_a(y))^2}.$$

  The D^2 *distance* (Torney et al., 1990) is $\sum_{a\in A_k \setminus A_l} (g_a(x) - g_a(y))^2$ for some $l \le k$. The D_2 *statistic* (Lippert et al., 2002) is the number of k-word matches of x, y.

- **Huang ensemble distance**

  Consider a genome, represented by a nucleotide sequence $s = (s_1, \ldots, s_l)$, of length l, where $s_i \in \{AC, G, T\}$. For $t = A, C, G, T$, define $w_t(s_i) = 1$ if $s_i = t$ and $w_t(s_1) = 0$, otherwise. The *natural vector* of s is defined to be the concatenation

$$(n_A, n_C, n_G, n_T, \mu_A, \mu_C, \mu_G, \mu_T, D_A, D_C, D_G, D_T)$$

  of three following vectors: the *counting vector* (n_A, n_C, n_G, n_T), where $n_t = \sum_{i=1}^{l} w_t(s_i)$, the *first moment of positions* $(\mu_A, \mu_C, \mu_G, \mu_T)$, where $\mu_t = \sum_{i=1}^{l} i\frac{w_t(s_i)}{n_t}$ and the *second moment of positions* (D_A, D_C, D_G, D_T), where $D_t = \sum_{i=1}^{l} (i - \mu_t)^2 \frac{w_t(s_i)}{l n_t}$.

The *k-mer vector* is $(m(1), \dots, m(4^k))$ where $m(j)$ is the number of times the j-th of 4^k possible strings of k nucleotides occurs as k consecutive elements in s.

A *multipartite*, i.e., consisting of several nucleic acid molecules, virus can be represented by a set of natural and k-mer counting vectors of its multiple genome segments. The **Huang ensemble distance** between such viruses X and Y is

$$\sqrt{\frac{N_{XY}^2}{\delta_N^2} + \frac{K_{XY}^2}{\delta_K^2}}$$

(Huang, 2016), where N_{XY}, K_{XY} are the **Hausdorff distances** between the sets of their natural vectors and between the sets of their k-mer counting vectors, and δ_N^2, δ_K^2 are the variances of the upper triangular matrix with elements N_{IJ} and K_{IJ} (for all pairs IJ of considered viruses), respectively.

N_{XY}, N_{XY} are $\max\{\max_{x\in X} \min_{y\in Y} d(x,y), \max_{y\in Y} \min_{x\in X} d(x,y)\}$, where $d(x,y)$ is the Euclidean distance of two natural or k-mer counting vectors $x \in X$, $y \in Y$.

- **Additive stem w-distance**

  Given an alphabet $\mathcal{A}$, let $w = w(a,b) > 0$ for $a, b \in \mathcal{A}$, be a weight function on it. The **additive stem w-distance** between two n-sequences $x, y \in \mathcal{A}^n$ is defined (D'yachkov and Voronina, 2008) by

$$D_w(x,y) = \sum_{i=1}^{n-1} (s_i^w(x,x) - s_i^w(x,y)),$$

  where $s_i^w(x,y) = w(a,b)$ if $x_i = y_i = a, x_{i+1} = y_{i+1} = b$ and $s_i^w(x,y) = 0$, otherwise. If all $w(a,b) = 1$, then $\sum_{i=1}^{n-1} s_i(x,y)$ is the number of common 2-blocks containing adjacent symbols in the longest common subsequence of x and y; then $D_w(x,y)$ is called a **stem Hamming distance**.

- **ACS-distance**

  Given an alphabet $\mathcal{A}$, the *average common substring length* between sequences $x = (x_1, \dots, x_m)$ and $y = (y_1, \dots, y_n)$ over $\mathcal{A}$ is (Ulitsky et al., 2006) $L(x,y) = \frac{1}{m}\sum_{i=1}^{m} l_i$, where l_i is the length of the longest substring $(x_i, \dots, x_{i-1+l_i})$ which matches a substring of y. So, $L(x,x) = \frac{m+1}{2}$.

  The **ACS-distance** is defined by

$$\frac{1}{2}\left(\frac{\log(n)}{L(x,y)} - \frac{\log(m)}{L(x,x)} + \frac{\log(m)}{L(y,x)} - \frac{\log(n)}{L(y,y)}\right).$$

  A similar distance was considered (Haubold et al., 2009) replacing the longest common substring by the shortest absent one.

23.3 Distances in Ecology, Biogeography, Ethology

Main distance-related notions in Ecology, Biogeography and Animal Behavior follow.

- **Niche overlap similarities**

  A *niche* is environmental space, while a *biotope* is a geographic space.

  Let $p(x) = (p_1(x), \ldots, p_n(x))$ be a *frequency vector* (i.e., all $p_i(x) \geq 0$ and $\sum_i p_i(x) = 1$) representing an ecological niche of species x, for instance, the proportion of resource i, $i \in \{1, \ldots, n\}$, used by species x.

  Four main **niche overlap similarities** of species x and y are:

  Schoener's D, introduced by Renkonen in 1938:

$$D(x, y) = 1 - \frac{1}{2} \sum_{i=1}^{n} |p_i(x) - p_i(y)|;$$

  cosine similarity (Chap. 17), called in Ecology (from 1973) *Pianka's O*:

$$O(x, y) = \frac{\langle p(x), p(y) \rangle}{||p(x)||_2 \cdot ||p(y)||_2};$$

  Hellinger I (i.e., **fidelity similarity**, cf. Chap. 14) and **Bray–Curtis** (or, since $p(x), p(y)$ are frequency vectors, *Renkonen percentage*) **similarity** (Chap. 17).

- **Ecological distance**

  Let a given species be distributed in subpopulations over a given *landscape*, i.e., a textured mosaic of *patches* (homogeneous areas of land use, such as fields, lakes, forest) and linear *frontiers* (river shores, hedges and road sides). The individuals move across the landscape, preferentially by frontiers, until they reach a different subpopulation or they exceed a maximum **dispersal distance**.

  The **ecological distance** between two subpopulations (patches) x and y is defined (Vuilleumier–Fontanillas, 2007) by

$$\frac{D(x, y) + D(y, x)}{2},$$

  where $D(x, y)$ is the distance an individual covers to reach patch y from patch x, averaged over all successful dispersers from x to y. If no such dispersers exist, $D(x, y)$ is defined as $\min_z(D(x, z) + D(z, x))$.

  Ecotopes are the smallest ecologically distinct features in a landscape mapping.

  Effective ecological distance (or *cost-distance*) is the Euclidean distance modified for the effect of landscape and behavior on the dispersal of an organism between locations in the landscape. Such functional distance can be computed as *least-cost path* using either *cost surface* (matrix between patches assigning degree of permeability depending on hostile habitat or physical barriers), or

resistance surface accounting for costs (resistance per unit distance) of passing through different landscape elements. Cf. **resistance metric** in Chap.15. Pinto–Kein, 2009, proposed *least-cost corridors* formed by multiple paths with similar costs, since animals, even birds, rarely move along straight-line paths in a landscape.

- **Biotope distance**

  The *biotopes* here are represented as binary sequences $x = (x_1, \dots, x_n)$, where $x_i = 1$ means the presence of the species i. The **biotope** (or **Tanimoto**, cf. Chap. 17) **distance** between biotopes x and y is defined by

$$\frac{|\{1 \le i \le n : x_i \ne y_i\}|}{|\{1 \le i \le n : x_i + y_i > 0\}|} = \frac{|X \Delta Y|}{|X \cup Y|},$$

  where $X = \{1 \le i \le n : x_i = 1\}$ and $Y = \{1 \le i \le n : y_i = 1\}$.

- **Prototype distance**

  Given a finite metric space (X, d) (usually, a Euclidean space) and a selected, as typical by some criterion, vertex $x_0 \in X$, called the *prototype*, the **prototype distance** of every $x \in X$ is the number $d(x, x_0)$.

  Usually, the elements of X represent phenotypes or morphological traits. The average of $d(x, x_0)$ over $x \in X$ estimates the corresponding *variability*.

- **Critical domain size**

  In Spatial Ecology, the **critical domain size** is (Kierstead and Slobodkin, 1953) the minimal amount of habitat, surrounded by a hostile matrix, required for a population to persist. For example, in the invasion and persistence of algal and insect populations in rivers, such a size is the minimal length of a river (with a given, less than the threshold, flow speed) that supports a population.

- **Island distance effect**

  An *island*, in Biogeography, is any area of habitat surrounded by areas unsuitable for the species on the island: true islands surrounded by ocean, mountains isolated by surrounding lowlands, lakes surrounded by dry land, isolated springs in the desert, grassland or forest fragments surrounded by human-altered landscapes.

  The **island distance effect** is that the number of species found on an island is smaller when the degree of isolation (distance to nearest neighbor and mainland) is larger. Also, organisms with high dispersal, such as plants and birds, are much more common on islands than are poorly dispersing taxa like mammals.

- **Dispersal distance**

  In Biology, the **dispersal distance** is a **range distance** to which a species maintains or expands the distribution of a population. It refers, say, to seed dispersal by pollination and to natal, breeding and migration dispersal. For animals, *natal dispersal* is permanent emigration from the natal range to a disjoint adult range, and **dispersal distance** is the distance between their barycenters.

  The dispersal distance is usually described by a *dispersal kernel* which gives the probability distribution of the distance traveled by any individual.

When *outcrossing* (gene flow) is used to increase genetic diversity of a plant species, the *optimal outcrossing distance* is the dispersal distance at which seed production is maximized. It is less than the mean pollen dispersal distance.

Plant height matters more than seed mass for its dispersal distance. Unusual way of wind dispersal include tumbleweeds.

Pollen from *Pinus sylvestris* can fly 100 km, but oceanic larvae dispersal is at least one order of magnitude greater than that of pollen-dispersing terrestrial biotas.

- **Long-distance dispersal**

  Long-distance dispersal (or *LDD*) refers to the rare events of biological dispersal on distances an order of magnitude greater than the median **dispersal distance**. For the regional survival of some plants, LDD is more important than local (median-distance) dispersal. The longest recorded distance traveled by a drift seed is 28,000 km by a Mary's bean from the Marshall Islands to Norway.

  LDD emerged in Biogeography as greater factor of biodiversity and species migration patterns than original *vicarience theory* (dispersal via land bridges) based on continental drift. Such relatively recent chance dispersal explain the fast spread of organisms in new habitats, for example, plant pathogens, invasive species and in paleocolonization events, such as the joining of North and South America 3 Ma ago, or Africa and India with Eurasia 30 and 50 Ma ago.

  Human colonization of Madagascar (isolated for 88 Ma) ≈2000 years ago may have resulted from an accidental transoceanic crossing; other animals arrived by rafting from Africa 60–70 Ma ago. LDD followed traders and explorers, especially, in Columbian Exchange after 1492.

  Transoceanic LDD by wind/water currents can explain strong floristic similarities among landmasses in the southern hemisphere. Monkey, rodents, and crocodiles dispersed 50–30 Ma ago to the Americas from Africa via the Atlantic.

  Free-living microbes occupy every niche but their biodiversity is low, because they are carried by wind thousands of km on dust particles protecting them from UV. Extreme example of such (or via underground rivers, before the continents split) LDD: sunlight-independent bacterium *Desulforudis audaxviator*, living 1–3.3 km deep in South Africa (the only species known to be alone in its ecosystem and radiation-relying), reached deep boreholes in eastern California.

  Some other LDD vehicles are: rafting by water (corals can traverse 40,000 km during their lifetime), migrating birds, human transport, ship ballast water, and extreme climatic events. Snails can travel hundreds of km inside bird guts: 1–10 % of eaten snails survive up to 5 h until being ejected in bird feces.

  Also, cancer invasion (spread from primary tumors invading new tissues) can be thought as an invasive species spread via LDD, followed by localized dispersal.

  The most invasive mammal species (besides humans) are: rabbits, black rats, gray squirrels, goats, pigs, deers, mice, cats, red foxes, mongooses. Invasive *Argentine ants* form the largest global insect mega-colony: they do not attack each other.

- **Migration distance (in Biogeography)**

  Migration distance is the distance between regular breeding and foraging areas within seasonal large-scale return movement of birds, fish, insects, turtles, seals, etc.

  The longest such recorded round-trip is 71,000 km pole-to-pole traveled each year by the Arctic tern. The highest migration altitude is 9 km by bar-headed goose. Longest each way migration for a mammal is ≈9800 km, traveled by a humpback whale from the Brazilian coast to Madagascar, and, for an insect, ≈4500 km by desert locust and Monarch butterfly.

  One of unsolved problems in Biology is: how do the descendants of Monarch butterfly, migrating from Canada to central Mexico for several generations, manage to return to a few small overwintering spots? Also, why the ancient murrelets fly almost 8000 km across entire North Pacific and back—for no obvious benefit?

  Migration differs from *ranging*, i.e., the movement of an animal beyond its home range which ceases when a suitable new home range (a resource: food, mates, shelter) is found. It differs also from foraging/commuting as occurs, say, for albatrosses or plankton. Wandering albatrosses, having the largest (3.63 m) wingspan, make several-days foraging round trips of up to 3000 km. Krill, 1–2 cm long, move up to 500 m vertically each night, to feed in the sunlit waters, where plants are abundant, while avoiding being seen by predators. *Mesopelagic* (living 0.2–1 km deep) fish also travel to upper layers at night.

  At the population level, migration involves displacement, while ranging/foraging result only in mixing. Entire species migrate slowly by shifting, because of rapid climate change, their geographical or elevation ranges. Chen et al., 2011, found that the mean travel poleward of over 1300 species, considered by them, was 17 km a decade; vertically, the mean had a species moving 11 m uphill.

  During ice ages species move to hotspots, say, volcanoes. In early Holocene, forests migrated northward, up to 5 km per decade, using LDD (by birds) and low-density founder populations. Root et al., 2003, claim that butterflies, birds and plants move towards the poles by 6.1 km per decade over the past 100 years.

  Lyons et al., 2015: during last 300 Mya, more pairs of land species with correlated co-occurrence were positively correlated than negatively correlated ones, and 6000 years ago this pattern was reversed. They explains it by barriers to dispersal introduced by increasing human population and the spread of agriculture.

- **Daily distance traveled**

  Daily distance traveled D (m/day) is an important parameter of the energy budget of ranging/foraging mammals.

  The *foraging efficiency* is the ratio $\frac{B}{C}$, where C, B (J/m) are the energy costs of travel and of acquiring energy. Over a day, the expected total net energy return is $D(B - C)$. The *locomotor cost* is the distance traveled per unit energy spent on locomotion. The limb length determines this cost in terrestrial animals but no

link with D has been observed. Pontzer, 2011, explains this paradox by high $\frac{B}{C}$ in most taxa: only for $\frac{B}{C} < 10$, would selection for limb length be needed.

Within species, over a lifetime, increased D is associated with decreased $B - C$, reproductive effort and maintenance. But among species, over evolutionary time, it is associated with a greater number of offspring and their total mass per lifetime.

The mean D traveled by carnivores is four times such distance by herbivores. Also, D and feeding/grooming time are much greater in larger groups of primates. Foraging radius, D and annual travel distance of Neanderthal was $\approx$ 75 % of that of humans.

- **Collective motion of organisms**

  Organisms aggregate to procure resources (pack-hunting), to find mates (plankton, plants) and to lower predation risk (meerkats, schools of sardines, flocks of starlings). Animals moving in large groups at the same speed and in the same direction, tend to have similar size and to be regularly spaced.

  The near-constant distance which an animal maintains from its immediate neighbors is called the **nearest-neighbor distance** (NDD). When NDD decreases, the mode of movement can change: marching locusts align, ants build bridges, etc.

  Moving in file when perception is limited to one individual (ants, caterpillars in processions up to 300, spiny lobsters in parallel chains of 3–30), animals use tactile cues or just perceive and follow the choice of the preceding individual, such as sheep in mountain path or cows in cattle-handling facilities. Penguins in the huddle move ("traveling wave", like the stop-and-go of cars in a traffic jam) trigger movements in their neighbors as soon as the threshold distance ($\approx$ 2 cm, i.e., twice the thickness of their compressive feather layer) is formed between two penguins.

  The greatest recorded group of moving animals was a swarm in US, 1875, by 12.5 trillion insects (Rocky Mountain locust, extinct by now) covering 510,000 km^2. A swarm by extant desert locusts in Kenya, 1954, covered 200 km^2.

  Flights of migratory pest insects occur usually at altitudes up to 1 km, and are downwind; they last for a few hours with displacement up tp 400 km. Flocks of *red-billed Quelea* (the most abundant wild bird species) take up to 5 h to fly past. Herring schools occupy up to 4.8 km^3 with density 0.5–1.0 fish per m^3. Jellyfish *Rhopilema nomadica* form swarms 100 km long.

  Schools of sardines, anchovy and krill, despite being variable in size, share a ratio $\frac{S}{V} = 3.3\ m^{-1}$ of surface area to volume; it has been interpreted as the optimal trade-off between predator avoidance and resource acquisition.

  The spatiotemporal movement patterns, emerging from such groups, result from interactions between individuals. This local mechanism can be *allelomimesis* ("do what your neighbor does"), social attraction (say, to the center of mass of neighbors), or the threat of cannibalism from behind (in running Mormon crickets and desert locusts), mass mate-searching (in burrow-dwelling crabs). Vicsek, 1995, modelled a swarm as a collection of particles moving with a constant

speed but adopting, if perturbation, at each time increment the average motion's direction of the neighbors.

Migrating birds tend to fly in a V, J, or W shaped formation. In energy-saving V-formation (or *skein*), they sync their flapping to hook the former bird's updraft. The birds flying at the front and the tips are rotated. The changes in distance between members and in direction propagate like sound waves: for distance better in bigger flocks, while for direction better in smaller flocks.

Most spectacular are aerial displays of flocks of starlings highly variable in shape. Scale-free behavioral correlation was observed: regardless of flock size, the correlations of a bird's orientation and velocity with the other birds did not vary and was near-instantaneous. Cf. *SOC* in **scale invariance** (Chap. 18).

Silverberg et al., 2013, discovered self-organized emergent behavior in *moshing* (when 100–100,000 fans at heavy metal concert form circles and then run together with abandon, bouncing off one another). In fact, the speed distribution of people closely matches that of molecules in a 2D gas at equilibrium and moshing corresponds to domination of the model's parameters by noise.

Such emerging, when their number increases, collective behavior can be seen as a *critical phase transition*; it was observed also for simple automatons.

Besides animals, collective directed motion occurs also in cellular populations. Some aggregated bacterial populations (say, foraging swarms of billions of *Paenibacillus vortex*) can migrate rapidly and coordinately over a surface. A *grex* is an slug-like aggregate 2–4 mm long of up to 100,000 amoebas formed when they are under stress. It moves as a unit, only forward, 1 mm/h. Other example of small-scale moving super-organism: oceanic *pyrosomes* (clonal colonies of zooids-tunicates).

In a multicellular organism, collective cell migration occurs (usually by *chemotaxis*: response to chemical concentration) throughout embryonic development, wound healing (fibroplasts and epithelial cells), immune response (leukocytes), and cancerous tumor invasion. Similarly to migration of songbirds, cancerous cells prepare for metastatic travel by gathering proteins near their leading edges.

During development, some cells migrate to very long distances. For example, newborn neurons in the adult brain can traverse $\frac{2}{3}$ of its length.

- **Distances in Animal Behavior**

  The first such distance was derived by Hediger for zoos; his *interanimal distance* is the maximum species-specific distance at which conspecifics approach each other. In 1955, he defined *flight distance* (run boundary), *critical distance* (attack boundary), *personal distance* (at which members of noncontact species feel comfortable) and *social distance* (at which within-species groups tolerate each other).

  The exact such distances are highly context dependent. An example: a tamer manipulate a semi-tamed lion moving in and out of its critical zone.

  For humans, flight and critical distances have been, with few exceptions, eliminated. So, Hall adapted above space boundaries; cf. his **distances between people** in Chap. 28. The main **distances in Animal Behavior** follow.

The **individual distance**: the distance which an animal attempts to maintain between itself and other animals. It ranges between "proximity" and "far apart" (for example, ≤ 8 m and ≥ 61 m in elephant social calls). Bell et al., 2012, found that gaining and maintaining a preferred interanimal distance, accounts for much of the variability in dodging by rats and field crickets.

The **group distance**: the distance which a group of animals attempts to maintain between it and other groups. Cf. the **nearest-neighbor distance**.

The **alert distance**: the distance from the disturbance source (say, a predator or a dominating conspecific) when the animal changes its behavior (say, turns towards as *perception advertisement*) in response to an approaching threat.

The **flight initiation distance** (or FID, *escape distance*): the distance from the disturbing stimulus when escape begins. FID, corrected for the *distance to refuge*, is a measure of animal's boldness.

The **reaction distance**: the distance at which the animal reacts to the appearance of prey; *catching distance*: the distance at which the predator can strike a prey.

The **detection distance**: the maximal distance from the observer at which the individual or cluster of them is seen, heard, or detected by some other remote way. For example, it is 2000 m for an eagle searching for displaying sage-grouse and 1450 m for a sage-grouse scanning for a flying eagle.

The **social recognition distance**: the distance over which a contact call can be identified as belonging to a family.

In the main nonresource-based mating system, *lek mating*, females in estrous visit a congregation of displaying males, the *lek* and mate preferentially with males of higher **lekking distance rank**, i.e., relative distance from male territory (the median of his positions) to the center of the lek. High-ranking individuals have smaller, centrally located (so, less far to travel and more secure) home ranges.

The **distance-to-shore**: the distance to the coastline used to study clustering of whale strandings (by distorted echo-location, anomalies of magnetic field, etc.).

The **sleeping distance** of a mating pair: for example, it is no further than 0.5 m in Arctic blue fox, but more than 2–2.5 m one month after copulation.

- **Snout-vent length**

  The **snout-vent length** (SVL) or *nose–cloaca distance* (NCD) is an animal's length taken from the tip of the nose (*snout*) to the cloaca's opening (*vent*) at the tail base.

  The **gape distance** is the width of the widely opened mouth of a vertebrate.

- **Animal proximity network**

  An *animal proximity network* is a digraph of individuals with a pair of them forming an edge or arc in the case of spatiotemporal co-occurrence using some range criteria: a mutual distance threshold or some distance rule (say, nearest neighbor) within a given distance around a focal individual.

  In general, the amount of time spent in proximity to another individual does not correlate with the proportion of social interactions between pairs of individuals. But proximity is a good proxy for interaction rates in mixed-species

bird flocks, for social information or disease transmission, and for some social behaviors, such as foraging, grooming, sleeping, mate guarding, and parent–offspring relationships.

- **Animal depth/distance perception**

  Many animals, including humans, have two eyes with overlapping visual fields that use parallax (cf. **parallax distance** in Chap. 26) for depth perception and distance estimation. Some animals (for example, pigeons) use *motion parallax* in which they move head to gain different viewpoints. Anoter example: the velocity of the mantis's head movement is kept constant during peering. So, the distance to the target (prey) is inversely proportional to the velocity of the retinal image.

  All animals have a binocular region (growing as eyes become more forward-facing) which allows for vision through the clutter, as long as the width of the objects causing clutter is less than the **interpupillary distance** (cf. Chap. 29) d.

  Changizi–Shimojo, 2008, suggested that the degree of binocular convergence is selected to maximize how much the animal can see. Most animals exist in noncluttered environments or surroundings where the cluttering objects are bigger in size than d. They tend to have sideways-facing eyes allowing panoramic vision. But humans and other large mammals evolved in leafy environments like forests and their forward-facing eyes (and smaller distance d) maximize ability to see.

  Still, the human eye sockets are much wider relative to their height and the outer margin is recessed much further back in the human skull, than those of the apes. So, unlike "forest view" of other apes, our "savannah eyes" can have a lateral view that is unimpeded by the bones of the skull.

  Larvae of the sunburst diving beetle (*Thermonectus marmoratus*) have 6 pairs of eyes. Four eyes of two frontal pairs (used to scan potential prey) have bifocal lenses and at least two 1D-retinas: distant and close-up. The two focused images produced by the lens sit at different distances and vertically separated.

- **Distance-related animal settings**

  Spatial fidelity zones specific to individuals (say, at a given distance from a colony center, or within a particular zone of the total foraging area) have been observed for some social insect species, molluscan communities, birds, etc.

  Home range is the area where an animal (or a group) lives and travels within. Within it, the area of intensive and exclusive use by resident animals is the *core area*. The *distance between range centroids* of two individuals (or groups) is a parameter used in studies of spatially based animal social systems. Cf. **dispersal distance**.

  An animal is **territorial** if it consistently occupies, marks and defends a *territory*, i.e., an area with a focused resource (say, a nest, den, mating site or sufficient food resources). Territories are held by an individual, a mated pair, or a group. An *extraterritorial foray* is the movement of a territorial animal into a conspecific's territory.*Dear enemy recognition* is the stronger response of a territorial animal to strangers than to its neighbors from adjacent territories.

  Lizards *Varanus panoptes* dig, in a spiral, the deepest known, ≤ 3.6 m, nests.

A linear relationship between the logarithm of faecal egg (of internal parasites) counts and the mean distance moved by a sheep per time step was found.

The **defense region** is the region that a male must defend in a mating competition to monopolize a female. It can be 1D (burrow, tunnel), 2D (dry land), bounded 3D (tree, coral reef), or open 3D (air, water). Puts, 2010, claims that 1D and 2D (as for humans) mating environments favor the evolution of contests.

The reliability of a threat display in animal contests is maintained by the *proximity risk*, i.e., the display is credible only within a certain distance of the opponent. This threshold distance is related to weaponry and the species-specific fighting technique. Here, greater formidability and dominance can be reached solely behaviorally; for example, an elephant's musth status overrides its body size and tusks.

The **landscape of fear** of a foraging animal is defined by the spatial variation of presumed predation risk. Its horizontal and vertical components correspond to terrestrial and aerial predators. It include clearness of sightlines (to spot predators), shrubs/trees/edge cover and the interplay of the distances to food and shelter. For example, small fish stay close to the coral reef when grazing seaweed; this creates "grazing halos" of bare sand, visible from space, around all reefs. Similar natural features are "fairy rings" of green eelgrass (up to 1500 m in width, off Denmark's coast), of mushrooms (10–600 m) and of barren sand (2–15 m, in Africa).

The **domain of danger** (DOD, or **Voronoi polygon**, cf. Chap. 20) of an animal, risking predation, in aggregation is the area closer to it than to any other group member. *Selfish herd theory* (Hamilton, 1971) posits that a cover-seeking dominant animal tends to minimize its DOD by occupying the center, thus diluting its risk by placing another individual between itself and a predator or parasite. Moreover, some fish bite a group member, when exposed to a searching predator.

During traveling, dominant animals are closer to the front of the herd. During foraging, their trajectories are shorter, more direct and more aligned both with their nearest neighbors and with the whole herd.

Romey et al., 2015: for beetles, *flash expansion of repulsive herd*, i.e., a rapid disassembly of a prey group detecting a predator, is away from the centroid rather than from density maximum or starter. The starter tend to be a female at the group's edge; she moved more quickly than others and favoured the group's centroid.

Distance senses include sight, hearing, and smell (they can be in stereo), while *contact senses* include taste, the senses of pressure, thermoception, and *internal senses* include the sense of balance and muscle stretch. The buzzard can see small rodents from a height of 4.6 km. The spotted hyaena hears noises from predators feeding on carcasses over distances of up to 10 km. The silkmoth detects pheromones up to 11 km distant. The grizzly bear smells food from up to 29 km away.

An example of unexplained **distance prediction** by animals is given (Vannini et al., 2008) by snails *Cerithidea decollata* migrating up and down mangrove

shores in synchrony with tidal phases. In the absence of visual cues and chemical marks, snails cluster just above the high water line, and the distance from the ground correlates better with the incoming tide level than with previous ones.

Ants initially wander randomly and upon finding food return to their colony while laying down pheromone trails. So, when one ant finds a **shortest path** to a food source, other (and eventually all) ants are likely to follow it. Inspired by this idea, the *ant colony optimization algorithm* (ACO) is a probabilistic technique for finding shortest paths through graphs; cf. **arc routing problems** in Chap. 15. Also, ants routinely find the maximal distance from all entrances to dispose of dead bodies.

The **distance effect avoidance** is the observed selection of some good distant source of interest over a poor but nearer one in the same direction. For example, females at a chorusing lek of anurians or arthropods may use the lower pitch of a bigger or better distant male's call to select it over a weaker but louder call nearby. High-quality males help them by timing their calls to precede or follow those of inferior males. Ant colonies can select a good distant nest over a poorer one in the way, even when it is 9 times closer. Ants compensate for the distance effect by increasing recruitment latencies and quorum thresholds at nearby poor nests. Another example: foraging vervet monkeys optimize travel distance when alone but prioritize high-reward food sites when in competition.

In land locomotion, animals crawl, walk, run, hop, climb or crawl, slither, undulate. In fluids (water, air) animals swim and fly by beating flagella, tails, wings, undulating their bodies, or actuating pumps. Some animals can switch the medium. Fish *Exocoetidae* can spend 45 s in flight gliding up to 200 m at altitudes of up to 6 m; using waves, it can span distances up to 400 m. Some squids fly in shoals covering up to 50 m at 6 m above the water. Squirrels *Petauristinae*, snakes *Chrysopelea* and lemurs *Dermoptera* can glide with small loss of height up to 200, 100 and 70 m, respectively. The deepest dive for a flying bird is 210 m by a thick-billed murre. The deepest (3 km) and longest (2.3 h) mammal's dive was recorded for a Cuvier's beaked whale in 2014. The human free-diving record is 253.2 m by Nitsch in 2012.

Flying and swimming animals can move through volumes with six degrees of freedom: 3 translational (left/right, forwards/backwards, up/down) and 3 rotational (pitch, roll, yaw). Surface-constrained animals have only three degrees: left/right, forwards/backwards and yaw; moving in 3D, they have higher place field resolution in the horizontal plane and showed a preference for movement in the horizontal.

Maximal relative speed (in body lengths per second) is 6.2, 16 and 322 for human (Usain Bolt, 2009), cheetah and a mite *Paratarsotomus macropalpis*. But Meyer-Vernet and Rospars, 2015, showed that it is (except flying and very large organisms) $\sim b_m \rho \sigma^{-1} \sim 10$ across 20 orders of magnitude in body mass. Here $\rho \approx 10^3$ kg m^{-3} is the density of liquid water, while $\sigma \approx 2 \times 10^5$ N m^{-2} and $b_m \approx 2 \times 10^3$ W kg^{-1}, roughly constant across life forms, are the applied force per unit cross-sectional area of tissue and maximum metabolic rate per unit of working tissue.

Navigating animals use an egocentric orientation mechanism and simple panoramic views, within which proximal objects dominate because their image on the retina change significantly with displacement. Animals rely on the spatial arrangement of the objects/landmarks across the scene rather than on their individual identification and geometric cues. Humans and, perhaps, chimpanzees and capuchin monkeys, possess, in addition, an allocentric reference system, centered on objects/features of the environment, and a more flexible geometric representation of space, with true distance and direction, i.e., closer to an abstract mental map.

Gaze monitoring and *pointing*: four great apes, canids and ravens follow another's head and eye orientation into distant space, even behind an obstacle. Moreover, bonobos and chimpanzees take barrier opacity into consideration. African elephants can use communicative intent of human pointing as a cue to find food. Horses use their facial expressions (direction of eyes and ears) to "talk" to other horses.

Great apes, dolphins, elephants, magpies recognise themselves in mirrors. *Metacognition* (cognitive self-awareness) was found in great apes, dolphins and rhesus monkeys. A basic *Theory of Mind* (ability to attribute mental states), mental time travel, meta-tool use and empathy are expected in primates and corvides. Ravens are as clever as chimpanzees, despite having much smaller brains.

Mammals, birds and octopuses possess neurological substrates generating consciousness. Chimpanzees have a system of intentional communication. But shared intentionality and cumulative culture seems to be uniquely human.

- **Animal communication**

  Only humans, songbirds, hummingbirds, parrots, cetaceans and bats have complex, learned vocalisation. Conceptual generalizations (bottlenose dolphins can transmit up to 9 km identity information independent of the caller's voice/location), syntax (calls of some monkeys, Bengal finches, Japanese great tits are built as "word sequences") and meta-communication ("play face" and tail-to-the-right signals in dogs that the subsequent aggressive signal is a play) have been observed.

  Matters of relevance *at a distance* (a distant food source or shelter) can be communicated by body language. For example, honeybees dancing convey (by duration of the waggle phase and orientation of the dance relative to the vertical) the polar coordinates (distance D to the goal and angle between the direction towards it and to that of the Sun's azimuth) of locations of interest. The mean number of waggings of bee's *waggle phases* increases with D. Also, wolves, before a hunt, howl to rally the pack, become tense and have their tails pointing straight. Dogs express their spatial needs by body language and vocalizations. Stiffness, pilorection, aggressive barking/lunging are *distance-increasing*, while play bow, tail wagging to the right, "positive" barking/lunging are *distance-decreasing signals*.

  A **distance pheromone** is a soluble (for example, in the urine) and/or evaporable substance emitted by an animal, as a chemosensory cue, in order to

send a message (on alarm, sex, food trail, recognition, etc.) to other members of the same species. In contrast, a *contact pheromone* is such an insoluble nonevaporable substance; it coats the animal's body and is a contact cue. The *action radius* of a distance pheromone is its attraction (or repulsion) range, the maximum distance over which animals can be shown to direct their movement to (or from) a source.

In species, such as carnivores occurring at low densities or having large home ranges, individuals are widely spaced and communicate via chemical broadcast signaling at *latrines*, i.e., collections of scent marks (feces, urine or glandular secretions), or via visually conspicuous landmarks of the boundary such as scratches and middens. Herrings communicate by farting. Shelter-dwelling caterpillars ballistically eject faecal pellets great distances (7–39 times their body length) at great speeds, in order to remove olfactory chemical cues for natural enemies.

The **communication distance** is the maximal distance at which the receiver can still get the signal. For example, a typical bird can detect a sound, coming from 300 m away amidst a background racket of human speech (roughly, 60 dB).

Animals can vary the signal amplitude and visual display with *receiver distance* in order to ensure signal transmission. For example, baleen whales have been observed calling more loudly, in order to compensate for human-generated noise.

Another example of *distance-dependent communication* is the protective coloration of some aposematic animals: it switches from *conspicuousness* (signaling nonedibility) to *crypsis* (camouflage) with increasing distance from a predator. Examples of interspecies communication of nonhuman animals, other than predator-prey signaling, are: eavesdropping, heterospecific alarm calls and cooperative hunting.

The main modes of animal communication are infrasound (< 20 Hz), sound, ultrasound (> 20 kHz), vision (light), chemical (odor), tactile, seismic and electrical. Infrasound, low-pitched sound (as territorial calls) and light in air can be long-distance. Some frogs, spiders, insects, small mammals have vibrotactile sense.

In a diverse ecosystem's soundscape, mammals tend to monopolize the low frequencies; birds call at higher pitches; and sound of insects is higher still.

A blue whale infrasound could (prior to noise pollution caused by ships) travel over 6000 km through the ocean water using the **SOFAR channel** (Chap. 25).

Most elephant communication is in the form of infrasonic rumbles which may be heard by conspecifics 5–10 km away. Also, they drum their soles on the ground, and resulting seismic waves can be detected as far as 16–32 km.

Many animals hear infrasound generated by earthquakes, tsunami and hurricanes before they strike. Elephants can hear storms 160–240 km away.

High-frequency sounds attenuate more rapidly with distance, more directional and vulnerable to scattering. But ultrasounds are used by bats (echo-location) and arthropods. Rodents use them to communicate to nearby receivers without alerting predators and competitors. Some anurans shift to ultrasound signals in

the presence of continuous background noise (such as waterfall, human traffic). Animals, including frogs, insects, birds and whales, increase the minimum frequency, amplitude or **signal-to-noise ratio** (Chap. 21) in the presence of antropogenic noise.

- **Plant long-distance communication**

  Long-distance signaling was observed from roots and mature leaves, exposed to an environmental stress, to newly developing leaves of a higher plant.

  This communication is done cell-to-cell through the plant vascular transpiration system. In this system, macromolecules (except for water, ions and hormones) carry nutrients and signals, via *phloem* and *xylem* tissues, only in one direction: from lower mature regions to shoots. The identity of long-distance signals in plants is still unknown but the existence of information macromolecules is expected.

  Besides the above vascular signaling, plants communicate chemically with each other or with mutualistic animals (pollinators, bodyguards, etc.). For example, plants respond to attack by herbivores or pathogens with the release of volatile compounds, informing neighboring plants and attracting predators of attackers.

  Some 80 % of plants are colonized by ectosymbiotic fungi that form a network of fine white threads, *mycorrhizae*, which take in water and minerals from the soil, and hand some over to the plant in exchange for nutrients. A mycorrhizal network can take over an entire forest and tie together plants of different species. Plants use this network as a signaling and kin (or host) detection system too. They assist neighbors or kin in deterring pests, attracting pollinators and nutrient uptake.

- **Internodal distance**

  A *node* on a plant stem is a joint where a leaf is attached. The **internodal distance** (or *internode length*) is the distance between two consecutive nodes.

  A *ramet* is an independent member of a clone. The **interramet distance** (or *propagule dispersal distance*) is the internodal distance in plant clonal species.

- **Leaf size**

  According to Boland et al., 2006, the leaf is *mesophyll, notophyll, microphyll, nanophyll*, if its length is > 12.7, 7.6–12.7, 2.5–7.6, < 2.5 cm, respectively.

- **Body size rules**

  Body size, measured as mass or length, is one of the most important traits of an organism. Food webs, describing "who eat whom" (cf. **trophic distance**), are *nearly interval*, i.e., the species can be ordered so that almost all the resources of each consumer are adjacent in the order. Zook et al., 2011, found that ordering by body size is the best proxy to produce this near-interval ordering.

  The lower limits (10 kg and 2 g) to body size is set by the size of offspring for marine and by energetic limitations for terrestrial mammals. The largest known sizes for them are 190 t and 16 t, but the upper limit is still unclear. The length ranges for mammals, fish, insects, vascular plants, algae, bacteria, virions are $[10^{-1}, 10^{2}]$, $[10^{-2}, 10^{1}]$, $[10^{-4}, 10^{-1}]$, $[10^{-2}, 10^{2}]$, $[10^{-5}, 10^{0}]$, $[10^{-7}, 10^{-3}]$, $[10^{-8}, 10^{-6}]$ m.

According to Payne et al., 2008, the maximum size of the Earth's organisms increased by 16 orders of magnitude over the last 3.5 billion years. 75 % of the increase happened in two great leaps (about 1900 and 600–400 Ma ago: the appearance of eukaryotic cells and multi-cellularity) due to leaps in the oxygen level, and each time it increased about million times. The average animal in the oceans today is 150 times larger in mass than the average one half a billion years ago.

Smith et al., 2010: the maximum size of mammals increased (from 2 g to 190 t) near-exponentially after the C-T (Cretaceous-Paleogene) extinction of the nonavian dinosaurs 65.5 Ma ago; with little food, only small, no larger than a cat, species survived on land. After this C-T event, homeothermic animals (mammals and birds) radiated globally from northern Asia and became dominant.

The maximum size of insects also followed O_2 level 350–150 Ma ago, reaching 71 cm. Then it dropped (while O_2 went up) with evolution of birds and 65 Ma ago with their specialization and evolution of bats. Larsson–Dececchi, 2013, explain the origin of birds by a change of body-to-limb length ratio in Maniraptoran dinosaurs: the hind legs shrank, while forelimbs got long enough to work as an airfoil. From 230–220 to 163 Ma ago, theropods shrinked (≈ 0.5 % of mass) to first birds.

Evans et al., 2012, claim that an increase in size (100, 1000, 5000 times) of land and marine mammals took 1.6, 5.1, 10 and 1, 1.3, 5 million generations, respectively. Mouse-sized mammals evolved into elephant-sized ones during 24 million generations, but decreasing in size occurred about 30 times faster.

Clauset and Erwin, 2008: 60 Ma of mammalian body size evolution can be explained by simple diffusion model of a trade-off between the short-term selective advantages (**Cope's rule**, common among mammals: a slight within-lineage drift toward larger masses) and long-term selective risks of increased size.

The size has costs as well as benefits; for example, reversals to unicellularity occurred at least 5 times in cyanobacteria. It favors the individual but renders the clade more susceptible to extinction via, for example, dietary specialization.

Large size enhances reproductive success, the ability to avoid predators and capture prey, and improves thermal efficiency. In large carnivores, bigger species dominate better over smaller competitors. Predator-prey mass ratio is typically around 10. But, for example, cookiecutter shark, only 0.5–1 m in length, preys on all larger animals in ocean, and the larvae of beetle *Epomis* preys on amphibians.

By mean body size (67 kg now and 50 kg in the Stone Age) humans are a small *megafauna* ($\geq$ 44 kg) species. A rapid average decline of ≈ 20 % in size-related traits was observed in human-harvested species.

Benthic (living on/in the bottom of a water body) animals are generally classified according to size: *microbenthos* $<$ 0.063 mm, *meiobenthos* 0.063–1 (or 0.5) mm, *macrobenthos* $>$ 1 (or 0.5) mm and, sometimes, *megabenthos* $>$ 10 mm.

Given below are the other main rules of large-scale Ecology involving body size.

Foster's (or *island*) **rule** is a principle that size of members of a species changes depending on the resources available in the environment. Damuth, 1993: there is an optimum mammal body size $\approx$ 1 kg for energy acquisition, and so island species should, in the absence of the usual competitors and predators, evolve to it.

Insular dwarfism is an evolutionary trend of the reduction in size of large mammals when their gene pool is limited to a very small environment (say, islands). One explanation is that smaller animals need fewer resources and reproduce faster.

Island gigantism is a form of natural selection where the size of animals isolated on an island increases dramatically over generations due the removal of constraints. Also, island bird species evolve smaller flight muscles and longer legs.

Abyssal gigantism is a tendency of deep-sea species to be larger than their shallow-water counterparts. For example, the colossal squid and the king-of-herrings (giant oarfish) can reach 14 and 17 m in length. It can be adaptation for scarcer food resources, greater pressure and lower temperature.

The **lilliput effect** is a reduction in the biota's size after mass extinctions.

1 °C of warming reduces the adult body mass of cold-blooded organisms by 2.5 % on average. For warm-blooded animals, **Allen's rule** holds: those from colder climates have shorter limbs than the equivalent ones from warmer climates.

Rensch's rule is that males are the larger sex in big-bodied species (such as humans) and the smaller sex in small-bodied species (such as spiders). It holds for plants also. Often, natural selection on females to maximize fecundity results in female-biased sexual size dimorphism, whereas sexual selection for large males promotes male-biased dimorphism. The males in some cichlid fish are up to 60 times larger than that of the females, while tremoctopus females may reach 2 m versus the males, at most a few cm long.

Size-assortative mating (positive correlation between male and female size among couples) has been found in crustaceans, insects, birds, reptiles, fishes and humans, for which it is a part of *homophily* (tendency to associate and bond with similar others). Humans have the largest, among apes, penises and breasts.

Cognitive and behavioral capacities do not correlate either with body or brain size, nor with their ratio, which is, say, $\frac{1}{7}$, $\frac{1}{40}$, $\frac{1}{2496}$ for small (0.06 mg) ant, human and shark. The *encephalization quotient* is the ratio of actual to predicted brain mass for a given size animal; it is the record 7.4–7.8 for humans. The number of neurons is $302, 85 \times 10^9, 2 \times 10^{11}$ in a nematode, human and elephant. Fish with smaller brain have more offspring. Echinoderms (say, starfish) lack a brain entirely.

Bromage et al., 2012, found a correlation between body mass and *RI* (*repeat interval*), i.e., the number of days between adjacent *striae of Retzius* (incremental growth lines seen in tooth) in primate's enamel. RI is also represented by the increments in bone. RI is an integer within $[1, 11]$; the mean RI is 8–9 in humans.

The *surface-to-volume ratio* $\frac{A}{V}$ is the main compactness measure for 3D shapes in Biology. Higher $\frac{A}{V}$ means increased exposure to the environment. It permits smaller cells to gather nutrients and reproduce very rapidly. Also, smaller animals in hot and dry climates lose heat better through the skin and cool the body. But lower $\frac{A}{V}$ (and so, larger size) improves temperature control: slower heat loss or gain. **Bergmann's rule** is a principle that, within a species, the body size increases with colder climate. For example, Northern Europeans on average are taller than Southern ones.

The *Hutchinson's ratio* is the ratio of the size differences between competing species when they were living together as compared to when they were isolated.

- **Allometry**

  Allometry concerns relative change in structure or function of organisms (within individuals, among individuals, and across groups/species) with change in body size (length l, or mass M). The dependence of a biological variable Y on body size is usually given by an empirical *allometric scaling law*, i.e., a power function $Y = Y_0 M^b$ or $Y = Y_0 l^b$, where b is the *scaling exponent* and Y_0 a constant.

  Geometrically similar (i.e., of the same basic shape) objects have proportional relationships between surface area A, volume V, and length l, i.e., $A' = A(\frac{l'}{l})^2$ and $V' = V(\frac{l'}{l})^3$, in terms of the *square–cube law*. Also, $M' = M(\frac{l'}{l})^3$ holds for the mass M if a scaled-up object maintains the same density.

  Isometric scaling occurs when the above proportions are preserved as size changes. Frogs grow isometrically, as well as Ediacaran biota.

  An isometrically scaling organism will have all V- (or M-), A-, and l-based properties change to the power $1, \frac{2}{3}, \frac{1}{3}$ of M, respectively.

  Allometric scaling is any change that deviates from isometry. Such scaling is *positive* or *negative* if the value is larger or smaller than predicted by isometry. Positive scaling occurs for some fishes, whose weight grows as about $l^{3.325}$.

  An example of negative allometric scaling is *Kleiber's law*: metabolic rate (V-based property) is proportional to $M^{0.75}$ over 27 orders of magnitude, from the molecular level up to the largest organisms. According to Garland, 1983, the speed of mammals tend to increase as $M^{0.17}$, and 119 kg is the optimal weight for the fastest runner.

  A unicellular organism of size l has metabolic activity roughly proportional to cell volume (so, to l^3) and flux of nutrient and energy dissipation proportional to cell envelope area (so, to l^2). Hence, l is close to their ratio. The size of viral particles is roughly proportional to the third root of the genome size.

  Let d, D denote mean size and distance between organisms. A proxy $\frac{D}{d}$ of animal abundance is very similar over a size span of 7 orders of magnitude. In fact, $\frac{D}{d} = \frac{44\,\mu}{3\,\mu}, \frac{390\,\mu}{40\,\mu}, \frac{5.8\,mm}{0.5\,mm}, \frac{35\,mm}{5\,mm}, \frac{50\,cm}{5\,cm}, \frac{300\,cm}{10\,cm}, \frac{100\,m}{1.5\,m}$, respectively, for bacteria, amoeba, nematodes, antropodes, shrews, birds and large mammals.

- **Size spectrum**

  The term **size spectrum** is used generally when comparing objects of a given class, say, shoes or phones. But mainly, it is (Sheldon–Parsons, 1967) the

relationship between body size of individuals and their abundance or biomass, regardless of their species, in a given (aquatic or soil) **size-based food web**.

For a population, the main considered sizes (lengths or masses) are: maximal, *asymptotic* (which individuals would reach if they were to grow indefnitely), of *maximal yield* (with highest biomass) and average in maturity. Example of corresponding *size-spectrum models*: Andersen and Beyer, 2006, derived proportionality of the number of individuals of given species and size to their asymptotic size raised to the power -2.05.

- **Trophic distance**

  Given an ecosystem, its *ecological network* is a digraph in which species are (biomass- or abundance-weighted) vertices with two of them being connected by arc or edge if there is a trophic or, respectively, symbiotic interaction. A *community food web* (or *ecological pyramid*) is a such digraph with only trophic arcs.

  The **trophic distance** from resource u to consumer v is the length of a shortest *food chain* (directed $(u - v)$ path) if it exists,

  The *trophic level* of a vertex v is 1 if it is a primary resource (usually, *producer* as plants, algae, phytoplankton) and 1 plus the trophic level of its principal diet, otherwise. The *fractional tropic level* of v is (Pauly–Palomares, 2005) 1 plus the weighted average (using stomach contents) trophic level of all its food items.

  The *mean trophic level* for fishery overall catch should be preserved to avoid *fishing down the food web*, when fisheries in a given ecosystem deplete the large predatory fish and end up with small fish and invertebrates.

  In a **size-based food web**, the layers are defined by body-size class rather than by trophic level. Community-based *predator-prey body mass ratios* (PPMR) and *energy transfer efficiency* (TE) are key parameters in such webs. In marine food webs, typically, PPMR $\in [100,\ 3000]$ and TE $\in [0.1,\ 0.13]$, i.e., 10–13 % of prey biomass is converted into predator production.

  An *energy* and *functional food webs* are weighted digraphs where arcs correspond to energy flow and interaction strength. Consumers at each level convert to tissue about 10 % of their food's chemical energy.

- **Insecticide distance effect**

  The main means of pest (termites, ants, etc.) control are chemical liquid insecticides and repellents. The efficiency of an insecticide can be measured by its **all dead distance**, i.e., the maximum distance from the standard toxicant source within which no targeted insects are found alive after a fixed period.

  The **insecticide distance effect** is that the toxicant is spread through the colony because insects groom and feed each other. The toxicant should act slowly in order to maximize this effect and minimize secondary repellency created by the presence of dying, dead and decaying insects. Nearly all animals, when they die, emit the same stench of fatty acids which acts as repellent and it is universal.

23.4 Other Biological Distances

Here we collect the main examples of other notions of distance and distance-related models used in Biology.

- **Immunologic distance**

  An *antigen* (or immunogen, pathogen) is any molecule eliciting an immune response. Once it gets into the body, the immune system either neutralizes its pathogenic effect or destroys the infected cells. The most important cells in this response are white blood cells: *T-cells* and *B-cells* responsible for the production and secretion of *antibodies* (specific proteins that bind to the antigen).

  When an antibody strongly matches an antigen, the corresponding B-cell is stimulated to divide, produce clones of itself that then produce more antibodies, and then differentiate into a plasma or memory cell. A secreted antibody binds to an antigen, and antigen-antibody complexes are removed.

  A mammal (usually a rabbit) when injected with an antigen will produce immunoglobulins (antibodies) specific for this antigen. Then *antiserum* (blood serum containing antibodies) is purified from the mammal's serum. The produced antiserum is used to pass on passive immunity to many diseases.

  Immunological distance procedures (*immunodiffusion* and, the mainly used now, *micro-complement fixation*) measure the relative strengths of the immunological responses to antigens from different taxa. This strength is dependent upon the similarity of the proteins, and the dissimilarity of the proteins is related to the evolutionary distance between the taxa concerned.

  The *index of dissimilarity* $id(x, y)$ between two taxa x and y is the factor $\frac{r(x,x)}{r(x,y)}$ by which the *heterologous* (reacting with an antibody not induced by it) antigen concentration must be raised to produce a reaction as strong as that to the *homologous* (reacting with its specific antibody) antigen.

  The **immunological distance** between two taxa is given by

$$100(\log id(x, y) + \log id(y, x)).$$

  It can be 0 for two closely related species. It is not symmetric in general.

  Earlier immunodiffusion procedures compared the amount of precipitate when heterologous bloods were added in similar amounts as homologous ones, or compared with the highest dilution giving a positive reaction.

  The name of the applied antigen (target protein) can be used to specify immunological distance, say, albumin, transferring lysozyme distances. Proponents of the *molecular clock hypothesis* estimate that one unit of albumin distance between two taxa corresponds to ≈ 0.54 Ma of their divergence time, and that one unit of **Nei standard genetic distance** corresponds to 18–20 Ma.

  Adams and Boots, 2006, call the *immunological distance* between two immunologically similar pathogen strains (actually, serotypes of dengue virus) their *cross-immunity*, i.e., 1 minus the probability that primary infection with one strain prevents secondary infection with the other. Lee and Chen, 2004, define

the *antigenic distance* between two influenza viruses to be the reciprocal of their *antigenic relatedness* which is (presented as a percentage) the geometric mean $\sqrt{\frac{r(x,y)}{r(x,x)}\frac{r(y,x)}{r(y,y)}}$ of two ratios between the heterologous and homologous antibody *titers*.

An antiserum *titer* is a measurement of concentration of antibodies found in a serum. Titers are expressed in their highest positive dilution.

- **Metabolic distance**

  Enzymes are proteins that *catalyze* (increase the rates of) chemical reactions.

  The **metabolic distance** (or *pathway distance*) between enzymes is the minimum number of metabolic steps separating two enzymes in the metabolic pathways.

- **Pharmacological distance**

  The *protein kinases* are enzymes which transmit signals and control cells using transfer of *phosphate groups* from high-energy donor molecules to specific target proteins. So, many drug molecules (against cancer, inflammation, etc.) are kinase inhibitors (blockers). Designed drugs should be *specific* (say, not to bind to $\geq 95\,\%$ of other proteins), in order to avoid toxic side-effects.

  Given a set $\{a_1, \ldots, a_n\}$ of drugs in use, the *affinity vector* of kinase x is defined as $(-\ln B_1(x), \ldots, -\ln B_n(x))$, where $B_i(x)$ is the *binding constant* for the reaction of x with drug a_i, and $B_i(x) = 1$ if no interaction was observed. The binding constants are the average of several experiments where the concentration of binding kinase is measured at equilibrium. The **pharmacological distance** (Fabian et al., 2005) between kinases x and y is the Euclidean distance $(\sum_{i=1}^{n}(\ln B_i(x) - \ln B_i(y))^2)^{\frac{1}{2}}$ between their affinity vectors.

  The *secondary structure* of a protein is given by the hydrogen bonds between its residues. A *dehydron* in a solvable protein is a hydrogen bond which is solvent-accessible. The *dehydron matrix* of kinase x with residue-set $\{R_1, \ldots, R_m\}$ is the $m \times m$ matrix $((D_{ij}(x)))$, where $D_{ij}(x)$ is 1 if residues R_i and R_j are paired by a dehydron, and is 0, otherwise. The **packing distance** (Maddipati–Fernándes, 2006) between kinases x and y is the Hamming distance $\sum_{1\leq i,j\leq m} |D_{ij}(x) - D_{ij}(y)|$ between their dehydron matrices; cf. **base pair distance** among **RNA structural distances**. The *environmental distance* (Chen, Zhang and Fernándes, 2007) between kinases is a normalized variation of their packing distance.

  Besides hydrogen bonding, residues in protein helices adopt backbone dihedral angles. So, the secondary structure of a protein much depends on its sequence of dihedral angles defining the backbone. Wang and Zheng, 2007, presented a variation of **Lempel–Ziv distance** between two such sequences.

- **Global distance test**

  The *secondary structures* of proteins are mainly composed of the α-helices, β-sheets and loops. Protein *tertiary structure* refers to the 3D structure of a single protein molecule. The α and β structures are folded into a compact globule.

  The **global distance test** (GDT) is a measure of similarity between two (model and experimental) proteins x and y with identical *primary structures*

(amino acid sequences) but different tertiary structures. GDT is calculated as the largest set of amino acid residues' α carbon atoms in x falling within a defined **cutoff distance** (Chap. 29) d_0 of their position y.

For proteins, in order for this set to define all intermolecular stabilizing (relevant short range) interactions, $d_0 = 0.5$ nm is usually sufficient. Sometimes, $d_0 = 0.6$ nm, in order to include contacts acting through another atom.

- **Migration distance (in Biomotility)**

  The **migration** (or *penetration*) **distance**, in cattle reproduction and human infertility diagnosis, is the distance in mm traveled by the vanguard spermatozoon during sperm displacement *in vitro* through a capillary tube filled with homologous cervical mucus or a gel mimicking it. Sperm swim 1–4 mm/min. 90 % of human sperm swim forward with small side-to-side movements, while ≈ 5 % swim in a faster-paced helical pattern and the remaining ≈ 5 % swim in a hyper-helical manner, where the sperm are more active but less directional.

  Such measurements, under different specifications (duration, temperature, etc.) of incubation, estimate the ability of spermatozoa to colonize the oviduct *in vivo*.

  In general, the term **migration distance** is used in biological measurements of directional motility using controlled migration; for example, determining the molecular weight of an unknown protein via its migration distance through a gel.

- **Penetration distance**

  The **penetration distance** is a general term used in (especially, biological) measurements for the distance from the given surface to the point where the concentration of the penetrating substance (say, a drug) in the medium (say, a tissue) had dropped to the given level. Several examples follow.

  During penetration of a macromolecular drug into the tumor interstitium, *tumor interstitial penetration* is the distance that the drug carrier moved away from the source at a vascular surface; it is measured in 3D to the nearest vascular surface.

  During the intraperitoneal delivery of cisplatin and heat to tumor metastases in tissues adjacent to the peritoneal cavity, the *penetration distance* is the depth to which the drug diffuses directly from the cavity into tissues. Specifically, it is the distance beyond which such delivery is not preferable to intravenous delivery.

  It can be the distance from the cavity surface into the tissues within which drug concentration is, for example, (a) greater, at a given time point, than that in control cells distant from the cavity, or (b) is much higher than in equivalent intravenous delivery, or (c) has a first peak approaching its plateau value within 1 % deviation.

  The *penetration distance* of a drug in the brain is the distance from the probe surface to the point where the concentration is roughly half its **far field** value.

  The *penetration distance* of chemicals into wood is the distance between the point of application and the 5 mm cut section in which the contaminant concentration is at least 3 % of the total.

  The *forest edge-effect penetration distance* is the distance to the point where invertebrate abundance ceased to differ from forest interior abundance.

Cf. **penetration depth distance** in Chap. 9, **penetration depth** in Chap. 24 and **distance sampling** in Chap. 17.

- **Capillary diffusion distance**

  One of the diffusion processes is *osmosis*, i.e., the net movement of water through a permeable membrane to a region of lower solvent potential. In the respiratory system (the alveoli of mammalian lungs), oxygen O_2 diffuses into the blood and carbon dioxide CO_2 diffuses out.

  The **capillary diffusion distance** is, similarly to **penetration distance**, a general term used in biological measurements for the distance, from the capillary blood through the tissues to the mitochondria, to the point where the concentration of oxygen has dropped to the given low level.

  This distance is measured as the average distance from the capillary wall to the mitochondria, or the distance between the closest capillary endothelial cell to the epidermis, or in percentage terms, say, the distance where a given percentage (95 % for maximal, 50 % for average) of the fiber area is served by a capillary.

  Another practical example: the *effective diffusion distance* of nitric oxide NO in microcirculation *in vivo* is the distance within which N concentration is greater than the equilibrium dissociation constant of the target enzyme for oxide action.

  Cf. the **immunological distance** for immunodiffusion and, in Chap. 29, the **diffusion tensor distance** among **distances in Medicine**.

- **Főrster distance**

  FRET (fluorescence resonance energy transfer; Főrster, 1948) is a distance-dependent quantum mechanical property of a *fluorophore* (molecule component causing its fluorescence) resulting in direct nonradiative energy transfer between the electronic excited states of two dye molecules, the donor fluorophore and a suitable acceptor fluorophore, via a dipole. In FRET microscopy, fluorescent proteins are used as noninvasive probes in living cells since they fuse genetically to proteins of interest.

  The efficiency of FRET transfer depends on the square of the donor electric field magnitude, and this field decays as the inverse sixth power of the intermolecular separation (the physical donor-acceptor distance). The distance at which this energy transfer is 50 % efficient, i.e., 50 % of excited donors are deactivated by FRET, is called the **Főrster distance** of these two fluorophores.

  Measurable FRET occurs only if the donor-acceptor distance is less than ≈ 10 nm, the mutual orientation of the molecules is favorable, and the spectral overlap of the donor emission with acceptor absorption is sufficient.

- **Gendron–Lemieux–Major distance**

  The **Gendron–Lemieux–Major distance** (2001) between two base-base interactions, represented by 4×4 *homogeneous transformation matrices* X, Y, is

$$\frac{S(XY^{-1}) + S(X^{-1}Y)}{2},$$

  where $S(M) = \sqrt{l^2 + (\theta/\alpha)^2}$, l is the translation length, θ is the rotation angle, and α is a scaling factor between the translation and rotation contributions.

- **Spike train distances**

A human brain has 85×10^9 *neurons* (nerve cells) each communicating with an average 1000 other neurons dozens of times per second. Most neurons are capable of making 10^4–10^6 individual microconnections. One human brain, using $\approx 10^{15}$ synapses, produces $\approx 6.4 \times 10^{18}$ nerve impulses per second.

The neuronal response to a stimulus is a continuous time series. It can be reduced, by a threshold criterion, to a simpler discrete series of *spikes* (short electrical pulses). A *spike train* is a sequence $x = (t_1, \ldots, t_s)$ of s events (neuronal spikes, or heart beats, etc.) listing absolute spike times or interspike time intervals. The main **distances between spike trains** $x = x_1, \ldots, x_m$ and $y = y_1, \ldots, y_n$ follow.

1. The **spike count distance** is defined by

$$\frac{|n-m|}{\max\{m,n\}}.$$

2. The **firing rate distance** is defined by

$$\sum_{1 \le i \le s} (x'_i - y'_i)^2,$$

where $x' = x'_1, \ldots, x'_s$ is the sequence of local firing rates of train $x = x_1, \ldots, x_m$ partitioned in s time intervals of length T_{rate}.

3. Let $\tau_{ij} = \frac{1}{2}\min\{x_{i+1} - x_i, x_i - x_{i-1}, y_{i+1} - y_i, y_i - y_{i-1}\}$ and $c(x|y) = \sum_{i=1}^{m}\sum_{j=1}^{n} J_{ij}$, where $J_{ij} = 1$ if $0 < x_i - y_i \le \tau_{ij}$, $= \frac{1}{2}$ if $x_i = y_i$ and $= 0$, otherwise. The **event synchronization distance** (Quiroga et al., 2002) is defined by

$$1 - \frac{c(x|y) + c(y|x)}{\sqrt{mn}}.$$

4. Let $x_{isi}(t) = \min\{x_i : x_i > t\} - \max\{x_i : x_i < t\}$ for $x_1 < t < x_m$, let $I(t) = \frac{x_{isi}(t)}{y_{isi}(t)} - 1$ if $x_{isi}(t) \le x_{isi}(t)$ and $I(t) = 1 - \frac{y_{isi}(t)}{x_{isi}(t)}$, otherwise. The time-weighted and spike-weighted **ISI distances** (Kreuz et al., 2007) are

$$\int_0^T |I(t)|dt \text{ and } \sum_{i=1}^{m} |I(x_i)|.$$

5. Various *information distances* were applied to spike trains: the **Kullback–Leibler distance**, and the **Chernoff distance** (Chap. 14). Also, if x and y are mapped into binary sequences, the **Lempel–Ziv distance** and a version of the **normalized information distance** (Chap. 11) are used.
6. The **Victor–Purpura distance** (1996) is a cost-based **editing metric** (i.e., the minimal cost of transforming x into y) defined by the following operations

with their associated costs: insert a spike (cost 1), delete a spike (cost 1), shift a spike by time t (cost qt); here $q > 0$ is a parameter. The **fuzzy Hamming distance** (Chap. 11), introduced in 2001, identifies cost functions of shift preserving the triangle inequality.

7. The **van Rossum distance**, 2001, is defined by

$$\sqrt{\int_0^\infty (f_t(x) - f_t(y))^2 dt},$$

where x is convoluted with $h(t) = \frac{1}{\tau} e^{-t/\tau}$ and $\tau \approx 12$ ms (best); $f_t(x) = \sum_0^m h(t - x_i)$. This and above distances are the most commonly used metrics.

8. Given two sets of spike trains labeled by neurons firing them, the **Aronov et al. distance** (2003) between them is a cost-based **editing metric** (i.e., the minimal cost of transforming one into the other) defined by the following operations: insert or delete a spike (cost 1), shift a spike by time t (cost qt), relabel a spike (cost k), where $q, k > 0$ are parameters.

- **Bursting distances**

Bursts refers to the periods in a spike train when the spike frequency is relatively high, separated by periods when it is relatively low or spikes are absent.

Given neurons $x_1, \ldots, x_n$ and SBEs (synchronized bursting events) $Y_1, \ldots, Y_m$ with similar patterns of neuronal activity, let C^{ij} denote the cross-correlation between the activity of a neuron in Y_i and Y_j maximized over neurons, and let C_{ij} denote the correlation between neurons x_i and x_j averaged over SBEs.

Baruchi and Ben-Jacob, 2004, defined the **interSBE distance** between Y_i and Y_j and the **interneuron distance** between x_i and x_j by $\frac{1}{m}(\sum_{s=1}^m (C^{is} - C^{js})^2)^{\frac{1}{2}}$ and $\frac{1}{n}(\sum_{s=1}^n (C_{is} - C_{js})^2)^{\frac{1}{2}}$, respectively.

- **Long-distance neural connection**

Unlike Computing, neural systems are not exclusively optimized for minimal global wiring, but for a variety of factors including the minimization of processing steps. Kaiser and Hilgetag, 2006, showed that, due to the existence of long-distance projections, the total wiring among 95 primate (Macaque) cortical areas could be decreased by 32 %, and the wiring of neuronal networks in the nematode *C. elegans* could be reduced by 48 % on the global level. For example, $>$ 10 % of the primate cortical projections connect components separated by $>$ 40 mm, while 69 mm is the maximal possible distance. For the global *C. elegans* network, some connections are almost as long as the entire organism.

Long-distance and long-lasting neural connections may be the architecture linking the separate regions/processes together during a single global conscious state.

In autism there are more local connections and more local processing, while the psychosis/schizophrenia spectrum is marked by more long-distance connections.

About 5 %, 10 %, 6.7 % of variation in individual intelligence is predicted by activity level in LPFC (lateral prefrontal cortex), by the strength of neural pathways connecting left LPFC to the rest of the brain and by overall brain size.

- **Long-distance cell communication**

  Human cell size is within [4–135] μm; typically, 10 μm. In *gap junctions*, the intercellular spacing is reduced from 25–450 nm to a gap of 1–3 nm, bridged by hollow tubes. Animal cells may communicate locally, either directly through gap junctions, or by cell-cell recognition (in immune cells), or (*paracrine signaling*) using messenger molecules that travel, by diffusion, only short distances. Mammal's, astrocytes form, via gap junctions, a network of neurons and vasculature. Neurons may use interferon signals transmitted over great distances to fend off viral infection.

  In *synaptic signaling*, the electrical signal along a neuron's axon triggers the release of a neurotransmitter to diffuse across the synapse through a gap junction. Signal transmission through the nervous system is a long-distance signaling. Slower long-distance signaling is done by hormones transported in the blood. A hormone reaches all parts of the body, but only target cells have receptors for it.

  Another means of long-distance cell communication, via TNTs (*tunneling nanotubes*), was found in 1999. TNTs are membrane tubes, 50–200 nm thick with length up to several cell diameters. Cells can send out several TNTs, creating a network lasting hours. TNTs can carry cellular components and pathogens (HIV and prions). Also, electrical signals can spread bidirectionally between TNT-connected cells (over distances 10–70 μm) through interposed gap junctions.

  Some bacteria gain energy by oxidizing H_2S via electron transfer, hundreds of cell-lengths away. Thousands of *Desulfobulbus* form cm-long conductive chains, transporting electrons from H_2S-rich marine sediment to the upper O_2-rich one.

- **Length constant**

  In an excitable cell (nerve or muscle), the **length constant** is the distance over which a nonpropagating, passively conducted electrical signal decays to $\frac{1}{e}$ (36.8 %) of its maximum.

  During a measurement, the **conduction distance** between two positions on a cell is the distance between the first recording electrode for each position.

- **Ontogenetic depth**

  The **ontogenetic depth** (or *egg-adult distance*) is (Nelson, 2003) the number of cell divisions, from the unicellular state (fertilized egg) to the adult metazoan capable of reproduction (production of viable gametes).

  The **mitotic length** is the number of intervening mitoses, from the normal (neither immortal nor malignant) cells in the immature precursor stage to their progeny in a state of *mitotic death* (terminal differentiation) and phenotypic maturity.

  Adult humans produce daily $\approx$ 200 billion red cells, 100 billion neutrophils and 50 billion other cells. About 7×10^{15} mature cells are produced in a human lifetime and these could be produced in 53 cell generations ($2^{53} \approx 9 \times 10^{15}$).

- **Interspot distance**.

  A *DNA microarray* is a technology consisting of an arrayed series of thousands of *features* (microscopic spots of DNA oligonucleotides, each containing picomoles of a specific DNA sequence) that are used as probes to hybridize a *target* (cRNA sample) under high-stringency conditions. Probe-target hybridization is quantified by fluorescence-based detection of fluorophore-labeled targets to determine the relative abundance of nucleic acid sequences in the target.

  The **interspot distance** is the **spacing distance** (Chap. 29) between features. Typical values are 375, 750, 1500 micrometers ($1\ \mu m = 10^{-6}$ m).

- **Read length**

  In gene sequencing, automated sequencers transform electropherograms (obtained by *electrophoresis* using fluorescent dyes) into a four-color chromatogram where peaks represent each of the DNA bases A, T, C, G. Chromosomes stained by some dyes show a 2D pattern of traverse bands of light and heavy staining.

  The **read length** is the length, in the number of bases, of the sequence obtained from an individual clone chosen. Computers then assemble those short blocks into long continuous stretches which are analyzed for errors, gene-coding regions, etc.

- **Action at a distance along DNA/RNA**

  An **action at a distance along DNA/RNA** happens when an event at one location on a molecule affects an event at a distant (say, more than 2500 base pairs) location on the same molecule.

  Many genes are regulated by distant (up to a million bp away and, possibly, located on another chromosome) or short (30–200 bp) regions of DNA, *enhancers*. Enhancers increase the probability of such a gene to be transcribed in a manner independent of distance and position (the same or opposite strand of DNA) relative to the transcription initiation site (the promoter).

  DNA supercoiling is the twisting of a DNA double helix around its axis, once every 10.4 bp of sequence (forming circles and figures of eight) because it has been bent, overwound or underwound. Such folding puts a long range enhancer, which is far from a regulated gene in **genome distance**, geometrically closer to the promoter.

  The *genomic radius of regulatory activity* of a genome is the genome distance of the most distant known enhancer from the corresponding promoter; in the human genome it is $\approx 10^6$ bp (for the enhancer of SSH, *Sonic Hedgehog* gene).

  There is evidence that genomes are organized into enhancer-promoter loops. But the long range enhancer function is not fully understood yet.

  Similarly, some viral RNA elements interact across thousands of intervening nucleotides to control translation, genomic RNA synthesis and mRNA transcription.

  Genes are controlled either locally (from the same molecule) by specialized *cis* regulators, or at a distance by *trans* regulators. Comparing genes in key brain regions of human and primates, the most drastic changes were found in *trans*-controlled genes.

- **Length variation in 5-HTTLPR**

  5-HTTLPR is a repeat polymorphic region in *SLC6A4*, the gene (on chromosome 17) coding for SERT (serotonin transporter) protein. This polymorphism has *short* (14 repeats) and *long* (16 repeats) variations. So, an individual can have short/short, short/long, or long/long genotypes at this location in the DNA.

  A short/short allele leads to less transcription for SLC6A4, and its carriers are more attuned and responsive to their environment; so, social support is more important for their well-being. They have less gray matter, more neurons and a larger thalamus. Whereas $\frac{2}{3}$ of East Asians have the short/short variant, only $\frac{1}{5}$ of Americans and Western Europeans have it.

  Other gene variants of central neurotransmitter systems—dopamine receptor (*DRD4 7R*), dopamine/serotonin breaking enzyme (*MAOA VNTR*) and μ-opioid receptor (*OPRM1 A118G*)—are also associated with novelty-seeking, plasticity and social sensitivity. They appeared < 0.08 Ma ago and spread into 20–50 % of the population. They generate anxiety and aggression, but could be selected for extending behavioral range and boosting resilience at the group level.
- **ER-mitochondria distance**

  The *endoplasmic reticulum* (ER) is a large membrane-bound compartment spread throughout the cytoplasm of eukaryotic cells. The interface between mitochondria and ER is a crucial hub for bidirectional communication regulating mitochondrial energy, lipid biosynthesis, calcium Ca2+ signalling, and cell death.

  Mitochondria are surrounded by tubules of the ER that lie preferentially within 200 nm apart, whereas 20 % of the mitochondrial surface is in direct contact with the ER. Mitochondria and ER are physically coupled by protein tethers. The size of these bridges between the two organelles are 10–25 nm in length. Altering this physical **ER-mitochondria distance** leads inevitably to cell dysfunction.

  When this distance is decreased, Ca(2+) overload occurs both in the cytosol and mitochondria. Qi–Shuai, 2016, proposed that the resultant death of neurons, which are responsible for memory and cognition, contributes to Alzheimer's disease.
- **Telomere length**

  The *telomeres* are the caps of repetitive DNA sequences ($(TTAGGG)_n$ in vertebrates cells) at both ends of each linear chromosome in the cell nucleus. They are long stretches of noncoding DNA protecting coding DNA. The number n of *TTAGGG* repeats is called the **telomere length** (TL); it is $\approx$2000 in humans. TL is a robust indicator of biological age and a prognostic marker of disease risk. A limit of life—about 120 years—can be defined by TL in blood stem cells.

  Every time a normal cell divides, its telomeres shorten (due to incomplete lagging strand DNA synthesis) and eventually they are so short that cell stops dividing, self-destructs, or tries to self-replicate and creates cancer. The *Hayflick limit* is the maximal number of divisions beneath which a normal cell will stop dividing, because of shortened telomeres or DNA damage, and die; for humans it is about 52.

  Human telomeres are 15–20 kb in length at birth and shorten gradually throughout life in dividing cells: they lose $\approx$ 100 bp, i.e., 16 repeats, at each

mitosis (i.e., every 20–180 min). But telomere length can increase: by transfer of repeats between telomers or by synthesizing new telomeric DNA from either an RNA template using the enzyme *telomerase*, or a DNA template using *alternative lengthening of telomeres* (ALT). In humans, telomerase acts only in germ, stem or actively dividing tumor cells; ALT occurs only in cancer cells.

Hydras, lobsters, planarian flatworms, trees maintain telomere lengths. Also, bacterial colonies and *Turritopsis dohrnii*, whose medusa form can revert to the polyp stage, are *biologically immortal*, i.e., there is no aging (sustained increase of mortality rate with age) since the Hayflick limit does not apply. Animals with negligible aging die mainly because of growth: they lose agility to get food. The oldest living animals are some sponges and black corals: 2000–10,000 years. The oldest known cell line is 11,000 years-old canine transmissible venereal tumor.

Phenoptsis is genetically programmed death of organism. It acts quickly in *semelparous* (capable of only single reproduction) species, say, Pacific salmon, cicada, mayflies, annual plants and some bamboo, arachnids, squids. Extreme examples: the male praying mantis ejaculates only after being decapitated by the female, and the *Adactyllidium* tick larvae kill their mother eating her from the inside out.

Aging is slow phenoptsis in other species. The telomere shortening is one of its main mechanisms. Vascular disease, osteoarthritis, cancer and menopause are other means of human phenoptsis. Human mortality doubles every 8 years. Mortality rate of people with cancer behave as if the cancer had aged them by 15 years.

- **Gerontologic distance**

  The **gerontologic distance** between individuals of ages x and y from a population with survival fraction distributions $S_1(t)$ and $S_2(t)$, respectively, is defined by

$$|\ln \frac{S_2(y)}{S_1(x)}|.$$

  A function $S(t)$ can be either an empirical distribution, or a parametric one based on modeling. The main survival functions $S(t)$ are: $\frac{N(t)}{N(0)}$ (where $N(t)$ is the number of survivors, from an initial population $N(0)$, at time t), e^{kt} (exponential model), $e^{\frac{a}{b}(1-e^{bt})}$ (Gompertz model), and $e^{-\frac{at^{b+1}}{b+1}}$ (Weibull model); here a and b are, respectively, age independent and age dependent mortality rate coefficients.

  But *late-life mortality deceleration* was observed for humans and fruit flies: the probability that organism's somatic cells become senescent tends to be independent of its age in the long-time limit. The one-year probability of death at advanced age asymptotically approaches 44 % for women and 54 % for men. Such a plateau is typical for many Markov processes. Human *species-specific life span* (age at which death rates of different populations converge) is close to 95 years.

Since 1840, life expectancy has risen linearly: almost three months per year for women and more slowly for men. But the age of super-long livers is linked to their genes rather than their lifestyle; at least 100 genes are linked to longevity.

Distances are used in Human Gerontology also to model the link between geographical distance and contact between adult children and their elderly parents.

Aging/death are adaptive species-specific trade-offs with reproduction. But the *Akela effect* (long post-reproductory period with intergenerational transfers) was observed, besides humans, in two species of toothed whales, Asian elephants, social aphids and, in zoo, Japanese macaques and chimpanzees.

- **Distance to death**

80 % of the persons, who die in any one year, are age 65 or older. Elderly persons think and talk readily about death, but perceived temporal nearness of it is not quantified by $\approx$ 50 % of them. Still this proximity determines one's attitude on it.

Gerstorf *et al., 2008*: relative to age-related decline, mortality-related one (i.e., **distance to death**) in reported life satisfaction account for more variance in the change of subjective well-being. At a point about 4 years before death of an old, i.e., 70+ years, person, this decline showed a 2-fold increase (3-fold for the *oldest old*, i.e., 85+ years) in steepness relative to the preterminal phase.

Bosworth *et al., 1999*: distance to death explains much of the variance in intellectual performance (verbal meaning, psychomotor speed, spatial and reasoning abilities) associated with age. Higher baseline intelligence test scores are associated with reduced risk of mortality and reduced effects of impending death on cognition.

The *terminal drop hypothesis* (Riegel–Riegel, 1972) states that death is preceded by a decrease in cognitive (especially, verbal) functioning over an $\approx$ 5 years period.

The *cascade model* (Birren–Cunningham, 1985) posits primary (normal), secondary (disease-related) and tertiary (distance to death) aging, which influence 3-rd, 2–3-rd and 1–3-rd, respectively, classes of intellectual function: *cristallilized abilities* (to think logically and solve problems knowledge-independently), *fluid abilities* (to use skills, knowledge and experience) and perceptual speed.

Borjigin et al., 2013, observed neural correlates of heightened conscious processing at near-death: a surge 30 s of coherence and connectivity in the dying rat's brain.

Micromort and *microlife* are the units of risk: 10^{-6} probability of death and half an hour ($\approx 10^{-6}$-th of 57 years) change of life expectancy, respectively.

The farthest from Earth that any human has died is about 167 km, when three cosmonauts on Soyuz 11 suffered a depressurization accident while returning to Earth. They were moving at about 7755 m/sec at the time, which is also the highest forward speed at which any human has ever died.

- **Distance running model**

  Bipedality is a key behavior of hominins which appeared 6–4.2 Ma ago. It allowed australopithecines to see approaching danger further off, to walk long distances and to use hands for gathering food. Our genus Homo emerged $\approx$ 2.5 Ma ago.

  The distance running model anthropogenesis, proposed in [BrLi04], claims that our capacity to run long distances in the savanna arised, prior to the invention of the spear, as adaptation for persistence hunting (by running prey to exhaustion) and scavenging (allowing to compete for widely dispersed carcasses).

  This model specifies how endurance running defined the human body form, producing balanced head, low/wide shoulders, narrow chest, short forearms and heels, large hip, etc. Even now, a good athlete can run at 20 km/h for several hours which is comparable to endurance specialists as, say, zebras and antelopes. By sweating we can dissipate body heat faster than any other large mammal and reach large sustainable distance. The capacity of humans to travel vast distances using little energy contributed also to the evolution of their complex social networks.

- **Distance coercion model**

  The **distance coercion model** ([OkBi08]) of the origin of uniquely human kinship-independent cooperation see all complex symbolic speech, cognitive virtuosity, transmission of fitness-relevant information, etc. as elements and effects of this cooperation catalyzed by advances in lethal projectile weapons.

  The model argues that such cooperation can arise only as a result of the pursuit of individual self-interest by animals who can project "death from a distance".

  Among rare organisms able to project coercive threat remotely, humans are the most efficient on long distances, say, to kill adult conspecifics up to 18–27 m by throwing a spear and up to 91 m by a bow. The chimpanzee and Neanderthal also could throw objects but not with human's precision.

  The model posits that this capacity, permitting to repel predators and scavenge their kills in the African savanna, briefly preceded the emergence of brain expansion and social support. Comparing with Neanderthals, evidence of a huge number of injuries suggests that their hunting involved dangerously close contact with large prey animals; they used conventional spears rather than true projectile weapons.

  Throwing and language capacities enabled humans to survive rapid climatic and environmental changes, to spread and to become the dominant large-scale species on the planet. Historical increases in social cooperation could be associated with prior acquisition of a new coercive technology; for instance, the bow and agricultural civilizations, gunpowder weaponry and the modern state.

Humans are most efficient enforcers of cooperation (even relying mainly on indirect cues): our cognitive abilities expanded the range of situations in which cooperation can be favored. Also, while the *strong reciprocity* (generous third-party enforcement) is prevalent in large societies, Marlowe et al., 2012, claim that motivated by the basic emotion of anger, humans-special tendency to retaliate on their own behalf, even at a cost, is sufficient to explain the origin of human cooperation.

- **Distance model of altruism**

  In Evolutionary Ecology, altruism is explained by kin selection, reciprocity, sexual selection, etc. The cooperation between nonrelatives was a driving force in some major transitions (say, from symbiotic bacteria to mitochondria, eukaryotes or multicellular organisms). Individual selection, including *social selection* in which fitness is influenced by the behaviors of others, interacts with group selection.

  The **distance model of altruism** ([Koel00]) claims that altruists spread locally, i.e., with small interaction distance and offspring dispersal distance, while the egoists invest in increasing of those distances. The intermediate behaviors are not maintained, and evolution will lead to a stable bimodal spatial pattern.

- **Distance grooming model of language**

  In primates, being groomed produces mildly narcotic effects, because it stimulates the production of the body's natural opiates, the *endogenous opioid peptides*. Kulahci et al., 2015, observed in lemurs vocal grooming-at-a-distance.

  Language, according to Dunbar, 1993, evolved in archaic *Homo sapiens* as more distance/time efficient replacement of social grooming. Their brain size expanded 0.5 Ma ago from 900 cm^3 in *Homo erectus* to 1300 cm^3, and they lived in large groups (over 120 individuals) requiring cohesion. Language allowed them to produce the reinforcing, social-bonding effects of grooming-at-a-distance and to use more efficiently the time available for social interaction.

  Language achieves this through information transfer, gossip and emotional means (say, laughter, facial expression, Duchenne smile). Many primate species extensively use contact calls such as the long-distance *pant-hoot* call of chimpanzees. Dunbar interprets such calls as a grooming-at-a-distance from which language evolved. But gestures are far more likely precursor of language than vocalizations.

  He deduced (from the link between group and brain sizes in primates) that human social networks tend to be structured in layers: 5 intimates (support clique), 15 best friends (sympathy group), active network of "persons" (50 good friends and 150 friends), 500 acquaintances, 1500 "people I recognize". One need to be in contact every week, month, half-year, year with groups 1–4, respectively. A natural group size (*Dunbar's number*) is 150 for humans and 50 for chimpanzees.

Dunbar explain above sizes by cognitive and time constraints on the number of relationships ego can maintain at a given level of intensity. The clique size correlates with the highest achievable order of *intentionality recursion*, in which mind states are reflexively attributed to others. 0-order means responses to stimuli (as bacteria and computers); 1-st order: belief about the real or imagined world (as most organisms with brains); 2-nd order: belief about the mental state of others; i-th order: as, for $i = 5$, in the sentence "I *think* that you *believe* that I *suppose* that we *understand* that Jane *wants*…". We operate usually at 3-rd and sometimes at 4-th, 5-th, 6-th or 7-th order. Language is essential for 4-th order recursion.

Chapter 24
Distances in Physics and Chemistry

24.1 Distances in Physics

Physics studies the behavior and properties of matter in a wide variety of contexts, ranging from the submicroscopic particles from which all ordinary matter is made (*Particle Physics*) to the behavior of the material Universe as a whole (*Cosmology*).

Physical forces which act at a distance (i.e., a push or pull which acts without "physical contact") are nuclear and molecular attraction and, beyond the atomic level, gravity (completed, perhaps, by anti-gravity), static electricity, and magnetism. Last two forces can be both push and pull, depending on the charges of involved bodies. The nucleon-nucleon interaction (or *residual strong force*) is attractive but becomes repulsive at very small distances keeping the nucleons apart. Dark matter is attractive while dark energy is repulsive (if they exist).

Distances on a relatively small scale are treated in this chapter, while large distances (as in Astronomy and Cosmology) are the subject of Chaps. 25 and 26.

The distances having physical meaning range from 1.6×10^{-35} m (**Planck length**) to 8.8×10^{26} m (estimated size of the observable Universe). We can see things of about $10^{-4} - 10^{21}$ m and measure them within $[10^{-18}, 10^{26}]$ m. The smallest measurable distance, time and weight are 10^{-18} m (by LHC), 10^{-17} sec and 10^{-24} g.

The Theory of Relativity, Quantum Theory and Newtonian laws permit us to describe and predict the behavior of physical systems in the range $10^{-15} - 10^{12}$ m, i.e., from proton to Solar System. Weakened description is still possible up to 10^{25} m.

The world appears Euclidean at distances less than about 10^{25} m (if gravitational fields are not too strong). Relativity and Quantum Theory effects, governing Physics on very large and small scales, are already accounted for in technology, say, of GPS satellites and nanocrystals of solar cells.

© Springer-Verlag Berlin Heidelberg 2016

M.M. Deza, E. Deza, *Encyclopedia of Distances*,
DOI 10.1007/978-3-662-52844-0_24

- **Moment**

  In Physics and Engineering, **moment** is the product of a quantity (usually, force) and a distance (or a power of it) to some point associated with that quantity.
- **Momentum**

  In classical mechanics, **momentum** $\mathbf{p} = (p_x, p_y, p_z)$ is the product $m\mathbf{v}$ of the mass m and velocity vector $\mathbf{v} = (v_x, v_y, v_z)$ of an object.

  In relativistic 4D mechanics, *momentum-energy* $(\frac{E}{c}, p_x, p_y, p_z)$, where c is the speed of light and $E = mc^2$ is energy, is compared with space-time (ct, x, y, z).
- **Displacement**

  In Mechanics, a *displacement* (or *relative position*) *vector* of a moving particle from its initial position P_i to the final position P_f, is the vector $\overrightarrow{P_iP_f} = \overrightarrow{0(P_f - P_i)}$, where O is a reference point (usually the origin of a coordinate system).

  A **displacement** is the length $||P_f - P_i||_2$ of this vector, i.e., the Euclidean distance from P_i to P_f. It is never greater than the distance traveled by a particle.
- **Acceleration distance**

  The **acceleration distance** is the minimum distance at which an object (or, say, flow, flame), accelerating in given conditions, reaches a given speed.
- **Mechanic distance**

  The **mechanic distance** is the position of a particle as a function of time t.

  For a particle, moving linearly with initial position x_0 and initial speed v_0, which is acted upon by a constant acceleration a, it and the speed are given by

$$x(t) = x_0 + v_0 t + \frac{1}{2}at^2 \quad \text{and} \quad v(t) = v_0 + at.$$

  So, the **acceleration distance** fallen under uniform acceleration a, in order to reach a speed v, is $\frac{v^2}{2a}$. A body is *free falling* if it is falling subject only to acceleration g by gravity; the **free fall distance** (distance fallen by it) is $y(t) = \frac{1}{2}gt^2$.
- **Terminal distance**

  The **terminal distance** is the distance of an object, moving linearly in a resistive medium, from an initial position to a stop.

  If object's initial position and speed are x_0, v_0, and the drag per unit mass in the medium is proportional to speed with constant of proportionality β, then the position and speed of a body are given by

$$x(t) = x_0 + \frac{v_0}{\beta}(1 - e^{-\beta t}) \quad \text{and} \quad v(t) = x'(t) = v_0 e^{-\beta t}.$$

  The speed decreases to 0, and the body reaches a *maximum terminal distance*

$$x_{terminal} = \lim_{t \to \infty} x(t) = x_0 + \frac{v_0}{\beta}.$$

For a body, moving from initial position (x_0, y_0) and speed (v_{x_0}, v_{y_0}), the position $(x(t), y(t))$ is $x(t) = x_0 + \frac{v_{x_0}}{\beta}(1 - e^{-\beta t})$, $y(t) = (y_0 + \frac{v_{y_0}}{\beta} - \frac{g}{\beta^2}) + \frac{v_{y_0}\beta - g}{\beta^2} e^{-\beta t}$. The horizontal motion ceases at a maximum terminal distance $x_{terminal} = x_0 + \frac{v_{x_0}}{\beta}$.

- **Ballistics distances**

  Ballistics is the study of the motion of *projectiles*, i.e., bodies which are propelled (or thrown) with some initial velocity, and then allowed to be acted upon by the forces of gravity and possible drag.

  The **trajectory**, **range** and **height** of a projectile are its parabolic path, total horizontal distance traveled and maximum upward distance reached. If projectile is launched on flat ground at velocity v and angle θ to the horizontal, then at the time t of motion, its horizontal and vertical positions are

$$x(t) = vt\cos\theta \quad \text{and} \quad y(t) = vt\cos\theta - \frac{1}{2}gt^2.$$

  So, the range, realized by the *time of flight* $t_{of} = \frac{2v\sin\theta}{g}$, and height are

$$x_{\max} = x(t_{of}) = \frac{v^2 \sin 2\theta}{g} \quad \text{and} \quad y_{\max} = y(\frac{1}{2}t_{of}) = \frac{v\sin^2\theta}{2g},$$

  which are maximized when $\theta = \pi/4$ and $\theta = \pi/2$, respectively.

  The *bullet drop* is the height it loses, because of gravity, between leaving the rifle and reaching the target. In order to ensure that the "zero" (point at which the bullet's path intersects with the *LOS*, line of sight, to the target) will be at a specific range, the shooter should set (using a *sight*, device mounted on the rifle) the *bore angle* between the rifle bore and the LOS. A properly adjusted rifle barrel and sight are said to be *zeroed* (or *sighted-in*). The shooter zeroes rifle at a standard *zero range* and then adjustments are made for other ranges.

  The **point-blank range** is the distance at which the bullet is expected to strike a target of a given size without adjusting the elevation of the firearm.

- **Interaction distance**

  The **impact parameter** is the perpendicular distance between the velocity vector of a projectile and the center of the object it is approaching.

  The **interaction distance** between two particles is the farthest distance of their approach at which it is discernible that they will not pass at the impact parameter, i.e., their distance of closest approach if they had continued to move in their original direction at their original speed.

  The *coefficient of restitution* (COR) of colliding objects A, B is the ratio of speeds after and before an impact, taken along its line. The collision is *inelastic* if COR< 1. COR^2 is the ratio of *rebound* and *drop* distances if A bounces off stationary B.

- **Mean free path (length)**

  The **mean free path (length)** of a particle (photon, atom or molecule) in a medium measures its probability to undergo a situation of a given kind K; it

is the average of an exponential distribution of distances until the situation K occurs. In particular, this average distance d is called:

nuclear collusion length if K is a nuclear reaction;
interaction length if K is an interaction which is neither elastic, nor quasi-elastic;
scattering length if K is a scattering event;
attenuation length (or *absorption length*) if K means that the probability $P(d)$, that a particle has not been absorbed, drops to $\frac{1}{e} \approx 0.368$, cf. **Beer-Lambert law**;
radiation length (or *cascade unit*) if K means that the energy of (high energy electromagnetic-interacting) relativistic charged particles drops by the factor $\frac{1}{e}$;
free streaming length if K means that particles become nonrelativistic.

In Gamma-ray Radiography, the *mean free path* of a beam of photons is the average distance a photon travels between collisions with atoms of the target material. It is $\frac{1}{\alpha\rho}$, where α is the material *opacity* and ρ is its density.

- **Neutron scattering length**

  In Physics, *scattering* is the random deviation or reflection of a beam of radiation or a stream of particles by the particles in the medium.

  In Neutron Interferometry, the **scattering length** a is the zero-energy limit of the scattering amplitude $f = -\frac{\sin\delta}{k}$. Since the *total scattering cross-section* (the likelihood of particle interactions) is $4\pi|f|^2$, it can be seen as the radius of a hard sphere from which a point neutron is scattered.

  The spin-independent part of the scattering length is the *coherent scattering length*. In order to expand the scattering formalism to absorption, the scattering length is made complex $a = a' - ia''$.

  Thomson scattering length is the *classical electron radius* $\approx 2.818 \times 10^{-15}$ m.

- **Inelastic mean free path**

  In Electron Microscopy, the **inelastic mean free path** (or IMFP) is the average total distance that an electron traverses between events of inelastic scattering, while the **effective attenuation length** (or EAL) is an experimental parameter reflecting the average net distance traveled.

  The EAL is the thickness in the material through which electron can pass with probability $\frac{1}{e}$ that it survives without inelastic scattering. It is about 20 % less than the IMFP due to the elastic scatterings which deflect the electron trajectories.

  Both are smaller than the total electron range which may be 10–100 times greater.

- **Sampling distance**

  In Electron Spectroscopy for chemical analysis, the **sampling distance** is the lateral distance between areas to be measured for characterizing a *surface*, i.e., the volume from which the photo-electrons can escape.

- **Debye screening distance**

  The **Debye screening distance** (or *Debye length*, *Debye–Hückel length*) is the distance over which a local electric field affects the distribution of mobile charge carriers (for example, electrons) present in the material (plasmas and other conductors).

  Its order increases with decreasing concentration of free charge carriers, from 10^{-4} m in gas discharge to 10^{5} m in intergalactic medium.
- **Range of a charged particle**

  The **range of a charged particle**, passing through a medium and ionizing, is the distance to the point where its energy drops to almost zero.
- **Gyroradius**

  The **gyroradius** (or *cyclotron radius*, *Larmor radius*) is the radius of the circular orbit of a charged particle in the presence of a uniform magnetic field.
- **Radius of gyration**

  The **radius of gyration** of a body about a given axis is the distance from this axis to the centre of gyration. It is the RMS (square root of the mean of the squares) of the distances from the axis of rotation to all the points in the body.
- **Inverse-square laws**

  An **inverse-square law** is any law stating that a quantity or intensity is inversely proportional to the square of the distance d from its source.

  Such law applies when some conserved quantity is evenly radiated outward from a point source in 3D space. The intensity of radiation passing through any unit area (directly facing the point source) is inversely proportional to d^2, since radiation is spread out over the surface area $4\pi d^2$ of a sphere.

  Newton's **law of universal gravitation** (checked above 6×10^{-5} m): the gravitational attraction between two point-like masses m_1, m_2 at distance d is

$$G\frac{m_1 m_2}{d^2},$$

  where $G = 6.67384(80) \times 10^{-11}$ $\mathrm{m^3 kg^{-1} s^{-2}}$ is the Newton *gravitational constant*.

  The existence of extra dimensions, postulated by M-theory, will be checked by LHC (Large Hadron Collider at CERN, near Geneva) based on the inverse proportionality of the gravitational attraction in nD space to the $(n-1)$-th degree of the distance between objects; if the Universe has a 4-th dimension, LHC will find out the inverse proportionality to the cube of the small interparticle distance.

  The effects of electric, magnetic, light, sound, and radiation phenomena also follows, an inverse-square law for large d. **Coulomb law**: the force of attraction or repulsion between two point-like objects with charges e_1, e_2 at distance d is given by

$$k_e\frac{e_1 e_2}{d^2},$$

where k_e is the *Coulomb constant* depending upon the medium that the charged objects are immersed in. The gravitational and electrostatic forces of two bodies with *Planck mass* m_P and $e_1 = e_2 = 1$ have equal strength.

The *irradiance* (power per unit area in the direction of propagation) of a spherical wavefront (light, sound, etc.) radiating from a point source decreases (assuming that there are no losses caused by absorption or scattering) inversely proportional to the square d^2 of the distance from the source (cf. **distance decay** in Chap. 29). However, for a radio wave, it decrease like $\frac{1}{d}$.

The **far field** is the region, where the emitter can be considered as a point source (so, inverse-square law holds), usually at a distance of more than 5–10 times the source diameter; the **near field** is the region closer to source.

For light, the distance, from which far field starts, is called **photometric distance**. Cf. **Fraunhofer distance** and, in Chap. 21, **acoustics distances**.

- **Fraunhofer distance**

The Maxwell equations, governing the field strength decay, can be approximated as d^{-3}, d^{-2} and d^{-1} for three regions surrounding an radiating antenna: the *reactive near field*, the *radiating near field* (or *Fresnel region*) and the **far field** (or *Fraunhofer region*). Cf. **inverse-square law**. The Fresnel region begins about at $0.62(\frac{D^3}{\lambda})^{\frac{1}{2}}$, where D is the largest dimension of the antenna and λ is the wavelength. The propagating waves start to dominate here, but only in the far field the distribution of the diffracted energy no longer change with distance.

The **Fraunhofer** (or *far field*, *Rayleigh*) **distance** is $\frac{2D^2}{\lambda}$, the distance where the far field begin. Cf. **acoustic distances** in Chap. 21.

In Optics, beam divergence is defined by its *radius*, i.e., for a Gaussian beam, the distance from the beam propagation axis where intensity drops to $\frac{1}{e^2} \approx 13.5\,\%$ of the maximum. The beam's *waist* (or *focus*) is the position on its axis where the radius is at its minimum. The *imaginary-distance BPM* (Jevick–Hermansson, 1989) refers to beam propagating the (complex electric) field along the imaginary axis.

The beam's **Rayleigh length** (or *Rayleigh range*) Rl is the distance from the waist (in the propagation direction) where the radius increases from w_0 to $\sqrt{2}w_0$, i.e., the beam propagates without diverging much. For Gaussian beams, $Rl = \frac{\pi w_0^2}{\lambda}$, where λ is the vacuum wavelength divided by the refractive index of the material. The Rayleigh length divides the near-field and *mid-field*; it is the distance from the waist at which the wavefront curvature is at a maximum. The divergence really starts in the far field where the beam radius is at least $10Rl$. The *confocal parameter* (or *depth of focus*) of the beam is $2Rl$. Cf. **lens distances** in Chap. 28.

- **Half-value layer**

Ionizing radiation consists of highly-energetic particles or waves (especially, X-rays, gamma rays and far ultraviolet light) which are progressively absorbed during propagation through the surrounding medium, via *ionization*, i.e., removing an electron from some of its atoms or molecules. The **half-value layer** is the depth within a material where half of the incident radiation is absorbed.

A basic rule of protection against ionizing radiation exposure: multiplying the distance from its source by a *distance factor r* decreases this exposure to $\frac{1}{r^2}$ of it.

In Maxwell Render light simulation software, the *attenuation distance* (or *transparency*) is the thickness of object that absorbs 50 % of light energy.

- **Range of fundamental forces**

The fundamental forces (or interactions) are gravity and electromagnetic, weak nuclear and strong nuclear forces. The **range** of a force is considered *short* if it decays (approaches 0) exponentially as the distance d increases.

Both electromagnetic force and gravity are forces of infinite range which obey **inverse-square laws**. The shorter the range, the higher the energy. Both weak and strong forces are very short range (about 10^{-17} m and 10^{-15} m, respectively) which is limited by the uncertainty principle.

At subatomic distances, Quantum Field Theory describes electromagnetic, weak and strong interactions with the same formalism but different constants. Quantum Electrodynamics describes electromagnetism via photon exchanges between charged particles and Quantum Chromodynamics describe strong interactions via gluon exchanges between quarks. Strong interaction force grows stronger with the distance. Three forces almost coincide at very large energy, but at large distances they are irrelevant compared with gravity. The number of fundamental particles increases on smaller distance scales. But at macroscopic scales, those particles can collectively create emerging phenomena, say, superconductivity.

General Relativity has been probed from submillimeter up to Solar System scales but at cosmological scale it require the presence of *dark matter* and *dark energy*. Maxwell's electromagnetism has been probed from atomic distances up to 1.3 AU (order of the **coherence lengths** of the magnetic fields dragged by the solar wind) but it does not explain magnetic fields found in galaxies, clusters and voids.

At cosmological scale, the repulsive force of putative *dark energy*, due to *vacuum energy* (or *cosmological constant*) overtakes gravity; cf. **metric expansion of space** in Chap. 26. Dark energy is the only substance known to act both on subatomic and cosmological scale. Its effect is measured only on a scale larger than superclusters. Khoury–Weltman, 2004, in order to explain dark energy, conjectured *fifth force* with range depending on density of matter in its environment, say, 1 mm in Earth's vicinity and 10^7 ly in cosmos. An alternative to dark energy: possible, in String Theory, modifications of gravity at ultra large distances (i.e., small curvatures) due to some specific compactification of extra dimensions.

Alexander-Katz et al., 2016, found a new kind of long-range interaction between particles, in a liquid medium, that is based entirely on their motions. A small number of magnetic metal microparticles a few μm across, were interspersed with a much larger quantity of inert particles of comparable size, all suspended in water. When a rotating magnetic field was applied, the metal particles would begin to spin and, even when separated by distances tens of times

their size, would migrate toward each other, through a slow series of motions. The attraction depends on the speed of spinning and amount of inert matter.

- **EM radiation wavelength range**

  The *wavelength* is the distance $\lambda = \frac{c}{f}$ the wave travels to complete one cycle.

  Electromagnetic (EM) **radiation wavelength range** is infinite and continuous in principle. The limits of short and long waves are the vicinity of the **Planck length** and the size of Universe, respectively.

  The wavelengths are: < 0.01 nm for gamma rays, 0.01–10 nm for X-rays, 100–400 nm for ultraviolet, 400–780 nm for visible light, 0.78–1000 μm for infrared (in lasers), 1–330 mm for microwave, 0.33–3000 m for radio frequency radiation, > 3 km for low frequency, and ∞ for static field.

  Besides gamma rays, X-rays and far ultraviolet, the EM radiation is *nonionizing*, i.e., passing through matter, it only *excites* electrons: moves them to a higher energy state, instead of removing them completely from an atom or molecule.

- **Compton wavelength**

  Compton scattering is the scattering of (X-ray or gamma ray) photons by electrons. It results in a decrease in energy (so, increase in wavelength) of the photon.

  Compton wavelength $\lambda_C(m)$ and **reduced Compton wavelength** $\overline{\lambda}_C(m)$ of a particle with rest mass m (where c is the speed of light, $\hbar$ is the *reduced Planck constant* $\frac{h}{2\pi}$ and l_P, m_P are Planck length and mass) are defined by

$$\frac{1}{2\pi}\lambda_C(m) = \overline{\lambda}_C(m) = \frac{\hbar}{mc} = \frac{m_P}{m} l_P.$$

- **Radiation attenuation with distance**

  Radiation is the process by which energy is emitted from a source and propagated through the surrounding medium. Radiant energy described in wave terms includes sound and electromagnetic radiation, such as light, X-rays and gamma rays. The incident radiation partially changes its direction, gets absorbed, and the remainder transmitted. The change of direction is *reflection*, *diffraction*, or *scattering* if the direction of the outgoing radiation is reversed, split into separate rays, or randomized (diffused), respectively. Scattering occurs in nonhomogeneous media.

  In Physics, *attenuation* is any process in which the flux density, power amplitude or intensity of a wave, beam or signal decreases with increasing distance from the energy source, as a result of absorption of energy and scattering out of the beam by the transmitting medium. It comes in addition to the divergence of flux caused by distance alone as described by the **inverse-square laws**.

  Attenuation of light is caused mainly by scattering and absorption of photons. The primary causes of attenuation in matter are the *photoelectric effect* (emission of electrons), *Compton scattering* (cf. **Compton wavelength**) and *pair production* (creation of an elementary particle and its antiparticle from a high-energy photon).

In Physics, *absorption* is a process in which atoms, molecules, or ions enter some bulk phase—gas, liquid or solid material; in *adsorption*, the molecules are taken up by the surface, not by the volume. *Absorption of EM radiation* is the process by which the energy of a photon is taken up (and destroyed) by, for example, an atom whose valence electrons make the transition between two electronic energy levels. The absorbed energy may be re-emitted or transformed into heat.

Attenuation is measured in units of decibels (dB) or *nepers* ($\approx$ 8.7 dB) per length unit of the medium and is represented by the medium *attenuation coefficient* α. When possible, specific absorption or scattering coefficient is used instead.

Attenuation (or *loss*) *of signal* is the reduction of its strength during transmission. In Signal Propagation, attenuation of a propagating EM wave is called the *path loss*. Path loss may be due to free-space loss, refraction, diffraction, reflection, absorption, aperture-medium coupling loss, etc. of antennas. Path loss in decibels is $L = 10n \lg d + C$, where n is the path loss exponent, d is the transmitter-receiver distance in m, and C is a constant accounting for system losses.

The *free-space path loss* (FSPL) is the loss in signal strength of an EM wave that would result from a line-of-sight path through free space, with no obstacles to cause reflection or diffraction. FSPL is $(\frac{4\pi d}{\lambda})^2$, where d is the distance from the transmitter and λ is the signal wavelength (both in m), i.e., in dB it is $10 \lg (FSPL) = 20 \lg d + 20 \lg f - 147.56$, where f is the frequency in Hz.

- **Beer–Lambert law**

The **Beer–Lambert law** is an empirical relationship for the *absorbance* Ab of a substance when a radiation beam of given frequency goes through it:

$$Ab = \alpha d = -\log_a T,$$

where $a = e$ or (for liquids) 10, d is the *path length* (distance the beam travels through the medium), $T = \frac{I_d}{I_0}$ is the *transmittance* (I_d and I_0 are the intensity of the transmitted and incident radiation), and α is the medium *opacity* (or *linear attenuation coefficient*, *absorption coefficient*); α is the fraction of radiation lost to absorption and/or scattering per unit length of the medium.

The *extinction coefficient* is $\frac{\lambda_w}{4\pi}\alpha$, where λ_w is the same frequency wavelength in a vacuum. In Chemistry, α is given as ϵC, where C is the absorber *concentration*, and ϵ is the *molar extinction coefficient*.

The **optical depth** is $\tau = -\ln \frac{I_d}{I_0}$, measured along the true (slant) optical path.

The **penetration depth** (or **attenuation length**, *mean free path*, *optical extinction length*) is the thickness d in the medium where the intensity I_d has decreased to $\frac{1}{e}$ of I_0; so, it is $\frac{1}{\alpha}$. Cf. **half-value layer**.

Also, in Helioseismology, the (meridional flow) *penetration depth* is the distance from the base of the solar convection zone to the location of the first reversal of the meridional velocity. In an information network, the *message*

penetration distance is the maximum distance from the event message traverses in the valid routing region.

The **skin depth** is the thickness d where the amplitude A_d of a propagating wave (say, alternating current in a conductor) has decreased to $\frac{1}{e}$ of its initial value A_0; it is twice the penetration depth. The *propagation constant* is $\gamma = -\ln \frac{A_d}{A_0}$.

The Beer–Lambert law can describe also the attenuation of solar or stellar radiation. The main components of the atmospheric light attenuation are: absorption and scattering by aerosols, Rayleigh scattering (from molecular oxygen O_2 and nitrogen Ni_2) and (only absorption) by carbon dioxide CO_2, O_2, nitrogen dioxide NiO_2, water vapor, ozone O_3. Cf. **atmospheric visibility distances** in Chap. 25.

The sea is nearly opaque to light: less than 1 % penetrates 100 m deep. Cf. **distances in Oceanography** in Chap. 25. In Oceanography, attenuation of light is the decrease in its intensity with depth due to absorption (by water molecules) and scattering (by suspended fine particles). The transparency of the water in oceans and lakes is measured by the *Secchi depth* d_S at which the reflectance equals the intensity of light backscattered from the water. Then $\alpha = \frac{10 d_S}{17}$ is used as the *light attenuation coefficient* in the Beer–Lambert law $\alpha d = -\ln \frac{I_d}{I_0}$, in order to estimate I_d, the intensity of light at depth d, from I_0, its intensity at the surface.

In Astronomy, attenuation of EM radiation is called *extinction* (or *reddening*). It arises from the absorption and scattering by the interstellar medium, the Earth's atmosphere and dust around an observed object.

The *photosphere* of a star is the surface where its optical depth is $\frac{2}{3}$. energy emitted. The *optical depth of a planetary ring* is the proportion of light blocked by the ring when it lies between the source and the observer.

- **Atmospheric depth**

  The total absorption along a slanted path through matter of density ρ at the angle θ from the vertical is measured by the **interaction depth**, i.e., $\frac{1}{\cos\theta} \int \rho(x) d(x)$.

  In particular, the **atmospheric depth** (or *effective thickness of the atmosphere*) at altitude h is defined as

$$A(h) = \frac{1}{\cos\theta} \int_h^\infty \rho(x) d(x).$$

  It is ≈ 11 times larger when the Sun is just above the horizon than at the shortest path (solar zenith). Vertical $A(h)$ is approximatively equal to the pressure divided by $g = 9.8\ \mathrm{m/s^2}$.

- **Arago distance**

  The *Arago point* is a *neutral point* (where the degree of polarization of skylight goes to zero) located $\approx 20°$ directly above the *antisolar point* (the point on the celestial sphere that lies directly opposite the sun from the observer) in relatively clear air and at higher elevations in turbid air.

So, the **Arago distance**, i.e., the angular distance from the antisolar point to the Arago point, is a measure of *atmospheric turbidity* (effect of aerosols in reducing the transmission of direct solar radiation).

Another useful measure of turbidity is *aerosol optical depth*, i.e., the **optical depth** due to extinction by the aerosol component of the atmosphere.

- **Sound attenuation with distance**

  Vibrations propagate through elastic solids and liquids, including the Earth, and consist of *elastic* (or *seismic*, *body*) *waves* and *surface* (occurring since it acts as an solid-gas interface) *waves*. Elastic waves are: primary (P) wave moving in the propagation direction of the wave and *secondary* (S) wave moving in this direction and perpendicular to it. Surface waves are: the *Love* wave moving perpendicular to the direction of the wave and the *Rayleigh* (R) wave moving in the direction of the wave and circularly within the vertical surface perpendicular to it. The attenuation of P- and S-waves is proportional to $\frac{1}{d^2}$ or $\frac{1}{d}$, when propagated by the surface or inside of an infinite elastic body. For the R-wave, it is proportional to $\frac{1}{\sqrt{d}}$.

  Sound propagates through gas (say, air) as a P-wave and attenuates over a distance, at a rate of $\frac{1}{d^2}$. The *far field* (cf. **Fraunhofer distance**) is the part of a sound field in which sound pressure (if it is the same in all directions) decreases according to the *inverse distance law* $\frac{1}{d}$; but sound intensity decreases as $\frac{1}{d^2}$.

  In natural media, further weakening occurs from *attenuation*, i.e., *scattering* (reflection of the sound in other directions) and *absorption* (conversion of the sound energy to heat). Cf. **critical distance** among **acoustics distances** in Chap. 21.

  The **sound extinction distance** is the distance over which its intensity falls to $\frac{1}{e}$ of its original value. For sonic boom intensities (say, supersonic flights), the lateral *extinction distance* is the distance where in 99 % of cases the sound intensity is lower than 0.1–0.2 mbar (10–20 pascals) of atmospheric pressure. Cf. earthquake *extinction length* in **distances in Seismology** (Chap. 25).

  Water is transparent to sound. Sound energy is absorbed (due to viscosity) and $\approx$ 6 % of it is scattered (due to water inhomogeneities). Absorbed less, low frequency sounds can propagate over large distances along lines of minimum sound speed. High frequency waves attenuate more rapidly. So, low frequency waves are dominant further from the source (say, a musical band or earthquake).

  Attenuation of ultrasound waves with frequency f MHz at a given distance r cm is αfr decibels, where α is the *attenuation coefficient* of the medium. It is used in Ultrasound Biomicroscopy; in a homogeneous medium (so, without scattering) α is 0.0022, 0.18, 0.85, 20, 41 for water, blood, brain, bone, lung, respectively.

- **Lighting distance**

  Sound travels through air at 330–350 m/s (depending on altitude, relative humidity, pressure, etc.), while the speed of light is $c \approx 300 \times 10^6$ m/s. In fact, structure of light pulses reduces their speed, even in a vacuum.

So, the **lighting distance** (of a lightning bolt from an observer) in km is $\approx \frac{1}{3}$ of the delay, in seconds, between observer's seeing it and hearing thunder.

- **Optical distance**

  The **optical distance** (or *optical path length*) is a distance dn traveled by light, where d is the physical distance in a medium and $n = \frac{c}{v}$ is the medium's *refractive index* (c, v are the speeds of an EM wave in a vacuum and in the medium). By *Fermat's principle* light follows the shortest optical path. Cf. **optical depth**.

  The **light extinction distance** is the distance where light propagating through a given medium reaches its *steady-state speed*, i.e., a characteristic speed that it can maintain indefinitely. It is proportional to $\frac{1}{\rho\lambda}$, where ρ is the density of the medium and λ is the wavelength, and it is very small for most common media.

- **Edge perimeter distance**

  In semiconductor technology, the **edge perimeter distance** is the distance from the edge of a *wafer* (thin slice with parallel faces cut from a semiconductor crystal) in a wafer carrier to the top face of the wafer carrier.

- **Proximity effects**

  In Electronic Engineering, an alternating current flowing through an electric conductor induces (via the associated magnetic field) eddy currents within the conductor. The *electromagnetic proximity effect* is the "current crowding" which occurs when such currents are flowing through several nearby conductors such as within a wire. It increases the alternating current resistance (so, electrical losses) and generates undesirable heating.

  In Nanotechnology, the *quantum* $\frac{1}{f}$ *proximity effect* is that the $\frac{1}{f}$ fundamental noise in a semiconductor sample is increased by the presence of another similar current-carrying sample placed in the close vicinity.

  The *superconducting proximity effect* is the propagation of superconductivity through a NS (normal-superconductor) interface, i.e., a very thin layer of "normal" metal behaves like a superconductor (that is, with no resistance) when placed between two thicker superconductor slices.

  In Lithography, if a material is exposed to an electronic beam, some molecular chains break and many electron scattering events occur. Any pattern written by the beam on the material can be distorted by this *E-beam proximity effect*.

  In LECD (localized electrochemical deposition) technique for fabrication of miniature devices, the electrode (anode) is placed close to the tip of a fabricated structure (cathode). Voltage is applied and the structure is grown by deposition. The *LECD proximity effect*: at small cathode-anode distances, migration overcomes diffusion, the deposition rate increases greatly and the products are porous.

  In Atomic Physics, the **proximity effect** refers to the intramolecular interaction between two (or more) functional groups (in terms of group contributions models of a molecule) that affects their properties and those of the groups located nearby.

  Cf. also *proximity effect (audio)* among **acoustics distances** in Chap. 21.

The term *proximity effect* is also used more abstractly, to describe some undesirable proximity phenomena. For example, the *proximity effect in the production of chromosome aberrations* (when ionizing radiation breaks double-stranded DNA) is that DNA strands can misrejoin if separated by less than $\frac{1}{3}$ of the diameter of a cell nucleus. The *proximity effect in innovation process* is the tendency to the geographic agglomeration of innovation activity.

- **Hopping distance**

  Hopping is atomic-scale long range dynamics that controls diffusivity and conductivity. For example, oxidation of DNA (loss of an electron) generates a radical cation which can migrate a long (more that 20 nm) distance, called the **hopping distance**, from site to site before it is trapped by reaction with water.

- **Atomic jump distance**

  In the solid state, the atoms are about closely packed on a rigid lattice. The atoms of some elements (carbon, hydrogen, nitrogen), being too small to replace the atoms of metallic elements on the lattice, are located in the interstices between metal atoms and they diffuse by squeezing between the host atoms.

  Interstitial diffusion is the only mechanism by which atoms can be transported through a solid substance while, in a gas or liquid, mass transport is possible by both diffusion and the flow of fluid (for example, convection currents).

  The **jump distance** is the distance an atom is moved through the lattice in a given direction by one exchange of its position with an adjacent lattice site.

  Some crystals can jump 1000 times their own length under light, since light energy rearranges atoms and builds strain, which is then explosively released.

  The **mean square diffusion distance** d_t from the starting point which a molecule will have diffused in time t, satisfies $d_t^2 = r^2 N = r^2 \nu t = 2nDt$, where r is the jump distance, N is the number of jumps (equal to νt assuming a fixed jump rate ν), $n = 1, 2, 3$ for $1, 2, 3$-dimensional diffusion, and $D = \frac{\nu r^2}{2n}$ is the *diffusivity* in cm^2/s.

  In diffusion alloy bonding, a **characteristic diffusion distance** is the distance between the joint interface and the site wherein the concentration of the diffusing substance (say, aluminum in high carbon-steel) falls to zero up to a given error.

- **Diffusion length**

  Diffusion is a process of spontaneous spreading of matter, heat, momentum, or light: particles move to lower chemical potential implying concentration change.

  In Microfluidics, the **diffusion length** is the distance from the point of initial mixing to the complete mixing point where the equilibrium composition is reached.

  In semiconductors, electron-hole pairs are generated and recombine. The (*minority carrier*) **diffusion length** of a material is the average distance a minority carrier can move from the point of generation until it recombines with majority carriers. Also, in electron transport by diffusion, the *diffusion length* is the distance over which concentration of free charge carriers injected into semiconductor falls to $\frac{1}{e}$ of its original value.

  Cf. **jump distance** and, in Chap. 23, **capillary diffusion distance**.

- **Thermal diffusion length**

  The heat propagation into material is represented by the **thermal diffusion length**, i.e., the propagation distance of the thermal wave producing an attenuation of the peak temperature to about 0.1 of the maximum surface value.

  The propagation of the laser-generated shock wave is approximated as blast wave (instantaneous, massless point explosion). The **expansion distance** is the distance between the surface of the target and the position of a blast wave; it depends on the energy converted into the plasma state.
- **Thermal entrance length**

  In heat transfer at a boundary (surface) within a fluid, the **thermal entrance length** is the distance required for the *Nusselt number* (ratio of convective to conductive heat transfer across normal to the boundary) associated with the pipe flow to decrease to within 5 % of its value for a fully developed heat flow.
- **Distance-to-spot ratio**

  The **distance-to-spot ratio** of an infrared temperature sensing device is the ratio of the distance to the object and the diameter of the $t°$ measurement area.
- **Bjerrum length**

  The **Bjerrum length** is the separation at which the electrostatic interaction between two elementary charges is comparable in magnitude to the thermal energy scale, k_B, T, where k_B is the Boltzmann constant and T is the temperature in kelvin.
- **Lagrangian radius**

  The **Lagrangian radius** of the particle is the distance from the explosion center to a particle at the moment the shock front passes through it.

  Cf. unrelated *Lagrangian radii* among the **radii of a star system** (Chap. 25).
- **Reynolds number**

  For an object of a characteristic length (Chap. 29) l, flowing with mean relative velocity v in a *fluid* (liquid or gas) of the density ρ and dynamic viscosity μ, the **Reynolds number** is the ratio $Re = \frac{\rho v l}{\mu}$ of inertial forces to viscous forces. The *flow* is *smooth* (or *laminar*) if Re is low (viscous forces dominate), *rough* (or *turbulent*) if Re is high (usually $Re \geq 10^5$) and *transitional* in between. In a *Stokes flow* (laminar flow with very low Re), the inertial forces are negligible.

  The *law of the wall* (von Kármán, 1930) states that the average velocity of a turbulent flow close to the *wall* (boundary of the fluid region) is proportional to $\ln y^+$, where the **wall distance** $y^+ = \frac{u'}{\nu} y$ is the distance y to the wall, made dimensionless with the friction velocity u' at the wall and fluid's kinematic viscosity ν.

  In swimming, Re is $10^{-5}, 4\times10^{-3}, 10^{-1}-10, 5\times10^4$ and 3×10^8 for bacterium, spermatozoa, small zooplankton, large fish and whale, respectively. In flying, Re is 30–4×10^4 for insects, 10^3–10^5 for birds, 1.6×10^6 for a glider and 2×10^9 for Boeing 747. Blood flow has $Re = 10^{-3}$, 140, 500 and 3.4×10^3 in capillary, vein, artery and aorta, respectively. Re is a *dimensionless parameter*, i.e., the units of measurement in it cancel out. Examples of other such flow parameters follow.

  The *Mach number Ma* is a ratio of the speed of flow to the speed of sound in a fluid. Ma is ratio of inertia to *compressibility* (volume change as a response to

a pressure). The flow is *subsonic*, *supersonic*, *transonic* or *hypersonic* if $Ma < 1, 0.8 \leq Ma \leq 1.5$ or $Ma \geq 5$, respectively. Ma governs *compressible* (i.e., those with $Ma > 0.3$) flows.

The *Froude number* $Fr = \frac{v}{\sqrt{gl}}$, where v, d, g are characteristic flow velocity, depth and external field (usually, gravity), is the ratio of the flow inertia to the external field; it governs open-channel flows. Alexander, 1984: legged animals moving with the same Froude number have similar gait patterns and *duty factors* (percentages of a stride when a foot touch the ground); cf. **gait distances** in Chap. 29.

The *lift* L and *drag* D are perpendicular and, respectively, parallel (to the oncoming flow direction) components of the force fluid flowing past the surface of a body exerts on it. In a flight without wind, the lift-to-drag ratio $\frac{L}{D}$ is the horizontal distance traveled divided by the altitude lost. $\frac{L}{D}$ is $4, 17, 20, 37$ for cruising house sparrow, Boeing 747, albatross, Lockheed U-2, respectively. Küchemann, 1978, found that range-maximizing L for high Ma is $\approx 4 + \frac{12}{Ma}$.

- **Turbulence length scales**

  Turbulence is the time dependent chaotic behavior of fluid flows. The turbulent field consists of the superposition of interacting *eddies* (coherent patterns of velocity, vorticity and pressure) of different length scales. The kinetic energy cascades from the eddies of largest scales down to the smallest ones generated from the larger ones through the nonlinear process of vortex stretching.

  The **turbulence length scales** are measures of the eddy scale sizes in turbulent flow. Such standard length scales for largest, smallest and intermediate eddy sizes are called **integral length scale**, **Kolmogorov microscale** and **Taylor microscale**, respectively. The corresponding ranges are called *energy-containing*, *dissipation* and *inertial* range.

  Integral length scale measures the largest separation distance over which components of the eddy velocities at two distinct points are correlated; it depends usually of the flow geometry. For example, the largest integral scale of pipe flow is the pipe diameter. For atmospheric turbulence, this length can reach several hundreds km. On intermediate Taylor microscale, turbulence kinetic energy is neither generated nor destroyed but is transferred from larger to smaller scales.

  At the smallest scale, the dynamics of the small eddies become independent of the large-scale eddies, and the rate at which energy is supplied is equal to the rate at which it is dissipated into heat by viscosity. The Kolmogorov length microscale is given by $\tau = (\frac{\nu^3}{\epsilon})^{\frac{1}{4}}$, where ϵ is the average rate of energy dissipation per unit mass and ν is the kinematic viscosity of the fluid. This microscale describe the smallest scales of turbulence before viscosity dominates.

  Similarly, the *Batchelor scale* (usually, smaller) describes the smallest length of fluctuations in scalar concentration before molecular diffusion dominates.

  Quantum turbulence is the chaotic motion of quantum fluids (say, *superfluids*) at high flow rates and close to absolute zero.

Turbulence is well described by the *Navier–Sokes equations*. Clay Mathematics Institute list the investigation, whether those equations in 3D always have a nonsingular solution, among the six US 1,000,000-valued open problems.

- **Meter of water equivalent**

  The **meter of water equivalent** (mwe) of a material is the thickness of that material that provides the equivalent shielding of 1 m of water.

  Also, the *mass balance* of a glacier is reported in mwe as the ratio of the volume (of water that would be obtained from melting the snow/ice) and area; it gives the change of thickness in water depth.

  Unrelated *centimeter of water* (cmH_2O) is the pressure $\approx$ 98.1 Pa (pascals) exerted by a column of water of 1 cm in height at 4° at acceleration g. A similar manometric unit of pressure is the *millimeter of mercury* (mmHg) $\approx$ 1 Torr $\approx$ 133.3 Pa.

- **Hydraulic diameter**

  For flow in a (in general, noncircular) pipe or tube, the **hydraulic diameter** is $\frac{4A}{P}$, where A is the cross-sectional area and P is the *wetted perimeter*, i.e., the perimeter of all channel walls that are in direct contact with the flow.

  So, in open liquid flow, the length exposed to air is not included in P. The hydraulic diameter of a circular tube is equal to its inside diameter. The **hydraulic radius** is (nonstandardly) defined as $\frac{1}{4}$ of the hydraulic diameter.

- **Hydrodynamic radius**

  The **hydrodynamic radius** (or *Stokes radius*, *Stokes–Einstein radius*) of a molecule, undergoing diffusion in a solution (homogeneous mixture of two or more substances), is the hypothetical radius of a hard sphere which diffuses with the same rate as the molecule. Cf. the **characteristic diameters** in Chap. 29.

- **Wigner–Seitz radius**

  The **Wigner–Seitz radius** is the radius of a sphere whose volume is equal to the mean volume $\frac{V}{n} = \frac{1}{n}$ per particle in a solid; n is the particle density.

  So, it is $(\frac{4}{3\pi n})^{\frac{1}{3}}$ an estimation of the mean interparticle distance.

- **Chromatographic migration distances**

  In thin layer Chromatography, the **solvent migration distance** is the distance d_{sl} traveled by the front line of the liquid or gas entering a chromatographic bed for *elution* (the process of using a solvent to extract an absorbed substance from a solid medium). The **migration distance of substance** is distance d_{sb} traveled by the center of a spot. The *retardation* and *retention factors* are $\frac{d_{sl}}{d_{sb}}$ and $\frac{d_{sl}}{d_{sb}} - 1$.

  The **retention distance** is a measure of equal-spreading of the spots on the chromatographic plate, defined via retention factors of sorted compounds.

- **Droplet radii**

  Let A be a small liquid droplet in equilibrium with a *supersaturated vapor*, i.e., a vapor which will begin to condense in the presence of nucleation centers.

  Let ρ_l, ρ_v be the liquid and vapor density, respectively, and let p_l, p_v be the liquid and vapor pressure. Let γ and γ_0 be the actual value at the surface of tension and planar limit value of surface tension. The **capillarity radius** R_c of A is defined by the *Young–Laplace equation* $\frac{\gamma_0}{R_e} = \frac{1}{2}(p_l - p_v)$.

The **surface of tension radius** (or **Kelvin–Laplace radius**, *equilibrium radius of curvature*) R_s is defined by $\frac{\gamma}{R_s} = \frac{1}{2}(p_l - p_v)$. The reciprocal of R_s is the mean curvature $H = \frac{1}{2}(k_1 + k_2)$ (cf. Chap. 8) of the *Gibbs surface of tension*, for which the Young–Laplace equation holds exactly for all droplet radii.

The **equimolar radius** (or *Gibbs adsorption radius*) R_e of A is the radius of a ball of *equimolar* (i.e., with the same *molar concentration*) volume. Roughly, this ball has uniform density ρ_l in the cubic cell of density ρ_v.

The **Tolman length** and the **excess equimolar radius** of the droplet A are $\delta = R_e - R_s$ and $\tau = R_e - R_c$, respectively.

On the other hand, the **cloud drop effective radius** is a weighted mean of the size distribution of cloud droplets.

- **Dephasing length**

  Intense laser pulses traveling through plasma can generate, for example, a wake (the region of turbulence around a solid body moving relative to a liquid, caused by its flow around the body) or X-rays. The **dephasing length** is the distance after which the electrons outrun the wake, or (for a given mismatch in speed of pulses and X-rays) laser and X-rays slip out of phase.

- **Healing length**

  A *Bose–Einstein condensate* (BEC) is a state of dilute gas of weakly interacting bosons confined in an external potential, and cooled to temperatures near absolute zero (0 K, i.e., −273.15 °C), so that a large fraction of them occupy the lowest quantum state of the potential, and quantum effects become apparent on a macroscopic scale. Examples of BEC are superconductors (materials loosing all electrical resistance if cooled below critical temperature), *superfluids* liquid states with no viscosity) and *supersolids* (spatially ordered materials with superfluid properties).

  The **healing length** of BEC is the width of the bounding region over which the probability density of the condensate drops to zero. For a superfluid, say, it is a length over which the wave function can vary while still minimizing energy.

- **Coupling length**

  In optical fiber devices mode coupling occurs during transmission by multimode fibers (mainly because of random bending of the fiber axis). Between two modes, a and b, the **coupling length** l_c is the length for which the complete power transfer cycle (from a to b and back) take place, and the **beating length** z is the length along which the modes accumulate a 2π phase difference. The resonant coupling effect is *adiabatic* (no heat is transferred) if and only if $l_c > z$. Furuya–Suematsu–Tokiwa, 1978, define the *coupling length* of modes a and b as the length of transmission at which the ratio $\frac{I_a}{I_b}$ of mode intensities reach e^2.

- **Localization length**

  Generally, the **localization length** is the average distance between two obstacles in a given scale.

  The localization scaling theory of metal-insulator transitions predicts that, in zero magnetic field, electronic wave functions are always localized in disordered 2D systems over a length scale called the **localization length**.

- **Thermodynamic length**

  Thermodynamic length (Weinhold, 1975) is a Riemannian metric defined on a manifold of equilibrium states of a thermodynamic system.

  It is a path function that measures the distance along a path in the state space. Cf. the **thermodynamic metrics** in Chap. 7.
- **Magnetic length**

  The **magnetic length** (or *effective magnetic length*) is the distance between the effective magnetic poles of a magnet.

  The *magnetic correlation length* is a magnetic-field dependent **correlation length**.
- **Correlation length**

  The **correlation length** (or *correlation radius*) is the distance from a point beyond which there is no further correlation of a physical property associated with that point. It is used mainly in statistical mechanics as a measure of the order in a system for phase transitions (fluid, ferromagnetic, nematic).

  For example, in a spin system at high temperature, the correlation length is $-\frac{\ln d \cdot C(d)}{d}$ where d is the distance between spins and $C(d)$ is the correlation function.

  In particular, the *percolation correlation length* is an average distance between two sites belonging to the same cluster, while the *thermal correlation length* is an average diameter of spin clusters in thermal equilibrium at a given temperature. In second-order phase transitions, the correlation length diverges at the *critical point*.

  In wireless communication systems with multiple antennas, **spatial correlation** is a correlation between a signal's direction and the average received signal gain.
- **Long range order**

  A physical system has **long range order** if remote portions of the same sample exhibit correlated behavior. For example, in crystals and some liquids, the positions of an atom and its neighbors define the positions of all other atoms.

  Examples of long range ordered states are: superfluidity and, in solids, magnetism, charge density wave, superconductivity. Most strongly correlated systems develop long range order in their ground state.

  Short range refers to the finite **correlation length**, say, to the first- or second-nearest neighbors of an atom.

  The system has **long range order**, *quasi-long range order* or is *disordered* if the corresponding correlation function decays at large distances to a constant, to 0 polynomially, or to 0 exponentially. Cf. **long range dependency** in Chap. 18.
- **Spatial coherence length**

  The **spatial coherence length** is the propagation distance from a coherent source to the farthest point where an electromagnetic wave still maintains a specific degree of coherence. This notion is used in Telecommunication Engineering (usually, for the optical regime) and in synchrotron X-ray Optics (the advanced characteristics of synchrotron sources provide highly coherent X-rays).

The spatial coherence length is about 20 cm, 100 m and 100 km for helium-neon, semiconductor and fiber lasers, respectively. Cf. *temporal coherence length* which describes the correlation between signals observed at different moments of time.

For vortex-loop phase transitions (superconductors, superfluid, etc.), **coherence length** is the diameter of the largest thermally excited loop. Besides coherence length, the second **characteristic length** (Chap. 29) in a superconductor is its **penetration depth**. If the ratio of these values (the *Ginzburg–Landau parameter*) is $< \sqrt{2}$, then the phase transition to superconductivity is of second-order.

- **Decoherence length**

  In disordered media, the **decoherence length** is the propagation distance of a wave from a coherent source to the point beyond which the phase is irreversibly destroyed (for example, by a coupling with noisy environment).

- **Critical radius**

  Critical radius is the minimum size that must be formed by atoms or molecules clustering together (in a gas, liquid or solid) before a new-phase inclusion (a bubble, a droplet, or a solid particle) is stable and begins to grow. Say, when atoms, under changes in temperature, pressure or composition (*doping*), get closer together in a solid, their electronic state levels broaden, overlap and hybridize. At a certain *critical distance*, a *Mott insulator-metal transition* occurs.

- **Binding energy**

  The **binding energy** of a system is the mechanical energy required to separate its parts so that their relative distances become infinite. For example, the binding energy of an electron or proton is the energy needed to remove it from the atom or the nucleus, respectively, to an infinite distance.

  In Astrophysics, *gravitational binding energy* of a celestial body is the energy required to disassemble it into dust and gas, while the lower *gravitational potential energy* is needed to separate two bodies to infinite distance, keeping each intact.

- **Metric theory of gravity**

  A **metric theory of gravity** assumes the existence of a symmetric metric (seen as a property of space-time itself) to which matter and nongravitational fields respond. Such theories differ by the types of additional gravitational fields, say, by dependency or not on the location and/or velocity of the local systems. General Relativity is one such theory; it contains only one gravitational field, the space-time metric itself, and it is governed by Einstein's partial differential equations. It has been found empirically that, besides Nordström's 1913 *conformally-flat scalar theory*, every other metric theory of gravity introduces auxiliary gravitational fields.

  A **bimetric theory of gravity** is (Rosen, 1973) a metric theory of gravity in which two, instead of one, metric tensors are used for, say, effective Riemannian and background Minkowski space-times. But usually, rather two frames (not two metric tensors) are considered. Cf. **multimetric** in Chap. 3.

The *Brans–Dicke theory* is a metric theory of gravity, in which $\frac{1}{G}$, where G is the gravitational constant, is replaced by a scalar field. Another direct competitor of General Relativity is affine *Einstein–Cartan–Sciama–Kibble theory* relaxing the assumption that the metric be torsion-free and interpreting spin as affine torsion. It supposes (Sakharov, 1967) *Induced Gravity* with space-time background emerging as a mean field approximation of underlying microscopic degrees of freedom. Such quantum gravity is implied by a *World Crystal model* of **quantum space-time**.

Østvang, 2001, proposed a quasi-metric framework for relativistic gravity.

Classical physics adequately describes gravity only for masses of 10^{-23} – 10^{30} kg.

- **Schwarzschild radius**

The **Schwarzschild radius** of a mass m is the radius $r_s(m) = \frac{2Gm}{c^2} = \frac{2m}{m_P} l_P$ of a sphere S such that, if m is compressed within S, it will become a *Schwarzschild* (i.e., uncharged and with angular momentum zero) *black hole*, and so, the escape speed from the surface of S would be the speed c of light.

For such hole, the radii of *photon sphere* (where photons are forced by gravity to travel in circular orbits), of *marginally bound orbit* (where a test particle starts to be gravitationally bound) and of *marginally stable orbit* (smallest circular orbit for material, usually the inner edge of the accretion cloud) are $\frac{3}{2} r_g$, $2r_g$ and $3r_g$.

A typical (stellar) black hole has mass $\approx 6\, M_\odot$ (where $M_\odot \approx 1.98 \times 10^{30}$ kg denotes the solar mass), diameter ≈ 18 km, temperature $\approx 10^{-8}$ K and lifetime $\approx 2 \times 10^{68}$ years. The mass of Sgr A^*, the black hole in the center of Milky Way is $4 \times 10^6 M_\odot$; its radius is at most 12.5 light-hours (45 AU). The masses of known stellar and supermassive black holes are within [3.8–15.7] and [5×10^4–3×10^{10}] suns, respectively. Most black holes do not exceed 0.1 % of the mass of their host galaxies, but the one in NGC 1277 reached $17 \times 10^9 M_\odot$ (14 % of this galaxy's mass).

The Schwarzschild radius of H1821+643 (black hole with largest precisely measured mass, $3 \times 10^{10} M_\odot$) is about 575 AU, 28 times the radius of Pluto's orbit.

The transition point separating neutron stars and black holes is expected within 1.7–2.7 $M_\odot$. *Neutron stars* are composed of the densest known form of matter. The radius of J0348-0432, the largest known ($2.04\, M_\odot$) neutron star is ≈ 10 km, i.e., only about twice its Schwarzschild radius.

The "mini" black hole would be a hypothetical *Planck particle* with mass $\sqrt{\pi} m_P$, for which $r_s(m) = \lambda_C(m)$ (cf. **Compton wavelength**), and radius $r_s(\sqrt{\pi} m_P) = 2\sqrt{\pi} l_P$. Cf. *planckeon* in **quantum space-time**; it should have radius $l_P = \overline{\lambda}_C(m_P)$ and mass m_P, for which $\overline{\lambda}_C(m) = \frac{1}{2} r_s(m)$.

A *quasar* (quasi-stellar radio source) is a compact region in the center of a massive galaxy surrounding its central supermassive black hole; its size is 10–10,000 times the Schwarzschild radius of the black hole.

The Schwarzschild radius of observable Universe is $\approx$ 10 Gly. So, Pathria–Good, 1972, then Poplawski, from 2010, proposed that the observable Universe is the interior of a black hole existing inside a larger universe, or multiverse.

- **Jeans length**

  The **Jeans length** (or *acoustic instability scale*) is (Jeans, 1902) the length scale $L_J = v_s t_g = \frac{v_s}{\sqrt{\rho G}}$ of a cloud (usually, of interstellar dust) where thermal energy causing the cloud to expand, is counteracted by self-gravity causing it to collapse. Here v_s, t_g, ρ are the speed of sound, gravitational free fall time and enclosed mass density. So, L_j is also the distance a sound wave would travel in the collapse time.

  The *Jeans mass* is the mass contained in a sphere of Jeans length diameter.

- **Acoustic metric**

  In Acoustics and Fluid Dynamics, the **acoustic metric** (or **sonic metric**) is a characteristic of sound-carrying properties of a given medium: air, water, etc.

  In General Relativity and Quantum Gravity, it is a characteristic of signal-carrying in a given *analog model* (with respect to Condensed Matter Physics) where, for example, the propagation of scalar fields in curved *space-time* is modeled (see, for example, [BLV05]) as the propagation of sound in a moving fluid, or slow light in a moving fluid dielectric, or *superfluid* (quasi-particles in quantum fluid).

  The passage of a signal through an acoustic metric modifies the metric; for example, the motion of sound in air moves air and modifies the local speed of the sound. Such "effective" (i.e., recognized by its "effects") **Lorentz metric** (Chap. 26) governs, instead of the background metric, the propagation of fluctuations: the particles associated to the perturbations follow geodesics of that metric.

  In fact, if a fluid is barotropic and inviscid, and the flow is irrotational, then the propagation of sound is described by an **acoustic metric** which depends on the density ρ of flow, velocity $\mathbf{v}$ of flow and local speed s of sound in the fluid. It can be given by the *acoustic tensor*

$$g = g(t, \mathbf{x}) = \frac{\rho}{s} \begin{pmatrix} -(s^2 - v^2) & \vdots & -\mathbf{v}^T \\ \cdots & & \cdots \\ -\mathbf{v} & \vdots & 1_3 \end{pmatrix},$$

  where 1_3 is the 3×3 identity matrix, and $v = ||\mathbf{v}||$. The *acoustic line element* is

$$ds^2 = \frac{\rho}{s}\left(-(s^2 - v^2)dt^2 - 2\mathbf{v}d\mathbf{x}dt + (d\mathbf{x})^2\right) = \frac{\rho}{s}\left(-s^2dt^2 + (d\mathbf{x} - \mathbf{v}dt)^2\right).$$

  The signature of this metric is $(3, 1)$, i.e., it is a **Lorentz metric**. If the speed of the fluid becomes supersonic, then the sound waves will be unable to come back, i.e., there exists a *mute hole*, the acoustic analog of a *black hole*.

The **optical metrics** are also used in analog gravity and effective metric techniques; they correspond to the representation of a gravitational field by an equivalent optical medium with magnetic permittivity equal to electric one.

- **Aichelburg–Sexl metric**

  In Quantum Gravity, the **Aichelburg–Sexl metric** (Aichelburg and Sexl, 1971) is a 4D metric created by a relativistic particle (having an energy of the order of the Planck mass) of momentum p along the x axis, described by its *line element*

$$ds^2 = dudv - d\rho^2 - \rho^2 d\phi^2 + 8p \ln \frac{\rho}{\rho_0} \delta(u) du^2,$$

  where $u = t - x, v = t + x$ are null coordinates, ρ and ϕ are standard polar coordinates, $\rho = \sqrt{y^2 + z^2}$, and ρ_0 is an arbitrary scale constant.

  This metric admits an nD generalization (de Vega and Sánchez, 1989), given by

$$ds^2 = dudv - (dX^i)^2 + f_n(\rho)\delta(u)du^2,$$

  where X^i are the traverse coordinates, $\rho = \sqrt{\sum_{1 \le i \le n-2} (X^i)^2}, f_n(\rho) = K(\frac{\rho}{\rho_0})^{4-n}$, $k = \frac{8\pi^{2-0.5n}}{n-4}\Gamma(0.5n-1)GP, n > 4, f_4 = 8GP \ln \frac{\rho}{\rho_0}$, P is the particle's momentum.

- **Quantum space-time**

  Quantum space-time is a generalization of the usual space-time in which some variables that ordinarily commute are assumed not to commute, form a different Lie algebra, and, as a result, some variables may become discrete. For example, noncommutative field theory supposes that, on sufficiently small (quantum) distances, the spatial coordinates do not commute, i.e., it is impossible to measure exactly the position of a particle with respect to more than one axis. Any noncommutative algebra with $\geq$ 4 generators could be interpreted as a quantum space-time.

  At Planck scale $l_P \approx 1.6 \times 10^{-35}$ m, "quantum foam" (Wheeler,1950) is expected: violent warping and turbulence of space-time, which loses the smooth continuous structure (apparent macroscopically) of a *Riemannian manifold*, to become discrete, fractal, nondifferentiable.

  Many models of *granular space* were proposed. *Planckeon* is (Markov, 1965) a hypothetical "grain of space" of size l_P and Planck rest mass m_P. In the *World Crystal model*, quantum space-time is a lattice with spacing of the order l_P, and matter creates defects generating curvature and all effects of General Relativity.

  A **quantum metric** is a general term used for a metric expected to describe the space-time at quantum scales. Cf. **Rieffel metric space**, **Fubini–Study distance** (Chaps. 7, 12), **quantum graph** (Chap. 15), statistical geometry of fuzzy lumps ([ReRo01]), quantization of the **semimetric cone** (Chap. 1) in [IKP90].

  Loop Quantum Gravity (LQG), *String Theory*, *Causal Sets* and *Black Hole Thermodynamics*, predict a quantum space-time at Planck scale. LQG predict,

moreover, that its geometry (area, volume) is quantized via **spin networks** (Chap. 15). Analyses of gamma ray bursts rule out quantum graininess at $> 10^{-48}$ m.

- **Distances between quantum states**

A **distance between quantum states** is a metric which is preferably preserved by unitary operations, monotone under quantum operations, stable under addition of systems and having clear operational interpretation.

The pure states correspond to the rays in the Hilbert space of wave functions. Every mixed state can be purified in a larger Hilbert space. The mixed quantum states are represented by *density operators* (i.e., positive operators of unit trace) in the complex projective space over the infinite-dimensional Hilbert space. Let X denote the set of all density operators in this Hilbert space. For two given quantum states, represented by $x, y \in X$, we mention the following main distances on X.

The **trace distance** is a metric on density matrices defined by

$$T(x,y) = \frac{1}{2}||x-y||_{tr} = \frac{1}{2}\mathrm{Tr}\sqrt{(x-y)^*(x-y)} = \frac{1}{2}\mathrm{Tr}\sqrt{(x-y)^2} = \frac{1}{2}\sum_i |\lambda_i|,$$

where λ_i are eigenvalues of the Hermitian matrix $x - y$. It is the maximum probability that a quantum measurement will distinguish x from y. Cf. the **trace norm metric** $||x - y||_{tr}$ in Chap. 12. When matrices x and y commute, i.e., are diagonal in the same basis, $T(x, y)$ coincides with **variational distance** in Chap. 14.

The **quantum fidelity similarity** is defined (Jorza, 1994) by

$$F(x,y) = (\mathrm{Tr}(\sqrt{x}y\sqrt{x}))^2 = (||\sqrt{x}\sqrt{y}||_{tr})^2.$$

When the states x and y are *classical*, i.e., they commute, $\sqrt{F(x,y)}$ is the classical **fidelity similarity** $\rho(P_1, P_2) = \sum_z \sqrt{p_1(z)p_2(z)}$ from Chap. 14.

When x and y are pure states, $F(x, y)$ is called *transition probability* and $\sqrt{F(x,y)} = |\langle x', y'\rangle|$ (where x', y' are the unit vectors representing x, y) is called *overlap*. In general, $F(x, y)$ is the maximum overlap between purifications of x and y. Useful lower and upper bounds for $F(x, y)$ are

$$\mathrm{Tr}(xy) + \sqrt{2((\mathrm{Tr}(xy))^2 - \mathrm{Tr}(xyxy))} \quad (\textit{subfidelity}) \text{ and}$$

$$\mathrm{Tr}(xy) + \sqrt{((\mathrm{Tr}(x))^2 - \mathrm{Tr}(x^2))((\mathrm{Tr}(y))^2 - \mathrm{Tr}(y^2))} \quad (\textit{super-fidelity}).$$

The **Bures distance** is $\sqrt{2(1 - \sqrt{F(x,y)})}$. The **Bures length** (or *Bures angle*) is arccos $\sqrt{F(x,y)}$; it is the minimal such distance between purifications of x and y. Cf. the **Bures metric** and **Fubini–Study metric** in Chap. 7. In general, the Riemannian **monotone metrics** in Chap. 7 generalize the **Fisher information**

metric on the class of probability densities (*classical* or commutative case) to the class of density matrices (*quantum* or noncommutative case). Fujiwara–Nagaoka, 1995, derived the *quantum Fisher metric*, coinciding, up to a scalar, on pure states with **Fubini–Study metric** on the associated projective Hilbert space.

The distances based on the *Shannon entropy* $H(p) = -\sum_i p_i \log p_i$ are generalized on quantum setting via the *von Neumann entropy* $S(x) = -\mathrm{Tr}(x \log x)$. Balian–Alhassid–Reinhardt, 1986 (see [Bali14]) defined a such metric by the Hessian of von Neumann entropy; cf. **Hessian metric** in Sect. 7.3.

The **sine distance** (Rastegin, 2006) is a metric defined by

$$\sin \min_{x',y'} (\arccos(|\langle x', y' \rangle|)) = \sqrt{1 - F(x,y)},$$

where x', y' are purifications of x, y. It holds $1 - \sqrt{F(x,y)} \leq T(x,y) \leq \sqrt{1 - F(x,y)}$.

Examples of other known metrics generalized to the class of density matrices are the **Hilbert–Schmidt norm metric**, **Sobolev metric** (Chap. 13) and **Monge–Kantorovich metric** (Chap. 21).

- **Action at a distance (in Physics)**

An **action at a distance** is the interaction, without known mediator, of two objects separated in space. Einstein used the term *spooky action at a distance* for quantum mechanical interaction (like *entanglement* and *quantum nonlocality*) which is instantaneous, regardless of distance. His **principle of locality** is: distant objects cannot have direct influence on one another, an object is influenced directly only by its immediate surroundings.

Alice–Bob distance is the distance between two entangled particles, "Alice" and "Bob". Quantum Theory predicts that the correlations based on quantum entanglement should be maintained over arbitrary Alice–Bob distances. But a *strong nonlocality*, i.e., a measurable action at a distance (a superluminal propagation of real, physical information) never was observed and is not expected. Salart et al., 2008, estimated that such signal should be 10,000 times faster than light.

At 2012, some quantum information—the polarization property of a photon—to its mate in an entangled pair of photons, was teleported over 143 km. But such photon systems transport only half of the information. Used with continuous variable systems, they are 100 % effective but limited to short distances.

Two-particle entanglement occurs in any temperature.

"Mental action at a distance" (say, telepathy, clairvoyance, distant anticipation, psychokinesis) is controversial because it challenge classical concepts of time/causality as well as space/distance.

The term *short range interaction* is used for the transmission of action at a distance by a material medium from point to point with a certain velocity dependent on properties of this medium. In Information Storage, the term *near-field interaction* is used for very short distance interaction using scanning probe techniques. *Near-field communication* is a set of standards-based technologies

enabling short range ($\leq$ 4 cm) wireless communication between electronic devices.

- **Macroscale entanglement/superposition**

  Quantum superposition is the addition of the amplitudes of wave-functions, occurring when an object simultaneously "possesses" two or more values for an observable quantity, say, the position or energy of a particle. If the system interacts with its environment in a *thermodynamically irreversible way* (say, the quantity is measured), then *quantum decoherence* occurs: the state randomly collapses onto one of those values. But it can happen also without any influence from the outside world.

  Superposition and *entanglement* (nonlocal correlation which cannot be described by classical communication or common causes) were observed at atomic scale. Entangling in time (a pair of photons that never existed at the same time) was observed as well. With increasing duration and size/complexity of objects, these quantum effects are lost: decoherence, due to many interactions at the molecular level, occurs. To find out this threshold, if any, is a hot research topic. Kasevich et al., 2015, got superposition on human scales: 54 cm apart for about 1 sec. Kaiser *et al.*, 2016, got it, for the oscillations of neutrinos, at 735 km.

  Nimmrichter and Hornberger, 2013 assign the *macroscopicity* μ to a quantum state, if the *equivalent* (in terms of ruling out even a minimal modification of Quantum Mechanics, which would predict a failure of the superposition principle on the macroscale) superposition state of a single electron last for 10^{τ} seconds. The record score so far is $\mu \approx 12$ and 24 looks reachable. But the Schrödinger's cat (seen as a 4-kg sphere of water) in a superposition, where it sits in two positions spaced 10 cm apart for 1 s, would score unconceivable 57.

  Szarek–Aubrun–Ye, 2013, found a threshold $k_0 \approx \frac{N}{5}$ such that two subsystems of k particles each of a system of N identical particles in a random pure state, typically share entanglement if $k > k_0$, and typically do not share it if $k < k_0$.

  "Warm" quantum coherence was observed in plant photosynthesis, animal magnetoreception, our sense of smell and microtubules inside brain neurons. Hameroff and Penrose, 2014: EEG rhythms (brain waves) and consciousness derive from quantum vibrations in microtubules, i.e., on the quantum-realm scale ($\sim$ 100 nm) rather than, or in addition to, the larger scale of neurons (4–100 μm).

  Schmied et al., 2016, got a special case of entanglement—*Bell correlation* (correlations between the spins)—of about 480 atoms in a Bose-Einstein condensate.

- **Entanglement distance**

  The **entanglement distance** is the maximal distance between two entangled electrons in a *degenerate* electron gas beyond which all entanglement is observed to vanish. *Degenerate matter* (say, a white dwarf star) is matter having so high density that the main contribution to its pressure arises from the *Pauli exclusion principle*: no two identical fermions may occupy the same quantum state together.

- **Tunneling distance**

  Quantum Tunneling is the quantum mechanical phenomenon where a particle tunnels through a barrier that it classically could not surmount.

  For example, in *STM* (Scanning Tunneling Microscope), electron tunneling current and a net electric current from a metal tip of STM to a conducting surface result from overlap of electron wavefunctions of tip and sample, if they are brought close enough together and an electric voltage is applied between them.

  The tip-sample current depends exponentially (about $exp(-d^{0.5})$) on their distance d, called **tunneling distance**. Formally, d is the sum of the radii of the electron delocalization regions in the donor and the acceptor atoms.

  By keeping the current constant while scanning the tip over the surface and measuring its height, the contours of the surface can be mapped out. The tunneling distance is longer ($<$ 1 nm) in aqueous solution than in vacuum ($<$ 0.3 nm).

24.2 Distances in Chemistry and Crystallography

Main chemical substances are ionic (held together by ionic bonds), metallic (giant close packed structures held together by metallic bonds), giant covalent (as diamond and graphite), or molecular (small covalent). Molecules are made of a fixed number of atoms joined together by covalent bonds; they range from small (single-atom molecules in the noble gases) to very large ones (as in polymers, proteins or DNA).

The largest known (55 tons and 12, 4 m in diameter) crystal is a selenite found in Naica Mine, Mexico. The largest stable synthetic molecule is PG_5 with a diameter of 10 nm and a mass equal to 2×10^8 hydrogen atoms.

The **interatomic distance** of two atoms is the distance (in angstroms or picometers, where $1\,\text{Å} = 10^{-10}$ m $=$ 10 pm) between their nuclei. The bond between helium atoms in molecules He_2 is the longest (54.6 Å) and weakest known; it is 0.75 Å in H_2. The $C - C$ *distance* (distance between two carbon atoms) in graphene is 1.42 Å. The *C-length* (number of carbon atoms) is *carbyne* (chain of carbon atoms) can reach 6400.

- **Atomic radius**

  Quantum Mechanics implies that an atom is not a ball having an exactly defined boundary. Hence, **atomic radius** is defined as the distance from the atomic nucleus to the outermost stable electron orbital in a atom that is at equilibrium. Atomic radii represent the sizes of isolated, electrically neutral atoms, unaffected by bonding.

  Atomic radii are estimated from **bond distances** if the atoms of the element form bonds; otherwise (like the noble gases), only **van der Waals radii** are used.

  The atomic radii of elements increase as one moves down the column (or to the left) in the Periodic Table of Elements. internuclear distance, Re is the equilibrium internuclear distance (bond length)

- **Bond distance**

  The **bond distance** (or *bond length*) is the equilibrium *internuclear distance* of two bonded atoms. For example, typical bond distances for carbon-carbon bonds in an organic molecule are 0.15, 0.13 and 0.12 pm (picometers 10^{-9} m) for single, double and triple bonds, respectively. The atomic nuclei repel each other; the **equilibrium distance** between two atoms in a molecule is the internuclear distance at the minimum of the electronic (or potential) energy surface.

  Depending on the type of bonding of the element, its atomic radius is called *covalent* or *metallic*. The *metallic radius* is one half of the **metallic distance**, i.e., the closest internuclear distance in a *metallic crystal* (lattice of metallic element).

  Covalent radii of atoms of elements that form covalent bonds are inferred from bond distances between pairs of covalently-bonded atoms. If the two atoms are of the same kind, then their covalent radius is one half of their bond distance. Covalent radii for other elements is inferred by combining the radii of those that bond with bond distances between pairs of atoms of different kind.
- **van der Waals contact distance**

  Intermolecular distance data are interpreted by viewing atoms as hard spheres. The spheres of two neighboring nonbonded atoms (in touching molecules or atoms) are supposed to just touch. So, their interatomic distance, called the **van der Waals contact distance**, is the sum of radii, called **van der Waals radii** (of *effective sizes*), of their hard spheres.

  The van der Waals contact distance corresponds to a "weak bond", when repulsion forces of electronic shells exceed London (attractive electrostatic) forces.
- **Molecular RMS radius**

  The **molecular RMS radius** (cf. **radius of gyration** in Sect. 24.1) is the root-mean-square distance of a molecule's atoms from their common center of gravity:

$$\sqrt{\frac{\sum_{1\le i\le n} d_{0i}^2}{n+1}} = \sqrt{\frac{\sum_i \sum_j d_{ij}^2}{(n+1)^2}},$$

  where n is the number of atoms in the molecule, d_{0i} is the Euclidean distance of the i-th atom from the center of gravity of the molecule (in a specified conformation), and d_{ij} is the Euclidean distance between the i-th and j-th atoms.

  The **mean molecular radius** is the number $\frac{\sum_i r_i}{n}$, where n is the number of atoms, and r_i is the Euclidean distance of the i-th atom from the centroid $\frac{\sum_j x_{ij}}{n}$ of the molecule (here x_{ij} is the i-th Cartesian coordinate of the j-th atom).
- **Molecular sizes**

  There are various descriptions of the **molecular sizes**; examples as follows.

  The *kinetic diameter* of a molecule (most applicable to transport phenomena) is its smallest effective dimension.

  The **effective diameter** of a molecule is the general extent of the electron cloud surrounding it as calculated in any of several ways.

Sometimes, it is defined as diameter of the sphere containing 98 % of the total electron density; then its half is close to the experimental **van der Waals radius**.

The **effective molecular radius** is the size a molecule displays in solution. For liquids and solids it is usually defined via packing density.

For a gas, molecular sizes can be estimated from the intermolecular separation, speed, mean free path and collision rate of gas molecules.

For example, in the model of kinetic theory of gases, assuming that molecules interact like hard spheres, the **molecular diameter** d is $\sqrt{\frac{m}{\pi\sqrt{2}\rho}}$, where m is the mass of molecule, l is mean free path and ρ is density.

- **Range of molecular forces**

  Molecular forces (or interactions) are the following electromagnetic forces: ionic bonds (charges), hydrogen bonds (dipolar), dipole-dipole interactions, London forces (the attraction part of van der Waals forces) and steric repulsion (the repulsion part of van der Waals forces). If the distance (between two molecules or atoms) is d, then (experimental observation) the potential energy function P relates inversely to d^n with $n = 1, 3, 3, 6, 12$ for the above five forces, respectively.

  The **range** (or the *radius*) of an interaction is considered *short* if P approaches 0 rapidly as d increases. It is also called *short* if it is at most 3 Å; so, only the range of steric repulsion is short (cf. **range of fundamental forces**).

  An example: for polyelectrolyte solutions, the long range ionic solvent-water force competes with the shorter range water-water (hydrogen bonding) force.

  In protein molecule, the range of London van der Waals force is $\approx$ 5 Å, and the range of hydrophobic effect is up to 12 Å, while the length of hydrogen bond is $\approx$ 3 Å, and the length of *peptide bond* is $\approx$ 1.5 Å.

- **Chemical distance**

  Various chemical systems (single molecules, their fragments, crystals, polymers, clusters) are well represented by graphs where vertices (say, atoms, molecules acting as monomers, molecular fragments) are linked by, say, chemical bonding, van der Waals interactions, hydrogen bonding, reactions path.

  In Organic Chemistry, a *molecular graph* $G = (V, E)$ is a graph representing a given molecule, so that the vertices $v \in V$ are atoms and the edges $e \in E$ correspond to electron pair bonds. The *Wiener number* of a molecule is one half of the sum of all pairwise distances between vertices of its molecular graph.The *Wiener polarity index* is the number of unordered vertex pairs at distance 3 in this graph. Cf. **Wiener-like distance indices** in Chap. 1.

  The (bonds and electrons) *BE-matrix* of a molecule is the $|V| \times |V|$ matrix $((e_{ij}))$, where e_{ii} is the number of free unshared valence electrons of the atom A_i and, for $i \neq j$, $e_{ij} = e_{ji} = 1$ if there is a bond between atoms A_i and A_j, and $= 0$, otherwise.

  Given two *stoichiometric* (i.e., with the same number of atoms) molecules x and y, their **Dugundji–Ugi chemical distance** is the **Hamming metric**

$$\sum_{1 \le i,j \le |V|} |e_{ij}(x) - e_{ij}(y)|,$$

and their **Pospichal–Kvasnička chemical distance** is

$$\min_{\pi} \sum_{1 \le i,j \le |V|} |e_{ij}(x) - e_{\pi(i)\pi(j)}(y)|,$$

where π is any permutation of the atoms. The above distance is equal to $|E(x)| + |E(y)| - 2|E(x,y)|$, where $E(x,y)$ is the edge-set of the maximum common subgraph of the molecular graphs $G(x)$ and $G(y)$. Cf. **Zelinka distance** in Chap. 15.

The **Pospichal–Kvasnička reaction distance**, assigned to a molecular transformation $x \to y$, is the minimum number of *elementary transformations* needed to transform $G(x)$ onto $G(y)$.

- **Molecular similarities**

  Given two 3D molecules x and y characterized by some structural (shape or electronic) property P, their similarities are called **molecular similarities**.

  The main electronic similarities correspond to some correlation similarities from Chap. 17. For example, the *Carbó similarity* (Carbó–Leyda–Arnau, 1980) is the **cosine similarity** (Chap. 17) defined by

$$\frac{\langle f(x), f(y) \rangle}{||f(x)||_2 \cdot ||f(y)||_2},$$

  where the *electron density function* $f(z)$ of a molecule z is the volumic integral $\int P(z)dv$ over the whole space.

  The *Hodgkin–Richards similarity* (1991) is defined (cf. the **Morisita–Horn similarity** in Chap. 17) by

$$\frac{2\langle f(x), f(y) \rangle}{||f(x)||_2^2 + ||f(y)||_2^2},$$

  where $f(z)$ is the electrostatic potential or electrostatic field of a molecule z.

  Petitjean, 1995, proposed to use the distance $V(x \cup y) - V(x \cap y)$, where the *volume* $V(z)$ of a molecule z is the union of *van der Waals spheres* of its atoms. Cf. **van der Waals contact distance** and, in Chap. 9, **Nikodym metric** $V(x \Delta y)$.

- **End-to-end distance**

  A *polymer* is a large macromolecule composed of repeating structural units connected by covalent chemical bonds.

  For a coiled polymer, the **end-to-end distance** (or *displacement length*) is the distance between the ends of the polymer chain. The maximal possible such distance (i.e., when the polymer is stretched out) is called *contour length*.

  The root-mean-square end-to-end distance of ideal linear or randomly branched polymer scales as $n^{0.5}$ or, respectively, $n^{0.25}$ if n is the number of monomers. For a polymer chain following a random walk in 3D, it is also 6 times **molecular RMS radius**. The **strand length** in Chap. 23 is the end-to-end distance for a special linear polymer, single-stranded RNA or DNA.

- **Persistence length**

  The **persistence length** of a polymer chain is the length over which correlations in the direction of the tangent are lost.

  The molecule behaves as a flexible elastic rod for shorter segments, while for much longer ones it can only be described statistically, like a 3D random walk. Cf. **correlation length**.

  Twice the persistence length is the *Kuhn length*, i.e., the length of hypothetical segments which can be thought of as if they are freely jointed with each other in order to form given polymer chain.
- **Bend radius**

  In Polymer Tubing, the **bend radius** of a tube is the distance from the center of an imaginary circle on which the arc of the bent tube falls to a point on that arc.
- **Intermicellar distance**

  Micelle is an electrically charged particle built up from polymeric molecules or ions and occurring in certain colloidal electrolytic solutions like soaps and detergents. This term is also used for a submicroscopic aggregation of molecules, such as a droplet in a colloidal system, and for a coherent strand or structure in a fiber.

  The **intermicellar distance** is the average distance between micelles.
- **Interionic distance**

  An *ion* is an atom that has a positive or negative electrical charge. The **interionic distance** is the distance between the centers of two adjacent (bonded) ions. **Ionic radii** are inferred from ionic bond distances in real molecules and crystals.

  The ion radii of *cations* (positive ions, for example, sodium Na^+) are smaller than the atomic radii of the atoms they come from, while *anions* (negative ions, for example, chlorine Cl^-) are larger than their atoms.
- **Repeat distance**

  Given a periodic layered structure, its **repeat distance** is the period, i.e., the spacing between layers (say, lattice planes, bilayers in a liquid-crystal system, or graphite sheets along the unit cell's hexagonal axis).

  A crystal lattice, the unit cell in it and cell spacing are called also a *repeat pattern*, *basic repeat unit* and *cell repeat distance* (or *lattice spacing*, *interplaner distance*).

  The *repeat distance* in a polymer is the ratio of the unit cell length along its axis of propagation to the number of monomeric units this length covers.
- **Metric symmetry**

  The full crystal symmetry is given by its *space group*.

  The **metric symmetry** of the crystal lattice is its symmetry without taking into account the arrangement of the atoms in the unit cell.

  In between lies the *Laue group* giving equivalence of different reflections, i.e., the symmetry of the crystal diffraction pattern. In other words, it is the symmetry in the *reciprocal space* (taking into account the reflex intensities).

The Laue symmetry can be lower than the metric symmetry (for example, an orthorhombic unit cell with $a = b$ is metrically tetragonal) but never higher.

There are seven *crystal systems—triclinic*, *monoclinic*, *orthorhombic*, *tetragonal*, trigonal, *hexagonal*, and *cubic* (or *isometric*). Taken together with possible *lattice centerings*, there are 14 *Bravais lattices*.

- **Homometric structures**

  Two structures of identical atoms are **homometric** if they are characterized by the same multiset of interatomic distances; cf. **distance list** in Chap. 1.

  Homometric crystal structures produce identical X-ray diffraction patterns.

  In Music, two rhythms with the same multiset of intervals are called **homometric**.

- **Dislocation distances**

  In Crystallography, a *dislocation* is a defect extending through a crystal for some distance (**dislocation path length**) along a *dislocation line*. It either forms a complete loop within the crystal or ends at a surface or other dislocation.

  The **mean free path** of a dislocation is (Gao et al., 2007), in 2D, the average distance between its origin and the nearest particle or, in 3D, the maximum radius of a dislocation loop before it reaches a particle in the slip plane.

  The **pinning distance** is the distance between two endpoints of a mobile dislocation, where one of the endpoints has to be within the volume. It is a characteristic length for the dislocation microstructure.

  The *Burgers vector* of a dislocation is a crystal vector denoting the direction and magnitude of the atomic displacement that occurs within a crystal when a dislocation moves through the lattice. A dislocation is called *edge*, *screw* or *mixed* if the angle between its line vector and the Burgers vector is 90°, 0° or otherwise, respectively. The **edge dislocation width** is the distance over which the magnitude of the displacement of the atoms from their perfect crystal position is greater than $\frac{1}{4}$ of the magnitude of the Burgers vector.

  The *dislocation density* ρ is the total length of dislocation lines per unit volume; typically, it is 10 km per cm^3 but can reach 10^6 km per cm^3 in a heavily deformed metal. The **average distance** between dislocations depends on their arrangement; it is $\rho^{-\frac{1}{2}}$ for a quadratic array of parallel dislocations. If the average distance decreases, dislocations start to cancel each other's motion.

  The **spacing dislocation distance** is the minimum distance between two dislocations which can coexist on separate planes without recombining spontaneously.

- **Dynamical diffraction distances**

  Diffraction is the apparent bending of propagating waves around obstacles of about the wavelength size. Diffraction from a 3D periodic structure such as an atomic crystal is called *Bragg diffraction*. It is a convolution of the simultaneous scattering of the probe beam (light as X-rays, or matter waves such as electrons or neutrons) by the sample and interference (superposition of reflections from crystal planes). Some materials, lacking 3D translational periodicity, still have aspects of **long range order**, that give rise to sharp Bragg reflections in their

X-ray diffraction patterns. Such distance doubling between layers of a material is called *c-axis periodicity*.

The *Bragg Law*, modeling diffraction as reflection from crystal planes of atoms, states that waves (with wavelength λ scattered under angle θ from planes at spacing d) interfere only if they remain in phase, i.e., $\frac{2d \sin\theta}{\lambda}$ is an integer.

The decay of intensity with depth traversed in the crystal occurs by *dynamical extinction*, redistributing energy within the wave field, and by *photoelectric absorption* (a loss of energy from the wave field to the atoms of the crystal).

The former *kinematic* theory works for imperfect crystals and estimates absorption. The *dynamical* (multiple diffraction) theory is used to model the *perfect* (no disruptions in the periodicity) crystals. It considers the incident and diffracted wave fronts as coupled/interacting parts of a wave field and the periodically varying electrical susceptibility of the medium so as to satisfy the Maxwell equations.

Dynamical theory distinguishes two cases: Laue (or *transmission*) and Bragg (or *reflection*) case, when the reflected wave is directed toward the inside and outside of the crystal. The wave field is represented by its *dispersion surface*. The inverse of the diameter of this surface is called (Autier, 2001) the **Pendellösung distance** Λ_L in the Laue case and the **extinction distance** Λ_B in the Bragg case.

At the exit face of the crystal, the wave splits into two single waves with different directions: incident 0-beam and diffracted H-beam. With increasing thickness of the crystal, the wave leaving it will first appear mainly in the 0-beam, then entirely in the H-beam at thickness $\frac{\Lambda_L}{2}$, and then it will oscillate between these beams with a period Λ_L, called the **Pendellösung length**; cf. similar **coupling length**.

The wave amplitude (and the intensity of the diffracted beam) is transferred back-and-forth once, i.e., the physical distance acquires a phase change of 2π. Pendellösung oscillations happen also in Bragg case, but with very rapidly decaying amplitudes, and *Pendellösung fringes* are visible only for θ close to 0^0 or 45^0.

Diffraction that involves multiple scattering events is called *extinction* since it reduces the observed integrated diffracted intensity. Extinction is very significant for perfect crystals and is then called *primary extinction*. In the Bragg case, the **primary extinction length** (James, 1964) is the inverse of the *extinction factor* (maximum extinction coefficient for the middle of the range of total reflection):

$$\frac{\pi V \cos\theta}{\lambda r_e |F| C},$$

where F, C (valued 1 or $\cos 2\theta$) are the structure and polarization factors, V is the volume of unit cell, $r_e \approx 2.81794 \times 10^{-15}$m is the *classical electron radius* and λ is the X-ray beam wavelength. The diffracted intensity with sufficiently large thickness no longer increases significantly with increased thickness.

The **extinction length** of an electron or neutron diffraction is $\frac{\pi V \cos\theta}{\lambda |F|}$. Half of it gives the number of atom planes needed to reduce the beam to 0 intensity.

The **X-ray penetration depth** (or *attenuation length*, *mean free path*, *extinction distance*) is (Wolfstieg, 1976) the depth into the material where the intensity of the diffracted beam has decreased e-fold. Cf. **penetration depth**.

In Gullity, 1956, *X-ray penetration depth* is the depth z such that $\frac{I_z}{I_\infty} = 1 - \frac{1}{e}$, where I_∞, I_z are the total diffraction intensities given from the whole specimen and, respectively, the range between the surface and the depth, z, from it.

- **X-ray absorption length**

  The *absorption edge* is a sharp discontinuity in the absorption spectrum of X-rays by an element that occurs when the energy of the photon is just above the **binding energy** of an electron in a specific shell of the atom.

  The **X-ray absorption length** of a crystal is the thickness s of the sample such that the intensity of the X-rays incident upon it at an energy 50 eV above the absorption edge is attenuated e-fold.

  For an X-ray laser, the *extinction length* is the thickness needed to fully reflect the beam; usually, it is a few microns while the absorption length is much larger.

  In Segmüller, 1968, the *absorption length* is $\frac{\sin\theta}{\mu}$, where μ is the linear absorption coefficient, and the beam enters the crystal at an angle θ.

- **Diamond-cutting distances**

  Diamond is the hardest natural gem and the only gemstone composed of a single element—carbon. Diamond takes a fine polish, which makes its surfaces highly reflective. Color in diamond (the rarest being red) is caused by structural irregularities, or trace elements. Diamonds are graded according to carat weight, clarity, color and cut. Diamonds are cut to maximize the play of light within the stone. Their beauty comes from a combination of *fire* (rainbow flash from within) and *brilliance* (burst of sparkling light). Both are a direct result of the cut.

  A faceted stone can be divided into an upper (*crown*) and lower (*pavilion*) section. The perimeter, where both parts meet, is referred to as the *girdle*. The **depth of a gemstone** is measured from the *table* (highest crown facet) to the *culet* (tip of the pavilion). On a round brilliant diamond, the **depth percentage** represents the ratio of the table-culet distance to the average girdle diameter.

  Normally, the table is the largest surface on a gemstone. On a round brilliant-cut diamond it forms an octagon, but some cutting styles do not have a table. The **table percentage** of a diamond represents the ratio of table width to overall stone width. A beautiful, well-cut stone will normally have a table percentage 53 − −64 %. A stone's *luster* (appearance of the surface dependent upon its reflecting qualities) is directly affected by its depth and table percentages.

Chapter 25
Distances in Earth Science and Astronomy

25.1 Distances in Geography

- **Spatial scale**

  In Geography, **spatial scales** are shorthand terms for distances, sizes and areas. For example, micro, meso, macro, mega may refer to local (0.001–1), regional (1–100), continental (100–10,000), global (>10,000) km, respectively.
- **Earth radii**

  The Earth's maximal and minimal *radii* (the center-surface distances) are 6384 km (the Chimborazo's summit) and 6353 km (the Arctic Ocean's floor). An object, moved from the 2-nd spot to the 1-st, will loose ≈ 1 % of its weight.

  In the ellipsoidal model, the Earth's *equatorial radius* (*semimajor axis*) a, is 6378 km and the *polar radius* (*semiminor axis*) b, is 6357 km. The equatorial and polar *radii of curvature* are $\frac{b^2}{a}$ and $\frac{a^2}{b}$. The *mean radius* is $\frac{2a+b}{3} = 6371$ km.

  The Earth's *authalic* and *volumetric radius* (the radii of the spheres with the same surface area and volume, respectively, as the Earth's ellipsoid) are 6371 and 6371 km; cf. the **characteristic diameters** in Chap. 29.

  In Telecommunications, the *effective Earth radius* is the radius of a sphere for which the distance to the radio horizon, assuming rectilinear propagation, is the same as that for the Earth with an assumed uniform vertical gradient of atmospheric refractive index. For the standard atmosphere, this radius is $\frac{4}{3}$ that of the Earth.
- **Great circle distance**

  The **great circle distance** (or **orthodromic distance**, *air line*) is the shortest distance between points x and y on the Earth's surface measured along a path on this surface. It is the length of the *great circle* arc, passing through x and y, in the spherical model of the planet. Cf. **spherical metric** in Chap. 6.

  Let δ_1, ϕ_1 be the latitude and the longitude of x, and δ_2, ϕ_2 be those of y; let r be the Earth's radius. Here $2r^2 = a^2 + b^2$, where a and b are the equatorial and

© Springer-Verlag Berlin Heidelberg 2016

M.M. Deza, E. Deza, *Encyclopedia of Distances*,
DOI 10.1007/978-3-662-52844-0_25

polar radii of the Earth. Then the great circle distance is equal to

$$r \arccos(\sin\delta_1 \sin\delta_2 + \cos\delta_1 \cos\delta_2 \cos(\phi_1 - \phi_2)).$$

In the spherical coordinates (θ, ϕ), where ϕ is the azimuthal angle and θ is the colatitude, the great circle distance between $x = (\theta_1, \phi_1)$ and $y = (\theta_2, \phi_2)$ is

$$r \arccos\left(\cos\theta_1 \cos\theta_2 + \sin\theta_1 \sin\theta_2 \cos(\phi_1 - \phi_2)\right).$$

For $\phi_1 = \phi_2$, the formula above reduces to $r|\theta_1 - \theta_2|$.

The **tunnel distance** between points x and y is the length of the line segment through 3D space connecting them. For a spherical Earth, this line is the chord of the great circle between the points.

The Earth resembles a flattened spheroid with extreme values for the radius of curvature of 6335.4 km at the equator and 6399.6 km at the poles. The *spheroidal distance* between points x and y is their distance in this spheroidal model.

The *geoid* (the shape the Earth would have if it was entirely covered by water and influenced by gravity alone) looks like a lumpy potato; cf. **potato radius**.

- **Loxodromic distance**

  A *loxodrome* (or, *rhumb line*) is a curve on the Earth's surface that crosses each meridian at the same angle. It is the path taken by a ship or plane maintaining a constant compass direction; it is a straight line on the Mercator projection.

  The **loxodromic distance** is a distance between two points on the Earth's surface on the rhumb line joining them. It is never shorter than the great circle distance.

  The **nautical distance** is the length in nautical miles of the rhumb line joining any two places on the Earth's surface. One nautical mile is equal to 1852 m.

- **Continental shelf distance**

  Article 76 of the United Nations Convention on the Law of the Sea (1999) defined the *continental shelf of a coastal state* (its sovereignty domain) as the seabed and subsoil of the submarine areas that extend beyond its *territorial sea* as the natural prolongation of its land territory to the outer edge of the continental margin. It postulated that the **continental shelf distance**, i.e., the **range distance** from the baselines from which the breadth of the territorial sea is measured to above the other edge, should be within 200–350 nautical miles (370–648 km), and gave rules of its (almost) exact determination.

  Territorial sea is a belt of coastal waters extending at most 22 km. Next 370 km form the *exclusive economic zone*; first 22 km of it form the *contiguous zone*.

  Example of arising problems: Canada, Denmark and Russia, all claim a large portion of the Arctic, including North Pole, arguing that underwater Lomonosov Ridge belongs to *their* extended continental shelf.

  Article 47 of the same convention postulated that, for an archipelagic state, the ratio of the area of its waters (sovereignty domain) to the area of its land, including atolls, should be between 1 to 1 and 9 to 1, and elaborated case-by-case rules.

There is no defined bottom underground and upper airspace limit for sovereignty. The international waters/seabed and celestial bodies are the common heritage of mankind for the signatories of the Law of the Sea and Outer Space (1967) treaties.

Among divided islands, the largest one (785,753 km^2) is New Guinea and the smallest one is Koiluoto (200 m × 110 m), shared by Finland and Russia.

- **Port-to-port distance**

  The **port-to-port distance** is the shortest great circle distance between two ports that does not intersect any land contours.

  Officially published **distance between ports** represent the shortest navigable route or longer routes using favorable currents and/or avoiding some dangers to navigation. Reciprocal distances between two ports may differ.

- **Airway distance**

  An *airway* is a designated route in the air. Low altitude (or *victor*) airways are those below 5500 m AMSL (above mean sea level). High altitudes (or *jet*) airways are those above 5500 m AMSL. **Airway distance** is the actual (as opposed to straight line) distance flown by the aircraft between two points, after deviations required by air traffic control and navigation along published routes.

  The *stage length* is the distance of a nonstop leg of an itinerary. *Radar altitude* is the height with respect to the terrain below.

- **Point-to-point transit**

  Point-to-point transit is a route structure (common among low-fare airlines) where a plane, bus or train travels directly to a destination, rather than going through a central hub as in a *spoke-hub network*.

  A **point-to-point telecommunication** is a connection restricted to two end-points as opposed to a *point-to-multipoint link* used in *hub and switch circuits*; cf. **flower-shop metric** in Chap. 19.

- **Lighthouse distance**

  The **lighthouse distance** is the distance from which the light from the lighthouse is first seen from of a sailboat. This distance (in feet) is $\approx 1.17(\sqrt{h_e}+\sqrt{h_l})$, where h_l is the lighthouse's height above tide level and h_e is the observer's eye level above sea. For $h_l = 0$, it estimates the **distance to horizon**.

- **Optical horizon**

  Optical (or, say, *neutrino*, *gravitational wave*) **horizon** is the farthest distance that any photon (respectively, neitrino and gravitational wave) can freely streem.

- **Distance to horizon**

  The *horizon* is the locus of points at which line of sight is tangent to the surface of the planet. At a height h above the surface of a spherical planet of radius R without atmosphere, the line-of-sight distance to the horizon is $d = \sqrt{(R+h)^2 - R^2}$, and the arc length distance to it along the curved planet's surface is $R\cos^{-1}(\frac{R}{R+h})$.

  Taking the equatorial radius 6378 km of the Earth as a typical value, gives $d \approx 357\sqrt{h}$ m for small $\frac{h}{R}$. Allowing for refraction, gives roughly $d \approx 386\sqrt{h}$ m.

  The *middle distance* is halfway between the observer and the horizon.

- **Radio distances**

  Marconi's law, 1897, claims that the maximum signalling distance of an antenna in meters is cH^2, where H is antenna's height and c is a constant.

  The *electrical length* is the length of a transmission medium or antenna element expressed as the number of wavelengths of the signal propagating in the medium. In coaxial cables and optical fibers, it is $\approx$ 1.5 times the physical length.

  The **electrical distance** is the distance between two points, expressed in terms of the duration of travel of an electromagnetic wave in free space between the two points. The *light microsecond*, $\approx$ 300 m, is a convenient unit of electrical distance.

  The main modes of electromagnetic wave (radio, light, X-rays, etc.) propagation are *direct wave* (line-of-sight), *surface wave* (interacting with the Earth's surface and following its curvature) and *skywave* (relying on refraction in the ionosphere).

  The **line-of-sight distance** is the distance which radio signals travel, from one antenna to another, by a *line-of-sight path*, where both antennas are visible to one another, and there are no metallic obstructions.

  The *radio horizon* is the locus of points in telecommunications at which direct rays from an antenna are tangential to the surface of the Earth. The **horizon distance** is the distance on the Earth's surface reached by a direct wave; due to ionospheric refraction or tropospheric events, it is sometimes greater than the distance to the visible horizon. In television, the **horizon distance** is the distance of the farthest point on the Earth's surface visible from a transmitting antenna.

  The **skip distance** is the shortest distance that permits a radio signal (of given frequency) to travel as a skywave from the transmitter to the receiver by reflection (hop) in the ionosphere.

  If two radio frequencies are used (for instance, 12.5 kHz and 25 kHz in maritime communication), the **interoperability distance** and **adjacent channel separation distance** are the range within which all receivers work with all transmitters and, respectively, the minimal distance which should separate adjacent tunes for narrow-band transmitters and wide-band receivers, in order to avoid interference.

  DX is amateur radio slang (and Morse code) for distance; **DXing** is a distant radio exchange (amplifiers required). Specifically, *DX* can mean **distance unknown**, short for DXing and a far-away station that is hard to hear.

  Radio waves need 138 ms to go round the world and $\approx$ 2.57 s to be reflected from the Moon. **Long delayed echoes** (LDEs) are radio echoes which return to the sender later than 2.7 s after transmission; it is a rare and not explained phenomenon.

- **Ground sample distance**

  In Remote Sensing of the surfaces of terrestrial objects of the Solar System, including the Earth, the **ground sample distance** (or *GSD*, *ground sampling distance*, *ground-projected sample interval*) is the spacing of areas represented by each pixel in a digital photo of the ground from air or space.

For example, in an image with GSD 22 m, provided by UK-DMC2 (a British Earth imaging satellite), each pixel represents a ground area of 22^2 m^2.

- **Map's distance**

  The **map's distance** is the distance between two points on the map (not to be confused with **map distance** from Chap. 23). The length of a curved line feature on a map is usually measured by an *opisometer* (or *curvimeter*).

  The **horizontal distance** is determined by multiplying the map's distance by the numerical scale of the map.

  Map resolution is the size of the smallest feature that can be represented on a surface; more generally, it is the accuracy at which the location and shape of map features can be depicted for a given map scale.

- **Equidistant map**

  An **equidistant map** is a map projection of Earth having a well-defined nontrivial set of *standard lines*, i.e., lines (straight or not) with constant scale and length proportional to corresponding lines on the Earth. Some examples are:

  Sanson–Flamsteed equatorial map: all parallels are straight lines;

  cylindric equidistant map: the vertical lines and equator are straight lines;

  an *azimuthal equidistant map* preserves distances along any line through the central point; a *Werner cordiform map* preserves, moreover, distances along any arc centered at that point.

  Maurer–Close (or *doubly equidistant*) *map* preserves distances from two central points. If those points are identical, the map is azimuthal equidistant.

  A *gnomonic map* displays all great circles as straight lines; so, it preserves the shortest route between two locations.

- **Distance cartogram**

  A **distance** (or *linear*) **cartogram** is a diagram or abstract map in which distances are distorted proportionally to the value of some thematic variable. Typically, it shows the relative travel times and directions from vertices in a network.

- **Tolerance distance**

  In GIS (computer-based Geographic Information System), the **tolerance distance** is the maximal distance between points which must be established so that gaps and overshoots can be corrected (lines snapped together) as long as they fall within it.

- **Space syntax**

  Space syntax is a set of theories and techniques (cf. Hiller–Hanson, 1984) for the analysis of spatial configurations complementing Transport Engineering and geographic accessibility analysis in a GIS (Geographical Information System).

  It breaks down space into components, analyzed as networks of choices, and then represents it by maps and graphs describing the relative connectivity and integration of parts. The basic notions of space syntax are, for a given space:

  isovist (or visibility polygon), i.e., the field of view from any fixed point;

  axial line, i.e., the longest line of sight and access through open space;

  convex space, i.e., the maximal inscribed convex polygon (all points within it are visible to all other points within it).

These components are used to quantify how easily a space is navigable, for the design of settings where way-finding is important such as museums, airports, hospitals. Space syntax has also been applied to predict the correlation between spatial layouts and social effects such as crime, traffic flow, sales per unit area, etc.

- **Defensible space**

  In landscape use, **defensible space** refers to the 30 m zone surrounding a structure that has been maintained/designed to reduce fire danger. The first 9 m ($\approx$ 30 feet) is where vegetation is kept to a minimum combustible mass. The remaining area 9–30 m is the *reduced fuel zone*, where fuels and vegetation should be separated (by thinning, pruning, etc.) vertically and/or horizontally.

- **Sanitation distances**

  The **drinking distance** of a dwelling is its distance from the closest source of water.

  A *latrine* is a communal facility containing (usually many) toilets. It should be at most 50 m away from dwellings to be served and at least 50 m away from communal food-storage and preparation. A latrine should be $\geq$ 30 m from water-storage and treatment facilities, as well as from surface water and shallow groundwater sources. A septic tank should be $\geq$ 15 m from a water supply well.

  The **vertical separation distance** is the distance between the bottom of the drain field of a sewage septic system and the underlying water table. This separation distance allows pathogens (disease-causing bacteria, viruses, or protozoa) in the effluent to be removed by the soil before it comes in contact with the groundwater.

- **Setback distance**

  In land use, a **setback** (or *buffer*) **distance** is the minimum horizontal distance at which a building or other structure must legally be from property lines, or the street, or a watercourse, or any other place which needs protection. Setbacks may also allow for public utilities to access the buildings, and for access to utility meters. Cf. also **buffer distance** and **clearance distance** in Chap. 29.

- **Shy distance**

  Shy distance is the space left between vehicles (or pedestrians and vehicles) as they pass each other.

- **Distance-based numbering**

  The **distance-based exit number** is a number assigned to a road junction, usually an exit from a freeway, expressing in miles (or km) the distance from the beginning of the highway to the exit. A *milestone* (or *kilometer sign*) is one of a series of numbered markers placed along a road at regular intervals.

  The *Kilometer Zero* (or *km* 0) is a particular location (usually in the nation's capital city), from which distances are traditionally measured. For France, it is on the square facing the entrance of Notre Dame cathedral in Paris. For Russia, it is in a short passage connecting Red Square with Manege Square in Moscow.

  Distance-based house addressing is the system when buildings and blocks are numbered according to the distance, i.e., the number of increments (feet or division of miles), from a given baseline. For example, the number 67*W*430

in Naperville, US, can express that the house is 67 miles west of downtown Chicago. One of the GIS-inspired guidelines: to use the address $n = \frac{d}{10} + 100$, where d is the distance in feet of the house from the reference point; roughly, $d = \frac{n}{500}$ miles.

Metes and bounds is a traditional system of land description (in Real Estate and town boundary determination) by courses and distances. *Metes* is a boundary defined by the measurement of each straight run specified as **displacement**, i.e., by the distance and direction. *Bounds* refers to a general boundary description in terms of local geography (along some watercourse, public road, wall, etc.). The boundaries are described in a running prose style, all the way around the parcel of land in sequence.

Surveying is the technique of determining the terrestrial and spatial position of points and the distances and angles between them; cf., for example, *Surveyor's Chain measures* among **imperial length measures** in Chap. 27.

- **Driveway distances**

  A *driveway* is a private road giving access from a public way. The main **driveway distances** follow.

  The *throat length* is the distance between the street and the end of the driveway inside the land development. It should be 200–250 feet (about 61–76 m or 15 car lengths) for shopping centers and 25–28, 9–15 m for small developments with or without signalized access.

  The optimal one-way *driveway width* is 4.5–5 m. Driveways entering a roadway at traffic signals should have two outbound lanes (for right and left turns) at least 7 m and an inbound lane at least 4.5 m wide. The normal width of residential driveways is 4.5–7.5 m.

  The *turn radius* is the extent that the edge of a commercial driveway is "rounded" to permit easier entry/exit by turning vehicles. In urban settings, it is 8–15 m.

- **Road sight distances**

  In Transportation Engineering, the *normal visual acuity* is the ability of a person to recognize a letter (or an object) of size 25 mm from a distance of 12 m.

  The **visibility distance** of a traffic control device is the maximum distance at which one can see it, while its **legibility distance** is the distance from which the driver can discern the intended message in order to have time to take the necessary action. For a safety sign, the **distance factor** is the ratio of the observation distance to the size of the symbol or text.

  The **clear sight distance** is the length of highway visible to a driver. The **safe sight distance** is the necessary sight distance needed to a driver in order to accomplish a fixed task. The main safe distances, used in Road Design, are:

  – the **stopping sight distance**—to stop the vehicle before reaching an unexpected obstacle;
  – the *maneuver sight distance*—to drive around an unexpected small obstacle;
  – the *road view sight distance*—to anticipate the alignment (eventually curved and horizontal/vertical) of the road (for instance, choosing a speed);

– the *passing sight distance*—to overtake safely (the distance the opposing vehicle travels during the overtaking maneuver).

The *safe overtaking distance* is the sum of four distances: the passing sight distance, the **perception-reaction distance** (between decision and action; cf. Chap. 25), the distance physically needed for overtaking and the buffer safety distance.

Also, adequate sight distances are required locally: at intersections and in order to process information on traffic signs. A warning "objects in mirror are closer than they appear" can be required on vehicle's passenger side mirrors.

In a traffic flow, the *spacing* (or *distance headway*) is the distance between corresponding points (front to front) of consecutive vehicles moving in the same lane, while the *clearance* is the spacing minus the length of the leading vehicle. The corresponding time measures are *headway* and *gap*.

- **Road travel distance**

The **road travel** (or *road*, *driving*, *wheel*, *actual*) **distance** between two locations (say, cities) of a region is the length of the shortest road connecting them.

Some GISs (Geographic Information Systems) approximate road distances as the l_p-metric with $p \approx 1.7$ or as a linear function of **great circle distances**; in the US the *distance factor* (multiplier) is ≈ 1.15 in an east–west direction and ≈ 1.21 in the north–south direction. Several relevant notions of distance follow.

The **GPS navigation distance**: the distance directed by GPS (Global Positioning System, cf. **radio distance measurement** in Chap. 29) navigation devices. But this shortest route, from the GPS system point of view, is not always the best, for instance, when it directs a large truck to drive through a tiny village; cf. the Talmudic little boy's paradox among **distance-related quotes** in Chap. 28.

The **official distance**: the officially recognized (by, say, an employer or an insurance company) driving distance between two locations that will be used for travel or mileage reimbursement. Distance data (shortest paths between locations) are taken from a large web map service (say, MapQuest, Google, Yahoo or Bing) which uses a variation of the *Dijkstra algorithm*; cf. **Steiner ratio** in Chap. 1.

The **distance between zip codes** (in general, postal or telephone area codes) is the estimated driving distance (or driving time) between two corresponding locations.

Time-distance and **cost-distance** are time and cost measures of how far apart places are. The **journey length** is a general notion of distance used as a reference in transport studies. It can refer to, say, the average distance traveled per person by some mode of transport (walk, cycle, car, bus, rail, taxi) or a statutory vehicle distance as in the evaluation of aircraft fuel consumption.

An *odometer* is an instrument that indicates distance traveled by a vehicle. A *hubometer* is such device mounted on the axle of a vehicle, while a *trip meter* is an electronic device recording such distance in any particular journey.

Distance-based (or *mileage-based*, *per-mile*) *pricing* means that vehicle charges are based on the amount a vehicle is driven during a time period.

Dead mileage is when a public transit vehicle operates without carrying or accepting passengers, such as when coming from a garage to begin its first trip of the day.

- **Death/kilometer**

  In countries collecting data on distance travelled, the traffic volume is measured in *vehicle-kilometrs* (calculated by odometer readings, traffic counts, driver survey or fuel consumption) or in *person-kilometers*, accounting for vehicle occupancy.

  The most objective indicator to describe risk on the road network is fatalities per billion vehicle-kilometrs, or fatalities per billion person-kilometrs.

  In the UK, the lifetime risk of dying according to various forms of transport is measured as relative traffic and crude death rate per 100 million vehicle-kilometrs.

  In French-speaking journalism, *loi du mort-kilomètre*, i.e., the *law of death-kilometer*, is the principle that information (especially on victims) is more or less important according to its proximity—geographic, temporal, emotional, or social—to the news medium's user. Cf. **distance to death** in Chap. 23 and **distant suffering** in Chap. 28.

- **Horizontal distance**

  The **horizontal distance** (or **ground distance**) is the distance on a true level plane between two points, such as scaled off the map (it does not take into account the relief between two points). There are two types of horizontal distance: **straight line distance** (the length of the straight line segment between two points as scaled off the map), and **distance of travel** (the length of the shortest path between two points as scaled off the map, in the presence of roads, rivers, etc.).

  The *thalweg* (valley way) of a river or valley is the deepest inline within it.

  The *stream gradient* is the slope measured (say, in m/km) by the ratio of drop in a stream per unit distance; the *relief ratio* is such average drop. The *gradient of a road* is the ratio of the vertical to the horizontal distance, measured in m/km or as slop tangent of the angle of the elevation. The *pitch* (or *slope*, *incline*) of a roof is the ratio of the rise to the roof span, expressed in cm/m.

- **Slope distance**

  The **slope distance** (or **slant distance**) is the inclined distance (as opposed to the true horizontal or vertical distance) between two points.

  In Engineering, the **rollout distance** is the distance that a boulder or rock took to finally reach its resting point after rolling down a slope. The *release height* is the height at which a boulder or rock was released in relation to a slope.

  Naismith's rule in mountaineering: eight units of walking flat distance are time-equivalent to one unit of climb on a typical decline 12°.

  Craeme *et al*, 2014, claim that the cost for an organism of mass M kg to walk uphill, gaining 100 m in altitude, is $2.94M$ kilojoules.

Walking uphill, humans and animals minimize metabolic energy expenditure; so, at critical slopes, they shift to zigzag walking. Langmuir's hiking handbook advises one to do it at 25°. Llobera and Sluckin, 2007, explain switchbacks in hill trails by the need to zigzag in order to maintain the critical slope, $\approx 16°$ uphill and $\approx 12.4°$ downhill. Skiing and sailing against the wind also require zigzagging.

The west face of Mount Thor, in the Canadian Arctic, is the Earth's greatest *vertical drop*: a uninterrupted wall 1250 m, with an average angle of 105°. The world record for the longest *rappel* (slope descent using ropes), 33 days, was set here in 2006. The world's highest unclimbed mountain is Gangkhar Puensum (7570 m) on the Bhutan-Tibet border. The most dangerous by fatality rate mountains are: Annapurna and K2, 10-th and 2-nd highest ones: 8091 and 8611.

- **Vertical distance**

  The **vertical distance** of a location is its height above or depth below a fixed *vertical datum*, i.e., reference surface, say, the Earth's surface, mean sea level (MSL) or its model. On other planets, the elevations of solid surface are measured relative to the mean radius.

  The terms *elevation* (or *geometric height*), *altitude* (or *geopotential height*) and *depth* are used for points/planes on the ground, in the air and below the surface, respectively. *AMSL*, *AGL*, *AAE* and (in Broadcasting) *HAAT* mean height above MSL, ground level, nearest aerodrome and average (surrounding) terrain, respectively. The *height of an aircraft* is its AGL, i.e., AMSL plus elevation of the ground.

  For measuring the height of land objects, the usual datum used is MSL, defined as the mean hourly water elevation taken over a specific 19 years cycle. Countries tend to choose MSL at one specific point to be used as the standard "zero elevation".

  Depths and tides on a nautical chart are measured relative to *chart datum*, defined as a level below which tide rarely falls: the lowest tide predictable from the effects of gravity, average lowest tide of each day, or (in waters with very low tidal ranges) MSL. Bridge clearances are given relative to a datum based on high tide.

  The *geoid* is a surface of a constant potential which is the best approximation, in a least-square sense, of the global MSL. The **orthometric height** of an object is its vertical distance above the geoid. Main nontidal datums are *gravimetric*, based on integral-mean gravity M between the geoid and the Earth's surface along some levelling line, and *ellipsoidal* one, used in satellite techniques.

  A **gravimetric height** of Earth's surface is $\frac{W_0-W}{M}$, where W, W_0 are the potentials of the Earth's gravity field on Earth's and geoid's levels. In particular, the *rigorous orthometric height* is the curved distance between the geoid and the Earth's surface along the *plumbline* (line orthogonal to the geoid). At present, there is no vertical datum, that is based on this height, due to difficulty in obtaining such M.

The minimal, maximal and average land heights are −418 m at the Dead Sea, 8848 m at the top of Mount Everest and 840 m, while the average and maximal depths of the ocean are 3680 m and 10,911 m (Challenger Deep in Mariana Trench). The surface's points closest (6353 km) and farthest (6384 km) from the Earth's center are the bottom of the Arctic Ocean and the summit of the Andean volcano Chimborazo (6268 m).

- **Prominence**

  In Topography, **prominence** (or *autonomous height*, *relative height*, *shoulder drop*) is a measure of the stature of a summit of a hill or mountain. The prominence of a peak is the minimum height of climb to the summit on any route from a higher peak (called the *parent peak*), or from sea level if there is no higher peak. The lowest point on that route is the *col*. So, the prominence of any island or continental highpoint is equal to its elevation above sea level.

  The highest mountains of the two largest isolated landmasses, Afro-Eurasia (Mount Everest) and the Americas (Aconcagua), have the most prominent peaks, 8848 m and 6962 m. But from its ocean base, the elevation of the Hawaiian volcano Mauna Kea (4205 m) is 10,203 m, and the mountain with the highest (5486 m) elevation from its land base is Mount McKinley (6193 m) in Alaska.

  The *topographic isolation* of a summit is the great circle distance to the nearest point of equal elevation; for Everest, it is 40,008 km (Earth's circumference between the poles). *Spire measure* (or *ORS*, short for *omnidirectional relief and steepness*) is a rough measure of the visual "impressiveness" of a peak. It averages out how high and steep a peak is in all directions above local terrain.

- **Special parallels and meridians**

  A network of *parallels* and *meridians* (lines of **latitude** and **longitude**, cf. Chap. 25) provides a locational system on Earth, using North Pole, South Pole (parallels 90°N and 90°S), rotation axis, and *equatorial plane* (an imaginary plane passing through Earth halfway between the poles and perpendicular to rotation axis).

  The *equator* is the imaginary midline, where the equatorial plane intersects Earth's surface. It is the parallel of 0° latitude separating North and South hemispheres.

  The *Prime meridian* and the *Date line* are internationally agreed at 0° and (with some bends, so as not to cross any land) ≈ 180° longitude; they form a great circle separating the Eastern and Western hemispheres. The point 0°, 0° is located in the Atlantic Ocean ≈ 614 km south of Accra, Ghana.

  A degree of latitude varies from 110.567 km apart at the equator to 111.699 km at the poles; each minute ($\frac{1}{60}$-th of a degree) is ≈ 1 mile. A degree of longitude shrinks from 111.321 km at the equator to 0 at the poles.

  The (solar) *terminator* (or, *circle of illumination*, *grey line*) is the great circle that divides Earth between a light half and a dark half. The *land hemisphere* is the hemisphere containing the largest possible area, ≈ $\frac{7}{8}$, of land. It is centered on 47°13′N 1°32′W (in the city of Nantes, France). The other half is the *water hemisphere*.

The *tropic of Cancer* and the *tropic of Capricorn* are parallels at which the Sun is directly overhead at the northern and the southern summer solstice, respectively. Their positions depend on the Earth's axial tilt. The region between them, centered on the equator, is the *tropics*. The regions around 25–30°N and S are *subtropics*, and the regions 30–35°N and S are *horse latitudes* (or *subtropical highs*).

Equatorial and *polar* regions are within a few degrees of the equator or a pole. The *Arctic circle* and the *Antarctic circle* are parallels at which the Sun does not appear above the horizon at the northern and the southern winter solstice.

The longest land, continuous land, continuous sea latitudes are 48°24′53N (10,726 km France–Ukraine–Kazakhstan–China), 78°35′S (7958 km Antarctica), 55°59′S (22,471 km). The longest land, continuous land, continuous sea longitudes are 22°E (13,035 km Russia–China–Thailand), 99°1′30"E (7590 km), 34°45′45"W (15,986 km). The longest continuous land and sea distances along a great circle are 13,573 km (Liberia–Suez Canal–China) and ≈32,000 km.

Many parallels and meridians, often named and/or approximated, represent political boundaries. For example, 49°N latitude is (much of, from British Columbia to Manitoba) the border between Canada and US, 38°N is the boundary between North and South Korea, and 60°S is the northern boundary of Antarctica in the Antarctic Treaty. 2°20′14.025″E longitude is the *Paris meridian* (historic rival of the Prime meridian through Greenwich), 52.5°E is the official meridian of Iran, and ≈ 70°E was agreed in 1941 by Nazi Germany and the Empire of Japan as division of their spheres of interest in Asia. The *Brandt Line* (Brandt, 1980), represents socio-economic and political divide between the "rich North" and the "poor South". It encircles the world at ≈ 30°N latitude, passing between North and Central America, north of Africa and the Middle East, then going north so as to exclude China, Mongolia, Korea and going south so as to include Australia.

- **Remotest places on Earth**

  In medieval geographies, *ultima Thule* was any distant place located beyond the borders of the known world. Eratosthenes (c. 276–195 BC), measuring the *oikoumene* (inhabited world), put its northern limit in a mythical island Thule.

  The remotest island is uninhabited Bouvet island in the South Atlantic Ocean. Its nearest (1600 km) land is Antarctica and nearest inhabited land is Tristan da Cunha, the remotest inhabited archipelago.

  Among other remotest (i.e., lacking normal transportation links) places on the Earth are: Kergelen (France), Pitcairn (UK), Svalbard (Norway) archipelagos, Easter (Chili), Foula (UK), Macquarie (Australia) islands, Motuo (China) county, McMurdo Station (Antarctica-US), La Rinconada (Peru, at an altitude of 5100 km) towns, Alert (Canada, 800 km below the North Pole) village.

  The *continental pole of inaccessibility* (*Point Nocean*), the point on land farthest (2514 km) from any ocean, lies in the Xinjiang, China, around 45°22′N 88°11′E. The *oceanic pole of inaccessibility* (*Point Nemo*), the point farthest (2690 km) from any land, lies in the South Pacific Ocean at 48°52.6′S 123°23.6′W.

The *northern pole of inaccessibility* (84°03′N 174°51′W) is the point on the Arctic Ocean pack ice, 661 km from the North Pole, farthest (1094 km) from any land mass. The *southern pole of inaccessibility* (82°06′S 54°58′E) is the point on the Antarctic, 878 km from the South Pole, farthest (1300 km) from the ocean.

For a country, accessibility to its coast from its interior is measured by the ratio of coastline length in meters to land area in km^2. This ratio is the highest (10,100) for Tokelau and the lowest nonzero (0.016) for the Democratic Republic of the Congo. Canada has the longest (202,080 km) coastline.

The largest *antipodal* (diametrically opposite) land masses are the Malay Archipelago–Amazon Basin, and east China + Mongolia, antipodal to Chile + Argentina. Capitals close to being antipodes are: Buenos Aires–Beijing, Madrid–Wellington, Lima–Bangkok, Quito–Singapore, Montevideo–Seoul.

Politically unaccessed areas include isolated people (as Sentinelese and $\approx$ 100 tribes in dense forests) and unclaimed areas (antarctic Marie Byrd Land, Bir Tawil).

The *geographical centre of Earth* is the superficial barycenter produced by treating the geoid as a sphere and each continent or island as a region of a thin shell of uniform density. It is at 40°52′N 34°34′E (180 km northeast of Ankara).

Counting as different only population centers at >1000 km, the *point of minimum aggregate travel* (or *geometric median*, cf. **Fréchet mean** in Chap. 25) of the world's population lies around Afghanistan-Kashmir. This point is closest, 5200 km of the mean great circle distance, to all humans, and its antipodal point is the farthest from mankind. But the closest, 5600 km, point to the world's entire wealth (measured in GNP) lies in southern Scandinavia.

In terms of altitude, the number of people decreases faster than exponentially with increasing elevation (Cohen–Small, 1998). Within 100 m of sea level, lies 15.6 % of all inhabited land but 33.5 % of the world population live there. Altitude of residence is, via hypoxia, a risk factor for psychological distress in bipolar disorder.

- **Latitudinal distance effect**

  Diamond, 1997, explained the larger spread of crops and domestic animals along an east–west, rather than north–south, axis by the greater longitudinal similarity of climates and soil types.

  Ramachandran and Rosenberg, 2006, confirmed that genetic differentiation increases (and so, cultural interaction decreases) more with *latitudinal distance* in the Americas than with *longitudinal distance* in Eurasia. Randler, 2008: within the same time zone, people in the east get up and go to bed earlier than people in the west.

  Turchin–Adams–Hall, 2006, observed that $\approx$ 80 % of land-based, contiguous historical empires are wider in the east–west compared to the north–south directions. Three main exceptions—Egypt (New Kingdom), Inca, Khmer—obey a more general rule of expansion within an ecological zone.

  Taylor et al., 2014: polyandry in species is more common in northern latitudes.

  The *latitudinal biodiversity gradient* (LBG) refers to the decrease in in both terrestrial and marine biodiversity, that occurs, the past 30 Ma, from the equator

to the poles for most fauna and flora. Its causes remain unresolved. Deep-time studies indicate that it might characterise cold icehouse climatic regimes,

Mace and Pagel, 1995 and 2004, found the same gradient for the density (number per range) of language groups and cultural variability. Around 60 % of the world's languages are found in the great belts of equatorial forest. Papua New Guinea (14 % of languages), sub-Saharan Africa and India have the largest linguistic diversity. The number of phonemes in a language decrease, but the number of color terms increase, from the equator to the poles.

25.2 Distances in Geophysics

- **Atmospheric visibility distances**

  Atmospheric extinction (or *attenuation*) is a decrease in the amount of light going in the initial direction due to *absorption* (stopping) and scattering (direction change) by particles with diameter 0.002–100 μm or gas molecules. The dominant processes responsible for it are *Rayleigh scattering* (by particles smaller than the wavelength of the incident light) and absorption by dust, ozone O_3 and water. For example, mountains in the distance look blue due to the Rayleigh scattering effect.

  In extremely clean air in the Arctic or mountainous areas, the visibility can reach 70–100 km. But it is often reduced by air pollution and high humidity: haze (in dry air) or mist (moist air). *Haze* is an atmospheric condition where dust, smoke and other dry particles (from farming, traffic, industry, fires, etc.) obscure the sky.

  The World Meteorological Organization classifies the horizontal obscuration into the categories of fog (a cloud in contact with the ground), ice fog, steam fog, mist, haze, smoke, volcanic ash, dust, sand and snow. Fog and mist are composed mainly of water droplets, haze and smoke can be of smaller particle size.

  Visibility of less than 100 m is usually reported as zero. The international definition of *fog*, *mist* and *haze* is a visibility of < 1 km, 1–2 km and 2–5 km.

  In the air pollution literature, **visibility** is the distance at which the contrast of a visual target against the background (usually, the sky) is equal to the threshold contrast value for the human eye, necessary for object identification, while **visual range** is the distance at which the target is just visible. Visibility can be smaller than the visual range since it requires recognition of the object.

  Visibility is usually characterized by either visual range or by the *extinction coefficient* (attenuation of light per unit distance due to four components: scattering and absorption by gases and particles in the atmosphere). It has units of inverse length and, under certain conditions, is inversely related to the visual range.

  Meteorological range (or *standard visibility*, *standard visual range*) is an instrumental daytime measurement of the (daytime sensory) visual range of a target. It is the furthest distance at which a black object silhouetted against

a sky would be visible assuming a 2 % threshold value for an object to be distinguished from the background. Numerically, it is ln 50 divided by the extinction coefficient.

In Meteorology, **visibility** is the distance at which an object or light can be clearly discerned with the unaided eye under any particular circumstances. It is the same in darkness as in daylight for the same air. **Visual range** is defined as the greatest distance in a given direction at which it is just possible to see and identify with the unaided eye in the daytime, a prominent dark object against the sky at the horizon, and at night, a known, unfocused, moderately intense light source.

The International Civil Aviation Organization defines the **nighttime visual range** as the greatest distance at which lights of 1000 candelas can be seen and identified against an unlit background. Daytime and nighttime ranges measure the atmospheric attenuation of contrast and flux density, respectively.

In Aviation Meteorology, the **runway visual range** is the maximum distance along a runway at which the runway markings are visible to a pilot after touchdown. It is measured assuming constant contrast and luminance thresholds.

Oblique visual range (or *slant visibility*) is the greatest distance at which a target can be perceived when viewed along a line of sight inclined to the horizontal.

- **Atmosphere distances**

  The **atmosphere distances** are the altitudes above Earth's surface (mean sea level) which indicate approximately the following specific (in terms of temperature, gravity, electromagnetism, etc.) layers of its atmosphere.

  Below 1–2 km: *planetary boundary layer*, where winds are directly retarded by surface friction. The reminder of the atmosphere: the *free atmosphere*.

  From 8 km: the death zone for human climbers (lack of oxygen).

  From the *Armstrong line* (18.900–19.350 km) water boils at 37 °C (low pressure) and a pressure suit is needed.

  Below 7–20 km (over the poles and equator, respectively): unstable *troposphere* in which temperature decreases with height (the weather and clouds occur here).

  Above the troposphere to $\approx$ 51 km: stable *stratosphere*, where the temperature increases with height (the ozone layer is at 19–48 km). The *tropopause* (its boundary with the troposphere) occurs at a pressure $\approx$ 0.1 bar.

  Above the stratosphere to 80–85 km: the *mesosphere*, in which temperature again decreases with height. Above the mesosphere to 500–1000 km: the *thermosphere*, where the temperature again increases with height.

  20–100 km: *near space* (or *upper atmosphere*), above airliners but below satellites.

  100 km: the *Kármán line* prescribed by Fédération Aéronautique International as the boundary separating Aeronautics and Astronautics, near and outer space.

  Above the thermosphere to $\approx$190,000 km : the *exosphere*, where molecules are still gravitationally bound but they can escape into space. Below the exosphere: the *homosphere*, where atmosphere has relatively uniform composition

since turbulence causes a continuous mixing. The reminder of the atmosphere: the *heterosphere*.

From 50–80 to 2000 km: the *ionosphere*, an electrically conducting region. From $\approx$ 160 km upwards: the *anacoustic zone*, where distances between air particles are so great that sound can no longer propagate; high-frequency sounds disappear first.

Up to 6–10 Earth radii on the sunward side: the *magnetosphere*, where Earth's magnetic field still dominates that of the solar wind. *Geospace* is the region from the beginning of ionosphere to the end of magnetosphere.

The altitude of the International Space Station is 278–460 km. 35,786 km: the altitude of geostationary (communication and weather) satellites. For observation and science satellites, it is 480–770 km and 4800–9700 km, respectively. Geocentric orbits with altitudes up to 2000 km, 2000–35,786 km and more than 35,786 km are called low, medium and high Earth orbits, respectively.

From 320,000 km: Moon's (at 356,000–406,700 km) gravity exceeds Earth's.

1,496,000 km = 0.011 AU: Earth's **Hill radius**, where Sun's gravity Earth's.

- **Wind distances**

  Examples of wind-related distances follow.

  Monin–Obukhov length: a rough measure of the height over the ground, where mechanically produced (by vertical wind shear) turbulence becomes smaller than the buoyant production of turbulent energy (dissipative effect of negative buoyancy). In the daytime over land, it is usually 1–50 m.

  The **aerodynamic roughness length** (or *roughness length*) z_0 is the height at which a wind profile assumes zero velocity.

  The **wind daily run** is the distance that results by integrating the wind speed, measured at a point, over 24 h. The fastest recorded wind speed near Earth's surface was 318 mph (i.e., 511.76 km/h) in Oklahoma, US, in 1999.

  Rossby radius of deformation is the distance that cold pools of air can spread under the influence of the *Coriolis force*, i.e., the apparent deflection of moving objects when they are viewed from a rotating reference frame. It is the length scale at which effects, caused by Earth's rotation and the inertia of the mass experiencing the effect, become as important as buoyancy or gravity wave effects in the evolution of the flow about some disturbance.

  The *aerial plankton* carried aloft by winds or convection, consists of bacteria, fungi, spores, pollen and small invertebrates. Even in the upper troposphere (8–15 km altitude), viable bacteria cells represent $\approx$ 20 % of $0.25 - -1$ μm-sized particles.

  The *jet streams* are fast flowing, narrow air currents found in the atmosphere. The strongest jet streams are, both west-to-east and in each hemisphere, the *Polar jet*, at 7–12 km above sea level, and the weaker *Subtropical jet* at 10–16 km.

  The *atmospheric rivers* are narrow (a few hundred km across but several thousand km long) corridors of atmospheric water vapor transport over mid-latitude ocean regions. They account for over 90 % of such global meridional daily transport.

A *teleconnection* refers to climate anomalies being related to each other at large, say, thousands of km distances. For example, teleconnection between sea level pressure at Tahiti and Darwin, Australia, defines ENSO (El Niño Southern Oscillation).

- **Distances in Oceanography**

  Sea-surface height (SSH) is the height of the ocean's surface. **Decay distance**: the distance through which ocean waves travel after leaving the generating area.

  Wavelength is the distance between the troughs at the bottom of consecutive waves. A wave's *height* and *amplitude* are its trough-crest and rest-crest distances.

  The **significant wave height** (SWH) is the mean height $H_{1/3}$ of the highest third of waves. More modern and very close value is four times the root-mean-square of the surface elevation. Unusual *rogue waves* are defined as those with height $> 2H_{1/3}$; the tallest recorded one (by ship USS Ramapo in 1933) was 34 m. A wave up to $11H_{1/3}$ is possible. Large internal waves occur at thermoline and saltwater-freshwater interface. A *hundred-year wave* is a statistically projected water wave, the height of which, on average, is met or exceeded once in a 100 years for a given location.

  The maximum horizontal distance inland and height reached there by tsunami waters are called the **run-up** (or *inundation*) **distance** and **run-up height**. It was 1100 and 525 m for the 1958 Lituya Bay, Alaska, megatsunami, the largest recorded.

  Deep water (or *short*, *Stokesian*) **wave**: a surface ocean wave that is traveling in water depth greater than one-quarter of its wavelength; the velocity of deep water waves is independent of the depth. **Shallow water** (or *long*, *Lagrangian*) **wave**: a surface ocean wave of length 25 or more times larger than the water depth.

  Littoral (or *intertidal*): the zone between high and low water marks. Sometimes, *littoral* refers to the zone between the shore and water depths of ≈ 200 m.

  Oceanographic (or *thermal*) **equator**: the zone of maximum sea surface temperature located near (generally, north) the geographic equator. Sometimes, it is defined more specifically as the zone within which the sea surface temperature exceeds 28 °C. Below about 500 m, all of the world's oceans are at about 1.1 °C.

  Standard depth: a depth below the sea surface at which water properties should be measured and reported (in m): 0, 10, 20, 30, 50, 75, 100, 150, 200, 250, 300, 400, 500, 600, 800, 1000, 1200, 1500, 2000, 2500, 3000, 4000, . . . , 9000, 10,000.

  Charted depth: the recorded vertical distance from the *lowest astronomical tide* (LAT, the lowest low water that can be expected in normal circumstances) to the seabed. **Drying height**: the vertical distance of the seabed that is exposed by the tide, above sea level at LAT. Actual depth of water is height of tide + charted depth or height of tide—drying height. **Tidal range**: the difference between the heights of high water and low water at any particular place. The empirical *rule*

of twelfths assigns 6 h for it and subdivides the range into 1, 2, 3, 3, 2, 1 twelfths per hour.

The **thermocline**, **halocline** and **pycnocline**: the layers where the water temperature, salinity and density, respectively, change rapidly with depth.

Depth of no motion: a reference depth in a body of water at which it is assumed that the horizontal velocities are practically zero. On a horizontal scale, *ocean fronts* are the boundaries between water masses with different properties.

Plankton (viruses, bacteria, phytoplankton, zooplankton and small pelagic larvae) aggregate at the clines, depth of no motion and persistent ocean fronts. $\approx$ 75 % of the water column's biomass consist of plankton organized in thin (<3–4 m) layers 1–12 km in horizontal extent. Standard proxies for phyto- and zooplankton abundance are chlorofill-a imagery and sound attenuation. Giant (up to 130,000 km^2) bacterial mats float in the oxygen minimum zone off Chili and Peru.

Depth of the effective sunlight penetration: the depth at which $\approx$ 1 % of solar energy penetrates; in general, it does not exceed 100 m. The ocean is opaque to electromagnetic radiation with a small window in the visible spectrum. But it is transparent to acoustic transmission.

Depth of compensation: the depth at which illuminance has diminished to the extent that oxygen production through photosynthesis and oxygen consumption through respiration by plants are equal. The maximum depth for photosynthesis depends on plants and weather. Within the *epipelagic zone* there is enough light for photosynthesis, and thus plants and animals are largely concentrated here.

Below the *mesopelagic zone* lies the **aphotic zone** which is not exposed to sunlight. Organisms there depend on "marine snow" (a continuous shower of mostly organic detritus, decaying creatures and feces, falling from above) and chemosynthesis. The *deep sea* is the layer in the ocean below thermocline, at the depth 1800 m or more.

The **pelagic zone** consists of all the sea other than that near the coast or the sea floor, while the *benthic zone* is the ecological region at the very bottom of the sea.

The ocean is divided into the following horizontal layers from the top down:

- From the surface down 200 m: *epipelagic* (sunlit zone);
- 200–1000 m: *mesopelagic* (twilight zone);
- 1000–4000 m: *bathypelagic* (dark zone);
- 4000–6000 m: *abyssopelagic* (abyss);
- below 6000 m: *hadalpelagic* (trenches).

The **deep sound** (or **SOFAR**, i.e., SOund Fixing And Ranging) **channel** is a layer of ocean water where the speed of sound is at a minimum ($\approx$1480 m/s), because water pressure, temperature and salinity cause a minimum of water density. Sound waves of low frequency, caught and bent here, can travel hundreds of km. In low and middle latitudes, the SOFAR channel axis lies 600–1200 m below the sea surface; it is deepest in the subtropics and comes to the surface in high latitudes.

The **SLD** (sonic layer depth) is the depth of maximum sound speed above this axis. The **best depth** for a submarine to avoid detection is SLD plus 100 m.

Mixing length: the distance at which an *eddy* (a circular movement of water) maintains its identity until it mixes. An eddy can reach 500 km across and persist for months. Cf. the **mean free path** and **diffusion length** in Chap. 24.

Mixed layer depth: the depth of the bottom of the *mixed layer*, i.e., a nearly isothermal surface layer of 40–150 m depth where water is mixed through wave action or thermohaline convection.

Depth of exponential mixing or **depth of homogeneous mixing** refers to a surface turbulent mixing layer in which the distribution of a constituent decreases exponentially, or is constant, respectively, with height.

Depth of frictional resistance: the depth at which the wind-induced current direction is 180° from that of the true wind.

The *fetch* (or *fetch length*): the horizontal distance along open water over which wave-generating wind or waves have traveled uninterrupted. In an enclosed body of water, the *fetch* is the distance between the points of minimum and maximum water-surface elevation. In Meteorology, the *fetch* is the distance upstream of a measurement site, receptor site, or region of interest that is relatively uniform.

The total volume of Earth's water is $\approx$ 1.39 billion km^3 (0.2 % Earth's mass) of which $\approx$ 96 % is liquid. For each sustained 1 °C increase in global temperature, the sea level could rise by 2.3 m. Global sea level will rise by at least 1 m by 2100. At 2016, it is higher than anytime during last 115,000 years.

The ocean on Ganymede (Jupiter's satellite and the largest Solar System's moon) has total volume 40 billion km^3 and depth 800 km (30 % of Ganymede's radius).

- **River length**

  Meaning of **river length**, i.e., the distance between source and mouth, depend on their definitions, *anabranches* (multiple channels), map scale, etc.

  The **maximal river length** is the length of the longest continuous river channel in a given river system, regardless of name. Here, a river's "true source" is considered to be the source of whichever tributary is farthest from the mouth.

  The world's longest rivers are Nile-Kagera ($\approx$6650–6853 km), Amazon-Ucayali-Apurmac ($\approx$6400–6992 km) and Yangtze ($\approx$6300–6418 km).

- **Soil distances**

  Soil is composed of particles of broken rock that have been altered by chemical and environmental processes that include weathering and erosion. It is a mixture of mineral and organic constituents that are in solid, gaseous and aqueous states. A *soil horizon* is a specific layer in the land area that is parallel to the soil surface and possesses physical characteristics which differ from the layers above and beneath. Each soil type usually has 3–4 horizons.

  – *A Horizon* (or *topsoil*): the upper layer (usually 5–20 cm) with most organic matter accumulation and soil life.

- *B Horizon* (or *subsoil*): the deeper layer accumulating by *illuviation* (action of rainwater), iron, clay, aluminum and organic compounds.
- *C Horizon*: the layer which is little affected by soil forming processes.
- *R Horizon*: the layer of partially weathered bedrock at the base of the soil profile.

The current average rate of erosion over the Earth's land is 30 B, where B is the *Bubnoff unit* of speed (for lowering of earth surfaces due to erosion) equal to 1 m in a million year, i.e., removing 1 m^3 of earth from an area of 1 km^2 in 1 year.

The *pedosphere* is the outermost layer of the Earth that is composed of soil and subject to soil formation processes. It lies below the vegetative cover of the biosphere and above the groundwater and *lithosphere* (outermost shell of the Earth).

Larger *Critical Zone* includes vegetation, the pedosphere, groundwater aquifer systems and ends in the bedrock where the biosphere and *hydrosphere* (combined mass of Earth's water) cease to make significant changes to the chemistry.

The *water table* (or *phreatic surface*) is the level at which the groundwater pressure is equal to atmospheric pressure.

The *cryosphere* is the part of the hydrosphere describing the Earth's ice: sea/lake/river ice, snow cover, glaciers, ice caps, ice sheets and frozen ground including permafrost. The Bentley Subglacial Trench in Antarctica is the world's deepest, 2555 m, ice.

The Earth is now in a warm phase of the 5-th (Quaternary) major Ice Age, which started 2.58 Ma ago, The last glacial expansion ended 11,700 years ago with the start of the Holocene. Next one is expected within coming 1500–10,000 years unless anthropogenic global warming will delay it. The planet has warmed by only 0.74 °C since the early 1900s.

- **Frost line (in Earth Science)**

  The **frost line** (or *freezing depth*) is the depth to which the groundwater in soil is expected to freeze. In polar locations with year-round permafrost, the *thaw depth* is the depth to which the permafrost is expected to thaw each summer.

  In tropical regions, *frost line* may refer to the vertical geographic elevation below which frost does not occur. The *climatic snow line* is the point above which snow and ice cover the ground throughout the year; seasonally, snow occurs much lower. Cf. **frost line (in Astrophysics)**.

- **Moho distance**

  The Earth's *oceanic crust* (or *sima* for Si and Mg in basaltic rocks) is the surface, 5–10 km thick, of the ocean basins. The *continental crust* (or *sial* for Si and Al) is the layer of granitic rocks, 20–90 km thick, forming continents and continental shelves. The *Moho interface* (or *Mohorovicić seismic discontinuity*) is the boundary between the crust and the mantle, where the velocity of seismic P-waves increases. The **Moho distance** is the crustal thickness, i.e., the distance from a surface's point to the *Moho interface* beneath it.

The world's lowest sea-drilled point was 10,680 m-deep (in the Gulf of Mexico) under 1259 m of water. The Japanese research vessel *Chikyu*, aiming to the Moho interface, drilled 7740 m below the sea level and 2466 m below the seafloor. Cf. the lowest point on dry land (the shore of Dead Sea: 418 m), deepest cave (Krubera, Caucasus: 2191 m and, Chavé Cave, Mexico, possibly, $\sim$ 2500 m), deepest mine (Mponeng gold mine, South Africa: about 4 km) and deepest drill (Kola Superdeep Borehole: 12,262 m). The temperature rises usually by 1° every 33 m.

The *Curie depth* is the depth (usually 10–50 km) where the temperature reaches the *Curie point* at which rocks lose their ferromagneticic properties.

The Earth's mantle extends from the Moho interface to the mantle-core boundary at $\approx$ 2890 km. The liquid outer core of radius 3480 km (i.e., Mars-sized) contains a solid iron inner core (expanding $\approx$ 0.5 mm per year) of radius 1220 km. The mantle is divided into the upper and lower one at $\approx$ 660 km. Main other seismic boundaries are at about 60–90 km, 50–150 km, 220 km (Hales, Gutenberg and Lehmann discontinuities) and 410 km, 520 km, 710 km.

The *lithosphere* comprises the crust and the rigid portion of the upper mantle that behaves elastically on large time scales. Its thickness is the depth of the isotherm $\approx$1000° of the transition between brittle and viscous behavior. The lithosphere is broken into *tectonic plates* which float on the more plastic part of the mantle, the *asthenosphere*, 100–200 km deep.

The Eurasian and African plates are moving at the rates of 2 and 2.15 cm per year. The maximum earthquakes occur on the boundaries of the major moving plates. The eastern part of Indo-Australian plate is moving north 5.6 cm per year while the western part (India) is moving (north-east) only 3.7 cm per year due to impediment by Himalayas. The sequence of earthquakes in 2012 off the coast of Sumatra indicates that this plate has broken up into 2 or 3 separate plates.

- **Distances in Seismology**

  The Earth's crust is broken into tectonic plates that move around (at some cm per year) driven by the thermal convection of the deeper mantle and by gravity. At their boundaries, plates stick most of the time and then slip suddenly.

  An *earthquake*, i.e., a sudden (several seconds) motion or trembling in the Earth, caused by the abrupt release of slowly accumulated strain, was, from 1906, seen mainly as a rupture (the sudden appearance, nucleation and propagation of a new crack or fault) due to elastic rebound. However, from 1966, it is seen within the framework of slippage along a pre-existing fault or plate interface, as the result of stick-slip frictional instability. One of most important parameters controlling fault instability is the **slip-weakening distance** D_c over which a fault weakens during its seismogenic motion. The coefficient of friction degrades linearly with slip until D_c is reached; then it stays constant.

  So, an earthquake happens when dynamic friction becomes less than static friction. The advancing boundary of the slip region is called the *rupture front*. The standard approach assumes that the fault is a definite surface of tangential displacement discontinuity, embedded in a liner elastic crust.

Most earthquakes occur at near-vertical faults but a magnitude 6.0 earthquake at Kohat, Pakistan, in 1992, moved a 80 km^2 swath of land 30 cm horizontally. Almost all (81 % and 17 %) world's largest earthquakes occur along the *Ring of Fire* (circum-Pacific seismic belt) and the *Alpide belt* (from Java to Sumatra through the Himalayas, the Mediterranean, and out into the Atlantic).

90 % of earthquakes are of tectonic origin, but they can also be caused by volcanic eruption, nuclear explosion and work in a large dam, well or mine. Earthquakes can be measured by **focal depth**, speed of slip, intensity (modified Mercali scale of earthquake effects), magnitude, acceleration (main destruction factor), etc.

The Richter scale of magnitude is computed from the amplitude and frequency of shock waves received by a seismograph, adjusted to account for the **epicentral distance**. An increase of 1.0 of this magnitude corresponds to an increase of 10 times in amplitude of the waves and $\approx$ 31 times in energy; the largest recorded value is 9.5 (Chile, 1960). Asteroid's impact in Yucatan 66 Ma ago was 12.55.

An earthquake first releases energy in the form of shock *pressure waves* that move quickly through the ground with an up-and-down motion. Next come shear S-waves which move along the surface, causing much damage: *Love waves* in a side-to-side fashion, followed by *Rayleigh waves* which have a rolling motion. The earthquake *extinction length* is the distance over which the S-wave energy is decreased by $\frac{1}{e}$.

Distance attenuation models (cf. **distance decay** in Chap. 29), used in Earthquake Engineering for buildings and bridges, postulate acceleration decay with an increase of some **site-source distance**, i.e., the distance between seismological stations and the crucial (for the given model) "central" point of the earthquake.

The simplest model is the *hypocenter* (or focus), i.e., the point inside the Earth from which an earthquake originates (the waves first emanate, the seismic rupture or slip begins). The *epicenter* is the point of the Earth's surface directly above the hypocenter. This terminology is also used for other catastrophes, such as an impact or explosion of a nuclear weapon, meteorite or comet but, for an explosion in the air, the term *hypocenter* refers to the point on the Earth's surface directly below the burst. A list of the main Seismology distances follows.

The **focal depth**: the distance between the hypocenter and epicenter. Earthquake is *shallow-*, *mid-* or *deep-focus* if it is $<$ 70 km, 70–300 km or 300–700 km.

The **hypocentral distance**: the distance from the station to the hypocenter.

The **epicentral distance** (or **earthquake distance**): the **great circle distance** from the station to the epicenter.

The **Joyner–Boore distance** (1981): the distance from the station to the closest point, located over the *rupture surface* (rupturing portion of the fault plane).

The **rupture distance**: the distance from the station to the closest point on the rupture surface. The **seismogenic depth distance**: the distance from the station

to the closest point of the rupture surface within the *seismogenic zone*, i.e., the depth range where the earthquake may occur; usually at depth 8–12 km.

The **crossover distance**: the distance on a seismic refraction survey time-distance chart at which the travel times of the direct and refracted waves are the same.

Also used are the distances from the station to:

- the center of static energy release and the center of static deformation of the fault plane;
- the surface point of maximal macroseismic intensity, i.e., of maximal ground acceleration (it can be different from the epicenter);
- the epicenter such that the reflection of body waves from the *Moho interface* (the crust-mantle boundary) contribute more to ground motion than directly arriving shear waves (it is called the *critical Moho distance*);
- the line extending the *fault trace* (top edge of the rupture) in both directions;
- the sources of noise and disturbances: oceans, lakes, rivers, railroads, buildings.

The **space-time link distance** between two earthquakes x and y is defined by

$$\sqrt{d^2(x,y) + C|t_x - t_y|^2},$$

where $d(x,y)$ is the distance between their epicenters or hypocenters, $|t_x - t_y|$ is the time lag, and C is a scaling constant needed to connect distance and time.

The *earthquake distance effect*: at greater distances from its center, the perception of an earthquake weaken and lower frequency shaking dominates it. Many animals hear infrasound of imminent earthquakes and feel primary P-waves.

Another space-time measure for catastrophic events is **distance between landfalls** for hurricanes hitting a US state. It is (Landreneau, 2003) the length of state's coastline divided by the number of hurricanes which have affected it from 1899.

Also, Shennan et al., 2015, compare archeological cultures by both, great circle distance between sites and Euclidean distance between median culture dates.

- **Plume height**

  In a volcanic eruption, **plume height** refers to the highest point the eruptive cloud reaches before it flattens out and begins to drift downwind.

  The Volcanic Explosivity Index (VEI) is a scale measuring known eruptions by their volume of ejecta and plume height from VEI 0 (1000 m^3, < 100 m) to *mega-colossal* (or *super-volcano*) VEI 8 (1000 km^3, > 50 km).

- **Weather distance records**

  For a tornado, maximum width of damage, highest elevation, longest path: 4000 m, 3650 m, 472 km. The longest transport of a surviving human and of an object: 398 m and 359 km (personal check).

Longest path of a tropical cyclone: 13,500 km; highest storm surge: 13 m.

Largest snowflake and hail diameter: 38 and 20 cm. Longest lighting bolt: 190 km.

Greatest minute, hour, day, month, year rainfall: 31.2 mm, 0.3 m, 1.82 m, 9.3 m, 26.47 m. Lowest and highest mean annual precipitation: 0.762 mm and 11.872 m.

- **Extent of Earth's biosphere**

  Life has adapted to every (except, perhaps, ocean vent locales $> 130\,^\circ$C) ecological niche possessing liquid water and a source of free energy (say, sunlight, plate tectonics, water-rock chemistry). The main physical factors are temperature and pressure; their range for known active life as $[-20^\circ,\ 122^\circ]$C and $[5 \times 10^{-2},\ 1.3 \times 10^3]$ bar. But the range, say, $[-30^\circ,\ 135^\circ]$C looks possible. The acidity/alkalinity range of known life is $[0, 11]$ on the pH scale, from acidic hot springs to soda lakes.

  In Jones–Lineweaver, 2010, the depth 5–10 km of the 122 °C isotherm and the altitude 10–15 km (a *tropopause* boundary of the vertical movement of particles) are the boundaries of active life. In Nussinov–Lysenko, 1991, the boundaries of biosphere are *Moho interface* (say, −30 km) and *Kármán line* (100 km).

  For humans, the typical bounds for main physiologic factors are: core temperature 35–38 °C, serum pH 7.35–7.45, plasma *osmolality* 270–290 mOsm/kg, fasting plasma glucose 3.3–5.6 mmol/l and serum calcium 2.2–2.6 mmol/l. But there are permanent human habitations at mean annual temperatures of 34.4 °C, −19.7 °C and at an altitude of 5.1 km. Birds usually fly at altitudes 0.65–1.8 km but a vulture collided, at 11.3 km, with an aircraft.

  A fish has been spotted at 8372 m down in the Puerto Rico Trench. Deepest multicellular life are worms found at depths up to 3.6 km in gold mines and up to 10.8 km in the Challenger Deep. Stoddard, 2015, expects microbial life up to 19 km deep since high pressure can offset the heat's destructive effects.

  Microbes, supported by chemosynthesis, have been found in cores drilled 5.3 km, in hydrothermal vents at 11 km depth and 2.5 km beneath ocean's floor. Such *deep biosphere* (1–10 % of the world's biomass and the Earth vastest) is expected below the surface of continents and bottom of the ocean up to isotherm 122 °C. Some of such microbes have doubling times in millennia, while *Vibrio natriegens* divide in 9.8 min. The same 19 deep-rock bacteria found to be similar worldwide.

  The ranges for latent life (*cryptobiosis*: reversible state of low or undetectable metabolism) are much larger. Fungi and bacterial spores were found at an altitude 18–41 km. Examples of survival limits follow.

  Some frogs, turtles and snakes survive the winter by freezing solid. A brine shrimp *Artemia* tolerates salt amounts of 25 %. Tardigrades, in cryptobiosis, survive −272 °C, 151 °C (a few minutes), −20 °C (30 years), pressure 6000 bar, radiation 6200 gray of gamma rays and 120 years without water. Fly's larva *Polypedilium vanderplanki* dehydrates, in dry period, to 3 % water content, and it can survive −270 °C, 102 °C, radiation 7000 g and 18 months in outer space

vacuum. Some Antarctic fungi and Alpine lichens survive 18 months in Mars-like conditions or space travel.

A parasitic leach *Ozobranchus jantseanus* survives −196 °C (24 h) and −90 °C during 32 months. Archea *Thermococcus gammatolerans* survive 30,000 gray. Bacteria growing under hypergravity 403,627 g were cultivated. A bacterium survived 2.5 years on the Moon. *Deinococcus radiodurans*, listed as the world's toughest bacterium, survive extreme cold, dehydration, vacuum, radiation and acid. A bacteria *Tersicoccus phoenicis* has only been found in two spacecraft assembly clean rooms and is resistant to the methods used to clean such facilities.

Millions of years old (nondormant, just slow metabolizing) microbs, reproducing only every 10,000 years, were found in ocean floor. Bacterial spores were revived after 34,000 years of stasis; it was claimed also for 40 Ma old spores. A 1300 years old lotus seed and 2000 year old seed from extinct Judean date palm were germinated. *Silene stenophylla* was grown from 31,800 years old fruit.

Among the proponents of *panspermia* (the hypothesis that life, via extremophile bacteria and crystallized viruses surviving in space, propagates throughout the Universe), Yang et al., 2009, expect microbe density to be $10^{-3} - 10^{-2}$ cells/m^3 at altitude 100 km and $10^{-6} - 10^{-4}$ at 500 km. A large amount is expected at the altitude of the ISS (278–460 km). Napier–Wickramasinghe, 2010, claim that $10^{14} - 10^{16}$ microorganisms ($\approx$ 10 tonnes) per year are ejected from Earth at survivable temperatures. Organics preserved in cometary amorphous ice and meteorite-formed glass can be transported from one planet to another. Also, microbes, if somehow protected from UV, survive in meteorites with transit time of a few years.

A total of 7.5×10^{15} terrestrial microbes could reach the Moon per year, and the Solar System could be surrounded by an expanding biosphere of radius $>$ 5 parsecs containing $10^{19} - 10^{21}$ microbes. No ubiquitous ultrasmall bacteria were found but large *Bacillus* and eukaryotes (5–100 μ fungal spores) have been isolated from the stratosphere 27 km up, too high to have been lifted from Earth's surface. So, some viable but nonculturable microbes could be incoming from space. Hoover, 2011, found microfossils similar to filamentous prokaryotes in CI1 (Alais, Ivuna and Orgueil) and CM2 (Murchison and Murray) meteorites.

Life on Mars, if any, is expected to be of the same origin (and, perhaps, earlier) as that on Earth, but it would have to be under at least 1 m of soil/rock to survive. Impact of icy comets crashing into Earth billions of years ago could have produced a variety of prebiotic or life-building compounds, including amino acids.

Interstellar panspermia, when the Sun passes a star-forming cloud, and even intergalactic panspermia, when galaxies collide, are debated. But on a cosmic scale, even enthusiasts of panspermia see it as a local, "a few megaparsecs", phenomenon.

25.3 Distances in Astronomy

A *celestial object* (or *celestial body*) is a term describing astronomical objects such as stars and planets. The *celestial sphere* is the projection of celestial objects into their apparent positions in the sky as viewed from the Earth. The *celestial equator* is the projection of the Earth's equator onto the celestial sphere. The *celestial poles* are the projections of Earth's North and South Poles onto the celestial sphere. The *hour circle* of a celestial object is the great circle of the celestial sphere, passing through the object and the celestial poles.

The *ecliptic* is the intersection of the plane, containing the Earth's orbit, with the celestial sphere: seen from the Earth, it is the path that the Sun appears to follow over the course of a year. The *vernal equinox point* (or the *First point in Aries*) is one of the two points on the celestial sphere, where the equator intersects the ecliptic: it is the position of the Sun at the time of the vernal equinox.

In Astronomy, the *horizon* is the horizontal plane through the eyes of the observer. The *horizontal coordinate system* is a celestial coordinate system using the observer's local horizon as the *fundamental plane*, the locus of points having an altitude of 0°. The horizon is the line separating Earth from sky; it divides the sky into the upper hemisphere that the observer can see, and the lower hemisphere that he cannot. The pole of the upper hemisphere (the point of the sky directly overhead) is called the *zenith*; the pole of the lower hemisphere is called the *nadir*.

Positions and distances are calculated with respect to the center of mass of a body, not with respect to the geometric center, or surface. In general, an **astronomical distance** is a distance from one celestial body to another measured in astronomical units or gygameters for planets, light-years (ly) or parsecs for stars, kiloparsecs at the galactic scale, in megaparsecs (Mpc) for nearby galaxies and in terms of redshift for distant galaxies.

The average distance between stars (in a galaxy) is several ly; it is about 4 ly in Milky Way and 6.57 ly in the solar neighborhood. The average distance between galaxies (in a cluster) is several Mpc, while between clusters of galaxies (in a supercluster) it is of order 10 Mpc. The large structures are groups of galaxies, clusters, galaxy clouds (or groups of clusters), superclusters, and supercluster complexes (or galaxy filaments, great walls). A range of structures: galaxies ($\sim$ 10 kpc), groups (0.3–1 Mpc), clusters (few Mpc), superclusters (10–100 Mpc).

The Universe appears as a collection of giant bubble-like voids separated by great walls, with the superclusters appearing as relatively dense nodes. The average density of stars is about 1.4 per 100 billion cubic light-years, i.e., the average distance between them is about 4150 light-years. The mean density of visible matter (i.e., galaxies) in the Universe is $\sim 10^{-31}$ g/cm^3, while 1 g/cm^3 is the mass density of water.

ESA's Herschel space observatory found that our galaxy is threaded with filamentary structures on every length scale, from a few to a hundreds light-years, revealing the "skeleton" of Milky Way. These filaments appear to have a universal

width of about one third of a light-year, and they seem to be the preferred sites for stellar birth.

- **Latitude**

  In spherical coordinates (r, θ, ϕ), the **latitude** is the **angular distance** δ from the xy plane (*fundamental plane*) to a point, measured from the origin; $\delta = 90° - \theta$, where θ is the **colatitude**.

  In a *geographic coordinate system* (or *earth-mapping coordinate system*), the **latitude** is the angular distance from the Earth's equator to an object, measured from the center of the Earth. Latitude is measured in degrees, from $-90°$ (South Pole) to $+90°$ (North Pole). *Parallels* are the lines of constant latitude. The **colatitude** is the angular distance from the Earth's North Pole to an object.

  The **celestial latitude** is an object's latitude (measured in degrees) on the celestial sphere from the intersection of the fundamental plane with the celestial sphere in a given *celestial coordinate system*. In the *equatorial coordinate system* the fundamental plane is the plane of the Earth's equator; in the *ecliptic coordinate system* the fundamental plane is the plane of the ecliptic; in the *galactic coordinate system* the fundamental plane is the plane of the Milky Way; in the *horizontal coordinate system* the fundamental plane is the observer's horizon.

  Geomagnetic latitude is a parameter analogous to geographic latitude, except that bearing is with respect to the magnetic poles. The intersection between the magnetic and rotation axes of the Earth is located $\approx$ 500 km North from its centre.

- **Longitude**

  In spherical coordinates (r, θ, ϕ), the **longitude** is the **angular distance** ϕ in the xy plane from the x axis to the intersection of a great circle, that passes through the point, with the xy plane.

  In a *geographic coordinate system* (or *Earth-mapping coordinate system*), the **longitude** is the angular distance measured eastward along the Earth's equator from the *Greenwich meridian* (or *Prime meridian*) to the intersection of the meridian that passes through the object. Longitude is measured in degrees, from $0°$ to $360°$. A *meridian* is a great circle, passing through Earth's North and South Poles; the meridians are the lines of constant longitude.

  The apparent longitude shift, 102 m east, at Greenwich is a local effect due to the direction of gravity there, and not a global shift in the longitude system.

  The **celestial longitude** is the longitude of a celestial object (measured in units of time) on the celestial sphere measured eastward, along the intersection of the fundamental plane with the celestial sphere in a given *celestial coordinate system*, from the chosen point. In the *equatorial coordinate system* the fundamental plane is the plane of the Earth's equator; in the *ecliptic coordinate system* it is the plane of the ecliptic; in the *galactic coordinate system* it is the plane of the Milky Way; and in the *horizontal coordinate system* it is the observer's horizon.

- **Declination**

  In the *equatorial* (or *geocentric*) *coordinate system*, the **declination** δ is the **celestial latitude** of a celestial object on the celestial sphere, measured from the celestial equator. Declination is measured in degrees, from $-90°$ to $+90°$.
- **Right ascension**

  In the *equatorial* (or *geocentric*) *coordinate system*, fixed to the stars, the **right ascension** *RA* is the **celestial longitude** of a celestial object on the celestial sphere, measured eastward along the celestial equator from the First point in Aries to the intersection of the hour circle of the celestial object. RA is measured in units of time with 1 h approximately equal to 15°.

  The time needed for one complete cycle of the precession of the equinoxes is called a *Platonic* (or *Great*) *year*); it is 257–258 centuries and slightly decreases. This cycle is important in Astrology. Also, it is close to the Maya calendar's longest cycle—5 *Great Periods* of 5125 years; cf. **distance numbers** in Chap. 29.

  The time (225–250 million Earth years) it takes the Solar System to revolve once around the center of the Milky Way (*Solar circle*) is called the *Galactic year*.
- **Hour angle**

  In the *equatorial* (or *geocentric*) *coordinate system*, fixed to the Earth, the **hour angle** HA is the **celestial longitude** of a celestial object on the celestial sphere, measured along the celestial equator from the observer's meridian to the intersection of the hour circle of the celestial object.

  HA gives the time elapsed since the celestial object's last transit at the observer's meridian (for $HA > 0$), or the time until the next transit (for $HA < 0$).
- **Polar distance (in Geography)**

  In the *equatorial* (or *geocentric*) *coordinate system*, the **polar distance** (or *codeclination*) *PD* is the **colatitude** of a celestial object, i.e., the **angular distance** from the celestial pole to a celestial object on the celestial sphere. Similarly as the **declination** δ, it is measured from the celestial equator: $PD = 90° \pm \delta$. An object on the celestial equator has $PD = 90°$.
- **Ecliptic latitude**

  In the *ecliptic coordinate system*, the **ecliptic latitude** is the **celestial latitude** (in degrees) of a celestial object on the celestial sphere from the ecliptic.

  The object's **ecliptic longitude** is its **celestial longitude** on the celestial sphere measured eastward along the ecliptic from the First point in Aries.
- **Zenith distance**

  In the *horizontal* (or *Alt/Az*) *coordinate system*, the **zenith distance** (or *North polar distance*, *zenith angle*) *ZA* is the object's **colatitude**, measured from the zenith.
- **Altitude**

  In the *horizontal* (or *Alt/Az*) *coordinate system*, the **altitude** *ALT* is the **celestial latitude** of an object from the horizon. It is the complement of the **zenith distance** *ZA*: $ALT = 90° - ZA$. Altitude is measured in degrees.

- **Azimuth**

  In the *horizontal* (or *Alt/Az*) *coordinate system*, the **azimuth** is the **celestial longitude** of an object, measured eastward along the horizon from the North point. Azimuth is measured in degrees, from 0° to 360°.
- **Morning width**

  Morning (or *rise*) **width** is the horizontal angular distance between the rise azimuth of a celestial body and the easterly direction.
- **Elliptic orbit distance**

  The **elliptic orbit distance** is the distance from a body in an elliptical orbit around a central body at a focus to that body. This distance is given by

$$r(\theta) = \frac{a(1-e^2)}{1+e\cos\theta} = a(1-e\cos E),$$

  where a, b are the *semimajor* and *semiminor* axes (halves of the major and minor diameters), e is the *eccentricity* $\sqrt{1-(\frac{b}{a})^2}$, and θ, E are the *true anomaly* (angle between the direction of periapsis and the current position of the body, as seen from the central body) and the *eccentric anomaly* $E = \arccos\frac{e+\cos\theta}{1+e\cos\theta}$. The *mean anomaly* is $F = 1 - e\sin E$. The **orbital distance** is mean $r(\theta)$ over E.

  The **periapsis distance** and **apoapsis distance** are the closest and farthest distances $r_{\min} = r(0) = a(1-e)$ and $r_{\max} = r(\pi) = a(1+e)$.

  For Earth's orbit, $e = 0.01671$; it wire the points at periapsis and apoapsis distances of an elliptical orbit around the Earth, while the *perihelion* and *aphelion* are such points around the Sun. The *periastron* and *apastron* of a double star are the closest and farthest points of the smaller star to its primary. ll reach a minimum, 0.00236, in 0.027 Ma.

  The *near-Earth objects* are asteroids, comets, spacecraft, and large meteoroids whose *perigee* is closer than 1.3 AU; the largest such asteroids are 1036 Ganymede and 433 Eros, about 34 km across. The *perigee* and *apogee* are the points at periapsis and apoapsis distances of an elliptical orbit around the Earth, while the *perihelion* and *aphelion* are such points around the Sun. The *periastron* and *apastron* of a double star are the closest and farthest points of the smaller star to its primary.

  In addition to a, e and F, the other three main parameters required to uniquely identify a *Kepler orbit* (ellipse, parabola, hyperbola, or straight line) are the *orbital inclination* (angle between reference and orbital planes), the *longitude of the ascending node* (angle Ω from a reference direction to the direction of the ascending node, measured in a reference plane), and the *argument of periapsis* (angle ω from the body's ascending node to its periapsis, measured in the direction of motion).

  Sedna, 2012VP113, and other distant detached Kuiper Belt objects exhibit unusual alignment in orbital planes and clustering around $\omega = 0$ if $a > 150$ AU and $\Omega = 113° \pm 13°$ if $a > 250$ AU. Batygin–Brown, 2016, explain it by *resonant coupling* with a hypothetical super-Earth, whose orbit lies in about the

same plane, but perihelion is 180° away from the perihelia of the minor bodies. This *Planet Nine* should have perihelion 200 AU and aphelion 1200 AU; so, $a = 700$ AU.

- **Minimum orbit intersection distance**

  The **minimum orbit intersection distance** (MOID) between two bodies is the distance between the closest points of their gravitational *Kepler orbits*.

  An asteroid or comet is a *potentially hazardous object* (PHO) if its Earth MOID is less than 0.05 AU and its diameter is at least 150 m. Impact with a PHO occurs on average around once per 10,000 years. The only known asteroid whose hazard could be above the background is 1950 DA (of mean diameter 1.2 km) which can, with probability $\frac{1}{300}$, hit Earth on March 16, 2880. Object up to about 25 m in size burn up in the atmosphere, and even the 50 to 80 m objects disintegrate before reaching Earth, although they can create a damaging airburst. The closest known geocentric distance for a comet was 0.0151 AU (Lexell's comet on July 1, 1770).

- **Impact distances**

  After an impact event, the falling debris forms an *ejecta blanket*, i.e., a generally symmetrical apron of ejecta that surrounds crater. About half the volume of ejecta falls within 2 radii from the center of the crater, and over 90 % falls within $\approx$ 5 radii. Beyond it, the debris are discontinuous and are called *distal ejecta*.

  Main parameter of an impact crater is the ratio of *rim-to-floor depth d* to the *rim-to-rim diameter D*. The *simple craters* are small with $\frac{1}{7} \leq \frac{d}{D} \leq \frac{1}{5}$ and a smooth bowl shape. If $D > D_0$, where the *transitional diameter* D_0 scales as the inverse power of the planet's surface gravity, the initially steep crater walls collapse gravitationally downward and inward, forming a complex structure. On Earth, $2 \leq D_0 \leq 4$ km depending on target rock properties; on the Moon, $15 \leq D_0 \leq 20$ km.

  The largest known (diameter of 300 km) and old (2023 Ma ago) *astrobleme* (meteorite impact crater) is Vredefort Dome, 120 km south-west of Johannesburg. It was the world's greatest known single energy release event and largest asteroid known to have impacted the Earth ($\approx$ 10 km). The diameter of MAPCIS crater in Australia is 600 km, but it is not confirmed impact crater.

  Sometimes, the term *impact distance* is used more generally as a **setback distance** from some possible hazard (say, explosion, toxic chemical release, odor from swine facilities) or from the action of some equipment (say, laser, homogenizer); Cf. **standoff distance** and **protective action distance** in Chap. 29.

- **Elongation**

  Elongation (or *digression*) is the angular distance in longitude of a celestial body from another around which it revolves (usually a planet from the Sun).

- **Lunar distance**

  The **lunar distance** is the **angular distance** between the Moon and another celestial object.

  In Astronomy, *new moon* (or *dark moon*) is a lunar phase that occurs at the moment of conjunction in **ecliptic longitude** with the Sun. If, moreover, the Sun,

Moon, and Earth are aligned exactly, a solar eclipse occurs. *Full moon* occurs when the Moon is on the opposite side of the Earth from the Sun. If, moreover, the Sun, Earth, and Moon are aligned exactly, a lunar eclipse occurs.

A *supermoon* (or *perigee-syzygy of the Earth-Moon-Sun system*) is the near-coincidence of a full moon or a new moon with the closest approach the Moon makes to the Earth on its orbit, resulting in its largest apparent size.

- **Sun-Earth-Moon distances**

  The Sun, Earth and Moon have masses 1.99×10^{30}, 5.97×10^{24}, 7.36×10^{22} kg and equatorial radii 695,500, 6378, 1738 km, respectively.

  Earth's axial tilt varies 22.1–24.5° about every 41,000 years, its rotation occurs about every 19,000 years and eccentricity cycles 0.003–0.058 about every 0.1 Ma.

  The Earth and the Moon are at a mean distance of 1 AU $\approx 1.496 \times 10^8$ km from the Sun. This distance increases at the present rate $\approx$ 15 cm per year.

  The Moon, at distance 0.0026 AU ($\approx$ 60 Earth radii $R_\oplus$), is within the **Hill radius** (1,496,000 km) of the Earth, but well outside of the **Roche radius** (9496 km).

  Asimov argued that the Earth-Moon system is a double planet because their diameter and mass ratios ($\approx$4:1 and $\approx$81:1) are smallest for a planet in the Solar System. Also, the Sun's gravitational effect on the Moon is more than twice that of Earth's. But the *barycenter* (common center of mass) of the Earth and Moon lies well inside the Earth, $\approx \frac{3}{4}$ of its radius.

  The Moon has a greater tidal influence on the Earth than the Sun. Because of tidal forces, the Moon is receding from the Earth at $\approx$ 3.8 cm per year. So, Earth's rotation is slowing, and Earth's day increases by $\approx$ 23 s every million years (excluding glacial rebounds). At present rate, the Moon's orbital distance will reach, $\approx$ 1 Ga from now, $67R_\oplus$, and Earth's axial tilt will become chaotic.

- **Opposition distance**

  A *syzygy* is a straight line configuration of three celestial bodies A, B, C. Then, as seen from A, B and C are in *conjunction*, and the passage of B in front of C is called *occultation* if the apparent size of B is larger, and *transit*, otherwise. *Appulse* is the closest approach of B and C as seen from A.

  If B and C are planets orbiting the star A, then C said to be in *opposition* to A, and the distance between B and C (roughly, their closest approach) is called their **opposition distance**. It can vary at different oppositions.

  A *greatest conjunction* is a conjunction of Jupiter and Saturn at or near their opposition to the Sun. The "Star of Bethlehem"—thought by Kepler to have appeared c. 7 BC—was theorized to be such triple conjunction and almost occultation of Saturn by Jupiter. The next such occultation will happen in 7541.

  The closest possible distance between Earth and a planet is 38 million km: the minimal opposition distance with Venus. The closest known approach between exoplanets is 0.0016 AU $\approx$ 240,000 km (by Kepler-70b and Kepler-70c).

  The closest known distance between two stars is 80,000 km in the binary HM Cancri; their orbital period is 5.4 min. The orbital period of exoplanet 2MASS J2126-8140 around a red dwarf star TYC 9486-927-1 takes nearly a million Earth

years. The largest and smallest known orbits of a planet around a single star are 6900 AU (by 2MASS J2126-8140) and 0.006 AU (by Kepler-70b).

- **Planetary aspects**

  In Astrology, an *aspect* is an angle (measured by the **angular distance** of ecliptic longitude, as viewed from Earth) the planets make to each other and other selected points in the *horoscope*, i.e., a chart representing the apparent positions and selected angles of the celestial bodies at the time of an event, say, a person's birth. Astrology claims a link between aspects and events in the human world.

  Major aspects are 1–10° (*conjunction*) and 90° (*square*), 180° (*opposition*) for which an *orb* (error) of 5–10° is usually allowed. Then follow $120 \pm 4°$ (*trine*), $60 \pm 4°$ (*sextile*) and (with orb 2°) 150° (*quincunx*), 45°, 135°, 72°, 144°. Other aspects are based on the division of the zodiac circle by 7, 9, 10, 11, 14, 16 or 24.

- **Primary-satellite distances**

  Consider two celestial bodies: a *primary* M and a smaller one m (a satellite, orbiting around M, or a secondary star, or a comet passing by).

  Let ρ_M, ρ_m and R_M, R_m be the densities and radii of M and m. The **Roche radius** (or *Roche limit*, *tidal radius*) of the pair (M, m) is the maximal distance between them within which m will disintegrate due to the tidal forces of M exceeding the gravitational self-attraction of m. This distance is $\approx 1.26 R_M \sqrt[3]{\frac{\rho_M}{\rho_m}}$ or $\approx 2.423 R_M \sqrt[3]{\frac{\rho_M}{\rho_m}}$ if m is rigid or fluid. The *Roche lobe* of a star is the region of space around the star within which orbiting material is gravitationally bound to it.

  The *tidal locking radius* of M is the distance at which the axial and orbital rotations of m become synchronized, i.e., the same side of m always faces M. The Moon is tidally locked by the Earth. Pluto and Charon are mutually tidally locked.

  Let $d(m, M)$ denote the **mean distance** between m and M, i.e., the arithmetic mean of their maximum and minimum distances; let S_m and S_M denote the masses of m and M. The barycenter of (M, m) is the point (in a focus of their elliptical orbits) where M and m balance and orbit each other. The distance from M to the barycenter is $d(m, M)\frac{S_m}{S_m + S_M}$. For the $(Earth, Moon)$ system, it is 4670 km (1710 km below the Earth's surface). Pluto and Charon, the largest of its five moons, form rather a *binary planet*, since their barycenter lies outside of either body.

  The *Hill sphere* of a body is the region in which it dominates the attraction of satellites. The **Hill radius** of m in the presence of M is $\approx d(m, M)\sqrt[3]{\frac{S_m}{3S_M}}$; within it m can have its own satellites. The Earth's Hill radius is 0.01 AU; in the Solar System, Neptune has the largest Hill radius, 0.775 AU.

  The pair (M, m) can be characterized by five **Lagrange points** L_i, $1 \le i \le 5$, where a third, much smaller body (say, a spacecraft) will be relatively stable because its centrifugal force is equal to the combined gravitational attraction of M and m, i.e., gravitational force of M and m balance out. These points are:

  L_1, L_2, L_3 lying on the line through the centers of M and m, so that $d(L_3, m) = 2d(M, m)$, $d(M, L_2) = d(M, L_1) + d(L_1, m) + d(m, L_2)$, $d(L_1, m) = d(m, L_2)$ (the

satellite SOHO is at the point L_1 of the Sun-Earth system, where the view of the Sun is uninterrupted; the satellites WMAP and Planck are at L_2);

L_4 and L_5 are the points forming equilateral triangles with the centers of M and m. These points are more stable; each of them forms with M and m a partial solution of the unsolved gravitational 3-*body problem*. Objects orbiting at L_4 or L_5 are called *Trojans of Greek* and *Trojan camp*, respectively. The Moon was created 4.5 Ga ago by head-on impact of a Mars-sized Trojan planetoid Theia on the Earth. The only known Sun-Earth Trojan is asteroid 2010 TK7, about 300 m across.

Other instances of the circular restricted 3-body problem are provided by planet–*co-orbital moons* and star–planet–*quasi-satellite* systems. *Co-orbital moons* are natural satellites that orbit at a very similar distance from their parent planet. Only Saturn's system is known to have them; it has three sets.

Orbital resonance occurs when the bodies orbital periods are in a close-to-integer ratio. For example, Pluto-Neptune are in a 2:3 ratio and Jupiter's moons Ganymede-Europa-Io are in a 1:2:4 ratio. Earth and Venus are in a *quasi-resonance* only 0.032 % away from 8:13. A *quasi-satellite* is an object in a 1:1 orbital resonance with its planet that stays close to the planet over many orbital periods. The largest of four known Earth's quasi-satellites is 3753 Cruithne, ≈ 5 km across.

The most tenuously linked long-distance binary in the Solar System is 2001 QW322: two icy bodies ($\approx$ 130 km in diameter) in the Kuiper Belt, at mean distance $> 10^5$ km, orbiting each other at 3 km/h. One of widest binaries is the Alpha Centauri system with Proxima separated from the A/B stars by 15,000 AU.

The elliptic restricted 3-body problem treats the *circumbinary* (orbiting two stars) planets such as Kepler-16b. A planet PH1 was found in a quadruple (binary pair) star system Kepler-64. Systems with up to 5 stars are known; most are triples.

- **Low-energy trajectory**

  The *Hohmann transfer orbit* is an elliptical orbit used to transfer between two circular orbits of different radii in the same plane. Currently, it is the favored method for getting a spacecraft into orbit around its destination. Leaving Earth's atmosphere, the craft makes, at high speed, a beeline for the destination; at approach, it slams on the brakes and starts to orbit the destination. Such a transfer is a highly effective, but it is time-specific and expensive, since it requires much energy.

  A **low-energy** (or *ballistic capture*) **trajectory** is a route in space that allows a spacecraft to change orbits using very little fuel. In such transfer to a planet, the craft is launched out ahead of the planet's orbital path. It would gradually slow and hold in place, waiting for the planet to swing by—the gravity of the planet pulls it into its orbit. Such transfers are very slow, and useful only for automated probes.

  Low-energy transfers follow the *Interplanetary Transport Network* (*ITN*), i.e., a collection of gravitationally determined pathways through the Solar System that

require very little energy (fuel) for an object to follow. The ITN uses **Lagrange points** as locations where trajectories are redirected using little or no energy.

- **Dynamical spacing**

  Let M, m_1, m_2 be the masses of a star and two adjacent planets orbiting it with semimajor axes a_1 and a_2. The *mutual Hill radius* of two planets is

$$R_H = \frac{a_1 + a_2}{2} \sqrt[3]{\frac{m_1 + m_2}{3M}}$$

  and their **dynamical spacing** is (Gladman, 1993; Chambers et al., 1996)

$$\Delta = \frac{|a_2 - a_1|}{R_H}$$

  .

  Fang–Margot, 2013, claim that on average $\Delta = 21.7$, and $\Delta < 10$ leads to instability in giga-year time span. In the Solar System, $\Delta > 26$ for terrestrial planets.

- **Titius–Bode law**

  The **Titius–Bode law**, 1766, is an empirical rule approximating the mean distance d_i of i-th planet from the Sun (its orbital *semimajor axis*) by $\frac{3k+4}{10}$ AU.

  Here 1 AU $\approx 1.5 \times 10^8$ km and $k_1 = 0 = 2^{-\infty}$ (for Mercury), $k_i = 2^{i-2}$ for $i \geq 2$, i.e., Venus, Earth, Mars, Ceres (the largest one in the Asteroid Belt, $\approx \frac{1}{3}$ of its mass), Jupiter, Saturn, Uranus, Pluto. (But Neptune does not fit in the law while Pluto fits Neptune's spot $k = 2^7$.) The best fit for the form (Wurm, 1787) $d_i = AC^{i-2} + B$ is given by $C \approx 1.925, A \approx 0.334, B = 0.382$. Cf. **elliptic orbit distance**.

  In the Solar System, the period ratios between adjacent orbits scatter around the dominant 5 : 2 ratio; it is 3 : 2 for Earth-Venus and 2 : 1 for Mars-Earth.

  A *generalized Titius–Bode relation* $d_i = AC^i$ for some A, C fits even better for many other exoplanet systems showing such preference towards near mean motion resonance; cf. **dynamical spacing**. It helps to locate undetected exoplanets.

  Hamano et al., 2013, claim that between 108 (as Venus) and 150 (as Earth) million km from the Sun, there is a critical distance explaining their difference. Venus has a similar size and bulk composition to those of Earth, but it lacks water. Earth solidified from its molten magma state within several million years, trapping water in rock and under its hard surface, while Venus got more of the Sun's heat and remained in molten state for ≈ 100 Ma giving time for any water to escape.

- **Planetary distance ladder**

  The scale of interstellar-medium dust, *chondrules* (round grains found in stony meteorites, the oldest solid material in the Solar System), *boulders* (rock with grain size of diameter ≥ 256 mm), *planetesimals* (kilometer-sized solid objects

in protoplanetary disks) and *protoplanets* (internally melted Moon-to-Mars-sized planetary embryos) is 10^{-6}, 10^{-3}, 10^{0}, 10^{3} and 10^{6} m.

In the Solar System's protoplanetary gas/dust disk, the binary electrostatic coagulation of dust/ice grains resulted in the creation, of planetesimals. Then gravity took over the accretion process. The growth was *runaway* (when $T_1 < T_2$, for growth time scales of the first and second most-massive bodies) at first and then (with $T_1 > T_2$ at some *transition radius*) it became *oligarchic*. A few tens of protoplanets were formed and then, by giant impacts, they were transformed into Earth and the other rocky planets. The process took $\approx$ 90 Ma from $\approx$ 4.57 to $\approx$ 4.48 Ga ago.

Brilliantov et al., 2015: if a system is comprised of particles that, colliding, can merge at low velocities and break at large velocities, the size distribution of particles abundance follow the inverse cubes law. Rare collisions of fast particles lead to a balance between aggregation and fragmentation. It explained Saturn's rings.

- **Potato radius**

  The basic shape-types of objects in the Universe are: an irregular dust, rounded "potatoes" (asteroids, icy moons), spheres (planets, stars, black holes), disks (Saturn's rings, galactic disks) and halos (elliptic galaxies, globular star clusters).

  At mean radius $R <$ few km, objects (dust, crystals, life forms) have irregular shape dominated by nonmass-dependent electronic forces. Solid objects with $R >$ 200–300 km are gravity-dominated spheres. If both energy E and angular momentum L are exported (by some dissipative processes), the object, if large enough, collapses into a sphere. If only E is exported, the shape is a disk. If neither E, nor L is exported, the shape is a *halo*, i.e., the body is spheroidal.

  If R ($R >$ few km) increases, there is a smooth size-dependent transition to more and more rounded potatoes until $\approx$200–300 km, where gravity begins to dominate. Ignoring surface tension, erosion and impact fragmentation, the potato shape comes mainly from a compromise between electronic forces and gravity. It also depends on the density and the structural yield strength of the (rocky or icy) material.

  Lineweaver and Norman, 2010, define the **potato radius** R_{pot} as this potato-to-sphere transition radius. They derived $R_{pot} = 300$ km for asteroids (Vesta, Pallas, Ceres have mean radius $R = 265, 275, 475$ km, respectively) and $R_{pot} = 200$ km for icy moons (Hyperion, Mimas, Miranda have $R = 135, 198, 235$ km, respectively). Mimas is the smallest body in the Solar System to be rounded, while Hyperion is the largest nonspherical one; their masses are 3.75×10^{19} and 5.62×10^{18} kg.

  In 2006, the IAU (International Astronomical Union) defined a *planet* as a orbiting body which has sufficient mass for its self-gravity to overcome rigid body forces so that it assumes a *hydrostatic equilibrium* (nearly round) shape and cleared the neighborhood around its orbit. If the body has not cleared its neighborhood, it is called a *dwarf planet*. The potato radius, at which self-gravity makes internal overburden pressures equal to the yield strengths of the material, marks the boundary of hydrostatic equilibrium used in above IAU definition.

Buchhave et al., 2014: planets smaller than 1.7 Earths are likely to be completely rocky, while those larger than 3.9 Earths are probably gas giants.

- **Frost line (in Astrophysics)**

  In Astrophysics, by analogy with **frost line (in Earth Science)**, the **frost** (or *snow*, *ice*) **line** is the distance from a star (or a nebula's protostar) where hydrogen compounds such as water, ammonia, methane condense into ice grains. It separates an inner region of rocky objects from an outer region of icy objects.

  Water and methane condensate at 180 K and 40 K, respectively. Sun's water-frost and methane-frost lines are roughly at 2.7 AU and 48 AU, i.e., in the Asteroid Belt (between the orbits of Mars and Jupiter) and the Kuiper Belt (at 30–55 AU). On the other hand, inside of $\approx$ 0.1 AU, rocky grains cannot exist: dust evaporates.

  Martin and Livio, 2012, claim that a giant planet like Jupiter should be in the right location outside of the frost line to produce an asteroid belt of the appropriate size, offering the potential for life on a nearby rocky planet like Earth.

- **Solar distances**

  Following a supernova explosion 4570 Ma ago in our galactic neighborhood, the Sun was formed 4567 Ma ago by rapid gravitational collapse of a fragment (about 1 parsec across) of a giant (about 20 parsecs) hydrogen molecular cloud.

  The mean distance of the Sun from Earth is 1 AU $\approx 1.496 \times 10^8$ km. The mean distance of the Sun from the Milky Way core is 27,200 light-years.

  The Sun is more massive than 95 % of nearby stars and its orbit around the Galaxy is less eccentric than $\approx$ 93 % of similar (i.e., of spectral types F, G, K) stars within 40 parsecs. The Sun's mass (99.86 % of the Solar System) is $\approx 1.988 \times 10^{30}$ kg.

  The Sun's radius is 6.955×10^5 km; it is measured from its center to the edge of the *photosphere* ($\approx$ 500 km thick layer below which the Sun is opaque to visible light). The Sun will expand $\approx$ 256 times in 7–8 Ga and then become a white dwarf.

  The Sun does not have a definite boundary, but it has a well-defined interior structure: the *core* extending from the center to $\approx$ 0.2 solar radii, the *radiative zone* at $\approx$0.2–0.8 solar radii, where thermal radiation is sufficient to transfer the intense heat of the core outward, the *tachocline* (transition layer) and the *convection zone*, where thermal columns carry hot material to the surface (photosphere) of the Sun.

  The principal zones of the *solar atmosphere* (the parts above the photosphere) are: temperature minimum, chromosphere, transition region, corona, and heliosphere.

  The *chromosphere*, a $\approx$ 3000 km deep layer, is more visually transparent. The *corona* is a highly rarefied region continually varying in size/shape; it is visible only during a total solar eclipse. The chromosphere-corona region is much hotter than the Sun's surface. Extending further, the corona becomes the *solar wind*, a very thin gas of charged particles that travels through the Solar System.

  The *heliosphere* is the teardrop-shaped region around the Sun created by the solar wind and filled with solar magnetic fields and outward-moving gas.

It extends from $\approx$ 20 solar radii (0.1 AU) outward 86–100 AU past the orbit of Pluto to the *heliopause*, its outermost edge, where the interstellar medium and solar wind pressures balance. The interstellar medium and solar wind are moving supersonically in opposite directions, towards and away from the Sun. The points, $\approx$ 80 AU and $\approx$ 230 AU from the Sun, where the solar wind and interstellar medium become subsonic, are the *termination shock* and *bow shock*, respectively.

The *tidal truncation radius* (100,000–200,000 AU, say, $\approx$ 2 ly from the Sun) is the outer limit of the *Oort Cloud*. It is the boundary of the Solar System, i.e., Sun's *Hill/Roche sphere*, where its gravity is overtaken by the galactic tidal force.

- **Dyson radius**

  The **Dyson radius** of a star is the radius of a hypothetical *Dyson sphere* around it, i.e., a megastructure (say, a system of orbiting star-powered satellites) meant to completely encompass a star and capture a large part of its energy output. The solar energy, available at distance d (measured in AU) from the Sun, is $\frac{1366}{d^2}$ watts/m^2. The inner surface of the sphere is intended to be used as a habitat.

  For example, at Dyson radius 300×10^6 km from the Sun a continuous structure with ambient temperature 20 °C (on the inner surface) and efficiency 3 % of power generation (by a heat flux to -3 °C on the outer surface) is conceivable.

- **Star's radii**

  The **corotation radius** of a star is the distance from it where the centrifugal force on a particle corotating with it balances the gravitational attraction, i.e., the accretion disk rotates at the same angular velocity as the star.

  The **Bondi-Hoyle accretion radius** is the radius where star's gravitational energy is larger than the kinetic energy and, so, at which material is bound to star.

  The **Hayashi radius** (or *Hayashi limit*) of a star is its maximum radius for a given mass. A star within *hydrostatic equilibrium* (where the inward force of gravity is matched by the outward pressure of the gas) cannot exceed this radius.

  The **Eddington radius** (or *Eddington limit*) of a star is the radius where the gravitational force inwards equals the continuum radiation force outwards, assuming hydrostatic equilibrium and spherical symmetry. A star exceeding it would initiate a very intense continuum driven stellar wind from its outer layers.

  The largest and smallest known stars, the red hypergiant UY Scuti and red dwarf OGLE-TR-122b, have respective radii 1708 ± 192 and 0.12 solar radii.

- **Galactocentric distance**

  A star's **galactocentric distance** (or *galactocentric radius*) is its **range distance** from the galactic center; it may also refer to a distance between two galaxies. The *galactic anticenter* is the point lying opposite, for an observer on Earth, this center.

  The Sun's present galactocentric distance is nearly fixed $\approx$ 8.4 kiloparsec, i.e., 27,400 light-years, but it may have been 2.5–5 kpc in the past. *Einasto's*

law, 1963, claims that the density $\rho(r)$ of a spherical stellar system (say, a galaxy or its halo) varies as $\exp(-Ar^{\alpha})$, where r is the distance from the center.

- **M31–M33 bridge**

  Braun and Thilker, 2004, discovered that the distance 782,000 light-years between Andromeda (M31) and Triangulum (M33) galaxies is spanned by a link consisting of about 500 million Sun's masses of ionized hydrogen.

  A third of all baryonic matter is in stars and galaxies; another $\frac{1}{3}$ is diffuse and thought to be in filamentary networks spread through space. Remaining $\frac{1}{3}$, called *warm-hot intergalactic medium* (WHIM), is expected to be of intermediate density. The **M31–M33 bridge** consists of WHIM, the first evidence of this medium. Such WHIM bridges are likely remnants of collisions between galaxies.

- **Radii of a star system**

  Given a star system, say, a galaxy or a *globular cluster* (a spherical collection of stars that orbits a galactic core as a satellite), its **half-light radius** (or **effective radius**) hr is the distance from the core within which half the total luminosity from the system, assumed to be circularly symmetric, is received. The **core radius** cr is the distance at which the apparent surface luminosity has dropped by half; so, $cr \leq hr$. If the luminosity profile rises steeply to a break, and then more slowly, we have the **break radius**. In general, **isophotal radius** is the size attributed to the system corresponding to a particular level of surface brightness.

  The **half-mass radius** $r_{0.5}$ is the radius from the core that contains half the total mass of the system. In general, the *Lagrangian radii* are the distances from the center at which various percentages of the total mass are enclosed.

  The **tidal radius** of a globular cluster is the distance from its center at which the external gravitation of the galaxy has more influence over the stars in the cluster than does the cluster itself.

  Unlike a star cluster, all galaxies are filled with and surrounded by a halo of dark matter acting (via gravity) as a sort of glue within and between galaxies. Thin tendrils of dark matter connect nodes of galaxy clusters, creating a cosmic web.

  The **virial radius** R_{vir} of a galaxy is the radius centered on it containing matter at 200 (sometimes, $18\pi^2 \approx 178$ or 130) times the critical (or, mean) density of the Universe. The mass within R_{vir} is a measure of the total mass inside a dark matter halo. Kravtsov, 2011, claim that $r_{0.5} \approx 0.015R_{vir}$. Also, Harris, 2013, explains speed anomalies of Earth's satellites by 0.005–008 % increase of its mass due to a dark matter's disk, 191 km thick and 70,000 km across, around the equator.

  The **Abell radius** of a cluster is $\frac{1.72}{z}$ arcminutes, where z is the cluster's redshift. At least 50 cluster's members should lie within this radius of its centre.

- **Habitable zone radii**

  A maximally Earth-like mean temperature is expected at the distance $\sqrt{\frac{L_{star}}{L_{sun}}}$ AU from a star, where L is the total radiant energy.

  The **habitable zone radii** of a star are the minimal and maximal orbital radii r, R such that liquid water may exist on a *terrestrial* (i.e., primarily composed of

silicate rocks or metals) planet orbiting within this range, so that life, constructed from carbon and reliant on liquid water, could develop there in a similar way as on the early Earth. For Sun, $[r,\ R]$ is [0.99, 1.70]; AU; it includes Earth and Mars. It moves outwards, according to Rushby et al., 2012, 0.1 Au every billion years. For best candidates—orange dwarf stars—HZ is within [0.5, 1] AU.

The **Kasting distance** (or *habitable zone distance*) of an exoplanet, at distance d from its star, is an index defined by

$$HZD(d) = \frac{2d - (R + r)}{R - r}.$$

So, $-1 \leq HZD(d) \leq 1$ correspond to $r \leq d \leq R$.

The above notion of surface habitability is modeled from temperature/humidity; the edges r, R of HZ are determined by loss of water and, respectively, by the maximum greenhouse provided by a CO_2 atmosphere. Among known exoplanets of 2–10 Earth's mass of our galaxy, good candidates for Earth-like habitability are GJ 667Cc, HD-85512b, Kepler-438b (24, 36, 470 ly away) orbiting, respectively, stars Gliese 667C, Gliese 370, Kepler-438 in the constellations Scorpius, Vela, Lyra.

Habitable zones are 10–14 times wider for subsurface life. Protected inside a warm mineral-rich rocks, it can be much more typical than Earth's surface life.

Instead of zones, habitability can be defined in terms of, say, geothermal vents on ocean floor, as on Saturn's moon Enceladus.

Petigra et al., 2013: *eta-Earth* of our galaxy, i.e., fraction of Sun-like stars with an *Earth-size* (1–2 Earth's radii) planet orbiting in habitable zones, is $22 \pm 8\,\%$, depending on the definition of HZ. There could be 4×10^{10} habitable Earth-size planets in the Milky Way with the nearest one being within 12 ly.

Our *galactic habitable zone* is (Lineweaver et al., 2004) a slowly expanding region between 7 and 9 kpc of **galactocentric distance**; so, the minimal and maximal radii are 22,000 and 28,000 ly. They used four prerequisites for complex life: the presence of a host star, enough heavy elements to form terrestrial planets, sufficient time (4 ± 1 Ga) for biological evolution and an supernovae-free environment.

Di Stefano et al., 2015, claim that the globular clusters (there are about 160 in Milky Way) could be best places to look for space-faring civilizations.

Most life-friendly are giant elliptical galaxies: their low rate of star formation means less supernovae and gamma bursts. Dwarf irregular galaxies are the least hospitable.

Behroozi–Peeples, 2015, claim that the Hubble volume, $\sim 10\ \mathrm{Mpc}^3$, contains $\sim 10^{20}$ Earth-like planets, $\sim 10^{21}$ will be formed in 100 Gyr to 1 Tyr from now and the likehood of us being the only civilisation the Universe will ever have is $< 8\,\%$.

- **Earth similarity index**

  The **Earth similarity index** of a planet P is (Schulze-Makuch et al., 2011):

$$ESI(P) = \prod_{i=1}^{n}(1 - |\frac{x_i(P) - x_i(E)}{x_i(P) + x_i(E)}|)^{\frac{w_i}{n}},$$

  where $x_i(P)$ is a planetary parameter (including surface temperature, escape velocity, mean radius, bulk density), $x_i(E)$ is the reference value for Earth (i.e., 14.85° C, 1,1,1), w_i is a weight (5.58, 0.70, 0.57, 1.07) and n is the number of parameters. ESI(P)= 1, 0.88, 0.85, 0.84, 0.70 for Earth, Kepler-438b, Kepler-296e, GJ 667Cc and Mars. Many exomoons and unconfirmed NASA Kepler candidates rank within $[0.76, 0.96]$. Terrestrial, but only simple extremophilic, life might be possible if ESI(P)> 0.6, while plants/animals may require > 0.8.

  The same authors proposed a *planetary habitability index* based on the presence of a stable substrate, atmosphere, magnetic field, available energy, appropriate chemistry and the potential for holding a liquid solvent, such as 100-km deep ocean beneath the surface of Jupiter's moon Europa and hydrocarbon lakes on Saturn's moon Titan. Unicellular life has been found in the most adverse conditions on Earth. So, the presence of extremophiles on Mars and, with very different biochemistry, on Europa and Titan is plausible. For primary producers (say, plants and cyanobacteria), Earth was more habitable 500 Ma ago, with less seasonal ice and deserts.

  Barnes et al., 2015, habitability index for star-transiting planet, observed by Kepler telescope, is based on orbital period, *transit depth* (planet-star ratio of areas), transit duration and host star's surface gravity, radius and effective temperature.

  Observing oxygen in a planet's atmosphere will indicate photosynthetic life since the photosynthesis is the only known process able to release O_2 in any real quantity. But the importance of oxygen and carbon can be a peculiarity of Earth life. For Oze et al., 2012, low (< 40) hydrogen/methane ratio indicate that life is likely present. Also, infrared, or heat, radiation can indicate an alien civilization.

- **SETI detection ranges**

  SETI (Search for Extra Terrestrial Intelligence) involves using radio telescopes to search for a possible alien radio transmission. The recorded signals are mostly random noise but in 1977 a strong signal (called WOW!) was received at $\leq$ 10 kHz of the frequency $\approx$1420.406 MHz (21 cm) of the hydrogen line. Also, a puzzling radio source SHGb02+14a was observed three times in 2003 at $\approx$1420 MHz.

  SETI detection ranges are the maximal distances over which detection is still possible using given frequency, antenna dish size, receiver bandwidth, etc. They are low for broadband signals from Earth (from 0.007 AU for AM radio up to 5.4 AU for EM radio) but reach 720 light-years for the S-Band of the world's largest (with dish's diameter 305 m) single-aperture radio telescope at Arecibo.

SETI searches in the microwave window 1–10 GHz (the part of the radio spectrum that can pass through the atmosphere), especially around the "waterhole" 1420–1666 MHz (21–18 cm) between hydrogen, H, and hydroxyl, OH.

All known signals with spectral width < 5 Hz arise from artificial sources; so, such extraterrestrial signal will indicate an intelligent civilization. SETI searched those narrow band signals in L-band (1.1–1.9 GHz) from 86 stars in the Kepler field of view hosting most life-promising exoplanets, but not found none. Tarter et al., 2013, deduce from it that the number of *Kardashev type II* (using all energy from their star; our total power consumption today is $\approx 0.01\,\%$ of the sunlight falling on Earth) civilizations in the Milky Way loud in L-band, is less than 1 in a million per sun-like star. The volume V of our galaxy is about $\pi(50{,}000^2)1000 \approx 7.9 \times 10^{12}$ (ly)^3. If N civilizations are distributed there uniformly with spacing d, then $d^3 = \frac{V}{N}$.

Active SETI (or *METI*) consists of sending radio or optical signals into space hoping that they will be picked up by an alien intelligence. The first radio signals from Earth to reach space were produced around 1940 but TV and radio signals decompose into static within 1–2 ly. In 1974 Arecibo telescope sent an elaborate radio signal aimed at the star cluster M13 located 25,000 ly away.

About the perceived risk of revealing the location of the Earth to an alien civilization, METI enthusiasts reply that an advanced civilization within a radius of 100 ly already knows of our existence due to electromagnetic signals leaking from TV, radio and radar. But now, with digital transmissions replacing analogue ones and virtually no radiation escaping into outer space, the Earth become electronically invisible to aliens. Still, a civilization even slightly more advanced than ours could detect the lights of our big cities from up to 500 light years away, using its sun as a gravitational lens. Also, some life (plants, lichens, algae, bacterial mats) can be recognized by its light signature from space.

Besides radio signals and light, nonmicrobial alien life can be discovered by analyzing the output of methane or oxygen in the atmosphere of exoplanets.

- **Voyager 1 distance**

  The Voyager 1 is a 722-kg robotic space probe launched by NASA in 1977; it has power to operate its radio transmitters until 2025 but only 69 kB of memory.

  It is currently the farthest man-made object from Earth, the first probe to leave the Solar System (in 2012) and the fastest probe (moving at $\approx$ 17 km/s or 3.6 AU/year). As of January 2016, **Voyager 1 distance** from Earth was 2.1×10^{10} km ≈ 134.4 AU, while for Voyager 2, it was ≈ 110.9 AU.

  Voyager 1 is moving now, until at least 2025, through a special region of interstellar space where magnetic fields are rotated away from true magnetic north.

  The NASA *Juno* spacecraft to Jupiter holds from 2016 solar power distance record. Its maximum distance from the Sun will be about 832 million km.

  Even though the NASA *New Horizons* was launched (in 2006, to see Pluto and Kuiper Belt) far faster, it will never be more distant from Earth than Voyager 1. Close flybys of Saturn and Titan gave Voyager 1 an advantage with their gravity assist. In 2038, New Horizons will reach, at 13 km/s, the distance of 100 AU.

The Earth-Moon distance ($\approx$ 1.28 light-seconds) can be covered, with current technologies, in $\approx$ 8 h. The distance from Earth to other planets ranges from 3 light-minutes to $\approx$ 4 light-hours. At Voyager 1's current rate, a journey to Proxima Centauri (the nearest known star, 4.24 ly away) would take 72,000 years.

Interstellar travel will be possible only with new technology, say, beamed-light sails, hydrogen-fuelled ramjet, nuclear pulse propulsion, warp drive, wormholes.

Human spaceflight beyond the close neighborhood in the Solar System looks, as now, unlikely, because of duration, cost and health threat due to microgravity, radiation and isolation. Also, long (more than a month) sojourns in space produce potentially serious brain anomalies and severe eyesight problems.

- **Earth in space**

  The Earth, spinning 0.5 km/s, orbits the Sun at 30 km/s. The Sun orbits the galactic center at 219 km/s and it moves at 16.5 km/s, with respect to the motion of its galactic neighborhood, towards Vega, a star in the constellation Lyra. There are 45 stars within 15 ly of the Solar System, the nearest one at 4.24 ly.

  The *Local Bubble* is a cavity, 300–800 ly across (with hydrogen density 0.05 atoms per cm^3, one tenth of the galactic density) in the *Local* (or *Orion-Cygnus*) *Arm* of the Milky Way. The Solar System has been traveling through this Bubble for the last 5–10 Ma and is located now close to its inner rim, about half-way along the Arm's length. From 0.044 to 0.15 Ma ago and for another 0.01–0.02 Ma, the Sun is traversing the *Local Interstellar Cloud* 30 ly across at 23 km/s.

  The Milky Way (0.1 Mly across and 1 kly thick) and Andromeda galaxies are 2.5 Mly apart and are approaching at 100–140 km/s. In $4 + 1.3 + 0.1$ Ga (3 consecutive collisions) they will merge to form the *Milkomeda*, new elliptical galaxy in which our Solar System would remain intact but Sun's **galactocentric distance** will be 0.16 Mly. Their stars will not collide but central black holes will merge.

  Our *Local Group* (LG) is a *poor* (small and not centered) cluster, 10 Mly across, consisting of Andromeda (M31), Milky Way (MW), Triangulum and about 50 small galaxies. It lies in the outskirts (on a small filament connecting the Fornax and Virgo clusters) of our small Local Supercluster (LSC), 110 Mly across and with a mass 10^{15} suns. The number of galaxies per unit volume, in the LSC, falls off with the square of the distance from its center, near the Virgo cluster.

  Tully and Courtois, 2014, defined superclusters (by analogy with drainage basins in Hydrology) via the relative velocities of galaxies: within a given supercluster, all galaxy motions will be directed inward, toward the center of mass. By new definition, LSC, Pavo-Indus Supercluster and Hydra-Centaurus Supercluster, containing *Great Attractor* (GrAt), formtogether "truly local" Supercluster, called *Laniakea*. Laniakea, about of diameter 520 Mly and mass 10^{17} suns, is centered in GrAt, toward which all its galaxies are moving at 630 km/s.

  The *Extended Local Group* is the LG plus the "nearby" (3.9 Mpc) Maffei and Sculptor groups. It belongs to our *Local Filament* (LF, or *Coma-Sculptor Cloud*), a branch of the Fornax-Virgo filament of the LSC.

The LF bounds the *Local Void* (LV), extending 60 Mpc from the edge of the LG. The *Local Sheet* (LS) is all LF's matter within 7 Mpc. The Milky Way and Andromeda are encircled by 12 large galaxies arranged in a ring about 24-Mly across.

With respect to the CMBR (cosmic microwave background radiation) filling the Universe almost uniformly, the Solar System, Milky Way, and LG velocities are 369, 600, 627 km/s. *Peculiar velocities* V_{pec} are the deviations from the Hubble expansion, i.e., $V_{pec} = V_{obs} - H_0 d$, where V_{obs} is the observed velocity, d is the distance and H_0 is the Hubble constant, $\approx$ 72 km/s for every Mpc. The Hubble flow, dominating at large distances, is negated by gravity at smaller distances; for example, its recession velocity is $<$ 1 mm/s at the edge of the Solar System.

According to Tully et al., 2007, the Local Sheet is moving as a unit with low internal dispersion; the LG moves at only 66 km/s with respect to the LS. The bulk flow of the LS is sharply discontinuous from the flows of other nearby structures. The vector of this flow has, with respect to the CMBR, amplitude 631 km/s. It can be decomposed into a vector sum of three quasi-orthogonal components: *local* (259 km/s away from the center of the Local Void), *intermediate* (185 km/s to the Virgo cluster) and *large* (455 km/s towards the *Great Attractor* (GrAt)).

All matter within 4.6 Mpc moves away from the Local Void at 268 km/s. It will collide, in $\approx$ 10 Ga, with the nearest adjacent filament, the Leo Spur. The Local Sheet moves toward the Virgo cluster, at the distance 17 Mpc. All matter within 50 Mpc moves at 600 km/s towards overdensities at 200 Mly (GrAt dominated by the Norma cluster) and 600 Mly (Shapley supercluster, roughly behind GrAt). Lebeskind et al., 2015, claim that a dark matter bridge of some 2000 galaxies, bound by voids, stretches from our Local Group to Virgo cluster.

Chapter 26
Distances in Cosmology and Theory of Relativity

26.1 Distances in Cosmology

The *Universe* is defined as the whole space-time continuum in which we exist, together with all the energy and matter within it.

Cosmology is the study of the large-scale structure of the Universe. Specific cosmological questions of interest include the *isotropy* of the Universe (on the largest scales, the Universe looks the same in all directions, i.e., is invariant to rotations), the *homogeneousness* of the Universe (any measurable property of the Universe is the same everywhere, i.e., it is invariant to translations), the density of the Universe, the equality of matter and antimatter, and the origin of density fluctuations in galaxies.

Hubble, 1929, discovered that all galaxies have a positive *redshift*, i.e., all galaxies, except for a few nearby galaxies like Andromeda, are receding from the Milky Way. By the Copernican principle (that we are not at a special place in the Universe), we deduce that all galaxies are receding from each other, i.e., we live in an expanding Universe, and the further a galaxy is away from us, the faster it is moving away (this is now called the *Hubble law*). The *Hubble flow* is the general outward movement of galaxies and clusters of galaxies resulting from the expansion of the Universe. It occurs radially away from the observer, and obeys the Hubble law. The gravitation in galaxies can overcome this expansion, but the clusters and superclusters (largest gravitationally bound objects) only slow the rate of their expansion.

In Cosmology, the prevailing scientific theory about the early development and shape of the Universe is the *Big Bang Theory*. The observation that galaxies appear to be receding from each other, combined with the General Theory of Relativity, leads to the construction that, as one goes back in time, the Universe becomes increasingly hot and dense, then leads to a gravitational singularity, at which all distances become zero, and temperatures and pressures become infinite.

© Springer-Verlag Berlin Heidelberg 2016

M.M. Deza, E. Deza, *Encyclopedia of Distances*,
DOI 10.1007/978-3-662-52844-0_26

The term *Big Bang* is used to refer to a hypothesized point in time when the observed expansion of the Universe began. Based on measurements of this expansion, it is currently believed that the Universe has an age of $\approx$ 13.82 Ga (billion years).

In Cosmology (or, more exactly, *astrometry*, the study of the positions, distances between, and motions of astronomical objects) there are many ways to specify the distance between two points, because in the expanding Universe, the distances between comoving objects are constantly changing, and Earth-bound observers look back in time as they look out in distance. But all distance measures somehow measure the separation between events on *radial null trajectories*, i.e., trajectories of photons which terminate at the observer. In general, the **cosmological distance** is a distance far beyond the boundaries of our Galaxy.

The geometry of the Universe is determined by several *cosmological parameters*: the *cosmic scale factor a*, the *Hubble constant H*, the *density* ρ and the *critical density* ρ_{crit} (the density required for the Universe to stop expansion and, eventually, collapse back onto itself), the *cosmological constant* Λ, the *curvature k of the Universe*. Many of these quantities are related under the assumptions of a given *cosmological model*. The most common cosmological models are the closed and open *Friedmann–Lemaître cosmological models* and the *Einstein–de Sitter cosmological model*.

This model assumes a homogeneous, isotropic, constant curvature Universe with zero cosmological constant Λ and pressure p. For constant mass M of the Universe, $H^2 = \frac{8}{3}\pi G\rho$, $t = \frac{2}{3}H^{-1}$, $a = \frac{1}{R_C}(\frac{9GM}{2})^{\frac{1}{3}}t^{\frac{2}{3}}$, where $G = 6.67 \times 10^{-11}\,\mathrm{m^3\,kg^{-1}\,s^{-2}}$ is the *gravitational constant*, $R_C = |k|^{-\frac{1}{2}}$ is the *radius of curvature*, and t is the age of the Universe.

The **scale factor** $a = a(t)$ is an expansion parameter, relating the size of the Universe $R = R(t)$ at time t to its size $R_0 = R(t_0)$ at time t_0 by $R = aR_0$.

The *Hubble constant H* is the constant of proportionality between the speed of expansion v and the size of the Universe R, i.e., $v = HR$. This equality is just the *Hubble law* with the Hubble constant $H = \frac{a'(t)}{a(t)}$. This is a linear redshift-distance relationship, where redshift is interpreted as recessional velocity v, typically expressed in km/s.

The current value of the Hubble constant is $H_0 = 71 \pm 4\,\mathrm{km\,s^{-1}\,Mpc^{-1}}$, where the subscript 0 refers to the present epoch because H changes with time. The *Hubble time* and the **Hubble distance** are defined by $t_H = \frac{1}{H_0} \approx 13.82$ Ga and $D_H = \frac{c}{H_0} \approx 4.24$ Gpc. The *Hubble volume* (or *Hubble sphere*) is the region, about 10^{13} Mpc^3, of the Universe surrounding an observer beyond which the recessional velocity exceeds the speed c of light, i.e., any object beyond *particle horizon* (4.4×10^{26} m = 47 light-Ga), is receding (due to the expansion of the Universe itself) at a rate greater than c.

The volume of observable Universe is the volume $\approx 4.1 \times 10^{34}$ cubic light-years, or $\approx 3.4 \times 10^{80}\,\mathrm{m}^3$, of Universe with a comoving size of $\frac{c}{H_0}$, i.e., a sphere with radius $\approx$ 14 Gpc (about 3 times larger than that of Hubble volume). It has mass $\approx 1.6 \times 10^{53}$ kg and contains $\approx 10^{23}$ stars (in at least 8×10^{10} galaxies) and $\approx 10^{80}$ atoms.

The mass density ρ (ρ_0 in the present epoch) and the value of the cosmological constant Λ are dynamical properties of the Universe; today $\rho \sim 9.47 \times 10^{-27}$ kg m^{-3} and $\Lambda \sim 10^{-52}$ m^{-2}. They can be made into dimensionless parameters Ω_M and Ω_Λ by $\Omega_M = \frac{8\pi G\rho_0}{3H_0^3}$, $\Omega_\Lambda = \frac{\Lambda}{3H_0^3}$. A third parameter $\Omega_R = 1 - \Omega_M - \Omega_\Lambda$ measures the "curvature of space". These parameters determine the geometry of the Universe if it is homogeneous, isotropic, and matter-dominated.

The velocity of a galaxy is measured by the *Doppler effect*, i.e., the fact that light emitted from a source is shifted in wavelength by the motion of the source. (The Doppler shift is reversed in some *metamaterials*: a light source moving toward an observer appears to reduce its frequency.) A relativistic form of the Doppler shift exists for objects traveling very quickly, and is given by $\frac{\lambda_{obser}}{\lambda_{emit}} = \sqrt{\frac{c+v}{c-v}}$, where λ_{emit} is the emitted wavelength, and λ_{obser} is the shifted (observed) wavelength. The change in wavelength with respect to the source at rest is called the *redshift* (if moving away), and is denoted by the letter z. The relativistic redshift z for a particle is given by $z = \frac{\Delta\lambda_{obser}}{\lambda_{emit}} = \frac{\lambda_{obser}}{\lambda_{emit}} - 1 = \sqrt{\frac{c+v}{c-v}} - 1$.

The cosmological redshift is directly related to the scale factor $a = a(t)$: $z + 1 = \frac{a(t_o)}{a(t_e)}$. Here $a(t_o)$ is the value of the scale factor at the time the light from the object is observed, and $a(t_e)$ is its value at the time it was emitted. It is usually chosen $a(t_o) = 1$, where t_o is the present age of the Universe.

- **Metric expansion of space**

  The **metric expansion of space** is the averaged increase of measured distances between objects in the Universe with time.

  It is not a motion of space and not a motion into pre-existing space. Only distances expand (and contract). The expansion has no center: all distances increase by the same factor, and every observer sees the same expanding cosmos. The observed *Hubble law* quantifies expansion from an observer. Expansion rate between two points in free space 1 m apart is 2.2×10^{-18} m/s.

  The mean distances between widely separated galaxies increase by $\approx$ 1 % every 140 million years. **FLRW metric** models, at large (superclusters of galaxies) scale, this expansion. On the scales of galaxies, there is no expansion since the metric of the local Universe has been altered by the presence of the mass of the galaxy. Full expansion, at the Hubble rate $\approx$7000 km/s, commences only at distances $\approx$ 100 Mpc. Superclusters are expanding but remain *gravitationally bound*, i.e., their expansion rate is decelerated.

  Expansion is thought to start due to cosmic inflation and then, due mainly to inertia. Its rate decelerated about 12 Ga ago due to gravity by dark and normal matter and then, from about 6 Ga ago when dark energy took over, accelerated. Now, for every megaparsec of distance from the observer, the rate of expansion increases by about 74 km/s. When the Universe doubles in volume, the dark energy doubles too. In 10^{11} years our galaxy will be the only one left in the observable Universe.

  The Universe was *radiation-dominated* with the **scale factor** $a(t) \sim t^{\frac{1}{2}}$ first $\approx$ 70,000 years, then *matter-dominated* with $a(t) \sim t^{\frac{2}{3}}$ until $\approx$ 4.5 Ma ago,

then *dark-energy-dominated* with $a(t) \sim \exp(Ht)$ and the Hubble constant $H = \sqrt{\frac{8\pi G\rho}{3}} = \sqrt{\frac{\Lambda}{3}}$. In fact, its expansion caused the matter surpass the radiation in energy density and further, when matter and radiation dropped to low concentrations, the repulsive *dark energy* (or *vacuum energy*) overtook the gravity of matter.

The most commonly accepted scenario for the future is the *Big Freeze*: continued expansion results in a universe that asymptotically approaches 0° K and the *Heat Death*, a state of maximum entropy in which everything is evenly distributed. Caldwell, 2003, claimed that the scale factor a will become infinite in the finite future, resulting in *Big Rip*, final singularity in which all distances diverge to ∞.

- **Zero-gravity radius**

  For a cluster of mass M, its **zero-gravity** (or *zero-velocity*, *turnover*) **radius** R_V is (Sandage, 1986, and Chernin–Teerikorpi–Baryshev, 2006) the distance r from the cluster's barycenter, where the radial force $\frac{GM}{r^2}$ of the point mass M gravity become equal to the radial force ($G2\rho_V\frac{4\pi}{3}r^3$ divided by r^2) of vacuum antigravity. So,

$$R_V^3 = \frac{3M}{8\pi\rho_V}.$$

  Here G is the *gravitational constant* and $\rho_V \approx 7 \times 10^{-30}$ g/cm^3 is the constant density of dark energy inferred from global observations of supernovae 1a.

  The **Einstein–Straus radius** R_M is the radius besides which expansion rate reach the global level. It is estimated that $\frac{R_M}{R_V}$ is 1.5–1.7 if the ratio of local and global density of dark energy is 0.1–1. If above ration is 1, then $R_M = R_V(1+z_V)$, where $z_V \approx 0.7$ is the global zero-acceleration redshift.

  For the *Local Group* (LG), containing Milky Way and of mass 2–3.5 $\times 10^{12}$ suns, above model corresponds to observed $R_V = 1.3$–1.55 Mpc and $R_M = 2.2$–2.6 Mpc. The Virgo cluster, dominating Local supercluster, contains over 1000 galaxies in a volume slightly larger than LG; its mass is $\approx 10^{15}$ suns and $R_V = 10.3$ Mpc.

- **Hubble distance**

  The **Hubble distance** (or **cosmic light horizon**, **Hubble radius**) is an increasing maximum distance $D_H = ct_H$ that a light signal could have traveled since the Big Bang, the beginning of the Universe. Here c is the speed of light and t_H is the *Hubble time* (or *age of the Universe*). It holds $t_H = \frac{1}{H_0}$, where H_0 is the *Hubble constant* which is estimated as $71 \pm 4\, km\, s^{-1} Mpc^{-1}$ at present. So, at present, $t_H \approx 4.32 \times 10^{17}$ s $\approx$ 13.82 Ga, and $D_H = \frac{c}{H_0} \approx$ 13.82 billion light-years $\approx 1.31 \times 10^{26}$ m $\approx$ 4.24 Gpc, i.e., 4.6×10^{61} **Planck lengths**.

  But we are observing now, due to the space expansion, objects much farther away than a static distance 13.82 Gly.

  For small $\frac{v}{c}$ or small distance d in the expanding Universe, the velocity is proportional to the distance, and all distance measures, for example, **angular**

diameter distance, **luminosity distance**, etc., converge. In the linear approximation, this reduces to $d \approx zD_H$. But for large $\frac{v}{c}$, the relativistic **Lorentz length contraction** $L = L_0\sqrt{1-(\frac{v}{c})^2}$, where L_0 is a **proper length**, of an object traveling at velocity v relative to an observer, become noticeable to that observer.

Above Hubble radius was measured (by the Wilkinson Microwave Anisotropy Probe) as a **light travel distance** to the source of *cosmic background radiation*. Other estimations: 13.1 Gly (calibrating the distances to supernovae of a standard brightness), 14.3 Gly (measuring radio galaxies of a standard size) and 14.5 Gly (basing on the abundance ratio of uranium/thorium chondritic meteorites, [Dau05]).

- **Cosmic sound horizon**

  Cosmic background radiation (CMB) is thermal radiation (strongest in the microwave region of the radio spectrum) filling the observable Universe almost uniformly. It originated $t_r \approx 380{,}000$ years after the Big Bang (or at a redshift of $z = 1100$), at *recombination*, when the Universe (ionized plasma of electrons and *baryons*, i.e., protons and neutrons) cooled to below 3000 K. (Now, the Universe's temperature is ≈ 1100 times cooler and its size is ≈ 1100 times larger.)

  The electrons and protons start to form neutral hydrogen atoms, allowing photons (trapped before by Thomson scattering) to travel freely. During next $\approx 100{,}000$ years radiation decoupled from the matter and the Universe became transparent.

  The plasma of photons and baryons can be seen as a single fluid. The gravitational collapse around "seeds" (point-like overdensities produced during inflation) into dark matter hierarchical halos was opposed by outward radiation pressure from the heat of photon-matter interactions. This competition created longitudinal (acoustic) oscillations in the photon-baryon fluid, analogic to sound waves, created in air by pressure differences, or to ripples in a pond.

  At recombination, the only remaining force on baryons is gravitation, and the pattern of oscillations (configuration of baryons and, at the centers of perturbations, dark matter) became frozen into the CMB. Baryon radiative cooling into gas and stars let this pattern of seeds to grow into structure of the Universe.

  More matter existed at the centers and edges of these waves, leading eventually to more galaxies there. Today, we detect the sound waves (regular, periodic fluctuations in the density of the visible baryonic matter) via the primary CMB anisotropies.

  These *baryon acoustic oscillations* (BAO) started at $t = 0$ (post-inflation) and stopped at $t = t_r$ (recombination). The **cosmic sound horizon** is the distance sound waves could have traveled. At recombination, it was $\approx c_s t_r \sim 100$ kpc, approximating the speed c_s of sound as $\frac{c}{\sqrt{3}}$.

  Expanding by factor $1 + z = 1100$, it is 120–150 Mpc today. It is a standard ruler; an excess of galaxy pairs separated by this horizon was confirmed. Cf. **cosmological distance ladder** and, in Chap. 24, **acoustic metric**.

- **GZK-horizon**

  Greisen and Kuzmin–Zatsepin, 1966, computed that a cosmic ray with kinetic energy over *GZK-limit* (5×10^{19} eV) traveling from its distant, over **GZK-horizon** (50 Mpc $\approx$ 163 Mly) source, will be absorbed (due to slowing interaction with photons of the CMB and associated mean path) and so never observed on Earth.

  Several cosmic rays apparently exceeding *GZK-limit* were observed; this *GZK-paradox* is still unexplained.

- **Comoving distance**

  The standard Big Bang model uses *comoving coordinates*, where the spatial reference frame is attached to the average positions of galaxies. With this set of coordinates, both the time and expansion of the Universe can be ignored and the shape of space is seen as a spatial hypersurface at constant cosmological time.

  The **comoving** (or *cosmological*) **distance** is a distance (denoted χ or d_{comov}) in comoving coordinates between two points in space at a single cosmological time, i.e., the distance between two *nearby* (close in redshift z) objects, which remains constant with epoch if these objects are moving with the Hubble flow.

  The (cosmological) **proper distance** d_{proper} is a distance between two nearby events in the frame in which they occur at the same time. It is the distance measured by a ruler at the time t_o of observation. It holds

$$d_{comov}(x, y) = d_{proper}(x, y) \cdot \frac{a(t_o)}{a(t_e)} = d_{proper}(x, y) \cdot (1 + z),$$

  where $a(t)$ is the **scale factor**. In the time t_o, i.e., at the present, $a = a(t_o) = 1$, and $d_{comov} = d_{proper}$, In general, $d_{proper}(t) = a(t)d_{comov}$, for a cosmological time t.

  The total **line-of-sight comoving distance** D_C from us to a distant object is computed by integrating the infinitesimal $d_{comov}(x, y)$ contributions between nearby events along the time ray from the time t_e, when the light from the object was emitted, to the time t_o, when the object is observed:

$$D_C = \int_{t_e}^{t_o} \frac{cdt}{a(t)}.$$

  In terms of redshift, D_C from us to a distant object is computed by integrating the infinitesimal $d_{comov}(x, y)$ contributions between nearby events along the radial ray from $z = 0$ to the object: $D_C = D_H \int_0^z \frac{dz}{E(z)}$, where D_H is the **Hubble distance**, and $E(z) = (\Omega_M(1 + z)^3 + \Omega_R(1 + z)^2 + \Omega_\Lambda)^{\frac{1}{2}}$.

  In a sense, the comoving distance is the fundamental distance measure in Cosmology, since all other distances can simply be derived in terms of it.

- **Proper motion distance**

  The **proper motion distance** (or **transverse comoving distance**, *contemporary angular diameter distance*) D_M is a distance from us to a distant object

defined as the ratio of the actual transverse velocity (in distance over time) of the object to its *proper motion* (in radians per unit time). It is given by

$$D_M = \begin{cases} D_H \frac{1}{\sqrt{\Omega_R}} \sinh(\sqrt{\Omega_R} D_C / D_H), & \text{for } \Omega_R > 0, \\ D_C, & \text{for } \Omega_R = 0, \\ D_H \frac{1}{\sqrt{|\Omega_R|}} \sin(\sqrt{|\Omega_R|} D_C / D_H), & \text{for } \Omega_R < 0, \end{cases}$$

where D_H is the **Hubble distance**, and D_C is the **line-of-sight comoving distance**. For $\Omega_\Lambda = 0$, there is an analytic solution (z is the *redshift*):

$$D_M = D_H \frac{2(2 - \Omega_M(1 - z) - (2 - \Omega_M)\sqrt{1 + \Omega_M z})}{\Omega_M^2 (1 + z)}.$$

The proper motion distance D_M coincides with the line-of-sight comoving distance D_C if and only if the curvature of the Universe is equal to zero. The **comoving distance** between two events at the same redshift or distance, but separated in the sky by some angle $\delta\theta$, is equal to $D_M \delta\theta$.

The distance D_M is related to the **luminosity distance** D_L and the **angular diameter distance** D_A by $D_M = (1 + z)^{-1} D_L = (1 + z) D_A$.

- **Luminosity distance**

  The **luminosity distance** D_L is a distance from us to a distant object defined by the relationship between the observed flux S and emitted luminosity L:

$$D_L = \sqrt{\frac{L}{4\pi S}}.$$

  This distance is related to the **proper motion distance** D_M and t the **angular diameter distance** by $D_L = (1 + z) D_M = (1 + z)^2 D_A$, where z is the *redshift*.

  The luminosity distance does take into account the fact that the observed luminosity is attenuated by two factors, the relativistic redshift and the Doppler shift of emission, each of which contributes an $(1 + z)$ attenuation: $L_{obser} = \frac{L_{emiss}}{(1+z)^2}$.

  The *corrected luminosity distance* $D_L^{'}$ is defined by $D_L^{'} = \frac{D_L}{1+z}$.

- **Distance modulus**

  The **distance modulus** is $DM = 5 \ln(\frac{D_L}{10pc})$, where D_L is the **luminosity distance**. The distance modulus is the difference between the *absolute magnitude* (the brightness that star would appear to have if it was at a distance of 10 parsec) and *apparent magnitude* (the actual brightness) of an astronomical object.

  Distance moduli are most commonly used when expressing the distances to other galaxies. For example, the Andromeda Galaxy's *DM* is 24.5, and the Virgo cluster has *DM* equal to 31.7. For a much smaller object (planet, comet or asteroid), the *absolute magnitude* is its apparent visual magnitude at zero phase angle and at unit (1 AU) heliocentric and geocentric distances. The brightest (with peak apparent magnitude -7.5) recorded stellar event was the supernova in 1006.

- **Angular diameter distance**

  The **angular diameter distance** (or *angular size distance*) D_A is a distance from us to a distant object defined as the ratio of an object's physical transverse size to its angular size (in radians). It is used to convert angular separations in telescope images into proper separations at the source. It is special for not increasing indefinitely as $z \to \infty$; it turns over at $z \sim 1$, and so more distant objects actually appear larger in angular size. D_A is related to the **proper motion distance** D_M and the **luminosity distance** D_L by $D_A = \frac{D_M}{1+z} = \frac{D_L}{(1+z)^2}$, where z is the *redshift*.

  The *distance duality* $\frac{D_L(z)}{D_A(z)} = (1+z)^2$ links D_L, based on the apparent luminosity of standard candles (for example, supernovae) and D_A, based on the *apparent size* ("visual diameter" measured as an angle) of standard rulers (for example, **cosmic sound horizon**). It holds for any general **metric theory of gravity** (Chap. 24) in any background in which photons travel on unique null geodesics.

  If the angular diameter distance is based on the representation of object diameter as angle × distance, the **area distance** is defined similarly according the representation of object area as solid angle × distance^2.

- **Einstein radius**

  General Relativity predicts *gravitational lensing*, i.e., deformation of the light from a *source* (a galaxy or star) in the presence of a *gravitational lens*, i.e., a body of large mass M (another galaxy, or a black hole) bending it.

  If the source S, lens L and observer O are all aligned, the gravitational deflection is symmetric around the lens. The **Einstein radius** is the radius of the resulting *Einstein* (or *Chwolson*) *ring*. In radians it is

$$\sqrt{M\frac{4G}{c^2}\frac{D(L,S)}{D(O,L)D(O,S)}},$$

  where $D(O,L)$ and $D(O,S)$ are the **angular diameter distances** of the lens and source, while $D(L,S)$ is the angular diameter distance between them.

- **Light travel distance**

  The **light travel** (or *look-back*) **distance** is a distance from us to a distant object, defined by $D_{lt} = cD_t$, where D_t is the difference $t_o - t_e$ between the time, when the object was observed, and the time, when the light from it was emitted. The *look-back time* D_t is a **proper time**, but D_{lt} is not a **proper distance**.

  D_{lt} is not a very useful distance, because it is hard to determine t_e, the age of the Universe at the time of emission of the light which we see. Cf. **Hubble radius**.

- **Parallax distance**

  Given an object O viewed along two different lines of sight, its *parallax* is the angle $p = AOB$ between its directions of view from the two ends of a baseline AB. If $AO \approx BO$ and p, AB are small, the distance $A0$ can be easily estimated.

Animals use their two eyes (*stereoopsis*) or two positions of moving head (*motion parallax*) as points A, B. Cf. **animal depth/distance perception** in Chap. 23.

In Astronomy, the **parallax distance** is a distance D_P from us to a distant object (say, a star) defined from measuring of *stellar parallaxes*, i.e., its apparent changes of position in the sky caused by the motion of the observer on the Earth.

Usually, it is the *annual* (or *heliocentric*) *paralllax*, i.e., p is the angle Earth-star-Sun (in arcseconds) subtended at a star by the longest baseline—mean radius $R = 1$ AU of the Earth's orbit around the Sun. So, this distance (in parsecs, corresponding to $p = 1$ arcsec) is given by $D_P = \frac{1}{\tan(p)} \approx \frac{1}{p}$, since p is usually very small.

- **Kinematic distance**

  The **kinematic distance** is the distance to a galactic source, which is determined from differential rotation of the galaxy: the *radial velocity* of a source directly corresponds to its **galactocentric distance**. But the *kinematic distance ambiguity* arises since, in our inner galaxy, any given galactocentric distance corresponds to two distances along the line of sight, *near* and *far* kinematic distances.

  This problem is solved, for some galactic regions, by measurement of their absorption spectra, if there is an interstellar cloud between the region and observer.

- **Radar distance**

  The **radar** (or *target*) **distance** D_R is a distance from us to a distant object, measured by a *radar*, i.e., a high frequency radio pulse sent out for a short interval of time. When it encounters a conducting object, sufficient energy is reflected back to allow radar to detect it. Since radio waves travel in air at close to their speed c (of light) in vacuum, one can calculate the distance D_R of the detected object from the round-trip time t between the transmitted and received pulses as

$$D_R = \frac{1}{2}ct.$$

  In general, *Einstein protocol* is to measure the distance between two objects A and B as $\frac{1}{2}c(t_3 - t_1)$. Here a light pulse is sent from A to B at time t_1 (measured in A), received at time t_2 (measured in B) and immediately sent back to A with a return time t_3 (measured with A).

- **Pulsar dispersion measure**

  A *pulsar* is an extraterrestrial source of radiation having a regular periodicity, detected as short bursts in, usually, the radio region of the spectrum.

  The **pulsar dispersion measure** (DM) is the integrated *column density* of free electrons (their number per unit area) between an observer and a pulsar. DM is shown by a pulse's broadening when it is observed over a finite bandwidth.

  The distance to the pulsar is $\frac{DM}{n_e}$, where n_e is the mean electron density.

- **Cosmological distance ladder**

  For measuring distances to astronomical objects, one uses a kind of "ladder" of different methods; each method applies only for a limited distance, and each method which applies for a larger distance builds on the data of the preceding methods.

  The starting point is knowing the distance from the Earth to the Sun; this distance is called one *astronomical unit* (*AU*), and is roughly 150 million km. Distances in the inner Solar System are measured by bouncing radar signals off planets or asteroids, and measuring the time until the echo is received.

  The next step in the ladder consists of simple geometrical methods; with them, one can go to a few hundred ly. The distance to nearby stars can be determined by their *parallaxes*: using Earth's orbit as a baseline, the distances to stars are measured by triangulation. This is accurate to about 1 % at 50 ly, 10 % at 500 ly.

  Using data acquired by the geometrical methods, and adding *photometry* (measurements of the brightness) and spectroscopy, one gets the next step in the ladder for stars so far away that their parallaxes are not measurable yet. The *distance-luminosity relation* is that the light intensity from a star is inversely proportional to the square of its distance; cf. **distance modulus**.

  For even larger distances, are used *standard candles*, i.e., several types of cosmological objects, for which one can determine their absolute brightness without knowing their distances. *Primary standard candles* are the *Cepheid* variable stars. They periodically change their size and temperature. There is a relationship between the brightness of these pulsating stars and the period of their oscillations, and this relationship can be used to determine their absolute brightness. Cepheids can be identified as far as in the Virgo cluster (60 Mly).

  Secondary standard candles are supernovae 1a (having equal peak brightness), red giant branch stars, active galactic nuclei and entire galaxies. Main other techniques to estimate the **angular diameter distance** to galaxies are *gravitational lensing* (cf. **Einstein radius**) and using *baryon acoustic oscillations* matter clustering (cf. **cosmic sound horizon**) as a standard ruler.

  For very large distances (hundreds of Mly or several Gly), the cosmological redshift and the Hubble law are used. A complication is that it is not clear what is meant by "distance" here, and there are several types of distances used here: **luminosity distance**, **proper motion distance**, **angular diameter distance**, etc.

  Depending on the situation, there is a large variety of special techniques to measure distances in Cosmology, such as *light echo*, *Bondi radar*, *RR Lyrae*, *maser* distances and *secular*, *statistical*, *expansion*, *spectroscopic* parallax distances.

  NASA's Chandra X-ray Observatory measures large distances via the delay of the halo of scattering material (interstellar dust grains) between the source and Earth. Also, frequency-dependent dispersion of *fast radio bursts* indicate the distance via amount of ionized plasma that lies between the burst's origin and Earth.

- **VLBI distance measurements**

  Very-long-baseline interferometry (VLBI) is a technique of radio astronomy.

In VLBI a signal from a compact bright astronomical radio source (say, *pulsar* or *maser*) is collected by an array of radio telescopes on Earth and in near space. The distance between the telescopes is then calculated using the time difference between the arrivals of the signals at different telescopes. Observations of an object made simultaneously by many telescopes are combined, emulating a telescope with a size equal to the maximum distance between the telescopes. VLBI arrays can be combined, increasing the resolution to, say, microarcseconds.

VLBI directly measure distance, via *annual parallax*, and proper motions.

26.2 Distances in Theory of Relativity

The *Minkowski space-time* (or *Minkowski space*, *Lorentz space-time*, *flat space-time*) is the usual geometric setting for the Einstein Special Theory of Relativity. In this setting the three ordinary dimensions of space are combined with a single dimension of time to form a 4D *space-time* $\mathbb{R}^{1,3}$ in the absence of gravity. See, for example, [Wein72] for details.

Vectors in $\mathbb{R}^{1,3}$ are called 4-*vectors* (or *events*). They can be written as (ct, x, y, z), where the first component is the unidirectional *time-like dimension* (c is the speed of light in vacuum, and t is the time), while the other three components are bidirectional *spatial dimensions*. Formally, c is a conversion factor from time to space.

In fact, c is the speed of gravitational waves and any massless particle: the *photon* (carrier of electromagnetism), the *gluon* (carrier of the strong force) and the *graviton* (theoretical carrier of gravity). It is the highest possible speed for any physical interaction in nature and the only speed independent of its source and the motion of an observer.

In the *spherical coordinates*, the events can be written as (ct, r, θ, ϕ), where r $(0 \leq r < \infty)$ is the *radius* from a point to the origin, ϕ $(0 \leq \phi < 2\pi)$ is the azimuthal angle in the xy plane from the x axis (*longitude*), and θ $(0 \leq \theta \leq \pi)$ is the polar angle from the z axis (*colatitude*). 4-vectors are classified according to the sign of their squared *norm*:

$$||v||^2 = \langle v, v \rangle = c^2t^2 - x^2 - y^2 - z^2.$$

They are said to be *time-like*, *space-like*, and *light-like* (*isotropic*) if their squared norms are positive, negative, or equal to zero, respectively. The set of all light-like 4-vectors forms the *light cone*. If the coordinate origin is singled out, the space can be broken up into three domains: domains of *absolute future* and *absolute past*, falling within the light cone, whose points are joined to the origin by time-like vectors with positive or negative value of time coordinate, respectively, and the domain of *absolute elsewhere*, falling outside of the light cone, whose points are joined to the origin by space-like vectors.

A *world line* of an object is the sequence of events that marks its time history. A world line is a *time-like* curve tracing out the path of a single point in the Minkowski

space-time, i.e., at any point its *tangent vector* is a time-like 4-vector. All world lines fall within the light cone, i.e., the curves whose tangent vectors are light-like 4-vectors correspond to the motion of light and other particles of zero rest mass.

World lines of particles at constant speed (equivalently, of free falling particles) are called *geodesics*. In Minkowski space they are straight lines. A geodesic in Minkowski space which joins two given events x and y, is the longest curve among all world lines which join these two events. This follows from the **Einstein time triangle inequality** (cf. **inverse triangle inequality** and, in Chap. 5, **reverse triangle inequality**):

$$||x + y|| \geq ||x|| + ||y||,$$

according to which a time-like broken line joining two events is shorter than the single time-like geodesic joining them, i.e., the **proper time** of the particle moving freely from x to y is greater than the **proper time** of any other particle whose world line joins these events. It holds also in Minkowski space extended to any number of spatial dimensions, assuming null or time-like vectors in the same time direction. It is called *twin paradox*.

The *space-time* is a 4D *manifold* which is the usual mathematical setting for the Einstein General Theory of Relativity, which is the generalization of Special Relativity to include gravitation. Here the three spatial components with a single time-like component form a 4D space-time in the presence of gravity. Gravity is equivalent to the geometric properties of space-time, and in the presence of gravity the geometry of space-time is curved. (Bean, 2009, found evidence that over extragalactic distances gravity exerts a greater pull on time than on space.) So, the space-time is a 4D curved manifold for which the tangent space to any point is the Minkowski space, i.e., it is a *pseudo-Riemannian manifold*—a manifold, equipped with a nondegenerate indefinite metric (called **pseudo-Riemannian metric** in Chap. 7) of signature (1,3).

In the General Theory of Relativity, gravity is described by the properties of the local geometry of space-time. In particular, the gravitational field can be built out of a **metric tensor**, a quantity describing geometrical properties space-time such as distance, area, and angle. Matter is described by its *stress-energy tensor*, a quantity which contains the density and pressure of matter. The strength of coupling between matter and gravity is determined by the gravitational constant G.

The *Einstein field equation* is an equation in the General Theory of Relativity, that describes how matter creates gravity and, conversely, how gravity affects matter. A solution of the Einstein field equation is a certain **Einstein metric** appropriated for the given mass and pressure distribution of the matter.

A *black hole* is an astrophysical object that is theorized to be created from the collapse of a neutron or "quark" star. The gravitational forces are so strong in a black hole that they overcome neutron degeneracy pressure and, roughly, collapse to a *singularity* (point of infinite density and space-time curvature). Even light cannot escape the gravitational pull of a black hole within the black hole's its *event horizon*.

Uncharged black holes are called *Schwarzschild* or *Kerr black holes* if their angular momentum is zero or not, respectively. Charged black holes are called *Kerr–Newman* or *Reissner–Nordström black holes* if they are spinning or not, respectively.

Universe and black hole both have singularities—in time and space, respectively. *Naked* (not surrounded by a black hole) singularities were not observed but they might exist also. **Kerr metric** and **Reissner–Nordström metric below** admit such case. Also, a *kugelblitz* is a putative black hole formed from energy as opposed to mass.

Experimentally, General Relativity is still untested for strong fields (such as near neutron-star surfaces or black-hole horizons) or over distances on a galactic scale and larger. Neither Newton law of gravitation was tested below 6×10^{-5} m.

Putative *gravitational waves* (fluctuations in the curvature of space-time propagating as a wave, predicted by Einstein), have been detected in 2014. Also predicted *frame-dragging effect* (the spinning Earth pulls space-time around with it) is under probe. The *geodetic effect*, confirming that space-time acts on matter, was found.

- **Minkowski metric**

  The **Minkowski metric** is a **pseudo-Riemannian metric**, defined on the *Minkowski space* $\mathbb{R}^{1,3}$, i.e., a 4D real vector space which is considered as the *pseudo-Euclidean space* of signature $(1, 3)$. It is defined by its **metric tensor**

$$((g_{ij})) = \begin{pmatrix} 1 & 0 & 0 & 0 \\ 0 & -1 & 0 & 0 \\ 0 & 0 & -1 & 0 \\ 0 & 0 & 0 & -1 \end{pmatrix}.$$

  The *line element* ds^2 of this metric are given by

$$ds^2 = c^2dt^2 - dx^2 - dy^2 - dz^2.$$

  In *spherical coordinates* (ct, r, θ, ϕ), one has $ds^2 = c^2dt^2 - dr^2 - r^2d\theta^2 - r^2 \sin^2 \theta d\phi^2$.

  The pseudo-Euclidean space $\mathbb{R}^{1,3}$ of signature $(1, 3)$ with the *line element*

$$ds^2 = -c^2dt^2 + dx^2 + dy^2 + dz^2$$

  can also be used as a space-time model of the Special Theory of Relativity.

  Above notion of *space-time* (Minkowski, 1908) was the first application of geometry to a nonlength-like quantity. But there were some precursors of such union of space and time. Lagrange, 1797, observed that with time as a 4-th coordinate, "one can regard mechanics as 4-dimensional geometry". Schopenhauer wrote in *On the Fourfold Root of the Principle of Sufficient Reason* (1813): "...it is only by the combination of Time and Space that the representation of coexistence arises." Poe wrote "Space and Duration are one" in *Eureka: A Prose Poem* (1848).

Wells wrote on the first page of *The Time Machine* (1895): 'Clearly,' the Time Traveler proceeded, 'any real body must have extension in four directions: it must have Length, Breadth, Thickness, and Duration ... There is no difference between Time and any of the tree dimensions of Space except that our consciousness moves along it". *Quechua*, the language of Inca and 8–10 million modern speakers, have a single concept, *pacha*, for the location in time and space.

- **Proper distance and time**

  In Relativistic Physics, **proper distance** and **proper time** between any two events are true physical distance and time difference: the spatial distance between them when the events are simultaneous and the temporal distance between them when the events occur at the same spatial location. They are the *invariant* (with respect to Lorentz transformations, describing a transition to a coordinate system associated with a moving body) intervals of a space-like path or pair of space-like separated events, and, respectively, of a time-like path or pair of time-like separated events.

  In General Relativity, **proper time** is the pseudo-Riemannian arc length of world lines in 4D-spacetime. In particular, in SR (Special Relativity), it is

$$\tau = \int_P \sqrt{dt^2 - c^{-2}(dx^2 + dy^2 + dz^2)},$$

  where t and x, y, z are time and spatial coordinates, while P is the path of the clock in space-time. In the subcase of inertial motion, it become

$$\Delta\tau = \sqrt{(\Delta t)^2 - c^{-2}((\Delta x)^2 + (\Delta y)^2 + (\Delta z)^2))},$$

  where Δ means "the change in" between two events. Cf. the **kinematic metric**.

  In SR, the **proper distance** between two space-like separated events is

$$\Delta\sigma = \sqrt{(\Delta x)^2 + (\Delta y)^2 + (\Delta z)^2 - c^2(\Delta t)^2}.$$

- **Proper length**

  In Special Theory of Relativity, the **proper** (or *rest*) **length** between two space-like separated events is the distance between them, such as measured in an inertial frame of reference in which the events are simultaneous. In contrast to invariant **proper distance**, such simultaneity depends on the observer.

  In a flat space-time, the proper length between two events is the proper length of a straight path between them. General Relativity consider the curved space-times in which may be more than one straight path (geodesic) between two events.

  So, the general **proper length** is defined as the path integral $\int_P \sqrt{-g_{ij}dx^i dx^j}$, where g_{ij} is the metric tensor for the space-time with signature $(1, 3)$, along the shortest curve joining the endpoints of the space-like path P at the same time.

- **Affine space-time distance**

  Given a space-time (M^4, g), there is a unique affine parametrization $s \to \gamma(s)$ for each light ray (i.e., light-like geodesic) through the observation event p_o, such that $\gamma(0) = p_o$ and $g(\frac{d\gamma}{dt}, U_o) = 1$, where U_o is the 4-velocity of the observer at p_o (i.e., a vector with $g(U_o, U_o) = -1$). In this case, the **affine space-time distance** is the *affine parameter* s, viewed as a distance measure.

  This distance is monotone increasing along each ray, and it coincides, in a small neighborhood of p_o, with the Euclidean distance in the rest system of U_o.
- **Lorentz metric**

  A **Lorentz metric** is a **pseudo-Riemannian metric** (i.e., **nondegenerate indefinite metric**, cf. Chap. 7) of signature $(1, p)$.

  The curved space-time of the General Theory of Relativity can be modeled as a *Lorentzian manifold* (a manifold equipped with a Lorentz metric) of signature $(1, p)$. The *Minkowski space* $\mathbb{R}^{1,p}$ with the flat **Minkowski metric** is a model of it, in the same way as Riemannian manifolds can be modeled on Euclidean space.

  Given a rectifiable non-space-like curve $\gamma : [0, 1] \to M$ in the space-time M, the *length* of the curve is defined as $l(\gamma) = \int_0^1 \sqrt{-\langle \frac{d\gamma}{dt}, \frac{d\gamma}{dt} \rangle} dt$. For a space-like curve, we set $l(\gamma) = 0$ and define the **Lorentz distance** between two points $p, q \in M$ as

$$\sup_{\gamma \in \Gamma} l(\gamma),$$

  if $p \prec q$, i.e., if the set Γ of *future directed* non-space-like curves from p to q is nonempty; otherwise, this distance is 0.

  The **Lorentz–Minkowski distance** is a **pseudo-Euclidean distance** (Chap. 7) $\sqrt{D(x, y)}$, where $D(x, y) = |x_1 - y_1|^2 - \sum_{2 \le i \le n} |x_i - y_i|^2$. The points are called *time-*, *space-*, *null-separated* if $D(x, y)$ is more, less or equal to 0, respectively, i.e., if they can be joined by a time-like, space-like or null path.
- **Distances on causal sets**

  Causal Set Theory is a fundamentally discrete approach to quantum gravity. A *causal set* (or *causet*) is a partially ordered set $(X, \preceq)$, which is *locally finite*, i.e., the *interval* $(x, y) = \{z \in X : x \prec z \prec y\}$ is finite for any $x, y \in X$. A *link* is a pair $x, y \in X$ such that $x \prec y$ and $(x, y) = \emptyset$. A *chain* is a subcauset such that $x \prec y$ or $y \prec x$ for any two its elements x, y.

  Given $x, y \in X$ with $x \prec y$, their **time-like distance** $d_t(x, y)$ is (Brightwell–Gregory, 1991) the *length* (number of links) in any *geodesic* between them, i.e., longest chain between and including x and y. Given two unrelated elements $x, y \in X$, their **naive space-like distance** is defined (Brightwell–Gregory, 1991) as

$$d_{ns}(x, y) = \min_{u,v \in X : u \prec (x,y) \prec v} d_t(u, v).$$

  Rideout–Wallden, 2013, modified $d_{ns}(x, y)$, replacing the minimum above with an average over suitably selected minimizing pairs.

The elements of X can be seen as events in a discrete space-time, where the partial order represent causal relationship. In a causet embedded in Minkowski space-time, the distance $d_t(x, y)$ is proportional to the **proper time**. A related discrete space-time is a random poset obtained by sampling from a compact domain in a space-time manifold. Cf. also **D-separation in Bayesian network** in Chap. 22.

- **Kinematic metric**

  Given a set X, a **kinematic metric** (or *abstract Lorentzian distance*) is (Pimenov, 1970) a function $\tau : X \times X \to \mathbb{R}_{\geq 0} \cup \{\infty\}$ such that, for all $x, y, z \in X$:

  1. $\tau(x, x) = 0$;
  2. $\tau(x, y) > 0$ implies $\tau(y, x) = 0$ (*antisymmetry*);
  3. $\tau(x, y), \tau(y, z) > 0$ implies $\tau(x, z) > \tau(x, y) + \tau(y, z)$ (**inverse triangle inequality** or *anti-triangle inequality*).

  The *space-time* set X consists of *events* $x = (x_0, x_1)$ where, usually, $x_0 \in \mathbb{R}$ is the *time* and $x_1 \in \mathbb{R}^3$ is the *spatial location* of the event x. The inequality $\tau(x, y) > 0$ means *causality*, i.e., x can influence y; usually, it is equivalent to $y_0 > x_0$ and the value $\tau(x, y) > 0$ can be seen as the largest (since it depends on the speed) **proper time** of moving from x to y.

  If the gravity is negligible, then $\tau(x, y) > 0$ implies $y_0 - x_0 \geq ||y_1 - x_1||_2$, and $\tau_p(x, y) = ((y_0 - x_0)^p - ||y_1 - x_1||_2^p)^{\frac{1}{p}}$ (as defined by Busemann, 1967) is a real number. For $p \approx 2$ it is consistent with Special Relativity observations.

  A kinematic metric is not our usual distance metric; also it is not related to the **kinematic distance** in Astronomy.

  But Zapata, 2013, proved that $\sup_z \max(|\tau(x, z) - \tau(y, z)|, |\tau(z, x) - \tau(z, y)|)$ is a continuous metric on a compact part of space-time and it generates the same topology as a nonphysical coordinate-dependent Euclidean distance $\sqrt{\sum_{i=2}^{4} |x_i - y_i|^2}$.

- **Galilean distance**

  The **Galilean distance** is a distance on $\mathbb{R}^n$ defined by

  $$|x_1 - y_1| \quad \text{if } x_1 \neq y_1,$$

  and by

  $$\sqrt{(x_2 - y_2)^2 + \cdots + (x_n - y_n)^2} \text{ if } x_1 = y_1.$$

  The space $\mathbb{R}^n$, equipped with the Galilean distance, is called *Galilean space*.

  For $n = 4$, it is a setting for the space-time of classical mechanics according to Galilei–Newton in which the distance between two events taking place at the points p and q at the moments of time t_1 and t_2 is defined as the time interval $|t_1 - t_2|$, while if $t_1 = t_2$, it is defined as the distance between the points p and q.

- **Einstein metric**

  In the General Theory of Relativity, describing how space-time is curved by matter, the **Einstein metric** is a solution to the Einstein field equation

$$R_{ij} - \frac{g_{ij}R}{2} + \Lambda g_{ij} = \frac{8\pi G}{c^4} T_{ij},$$

  i.e., a **metric tensor** $((g_{ij}))$ of signature $(1, 3)$, appropriated for the given mass and pressure distribution of the matter. Here $E_{ij} = R_{ij} - \frac{g_{ij}R}{2} + \Lambda g_{ij}$ is the *Einstein curvature tensor*, R_{ij} is the *Ricci curvature tensor*, R is the *Ricci scalar*, and T_{ij} is a *stress-energy tensor*. *Empty space* (*vacuum*) is the case of $R_{ij} = 0$.

  Einstein introduced in 1917 the *cosmological constant* Λ to counteract the effects of gravity on ordinary matter and keep the Universe *static*, i.e., with **scale factor** always being 1. He put $\Lambda = \frac{4\pi G\rho}{c^2}$. The static Einstein metric for a homogeneous and isotropic Universe is given by the *line element*

$$ds^2 = -dt^2 + \frac{dr^2}{(1 - kr^2)} + r^2(d\theta^2 + \sin^2\theta d\phi^2),$$

  where k is the curvature of the space-time. The radius of this curvature is $\frac{c}{\sqrt{4\pi G\rho}}$ and numerically it is of the order 10 Gly. Einstein from 1922 call this model his "biggest blunder" but Λ was reintroduced in modern dynamic models as dark energy.

- **de Sitter metric**

  The **de Sitter metric** is a maximally symmetric vacuum solution to the Einstein field equation with a positive cosmological constant Λ, given by the *line element*

$$ds^2 = dt^2 + e^{2\sqrt{\frac{\Lambda}{3}}t}(dr^2 + r^2 d\theta^2 + r^2 \sin^2\theta d\phi^2).$$

  Expansion of Universe is accelerating at the rate consistent with $\Lambda \sim 10^{-123}$, but Hartie–Hawking–Hertog, 2012, gave a quantum model of it with $\Lambda < 0$.

  The most symmetric solutions to the Einstein field equation in a vacuum for $\Lambda = 0$ and $\Lambda < 0$ are the flat **Minkowski metric** and the **anti de Sitter metric**.

  The n-dimensional *de Sitter space* dS_n and *anti de Sitter space* AdS_n are Lorentzian manifold analogs of elliptic and hyperbolic space, respectively.

  In order to explain the *hierarchy problem* (why the weak nuclear force is 10^{32} times stronger than gravity?), Randall and Sundram, 1999, proposed that Universe is 5D anti de Sitter space AdS_5 with elementary particles, except for the graviton, being on a $(3 + 1)$-D brane or branes. This **Randall–Sundrum metric** is $ds^2 = e^{-2ky} g_{ab} dx^a dy^b + dy^2$, where k is of order the Planck scale ($\sim 10^{-35}$ m) and x^a, y are coordinates in 4D and extra-dimension.

- **BTZ metric**

  The **BTZ metric** (Banados, Teitelboim and Zanelli, 2001) is a black hole solution for $(2+1)$-dimensional gravity with a negative cosmological constant Λ.

  There are no such solutions with $\Lambda = 0$. BTZ black holes without any electric charge are locally isometric to *anti de Sitter space*.

  This metric is given by the *line element*

$$ds^2 = -k^2(r^2 - R^2)dt^2 + \frac{1}{k^2(r^2 - R^2)}dr^2 + r^2 d\theta^2,$$

  where R is the black hole radius, in the absence of charge and angular momentum.

- **Schwarzschild metric**

  The **Schwarzschild metric** is a vacuum solution to the *Einstein field equation* around a spherically symmetric mass distribution; this metric represents the Universe around a black hole of a given mass, from which no energy can be extracted.

  It was found by Schwarzschild, 1915, only a few months after the publication of the Einstein field equation, and was the first exact solution of this equation.

  The *line element* of this metric is given by

$$ds^2 = \left(1 - \frac{r_g}{r}\right)c^2 dt^2 - \frac{1}{\left(1 - \frac{r_g}{r}\right)}dr^2 - r^2(d\theta^2 + \sin^2\theta d\phi^2),$$

  where $r_g = \frac{2Gm}{c^2}$ is the *Schwarzschild radius* and m is the mass of the black hole.

  This solution is only valid for radii larger than r_g, as at $r = r_g$ there is a coordinate singularity. This problem can be removed by a transformation to a different choice of space-time coordinates, called *Kruskal–Szekeres coordinates*. As $r \to +\infty$, the Schwarzschild metric approaches the **Minkowski metric**.

- **Kottler metric**

  The **Kottler metric** is the unique spherically symmetric vacuum solution to the Einstein field equation with a cosmological constant Λ. It is given by

$$ds^2 = -\left(1 - \frac{2m}{r} - \frac{\Lambda r^2}{3}\right)dt^2 + \left(1 - \frac{2m}{r} - \frac{\Lambda r^2}{3}\right)^{-1} dr^2 + r^2(d\theta^2 + \sin^2\theta d\phi^2).$$

  It is called also the **Schwarzschild–de Sitter metric** for $\Lambda > 0$ and **Schwarzschild–anti de Sitter metric** for $\Lambda < 0$. Cf. **Delaunay metric** in Chap. 7.

- **Reissner–Nordström metric**

  The **Reissner–Nordström metric** is a vacuum solution to the Einstein field equation around a spherically symmetric mass distribution in the presence of a charge; it represents the Universe around a charged black hole. This metric is

given by

$$ds^2 = \left(1 - \frac{2m}{r} + \frac{e^2}{r^2}\right) dt^2 - \left(1 - \frac{2m}{r} + \frac{e^2}{r^2}\right)^{-1} dr^2 - r^2(d\theta^2 + \sin^2\theta d\phi^2),$$

where m is the mass of the hole, e is the charge ($e < m$), and we have used units with the speed c of light and the *gravitational constant* G equal to one.

- **Kerr metric**

  The **Kerr metric** (or **Kerr–Schild metric**) is an exact solution to the Einstein field equation for empty space (vacuum) around an axially symmetric, rotating mass distribution, This metric represents the Universe around a rotating black hole. Its *line element* is given (in *Boyer–Lindquist form*) by

$$ds^2 = \rho^2 \left(\frac{dr^2}{\Delta} + d\theta^2\right) + (r^2 + a^2)\sin^2\theta d\phi^2 - dt^2 + \frac{2mr}{\rho^2}(a\sin^2\theta d\phi - dt)^2,$$

  where $\rho^2 = r^2 + a^2\cos^2\theta$ and $\Delta = r^2 - 2mr + a^2$. Here m is the mass of the black hole and a is the angular velocity as measured by a distant observer.

  The **Schwarzschild metric** is the Kerr metric with $a = 0$. A black hole is rotating if radiation processes are observed outside its *Schwarzschild radius* (the event horizon radius as dependent on the mass only) but inside its *Kerr radius* (where the rotational kinetic energy is comparable with the rest energy). For the Earth, those radii are about 1 cm and 3 m, respectively.

  In 2013, the spin of a black hole was directly measured for the first time: the central black hole of the galaxy NGC 1365 rotates at 84 % of the speed c of light.

- **Kerr–Newman metric**

  The **Kerr–Newman metric** is an exact, unique and complete solution to the Einstein field equation for empty space (vacuum) around an axially symmetric, rotating mass distribution in the presence of a charge, This metric represents the Universe around a rotating charged black hole. Its *line element* is given by

$$ds^2 = -\frac{\Delta}{\rho^2}(dt - a\sin^2\theta d\phi)^2 + \frac{\sin^2\theta}{\rho^2}((r^2 + a^2)d\phi - adt)^2 + \frac{\rho^2}{\Delta}dr^2 + \rho^2 d\theta^2,$$

  where $\rho^2 = r^2 + a^2\cos^2\theta$ and $\Delta = r^2 - 2mr + a^2 + e^2$. Here m is the mass of the black hole, e is the charge, and a is the angular velocity.

  The Kerr–Newman metric becomes the **Kerr metric** if the charge is 0 and the **Reissner–Nordström metric** if the angular momentum is 0.

- **Ozsváth–Schücking metric**

  The **Ozsváth–Schücking metric** (1962) is a rotating vacuum solution to the field equations having in Cartesian coordinates the form

$$ds^2 = -2[(x^2 - y^2)\cos(2t) - 2xy\sin(2t)]dt^2 + dx^2 + dy^2 - 2dtdz.$$

- **Static isotropic metric**

  The **static isotropic metric** is the most general solution to the Einstein field equation for empty space (vacuum); this metric can represent a static isotropic gravitational field. The *line element* of this metric is given by

$$ds^2 = B(r)dt^2 - A(r)dr^2 - r^2(d\theta^2 + \sin^2\theta d\phi^2),$$

  where $B(r)$ and $A(r)$ are arbitrary functions.

- **Eddington–Robertson metric**

  The **Eddington–Robertson metric** is a generalization of the **Schwarzschild metric** which allows that the mass m, the *gravitational constant* G, and the density ρ are altered by unknown dimensionless parameters α, β, and γ (all equal to 1 in the *Einstein field equation*). The *line element* of this metric is given by

$$ds^2 = \left(1 - 2\alpha\frac{mG}{r} + 2(\beta - \alpha\gamma)\left(\frac{mG}{r}\right)^2 + \dots\right)dt^2 - \left(1 + 2\gamma\frac{mG}{r} + \dots\right)dr^2 -$$

$$-r^2(d\theta^2 + \sin^2\theta d\phi^2).$$

- **Janis–Newman–Wincour metric**

  The **Janis–Newman–Wincour metric** is the most general spherically symmetric static and asymptotically flat solution to the Einstein field equation coupled to a massless scalar field. It is given by the *line element*

$$ds^2 = -\left(1 - \frac{2m}{\gamma r}\right)^{\gamma} dt^2 + \left(1 - \frac{2m}{\gamma r}\right)^{-\gamma} dr^2 + \left(1 - \frac{2m}{\gamma r}\right)^{1-\gamma} r^2(d\theta^2 + \sin^2\theta d\phi^2),$$

  where m and γ are constants. For $\gamma = 1$ one obtains the **Schwarzschild metric**. In this case the scalar field vanishes.

- **FLRW metric**

  The **FLRW** (Friedmann–Lemaître–Robertson–Walker) **metric** is a exact solution to the Einstein field equation for a simply connected, homogeneous, isotropic expanding (or contracting) Universe filled with a constant density and negligible pressure. This metric represents a matter-dominated Universe filled with a *dust* (pressure-free matter); it models the **metric expansion of space**.

  Its *line element* is usually written in the *spherical coordinates* (ct, r, θ, ϕ):

$$ds^2 = c^2dt^2 - a(t)^2\left(\frac{dr^2}{1 - kr^2} + r^2(d\theta^2 + \sin^2\theta d\phi^2)\right),$$

  where $a(t)$ is the **scale factor** and k is the *curvature* of the space-time.

- **Vaidya metric**

  The **Vaidya metric** is a inhomogeneous solution to Einstein field equation describing a spherically symmetric space-time composed purely of radially propagating radiation. It has been used to describe the radiation emitted by a shining star, by a collapsing star and by evaporating black hole.

  The Vaidya metric is a nonstatic generalization of the **Schwarzschild metric** and the radiation limit of the **LTB metric**. Let $M(u)$ be the mass parameter; the *line element* of this metric (Vaidya, 1953) is given by

$$ds^2 = -[1 - 2\frac{M(u)}{r}]du^2 + 2dudr + r^2(d\theta^2 + \sin^2\theta d\phi^2).$$

- **LTB metric**

  The **LTB** Lemaître–Tolman–Bondi) **metric** is a solution to the Einstein field equation describing a spherical (finite or infinite) cloud of *dust* (pressure-free matter) that is expanding or collapsing under gravity.

  The LTB metric describes an inhomogeneous space-time expected on very large (Gpc) scale. It generalizes the **FLRW metric** and the **Schwarzschild metric**.

  The *line element* of this metric in the *spherical coordinates* is:

$$ds^2 = dt^2 - \frac{(R')^2}{1 + 2E}dr^2 - R^2(d\theta^2 + \sin^2\theta d\phi^2),$$

  where $R = R(t, r)$, $R' = \frac{\partial R}{\partial r}$, $E = E(r)$. The shell $r = r_0$ at a time $t = t_0$ has an area $4\pi R^2(r_0, t_0)$, and the areal radius R evolves with time as $\frac{\partial R}{\partial t} = 2E + \frac{2M}{R}$, where $M = M(r)$ is the gravitational mass within the comoving sphere at radius r.

- **Kantowski–Sachs metric**

  The **Kantowski–Sachs metric** is a solution to the Einstein field equation, given by the *line element*

$$ds^2 = -dt^2 + a(t)^2dz^2 + b(t)^2(d\theta^2 + \sin\theta d\phi^2),$$

  where the functions $a(t)$ and $b(t)$ are determined by the Einstein equation. It is the only homogeneous model without a 3D transitive subgroup.

  In particular, the Kantowski–Sachs metric with the *line element*

$$ds^2 = -dt^2 + e^{2\sqrt{\Lambda}t}dz^2 + \frac{1}{\Lambda}(d\theta^2 + \sin^2\theta d\phi^2)$$

  describes an anisotropic Universe with two spherical dimensions having a fixed size during the cosmic evolution and exponentially expanding 3-rd dimension.

- **Bianchi metrics**

  The **Bianchi metrics** are solutions to the Einstein field equation for cosmological models that have spatially homogeneous sections, invariant under the action of a 3D Lie group, i.e., they are real 4D metrics with a 3D isometry group, transitive on 3-surfaces. Using the Bianchi classification of 3D Lie algebras over Killing vector fields, we obtain the nine types of Bianchi metrics.

  Each Bianchi model B defines a transitive group G_B on some 3D simply connected manifold M; so, the pair (M, G) (where G is the maximal group acting on X and containing G_B) is one of eight Thurston *model geometries* if M/G' is compact for a discrete subgroup G' of G. In particular, Bianchi type IX corresponds to the geometry S^3. Only the model geometry $S^2 \times \mathbb{R}$ is not realized in this way.

  The Bianchi type I metric is a solution to the Einstein field equation for an anisotropic homogeneous Universe, given by the *line element*

$$ds^2 = -dt^2 + a(t)^2 dx^2 + b(t)^2 dy^2 + c(t)^2 dz^2,$$

  where the functions $a(t)$, $b(t)$, and $c(t)$ are determined by the Einstein equation. It corresponds to flat spatial sections, i.e., is a generalization of the **FLRW metric**.

  The Bianchi type IX metric, or **Mixmaster metric** (Misner, 1969), exhibits chaotic dynamic behavior near its curvature singularities.

- **Kasner metric**

  The **Kasner metric** is a Bianchi type I metric, which is a vacuum solution to the Einstein field equation for an anisotropic homogeneous Universe, given by

$$ds^2 = -dt^2 + t^{2p_1} dx^2 + t^{2p_2} dy^2 + t^{2p_3} dz^2,$$

  where $p_1 + p_2 + p_3 = p_1^2 + p_2^2 + p_3^2 = 1$.

  The equal-time slices of Kasner space-time are spatially flat, but space contracts in one dimension (i with $p_i < 0$), while expanding in the other two. The volume of the spatial slices is proportional to t; so, $t \to 0$ can describe either a Big Bang or a *Big Crunch*, depending on the sense of t.

- **GCSS metric**

  A **GCSS** (i.e., **general cylindrically symmetric stationary**) **metric** is a solution to the *Einstein field equation*, given by the *line element*

$$ds^2 = -f dt^2 + 2k dt d\phi + e^{\mu}(dr^2 + dz^2) + l d\phi^2,$$

  where the space-time is divided into two regions: the interior, with $0 \le r \le R$, to a cylindrical surface of radius R centered along z, and the exterior, with $R \le r < \infty$. Here f, k, μ and l are functions only of r, and $-\infty < t, z < \infty$, $0 \le \phi \le 2\pi$; the hypersurfaces $\phi = 0$ and $\phi = 2\pi$ are identical.

- **Lewis metric**

  The **Lewis metric** is a **cylindrically symmetric stationary metric** which is a solution to the *Einstein field equation* for empty space (vacuum) in the exterior of a cylindrical surface. The *line element* of this metric has the form

$$ds^2 = -fdt^2 + 2kdtd\phi - e^{\mu}(dr^2 + dz^2) + ld\phi^2,$$

  where $f = ar^{-n+1} - \frac{c^2}{n^2a}r^{n+1}$, $k = -Af$, $l = \frac{r^2}{f} - A^2 f$, $e^{\mu} = r^{\frac{1}{2}(n^2-1)}$ with $A = \frac{cr^{n+1}}{naf} + b$. The constants n, a, b, and c can be either real or complex, the corresponding solutions belong to the *Weyl class* or *Lewis class*, respectively. In the last case, such metrics form a subclass of the *Kasner type metrics*.
- **van Stockum dust metric**

  The **van Stockum dust metric** is a stationary cylindrically symmetric solution to the Einstein field equation for empty space (vacuum) with a rigidly rotating infinitely long dust cylinder. The *line element* of this metric for the interior of the cylinder is given (in comoving, i.e., corotating, coordinates) by

$$ds^2 = -dt^2 + 2ar^2 dtd\phi + e^{-a^2r^2}(dr^2 + dz^2) + r^2(1 - a^2r^2)d\phi^2,$$

  where $0 \le r \le R$, R is the radius of the cylinder, and a is the angular velocity of the dust particles. There are three vacuum exterior solutions (i.e., **Lewis metrics**) that can be matched to the interior solution, depending on the mass per unit length of the interior (the *low mass case*, the *null case*, and the *ultrarelativistic case*).

  Under some conditions (for example, if $ar > 1$), the existence of *closed time-like curves* (and, hence, time-travel) is allowed.
- **Levi-Civita metric**

  The **Levi-Civita metric** is a static cylindrically symmetric vacuum solution to the Einstein field equation, with the *line element*, given (in the Weyl form) by

$$ds^2 = -r^{4\sigma}dt^2 + r^{4\sigma(2\sigma-1)}(dr^2 + dz^2) + C^{-2}r^{2-4\sigma}d\phi,$$

  where the constant C refers to the deficit angle, and σ is a parameter.

  In the case $\sigma = -\frac{1}{2}$, $C = 1$ this metric can be transformed either into the *Taub's plane symmetric metric*, or into the *Robinson–Trautman metric*.
- **Weyl–Papapetrou metric**

  The **Weyl–Papapetrou metric** is a stationary axially symmetric solution to the Einstein field equation, given by the *line element*

$$ds^2 = Fdt^2 - e^{\mu}(dz^2 + dr^2) - Ld\phi^2 - 2Kd\phi dt,$$

  where F, K, L and μ are functions only of r and z, $LF + K^2 = r^2$, $\infty < t, z < \infty$, $0 \le r < \infty$, and $0 \le \phi \le 2\pi$; the hypersurfaces $\phi = 0$ and $\phi - 2\pi$ are identical.

- **Bonnor dust metric**

  The **Bonnor dust metric** is a solution to the *Einstein field equation* which is an axially symmetric metric describing a cloud of rigidly rotating dust particles moving along circular geodesics about the z axis in hypersurfaces of $z =$ *constant*. The *line element* of this metric is given by

$$ds^2 = dt^2 + (r^2 - n^2)d\phi^2 + 2ndtd\phi + e^{\mu}(dr^2 + dz^2),$$

  where, in Bonnor comoving (i.e., corotating) coordinates, $n = \frac{2hr^2}{R^3}$, $\mu = \frac{h^2r^2(r^2-8z^2)}{2R^8}$, $R^2 = r^2 + z^2$, and h is a rotation parameter.

  As $R \to \infty$, the metric coefficients tend to Minkowski values.

- **Weyl metric**

  The **Weyl metric** is a general static axially symmetric vacuum solution to the Einstein field equation given, in Weyl canonical coordinates, by the *line element*

$$ds^2 = e^{2\lambda}dt^2 - e^{-2\lambda}\left(e^{2\mu}(dr^2 + dz^2\right) + r^2d\phi^2),$$

  where λ and μ are functions only of r and z such that $\frac{\partial^2\lambda}{\partial r^2} + \frac{1}{r}\cdot\frac{\partial\lambda}{\partial r} + \frac{\partial^2\lambda}{\partial z^2} = 0$, $\frac{\partial\mu}{\partial r} = r(\frac{\partial\lambda^2}{\partial r} - \frac{\partial\lambda^2}{\partial z})$, and $\frac{\partial\mu}{\partial z} = 2r\frac{\partial\lambda}{\partial r}\frac{\partial\lambda}{\partial z}$.

- **Zipoy–Voorhees metric**

  The **Zipoy–Voorhees metric** (or γ-*metric*) is a **Weyl metric**, obtained for $e^{2\lambda} = \left(\frac{R_1+R_2-2m}{R_1+R_2+2m}\right)^{\gamma}$, $e^{2\mu} = \left(\frac{(R_1+R_2+2m)(R_1+R_2-2m)}{4R_1R_2}\right)^{\gamma^2}$, where $R_1^2 = r^2+(z-m)^2$, $R_2^2 = r^2 + (z+m)^2$. Here λ corresponds to the Newtonian potential of a line segment of mass density $\gamma/2$ and length $2m$, symmetrically distributed along the z axis.

  The case $\gamma = 1$ corresponds to the **Schwartzschild metric**, the cases $\gamma > 1$ ($\gamma < 1$) correspond to an oblate (prolate) spheroid, and for $\gamma = 0$ one obtains the flat Minkowski space-time.

- **Straight spinning string metric**

  The **straight spinning string metric** is given by the *line element*

$$ds^2 = -(dt - ad\phi)^2 + dz^2 + dr^2 + k^2r^2d\phi^2,$$

  where a and $k > 0$ are constants. It describes the space-time around a straight spinning string. The constant k is related to the string's mass-per-length μ by $k = 1–4\mu$, and the constant a is a measure of the string's spin. For $a = 0$ and $k = 1$, one obtains the **Minkowski metric** in cylindrical coordinates.

- **Tomimatsu–Sato metric**

  A **Tomimatsu–Sato metric** ([ToSa73]) is one of the metrics from an infinite family of spinning mass solutions to the Einstein field equation, each of which has the form $\xi = U/W$, where U and W are some polynomials.

  The simplest solution has $U = p^2(x^4 - 1) + q^2(y^4 - 1) - 2ipqxy(x^2 - y^2)$, $W = 2px(x^2 - 1) - 2iqy(1 - y^2)$, where $p^2 + q^2 = 1$. The *line element* for it is

given by

$$ds^2 = \Sigma^{-1}\left((\alpha dt + \beta d\phi)^2 - r^2(\gamma dt + \delta d\phi)^2\right) - \frac{\Sigma}{p^4(x^2-y^2)^4}(dz^2 + dr^2),$$

where $\alpha = p^2(x^2-1)^2+q^2(1-y^2)^2$, $\beta = -\frac{2q}{p}W(p^2(x^2-1)(x^2-y^2)+2(px+1)W)$, $\gamma = -2pq(x^2-y^2)$, $\delta = \alpha + 4((x^2-1)+(x^2+1)(px+1))$, $\Sigma = \alpha\delta - \beta\gamma = |U+W|^2$.

- **Gödel metric**

  The **Gödel metric** is an exact solution to the Einstein field equation with cosmological constant for a rotating Universe, given by the *line element*

$$ds^2 = -(dt^2 + C(r)d\phi)^2 + D^2(r)d\phi^2 + dr^2 + dz^2,$$

  where (t, r, ϕ, z) are the usual *cylindrical coordinates*.

  The *Gödel Universe* is homogeneous if $C(r) = \frac{4\Omega}{m^2}\sinh^2\left(\frac{mr}{2}\right)$, $D(r) = \frac{1}{m}\sinh(mr)$, where m and Ω are constants. The Gödel Universe is singularity-free. But there are *closed time-like curves* through every event, and hence time-travel is possible here. The condition required to avoid such curves is $m^2 > 4\Omega^2$.

- **Conformally stationary metric**

  The **conformally stationary metrics** are models for gravitational fields that are time-independent up to an overall conformal factor. If some global regularity conditions are satisfied, the space-time must be a product $\mathbb{R} \times M^3$ with a (Hausdorff and paracompact) 3-manifold M^3, and the *line element* of the metric is given by

$$ds^2 = e^{2f(t,x)}(-(dt + \sum_\mu \phi_\mu(x)dx_\mu)^2 + \sum_{\mu,\nu} g_{\mu\nu}(x)dx_\mu dx_\nu),$$

  where $\mu, \nu = 1, 2, 3$. The conformal factor e^{2f} does not affect the light-like geodesics apart from their parametrization, i.e., the paths of light rays are completely determined by the Riemannian metric $g = \sum_{\mu,\nu} g_{\mu\nu}(x)dx_\mu dx_\nu$ and the one-form $\phi = \sum_\mu \phi_\mu(x)dx_\mu$ which both live on M^3.

  In this case, the function f is called the *redshift potential*, the metric g is called the **Fermat metric**. For a static space-time, the geodesics in the Fermat metric are the projections of the null geodesics of space-time.

  In particular, the **spherically symmetric and static metrics**, including models for nonrotating stars and black holes, *wormholes*, *monopoles*, *naked singularities*, and (boson or fermion) stars, are given by the *line element*

$$ds^2 = e^{2f(r)}(-dt^2 + S(r)^2dr^2 + R(r)^2(d\theta^2 + \sin^2\theta d\phi^2)).$$

  Here, the one-form ϕ vanishes, and the Fermat metric g has the special form

$$g = S(r)^2dr^2 + R(r)^2(d\theta^2 + \sin^2\theta d\phi^2).$$

For example, the conformal factor $e^{2f(r)}$ of the **Schwartzschild metric** is equal to $1 - \frac{2m}{r}$, and the corresponding Fermat metric has the form

$$g = (1 - \frac{2m}{r})^{-2}(1 - \frac{2m}{r})^{-1}r^2(d\theta^2 + \sin\theta d\phi^2).$$

- **pp-wave metric**

  The **pp-wave metric** is an exact solution to the Einstein field equation, in which radiation moves at the speed c of light. The *line element* of this metric is given (in Brinkmann coordinates) by

$$ds^2 = H(u, x, y)du^2 + 2dudv + dx^2 + dy^2,$$

  where H is any smooth function. The term "pp" stands for *plane-fronted waves with parallel propagation* introduced by Ehlers–Kundt, 1962.

  The most important class of particularly symmetric pp-waves are the **plane wave metrics**, in which H is quadratic. The *wave of death*, for example, is a *gravitational* (i.e., the space-time curvature fluctuates) plane wave exhibiting a strong nonscalar null curvature singularity which propagates through an initially flat space-time, progressively destroying the Universe.

  Examples of axisymmetric pp-waves include the *Aichelburg–Sexl ultraboost* modeling the motion past a spherically symmetric gravitating object at nearly c, and the *Bonnor beam* modeling the gravitational field of an infinitely long beam of incoherent electromagnetic radiation. The Aichelburg–Sexl wave is obtained by boosting the Schwarzschild solution to the speed c at fixed energy, i.e., it describes a Schwarzschild black hole moving at c. Cf. **Aichelburg–Sexl metric** (Chap. 24).

- **Bonnor beam metric**

  The **Bonnor beam metric** is an exact solution to the Einstein field equation which models an infinitely long, straight beam of light. It is an **pp-wave metric**.

  The interior part of the solution (in the uniform plane wave interior region which is shaped like the world tube of a solid cylinder) is defined by the *line element*

$$ds^2 = -8\pi mr^2du^2 - 2dudv + dr^2 + r^2d\theta^2,$$

  where $-\infty < u, v < \infty$, $0 < r < r_0$, and $-\pi < \theta < \pi$. This is a null dust solution and can be interpreted as incoherent electromagnetic radiation.

  The exterior part of the solution is defined by

$$ds^2 = -8\pi mr_0^2(1 + 2\log(r/r_0))du^2 - 2dudv + dr^2 + r^2d\theta^2,$$

  where $-\infty < u, v < \infty$, $r_0 < r < \infty$, and $-\pi < \theta < \pi$.

- **Plane wave metric**

  The **plane wave metric** is a vacuum solution to the Einstein field equation, given by the *line element*

$$ds^2 = 2dwdu + 2f(u)(x^2 + y^2)du^2 - dx^2 - dy^2.$$

  It is conformally flat, and describes a pure radiation field. The space-time with this metric is called the *plane gravitational wave*. It is an **pp-wave metric**.
- **Wils metric**

  The **Wils metric** is a solution to the *Einstein field equation*, given by

$$ds^2 = 2xdwdu - 2wdudx + \left(2f(u)x(x^2 + y^2) - w^2\right) du^2 - dx^2 - dy^2.$$

  It is conformally flat, and describes a pure radiation field which is not a *plane wave*.
- **Koutras–McIntosh metric**

  The **Koutras–McIntosh metric** is a solution to the Einstein field equation, given by the *line element*

$$ds^2 = 2(ax+b)dwdu - 2awdudx + \left(2f(u)(ax + b)(x^2 + y^2) - a^2w^2\right) du^2 - dx^2 - dy^2.$$

  It is conformally flat and describes a pure radiation field which, in general, is not a *plane wave*. It gives the **plane wave metric** for $a = 0$, $b = 1$, and the **Wils metric** for $a = 1$, $b = 0$.
- **Edgar–Ludwig metric**

  The **Edgar–Ludwig metric** is a solution to the *Einstein field equation*, given by

$$ds^2 = 2(ax + b)dwdu - 2awdudx +$$

$$+ \left(2f(u)(ax + b)(g(u)y + h(u) + x^2 + y^2) - a^2w^2\right) du^2 - dx^2 - dy^2.$$

  This metric is a generalization of the **Koutras–McIntosh metric**. It is the most general metric which describes a conformally flat pure radiation (or null fluid) field which, in general, is not a *plane wave*. If plane waves are excluded, it has the form

$$ds^2 = 2xdwdu - 2wdudx + \left(2f(u)x(g(u)y + h(u) + x^2 + y^2) - w^2\right) du^2 - dx^2 - dy^2.$$

- **Bondi radiating metric**

  The **Bondi radiating metric** describes the asymptotic form of a radiating solution to the Einstein field equation, given by the *line element*

$$ds^2 = -\left(\frac{V}{r}e^{2\beta} - U^2r^2e^{2\gamma}\right) du^2 - 2e^{2\beta}dudr - 2Ur^2e^{2\gamma}dud\theta + r^2(e^{2\gamma}d\theta^2 + e^{-2\gamma}\sin^2\theta d\phi^2),$$

where u is the retarded time, r is the **luminosity distance**, $0 \le \theta \le \pi$, $0 \le \phi \le 2\pi$, and U, V, β, γ are functions of u, r, and θ.

- **Taub–NUT de Sitter metric**

  The **Taub–NUT de Sitter metric** (cf. **de Sitter metric**) is a positive-definite (i.e., Riemannian) solution to the Einstein field equation with a cosmological constant Λ, given by the *line element*

$$ds^2 = \frac{r^2 - L^2}{4\Delta} dr^2 + \frac{L^2 \Delta}{r^2 - L^2} (d\psi + \cos\theta d\phi)^2 + \frac{r^2 - L^2}{4} (d\theta^2 + \sin^2\theta d\phi^2),$$

  where $\Delta = r^2 - 2Mr + L^2 + \frac{\Lambda}{4}(L^4 + 2L^2 r^2 - \frac{1}{3} r^4)$, L and M are parameters, and θ, ϕ, ψ are the *Euler angles*.

  If $\Lambda = 0$, one obtains the **Taub–NUT metric** (Chap. 7).

- **Eguchi–Hanson de Sitter metric**

  The **Eguchi–Hanson de Sitter metric** (cf. **de Sitter metric**) is a positive-definite (i.e., Riemannian) solution to the Einstein field equation with a cosmological constant Λ, given by the *line element*

$$ds^2 = \left(1 - \frac{a^4}{r^4} - \frac{\Lambda r^2}{6}\right)^{-1} dr^2 + \frac{r^2}{4} \left(1 - \frac{a^4}{r^4} - \frac{\Lambda r^2}{6}\right) (d\psi + \cos\theta d\phi)^2 +$$

$$+ \frac{r^2}{4} (d\theta^2 + \sin^2\theta d\phi^2),$$

  where a is a parameter, and θ, ϕ, ψ are the *Euler angles*.

  If $\Lambda = 0$, one obtains the **Eguchi-Hanson metric**.

- **Barriola–Vilenkin monopole metric**

  The **Barriola–Vilenkin monopole metric** is given by the *line element*

$$ds^2 = -dt^2 + dr^2 + k^2 r^2 (d\theta^2 + \sin^2\theta d\phi^2),$$

  with a constant $k < 1$. There is a deficit solid angle and a singularity at $r = 0$; the plane $t = constant$, $\theta = \frac{\pi}{2}$ has the geometry of a cone.

  This metric is an example of a conical singularity; it can be used as a model for *monopole*, i.e., a hypothetical isolated magnetic poles. It has been theorized that such things might exist in the form of tiny particles similar to electrons or protons, formed from topological defects in a similar manner to cosmic strings.

  Cf. **Gibbons–Manton metric** in Chap. 7.

- **Bertotti–Robinson metric**

  The **Bertotti–Robinson metric** is a solution to the Einstein field equation in a universe with a uniform magnetic field. The *line element* of this metric is

$$ds^2 = Q^2 (-dt^2 + \sin^2 t dw^2 + d\theta^2 + \sin^2\theta d\phi^2),$$

  where Q is a constant, $t \in [0, \pi]$, $w \in (-\infty, +\infty)$, $\theta \in [0, \pi]$, and $\phi \in [0, 2\pi]$.

- **Wormhole metric**

  A *wormhole* is a hypothetical region of space-time containing a *world tube* (the time evolution of a closed surface) that cannot be continuously deformed to a *world line* (the time evolution of a point).

  Wormhole metric is a theoretical distortion of space-time in a region of the Universe that would link one location or time with another, through a "shortcut", i.e., a path that is shorter in distance or duration than would otherwise be expected. A wormhole geometry can only appear as a solution to the Einstein equations if the *stress-energy tensor* of matter violates the *null energy condition* at least in a neighborhood of the wormhole throat.

  Einstein–Rosen bridge (1935) is a *nontraversable* (unstable) wormhole formed from either black hole or spherically symmetric vacuum regions; it possesses a singularity and impenetrable event horizon. Traversable wormholes, as well as *warp drive* (faster-than-light propulsion system) and *time machines*, permitting journeys into the past, require bending of space-time by *exotic matter* (negative mass or energy).

  Whereas the curvature of space produced by the attractive gravitational field of ordinary matter acts like a converging lens, negative energy acts like a diverging lens. The negative mass required for engineering, say, a wormhole of throat diameter 4.5 m, as in Stargate's inner ring (from TV franchise *Stargate*), is $\approx -3\times 10^{27}$ kg. But oscillating warp and tweaking wormhole's geometry (White, 2012) can greatly reduce it. Also, negative energy can be created (Butcher, 2014) at the centre of a wormhole if its throat is orders of magnitude longer than its mouth.

  Lorentzian wormholes, not requiring exotic matter to exist, were proposed, using higher-dimensional extensions of Einstein's theory of gravity, by Bronnikov–Kim, 2002, and Kanti–Kleihaus–Kunz, 2011. Still, only atomic-scale wormholes would be practical to build, using them solely for superluminal information transmission.

  Lorentzian wormholes can be seen as maximally entangled states of two black holes in a *Einstein–Podolsky–Rosen correlation*, i.e., *nonclassical* one (it cannot be approximated by convex combinations of product states). Maldacena–Susskind, 2013: any two entangled quantum subsystems (cf. Chap. 24) are connected by a such wormhole. For Sonner, 2013, gravity might emerge from quantum entanglement.

- **Morris–Thorne metric**

  The **Morris–Thorne metric** (Morris–Thorne, 1988) is a traversable **wormhole metric** which is a solution to the Einstein field equation with the *line element*

$$ds^2 = e^{\frac{2\Phi(w)}{c^2}} c^2 dt^2 - dw^2 - r(w)^2(d\theta^2 + \sin^2\theta d\phi^2),$$

  where $w \in [-\infty, +\infty]$, r is a function of w that reaches some minimal value above zero at some finite value of w, and $\Phi(w)$ is a gravitational potential

allowed by the space-time geometry. It is the most general static and spherically symmetric metric able to describe a stable and traversable wormhole.

Morris–Thorne–Yurtsever, 1988, stated that two closely spaced ($10^{-9} - 10^{-10}$ m) concentric thin charged hollow spheres the size of 1 AU can create negative energy, required for engineering this wormhole, using the quantum *Casimir effect*.

- **Alcubierre metric**

  The **Alcubierre metric** (Alcubierre, 1994) is a **wormhole metric** which is a solution to the Einstein field equation, representing *warp drive space-time* where the existence of *closed time-like curves* is allowed. The Alcubierre construction corresponds to a *warp* (i.e., faster than light) drive in that it causes space-time to contract in front of a spaceship bubble and expand behind, thus providing the spaceship with a velocity that can be much greater than the speed of light relative to distant objects, while the spaceship never locally travels faster than light.

  In this case, only the relativistic principle that a space-traveler may move with any velocity up to, but not including or exceeding, the speed of light, is violated.

  Also, light has another speed, *phase velocity*, measured by how fast a wavelength's crests move. This speed depends on the material it's moving through.

  The *line element* of this metric has the form

$$ds^2 = -dt^2 + (dx - vf(r)dt)^2 + dy^2 + dz^2,$$

  where $v = \frac{dx_s(t)}{dt}$ is the apparent velocity of the warp drive spaceship, $x_s(t)$ is spaceship trajectory along the coordinate x, the radial coordinate is $r = ((x - x_s(t))^2 + y^2 + z^2)^{\frac{1}{2}}$, and $f(r)$ an arbitrary function subject to the conditions that $f = 1$ at $r = 0$ (the location of the spaceship) and $f(\infty) = 0$.

  Another warp drive space-time was proposed by Krasnikov, 1995. **Krasnikov metric** in the 2D subspace t, x is given by the *line element*

$$ds^2 = -dt^2 + (1 - k(x,t))dxdt + k(x,t)dx^2,$$

  where $k(x,t) = 1 - (2 - \delta)\theta_\epsilon(t - x)(\theta_\epsilon(x) - \theta_\epsilon(x + \epsilon - D))$, D is the distance to travel, θ_ϵ is a smooth monotonic function satisfying $\theta_\epsilon(z) = 1$ at $z > \epsilon$, $\theta_\epsilon(z) = 0$ at $z < 0$ and δ, ϵ are arbitrary small positive parameters.

- **Misner metric**

  The **Misner metric** (Misner, 1960) is a metric, representing two black holes, instantaneously at rest, whose throats are connected by a *wormhole*. The *line element* of this metric has the form

$$ds^2 = -dt^2 + \psi^4(dx^2 + dy^2 + dz^2),$$

where the *conformal factor* ψ is given by

$$\psi = \sum_{n=-N}^{N} \frac{1}{\sinh(\mu_0 n)} \frac{1}{\sqrt{x^2 + y^2 + (z + \coth(\mu_0 n))^2}}.$$

The parameter μ_0 is a measure of the ratio of mass to separation of the throats (equivalently, a measure of the distance of a loop in the surface, passing through one throat and out of the other). The summation limit N tends to infinity.

The topology of the *Misner space-time* is that of a pair of asymptotically flat sheets connected by a number of wormholes. In the simplest case, it can be seen as a 2D space $\mathbb{R} \times S^1$, in which light progressively tilts as one moves forward in time, and has *closed time-like curves* (so, time-travel is possible) after a certain point.

- **Rotating *C*-metric**

  The **rotating *C*-metric** is a solution to the *Einstein–Maxwell equations*, describing two oppositely charged black holes, uniformly accelerating in opposite directions. The *line element* of this metric has the form

$$ds^2 = A^{-2}(x+y)^{-2}\left(\frac{dy^2}{F(y)} + \frac{dx^2}{G(x)} + k^{-2}G(X)d\phi^2 - k^2A^2F(y)dt^2\right),$$

  where $F(y) = -1 + y^2 - 2mAy^3 + e^2A^2y^4$, $G(x) = 1 - x^2 - 2mAx^3 - e^2A^2x^4$, m, e, and A are parameters related to the mass, charge and acceleration of the black holes, and k is a constant fixed by regularity conditions.

  This metric should not be confused with the ***C*-metric** from Chap. 11.

- **Myers–Perry metric**

  The **Myers–Perry metric** describes a 5D rotating black hole. Its *line element* is

$$ds^2 = -dt^2 + \frac{2m}{\rho^2}(dt - a\sin^2\theta d\phi - b\cos^2\theta d\psi)^2 +$$

$$+\frac{\rho^2}{R^2}dr^2 + \rho^2 d\theta^2 + (r^2 + a^2)\sin^2\theta d\phi^2 + (r^2 + b^2)\cos^2\theta d\psi^2,$$

  where $\rho^2 = r^2 + a^2\cos^2\theta + b^2\sin^2\theta$, and $R^2 = \frac{(r^2+a^2)(r^2+b^2)-2mr^2}{r^2}$. Above black hole is asymptotically flat and has an event horizon with S^3 topology.

  Emparan and Reall, 2001, using the possibility of rotation in several independent rotation planes, found a 5D *black ring*, i.e., asymptotically flat black hole solution with the event horizon's topology of $S^1 \times S^2$.

- **Ponce de León metric**

  The **Ponce de León metric** (1988) is a 5D metric, given by the *line element*

$$ds^2 = l^2dt^2 - (t/t_0)^2 pl^{\frac{2p}{p-1}}(dx^2 + dy^2 + dz^2) - \frac{t^2}{(p-1)^2}dl^2,$$

where l is the 5-th (space-like) coordinate. This metric represents a 5D apparent vacuum. It is not flat but embed the flat 4D **FLRW metric**.

- **Kaluza–Klein metric**

  The **Kaluza–Klein metric** is a metric in the *Kaluza–Klein model* of 5D space-time which seeks to unify classical gravity and electromagnetism.

  Kaluza, 1921 (but sent to Einstein in 1919), found that, if the Einstein theory of pure gravitation is extended to a 5D space-time, the Einstein field equation can be split into an ordinary 4D gravitation tensor field, plus an extra vector field which is equivalent to the Maxwell equation for the electromagnetic field, plus an extra scalar field known as the *dilation* (or *radion*).

  Klein, 1926, assumed that the 5-th dimension (i.e., 4-th spatial dimension) is curled up in a circle of an unobservable size, below 10^{-20} m. Almost all modern higher-dimensional unified theories are based on Kaluza–Klein approach.

  An alternative proposal is that the extra dimension(s) is extended, and the matter is trapped in a 4D submanifold. In a model of a such large extra dimension, the 5D metric of a universe can be written in Gaussian normal coordinates as

$$ds^2 = -(dx_5)^2 + \lambda^2(x_5) \sum_{\alpha,\beta} \eta_{\alpha\beta} dx_\alpha dx_\beta,$$

  where $\eta_{\alpha\beta}$ is the 4D **metric tensor** and $\lambda^2(x_5)$ is any function of the 5-th coordinate.

  In particular, the *STM* (space-time-matter) *theory* (Wesson and Ponce de León, 1992) relate the 5-th coordinate to mass via either $x_5 = \frac{Gm}{c^2}$ or $x_5 = \frac{h}{mc}$, where G is the *Newton gravitational constant* and h is the *Planck constant*.

  The **Ponce de León metric** is a STM solution. In STM (or *induced matter*) theory, the 4D curvature arises not due to the distribution of matter in the Universe (as claims Relativity Theory) but because the Universe is embedded in some higher-dimensional vacuum manifold M, and all the matter in our world can be thought of as being manifestations of the geometrical properties of M.

  Wesson and Seahra, 2005, claim that the Universe may be a 5D black hole. Life is not excluded since in 5D there is no physical plughole and the "tidal" forces are negligible. Suitable manifolds for such STM theory are given by two isometric solutions of the 5D vacuum field equations: *Liu–Mashhoon–Wesson metric* and *Fukui–Seahra–Wesson metric*; both embed 4D **FLRW metric**.

- **Carmeli metric**

  The **Carmeli metric** (Carmeli, 1996) is given by the *line element*

$$ds^2 = dx^2 + dy^2 + dz^2 - \tau^2 dv^2,$$

  where $\tau = \frac{1}{H}$ is the inverse of *Hubble constant* and v is the *cosmological recession velocity*. So, comparing with the **Minkowski metric**, it has τ and velocity v, instead of c and time t. This metric was used in *Carmeli's Relativity Theory* which is intended to be better than General Relativity on cosmological scale.

The Carmeli metric produces the *Tulli–Fisher type relation* in spiral galaxies: 4-th power of the rotation speed is proportional to the mass of galaxy; it obviate the need for dark matter. This metric predicts also cosmic acceleration.

Including *icdt* component of the **Minkowski metric**, gives the **Kaluza–Klein–Carmeli metric** (Harnett, 2004) defined by

$$ds^2 = dx^2 + dy^2 + dz^2 - c^2dt^2 - \tau^2 dv^2.$$

- **Prasad metric**

A *de Sitter Universe* can be seen as the sum of the external and internal space.

The internal space has a negative constant curvature $-\frac{1}{r^2}$ and can be characterized by the symmetry group $SO_{3,2}$. The **Prasad metric** of this space is given, in hyperspherical coordinates, by the *line element*

$$ds^2 = r^2 \cos^2 t(d\chi^2 + \sinh^2 \chi(d\theta^2 + \sin^2 \theta d\phi^2)) - r^2 dt^2.$$

The value $\sin \chi$ is called *adimensional normalized radius* of the de Sitter Universe.

The external space has constant curvature $\frac{1}{R^2}$ and can be characterized by the symmetry group $SO_{4,1}$. Its metric has the *line element* of the form

$$ds^2 = R^2 \cosh^2 t(d\chi^2 + \sin^2 \chi(d\theta^2 + \sin^2 \theta d\phi^2)) - R^2 dt^2.$$

Part VII
Real-World Distances

Chapter 27
Length Measures and Scales

The term *length* has many meanings: distance, extent, linear measure, span, reach, end, limit, etc.; for example, the length of a train, a meeting, a book, a trip, a shirt, a vowel, a proof. The *length* of an object is its linear extent, while the *height* is the vertical extent, and *width* (or *breadth*) is the side-to-side distance at 90° to the length, wideness. The *depth* is the distance downward, distance inward, deepness, profundity, drop.

The ancient Greek mathematicians saw all numbers as lengths (of segments), areas or volumes. In Mathematics, a **length function** is a function $l : G \to \mathbb{R}_{\geq 0}$ on a group $(G, +, 0)$ such that $l(0) = 0$ and $l(g) = l(-g)$, $l(g + g') \leq l(g) + l(g')$ for $g, g' \in G$.

In Engineering and Physics, "length" usually means "distance". **Unit distance** is a distance taken as a convenient unit of length in a given context.

In this chapter we consider length only as a measure of physical distance. We give selected information on the most important length units and present, in length terms, a list of interesting physical objects.

27.1 Length Scales

The main length measure systems are: Metric, Imperial (British and American), Japanese, Thai, Chinese Imperial, Old Russian, Ancient Roman, Ancient Greek, Biblical, Astronomical, Nautical, and Typographical.

There are many other specialized length scales; for example, to measure cloth, shoe size, gauges (such as interior diameters of shotguns, wires, jewelry rings), sizes for abrasive grit, sheet metal thickness, etc.

Many units express relative or inverse distances. Quantities measured in **reciprocal length** include: radius of curvature, density of a linear feature in an area, surface-area-to-volume ratio, vector's magnitude (in Crystallography and Spectroscopy),

© Springer-Verlag Berlin Heidelberg 2016

M.M. Deza, E. Deza, *Encyclopedia of Distances*,
DOI 10.1007/978-3-662-52844-0_27

optical power (cf. **lens distances** in Chap. 29), absorption (or attenuation) coefficient (cf. Chap. 24), gain (in Laser Physics). Common units used for such measures are inverse meter m^{-1} (called *diopter* in Optics), cm^{-1} and cycles per unit length (for spatial frequency).

Some units express nonlength quantities in length terms. For example, the *denudation rate* (wearing down of the Earth's surface) is measured in cm per 1000 years. Cf. also **meter of water equivalent** in Chap. 24.

- **International Metric System**

  The **International Metric System** (or SI, short for *Système International*), also known as MKSA (meter–kilogram–second–ampere), is a modernized version of the system of units, established by the *Treaty of the Meter* from 20 May 1875, which provides a logical and interconnected framework for all measurements in science, industry and commerce. The system is built on a foundation consisting of the following seven *SI base units*, assumed to be mutually independent:

  (1) length: **meter** (m); it is equal to the distance traveled by light in a vacuum in 1/299,792,458 of a second; (2) time: *second* (s); (3) mass: *kilogram* (kg); (4) temperature: *kelvin* (K); (5) electric current: *ampere* (A); (6) luminous intensity: *candela* (cd); (7) amount of substance: *mole* (mol).

  Meter, second, candela are already defined in terms of fundamentals of nature. Kilogram, kelvin, mole and ampere are expected to be redefined in terms of the Planck, Boltzmann, Avogadro constants and the charge of proton, respectively.

  Meter is defined as a **proper length** (the length of the object in its rest frame, cf. Sect. 26.2). So, it is well defined only over short distances where relativistic effects are negligible (cf. **Lorentz length contraction** in Sect. 26.1), and all cosmic distances, given in meters, are approximations.

  Originally, on March 26, 1791, the *mètre* (French for meter) was defined as $\frac{1}{10{,}000{,}000}$ of the distance from the North Pole to the equator along the Dunkirk-Barcelona meridian. The name *mètre* was derived from the Greek *metron* (measure). In 1799 the standard of *mètre* became a meter-long platinum-iridium bar kept in Sèvres, a town outside Paris, for people to come and compare their rulers with. (The metric system, introduced in 1793, was so unpopular that Napoleon was forced to abandon it and France returned to the *mètre* only in 1837.) In 1960–1983, the **meter** was defined in terms of wavelengths.

  The initial metric unit of mass, the *gram*, was defined as the mass of one cubic centimeter of water at its temperature of maximum density. A *metric ton* (or *metric tonne*, *tonne*) is a unit of mass equal to 1000 kg; this non-SI unit is used instead of the SI term *megagram* (10^6 grams). For capacity, the *litre* (liter) was defined as the volume of a cubic decimeter.

- **Metrication**

  The **metrication** is an ongoing (especially, in the US, the UK and Caribbean countries) process of conversion to the **International Metric System**, SI. Only the US, Liberia and Myanmar have not fully switched to SI.

For example, the US uses only miles for road distance signs (milestones). Altitudes in aviation are usually described in feet, and resolutions of output devices are specified in *dpi* (dots per inch). In shipping, nautical miles and knots are used; both are accepted for use with SI.

Hard metric means designing in the metric measures from the start and conformation, where appropriate, to internationally recognized sizes and designs.

Soft metric means multiplying an inch-pound number by a metric conversion factor and rounding it to an appropriate level of precision; so, the soft converted products do not change size. The *American Metric System* consists of converting traditional units to embrace the uniform base 10 used by the Metric System.

Such SI-Imperial hybrid units, used in soft metrication, are, for example, *kiloyard* (914.4 m), *kilofoot* (304.8 m), *mil* or *milli-inch* (25.4 micron), and *min* or *microinch* (25.4 nm). The *metric inch* (2.5 cm $\approx$ 1 inch) and *metric foot* (30 cm) were used in some Soviet computers when building from American blueprints.

In athletics and skating, races of 1500 m or 1600 m are often called *metric miles*. Examples of traditional units adapted to the meter are Chinese *li* = 500 m = 1500 *chi* (Chinese feet), Thai *wa* = 2 m = 4 *sok*, Vietnamese *xich* = 1 m = 1000 *ly*.

- **Meter, in Poetry and Music**

  In Poetry, *meter* (or *cadence*) is a measure of rhythmic quality, the regular linguistic sound patterns of a verse or line in it. The meter of a verse is the number of lines, the number of syllables in each line and their arrangement as sequences of *feet*. Each foot is a specific sequence of syllable types—such as unstressed/stressed or long/short. Fussell, 1965, define four types of meter: syllabic, accentual, accentual-syllabic and quantitative, where patterns are based on *syllable weight* (number and/or duration of segments in the rhyme) rather than stress.

  Hypermeter is part of a verse with an extra syllable; *metromania* is a mania for writing verses and *metrophobia* is a fear/hatred of poetry.

  In Music, *meter* (or *metre*) is the regular rhythmic patterns of a musical line, the division of a composition into parts of equal time, and the subdivision of them. It is derived from the poetic meter of song. Different tonal preferences in voiced speech are reflected in music; it explains why Eastern and Western music differ.

  Metrical rhythm is where each time value is a multiple or fraction of a fixed unit (*beat*) and normal accents re-occur regularly providing systematic grouping (*measures*). *Isometre* is the use of a *pulse* (unbroken series of periodically occurring short stimuli) without a regular meter, and *polymetre* is the use of two or more different meters simultaneously, whereas *multimetre* is using them in succession.

  A rhythmic pattern/unit is either *intrametric* (confirming the pulses on the metric level), or *contrametric* (syncopated, not following the beat/meter), or *extrametric* (irregular with respect to the metric structure of the piece).

Rhythms/chords with the same multiset of intervals/distances are called *homometric*.

A temporal pattern is *metrically represented* if it can be subdivided into equal time intervals. A *metronome* is any device that produces regular, metrical ticks (beats); *metronomy*: measurement of time by a metronome or, in general, an instrument.

- **Meter-related terms**

We present this large family of terms by the following examples (besides the unit of length and use in Poetry and Music).

Metrograph: a device attached to a locomotive to record its speed and the number and duration of its stops. Cf. unrelated *metrography* in Medicine (Chap. 29).

Metrogon: a high resolution, low-distortion, extra-wide field photographic lens design used extensively in aerial photography.

The names of various measuring instruments contain *meter* at the end, say, *ammeter*, *gas meter*, *multimeter* (or *volt-ohm meter*).

Metrosophy: a cosmology based on strict number correspondences.

Metrology: the science of, or a system of, weights and measures.

A **metric meterstick** is a rough rule of thumb for comprehending a metric unit; for example, 5 cm is the side of a matchbox, and 1 km is $\approx$ 10 minutes' walk.

Metering: an equivalent term for a *measurement* (assignment of numbers to objects or events); *micrometry*: measurement under the microscope; *hypsometry*: measurement of heights; *telemetry*: technology that allows remote measurement; *archeometry*: the science of exact measuring referring to the remote past.

Hedonimetry: the study of happiness as a measurable economic asset; *psychometry*: alleged psychic power enabling one to divine facts by handling objects.

Psychometrics: the theory and technique of psychological measurement; *psychrometrics*: the determination of physical and thermodynamic properties of gas-vapor mixtures; *biometrics*: the identification of humans by their characteristics or traits; *cliometrics*: the systematic application of econometric techniques and other formal or mathematical methods to the study of history.

Metric, as a nonmathematical term, is a standard unit of measure (for example, *font metrics* refer to numeric values relating to size and space in the font) or, more generally, part of a system of parameters; cf. **quality metrics** in Chap. 29.

Antimetric matrix: a square matrix A with $A = -A^T$; an *antimetric electrical network* is one that exhibits antisymmetrical electrical properties.

Isometropia: equality of refraction in both eyes; *hypermetropia* is farsightedness.

Isometric particle: a virus which (at the stage of virion capsid) has icosahedral symmetry. *Isometric process*: a thermodynamic process at constant volume.

Metrohedry: overlap in 3D of the lattices of twin domains in a crystal.

Multimetric crystallography: to consider (Janner, 1991), in addition to the Euclidean metric tensor, *pseudo-Euclidean tensors* (hyperbolic rotations)

attached to the same basis; cf. **pseudo-Euclidean distance** in Chap. 7 and **multimetric** in Chap. 3.

Metria: a genus of moths of the *Noctuidae* family.

Metrio: Greek coffee with one teaspoon of sugar (medium sweet). In Anthropology, *metriocranic* means having a skull that is moderately high compared with its width, with a breadth-height index 92–98.

Metroid: the name of a series of video games produced by Nintendo and *metroids* are a fictional species of parasitic alien creatures from those games.

Examples of companies with a meter-related name are: Metron, Metric Inc., MetaMetrics Inc., Metric Engineering, Panametric, Prometric, Unmetric, World Wide Metric. *Metric* is also a Canadian New Wave rock band.

- **Metric length measures**

  kilometer (km) = 1000 meters = 10^3 m;
  meter (m) = 10 decimeters = 10^0 m;
  decimeter (dm) = 10 centimeters = 10^{-1} m;
  centimeter (cm) = 10 millimeters = 10^{-2} m;
  millimeter (mm) = 1000 micrometers = 10^{-3} m;
  micrometer (or non-SI *micron*; μm) = 1000 nanometers = 10^{-6} m;
  nanometer (or non-SI 10 *angstroms* Å; nm) = 1000 picometers = 10^{-9};
  picometer (pm) = 1000 femtometers = 10^{-12} m;
  femtometer (or non-SI *fermi*; fm) = 1000 attometers = 10^{-15} m.

  The numbers 10^{3t} ($t = -8, \ldots, -1, 1, \ldots, 8$) are given by *metric prefixes*: yocto-(y), zepto-(z), atto-(a), femto-(f), pico-(p), nano-(n), micro-(μ), milli-(m), kilo-(k), mega-(M), giga-(G), tera-(T), peta-(P), exa-(E), zetta-(Z), yotta-(Y), respectively, while 10^t ($t = -2, -1, 1, 2$) are given by centi-(c), deci-(d), deca-(da), hecto-(h).

  But for plankton's size femto-, pico-, nano-, micro-, meso-, macro-, mega- mean $< 0.2\mu$, 0.2–2μ, 2–20μ, 20–200μ, 0.2–20 mm, 20–200 mm, $>$ 200 mm.

  In computers, a *bit* (binary digit) is the basic unit of information, a *byte* (or *octet*) is 8 bits, and 10^{3t} bytes for $t = 1, \ldots, 8$ are kilo-(KB), mega-(MB), giga-(GB), ..., yottabyte (YB), respectively. Sometimes (because of $2^{10} = 1024 \approx 10^3$) the binary terms kibi-(KiB), mebi-(MiB), gibibyte (GiB), etc., are used for 2^{10t} bytes.

- **Imperial length measures**

  The **Imperial length measures** (as slightly adjusted by a treaty in 1959) are:
  (land) *league* = 3 international miles;
  (international) *mile* = 5280 feet = 1609.344 m;
  (US survey) *mile* = 5280 US feet ≈ 1609.347 m;
  data (or *tactical*) *mile* = 6000 feet = 1828.8 m and *radar mile* = 12.204 μs (time it takes a radar pulse to travel one data mile forth and back);
  (international) *yard* = 0.9144 m = 3 *feet* = $\frac{1}{2}$ *fathom*;
  (international) *foot* = 0.3048 m = 12 *inches*;
  (international) *inch* = 2.54 cm = 12 *lines*;

(a unit of measure of height of equipment) *rack unit* $= \frac{7}{4}$ inch;

(a unit of measure in advertising space) *agate line* $\approx \frac{1}{14}$ inch;

(a unit of computer mouse movement) *mickey* $= \frac{1}{200}$ inch;

mil (British *thou*) $= \frac{1}{1000}$ inch; *mil* is also an angular measure $\frac{\pi}{3200} \approx 0.001$ radian.

In addition, *Surveyor's Chain measures* are: *furlong* $= 10$ chains $= \frac{1}{8}$ mile; *chain* $= 100$ links $= 66$ feet; *rope* $= 20$ feet; *rod* (or *pole*) $= 16.5$ feet; *link* $= 7.92$ inches. Mile, furlong and fathom come from the slightly shorter Greco-Roman milos (milliare), stadion and orguia, mentioned in the New Testament.

For measuring cloth, old measures are used: *bolt* $= 40$ yards; *goad* $= \frac{3}{2}$ yard; *ell* $= \frac{5}{4}$ yard $= 45$ inches; *quarter* $= \frac{1}{4}$ yard; *finger* $= \frac{1}{8}$ yard; *nail* $= \frac{1}{16}$ yard.

Other old English units of length: *barleycorn* $= \frac{1}{3}$ inch; *digit* $= \frac{3}{4}$ inches and *palm*, *hand*, *shaftment*, *span*, *cubit* $= 3, 4, 6, 9, 18$ inches, respectively.

- **Cubit**

The **cubit**, originally the length of the forearm from the elbow to the tip of the middle finger, was the ordinary unit of length in the ancient Near East which varied among cultures and with time. It is the oldest recorded measure of length.

The cubit was used, in the temples of Ancient Egypt from at least 2700 BC, as follows: 1 *ordinary Egyptian cubit* $= 6$ *palms* $= 24$ *digits* $= 45$ cm (18 inches), and 1 *royal Egyptian cubit* $= 7$ *palms* $= 28$ *digits* ≈ 52.6 cm. Relevant Sumerian measures were: 1 *ku* $= 30$ *shusi* $= 25$ *uban* $= 50$ cm, and 1 *kus* $= 36$ *shusi*.

Biblical measures of length are the *cubit* and its multiples by $4, \frac{1}{2}, \frac{1}{6}, \frac{1}{24}$ called *fathom*, *span*, *palm*, *digit*, respectively. But the length of this cubit is unknown; it is estimated now as ≈ 44.5 cm (as Roman *cubitus*) for the common cubit, used in commerce, and 51–56 cm for the sacred one, used for building.

The *Talmudic cubit* is 48–57.6 cm. The *pyramid cubit* (25.025 inches $\approx$ 63.567 cm), derived in Newton's Biblical studies, is supposed to be the basic one in the dimensions of the Great Pyramid and far-reaching numeric relations on them.

Thom, 1955, claim that the *megalithic yard*, 82.966 cm, was the basic unit used for stone circles in Britain and Brittany c. 3500 BC. Butler–Knight, 2006, derived this unit as $1/(360 \times 366^2)$-th of 40,075 km (the Earth's equatorial circumference), linking it to the putative Megalithic 366-degree circle and Minoan 366-day year. Such a "366 geometry" is a part of the pseudoscientific metrology

- **Nautical length units**

The main **nautical length units** (also used in aerial navigation) are:

sea league $= 3$ sea (nautical) miles;

nautical mile $= 1852$ m (originally defined as 1 min of arc of latitude);

geographical mile ≈ 1855.32 m (the average distance on the Earth's surface, represented by 1 min of arc along the Earth's equator);

(international) *short cable length* $= \frac{1}{10}$ nautical mile $= 185.2$ m ≈ 101 fathoms;

(US customary) *cable length* = 120 fathoms = 720 feet = 219.456 m;
fathom = 6 feet = 1.8288 m.

- **Preferred design sizes**

Objects are often manufactured in a series of sizes of increasing magnitude. In Industrial Design, *preferred numbers* are standard guidelines for choosing such product sizes within given constraints of functionality, usability, compatibility, safety or cost. **Preferred design sizes** are such lengths, diameters and distances.

Four basic *Renard's series* of preferred numbers divide the interval from 10 to 100 into 5, 10, 20, or 40 steps, with the factor between two consecutive numbers being constant (before rounding): the 5-th, 10-th, 20-th, or 40-th root of 10. Since the **International Metric System** (SI) is decimally-oriented, the International Organization for Standardization (ISO) adopted Renard's series as the main preferred numbers for use in setting metric sizes. But, for example, the ratio between adjacent terms (i.e., notes) in the Western musical scale is 12-th root of 2.

In the widely used ISO paper size system, the height-to-width ratio of all pages is the *Lichtenberg ratio*, i.e., $\sqrt{2}$. The system consists of formats An, Bn and (used for envelopes) Cn with $0 \le n \le 10$, having widths $2^{-\frac{1}{4}-\frac{n}{2}}$, $2^{-\frac{n}{2}}$ and $2^{-\frac{1}{8}-\frac{n}{2}}$, respectively. The above measures are in m; so, the area of An is 2^{-n} m^2. They are rounded and expressed usually in mm; for example, format A4 is 210×297 and format B7 (used also for EU and US passports) is 88×125.

- **Typographical length units**

PostScript point = $\frac{1}{72}$ inch = 100 gutenbergs = 0.3527777778 mm;
TeX point (or *printer's point*) = $\frac{1}{72.27}$ inch = 0.3514598035 mm;
ATA point (or *Anglo-Saxon point*) = $\frac{1}{72.272}$ inch = 0.3514598 mm;
point (Didot, European) = 0.37593985 mm, *cicero* = 12 points Didot;
pica (Postscript, TeX or ATA) = 12 points in the corresponding system;
twip = $\frac{1}{20}$ of a point in the corresponding system.

In display systems, *twip* is $\frac{1}{1440}$ inch, and *himetric* is 0.01 mm.

- **Astronomical system of units**

The **astronomical system of units** (or, formally, *IAU (1976) System of Astronomical Constants*) is a system of measurement developed for use in astronomy by the IAU (International Astronomical Union).

It is based on units of length (AU), mass ($M_\odot$), and time (day). The speed of light in IAU is defined as $c_0 = 299{,}792{,}458$ m/s.

The *astronomical unit of time* is the day $D = 24 \times 60^2 = 86{,}400$ s. 365.25 days make up one *Julian year*.

The *astronomical unit of mass* is the mass of the Sun: $M_\odot = 1.98892 \times 10^{30}$ kg.

The *astronomical unit of length* (*AU* or *ua*) is $c_0 t_A = 149{,}597{,}870{,}691 \pm 3$ m $\approx$ mean Earth–Sun distance; here t_A is the transit time of light across 1 AU.

Among derived units are *light-year* $c_0 D \times 365.25 = 0.94607304725808 \times 10^{16}$ m and *parsec* $\frac{648{,}000}{\pi}$ AU $\approx 206{,}264.81$ AU $\approx 3.085677581 \times 10^{16}$ m.

- **Length units in Astronomy**

  The **Hubble distance** (Chap. 26) or *Hubble length* is $D_H = \frac{c}{H_0} \approx 1.31 \times 10^{26}$ m ≈ 4.237 Gpc ≈ 13.82 Gly (used to measure distances $d > \frac{1}{2}$ Mpc in terms of redshift z: $d = zD_H$ if $z \leq 1$, and $d = \frac{(z+1)^2-1}{(z+1)^2+1} D_H$, otherwise).

  gigaparsec (Gpc) $= 10^3$ megaparsec (Mpc) $= 10^6$ kiloparsec (kpc) $= 10^9$ parsecs;
  hubble (or light-gigayear, light-Ga, Gly) $= 10^3$ million light-years (Mly);
  siriometer $= 10^6$ AU ≈ 15.813 ly (about twice the Earth-Sirius distance);
  parsec (pc) $= \frac{648{,}000}{\pi} \approx 206{,}265$ AU ≈ 3.262 light-years $= 3.086 \times 10^{16}$ m;
  light-year (ly) $\approx 9.461 \times 10^{15}$ m $\approx \pi \times 10^7$ light-seconds ≈ 0.307 parsec;
  spat (used formerly) $= 10^{12}$ m $= 10^3$ gigameters ≈ 6.685 AU;
  astronomical unit (AU) $\approx 1.496 \times 10^{11}$ m ≈ 499 light-seconds;
  light-second $\approx 2.998 \times 10^8$ m (the Earth-Moon distance is ≈ 1.28 light-seconds);
  radii of Moon, Earth, Jupiter and Sun: 1737, 6371, 69,911 and 695,510 km;
  picoparsec ≈ 30.86 km; cf. other funny units such as *sheppey* 1.4 km (closest distance at which sheep remain picturesque), *beard-second* 5 nm (distance that a beard grows in a second), *microcentury* ≈ 52.5 min (lecture's length), *nanocentury* $\approx \pi$ sec.

- **Natural length units**

  Natural units are units of measurement based only on physical constants, for example, the speed c of light, gravitational constant G, reduced Planck constant $\hbar$, *Boltzmann constant* k_B, *Coulomb's constant* k_e, proton's *elementary charge* e, *fine-structure constant* $\alpha = \frac{e^2 k_e}{\hbar c} \approx \frac{1}{137}$ and masses m_e, m_p of electron and proton.

  Planck length (smallest measurable length) is $l_P = \sqrt{\frac{\hbar G}{c^3}} \approx 1.6162 \times 10^{-35}$ m. (The *Stoney length*, used formerly, is $\sqrt{\alpha} l_P$.) l_P is the **reduced Compton wavelength** $\overline{\lambda}_C(m) = \frac{m_P}{m} l_P$, and also half of the **Schwarzschild radius** $r_s(m) = 2Gmc^{-2}$ (Chap. 24) for $m = m_P$ (*Planck mass*) $= \sqrt{\frac{\hbar c}{G}} \approx 2.18 \times 10^{-8}$ kg ≈ 22 mg.

  The remaining base Planck units are *Planck time* $t_p = \frac{l_P}{c} \approx 5.39 \times 10^{-44}$ s, *Planck temperature* $T_P = \frac{m_P c^2}{k_B} \approx 1.42 \times 10^{32}$ K, and *Planck charge* $q_P = \sqrt{\frac{\hbar c}{k_e}} = \frac{e}{\sqrt{\alpha}} \approx 1.88 \times 10^{-18}$ C. The *Planck area* A_P is l_P^2, *Planck energy* E_P is $m_P c^2 \approx 1.22 \times 10^{28}$ eV ≈ 500 kWh, and *Planck density* ρ_P is $m_{\mathrm{Pl}} l_P^{-3} \approx 5.16 \times 10^{96}$ kg/m^3. Only black holes exceed ρ_P; some theories (for example, *Landau poles*) allow to exceed T_P.

  The Planck units come by a normalization of the *geometrized units* for the expressing SI units second, kilogram, kelvin and coulomb as c, $\frac{G}{c^2}$, $\frac{Gk_B}{c^4}$ and $\frac{\sqrt{Gk_e}}{c^2}$ m, respectively.

  The length unit of Quantum Chromodynamics (or strong interactions) is $\overline{\lambda}_C(m_p) \approx 2.103 \times 10^{-16}$ m. The majority of lengths, used in experiments on

nuclear fundamental forces, are integer multiples of $\lambda_C(m_p) = 2\pi\overline{\lambda}_C(m_p) \approx 1.32$ fm.

X unit $\approx 1.002 \times 10^{-13}$ m ≈ 0.1 pm measures wavelengths of X- and gamma rays.

The atomic unit of length is the **Bohr radius** (or *bohr*) $\alpha_0 \approx 5.292 \times 10^{-11}$ m ≈ 53 pm $= 0.53$ Å, the most probable distance between the proton and electron in a hydrogen atom. It is $\alpha^{-1}\overline{\lambda}_C(m_e) = \alpha^{-2} r_e$, where $r_e \approx 2.818 \times 10^{-15}$ m is the **Thomson scattering length** (Chap. 24), i.e., the *classical electron radius*.

In the units of Particle Physics, $1/rmeV = 10^{-9}$/GeV is $\frac{\hbar c}{\text{eV}} = \frac{E_P}{\text{eV}} l_P \approx 1.97 \times 10^{-7}$ m.

- **Length scales in Physics**

  In Physics, a **length scale** (or **distance scale**) is a distance range determined with the precision of a few orders of magnitude, within which given phenomena are consistently described by a theory. Roughly, the scales $< 10^{-15}$, 10^{-15}–10^{-6}, $10^{-6} - 10^{6}$ and $> 10^{6}$ m are called *subatomic*, *atomic to cellular* (microscopic), *human* (macroscopic) and *astronomical*, respectively.

  Bacteria (and human ovums) are roughly on the geometrical mean (10^{-4} m) of Nature's hierarchy of sizes. Dawkins, 2006, used term **middle world** for our realm between two counterintuitive extreme levels of existence: the microscopic world of quarks/atoms and the Universe at the galactic/universal level. The limit scales correspond to the **Planck length** l_P and **Hubble distance** $\approx 4.6 \times 10^{61}\, l_P$.

  In terms of their constituents, Chemistry (molecules, atoms), Nuclear (say, proton, electron, photon), Hadronic (exited states) and Standard Model (quarks and leptons) are applicable at scales $\geq 10^{-10}$, $\geq 10^{-14}$, $\geq 10^{-15}$ and $\geq 10^{-18}$ m.

  At the *meso-* (or *nanoscopic*) *scale*, $10^{-9} - 10^{-7}$ m, materials and phenomena can be described continuously and statistically, and average macroscopic properties (say, temperature and entropy) are relevant. At the *atomic scale*, $\sim 10^{-10}$ m $= 1$ Å, the atoms should be seen as separated. The *electroweak scale*, $\sim 10^{-18}$ m (100–1000 GeV, in terms of energy) will be probed by the LHC (Large Hadron Collider). The *Planck scale* (Quantum Gravity), $\sim 10^{-35}$ m ($\sim 10^{19}$ GeV) is not yet accessible.

  Belenchia et al., 2015, gave upper bound $10^{-29} - 10^{-22}$ m of *nonlocality scale* for Quantum Gravity induced nonlocality via opto-mechanical quantum oscillators.

  Both, uncertainty principle from Quantum Mechanics and gravitational collapse (black hole formation) from classical General Relativity, indicate some minimum length of order the Planck length l_P where the notion of distance loses operational meaning. Also, *doubly special relativity* adds minimum length and maximum energy scales to observer-independent maximum velocity c.

  At short distances, classical geometry is replaced by "quantum geometry" described by 2D conformal field theory (CFD). As two points are getting closer together, the vacuum fluctuations of the gravitational field make the distance between them fluctuate randomly, and its mean value tends to a limit, of the order of l_P. So, no two events in space-time can ever occur closer together.

In String Theory, space-time geometry is not fundamental and, perhaps, it only emerges at larger distance scales. The *Maldacena duality* is the conjectured equivalence between an M-theory defined on a ("large, relativistic") space, and a (quantum, without gravity) CFD defined on its (lower dimensional) conformal boundary.

The Big Bang paradigm supposes a minimal length scale and a smooth distribution (homogeneous and isotropic) at a large scale. For Vilenkin et al., 2011, the main theories admitting "before the Big Bang" (*cyclical universe*, *eternal inflation*, *multiverse*, *cosmic egg*) still require a beginning. For Hartle–Hawkings, 1983, time emerged continuously from space after the Universe was at the age t_P.

- **Glashow's snake**

  Uroboros, the snake that bites in its own tail, is an ancient symbol representing the fundamental in different cultures: Universe, eternal life, integration of the opposite, self-creation, etc. **Glashow's snake** is a sketch of the cosmic uroboros by Glashow, 1982, arraying four fundamental forces and the distance scales over which they dominate (62 orders of magnitude from the *Planck scale* $\sim 10^{-35}$ m to the *cosmological scale* $\sim 10^{26}$ m) in clock-like form around the serpent. The dominating forces are:

  1. gravity: in the *macrocosmos* from cosmic to planetary distances;
  2. electromagnetism: from mountains to atoms (say, within $[10^{-10}, 2 \times 10^5]$ m);
  3. weak and strong forces: in the *microcosmos* inside the atom (say, $< 10^{-12}$ m).

  No objects are known within $[10^{-14}, 10^{-10}]$ m (the largest nucleus and smallest atom). As distances decrease and energies increase, the last three forces become equivalent around the length 10^{-28} m. Then gravity is included (super-unification happens) linking the largest and smallest: the snake swallows its tail.

  Also, a symmetry between small and large distances, called *T-duality*, claims: two superstring theories are *T-dual* if one compactified on a space of large volume is equivalent to the other compactified on a space of small volume.

  Cosmic inflation (expansion by a factor of at least 10^{78} in volume, to the size of a grain of sand, from 10^{-36} to $\approx 10^{-32}$ second after the Big Bang) may have created the large scale of the Universe out of quantum-scale fluctuations. Strong and weak forces describe both atomic nuclei and energy generation in stars. Cf. **range of fundamental forces** in Chap. 24.

  In *Conformal Cyclic Cosmology* (Penrose, 2010), the Universe is a sequence of *aeons* (space-times with **FLRW metrics** g_i), where the future time-like singularity of each aeon is the Big Bang singularity of the next. In an eaon's beginning and end, distance and time do not exist; only *conformal* (preserving angles) geometry holds. Any eaon is attached to the next one by a conformal rescaling $g_{i+1} = \Omega^2 g_i$.

27.2 Orders of Magnitude for Length

In this section we present a selection of such orders of length, expressed in meters.

$1.616252(81) \times 10^{-35}$: Planck length;
10^{-34}: length of a putative *string* in *M-theory* which supposes that all forces and elementary particles arise by vibration of such strings (but there is no even agreement that there are smallest fundamental objects);
1.01×10^{-25}: *Schwarzschild radius* ($\frac{2Gm}{c^2}$: the value below which mass m collapses into a black hole) of an average (68 kg) human;
$10^{-24} = 1$ **yoctometer**: effective cross-section radius of 1 MeV neutrinos is 2×10^{-23};
10^{-22}: a certain quantum roughness starts to show up, while the space appears completely smooth at the scale of 10^{-14};
$10^{-21} = 1$ **zeptometer**: *preons*, hypothetical components of quarks/leptons;
$10^{-18} = 1$ **attometer**: size of up quark and down quarks; sizes of strange, charm and bottom quarks are 4×10^{-19}, 10^{-19} and 3×10^{-20};
$10^{-15} = 1$ **femtometer** (or *fermi*);
1.75×10^{-15} and 1.5×10^{-14}: diameter of the smallest (H, hydrogene) and largest (U, uranium-234) nucleus;
1.68×10^{-15}: diameter of proton, range of the weak nuclear force;
$10^{-12} = 1$ **picometer**: distance between atomic nuclei in a white dwarf star;
10^{-11}: wavelength of the hardest (shortest) X-rays and longest gamma rays;
0.62 Å and 5.2 Å: diameter of the smallest (helium) and largest (caesium) atom;
$10^{-10} = 1$ Å (angstrom): diameter of a typical atom;
0.74 Å and 1000 Å: diameter of the smallest (H_2) and largest (a SiO_2) molecule;
1.54 Å: length of a typical covalent bond (C-C);
3.4 Å: distance between base pairs in a DNA molecule;
$10^{-9} = 1$ **nanometer**: diameter of typical molecule;
10^{-8}: wavelength of softest X-rays and most extreme ultraviolet;
1.1×10^{-8}: diameter of prion (smallest self-replicating biological entity);
in 2012;
9×10^{-8}: human immunodeficiency virus, HIV; in general, capsid sizes of known viruses range from 1.7×10^{-8} (*Porsine circovirus*) to 1.5×10^{-6} (*pithovirus sibericum*);
10^{-7}: size of chromosomes and largest particle fitting through a surgical mask;
2×10^{-7}: limit of resolution of the light microscope;
$3.8–7.6 \times 10^{-7}$: wavelength of visible (to humans) light;
$10^{-6} = 1$ **micrometer** (or *micron*);
$10^{-6} - 10^{-5}$: diameter of a typical bacterium; known (nondormant) bacteria range from $2–3 \times 10^{-7}$ (*Mycoplasma genitalium*) to 7.5×10^{-4} (*Thiomargarita Namibiensis*);
8.5×10^{-6}: size of *Ostreococcus*, the smallest free-living eukaryotic unicellular organism, while the length of a nerve cell of the Colossal Squid can reach 12 m;
10^{-5}: typical size of (a fog, mist, or cloud) water droplet;

10^{-5}, 1.5×10^{-5}, and 2×10^{-5}: widths of cotton, silk, and wool fibers;
2×10^{-4}: approximately, the lower limit for the human eye to discern an object;
5×10^{-4}: diameter of a human ovum, grain of salt;
$10^{-3} = 1$ **millimeter**;
5×10^{-3}: length of average red ant; in general, insects range from 1.39×10^{-4} (*Dicopomorpha echmepterygis*, the smallest animal) to 5.67×10^{-1} (*Phobaeticus chani*); the smallest flying insects are on the order of 10^{-3} in length;
$7.7 \times 10^{-3}, 5 \times 10^{-2}$ and 9.2×10^{-2}: length of the smallest ones: vertebrate (frog *Paedophryne amauensis*), warm-blooded vertebrate (bee hummingbird *Mellisuga helenae*) and primate (lemur *Microcebus berthae*);
8.9×10^{-3}: Schwarzschild radius of the Earth;
$10^{-2} = 1$ **centimeter**;
5.8×10^{-2}: length of uncoiled sperm of the fruit fly *Drosophila bifurca* (it is 20 fly's bodylengths and the longest sperm cell of any known organism);
$10^{-1} = 1$ **decimeter**: wavelength of the lowest microwave and highest UHF radio frequency, 3 GHz;
1 **meter**: wavelength of the lowest UHF and highest VHF radio frequency, 300 MHz;
1.5: average ground level of the Maldives above sea level;
2.77–3.44: wavelength of the broadcast radio FM band, 108–87 MHz;
5.5 and ≈ 3: height of the tallest animal (giraffe) and extinct primate *Gigantopithecus*;
$10 = 1$ **decameter**: wavelength of the lowest VHF and highest shortwave radio frequency, 30 MHz;
$20, 33, 37$ and 55: lengths of the longest animals (tapeworm *Diphyllobothrium Klebanovski*, blue whale, lion's mane jellyfish and bootlace worm *Lineus longissimus*);
99.6: height of the world's tallest flowering plant, a tasmanian *Eucalyptus* Centurion (after 100 m, the distribution of the products of photosynthesis become impossible);
$100 = 1$ **hectometer**: wavelength of the lowest HF (high radio frequency) and highest MF (medium radio frequency), 3 MHz;
115.5: height of the world's tallest living tree, a californian *sequoia* Hyperion;
$139, 324, 541, 830, 1007$ and 8.5: heights of the Great Pyramid of Giza, Eiffel Tower in Paris, One World Trade Center in New York, Burj Khalifa skyscraper in Dubai, Kingdom Tower, planned in Jeddah for 2019, and 11,000 years-old Tower of Jericho;
187–555: wavelength of the broadcast radio AM band, 1600–540 kHz;
340: distance which sound travels in air in 1 s;
$10^3 = 1$ km;
2.954×10^3: Schwarzschild radius of the Sun;
$10^4 = 1$ *miriameter* (used formerly): *scandinavian mile* (Norwegian/Swedish *mil*);

8848 and 10,911: the highest (Mount Everest) and deepest (Mariana Trench) points on the Earth's surface;
$5 \times 10^4 = 50$ km: the maximal distance at which the light of a match can be seen (at least 10 photons arrive on the retina during 0.1 s);
$1.11 \times 10^5 = 111$ km: one degree of latitude on the Earth;
$1.5 \times 10^4 - 1.5 \times 10^7$: wavelengths of sound audible to humans (20 Hz to 20 kHz);
1.37×10^5 and 1.9×10^6: length of the world's longest tunnel, Delaware Aqueduct, New York, and of longest street, Jounge Street, Ontario;
2×10^5: wavelength of a typical tsunami;
$10^6 = 1$ **megameter**, thickness of Earth's atmosphere;
2.22×10^6: diameter of Typhoon Tip (northwest Pacific Ocean, 1979), the most intense tropical cyclone on record;
2.37×10^6: diameter of Pluto at 39.54 AU from the Sun; the smallest dwarf planet is Ceres (the largest asteroid in the Asteroid Belt) of diameter 9.42×10^5 and at 2.77 AU;
3.47×10^6: diameter of the Moon;
9.3×10^6 and 2.1×10^7: length of Trans-Siberian Railway and China's Great Wall;
1.28×10^7 and 4.01×10^7: Earth's equatorial diameter and length of the equator;
4.5×10^7: distance from which Earth's good-looking photograph, *The Blue Marbre*, was taken in 1972 by the Apollo 17 mission. Other famous Earth's images are *Earthrise* (1968, by the Apollo 8), *Pale Blue Dot* (0.12 pixel against the space's vastness; 1990, by Voyager 1) and one from Saturn's neighborhood (2013, by NASA's Cassini).
1.4×10^8: mean diameter of Jupiter;
1.67×10^8: diameter of OGLE-TR-122b, the smallest known star;
$\approx 3 \times 10^8$ (299,792.458 km): distance traveled by light in 1 s;
3.84×10^8: Moon's orbital distance from the Earth;
4.002×10^8: the farthest distance a human has ever been from Earth (Appolo 13 mission, 1970, passed over the far side of the Moon);
$10^9 = 1$ **gigameter**;
1.39×10^9: Sun's diameter and orbital distance of a planet with 3.3-h "year";
6.37×10^9: distance at which Earth's gravity becomes $\frac{1}{1{,}000{,}000}$ of that on its surface;
5.83×10^{10}: orbital distance of Mercury from the Sun;
1.496×10^{11} (1 astronomical unit, AU): mean Earth-Sun distance;
≈ 2.8 AU (near the middle of the Asteroid Belt): Sun's water **frost line** (the distance where it is cold enough, $\approx -123\,°\text{C}$, for water to condense into ice), separating terrestrial and jovian planets; it is the radius of the inner Solar System;
5.7×10^{11}: length of the longest observed comet tail (Hyakutake, 1996); the Great Comet of 1997 (Hale–Bopp) has biggest known nucleus (> 60 km);
$10^{12} = 1$ **terameter** (formerly, *spat*);
15.8 AU: diameter of the largest known star, red supergiant UY Scuti;
30.1 AU: radius of the outer Solar System (orbital distance of Neptune);

50 AU: distance from the Sun to the *Kuiper cliff*, the abrupt outer boundary of the *Kuiper Belt* (the region of trans-Neptunian objects around Sun).
936 AU: aphelion of Sedna, the farthest known Solar System object (its orbital period is $\approx$ 11,400 years); it and 2012 VP_{113} (having the farthest known—80, 5 AU—perihelion in the Solar System) are only known objects within the *Oort Cloud*;
$10^{15} = 1$ **petameter**;
50,000–200,000 AU: distance from the Sun to the boundaries of the Oort Cloud;
52,000 AU = 0.82 ly: the only known close flyby of Solar System by a star (*Scholz's binary* of dwarfs passed the Oort Cloud about 70,000 years ago);
1.3 parsec $\approx 4 \times 10^{16} \approx 4.24$ ly: distance to Proxima Centauri, the nearest star;
$\approx 6.15 \times 10^{17}$: radius of humanity's radio bubble, caused by high-power TV broadcasts leaking through the atmosphere into outer space;
$10^{18} = 1$ **exameter**;
$1.57 \times 10^{18} \approx 50.9$ pc, ≈ 250 pc, 46 pc: distances to supernova 1987A, to rapidly rotating neutron star Geminga (remains of a supernova 0.3 Ma ago which created the Local Bubble), to IK Pegasi B (nearest known supernova candidate). A supernova within 10–20 pc would be a catastrophic event for the Earth's life;
$2.59 \times 10^{20} \approx 8.4$ kpc $\approx$ 27,400 ly: distance from the Sun to the geometric center of our Milky Way galaxy (in Sagittarius A^*, "our" supermassive black hole);
12.9 kpc and 52.8 kpc: distances to the closest (Canis Major Dwarf) and the largest (Large Magellanic Cloud) of 26 satellite galaxies of the Milky Way;
$9.46 \times 10^{20} \approx 30.66$ kpc $\approx 10^5$ ly: diameter of the Milky Way. The largest known galaxy, C 1101, at the center of the cluster Abell 2029, is ≈ 6 Mly across;
$10^{21} = 1$ **zettameter**;
$2.23 \times 10^{22} = 725$ kpc = 2.54 Mly: distance to Andromeda (M31), the closest (and approaching at 100–140 km/s) large galaxy; also, it is the farthest permanently visible to the naked eye object;
$5.7 \times 10^{23} = 59$ Mly: distance to Virgo, the nearest (and approaching) major cluster;
$10^{24} = 1$ **yottameter**;
$2 \times 10^{24} = 60$ Mpc = 110 Mly: diameter of the Local (or Virgo) supercluster;
1.2 Gly: maximal size of structure compatible with the cosmological principle (that distribution of matter is homogeneous and isotropic on a large enough scale);
1.3 Gly, 5.6 Gly and 10 Gly: diameters of the *Canes Venatici Supervoid* (largest known), Giant GRB Ring (largest known regular formation) and Hercules-Corona Borealis Great Wall of GRB (largest known superstructure);
7.5 Gly: the gamma ray burst GRB 080319B, farthest visible, $\approx$ 30 s in 2008, to the naked eye object (GRB 980425, at $\approx$ 40 Mpc, is closest known);
13.14 Gly: the gamma ray burst GRB 090429B (farthest event, ever observed);
13.4 Gly ($z = 11.1$): distance to the farthest known object, galaxy GN-z11;
$1.3 \times 10^{26} = 13.82$ Gly = 4.24 Gpc: **Hubble radius** of the Universe measured as the **light travel distance** to the source of CMB radiation;

$4.4\times10^{26} = 47$ Gly $= 14.4$ Gpc: *particle horizon* (present radius of the Universe measured as a **comoving distance**); it is larger than the Hubble radius, since the Universe is expanding). It is $\approx 2\,\%$ larger than the radius of the *visible universe* including only signals emitted later than $\approx$ 380,000 years after the Big Bang;

The size of whole Universe can be now much larger than the size of the observable one, even infinite, if its curvature is 0. If the Universe is finite but unbounded or if it is nonsimply connected, then it can be smaller than the observable one.

Projecting into the future: the scale of the Universe will be 10^{31} in 10^{14} years (last red dwarf stars die) and 10^{37} in 10^{20} years (stars have left galaxies). If protons decay, their half-life is $\geq 10^{35}$ years; their estimated number in the Universe is 10^{77};

The Universe, in the current *Heat Death* scenario, achieves beyond 10^{1000} years such a low-energy state that quantum events become major macroscopic phenomena, and space-time loses its meaning again, as below the Planck time/length;

The hypothesis of parallel universes estimates that one can find another identical copy of our Universe within the distance $10^{10^{118}}$ m.

Chapter 28
Distances in Applied Social Sciences

In this chapter we present selected distances used in real-world applications of Human Sciences. In this and the next chapter, the expression of distances ranges from numeric (say, in m) to ordinal (as a degree assigned according to some rule) and nominal.

Depending on the context, the distances are either practical ones, used in daily life and work outside of science, or uncountable ones, used figuratively, say, as metaphors for remoteness (being apart, being unknown, coldness of manner, etc.).

28.1 Distances in Perception and Psychology

- **Distance ceptor**

  A **distance ceptor** is a nerve mechanism of one of the organs of special sense whereby the subject is brought into relation with his distant environment.
- **Oliva et al. perception distance**

  Let $\{s_1, \ldots, s_n\}$ be the set of stimuli, and let q_{ij} be the conditional probability that a subject will perceive a stimulus s_j, when the stimulus s_i was shown; so, $q_{ij} \geq 0$, and $\sum_{j=1}^{n} q_{ij} = 1$. Let q_i be the probability of presenting the stimulus s_i.

  The **Oliva et al. perception distance** ([OSLM04]) between stimuli s_i and s_j is

$$\frac{1}{q_i + q_j} \sum_{k=1}^{n} \left| \frac{q_{ik}}{q_i} - \frac{q_{jk}}{q_j} \right| .$$

- **Representational dissimilarity matrix**

  Representational dissimilarity matrix (or RDM) is a square matrix indexed horizontally and vertically by the stimuli (or experimental conditions) and containing a dissimilarity index in each cell, which compares the two brain-activity patterns associated with stimuli labeling the row and column.

© Springer-Verlag Berlin Heidelberg 2016

M.M. Deza, E. Deza, *Encyclopedia of Distances*,
DOI 10.1007/978-3-662-52844-0_28

If the same activity pattern estimates are used for the vertical and horizontal dimensions, the RDM is symmetric about a diagonal of zeros. If independent pattern estimates are used for the vertical and horizontal dimensions, the RDM contains entries comparing independent pattern estimates for identical stimuli (reflecting measurement noise) along its diagonal, and two alternative dissimilarity estimates for each stimulus pair in symmetric off-diagonal positions.

- **Visual space**

  Visual space refers to a stable perception of the environment provided by vision, while **haptic space** (or *tactile space*) and **auditory space** refer to such internal representation provided by the senses of pressure perception and audition. The geometry of these spaces and the eventual mappings between them are unknown. But Lewin et al., 2012, found that sensitivity to touch is heritable, and linked to hearing. The main observed kinds of distortion of vision and haptic spaces versus physical space follow; the first three were observed for auditory space also.

  – *Distance-alleys*: lines with corresponding points perceived as equidistant, are, actually, some hyperbolic curves. Usually, the parallel-alleys are lying within the distance-alleys and, for visual space, their difference is small at > 1.5 m.
  – *Oblique effects*: performance of certain tasks is worse when the orientation of stimuli is oblique rather than horizontal or vertical.
  – *Equidistant circles*: the **egocentric distance** is direction-dependent; the points perceived as equidistant from the subject lie on egg-like curves, not on circles.

  These effects and **size-distance invariance hypothesis** should be incorporated in a good model of visual space. In a visual space the distance d and direction are defined from the self, i.e., as the **egocentric distance**. There is evidence that visual space is almost affine and, if it admits a metric d, then d is a **projective metric**, i.e., $d(x, y) + d(y, z) = d(x, z)$ for any perceptually collinear points x, y, z.

  The main models for visual space are a Riemannian space of constant negative curvature (cf. **Riemannian color space** in Chap. 21), a general Riemannian/Finsler space, or an affinely connected (so, not metric, in general) space ([CKK03]).

  An *affine connection* is a linear map sending two vector fields into a third one. The expansion of perceived depth on near and its contraction at far distances hints that the mapping between visual and physical space is not affine.

  Amedi et al., 2002, observed the convergence of visual and tactile shape processing in the human lateral occipital complex. The *vOICe technology* (OIC for "Oh I see!") explores cross-modal binding for inducing visual sensations through sound (mental imagery and artificial synesthesia). Some blind people "see" by echolocation. The cane extends peri-hand space of blind users and, in general, extrapersonal or far space can remap as peripersonal or near space when using tools.

  Weber's illusion: two tactile points are perceived as further apart on body parts with higher tactile sensitivity,

- **Length-related illusions**

  The most common optical illusions distort size or length. For example, in the *Müller–Lyer illusion*, one of two lines of equal length appear shorter because of the way the arrows on their ends are oriented. Pigeons and parrots also are susceptible to it. Segall et al., 1963, found that the mean fractional misperception varies cross-culturally from 1.4 % to 20.3 % with maximum for Europeans. Also, urban residents and younger subjects are much more susceptible to this illusion.

  In the *Luckiech–Sander illusion* (1922), the diagonal bisecting the larger, left-hand parallelogram appears to be longer than the diagonal bisecting the smaller, right-hand parallelogram, but is in fact of the same length.

  The perspective created in *Ponzo illusion* (1911) increases the perceived distance and so, compliant with **Emmert's size-distance law**, perceived size increases.

  The *Moon illusion* (mentioned in clay tablets at Nineveh in the seventh century BC) is that the Moon, despite the constancy of its visual angle ($\approx 0.52°$), at the horizon may appear to be about twice the zenith Moon. This illusion (and similar *Sun illusion*) could be cognitive: the zenith moon is perceived as approaching. (Plug, 1989, claim that the *distance to the sky*, assumed unconsciously, is about 10–40 m cross-culturally and independent of the consciously perceived distance.) The *Ebbenhouse illusion*: the diameter of the circle, surrounded by smaller circles, appears to be larger than one of the same circle nearby, surrounded by larger circles.

  In *vista paradox* (Walker–Rupich–Powell, 1989), a large distant object viewed through a window appears to both shrink in size and recede in distance as the observer approaches; a similar framing effect works in the *coffee cup illusion* (Senders, 1966). In the *Pulfrich depth illusion* (1922), lateral motion of an object is interpreted as having a depth component.

  An *isometric illusion* (or *ambiguous figure*) is a shape that can be built of same-length (i.e., isometric) lines, while relative direction between its components are not clearly indicated. The *Necker Cube* is an example.

  The *Charpentier size-weight illusion* (1891): the larger of two graspable/liftable objects of equal mass is misperceived to be less heavy than the smaller.

- **Size-distance invariance hypothesis**

  The SDIH (**size-distance invariance hypothesis**) by Gilinsky, 1951, is that $\frac{S'}{D'} = C\frac{S}{D}$ holds, where S, D are the physical and S', D' are perceived size and distance of visual stimulus, while C is an observer constant. A simplified formula is $\frac{S'}{D'} = 2\tan\frac{\alpha}{2}$, where α is the angular size of the stimulus.

  A version of SDIH is the **Emmert's size-distance law**: $S' = CD'$. This law accounts for *size constancy*: object's size is perceived to remain constant despite changes in the retinal image (more distant objects appear smaller because of perspective). The Müller–Lyer and Ponzo illusions are examples of size constancy.

  The Moon and Ebbenhouse illusions are called **size-distance paradoxes** since they unbalance SDIH. They are misperceptions of visual angle and examples of

distance constancy: distance is perceived constant despite changes in the retinal image.

If an observer's head translates smoothly through a distance K as he views a stationary target point at pivot distance D_p, then the point will appear to move through a displacement W' when it is perceived to be at a distance D'. The **apparent distance/pivot distance hypothesis** (Gogel, 1982): it holds $\frac{D'}{D_p} + \frac{W'}{K} = 1$.

The **size-distance centration** is the overestimation of the size of objects located near the focus of attention and underestimation of it at the periphery.

Hubbard and Baiard, 1988, gave to subjects name and size S of a familiar object and asked imaged distances d_F, d_O, d_V. Here the object mentally looks to be of the indicated size at the *first-sight distance* d_F. The object become, while mentally walking (zooming), too big to be seen fully with zoom-in at the *overflow distance* d_O, and too small to be identified with zoom-out at the *vanishing point distance* d_V. Consistently with SDIH, d_F was linearly related to S. For d_O and d_V, the relation were the power functions with exponents about 0.9 and 0.7. The time needed to imagine d_O increased slower than linearly with the *scan distance* $d_O - d_F$.

Konkle and Oliva, 2011, found that the real-world objects have a consistent visual size at which they are drawn, imagined, and preferentially viewed. This size is proportional to the logarithm of the object's assumed size, and is characterized by the ratio of the object and the frame of space around it. This size is also related to the first-sight distance d_F and to the typical distance of viewing and interaction. A car at a typical viewing distance of 9.15 m subtends a visual angle of 30°, whereas a raisin held at an arm's length subtends 1°. Cf. the **optimal eye-to-eye distance** and, in Chap. 29, the *TV viewing distance* in the **vision distances**.

Similarly, Palmer et al., 1981, found that in goodness judgments of photographs of objects, the $\frac{3}{4}$ *perspective* (or 2.5 *view*, *pseudo-3D*), in which the front, side, and top surfaces are visually present, were usually ranked highest. Cf. the *axonometric projection* in the **representation of distance in Painting**.

- **Egocentric distance**

  The **egocentric distance** is the perceived absolute distance from the self (observer or listener) to an object or a stimulus; cf. **subjective distance**. Usually, such visual distance underestimates the actual physical distance to far objects, and overestimates it for near objects. Such distortion decreases in a lateral direction.

  In Visual Perception, the *action space* of a subject is 1–30 m; the smaller and larger spaces are called the *personal space* and *vista space*, respectively.

  The **exocentric distance** is the perceived relative distance between objects.

- **Distance cues**

  The **distance cues** are cues used to estimate the **egocentric distance**.

  For a listener at a fixed location, the main auditory distance cues include: *intensity*, *direct-to-reverberant energy ratio* (in the presence of sound reflecting surfaces), *spectrum* and *binaural differences*; cf. **acoustics distances** in Chap. 21.

For an observer, the main visual distance cues include:

- *relative size*, *relative brightness*, *light and shade*;
- *height in the visual field* (in the case of flat surfaces lying below the level of the eye, the more distant parts appear higher);
- *interposition* (when one object partially occludes another from view);
- *binocular disparities*, *convergence* (depending on the angle of the optical axes of the eyes), *accommodation* (the state of focus of the eyes);
- *aerial perspective* (distant objects become bluer and paler), *distance hazing* (distant objects become decreased in contrast, more fuzzy);
- *motion perspective* (stationary objects appear to a moving observer to glide past).

Examples of the techniques which use the above distance cues to create an optical illusion for the viewer, are:

- *distance fog*: a 3*D* computer graphics technique such that objects farther from the camera are progressively more blurred (obscured by haze). It is used, for example, to disguise the too-short **draw distance**, i.e., the maximal distance in a 3D scene that is still drawn by the rendering engine;
- *forced perspective*: a technique to make objects appear either far away, or nearer depending on their positions relative to the camera and to each other.
- *lead room*: space left in the direction the subject is facing or moving.

- **Subjective distance**

  The **subjective distance** (or *cognitive distance*) is a mental representation of actual distance molded by an individual's social, cultural and general life experiences; cf. **egocentric distance**. Cognitive distance errors occur either because information about two points is not coded/stored in the same branch of memory, or because of errors in retrieval of this information.

  For example, the length of a route with many turns and landmarks is usually overestimated. In general, the filled or divided space (distance or area) appears greater than the empty or undivided one. Also, affective signals of threat and disgust increase and decrease, respectively, perceived proximity.

  Human mental maps, used to find out distance and direction, rely mainly, instead of geometric realities, on real landscape understanding, via webs of landmarks.

  Ellard, 2009, suggests that this loss of natural navigation skills, coupled with the unique ability to imagine themselves in another location, may have given modern humans the freedom to create a reality of their own.

- **Geographic distance biases**

  Sources of distance knowledge are either symbolic (maps, road signs, verbal directions) or directly perceived ones during locomotion: environmental features (visually-perceived turns, landmarks, intersections, etc.), travel time/effort.

  They relate mainly to the perception and cognition of **environmental distances**, i.e., those that cannot be perceived in entirety from a single point of view but can still be apprehended through direct travel experience.

Examples of **geographic distance biases** (subjective distance judgments) are:

- observers are quicker to respond to locations preceded by locations that were either close in distance or were in the same region;
- distances are overestimated when they are near to a reference point; for example, intercity distances from coastal cities are exaggerated;
- subjective distances are often asymmetrical as the perspective varies with the reference object: a small village is considered to be close to a big city while the big city is likely to be seen as far away from it;
- traveled routes segmented by features are subjectively longer than unsegmented routes; moreover, longer segments are relatively underestimated;
- increasing the number of pathway features encountered and recalled by subjects leads to increased distance estimates;
- structural features (such as turns and opaque barriers) breaking a pathway into separate vistas strongly increase subjective distance (suggesting that distance knowledge may result from a process of summing vista distances) (turns are often memorized as straight lines or right angles);
- *Chicago-Rome illusion*: belief that some European cities are located far to the south of their actual location; in fact, Chicago and Rome are at the same latitude (42°), as are Philadelphia and Madrid (40°), etc.;
- *Miami-Lima illusion*: belief that US east coast cities are located to the east of the west coast cities of South America; in fact, Miami is 3° west of Lima.

Such illusions could be perceptually based mental representations that have been distorted through normalization and/or conceptual nonspatial plausible reasoning.

Thorndyke and Hayes-Roth, 1982, compared distance judgments of people with navigation- and map-derived spatial knowledge. Navigation-derived route distance estimates were more accurate than Euclidean judgments, and this difference diminished with increased exploration. The reverse was true for map subjects, and no improvement was observed in the map learning.

Turner–Turner, 1997, made a similar experiment in a plane virtual building. Route distances were much underestimated but exploration-derived Euclidean judgments were good; repeated exposure did not help. The authors suggest that exploration of virtual environments is similar to navigation in the real world but with a restricted field of view, as in tunnels, caves or wearing a helmet, watching TV.

Krishna et al., 2008, compared spatial judgments of *self-focused* ("Western") and *relationship-focused* ("Eastern") people. The former ones were more likely to misjudge distance (when multiple features should be considered), to pay attention to only focal aspects of stimuli and ignore the context and background information.

- **Psychogeography**

  Psychogeography is (Debord, 1955) the study of the precise laws and specific effects of the geographical environment, consciously organized or not, on the

emotions and behavior of individuals. An example of related notions is a *desire path* (or *social trail*), i.e., a path developed by erosion caused by animal or human footfall, usually the shortest or easiest route between an origin and destination.

Also, the psychoanalytic study of spatial representation within the unconscious construction of the social and physical world is called *Psychogeography*. In general, *Depth Psychology* refer to unconscious-accounting approaches to therapy and research.

- **Psychological Size and Distance Scale**

  The CID (*Comfortable Interpersonal Distance*) scale by Duke and Nowicky, 1972, consists of a center point 0 and eight equal lines emanating from it. Subjects are asked to imagine themselves on the point 0 and to respond to descriptions of imaginary persons by placing a mark at the point on a line at which they would like the imagined person to stop, that is, the point at which they would no longer feel comfortable. CID is then measured in mm from 0.

  The GIPSDS (**Psychological Size and Distance Scale**) by Grashma and Ichiyama, 1986, is a 22-item rating scale assessing interpersonal status and affect. Subjects draw circles, representing the drawer and other significant persons, so that the radii of the circles and the distances between them indicate the thoughts and feelings about their relationship. These distances and radii, measured in mm, represent the **psychological distance** and status, respectively. Cf. related questionnaire on http://www.surveymonkey.com/s.aspx?sm=Nd8c_2fazsxMZfK9ryhvzPlw_3d_3d

- **Visual Analogue Scales**

  In Psychophysics and Medicine, a **Visual Analogue Scale** (or *VAS*) is a self-report device used to measure the magnitude of internal states such as pain and mood (depression, anxiety, sadness, anger, fatigue, etc.) which range across a continuum and cannot be measured directly. Usually, VAS is a horizontal (or vertical, for Chinese subjects) 10 cm line anchored by word descriptors at each end.

  The *VAS score* is the distance, measured in mm, from the left hand (or lower) end of the line to the point marked by the subject. The VAS tries to produce *ratio data*, i.e., ordered data with a constant scale and a natural zero.

  Amongst scales used for pain-rating, the VAS is more sensitive than the simpler verbal scale (six descriptive or activity tolerance levels), the Wong–Baker facial scale (six grimaces) and the numerical scale (levels $0, 1, 2, \ldots, 10$). Also, it is simpler and less intrusive than questionnaires for measuring internal states.

- **Psychological distance**

  CLT (*construal level theory*) (Liberman–Trope, 2003, defines **psychological distance** from an event or object as a common meaning of spatial ("where"), temporal ("when"), social ("who") and hypotheticality ("whether") distance from it.

  Expanding spatial, temporal, social and hypotheticality horizons in human evolution, history and child development is enabled by our capacity for *mental construals*, i.e., abstract mental representations. Any event or object can be represented at *lower-level* (concrete, contextualized, secondary) or *higher-level* (abstract, more schematic, primary) construal.

More abstract construals lead to think of more distant (spatially, temporally, socially, hypothetically) objects and vice versa; cf., say, **temporal distance**.

CLT implied that the four dimensions are functionally similar. For example, increase of distance in only one dimension leads to greater moral concern. Zhang and Wang, 2008, observed that stimulating people to consider spatial distance influences their judgments along three other dimensions, but the reverse is not true.

It is consistent with a claim by Boroditsky, 2000, that the human cognitive system is structured around only concepts emerging directly out of experience, and that other concepts are then built in a metaphorical way. Williams and Bargh, 2008, also claim that psychological distance is a derivative of spatial distance. Spatial concepts such as "near/far" are present at 3 to 4 months of age since the relevant information is readily available to the senses, whereas abstract concepts related to internal states are more difficult to understand. Also, spatial relations between oneself, one's caretakers and potential predators have primary adaptive significance.

- **Temporal distance**

  Temporal distance is a type of **psychological distance** altering individuals' construals of future or past events (Trope–Liberman, 2003). Immediate events trigger concrete construals, which are characterized by an emphasis on details.

  People construe events at greater temporal distance in terms of their abstract, central, goal-related features and pro-arguments, while nearer events are treated situation-specifically at a lower level of counter-arguments. Examples are: greater moral concern over a distant future event, more likely forgiveness by a victim of an earlier transgression, more intense affective consumer's reaction when a positive outcome is just missed. Also, temporal distance relates to our conceptions of the self. Actor perspective dominates the simulation of a near-future event; it switches to a third-person depiction when the event is located in the distant future.

  Spronken et al., 2016, found that in mind-wandering, future-oriented thoughts are more positive compared to past-oriented thoughts. Also, thoughts about the distant past and future are more positive than thoughts about the near past and future, and the frequency of positive thoughts increases with temporal distance.

- **Time-distance relation (in Psychology)**

  People often talk about time using spatial linguistic metaphors (a long vacation, a short concert) but much less talk about space in terms of time. This bidirectional but asymmetric relation suggests that spatial representations are primary, and are later co-opted for other uses such as time.

  Casasanto and Boroditsky, 2008, showed that people, in tasks not involving any linguistic stimuli or responses, are unable to ignore irrelevant spatial information when making judgments about duration, but not the converse. So, the metaphorical space-time relationship observed in language also exists in our more basic representations of distance and duration. Mentally representing time as a linear spatial path may enable us to conceptualize abstract (as moving a meeting forward, pushing a deadline back) and impossible (as time-travel) temporal events.

In Psychology, the *Kappa effect* is that among two journeys of the same duration, one covering more distance appears to take longer, and the *Tau effect* is that among two equidistant journeys, one taking more time to complete appears to have covered more distance. Jones–Huang, 1982, see them as effects of *imputed velocity* (subjects impute uniform motion to discontinuous displays) on judgments of both time and space, rather than direct effect of time (distance) on distance (time) judgment.

Fleet–Hallet–Jepson, 1985, found spatiotemporal inseparability in early visual processing by retinal cells. Maruya–Sato, 2002, reported a new illusion (the time difference of two motion stimuli is converted in the illusory spatial offset) indicating interchangeability of space and time in early visual processing. Simner–Mayo–Spiller, 2009, tested ten individuals with time-space synaesthesia.

The differences appear at the level of higher processing because of different representations: space is represented in retinotopic maps within the visual system, while time is processed in the cerebellum, basal ganglia and cortical structures. Evidence from lesion and human functional brain imaging/interference studies point towards the posterior parietal cortex as the main site where spatial and temporal information converge and interact with each other. Cf. also **spatial-temporal reasoning**.

In human-computer interaction, *Fitts' law* claims that the average time taken to position a mouse cursor over an on-screen target is $a + b \log_2(1 + \frac{D}{W})$, where D is the distance to the center of the target, W is the width (along the axis of motion) of the target and a, b represent the start/stop time and device's speed.

People in the West construct diagonal mental timelines (running from bottom left to the top right); those with damaged right side of their brain have trouble imagining past, i.e., timeline's left side.

Núñez, 2012, found that our spatial representation of time is not innate but learned. The Aymara of the Andes place the past in front and the future behind. The Pormpuraaw of Australia place the past in the east and the future in the west. Some Mandarin speaker have the past above and future below.

For the Yupno of Papua New Guinea, past and future are arranged as a nonlinear 3D bent shape: the past downhill and the future uphill of the local river. Inside of their homes, Yupno point towards the door when talking about the past, and away from the door to indicate future. Yupno also have a native counting system and number concepts but they ignore the number-line concept. They place numbers on the line but only in a categorical manner, ignoring line's extension.

- **Symbolic distance effect**

  In Psychology, (symbolic) **distance effect** is the phenomenon that the brain compares two abstract concepts, represented as a continuous space, with higher accuracy and faster reaction time if they differ more on the relevant dimension. For example, the performance of subjects when comparing a pair of positive numbers (x, y) decreases for smaller $|x - y|$ (*behavioral numerical distance effect*).

  The related *magnitude effect* is that performance decreases for larger $\min\{x, y\}$. For example, it is more difficult to measure a longer distance (say,

100 m) to the nearest mm than a short distance (say, 1 cm). Those effects correspond to *Weber law. They* are valid also for congenitally blind people; they learn spatial relations via tactile input (interpreting, say, numerical distance by placing pegs in a peg board).

A current explanation is that there exists a mental line of numbers (MNL) which is oriented from left to right (as $2, 3, 4$) and nonlinear (more mental space for smaller numbers). So, close numbers are easier to confuse since they are represented on the MNL at adjacent and not always precise locations. Possible MNL's, explaining such confusion, are *linear-scalar* (the psychological distance $d(a, a+1)$ between adjacent values is constant but the amount of noise increases as ka) or *logarithmic* (amount of noise is constant but $d(a, a+1)$ decreases logarithmically).

Related *SNARC* (spatial-numerical association of response codes) *effect* is that smaller (or larger) numbers are responded to more easily with responses toward a left (or, respectively, right) location. Also, smaller numbers promote a left-oriented gaze-direction whereas the opposite is true for higher numbers. Similar spatial-musical association *SMARC* and a mental line of pitches were observed. The same (from left to right) mental number line ability was found in three-day-old chicks.

In general, human cognition is often body-based, i.e., conceptual thinking relies on simulations of perceptual symbols. There is now increasing evidence that abstract concepts are also grounded in sensory-motor representations through metaphors. For example, power/status mapped to verticality, physical force to size, social proximity to temperature, and social distance to spatial distance.

- **Law of proximity**

  Gestalt Psychology is a theory of mind and brain of the Berlin School, in which the brain is holistic, parallel and self-organizing. Perceptual organization is composed of grouping and segregation. The visual grouping of discrete elements is determined by proximity, similarity, common fate, good continuation, closure (Wertheimer, 1923), and, more recently, common region, connectedness or synchrony.

  In particular, the **law of proximity** is that spatial or temporal proximity of elements may induce the mind to perceive a collective or totality.

- **Emotional distance**

  The **emotional distance** is the degree of emotional detachment (toward a person, group or events), aloofness, indifference by personal withdrawal, reserve.

  The Bogardus Social Distance Scale (cf. **social distance**) measures the distance between two groups by averaged emotional distance of their members.

  Spatial empathy is the awareness that an individual has to the proximity, activities, and comfort of people surrounding him.

  The *propinquity effect* is the tendency for people to get emotionally involved with those who have higher *propinquity* (physical/psychological proximity) with them, i.e., whom they encounter often. Walmsley, 1978, proposed that emotional involvement decreases as $d^{-\frac{1}{2}}$ with increasing **subjective distance** d.

- **Psychical distance**

  Psychical (or *psychic*) **distance** is a term having no commonly accepted definition. In several dictionaries, it is a synonym for the **emotional distance**. This term was introduced in [Bull12] to define what was called later the **aesthetic distance** (cf. the **antinomy of distance**) as a degree of the emotional involvement that a person, interacting with an aesthetic artifact or event, feels towards it.

  In Marketing, the psychic distance mean the level of attraction or detachment to a particular country resulting from the degree of uncertainty felt about it.

- **Distancing**

  Distancing (from the verb *to distance*, i.e., to move away from or to leave behind) is any behavior or attitude causing to be or appearing to be at a distance.

  Uncountable noon **distantness** (or **farness**) is the state or quality of being distant, remote, far-off, way in the distance. Archaic meaning: distant parts or regions.

  Distancy, **farawayness**, **distaunce** are rare/obsolete synonyms for distance, while **indistancy** is either nearness, or lack (or want) of distance (or separation).

  Self-distance is the ability to critically reflect on yourself and your relations from an external perspective; not to confound with mathematical notions of **self-distance** in Chaps. 1 and 17.

  Outdistancing means to outrun, especially in a long-distance race, or, in general, to surpass by a wide margin, especially through superior skill or endurance.

  In Martial Arts, **distancing** is the selection of an appropriate *combat range*, i.e., distance from the adversary. For other examples of spatial distancing; cf. **distances between people** and, in Chap. 29, **safe distancing** from a risk factor.

  Social distancing during pandemic refers to focused measures to increase the physical distance between individuals, or activity restrictions, such as increasing distance between student desks, canceling sports activities, and closing schools.

  In *Mediation* (a form of alternative dispute resolution), **distancing** is the impartial and nonemotive attitude of the mediator versus the disputants and outcome.

  In Psychoanalysis, **distancing** is the tendency to put persons and events at a distance. It concerns both the patient and the psychoanalyst.

  In Developmental Psychology, **distancing** (Werner–Kaplan, 1964, for deaf-blind patients) is the process of establishing the individuality of a subject as an essential phase (prior to symbolic cognition and linguistic communication) in learning to treat symbols and referential language. For Sigel (1970, for preschool children), **distancing** is the process of the development of cognitive representation: cognitive demands by the teacher or the parent help to generate a child's representational competence. **Distancing from role identities** is the first step of 7-th (individualistic) of nine stages of ego development in Loevinger, 1976.

  In the books by Kantor, **distancing** refers to APD (Avoidant Personality Disorder): fear of intimacy and commitment in confirmed bachelors, "femmes

fatales", etc. **Associational distancing** refers to individual's dissociation with those in the group inconsistent with his desired social identity.

The **distancing language** is phrasing used by a person to avoid thinking about the subject or content of his own statement (for example, referring to death).

Distancing by scare quotes is placing quotation marks around an item (single word or phrase) to indicate that the item does not signify its literal or conventional meaning. The purpose could be to distance the writer from the quoted content, to alert the reader that the item is used in an unusual way, or to represent the writer's concise paraphrasing. **Neutral distancing** convey a neutral writer's attitude, while distancing him from an item's terminology, in order to call attention to a neologism, jargon, a slang usage, etc; sometimes italics are used for it.

Cf. **technology-related distancing**, **antinomy of distance**, **distanciation**.

28.2 Distances in Economics and Human Geography

- **Technology distances**

  The **technological distance** between two firms is a distance (usually, χ^2- or **cosine distance**) between their *patent portfolios*, i.e., vectors of the number of patents granted in (usually, 36) technological subcategories. Other measures are based on the number of patent citations, co-authorship networks, etc.

  Granstrand's **cognitive distance** between two firms is the **Steinhaus distance** $\frac{\mu(A\triangle B)}{\mu(A\cup B)} = 1 - \frac{\mu(A\cap B)}{\mu(A\cup B)}$ between their technological profiles (sets of ideas) A and B seen as subsets of a *measure space* $(\Omega, \mathcal{A}, \mu)$.

  Olsson, 2000, defined the metric space (I, d) of all ideas (as in human thinking), $I \subset \mathbb{R}^n_+$, with some **intellectual distance** d. The closed, bounded, connected *knowledge set* $A_t \subset I$ extends with time t. New elements are, normally, convex combinations of previous ones: *innovations* within gradual technological progress. Exceptionally, breakthroughs (Kuhn's paradigm shifts) occur.

  The similar notion of *thought space* (of ideas/knowledge and relationships among them in thinking) was used by Sumi et al., 1997, for computer-aided thinking with text; they proposed a system of mapping text-objects into metric spaces.

  Introduced by Patel, 1965, the **economic distance** between two countries is the time (in years) for a lagging country to catch up to the same per capita income level as the present one of an advanced country. Nazarczuk, 2015, adapted this notion as the *regional economic distance* and defined the *relative regional distance* as the mean number of years necessary to achieve the reference area GDP per capita, taking into consideration the growth rate of the reference area.

  Introduced by Fukuchi–Satoh, 1999, the **technology distance** between countries is the time (in years) when a lagging country realizes a similar technological structure as the advanced one has now. The basic assumption of the *Convergence Hypothesis* is that this distance between two countries is smaller than the economic one.

- **Production Economics distances**

  In quantitative Economics, a *technology* is modeled as a set of pairs (x, y), where $x \in \mathbb{R}^m_+$ is an *input* vector, $y \in \mathbb{R}^m_+$ is an *output* vector, and x can produce y. Such a set T should satisfy standard economical regularity conditions.

  The **directional distance function** of input/output x, y toward a (projected and evaluated) direction $(-d_x, d_y) \in \mathbb{R}^m_- \times \mathbb{R}^m_+$ is (Chambers–Chung–Färe, 1996)

$$\sup\{k \geq 0 : ((x - kd_x), (y + kd_y)) \in T\}.$$

  For $d_x = x, d_y = y$, it is a scaled version of the **Shephard input distance function** (Shephard, 1953 and 1970) $\sup\{k \geq 0 : (x, \frac{y}{k}) \in T\}$.

  The *frontier* $f_s(x)$ is the maximum feasible output of a given input x in a given system (or year) s. The **distance to frontier** (Färe–Crosskopf–Lovell, 1994) of a production point (x, y), where $y = g_s(x)$), is $\frac{g_s(x)}{f_s(x)}$.

  The *Malmquist index* measuring the change in TFP (total factor productivity) between periods s, s' (or comparing to another unit in the same period) is $\frac{g'_s(x)}{f_s(x)}$. The *distance to frontier* is the inverse of TFP in a given industry (or of GDP per worker in a given country) relative to the existing maximum (the frontier, usually, US). In general, the term *distance-to-target* is used for the deviation in percentage of the actual value from the planned one.

  Consider a *production set* $T \subset \mathbb{R}^{n_1} \times \mathbb{R}^{n_2}$ (input, output). The measure of the technical efficiency, given by Briec–Lemaire, 1999, is the point-set distance $\inf_{y \in we(T)} ||x - y||$ (in a given norm $||.||$ on $\mathbb{R}^{n_1+n_2}$) from $x \in T$ to the *weakly efficient set* $we(T)$. It is the set of minimal elements of the poset $(T, \preceq)$ where the *partial order* $\preceq$ ($t_1 \preceq t_2$ if and only if $t_2 - t_1 \in K$) is induced by the cone $K = int(\mathbb{R}^{n_1}_{>0} \times \mathbb{R}^{n_2}_{>0}) + \{0\}$.

- **Distance to default**

  A *call option* is a financial contract in which the buyer gets, for a fee, the right to buy an agreed quantity of some commodity or financial instrument from the seller at a certain time (the expiration date) for a certain price (the *strike price*).

  Let us see a firm's equity E as a call option on the firm's assets A, with the total *liabilities* (debt) L being the strike price, i.e., $E = \max(0, A - L)$ with $A < L$ meaning the firm's default. Applying Black–Sholes, 1973, and Merton, 1974, option pricing formulas, the **distance to default** t periods ahead is defined by

$$D2D_t = \frac{\ln \frac{A_t}{D} + t(\mu_A - \frac{1}{2}\sigma_A^2)}{\sigma_A \sqrt{t}},$$

  where μ_A is the rate of growth of A and σ_A is its *volatility* (standard deviation of yearly logarithmic returns). A Morningstar's credit score is $cs = \frac{7}{2}(D2D + SS) + 8BR + CC \times \max(D2D, SS, BR)$, where SS, BR and CC are the solvency, business risk and cash flow cushion scores. The resulting credit rating AAA, AA, A, BBB etc., corresponds to cs within $[16, 23), [23, 61), [61, 96)$, etc.

- **Action distance**

  The **action distance** is the distance between the set of information generated by the Active Business Intelligence system and the set of actions appropriate to a specific business situation. Action distance is the measure of the effort required to understand information and to effect action based on that information. It could be the physical distance between information displayed and action controlled.

- **Effective trade distance**

  There is large border effect of political boundaries on the volume of trade and on relative prices. The border introduces costs related to tariffs, market regulations, differences in product packages and languages.

  Engel–Rogers, 1996, showed that the dispersion of prices within a country is orders of magnitude smaller than across countries, and estimated that the US-Canadian border was equivalent to a distance of 120,000 km. McCallum, 1995, found that inter-provincial trade within Canada was, on average, 22 times larger that the trade of any province with any State from US. Cf. **impact of distance on trade**.

  Borraz et al., 2012, showed that the "online border" in E-commerce is equivalent to the average distance from the online warehouse to the offline stores.

  [HeMa02] defined the **effective trade distance** between countries x and y with populations $x_1, \ldots, x_m$ and $y_1, \ldots, y_n$ of their main agglomerations as

$$\left(\sum_{1\le i\le m} \frac{x_i}{\sum_{1\le t\le m} x_t} \sum_{1\le j\le n} \frac{y_j}{\sum_{1\le t\le n} y_t} d_{ij}^r\right)^{\frac{1}{r}},$$

  where d_{ij} is the bilateral distance (in km) of the corresponding agglomerations x_i, y_i, and r measures the sensitivity of trade flows to d_{ij}.

  As an **internal distance of a country**, measuring the average distance between producers and consumers, [HeMa02] proposed $0.67\sqrt{\frac{area}{\pi}}$.

- **Impact of distance on trade**

  Bilateral trade decreases with distance; this effect slightly increased over the last century. Webb, 2007, claims that an average distance of trade in 1962 of 4790 km changed only to 4938 km in 2000.

  The relationship between shipments and distance, found in Hillberry–Hummels, 2008, is highly nonlinear: at the beginning, there is a sharp reduction in value with distance; but, once a distance-threshold is achieved the negative effect vanishes.

  An example of used measures is the average distance traveled by heavy trucks between actual origins and destinations in their deliveries of commodities.

  Frankel–Rose, 2000, estimated impact of certain distance variables on trade, for example, +340 %, +200 %, +80 %, +0.8 %,-0.2 %,-1.1 % for common currency, common language, common border, economic size (1 % GDP increase), physical size (1 % increase), physical distance (1 % increase), respectively.

  Using the **gravity models** with 16 *CAGE* (cultural, administrative, geographic, economic) distances between countries, Ghemawat, 2004, developed *CAGE Distance Framework* for managers considering international strategies.

His distances are *cultural* (different languages, ethnicities, religions, social norms), *administrative* (absence of shared monetary or political association, institutional weakness), *geographic* (physical remoteness, different climates, lack of common border or waterway access, weak transportation or communication links) and *economic* (difference in consumer incomes, cost and quality of natural, financial, human resources).

Most affected industries are: meat, cereals, tobacco (by linguistic ties), gold, electricity, textile (by preferential trading agreements), electricity, gas, live animals (by physical remoteness). The wealth difference decreases trade in metals, fertilisers, meat, but increases trade in coffee, tea, animal oils, office machines.

- **Long-distance trade routes**

  Examples of such early historic routes are the *Amber Road* (from northern Africa to the Baltic Sea), *Via Maris* (from Egypt to modern day Iran, Iraq, Turkey, Syria), the route *from the Varangians to the Greeks* (from Scandinavia across Kievan Rus' to the Byzantine Empire), the *Incense Road* (from Mediterranean ports across the Levant and Egypt through Arabia to India), Roman-Indian routes, Trans-Saharan trade, *Grand Trunk Road* (from Calcutta to Peshawar) and the *Ancient Tea Route* (from Yunnan to India via Burma, to Tibet and to central China).

  The *Silk Road* was, from the second century BC, a network of trade routes connecting East, South, and Western Asia with the Mediterranean world, North/Northeast Africa and Europe. Extending 6500 km, it enabled traders to transport goods, slaves and luxuries such as silk, other fine fabrics, perfumes, spices, medicines, jewels, as well as the spreading of knowledge, ideas, cultures, plants, animals and diseases. But the Silk Road became unsafe and collapsed in the tenth century after the fall of the Tang Dynasty of China, the destruction of the Khazar Khaganate and, later, the Turkic invasions of Persia and the Middle East.

  During fifth to tenth centuries, the *Radhanites* (medieval Jewish merchants) dominated trade between the Christian and Islamic worlds, covering much of Europe, North Africa, Middle East, Central Asia and parts of India and China. They carried commodities combining small bulk and high demand (spices, perfumes, jewelry, silk). The *Maritime Republics* (mercantile Italian city-states, especially Genoa, Venice, Pisa, Amalfi) dominated long-distance trade during tenth to thirteenth centuries. The spice trade from Asia to Europe became, via new sea routes, a Portuguese monopoly (fifteenth to seventeenth centuries) replaced by the Dutch, and soon after the English and the French. During thirteenth to seventeenth centuries, the *Hanseatic League* v(an alliance of trading cities and their guilds) dominated trade along the coast of Northern Europe.

- **Relational proximity**

  Economic Geography considers to nongeographical types of proximity (organizational, institutional, cognitive, etc.). In particular, **relational proximity** (or trust-based interaction between actors) is an inclusive concept of the benefits

derived from spatially localized sets of economic activities. It generates relational capital through the dynamic exchange of locally produced knowledge.

The five dimensions of relational proximity are proximity: of contact (directness), through time (continuity, stability), in diversity (multiplicity, scope), in mutual respect and involvement (parity), of purpose (commonality).

Individuals are close to each other in a relational sense when they share the same interaction structure, make transactions or realize exchanges. They are *cognitively close* if they share the same conventions and have common values and representations (including knowledge and technological capabilities).

Bouba-Olga and Grossetti, 2007, divide socio-economic proximity into relational one (role of social networks) and *mediation proximity* (role of newspapers, directories, Internet, agencies, etc.). Tranos and Nijkamp, 2013: physical distance and relational proximities have a significant impact on Internet's infrastructure.

- **Migration distance (in Economics)**

  The **migration distance**, in Economic Geography, is the distance between the geographical centers of the municipalities of origin and destination.

  Ravenstein's 2-nd and 3-rd laws of migration (1880) are that the majority of migrants move a short distance, while those move longer distances tend to choose big-city destinations. About 80 % of migrants move within their own country.

  Migration tends to be an act of aspiration; it generally improves migrant's wealth and lifestyle. *Existential migrants* refer to voluntary noneconomic expatriates with "existential wanderlust". Madison, 2006, defines them as seeking greater possibilities for self-actualising, exploring foreign cultures in order to assess own identity, and ultimately grappling with issues of home/belonging in the world generally.

- **Commuting distance**

  The **commuting distance** is the distance (or travel time) separating work and residence when they are located in separated places (say, municipalities).

  The **acceptable commute distance**, in Real Estate, is the distance that can be covered in an acceptable travel time and increases with better connectivity.

- **Consumer access distance**

  Consumer access distance is a distance measure between the consumer's residence and the nearest provider where he can get specific goods or services (say, a store, market or a health service). For example, *food miles* refers to the distance food is transported from the time of its production until it reaches consumers.

  Measures of geographic access and spatial behavior include distance measures (**map's distance**, **road travel distance**, perceived travel time, etc.), **distance decay** (decreased access with increasing distance) effects, transportation availability and *activity space* (the area of $\approx \frac{2}{3}$ of the consumer's routine activities).

  For example, by US Medicare standards, consumers in urban, suburban, rural areas should have a pharmacy within $2, 5, 15$ miles, respectively. The patients residing outside of a 15-miles radius of their hospital are called *distant patients*. Food grown within 100 miles of its point of purchase or consumption is *local food*.

Similar studies for retailers revealed that the negative effect of distance on store choice behavior was (for all categories of retailers) much larger when this behavior was measured as "frequency" than when it was measured as "budget share".

- **Distance decay (in Spatial Interaction)**

  In general, **distance decay** or the **distance effect** (Chap. 29) is the attenuation of a pattern or process with distance. In Spatial Interaction, **distance decay** is the mathematical representation of the inverse ratio between the quantity of obtained substance and the distance from its source.

  This decay measures the effect of distance on accessibility and number of interactions between locations. For example, it can reflect a reduction in demand due to the increasing travel cost. The quality of streets and shops, height of buildings and price of land decrease as distance from the center of a city increases.

  The *bid-rent distance decay* induces, via the cost of overcoming distance, a class-based spatial arrangement around a city: with increasing distance (and so decreasing rent) commercial, industrial, residential and agricultural areas follow.

  In location planning for a service facility (fire station, retail store, transportation terminal, etc.), the main concerns are *coverage standard* (the maximum distance, or travel time, a user is willing to overcome to utilize it) and distance decay (demand for service decays with distance).

  An example of related *size effect*: doubling the size of a city leads usually to a 15 % decrease of resource use (energy, roadway amount, etc.) per capita, a rise of $\approx$ 15 % in socio-economic well-being (income, wealth, the number of colleges, etc.), but also in crime, disease and average walking speed. Bettencourt et al., 2007, observed that "social currencies" (information, innovation, wealth) typically scale superlinearly with city size, while basic needs (water and household energy consumption) scale linearly and transportation/distribution infrastructures scale sublinearly.

  Distance decay is related to **friction of distance** which posits that in Geography, the *absolute distance* (say, in km) requires some amount of effort, money, time and/or energy to overcome. The corresponding cost is called *relative distance*; it describes the amount of social, cultural, or economic connectivity between two places.

- **Gravity models**

  The general **gravity model** for social interaction is given by the *gravity equation*

$$F_{ij} = a\frac{M_i M_j}{D_{ij}^b},$$

  where F_{ij} is the "flow" (or "gravitational attraction", *interaction*, *mass-distance function*) from location i to location j (alternatively, between those locations), D_{ij} is the "distance" between i and j, M_i and M_j are the relevant economic "masses" of i and j, and a, b are parameters. Cf. Newton's **law of universal gravitation**

in Chap. 24, where $b = 2$. The first instances were formulated by Reilly (1929), Stewart (1948), Isard (1956) and Tinbergen (1962).

If F_{ij} is a monetary flow (say, export values), then M is GDP (gross domestic product), and D_{ij} is the distance (usually the **great circle distance** between the centers of countries i and j). For trade, the true distances are different and selected by economic considerations. But the distance is a proxy for transportation cost, the time elapsed during shipment, cultural distance, and the costs of synchronization, communication, transaction. The **distance effect on trade** is measured by the parameter b; it is 0.94 in Head, 2003, and 0.6 in Leamer–Levinsohn, 1994.

If F_{ij} is a people (travel or migration) or message flow, then M is the population size, and D_{ij} is the travel or communication cost (distance, time, money).

If F_{ij} is the force of attraction from location i to location j (say, for a consumer, or for a criminal), then, usually $b = 2$. Reilly's *law of retail gravitation* is that, given a choice between two cities of sizes M_i, M_j and at distances D_i, D_j, a consumer tends to travel further to reach the larger city with the equilibrium point defined by

$$\frac{M_i}{D_i^2} = \frac{M_j}{D_j^2}.$$

- **Nearness principle**

  The **nearness principle** (or Zipf's *least effort principle*, in Psychology) is the following basic geographical heuristic: given a choice, a person will select the route requiring the least expenditure of effort, i.e., path of least resistance.

  This principle is used, for example, in transportation planning and locating of serial criminals: they tend to commit their crimes fairly close to where they live.

  The **first law of geography** (Tobler, 1970) is: "Everything is related to everything else, but near things are more related than distant things".

- **Distances in Criminology**

  Geographic profiling (or *geoforensic analysis*) aims to identify the spatial behavior (target selection and likely *offender's heaven*, i.e., the residence or workplace) of a serial criminal as it relates to the spatial distribution of linked crime sites.

  The **offender's buffer zone** is an area surrounding the offender's heaven, from which little or no criminal activity will be observed; usually, such a zone occurs for premeditated personal offenses. The primary streets and network arterials that lead into the buffer zone tend to intersect near the estimated offender's heaven. A 1 km buffer zone was found for the UK serial rapists. Most personal offenses occur within about 2 km from the offender's heaven, while property thefts occur further away.

  Given n crime sites (x_i, y_i), $1 \le i \le n$ (where x_i and y_i are the latitude and longitude of the i-th site), the *Newton–Swoope Model* predicts the offender's heaven to be within the circle around the point $(\frac{\sum_i x_i}{n}, \frac{\sum_i y_i}{n})$ with the search

radius being

$$\sqrt{\frac{\max|x_{i_1} - x_{i_2}| \cdot \max|y_{i_1} - y_{i_2}|}{\pi(n-1)^2}},$$

where the maxima are over (i_1, i_2), $1 \le i_1 < i_2 \le n$. The *Ganter–Gregory Circle Model* predicts the offender's heaven to be within a circle around the first offense crime site with diameter the maximum distance between crime sites.

The *centrographic models* estimate the offender's heaven as a *center*, i.e., a point from which a given function of travel distances to all crime sites is minimized; the distances are the Euclidean distance, the Manhattan distance, the **wheel distance** (i.e., the actual travel path), perceived travel time, etc. Many of these models are the reverse of Location Theory models aiming to maximize the placement of distribution facilities in order to minimize travel costs. These models (*Voronoi polygons*, etc.) are based on the **nearness principle** (*least effort principle*).

The **journey-to-crime decay function** is a graphical **distance curve** used to represent how the number of offenses committed by an offender decreases as the distance from his/her residence increases. Such functions are variations of the center of gravity functions; cf. **gravity models**.

For detection of criminal, terrorist and other hidden networks, there are many data-mining techniques which extract latent associations (distances and **near-metrics** between people) from graphs of their co-occurrence in relevant documents, events, etc. In, say, drug cartel networks, better to remove *betweeners* (not well-connected bridges between groups, as paid police) instead of hubs (kingpins).

Electronic tagging consist of a device attached to a criminal or vehicle, allowing their whereabouts to be monitored using GPS. An *ankle monitor* (or *tether*) is a such tracking device that individuals under house arrest or parole are often required to wear. The *range of a tether* (or *inclusion zone*, 10–50 m) depends usually on the gravity of the crime; it is set by the offender's probation officer.

- **Drop distance**

  In judicial hanging, the **drop distance** is the distance the executed is allowed to fall. In order to reduce the prisoner's physical suffering (to about a third of a second), this distance is pre-determined, depending on his/her weight, by special *drop tables*. For example, the (US state) Delaware protocol prescribes, in pounds/feet, about 252, 183 and 152 cm for at most 55, 77 and at least 100 kg. Unrelated *hanging distance* is the minimum (horizontal) distance needed for hanging a hammock.

  In Biosystems Engineering, a ventilation jet *drop distance* is defined as the horizontal distance from an air inlet to the point where the jet reaches the occupational zone. In Aviation, an airlift *drop distance* (or *drop height*) is the

vertical distance between the aircraft and the drop zone over which the airdrop is executed.

- **Distance telecommunication**

  Distance telecommunication is the transmission of signals over a distance for the purpose of communication. In modern times, this process almost always involves the use of electromagnetic waves by transmitters and receivers.

  Nonelectronic visual signals were sent by fires, beacons, smoke signals, then by mail, pigeon post, hydraulic semaphores, heliographs and, from the fifteenth century, by maritime flags, semaphore lines and signal lamps.

  Audio signals were sent by drums, horns (cf. **long-distance drumming** in Chap. 21) and, from nineteenth century, by telegraph, telephone, and radio.

  Advanced electrical/electronic signals are sent by television, videophone, fiber optical telecommunications, computer networking, analog cellular mobile phones, SMTP email, Internet and satellite phones.

- **Distance supervision**

  Distance supervision refers to the use of interactive distance technology (landline and cell phones, Email, chat, text messages to cell phone and instant messages, video teleconferencing, Web pages) for live (say, work, training, psychological umbrella, mental health worker, administrative) supervision.

  Such supervision requires tolerance for ambiguity when interacting in an environment that is devoid of nonverbal information.

- **Distance education**

  Distance education is the process of providing instruction when students and instructors are separated by physical distance, and technology is used to bridge the gap. *Distance learning* and *distance* (or *online*) degrees are the desired outcomes. A *semi-distance program* is one combining online and residential courses.

  The **transactional distance** (Moore, 1993) is a perceived degree of separation during interaction between students and teachers, and within each group. This distance decreases with *dialog* (a purposeful positive interaction meant to improve the understanding of the student), with larger autonomy of the learner, and with lesser predetermined structure of the instructional program.

  Vygotsky's *zone of proximal development* is the distance between the actual developmental level as determined by independent problem solving and the level of potential development as determined through problem solving under adult guidance, or in collaboration with more capable peers.

- **Distance selling**

  Distance selling, as opposed to face-to-face selling in shops, covers goods or services sold without face-to-face contact between supplier and consumer but through *distance communication means*: press adverts with order forms, catalog sales, telephone, tele-shopping, e-commerce (via Internet), m-commerce (via mobile phone). Examples of the relevant legislation are Consumer Protection (Distance Selling) Directive 97/7/EC and Regulations 2000 in EU.

  The main provisions are: clear prior information before the purchase, its confirmation in a durable medium, delivery within 30 days, "cooling-off" period

of seven working days during which the consumer can cancel the contract without any reason and penalty. Exemptions are: *Distance marketing* (financial services sold at distance), business-to-business contracts and some purchases (say, of land, or at an auction, or from vending machines).

- **Approximative human-scale distances**

  An **arm's length** is a distance (about 0.7 m, i.e., within **personal distance**) sufficient to exclude intimacy, i.e., discouraging familiarity or conflict; its analogs are: Italian *braccio*, Turkish *pik*, and Old Russian *sazhen*.

  The **reach distance** is the difference between the maximum reach and arm's length. The **striking** (or *handshaking*) **distance** is a short, easily reachable distance.

  The **whiffing** (or **spitting**, **poking**) **distance** is a very close distance.

  A **stone's throw** is a distance of about 25 fathoms (46 m).

  The **hailing** (or **shouting**, **calling**) **distance** is the distance within which the human voice can be heard. **Far cry**: distance estimated in audibility's terms.

  The **Goldilocks distance** is the "just right" one; cf. the **Kasting distance** in Sect. 25.3.

  The **walking distance** is the context-depending distance normally reachable by walking. In Japan, its standard unit is 80 m, i.e., one minute walking time. Some the UK high schools define 2 and 3 miles as the statutory walking distance for children younger and older than 11 years.

  Pace out means to measure distance by *pacing* (walking with even steps).

- **Walkability distances**

  Walkability is (Abley, 2005) the extent to which the environment is friendly to the presence of people living, shopping, visiting, or spending time in an area.

  Walk Score is a walkability index based on the Euclidean distance to amenities such as businesses, schools, parks, and other common destinations within 20 minutes' walk (1 mile $=$ 5280 feet $\approx$ 1.609 km) of a given starting point. The algorithm awards points based on the distance to the closest amenity in each category.

  The number of points declines from maximum to 0 as the distance runs from 0.4 km (5 minutes' walk) to 1.6 km. Each category is weighted equally and the points are summed and normalized to yield a score from 0 to 100.

  Walk Score also measures pedestrian friendliness by analyzing population density, block length and intersection density. Scores 0 to 49 mean that almost all or most daily errands require a car, and scores 90 to 100 signify a "walker's paradis".

  Walkability is a central principle of *New Urbanism*. In particular, the (urban-to-rural) *transect* is (Duany, 2000) a series of zones that transition from the natural landscape to the dense urban core: T_1 (natural), T_2 (rural), T_3 (suburban), T_4 (general urban), T_5 (urban center), T_6 (downtown).

  Block length and building height for $T_3 - T_6$ are, respectively: 700–800, 600, 500, $\leq$ 400 feet and 1–2, 2–3, 2–4, $\geq$ 4 floors. Each zone is *self-similar* in that it contains a similar transition from the edge to the center of the neighborhood.

  A **walking radius** is a typical urban walking distance from a given starting point to transit or before driving. It was estimated as 400 m for the US, and larger for Europe. For the US the blog *Walk Appeal* defines the following urban

walking radii: W_6 (2 miles on a highway), W_5 (0.75 mile on a main street, in T_5), W_4 (0.25 mile on a neighborhood street, in T_4), W_3 (0.1 mile on a suburban street, in T_3), W_2 (250 feet on a subdivision street), W_1 (100 feet in parking lot), W_0 (unwalkable).

- **Optimal eye-to-eye distance**

  The **optimal eye-to-eye distance** between two persons was measured for some types of interaction. For example, such an optimal viewing distance between a baby and its mother's face, with respect to the immature motor and visual systems of the newborn, is 20–30 cm. During the first weeks of life the accommodation system does not yet function and the lens of the newborn is locked at the **focal distance** of about 19 cm. At ages 8–14 months, babies are judging distances well; they fear a distance with mother (separation anxiety stage) and strangers. Also, left-sided cradling/holding preference have been found in humans and great apes.

- **Language style matching**

  During conversation, texting, emailing, and other forms of interactive communication, people unconsciously mimic their partners' language use patterns.

  The *LSM* (language style matching) *score* of a dyad $(1, 2)$ of persons, with respect to a *function word type* $k, 1 \leq k \leq 9$, is $LSM_i = 2\frac{\min(l_{1k}, l_{2k})}{l_{1k}+l_{2k}}$, where l_{ik} $(i = 1, 2)$ is the percentage of person i's words of type k. Each dyad's total *LSM* is the mean of its LSM_i across the nine types of *function words*: auxiliary verbs (say, *am*, *will*, *have*), articles, common adverbs (say, *hardly*, *often*), personal pronouns, indefinite pronouns, prepositions, negations, conjunctions (say, *and*, *but*) and quantifiers.

  LSM is high within the first 15–30 s of any interaction and is generally unconscious. Women use conjunctions at much higher rates.

  LSM predicts successful hostage negotiations (Taylor–Thomas, 2008), task group cohesiveness (Gonzales–Hancock–Pennebaker, 2010), and the formation and persistence of romantic relationships (Ireland et al., 2011).

  However (Manson et al., 2013), the probability of diad's cooperation in a post-conversation one-shot prisoner's dilemma, is positively related, instead of LSM, to the convergence of their speech rates (mean syllable duration).

- **Distances between people**

  In [Hall69], four interpersonal bodily distances were introduced: the *intimate distance* for lovers, childrens, pets (from touching to 46 cm), the *personal-casual distance* for conversations among friends (46–120 cm), the *social-consultative distance* for conversations among acquaintances (1.2–3.7 m), and the *public-audience distance* for public speaking (over 3.7 m). To each of those *proxemics distances*, there corresponds an intimacy/confidence degree and appropriated sound level.

  The distance which is appropriate for a given social situation depends on culture, gender and personal preference. For example, under Islamic law, proximity (being in the same room or secluded place) between a man and a woman is permitted only in the presence of their *mahram* (a spouse or anybody from the same sex or a pre-puberty person from the opposite sex). For an average

westerner, personal space is about 70 cm in front, 40 cm behind and 60 cm on either side.

In interaction between strangers, the interpersonal distance between women is smaller than between a woman and a man. The bonding hormone oxytocin discourages partnered (but not a single) men from getting close to a female stranger; they, if were given oxytocin, stayed 10–15 cm farther from the attractive woman.

An example of other cues of nonverbal communication is given by angles of vision which individuals maintain while talking. The **people angular distance in a posture** is the spatial orientation, measured in degrees, of an individual's shoulders relative to those of another; the position of a speaker's upper body in relation to a listener's (for example, facing or angled away). Speaker uses 45° open position in order to make listener feel comfortable and direct body point in order to exert pressure. In general, to approach men directly from the front or women from behind is rude. Also, this distance reveals how one feels about people nearby: the upper body unwittingly angles away from disliked persons and during disagreement.

Eye-contact decreases with spatial proximity. Persons stand closer to those whose eyes are shut. The *Steinzor effect* is the finding that members of leaderless discussion groups seated in circles, are most apt to address remarks to or to get responses from persons seated opposite or nearly opposite them, while in the presence of a strong leader, it happens with persons seated alongside or nearly alongside.

Distancing behavior of people can be measured, for example, by the *stop distance* (when the subject stops an approach since she/he begins to feel uncomfortable), or by the *quotient of approach*, i.e., the percentage of moves made that reduce the interpersonal distance to all moves made.

Humans and monkeys with amygdala lesions have much smaller than average preferred interpersonal distance. *Peripersonal*, i.e., within reach of any limb of an individual, *space* is located dorsally in the parietal lobe whereas *extrapersonal* (outside his reach) *space* is located ventrally in the temporal lobe.

- **Death of Distance**

  Death of Distance is the title of the influential book [Cair01] arguing that the telecommunication revolution (the Internet, mobile telephones, digital TV, etc.) initiated the "death of distance" implying fundamental changes: three-shift work, lower taxes, prominence of English, outsourcing, new ways of government control and citizens communication, but also management-at-a-distance and concentration of elites within the "latte belt". Physical distance (and so, Economic Geography) do not matter; we all live in a "global village". Friedman, 2005, announced: "The world is flat". Gates, 2006, claimed: "With the Internet having connected the world together, someone's opportunity is not determined by geography". The proportion of long-distance relationships in foreign relations increased.

  Similarly (see [Ferg03]), steam-powered ships and the telegraph (as railroads previously and cars later) led, via falling transportation/communication costs, to

the "annihilation of distance" in the nineteenth and twentieth centuries. Heine wrote in 1843: "Space is killed by the railways, and we are left with time alone".

Further in the past, archaeological evidence points out the appearance, ≈ 0.14 Ma ago, long-distance (up to 300 km) trade, and, ≈ 0.04 Ma ago, the innovation of projectile weapons and traps which allowed humans to kill large game (and other humans) from a safe distance.

But already Orwell, 1944, dismissed as "shallowly optimistic" the the phrases "airplane and radio have abolished distance" and "all parts of the world are now interdependent". Heidegger wrote in 1950: "All distances in time and space are shrinking…The peak of this abolition of every possibility of remoteness is reached by television…" but "The frank abolition of all distances brings no nearness". Edgerton, 2006, claims that new technologies foster self-sufficiency and isolation instead.

Modern technology eclipsed distance only in that the time to reach a destination has (usually) shrunk. Distances still matter for, say, a company's strategy on the emerging markets (cf. **impact of distance on trade**) and for political legitimacy. "Tyranny of distance" still affects small island states in the Pacific.

Partridge et al., 2007, report that proximity to higher-tiered urban centers (with their higher-order services, urban amenities, higher-paying jobs, lower-cost products) increasingly favors local job growth. Increased access to services and knowledge exchange requires more face-to-face interaction and so, an increase in the role of distance. Economic and innovation activity are highly localized spatially and tend to agglomerate more. Also, the social influence of individuals, measured by the frequency of memorable interactions, is heavily determined by distance. Goldenberg–Levy, 2009, show that the IT (Information Technology) revolution which occurred in the 1990s, increased local social interactions (as email, Facebook communication, baby name diffusion) to a greater degree than long-distance ones.

In military affairs, Boulding, 1965, and Bandow, 2004, argued that twentieth century technology reduced the value of proximity for the projection of military power because of "a very substantial diminution in the cost of transportation of armed forces" and "an enormous increase in the range of the deadly projectile". It was used as partial justification for the withdrawal of US forces from overseas bases in 2004. But Webb, 2007, counter-argues that any easing of transport is countered by increased strain put upon its modes since both sides will take advantage of the falling costs to send more supplies. Also, the greatest movement of logistics continues to be conducted by sea, with little improvement in speed since 1900.

- **Technology-related distancing**

  The *Moral Distancing Hypothesis* postulates that technology increases the propensity for unethical conduct by creating a **moral distance** between an act and the moral responsibility for it.

  Print technologies divided people into separate communication systems and distanced them from face-to-face response, sound and touch. TV involved

audile-tactile senses and made distance less inhibiting, but it exacerbated *cognitive distancing*: story and image are biased against space/place and time/memory.

This distancing has not diminished with computers but interactivity has increased. In terms of Hunter: technology only re-articulates *communication distance*, because it also must be regarded as the space between understanding and not. The collapsing of spatial barriers diminishes economic but not social and cognitive distance.

The *Psychological Distancing Model* in [Well86] relates the immediacy of communication to the number of information channels: sensory modalities decrease progressively as one moves from face-to-face to telephone, videophone, and e-mail. Skype communication is rated higher than phone since it creates a sense of co-presence. People phone with bad news but text with good news.

Online settings tend to filter out social and relational cues. The lack of instant feedback (since e-mail communication is asynchronous) and low bandwidth limit visual/aural cues. For example, moral and cognitive effects of distancing in online education are not known at present. Also, the shift from face-to-face to online communication can diminish social skills, lead to smaller and more fragmented networks and so, increase feeling of isolation and alienation. But it can be only a bias, based on traditional spatiotemporal assumptions that farness translates into an increase in mediation and results in blurring of the communication.

Virtual distance is the perceived distance between individuals when their primary way of communication is not face-to-face. The main markers of virtual distance are physical, operational and affinity distances.

Mejias, 2005, define *epistemological distance* and *ontological distance* between things as the difference, respectively, in degree of knowledge justification and in ability of subjects to act upon things. He argue that we should strive towards ontological nearness, using modern information and communication technologies to manipulate temporal/spatial and epistemological distances to attain this goal.

Mejias, 2007, see some new advantages in "uniform distancelessness", deplored by Heidegger. *Networked proximity* (nearness mediated through new technology) provides shift from physical proximity to informational availability as the main measure of social relevance. It facilitates new kinds of spatially unbound community, and these emerging forms of sociality could be no less meaningful than the older ones. Networked sociality reconfigures distance rather than eliminates it.

28.3 Distances in Sociology and Language

- **Sociometric distance**

  The **sociometric distance** refers to some measurable degree of mutual or social perception, acceptance, and understanding. Hypothetically, greater sociometric distance is associated with more inaccuracy in evaluating a relationship.

- **Social distance**

  In Sociology, the **social distance** is the extent to which individuals or groups are removed or excluded from participating in one another's lives; a degree of understanding and intimacy which characterize personal and social relations generally. This notion was originated by Simmel in 1903; in his view, the social forms are the stable outcomes of distances interposed between subject and object.

  For example (Mulgan, 1991), the centers of global cities are socially closer to each other than to their own peripheries. In general, the notion of social distance is conceptualized in affective, normative or interactive way, i.e., in terms of sympathy the members of a group feel for another group, norms to define in- and outsider, or the frequency/intensity of interactions between two groups.

  The *Social Distance Scale* by Bogardus, 1947, offers the following response items: would marry, would have as a guest in my household, would have as next door neighbor, would have in neighborhood, would keep in the same town, would keep out of my town, would exile, would kill; cf. **emotional distance**. The responses for each (say, ethnic/racial) group are averaged across all respondents which yields (say, racial) distance quotient ranging from 1.00 to 8.00.

  Dodd and Nehnevasja, 1954, attached distances of 10^t m, $0 \leq t \leq 7$, to eight levels of the Bogardus scale. Many studies on conflicts in ex-Yugoslavia consider *ethnic distance* defined via some modified Bogardus scale, i.e., in terms of acceptance of a particular relation with an abstract person from the other group. Caselli and Coleman, 2012, defined *ethnic distance* as the cost to be born by a member of one group to successfully pass himself as a member of the other group.

  An example of relevant models: Akerlof ([Aker97]) defines an *agent* x as a pair (x_1, x_2) of numbers, where x_1 represents the initial, i.e., inherited, social position, and the position expected to be acquired, x_2. The agent x chooses the value x_2 so as to maximize

$$f(x_1) + \sum_{y \neq x} \frac{e}{(h + |x_1 - y_1|)(g + |x_2 - y_1|)},$$

  where e, h, g are parameters, $f(x_1)$ represents the intrinsic value of x, and $|x_1 - y_1|$, $|x_2 - y_1|$ are the inherited and acquired *social distances* of x from any agent y (with the social position y_1) of the given society.

  Hoffman, Cabe and Smith, 1996, define *social distance* as the degree of reciprocity that subjects believe exists within a social interaction.

- **Rummel sociocultural distances**

  [Rumm76] defined the main sociocultural distances between two persons as follows.

  – **Personal distance**: one at which people begin to encroach on each other's territory of personal space.
  – **Psychological distance**: perceived difference in motivation, temperaments, abilities, moods, and states (subsuming **intellectual distance**).

- **Interests-distance**: perceived difference in wants, means, and goals (including **ideological distance** on socio-political programs).
- **Affine distance**: degree of sympathy, liking or affection between the two.
- **Social attributes distance**: differences in income, education, race, sex, etc.
- **Status-distance**: differences in wealth, power, and prestige (including **power distance**).
- **Class-distance**: degree to which one person is in general authoritatively superordinate to the other.
- **Cultural distance**: differences in meanings, values and norms reflected in differences in philosophy-religion, science, ethics, law, language, and fine arts.

- **Cultural distance**

  The **cultural distance between countries** $x = (x_1, \ldots, x_5)$ and $y = (y_1, \ldots, y_5)$ (usually, US) is derived (in [KoSi88]) as the following composite index

$$\sum_{i=1}^{5} \frac{(x_i - y_i)^2}{5V_i},$$

  where V_i is the variance of the index i, and the five indices represent ([Hofs80]):

1. Power distance (preferences for equality);
2. Uncertainty avoidance (risk aversion);
3. Individualism versus collectivism;
4. Masculinity versus femininity (gender specialization);
5. Confucian dynamism (long-term versus short-term orientation).

  The above **power distance** measures the extent to which the less powerful members of institutions and organizations within a country expect and accept that power is distributed unequally, i.e., how much a culture has respect for authority. For example, Latin Europe and Japan fall in the middle range.

  But for Shenkar–Luo–Yeheskel, 2008, above distance is merely a measure of how much a country strayed from the core culture of the multinational enterprise. They propose instead (especially, as a regional construct) the *cultural friction* linking goal incongruity and the nature of cultural interaction.

  In order to explain multinational enterprise behavior, Kostova, 1999, introduced the *institutional distance* between its home and host countries as the difference in their regulative, cognitive, and normative institutions. Habib–Zurawicki, 2002, consider effects of the *corruption distance*, i.e., such difference in corruption levels.

  Wirsing, 1973, defined *social distance* as a "symbolic gap" between rulers and ruled designed to set apart the political elite from the public. It consists of reinforced and validated ideologies (a formal constitution, a historical myth, etc.).

Davis, 1999, theorized social movements (in Latin America) in terms of their shared distance from the state: geographically, institutionally, socially (class position and income level) and culturally.

The Inglehart–Welzel *cultural map of the world* represent countries as points on $\mathbb{R}^2$, in which the two dimensions (*traditional/secular-rational* and *survival/self-expression*) explain $> 70\,\%$ of cross-national variance in 10 indicators.

- **Trust radius**

  People's **trust radius** is the width of the *cooperation circle* (people among whom a certain trust level exists), while *trust level* is the intensity with which people trust other people. The relation between them is weak. Individualism/collectivism is associated with a broader/narrower trust radius. A given level of trust can be broad/narrow if trust is mostly out-group/in-group connoted.

  Delhey–Newton–Welzel, 2011, distinguish *in-group trust* (trust in your family, your neighborhood, people you know personally) from *out-group trust* (people you meet for the first time, people of another religion, of another nationality). Respondents were asked whether "most people can be trusted" or "you need to be very careful in dealing with people." Then this generalized trust was regressed on out-group and in-group trust via the degree of in-group/out-group connotation of the term *most people*. If this term is more in-group connoted, trust radius is narrow, and it is broad otherwise. Quantification of trust radius occurs by estimating linear regression models, separately for all countries in the sample, employing level of trust in *most people* as the dependent variable and scaled measures of in-group and out-group trust levels as the independent variables.

  The trust radius is calculated as (rescaled to fit a $[0, 1]$ scale) the difference of the estimated coefficients for out-group and in-group trust. Swiss residents got the widest trust radius (followed by Italy, Slovenia, Sweden, Australia), while Thai residents rank lowest (with Morocco, Burkina Faso, and China).

  An unrelated term, the *margin of error*, is usually defined as the *radius* (or half the width) *of a confidence interval* for a particular statistic or observational error. *Confidence level* is usually $90\,\%$, $99\,\%$ or, typically, $95\,\%$.

- **Political distance**

  A finite metric space $(X = \{x_1, \ldots, x_n\}, d)$ can be seen as a *political space* with the points and distance seen as positions (policy proposals) and some **ideological distance**, respectively. Usually, (X, d) is a subspace of $([0, 1]^m, ||x - y||_2)$.

  Let $\{v_1, \ldots, v_n\}$ be the vote shares of all candidates $\{c_1, \ldots, c_n\}$ of an election or, say, allocated seat shares of all competing parties; so, $\sum_{i=1}^{n} v_i = 1$. The *index of political diversity* (Ortuño-Ortin and Weber, 2008) is $\sum_{1 \le i < j \le n} v_i v_j d(x_i, x_j)$.

  The **mean minimum political distance**, cf. http://wiki.electorama.com/wiki, is (the case $m = 1$ of) $\sum_{i=1}^{n} v_i \min_{j \in E} d(x_i, y)$, where $E = \{1 \le i \le n : c_i \text{ is elected}\}$. Cf. **distance-rationalizable voting rule** in Chap. 11.

- **Surname distance model**

  A **surname distance model** was used in [COR05] in order to estimate the preference transmission from parents to children by comparing, for 47 provinces of mainland Spain, the 47×47 distance matrices for **surname distance** with those of **consumption distance** and **cultural distance**.

  The distances were l_1-distances $\sum_i |x_i - y_i|$ between the frequency vectors (x_i), (y_i) of provinces x, y, where z_i is, for the province z, either the frequency of the i-th surname (**surname distance**), or the budget share of the i-th product (**consumption distance**), or the population rate for the i-th cultural issue, say, rate of weddings, newspaper readership, etc. (**cultural distance**), respectively.

  Other (matrices of) distances considered there are:

  – *geographical distance* (in km, between the capitals of two provinces);
  – *income distance* $|m(x) - m(y)|$, where $m(z)$ is mean income in the province z;
  – *climatic distance* $\sum_{1 \le i \le 12} |x_i - y_i|$, where z_i is the average temperature in the province z during the i-th month;
  – *migration distance* $\sum_{1 \le i \le 47} |x_i - y_i|$, where z_i is the percentage of people (living in the province z) born in the province i.

  Strong *vertical preference transmission*, i.e., correlation between surname and consumption distances, was detected only for food items.

- **Distance as a metaphor**

  Lakoff and Núñez, 2000, claim that mathematics emerged via conceptual metaphors grounded in the human body, its motion through space and time, and in human sense perceptions: change is motion, arithmetic is motion along a path, etc.

  For them, the mathematical idea of distance comes from the activity of measuring, and the corresponding technique consists of rational numbers and metric spaces. The idea of proximity/connection comes from connecting and corresponds to topological space. The idea of subtraction mathematizes the ordinary idea of distance.

- **Metaphoric distance**

  A **metaphoric distance** is any notion in which a degree of similarity between two difficult-to-compare things is expressed using spatial notion of distance as an implicit bidirectional and understandable metaphor. Some examples are:

  Internet and Web bring people closer: proximity in subjective space is at-handiness;

  professional distance: teacher-student, therapist-patient, manager-employee;

  financial distance: degree of separation in couple's money/property arrangements;

  competitive distance (incomparability) between two airline product offerings;

  metaphoric distance that a creative thinker takes from the problem, i.e., degree of intuitivity, required to evolve/reshape concepts into new ideas.

  The **distance-similarity metaphor** (Montello et al., 2003) is a design principle, where relatedness in nonspatial data is projected onto distance, so that semantically similar documents are placed closer to one another in an

information space. It is the inverse of the Tobler's **first law of geography**; cf. **nearness principle**. This metaphor is used in Data Mining, Pattern Recognition and **Spatialization**.

Comparing the linguistic metaphor *proximity→similarity* with its mental counterpart, Casasanto (2008), found that stimuli (pairs of words or pictures) presented closer together on the computer screen were rated more similar in conceptual judgments of abstract entities or unseen object properties but, less similar in perceptual judgments of visual appearance of faces and objects.

- **Spatial cognition**

  Spatial cognition concerns the knowledge about spatial properties of objects and events: location, size, distance, direction, separation/connection, shape, pattern, and movement. For instance, it consider navigation (locomotion and way-finding) and orientation during it: recognition of landmarks and *path integration* (an internal measuring/computing process of integrating information about movement).

  Spatial cognition addresses also our (spatial) understanding of the World Wide Web and computer-simulated virtual reality.

  Men surpass women on tests of spatial relations, mental rotation and targeting, while women have better fine motor skills and spatial memory for immobile objects and their location. Such selection should come from a division of labor in Pleistocene groups: hunting of mobile prey for men and gathering of immobile plant foods for women. Women's brains are 10–15 % smaller than men's, but their frontal lobe (decision-making, problem-solving), limbic cortex (emotion regulation) and hippocampus (spatial memory) are proportionally larger, while the parietal cortex (spatial perception) and amygdala (emotional memory) are smaller. Men's brains contain stronger front-to-rear connections (suggesting greater synergy between perception and action) while those of women are better connected from left to right (facilitating emotional processing and the ability to infer others' intentions).

  One of the *cultural universals* (traits common to all human cultures) is that men on average travel greater distances over their lifetime. They are less likely than women to migrate within the country of their birth but more likely to emigrate.

- **Size representation**

  Konkle and Oliva, 2012, found that object representations is differentiated along the ventral temporal cortex by their real-world size. Both big and small objects activated most of temporal cortex but fMRI (cf. **brain distances**) voxels with a big- or small-object preference were consistently found along its medial or, respectively, lateral parts. These parts overlapped with the regions known to be active when identifying spaces to interact with (say, streets, elevators, cars, chairs) or, respectively, processing information on tools, ones we usually pick up.

  Different-sized objects have different action demands and typical interaction distances. Big/small preferences are object-based rather than retinotopic or conceptual. They may derive from systematic biases, say, eccentricity biases and size-dependent biases in the perceptual input and in functional requirements

for action. For example, over the viewing experience, in the lifetime or over evolutionary time, the smaller objects tend to be rounder, while larger objects tend to extend more peripherally on the retina. Cf. the **size-distance invariance hypothesis** and, in Chap. 29, **neurons with spatial firing properties**.

- **Spatialization**

  Spatialization (Lefebvre, 1991) refer to the spatial forms that social activities and material things, phenomena or processes take on. It includes cognitive maps, cartography, everyday practice and imagination of possible spatial worlds.

  One of the debated definitions of consciousness: it is a notion of self in space and an ability to make decisions based on previous experience and the current situation. Self-awareness permits to evaluate the distance that separates one from his objectives and to adjust his behavior in order to approach those aims.

  We usually give the upper face or upper torso as *egocenter* (spatial seat of self).

  The term *spatialization* is also used for information display of nonspatial data.

- **Spatial reasoning**

  Spatial reasoning is the domain of spatial knowledge representation: spatial relations between spatial entities and reasoning based on these entities and relations.

  As a modality of human thought, spatial reasoning is a process of forming ideas through the spatial relationships between objects (as in Geometry), while verbal reasoning is the process of forming ideas by assembling symbols into meaningful sequences (as in Language, Algebra, Programming). *Spatial intelligence* is the ability to comprehend 2D and 3D images and shapes.

  Luria, 1973, called the ability to derive the abstract concepts from spatially organized heteromodal information, the *quasi-spatial synthesis*.

  Spatial-temporal reasoning (or *spatial ability*) is the capacity to visualize spatial patterns, to manipulate them mentally over a time-ordered sequence of spatial transformations and to draw conclusions about them from limited information.

  Specifically, *spatial visualization ability* is the ability to manipulate mentally 2D and 3D figures. *Spatial skills* is the ability to locate objects in a 3D-world using sight or touch. *Spatial acuity* is the ability to discriminate two closely-separated points or shapes (say, two similar polygons with different numbers of sides).

  Visual thinking (or *visual/spatial learning*, *picture thinking*) is the common (about 60 % of the general population) phenomenon of thinking through visual processing. Spatial-temporal reasoning is prominent among visual thinkers, as well as among *kinesthetic learners* (who learn through body mapping and physical patterning) and *logical thinkers* (mathematical/systems thinking) who think in patterns and relationships and may work without this being pictorially.

  In Computer Science, spatial-temporal reasoning aims at describing, using abstract relation algebras, the common-sense background knowledge on which human perspective of physical reality is based. It provides rather inexpensive reasoning about entities located in space and time.

- **Spatial language**

  Spatial language consists of natural-language spatial relations used to indicate where things are, and so to identify or refer to them. It usually expresses imprecise and context-dependent information about space.

  Among spatial relations there are *topological* (such as on, to, in, inside, at), *path-related* (such as across, through, along, around), *distance-related* and more complex ones (such as right/left, between, opposite, back of, south of, surround).

  A **distance relation** is a spatial relation which specifies how far the object is away from the reference object: near, far, close, etc.

  The **distance concept of proximity** (Pribbenow, 1992) is the area around the RO (reference object) in which it can be used for localization of the LO (local object), so that there is visual access from RO and noninterruption of the spatial region between objects, while LO is less directly related to a different object. Such proximity can differ with physical distance as, for example, in "The Morning Star is to the left of the church". The area around RO, in which a particular relation is accepted as a valid description of the distance between objects, is called the *acceptance area*.

  Pribbenow, 1991, proposed five distance distinctions: *inclusion* (acceptance area restricted to projection of RO), *contact/adjacency* (immediate neighborhood of RO), *proximity*, *geodistance* (surroundings of RO) and *remoteness* (the complement of the proximal region around RO).

  For Jackendorff–Landau, 1992, there are 3 degrees of distance distinctions in English: interior of RO (*in*, *inside*), exterior but in contact (*on*, *against*), proximate (*near*), plus corresponding negatives, such as *outside*, *off of*, *far from*.

  A spatial reference system is mainly egocentric, or relative (such as *right*, *back*) for the languages spoken in industrialized societies, while the languages spoken in small scale societies rely rather on an allocentric, or absolute set of coordinates.

  Language affects our sense of space and time. Guugu Yimithirr in Australia do not have words for relative space, like left and right, but they unusually well keep track where they are, using their terms for north, south, east and west.

  Semantics of spatial language is considered, say, in Linguistics, Cognitive Psychology, Anatomy, Robotics, Artificial Intelligence, Computer Vision and Geographic Information Systems. An example of far-reaching applications is Grove's *clean space*, a neuro-linguistic psychotherapy based on the spatial metaphors produced by (or extracted from) the client on his present and desired "space" (state).

- **Language distance from English**

  Such measures are based either on a typology (comparing formal similarities between languages), or language trees, or performance (mutual intelligibility and learnability of languages). For example, Rutheford, 1983, defined **distance from English** as the number of differences from English in the following three-way typological classification: subject/verb/object order, topic-prominence/subject-prominence and pragmatic word-order/grammatical word-order. It gives distances 1, 2, 3 for Spanish, Arabic/Mandarin, Japanese/Korean.

Borland, 1983, compared several languages of immigrants by their acquisition of four areas of English syntax: copula, predicate complementation, negation and articles. The resulting ranking was English, Spanish, Russian, Arabic, Vietnamese.

Elder–Davies, 1998, used ranking based on the following three main types of languages: isolating, analytic or root (as Chinese, Vietnamese), inflecting, synthetic or fusional (as Arabic, Latin, Greek), agglutinating (as Turkish, Japanese). It gave ranks $1, 2, 4, 5$ for Romance, Slavic, Vietnamese/Khmer, Japanese/Korean, respectively, and 3 for Chinese, Arabic, Indonesian, Malay.

The **language distance index** (Chiswick–Miller, 1998) is the inverse of the *language score* of the average speaking proficiency, after 24 weeks of instruction, of English speakers learning this language. This score was measured at regular intervals by increments of 0.25; it ranges from 1 (hardest to learn) to 3 (easiest to learn). The score was, for example, 1.00, 1.25, 1.50, 1.75, 2.00, 2.25, 2.50, 2.75, 3.00 for Japanese, Cantonese, Mandarin, Hindi, Hebrew, Russian, French, Dutch, Afrikaans.

In addition to the above distances, based on syntax, and **linguistic distance**, based on pronunciation, see the lexical semantic distances in Chap. 22.

Cf. **clarity similarity** in Chap. 14, **distances between rhythms** in Chap. 21, **Lasker distance** in Chap. 23 and **surname distance model** in Chap. 28.

Translations of the English noun *distance*, for example, into French, Italian, German, Swedish, Spanish, Interlingua, Esperanto are: distance, distanza, distanz, distans, distancia, distantia, distanco.

The word *distance* has Nr. 625 in the list (Wiktionary:Frequency lists/PG/2006/04) of the common English words in the books found on Project Gutenberg. It has Nrs. 835, 1035, 2404 in contemporary poetry, fiction, TV/movie and overall Nrs. 1513 (written), 1546 (spoken). It comes from Latin *distantia* (distance, farness, difference) and *distans*, present participle of *distare*: *di* (apart) + *stare* (to stand).

The **longest English word** (noncoined and nontechnical) is *antidisestablishmentarianism* (28 letters). Examples of funny distance-related words in *Urban Dictionary* (Web-based dictionary of slang in English) are: *distading* (start and give up on many goals in quick succession), *distarnated* (having no friends and being hated by everyone), *distanitus* (illness one suffer from spotting a person which looks really good from across the room but is a butterface at 5 feet distance), *disstance* (space provided when someone is *dissing*, i.e., show disrespect for, someone else).

- **Editex distance**

  The main phonetic encoding algorithms are (based on English language pronunciation) *Soundex*, *Phonix* and *Phonex*, converting words into one-letter three-digit codes. The letter is the first one in the word and the three digits are derived using an assignment of numbers to other word letters. Soundex and Phonex assign:

  0 to *a, e, h, i, o, u, w, y*; 1 to *b, p, f, v*; 2 to *c, g, j, k, q, s, x, z*; 3 to *d, t*; 4 to *l*; 5 to *m, n*; 6 to *r*.

Phonix assigns the same numbers, except for 7 (instead of 1) to *f* and *v*, and 8 (instead of 2) to *s, x, z*.

The **Editex distance** (Zobel–Dart, 1996) between two words x and y is a cost-based **editing metric** (i.e., the minimal cost of transforming x into y by substitution, deletion and insertion of letters). For substitutions, the costs are 0 if two letters are the same, 1 if they are in the same letter group, and 2, otherwise.

The *syllabic alignment distance* (Gong–Chan, 2006) between two words x and y is another cost-based **editing metric**. It is based on Phonix, the identification of syllable starting characters and seven edit operations.

- **Phone distances**

  A *phone* is a sound segment having distinct acoustic properties, and is the basic sound unit. A *phoneme* is a minimal distinctive feature/unit in the language (a set of phones which are perceived as equivalent to each other in a given language).

  The number of phonemes (consonants) range, among about 7102 languages spoken now, from 11 (6) in Rotokas to 112 (77) in Taa (languages spoken by about 4000 people in Papua New Guinea and Botswana, respectively).

  The main classes of the **phone distances** (between two phones x and y) are:

  – *Spectrogram-based distances* which are physical-acoustic distortion measures between the sound spectrograms of x and y;
  – *Feature-based phone distances* which are usually the **Manhattan distance** $\sum_i |x_i - y_i|$ between vectors (x_i) and (y_i) representing phones x and y with respect to a given inventory of phonetic features (for example, nasality, stricture, palatalization, rounding, syllabicity).

  The **Laver consonant distance** refers to the improbability of confusing 22 consonants among $\approx$ 50 phonemes of English, developed by Laver, 1994, from subjective auditory impressions. (Chen–Wang–Jia–Dang, 2013, considered similar perception distance between two types of Chinese initials.) The smallest distance, 15 %, is between phonemes $[p]$ and $[k]$, the largest one, 95 %, is, for example, between $[p]$ and $[z]$. Laver also proposed a quasi-distance based on the likelihood that one consonant will be misheard as another by an automatic speech-recognition system.

  Each vowel can be represented by a pair (F_1, F_2) of resonant frequencies of the vocal tract (first and second formants). For example, $[u]$, $[a]$, $[i]$ are represented by $(350, 800)$, $(850, 1150)$, $(350, 1700)$ in *mels* (Chap. 21). The International Phonetic Alphabet identifies seven levels of *height* (F_1) and five levels of *backness* (F_2).

  Chang et al., 2013, produced English language map of the brain; they found the set of neurons in the sensorimotor cortex which controls muscles (in the tongue, lips, jaw, larynx) and fires in unique combination for each sound.

- **Phonetic word distance**

  The **phonetic word** (or *pronunciation*, *Levenstein phonological*) **distance** between two words x and y seen as strings of phones is the **Levenstein metric** with costs (Chap. 11): the minimal cost of transforming x into y by

substitution, deletion and insertion of phones. Given a **phone distance** $r(u, v)$ on the International Phonetic Alphabet with the additional phone 0 (silence), the cost of substitution of phone u by v is $r(u, v)$, while $r(u, 0)$ is the cost of insertion or deletion of u.

Levenstein orthographic distance (or *LPD*) is the same measure, but operating on letters instead of phonemes. Words with larger mean LPD to (but smaller mean frequency of) its 20 closest neighbors are easier to recognize.

The average adult has a vocabulary of about 40,000–50,000 words.

- **Linguistic distance**

  The **linguistic distance** between two languages is a term loosely used to describe their difference. The mutual intelligibility of the two languages depends on the degree of their lexical, phonetical, morphological, and syntactical similarity.

  The **lexical similarity** is the percentage of *common* (similar in form and meaning) words in their standardized wordlists. English was evaluated to have a lexical similarity of 60 %, 27 %, 24 % with German, French and Russian, respectively. Cf. **language distance index**, **language distance effect**, **Swadesh similarity**.

  Specifically, the **linguistic** (**dialectal**) **distance** between language varieties X and Y is the mean, for a fixed sample S of notions, **phonetic word distance** between *cognate* (i.e., having the same meaning) words s_X and s_Y, representing the same notion $s \in S$ in X and Y, respectively.

  One example of a *dialect continuum* (as *ring species* in Biology) is Dutch-German: their mutual intelligibility is small but a chain of dialects connects them.

- **Swadesh similarity**

  The *Swadesh word list* of a language (Swadesh, 1940–1950) is a list of vocabulary with (usually, 100) basic words which are acquired by the native speakers in early childhood and supposed to change very slowly over time. The **Swadesh similarity** between two languages is the percentage of *cognate* (having similar meaning and sound) words in their Swadesh lists. *Glottochronology* is a method of assessing the temporal divergence of two languages based on this similarity.

  The first 12 items of the original final Swadesh list: *I, you, we, this, that, who?, what?, all, many, one, two*. Cf. the first 12 most frequently used English words: *the, of, and, a, to, in, is, you, that, it, he, was* in all printed material and *I, the, and, to, a, of, that, in, it, my, is, you* across both spoken and written texts.

  Acerbi et al., 2013: the frequency of emotional words declined in English-language books over twentieth century, but the use of fear-related words increased from 1980. The *half-life* of a word is the number of years after which it has a 50 % probability of having been replaced by a new noncognate word; rougly, it is within 750–20,000 years, say, 9000, 3200, 1900. *stab*, *bird*, *we*.

  Pagel et al., 2013, suggest existence of a *proto-Eurasian mother tongue*. For example, they list 15,000 years old words cognate in at least 4 Eurasiatic language families: thou, I, not, that, we, to give, who, this, what, man/male, ye, old, mother, to hear, hand, fire, to pull, black, to flow, bark, ashes, to spit, worm.

- **Language distance effect**

  In Foreign Language Learning, Corder, 1981, conjectured the existence of the following **language distance effect**: where the mother tongue (L1) is structurally similar to the target language, the learner will pass more rapidly along the developmental continuum (or some parts of it) than where it differs; moreover, all previous learned languages have a facilitating effect.

  Ringbom, 1987, added: the influence of the L1 is stronger at early stages of learning, at lower levels of proficiency and in more communicative tasks. But such correlation could be indirect. For example, the written form of modern Chinese does not vary among the regions of China, but the spoken languages differ sharply, while spoken German and Yiddish are close but have different alphabets.

- **Long-distance dependence (in Language)**

  In Language, **long-distance dependence** (or *syntactic binding*) is a construction, including wh-questions (such as "Who do you think he likes"), topicalizations (such as "Mary, he likes"), *easy*-adjectives (such as "Mary is easy to talk to"), relative clauses (such as "I saw the woman who I think he likes")—which permits an element in one position (*filler*) to fulfill the grammatical role associated with another nonadjacent position (*gap*). The *filler-gap distance*, in terms of the number of intervening clauses or words between them in a sentence, can be arbitrary large. Cf. **long range dependence** in Chap. 18.

  An *anaphora* is a subsequent reference to an entity already introduced in discourse. In order to be interpreted, anaphora must get its content from an antecedent in the sentence which in English is usually syntactically local as in "Mary excused *herself*". A **long-distance anaphora** is an anaphora with antecedent outside of its local domain, as in "The players told us stories about *each other*". Its resolution (finding what it refers to) is a hard problem of machine translation.

  The **anaphoric distance** is (Ariel, 1990) the number of words between an anaphora and its antecedent. The **referential distance** (or **textual distance**) is (Givón, 1983) the amount of clauses between them. In general, each text can be represented as a tree in which *discourse units* (normally, clauses) are vertices and *rhetorical relations* (sequence, joint, cause, elaboration, etc.) are edges.

  The **rhetorical distance** between two discourse units is (Fox, 1987) the minimal number of "sequence"-edges on a path between them.

28.4 Distances in Philosophy, Religion and Art

- **Zeno's distance dichotomy paradox**

  This paradox by the pre-Socratic Greek philosopher Zeno of Elea claims that it is impossible to cover any distance, because half the distance must be traversed first, then half the remaining distance, then again half of what remains, and so on.

The paradoxical conclusion is that travel over any finite distance can neither be completed nor begun, and so all motion must be an illusion.

But, in fact, dividing a finite distance into an infinite series of small distances and then adding the all together gives back the finite distance one started with.

- **Space (in Philosophy)**

  The present Newton–Einstein notion of **space** was preceded by Democritus' (c. 460–370 BC) *Void* (the infinite container of objects), Plato's (c. 424–348 BC) *Khora* (an interval between being and nonbeing in which Forms materialize) and Aristotle's (380–322 BC) *Cosmos* (a finite system of relations between objects). Cf. **Minkowski metric** (Chap. 26) for the origin of the space-time concept.

  Like the Hindu doctrines of Vedanta, Spinoza (1632–77) saw our Universe as a mode under two (among an infinity of) attributes, *Thought* and *Extension*, of *God* (unique absolutely infinite, eternal, self-caused substance, without personality and consciousness). These parallel (but without causal interaction) attributes define how substance can be understood: to be composed of thoughts and physically extended in space, i.e., to have breadth and depth. So, the Universe is deterministic.

  For Newton (1642–1727) space was absolute: it existed permanently and independently of whether there is any matter in it. It is a framework of creation, stage setting within which physical phenomena occur. For Leibniz's (1646–1716) space was a collection of relations between objects, given by their distance and direction from one to another, i.e., an idealized abstraction from the relations between individual entities or their possible locations which must therefore be discrete.

  For Kant (1724–1804) space is not substance or relation, but a part of an unavoidable systematic framework used by the humans to organize their experiences. Disagreement continues between philosophers over whether space is an entity, a relationship between entities, or part of a conceptual framework.

  In *biocentric cosmology* (Lanza, 2007), build on quantum physics, space is a form of our animal understanding and does not have an observer-independent reality, while time is the process by which we perceive changes in the Universe. Also, space-time could be not fundamental, but emerging from a deeper quantum reality.

  Free space refers to a perfect vacuum, devoid of all particles; it is excluded by the uncertainty principle. The quantum vacuum is devoid of atoms but contains subatomic short-lived particles—photons, gravitons, etc.

  A *parameter space* is the set of values of parameters in a mathematical model.

  In Mathematics and Physics, the *phase space* (Gibbs, 1901) is a space in which all possible states of the system are represented as unique points; cf. Chap. 18.

- **Kristeva nonmetric space**

  Kristeva, 1980, considered the basic psychoanalytic distinction (by Freud) between pre-Oedipal and Oedipal aspects of personality development. Narcissistic identification and maternal dependency, anarchic component drives, polymorphic erotogenicism, and primary processes characterize the pre-Oedipal.

Paternal competition and identification, specific drives, phallic erotogenicism, and secondary processes characterize Oedipal aspects.

Kristeva describes the pre-Oedipal feminine phase by an enveloping, amorphous, "nonmetric" space (Plato's *khora*) that both nourishes and threatens; it also defines and limits self-identity. She characterizes the Oedipal male phase by a metric space (Aristotle's *topos*); the self and the self-to-space are more precise and well defined in topos. Kristeva insists also on the fact that the semiotic process is rooted in feminine libidinal, pre-Oedipal energy which needs channeling for social cohesion.

Deleuze–Guattari, 1980, divide *multiplicities* (networks, manifolds, spaces) into *striated* (metric, hierarchical, centered, numerical) and *smooth* ("nonmetric, rhizomic, those that occupy space without counting it and can be explored only by legwork").

The above French post-structuralists use the metaphor of *nonmetric* in line with a systematic (but generating controversy) use of topological terms by the psychoanalyst Lacan. In particular, he sought the space *J* (of *Jouissance*, i.e., sexual relations) as a metric space and used metaphorically the *Heine–Borel theorem* (that closed and bounded subspaces of Euclidean spaces are their only compact subspaces).

Back to Mathematics, when a notion, theorem or algorithm is extended from metric to general distance space, the latter is called **nonmetric space**.

- **Emerson distance between persons**

  We call the **Emerson distance between persons** the separation between "gods", which was required by an American poet and philosopher Ralph Waldo Emerson (1803–82) in his Essay 16 *Manners*: "Let the incommunicable objects of nature and the metaphysical isolation of man teach us independence... We should meet each morning, as from foreign countries, and spending the day together, should depart at night, as into foreign countries. In all things I would have the island of a man inviolate. Let us sit apart as the gods, talking from peak to peak all round Olympus... Lovers should guard their strangeness... Every natural function can be dignified by deliberation and privacy." At the end of his 1836 book *Nature*, Emerson also wrote: "Every spirit builds itself a house; and beyond its house, a world; and beyond its world, a heaven... Build, therefore, your own world."

  Similar dignified separation is mentioned in quotes from the Russian philosopher Mikhail Bakhtin (1895–1975): "The feeling of respect creates a distance, both in relation to the other person, and in relation to one's own self", and the Bohemian-Austrian poet Rainer Maria Rilke (1875–1926): "Once the realization is accepted that even between the closest human beings infinite distances continue, a wonderful living side by side can grow, if they succeed in loving the distance between them which makes it possible for each to see the other whole against the sky."

- **Nietzsche's Ariadne distance**

  The German philosopher Friedrich Wilhelm Nietzsche (1844–1900), treated distance in a sensual/erotic way. In "On the Genealogy of Morals" (1887) he wrote:

  "The pathos of nobility and distance… the fundamental total feeling on the part of a higher ruling nature in relation to a lower nature, to a 'beneath' – that is the origin of the opposition between 'good' and 'bad.'"

  His Zarathustra favors *fernstenliebe* (love of the farthest) over Christian love of the neighbor. Moreover, *fernstenliebe* is to love neither objects, nor ends—but rather, distance/endlessness itself, which makes all distances recur and perpetuate themselves.

  The courtly troubadours of the twelfth century valued eroticization of the unattainable object, while for German romanticism (for example, Novalis, Schopenhauer, Wagner) there can be no satisfaction in erotic relations, or in life itself, as long as distance remains. In Wagner's opera, Tristan laments: "Blessed nearness, tedious distance."

  Kuzma, 2013, claims that Nietzsche, by the early 1880s, "rehabilitated erotic distance", in response to its denigration and the consummatory idealism and passive nihilism of the German romantic tradition. This rehabilitation of courtly love culminated in the concept of an absolute separation and eternal recurrence.

  According to Kuzma, Ariadne in '*Thus Spoke Zarathustra* (1883–1885) is not only the symbol of the human soul and life, but Nietzsche's privileged name for absolute, infinite spatially and eternal distance itself, for an eternity conceived in the absence of every end, any possible object to attain and every Other to love. To desire Ariadne, is to desire the incessant prolongation of longing in the absence of all fulfilment. Zarathustra does not seek rest, consummation, and release, but affirms a sort of metaphysical *coitus reservatus*, the eternal prolongation of boundless and unresolved desire, implying "voluptuousness of the future" and "love of fate".

  The eternal recurrence requires spatial or temporal infinity. Nietzsche, in his posthumous notes, posits finite matter and infinite cyclical time.

- **Heidegger's de-severance distance**

  The German philosopher Martin Heidegger (1889–1976), sought space in terms of limit and event of placing, not merely a location. He wrote: "space is something that has been spaced, or made room for, and that which is let into its bounds".

  His main notion, *Dasein* (Being there), means Being-in-the-world, as opposed to the Cartesian abstract agent, a subject, or the objective world alone. Dasein is revealed by projection into, and engagement with, a personal world, one's environment. It is *ontically* (in factual existence) closest to itself, yet ontologically farthest.

  For Heidegger, Dasein dwells spatially in the world, but in the *equipmental space* (functional places, defined by Dasein-centered totalities of involvements) rather than in physical, Cartesian space, and this spatiality is characterized by *de-severance*, where "*de-severing* amounts to making the farness vanish—that

is, making the remoteness of something disappear, bringing it close". Not only reducing physical distance, de-severance is the *reach* of Dasein's skilled practical activity.

An entity is *nearby* if it is readily available for some such activity, and *far away* if it is not. Nearness comes into being when the thing is examined. We reach it through things; it is nearness that makes the thingness of the thing appear. Cf. *Heidegger's Topology* (MIT Press, 2007) by Malpas. The following quotes (of 1924, 1954, 1966, 1971) illustrate **Heidegger's de-severance distance**:

"Man, as existing transcendence abounding in and surpassing toward possibilities, is a creature of distance. Only through the primordial distances he establishes toward all being in his transcendence does a true nearness to things flourish in him."

"Longing is the agony of the nearness of the distant."

"Then thinking would be coming-into-the-nearness-of distance."

"What is this uniformity in which everything is neither far nor near – is, as it were, without distance? Everything gets lumped together into uniform distancelessness."

Cf. the **technology-related distancing** and **death of distance** in Sect. 28.2.

French philosopher/writer Maurice Blanchot (1907–2003) considered Nietzsche, Heidegger and Lévinas via their metaphorics of distance. For example, he wrote:

"A distance is synonymous with extreme non-coincidence."

"Far and near are dimensions of what escapes presence as well as absence under attraction of [impersonal] 'it'. It draws away, draws close, the same ghostly affirmation, the same premises of non-presence."

"To the proximity of the most distant, to the pressure of what is lightest, … to the contact of that which is never arrives, it is by friendship that I can respond, … the response of passivity to the non-presence of unknown [stranger]".

- **Lévinas distance to Other**

  We call the **Lévinas distance to Other** a primary distance between the individuals in their face-to-face encounter, which the French philosopher and Talmudic scholar Emmanuel Lévinas (1906–95) discusses in his book *Totality and Infinity*, 1961.

  Lévinas considers the precognitive relation with the Other: the Other, appearing as the Face, gives itself priority, its first demand even before I react to, love or kill it, is: "thou shalt not kill me". This Face is not an object but pure expression affecting me before I start meditating on it and passively resisting the desire that is my freedom. In this asymmetrical relationship—being silently summoned by the exposed Face of the Other ("widow, orphan, or stranger") and responding by responsibility for the Other without knowing that he will reciprocate—Lévinas (in line of *Misnagdim Judaism* ethics) finds the meaning of being human and concerned about justice. For him, this ethical duty is prior to pursuit of knowledge and ontology of nature.

  According to him, before covering the distance separating the *existent* (the lone subject) from the Other, one must first go from anonymous existence to

the existent, from "there is" (swarming of points) to the Being (lucidity of consciousness localized here-below). Lévinas' ethics spans the distance between the foundational chaos of "there is" and the objective or intersubjective world. Ethics marks the primary situation of the face-to-face, whereas morality comes later as a set of rules emerging in the social situation if there are more than two people face-to-face. And, for Lévinas, the scriptural/traditional God is the Infinite Other.

- **Distant suffering**

  Normally, physical distance is inversely related to charitable inclinations. But the traditional morality of "universal" proximity (geographic, age, familial, etc.) and pity not works in contemporary life. Most important actions happen on distance and the *mediation* (capacity of the media to involve us emotionally and culturally) address our concern for the "other". Cf. **death/kilometer** in Chap. 25.

  The nonuniversal quality of humanity should be constructed. So, mass media, NGO's, aid agencies, live blogs, and celebrity advocacy use imagery in order to encourage audiences to acknowledge, care and act for far away vulnerable others.

  For Chouliaraki, 2006, the current mediation replaced earlier claims to our "common humanity" by artful stories that promise to make us better people. As suffering becomes a spectacle of sublime artistic expression, the inactive spectator can merely gaze in disbelief. Arising voyeuristic altruism is motivated by self-empowerment: to realize our own humanity while keeping the humanity of the sufferer outside the remit of our judgement and imagination, i.e., keeping **moral distance**. Chouliaraki calls it *narcissistic self-distance* or *improper distance*.

  Silverstone's (2002) **proper distance in mediation** refers to the degree of proximity required in our mediated interrelationships if we are to create a sense of the other sufficient not just for reciprocity but for a duty of care, obligation and understanding. It should be neither too close to the particularities or the emotionalities of specific instances of suffering, nor too far to get a sense of common humanity as well as intrinsic difference. Cf. **Lévinas distance** and **antinomy of distance**.

  Silverstone and Chouliaraki call to represent sufferers as active, autonomous and empowered individuals. They advocate *agonistic solidarity*, treating the vulnerable other as other with her/his own humanity. It requires "an intellectual and aesthetic openness towards divergent cultural experiences, a search for contrasts rather than uniformity" (Hannerz, 1990). For Arendt, 1978, the imagination enables us to create the distance which is necessary for an impartial judgment,

  But for Dayan, 2007, a climactic Lévinasian encounter with Other is not dualistic: there are many others awaiting my response at any given moment. So, proper distance should define the point from which one is capable of equitably hearing their respective claims, and it involves the reintroduction of actual distance.

- **Moral distance**

  The **moral distance** is a measure of moral indifference or empathy toward a person, group of people, or events. Abelson, 2005, refers to moral distance as the emotional closeness between agent and beneficiary.

  But Aguiar, Brañas-Garza and Miller, 2008, define it as the degree of moral obligation that the agent has towards the recipient. So, for them the social distance is only a case of moral distance in which anonymity plays a crucial, negative role.

  The **ethical distance** is a distance between an act and its ethical consequences, or between the moral agent and the state of affairs which has occurred.

  The (moral) *distancing* is a separation in time or space that reduces the empathy that a person may have for the suffering of others, i.e., that increases moral distance. In particular, **distantiation** is a tendency to distance oneself (physically or socially, by segregation or congregation) from those that one does not esteem. Cf. **distanciation**. On the other hand, the *good distancing* (Sartre, 1943, and Ricoeur, 1995) means the process of deciding how long a given ethical link should be.

- **Simone Weil distance**

  We call **Simone Weil distance** a kind of moral God-cross radius of the Universe which the French philosopher, Christian mystic, social activist and self-hatred Jewess, Simone Weil (1909–43) introduced in "The Distance", one of the philosophico-theological essays comprising her *Waiting for God* (Putnam, New York, 1951).

  She connects God's love to the distance; so, his absence can be interpreted as a presence: "every separation is a link" (Plato's *metaxu*). She wrote: "God did not create anything except love itself, and the means to love… Because no other could do it, he himself went the greatest possible distance, the infinite distance. This distance between God and God, this supreme tearing apart, this agony beyond all others, this marvel of love, is the crucifixion."

  In her peculiar Christian theodicy, "evil is the form which God's mercy takes in this world", and the crucifixion of Christ (the greatest love/distance) was necessary "in order that we should realize the distance between ourselves and God … for we do not realize distance except in the downward direction". Weil's *God-cross* (or *creator-creature*) distance recalls the old question: can we equate distance from God with proximity to Evil? Her main drive, purity, consisted of maximizing **moral distance** to Evil, embodied for her by "the social, Rome and Israel".

  Cf. Irenaeus (second century) God-humans **epistemic distance**, which must be far enough that belief in God remains a free choice. In Irenaean teodicy, God created both, evil/suffering and free will, allowing us moral choices and development.

  Cf. Pascal's (1669) *God-man-nothing* distances in *Pensées*, note 72: "…what is man in Nature? A nothing in relation to infinity, all in relation to nothing, a central point between nothing and all and infinitely far from understanding either".

Cf. Montaigne's (1580) *nothing-smallest* and *smallest-largest* distances in *Essais, III:11 On the lame*: "Yet the distance is greater from nothing to the minutest thing in the world than it is from the minutest thing to the biggest."

Cf. Tipler's (2007) *Big Bang–Omega Point* time/distance with Initial and Final singularities seen as God-Father and God-Son. Tipler's *Omega point* (technological singularity) is a variation of prior use of the term (Teilhard de Chardin, 1950) as the supreme point of complexity and consciousness: the Logos, or Christ.

Calvin's (1537) *Eucharistic theology* (doctrine on the meaning of bread and vine that Christ offered to his disciples during the last supper before his arrest) also relies on spatial distance as a metaphor that best conveys the separation of the world from Christ and of the earthly, human from the heavenly, divine.

Weil's approach reminds that of the Lurian (about 1570) kabbalistic notions: *tzimtzum* (God's concealment, withdrawal of a part, creation by self-delimitation) and *shattering of the vessels* (evil as impure vitality of husks, produced whenever the force of separation loses its distancing function and giving man the opportunity to choose between good and evil). The purpose is to bridge the distance between Infiniteness of God (or Good) and the diversity of existence, without falling into the facility of dualism (as manicheanism and gnosticism). It is done by postulating intermediate levels of being (and purity) during emanation (unfolding) within the divine and allowing humans to participate in the redemption of the Creation.

So, a possible individual response to the Creator is purification and *ascent*, i.e., the spiritual movement through the levels of emanation in which the coverings of impurity, that create distance from God, are removed progressively.

Besides, the song "From a Distance", written by Julie Gold in 1985 , is about how God is watching us and how, despite the distance (physical and emotional) distorting perceptions, there is still a little peace and love in this world.

- **Golgotha distance**

  The exact locations of the Praetorium, where Pilate judged Jesus, and Golgotha, where he was crucified, as well as of the path that Jesus walked, are not known. At present, the Via Dolorosa (600 m from the Antonia Fortress west to the Church of the Holy Sepulchre) in the Old City of Jerusalem, held to be this path.

  The first century Jerusalem was about 500 m east to west and 1200 m north to south. Herod's palace (including Praetorium) was about 600 m from Golgotha and 400 m from the Temple. The **Golgotha distance** (total distance from Gethsemane, where Jesus was arrested, to the Crucifixion) was about 1500 m.

  Another New Testament's distance is mentioned in Apocalypse: "And the angel thrust in his sickle into the earth, and gathered the vine of the earth, and cast it into the great winepress of the wrath of God. And the winepress was trodden without the city [Jerusalem], and blood came out of the winepress, even unto the horse bridles, by the space of 1600 furlongs [200 miles]" (Revelation 14:19–20). It can hint to the whole length of the land of Israel, computable as 1600 studia.

- **Distance to Heaven**

  Below are given examples of distances and lengths which old traditions related (sometimes as a metaphor) to such notions as God and Heaven.

  In the Hebrew text *Shi'ur Qomah* (*The Measure of the Body*), the height of the *Holy Blessed One* is 236×10^7 *parasangs*, i.e., 14×10^{10} (divine) *spans*. In the Biblical verse "Who has measured the waters in the hollow of his hand and marked off the heaven with a span" (Isaiah 40:12), the size of the Universe is one such span.

  The age/radius of the Universe is 13.82 billion ly. *Sefer HaTemunah* (by Nehunia ben Hakane, first century) and *Otzar HaChaim* (by Yitzchok deMin Acco, thirteenth century) deduced that the world was created *in thought* 42,000 divine years, i.e., $42{,}000 \times 365{,}250 \approx 15.3$ billion human years, ago. It counts, using the 42-letter name of the God at the start of Genesis, that now we are in the 6-th of the 7 cosmic *sh'mitah* cycles, each one being 7000 divine years long. *Tohu va-bohu* (formless and empty) followed and 6000 years ago the creation of the world *in deed* is posited.

  In the Talmud (Pesahim, 94), the Holy Spirit points out to "impious Nebuchadnezzar" (planning "to ascend above the heights of the clouds like the Most High"): "The distance from earth to heaven is 500 year's journey alone, the thickness of the heaven again 500 years…". This heaven is the *firmament* plate, and the journey is by walking. Seven other heavens, each 500 years thick, follow and the feet of the holy Creatures are equal to the whole…Their ankles, wings, necks, heads and horns are each consecutively equal to the whole." Finally, "upon them is the Throne of Glory which is equal to the whole". The resulting journey of 4,096,000 years amounts, at the rate of 80 miles ($\approx$ 129 km) per day, to $\approx$2600 AU, i.e., $\approx \frac{1}{100}$ of the actual distance to Proxima Centauri, the nearest other star. Also, in Talmud, the width of *Jacob's Ladder* (bridge to Heaven that Jacob dreams about, described in the Book of Genesis) is computed as 8000 parasangs.

  On the other hand, *Baraita de Massechet Gehinom* affirms in Section VII.2 that Hell consists of 7 cubic regions of side 300 year's journey each; so, 6300 years altogether. According to the Christian Bible (Chap. 21 of the Book of Revelation), New Heavenly Jerusalem (a city that is or will be the dwelling place of the Saints) is a cube of side 12,000 furlongs ($\approx$ 2225 km), or a similar pyramid or spheroid.

  Islamic tradition (Dawood, Book 40, Nr. 470) also attributes a journey of 71–500 years (by horse, camel or foot) between each *samaa'a* (the ceiling containing one of the seven luminaries: Moon, Mercury, Venus, Sun, Mars, Jupiter, Saturn). Besides 7 heavens (as in Judaism and Hinduism), Shia Islam and Sufism have 7 depths of esoteric meanings of Quran, with only God knowing the 4-th meaning.

  The Vedic text (Pancavimsab Brahmana, c. 2000 BC) states that the distance to Heaven is 1000 Earth diameters and the Sun (the middle one among seven luminaries) is halfway at 500 diameters. A similar ratio 500–600 was expected

till the first scientific measurement of 1 AU (mean Earth-Sun distance) by Cassini and Richter, 1672. The actual ratio is $\approx$ 11,728.

The sacred Hindu number 108 ($=6^2+6^2+6^2=\prod_{1\le i\le 3} i^i$), connected to the Golden Ratio as the interior angle 108° of a regular pentagon, is traced to the following Vedic values: 108 Sun's diameters for the Earth-Sun distance and 108 Moon's diameters for the Earth-Moon distance. The actual values are (slightly increasing) $\approx$ 107.6 and $\approx$ 110.6; they could be computed during an eclipse, since the angular size of the Moon and Sun, viewed from the Earth, is almost identical.

Also, the ratio between the Sun and Earth diameters is $\approx$ 108.6, but it is unlikely that Vedic sages knew this. In Ayurveda, the devotee's distance to his "inner sun" (God within) consists of 108 steps; it corresponds to 108 beads of *mala* (rosary): by saying beads, the devotee does a symbolic journey from his body to Heaven.

In Bhagavata, the total diameter of the Universe is about 6.4 billion km.

- **Swedenborg heaven distances**

  The Swedish scientist and visionary Emanuel Swedenborg (1688–1772), in Section 22 (Nos. 191–199, *Space in Heaven*) of his main work *Heaven and Hell* (1952, first edition in Latin, London, 1758), posits: "distances and so, space, depend completely on interior state of angels". A move in heaven is just a change of such a state, the length of a way corresponds to the will of a walker, approaching reflects similarity of states. In the spiritual realm and afterlife, for him, "instead of distances and space, there exist only states and their changes".

- **Safir distance**

  According to Islamic law, a traveler may shorten the prayers, combine them, and be permitted to break the fast of Ramadan if the travel (*safir*) exceeds some minimum distance. Hanafi, the largest Sunni school of jurisprudence, define such **safir distance** as 3 days of continuous journey (in the great part of the day and at a moderate speed) or 15 *farsakh* (ancient unit of length, called also *parasang*).

  Three other main schools define it as 2 days of such journey or as 16 farsakh, computed differently. This distance is usually approximated as 80 or 83 km and applied for travel by camel, car, plane or ship. Another strong opinion, by Ibn Taymiyya, claims that safir is not merely a distance but also a state of mind, an exposure to the wilderness; so, any distance customarily considered traveling is safir.

- **Sabbath distance**

  The **Sabbath distance** (or *rabbinical mile*) is a **range distance**: 2000 Talmudic cubits (960–11,152 m, cf. **cubit** in Chap. 27) which an observant Jew should not exceed in a public thoroughfare from any given private place on the Sabbath day. It is about the distance covered by an average man in 18 min.

  Other Israelite/Talmudic length units are: a day's march, parsa, stadium (40, 4, $\frac{2}{15}$ of the rabbinical mile, respectively), and span, hasit, palm, thumb, middle finger, little finger ($\frac{1}{2}$, $\frac{1}{3}$, $\frac{1}{6}$, $\frac{1}{24}$, $\frac{1}{30}$, $\frac{1}{36}$ of the Talmudic cubit, respectively).

- **Bible code distance**

  Witztum, Rips and Rosenberg, 1994, claimed to have discovered a meaningful subtext of the Book of Genesis, formed by uniformly spaced letters. The text was seen as written on a cylinder on which it spirals down in one long line. Many reactions followed, including criticism by McKay, Bar-Natan, Bar-Hillel and Kalai, 1999, in the same journal *Statistical Science*.

  The following **Bible code distance** d_t between two letters, that are t positions apart in the text, was used. Let h be the circumference of the cylinder, and let q and r be the quotient and reminder, respectively, when t is divided by h, i.e., $t = qh + r$ with $0 \leq r \leq h - 1$. Then $d_t = \sqrt{q^2 + r^2}$ if $2q \leq h$, and $d_t = \sqrt{(q+1)^2 + (r-h)^2}$, otherwise. It is, approximatively, the shortest distance between those letters along the cylinder surface; cf. **cylindrical distance** (Chap. 20).
- **Distance numbers**

  On Maya monuments usually only one anchor event is dated absolutely, in the linear *Mesoamerican Long Count calendar* by the number of days passed since the mythical creation on August 11, 3114 BC of the fourth world, which completed a *Great Period* of 13 b'ak'tuns ($\approx$ 5125 years) on December 21, 2012.

  The other events were dated by adding to or subtracting from the anchor date some **distance numbers**, i.e., periods from the cyclical 52-year *Calendar Round*.
- **Antinomy of distance**

  The **antinomy of distance**, as introduced in [Bull12] for aesthetic experiences by the beholder and artist, is that both should find the right amount of **emotional distance** (neither too involved, nor too detached), in order to create or appreciate art. The fine line between objectivity and subjectivity can be crossed easily, and the amount of distance can fluctuate in time.

  The **aesthetic distance** is a degree of emotional involvement of the individual, who undergoes experiences and objective reality of the art, in a work of art. It refers to the gap between the individual's conscious reality and the fictional reality presented in a work of art. It means also the frame of reference that an artist creates, by the use of technical devices in and around the work of art, to differentiate it psychologically from reality; cf. **distanciation**.

  Some examples are: the perspective of a member of the audience in relation to the performance, the psychological/emotional distance between the text and the reader, the *actor-character distance* in the Stanislavsky system of acting.

  Antinomy between inspiration and technique (embracement and estrangement) in performance theory is called the *Ion hook* since Ion of Ephesus (a reciter of rhapsodic poetry, in a Platon's dialog) employed a double-consciousness, being ecstatic and rational. The acting models of Stanislavsky and Brecht are, respectively, incarnating the role truthfully and standing artfully distanced from it. Cf. **role distance**.

  [Morg76] defines pastoral ecstasy as the experience of *role-distancing*, or the authentic self's supra-role suspension, i.e., the capacity of an individual to stand outside or above himself for purposes of critical reflection. Morgan concludes:

"The authentic self is an *ontological possibility*, the social self is an *operational inevitability*, and awareness of both selves and the creative coordination of both is the gift of ecstasy". Cf. **Lévinas distance to Other**.

The **historical distance**, in terms of [Tail04], is the position the historian adopts *vis-à-vis* his objects—whether far-removed, up-close, or somewhere in between; it is the fantasy through which the living mind of the historian, encountering the inert and unrecoverable, positions itself to make the material look alive. The antinomy of distance appears because historians engage the past not just intellectually but morally/emotionally. The formal properties of historical accounts are influenced by the affective, ideological and cognitive commitments of their authors.

A variation of the antinomy of distance appears in critical thinking: the need to put some emotional and **epistemic** (intellectual) distance between oneself and ideas, in order to better evaluate their validity and avoid *illusion of explanatory depth* (to fail see the trees for the forest). A related problem is how much distance people must put between themselves and their pasts in order to remain psychologically viable; Freud showed that often there is no such distance with childhoods.

- **Role distance**

  In Sociology, Goffman, 1961, using a dramaturgical metaphor, defined **role distance** (or *role distancing*) as actions which effectively convey some disdainful detachment of the (real life) performer from a role he is performing. An example of social role distancing is when a teacher explains to students that his disciplinary actions are due only to his role as a teacher.

  Goffman observed that children are able to merge doing and being, i.e., *embracement of the performer's role*, only from 3–4 years. Starting from about 5, their role distance (distinguishing being from doing) appears and expands, especially, at age 8, 11 and adult years.

  Besides role embracement and role distance, one can play a role cynically in order to manage the outcomes of the situation (impression management). The most likely cause of role distancing is *role conflict*, i.e., the pressure exerted from another role to act inconsistently from the expectations of the first role.

  A *frame* is a type of role (participant, observer, authority, critic, artist, etc.) given to a person in relation to a given event. The **frame distance**, introduced by Heathcote, 1980, in teaching drama, refer to a specific (implied by the frame) responsibility, interest, attitude and behavior of a person/student in this event/drama.

- **Distanciation**

  In scenic art and literature, **distanciation** (Althusser, 1968, on Brecht's *alienation effect*) consists of methods to disturb purposely (in order to challenge basic codes and conventions of spectator/reader) the *narrative contract* with him, i.e., implicit clauses defining logic behavior in a story. The purpose is to differentiate art psychologically from reality, i.e., to create some **aesthetic distance**.

For Bakhtin, the mandate to "be outside" that which you create is a matter of subject-subject (as opposed to subject-object) relations. For Shklovsky the distancing of an object sharpens our perception and stimulates senses, thereby arousing us to artistic (as opposed to dull everyday) experience.

One of the distanciation devices is *breaking of the fourth wall*, when the actor/author addresses the spectators/readers directly through an imaginary screen separating them. The *fourth wall* is the conventional boundary between the fiction and the audience. It is a part of the *suspension of disbelief* between them: the audience tacitly agrees to provisionally suspend their judgment in exchange for the promise of entertainment. Cf. **distancing** and **distantiation**.

- **Narrative distance**

  The author creates a persona of *narrator*, who tell the story, usually, from the point of view of first- or third-person. **Narrative distance** is (Genette, 1980) the distance between the narrator and the story's characters, setting, events and objects.

  The closest possible distance—the narrator reports on the thoughts and feeling (even unconscious ones) of the characters, while the farthest distance—reporting only actions and situations. The author can vary this distance; say, the third-person omniscient narrator can zoom in and out of character's perspectives.

- **Ironic distance**

  Rhetorical writer or speaker does not allow audience to maintain an objective or fixed distance from the story. He intrude to distance himself from characters in a story or from his own remarks. **Ironic distance** refers to the narrative irony: distance of knowledge between author/narrator/character/reader.

  As a literary device, irony implies a distance between what is said and what is meant. Irony is also the art of juxtaposing incongruous parts; so, an *ironic distance* also mean the closeness between two things that never meet.

- **Epistemic distance**

  Epistemic (or *intellectual*) **distance** from something refers to the degree of difficulty involved in knowing it. For example, conditional rhetorical constructions are used in discourse, in order to indicate this distance. Mejias (2005) *epistemological distance* between things is the difference in degree of knowledge justification.

- **Representation of distance in Painting**

  In Western Visual Arts, the *distance* is the part of a picture representing objects which are the farthest away, such as a landscape; it is the illusion of 3D depth on a flat picture plane. The *middle distance* is the central part of a scene between the foreground and the background (implied horizon).

  Perspective projection draws distant objects as smaller to provide additional realism by matching the decrease of their visual angle; cf. Chap, 6. A *vanishing point* (or *point of distance*) is a point at which parallel lines receding from an observer seem to converge. (For a meteor shower, the *radiant* is the point in the sky, from which meteors appear to originate.) *Linear perspective* is a drawing with 1–3 vanishing points; usually, they are placed on the horizon and equipartition it.

In a *curvilinear perspective*, there are ≥ 4 vanishing points; usually, they are mapped into and equipartition a *distance circle*. 0-*point perspective* occurs if the vanishing points are placed outside the painting, or if the scene (say, a mountain range) does not contain any parallel lines. Such perspective can still create a sense of *depth* (3D distance) as in a photograph of a mountain range.

In a *parallel projection*, all sets of parallel lines in 3D object are mapped to parallel lines in 2D drawing. This corresponds to a perspective projection with an infinite *focal length* (the distance from the image plane to the projection point).

Axonometric projection is parallel projection which is *orthographic* (i.e., the projection rays are perpendicular to the projection plane) and such that the object is rotated along one or more of its axes relative to this plane. The main case of it, used in Engineering Drawing, is **isometric projection** in which the angles between three projection axes are the same, or $\frac{2\pi}{3}$.

In Chinese Painting, the *high-distance*, *deep-distance* or *level-distance* views correspond to picture planes dominated, respectively, by vertical, horizontal elements or their combination. Instead of the perspective projection of a "subject", assuming a fixed position by a viewer, Chinese classic hand scrolls (up to 10 m in length) used axonometric projection. It permitted them to move along a continuous/seamless visual scenario and to view elements from different angles. It was less faithful to appearance and allowed them to present only three (instead of five) of six surfaces of a normal interior. But in Chinese Painting, the focus is rather on symbolic and expressionist representation.

- **Scale in art**

  In drawing, the **scale** refers to the proportion or ratio that defines the size relationships. It is used to create the illusion of correct size relationships between objects and figures. The *relative scale* is a method used to create and determine the spatial position of a figure or object in the 3D picture plane: objects that are more distant to the viewer are drawn smaller in size. In this way, the relative size of an object/figure creates the illusion of space on a flat 2D picture.

  In an architectural composition, the **scale** is the two-term relationship of the parts to the whole which is harmonized with a third term—the observer. For example, besides the proportions of a door and their relation to those of a wall, an observer measures them against his own dimensions.

  The **scale** of an outdoor sculpture, when it is one element in a larger complex such as the facade of a building, must be considered in relation to the scale of its surroundings. In *flower arrangement* (floral decoration), the **scale** indicates relationships: the sizes of plant materials must be suitably related to the size of the container and to each other.

  The *hierarchical scale* in art is the manipulation of size and space in a picture to emphasize the importance of a specific object. Manipulating the scales was the theme of *Measure for Measure*, an art/science exhibition at the Los Angeles Art Association in 2010. Examples of the interplay of the small and the large in literature are Swift's *Gulliver's Travels* and Carrol's *Through the Looking Glass*. In the cinema, the spectator can easily be deceived about the size of objects, since scale constantly changes from shot to shot.

In Advertising and Packaging, the size changes the meaning or value of an object. The idea that "bigger is better" is validated by the sales of sport utility vehicles, super-sized soft drinks and bulk food at Wal-Mart.

In reverse, the principle "small is beautiful" is often used to champion small, appropriate objects and technologies that are believed to empower people more. For example, small-sized models sell the benefits of diet programs and fitness regimes designed to scale back people's proportions. Examples of Japanese miniaturization culture are bonsai and many small/thin portable devices.

- **Distances in Interior Design**

  In Interior Design, the *scale* refer to how an item relates to the size of the room or the owner, and the *proportion* refer to the shape of an item and how it relates to other objects in the room. The vertical, horizontal, diagonal and curved lines give a room a feeling of formalness, casualness, transition and sensuality, respectively. Other required space relationships are *balance* (equal weight between objects on either side of a room) and *rhythm* (repetition of patterns, color, or line).

  Workplane is the height at which an activity takes place; it is about 90, 75–90 and 75 cm for a kitchen, bath and a dining room or desk. In a kitchen, the perimeter of the *work triangle* formed by sink, cooking surface and refrigerator ideally should be 3.5–7.5 m. In a living room, the triangle of *focal points* to emphasize is formed usually at the door or fireplace, TV, big window, sofa. Other examples of recommended distances are: 35–45 cm between the sofa (or chairs) and coffee table, 60 cm between dining chairs and at least 90 cm for traffic lanes.

  Used in lighting calculations, the **room cavity ratio** (or RCR) is $\frac{5hP}{2A}$, where h, P, A are the ceiling height, perimeter and area of the room. So, $RCR = \frac{5h(l+w)}{lw}$ for a rectangular room of length l and width w.

- **Spatialism**

  Spatialism (or *Spazialismo*) is an art movement founded by Lucio Fontana in Milan in 1947, intended to synthesize space, color, sound, movement and time into a new "art for the Space Age". Instead of the illusory virtual space of traditional *easel* (i.e., of a size and on a material suitable for framing) painting, he proposed to unite art and science to project color and form into real space by the use of up-to-date techniques, say, TV and neon lighting. His *Spatial Concept* series consisted of holes or slashes, by a razor blade, on the surface of monochrome paintings.

- **Spatial music**

  Spatial music refers to music and sound art (especially, electroacoustic), in which the location and movement of sound sources, in physical or virtual space, is a primary compositional parameter and a central feature for the listener.

  Space music is gentle, harmonious sound that facilitates the experience of contemplative spaciousness. Engaging the imagination and generating serenity, it is particularly associated with ambient, New Age, and electronic music.

- **Distance-named cultural products**

  Far Near Distance is the name of the program of the House of World Cultures in Berlin which presents contemporary positions of Iranian artists. Examples of similar use of distance terms in modern popular culture follow.

  "Some near distance" and "Zero/Distance" are the titles of art exhibitions of Mark Lewis (Bilbao, 2003) and Jim Shrosbree (Des Moines, Iowa, 2007). "A Near Distance" is a paper collage by Perle Fine (New York, 1961); "Quiet Distance" is a fine art print by Ed Mell. "Distance" is a Windows/Mac/Linux survival racing game; "Dream Drop Distance" is a video game for Nintendo.

  "Distance" is a Japanese film directed by Hirokazu Koreeda (2001) and an album of Utada Hikaru (her famous ballad is called "Final Distance"). It is also a song by Christina Perry, the stage name of a musician Greg Sanders and the name of the rock/funk band led by Bernard Edwards. "The Distance" is a US film directed by Benjamin Busch (2000), an album by the band "Silver Bullet" and a song by the band "Cake". "Near Distance" is a musical composition by Chen Yi (New York, 1988) and lyrics by the quartet "Puressence".

  "Distance to Fault", "Distance from Shelter", "Long Distance Calling" are the rock bands. Among popular albums are "The Tyranny of Distance", "The Great Cold Distance", "Close the Distance", "The Distance to Here", "Love and Distance", "Long Distance Voyager" and "The Crawling Distance", "This Magnificent Distance" by the bands "Washington, D.C.", "Katatonia", "Go Radio", "Live", "The Helio Sequence", "The Moody Blues" and Robert Pollard, Chris Robinson.

  The terms *near distance* and *far distance* are also used in Ophthalmology and for settings in some sensor devices.

- **Distance-related quotes**

  - "Respect the gods and the devils but keep them at a distance." (Confucius)
  - "Sight not what's near through aiming at what's far." (Euripides)
  - "It is when suffering seems near to them that men have pity." (Aristotle)
  - "Distance in space or time weakened all feelings and all sorts of guilty conscience." "Distance is a great promoter of admiration." (Denis Diderot)
  - "Our main business is not to see what lies dimly at a distance, but to do what lies clearly at hand." (Thomas Carlyle)
  - "We can only see a short distance ahead, but we can see plenty there that needs to be done." (Alan Turing)
  - "The foolish man seeks happiness in the distance; the wise grows it under his feet."(Julius Robert Oppenheimer)
  - "The very least you can do in your life is to figure out what you hope for. And the most you can do is live inside that hope. Not admire it from a distance but live right in it, under its roof." (Barbara Kingsolver)
  - "Better is a nearby neighbor, than a far off brother." (Proverbs 27:10, Bible)
  - "These [patriarchs] all died in faith without receiving the things promised [Canaan, Messiah, Gospel], but they saw them and welcomed them from

a distance, admitting that they were strangers and pilgrims on the earth." (Hebrews 11:13, Bible)

- "By what road", I asked a little boy, sitting at a cross-road, "do we go to the town?"—"This one", he replied, "is short but long and that one is long but short". I proceeded along the "short but long road". When I approached the town, I discovered that it was hedged in by gardens and orchards. Turning back I said to him, "My son, did you not tell me that this road was short?"—"And", he replied, "Did I not also tell you: "But long"?" (Erubin 53b, Talmud)
- "The Prophet Muhammad was heard saying: "The smallest reward for the people of paradise is an abode where there are 80,000 servants and 72 wives, over which stands a dome decorated with pearls, aquamarine, and ruby, as wide as the distance from Al-Jabiyyah [a Damascus suburb] to Sana'a [Yemen]." (Hadith 2687, Islamic Tradition)
- "The closer the look one takes at the world, the greater distance from which it looks back." (Karl Kraus)
- "Telescopes and microscopes are designed to get us closer to the object of our studies. That's all well and good. But it's as well to remember that insight can also come from taking a step back." (New Scientist, March 31, 2012)
- "Where the telescope ends, the microscope begins. Which of the two has the grander view?" (Victor Hugo)
- "Nature uses only the longest threads to weave her patterns." (Richard Feynman)
- "We're about eight Einsteins away from getting any kind of handle on the universe." (Martin Amis)
- "It is true that when we travel we are in search of distance. But distance is not to be found. It melts away. And escape has never led anywhere . . . What are we worth when motionless, is the question." (Antoine de Saint-Exupéry)
- "If you want to build a ship, don't drum up people to collect wood and don't assign them tasks and work, but rather teach them to long for the endless immensity of the sea." (Antoine de Saint-Exupéry)
- "Ships at a distance have every man's wish on board." (Zora Neale Hurston)
- "If you've never stared off in the distance, then your life is a shame." (Adam Duritz)
- "Every once in a while, people need to be in the presence of things that are really far away." (Ian Frazier)
- "Only those who will risk going too far can possibly find out how far one can go." (Thomas Stearns Eliot)
- "Distance is to love like wind is to fire . . . it extinguishes the small and kindles the great." (source unknown)
- "I could never take a chance of losing love to find romance
  In the mysterious distance between a man and a woman." (Performed by U2)
- "In true love the smallest distance is too great, and the greatest distance can be bridged." (Hans Nouwens)

- "Love is like a landscape which doth stand
  Smooth at a distance, rough at hand." (Robert Hegge)
- "Life is like a landscape. You live in the midst of it but can describe it only from the vantage point of distance." (Charles Lindbergh)
- "Distance between two people is only as one allows it to be." (source unknown)
- "It is only the mountains which never meet." (french proverb)
- "Nothing makes Earth seem so spacious as to have friends at a distance; they make the latitudes and longitudes." (Henri David Thoreau)
- "Distance can endear friendship, and absence sweeteneth it." (James Howell)
- "The word is distance within non-distance, that is, the width of a gap that every letter stresses while bridging it. What is said is always said in relation to what will never be expressed. At these limits we recognize ourselves." (Edmond Jabès)
- "The poet's other readers are the ancient poets, who look upon the freshly written pages from an incorruptible distance. Their poetic forms are permanent, and it is difficult to create new forms which can approach them." (Salvatore Quasimodo)
- "Sad things are beautiful only from a distance . . . From a distance of 130 years i'm going to distance myself until the world is beautiful. . . " (Tao Lin)
- "Dying away into the distance, prose turns into poetry, speech into vocalise, language into music." (Berthold Hoeckner)
- "Everything becomes romantic and poetic, if one removes it to a distance . . . Distant philosophy sounds like poetry – for each call into the distance becomes a vowel . . . Everything becomes poetry – poem from afar." (Novalis)
- "The appropriated way to determine whether a painting is melodious is to look at it from a distance so as to be unable to comprehend its subject or its lines." (Charles Baudelaire)
- "There is no object so large . . . that at great distance from the eye it does not appear smaller than a smaller object near." (Leonardo da Vinci)
- "Distance lends enchantment to the view,
  And robes the mountain in its azure hue." (Thomas Campbell)
- "There are charms made only for distant admiration."
  "Distance has the same effect on the mind as on the eye." (Samuel Johnson)
- "Age, like distance, lends a double charm." (Oliver Wendell Holmes)
- "Distance not only gives nostalgia, but perspective, and maybe objectivity." (Robert Morgan)
- "It is the just distance between partners who confront one another, too closely in cases of conflict and too distantly in those of ignorance, hate and scorn, that sums up rather well, I believe, the two aspects of the act of judging. On the one hand, to decide, to put an end to uncertainty, to separate the parties; on the other, to make each party recognize the share the other has in the same society." (Paul Ricoeur)
- "Authority doesn't work without prestige, or prestige without distance." (Charles de Gaulle)

- "The human voice can never reach the distance that is covered by the still small voice of conscience." (Mohandas Gandhi)
- "A smile is the shortest distance between two people." (Victor Borge)
- "The shortest distance between two points is under construction." (Leo Aikman)
- "A straight line may be the shortest distance between two points, but it is by no means the most interesting." (Third Doctor from BBC TV series *Doctor Who*)
- "In politics a straight line is the shortest distance to disaster." (John P. Roche)
- "Fret not where the road will take you. Instead concentrate on the first step. That is the hardest part and that is what you are responsible for. Once you take that step let everything do what it naturally does and the rest will follow. Do not go with the flow. Be the flow." (Shams Tabrisi)
- "The distance is nothing; only the first step that is difficult." (Marie du Deffand)
- "A perfect run has nothing to do with distance. It's when your stride feels comfortable." (Sean Astin)
- "Fill the unforgiving minute with sixty seconds worth of distance run." (Rudyard Kipling)
- "The distance between dreams and reality is called Discipline." (Albert Wright)
- "The distance between who you are and who you might be is closing." (Jan Chipchase)
- "Everywhere is within walking distance if you have the time." (Steven Wright)
- "Time is the longest distance between two places." (Tennessee Williams)
- "There is an immeasurable distance between late and too late." (Og Mandino)
- "They couldn't hit an elephant at this distance." (last words of John Sedgwick, seconds before he was mortally wounded)
- "The distance that the dead have gone does not at first appear;
  Their coming back seems possible for many an ardent year." (Emily Dickinson)
- "A vast similitude interlocks all . . . All distances of place however wide,
  All distances of time, all inanimate forms, all souls . . . " (Walt Whitman)

Chapter 29
Other Distances

In this chapter we group together distances and distance paradigms which do not fit in the previous chapters, being either too practical (as in equipment), or too general, or simply hard to classify.

29.1 Distances in Medicine, Anthropometry and Sport

- **Distances in Medicine**

  Some examples from this vast family of physical distances follow.

  In Dentistry, the **interocclusal distance**: the distance between the occluding surfaces of the maxillary and mandibular teeth when the mandible is in a physiologic rest position. The **interarch** and **interridge distances**: the vertical distances between the maxillary and mandibular arches, or, respectively, ridges.

  The **intercanine distance**: the distance between the distal surfaces of the maxillary canines on the curve (the circumference of six maxillary anterior teeth).

  The **interincisor distance**: the distance between the upper and lower incisors.

  The **interproximal distance**: the **spacing distance** between adjacent teeth; *mesial drift* is the movement of the teeth slowly toward the front of the mouth with the decrease of the interproximal distance by wear.

  The **biologic width**: the distance between the deepest point of the gingival sulcus and the alveolar bone crest. The *crown-to-root-ratio*: the ratio of the length of the part of a tooth that appears above the alveolar bone versus what lies below it.

  The **interbrow distance**: the distance between the eyebrows.

  The **interaural** (or *biauricular*) **distance**: the distance between the ears.

  Lumbar spinal canal (LSC) is the tunnel that the spinal cord and nerves pass through. The **LSC diameter** is the longest horizontal distance between any two points on the lumbar edge; normally, it is 15–27 mm.

© Springer-Verlag Berlin Heidelberg 2016

M.M. Deza, E. Deza, *Encyclopedia of Distances*,
DOI 10.1007/978-3-662-52844-0_29

The **rectosacral distance**: the shortest distance from the rectum to the *sacrum* (triangular bone at the base of the spine, inserted between the two hip bones) between the 3-rd and 5-th sacral vertebra. It is at most 10 mm in adults.

The **anogenital distance** (or AGD): the length of the *perineum*, i.e., the region between the anus and genital area (the anterior base of the penis for a male). For a male it is 5 cm in average (twice what it is for a female). ARD is a measure of physical masculinity and, for a male, lower ARD correlates with lower fertility.

The **internipple distance**: the distance between nipples. "Ideally", the nipples and sternal notch form an equilateral triangle with a side of 21 cm, and the nipples are at the middle of the humeral shoulder-elbow distance. The average *areolar diameter* is 38 mm for a mature woman and 25 mm for a male.

The **intercornual distance**: the distance between uterine horns (2–4 cm). The **C-V distance**: clitoris-vagina distance (2.3–3 cm); < 2.5 cm tend to yield reliable orgasms from intercourse alone, while > 3 cm almost exclude it. The *clitoral index* (CI): product of the crosswise (3–4 mm) and lengthwise (4–5 mm) widths of the external portion of the clitoris; CI is a measure of virilization in women. Mean *vaginal depth* (cervix-introitus) is 7–8 cm, increasing to 11–13 cm during sexual arousal. For a human penis, mean *flaccid and erect lengths* are 9.16 and 13.2 cm.

A **pelvic diameter** is any measurement that expresses the diameter of the birth canal in the female. For example, the *diagonal conjugate* (13 cm) joins the posterior surface of the pubis to the tip of the sacral promontory, and the *true* (or *obstetric*, *internal) conjugate* (11.5 cm) is the anteroposterior diameter of the pelvic inlet.

In Obstetrics, the **fundal height** is the size the mother's uterus (the distance between the tops of uterus and pubic bone) used to assess fetal growth and development during pregnancy. The **crown-rump length** is the length of human embryos/fetuses (the distance, determined from ultrasound imagery, from the top of the head to the bottom of the buttocks) used to estimate gestational age.

Metra and uterus are (Greek and Latin) medical terms for the womb. *Metropathy* is any disease of the uterus, say, *metritis* (inflammation), *metratonia* (atony), *metrofibroma*. *Metrometer* is an instrument measuring the womb's size. *Metrography* (or *hysterography*) is a radiographic examination of the uterine cavity filled with a contrasting medium. Cf. **meter-related terms** in Chap. 27.

In Radiography, the **teardrop distance**: the distance from the lateral margin of the pelvic teardrop to the most medial aspect of the femoral head; a widening of ≥ 1 mm indicates excess hip joint fluid and so inflammation. The **intertrochanteric distance**: the distance between femurs. The **interpediculate distance**: the distance between the vertebral pedicles. The **source-skin distance**: the distance from the focal spot on the target of the X-ray tube to the subject's skin.

In *Intubation* (insertion of a tube into a body canal or hollow organ, to maintain an opening or passageway), the **insertion distance**: the distance from the body aperture at which the tubing is advanced. The *French size* of a catheter with external diameter D is $\pi D \approx 3D$; so, 20 F means $D = 6.4$ mm.

In Anesthesia, the **thyromental distance** (or TMD): the distance from the upper edge of the thyroid cartilage (laryngeal notch) to the *menton* (tip of the chin). The **sternomental distance**: the distance from the upper border of the manubrium sterni to the menton. The **mandibulo-hyoid distance**: mandibular length from menton to hyoid. When the above distances are less than 6–6.5 cm, 12–12.5 cm and 4 cm, respectively, a difficult intubation is indicated.

The *depth of anesthesia* is a number expressing the likehood of awareness by the degree of slowing and irregularity in electroencephalogram (EEG) signals. Also, at loss of consciousness, high frequency (12–35 Hz) brain waves are replaced by two (low, < 1 Hz, and alpha, 8–12 Hz) superimposed waves. Even beyond a flat line EEG, some neuronal spikes come to the cortex from the hippocampus.

The **sedimentation distance** (or ESR, *erythrocyte sedimentation rate*): the distance red blood cells travel in 1 h in a sample of blood as they settle to the test tube's bottom. ESR indicates inflammation and increases in many diseases.

The **stroke distance**: the distance a column of blood moves during each heart beat, from the aortic valve to a point on the arch of the aorta.

The **distance between the lesion and aortic valve** being < 6 mm, is an important predictor, available before surgical resection of DSS (discrete subaortic stenosis), or reoperation for recurrent DSS. The **aortomesenteric distance** (between aorta and superior mesenteric artery) correlates with the *body mass index*.

The **aortic diameter**: the maximum diameter of the outer contour of the aorta. It, as well as the cross-sectional diameter of the left ventricle, varies between the ends of the *systole* (the time of ventricular contraction) and *diastole* (the time between contractions). The smallest and largest cardiac dimensions are LVE (left ventricle end-) *systolic* and *diastolic diameters*; the *strain* is the ratio between them.

The **dorsoventral interlead distance** of an implanted pacemaker or defibrillator: the horizontal separation of the right and left ventricular lead tips on the lateral chest radiograph, divided by the *cardiothoracic ratio* (ratio of the cardiac width to the thoracic width on the posteroanterior film).

The **distance factor** is a crude measure $\frac{l}{d} - 1$ of arterial tortuosity, where l is the vessel length and d is the Euclidean distance between its endpoints.

In Nerve Regeneration by transplantation of cultured stem cells, the **regeneration distance** is the distance between the point of insertion of the proximal stump and the tip of the most distal regenerating axon.

The *small-for-size syndrome* (SFSS) is acute liver failure resulting from the transplantation of a too small (usually $< 0.8\,\%$ of recipient weight) *graft* (donor liver).

A **distant flap** is a procedure moving tissue (skin, muscle, bone, or some combination) from one part of the body, where it is dispensable, to another part.

The length of the alimentary (mouth-to-anus) tract is ≈ 9 m in a dead and, due to muscle tone, 5–6 m in a leaving human. Transit takes 30–50 h.

In Laser Treatments, the **extinction length** and **absorption length** of the vaporizing beam are the distances into the tissue along the ray path over which 90 % (or 99 %) and 63 %, respectively, of its radiant energy is absorbed.

In Ophthalmic Plastic Surgery, the **marginal reflex distances** MRD_1 and MRD_2 are the distances from the center of the pupil (identified by the corneal reflex created by shining a light on the pupil) to the margin of the upper or lower eyelid, while the **vertical palperbal fissure** is the distance between these eyelids.

The main distances used in Ultrasound Biomicroscopy (for glaucoma treatment) are the **angle-opening distance** (from the corneal endothelium to the anterior iris) and the **trabecular ciliary process distance** (from a particular point on the *trabecular mesh-work* to the *ciliary process*).

In Medical Statistics, *length bias* is a selection bias that can occur when the lengths of intervals are analyzed by selecting random intervals in space or time. This process favors longer intervals, thus skewing the data. For example, screening over-represents less aggressive disease, say, slower-growing tumors.

- **Distances in Oncology**

  In Oncology, the **tumor radius** is the mean radial distance R from the tumor origin (or its center of mass) to the tumor-host interface (the tumor/cell colony border). The cell proliferation along $[0, R]$ is ≈ 0 up to some r_0, then increases only linearly up to some r_1, and it happens mainly within $[r_1, R]$.

  The **tumor diameter** is the greatest vertical diameter of any section; the *tumor growth* is the geometric mean of its three perpendicular diameters. The *average diameter* is $\frac{L+W+H}{3}$ where L, W, H are the longest length, width and height.

  Tubiana, 1986, claims that for each tumor type a critical tumor diameter and mass for metastatic spread exists and this threshold may be reached before the primary tumor is detectable. For breast cancer, metastases were found in 50 % of the women whose primary tumor had a diameter of 3.5 cm, i.e., a mass ≈ 22 g.

  In the *tumor, node, metastasis* (TNM) classification, describing the stage of cancer in a patient's body, the parameter T is the **tumor size** (direct extent of the primary tumor) by the categories T-1, T-2, T-3, T-4. In breast cancer, T-1, T-2, T-3 are $< 2, 2–5, > 5$ cm and T-4 is a tumor of any size that has broken through the skin, or is attached to the chest wall. A *clinical size* is 10^9–10^{11} cells.

  In Oncological Surgery, the **margin distance** (or *margins of resection*) is the distance between a tumor and the ink-marked edge of *tumor bed*, i.e., normal-appearing tissue surrounding tumor that is removed along with it in order to prevent local recurrence. If the margins, as checked by a pathologist under microscope, are *positive* (cancer cells are found in the ink), then more surgery is needed. The margins are *negative* (or *clear*, *clean*) if no cancer cells are found "close" to the ink.

  The **perfusion distance** is the shortest distance between the infusion outlet and the surface of the electrodes during radio-frequency tumor ablation.

  In Radiation Oncology, the **maximum heart distance** MHD is the maximum distance of the heart contour (as seen in the beam's eye view of the medial tangential field) to the medial field edge, and the **central lung distance** CLD is the distance from the dorsal field edge to the thoracic wall. An "L-bar"

armrest, used to position the arm during breast cancer irradiation, decreases these distances.

A **distant cancer** (or relapse, metastasis) is a cancer that has spread from the original (primary) tumor to distant organs or distant lymph nodes. It can happen by **long-distance dispersal** (Chap. 23) and by dividing of *cancer stem cell*. DDFS (Distant Disease-free Survival) is the time until such an event.

According to Hanahan–Weinberg, 2000, tumor progress via evolution-like process of genetic changes which can be grouped into six hallmarks. Tumorigenesis requires a mutation pathway of 4–6 events among them to occur in the lineage of one cell. Spencer et al., 2006, define *tumor heterogeneity* as

$$\frac{2}{n(n-1)} \sum_{1 \le i < j \le p} n_i n_j d_{ij},$$

where $n = \sum_{1 \le i \le p} n_i$, p, n_i are the numbers of cells in a tumor, of distinct pathways, of cells with i-th pathway, and d_{ij} is the **ancestral path distance** (cf. **pedigree-based distances** in Chap. 23) between i-th and j-th pathways.

Similarly, the *distance to flu pandemic* is, say, the length of mutation pathway for a virus strain to become airborne transmissible among humans.

- **Distances in Rheumatology**

  The main such distances (measured in cm to the nearest 0.1 cm) follow.

  Occiput wall distance: the distance from the patient's occiput to the wall during maximal effort to touch the head to the wall, without raising the chin above its usually carrying level (when heels and, if possible, the back are against the wall).

  Modified Schober test: the distance between two marked points (a point over the spinous process of *L5* and the point 10 cm above) measured when the patient is extending his lumbar spine in a neutral position and then when he flexes forward as far as possible. Normally, the 10 cm distance increases to $\ge$ 16 cm.

  Lateral spinal flexion: the distance from the middle fingertip to the floor in full lateral flexion without flexing forward or bending the knees or lifting the heels and attempting to keep the shoulders in the same place.

  Chest expansion: the difference between full expiration and full inspiration, measured at the nipples.

  Intermalleolar distance: the distance between the medial malleoli when the patient (supine, the knees straight and the feet pointing straight up) is asked to separate the legs as far as possible.

- **Distance healing**

  Distance (or *distant*, *remote*) **healing** is defined (Sicher–Targ, 1998) as a conscious, dedicated act of mentation attempting to benefit another person's physical or emotional well-being at a distance. Cf. **action at a distance** in Chap. 24.

It includes prayer (intercessory, supplicative and nondirected), spiritual/mental healing and strategies purporting to channel some supra-physical energy (*noncontact therapeutic touch*, *Reiki healing*, *external qigong*).

Distant healing is part of popular alternative/complementary medicine but it is highly controversial: some positive results are attributed to a placebo effect. However, such rejection (as well as for homeopathy) is also a matter of belief.

In Chinese Medicine, the life-energy, *qi*, flow through 20 *meridians* connecting about 400 acupuncture points. Many *trigger points* (hyperirritable muscle spots) and *pressure points* in martial arts are related to above points. Many meridians are located along connective-tissue planes between muscles or muscle and bone.

In Ayurveda, the life force, *prana*, flow through $> 72{,}000$ *nadis* connecting *chakras* (intensity points); it also lists 13 internal *srotas* (physical body channels) and, by the number of orifices, 9 external ones for males and 12 for females. The main 13 chakras are evenly spaced, using the **interpupillary distance** as the unit. The root chakra is at the base of the spine, followed by chakras at the sex, navel, solarplexis, heart (two), Adam's apple, chin's tip, nose's tip, third eye, just above the forehead, the crown, one hand length above the head.

Distance medicine technologies are used to transmit/treat patient information, to submit prescriptions, to create distributive patient care and distributive learning. Examples of telephonic communication with patients are in: follow-up care, reminders, interactive systems, screening and access in hospital use.

- **Brain distances**

  fMRI (functional Magnetic Resonance Imaging) measures, using MRI technology, brain activity by detecting changes associated with blood flow.

  dMRI (diffusion MRI) noninvasively produces *in vivo* images of brain tissues weighted by their water diffusivity. The image intensities at each position are attenuated proportionally to the strength of diffusion in the direction of its gradient. Diffusion in tissues is described by a diffusivity tensor. Tensor data are displayed, for each voxel, by ellipsoids; their length in any direction is the diffusion distance molecules cover in a given time in this direction. The **diffusion tensor distance** is the length from the center to the surface of the diffusion tensor.

  In brain MRI, the distances considered for *cortical maps* (i.e., outer layer regions of cerebral hemispheres representing sensory inputs or motor outputs) are: MRI **distance map** from the GW (gray/white matter) interface, **cortical distance** (say, between activation locations of spatially adjacent stimuli), **cortical thickness** (the shortest distance between the GW the boundary and the innermost surface of *pia mater* enveloping the brain) and *lateralization metrics*. In fact, language, for example, tends to be on the left, attention more on the right side of the brain.

  The cortical thickness of Einstein's brain is 2.1 mm, while the average one is 2.6 mm; the resulting closer packing of neurons may speed up communication between them. This brain had a relatively larger (and more intricately folded) prefrontal cortex and an unusually high glia-to-neuron ratio. Also, the *corpus*

callosum is thicker in many areas, indicating greater connectivity between the two hemispheres.

Stereotaxic coordinates of a point p in the human brain are given by a triple (x_p, y_p, z_p) in mm (Talairach–Tournoux, 1988), where the *anterior commissure* is the origin $(0, 0, 0)$. The dimensions x, y, z refer to the left-right (LR), posterior-anterior (PA) and ventro-dorsal (VD or inferior-superior) orthogonal axes with positive values for the right hemisphere, anterior part and dorsal part. The **Talairach distance** of a point p is its Euclidean distance $\sqrt{x_p^2 + y_p^2 + z_p^2}$ from the origin.

Among proto-humans, only Neanderthals had a larger (11.6 %) brain than *Homo sapiens*; we got the brain-size increasing gene 0.037 Ma ago. But over the last 0.03 Ma our brains have been shrinking, while craniums have been increasing. Our brain reaches its full size by age 20 and then shrinks (faster for men) by about 1 % per year. Brain accounts for $\frac{1}{5}$ of the total ($\approx$ 100 W) body energy consumption.

Network models (of human brain in a living person) derived from resting state fMRI and dMRI are similar and strongly correlate. Siegelmann et al., 2015, defined the **connectivity-distance** (or *network depth*) of a brain area, as increase in its average connectivity from sensory cortex inputs, derived from those MRI data. This depth is expected to be a proxy for an increase in number of sequential synapses, processing time and to correlate with degree of abstractness of cognitive behaviors.

- **Dysmetria**

  Dysmetria is a symptom of a cerebellar disorder or syndrome, expressed in a lack of coordination of movement typified by the undershoot (*hypometria*) or overshoot (*hypermetria*) of the intended position with the hand, arm, leg, or eye.

  More generally, *dysmetria* can refer to an inability to judge distance or scale, which is also one of symptoms of dyscalculia. The **distance constancy** (Chap. 28) is poor in schizophrenics; so, their visual perception is lacking in depth.

  Alice in Wonderland syndrome, affecting mainly children, is that objects appear either much smaller (*micropsia*) or larger (*macropsia*) than they are. Micropsia appear also in *Charles Bonnet syndrome*, affecting mainly vision-impaired elderly.

- **Space-related phobias**

  Several **space-related phobias** have been identified: *agoraphobia*, *astrophobia*, *claustrophobia*, *cenophobia*, and *acrophobia*, *bathophobia*, *gephyrophobia*, *megalophobia* which are, respectively, fear of open, celestial, enclosed, empty spaces, and heights, depths, bridges, large/oversized objects. *Autoscopy* (or *out-of-body experience*) is the hallucination of seeing one's own body at a distance.

  Among neuropsychological spatial disorders are: *Balint's syndrome* (inability to localize objects in space), *hemispatial neglect* (bias of attention to and awareness of the side of the hemispheric lesion) and *allochiria* (left-right disorientation).

Topographical disorientation is the inability to orient in the surrounding as a result of focal brain damage. Such agnosia with respect to self, to landmarks, to external environment, to new environments is called *egocentric*, *landmark*, *heading*, *anterograde*, respectively. *Dromosagnosia* is the loss of direction while driving.

In Chap. 28, among applications of **spatial language** is mentioned Grove's *clean space*: a neuro-linguistic psychotherapy based on the spatial metaphors produced by the client on his present and desired "space" (state).

- **Neurons with spatial firing properties**

  Known types of **neurons with spatial firing properties** are listed below; cf. also **spike train distances** in Chap. 23.

  Many mammals have in several brain areas *head direction cells*: neurons which fire only when the animal's head points in a specific direction.

  Place cells are principal neurons in the hippocampus that fire strongly whenever an animal is in a specific location (the cell's *place field*) in an environment.

  Grid cells are neurons in the entorhinal cortex that fire periodically and at very regular distances as an animal walks. Grid cells measure distance while place cells indicate location. But only place cells are sensitive (albeit weakly) to height.

  Spatial view cells are neurons in the hippocampus which fire when the animal views a specific part of an environment. They differ from head direction cells since they represent not a global orientation, but the direction towards a specific object. They also differ from place cells, since they are not localized in space.

  Border cells are neurons in the entorhinal cortex that fire when a border is present in the proximal environment.

  Mirror cells are neurons that fire both when an animal acts and when it observes the same action performed by another.

  Head direction cells of rats are fully developed before pups open their eyes and become mobile. Next to mature are place cells followed by grid cells. All navigational cell types mature before rat adolescence (about 30 days of age).

  The smallest processing module of cortical neurons is a *minicolumn*—a vertical column (of diameter 28–40 microns) through the cortical layers of the brain, comprising 80–120 neurons that seem to work as a team. There are about 2×10^8 minicolumns in humans. Smaller minicolumns (as observed in scientists and in people with autism) mean that there are more processing units within any given cortical area; it may allow for better signal detection and more focused attention.

- **Vision distances**

  The *interocular distance* is the distance between the centers of rotation of the eyeballs of an individual or between the oculars of optical instruments.

  The **interpupillary distance** (or *binocular pupillary distance*) is the distance (50–75 mm) between the centers of the pupils of the two eyes. The *monocular pupillary distance* is the distance from the center of the nose to the pupil.

Stereoacuity is the smallest detectable depth difference that can be seen in binocular vision.

Involuntary *pupil's diameter* dilation of 0.5 mm can indicate interest, attention or sexual stimulation. Straight (homosexual) observers' pupils increase linearly as the amount of clothing on opposite (same, respectively) sex models decreases.

The *near acuity* is the eye's ability to distinguish an object's shape and details at a near distance such as 40 cm; the **distance acuity** is the ability to do it at a far distance such as 6 m. The **distance vision** is a vision for objects that are at least 6 m from the viewer. *Optical near devices* are designed for magnifying close objects and print; **distance devices** are for magnifying things in the distance.

The *near distance* is the distance between the object and *spectacle* (eyeglasses) planes. The *vertex distance*: the distance between a person's glasses (spectacles planes) and their eyes (the corneal). The *infinite distance*: a distance of at least 6 m; so called because rays entering the eye from an object at that distance are practically as parallel as if they came from an infinitely far point.

The *default accommodation distance* (or *resting point of accommodation*, *RPA distance*) is the distance at which the eyes focus if there is nothing to focus on.

The *RPV distance* (or *resting point of vergence*) is the distance at which the eyes are set to *converge* (turn inward toward the nose) when there is no close object to converge on. It averages about 1.15 m when looking straight ahead and in to about 0.9 m with a 30° downward gaze angle. Ergonomists recommend the RPV distance as the eye-screen distance in sustained viewing, in order to minimize eyestrain.

The *least distance of distinct vision* (or *reference seeing distance*) is the minimum comfortable distance (usually, 25 cm) between the eye and a visible object. Ideal focus distances for reading and writing are within 37–62 cm from the eyes.

The **Harmon distance** (or *elbow distance*) is the optimal visual distance for reading and other near work. It is the distance from the elbow on the desk to the first *knuckle* (prominence of a joint connecting the finger to the hand).

The ideal *TV viewing distance* is 1.9 times the screen width, since then this width occupies a 30° angle from the viewing position. For multiple-row seating in the home theater, a viewing angle 26–36° is recommended.

The **Lechner distance** is the optimal viewing distance at which the human eye can best process the details given by High Definition TV resolution. For example, it is about 1.7 or 2.7 m for a 1080 HD TV with a screen size of 42 or 69 inches.

Lateral masking (or *crowding*) is impairment of peripheral object identification by *flankers* (nearby objects). *Critical spacing* (or *crowding distance*) is the minimum target-flanker distance that does not produce crowding of a target of fixed size.

The *throw distance* is the distance that the projector needs to be from the screen to project the optimum image. The *viewing-distance factor* is a ratio of the width of a projected image to the maximum acceptable viewer's distance from it.

The **laser hazard distance** is the safe viewing distance for direct exposure to visible laser beams.

- **Gait distances**

  Gait stride is the distance traveled between successive footfalls of the same foot. It is the double of the *step length* (distance traveled while a foot is on the ground).

  Stride width (or *walking base*) is the side-to-side distance between the line of the two feet. Normally, it is 3–8 cm for adult but it increases with gait instability.

  The *Gait Deviation* (from normality) *Index* GDI is (Schwartz–Rosumalski, 2008) the **standardized Euclidean distance** (Chap. 17) in the 15D gait feature space between the abnormal state vector of a patient and the closest matching normal (mean of controls) state vector.

  The length of cane, when it is needed, should extend the distance from the distal wrist crease to the ground, when the person is placing arms at the sides.

  The average walking speed is 1–1.5 m/s; above 2 m/s, it is more efficient to run. Cadence for normal adults is 100–117 steps/min at preferred speed. As the body moves forward, its center of gravity moves vertically and laterally, with average displacement 5 cm and 6 cm, in a smooth sinusoidal pattern.

  Wearing high heels by women exaggerate some sex specific elements of female gait: greater pelvic rotation, increased lateral pelvic tilt, shorter strides and higher cadence. Millipedes have smooth wave-like polypedal gait. Some millipeds *Illacme* have 750 legs. No species with larger or odd number of legs are known.

  Most insects have a *tripod gait*, with front and back legs on one side moving in sync with the middle leg on the other side. But some dung beetles can gallop.

  Humans, birds and (occasionally) apes walk bipedally. Humans, birds, many lizards and (at their highest speeds) cockroaches run bipedally. But (Alexander, 2004) no animal walks or runs as we do: the trunk erect, almost straight knees at mid-stance, striking the ground with the heel alone and two-peaked force pattern in fast walking. Our walking, but not running, is relatively economical metabolically.

  A *pedometer* is a device, usually portable and electronic or electromechanical, that counts each step a person takes by detecting the motion of the person's hands or hips. Modern activity trackers, such as the Fitbit Tracker, Misfit Wearables and Razer Nabu, count the number of steps and, using it, distance walked or run.

- **Biodistances for nonmetric traits**

  In Physical Anthropology and Human Osteology (including Forensic Anthropology and Paleoanthropology), the *biodistances* (or *biological distances*) are the measures of relatedness between and within human groups, living or past, based on human cranial, skeletal or dental variation.

  Nonmetric traits are skeletal **nonmetric data** (binary, nominal or ordinal, cf. Chap. 17). The main distance statistics used to compare them between populations x and y are *Mahalanobis* D^2 *statistics*, i.e., square **Mahalanobis**

distance (Chap. 17) and, when the data are incomplete, the **mean measure of divergence**:

$$MMD = \frac{1}{n}\sum_{i=1}^{n}((\phi_{xi} - \phi_{yi})^2 - 4\frac{N_{xi} + N_{yi} + 1}{(2N_{xi} + 1)(2N_{yi} + 1)}).$$

Here, n is the number of traits used in the comparison, ϕ_{xi} and ϕ_{yi} are the transformed frequencies in radians of the i-th trait in the groups x, y, and N_{xi} and N_{yi} are the numbers of individuals scored for the i-th trait in the two groups.

The frequencies ϕ are obtained (in radians) from observed trait frequencies $\frac{k}{n}$ by the *Freeman–Tukey arcsine transformation*. The MMD can be negative. The *standardized MMD* (SMMD) is obtained by dividing MMD by its standard deviation.

- **Body distances in Anthropometry**

  Besides weight and circumference, the main metric (i.e., linear continuous, cf. Chap. 17) measurements in Anthropometry are between some body landmark points or planes. The main vertical distances from a standing surface are:

  – *stature* (to the top of the head);
  – *C7 level height* (to the first palpable vertebra from the hairline down, C7);
  – *acromial height* (to the *acromion*, i.e., the lateral tip of the shoulder);
  – *L5 level height* (to the first palpable vertebra from the tailbone up, L5);
  – *knee height* (to the *patella*, i.e., kneecap plane).

  The genotype gives 60 % of the phenotypic variation of human height (stature). It was about 1.63 and 1.83 m for *Neanderthal* 0.07 Ma ago and *Homo erectus* 1.8 Ma ago. The height of the average modern man ranges from 1.37 (Mbuti people of the Democratic Republic of the Congo) to 1.84 m (the Dutch). There is small (0.15–0.20) correlation between IQ and height within national populations.

  Examples of other body distances are:

  – *sitting height*: the distance from the top of the head to the sitting surface;
  – *popliteal* (or *stool*) height (seated): the distance between the underside of the foot to the underside of the thigh at the knee;
  – *hip breadth* (seated): the lateral distance at the widest part of the hips;
  – *biacromial breadth*: the distance between the acromions;
  – *buttock-knee length* : the distance from the buttocks to the patella;
  – *total foot length*: the maximum length of the right foot;

  In the thigh, there are the longest ones in the human body: bone (*femur*), muscle (*sartorius*) and nerve (*sciatic*).

- **Head and face measurement distances**

  The main linear dimensions of the cranium in Archeology are: lengths (of temporal bone, of tympanic plate, glabella-opistocranion), breadths (maximum cranial, minimum frontal, biauricular, mastoid), heights (of temporal bone, basion-bregma), thickness of the tympanic plate, and bifrontomolar-temporal distance.

Main viscerocranium measurements in Craniofacial Anthropometry are the *head width*, i.e., the (horizontal) maximum breadth of the head above the ears, and the *head length* (or *head depth*): the horizontal distance from the *nasion* (the top of the nose between the eyes) to the *opistocranion* (the most prominent point on the back of the head). The *cephalic index* of a skull is the percentage of width to length.

The **face length** *FL*: the distance between the *trichion* (midpoint on the forehead) and the *gnathion* (the lowest point of the midline of the lower jaw). It is divided by nasion and *subnasale* lines into three ("ideally", equal) parts. The *upper face height UFH* is the distance between brow and upper lip; *LFH* is the *lower face height*.

The **intercanthal distance** *IC* and **outercanthal distance** *OC*: the distances between inner or outer *canthi* (corners of eyes). The **face width** *FW* (or *bizygomatic width*) is the maximum distance between lateral surfaces of the cheeks. Let EW be the eye width and *NW* be the nose width (or **interalar distance**).

According to Schmid–Marx–Samal, 2007, among neoclassical canons of face, proposed by artists, the most related to attractiveness are: IC = NW = EW, FW = 4× NW and nose length = ear length = forehead height = LFH. Among aesthetically pleasing facial golden ratios $\frac{1+\sqrt{5}}{2} \approx 1.618$ are: mouth width (or lips-chin distance) to IC (or NW), ear length to NW and the *superior facial index* $\frac{UFH}{FW}$.

According to Lefevre et al., 2013, the ratios FWHR= $\frac{FW}{UFH}$ and $\frac{FW}{LFH}$ correlate with "maleness" (testosterone in mating context, aggression, status-striving etc.). On average, men have much larger faces (below the pupils), lips and chins; wider cheekbones, jaws and nostrils; and longer lower faces, but much lower eyebrows.

In Face Recognition, the sets of (vertical and horizontal) *cephalofacial dimensions*, i.e., distances between *fiducial* (standard of reference for measurement) facial points, are used. For example, the following five independent facial dimensions are derived in [Fell97] for facial gender recognition: *IC*, *NW*, *FW* and (vertical ones) eye-to-eyebrow distance *EB* and distance *EM* between eye midpoint and horizontal line of mouth. "Femaleness" relies on large *IC*, *EB* and small *NW*, *FW*, *EM*. In general, a face with larger *EB* is perceived as baby-like and less dominant.

Humans have the innate ability to recognize and distinguish (friend from foe) between faces from a distance. Facial attractiveness is a cultural construct found in all extant societies, and males strongly prefer neotenous facial features in females.

Pallett–Link–Lee, 2009, claim that Caucasian females with $EM \approx 36\,\%$ of *FL* and the **interpupillary distance** $\approx 46\,\%$ of *FW*, have the both, most attractive and average, faces. On the other hand, Japanese standards of beautiful eyes changed with Westernization (comparing Meiji and modern portraits): the mean ratios to *corneal diameter* (horizontal white-to-white distance) of eye height and upper lid-to-eyebrow distance are moved from 0.62 and 2.21 to 0.82 and 1.36.

Among the symmetry pairs, main contributors to attractiveness are the nose, mouth and upper tips of the lips. Comparing 3D facial scans with their mirror images, Djordjevic et al., 2011, found that on average, males and females have 53.5 % and 58.5 % symmetry of the whole face. Cf. **distances from symmetry** in Chap. 21. Alare and pogonio were the most and the least symmetric landmark.

Modifying traditional canons of Facial Plastic Surgery (based on horizontal and vertical planes in 2D), Young, 2008, asserts that the iris, nasal tip and lower lip are the most prominent structures within the eye, nose and mouth. All distances which he proposed as elements of facial beauty are multiples of the diameter of the iris.

- **Gender-related body distance measures**

  The main gender-specific body configuration features are:

  for females, WHR (*waist-to-hip ratio*), LBR (*leg-to-body ratio*) and BMI (*body mass index*), i.e., the ratio of the weight in kg and squared height in m^2;

  for males, height, SHR (*shoulder-to-hip ratio*) and WCR (*waist-to-chest ratio*);

  androgen equation (three times the shoulder width minus one times the pelvic width) and HGS (hand grip strength), which are higher for males;

  right *second-to-fourth digit* (index to ring finger) *ratio 2D-4D*, which is lower (as well as prenatal testosterone is higher) for males in the same population;

  anogenital distance (cf. **distances in Medicine**), which is larger for males;

  person's *center of mass* (slightly below the belly button), higher for males.

  The *angle of lumbar curvature* θ is the angle between the thoracic back and buttocks. Its mean value is 43.25° for men, 47.19° for women and 45.5° for reproductively viable women. This wedging in third-to-last lumbar vertebra shifts the center of mass of pregnant woman back over hips, reducing hip torque by over 90 %. But excessive θ (hyperlordosis) also lead to muscular fatigue and lower back pain; the optimal θ is 45.5°. Men prefer the women for whom the buttocks protrusion θ is close to optimal and attributable to vertebral wedging, not buttock mass.

  The main predictor for developmental instability, increasing with age, is FA (*fluctuating asymmetry*), i.e., the degree to which the size of bilateral body parts deviates from the population mean, aggregated across several traits. Women (men) prefer the odors, faces and voices of men (women) with lower FA. Old men (but not women) with lower facial FA have better cognitive ability and reaction time.

  BMI and WHR indicate the percentage of body fat and fat distribution, respectively; they are used in medicine to assess risk factors. A WHR of 0.7 for women and 0.9 for men correlates with general health and fertility. As a cue to female body attractiveness for men, the ideal WHR varies from 0.6 in China to 0.85 in Africa. In general, men tend to prefer BMI 17–20 in women; it correspond, usually, to women of 18–20 yers old.

  In Fan et al., 2005, the main visual cue to male body attractiveness is VHI (*volume-to-height index*), i.e., the ratio of the volume in liters and squared height in m^2. Mautz et al., 2013, claim that women prefer taller men with higher SHR

and FPL (flaccid penis length), but attractiveness increased quickly until FPL reached 7.6 cm and then began to slow down. Stulp et al., 2013, found that on average among speed-daters, women choose 25 cm taller men, while men choose only 7 cm shorter women, resulting in suboptimal (19 cm) pair formation.

In terms of somatotype, women prefer mesomorphs (muscular men) followed by ectomorphs (lean men) and endomorphs (heavily-set men).

In terms of BWH (bust-waist-hips), the average Playboy centrifold 1955–1968 has (90.8, 58.6, 89.3) cm, close to the ideal hourglass figures (90, 60, 90) cm and (36, 24, 36) inch. But dietitians advocate waistline 80–85 cm and at most half-height.

In conversation, women are better at detecting mismatch between meaning and *prosody* (intonation and rhythm of speech), but worse at vocabulary's variety. Men's vocal cords are larger and their vocal tracts are longer than women's; so, they speak about an octave lower. In English, women use less nonstandard forms and often use different color terms and descriptive phrases from men. Pirahã (Amazon's tribe) men use larger articulatory space and, say, only men use "s".

Used as obesity indices, WC, ICO=WC/height and (proposed by Krakauer–Krakauer, 2012) ABSI=WC/(BMI$^{\frac{2}{3}}$height$^{\frac{1}{2}}$) are better predictors of mortality than BMI.

- **Sagittal abdominal diameter**

  Sagittal abdominal diameter (SAD) is the distance between the back and the highest point of the abdomen, measured while standing. It is a measure of visceral obesity. Normally, SAD should be under 25 cm. SAD$>$ 30 cm correlates to insulin resistance and increased risk of cardiovascular and Alzheimer's diseases.

  A related measurement is SAH, the abdominal height as measured in the supine position. *Inter-recti distance* (IRD) is the width of the *linea alba* (a fibrous structure that runs down the midline of the abdomen).

- **Body distances for clothes**

  Humans lost body hair around 1 Ma ago and began wearing clothes $\approx$ 0.17 Ma ago.

  The European standard EN 13402 "Size designation of clothes" defined, in part EN 13402-1, a standard list of 13 body dimensions (measured in cm) together with a method for measuring each one on a person. These are: body mass, height, foot length, arm length, inside leg length, and girth for head, neck, chest, bust, under-bust, waist, hip, hand. Examples of these definitions follow.

  Foot length: horizontal distance between perpendiculars in contact with the end of the most prominent ones, toe and part of the heel, measured with the subject standing barefoot and the weight of the body equally distributed on both legs.

  Arm length: distance from the armscye/shoulder line intersection (acromion), over the elbow, to the far end of the prominent wrist bone (ulna), with the subject's right fist clenched and placed on the hip, and with the arm bent at 90°.

  Inside leg length: distance between the crotch and the soles of the feet, measured in a straight vertical line with the subject erect, feet slightly apart, and the weight of the body equally distributed on both feet.

For clothes where a larger step size is sufficient to select the right product, the standard also defines a letter code: XXS, XS, S, M, L, XL, XXL, 3XL, 4XL or 5XL. This code represents the bust girth for women and the chest girth for men.

Vanity sizing (or *size deflation*) is the marketing phenomenon of ready-to-wear clothing of the same nominal size becoming bigger in physical size over time.

- **Distance handling**

  Distance handling refers to the training of gun dogs (to assist hunters in finding and retrieving game) or sport dogs (for canine agility courses) where a dog should be able to work away from the handler.

  In agility training, the *lateral distance* is the distance that the dog maintains parallel to the handler, and the *send distance* is the distance that the dog can be sent straight away from the handler.

- **Racing distances**

  In Racing, **length** is an informal unit of distance to measure the distance between competitors; for example, in boat-racing it is the average length of a boat.

  The **horse-racing distances** and winning margins are measured in terms of the **horses** (or **lengths**, i.e., lengths of a horse, $\approx$ 8 feet (2.44 m), ranging from half the length to the **distance**, i.e., more than 20 lengths. The *length* is often interpreted as a unit of time equal to $\frac{1}{5}$ second. Smaller margins are: *short-head*, *head*, or *neck*. A *distance flag* is a flag held at a distance pole in a racecourse.

  The distances a horse travels without stops (15–25 km) and it travels in a day (40–50 km) or hour (6 km) were used as Tatar and Persian units of length.

- **Triathlon race distances**

  The **Ironman distance** (or **Ultra distance**) started in Hawaii, 1978, is a 3.86 km swim followed by a 180 km bike and a 42.195 km (*marathon distance*) run.

  The international **Olympic distance** started in Sydney, 2000, is 1.5 km (*metric mile*), 40 km and 10 km of swim, cycle and run, respectively.

  Next to it are the **Sprint distance** 0.75, 20, 5 km, the **Long Course** (or *Half Ironman*) 1.9, 90, 21.1 km and the *ITU long distance* 3, 80, 20 km.

- **Running distances**

  In Running, usually, *sprinting* is divided into 100, 200, 400 m, *middle distance* into 800, 1500, 3000 m and *long distance* into 5, 10 km.

  LSD (long slow distance) is a is a form of aerobic endurance training in running and cycling, in which distances longer, than those of races, are covered, but at a slower pace.

  Fartlek (or *speed play*) is an approach to distance-running training involving variations of pace and aimed at enhancing the psychological aspects of conditioning.

  Race-walking is divided into 10, 20, 50 km, and *relay races* into $4 \times 100, 4 \times 200, 4 \times 300, 4 \times 400$ m. *Distance medley relay* is made up of 1200, 400, 800, 1600 m legs.

Besides track running, runners can compete on a measured course, over an established road (*road running*), or over open or rough terrain (*cross-country running*).

Roughly, 4 units of running distance are time-equivalent to 1 unit of swimming distance. Also, one have to walk about twice the distance to burn the same amount of calories as running it. Running workout times should be multiplied by 3.5 when aiming for a similar training effect from cycling. A multiple of 0.75–1 should be used for an indoor rowing-to-running ratio.

- **Distance swimming**

  Distance swimming is any swimming race $>$ 1.5 km; usually, within 24–59 km.

  DPS (distance per swim stroke) is a metric of swimming efficiency used in training. In Rowing, *run* is the distance the boat moves after a stroke.

- **Distance jumping**

  The four Olympic jumping events are: *long jump* (to leap horizontally as far as possible), *triple jump* (the same but in a series of three jumps), *high jump* (to reach the highest vertical distance over a horizontal bar), and *pole vault* (the same but using a long, flexible pole).

  The world's records, as in 2013: 8.95 , 18.29 , 2.45, and 6.14 m, respectively.

- **Distance throwing**

  The four Olympic throwing events are: shot put, discus, hammer, and javelin.

  The world's records, as in 2013: 23.12 , 74.08 , 86.74 m, and 98.48 m, respectively.

  As in 2013, the longest throws of an object without any velocity-aiding feature are 427.2 m with a boomerang and 406.3 m with a flying ring *Aerobie*.

  Distance casting is the sport of throwing a fishing line with an attached sinker (usually, on land) as far as possible.

  Darts is a sport and a pub game in which darts are thrown at a *dartboard* (circular target) fixed to a wall so that the bullseye is 172.72 cm from the floor. The *oche* (line behind which the throwing player must stand) is 236.86 cm from the dartboard.

- **Archery target distances**

  FITA (Federation of International Target Archery, organizing world championships) **target distances** are 90, 70, 50, 30 m for men and 70, 60, 50, 30 m for women, with 36 arrows shot at each distance. Farthest accurate shot is 200 m.

  In Archery, *brace height* (or *fistmele*) is the distance from the string, when the bow is strung, to the pivot point of the bow's grip, i.e., the handle of a bow.

- **Bat-and-ball game distances**

  The best known bat-and-ball games are bowling (cricket) and baseball. In cricket, the field position of a player is named roughly according to its polar coordinates: one word (*leg, cover, mid-wicket*) specifies the angle from the batsman, and this word is preceded by an adjective describing the distance from the batsman. The *length* of a delivery is how far down the *pitch* (central strip of the cricket field) towards the batsman the ball bounces.

This distance is called *deep* (or *long*), *short* and *silly distance* if it is, respectively, farther away, closer and very close to the batsman. The distance further or closer to an extension of an imaginary line along the middle of the pitch bisecting the stumps, is called *wide* or *fine distance*, respectively.

In baseball, a *pitch* is the act of throwing a baseball toward home plate to start a play. The standard professional *pitching distance*, i.e., the distance between the front (near) side of the pitching rubber, where a pitcher start his delivery, and home plate is 60 feet 6 inches ($\approx$ 18.4 m). The distance between bases is 90 feet.

- **Three-point shot distance**

  In basketball, the *three-point line* is an arc at a set radius, called **three-point shot distance**, from the basket. A field goal made from beyond this line is worth three points. In international basketball, this distance is 6.25 m.

  Goals in *indoor soccer* are worth 1, 2 or 3 points depending upon distance.

- **Football distances**

  In *association football* (or *soccer*), the average distance covered by a player in a men's professional game is 9–10 km. It consists of about 36 % jogging, 24 % walking, 20 % cruising submaximally, 11 % sprinting, 7 % moving backwards and 2 % moving in possession of the ball. The ratio of low- to high-intensity exercise is about 2.2:1 in terms of distance, and 7:1 in terms of time.

  In *American football*, one *yard* means usual yard (0.9144 m) of the distance in the direction of one of the two goals. A field is 120 yards long by 53.3 yards wide. A team possessing the ball should advance at least the *distance* (10 yards) in order to get a new set of (4 or 3) *downs*, i.e., periods from the time the ball is put into play to the time the play is whistled over by the officials. *Yardage* is the amount of yards gained or lost during a play, game, season, or career.

- **Golf distances**

  In golf, *carry* and *run* are the distances the ball travels in the air and once it lands.

  The golfer chooses a golf club, grip, and stroke appropriate to the distance. The *drive* is the first shot of each hole made from the area of *tees* (peg markers) to long distances. The *approach* is used in long- to mid-distance shots.

  The *chip* and *putt* are used for short-distance shots around and, respectively, on or near the green. The maximum distance a typical golfer can hit a ball with a particular club is the club's *hitting distance*.

  A typical *par* (standard score) 3, 4, 5 holes measure 229, 230–430, $\geq$431 m. The greatest recorded drive distance, carry, shot with one hand are 471, 419, 257 m.

  Some manufacturers stress the large range of a device in the product name, say, *Ultimate Distance* golf balls (or softball bates, spinning reels, etc.).

- **Fencing distances**

  In combative sports and arts, *distancing* is the appropriate selection of the distance between oneself and a combatant throughout an encounter.

  For example, in fencing, the *distance* is the space separating two fencers, while the distance between them is the *fencing measure*.

A *lunge* is a long step forward with the front foot. A *backward spring* is a leap backwards, out of distance, from the lunge position.

The following five distances are distinguished: *open distance* (farther than advance-lunge distance), *advance-lunge distance*, *lunging distance*, *thrusting distance* and *close quarters* (closer than thrusting distance).

In Japanese martial arts, **maai** is the *engagement distance*, i.e., the exact position from which one opponent can strike the other, after factoring in the time it will take to cross their distance, angle and rhythm of attack. In kendo, there are three maai distances: *to-ma* (long distance), *chika-ma* (short distance) and, in between, *itto-ma* $\approx$ 2 m, from which only one step is needed in order to strike.

- **Distance in boxing**

  The distance is boxing slang for a match that lasts the maximum number (10 or 12) of scheduled rounds. The longest boxing match (with gloves) was on April 6–7, 1893, in New Orleans, US: Bowen and Burke fought 110 rounds for 7.3 h.

- **Soaring distances**

  Soaring is an air sport in which pilots fly unpowered aircraft called *gliders* (or *sailplanes*) using currents of rising air in the atmosphere to remain airborne.

  The *Silver Distance* is a 50 km unassisted straight line flight. The *Gold* and *Diamond Distance* are cross-country flights of 300 km and over 500 km, respectively.

  Possible courses—*Straight*, *Out-and-Return*, *Triangle* and 3 *Turnpoints Distance*—correspond to 0, 1, 2 and 3 turnpoints, respectively.

  Using open class gliders, the world records in free distance, in absolute altitude and in gain of height are: 3008.8 km (by Olhmann and Rabeder, 2003), 15,460 m (by Fossett and Enevoldson, 2006) and 12,894 m (by Bikle, 1961). The distance record with a paraglider is 501.1 km (by Hulliet, 2008).

  Eustace jumped in 2014 from a balloon at 41,419 m, setting world records in exit altitude and total free fall distance. But, since Eustace used a stabilizing drogue parachute while Baumgartner, 2012, did not, their free fall distance and vertical speed records are in different categories. A stewardess Vesna Vulović survived in 1972 a fall of 10 km, when JAT Flight 367 was brought down by explosives.

- **Aviation distance records**

  Absolute general aviation world records in flight distance without refueling and in altitude are: 41,467.5 km by Fossett, 2006, and 37,650 m by Fedotov, 1977.

  Distance and altitude records for free manned balloons are, respectively: 40,814 km (by Piccard and Jones, 1999) and 41,425 m (by Eustace, 2014).

  The general flight altitude record is 112,010 m by Binnie, 2004, on a rocket plane.

  The longest (13,804 km during 16 h 55 min) nonstop scheduled passenger route in 2015 was Qantas Flight 8 from Dallas to Sydney.

  The *Sikorsky prize* (US $250,000) will be awarded for the first flight of a human-powered helicopter which will reach an altitude of 3 m, stay airborne for

at least 1 min remaining within 10m×10m square. In 2012, a craft (32.2 kg) by a team at the University of Maryland flew 50 s at 61 cm up.

- **Amazing greatest distances**

  Examples of such distances among Guinness world records are the greatest distances:

  – being fired from a cannon (59 m),
  – walked unsupported on tightrope (130 m),
  – run on a static cycle in 1 min (2.04 km),
  – moon-walked (as Michael Jackson) in 1 h (5.125 km),
  – covered three-legged (the left leg of one runner strapped to the right leg of another runner) in 24 h (33 km),
  – jumped with a pogo stick (37.18 km),
  – walked with a milk bottle balanced on the head (130.3 km),
  – covered by a car driven on its side on two wheels (371.06 km),
  – hitchhiked with a fridge (1650 km).

  Amazing race *The* 2904 is to drive the 2904 miles from New York City to San Francisco for $2904 including the vehicle, fuel, food, tolls, repairs and tickets.

- **Isometric muscle action**

  An **isometric muscle action** refers to exerting muscle strength and tension without producing an actual movement or a change in muscle length.

  Isometric action training is used mainly by weightlifters and bodybuilders. Examples of such *isometric exercises*: holding a weight at a certain position in the range of motion and pushing or pulling against an immovable external resistance.

29.2 Equipment Distances

- **Motor vehicle distances**

  The **safe following distance**: the reglementary distance from the vehicle ahead of the driver. For reglementary perception-reaction time of at least 2 s (the *two-second rule*), this distance (in m) should be $0.56 \times v$, where v is the speed (in km/h). Sometimes the *three-second rule* is applied. The stricter rules are used for heavy vehicles (say, at least 50 m) and in tunnels (say, at least 150 m).

  The **perception-reaction distance** (or **thinking distance**): the distance a vehicle travels from the moment the driver sees a hazard until he applies the brakes (corresponding to human perception time plus reaction time). Physiologically, it takes 1.3–1.5 s, and the brake action begins 0.5 s after application.

  The **braking distance**: the distance a motor vehicle travels from the moment the brakes are applied until the vehicle completely stops.

  The (total) **stopping distance**: the distance a motor vehicle travels from where the driver perceives the need to stop to the actual stopping point (corresponding to the vehicle reaction time plus the vehicle braking capability).

The **crash distance**: (or *crushable length*): the distance between the driver and the front end of a vehicle in a frontal impact (or, say, between the pilot and the first part of an airplane to impact the ground).

The **skidding distance** (or *length of the skid mark*): the distance a motor vehicle *skidded*, i.e., slid on the surface of the road (from the moment of the accident, when a wheel stops rolling) leaving a rubber mark on the road.

The **cab-to-frame** (or **cab-to-end**, *CF*, *CE*): the distance from back of a truck's cab to the end of its frame.

The **distance to empty** (or *DTE*) displays the estimated distance the vehicle can travel before it runs out of fuel. The warning lamp start blinking at 80 km.

The **acceleration-deceleration distance** of a vehicle, say, a car or aircraft, is (Drezner–Drezner–Vesolowsky, 2009) the cruising speed v times the travel time. For a large origin-destination distances d, it is $d + \frac{v^2}{2}(\frac{1}{a} + \frac{1}{b})$, where a is the acceleration at the beginning and $-b$ is the deceleration at the end.

- **Aircraft distances**

The maximum distance the aircraft can fly without refueling is called the **maximum range** if it fly with its maximum cargo weight and the **ferry range** if it fly with minimum equipment.

For a warplane, the *combat range* is the maximum distance it can fly when carrying ordnance, and the *combat radius* is a the maximum distance it can travel from its base, accomplish some objective, and return with minimal reserves.

The FAA **lowest safe altitude**: 1000 feet (305 m) above the highest obstacle within a horizontal distance of 2000 feet.

A **ceiling** is the maximum *density altitude* (height measured in terms of air density) an aircraft can reach under a set of conditions.

A *flight level* (FL) is specific barometric pressure, expressed as a nominal altitude in hundreds of feet, assuming standard sea-level pressure datum of 1013.25 hPa.

The *transition altitude* is the altitude above sea level at which aircraft change from the use of altitude to the use of FL's; in the US and Canada, it is 5500 m).

The **gust-gradient distance**: the horizontal distance along an aircraft flight path from the edge of the *gust* (sudden, brief increase in the speed of the wind) to the point at which the gust reaches its maximum speed.

The **distance-of-turn anticipation**: the distance, measured parallel to the anticipated course and from the earliest position at which the turn will begin, to the point of route change.

The **landing distance available** (LDA): the length of runway which is declared available and suitable for the ground run of an airplane landing. The **landing roll**: the distance from the point of touchdown to the point where the aircraft can be brought to a stop or exit the runway. The **actual landing distance** (ALD): the distance used in landing and braking to a complete stop (on a dry runway) after crossing the runway threshold at 50 feet (15.24 m); it can be affected by various operational factors. The FAA **required landing distance**

(used for dispatch purposes): a factor of 1.67 of ALD for a dry runway and 1.92 for a wet runway.

The **takeoff run available** (TORA): the *runway distance* (length of runway) declared suitable for the ground run of an airplane takeoff. The **takeoff distance available** (TODA): TORA plus the length of the clearway, if provided. The **emergency distance** (ED or *accelerate-stop distance*): the runway plus *stopway length* (able to support the airplane during an aborted takeoff) declared suitable for the acceleration and deceleration of an airplane aborting a takeoff.

The **arm's distance**: the horizontal distance that an item of equipment is located from the *datum* (imaginary vertical plane, from which all horizontal measurements are taken for balance purposes, with the aircraft in level flight attitude).

In the parachute deployment process, the **parachute opening distance** is the distance the parachute system dropped from pulling to full inflation of the canopy, while the **inflation distance** is measured from *line stretch* (when the suspension lines are fully extended) to full inflation.

Wing's aspect ratio (of an aircraft or bird) is the ratio $AR = \frac{b^2}{S}$ of the square of its span to the area of its planform. If the length of the *chord* (straight line joining the leading and trailing edges of an airfoil) is constant, then AR is length-to-breadth **aspect ratio**; cf. Chap. 1. A better measure of the aerodinamic efficiency is the *wetted aspect ratio* $\frac{b^2}{S_w}$, where S_w is the entire surface area exposed to airflow.

- **Ship distances**

  Endurance distance: the total distance that a ship or ground vehicle can be self-propelled at any specified endurance speed.

  Distance made good: the distance traveled by the boat after correction for current, *leeway* (the sideways movement of the boat away from the wind) and other errors that may be missed in the original distance measurement.

  Log: a device to measure the distance traveled which is further corrected to a distance made good. Hitherto, sea distances were measured in units of a day's sail.

  Leg (nautical): the distance traveled by a sailing vessel on a single tack.

  Berth: a safety margin to be kept from another vessel or from an obstruction.

  Length overall (LOA): the maximum length of a vessels's hull along the waterline.

  Length between perpendiculars (LPP): the length of a vessel along the waterline from the main bow perpendicular member to the main stern perpendicular member.

  Freeboard: the height of a ship's hull above the waterline. *Draft* (or *draught*): the vertical distance between the waterline and the keel (bottom of the hull).

  GM-distance (or *metacyclic height*) of a ship: the distance between its center of gravity G and the *metacenter*, i.e., the projection of the *center of buoyancy* (the center of gravity of the volume of water which the hull displaces) on the centerline of the ship as it heels. This distance, 1–2 m, determines ship's stability.

Distance line (in Diving): a marker (say, 50 m of thin polypropylene line) of the shortest route between two points. It is used, as Ariadne's thread, to navigate back to the start in conditions of low visibility, water currents or *penetration diving* into a space (cave, wreck, ice) without vertical ascent back.

- **Distance-to-fault**

  In Cabling, DTF (**distance-to-fault**) is a test using time or frequency domain reflectometers to locate a fault, i.e., discontinuity caused by, say, a damaged cable, water ingress or improperly installed/mated connectors.

  The amount of time a pulse (output by the tester into the cable) takes for the signal (reflected by a discontinuity) to return can be converted to distance along the line and provides an approximate location of the reflection point.

  Protective *distance relays* respond to the voltage and current. The *impedance* (their ratio) per km being constant, these relays respond to the relay-fault distance.

- **Distances in Forestry**

  In Forestry, the **diameter at breast height** (d.b.h.) is a standard measurement of a standing tree's diameter taken at 4.5 feet ($\approx$ 1.37 m) above the ground. The *diameter at ground line* (d.g.l.) is the diameter at the estimated cutting height. The *diameter outside bark* (d.o.b.) is a measurement in which the thickness of the bark is included, and d.i.b. is a measurement in which it is excluded.

  The *crown height* is the vertical distance of a tree from ground level to the lowest live branch of the crown. The *merchantable height* is the point on a tree to which it is salable. A log is a length of tree suitable for processing into a wood product.

  Optimum road spacing is the distance between parallel roads that gives the lowest combined cost of *skidding* (log dragging) and road construction costs per unit of log volume. The *skid distance* is the distance logs are dragged.

  A *yarder* is a piece of equipment used to lift and pull logs by cable from the felling site to a landing area or to the road's side. The **yarding distance** is the distance from which the yarder takes logs. The **average yarding distance** is the total yarding distance for all turns divided by the total number of turns.

  A *spar tree* is a tree used as the highest anchor point in a cable logging setup. A *skyline* is a cableway stretched between two spar trees and used as a track for a log carriage. The distance spanned by a skyline is called its *reach*.

  Understory is the area of a forest which grows at the lowest height level between the forest *floor* and the *canopy* (layer formed by mature tree crowns and including other organisms). Perhaps, a half of all life on Earth could be found in canopy. The *emergent layer* contains a small number of trees which grow above the canopy.

- **Distance in Military**

  In the Military, the term **distance** usually has one the following meanings:

  the space between adjacent individual ships or boats measured in any direction between foremasts;

  the space between adjacent men, animals, vehicles, or units in a formation measured from front to rear;

the space between known reference points or a ground observer and a target, measured in m (artillery), or in units specified by the observer. This distance along an imaginary straight line from the spotter is called *observer-target distance*.

In amphibious operations, the *distant retirement area* is the sea area located to seaward of the landing area, and the *distant support area* is the area located in the vicinity of the landing area but at considerable distance seaward of it.

Strategic depth refers to the distances between the front lines and the combatants' industrial and population core areas.

In military service, a **bad distance** of the troop means a temporary intention to extract itself from war service. This passing was usually heavily punished and equated with that of *desertion* (an intention to extract itself durably).

In US military slang, BFE (Big Fucking Empty) is an extremely distant or isolated deployment or location; used mostly about the disgust at the distance or remoteness. Also, a *klick* means a distance of 1 km.

- **Interline distance**

  In Engineering, the **interline distance** is the minimum distance permitted between any two buildings within an explosives operating line, in order to protect buildings from propagation of explosions due to the blast effect.

- **Scaled distance**

  The **scaled distance** (*SD*) is the parameter used to measure the level of vibration from a blast, when effects of the frequency characteristics are discounted.

  The minimum safe distance from a blast to a monitoring location is $SD \times \sqrt{W}$, where W denotes the maximum per delay (instantaneous) charge weight.

- **Standoff distance**

  The **standoff distance** is the distance of an object from the source of an explosion (in Warfare), or from the delivery point of a laser beam (in laser material processing). Also, in Mechanics and Electronics, it is the distance separating one part from another; for example, for insulating (cf. **clearance distance**), or the distance from a noncontact length gauge to a measured material surface.

- **Buffer distance**

  In Nuclear Warfare, the **horizontal buffer distance** is the distance which should be added to the radius of safety in order to be sure that the specified degree of risk will not be exceeded. The **vertical buffer distance** is the distance which should be added to the fallout safe-height of a burst, in order to determine a desired height of burst so that militari significant fallout will not occur.

  The term *buffer distance* is also used more generally as, for example, the buffer distance required between sister stores or from a high-voltage line.

  Cf. **clearance distance** and, in Chap. 25, **setback distance**.

- **Offset distance**

  In Nuclear Warfare, the **offset distance** is the distance the desired (or actual) ground zero is offset from the center of the area (or point) target.

In Computation, the *offset* is the distance from the beginning of a string to the end of the segment on that string. For a vehicle, the **offset** of a wheel is the distance from its hub mounting surface to the centerline of the wheel.

The term *offset* is also used for the **displacement** vector (Chap. 24) specifying the position of a point or particle in reference to an origin or to a previous position.

- **Range of ballistic missile**

  Main **ranges of ballistic missiles** are *short* (at most 1000 km), *medium* (1000–3500 km), *long* (3500–5500 km) and *intercontinental* (at least 5500 km).

  Tactical and *theatre* ballistic missiles have ranges 150–300 and 300–3500 km.
- **Proximity fuse**

  The **proximity fuse** is a fuse that is designed to detonate an explosive automatically when close enough to the target.
- **Sensor network distances**

  The **stealth distance** (or *first contact distance*): the distance traveled by a moving object (or intruder) until detection by an active sensor of the network (cf. **contact quasi-distances** in Chap. 19); the *stealth time* is the corresponding time.

  The **first sink contact distance**: the distance traveled by a moving object (or intruder) until the monitoring entity can be notified via a sensor network.

  The **miss distance**: the distance between the lines of sight representing estimates from two sensor sites to the target (cf. the **line-line distance** in Chap. 4).

  The **sensor tolerance distance**: a **range distance** within which a localization error is acceptable to the application (cf. the **tolerance distance** in Chap. 25).

  The actual distances between some pairs of sensors can be estimated by the time needed for a two-way communication. The positions of sensors in space can be deduced (cf. **Distance Geometry Problem** in Chap. 15) from those distances.
- **Proximity sensors**

  Proximity (or *distance*) **sensors** are varieties of ultrasonic, laser, photoelectric and fiber optic sensors designed to measure the distance from itself to a target. For such laser range-finders, a special *distance filter* removes measurements which are shorter than expected, and which are therefore caused by an unmodeled object. The *blanking distance* is the minimum range of an ultrasonic proximity sensor.

  The *detection distance* is the distance from the detecting surface of a sensor head to the point where a target approaching it is first detected. The *maximum operating distance* is its maximum detection distance from a standard modeled target, disregarding accuracy. The *stable detection range* is the detectable distance range in which a standard detected object can be stably detected with respect to variations in the operating ambient temperature and power supply.

  The *resolution* is the smallest change in distance that a sensor can detect. The *span* is the working distance between measurement range endpoints over which the sensor will reliably measure displacement. The *target standoff* is the distance from the face of the sensor to the middle of the span.

Distance constant of a metereological sensor is the length of fluid flow past required to cause it to respond to 63.2 % (i.e., $1 - \frac{1}{e}$) of a step change in speed.

- **Precise distance measurement**

  The resolution of a TEM (transmission electronic microscope) is about 0.2 nm (2×10^{-10} m). This resolution is 1000 times greater than a light microscope and about 500,000 times greater than that of a human eye which is 576 mega pixel. However, only nanoparticles can fit in the vision field of an electronic microscope.

  The methods, based on measuring the wavelength of laser light, are used to measure macroscopic distances nontreatable by an electronic microscope. But the uncertainty of such methods is at least the wavelength of light, say, 633 nm.

  The recent adaptation of *Fabry–Perot metrology* (measuring the frequency of light stored between two highly reflective mirrors) to laser light permits the measuring of relatively long (up to 5 cm) distances with an uncertainty of only 0.01 nm.

  The main devices used for low accuracy distance measurement are the rulers, engineer's scales, calipers and surveyor's wheels.

- **Laser distance measurement**

  Lasers measure distances without physical contact. They allow for the most sensitive and precise length measurements, for extremely fast recording and for the largest measurement ranges. The main techniques used are as follows.

  Triangulation (cf. **laterations**) is useful for distances from 1 mm to many km. *Pulse measurements*, used for large distances, measure the time of flight of a laser pulse from the device to some target and back. The *phase shift method* uses an intensity-modulated laser beam. *Frequency modulation methods* involve frequency-modulated laser beams. *Interferometers* allow for distance measurements with an accuracy which is far better than the wavelength of the light used.

  The main advantage of laser distance measurement is that laser light has a very small wavelength, allowing one to send out a much more concentrated probe beam and thus to achieve a higher transverse spatial resolution.

- **Radio distance measurement**

  DME **distance measuring equipment**) is an air navigation technology that measures distances by timing the propagation delay of UHF signals to a *transponder* (a receiver-transmitter that will generate a reply signal upon proper interrogation) and back. DME will be phased out by global satellite-based systems: GPS (US), GLONASS (Russia), BeiDou (China) and Galileo (EU).

  The GPS (Global Positioning System) is a radio navigation system which permits one to get her/his position on the globe with accuracy of 10 m. It consists of 32 satellites and a monitoring system operated by the US Department of Defense. The nonmilitary part of GPS can be used by the purchase of an adequate receiver.

  The **GPS pseudo-distance** (or *pseudo-range*) is an approximation (since the receiver clock is not so perfect as the clock of a satellite) of the distance between

a satellite and a GPS receiver by the travel time of a satellite time signal to a receiver multiplied by the propagation time of the radio signal.

The receiver uses **trilatelation** in order to calculate its position (latitude, longitude, altitude) and speed by solving a system of equations using its pseudo-distances from 4 to 7 satellites and their positions. Cf. **radio distances** in Chap. 25.

- **Laterations**

  Lateration (or *ranging*) is the determination of the distance from one location or position to another one. Usually, the term *ranging* is used for moving objects, while *surveying* is used for static terrestrial objects. Active ranging systems operate with unilateral transmission and passive reflections, such as SONAR (SOund Navigation And Ranging), RADAR (RAdio Detection) and LIDAR (Light Detection).

  A *rangefinder* is a device for measuring distance from the observer to a target. Among applications are surveying, navigation, ballistics and photography.

  Triangulation is the process of locating a point P as the third point of a triangle with one known side (say, $[A, B]$ of length l) and two known angles (say, $\angle PAB = \alpha$ and $\angle PBA = \beta$). In $\mathbb{R}^2$, the perpendicular distance between P (say, a ship) and $[A, B]$ (say, a shore) is $\frac{l \sin\alpha \sin\beta}{\sin(\alpha+\beta)}$. Cf. point-line distance in Chap. 4.

  Technically more complicated, **trilateration** is locating a (possibly, moving) object P, using only its distances to known locations A_1, A_2 and A_3 (for example, to stations, beacons or satellites), as the overlap of $2D$ or $3D$ spheres, centered on them and having radii $d(P, A_1), d(P, A_2), d(P, A_3)$, respectively. Using additional stations, as in GPS, permits double-checking of the measurements. Cf. the **metric basis** in Chap. 1.

  More accurate generally, **multilateration** is locating a moving object P, using only two pairs (A_1, A_2), (B_1, B_2) of known locations, as the intersection of two curves defined by the relative distances $d(P, A_1) - d(P, A_2)$ and $d(P, B_1) - d(P, B_2)$, respectively.

- **Transmission distance**

  The **transmission distance** is a **range distance**: for a given signal transmission system (fiber optic cable, wireless, etc.), it is the maximal distance the system can support within an acceptable path loss level.

  For a given network of contact that can transmit an infection (or, say, an idea with the belief system considered as the immune system), the **transmission distance** is the path metric of the graph, in which edges correspond to events of infection and vertices are infected individuals. Cf. **forward quasi-distance** in Chap. 22.

- **Delay distance**

  The **delay distance** is a general term for the distance resulting from a given delay. For example, in a meteorological sensor, the *delay distance* is the length of a column of air passing a wind vane, such that the vane will respond to 50 % of a sudden angular change in wind direction. When the energy of a neutron is measured by the delay (say, t) between its creation and detection, the *delay distance* is $vt - D$, where v is its velocity and D is the source-detector distance.

In evaluations of visuospatial working memory (when the subjects saw a dot, following a 10-, 20-, or 30-s delay, and then drew it on a blank sheet of paper), the *delay distance* is the distance between the stimulus and the drawn dot.

- **Master-slave distance**

  Given a design (say, remote manipulation, surveillance, or data transmission system) in which one device (the *master*) fully controls one or more other devices (the *slaves*), the **master-slave distance** is a measure of distance between the master and slave devices. Cf. also Sect. 18.2.

- **Flow distance**

  In a manufacturing system, a group of machines for processing a set of jobs is often located in a serial line along a path of a transporter system.

  The **flow distance** from machine i to machine j is the total flow of jobs from i to j times the physical distance between machines i and j.

- **Single row facility layout**

  The **SRFLP** (or **single row facility layout problem**) is the problem of arranging (finding a permutation of) n departments (disjoint intervals) with given lengths l_i on a straight line so as to minimize the total weighted distance $\sum_{i=1}^{n-1} \sum_{i=j+1}^{n} w_{ij} d_{ij}$ between all department pairs. Here w_{ij} is the average daily traffic between two departments i and j, and d_{ij} is their **centroid distance**.

  Among applications of SRFLP, there are arranging machines in a manufacturing system, rooms on a corridor and books on a shelf.

- **Distance hart**

  In Technical Drawing, the **distance hart** means the distance from the center (the heart) of an object, as, for example, the distance hart of the toilet seat to the wall.

  The **center-to-center distance** (or **on-center**, *O.C.*) is the distance between the centers of two adjacent members (say, columns or pillars). Cf. **centroid linkage**, **centroid distance** in Chaps. 17, 19 and *center* **gear distance**.

- **Push distance**

  Precise machining of bearing rings should be preceded by part centering. In such a centering system, the **push distance** is the distance the slide must move towards the part in order to push it from its off-center position to the center of rotation.

- **Engine compression distance**

  Piston motors convert the compressed air energy to mechanical work through motion. **Engine compression distance** (or *compression height*) is the distance from the centerline of the wrist pin to the top deck of the piston.

- **Shift distance**

  A *penetrometer* is a device to test the strength of a material, say, soil. The penetrometer (usually cone-shaped) is pressed against material and the depth of the resulting hole is measured. The **shift distance** (or *friction-bearing offset*) is the distance between the cone's base and the mid-height of the friction sleeve above it.

- **Throat distance**

  The *swing* (size) of a drill/boring press is twice the **throat distance**, the distance from the center of the spindle to the column's edge.
- **Collar distance**

  In Mining, the **collar distance** is the distance from the top of the powder column to the collar of the blasthole, usually filled with stemming.
- **Quenching distance**

  Quenching is the rapid cooling of a workpiece; the **quenching distance** is the diameter of smallest hole a flame can travel through.

  The *run-up length* is the distance between initiation of a flame and onset of detonation (supersonic combustion wave). *Markstein number* is the *Markstein length*, measuring the effect of curvature on a flame, divided by the flame thickness.
- **Feeding distance**

  Carbon steel shrinks during solidification and cooling. In order to avoid resulting porosity, a **riser** (a cylindric liquid metal reservoir) provides liquid feed metal until the end of the solidification process.

  A riser is evaluated by its **feeding distance** which is the maximum distance over which a riser can supply feed metal to produce a radiographically sound (i.e., relatively free of internal porosity) casting. The **feeding length** is the distance between the riser and the furthest point in the casting fed by it.
- **Etch depth**

  Laser etching into a metal substrate produces craters. The **etch depth** is the central crater depth averaged over the apparent roughness of the metal surface.
- **Approach distance**

  In metal cutting, the **approach distance** is the linear distance in the direction of feed between the point of initial cutter contact and the point of full cutter contact.
- **Input and output distances**

  The **input distance** d_{in} of a machine M is a distance machine is moved by the *input* (applied on it) force F_{in}. The **output distance** d_{out} is a distance the *output* (exerted by it) force F_{out} results in. The *mechanical advantage* of M is $\frac{F_{out}}{F_{in}} = \frac{d_{in}}{d_{out}}$.

  For example, the *effort* (or *resistance*) *distance* and *load distance* on a lever are the distances from the fulcrum to the resistance and load, respectively.
- **Instrument distances**

  Examples of such distances follow.

  The *K-distance*: the distance from the outside fiber of a rolled steel beam to the web toe of the fillet of a rolled shape.

  The *end distance* and *edge distance* are the distances from a fastener (say, bolt, screw, rivet, nail) to the end and, respectively, edge of treated material.

  The *calibration distance*: the standard distance used in the process of adjusting the output or indication on a measuring instrument.

- **Gear distances**

  Given two meshed gears, the distance between their centers is called the *center distance*. Examples of other distances used in basic gear formulas follow.

  Pitch diameter: the diameter of the *pitch circle* (the circle whose radius is equal to the distance from the center of the gear to the pitch point).

  Addendum: the radial distance between the pitch circle and the top of the teeth.

  Dedendum: the depth of the tooth space below the pitch line. It should be greater than the addendum of the mating gear to provide *clearance*.

  Whole depth: the total depth of a tooth space, equal to addendum plus dedendum.

  Working depth: the depth of engagement (i.e., the sum of addendums) of two gears.

  Backlash: the play between mating teeth.
- **Threaded fastener distances**

  Examples of distances applied to nuts, screws and other threaded fasteners, follow.

  Pitch: the nominal distance between two adjacent thread roots or crests.

  Ply: a single thickness of steel forming part of a structural joint.

  Grip length: the total distance between the underside of the nut to the bearing face of the bolt head.

  Effective nut radius: the radius from the center of the nut to the point where the contact forces, generated when the nut is turned, can be considered to act.

  Effective diameter (or *pitch diameter*): the diameter of an imaginary cylinder coaxial with the thread which has equal metal and space widths.

  Virtual effective diameter: the effective diameter of a thread, allowing for errors in pitch and flank angles. *Nominal diameter*: the external diameter of the threads.

  Major and *minor diameters* are the diameters of imaginary cylinders parallel with the crests of the thread (i.e., the distance, crest-to-crest for an external or root-to-root for an internal thread), or, respectively, just touching the roots of an external (or the crests of an internal) thread.

  Thread height: the distance between thread's minor and major diameters measured radially. *Thread length*: the length of the portion of the fastener with threads.
- **Distance spacer**

  A **distance spacer** is a device for holding two objects at a given distance from each other. Examples of such components are: male-female *distance bolt*, *distance bush*, *distance ring*, *distance plate*, *distance sleeve*, *distance finger*, *distance gauge*.
- **Sagging distance**

  The brazeability of brazing sheet materials is evaluated by their **sagging distance**, i.e., the **deflection** of the free end of the specimen sheet after brazing.
- **Haul distance**

  In Engineering, the **haul distance** is the average distance material is transported from where it originates to where it is deposited.

- **Deflection**

  In Engineering, **deflection** is the degree, in distance or angle, to which a structural part is displaced under a load/stress.

  In general, it can be a specified amount of deviation, say, the distance an elastic body or spring moves when subjected to a force, the amount by which a propagating wave or a projectile's trajectory is bent, and so on.

- **Distances in Structural Engineering**

  Examples of such distances related to superstructures (mainly, bridges and buildings) follow; cf. also **bar-and-joint framework** in Chap. 15.

  For a building, its *length* is the distance between out ends of wall steel lines, *width* is the distance from outside of *eave strut* (piece spanning columns at roof's edge) of one sidewall to outside of eave strut of the opposite sidewall, *height* is the distance from finished floor level to the top outer point of the eave strut.

  A *bay* refers the space between architectural elements. *Bay depth* is the distance from the building's corridor wall to the outside window. *End bay length* is the distance from outside of the outer *flange* (longitudinal part of a beam) of endwall columns to centerline of the first interior frame column. *Interior bay length* is the distance between the centerlines of two adjacent interior main frame columns.

  Clear height (or *head room*) is the vertical distance from the floor to the bottom of the lowest hanging overhead obstruction, allowable for passage.

  A *beam* is a structural element that is capable of withstanding load primarily by resisting bending; *girder* is a support beam used in construction. A *truss* is a framed or jointed structure designed to act as a beam while each of its members is primarily subjected to longitudinal stress only. Given a truss or girder, its *effective length* is the distance between the points of support, *effective depth* is the perpendicular distance between the gravity lines, and *economic depth* is the depth, which will give satisfactory results from all standpoints and involving the least expenditure of money for properly combined first cost, operation, maintenance and repairs.

  Effective span is the distance between supports (centres of bearings) in any structure. The **bearing distance** is the length of a beam between its bearing supports.

  For a bridge, its *effective span* is the center-to-center distance of end pins, *structural height* is the maximum vertical distance from the uppermost point down to the lowest visible point, while the *deck height* is the maximum vertical distance from the *deck* (road bed) down to the ground or water surface.

  Clear headway: the vertical distance from the lowest part of the superstructure to the ground or water surface; it is the measure of height of the tallest vehicle that could pass through the bridge. *Clear waterway*: the horizontal distance over the water, measured perpendicularly to the centrelines of adjacent piers.

- **Clearance distance**

  In Civil Engineering and Safety, a **clearance distance** (or *separation distance*, *clearance*) is a physical distance or unobstructed space tolerance between the

loading and structural gauges as, for example, the distance between the lowest point on the vehicle and the road (*ground clearance*).

For vehicles going in a tunnel or under a bridge, the *clearance* is the difference between the *structure gauge* (minimum size of tunnel or bridge) and the vehicles' *loading gauge* (maximum size). A clearance distance can be prescribed by a code or a standard between a piece of equipment containing potentially hazardous material (say, fuel) and other objects (buildings, equipment, etc.) and the public. Or, say, no vehicle should parked nearer than 15 feet (4.6 m) from a fire hydrant.

In general, *clearance* refers to the distance to the nearest "obstacle" as defined in a context. It can be either a *tolerance* (the limit of an acceptable unplanned deviation from the nominal or theoretical dimension), or an *allowance* (planned deviation). Cf. **buffer distance** and **setback distance** in Chap. 25.

- **Creepage distance**

  The **creepage distance** is the shortest path distance along the surface of an insulation material between two conductive parts, while the shortest (straight line) distance between them is *clearance distance*; cf. the general term above.
- **Spark distance**

  The simplest way of measuring high voltages is by their **spark distance** (or **maximum spark length**). It is the length d of the gap between two electrodes in a gas, at which given voltage V becomes the *breakdown voltage*, i.e., starts a discharge or electric arc (a spark jumps over). Spark distance depends on the pressure p of gas and many other factors. The *Paschen's law* estimate V as a function of pd.
- **Humidifier absorption distance**

  The **absorption distance** of a (water centrifugal atomizing) humidifier is the list of minimum clearance dimensions needed to avoid condensation.
- **Spray distance**

  The **spray distance** is the distance maintained between the nozzle tip of a thermal spraying gun and the surface of the workpiece during spraying.
- **Protective action distance**

  The **protective action distance** is the distance downwind from an incident (say, a spill involving dangerous goods which are considered toxic by inhalation) in which persons may become incapacitated.

  The *screening distance* in a forest fire is the downwind distance which should be examined for possible smoke-sensitive human sites. The *spot fire distance* is the maximum distance between a source of firebrands (a group of burning trees) and a potential *spot fire* (a fire started by flying sparks or embers from the main fire). The *response distance* is the distance to fire traveled by fire companies.

  The notion of *mean distance between people and any hazardous event* operates also at a large scale: expanding the living area of human species (say, space colonization) will increase this distance and prevent many human extinction scenarios.
- **Fringe distance**

  Usually, the **fringe distance** is the spacing between *fringes*, for example, components into which a spectral line splits in the presence of an electric

or magnetic field (*Stark* and *Zeeman effects*, respectively, in Physics) or dark and light regions in the interference pattern of light beams (cf., in Chap. 24, *Pendellösung fringes* in **dynamical diffraction distances**).

For an interferometer, the fringe distance is the value $\frac{\lambda}{2\sin\alpha}$, where λ is the laser wavelength and α is the beam angle, while the **shear distance** is the spacing between two, due to the thickness of the plate, reflections.

In Image Analysis, there is also the *fringe distance* (Brown, 1994) between binary images (cf. **pixel distance** in Chap. 21).

- **Ranged weapon**

  A **ranged** (or *distance*) **weapon** is any weapon that can harm targets at distances greater than hand-to-hand distance; it can be thrown or used to fire projectiles at targets. A weapon intended to be used in hand-to-hand combat is called a *melee weapon*. But spears, knives, daggers can be used for both throwing and stabbing.

  The **maximum effective range** of a weapon is the greatest distance fired and able to produce casualties or damage consistently. The **effective weapon distance** is the actual distance (as opposed to maximal range) over which it is usually deployed. For given game and rifle type, the *effective hunting distance* (or *killing distance*) is the maximal range of a "clean kill."

- **Shooting distance**

  The **shooting distance** (or *shot distance*) is the distance achieved by, say, a bullet or a golf ball after a shot.

  The range of a Taser projectile delivering an incapacitating shock is called the *shocking distance*. Longest confirmed sniper kill at 2016 was 2475 m.

  For a shooting range, *firing distance* is the distance between the firing line and the target line. In shooting incident reconstruction, *firing distance* (or *muzzle-to-target distance*) is the distance from the muzzle of the firearm to the victim's clothing.

  In photography, the *shooting distance* is the camera-subject distance.

- **Lens distances**

  A convex lens is converging/magnifying; a concave one is diverging/reducing.

  The **focal distance** (*effective focal length*): the distance from the optical center of a lens (or a curved mirror) to the focus (to the image). Its reciprocal measured in m is called the *diopter* and is used as a unit of measurement of the (refractive) power of a lens; roughly, the magnification power of a lens is $\frac{1}{4}$ of its diopter.

  The *lens effective diameter* is twice the longest lens radius measured from its center to the apex of its edge. The *back focal length* is the distance between the rear surface of a lens and its image plane; the *front focal length* is the distance from the vertex of the first lens to the front focal point.

  Depth of field (DoF): the distance in the object plane (in front of and behind the object) over which the system delivers an acceptably sharp image, i.e., the region where blurring is tolerated at a particular resolution.

  The *depth of focus*: the range of distance in the image plane (the eyepiece, camera, or photographic plate) over which the system delivers an acceptably sharp image.

The *vertex depth* (or *sagitta*) is the depth of the surface curve on a lens measured over a specific diameter. Given a circle, the *apothem* is the perpendicular distance from the midpoint of a chord to the circle's center; it is the radius minus the *sagitta*.

The **working distance**: the distance from the front end of a lens system to the object when the instrument is correctly focused; it is used to modify the DoF. For a flashlight, it is the distance at which the *illuminance* (maximum light falling on a surface) would fall to 0.25 lux as, say, a full moon on a clear night.

The *register distance* (or *flange distance*): the distance between the flange (protruding rim) of the lens mount and the plane of the film image.

The *conjugate image distance* and *conjugate object distance*: the distances along the optical axis of a lens from its principal plane to the image and object plane, respectively. When a converging lens is placed between the object and the screen, the sum of the inverses of those distances is the inverse focal distance.

A *circle of confusion* (CoC) is an optical spot caused by a cone of light rays from a lens not coming to a perfect focus; in photography, it is the largest blur circle that will still be perceived as a point when viewed at a distance of 25 cm.

The *close* (or *minimum*, *near*) *focus distance*: the closest distance to which a lens can approach the subject and still achieve focus.

The **hyper-focal distance**: the distance from the lens to the nearest point (*hyper-focal point*) that is in focus when the lens is focused at infinity; beyond this point all objects are well defined and clear. It is the nearest distance at which the far end of the **depth of field** stretches to infinity (cf. **infinite distance**).

Eye relief: the distance an optical instrument can be held away from the eye and still present the full field-of-view. The *exit pupil width*: the width of the cone of light that is available to the viewer at the exact eye relief distance.

- **Distances in Stereoscopy**

  A method of 3D imaging is to create a pair of 2D images by a two-camera system.

  The *convergence distance* is the distance between the *baseine* of the camera center to the *convergence point* where the two lenses should converge for good stereoscopy. This distance should be 15–30 times the **intercamera distance**.

  The *intercamera distance* (or *baseline length*, *interocular lens spacing*) is the distance between the two cameras from which the left and right eye images are rendered.

  The *picture plane distance* is the distance at which the object will appear on the *picture plane* (the apparent surface of the image). The *window* is a masking border of the screen frame such that objects, which appear at (but not behind or outside) it, appear to be at the same distance from the viewer as this frame. In human viewing, the picture plane distance is about 30 times the **intercamera distance**.

- **Distance-related shots**

  A film *shot* is what is recorded between the time the camera starts (the director's call for "action") and the time it stops (the call to "cut").

The main **distance-related shots** (camera setups) are:

- *establishing shot*: a shot, at the beginning of a sequence which establishes the location of the action and/or the time of day;
- *long shot*: a shot taken from at least 50 yards (45.7 m) from the action;
- *medium shot*: a shot from 5 to 15 yards (4.6–13.7 m), including a small entire group, which shows group/objects in relation to the surroundings;
- *close-up*: a shot from a close position, say, the actor from the neck upwards;
- *two-shot*: a shot that features two persons in the foreground;
- *insert*: an inserted shot (usually a close up) used to reveal greater detail.

29.3 Miscellany

- **Range distances**

  In Mathematics, *range* is the set of values of a function or variable; specifically, it means the difference (or interval, area) between a maximum and minimum.

  The **range distances** are practical distances emphasizing a maximum distance for effective operation such as vehicle travel without refueling, a bullet range, visibility, movement limit, home range of an animal, etc. For example, the range of a risk factor (toxicity, blast, etc.) indicates the minimal **safe distancing**.

  The **operating distance** (or *nominal sensing distance*) is the range of a device (for example, a remote control) which is specified by the manufacturer and used as a reference. The **activation distance** is the maximal distance allowed for activation of a sensor-operated switch.

- **Spacing distances**

  The following examples illustrate this large family of practical distances emphasizing a minimum distance; cf. **minimum distance**, nearest-neighbor **distance in Animal Behavior**, **first-neighbor distance** in Chaps. 16, 23, 24, respectively.

  The **miles in trail**: a specified minimum distance, in nautical miles, required to be maintained between airplanes. *Seat pitch* and *seat width* are airliner distances between, respectively, two rows of seats and the armrests of a single seat.

  The **isolation distance**: a specified minimum distance required (because of pollination) to be maintained between variations of the same species of a crop in order to keep the seed pure (for example, ≈ 3 m for rice).

  The **legal distance**: a minimum distance required by a judicial rule or decision, say, a distance a sex offender is required to live away from school.

  In a restraining order, **stay away** means to stay a certain distance (often 300 yards, i.e., 275 m) from the protected person. A general **distance restriction**: say, a minimum distance required for passengers traveling on some long distance trains in India, or a distance from a voting facility where campaigning is permitted.

The **stop-spacing distance**: the interval between bus stops; such mean distance in US light rail systems ranges from 500 (Philadelphia) to 1742 m (Los Angeles).

The **character spacing**: the interval between characters in a given computer font.

The **just noticeable difference** (JND): the smallest perceived percent change in a dimension (for distance/position, etc.). *Weber's law* states that JND between two stimuli is proportional to their magnitude (and the subject's sensitivity).

- **Cutoff distances**

  Given a range of values (usually, a length, energy, or momentum scale in Physics), *cutoff* (or *cut-off*) is the maximal or minimal value, as, for example, Planck units.

  A **cutoff distance** is a cutoff in a length scale. For example, infrared and ultraviolet cutoff (the maximal and minimal wavelength that the human eye takes into account) are *long-distance* and *short-distance cutoff*, respectively, in the visible spectrum. Cutoff distances are often used in Molecular Dynamics.

  A similar notion of a **threshold distance** refers to a limit, margin, starting point distance (usually, minimal) at which some effect happens or stops. Some examples are the threshold distance of sensory perception, neuronal reaction or, say, upon which a city or road alters the abundance patterns of the native bird species.

- **Quality metrics**

  A **quality metric** (or, simply, *metric*) is a standard unit of measure or, more generally, part of a system of parameters, or systems of measurement. This vast family of measures (or standards of measure) concerns different attributes of objects. In such a setting, our distances and similarities are rather "similarity metrics", i.e., metrics (measures) quantifying the extent of relatedness between two objects.

  Examples include academic metrics, crime statistics, corporate investment metrics, economic metrics (indicators), education metrics, environmental metrics (indices), health metrics, market metrics, political metrics, properties of a route in computer networking, software metrics and vehicle metrics.

  For example, the site http://metripedia.wikidot.com/start aims to build an Encyclopedia of IT (Information Technology) performance metrics. Some examples of nonequipment quality metrics are detailed below.

  Landscape metrics evaluate, for example, greenway patches in a given landscape by *patch density* (the number of patches per km^2), *edge density* (the total length of patch boundaries per hectare), *shape index* $\frac{E}{4\sqrt{A}}$ (where A is the total area, and E is the total length of edges), connectivity, diversity, etc.

  Morphometrics evaluate the forms (size and shape) related to organisms (brain, fossils, etc.). For example, the roughness of a fish school is measured by its *fractal dimension* $2\frac{\ln P - \ln 4}{\ln A}$ where P, A are its perimeter (m) and surface (m^2).

Management metrics include: surveys (say, of market share, sales increase, customer satisfactions), forecasts (say, of revenue, contingent sales, investment), R&D effectiveness, absenteeism, etc.

Risk metrics are used in Insurance and, in order to evaluate a portfolio, in Finance.

Importance metrics rank the relative influence such as, for example:

- *PageRank* of Google ranking web pages;
- ISI (now Thomson Scientific) *Impact Factor* of a journal measuring, for a given two-year period, the number of times the average article in this journal is cited by some article published in the subsequent year;
- Hirsch's *h-index* of a scholar: the largest number h such that h of his/her publications have at least h citations;
- and his/her i10-*index*: the number of publications with at least 10 citations.

- **Heterometric and homeometric**

  The adjective **heterometric** means involving or dependent on a change in size, while **homeometric** means independent of such change.

  Those terms are used mainly in Medicine; for example, *heterometric* and *homeometric autoregulation* refer to intrinsic mechanisms controlling the strength of ventricular contractions that depend or not, respectively, on the length of myocardial fibers at the end of diastole; cf. **distances in Medicine**.

- **Distal and proximal**

  The antipodal notions near (close, nigh) and far (distant, remote) are also termed *proximity* and *distality*.

  The adjective **distal** (or *peripheral*) is an anatomical term of location (on the body, the limbs, the jaw, etc.); corresponding adverbs are: distally, distad.

  For an *appendage* (any structure that extends from the main body), **proximal** means situated towards the point of attachment, while **distal** means situated around the furthest point from this point of attachment. More generally, as opposed to *proximal* (or *central*), *distal* means: situated away from, farther from a point of reference (origin, center, point of attachment, trunk). As opposed to *mesial* it means: situated or directed away from the midline or mesial plane of the body.

  Proximal and distal *demonstratives* are words indicating *place deixis*, i.e., a spatial location relative to the point of reference. Usually, they are two-way as *this/that*, these/those or *here/there*, i.e., in terms of the dichotomy near/far from the speaker. But, say, Korean, Japanese, Spanish, and Thai make a three-way distinction: proximal (near to the speaker), medial (near to the addressee) and distal (far from both). English had the third form, *yonder* (at an indicated distance within sight), still spoken in Southern US. Cf. **spatial language** in Chap. 28.

  A **distal stimulus** is an real-word object or event, which, by some physical process, stimulates the body's sensory organs. Resulting raw pattern of neural activity is called the **proximal stimulus**. *Perception* is the constructing mental representations of distal stimuli using the information available in proximal stimuli.

A *proximate cause* is an event which is closest to, or immediately responsible for causing, some observed result. This exists in contrast to a higher-level *ultimate* (or *distal*) *cause* which is usually thought of as the "real" reason something occurred.

Tinbergen's (1960) *proximate* and *ultimate questions* about behavior are "how" an organism structures function? and "why" a species evolved the structures it has?

- **Distance effect**

  The **distance effect** is a general term for the change of a pattern or process with distance. Usually, it is the result of **distance decay**. For example, a static field attenuates proportionally to the inverse square of the distance from the source.

  Another example of the distance effect is a periodic variation (instead of uniform decrease) in a certain direction, when a *standing wave* occurs in a time-varying field. It is a wave that remains in a constant position because either the medium is moving in the opposite direction, or two waves, traveling in opposite directions, interfere; cf. **Pendellösung length** in Chap. 24.

  The distance effect, together with the size (source magnitude) effect determine many processes; cf. **island distance effect**, **insecticide distance effect** in Chap. 23 and **symbolic distance effect**, **distance effect on trade** in Chap. 28.

- **Distance decay**

  The **distance decay** is the attenuation of a pattern or process with distance. Cf. **distance decay (in Spatial Interaction)** in Chap. 28.

  Examples of distance-decay curves: Pareto model $\ln I_{ij} = a - b \ln d_{ij}$, and the model $\ln I_{ij} = a - b d_{ij}^p$ with $p = \frac{1}{2}$, 1, or 2 (here I_{ij} and d_{ij} are the interaction and distance between points i, j, while a and b are parameters). The *Allen curve* gives the exponential drop of frequency of all communication between engineers as the distance between their offices increases, i.e., face-to-face probability decays.

  A **mass-distance decay curve** is a plot of "mass" decay when the distance to the center of "gravity" increases. Such curves are used, say, to determine an *offender's heaven* (the point of origin; cf. **distances in Criminology**) or the galactic mass within a given radius from its center (using *rotation-distance curves*).

- **Distance factor**

  A **distance factor** is a multiplier of some straight-line distance needed to account for additional data. For example, 10 % increase of aircraft weight implies 20 % increase, i.e., a distance factor of 1.2, in needed take-off distance.

- **Propagation length**

  For a pattern or process attenuating with distance, the **propagation length** is the distance to decay by a factor of $\frac{1}{e}$.

  Cf. **radiation length** and the **Beer–Lambert law** in Chap. 24.

  A **scale height** is a distance over which a quantity decreases by a factor of e.

- **Incremental distance**

  An **incremental distance** is a gradually increasing (by a fixed amount) one.

- **Distance curve**

  A **distance curve** is a plot (or a graph) of a given parameter against a corresponding distance. Examples of distance curves, in terms of a process under consideration, are: **time-distance curve** (for the travel time of a wave-train, seismic signals, etc.), *height-run distance curve* (for the height of tsunami wave versus wave propagation distance from the impact point), *drawdown-distance curve*, *melting-distance curve* and *wear volume-distance curve*.

  A **force-distance curve** is, in SPM (scanning probe microscopy), a plot of the vertical force that the tip of the probe applies to the sample surface, while a contact-AFM (Atomic Force Microscopy) image is being taken. Also, *frequency-distance* and *amplitude-distance* curves are used in SPM.

  The term *distance curve* is also used for charting growth, for instance, a child's height or weight at each birthday. A plot of the rate of growth against age is called the **velocity-distance curve**; this term is also used for the speed of aircraft. Example of a constant rate of growth: in a month, human (hear or body) hair grow 15 and 8.1 mm, while nails (finger and toe) grow 3.5 and 1.6 mm.

- **Distance sensitivity**

  Distance sensitivity is a general term used to indicate the dependence of something on the associated distance. It could be, say, commuting distance sensitivity of households, traveling distance sensitivity of tourists, distance sensitive technology, distance sensitive products/services and so on.

- **Characteristic diameters**

  Let X be an irregularly-shaped 3D object, say, Earth's spheroid or a particle. A **characteristic diameter** (or **equivalent diameter**) of X is the diameter of a sphere with the same geometric or physical property of interest. Examples follow.

  The **authalic diameter** and **volumetric diameter** (*equivalent spherical diameter*) of X are the diameters of the spheres with the same surface area and volume. The **Heywood diameter** is the diameter of a circle with the same projection area. Cf. the **Earth radii** in Chap. 25 and the **shape parameters** in Chap. 21.

  The **Stokes diameter** is the diameter of the sphere with the same gravitational velocity as X, while the **aerodynamic diameter** is the diameter of such sphere of unit density. Cf. the **hydrodynamic radius** in Chap. 24.

  Equivalent *electric mobility*, *diffusion* and *light scattering* diameters of a particle X are the diameters of the spheres with the same electric mobility, penetration and intensity of light scattering, respectively, as X.

- **Characteristic length**

  A **characteristic length** (or *scale*) is a convenient reference length of a given configuration, such as the overall length of an aircraft, the maximum diameter or radius of a body of revolution, or a chord or span of a lifting surface.

  In general, it is a length that is representative of the system (or region) of interest, or the parameter which characterizes a given physical quantity in, say, Heat Transfer or Fluid Mechanics. For complex shapes, it is defined as the volume of the body divided by the surface area. For example, for a rocket engine, it is the ratio of the volume of its combustion chamber to the area of the nozzle's

throat, representing the average distance that the products of burned fuel must travel to escape.

- **True length**

  In Engineering Drawing, **true length** is any distance between points that is not foreshortened by the view type. In 3D, lines with true length are parallel to the projection plane, as, for example, the base edges in a top view of a pyramid.

- **Path length**

  In general, a path is a line representing the course of actual, potential or abstract movement. In Topology, a path is a certain continuous function; cf. parametrized **metric curve** in Chap. 1.

  In Physics, **path length** is the total distance an object travels, while *displacement* is the net distance it travels from a starting point. Cf. **displacement**, **inelastic mean free path**, **optical distance** and **dislocation path length** in Chap. 24. In Chemistry, (cell) **path length** is the distance that light travels through a sample in an analytical cell.

  In Graph Theory, **path length** is a discrete notion: the number of vertices in a sequence of vertices of a graph; cf. **path metric** in Chap. 1. Cf. **Internet IP metric** in Chap. 22 for **path length** in a computer network. Also, it means the total number of machine code instructions executed on a section of a program.

- **Middle distance**

  The **middle distance** is a general term. It can be a precise distance (cf. **running distances**), the halfway between the observer and the horizon (cf. **distance to horizon** in Chap. 25), implied horizon of a scene (cf. **representation of distance in Painting** in Chap. 28), or the place that you can see when you are not quite focusing on the world around you (Urban Dictionary of slang). Another example: goals in the middle distance (1 block to 2 miles) are places one might walk to.

- **Long-distance**

  The term **long-distance** usually refers to telephone communication (long-distance call, operator) or to covering large distances by moving (long-distance trail, running, swimming, riding of motorcycles or horses, etc.) or, more abstractly: long-distance migration, commuting, supervision, relationship, etc. For example, a *long-distance relationship* (LDR) is typically an intimate relationship that takes place when the partners are separated by a considerable distance.

  For example, a *long-distance* (or *distance*) *thug* has two meanings: 1. a person that is a coward in real life, but gathers courage from behind the safety of a computer, phone, or through e-mail; and 2. a hacker, spammer, or scam artist that takes advantage of the Internet to cause harm to others from a distance.

  Cf. **long-distance dispersal**, **animal** and **plant long-distance communication**, **long range order**, **long range dependence**, **action at a distance** (in Computing, Physics, along DNA).

  DDD (or *direct distance dialing*) is any switched telecommunication service (like 1+, 0 + +, etc.) that allows a call originator to place long-distance calls directly to telephones outside the local service area without an operator.

The term *short-distance* is rarely used. Instead, the adjective **short range** means limited to (or designed for) short distances, or relating to the near future. Finally, **touching**, for two objects, is having (or getting) a zero distance between them.

- **Long-distance intercourse**

  Long-distance intercourse (coupling at a distance) is found often in Native American folklore: Coyote, the Trickster, is said to have lengthened his penis to enable him to have intercourse with a woman on the opposite bank of a lake.

  A company Distance Labs has announced the "intimate communication over a distance", an interactive installation *Mutsugoto* which draws, using a custom computer vision and projection system, lines of light on a body of a person. Besides light, haptic technology provides a degree of touch communication between remote users. A company Lovotics created *Kissinger*, a messaging device wirelessly sending kisses. Other devices can send hugs, strokes and squeezes over the internet by making companion devices respond with vibrations and temperature changes.

  In Nature, the *acorn barnacle* (small sessile crustacean) have the largest penis-body size ratio (up to 10 when extended) of any animal. The squid *Onykia ingens* have largest ratio among mobile animals. The male octopus *Argonauta* use a modified arm, the *hectocotylus*, to transfer sperm to the female *at a distance*; this tentacle detaches itself from the body and swims—under its own power—to the female.

  Also, many aquatic animals (say, coral, hydra, sea urchin, bony fish) and amphibians reproduce by external fertilization: eggs and sperm are released into the water. Similar transfer of sperm at a distance is pollination (by wind or organisms) in flowering plants. Another example is *in vitro* fertilization in humans.

  The shortest range intercourse happens in anglerfish. The male, much smaller, latches onto a female with his sharp teeth, fuses inside her to the blood-vessel level and degenerates into a pair of testicles. It releases sperm when the female (with about 6 males inside) releases eggs. But female-male pairings of a parasitic worm *Schistosoma mansoni* is monogamous: the male's body forms a channel, in which it holds the longer and thinner female for their entire adult lives, up to 30 years. Two worms *Diplozoon paradoxum* fuse completely for lifetime of cross-fertilization.

- **Go the distance**

  Go the (full) **distance** is a general distance idiom meaning to continue to do something until it is successfully completed.

  An *unbridgeable distance* is a distance (seen as a spatial or metaphoric extent), impossible to span: a wide unbridgeable river, chasm or, in general, differences.

Newnes Radio and RF Engineering
Pocket Book

Newnes Radio and RF Engineering Pocket Book

3rd edition

Steve Winder
Joe Carr

Newnes

OXFORD AMSTERDAM BOSTON LONDON NEW YORK PARIS
SAN DIEGO SAN FRANCISCO SINGAPORE SYDNEY TOKYO

Newnes
An imprint of Elsevier Science
Linacre House, Jordan Hill, Oxford OX2 8DP
225 Wildwood Avenue, Woburn, MA 01801-2041

First published 1994
Reprinted 2000, 2001
Second edition 2000
Third edition 2002

Copyright © 1994, 2000, 2002, Steve Winder. All rights reserved

The right of Steve Winder to be identified as the author of this work has been asserted in accordance with the Copyright, Designs and Patents Act 1988

No part of this publication may be reproduced in any material form (including photocopying or storing in any medium by electronic means and whether or not transiently or incidentally to some other use of this publication) without the written permission of the copyright holder except in accordance with the provisions of the Copyright, Designs and Patents Act 1988 or under the terms of a licence issued by the Copyright Licensing Agency Ltd, 90 Tottenham Court Road, London, England W1T 4LP. Applications for the copyright holder's written permission to reproduce any part of this publication should be addressed to the publisher

British Library Cataloguing in Publication Data
A catalogue record for this book is available from the British Library

ISBN 0 7506 5608 5

For information on all Newnes publications
visit our website at www.newnespress.com

Typeset by Laserwords Private Limited, Chennai, India.
Printed and bound in Great Britain

Contents

Preface to second edition xi

Preface to third edition xiii

1 Propagation of radio waves 1
- 1.1 Frequency and wavelength 1
- 1.2 The radio frequency spectrum 1
- 1.3 The isotropic radiator 3
- 1.4 Formation of radio waves 3
- 1.5 Behaviour of radio waves 7
- 1.6 Methods of propagation 13
- 1.7 Other propagation topics 18
- References 24

2 The decibel scale 25
- 2.1 Decibels and the logarithmic scale 25
- 2.2 Decibels referred to absolute values 25

3 Transmission lines 35
- 3.1 General considerations 35
- 3.2 Impedance matching 35
- 3.3 Base band lines 36
- 3.4 Balanced line hybrids 36
- 3.5 Radio frequency lines 37
- 3.6 Waveguides 45
- 3.7 Other transmission line considerations 47
- References 51

4 Antennas 52
- 4.1 Antenna characteristics 52
- 4.2 Antenna types 56
- 4.3 VHF and UHF antennas 60
- 4.4 Microwave antennas 69
- 4.5 Loop antennas 73
- References 78

5 Resonant circuits 79
- 5.1 Series and parallel tuned circuits 79
- 5.2 Q factor 81
- 5.3 Coupled (band-pass) resonant circuits 81
- References 84

6 Oscillators 85
6.1 Oscillator requirements 85
6.2 Tunable oscillators 85
6.3 Quartz crystal oscillators 87
6.4 Frequency synthesizers 89
6.5 Caesium and rubidium frequency standards 93
References 94

7 Piezo-electric devices 95
7.1 Piezo-electric effect 95
7.2 Quartz crystal characteristics 97
7.3 Specifying quartz crystals 101
7.4 Filters 102
7.5 SAW filters and resonators 105
References 109

8 Bandwidth requirements and modulation 110
8.1 Bandwidth of signals at base band 110
8.2 Modulation 112
8.3 Analogue modulation 113
8.4 Digital modulation 123
8.5 Spread spectrum transmission 129
References 131

9 Frequency planning 132
9.1 International and regional planning 132
9.2 National planning 132
9.3 Designations of radio emissions 134
9.4 Bandwidth and frequency designations 135
9.5 General frequency allocations 135
9.6 Classes of radio stations 139
9.7 Radio wavebands 142
Reference 142

10 Radio equipment 143
10.1 Transmitters 143
10.2 Receivers 148
10.3 Programmable equipment 157
References 158

11 Microwave communication 159
11.1 Microwave usage 159
11.2 Propagation 159

11.3 K factor 161
11.4 Fresnel zones, reflections and multi-path fading 161
11.5 Performance criteria for analogue and digital links 164
11.6 Terminology 165
11.7 Link planning 165
11.8 Example of microwave link plan 165
Reference 166

12 Information privacy and encryption 167
12.1 Encryption principles 167
12.2 Speech encryption 168
12.3 Data encryption 169
12.4 Code division multiple access (CDMA) or spread spectrum 172
12.5 Classification of security 172
References 172

13 Multiplexing 173
13.1 Frequency division multiplex 173
13.2 Time division multiplex (TDM) 174
13.3 Code division multiple access (CDMA) 177
Reference 178

14 Speech digitization and synthesis 179
14.1 Pulse amplitude modulation 179
14.2 Pulse code modulation 179
14.3 ADPCM codecs 181
14.4 The G728 low delay CELP codec 181
14.5 The GSM codec 182
References 182

15 VHF and UHF mobile communication 183
15.1 Operating procedures 183
15.2 Control of base stations 186
15.3 Common base station (CBS) operation 186
15.4 Wide area coverage 187

16 Signalling 194
16.1 Sub-audio signalling 194
16.2 In-band tone and digital signalling 195
16.3 Digital signalling 197
16.4 Standard PSTN tones 198
References 199

17 Channel occupancy, availability and trunking 200
17.1 Channel occupancy and availability 200
17.2 Trunking 201
17.3 In-band interrupted scan (IBIS) trunking 203
17.4 Trunking to MPT 1327 specification 203
References 204

18 Mobile radio systems 205
18.1 Paging 205
18.2 Cordless telephones 206
18.3 Trunked radio 207
18.4 Analogue cellular radio-telephone networks 208
18.5 Global system mobile 209
18.6 Other digital mobile systems 211
18.7 Private mobile radio (PMR) 213
18.8 UK CB radio 213
References 213

19 Base station site management 214
19.1 Base station objectives 214
19.2 Site ownership or accommodation rental? 214
19.3 Choice of site 214
19.4 Masts and towers 215
19.5 Installation of electronic equipment 216
19.6 Earthing and protection against lightning 217
19.7 Erection of antennas 219
19.8 Interference 221
19.9 Antenna multi-coupling 225
19.10 Emergency power supplies 226
19.11 Approval and certification 227
References 227

20 Instrumentation 229
20.1 Accuracy, resolution and stability 229
20.2 Audio instruments 230
20.3 Radio frequency instruments 231
References 235

21 Batteries 236
21.1 Cell characteristics 236
21.2 Non-rechargeable, primary batteries 238
21.3 Rechargeable batteries 242

22 Satellite communications 246
22.1 Earth orbits 246
22.2 Communications by satellite link 248
22.3 Proposed satellite television formats 248
22.4 Global positioning system (GPS) 252
References 255

23 Connectors and interfaces 256
23.1 Audio and video connectors 256
23.2 Co-axial connector 258
23.3 Interfaces 268
Reference 280

24 Broadcasting 281
24.1 Standard frequency and time transmissions 281
24.2 Standard frequency formats 283
24.3 UK broadcasting bands 284
24.4 BBC VHF test tone transmissions 284
24.5 Engineering information about broadcast services 287
24.6 Characteristics of UHF terrestrial television systems 288
24.7 Terrestrial television channels 291
24.8 Terrestrial television aerial dimensions 294
24.9 AM broadcast station classes (USA) 295
24.10 FM broadcast frequencies and channel numbers (USA) 296
24.11 US television channel assignments 299
24.12 License-free bands 301
24.13 Calculating radio antenna great circle bearings 302

25 Abbreviations and symbols 307
25.1 Abbreviations 307
25.2 Letter symbols by unit name 313
25.3 Electric quantities 321

26 Miscellaneous data 323
26.1 Fundamental constants 323
26.2 Electrical relationships 323
26.3 Dimensions of physical properties 324
26.4 Fundamental units 324
26.5 Greek alphabet 325

26.6 Standard units 325
26.7 Decimal multipliers 327
26.8 Useful formulae 327
26.9 Colour codes 334
Index 337

Preface to second edition

This edition of the *Newnes Radio and RF Engineer's Pocket Book* is something special. It is a compendium of information of use to engineers and technologists who are engaged in radio and RF engineering. It has been updated to reflect the changing interests of those communities, and reflects a view of the technology like no other. It is packed with information!

This whole series of books is rather amazing with regard to the range and quality of the information they provide, and this book is no different. It covers topics as diverse as circuit symbols and the abbreviations used for transistors, as well as more complex things as satellite communications and television channels for multiple countries in the English speaking world. It is a truly amazing work.

We hope that you will refer to this book frequently, and will enjoy it as much as we did in preparing it.

John Davies
Joseph J. Carr

Acknowledgements

I gratefully acknowledge the ready assistance offered by the following organizations: Andrew Ltd, Aspen Electronics Ltd, BBC, British Telecommunications plc, Farnell Instruments Ltd, Independent Television Authority, International Quartz Devices Ltd, Jaybeam Ltd, MACOM Greenpar Ltd, Marconi Instruments Ltd, Panorama Antennas Ltd, Radiocommunications Agency, the Radio Authority, RTT Systems Ltd. A special thanks goes to my wife Dorothy for once again putting up with my months of seclusion during the book's preparation.

Preface to third edition

This, the third edition of the *Newnes Radio and RF Engineering Pocket Book* has been prepared with a tinge of sadness. Joe Carr, who edited the second edition, has died since the last edition was published. Although I did not know Joe personally, his prolific writing over recent years has impressed me. His was a hard act to follow.

I have updated this book to be more international. Thus the long tables giving details of British television transmitters have been removed (they are available on the Web). Details of the European E1 multiplexing system have been supplemented by a description of the US and Japanese T1 system. There are many more general updates included throughout.

Steve Winder

1 Propagation of radio waves

1.1 Frequency and wavelength

There is a fixed relationship between the frequency and the wavelength, which is the distance between identical points on two adjacent waves (*Figure 1.1*), of any type of wave: sound (pressure), electromagnetic (radio) and light. The type of wave and the speed at which the wavefront travels through the medium determines the relationship. The speed of propagation is slower in higher density media.

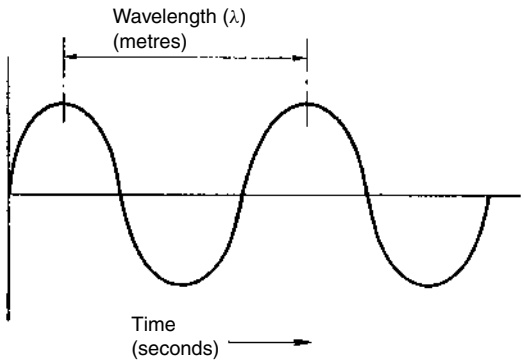

Figure 1.1 Frequency and wavelength

Sound waves travel more slowly than radio and light waves which, in free space, travel at the same speed, approximately 3×10^8 metres per second, and the relationship between the frequency and wavelength of a radio wave is given by:

$$\lambda = \frac{3 \times 10^8}{f} \text{ metres}$$

where λ is the wavelength and f is the frequency in hertz (Hz).

1.2 The radio frequency spectrum

The electromagnetic wave spectrum is shown in *Figure 1.2*: the part usable for radio communication ranges from below 10 kHz to over 100 GHz.

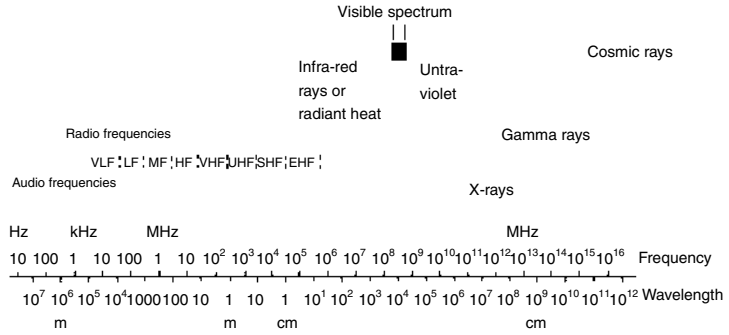

Figure 1.2 The electromagnetic wave spectrum

The radio spectrum is divided into bands and the designation of the bands, their principal use and method of propagation is shown in *Table 1.1*. Waves of different frequencies behave differently and this, along with the amount of spectrum available in terms of radio communication channels in each band, governs their use.

Table 1.1 Use of radio frequencies

Frequency band	*Designation, use and propagation*
3–30 kHz	Very low frequency (VLF). Worldwide and long distance communications. Navigation. Submarine communications. Surface wave.
30–300 kHz	Low frequency (LF). Long distance communications, time and frequency standard stations, long-wave broadcasting. Ground wave.
300–3000 kHz	Medium frequency (MF) or medium wave (MW). Medium-wave local and regional broadcasting. Marine communications. Ground wave.
3–30 MHz	High frequency (HF). 'Short-wave' bands. Long distance communications and short-wave broadcasting. Ionospheric sky wave.
30–300 MHz	Very high frequency (VHF). Short range and mobile communications, television and FM broadcasting. Sound broadcasting. Space wave.
300–3000 MHz	Ultra high frequency (UHF). Short range and mobile communications. Television broadcasting. Point-to-point links. Space wave. Note: The usual practice in the USA is to designate 300–1000 MHz as 'UHF' and above 1000 MHz as 'microwaves'.
3–30 GHz	Microwave or super high frequency (SHF). Point-to-point links, radar, satellite communications. Space wave.
Above 30 GHz	Extra high frequency (EHF). Inter-satellite and micro-cellular radio-telephone. Space wave.

1.3 The isotropic radiator

A starting point for considering the propagation of radio- or lightwaves is the isotropic radiator, an imaginary point source radiating equally in all directions in free space. Such a radiator placed at the centre of a sphere illuminates equally the complete surface of the sphere. As the surface area of a sphere is given by $4\pi r^2$ where r is the radius of the sphere, the brilliance of illumination at any point on the surface varies inversely with the distance from the radiator. In radio terms, the power density at distance from the source is given by:

$$P_{\mathrm{d}} = \frac{P_{\mathrm{t}}}{4\pi r^2}$$

where P_{t} = transmitted power.

1.4 Formation of radio waves

Radio waves are electromagnetic. They contain both electric and magnetic fields at right angles to each other and also at right angles to the direction of propagation. An alternating current flowing in a conductor produces an alternating magnetic field surrounding it and an alternating voltage gradient – an electric field – along the length of the conductor. The fields combine to radiate from the conductor as in *Figure 1.3*.

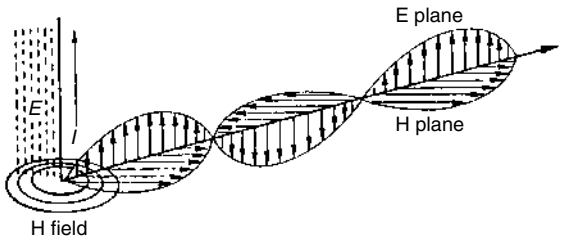

Figure 1.3 Formation of electromagnetic wave

The plane of the electric field is referred to as the E plane and that of the magnetic field as the H plane. The two fields are equivalent to the voltage and current in a wired circuit. They are measured in similar terms, volts per metre and amperes per metre, and the medium through

which they propagate possesses an impedance. Where $E = ZI$ in a wired circuit, for an electromagnetic wave:

$$E = ZH$$

where
E = the RMS value of the electric field strength, V/metre
H = the RMS value of the magnetic field strength, A/metre
Z = characteristic impedance of the medium, ohms

The voltage is that which the wave, passing at the speed of light, would induce in a conductor one metre long.

The characteristic impedance of the medium depends on its permeability (equivalent of inductance) and permittivity (equivalent of capacitance). Taking the accepted figures for free space as:

$\mu = 4\pi \times 10^{-7}$ henrys (H) per metre (permeability) and

$\varepsilon = 1/36\pi \times 10^{9}$ farads (F) per metre (permittivity)

then the impedance of free space, Z, is given by:

$$\sqrt{\frac{\mu}{\varepsilon}} = 120\pi = 377 \text{ ohms}$$

The relationship between power, voltage and impedance is also the same for electromagnetic waves as for electrical circuits, $W = E^2/Z$.

The simplest practical radiator is the elementary doublet formed by opening out the ends of a pair of wires. For theoretical considerations the length of the radiating portions of the wires is made very short in relation to the wavelength of the applied current to ensure uniform current distribution throughout their length. For practical applications the length of the radiating elements is one half-wavelength ($\lambda/2$) and the doublet then becomes a dipole antenna (*Figure 1.4*).

When radiation occurs from a doublet the wave is polarized. The electric field lies along the length of the radiator (the E plane) and the magnetic field (the H plane) at right angles to it. If the E plane is vertical, the radiated field is said to vertically polarized. Reference to the E and H planes avoids confusion when discussing the polarization of an antenna.

Unlike the isotropic radiator, the dipole possesses directivity, concentrating the energy in the H plane at the expense of the E plane. It effectively provides a power gain in the direction of the H plane

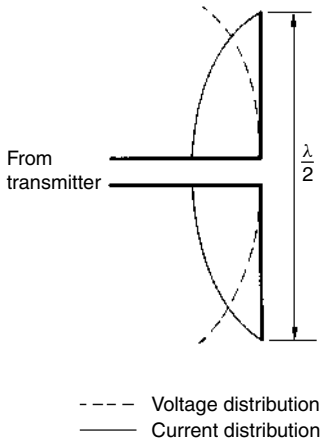

Figure 1.4 Doublet (dipole) antenna

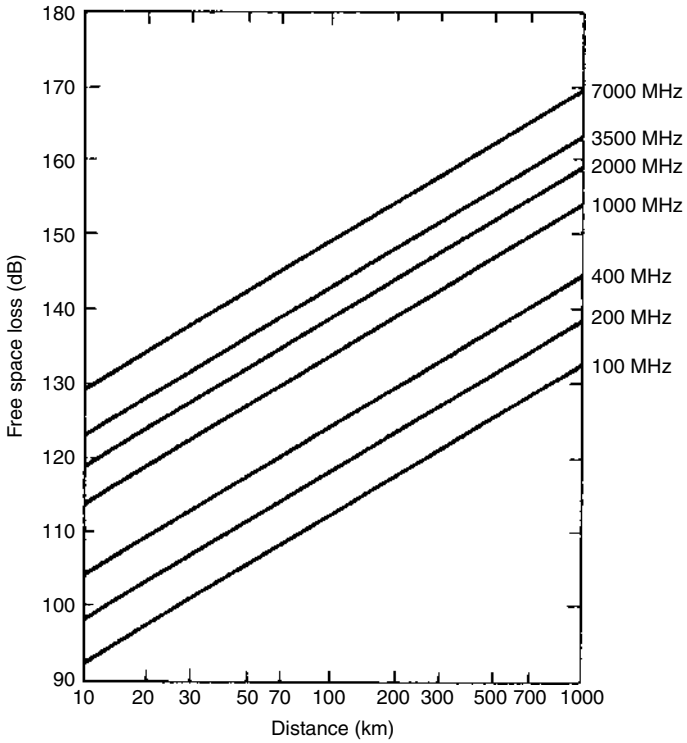

Figure 1.5 Free space loss vs. distance and frequency

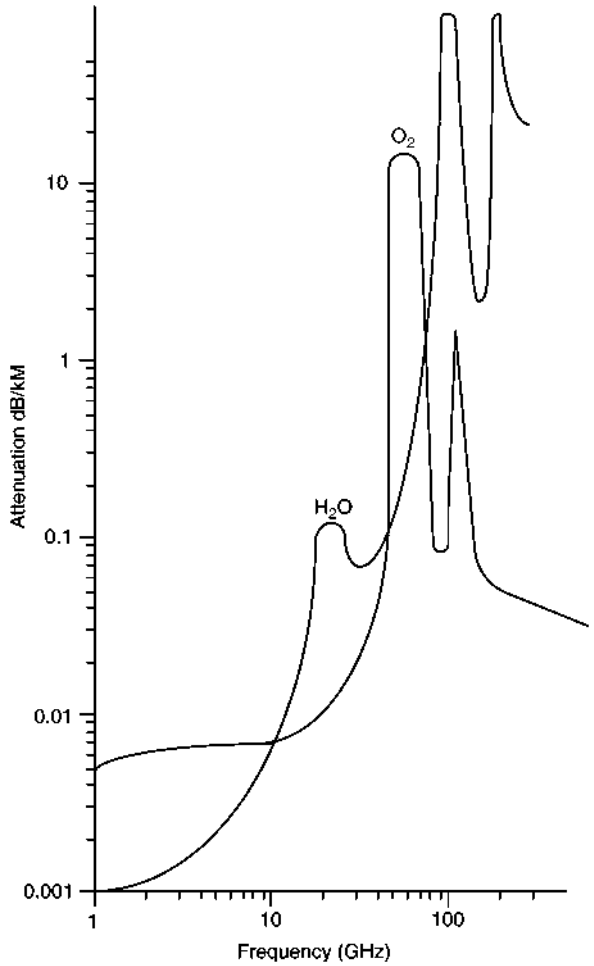

Figure 1.6 Major loss of microwave communications and radar systems due to atmospheric attenuation

compared with an isotropic radiator. This gain is 1.6 times or 2.15 dBi (dBi means dB relative to an isotropic radiator).

For a direct ray the power transfer between transmitting and receiving isotropic radiators is inversely proportional to the distance between them *in wavelengths*. The free space power loss is given by:

$$\text{Free space loss, dB} = 10\log_{10}\frac{(4\pi d)^2}{\lambda^2}$$

where d and λ are in metres, or:

$$\text{Free space loss (dB)} = 32.4 + 20 \times \log_{10} d + 20 \times \log_{10} f$$

where d = distance in km and f = frequency in MHz.

The free space power loss, therefore, increases as the square of the distance and the frequency. Examples are shown in *Figure 1.5*.

With practical antennas, the power gains of the transmitting and receiving antennas, in dBi, must be subtracted from the free space loss calculated as above. Alternatively, the loss may be calculated by:

$$\text{Free space loss (dB)} = 10 \log_{10} \left[\frac{(4\pi d)^2}{\lambda^2} \times \frac{1}{G_t \times G_r} \right]$$

where G_t and G_r are the respective actual gains, not in dB, of the transmitting and receiving antennas.

A major loss in microwave communications and radar systems is atmospheric attenuation (see *Figure 1.6*). The attenuation (in decibels per kilometre (dB/km)) is a function of frequency, with especial problems showing up at 22 GHz and 64 GHz. These spikes are caused by *water vapour* and *atmospheric oxygen* absorption of microwave energy, respectively. Operation of any microwave frequency requires consideration of atmospheric losses, but operation near the two principal spike frequencies poses special problems. At 22 GHz, for example, an additional 1 dB/km of loss must be calculated for the system.

1.5 Behaviour of radio waves

1.5.1 Physical effects

The physical properties of the medium through which a wave travels, and objects in or close to its path, affect the wave in various ways.

Absorption

In the atmosphere absorption occurs and energy is lost in heating the air molecules. Absorption caused by this is minimal at frequencies below about 10 GHz but absorption by foliage, particularly when wet, is severe at VHF and above.

Waves travelling along the earth's surface create currents in the earth causing ground absorption which increases with frequency. A horizontally polarized surface wave suffers more ground absorption than a vertically polarized wave because of the 'short-circuiting' by

the ground of the electric field. Attenuation at a given frequency is least for propagation over water and greatest over dry ground for a vertically polarized wave.

Refraction and its effect on the radio horizon

As radio waves travel more slowly in dense media and the densest part of the atmosphere is normally the lowest, the upper parts of a wave usually travel faster than the lower. This refraction (*Figure 1.7*) has the effect of bending the wave to follow the curvature of the earth and progressively tilting the wavefront until eventually the wave becomes horizontally polarized and short-circuited by the earth's conductivity.

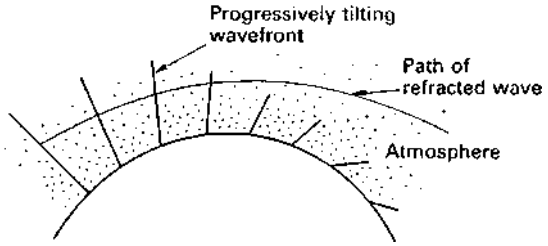

Figure 1.7 Effects of refraction

Waves travelling above the earth's surface (space waves) are usually refracted downwards, effectively increasing the radio horizon to greater than the visual.

The refractive index of the atmosphere is referred to as the *K* factor; a *K* factor of 1 indicates zero refraction. Most of the time *K* is positive at 1.33 and the wave is bent to follow the earth's curvature. The radio horizon is then 4/3 times the visual. However, the density of the atmosphere varies from time to time and in different parts of the world. Density inversions where higher density air is above a region of low density may also occur. Under these conditions the *K* factor is negative and radio waves are bent away from the earth's surface and are either lost or ducting occurs. A *K* factor of 0.7 is the worst expected case.

Ducting occurs when a wave becomes trapped between layers of differing density only to be returned at a great distance from its source, possibly creating interference.

Radio horizon distance at VHF/UHF

The radio horizon at VHF/UHF and up is approximately 15% further than the optical horizon. Several equations are used in calculating the

distance. If D^- is the distance to the radio horizon, and H is the antenna height, then:

$$D = k\sqrt{H}$$

- When D is in statute miles (5280 feet) and H in feet, then $k = 1.42$.
- When D is in nautical miles (6000 feet) and H in feet, then $k = 1.23$.
- When D is in kilometres and H is in metres, then $k = 4.12$.

Repeating the calculation for the receiving station and adding the results gives the total path length.

Diffraction

When a wave passes over on the edge of an obstacle some of its energy is bent in the direction of the obstacle to provide a signal in what would otherwise be a shadow. The bending is most severe when the wave passes over a sharp edge (*Figure 1.8*).

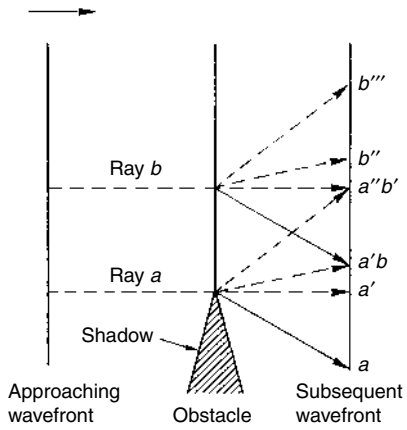

Figure 1.8 Effects of diffraction

As with light waves, the subsequent wavefront consists of wavelets produced from an infinite number of points on the wavefront, rays *a* and *b* in *Figure 1.8* (Huygens' principle). This produces a pattern of interfering waves of alternate addition and subtraction.

Reflection

Radio waves are reflected from surfaces lying in and along their path and also, effectively, from ionized layers in the ionosphere – although

most of the reflections from the ionized layers are actually the products of refraction. The strength of truly reflected signals increases with frequency, and the conductivity and smoothness of the reflecting surface.

Multi-path propagation

Reflection, refraction and diffraction may provide signals in what would otherwise be areas of no signal, but they also produce interference.

Reflected – or diffracted – signals may arrive at the receiver in any phase relationship with the direct ray and with each other. The relative phasing of the signals depends on the differing lengths of their paths and the nature of the reflection.

When the direct and reflected rays have followed paths differing by an odd number of half-wavelengths they could be expected to arrive at the receiver in anti-phase with a cancelling effect. However, in the reflection process a further phase change normally takes place. If the reflecting surface had infinite conductivity, no losses would occur in the reflection, and the reflected wave would have exactly the same or opposite phase as the incident wave depending on the polarization in relation to the reflecting surface. In practice, the reflected wave is of smaller amplitude than the incident, and the phase relationships are also changed. The factors affecting the phasing are complex but most frequently, in practical situations, approximately 180° phase change occurs on reflection, so that reflected waves travelling an odd number of half-wavelengths arrive in phase with the direct wave while those travelling an even number arrive anti-phase.

As conditions in the path between transmitter and receiver change so does the strength and path length of reflected signals. This means that a receiver may be subjected to signal variations of almost twice the mean level and practically zero, giving rise to severe fading. This type of fading is frequency selective and occurs on troposcatter systems and in the mobile environment where it is more severe at higher frequencies. A mobile receiver travelling through an urban area can receive rapid signal fluctuations caused by additions and cancellations of the direct and reflected signals at half-wavelength intervals. Fading due to the multi-path environment is often referred to as Rayleigh fading and its effect is shown in *Figure 1.9*. Rayleigh fading, which can cause short signal dropouts, imposes severe restraints on mobile data transmission.

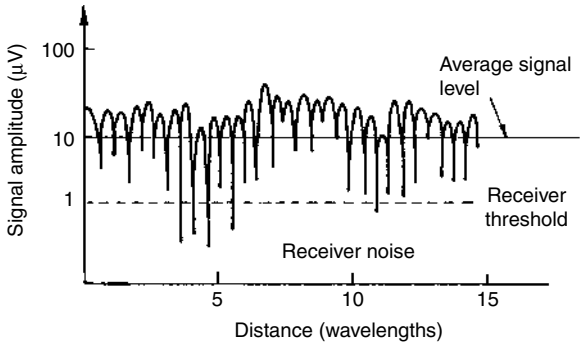

Figure 1.9 Multi-path fading

Noise

The quality of radio signals is not only degraded by the propagation losses: natural or manmade electrical noise is added to them, reducing their intelligibility.

Atmospheric noise includes static from thunderstorms which, unless very close, affects frequencies below about 30 MHz and noise from space is apparent at frequencies between about 8 MHz to 1.5 GHz.

A type of noise with which radio engineers are continually concerned is thermal. Every resistor produces noise spread across the whole frequency spectrum. Its magnitude depends upon the ohmic value of the resistor, its temperature and the bandwidth of the following circuits. The noise voltage produced by a resistor is given by:

$$E_n = \sqrt{4kTBR}$$

where

E_n = noise voltage, V(RMS)
k = Boltzmann's constant
= 1.38×10^{-23} joules/kelvin
T = temperature in degrees K
B = bandwidth of measurement, Hz
R = resistance in ohms

An antenna possesses resistance and its thermal noise, plus that of a receiver input circuit, is a limiting factor to receiver performance.

Noise is produced in every electronic component. Shot noise – it sounds like falling lead shot – caused by the random arrival of electrons at, say, the collector of a transistor, and the random division of electrons at junctions in devices, add to this noise.

Doppler effect

Doppler effect is an apparent shift of the transmitted frequency which occurs when either the receiver or transmitter is moving. It becomes significant in mobile radio applications towards the higher end of the UHF band and on digitally modulated systems.

When a mobile receiver travels directly towards the transmitter each successive cycle of the wave has less distance to travel before reaching the receiving antenna and, effectively, the received frequency is raised. If the mobile travels away from the transmitter, each successive cycle has a greater distance to travel and the frequency is lowered. The variation in frequency depends on the frequency of the wave, its propagation velocity and the velocity of the vehicle containing the receiver. In the situation where the velocity of the vehicle is small compared with the velocity of light, the frequency shift when moving directly towards, or away from, the transmitter is given to sufficient accuracy for most purposes by:

$$f_d = \frac{V}{C} f_t$$

where
f_d = frequency shift, Hz
f_t = transmitted frequency, Hz
V = velocity of vehicle, m/s
C = velocity of light, m/s

Examples are:

- 100 km/hr at 450 MHz, frequency shift = 41.6 Hz
- 100 km/hr at 1.8 GHz – personal communication network (PCN) frequencies – frequency shift = 166.5 Hz
- Train at 250 km/hr at 900 MHz – a requirement for the GSM pan-European radio-telephone – frequency shift = 208 Hz

When the vehicle is travelling at an angle to the transmitter the frequency shift is reduced. It is calculated as above and the result multiplied by the cosine of the angle of travel from the direct approach (*Figure 1.10*).

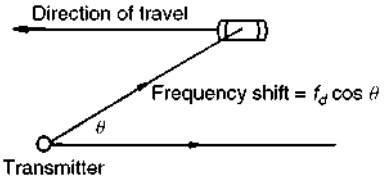

Figure 1.10 Doppler frequency shift and angle to transmitter

In a radar situation Doppler effect occurs on the path to the target and also to the reflected signal so that the above formula is modified to:

$$f_{\mathrm{d}} = \frac{2V}{C} f_{\mathrm{t}}$$

where f_{d} is now the total frequency shift.

1.6 Methods of propagation

The effects of all of the above phenomena vary with frequency and are used in the selection of frequencies for specific purposes. The behaviour of waves of different frequencies gives rise to the principal types of wave propagation.

Ground wave propagation

Waves in the bands from very low frequencies (VLF, 3–30 kHz), low frequencies (LF, 30–300 kHz) and medium frequencies (MF, 300–3000 kHz) travel close to the earth's surface: the ground wave (*Figure 1.11*). Transmissions using the ground wave must be vertically polarized to avoid the conductivity of the earth short-circuiting the electric field.

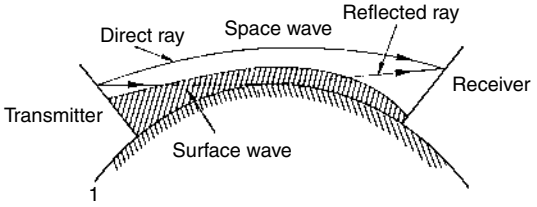

Figure 1.11 Components of the ground wave

The ground wave consists of a surface wave and a space wave. The surface wave travels along the earth's surface, and is attenuated by ground absorption and the tilting of the wavefront due to diffraction.

The losses increase with frequency and thus VLF radio stations have a greater range than MF stations. The attenuation is partially offset by the replacement of energy from the upper part of the wave refracted by the atmosphere.

The calculation of the field strength of the surface wave at a distance from a transmitter is complex and affected by several variables. Under plane earth conditions and when the distance is sufficiently short that the earth's curvature can be neglected the field intensity is given by:

$$E_{su} = \frac{2E_0}{d}A$$

where

E_{su} = field intensity in same units as E_0

d = distance in same units of distance as used in E_0

A = a factor calculated from the earth losses, taking frequency, dielectric constant and conductivity into account

E_0 = the free space field produced at unit distance from the transmitter. (With a short (compared with $\lambda/4$) vertical aerial, $2E_0 = 300\sqrt{P}$ mV/m at 1 km where P is the radiated power in kW.) (Terman, 1943)

For a radiated power of 1 kW and ground of average dampness, the distance at which a field of 1 mV/m will exist is given in *Table 1.2*.

Table 1.2 Distance at which a field of 1 mV/m will exist for a radiated power of 1 kW and ground of average dampness

Frequency	*Range (km)*
100 kHz	200
1 MHz	60
10 MHz	6
100 MHz	1.5

The direct and reflected components of the ground wave produce multi-path propagation and variations in received single strength will arise depending on the different path lengths taken by the two components. When the transmitting and receiving antennas are at ground level the components of the space wave cancel each other and the surface wave is dominant. When the antennas are elevated, the space wave becomes increasingly strong and a height is eventually reached where the surface wave has a negligible effect on the received signal strength.

Sky wave propagation

High frequency (HF) waves between 3 MHz and 30 MHz are effectively reflected by ionized layers in the ionosphere producing the sky wave. Medium frequency waves may also be reflected, but less reliably.

The ionosphere contains several layers of ionized air at varying altitudes (*Figure 1.12*). The heights and density of the layers vary diurnally, seasonally and with the incidence of sunspot activity. The E and F_2 layers are semi-permanent while the F_1 layer is normally only present during daytime.

Radio waves radiated at a high angle and reflected by these layers return to earth at a distance from the transmitter. The HF reflection

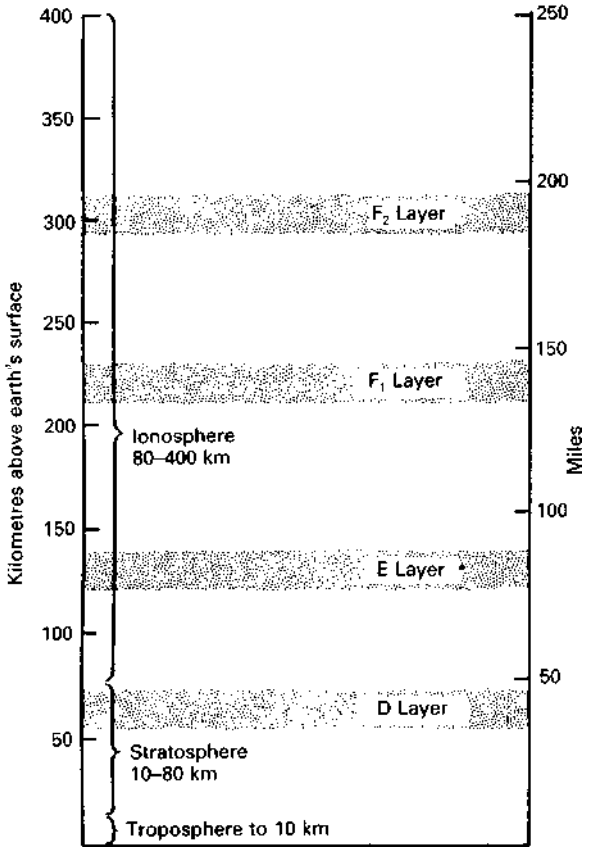

Figure 1.12 The ionosphere

process is in reality one of refraction in layers possessing a greater free electron density than at heights above or below them. The speed of propagation is slowed on entering a layer and the wave is bent and, if of a suitable frequency and angle of incidence, returned to earth (*Figure 1.13*). The terms used are defined as follows:

- *Virtual height*. The height at which a true reflection of the incident wave would have occurred (*Figure 1.13*).
- *Critical frequency* (f_c). The highest frequency that would be returned to earth in a wave directed vertically at the layer.
- *Maximum usable frequency* (muf). The highest frequency that will be returned to earth for a given angle of incidence. If the angle of incidence to the normal is θ, the muf $= f_c / \cos\theta$.
- *Skip distance*. The minimum distance from the transmitter, along the surface of the earth, at which a wave above the critical frequency will be returned to earth (*Figure 1.12*). Depending on the frequency, the ground wave will exist at a short distance from the transmitter.
- *Sporadic E-layer reflections*. Reflections from the E layer at frequencies higher than those which would normally be returned to earth. They appear to be reflections from electron clouds having sharp boundaries and drifting through the layer. As the name implies the reflections are irregular but occur mostly in summer and at night.

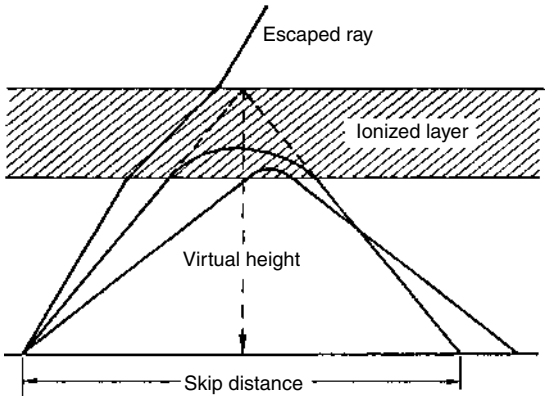

Figure 1.13 Sky wave propagation

Space wave propagation

The space wave travels through the troposphere (the atmosphere below the ionosphere) between the transmitter and the receiver. It contains

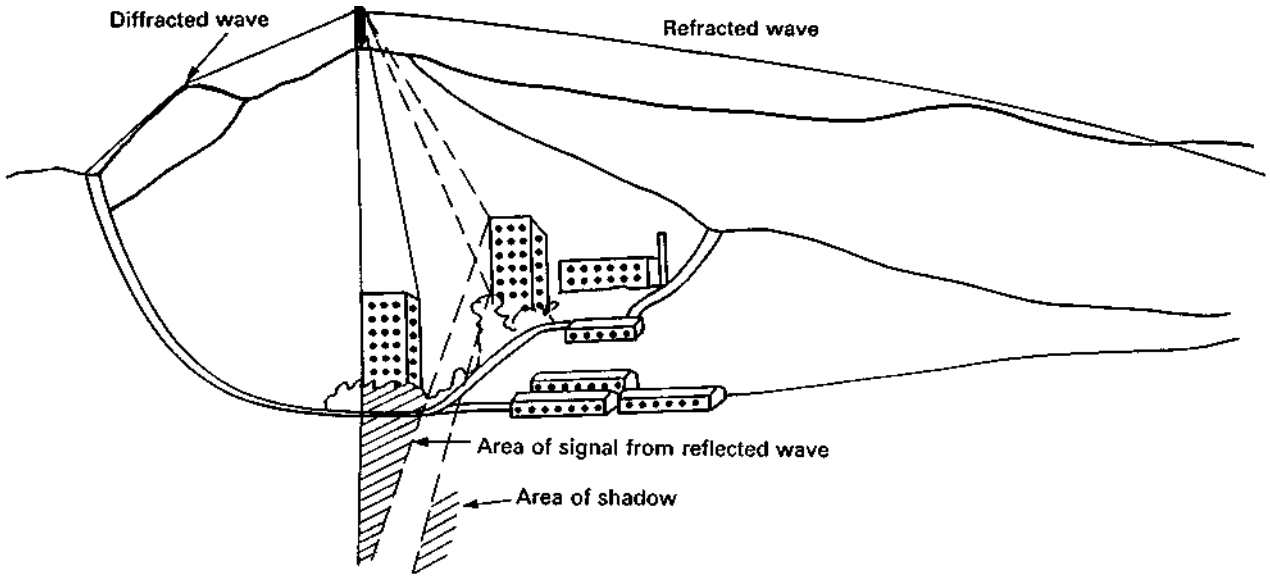

Figure 1.14 Pictorial representation of radio coverage from a base station

both direct and reflected components (see *Figure 1.11*), and is affected by refraction and diffraction. The importance of these effects varies with frequency, the nature of the terrain and of objects close to the direct path, and the type of communication, e.g. data. Apart from medium-wave broadcasting, space waves are used mainly for communications using frequencies of VHF and upwards.

The range of space waves is the radio horizon. However, places of little or no signal can arise in the lee of radio obstacles. Fortunately, they may be filled with either reflected or diffracted signals as depicted in *Figure 1.14*.

Tropospheric scatter

The tropospheric, or forward, scatter effect provides reliable, over the horizon, communication between fixed points at bands of ultra and super high frequencies. Usable bands are around 900, 2000 and 5000 MHz and path lengths of 300 to 500 km are typical.

The mechanism is not known with certainty but reflections from discontinuities in the dielectric constant of the atmosphere and scattering of the wave by clouds of particles are possibilities. It is an inefficient process, the scattered power being -60 to -90 dB relative to the incident power, so high transmitter powers are necessary. The phenomenon is regularly present but is subject to two types of fading. One occurs slowly and is due to variations of atmospheric conditions. The other is a form of Rayleigh fading and is rapid, deep and frequency selective. It is due to the scattering occurring at different points over a volume in the atmosphere producing multipath propagation conditions.

Troposcatter technique uses directional transmitting and receiving antennas aimed so that their beams intercept in the troposphere at the mid-distance point. To overcome the fading, diversity reception using multiple antennas spaced over 30 wavelengths apart is common.

1.7 Other propagation topics

Communications in the VHF through microwave regions normally takes place on a 'line-of-sight' basis where the radio horizon defines the limit of sight. In practice, however, the situation is not so neat and simple. There is a transition region between the HF and VHF where long distance ionospheric 'skip' occurs only occasionally. This effect is seen above 25 MHz, and is quite pronounced in the 50 MHz region. Sometimes the region behaves like line-of-sight VHF, and at others like HF shortwave.

1.7.1 Scatter

There are a number of scatter modes of propagation. These modes can extend the radio horizon a considerable amount. Where the radio horizon might be a few tens of kilometres, underscatter modes permit very much longer propagation. For example, a local FM broadcaster at 100 MHz might have a service area of about 40 miles, and might be heard 180 miles away during the summer months when *Sporadic-E* propagation occurs. One summer, a television station in Halifax, Nova Scotia, Canada, was routinely viewable in Washington, DC in the United States during the early morning hours for nearly a week.

Sporadic-E is believed to occur when a small region of the atmosphere becomes differentially ionized, and thereby becomes a species of 'radio mirror'. Ionospheric scatter propagation occurs when clouds of ions exist in the atmosphere. These clouds can exist in both the ionosphere and the troposphere, although the tropospheric model is more reliable for communications. A signal impinging this region may be scattered towards other terrestrial sites which may be a great distance away. The specific distance depends on the geometry of the scenario.

There are at least three different modes of scatter from ionized clouds: *back scatter, side scatter*, and *forward scatter*. The back scatter mode is a bit like radar, in that signal is returned back to the transmitter site, or in regions close to the transmitter. Forward scatter occurs when the reflected signal continues in the same azimuthal direction (with respect to the transmitter), but is redirected toward the Earth's surface. Side scatter is similar to forward scatter, but the azimuthal direction might change.

Unfortunately, there are often multiple reflections from the ionized cloud, and these are shown as 'multiple scatter' in *Figure 1.15*. When these reflections are able to reach the receiving site, the result is a rapid, fluttery fading that can be of quite profound depths.

Meteor scatter is used for communication in high latitude regions. When a meteor enters the Earth's atmosphere it leaves an ionized trail of air behind it. This trail might be thousands of kilometres long, but is very short lived. Radio signals impinging the tubular metre ion trail are reflected back towards Earth. If the density of meteors in the critical region is high, then more or less continuous communications can be achieved. This phenomenon is noted in the low VHF between 50 and about 150 MHz. It can easily be observed on the FM broadcast band if the receiver is tuned to distant stations that are barely audible. If the geometry of the scenario is right, abrupt but short-lived peaks in the signal strength will be noted.

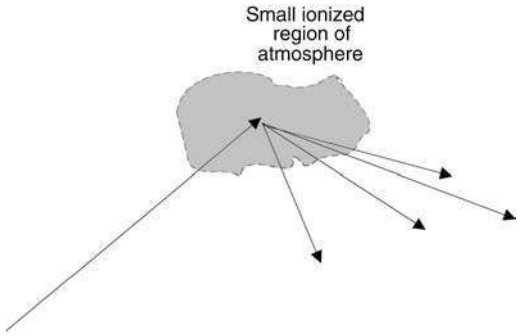

Figure 1.15 Multiple scatter

1.7.2 Refraction modes

Refraction is the mechanism for most tropospheric propagation phenomena. The dielectric properties of the air, which are set mostly by the moisture content, are a primary factor in tropospheric refraction. Refraction occurs in both light or radio wave systems when the wave passes between mediums of differing density. Under that situation, the wave path will bend an amount proportional to the difference in density of the two regions.

The general situation is typically found at UHF and microwave frequencies. Because air density normally decreases with altitude, the top of a beam of radio waves typically travels slightly faster than the lower portion of the beam. As a result, those signals refract a small amount. Such propagation provides slightly longer surface distances than are normally expected from calculating the distance to the radio horizon. This phenomenon is called *simple refraction*, and is described by the *K factor*.

Super refraction

A special case of refraction called super refraction occurs in areas of the world where warmed land air flows out over a cooler sea (*Figure 1.16*). Examples of such areas are deserts that are adjacent to a large body of water: the Gulf of Aden, the southern Mediterranean, and the Pacific Ocean off the coast of Baja, California. Frequent VHF/UHF/microwave communications up to 200 miles are reported in such areas, and up to 600 miles have reportedly been observed.

Ducting

Another form of refraction phenomenon is weather related. Called *ducting*, this form of propagation is actually a special case of super

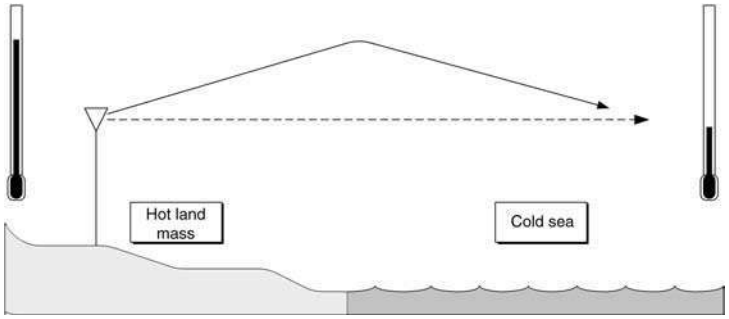

Figure 1.16 An example of super refraction

refraction. Evaporation of sea water causes temperature inversion regions to form in the atmosphere. That is, layered air masses in which the air temperature is greater than in the layers below it (note: air temperature normally decreases with altitude, but at the boundary with an inversion region, it begins to increase). The inversion layer forms a 'duct' that acts similarly to a waveguide. Ducting allows long distance communications from lower VHF through microwave frequencies; with 50 MHz being a lower practical limit, and 10 GHz being an ill-defined upper limit. Airborne operators of radio, radar, and other electronic equipment can sometimes note ducting at even higher microwave frequencies.

Antenna placement is critical for ducting propagation. Both the receiving and transmitting antennas must be either: (a) physically inside the duct (as in airborne cases), or (b) able to propagate at an angle such that the signal gets trapped inside the duct. The latter is a function of antenna radiation angle. Distances up to 2500 miles or so are possible through ducting.

Certain paths, where frequent ducting occurs, have been identified: in the United States, the Great Lakes region to the southeastern Atlantic seaboard; Newfoundland to the Canary Islands; across the Gulf of Mexico from Florida to Texas; Newfoundland to the Carolinas; California to Hawaii; and Ascension Island to Brazil.

Subrefraction

Another refractive condition is noted in the polar regions, where colder air from the land mass flows out over warmer seas (*Figure 1.17*). Called *subrefraction*, this phenomena bends EM waves away from the Earth's surface – thereby reducing the radio horizon by about 30 to 40%.

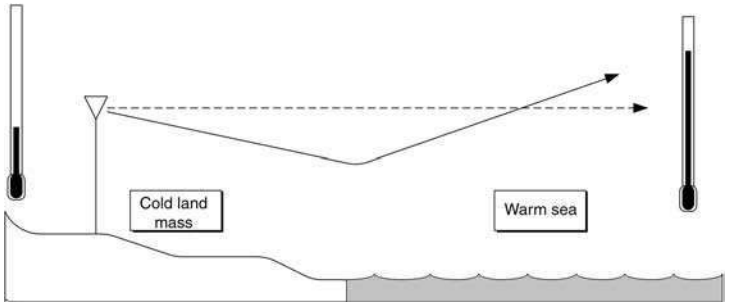

Figure 1.17 An example of subrefraction

All tropospheric propagation that depends upon air-mass temperatures and humidity shows diurnal (i.e. over the course of the day) variation caused by the local rising and setting of the sun. Distant signals may vary 20 dB in strength over a 24-hour period. These tropospheric phenomena explain how TV, FM broadcast, and other VHF signals can propagate great distances, especially along seacoast paths, sometimes weak and sometimes nonexistent.

1.7.3 Great circle paths

A great circle is the shortest line between two points on the surface of a sphere, such that it lays on a plane through the Earth's centre and includes the two points. When translated to 'radiospeak', a great circle is the shortest path on the surface of the Earth between two points. Navigators and radio operators use the great circle for similar, but different, reasons. Navigators use it in order to get from here to there, and radio operators use it to get a transmission path from here to there.

The heading of a directional antenna is normally aimed at the receiving station along its great circle path. Unfortunately, many people do not understand the concept well enough, for they typically aim the antenna in the wrong direction. For example, Washington, DC in the USA is on approximately the same latitude as Lisbon, Portugal. If you fly due east, you will have dinner in Lisbon, right? Wrong. If you head due east from Washington, DC, across the Atlantic, the first landfall would be West Africa, somewhere between Ghana and Angola. Why? Because the great circle bearing 90 degrees takes us far south. The geometry of spheres, not flat planes, governs the case.

Long path versus short path

The Earth is a sphere (or, more precisely, an 'oblique spheroid'), so from any given point to any other point there are two great circle

paths: the long path (major arc) and the short path (minor arc). In general, the best reception occurs along the short path. In addition, short path propagation is more nearly 'textbook', compared with long path reception. However, there are times when long path is better, or is the only path that will deliver a signal to a specific location from the geographic location in question.

Grey line propagation

The Grey line is the twilight zone between the night and daytime halves of the earth. This zone is also called the *planetary terminator*. It varies up to +23 degrees either side of the north–south longitudinal lines, depending on the season of the year (it runs directly north–south only at the vernal and autumnal equinoxes). The D-layer of the ionosphere absorbs signals in the HF region. This layer disappears almost completely at night, but it builds up during the day. Along the grey line, the D-layer is rapidly decaying west of the line, and has not quite built up east of the line.

Brief periods of abnormal propagation occur along the grey line. Stations on either side of the line can be heard from regions, and at distances, that would otherwise be impossible on any given frequency. For this reason, radio operators often prefer to listen at dawn and dusk for this effect.

1.7.4 Scatter propagation modes

Auroral propagation

The auroral effect produces a luminescence in the upper atmosphere resulting from bursts of particles released from the sun 18 to 48 hours earlier. The light emitted is called the northern lights and the southern lights. The ionized regions of the atmosphere that create the lights form a radio reflection shield, especially at VHF and above, although 15 to 20 MHz effects are known. Auroral propagation effects are normally seen in the higher latitudes, although listeners in the southern tier of states in the USA and Europe are often treated to the reception of signals from the north being reflected from auroral clouds. Similar effects exist in the southern hemisphere.

Non-reciprocal direction

If you listen to the 40 metre (7–7.3 MHz) amateur radio band receiver on the East Coast of the United States, you will sometimes hear European stations – especially in the late afternoon. But when the

US amateur tries to work those European stations there is no reply whatsoever. The Europeans are unable to hear the US stations. This propagation anomaly causes the radio wave to travel different paths dependent on which direction it travels, i.e. an east–west signal is not necessarily the reciprocal of a west–east signal. This anomaly can occur when a radio signal travels through a heavily ionized medium in the presence of a magnetic field, which is exactly the situation when the signal travels through the ionosphere in the presence of the Earth's magnetic field.

References

Belcher, R. *et al.* (1989). *Newnes Mobile Radio Servicing Handbook*. Butterworth-Heinemann, Oxford.

Kennedy, G. (1977). *Electronic Communications Systems*. McGraw-Hill Kogashuka, Tokyo.

Terman, F.E. (1943). *Radio Engineers' Handbook*. McGraw-Hill, London.

2 The decibel scale

2.1 Decibels and the logarithmic scale

The range of powers, voltages and currents encountered in radio engineering is too wide to be expressed on linear scale. Consequently, a logarithmic scale based on the decibel (dB, one tenth of a bel) is used. The decibel does not specify a magnitude of a power, voltage or current but a ratio between two values of them. Gains and losses in circuits or radio paths are expressed in decibels.

The ratio between two powers is given by:

$$\text{Gain or loss, dB} = 10 \log_{10} \frac{P_1}{P_2}$$

where P_1 and P_2 are the two powers.

As the power in a circuit varies with the square of the voltage or current, the logarithm of the ratio of these quantities must be multiplied by twenty instead of ten. To be accurate the two quantities under comparison must operate in identical impedances:

$$\text{Gain or loss, dB} = 20 \log_{10} \frac{V_1}{V_2}$$

To avoid misunderstandings, it must be realized that a ratio of 6 dB is 6 dB regardless of whether it is power, voltage or current that is referred to: if it is power, the ratio for 6 dB is four times; if it is voltage or current, the ratio is two times (*Table 2.1*).

2.2 Decibels referred to absolute values

While the decibel scale expresses ratios only, if a reference value is added to the statement as a suffix it can be used to refer to absolute values. For example, a loss of 10 dB means a reduction in power to a level equal to one tenth of the original and if the statement is −10 dBm the level referred to is 1/10 of a milliwatt. Commonly used suffixes and, where applicable, their absolute reference levels are as follows. *Table 2.2* shows the relative levels in decibels at 50 ohms impedance.

Table 2.1 The decibel figures are in the centre column: figures to the left represent decibel loss, and those to the right decibel gain. The voltage and current figures are given on the assumption that there is no change in impedance

Voltage or current ratio	*Power ratio*	*dB* ← − + →	*Voltage or current ratio*	*Power ratio*
1.000	1.000	0	1.000	1.000
0.989	0.977	0.1	1.012	1.023
0.977	0.955	0.2	1.023	1.047
0.966	0.933	0.3	1.035	1.072
0.955	0.912	0.4	1.047	1.096
0.944	0.891	0.5	1.059	1.122
0.933	0.871	0.6	1.072	1.148
0.912	0.832	0.8	1.096	1.202
0.891	0.794	1.0	1.122	1.259
0.841	0.708	1.5	1.189	1.413
0.794	0.631	2.0	1.259	1.585
0.750	0.562	2.5	1.334	1.778
0.708	0.501	3.0	1.413	1.995
0.668	0.447	3.5	1.496	2.239
0.631	0.398	4.0	1.585	2.512
0.596	0.355	4.5	1.679	2.818
0.562	0.316	5.0	1.778	3.162
0.501	0.251	6.0	1.995	3.981
0.447	0.200	7.0	2.239	5.012
0.398	0.159	8.0	2.512	6.310
0.355	0.126	9.0	2.818	7.943
0.316	0.100	10	3.162	10.00
0.282	0.0794	11	3.55	12.6
0.251	0.0631	12	3.98	15.9
0.224	0.0501	13	4.47	20.0
0.200	0.0398	14	5.01	25.1
0.178	0.0316	15	5.62	31.6
0.159	0.0251	16	6.31	39.8
0.126	0.0159	18	7.94	63.1
0.100	0.0100	20	10.00	100.0
3.16×10^{-2}	10^{-3}	30	3.16×10	10^{3}
10^{-2}	10^{-4}	40	10^{2}	10^{4}
3.16×10^{-3}	10^{-5}	50	3.16×10^{2}	10^{5}
10^{-3}	10^{-6}	60	10^{3}	10^{6}
3.16×10^{-4}	10^{-7}	70	3.16×10^{3}	10^{7}
10^{-4}	10^{-8}	80	10^{4}	10^{8}
3.16×10^{-5}	10^{-9}	90	3.16×10^{4}	10^{9}
10^{-5}	10^{-10}	100	10^{5}	10^{10}
3.16×10^{-6}	10^{-11}	110	3.16×10^{5}	10^{11}
10^{-6}	10^{-12}	120	10^{6}	10^{12}

Table 2.2 Relative levels in decibels at 50 ohms impedance

dB μV	*Voltage*	*dBV*	*dBm*	*dBW*	*Power*
−20	100 nV	−140	−127	−157	200 aW
−19	115	−139	−126	−156	250
−18	125	−138	−125	−155	315
−17	140	−137	−124	−154	400
−16	160	−136	−123	−153	500
−15	180	−135	−122	−152	630
−14	200	−134	−121	−151	800
−13	225	−133	−120	−150	1 fW
−12	250	−132	−119	−149	1.25
−11	280	−131	−118	−148	1.6
−10	315	−130	−117	−147	2.0
−9	355	−129	−116	−146	2.5
−8	400	−128	−115	−145	3.15
−7	450	−127	−114	−144	4.0
−6	500	−126	−113	−143	5.0
−5	565	−125	−112	−142	6.3
−4	630	−124	−111	−141	8.0
−3	710	−123	−110	−140	10
−2	800	−122	−109	−139	12.5
−1	900	−121	−108	−138	16
0	1 μV	−120	−107	−137	20
1	1.15	−119	−106	−136	25
2	1.25	−118	−105	−135	31.5
3	1.4	−117	−104	−134	40
4	1.6	−116	−103	−133	50
5	1.8	−115	−102	−132	63
6	2.0	−114	−101	−131	80
7	2.25	−113	−100	−130	100
8	2.5	−112	−99	−129	125
9	2.8	−111	−98	−128	160
10	3.15	−110	−97	−127	200
11	3.55	−109	−96	−126	250
12	4.0	−108	−95	−125	315
13	4.5	−107	−94	−124	400
14	5.0	−106	−93	−123	500
15	5.65	−105	−92	−122	630
16	6.3	−104	−91	−121	800
17	7.1	−103	−90	−120	1 pW
18	8.0	−102	−89	−119	1.25
19	9.0	−101	−88	−118	1.6
20	10.0	−100	−87	−117	2.0
21	11.5	−99	−86	−116	2.5
22	12.5	−98	−85	−115	3.15
23	14	−97	−84	−114	4.0
24	16	−96	−83	−113	5.0
25	18	−95	−82	−112	6.3

(*continued overleaf*)

Table 2.2 (*continued*)

dB μV	*Voltage*	*dBV*	*dBm*	*dBW*	*Power*
26	20	−94	−81	−111	8.0
27	22.5	−93	−80	−110	10
28	25	−92	−79	−109	12.5
29	28	−91	−78	−108	16
30	31.5	−90	−77	−107	20
31	35.5	−89	−76	−106	25
32	40	−88	−75	−105	31.5
33	45	−87	−74	−104	40
34	50	−86	−73	−103	50
35	56.5	−85	−72	−102	63
36	63	−84	−71	−101	80
37	71	−83	−70	−100	100
38	80	−82	−69	−99	125
39	90	−81	−68	−98	160
40	100	−80	−67	−97	200
41	115	−79	−66	−96	250
42	125	−78	−65	−95	315
43	140	−77	−64	−94	400
44	160	−76	−63	−93	500
45	180	−75	−62	−92	630
46	200	−74	−61	−91	800
47	225	−73	−60	−90	1 nW
48	250	−72	−59	−89	1.25
49	280	−71	−58	−88	1.6
50	315	−70	−57	−87	2.0
51	355	−69	−56	−86	2.5
52	400	−68	−55	−85	3.15
53	450	−67	−54	−84	4.0
54	500	−66	−53	−83	5.0
55	565	−65	−52	−82	6.3
56	630	−64	−51	−81	8.0
57	710	−63	−50	−80	10
58	800	−62	−49	−79	12.5
59	900	−61	−48	−78	16
60	1 mV	−60	−47	−77	20
61	1.15	−59	−46	−76	25
62	1.25	−58	−45	−75	31.5
63	1.4	−57	−44	−74	40
64	1.6	−56	−43	−73	50
65	1.8	−55	−42	−72	63
66	2.0	−54	−41	−71	80
67	2.25	−53	−40	−70	100
68	2.5	−52	−39	−69	125
69	2.8	−51	−38	−68	160
70	3.15	−50	−37	−67	200
71	3.55	−49	−36	−66	250
72	4.0	−48	−35	−65	315

Table 2.2 (*continued*)

dB μV	*Voltage*	*dBV*	*dBm*	*dBW*	*Power*
73	4.5	−47	−34	−64	400
74	5.0	−46	−33	−63	500
75	5.65	−45	−32	−62	630
76	6.3	−44	−31	−61	800
77	7.1	−43	−30	−60	1 μW
78	8.0	−42	−29	−59	1.25
79	9.0	−41	−28	−58	1.6
80	10 mV	−40	−27	−57	2.0
81	11.5	−39	−26	−56	2.5
82	12.5	−38	−25	−55	3.15
83	14	−37	−24	−54	4.0
84	16	−36	−23	−53	5.0
85	18	−35	−22	−52	6.3
86	20	−34	−21	−51	8.0
87	22.5	−33	−20	−50	10
88	25	−32	−19	−49	12.5
89	28	−31	−18	−48	16
90	31.5	−30	−17	−47	20
91	35.5	−29	−16	−46	25
92	40	−28	−15	−45	31.5
93	45	−27	−14	−44	40
94	50	−26	−13	−43	50
95	56.5	−25	−12	−42	63
96	63	−24	−11	−41	80
97	71	−23	−10	−40	100
98	80	−22	−9	−39	125
99	90	−21	−8	−38	160
100	100	−20	−7	−37	200
101	115	−19	−6	−36	250
102	125	−18	−5	−35	315
103	140	−17	−4	−34	400
104	160	−16	−3	−33	500
105	180	−15	−2	−32	630
106	200	−14	−1	−31	800
107	225	−13	0	−30	1 mW
108	250	−12	1	−29	1.25
109	280	−11	2	−28	1.6
110	315	−10	3	−27	2.0
111	355	−9	4	−26	2.5
112	400	−8	5	−25	3.15
113	450	−7	6	−24	4.0
114	500	−6	7	−23	5.0
115	565	−5	8	−22	6.3
116	630	−4	9	−21	8.0
117	710	−3	10	−20	10
118	800	−2	11	−19	12.5

(*continued overleaf*)

Table 2.2 (*continued*)

dB μV	*Voltage*	*dBV*	*dBm*	*dBW*	*Power*
119	900	−1	12	−18	16
120	1 V	0	13	−17	20
121	1.15	1	14	−16	25
122	1.25	2	15	−15	31.5
123	1.4	3	16	−14	40
124	1.6	4	17	−13	50
125	1.8	5	18	−12	63
126	2.0	6	19	−11	80
127	2.25	7	20	−10	100
128	2.5	8	21	−9	125
129	2.8	9	22	−8	160
130	3.15	10	23	−7	200
131	3.55	11	24	−6	250
132	4.0	12	25	−5	315
133	4.5	13	26	−4	400
134	5.0	14	27	−3	500
135	5.65	15	28	−2	630
136	6.3	16	29	−1	800
137	7.1	17	30	0	1 W
138	8.0	18	31	1	1.25
139	9.0	19	32	2	1.6
140	10	20	33	3	2.0
141	11.5	21	34	4	2.5
142	12.5	22	35	5	3.15
143	14	23	36	6	4.0
144	16	24	37	7	5.0
145	18	25	38	8	6.3
146	20	26	39	9	8.0
147	22.5	27	40	10	10
148	25	28	41	11	12.5
149	28	29	42	12	16
150	31.5	30	43	13	20
151	35.5	31	44	14	25
152	40	32	45	15	31.5
153	45	33	46	16	40
154	50	34	47	17	50
155	56.5	35	48	18	63
156	63	36	49	19	80
157	71	37	50	20	100
158	80	38	51	21	125
159	90	39	52	22	160
160	100	40	53	23	200
161	115	41	54	24	250
162	125	42	55	25	315
163	140	43	56	26	400
164	160	44	57	27	500
165	180	45	58	28	630

Table 2.2 (*continued*)

dB μV	*Voltage*	*dBV*	*dBm*	*dBW*	*Power*
166	200	46	59	29	800
167	225	47	60	30	1 kW
168	250	48	61	31	1.25
169	280	49	62	32	1.6
170	315	50	63	33	2.0
171	355	51	64	34	2.5
172	400	52	65	35	3.15
173	450	53	66	36	4.0
174	500	54	67	37	5.0
175	565	55	68	38	6.3
176	630	56	69	39	8.0
177	710	57	70	40	10
178	800	58	71	41	12.5
179	900	59	72	42	16
180	1 kV	60	73	43	20

Decibel glossary

dBa stands for dB 'adjusted'. This is a weighted circuit noise power referred to −85 dBm, which is 0 dBa. (Historically measured with a noise meter at the receiving end of a line. The meter is calibrated on a 1000 Hz tone such that 1 mW (0 dBm) gives a reading of +85 dBm. If the 1 mW is spread over the band 300–3400 Hz as random white noise, the meter will read +82 dBa.)

dBa0 circuit noise power in dBa referred to, or measured at, a point of zero relative transmission level (0 dBr). (A point of zero relative transmission level is a point arbitrarily established in a transmission circuit. All other levels are stated relative to this point.) It is preferable to convert circuit noise measurement values from dBa to dBa0 as this makes it unnecessary to know or to state the relative transmission level at the point of measurement.

dBd used for expressing the gain of an antenna referred to a dipole.

dBi used for expressing the gain of an antenna referred to an isotropic radiator.

dB μV decibels relative to 1 microvolt.

dbm decibels relative to 1 milliwatt. The term dBm was originally used for telephone and audio work and, when used in that context, implies an impedance of 600 Ω, the nominal impedance of a telephone line. When it is desired to define a relative transmission level in a circuit, dBr is preferred.

Table 2.3 Binary decibel values

Bits	*Max. value*	*Decibels (dB)*
1	2	6.02
2	4	12.04
3	8	18.06
4	16	24.08
5	32	30.10
6	64	36.12
7	128	42.14
8	256	48.16
9	512	54.19
10	1024	60.21
11	2048	66.23
12	4096	72.25
13	8192	78.27
14	16 384	84.29
15	32 768	90.31
16	65 536	96.33
17	131 072	102.35
18	262 144	108.37
19	524 288	114.39
20	1 048 576	120.41
21	2 097 152	126.43
22	4 194 304	132.45
23	8 388 608	138.47
24	16 777 216	144.49
25	33 554 432	150.51
26	67 108 864	156.54
27	134 217 728	162.56
28	268 435 456	168.58
29	536 870 912	174.60
30	1 073 741 824	180.62
31	2 147 483 648	186.64
32	4 294 967 296	192.66

dBm0 dBm referred to, or measured at, a point of zero transmission level.

dBmp a unit of noise power in dBm, measured with psophometric weighting. $\text{dBmp} = 10\log_{10}\text{pWp} - 90 = \text{dBa} - 84 = \text{dBm} - 2.5$ (for flat noise 300–3400 Hz).
pWp = picowatts psophometrically weighted.

dBm0p the abbreviation for absolute noise power in dBm referred to or measured at a point of zero relative transmission level, psophometrically weighted.

dBr means dB 'relative level'. Used to define transmission level at various points in a circuit or system referenced to the zero transmission level point.

dBrn a weighted circuit noise power unit in dB referenced to 1 pW (−90 dBm) which is 0 dBrn.
dBrnc weighted noise power in dBrn, measured by a noise measuring set with 'C-message' weighting.
dBrnc0 noise measured in dBrnc referred to zero transmission level point.
dBu decibels relative to 0.775 V, the voltage developed by 1 mW when applied to 600 Ω. dBu is used in audio work when the impedance is not 600 Ω and no specific impedance is implied.
dbV decibels relative to 1 volt.
dbW decibels relative to 1 watt.

Note: To convert dBm to dB μV add 107 (e.g. −20 dBm = −20 + 107 = 87 dB μV.

The beauty of decibel notation is that system gains and losses can be computed using addition and subtraction rather than multiplication and division. For example, suppose a system consists of an antenna that delivers a −4.7 dBm signal at its terminals (we conveniently neglect the antenna gain by this ploy). The antenna is connected to a 40 dB low-noise amplifier (A1) at the head end, and then through a 370 metre long coaxial cable to a 20 dB gain amplifier (A2), with a loss (L1) of −48 dB. The amplifier is followed by a bandpass filter with a −2.8 dB insertion loss (L2), and a −10 dB attenuator (L3). How does the signal exist at the end of this cascade chain?

S1	−4.7 dBm
A1	40.0 dB
A2	20.0 dB
L1	−48.0 dB
L2	−2.8 dB
L3	−10.0 dB
Total:	−5.5 dBm

Converting dBm to watts

$$P = \frac{10^{\mathrm{dBm}/10}}{1000}$$

Converting any dB to ratio

Power levels: $\dfrac{P1}{P2} = 10^{\mathrm{dB}/10}$

Voltage levels: $\frac{V1}{V2} = 10^{\mathrm{dB}/20}$

Current levels: $\frac{I1}{I2} = 10^{\mathrm{dB}/20}$

Binary decibel values

Binary numbers are used in computer systems. With the digitization of RF systems it is necessary to understand the decibel values of binary numbers. These binary numbers might be from an analogue-to-digital converter (ADC or A/D) that digitizes the IF amplifier output, or a digital-to-analogue converter (DAC or D/A) used to generate the analogue signal in a direct digital synthesis (DDS) signal generator.

3 Transmission lines

3.1 General considerations

The purpose of any transmission line is to transfer power between a source and a load with the minimum of loss and distortion in either amplitude, frequency or phase angle.

Electrons travel more slowly in conductors than they do in free space and all transmission lines contain distributed components: resistance, inductance and capacitance. Consequently, lines possess an impedance which varies with frequency, and loss and distortion occur. Because the impedance is not constant over a wide frequency band the insertion loss will not be the same for all frequencies and frequency distortion will arise. A wavefront entering a line from a source takes a finite time to travel its length. This transit time, because of the distributed components, also varies with frequency and creates phase distortion.

3.2 Impedance matching

To transfer the maximum power from a generator into a load the impedance of the load and the internal impedance of the generator – and any intervening transmission line – must be equal.

Figure 3.1 illustrates the simplest case of a generator of internal impedance Z_s equal to 5 ohms and producing an e.m.f. of 20 volts.

When loads of varying impedance, Z_1, are connected the output voltage, V (p.d.) and the power in the load, P_1, varies as follows:

$Z_1 = 5\,\Omega \quad I = 20/10 = 2\,\text{A} \quad V = 10\,\text{V}$
$Z_1 = 3\,\Omega \quad I = 2.5\,\text{A} \quad V = 7.5\,\text{V}$
$Z_1 = 8.33\,\Omega \quad I = 1.5\,\text{A} \quad V = 12.5\,\text{V}$

$P_1 = V^2/Z_1 = 100/5 = 20\,\text{W}$
$P_1 = V^2/Z_1 = 56.25/3 = 18.75\,\text{W}$
$P_1 = V^2/Z_1 = 156.25/8.33 = 18.75\,\text{W}$

When dealing with alternating current and when transmission lines, particularly at radio frequencies, are interposed between the source and the load, other factors than the power transfer efficiency must also be considered.

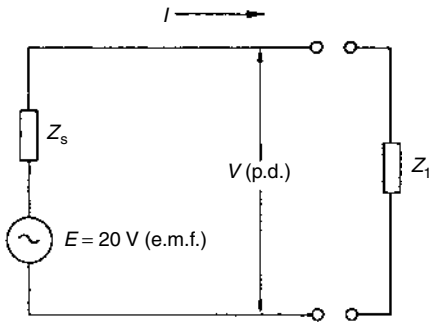

Figure 3.1 Impedance matching

3.3 Base band lines

These are the lines which generally operate at comparatively low frequencies carrying information at base band, e.g. speech, music, video or data. Generally provided by the telecommunications or telephone companies, usually on a rental basis, they are no longer likely to be hard wired, solid copper lines, although these may still be obtainable for lengths below about 10 km within one exchange area. Longer lines will probably be multiplexed, and comprised of radio and optical circuits over part of their length.

Baseband line impedance may vary between 450 Ω and 750 Ω. Nominal impedance is 600 Ω. Most line parameters are specified when measured between 600 Ω non-reactive impedance.

3.4 Balanced line hybrids

Radio transmitters and receivers are often controlled over a two-wire line. To facilitate this a balanced line hybrid circuit, consisting of two transformers connected back to back as in *Figure 3.2*, is inserted between the transmitter and receiver, and the line.

A signal from the receiver audio output is fed to winding L_1 of transformer T_1 which induces voltages across L_2 and L_3. The resultant line current also flows through L_4 and produces a voltage across L_6 which would appear as modulation on the transmitter but for the anti-phase voltage appearing across L_5. To ensure that the voltages cancel exactly a variable resistor, and often a capacitor to equalize the frequency response, is connected between L_2 and L_5.

A signal arriving via the line is applied to the transmitter as modulation; that it is also applied to the receiver poses no problem.

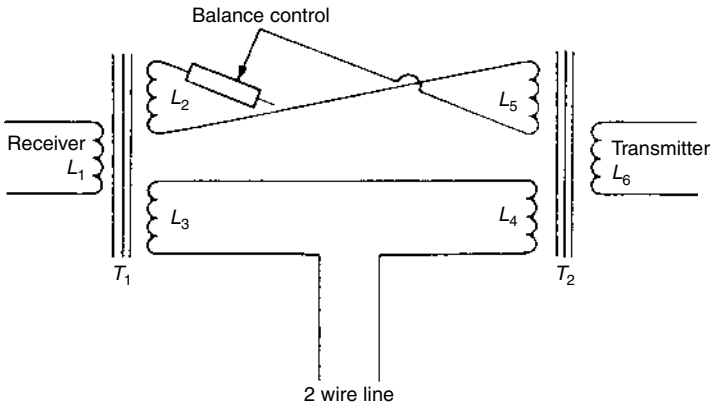

Figure 3.2 Balanced line hybrid

3.5 Radio frequency lines

Radio frequency transmission lines possess similar electrical characteristics to base band lines. However, they may be carrying large powers and the effects of a mismatched load are much more serious than a loss of transferred power. Three types of wire RF line are commonly used: a single wire with ground return for MF and LF broadcast transmission, an open pair of wires at HF and co-axial cable at higher frequencies. Waveguides are used at the higher microwave frequencies. RF lines exhibit an impedance characterized by their type and construction.

3.5.1 Characteristic impedance, Z_0

The physical dimensions of an RF transmission line, the spacing between the conductors, their diameters and the dielectric material between them, determine the characteristic impedance of the line, Z_0, which is calculated for the most commonly used types as follows.

Single wire with ground return (*Figure 3.3(a)*):

$$Z_0 = 138 \log_{10} \frac{4h}{d} \text{ ohms}$$

2-wire balanced, in air (*Figure 3.3(b)*):

$$Z_0 = \frac{276}{\sqrt{\varepsilon_p}} \log_{10} \frac{2s}{d} \text{ ohms}$$

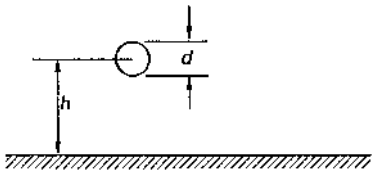

(a) Single wire, ground return line

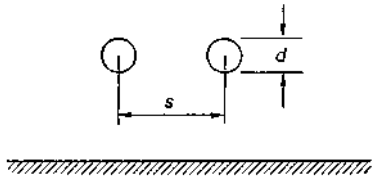

(b) 2-wire balanced air dielectric line

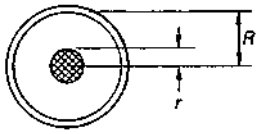

(c) Co-axial cable

Figure 3.3

Co-axial (*Figure 3.3(c)*):

$$Z_0 = \frac{138}{\sqrt{\varepsilon_r}} \log_{10} \frac{R}{r} \text{ ohms}$$

where dimensions are in mm and ε_r = relative permittivity of continuous dielectric.

3.5.2 Insertion loss

The loss in RF cables is quoted in specifications as attenuation in dB per unit length at specific frequencies, the attenuation increasing with frequency. The electrical specifications for cables having a braided outer conductor are given in *Tables 3.1* and *3.2*. Those for the now commonly used foam dielectric, solid outer conductor cables are provided in *Table 3.3*.

Table 3.1 RF cables USA RG and URM series

RG number	Nominal impedance Z_0 (ohms)	Overall diameter (inches)	Velocity factor	Attenuation (dB per 100 ft)					Capacity (pF/ft)	Maximum operating voltage RMS
				1 MHz	10 MHz	100 MHz	1000 MHz	3000 MHz		
RG-6A/U	75.0	0.332	0.659	0.21	0.78	2.9	11.2	21.0	20.0	2700
RG-11A/U	75.0	0.405	0.66	0.18	0.7	2.3	7.8	16.5	20.5	5000
RG-12A/U	75.0	0.475	0.659	0.18	0.66	2.3	8.0	16.5	20.5	4000
RG-16/U	52.0	0.630	0.670	0.1	0.4	1.2	6.7	16.0	29.5	6000
RG-34A/U	75.0	0.630	0.659	0.065	0.29	1.3	6.0	12.5	20.5	5200
RG-34B/U	75.0	0.630	0.66	–	0.3	1.4	5.8	–	21.5	6500
RG-35A/U	75.0	0.945	0.659	0.07	0.235	0.85	3.5	8.60	20.5	10 000
RG-54A/U	58.0	0.250	0.659	0.18	0.74	3.1	11.5	21.5	26.5	3000
RG-55/U	53.5	0.206	0.659	0.36	1.3	4.8	17.0	32.0	28.5	1900
RG-55A/U	50.0	0.216	0.659	0.36	1.3	4.8	17.0	32.0	29.5	1900
RG-58/U	53.5	0.195	0.659	0.33	1.25	4.65	17.5	37.5	28.5	1900

(*continued overleaf*)

Table 3.1 (*continued*)

RG number	Nominal impedance Z_0 (ohms)	Overall diameter (inches)	Velocity factor	Attenuation (dB per 100 ft)					Capacity (pF/ft)	Maximum operating voltage RMS
				1 MHz	10 MHz	100 MHz	1000 MHz	3000 MHz		
RG-58C/U	50.0	0.195	0.659	0.42	1.4	4.9	24.0	45.0	30.0	1900
RG-59A/U	75.0	0.242	0.659	0.34	1.10	3.40	12.0	26.0	20.5	2300
RG-59B/U	75	0.242	0.66	–	1.1	3.4	12.0	–	21	2300
RG-62A/U	93.0	0.242	0.84	0.25	0.85	2.70	8.6	18.5	13.5	750
RG-83/U	35.0	0.405	0.66	0.23	0.80	2.8	9.6	24.0	44.0	2000
RG-174A/U	50	0.1	0.66	1.83	3.35	11.0	32.0	64.0	30.0	1400
RG-188A/U	50	0.11	0.66	–	–	10.0	30.0	–	–	1200
*RG-213/U	50	0.405	0.66	0.16	0.6	1.9	8.0	–	29.5	5000
†RG-218/U	50	0.870	0.66	0.066	0.2	1.0	4.4	–	29.5	11 000
‡RG-220/U	50	1.120	0.66	0.04	0.2	0.7	3.6	–	29.5	14 000
URM43	50	0.116	0.66	0.396	1.25	3.96	–	–	30.0	2600
URM70	75	0.128	0.66	0.457	1.46	4.63	–	–	20.5	1800
URM76	50	0.116	0.66	0.457	1.46	4.72	–	–	30.0	2600

*Formerly RG8A/U.
†Formerly RG17A/U.
‡Formerly RG19A/U.

Table 3.2 British UR series

UR number	Nominal impedance Z_0 (ohms)	Overall diameter (inches)	Inner conductor (inches)	Capacity (pF/ft)	Maximum operating voltage RMS	Attenuation (dB per 100 ft)				Nearest RG equivalent
						10 MHz	100 MHz	300 MHz	1000 MHz	
43	52	0.195	0.032	29	2750	1.3	4.3	8.7	18.1	58/U
57	75	0.405	0.044	20.6	5000	0.6	1.9	3.5	7.1	11A/U
63*	75	0.855	0.175	14	4400	0.15	0.5	0.9	1.7	
67	50	0.405	7/0.029	30	4800	0.6	2.0	3.7	7.5	213/U
74	51	0.870	0.188	30.7	15 000	0.3	1.0	1.9	4.2	218/U
76	51	0.195	19/0.0066	29	1800	1.6	5.3	9.6	22.0	58C/U
77	75	0.870	0.104	20.5	1 25 000	0.3	1.0	1.9	4.2	164/U
79*	50	0.855	0.265	21	6000	0.16	0.5	0.9	1.8	
83*	50	0.555	0.168	21	2600	0.25	0.8	1.5	2.8	
85*	75	0.555	0.109	14	2600	0.2	0.7	1.3	2.5	
90	75	0.242	0.022	20	2500	1.1	3.5	6.3	12.3	59B/U

All the above cables have solid dielectric with a velocity factor of 0.66 with the exception of those marked with an asterisk, which are helical membrane and have a velocity factor of 0.96.

Table 3.3 Foam dielectric, solid outer conductor co-axial RF cables 50 ohms characteristic impedance

	Superflexible FS-J series		*LDF series*	
Cable type	FSJ1-50A 1/4″	FSJ4-50B 1/2″	LDF2-50 3/8″	LDF4-50A 1/2″
Min. bending radius, in. (mm)	1.0 (25)	1.25 (32)	3.75 (95)	5.0 (125)
Propagation velocity, %	84	81	88	88
Max. operating frequency, GHz	20.4	10.2	13.5	8.8
Att. dB/100 ft (dB/100 m)				
50 MHz	1.27 (4.17)	0.732 (2.40)	0.75 (2.46)	0.479 (1.57)
100 MHz	1.81 (5.94)	1.05 (3.44)	1.05 (3.44)	0.684 (2.24)
400 MHz	3.70 (12.1)	2.18 (7.14)	2.16 (7.09)	1.42 (4.66)
1000 MHz	6.00 (19.7)	3.58 (11.7)	3.50 (11.5)	2.34 (7.68)
5000 MHz	14.6 (47.9)	9.13 (30.0)	8.80 (28.9)	5.93 (19.5)
10 000 MHz	21.8 (71.5)	15.0 (49.3)	13.5 (44.3)	N/A N/A
Power rating, kW at 25°C (77°F)				
50 MHz	1.33	3.92	2.16	3.63
100 MHz	0.93	2.74	1.48	2.53
400 MHz	0.452	1.32	0.731	1.22
1000 MHz	0.276	0.796	0.445	0.744
5000 MHz	0.11	0.30	0.17	0.29
10 000 MHz	0.072	0.19	0.12	N/A

The claimed advantages of foam dielectric, solid outer conductor cables are:

1. Lower attenuation
2. Improved RF shielding, approximately 30 dB improvement
3. High average power ratings because of the improved thermal conductivity of the outer conductor and the lower attenuation.

A disadvantage is that they are not so easy to handle as braided cables.

3.5.3 Voltage standing wave ratio (VSWR)

When an RF cable is mismatched, i.e. connected to a load of a different impedance to that of the cable, not all the power supplied to the

cable is absorbed by the load. That which does not enter the load is reflected back down the cable. This reflected power adds to the incident voltage when they are in phase with each other and subtracts from the incident voltage when the two are out of phase. The result is a series of voltage – and current – maxima and minima at half-wavelength intervals along the length of the line (*Figure 3.4*). The maxima are referred to as antinodes and the minima as nodes.

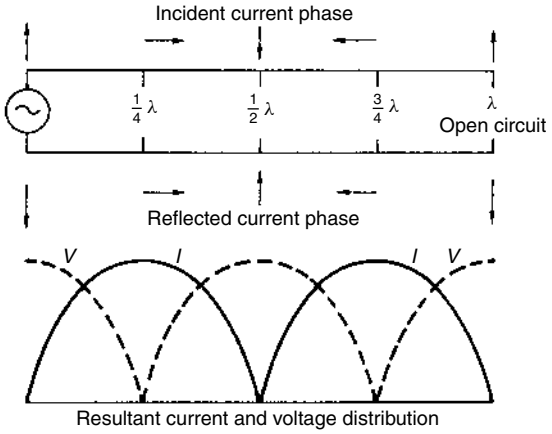

Figure 3.4 Formation of standing waves

The voltage standing wave ratio is the numerical ratio of the maximum voltage on the line to the minimum voltage: VSWR = V_{max}/V_{min}. It is also given by: VSWR = R_L/Z_0 or Z_0/R_L (depending on which is the larger so that the ratio is always greater than unity) where R_L = the load resistance.

The return loss is the power ratio, in dB, between the incident (forward) power and the reflected (reverse) power.

The reflection coefficient is the numerical ratio of the reflected voltage to the incident voltage.

The VSWR is 1, and there is no reflected power, whenever the load is purely resistive and its value equals the characteristic impedance of the line. When the load resistance does not equal the line impedance, or the load is reactive, the VSWR rises above unity.

A low VSWR is vital to avoid loss of radiated power, heating of the line due to high power loss, breakdown of the line caused by high voltage stress, and excessive radiation from the line. In practice, a VSWR of 1.5:1 is considered acceptable for an antenna system, higher ratios indicating a possible defect.

3.5.4 Transmission line filters, baluns and matching circuits

Use can be made of standing waves on sections of line to provide filters and RF transformers. When a line one-quarter wavelength long (aλ/4 stub) is open circuit at the load end, i.e. high impedance, an effective short-circuit is presented to the source at the resonant frequency of the section of line, producing an effective band stop filter. The same effect would be produced by a short-circuited λ/2 section. Unbalanced co-axial cables with an impedance of 50 Ω are commonly used to connect VHF and UHF base stations to their antennas although the antennas are often of a different impedance and balanced about ground. To match the antenna to the feeder and to provide a balance to unbalance transformation (known as a balun), sections of co-axial cable are built into the antenna support boom to act as both a balun and an RF transformer.

Balun

The sleeve balun consists of an outer conducting sleeve, one quarter-wavelength long at the operating frequency of the antenna, and connected to the outer conductor of the co-axial cable as in *Figure 3.5*. When viewed from point Y, the outer conductor of the feeder cable and the sleeve form a short-circuited quarter-wavelength stub at the operating frequency and the impedance between the two is very high. This effectively removes the connection to ground for RF, but not for DC, of the outer conductor of the feeder cable permitting the connection of the balanced antenna to the unbalanced cable without short-circuiting one element of the antenna to ground.

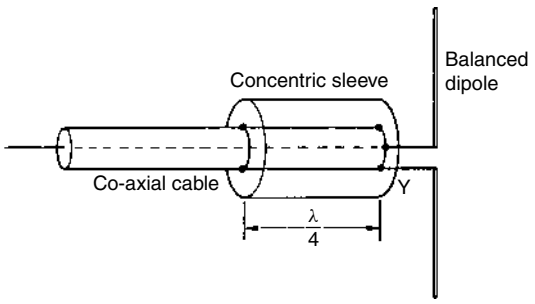

Figure 3.5 Sleeve balun

RF transformer

If a transmission line is mismatched to the load variations of voltage and current, and therefore impedance, occur along its length (standing

waves). If the line is of the correct length an inversion of the load impedance appears at the input end. When a λ/4 line is terminated in other than its characteristic impedance an impedance transformation takes place. The impedance at the source is given by:

$$Z_s = \frac{{Z_0}^2}{Z_L}$$

where
Z_s = impedance at input to line
Z_0 = characteristic impedance of line
Z_L = impedance of load

By inserting a quarter-wavelength section of cable having the correct characteristic impedance in a transmission line an antenna of any impedance can be matched to a standard feeder cable for a particular design frequency. A common example is the matching of a folded dipole of 300 Ω impedance to a 50 Ω feeder cable.

Let $Z_s = Z_0$ of feeder cable and $Z_0^{'}$ = characteristic impedance of transformer section. Then:

$$Z_0 = \frac{{Z_0^{'}}^2}{Z_L}$$

$$Z_0^{'} = \sqrt{Z_0 Z_L}$$

$$= \sqrt{300 \times 50} = 122\,\Omega$$

3.6 Waveguides

At the higher microwave frequencies waveguides which conduct electromagnetic waves, not electric currents, are often used. Waveguides are conductive tubes, either of rectangular, circular or elliptical section which guide the wave along their length by reflections from the tube walls. The walls are not used as conducting elements but merely for containment of the wave. Waveguides are not normally used below about 3 GHz because their cross-sectional dimensions must be comparable to a wavelength at the operating frequency. The advantages of a waveguide over a co-axial cable are lower power loss, low VSWR and a higher operating frequency, but they are more expensive and difficult to install.

In a rectangular waveguide an electromagnetic wave is radiated from the source at an angle to the direction of propagation and is

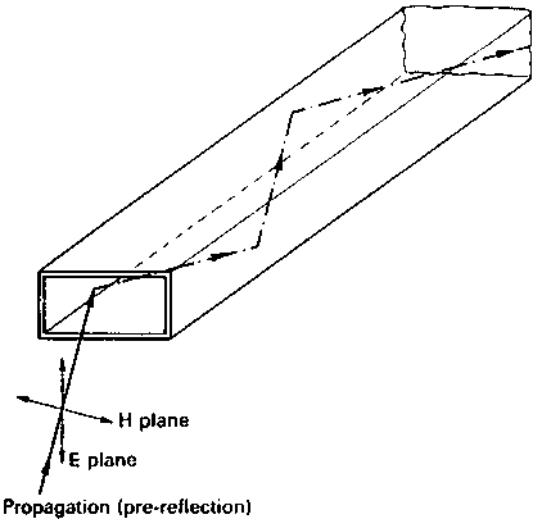

Figure 3.6 Propagation in rectangular waveguide

bounced off the walls (*Figure 3.6*). If the wave were transmitted directly along the length of the guide the electric field would be parallel to one of the walls and be short-circuited by it. Radiating the wave at an angle to the walls creates the maximum field at the centre of the guide and zero at the walls, if the dimensions of the guide are correct for the frequency. However, because the wave does not travel directly along the length of the guide, the speed of propagation is less than in space.

In an electro-magnetic wave the electric and magnetic fields, and the direction of propagation, are mutually perpendicular (see *Figure 1.3*) and such a wave may therefore be thought of as transverse electro-magnetic (TEM). In a waveguide though, because of the short-circuiting effect of the walls, a TEM wave cannot exist. A method of making the wave either transverse electric or transverse magnetic is needed.

When a wave is propagated by a reflection either the magnetic or the electric field is changed. The changed field will now contain the normal component perpendicular to the direction of propagation and a component in its direction, i.e. the wave is no longer wholly transverse. It must be either transverse electric or transverse magnetic. The terminology used to distinguish the type of wave differs: the American system uses the field which behaves as it would in free space to describe the type of wave, e.g. when there is no electric field in the direction of propagation the wave is called TE and the

mode with no magnetic field in the direction of propagation, TM; the European system uses the field that is modified and an American TE wave is a European TM wave. In the European system H and E may also be used in lieu of (American) TE and TM.

The behaviour of waves in circular waveguides is similar to that in rectangular guides. Circular waveguides minimize feeder attenuation and are particularly suitable for long vertical runs. A single circular waveguide can carry two polarizations with a minimum isolation of 30 dB. Circular waveguides are recommended where attenuation is critical or where multi-band capability is needed.

Elliptical waveguides have the advantages of flexibility, the availability of long continuous runs and reduced cost.

3.7 Other transmission line considerations

3.7.1 Noise factor of coaxial cable transmission line

Any lossy electrical device, including coaxial cable, produces a noise level of its own. The noise factor of coaxial line is:

$$F_{\mathrm{N(COAX)}} = 1 + \frac{(L-1)T}{290}$$

where

$F_{\mathrm{N(COAX)}}$ is the noise factor of the coax
L is the loss expressed as a linear quantity
T is the physical temperature of the cable in Kelvins

The linear noise factor due to loss can be converted to the noise figure by $10\log(F_{\mathrm{N(COAX)}})$, which can be added to the system noise decibel for decibel.

The attenuation loss figure published in manufacturers' tables is called the *matched line loss* (L_{M}) because it refers to the situation where the load and characteristic impedance of the line are equal. But we also have to consider the *Total Line Loss* (TLL), which is:

$$\mathrm{TLL} = 10\log\left[\frac{B^2 - C^2}{B(1-C^2)}\right]$$

where

B = antilog L_{M}
$C = (\mathrm{SWR_{LOAD}} - 1)/(\mathrm{SWR_{LOAD}} + 1)$
$\mathrm{SWR_{LOAD}}$ is the VSWR at the load end of the line

3.7.2 Types of coaxial cable

Coaxial cable consists of two cylindrical conductors sharing the same axis (hence 'co-axial') and separated by a dielectric. For low frequencies (in flexible cables) the dielectric may be polyethylene or polyethylene foam, but at higher frequencies Teflon® and other materials are used. Also used in some applications, notably high powered broadcasting transmitters, are dry air and dry nitrogen.

Several forms of coaxial line are available. Flexible coaxial cable discussed earlier in this chapter is perhaps the most common form. The outer conductor in such cable is made of either braided wire or foil. Again, television broadcast receiver antennas provide an example of such cable from common experience. Another form of flexible or semi-flexible coaxial line is *helical line* (*Figure 3.7*) in which the outer conductor is spiral wound. This type of coaxial cable is usually 2.5 or more centimetres in diameter.

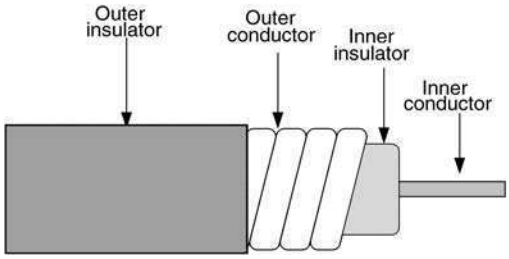

Figure 3.7 The helical line

Hardline is coaxial cable that uses a thin-walled pipe as the outer conductor. Some hardline coax used at microwave frequencies has a rigid outer conductor and a solid dielectric. *Gas-filled line* is a special case of hardline that is hollow (*Figure 3.8*), the centre conductor

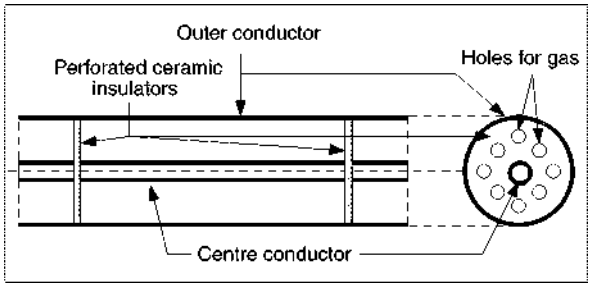

Figure 3.8 Gas-filled line

being supported by a series of thin ceramic or Teflon insulators. The dielectric is either anhydrous (i.e. dry) nitrogen or some other inert gas.

Some flexible microwave coaxial cable uses a solid 'air-articulated' dielectric (*Figure 3.9*), in which the inner insulator is not continuous around the centre conductor, but rather is ridged. Reduced dielectric losses increase the usefulness of the cable at higher frequencies. Double shielded coaxial cable (*Figure 3.10*) provides an extra measure of protection against radiation from the line, and EMI from outside sources from getting into the system.

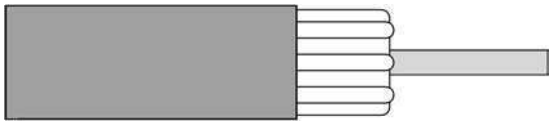

Figure 3.9 Solid 'air-articulated' dielectric

Figure 3.10 Double shielded coaxial cable

3.7.3 Transmission line noise

Transmission lines are capable of generating noise and spurious voltages that are seen by the system as valid signals. Several such sources exist. One source is coupling between noise currents flowing in the outer and inner conductors. Such currents are induced by nearby electromagnetic interference and other sources (e.g. connection to a noisy ground plane). Although coaxial design reduces noise pick-up compared with parallel line, the potential for EMI exists. Selection of high-grade line, with a high degree of shielding, reduces the problem.

Another source of noise is thermal noise in the resistances and conductances of the line. This type of noise is proportional to resistance and temperature.

There is also noise created by mechanical movement of the cable. One species results from movement of the dielectric against the two conductors. This form of noise is caused by electrostatic discharges in much the same manner as the spark created by rubbing a piece of plastic against woollen cloth.

A second species of mechanically generated noise is piezoelectricity in the dielectric. Although more common in cheap cables, one

should be aware of it. Mechanical deformation of the dielectric causes electrical potentials to be generated.

Both species of mechanically generated noise can be reduced or eliminated by proper mounting of the cable. Although rarely a problem at lower frequencies, such noise can be significant at microwave frequencies when signals are low.

3.7.4 Coaxial cable capacitance

A coaxial transmission line possesses a certain capacitance per unit of length. This capacitance is defined by:

$$C = \frac{24\varepsilon}{\log(D/d)} \frac{\text{pF}}{\text{Metre}}$$

where

C is the capacitance
D is the outside conductor diameter
d is the inside conductor diameter
ε is the dielectric constant of the insulator.

A long run of coaxial cable can build up a large capacitance. For example, a common type of coax is rated at 65 pF/metre. A 150 metre roll thus has a capacitance of (65 pF/m) (150 m), or 9750 pF. When charged with a high voltage, as is done in performing breakdown voltage tests at the factory, the cable acts like a charged high voltage capacitor. Although rarely if ever lethal to humans, the stored voltage in new cable can deliver a nasty electrical shock and can irreparably damage electronic components.

3.7.5 Coaxial cable cut-off frequency (F_c)

The normal mode in which a coaxial cable propagates a signal is as a transverse electromagnetic (TEM) wave, but others are possible – and usually undesirable. There is a maximum frequency above which TEM propagation becomes a problem, and higher modes dominate. Coaxial cable should not be used above a frequency of:

$$F_{\text{CUT-OFF}} = \frac{1}{3.76(D+d)\sqrt{\varepsilon}}$$

where

F is the TEM mode cut-off frequency
D is the diameter of the outer conductor in mm

d is the diameter of the inner conductor in mm
ε is the dielectric constant

When maximum operating frequencies for cable are listed it is the TEM mode that is cited. Beware of attenuation, however, when making selections for microwave frequencies. A particular cable may have a sufficiently high TEM mode frequency, but still exhibit a high attenuation per unit length at X or Ku-bands.

References

Andrew Antennas, (1991). *Catalogue 35*, Illinois.
British Telecommunications (1992). *Connect Direct, private circuits*. BT, London.
Kennedy, G. (1977). *Electronic Communications Systems*. McGraw-Hill Kogashuka, Tokyo.
Terman, F.E. (1943), *Radio Engineers' Handbook*, McGraw-Hill, London.
Winder, S.W. (2001). *Newnes Telecommunications Pocket Book*. Butterworth-Heinemann, Oxford.

4 Antennas

4.1 Antenna characteristics

4.1.1 Bandwidth

Stated as a percentage of the nominal design frequency, the bandwidth of an antenna is the band of frequencies over which it is considered to perform acceptably. The limits of the bandwidth are characterized by unacceptable variations in the impedance which changes from resistive at resonance to reactive, the radiation pattern, and an increasing VSWR.

4.1.2 Beamwidth

In directional antennas the beamwidth, sometimes called half-power beamwidth (HPBW), is normally specified as the total width, in degrees, of the main radiation lobe at the angle where the radiated power has fallen by 3 dB below that on the centre line of the lobe (*Figure 4.1A*).

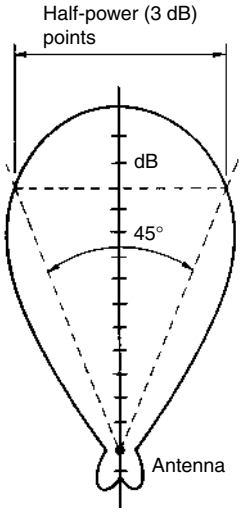

Figure 4.1A Half-power beamwidth

4.1.3 Directivity and forward gain

All practical antennas concentrate the radiated energy in some directions at the expense of others. They possess directivity but are

completely passive; they cannot increase the power applied to them. Nevertheless, it is convenient to express the enhanced radiation in some directions as a power gain.

Antenna gain may be quoted with reference to either an isotropic radiator or the simplest of practical antennas, the dipole. There is a difference of 2.15 dB between the two figures. A gain quoted in dBi is with reference to an isotropic radiator and a gain quoted in dBd is with reference to a dipole. When gain is quoted in dBi, 2.15 dB must be subtracted to relate the gain to that of a dipole.

4.1.4 Effective height or length

The current flowing in an antenna varies along its length (see *Figure 1.4*). If the current were uniform along the length of an antenna it would produce a field appropriate to its physical length, and the effective height or length of the antenna would be its physical length. In practice, because the current is not uniform, the effective length is less than the physical length and is given by:

$$l_{\text{eff}} = \frac{l_{\text{phys}} \times I_{\text{mean}}}{I}$$

where

l_{eff} = effective length
l_{phys} = physical length
I = current at feed point

With an antenna which is short in comparison with a wavelength the current can be considered to vary linearly over its length and $I_{\text{mean}} = I/2$. Because the apparent length of a vertical radiator is twice that of its physical dimension due to the mirror image formed below the ground, the effective length of an electrically short vertical antenna may be approximated to be its physical length.

4.1.5 Effective radiated power (erp)

This is the power effectively radiated along the centre line of the main lobe. It is the power supplied to the antenna multiplied by the antenna gain with reference to a dipole.

4.1.6 Radiation resistance and efficiency

The power radiated by an antenna can conveniently be expressed in terms of the value of a resistor which would dissipate the same power

that the antenna radiates. This value is referred to as the radiation resistance and is defined as the ratio of the power radiated to the square of the current at the feed point. The efficiency is the ratio of the power radiated to that lost in the antenna. It is given by:

$$\text{eff} = \frac{R_r}{R_r + R_L} \times 100\%$$

where R_r is the radiation resistance and R_L represents the total loss resistance of the antenna. The sum of the two resistances is the total resistance of the antenna and, for a resonant antenna, is also the impedance.

4.1.7 Front-to-back ratio

The ratio, in dB, of the strength of the radiation (or received signal) in the forward (desired) direction to that in the reverse (unwanted) direction. The front-to-back ratio of the antenna shown in *Figure 4.1A* is 13 dB.

4.1.8 Impedance

The impedance of an antenna is that presented to the feeder cable connecting it to the transmitter or receiver. It is the result of the vectorial addition of the inductive, capacitive and resistive elements of the antenna. Each resonant antenna possesses an impedance characteristic of the type, and when an antenna operates at its resonant frequency the reactive elements cancel out and the impedance becomes resistive. The radiation resistance plus the losses in the antenna, i.e. the series resistance of the conductors, the shunt resistance of the base material and losses in nearby objects, form the resistive portion of the impedance.

4.1.9 Polarization

The radiated field from an antenna is considered to be polarized in the plane of the length of the conductors which is the plane of the electric field, the E plane. Confusion arises when reference is made to vertical or horizontal polarization and it is preferable when referring to polar diagrams to use the E and H plane references.

Circular polarization, produced by crossed dipoles or helical wound antennas, is occasionally used for point-to-point work at VHF and above to reduce multi-path propagation losses.

Cross polarization discrimination defines how effectively an antenna discriminates between a signal with the correct polarization, i.e. mounted with the elements in the same plane, and one operating at the same frequency with the opposite polarization. 20 dB is typical.

4.1.10 Radiation pattern

A plot of the directivity of an antenna showing a comparison of the power radiated over 360°. Two polar diagrams are required to show the radiation in the E and H planes. The polar diagrams may be calibrated in either linear (voltage) or logarithmic (decibel) forms.

4.1.11 Voltage standing wave ratio (VSWR)

Most VHF and UHF antennas contain an impedance matching device made up of lengths of co-axial cable. Thus the VSWR (see Chapter 3) of these types of antenna varies with the operating frequency, more so than the bandwidth of the antenna alone would produce. At the centre design frequency, the VSWR should, theoretically, be 1:1 but in practice a VSWR less than 1.5:1 is considered acceptable.

4.1.12 Receive aperture

Receiving antennas also possess a property called aperture, or capture area. This concept relates the amount of power that is delivered to a matched receiver to the power density (watts per square metre). The aperture is often larger than the physical area of the antenna, as in the case of the half-wavelength dipole (where the wire fronts a very small physical area), or less as in the case of a parabolic reflector used in microwave reception. *Figure 4.1B* shows the capture area of a half-wavelength (0.5λ) dipole. It consists of an ellipse with major axes of 0.51λ and 0.34λ. The relationship between gain and aperture is:

$$A_e = \frac{G\lambda^2}{4\pi n}$$

where

A_e is the effective aperture
G is the gain
λ is the wavelength of the signal
n is the aperture effectiveness ($n = 1$ for a perfect no-loss antenna, real values are typically 0.3 to 0.55

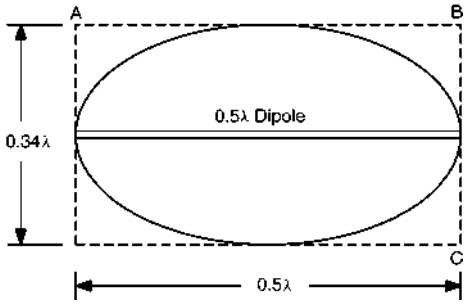

Figure 4.1B Capture area of half-wavelength (0.5λ) dipole

4.2 Antenna types

4.2.1 The dipole

The half-wavelength (λ/2) dipole as described in Section 1.4 is the antenna on which many others are based. *Figure 4.2* shows the relative radiation in the E and H planes of a dipole in free space.

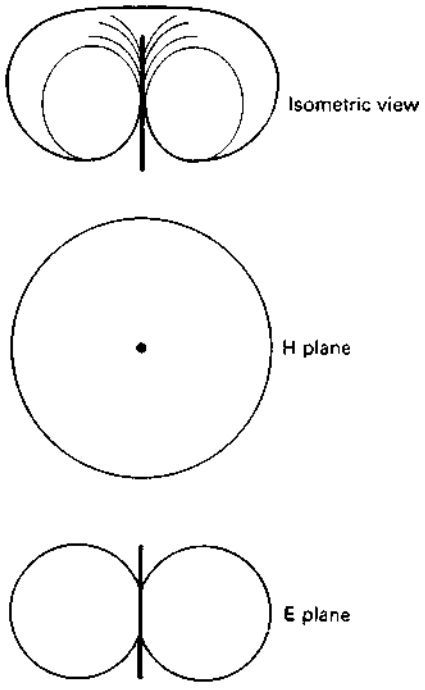

Figure 4.2 Radiation patterns of a half-wave dipole

The impedance of a half-wavelength dipole is 72 Ω; that of a full wavelength or folded dipole is 300 Ω.

4.2.2 The quarter-wavelength vertical radiator

The quarter-wavelength (λ/4) vertical radiator is a commonly used antenna for MF broadcasting and for VHF and UHF mobile radio applications. It is derived from the λ/2 dipole and it is assumed that a mirror image of the radiator is formed below the ground to complete the λ/2 structure of the dipole as in *Figure 4.3*. The radiation pattern of a λ/4 vertical radiator mounted close to a perfect earth shows a strong similarity to that of a dipole. The effect of reducing the size and conductivity of the ground plane raises the angle of radiation.

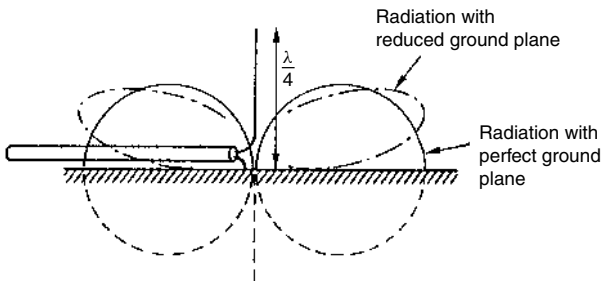

Figure 4.3 Quarter-wavelength vertical radiator

The impedance of a perfect λ/4 vertical radiator is 36 Ω but reducing the effectiveness of the ground plane raises the impedance.

4.2.3 LF, MF and HF antennas

Because of the physical lengths involved, LF and MF antennas are usually non-resonant and their impedances do not conform to the resistive 70 Ω or 36 Ω of the basic resonant types. The impedance of a non-resonant antenna is usually higher and reactive so an antenna tuning or matching unit is used to couple the antenna efficiently to the transmission line and also act as filter to reduce out-of-band radiations. The matching unit comprises a tuned circuit with either a tap on the coil at the correct impedance point or a separate coupling coil to feed the antenna.

Obtaining an adequate length is always the problem with low frequency antennas and various methods have been used based mainly on the λ/4 radiator. The horizontal section of the inverted L (*Figure 4.4*) extends the effective length but, as the ground wave is much used at

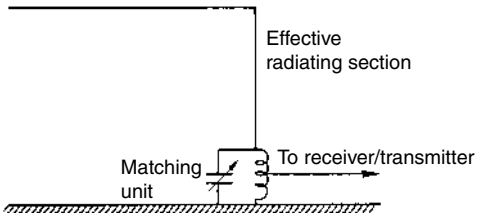

Figure 4.4 Inverted L antenna

the lower frequencies, these antennas are intended for vertical polarization and it is therefore only the down-lead which radiates, or receives, effectively. An alternative method of increasing the effective height of a vertical radiator is to provide a capacitance top where the system of horizontal conductors provides a high capacitance to ground. This prevents the current falling to zero at the top of the antenna, maintaining a higher mean current and so increasing the antenna's effective length.

Dipoles used at HF are mounted horizontally because of their length and have directivity in the horizontal (E) plane. Propagation is mainly by the sky wave and the omni-directional properties in the vertical (H) plane, modified by ground reflections, produce wide angle upwards radiation.

4.2.4 Directional arrays

Broadside array

A broadside array consists of several radiators spaced uniformly along a line, each carrying currents of the same phase. When each radiator has an omni-directional pattern, and the spacing between radiators is less than $3\lambda/4$, maximum radiation occurs at right angles to the line of the array. The power gain is proportional to the length of the array, provided that the length is greater than two wavelengths; this means, effectively, the number of radiators. *Figure 4.5* shows a typical H plane polar diagram for an array with vertically mounted radiators and a spacing of $\lambda/2$.

End-fire array

Physically an end-fire array is identical to a broadside except for the feeding arrangements and the spacing of the elements. In an end-fire array the radiators are fed with a phase difference between adjacent radiators equal in radians to the spacing between them in wavelengths.

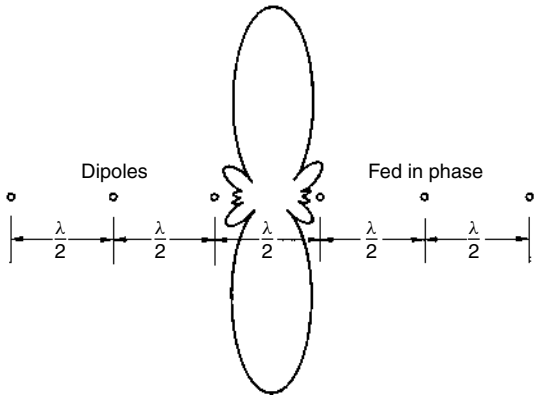

Figure 4.5 Broadside array

A spacing of λ/4 requires a phase shift of 90° between adjacent radiators. *Figure 4.6* shows a typical radiation pattern. An end-fire array concentrates the power in both the E and H planes and the maximum radiation is in the direction of the end of the array with the lagging phase.

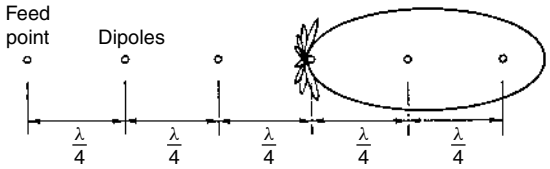

Figure 4.6 End-fire array

Rhombic antenna

A rhombic is a wide band, directional antenna comprised of four non-resonant wire antennas, each several wavelengths long, arranged as shown in *Figure 4.7(a)* which also shows the radiation pattern for each leg of the rhombus. The lobe angle θ can be varied by adjusting the length, in wavelengths, of each radiator. The antenna has greater directivity than a single wire and can be terminated by an appropriate value resistor to ensure non-resonance and a wide bandwidth. However, because it must be terminated in a resistance equal to the characteristic impedance of the conductors, it cannot be more than 50% efficient. It also exhibits considerable side lobes of radiated power. Rhombics are used for sky wave working at HF and more than one frequency is allocated to allow for varying propagation conditions. The conductors of a rhombic are normally horizontal and the horizontal directivity is

determined by the tilt angle, β in *Figure 4.7(a)*. If the lobe angle θ is equal to $(90 - \beta)^\circ$ the radiation in the A lobes cancels, while that from the B lobes, which point in the same direction, is added. The resultant pattern in the horizontal plane is shown in *Figure 4.7(b)*. The vertical directivity is controlled by the height of the conductors above the ground.

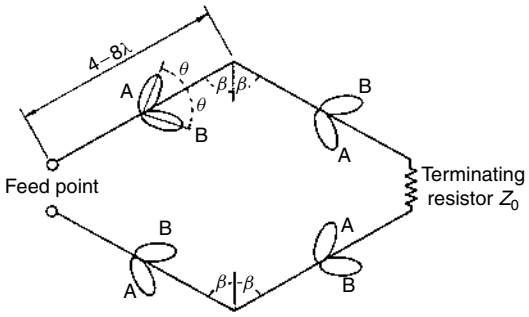

(a) Rhombic antenna

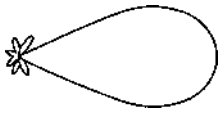

(b) Radiation pattern of rhombic

Figure 4.7

Log-periodic antenna

An alternative, usable from HF through UHF, to the rhombic for wide band operation is the log-periodic antenna. It is comprised of several dipoles of progressive lengths and spacings as in *Figure 4.8*, and is resonant over a wide frequency range and may be mounted with either polarization. The dipoles are fed via the support booms and this construction ensures that the resultant phasing of the dipoles is additive in the forward direction producing an end-fire effect. However, because at any one frequency only a few of the dipoles are close to resonance, the forward gain of the antenna is low considering the number of elements it contains.

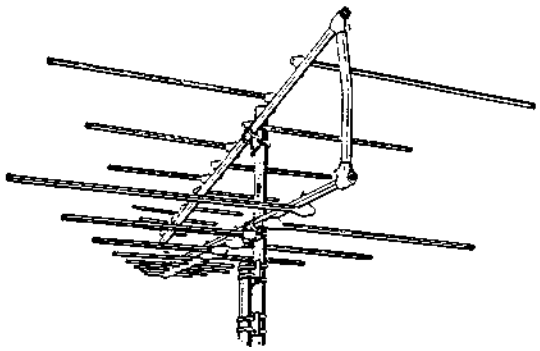

Figure 4.8 Log-periodic antenna at VHF frequency

4.3 VHF and UHF antennas

4.3.1 Base station antennas

Apart from entertainment broadcasting and mobile telephony, most VHF and UHF systems use vertical polarization and a dipole – or to prevent noise from rain static, the folded dipole – with the conductors mounted vertically is a frequently used antenna for VHF and UHF base station installations. Unfortunately it is often mounted on the side of the support structure in a manner which seriously affects its omnidirectional radiation pattern. Where practical, there should be a minimum spacing of one wavelength between the structure and the rearmost element of the antenna.

To obtain a good omni-directional pattern either an end-fed dipole (*Figure 4.9*) or a unipole antenna (*Figure 4.10*) protruding from the top of the mast or tower is the best option. A unipole is a variation of the vertical quarter-wave radiator and provides a low angle of radiation.

To reduce the likelihood of co-channel interference directional antennas are often necessary. The simplest of these is the combination of a $\lambda/2$ dipole and reflector shown in *Figure 4.11*. The reflector is slightly longer than the dipole and spaced one quarter-wavelength from it. The portion of the signal radiated by the dipole in the direction of the reflector is received and re-transmitted by the reflector, with a 180° phase change occurring in the process. The signal re-transmitted

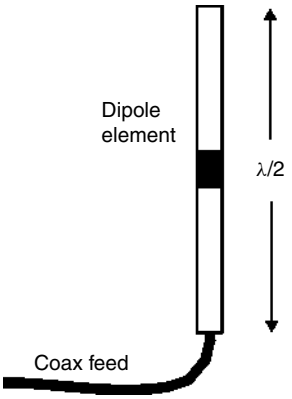

Figure 4.9 Type EDV end-fed antenna (by kind permission of C and S Antennas Ltd)

to the rear of the antenna – the direction of the reflector – cancels the signal from the dipole, that towards the front of the antenna adds to the signal from the dipole giving the radiation pattern shown. The power gain of a dipole and reflector, a two-element array, is 3 dBd.

Directivity can be increased by adding directors forward of the dipole, the result is a Yagi–Uda array. The limit to the number of radiators is set by physical constraints and the reduction of bandwidth produced by their addition. At low VHF, a 3-element array is about the practical maximum, while at 1500 MHz, 12-element arrays are commonplace. As a rule of thumb, doubling the number of elements in an array increases the forward gain by 3 dB. Where the maximum front-to-back ratio is essential the single rod reflector can be replaced by a corner reflector screen.

Co-linear antennas provide omni-directional characteristics and power gain in the H plane. A co-linear consists of a number of dipoles stacked vertically and, in the normal configuration, fed so that they radiate in phase and the maximum power is radiated horizontally. *Figure 4.12* shows alternative feeding arrangements. One advantage of the co-linear is that the horizontal angle of radiation can be tilted to about 15° downwards by changing the phasing of the elements. The gain of a co-linear is limited, because of the physical lengths involved and losses in the feeding arrangements to 3 dBd at VHF and 6 dBd at UHF.

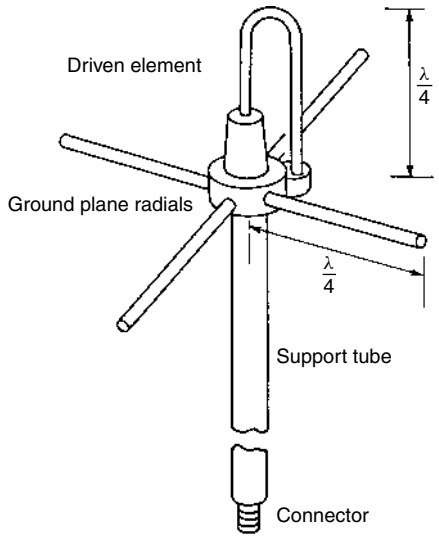

Figure 4.10 Folded unipole antenna

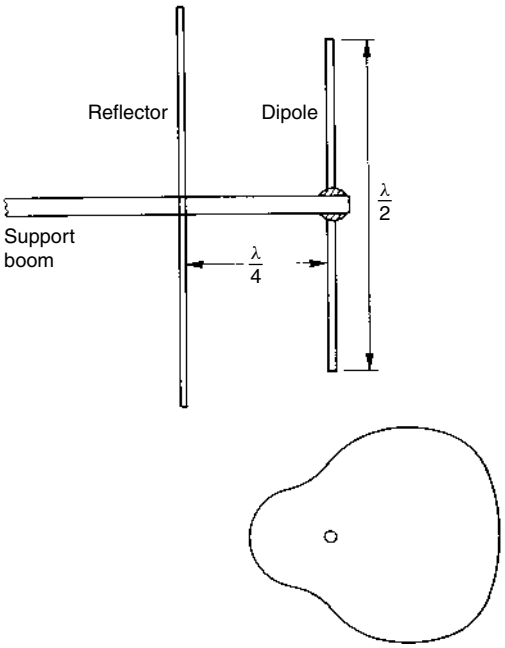

Figure 4.11 Dipole and reflector

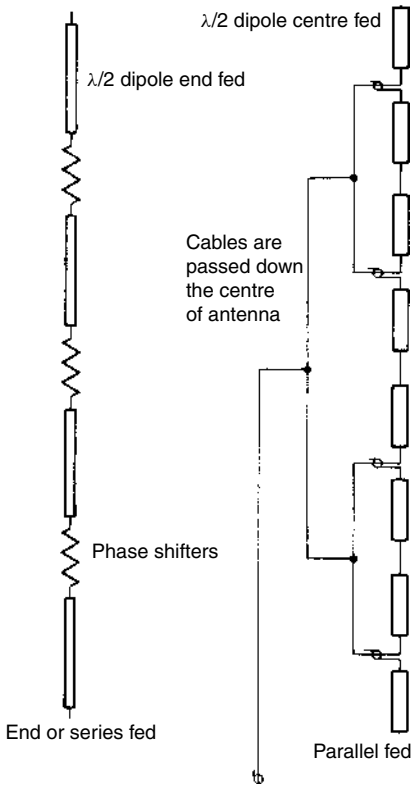

Figure 4.12 General construction of co-linears

Figure 4.13 shows a slot antenna cut into a flat metal sheet. Current (I) injected at the centre of the slot flows around the edge and creates a vertical electric field. The radiated field pattern is like a dipole.

The type of slot antenna typically used for mobile telephony base stations is a cylindrical waveguide with slots cut width-wise. Current flowing along the waveguide creates an electric field along the length of the cylinder. The radiation pattern produced by a slot antenna cut into a cylinder is directional, with the main beam perpendicular to the slot. Using two slot antennas side by side provides radio coverage over a 120° sector. Three pairs of slot antennas placed around a mast gives three sectors that can operate at different frequencies.

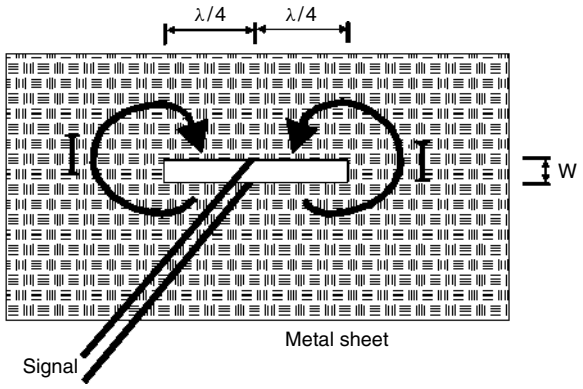

Figure 4.13 Slot antenna

A wide-band alternative to the log-periodic is the conical (discone) antenna (*Figure 4.14*). It provides unity gain, is omni-directional and has a bandwidth of approximately 3:1, depending on the designed frequency range. In practice there has been a tendency to expect these antennas to perform outside their specified bandwidths with unsatisfactory results.

Stacking and baying

A method of increasing an antenna's directivity is to mount two or more antennas vertically above one another (stacking) or side-by-side (baying), and to feed them so that they radiate in phase. Stacking two dipoles vertically increases the directivity in the E plane and baying them increases the directivity in the H plane, approximately halving the beamwidth in each case.

An array of two stacked plus two bayed antennas approximately halves the beamwidth in both planes.

4.3.2 Mobile antennas

The aerial is the least expensive, and most abused, component of a mobile radio installation. Frequently installed in a manner which does not produce optimum performance it can have a profound effect on the performance of the whole installation.

Most mobile antennas consist of a metal rod forming a quarter-wavelength radiator. The ideal mounting position is the centre of a

metallic roof, and as the area of the ground plane is reduced the radiation pattern changes and more of the energy is radiated upwards (not always a bad thing in inner city areas); also, the impedance rises.

The effect of the mounting position on the H plane radiation can be dramatic, resulting in ragged radiation patterns and, in some directions, negligible radiation. Advice on the installation of mobile antennas and the polar diagrams produced by typical installations are illustrated in MPT 1362, *Code of Practice for Installation of Mobile Radio Equipment in Land Based Vehicles*.

As the installation moves away from the ideal and the antenna impedance rises a mismatch is introduced between the antenna and the feeder with the consequent production of standing waves on the feeder. Under high VSWR conditions the cable is subject to higher voltage stresses and it also behaves as an aerial radiating some of the reflected power. This spurious radiation adds to the radiation from the antenna in some directions but subtracts from it in others giving rise to jagged radiation patterns or deep nulls in radiated signal.

Mobile antennas providing a small amount of gain, typically 3 dB and obtained by narrowing the radiation lobes, are on the market. These have a length of 5/8 wavelength and, because the extra length makes the impedance capacitive at the operational frequency, a loading coil is inserted at the lower end of the element to cancel the capacitive reactance. An adjustable metallic disk towards the base of the whip is often provided for tuning purposes. Note that gain figures quoted for mobile antennas are usually with reference to a quarter-wave whip.

Low profile antennas

Low profile antennas are available for use at UHF. They have a built-in ground plane approximately 150 mm in diameter and a height of some 30 mm and have obvious applications for use on high vehicles and, although not strictly covert, where a less obtrusive antenna is required. They are fitted with a tuning screw and when adjusted to resonance a VSWR of better than 1.2:1 is quoted by one maker and a bandwidth of 10 MHz at a VSWR of 2:1. *Figure 4.15* shows the radiation pattern for one type.

Motor-cycle antennas

The installations of antennas on motor cycles poses problems because of the absence of a satisfactory ground plane. One frequently used method is to employ a 5/8 wavelength whip and loading coil. Another

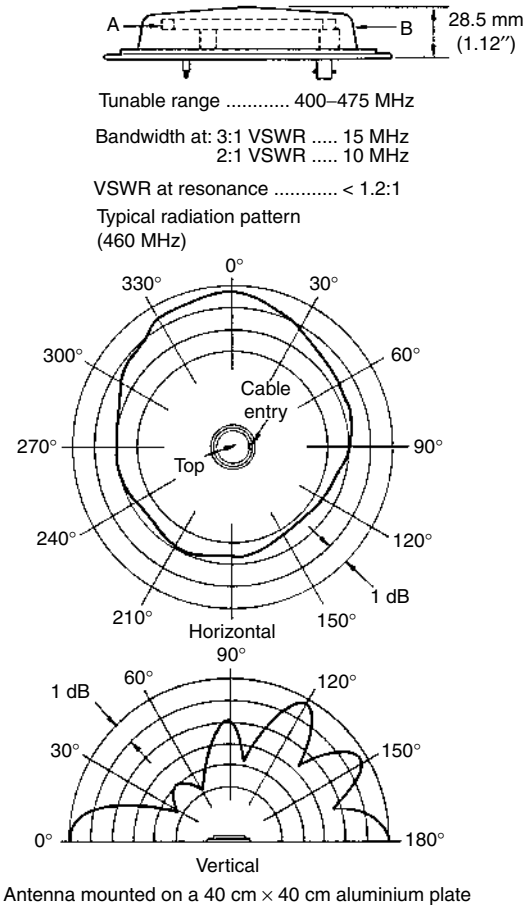

Figure 4.15 Low profile UHF antenna (by kind permission of Panorama Antennas Ltd)

method uses a pair of grounded downwards-pointing rods to form the lower half of a dipole.

Hand-portable antennas

Again, because of the lack of a ground plane high performance antennas are difficult to provide for hand-portables, particularly at VHF. Body-worn sets may have an antenna incorporated in the microphone lead but the high current portion of the antenna must then be at a low height and in some directions the radiation must pass through the body, which is highly absorbent, to reach the base station. Helical

antennas are frequently used on hand-held sets to reduce the physical length. Useful operating tips are to face the base station when using the radio in low signal areas, while placing the set on a nearby car roof effectively increases the performance of the antenna.

Safety

There are two safety aspects to consider when installing mobile antennas: physical and electrical. The physical considerations are that the antenna must be incapable of inflicting injury when it is in its correct position, and also when it has been bent or damaged. Rear wing mounted antennas need particular care in their positioning; a Band 111 aerial tip is just about eye height when bending over an open boot lid. The same considerations apply to hand-portables, helical antennas being perhaps safer than whips because they are thicker and thus more easily seen. They also have rounded tips.

The electrical dangers are from radiation affecting the body either directly – radiation from a hand-portable helical into the eye is a possible example – or indirectly by affecting electronic equipment. The danger of radiation affecting equipment in the vehicle is increased when the VSWR is high because of increased radiation from the feeder. Advice should be sought from the Radiological Protection Board.

4.4 Microwave antennas

The small antenna elements at microwaves facilitate the construction of highly directive, high gain antennas with high front-to-back ratios.

At frequencies below about 2 GHz, 12- to 24-element Yagi arrays, enclosed in plastic shrouds for weather protection, may be used. At higher frequencies, antennas with dish reflectors are the norm.

The aperture ratio (diameter/wavelength) of a dish governs both its power gain and beamwidth. The power gain of a parabolic dish is given to a close approximation by:

$$\text{Gain} = 10 \log_{10} 6(D/\lambda)^2 \times N, \text{dBi}$$

where $D =$ dish diameter and $N =$ efficiency. Dimensions are in metres. The half-power beam width (HPBW) in degrees is approximately equal to $70\lambda/D$.

A microwave antenna with its dish reflector, or parasitic elements in the case of a Yagi type, is a large structure. Because of the very narrow beamwidths – typically 5° for a 1.8 m dish at 2 GHz – both

the antenna mounting and its supporting structure must be rigid and able to withstand high twisting forces to avoid deflection of the beam in high winds. Smooth covers, radomes, fitted to dishes and the fibre-glass shrouds which are normally integral with Yagis designed for these applications considerably reduce the wind loading and, for some antenna types, increase the survival wind speed.

The electrical performance of a selection of microwave antennas is given in *Table 4.1* and the wind survival and deflection characteristics in *Table 4.2* (Andrew Antennas, 1991).

Table 4.1 2.1–2.2 GHz antennas – electrical characteristics

Type number	*Dia. (m)*	*Gain (dBi)*			*Beam width (deg.)*	*Cross pol. disc (dB)*	*F/B ratio (dB)*	*VSWR max.*
		Bottom	*Mid-band*	*Top*				
Ultra High Performance Antenna, F-Series Unpressurized – Radome Inc.								
Single polarized								
UHP8F-21	2.4	31.9	32.1	32.3	4.2	32	61	1.10
UHP10F-21	3.0	33.7	33.9	34.0	3.6	33	64	1.10
UHP12F-21	3.7	35.4	35.6	35.8	2.9	32	65	1.10
Dual polarized								
UHX8F-21	2.4	31.9	32.1	32.3	4.2	30	58	1.20
UHX10F-21A	3.0	33.8	34.0	34.2	3.6	32	62	1.20
UHX12F-21A	3.7	35.4	35.6	35.8	2.8	32	67	1.20
High Performance Antenna, F-Series Unpressurized – Radome Inc.								
Single polarized								
HP6F-21B	1.8	29.4	29.6	29.8	5.5	30	46	1.12
HP8F-21A	2.4	31.9	32.1	32.3	4.1	30	53	1.12
HP10F-21A	3.0	33.8	34.0	34.2	3.4	32	55	1.12
HP12F-21A	3.7	35.4	35.6	35.8	2.9	32	56	1.12
Standard Antenna, F-Series Unpressurized								
Single polarized								
P4F-21C	1.2	26.4	26.6	26.8	7.6	30	36	1.15
P6F-21C	1.8	29.8	30.0	30.2	4.9	30	39	1.12
P8F-21C	2.4	32.3	32.5	32.7	3.8	30	40	1.12
P10F-21C	3.0	34.0	34.2	34.4	3.4	30	44	1.12
Grid Antenna, F-Series Unpressurized								
Single polarized								
GP6F-21A	1.8	29.6	29.8	30.0	5.4	31	36	1.15
GP8F-21A	2.4	32.0	32.2	32.4	4.0	35	39	1.15
GP10F-21A	3.0	34.0	34.2	34.4	3.3	40	42	1.15
GP12F-21	3.7	35.5	35.7	35.9	2.8	40	44	1.15

With shrouded Yagis and some dishes low loss foam-filled cables are generally used up to about 2 GHz although special connectors may

Table 4.2 Wind survival and deflection characteristics

Antenna types	*Survival ratings*		*Max. deflection in 110 km wind (degrees)*
	Wind velocity (km/h)	*Radial ice (mm)*	
P4F Series			
Without Radome	160	12	0.1
With Radome	185	12	0.1
Standard Antennas (except P4F Series)			
Without Radome	200	25	0.1
With Standard Radome	200	25	0.1
UHX, UMX, UGX Antennas	200	25	0.1

be required. At higher frequencies, air-spaced or pressurized nitrogen-filled cables are frequently used with waveguides as an alternative.

4.4.1 Omnidirectional normal mode helix

The normal mode helix antenna shown in *Figure 4.16* produces an omnidirectional pattern when the antenna is mounted vertically. The diameter (D) of the helical coil should be one-tenth wavelength ($\lambda/10$), while the pitch (i.e. S, the distance between helix loops) is one-twentieth wavelength ($\lambda/20$). An example of the normal mode helix is the 'rubber ducky' antenna used on VHF/UHF two-way radios and scanners.

4.4.2 Axial mode helical antenna

An axial mode helical antenna is shown in *Figure 4.17*. This antenna fires 'off-the-end' in the direction shown by the arrow. The helix is mounted in the centre of a ground plane that is at least 0.8λ across. For some UHF frequencies some manufacturers have used aluminum pie pans for this purpose. The helix itself is made from either heavy copper wire (solid, not stranded) or copper or brass tubing. The copper tubing is a bit easier to work. The dimensions are:

$$D \approx \lambda/3$$

$$S \approx \lambda/4$$

$$\text{Length} \approx 1.44\lambda$$

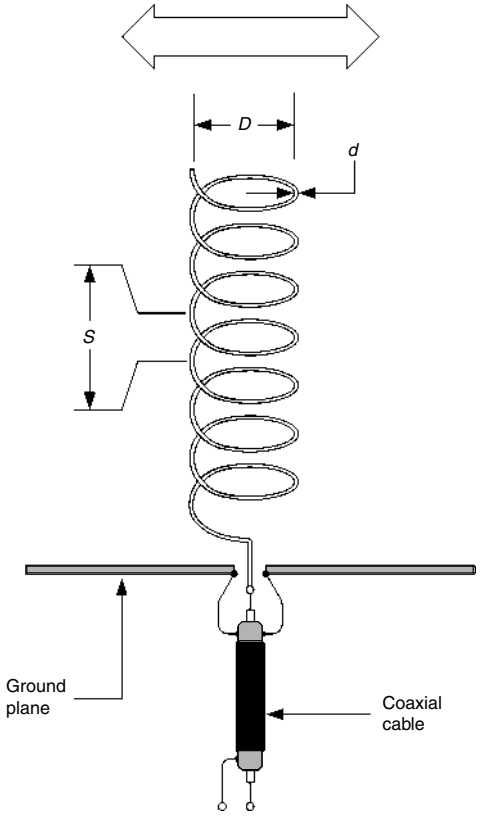

Figure 4.16 Normal mode helix antenna

A 'rule of thumb' for the circumference is that maximum gain is obtained when circumference C is:

$$C = 1.066 + [(N - 5) \times 0.003]$$

4.4.3 Small loop antennas

Small loop antennas are used mostly for receiving, although some designs are also used for transmitting. One application for the small loop antenna is radio direction finding (RDF). Another use is for providing a small footprint antenna for people who cannot erect a full sized receiving antenna. Perhaps the greatest use of the small loop antenna is for receiving stations on crowded radio bands. The small loop antenna has very deep nulls that make it easy to null out interfering co-channel and adjacent channel signals.

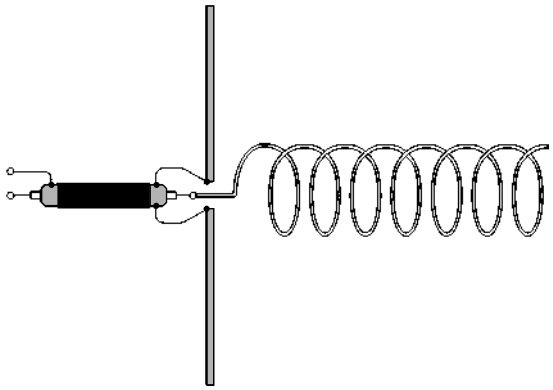

Figure 4.17 Axial mode helical antenna

4.5 Loop antennas

4.5.1 Small loop antennas defined

Large loop antennas are those with overall wire lengths of 0.5λ to more than 2λ. Small loop antennas, on the other hand, have an overall wire length that is much less than one wavelength (1λ). According to a Second World War US Navy training manual such antennas are those with an overall length of $\leq$0.22λ. Jasik's classic 1961 text on radio antennas uses the figure $\leq$0.17λ, while John Kraus (1950) used the figure $\leq$0.10λ. An amateur radio source, *The ARRL Antenna Book*, recommends $\leq$0.085λ for small loop antennas. For the purposes of our discussion we will use Kraus's figure of $\leq$0.10λ.

A defining characteristic of small loops versus large loops is seen in the current distribution. In the small loop antenna the current flowing in the loop is uniform in all portions of the loop. In the large loop, however, the current varies along the length of the conductor, i.e. there are current nodes and antinodes.

The small loop antenna also differs from the large loop in the manner of its response to the radio signal. A radio signal is a transverse electromagnetic (TEM) wave, in which magnetic and electrical fields alternate with each other along the direction of travel. The large loop, like most large wire antennas, respond primarily to the *electrical field* component of the TEM, while small loops respond mostly to the *magnetic field* component. The importance of this fact is that it means the small loop antenna is less sensitive to local electromagnetic interference sources such as power lines and appliances. Local EMI consists largely of electrical fields, while radio signals have both magnetic and

electrical fields. With proper shielding, the electrical response can be reduced even further.

4.5.2 Small loop geometry

Small loop antennas can be built in any of several different shapes (*Figure 4.18*). Popular shapes include hexagonal (*Figure 4.18A*), octagonal (*Figure 4.18B*), triangular (*Figure 4.18C*), circular (*Figure 4.18D*) and square (*Figure 4.18E*).

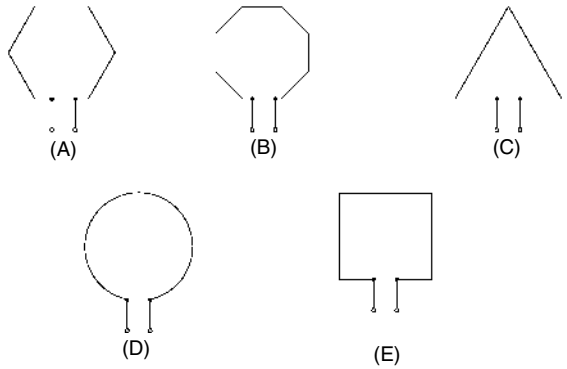

Figure 4.18 Small loop antennas: (A) hexagonal, (B) octagonal, (C) triangular, (D) circular and (E) square

The far-field performance of small loop antennas is approximately equal provided that $A^2 \leq \lambda/100$, where A is the loop area and λ is the wavelength of the desired frequency.

The 'standard' loop used in this discussion is the square loop depicted in *Figure 4.19*. There are two forms of winding used: *depth wound* and *spiral wound*. The difference is that the depth wound has its turns in different parallel planes, while in the spiral wound version all of the turns are in the same plane. The spiral wound loop theoretically has a deeper null than depth wound, but in practical terms there is usually little difference.

The length of each side of the loop is designated A, while the depth or width is designated B. These dimensions will be used in equations shortly. The constraint on the dimensions is that A should be $\leq 0.10\lambda/4$ and $B \leq A/5$.

The loop may be either tuned or untuned. The differences between tuned and untuned will be discussed shortly.

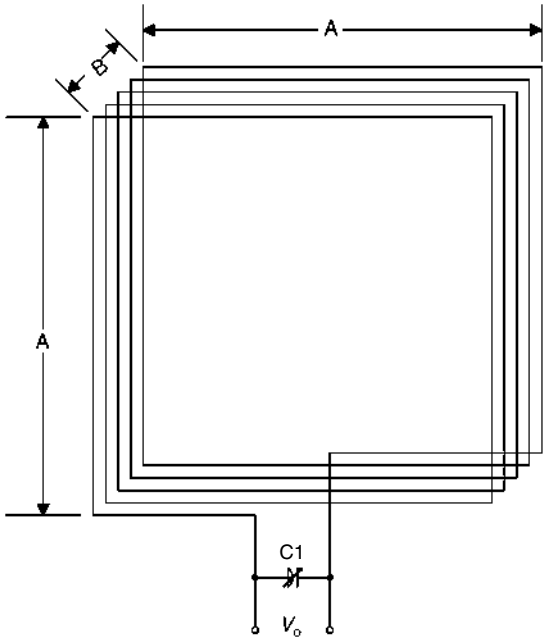

Figure 4.19 Square loop

4.5.3 Small loop antenna patterns

Small loop antennas have patterns opposite those of large loops. The minima, or 'nulls', are perpendicular to the plane of the loop, while the maxima are off the ends. *Figure 4.20* shows the directions of maximum and minimum response. The loop antenna is viewed from above. The nulls are orthogonal to the loop axis, while the maxima are along the loop axis.

The fact that the small loop pattern has nulls perpendicular to the loop axis, i.e. perpendicular to the plane of the loop, is counterintuitive to many people. The advancing radio wave produces alternating regions of high and low amplitude. A *potential difference* exists between any two points. When the loop is aligned such that its axis is parallel to the isopotential lines low signal levels are induced into the loop. If the turns of the loop cut several isopotential lines, a larger signal is induced from this direction.

4.5.4 Signal voltage (V_o) developed by the loop

The actual signal voltage (V_o) at the output of the terminals of an untuned loop is a function of the direction of arrival of the signal (α),

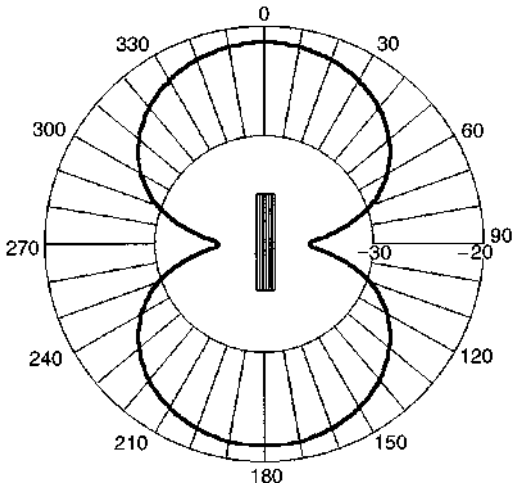

Figure 4.20 Small loop azimuth

as well as the strength of the arriving signal and the design of the loop. The angle α is formed between the loop axis and the advancing isopotential lines of the radio signal.

The output voltage of an untuned loop is:

$$V_o = \frac{2\pi ANE_f \cos\alpha}{\lambda}$$

While the output voltage of a tuned loop is:

$$V_o = \frac{2\pi ANQE_f \cos\alpha}{\lambda}$$

where

V_o is the output voltage of an untuned loop in volts (V)
A is the length of one side of the loop
N is the number of turns in the loop
E_f is the strength of the incoming signal in volts per metre (V/m)
α is the angle between the advancing wavefront and the loop axis
λ is the wavelength of the radio signal in metres (m), i.e. the reciprocal of the frequency ($\lambda = 1/F$)
Q is the loaded Q (figure of merit) of the tuned circuit formed by C1 and the loop inductance (typically 10 to 100)

4.5.5 *Effective height*

Loop antennas are sometimes described in terms of the *effective height* (H_{eff}) of the antenna. This number is a theoretical construct that compares the output voltage of a small loop with a vertical piece of the same kind of wire that has a height of:

$$H_{\text{eff}} = \frac{2\pi NA}{\lambda}$$

where H_{eff} is the effective height in metres, and all other terms are as defined above.

Loop inductance

A loop antenna essentially forms a coil of wire (or other conductor), so will have inductance. There are several methods for calculating loop inductance, but the most common are the *Grover equation* and the *Patterson equation*.

Grover equation:

$$L_{\mu\text{H}} = \left[K_1 N^2 A \text{Ln}\left[\frac{K_2 AN}{(N+1)B}\right]\right] + K_3 + \left[\frac{K_4(N+1)B}{AN}\right]$$

where all terms are as previously defined, except $K_1 - K_4$, which are defined in *Table 4.3*.

Table 4.3 *K* factors for calculating loop inductance

Shape	K_1	K_2	K_3	K_4
Triangle	0.006	1.1547	0.65533	0.1348
Square	0.008	1.4142	0.37942	0.3333
Hexagon	0.012	2.00	0.65533	0.1348
Octagon	0.016	2.613	0.75143	0.07153

Patterson equation:

$$L\mu\text{H} = (0.00508A) \times \left[2.303 \log\left(\frac{4A}{d}\right) - \phi\right]$$

where
d is the conductor diameter
ϕ is a factor found in *Table 4.4*

Table 4.4 ϕ Factor for calculating loop inductance

Shape	*Factor (ϕ)*
Circle	2.451
Octagon	2.561
Hexagon	2.66
Pentagon	2.712
Square	2.853
Triangle	3.197

Of these equations, most people will find that the Grover equation most accurately calculates the actual inductance realized when a practical loop is built.

References

Andrew Antennas (1991). *Catalog 35*. Illinois.
Belcher, R. *et al*. (1989). *Newnes Mobile Radio Servicing Handbook*. Butterworth-Heinemann, Oxford.
Davies, J. (1987). *Private Mobile Radio – A Practical Guide*. Heinemann, London.
Green, D.C. (1979). *Radio systems, Vols II and III*. Pitman, London.
Kennedy, G. (1977). *Electronic Communication Systems*. McGraw-Hill Kogashuka, Tokyo.
Terman, F.E. (1943). *Radio Engineers' Handbook*. McGraw-Hill, London.

5 Resonant circuits

5.1 Series and parallel tuned circuits

Tuned resonant circuits composed of inductance and capacitance are used to generate alternating voltages of a specific frequency and to select a wanted frequency or band of frequencies from the spectrum. *Figure 5.1* contains the diagrams of series and parallel resonant circuits including the resistances which account for the losses present in all circuits. In practice the greatest loss is in the resistance of the inductor, R_L, with a smaller loss, r_c, occurring in the dielectric of the capacitor.

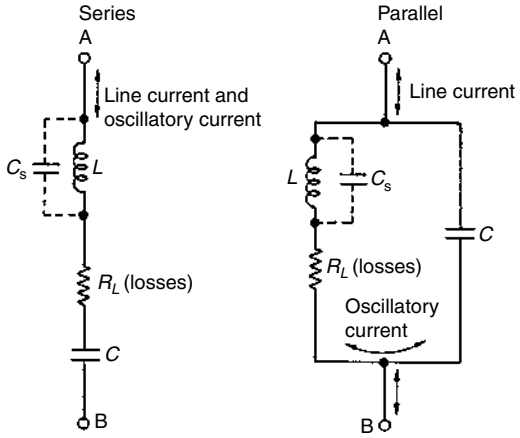

Figure 5.1 Series and parallel resonant circuits

5.1.1 Series resonance

Off resonance, the series circuit exhibits a high impedance to a voltage applied across A and B. This impedance is formed by the vectorial addition of the reactances of the inductance and capacitance at the applied frequency plus the resistances. Ignoring the dielectric losses and the very small stray shunt capacitance C_s, the resonant impedance is given by:

$$Z = \sqrt{R^2 + \left(\omega L - \frac{1}{\omega C}\right)^2}$$

where
R = resistance of components in ohms
$\omega = 2\pi \times$ frequency in hertz
L = inductance in henries
C = capacitance in farads

At resonance the reactances cancel out and the impedance falls to approximately the value of the resistance, R, and a maximum line current will flow. *Figure 5.2* shows the response curves of series and parallel circuits near resonance. The resonant frequency is given by:

$$f = \frac{1}{2\pi\sqrt{LC}}$$

where
f = resonant frequency in hertz
L = inductance in henries
C = capacitance in farads

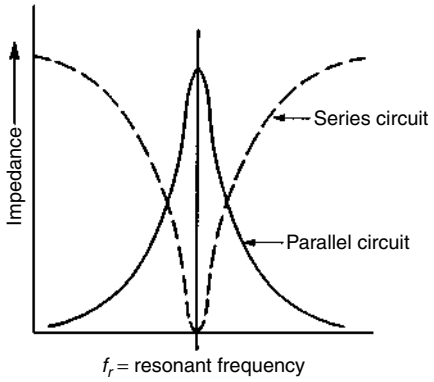

Figure 5.2 Variation of impedance around resonance with series and parallel tuned circuits

5.1.2 Parallel resonance

At resonance, calculated by using the same formula as for a series circuit, the impedance of a parallel tuned circuit is also resistive, and the circulatory current in the circuit is high producing the maximum voltage across the inductance and capacitance. Consequently, at resonance the minimum line current flows. The impedance at resonance

or dynamic resistance of a parallel tuned circuit of moderate to high Q is given by:

$$R_{\mathrm{d}} = \frac{L}{CR}$$

where
R_{d} = dynamic resistance of circuit
R = resistance of components in ohms
L = inductance in henries
C = capacitance in farads

5.2 Q factor

The voltages across the inductor and capacitor in a circuit at resonance are substantially opposite in phase (the loss resistances affect the phasing slightly) and cancel each other. The voltage developed across the inductor, usually the lossiest component, compared with the voltage applied in series to the circuit, is a measure of the 'goodness' of the circuit. This ratio is often referred to as the magnification factor, Q, of the circuit. The Q factor is calculated from:

$$Q = \frac{\omega L}{R} \text{ or } \frac{1}{\omega CR}$$

where L and C are in henries and farads respectively.

5.3 Coupled (band-pass) resonant circuits

5.3.1 Methods of coupling

Radio signals carrying intelligence occupy a band of frequencies and circuits must be able to accept the whole of that band whilst rejecting all others. When tuned circuits are coupled together in the correct manner they form such a band-pass circuit. The coupling may be either by mutual inductance between the two inductances of the circuits as in *Figure 5.3* or through discrete electrical components as in *Figure 5.4*.

Mutual inductance can be defined in terms of the number of flux linkages in the second coil produced by unit current in the first coil. The relationship is:

$$M = \frac{\text{flux linkages in 2nd coil produced by current in 1st coil}}{\text{current in 1st coil}} \times 10^{-8}$$

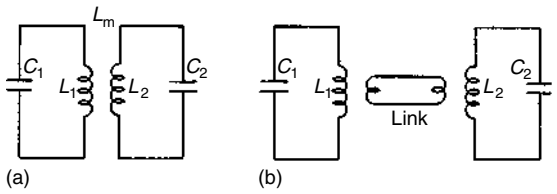

Figure 5.3 Mutual inductance (low impedance) coupling

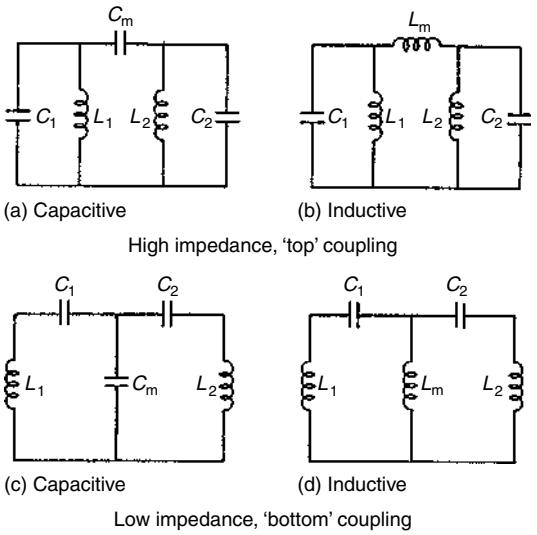

Figure 5.4 Electrical coupling

where $M =$ mutual inductance in henries. The e.m.f. induced in the secondary is $e_2 = -j\omega M I_1$ where I_1 is the primary current.

The maximum value of mutual inductance that can exist is $\sqrt{L_1 L_2}$ and the ratio of the actual mutual inductance to the maximum is the coefficient of coupling, k:

$$k = \frac{M}{\sqrt{L_1 L_2}}$$

The maximum value of k is 1 and circuits with a k of 0.5 or greater are said to be close coupled. Loose coupling refers to a k of less than 0.5.

An advantage of coupling using discrete components is that the coupling coefficient is more easily determined. Approximations for k for the coupling methods shown in *Figure 5.4* are:

(a) $k = \dfrac{C_m}{\sqrt{C_1 C_2}}$ where C_m is much smaller than $(C_1 C_2)$

(b) $k = \dfrac{\sqrt{L_1 L_2}}{L_m}$ where L_m is much larger than $(L_1 L_2)$

(c) $k = \dfrac{\sqrt{C_1 C_2}}{C_m}$ where C_m is much larger than $(C_1 C_2)$

(d) $k = \dfrac{L_m}{\sqrt{L_1 L_2}}$ where L_m is much smaller than $(L_1 L_2)$

5.3.2 Response of coupled circuits

When two circuits tuned to the same frequency are coupled their mutual response curve takes the forms shown in *Figure 5.5*, the actual shape depending on the degree of coupling.

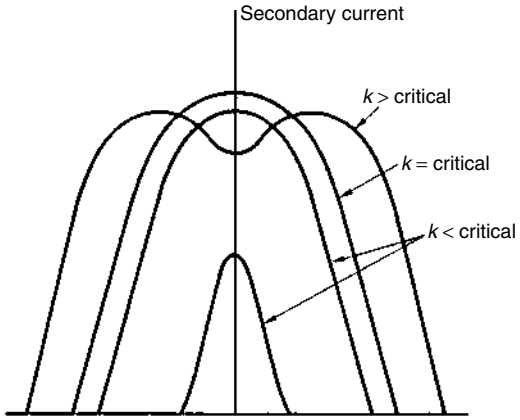

Figure 5.5 Effect of degree of coupling

When coupling is very loose the frequency response and the current in the primary circuit are very similar to that of the primary circuit alone. Under these conditions the secondary current is small and the secondary response curve approximates to the product of the responses of both circuits considered separately.

As coupling is increased the frequency response curves for both circuits widen and the secondary current increases. The degree of coupling where the secondary current attains its maximum possible value is called the critical coupling. At this point the curve of the primary circuit shows two peaks, and at higher coupling factors the

secondary response also shows two peaks. The peaks become more prominent and further apart as coupling is increased, and the current at the centre frequency decreases.

References

Langford-Smith, F. (1955). *Radio Designer's Handbook*, Iliffe and Sons, London.
Terman, F.E. (1943). *Radio Engineers' Handbook*. McGraw-Hill, London.

6 Oscillators

6.1 Oscillator requirements

Oscillators generate the frequencies used in radio and electronic equipment. The performance of those which determine the operating frequencies of radio systems is tremendously important. Most oscillators must:

- Generate a precise frequency of high purity.
- Be highly stable, i.e. produce an output constant in frequency and level despite changes in temperature, supply voltage and load.
- Be tunable in frequency.
- Produce minimum noise and microphony (fluctuations in frequency with vibration).

These requirements conflict. A readily tunable oscillator cannot be precise and highly stable, and compromises must be made; either a less stringent specification must be accepted where permissible or the facility for tuning restricted.

Not all oscillators need to produce a pure output, devoid of spurious frequencies. The clock generators in digital circuitry, for instance, produce square waves, but a radio transmitter carrier generator and receiver local oscillator must produce a pure sine wave output if spurious radiations and receiver responses are to be avoided.

6.2 Tunable oscillators

An oscillator is an amplifier with a portion of the output fed back to the input. The feedback must be positive, i.e. in phase with the input, and the loop gain, input back to input via the feedback loop, must be sufficient to overcome the losses in the circuit.

Most radio frequency oscillators – and some audio ones – use inductance and capacitance (LC) tuned circuits as the frequency determining elements. *Figure 6.1* shows two commonly used basic circuits, the Hartley and the Colpitts.

The frequency is determined by the values of L and C_1 (the combined values of C_1 in the Colpitts circuit) and the amount of feedback by the collector choke and C_2. Such circuits produce a very pure output but, principally because the physical dimensions of the frequency

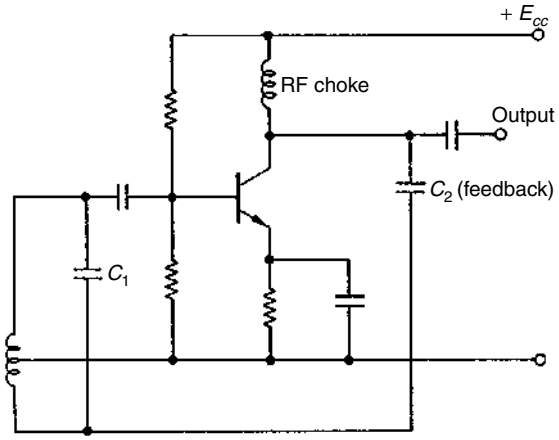

(a) Hartley circuit

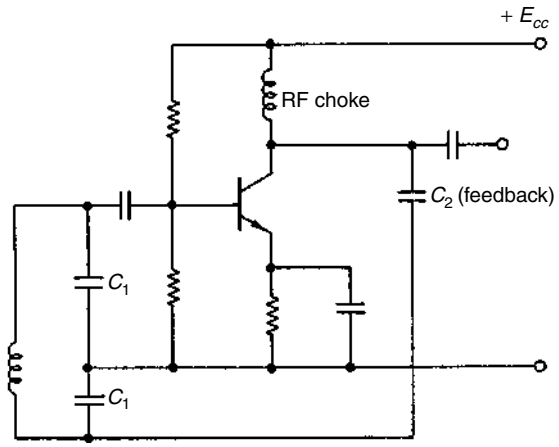

(b) Colpitts circuit

Figure 6.1 Hartley and Colpitts oscillators

determining components change with temperature, the accuracy of the set frequency is doubtful and is not very stable. Temperature compensation can be applied by selecting a capacitor for C_1 with the correct negative temperature coefficient (assuming that the inductance increases with temperature), inserting temperature compensation for the rise in collector current with temperature and stabilizing the supply voltage. In the design of equipment an oscillator should be built into an area of low temperature change.

6.3 Quartz crystal oscillators

The problems of frequency accuracy and stability are largely overcome by using a quartz crystal as the frequency determining element (see Chapter 7).

Figure 6.2(a) shows a circuit for an oscillator using the crystal's parallel resonant mode. In this circuit, the rising voltage developed across R_e on switch-on is applied via C_1 to the base accelerating the rise of current through the transistor. When saturation is reached the voltage across R_e becomes static and the voltage on the base falls, reducing the transistor current. The oscillations are only sustained

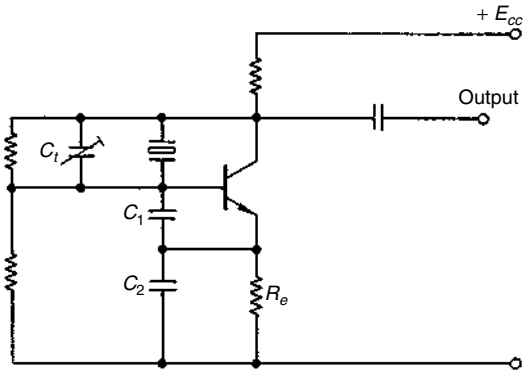

(a) Parallel resonant

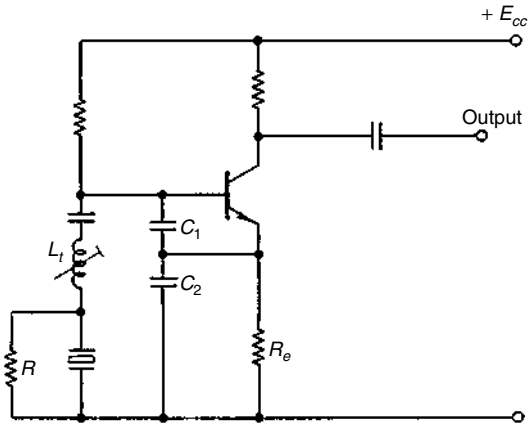

(b) Series resonant

Figure 6.2 Quartz crystal oscillators

at the parallel resonant frequency of the crystal where it presents a high impedance between base and collector. C_t enables the parallel resonance of the crystal to be adjusted to a precise frequency.

Figure 6.2(b) shows a series resonant crystal oscillator and here L_t is the tuning inductor of a Colpitts oscillator. The loop gain is adjusted so that the circuit will oscillate only at the series resonant frequency of the crystal where it presents a very low resistance. At other frequencies the crystal presents an increasing impedance in series with L_t, shunted by R which can be of a low value. When first setting the oscillator, L_t is adjusted, with the crystal short-circuited, for oscillation at a frequency close to that desired. The short-circuit is then removed and L_t used as a fine trimmer.

The same circuit will operate at the parallel resonant frequency of the crystal by making C_1 equal to the crystal load capacitance.

The maximum frequency error permitted by the British Radiocommunications Agency specification MPT 1326 for mobile radio equipment designed for 12.5 kHz channel separation in the band 100–300 MHz is plus or minus 1.5 MHz. This is an overall accuracy of 0.0005% over the temperature range $-10\,^{\circ}$C to $+55\,^{\circ}$C. Well-designed standard crystal oscillators meet this specification, but higher stability can be obtained by operating the crystal in an oven at a constant higher temperature.

Until recently equipment which was required to change operating frequency quickly was fitted with several crystals, one for each operating frequency, and a change of frequency was made by selecting the appropriate crystal. Frequency synthesizer circuits are now normally used for such applications.

6.3.1 Overtone oscillators

Piezoelectric crystals can oscillate at more than one frequency. The oscillations of a crystal slab are in the form of *bulk acoustic waves* (BAWs), and can occur at any frequency that produces an odd half-wavelength of the crystal's physical dimensions (e.g. $1\lambda/2$, $3\lambda/2$, $5\lambda/2$, $7\lambda/2$, $9\lambda/2$, where the fundamental mode is $1\lambda/2$). Note that these frequencies are not exact harmonics of the fundamental mode, but are actually valid oscillation modes for the crystal slab. The frequencies fall close to, but not directly on, some of the harmonics of the fundamental (which probably accounts for the confusion). The overtone frequency will be marked on the crystal, rather than the fundamental (it is rare to find fundamental mode crystals above 20 MHz or so, because their thinness makes them more likely to fracture at low values of power dissipation).

The problem to solve in an overtone oscillator is encouraging oscillation on the correct overtone, while squelching oscillations at the fundamental and undesired overtones. Crystal manufacturers can help with correct methods, but there is still a responsibility on the part of the oscillator designer. It is generally the case that overtone oscillators will contain at least one $L-C$ tuned circuit in the crystal network to force oscillations at the right frequency.

6.4 Frequency synthesizers

Frequency synthesizers offer the stability of a quartz crystal oscillator combined with the facility to change operating frequency rapidly. They are essential for equipment operating on trunked or cellular networks where the frequency of the mobiles is changed very rapidly on instructions from the network.

6.4.1 Voltage controlled oscillators

The advent of the variable capacitance diode (varicap), where the capacitance across the diode varies according to the applied DC voltage, made the frequency synthesizer a practicality.

When a varicap diode replaces the tuning capacitor in an oscillator the circuit becomes a DC-voltage-controlled oscillator (VCO). The two varicaps in *Figure 6.3* are used to minimize harmonic production and to obtain a greater capacitance change per volt.

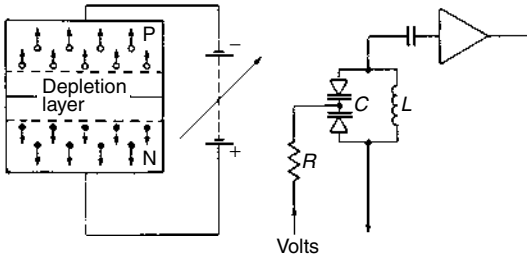

Figure 6.3 Voltage variable capacitance diode

The VCO is the circuit that directly generates the output frequency of a frequency synthesizer but, by itself, inherits the problem of frequency stability. To overcome this, the frequency and phase of the VCO are compared with those of a crystal-controlled high stability oscillator. Any frequency or phase difference between the two oscillators creates a DC voltage of the correct sense to change the frequency of the VCO to agree with that of the crystal oscillator.

While the stability of the crystal oscillator is transferred to the synthesizer output, additional noise is produced close to the operational frequency and the elimination of microphony requires careful physical design.

6.4.2 Phase-locked loops

Figure 6.4(a) and *(b)* are diagrams of a simple phase-locked loop (PLL). The outputs of both the crystal oscillator and the voltage-controlled oscillator are fed to the phase comparator which produces pulses whenever there is a frequency or phase difference between the two inputs. The pulses will be either positive or negative depending on the sense of the difference, and their width is dependent upon the magnitude of the differences. The pulses are then fed to a low pass loop filter which smooths them. If the time constant of the filter is sufficiently long it will completely remove the pulses and produce a DC output proportionate to the input pulse width which is applied to the VCO in the right sense to correct the frequency error. To enable the pulses to swing the VCO frequency in either direction, a small bias voltage of about 4 volts is applied to the varicap.

Identical frequencies have been selected for both oscillators in *Figure 6.4* but in practice this is seldom the case. More frequently, the

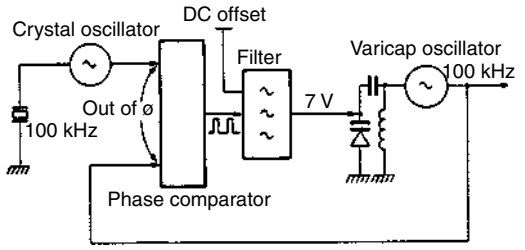

(a)

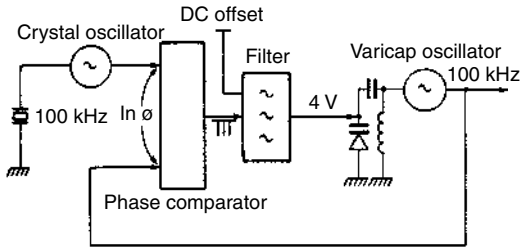

(b)

Figure 6.4 Simple phase-locked loop

VCO runs at a higher frequency than the crystal oscillator and a divider is used to equate the frequencies applied to the phase comparator (*Figure 6.5*). Changing the division ratio provides a convenient means of tuning the oscillator.

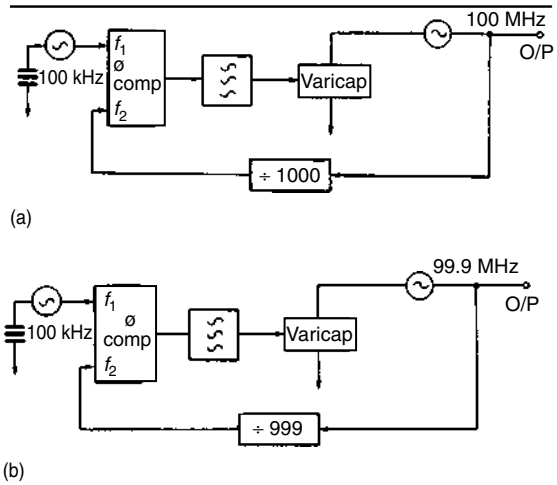

Figure 6.5 Frequency variable phase-locked loop

While the division ratio is 1000, the VCO will run at 100 MHz but if the division ratio is changed to 999 the comparator will produce pulses which, when converted to a DC voltage by the loop filter, will change the frequency of the VCO to 99.9 MHz, and the loop will lock at this new frequency.

The design of the loop filter is critical. Too long a time constant lengthens the settling time when changing frequency, yet if it is too short any deliberate frequency modulation will be removed. In practice, a relatively long time constant is chosen which is shortened by a 'speed up' circuit introduced whenever a channel change is called for.

The above values would enable a radio operating on a system with a channel separation of 100 kHz to change channel, but mobile radio channel separations are 25 kHz, 12.5 kHz or even 6.25 kHz at frequencies from 50 MHz to at least 900 MHz. To change channel at these frequencies a synthesizer must use a high division ratio. With a reference frequency applied to the comparator of 6.25 kHz and an operating frequency of, say, 450 MHz, the frequency select divider must have a ratio of 72 000, and be programmable in steps of 1 with a minimum operating speed of at least 900 MHz. A problem is then that the technology capable of meeting these requirements, emitter

coupled logic (ECL), is power hungry, and the preferred LSI low power technology, CMOS, has a maximum operating speed of about 30 MHz. A simple ECL pre-scaler to bring the VCO frequency to about 30 MHz needs a ratio of 20 (500 MHz to 25 MHz). However, every change of 1 in the CMOS divider ratio then changes the total division ratio by 20. The solution is to use a dual modulus pre-scaler.

6.4.3 Dual modulus pre-scaler

The division ratio of the dual modulus pre-scaler (*Figure 6.6*) is programmable between two consecutive numbers, e.g. 50 and 51 (P and $P + 1$) and, in conjunction with two CMOS dividers, ÷A and ÷N, provides a fully programmable divider.

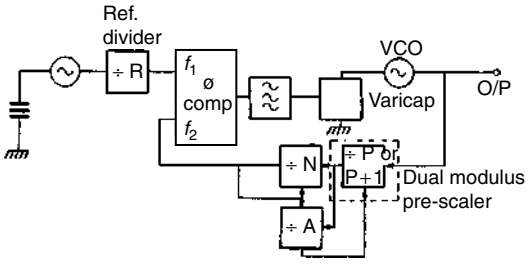

Figure 6.6 Programmable frequency synthesizer

The A and N dividers are pre-loaded counters. These count down and when the count value reaches zero they produce an output which changes the division ratio of the pre-scaler. The total division ratio, N_t, is decided by the initial programmed contents of the A and N counters and the setting of the pre-scaler. The initial content of the A counter must be less than that of the N counter.

Consider the pre-scaler set to divide by $P + 1$. For every count of $P + 1$, the contents of the A and N counters are reduced by 1 until the contents of the A counter are zero. The difference between the original contents of the A and N counters, $N - A$, remains in the N counter, and the total count, N_t, up to now, is $A(P + 1)$. At this point the division ratio of the pre-scaler is changed to P. Now, for every P count, the contents of the N counter are reduced by 1 until zero is reached. Under these conditions the total division ratio is given by:

$$\begin{aligned} N_t &= A(P + 1) + (N - A)P \\ &= AP + A + NP - AP \\ &= NP + A \end{aligned}$$

For example, let $P = 50$ so $P + 1 = 51$, let $N = 10$ and $A = 7$. Then:

$$N_t = 10 \times 50 + 7 = 507$$

Now, change A to 6:

$$N_t = 10 \times 50 + 6 = 506$$

a change of N_t by 1.

Programming a divider

Example:

$$\text{VCO frequency} = 455.6\,\text{MHz}$$

$$\text{Reference frequency} = 12.5\,\text{kHz}$$

Calculate N_t, and the numbers which must be programmed into the A and N counters, assuming $P = 50$:

1. Calculate $N_t = 455.6\,\text{MHz}/12.5\,\text{kHz} = 36\,448$.
2. Divide N_t by P: $36\,488/50 = 728.96$. Make $N = 728$.
3. For A, multiply fraction by P: $0.96 \times 50 = 48$.
4. Check $N_t = NP + A = 728 \times 50 + 48 = 36\,448$.
   Change A to 47: $NP + A = 728 \times 50 + 47 = 36\,447$.
   $36\,447 \times 12.5\,\text{kHz} = 455.5875\,\text{MHz}$, the adjacent 12.5 kHz channel.

6.4.4 Direct digital synthesis

A method of direct digital frequency synthesis replaces the voltage-controlled oscillator by a numerically controlled oscillator (NCO) where the function of the VCO is digitally synthesized.

The direct digital synthesizer generates an analogue sine wave from digital sine wave samples applied to a digital to analogue (D/A) converter. There are limitations to the method in terms of bandwidth and spectral purity.

6.5 Caesium and rubidium frequency standards

Where extra high stability is required for, say, laboratory standards or in quasi-synchronous wide area coverage systems, oscillators utilizing the atomic resonances of substances like caesium and rubidium, although expensive, may be employed.

Caesium oscillators are used to provide standard frequencies such as 1, 5 and 10 MHz with accuracies of $\pm 7 \times 10^{-12}$ over a temperature range of 0 to 50 °C with a long-term stability of 2×10^{-12}.

Rubidium oscillators are used to provide secondary standards and in some quasi-synchronous radio systems. Their accuracy is less than that of caesium, the long-term drift being of the order of 1×10^{-11} per month.

References

Belcher, R. *et al*. (1989). *Newnes Mobile Radio Servicing Handbook*. Butterworth-Heinemann, Oxford.

Winder, S.W. (2001). *Newnes Telecommunications Pocket Book*. Butterworth-Heinemann, Oxford.

7 Piezo-electric devices

7.1 Piezo-electric effect

When electrical stress is applied to one axis of a quartz crystal it exhibits the piezo-electric effect: a mechanical deflection occurs perpendicular to the electric field. Equally, a crystal will produce an e.m.f. across the electrical axis if mechanical stress is applied to the mechanical axis. If the stress is alternating – the movement of the diaphragm of a crystal microphone is an example – the e.m.f. produced will be alternating at the frequency of the movement. If the stress alternates at a frequency close to the mechanical resonance of the crystal as determined by its dimensions, then large amplitude vibrations result. Polycrystalline ceramics possess similar qualities.

Quartz crystals used for radio applications are slices cut from a large, artificially grown crystal. The slices are then ground to the appropriate size to vibrate at a desired frequency. The performance of an individual slice – the crystal as the end user knows it – depends upon the angle at which it was cut from the parent crystal.

Each crystal slice will resonate at several frequencies and if the frequency of the stimulus coincides with one of them the output, electrical or mechanical, will be very large.

The vibrations occur in both the longitudinal and shear modes, and at fundamental and harmonic frequencies determined by the crystal dimensions.

Figure 7.1A shows a typical natural quartz crystal. Actual crystals rarely have all of the planes and facets shown. There are three *optical axes* (X, Y and Z) in the crystal used to establish the geometry and locations of various cuts. The actual crystal segments used in RF circuits are sliced out of the main crystal. Some slices are taken along the optical axes, so are called Y-cut, X-cut and Z-cut slabs. Others are taken from various sections, and are given letter designations such as BT, BC, FT, AT and so forth.

7.1.1 Equivalent circuit of a quartz crystal

A quartz crystal behaves similarly to a very high Q tuned circuit and the equivalent circuit of a crystal is shown in *Figure 7.1B*.

C_1 and L_1 are equivalent to the inductance and capacitance of a conventional tuned circuit and R_1 represents the losses in the quartz

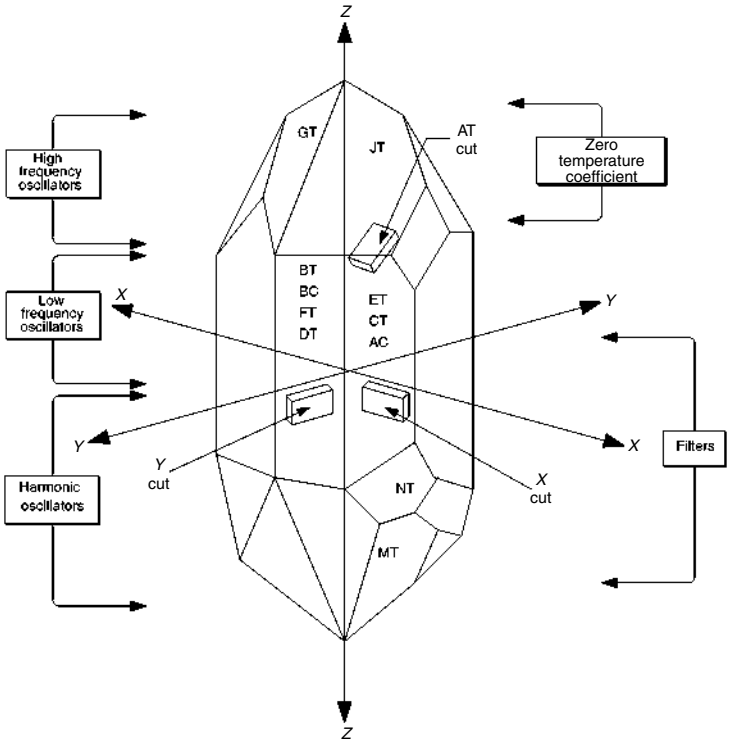

Figure 7.1A Natural quartz crystal

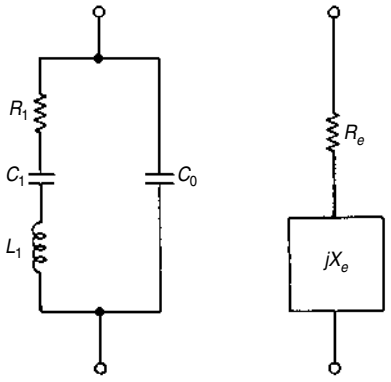

Figure 7.1B Equivalent circuit of a crystal

and the mounting arrangements. C_0, typically 3–15 pfd, represents the shunt capacitance of the electrodes in parallel with the can capacitance. If the oscillatory current is considered, the resonant frequency is decided by the values of C_0 in series with C_1, L_1 and R_1, and all crystals basically resonate in a series mode. *Figure 7.2* illustrates the changes in impedance close to resonance. However when a high impedance, low capacitance, load is connected across the crystal terminals it behaves as a parallel tuned circuit exhibiting a high resistance at the resonant frequency. A crystal operating in the parallel mode oscillates at a higher frequency than that of series resonance.

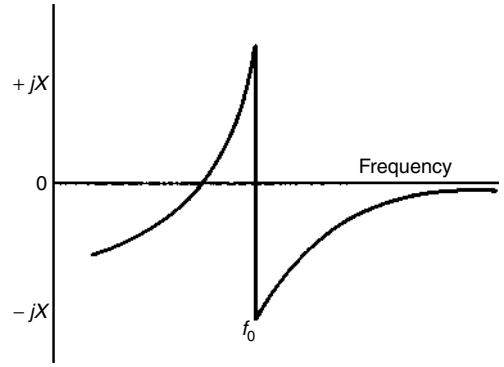

Figure 7.2 Crystal reactance close to resonance

A crystal will resonate at its fundamental frequency or at one or more of its harmonics. As the desired resonant frequency is increased, a crystal slice operating at its fundamental frequency becomes extremely thin and fragile. Consequently, overtone crystals are composed of larger slices of quartz operating close to, but not necessarily at, an exact harmonic of the fundamental frequency. Crystals operating at the 3rd, 5th and 7th harmonics are often employed at frequencies above approximately 25 MHz.

7.2 Quartz crystal characteristics

7.2.1 Resonant frequency

The resonant frequency is determined by the mass of the finished crystal which can be adjusted by grinding and the deposition of gold or other metal onto the crystal faces during manufacture. The adjustment is made to suit the intended method of operation, series or parallel, and at a specific temperature, usually 25°C. When parallel mode is

specified, allowance is made for the load or circuit capacitance, usually 20–30 pfd, in parallel with C_0.

7.2.2 Frequency stability

Temperature coefficient

A crystal's resonant frequency varies with temperature and this temperature coefficient is determined by the angle at which the slice was cut from the parent crystal. Commonly used cuts are AT and BT. Because of its better performance AT is the most common.

Typical examples of the temperature coefficients for these are shown in *Figure 7.3*.

The temperature coefficient is specified, usually in parts per million (ppm) per degree C, or as a percentage, over a defined temperature range. The standard European temperature range is -10°C to $+60^{\circ}$C. A crystal designed for a restricted temperature range has a better

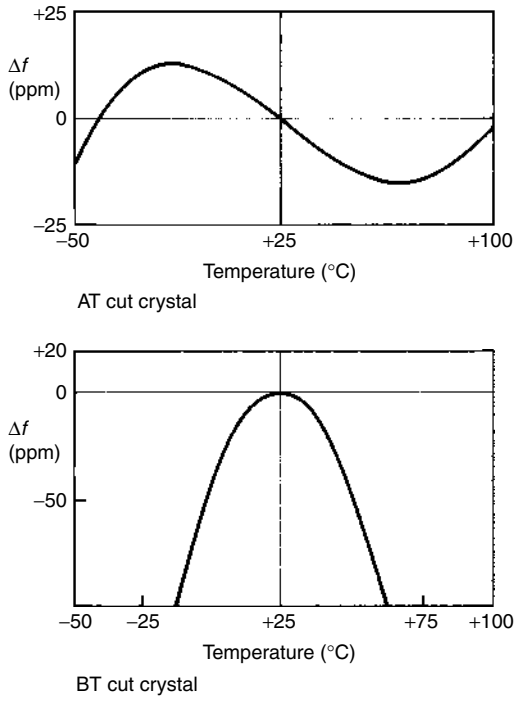

Figure 7.3 Frequency vs. temperature curves AT and BT cut crystals

stability over that range than one designed for operation over a wide temperature range will have when used over a restricted range.

For higher frequency stability crystals may be operated in a temperature-controlled oven operating at a more constant high temperature.

Common frequency tolerance specifications are $\pm 0.005\%$ or 0.0025% from $-55^{\circ}C$ to $+105^{\circ}C$. These include the frequency errors from all sources, including the calibration tolerance; thus, the temperature coefficient is slightly better than these figures.

Ageing

The resonant frequency shifts with age from that set at production, following a curve similar to that in *Figure 7.4*. Initially the frequency shift for a given period of time is rapid but slows with age. The frequency may shift in either direction, and although it is possible to specify crystals ageing in one direction – high stability oscillators for quasi-synchronous transmission systems is an application – they are selected from a batch, not specifically manufactured. Once a crystal has been operated, a subsequent long period of inactivity can produce a glitch in the ageing curve followed by a higher rate of change for a short time.

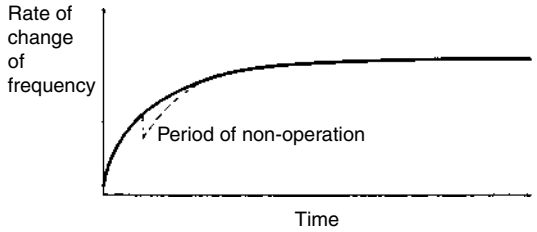

Figure 7.4 Effect of ageing

7.2.3 Load capacitance and pullability

When a crystal is operated in the parallel mode across a low capacitance load the results are a higher frequency and larger output voltage to the load. Increasing the load capacitance causes a reduction in frequency approaching that of series resonance.

The change in frequency that can be achieved by varying the load capacitance – a small trimmer capacitor is often connected across the crystal for this purpose – is the crystal's pullability. A typical pullability is from -1 ppm/pfd to -20 ppm/pfd for a total shunt capacitance of 40 pfd ($C_0 + C_{load}$).

7.2.4 Activity, effective series resistance (ESR) and Q

All these characteristics are interrelated. A crystal's activity, its vibrational response, can be quoted in terms of the effective series resistance. A higher effective series resistance implies lower activity, lower output and lower Q. The usual range of ESRs is from 20 Ω to 100 Ω although higher values occur in some low frequency crystals. Some manufacturers may quote activity levels for crystals for use in a parallel mode as effective parallel resistance (EPR). The EPR is the value of the resistor which, if connected in lieu of the crystal in an oscillator, would give the same output level as the crystal. The higher the EPR, the greater the crystal activity and Q.

7.2.5 Spurious responses

Crystals will resonate at frequencies other than those of the fundamental and harmonic modes for which they were designed; *Figure 7.5* shows the overtone (harmonic) and some typical spurious responses. The spurious responses of overtone crystals can occur with very little separation from the desired overtone frequency requiring very careful oscillator design if they are to be avoided.

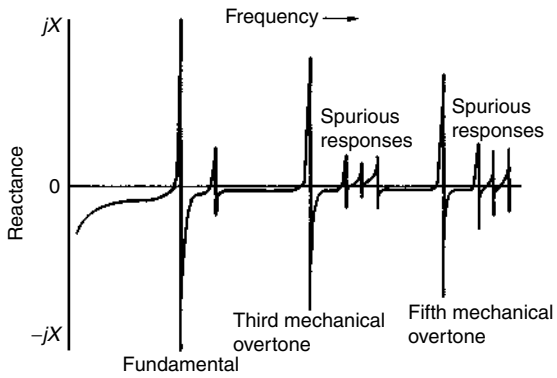

Figure 7.5 Overtone response of a quartz crystal

7.2.6 Case styles

A wide range of mounting styles is available. The American military nomenclature is widely used to describe them and *Figure 7.6* shows the outlines of some of the more popular styles.

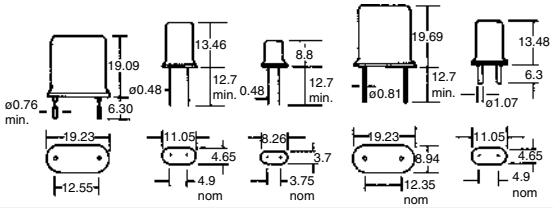

Solder seal	HC6/U AA	HC18/U J	– –	HC33/U BF	HC25/U CX	MIL IEC
Cold weld	HC36/U DNC	HC43/U DPC	HC45/U EBC	HC47/U AC	HC42/U DQ	MIL IEC
Glass	HC27/U DA	HC26/U CY	– –	– –	HC29/U CZ	MIL IEC
Res weld	HC48/U DNR	HC43/U DPR	HC45/U EBR	HC51/U RF	HC50/U RX	MIL IEC

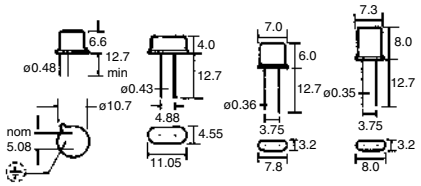

Solder seal	– –	– –	– –	– –		MIL IEC
Cold weld	HC35/U DKC	– –	– –	– –		MIL IEC
Glass	– –	– –	– –	– –		MIL IEC
Res weld	HC35/U DKR	HC49/4H –	– UM-5	– UM-1		MIL IEC

Figure 7.6 Crystal case styles

7.3 Specifying quartz crystals

The details which must be specified when ordering crystals are:

1. *Frequency*. Normally specified in kHz up to 9999.999 kHz and in MHz from 10.0 MHz upwards except for integer values which are all specified in MHz. The frequency must be described to seven significant figures, otherwise any figure that might follow those given will be taken as zero.
2. *Mounting or holder style*.
3. *Frequency tolerance*. This is the cutting or calibration tolerance acceptable at 25°C. It should be borne in mind that cost rises with increased manufacturing accuracy and a slight adjustment (pullability) is possible in the circuit.

4. *Frequency stability*. Normally specified as a plus or minus value measured over a defined temperature range. A crystal designed for a restricted range has a better performance over that range than one designed for a wider range so it is important not to overspecify.
5. *Temperature range*. The range over which the crystal is required to operate and meet the performance specified in 4. Standard temperature ranges are:

   0 to 5°C
   −10 to 60°C
   −20 to 70°C
   −30 to 80°C
   −40 to 90°C
   −55 to 105°C
   −55 to 125°C

   It is sufficient when ordering from some manufacturers to quote only the lower temperature limit.

   For ovened operation the quoted figure, say 80°C, would denote the oven temperature.
6. *Circuit condition*. This specifies the shunt capacitance that the circuit will place across the crystal in parallel mode operation.
7. *Drive level*. The maximum power that the crystal can safely dissipate. 1 mW is a typical value for crystals used in radio transmitters and receivers.

A typical specification therefore reads:

16.66667 MHz	HC49	20	30	10	30
1	2	3	4	5	6

referring to the items listed above

When the crystal is for operation in series mode, it is usually sufficient to replace the last figure with ‘S’. The drive level is not normally specified in the ordering details.

7.4 Filters

Both quartz and ceramic materials are used in the production of radio frequency filters. Ceramic filters do not have the same performance as quartz but have the advantages of a lower cost. They are used at lower frequencies and where the higher stability and lower spurious responses of quartz are not essential.

Crystal filters are obtainable at frequencies up to about 45 MHz. Most of these use either a number of discrete crystals arranged in the form of a lattice or a monolithic structure. A single crystal will behave as an extremely narrow band filter and it is possible to use a crystal bar in this way down to a very few kilohertz.

The characteristics of filters can be divided into groups affecting the performance (*Figure 7.7*).

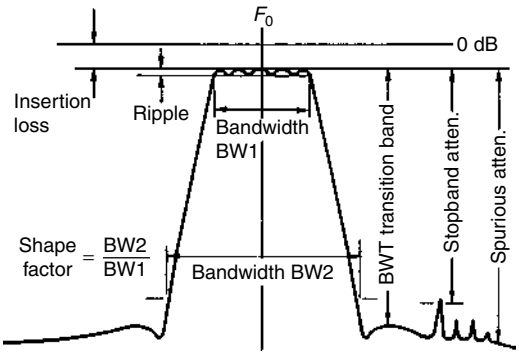

Figure 7.7 Filter characteristics

7.4.1 Passband performance

- *Insertion loss*. The loss at centre frequency, in dB, resulting from the insertion of the filter in a transmission system.
- *Flat loss*. The insertion loss at the frequency of minimum loss within the passband.
- *Attenuation*. The loss of a filter at a given frequency measured in dB.
- *Passband (bandwidth, BW_1)*. The range of frequencies attenuated less than a specified value, typically 3 or 6 dB.
- *Centre frequency* (f_0). The arithmetic mean of the passband limits.
- *Fractional bandwidth*. A specified frequency, typically the minimum loss point or F_0, from which all attenuation measurements are made.
- *Ripple*. The amplitude difference, in dB, between the maximum peak and minimum passband valley. Both the peak and the valley are defined by a surrounding change in slope, i.e. sign of the amplitude response. This is very important as a high ripple, particularly between a peak and the adjacent trough, produces rapid phase changes as the signal moves across the

passband resulting in audio distortion and corruption in digital signals.

7.4.2 Stopband performance

- *Attenuation*. The output of a filter at a given frequency relative to the defined insertion loss reference.
- *Stopband*. The range of frequencies attenuated by a greater amount than some specified minimum level of attenuation.
- *Transition band (bandwidth, BW_2)*. The range of frequencies differently attenuated between the passband and stopband limits.
- *Shape factor*. The ratio of the bandwidth at some point within the transition region, typically 60 dB, to the specified passband bandwidth. It is given by:

$$\text{Shape factor } \frac{BW_2}{BW_1}$$

- *Spurious attenuation*. The specified minimum level of attenuation received by all non-harmonic related resonances of each crystal resonator within the filter network.

7.4.3 Time domain performance

- *Insertion phase*. The phase shift at the output load (measured at the reference frequency) resulting from the insertion of the filter.
- *Differential phase*. The measurement of phase at a given frequency relative to the phase at the reference frequency.
- *Phase linearity*. The phase error in degrees between the phase points and a straight line drawn through the phase points.
- *Group delay*. The time by which a signal will be delayed before it appears at the filter output, i.e. the derivative of phase with respect to frequency.
- *Differential delay*. The measurement of delay at a given frequency relative to the reference frequency.

7.4.4 Source and load impedance

- *Source impedance*. The impedance of the circuit driving the filter, measured at the reference frequency.
- *Load impedance*. The impedance of the circuit terminating the filter at its output, measured at the reference frequency.

7.4.5 Non-linear effects

- *Maximum input level*. The driving point power, voltage or current level above which intolerable signal distortion or damage to the device will result.
- *Drive level stability*. The ability of the filter to return within a specified tolerance of its original insertion loss, at a specified drive level, after experiencing changing environmental and/or drive level conditions.
- *Drive level linearity*. The maximum permissible variation in insertion loss, per dB change in drive level, measured over a specific dynamic range.
- *Inband intermodulation distortion*. The attenuation, in dB, of third and higher order signal products, inband, relative to the power level of two signals placed within the passband.
- *Out-of-band intermodulation distortion*. The attenuation, in dB, of third and higher order signal products, inband, relative to the power level of two signals placed in the stopband, or one signal in the transition region and the other in the stopband.

A manufacturer's specifications for two stock 10.7 MHz filters are given in *Table 7.1*.

Table 7.1 Manufacturers' specifications for two stock 10.7 MHz filters

Centre freq.	*Passband width (plus/minus)*	*Attenuation bandwidth*	*Ripple (max)*	*Ins. loss (max)*	*Term. impedance ΩS/pfd*
10.7 MHz	3.75 kHz (6 dB)	8.75 kHz (45 dB)	2.0 dB	3.0 dB	1.5k/1
		12.5 kHz (60 dB)			
10.7 MHz	7.5 kHz (6 dB)	15.0 kHz (60 dB)	2.0 dB	4.0 dB	3k/1
		20.0 kHz (80 dB)			

7.5 SAW filters and resonators

The piezo-electric effect that some ceramic materials such as lithium niobate exhibit enables useful applications, such as pressure sensors and audible alarms. When piezo-electric material has an electric field applied across it, usually through metal electrodes, the material changes shape. This often takes the form of local material expansion or contraction (depending on the polarity of the applied voltage). In the case of the audible alarm, the material expansion and contraction

modulates the air pressure to give an audible tone if the electric field is alternating at audio frequencies.

One form of the piezo-electric effect is the SAW (surface-acoustic-wave) phenomenon, in which signals travel due to an acoustic wave in the ceramic material. To see this effect the piezo-electric material has one side bonded to a metal plate. The upper surface has metal electrodes applied to it, to provide an electric energizing force. The surface wave is created when a material is forced to expand (by the piezo-electric effect) beneath the metal electrodes. Physical bonds between molecules then force adjacent material to expand and this expansion propagates through the material.

The piezo-electric effect is bi-directional, so that if the material between electrodes changes shape, an electric field is generated between the electrodes. This is the effect seen when a piezo-electric gas lighter is used: a sudden force across a piezo-electric element generates high voltages that force a spark to be produced. In the SAW device, the acoustic wave travels along the material and deforms the piezo-electric material between a second set of electrodes, which are located at the other end of the piezo-electric material. A voltage is then formed between these electrodes. By having two sets of electrodes, known as transducers, at opposite ends of a piece of piezo-electric material, a signal can be transmitted through the material by applying a voltage at one end and detecting it at the other.

The range of frequencies that propagate through the piezo-electric material can be controlled by suitable transmit and receive transducer spacing. The propagation frequencies can be further controlled by applying additional metallized areas (described later) between the transmit and receive transducers. Thus SAW devices could be used to make compact and low-cost filters.

SAW resonators use piezo-electric material that is free to vibrate in one direction. The speed of wave propagation and the dimensions of the material are such that the wave reflects back and forth, resonating at a certain frequency. This can replace quartz crystals in many oscillator circuits, where the frequency accuracy is not critical.

7.5.1 Fundamentals of SAW transversal filters

In its simplest form, a transversal SAW filter consists of two transducers with inter-digital arrays of thin metal electrodes deposited on a piezoelectric substrate, such as quartz or lithium niobate (see *Figure 7.8*). The electrodes that comprise these arrays are arranged to have alternate polarities, so that an RF signal voltage of the proper

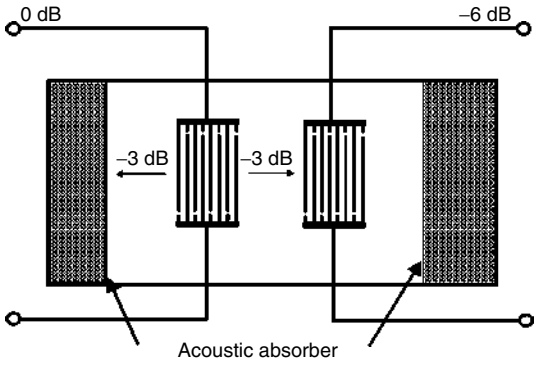

Figure 7.8 Simple transversal SAW filter configuration

frequency applied across them causes the surface of the crystal to alternately expand and contract along its length. This generates the Rayleigh wave, or surface wave, as it is more commonly called.

These inter-digital electrodes are generally spaced at half or quarter wavelength of the operating centre frequency. Since the surface wave or acoustic velocity is 10^5 slower than the speed of light, an acoustic wavelength is much smaller than its free space electromagnetic counterpart. For example, a CW signal at 1000 MHz with a free space wavelength of 300 mm would have a corresponding acoustic wavelength of about 3 μm. This wavelength compressing effect results in the SAW filter's unique ability to provide considerable signal processing or delay in a very small volume.

The wavelength compressing effect of the piezo-electric material has the effect of producing physical limitations at very high and low frequencies. At very high frequencies the electrodes become too narrow to fabricate with standard photo-lithographic techniques. At low frequencies the devices become impracticably large. Consequently, SAW devices are most typically used over the frequency range 10 MHz to about 3 GHz.

The basic SAW transducer is a bi-directional radiator. That is, half of the power (or −3 dB) is directed towards the output transducer while the other half is radiated towards the end of the crystal and is lost. By reciprocity, only half of the intercepted acoustic energy at the output is reconverted to electrical energy; hence, the inherent 6 dB loss associated with this structure (refer to *Figure 7.8*). Numerous second-order effects, such as coupling efficiency, resistive losses, and impedance mismatch, raise the insertion loss of practical filters to about 15 to 30 dB.

A new low-loss structure is the single-phase unidirectional transducer (SPUDT). Unlike the traditional three-phase unidirectional filters, the SPUDT devices are generally as straightforward to fabricate as ordinary bi-directional transducers. In addition, the required impedance matching network is greatly simplified, usually consisting of an L-C network on each port. Most SPUDT structures contain acoustic reflectors within the inter-digital pattern, illustrated schematically in *Figure 7.9* as wider electrodes. These internal reflectors serve to redirect most of the acoustic energy that is normally lost in a conventional bi-directional device. Second-order effects tend to limit the practical insertion loss to about 5 to 12 dB.

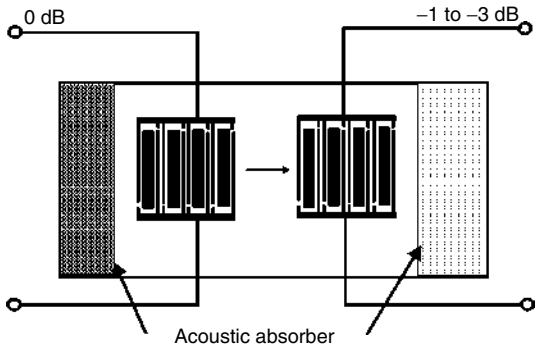

Figure 7.9 Single-phase unidirectional filter configuration

7.5.2 SAW device design

A better understanding of SAW device operation can be obtained by understanding how they are designed. SAW filters use finite impulse response design techniques, which are very similar to those used for digital filters. Hence, the Fourier transform is used to relate the time and frequency responses of the transducers and resultant filter. The desired total frequency response characteristics are used to find the impulse responses for the two transducers. These two impulse response shapes are then etched onto the surface of a metallized piezo-electric substrate to form transducers. When an impulse is applied to the transducer, the output wave shape is the same as the shape of the metallized transducer pattern.

To illustrate this relationship, the following examples may be valuable. First, consider the case of the uniform-overlap (or unweighted) transducer as shown in *Figure 7.10*. Since all fingers have the same

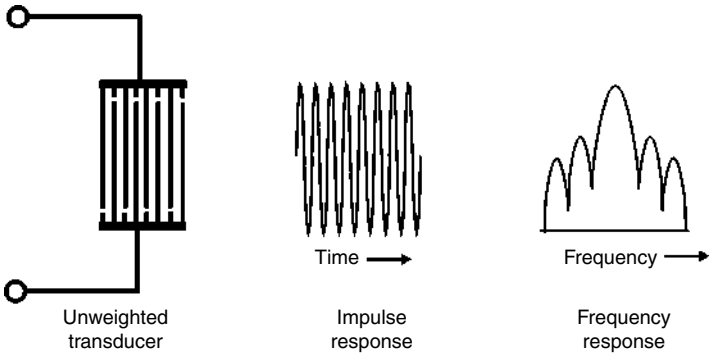

Figure 7.10 Uniform-overlap transducer

length, the impulse response envelope of this transducer is a rectangle. The Fourier transform of a rectangle is a $\sin(x)/x$ function with a 4 dB bandwidth roughly equal to the reciprocal of its time length. This illustrates the important trade-off between bandwidth and size, the narrower the bandwidth: the longer the transducer.

The $\sin(x)/x$ response has 13 dB first side-lobe attenuation, which results in 26 dB of rejection when two of these unweighted transducers are cascaded on the substrate. The 26 dB frequency rejection and poor skirt selectivity make the unweighted transducer suitable for delay lines, but unsuitable for most filter applications where more rejection is needed close to the passband edge.

According to Fourier transform theory, to obtain the rectangular frequency response, a transducer must be built that is infinitely long with electrode lengths that have $\sin(x)/x$ weighting. This is impossible, but the principle behind this example will always hold true: the steeper the skirts (the more rectangular the response) for a given bandwidth, the longer the device must be. The longest possible SAW device would exhibit a narrow bandwidth with a very steep roll-off. The transducer pattern must be limited in length but a gradual tailing off to zero length of the outer electrodes provides close to ideal performance (akin to the windowing function in digital FIR filters).

References

Crystal Product Data Book (1993). International Quartz Devices Ltd, Crewkerne, Somerset.

Winder, S.W. (2001). *Newnes Telecommunications Pocket Book*. Butterworth-Heinemann, Oxford.

8 Bandwidth requirements and modulation

8.1 Bandwidth of signals at base band

8.1.1 Analogue signals

The amount of information and the speed at which it is transmitted determines the base bandwidth occupied by a signal. For analogue signals, the base bandwidth is the range of frequencies contained in the signal; it is not the same as that occupied by a radio frequency carrier modulated by the signal. Examples of base bandwidths are given in *Table 8.1*.

Table 8.1 Base bandwidths

Application	*Frequency range (Hz)*
Speech	
High fidelity reproduction	15–15 000
Good fidelity	150–7000
Public address	200–5000
Restricted bass and treble	500–4000
Toll quality (good quality telephone line)	300–3400
Communications quality (radio communication)	300–3000
Mobile radio (12.5 kHz channel separation)	300–2700
Music (for FM broadcasting)	30–15 000
Video	60 Hz–4.2 MHz

8.1.2 Digital signals

Bit rate (b/s) and baud rate are terms used to specify the speed of transmitting digital information. Where the duration of all the signalling elements is identical the terms are synonymous, but not where the duration of the information bits differs.

As the term implies, the bit rate is the number of bits transmitted per second but the baud rate (after J.M.E. Baudot, the code's inventor) is the reciprocal of the length, in seconds, of the shortest duration signalling element. *Figure 8.1(a)* shows a binary code pattern where

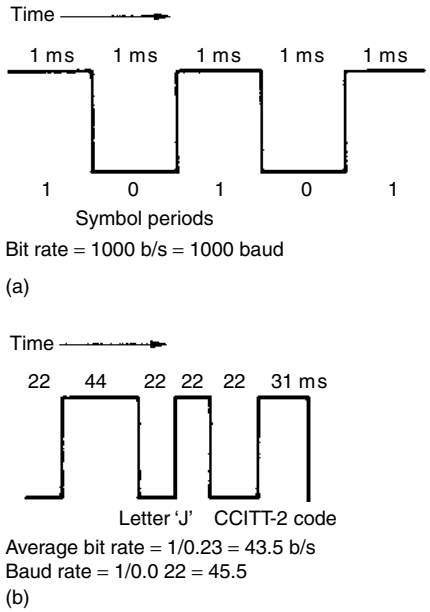

Figure 8.1 Bit rate and baud rate

all the bits are of equal duration, in this case 1 millisecond; the bit rate is 1000 per second and the baud rate is $1/0.001 = 1000$ also.

On telegraphy systems all the bits may not be of the same duration and *Figure 8.1(b)* shows the pattern for the letter 'J' in the CCITT-2 code as used for teletype. In this code a letter is composed of 5 elements, each of 22 ms duration, but each letter is preceded by a space of 22 ms and followed by a mark of 31 ms. The duration of each character is 163 ms – the time for 7.5 elements – but is comprised of only 7 bits.

The baud rate is $1/0.022 = 45.5$ baud.

The average bit duration is $163/7 = 23.29$ ms.

The average bit rate is $1/0.023 = 43.5$ bits per second.

If the bandwidth were under consideration the baud rate, being faster, would be the figure to use.

A stream of binary coded information is composed of pulses where, say, a pulse (mark) represents digit 1 and the absence of a pulse (space) represents digit 0. The highest frequency contained in the information is determined by the bit – or baud – rate. Because a series of 1s

or 0s may be consecutive in the data stream, the pulse repetition rate will vary throughout the message although the bit rate will be constant, and over a long period of time as many spaces will be sent as pulses. Transmitting either a stream of spaces or of marks requires no bandwidth; it is only when a change of state occurs that frequencies are produced. In the duration of one cycle (*Figure 8.1(a)*) two bits may be carried and the maximum *fundamental* frequency contained in the wave is one-half the number of bits per second, i.e. the channel capacity, bits/second, equals twice the bandwidth in hertz.

8.1.3 Channel capacity – Hartley – Shannon theorem

Channel capacity as stated by Hartley's law is, in the absence of noise:

$$C = 2\delta f \log_2 N$$

where
C = channel capacity, bits per second
δf = channel bandwidth, Hz
N = number of coding levels (2 in binary system)

When noise is present, the channel capacity calculated according to the Hartley–Shannon theorem is:

$$C = \delta f \log_2(1 + S/N)$$

where S/N = the ratio of total signal power to total noise power at the receiver input within the bandwidth, δf.

8.2 Modulation

For radio transmission, the low frequency information signal is carried on a radio frequency wave and it must change (modulate) that carrier. The modulation may change the amplitude, frequency or phase of the carrier. Modulation aims to achieve:

1. the transfer of information with the minimum distortion or corruption
2. the modulation of the carrier with the minimum loss of power
3. efficient use of the frequency spectrum.

8.3 Analogue modulation

8.3.1 Amplitude modulation (AM)

There are a number of methods of modulation where the amplitude of the carrier is varied by the information signal but the most commonly used is double sideband AM (DSB). *Figure 8.2* shows a radio frequency carrier modulated by a low frequency signal.

The amount or depth of modulation is expressed as percentage ratio, $m\%$, of the maximum to minimum amplitude:

$$\text{Mod. depth} = m\% = \frac{\text{max. amplitude} - \text{min. amplitude}}{\text{max. amplitude} + \text{min. amplitude}} \times 100\%$$

When the modulation is increased to the point where the minimum amplitude falls to zero, 100% modulation occurs. Any further increase in modulation produces spurious, out-of-band frequencies (AM splash), a source of interference for other radio users. For this reason, the depth of amplitude modulation is usually limited to 70%.

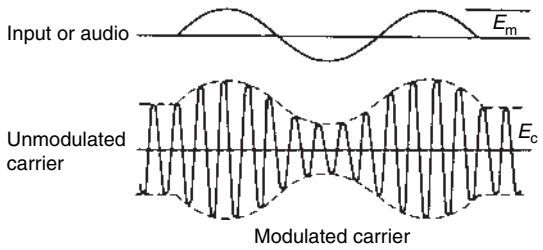

Figure 8.2 Amplitude modulation

An alternative expression for modulation depth is in terms of a modulation index from 0 to 1. The peak carrier voltage in *Figure 8.2* is E_c and the peak modulation voltage, E_m. The modulation index, m, is:

$$m = \frac{E_m}{E_c}$$

Amplitude modulation produces a band of frequencies above and below the carrier frequency – the upper and lower sidebands. The width of each sideband is equal to the highest modulating frequency so the bandwidth of an AM wave is $2 \times$ the highest modulating frequency. To conserve spectrum, the range of modulating frequencies

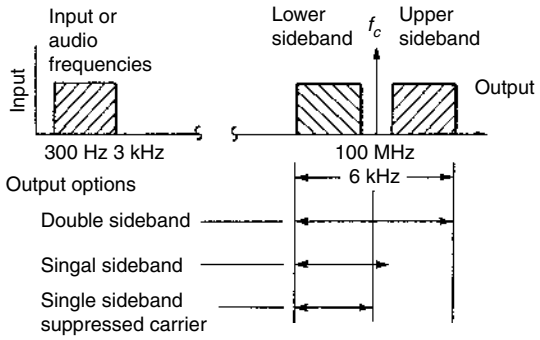

Figure 8.3 Amplitude modulation – sidebands

is restricted. For example, radio communication quality speech is limited to 300 Hz to 3000 Hz. The bandwidth occupied by a double sideband, amplitude modulated carrier for this service is 6 KHz (*Figure 8.3*).

Power relationships in an AM wave

The total power in an AM wave is the sum of powers of the carrier, the upper sideband and lower sideband:

$$P_t = \frac{E_{carr}{}^2}{R} + \frac{E_{lsb}{}^2}{R} + \frac{E_{usb}{}^2}{R}$$

where all values are RMS and R is the resistance in which the power is dissipated. From the peak voltages shown in *Figure 8.2* the power in the unmodulated carrier is:

$$P_c = \frac{E_c/\sqrt{2}\,^2}{R} = \frac{E_c{}^2}{2R}$$

The power in the sidebands

$$P_{lsb} = P_{usb} = \left(\frac{mE_c/2}{\sqrt{2}}\right)^2 \div R = \frac{m^2 E_c{}^2}{8R}$$

$$= \frac{m^2}{4}\frac{E_c{}^2}{2R}$$

The ratio of the total power in the wave to the carrier power is:

$$\frac{P_t}{P_c} = 1 + \frac{m^2}{2}$$

As m cannot exceed 1, the maximum RMS power in the wave is $P_t = 1.5P_c$; but if m reaches 1, the peak sum of E_c and E_m is $2E_c$ and so the instantaneous peak power is $2P_c$. Circuitry must be capable of handling this power level without distortion.

Double sideband amplitude modulation wastes power and spectrum. Two-thirds of the power is in the carrier which conveys no information and one sideband is discarded in the receiver. Also, the modulation must be accomplished either in the final power amplifier of the transmitter necessitating a high power modulator, or in an earlier, low power stage when all subsequent amplifiers must operate in a linear, but inefficient, mode.

8.3.2 Double sideband suppressed carrier (DSBSC)

In an amplitude modulated wave the carrier conveys no information yet contains 2/3 of the transmitted power. It is possible to remove the carrier by using a balanced modulator (*Figure 8.4*), and improve the power efficiency by this amount.

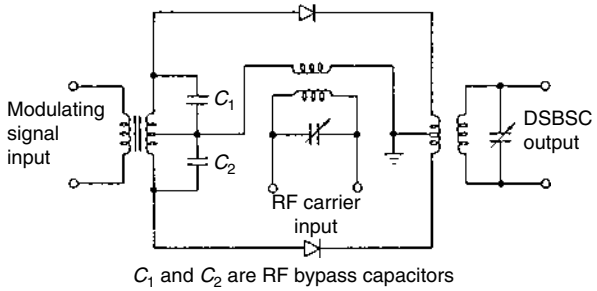

Figure 8.4 Balanced modulator

In a balanced modulator, the modulating voltage is fed in push–pull to a pair of matched diodes or amplifiers while the carrier is fed to them in parallel. The carrier components in the output cancel leaving the two sidebands. The result is a double sideband suppressed-carrier (DSBSC) wave, which is not sinusoidal, formed by the sum of the two sidebands. The carrier must be re-introduced in the receiver and its accuracy in both frequency and phase is critical.

8.3.3 Single sideband suppressed carrier (SSB or SSBSC)

The advantages of single sideband suppressed carrier transmission over double sideband AM are:

- removal of the carrier saves 2/3 of the total power
- removal of one sideband saves 50% of the remaining power
- an SSBSC transmitter only produces power when modulation is present
- the occupied bandwidth is halved; a spectrum saving
- the received signal-to-noise ratio is improved by 9 dB for a 100% modulated carrier. Halving the bandwidth accounts for 3 dB, the remainder from the improved sideband power to total power ratio. The S/N ratio improves further with lower modulation levels
- reduced susceptibility to selective fading and consequent distortion.

Two methods of generating a single sideband wave are in general use. One filters out the unwanted sideband after removal of the carrier by a balanced modulator. The other is a phase shift method (*Figure 8.5*). Here, the modulating signal is fed to two balanced modulators with a 90° phase difference. The output from both modulators contains only the sidebands but, while both upper sidebands lead the input carrier voltage by 90°, one of the lower sidebands leads it by 90° and the other lags it by 90°. When applied to the adder, the lower sidebands cancel each other while the upper sidebands add.

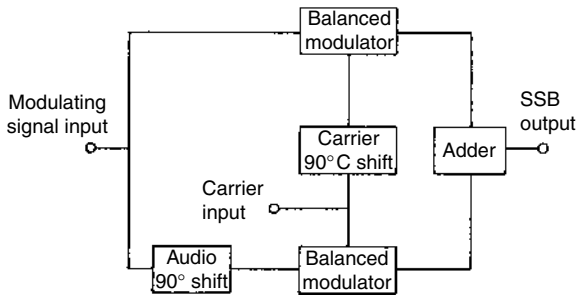

Figure 8.5 Phase shift production of single sideband

A single sideband AM wave modulated by a sinusoid consists of a constant amplitude signal whose frequency varies with the frequency of the modulating wave. Note that this is not the same as FM: the frequency in SSB does not swing to either side of the carrier. It is higher than the carrier frequency if the upper sideband is transmitted, and lower if the lower sideband is selected. The single sideband waveform is sinusoidal and, although the frequency of the reintroduced carrier must be highly accurate (±2 Hz), the phase is

unimportant making a single sideband receiver less complex than one for DSBSC.

On some systems a pilot carrier is transmitted and the transmitter output power is then specified in terms of peak envelope power (pep), the power contained in a wave of amplitude equal to the pilot carrier and transmitted sideband power. Where no pilot carrier is transmitted, the power is specified as peak sideband power (psp).

8.3.4 Frequency modulation (FM)

Both frequency and phase modulation (both may be referred to as angle modulation) effectively vary the frequency of the carrier rather than its amplitude. Frequency modulation varies the carrier frequency directly but its amplitude remains constant regardless of the modulating voltage. Angle modulation is employed at VHF and above for both communications and broadcasting services.

When frequency modulated, a carrier frequency either increases or decreases when the modulation voltage is positive and varies in the opposite sense when the modulating voltage is negative (*Figure 8.6*). The amount of modulation, i.e. the 'deviation' of the carrier from its nominal frequency, is proportional to the amplitude, and not the frequency, of the modulating voltage. The modulation index, M, is defined as the deviation divided by the modulating frequency:

$$M = \frac{f_\mathrm{d}}{f_\mathrm{m}} \text{ or } \frac{\omega_\mathrm{d}}{\omega_\mathrm{m}}$$

where

f_d = deviation in hertz

f_m = modulating frequency in hertz

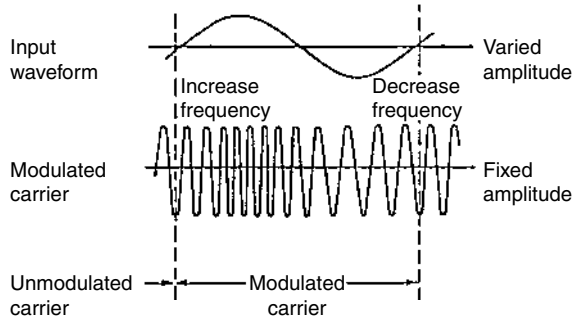

Figure 8.6 Frequency modulation

$\omega_d = 2\pi f_d$ = deviation in radians
$\omega_m = 2\pi f_m$ = modulating frequency in radians

The 'deviation ratio', D, is given by:

$$D = \frac{f_{d(max)}}{f_{m(max)}}$$

The peak deviation is the maximum amount of modulation occurring (equivalent to 100% amplitude modulation). With FM, this is limited only by the need to conserve spectrum; there is no technical limit where distortion occurs, as with 100% AM. The maximum permitted deviation for a service is determined by regulation.

The bandwidth of a frequency modulated signal is made up of the carrier and a series of sidebands, sometimes referred to as sidecurrents, spaced apart from each other at the modulating frequency. The number of sidebands is proportional to the modulation index and their amplitudes decrease with spacing from the carrier. It is generally considered satisfactory to transmit those sidebands $M + 1$ in number, with amplitudes greater than 10% of that of the carrier for that modulation index (*Figure 8.7*). The sidebands occur on both sides of the carrier and:

$$\text{1st order sidebands} = f_c \pm f_m$$

$$\text{2nd order sidebands} = f_c \pm 2f_m, \text{ etc.}$$

When the modulation index approaches 6 a good approximation of the bandwidth (δf) required for an FM transmission is $2(f_d + f_m)$ Hz. For example, speech 300–3000 Hz, max deviation 15 kHz (relevant to a VHF, 50 kHz channel spacing system):

$$\delta f = 2(f_d + f_m) = 2(15 + 3)\,\text{kHz} = 36\,\text{kHz}$$

$$M = 15/3 = 5$$

The bandwidth is also given by $\delta f = f_m \times$ highest needed sideband $\times$ 2. From Bessel functions (*Figure 8.7*), a modulation index of 5 requires the 6th order sideband to be transmitted ($M + 1$). Therefore:

$$\delta f = f_m \times 6 \times 2 = 3 \times 6 \times 2 = 36\,\text{kHz}$$

For specific values of M the carrier of an FM wave disappears. The successive disappearances and the modulation index are given in *Table 8.2*.

Table 8.2 Successive disappearances and modulation index

Order of disappearance	*Modulation index M*
1	2.40
2	5.52
3	8.65
4	11.79
5	14.93
6	18.07
$n(n > 6)$	$18.07 + \pi(n - 6)$

Systems where the modulation index exceeds $\pi/2$ are considered to be wide band FM (WBFM), those with a modulation index lower than $\pi/2$, narrow band FM (NBFM). The bandwidth of an NBFM signal is $2f_{\mathrm{m(max)}}$.

Pressure on spectrum necessitates narrower channel spacings for communications and, at VHF, 12.5 kHz is normal with ± 2.5 kHz as the maximum permitted deviation. Lower standards of performance with a restricted modulation index and a highest modulating frequency of 3 kHz have had to be accepted.

For transmitters used on 12.5 kHz channel spaced systems the highest modulating frequency is, in practical terms, 2700 Hz because the specification requires the frequency response to fall above 2.55 kHz.

The modulation index on such systems, assuming a highest modulating frequency of 3 kHz, is $2.5/3 = 0.8333$ ($<\pi/2$ and so system is NBFM) and the amplitude of the 2nd order sideband is $<10\%$ of carrier amplitude (*Figure 8.7*), so the bandwidth $= 2f_{\mathrm{m(max)}} = 6$ kHz.

8.3.5 Phase modulation

The end result of phase modulation is frequency modulation, but the method of achieving it and the definition of the modulation index is different. Phase modulation is used in VHF and UHF transmitters where the carrier frequency is generated directly by a crystal oscillator. The frequency of a crystal oscillator can be varied by only a few radians but if the oscillator frequency is multiplied to produce the final carrier frequency the phase variation is also multiplied to produce a frequency deviation.

In frequency modulation deviation is proportional to the modulating voltage, but in phase modulation the frequency deviation is proportional to both the modulating voltage and frequency.

The phase modulation, ϕ_d radians, equals the modulation index so, for phase modulation, the modulation index is $\phi_d = \omega_d/\omega_m$.

Phase modulation has, therefore, a frequency response for the deviation that rises at 6 dB per octave of the modulating frequency. The flat frequency response of FM can be produced on a phase modulated transmitter by installing a filter with a response falling at 6 dB per octave in the audio amplifier, and the rising response of PM can be produced in an FM transmitter with a rising response filter.

8.3.6 Pre- and de-emphasis

Phase modulation, and FM modified to give a rising frequency response (pre-emphasis), offer an improved signal-to-noise ratio in the receiver. The +6 dB per octave response produced in the transmitter is restored to a flat response in the receiver by a −6 dB per octave filter in the audio circuitry which reduces both the enhanced levels of the higher speech frequencies and the high frequency noise (de-emphasis).

8.3.7 Merits of amplitude and frequency modulation

The advantages and disadvantages of AM and FM are given in *Table 8.3*.

Table 8.3 Advantages and disadvantages of AM and FM

	Advantages	*Disadvantages*
AM	Simple modulators and de-modulators	Susceptible to man-made noise
	Narrower bandwidth than wide-band FM	Audio strength falls with decreasing RF signal strength
		Inefficient power usage
		Limited dynamic range
		Transmitter output power not easily adjusted
FM	Less susceptible to noise	Wider bandwidth
	Constant audio level to almost the end of radio range	
	Capture effect in receiver	Capture effect may be undesirable, e.g. aviation communications
	More power-efficient	
	Transmitter output power easily adjustable	

8.3.8 Stereo FM radio

An important advantage of FM over AM radio broadcasting is the availability of stereo sound. This requires the transmission and

reception of the left and right audio signals, to produce a stereo image. However, the introduction of stereo had to be achieved while still catering for large numbers of listeners who wanted to continue receiving in mono. The introduction of stereo FM radio had to go unnoticed by anyone using old mono radios. Without this condition, a simpler method could have been chosen.

The standard FM stereo system used by broadcasters around the world is illustrated in the block diagram of *Figure 8.8*. It uses frequency division multiplexing (FDM) to combine the two signals of the left and right channels. The signals are filtered to limit the bandwidth to 15 kHz. The left (L) and right (R) signals are then added to produce a sum signal and subtracted one from the other to produce a difference signal.

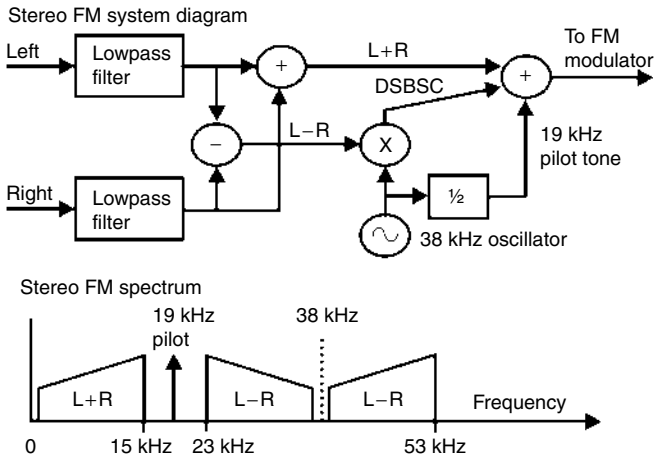

Figure 8.8 FM stereo transmitter

The sum signal provides a monophonic signal, which provides a baseband signal for the frequency modulator. This was the technique used in mono FM and thus was the obvious choice for stereo FM, to allow backward compatibility. An mono FM radio can receive this signal and recover the combined L and R channels, thereby satisfying the requirement for providing unchanged service to mono radios.

The difference signal is used to amplitude modulate a 38 kHz sinewave. By utilizing a balanced mixer, double sideband suppressed carrier (DSBSC) is generated. However, the modulation method must take into account the ease of demodulation. In particular, demodulating a DSBSC signal can be difficult. Both frequency and phase of the carrier are needed to perform faithful demodulation.

In the stereo system the DSBSC demodulation problem is dealt with by including a 19 kHz pilot tone in the broadcast. This tone is generated by a divide-by-two frequency converter circuit, which takes the 38 kHz carrier and produces the 19 kHz pilot tone. The 19 kHz pilot tone falls midway in the spectral region between the mono sum signal (up to 15 kHz) and below the DSBSC difference signal information. The DSBSC signal extends from 23 kHz to 53 kHz, since the input modulating signals are band limited to 15 kHz. The DSBSC output is added to the baseband (L and R sum) signal and the 19 kHz pilot tone before being sent to the FM modulator.

A mono FM receiver ignores the stereo information by using a filter after its FM demodulator to block everything above 15 kHz. It passes the combined L and R channel signal, which is monophonic.

A stereo receiver has an additional circuit after the FM demodulator to detect and demodulate the DSBSC signal. The stereo receiver detects a 19 kHz pilot tone and uses this to generate a 38 kHz signal. This is then used to demodulate the DSBSC signal that carries the L and R channel difference information. The stereo receiver then has both the sum and difference signals, which is all that is needed to recreate the separate left and right signals. Separation is achieved by adding and subtracting sum and difference signals.

The noise power spectral density of a demodulated FM signal tends to increase with the square of the modulation frequency. This is why pre-emphasis is used to boost the high frequency baseband signals for maintaining the signal-to-noise ratio of the transmitted signal. However, this means that there will be more noise in the 23 kHz to 53 kHz band used for the difference signal than for the 0–15 kHz band used for the sum signal. Consequently a significantly higher input signal level is required to receive a stereo transmission compared with a mono signal for the same output signal-to-noise ratio. Thus stereo reception requires far higher radio signal levels than for mono reception and is more susceptible to interference from other radio sources.

8.4 Digital modulation

8.4.1 Data processing

Filtering

A data pulse with a sharp rise- and fall-time produces harmonic frequencies and requires a wide bandwidth if it is to maintain its

shape during transmission. Consequently, to transmit the data over a limited bandwidth the pulses must be shaped to reduce the harmonic content as much as possible without impairing the intelligibility of the signal. This is accomplished by the use of low-pass (Gaussian) filters of which the result is a string of smoother pulses, often referred to as 'tamed' (*Figure 8.9(b)*). Tamed FM permits high data rates within a limited channel bandwidth whilst maintaining acceptable adjacent channel interference levels.

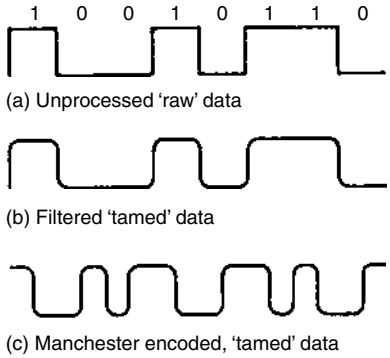

Figure 8.9 Data processing

Manchester encoding

A serious problem with the transmission of binary data is that unless the clocks in the transmitter and receiver are synchronous the digits become confused, particularly where a continuous string of 1s or 0s occurs. Manchester encoding makes 1s change state from 1 to 0, and 0s from 0 to 1 during each digit period (*Figure 8.9(c)*), facilitating the synchronization of the clocks and rendering the digits more easily recognizable.

Gray coding

For binary data the number of signalling levels is not restricted to two (mark and space). Multi-level signalling has the advantage that one signalling element carries the information for more than one information bit, thus reducing the bandwidth requirement.

If the number of levels is increased to m, where $m = 2^n$ (i.e. $n = \log_2 m$), the m-level data symbol is represented by n binary digits of 0 or 1 (see quaternary phase shift keying, Section 8.4.5). For example, in a quaternary data signal, $m = 4 = 2^2$ giving the binary sequences 00, 01, 10, 11 for each signalling level. This process is Gray coding

where there is only one digit difference for each transition between adjacent levels. The number of levels is not restricted to four and 16 level quadrature amplitude modulation (QAM), where $n = 4$, is an efficient system.

In a Gray coded signal where each element contains n bits ($n = \log_2 m$) and the signalling element rate is B bauds (elements per second), the transmission rate is $B \log_2 m$ bits per second.

8.4.2 On/off and amplitude shift keying

On/off keying

The earliest modulation method. A continuous radio frequency wave (CW) is interrupted in a recognizable pattern (Morse code). To provide audibility the carrier is heterodyned with a beat frequency oscillator (BFO) in the receiver. The use of a modulated continuous wave (MCW) eliminates the need for a BFO but the bandwidth of the signal is increased. The problem with on/off keying is the lack of a reference level. If the signal strength temporarily falls below the sensitivity threshold of the receiver it appears to the operator as a series of spaces.

Binary amplitude shift keying (ASK or BASK)

This shifts the level of an audio frequency subcarrier which then modulates a radio frequency carrier.

Because the level of a subcarrier is changed, AM sidebands are produced. Also, because the keyed waveform is non-sinusoidal harmonics occur. The occupied sub-carrier bandwidth for ASK is:

$$\text{Bandwidth} = 2B$$

where B = bit repetition rate (bits/second).

When the RF carrier is modulated its bandwidth is $2(f_c + B)$ where f_c = subcarrier frequency.

8.4.3 Frequency shift keying (FSK)

Although used for conveying digital information, frequency shift keying in reality employs frequency modulation. In its original form, developed for HF transmission, FSK changes the carrier frequency to indicate a 1 or a 0 but retains the nominal carrier frequency as a reference and to represent a mark. A downwards shift of carrier frequency by 170 Hz represents a space in the HF radio system.

Table 8.4 Standard ITU-T frequencies for various bit rates

Bit rate (bps)	*Frequencies*		*Subcarrier frequency*
	0	*1*	
600	1700	1300	1500
1200	2100	1300	1700
up to 300	1180	980	1080
	1850	1650	1750

Modern FSK uses two different modulation frequencies to represent 1s and 0s. If intersymbol interference (ISI) is to be avoided the separation of the tones must be more than half the bit rate, and a factor of 0.7 is often used. Standard ITU-T frequencies for various bit rates are given in *Table 8.4*.

The base bandwidth requirement is:

$$\text{Bandwidth} = f_2 - f_1 + 2B$$

The bandwidth of a modulated carrier is:

$$\text{RF bandwidth} = 2(f_2 + B)(\text{narrow band FM})$$

Minimum shift keying (MSK) is a form of FSK where the frequency deviation is equal to half the bit rate.

Gaussian minimum phase shift keying (GMSK)

Similar to MSK, the Gaussian filters improve the adjacent channel performance against a small cost (approximately 1%) in ISI while achieving high data transmission rates.

8.4.4 Fast frequency shift keying (FFSK)

Fast frequency shift keying may either amplitude or frequency modulate the carrier. In binary FFSK, the data is changed in a modem to tones of 1800 Hz to represent binary 0 and 1200 Hz to represent binary 1. During transmission a binary 1 consists of 1 cycle of 1200 Hz, f_1, and a 0, $1\frac{1}{2}$ cycles of 1800 Hz, f_2, i.e. a bit rate of 1200 bps. For acceptable intersymbol interference the distance between the tones cannot be less than half the bit rate and the 600 Hz separation in FFSK represents the fastest signalling speed – hence the description – and minimum bandwidth. For this reason it is sometimes called minimum frequency shift keying (MFSK). The base bandwidth is the same as

for FSK, but the RF bandwidth depends upon the system deviation. For example, on a 12.5 kHz channel spaced system carrying FFSK and complying with Radiocommunications Agency Code of Practice MPT 1317, deviation = 60% of system deviation = 1.5 kHz:

$$f_1 = 1200\,\text{Hz}$$

$$f_2 = 1800\,\text{Hz}$$

$$B = 1200\,\text{bps}$$

$f_{\max} = f_2 + B = 3\,\text{kHz}$ and the mod. index $m = \text{max. dev.}/f_{\max} < \pi/2$ so the system is NBFM and the bandwidth $= 2(f_2 + B) = 6\,\text{kHz}$.

Where more data states than binary are to be transmitted, multistate FSK (M-ary FSK) is also possible where M may be up to 32 states.

Both FFSK and M-ary FSK are well suited to radio transmission as the change of state occurs while the signals are passing through zero, avoiding sudden phase changes (*Figure 8.10(a)*).

The minimum distance between the tones used in FFSK of 0.5 times the bit rate is not ideal for immunity to intersymbol interference (ISI).

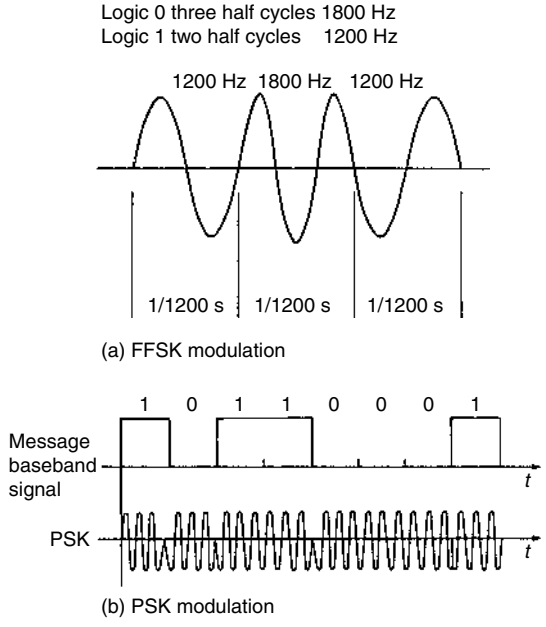

Figure 8.10 FFSK and PSK

A separation of 0.7 times the bit rate would improve the ISI but increase the bandwidth.

8.4.5 Phase shift keying

There are several variants of phase shift keying. Binary phase shift keying (BPSK or PSK) changes the phase of the carrier by 180° at the zero crossing point (*Figure 8.10(b)*). No carrier frequency is present with PSK as half the time the carrier is multiplied by +1 and the other half by −1 and cancels out, but the reference phase of the carrier must be re-inserted at the receiver. The bandwidths occupied are the same as for ASK, i.e.:

$$\text{Baseband} = 2B$$

$$\text{RF bandwidth (AM or NBFM)} = 2(f_c + B)$$

Differential phase shift keying (DPSK) advances the phase 90° or 270° at each change of logic state (*Figure 8.11*). Changing phase only at a

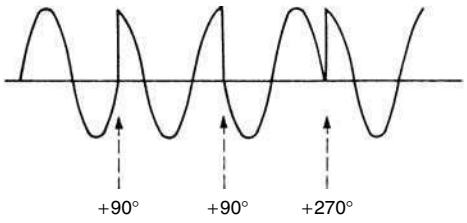

Data	Phase change
0	+90°
1	+270°

(a) DPSK modulation

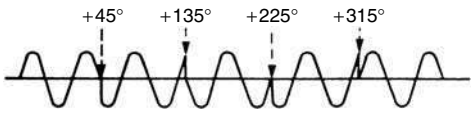

Dibit	Phase change
00	+45°
01	+135°
11	+225°
10	+315°

(b) QPSK modulation

Figure 8.11 DPSK and QPSK

change of logic state saves bandwidth which, for DPSK, is equal to the bit rate.

An important advantage of both FFSK and PSK over FSK is that because the moment of change is predefined it is possible to recover data more accurately. However, the transition between signalling states is not smooth requiring large and rapid phase shifts. Multilevel systems with less phase shift between elements are preferable.

Quaternary, or quadrature, phase shift keying (QPSK) is a four-level Gray-coded signalling method with 90° phase shift between adjacent signalling elements (*Figure 8.11(b)*). If the signal is considered as a vector the points at $\pi/4$ (45°), $3\pi/4$ (135°), $5\pi/4$ (225°) and $7\pi/4$ (315°) represent the transition points between states and the binary data.

8.5 Spread spectrum transmission

The spread spectrum technique spreads the carrier containing the information over a very wide bandwidth, typically 1.25 MHz, using pseudo-noise generation techniques as described in Chapter 12. The transmitter uses what is in effect a digital key to spread the bandwidth and the receiver is equipped with an identical key for despreading. A number of users with different keys can occupy the same band at the same time. The system operates well in poor signal-to-noise or high interference environments.

A continuous wave (CW) transmission concentrates all the radiated energy on a single frequency (*Figure 8.12*). Amplitude modulation and narrow band FM widen the radiated bandwidth, reducing the energy at the carrier frequency and per kHz. Wide band FM carries the process a stage further until with spread spectrum the band width is increased to the extent that the signal almost disappears into the noise floor.

Spreading of the bandwidth is achieved by multiplying the digitally modulated signal by a spreading code at a much higher bit rate (100–1000 times the signal bit rate). This is done by combining the signal with the output of a random code generator running at 2 or 3 orders of magnitude faster than the binary signal rate. *Figure 8.13* is a block diagram of a spread spectrum system. A clock running at the spreading rate R_c is used to drive both the spreading generator and, after frequency division, the data encoder. The carrier is first BPSK modulated by the encoded data and then in a balanced modulator (the spreading correlator) by the high rate code from the spreading generator. The resultant transmitted bits are referred to as chips to distinguish them from data bits. In the receiver, the clock pulses R_c are recovered and used to drive both the despreading generator and decoder.

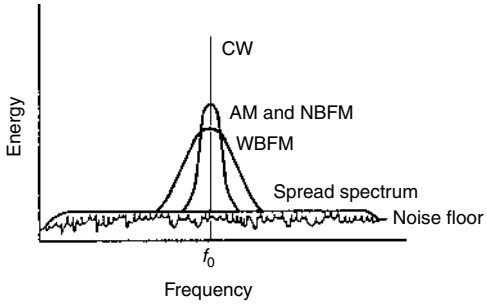

Figure 8.12 Comparative energy dispersal

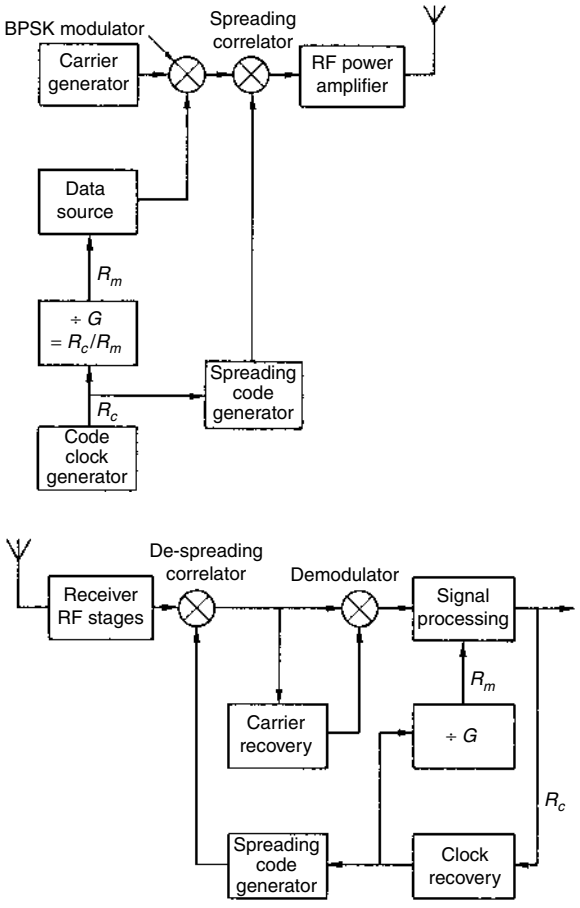

Figure 8.13 CDMA (spread spectrum) system

Many users can be accommodated by allocating each a unique spreading code. It is common to use a pseudo-noise (PN) generator to multiply the bit rate and then to modulate the carrier with either FSK or PSK.

Although spread spectrum is a digital system, in quality of signal there are similarities with analogue:

Analogue	*Digital*
Signal/noise ratio	Energy per bit, E_b/N_o
Intelligibility, signal/ noise + distortion	Bit error rate

References

Belcher, R. *et al*. (1989). *Newnes Mobile Radio Servicing Handbook*. Butterworth-Heinemann, Oxford.

Kennedy, G. (1977). *Electronic Communications Systems*, McGraw-Hill Kogashuka, Tokyo.

Winder, S.W. (2001). *Newnes Telecommunications Pocket Book*. Butterworth-Heinemann, Oxford.

9 Frequency planning

9.1 International and regional planning

The International Telecommunications Union (ITU) administers the planning and regulation of the radio frequency spectrum on a worldwide basis through the World Administrative Radio Conferences.

For planning purposes the world is divided into three regions as shown in *Figure 9.1*. The boundaries are formed by geographical features suited to the purpose such as seas, high mountain ranges or uninhabited remote areas.

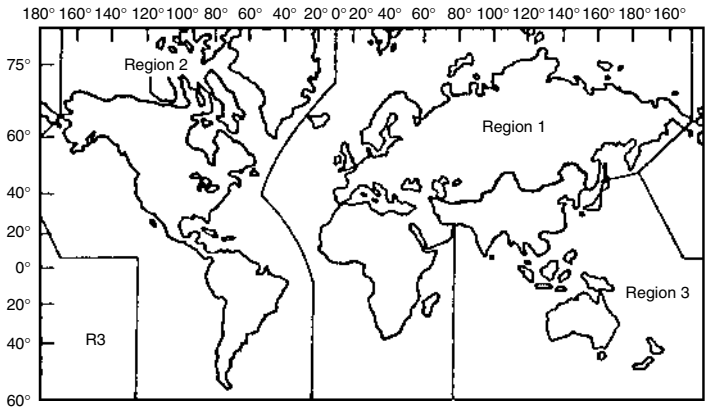

Figure 9.1 ITU defined regions. For purposes of international allocations of frequencies the world has been divided into three regions

The World Administrative Radio Conferences decide the use of blocks of the spectrum, e.g. sound broadcasting, television, marine communications, and the countries permitted to use the blocks for those allotted purposes.

9.2 National planning

Having been allocated blocks of frequencies for a particular type of use, the administration of each country determines the method of allocating frequency bands from each block to the user categories within their country. Every country has a radio regulatory department within

its administration. In the UK this is the Radiocommunications Agency of the Department of Trade and Industry.

9.2.1 The role of the Radiocommunications Agency

The aims of the Radiocommunications Agency in the UK, and, in general, the radio regulatory bodies of other countries are:

1. To ensure that the radio frequency spectrum is used in ways which maximize its contribution to national social and economic welfare, having regard to safety of life factors.
2. To make the maximum amount of spectrum available for commercial use.
3. To provide an expert service to government as a whole in the field of radio regulation.

The first stage of national planning is the assignment of the radio frequencies (channels) within a geographic area. Both the allocation of the blocks to users and the geographic assignment of channels if not wisely carried out can result in spectrum pollution – intermodulation products are one source (see Chapter 19) – and unacceptable interference between services and users. The incorrect allocation of blocks may not only cause interference in the home country but, even at VHF and UHF, between adjacent countries. Incorrect assignment of channels causes a more local problem but, depending on the frequencies involved, the undesirable effects can spread over a wide area.

The second stage of national planning is the assignment of discrete channels for use on multi-user sites where the selection of incompatible frequencies causes interference, receiver de-sensitization and, possibly, blocking, and intermodulation products.

Not all channels are allocated directly by the regulatory body. Blocks of channels, usually comprised of two frequencies, may be issued to responsible user organizations: the Home Office for the police and fire services is an example. These organizations then become responsible for the frequency planning and allocation within their user group.

Additional to the allocation of frequencies, the Radiocommunications Agency through the licensing procedure regulates the use of base station sites, the maximum transmitter power, and antenna directivity for each service. It also prepares and publishes technical specifications with which all equipment must comply. A list of the current specifications, of which single copies can be obtained, is available from

The Information and Library Service, Radiocommunications Agency, Wyndham House, 189 Marsh Wall, London E14 9SX.

The Radio Investigation Service (RIS) is the branch of the Agency which, in addition to investigating interference, inspects all radio installations prior to commissioning and, if in order, issues an inspection certificate. No station is permitted to operate without a certificate and may not be modified subsequent to the issue of the certificate.

Current policy throughout Europe is leading towards the de-regulation of radio communications while safeguarding the protection from interference. Allocation of frequencies by pricing is also under consideration on the basis that a scarce resource, the spectrum, will be allocated to the users having the greatest need.

9.3 Designations of radio emissions

Radio emissions should be expressed in a three-symbol code form, which defines the exact nature of carrier, signal and transmitted information. The first symbol defines the carrier, the second symbol defines the signal, and the third symbol defines the information.

First symbol

A	Double-sideband amplitude-modulated
B	Independent sideband amplitude-modulated
C	Vestigial sideband amplitude-modulated
D	Amplitude- and angle-modulated simultaneously, or in a predefined sequence
F	Frequency modulated
G	Phase modulated
H	Single-sideband, full carrier
J	Single-sideband, suppressed carrier
K	Amplitude-modulated pulse sequence
L	Width-modulated pulse sequence
M	Position phase modulated pulse sequence
N	Unmodulated carrier
P	Unmodulated pulse sequence
Q	Pulse sequence in which carrier is angle-modulated during the pulse period
R	Single-sideband, reduced or variable level carrier
V	Pulse sequence with a combination of carrier modulations, or produced by other means
W	Carrier is modulated by two or more of angle, amplitude, and pulse modes, simultaneously or in a defined sequence
X	Other cases

Second symbol

0	No modulating signal
1	Digital signal without modulating sub-carrier
2	Digital signal with modulating sub-carrier
3	Analogue signal
7	Two or more channels with digital signals
8	Two or more channels with analogue signals
9	Composite system with one or more channels of digital signals and one or more channels of analogue signals
X	Other cases

Third symbol

A	Aural telegraph
B	Automatic telegraph
C	Facsimile
D	Data
E	Telephony (and sound broadcasting)
F	Television
N	No information transmitted
W	Combination of any of the above
X	Other cases

9.4 Bandwidth and frequency designations

A four symbol code should be used to express bandwidth and frequency to three significant figures. A letter to denote the unit of frequency is placed in the position of the decimal point, where the letters and bandwidths are:

Letter	Bandwidth
H	Below 1000 Hz
K	Between 1 and 999 kHz
M	Between 1 and 999 MHz
G	Between 1 and 999 GHz

So, a frequency of 120 Hz is 120H, while a frequency of 12 Hz is 12H0 etc.

9.5 General frequency allocations

VLF, LF, MF (frequency in kHz)

10.0	140.5	Fixed; maritime; navigation
140.5	283.5	Broadcast

255.0	526.5	Radio navigation; fixed
526.0	1606.5	Broadcast
1606.5	1800.0	Maritime and land mobile; fixed
1810.0	1850.0	Amateur (shared in UK)
1850	2000	Amateur
1850	2045	Fixed; mobile
2045	2173.5	Maritime mobile; fixed
2160	2170	Radiolocation
2173.5	2190.5	Mobile
2190.5	2194	Maritime
2194	2625	Fixed; mobile
2300	2498	Broadcast
2625	2650	Maritime mobile
2650	2850	Fixed; mobile
2850	3155	Aero mobile

HF (frequency in kHz)

3155	3400	Fixed; mobile
3200	3400	Broadcast
3400	3500	Aero mobile
3500	3800	Amateur, fixed; mobile
3800	4000	Amateur (region 2 only)
3800	3900	Fixed; mobile
3800	3950	Aero mobile
3950	4000	Fixed; broadcast
4000	4063	Fixed; maritime mobile
4063	4438	Maritime mobile
4438	4650	Fixed; mobile
4650	4750	Aero mobile
4750	5060	Fixed; mobile; broadcast
5060	5480	Fixed; mobile
5450	5730	Aero mobile
5730	5950	Fixed; mobile
5950	6200	Broadcast
6200	6525	Maritime mobile
6525	6765	Aero mobile
6765	7000	Fixed; mobile
7000	7100	Amateur
7100	7300	Amateur (region 2 only)
7100	7300	Broadcast (regions 1 and 3)
7300	8195	Fixed
8100	8815	Maritime mobile
8815	9040	Aero mobile

9040	9500	Fixed
9500	10 000	Broadcast
10 000	10 100	Aero mobile
10 100	11 175	Fixed
10 100	10 150	Amateur
11 175	11 400	Aero mobile
11 400	11 650	Fixed
11 650	12 050	Broadcast
12 050	12 230	Fixed
12 230	13 200	Maritime mobile
13 200	13 360	Aero mobile
13 360	13 600	Fixed
13 600	13 800	Broadcast
13 800	14 000	Fixed
14 000	14 350	Amateur
14 350	15 000	Fixed
15 000	15 100	Aero mobile
15 100	15 600	Broadcast
15 600	16 360	Fixed
16 360	17 410	Maritime mobile
17 410	17 550	Fixed
17 550	17 900	Broadcast
17 900	18 030	Aero mobile
18 030	18 068	Fixed
18 068	18 168	Amateur
18 168	18 780	Fixed
18 780	18 900	Maritime mobile
18 900	19 680	Fixed
19 680	19 800	Maritime mobile
19 800	21 000	Fixed
21 000	21 450	Amateur
21 450	21 850	Broadcast
21 850	21 870	Fixed
21 870	22 000	Aero mobile
22 000	22 855	Maritime mobile
22 855	23 200	Fixed; mobile
23 200	23 350	Aero mobile
23 350	24 890	Fixed; mobile
24 890	24 990	Amateur
25 010	25 070	Fixed; mobile
25 070	25 210	Maritime mobile
21 210	25 550	Fixed; mobile

25 550	25 670	Radio astronomy
25 670	26 100	Broadcast
26 100	26 175	Maritime mobile
26 175	28 000	Fixed; mobile
28 000	29 700	Amateur
29 700	30 000	Fixed; mobile

VHF, UHF (frequencies in MHz)

30.0	50.0	Fixed; mobile
47.0	68.0	Broadcast (TV)
50.0	52.0	Amateur (UK)
50.0	54.0	Amateur (regions 2 and 3)
68.0	74.8	Fixed; mobile
70.0	70.5	Amateur (UK)
74.8	75.2	Aero navigation
75.2	87.5	Fixed; mobile
87.5	108	Broadcast (FM)
108	118	Aero navigation
118	137	Aero mobile
137	138	Spacecraft; satellites
138	144	Aero mobile; space research
144	146	Amateur
146	148	Amateur (regions 2 and 3 only)
146	174	Fixed; mobile
156	174	Maritime mobile
174	230	Broadcast (TV)
220	225	Amateur (USA)
230	328.6	Fixed; mobile
328.6	335.4	Aero navigation
335.4	400	Fixed; mobile
400	410	Space research; meteorology
410	430	Fixed; mobile
430	440	Amateur; radiolocation
440	470	Fixed; mobile
470	855	Broadcast (TV)
855	1300	Fixed; mobile
902	928	Amateur (USA)
934	935	Citizens band (UK)
1240	1325	Amateur
1300	1350	Aero navigation
1350	1400	Fixed; mobile
1400	1429	Space (uplink); fixed
1429	1525	Fixed; mobile

1525	1600	Space (downlink)
1600	1670	Space (uplink)
1670	1710	Space (downlink)
1710	2290	Fixed; mobile
2290	2300	Space (downlink); fixed
2300	2450	Amateur; fixed
2310	2450	Amateur (UK)
2300	2500	Fixed; mobile
2500	2700	Fixed; space (downlink)
2700	3300	Radar
3300	3400	Radiolocation; amateur
3400	3600	Fixed; space (uplink)
3600	4200	Fixed; space (downlink)
4200	4400	Aero navigation
4400	4500	Fixed; mobile
4500	4800	Fixed; space (downlink)
4800	5000	Fixed; mobile
5000	5850	Radio navigation; radar
5650	5850	Amateur
5850	7250	Fixed; space (uplink)
7250	7900	Fixed; space (downlink)
7900	8500	Fixed; mobile; space
8500	10 500	Radar; navigation
10 000	10 500	Amateur
10 700	12 700	Space (downlink); fixed
12 700	15 400	Space (uplink); fixed
17 700	20 000	Space (up/down); fixed
24 000	24 250	Amateur

9.6 Classes of radio stations

AL	Aeronautical radionavigation land station
AM	Aeronautical radionavigation mobile station
AT	Amateur station
AX	Aeronautical fixed station
BC	Broadcasting station, sound
BT	Broadcasting station, television
CA	Cargo ship
CO	Station open to official correspondence exclusively
CP	Station open to public correspondence
CR	Station open to limited public correspondence
CV	Station open exclusively to correspondence of a private agency

DR Directive antenna provided with a reflector
EA Space station in the amateur-satellite service
EB Space station in the broadcasting-satellite service (sound broadcasting)
EC Space station in the fixed-satellite service
ED Space telecommand space station
EE Space station in the standard frequency-satellite service
EF Space station in the radiodetermination-satellite service
EG Space station in the maritime mobile-satellite service
EH Space research space station
EJ Space station in the aeronautical mobile-satellite service
EK Space tracking space station
EM Meteorological-satellite space station
EN Radionavigation-satellite space station
EO Space station in the aeronautical radionavigational-satellite service
EQ Space station in the maritime radionavigation-satellite service
ER Space telemetering space station
ES Station in the intersatellite service
EU Space station in the land mobile-satellite service
EV Space station in the broadcasting-satellite service (television)
EW Space station in the earth exploration-satellite service
EX Experimental station
EY Space station in the time signal-satellite service
FA Aeronautical station
FB Base station
FC Coast station
FL Land station
FP Port station
FR Receiving station only, connected with the general network of telecommunication channels
FS Land station established solely for the safety of life
FX Fixed station
GS Station on board a warship or a military or naval aircraft
LR Radiolocation land station
MA Aircraft station
ME Space station
ML Land mobile station
MO Mobile station
MR Radiolocation mobile station

MS	Ship station
ND	Non-directional antenna
NL	Maritime radionavigation land station
OD	Oceanographic data station
OE	Oceanographic data interrogating station
OT	Station open exclusively to operational traffic of the service concerned
PA	Passenger ship
RA	Radio astronomy station
RC	Non-directional radio beacon
RD	Directional radio beacon
RG	Radio direction-finding station
RM	Maritime radionavigation mobile station
RT	Revolving radio beacon
SM	Meteorological aids station
SS	Standard frequency and time signal station
TA	Space operation earth station in the amateur-satellite service
TB	Fixed earth station in the aeronautical mobile-satellite service
TC	Earth station in the fixed-satellite service
TD	Space telecommand earth station
TE	Transmitting earth station
TF	Fixed earth station in the radiodetermination-satellite service
TG	Mobile earth station in the maritime mobile-satellite service
TH	Earth station in the space research service
TI	Earth station in the maritime mobile-satellite service at a specified fixed point
TJ	Mobile earth station in the aeronautical mobile-satellite service
TK	Space tracking earth station
TL	Mobile earth station in the radiodetermination-satellite service
TM	Earth station in the meteorological-satellite service
TN	Earth station in the radionavigation-satellite service
TO	Mobile earth station in the aeronautical radionavigation-satellite service
TP	Receiving earth station
TQ	Mobile earth station in the maritime radionavigation-satellite service
TR	Space telemetering earth station
TS	Television, sound channel
TT	Earth station in the space operation service

TU Mobile earth station in the land mobile-satellite service
TV Television, vision channel
TW Earth station in the earth exploration-satellite service
TX Fixed earth station in the maritime radionavigation-satellite service
TY Fixed earth station in the land mobile-satellite service
TZ Fixed earth station in the aeronautical radionavigation-satellite service

9.7 Radio wavebands

Frequency band	*Frequency*	*Wavelength*	*Waveband definition*
VLF	3 to 30 kHz	1 00 000 to 10 000 m	myriametric
LF	30 to 300 kHz	10 000 to 1000 m	kilometric
MF	300 to 3000 kHz	1000 to 100 m	hectometric
HF	3 to 30 MHz	100 to 10 m	decametric
VHF	30 to 300 MHz	10 to 1 m	metric
UHF	300 to 3000 MHz	1 to 0.1 m	decimetric
SHF	3 to 30 GHz	10 to 1 cm	centimetric
EHF	30 to 300 GHz	1 to 0.1 cm	millimetric
EHF	300 to 3000 GHz	0.1 to 0.01 cm	decimillimetric

Reference

Pannell, W.M. (1979). *Frequency Engineering in Mobile Radio Bands.* Granta Technical Editions, Cambridge.

10 Radio equipment

10.1 Transmitters

10.1.1 Transmitter functions

The functions of all transmitters and the terminology used to describe them, irrespective of the modulation method, are:

1. To generate the radio frequency carrier and amplify it to an appropriate power level; the RF power output.
2. To modulate the carrier with the intelligence to the pre-determined level; the modulation depth for AM, the deviation for FM or PM. The process must introduce the minimum noise and distortion, and prevent the modulation from exceeding the permitted level.
3. Radiate the minimum signals at frequencies outside the permitted bandwidth. Out-of-band or spurious radiation is strictly controlled by the Radiocommunications Agency MPT specifications.

10.1.2 Amplitude-modulated transmitters

Figure 10.1 is a block diagram of an amplitude modulated transmitter; in this case a quartz crystal oscillator generates the carrier frequency, although a frequency synthesizer could equally well be used. The carrier frequency in an AM transmitter is usually generated either at the transmitted frequency or one of its subharmonics; 2nd, 3rd or 6th subharmonic frequencies are typical choices depending on the final frequency.

The output of the oscillator is amplified to the level of the specified power output and if the oscillator runs at a subharmonic a frequency multiplier stage will be included, as in *Figure 10.1*, in the amplifier chain before the final stage, the power amplifier (PA). A tuned filter in the aerial circuit removes from the output unwanted frequencies which might cause interference with other users. A matching circuit correctly matches the impedance of the filter circuit to that of the aerial to ensure maximum power transfer.

In the audio circuits, the speech input from the microphone is processed by controlling the range of frequencies it contains and limiting its amplitude. This eliminates the risk of over-modulation and the production of out-of-band frequencies. Over-modulation produces

out-of-band frequencies in any transmitter, but with AM once 100% modulation is exceeded frequencies are produced across a wide range of the spectrum: a disastrous situation for other users. After processing, the audio is amplified in an AM transmitter to a high level and applied to the RF power amplifier to vary its output in the form illustrated in *Figure 8.2*.

AM transmitters are power inefficient. The RF PA cannot operate in class C. It must be linear so as not to distort the speech, and the audio, when it is the power amplifier which is modulated, must be amplified to a high power. If the modulation is applied at a lower power level (in an early stage of the amplifier chain) all the subsequent amplifiers must operate in a linear, but inefficient, manner.

The power output of an AM transmitter is normally specified in terms of the RMS value of the carrier power but the average and peak powers will depend on the depth of modulation, 100% modulation producing a peak power of twice the carrier peak power (see Chapter 8).

10.1.3 Angle modulated transmitters

Figure 10.2 is a block diagram of a frequency modulated transmitter using a frequency synthesizer for carrier generation. The frequency is generated at the final frequency and RF amplifiers raise the power level to that specified for the transmitter output. When a crystal oscillator is used for carrier generation, it must operate at a very low frequency because a quartz crystal oscillator can be frequency modulated by a few radians only. Several stages of the RF amplifier chain then operate as frequency multipliers. Similar filter and aerial matching circuits to those of an AM transmitter are necessary in the output arrangements of the transmitter.

The audio processing circuitry is similar to that for AM transmitters but the modulation (deviation) is applied to a stage operating at a very low RF power level (directly to the VCO in a synthesizer-equipped transmitter and immediately following the crystal oscillator in a direct crystal controlled one); high power audio is not necessary. An additional simple circuit in an FM transmitter may be included to enhance the higher audio frequencies at a rate of 6 dB/octave. This is pre-emphasis and has the merit of improving the level of speech to noise at the receiver (signal-to-noise ratio). The audio level must still be limited because, while the effect of over-deviation is not as disastrous as over-modulation in an AM transmitter, increasing deviation produces a steadily increasing range of frequencies, known as side-currents, outside the permitted bandwidth.

Angle modulated transmitters are more power efficient than amplitude modulated because the modulation is applied at a low power level and also, as no audio frequencies are directly present in the RF amplifier and PA stages, these can operate efficiently in class C.

Phase modulated (PM) transmitters, because the phase shift with modulation is very small, generate the carrier at a very low frequency and use direct crystal control. The frequency is then multiplied many times, thirty-two to thirty-six is common, up to the final frequency. After multiplication, the phase modulation which was originally a few radians has effectively become frequency modulation. The phase modulation process produces pre-emphasis inherently. As far as the user is concerned there is no practical difference between phase modulation and frequency modulation with added pre-emphasis.

10.1.4 Transmitter specifications

In the UK, the Radiocommunications Agency issues specifications with which all equipment must comply. Other countries have their own regulatory bodies, such as the FCC in the USA. These specifications are concerned principally with the prevention of interference and obtaining the maximum use of the frequency spectrum. The characteristics defined in the MPT specifications and other features which affect the user, apart from the physical dimensions, are:

- *Supply voltage*.
- *Operational frequency band*.
- *Modulation method*.
- *Channel separation*.
- *RF power output and impedance*. Output ranges from about 0.5 W to 5 W for hand-portables and 5 W to 25 W for mobiles. The maximum power permitted on a system will be specified in the Licence. Output impedance is commonly 50 Ω.
- *Spurious emissions*. The level of these is critical for the prevention of interference with other users on different frequencies. The limit for VHF and UHF is a maximum of 0.25 μW.
- *Residual noise*. Not always quoted by manufacturers, it is the noise level existing on an unmodulated carrier. A typical figure is better than −40 dB referred to full deviation.
- *Audio frequency distortion*. Typically <3% and usually measured with a modulating frequency of 1 kHz at 60% modulation.
- *Audio frequency response*. This is the variation of modulation level over the audio frequency spectrum. Typically within +1 dB to −3 dB over a frequency range of 300 to 3000 Hz (2.55 kHz for 12.5 kHz

channel spacing equipment). It may be quoted with reference to a pre-emphasis curve.

- *Switching bandwidth*. This is the frequency range over which the transmitter will operate without retuning and without degradation of performance. Much equipment is now specified to cover a complete frequency band, e.g. 146–174 MHz, without retuning.

10.2 Receivers

10.2.1 Receiver functions

A receiver's functions are:

- Detect a weak signal; the minimum level, which may be as low as 0.25 microvolts, defines the receiver sensitivity.
- Amplify a received signal and maintain the information contained in a minimum strength signal at a minimum of 12 dB above the electrical noise level (signal-to-noise ratio). If the audio distortion produced in the receiver is also taken into account the above figure becomes the signal-to-noise + distortion (Sinad) ratio. As the signal is increased, the ultimate Sinad should attain 50 to 55 dB.
- Separate the wanted signal from any unwanted ones which may be very close in frequency (the adjacent channel may be 12.5 kHz away at UHF); the selectivity.
- Recover the information from the carrier; demodulation.
- Amplify the audio information to a level suitable for operating a loudspeaker; the audio power output. The audio amplification must introduce the minimum distortion.
- Disenable the audio amplifiers in the absence of signal to cut out the electrical noise. This is done by the mute or squelch circuit.

10.2.2 Types of receiver

It is possible to amplify directly the incoming RF signal to a level suitable for demodulation. This is done in a tuned radio frequency (TRF) receiver, but these are seldom used today because of the problems of obtaining sufficient selectivity and gain at one radio frequency, and the difficulty of retuning a number of RF stages to change frequency. Almost all receivers designed for analogue communications now operate on the superheterodyne principle where the incoming radio frequency is converted to a lower, more manageable, intermediate frequency (IF). The fixed IF means that only the oscillator and, possibly, one RF amplifier stage need retuning for a change of channel.

The lower frequency of the IF facilitates the acquisition of adequate gain with stability and selectivity.

There is little difference in the layout of receivers for AM and FM except that the circuits perform their functions differently. *Figure 10.3* is a block diagram of a typical FM receiver with a crystal controlled local oscillator.

When two frequencies are applied to a non-linear circuit such as the mixer, they combine to produce other frequencies, their sum and difference being the strongest. The superheterodyne mixes a locally generated frequency with the received signal to produce a, usually lower, frequency retaining the modulation of the received signal. Commonly used values for this intermediate frequency (IF) are 465 kHz for MF and HF receivers and 10.7 MHz for VHF and UHF. At these fixed frequencies the necessary high amplification with low noise and stability and the required selectivity are easier to obtain. The local oscillator (injection) frequency = signal frequency ± IF frequency.

Superheterodyne receivers are susceptible to a particular form of interference. Assume a local oscillator frequency of 149.3 MHz is mixed with a wanted signal of 160 MHz to produce the IF frequency of 10.7 MHz. A signal of 138.6 MHz would also combine with the local oscillator to produce 10.7 MHz. The frequency of this spurious response is the image, or second channel frequency. The IF amplifier cannot discriminate against it so some degree of selectivity must also be provided in the RF amplifier and input circuitry. Intermediate frequencies are chosen which are a compromise between ease of obtaining adjacent channel discrimination and image frequency rejection.

The IF amplifier contains a block filter, either crystal or ceramic (see *Figure 7.7*), necessary to discriminate between channels adjacent in frequency. The design of the filter is crucial. It must be wide enough to accommodate the band of frequencies present in the modulation plus an allowance for frequency drift and its response over this band must be uniform with minimal ripple, particularly if data is to be received, yet its response must be of the order of −100 dB at the frequency of the adjacent channel.

Apart from the demodulator the main difference between AM and FM receivers lies in the operation of the IF amplifier. The IF stages in an AM receiver are linear, although their gain is variable. Part of the IF amplifier output is rectified and used to control the gain to provide automatic gain control (AGC). An increase of signal above a predetermined level, with delayed AGC, causes a reduction in IF gain maintaining a sensibly constant audio output level.

The IF amplifier in a FM receiver possesses a very high gain, some 100 dB, and is non-linear. On receipt of a signal, or even with only the receiver noise, it runs into limitation, cutting off both positive and negative peaks of the signal or noise. This gives FM its constant level audio output over a wide range of signal levels. It also produces the capture effect where a strong signal, fully limiting, completely removes a weaker signal. A signal difference of some 6 dB is required to provide effective capture.

Most receivers employ only one change of frequency, single superheterodynes, but double superheterodynes are occasionally used at VHF and above. A double superheterodyne changes the frequency twice, perhaps to 10.7 MHz for the first IF and then, using a fixed frequency crystal second local oscillator, to a lower, often 1.2 MHz or thereabouts, second IF. The result is greater gain and selectivity but the incorporation of a second oscillator and mixer increases the number of possible spurious responses.

A variation of a very old receiver circuit, the Autodyne, forgotten in about 1914, is now finding favour in receivers for digitally modulated signals. Under its new names of Homodyne or zero-IF receiver it lends itself to the purpose. In this type of receiver the local oscillator runs at the same frequency as the incoming signal, hence the zero-IF. Frequency or phase shifts of the incoming signal representing the data emerge from the mixer at base band and are applied directly to the processing circuits.

In a communications receiver the noise generated in the aerial and RF stages in the absence of a signal is amplified to what may be, when demodulated, an unacceptable level. To eliminate the annoyance the loudspeaker is switched off during no-signal periods by a squelch or mute circuit. The mute circuit rectifies the high frequency noise at the demodulator and uses it to switch off the audio amplifier. When a signal is received the limiting action of the IF amplifier of an FM receiver depresses the noise in favour of the signal. Some AM mobile receivers use additional FM circuitry to provide improved mute action.

10.2.3 Noise figure

An ideal receiver would generate no noise and the signal-to-noise ratio, in a receiver of given bandwidth, would be determined by the level of the signal at the base of the antenna compared with the noise produced in the antenna. The noise factor of the ideal receiver is the number of times the signal power must exceed the antenna noise power to

produce a 1:1 ratio at the receiver. It is given by (see Section 1.5.1):

$$\frac{e^2_{\text{antenna}}(\text{e.m.f.})}{4kTBR}$$

When the receiver input impedance is matched to the antenna impedance, half the power is dissipated in the antenna and the noise factor is 2 (3 dB). In a practical receiver, the noise generated in the RF amplifier is the most significant, and the noise figure is the sum of the RF amplifier noise plus all the preceding losses. Figures between 4 and 6 dB are common and the higher the noise figure, the worse the receiver sensitivity.

Signal-to-noise ratio (SNR, S/N or S_N)

Receivers are evaluated for quality on the basis of *signal-to-noise ratio* (S/N or 'SNR'), sometimes denoted S_N. The goal of the designer is to enhance the SNR as much as possible. Ultimately, the minimum signal level detectable at the output of an amplifier or radio receiver is that level which appears just above the noise floor level. Therefore, the lower the system noise floor, the smaller the *minimum allowable signal*.

Noise factor, noise figure and noise temperature

The noise performance of a receiver or amplifier can be defined in three different, but related, ways: *noise factor* (F_N), *noise figure* (NF) and *equivalent noise temperature* (T_E); these properties are definable as a simple ratio, decibel ratio or Kelvin temperature, respectively.

Noise factor (F_N). For components such as resistors, the noise factor is the ratio of the noise produced by a real resistor to the simple thermal noise of an ideal resistor.

The noise factor of a radio receiver (or any system) is the ratio of output noise power (P_{NO}) to input noise power (P_{NI}):

$$F_N = \left[\frac{P_{NO}}{P_{NI}}\right]_{T=290/K}$$

In order to make comparisons easier the noise factor is usually measured at the standard temperature (T_o) of 290 K (standardized room temperature); although in some countries 299 K or 300 K are commonly

used (the differences are negligible). It is also possible to define noise factor F_N in terms of the output and input signal-to-noise ratios:

$$F_N = \frac{S_{NI}}{S_{NO}}$$

where
S_{NI} is the input signal-to-noise ratio
S_{NO} is the output signal-to-noise ratio

Noise figure (NF). The *noise figure* is the frequency used to measure the receiver's 'goodness', i.e. its departure from 'idealness'. Thus, it is a *figure of merit*. The noise figure is the noise factor converted to decibel notation:

$$\mathrm{NF} = 10 \log(F_N)$$

where
NF is the noise figure in decibels (dB)
F_N is the noise factor
log refers to the system of base-10 logarithms

Noise temperature (T_e). The noise 'temperature' is a means for specifying noise in terms of an equivalent temperature. That is, the noise level that would be produced by a resistor at that temperature (expressed in degrees Kelvin). Evaluating the noise equations shows that the noise power is directly proportional to temperature in degrees Kelvin, and also that noise power collapses to zero at the temperature of Absolute Zero (0 K).

Note that the equivalent noise temperature T_e is *not* the physical temperature of the amplifier, but rather a theoretical construct that is an *equivalent* temperature that produces that amount of noise power in a resistor. The noise temperature is related to the noise factor by:

$$T_e = (F_N - 1)T_o$$

and to noise figure by

$$T_e = K T_o \log^{-1}\left[\frac{\mathrm{NF}}{10}\right] - 1$$

Noise temperature is often specified for receivers and amplifiers in combination with, or in lieu of, the noise figure.

Noise in cascade amplifiers

A noise signal is seen by any amplifier following the noise source as a valid input signal. Each stage in the cascade chain amplifies both signals and noise from previous stages, and also contributes some additional noise of its own. Thus, in a cascade amplifier the final stage sees an input signal that consists of the original signal and noise amplified by each successive stage plus the noise contributed by earlier stages. The overall noise factor for a cascade amplifier can be calculated from *Friis' noise equation*:

$$F_{\mathrm{N}} = F_1 + \frac{F_2 - 1}{G1} + \frac{F_3 - 1}{G1G2} + \cdots + \frac{F_{\mathrm{N}} - 1}{G1G2 \cdots G_{n-1}}$$

where

F_{N} is the overall noise factor of N stages in cascade
F_1 is the noise factor of stage-1
F_2 is the noise factor of stage-2
F_{N} is the noise factor of the nth stage
$G1$ is the gain of stage-1
$G2$ is the gain of stage-2
$G_{\mathrm{n-1}}$ is the gain of stage $(n - 1)$.

As you can see from Friis' equation, the noise factor of the entire cascade chain is dominated by the noise contribution of the first stage or two. High gain, low noise radio astronomy RF amplifiers typically use low noise amplifier (LNA) circuits for the first stage or two in the cascade chain. Thus, you will find an LNA at the feedpoint of a satellite receiver's dish antenna, and possibly another one at the input of the receiver module itself, but other amplifiers in the chain might be more modest (although their noise contribution cannot be ignored at radio astronomy signal levels).

The matter of signal-to-noise ratio (S/N) is sometimes treated in different ways that each attempts to crank some reality into the process. The signal-plus-noise-to-noise ratio (S + N/N) is found quite often. As the ratios get higher, the S/N and S + N/N converge (only about 0.5 dB difference at ratios as little as 10 dB). Still another variant is the SINAD (signal-plus-noise-plus-distortion-to-noise) ratio. The SINAD measurement takes into account most of the factors that can deteriorate reception.

10.2.4 Signal-to-noise ratio and bandwidth

To obtain the maximum signal-to-noise ratio the bandwidth of every circuit must be designed to admit its operational band of frequencies only. The wider its bandwidth the more noise a circuit admits, and the more the bandwidth exceeds that needed, the worse becomes the signal-to-noise ratio. There is a linear ratio between bandwidth and noise power admitted: doubling the bandwidth doubles the noise power.

Improvements in local oscillator crystal frequency stability has resulted in improved signal-to-noise ratios by reducing the necessary width of the IF filter.

Demodulation, the recovery of the audio from the IF bandwidth affects the signal-to-noise ratio. The relationship is complex, but consider two examples. First, for 12.5 kHz channel spacing FM:

The audio frequency range is 300 Hz to 3000 Hz
Bandwidth, $b = 2700$ Hz
The modulation index $M = f_{\mathrm{d(max)}}/f_{\mathrm{m(max)}}$
Signal/noise out $= 3M^2/2b\times$ signal/noise in
For a 12.5 kHz PMR channel:
$M = 2500/3000 = 0.83$
$b = 2.7$ kHz
$3M^2/2b = 0.38$
A 0.38 times reduction in power is -4.8 dB. Demodulation in this case worsens the signal-to-noise ratio by some 5 dB, and if a signal-to-noise ratio of 12 dB is required at the loudspeaker, 17 dB is needed at the input to the demodulator.

When channel separations were 25 kHz, and deviation 5 kHz, the situation was:

Audio frequency range, 300 Hz to 3000 Hz
Bandwidth, $b = 2700$ Hz
For a 50 kHz channel:
$M = 5000/3000 = 1.66$
$b = 2.7$ kHz
$3M^2/2b = 1.54$
A 1.54 times gain in power is $+1.8$ dB. In this case the demodulation improved the signal-to-noise ratio slightly. Reducing the bandwidth would have the same effect.

For AM, the signal-to-noise ratio is dependent on the modulation depth. The demodulation process reduces the signal-to-noise ratio by

6 dB but the recovered audio is less than the IF bandwidth by a factor of 3:1 which compensates for the demodulation loss. Reducing the modulation depth degrades the signal-to-noise ratio by 6 dB for every halving of the modulation depth.

10.2.5 Receiver specifications

The important features of receiver specifications are:

- *Sensitivity*. The minimum signal to which a receiver will respond. For an AM receiver, the generally accepted standard is the signal (30% modulated with sinusoidal tone, either 400 Hz or 1 kHz) required to provide an audio output of 50 mW. For an FM receiver, the standard is the unmodulated signal required to produce a 20 dB reduction in noise. A typical figure is 0.25 μV (p.d.) for 20 dB quieting. However, sensitivity is often quoted in terms of either the signal-to-noise ratio or Sinad so, in modern parlance, sensitivity and signal-to-noise ratio are sometimes considered to be synonymous.
- *Signal-to-noise ratio (may be quoted as Sinad, signal-to-noise and distortion)*. Typically 0.3 μV (p.d.) for 12 dB Sinad.
- *Spurious response attenuation*. Typically better than 80 dB.
- *Adjacent channel selectivity*. Better than 65 dB at 12.5 kHz channel spacing.
- *Cross modulation*. The modulation, in the receiver, of a wanted signal by a stronger, unwanted signal. It is usually caused by non-linearity in the receiver RF stages.
- *Blocking and de-sensitization*. The reduction in sensitivity of a receiver due to overloading of the RF stages when a strong signal is applied. A blocked receiver may take an appreciable time to recover.
- *Audio frequency response*. Typically within +1 dB to −3 dB of a 6 dB/octave de-emphasis curve from 300 Hz to 3000 Hz (2.55 kHz for 12.5 kHz channel spacing, above which the response falls more rapidly).
- *Audio output*. Typically 3–4 W. For hand-portables, 100–500 mW. (Distortion may also be quoted, typically better than 5%.)
- *Switching bandwidth*. As for transmitter.
- *Duplex separation*. For a receiver/transmitter combination, the minimum separation between the receiving and transmitting frequencies which will permit duplex operation with minimal degradation of the receiver performance.

10.3 Programmable equipment

The current trend is for many of the functions of radio equipment – even down to the control buttons on the front panel – to be software controlled. In one manufacturer's equipment the only screwdriver-adjustable control is that for setting maximum deviation; this is insisted upon by the Radiocommunications Agency for use in the UK.

Software control enables radio sets to be cloned so that once a single piece of equipment is programmed with its frequencies, power output, selective calling, etc., the whole of a fleet of mobiles can be identically programmed in a short time. Some of the functions can be programmed by the user, but not all, and different manufacturers permit different degrees of programming.

The functions are allocated degrees of priority which determine which functions can be changed by each class of person. Again, some of the priorities may be altered by the user but the highest priority functions are installed in a programmable read only memory (PROM) by the manufacturer and can only be altered by replacing the PROM, in most instances a job for the manufacturer.

The essential equipment for major reprogramming is an IBM or equivalent computer and the equipment manufacturer's software which is supplied as a package complete with hardware interface and instructions.

Cloning may be carried out using an inter-connecting cable between the equipment, or restricted reprogramming via a unit supplied by the equipment manufacturer for the purpose.

The functions which may be programmed from a computer are:

- Channel frequencies.
- Transmitter power and deviation.
- Receiver squelch setting (referred to Sinad ratio). Selective calling details including encode or decode only, type of signalling, extension of first tone and call sign.
- Transmission time out timer.
- Channel busy light. Transmitter inhibit on busy channel.
- Alert tones. Tone decoder indicator.
- Low battery indicator. Battery saver.

Restricted reprogramming may include:

- Channel frequencies, including any offsets.
- Lock out of any channels.

- Channel spacing.
- Channel search priority.
- Frequency stability.
- Signalling type.
- Control functions.
- Synthesizer reference crystal (the frequency can be trimmed to compensate for ageing).
- Transmitter power.
- CTCSS (encode and decode).
- Timers.
- Alerts.

Pagers are also programmable. The functions which can be changed include:

- Code number.
- Alert tone/vibrator/repeat.
- Urgency.
- Out of range warning.
- Printer on/off.
- Language of display.

References

Belcher, R. *et al*. (1989). *Newnes Mobile Radio Servicing Handbook*. Butterworth-Heinemann, Oxford.
Langford-Smith, F. (1955). *Radio Designer's Handbook*, Iliffe, London.

11 Microwave communication

11.1 Microwave usage

Microwaves are loosely considered to be those at frequencies between 1 GHz (30 cm) and 100 GHz (0.3 cm). Principal ground communications usage is for point-to-point links carrying information and control signals on systems such as multiplexed communication – including data networks, telemetry and mobile radio. The propagation of the higher frequencies, 30–100 GHz, is being studied for possible future use in micro-cellular radio-telephone systems. These higher frequencies are also used for satellite communications and radar applications. Microwave frequencies up to 3 GHz have now been reserved for mobile use.

11.2 Propagation

The path loss is higher at microwave frequencies than at VHF and UHF: *Figure 1.5* charts the free space loss between isotropic radiators for microwaves at frequencies of 1, 2, 3.5 and 7 GHz over distances of 10 to 1000 km. The free-space loss between isotropic radiators is given by

$$\text{Free space loss, d}B = 32.4 + 20\log_{10} d + 20\log_{10} f$$

where d is in km and f in MHz.

The free-space loss between practical antennas is given by:

$$\text{Loss, dB} = 10\log_{10}\left(\frac{(4\pi d)^2}{\lambda^2}\frac{1}{G_t G_r}\right)$$

where

d = path length, metres
λ = wavelength, metres
G_t = power gain of transmitting antenna
G_r = power gain of receiving antenna

The antenna gains are expressed relative to an isotropic radiator (not in dB).

Absorption varies with atmospheric humidity, and as energy is also absorbed by the ground the path height therefore has an effect

on the losses. Absorption by rain is a factor at the higher frequencies but, although considered to be insignificant below about 3 GHz, it has an indirect effect. Wet foliage, for example, produces considerable absorption at frequencies as low as 450 MHz.

Waves of millimetric lengths are special cases and narrow bands of very high absorption due to resonance effects exist at 22 and 183 GHz for water vapour, and 60 and 119 GHz for oxygen. Non-resonant attenuation occurs due to scatter from rain, hail and snow. The attenuation increases with frequency as the wavelength approaches the dimensions of a raindrop. Bands of very low absorption, 'atmospheric windows', where the water vapour and oxygen attenuations are very low occur at 37, 97, 137 and 210 GHz.

Objects close to a path may severely affect the received signal and a proposed path must be examined for the likely effects of these at the planning stage. The effects may be due either to diffraction bending the wave away from the line of sight between the antennas, or reflection causing multi-path signals.

The additional losses in a microwave path caused by objects either intruding into the first Fresnel zone or close to it, and which exhibit 'knife-edge' or 'smooth-sphere' characteristics, are shown in *Figure 11.1*. A negative F/F_1 indicates an intrusion. When the path clearance exceeds 0.6 times the first Fresnel zone radius, the free space loss is achieved.

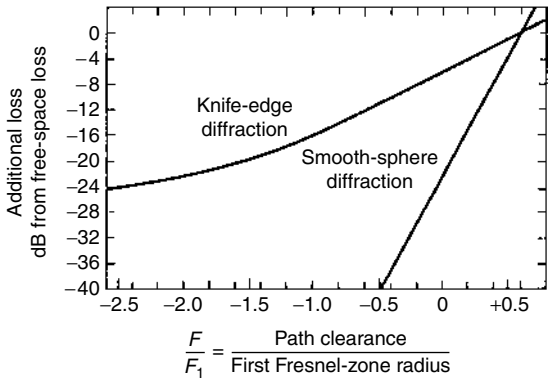

Figure 11.1 Knife-edge and smooth-sphere diffraction

Refraction also affects microwave propagation and temperature inversions may cause ducting resulting in a loss of signal and, possibly, interference. When ducting occurs, a layer of air of low refractive index is formed between two highly refractive layers and a wave may

be trapped between them. Under these conditions a signal can be carried an abnormal distance before it can return to Earth resulting in loss of signal at the intended receiver and possibly interference at a distant one on the same frequency.

11.3 *K* factor

The degree and sense of refraction of wave is related to a factor known as K. Refraction normally bends the wave downwards, extending the range, but the refractive index of the atmosphere varies from place to place and with time and height. At times, during an atmospheric inversion for instance, and in some places on the earth the effect is reversed:

When no bending occurs, $K = 1$.
When $K > 1$, the bending is downwards, effectively increasing the Earth's radius.
When $K < 1$, the bending is upwards, effectively reducing the Earth's radius.

For most of the time $K > 1$, 1.33 being accepted as the normal factor, but for small periods K may be less than one.

For a point-to-point link, the path between the transmitting and receiving sites should be a clear line of sight, although by making allowances for refraction, the Earth's radius has, up to now, generally been considered to be effectively increased by the factor of 1.33. However, in the interests of reliability a decrease to 0.7 times the radius (the minimum K factor considered likely to occur) is now often used in link planning. When a link has been planned using a higher K factor, a temporary reduction of K not only reduces the radio horizon but effectively raises objects close to the path, possibly to the point where they become significantly close to the first Fresnel zone.

It is usual when planning a link to plot the profile of a path on paper with curved horizontal graduations to represent the amended Earth's radius. The radio beam can then be drawn as a straight line between the antenna locations. *Figure 11.2* is an example.

11.4 Fresnel zones, reflections and multi-path fading

Signals which arrive at the receiver by more than one path as the results of reflection or diffraction may arrive in any phase relationship

to the direct wave. When they arrive anti-phase to the direct wave, cancellations result. The intensity and phase of the spurious signal may not be constant, thus providing random multi-path fading.

Where a carefully drawn profile of a link path shows there to be a clear line of sight, the effect of waves reflected or diffracted from objects close to the line of the direct wave must then be considered. The effect of these indirect waves can be predicted by calculating where the reflection occurs in relation to a series of ellipsoids which can be drawn around the line-of-sight path between the transmitting and receiving antennas. These ellipsoids, known as the Fresnel zones, contain the points where reflected waves will follow a path of constant length, as shown in *Figure 11.3*.

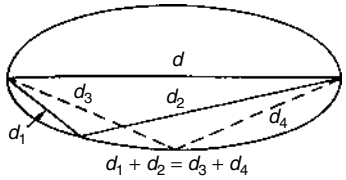

Figure 11.3 Fresnel zone: reflected path lengths

Waves reflected at the odd-numbered Fresnel zones will travel an odd number of half-wavelengths further than the direct wave but, because a 180° phase change usually occurs in the reflection process, will arrive at the receiver in phase with the direct wave. Waves reflected at even-numbered zones will arrive anti-phase to the direct wave with a cancelling effect. The effect of reflected waves diminishes with reflections from the higher order zones. The radius of a Fresnel zone in metres at the point of intrusion is given by:

First zone, F_1:

$$F_1 = 31.6\sqrt{\frac{\lambda d_1 d_2}{d}}$$

or

$$F_1 = 548\sqrt{\frac{d_1 d_2}{f d}}$$

where

F_1 = radius in metres at point of intrusion
$d_1 + d_2 = d$ (path length in km)
λ = wavelength in metres
f = frequency in MHz

Second zone:

$$F_2 = \sqrt{2} \times F_1$$

Third zone:

$$F_3 = \sqrt{3} \times F_1$$

and so on.

The degree of reflection from an object depends on its nature, the greatest reflection occurring from smooth flat ground or water. Where a path lies over the sea, variations in the path length of a reflected wave due to tides may render a path unusable. When the height of the antenna closest to the sea is varied, the *effect* of the reflected wave passes through a series of minima and maxima and adjustment of the height of that antenna can reduce or, occasionally, overcome the effect.

Atmospheric conditions change giving rise to fading and variations of the multi-path effects. The reliability of a link may be crucial to the success of a complete system and, where a critical path in terms of performance exists, long-term tests are advisable to ensure that variations of propagation do not reduce the reliability to an unacceptable level. Paths which contain obstacles in the line of sight which will cause additional losses are obviously suspect. So are those where objects or large stretches of water or flat ground which might produce diffraction or reflections of the wave lie close to the line of sight.

11.5 Performance criteria for analogue and digital links

The transmission quality for analogue modulated systems is based on the signal-to-noise ratio. The noise is specified relative to a standard test tone level and is commonly expressed as either picowatts psophometrically weighted (pWp) or decibels (dB) of C-message weighted noise above a reference noise level of −90 dBm (defined as 0 dBrnc0). Typical objectives range from 28 dBrnc0 for long-haul routes to 34 dBrnc0 for short-haul routes. When the signal fades the noise increases until the threshold noise level is reached. When the threshold (typically 55 to 58 dBrnc0) is exceeded, the transmission quality is considered unacceptable.

With digitally modulated systems the bit error rate (BER) is the measure of transmission quality. The bit error rate is the number of bit errors per total received averaged over a period of time. If the transmission rate is 10 Mbits per second and 100 bit errors occur over a 100

second period, the BER is 10^{-7}, an average of 1 error in 10^6 bits. The acceptable level of transmission is determined by the type of traffic.

For PCM voice traffic, bit errors manifest themselves as clicks and a threshold of 10^{-6} (1 click approximately every 15 seconds) is usually considered acceptable. At this threshold the speech is intelligible, but beyond it the clicks become annoying and intelligibility falls rapidly.

For data with error correction a higher BER of 10^{-8} is normally acceptable (Communications International, 1989).

11.6 Terminology

A number of different units are used worldwide to define the performance and transmission levels of a radio relay system (for decibel definitions see Chapter 2). Important international definitions and units are:

- *Zero transmission reference point*. This is a point arbitrarily established in a transmission circuit, with all other levels in the circuit being stated with reference to this point. Its relative level is 0 dBr.
- *Standard test tone*. The standard test tone for use at audio circuit points is defined as a power of 1 milliwatt (0 dBm) at a frequency of 1000 Hz applied at the zero transmission reference level point.

11.7 Link planning

Planning a link involves producing a profile of the path and calculating the net loss in the system to arrive at a transmitter output power which will produce the designed signal-to-noise ratio at the receiver. A simple example using the profile of *Figure 11.2* is shown in Section 11.8.

Transmission lines and waveguides are discussed in Chapter 3 and microwave antennas in Chapter 4.

11.8 Example of microwave link plan

Frequency: 2000 MHz		
Antenna type, station A: P6F-17C	height agl.	20 m
Antenna type, station B: P6F-17C	height agl.	20 m
Feeder type, station A: LDF5P50A	loss, dB/100 m	6.46
Total length, antenna to equipment		30 m
Feeder type, station B: LDF5P50A	loss, dB/100 m	6.46
Total length, antenna to equipment		30 m

Performance	
Path length: 20 km, therefore clear path loss	124.0 dBi
Obstruction loss	0.0 dB
Feeder loss, station A:	1.9 dB
Feeder loss, station B:	1.9 dB
Feeder tail loss, total for link	1.5 dB
Connector loss, total for link	1.5 dB
Total loss	**130.8 dB**
Gain, antenna A	28.6 dB
Gain, antenna B	28.6 dB
Total gain	**57.2 dB**
Nett loss (total loss – total gain)	**73.6 dB**
Receiver threshold for max. signal/noise	−125.0 dBW
Design fade margin	+30.0 dB
Design receiver input level (threshold – fade margin)	**−95.0 dB**
Transmitter output power (receiver input – nett loss)	**−21.4 dBW**

Reference

Krzyczkowski, M. (1989). *Communications International*, August.

12 Information privacy and encryption

12.1 Encryption principles

Radio communication was never secret, but since the advent of fast frequency scanning receivers the ability to overhear, even on cellular radio telephones, is within easy reach of anyone. Privacy systems are, however, available which will deter the casual listener and gain time against the determined eavesdropper.

Messages, which may be either speech or data, are encrypted to prevent both eavesdropping and the injection of spurious information. The aim is to make the encryption and decryption as easy and inexpensive as possible for authorized users and time-consuming, difficult and costly for the eavesdropper (cryptanalyst). *Figure 12.1* shows a standard cryptographic channel.

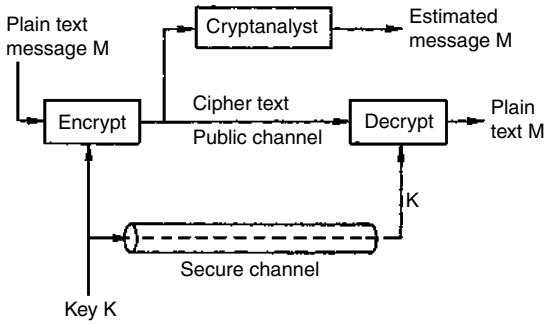

Figure 12.1 Cryptographic channel

A plain text message M (speech, written or digital) is encrypted by mixing with a key K to produce a cipher text. The cipher text may be transmitted over a channel which is accessible to the public and hence to the cryptanalyst. The key is issued via a secure channel to the authorized recipient who uses it to decipher the message. The cryptanalyst without access to the key attempts to derive the maximum information from the cipher text to enable him or her to estimate the content of the message.

One key may be used continuously or for long periods or, to increase the cryptanalyst's confusion, the key may be changed frequently, perhaps even for each character of the message. A sequence of

key changes which repeats after a fixed number of characters produces what is known as periodic encryption.

Encryption may be either symmetrical or asymmetrical. Symmetrical encryption uses the same key for both encryption and decryption. Asymmetrical encryption uses a different key for each process, thus providing for different levels of authorization. Encryption keys may be supplied to many persons who are authorized to transmit encrypted messages but decryption keys may be issued to only a few authorized recipients.

12.2 Speech encryption

The encryption of speech offers fewer possibilities than does the encryption of written or digital data messages. The simplest method of encrypting speech is scrambling by inverting the speech frequencies; *Figure 12.2* shows this process.

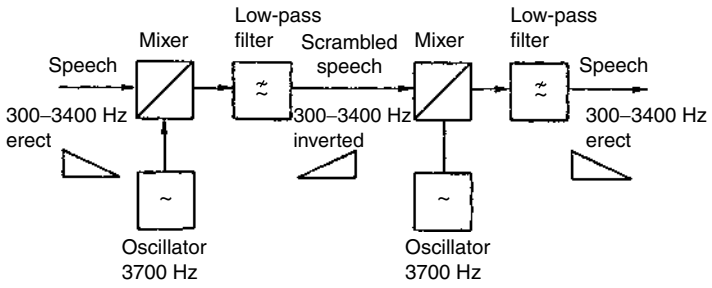

Figure 12.2 Speech inversion

The speech, contained in the band 300–3400 Hz, is mixed with a key frequency of 3700 Hz producing an erect, upper side band from 4000–7100 Hz, and an inverted, lower side band where the 300 Hz components of speech have become 3400 Hz and the 3400 Hz have been inverted to 300 Hz. The upper side band is rejected by a lowpass filter and the inverted lower side band is transmitted. In the receiver the scrambled speech is mixed again with 3700 Hz to produce an erect side band – the original non-inverted speech message.

Simple inverted speech is easily unscrambled. There is little choice of key frequency and if the eavesdropper uses a slightly different frequency the pitch is changed but the speech is readable. Also, if the centre frequencies only of the inverted band are selected by means of a band-pass filter, inverted speech becomes intelligible.

A sophistication which renders the speech more secure divides the speech band into sections and transmits them separately using a different key frequency for each band (audio frequency hopping). The divisions of the speech band may also be treated as blocks and transposed in time according to a user-programmable pattern to create further confusion in the mind of the eavesdropper.

The most up-to-date methods of speech scrambling convert the speech into digital form by either pulse code modulation (PCM) or some other method. The digits corresponding to the speech may then be either transmitted as frequency modulation, e.g. FFSK, on an analogue radio system or, possibly after further encryption, transmitted directly on a digital system. Digitized speech creates improved security not only by the digitization itself but by offering the higher encryption capabilities of data.

The price to be paid for security with analogue encryption is a degradation of the received signal-to-noise ratio by 9 dB, effectively reducing the range of a transmitter by approximately 40%.

12.3 Data encryption

Digital data may be encrypted by changing the digits, perhaps adding superfluous digits, and transmitting the resultant cipher message either in blocks of a fixed size or as a stream.

Block encryption treats the blocks in the same way as in the encryption of speech, with different keys being used for each block – or each character – and the blocks re-distributed in time.

Stream encryption has no fixed block size and each plain text bit, M_i, is encrypted with the ith element, K_i, of a pseudo-random, sometimes called pseudo-noise (PN), key.

Figure 12.3 shows two methods of generating pseudo-random keys or pseudo-noise. The first, *Figure 12.3(a)*, operates as follows. At each clock pulse the contents of the pre-loaded four-stage shift register are stepped forward from left to right. Immediately after the shift, the output bit is fed back into the 1st and 2nd stages. It introduces a new bit into stage 1, and is added by modulo 2 addition to the new content of stage 2, producing a new set of contents. The initial loading of 1100 emerges as a pseudo-random 15 bit sequence which then repeats. The periodicity of the sequence is given by:

$$\text{Sequence length, characters} = 2^N - 1$$

where N = the number of stages in the shift register.

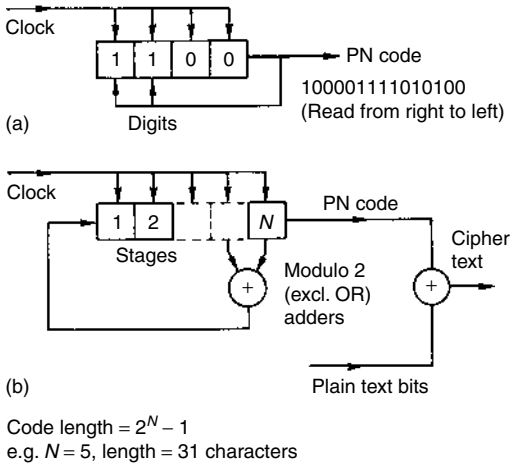

Figure 12.3 Pseudo-noise (PN) generation

For a four-stage register, therefore, the sequence repeats after 15 bits and is shown in *Figure 12.3(a)*.

A more commonly used method combines the outputs of two or more of the earlier stages in a modulo 2 adder and feeds the result back to the input of the register as in *Figure 12.3(b)*.

To form the cipher text the resultant pseudo-random key is mixed with the original data message in a second modulo 2 adder. If the clock rate for the shift register is the same as the bit rate of the plain text message, the plain text bits are exchanged for those of the modulo 2 sum, but if the shift register runs faster than the plain text bit rate, additional bits are added into the cipher text. This is more common and extends the time taken by a cryptanalyst to estimate the message. The price to be paid for the improved security is either a slower effective bit rate for the message or a higher overall bit rate and hence an increased bandwidth requirement.

Mixing the cipher text with the output from an identical PN generator in the receiver recovers the original text.

Modulo 2 addition

A modulo 2 adder is an exclusive-OR gate which produces a logic 1 output whenever either of the inputs is at logic 1 and the other is at logic 0. When both inputs are identical, the exclusive-OR gate produces a logic 0 output.

The truth table for an exclusive-OR gate is:

Input		*Output*
A	*B*	*Y*
0	0	0
0	1	1
1	0	1
1	1	0

Modulo addition is not limited to two inputs. Any quantity of binary numbers may be added: if there is an odd number of logic 1s in a column, the adder produces a logic 1 output, if an even number, i.e. no remainder in the binary addition, the output is logic 0.

Synchronous encryption

The key is generated independently of the message from a previously loaded register. If a character is lost during transmission of a synchronous text, resynchronization of transmitter and receiver key generators is necessary before transmission can continue.

Self-synchronous encryption

The key for each character is derived from a fixed number of previous characters of the plain text message. For example, the shift register is pre-loaded with the plain text characters so that in a four-stage register the key used for encrypting the 4th character will be the 4th previous message character. If a self-synchronized transmission loses a character, the system automatically re-synchronizes the same number of characters (in this case four) later.

Written messages may be encrypted using one of the classical mechanical methods of rearrangement of the letters before digital encryption.

When sufficient RF channels exist frequency hopping is a further possibility, and the spread spectrum technique, where the signal energy is spread over a very wide band of frequencies, not only offers very high security but also makes detection of the signal difficult. The shift register techniques described above are also used for generation of the frequency hopping sequence and the spreading of the base band frequencies.

12.4 Code division multiple access (CDMA) or spread spectrum

The extension of pseudo-random key or noise generation is code division multiple access or spread spectrum transmission, described in Chapter 8. The spread spectrum technique provides an extremely high level of security by reducing the radiated energy at any one frequency to very little above the ambient noise level by spreading the transmission over a very wide band. The transmitter uses what is in effect an extended digital key to spread the bandwidth and the receiver is equipped with an identical key for de-spreading. The transmission almost disappears into the noise and, without the appropriate key, the existence of a spread spectrum signal is very difficult to detect.

12.5 Classification of security

Unconditionally secure

Those systems where the cryptanalyst has insufficient information to estimate the content of the cipher regardless of the amount of time and computation facilities available. This is only realistic when using what is known as a one-time pad where the key is used once and once only.

Computationally secure

Encryption systems are specified in terms of the amount of time taken by a cryptanalyst to estimate the cipher's contents using the state of the art techniques. Unless an extremely long periodicity is used for a progressive key – months and even years in some instances – requiring many stages in the shift register, it is possible for a cryptanalyst who knows, or can estimate, a small part of the message to calculate all the parameters necessary to decipher the message. However, stream encryption with a pseudo-random key approaches perfect secrecy for a finite number of messages.

References

Chambers, W.G. (1985). *Basics of Communications and Coding*. Oxford University Press, Oxford.

Sklar, B. (1988). *Digital Communications*. Prentice Hall, Englewood Cliffs, NJ.

13 Multiplexing

Multiplexing enables several information (speech or data) channels to be carried simultaneously over one bearer, a wide band, single frequency microwave radio link for example. Both frequency and time division multiplex are common methods. On trunked radio systems where channels are allocated to users on demand the multiplexing is referred to as frequency- or time-division multiple access (FDMA, TDMA).

Frequency division multiplexing (FDM) used to be a common technique for sharing analogue trunk circuits between 12 (or multiples of 12) separate channels. This is an analogue technique that been superseded by the use of digital trunk circuits, where digital multiplexing is employed. FDM is still used on some satellite and microwave links, although most links are now using digital techniques. Some systems such as cellular telephones use separate transmit and receive frequencies, which is known as frequency division duplexing (FDD).

13.1 Frequency division multiplex

Frequency division multiplex divides a broad band of frequencies into slots, each wide enough to accommodate an information channel. This is achieved by amplitude modulating a higher frequency subcarrier with each speech signal to form groups of channels.

Each speech channel contains frequencies between 300 and 3400 Hz plus, in some systems, an out-of-band signalling tone of 3825 Hz and a guard band. Each channel modulates a base band subcarrier spaced at 4 kHz intervals upwards from 64 kHz. This produces an upper and lower side band from each channel (*Figure 13.1*). The carrier and upper side band are removed by filters and the lower (inverted) side band is transmitted. At the receiver, the base band frequencies are again mixed with the same subcarrier frequency to restore the original speech. The subcarrier frequencies are maintained to an accuracy of ± 1 Hz which creates the ± 2 Hz frequency translation error quoted in some telephone line specifications.

Twelve such channels form a ITU-T basic group B occupying the band between 60 and 108 kHz. This basic group B may now be

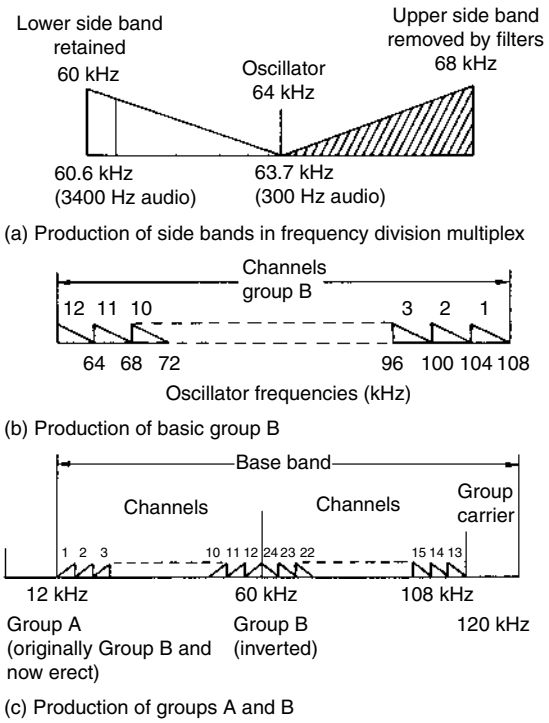

Figure 13.1 Frequency division multiplex

mixed with 120 kHz to produce a lower side band of 12 to 60 kHz, now basic group A. Filters leave 60 to 108 kHz free for a new basic group B.

The process may be repeated by using five basic groups to modulate still higher-frequency carriers, to produce super- and hypergroups.

For FDM data communications, the bearer circuit bandwidth of 3000 Hz is divided into 12 channels each of 240 Hz bandwidth. Data is transmitted at 110 bits per second allowing a send-and-receive channel in each block of 240 Hz.

13.2 Time division multiplex (TDM)

A time division multiplex system conveys digital data, and speech must first be converted to data. TDM allocates short-duration time slots within a wider time frame to each information channel. For example, a continuous stream of data sent over a link at a rate of 2400 bit/s

could convey the information contained in four 600 bit/s channels in short sequential bursts.

If the duration of one input bit is 1/600 s or 1.666 ms, a seven-bit character occupies 11.66 ms and 85 such characters can be sent per second. If the transmitted rate can be speeded up each bit sent at 2400 bit/s has a duration of 416 μs and 343 seven-bit characters can be sent per second. Such a system is shown in *Figure 13.2*. The data is stored in the buffers at the transmitter and the clock pulses are applied to each store/gate sequentially allowing one character from each data channel to be transmitted at a rate of 2400 bit/s. Perfect synchronization must be maintained between all channels and the transmitter and receiver to avoid data errors.

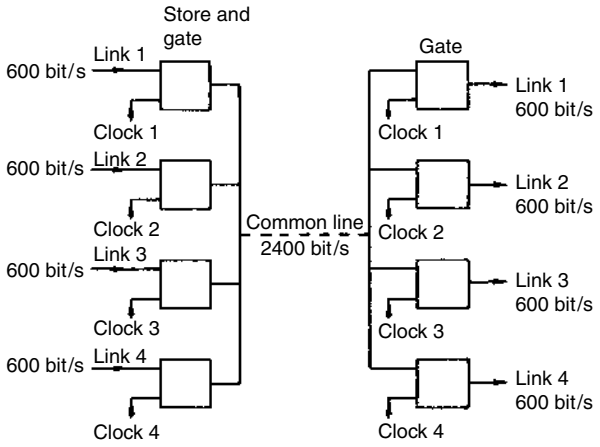

Figure 13.2 Time division multiplex

The principle is illustrated in *Figure 13.3* where a 1 s time frame at 2400 bit/s contains 343 time slots, each of 2.92 ms and containing a character from a specific information channel. Every second, therefore:

channel A would occupy slots 1, 5, 9, . . ., 337

channel B would occupy slots 2, 6, 10, . . ., 338

channel C would occupy slots 3, 7, 11, . . ., 339

channel D would occupy slots 4, 8, 12, . . ., 340

This leaves three blank slots; in practice slots are also allocated for preamble, address and synchronization purposes.

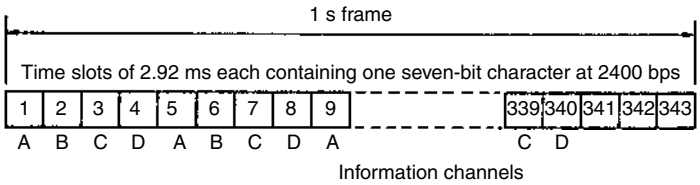

Figure 13.3 TDM time frame

13.2.1 European E1 multiplexing

The digital base band signal adopted in Europe operates at 64 kbit/s and the multiplexed signal at 2048 kbit/s. An eight-bit word or sample of a PCM voice channel (see Chapter 14) occupies 3.9 μs, and the interval between successive samples of a channel is 125 μs, the time frame duration. Therefore, the number of channels (time slots) that can be accommodated in one frame is $125/3.9 = 32$. Thirty of the slots are used for information channels and two for control purposes (*Figure 13.4*).

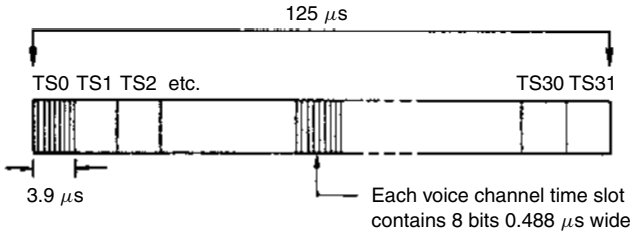

Figure 13.4 TS0, TS16 are used for signalling; TS1–TS15 and TS17–TS31 are used for voice channels

In the European E1 system, timeslots are numbered 0 to 32. Timeslot zero (TS0) is used for synchronization and TS16 is used for signalling. The signalling channel is therefore operating at 64 kbit/s. Digitized voice is carried in the remaining 30 timeslots. Voice channels 1 to 15 are carried over TS1–15. Voice channels 16–30 are carried over TS17–31.

13.2.2 American T1 (D1) multiplexing

The American T1 system is a 1.544 Mbit/s transmission system. The data format should be referred to as DS-1, but T1 is sometimes used instead. Timeslots (TS), or channels, in this system are numbered 1 to 24; there are 23 available to carry traffic and TS24 is used for synchronization. Each timeslot carries 8 bits, sampled at 8 kHz. An

additional bit is sent at the end of each frame (known as the frame-bit or F-bit) so there are 24, 8-bit timeslots, plus 1 bit = 193 bits per frame.

The synchronization word sent in TS24 is coded as 1 0 1 1 1 Y R 0. The Y and R are dependent upon the data multiplexer and are for the manufacturer's use.

Signalling information is transmitted using 'stolen' bits from each channel, rather than using a separate timeslot as in the European E1 system. Bits are not stolen from timeslots in every frame, because this would degrade the quality of a voice channel. Instead, the least significant bit of every sixth frame is used for signalling. Thus the effective word length of the encoded voice is 7.833 bits, rather than 8 bits of the E1 system.

There are two virtual signalling channels (A and B) created by the use of stolen bits. Signalling Channel A is derived from bits stolen from timeslots during the sixth frame. Signalling Channel B is derived from bits stolen from timeslots during the twelfth frame. This is repeated for every superframe. Each channel has a data rate of 24 bits per 12 frames (1.5 ms), or 16 kbit/s, giving 32 kbit/s signalling in total. Although this data rate is half that of the E1 system, there are only 23 voice channels instead of the 30 used in the E1 system.

The F-bit is used to identify the frame, which is important when extracting the signalling information. Because only one in six frames are used for signalling, it is vital to know which ones carry the information and which ones carry voice traffic. Also there are two signalling channels and these must be separated at the receiver end of the system. A six bit data pattern of 1 0 0 0 1 1 is transmitted, followed by the inverse: 0 1 1 1 0 0. The complete 12-frame sequence is known as a superframe.

13.3 Code division multiple access (CDMA)

Spread spectrum transmission (described in Chapter 8) is a form of multiplexing. In addition to high security it permits multiple occupation of the wide – typically 1.25 MHz – frequency band. A number of users possessing keys of low correlation can occupy the same band at the same time. The system operates well in poor signal-to-noise or high interference environments.

Digital signals can be multiplexed by coding each source individually. Instead of transmitting logical 1's and 0's, a data pattern is assigned to each bit. The pattern for a logical 1 could be a ten-bit word (e.g. 1011010011); a separate pattern would represent a

logical 0. Correlation (i.e. pattern matching) between a known signal and a signal received with a certain code gives an indication of whether the bit received is a 1 or a 0. This technique allows the occasional error in the data path without affecting the received bit. More often, it allows several users to transmit at the same frequency. Each user is allocated a different data pattern so that only the correct person will be able to decode the signal; all other signals will be ignored.

Reference

Winder, S.W. (2001). *Newnes Telecommunications Pocket Book*. Butterworth-Heinemann, Oxford.

14 Speech digitization and synthesis

14.1 Pulse amplitude modulation

The digitization of analogue waveforms by pulse code modulation is accomplished in two stages. First the waveform is sampled to produce pulse amplitude modulation (PAM). Short-duration samples are taken at regular intervals which are long compared with the sampling time but short in relation to the highest signal frequency. The result is a train of pulses whose amplitude envelope is the same as the analogue waveform. The envelope (*Figure 14.1*) will contain:

- clock frequency f_c, the sampling rate
- all the signal frequencies contained in the waveform from the lowest, f_1, to the highest, f_2
- upper and lower side bands, $(f_c - f_2)$ to $(f_c - f_1)$ and $(f_c + f_1)$ to $(f_c + f_2)$
- harmonics of f_c and the upper and lower side band frequencies
- a DC component equal to the mean value of the PAM waveform.

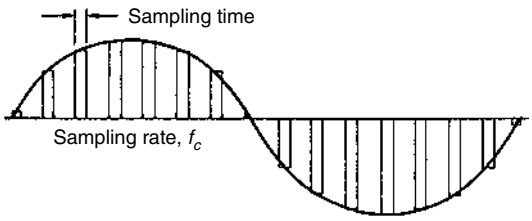

Figure 14.1 Pulse amplitude modulation

The envelope contains the original signal frequencies and can be demodulated by a low-pass filter which will pass f_2 but not the clock frequency. The clock frequency must therefore be higher than $2f_2$. For line communications in the UK a clock frequency of 8 kHz is used with a maximum modulating frequency of 3400 Hz.

14.2 Pulse code modulation

To overcome the susceptibility of PAM signals to corruption of the amplitude waveform by noise and interference, the waveform is processed further to produce pulse code modulation (PCM) before transmission.

In this process the magnitude of the PAM samples with respect to a fixed reference is quantized and converted to a digital (data) signal. Quantizing rounds off the instantaneous sample pulse amplitude to the nearest one of a number of adjacent voltage levels. *Figure 14.2* illustrates the process for an eight-level system. In the figure the amplitude at t_0 is 2, between 4 and 5 at t_1, between 5 and 6 at t_2, etc. After quantization the values would be 2 at t_0, 5 at t_1, 5 at t_2 and so on. The difference between the amplitude levels and the rounded-off values is the quantization noise or distortion.

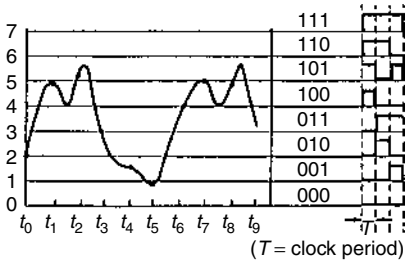

Figure 14.2 Eight-level pulse code modulation

The binary pulse train – leaving a one-bit synchronizing space between each number – for this example would be as in *Figure 14.3*.

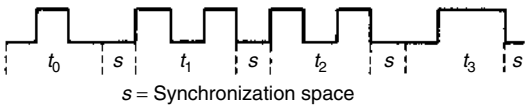

Figure 14.3 Binary pulse train (from *Figure 14.2*)

The number of quantizing levels is 2^n and the highest denary number represented is $(2^n - 1)$ where n is the number of bits used to represent each sample. If each train of pulses is accompanied by one synchronizing bit, the number of bits per sample is $(n + 1)$. If the sampling rate is f_c, the transmitted bit rate is $(n + 1) f_c$. For example, an eight-bit word – including the synch. bit – is commonly used to represent a sample, so, with a clock frequency of 8 kHz:

$$\text{number of quantizing levels} = 2^7 = 128$$

$$\text{sampling rate, } f_c = 8\,\text{kHz}$$

$$\text{therefore transmitted bit rate} = (n + 1) f_c$$

$$= 64\,\text{kb/s}$$

The maximum frequency of the pulses will be when transmitting alternate 1s and 0s, and the occupied bandwidth, $\frac{1}{2} \times$ bit rate, 32 kb/s.

Quantization as described above is linear, i.e. the spacing of the quantization levels is the same over the range of pulse amplitudes. This produces a poor signal-to-noise ratio for low-level signals which is improved by the use of more closely-spaced levels at small signal amplitudes than at large amplitudes. Where non-linear quantization is used the most significant bit of the sample character identifies the polarity of the signal.

If linear quantization is used then about 12 bits per sample are needed to give a good voice quality, which requires a bit rate of about 96 kbits/s. For coding speech using non-linear quantization 8 bits per sample is sufficient, which requires a bit rate of 64 kbits/s. Two slightly different non-linear PCM codecs were standardized in the 1960s. In America u-law coding is the standard, but in Europe A-law coding is used.

14.3 ADPCM codecs

Adaptive differential pulse code modulation (ADPCM) codecs are waveform codecs which quantize the difference between the speech signal and a prediction of the speech signal. If the prediction is accurate, then the difference between the real and predicted speech samples will be small. The signal will be accurately quantized with fewer bits than would be needed using standard PCM. At the decoder the quantized difference signal is added to the predicted signal to give the reconstructed speech signal.

The performance of the codec is aided by using adaptive prediction and quantization. The predictor and difference quantizer adapt themselves to the changing characteristics of the speech being coded.

The CCITT (now ITU-T) standardized a 32 kbits/s ADPCM, known as G721, in the 1980s. The quality of the reconstructed speech was almost as good as that from standard 64 kbits/s PCM codecs. Since then G726 and G727 codecs operating at 40, 32, 24 and 16 kbits/s were standardized.

14.4 The G728 low delay CELP codec

At bit rates of around 16 kbits/s and lower the quality of waveform codecs falls rapidly. Thus, at these rates, CELP codecs and their derivatives, tend to be used. CELP stands for Code Excited Linear Prediction. A code representing a voice pattern is transmitted, rather

than coding short samples of voice signal. The code is calculated by looking at the long-term changes in the voice and then predicting how the voice pattern will change. Since the pattern takes some time to establish, CELP codecs produce a delay.

A backward adaptive CELP codec was standardized in 1992 as G728. This codec uses backward adaptation in its calculations. This means that, rather than buffer 20 ms or so of the input speech for its calculations, the pattern of previous speech is used. This means that the G728 codec has to analyse fewer samples than traditional CELP codecs. The G728 codec uses only 5 samples giving it a total delay of less than 2 ms.

14.5 The GSM codec

The 'Global System for Mobile communications' (GSM) is a digital mobile radio system which is extensively used throughout Europe, and also in many other parts of the world. The GSM codec provides good quality speech, although not as good as the slightly higher rate G728 codec.

The GSM full rate speech codec operates at 13 kbits/s and uses a regular pulse excited (RPE) codec. This codec has short-term and long-term predictors to estimate how the voice pattern will change over time.

The input speech is split up into 20 ms long sections, called frames, and for each frame a set of eight filter coefficients are calculated for the short-term predictor. Each frame is then divided into four 5 ms sub-frames, and for each sub-frame the encoder calculates the delay and gain needed for the codec's long term predictor. Finally, after both short and long term prediction has been applied, the residual signal is quantized for each sub-frame. The filter coefficients for the short term predictor, the delay and gain of the long-term predictor and the coded residual signal are all transmitted. The receiver uses all these values to reconstruct the signal.

References

Kennedy, G. (1977). *Electronic Communications Systems*, McGraw-Hill Kogashuka, Tokyo.

Winder, S.W. (2001). *Newnes Telecommunications Pocket Book*, Butterworth-Heinemann, Oxford.

15 VHF and UHF mobile communication

Mobile communication operating throughout the VHF and UHF bands is expanding rapidly and, although the fastest growth has been in the radio-telephone field, interest in private mobile radio (PMR) is undiminished. Most of the procedures described for PMR are applicable to many other branches of radio communication, so traditional PMR is considered here. Other systems are discussed in later chapters.

A private mobile radio system, comprising a base station and mobiles, is one that is effectively owned by the user and, under the conditions of the licence, may only be operated by the user's own staff for his or her own business. Airtime cannot be leased to other persons.

15.1 Operating procedures

Frequencies are normally allocated in pairs, one for the up-link to the base station and one for the down-link to the mobile (not to be confused with a radio link used for control purposes). Such a pair of frequencies, spaced sufficiently apart to permit simultaneous transmission and reception by a station, comprises the radio channel. Occasionally, for special purposes and for small, low-power, and possibly temporary, operations a single frequency only may be allocated. The mountain rescue teams are an example.

The methods of operating are as follows.

Single-frequency simplex

This method uses a common frequency for transmission and reception by all stations operating on the system (*Figure 15.1*). Transmission

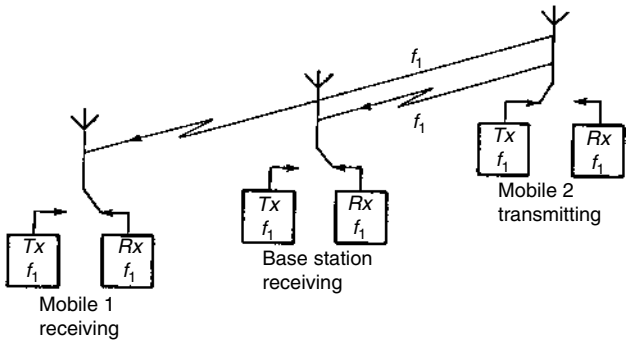

Figure 15.1 Single-frequency simplex

and reception cannot take place simultaneously at a station, and a receiver is switched off whenever the transmit switch is operated. This prevents blocking of the receiver by the transmitter and acoustic feedback occurring. The method allows all stations within range to hear both sides of a conversation and to relay messages to more distant stations; an obvious advantage for mountain rescue.

At the end of a transmission an operator must say 'over' and switch off the transmitter to hear the reply. A conversation must end with the word 'out' so that other stations are aware that the system is unoccupied.

Two-frequency simplex

Separate frequencies are used for transmission and reception but whilst a station is transmitting its receiver is still switched off (*Figure 15.2*). Mobiles hear only the base station and, therefore, the relaying of messages is not possible. A further disadvantage is that because mobiles hear only the base station, they may be unaware of the system occupancy and transmit, interfering with an existing conversation. The advantage of two-frequency simplex is the avoidance of receiver blocking or de-sensitization, not only from the associated transmitter but also, at base stations where several channels within the same band are located, from nearby transmitters.

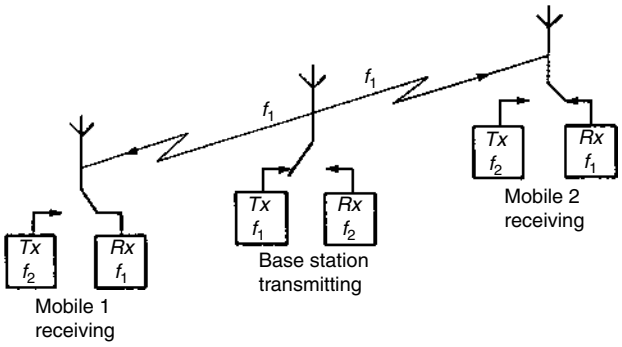

Figure 15.2 Two-frequency simplex

Duplex and semi-duplex

Separate frequencies are used for transmission and reception and, in full duplex, all stations can transmit and receive simultaneously as in a two-way telephone conversation (*Figure 15.3*). While a station is transmitting, its receiver audio output is switched from the loudspeaker

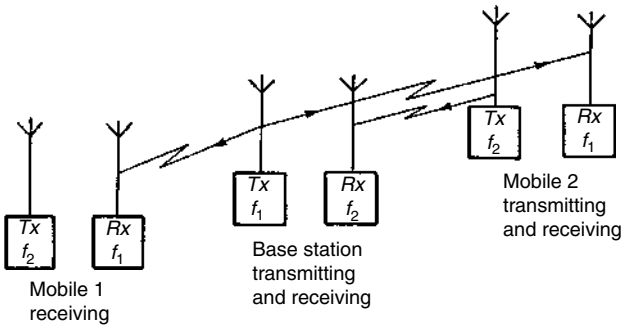

Figure 15.3 Duplex

to an earpiece to prevent acoustic feedback. A mobile cannot receive other mobiles directly but full duplex enables all stations to break in on a conversation in an emergency or to query part of a message; it also facilitates the use of talk-through where mobiles can speak to each other via the base station. To maintain awareness of system occupancy the base station may transmit a series of pips as an engaged signal during pauses in the despatcher's speech.

Many systems operate semi-duplex where only the base station operates a duplex procedure and the mobiles use a simplex procedure. This avoids the higher cost of duplex mobiles and offers most of the facilities of duplex, except that a despatcher cannot break in on a transmitting mobile.

Open channel/'All informed'

All mobiles hear all the calls from control, i.e. no selective calling is in operation.

Selective calling

Mobile receivers remain quiescent until specifically addressed; the opposite of open channel working. Individual mobiles, groups and a whole fleet may be addressed.

Auto-acknowledgement

When selectively called a mobile automatically transponds, sending the code for its address and, possibly, its status information. Mobiles can only acknowledge when individually addressed; auto-acknowledgement on group and fleet calls is prevented to avoid mobiles transponding simultaneously.

Status updating

The transmission, automatically or manually, of the data denoting the mobile's current status.

Call stacking

The storage of calls from mobiles and their presentation in call order to the despatcher. Arrangements are usually made to raise urgent calls to the top of the stack with an enhanced display.

15.2 Control of base stations

Where adequate radio signals over the desired service area of the system can be provided by one base station sited at the control point, it can be easily controlled, either directly from the front panel or over a multi-way cable.

In many instances, to obtain adequate coverage, the base station must be sited on high ground remote from the control point. Then, either a land line or a radio link, both of which will today probably be digital and the link microwave, must be used for control. A land line will most likely be rented but radio links are favoured by those users who insist on the complete system being under their direct control.

15.3 Common base station (CBS) operation

An economic method of providing mobile communication for users with a small quantity of mobiles and light traffic is a common base station or community repeater system. Although still referred to as private mobile radio, the base station is shared by several users who pay a fixed subscription for the service irrespective of airtime used. The station is controlled by radio using tone-controlled talk-through or what is sometimes called reverse frequency trigger (not normally permitted on a true PMR system). *Figure 15.4* shows the layout of a single-station CBS system. Each participant's office contains a fixed transmitter/receiver operating on the same frequencies as a mobile and equipped with CTCSS. Different CTCSS tones are assigned to each user to ensure privacy. All office stations must use a directional antenna so that they access only the base station to which they subscribe.

When a user transmits, from either the office station or a mobile, the base station, on receipt of a signal containing a valid CTCSS tone,

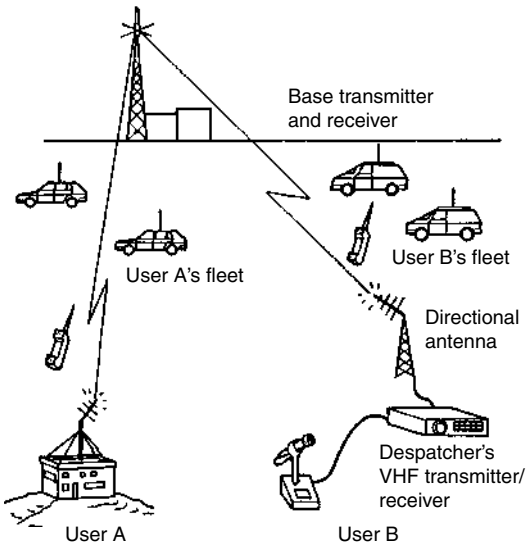

Figure 15.4 Common base station system

enters a talk-through mode. The caller's CTCSS tone is retransmitted and, in turn, opens the mute on all that user's mobiles allowing communication via talk-through. Mobiles are equipped with 'busy' lamps to indicate whenever the system is engaged, and transmission time-out timers to prevent excessively long calls excluding other users.

15.4 Wide area coverage

Where the desired service area for one radio channel is larger than can be covered by a single base station the way in which the base stations are to be controlled requires special consideration. Crucial aspects are the presentation of the best received signal from a mobile to the control operator or despatcher and the selection of the transmitter most likely to provide the best signal at the location of the mobile.

Receiver voting

Well-proven receiver voting circuits which present the best received signal to the despatcher have been used for many years. These circuits sample the signals received from a mobile at each base station and, by means of coded information–which may be either digital or in the form of continuous tones–enable equipment at the control centre to automatically select the best. The selection may be made by comparing

either the signal-to-noise ratio or the signal strength of the received signal. If the information is to be used solely to select the best signal in terms of readability, the signal-to-noise ratio is probably the better characteristic to use, but if the information is also to be used to select a base transmitter, the signal strength could be considered more satisfactory. Some systems utilize both types of information.

A typical 3-station voting system is shown in *Figure 15.5* where signal sampling and vote encoding occur at the receiving sites and the coded information is passed over the base station control system to the control centre. This method is necessary when the selection is made on a signal strength basis, but where the signal-to-noise ratio is used for the selection the sampling and encoding can be done at the control centre taking into account the noise occurring in the control network. Receiver voting systems operate very quickly, and changes

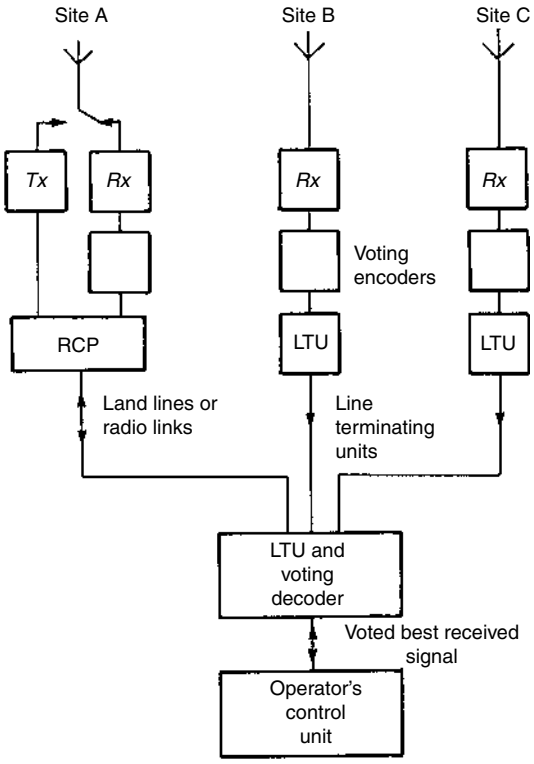

Figure 15.5 Radio scheme with one transmit/receive plus two receiver-only stations with voting

of the selected receiving site may occur several times during a message without the despatcher's awareness.

The broadcast transmit and receive paths are not always reciprocal, for instance when low power hand-portables are integrated with higher power vehicular mobiles. In these circumstances the use of additional receiver-only fill-in stations is an economic and satisfactory proposition.

Base transmitter control poses a problem much more difficult to resolve. The selection of a base transmitter to communicate with a mobile whose precise whereabouts may be unknown, the broadcasting of messages to all, or groups of, mobiles whose locations may be widespread, and the provision of talk-through between mobiles are all facilities required on major systems, and difficult to provide satisfactorily. Apart from trunking, which can be economic only on very large networks, there are three traditional methods of operating the base transmitters on wide area schemes: manual selection, automatic selection and simultaneous transmission from more than one transmitter.

Manual transmitter selection

On many systems the despatchers select the transmitters manually. It is the simplest and least expensive method but has serious disadvantages:

1. Making the selection may entail trying a number of transmitters before sending the message, increasing the operator's work load and wasting air time.
2. Mobiles outside the service area of the selected transmitter may call, interrupting an existing conversation, either because they are unaware that the system is engaged or have received a poor signal that they believe may have been intended for them. Transmitting bursts of 'engaged' pips sequentially over the unselected transmitters during pauses in the despatcher's speech alleviates the first situation; the use of selective calling overcomes the second.
3. Broadcast messages must be transmitted on each transmitter in turn and talk-through between mobiles which are not in the service area of the same transmitter is not practicable.

Automatic transmitter selection

Selecting the transmitters automatically, or semi-automatically, is an improvement over manual selection. On a system where the mobiles are not equipped with selective calling and automatic acknowledgement of a call, automatic selection of transmitters can only occur on

receipt of a call from a mobile. The transmitter through which to reply is then selected by the receiver voting system at the same time as it selects the signal to present to the despatcher. The selection is made at the start of the call and, because of the switching times involved, the transmitter selected is retained for the duration of the call. On these open channel systems, a calling despatcher must initially manually select a transmitter.

On systems where selective calling and auto-acknowledgement of a call are provided, the system can be made fully automatic by transmitting the data corresponding to a mobile's call sign from each transmitter in turn until a satisfactory acknowledgement is received. The successful transmitter is then retained for the duration of the conversation and, at its conclusion, is usually the one used to commence another call.

Such a system overcomes the disadvantage of the need to manually select the transmitter but the problems with mobiles outside the service area of the selected transmitter, and of broadcasting and talk-through, remain.

Simultaneous transmission

Operationally, simultaneous transmission from all sites is ideal and, under various names such as Spaced Carrier, Simulcast and Quasi-synch., has been around since the mid-1940s. Its operational value is proven but systems require special care in their planning, adjustment and subsequent maintenance.

An early form of simultaneous transmission was the amplitude modulated spaced carrier system. Used very successfully at VHF on systems using 25 kHz channel separation, the transmitter carrier frequencies were separated by 7 kHz – above the mobile receivers' audio pass-band. With the reduction of channel spacings to 12.5 kHz, spaced carrier operation on this basis was no longer possible and alternatives are to either synchronize, or very nearly synchronize, the carrier frequencies. There are, however, undesirable effects of synchronous and quasi-synchronous transmission but, with care, these can be reduced to an acceptable level. They are:

1. The beat note between transmitters being audible in the mobile receiver.
2. Variations in signal level due to interference patterns between signals from more than one transmitter.
3. Distortion due to audio phase differences and differing modulation levels when signals of comparable strength are received from more than one transmitter.

The beat note is easily dealt with. It is rendered unobjectionable either by placing it outside the mobile receiver audio pass-band – which is the usual method – or by synchronizing the transmitter carrier frequencies so that no beat note is produced. Synchronization, however, raises other problems, which are particularly severe at VHF but less so at UHF.

The spaced carrier system placed the beat note above the receiver pass-band, but modern systems place it below. This means that the beat note between the lowest and highest carrier frequencies must be below about 150 Hz if it is to be unobtrusive. Tests have shown the optimum carrier separation to be from 0.5 Hz to 4 Hz between any two transmitters using amplitude modulation, and from 5 Hz to 40 Hz between adjacent frequency transmitters using angle modulation.

Two transmitters on the same or closely-spaced frequencies produce deep nulls in the received signal in the areas where they provide almost equal strength signals. This is a natural phenomenon and the effect can only be reduced by the correct siting of stations and antenna configurations. Because of the longer wavelength the effect is more detrimental at VHF than UHF. Where the frequencies are quasi-synchronous the interference pattern is continually moving, but with synchronized carriers the pattern is virtually stationary and at low band VHF wavelengths it is possible to stop a vehicle in a place of semi-permanent zero signal. While moving slowly in an area of equal signal strengths from two transmitters, the cancellations become very objectionable. At 450 MHz the distance between the nulls is so short that it is almost impossible to remain in one, and while moving they are unnoticed. Strong signals in the overlap areas minimize the time that the signals fall below the receiver noise threshold at each cancellation. They are the key to reducing the annoyance from the cancellations. Amplitude modulated systems have an advantage in that the receivers produce less severe bursts of noise during the signal nulls.

The audio distortion, provided the equipment does not introduce significant additional harmonic distortion, is attributable to audio phase differences in the signals received from more than one transmitter. For the distortion to be severe, the received signals must differ by less than 6 dB on an angle modulated system; capture effect in the receiver removes the audible effects at greater differences.

The phase differences arise from differing audio characteristics in all the circuits in the path including land lines, radio links and control equipment. Common to all systems are the phase differences due to the different path lengths from the control centre to a receiving mobile, but where land lines or multiplexed circuits are used for the control

of the base stations, variable bulk and group delays and frequency translation errors can present serious difficulties. Tests have shown AM to be slightly more tolerant than angle modulation in respect of this type of distortion, phase delays of 100 μs being acceptable with AM compared with 70 μs with FM.

Differing path lengths between the control centre to the transmitting sites can be equalized by installing audio delay circuits at the transmitters. The path lengths from each transmitting site to all the places where equal signals occur must then be less than about 21 km (equivalent to 70 μs) for acceptable quality. Modern techniques enable delays to be dynamically equalized to compensate for variations in the path.

Figure 15.6 shows the layout of a multi-station scheme including the audio delays. However, signals do not confine themselves to neat

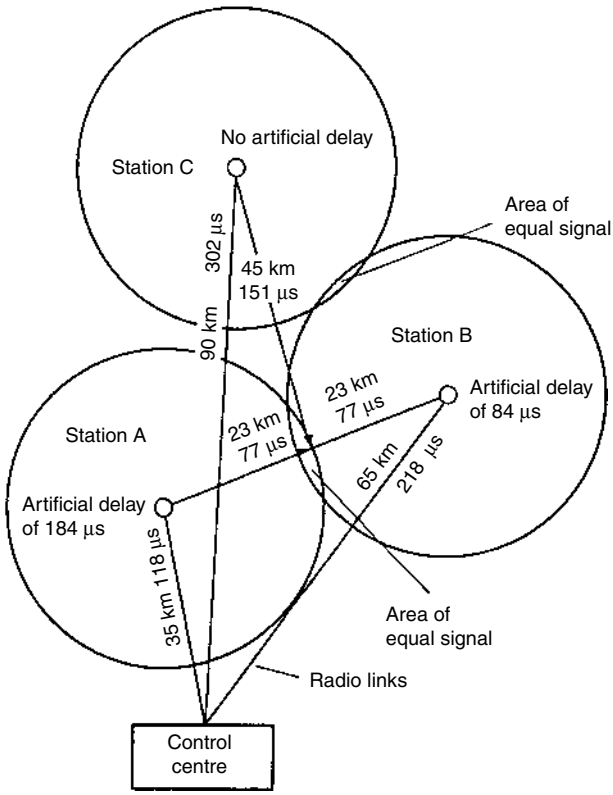

Figure 15.6 Quasi-synchronous transmitter system

circles and the worst situation is where the signals from two transmitters arrive at a mobile more or less equal in strength and phase. In this situation, apart from the ripple caused by the carrier frequency offset of the transmitters, a satisfactory signal would still be received but, occasionally, the presence of a weaker signal from a third, distant station (C in *Figure 15.6*) intrudes during the cancellation periods and, because of its long path length, introduces severe distortion. The area where this situation occurs is often small and the areas of overlap can usually be moved slightly by adjustment of either the transmitter power or antenna directivity.

16 Signalling

Many radio receivers are required to respond to instructions sent to them over the radio channel to which they are tuned. Several methods of signalling these instructions are in use, from the continuous tones used for controlling the receiver mute operation to the rapid data to initiate channel changes and transmitter power control on cellular radio-telephones.

16.1 Sub-audio signalling

The slowest signalling system uses continuous sub-audio frequency tones. Known as continuous tone controlled signalling (previously squelch) system (CTCSS) its performance, in the UK, is specified in Radiocommunications Agency specification MPT 1306. The most common use for the system is to control receiver mute opening. Permitting a mute to open only on receipt of an authorized signal, its use enables privacy between users to be maintained on shared systems, common base station systems for example, and reduces the annoyance factor from interference in the absence of a signal. Thirty-two tones are permitted and assigned by the Radiocommunications Agency (*Table 16.1*).

Table 16.1 CTCSS tones and modulation levels

67.0	110.9	146.2	192.8
71.9	114.8	151.4	203.5
77.0	118.8	156.7	210.7
82.5	123.0	162.2	218.1
88.5	127.3	167.9	225.7
94.8	131.8	173.8	233.6
103.5	136.5	179.9	241.8
107.2	141.3	186.2	250.3

The tones are transmitted at very low modulation levels (*Table 16.2*).

Table 16.2 Modulation levels

System channel spacing	*Amplitude modulation Modulation depth (%)*	*Angle modulation Peak deviation ± Hz*
25 kHz	10 to 20	400 to 800
12.5	10 to 20	200 to 400

16.2 In-band tone and digital signalling

16.2.1 Dual tone multi-frequency (DTMF)

Developed for telephone work, dual tone multi-frequency signalling has crept into some radio systems but is slow to operate compared with other in-band systems. Two tones are transmitted simultaneously to represent each digit. In the UK they conform to the MF4 code (*Table 16.3*).

Table 16.3 MF4 code of DTMF tones

Digit	*Frequencies (Hz)*	
1	697	1209
2	697	1336
3	697	1477
4	770	1209
5	770	1336
6	770	1477
7	852	1209
8	852	1336
9	852	1477
0	941	1336
*	941	1209
#	941	1477

Some push button telephones signal to the local exchange by generating a combination of two frequencies. Each row and each column of the push button keypad is connected to an oscillator of set frequency. When any push button is pressed, tones corresponding to its row and column frequencies are therefore generated. The row and column oscillator frequencies are as shown below:

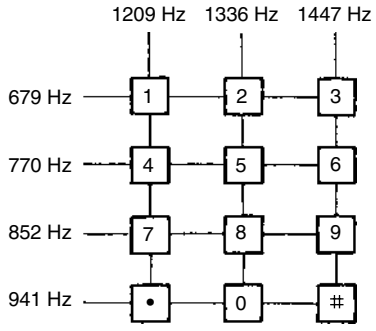

16.2.2 5-tone signalling

So-called 5-tone signalling uses a series of tones – usually five but other quantities are used in some systems. The system is popular for selective calling and addressing purposes (*Table 16.4*). There are a range of tones established by various organizations but, although the tones in each series may be assigned to each digit, equipment manufacturers sometimes amend the code and the usage. The relevant Radiocommunications Agency document is MPT 1316, *Code of Practice, Selective Signalling for use in the Private Mobile Radio Services*.

Table 16.4 5-tone codes

Standard	*ZVEI*	*DZVEI*	*EIA*	*CCIR/ EEA*	*CCITT*	*EURO*
Tone duration (ms)	70	70	33	100/ 40	100	100
Pause duration (ms)	0	0	0	0	0	0
Code/digit	Tone frequency (Hz)					
0	2400	970	600	1981	400	980
1	1060	1060	741	1124	697	903
2	1160	1160	882	1197	770	833
3	1270	1270	1023	1275	852	767
4	1400	1400	1164	1358	941	707
5	1530	1530	1305	1446	1209	652
6	1670	1670	1446	1540	1335	601
7	1830	1830	1587	1640	1477	554
8	2000	2000	1728	1747	1633	511
9	2200	2200	1869	1860	1800	471
Repeat	2600	2400	459	2110	2300	1063
Alarm	2800	2600		2400		
Free-tone						1153
Group tone	970	825	2151	1055		

ZVEI Zuverein der Electronisches Industrie. Designed to operate on 20 kHz channel spaced systems. On 12.5 kHz channel spaced systems transmission of 2800 Hz creates difficulty and depressed ZVEI (DZVEI) was adopted and recommended in MPT 1316.

EIA Electrical Industries Association.

CCIR Committee Consultatif International Radio Communication. The longer tone duration offers robustness against corruption but is slow to operate. Originally designed for marine use, each digit was transmitted twice to ensure reliability.

EEA Electronic Engineering Association. Recommended in MPT 1316.

CCITT International Telegraph and Telephone Consultative Committee.

16.3 Digital signalling

FFSK

Many analogue modulated systems use digital signalling in the form of 1200 bit/s fast frequency shift keying which is faster than 5-tone but less robust.

DCS

Digitally coded squelch (DCS) is a digital, but slower, alternative to CTCSS. It is not in current use in the UK. DCS continuously repeats the constant binary bit pattern of a 23 bit word. Golay error coding reduces the number of data bits to 12 of which 3 initiate the Golay sequence leaving 9 information bits, i.e. a 9 bit word. With a 9 bit word, $2^9 = 512$ codes are possible but, because of problems with the frequencies produced, the codes with 7 or more 1s or 0s in succession are discarded leaving 104 'clean codes'. The transmitted rate is 134 bit/s and the highest fundamental frequency is therefore 67 Hz. The lowest fundamental frequency is produced when 6 zeros follow 6 ones = 1/6th of the fundamental frequency = 11.7 Hz. The important harmonics are:

$$\text{third} = 201\,\text{Hz}$$

$$\text{fifth} = 335\,\text{Hz}$$

$$\text{seventh} = 469\,\text{Hz}$$

The seventh harmonic is well within the audio pass band of most receivers but at 3 octaves from the fundamental is relatively weak.

16.4 Standard PSTN tones

	Signal			
	UK		*USA*	
Tone	*Frequency*	*Sequence*	*Frequency*	*Sequence*
Number unobtainable	400 Hz	Continuous	500 + 600 Hz	Interrupted every second
Number busy	400 Hz	0.75 s on, 0.75 s off	480 + 620 Hz	Interrupted once per second
System busy	400 Hz	0.4 s on, 0.35 s off, 0.225 s on, 0.525 s off	480 + 620 Hz	Interrupted twice per second
Dial tone	50 Hz 33.3 Hz		350 + 440 Hz	
Ringing tone	400 Hz, or 400 + 450 Hz, modulated by 17, 25, or 50 Hz	0.4 s on, 0.2 s off, 0.4 s on, 2 s off	440 + 480 Hz	Interrupted once per second
Pay tone	400 Hz	0.125 s on, 0.125 s off		
Time tones	900 Hz	0.15 s on, 0.85 s off. Three times every three minutes		
Recorder warning			1400 Hz	One burst, every 15 s

References

Belcher, R. *et al*. (1989). *Newnes Mobile Radio Servicing Handbook*. Butterworth-Heinemann, Oxford.

Winder, S.W. (2001). *Newnes Telecommunications Pocket Book*. Butterworth-Heinemann, Oxford.

17 Channel occupancy, availability and trunking

17.1 Channel occupancy and availability

The usefulness of any communications network depends on successful calls. Assuming that no calls fail for technical reasons, the success rate depends on the amount of traffic on the channel and how well it is managed. Channel occupancy is a measure of the amount of traffic carried and is affected by:

1. the number of subscribers (mobiles on a radio network)
2. the number of calls per subscriber in a given time
3. the average duration of each message.

The occupancy of any system varies hourly, daily and possibly seasonally. To be successful the network must be able to cope with the traffic during the periods of highest occupancy and, when considering occupancy it is usual to examine the conditions over one hour, the 'busy hour'. The occupancy of a channel can be expressed as a percentage:

$$\text{Channel occupancy} = \frac{nct}{36}\%$$

where

n = number of subscribers (on a mobile radio system, mobiles on watch)

c = call rate (number of calls per subscriber in 1 hour)

t = average message duration in seconds

Occupancy may also be expressed in erlangs where continuous traffic, i.e. 100% occupancy over a specified period, is 1 erlang. Less than 100% occupancy is expressed as a decimal fraction, e.g. 30% occupancy is 0.3 erlang. Demand may also be expressed in traffic units, A:

$$A = \frac{Ct}{T} \text{ erlangs}$$

where C is the number of calls in time T and t is the mean call duration.

The amount of congestion occurring on a system can be defined by the grade of service it offers. Grade of service is expressed as a

percentage in terms of the probability of meeting either congestion or waiting more than a specified delay before a call can be established. Erlang's formula is:

$$\text{Grade of service} = \frac{A^N/N!}{1 + A + A^2/2! + A^3/3! + \cdots + A/N!}$$

where A is the number of traffic units (erlangs) and N is the number of outlets (trunked channels).

The probability that delayed calls will have to wait more than a specified time ($W > t$) is:

$$P(W > t) = \exp\left(-\frac{(C - A)t}{H}\right)$$

where
A = traffic units (erlangs)
C = number of trunked channels
H = mean call duration in busy hour

The above assumes that:

1. the number of users is infinite
2. the intervals between calls are random
3. call durations are random
4. call set-up times are negligible
5. delayed calls are queued so that they are dealt with on a first come, first served basis.

The number of potential radio users is continuously growing and any technique that makes more effective use of the finite radio spectrum is welcome. Whenever technology has permitted, higher frequencies and reduced channel spacings have been employed in the attempt to meet the demand. A method of making more effective use of the available spectrum is trunking.

17.2 Trunking

The generally accepted term for the automatic allocation of communication channels to subscribers on demand is trunking, and a 'trunked radio system' is one in which many users share the use of a common pool of radio channels. Channels from the pool are allocated to users on demand and as they become unoccupied; no channels are allocated to specific users or groups of users.

When making a telephone call, provided the speech quality is good it is immaterial which route the call takes. The same applies to radio; providing the message reaches the right person quickly, the radio frequency which carries it does not matter.

Most trunked radio systems use a calling channel on which calls are requested. When a call is established and accepted a working channel from the pool is allocated for the duration of the call and at its termination the channel is returned to the pool for re-allocation to another user. The important principle is that any user has access to any free channel. This has the advantage that more mobiles per channel can be accommodated, or a better grade of service, i.e. less waiting time for access, can be provided. Basic trunked systems are unsuitable where everyone using the system needs to be a party to every call but the latest trunked mobile radio system arrange, on receipt of a call, to assign a working channel to a particular group of mobiles where they operate within the service area of one base station. They then operate on an 'all informed' basis.

Trunking provides the most benefit when the number of channels required is greater than the number assigned to the system. The effective gain in the number of mobiles that can be accommodated on a trunked system is illustrated by the following example:

> *A single radio channel with an efficient signalling system offering a 30% grade of service can accommodate 90 mobiles with a mean waiting time of 20 seconds if each mobile makes 1 call. Twenty non-trunked channels cater for 1800 mobiles. A 20 channel trunked system under the same conditions can accommodate 3430 mobiles with a mean waiting time of 16.4 seconds, a trunking gain of over 170 mobiles per channel.*

The mobile transmitter/receivers used on trunked systems are more complex than those used on systems where channels are permanently allocated because the mobiles must either scan the channels searching for an available one or one containing a call directed to them, or listen continuously on a channel designated for calling. In the latter case when a call is initiated, a complex 'handshake' procedure occurs and the mobile is automatically switched to the channel allocated for that conversation. The band III public access mobile radio (PAMR) networks use a calling channel and many common base station (CBS) systems use channel scanning methods with no calling channel.

Working channels may be assigned for the duration of conversation, which is message trunking, or for the duration of a transmission, which is transmission trunking. With either type of trunking the channel is not returned to the pool immediately the signal from the mobile is lost; some waiting time is essential to cater for short-term signal

dropouts but with message trunking the channel is retained for a longer period of time to allow the complete conversation to take place. On a very busy system this is wasteful and, on a system with very rapid signalling, transmission trunking may be used. Then the use of the working channel is lost very soon after the cessation of transmission and a new working channel assigned on its resumption. Some networks automatically migrate from message trunking to transmission as traffic increases.

17.3 In-band interrupted scan (IBIS) trunking

IBIS trunking is a method which is finding favour for common base station applications. All channels are used for communication with no dedicated calling channel, thus making the most effective use of the channels available.

On a CBS system all users access the base station, which operates talk-through, by radio. Each user is allocated his own continuously coded squelch system (CTCSS) tone to access the base station and to prevent overhearing by other users. A trunked common base station contains the transmitters and receivers for a number of radio channels and when the system is quiescent transmits bursts of an in-band (speech band) free-tone – 1953 Hz is one that is used – on one channel only. The mobiles, which are fitted with decoders to recognize both the free-tone and their CTCSS tone, scan all channels looking for one containing free-tone onto which they lock. Should the mobile operator press the transmit button the transmitter will only be enabled when the mobile receiver is on a channel containing either the free-tone or its CTCSS code. As soon as the channel becomes occupied the base station commences to radiate free-tone on another channel and mobiles of other user groups re-lock onto the new free channel. When either a mobile or the control station, which is a fixed mobile, makes a call it is on the channel radiating free-tone and the transmission contains the CTCSS code allocated to that user group. The repeater re-transmits the CTCSS code which activates the calling mobile and all other mobiles within that group. Mobiles of other user groups sensing the alien CTCSS tone leave the channel and continue scanning for a free channel. If all channels are engaged, the caller hears a 'busy' tone and must try again later.

17.4 Trunking to MPT 1327 specification

Specification MPT 1327 produced by the Radiocommunications Agency lays down a signalling standard for trunked private land

mobile radio systems. The system uses fast frequency shift keying (FFSK) at 1200 bit/s with time division random access. The mobiles operate two-frequency semi-duplex and the base stations or trunking system controller (TSC) operate full duplex. A calling channel is used for call establishment but may be either dedicated or nondedicated. After a call is established messages are transmitted over a traffic (working) channel. The basic components of the signalling format, in sequence, are:

1. The link establishment time (LET), a period of transmission of undefined modulation.
2. A preamble comprising a sequence of bit reversals 1010. . .10, minimum 16 bits and ending with a binary zero for the receiver data demodulator to achieve synchronization.
3. A message. A contiguous transmission of a synchronization sequence, address codeword and, where appropriate, data codewords.
4. A hangover bit, H, of either binary zero or binary one, added to the last transmitted message identifying the end of signalling transmission.

The message synchronization sequence for both control and message channels consists of 16 bits, the first bit being a binary one on a control channel and binary zero on a traffic channel.

Messages, whether address or data, are transmitted in 64 bit codewords. The first bit, bit 1, indicates the status of the codeword. Binary one denotes an address word, binary zero, a message word. Bits 2–48 are the information field and bits 49–64 are check bits.

References

Macario, R.C.V. (1991). *Personal and Mobile Radio Systems*. Peter Peregrinus, London.

Parsons, J.D. and Gardiner, J.G. (1989). *Mobile Communication Systems*. Blackie, London and Glasgow.

Radiocommunications Agency (1991). MPT 1327, *A Signalling Standard for Trunked Private Land Mobile Radio Systems*.

Radiocommunications Agency (1993). MPT 1318, *Engineering Memorandum, Trunked Systems in the Land Mobile Radio Service*.

Winder, S.W. (2001). *Newnes Telecommunications Pocket Book*. Butterworth-Heinemann, Oxford.

18 Mobile radio systems

18.1 Paging

Where an immediate reply to a message is not essential, paging systems, which are basically a one-way path from controller to mobile, are an economic option. Paging is also spectrally economic, only one frequency being required and messages being of very short duration. The recipient of a call may be merely alerted by means of a tone emitted by the paging receiver or, if silent alert is required, a vibration. Alternatively, pagers displaying, and storing, alpha-numeric messages are readily available. Message handling services are also offered on some paging systems.

On-site paging systems are usually owned or rented by the user and consist of either a radio base station or, in the case of a non-radio system, an inductive loop around the perimeter of the service area. The details of on-site paging systems and the Radiocommunications Agency specifications governing them are:

RF frequencies:

on-site, 26 MHz and 31 MHz bands, MPT 1365
49.0–49.5 MHz, MPT 1335
160–161 MHz
458–459 MHz, MPT 1305

Channel spacings:

12.5 kHz in the VHF bands and 25 kHz in UHF band

Modulation:

FM, FFSK data

Wide area, national or international systems are generally owned by a network provider to whom the user subscribes for the service. There are frequencies allocated in the high VHF and UHF bands. The appropriate specifications are MPT 1308 for receivers and MPT 1325 for transmitters.

The Post Office Code Standardization Group (POCSAG) standard which has been adopted by the CCITT allows the transmission of messages at a rate of 10 calls per second and a capacity of 1 million pagers with up to four alternative addresses per pager. The recommended bit speed is 512 bit/s with direct FSK deviating the transmitter frequency

by ±4.5 kHz. Positive deviation indicates a binary zero and negative deviation a binary one.

In America the Golay sequential code is widely used for paging addressing. The format for tone-only paging consists of 12 address bits followed by 11 parity bits for each 23 bit word. Two bit rates are used, 300 bit/s for address codewords and 600 bit/s for message codewords.

There are European paging and message systems in operation including Euromessage and the frequency agile European Radio Message Service (ERMES).

18.2 Cordless telephones

CT1

The first generation of cordless telephone, still very popular in the UK, is designed to serve the domestic environment with a range of 100 m. The base station transmits on one of eight frequencies between 1.6 MHz and 1.8 MHz, and the handset on one of eight frequencies in the 47 MHz band. Frequency modulation is used with a deviation of ±4 kHz at the base station and 2.5 kHz at the handset. MPT 1322 applies and permits an erp of 10 mW at both the base station and the handset.

CT2

The second generation of cordless telephone. The services, under various names, telepoint, phonezone, etc. were planned to provide for the general public a lower cost alternative to the cellular radiotelephone networks which were seen at the time as a businessman's preserve. However, the low market uptake caused their demise in the UK although services are thriving in some European and Far Eastern countries.

One hand-portable transmitter/receiver can operate to a local base station installed in the home or office, or through one of a number of multi-channel base stations with a range of approximately 200 m installed in public places. While away from the local base station the subscriber must initiate a call: calls cannot be made from the PSTN to a CT2 subscriber's handset.

The operational frequencies are in the band 864.1 to 868.1 MHz and employ time division multiple access. Speech is digitized at 32 kbit/s, stored, and then transmitted at 64 kbit/s in 1 ms slots. This leaves the alternate 1 ms slots available for the digitized and stored

speech of a reply. Duplex operation is achieved in this way on a single radio frequency.

Inter-operability between networks was to be ensured by specification MPT 1375 *Common Air Interface*.

Digital European cordless telephone (DECT)

A pan-European system complying with an ETSI standard, DECT operates in the 1880 to 1900 MHz band. It offers data handling facilities and the ability for a subscriber to receive calls while away from the local base station. The techniques are similar to those used for GSM although, because the mobile is virtually stationary, the constraints on data transmission are less severe and no hand-off is required. The 20 MHz RF bandwidth is divided into 13 carriers spaced at 1.7 MHz intervals, each carrier containing 12 TDMA channels with GMSK modulation.

CT3 is developed from DECT and operates in the band 800 to 900 MHz. Each 8 MHz section of that band is divided into 1 MHz blocks, each containing sixteen 1 ms time slots.

18.3 Trunked radio

Bank III trunked radio

So-called because it occupies part of the now redundant television band III, 174 to 225 MHz, and often referred to as private mobile radio, this is a subscriber access system. The network has almost nationwide coverage in the UK, arranged on both local and regional bases. The network permits radio communication between a fixed office station and mobiles, mobile to mobile, and limited access from mobiles to the PSTN.

The relevant Radiocommunications Agency specifications are:

MPT 1323	*Angle-modulated Radio Equipment for Use at Base and Mobile Stations Private Mobile Radio Service Operating in the Frequency Band 174–225 MHz.*
MPT 1327	*A Signalling Standard for Trunked Private Land Mobile Radio Systems.*
MPT 1343	*System Interface Specification for Radio Units to be Used with Commercial Trunked Networks Operating in Band III sub-band 2.*
MPT 1347	*Radio Interference Specification for Commercial Trunked Networks Operating in Band III sub-band 2.*

MPT 1352 *Test Schedule. For Approval of Radio Units to be Used with Commercial Trunked Networks Operating in Band III sub-band 2.*

Frequency modulation is used with FFSK signalling, a channel spacing of 12.5 kHz and TDMA techniques (Section 17.4).

Trans-European trunked radio (TETRA)

A new European standard for digital trunking. The system is aimed at PMR users and will employ TDMA with four users sharing a 25 kHz radio channel with the option of two users on a 12.5 kHz channel. Speech will be digitally encoded at 4.8 kbit/s and transmitted at 36 kbit/s (gross bit rate including error correction overhead) using $\pi/4$ differential quaternary phase shift keying (DQPSK).

Digital short range radio (DSRR)

This utilizes trunking techniques but with no infra-structure of control or switching centres; mobiles work to mobiles via a locally installed repeater. It offers great potential for short-term hire for local events. The band 933 to 935 MHz has been allocated to the service and accommodates 76 traffic and 2 control channels separated by 25 kHz. The operating procedure may be either single-frequency simplex or two-frequency semi-duplex. Mobiles remain on standby waiting to receive their selective signalling code (SSC) on one of the two control channels; mobiles with even serial numbers normally listen on control channel 26 and those with odd serial numbers on control channel 27. A mobile wishing to initiate a call first scans for a free traffic channel and, having obtained one, selectively addresses the intended recipients of the call over the relevant control channel. The recipient mobiles are then instructed automatically by the system to go to the appropriate traffic channel.

The modulation is GMSK at 4 kbit/s for addresses and 16 kbit/s for speech and data messages. The maximum transmitter erp is 4 W.

18.4 Analogue cellular radio-telephone networks

Analogue networks are becoming obsolete and are being replaced by digital cellular networks. There are no analogue networks operating in the UK and the frequency bands that they used to occupy are now reassigned to GSM operators.

However some countries still have an analogue service based on AMPS or TACS. These provide national coverage with roaming facility and hand-off from cell to cell as a mobile travels across the network, calling for more complex signalling than local trunking.

The control system must know at all times the location of all operational mobiles. It does this by continuously monitoring signal strength and instructing the mobile to change channel as it crosses cell boundaries.

To permit the maximum re-use of frequencies mobiles are instructed by the system controller to reduce transmitted power to the minimum necessary for acceptable communications in either eight or five steps, depending on the mobile classification, to 0.01 W. Mobiles are classified by their maximum effective radiated power output:

Class 1	10 W erp, vehicle mounted
Class 2	4 W erp, transportable
Class 3	1.6 W erp, transportable
Class 4	0.6 W erp, hand-portable

The channel separation is 25 kHz with a peak speech deviation of ±9.5 kHz. Signalling is by Manchester encoded PSK at 8 kbit/s with 6.4 kHz deviation.

To discriminate between stations transmitting on the same RF channel an FM supervisory audio tone (SAT) is transmitted concurrently with speech at ±1.7 kHz deviation. There are three such tones: 5970, 6000 and 6030 Hz.

An FM signalling tone (ST) of 8 kHz transmitted for 1.8 seconds (deviation = ±6.4 kHz) indicates the clear-down of a conventional telephone call.

The advanced mobile phone service (AMPS) is the American cellular system designed for 30 kHz channel spacing with a 10 kbit/s signalling rate. TACS is based on the AMPS system but modified for reduced channel spacing. Narrower channel spacing systems (NAMPS and NTACS) are also found in some countries.

18.5 Global system mobile

Global system mobile (GSM), formerly known as Groupe Speciale Mobile, is the pan-European digital cellular radio-telephone service. The operational requirements for GSM are severe, e.g. it must operate satisfactorily to a person walking, or in a slowly moving vehicle, in a street where much of the furnishings will introduce multi-path fading,

and operate to a train travelling at 250 km/hr where Doppler frequency shift becomes significant. To reduce the corruption, a high degree of error detection and correction must be applied which increases the occupied bandwidth. To compensate, to some extent, for this, the system takes full advantage of the redundancy in speech to reduce the bandwidth during synthesis.

GSM operates full duplex in the band 890–915 MHz, up-link and 935–960 MHz, down-link.

A combination of FDMA and TDMA is employed. Each allocated band of 25 MHz is divided into 125 carriers spaced 200 kHz apart. The subdivision of each transmitted bit stream into 8 TDM time slots of 540 μs gives 8 channels per carrier and 1000 channels overall. Modulation is Gaussian minimum shift keying (GMSK).

Speech synthesis is by speech codec using linear predictive coding. It produces toll quality speech at 13 kbit/s.

18.5.1 Emergency locator service

The FCC in the US has placed a requirement on mobile phone operators to provide an emergency location service, referred to as E911. The aim is to locate people who need emergency services, but are not able to indicate their location either through injury or through lack of local knowledge. The locator service may also deter hoax calls (or help to catch people making hoax calls) and could have commercial applications in providing directions to businesses such as garages and restaurants.

There are two options: handset based solutions or network-based solutions. The handset-based solutions generally rely on signals picked up from the global positioning system (GPS). Network-based solutions rely on the timing difference in the arrival of signals from neighbouring cell sites. In network based solutions, the E911 requirement is for the mobile phone to be located within 100 metres at least 67% of the time and to within 300 metres in 95% of cases. In handset-based solutions, the location distances are 50 metres and 100 metres, respectively.

18.5.2 Data over GSM

Standard GSM data service allows a maximum of 9600 baud data rate transmission. An enhanced data rate of 14.4 kbps is also possible with some terminals.

The data link can be either synchronous or asynchronous and the data is conveyed through the network using an ISDN-based data protocol, the ITU-T standard V.110 rate adaptation scheme. Asynchronous transmission requires start and stop bits to be added, so the net data rate is reduced to 7680 bits per second (bps). Synchronous transmission potentially allows a faster data rate, but error checking is employed that requests re-transmission of data when errors are identified and this can produce a lower overall data throughput.

18.5.3 High-speed circuit switched data (HSCSD)

HSCSD allows higher data rates by combining up to four 14.4 kbps data channels together. A maximum data rate of 57.6 kbps is possible.

18.5.4 General packet radio service (GPRS)

GPRS combines up to eight 14.4 kbps channels to give data rates of up to 115.2 kbps. At these rates, Internet browsing is possible. GPRS supports X.25 and IP based transmission, which includes wireless application protocol (WAP) data.

18.6 Other digital mobile systems

Second generation mobile systems are digital systems. The GSM system has been described in Section 18.5. This section describes the GSM1800 system, the personal communications system (PCS1900, sometimes known as personal communications network or PCN) and third generation systems.

18.6.1 GSM1800 (DCS1800)

The GSM1800 system operates in the 1840–1880 MHz band, with a carrier spacing of 200 kHz. Each carrier gives multiple access through time division multiple access (TDMA). It is a lower power version of GSM900, which operates in the 900 MHz band. A GSM1800 handset has a maximum power output level of 1 watt, rather than the 2 watts of a GSM900 handset.

Voice coding can be either: half-rate using VSELP at 5.6 kbps, full-rate using RPE-LTP at 13 kbps, or enhanced full rate (EFR) using ACELP at 12.2 kbps. Convolutional coding is used at a rate of $\frac{1}{2}$ to reduce the effects of noise and errors on the radio channel. The radio carrier modulation is Gaussian minimum shift keying (GMSK).

18.6.2 PCS1900 (IS-136, or PCN)

The personal communications system (PCS) is based on GSM and used time division multiplexing to provide separate channels over each radio frequency. Convolutional coding is used at a rate of $\frac{1}{2}$ to reduce the effects of noise and errors on the radio channel. Each carrier is spaced 30 kHz apart and offset quadrature phase-shift keying (OQPSK) is used to modulate the carrier.

The voice-coder (vocoder) used by PCS1900 is either full-rate using VSELP at 7.95 kbps or enhanced full rate (EFR) that uses ACELP at 7.4 kbps. The EFR scheme was developed for use in PCS1900 and has since been adopted by both GSM900 and GSM1800 networks because it improves the audio quality. Previously, GSM used either a half-rate (HR) or full-rate (FR) vocoder.

18.6.3 Third generation systems

The so-called 3G systems have been described using a number of terms: UMTS, IMT-2000, cdma-2000, w-cdma, etc. There are variations between the proposed standards, but in general they all use code division multiple access (CDMA), convolutional coding, quadrature phase shift keying and time or frequency division duplexing.

Third generation systems will operate in the 1885–2025 MHz band and in the 2110–2200 MHz band. Initially the lower band between 1980 and 2010 MHz will not be allocated, nor will the upper band between 2170 and 2200 MHz. However, the full bands will be available when existing services in these bands can be moved (such as PCS1900, PHS and DECT).

The code division multiple access (CDMA) modulation scheme allows several channels to occupy the same frequency band. CDMA is a form of spread spectrum encoding. The digitized speech signals are coded using a unique code, known as a spreading code, so that one bit of speech code produces many encoded bits. When demodulated and mixed with the same spreading code, the original data is recovered. Receivers that use a different spreading code are unable to recover this data, but they are able to recover data intended for them.

18.7 Private mobile radio (PMR)

These systems are privately owned or rented and may be used only by the owner's own staff for the purpose of the owner's business. The leasing of air-time is forbidden. Common base station or community

repeater systems where several users subscribe to, and use, the station is often also referred to as PMR.

18.8 UK CB radio

27 MHz band: 27.60125 to 27.99125 MHz

40 channels at 10 kHz spacing.
Max. erp, 2 W; max. transmitter output power, 4 W.
Antenna: single rod or wire, 1.5 m overall length, base loaded.
If mounted higher than 7 m transmitter output to be reduced at least 10 dB.
Modulation: FM only, deviation ±2.5 kHz max.

934 MHz band: 934.025 to 934.975 MHz

20 channels at 50 kHz spacing (may be reduced later to 25 kHz).
If synthesizer used spacing may be 25 kHz on precise channel frequencies specified.
Max. erp, 25 W; max. transmitter output power 8 W. If antenna integral, max. erp, 3 W.
Antenna: may have up to four elements, none exceeding 17 cm.
If mounted higher than 10 m, transmitter output to be reduced at least 10 dB.
Modulation: FM only, deviation ±5.0 kHz max.

Spurious emissions: for both bands, not exceeding 0.25 μW except for specified frequency bands where the limit is 50 n W.

For latest full specifications see publications MPT 1320 (27 MHz band) and MPT 1321 (934 MHz band) obtainable from the Information and Library Service of the Radiocommunications Agency.

References

Belcher, R. *et al*. (1989). *Newnes Mobile Radio Servicing Handbook*. Butterworth-Heinemann, Oxford.
Macario, R.C.V. (1991). *Personal and Mobile Radio Systems*. Peter Peregrinus, London.
Winder, S.W. (2001). *Newnes Telecommunications Pocket Book*. Butterworth-Heinemann, Oxford.

19 Base station site management

The information in this chapter applies mainly to sites for stations operating at VHF and above. Some conditions will be different for stations working at lower frequencies due to the generally physically larger transmitters and antennas.

19.1 Base station objectives

The objectives of a radio base station are:

1. To provide an adequate service over the whole of the desired service area in a well-defined manner. Special consideration must be given to those areas where, because of their location, weak signals or a high ambient electrical noise level might be expected.
2. To create the minimum interference with other radio users and be designed to receive the minimum from other users.
3. To be electromagnetically compatible with neighbouring installations, possibly on the same site.
4. To create the minimum impact on the environment.

19.2 Site ownership or accommodation rental?

The question of whether to privately develop a base station site or rent space on someone else's site may be resolved by the planning authorities rather than the developer. Before planning consent will be given the developer must normally prove that no existing site will meet the requirements. However, assuming that land is available and planning consent might be forthcoming, other factors to consider are costs, both initial and recurring, and access for services, materials during building and tower erection and for maintenance during bad weather (*Table 19.1*).

19.3 Choice of site

The first stage in selecting a site is to look for an existing site which might appear to cover the service area. Information may be available from the operators of such sites regarding their coverage, and coverage tests may be made or computer predictions obtained. For a

Table 19.1 Factors affecting the decision to own or rent

	Ownership	*Rental*
Initial costs	Legal charges Land clearance Provision of services Erection of buildings and mast or tower Installation of equipment Provision of standby power	Legal charges Connection fee Installation of equipment Provision of standby power
Recurring costs	Maintenance of site Power Insurance (other than radio equipment)	Rental Normally included in rental Normally included in rental
Other considerations	Very long commissioning time Site under user's control Space may be leased to other users creating revenue	Very short commissioning time Site under landlord's control Accommodation will be shared with other users (install equipment in locked cabinet to preserve security)

receiving site the ambient noise level at the base station must also be considered. It should be realized that a site, or an antenna, can be too high, particularly when coverage is required at very short range or if interference from other users is likely to occur. Antennas radiate the minimum signal along the line of their elements so that vertically polarized antennas, i.e. with the E plane vertical, provide very little, if any, signal immediately below them. This creates a hole in the coverage, 'the Polo mint effect', close to the antenna.

Where there is capacity on an existing site the possibilities are:

1. Sharing an existing lightly used radio channel, e.g. common base station.
2. Sharing equipment space in an existing building or providing own building or extension on a communal site.
3. Sharing an antenna by means of multi-coupling or erecting own antenna on existing structure.

19.4 Masts and towers

Apart from short, unguyed poles mounted on the side of buildings, antenna supports fall into two types: guyed masts and self-supporting towers.

A guyed mast may be a single pole, or a square or triangular section lattice structure. The range of single-pole masts includes those of about 4 m maximum height mounted on chimney stacks and secured by wire lashings, and poles supported on the ground or the roof of a building. The latter types may be up to 30 m high. They are usually constructed from steel or aluminium hollow tubular sections – the bottom section is invariably steel – with a set of guys at about every 5 m. Mast erection is specialist work but to estimate the approximate height that a site can accommodate, a four-guy, single-pole mast requires a minimum spacing for the anchorage points in the form of a square with sides equal to half the height of the mast. The guys may be of steel, possibly plastic-coated, or more likely of synthetic fibre. Steel guys may affect the directivity of antennas in close proximity, and if the guys corrode at their fixing points, intermodulation interference may result.

Self-supporting towers come in all heights up to many hundreds of feet and may be made of a variety of materials from steel sections to concrete.

The factors determining the type of structure to be erected are the number and types of antenna, and the site conditions.

Antenna considerations:

- Physical dimensions and space requirements.
- Weight.
- Wind loading.
- Directivity. For example, the beam width of a 6.5 GHz, 3.0 m dia. microwave dish is 0.9 degrees. A tower supporting such an antenna must twist, therefore, less than about 0.3 degrees in the highest wind likely to be experienced at the site.
- Access for riggers to antenna mounting positions.

Site conditions:

- Availability of space for tower footings, and guys and anchorages if a mast is contemplated.
- Stability and type of ground.
- Weather conditions. High winds. Accumulation of ice and snow. Build-up of ice increases wind loading of antenna – and of mast or tower – considerably. There is no point in using grid microwave antennas where icing is likely to occur.
- Aesthetic and planning consent considerations.

19.5 Installation of electronic equipment

For radio equipment, safety is one of the first priorities and in addition to the electrical considerations, physical hazards must be avoided.

Adequate working space must be provided around the equipment racks. Much equipment is now wall-mounted but tall, floor-standing cabinets must be firmly bolted down to prevent toppling when units are partially withdrawn for servicing and cables need to be routed safely. Overhead cable trays are generally considered the most satisfactory method but, to avoid interaction, it is recommended that cables for the various functions be segregated to reduce cross-talk and interference. Where cabling enters a cabinet at floor level, mounting the cabinet on a hollow plinth and running the cables through the plinth avoids damage to the cables and persons tripping over them.

For low voltage installations (see classifications below) the IEE wiring regulations apply. For high voltage installations, recommendations are given in BS 6701: part 1: 1990 which also covers accommodation, lighting levels and access arrangements.

Classification of installations:

- *Extra low voltage*. Normally not exceeding 50 V AC or 120 V DC.
- *Low voltage*. Exceeding 50 V AC or 120 V DC but not exceeding 1000 V AC or 1500 V DC between conductors, or 600 V AC or 900 V DC between conductors and earth.
- *High voltage*. Exceeding 1000 V AC or 1500 V DC between conductors, or 600 V AC or 900 V DC between conductors and earth.

19.6 Earthing and protection against lightning

Recommendations for earthing are given in BS 7430: 1991. This document covers the earthing of equipment and the principles of earthing for protection against lightning. All equipment metalwork must be bonded together and connected to the electricity supply earth point, the main earth terminal. In addition a connection must be made to the earthing system provided for protection against the effects of lightning.

Antenna systems by their nature are vulnerable to lightning strikes. Nearby taller structures may reduce the risk but precautions must still be taken. The zone of protection – a cone with its apex at the tip of the protecting structure and its base on the ground forming an angle of 45° to the perpendicular – does not necessarily protect structures above 20 m high. BS 6651: 1985 is the *Code of Practice for the Protection of Structures against Lightning*. Lightning protection begins at the top of the mast or tower where, ideally, the highest item should be a finial bonded to the tower. However, a finial mounted alongside an omnidirectional antenna will affect is radiation pattern. Grounded antennas are preferred and the outer conductor of each feeder cable must be

bonded to the tower at the top and bottom of its vertical run. Grounding kits for the purpose are obtainable. The feeder cables must also be bonded to an earthing bar at their point of entry to the equipment building. The codes of practice should be consulted regarding the routes to be taken by earthing tape and the methods of jointing. An important point is that neither very sharp bends nor 'U' bends are created.

The legs of the tower must be bonded together with earthing tape and each leg connected to an earthing system which may consist of a buried plate or rods. Several rods may be necessary for each subsystem to attain the specified earth resistance of not more than 10 ohms. The rods should, except in rock, be driven into ground which is not made up or backfilled or likely to dry out. Where several rods are necessary to achieve the specified earth resistance these should be spaced well apart, the reduction in earth resistance being small with parallel rods closely spaced. Joints to facilitate testing of each subsystem separately must be provided either above ground or in a purpose-built pit or chamber. *Figure 19.1* shows a typical earthing system.

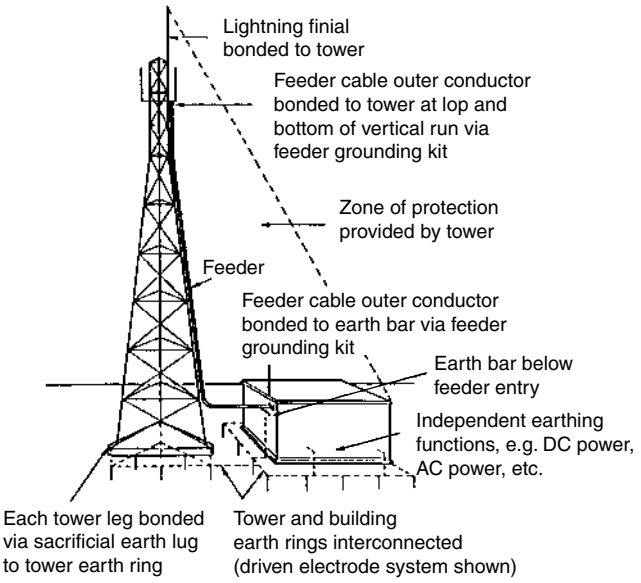

Figure 19.1 Typical example of good earthing practice (© Crown Copyright 1991, Radiocommunications Agency)

The system should be tested regularly, at least annually, and the results recorded in a lightning protection system log book. The test comprises:

1. Measurement of the resistance to earth of each termination network and each earth electrode.
2. Visual inspection of all conductors, bonds and joints or their measured electrical continuity.

BS 7430 recommends the method of testing.

Other vulnerable systems are overhead cables for either the electricity supply or telephone and control purposes.

19.7 Erection of antennas

The installation of the antenna probably influences the performance of a radio system more than any other part. The heights involved render supervision of the installation difficult and, although antennas are relatively inexpensive, labour charges raise the cost of their replacement, and bad weather may delay rigging work. It is therefore important that good quality antennas are specified and that the initial installation is correct. In addition to the physical mounting arrangements, the dispositions of antennas on the structure are important. Some aspects are detailed below and MPT 1331 contains more information.

19.7.1 Directivity

The radiation pattern diagrams provided in the antenna manufacturers' catalogues are produced by an isolated antenna. They can be greatly affected by the proximity of the support structure, e.g. if a dipole is mounted close to the leg of a tower, the leg behaves as a reflector and the radiation pattern of the antenna approaches that of two-element Yagi. The less directional the antenna, the worse the effect. Omni-directional antennas should not be mounted on the side of a mast or tower if it can be avoided. If an omni-directional antenna must be so mounted it should be spaced two wavelengths from it. This is difficult to achieve at the lower frequencies considering the antenna dimensions, weight and windloading. The rear element of a Yagi antenna must be one wavelength clear of the structure. To obtain a nominally omni-directional pattern a better, albeit expensive, solution is to mount a number of antennas, phased correctly, around the tower.

All antennas should point directly away from the structure, i.e. at right angles to the side of the tower.

The proximity of metalwork also adversely affects the VSWR of an antenna, causing standing waves with their additional voltage stresses on the feeder and possibly producing interference.

19.7.2 Practical aspects of antenna installation

All installation components must be made from compatible materials, electrically dissimilar metals, e.g. steel and brass, brass and aluminium, being avoided at all costs; they will corrode and cause intermodulation. Preferred materials are aluminium, and galvanized or stainless steel. Mounting brackets must be secure – remembering that antennas and feeders vibrate – but not overtightened so as to distort and weaken antenna support booms.

Connectors of the correct impedance, and preferably with a captive centre pin, are vital. Type N connectors are available at either 50 or 70 ohms impedance, are robust and can be used at frequencies up to 10 GHz. UHF 83 series connectors, although very robust, are of imprecise impedance and, from first-hand experience of interference aggravated by a UHF 83 used to connect an antenna feeder to a receiver tail, should not be used on base station installations. Assembly instructions for a range of connectors are shown in Chapter 23. All joints must be waterproofed, preferably by first wrapping with a self-amalgamating tape for two inches either side of the joint, then a layer of PVC tape covered by a further layer of Sylglass or Denso tape. When installing feeder cables the required length should be loosely coiled and taken up the tower and paid out as it is secured, working from top to bottom. It must not be dragged from a drum on the ground. Feeders must be cleated at the intervals specified by the manufacturer. Route cables where they are easily accessible but least likely to suffer physical damage.

Health and safety

Apart from the physical risks to riggers, there are radiation hazards. Large amounts of RF power may be radiated from antenna systems and research is continuing into its effects on health. The most recent recommendations of the National Radiological Protection Board and the Department of Trade and Industry should be sought and followed. Riggers should be aware of the power levels present on a structure before climbing, and equipment switched off where levels are considered unsafe.

19.7.3 Antenna checking and fault finding

The majority of VHF and UHF antennas present a short-circuit across the antenna and to ground as a means of reducing their vulnerability to static charges. An ohmmeter applied to the lower end of the feeder will

indicate a circuit through the feeder and antenna but may also indicate a short-circuit or low resistance fault, water in the feeder for instance. Most antenna system faults increase the VSWR present on the feeder cable. A good antenna, operating within its design bandwidth, exhibits a VSWR of 1:1. When connected to a length of co-axial cable this may be raised and a VSWR of 1.5:1 for the system is generally considered acceptable. However, faults can be masked by conditions occurring on the feeder, and a measurement taken with a standing wave, or forward and reflected power meter at the bottom of the feeder, may not indicate the true condition of the antenna. A measurement taken with an accurate dummy resistive load connected to the top of the feeder will prove the cable, and a measurement of the VSWR should also be taken directly at the antenna. A record of the VSWR at installation and any subsequent measurements is helpful.

19.8 Interference

There are two sources of radio interference induced by antenna systems. One occurs from strong signals radiated by either the system's own transmitter antenna or from a co-sited system operating on a close neighbouring frequency. The other source is intermodulation, 'rusty bolt effect', the mixing of two or more signals to produce the interfering frequency.

19.8.1 Antenna isolation

One solution to the problem of direct radiation is to space the antennas so that there is sufficient isolation between them. Because minimum radiation is present immediately below and above the ends of the elements of vertically polarized antennas, maximum isolation occurs when such antennas are mounted in a vertical line. Maximum radiation, and hence minimum isolation, occurs when antennas are mounted side-by-side. The degree of isolation depends on the spacing but a figure of 40–45 dB between a transmitter and a receiver antenna, and 20–25 dB between transmitting antennas, should be the target. To achieve 25 dB isolation requires a vertical separation of 0.9 wavelengths between the centres of vertically polarized dipoles; 45 dB requires a vertical separation of 3 wavelengths. The spacing for horizontal separation of vertically polarized antennas is 2.5 wavelengths for 25 dB isolation and 25 wavelengths for 45 dB. To preserve this isolation the feeder cables should also be separated over their routes.

Antenna multi-coupling

A precise method of controlling the RF isolation between mutually sited systems where the frequencies are moderately spaced is for several systems to share one antenna by using multi-coupling techniques (see Section 19.9).

19.8.2 Intermodulation

Any two or more RF signals applied to a non-linear device intermodulate, that is, they combine to form additional frequencies. *Table 19.2* lists the combinations for two input frequencies. It must be remembered that the side frequencies produced by modulation of the original carriers will also be present.

Table 19.2 Low order intermodulation products

2nd	$A + B$	5th	$3A + 2B$	7th	$4A + 3B$
	$A - B$		$3B + 2A$		$4B + 3A$
			$3A - 2B^*$		$4A - 3B^*$
3rd	$2A + B$		$3B - 2A^*$		$4B - 3A^*$
	$2A - B^*$		$4B + A$		$5A + 2B$
	$2B + A$		$4A + B$		$5B + 2A$
	$2B - A^*$		$4A - B$		$5A - 2B$
			$4B - A$		$5B - 2A$
4th	$2A + 2B$				$6A + B$
	$2A - 2B$	6th	$5A + B$		$6B + A$
	$2B + 2A$		$5B + A$		$6A - B$
	$2B - 2A$		$5A - B$		$6B - A$
	$3A + B$		$5B - A$		
	$3A - B$		$4B + 2A$		
	$3B + A$		$4B + 2B$		
	$3B - A$		$4B - 2A$		
			$4B - 2B$		
			$3A + 3B$		
			$3A - 3B$		
			$3B - 3A$		

*indicates in-band products. No eighth-order products fall in-band but ninth-order in-band products are produced by:

$5A - 4B$

$5B - 4A$

19.8.3 Control of intermodulation

A clue to the source of interference will be obtained from examination of the relationship of all frequencies produced on site, and also those produced nearby. That the side frequencies produced by modulation

must be considered was proved in an intermodulation situation where the interference was only received when a nearby band III television transmitter radiated a peak white signal.

Corroded joints in metalwork close to the site, receiver RF stages subjected to very large signals and transmitter output stages are all non-linear devices and can create intermodulation.

Regular maintenance of the metalwork around the site reduces the chances of intermodulation from this source, but it is difficult to see and eliminate all corrosion on an inspection. Should interference from this cause be suspected after elimination of the other sources, a successful method of locating the offending joint requires a receiver tuned to the interfering signal and fitted with a whip antenna. While receiving the interference, a very sharp null in signal strength occurs when the tip of the whip points directly at the source of the signal.

Receiver RF amplifiers are usually designed to cope with small signals. When a strong signal radiated from a nearby transmitter is received the stage may well be overloaded and driven into non-linearity, or even into a blocked state where the receiver is effectively dead and may take some seconds to recover after the signal is removed. In the non-linear state the receiver is in an ideal condition to create intermodulation. If this situation is suspected a method of identifying it is to install a variable RF attenuator in the antenna feed to the suspect receiver. With zero attenuation the interference will be received but, if the receiver is the cause, increasing attenuation will produce little reduction of the interference until a point is reached where the interference suddenly disappears – the receiver at this point has re-entered a linear state. If the interference reduces gradually to zero with increased attenuation, the source is elsewhere.

Most amplifiers are designed to be linear, that is, the output signal level will follow that of the input signal. However, with a sufficiently high input signal overloading occurs, the amplifier becomes non-linear and compression of the signal results (*Figure 19.2*). The point where 1 dB of compression occurs is a commonly referred to amplifier parameter. If the input level is increased further the gain of the amplifier is reduced until saturation is reached when the output level can no longer increase.

At the onset of non-linearity harmonics and intermodulation, if any other frequencies are present, are produced. The strength of these rises rapidly with an increase of input, and the point where an extension of the almost linear portion of their curve crosses an extension of the linear gain line of the amplifier is the third-order intercept – usually it is only the third-order products which are considered for this purpose.

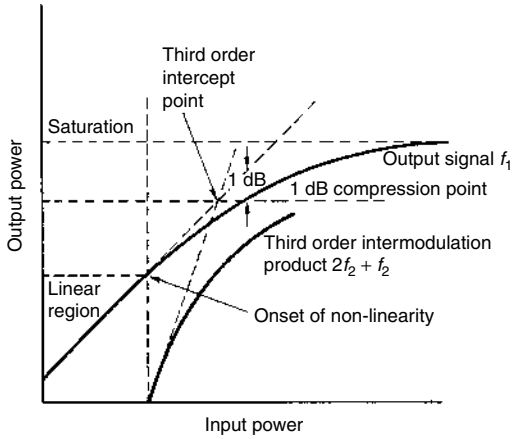

Figure 19.2 Production of intermodulation

The class C operated output stages of transmitters are by design non-linear. Strong signals from a neighbouring transmitter or antenna applied via the antenna feed will mix with the transmitted frequency to create intermodulation products. Increased isolation between antennas and feeders may be the simplest remedy. Alternatively, a circulator or filters may be connected to the output of the transmitter,

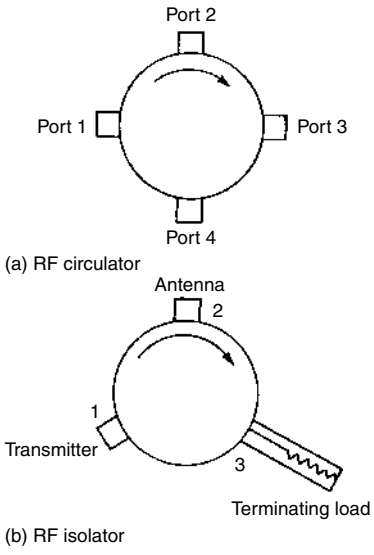

Figure 19.3 RF circulator and isolator

and the possibility of direct radiation from transmitters must not be ignored.

A circulator is a uni-directional device with either three or four ports as shown in *Figure 19.3(a)*. A signal entering at port 1 will leave at port 2 but not at ports 3 or 4. Similarly, a signal entering at port 2 will leave at port 3 but not ports 1 or 4. Circulators are used for combining the outputs of transmitters for application to a single antenna but if a three-port circulator is connected as in *Figure 19.3(b)* it forms an isolator. Typical isolation over a 1.5% bandwidth is 20–30 dB with an insertion loss of 0.7 dB.

19.9 Antenna multi-coupling

The sharing of antennas and feeders between a number of co-sited services is not only a precise method of controlling frequency isolation, it is an economic solution to the problems of antenna and tower management. An antenna may be shared between a number of receivers or transmitters, or shared simultaneously by both receivers and transmitters. Receiver sharing requires a splitter, i.e. a filter, to separate the frequencies for each receiver and an amplifier to make up the filter losses. Transmitters can share an antenna through circulator/isolators and filters. To obtain the required selectivity, stability

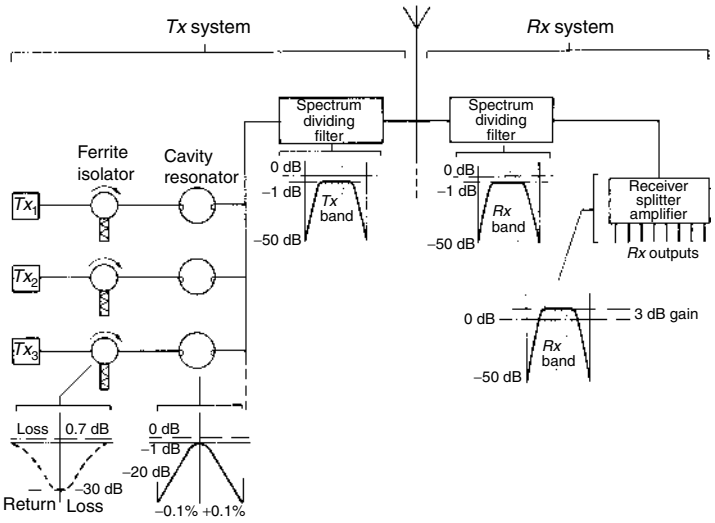

Figure 19.4 Typical sub-band transmitter/receiver sharing (© Crown Copyright 1991, Radiocommunications Agency)

and power handling capability the filters are often solidly constructed cavity resonators with an insertion loss of 1 dB and a bandwidth of 0.1% to the −20 dB points. *Figure 19.4* shows the layout of a transmitter/receiver sharing system.

19.10 Emergency power supplies

The installation of equipment to provide power for all the equipment on a site during a failure of the public supplies has declined in recent years. But although lengthy power failures seem to be a thing of the past, they could recur, and electricity supplies do still fail for short periods. To provide a complete supply for large station necessitates a standby generator. On smaller stations batteries may be capable of supplying the demands of the electronic equipment and emergency lighting for one or two hours. The trend on multi-user shared sites appears to be for the individual user to provide the emergency power, derived from batteries, for his own equipment. Factors to consider are:

1. Standby motor generators are expensive. They need housing, ventilation and fuel storage. They take time to start up, 45 seconds being typical.
2. Uninterruptible power supplies (UPS). Where no interruptions can be tolerated the most efficient supply is provided by batteries alone but the equipment must be designed to operate directly from a DC, low voltage supply.

   To supply power at 220/240 V AC an inverter is the accepted method. Double inverters permanently charge a battery from the AC supply and the battery drives an oscillator to reproduce the AC supply voltage, a very inefficient process. Also, should any item of the inverter break down the supply is lost. This is overcome in some inverters by a switch which transfers the load to the public supply when a failure of the inverter occurs. Single inverters charge a battery and supply the equipment directly from the public supply until a failure occurs. When this happens the supply changes over to the battery and oscillator. Single inverters are more efficient but there is a short break in supply while the change-over occurs. Adequate stabilization and filtering to avoid disturbances on the supply must be provided. One possible hazard with all inverter supplies is that where more than one inverter is used, the outputs of the inverters are unlikely to be in phase and a 480 V difference could exist between the supplies for two items of equipment.

For all battery-operated supplies correct charging of the battery is crucial. Nickel–cadmium batteries require constant-current charging with a fall to the trickle rate when fully charged and sophisticated circuitry is needed to identify the precise point of full charge (see Section 21.3.2).

Lead acid batteries produce hydrogen if over-charged so their storage must be designed so that no danger, either to personnel or of explosion, exists. For reliability, natural ventilation is preferred to forced. Recommendations for the accommodation of lead acid batteries other than sealed are given in BS 6133: 1985. Batteries which gas also need more frequent maintenance. Because of the reduction in performance of batteries at low temperatures the ambient temperature of the battery storage room should not fall below 4°C, and to reduce water evaporation lead acid batteries should not be run continuously above 40°C.

The period of time over which a lead acid battery must be fully recharged determines the capacity of the battery more than the period of time over which it must supply power. Because of the need to reduce the charge rate – to avoid gassing – to a very low level as the battery approaches full charge, the last 15% of capacity takes a very long time to acquire (see Section 21.3).

19.11 Approval and certification

No base radio station may be operated in the UK prior to inspection of the installation by the Radio Investigation Service of the Radiocommunications Agency and the issue of their certificate of approval. The installation may not subsequently be modified without re-approval and certification.

References

Belcher R. *et al*. (1989). *Newnes Mobile Radio Servicing Handbook.* Butterworth-Heinemann, Oxford.

BS 6651: 1985. *Code of Practice for the Protection of Structures against Lightning.*

BS 6701: Part 1:1990. *Code of Practice for Installation of Apparatus Intended for Connection to Certain Telecommunications Systems.*

BS 7430: 1991. *Code of Practice for Earthing. Earthing of Telecommunications Installations.* International Telecommunications Union.

MPT 1331. *Code of Practice For Radio Site Engineering.*

MPT 1351. *Code of Practice For Repeater Operation at Communal Sites.*

MPT 1367. *Guidance Note to Legal Requirements Covering the Installation and use of Radio Apparatus and other Apparatus Generating Radio Frequency Emissions.*

MPT 1368. *Code of Practice for the Inspection of a Land Mobile Radio System for Conformity with the Wireless Telegraphy Act Licence and Performance Specification.*

Note: MPT documents are available from the Radiocommunications Agency (UK).

20 Instrumentation

20.1 Accuracy, resolution and stability

All measurements are subject to error and two instruments applied to the same piece of equipment under test may give a different answer. Tolerances must therefore be accepted. The errors arise from the following sources:

1. Human error, e.g. precision in reading a scale, use of incorrect instrument or range setting for the purpose.
2. The accuracy to which the instrument is able to display the result of a measurement or, in the case of a generator, the frequency or output level.
3. Accuracy of calibration.
4. Tolerances in the components used in the construction of the instrument. Variations in the load applied to the instrument.
5. Variations caused by long-term drift in the values of components.
6. Variations due to temperature and supply voltage fluctuations, and the warm-up time required by some instruments.
7. An effect on the circuit under test by the connection of the instrument.

There is an important difference between the accuracy and the resolution of an instrument. The accuracy is a statement of the maximum errors which may occur from the causes in statements 3 to 6 above. In instrument specifications, stability defined by statements 5 and 6 is usually quoted separately.

The accuracy of analogue measuring instruments is normally quoted as a percentage of full scale deflection (FSD). This is the accuracy of the instrument movement and components plus the scale calibration. The scale graduations, though, may not permit the user to determine the reading to the accuracy of the instrument perhaps because the graduations are cramped or parallax reading error occurs. These factors decide the resolution or precision of reading.

The accuracy of instruments with digital displays is usually quoted as a percentage of the reading plus or minus one count or one digit. While digital instruments are generally more accurate than their analogue counterparts, the fact that the least significant figure may be in error affects the resolution. *Figure 20.1* shows how this can arise. Most digital instruments use a gating process to switch the input to

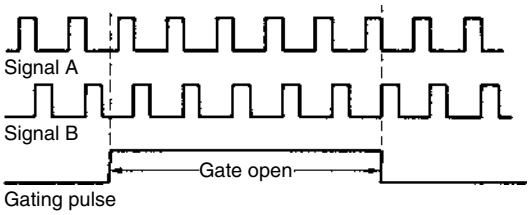

Figure 20.1 Gating error introduced by signal phasing

the measuring circuitry for the appropriate period of time. The gating time itself may vary and affect the accuracy, but even with a perfectly accurate and stable gating time, the phase of the input signal at the time of switching affects the number of pulses passing through the gate and thus the resolution.

Performance figures taken from a number of manufacturer's catalogues are listed below. They show only the more important features of the specifications and are typical of those for high quality instruments used in radio work.

20.2 Audio instruments

20.2.1 Output power meters

Those for radio applications measure RMS audio power and are usually calibrated in watts and dBW or dBm. They usually contain a dummy load resistor of adjustable impedance as a substitute for the receiver loudspeaker when in use.

20.2.2 Distortion factor and Sinad meters

These may be separate instruments or combined, and may also be incorporated within an audio output power meter. Both operate on the same principle. An audio input amplifier, with automatic gain control to give a fixed reference level at its output, applies the output from the unit under test, first to a notch filter to remove the test frequency of 1000 Hz, then to an AC voltmeter. The voltmeter is calibrated in percentage distortion or dB Sinad.

In testing a receiver Sinad ratio, the instrument is connected across the loudspeaker or equivalent dummy load. An RF signal generator connected to the antenna socket is adjusted to apply a moderately high level signal modulated with a 1 kHz tone – which must be pure and match the notch filter in the Sinad meter – at 60% of the system peak modulation. To be correct, the receiver volume control is adjusted

to give the rated audio output but if only Sinad sensitivity is being measured a lower level is acceptable. The Sinad meter will now display the combined level of all the frequencies except 1000 Hz present in the receiver's output. These are the noise and distortion products. With the high level input applied these will be low and the meter deflection will be small indicating a high Sinad ratio. The RF input level is now reduced until the meter reads 12 dB (the standard reference) and the RF level, μV or dBm, is the Sinad sensitivity for the receiver.

The oscillator to produce the test tone may be included in the meter and filters may be provided to comply with various weightings.

20.2.3 Audio signal generators

The instrument provides an output for synchronizing to an external standard and a TTL compatible output. A high power version capable of delivering 3 watts into a 3 Ω load in the audio band is available.

20.3 Radio frequency instruments

20.3.1 RF power meters

Direct reading RF power meters either contain a non-reactive load or use an external load and may be calibrated in watts or dBm. RF calorimeters convert the RF energy into heat and measure the temperature of the heated element. At low powers, 'dry' calorimeters are used but their long thermal time constant inhibits their use at high power levels. To measure high powers 'flow' calorimeters, where a fluid flows around a closed system and the output temperature of the fluid is measured, are used. Power can be determined from:

$$P = F(T_{\text{out}} - T_{\text{in}})c(T)$$

where

P = power
F = mass flow rate of the fluid
$c(T)$ = the fluid's specific heat
T_{in} = temperature of the fluid entering the load
T_{out} = temperature of the fluid after being heated by the load

Thruline type instruments require an external load which may be either an antenna system or a load resistor. This type of meter reads forward and reflected power and, in some instruments, VSWR directly.

20.3.2 RF signal generators

The range of instruments designed for use on specific systems, e.g. cellular and digitally modulated, is so wide that manufacturers' catalogues must be consulted for each application. In addition to the accuracy of the carrier frequency and output level, RF leakage, spectral purity and modulation noise levels are important. The output level may be calibrated in μV, dBV or dBm, and may refer to either an unterminated instrument (p.d.) or terminated in a load equal to the output impedance of the generator (e.m.f.). If the instrument is calibrated in p.d., the output voltage must be halved when the instrument is terminated in an equal impedance.

The 50 ohm output impedance of many signal generators matches the input impedance of most VHF and UHF receivers directly. To simulate the impedance of antennas at HF and below a dummy antenna is usually inserted between the generator and the receiver under test. *Figure 20.2* shows the circuit of a standard dummy antenna.

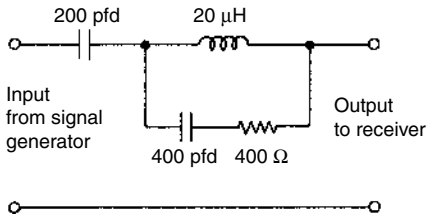

Figure 20.2 Standard dummy antenna

20.3.3 Frequency counters

Instruments are necessary to measure not only the precise frequencies of transmitters and receiver local oscillators but also those of low frequency signalling tones. Consequently they have a wide operating range.

The output of a transmitter must never be connected directly into a counter. The signal should either be obtained off-air or through a 'sniffer', appropriate for the frequency range, which siphons off a fragment of the transmitter output. It is also essential to ensure that the frequency displayed is the fundamental and not a harmonic or some other spurious frequency.

20.3.4 Modulation meters

The remarks in the above section relating to the connection of a transmitter and the selection of the fundamental frequency apply equally to modulation meters.

20.3.5 Spectrum analysers

Today's tight regulation of spectrum usage makes a spectrum analyser an essential tool for the precise alignment of radio equipment and for the measurement of modulation products and the noise content of signals.

A spectrum analyser is essentially a superheterodyne receiver with an adjustable IF bandwidth which sweeps across a portion of the frequency spectrum in synchronism with the horizontal trace of a cathode ray tube display. A signal at any frequency within the swept band will, while it remains within the IF passband, appear as a vertical displacement of the display trace. The design of the filter is crucial but must be a compromise. An analyser using multiple filters permits fast measurement but low resolution; a single filter offers high resolution but slower response time. Also, the shape factor of a wide filter inhibits the display of low level signals close to the centre frequency of the filter and a narrow filter, while permitting the display of these signals, may fail to display transients. The bandwidth determines the sweep speed, narrower bandwidths requiring slower speeds.

The possibility exists of spurious signals, e.g. intermodulation, being produced within the analyser with large input signals. A method of reducing the possibility is to insert a circulator and a notch filter

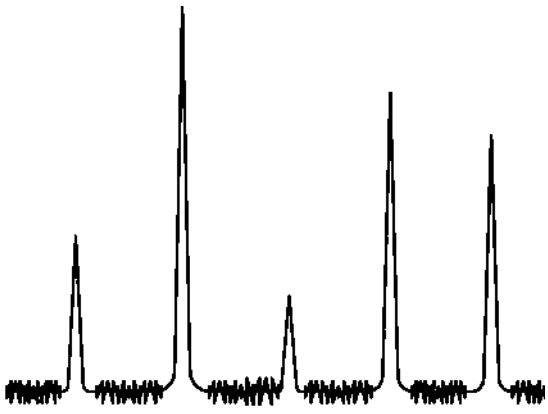

Figure 20.3 Amplitude-vs-frequency spectrum analyser display

between the unit under test and the analyser input to reduce the fundamental frequency amplitude. The circulator must be installed between the filter and the unit under test to absorb the reverse power produced by the impedance variations of the filter.

Many instruments are programmable and suitable for incorporation in automatic testing (ATE) systems, and instruments with similar features to those described are also offered in a combination test set form.

20.3.6 Network analysers

A network analysers examines *incident, reflected* and *transmitted* signals through a circuit or device, and displays the magnitude and phase of these signals. A spectrum analyser, on the other hand, measures only one channel, and displays magnitude and frequency.

Figure 20.4 shows an optical analogy to the network analyser. A 'device' of different optical density than ambient is in the path of an incident ray of light (R). When the light hits the surface, part of it is reflected (A) and part is transmitted through the 'devices' (even though refracted a bit).

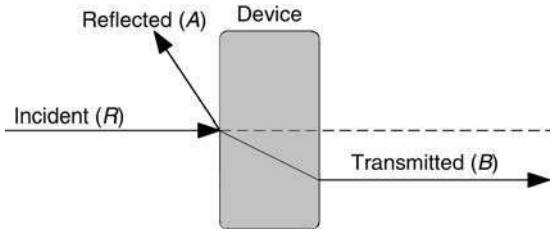

Figure 20.4 Optical analogy to network analyser

A network analyser consists of a three-channel RF receiver and a display. The incident signal is considered the *reference signal*, so is designated the R-channel. The other two channels receive the reflected signal on the A-channel, and the transmitted signal on the B-channel.

The uses of scalar and vector network analysers differ from the uses of spectrum analysers. The spectrum analyser measures external signals of unknown frequency and modulation type. Even when a tracking generator is added, to allow the spectrum analyser to perform stimulus-response tests, the spectrum analyser cannot do the job of the network analyser. The network analyser, by contrast, contains a known signal source, and is capable of sweeping a range of frequencies and power output levels. It can also perform ratio measurements.

References

Belcher, R. *et al*. (1989). *Newnes Mobile Radio Servicing Handbook*. Butterworth-Heinemann, Oxford.
Bird Electronic Corp., Catalog GC-92.
Farnell Instruments Ltd, Catalogue, 1993.
Marconi Instruments Ltd, Test and Measurement Instrument Systems 1993/94.
RTT Systems Ltd, Catalogue, 1993.
Winder, S.W. (2001). *Newnes Telecommunications Pocket Book*. Butterworth-Heinemann, Oxford.

21 Batteries

21.1 Cell characteristics

Batteries are composed of cells which exhibit characteristics peculiar to their chemical constituents and construction. Common features, important to users, are their ability to store energy within a small space and with the least weight, and to release it at an adequate rate for the purpose under consideration.

21.1.1 Capacity

The amount of energy a battery can store is measured in ampere hours (Ah) at a specified discharge rate. For large cells this is usually the 10 hour rate but American practice, which is now almost universal, at least for smaller cells, is to use the 1 hour rate. It is important, therefore, to be certain which rate is referred to. The capacity reduces as the rate of discharge increases. Thus a battery of 60 ampere hours capacity at the 10 hour rate will provide 6 amps for ten hours before reaching the point at which it is considered to be discharged. If a current of 12 amps is taken, the battery will become discharged in less than 5 hours, and if the current is 3 amps, it will last longer than 20 hours. The rate of discharge is often referred to in terms of the C-rate which may be expressed in several ways. 1C, C or C_1 are numerically the same as the rated capacity, e.g. a 500 mA Nicad cell supplying 500 mA, which may be expressed as C, 1C or C_1 continuously will be discharged in approximately 1 hour. If the cell supplies current at a reduced rate, 0.5 C, 0.5 C_1, or C/2, i.e. 250 mA, it will last approximately 125 minutes. The subscript, e.g. C_5, indicates the hourly discharge rate.

The terminal voltage at which a cell is considered discharged also varies with the discharge rate; a lead acid cell discharged at 1C is considered to be discharged when the terminal voltage falls to 1.75 V. At C_{10} the cell is considered to be discharged at 1.85 V.

The capacity of a battery or cell may also be specified at a given ambient temperature, usually 20°C. Lower temperatures reduce the effective capacity and maximum current off-take, higher temperatures increase them slightly.

For radio use battery duration may be quoted in terms of standby, receive and talk time. The duty cycle obviously varies from user to

user but a useful standard for a radio-telephone is 90% standby, 5% receive and 5% transmit. On an open channel PMR system, 80%/15%/5% is more typical. Measuring the current drains during these activities enables the battery requirements to be calculated.

21.1.2 Internal resistance

The maximum instantaneous current which a battery can deliver is determined by its internal resistance. In this respect a battery behaves like any other generator (see Section 21.3.2), where increasing load currents produce an increasing voltage drop across the internal resistance. The internal resistance of a battery is seldom specified, but for a battery in good condition it is extremely low (one quoted figure is 15 mΩ for a fully charged 500 mAh Nicad cell) and the voltage drop in the connecting leads will govern the maximum withdrawable current. Equally, the resistance of the meter used will affect the measurement of charge or discharge currents. If using an analogue meter, the older low resistance types are preferable (I keep a model 40 Avometer, 0.03 Ω int. res. on 12 amp range, for the purpose). Low current-rating fuses also present a resistance higher than that of a battery (4 Ω measured for a 250 mA fuse, 0.5 Ω for a 1 A) and, probably, the connecting leads.

21.1.3 Power:weight and volume ratios

It is the battery that now limits the size to which radio equipment can be reduced. Recent developments have increased the power to weight and power to volume ratios which are possible. Typical ratios are referred to in the sections dealing with individual battery types.

21.1.4 Recharging conditions

The initial charge rate is the current flowing through a discharged battery to replace the charge in a specified time. Unless supplied from a constant current charger the current will fall as the battery voltage rises, but as full charge is approached the charge rate is usually reduced to a trickle or finishing charge rate.

Trickle charging maintains the cells in a fully charged condition by passing a very small current through them sufficient merely to replace any self-discharge losses through leakage.

Finishing charge is a rate to which the charging current is reduced when a battery reaches about 85% of its full capacity. It is a rate at which gassing is unlikely to occur.

Float charging maintains the cell voltage at its nominal while it is supplying continuous and variable loads.

21.2 Non-rechargeable, primary batteries

While rechargeable batteries are the obvious choice for use in equipment which is in use continuously, disposable types have economic and logistic advantages for some applications – the batteries are more expensive long term but no charger is needed. Also primary batteries have up to 4 times the available capacity of their nickel cadmium equivalents with less weight. Details of disposable batteries with some standard nickel-cadmium rechargeable equivalents are given in *Table 21.1*.

Lithium primary batteries are now available and have the following qualities:

1. A high cell voltage of 3.6 V on load. The voltage is constant – after an initial fall when load is first applied – until discharged when a rapid fall occurs.
2. An operating temperature range of -55°C to $+75^{\circ}$C is possible.
3. Energy densities up to 630 mWh/g. A standard AA size cell has a power/weight ratio of 340 mWh/g.
4. Long shelf life. Ten years at room temperature for a 10% fall in capacity is envisaged.

They have a disadvantage in that fire, explosion or severe burns may result if the batteries are mistreated. They must not be recharged, disassembled, heated above 100°C, incinerated or the contents exposed to water.

One use of lithium batteries is as a power source for memories but protection against charging is needed. *Figure 21.1* shows a typical circuit.

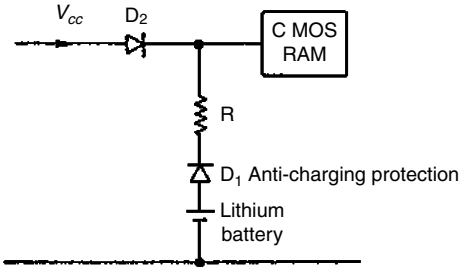

Figure 21.1 Typical lithium battery application

21.3 Rechargeable batteries

21.3.1 Lead acid batteries

Lead acid batteries, whether of free electrolyte or low-maintenance sealed construction, have a nominal terminal voltage on load of 2.0 V per cell. This voltage falls on load in a gradual curve, shown in *Figure 21.2*, until the discharged voltage of between 1.75 and 1.85 volts per cell is reached.

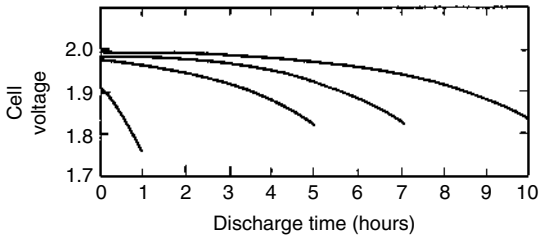

Figure 21.2 Typical lead acid cell discharge characteristics

A discharged battery will, because of its inefficiencies, require a recharge equal to the amperes × hours discharged +11%, e.g. a cell discharged at 5 amps for 10 hours will require a recharge of 55.5 ampere hours with a constant current at the 10 hour rate. Because of the reducing current as full charge is approached a recharge time of 1.4 to 1.5 times the capacity to be restored is more practical. The final on-charge cell voltage can increase to approximately 2.7 volts. Gassing occurs and hydrogen is liberated when the cell voltage reaches 23 V but provided the charging current is sufficiently low above this point gassing will be avoided. This lower charge rate, the 'finishing rate' can be applied by maintaining the charging voltage at about 2.4 volts when the battery will automatically limit the charging current. The specific gravity of the electrolyte in a fully charged cell is between 1.205 and 1.215.

The trickle charge current must be low enough to avoid gassing. A current of 7% of the 10 hour capacity is typical.

Float charging should maintain a cell voltage of approximately 2.2 volts.

The power:weight ratio of lead acid batteries is poor, a small (4 Ah), 6.0 V, sealed lead acid battery having a power:weight ratio of 26 mWh/g.

21.3.2 Nickel-cadmium (Nicad) batteries

At present the Nicad is probably the most commonly used rechargeable battery for portable applications. A standard size AA cell has a power:weight ratio of 27 mWh/g. The on-load Nicad cell voltage, after an initial fall from the on-charge voltage of between 1.3 and 1.4 V, remains substantially constant at about 1.2 V until the discharged voltage of 0.9 to 1.1 V is reached. Thereafter the voltage falls rapidly. This is illustrated in *Figure 21.3*. While the constant voltage is ideal during discharge it poses a problem in that it is difficult to reliably measure the intermediate state of charge which created difficulties with recharging. A Nicad battery which is repeatedly partially discharged and then recharged may, after many cycles, behave as though it were fully discharged when the repeated recharge condition is reached (the memory effect) and, with a fixed time charger, the possibility of over-charging is present. One solution fully discharged all batteries after use to a predetermined level, typically 1.1 V per cell, and then recharged them at a constant current for a fixed period of time. Unfortunately, this procedure shortened the life of the batteries; *Figure 21.4* shows the life expectancy of a cell with repeated discharges. The present solution is to charge the batteries automatically to the fully charged state and then reduce the current to the trickle charge level. Batteries which are subjected to repeated partial discharge may then be occasionally fully discharged to obviate the memory effect.

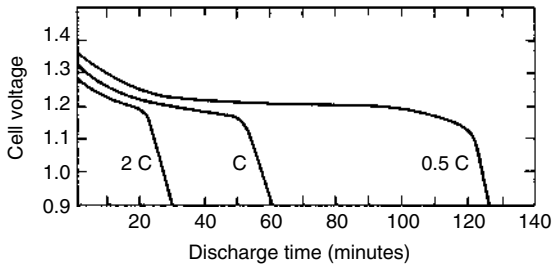

Figure 21.3 Typical Nicad cell discharge characteristics

Constant current, automatic charging is recommended. Chargers vary in complexity, some detecting the end-of-charge point by sensing a variation of voltage. At end of charge the cell voltage first rises and then falls slightly as in *Figure 21.5*. More sophisticated chargers also sense the cell case temperature which rises during charge. Batteries are available for standard charging at the ten hour rate where 14 to

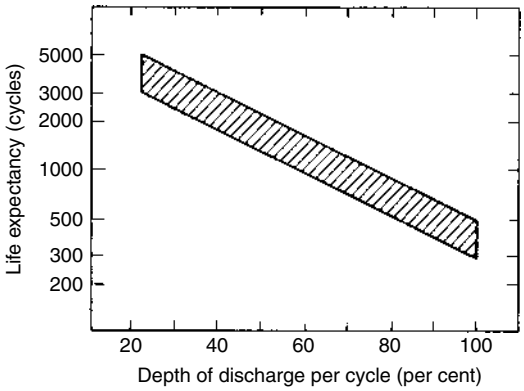

Figure 21.4 Nicad cell: effect of repeated discharge vs. cell life

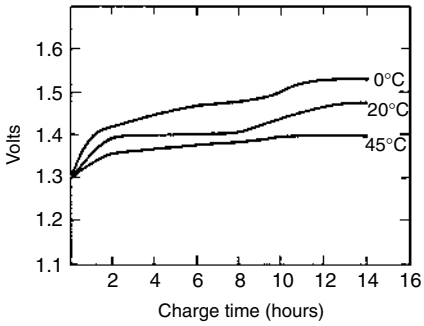

(a) Standard charge, C/10 × 15 hrs

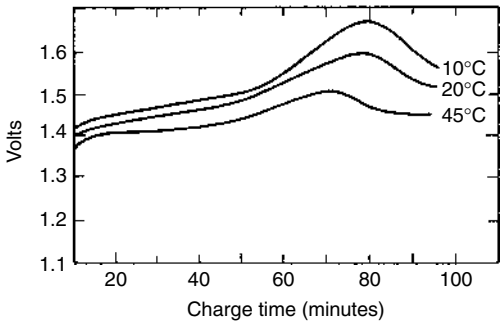

(b) Rapid charge, 1 C × 90 mins

Figure 21.5 Nicad cell: discharging characteristics

15 hours will be required to recharge a fully discharged battery, fast charging at 5 C and rapid charging at C rate.

Cells may be fitted with a re-sealing one-way vent which opens at about 200 psi and closes at about 175 psi to relieve any excess internal pressure caused by a fault or abuse.

22 Satellite communications

22.1 Earth orbits

Communications satellites are required to illuminate the earth with radio signals and their orbits are chosen according to the size and location of the part of the earth's surface they must light up.

A satellite orbiting the earth is continuously pulled by a centripetal force, in this case gravity, towards the centre of the earth. It is also pulled by centrifugal force to leave its orbit at a tangent. When these opposing forces are equal in magnitude the satellite is in a stable orbit. There is, then, for a given height (the radius of the path minus the radius of the earth, 6378 km), a velocity at which the conditions for stable orbit apply, and which determines the orbiting time.

22.1.1 Geostationary orbits

Satellites relay information from ground stations, either fixed or mobile, or between satellites. It is an advantage for some purposes, therefore, to use satellites with an orbit time identical to that of the earth so that no tracking from the ground stations is needed. Geostationary satellites have the same angular velocity as the earth making them appear to be stationary. Their height is 35 788 km and four such satellites cover the earth from latitude 81.3°N to 81.3°S as in *Figure 22.1*.

The disadvantages of geostationary satellites are that they are in a high earth orbit (HEO) resulting in a signal delay of 240 ms for the complete go and return path. Also they are in an equatorial orbit so that signals to the higher latitudes travel at a shallow angle to the earth's surface rendering them unsuitable for mobile use where communications must be achieved at street level in cities.

As each satellite covers a large portion of the earth, the design of their antennas to permit repeated frequency re-use is important and antennas with small, steerable footprints have been developed for this purpose. An advantage, in addition to the lack of tracking, is that the shadowing by the earth is minimal so that solar power cells receive almost continuous illumination.

22.1.2 Elliptical orbits

A polar orbit, where the satellite follows a North/South track, provides the opportunity to survey the earth in a series of strips. The satellites

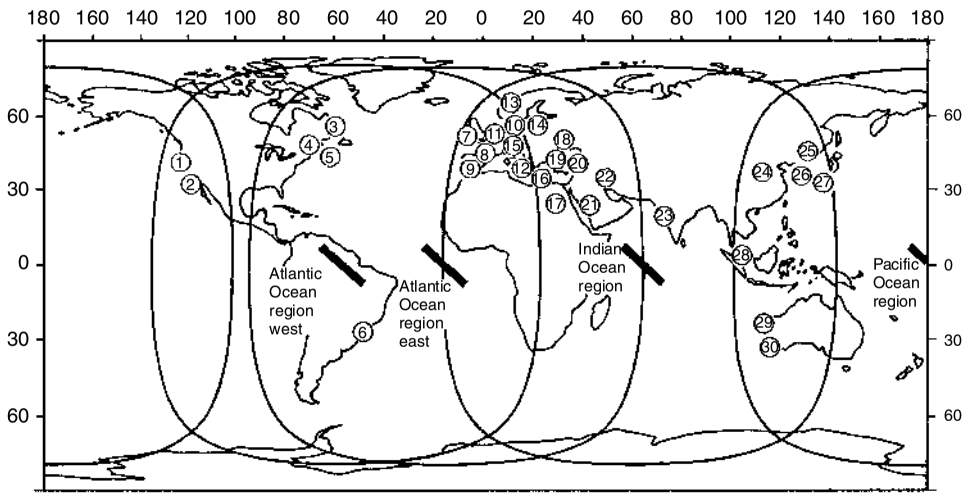

Land earth station services	Inmarsat-A	Inmarsat-C	Inmarsat-Aero
1. Niles Canyon	•		•
2. Santa Paula	•	•	•
3. Laurentides			•
4. Southbury	•	•	•
5. Staten Island	•		
6. Tangua	•		
7. Goonhilly	•	•	•
8. Pleumeur Bodou	•	•	
9. Ausseguel			•
10. Blavand		•	
11. Burum	•	•	
12. Fucino	•		
13. Elk	•	•	•
14. Psary	•		
15. Raisting	•	•	
16. Thermopylae	•		
17. Maadi	•		
18. Odessa	•		
19. Anatolia	•		
20. Ata	•		
21. Jeddah	•		
22. Boumehen	•		
23. Arvi	•		
24. Beijing	•		
25. Nakhodka	•		
26. Kumsan	•		
27. Yamaguchi	•		•
28. Singapore	•	•	•
29. Perth	•	•	•
30. Ganagara	•		

Figure 22.1 Immarsat coverage and GES locations

used for this purpose are in low each orbit (LEO) and consequently have a high velocity. Their orbit time is approximately 1.5 hours and between successive orbits the earth has rotated 22.5°. Sixteen orbits are therefore needed to scan the earth's surface. Until recently polar orbits were used only for optical surveillance but now several projects for radio communication are either in the early stages of installation or under development. These use a number of satellites so that for mobile communications, for instance, there is a satellite continuously in view. Tracking of these extremely fast satellites by the ground stations, which may themselves be moving, along with Doppler effect has been a major obstacle which is now being overcome.

22.2 Communications by satellite link

Satellites are radio links and receive signals from the ground and other satellites which they must re-transmit. The signals from ground stations are comparatively weak and require high power amplification for onward transmission. As the satellite's receive and transmit antennas must be close together, the possibility of RF instability prohibits on-frequency repetition. The up-link, from ground station to satellite, must therefore be converted to another before re-transmission. The up-link frequency is normally higher than the down-link and the frequency converter is referred to as a 'down-converter'.

The frequency bands used for communications purposes are listed in *Table 22.1*.

Satellite television

The broadcasting of television may be via either communications satellites or Direct Broadcasting by Satellite (DBS) satellites. The positions of non-DBS satellites relative to the UK are shown in *Figure 22.2* and *Table 22.2* lists the European channels. *Figure 22.3* shows the world allocations of DBS satellites and *Tables 22.3* and *22.4* list the channel frequencies and national allocations. The frequency plan for the Astra satellite is in *Table 22.5*.

22.3 Proposed satellite television formats

Most current European satellite television programmes (non-DBS) are broadcast as fairly standard PAL signals, FM modulated into the satellite channel. DBS transmissions, and those from Astra satellite, will probably be of a multiplexed analogue component (MAC) format. In MAC, data corresponding to sound tracks and subtitles, etc., an

Table 22.1 Communications satellite frequencies

Frequency band (GHz)	*Link*	*European telecom links*	*International telecom links*
1.5–1.6	Down	Mobile	
1.6–1.7	Up	Mobile	
3.4–4.2	Down	Fixed	Fixed
4.5–4.8	Down	Fixed	Fixed
5.9–7.0	Up	Fixed	Fixed
10.7–11.7	Down	Fixed (+ Non-DBS television)	
11.7–12.5	Down	Fixed (+ television)	
12.5–12.75	Down	Fixed (private links)	
12.75–13.75	Up	Fixed (private links)	
14.0–14.8	Up	Fixed	
17.3–18.3	Up	Fixed	
17.7–20.2	Down	Fixed	
20.2–21.2	Down	Mobile	
27.0–30.0	Up	Fixed	
30.0–31.0	Up	Mobile	
22.5–23.55		Allocated for intersatellite links	
32.0–33.0		Allocated for intersatellite links	
54.25–58.2		Allocated for intersatellite links	
59.0–64.0		Allocated for intersatellite links	

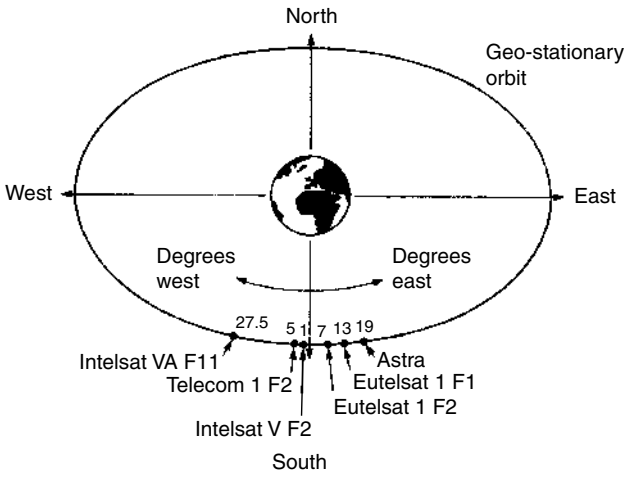

Figure 22.2 Non-DBS satellite television: positions of the main non-DBS satellites relevant to the UK

Table 22.2 European satellite television channels broadcast via communications satellites

Channel	Frequency (GHz)	Polarization	Audio sub-carrier	Video standard	Satellite
3Sat	11.175	H	6.65	PAL	Eutelsat 1 F1
Anglovision	11.515	V	6.6	PAL	Intelsat VA-F11
Arts Channel	11.135	H	6.6	PAL	Intelsat VA-F11
BBC1/2	11.175	H	6.65	PAL	Intelsat VA-F11
CanalJ	12.564	V	5.8	PAL	Telecom 1 F2
Children's Channel	11.015	H	6.6	PAL	Intelsat VA-F11
CNN	11.155	V	6.65	PAL	Intelsat VA-F11
Filmnet	11.140	V	6.6	PAL	Eutelsat 1 F1
Moscow 1	3.675	–	7.0	SECAM	Gorizont-12
Moscow 2	3.0	–	7.0	SECAM	Gorizont-7
Infofilm & Video	11.015	H	6.6	PAL	Intelsat F2
La Cinq	12.606	V	5.8	SECAM	Telecom 1 F2
Lifestyle	11.135	H	6.6	PAL	Intelsat VA-F11
M6	12.648	V	5.8	SECAM	Telecom 1 F2
MTV	10.975	H	6.65	PAL	Intelsat VA-F11
Norsk Rikskringkasti	11.644	H	Digital	C-MAC	Eutelsat 1 F2
Premiere	11.015	H	6.6	PAL	Intelsat VA-F11
RAI-Uno	11.007	H	6.6	PAL	Eutelsat 1 F1
RTL-Plus	11.091	V	6.65	PAL	Eutelsat 1 F1
SAT1	11.507	V	6.65	PAL	Eutelsat 1 F1
Satellite Information	11.575	H	Digital	B-MAC	Intelsat VA-F11
Screensport	11.135	H	6.6	PAL	Intelsat VA-F11
Skychannel	11.650	H	6.65	PAL	Eutelsat 1 F1
Superchannel	10.674	V	6.65	PAL	Eutelsat 1 F1
SVT-2	11.178	H	Digital	C-MAC	Intelsat F2
SVT-2	11.133	H	Digital	C-MAC	Intelsat F2
Teleclub	11.987	V	6.5	PAL	Eutelsat 1 F1
TV5	11.472	H	6.65	PAL	Eutelsat 1 F1
Worldnet	11.512	H	6.65	PAL	Eutelsat 1 F1
Worldnet	11.591	H	6.6	SECAM	Eutelsat 1 F1
Worldnet	12.732	V	5.8	NTSC	Telecom 1 F2

analogue signal corresponding to chrominance and an analogue signal corresponding to luminance are transmitted separately in each broadcast line of the picture.

In order to achieve multiplexing of the three parts of the format, time compression of chrominance and luminance signals occurs before

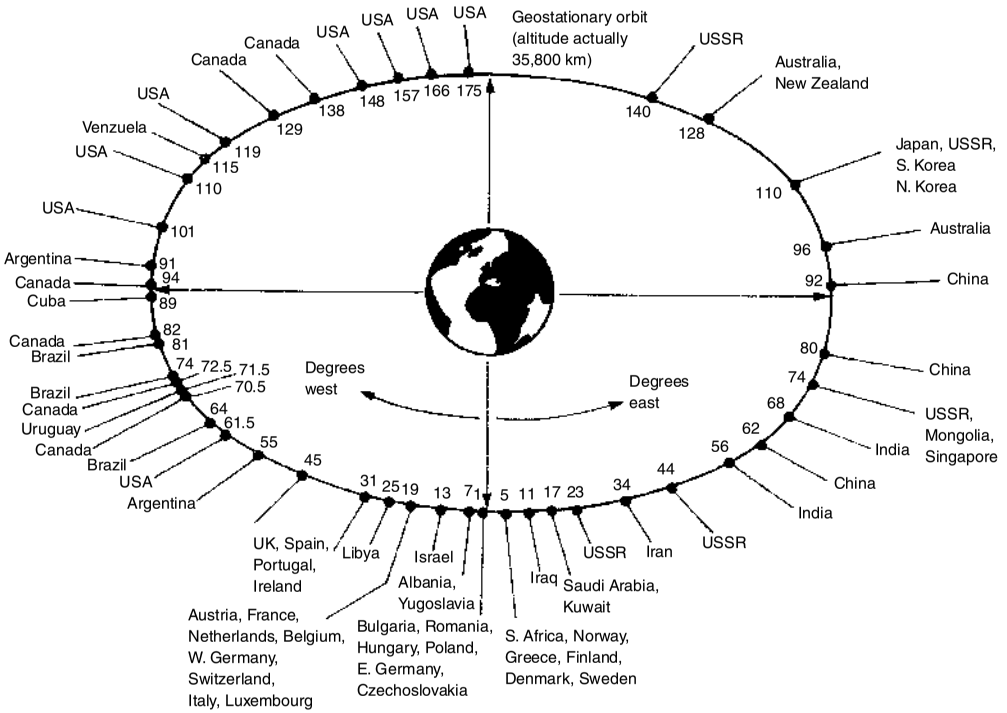

Figure 22.3 World allocations of DBS satellite positions

Table 22.3 DBS television channels

Channel number	Frequency (GHz)		
1	11.72748	21	12.11108
2	11.74666	22	12.13026
3	11.76584	23	12.14944
4	11.78502	24	12.16862
5	11.80420	25	12.18780
6	11.82338	26	12.20698
7	11.84256	27	12.22616
8	11.86174	28	12.24534
9	11.88092	29	12.26452
10	11.90010	30	12.28370
11	11.91928	31	12.30288
12	11.93846	32	12.32206
13	11.95764	33	12.34124
14	11.97682	34	12.36042
15	11.99600	35	12.37960
16	12.01518	36	12.39878
17	12.03436	37	12.41796
18	12.05354	38	12.43714
19	12.07272	39	12.45632
20	12.09190	40	12.47550

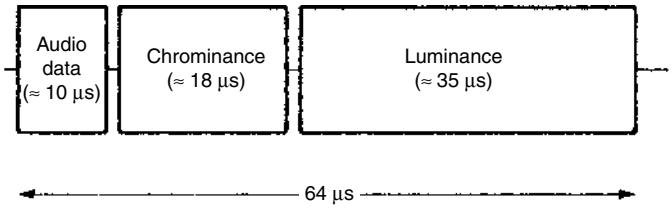

transmission, and they must be reconstituted at the receiver. Two main variations of the MAC format have been selected for European broadcasters, D-MAC and D2-MAC. They differ basically in the number of data channels, and hence the overall bandwidth required. Both modulate video signals in FM, and data signals in duobinary FM.

22.4 Global positioning system (GPS)

This system uses an American government satellite network comprised of 24 satellites in three circular orbits at a height of 20 000 km and with twelve-hour periods. At least six satellites should be visible from any point around the earth at any one time.

Table 22.4 Direct broadcast by satellite (DBS) television. European allocation of satellite positions, channel and polarizations

		Orbital position		
Band	*5° E*	*19° W*	*31° W*	*37° W*
11.7–12.1 GHz RH polarized	*Turkey:* CH. 1, 5, 9, 13, 17 *Greece:* CH. 3, 7, 11, 15, 19	*France:* CH. 1, 5, 9, 13, 17 *Luxembourg:* CH. 3, 7, 11, 15, 19	*Eire:* CH. 2, 6, 10, 14, 18 *UK:* CH. 4, 8, 12, 16, 20	*San Marino:* CH. 1, 5, 9, 13, 17 *Lichtenstein:* CH. 3, 7, 11, 15, 19
11.7–12.1 GHz LH polarized	*Finland:* CH. 2, 6, 10 *Norway:* CH. 14, 18 *Sweden* CH. 4, 8 *Denmark:* CH. 12, 16, 20	*Germany:* CH. 2, 6, 10, 14, 18 *Austria:* CH. 4, 8, 12, 16, 20	*Portugal:* CH. 3, 7, 11, 15, 19	*Andorra:* CH. 3, 8, 12, 16, 20
12.1–12.5 GHz RH polarized	*Cyprus:* CH. 21, 25, 29, 33, 37 *Iceland, etc.:* CH. 23, 27, 31, 35, 39	*Belgium:* CH. 21, 25, 29, 33, 37 *Netherlands:* CH. 23, 27, 31, 35, 39		*Monaco:* CH. 21, 25, 29, 33, 37 *Vatican* CH. 23, 27, 31, 35, 39
12.1–12.5 GHz LH polarized	*Nordic group** CH. 22, 24, 26, 28 30, 32, 36, 40 *Sweden:* CH. 34 *Norway:* CH. 38	*Switzerland:* CH. 22, 26, 30, 34, 38 *Italy:* CH. 24, 28, 32, 36, 40	*Iceland:* CH. 21, 25, 29, 33, 37 *Spain:* CH. 23, 27, 31, 35, 39	

*Wide beam channels: Denmark, Finland, Norway, Sweden.

Each satellite transmits continuously updated information about its orbit on two frequencies, 1227 MHz and 1575 MHz. One radio channel carries two pseudo-random codes, one very long and the other very short. The second channel is modulated only with the short code. The codes enable the satellite to be positively identified, and the distance from a receiver on, or close to, the earth to be calculated.

A receiver's position, in three-dimensional space, is identified by measuring and calculating the distance from three satellites. The short codes provide the initial fix but increased precision is obtained from the long codes. There is an error due to time variations arising from various sources of which satellite speed is one, but taking a measurement from a fourth satellite enables a correction factor to be applied.

Receivers which utilize only the short PN codes provide a resolution accurate to about 100 m. Those which can process the long codes provide a fix accurate to about 45 m.

References

Lewis, G.E. (1988). *Communication Services via Satellite*. BSP Professional Books, Oxford.

Long, M. *The 1993/1994 World Satellite Annual*. Mark Long Enterprises Inc., Ft Lauderdale, USA.

23 Connectors and interfaces

23.1 Audio and video connectors

Audio connectors

The DIN standards devised by the German Industrial Standards Board are widely used for the connection of audio equipment. The connectors are shown below. The 3-way and 5-way 45 are the most common and connections for those are listed.

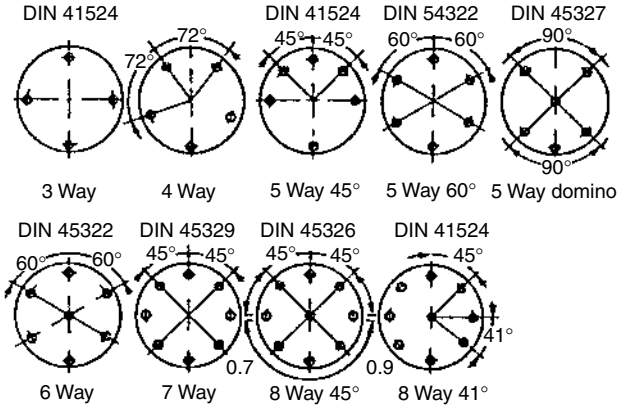

	Mono	*Stereo*
Microphone	Input 1 O V 2 Pin 3 available for polarizing voltage	Input LH 1 Input RH 4 O V 2 Pins 3 and 5 available for polarizing voltage
Tape recorder inputs and monitor outputs	Input 1 O V 2 Output 3	Input LH 1 Input R4 4 O V 2 Output LH 3 Output RH 5

	Mono	*Stereo*
Tape recorder replay output	Output, low Z1 O V 2 Output, high Z3	Output LH, low Z1 Output RH, low Z4 O V 2 Output LH, high Z3 Output RH, high Z5
Amplifiers	Output to tape 1 O V 2 Input from tape 3	Output LH 1 Output RH 1 O V 2 Input LH 3 Input RH 5

Variations on the above exist between different manufacturers.

Videorecorder/televisions/camera connectors

Standard pin configurations for videorecorders, televisions and videocameras are shown below. Many follow standard DIN connector pinouts, but videocamera and SCART connectors differ significantly.

(a) 5-pin DIN

1,4 Audio in
2 Chassis
3,5 Audio out or stereo
1 L audio in
2 Chassis
3 L audio out
4 R audio in
5 R audio out

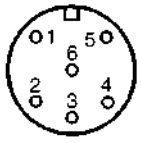

(b) 6-pin DIN

1 AV select, For VCR high = all outputs, low = all inputs, Opposite for TV set
2 Video in/out
3 Chassis
4 L audio in/out
5 12 V
6 R audio in/out

(c) 7-pin DIN

1 L audio in
2 Chassis
3 L audio out
4 R audio in
5 R audio out
6 Remote control data
7 Chassis

SCART (BS 6552)

SCART connectors, also known as Peritelevision or Euroconnector connectors, feature two control systems which allow remote control over the television's or videorecorder's functions.

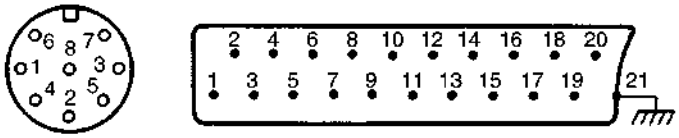

(d) 8-pin DIN (e) SCART

1 L audio in
2 Remote control data
3 R audio in
4 Chassis (audio)
5 Chassis (remote control)
6 Chassis (video)
7 Chassis (audio)
8 Video in

1 R audio out
2 R audio in
3 L audio out
4 Chassis (audio)
5 Chassis (B video)
6 L video in
7 B video in
8 Source switching

9 Chassis (G video)
10 Data bus
11 G video in
12 Data bus
13 Chassis (data bus)
14 Chassis (data bus)
15 R video in

16 Fast video blanking
17 Chassis (composite video)
18 Chassis (fast video blanking)
19 Composite video out
20 Composite video in

The simplest is a source switching input (pin 8) in which an external source (videorecorder, computer, etc.) can, by issuing a 12 volt signal, cause the television to switch to baseband inputs.

A more complex control system, called *domestic data bus* (D^2B), is given through pins 10 and 12, in which serial data can be passed between controlling microprocessors in the television and external equipment. No standard yet exists for D^2B.

23.2 Co-axial connector

The most commonly used connectors for RF cables are:

Type	*Impedance, Z_0 (ohms)*	*Max. VSWR to (frequency GHz)*	*Maximum proof RF voltage*	*Notes*
N	50 or 75	1.30 (4)	1.5 kV (5 MHz at sea level)	Screw together

Type	*Impedance, Z_0 (ohms)*	*Max. VSWR to (frequency GHz)*	*Maximum proof RF voltage*	*Notes*
BNC	50 or 75	1.01 (1) 1.30 (4)	1 kV (5 MHz at sea level)	Miniature. Bayonet fitting
TNC	50 or 75	As BNC	As BNC	Miniature. Robust screw together
SMB	50	1.46 (4)	1.5 kV (At sea level. Cable dependent)	Sub-miniature. Snap together
SMC	50	1.41 (4) 1.69 (10)	As SMB	Sub-miniature. Screw together
SMD	50	As SMB	As SMB	Sub-miniature. Push together
BT 43	75			Developed from SMB range for use in telecomms and data transmission
7–16	50	1.3 (5 GHz)	2.7 (connector)	Suitable for medium to high power applications in the cellular and broadcast industries. Screw together
PL259/ SO239/ UHF 83	50	–	500 (pk)	Non-constant imp. High VSWR makes it unsuitable for use above 144 MHz and for extending RF cables. Very robust. Screw together
C	75	–	–	Bayonet fitting

Type	*Impedance, Z_0 (ohms)*	*Max. VSWR to (frequency GHz)*	*Maximum proof RF voltage*	*Notes*
F	50	–	–	American CCTV connector used on some 144 MHz hand-portable transceivers. Plugs use inner conductor of cable as centre pin
Belling Lee	50	–	–	British TV antenna connector. Aluminium versions may corrode when used outdoors
GR	50	1 MHz max. frequency	–	Constant imp. sexless connector
Phono	–	–	–	American connector for audio use

Examples of assembly instructions for co-axial RF connectors (by kind permission of M/ACOM Greenpar Ltd.)

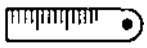

Measuring instrument – a rule is shown, but better results are obtained by using a Vernier gauge

Stout trimming blade, suitable for cutting copper wire braid

Crimping tool

Soldering iron

Side cutters, also for trimming braid

Spanner, of the relevant size for the connector

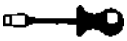

Small screwdriver

Hacksaw, sometimes appropriate for semi-rigid cable, although for repetitive operations a power trimmer should be considered

Assembly instructions Type N

Cable types:

50 ohm: PSF1/4M (BBC), RG 8A/U, RG 213/U, URM 67

75 ohm: RG 11A/U, RG 63B/U, RG 114A/U, URM 64

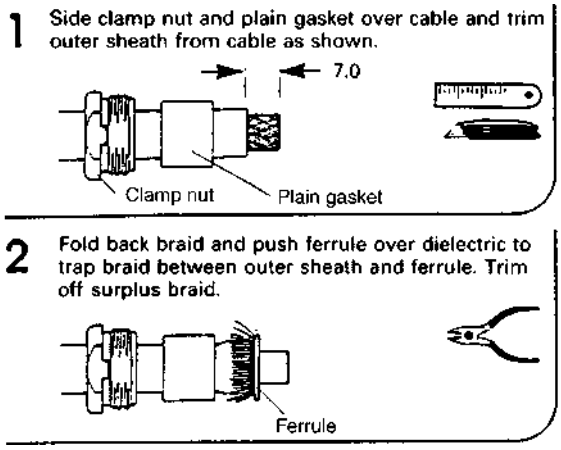

3 Trim back dielectric and check the length of the protruding centre conductor.

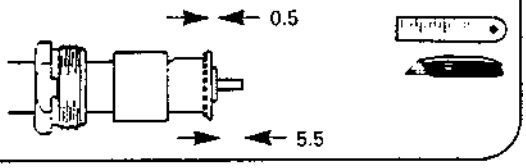

4 Tin centre conductor, then slide rear insulator over dielectric, to butt against ferrule.

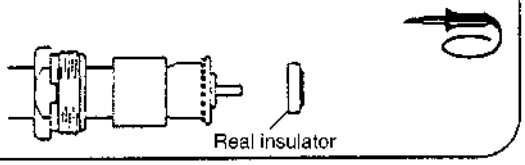

5 Fit contact (male for plugs, female for jacks) onto centre conductor. Hold cable and contact tightly together and solder.

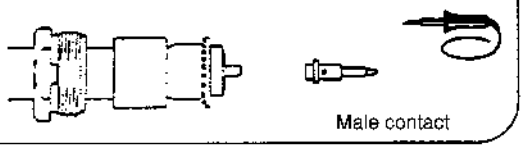

6 Slide plain gasket and clamp nut up to ferrule trapping braid. Fit front insulator over contact to butt against rear insulator and press sub-assembly into body as far as possible.

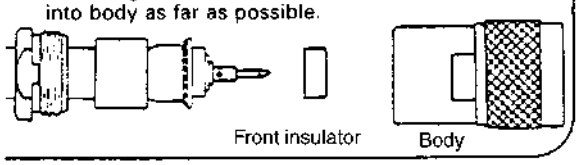

7 Engage and tighten clamp nut.

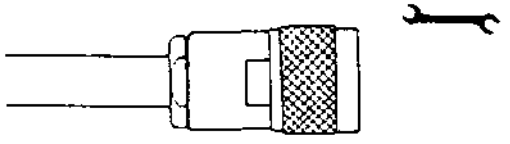

1 Slide crimp sleeve over cable

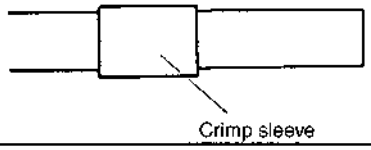

2 Trim back outer sheath and braid to dimensions shown. Any foils adjacent to the dielectric should be left in place but trimmed 1.5 mm from the face of the dielectric

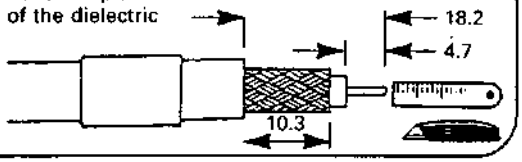

3 Fit contact (male for plugs, female for jacks) over centre conductor to butt against dielectric and crimp.

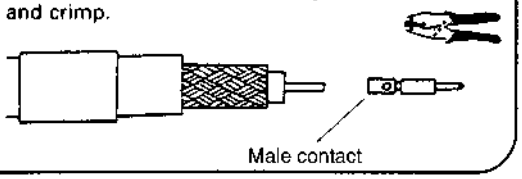

4 Push fit sub-assembly into body until contact clicks into insulator. In all cases, braids (and any intermediate foils) slide over ferrule while any foil adjacent to the dielectric should enter the ferrule bore.

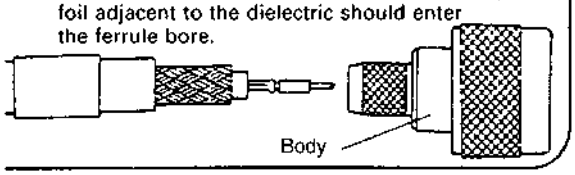

5 Slide crimp sleeve forward over braid and ferrule to butt against rear of the connector and crimp.

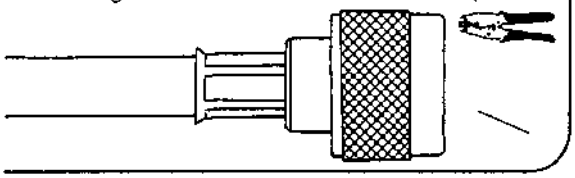

Assembly instructions Type BNC

Cable types:
RG 58C/U, RG 141A/U, URM 43, URM 76

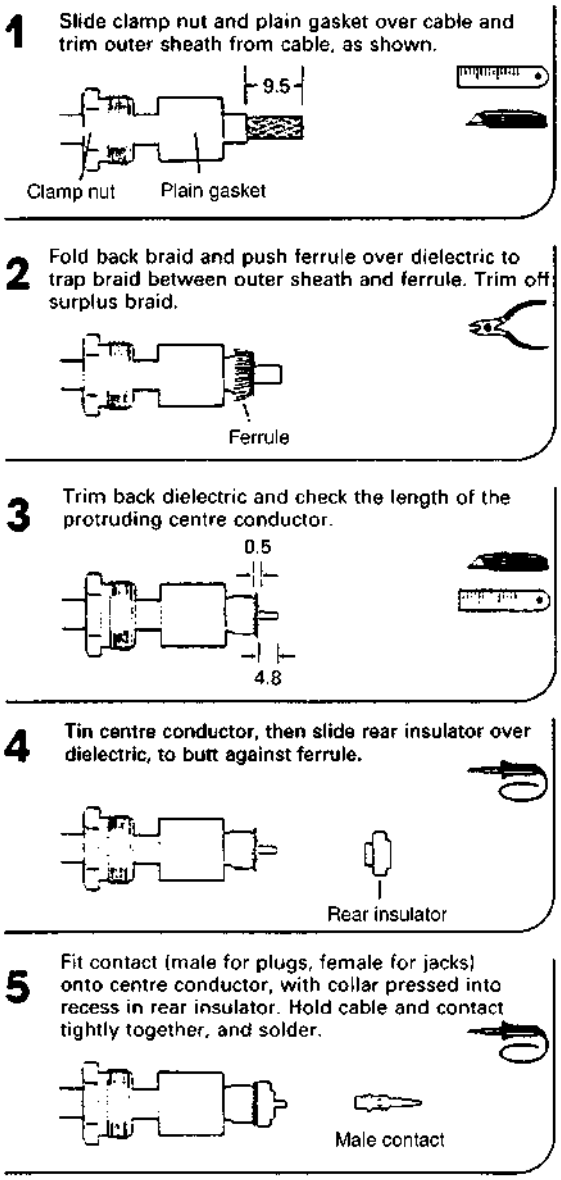

6 Slide plain gasket and clamp nut up to ferrule, trapping braid. Fit front insulator over contact to butt against rear insulator and press sub-assembly into body as far as possible.

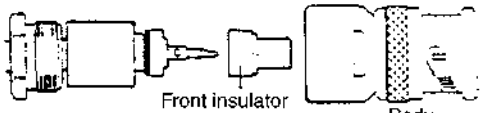

7 Engage and tighten clamp nut

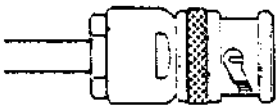

1 Slide metal crimp sleeve over cable, trim outer sheath from cable as shown.

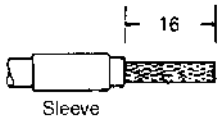

2 Trim back braid and dielectric to the dimensions shown.

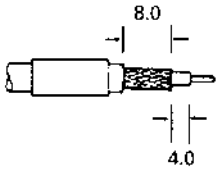

3 Fit contact over centre conductor to butt against the dielectric, then crimp.

4 Press sub-assembly into body, until contact clicks into place and ensuring that the knurled ferrule is inserted between the dielectric and braid.

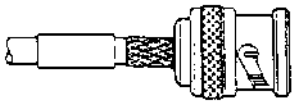

5 Slide the sleeve along the cable, until it butts against the body sub-assembly. Crimp, using the tool listed below.

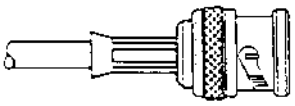

Note: A plug is shown, but these instructions are relevant to both plugs and jacks. The shape of contacts and insulators may also vary from the drawings shown.

Assembly instructions Types SMB/SMC/SMD

Cable types:

TM 3306, RG174A/U, RG188A/U, RG316/U
TM 3263, RG178B/U, RG196A/U, URM 110

1 Slide clamp nut, a washer, a gasket and the other washer over the cable trim outer sheath to dimension shown.

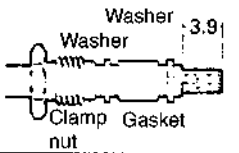

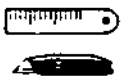

2 Fold back braid. Push ferrule over dielectric to trap braid between outer sheath and ferrule.

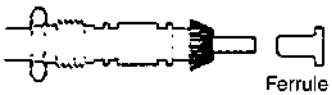

3 Trim off surplus braid. Trim dielectric flush with ferrule and check length of centre conductor. Tin centre conductor.

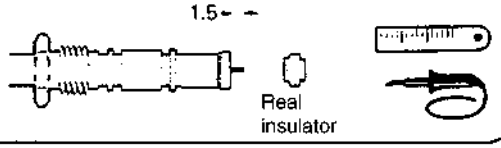

4 Side rear insulator over centre conductor until it butts against ferrule.

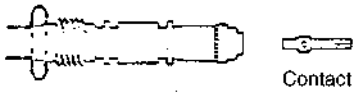

5 Fit contact onto centre conductor until it butts against rear insulator. Hold cable and contact tightly together and solder.

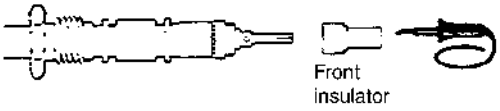

6 Fit front insulator over contact until it butts against internal shoulder.

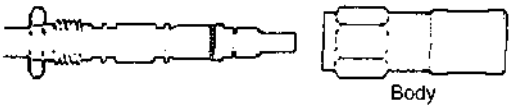

7 Press sub-assembly into body as far as possible. Engage and tighten clamp nut.

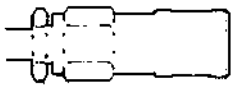

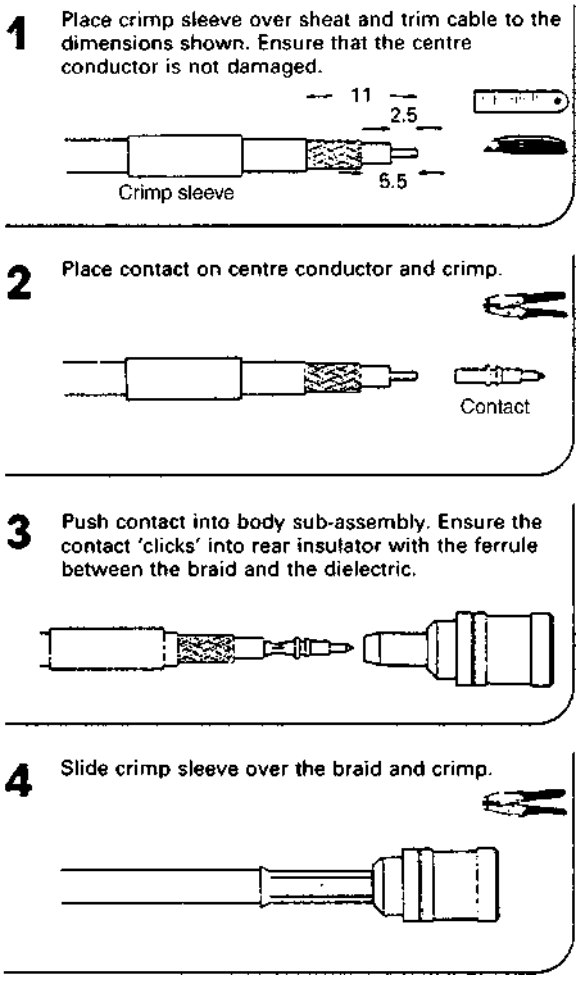

23.3 Interfaces

23.3.1 Connectors and connections

Data interchange by modems

When transmitting and receiving data across telephone or other circuits, the equipment which actually generates and uses the data (e.g. a computer or VDU terminal) is known as *data terminating equipment* (DTE). The equipment which terminates the telephone line and

converts the basic data signals into signals which can be transmitted is known as *data circuit-terminating equipment* (DCE). As far as the user is concerned the interface between DTE and DCE is the most important. ITU-T recommendation V24 defines the signal interchanges and functions between DTE and DCE; these are commonly known as the 100 series interchanges circuits:

Interchange circuit		*Data*		*Control*		*Timing*	
Number	*Name*	*From DCE*	*To DCE*	*From DCE*	*To DCE*	*From DCE*	*To DCE*
101	Protective ground or earth						
102	Signal ground or common return						
103	Transmitted data		•				
104	Received data	•					
105	Request to send				•		
106	Ready for sending			•			
107	Data set ready			•			
108/1	Connect data set to line				•		
108/2	Data terminal ready				•		
109	Data channel received line signal detector			•			
110	Signal quality detector			•			
111	Data signalling rate selector (DTE)				•		
112	Data signalling rate selector (DCE)			•			
113	Transmitter signal element timing (DTE)						•

Interchange circuit		*Data*		*Control*		*Timing*	
Number	*Name*	*From DCE*	*To DCE*	*From DCE*	*To DCE*	*From DCE*	*To DCE*
114	Transmitter signal element timing (DCE)					•	
115	Receiver signal element timing (DCE)					•	
116	Select stand by				•		
117	Standby indicator			•			
118	Transmitted backward channel data		•				
119	Received backward channel data	•					
120	Transmit backward channel line signal				•		
121	Backward channel ready			•			
122	Backward channel received line signal detector			•			
123	Backward channel single quality detector			•			
124	Select frequency groups				•		
125	Calling indicator			•			
126	Select transmit frequency				•		
127	Select receive frequency				•		

Interchange circuit		*Data*		*Control*		*Timing*	
Number	*Name*	*From DCE*	*To DCE*	*From DCE*	*To DCE*	*From DCE*	*To DCE*
128	Receiver signal element timing (DTE)						•
129	Request to receive				•		
130	Transmit backward tone				•		
131	Received character timing					•	
132	Return to non-data mode				•		
133	Ready for receiving				•		
134	Received data present			•			
191	Transmitted voice answer				•		
192	Received voice answer			•			

Modem connector pin numbers

The connectors used with 100 series interchange circuits and its pin assignments are defined by international standard ISO 2110 and are (for modems following the ITU-T recommendations V21, V23, V26, V26bis, V27 and V27bis) as follows:

Pin number	Interchange circuit numbers			Pin Name
	V21	V23	V26/ V27	
1	*1	*1	*1	Ground
2	103	103	103	TXD
3	104	104	104	RXD
4	105	105	105	RTS
5	106	106	106	RFS
6	107	107	107	DSR
7	102	102	102	Signal return
8	109	109	109	Signal DET
9	*N	*N	*N	
10	*N	*N	*N	
11	126	*N	*N	STF
12	*F	122	122	
13	*F	121	121	
14	*F	118	118	
15	*F	*2	114	
16	*F	119	119	
17	*F	*2	115	
18	141	141	141	
19	*F	120	120	
20	108/1-2	108/1-2	108/1-2	DTR
21	140	140	140	
22	125	125	125	Call ind.
23	*N	111	111	
24	*N	*N	113	
25	142	142	142	

Notes:

*1 Pin 1 is assigned for connecting the shields between tandem sections of shielded cables. It may be connected to protective ground or signal ground.

*F Reserved for future use.

*N Reserved for national use.

9-Pin connector		
Pin number	*Pin name*	*Description*
1	DCD	Data carrier detect
2	RXD	Receive data
3	TXD	Transmit data
4	DTR	Data terminal ready
5	GND	Ground
6	DSR	Data set ready
7	RTS	Ready to send
8	CTS	Clear to send
9	RI	Ring indicator

Automatic calling

A similar series of interchange circuits is defined in ITU-T recommendation V25 for automatic calling answering between modems over the telephone network. This is the 200 series interchange circuits:

Interchange circuit

Number	*Name*	*From DCE*	*To DCE*
201	Signal ground	•	•
202	Call request		•
203	Data line occupied	•	
204	Distant station connected	•	
205	Abandon call	•	
206	Digit signal (2^0)		•
207	Digit signal (2^1)		•
208	Digit signal (2^2)		•
209	Digit signal (2^3)		•
210	Present next digit	•	
211	Digit present		•
213	Power indication	•	

RS 232C

The EIA equivalent of CCITT V24 interface is the RS 232C specification, which similarly defines the electrical interface between DTE and DCE. Although the two have different designations, they are to all practical purposes equivalent. The RS 232C interchange circuits are:

Interchange circuit		*Data*		*Control*		*Timing*	
Mnemonic	*Name*	*From DCE*	*To DCE*	*From DCE*	*To DCE*	*From DCE*	*To DCE*
AA	Protective ground						
AB	Signal ground/common return						
BA	Transmitted data		•				
BB	Received data	•					
CA	Request to send				•		
CB	Clear to send			•			
CC	Data set ready			•			
CD	Data terminal ready				•		
CE	Ring indicator			•			
CF	Received line signal detector			•			
CG	Signal quality detector			•			
CH	Data signal rate selector (DTE)				•		
CI	Data signal rate selector (DCE)			•			
DA	Transmitter signal element timing (DTE)						•
DB	Transmitter signal element timing (DCE)					•	
DD	Receiver signal element timing (DCE)					•	

Interchange circuit		*Data*		*Control*		*Timing*	
Mnemonic	*Name*	*From DCE*	*To DCE*	*From DCE*	*To DCE*	*From DCE*	*To DCE*
SBA	Secondary transmitted data		•				
SBB	Secondary received data	•					
SCA	Secondary request to send				•		
SCB	Secondary clear to send			•			
SCF	Secondary received line signal detector			•			

RS 449

The EIA RS 232C standard, although the most common, is by no means perfect. One of its main limitations is the maximum data rate −18.2 K baud. Various improved interchange circuits (RS 422, RS 423) have been developed. The RS 449 standard is capable of very fast data rates (up to 2 Mbaud):

Interchange circuit		*Data*		*Control*		*Timing*	
Mnemonic	*Name*	*From DCE*	*To DCE*	*From DCE*	*To DCE*	*From DCE*	*To DCE*
SG	Single ground						
SC	Send common						
RC	Receive common						
IS	Terminal in service				•		
IC	Incoming call			•			
TR	Terminal ready				•		

Interchange circuit			*Data*		*Control*		*Timing*	
	Mnemonic	*Name*	*From DCE*	*To DCE*	*From DCE*	*To DCE*	*From DCE*	*To DCE*
Primary channel	DM	Data mode			•			
	SD	Send data		•				
	RD	Receive data	•					
	TT	Terminal timing						•
	ST	Send timing					•	
	RT	Receive timing					•	
	RS	Request to send				•		
	CS	Clear to send			•			
	RR	Receiver ready			•			
	SQ	Signal quality			•			
	NS	News signal				•		
	SF	Select frequency				•		
	SR	Signalling rate selector				•		
	SI	Signalling rate indicator			•			
Secondary channel	SSD	Secondary send data		•				
	SRD	Secondary receive data	•					
	SRS	Secondary request to send				•		
	SCS	Secondary clear to send			•			
	SRR	Secondary receiver ready			•			
	LL	Local loopback				•		
	RL	Remote loopback				•		
	TM	Test mode			•			
	SS	Select standby				•		
	SB	Standby indicator			•			

Centronics interface

Most personal computers use the Centronics parallel data transfer to a printer. The pin connections of the connector, abbreviations and signal descriptions are shown.

All signals are standard TTL, although not all signals necessarily exist in any given interface.

Pin number	*Abbreviation*	*Signal description*
1	STROBE	Strobe
2	DATA1	Data line 1
3	DATA2	Data line 2
4	DATA3	Data line 3
5	DATA4	Data line 4
6	DATA5	Data line 5
7	DATA6	Data line 6
8	DATA7	Data line 7
9	DATA8	Data line 8
10	ACKNLG	Acknowledge data
11	BUSY	Busy
12	PE	Paper end
13	SLCT	Select printer
14	AUTO FEED XT	Automatic line feed at end of line
15	NC	No connection
16	OV	Logic ground
17	CHASSIS GND	Printer chassis (not necessarily the same as logic ground)
18	NC	No connection
19 to 30	GND	Single ground
31	INIT	Initialize
32	ERROR	Error
33	GND	Signal ground
34	NC	No connection
35	Logic 1	Logic 1
36	SLCT IN	Select input to printer

RS 232C/RS 449/V24 comparison

RS 232C		*RS 449*		*V24*	
AB	Signal ground	SG	Signal ground	102	Signal ground
		SC	Send common	102a	DTE common
		RC	Receive common	102b	DCE common
		IS	Terminal in service		
CE	Ring indicator	IC	Incoming call	125	Calling indicator
CD	Data terminal ready	TR	Terminal ready	108/2	Data terminal ready
CC	Data set ready	DM	Data mode	107	Data set ready
BA	Transmitted data	SD	Send data	103	Transmitted data
BB	Receive data	RD	Receive data	104	Received data
DA	Transmitter signal element Timing (DTE source)	TT	Terminal timing	113	Transmitter signal element Timing (DTE source)
DB	Transmitter signal element Timing (DCE source)	ST	Send timing	114	Transmitter signal element Timing (DCE source)
DD	Receiver signal element timing	RT	Receive timing	115	Receiver signal element timing (DCE source)
CA	Request to send	RS	Request to send	105	Request to send
CB	Clear to send	CS	Clear to send	106	Ready for sending
CF	Received line single detector	RR	Receiver ready	109	Data channel received line signal detector

CG	Signal quality detector	SQ	Signal quality	110	Data signal quality detector
		NS	New signal		
		SF	Select frequency	126	Select transmit frequency
CH	Data signal rate selector (DTE source)	SR	Signalling rate selector	111	Data signalling rate selector (DTE source)
CI	Data signal rate selector (DCE source)	SI	Signalling rate indicator	112	Data signalling rate selector (DCE source)
SBA	Secondary transmitted data	SSD	Secondary send data	118	Transmitted backward channel data
SBB	Secondary received data	SRD	Secondary receive data	119	Received backward channel data
SGA	Secondary request to send	SRS	Secondary request to send	120	Transmit backward channel line signal
SCB	Secondary clear to send	SCS	Secondary clear to send	121	Backward channel ready
SCF	Secondary received line signal detector	SRR	Secondary receiver ready	122	Backward channel received line signal detector
		LL	Local loopback	141	Local loopback
		RL	Remote loopback	140	Remote loopback
		TM	Test mode	143	Test indicator
		SS	Select standby	116	Select standby
		SB	Standby indicator	117	Standby indicator

Reference

M/ACOM Greenpar Ltd, catalogue 1993.

24 Broadcasting

24.1 Standard frequency and time transmissions

Frequency (mHz)	*Wavelength (m)*	*Code*	*Station location*	*Country*	*Power (kW)*
60 kHz	5000	MSF	Rugby	England	–
–	–	WWVB	Colorado	USA	–
75 kHz	4000	HBG	–	Switzerland	–
77.5 kHz	3871	DCF77	Mainflingen	DDR	–
1.5	200	HD210A	Guayaquil	Ecuador	–
2.5	120	MSF	Rugby	England	0.5
–	–	WWV	Fort Collins	USA	2.5
–	–	WWVH	Kekaha	Hawaii	5
–	–	ZLF	Wellington	New Zealand	–
–	–	RCH	Tashkent	USSR	1
–	–	JJY	–	Japan	–
–	–	ZUO	Olifantsfontein	South Africa	–
3.33	90.09	CHU	Ottawa	Canada	3
3.81	78.7	HD201A	Guayaquil	Ecuador	–
4.5	66.67	VNG	Victoria	Australia	–
4.996	60.05	RWM	Moscow	USSR	5
5	60	MSF	Rugby	England	0.5
–	–	WWVB	Fort Collins	USA	10
–	–	WWVH	Kekaha	Hawaii	10
–	–	ATA	New Delhi	India	–
–	–	LOL	Buenos Aires	Argentina	2
–	–	IBF	Turin	Italy	5
–	–	RCH	Tashkent	USSR	1
–	–	JJY	–	Japan	–
–	–	ZUO	Olifantsfontein	South Africa	–
5.004	59.95	RID	Irkutsk	USSR	1
6.10	49.2	YVTO	Caracas	Venezuela	–
7.335	40.9	CHU	Ottawa	Canada	10
7.5	40	VNG	Lyndhurst	Australia	5

Frequency (mHz)	*Wavelength (m)*	*Code*	*Station location*	*Country*	*Power (kW)*
7.6	39.4	HD210A	Guayaquil	Ecuador	–
8	37.5	JJY	–	Japan	–
8.1675	36.73	LQB9	Buenos Aires	Argentina	5
9996	30.01	RWM	Moscow	USSR	–
10	30	MSF	Rugby	England	0.5
–	–	WWVB	Fort Collins	USA	10
–	–	WWVH	Kekaha	Hawaii	10
–	–	BPM	Xian	China	–
–	–	ATA	New Delhi	India	–
–	–	JJY	–	Japan	–
–	–	LOL	Buenos Aires	Argentina	2
–	–	RTA	Novosibirsk	USSR	5
–	–	RCH	Tashkent	USSR	1
10.004	29.99	RID	Irkutsk	USSR	1
12	25	VNG	Lyndhurst	Australia	10
14.67	20.45	CHU	Ottawa	Canada	3
14.996	20.01	RWM	Moscow	USSR	8
15	20	WWVB	Fort Collins	USA	10
–	–	WWVH	Kekaha	Hawaii	10
–	–	LOL	Buenos Aires	Argentina	2
–	–	RTA	Novosibirsk	USSR	5
–	–	BPM	Xian	China	–
–	–	ATA	New Delhi	India	–
–	–	JJY	–	Japan	–
15.004	19.99	RID	Irkutsk	USSR	1
16.384	18.31	–	Allouis	France	2000
15.55	17.09	LQC20	Buenos Aires	Argentina	5
20	15	WWVB	Fort Collins	USA	2.5
100	3	ZUO	Olifantsfontein	South Africa	–

24.2 Standard frequency formats

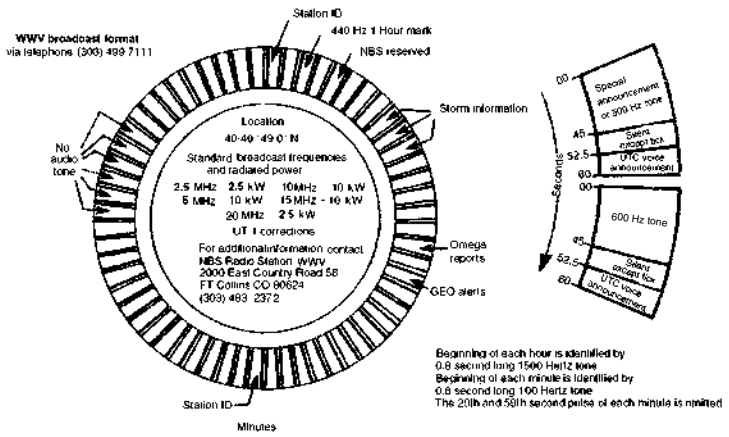

MSF Rugby

Time is inserted in the 60 kHz transmission in two ways, illustrated below.

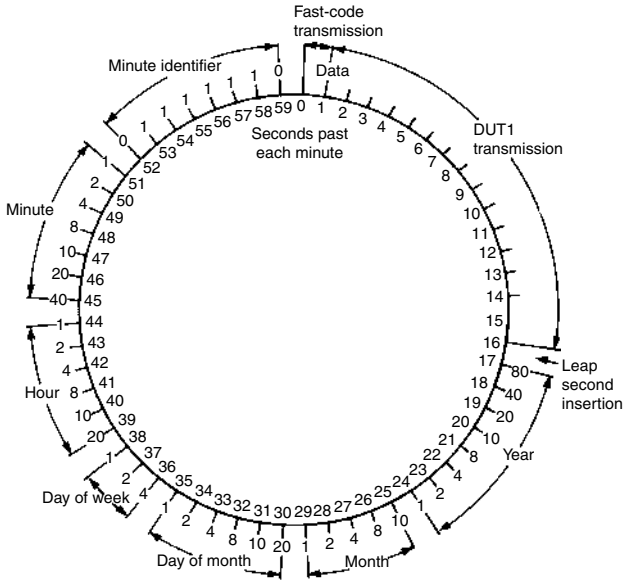

Slow code time and date information is transmitted between the 17th and 59th seconds of the minute-long cycle, in normal BCD coding. *Fast code* time and date BCD coded information is inserted into a 500 ms window in the first second of each minute-long cycle, as illustrated below.

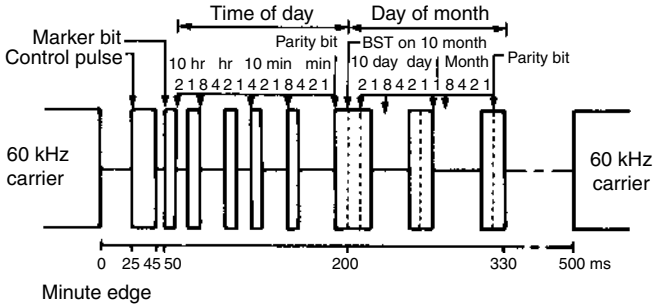

24.3 UK broadcasting bands

Frequency band	*Frequency*	*Use*
Long wave	150–285 kHz (2000–1053 m)	AM radio
Medium wave	525–1605 kHz (571–187 m)	AM radio
Band II (VHF)	88–108 MHz	FM radio
Band IV (UHF)	470–582 MHz (channels 21 to 34)	TV
Band V (UHF)	614–854 MHz (channels 39 to 68)	TV
Band VI (SHF)	11.7–12.5 GHz (channels 1 to 40)	Satellite TV

24.4 BBC VHF test tone transmissions

Transmission starts about 4 minutes after the end of Radio 3 programmes on Mondays and Saturdays.

Time min.	*Left channel*	*Right channel*	*Purpose*
–	250 Hz at zero level	440 Hz at zero level	Identification of left and right channels and setting of reference level
2	900 Hz at +7 dB	900 Hz at +7 dB, antiphase to left channel	Adjustment of phase of regenerated subcarrier (see Note 4) and check of distortion with L−R signal only
6	900 Hz at +7 dB	900 Hz +7 dB, in phase with left channel	Check of distortion with L + R signal only
7	900 Hz at +7 dB	No modulation	Check of L to R cross-talk
8	No modulation	900 Hz at +7 dB	Check of R to L cross-talk
9	Tone sequence at −4 dB: 40 Hz 6·3 kHz 100 Hz 10 kHz 500 Hz 12.5 kHz 1000 Hz 14 kHz This sequence is repeated	No modulation	Check of L-channel frequency response and L to R cross-talk at high and low frequencies
11′40″	No modulation	Tone sequence as for left channel	Check of R-channel frequency response and R to L cross-talk at high and low frequencies

Time min.	*Left channel*	*Right channel*	*Purpose*
14′20″	No modulation	No modulation	Check of noise level in the presence of pilot
15′20″	End of test transmissions		

Notes:

1. This schedule is subject to variation or cancellation to accord with programme requirements and essential transmission tests.
2. The zero level reference corresponds to 40% of the maximum level of modulation applied to either stereophonic channel before pre-emphasis. All tests are transmitted with pre-emphasis.
3. Periods of tone lasting several minutes are interrupted momentarily at one-minute intervals.
4. With receivers having separate controls of subcarrier phase and crosstalk, the correct order of alignment is to adjust first the subcarrier phase to produce maximum output from either the L or the R channel and then to adjust the crosstalk (or 'separation') control for minimum crosstalk between channels.
5. With receivers in which the only control of crosstalk is by adjustment of subcarrier phase, this adjustment of subcarrier phase, this adjustment should be made on the crosstalk checks.
6. Adjustment of the balance control to produce equal loudness from the L and R loudspeakers is best carried out when listening to the announcements during a stereophonic transmission, which are made from a centre-stage position. If this adjustment is attempted during the tone transmissions, the results may be confused because of the occurrence of standing-wave patterns in the listening room.
7. The outputs of most receivers include significant levels of the 19-kHz tone and its harmonics, which may affect signal-level meters. It is important, therefore, to provide filters with adequate loss at these frequencies if instruments are to be used for the above tests.

24.5 Engineering information about broadcast services

Information about all BBC services as well as advice on how best to receive transmissions (including television) can be obtained from:

British Broadcasting Corporation
Engineering Liaison
White City
201 Wood Lane
London W12 7TS

Telephone: 020 8752 5040

Transmitter service maps for most main transmitters can also be supplied, but requests for maps should be accompanied by a stamped addressed A4 sized envelope.

Similarly, information about all IBA broadcast services can be obtained from:

Radio:
Radiocommunications Agency
Wyndham House
189 Marsh Wall
London E14 9SX

Telephone: 020 7211 0211

Television:
The Independent Television Commission
Kings Worthy Court
Kings Worthy
Winchester
Hants SO23 7QA

Telephone: 01962 848647

24.6 Characteristics of UHF terrestrial television systems

24.6.1 World systems

System	*Number of lines*	*Channel width (MHz)*	*Vision bandwidth (MHz)*	*Vision/sound separation (MHz)*	*Vestigial side-band (MHz)*	*Vision modulation*	*Sound modulation*	*Field frequency*
A	625	8	5.5	+6	1.25	Neg.	FM	50
B	625	8	5.0	+5.5	1.25	Neg.	FM	50
C	625	8	5.0	+5.5	0.75	Neg.	FM	50
D	625	8	6.0	+6.5	1.25	Pos.	AM	50
E	625	8	6.0	+6.5	0.75	Neg.	FM	50
F	525	6	4.2	+4.5	1.25	Neg.	FM	60

A – UK and Eire
B – Eastern Europe
C – Most of Western Europe, Australia, New Zealand
D – France
E – Russia and Eastern Europe
F – USA, most of Central and South America, Japan

24.6.2 European systems

Country	*System*	*Colour*
Austria	C	PAL
Belgium	B	PAL
Bulgaria	No UHF system	
Cyprus	C	PAL
Czechoslovakia	E	SECAM
Denmark	No UHF system	PAL
Finland	C	PAL
France	D	SECAM
Germany	C	PAL

Country	*System*	*Colour*
German DR	C	SECAM
Greece	B	PAL
Holland	C	PAL
Hungary	E	SECAM
Iceland	No UHF system	
Ireland	A	PAL
Italy	C	PAL
Luxembourg	D	SECAM
Malta	B	PAL
Monaco	D	SECAM
Norway	C	PAL
Poland	E	SECAM
Portugal	C	PAL
Romania	E	PAL
Spain	C	PAL
Sweden	C	PAL
Switzerland	C	PAL
Turkey	No UHF system	
UK	A	PAL
USSR	E	SECAM
Yugoslavia	B	PAL

24.6.3 UK 625-line television system specification

Channel bandwidth	8 MHz
Upper sideband (vision signal)	5.5 MHz
Lower sideband (vision signal)	1.25 MHz
Vision modulation	AM negative
Sound modulation	FM
Sound deviation (max.)	±50 kHz
Sound pre-emphasis	50 μs
Sound carrier relative to vision carrier	+
Aspect ratio	4:3
Blanking and black level	76%
White level	20% peak
Sync. level	100% peak
Video bandwidth	5.5 MHz

Field frequency	50 Hz
Line frequency	15 625 Hz
Field sync. signal	5 equalizing then 5 broad pulses, followed by 5 equalizing pulses in 7.5 line periods
Field sync. and flyback intervals	2 × 25 line periods
Line period (approx.)	64 μs
Line syn. pulses (approx.)	4.7 μs
Line blanking (approx.)	12 μs
Field sync. pules (broad)	27.3 μs
Field sync. pulses (equalizing)	2.3 μs
Colour subcarrier frequency	4.43361875 MHz
Burst duration	2.25 μs
Burst amplitude	equal to sync
Burst phase	180° ± 45°

24.6.4 UK 625-line television system field blanking details

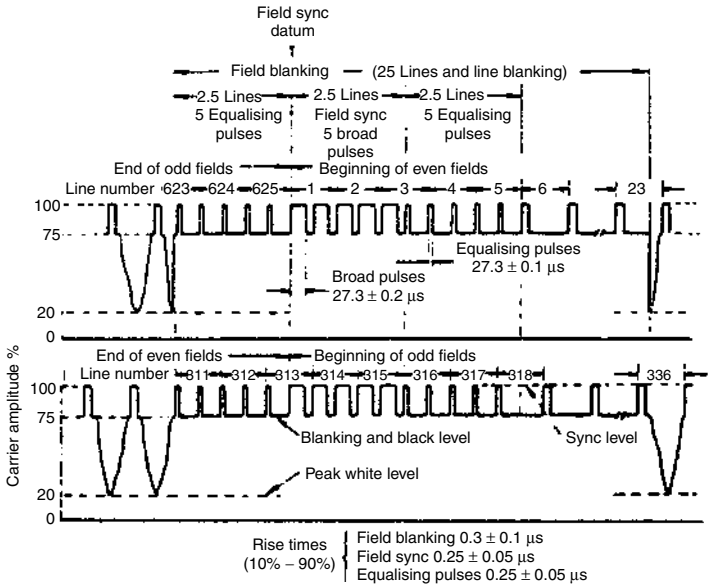

24.7 Terrestrial television channels

UK

	Frequency (MHz)			*Frequency (MHz)*	
Channel	*Vision*	*Sound*	*Channel*	*Vision*	*Sound*
39	615.25	621.25	54	735.25	741.25
40	623.25	629.25	55	743.25	749.25
41	631.25	637.25	56	751.25	757.25
42	639.25	645.25	57	759.25	765.25
43	647.25	653.25	58	767.25	773.25
44	655.25	661.25	59	775.25	781.25
45	663.25	669.25	60	783.25	789.25
46	671.25	677.25	61	791.25	797.25
47	679.25	685.25	62	799.25	805.25
48	687.25	693.25	63	807.25	813.25
49	695.25	701.25	64	815.25	821.25
50	703.25	709.25	65	823.25	829.25
51	711.25	717.25	66	831.25	837.25
52	719.25	725.25	67	839.25	845.25
53	727.25	733.25	68	847.25	853.25

Republic of Ireland

	Frequency (MHz)			*Frequency (MHz)*	
Channel	*Vision*	*Sound*	*Channel*	*Vision*	*Sound*
IA	45.75	51.75	IF	191.25	197.25
IB	53.75	59.75	IG	199.25	205.25
IC	61.75	67.75	IH	207.25	213.25
ID	175.25	81.25	IJ	215.25	221.25
IE	183.25	189.25			

South Africa

Channel	Frequency (MHz)		Channel	Frequency (MHz)	
	Vision	*Sound*		*Vision*	*Sound*
4	175.25	181.25	9	215.25	221.25
5	183.25	189.25	10	223.25	229.25
6	191.25	197.25	11	231.25	237.25
7	199.25	205.25	13	247.43	253.43
8	207.25	213.25			

Australia

Channel	Frequency (MHz)		Channel	Frequency (MHz)	
	Vision	*Sound*		*Vision*	*Sound*
0	46.25	51.75	6	175.25	180.75
1	57.25	62.75	7	182.25	187.75
2	64.25	69.75	8	189.25	194.75
3	86.25	91.75	9	196.25	201.75
4	95.25	100.75	10	209.25	214.75
5	102.25	107.75	11	216.25	221.75
5A	138.25	143.75			

New Zealand

Channel	Frequency (MHz)		Channel	Frequency (MHz)	
	Vision	*Sound*		*Vision*	*Sound*
1	45.25	50.75	6	189.25	194.75
2	55.25	60.75	7	196.25	201.75
3	62.25	67.75	8	203.25	208.75
4	175.25	180.75	9	210.25	215.75
5	182.25	187.75			

USA

Channel	Frequency (MHz)		Channel	Frequency (MHz)	
	Vision	*Sound*		*Vision*	*Sound*
2	55.25	59.75	43	645.25	649.75
3	61.25	65.75	44	651.25	655.75
4	67.25	71.75	45	657.25	661.75
5	77.25	81.75	46	663.25	667.75
6	83.25	87.75	47	669.25	673.75
7	175.25	179.75	48	675.25	679.75
8	181.25	185.75	49	681.25	685.75
9	187.25	191.75	50	687.25	691.75
10	193.25	197.75	51	693.25	697.75
11	199.25	203.75	52	699.25	703.75
12	205.25	209.75	53	705.25	709.75
13	211.25	215.75	54	711.25	715.75
14	471.25	475.75	55	717.25	721.75
15	477.25	481.75	56	723.25	727.75
16	483.25	487.75	57	729.25	733.75
17	489.25	493.75	58	735.25	739.75
18	495.25	499.75	59	741.25	745.75
19	501.25	505.75	60	747.25	751.75
20	507.25	511.75	61	753.25	757.75
21	513.25	517.75	62	759.25	763.75
22	519.25	523.75	63	765.25	769.75
23	525.25	529.75	64	771.25	775.75
24	531.25	535.75	65	777.25	781.75
25	537.25	541.75	66	783.25	787.75
26	543.25	547.75	67	789.25	793.75
27	549.25	553.75	68	795.25	799.75
28	555.25	559.75	69	801.25	805.75
29	561.25	565.75	70	807.25	811.75
30	567.25	571.75	71	813.25	817.75
31	573.25	577.75	72	819.25	823.75
32	579.25	583.75	73	825.25	829.75
33	585.25	589.75	74	831.25	835.75
34	591.25	595.75	75	837.25	841.75
35	597.25	601.75	76	843.25	847.75
36	603.25	607.75	77	849.25	853.75
37	609.25	613.75	78	855.25	859.75
38	615.25	619.75	79	861.25	865.75
39	621.25	625.75	80	867.25	871.75
40	627.25	631.75	81	873.25	877.75
41	633.25	637.75	82	879.25	883.75
42	639.25	643.75	83	885.25	889.75

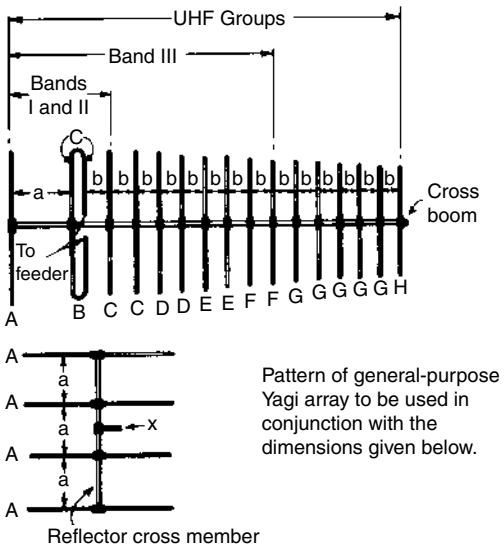

Pattern of general-purpose Yagi array to be used in conjunction with the dimensions given below.

24.9 AM broadcast station classes (USA)

The US AM broadcast band is 540 kHz to 1700 kHz, with 10 kHz channel spacings with centre frequencies divisible by ten (e.g. 780 kHz or 1540 kHz). Other countries in the western hemisphere operate on either 10 kHz channel spacings with frequencies ending in '5', or 9 kHz spacing. The Domestic Class is generally the class of station defined in 47 CFR Section 73.21. The Region 2 Class is generally the class of station as defined in the Region 2 [Western Hemisphere] AM Agreement. This class also corresponds to the class in the 1984 US–Canadian AM Agreement and the 1986 US–Mexican Agreement.

24.9.1 Class A station

A Class A station is an unlimited time station (that is, it can broadcast 24 hours per day) that operates on a clear channel. The operating power shall not be less than 10 kilowatts (kW) or more than 50 kW.

24.9.2 Class B station

A Class B station is an unlimited time station. Class B stations are authorized to operate with a minimum power of 250 watts and a maximum power of 50 kW. (If a Class B station operates with less than 250 W, the RMS must be equal to or greater than 141 mV/m at 1 km

for the actual power.) If the station is authorized to operate in the expanded band (1610 to 1700 kHz), the maximum power is 10 kW.

24.9.3 Class C station

A Class C station is an unlimited time station that operates on a local channel. The power shall not be less than 250 W nor more than 1 kW. Class C stations that are licensed to operate with 100 W may continue to operate as licensed.

24.9.4 Class D station

A Class D station operates either daytime, limited time, or unlimited time with a night-time power less than 250 W and an equivalent RMS antenna field less than 141 mV/m at 1 km for the actual power. Class D stations shall operate with daytime powers not less than 0.250 kW nor more than 50 kW. *Note*: If a station is an existing daytime-only station, its class will be Class D.

24.10 FM broadcast frequencies and channel numbers (USA)

From US Code USC 47 CFR 73. The FM broadcast band consists of that portion of the radio frequency spectrum between 88 MHz and 108 MHz. It is divided into 100 channels of 200 kHz each. For convenience, the frequencies available for FM broadcasting (including those assigned to non-commercial educational broadcasting) are given numerical designations which are shown in the table below:

Frequency (MHz)	*Channel No.*
88.1	201
88.3	202
88.5	203
88.7	204
88.9	205
89.1	206
89.3	207
89.5	208
89.7	209
89.9	210
90.1	211
90.3	212
90.5	213

Frequency (MHz)	*Channel No.*
90.7	214
90.9	215
91.1	216
91.3	217
91.5	218
91.7	219
91.9	220
92.1	221
92.3	222
92.5	223
92.7	224
92.9	225
93.1	226
93.3	227
93.5	228
93.7	229
93.9	230
94.1	231
94.3	232
94.5	233
94.7	234
94.9	235
95.1	236
95.3	237
95.5	238
95.7	239
95.9	240
96.1	241
96.3	242
96.5	243
96.7	244
96.9	245
97.1	246
97.3	247
97.5	248
97.7	249
97.9	250
98.1	251
98.3	252
98.5	253

Frequency (MHz)	*Channel No.*
98.7	254
98.9	255
99.1	256
99.3	257
99.5	258
99.7	259
99.9	260
100.1	261
100.3	262
100.5	263
100.7	264
100.9	265
101.1	266
101.3	267
101.5	268
101.7	269
101.9	270
102.1	271
102.3	272
102.5	273
102.7	274
102.9	275
103.1	276
103.3	277
103.5	278
103.7	279
103.9	280
104.1	281
104.3	282
104.5	283
104.7	284
104.9	285
105.1	286
105.3	287
105.5	288
105.7	289
105.9	290
106.1	291
106.3	292
106.5	293

Frequency (MHz)	*Channel No.*
106.7	294
106.9	295
107.1	296
107.3	297
107.5	298
107.7	299
107.9	300

24.11 US television channel assignments

Channel No.	*Frequency (MHz)*
1	(No Ch. 1 assigned)
2	54–60
3	60–66
4	66–72
5	76–82
6	82–88
7	174–180
8	180–186
9	186–192
10	192–198
11	198–204
12	204–210
13	210–216
14	470–476
15	476–482
16	482–488
17	488–494
18	494–500
19	500–506
20	506–512
21	512–518
22	518–524
23	524–530
24	530–536
25	536–542
26	542–548
27	548–554

Channel No.	*Frequency (MHz)*
28	554–560
29	560–566
30	566–572
31	572–578
32	578–584
33	584–590
34	590–596
35	596–602
36	602–608
37	608–614
38	614–620
39	620–626
40	626–632
41	632–638
42	638–644
43	644–650
44	650–656
45	656–662
46	662–668
47	668–674
48	674–680
49	680–686
50	686–692
51	692–698
52	698–704
53	704–710
54	710–716
55	716–722
56	722–728
57	728–734
58	734–740
59	740–746
60	746–752
61	752–758
62	758–764
63	764–770
64	770–776
65	776–782
66	782–788
67	788–794

Channel No.	*Frequency (MHz)*
68	794–800
69	800–806

Notes:

1. In Alaska, television broadcast stations operating on Channel 5 (76–82 MHz) and on Channel 6 (82–88 MHz) shall not cause harmful interference to and must accept interference from non-Government fixed operations authorized prior to 1 January 1982.
2. Channel 37, 608–614 MHz is reserved exclusively for the radio astronomy service.
3. In Hawaii, the frequency band 488–494 MHz is allocated for non-broadcast use. This frequency band (Channel 17) will not be assigned in Hawaii for use by television broadcast stations.

24.12 License-free bands

In Europe there are a number of license-free bands that can be used by anyone. However, there are restrictions on the use of these bands, both in terms of the application and the transmitted power. In particular, the manufacturer of transmitters operating in these bands must certify the equipment as meeting the required emission limits.

49.82 to 49.98 MHz – general purpose
173.2 to 173.35 MHz – telemetry. Note: 173.225 MHz is for short range alarms only
433.05 to 434.79 MHz – telemetry and vehicle security
458.5 to 458.95 MHz – industrial or commercial telemetry
868 to 870 MHz – general purpose.

Worldwide agreement has resulted in two bands, at 2.4 GHz and 5 GHz, being allocated to wireless LANs. Both of these bands are for industrial, scientific and medical (ISM) use.

The 2.4 GHz allocation covers 2.4 to 2.4835 GHz. Restrictions on the use of this ISM band include the use of carrier frequency hopping in step multiples of 1 MHz. This band is used by wireless LANs operating under IEEE802.11B and Bluetooth.

The IEEE802.11B standard uses 5 MHz carrier frequency steps, with some international variations. Europe allows the use of 13 channels (channel 1 to 13, with centre frequencies 2412 MHz to 2472 MHz), but

the USA only allows the use of 11 channels (channel 1 to 11, with centre frequencies 2412 MHz to 2462 MHz). In Japan only channel 14 is allowed (no hopping), using a carrier centre frequency of 2477 MHz.

Bluetooth uses 79 hop frequencies, with multiples of a 1 MHz step size. The lowest carrier frequency is at 2402 MHz (channel 0) and the highest is 2480 MHz (channel 78). The frequency hopping pattern is psuedo-random, with 1600 hops per second.

The 5 GHz allocation is actually two sub-bands, one covering 5.15 to 5.35 GHz and the other covering 5.47 GHz to 5.725 GHz. The higher frequency ISM band allows 1 watt radiated power, rather than the 200 mW limit of the lower frequency band. As with the 2.4 GHz ISM band, sources in the 5 GHz band must use carrier frequency hopping with 5 MHz steps.

24.13 Calculating radio antenna great circle bearings

Aiming radio antennas to target a particular area of the world requires calculation of the *great circle bearing* between your location and the other stations' location. That bearing is calculated from some simple spherical trigonometry using a hand-held calculator or a computer program. Before talking about the maths, however, we need to establish a frame of reference that makes the system work.

24.13.1 Latitude and longitude

The need for navigation on the surface of the Earth caused the creation of a grid system uniquely to locate points on the surface of our globe. *Longitude* lines run from the north pole to the south pole, i.e. from north to south.

The reference point (longitude zero), called the *prime meridian*, runs through Greenwich, England. The longitude of the prime meridian is 0 degrees. Longitudes west of the prime meridian are given a plus sign (+), while longitudes east of the prime are given a minus (−) sign. If you continue the prime meridian through the poles to the other side of the Earth it has a longitude of 180 degrees. Thus, the longitude values run from −180 degrees to +180 degrees, with ±180 degrees being the same line.

The observatory at Greenwich is also the point against which relative time is measured. Every 15 degree change of longitude is equivalent to a one hour difference with the Greenwich time. To the west, subtract one hour for each 15 degrees and to the east add one

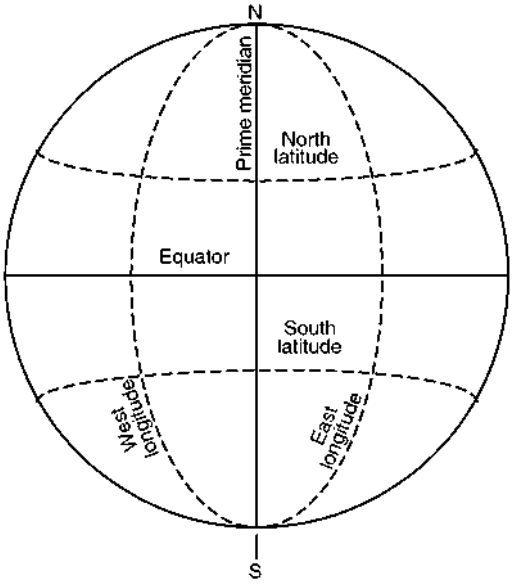

Figure 24.1 Lines of longitude and latitude

hour for each 15 degrees. Thus, the time on the East Coast of the United States is −5 hours relative to Greenwich time. At one time, we called time along the prime meridian *Greenwich mean time* (GMT), also called *Zulu time* to simplify matters for CW operators.

Latitude lines are measured against the equator, with distances north of the equator being taken as positive, and distances south of the equator being negative. The equator is 0 degrees latitude, while the north pole is +90 degrees latitude and the south pole is −90 degrees latitude.

Long ago navigators learned that the latitude can be measured by 'shooting' the stars and consulting a special atlas to compare the angle of certain stars with tables that translate to latitude numbers. The longitude measurement, however, is a bit different. For centuries sailors could measure latitude, but had to guess longitude (often with tragic results). In the early eighteenth century, the British government offered a large cash prize to anyone who could design a chronometer that could be taken to sea. By keeping the chronometer set accurately to Greenwich mean time, and comparing GMT against local time (i.e. at a time like high noon when the position of the sun is easy to judge), the longitude could be calculated. If you are interested in this subject, then most decent libraries have books on celestial navigation.

24.13.2 The great circle

On the surface of a globe, a curved line called a *great circle path* is the shortest distance between two points.

Consider two points on a globe: 'A' is your location, while 'B' is the other station's location. The distance 'D' is the great circle path between 'A' and 'B'.

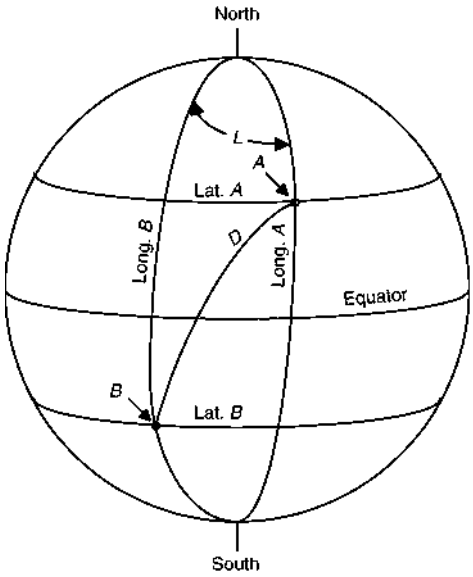

Figure 24.2 Great circle path

The great circle path length can be expressed in either degrees or distance (e.g. miles, nautical miles or kilometres). To calculate the distance, it is necessary to find the difference in longitude (L) between your longitude (LA) and the other station's longitude (LB): $L = LA - LB$. Keep the signs straight. For example, if your longitude (LA) is 40 degrees, and the other station's longitude (LB) is -120 degrees, then $L = 40 - (-120) = 40 + 120 = 160$. The equation for distance (D) is:

$$\cos D = (\sin A \times \sin B) + (\cos A \times \cos B \times \cos L)$$

where:

D is the angular great circle distance
A is your latitude
B is the other station's latitude.

To find the actual angle, take the arccos of the above equation, i.e.

$$D = \arccos(\cos D)$$

In the next equation you will want to use D in angular measure, but later on will want to convert D to miles. To do this, multiply D in degrees by 69.4. Or, if you prefer metric measures, then $D \times 111.2$ yields kilometres. This is the approximate distance in statute miles between 'A' and 'B'.

To find the bearing from true north, work the equation below:

$$C = \arccos\left[\frac{\sin B - (\sin A \times \cos D)}{(\cos A \times \sin D)}\right]$$

However, this equation won't always give you the right answer unless you make some corrections.

The first problem is the 'same longitude error', i.e. when both stations are on the same longitude line. In this case, $L = LA - LB = 0$. If LAT $A >$ LAT B, then $C = 180$ degrees, but if LAT $A <$ LAT B, then $C = 0$ degrees. If LAT $A =$ LAT B, then what's the point of all these calculations?

The next problem is found when the condition $-180^\circ \leq L \leq +180^\circ$ is not met, i.e. when the absolute value of L is greater than 180°, ABS$(L) > 180^\circ$. In this case, either add or subtract 360 in order to make the value between $\pm 180^\circ$:

$$\text{If } L > +180, \text{ then } L = L - 360$$

$$\text{If } L < -180, \text{ then } L = L + 360$$

One problem seen while calculating these values on a computer or hand calculator is the fact that the sin(X) and cos(X) cover different ranges. The sin(X) function returns values from 0° to 360°, while the cos(X) function returns values only over 0° to 180°. If L is positive, then the result bearing C is accurate, but if L is negative then the actual value of $C = 360 - C$. The following test is necessary:

$$\text{If } L < 0 \text{ then}$$

$$L = 360 - L$$

$$\text{Else } L = L$$

$$\text{End if}$$

Another problem is seen whenever either station is in a high latitude near either pole ($\pm 90^{\circ}$), or where both locations are very close together, or where the two locations are antipodal (i.e. on opposite points on the Earth's surface). The best way to handle these problems is to use a different equation that multiplies by the cosecant of D (i.e. cosec(D)), rather than dividing by sine of D (i.e. sin(D)).

25 Abbreviations and symbols

25.1 Abbreviations

Many abbreviations are found as either capital or lower case letters, depending on publishers' styles. Symbols should generally be standard, as shown.

A	Ampere or anode
ABR	Auxiliary bass radiator
a.c.	Alternating current
Ack	Acknowledgement
A/D	Analogue to digital
ADC	Analogue to digital converter
Ae	Aerial
a.f.	Audio frequency
a.f.c.	Automatic frequency control
a.g.c.	Automatic gain control
a.m.	Amplitude modulation
AMPS	Advanced mobile phone system
ANSI	American National Standards Institute
ASA	Acoustical Society of America
ASCII	American Standard Code for Information Interchange
a.t.u.	Aerial tuning unit
AUX	Auxiliary
a.v.c.	Automatic volume control
AWG	American Wine Gauge
b	Base of transistor
BAF	Bonded acetate fibre
B & S	Brown & Sharpe (U.S.) wire gauge
b.p.s.	Bits per second
BR	Bass reflex
BSI	British Standards Institution
BW	Bandwidth
C	Capacitor, cathode, centigrade, coulomb
c	Collector of transistor, speed of light
CB	Citizen's band
CCD	Charge coupled device
CCIR	International Radio Consultative Committee

CCITT	International Telegraph and Telephone Consultative Committee
CCTV	Closed circuit television
CDMA	Code division multiple access
chps	Characters per second
CISPR	Comité International Special Des Peturbations (radio interference standards body)
CLK	Clock signal
CMOS	Complementary metal oxide semiconductor
CrO_2	Chromium dioxide
CPU	Central processor unit
CTCSS	Continuous tone controlled signalled system
CTD	Charge transfer device
c.w.	Continuous wave
D	Diode
d	Drain of an f.e.t.
D/A	Digital to analogue
DAC	Digital to analogue converter
dB	Decibel
d.c.	Direct current
DCC	Double cotton covered
DCE	Data circuit-terminating equipment
DCS	Digital Communications Service
DF	Direction finding
DIL	Dual-in-line
DIN	German standards institute
DMA	Direct memory access
DPDT	Double pole, double throw
DPSK	Differential phase shift keying
DPST	Double pole, single throw
dsb	or dsbam. Double sideband amplitude modulation
DSRR	Digital short range radio
DTE	Data terminal equipment
DTL	Diode-transistor logic
DTMF	Dual tone multi-frequency
DX	Long distance reception
e	Emitter of transistor
EAROM	Electrically alterable read only memory
ECL	Emitter coupled logic
EDGE	Enhanced Data for GSM Evolution
e.h.t.	Extremely high tension (voltage)

EIRP	Effective Isotropic Radiated Power
e.m.f.	Electromotive force
en	Enamelled
EPROM	Erasable programmable read only memory
EQ	Equalization
EROM	Erasable read only memory
ERP	Effective radiated power
ETACS	Extended total access communications system
F	Farad, fahrenheit or force
f	Frequency
FDD	Frequency Division Duplex
FDM	Frequency division multiplex
FDMA	Frequency division multiple access
Fe	Ferrous
FeCr	Ferri-chrome
f.e.t.	Field effect transistor
FFSK	Fast frequency shift keying
f.m.	Frequency modulation
f.r.	Frequency response or range
f.s.d.	Full-scale deflection
FSK	Frequency shift keying
G	Giga (10^9)
g	Grid, gravitational constant
GMSK	Gaussian minimum shift keying
GSM	Global system mobile
H	Henry
h.f.	High frequency
Hz	Hertz (cycles per second)
I	Current
IB	Infinite baffle
i.c.	Integrated circuit
IF	Intermediate frequency
IHF	Institute of High Fidelity (U.S.)
I^2L(HL)	Integrated injection logic
i.m.d.	Intermodulation distortion
i/p	Input
i.p.s.	Inches per second
K	Kilo, in computing terms ($= 2^{10} = 1024$), or degrees Kelvin
k	Kilo (10^3) or cathode
L	Inductance or lumens
l.e.d.	Light emitting diode

l.f.	Low frequency
LIN	Linear
LOG	Logarithmic
LS	Loudspeaker
LSI	Large scale integration
l.w.	Long wave (approx. 1100–2000 m)
M	Mega (10^6)
m	Milli (10^{-3}) or metres
m.c.	Moving coil
MHz	Megahertz
mic	Microphone
MOS	Metal oxide semiconductor
MPU	Microprocessor unit
MPX	Multiplex
MSC	Mobile Switching Centre
MSK	Minimum shift keying
m.w.	Medium wave (approx. 185–560 m)
n	Nano (10^9)
NAB	National Association of Broadcasters
Ni-Cad	Nickel-cadmium
n/c	Not connected; normally closed
n/o	Normally open
NMOS	Negative channel metal oxide semiconductor
NRZ	Non-return to zero
o/c	Open channel; open circuit
o/p	Output
op-amp	Operational amplifier
p	Pico (10^{-12})
PA	Public address
PABX	Private automatic branch exchange
PAL	Phase alternation, line
p.a.m.	Pulse amplitude modulation
PCB	Printed circuit board
PCM	Pulse code modulation
PCN	Personal communications network
PCS	Personal communication system
PLA	Programmable logic array
PLL	Phase locked loop
pm	Phase modulation
PMOS	Positive channel metal oxide semiconductor
P.P.M.	Peak programme meter
p.r.f.	Pulse repetition frequency

PROM	Programmable read only memory
PSK	Phase shift keying
PSS	Packet SwitchStream
PSTN	Public Switched Telephone Network
PSU	Power supply unit
PTFE	Polytetrafluoroethylene
PU	Pickup
PUJT	Programmable unijunction transistor
Q	Quality factor; efficiency of tuned circuit, charge
QAM	Quadrature (or quaternary) amplitude modulation
QPSK	Quadrature (or quaternary) phase shift keying
R	Resistance
RAM	Random access memory
RCF	Recommended crossover frequency
r.f.	Radio frequency
r.f.c.	Radio frequency choke (coil)
RFI	Radio frequency interference
RIAA	Record Industry Association of America
r.m.s.	Root mean square
ROM	Read only memory
RTL	Resistor transistor logic
R/W	Read/write
RX	Receiver
S	Siemens
s	Source of an f.e.t.
s/c	Short circuit
SCR	Silicon-controlled rectifier
s.h.f.	Super high frequency
SI	International system of units
S/N	Signal-to-noise.
SPL	Sound pressure level
SPDT	Single pole, double throw
SPST	Single pole, single throw
ssb	Single sideband amplitude modulation
ssbdc	Single sideband diminished carrier
ssbsc	Single sideband suppressed carrier
SSI	Small scale integration
s.w.	Short wave (approx. 10–60 m)
s.w.g.	Standard wire gauge
s.w.r.	Standing wave ratio
T	Tesla

TACS	Total access communications system
TDD	Time division duplex
TDM	Time division multiplex
TDMA	Time division multiple access
t.h.d.	Total harmonic distortion
t.i.d.	Transient intermodulation distortion
TR	Transformer
t.r.f.	Tuned radio frequency
TRS	Transmitter repeater station
TTL	Transistor transistor logic
TTY	Teletype unit
TVI	Television interface; television interference
TX	Transmitter
UART	Universal asynchronous receiver transmitter
u.h.f.	Ultra high frequency (approx. 470–854 MHz)
u.j.t.	Unijunction transistor
ULA	Uncommitted logic array
V	Volts
VA	Volt-amps
v.c.a.	Voltage controlled amplifier
v.c.o.	Voltage controlled oscillator
VCT	Voltage to current transactor
v.h.f.	Very high frequency (approx. 88–216 MHz)
v.l.f.	Very low frequency
VSB	Vestigial side band
VSWR	Voltage standing wave ratio
VU	Volume unit
W	Watts
WAP	Wireless application protocol
Wb	Weber
W/F	Wow and flutter
WML	Wireless mark-up language
w.p.m.	Words per minute
X	Reactance
Xtal	Crystal
Z	Impedance
ZD	Zener diode

25.2 Letter symbols by unit name

Unit	*Symbol*	*Notes*
ampere	A	SI unit of electric current.
ampere (turn)	At	SI unit of magnetomotive force.
ampere-hour	Ah	
ampere per metre	$A\,m^{-1}$	SI unit of magnetic field strength.
angstrom	Å	$1\ Å = 10^{-10}\,m$.
apostilb	asb	$1\,asb(1/\pi)cd\ m^{-2}$ A unit of luminance. The SI unit, candela per square metre, is preferred.
atmosphere:		
standard atmosphere	atm	$1\,atm = 101\,325\,N\ m^{-2}$.
technical atmosphere	at	$1\ at = 1\,kgf\ cm^{-2}$.
atomic mass unit (unified)	u	The (unified) atomic mass unit is defined as one-twelfth of the mass of an atom of the ^{12}C nuclide. Use of the old atomic mass unit (amu), defined by reference to oxygen, is deprecated.
bam	b	$1\,b10^{-28}\,m^2$.
bar	bar	$1\,bar = 100\,000\,N\ m^{-2}$.
baud	Bd	Unit of signalling speed equal to one element per second.
becquerel	Bq	$1\ Bq = 1\,s^{-1}$. SI unit of radioactivity.
bel	B	
bit	b	
British thermal unit	Btu	

Unit	*Symbol*	*Notes*
calorie (International Table calorie)	cal_{IT}	1 $cal^{\circ} - = 4.1868$ J. The 9th Conférence Générale des Poids et Mesures adopted the joule as the unit of heat, avoiding the use of the calorie as far as possible.
calorie (thermochemical calorie)	cal	1 cal = 4.1840 J. (See note for International Table calorie.)
candela	cd	SI unit of luminous intensity.
candela per square inch	cd in^{-2}	Use of the SI unit, candela per square metre, is preferred.
candela per square metre	cd m^{-2}	SI unit of luminance. The name nit has been used.
candle		The unit of luminous intensity has been given the name *candela*; use of the word *candle* for this purpose is deprecated.
centimetre	cm	
circular mil	cmil	1 cmil = $(\pi/4)10^{-6}$ in^2.
coulomb	C	SI unit of electrical charge.
cubic centimetre	cm^3	
cubic foot	ft^3	
cubic foot per minute	ft^3 min^{-1}	
cubic foot per second	ft^3 s^{-1}	
cubic inch	in^3	
cubic metre	m^3	
cubic metre per second	m^3 s^{-1}	
cubic yard	yd^3	
curie	Ci	Unit of activity in the field of radiation dosimetry.
cycle	c	
cycle per second	c s^{-1}	Deprecated. Use hertz.
decibel	dB	
degree (plane angle)	$^{\circ}$	

Unit	*Symbol*	*Notes*
degree (temperature):		Note that there is no space between the symbol ° and the letter. The use of the word *centigrade* of the Celsius temperature scale was abandoned by the Conférence Générale des Poids et Mesures in 1948.
degree Celsius	°C	
degree Fahrenheit	°F	
degree Kelvin		See Kelvin.
degree Rankine	°R	
dyne	dyn	
electronvolt	eV	
erg	erg	
erlang	E	Unit of telephone traffic.
farad	F	SI unit of capacitance.
foot	ft	
footcandle	fc	Use of the SI unit of illuminance, the lux (lumen per square metre), is preferred.
footlambert	fL	Use of the SI unit, the candela per square metre, is preferred.
foot per minute	ft min^{-1}	
foot per second	ft s^{-1}	
foot per second squared	ft s^{-2}	
foot pound-force	ft lb_f	
gal	Gal	1 Gal = 1 cm s^{-2}.
gallon	gal	The gallon, quart, and pint differ in the US and the UK, and their use is deprecated.
gauss	G	The gauss is the electromagnetic CGS (Centimetre Gram Second) unit of magnetic flux density. The SI unit, tesla, is preferred.
gigaelectronvolt	GeV	

Unit	*Symbol*	*Notes*
gigahertz	GHz	
gilbert	Gb	The gilbert is the electromagnetic CGS (Centimetre Gram Second) unit of magnetomotive force. Use of the SI unit, the ampere (or ampere-turn), is preferred.
grain	gr	
gram	g	
gray	Gy	1 Gy = 1 J kg^{-1}. SI unit of absorbed dose.
henry	H	
hertz	Hz	SI unit of frequency.
horsepower	hp	Use of the SI unit, the watt, is preferred.
hour	h	Time may be designated as in the following example; $9^{h}46^{m}30^{s}$.
inch	in	
inch per second	in s^{-1}	
joule	J	SI unit of energy.
joule per Kelvin	$J K^{-1}$	SI unit of heat capacity and entropy.
Kelvin	K	SI unit of temperature (formerly called *degree Kelvin*). The symbol K is now used without the symbol°.
kiloelectronvolt	KeV	
kilogauss	kG	
kilogram	kg	SI unit of mass.
kilogram-force	kg_f	In some countries the name *kilopond* (kp) has been adopted for this unit.
kilohertz	kHz	
kilohm	kΩ	
kilojoule	kJ	
kilometre	km	

Unit	*Symbol*	*Notes*
kilometre per hour	km h^{-1}	
kilopond	kp	See kilogram-force.
kilovar	kvar	
kilovolt	kV	
kilovoltampere	kVA	
kilowatt	kW	
kilowatthour	kWh	
knot	kn	1 kn = 1 nmi h^{-1}.
lambert	L	The lambert is the CGS (Centimetre Gram Second) unit of luminance. The SI unit, candela per square metre, is preferred.
litre	l	
litre per second	l s^{-1}	
lumen	lm	SI unit of luminous flux.
lumen per square foot	lm ft^{-2}	Use of the SI unit, the lumen per square metre, is preferred.
lumen per square metre	lm m^{-2}	SI unit of luminous excitance.
lumen per watt	lm W^{-1}	SI unit of luminous efficacy.
lumen second	lm s	SI unit of quantity of light.
lux	lx	1 lx = 1 lm m^{-2}. SI unit of illuminance.
maxwell	Mx	The maxwell is the electromagnetic CGS (Centimetre Gram Second) unit of magnetic flux. Use of the SI unit, the weber, is preferred.
megaelectronvolt	MeV	
megahertz	MHz	
megavolt	MV	
megawatt	MW	
megohm	MΩ	
metre	m	SI unit of length.
mho	mho	1 mho = 1 Ω^{-1} = 1 S.
microampere	μA	
microbar	μbar	

Unit	*Symbol*	*Notes*
microfarad	μF	
microgram	μg	
microhenry	μH	
micrometre	μm	
micron		The name *micrometre* (μm) is preferred.
microsecond	μS	
microwatt	μW	
mil	mil	1 mil = −0.001 in.
mile		
nautical	nmi	
statute	mi	
mile per hour	mi h^{-1}	
milliampere	mA	
millibar	mbar	mb may be used.
milligal	mGal	
milligram	mg	
millihenry	mH	
millilitre	ml	
millimetre	mm	
conventional millimetre of mercury	mm Hg	1 mm Hg = 133.322 N m^{-2}.
millimicron		The name *nanometre* (nm) is preferred.
millisecond	ms	
millivolt	mV	
milliwatt	mW	
minute (plane angle)	…′	
minute (time)	min	Time may be designated as in the following example: $9^h46^m30^s$.
mole	mol	SI unit of amount of substance.
nanoampere	nA	
nanofarad	nF	
nanometre	nm	
nanosecond	ns	
nanowatt	nW	
nautical mile	nmi	

Unit	*Symbol*	*Notes*
neper	Np	
newton	N	SI unit of force.
newton metre	Nm	
newton per square metre	$N\,m^{-2}$	See pascal.
nit	nt	$1\,nt = 1\,cd\,m^{-2}$. See candela per square metre.
oersted	Oe	The oersted is the electromagnetic CGS (Centimetre Gram Second) unit of magnetic field strength. Use of the SI unit, the ampere per metre, is preferred.
ohm	Ω	SI unit of electrical resistance.
ounce (avoirdupois)	oz	
pascal	Pa	SI unit of pressure or stress. $1\,Pa = 1\,N\,m^{-2}$.
picoampere	pA	
picofarad	pF	
picosecond	ps	
picowatt	pW	
pint	pt	The gallon, quart, and pint differ in the US and the UK, and their use is deprecated.
pound	lb	
poundal	pdl	
pound-force	lb_f	
pound-force feet	lb_f ft	
pound-force per square inch	$lb_f\,in^{-2}$	
pound per square inch		Although use of the abbreviation psi is common, it is not recommended. See pound-force per square inch.

Unit	*Symbol*	*Notes*
Quart	qt	The gallon, quart, and pint differ in the US and the UK, and their use is deprecated.
rad	rd	Unit of absorbed dose in the field of radiation dosimetry.
revolution per minute	$r\ min^{-1}$	Although use of the abbreviation rpm is common, it is not recommended.
revolution per second	$r\ s^{-1}$	
roentgen	R	Unit of exposure in the field of radiation dosimetry.
second (plane angle)	$\ldots''$	
second (time)	s	SI unit of time. Time may be designated as in the following example: $9^h46^m30^s$.
siemens	S	SI unit of conductance. $1\,S = 1\ \Omega^{-1}$.
square foot	ft^2	
square inch	in^2	
square metre	m^2	
square yard	yd^2	
steradian	sr	SI unit of solid angle.
stilb	sb	$1\,sb = 1\,cd\ cm^{-2}$. A CGS unit of luminance. Use of the SI unit, the candela per square metre, is preferred.
tesla	T	SI unit of magnetic flux density. $1\,T = 1\,Wb\ m^{-2}$.
tonne	t	$1\,t = 1000\,kg$.
(unified) atomic mass unit	u	See atomic mass unit (unified).
var	var	Unit of reactive power.
volt	V	SI unit of electromotive force.
voltampere	VA	SI unit of apparent power.
watt	W	SI unit of power.
watthour	Wh	

Unit	*Symbol*	*Notes*
watt per steradian	W sr^{-1}	SI unit of radiant intensity.
watt per steradian square metre	W (sr $m^2)^{-1}$	SI unit of radiance.
weber	Wb	SI unit of magnetic flux. 1 Wb = 1 V s.
yard	yd	

25.3 Electric quantities

Quantity	*Symbol*	*Unit*	*Symbol*
Admittance	Y	siemens	S
Angular frequency	ω	hertz	Hz
Apparent power	S	watt	W
Capacitance	C	farad	F
Charge	Q	coulomb	C
Charge density	ρ	coulomb per square metre	C m^{-2}
Conductance	G	siemens	S
Conductivity	κ, γ, σ	siemens per metre	S m^{-1}
Current	I	ampere	A
Current density	j, J	ampere per square metre	A m^{-2}
Displacement	D	coulomb per square metre	C m^{-2}
Electromotive force	E	volt	V
Energy	E	joule	J
Faraday constant	F	coloumb per mole	C mol^{-1}
Field strength	E	volt per metre	V m^{-1}
Flux	ψ	coulomb	C
Frequency	v, f	hertz	Hz
Impedance	Z	ohm	Ω
Light, velocity of in a vacuum	c	metre per second	m s^{-1}
Period	T	second	s
Permeability	μ	henry per metre	H m^{-1}
Permeability of space	μ_o	henry per metre	H m^{-1}
Permeance	Λ	henry	H

Quantity	*Symbol*	*Unit*	*Symbol*
Permittivity	ε	farad per metre	$\mathrm{F\,m^{-1}}$
Permittivity of space	ε_o	farad per metre	$\mathrm{F\,m^{-1}}$
Phase	ϕ	–	–
Potential	V, U	volt	V
Power	P	watt	W
Quality factor	Q	–	–
Reactance	X	ohm	Ω
Reactive power	Q	watt	W
Relative permeability	μ_r	–	–
Relative permittivity	ε_r	–	–
Relaxation time	τ	second	s
Reluctance	R	reciprocal henry	$\mathrm{H^{-1}}$
Resistance	R	ohm	Ω
Resistivity	ρ	ohm metre	Ω m
Susceptance	B	siemens	S
Thermodynamic temperature	T	kelvin	K
Time constant	τ	second	s
Wavelength	λ	metre	m

26 Miscellaneous data

26.1 Fundamental constants

Constant	*Symbol*	*Value*
Boltzmann constant	k	$1.38062 \times 10^{-23}\ \mathrm{J\,K^{-1}}$
Electron charge, proton charge	e	$\pm 1.60219 \times 10^{-19}\ \mathrm{C}$
Electron charge-to-mass ratio	e/m	$1.7588 \times 10^{11}\ \mathrm{C\,kg^{-1}}$
Electron mass	m_e	$9.10956 \times 10^{-31}\ \mathrm{kg}$
Electron radius	r_e	$2.81794 \times 10^{-15}\ \mathrm{m}$
Faraday constant	F	$9.64867 \times 10^{4}\ \mathrm{C\,mol^{-1}}$
Neutron mass	m_n	$1.67492 \times 10^{-27}\ \mathrm{kg}$
Permeability of space	μ_o	$4\pi \times 10^{-7}\ \mathrm{H\,m^{-1}}$
Permittivity of space	ε_o	$8.85419 \times 10^{-12}\ \mathrm{F\,m^{-1}}$
Planck constant	h	$6.6262 \times 10^{-34}\ \mathrm{J\,s}$
Proton mass	m_p	$1.67251 \times 10^{-27}\ \mathrm{kg}$
Velocity of light	c	$2.99793 \times 10^{8}\ \mathrm{m\,s^{-1}}$

26.2 Electrical relationships

Amperes $\times$ ohms = **volts**
Volts $\div$ amperes = **ohms**
Volts $\div$ ohms = **amperes**
Amperes $\times$ volts = **watts**
$(\text{Amperes})^2 \times$ ohms = **watts**
$(\text{Volts})^2 \div$ ohms = **watts**
Joules per second = **watts**
Coulombs per second = **amperes**
Amperes $\times$ seconds = **coulombs**
Farads $\times$ volts = **coulombs**
Coulombs $\div$ volts = **farads**
Coulombs $\div$ farads = **volts**
Volts $\times$ coulombs = **joules**
Farads $\times (\text{volts})^2$ = **joules**

26.3 Dimensions of physical properties

Length: metre [L]. Mass: kilogram [M]. Time: second [T]. Quantity of electricity: coulomb [Q]. Area: square metre [L^2]. Volume: cubic metre [L^3].

Velocity: metre per second	$[LT^{-1}]$
Acceleration: metre per second^2	$[LT^{-2}]$
Force: newton	$[MLT^{-2}]$
Work: joule	$[ML^2T^{-2}]$
Power: watt	$[ML^2T^{-3}]$
Electric current: ampere	$[QT^{-1}]$
Voltage: volt	$[ML^2T^{-2}Q^{-1}]$
Electric resistance: ohm	$[ML^2T^{-1}Q^{-2}]$
Electric conductance: siemens	$[M^{-1}L^{-2}TQ^2]$
Inductance: henry	$[ML^2Q^{-2}]$
Capacitance: farad	$[M^{-1}L^{-2}T^2Q^2]$
Current density: ampere per metre^2	$[L^{-2}T^{-1}Q]$
Electric field strength: volt per metre	$[MLT^{-2}Q^{-1}]$
Magnetic flux: weber	$[MLT^2T^{-1}Q^{-1}]$
Magnetic flux density: tesla	$[MT^{-1}Q^{-1}]$
Energy: joule	$[ML^2T^{-2}]$
Frequency: hertz	$[T^{-1}]$
Pressure: pascal	$[ML^{-1}T^{-2}]$

26.4 Fundamental units

Quantity	*Unit*	*Symbol*
Amount of a substance	mole	mol
Charge	coulomb	C
Length	metre	m
Luminous intensity	candela	cd
Mass	kilogram	kg
Plane angle	radian	rad
Solid angle	steradian	sr
Thermodynamic temperature	kelvin	K
Time	second	s

26.5 Greek alphabet

Capital letters	*Small letters*	*Greek name*	*English equivalent*	*Capital letters*	*Small letters*	*Greek name*	*English equivalent*
A	α	*Alpha*	a	N	ν	*Nu*	n
B	β	*Beta*	b	Ξ	ξ	*Xi*	x
Γ	γ	*Gamma*	g	O	*o*	*Omicron*	*ŏ*
Δ	δ	*Delta*	d	Π	π	*Pi*	p
E	ε	*Epsilon*	e	P	ρ	*Rho*	r
Z	ζ	*Zeta*	z	Σ	σ	*Sigma*	s
H	η	*Eta*	é	T	τ	*Tau*	t
Θ	θ	*Theta*	th	Y	υ	*Upsilon*	u
I	ι	*Iota*	i	Φ	ϕ	*Phi*	ph
K	κ	*Kappa*	k	X	χ	*Chi*	ch
Λ	λ	*Lambda*	l	Ψ	ψ	*Psi*	ps
M	μ	*Mu*	m	Ω	ω	*Omega*	ö

26.6 Standard units

Ampere Unit of electric current, the constant current which, if maintained in two straight parallel conductors of infinite length of negligible circular cross-section and placed one metre apart in a vacuum, will produce between them a force equal to 2×10^{-7} newton per metre length.

Ampere-hour Unit of quantity of electricity equal to 3 600 coulombs. One unit is represented by one ampere flowing for one hour.

Candela Unit of luminous intensity. It is the luminous intensity, in the perpendicular direction, of a surface of $1/600\,000\,\mathrm{m}^{-2}$ of a full radiator at the temperature of freezing platinum under a pressure of 101 325 newtons m^{-2}.

Coulomb Unit of electric charge, the quantity of electricity transported in one second by one ampere.

Decibel (dB) Unit of acoustical or electrical power ratio. Although the bel is officially the unit, this is usually regarded as being too large, so

the decibel is preferred. The difference between two power levels is P_1 and P_2, is given as

$$10 \log_{10} \frac{P_1}{P_2} \text{ decibels}$$

Farad Unit of electric capacitance. The capacitance of a capacitor between the plates of which there appears a difference of potential of one volt when it is charged by one coulomb of electricity. Practical units are the microfarad (10^{-6} farad), the nanofarad (10^{-9} farad) and the picofarad (10^{-12} farad).

Henry Unit of electrical inductance. The inductance of a closed circuit in which an electromotive force of one volt is produced when the electric current in the circuit varies uniformly at the rate of one ampere per second. Practical units are the microhenry (10^{-6} henry) and the millihenry (10^{-3} henry).

Hertz Unit of frequency. The number of repetitions of a regular occurrence in one second.

Joule Unit of energy, including work and quantity of heat. The work done when the point of application of a force of one newton is displaced through a distance of one metre in the direction of the force.

Kilovolt-ampere 1000 volt-amperes.

Kilowatt 1000 watts.

Light, velocity of Light waves travel at 300 000 kilometres per second (approximately). Also the velocity of radio waves.

Lumen $\mathbf{m}^{-2}$, lux Unit of illuminance of a surface.

Mho Unit of conductance, see Siemens.

Newton Unit of force. That force which, applied to a mass of one kilogram, gives it an acceleration of one metre per second per second.

Ohm Unit of electric resistance. The resistance between two points of a conductor when a constant difference of potential of one volt, applied between these two points, produces in the conductor a current of one ampere.

Pascal Unit of sound pressure. Pressure is usually quoted as the root mean square pressure for a pure sinusoidal wave.

Siemens Unit of conductance, the reciprocal of the ohm. A body having a resistance of 4 ohms would have a conductance of 0.25 siemens.

Sound, velocity of Sound waves travel at 332 metres per second in air (approximately) at sea level.

Tesla Unit of magnetic flux density, equal to one weber per square metre of circuit area.

Volt Unit of electric potential. The difference of electric potential between two points of a conducting wire carrying a constant current of one ampere, when the power dissipated between these points is equal to one watt.

Volt-ampere The product of the root-mean-square volts and root-mean-square amperes.

Watt Unit of power, equal to one joule per second. Volts times amperes equals watts.

Weber Unit of magnetic flux. The magnetic flux which, linking a circuit of one turn, produces in it an electromotive force of one volt as it is reduced to zero at a uniform rate in one second.

26.7 Decimal multipliers

Prefix	*Symbol*	*Multiplier*	*Prefix*	*Symbol*	*Multiplier*
tera	T	10^{12}	centi	c	10^{-2}
giga	G	10^{9}	milli	m	10^{-3}
mega	M	10^{6}	micro	μ	10^{-6}
kilo	k	10^{3}	nano	n	10^{-9}
hecto	h	10^{2}	pico	p	10^{-12}
deka	da	10	femto	f	10^{-15}
deci	d	10^{-1}	atto	a	10^{-18}

26.8 Useful formulae

Boolean Algebra (laws of)

Absorption:

$$A + (A.B) = A$$
$$A.(A + B) = A$$

Annulment:	$A + 1$	$=$	1
	$A.0$	$=$	0
Association:	$(A + B) + C$	$=$	$A + (B + C)$
	$(A.B).C$	$=$	$A.(B.C)$
Commutation:	$A + B$	$=$	$B + A$
	$A.B$	$=$	$B.A$
Complements:	$A + \bar{A}$	$=$	1
	$A.\bar{A}$	$=$	0
De Morgan's:	$\overline{(A + B)}$	$=$	$\bar{A}.\bar{B}$
	$\overline{(A.B)}$	$=$	$\bar{A} + \bar{B}$
Distributive:	$A.(B + C)$	$=$	$(A.B) + (A.C)$
	$A + (B.C)$	$=$	$(A + B).(A + C)$
Double negation:	$\bar{\bar{A}}$	$=$	A
Identity:	$A + O$	$=$	A
	$A.1$	$=$	A
Tautology:	$A.A$	$=$	A
	$A + A$	$=$	A

Capacitance

The capacitance of a parallel plate capacitor can be found from

$$C = \frac{0.885\,KA}{d}$$

C is in picofarads, K is the dielectric constant (air = 1). A is the area of the plate in square cm and d the thickness of the dielectric.

Calculation of overall capacitance with:
Parallel capacitors $-C = C_1 + C_2 + \cdots$
Series capacitors $-\dfrac{1}{C} = \dfrac{1}{C_1} + \dfrac{1}{C_2} + \cdots$

Characteristic impedance

$$\text{(open wire) } Z = 276 \log \frac{2D}{d} \text{ohms}$$

where

$D =$ wire spacing
$d =$ wire diameter
} in same units.

$$\text{(coaxial) } Z = \frac{138}{\sqrt{(K)}} \log \frac{d_o}{d_i} \text{ ohms}$$

where K = dielectric constant, d_o = outside diameter of inner conductor, d_i = inside diameter of outer conductor.

Dynamic resistance

In a parallel-tuned circuit at resonance the dynamic resistance is

$$R_d = \frac{L}{Cr} = Q\omega L = \frac{Q}{\omega C} \text{ ohms}$$

where L = inductance (henries), C = capacitance (farads), r = effective series resistance (ohms). $Q = Q$-value of coil, and $\omega = 2\pi \times$ frequency (hertz).

Frequency – wavelength – velocity

(See also Resonance)
The velocity of propagation of a wave is

$$v = f\lambda \text{ metres per second}$$

where f = frequency (hertz) and λ = wavelength (metres).

For electromagnetic waves in free space the velocity of propagation v is approximately 3×10^8 m/sec, and if f is expressed in kilohertz and λ in metres

$$f = \frac{300\,000}{\lambda} \text{ kilohertz} \qquad f = \frac{300}{\lambda} \text{ megahertz}$$

or

$$\lambda = \frac{300\,000}{f} \text{ metres} \qquad \lambda = \frac{300}{f} \text{ metres}$$

f in kilohertz $\qquad$ f in megahertz

Impedance

The impedance of a circuit comprising inductance, capacitance and resistance in series is

$$Z = \sqrt{R^2 + \left(\omega L - \frac{1}{\omega C}\right)^2}$$

where R = resistance (ohms), $\omega = 2\pi \times$ frequency (hertz). L = inductance (henries), and C = capacitance (farads).

Inductance

Single layer coils

$$L(\text{in microhenries}) = \frac{a^2N^2}{9a + 10l} \text{ approximately}$$

If the desired inductance is known, the number of turns required may be determined by the formula

$$N = \frac{5L}{na^2}\left[1 + \sqrt{\left(1 + \frac{0.36n^2a^3}{L}\right)}\right]$$

where N = number of turns, a = radius of coil in inches, n = number of turns per inch. L = inductance in microhenries (μH) and l = length of coil in inches.

Calculation of overall inductance with:
Series inductors $-\mathrm{L} = \mathrm{L}_1 + \mathrm{L}_2 + \cdots$
Parallel inductors $-\dfrac{1}{\mathrm{L}} = \dfrac{1}{\mathrm{L}_1} + \dfrac{1}{\mathrm{L}_2} + \cdots$

Meter conversions

Increasing range of ammeters or milliammeters
Current range of meter can be increased by connecting a shunt resistance across meter terminals. If R_m is the resistance of the meter; R_s the value of the shunt resistance and n the number of times it is wished to multiply the scale reading, then

$$R_\mathrm{s} = \frac{R_\mathrm{m}}{(n-1)}$$

Increasing range of voltmeters
Voltage range of meter can be increased by connecting resistance in series with it. If this series resistance is R_s and R_m and n as before, then $R_\mathrm{s} = R_\mathrm{m} \times (n-1)$.

Negative feedback

Voltage feedback

$$\text{Gain with feedback} = \frac{A}{1 + Ab}$$

where A is the original gain of the amplifier section over which feedback is applied (including the output transformer if included) and b is the fraction of the output voltage fed back.

$$\text{Distortion with feedback} = \frac{d}{1 + Ab} \text{ approximately}$$

where d is the original distortion of the amplifier.

Ohm's Law

$$I = \frac{V}{R} V = IR \; R = \frac{V}{I}$$

where I = current (amperes), V = voltage (volts), and R = resistance (ohms).

Power

In a d.c. circuit the power developed is given by

$$W = VI = \frac{V^2}{R} = I^2 R \text{ watts}$$

where V = voltage (volts), I = current (amperes), and R = resistance (ohms).

Power ratio

$$P = 10 \log \frac{P_1}{P_2}$$

where P = ratio in decibels, P_1 and P_2 are the two power levels.

Q

The Q value of an inductance is given by

$$Q = \frac{\omega L}{R}$$

Radio horizon distance

The radio horizon at VHF/UHF and up is approximately 15% further than the optical horizon. Several equations are used in calculating the distance. If D is the distance to the radio horizon, and H is the antenna height, then:

$$D = k\sqrt{H}$$

1. When D is in statute miles (5280 feet) and H in feet, then $K = 1.42$.
2. When D is in nautical miles (6000 feet) and H in feet, then $K = 1.23$.
3. When D is in kilometres and H is in metres, then $K = 4.12$.

Reactance

The reactance of an inductor and a capacitor respectively is given by

$$X_{\mathrm{L}} = \omega L \text{ ohms} \qquad X_{\mathrm{C}} = \frac{1}{\omega C} \text{ ohms}$$

where $\omega = 2\pi \times$ frequency (hertz), $L =$ inductance (henries), and $C =$ capacitance (farads).

The total resistance of an inductance and a capacitance in series is $X_{\mathrm{L}} - X_{\mathrm{C}}$.

Resistance

Calculation of overall resistance with:
Series resistors $-\ \mathrm{R} = \mathrm{R}_1 + \mathrm{R}_2 + \cdots$

Parallel resistors $-\ \dfrac{1}{\mathrm{R}} = \dfrac{1}{\mathrm{R}_1} + \dfrac{1}{\mathrm{R}_2} + \cdots$

Resonance

The resonant frequency of a tuned circuit is given by

$$f = \frac{1}{2\pi\sqrt{LC}} \text{ hertz}$$

where $L =$ inductance (henries), and $C =$ capacitance (farads). If L is in microhenries (μH) and C is picofarads, this becomes

$$f = \frac{10^6}{2\pi\sqrt{LC}} \text{ kilohertz}$$

The basic formula can be rearranged

$$L = \frac{1}{4\pi^2 f^2 C} \text{ henries} \qquad C = \frac{1}{4\pi^2 f L} \text{ farads}$$

Since $2\pi f$ is commonly represented by ω, these expressions can be written

$$L = \frac{1}{\omega^2 C} \text{ henries} \qquad C = \frac{1}{\omega^2 L} \text{ farads}$$

Time constant

For a combination of inductance and resistance in series the time constant (i.e. the time required for the current to reach 63% of its final value) is given by

$$\tau = \frac{L}{R} \text{ seconds}$$

where L = inductance (henries), and R = resistance (ohms).

For a combination of capacitance and resistance in series the time constant (i.e. the time required for the voltage across the capacitance to reach 63% of its final value) is given by

$$\tau = CR \text{ seconds}$$

where C = capacitance (farads), and R = resistance (ohms).

Transformer ratios

The ratio of a transformer refers to the ratio of the number of turns in one winding to the number of turns in the other winding. To avoid confusion it is always desirable to state in which sense the ratio is being expressed: e.g. the 'primary-to-secondary' ratio n_p/n_s. The turns ratio is related to the impedance ratio thus

$$\frac{n_p}{n_s}\sqrt{\frac{Z_p}{Z_s}}$$

where n_p = number of primary turns, n_s = number of secondary turns, Z_p = impedance of primary (ohms), and Z_s = impedance of secondary (ohms).

Wattage rating

If resistance and current values are known,

$$W = I^2 R \text{ when } I \text{ is in amperes}$$

or

$$W = \frac{\text{milliamps}^2}{1\ 000\ 000} \times R$$

If wattage rating and value of resistance are known, the safe current for the resistor can be calculated from

$$\text{milliampers} = 1.000 \times \sqrt{\frac{\text{watts}}{\text{ohms}}}$$

Wavelength of tuned circuit

Formula for the wavelength in metres of a tuned oscillatory circuit is: $1885\sqrt{LC}$, where L = inductance in microhenries and C = capacitance in microfarads.

26.9 Colour codes

26.9.1 Resistor and capacitor colour coding

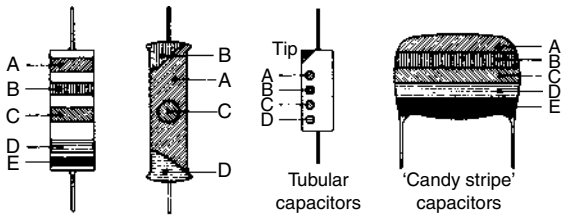

Resistors | Resistors (old type) | Tubular capacitors | 'Candy stripe' capacitors

Tantalum capacitors

	1	2	3	4
Black	–	0	× 1	10 V
Brown	1	1	× 10	
Red	2	2	× 100	
Orange	3	3	–	
Yellow	4	4	–	6.3 V
Green	5	5	–	16 V
Blue	6	6	–	20 V
Violet	7	7	–	
Grey	8	8	× 0.01	25 V
White	9	9	× 0.1	3 V
				(Pink 35 V)

26.9.2 Resistor and capacitor letter and digit code table **(BS 1852)**

Resistor values are indicated as follows:

0.47 Ω	marked	R47
1 Ω		1R0
4.7 Ω		4R7
47 Ω		47R
100 Ω		100R
1 kΩ		1K0
10 kΩ		10K
10 MΩ		10M

A letter following the value shows the tolerance.

F = ±1%; G = ±2%; J = ±5%; K = ±10%; M = ±20%; R33M = 0.33Ω ± 20%; 6K8F = 6.8 kΩ ± 1%.

Capacitor values are indicated as:

0.68 pF	marked	p68
6.8 pf		6p8
1000 pF		1n0
6.8 nf		6n8
1000 nF		1μ0
6.8 μF		6μ8

Tolerance is indicated by letters as for resistors. Values up to 999 pF are marked in pF, from 1000 pf to 999 000 pF (= 999 nF) as nF (1000 pF = InF) and from 1000 nF (= 1 μF) upwards as μF.

Some capacitors are marked with a code denoting the value in pF (first two figures) followed by a multiplier as a power of ten (3 = 10^3). Letters denote tolerance as for resistors but C = ±0.25 pf. E.g. 123 J = 12 pF × 10^3 ± 5% = 12 000 pF (or 0.12 μF).

STAN GIBILISCO

THE ILLUSTRATED DICTIONARY OF Electronics

EIGHTH EDITION

Audio/Video
Consumer Electronics
Wireless Technology

Front 4/9/01 4:38 PM Page i

The Illustrated Dictionary of Electronics

This page intentionally left blank.

Front 4/9/01 4:38 PM Page iii

The Illustrated Dictionary of Electronics

Eighth Edition

Stan Gibilisco
Editor-in-Chief

McGraw-Hill

New York Chicago San Francisco Lisbon London Madrid
Mexico City Milan New Delhi San Juan Seoul
Singapore Sydney Toronto

Cataloging-in-Publication Data is on file with the Library of Congress

McGraw-Hill

A Division of The McGraw-Hill Companies

Copyright © 2001 by The McGraw-Hill Companies, Inc. All rights reserved. Printed in the United States of America. Except as permitted under the United States Copyright Act of 1976, no part of this publication may be reproduced or distributed in any form or by any means, or stored in a data base or retrieval system, without the prior written permission of the publisher.

1 2 3 4 5 6 7 8 9 0 AGM/AGM 0 9 8 7 6 5 4 3 2 1

P/N 0-07-137237-7

ISBN 0-07-137236-9

The sponsoring editor for this book was Scott Grillo, and the production supervisor was Pamela Pelton. It was set in Bookman by Techbooks.

Printed and bound by Quebecor/Martinsburg.

McGraw-Hill books are available at special quantity discounts to use as premiums and sales promotions, or for use in corporate training programs. For more information, please write to the Director of Special Sales, McGraw-Hill, Two Penn Plaza, New York, NY 10121-2298. Or contact your local bookstore

Information in this book has been obtained by the publisher from sources believed to be reliable. However, neither the publisher nor the authors guarantee the accuracy or completeness of any information published herein. Neither the publisher nor the authors shall be responsible for any errors, omissions, or damages arising out of use of this information. This work is published with the understanding that the publisher and authors are supplying information but are not attempting to render professional services in any way, shape or form. If such services are required, the assistance of an appropriate professional should be sought.

This book is printed on recycled, acid-free paper containing a minimum of 50 percent recycled de-inked fiber.

Front 4/9/01 4:38 PM Page v

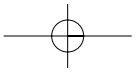

To Tony, Tim, and Samuel
from Uncle Stan

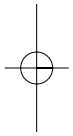

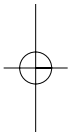

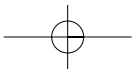

This page intentionally left blank.

Contents

Preface *ix*
Acknowledgments *xi*

Dictionary 1
Appendix A Schematic Symbols 773
Appendix B Tables and Data 787

Copyright 2001 The McGraw-Hill Companies, Inc. Click Here for Terms of Use

This page intentionally left blank.

Preface

The Illustrated Dictionary of Electronics—8th Edition has been revised, clarified, and updated, reflecting technological advances of recent years. New definitions have been added in the fields of wireless technology, robotics, and artificial intelligence. Every effort has been made to be concise and accurate, without "talking down" to the reader.

Many definitions contain cross references (indicated in ALL CAPITALS); these provide recommended additional information or allow comparison with related terms. Expressions of special significance are printed in italics. Electronics abbreviations are included in the text; the full terms are stated as definitions.

While an effort has been made to avoid superfluous mathematics, equations are sometimes necessary to completely and effectively define a term. Mathematics beyond the high-school level has not been used.

Appendix A contains the standard symbols used in electrical and electronic diagrams. These symbols are used in illustrations throughout this dictionary. Appendix B contains the following data tables:

1. Conversion between electrical systems
2. Greek alphabet
3. Mathematical functions and operations
4. Prefix multipliers
5. Resistor color code

Suggestions for future editions are welcome.

Stan Gibilisco
Editor-in-Chief

Copyright 2001 The McGraw-Hill Companies, Inc. Click Here for Terms of Use

This page intentionally left blank.

Front 4/9/01 4:38 PM Page xi

Acknowledgments

Illustrations in this book were generated with *CorelDRAW*. Some clip art is courtesy of Corel Corporation, 1600 Carling Avenue, Ottawa, Ontario, Canada K1Z 8R7.

Copyright 2001 The McGraw-Hill Companies, Inc. Click Here for Terms of Use

This page intentionally left blank.

Front 4/9/01 4:38 PM Page xiii

The Illustrated Dictionary of Electronics

This page intentionally left blank.

5059F-pA_1-55 4/9/01 4:41 PM Page 1

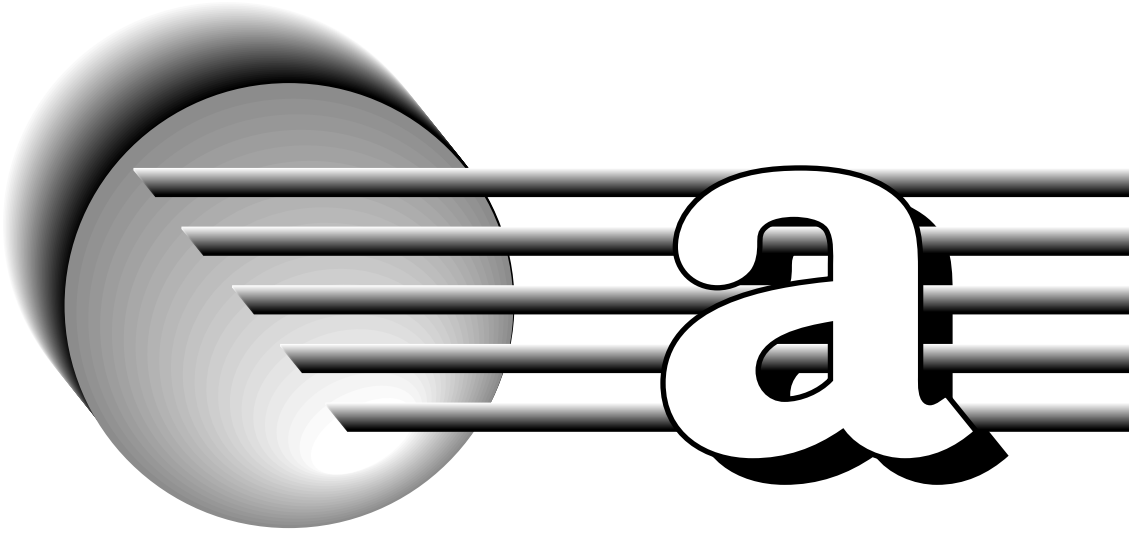

A **1.** Symbol for GAIN. **2.** Symbol for AREA. **3.** Symbol for AMPERE (SI unit for current).

A− Symbol for negative terminal of filament-voltage source in a vacuum-tube circuit.

A+ Symbol for positive terminal of filament-voltage source in a vacuum-tube circuit.

a **1.** Abbreviation of ATTO- (prefix). **2.** Abbreviation of AREA. **3.** Abbreviation of ACCELERATION. **4.** Abbreviation of ANODE. **5.** Obsolete abbreviation of cgs prefix AB-.

aA **1.** Abbreviation of *attoampere.* **2.** Obsolete for ABAMPERE.

AAAS Abbreviation for *American Association for the Advancement of Science.*

AAC Abbreviation of *automatic aperture control* (NASA).

AAS Abbreviation of *advanced antenna system* (NASA).

AASR Abbreviation of *airport and airways surveillance radar.*

AB Abbreviation of *acquisition beacon* (NASA).

A-B In sound and acoustics, the direct comparison of two sources of sound by alternately turning on one and the other.

ab- **1.** Prefix that transforms the name of a practical electrical unit to that of the equivalent electromagnetic cgs unit (e.g., ABAMPERE, ABOHM, ABVOLT). See individual entries of such cgs units. **2.** Abbreviation for ABSOLUTE.

abac A graphic device for the solution of electronics problems. Also see ALIGNMENT CHART.

abampere The unit of current in the cgs electromagnetic system. One abampere equals 10 amperes and corresponds to 1 abcoulomb per second.

Abbe condenser **1.** In microscopy, a special two-piece lens that has enhanced light-gathering power. **2.** A similar focusing device in an electromagnetic antenna.

abbreviated dialing In telephone systems, special circuits requiring fewer-than-normal dialing operations to connect subscribers.

abc **1.** Abbreviation of AUTOMATIC BASS COMPENSATION, a system for boosting the volume of bass sounds at low amplifier gain. **2.** Abbreviation of AUTOMATIC BIAS CONTROL. **3.** Abbreviation of AUTOMATIC BRIGHTNESS CONTROL. **4.** Abbreviation of AUTOMATIC BRIGHTNESS COMPENSATION.

abcoulomb The unit of electrical quantity in the cgs electromagnetic system. One abcoulomb equals 10 coulombs and is the quantity of electricity that flows past any point in a circuit in one second when the current is one abampere.

aberration **1.** Distortion from perfect shape in a lens or reflecting mirror or antenna dish. **2.** A small error in the determination of the direction of a source of electromagnetic energy, on account of the motion of the source and/or the detecting apparatus. **3.** A small displacement in the apparent positions of the stars from month to month on account of the earth's orbital motion.

ABETS Acronym for *airborne beacon electronic test set* (NASA).

abfarad The unit of capacitance in the cgs electromagnetic system. One abfarad equals 10^9 farads and is the capacitance across which a charge of 1 abcoulomb produces a potential of 1 abvolt.

abhenry The unit of inductance in the cgs electromagnetic system. One abhenry equals 10^{-9} henry

Copyright 2001 The McGraw-Hill Companies, Inc. Click Here for Terms of Use

5059F-pA_1-55 4/9/01 4:41 PM Page 2

and is the inductance across which a current that changes at the rate of 1 abampere per second induces a potential of 1 abvolt.

ABL Abbreviation of *Automated Biology Laboratory* (NASA).

abmho The obsolete unit of conductance and of conductivity in the cgs electromagnetic system. Replaced with ABSIEMENS.

abnormal dissipation Power dissipation higher or lower than the customary level, usually an overload.

abnormal oscillation **1.** Oscillation where none is desired or expected, as in an amplifier. **2.** Oscillation at two or more frequencies simultaneously when single-frequency operation is expected. **3.** Oscillation at an incorrect frequency. **4.** Parasitic oscillation.

abnormal propagation **1.** The chance shifting of the normal path of a radio wave, as by displacements in the ionosphere, so that reception is degraded. **2.** Unintentional radiation of energy from some point other than the transmitting antenna. **3.** Propagation over a path or in a direction not expected.

abnormal reflections Sharp, intense reflections at frequencies higher than the critical frequency of the ionosphere's ionized layer.

abnormal termination The shutdown of a running computer program or other process. Caused by the detection of an error by the associated hardware that indicates that some ongoing series of actions cannot be executed correctly.

abnormal triggering The false triggering or switching of a circuit or device, such as a flip-flop, by some undesirable source instead of the true trigger signal. Electrical noise pulses often cause abnormal triggering.

abohm The unit of resistance and of resistivity in the cgs electromagnetic system. One abohm equals 10^{-9} ohms and is the resistance across which a steady current of 1 abampere produces a potential difference of 1 abvolt.

abort To deliberately terminate an operation, experiment, process, or project before it has run its normal course.

AB power pack **1.** A portable dry-cell or wet-cell array containing both A and B batteries in one package. **2.** An ac-operated unit in one package for supplying A and B voltages to equipment normally operated from batteries.

abrasion machine An instrument for determining the abrasive resistance of a wire or cable.

abrasion resistance A measure of the ability of a wire or wire covering to resist mechanical damage.

ABS A basic programming abbreviation for the absolute value (of a number, variable, or expression).

abscissa **1.** The independent variable in a function. **2.** The axis (usually horizontal) on the graph of a function that indicates the independent variable.

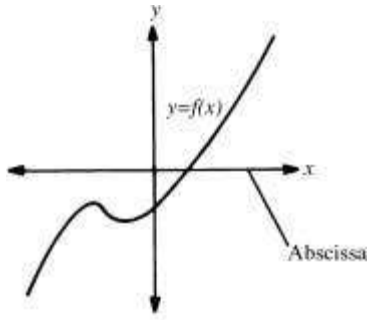

abscissa

absence-of-ground searching selector A rotary switch that searches for an ungrounded contact in a dial telephone system.

absiemens The unit of conductance or conductivity in the cgs electromagnetic system. One absiemens equals 10^9 siemens and is the conductance through which a potential of 1 abvolt forces a current of 1 abampere.

absolute **1.** A temperature scale in which zero represents the complete absence of heat. Units of measure are same as units on Celsius and Fahrenheit scales. See ABSOLUTE SCALE. **2.** Independent of any arbitrarily assigned units of measure or value.

absolute accuracy The full-scale accuracy of a meter with respect to a primary (absolute) standard.

absolute address In a digital computer program, the location of a word in memory, as opposed to location of the word in the program.

absolute code A computer code in which the exact address is given for storing or locating the reference operand.

absolute coding In computer practice, coding that uses absolute addresses.

absolute constant A mathematical constant that has the same value wherever it is used.

absolute delay The time elapsing between the transmission of two synchronized signals from the same station or from different stations, as in radio, radar, or loran. By extension, the time interval between two such signals from any source, as from a generator.

absolute digital position transducer A digital position transducer whose output signal indicates absolute position. (See ENCODER.)

absolute efficiency The ratio X_x/X_s, where X_x is the output of a given device, and X_s is the output of an ideal device of the same kind under the same operating conditions.

absolute encoder system A system that permits the encoding of any function (linear, nonlinear, continuous, step, and so on) and supplies a nonambiguous output.

absolute error The difference indicated by the approximate value of a quantity minus the actual

5059F-pA_1-55 4/9/01 4:41 PM Page 3

value. This difference is positive when the approximate value is higher than the exact value, and it is negative when the approximate value is lower than the exact value. Compare RELATIVE ERROR.

absolute gain Antenna gain for a given orientation when the reference antenna is isolated in space and has no main axis of propagation.

absolute humidity The mass of water vapor per unit volume of air. Compare RELATIVE HUMIDITY.

absolute instruction A computer instruction that states explicitly and causes the execution of a specific operation.

absolute magnitude For a complex number quantity, the vector sum of the real and imaginary components (i.e., the square root of the sum of the squares of those components). Also see ABSOLUTE VALUE and IMPEDANCE.

absolute maximum rating The highest value a quantity can have before malfunction or damage occurs.

absolute maximum supply voltage The highest supply voltage that can be applied to a circuit without permanently altering its characteristics.

absolute measurement of current Measurement of a current directly in terms of defining quantities. **1.** TANGENT GALVANOMETER method: Current is proportional to the tangent of the angle of deflection of the needle of this instrument. Deflection depends on torque, resulting from the magnetic field produced by current in the galvanometer coil acting against the horizontal component of the earth's magnetic field. **2.** ELECTRODYNAMOMETER method: With this 2-coil instrument, current is determined from the observed deflection, the torque of the suspension fiber of the movable coil, and the coil dimensions.

absolute measurement of voltage Measurement of a voltage directly in terms of defining quantities. **1.** CALORIMETRIC method: A current-carrying coil immersed in water raises the temperature of the water. The difference of potential that forces the current through the coil then is determined in terms of the equivalent heat energy. **2.** Disk-electrometer method: In this setup, a metal disk attached to one end of a balance beam is attracted by a stationary disk mounted below it, the voltage being applied to the two disks. The other end of the beam carries a pan into which accurate weights are placed. At balance, the voltage is determined in terms of the weight required to restore balance, the upper-disk area, and the disk separation.

absolute minimum resistance The resistance between the wiper and the nearer terminal of a potentiometer, when the wiper is as close to that terminal as physically possible. All potentiometers have two such specifications, one for each end terminal.

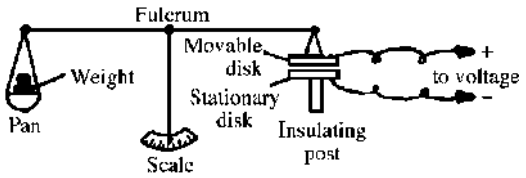

absolute measurement of voltage, 2

absolute Peltier coefficient The product of the absolute Seebeck coefficient and absolute temperature of a material.

absolute pitch A tone in a standard scale, determined according to the rate of vibration, independent of other tones in the range of pitch.

absolute pressure Pressure (force per unit area) of a gas or liquid determined with respect to that of a vacuum (taken as zero).

absolute-pressure transducer A transducer actuated by pressure from the outputs of two different pressure sources, and whose own output is proportional to the difference between the two applied pressures.

absolute scale **1.** A scale in which the zero value indicates the lowest physically possible value that a parameter can attain. **2.** A standard scale for measurement of a quantity. **3.** A universally agreed-upon scale for the determination of a variable quantity. **4.** The Kelvin temperature scale. **5.** The Rankine temperature scale.

absolute Seebeck coefficient The quotient, as an integral from absolute zero to the given temperature, of the Thomson coefficient of a material divided by its absolute temperature.

absolute spectral response The frequency output or response of a device in absolute power units (such as milliwatts) as opposed to relative units (such as decibels).

absolute system of units A system of units in which the fundamental (ABSOLUTE) units are those expressing length (l), mass (m), charge (q), and time (t). All other physical units, including practical ones, are then derived from these absolute units.

absolute temperature Temperature measured on either the Kelvin or Rankine scales, where zero represents the total absence of heat energy.

absolute temperature scale **1.** The Kelvin temperature scale, in which the divisions are equal in size to 1° Celsius, and the zero point is absolute zero, the coldest possible temperature, approximately –273.16° Celsius. **2.** The Rankine temperature scale, in which the divisions are equal in size to 1° Fahrenheit, and the zero point is absolute zero or approximately –459.7° Fahrenheit.

absolute tolerance The value of a component as it deviates from the specified or nominal value. It is usually expressed as a percentage of the specified value.

5059F-pA_1-55 4/9/01 4:41 PM Page 4

absolute units Fundamental physical units (see ABSOLUTE SYSTEM OF UNITS) from which all others are derived. See, for example, AMPERE, OHM, VOLT, and WATT.

absolute value The magnitude of a quantity without regard to sign or direction. The absolute value of a is written $|a|$. The absolute value of a positive number is the number itself; thus, $|10|$ equals 10. The absolute value of a negative number is the number with its sign changed: $|-10|$ equals 10.

absolute-value circuit A circuit that produces a unipolar signal in response to a bipolar input and in proportion to the absolute value of the magnitude of the input.

absolute-value computer A computer in which data is processed in its absolute form; i.e., every variable maintains its full value. (Compare to INCREMENTAL COMPUTER.)

absolute-value device In computer practice, a device that delivers a constant-polarity output signal equal in amplitude to that of the input signal. Thus, the output signal always has the same sign.

absolute zero The temperature –273.16°C (−459.7°F and 0 Kelvin). The coldest possible temperature, representing the complete absence of heat energy.

absorbed wave A radio wave that dissipates in the ionosphere as a result of molecular agitation. This effect is most pronounced at low and medium frequencies.

absorptance The amount of radiant energy absorbed in a material; equal to 1 minus the transmittance.

absorption The taking up of one material or medium by another into itself, as by sucking or soaking up. Also, the retention of one medium (or a part of it) by another medium, through which the first one attempts to pass. See, for example, ABSORBED WAVE, ABSORPTION COEFFICIENT, DIELECTRIC ABSORPTION. Compare ADSORPTION.

absorption band See ABSORPTION SPECTRUM.

absorption circuit A circuit that absorbs energy from another circuit or from a signal source—especially a resonant circuit, such as a wavemeter or wavetrap.

absorption current In a capacitor, the current resulting from absorption of energy by the dielectric material.

absorption dynamometer A power-measuring instrument in which a brake absorbs energy from a revolving shaft or wheel.

absorption fading Fading of a radio wave, resulting from (usually) slow changes in the absorption of the wave in the line of propagation.

absorption frequency meter See WAVEMETER.

absorption line See ABSORPTION SPECTRUM.

absorption loss **1.** Transmission loss caused by dissipation of electrical energy, or conversion of it into heat or other forms of energy. **2.** Loss of all or part of a skywave because of absorption by the ionosphere. Also called *ionospheric absorption* or *atmospheric absorption*.

absorption marker A small blip introduced onto an oscilloscope trace to indicate a frequency point. It is so called because it is produced by the action of a frequency-calibrated tuned trap, similar to an absorption wavemeter.

absorption modulation Amplitude modulation of a transmitter or oscillator by means of an audio-frequency-actuated absorber circuit. In its simplest form, the modulator consists of a few turns of wire coupled to the transmitter tank coil and connected to a carbon microphone. The arrangement absorbs energy from the transmitter at a varying rate as the microphone changes its resistance in accordance with the sound waves it receives.

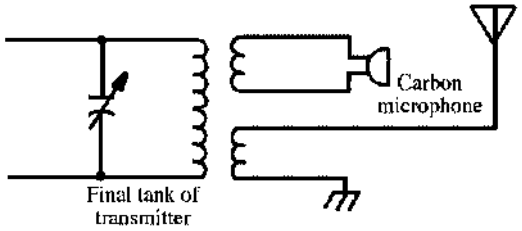

absorption modulation

absorption spectrum For electromagnetic waves, a plot of absorption coefficient (of the medium of propagation) versus frequency. Also called EMISSION SPECTRUM.

absorption trap See WAVETRAP.

absorption wavemeter A resonant-frequency indicating instrument that is inductively coupled to the device under test.

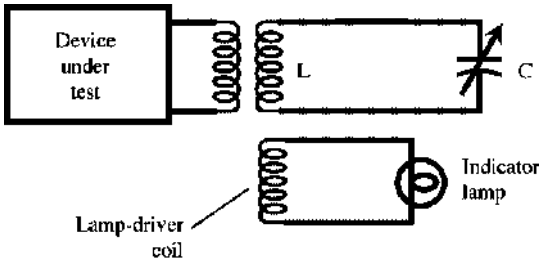

absorption wavemeter

absorptivity In audio and microwave technologies, a measure of the energy absorbed by a given volume of material.

A-B test Comparison of two sounds by reproducing them in alternating succession.

5059F-pA_1-55 4/9/01 4:41 PM Page 5

abvolt The unit of potential difference in the cgs electromagnetic system. One abvolt equals 10^{-8} V and is the difference of potential between any two points when 1 erg of work is required to move 1 abcoulomb of electricity between them.

abwatt The unit of power in the cgs electromagnetic system. One abwatt equals 10^{-7} W and is the power corresponding to 1 erg of work per second.

ac **1.** Abbreviation of ALTERNATING CURRENT. **2.** Abbreviation of ATTITUDE CONTROL. **3.** Abbreviation of AERODYNAMIC CENTER. **4.** A suffix meaning AUTOMATIC CALCULATOR or AUTOMATIC COMPUTER.

a/c **1.** Abbreviation of AIRCRAFT. **2.** Abbreviation of AIR CONDITIONING.

Ac Symbol for ACTINIUM.

ACA Abbreviation of *automatic circuit analyzer.*

ac base current Symbol, $I_{B(ac)}$. The ac component of base current in a bipolar transistor.

ac base resistance Symbol, $R_{B(ac)}$. The dynamic base resistance in a bipolar transistor.

ac base voltage Symbol, $V_{B(ac)}$. The ac component of base voltage in a bipolar transistor. It is the ac input signal voltage in a common-emitter amplifier or emitter-follower amplifier.

ac bias In a tape recorder, the high-frequency current that passes through the recording head to linearize operation.

acc **1.** Abbreviation of AUTOMATIC CHROMINANCE CONTROL. **2.** Abbreviation of AUTOMATIC COLOR COMPENSATION. **3.** Abbreviation of ACCELERATION.

ac cathode current Symbol, $I_{K(ac)}$. The ac component of cathode current in an electron tube.

ac cathode resistance Symbol, $R_{K(ac)}$. The dynamic cathode resistance in an electron tube. $R_{K(ac)}$ equals dV_K/dI_K for a constant value of V_G.

ac cathode voltage Symbol, $V_{K(ac)}$. The ac component of cathode voltage in an electron tube. It is the ac output signal voltage in cathode-follower and grounded-grid amplifiers.

accelerated life test A test program that simulates the effects of time on devices or apparatus, by artificially speeding up the aging process.

accelerated service test A service or bench test in which equipment or a circuit is subjected to an extreme condition in an attempt to simulate the effects of average use over a long time.

accelerating conductor or relay A conductor or relay that prompts the operation of a succeeding device in a starting mode according to established conditions.

accelerating electrode In a cathode-ray tube or klystron, the electrode to which the accelerating voltage is applied.

accelerating time The elapsed time that starts when voltage is applied to a motor, and ends when the motor shaft reaches maximum speed.

accelerating voltage A positive high voltage applied to the accelerating electrode of a cathode-ray tube to increase the velocity of electrons in the beam.

acceleration at stall The angular acceleration of a servomotor at stall, determined from the stall torque and the moment of inertia of the motor's rotor.

acceleration derivative Acceleration (a) expressed as the second derivative of distance (s) with respect to time (t): a equals d^2s/dt^2.

acceleration potential See ACCELERATING VOLTAGE.

acceleration switch A switch that operates automatically when the acceleration of a body to which it is attached exceeds a predetermined rate in a given direction.

acceleration time The time required by a computer to take in or deliver information after interpreting instructions. Compare ACCESS TIME.

acceleration torque During the accelerating period of a motor, the difference between the torque demanded and the torque actually produced by the motor.

acceleration voltage The potential between accelerating elements in a vacuum tube, the value of which determines average electron velocity.

accelerometer A transducer whose output voltage is proportional to the acceleration of the moving body to which it is attached.

accentuation The emphasis of a desired band of frequencies, usually in the audio-frequency spectrum.

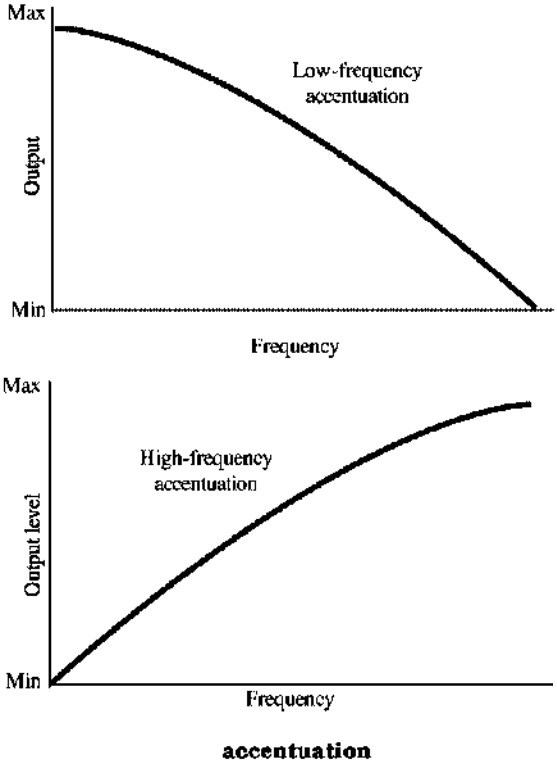

accentuation

5059F-pA_1-55 4/9/01 4:41 PM Page 6

accentuator A circuit or device, such as a filter, tone control, or equalizer, used to emphasize a band of frequencies, usually in the audio-frequency spectrum. Also see ACCENTUATION.

acceptable-environmental-range test A test to disclose the environmental conditions that equipment can endure while maintaining at least the minimum desired reliability.

acceptable quality level Abbreviation, AQL. A percentage that represents an acceptable average of defective components allowable for a process, or the lowest quality that a supplier is permitted to regularly present for acceptance.

acceptance sampling plan A probabilistic method of sampling a quantity of units from a lot, and determining from the sample whether to accept the lot, reject the lot, or perform another sampling.

acceptance test A test performed on incoming equipment or on submitted samples to determine if they meet tester's or supplier's specifications.

acceptor **1.** Any device or circuit, such as a series-resonant circuit, that provides relatively easy transmission of a signal, in effect accepting the signal. **2.** A hole-rich impurity added to a semiconductor to make the latter p-type. It is so called because its holes can accept electrons. Compare DONOR.

acceptor circuit See ACCEPTOR, **1.**

acceptor impurity See ACCEPTOR, **2.**

access **1.** To gain entrance to something, such as the interior of the cabinet of a high-fidelity amplifier. **2.** In a computer, the action of going to a specific memory location for the purpose of data retrieval. **3.** A port or opening into a piece of equipment, placed there to make the equipment easy to maintain and repair.

access arm A mechanical device that positions the read/write mechanism in a computer storage unit.

access control register A register that is part of a computer protection system that prevents interference between different software modules.

access method A method of transferring information or data from main storage to an input/output unit.

access right The access status given to computer system users that indicates the method of access permitted (e.g., read a file only or write to a file).

access time The time required by a computer to begin delivering information after the memory or storage has been interrogated.

accidental error An unintentional error committed by a person making measurements and recording data.

accidental triggering The undesired chance-operation of a flip-flop or other switching circuit caused by a noise pulse or other extraneous signal.

ac collector current Symbol, $I_{C(ac)}$. The ac component of collector current in a bipolar transistor.

ac collector resistance Symbol, $R_{C(ac)}$. The dynamic collector resistance of a bipolar transistor. $R_{C(ac)}$ equals dV_C/dI_C for a constant value of base current I_B (in a common-emitter circuit) or emitter current I_E (in a common-base circuit).

ac collector voltage Symbol, $V_{C(ac)}$. The ac component of collector voltage in a bipolar transistor. The ac output signal voltage in a common-emitter or common-base amplifier.

accompanying audio channel The RF signal that supplies television sound. Also called *Cochannnel sound frequency.*

ac component In a complex wave (i.e., one containing both ac and dc), the alternating, fluctuating, or pulsating part of the combination. Compare DC COMPONENT.

accordion A printed-circuit connector contact with a Z-shaped spring that allows high deflection with low fatigue.

ac-coupled flip-flop A flip-flop that is operated by the rise or fall of a clock pulse.

ac coupling Transformer coupling or capacitive coupling, which transmit ac, but not dc. Compare DIRECT COUPLING.

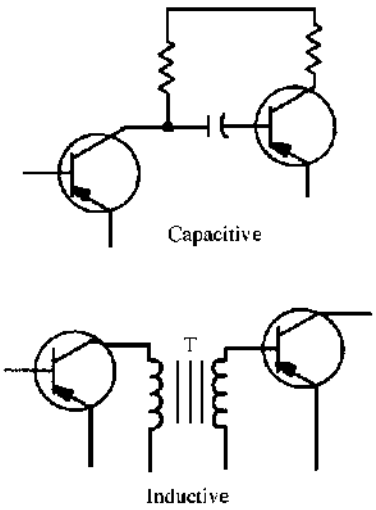

ac coupling

accumulator **1.** In a digital computer, a circuit or register device that receives numbers, totals them, and stores them. **2.** Storage battery.

accuracy **1.** Precision in the measurement of quantities and in the statement of physical characteristics. **2.** Degree of precision. Usually expressed, in terms of error, as a percentage of the specified value (e.g., 10 V plus or minus 1%), as a percentage of a range (e.g., 2% of full scale), or as parts (e.g., 100 parts per million).

accuracy rating The maximum error in an instrument, given as a percentage of the full-scale value.

5059F-pA_1-55 4/9/01 4:41 PM Page 7

accw Abbreviation of ALTERNATING-CURRENT CONTINUOUS WAVE.

ac/dc Abbreviation of ALTERNATING CURRENT/DIRECT CURRENT. Pertains to equipment that will operate from either ac utility power or a dc power source. A notebook computer is a good example.

ac directional overcurrent relay A relay that works on a specific value of alternating overcurrent that is rectified for a desired polarity.

ac drain current Symbol, $I_{D(ac)}$. The ac component of drain current in a field-effect transistor.

ac drain resistance Symbol, $R_{D(ac)}$. The dynamic drain resistance in a field-effect transistor; $R_{D(ac)}$ equals dV_D/dI_D for a constant value of gate voltage V_G.

ac drain voltage Symbol, $V_{D(ac)}$. The ac component of drain voltage in a field-effect transistor. The ac output signal voltage in a common-source FET amplifier.

ac dump The removal of all ac power from a system or component.

ac emitter current Symbol, $I_{E(ac)}$. The ac component of emitter current in a bipolar transistor.

ac emitter resistance Symbol, $R_{E(ac)}$. The dynamic emitter resistance of a bipolar transistor; $R_{E(ac)}$ equals dV_E/dI_E for a constant value of base current I_B (in an emitter-follower circuit) or collector voltage V_{CC} (in a common-base circuit).

ac emitter voltage Symbol, $V_{E(ac)}$. The ac component of emitter voltage in a bipolar transistor. The ac input signal voltage in a common-base amplifier; the ac output signal voltage in an emitter-follower amplifier.

ac equipment An apparatus designed for operation from an ac power source only. Compare DC EQUIPMENT and AC/DC.

ac erasing In tape recording, the technique of using an alternating magnetic field to erase material already recorded on the tape.

ac erasing head Also called *ac erase head.* In tape and wire recording, a head that carries alternating current to erase material already recorded on the tape or wire. Also see AC ERASING.

acetate Cellulose acetate, a tough thermoplastic material that is an acetic acid ester of cellulose. It is used as a dielectric and in the manufacture of photographic films.

acetate base **1.** The cellulose acetate film that served as the base for the magnetic oxide coating in early recording tape. Most such tapes today are of polyester base. **2.** The cellulose acetate substrate onto which certain photosensitive materials are deposited for lithographic reproduction. Also see ACETATE and ANCHORAGE.

acetate tape Recording tape consisting of a magnetic oxide coating on a cellulose acetate film. Also see ACETATE BASE.

ac gate voltage Symbol, $V_{G(ac)}$. The ac component of gate voltage in a field-effect transistor. The ac input signal voltage.

ac generator **1.** A rotating electromagnetic machine that produces alternating current (e.g., a dynamo or alternator). **2.** An oscillator or combination of an oscillator and an output amplifier.

ac grid voltage Symbol, $V_{G(ac)}$. The ac component of control grid voltage in an electron tube. The ac input signal voltage in a common-cathode amplifier or cathode follower.

A channel The left channel of a two-channel stereo system.

achieved reliability A statement of reliability based on the performance of mass-produced parts or systems under similar environmental conditions. Also called OPERATIONAL RELIABILITY.

achromatic **1.** Without color. In a TV image, the tones from black through gray to white. The term occasionally refers to black-and-white television, although MONOCHROMATIC is more often used in this sense.

achromatic locus Also called *achromatic region.* An area on a chromaticity diagram that contains all points, representing acceptable reference white standards.

achromatic scale A musical scale without accidentals.

ACIA Abbreviation of *asynchronous communications interface adapter.*

acicular Pertaining to the shape of magnetic particles on recording tape. Under magnification, these particles look like thin rods.

acid A substance that dissociates in water solution and forms hydrogen (H) ions (e.g., sulfuric acid). Compare BASE, **2.**

acid depolarizer Also called *acidic depolarizer.* An acid, in addition to the electrolyte, used in some primary cells to slow the process of polarization.

ac line A power line that delivers alternating current only.

ac line filter A filter designed to remove extraneous signals or electrical noise from an ac power line, while causing virtually no reduction of the power-line voltage or power.

ac line voltage The voltage commonly delivered by the commercial power line to consumers. In the United States, the two standards are 117 V and 234 V (~ about 5 percent). The lower voltage is used by most appliances; the higher voltage is intended for appliances and equipment that draws high power, such as electric ovens, cooking ranges, clothes dryers, and amateur-radio amplifiers. In Europe, 220 V is the common standard.

aclinic line Also called *magnetic equator.* An imaginary line drawn on a map of the world or of an area that connects points of zero inclination (dip) of the needle of a magnetic compass.

ACM Abbreviation for *Association for Computing Machinery.*

ac magnetic bias See AC BIAS.

5059F-pA_1-55 4/9/01 4:41 PM Page 8

ac meter A meter that is intended to work only on alternating current or voltage. Such meters include iron-vane and rectifier types.

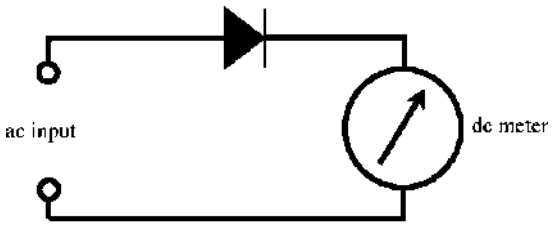

ac meter

ac noise **1.** Electromagnetic interference originating in the ac power lines. **2.** Electrical noise of a rapidly alternating or pulsating nature.

ac noise immunity In computer practice, the ability of a logic circuit to maintain its state, despite excitation by ac noise.

acous Abbreviation for ACOUSTIC.

acoustic Pertaining to audible sound disturbances, usually in air (versus audio-frequency currents or voltages).

acoustic absorption The assimilation of energy from sound waves passing through or reflected by a given medium.

acoustic absorption loss That portion of sound energy lost (as by dissipation in the form of heat) because of ACOUSTIC ABSORPTION.

acoustic absorptivity The ratio of sound energy absorbed by a material to sound energy striking the surface of the material.

acoustic attenuation constant The real-number component of the complex acoustical propagation constant, expressed in nepers per unit distance.

acoustic burglar alarm An alarm that receives the noise made by an intruder. The alarm device responds to the impulses from concealed microphones.

acoustic capacitance The acoustic equivalent of electrical capacitance.

acoustic clarifier In a loudspeaker system, a set of cones attached to the baffle that vibrate to absorb and suppress sound energy during loud bursts.

acoustic communication Communications by means of sound waves. This can be through the atmosphere, or it can be through solids or liquids, such as a taut wire, a body of water, or the earth.

acoustic compliance COMPLIANCE in acoustic transducers, especially loudspeakers. It is equivalent to electrical capacitive reactance.

acoustic consonance An effect that occurs when two objects are near each other but not in physical contact, and both have identical or harmonically related resonant frequencies. An example is shown by two tuning forks with identical fundamental frequencies. If one fork is struck and then brought near the other, the second fork will begin vibrating. If the second fork has a fundamental frequency that is a harmonic of the frequency of the first fork, the second fork will vibrate at its own resonant frequency. See HARMONIC, RESONANCE.

acoustic coupling Data transfer via a sound link between a telephone and a pickup/reproducer. Was once common in computer terminals and facsimile machines. This scheme has been largely replaced by hard wiring and optical coupling.

acoustic damping The deadening or reduction of the vibration of a body to eliminate (or cause to die out quickly) sound waves arising from it.

acoustic delay line Any equivalent of a special transmission line that introduces a useful time delay between input and output signals. In one form, it consists of a crystal block or bar with an input transducer at one end and an output transducer at the other. An electrical input signal in the first transducer sets up sound waves that travel through the interior of the crystal; the piezoelectric reaction of the crystal to sound vibrations sets up an output voltage in the second transducer. The delay is caused by the time required for the acoustic energy to travel the length of the crystal bar.

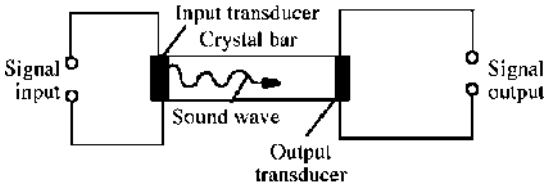

acoustic delay line

acoustic depth finder A direct-reading device for determining the depth of a body of water, or for locating underwater objects via sonic or ultrasonic waves transmitted downward and reflected back to the instrument.

acoustic dispersion Variation of the velocity of sound waves, depending on their frequency.

acoustic elasticity **1.** In a loudspeaker enclosure, the compressibility of air behind the vibrating cone of the speaker. **2.** In general, the compressibility of any medium through which sound passes.

acoustic electric transducer A transducer, such as a microphone or hydrophone, that converts sound energy into electrical energy. Compare ELECTRICAL/ACOUSTIC TRANSDUCER. Also see ACOUSTIC TRANSDUCER.

acoustic feedback A usually undesirable effect that occurs when sound waves from a loudspeaker (or other reproducer) reach a microphone (or other input transducer) in the same system.

5059F-pA_1-55 4/9/01 4:41 PM Page 9

This can cause an amplifier to oscillate, with a resultant rumbling, howling, or whistling.

acoustic filter Any sound-absorbing or transmitting arrangement, or combination of the two, that transmits sound waves of desired frequency while attenuating or eliminating others.

acoustic frequency response The sound-frequency range as a function of sound intensity. A means of describing the performance of an acoustic device.

acoustic generator A device that produces sound waves of a desired frequency and/or intensity. Examples are electrical devices (headphones or loudspeakers operated from a suitable oscillator, buzzer, bell, or flame) and mechanical devices (tuning forks, bells, string, or whistles).

acoustic grating A set of bars or slits that are parallel to one another and arranged a fixed distance apart so that an interference pattern forms as sound passes through. Used to determine the wavelength of acoustic waves.

acoustic homing system **1.** A system that uses a sound signal for guidance purposes. **2.** A guidance method in which a missile homes in on noise generated by a target.

acoustic horn A tapered tube (round or rectangular, but generally funnel-shaped) that directs sound and, to some extent, amplifies it. So called to distinguish it from a microwave horn.

acoustic howl See ACOUSTIC FEEDBACK.

acoustician **1.** A person skilled in acoustics (an acoustics technician). **2.** An AUDIOLOGIST.

acoustic impedance Unit, ACOUSTIC OHM. The acoustic equivalent of electrical impedance. Like the latter, acoustic impedance is the total opposition encountered by acoustic force. Also like electrical impedance, acoustic impedance has resistive and reactive components: ACOUSTIC RESISTANCE and ACOUSTIC REACTANCE.

acoustic inductance Also called *inertance.* The acoustic equivalent of electrical inductance.

acoustic inertance See ACOUSTIC INDUCTANCE.

acoustic inhibition See AUDITORY INHIBITION.

acoustic intensity See SOUND INTENSITY.

acoustic interferometer An instrument that evaluates the frequency and velocity of sound waves in a liquid or gas, in terms of a standing wave set up by a transducer and reflector as the frequency or transducer-to-reflector distance varies.

acoustic labyrinth A loudspeaker enclosure whose internal partitions form a maze-like path or "tube" lined with sound-absorbing material. The tube effectively runs from the back of the speaker down to where it terminates in a MOUTH or PORT that opens at the front of the enclosure. The labyrinth provides an extremely efficient reproduction system because of its excellent acoustic impedance-matching capability.

acoustic lens A system of barriers that refracts sound waves the way that an optical lens does with light waves.

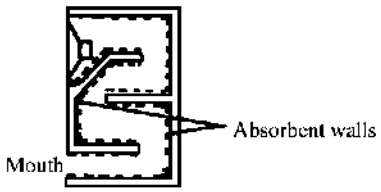

acoustic labyrinth

acoustic line Baffles or other such structures within a speaker that act as the mechanical equivalent of an electrical transmission line to enhance the reproduction of very low bass frequencies.

acoustic load A device that serves simultaneously as the output load of an amplifier and as a transducer of electrical energy into acoustic energy (e.g., headphones or a loudspeaker).

acoustic memory In a computer, a volatile memory element employing an acoustic delay line, often incorporating quartz or mercury as the transmission and delay element.

acoustic mirage A type of sound distortion in which the listener experiences the illusion of two sound sources when there is only one. The phenomenon is caused by the effect of a large temperature gradient in the air or water through which the sound passes.

acoustic mode Crystal-lattice vibration without producing an oscillating dipole.

acoustic noise Interferential (usually disagreeable) sounds carried by the air (or other propagation medium) to the ear or to an acoustic transducer. This is in contrast to electrical noise, which consists of extraneous current or voltage impulses and is inaudible until converted into sound.

acoustic ohm The unit of acoustic resistance, reactance, or impedance. One acoustic ohm equals the volume velocity of 1 cm/s produced by a sound pressure of 1 microbar (0.1 Pa). Also called *acoustical ohm.*

acoustic phase constant The imaginary-number component of the complex acoustic propagation constant expressed in radians per second or radians per unit distance.

acoustic phase inverter A bass reflex loudspeaker enclosure.

acoustic pressure **1.** The acoustic equivalent of electromotive force, expressed in dynes per square centimeter; also called *acoustical pressure.* **2.** Sound pressure level.

acoustic propagation The transmission of sound waves, or subaudible or ultrasonic waves, as a disturbance in a medium, rather than as an electric current or electromagnetic field.

acoustic radiator A device that emits sound waves. Examples are the cone of a loudspeaker, the diaphragm of a headphone, and the vibrating reed of a buzzer.

5059F-pA_1-55 4/9/01 4:41 PM Page 10

acoustic radiometer An instrument for measuring the intensity of a sound wave (see SOUND INTENSITY) in terms of the unidirectional steady-state pressure exerted at a boundary as a result of absorption or reflection of the wave.

acoustic reactance Unit, ACOUSTIC OHM. The imaginary-number component of ACOUSTIC IMPEDANCE. It can take the form of ACOUSTIC CAPACITANCE or ACOUSTIC INDUCTANCE.

acoustic reflectivity The ratio F_r/F_i, where F_r is the rate of flow of sound energy reflected from a surface and F_i is the rate of flow of sound energy incident to the surface.

acoustic refraction The deflection of sound waves being transferred obliquely between media that transmit sound at different speeds.

acoustic regeneration See ACOUSTIC FEEDBACK.

acoustic resistance Unit, ACOUSTIC OHM. The real-number component of ACOUSTIC IMPEDANCE. The opposing force that causes acoustic energy to be dissipated in the form of heat. It is attributed to molecular friction in the medium through which sound passes. See ACOUSTIC OHM.

acoustic resonance In an enclosed chamber with walls that reflect sound waves, resonance that occurs at certain wavelengths because the echoes combine in and out of phase. Speaker enclosures almost always have resonance at certain frequencies. This effect can be used to an advantage when it is necessary to get good bass (low-frequency) response from a relatively small speaker.

acoustic resonator **1.** A chamber, such as a box, cylinder, or pipe, in which an air column resonates at a particular frequency. **2.** A piezoelectric, magnetostrictive, or electrostrictive body that vibrates at a resonant audio frequency that is governed by the mechanical dimensions of the body when an audio voltage at that frequency is applied.

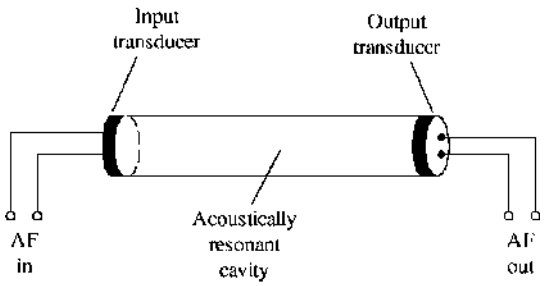

acoustic resonator, 1

acoustics **1.** The physics of sound. The study and applications of acoustic phenomena. **2.** The qualities of an enclosure or sound chamber (room, auditorium, or box) that describe how sound waves behave in it.

acoustic scattering The spreading of a sound wave in many directions as a result of diffraction, reflection, or refraction.

acoustic suspension A loudspeaker design that allows exceptional low-frequency reproduction for a fairly small physical size. An airtight enclosure is used to increase the tension on the speaker cone.

acoustic system **1.** A coordinated array of acoustic components (e.g., acoustic filters, resonators, etc.) that responds to sound energy in a predetermined manner. **2.** An audio-frequency system in which sound energy is converted into electrical energy, processed, and then reconverted into sound energy for a clearly defined purpose.

acoustic telegraph A telegraph that gives audible signals, as opposed to visual signals or printed messages.

acoustic transducer **1.** Any device, such as headphones or a loudspeaker, for converting audio-frequency electrical signals into sound waves. **2.** Any device, such as a microphone, for converting sound waves into alternating, pulsating, or fluctuating currents.

acoustic transmission The direct transmission of sound energy without the intermediary of electric currents.

acoustic transmission system A set of components designed to generate acoustic waves.

acoustic transmissivity Also called *acoustic transmitivity.* The ratio e_t/e_i, where e_t is the sound energy transmitted by a medium, and e_i is the incident sound energy reaching the surface of the medium. Acoustic transmissivity is proportional to the angle of incidence.

acoustic treatment Application of sound-absorbing materials to the interior of an enclosure or room to control reverberation.

acoustic wave The traveling vibration, consisting of molecular motion, via which sound is transmitted through a gas, liquid or solid. Usually refers to sound waves in air.

acoustic wave filter See ACOUSTIC FILTER.

acoustoelectric effect The generation of a voltage across the faces of a crystal by sound waves traveling longitudinally through the crystal.

acoustoelectronics A branch of electronics concerned with the interaction of sound energy and electrical energy in devices, such as surface-wave filters and amplifiers. In such devices, electrically induced acoustic waves travel along the surface of a piezoelectric chip and generate electrical energy. Also called *praetersonics* and *microwave acoustics.*

ac plate current Symbol, $I_{P(ac)}$. The ac component of plate current in a vacuum tube.

ac plate resistance Symbol, $R_{P(ac)}$. The dynamic plate resistance of an electron tube. $R_{P(ac)}$ equals dE_P/dI_P, where E_P is the plate voltage and I_P is the plate current, for a constant value for grid voltage E_G.

5059F-pA_1-55 4/9/01 4:41 PM Page 11

ac plate voltage Symbol, $E_{P(ac)}$. The ac component of plate voltage in an electron tube. The ac output-signal voltage in a common-cathode amplifier.

ac power Symbol, P_{ac}. Unit, watt (W). The power acting in an ac circuit, P_{ac} equals $EI \cos q$, where E is in volts, I in amperes, and q is the phase angle. Compare DC POWER. Also see POWER.

ac power supply A power unit that supplies ac only (e.g., ac generator, vibrator-transformer, oscillator, or inverter). Compare DC POWER SUPPLY.

acquisition **1.** The gathering of data from transducers or a computer. **2.** Locating the path of an orbiting body for purposes of collecting telemetered data. **3.** Orienting an antenna for optimum pickup of telemetered data.

acquisition and tracking radar An airborne or ground radar, which locks in on a strong signal and tracks the body that reflects (or transmits) the signal.

acquisition radar A radar that spots an oncoming target and supplies position data regarding the target to a fire-control or missile-guidance radar, which then tracks the target.

acr **1.** Abbreviation of AUDIO CASSETTE RECORDER. **2.** Abbreviation of AUDIO CASSETTE RECORDING SYSTEM.

ac reclosing relay The controlling component in an alternating-current circuit breaker. It causes the breaker to reset after a specified period of time.

ac relay A relay designed to operate on alternating current without chattering or vibrating.

ac resistance Pure resistance in an ac circuit. Unlike reactance and impedance, which are also forms of opposition to the flow of current, ac resistance introduces no phase shift.

acronym A word formed from letters or syllables taken from other applicable words of a multiword term. Acronyms are convenient for naming new devices and processes in electronics. Usually, a term is considered an acronym only when it is spelled in all-capital letters; once the term is accepted and popularized, it is written as a conventional word and is no longer thought of as an acronym. For example, *LASER* was once an acronym for light amplification by the stimulated emission of radiation. By the popularization process, the acronym became a conventional word from which other terms (such as the verb "lase") were derived.

acrylic resin A synthetic resin used as a dielectric and in electronic encapsulations. It is made from acrylic acid or one of its derivatives.

ACS Abbreviation of *automatic control system.*

ac source current Symbol, $I_{S(ac)}$. The ac component of source current in a field-effect transistor.

ac source resistance Symbol, $R_{S(ac)}$. The dynamic source resistance in a field-effect transistor; $R_{S(ac)}$ equals dV_S/dI_S for a constant value of V_G.

ac source voltage Symbol, $V_{S(ac)}$. The ac component of source voltage in a field-effect transistor. The ac output-signal voltage in a source-follower (grounded-drain) FET amplifier.

acss Abbreviation of *analog computer subsystem.*

ac time overcurrent relay A device with a certain time characteristic, which breaks a circuit when the current exceeds a certain level.

actinic rays Short-wavelength light rays in the violet and ultraviolet portion of the spectrum that give conspicuous photochemical action.

actinism The property whereby radiant energy (such as visible and ultraviolet light, X-rays, etc.) causes chemical reactions.

actinium Symbol, Ac. A radioactive metallic element. Atomic number, 89. Atomic weight, 227.

actinodielectric Exhibiting a temporary rise in electrical conductivity during exposure to light.

actinoelectric effect The property whereby certain materials (such as selenium, cadmium sulfide, germanium, and silicon) change their electrical resistance or generate a voltage on exposure to light. Also see ACTINODIELECTRIC.

actinometer An instrument for measuring the direct heating power of the sun's rays or the actinic power of a light source.

action current A small transient current that flows in a nerve in the human body as a result of stimulation.

activate To start an operation, usually by applying an appropriate enabling signal.

activation **1.** Supplying electrolyte to a battery cell to prepare the cell for operation. **2.** Causing the acceleration of a chemical reaction.

activation time In the activation of a battery cell (see ACTIVATION, **1**), the interval between addition of the electrolyte and attainment of full cell voltage.

activator A substance added to an accelerator (see ACCELERATOR, **3**) to speed the action of the accelerator.

active Pertaining to a circuit or device that requires a power supply for its operation. This differs from a passive circuit or device, which operates with no external source of power.

active antenna An antenna that uses a small whip, loop, or ferrite loopstick with a high-gain amplifier for receiving at very-low, low, medium, and high radio frequencies (approximately 9 kHz to 30 MHz).

active area The forward-current-carrying portion of the rectifying junction of a metallic rectifier.

active arm See ACTIVE LEG.

active balance In telephone repeater operation, the sum of return currents at a terminal network balanced against the local circuit or drop resistance.

active chord mechanism Abbreviation, ACM. In robots, an electromechanical gripper capable of conforming to irregular objects. It has a structure similar to the human spine, with numerous small, rigid links connected by hinges.

5059F-pA_1-55 4/9/01 4:41 PM Page 12

active communications satellite A satellite containing receivers (which pick up beamed electromagnetic signals from a ground point and amplify them) and transmitters (which send signals back to the surface of the earth). Also called *active comsat.* Compare PASSIVE COMMUNICATIONS SATELLITE.

active component **1.** A device capable of some dynamic function (such as amplification, oscillation, or signal control) that usually requires a power supply for its operation. Examples include bipolar transistors, field-effect transistors, and integrated circuits. Compare PASSIVE COMPONENT. **2.** In an ac circuit, a quantity that contains no reactance so that the current is in phase with the voltage.

active component of current See ACTIVE CURRENT.

active computer A computer in an installation or network that is processing data.

active comsat See ACTIVE COMMUNICATIONS SATELLITE.

active control system A device or circuit that compensates for irregularities in the operating environment.

active current In an ac circuit, the current component that is in phase with the voltage. This is in contrast to reactive current, which is not in phase with the voltage, and is "inactive," with respect to power in the circuit. The active current is equal to the average power divided by the effective voltage.

active decoder An automatic ground-station device that gives the number or letter designation of a received radio beacon reply code.

active device **1.** An electronic component, such as a transistor that needs a power supply, and/or that is capable of amplifying. **2.** Broadly, any device (including electromechanical relays) that can switch (or amplify) by application of low-level signals.

active electric network A network containing one or more active devices or components, usually amplifiers or generators, in addition to passive devices or components.

active element The driven or RF-excited element in a multielement antenna or antenna array.

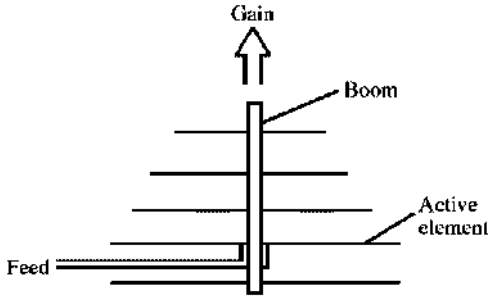

active element

active file A computer file in use (i.e., one that is being updated or referred to).

active filter A bandpass, bandstop, highpass or lowpass filter, consisting of resistors, capacitors, and operational amplifiers, arranged to pass a desired frequency response. Commonly used at audio frequencies.

active infrared detection Detection of infrared rays reflected from a target to which they were beamed.

active jamming Transmission or retransmission of signals for the purpose of disrupting communications.

active junction A pn junction in a semiconductor device that has been created by a diffusion process.

active leg An element within a transducer that changes one or more of its electrical characteristics in response to the input signal of the transducer. Also called *active arm.*

active lines In a U.S. television picture, the lines (approximately 488) that make up the picture. The remaining 37 of the 525 available lines are blanked and are called INACTIVE LINES.

active material **1.** In a storage cell, the chemical material in the plates that provides the electrical action of the cell, as distinguished from the supporting material of the plates themselves. **2.** A radioactive substance. **3.** The phosphor coating of a cathode-ray tube screen. **4.** The material used to coat an electron-tube cathode.

active mixer A signal mixer using one or more active components, such as transistors or integrated circuits. An active circuit provides amplification, input-output isolation, and high input impedance, in addition to the mixing action. Compare PASSIVE MIXER.

active modulator A modulator using one or more active components, such as transistors or integrated circuits. An active circuit provides gain, input-output isolation, and high input impedance, in addition to modulation. Compare PASSIVE MODULATOR.

active network See ACTIVE ELECTRIC NETWORK.

active pressure The electromotive pressure that produces a current in an ac circuit.

active pull-up An arrangement using a transistor as a pull-up resistor replacement in an integrated circuit, providing low output impedance and low power consumption.

active RC network **1.** A resistance-capacitance (RC) circuit that contains active components (transistors or integrated circuits), as well as passive components (capacitors and resistors). **2.** An RC network in which some or all of the resistors and capacitors are simulated by the action of active components.

active repair time The time during which maintenance is done on a system and the system is out of operation.

5059F-pA_1-55 4/9/01 4:41 PM Page 13

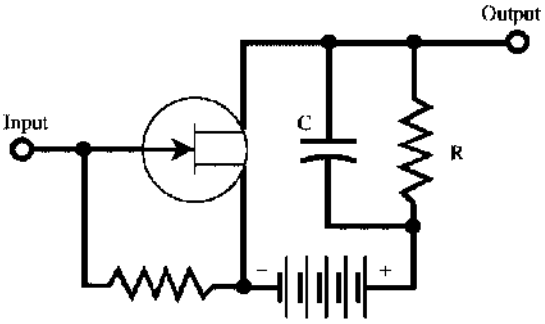

active RC network

active satellite See ACTIVE COMMUNICATIONS SATELLITE.

active sensor In an electronic security system, a transducer that generates an electromagnetic field or acoustic-wave field, and detects changes in the field resulting from the presence or movement of objects in the vicinity.

active substrate In an integrated circuit, a substrate consisting of single-crystal semiconductor material into which the components are formed; it acts as some or all of the components. This is in contrast to a substrate consisting of a dielectric, where the components are deposited on the surface.

active system A radio and/or radar system that requires transmitting equipment to be carried in a vehicle.

active tracking system A system in which a transponder or responder on board a vehicle retransmits information to tracking equipment (e.g., *azusa*, *secor*).

active transducer **1.** A transducer that contains an active device, such as a transistor or integrated circuit, for immediate amplification of the sensed quantity. **2.** A transducer that is itself an active device.

active wire In the armature of a generator, a wire experiencing induction and, therefore, is delivering voltage.

activity **1.** Intensity of, as well as readiness for, oscillation in a piezoelectric crystal. **2.** Radioactive intensity. **3.** Intensity of thermal agitation. **4.** Thermionic emission of electrons.

activity ratio The ratio of active to inactive records in a computer file.

ac transducer A transducer that either requires an ac supply voltage or delivers an ac output signal—even when operated from a dc supply.

ac transmission The use of an alternating voltage to transfer power from one point to another, usually from generators to a distribution center, and generally over a considerable distance.

actual ground The ground as "seen" by an antenna. The actual ground surface is not necessarily in the same physical location as the true ground surface (i.e., the earth itself). An actual ground can be an artificial ground plane, such as that provided in some antenna structures. Actual ground can also be modified by nearby rooftops, buildings, guy wiring, and utility wiring.

actual height The highest altitude where radio wave refraction actually occurs.

actual power Also called active or AVERAGE POWER. Symbol, P_{avg}. In a resistive circuit under sine-wave conditions, average power is the product of the rms voltage and the rms current. It is also equal to half the product of the maximum current and maximum voltage.

actuating device A device or component that operates electrical contacts to affect signal transmission.

actuating system **1.** An automatic or manually operated system that starts, modifies, or stops an operation. **2.** A system that supplies energy for ACTUATION.

actuating time Also called *actuation time.* The time interval between generation of a control signal, or the mechanical operation of a control device, and the resulting ACTUATION.

actuation **1.** The starting, modification, or termination of an operation or process. **2.** Activation of a mechanical or electromechanical switching device.

actuator An electromechanical device that uses electromagnetism to produce a longitudinal or rotary thrust for mechanical work. It is often the end (load) device of a servosystem.

ACU Abbreviation of *automatic calling unit.*

ac voltage A voltage, the average value of which is zero, that periodically changes its polarity. In one cycle, an ac voltage starts at zero, rises to a maximum positive value, returns to zero, rises to a maximum negative value, and finally returns to zero. The number of such cycles per second is termed the *ac frequency.*

ac voltmeter See AC METER.

acyclic machine Also called ACYCLIC GENERATOR. A dc generator in which voltage induced in the active wires of the armature is always of the same polarity.

A/D Abbreviation for ANALOG-TO-DIGITAL. See ANALOG-TO-DIGITAL CONVERSION.

Ada A microcomputer language designed primarily for use in multi-computer systems, where each small computer communicates with the others, providing some of the advantages of a larger computer.

Adam A communications code word sometimes used for phonetic verbalizing of the letter A. More commonly, ALPHA is used.

adapter **1.** A fitting used to change either the terminal scheme or the size of a jack, plug, or socket to that of another. **2.** A fitting used to provide a transition from one type or style of conductor to another (e.g., waveguide to coaxial line). **3.** An

5059F-pA_1-55 4/9/01 4:41 PM Page 14

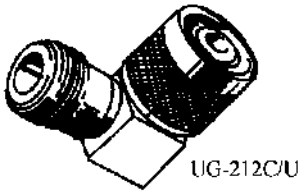

adapter

auxiliary system or unit used to extend the operation of another system (e.g., a citizens-band adapter for a broadcast receiver).

adaptive communication A method of communication that adjusts itself according to the particular requirements of a given time.

adaptive suspension vehicle Abbreviation, ASV. A specialized robot that moves on mechanical legs, rather than on wheels. It generally has six legs and resembles an insect. It is designed to move over extremely irregular or rocky terrain, and to carry a human passenger.

adaptivity The ability of a system to respond to its environment by changing its performance characteristics.

adc Abbreviation of ANALOG-TO-DIGITAL CONVERTER.

Adcock antenna A directional antenna system consisting of two vertical antennas, spaced in such a way that the whole array behaves like a loop antenna. Its members are connected and positioned so that it discriminates against horizontally polarized waves, and delivers output that is proportional to the vector difference of signal voltages induced in the two vertical arms.

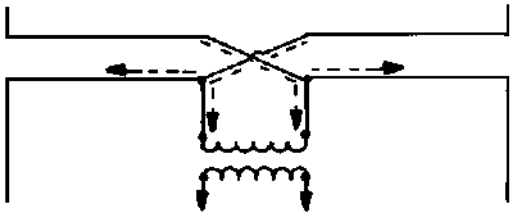

Adcock antenna

Adcock direction finder A radio direction-finding system based on the directivity of the ADCOCK ANTENNA.

Adcock radio range A radio range system with four ADCOCK ANTENNAS situated at the corners of a square, and a fifth antenna at the center of the square.

add-and-subtract relay A stepping relay that can be switched either uprange (add) or downrange (subtract).

addend In a calculation, any number to be added to another. Compare AUGEND.

addend register In a digital computer, the register that stores the addend.

adder **1.** In a digital computer, the device or circuit that performs binary addition. A HALF ADDER is a two-input circuit that can produce a sum output and a carry output, but it cannot accommodate a carry signal from another adder. A FULL ADDER can accommodate a carry input, as well as two binary signals to be added. Also see ANALOG ADDER. **2.** A circuit in a color TV receiver that amplifies the receiver primary matrix signal.

additive **1.** The character or characters added to a code to encipher it. **2.** In a calculation, an item that is to be added. **3.** An ingredient, usually in a small quantity, added to another material to improve the latter in quality or performance.

additive color A color formed by combining the rays from two or three primary-colored lights onto a single neutral surface. For example, by projecting a red and a green beam onto a neutral screen, a yellow additive color results.

additive primaries Primary colors that form other colors in a mixing of light (see ADDITIVE COLOR), but are not themselves formed by mixing other additive primaries. For example, red, green, and blue are the additive primaries used in color television. Through appropriate mixing, these colors can be used to generate an unlimited variety of other colors. Compare SUBTRACTIVE PRIMARIES, which form the color spectrum by mixing pigments rather than lights. In additive systems, each superimposed primary color increases the total light output from the reflecting (viewing) surface; in subtractive systems, each superimposed primary decreases the total reflectivity. Thus, equal combination of additive primaries produces gray or white, and equal combination of subtractive primaries produces gray or black.

addition record An extra data store created in a computer during processing.

address **1.** In computer operations, a usually numerical expression designating the location of material within the memory or the destination of such material. **2.** The accurately stated location of information within a computer; a data point within a grid, matrix, or table; a station within a network. **3.** In computer operations, to select the location of stored information.

address comparator A device that ensures that the address being read is correct.

address computation In digital computer operations, the technique of producing or modifying only the address part of an instruction.

address field In a computer, the part of the instruction that gives the address of a bit of data (or a word) in the memory.

address generation The programmed generation of numbers or symbols used to retrieve records from a randomly stored direct-access file.

5059F-pA_1-55 4/9/01 4:41 PM Page 15

address indirect An address that specifies a storage location that contains another address.

address memory The memory sections in a digital computer that contain each individual register.

address modification In computer operations, altering only the address portion of an instruction; if the command or instruction routine is then repeated, the computer will go to the new address.

address part In a digital computer instruction, the part of an expression that specifies the location. Also called ADDRESS FIELD.

address register In a computer, a register in which an address is stored.

add/subtract time In a computer, the time required to perform addition or subtraction, excluding the time required to get the quantities from storage and to enter the sum or difference into storage.

add time In computer operations, the time required to perform addition, excluding the time required to get the quantities from storage and to enter the sum into storage.

a/d converter A device that changes an analog quantity into a digital signal. See ANALOG-TO-DIGITAL CONVERSION.

ADF Abbreviation of AUTOMATIC DIRECTION FINDER.

ADI Abbreviation of ALTERNATE DIGIT INVERSION.

adiabatic damping In an accelerator (see ACCELERATOR, **1**), reduction of beam size as beam energy is increased.

adiabatic demagnetization A technique using a magnetic field to keep a substance at a low temperature, sometimes within a fraction of a degree of absolute zero.

adjacency A character-recognition condition in which the spacing reference lines of two characters printed consecutively in line are closer than specified.

adjacent- and alternate-channel selectivity The selectivity of a receiver or radio-frequency (RF) amplifier, with respect to adjacent-channel and alternate-channel signals. That is, the extent to which a desired signal is passed, and nearby unwanted signals are rejected.

adjacent audio channel See ADJACENT SOUND CHANNEL.

adjacent channel The channel (frequency band) immediately above or below the channel of interest.

adjacent-channel attenuation The reciprocal of the *selectivity ratio* of a radio receiver. The selectivity ratio is the ratio of the sensitivity of a receiver (tuned to a given channel) to its sensitivity in an adjacent channel or on a specified number of channels removed from the original.

adjacent-channel interference In television or radio reception, the interference from stations on adjacent channels. A common form arises from the picture signal in the next higher channel and the sound signal in the next lower channel.

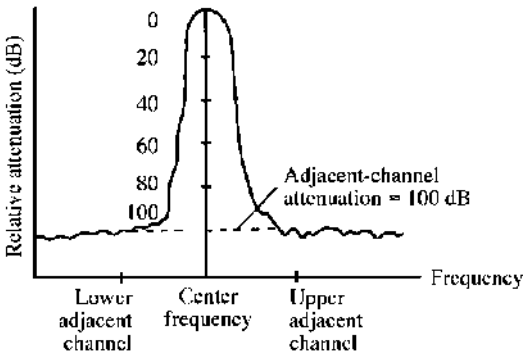

adjacent-channel attenuation

adjacent-channel selectivity The extent to which a receiver or tuned circuit can receive on one channel and reject signals from the nearest outlying channels.

adjacent sound channel In television, the radio-frequency (RF) channel containing the sound modulation of the next lower channel.

adjacent video carrier In television, the radio-frequency (RF) carrier containing the picture modulation of the next higher channel.

adjustable component Any circuit component whose main electrical value can be varied at will (e.g., a variable capacitor, inductor, resistor, or load).

adjustable instrument **1.** An instrument whose sensitivity, range, or response can be varied at will (e.g., multirange meter or wideband generator). **2.** An instrument that requires adjustment or manipulation to measure a quantity (e.g., bridge, potentiometer, or attenuator).

adjustable motor tuning An arrangement that allows the motor tuning of a receiver to be confined to a portion of the frequency spectrum.

adjustable resistor A wirewound resistor in which the resistance wire is partially exposed to allow varying the component's value.

adjustable voltage divider A wirewound resistor with terminals that slide on exposed resistance wire to produce various voltage values.

adjusted circuit A circuit in which leads that are normally connected to a circuit breaker are shunted so that current can be measured under short-circuit conditions without breaker tripping.

adjusted decibels Noise level (in decibels) above a reference noise level (designated arbitrarily as zero decibels) measured at any point in a system with a noise meter that has previously been adjusted for zero (at reference), according to specifications.

5059F-pA_1-55 4/9/01 4:41 PM Page 16

admittance Symbol, *Y*. Unit, siemens (formerly mho). The property denoting the comparative ease with which an alternating current flows through a circuit or device. Admittance is the reciprocal of impedance (*Z*): $Y = 1/Z$.

adp **1.** Abbreviation of AMMONIUM DIHYDROGEN PHOSPHATE, a piezoelectric compound used for sonar crystals. **2.** Abbreviation of AUTOMATIC DATA PROCESSING.

adsorption Adhesion of a thin layer of molecules of one substance to the surface of another without absorption. An example is adsorption of water to the surface of a dielectric. This term is often confused with ABSORPTION because the spellings of the two words are almost identical. Compare ABSORPTION.

adu Abbreviation of *automatic dialing unit.*

advanced-class license An amateur-radio license conveying all operating privileges, except for a few small bands that are allocated to extra-class licensees. The second-highest class of amateur license.

advance information Data published prior to the actual production or availability of a manufactured component, circuit, or system. Advance information is often only an approximate reflection of the expected characteristics of a device.

advance wire A resistance wire used in thermocouples and precision applications. It is an alloy of copper and nickel, which has high resistivity and a negligible temperature coefficient of resistance.

aeolight A glow lamp using a cold cathode and a mixture of inert gases. Because its illumination can be regulated with an applied signal voltage, it is sometimes used as a modulation indicator for motion-picture sound recording.

aerial See ANTENNA.

aerial cable A wire or cable run through the air, using support structures, such as towers or poles.

aerodiscone antenna A miniature discone antenna designed for use on aircraft.

aerodynamics The science dealing with forces exerted by air and other gases in motion—especially upon bodies (such as aircraft) moving through these gases.

aerogram See RADIOGRAM.

aeromagnetic Pertaining to terrestrial magnetism, as surveyed from a flying aircraft.

aeronautical advisory station A civil defense and advisory communications station in service for the use of private aircraft stations.

aeronautical broadcasting service The special service that broadcasts information regarding air navigation and meteorological data pertinent to aircraft operation.

aeronautical broadcast station A station of the aeronautical broadcasting service.

aeronautical fixed service A fixed radio service that transmits information regarding air navigation and flight safety.

aeronautical fixed service station A station that operates in the aeronautical fixed service.

aeronautical ground station A land station that provides communication between aircraft and ground stations.

aeronautical marker-beacon signal A distinctive signal that designates a small area above a beacon transmitting station for aircraft navigation.

aeronautical marker-beacon station A land station that transmits an aeronautical marker-beacon signal.

aeronautical mobile service A radio service consisting of communications between aircraft, and between aircraft and ground stations.

aeronautical radio-beacon station An aeronautical radio-navigation land station that transmits signals used by aircraft and other vehicles to determine their position.

aeronautical radionavigation services Services provided by stations transmitting signals used in the navigation of aircraft.

aeronautical radio service A service that encompasses aircraft-to-aircraft, aircraft-to-ground, and ground-to-aircraft communications important to the operation of aircraft.

aeronautical station A station on land, and occasionally aboard ship, operating in the aeronautical mobile service.

Aeronautical Telecommunication Agency The agency that administers the operation of stations in the aeronautical radio service.

aeronautical telecommunications Collectively, all of the electronic and nonelectronic communications used in the aeronautical service.

aeronautical utility land station A ground station in an airport control tower that provides communications having to do with the control of aircraft and other vehicles on the ground.

aeronautical utility mobile station At an airport, a mobile station that communicates with aeronautical utility land stations and with aircraft and other vehicles on the ground.

aerophare See RADIO BEACON.

aerospace **1.** The region encompassing the earth's atmosphere and extraterrestrial space. **2.** Pertaining to transport and travel in the earth's atmosphere and in outer space. This includes aircraft, orbiting space vessels, and interplanetary spacecraft.

AES Abbreviation for *Audio Engineering Society.*

AEW Abbreviation of *airborne (or aircraft) early warning.*

aF Abbreviation of ATTOFARAD.

AF Abbreviation of AUDIO FREQUENCY.

AFC **1.** Abbreviation of AUTOMATIC FREQUENCY CONTROL. **2.** Abbreviation of AUDIO-FREQUENCY CHOKE.

affirmative In voice communications, a word often used for "yes"—especially when interference is present or signals are weak.

5059F-pA_1-55 4/9/01 4:41 PM Page 17

AFIPS Acronym for *American Federation of Information Processing Societies.*

afpc Abbreviation of *automatic frequency/phase control.*

AFSK Abbreviation of AUDIO-FREQUENCY-SHIFT KEYING.

afterglow The tendency of the phosphor of a cathode-ray-tube screen to glow for a certain time after the cathode-ray beam has passed. Also see PERSISTENCE.

afterpulse An extraneous pulse in a multiplier phototube (photomultiplier), induced by a preceding pulse.

AF transformer See AUDIO-FREQUENCY TRANSFORMER.

a/g Abbreviation of AIR-TO-GROUND.

AGC Abbreviation of AUTOMATIC GAIN CONTROL.

AGE Abbreviation of AEROSPACE GROUND EQUIPMENT.

agent An active force, condition, mechanism, or substance that produces or sustains an effect. Thus, a sudden voltage rise is a triggering agent in certain bistable circuits; arsenic is a doping agent in semiconductor processing; the slow cooling of a heated metal to improve ductility is an ANNEALING AGENT.

aging **1.** An initial run of a component or circuit over a certain period of time shortly after manufacture to stabilize its characteristics and performance. **2.** The changing of electrical characteristics or of chemical properties over a protracted period of time.

agonic line An imaginary line connecting points on the earth's surface at which a magnetic needle shows zero declination (i.e., points to true geographic north).

AGREE Acronym for *Advisory Group on Reliability of Electronics Equipment.*

Ah Abbreviation of AMPERE-HOUR. Depending on the standard used, the abbreviation can be amp-hr, a-h, a-hr, or A-h.

aH Abbreviation of ATTOHENRY.

aided tracking In radar and fire control, a system in which manual correction of target tracking error automatically corrects the rate of movement of the tracking mechanism.

AIEE Abbreviation for *American Institute of Electrical Engineers*, now consolidated with the IRE, forming the IEEE.

AIP Abbreviation for *American Institute of Physics.*

air The mixture of gases that constitutes the earth's atmosphere and figures prominently in the manufacture and operation of numerous electronic devices. By volume, air contains about 21 percent oxygen, 78 percent nitrogen, and lesser amounts of argon, carbon dioxide, helium, hydrogen, krypton, neon, and xenon. It also contains varying amounts of water vapor, and in smoggy areas, carbon monoxide and the oxides of sulfur and nitrogen.

airborne intercept radar A type of short-range radar used aboard fighter and interceptor aircraft for tracking their targets.

airborne long-range input Equipment aboard aircraft, for the purpose of facilitating the use of long-range missiles.

airborne noise See ACOUSTIC NOISE.

airborne radar platform Surveillance and altitude-finding radar used aboard aircraft.

air capacitor A capacitor in which air is the dielectric between two sets of conductive plates. Also called *air-dielectric capacitor.*

aircarrier aircraft station On an aircraft, a radio station that is involved in carrying people for hire or in transporting cargo.

air cell A primary electrochemical cell in which the positive electrode is depolarized by reduced oxygen in the air.

air cleaner See DUST PRECIPITATOR.

air column The open space inside an acoustic chamber, pipe, or horn.

air-cooled component A component, such as a power transistor, that is cooled by circulating air, compared with one cooled by a circulating liquid, such as water or oil.

air-cooled transistor A transistor (particularly a power transistor) from which the heat of operation is drawn away, through radiation and convection, into the surrounding air. The transistor is usually mounted on a heatsink or fitted with fins.

air-cooled tube An electron tube from which heat is drawn away, mainly via convection, into the surrounding air. A device called a *chimney* can be placed around the tube, through which air is blown by a fan. Cool air enters through the bottom of the assembly, and hot air escapes from the top.

air-core inductor A coil of wire wound around a hollow cylindrical form or in a loop, designed to introduce inductive reactance into a circuit or system. In practice, the maximum attainable inductance is approximately 1 mH. This type of inductor is used in some wireless transmitters, receivers, and antenna networks. The component can be designed for high current-carrying capacity by using heavy-gauge wire and a large winding radius. The magnetic lines of flux extend considerably beyond the interior of the coil, especially along the winding axis. This increases the likelihood of mutual inductance between the coil and surrounding electrical components, devices, or circuits.

air-core transformer A transformer without a ferromagnetic core, so called because air is the only material at the center of (and immediately surrounding) the transformer coils.

aircraft bonding The practice of solidly connecting, for electrical purposes, the metal parts of an aircraft, including the engine.

5059F-pA_1-55 4/9/01 4:41 PM Page 18

aircraft flutter Rapid, repetitive fading and intensifying of a received radio or television signal, resulting from reflections of the signal by passing aircraft.

aircraft station A nonautomatic radio communications station installed on an aircraft.

air-dielectric coax A special type of COAXIAL CABLE designed to have minimum loss. The space between inner and outer conductors is mostly empty (i.e., air-filled). Some such cables are sealed and filled with an inert gas. The inner conductor is held away from the inner wall of the outer conductor by beads, washers, or a spiral-wound filament of high-grade dielectric material, such as polyethylene.

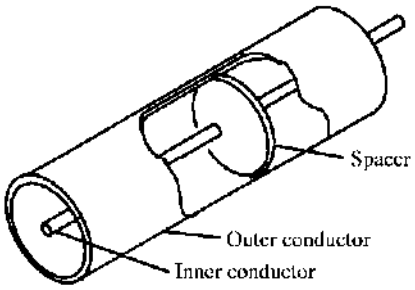

air-dielectric coax

air environment Pertaining to communications equipment aboard aircraft.

airflow The path or movement of air in, through, or around an electronic device or piece of equipment—especially pertaining to an AIR-COOLED COMPONENT.

air gap **1.** A narrow space between two parts of a magnetic circuit (e.g., the gap in the core of a filter choke). Often, this gap is filled with a nonmagnetic material, such as plastic, for mechanical support. **2.** The space between two or more magnetically coupled or electrostatically coupled components. **3.** A device that gets its name from the narrow gap between two small metal balls, needle points, or blunt rod tips therein. When an applied voltage is sufficiently high, a spark discharges across the gap.

air/ground control radio station A station for aeronautical telecommunications related to the operation and control of local aircraft.

air-insulated line **1.** An open-wire feeder or transmission line. Typically, the line consists of two parallel wires held apart by separators (bars or rods of high-grade dielectric material) situated at wide intervals. **2.** AIR-DIELECTRIC COAX.

air-moving device A mechanical device, such as a specially designed fan or blower, used to facilitate air cooling of electronic components.

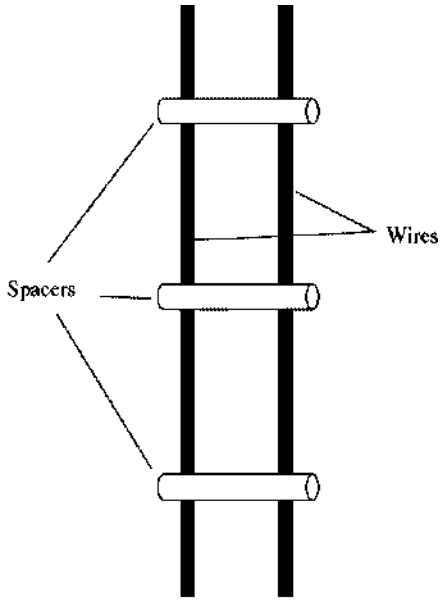

air-insulated line, 1

airport beacon A radio or light beacon that marks the location of an airport.

airport control station A station that provides communications between an airport control tower and aircraft in the vicinity.

airport surveillance radar An air-traffic-control radar that scans the airspace within about 60 miles (approximately 100 kilometers) of an airport, and displays in the control tower the location of all aircraft below a certain altitude and all obstructions in the vicinity.

air-position indicator An airborne computer system that, using airspeed, aircraft heading, and elapsed time, furnishes a continuous indication of the position of the aircraft. The indication is affected by high-altitude winds. Compare GROUND-POSITION INDICATOR.

air-to-air communication Radio transmission from one aircraft to another in flight. Compare AIR-TO-GROUND COMMUNICATION and GROUND-TO-AIR COMMUNICATION.

air-to-ground communication Radio transmission from an aircraft in flight to a station located on the ground. Compare AIR-TO-AIR COMMUNICATION and GROUND-TO-AIR COMMUNICATION.

air-to-ground radio frequency The carrier frequency, or band of such frequencies, allocated for transmissions from an aircraft to a ground station.

airwaves **1.** Radio waves. The term is slang, but is widely used. It probably came from the public's

5059F-pA_1-55 4/9/01 4:41 PM Page 19

mistaken notion that radio signals are propagated by the air. **2.** Skywaves.

Al Symbol for ALUMINUM.

alabamine See ASTATINE.

alacratized switch A mercury switch in which the tendency of the mercury to stick to the parts has been reduced.

alarm **1.** An electronic security system. **2.** A silent and/or audible alert signal transmitted by an electronic security system when an intrusion occurs. **3.** A silent and/or audible signal that informs personnel of the occurrence of an equipment malfunction.

alarm circuit A circuit that alerts personnel to a system malfunction, a detected condition, or an intruder.

alarm condition **1.** An intrusion or equipment malfunction that triggers an alarm circuit. **2.** The operation of an alarm circuit that occurs in response to an intrusion or equipment malfunction.

alarm hold A device that keeps an alarm sounding once it has been actuated.

alarm output The signal sent from an alarm circuit to a siren, buzzer, computer, or other external device to alert personnel to an ALARM CONDITION.

alarm relay A relay that is actuated by an alarm device.

A-law A form of companding law frequently used in European electronics (the mu-law is more often used in North America). A nonlinear transfer characteristic in companding circuits. It can be continuous, or can be a piecewise linear approximation of a continuous function.

A-law companded Companding by means of an 8-bit binary code following the A-LAW, a specific companding function.

albedo For an unpolished surface, the ratio of reflected light to incident light. It can vary from 0.0 to 1.0, or from 0 to 100 percent.

albedograph An instrument for measuring the albedo of planets.

ALC Abbreviation of AUTOMATIC LEVEL CONTROL.

alerting device An audible alarm that includes a self-contained solid-state audio oscillator. Powered from the ac line or a battery, the device produces a raucous noise when actuated.

Alexanderson antenna A very-low-frequency (VLF) and low-frequency (LF) vertically polarized antenna, designed to minimize ground losses in structures of manageable height. It usually consists of several wires, each quarter-wave resonant with a loading coil, and all connected together at the apex of a tower. The antenna is fed between the ground and the base of one of the wires.

Alford antenna A loop antenna, in a square configuration, with the corners bent toward the center to lower the impedance at the current nodes.

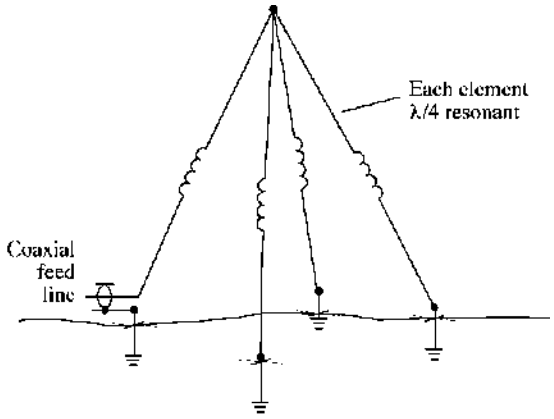

Alexanderson antenna

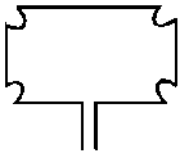

Alford antenna

algebraic adder In computer operations, an adder that provides the algebraic sum, rather than the arithmetic sum, of the entered quantities.

algebraic operation A form of electronic calculator operation, in which the keystrokes proceed in an intuitive sequence, following the way in which the calculation is written down. Compare REVERSE POLISH NOTATION.

algebraic sum The sum of two or more quantities with consideration of their signs. Compare ARITHMETIC SUM.

algorithm A step-by-step procedure for solving a problem, (e.g., the procedure for finding the square root of a number). It can be expressed in a line-by-line instruction set or as a flowchart.

algorithmic language A computer language used to describe a numeral or algebraic process.

alias A label that is an alternate term for items of the same type; a label and several aliases can identify the same data element in a computer program.

aliasing **1.** In analog-to-digital (A/D) conversion, a false output signal that results from a sampling rate that is too slow. Ideally, the sampling rate is at least twice the highest input signal frequency. **2.** Sawtooth-like irregularities, also called *jaggies*, which are sometimes introduced into a bit-mapped computer image when it is changed in size.

aliasing noise A form of signal distortion caused by a signal with an excessive bandwidth.

5059F-pA_1-55 4/9/01 4:41 PM Page 20

align **1.** To adjust (i.e., to preset) the circuits of an electronic system, such as a receiver, transmitter, or test instrument, for predetermined response. **2.** To arrange elements in a certain precise orientation and spacing, relative to each other, as in a Yagi antenna. **3.** To orient antennas so that they are in line of sight, with respect to each other.

alignment The process of ensuring that equipment, components, or systems are adjusted, both physically and electronically, for the most efficient possible performance.

alignment chart A line chart for the simple solution of electronic problems. It is so called because its use involves aligning numerical values on various scales, the lines intersecting at the solution on another scale. Also called *nomograph*.

alignment pin A pin or protruding key, usually in the base of a removable or plug-in component, to ensure that the latter will be inserted correctly into a circuit. Often, the pin mates with a keyway, notch, or slot.

alignment tool A specialized screwdriver or wrench (usually nonmagnetic) used to adjust padder or trimmer capacitors or inductor cores.

alive See LIVE.

alkali See BASE, **2.**

alkali metals Metals whose hydroxides are bases (alkalis). The group includes cesium, francium, lithium, potassium, rubidium, and sodium.

alkaline battery **1.** A battery composed of alkaline cells and characterized by a relatively flat discharge curve under load.

alkaline cell A common non-rechargeable electrochemical cell that employs granular zinc for the negative electrode, potassium hydroxide as the electrolyte, and a device called a *polarizer* as the positive electrode. Produces approximately 1.5 volts under no-load conditions. The geometry of construction is similar to that of the zinc–carbon cell, but it can deliver current effectively at lower temperatures. Cells of this type have shelf lives longer than zinc–carbon cells; they also have greater energy-storage capacity per unit volume, but they are more expensive than zinc–carbon cells. They are used in calculators, transistor radios, and cassette tape and compact-disc players. Compare ZINC–CARBON CELL.

alkaline-earth metals The elemental metals barium, calcium, strontium, and sometimes beryllium, magnesium, and radium, some of which are used in vacuum tubes.

alkaline earths Substances that are oxides of the alkaline-earth metals. Some of these materials are used in vacuum tubes.

all-diffused A type of INTEGRATED CIRCUIT in which both active and passive elements have been fabricated by diffusion and related processes.

Allen screw A screw fitted with a six-sided (hexagonal) hole.

Allen wrench A tool used to tighten or loosen an Allen screw. It is a hexagonal rod and is available in various sizes.

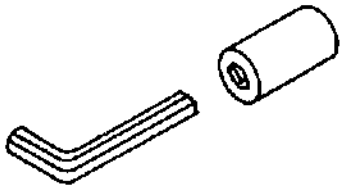

Allen screw and wrench

alligator clip A spring-loaded clip with jagged teeth, designed to be used for temporary electrical connections.

allocate **1.** To assign (especially through legislation) operating frequencies or other facilities or conditions needed for scientific or technical activity; see, for example, ALLOCATION OF FREQUENCIES. **2.** In computer practice, to assign locations in the memory or registers for routines and subroutines.

allocated channel A frequency channel assigned to an individual or group.

allocated-use circuit **1.** A circuit in which one or more channels have been authorized for the exclusive use of one or more services. **2.** A communications link assigned to users needing it.

allocation of frequencies See RADIO SPECTRUM.

allocator A telephone system distributor associated with the finder control group relay assembly. It reserves an inactive line-finder for another call.

allophone A variation in the sound of a phoneme, depending on what comes before and/or after the phoneme in the course of speech. Important in speech recognition and synthesis. There are 128 different phoneme variations in the English language. See PHONEME.

alloter relay A telephone system line-finder relay that reserves an inactive line-finder for the next incoming call from the line.

allotropic Pertaining to a substance existing in two forms.

alloy A metal that is a mixture of several other metals (e.g., brass from copper and zinc), or of a metal and a nonmetal.

alloy deposition In semiconductor manufacture, depositing an alloy on a substrate.

alloy-diffused transistor A transistor in which the base is diffused and the emitter is alloyed. The collector is provided by the semiconductor substrate into which alloying and diffusion are affected. Compare ALLOY TRANSISTOR and DIFFUSE TRANSISTOR.

alloy diode A junction-type semiconductor diode in which a suitable substance (such as p-type) is alloyed into a chip of the opposite type (such as

5059F-pA_1-55 4/9/01 4:41 PM Page 21

n-type) to form the junction. Also called *alloy-junction diode.*

alloy junction In a semiconductor device, a positive/negative (pn) junction formed by alloying a suitable material (such as indium) with the semiconductor (silicon or germanium).

alloy transistor A transistor whose junctions are created by alloying. Also see ALLOY JUNCTION.

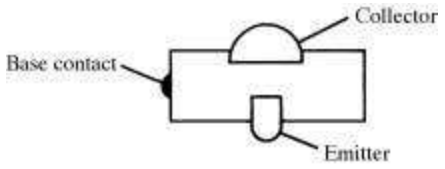

alloy transistor

all-pass filter Also called *all-pass network.* A filter that (ideally) introduces a desired phase shift or time delay, but has zero attenuation at all frequencies.

all-relay central office In telephone service, an automatic central-office switchboard that uses relay circuits to make line interconnections.

all-wave Pertaining to a wide operating-frequency range. Few systems are literally all-wave. For example, a so-called "all-wave radio receiver" might cover 500 kHz to 30 MHz only.

all-wave antenna An antenna that can be operated over a wide frequency range with reasonable efficiency and preferably without needing readjustment. Examples are the DISCONE ANTENNA and the LOG-PERIODIC ANTENNA.

all-wave generator A signal generator that will supply output over a wide range of frequencies.

all-wave receiver A radio receiver that can be tuned over a very wide range of frequencies, such as 10 kHz to 70 MHz.

allyl plastics Plastics, sometimes used as dielectrics or for other purposes in electronics, based on resins made by polymerization of monomers (such as diallyl phthalate) that contain allyl groups.

alnico Coined from the words aluminum, nickel, and cobalt. An alloy used in strong permanent magnets, it contains the constituents noted plus (sometimes) copper or titanium.

alpha **1.** Symbol, α. The current gain of a common-base-connected bipolar transistor. It is the ratio of the differential of collector current to the differential of emitter current; $\alpha = dI_C/dI_E$. For a junction transistor, alpha is always less than unity, but very close to it. **2.** In voice communications, the phonetic representation of the letter A.

alphabet The set of all characters in a natural language.

alphabetic coding In computer practice, an abbreviation system for coding information to be fed into the computer. The coding contains letters, words, and numbers.

alphabetic-numeric Also called *alphabetical-numerical* and *alphanumeric.* In computer operations, pertaining to letters of the alphabet and special characters, and to numerical digits.

alpha cutoff frequency Also called *alpha cutoff.* In a bipolar transistor circuit, the frequency at which the alpha (current gain) becomes 0.707 (70.7 percent) of its value at 1 kHz. A bipolar transistor can have considerable gain at its alpha cutoff. This specification denotes how rapidly a transistor loses gain as the frequency increases, an important consideration in the design of radio-frequency (RF) amplifiers. See ALPHA. Compare GAIN BANDWIDTH PRODUCT.

alpha decay The decay of a substance in which the nuclei of the atoms emit alpha particles, resulting in a change of the atomic number and atomic weight of the substance over a period of time.

alphanumeric See ALPHABETIC-NUMERIC.

alphanumeric code In computer operations or in communications, a code composed of, or using, both letters and numbers.

alphanumeric readout A type of digital readout that displays both letters and numerals.

alpha particle A nuclear particle bearing a positive charge. Consisting of two protons and two neutrons, it is given off by certain radioactive substances. Compare BETA RAYS and GAMMA RAYS.

alpha system An alphabetic code-signaling system.

alphatron An ionizing device in which the radiation source is an emitter of alpha particles.

alteration An inclusive-OR operation.

alternate channel In communications, a channel situated two channels higher or lower than a given channel. Compare ADJACENT CHANNEL.

alternate-channel interference Interference caused by a transmitter operating in the channel beyond an adjacent channel. Compare ADJACENT-CHANNEL INTERFERENCE.

alternate digit inversion In multiplex equipment, a method of switching the binary signals to the opposite state, in accordance with A-law companding.

alternate frequency A frequency allocated as an alternative to a main assigned frequency and used under certain specified conditions.

alternate-mark inversion signal A signal that conveys bits in which the successive signals are of opposite polarity (positive, then negative, then positive, etc.). They are equal in absolute value amplitude.

alternate mode The technique of displaying several signals on an oscilloscope screen by rapidly switching the signals in sequence at the end of each sweep.

alternate routing A secondary, or backup, communications path, used when primary (normal) routing is impossible.

alternating-charge characteristic In a nonlinear capacitor, the relationship between the instanta-

5059F-pA_1-55 4/9/01 4:41 PM Page 22

neous charge and the instantaneous value of an alternating voltage.

alternating current Abbreviation, ac. A current that periodically reverses its direction of flow. In one cycle, an alternation starts at zero, rises to a maximum positive level, returns to zero, rises to a maximum negative level, and again returns to zero. The number of such cycles completed per second is termed the *ac frequency.* Also see CURRENT.

alternating-current continuous wave An amplitude-modulated signal resulting from the operation of an oscillator or RF amplifier with raw ac voltage.

alternating current/direct current See AC/DC.

alternating-current erasing head See AC ERASING HEAD.

alternating-current pulse A short-duration ac wave.

alternating-current transmission **1.** The propagation of alternating currents along a length of conductor—especially for power-transfer purposes. **2.** A means of picture transmission in which a given signal strength produces a constant value of brightness for a very short time.

alternating voltage Also called *alternating-current voltage.* See AC VOLTAGE.

alternation In ac practice, a half cycle. In a complete cycle, there are two alternations, one in the positive direction and one in the negative direction.

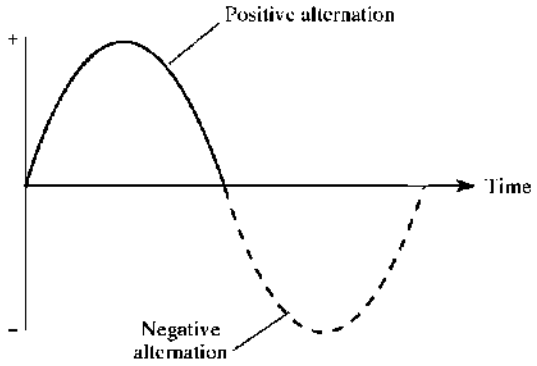

alternation

alternative denial A NOT-AND operation.

alternator Any mechanically driven machine for generating ac power. Sometimes specifically one having a permanent-magnet rotor, such as a *magneto.*

altimeter station An airborne transmitter whose signals are used to determine the altitude of aircraft.

altitude **1.** The vertical distance of an object above sea level. **2.** The vertical distance of an object above the earth's surface. **3.** The angle, measured in degrees, with respect to the horizon, at which a highly directional antenna is pointed.

altitude delay In a plan-position-indicating type of radar, the sync delay introduced between transmission of the pulse and start of the trace on the indicator screen to eliminate the altitude circle in the display.

ALU Abbreviation of ARITHMETIC AND LOGIC UNIT.

alumel An alloy used in the construction of one type of THERMOCOUPLE. It is composed of nickel (three parts) and aluminum (one part).

alumina An aluminum-oxide ceramic used in electron tube insulators and as a substrate in the fabrication of thin-film circuits.

aluminum Symbol, Al. An elemental metal. Atomic number, 13. Atomic weight, 26.98. Aluminum is widely used in electronics, familiar instances being chassis, wire, shields, semiconductor doping, and electrolytic-capacitor plates.

aluminum antimonide Formula, AlSb. A crystalline compound useful as a semiconductor dopant.

aluminized screen A television picture-tube screen with a thin layer of aluminum deposited on its back to brighten the image and reduce ion-spot formation.

Am Symbol for AMERICIUM.

A/m Abbreviation of *ampere per meter:* the SI unit of magnetic field strength.

AM **1.** Abbreviation of *amplitude modulator.* **2.** Abbreviation of AMPLITUDE MODULATION.

amalgam An alloy of a metal and mercury. Loosely, any combination of metals.

amateur **1.** A nonprofessional, usually noncommercial devotee of any technology (i.e., a hobbyist). **2.** A licensed radio operator legally authorized to operate a station in the AMATEUR SERVICE.

amateur band Any band of radio frequencies assigned for noncommercial use by licensed radio amateurs (see AMATEUR, **2**). In the United States, numerous such bands are above 1.8 MHz (160 meters). Also see AMATEUR SERVICE and AMATEUR STATION.

amateur call letters Call letters assigned by a government licensing authority—especially to amateur stations. Call-letter combinations consist of a letter prefix denoting the country in which the station is situated, plus a number designating the location within the country, and two or more letters identifying the particular station. For example: W6ABC: W (or K) = United States, 6 = California, and ABC = identification of individual licensee (issued alphabetically, except under special circumstances).

amateur callsign See AMATEUR CALL LETTERS.

amateur extra-class license The highest class of amateur-radio operator license in the United States. It conveys all operating privileges.

5059F-pA_1-55 4/9/01 4:41 PM Page 23

amateur radio **1.** A general term, referring to the practice of operation, experimentation, and other work in and related to the amateur service. **2.** The hardware that comprises an amateur radio station. **3.** A radio receiver, transmitter, or transceiver that is specifically designed for operation in the amateur bands.

amateur radio operator Also called *radio ham* or *ham radio operator*. An individual licensed to transmit radio signals in the amateur service.

amateur service A two-way radio service, existing purely for hobby purposes (i.e., without pecuniary interest).

amateur station A radio station licensed in the AMATEUR SERVICE.

amauroscope An electronic aid to the blind, in which photocells in a pair of goggles receive light images. Electric pulses proportional to the light are impressed upon the visual receptors of the brain through electrodes in contact with nerves above each eye.

amber A yellow or brown fossil resin that is historically important in electronics. It is the first material reported to be capable of electrification by rubbing (Thales, 600 BC). Also, the words *electricity*, *electron*, and *electronics* are derived from the Greek name for amber, *elektron.*

ambience The acoustic characteristic of a room, in terms of the total amount of sound reaching a listener from all directions.

ambient An adjective meaning "surrounding." Often used as a noun in place of the adjective-noun combination (thus, "10 degrees above ambient," instead of "10 degrees above ambient temperature").

ambient humidity The amount of moisture in the air at the time of measurement or operations in which dampness must be accounted for.

ambient level The amplitude of all interference (acoustic noise, electrical noise, illumination, etc.) emitted from sources other than that of a signal of interest.

ambient light Also called *ambient illumination.* Room light or outdoor light incident to a location at the time of measurement or operations.

ambient-light filter In a television receiver, a filter mounted in front of a picture-tube screen to minimize the amount of ambient light reaching the screen.

ambient noise **1.** In electrical measurements and operation, background electrical noise. **2.** In acoustical measurements and operations, audible background noise.

ambient pressure Surrounding atmospheric pressure.

ambient temperature The temperature surrounding apparatus and equipment (e.g., room temperature).

ambient-temperature range **1.** The range over which ambient temperature varies at a given location. **2.** The range of ambient temperature that will cause no malfunction of, or damage to, a circuit or device.

ambiguity **1.** Any unclear, illogical, or incorrect indication or result. **2.** The seeking of a false null by a servo. **3.** In digital computer operations, an error resulting from improper design of logic.

ambiguous count In digital counters, a clearly incorrect count. See ACCIDENTAL TRIGGERING.

ambisonic reproduction A close approximation of the actual directional characteristics of a sound in a given environment. The reproduced sound almost exactly duplicates the sound in the actual environment in which it was recorded.

American Morse code (Samuel F. B. Morse, 1791–1872). Also called *Railroad Morse.* A telegraph code, at one time used on wire telegraph lines in the United States. It differs from the *Continental code*, also called the *International Morse Code*, which is used in radiotelegraphy. Compare CONTINENTAL CODE.

American National Standards Institute Acronym, ANSI. An industrial group in the United States that encourages companies to manufacture devices and equipment in accordance with certain standards. The objective is to minimize hardware incompatibility problems.

American Radio Relay League A worldwide organization of amateur radio operators, headquartered in Newington, Connecticut. The official publications are the monthly magazines, *QST* and *QEX.* They also publish numerous books and other educational materials.

American Standards Association Abbreviation, ASA. At one time, the name of the national association in the U.S. devoted to the formation and dissemination of voluntary standards of dimensions, performance, terminology, etc. See ANSI.

American wire gauge Abbreviation, AWG. Also called *Brown and Sharpe gauge* or *B & S gauge.* The standard American method of designating wire sizes. Wire is listed according to gauge number from 0000 (460 mils diameter) to 40 (3.145 mils diameter).

americium Symbol, Am. A radioactive elemental metal first produced artificially in the 1940s. Atomic number, 95. Atomic weight, 243.

AM/FM receiver A radio set that can receive either amplitude-modulated or frequency-modulated signals. Usually, a band switch incorporates the demodulation-selection circuitry so that as the frequency range is changed, the appropriate detector is accessed.

AM/FM transmitter A radio transmitter whose output signal can be frequency- or amplitude-modulated by a panel selector switch.

AM/FM tuner A compact radio receiver unit that can handle either amplitude- or frequency-modulated signals, and delivers low-amplitude output to a high-fidelity audio power amplifier. Compare AM TUNER and FM TUNER.

5059F-pA_1-55 4/9/01 4:41 PM Page 24

Character	*Symbol*	*Character*	*Symbol*
A	. —	U	. . —
B	— . . .	V	. . . —
C	— . — .	W	. — —
D	— . .	X	— . . —
E	.	Y	— . — —
F	. . — .	Z	— — . .
G	— — .	1	. — — — —
H	. . . .	2	. . — — —
I	. .	3	. . . — —
J	. — — —	4	. . . . —
K	— . —	5	. . . . .
L	— . . —	6	— . . . .
M	— —	7	— — . . .
N	— .	8	— — — . .
O	— — —	9	— — — — .
P	. — — .	0	— — — — —
Q	— — . —	period	. — . — . —
R	. — .	comma	— — . . — —
S	. . .	question	. . — — . .
T	—	mark	— . . . —

American Morse Code

American Wire Gauge (AWG) Diameters

AWG	Millimeters	Inches	AWG	Millimeters	Inches
1	7.35	0.289	21	0.723	0.0285
2	6.54	0.257	22	0.644	0.0254
3	5.83	0.230	23	0.573	0.0226
4	5.19	0.204	24	0.511	0.0201
5	4.62	0.182	25	0.455	0.0179
6	4.12	0.163	26	0.405	0.0159
7	3.67	0.144	27	0.361	0.0142
8	3.26	0.128	28	0.321	0.0126
9	2.91	0.115	29	0.286	0.0113
10	2.59	0.102	30	0.255	0.0100
11	2.31	0.0909	31	0.227	0.00894
12	2.05	0.0807	32	0.202	0.00795
13	1.83	0.0720	33	0.180	0.00709
14	1.63	0.0642	34	0.160	0.00630
15	1.45	0.0571	35	0.143	0.00563
16	1.29	0.0508	36	0.127	0.00500
17	1.15	0.0453	37	0.113	0.00445
18	1.02	0.0402	38	0.101	0.00398
19	0.912	0.0359	39	0.090	0.00354
20	0.812	0.0320	40	0.080	0.00315

AMI See ALTERNATE-MARK INVERSION SIGNAL.

A-minus Also, A-. The negative terminal of an A battery, or pertaining to the part of a circuit connected to that terminal.

ammeter An instrument used to measure the amount of current (in amperes) flowing in a circuit.

ammeter shunt A resistor connected in parallel with an ammeter to increase its current range. Also see AYRTON-MATHER GALVANOMETER SHUNT.

ammeter-voltmeter method The determination of resistance or power values from the measurement of voltage (E) and current (I). For resistance, $R = E/I$; for power, $P = EI$.

ammonium chloride Formula, NH_4Cl. The electrolyte in the carbon-zinc type of primary cell. Also called SAL AMMONIAC.

AMNL Abbreviation of AMPLITUDE-MODULATION NOISE LEVEL.

amortisseur winding **1.** A winding that acts against pulsation of the magnetic field in an electric motor. **2.** A winding that acts to prevent oscillation in a synchronous motor.

amorphous substance A noncrystalline material.

amp **1.** Slang for AMPERE. **2.** Slang for AMPLIFIER—especially in audio high-fidelity applications.

ampacity Current-carrying capacity expressed in amperes.

amperage The strength of an electric current (i.e., the number of amperes).

ampere (Andre Marie Ampere, 1775-1836). Abbreviations, A (preferred), a, amp. The SI base unit of current intensity (I). The ampere is the constant current that, if maintained in two straight parallel conductors of infinite length and of negligible circular cross section and placed 1 meter apart in a vacuum, would produce between the conductors a force of 2×10^{-7} newton per meter. One ampere flows through a 1-ohm resistance when a potential of 1 volt is applied; thus $I = E/R$. Also see MICROAMPERE, MILLIAMPERE, NANOAMPERE, and PICOAMPERE.

ampere balance A device consisting of two conductors in which the force between them (caused by current) is balanced against the gravitational force exerted on an object in the gravitational field of the earth. Used for the precise determination of current of large dimension, or of the size of the ampere.

ampere-hour Abbreviations: Ah, amp-hr. The quantity of electricity that passes through a circuit in one hour when the rate of flow is one ampere. Also see BATTERY CAPACITY.

ampere-hour meter An instrument for measuring ampere-hours. It contains a small motor driven by the current being measured and which moves a point on an ampere-hour scale. The motor speed is proportional to the current. The position of the pointer is proportional to current and elapsed time.

Ampere's law Current flowing in a wire generates a magnetic flux that encircles the wire in the clockwise direction when the current is moving away from the observer.

ampere-turn Symbol, NI. A unit of magnetomotive force equal to 1 ampere flowing in a single-turn coil. The ampere-turns value for any coil is obtained by multiplying the current (in amperes) by the number of turns in the coil.

Amperian whirl The stream of electrons in a single-turn, current-conducting wire loop acting as an elementary electromagnet.

5059F-pA_1-55 4/9/01 4:41 PM Page 25

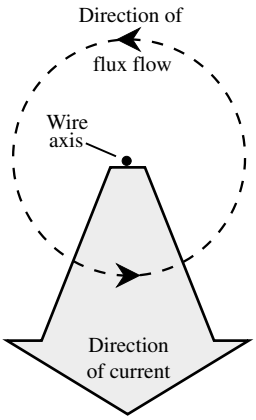

Ampere's Law

amp-hr One style of abbreviating AMPERE-HOUR. Also, Ah.

amplidyne A dynamo-like rotating dc machine that can act as a power amplifier because the response of the output voltage to changes in field excitation is quite rapid. Used in servo systems.

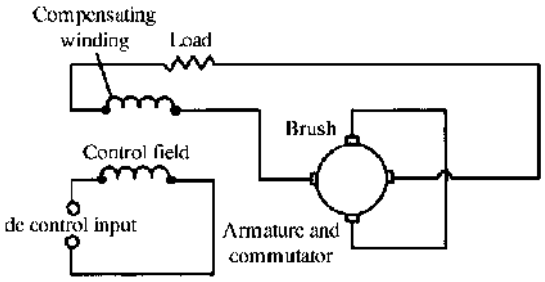

amplidyne

amplification **1.** The process of increasing the magnitude of a signal. This entails an input signal controlling a local power supply to produce a larger output signal. Depending on the kind of input and output signals, amplification can be categorized as CURRENT, VOLTAGE, POWER, or some combination of these. **2.** The qualitative signal increase resulting from the process in **1. 3.** The quantitative signal increase (resulting from the process in **1**), expressed as a factor (such as 100) or in terms of *decibels* (dB). See AMPLIFICATION FACTOR and DECIBEL.

amplification factor **1.** The ratio of the output voltage, current, or power to the input voltage, current, or power of an AMPLIFIER circuit. For voltage or current, this ratio has meaning only when the input and output impedances are identical. **2.** The number of decibels by which an AMPLIFIER circuit increases the amplitude of a signal. For voltage or current, this figure has meaning only when the input and output impedances are identical. See DECIBEL. **3.** The ALPHA or BETA of a bipolar transistor. **4.** In the operation of an electron tube, the ratio of the derivative (instantaneous rate of change) of the plate voltage to the derivative of the grid voltage, for zero change in plate current.

amplified ALC Abbreviation, AALC. An automatic-level-control (ALC) system that uses the amplification of the fed-back control signal. It is used in RF power amplifiers, particularly single-sideband (SSB) linear amplifiers, to prevent overmodulation and nonlinearity.

amplified back bias A declining voltage developed across a fast-time-constant circuit in an amplifier stage and fed back into a preceding stage.

amplifier Any device that increases the magnitude of an applied signal. It receives an input signal and delivers a larger output signal that, in addition to its increased amplitude, is a replica of the input signal. Also see CURRENT AMPLIFIER, POWER AMPLIFIER, and VOLTAGE AMPLIFIER.

amplifier diode Any semiconductor that can provide amplification in a suitable circuit or microwave system. See DIODE AMPLIFIER.

amplifier distortion A change in the waveform of a signal, arising within an amplifier that is operated in compliance with specified conditions.

amplifier input **1.** The terminals and section of an amplifier that receive the signal to be amplified. **2.** The signal to be amplified.

amplifier noise Collectively, all extraneous signals present in the output of an amplifier when no working signal is applied to the amplifier input terminals.

amplifier nonlinearity A condition in which the amplifier output signal does not exhibit a linear relationship to the corresponding input signal. Some amplifiers are designed to operate in a linear manner at all times, but many amplifier types need not function in this manner to be effective. Also see AMPLIFIER DISTORTION and LINEAR AMPLIFIER.

amplifier output **1.** The terminals and section of an amplifier that deliver the amplified signal for external use. **2.** The amplified signal.

amplifier power The power level of the output signal delivered by an amplifier (also called OUTPUT POWER), or the extent to which the amplifier increases the power of the input signal (also called POWER AMPLIFICATION).

amplifier response The performance of an amplifier throughout a specified frequency band. Factors usually included are gain, distortion, amplitude versus frequency, and power output.

amplify To perform the functions of amplification (see AMPLIFICATION, **1**).

5059F-pA_1-55 4/9/01 4:41 PM Page 26

amplifying delay line A delay line that causes amplification of signals in a circuit intended for pulse compression.

amplistat A self-saturating magnetic amplifier.

amplitron A backward-wave amplifier used in microwave circuits.

amplitude The extent to which an alternating or pulsating current or voltage swings, positively and negatively, from zero or from a mean value.

amplitude-controlled rectifier A thyratron- or thyristor-based rectifier circuit.

amplitude density distribution A mathematical function giving the probability that, at a given instant in time, a fluctuating voltage has a certain value.

amplitude distortion In an amplifier or network, the condition in which the output-signal amplitude exhibits a nonlinear relationship to the input-signal amplitude.

amplitude error **1.** The error in measuring the amplitude of a signal, normally expressed as a percentage of signal amplitude or as a percentage of full scale. **2.** The frequency at which the output amplitude of a signal is in error by 1% with amplitude at 10% of full scale.

amplitude factor For an ac wave, the ratio of the peak value to the rms value. The amplitude factor of a sine wave is equal to the square root of 2 = 1.4142136.

amplitude fading In the propagation of electromagnetic waves, a condition in which the amplitudes of all components of the signal (i.e., carrier and sidebands) increase and decrease uniformly. Compare SELECTIVE FADING.

amplitude/frequency response Performance of an amplifier throughout a specified range, as exhibited by a plot of output-signal amplitude versus frequency for a constant-amplitude input signal.

amplitude gate A transducer that transmits only those portions of an input wave that lie within two close-spaced amplitude boundaries; also called *slicer*.

amplitude limiter A circuit, usually with automatic gain control (AGC), that keeps an amplifier output signal from exceeding a certain level, despite large variations in input-signal amplitude. A dc-biased diode performs passive limiting action via *clipping*.

amplitude-modulated generator A signal generator whose output is amplitude modulated. Usually, this instrument is an RF generator that is modulated at an audio frequency.

amplitude-modulated transmitter A radio-frequency transmitter whose carrier is varied in amplitude, according to the rate of change of some data-containing signal (such as voice, music, facsimile, television pictures, control signals, or instrument readings).

amplitude modulation Abbreviation, AM. A method of conveying intelligence in wireless communications and broadcasting. The modulating-signal energy appears at sideband frequencies above and below, and very close to, the carrier frequency. These sideband signals carry all the information. The extent of modulation is expressed as a percentage, from 0, which represents an unmodulated carrier, to 100, which represents full modulation. In a signal modulated 100 percent, one-third of the power is used to convey the data; the other two-thirds is consumed by the carrier. This form of modulation is essentially outmoded, although it is still used in the standard broadcast band from 535 to 1605 kHz. See FREQUENCY MODULATION, PHASE MODULATION, SINGLE SIDEBAND.

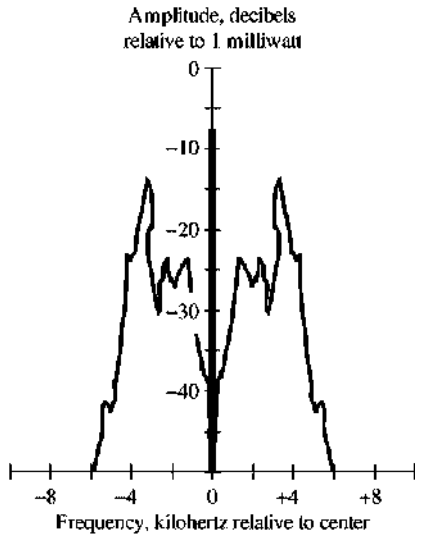

amplitude modulation

amplitude-modulation noise Spurious amplitude modulation of a carrier wave by extraneous signals and random impulses, rather than by the intended data-containing signal.

amplitude noise In radar, amplitude fluctuations of an echo returned by a target. This noise limits the precision of the system.

amplitude of noise The level of random noise in a system. The amplitude of noise is measured in the same way that signal amplitude is measured.

amplitude range The maximum-to-minimum amplitude variation of a signal. It can be expressed as a direct numerical ratio or in decibels.

amplitude response The maximum output obtainable at various frequencies over the range of an instrument operating under rated conditions.

amplitude selection The selection of a signal, according to its correspondence to a predetermined amplitude or amplitude range.

5059F-pA_1-55 4/9/01 4:41 PM Page 27

amplitude separator In a television receiver, a circuit that separates the control pulses from the composite video signal.

amplitude suppression ratio The ratio of an undesired output of a frequency-modulated (FM) receiver to the desired output, when the test signal is amplitude modulated and frequency modulated simultaneously.

amplitude-versus-frequency distortion Distortion resulting from varying gain or attenuation of an amplifier or network, with respect to signal frequency.

AMTOR A form of amateur-radio data communications, in which the accuracy of a group of characters in a message is checked periodically by the receiving station. If an error appears likely, then the receiving station sends an instruction to the transmitting station to retransmit that particular group of characters. Characters are sent in bunches with pauses for possible inquiries from the receiving station.

AM tuner A compact radio receiver unit that handles amplitude-modulated signals and delivers low-amplitude audio output to a high-fidelity amplifier. Compare AM/FM TUNER and FM TUNER.

amu Abbreviation of *atomic mass unit.*

amusement robot An electromechanical robot, often computer-controlled, that is intended for use as a toy.

AN- A prefix designator used by American military services to indicate commonality.

anacoustic Pertaining to the lack of sound or absence of reverberation or transmission of sonic waves.

analog **1.** A quantity that corresponds, point for point or value for value, to an otherwise unrelated quantity. Thus, voltage is the analog of water pressure, and current is the analog of water flow. **2.** Varying over a continuous range and, therefore, capable of attaining an infinite number of values or levels. Compare DIGITAL.

analog adder An analog circuit or device that receives two or more inputs and delivers an output equal to their sum.

analog adder/subtracter An analog circuit or device that receives two or more inputs and delivers an output equal to their sum or difference (in any combination), as desired.

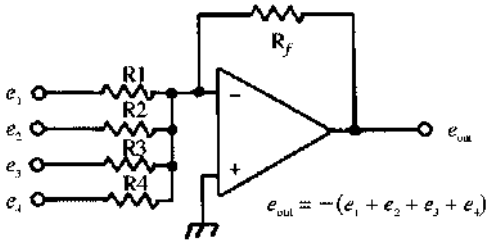

analog adder (inverting)

analog channel In an ANALOG COMPUTER, an information channel in which the extreme limits of data magnitude are fixed, and the data can have any value between the limits.

analog communications Any form of communications in which a carrier, generally an electromagnetic wave or high-frequency current, is varied in a continuous and controlled way by a data-containing signal. See ANALOG, **2.**

analog computer A computer in which input and output quantities are represented as points on continuous (or small-increment) scales. To represent these quantities, the computer uses voltages or resistances that are proportional to the numbers to be worked on. When the quantities are nonelectrical (such as pressure or velocity), they are made analogous by proportional voltages or resistances.

analog data **1.** Data represented in a quantitatively analogous way. Examples are the deflection of a movable-coil meter, the positioning of a slider on a slide rule, and the setting of a variable resistor to represent the value of a nonelectrical quantity. Also see ANALOG. **2.** Data displayed along a smooth scale of continuous values (as by a movable-coil meter), rather than in discrete steps (as by a digital meter).

analog differentiator An analog circuit or device whose output waveform is the derivative of the input-signal waveform, with respect to time.

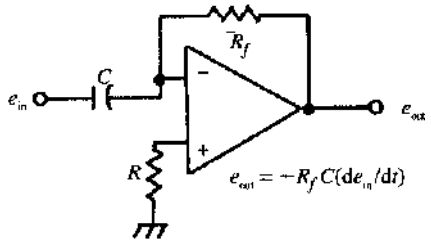

analog differentiator

analog divider An analog circuit or device that receives two inputs and delivers an output equal to their quotient.

analog electronics Electronic techniques and equipment that is based on uniformly changing signals, such as sine waves, and often having continuous-scale indicators, such as D'Arsonval meters. Compare DIGITAL ELECTRONICS.

analog information Approximate numerical information, as opposed to digital information, which is assumed to be exact.

analog integrator An analog circuit or device whose output waveform is the integral of the input signal waveform, with respect to time.

5059F-pA_1-55 4/9/01 4:41 PM Page 28

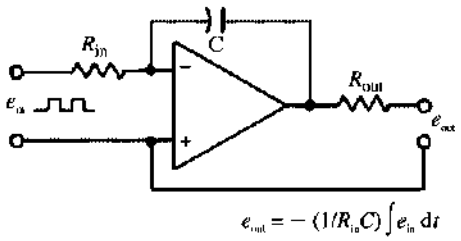

analog integrator

analog inverting adder An analog adder that delivers a sum with the opposite sign to that of the input quantities.

analog meter An indicating instrument that uses a movable-coil arrangement or the equivalent, causing a rotating pointer to indicate a particular value on a graduated printed scale. Compare DIGITAL METER.

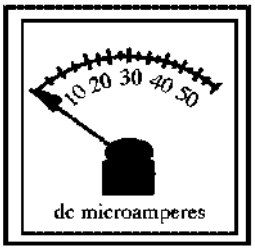

analog meter

analog multiplexer **1.** A multiplexer used with analog signals (see MULTIPLEXER). **2.** An analog time-sharing circuit.

analog multiplier An analog circuit or device that receives two or more inputs and delivers an output equal to their product.

analog network A circuit that permits mathematical relationships to be shown directly by electric or electronic means.

analogous pole In a PYROELECTRIC MATERIAL, the end or face having the positive electric charge.

analog output An output quantity that varies smoothly over a continuous range of values, rather than in discrete steps.

analog record Also called *analog recording.* A record or recording method in which some property of the recorded material, such as displacement or magnetization, varies over a continuous range that is relative to time and/or physical position.

analog recorder Any recorder, such as a recording oscillograph, potentiometric recorder, electroencephalograph, electrocardiograph, or lie detector, that produces an analog record. The counterpart is a digital recorder, which produces a readout in discrete numbers (printed or visually displayed).

analog representation Representation of information within a smooth, continuous range, rather than as separate (discrete) steps or points.

analog signal A signal that attains an infinite number of different amplitude levels, as opposed to one that can attain only a finite number of levels as a function of time.

analog subtracter An analog circuit or device that receives two inputs and delivers an output equal to their difference.

analog summer See ANALOG ADDER.

analog switch A switching device that will only pass signals that are faithful analogs of transducer parameters.

analog-to-digital conversion **1.** A process in which an analog signal (such as a voice waveform) is changed into a digital or binary signal that conveys the same information. This process is commonly used in digital computers to encode sounds and images. It is also used in communications systems to improve efficiency, minimize the necessary bandwidth, and optimize the signal-to-noise ratio. **2.** A process in which continuous mechanical motion is encoded into a digital or binary electronic signal.

analog-to-digital converter Any circuit or device that performs ANALOG-TO-DIGITAL CONVERSION.

analysis **1.** The rigorous determination of the constants and modes of operation for electronic equipment. Compare SYNTHESIS. **2.** A branch of mathematics dealing with point sets, relations, and functions.

analytical engine A primitive mechanical calculating machine, invented in 1833 by Charles Babbage.

analyzer **1.** Any instrument that permits analysis through close measurements and tests (e.g., distortion analyzer, WAVE ANALYZER, or gas analyzer). **2.** A computer program used for debugging purposes; it analyzes other programs and summarizes references to storage locations. **3.** An analysis interface to an oscilloscope.

anastigmatic yoke Also called *full-focus yoke.* In a television (TV) receiver, a deflection yoke with a cosine winding for better focus at the edges of the picture.

anchorage In plastic recording tape, the adhesion of the magnetic oxide coating to the surface of the tape.

ancillary equipment Equipment that does not directly enter into the operation of a central system. Examples are input/output components of a computer and test instruments attached to a system.

AND circuit In digital systems and other switching circuits, a logic gate whose output is high (logic 1) only when all input signals are high. Otherwise the output is low (logic 0). Compare OR CIRCUIT.

5059F-pA_1-55 4/9/01 4:41 PM Page 29

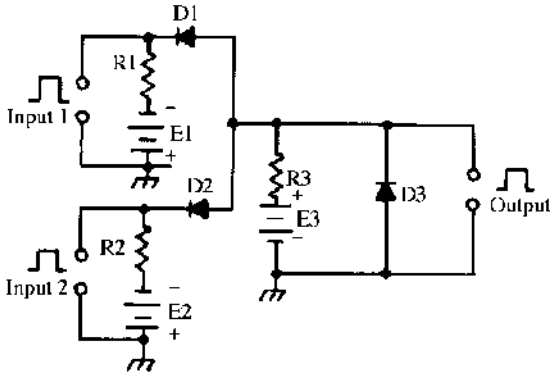

AND circuit

Anderson bridge An ac bridge circuit with six impedances, permitting the value of an unknown inductance to be determined in terms of a standard capacitance.

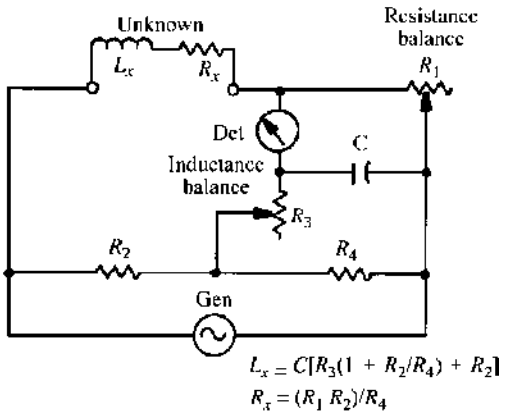

Anderson bridge

AND gate **1.** AND circuit. **2.** In a TV receiver, an AND circuit that holds the keyed-AGC signal off until a positive horizontal flyback pulse and a horizontal sync pulse appear simultaneously at the input.

android A sophisticated robot built in humanoid form. Usually, it propels itself by rolling on wheels or on a track drive. A rotatable head contains position sensors, a machine vision system, and/or a machine hearing system. Mechanical arms are equipped with end effectors to perform various tasks. The most advanced androids have self-contained computer control systems.

anechoic Pertaining to the absence of echoes. Examples: ANECHOIC CHAMBER, *anechoic enclosure,* or *anechoic room.*

Truth Table

A	B	C
0	0	0
0	1	0
1	0	0
1	1	1

AND gate

anechoic chamber An enclosure that does not reflect sound waves that approach its walls. Such a chamber is used to test certain audio devices.

anemograph An electromechanical device that produces a recording of wind speed versus time. Generally, it consists of an ANEMOMETER connected to a PEN-AND-INK RECORDER via a suitable electronic interface.

anemometer An instrument that measures or indicates wind speed, or speed and direction (velocity).

angel **1.** An extraneous image, usually of short duration, on a cathode-ray-tube (CRT) display. The term applies particularly to anomalies in a radar image caused by low-atmospheric reflection, birds, or other mobile objects. **2.** Air-deployed metallic debris, also known as *chaff,* designed to create radar echoes as a decoy or diversion tactic.

angle jamming A radar jamming technique in which the return echo is jammed with a signal containing improper azimuth or elevation angle components.

angle modulation Variation of the angle of a sine-wave carrier in response to the modulating source, as in FREQUENCY MODULATION and PHASE MODULATION.

angle noise In radar reception, the interference resulting from variations in the angle at which an echo arrives from the target.

angle of arrival The angle which the line of propagation of an incoming radio wave makes with the surface of the earth. Compare ANGLE OF DEPARTURE.

angle of azimuth The horizontal angle between the viewer and object or target, usually measured clockwise from north.

angle of beam The angle enclosing most of the transmitted energy in the radiation from a directional antenna. It is usually measured between the *half-power points* in the main lobe of the directional pattern. This angle can be measured in the horizontal (azimuth) plane or in the vertical (elevation) plane.

5059F-pA_1-55 4/9/01 4:41 PM Page 30

angle of conduction **1.** Also called *angle of flow.* The number of degrees of an excitation-signal cycle during which output (drain, collector or plate) current flows in an amplifier circuit. **2.** The number of degrees of any sine wave at which conduction of a device (e.g., a diode) begins.

angle of convergence **1.** In any graphical representation, the angle formed by any two lines or plots that come together at a point. **2.** The angle formed by the light paths of two photocells focused on the same object.

angle of declination The angle between the horizon and a descending line. Compare ANGLE OF ELEVATION.

angle of deflection In a cathode-ray tube, the angle between the electron beam at rest and a new position resulting from deflection.

angle of departure The angle, relative to the horizon, made by the line of propagation of a transmitted radio wave. Compare ANGLE OF ARRIVAL.

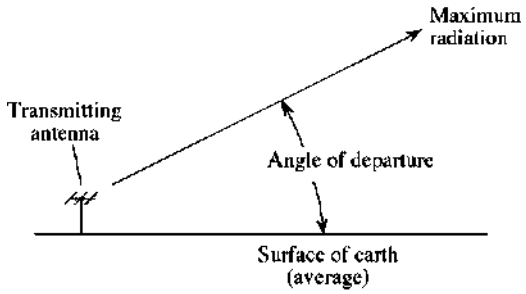

angle of departure

angle of depression See ANGLE OF DECLINATION.

angle of divergence In a cathode-ray tube, the angle formed by the spreading of an undeflected electron beam as it extends from the gun to the screen.

angle of elevation The angle that an ascending line subtends, with respect to the horizon. Compare ANGLE OF DECLINATION.

angle of flow See ANGLE OF CONDUCTION.

angle of incidence The angle, measured relative to the perpendicular (orthogonal) to a surface or boundary, subtended by an approaching ray. Compare ANGLE OF REFLECTION and ANGLE OF REFRACTION.

angle of lag The phase difference (in degrees or radians) whereby one component follows another in time, both components being of the same frequency. Compare ANGLE OF LEAD. Also see PHASE ANGLE.

angle of lead The phase difference (in degrees or radians) whereby one component precedes another in time, both components being of the same frequency. Compare ANGLE OF LAG. Also see PHASE ANGLE.

angle of radiation **1.** The angle, measured with respect to the horizon, at which the principal lobe of an electromagnetic wave leaves a transmitting antenna. **2.** The angle, measured relative to the horizon, of a receiving or transmitting antenna's optimum sensitivity.

angle of reflection The angle, measured relative to the perpendicular (orthogonal) to a surface, subtended by a ray leaving the surface after having been reflected from it. Compare ANGLE OF INCIDENCE.

angle of refraction The angle, measured relative to the perpendicular (orthogonal) to a boundary between two different media, subtended by a ray leaving the boundary after having been refracted thereat. Compare ANGLE OF INCIDENCE.

angle tracking noise Noise in a servo system that results in a tracking error.

angstrom (Anders J. Angstrom, 1814–1874). A unit of length used to describe certain extremely short waves and microscopic dimensions; 1 angstrom equals 10^{-4} microns (10^{-10} meters).

angular deviation loss The ratio of microphone or loudspeaker response on the principal axis of response to the response at a designated angle from that axis. Expressed in decibels.

angular difference See PHASE ANGLE.

angular displacement In an ac circuit, the separation, in degrees, between two waves. See PHASE ANGLE.

angular frequency The frequency of an ac signal, expressed in *radians per second (rad/sec)* and approximately equal to $6.28f$, where f is the frequency in Hertz.

angular length Length, as along the horizontal axis of an ac wave or along the standing-wave pattern on an antenna, expressed as the product of radians and wavelength.

angular-mode keys On a calculator or computer, the DEG, RAD, and GRAD keys for expressing or converting angles in DEGREES, RADIANS, and GRADS, respectively.

angular phase difference For two sinusoidal waves, the phase difference, expressed in degrees or radians.

angular rate In navigation, the rate of bearing change, expressed in degrees or radians.

angular resolution The ability of a radar to distinguish between two targets by angular measurement.

angus pen recorder An instrument that makes a permanent record of the time whenever a channel is used.

anharmonic oscillator An oscillating device in which the force toward the balance point is not linear, with respect to displacement.

anhysteresis The magnetization of a material by a unidirectional field containing an alternating field component of gradually decreasing amplitude.

5059F-pA_1-55 4/9/01 4:41 PM Page 31

anhysteretic state The condition of a substance after it has been subjected to a strong magnetic field, the intensity of which alternates in direction and diminishes gradually to zero.

animism A belief or philosophy, held especially in Eastern civilizations, such as Japan, that all things contain an essence of life. This theory renders irrelevant the question of whether or not machines, such as computers and robots can be "alive."

anion A negative ion. Also see ION.

anisotropic Pertaining to the tendency of some materials to display different magnetic and other physical properties along different axes.

ANL Abbreviation of AUTOMATIC NOISE LIMITER.

anneal To heat a metal to a predetermined temperature and let it cool slowly. The operation prevents brittleness and often stabilizes electrical characteristics.

annealed laminations Core laminations for transformers or choke coils that have been annealed.

annealed shield A magnetic shield for cathode-ray tubes, that has been processed by annealing.

annealed wire Soft-drawn wire that has been subjected to annealing.

annotations **1.** Marking on copies of original engineering-installation documents to show changes made during the installation. **2.** Any set of comments or notes accompanying a program, an equipment or system, or a process.

annular **1.** Pertaining to the region between two concentric circles that lie in the same plane; ring-shaped. **2.** Pertaining to two or more concentric circles that lie in a common plane.

annular conductor A number of wires stranded in three concentric layers of alternating twists around a hemp core.

annular transistor A mesa transistor in which the base and collector take the form of concentric rings around a central emitter.

annulling network A subcircuit that shunts a filter to cancel reactive impedance at the extreme ends of the pass band of the filter.

annunciation relay A relay that indicates whether or not a circuit is carrying current.

annunciator A device that produces loud sound and/or conspicuous light to attract attention (e.g., the electronic siren in an automotive security system).

anode **1.** The positive electrode of a vacuum tube or solid-state device (i.e., the electrode toward which electrons move during current flow). **2.** In an electrochemical cell, the electrode that loses electrons by oxidation. This is usually the negative electrode.

anode balancing coil Mutually coupled windings used to maintain equal currents in parallel anodes operating from a common transformer terminal.

anode current Current flowing in the anode circuit of a device.

anode efficiency Also called *plate efficiency*. In a power amplifier using an electron tube, the ratio P_o/P_i, where P_o is the output power in watts and P_i is the dc anode power input in volt-amperes.

anode power input Symbol, $P_{A(input)}$. The product of anode current and anode voltage.

anode power supply The ac or positive dc power supply unit that delivers current and voltage to the anode of a device.

anode saturation The point beyond which a further increase in anode voltage does not produce an increase in anode current.

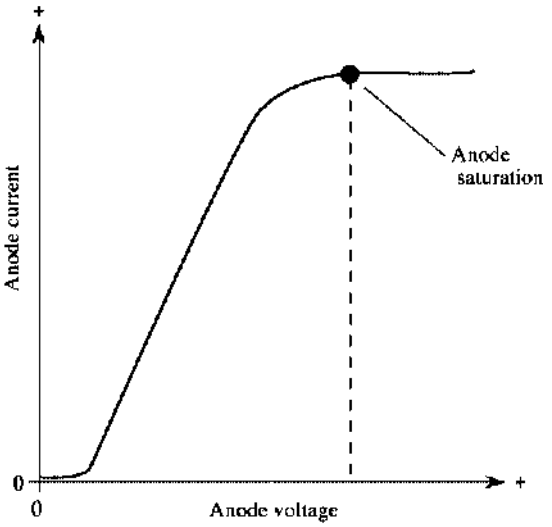

anode saturation

anode strap In a multicavity magnetron, a metal strap connecting the anodes.

anode terminal **1.** In a diode, the terminal to which a positive dc voltage must be applied for forward bias. Compare CATHODE TERMINAL. **2.** In a diode, the terminal at which a negative dc voltage appears when the device is used as an ac rectifier. Compare CATHODE TERMINAL. **3.** The terminal that is connected internally to the anodic element of any device.

anode voltage Symbol, E_A or V_A. The difference in potential between the anode and cathode of a device.

anodic Pertaining to the anode of a device, or to anode-like effects.

anodizing An electrolytic process in which a protective oxide film is deposited on the surface of a metallic body acting temporarily as the anode of the electrolytic cell.

anomalous dispersion Dispersion of electromagnetic radiation that is characterized by a decrease in refractive index with increase in frequency.

anomalous propagation **1.** The low-attenuation propagation of UHF or microwave signals through

5059F-pA_1-55 4/9/01 4:41 PM Page 32

atmospheric layers. **2.** Unusual, bizarre, or unexplainable electromagnetic-wave propagation (e.g., apparent F-layer ionospheric effects in the FM broadcast band). **3.** Rapid fluctuation of a sonar echo because of variations in propagation.

anoxemia toximeter An electronic instrument for measuring or alerting against the onset of anoxemia (deficiency of oxygen in the blood)—especially in airplane pilots.

AN radio range A navigational facility entailing four zones of equal signal strength. When the aircraft deviates from course, an aural Morse-code signal, A (DIT DAH) or N (DAH DIT) is heard; but when the aircraft is on course, a continuous tone is heard.

ANSI Acronym for *American National Standards Institute.*

AN signal The signal provided by an AN radio range to apprise aircraft pilots of course deviation.

answerback The automatic response of a terminal station to a remote-control signal.

answer cord In a telephone system, the cord used for answering subscribers' calls and incoming trunk calls.

answering machine A device that automatically answers a telephone and records an audio message from the caller.

answer lamp A telephone switchboard lamp that lights when an answer cord is plugged into a line jack; it switches off when the telephone answers and lights when the call is completed.

ant Abbreviation of ANTENNA.

antenna In a communications system, a specialized transducer that converts incoming electromagnetic fields into alternating electric currents having the same frequencies (*receiving antenna*), or converts an alternating current at a specific frequency into an outgoing electromagnetic field at the same frequency (*transmitting antenna*). An antenna can be a simple wire or rod, or a complicated structure. Thousands of geometries and specifications are possible. The optimum antenna type for a given situation depends on the communications frequency, the distance to be covered, and various other factors.

antenna ammeter An RF ammeter, usually of the thermocouple type, employed to measure current flowing to a transmitting antenna.

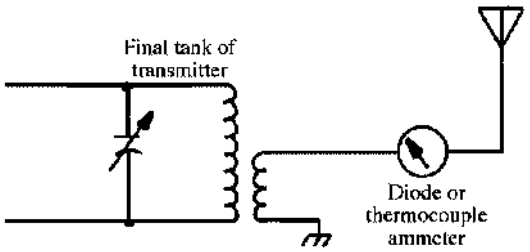

antenna ammeter

antenna amplifier **1.** A radio-frequency amplifier, often installed at the antenna, used to boost signals before they reach a receiver (also called an *RF preamplifier*). **2.** Occasionally, the first RF amplifier stage of a receiver, also known as the *front end.*

antenna array See ARRAY.

antenna bandwidth The frequency range throughout which an antenna will operate at a specified efficiency without needing alteration or adjustment.

antenna beamwidth A measure of the extent to which a directional antenna focuses a transmitted electromagnetic field, or focuses its response to incoming electromagnetic fields. Expressed as the angle in degrees between opposite *half-power points* in the main lobe of the directional pattern. Usually determined in the horizontal plane, but occasionally in the vertical plane.

antenna coil The primary coil of the input RF transformer of a receiver, or the secondary coil of the output RF transformer of a transmitter.

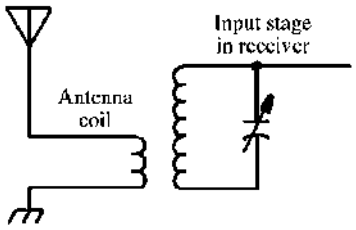

antenna coil

antenna coincidence The condition in which two directional antennas are pointed directly toward each other.

antenna-conducted interference Extraneous signals generated in a transmitter or receiver and presented to the antenna, from which they are radiated.

antenna core A ferrite rod or slab around which a coil of wire is wound to act as a self-contained antenna, usually in a miniature receiver.

antenna coupler A device consisting of an inductor, RF transformer, or a combination of inductor(s) and capacitor(s), used to match the impedance of an antenna to that of a transmitter or receiver. Also known as a *transmatch* or *antenna tuner.*

antenna coupling Inductive and/or capacitive coupling used to optimize the transfer of energy from an antenna to a receiver, or from a transmitter to an antenna.

antenna current **1.** Radio-frequency current flowing from a transmitter into an antenna. **2.** Radio-frequency current flowing from a receiving antenna into a receiver.

5059F-pA_1-55 4/9/01 4:41 PM Page 33

antenna detector A circuit that warns aircraft personnel that they are being observed by radar. It picks up the radar pulses and actuates a warning light or other device.

antenna diplexer A coupling device that permits several transmitters to share one antenna without troublesome interaction. Compare ANTENNA DUPLEXER.

antenna directivity The directional characteristics of a transmitting or receiving antenna, usually expressed qualitatively (e.g., *omnidirectional*, *bidirectional*, or *unidirectional*). A more precise expression is ANTENNA BEAMWIDTH.

antenna director In a directional antenna, a PARASITIC ELEMENT situated in front of the radiator and separated from it by an appropriate fraction of a wavelength. Its function is to intensify radiation in the direction of transmission. Compare ANTENNA RADIATOR and ANTENNA REFLECTOR.

antenna duplexer A circuit or device permitting one antenna to be shared by two transmitters without undesirable interaction.

antenna effect The tendency of wires or metallic bodies to act as antennas (i.e., to radiate or receive radio waves).

antenna efficiency The ratio of radio-frequency energy supplied to a wireless transmitting antenna, to the energy radiated into space. Electrically, the radiation resistance of the antenna (R_R) appears in series with loss resistance (R_L). The efficiency *Eff* of the antenna can be determined by the following formula:

$$Eff = R_R/(R_R + R_L)$$

As a percentage,

$$Eff_{\%} = 100\ (R_R/(R_R + R_L)$$

The efficiency is always less than 1 (100 percent) because, in practice, the loss resistance can never be reduced to zero.

antenna factor A factor (in decibels) added to an RF voltmeter reading to find the true open-circuit voltage induced in an antenna.

antenna field The electromagnetic field immediately surrounding an antenna.

antennafier Low-profile antenna/amplifier device, sometimes used with portable communications systems. Also called an *active antenna.*

antenna front-to-back ratio For a directional antenna, the ratio of field strength in front of the antenna (i.e., directly forward in the line of maximum directivity) to field strength in back of the antenna (i.e., 180 degrees from the front), as measured at a fixed distance from the radiator. It is usually specified in decibels.

antenna gain For a given antenna, the ratio of signal strength (received or transmitted) to that obtained with a comparison antenna, such as a simple dipole. Generally specified in decibels.

antenna ground system The earth, counterpoise, guy wires, radials, and/or various conducting objects in the vicinity of an antenna which, taken together, form the radio-frequency (RF) ground system against which the antenna operates. Some antennas require an extensive ground system to function efficiently; others need no ground system.

antenna/ground system An arrangement embodying both an antenna and a low-resistance connection to the earth, as opposed to an antenna system that involves no connection to earth.

antenna height **1.** The height of an antenna above the surface of the earth immediately beneath the driven element(s). **2.** The height of an antenna above the effective radio-frequency (RF) ground immediately beneath the driven element(s). **3.** The height of an antenna above average terrain, determined against the mean altitude of a number of points on the earth's surface that lie within a certain radius of the antenna structure. Also called *height above average terrain (HAAT).*

antenna impedance The complex-number impedance that an antenna presents to a transmission line. It can vary over a tremendous range, and depends on the antenna type, antenna size, antenna height, operating frequency, and various other factors.

antenna-induced potential Also called *antenna-induced microvolts.* The voltage across the open-circuited terminals of an antenna.

antenna lens Also called *lens antenna.* A radiator designed to focus microwave energy in much the same manner that an optical lens focuses light rays. Lens antennas are made from dielectric materials and/or metals.

antenna loading **1.** The insertion of inductance in antenna elements to lower the resonant frequency of the system without necessarily making the system physically larger or the elements longer. **2.** The insertion of capacitance in antenna elements to raise the resonant frequency of the system without necessarily making the system physically smaller or the elements shorter.

antenna lobe A well-defined region in the radiation pattern of an antenna in which radiation is most intense, or in which reception is strongest. Also see ANTENNA PATTERN.

antenna matching The technique of establishing a satisfactory relationship between the antenna impedance and the transmission-line or transmitter-output impedance, for maximum transfer of power into the antenna. Also, the matching of antenna impedance to receiver-input impedance, for delivery of maximum energy to the receiver.

antennamitter An antenna/oscillator combination that serves as a low-power transmitter.

antenna pattern A polar plot of antenna performance that shows field strength versus angle of azimuth, with the antenna at the center. It is usually specified in the horizontal plane.

5059F-pA_1-55 4/9/01 4:41 PM Page 34

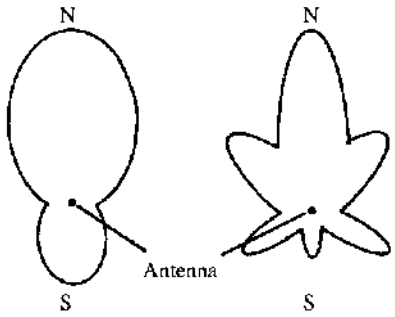

antenna patterns

antenna polarization The orientation of electric lines of flux, with respect to the surface of the earth, for which an antenna is most efficient. A vertical antenna radiates and receives vertically polarized waves. A horizontal antenna radiates and receives horizontally polarized waves broadside to itself, and vertically polarized waves at high elevation angles off its ends. In other directions, the polarization is slanted at various angles.

antenna power Symbol, P_{ant}. The RF power developed in an antenna by a transmitter; P_{ant} equals I^2R, where I is the antenna current and R is the antenna resistance at point I is measured.

antenna power gain The ratio of the maximum effective radiated power (ERP) from a wireless transmitting antenna to the ERP from a reference antenna, expressed in decibels (dB). If the ERP from an antenna under test is P_T watts and the ERP from the reference antenna is P_R watts, then the gain G_{dB} is:

$$G_{dB} = 10 \log_{10} (P_T/P_R)$$

Power gain is always measured in the direction in which the test antenna performs the best. The reference antenna, usually a dipole, is chosen with a gain assumed to be unity, or 0 dB. Gain relative to a dipole is expressed in dBd (decibels relative to a dipole). Alternatively, the reference antenna can be an isotropic radiator, in which case the gain is expressed in dBi (decibels relative to an isotropic radiator). Gain figures in dBd and dBi differ by a constant amount as follows:

$$G_{dBi} = 2.15 + G_{dBd}$$

antenna preamplifier A highly sensitive amplifier used to enhance the gain of a receiver. It is usually used at the very high frequencies and above.

antenna radiation The propagation of radio waves by a transmitting antenna.

antenna radiator The element of an antenna that receives RF energy from the transmitter and radiates waves into space. Also known as the *driven element*. Compare ANTENNA DIRECTOR and ANTENNA REFLECTOR.

antenna range **1.** The frequency band, communication distance characteristically covered, or other continuum of values that specify the operating limits of an antenna. **2.** The region immediately surrounding an antenna in which tests and measurements usually are made. Sometimes called ANTENNA FIELD.

antenna reflector In a directional antenna, a PARASITIC ELEMENT situated behind the radiator and separated from the latter by an appropriate fraction of a wavelength. Its function is to intensify radiation in the direction of transmission. Compare ANTENNA DIRECTOR and ANTENNA RADIATOR.

antenna relay In a radio station, a low-loss, heavy-duty relay that enables the antenna to be switched between transmitter and receiver.

antenna resistance The resistive component of ANTENNA IMPEDANCE.

antenna resonant frequency The frequency, or narrow band of frequencies, at which an antenna's impedance appears resistive.

antenna stage **1.** The first RF amplifier stage of a receiver. **2.** Occasionally, the final RF amplifier of a transmitter.

antenna switch In a radio station, a low-loss, heavy-duty switch that enables the antenna to be connected to transmitter, receiver, or safety ground.

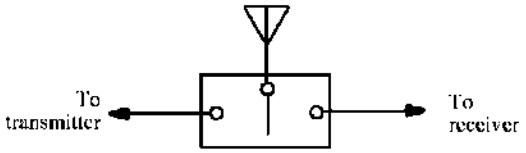

antenna switch (single-pole, double-throw)

antenna system Collectively, an antenna and all of the auxiliary electrical and mechanical devices needed for its efficient operation, including couplers, tuners, transmission lines, supports, insulators, and rotator.

antenna terminals **1.** The points at which a transmission line is attached to an antenna. **2.** The signal input terminals of a receiver. **3.** The signal output terminals of a transmitter.

antennaverter An antenna and converter combined into a single circuit, intended for connection to the antenna terminals of a receiver to allow operation on frequencies outside the band for which the receiver has been designed.

antenna wire **1.** The radiator element of a wire-type antenna. **2.** A strong solid or stranded wire (e.g., hard-drawn copper, copper-clad steel, or phosphor-bronze) used for antennas.

anthropomorphism The perception, by people, of machines as having human qualities. This can

5059F-pA_1-55 4/9/01 4:41 PM Page 35

lead to emotional attachment to hardware, such as computers and robots. The more sophisticated the apparatus, in general, the more powerful this perception can become.

antialiasing filter A low-pass or bandpass filter that limits the bandwidth of an input signal to prevent *aliasing* and its effects. See ALIASING, **1**.

anticapacitance switch A switch whose members are thin blades and stiff wires widely separated to minimize capacitance between them.

anticathode The target electrode of an X-ray tube.

Anticipatory Sciences A group of *futurists*, people who attempt to predict the course of technology. Some futurists believe that progress will continue until, for example, homes become fully automated and artificial intelligence reaches a level comparable to human intelligence. Other futurists believe that such things are highly improbable.

anticlutter circuit A supplementary circuit in a radar receiver that minimizes the effect of extraneous reflections that would obscure the image of the target.

anticlutter gain control In a radar receiver, a circuit that automatically raises the gain of the receiver slowly to maximum after each transmitter pulse to reduce the effect of clutter-producing echoes.

anticoincidence Noncoincidental occurrence of two or more signals. Compare COINCIDENCE.

anticoincidence circuit In computers and control systems, a circuit that delivers an output signal only when two or more input signals are not received simultaneously. Compare COINCIDENCE CIRCUIT. Also see NAND CIRCUIT.

anticoincidence operation An exclusive-OR operation.

anticollision radar A vehicular radar system that is used to minimize the probability of a collision with another vehicle, whether or not that other vehicle has a similar system.

antiferroelectric **1.** Pertaining to the property wherein the polarization curve of certain crystalline materials shows two regions of symmetry. **2.** A material that exhibits the aforementioned property.

antiferromagnetic Pertaining to the behavior of materials in which, at low temperatures, the magnetic moments of adjacent atoms point in opposite directions.

antihunt The condition in which *hunting* is counteracted, usually by removing overcorrection in automatic control or compensation systems.

antihunt circuit **1.** A circuit that minimizes or eliminates hunting. Also see ANTIHUNT. **2.** In a television (TV) receiver, a circuit that stabilizes an automatic frequency control (afc) system.

antijamming Pertaining to communications systems that are resistant to, or that counteract, the effects of *jamming.*

antilogarithm Abbreviated, antilog or $\log^{-1}$. The number corresponding to a given logarithm. For example, log 10,000 = log 10^4 = 4, and thus antilog 4 = 10^4 = 10,000.

antilogous pole In a PYROELECTRIC MATERIAL, the end that becomes negatively charged as the temperature rises.

antimagnetic Pertaining to materials having extremely low RETENTIVITY.

antimatter Pertaining to particles that are the counterparts of conventional particles (i.e., positrons instead of electrons, antineutrons instead of neutrons, and antiprotons instead of protons). When a particle meets its antiparticle, the two annihilate, releasing energy. Also see ANTIPARTICLE.

antimicrophonic See NONMICROPHONIC.

antimony Symbol, Sb. A metalloidal element. Atomic number, 51. Atomic weight, 121.76. Often used as n-type dopant in semiconductor manufacture.

antineutrino The antiparticle of the NEUTRINO, emitted as a result of radioactive decay.

antineutron An uncharged particle with a mass equal to that of the neutron, but with a magnetic moment in the direction opposite that of the neutron.

antinode A point of maximum amplitude in a standing wave.

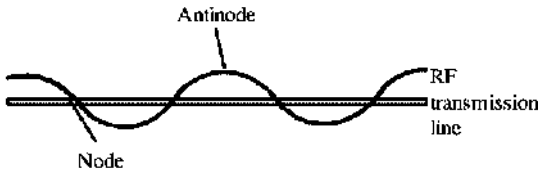

antinode

antinoise carrier-operated circuit A circuit that cuts off the audio output of a receiver while the station transmitter is in use. This can be accomplished in the automatic-gain-control (AGC) circuit of the receiver, or in the speaker or audio line. The circuit is actuated by energy from the transmitted signal.

antinoise microphone Any microphone that discriminates against acoustic noise (e.g., a *lip microphone* or *throat microphone*).

antinucleon A particle with the mass of a nucleon, but with the opposite electrical charge and direction of magnetic moment. Compare NUCLEON.

antioxidant A material, such as a lacquer coat or an inactive oxide layer, that prevents or slows oxidation of a material exposed to air.

antiparticle A subatomic particle opposite in character to conventional particles, such as electrons, neutrons, protons. Antiparticles constitute *antimatter.* Also see ANTINEUTRINO, ANTINEUTRON, ANTINUCLEON, ANTIPROTON, and POSITRON.

5059F-pA_1-55 4/9/01 4:41 PM Page 36

antiphase The property of being in phase opposition (180 degrees out of phase).

antipincushioning magnets In some television (TV) receivers, a pair of corrective magnets in the deflection assembly on the picture tube that eliminate *pincushion distortion* (disfigurement of the raster so that it resembles a pincushion—a rectangle with its sides bowed in).

antiproton A subatomic particle with a mass equal to that of the proton, but with opposite electrical charge.

antiquark An ANTIPARTICLE of a QUARK.

antirad substance A material that protects against damage caused by atomic radiation.

antiresonance 1. Parallel resonance. **2.** The condition of being detuned from a resonant frequency.

antiresonant circuit See PARALLEL-RESONANT CIRCUIT.

antiresonant frequency 1. The resonant frequency of a parallel-resonant circuit. **2.** In a piezoelectric crystal, the frequency at which impedance is maximum (as in a parallel-resonant circuit).

antisidetone Pertaining to the elimination in telephone circuits of interference between the microphone and earphone of the same telephone.

antistickoff voltage The low voltage applied to the coarse synchro control transformer rotor winding in a dual-speed servo system to eliminate ambiguous behavior in the system.

antitransmit/receive switch Abbreviated *ATR.* In a radar installation, an automatic device to prevent interaction between transmitter and receiver.

antivirus program A computer program or utility designed to detect and eliminate viruses and Trojan horses in a computer system.

antivoice-operated transmission Radio communications that use a voice-activated circuit as a transmitter interlock during reception on the companion receiver.

apc 1. Abbreviation of *automatic picture control.* **2.** Abbreviation of AUTOMATIC PHASE CONTROL.

aperiodic Characterized by a lack of predictable repetitive behavior. For example, the *sferics* or "static" electromagnetic interference caused by lightning.

aperiodic current The unidirectional current that follows an electromagnetic disturbance in an LCR circuit, in which R is equal to or higher than the critical circuit resistance.

aperiodic damping Damping of such a high degree that the damped system, after disturbance, comes to rest without oscillation or hunting.

aperiodic discharge A discharge in which current flowing in an LCR circuit is unidirectional, rather than oscillatory. For this condition, $1/LC$ is less than or equal to $R^2/4L^2$.

aperiodic function A nonrepetitive function (e.g., a hyperbolic trigonometric function).

aperture 1. The larger, normally open end of a horn antenna or horn loudspeaker. **2.** An opening in an opaque disk or mask that passes a predetermined amount of light or other radiant energy. **3.** The portion of a directional antenna through which most of the radiated energy passes.

aperture angle For an antenna or telescope or microscope, the half angle formed by the radius of the detecting instrument, as viewed from the source.

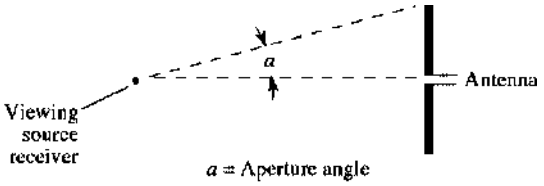

aperture angle

aperture antenna An antenna whose beamwidth depends on the size of a horn, reflector, or lens.

aperture compensation In a television (TV) camera, the minimizing of APERTURE DISTORTION by widening the video-amplifier passband.

aperture distortion In a television (TV) camera tube, a form of distortion that occurs when the scanning beam covers several mosaic elements simultaneously. This condition, caused by excessive beam thickness, results in poor image resolution.

aperture mask In a three-gun color picture tube, a thin, perforated sheet mounted behind the viewing screen to ensure that a particular color phosphor will be excited only by the beam for that color. Also called *shadow mask.*

aperture synthesis In telescopes, a method of obtaining high resolution using several small antennas separated by great distances. The small antennas are moved around to simulate the resolving power of a much larger antenna that would, in practice, be impossible or impractical to construct.

aphelion 1. The point at which a solar-orbiting satellite attains its highest altitude. It occurs once for every complete orbit. At this point, the satellite travels slower than at any other point in the orbit. **2.** The altitude, measured from the sun's surface or the sun's center, of a solar-orbiting satellite at its most distant point.

APL Abbreviation for *A Programming Language.* A high-level computer language designed for ease of use, and characterized by the requirement for a special character set.

apl 1. Abbreviation of *average picture level.* **2.** Abbreviation of *automatic phase lock.*

A plus Also, A+. The positive terminal of an A battery. Also, pertaining to the part of a circuit connected to that terminal.

5059F-pA_1-55 4/9/01 4:41 PM Page 37

apogee **1.** The point at which an earth-orbiting satellite attains its highest altitude. It occurs once for every complete orbit. At this point, the satellite travels slower than at any other point in the orbit. **2.** The altitude, measured from the earth's surface or the earth's center, of an earth-orbiting satellite at its most distant point.

A power supply A term sometimes used to denote the unit that supplies energy to a vacuum-tube filament. Compare B POWER SUPPLY.

apparent bearing In radio-direction finding, the uncorrected direction from which a signal appears to arrive.

apparent power In an ac circuit, the power value obtained by multiplying the current by voltage (*P* equals *IE*), with no consideration of the effects of phase angle. Compare TRUE POWER.

apparent power loss The loss in an ammeter or voltmeter, caused by the imperfection of the instrument. At full scale, the ammeter has a certain voltage across its terminals; the apparent power loss is the current multiplied by this voltage. A voltmeter carries a small current; the apparent power loss is the product of the current and the indicated voltage.

appearance potential The potential through which an electron must move to produce a certain ion from the atom with which it is associated.

applause meter An instrument consisting essentially of a microphone, audio amplifier, and indicating meter (reading directly in sound level). It is so called because of its familiar use in measuring audience response, as indicated by loudness of applause.

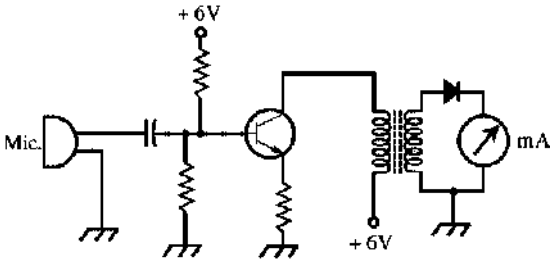

applause meter

Applegate diagram For a velocity-modulated tube, a plot of the positions of electron bunches in the drift space versus time.

Appleton layer Collectively, the F1 and F2 layers of the ionosphere, at a height between 150 and 400 kilometers above the surface of the earth.

apple tube A color picture tube, used in television, with the red, blue, and green phosphor in vertical strips.

appliance Electrical equipment in general. This might include any home-operated device.

application A task or job for which an electronic device or system is used. It especially pertains to personal-computer software that has practical usefulness.

application factor A factor involved in determining the failure rate of a circuit or system affected by unusual operating conditions.

application schematic diagram A diagram of pictorial symbols and lines that illustrate the interrelationship of functional circuit blocks in a specific program mode.

applicators **1.** In dielectric heating, the electrodes between which the dielectric body is placed and the electrostatic field developed. **2.** In medical electronics, the electrodes applied to a patient undergoing diathermy or ultrasonic therapy.

applied voltage The voltage presented to a circuit point or system input, as opposed to the voltage drop resulting from current flow through an element.

applique circuit A circuit for adapting equipment to a specialized job.

approach-control radar A radar installation serving a ground-controlled approach (GCA) system.

approximate data **1.** Data obtained through physical measurements. Such data can never be exact; all measurements are subject to error. **2.** Loosely estimated data or imprecise calculations.

AQL Abbreviation of ACCEPTABLE QUALITY LEVEL. A statistically defined quality level, defined in terms of percent defective, accepted on an average of 95 percent of the time.

Aquadag A tradename for a material that consists of a slurry of fine particles of graphite. Aquadag forms a conductive coating on the inside and outside walls of some cathode-ray tubes.

aqua pura Pure water; in most instances, distilled water. Formula, H_2O. Pure water is a nonconductor with a dielectric constant of about 81.

Ar Symbol for ARGON.

arbitrary function fitter A circuit or device, such as a potentiometer, curve changer, or analog computer element, providing an output current or voltage that is some preselected function of the input current or voltage.

arc **1.** A luminous sustained discharge between two electrodes. Because it is sustained, rather than intermittent, an arc is distinguished from a spark discharge, the latter being a series of discharges (sparks)—even when it appears continuous. **2.** In graphical presentations, a section of curved line, as of a circle.

arc angle The angle in degrees traced out by a circular arc if the center point of the circle is considered to be the vertex of an angle formed by two rays intersecting the arc at designated points.

arc cosecant Abbreviated arc csc or csc^{-1}. **1.** The inverse of the *cosecant* function. **2.** The angle, in

5059F-pA_1-55 4/9/01 4:41 PM Page 38

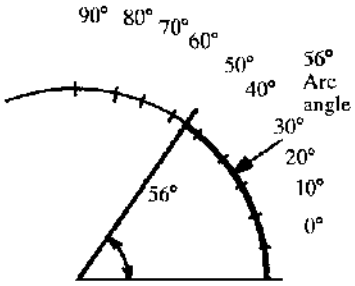

arc angle

radians or degrees, corresponding to a given cosecant.

arc cosine Abbreviated arc cos or $\cos^{-1}$. **1.** The inverse of the *cosine* function. **2.** The angle, in radians or degrees, corresponding to a given cosine.

arc cotangent Abbreviated arc cot or $\cot^{-1}$. **1.** The inverse of the *cotangent* function. **2.** The angle, in radians or degrees, corresponding to a given cotangent.

arc failure **1.** Damage to, and/or failure of, insulation or a dielectric as a result of ARCOVER. **2.** Failure of make-and-break contacts through damage caused by arcover.

arc function An *inverse trigonometric function.* See ARC COSECANT, ARC COSINE, ARC COTANGENT, ARC SECANT, ARC SINE, and ARC TANGENT.

arc furnace A high-temperature electric furnace in which heat is produced by one or more electrical arcs.

architecture The functional design elements of a computer—especially the components of the *central processing unit (CPU)* and the manner in which these elements interact.

archived file A computer file stored on some backup medium, such as magnetic tape, diskette, or CD-ROM (compact disk, read-only memory), rather than being held on the hard disk. Such a file will be apart from the operating system's catalog of current files, but can be reconstituted as needed.

archives A complete, periodically updated set of ARCHIVED FILES.

arcing See ARCOVER.

arcing contacts Make-and-break contacts between which an arc occurs when they are separated.

arcing ring A metal ring placed around an insulator in a high-voltage electrical system. This keeps an arc from charring or breaking the insulator.

arcing time The elapsed time between the breaking of contacts and the end of the arc between the contacts.

arc lamp An electric lamp in which a brilliant arc jumps between the tips of two rods (originally carbon).

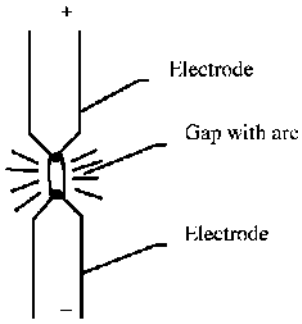

arc lamp

arc length The length along a given arc, usually a part of the circumference of a circle. If the circle has circumference C and the arc measures x degrees, then the arc length is $Cx/360$ units.

arc minute See MINUTE.

arc oscillation Oscillations that can occur when opening relay contacts arc.

arcover The occurrence of an electrical ARC between electrodes, contacts, or capacitive plates.

arcover voltage The voltage at which disruptive discharge occurs, typically accompanied by an arc.

arc resistance The ability of a material, usually a dielectric, to resist damage from arcing. This property is commonly expressed as the length of time between the start of the arc and the establishment of a conductive path through the material.

arc secant Abbreviated arc sec or $\sec^{-1}$. **1.** The inverse of the *secant* function. **2.** The angle, in radians or degrees, that corresponds to a given secant.

arc second See SECOND.

arc sensor A device for detecting visible arcs and excessive reflected power in microwave systems.

arc sine Abbreviated arc sin or $\sin^{-1}$. **1.** The inverse of the *sine* function. **2.** The angle, in radians or degrees, that corresponds to a given sine.

arc suppression Extinguishing an arc discharge. Disruptive arcs in electronic circuits are suppressed by means of auxiliary diodes or resistor-capacitor networks.

arc-suppressor diode A semiconductor diode used to prevent arcing between make-and-break contacts.

arc tangent Abbreviated arc tan or $\tan^{-1}$. **1.** The inverse of the *tangent* function. **2.** The angle, in radians or degrees, corresponding to a given tangent.

arcthrough The puncturing of a material by an arc.

area code In the United States, a three-digit number that indicates the location, according to specified assigned districts, of a telephone sub-

5059F-pA_1-55 4/9/01 4:41 PM Page 39

scriber. When making a long-distance call, the area code of the desired station must be given in addition to the seven-digit telephone number.

area protection Coverage of a defined region, in terms of area or volume, by an alarm system.

area redistribution A scheme to determine the effective duration of an irregularly shaped pulse. A rectangle is constructed whose height is equal to the peak height of the pulse, as displayed on an oscilloscope. The rectangle width is adjusted until the area of the rectangle is the same as the area under the curve representing the pulse. The width of the rectangle then represents the effective duration of the pulse.

area search The scanning of a large group of computer records for those of a major category or class.

area sensor A transducer, used with an alarm system, that protects a defined region or volume, such as an office or bedroom.

Argand diagram Named after Jean Robert Argand, (1768-1822) of Geneva, for his work on the graphical representation of complex numbers. A graphical illustration of a complex number in the form $A + jB$, where the real-number (A) axis is perpendicular to the imaginary-number (jB) axis. The value j is the square root of -1, the unit imaginary number. The axes are perpendicular, usually with the A axis horizontal. The length of the line from the point (0,0) to the point (A,jB) is the amplitude of the vector $\mathbf{X} = A + jB$. The direction is specified as the angle, in degrees or radians, of the vector measured counterclockwise from the A axis.

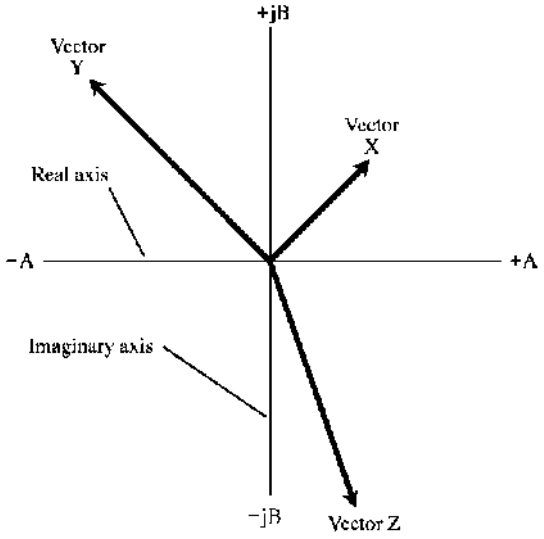

Argand diagram

argon Symbol, Ar. An inert gaseous element. Atomic number, 18. Atomic weight, 39.94. Argon, present in small amounts in the earth's atmosphere, is used in various specialized devices, such as lasers.

argon laser A laser whose tube is filled with argon gas. It generates coherent light at specific wavelengths that are characteristic of elemental argon.

argument **1.** The direction angle of a polar vector. **2.** An independent variable whose value determines the value of a function.

arithmetic address An address obtained by performing an arithmetic operation on another address.

arithmetic and logic unit Abbreviation, ALU. The part of a digital computer containing the circuits that perform calculations and logic operations; distinguished from mass storage, input/output, and peripheral units.

arithmetic circuit Also called *arithmetic element.* In a digital computer, a circuit that is involved in the execution of calculations. Included are adders, storage registers, accumulators, subtracters, and multipliers.

arithmetic mean The average of a group of quantities, obtained by dividing their sum by the number of quantities.

arithmetic operation In digital computer practice, a numerical process performed: addition, subtraction, multiplication, division, comparison.

arithmetic progression A mathematical series in which each term following the first is obtained by adding a constant quantity to the preceding one. For example, $S = 1, 2, 3, 4, \ldots n$. Compare GEOMETRIC PROGRESSION.

arithmetic shift In a digital computer, the multiplication or division of a quantity by a power of the base used in the notation.

arithmetic sum The sum of two or more quantities disregarding their signs. Compare ALGEBRAIC SUM.

arithmetic symmetry A filter response that is exactly symmetrical about the center frequency when the frequency scale is linear.

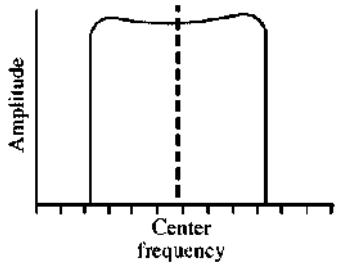

arithmetic symmetry

5059F-pA_1-55 4/9/01 4:41 PM Page 40

arm **1.** Any of the distinct branches of a circuit or network. Also called *leg.* **2.** A movable element in a device, usually containing a contact for switching.

armature **1.** The rotating member of a motor. **2.** The rotating member of some types of electro-mechanical generator. **3.** The movable member of a relay, bell, buzzer, or gong. **4.** The movable member of an actuator. **5.** The soft-iron *keeper* placed across the poles of a permanent magnet to conserve power.

armature coil A coil of insulated wire wound on a ferromagnetic core to provide the electromagnetic properties of an armature. In a motor or generator, the armature coil is distinguished from the FIELD COIL.

armature core The ferromagnetic core upon which the armature coil of a motor or generator is wound.

armature gap **1.** In a motor or generator, the space between an armature core and the pole of a field magnet. **2.** In a relay, the space between the armature and the relay-coil core.

armature hesitation A momentary delay in the movement of a relay.

armature-hesitation contact chatter Undesired (usually rapid, repetitive) making and breaking of relay contacts. Generally caused by armature hesitation.

armature-impact contact chatter Undesired (usually rapid, repetitive) making and breaking of relay contacts, caused by *contact bounce* when the armature strikes the relay core (closure) or backstop (opening).

armature relay A relay that uses an electromagnet to pull a lever toward or away from a set of fixed contacts.

armature travel The distance traveled by an armature during relay operation.

armor A protective metal cable covering.

Armstrong FM system (Edwin H. Armstrong, 1890–1954). A phase-shift method of frequency modulation. See PHASE MODULATION.

armature voltage control A means of controlling motor speed by changing the applied armature winding voltage.

armchair copy An amateur radio term for reception of exceptionally clear signals.

arming the oscilloscope sweep Enabling an oscilloscope to trigger on the next pulse by closing a switch.

Armstrong oscillator (Edwin H. Armstrong, 1890–1954). An oscillator circuit that uses inductive feedback between the output and input. Either the output coil or the input coil can be tuned to set the oscillator frequency. The amount of positive feedback is controlled by varying the coupling between the coils.

Armstrong superheterodyne circuit See SUPERHETERODYNE CIRCUIT.

Armstrong superregenerative circuit See SUPERREGENERATIVE CIRCUIT.

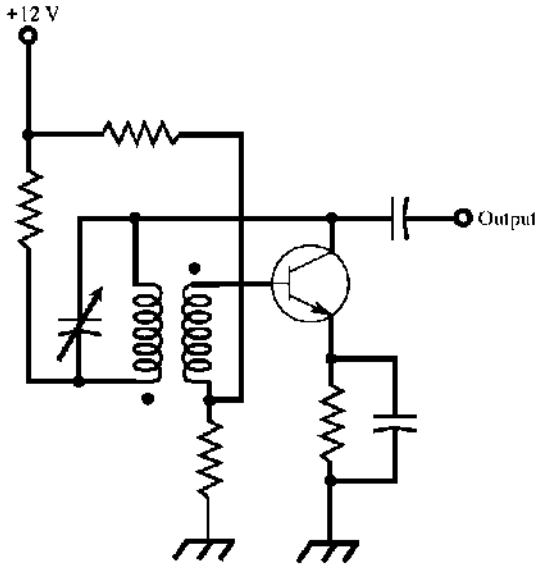

Armstrong oscillator

ARPA Acronym for *Advanced Research Projects Agency,* a subsidiary of the U.S. Department of Defense.

array **1.** A directive antenna that consists of an assembly of properly dimensioned and spaced elements, such as radiators, directors, and reflectors. **2.** A coordinated group or matrix of components, such as diodes, resistors, memory cells, etc., often enclosed in one capsule. **3.** Subscripted variables representing data arranged so that a program can examine the array and extract data relevant to a particular subscript.

array device A group of similar or identical components that are connected together in a certain fashion, to perform a specific task.

arrester **1.** A device used to protect an installation from lightning. It consists of a varistor or an air gap connected between an antenna or power line and an earth ground. The device passes little or no current under ordinary conditions, but passes heavy current to ground during a lightning stroke. Also called LIGHTNING ARRESTER. **2.** A self-restoring protective device used to reduce voltage surges on power lines.

ARRL Abbreviation for *American Radio Relay League.*

arrowhead A wideband, log-periodic antenna with linear polarization.

ARS Abbreviation of *Amateur Radio Service.*

arsenic Symbol, As. A metalloidal element. Atomic number, 33. Atomic weight, 74.91. Arsenic is familiar as an n-type dopant in semiconductor processing.

5059F-pA_1-55 4/9/01 4:41 PM Page 41

ARSR Abbreviation of *air route surveillance radar.*

articulation A measure of the effectiveness of voice communications, expressed as the percentage of speech units understood by the listener when the effect of context is negligible.

artificial antenna See DUMMY ANTENNA.

artificial ear A microphone-type sensor, equivalent to the human ear, used to measure sound pressures.

artificial echo **1.** In radar practice, the reflections of a transmitted pulse returned by an artificial target. **2.** A signal from a pulsed radio-frequency (RF) generator, delayed to simulate an echo.

artificial ground The effective ground provided by the radials or disk of a ground-plane antenna, as opposed to actual ground (the earth itself). Compare TRUE GROUND.

artificial horizon In aircraft instrumentation, a device that displays lines showing the position of the aircraft in flight, with reference to the horizon.

artificial intelligence Abbreviation, AI. **1.** A specialized field of computer science overlapping with electronics, biology, physiology, and other sciences, concerning attempts to develop advanced computer systems that can emulate the processes of the human mind. **2.** The ability of a computer to learn from its mistakes, refine its own processes, and perhaps ultimately reason in a humanlike manner.

artificial ionization An artificial reflecting layer that is created in the atmosphere to provide a skip condition.

artificial language A language that is not commonly used, but has been devised for efficiency in a particular situation—especially in a computer system.

artificial life **1.** The ultimate endpoint of ARTIFICIAL INTELLIGENCE, wherein machines acquire qualities, such as wisdom and the capability to feel emotions. The state of the art is currently nowhere near this point. **2.** A hypothetical machine or set of machines with lifelike qualities, including human-level intelligence, wisdom, and emotion.

artificial stimulus An electronic method of robot guidance and navigation using radar, sonar, vision systems, edge detection, and/or beacons.

artificial transmission line A network of capacitors and inductors with characteristics similar to those of the more bulky transmission line it replaces in tests and measurements. It also serves as a time-delay or phase-shift device and as a pulse-forming network.

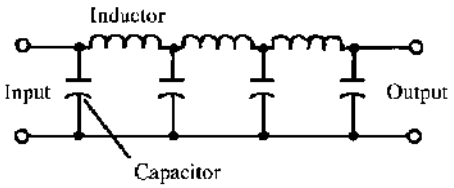

artificial transmission line

artificial voice A device used to test and calibrate noise-canceling microphones, consisting essentially of a small loudspeaker that has a baffle whose acoustical properties simulate those of the human head.

artos stripper A machine that cuts and strips wire for the fabrication of multiconductor cables.

artwork **1.** In the manufacture of printed circuits, the scaled drawings from which the mask or etch pattern is obtained photographically. **2.** Collectively, the illustrations depicting an electronic circuit, device, or system.

As Symbol for ARSENIC.

ASA Abbreviation of AMERICAN STANDARDS ASSOCIATION.

asbestos A nonflammable fibrous material consisting of calcium and magnesium silicates that is used for high-temperature insulation.

A-scan A radar-screen presentation in which the horizontal time axis displays distance or range, and the vertical axis displays the amplitude of signal pulse and echo pulses.

ascending node For a satellite orbiting the earth or another planet, any point at which the groundtrack crosses the equator as it moves from the southern hemisphere into the northern hemisphere. This node generally changes for each succeeding orbit, because the earth or planet rotates underneath the orbit of the satellite. Compare DESCENDING NODE.

ascending pass For a specific point on the earth's surface, the time during which an artificial communications satellite is accessible when its latitude is moving northward. The duration of accessibility depends on the altitude of the satellite, and on how close its groundtrack comes to the earth-based point. Compare DESCENDING PASS.

ASCII Acronym (pronounced "*ask*-ee") for *American Standard Code for Information Interchange.*

ASI Abbreviation for *American Standards Institute.*

A-scope A radar system that displays an A-SCAN.

Askarel A synthetic, nonflammable liquid dielectric.

aspect ratio The width-to-height ratio of a video image, generally three units high by four units wide.

asperities On the surface of an electrode, tiny points at which the electric field is intensified and from which discharge is highly probable.

ASR **1.** Abbreviation of AIRBORNE (or AIRPORT) surveillance radar. **2.** Abbreviation of AUTOMATIC SEND/ RECEIVE.

ASRA Acronym for *automatic stereophonic recording amplifier.*

assemble **1.** To gather subprograms into a complete digital computer program. **2.** To translate a

5059F-pA_1-55 4/9/01 4:41 PM Page 42

Symbols for ASCII teleprinter code

First four signals	*Last three signals*							
	000	*001*	*010*	*011*	*100*	*101*	*110*	*111*
0000	NUL	DLE	SPC	0		P	/	p
0001	SOH	DC1	!	1	A	Q	a	q
0010	STX	DC2	"	2	B	R	b	r
0011	ETX	DC3	#	3	C	S	c	s
0100	EOT	DC4	$	4	D	T	d	t
0101	ENQ	NAK	%	5	E	U	e	u
0110	ACK	SYN	&	6	F	V	f	v
0111	BEL	ETB	'	7	G	W	g	w
1000	BS	CAN	(	8	H	X	h	x
1001	HT	EM	)	9	I	Y	i	y
1010	LF	SUB	*	:	J	Z	j	z
1011	VT	ESC	+	;	K	[	k	{
1100	FF	FS	,	<	L	/	l	/
1101	CR	GS	–	=	M	]	m	}
1110	SO	RS	.	>	N		n	~
1111	SI	US	|	?	O	-	o	DEL

ACK: acknowledge
BEL: bell
BS: back space
CAN: cancel
CR: carriage return
DC1: device control no. 1
DC2: device control no. 2
DC3: device control no. 3
DC4: device control no. 4
DEL: delete
DLE: data link escape
ENQ: enquiry
EM: end of medium
EOT: end of transmission
ESC: escape
ETB: end of transmission block
ETX: end of text
FF: form feed
FS: file separator
GS: group separator
HT: horizontal tab
LF: line feed
NAK: do not acknowledge
NUL: null
RS: record separator
SI: shift in
SO: shift out
SOH: start of heading
SPC: space
STX: start of text
SUB: substitute
SYN: synchronous idle
US: unit separator
VT: vertical tab

symbolic program language into a machine (binary) language program by substituting operation codes and addresses.

assembly **1.** A finished unit that can be either a practical working model or a dummy, a prototype, or a final model; an integrated aggregation of subunits. **2.** A low-level computer source-code language that uses crude mnemonics that are easier to remember than the *machine-language* equivalents.

assembly language A source code that uses mnemonic instructions. (See ASSEMBLY, **2.**)

assembly program The program that operates on a symbolic-language program to produce a machine language program in the process of assembly. Also called *assembler.*

assembly robot A form of *industrial robot* that puts hardware together. Such a robot is generally a component of an *automated integrated manufacturing system (AIMS).* The robot can do repetitive work at high speed and precision for long periods of time.

assign To reserve part of a computing system for a specific purpose, normally for the duration of a program run.

assigned frequency The radio carrier frequency or band of frequencies designated for a transmitting station by a licensing authority. Also see RADIO SPECTRUM.

associative memory Computer memory in which locations are identified by content, rather than by specific address.

assumed decimal point A decimal point that does not occupy an actual computer storage space, but is used by the computer to align values for calculation; the decimal point is assumed to be at the right unless otherwise specified.

astable Having two temporary states; BISTABLE.

astable circuit A circuit that has two unstable states, and whose operation is characterized by alternation between those states at a frequency determined by the circuit constants.

astable multivibrator A free-running multivibrator. The common circuit uses two bipolar or field-effect transistors, their inputs and outputs being cross coupled. Conduction switches alternately between the two.

astatic **1.** Without fixed position or direction. **2.** In a state of neutral equilibrium.

astatic galvanometer A galvanometer with a movable element consisting of two identical magnetized needles mounted nonparallel on the same suspension. Each needle is surrounded by a coil. The coils are wound in opposite directions, and are connected in series to the current source. A large permanent magnet provides the field against which the needle assembly rotates. The instrument functions independently of the geomagnetic field.

astatine Symbol, At. A radioactive elemental halogen produced from radioactive decay. Atomic number, 85. Atomic weight, 210. Formerly called *alabamine.*

A station One of the two stations in the transmitting system of LORAN (long-range navigation).

astigmatism A focusing fault in a cathode-ray tube (CRT), in which electrons in different axial planes focus at different points.

ASTM Abbreviation for *American Society for Testing and Materials.*

astrionics The design, production, and application of electronic devices and systems for use in space vehicles and space navigation.

5059F-pA_1-55 4/9/01 4:41 PM Page 43

astronomical unit Abbreviation, AU. A unit of distance equal to 1.496×10^8 kilometers (9.296×10^7 miles). Approximately equal to the mean distance between the earth and the sun.

A supply See A POWER SUPPLY.

asymmetrical cell A photocell exhibiting ASYMMETRICAL CONDUCTIVITY.

asymmetrical communications **1.** Two-way communications in which the volume of transmitted data is much greater in one direction than in the other. **2.** Two-way communications in which the speed of transmitted data is much greater in one direction than in the other. Compare SYMMETRICAL COMMUNICATIONS.

asymmetrical conductivity A condition in which a device conducts well in one direction, but poorly in the other direction. A rectifier diode is a common example of a component that exhibits this effect.

asymmetrical distortion In a binary system, lengthening or shortening of one of the states, by comparison to the theoretical or ideal duration.

asymmetrical FET A FIELD-EFFECT TRANSISTOR in which the source and drain cannot be interchanged without degrading performance.

asymmetrical multivibrator An unbalanced multivibrator (i.e., one in which the circuit halves are not identical). If the time constants of the halves are different, the output pulses will be short and widely separated.

asymmetrical sideband See VESTIGIAL SIDEBAND.

asymmetrical sideband transmission See VESTIGIAL SIDEBAND TRANSMISSION.

asymmetrical wave A wave whose upper (positive half-cycle) and lower (negative half-cycle) portions have different amplitudes or shapes. Also called *asymmetric wave.*

asymmetry control An adjustment in a device intended for measuring the pH (acidity/alkalinity). This corrects the inaccuracies that results from the differences between the electrodes.

asymptote In analytical geometry, a fixed straight line or ray *L* with a special relationship to a curve or part of a curve *K* that recedes to infinity. As the distance from the origin (0,0) increases without limit, the separation between *K* and *L* approaches zero, but *K* and *L* never actually meet.

asymptotic breakdown voltage A voltage that will cause *dielectric breakdown* if applied continuously for a sufficiently long time.

asymptotic expression An expression having a very small error in terms of percentage.

asynchronous **1.** Not synchronous, i.e., nonrecurrent (as in out-of-phase waves). **2.** A mode of computer operation in which the completion of one operation starts another.

asynchronous device A device not regulated by the system in which it is used, as far as its operating frequency or rate is concerned.

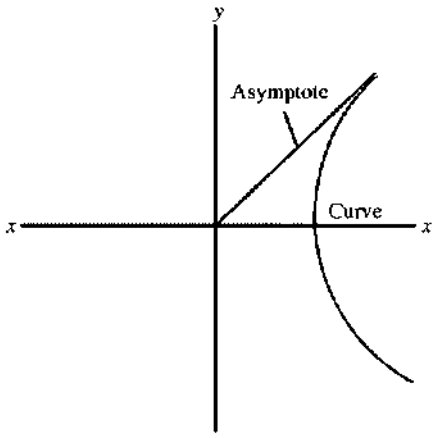

asymptote

asynchronous input In digital circuitry, any flip-flop input at which a pulse can affect the output independently of the clock.

asychronous motor An ac motor whose speed is not proportional to the supply frequency.

asynchronous transmission Data transmission in which each character or symbol begins with a start signal and ends with a stop signal. This eliminates the need for the data to be sent at a uniform speed.

asynchronous vibrator In a vibrator-type portable power supply, a vibrator that only makes and breaks the primary circuit of the step-up transformer. This is in contrast to the synchronous vibrator, which also makes and breaks the secondary circuit in synchronism with the primary. Also called NONSYNCHRONOUS VIBRATOR.

AT A quartz crystal cut wherein the angle between the x-axis and the crystal face is 35 degrees.

At Symbol for astatine.

AT-cut crystal A piezoelectric crystal cut at a 35-degree angle, with respect to the optical axis of the quartz. The frequency of such a crystal does not appreciably change with variations in temperature.

atmosphere **1.** The gas surrounding a planet, particularly the air sheathing the earth. **2.** Abbreviation, atm. A unit of pressure equal to 1.013×10^6 dynes per square centimeter (about 14.7 pounds per square inch).

atmospheric absorption **1.** The conversion of electromagnetic energy into heat, with resulting loss, as the energy passes through the earth's atmosphere. The extent of this effect depends on the wavelength. **2.** See ABSORPTION LOSS, **2.**

atmospheric absorption noise Noise, principally above 1 GHz, resulting from atmospheric absorption (see ABSORPTION LOSS, **2**).

5059F-pA_1-55 4/9/01 4:41 PM Page 44

atmospheric bending The refraction or reflection of electromagnetic waves by the troposphere or ionosphere. See ATMOSPHERIC REFLECTION.

atmospheric duct A tropospheric stratum, often associated with temperature inversions, lake effects, or weather fronts, through which electromagnetic energy at ultra-high and microwave frequencies is efficiently propagated for long distances.

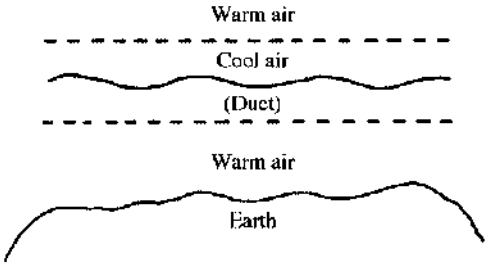

atmospheric duct

atmospheric electricity Static electricity present in the atmosphere, which evidences itself in disturbance of radio communications and in displays of lightning.

atmospheric noise Receiver noise resulting from ATMOSPHERIC ELECTRICITY. Also called *sferics* or *static*.

atmospheric pressure Abbreviation, atm press. **1.** The pressure exerted by the earth's atmosphere, as indicated by a barometer at sea level; normally between 29 and 31 inches of mercury. **2.** A pressure of 1.013×10^6 dynes per square centimeter. See ATMOSPHERE, **2.**

atmospheric radio wave See SKYWAVE.

atmospheric radio window The band of frequencies (approximately 10 MHz to 10 GHz), including radio waves that can penetrate the earth's troposphere and ionosphere.

atmospheric reflection The return of a radio wave to earth, resulting from reflection by an ionized portion of the atmosphere.

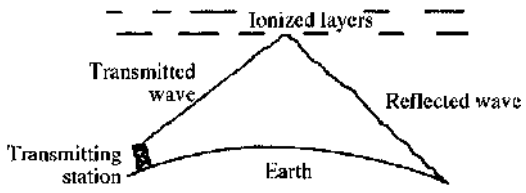

atmospheric reflection

atmospheric refraction **1.** Downward bending of radio waves as a result of variations in the dielectric constant of the troposphere. **2.** Downward bending of radio waves in the ionosphere, resulting in long-range propagation at high frequencies.

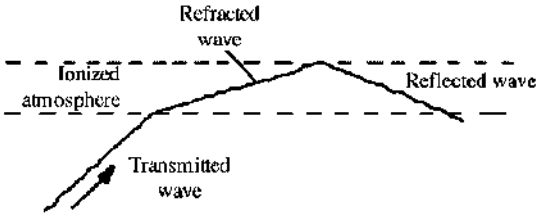

atmospheric refraction

atmospheric scatter **1.** The scattering of very-high frequency (VHF) and ultra-high frequency (UHF) radio waves by the lower atmosphere. **2.** Communication via scattering of VHF and UHF radio waves in the lower atmosphere.

atmospherics See ATMOSPHERIC NOISE.

atom **1.** The smallest material particle that displays the unique characteristics and properties of an element. Atoms consist of a dense, positively charged central nucleus, around which less-massive, negatively charged electrons "swarm" at definite levels called *shells*. Also see BOHR ATOM and RUTHERFORD ATOM. **2.** In a computer-compiling operation, an operator or operand.

atomechanics The physics of electron movement.

atomic battery A battery in which atomic energy is converted into electrical energy.

atomic charge The electrification (i.e., the electron charge) exhibited by an ion.

atomic clock Also called *atomic time standard*. A highly accurate electronic clock, driven by the characteristic oscillations of certain atoms.

atomic energy Energy released by the FUSION or FISSION of atomic nuclei. Also see ATOMIC POWER.

atomic fission See FISSION.

atomic frequency The natural vibration frequency of an atom.

atomic fusion See FUSION.

atomic pile See REACTOR, **2.**

atomic mass unit Abbreviated amu. A unit that expresses the relative mass of an elemental *isotope*. One amu is equal to 1/12 of the atomic mass of carbon 12 (C12). A neutron has a mass of roughly one amu.

atomic migration The transfer or "wandering" of a valence electron between or among atoms in a single molecule.

atomic number The number of protons in the nucleus of an atom. Also, the number of electrons if the atom is electrically neutral. For example, the atomic number for copper is 29, indicating 29 protons in the nucleus. An electrically neutral atom of copper has 29 electrons. The atomic number uniquely identifies an element.

atomic radiation The emission of radiant energy by radioactive substances.

5059F-pA_1-55 4/9/01 4:41 PM Page 45

atomic reactor See REACTOR, **2.**

atomic theory The scientific theory that all matter is composed ultimately of *atoms*, which are the smallest particles retaining the identity of an element. Atoms combine to form *molecules*, the smallest particles that retain the identity of a compound. Atoms themselves contain minute *subatomic particles*, some of which carry electric charges. See BOHR ATOM and RUTHERFORD ATOM.

atomic time **1.** A means of time determination that makes use of the resonant vibrations of certain substances, such as cesium. **2.** Synchronized astronomical time, as determined by an ATOMIC CLOCK.

atomic unit of energy In a hydrogen atom, the potential energy of the electron in the lowest-energy shell, as averaged over a certain length of time. The shell represents the mean energy of the electron.

atomic weight **1.** The mass of a particular atom in ATOMIC MASS UNITS (amu). **2.** A number characterizing the average mass of individual atoms for a specific isotope of an element. Thus, carbon 12 (C12) has an atomic weight of 12, oxygen 16 (O16) has an atomic weight of approximately 16, and uranium 238 (U238) has an atomic weight of about 238.

atomistics The science of the atom and atomic energy. Also called *atomics.*

attack **1.** The rise of a pulse from zero to maximum amplitude. **2.** The time required for a pulse to rise from zero to maximum amplitude. **3.** The initialization of a circuit voltage or current for a certain purpose, such as an automatic gain control. **4.** The rise of a musical note from zero to full volume.

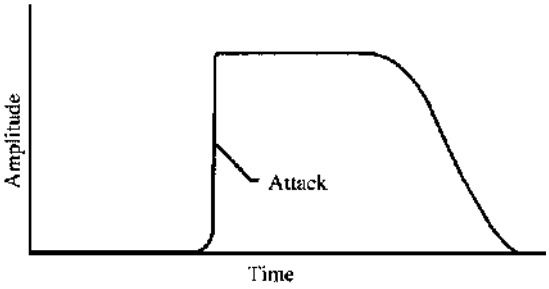

attack

attack time The time required for an applied signal that suddenly increases in amplitude to reach 63.2 percent of its final, stable value.

attemperator An automatic temperature-controlling device; a *thermostat.*

attention display A computer-generated chart or graph, displayed as an alert signal concerning a particular situation.

attenuate To reduce in amplitude.

attenuation A reduction of signal amplitude.

attenuation characteristic Also called *attenuation constant.* **1.** In an amplifier, network, or component, the decrease in signal amplitude as a function of frequency, usually expressed in decibels per octave. **2.** In a transmission line, the decrease in signal amplitude per unit length. Usually expressed in decibels per 100 feet, decibels per mile, or decibels per kilometer.

attenuation constant See ATTENUATION CHARACTERISTIC.

attenuation distortion A type of distortion characterized by variation of attenuation with frequency within a given frequency range.

attenuation equalizer An equalizer that stabilizes the transfer impedance between two ports at all frequencies within a specified frequency band.

attenuation-frequency distortion Distortion characterized by the attenuation of the frequency components in a complex waveform. Frequency-sensitive RC networks (such as a Wien bridge) exhibit this type of distortion when they attenuate a fundamental and each harmonic unequally.

attenuation network A combination of components (R, C, or L singly or in any necessary combination) that provide constant signal attenuation with negligible phase shift throughout a frequency band.

attenuation ratio The ratio indicating a relative current, voltage, power or energy decrease. For example, for voltage, $E_{input}/E_{output} = 6/2 = 3{:}1 = 3$.

attenuator A device for reducing signal amplitude in precise, predetermined steps, or smoothly over a continuous range. A network of resistors, capacitors, or both. The simplest attenuator consists of one or more noninductive resistors.

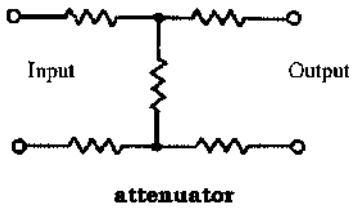

attenuator

attitude The position of an aircraft or space vehicle relative to a (usually terrestrial) reference point, often determined with electronic instruments.

atto- Abbreviated, a. A prefix meaning 10^{-18} or multiplication by 10^{-18}.

attofarad Abbreviation, aF. An extremely small unit of low capacitance; 1 aF equals 10^{-18} F.

attracted-disk electrometer A device to measure potential difference consisting of two parallel metal disks—one of which is connected to a tension spring. The force between the disks indicates the magnitude of the electric field.

5059F-pA_1-55 4/9/01 4:41 PM Page 46

attraction The drawing together or pulling toward, as in the attraction between electric charges or magnetic poles. Dissimilar charges and poles attract each other (electric plus to minus, magnetic north to south). Compare REPULSION.

ATV Abbreviation of *amateur television*, used in the Amateur Radio Service.

AU Abbreviation of ASTRONOMICAL UNIT.

Au Symbol for GOLD.

audibility The quality of being detectable by the human ear. In a healthy listener, the *threshold of audibility* is extremely low; at the threshold, the pressure of a sound wave varies from normal by approximately 10^{-4} pascal. The frequency range of human audibility extends roughly from 20 Hz to 20 kHz.

Sound	*Audibility (dB)*
Threshold of hearing	0
Whisper	10–20
Electric fan at 10 feet	30–40
Running water at 10 feet	40–60
Speech at 5 feet	60–70
Vacuum cleaner at 10 feet	70–80
Passing train at 50 feet	80–90
Jet at 1000 feet altitude	90–100
Rock band on stage	110–120
Air hammer at 5 feet	130–140

audibility table

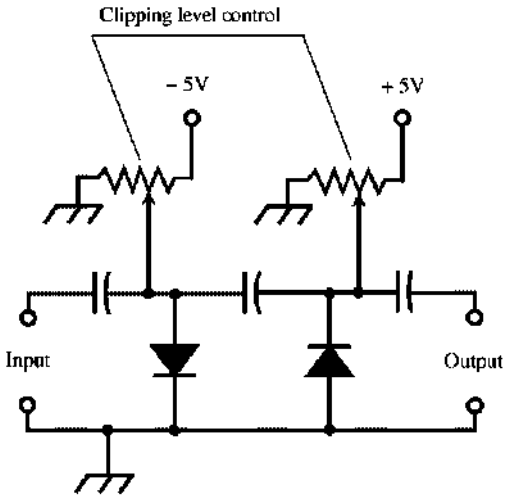

audio clipping

audibility curve A graph (such as the *Fletcher-Munson curve*) that depicts the range of human hearing in terms of frequency versus the sound pressure at the threshold of AUDIBILITY.

audible Detectable by the human ear.

audible alarm device An ANNUNCIATOR that produces an easily identifiable sound in response to an ALARM CONDITION in a security system.

audible frequency See AUDIO FREQUENCY.

audible tone A vibration of air molecules that can be detected by the human ear, and with periodic properties, such as a sine-wave vibration.

audio **1.** Pertaining to the spectrum of frequencies corresponding to the human hearing range (about 20 Hz to 20 kHz), or to equipment or performance associated with that spectrum. **2.** Any disturbance, such as a current or compression wave, falling within the range of about 20 Hz to 20 kHz. **3.** AUDIO FREQUENCY.

audio amplifier See AUDIO-FREQUENCY AMPLIFIER.

audio band The range (band) of audio frequencies.

audio channel **1.** The portion of a complex signal or waveform used to convey audio information exclusively. **2.** The audio-frequency section of a transmitter or receiver (as opposed to the radio-frequency section). **3.** A radio channel of fixed frequency that is reserved for voice communications.

audio clipping Brute-force limiting of the amplitude of an audio signal, usually accomplished using semiconductor diodes to prevent the positive and negative peak amplitudes from exceeding a certain level.

audio component The audio-frequency portion of any wave or signal.

audio converter A circuit in which a received radio-frequency (RF) signal is heterodyned with a local RF oscillator signal to produce an audio-frequency (AF) beat-note output. The beat note is then amplified by an AF amplifier. It is used especially by amateur radio operators in the reception of continuous-wave (CW) radiotelegraphy, radioteletype, and packet radio at high frequencies.

audio frequency A frequency lying within the audible spectrum. Abbreviated AF. See AUDIO-FREQUENCY SPECTRUM.

audio-frequency amplifier An amplifier that operates in part or all of the frequency range 20 Hz to 20 kHz. High-fidelity amplifiers function over a somewhat wider range (e.g., 10 Hz to 50 kHz).

audio-frequency choke An inductor (usually having a ferromagnetic core) that blocks audio-frequency current, but passes direct current.

audio-frequency feedback **1.** Electrical FEEDBACK (positive and/or negative) that affects audio-frequency circuits. **2.** ACOUSTIC FEEDBACK.

audio-frequency filter A filter of any type that operates on any part of the frequency range 20 Hz to 20 kHz.

5059F-pA_1-55 4/9/01 4:41 PM Page 47

audio-frequency meter An instrument to measure frequencies in the audio-frequency spectrum (approximately 20 Hz to 20 kHz). Three types are commonly used:

- ***Analog*** Gives direct indications of frequency on the scale of a D'Arsonval meter; the usual range is 20 Hz to 100 kHz.
- ***Digital*** Gives direct indications of frequency by means of readout lamps; the usual range is 1 Hz to 15 MHz. This instrument is useful also as a radio-frequency meter.
- ***Bridge*** Consists of a frequency-sensitive bridge, such as a Wien bridge, with a null-indicating meter. The operator balances the bridge and reads the unknown frequency from the dial of the balance control.

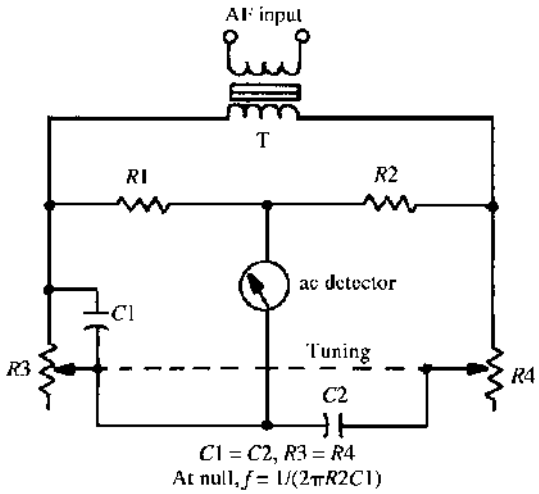

audio-frequency meter

audio-frequency noise Any electrical noise signal causing interference within the audio-frequency spectrum.

audio-frequency oscillator See AUDIO OSCILLATOR.

audio-frequency peak limiter Any circuit or device, such as a biased diode, that performs the function of audio limiting.

audio-frequency-shift keying Abbreviation, AFSK. Frequency-shift keying that is done at audio frequencies (below approximately 20 kHz) rather than at radio frequencies. There are two audio sine-wave signals, one for logic 1 (*high* or *mark*) pulses and the other for the logic 0 (*low* or *space*) pulses. This scheme is commonly used with telephone modems where the signal bandwidth is severely limited by circuit characteristics. At typical data speeds in twisted-pair telephone lines (usually 28.8 or 57.6 kbps), signals of this type sound like a hiss or roar. Compare FREQUENCY-SHIFT KEYING.

audio-frequency-shift modulator A modulator for audio-frequency-shift keying of a signal.

audio-frequency spectrum The band of frequencies extending from roughly 20 Hz to 20 kHz. High-fidelity component specifications extend this range somewhat in both directions (e.g., from 10 Hz to 50 kHz).

audio-frequency transformer Abbreviation, AF transformer. A device used for the purpose of matching impedances at frequencies within the range of human hearing (up to approximately 20 kHz). This ensures the most efficient possible transfer of power between stages of audio amplification, between an amplifier and a speaker or headset, or between a microphone and an audio preamplifier. These transformers are available with various power ratings and impedance-matching ratios. Some devices are tailored to have a certain attenuation-versus-frequency response. At audio frequencies, transformers are physically similar to the alternating-current transformers used in power supplies. They are wound on laminated or powdered-iron cores. Compare RADIO-FREQUENCY TRANSFORMER.

audio-frequency transistor A transistor that is usually used only at audio frequencies.

audiogram A graph used to rate hearing, used by audiologists and audiometrists.

audio image In a direct-conversion receiver, a response to a signal on one side of (above or below) the local-oscillator (LO) frequency, when the operator is listening to a signal on the other side of the LO frequency. These responses are reduced or eliminated in single-signal receivers.

audio-level meter An ac meter for monitoring signal amplitude in an audio-frequency system. It can indicate in volts, decibels, volume units (VU), or arbitrary units, and is often permanently connected in the circuit.

audio limiter A limiter or clipper operated in the audio-frequency (AF) channel of a receiver or transmitter to hold the output-signal amplitude constant, or to minimize the effect of noise peaks.

audiologist A person skilled in testing hearing (i.e., in using audiometers and other electronic instruments) and evaluating their indications for the fitting of hearing aids.

audiometer An instrument used for hearing tests, which consists of a specialized audio-frequency (AF) amplifier with calibrated attenuators, output meter, and signal source.

audiometrist A person skilled in the use of audiometers and other electronic instruments that measure sound and human hearing, and who deals with attendant health and behavior problems. Compare ACOUSTICIAN and AUDIOLOGIST.

audio mixer An amplifier circuit for blending two or more audio-frequency (AF) signals, such as those delivered by microphones or receivers.

5059F-pA_1-55 4/9/01 4:41 PM Page 48

audio oscillator **1.** An oscillator that delivers an output signal in the frequency range 20 Hz to 20 kHz. **2.** An audio-frequency (AF) signal generator. Some instruments of this type operate above and below the limits of the common audio-frequency spectrum (e.g., 1 Hz to 1 MHz).

audio output The output of an audio-frequency oscillator or amplifier. It can be measured in terms of peak or rms volts, amperes, or watts.

audiophile A sound-reproduction hobbyist.

audio power Alternating-current power at frequencies roughly between 20 Hz and 20 kHz. When used in connection with transmitters and other modulated radio-frequency (RF) equipment, the term refers to modulator power output.

audio response unit A device that links digitized responses, held in computer storage, to a telephone set or line to answer incoming calls and inquiries.

audio signal generator See AUDIO OSCILLATOR, **2.**

audio spectrum The range of sine-wave frequencies detectable by the human ear when they occur as acoustic vibrations. This range is about 20 Hz to 20 kHz.

audio squelch A squelch circuit that operates only on the audio channel of a receiver.

audio system **1.** The portion of any electronic assembly that is used to process sound. **2.** Special computer equipment capable of storing and processing digitized audio-frequency (AF) data.

audiotape Magnetic tape for the recording and reproduction of data in the audio-frequency (AF) range.

audio taper In potentiometers, a semilogarithmic variation of resistance versus rotation. Used in volume and tone controls for audio circuits. At midposition (the halfway point), the counterclockwise portion of the device has about 1/10 the resistance of the clockwise portion. A listener will hear sound at half-volume because of the logarithmic nature of the human audibility curve.

audio-visual Pertaining to a combination of sound and sight (e.g., television and sound motion pictures).

auditory backward inhibition A subjective phenomenon, in which a sound is erased from the memory of a listener by a second sound arriving about 60 milliseconds later.

auditory inhibition The tendency of sound waves to be partially or totally canceled by the ears/mind of a listener, depending on the waves' intensity, relative phase, and/or direction of impact.

auditory mirage See ACOUSTIC MIRAGE.

audit trail A history of the processes relating to a record, transaction, or file in a computer system. Created during the routine processing of data, the trail is stored as a file. The audit trail allows auditing of the system or the subsequent recreation of files.

augend In a calculation, the number to which another is to be added. Compare ADDEND.

augend register In a digital computer, the register that stores the augend. Compare ADDEND REGISTER.

aural Pertaining to sound actually heard, as opposed to sound that exists only as audio-frequency currents or waves.

aurora A phenomenon sometimes called the *northern lights* or *southern lights*, as seen in the night sky. In the Northern Hemisphere, it is known as *Aurora Borealis*; in the Southern Hemisphere, it is called *Aurora Australis.* It generally occurs a few hours after a solar flare, when charged particles, emitted from the sun, arrive at the earth, and are accelerated in the vicinity of the the geomagnetic poles.

auroral absorption Radio wave absorption by an aurora.

auroral flutter Rapid fading of a signal at high or very high frequencies, so-called because it often imparts a fluttering quality to the signal that is caused by phase distortion and Doppler shift when the waves are reflected from the aurora.

auroral interference **1.** Interference to high-frequency radio propagation and also occasionally to medium-frequency and low-frequency propagation, caused by the activity of the aurora. **2.** Auroral flutter on a signal.

auroral opening A condition in which radio communication becomes possible via AURORAL PROPAGATION. It can occur when communication between two points is normally impossible at a certain frequency. Auroral openings allow long-distance communication well into the very-high-frequency (VHF) spectrum.

auroral propagation Reflection of radio signals from aurora that occur during geomagnetic storms. Theoretically, auroral propagation is possible when the aurora are active, between any two points on the earth's surface from which the same part of the aurora lie on a line of sight. This type of propagation seldom occurs when one end of the

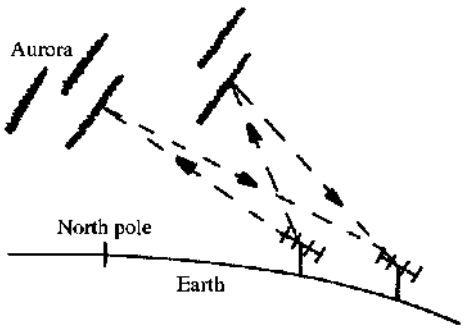

auroral propagation

5059F-pA_1-55 4/9/01 4:41 PM Page 49

circuit is at a latitude less than 35 degrees north or south of the equator. Auroral propagation can take place at frequencies well above 30 MHz. It is characterized by deep, rapid fading and random phase modulation of reflected signals.

auroral reflection The return of electromagnetic waves that have been beamed toward an aurora. Most often observed between 15 MHz and 150 MHz.

authorized access switch A device that disables a security system in a defined region or volume so that authorized personnel can enter without triggering an alarm condition.

authorized channel The carrier frequency or band assigned to a transmitting station by a licensing authority. Also see RADIO SPECTRUM.

autoalarm A device that is actuated from a received signal to alert a radio or computer network operator to the existence of a message.

autobaud **1.** In digital communications, a function that allows the equipment to adjust itself to the speed of the terminal. **2.** Any digital communications equipment capable of automatically adjusting to the speed of the terminal.

autocondensation The application of radio-frequency (RF) energy to the human body for medical purposes. The living organs serve as an impedance or load, across which the RF is applied.

autoconduction The application of radio-frequency (RF) currents into the body, by placing the living organ inside a coil and supplying the coil with RF. Used for medical purposes.

autocorrelation function A measure of the similarity between delayed and undelayed versions of a signal, expressed as a delay function.

autodyne reception Radio reception of cw signals by means of an oscillating detector. This is in contrast to heterodyne reception, in which a local oscillator (LO) generates an audio beat note with the cw signal in a separate detector.

autoionization A two-phase process of atomic ionization. The atom is excited beyond its ionization potential, and then it is allowed to deionize, causing the emission of an electron. The result is a positively charged atom (positive ion).

automated communications The transfer of data without the use of operating personnel; generally done with computers connected to communications equipment.

automated guided vehicle Abbreviation, AGV. A robot cart that runs without a driver. It uses an electric engine and is guided by the magnetic field produced by a current-carrying wire embedded in the floor or pavement. Alternatively, the robot can run on a track.

automated home A residence in which many, or most, of the routine chores are done by computers and/or robots. Examples of such tasks are dishwashing, doing the laundry, mowing the lawn, blowing snow, and vacuuming the floors.

automated integrated manufacturing system Acronym, AIMS. An assembly line or factory that uses robots, often controlled by one or more computers, to perform specific tasks that result in the production of various hardware items.

automatic Self-regulating, independent of human intervention. Some periodic adjustment might be needed.

automatic base bias A method of obtaining base bias in a bipolar transistor, where a resistor develops a voltage drop because of the current flowing through it. The resistor is usually placed in the emitter circuit, raising the emitter above ground potential.

automatic bass compensation Also called *bass boost.* In audio high-fidelity systems, a resistor-capacitor (RC) network that increases the relative amplitude of the bass at low volume levels. This compensates for the ear's inefficiency at low frequencies. The function can be automatically actuated by the setting of the volume control, or it can be switched manually on and off.

automatic bias In an amplifier, dc base/gate/grid bias obtained from the voltage drop produced by collector/drain/plate current flowing through a resistor common to the input and output. This resistor is usually shunted by a capacitor and placed in the emitter/source/cathode circuit.

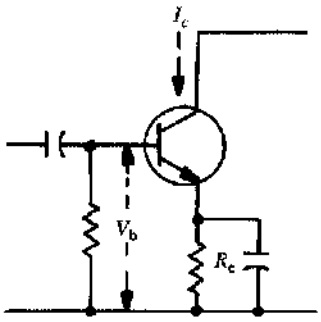

automatic bias

automatic brightness control A circuit that uses the same principles used in AUTOMATIC GAIN CONTROL (AGC) to hold steady the average brightness of a television (TV) picture.

automatic carriage Typewriters, automatic key punches, and other devices that can control automatically the spacing and feeding of paper, cards, and forms.

automatic check **1.** In a digital computer, the automatic inspection of operation and performance by a self-contained subsystem. **2.** The circuit or device for performing this inspection.

automatic chrominance control In a color television (TV) receiver, a subcircuit that controls the

5059F-pA_1-55 4/9/01 4:41 PM Page 50

gain of the chrominance bandpass amplifier by automatically adjusting its bias.

automatic circuit breaker Any device that opens a circuit automatically when the flow of current becomes excessive. The breaker generally resets automatically after a specified length of time, or after power has been temporarily removed from the circuit.

automatic coding The use of a computer to determine the steps for solving a problem, before the actual program for the problem is written. This can help software engineers develop long and/or complex computer programs.

automatic contrast control A circuit that automatically adjusts the gain of the video IF and RF stages of a television (TV) receiver to preserve good picture contrast.

automatic controller In servo systems, any of several circuits or devices that samples a variable signal, compares it with a standard (reference) signal, and delivers a control or correction signal to an actuator.

automatic crossover **1.** Current limiting in a power supply. **2.** A device that switches a circuit from one operating mode to another automatically when conditions change in a predetermined manner.

automatic current limiter A circuit or device for holding the output current of a power supply to a safe value during overload.

automatic current regulator A circuit or device that holds the output current of a generator or power supply to a predetermined value, in spite of wide variations in load resistance.

automatic cutout A device that shuts down a circuit or system when the safe limits of operation are exceeded. A circuit breaker is an example of such a device, as is a thermostat in a power amplifier.

automatic data processing Abbreviation, ADP. The use of computers and accessories for calculations and tabulations using data gathered automatically by the system.

automatic degausser A system for automatically demagnetizing the picture tube in a color television (TV) receiver.

automatic dialing unit Abbreviated, ADU. A device that automatically generates dialing digits. Many telephone sets have these devices, some of which can be programmed for several different telephone numbers, including country codes and area codes.

automatic dictionary A computer system component that substitutes codes for words and phrases in information retrieval systems. In language-translating systems, it provides word-for-word substitutions.

automatic direction finder Abbreviated ADF. A specialized receiver/antenna combination for automatically showing the direction from which a signal arrives.

automatic error correction A technique of correcting transmission errors using error-detecting and error-correcting codes and, usually, automatic retransmission.

automatic exchange A transmission exchange in which interterminal communications are accomplished without operators.

automatic focusing A method of focusing a picture tube automatically, in which a resistor connects the focusing anode to the cathode; thus, no external focusing voltage is necessary.

automatic frequency control Abbreviation, AFC. A system that keeps a circuit automatically tuned to a desired signal frequency. A detector (such as a discriminator) operated from the tuned circuit delivers a dc output voltage only when the circuit is operating above or below the signal frequency; otherwise, it has zero dc output. The dc output, when present, alters the capacitance of a varactor in the tuned circuit to retune the stage to the desired frequency.

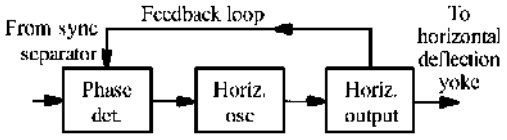

automatic frequency control (used in typical TV receiver)

automatic gain control Abbreviated AGC. A system that holds the output of a receiver or amplifier substantially constant despite input-signal amplitude fluctuations. A rectifier samples the ac signal output and delivers a dc signal proportional to that output. The dc signal is filtered, and the smoothed-out voltage is applied in correct polarity as bias to one or more preceding stages to reduce their gain. The stronger the signal entering the system, the greater the reduction in gain. As a result, weak signals are amplified much more than strong ones. Various forms of this scheme are used in many types of amplifiers and communications systems.

automatic gate bias A method of obtaining gate bias in a FET, where a resistor develops a voltage drop because of the current flowing through it. The resistor is usually placed in the source circuit, raising the source above ground potential.

automatic height control In a television (TV) receiver, a system that automatically maintains the height of the picture, despite signal-amplitude fluctuations, power-line voltage changes, and gain variations.

automatic intercept A telephone answering machine. It allows messages to be recorded when the subscriber is not able to answer the telephone.

5059F-pA_1-55 4/9/01 4:41 PM Page 51

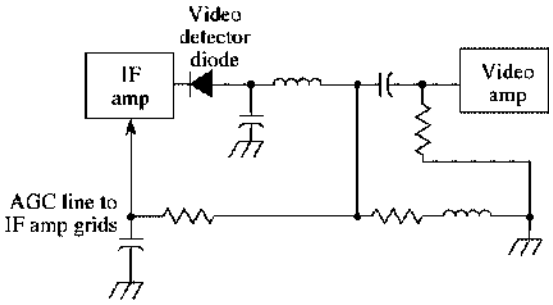

automatic gain control (used in typical TV receiver)

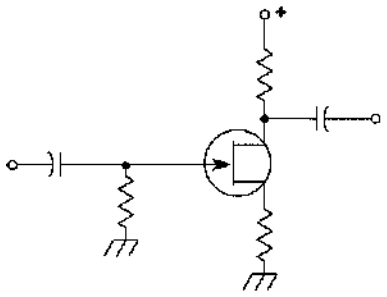

automatic gate bias

automatic interrupt A program interruption caused by hardware or software acting in response to some event independent of the program.

automatic level compensation See AUTOMATIC GAIN CONTROL.

automatic level control Abbreviation, ALC. **1.** A circuit that adjusts the input gain of a magnetic-tape recording device to compensate for changes in the loudness of the sound reaching the microphone. **2.** A form of AUTOMATIC GAIN CONTROL used in single-sideband (SSB) radio transmitters to maintain linearity while increasing the level of the average power relative to the peak power.

automatic line feed In the digital transmission of printed matter, the automatic insertion of a line feed (LF) character immediately following every carriage return (CR) character.

automatic modulation control Abbreviation, AMC. In a frequency-modulated (FM) radio transmitter, a form of AUTOMATIC GAIN CONTROL that regulates the gain of the audio amplifiers to compensate for fluctuating audio input amplitude. This prevents overdeviation while optimizing signal intelligibility.

automatic noise limiter Abbreviation, ANL. Any of several circuits for clipping noise peaks exceeding a predetermined maximum received-signal amplitude.

automatic phase control In a color television (TV) receiver, a circuit that synchronizes the burst signal with the 3.58-MHz color oscillator.

automatic pilot An electronic device, often computer-controlled, that automatically keeps a ship, airplane, or space vehicle on course.

automatic polarity In an electronic metering device, a means of automatically switching the input polarity of the instrument when the input signal polarity is shifted. Also called *bipolar operation.*

automatic programming See AUTOMATIC CODING.

automatic protective device A circuit or device (such as a fuse, circuit breaker, limiter, or regulator) that protects another circuit or device by automatically removing, reducing, or increasing the current or voltage during overload or underload.

automatic radio compass See AUTOMATIC DIRECTION FINDER.

automatic ranging In a metering device, the automatic adjustment or optimization of the full-scale range to compensate for large changes in the input parameter.

automatic regulation **1.** *Voltage regulation.* In a power supply, the automatic holding of the output voltage to a constant value, despite variations in the input voltage or load resistance. **2.** *Current regulation.* In a power supply, the automatic holding of the output current to a constant value, despite variations in the input voltage or load resistance.

automatic relay The relaying of messages automatically from one station to another via intermediate points, without the need for human operators.

automatic repeater station A station that receives signals and simultaneously retransmits them, usually on a different frequency.

automatic reset **1.** The self-actuated restoration of a circuit or device to a given state (e.g., the state of rest). **2.** A circuit or device that restores another circuit or device to a given state.

automatic scanning **1.** The automatic (usually repetitive) tuning or adjustment of a circuit or system throughout a given frequency range. In a radio receiver, the system can be programmed to pause or stop at occupied channels, passing over vacant ones; or it can be programmed to pause or stop at vacant channels, passing over occupied ones. **2.** The repetitive sweep of a cathode-ray-tube (CRT) electron beam.

automatic scanning receiver Also called PANORAMIC RECEIVER. A radio receiver that is automatically tuned (usually repetitively) over a frequency band. Such a receiver either homes in on a signal when one is found, or displays on a cathode-ray-tube (CRT) screen the distribution of signals in the band.

automatic secure voice communications A wideband and narrowband voice-digitizing application

5059F-pA_1-55 4/9/01 4:41 PM Page 52

to a security network that provides encoded voice communications.

automatic send/receive set A teletypewriter or terminal that is capable of receiving and transmitting.

automatic sensitivity control **1.** A self-actuating circuit using principles similar to those used in AUTOMATIC GAIN CONTROL. It varies the sensitivity of the radio-frequency (RF) and intermediate-frequency (IF) sections of a receiver in inverse proportion to the strength of a received signal. **2.** In a bridge null detector, a circuit similar to the one described in **1**, which operates ahead of the detector, varying the sensitivity of the latter automatically.

automatic sequencing The ability of a digital computer to perform successive operations without additional instructions from the operator.

automatic short-circuiter A device that automatically short-circuits the commutator bias in some single-phase commutator motors.

automatic short-circuit protection A circuit that allows the output of a power supply to be short-circuited without damage to the components in the supply. It usually consists of a current-limiting device.

automatic shutoff A switching arrangement that automatically shuts off a device or circuit under certain specified conditions.

automatic switch center A telephone-switching network that routes calls to their destinations without the need for a human operator.

automatic target control For a vidicon television camera tube, a circuit that automatically adjusts the target voltage in proportion to brightness of the scene.

automatic telegraph reception Telegraph reception providing a direct printout of the received information, without intervention by an operator.

automatic telegraph transmission Telegraph transmission originating from tapes, disks, or other records, rather than from a hand-operated key.

automatic telegraphy Communications that utilize automatic telegraph transmission and reception.

automatic time switch A time-dependent circuit or device that opens or closes another circuit at the end of a predetermined time interval.

automatic tracking A method of keeping a radar beam automatically fixed on a target.

automatic trip A circuit breaker that automatically opens a circuit.

automatic tuning A process whereby a circuit tunes itself to a predetermined frequency upon receiving a command signal.

automatic voltage regulator A circuit that keeps the output of a power supply constant, despite the load resistance or input voltage to the supply.

automatic volume control Abbreviated AVC. The use of AUTOMATIC GAIN CONTROL in an audio amplifier system.

automatic zero In an electronic meter, a means of automatically setting the indicator to zero in the absence of an input signal.

automation **1.** The control of machines or processes by self-correcting electronic systems. See ROBOT. **2.** The use of robots and/or computers, rather than human beings, to perform repetitive tasks. **3.** The use of robots and/or computers to assist human beings in industrial, office, governmental, and educational work.

automaton A simple robot that performs a task or set of tasks without artificial intelligence (AI). These machines have existed for decades. Compare ANDROID.

automonitor In digital computer operations, to require the machine to supply a record of its information-handling operations. Also, the program for such instructions.

automotive battery A set of four or eight rechargeable lead-acid cells connected in series and housed in a common enclosure. The electrolyte is a free-flowing liquid acid. Provides approximately 6 volts (four cells) or 12 volts (eight cells) under no-load conditions when fully charged. The high mass results in large energy-storage capacity. These batteries must be handled with care and always kept in an upright position to prevent spillage of the acid. See LEAD-ACID BATTERY, LEAD-ACID CELL.

autonomous robot A self-contained robot with an independent computerized control system. It moves under its own power, usually by rolling on wheels or a track drive. Compare INSECT ROBOT.

autopatch A remotely controllable device that interconnects a radio-communications system into a telephone network.

autopilot A self-correcting control and guidance device for the automatic management of an aircraft or missile.

autoranging See AUTOMATIC RANGING.

autosyn A device or system that operates on the principle of the synchronous ac motor, in which the position of the rotor in one motor (the transmitter) is assumed by the rotor in a distant motor (the receiver) to which the first is connected.

auto tracking A method of controlling the output voltages of many different power supplies simultaneously.

autotransducter A type of magnetic amplifier whose power windings serve also as control windings.

autotransformer A single-winding transformer in which the primary coil is a fraction of the entire winding for voltage step-up, or the secondary coil is a fraction of the entire winding for voltage step-down.

auxiliary circuit A circuit that is supplementary to the main system.

auxiliary contacts In switches and relays, contacts that are supplementary to the main contacts and are usually actuated with them.

5059F-pA_1-55 4/9/01 4:41 PM Page 53

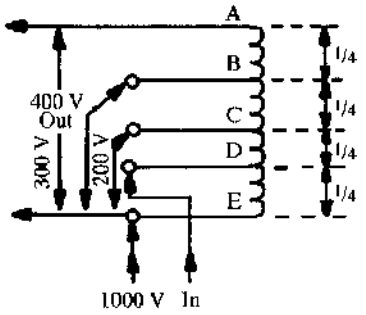

autotransformer

auxiliary equipment **1.** Also known as *peripherals.* An apparatus not directly governed by the central processing unit of a digital computer, such as a printer or personal robot. **2.** Peripheral equipment in any system. **3.** Backup equipment.

auxiliary memory In a digital computer, a unit that is supplementary to the main memory, which it augments.

auxiliary receiver Also called *standby receiver.* In a radio communications system, a receiver that is available for use if the main receiver fails.

auxiliary relay **1.** A standby relay. **2.** A relay whose operation supports that of another relay. **3.** A relay that is actuated by the operation of another relay.

auxiliary switch **1.** A standby switch. **2.** A switch wired in series or parallel with another switch. **3.** A switch that is operated by another switch.

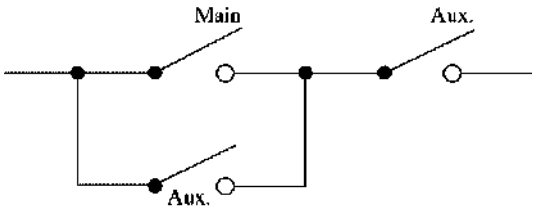

auxiliary switch, 2

auxiliary transmitter Also called *standby transmitter.* In a radio communications system, a transmitter that is available for use if the main transmitter fails.

a/v Abbreviation of AUDIO-VISUAL.

aV Abbreviation of *attovolt.*

availability The proportion of time during which an apparatus is operating correctly. It is usually given as a percentage.

available conversion gain The ratio of the input power to the output power of a transducer or converter. It is generally given in decibels.

available gain The ratio P_o/P_i, where P_i is the available power at the input of a circuit and P_o is the available power at the output.

available line The percentage of the length of a facsimile scanning line that is usable for picture signals.

available power The mean square of the open-circuit terminal voltage of a linear source divided by four, times the resistive component of the source impedance. The available power is the maximum power delivered to a load impedance, equal to the conjugate of the internal impedance of the power source.

available power gain In a power transistor, the ratio of available transistor output power to the power available from the generator. It depends on the generator resistance, but not on the transistor load resistance.

available signal-to-noise ratio The ratio P_s/P_n, where P_s is the available signal power at a given point in a system and P_n is the available random-noise power at that point.

available time **1.** The time during which a computer is available and ready for immediate use. **2.** The amount of time a computer is available to an individual.

avalanche The phenomenon in semiconductors operated at high reverse bias voltage, whereby carriers acquire sufficient energy to produce new electron-hole pairs as they collide with atoms. The action causes the reverse current to increase sharply.

avalanche breakdown In a semiconductor P-N junction, a condition that occurs when the reverse bias voltage exceeds a certain value. If the electric field in the vicinity of the junction becomes strong enough, charge carriers are dislodged from the atoms and the carriers (electrons and holes) flow freely across the P-N junction in the opposite direction from normal. The mini-

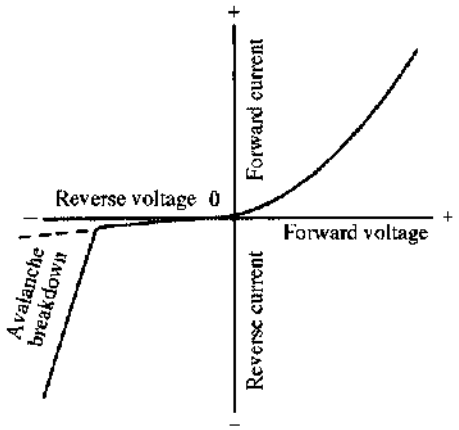

avalanche breakdown

5059F-pA_1-55 4/9/01 4:41 PM Page 54

mum reverse-bias voltage required to cause this phenomenon varies among different kinds of diodes. Some diodes are manufactured to have precise avalanche voltages. See ZENER DIODE.

avalanche conduction In a semiconductor junction, the enhanced reverse-bias conduction caused by a condition of AVALANCHE.

avalanche current The high current that flows through a semiconductor junction when AVALANCHE occurs.

avalanche diode See ZENER DIODE.

avalanche impedance The reduced impedance of a diode during avalanche.

avalanche noise Electrical noise generated in a junction diode operated at the point at which avalanche just begins.

avalanche transistor A transistor that operates at a high value of reverse-bias voltage, causing the pn junction between the emitter and base to conduct because of avalanche breakdown.

avalanche voltage In a semiconductor P-N junction, the minimum applied reverse-bias voltage that produces AVALANCHE BREAKDOWN.

AVC Abbreviation of *automatic volume control.*

avdp Abbreviation for *Avoirdupois*, a weight-measurement scheme that is used in English-speaking countries and is based on the pound.

average absolute pulse amplitude The average (disregarding algebraic sign) of the absolute amplitudes of a pulse, taken over the duration of the pulse.

average brightness The average brilliance of a television (TV) picture, cathode-ray-tube (CRT) computer display, or oscilloscope image.

average calculating operation The operating time considered typical for a computer calculation (i.e., one that is longer than an addition and shorter than a multiplication); it is frequently taken as the average of nine additions and one multiplication.

average current Abbreviation, I_{avg}. The average value of alternating current flowing in a circuit. Taking polarity into account, this value is zero for a pure sine wave. For other waveforms, it can vary. When polarity is not considered, the sine-wave value of I_{avg} is equal to 0.637 times I_{pk}, the peak value of current; $I_{avg} = 0.637\ I_{pk}$.

average life See MEAN LIFE.

average noise figure The ratio of the total noise output from a circuit to the thermal noise output at 290 degrees Kelvin. It is usually expressed in decibels, with the noise taken at all frequencies.

average power The average value of power in an ac circuit. In a resistive circuit, it is the square of the effective (rms) current times the resistance; $P_{avg} = (I_{rms})^2R$ (for sine waves).

average pulse amplitude Also called *effective pulse amplitude.* The value obtained by integrating the pulse amplitude, with respect to time, from the start of the pulse to its end, then dividing this integral by the pulse duration.

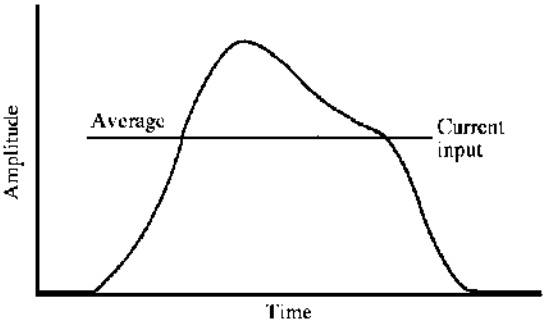

average pulse amplitude

average rectified current Abbreviation, I_{avg}. The average value of rectifier output current before filtering. For a full-wave rectifier with a sine wave input and a resistive load, I_{avg} is equal to the maximum current I_m multiplied by 0.637.

average rectified voltage Abbreviation, E_{avg}. The average value of rectifier output voltage before filtering. For a full-wave rectifier with a sine-wave input and a resistive load, E_{avg} is maximum voltage E_m multiplied by 0.637.

average value **1.** The *arithmetic mean* of two or more quantities. **2.** The *geometric mean* of two or more quantities. **3.** The *harmonic mean* of two or more quantities. **4.** In ac operation, the average current, voltage, or power.

average voltage Abbreviation, E_{avg}. The average value of ac voltage in a circuit. Taking polarity into account, this value is zero for a pure sine wave. For other waveforms, it can vary. When polarity is not considered, the sine-wave value of E_{avg} is equal to 0.637 times E_{pk}, the peak value of voltage.

avg Abbreviation of *average.*

aviation channels Frequency channels assigned to the AVIATION SERVICES.

Aviation services The radio-communication services used by aeronautical-mobile and radio navigation personnel.

avigation Acronym for *aviation navigation.* Aircraft navigation by means of electronic equipment.

avionics Acronym for *aviation electronics.* The design, production, and application of electronic devices and systems for use in aviation, navigation, and astronautics.

Avogadro's constant (Amedeo Avogadro, 1776–1856.) Symbol, NA. The number of molecules in a kilogram-molecular weight of any substance; NA equals 6.025×10^{26} (kg-mole)$^{-1}$.

A voltage The filament voltage in a vacuum-tube circuit.

aW Abbreviation of *attowatt.*

AWG Abbreviation of AMERICAN WIRE GAUGE.

AX.25 A signal format used in some digital communications systems, notably amateur *packet radio.*

5059F-pA_1-55 4/9/01 4:41 PM Page 55

axial leads The centrally located leads emanating from the ends of cylindrical components, such as resistors and diodes.

axial ratio The ratio of the minor to major axes of a waveguide's polarization ellipse.

axis **1.** A coordinate in a graphical presentation or display (e.g., horizontal and vertical axes in a rectangular coordinate system). **2.** The real or imaginary straight line around which a body rotates, or the line that passes through the center of a symmetrical arrangement (line of symmetry).

axis of abscissas The horizontal axis (x-axis) of a rectangular-coordinate graph or screen. Compare AXIS OF ORDINATES.

axis of imaginaries The vertical axis of the complex plane in which rectangular vectors lie. Compare AXIS OF REALS.

axis of ordinates The vertical (y-axis) of a rectangular-coordinate graph or screen. Compare AXIS OF ABSCISSAS.

axis of reals The horizontal axis of the complex plane in which rectangular vectors lie. Compare AXIS OF IMAGINARIES.

Ayrton-Mather galvanometer shunt A step-adjustable universal shunt resistor for varying the sensitivity of a galvanometer. It has the virtue of keeping the galvanometer critically damped. The shunt is also useful in multirange milliammeters, microammeters, and ammeters. The sensitive meter movement is never without a shunting resistor during range switching.

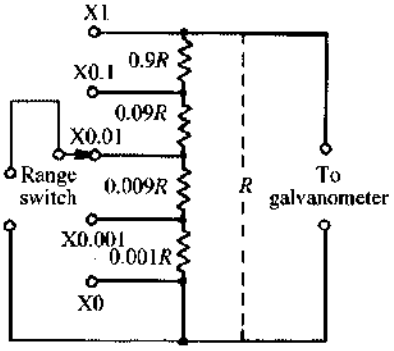

Ayrton-Mather galvanometer shunt

Ayrton-Perry winding A noninductive winding comprising two inductors conducting current in opposite directions; the opposing flow cancels the magnetic field.

azel display A plan-position display that incorporates two different radar traces on a single cathode-ray tube (CRT), one giving bearing, the other elevation.

azimuth Also called *compass direction.* Angular measurement in the horizontal plane, clockwise from north. It is important in radio and television communications, navigation, direction finding, land surveying, and radar.

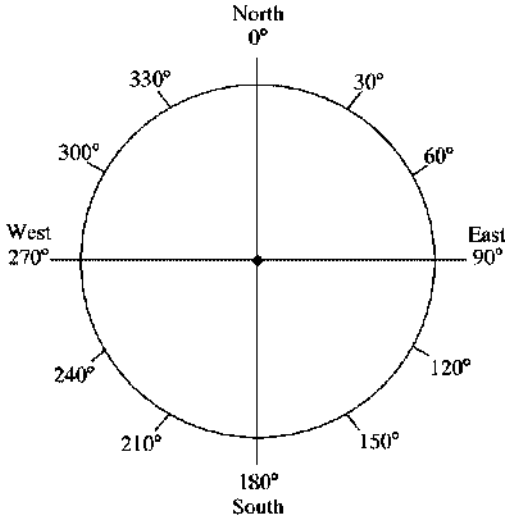

azimuth

azimuth alignment In a tape recorder, the alignment of record and playback head gaps so that their centerlines are parallel.

azimuth blanking In a radar system, blacking-out of the image as the antenna sweeps across a specified range of azimuth angles. Effectively eliminates nuisance echoes from stationary, permanent objects (such as tall buildings or communications towers).

azimuth resolution In a radar system, the minimum azimuth separation of two targets whose range (distance from the station) are equal that is required for the system to show two echoes, rather than one. It is generally measured in degrees.

azusa An electronic tracking system, in which a single station provides slant range and two direction cosines for a distant airborne object. This accurately defines the coordinates of the distant object in three-dimensional space.

5059F-pB_56-92 4/9/01 4:45 PM Page 56

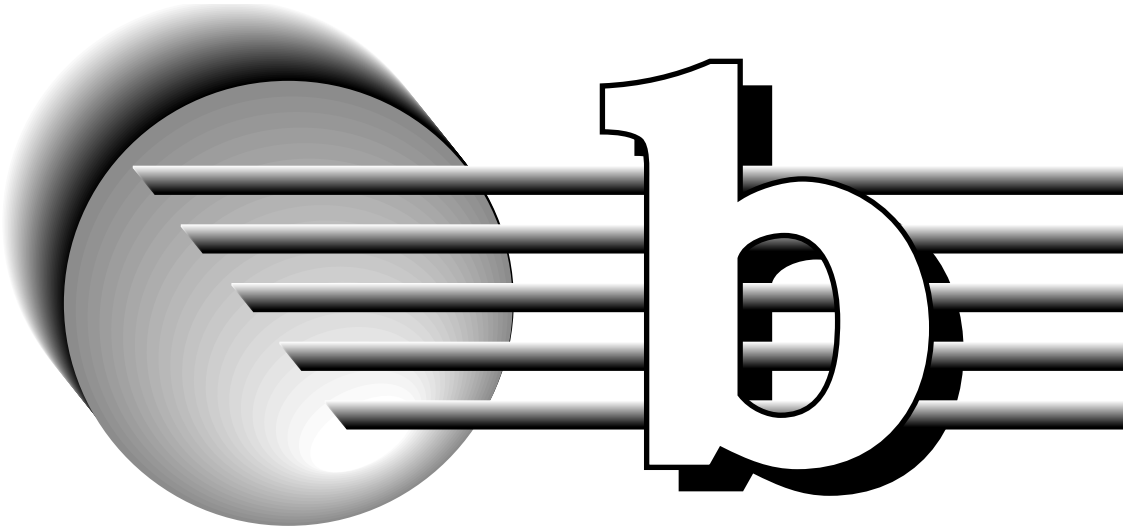

B **1.** Symbol for SUSCEPTANCE. **2.** Symbol for FLUX DENSITY. **3.** Abbreviation of BATTERY. **4.** Symbol for BORON. **5.** Symbol for base of transistor (see BASE, **1**). **6.** Abbreviation of BASS. **7.** Abbreviation of BEL. **8.** Anode voltage or main operating voltage in any circuit (when used with sign). Also see B VOLTAGE.

b **1.** Symbol for SUSCEPTANCE. **2.** Symbol for base of transistor (see BASE, **1**). **3.** Abbreviation of BASS. **4.** Symbol for BARN.

B&S See AMERICAN WIRE GAUGE.

B5-cut crystal A piezoelectric plate cut from a quartz crystal in such a way that the face of the plate is at an angle, with respect to the z-axis of the crystal. This type of crystal has good frequency stability under conditions of changing temperature.

BA Abbreviation of BATTERY. Also see B and BAT.

Ba Symbol for BARIUM.

babbit A relatively soft, tin-base alloy of various compositions. One composition contains 7.4% antimony, 3.7% copper, and 88.9% tin.

babble Interference caused by *crosstalk* from a number of channels.

babble signal A jamming signal containing babble components. See BABBLE and JAMMING.

BABS Abbreviation of BLIND-APPROACH BEACON SYSTEM.

baby monitor A short-range radio transmitter and receiver that can be used to listen at a distance to the sounds in an infant's room. The transmitter contains a sensitive microphone, a whip antenna, and a power supply. The unit can be placed on a table or desk, or even on the floor near the baby's crib. The receiver is similar to a handheld "walkie-talkie." It is battery-powered and can be carried around. It has an inductively loaded, short "rubber duckie" antenna similar to the antennas on cordless telephone sets. The receiver can pick up signals from the transmitter at distances of up to about 200 feet. The radio-frequency signals pass easily through walls, ceilings, and floors.

back bias **1.** A feedback signal (negative or positive). **2.** Reverse bias (also see BIAS). **3.** A reverse bias voltage, obtained from a voltage divider connected between a voltage source and ground.

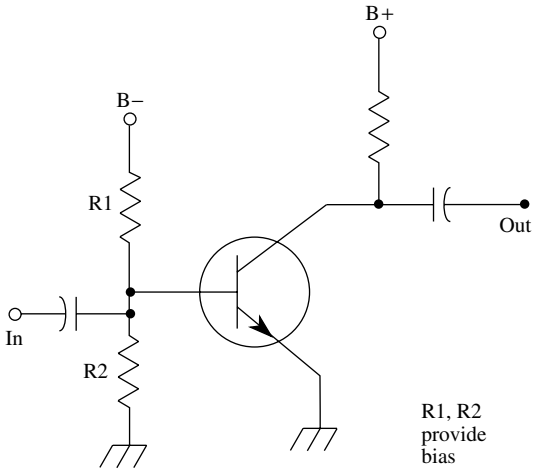

back bias, 3

Copyright 2001 The McGraw-Hill Companies, Inc. Click Here for Terms of Use

5059F-pB_56-92 4/9/01 4:45 PM Page 57

backbone A form of transmission line with capacitive connections between the generator and the load.

back conduction Conduction of current in the reverse direction, as across a semiconductor junction that is reverse-biased.

back contact A contact that closes a circuit when a relay, switch, or jack is in its normal rest position.

back current Symbol, I_b. The normally small current flowing through a reverse-biased pn semiconductor junction. Also called *reverse current* and *inverse current*. Compare FORWARD CURRENT.

back diode A semiconductor diode that is normally back-biased (reverse-biased).

back echo An echo resulting from the rear lobe of an antenna radiation pattern.

back emf See BACK VOLTAGE.

Back-Goudsmit effect See ZEEMAN EFFECT.

background **1.** The context or supporting area of a picture (e.g., the background of a television picture). **2.** Background noise.

background control In a color television receiver, a potentiometer used to set the dc level of the color signal at one input of the three-gun picture tube.

background count Residual response of a radioactivity counter in an environment as free as practicable of radioactivity. This background is caused largely by cosmic rays and inherent radioactivity of surrounding buildings and other bodies.

background job A low-priority, relatively long-running computer program that can be interrupted so that a higher-priority program can be run.

background noise Electrical noise inherent to a particular circuit, system, or device that remains when no other signal is present.

background processing In a computer, the running of programs having low priority.

background radiation Nuclear radiation from materials in the environment. Also see BACKGROUND COUNT.

background response The response of a radiation detector to background radiation.

backing store In a computer, a device that stores large amounts of information. In most small computers, this is done via MAGNETIC DISK and/or MAGNETIC TAPE. A backing store can also be an optical storage medium, such as CD-ROM (compact disk, read-only memory).

backlash **1.** Slack or lag in action of moving parts. Example: delay between initial application of a force (such as that required to turn a knob) and movement of a part or device (e.g., a potentiometer or variable capacitor). **2.** On a mechanical analog tuning dial, an arc within which slack or lag is discernible.

backloaded horn A loudspeaker enclosure in which the front of the speaker cone feeds sound directly into the listening area, and the rear of the cone feeds sound into the same area through a folded horn.

backloading In a cascaded series of amplifiers, the tendency of loading effects to be passed to earlier stages. A change in the output impedance of a final amplifier circuit, for example, could also result in a change in the output impedance of the driver circuit, and perhaps even in a change in the output impedance of the predriver.

back lobe In the pattern of a directional antenna, the lobe directly opposite the major lobe, representing the radiation or response in or from a direction 180 degrees from that in which the gain is greatest.

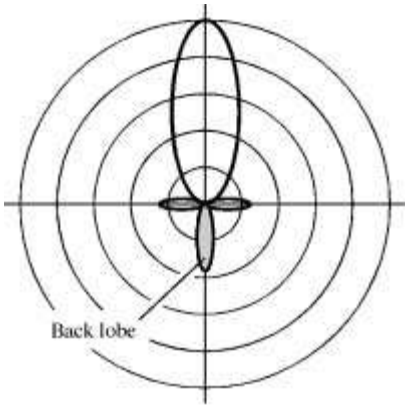

back lobe

backplate A flat electrode in a television (TV) camera tube that receives the stored-charge image via capacitive coupling.

back porch In a television (TV) horizontal sync pulse, the time interval between the end of the rise of the blanking pedestal and the beginning of the rise of the sync pulse. That portion of the flat top of the blanking pedestal behind the sync pulse. Compare FRONT PORCH.

back-porch effect In transistor operation, the continuation of collector-current flow for a short time after the input signal has fallen to zero.

back-porch tilt The departure of the top edge of a back porch from true horizontal.

back pressure sensor A device that detects and measures the torque that a motor is applying, and produces a signal whose amplitude is proportional to the torque. This signal can be used for various purposes. In a robotic device, for example, the sensor output can be fed back to the motor control to limit the applied force.

back resistance Symbol, R_b. The resistance of a reverse-biased pn semiconductor junction. Also called REVERSE RESISTANCE.

5059F-pB_56-92 4/9/01 4:45 PM Page 58

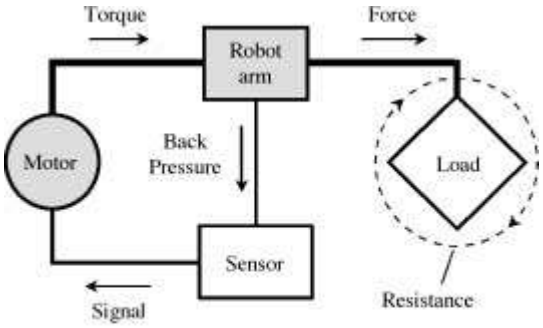

back pressure sensor

back scatter Scattering of a wave back toward a radio transmitter from points beyond the skip zone. This phenomenon is caused by ionospheric reflection. Compare FORWARD SCATTER.

backstop A contact or barrier (such as a screw or post) that serves to limit the BACKSWING of the armature of a relay.

backswing **1.** The tendency of a pulse to overshoot, or reverse direction after completion. Backswing is measured in terms of the overshoot amplitude as a percentage of the maximum amplitude of the pulse. **2.** The extent to which a relay armature moves back from a contact when the relay contacts are open.

back-to-back connection The connection of diodes or rectifiers in reverse parallel (i.e., the anode of one to the cathode of the other) across a signal line to pass both half cycles of ac in certain control circuits.

back-to-back sawtooth A symmetrical sawtooth wave in which the rise slope is equal to the fall slope. Also called *triangular wave* and *pyramidal wave.*

backup **1.** An element, such as a circuit component, that is used to replace a main component, in case of main-component failure. **2.** Any process or scheme that serves to maintain operation of a system in case of main-component failure. **3.** A battery that maintains volatile memory data stored in one or more integrated circuits. **4.** A computer file, or set of files, stored in a nonvolatile medium, such as diskettes or magnetic tape, to prevent catastrophic data loss in the event of hard-disk failure. **5.** A battery or alternative power source that keeps an alarm system operational in the event of a utility power failure.

backup battery **1.** In a computer or microcomputer-controlled electronic device, a source of voltage to preserve volatile memory data if the power is removed. **2.** A battery used for powering a system in the event that the main power source should fail.

backup facility In an electrical or communications system, a facility that is intended for use when the primary, or main, facility is not operational.

back voltage **1.** Voltage induced in an inductor by the flow of current through the inductor, so called because its polarity is opposite to that of the applied voltage. Also called *counter emf.* **2.** A voltage used to obtain bucking action (e.g., the voltage used to zero the meter in an electronic voltmeter circuit). **3.** Reverse voltage applied to a semiconductor junction.

backwall In a pot core, the plate or disk that connects the sleeve and center post to close the magnetic circuit.

backward diode A semiconductor diode manufactured in such a way that its high-current flow occurs when the junction is reverse biased. Such a diode is also a negative-resistance device.

backward-wave oscillator Abbreviation, BWO. A microwave oscillator tube similar to the *traveling-wave tube.* Like the traveling-wave tube, the BWO contains a helical transmission line. In the electron beam, electron bunching results from interaction between the beam and the electromagnetic field, and reflection occurs at the collector. The wave moves backward from collector to cathode, and oscillation is sustained because the backward wave is in phase with the input. Output is taken from the cathode end of the helix.

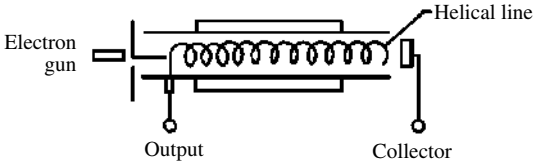

backward-wave oscillator

back wave The oscillator signal present in an amplifier-keyed, continuous-wave (CW), Morse-code transmitter. Normally, this signal is at the same frequency as the transmitter output, but is not sufficiently strong to be radiated over the air.

back-wave radiation The condition wherein a back wave is strong enough to be heard on a continuous-wave (CW) keyed signal at the receiving station. This results from ineffective amplifier keying.

baffle A board on which a loudspeaker is mounted to separate acoustic radiation from the back of the cone from radiation emanating from the front. The baffle improves bass response by increasing the wavelength (lowering the frequency) at which phase cancellation occurs.

baffle plate **1.** See BAFFLE. **2.** A metal plate mounted in a waveguide to reduce the cross-sectional area.

bail A wire loop or chain that holds one member of a two-member assembly to prevent loss (e.g., the short chain holding the dust cap of a jack).

5059F-pB_56-92 4/9/01 4:45 PM Page 59

Bakelite The trade name for a specialized plastic dielectric material. Its chemical composition is *phenol-formaldehyde* resin.

baker An obsolete phonetic alphabet code word for letter B. BRAVO is commonly used instead.

baking-out In the process of evacuating a system, the procedure of heating the system to a high temperature to drive out gases occluded in the glass and metal parts.

balance **1.** See BRIDGE. **2.** To null a bridge or similar circuit. **3.** To equalize loads, voltages, or signals between two circuits or components. **4.** In a high-fidelity stereo sound system, a control or set of controls that adjusts the relative loudness of the left and right channels. **5.** Alignment of a *balanced modulator* for minimum carrier output amplitude. **6.** A condition in which two branches of a circuit have identical impedances, relative to ground.

balance coil **1.** A type of autotransformer that enables a three-wire ac circuit to be supplied from a two-wire line. A series of taps around the center of the winding enables the circuit to be compensated for unequal loads. **2.** See BALANCING COIL.

balance control A variable component, such as a potentiometer or variable capacitor, that is used to balance bridges, null circuits, or loudspeakers.

balanced Having identical impedances, with respect to ground.

balanced amplifier Any amplifier with two branches that have identical impedances, with respect to ground. Usually, the two branches are in phase opposition (180 degrees out of phase).

balanced antenna An antenna system where two halves are exact replicas of each other, geometrically and electrically. Such an antenna normally must either be fed with a balanced transmission line or with a coaxial cable and balun.

balanced antenna system A balanced antenna, fed with a balanced transmission line, that has currents of equal magnitude in each side. An example is a half-wave dipole at uniform height above electrical ground, fed at the center with parallel-wire line. It is important that the transmission line runs away from the antenna at a right angle for at least ¼ wavelength, preferably ½ wavelength or more, to prevent line imbalance caused by currents induced from the radiated field.

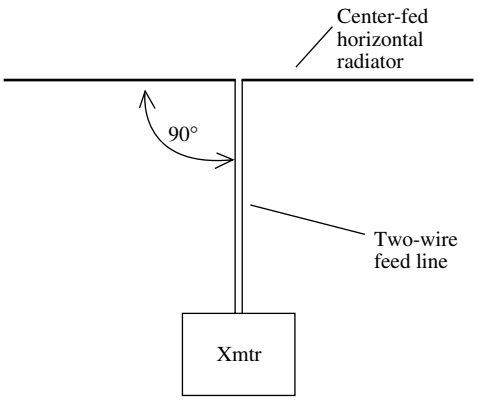

balanced antenna system

balanced bridge Any four-leg bridge circuit in which all legs are identical in all electrical respects.

balanced circuit **1.** A circuit that has its electrical midpoint grounded, as opposed to the *single-ended circuit*, which has one side grounded. **2.** A bridge circuit in the condition of null.

balanced converter See BALUN.

balanced currents Currents with the same value. In the two conductors of a balanced transmission line, these currents are equal in amplitude and opposite in phase at every point along the line.

balanced delta A set of coils or generators in a three-phase system, connected so that the currents in any two coils differ in phase by 120 degrees.

balanced detector A symmetrical demodulator, such as a full-wave diode detector or a discriminator.

balanced electronic voltmeter An electronic voltmeter circuit in which two matched transistors are connected in a four-arm bridge arrangement. The drift in one half of the circuit opposes that in the other half; the resulting drift of the zero point is virtually eliminated.

balanced filter A filter consisting of two identical sections, one in each branch of a balanced system, such as a parallel-wire transmission line.

balanced input An input circuit whose electrical midpoint is grounded. Compare SINGLE-ENDED INPUT.

balanced input transformer An input transformer in which the center tap of the primary winding is grounded.

balanced line A pair of parallel wires that possesses a uniform characteristic impedance. The two conductors are of the same material and have identical diameters. The distance between them is constant. In a balanced two-wire line, the currents in the two conductors are of equal amplitude and opposite phase.

balanced lines In high-fidelity audio systems, a cable that consists of two parallel conductors surrounded by a single braid. The parallel wires carry the audio-frequency (AF) signals, and the braid is grounded for shielding.

balanced loop antenna A loop antenna with a grounded electrical midpoint, determined by the junction of two identical series-connected capacitors shunting the loop.

balanced low-pass filter A low-pass filter used in a balanced system or balanced transmission line.

5059F-pB_56-92 4/9/01 4:45 PM Page 60

balanced method A system of instrumentation in which a zero-center scale is used. The reading can be either side of the zero reading.

balanced modulator A symmetrical modulator circuit using bipolar transistors, field-effect transistors, an integrated circuit, or diodes as principal components, that delivers an output signal containing the sidebands, but not the carrier. It is commonly used to generate a double-sideband (DSB) signal that can be filtered to obtain a single-sideband (SSB) signal.

balanced multivibrator A switching oscillator circuit in which the two halves are identical in configuration, and as nearly identical as practicable in performance.

balanced network Any network intended to be used with a balanced system or balanced transmission line. It is characterized by a pair of terminals, each of which shows the same impedance with respect to ground.

balanced oscillator A PUSH-PULL OSCILLATOR.

balanced output Output balanced against ground (e.g., where the electrical midpoint of the output circuit is grounded).

balanced output transformer **1.** A push-pull output transformer with a center-tapped primary winding. **2.** An output transformer with a grounded center tap on its secondary winding.

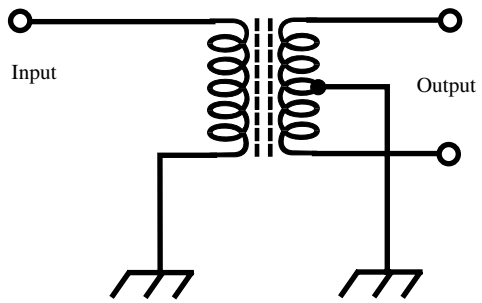

balanced output transformer, 2.

balanced probe A probe, such as one for an electronic voltmeter or oscilloscope, that has a balanced input and (usually) a single-ended output.

balanced-tee trap A wavetrap constructed in a T configuration, with a resonant section in each conductor of a balanced transmission line.

balanced telephone line A telephone transmission line that has two sides, similar to a balanced radio-frequency transmission line. Either side has the same impedance, with respect to ground.

balanced termination A load device (or the practice of using such a device) in which the sections provide identical termination for each of the sections or conductors of a balanced system, such as a balanced line.

balanced-to-unbalanced transformer See BALUN.

balanced transmission line See BALANCED LINE.

balanced varactor tuning A two-varactor, back-to-back circuit for adjusting the value of a capacitor using an applied dc voltage. This arrangement has an advantage over a single-varactor (unbalanced) circuit, because high-tuned-circuit Q is maintained and harmonic generation is reduced.

balanced voltages In any symmetrical system, such as a balanced line or push-pull circuit, two or more input or output voltages that are adjusted to have the same amplitude and (usually) opposite phase.

balanced-wire circuit A circuit or conductor system with identical halves that are symmetrical, with respect to ground and to other conductors.

balancing circuit See BUCKING CIRCUIT.

balancing coil In a receiver, a center-tapped antenna coil that is balanced to ground to eliminate MARCONI EFFECT.

ballast **1.** A component that is used to stabilize the current flow through, or operation of, a circuit, stage, or device. **2.** An iron-core choke connected in series with one of the electrodes in a fluorescent or other gas-discharge lamp.

ballast resistor **1.** A nonlinear inductive power resistor whose voltage-current (EI) characteristic is such that current through the resistor is independent of voltage over a useful range. This feature enables the ballast resistor to act as an automatic voltage regulator when it is simply connected in series with a power supply and load. **2.** A small (usually high-resistance) resistor operated in series with a glow lamp, such as a neon lamp, to prevent overload.

ballast transformer A misnomer often used in place of BALLAST, **2.**

ballistic galvanometer An undamped galvanometer that is used particularly to observe electric charges by noting the single throw resulting from the momentary flow of current through the galvanometer coil.

ballistics The electronics-supported science concerned with the motion of projectiles and similar bodies in air or space.

balloon antenna A vertical antenna consisting of a wire or wires held aloft by a captive balloon. Occasionally, used by radio amateurs and shortwave listeners at low and medium frequencies. A potentially dangerous antenna because of large static-electric buildup, a tendency to attract lightning, the possibility of its breaking loose, and the risk of accidental contact with high-voltage power lines.

balop Contraction of BALOPTICON.

balopticon An opaque-picture projecting system in which the picture is viewed by a television (TV) camera, such as a vidicon, and displayed by a picture tube. Also called *balop.*

balun A specialized impedance-matching radio-frequency (RF) transformer. It is a wideband device,

5059F-pB_56-92 4/9/01 4:45 PM Page 61

usually providing a 1:1 or 1:4 impedance ratio and available in several different forms. It is so called because it has an unbalanced input suitable for coaxial transmission lines, and a balanced output suitable for dipole, Yagi, and quad antennas.

banana jack The female half of a two-part quick-connector combination. Splicing of a circuit is completed by inserting a BANANA PLUG into this jack.

banana plug The male half of a two-part quick-connector combination, with sides usually composed of flat springs that ensure contact with the female BANANA JACK into which it is inserted.

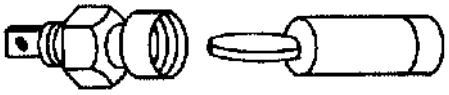

banana jack and plug

band **1.** A continuous range of radio or television communications frequencies or wavelengths, usually designated by the lowest and highest frequencies, or the approximate wavelength (e.g., the 20-meter amateur radio band). **2.** A set of discrete radio or television frequency channels within a specified range (e.g., the standard AM broadcast band). **3.** A range of wavelengths for infrared, visible, ultraviolet, X-ray, or gamma-ray energy. **4.** A range of energy levels. **5.** A colored stripe on a resistor or capacitor that forms part of the code that indicates component value and tolerance.

band center **1.** In a given radio or television communications band, the arithmetic mean of the lowest and highest frequencies. **2.** In a given band, the geometric mean of the longest and shortest wavelengths.

band-elimination filter See BAND-REJECTION FILTER.

band gap In any atom, the difference in electron energy between the conduction and valence bands.

bandpass **1.** The frequency limits between which a BANDPASS FILTER or BANDPASS AMPLIFIER transmits ac energy with negligible loss. **2.** The ability to allow passage of signals at a given frequency or band of frequencies while blocking other signals. Compare BANDSTOP.

bandpass amplifier An amplifier that is tuned to pass only those frequencies between preset limits.

bandpass coupling A coupling circuit with a flat-topped frequency response so that a band of frequencies, rather than a single frequency, is coupled into a succeeding circuit. Also see BANDPASS, **1.**

bandpass filter Any resonant circuit, or combination of resonant circuits, designed to discriminate against all frequencies except a specific frequency f_0, or a band of frequencies between two limiting frequencies f_0 and f_1. In a parallel inductance-capacitance (LC) circuit, the device exhibits high impedance at the desired frequency or frequencies and a low impedance at unwanted frequencies. In a series configuration, the filter has a low impedance at the desired frequency or frequencies and a high impedance at unwanted frequencies. Compare BAND-REJECTION FILTER, HIGH-PASS FILTER, LOW-PASS FILTER.

bandpass flatness The degree to which a bandpass device's attenuation-versus-frequency curve is a straight line with zero slope within the passband.

band pressure level The net acoustic pressure of a sound source within a specified frequency range (band).

band-rejection filter Also called a *band-stop filter*. Any resonant circuit, or combination of resonant circuits designed to discriminate against a specific frequency f_0, or a band of frequencies between two limiting frequencies f_0 and f_1. In a parallel inductance-capacitance (LC) circuit, the device exhibits high impedance at the desired frequencies, and a low impedance at the unwanted frequency or range of frequencies. In a series configuration, the filter has a low impedance at the desired frequencies and a high impedance at the unwanted frequency or range of frequencies. Compare BANDPASS FILTER, HIGH-PASS FILTER, LOW-PASS FILTER, NOTCH FILTER.

band selector Any switch or relay that facilitates switching the frequency of a radio transmitter, receiver, or transceiver among various bands.

bandset capacitor In some older communications receivers, a variable capacitor is used to preset the tuning range in each band to correspond to graduations on the tuning dial. This capacitor is a trimmer or padder operated in conjunction with the main tuning capacitor.

bandspreading In some older communications receivers, the process of widening the tuning range within a given frequency band to cover the entire dial. Otherwise, the band would occupy only a portion of the dial, and tuning would be difficult. It is usually accomplished with a BANDSPREAD TUNING CONTROL whose range is preset via the main tuning control and/or a BANDSET CAPACITOR.

bandspread tuning control An analog adjustment in some older communications receivers that allows continuous tuning over a desired band of frequencies. This control is separate from the main tuning control.

bandstop **1.** The frequency limits between which a BAND-REJECTION FILTER blocks, or greatly attenuates, ac energy. **2.** The ability to suppress or block signals of a given frequency or band of frequencies, while allowing signals of other frequencies to pass with little or no attenuation. Compare BANDPASS.

5059F-pB_56-92 4/9/01 4:45 PM Page 62

bandstop filter See BAND-REJECTION FILTER.

band suppression **1.** The property of blocking, or greatly attenuating, signals within a specific frequency band. **2.** The frequency limits between which a device or circuit rejects or blocks ac energy, while passing energy at other frequencies with negligible loss.

band-suppression filter See BAND-REJECTION FILTER.

bandswitch A low-reactance selector switch (usually rotary) that facilitates changing the tuning range of a radio receiver, transmitter or transceiver from one band of frequencies to another.

bandswitching In a receiver, transmitter, or test instrument, the process of switching self-contained tuned circuits to change from one frequency spectrum to another within the range of the device's intended operation.

bandwidth **1.** For a communications or data signal, a measure of the amount of spectrum space the signal occupies. Usually, it is given as the difference between the frequencies at which the signal amplitude is nominally 3 dB down with respect to the amplitude at the center frequency. These frequencies represent the half-power points of the amplitude-versus-frequency function. In general, the bandwidth increases as the data rate (in bits per second, baud, or words per minute) increases. **2.** Also called NECESSARY BANDWIDTH. The minimum amount of spectrum space normally required for effective transmission and reception of a communications or data signal. **3.** See BANDPASS, **1.**

bank A collection of usually similar components used in conjunction with each other, usually in a parallel configuration. Some examples are resistor bank, lamp bank, and transformer bank.

banked transformers Parallel-operated transformers.

bankwound coil A coil wound in such a way that most of its turns are not side by side, thus reducing the inherent distributed capacitance.

bar **1.** Abbreviation, b. The cgs unit of pressure, in which 1 b = 10^5 pascals per square centimeter. **2.** A horizontal or vertical line produced on a television (TV) screen by a bar generator and used to check linearity. **3.** A thick plate of piezoelectric crystal. **4.** A solid metal conductor, usually uninsulated, of any cross section. **5.** A silicon ingot from which semiconductor devices can be fabricated.

BAR Abbreviation of BUFFER ADDRESS REGISTER.

bar code A printed pattern that contains data that can be recovered by laser scanning. It is commonly used for the pricing and identification of store merchandise. It can also be used by an assembly or maintenance robot as an aid to identifying tools.

bar-code reader A laser scanning device that recovers the data from a tag that contains a BAR CODE. The laser beam moves across the tag. The beam is reflected from the white regions between the lines, but is absorbed by the dark lines themselves. This produces modulation of the reflected beam by the data contained in the tag.

bare conductor A conductor with no insulating covering, a common example being bare copper wire.

bar generator A special type of radio-frequency signal generator that produces horizontal or vertical bars on the screen of a television receiver. It is used in adjustment of horizontal and vertical linearity.

bar graph A graphical presentation of data, in which numerical values are represented by horizontal bars of width that correspond to the values. This type of graph is nonstandard in the sense that the ordinate is horizontal, whereas it is usually vertical. Compare COLUMNAR GRAPH.

bar-graph meter See BAR METER.

barium Symbol, Ba. An elemental metal of the alkaline-earth group. Atomic number, 56. Atomic weight, 137.36. It is present in some compounds used as dielectrics (e.g., barium titanate).

barium-strontium oxides The combined oxides of barium and strontium used as coatings of vacuum-tube cathodes to increase electron emission at relatively low temperatures.

barium strontium titanate A compound of barium, strontium, oxygen, and titanium that is used as a ceramic dielectric material. It exhibits ferroelectric properties and is characterized by a high dielectric constant.

barium titanate Formula, $BaTi0_2$. A ceramic used as the dielectric in ceramic capacitors. It exhibits high dielectric constant and some degree of ferroelectricity.

Barkhausen effect The occurrence of minute jumps in the magnetization of a ferromagnetic substance as the magnetic force is increased or decreased over a continuous range.

Barkhausen interference Interference that results from oscillation because of the BARK-HAUSEN EFFECT.

bar magnet A relatively long permanent magnet in the shape of a bar with a rectangular or square cross section.

bar meter A digital meter that displays a quantity, such as signal strength, incrementally, using a set of LEDs or LCDs arranged in a straight line. Its main advantage is that it has no moving parts, yet (unlike direct-readout digital meters) gives the viewer some impression of the way a rapidly fluctuating quantity changes. Its chief

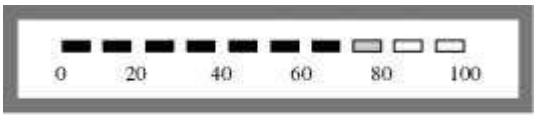

bar meter

5059F-pB_56-92 4/9/01 4:45 PM Page 63

disadvantage is that it does not provide a precise indication.

barn Symbol, b. A non-SI unit of nuclear cross section equal to 100 square femtometers or 10^{-24} square centimeters. This unit is approved as compatible with SI (International System of Units).

Barnett effect The development of a small amount of magnetization in a long iron cylinder that is rotated rapidly about its longitudinal axis.

barograph A recording barometer, using either a drum recorder (pen recorder) or a computer to store the data as a function of atmospheric pressure versus time.

barometer An instrument for measuring atmospheric pressure.

barometer effect A relation that appears to exist between the intensity of *cosmic rays* and the atmospheric pressure. It is an inverse relation; that is, increasing pressure seems to correlate with reduced intensity of cosmic rays. It is said to be approximately to 1 or 2% per centimeter of mercury.

barometric pressure The atmospheric pressure, usually given in inches of mercury. The average barometric pressure at the surface of the earth is just under 30 inches of mercury.

bar pattern A series of spaced lines or bars (horizontal, vertical, or both) produced on a television picture screen by means of a BAR GENERATOR. It is useful in adjusting horizontal and vertical linearity of the picture.

barrage array An antenna array in which a string of collinear elements are vertically stacked. The end quarter wavelength of each string is bent in to meet the end quarter wavelength of the opposite radiator to improve balance.

barrage jamming The jamming of many frequencies, or an entire band, at the same time.

barrell distortion Television picture distortion consisting of horizontal and vertical bulging.

barrier **1.** The carrier-free space-charge region in a semiconductor pn junction. **2.** An insulating partition placed between two conductors or terminals to lengthen the dielectric path.

barrier balance The state of near equilibrium in a semiconductor pn junction (after initial junction forming), entailing a balance of majority and minority charge carrier currents.

barrier capacitance **1.** The capacitance in a bipolar transistor between the emitter and collector. It varies with changes in applied voltage, and also with the junction temperature. **2.** The capacitance across any pn junction that is reverse-biased.

barrier height The difference in voltage between opposite sides of a barrier in a semiconductor material.

barrier layer See BARRIER, **1.**

barrier-layer cell A photovoltaic cell, such as the copper oxide or selenium type, in which photons striking the barrier layer produce the potential difference.

barrier potential The apparent internal dc potential across the barrier (see BARRIER, **1**) in a pn junction.

barrier strip A terminal strip having a barrier (see BARRIER, **2**) between each pair of terminals.

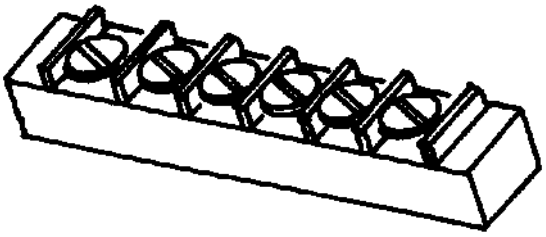

barrier strip

barrier voltage The voltage required for the initiation of current flow through a pn junction.

Bartlett force See EXCHANGE FORCE.

baryon A subatomic particle made up of three quarks.

base **1.** In a bipolar transistor, the intermediate region between the emitter and collector, which usually serves as the input or controlling element of transistor operation. **2.** A substance that dissociates in water solution and forms hydroxyl (OH) ions. For example, sodium hydroxide. **3.** The constant figure upon which logarithms are computed (10 for common logs, 2.71828 for natural logs). **4.** The radix of a number system (e.g., base 10 for the decimal system, base 8 for the octal system, base 16 for the hexadecimal system, and base 2 for the binary system). **5.** A fixed nonportable radio communications installation.

base address The number in a computer address that serves as the reference for subsequent address numbers.

baseband The frequency band of the modulating signal in a communications, broadcast, or data transmitter. For voice communications, this is generally the range of voice frequencies necessary for intelligible transmission. For high-fidelity music broadcasting, it is approximately the range of human hearing. For fast-scan television, it ranges up to several megahertz. It can be restricted or expanded, depending on the nature of the transmitted signal. See BASEBAND FREQUENCY RESPONSE.

baseband frequency response **1.** The amplitude-versus-frequency characteristic of the audio-frequency (AF) or composite video section of a transmitter that defines the BASEBAND, or range of modulating frequencies. **2.** The range of frequencies over which a radio transmitter can be modulated to convey information. For single sideband (SSB), it is approximately 300 Hz to 3 kHz; for high-fidelity, frequency-modulated (FM) music

5059F-pB_56-92 4/9/01 4:45 PM Page 64

transmission, it is about 10 Hz to 20 kHz or 30 kHz; for fast-scan television, it consists of frequencies up to several megahertz. This range is determined by bandpass and/or lowpass filters in the AF or composite video section of the transmitter.

base bias The steady dc voltage applied to the base electrode of a transistor to determine the operating point along the transistor characteristic curve.

base-bulk resistance The resistance of the semiconductor material in the base layer of a bipolar transistor.

base-charging capacitance In the common-emitter connection of a bipolar transistor, the internal capacitance of the base-emitter junction.

base current Symbol, I_B. Current flowing through the base electrode of a bipolar transistor. Also see AC BASE CURRENT and DC BASE CURRENT.

base electrode See BASE, **1.** Also called *base element.*

base element **1.** Base electrode. **2.** One of the basic metals, such as iron or tin, that are not generally considered precious (as opposed to NOBLE).

base-e logarithm See NAPIERIAN LOGARITHM.

base film The plastic substrate of a magnetic recording tape.

base frequency **1.** The frequency of the principal, or strongest, component in a complex signal or waveform; also called *basic frequency.* **2.** The frequency of operation of a base-station transmitter when the receiver is tuned to a second channel.

base-input circuit A common-collector circuit, common-emitter circuit, or emitter follower.

base insulator A stout dielectric insulator, used to support a heavy conducting element and keep the conductor isolated from other possible conductors or conductive paths.

base line In visual alignment procedures involving an oscilloscope and radio-frequency (RF) sweep generator, a zero-voltage reference line developed by the generator as a horizontal trace on the oscilloscope screen.

baseline stabilizer A clamping circuit that holds the reference voltage of a waveform to a predetermined value. Also called DC RESTORER.

base-loaded antenna A usually vertical antenna or radiating element, the electrical length of which is adjusted by means of a loading coil or tuned circuit in series with, and positioned at the bottom of, the antenna or radiator.

base material In printed circuits, the dielectric material used as a substrate for the metal pattern. Also called *base medium.*

base notation The numbering or radix system used in any application (as octal, decimal, binary, or hexadecimal).

base number See BASE, **4.**

base pin One of the straight prong-like terminals on an electrical or electronic component; it is used to provide support for the device and to allow a physical connection between the socket terminal, into which it fits, and one of the internal electrodes of the device.

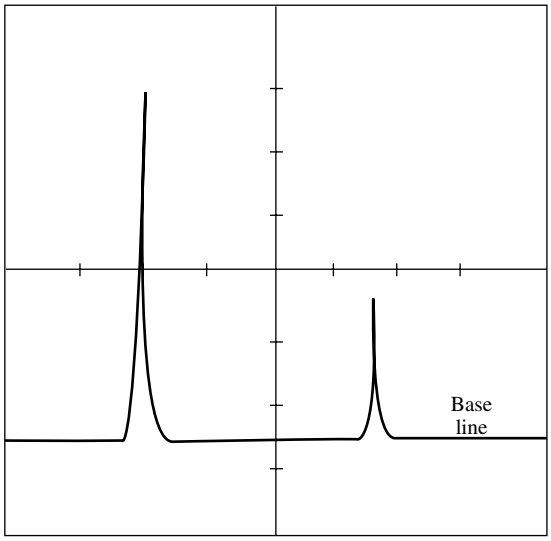

base line

base plate The chassis plate upon which components are mounted before wiring.

base potential See BASE VOLTAGE.

base region See BASE, **1.**

base resistance Symbol, R_B. Resistance associated with the base electrode of a bipolar transistor. Also see AC BASE RESISTANCE and DC BASE RESISTANCE.

base resistor The external resistor connected to the base of a bipolar transistor. In the common-emitter circuit, the base resistor is analogous to the gate resistor of a field-effect transistor (FET) circuit.

base spreading resistance Symbol, r_{BB}. In a bipolar transistor, the bulk-material resistance of the base region between the collector junction and emitter junction.

base station The head station or fixed home station in a communication network.

base-10 logarithm Abbreviation, $\log_{10}$. A logarithm based on the decimal number 10. If $\log_{10}(x) = y$, then $10^y = x$. Base-10 logarithms are commonly used in engineering. Compare NAPIERIAN LOGARITHM.

base voltage Symbol, V_B. The voltage at the base electrode of a bipolar transistor. Also see AC BASE VOLTAGE and DC BASE VOLTAGE.

BASIC Acronym for BEGINNER'S ALL-PURPOSE SYMBOLIC INSTRUCTION CODE, a relatively primitive, but versatile and easy-to-learn computer language developed at Dartmouth College.

5059F-pB_56-92 4/9/01 4:45 PM Page 65

basic frequency **1.** The FUNDAMENTAL FREQUENCY of a signal, as opposed to one of its harmonics. **2.** See BASE FREQUENCY, **1.**

basic protection Devices and procedures essential to minimize the risk of damage to electronic equipment, and/or injury or death to its operators, as a result of lightning. Hardware provisions include a substantial earth ground, heavy-gauge grounding wire, lightning arrestors for antennas, and transient suppressors for power connections. The safest procedure is to disconnect and ground all antennas, and unplug all equipment from utility outlets, during electrical storms and/or when the apparatus is not in use. Radio communications equipment with outdoor antennas, in particular, should not be operated during thunderstorms.

basket The structure that supports the cone in an acoustic loudspeaker.

basket-weave coil A type of single-layer inductor in which adjacent turns do not parallel each other around the circumference, but zigzag oppositely as a strand does in the woven pattern of a basket. This reduces distributed capacitance.

bass Low audio frequencies (AF) corresponding to low-frequency musical notes or sounds.

bass boost **1.** The special emphasis given to low audio frequencies (the bass notes) by selective circuits in audio systems. **2.** The technique of increasing the loudness of the bass, relative to the higher audio frequencies, to render a more faithful reproduction of sound at low volume levels.

bass compensation See BASS BOOST, **2.**

bass control **1.** A manually variable potentiometer for adjusting bass boost of an amplifier or sound system. **2.** The arrangement of components that are required to achieve amplitude variation of bass in an audio signal.

bass port In a loudspeaker, a hole in the cabinet that enhances the low-frequency (bass) sound output. Used in high-fidelity audio systems.

bass-reflex enclosure A loudspeaker cabinet with a critically dimensioned duct or port that allows back waves to be radiated in phase with front waves, thus averting unwanted acoustic phase cancellation.

bass-reflex loudspeaker A loudspeaker mounted in a bass reflex enclosure. Also see ACOUSTICAL PHASE INVERTER.

bass-resonant frequency The low frequency at which a loudspeaker or its enclosure displays resonant vibration.

bass roll-off **1.** The attenuation of the low-frequency (bass) component in a high-fidelity audio signal. **2.** A control that allows adjustable attenuation of the low-frequency component in a high-fidelity audio signal.

bass suppression In speech transmission, the removal of all frequencies below about 300 Hz, on the assumption that those frequencies contribute little to intelligibility. This suppression permits the speech level to be increased without overmodulating a transmitter. It also allows smaller audio transformers to be used because transformer core size must increase as the frequency it passes decreases.

bassy In audio and high-fidelity applications, a sound in which the low-frequency components, below about 500 Hz, are overly predominant.

BAT Abbreviation of BATTERY.

batch fabrication process The manufacture of devices in a single batch from materials of uniform grade. Particularly, the manufacture of a large number of semiconductor devices from one batch of semiconductor material by means of carefully controlled, identical processes.

batch processing In digital-computer operations, the processing of quantities of similar information during a single run.

bat-handle switch A toggle switch, the lever of which is relatively long and thick, and is shaped like a baseball bat.

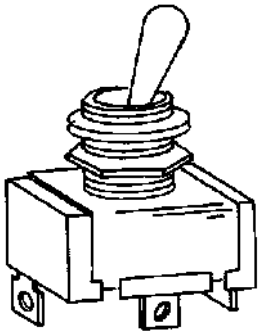

bat-handle switch

bathtub capacitor A (usually oil-filled) capacitor housed in a metal can that looks like a miniature bathtub.

bathyconductorgraph An instrument that is used to measure the electrical conductivity of seawater.

bathythermograph An instrument that plots a graph of temperature versus depth in a body of water, such as a lake or an ocean.

batten Supporting bars or braces that hold a loudspeaker in place within its cabinet, and/or that hold the cabinet panels in place.

battery Abbreviations, B, BA. BAT. A device consisting of two or more interconnected electrochemical or photovoltaic cells that generate dc electricity. The cells can be connected in series to supply a desired voltage, in parallel to supply a desired current-delivering capability, or in series-parallel to obtain a desired voltage and current-delivering capability. Also see CELL, EDISON BATTERY, LEAD-ACID BATTERY, PHOTO-

5059F-pB_56-92 4/9/01 4:45 PM Page 66

VOLTAIC CELL, PRIMARY BATTERY, and STORAGE BATTERY.

battery acid **1.** A chemical acid, such as sulfuric acid, used as the electrolyte of a battery. **2.** Colloquially, any cell or battery electrolyte, whether acid, base, or salt.

battery capacity The current-supplying capability of a battery, usually expressed in ampere-hours (Ah).

battery cell See CELL, **1.**

battery charger **1.** A specialized dc power supply, usually embodying a stepdown transformer, rectifier, and filter. It is used to charge a storage battery from an ac power line. **2.** A motor-generator combination used to charge a storage battery from an ac power line. **3.** A combination of solar cells, generators, or other voltaic transducers, that are used to charge a storage battery with dc obtained from a nonelectrical energy source.

battery clip **1.** A heavy-duty metallic clamp that is used for quick, temporary connection to a large cell terminal, such as that of a lead-acid storage battery. **2.** A small connector of the snap-fastener type, used for quick connection to a small power source, such as a transistor-radio battery.

battery eliminator A specialized dc power supply, usually embodying a transformer, rectifier, and filter, that permits battery-powered equipment to be operated from an ac power line.

battery holder **1.** A case or container of any kind for holding a cell or battery. **2.** A shelf for holding a cell or battery. **3.** A small, metal bracket-type device for holding a cell or battery between two contacts.

battery life **1.** The ampere-hour or watt-hour capacity of a battery. **2.** The number of times that a rechargeable electrochemical battery can be cycled before it becomes unusable. **3.** The nominal length of time (e.g., hours, days, or weeks) that an electrochemical battery will function effectively in a given application before it must be discarded or recharged.

battery memory See MEMORY DRAIN.

battery receiver A usually portable radio or television receiver operated from self-contained batteries.

battery substitute See BATTERY ELIMINATOR.

bat wing On a television (TV) or frequency-modulation (FM) broadcast receiving antenna, a metallic element with a shape that resembles that of a bat's wing.

baud A unit of communications processing speed in telegraphy and digital data communications systems. Often confused with *bits per second* (bps). Baud refers to the number of times per second that a signal changes state. The speed in bps is generally higher than the speed in baud, sometimes by a factor of several times. Compare BITS PER SECOND.

Baudot code A machine communications code that uses five parallel binary digits of equal length, the interpretation of which depends on the history of the previous transmission or an additional case bit.

baud rate **1.** A colloquial expression for data speed in BAUD. **2.** Colloquial, and technically inaccurate, expression for data speed in BITS PER SECOND.

Baume (Antione Baume, 1728–1804). Abbreviation, Be. Pertaining to the *Baume scales* for hydrometers. The two such scales are for liquids heavier than water and for liquids lighter than water.

bay One of several sections of a directional antenna array.

bayonet base The insertable portion of a plug-in component (e.g., a lamp) that has a projecting pin that fits into a slot or keyway in the shell of the socket into which the component is inserted.

bayonet socket A socket with a suitably slotted shell for receiving the bayonet base of a plug-in component.

bazooka A linear BALUN, in which a quarter wavelength of metal sleeving surrounds a coaxial feeder, and is shorted to the outer conductor of the feeder to form a shorted quarter-wave section.

bb Abbreviation of BLACKBODY.

BBC Abbreviation of *British Broadcasting Corporation*.

BBM Abbreviation of BREAK BEFORE MAKE.

b-box The index register of a computer.

BC Abbreviation of BROADCAST.

BCD Abbreviation of BINARY-CODED DECIMAL.

BCFSK Abbreviation of BINARY CODE FREQUENCY-SHIFT KEYING.

B channel One of the channels of a two-channel stereophonic system. Compare A CHANNEL.

BCI Abbreviation of BROADCAST INTERFERENCE.

BCL Amateur radio abbreviation of BROADCAST LISTENER.

BCN Abbreviation of BEACON.

BCO Abbreviation of BINARY-CODED OCTAL.

BCST Abbreviation of BROADCAST.

BDC Abbreviation of BINARY DECIMAL COUNTER.

B display A radar display in which the target is represented by a bright spot on a rectangular-coordinate screen. Compare A DISPLAY and J DISPLAY.

Be Symbol for BERYLLIUM.

Be Abbreviation of BAUME.

beacon **1.** A beam of radio waves, or a radio signal, that is used for navigation and/or direction finding. **2.** A transmitter that radiates a beam of radio waves, or a radio signal, as an aid in navigation and/or direction finding. **3.** A signal transmitted continuously on a specific frequency, to help radio operators ascertain propagation conditions. **4.** A station or transmitter that generates and radiates a signal to help radio operators determine propagation conditions. **5.** In robotics, a device or system that aids in navigation. For example, tricorner reflectors can be positioned in strategic locations, and a mobile robot equipped with a

5059F-pB_56-92 4/9/01 4:45 PM Page 67

scanning infrared laser. The robot controller determines the distance to any given reflector by measuring the time required for the laser beam to return. In this way, two mirrors can allow the robot to locate its position in two dimensions; three mirrors can facilitate position determination in three-dimensional space.

beacon direction finder A direction finder using a signal received from a beacon station.

beacon receiver A receiver that is specially adapted for the reception of beacon signals (see BEACON, **1** and **3**).

beacon station **1.** A station broadcasting beacon signals (see BEACON, **1** and **3**) for direction finding, navigation, and/or determination of radio-wave propagation conditions. **2.** Sometimes, a radar transmitting station.

beacon transmitter A transmitter specially adapted for the transmission of beacon signals (see BEACON, **1** and **3**).

bead **1.** A small ferromagnetic ring that is used as a passive decoupling choke by slipping it over the input power leads of a circuit or stage, or around a coaxial transmission line. **2.** A magnetic memory element in a ferrite-core matrix.

beaded coax A low-loss, coaxial transmission line, in which the inner conductor is separated from the outer conductor by means of spaced dielectric beads.

beaded support A plastic or dielectric bead that is used to support the inner conductor of an air-insulated transmission line of coaxial construction.

bead thermistor A thermistor consisting essentially of a small bead of temperature-sensitive resistance material into which two leads are inserted.

beam **1.** The more-or-less narrow pattern of radiation from a directional antenna. **2.** A directional antenna—especially a YAGI ANTENNA. **3.** The stream or cloud of electrons emitted by the cathode in an electron tube—especially a BEAM POWER TUBE.

beam alignment **1.** The lining-up of a directional transmitting antenna with a directional receiving antenna for maximum signal transfer. **2.** In a television (TV) camera tube, the lining-up of the electron beam so that it is perpendicular to the target. **3.** In a cathode-ray tube, the positioning of the electron rays so that they converge properly on the screen, regardless of the deflection path.

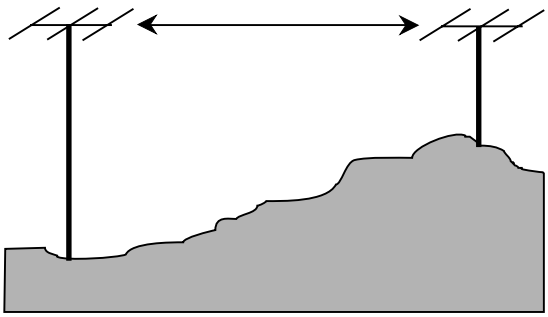

beam alignment

beam angle In the radiation from an antenna, the direction of most intense radiation, the side limits of which are determined by the points at which the field strength drops to half the value in the principal direction.

beam antenna **1.** A multielement directional antenna, consisting of a half-wave driven dipole and one or more parasitic elements. See YAGI ANTENNA. **2.** Any directional antenna used for transmitting and receiving radio-frequency (RF) signals.

beam bender **1.** In a television (TV) picture tube, the ion-trap magnet. **2.** Deflection-plate correction device or circuit.

beam bending Deflection of an electron beam by electric or magnetic fields.

beam blanking See BLANK, **2.**

beam convergence The meeting, at a shadow-mask opening, of the three electron beams in a three-color television picture tube. See BEAM ALIGNMENT, **3.**

beam coupling A method of producing an alternating current between two electrodes by passing a density-modulated beam of electrons between the electrodes. This, in effect, demodulates the electron beam, recovering the information.

beam crossover Either of the half-power points in the beam of a directional antenna, usually in the horizontal plane. The reference point is considered to be the direction of maximum radiation.

beam current The current represented by the flow of electrons in the beam of a cathode-ray tube.

beam cutoff In an oscilloscope or television picture tube, the complete interruption of the electron beam, usually as a result of highly negative control-grid bias.

beam deflector A deflection plate in an oscilloscope tube.

beam efficiency In a cathode-ray tube, the ratio of the number of electrons generated by the gun to the number reaching the screen. The efficiency is high in electromagnetic-deflection tubes and lower in electrostatic-deflection tubes.

beam lead In an integrated circuit, a relatively thick and strong lead that is deposited in contact with portions of the thin-film circuit. It provides stouter connections than continuations of the thin film would provide.

beam-lead isolation In an integrated circuit, reduction of distributed capacitance and other interaction through use of beam leads.

beam modulation See INTENSITY MODULATION.

beam parametric amplifier A PARAMETRIC AMPLIFIER in which the variable-reactance component is supplied by a modulated electron beam.

5059F-pB_56-92 4/9/01 4:45 PM Page 68

beam-positioning magnet In a three-gun color television picture tube, a permanent magnet that is used to position one of the electron beams correctly, with respect to the other two.

beam power tube A tetrode or pentode vacuum tube, in which special deflector plates concentrate the electrons into beams in their passage from cathode to plate. The beam action greatly increases plate current at a given plate voltage. It is used in some radio-frequency (RF) power amplifiers.

beam-rider control system A missile-guidance system in which a control station sends a radio beam to a missile. The beam is moved in such a way that as the missile stays within the beam, it hits the target.

beam-rider guidance **1.** An aircraft landing guidance system, in which the aircraft follows a radio beam in its glide path. **2.** The circuitry in a guided missile using a beam-rider control system.

beam splitter A device used to divide a light beam (as by a transparent mirror) into two components, one transmitted and the other reflected; hence, a BEAM-SPLITTING MIRROR.

beam splitting In radar, a method of calculating the mean azimuth of a target from the azimuth at which the target is first revealed by one scan, and the azimuth at which the target information ceases.

beam-splitting mirror In an oscilloscope-camera system, a tilted, transparent mirror that allows rays to pass horizontally from the oscilloscope screen to the camera and to be reflected vertically to the viewer's eye.

beamwidth of antenna The angular width of the main lobe of the pattern of radiation from a directional antenna. Generally, it is measured between the half-power points in the horizontal plane. Occasionally, it is measured in the vertical plane.

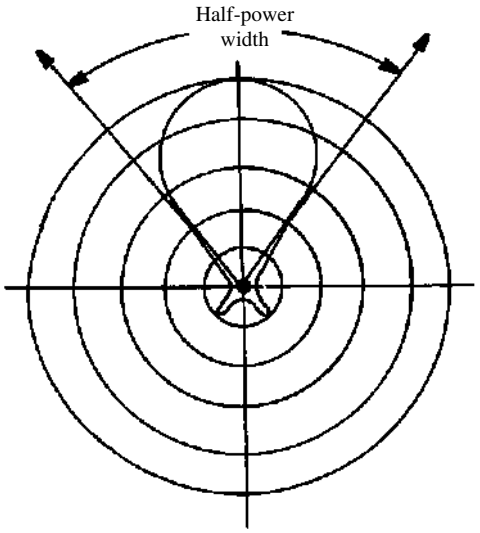

beamwidth of antenna

bearing The direction of an object or point expressed in degrees within a 360° horizontal clockwise boundary, with the center of the circle serving as the observation point.

bearing resolution In radar operations, the minimum horizontal separation of two targets, in degrees, that permits the individual targets to be displayed as two echoes, rather than one.

beat Any one of the series of pulsations constituting a beat note, which results from heterodyning one signal against another.

beat frequency Either of two frequencies f_{C1} and f_{C2} resulting from the mixing of two signals of different frequencies f_A and f_B. Frequency f_{C1} is the sum of the two input frequencies; $f_{C1} = f_A + f_B$. Frequency f_{C2} is the difference; $f_{C2} = f_A - f_B$ when f_A is the higher of the two input frequencies.

beat-frequency oscillator Abbreviation, BFO. An oscillator used to set up audible beat frequencies with an incoming received signal and installed in the intermediate-frequency (IF) stages of a superheterodyne communications receiver. For single-sideband (SSB) reception, the BFO is set at the frequency of the received suppressed carrier. In continuous-wave (CW) Morse code reception, the BFO is set at a frequency that differs from that of the incoming signal by about 400 to 1000 Hz. The resulting tone has an audio frequency equal to the difference between the BFO frequency and the received signal carrier frequency. For reception of frequency-shift-keyed (FSK) signals, the BFO is set to such a frequency that the resulting audio beat notes are appropriate for the mark and space inputs of a terminal unit or modem.

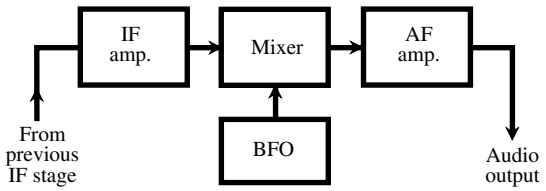

beat-frequency oscillator

beating **1.** Also called *heterodyning.* The combination of signals of different frequencies resulting in sum and difference frequencies. **2.** The fluttering noise heard when two audio tones, very close in frequency and very similar in amplitude, are emitted at the same time.

beat marker In the visual (oscilloscopic) alignment of a tuned circuit, a marker pip that results from the beat note between the sweep-generator signal and the signal from a marker oscillator.

5059F-pB_56-92 4/9/01 4:45 PM Page 69

beat note The sum or difference frequency that results from the heterodyning of two signals or, under some conditions, of more than two signals.

beat-note reception **1.** Reception in which a radio-frequency carrier is made audible by heterodyning it with a beat-frequency oscillator (BFO) to produce an audible beat note. **2.** Superheterodyne reception (see SUPERHETERODYNE CIRCUIT).

beat tone A beat note in which the frequency is within the range of hearing.

beaver tail A flat or elongated radar beam, wide in the azimuth plane. Primarily used to determine the altitude of a target. The beam is moved up and down to find the target elevation.

Becquerel effect A phenomenon in which a voltage is produced when radiant energy, such as infrared, visible light, ultraviolet, or X-rays, falls on one electrode in an electrolytic cell.

bedspring A directional antenna consisting of a broadside array with a flat reflector and one or more helical driven elements.

beep A test or control signal, usually of single tone and short duration.

beeper **1.** A pocket- or hand-carried transceiver—especially one for maintaining two-way contact with personnel who are away from their base. **2.** An acoustic transducer that produces a beep in response to an input signal.

beetle A urea formaldehyde plastic used as a dielectric material and as a container material.

bel Abbreviation, B. The basic logarithmic unit (named for Alexander Graham Bell) for expressing gain or loss ratios. One bel is equivalent to a power gain of 10. Also see DECIBEL.

bell An electric alarm device consisting of a metallic gong that emits a ringing sound when it is struck by an electrically vibrated clapper.

Bellini-Tosi direction finder A direction finder in which the sensing element consists of two triangular vertical antennas crossed at right angles, the antennas being open at the top and accordingly not acting as conventional coil antennas.

bell-shaped curve A statistical curve (so called from its characteristic shape) that exhibits a *normal distribution* of data. Typically, the curve describes the distribution of errors of measurement around the real value.

bell transformer A (usually inexpensive) stepdown transformer that operates an electric bell or similar alarm or signaling device from the ac power line.

bell wire Insulated 18-gauge (AWG) solid copper wire, so called because of its principal early use in the wiring of electric-bell circuits.

belt generator Also known as a *Van de Graaff generator.* A very-high-voltage electrostatic generator, a principal part of which is a fast-traveling endless belt of dielectric material. At the lower end, charges of one sign are sprayed on the belt at 10 to 100 kV dc and are carried to the inside of a hollow metal sphere at the upper end, where they are removed and spread to the surface of the sphere, which they raise to a potential up to several million volts.

benchmark A test standard to measure product performance.

benchmark routine A routine designed to evaluate computer software and/or hardware, producing a good indication of how well the software or hardware will perform in real-life situations. In particular, tests *instructions per second* and *throughput*, thereby producing an indication of the overall computer power in applications, such as word processing, database, spreadsheet, graphics, animation, and mathematical calculations.

bench test An extensive checkout of a piece of equipment in the test laboratory—either to find an intermittent problem, or to check for reliability.

bend An angular shift in the lengthwise direction of a waveguide.

bending effect **1.** The downward refraction of a radio wave by the ionosphere. **2.** The low-atmosphere turning of a radio wave downward by temperature discontinuity and atmospheric inversions.

Benito A continuous-wave method of measuring the distance of an aircraft from the ground, involving the transmission of an audio-modulated signal from ground and the retransmission back to ground by the aircraft. The phase shift between the two signals is proportional to the distance to the aircraft.

bent antenna An antenna that has its driven element bent, usually near the ends and at right angles, to conserve space.

bent gun A television picture tube neck arrangement having an electron gun that is slanted to direct the undesired ion beam toward a positive electrode, but which allows the electron beam to pass to the screen. This prevents the ion beam from "burning" a permanent spot on the phosopor of the screen.

Be0 Formula for beryllium oxide. Also see BERYLLIA.

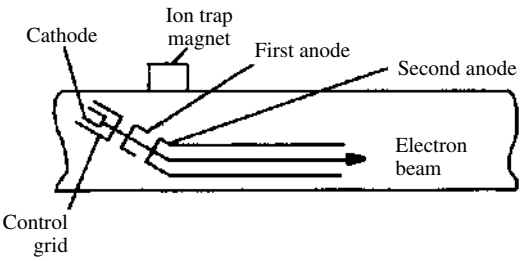

bent gun

5059F-pB_56-92 4/9/01 4:45 PM Page 70

berkelium Symbol, Bk. A radioactive elemental metal produced artificially. Atomic number, 97. Atomic weight, 247.

beryllia Formula, Be0. Beryllium oxide, used in various forms as an insulator and structural element (as in resistor cores).

beryllium Symbol, Be. An elemental metal. Atomic number, 4. Atomic weight, 9.01218. Beryllium is present in various dielectrics and alloys used in electronic components.

Bessel functions Sophisticated mathematical functions for dealing with periodic electronic phenomena in which the waveform often displays decrement. Also called *cylindrical functions.*

beta Symbol, β. The current gain of a common-emitter bipolar transistor stage. It is the ratio of the induced change of collector current to the applied change of base current: $\beta = dIC/dIB$.

beta circuit The output-input feedback circuit in an amplifier.

beta cutoff frequency The frequency at which the current amplification of a bipolar transistor falls to 70.7% of its low-frequency value.

beta particles Minute radioactive subatomic bits identical to the electron or positron, and emitted by some radioactive materials. Also see BETA RAYS.

beta rays Rays emitted by the nuclei of radioactive substances, consisting of a stream of beta particles (i.e., electrons or positrons) that move at velocities up to 299.8 million meters per second. Compare ALPHA PARTICLE and GAMMA RAYS.

beta-to-alpha conversion For a bipolar transistor, the conversion of current amplification expressed as beta (β) to current amplification expressed as alpha (α): $\alpha = \beta/(\beta + 1)$.

betatron A particle accelerator in which injected electrons are given extreme velocity by being propelled in circular paths in a doughnut-shaped glass container. The term comes from the fact that high-speed electrons constitute BETA PARTICLES.

beta videocassette recorder The earliest scheme for videocassette recording, developed by Sony corporation in the 1970s. Compare *VHS videocassette recorder.*

beta zinc silicate phosphor Formula, $(Zn0 + Si0_2)$:Mn. A phosphorescent substance used to coat the screen of a cathode-ray tube. The fluorescence is green-yellow.

BeV Abbreviation of *billion electronvolts.* Also see ELECTRONVOLT, GEV, MEV, and MILLION ELECTRONVOLTS. This abbreviation has been supplanted by the SI (International System of Units) abbreviation GeV, for GIGAELECTRONVOLTS.

bevatron An accelerator (see ACCELERATOR, **1**) similar to the synchrotron, which accelerates particles to levels greater than 10 GeV.

Beverage antenna (Harold H. Beverage.) A nonresonant, directional long-wire antenna, erected a few feet above ground and run in a straight line for one to several wavelengths. It is generally used for reception at low and medium frequencies, the best response is to vertically polarized signals arriving from one or both directions in line with the wire. It can be left unterminated for bidirectional response, or it can be terminated at its far end by a noninductive resistor of about 600 ohms for a unidirectional response.

beyond-the-horizon propagation See FORWARD SCATTER.

bezel A faceplate for an electronic instrument, usually having a fitted rim and cutouts for knobs, switches, jacks, etc.

BFO Abbreviation of BEAT-FREQUENCY OSCILLATOR.

BG Abbreviation of BIRMINGHAM WIRE GAUGE. Also abbreviated BWG.

B-H curve A plot showing the *B* and *H* properties of a magnetic material. Magnetizing force *H* is plotted along the horizontal axis, and flux density *B* is plotted along the vertical axis.

B-H loop See BOX-SHAPED LOOP.

B-H meter Any instrument for displaying or evaluating the hysteresis loop of a magnetic material.

bhp Abbreviation of *brake horsepower.*

Bi Symbol for BISMUTH.

bias **1.** Any parameter of which the value is set to a predetermined level to establish a threshold or operating point. Although it is common to think of bias currents and bias voltages, other parameters (e.g., capacitance, resistance, illumination, magnetic intensity, etc.) can serve as biases. **2.** In a high-fidelity audio system, a circuit in a tape recorder/player that optimizes performance for a particular type of recording tape.

bias current A steady, constant current that presets the operating threshold or operating point of a circuit or device, such as a transistor, diode, or magnetic amplifier. Compare BIAS VOLTAGE.

bias current drift The ratio of a change in input bias current to a change in ambient temperature, generally expressed in nanoamperes per degree Celsius.

bias distortion Distortion caused by operation of a tube or transistor with incorrect bias so that the response of the device is nonlinear.

biased diode A diode having a dc voltage applied in either forward or reverse polarity. Current flows readily through the forward-biased diode; the reverse-biased diode appears as an open circuit. The biased diode is the basis of clippers, limiters, slicers, and similar circuits.

biased off In a circuit or device, the state of cutoff caused by application of a control-electrode bias. Examples include collector-current cutoff (when the dc base bias of a bipolar transistor reaches a critical value), and drain-current cutoff (when the dc gate bias reaches a critical value in a field-effect transistor).

5059F-pB_56-92 4/9/01 4:45 PM Page 71

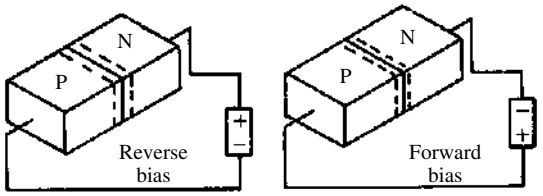

biased diodes

biased search A scheme that a mobile robot can use to find its way to a destination or target, by deliberately searching off to the side and then homing in as the approach progresses. It is so called because the general nature of the initial error (bias) is known, although its exact extent need not be known.

bias oscillator In a magnetic recorder, an oscillator operated at a frequency in the 40-kHz to 100-kHz range to erase prerecorded material and bias the system magnetically for linear recording.

bias resistor A usually fixed resistor, such as the source resistor in a field-effect-transistor (FET) circuit or the emitter resistor in a bipolar-transistor circuit, across which a desired bias voltage is developed by current flowing through the resistor.

bias set A control, such as a potentiometer or variable autotransformer, that facilitates manual adjustment of the dc bias of a circuit.

bias stabilization **1.** The maintenance of a constant bias voltage, despite variations in load impedance or line voltage. It is usually accomplished by means of automatic voltage regulation. **2.** The stabilization of transistor dc bias voltage by means of resistance networks or through the use of barretters, diodes, or thermistors.

bias supply **1.** Batteries that provide bias voltage or current for bipolar or field-effect transistors. **2.** A line-operated unit for supplying dc bias and consisting of a transformer, rectifier, and high-grade filter.

bias voltage A steady voltage that presets the operating threshold or operating point of a circuit or device, such as a transistor. Compare BIAS CURRENT.

bias windings The dc control windings of a saturable reactor or magnetic amplifier.

biconical antenna A form of broadband antenna, consisting of two conical sections joined at the apexes. The cones are at least ¼ wavelength in diagonal height. The vertex angles of the cones can vary, although the apex angle is usually the same in each cone. The vertex angle affects the feedpoint impedance. Such an antenna radiates, and responds optimally to, signals with polarization parallel to the axis of the cones.

biconical horn antenna A double-horn microwave antenna that radiates along relatively sharp front and back beams.

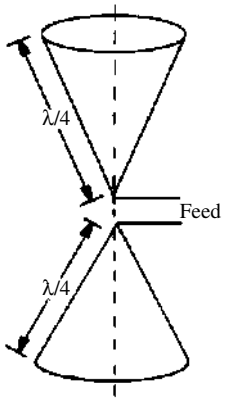

biconical antenna

bidecal base The 20-pin base of a cathode-ray tube. Also see DIHEPTAL, DUODECAL, and MAGNAL.

bidirectional Radiating or receiving (usually equally) from opposite directions (e.g., front-and-back radiation from an antenna or loudspeaker, or front-and-back pickup with an antenna or microphone).

bidirectional antenna An antenna with a directional pattern that consists of maximum lobes 180 degrees apart.

bidirectional bus In computers, a data path over which both input and output signals are routed.

bidirectional bus driver In a microcomputer, a signal-driving device that permits direct connection of a buffer-to-buffer arrangement on one end (the interface to I/O, memories, etc.) and data inputs and outputs on the other. This device permits bidirectional signals to pass and provides drive capability in both directions.

bidirectional counter A counter that can count consecutively up from a given number or down from that number. Also called UP-DOWN COUNTER.

bidirectional current A current that flows in both directions. Utility alternating current (ac) is a common example.

bidirectional loudspeaker A loudspeaker that delivers sound waves to the front and rear.

bidirectional microphone A microphone that picks up sound waves equally well from the front and rear.

bidirectional transistor A symmetrical transistor (i.e., one in which the two main current-carrying electrodes can be interchanged without influencing device performance). Some field-effect transistors (FETs) are of this type; the drain and the source can be interchanged.

bifilar electrometer An electrometer in which the sensitive element consists of two long platinized-quartz fibers. When an electric potential is ap-

5059F-pB_56-92 4/9/01 4:45 PM Page 72

plied, the fibers separate by a distance proportional to the voltage.

bifilar resistor A wirewound resistor with two oppositely wound filaments. The nature of the winding tends to cancel the inductance, making the device useful at a much higher frequency than an ordinary wirewound resistor.

bifilar transformer A transformer in which unity coupling is approached by interwinding the primary and secondary coils (i.e., the primary and secondary turns are wound side by side and in the same direction).

bifilar winding **1.** A method of winding a coil (such as a resistor coil) in the shape of a coiled hairpin so that the magnetic field is self-canceling and the inductance is minimized. **2.** A method of winding transformers to minimize leakage reactance.

bifilar winding

bifurcated contact A forked contact whose parts act as two contacts in parallel for increased reliability.

bilateral amplifier An amplifier that transmits or receives in either direction equally well (i.e., the input and output can be exchanged at will).

bilateral antenna A bidirectional antenna, such as a loop antenna or a half-wave dipole.

bilateral element A circuit element or component (as a capacitor, resistor, or inductor) that transmits energy equally well in either direction. Compare UNILATERAL ELEMENTS.

bilateral network A network, usually passive and either balanced or unbalanced, that has BILATERAL SYMMETRY. Thus, the input and output terminals can be exchanged without affecting the performance of the network in any way.

bilateral symmetry **1.** Exhibiting symmetry, with respect to a vertical line or plane. **2.** For a network, having the property that if the input and output are reversed, the circuit behavior remains precisely the same. See BILATERAL NETWORK. **3.** For an amplitude-versus-frequency response curve, having the property that the right-hand and left-hand halves are mirror images of each other.

billboard antenna A phased group of dipole antennas that lie in one plane. A reflector might be used behind the entire array.

bilobe pattern An antenna radiation pattern consisting of two major lobes in a given plane, usually the horizontal plane. Often the lobes exist in opposite directions relative to each other, as in a half-wave dipole. But they can be at varying angles, as in a long-wire antenna.

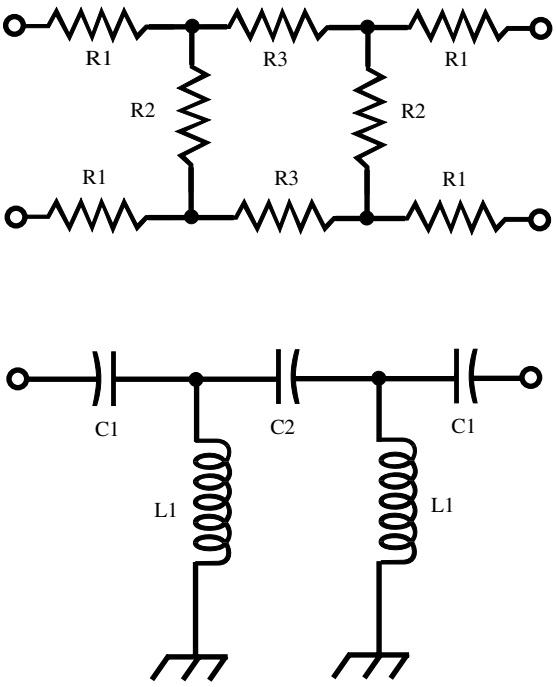

bilateral network

bimetal A union of two dissimilar metals—especially those having a different temperature coefficient of expansion. The two are usually welded together over their entire surface.

bimetallic element A strip or disk of bimetal. When the element is heated, it bends in the direction of the metal that has the lower temperature coefficient of expansion; when cooled, it unbends. Usually, an electrical contact is made at one extreme or the other so that the element can serve as a thermostat.

bimetallic switch A temperature-sensitive switch based on a bimetallic element.

bimetallic thermometer A thermometer based on a bimetallic element that is mechanically coupled (as through a lever and gear system) to a pointer that moves over a temperature scale.

bimetallic thermostat A thermostat in which a bimetallic element closes or opens a pair of switch contacts.

bimorphous cell A piezoelectric transducer that consists of two crystal plates, such as Rochelle salt, bound intimately face to face. In a crystal microphone, vibration of the transducer results in a voltage output; in a crystal headphone, an ac signal voltage impressed on the transducer causes vibratory mechanical motion.

5059F-pB_56-92 4/9/01 4:45 PM Page 73

BiMOS A combination of bipolar and MOSFET transistors in an integrated circuit. Thus, a typical BiMOS device can have MOSFET input for high impedance and bipolar output for low impedance.

binant electrometer An electrometer in which a thin platinum vane ("the needle") is suspended within two halves of a metal pillbox-shaped container. The halves or binants are biased with a dc voltage of 1 to 12 V, and the unknown voltage is applied to the vane. It is also called DUANT ELECTROMETER and HOFFMAN ELECTROMETER.

binary **1.** Pertaining to the base-2 number system. Thus, binary arithmetic uses two digits: 0 and 1. **2.** Pertaining to two-element chemical compounds.

binary arithmetic Mathematical operations performed using only the digits 0 and 1.

binary cell In a computer memory, an element that can display either of two stable states.

binary chain A cascade of binary elements, such as flip-flops, each unit of which affects the stable state of the succeeding unit in sequence.

binary channel Any channel whose use is limited to two symbols.

binary code A system of numbers representing quantities by combinations of 1 and 0; a binary-number system.

binary-coded decimal notation In digital computer operations, a system of notation in which each digit of a decimal number is represented by its binary equivalent. Thus, the decimal number 327 in BCD notation becomes 0011 0010 0111. (By contrast, in pure binary notation, 327 is 101000111.)

binary-coded octal notation A method of numbering in which each base-8 digit is represented by a binary number from 000 to 111.

binary-controlled gate circuit A gate circuit controlled by a binary stage. An example is a gating transistor that receives its on/off pulses from a flip-flop.

binary counter A counter circuit consisting of a cascade of bistable stages. Each stage is a scale-of-two counter because its output is on for every second input pulse. At any instant, the total binary count in a multistage counter thus is shown by the on and off states of the various stages in sequence.

binary decoder A device or stage that accepts binary signals on its input lines, and provides a usually exclusive output (representing a decimal digit, for example).

binary digit See BIT.

binary number system The base-two system of notation. This system uses only two symbols, 0 and 1, and accordingly is easily applied to two-position switches, relays, and flip-flops.

binary preset switch In a binary counter or binary control circuit, a selector switch that allows the circuit to be preset to deliver an output pulse only after a predetermined number of input pulses.

binary relay See BISTABLE RELAY.

binary scaler In its simplest form, a single two-stage device, such as a flip-flop, which functions as a divide-by-two counter, because one output pulse results from every two input pulses. Higher-order scaling is obtained by cascading stages.

binary search A system of search entailing the successive division of a set of items into two parts and the rejection of one of the two until all items of the sought-for kind are isolated.

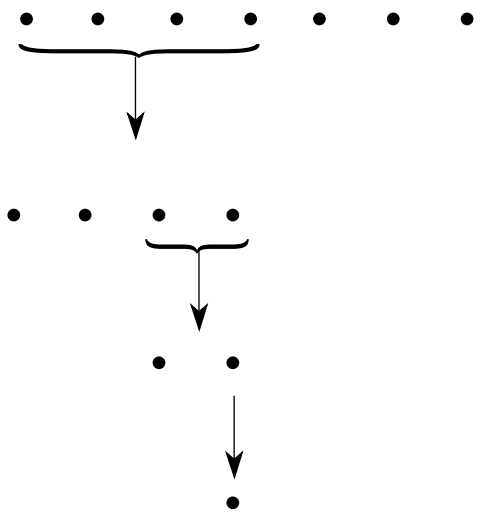

binary search

binary signal Any signal that can attain either of two states. Such a signal is always a digital signal.

binary-to-decimal conversion **1.** The automatic conversion of a number represented by a series of binary pulses into the corresponding decimal number, which then is displayed by a readout device. **2.** The arithmetic operation of converting a binary number into a decimal number; this can be done by noting the powers of 2 represented by the various binary digits in a number, and then adding the decimal values of these powers.

binary word A binary numeral that has a particular meaning, agreed upon by convention. For example, the letters A through Z can be represented by binary numbers 00001 through 11010; a word can be represented by several blocks of five digits.

binaural Literally, two-eared. In sound recording and reproduction, the transcription of a broad sound source using two microphones spaced at approximately the distance between the ears on a human head, and played back using headphones

5059F-pB_56-92 4/9/01 4:45 PM Page 74

to re-create the stereo effect. The technique evolved into multichannel stereophonic reproduction.

binaural machine hearing Also called *stereo machine hearing.* The ability of a machine, such as a robot, to sense the direction and distance to a source of sound, using two acoustic transducers and a computer to process their output signals. The machine determines the location of the sound source by comparing the relative amplitude and phase of the signals from the two transducers. It functions according to the same principle as human hearing, in which a person can determine the general direction and distance to a sound source by subconsciously comparing the relative amplitude and phase of the sounds arriving at the left and right ears.

binaural sound The equivalent of a listener hearing a concert through a pair of earholes; it takes earphones to reproduce the signal. If speakers are substituted for the earphones, the listener hears monophonically, as if standing back several feet from the earholes.

binder A material (such as lacquer) that acts as a holder and cohesive medium for the particles of another material. It is used in carbon resistors, ceramic dielectric bodies, powder cores, and resistive and metallic paints.

binding energy A property of the nucleus of an atom. The binding energy of a nucleus is equal to the difference between the nuclear weight and the sum of the weights of the lighter particles making up the nucleus. The nucleus is stable when the binding energy is high.

binding force Any one of the electrostatic forces that bind crystals together.

binding post A screw-type terminal of various styles, often having a hole into which a wire or tip can be inserted and gripped. It is used for temporary indoor connections only.

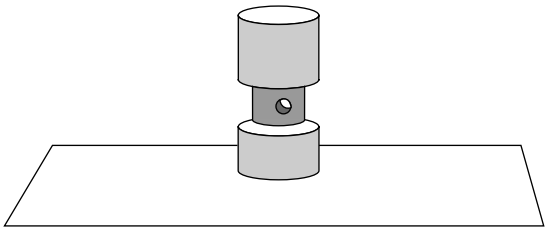

binding post

binistor A semiconductor switching device that exhibits two stable states and also negative resistance.

binocular machine vision Also called *stereoscopic machine vision.* The ability of a machine vision system to provide depth and perspective data. Uses two optical sensors spaced a fixed distance apart. The left sensor sees a slightly different image than the right sensor. These two images are combined and processed by a computer, allowing the machine (such as a mobile robot) to determine the distances to various objects in its environment. Functions on the same principle as stereoscopic human vision.

bin picking In robotics, the selection of a particular object from a container (bin) in which there are many objects. Can be done using object recognition, bar coding, or passive transponders. It requires a sensor, operating in conjunction with a computer that processes the sensed data and controls the movements of the robot.

binomial An algebraic expression containing two terms joined by a plus or minus sign. Examples: $a^2 + b^2$, $3x^3 - 6x$.

binomial theorem The theorem, proven by Isaac Newton, permits a binomial to be raised to any desired power without performing the multiplications. In electronics, *power series* are convenient for expressing such expressions.

biochemical cell A fuel-cell energy source in which electricity is generated chemically through the oxidation of biological substances. Also called *biochemical fuel cell.*

biochip **1.** A natural, living organism with a physical structure that in some way resembles that of an electronic *integrated circuit (IC).* **2.** A theoretical possibility, according to some scientists, but not yet a practical reality: An IC manufactured by a laboratory process that mimics the way in which nature builds living organisms. A form of *artificial life,* harnessed for electronic and/or computing applications.

bioelectricity **1.** Electric currents in living tissues, generated by the organism and not applied by external means. **2.** The science or study of such currents.

bioelectrogenesis The study and application of electricity generated by living animals, including humans, in the powering and control of electronic devices.

bioelectronics Electronics in relation to the life sciences—especially the electronic instrumentation of biological experiments.

bioengineering **1.** The engineering of equipment, such as electron microscopes, electroencephalographs, centrifuges, irradiators, etc., for study and experimentation in the life sciences. **2.** The engineering of equipment, such as pacemakers, hearing aids, X-ray apparatus, shock-therapy units, etc., for aid or support-of-life processes.

biofeedback A technique in which changes in skin temperature and resistance are detected and displayed by an electronic device.

biofeedback monitor A system that provides an indication of skin temperature and resistance to a user. Because skin temperature and resistance are affected by emotions, such as fear, nervous-

5059F-pB_56-92 4/9/01 4:45 PM Page 75

ness, anger, etc., these monitors might be of value to people who wish to gain improved control of their emotions, and thus perhaps minimize the physiological effects of stress.

biological robot Believed by some researchers to be possible, but not yet a practical reality: A living organism created by biological cloning, whose brain has been programmed exactly as a computer is programmed.

biological shield An absorbent shield that blocks or attenuates ionizing radiation to protect personnel working near radioactive materials.

bioluminescence **1.** The emission of light by a living organism. **2.** The light itself so produced by living organisms.

biomechanism An electromechanical device that simulates the workings of some part of a living being's body. Examples are electromechanical hands, arms, and legs. Such a device is often difficult to distinguish from its biological counterpart when obscured by clothing.

biomechatronics A contraction of the words *bio*logy, *mecha*nics and elec*tronics*. Research, development and manufacturing that encompasses aspects of all three fields. This is especially important in robotics.

biometrics Mathematics, and in particular, statistics and probability, applied to biology.

biometric security system An advanced intrusion-prevention system that measures biological characteristics of the people who are authorized to enter a property. Such a machine can employ vision systems, object recognition, and/or pattern recognition to check a person's face. The machine might use speech recognition to identify people by the waveforms of their voices. It might record a hand print, a fingerprint, or an iris print, or a combination of all these things. A powerful computer analyzes the data obtained by the sensors and determines whether the person is authorized to enter the premises.

bionics The study, design, and application of microelectronic systems that simulate the functions of living organisms.

biotelemetry The use of telemetry to collect data from living organisms or to direct their movement.

biotelescanner An instrument that monitors body functions via radio, from a great distance.

Biot/Savart law A principle of electromagnetism that expresses the intensity of magnetic field H in the vicinity of a long, straight wire carrying a steady current I. The basic formula is $H = 2I/r$, where H is in oersteds, I is in amperes, and r is the distance in centimeters from the wire.

bip Abbreviation of *binary image processor.*

biphase half-wave rectifier An alternative term for FULL-WAVE RECTIFIER; also, each leg of a two-diode full-wave rectifier.

BIPM Abbreviation of *International Bureau of Weights and Measures.*

bipolar The condition of possessing two pole sets. In a conventional (non-FET) transistor, one pole set exists between the base and collector, and another pole set exists between the base and emitter.

bipolar driving unit A magnetic headphone or loudspeaker in which both poles (north and south) of a magnet actuate a diaphragm or lever.

bipolar operation See AUTOMATIC POLARITY.

bipolar transistor A two-junction transistor whose construction takes the form of a pnp or an npn "sandwich." Such devices are current-operated, compared with field-effect transistors, which are voltage-operated. The bipolar transistor (of which the familiar npn and pnp types are examples) uses both electron and hole conduction.

biquinary code A variety of binary-coded-decimal notation in which seven bits are used to represent each decimal digit. A number is written in two groups of bits: a two-bit group followed by a five-bit group. The positional values are 5 and 0 for the two-bit group, and 4, 3, 2, 1, and 0 for the five-bit group.

biquinary decade A decade counter that consists of a binary stage, followed by a quinary stage.

bird **1.** Slang for orbiting SATELLITE. **2.** Slang for *guided missile.*

birdie **1.** A spurious beat note in a superheterodyne receiver. So called because of the characteristic chirping sound it makes as the operator tunes by the frequency on which it occurs. **2.** A parasitic oscillation in a radio transmitter, also called a *spurious emission* or *spur.*

Birmingham wire gauge Abbreviation, BWG. Also called *Stubs gauge.* A method of designating the various sizes of solid wire. BWG diameters are somewhat larger than corresponding AMERICAN WIRE GAUGE diameters for a given wire-size designator.

Birmingham Wire Gauge (BWG) Diameters

BWG	Millimeters	Inches
1	7.62	0.300
2	7.21	0.284
3	6.58	0.259
4	6.05	0.238
5	5.59	0.220
6	5.16	0.203
7	4.57	0.180
8	4.19	0.165
9	3.76	0.148
10	3.40	0.134
11	3.05	0.120
12	2.77	0.109
13	2.41	0.095
14	2.11	0.083
15	1.83	0.072
16	1.65	0.064
17	1.47	0.058
18	1.25	0.049
19	1.07	0.042
20	0.889	0.035

5059F-pB_56-92 4/9/01 4:45 PM Page 76

bismuth Symbol, Bi. A metallic element. Atomic number, 83. Atomic weight, 209.

bismuth flux meter A flux meter in which the sensor contains a length of bismuth wire, which acts as a magnetoresistor.

bismuth thermocouple A thermocouple that uses the junction between bismuth and antimony wires. Used in thermocouple-type meters.

bistable Having two stable states.

bistable device Any device, such as a flip-flop, the operation of which exhibits two stable states and which can be switched at will from one state to the other.

bistable multivibrator A multivibrator, the operation of which exhibits two stable states. More commonly known as a FLIP-FLOP. These circuits are abundant in digital electronic equipment. Compare ASTABLE MULTIVIBRATOR and MONOSTABLE MULTIVIBRATOR.

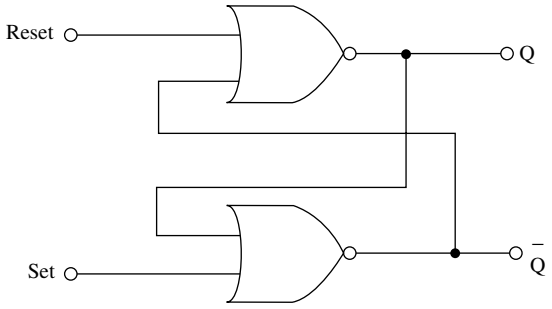

bistable multivibrator

bistable relay A relay that has two stable states: open and closed. Successive actuating pulses open and close the relay, two consecutive pulses being required to return the relay to a given state. Also called *binary relay, relay flip-flop,* and *electromechanical flip-flop.*

bistatic radar A radar set in which the transmitting and receiving antennas are separate.

bistate Having two states. Example: the performance of a FLIP-FLOP.

bit An acronym formed from the words *binary digit.* The smallest or elementary unit of data in digital electronics. Represented either by logic 0 (low) or logic 1 (high). These states can be represented by any dichotomy, such as off/on, false/true, minus/plus, dark/bright, red/green, etc.

BIT Abbreviation of *built-in test.*

bit density The number of digital bits per unit area or volume, as the number of bits per square centimeter of magnetic tape.

BITE Abbreviation of built-in test equipment.

bit rate The speed in BITS PER SECOND (bps) at which digital data bits are transmitted or handled.

bit-slice processor A microprocessor whose word or byte capacity is achieved through the use of interrelated smaller capacity processors (e.g., a 16-bit unit derived from eight 2-bit "slices").

bits per second Abbreviation, bps. An expression of digital data speed. Commonly used in computer communications. This unit is often confused with, and improperly called, the *baud.* There is generally a difference between the speed of a signal in baud, and the speed of the same signal in bps. Compare BAUD.

bitter pattern A pattern produced in a suspension of ferromagnetic powder in the presence of an imperfection in a magnet. The pattern appears as an irregularity that is easy to see.

Bjerknes' equation An expression for the total (primary plus secondary) decrement of a tuned circuit, based on measurements of the tank current at the resonant frequency and at a frequency near resonance.

BK **1.** Radiotelegraph signal for BREAK. **2.** Abbreviation of BREAK-IN.

Bk Symbol for BERKELIUM.

black-and-white Also called *monochrome* and *gray-scale.* Any system of image reproduction, transmission, or reception in which the image is composed of opaque elements (black) and white or bright areas, as in noncolor television reception.

black area An area in which there is only an encrypted signal.

blackboard system A method via which computers can recognize, and to some extent determine the meaning of, spoken words and visual images. Incorporates machine vision and/or machine hearing in conjunction with artificial intelligence (AI). Incoming voices and/or images are digitized and entered into a large-capacity random-access memory (RAM). The data is evaluated by sophisticated software to determine the most logical or probable interpretations of the sounds and images.

blackbody An ideal surface or object, that completely absorbs energy of any wavelength that strikes it. Such an object is a theoretically perfect radiator of energy at all wavelengths.

blackbody radiation Electromagnetic radiation from a heated ideal BLACKBODY. This radiation is conceived as covering the entire ELECTROMAGNETIC FREQUENCY SPECTRUM. It can be expressed graphically as a characteristic curve with a peak at a wavelength that depends on the absolute temperature of the object. As the absolute temperature increases, the peak occurs at progressively shorter wavelengths (higher frequencies). This enables radio astronomers to get a reasonably good idea of the temperatures of distant celestial objects, such as planets.

black box **1.** Any "box" or "block" that can be included in an analysis or synthesis based upon the BLACK-BOX CONCEPT. **2.** Any functional unit (such as a module) whose operating characteristics are known, and that can be inserted into

5059F-pB_56-92 4/9/01 4:45 PM Page 77

a system in development or maintenance operations. **3.** Any subcircuit or stage that can be specified in total as required in a system, in terms of its known or prescribed performance, but whose internal structure need not be known.

black-box concept A technique for development of equivalent circuits and of considering their operation. The "box" has a pair of input terminals and a pair of output terminals; one input terminal is often common to one output terminal. The contents of the box need not be known, but from the input and output current and voltage relationships, its nature can be determined. Moreover, from the available input signal and desired output signal, the internal circuit of the box can be specified. Integrated circuits (ICs) are often treated as black boxes by engineers designing complex electronic equipment.

black compression Attenuation of the level of dark areas in a television picture.

blacker than black The video-signal amplitude region above the level that just darkens the screen. Signal information (such as control pulses) in this region are therefore not seen.

black light **1.** Ultraviolet radiation—especially when used to cause visible fluorescence in certain materials. **2.** A lamp that produces a principal portion of its radiation in the ultraviolet region, causing visible fluorescence of certain substances. Such lamps are used in some scientific experiments, and also for creating special effects at presentations or parties. It is hazardous to look directly at the output of such a lamp with unprotected eyes.

blackout **1.** A complete interruption of ac utility power to numerous customers at the same time. **2.** A complete cessation of ionospheric radio-wave propagation, such as might be caused by a solar flare. **3.** Complete blanking of the screen of an oscilloscope or picture tube.

black reference In a television signal, the blanking level of pulses, beyond which the sync pulse is in the *blacker-than-black* region.

black reference level In a television signal, the voltage threshold of the BLACK REFERENCE (i.e., its level above zero volts).

black transmission A system of picture or facsimile transmission in which the maximum copy darkness corresponds to the greatest amplitude (in an amplitude-modulated transmitter) or the lowest instantaneous frequency (in a frequency-modulated transmitter). Compare WHITE TRANSMISSION.

blank **1.** A piezoelectric plate cut from a quartz crystal, but not yet finished to operate at a desired frequency. **2.** To obscure or interrupt a signal or electron beam (usually momentarily), as in z-axis blanking in an oscilloscope. **3.** A silicon wafer cut from a large slab, containing dopants only. **4.** A magnetic diskette or tape on which nothing is recorded. **5.** An optical diskette on which nothing is recorded. **6.** A location (such as a symbol or space) that is used to verify proper data character grouping and values.

blanketing A form of radio interference accompanied by severe degradation of reception, virtually unaffected by tuning, over a wide range of frequencies. An example is ac line noise caused by an arcing power transformer or electrical appliance in the vicinity of a receiving antenna. It tends to occur most often at low, medium, and high frequencies.

blanking Obscuring or momentary elimination of a signal (see BLANK, **2**).

blanking interval The short period during which the electron beam of a cathode-ray tube is cut off so that the beam can return to its start position without creating a trace on the screen.

blanking level The discrete, predetermined level (usually a threshold voltage) at which BLANKING occurs.

blanking pedestal In the horizontal pulse of a television signal, the lower portion between zero volts and the blanking level.

blanking pulse A pulse that produces momentary blanking (see BLANK, **2**).

blanking time The time interval during which the electron beam of a cathode-ray tube is interrupted by a blanking signal.

blank tape **1.** Magnetic tape that has never been subjected to the recording process and that is substantially free from noise. **2.** Magnetic tape from which all preexisting information has been erased.

blasting **1.** Severe overloading of a sound system, usually caused by setting the volume control at or near maximum and then applying a significant input signal to the amplifier. Accompanied by distortion, in its worst form, it can cause damage to speakers and/or headsets. **2.** In a communications receiver, the result of a strong signal coming in unexpectedly when the automatic gain control (AGC) has been switched off, and the audio-frequency (AF) and radio-frequency (RF) gain controls are set high for reception of weak signals.

bleeder A resistor or group of resistors, used permanently to drain current from charged capacitors. It establishes the predetermined initial load level for a power supply or signal source, and it serves as a safety device in high-voltage power supplies.

bleeder current The current normally flowing through a bleeder.

bleeder divider A network of resistors, series-strung across the output of a power supply or its regulator. As a load resistor, the bleeder improves regulation and protects against no-load voltage surges. The resistor junctions allow various voltages to be drawn from the supply.

bleeder power Power dissipated as heat in a bleeder.

bleeder resistor See BLEEDER.

5059F-pB_56-92 4/9/01 4:45 PM Page 78

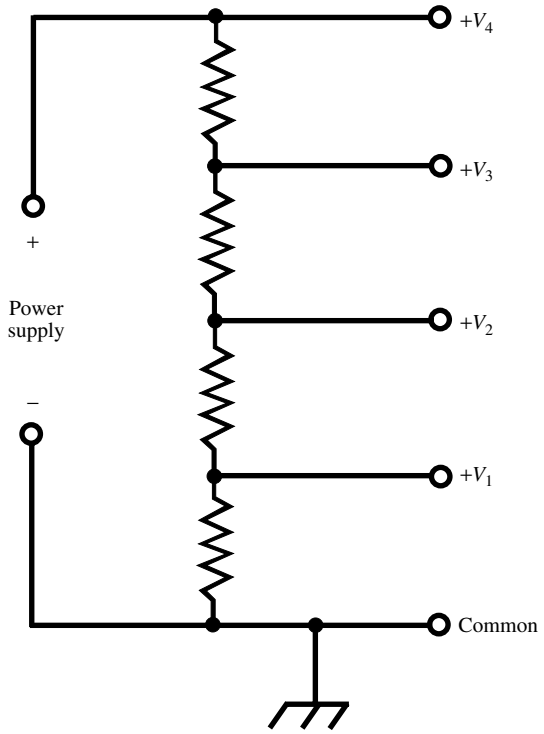

bleeder divider

bleeder temperature The operating temperature in a bleeder. It is generally high because of power dissipation in the form of heat.

bleeding whites A flowing of the white areas of a television picture into the black areas; an overload condition.

blemish See BURN.

blind flight The flying of aircraft entirely by means of instruments and electronic communications.

blind landing Landing of an aircraft entirely by means of instruments and electronic commnications.

blind zone **1.** In radar operations, an area that gives no echoes. **2.** Skip zone (see ZONE OF SILENCE).

blip **1.** The pulse-like figure on a radar scan, indicating the transmission or reflection (see A-SCAN and J-SCAN). Also called PIP. **2.** In visual alignment of a tuned circuit using a sweep generator and marker generator, the pulse or dot produced on the response curve by the marker signal. **3.** A short, momentary signal pulse, such as a single Morse dot.

BLIP Abbreviation for *background-limited infrared photoconductor.*

blip-scan ratio The number of radar scans necessary to show a visible blip, or echo, on a radar screen.

Bloch functions Solutions of the *Schrodinger wave equation* for a single electron surrounded by an electric field. The field varies periodically with distance from the source.

Bloch wall The transition layer between adjacent ferromagnetic domains (see DOMAIN).

block **1.** A group of data words or digits. **2.** A group of memory storage spaces. **3.** A circuit that operates as an identifiable unit. **4.** The symbol for a circuit, stage, unit, or device in a BLOCK DIAGRAM.

block diagram A simplified diagram of an electronic system, in which circuits, stages, units, or devices are shown as two-dimensional boxes with the internal wiring and detail circuitry omitted. This makes it possible to clearly show the interconnection among circuits, stages, units or devices. It also provides a concise rendition of the overall functional concept of the system.

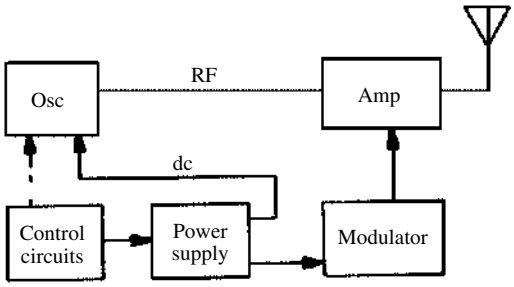

block diagram (of a radio transmitter)

blocked impedance The input impedance of a transducer, whose output load is a theoretically infinite impedance.

blockette In a computer, the subdivision of a character block that is handled as a unit during data transfer.

blocking action Obstruction of circuit action, usually abrupt, through internal action or by the application of an external signal. Thus, the operation of an amplifier can be blocked (output reduced to zero) by an input signal or by excessive feedback, either of which overloads the input.

blocking capacitor A capacitor inserted into a circuit to prevent the passage of direct current while easily passing alternating current.

blocking choke Any inductor, such as a choke coil, that is used to prevent the flow of an alternating current while allowing direct current to pass with little resistance.

blocking interference Radio interference from signals strong enough to reduce the receiver output through blocking action.

5059F-pB_56-92 4/9/01 4:45 PM Page 79

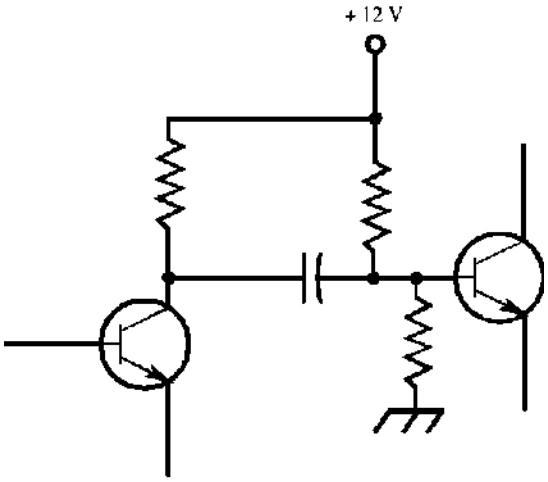

blocking capacitor

blocking oscillator An oscillator that turns itself off after one or more cycles. It does this as a result of an accumulation of negative charge on its input electrode (base of a bipolar transistor or gate of a field-effect transistor). The action is repetitive. In the self-pulsing type of blocking oscillator, a series of pulses consisting of trains of sine waves with intervening spaces is generated. In the single-swing type of blocking oscillator, the output consists of a series of single cycles with long intervals between them.

blocking oscillator synchronization **1.** In the BLOCKING OSCILLATOR used in the vertical deflection circuit of a television receiver, the oscillator is synchronized with vertical sync pulses arriving in the video signal. **2.** Synchronization of the repetition rate of any blocking oscillator with a suitable external control signal.

blocking system In a telephone system, a method of dealing with the condition of having more subscribers than connection paths. Allocation is made on a demand basis. If all channels are in use, it is impossible to make new calls. This prevents excessive degradation of the quality of existing connections.

block length The number of characters, bits, or words that compose a defined unit word or character group.

block transfer The conveyance of a word or character grouping in a computer register to another register or a peripheral device.

blooming On a cathode-ray-tube (CRT) screen, an enlargement of the electron-beam spot, caused by poor focusing. This results in poor image resolution.

blooper **1.** A radio receiver that is in oscillation, and is transmitting a signal that causes interference. **2.** A parasitic oscillation in a radio transmitter. **3.** In broadcasting, a statement in which a radio or television announcer makes an embarrassing error or breach of etiquette.

blow The opening of a fuse or circuit breaker as a result of excessive current.

blower A fan used to remove heat from electronic circuits. These are often used in tube-type radio-frequency (RF) power amplifiers, where much heat is generated, and in computers to cool the microprocessor and surrounding components.

blowout **1.** An alternate term for BURNOUT. **2.** The forceful opening of a circuit breaker. **3.** The extinguishing of an arc.

blowout coil An electromagnet that provides a field to extinguish an arc.

blowout magnet A permanent magnet that provides a field to extinguish an arc.

blst Abbreviation of *ballast.*

blue-beam magnet In a color television picture-tube assembly using three electron guns, a small permanent magnet to adjust the static convergence of the beam for blue phosphor dots.

blue box An accessory device (sometimes unlawfully used) that generates tones that switch a telephone circuit in the placing of calls.

blue glow **1.** In a neon lamp, a bluish light that results from high-voltage arcing. **2.** The normal color of the gas discharge in an argon glow lamp. **3.** The bluish glow between anode and cathode of a gassy vacuum tube. **4.** The normal color of the discharge that fills a mercury-vapor tube.

blue gun The electron in a three-gun color picture tube, the beam from which strikes the blue phosphor dots.

blueprint **1.** A type of contact-print reproduction in which a sheet of sensitized paper is exposed to an image on a translucent or transparent film, under strong light, and is then developed and fixed. Although this process is still used to reproduce electronic illustrations and typescripts, it has been superseded largely by other (dry) processes. **2.** Loosely, any plan or design for the development of a system.

blue restorer In a three-gun color television circuit, the dc restorer in the blue channel.

blue ribbon program A computer program that has been hand-prepared and debugged completely before its first computer run.

blue video voltage The signal voltage presented to the grid of the blue gun of a three-gun color picture tube.

blurring **1.** BLOOMING. **2.** A defocusing of a television picture or oscilloscope trace. **3.** An obscuring of a signal by echoes or trailing (e.g., the slow decrement of a Morse code signal element).

B-minus Also called *B-negative.* The negative terminal of a B-power supply.

BNC Abbreviation of *bayonet Neill-Concelman.* A type of coaxial connector that can be quickly con-

5059F-pB_56-92 4/9/01 4:45 PM Page 80

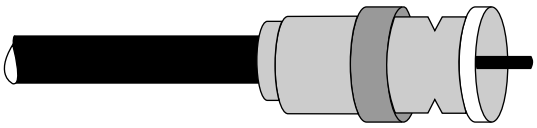

BNC

nected and disconnected. It is commonly used with test equipment.

B-negative Alternative expression for B-MINUS.

BNL Abbreviation of *Brookhaven National Laboratory.*

BO Abbreviation of *beat oscillator.* Also abbreviated BFO.

board **1.** A panel containing patch jacks. **2.** A printed circuit.

boat A type of crucible in which a semiconductor material is melted and sometimes processed. The material of which the boat is made (e.g., graphite) does not react with or contaminate the semiconductor material.

bobbin **1.** A usually nonmetallic spool on which a coil is wound. **2.** The form onto which the voice coil of a loudspeaker is wound.

Bode plot A pair of curves plotted to the same frequency axis, one showing the gain of a network or amplifier and the other showing its phase shift. Phase and amplitude of active and passive networks can be exhibited. Also called *Bode curve* and *Bode diagram.*

body-antenna effect The tendency of the human body to act as a receiving antenna when a finger is touched to the antenna input terminal of a receiver or when a hand (or the whole body) is brought close enough to the circuit to provide capacitive coupling.

body capacitance Capacitance between the body of the operator (as one plate of an equivalent capacitor) and a piece of electronic equipment (as the other plate). This phantom capacitance is often the cause of detuning and of the injection of interfering signals and noise because the body acts as a pickup antenna.

body electrode **1.** An electrode attached to the human body (or to the body of a laboratory animal) to conduct body-generated currents to an instrument, as in cardiography, electroencephalography, and myography. **2.** An electrode attached to the human body (or to the body of a laboratory animal) to conduct currents into the body, as in shock therapy and skin-resistance measurement.

body leakage Leakage of current through the bulk or body of a dielectric material, as opposed to SURFACE LEAKAGE.

body temperature In a thermistor, a rating that represents the temperature measured on the surface of the device. It is any combination of ambient temperature, power dissipation, and operation of the internal heater element (if the thermistor has one).

bof Abbreviation of *barium oxide ferrite.*

boffle A loudspeaker enclosure consisting of stretched screens that are sound absorbing and elastic.

bogie Also called *bogey.* **1.** The exact value of a specified characteristic. Thus, if resistance is given as 1 kΩ ±0.5%, the bogie value is 1 kΩ. **2.** The average value (i.e., the ARITHMETIC MEAN). **3.** A false or unidentified echo on a radar screen.

Bohr atom The concept of the nature of the atom, proposed by Niels Bohr in 1913 partly to explain why the electrons in the Rutherford atom do not fly off into space or fall into the nucleus. The Bohr theory places the electrons in permissible orbits where they cannot radiate energy (see BOHR RADIUS). They can radiate or absorb energy, however, if they go to a lower orbit or to a higher orbit, respectively. Compare RUTHERFORD ATOM.

bohrium Symbol, Bh. Also called *unnilseptium* (Uns). Atomic number, 107. The most common isotope has atomic weight 262. Classified as a transition metal. It is human-made and is not known to occur in nature.

Bohr radius Symbol, a_0. A physical constant whose value is approximately 5.291772×10^{-11} meter.

boiling point Abbreviation, bp. The temperature at which a liquid vaporizes. The boiling point of water in air at a pressure of one atmosphere is 100°C or 212°F.

bolometer Any device that is essentially a small, nonrectifying, temperature-sensitive resistor that can be used for heat sensing, radio-frequency power measurement, curve changing, demodulation, circuit protection, etc. Included in this category are the BARRETTER, the THERMISTOR, and the wire-type FUSE.

bolometer bridge A dc bridge in which a bolometer is one of the four arms. The bridge is balanced first with the bolometer cold. The bolometer then is excited with a radio-frequency (RF) current, whereupon the resultant heating changes the bolometer resistance. The bridge is rebalanced for the new resistance. The RF power driving the bolometer is determined according to a predetermined function of bridge settings versus RF input power.

Boltzmann constant Symbol, *k.* A figure that enters into the calculation of thermionic emission and of thermal noise factor. It represents the temperature equivalent of work function, in electron volts per Kelvin (eV/K) or joules per Kelvin (J/K). The values are approximately:

$$k = 8.617 \times 10^{-5}\ \text{eV/K} = 1.38 \times 10^{-23}\ \text{J/K}$$

Boltzmann's principle A description of the statistical distribution of large numbers of tiny particles under the influence of a force, such as an electric or magnetic field. When the system is in

5059F-pB_56-92 4/9/01 4:45 PM Page 81

statistical equilibrium, the number of particles in any portion of the field is given by:

$$N_E = N_{0e}^{-E/kT}$$

where E is the potential energy of a particle in the observed area, N_0 is the number of particles per unit volume in a part of the field where E is zero, k is the BOLTZMANN CONSTANT, T is the absolute temperature of the system of particles, and e is approximately equal to 2.718.

bombardment The usually forceful striking of a target with rays or a stream of particles.

bond **1.** An area in which two or more items are securely and intimately joined. **2.** The attractive force that holds an atomic or subatomic particle or particle group together.

bonded-barrier transistor A bipolar transistor in which the connection at the base region is alloyed.

bonded negative-resistance diode A diode that displays a negative-resistance characteristic over part of its current curve. This results from avalanche breakdown.

bond energy In a molecule, the energy necessary to break an atomic bond.

bonding **1.** The formation of bonds between adjacent atoms in a crystalline material, such as a semiconductor. See specifically COVALENT BINDING FORCES, IONIC BINDING FORCES, and METALLIC BINDING FORCES. **2.** The secure fastening together of conducting surfaces, as by soldering or brazing, to produce a high-conductance, leak-free continuum.

bond strength The minimum stress required to separate a material from another to which it is bonded.

bone-conduction transducer A device used in place of the earphone in a hearing aid to convey sound energy to the bone structure of the head.

Bongard problem A method of evaluating how well a machine vision system can differentiate among patterns. Similarities and differences are noted between objects in two sets of boxes. It was developed for object-recognition systems, mainly for use in intelligent robots.

book capacitor A variable capacitor in which the metal plates are bonded along one edge and separated from each other by means of mica sheets. The capacitance is varied by opening and closing the assembly book fashion. It is used as a padder or trimmer.

Boolean algebra A system of symbolic logic. Statements are represented as symbols, usually variables such as *x*, *y*, and *z*. The logical AND operation is represented by multiplication; the logical inclusive OR operation is represented by addition; the logical NOT operation is represented by a minus sign or a line over the element symbol. The system has rules, definitions and axioms via which *theorems* can be derived. Used by engineers in the design of digital electronic circuits.

Boolean truth table

		AND	*NOT*	*OR*
x	y	xy	x	$x + y$
0	0	0	1	0
0	1	0	1	1
1	0	0	0	1
1	1	1	0	1

Boolean function In mathematical logic, a function that makes use of BOOLEAN ALGEBRA.

Boolean theoreams

1. $x + 0 = x$ (additive identity)
2. $x1 = x$ (multiplicative idenity)
3. $x + 1 = 1$
4. $x0 = 0$
5. $x + x = x$
6. $xx = x$
7. $(x')' = x$ (double negation)
8. $x + x' = 1$
9. $x'x = 0$
10. $x + y = y + x$ (commutativity of addition)
11. $xy = yx$ (commutativity of multiplication)
12. $x + xy = x$
13. $xy' + y = x + y$
14. $x + y + z = (x + y) + z = x + (y + z)$ (associativity of addition)
15. $xyz = (xy)z = x(yz)$ (associativity of multiplication)
16. $x(y + z) = xy + xz$ (distributivity)
17. $(x + w)(y + z) = xy + xz + wy + wz$ (distributivity)

boom **1.** A horizontal support for a microphone, enabling the microphone to be suspended over a sound source, but out of the sight of a camera. **2.** A horizontal support for a small antenna that is undergoing tests or sampling the field of another antenna. **3.** The supporting element in a Yagi, quad, or log-periodic antenna. It establishes the center of gravity and directional axis of the radiation pattern. The driven element(s) and parasitic element(s) are attached, usually at right angles.

boost capacitor In the damper circuit of a television receiver, the capacitor that is used to boost the B-plus voltage. Also called *booster capacitor.*

boost charge A high-current, short-interval charge used to revitalize a storage battery quickly. Also called *booster charge.*

booster **1.** Any device used to increase the amplitude of a signal (e.g., as an amplifier or preamplifier) or of an energy source (e.g., to boost the output of a power supply). **2.** A radio-frequency preamplifier used ahead of a television receiver.

5059F-pB_56-92 4/9/01 4:45 PM Page 82

booster battery **1.** A battery used to forward bias a diode detector into a favorable region of its conduction curve, or to bias a bolometer into the square-law region of its response. **2.** A battery supplying power to a booster.

booster gain The amplification (usually in terms of voltage gain) provided by a booster (see especially BOOSTER, **2**).

boot **1.** The powering-up routine in a digital computer, in which the machine executes a series of programs to get itself ready for use. **2.** The resetting of a computer, by pressing certain keyboard keys (e.g., CTRL-ALT-DEL), pressing a reset button, or by powering-down, waiting about two minutes, and then powering-up again. **3.** To install a computer diskette and instruct the computer to execute one or more programs on the diskette. **4.** A usually flexible protective nipple or jacket pulled over a cable or connector, so called from its resemblance to a foot boot.

boot loader A form of computer program that operates on the BOOTSTRAP ROUTINE.

bootstrap A technique for making a device or process achieve a condition through its own actions; see BOOTSTRAP CIRCUIT, for example.

bootstrap circuit A specialized form of follower circuit that presents very high input impedance. Its chief feature is the return of the control-element resistor to a tap on the source or emitter resistor. The technique takes its name from the figurative notion that such a circuit "lifts its input impedance by its own bootstraps."

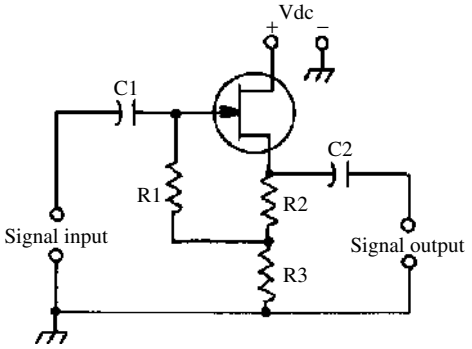

bootstrap circuit
(with junction-type field-effect transistor)

bootstrap routine **1.** Also called *bootstrap program.* In a digital computer, and especially in a personal computer, the routine that the machine follows when first powered-up. See BOOT, **1.** **2.** In a digital computer, a routine in which the first few instructions put in storage are later used to complete the routine, as supplemented by some operator instruction. **3.** A portion of a computer program that is used to establish an alternate version of the program.

borax-aluminum cell An electrolytic cell that consists essentially of an aluminum electrode and a lead electrode in a saturated solution of sodium tetraborate (borax). After electroforming, such a cell can be used either as a rectifier or as an electrolytic capacitor.

boric acid Formula, H_3BO_3. A compound used variously in electronics—especially as the electrolyte in electrolytic capacitors.

bornite Formula, Cu_5FeS_4. A natural mineral that is a sulfide of copper and iron. Its crystalline structure made it important in early semiconductor diodes (crystal detectors).

boron Symbol, B. A metalloidal element. Atomic number, 5. Atomic weight, 10.82. It is used as a dopant in semiconductor processing.

bot **1.** Abbreviation for *beginning of tape.* **2.** Abbreviation of *bottom.*

bottoming Excessive movement of the cone of a loudspeaker or the diaphragm of a headphone so that the magnet or supporting structure is struck by the moving-coil piston assembly. It produces a clapping sound, particularly on bass (low-frequency) audio peaks.

bounce **1.** The springback or vibration of the armature of a relay on closure. **2.** An abnormal, abrupt change in the brightness of the image in a television receiver or cathode-ray-tube (CRT) computer monitor.

boundary **1.** In a polycrystalline substance, the area of contact between adjacent crystals. **2.** The area of meeting of two regions (such as n and p) in a semiconductor.

boundary defect A condition in which a piezoelectric crystal has two regions, intersecting in a plane, with different polarizations.

boundary effect In audio systems, a pheno-menon in which the proximity of an acoustic transducer to a flat surface enhances the pickup and/or transmission of sound. Occurs because of reflection of acoustic waves from the surface.

bound charge The portion of the electric charge on a conductor that does not escape to ground when the conductor is grounded. This occurs because of induction from neighboring charge carriers. Compare FREE CHARGE.

bound electron An electron held tightly in its orbit within an atom so that it is not ordinarily free to drift between atoms and contribute to electric current flow.

bow-tie antenna A center-fed antenna in which the two horizontal halves of the radiator are triangular plates that resemble a bow tie. A flat reflector consisting of closely spaced horizontal wires is mounted behind the triangles.

bow-tie test An oscilloscope-display checkout of a single-sideband (SSB) signal, in which the appearance of the display indicates the signal quality. The transmitter output signal is fed to the

5059F-pB_56-92 4/9/01 4:45 PM Page 83

vertical deflection plates of the oscilloscope. The exciter audio output is fed to the horizontal sweep input of the scope.

boxcars Long pulses with short separating spaces between them.

box-shaped loop The characteristic square-loop hysteresis curve (B-H loop) that result when a sine wave of current is used to magnetize a sample of magnetic material. In this plot, which covers all four quadrants, the horizontal axis (H) displays magnetizing force, and the vertical axis (B) displays magnetization. Also see HYSTERESIS.

Boys radiomicrometer A detector for radiant energy. The device consists of a thermocouple and a galvanometer. When energy falls on the thermocouple, a voltage is produced, and this is measured by the galvanometer.

bp **1.** Abbreviation of BOILING POINT. **2.** Abbreviation of BANDPASS.

bpi Abbreviation of *bits per inch.*

B-plus Also called *b-positive.* **1.** Symbol, B+. The positive dc voltage required for certain electrodes of vacuum tubes, transistors, etc. **2.** The positive terminal of a B power supply.

B positive See B-PLUS.

B power supply A name used sometimes for the unit that supplies high-voltage dc energy to a vacuum tube plate or screen circuit.

bps Abbreviation of BITS PER SECOND.

Br Symbol for BROMINE.

bracketing A troubleshooting routine characterized by isolating progressively smaller areas in a circuit or chain of stages until the defective subcircuit or stage is located.

Bradley detector A locked-oscillator circuit that was once used as an FM detector.

braid **1.** A woven network of fine metal wires used for grounding purposes. It is usually made of fine copper conductors. The increased surface-area-to-volume ratio improves the conductivity, at radio frequencies, over a single conductor that has the same cross-sectional area. Braid can be tinned (saturated with solder) to retard corrosion. **2.** It is also called a *shield.* The outer conductor in prefabricated coaxial cable.

braided wire A length of braid. Used for grounding or shielding purposes.

brain waves Alternating or pulsating voltages that are caused by electrical activity in the brain of an animal or human being. The voltages can be picked up by electrodes attached to the scalp, and amplified to be viewed on a cathode-ray-tube (CRT) screen, heard by headphones or speakers, or traced by an electroencephalograph.

branch **1.** Any one of the separate paths of a circuit. With respect to the layout of its components, a branch can be series, parallel, series-parallel, parallel-series, or any combination of these. It is also called a LEG. **2.** See BRANCH CIRCUIT.

branch circuit In electrical wiring, a group of outlets served through a single cutout from a source of power-line ac voltage. The source can be a distribution center, subdistribution center, main, or submain. Interior lighting circuits are usually branch circuits because many lights are connected to one circuit controlled by a single fuse or circuit breaker.

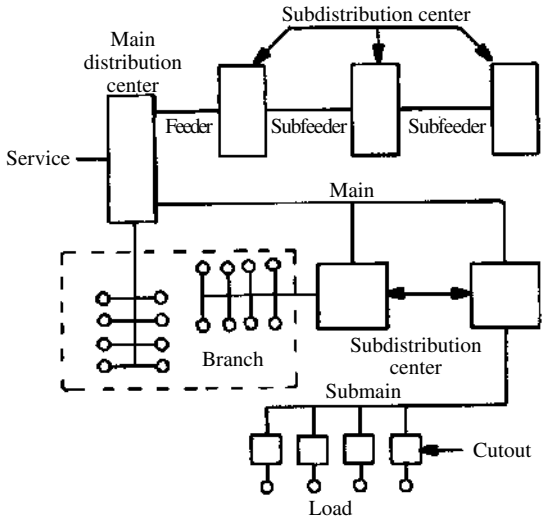

branch circuit (enclosed in broken lines)

branch current Current flowing through a branch of a circuit, whose magnitude, with respect to the total current of the circuit depends on the nature of the branch.

branched In molecular polymers, the condition of side chains being attached to the main chain.

branched windings Forked windings of a polyphase transformer.

branching In robotics and artificial intelligence (AI), a set of routines or programs containing points at which a computer must select from among two or more alternatives. Such routines are used in critical processes, such as the manufacture of precision equipment.

branch point See JUNCTION POINT.

branch voltage The voltage, or voltage drop, across a branch of a circuit.

brass **1.** An alloy of copper and zinc that is widely used in electronics. Compared to annealed copper, this metal has four times the resistivity (or ¼ the conductivity), half the temperature coefficient, more than twice the tensile strength, and a lower melting point (900°C). **2.** A colloquialism for an old-fashioned, straight telegraph key.

brass pounder **1.** Colloquialism for telegraph operator or radiotelegraph operator. **2.** A radio ama-

5059F-pB_56-92 4/9/01 4:45 PM Page 84

teur who handles large amounts of message traffic, particularly via Morse code. **3.** A radio amateur proficient in Morse code operation.

Braun electroscope An electroscope consisting essentially of a fixed metal vane to which a movable needle is fastened at a pivot. The repulsion between the two, when an electric charge is applied, causes the needle to move over a calibrated scale.

bravo Phonetic representation of the letter B.

brazing The joining of two metal (usually iron or steel) parts together with a suitable melted copper-alloy metal. Compare SOLDERING.

breadboard **1.** A perforated board, a chassis, or any basic framework on which electronic components can be mounted and quickly wired for the preliminary test of a circuit. It is so called because the first such foundation units of this sort actually were wooden breadboards. **2.** Any preproduction electronic prototype circuit. **3.** To set up a circuit on a breadboard.

breadboard model **1.** The preliminary model of an electronic device, often built on a breadboard (see BREADBOARD, **1**). **2.** Loosely, any prototype.

break **1.** An open circuit. **2.** To open a circuit. **3.** In communications, a word indicating a desire to transmit on a wavelength already occupied by radio traffic. **4.** See BREAK-IN, **1**.

break-before-make contacts Contacts, especially in a rotary selector switch, that open one circuit before closing the next one.

breakdown **1.** Failure of a circuit or device, caused mainly by excessive voltage, current, or power. A sudden high current, however, does not always indicate failure. **2.** AVALANCHE BREAKDOWN. **3.** The separation of an electronics problem or project into its constituent parts for an easier solution.

breakdown diode See ZENER DIODE.

breakdown region The region, in a pn junction, in which avalanche breakdown occurs.

breakdown strength See DIELECTRIC STRENGTH.

breakdown voltage **1.** The voltage at which current suddenly passes in destructive amounts through a dielectric. **2.** The voltage at which a gas suddenly ionizes, as in a gas tube. **3.** The voltage at which the reverse current of a semiconductor junction suddenly rises to a high value (nondestructive if the current is limited). See AVALANCHE BREAKDOWN.

break-in **1.** A technique of radio communication in which one station interrupts a transmission from another station, rather than waiting until the end of the latter's transmission. **2.** Also called *full break-in.* In a radio communications transceiver or transmitter/receiver combination, extremely rapid transmit/receive switching, approaching *full duplex* communications. Every pause in transmission, even of only a few milliseconds, creates a "receive window" allowing reception between spoken words or Morse code elements. **3.** BURN-IN.

breaking current The momentary current that flows when the contacts of a switch or relay are broken.

break-in keying A system of radiotelegraph keying in which the receiver is in operation whenever the key is open. See BREAK-IN, **2.**

break-in operation In radiotelegraph or single-sideband (SSB) communications, the practice of interrupting at any time to "talk back" to the other transmitting station. This operation is made possible by high-speed transmit/receive switching. See BREAK-IN, **2.**

break-in relay An electromechanical or solid-state relay that enables break-in operation. Largely supplanted by solid-state switching devices.

breakover point In a silicon-controlled rectifier, the source-voltage value at which the load current is suddenly triggered to its steep climb. Also called TRIGGERING POINT.

breakover voltage In a silicon-controlled rectifier with open gate circuit, the anode voltage at which anode current is initiated.

breakpoint A point in a computer program when, for the purpose of obtaining information for the program's analysis, the sequence of operations is interrupted by an operator or a monitor program.

breakpoint frequencies The upper- and lower-frequency points at which the gain-versus-frequency response of an amplifier or network departs from flatness.

breakpoint instruction An instruction that stops a computer.

breakthrough **1.** A new discovery, insight, or solution to a problem that results in an advancement in the state of the art. **2.** See PUNCHTHROUGH. **3.** See BREAKDOWN, **1. 4.** See AVALANCHE BREAKDOWN.

break time The time taken for a relay to drop out completely or a switch to open. Compare MAKE TIME.

breathing Slow, rhythmic pulsations of a quantity, such as current, voltage, brightness, beat note, etc.

breezeway In a sync pulse in NTSC color television, the part of the back porch between the trailing edge of the pulse and the color burst.

B-register An index register in a computer for storing words that are used to change an instruction before it is executed by the program.

Bremsstrahlung radiation The radiation emitted by a charged particle whose speed is altered when it passes through the electric field in the vicinity of an atomic nucleus.

brevity code A code not intended to conceal information, but to shorten the number of characters in a message or data file. The Q SIGNALS are an example of a brevity code used in communications. In computer data transfer and communications, brevity codes allow compression, speeding up the transfer rate and reducing the storage space for a given amount of data.

5059F-pB_56-92 4/9/01 4:45 PM Page 85

Brewster angle From BREWSTER'S LAW, the polarizing angle at which the reflected and refracted rays of incident light are perpendicular to each other.

Brewster's law (Sir David Brewster, 1781–1868). For any dielectric reflector, the relationship in which the refractive index is equal to the tangent of the polarizing angle.

bridge **1.** A network, usually consisting of four branches, connected so that an input signal can be applied between two opposite points and the output taken between the other two opposite points. When the component values are in a certain ratio, the voltage between the output points is zero, and the bridge is said to be balanced or set to null. **2.** A circuit such as that described in (**1**) used for electrical measurements. **3.** An audio or servo amplification system in which the load is driven from two outputs having opposite polarity, neither of which are at ground potential. **4.** A communications path between or among two or more networks. This allows the subscribers in any network to obtain data from, or send data to, any other network, in effect creating a network of networks.

bridge balance control A potentiometer, variable capacitor, or variable inductor that is used to adjust a bridge circuit to balance.

bridge-connected amplifier **1.** A dc amplifier stage in which the transistors and resistors are connected in a four-arm bridge circuit, with respect to dc. When the bridge is initially balanced, all dc is eliminated in the output load. The input signal unbalances the bridge, which results in an amplified output signal in the load. **2.** An amplifier pair having opposing outputs across which a load can be bridged to obtain twice the power output of either amplifier alone.

bridged differentiator See HALL NETWORK.

bridge detector The output-indicating device (e.g., meter, oscilloscope, or headphones) that indicates whether a bridge is balanced or unbalanced. Also called *null detector* or *null indicator.*

bridged integrator A null network that consists of a two-stage resistance-capacitance (RC) integrator circuit bridged by a capacitor. This network produces a shallow null at a single frequency determined by the *R* and *C* values in the integrator. Compare HALL NETWORK.

bridged-tee attenuator An attenuator consisting of a tee section, between the input and output of which is bridged a single-series arm.

bridged-tee circuit Any circuit (of resistors, capacitors, inductors, or a combination of these) that consists of a tee section, bridged by a single-series section, from input to output.

bridged-tee null network A bridged-tee circuit of resistance (*R*) and capacitance (*C*), proportioned so that at some setting of the *R* and *C* values, the output of the circuit is zero.

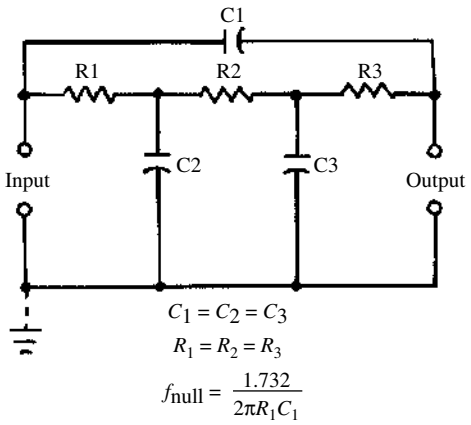

bridged integrator

bridged-tee oscillator A low-distortion oscillator circuit whose frequency is determined by a bridged-tee null network inserted into the negative-feedback path of the circuit.

bridge feedback A combination of current feedback and voltage feedback around an amplifier circuit. It is so called because, in the feedback circuit, the resistors and the output resistance of the amplifier form a four-arm bridge.

bridge generator The power source (e.g., a battery or oscillator) that supplies the signal to a BRIDGE used for electrical measurements.

bridge indicator See BRIDGE DETECTOR.

bridge oscillator See BRIDGE GENERATOR.

bridge rectifier A full-wave rectifier circuit in which four rectifying diodes are connected in a bridge configuration. Each half-cycle of ac input is rectified by a pair of diodes in opposite quarters of the bridge and in series with each other. The bridge does not require a transformer with a center-tapped secondary, as does the FULL-WAVE, CENTER-TAP RECTIFIER circuit.

bridge source See BRIDGE GENERATOR.

bridge-type meter A frequency-sensitive bridge (such as the Wien bridge) that can be used to measure audio frequency. Because the bridge can be balanced at only one frequency at a time,

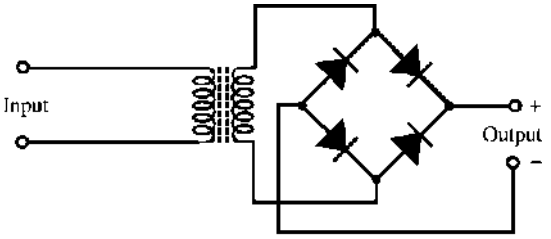

bridge rectifier

5059F-pB_56-92 4/9/01 4:45 PM Page 86

its adjustable arm can be calibrated to read the frequency directly.

bridge-type impedance meter An impedance-measuring circuit in which unknown impedance *Z* is connected in series with a calibrated variable resistor R. An ac voltage is applied to the series circuit. The separate voltage drops across the resistor and impedance are measured successively as the value of *R* is varied. When the two voltage drops are identical, *Z* equals *R*, and the impedance can be read from a calibrated dial on the variable-resistor control.

bridge-type oscillator A resistance-capacitance (RC) tuned oscillator in which a Wien bridge is used as the frequency-determining circuit in the feedback loop.

bridge-type power meter **1.** See BOLOMETER BRIDGE. **2.** A four-arm bridge specially designed to operate at radio frequencies. At null, the impedance of the unknown is read directly from the balancing dial or calculated from bridge constants. This instrument is used to measure the impedance of circuit components, antennas, and transmission lines.

bridge-type SWR meter A four-arm bridge that is specially designed to operate at radio frequencies. At null, the standing-wave ratio (SWR) is calculated from the bridge resistance values or read from a direct-reading scale on the null-indicating meter.

bridging amplifier An amplifier whose input impedance is so high that it can be considered infinite for practical purposes. Thus, the amplifier can be connected across a load or line without significantly affecting the operation of the system.

bridging coupler A voltage-dependent resistor that permits an occasionally used device (such as a bell) to be connected permanently across a regularly used device (such as a telephone) without continuously short-circuiting the latter. Thus, the bridging coupler ordinarily has very high resistance; but when the line voltage is momentarily raised, the resistance lowers and the occasionally used device is actuated (e.g., the bell rings).

bridging gain The gain of a bridging amplifier expressed as the ratio (in decibels) of the power developed in the amplifier load to the power in the load to which the input terminals of the amplifier are connected.

bridging loss The loss that results from the shunting of a speaker, microphone, earphone, or other transducer by a resistor, capacitor, or inductor. Generally, the loss is expressed as a power ratio in decibels.

Briggsian logarithm (Henry Briggs, 1556-1631). A base-10 logarithm, generally known as a COMMON LOGARITHM. Compare NAPIERIAN LOGARITHM.

brightness SI unit, candela per square meter (cd/m^2); cgs unit, lambert (L). The quantity of light, per unit area, emitted or reflected perpendicular to a light-emitting surface.

brightness control **1.** In a computer monitor, television receiver, or oscilloscope, a potentiometer that varies the negative bias voltage on the control grid of the cathode-ray tube (CRT). The brightness of the image is inversely proportional to this negative bias voltage. **2.** The control of the brightness of an illuminated area.

brilliance See BRIGHTNESS.

brilliance control **1.** The BRIGHTNESS CONTROL in a television receiver or computer monitor. **2.** The brightness control in a cathode-ray oscilloscope. **3.** A control for adjusting the level of the tweeter output in a speaker system.

British Standard wire gauge Abbreviation, NBS SWG. A classification of wire sizes sometimes used in England, Australia, and New Zealand. The higher the number, the thinner the wire. The designator does not take into account any coatings on the wire, such as enamel, rubber, or plastic insulation. In the United States, the *American wire gauge* is more often used. See AMERICAN WIRE GAUGE.

British Standard Wire Gauge (NBS SWG) Diameters

NBS SWG	Millimeters	Inches
1	7.62	0.300
2	7.01	0.276
3	6.40	0.252
4	5.89	0.232
5	5.38	0.212
6	4.88	0.192
7	4.47	0.176
8	4.06	0.160
9	3.66	0.144
10	3.25	0.128
11	2.95	0.116
12	2.64	0.104
13	2.34	0.092
14	2.03	0.080
15	1.83	0.072
16	1.63	0.064
17	1.42	0.056
18	1.22	0.048
19	1.02	0.040
20	0.91	0.036
21	0.81	0.032
22	0.71	0.028
23	0.61	0.024
24	0.56	0.022
25	0.51	0.020
26	0.46	0.018
27	0.42	0.0164
28	0.38	0.0148
29	0.345	0.0136
30	0.315	0.0124
31	0.295	0.0116
32	0.274	0.0108

5059F-pB_56-92 4/9/01 4:45 PM Page 87

NBS SWG	Millimeters	Inches
33	0.254	0.0100
34	0.234	0.0092
35	0.213	0.0084
36	0.193	0.0076
37	0.173	0.0068
38	0.152	0.0060
39	0.132	0.0052
40	0.122	0.0048

British thermal unit Abbreviation, Btu. The amount of heat required to raise the temperature of a pound of water by one degree Fahrenheit, in an ambient environment of slightly greater than 39°F.

broadband Also called *wideband.* Possessing a characteristic wide bandwidth or range of operating frequencies. This term can be applied at audio frequencies (AF) or radio frequencies (RF), and is frequently used to describe the performance of oscillators, amplifiers, antennas, and various types of networks. The term can also be applied to describe the nature of electromagnetic emissions or noise. Examples are given in the following several definitions. Compare NARROWBAND.

broadband amplifier An amplifier that has very wide frequency response, such as 10 Hz to 10 MHz. Examples are an instrument amplifier and a video amplifier.

broadband antenna An antenna that operates satisfactorily over a comparatively wide band of frequencies without requiring retuning at individual frequencies. Examples are the log-periodic and discone antennas.

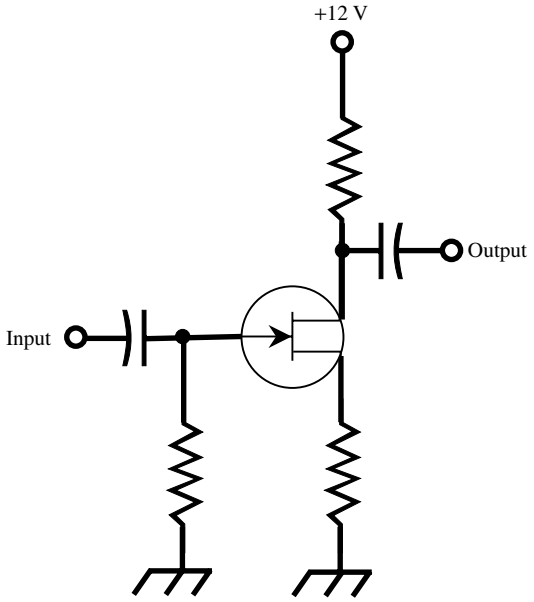

broadband amplifier

broadband electrical noise Electrical noise that is present over a wide frequency spectrum (e.g., 3 kHz to 30 MHz).

broadband I-F An intermediate-frequency (IF) amplifier or amplifier chain. The wide frequency response is important when an increased bandpass is preferred to high selectivity, as in high-fidelity radio tuners.

broadband interference Interference, other than noise, that is present over a wide band of frequencies. An example is over-the-horizon shortwave radar, recognizable by its characteristic "woodpecker" sound in communications receivers at high frequencies.

broadband Klystron A Klystron oscillator with a broadbanded tuned circuit.

broadband tuning Receiver tuning characterized by a selectivity curve having a pronounced flat top or broad nose that passes a wide band of frequencies. Also called *broadband response.*

broadcast **1.** A radio-frequency transmission of an intelligence-bearing signal that is directed to numerous unspecified receiving stations. **2.** The transmission or dissemination of signals to a large, unspecified number of receiving stations.

broadcast band Any band of frequencies allocated for broadcasting (see BROADCAST SERVICE, **1**), but particularly the U.S. standard amplitude-modulation (AM) and frequency-modulation (FM) radio broadcast bands at 535 to 1605 kHz (AM) and 88 to 108 MHz (FM).

broadcasting The dissemination of signals for reception by the general public, not for communications purposes.

broadcast interference Abbreviation, BCI. Interference to normal reception by broadcast receivers, usually arising from signals emitted by other stations.

broadcast receiver A receiver intended primarily to pick up standard broadcast stations. Also see BROADCAST BAND.

broadcast service **1.** Any radio transmitting service (including television) that exists for the purpose of sending out electromagnetic signals for general reception, rather than addressing them to specific receiving stations. **2.** The service provided by a station operating in the broadcast band.

broadcast station Any station in the broadcast service, but especially one assigned to operate in the standard U.S. broadcast bands. Also called *broadcasting station.*

broadcast transmitter A radio transmitter designed specifically for, and operated in, the broadcast service.

broad response Slow deflection of an indicator, such as a meter, over a relatively wide range of values of the input quantity.

5059F-pB_56-92 4/9/01 4:45 PM Page 88

broadside In a perpendicular direction; for example, broadside radiation from an antenna.

broadside antenna See BROADSIDE ARRAY.

broadside array Also called *broadside antenna.* A phased group of antennas arranged so maximum radiation occurs in directions perpendicular to the plane containing the driven elements. This requires that all of the antennas be fed in phase. The elements can be half-wave dipoles or full-wave, center-fed conductors. Full-wave elements have a slight gain over half-wave elements. At high frequencies, this type of array is usually constructed from two driven antennas. At very-high and ultra-high frequencies there can be several driven antennas. The antennas can each consist of a single element, or they can be Yagis, loops, or other systems with individual directive properties. In general, the larger the number of elements in the entire array, the greater the gain and directivity.

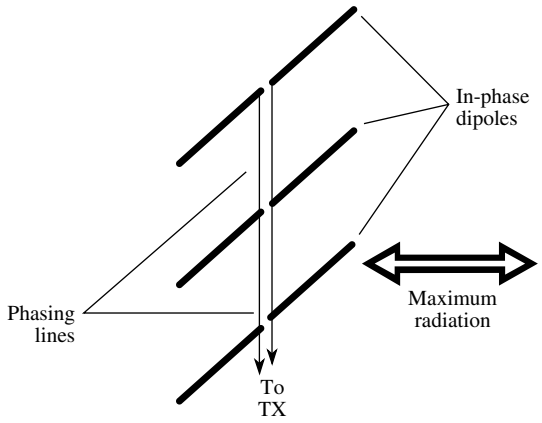

broadside array

broad tuning Tuning that is characterized by pronounced signal width, often resulting in adjacent-channel interference. A common cause of such impaired selectivity is low Q in the tuned circuit(s).

Broca galvanometer A device consisting of an astatic magnetic arrangement, with a coil enclosing central consequent poles. The device is characterized by fast response and high sensitivity.

bromine Symbol, Br. A nonmetallic element of the halogen family. Atomic number, 35. Atomic weight, 79.90.

bronze An alloy of copper and tin that has various uses in electronics. Also see PHOSPHOR BRONZE.

Brown and Sharpe gauge See AMERICAN WIRE GAUGE.

Brownian movement (Robert Brown, 1773–1858). Random movement of microscopic particles—especially in solutions. It occurs because of collisions of molecules with the particles. Einstein showed, in his early work, a connection between this movement and the *Boltzmann constant.*

brownout A deliberate lowering of line voltage by a power company to reduce load demands. Minor events of this type often pass unnoticed by the average consumer. More pronounced events produce observable effects, such as shrinkage of television and cathode-ray-tube (CRT) computer-display images.

Bruce antenna A vertical collinear array that consists of several resonant sections connected by short, rigid, parallel-conductor stubs. The currents in the radiating sections are in phase. Maximum radiation and response occur broadside to the antenna (omnidirectional in the horizontal plane). Polarization is vertical. The antenna produces gain at low radiation and response angles, and is commonly used in repeater installations and fixed communications stations at very-high frequencies (VHF) and ultra-high frequencies (UHF).

brush A usually metal or carbon strip, blade, or block, that slides in contact with another part, as in a motor commutator.

brush discharge Also called *Saint Elmo's fire.* A cloud of repelled ions around the tip of a pointed conductor charged to a high voltage. It often produces a visible glow in the air.

brush holder The housing for a brush in a motor, generator, rheostat, slip-ring junction in a rotating data-transmission system, etc.

brute force **1.** The transmission of a signal of excessive or unnecessary power. **2.** An inefficient approach to a problem, which might solve the problem, but requires far more energy, effort, or computer memory/storage space than the minimum needed to accomplish the same result.

brute-force filter A pi-type lowpass dc power supply filter, so called because of the extremely large inductances and capacitances that are generally used.

brute supply An unregulated power supply.

B-scope A cathode-ray tube (CRT), used in radar, that presents a B DISPLAY.

B service A teletype communication system operated by the Federal Aviation Administration (FAA).

B-supply The dc power supply that provides anode operating voltages, such as plate and screen voltages in a vacuum-tube radio-frequency (RF) power amplifier.

BT-cut crystal A piezoelectric plate cut from a quartz crystal at an angle of rotation (relative to the x-axis) of -49°. It has a zero temperature coefficient of frequency at approximately 25°C. Also see CRYSTAL AXES and CRYSTAL CUTS.

Btu Abbreviation of BRITISH THERMAL UNIT.

BuAer Abbreviation of *Bureau of Aeronautics.*

bubble memory In digital-computer practice, a special type of static magnetic memory. The mag-

5059F-pB_56-92 4/9/01 4:45 PM Page 89

netic material is divided into regions that are magnetized in different directions. So called because the flux lines of the tiny magnetized regions are shaped somewhat like, and move around after the fashion of, bubbles on the surface of a glass of soda.

bubble shift register A shift register that uses a magnetic bubble (see BUBBLE MEMORY) that can be moved sequentially from electrode to electrode on a wafer.

bubbling See MOTORBOATING.

bucket A computer memory or a designated location in such a memory.

bucking The process of counteracting one quantity, such as a current or voltage, via series or parallel application of a similar quantity that has opposite polarity (180 degrees out of phase).

bucking circuit **1.** A circuit used to obtain bucking action. The simplest form is a battery and potentiometer that supply a variable voltage of polarity opposite to that of the voltage to be bucked. A more sophisticated form is an ac transformer, the secondary of which is connected in series and out of phase with the ac utility line. **2.** The zero-set circuit in an electronic voltmeter.

bucking coil A coil placed and positioned so that its magnetic field partially or completely cancels the field of another coil. Troublesome hum fields sometimes are neutralized with such a coil.

bucking voltage See BACK VOLTAGE, **2.**

buckling The warping of storage-battery plates, usually resulting from excessive charge or discharge.

buckshot In an amplitude-modulated (AM) or single-sideband (SSB) radio transmission, broadband signal splatter caused by excessive modulation, or detuned multiplier circuits.

buffer **1.** An amplifier used principally to match two dissimilar impedance points and isolate one stage from a succeeding one in a cascaded system, and thus to prevent undesirable interaction between the two. **2.** In a digital computer, a storage site used temporarily during data transfers to compensate for differences in data flow rates. **3.** In digital-computer operations, a follower stage that is used to drive a number of gates without overloading the preceding stage.

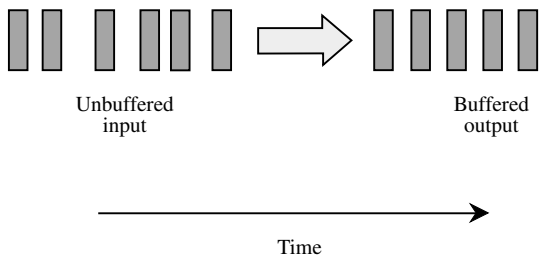

buffer, 2.

buffer amplifier See BUFFER, **1.**

buffer capacitor A high-voltage fixed capacitor that is placed across a transformer secondary to suppress voltage spikes and sharp waveforms—especially when the input is a square wave.

buffer circuit **1.** In a data system that uses a keyboard, an electronic circuit that allows the operator to type ahead of the data output. **2.** See BUFFER, **1**, **2** and **3.**

buffered output An output (power, signal, etc.) that is delivered from the generating device through an isolating stage, such as a buffer amplifier. This arrangement protects the device from variations in the external load. Compare UNBUFFERED OUTPUT.

buffer storage **1.** A buffer that is used to interface between data systems with different rates of transmission. **2.** See BUFFER, **2.**

bug **1.** Slang for WIRETAP, **1. 2.** Slang for circuit fault, **1**. **3.** A semiautomatic key that some radiotelegraph operators use to send Morse code.

bug key See BUG, **3.**

building-block technique The process of assembling electronic equipment by quickly connecting together already completed stages (in the form of boxes or blocks) and supplying power and signals to the setup. Also called *modular technique* and *modular construction.*

building-out circuit A short section of transmission line shunting another line; it is used for impedance matching. Also called *building-out section.*

buildup **1.** The process whereby the voltage of a rotating generator starts at a point that is determined by the residual magnetism of the machine, and gradually increases to a voltage representing the point at which the resistance line crosses the magnetization curve. **2.** The (usually gradual) accumulation of a quantity (e.g., the buildup of charge in a capacitor).

bulb A globe-like container having any of a number of characteristic shapes from spherical to tubular and usually evacuated, for enclosing the elements of an electron device, such as a vacuum tube, gas tube, photocell, or lamp.

bulge **1.** A nonlinear attenuation-versus-frequency curve in a transmission line. **2.** A localized nonlinearity in a function.

bulk The body or mass of a semiconductor specimen, as opposed to junctions within the specimen. Current flows through a junction, but it can also flow, more or less, through the mass of semiconductor wafer into which the junction has been formed.

bulk effect An effect, such as current, resistance, or resistivity, observed in the overall body of a sample of material, as opposed to a region within the material or on its surface. Thus, a silicon diode can display junction resistance (i.e., resistance offered by a junction processed in a wafer of silicon), as well as bulk resistance (i.e., the effec-

5059F-pB_56-92 4/9/01 4:45 PM Page 90

tive resistance of all paths around the junction, through the mass of the wafer). Compare SURFACE EFFECT.

bulk-erased tape Recording tape whose signal content has been removed via a bulk eraser.

bulk-erase noise **1.** The residual magnetic impulses that remain on a magnetic tape after it has been bulk-erased. **2.** Noise generated by bulk-erased tape when the latter passes through deenergized record or erase heads in a tape machine.

bulk eraser A type of power-line-frequency degausser that erases an entire reel of magnetic tape without requiring that the tape be unreeled and passed continuously under an erase head. This saves considerable time, but often leaves some BULK-ERASE NOISE on the tape. Also called BULK DEGAUSSER.

bulletin board In personal computing or amateur packet communications, a system that allows subscribers to leave messages for each other for access via a *modem* or *terminal node controller.*

bulletin station A station intended for the transmission of bulletins of interest to certain parties, such as military personnel or amateur radio operators. An example is W1AW in Newington, Connecticut, an amateur radio station that transmits bulletins and code practice.

buncher In a Klystron, a cavity resonator that contains two grids mounted parallel to the electron stream. The electrostatic field of the grids alternately accelerates and retards the electrons, velocity-modulating the stream into bunches.

buncher grids In a Klystron, the closely spaced grids that velocity-modulate the electron beam into successive bunches.

buncher resonator In a velocity-modulated tube, such as a Klystron, the input cavity resonator.

buncher voltage The radio-frequency (RF) grid-to-grid voltage in the buncher resonator of a Klystron.

bunching The production of electron bunches in a velocity-modulated tube, such as a Klystron. Also see BUNCHER.

bunch stranding A technique for combining several thin wires into a single thick wire. Often used in guy wires and electrical conductors to improve tensile strength and flexibility. At radio frequencies, bunch stranding also improves electrical conductivity by increasing the ratio of surface area to cross-sectional area. This minimizes losses caused by *skin effect.*

Bunet's formula A formula for calculating the inductance of a multilayer air-core coil that has a diameter less than three times the length:

$$L = a^2N^2/(9a + 10l + 8.4c + 3.2cl/a)$$

where N is the number of turns, a is the average coil radius, c is the winding thickness, and l is the length of the coil.

Bunsen cell A cell consisting of a zinc rod in a sulfuric acid solution contained in a porous pot, which is in a nitric acid solution. The zinc rod serves as the negative pole; the positive pole is a piece of hard carbon. The cell produces about 1.9 volts and delivers relatively high current.

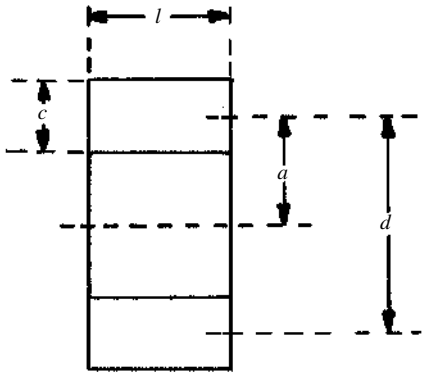

Bunet's formula

burden See VOLTAGE BURDEN.

burn **1.** A blemish on the screen of a cathode-ray tube (CRT), caused by destruction of the phosphor there. This results from prolonged focusing of an intense electron beam in one spot. **2.** A blemish on the screen of a television picture tube, usually resulting from ions that reach the screen when the ion trap is not working correctly.

burn-in A long, thorough, carefully controlled preliminary test of a component, device, or system, to stabilize its electrical characteristics after manufacture and to ensure that it will function according to rated specifications. An important test for equipment whose reliability must be guaranteed, such as an emergency communications transceiver.

burnout **1.** Failure of a conductor or component caused by overheating from excess current or voltage. **2.** The open-circuiting of a fuse. **3.** Electrical failure of any type.

burst **1.** The abrupt ionization of the gas in an ionization chamber by cosmic rays. **2.** An abrupt increase in the amplitude of a signal. Also, the type of signal that results from burst action. **3.** See COLOR BURST.

burst amplifier In a color-television receiver, the amplifier that separates the burst pulse from the video signals and amplifies the former. See COLOR BURST.

burst gate timing In a color-television receiver, the timing of the gating pulse with the input signal of the burst amplifier.

burst generator A signal generator delivering a burst output (see BURST, **2**) for testing various types of equipment. Its output is intermediate between sine waves and square waves, and is convenient for rapidly appraising the perfor-

5059F-pB_56-92 4/9/01 4:45 PM Page 91

mance of such devices as amplifiers, filters, electronic switches, transducers, and loudspeakers.

burst transmission A short transmission at high speed. This method of transmission saves time, but increases the necessary bandwidth of a signal by the same factor as the ratio of the high speed to the original speed.

bus **1.** A main conductor in a circuit. A bus can be high in the sense that its potential is above or below ground, or it can be low or at ground reference. **2.** In computer operations, a common group of paths over which input and output signals are routed.

bus driver A buffering device designed to increase the driving capability of a microprocessor, which itself might be capable of driving no more than a single load.

business machine Any piece of electronic or electromechanical equipment used mainly, or entirely, for business purposes. Examples are photocopiers, facsimile (fax) machines, printers, and computers.

busing The parallel interconnection of circuits.

busy test A check conducted to find out whether or not a certain telephone subscriber line is in use.

busy tone Also called *busy signal.* An intermittent tone that indicates that the subscriber line being called is in use.

Butler oscillator An oscillator that consists of a two-stage amplifier with a quartz crystal in the positive-feedback path from output to input.

butterfly capacitor A plate-type variable capacitor that has two stator sections and a single rotor section common to the two stators. External connections are made to the stators only. Thus, no wiping contact is required to the rotor, and the troubles associated with such a contact are avoided. The butterfly capacitor is actually two variable capacitors in series. The unit is so called from the shape of its rotor.

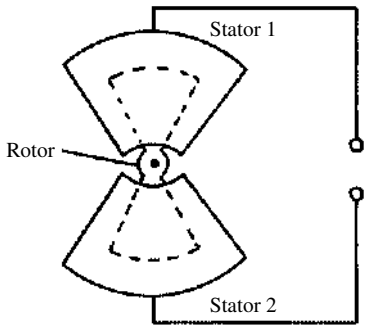

butterfly capacitor

butterfly circuit A combination of a butterfly capacitor and a ring, of which the stator plates of the capacitor are an integral part. The resulting structure is a compact variable-frequency tuned circuit. The ring supplies the inductance, and the butterfly supplies the capacitance. It is also called *butterfly tank* and *butterfly resonator.*

Butterworth filter A high-pass, low-pass, bandpass or band-rejection filter, characterized by a flat passband (absence of passband ripple) and high attenuation at frequencies far removed from the passband.

Butterworth function A mathematical function that is used in the design of a BUTTERWORTH FILTER.

button **1.** Usually, a small switch that is actuated by finger pressure. It is also called pushbutton and pushbutton switch. Sometimes, the term is applied only to the insulated knob or pin which is pushed to operate the switch. **2.** A tiny lump of impurity material, placed on the surface of a semiconductor wafer for alloying with the wafer to form a junction. See ALLOY JUNCTION. **3.** The carbon element(s) in a BUTTON MICROPHONE.

button capacitor A button-shaped ceramic or silvered-mica fixed capacitor. Because of its disk shape and mode of terminal connection, it offers very low internal inductance.

button microphone A microphone in which a button-shaped carbon element is attached to a diaphragm, which is set into vibration by sound waves. This motion causes the button resistance to vary, modulating a direct current that passes

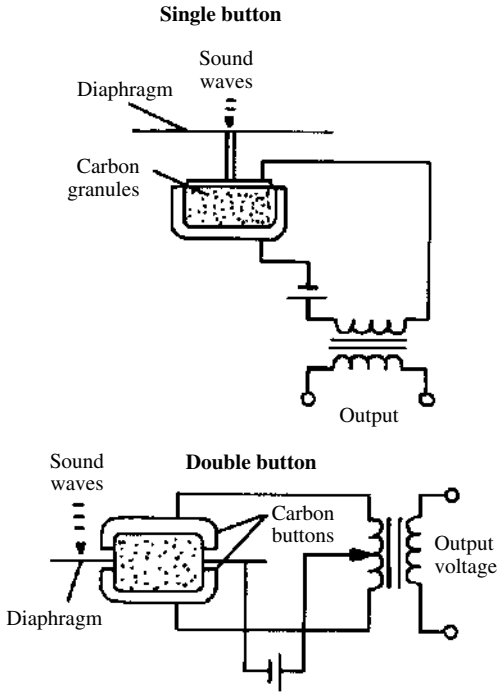

button microphone

5059F-pB_56-92 4/9/01 4:45 PM Page 92

through the button. A single-button microphone has only one button, whereas a double-button microphone has two—one mounted on each side of the center of the diaphragm.

buzz **1.** A low-pitched rough sound with high-frequency components, usually the result of electrical interference from nonsinusoidal voltages generated by neighboring equipment or devices. **2.** The waveform associated with such a sound. **3.** Fastening two conducting surfaces by a KELLIE BOND.

buzzer A nonringing device used principally to generate sound other than that achievable with sine waves. In an electromechanical vibrating-reed buzzer, the reed acts as an armature, which is mounted close to the core of an electromagnet. At quiescence, the reed rests against a stationary contact. When voltage is applied to the electromagnet, the reed is attracted to the core, moving away from the contact; but this breaks the circuit, the magnetism ceases, and the reed springs back to the contact. The action is repeated continuously at a frequency that depends on the reed dimensions and its distance from the core.

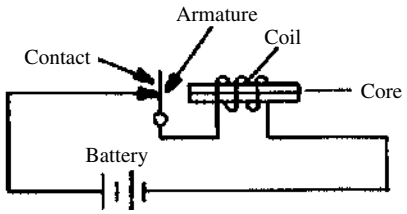

buzzer

BV Abbreviation of BREAKDOWN VOLTAGE.

B voltage The dc voltage required by certain electrodes of vacuum tubes and transistors. It especially pertains to voltages required by the plate and screen of a vacuum tube, as opposed to the filament voltage and control-grid voltage.

bw **1.** Abbreviation of *bandwidth*. 2. Abbreviation of *black-and-white*.

BWA Abbreviation of *backward-wave amplifier*.

BWG Abbreviation of BIRMINGHAM WIRE GAUGE.

BWO Abbreviation of BACKWARD-WAVE OSCILLATOR.

BX Symbol and abbreviation for armored and insulated flexible electrical cable.

bypass A route (either intended or accidental) through which current easily flows around a component or circuit instead of through it.

bypass capacitor A capacitor that is used to conduct an alternating current around a component or group of components. Often the ac is removed from an ac/dc signal, the dc being free to pass through the bypassed component.

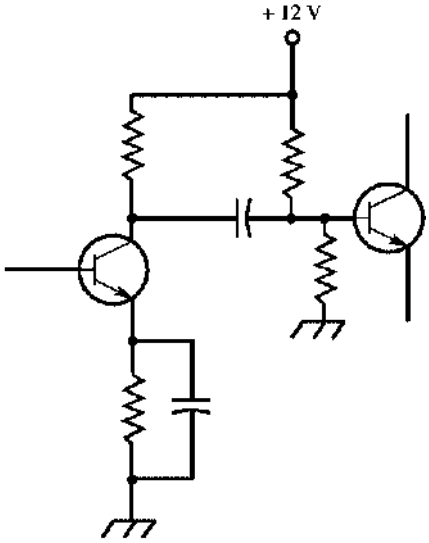

bypass capacitor

B-Y signal In a color television receiver, the color-difference signal which, when combined with a luminance (Y) signal, forms a blue primary signal for the three-gun picture tube.

byte In digital-computer and data-communications operations, a unit of data consisting of eight contiguous bits. In packet communications, the term *octet* is often used.

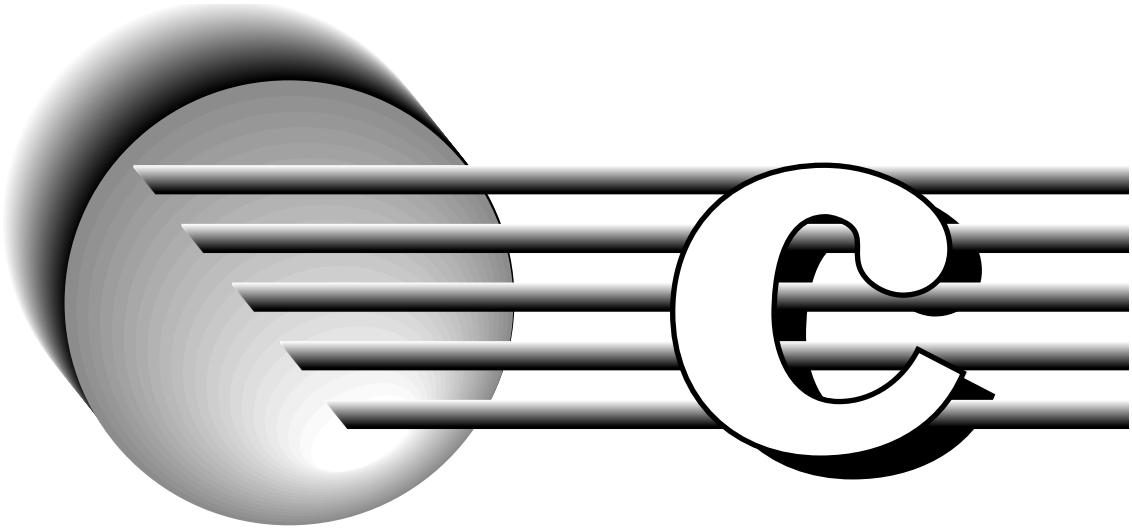

C **1.** Abbreviation of CAPACITANCE. **2.** Symbol for COLLECTOR of a transistor. **3.** Symbol for CARBON. **4.** Abbreviation of CELSIUS. **5.** Symbol for COULOMB. **6.** Abbreviation of CALORIE.

c **1.** Abbreviation of CENTI. **2.** Abbreviation of CENTS. **3.** Symbol for CAPACITANCE. **4.** Symbol for SPEED OF LIGHT in a vacuum.

Ca Symbol for CALCIUM.

cabinet An enclosure for a piece of apparatus. It might or might not incorporate electromagnetic shielding.

cable **1.** A usually flexible (but sometimes rigid) medium, via which electrical power or signals are transferred. Although the term is occasionally applied to a single conductor, especially when it is a braid or weave of a number of wires, cable usually means a bundle of separate, insulated wires or strands of fiberoptic material. **2.** CABLEGRAM.

cable address A code word that specifies the recipient of a CABLEGRAM.

cable assembly A special-purpose cable with connectors.

cable attenuation Reduction of signal intensity along a cable, usually expressed in decibels per foot, hundred feet, mile, etc.

cable capacitance Capacitance between conductors in a cable or between conductors and the outer sheath of a cable. **2.** Sometimes, capacitance between a cable and earth.

cable clamp A support device for cable runs in equipment and systems.

cable communications Telegraphy or telegraphy via a (usually undersea) cable.

cable connector A connector, such as a coaxial fitting, that joins cable circuits or connects a cable to a device.

cabled wiring Insulated leads connecting circuit points; they are tied together with lacing cord or with spaced fasteners.

cablegram A (usually printed) message transmitted or received via undersea cable. Compare RADIOGRAM and TELEGRAM.

cable loss See CABLE ATTENUATION.

cable run The path taken by a cable.

cable splice **1.** An electrical attachment between two sections of cable that has identical or similar construction, with or without the use of connectors. **2.** To electrically attach two sections of cable that have identical or similar construction, with or without the use of connectors.

cable tie A short piece of wire or plastic that holds wires or cables in a bundle.

cable TV See COMMUNITY-ANTENNA TELEVISION.

cache memory A short-term, high-speed, high-capacity computer memory. Similar to a scratchpad or read-write memory.

CAD Acronym for *computer-aided design.*

CAD/CAM Acronym for *computer-aided design and manufacturing.*

cadmium Symbol, Cd. A metallic element. Atomic number, 48. Atomic weight, 112.41. Many electronic structures are cadmium plated for protection.

cadmium borate phosphor Formula, (CdO + B_2O_3): Mn. A substance used as a phosphor coating on the screen of cathode-ray tubes. The characteristic fluorescence is green-orange.

cadmium cell Also called *Weston standard cell.* An electrochemical standard cell used as a reference voltage source. Produces 1.0186 volt at 20°C.

Copyright 2001 The McGraw-Hill Companies, Inc. Click Here for Terms of Use

5059F-pC-93-162 4/9/01 4:51 PM Page 94

cadmium plating The process of coating a conductor or component with cadmium to increase its resistance to corrosion.

cadmium selenide photocell A photoconductive cell in which cadmium selenide is the light-sensitive material.

cadmium silicate phosphor Formula, ($CdO + SiO_2$). A substance used as a phosphor coating on the screen of cathode-ray tubes; the characteristic fluorescence is orange-yellow.

cadmium standard cell See STANDARD CELL.

cadmium sulfide photocell A photoconductive cell in which cadmium sulfide is the light-sensitive material.

cadmium tungstate phosphor Formula, $CdO + WO_3$. A substance used as a phosphor coating on the screen of cathode-ray tubes; the characteristic fluorescence is light blue.

cage A completely shielded enclosure, such as a screen room, which is covered with a grounded fine-mesh conductive screen on all sides.

cage antenna An antenna, usually center-fed and balanced, that consists of multiple parallel conductors arranged in a cylindrical cage configuration. The cage results in a much broader bandwidth than is the case with an antenna made up of a single conductor. Cage antennas are typically used at frequencies between about 10 and 200 MHz.

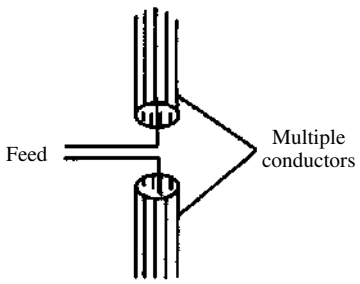

cage antenna

CAI Abbreviation for *computer-assisted instruction*.

CAL An acronym for *conversional algebraic language*, a general-purpose problem-oriented computer programming language used in time-sharing systems.

calcium Symbol, Ca. A metallic element of the alkaline-earth group. Atomic number, 20. Atomic weight, 40.08.

calcium phosphate phosphor Formula, $Ca_3(PO_4)_2$. A substance used as a phosphor coating on the screen of long-persistence cathode-ray tubes; the characteristic fluorescence is white, as is the phosphorescence.

calcium silicate phosphor Formula, ($CaO + SiO_2$): Mn. A substance used as a phosphor coating on the screen of cathode-ray tubes; the characteristic fluorescence ranges from green to orange.

calcium tungstate phosphor Formula, $CaWO_4$. A substance used as a phosphor coating on the screen of short-persistence cathode-ray tubes; the characteristic fluorescence is blue, as is the phosphorescence.

calculate To perform the steps of an intricate mathematical operation. Compare COMPUTE.

calculating punch A data-processing peripheral that reads punched cards, makes calculations, and punches new data into those cards or new cards.

calculator A machine that performs mathematical operations, especially arithmetic. Typically, the device is a small box with buttons and a miniature numeric display. Used only in mathematical applications. In contrast, a COMPUTER can be used for a much wider variety of jobs, such as word processing, graphics, and data-base. Many personal computers have calculator programs; the "buttons" are actuated by pointing and clicking with a mouse.

calculus **1.** The symbology and rules comprising a system of logic, such as BOOLEAN ALGEBRA. **2.** A branch of mathematical analysis concerned with rates of change and accumulation. See DIFFERENTIAL CALCULUS and INTEGRAL CALCULUS.

calendar age The age of a piece of equipment, measured since the date of manufacture. Specified in years, months, and days. The actual manufacture date might alternatively be given.

calendar time The time available in a working period [i.e., a 40-hour work week represents a calendar time of 120 hours (five days times 24 hours per day)].

calibrate To compare and bring into agreement with a standard.

calibrated measurement **1.** A measurement made with an instrument that has been calibrated with a standard reference source. **2.** A measurement that is corrected for instrument error.

calibrated meter An analog or digital meter that has been adjusted to agree as closely as possible with a reference source.

calibrated scale **1.** A scale whose graduations have been carefully checked for accuracy (i.e., they correspond to the true values of the quantity that they represent). The scale is graduated to read directly in units of the quantity, such as milliamperes, kilohertz, volts, etc. **2.** A scale with fixed, plain numeric graduations (e.g., 0 to 100) that do not directly indicate the magnitude of a quantity, but that can be converted to various quantities via graphs, nomographs, tables, or charts. See CALIBRATION CURVE.

calibrated sweep In an oscilloscope, a sweep circuit calibrated to indicate sweep frequency or time at all control settings.

5059F-pC-93-162 4/9/01 4:51 PM Page 95

calibrated triggered sweep In an oscilloscope, a triggered sweep circuit calibrated in terms of sweep time or frequency.

calibration **1.** Determining the accuracy with which an instrument indicates a quantity. **2.** Determining the degree to which the response of a circuit or device corresponds to desired performance. **3.** Marking a scale to show actual values of a quantity in the form of a direct readout. For example, the scale of an analog meter might be calibrated in milliamperes (mA) from 0 to 50 in increments of 1 mA.

calibration accuracy **1.** A quantitative expression of the agreement between the value of a quantity, as indicated by an instrument, and the true value. Usually expressed as the maximum percentage of the true value by which the indicated value can be expected to deviate in either direction (e.g., ±0.5 percent). **2.** The precision of a direct-reading meter in terms of its full-scale deflection (e.g., ±2.0 percent of full scale).

calibration curve A graph showing the relation between the actual values of a quantity and the setting or indication of an instrument or component. Usually plotted in rectangular coordinates.

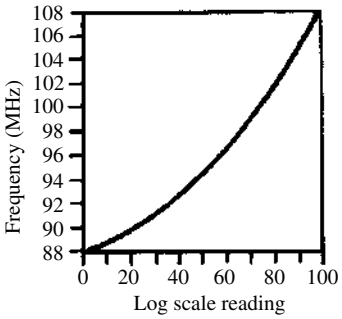

calibration curve

calibration marker A pip or blip, superimposed on a pattern displayed on a cathode-ray-tube (CRT) screen, to identify a point closely as to frequency, voltage, distance, or some similar term.

calibrator A device used to perform a calibration (e.g., a signal generator).

calibrator crystal A highly accurate and stable quartz crystal, used in an oscillator as a frequency standard. An example is the 100-kHz crystal oscillator and harmonic generator used in some communications receivers.

californium Symbol, Cf. A radioactive element produced artificially. Atomic number, 98. Atomic weight, 251.

call **1.** In communications, a transmission by a station for the purpose of either alerting a particular receiving station for which there is a message, or alerting all receiving stations to prepare them for a general broadcast message. **2.** In a computer program, a branch to a closed subroutine; also, to branch to such a subroutine.

call direction code Abbreviation, CDC. In telegraph networks, a special code that, when transmitted to a terminal, causes the teleprinter to be automatically switched on.

calling sequence **1.** Computer program instructions needed to establish the conditions for a call (see CALL, **2**). **2.** Subroutine instructions providing a link to the main program.

call instruction A computer program instruction that makes a program controller branch to a subroutine; it also locates and identifies the parameters needed for the subroutine's execution. Also known as *subroutine call.*

call letters Letters and/or numbers assigned to, and used to identify, licensed radio stations.

calorie Abbreviation, cal or C. The amount of heat energy, at a pressure of 1 atmosphere, that will raise the temperature of 1 gram of water by 1 degree Celsius.

calorimeter An instrument for measuring heat energy. By adaptation, a calorimeter can be used to measure radio-frequency (RF) power—especially at microwave frequencies (see CALORIMETRIC POWER METER).

calorimeter system See CALORIMETRIC POWER METER.

calorimetric power meter A specialized form of wattmeter, in which the power to be measured is dissipated in an oil or water bath that has a known and fixed mass. The wattage is determined indirectly, by measuring the extent to which the temperature of the liquid increases in a certain amount of time.

CAM **1.** Abbreviation of *computer-aided manufacturing.* **2.** Abbreviation of *content-addressed memory.*

cambric Finely woven cotton or linen used for insulation. One type of spaghetti (conductor insulation), for example, is varnished cambric tubing.

camera cable A multiwire cable that conducts the video signal from a television camera to control equipment.

camera chain In television, the camera and the equipment immediately associated with it, excluding the transmitter and its peripherals.

camera signal The output signal delivered by a television camera.

camera tube Any video pickup tube, such as an iconoscope or orthicon, that converts light reflected by a scene into a corresponding television signal.

Campbell bridge A circuit that is used for comparing mutual inductance with capacitance.

camp-on In a telephone system, a method of engaging a line that is busy until it becomes available for use.

CAN Abbreviation of CANCEL CHARACTER.

5059F-pC-93-162 4/9/01 4:51 PM Page 96

can **1.** A metal enclosure or container roughly resembling a tin can (though not necessarily cylindrical), used for shielding or potting components. **2.** Colloquial expression for HEADPHONE.

Canada balsam A transparent cement derived from the turpentine distilled from balsam fir resin. It is useful in optical technology and in certain areas of electro-optics.

Canadian Standards Association The Canadian equivalent of the *National Bureau of Standards* in the United States. An agency that publishes agreed-on standards for industries.

cancel character **1.** IGNORE CHARACTER. **2.** A control character indicating that the associated data is erroneous.

cancellation The elimination of one quantity by another, as when a voltage is reduced to zero by another voltage of equal magnitude and opposite sign.

candela Symbol, cd. The SI unit of luminous intensity; 1 cd represents 1⁄60 of the radiating power of one square centimeter of a perfect radiator at the temperature of freezing platinum.

candle Abbreviation, c. Also called *international candle.* A unit of light intensity that is the value of emission by the flame of a sperm-whale-oil candle burning at the rate of 7.776 grams per hour.

candle power Abbreviation, cp. Luminous intensity in international candles: the luminous intensity resulting from the burning of a sperm-whale-oil candle at 7.776 grams per hour.

candoluminescence White light produced without extreme heat.

cannibalization The deliberate use of parts from operational equipment to temporarily repair or maintain other equipment. It is a last-resort, emergency measure.

cap **1.** Abbreviation of CAPACITANCE. **2.** Abbreviation of CAPACITOR.

capacimeter See CAPACITANCE METER.

capacitance Symbol, C. Unit, farad. The property exhibited by two conductors separated by a dielectric, whereby an electric charge becomes stored between the conductors. Capacitance is thought of as analogous to mechanical elasticity. Also see FARAD.

capacitance bridge A four-arm ac bridge for gauging capacitance against a standard capacitor. In its simplest form, it has a standard capacitor in one arm and resistors in the other three.

capacitance coupling The transfer of ac energy between two circuits or devices by a capacitor or capacitance effect. Also see COUPLING.

capacitance diode See VARACTOR.

capacitance divider An alternating-current voltage divider that uses capacitors, rather than resistors. It is used in certain oscillators, such as the Colpitts type.

capacitance filter A filter consisting of only a high-capacitance capacitor. Because the capacitor cannot discharge instantaneously, it tends to maintain its voltage and smooth out the ripples in the voltage applied to it.

capacitance-inductance bridge A combination ac bridge that can be used for either capacitance or inductance measurement. Both capacitance and inductance can be measured in terms of a standard capacitance; however, some of these bridges use standard inductors in the inductance-measuring mode.

capacitance meter A direct-reading meter for measuring capacitance. In most available types, a stable ac voltage is applied to the meter circuit, to which an unknown capacitor is connected in series; meter deflection is roughly proportional to the reactance of the capacitor. Also called MICROFARAD METER.

capacitance ratio In a variable capacitor, the ratio of maximum to minimum capacitance.

capacitance relay A relay circuit that operates from a small change in its own capacitance. It consists of an RF oscillator whose tank capacitance is very low. When a finger is brought near the circuit's short pickup antenna, the attendant increase in capacitance detunes the oscillator, activating the relay. Also called PROXIMITY RELAY and PROXIMITY SWITCH.

capacitance-resistance bridge A combination ac bridge that can be used for either capacitance or resistance measurement. The unknown resistance is measured against a standard resistor; the unknown capacitance against a standard capacitor.

capacitance sensor See CAPACITANCE TRANSDUCER.

capacitive amplifier See DIELECTRIC AMPLIFIER.

capacitive attenuator An ac attenuator whose elements are capacitors in any desired combination of fixed and/or variable units. The desired attenuation is afforded by the capacitance ratio.

capacitive coupling A means of coupling between circuits that uses a series capacitor for direct-current blocking. The signal passes through the capacitor, but the blocking effect allows different bias voltages to be applied to the two stages.

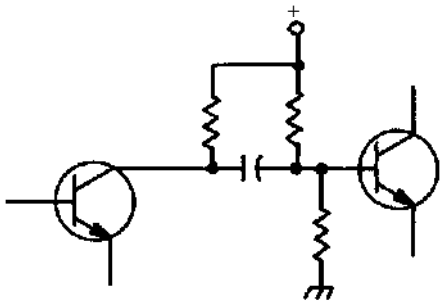

capacitive coupling

5059F-pC-93-162 4/9/01 4:51 PM Page 97

capacitive diaphragm A metal plate deliberately placed in a waveguide to introduce capacitive reactance and, thereby, cancel an inductive reactance.

capacitive-discharge ignition An electronic ignition system for automotive engines. Provides nearly constant high voltage, regardless of engine speed. A dc-to-dc step-up converter charges a large capacitor (typically to 300 volts) when the distributor breaker points are closed; when they are open, the capacitor discharges through the ignition coil, thereby generating an ignition pulse of several thousand volts.

capacitive division Reduction of an ac voltage by a capacitive voltage divider.

capacitive feedback Feeding energy back from the output to the input of an amplifier or oscillator through a capacitor.

capacitive-input filter A smoothing filter for ac power supplies, in which the element closest to the rectifier is a capacitor, regardless of the components or circuits placed subsequently.

capacitive load A load consisting of a capacitor or a predominantly capacitive circuit.

capacitive loading In an antenna, the addition of capacitance in series with the element(s). This raises the resonant frequency for a radiator having a given physical length. It can also serve to increase the physical length required for a radiator having a specified resonant frequency. Compare INDUCTIVE LOADING.

capacitive post A protrusion inside a waveguide for the purpose of introducing capacitive reactance to cancel an inductive reactance.

capacitive potentiometer See CAPACITIVE VOLTAGE DIVIDER.

capacitive pressure sensor A pressure sensor that uses a radio-frequency oscillator and a pair of metal plates separated by dielectric foam. The circuit is designed so a change in the capacitance between the plates causes the oscillator frequency to change. This change is sensed. A signal is sent to an analog-to-digital converter (ADC) and then to a microcomputer that calculates the extent of the pressure.

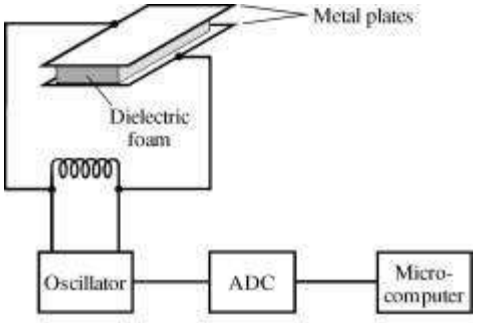

capacitive pressure sensor

capacitive proximity sensor A transducer used in mobile robots that detects the presence of certain kinds of objects. It consists of an oscillator whose frequency is determined by an inductance-capacitance (LC) circuit to which a metal plate is connected. When a conducting or partially conducting object comes near the plate, the mutual capacitance changes the oscillator frequency. This change is detected and sent to the robot controller.

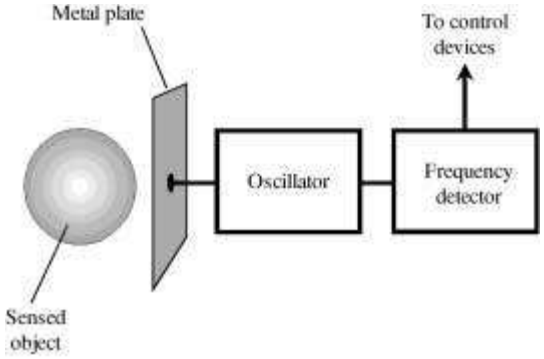

capacitive proximity sensor

capacitive reactance Symbol, X_C. Unit, ohm. The reactance exhibited by an ideal capacitor, considered as a negative pure-imaginary quantity; $X_C = -j/(6.28fC)$, where f is the frequency in hertz, C is the capacitance in farads, and j is the unit imaginary number (the square root of –1). Alternatively, f can be specified in megahertz and C in microfarads. In a pure capacitive reactance, current leads voltage by 90 degrees. Also see CAPACITANCE, CAPACITOR, and REACTANCE.

capacitive speaker See ELECTROSTATIC SPEAKER.

capacitive transducer A transducer consisting essentially of a refined variable capacitor whose value is varied by a quantity under test, such as pressure, temperature, liquid level, etc.

capacitive tuning Variable-capacitor tuning of a circuit.

capacitive voltage divider A capacitive attenuator usually consisting of two series-connected capacitors whose values are such that an applied ac voltage is divided across them in the desired ratio.

capacitive welding An electronic welding system in which energy stored in a capacitor is discharged through the joint to be welded. This develops the heat necessary for the operation.

capacitive window A pair of capacitive diaphragms used in a waveguide to introduce capacitive reactance.

5059F-pC-93-162 4/9/01 4:51 PM Page 98

capacitor A passive electronic-circuit component consisting of, in basic form, two metal electrodes or plates separated by a dielectric (insulator).

capacitor amplifier See DIELECTRIC AMPLIFIER.

capacitor antenna See CONDENSER ANTENNA.

capacitor bank A network of capacitors connected in combination, yielding a desired characteristic.

capacitor braking The connection of a capacitor to the winding of a motor after the removal of power, to speed up the process of braking.

capacitor color code See COLOR CODE.

capacitor decade See DECADE CAPACITOR.

capacitor-discharge ignition CAPACITIVE-DISCHARGE IGNITION.

capacitor filter In a direct-current power supply, a filter consisting simply of a capacitor connected in parallel with the rectifier output.

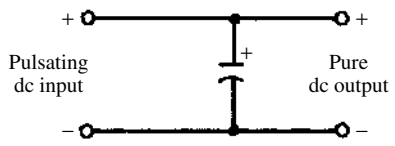

capacitor filter

capacitor-input filter A filter whose input component is a capacitor. The capacitor-input power-supply filter is distinguished by its relatively high dc output voltage, but somewhat poorer voltage regulation, compared with the CHOKE-INPUT FILTER.

capacitor leakage Direct current flowing through the dielectric of a capacitor. In a good nonelectrolytic capacitor, this current is normally less than 1 microampere. In an electrolytic capacitor, it can be up to several milliamperes, depending on the capacitance and the applied voltage.

capacitor loudspeaker See ELECTROSTATIC SPEAKER.

capacitor microphone See CONDENSER MICROPHONE.

capacitor motor An ac motor that uses a capacitor in series with an auxiliary field winding for starting purposes. Initially out-of-phase current in the auxiliary field (starting winding) causes a rotating field that turns the rotor. When the rotor reaches a safe speed, a centrifugal switch disconnects the capacitor and auxiliary field, and the motor continues running as an induction motor.

capacitor series resistance The ohmic loss in a capacitor. It results partly from conductor losses, and partly from losses in the dielectric material.

capacitor substitution box An enclosed assortment of selected-value capacitors arranged to be switched one at a time to a pair of terminals. In troubleshooting and circuit development, any of several useful fixed capacitance values can be thus obtained.

capacitor voltage **1.** The voltage at the terminals of a capacitor. **2.** The maximum voltage rating of a capacitor.

capacitor voltmeter See ELECTROSTATIC VOLTMETER.

capacity **1.** A measure of a cell's or battery's ability to supply current during a given period. **2.** CAPACITANCE. **3.** The number of bits or bytes a computer storage device can hold. **4.** The limits of numbers that a register can process.

capacity lag In an automatic control system, a delay caused by the storing of energy by the components. For example, in a heating system, capacity lag results from the time taken to heat the air or fluid after the thermostat turns on the heat.

capillary electrometer A sensitive voltage indicator, consisting of a column of mercury in a transparent capillary tube, in which is suspended a small drop of acid. When a voltage is applied to both ends of the mercury column, the acid drop moves toward the low-potential end of the column over a distance proportional to the voltage.

capstan The driven spindle or shaft of a magnetic tape recorder or transport.

capture area The effective ability of a radio antenna to pick up electromagnetic signals. The larger the capture area, the greater the antenna gain.

capture effect **1.** In frequency-modulation (FM) radio receivers, the effect of domination by the stronger of two signals, or by the strongest of several signals, on the same frequency. **2.** In an automatic-frequency-control system, the tendency of the receiver to move toward the strongest of several signals near a given frequency. **3.** In general, the tendency of one effect to totally predominate over other effects of lesser amplitude.

capture ratio A measure of frequency-modulation (FM) tuner selectivity: The amplitude difference, in decibels, between unwanted signals and the one being tuned in.

carbon Symbol, C. A nonmetallic element. Atomic number, 6. Atomic weight, 12.011. Carbon, besides being an invaluable material in electronics, is an important constituent of organic compounds.

carbon arc The arc between two electrified pencils of carbon or, as in an arc converter, between a carbon pencil and a metal electrode.

carbon brush A contact made of carbon or some mixture of carbon and another material, used in motors, generators, variable auto-transformers, rheostats, and potentiometers.

carbon-button amplifier An audio-frequency amplifier having as the active component an earphone whose diaphragm is attached to a carbon microphone button. The input signal applied to the earphone makes its diaphragm vibrate. The vibrating button modulates a local

5059F-pC-93-162 4/9/01 4:51 PM Page 99

direct current. Amplification results from the large ratio of modulated local current to input-signal current.

carbon-composition resistor A non-inductive resistor made from a mixture of finely powdered carbon with a non-conductive substance, usually phenolic. The resulting clay-like material is pressed into a cylindrical shape, and wire leads are inserted in the ends. The resistance depends on the ratio of carbon to the non-conducting material, and on the physical distance between the wire leads. This type of resistor is useful from direct current to ultra-high radio frequencies. Compare FILM RESISTOR, WIREWOUND RESISTOR.

carbon/disk rheostat A rheostat consisting of a stack of carbon disks or washers, arranged so that a controllable pressure can be exerted on the stack. As a knob is turned, a screw increases or decreases the pressure, varying the total resistance of the stack.

carbon-film resistor A stable resistor whose resistance element is a film of carbon, vacuum-deposited on a substrate, such as a ceramic.

carbonization The application of a coat of carbon onto an electrode, either by electroplating or by any other means.

carbon microphone A microphone that includes one or two carbon buttons. See BUTTON MICROPHONE.

carbon-paper recorder A recorder in which a signal-actuated stylus writes, by impression only, through a sheet of carbon paper onto a plain sheet underneath. This eliminates the need for an ink-carrying stylus.

carbon-pile regulator A voltage regulator in which a stack of carbon disks or washers is in series with the shunt field. The pile resistance and field current depend on pressure applied to the pile by a wafer spring acting through a movable iron armature. Voltage drops increase the pressure and voltage rises decrease the pressure, thus regulating the generator with which it is associated.

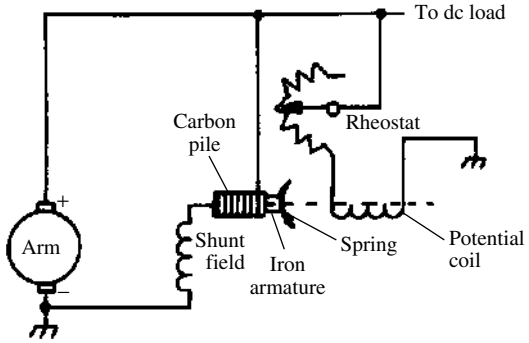

carbon-pile regulator

carbon-pile rheostat See CARBON-DISK RHEOSTAT.

carbon recording 1. A record made with a CARBON-PAPER RECORDER. **2.** The use of a carbon-paper recorder in data acquisition, facsimile, communications, and similar applications.

carbon resistor A resistor made from carbon, graphite, or some composition that contains carbon.

carbon/silicon-carbide thermocouple A thermocouple that is a junction between carbon and silicon carbide.

carbon transfer recording A method of facsimile reception in which the image is reproduced by carbon particles sprayed on the paper, a process controlled by the received signal.

carbon-zinc cell See ZINC-CARBON CELL.

Carborundum Formula, SiC. Trade name for a synthetic silicon carbide used as a semiconductor, refractory, or abrasive. Also see SILICON CARBIDE.

Carborundum crystal Trade name for a characteristically superhard crystal of silicon carbide.

Carborundum varistor A voltage-dependent resistor made from Carborundum.

carcinotron A special kind of oscillator tube used at ultra-high and microwave frequencies.

card 1. A usually thin, rectangular board containing a PRINTED CIRCUIT, often equipped with an edge connector that makes it easy to install, remove, or replace. Common in electronic and computer equipment having modular construction. **2.** The usually flat, thin insulating strip on which a resistor element is wound.

cardiac monitor An electronic device that displays or records electrical impulses from the heart for medical observation or diagnosis.

cardiac pacemaker An electrical cardiac stimulator that causes the heart to beat at certain intervals. Used when the patient has heart disease that prevents the heart from regulating itself.

cardiac stimulator An electronic device (sometimes implanted in the subject) that supplies electric pulses to stimulate heart action. Also called DEFIBRILLATOR and PACEMAKER.

card image In memory storage, the data contained on a single card.

cardiogram ELECTROCARDIOGRAM.

cardiograph ELECTROCARDIOGRAPH.

cardioid diagram A polar response curve in the shape of a cardioid pattern.

cardioid microphone A microphone with a (roughly) heart-shaped sound-field pickup pattern.

cardioid pattern A radiation/response pattern with one sharp null in the direction opposite the single main lobe. The lobe is extremely broad. In two dimensions, the curve is shaped somewhat like a "Valentine" heart.

cardiotachometer A device that indicates the pulse rate.

cardistimulator See CARDIAC STIMULATOR.

5059F-pC-93-162 4/9/01 4:51 PM Page 100

Carey-Foster bridge A special version of the slide-wire bridge that is useful for measuring an unknown resistance, whose value is close to that of a standard resistance.

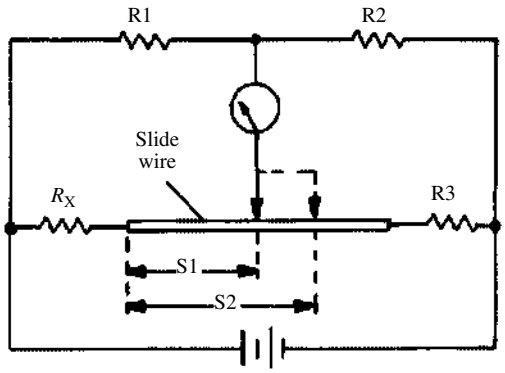

Carey-Foster bridge

Carey-Foster mutual inductance bridge An ac bridge that permits the measurement of mutual inductance in terms of a standard capacitor.

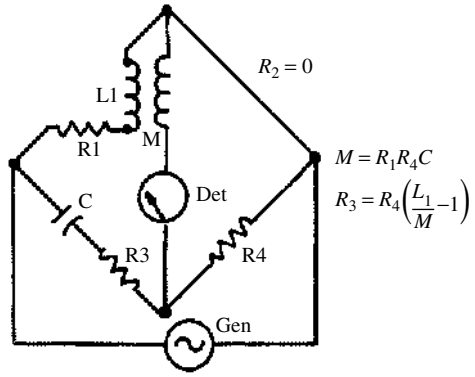

Carey-Foster mutual inductance bridge

carnauba wax A wax obtained from the Brazilian wax palm. Used as an electrical insulator, and as the dielectric in some electrets.

Carnot theorem In thermodynamics, the proposition that in a reversible cycle, all available energy is converted into mechanical work. Also called *Carnot's principle*.

carrier **1.** See CARRIER WAVE. **2.** See CHARGE CARRIER.

carrier amplifier See DIELECTRIC AMPLIFIER.

carrier beating **1.** The mixing of two radio-frequency carriers that are separated by a small amount of frequency, resulting in an audible tone in a receiver. **2.** A heterodyne in a facsimile or television signal, resulting in a pattern of cross hatches in the received image.

carrier choke A radio-frequency (RF) choke, inserted in a line to block a carrier component.

carrier chrominance signal For conveying color television information, sidebands of a modulated chrominance subcarrier.

carrier color signal For conveying color information in color television transmission, the sidebands of a modulated chrominance subcarrier (plus the unsuppressed chrominance subcarrier) added to the monochrome signal.

carrier concentration In a semiconductor material, the number of charge carriers per unit volume.

carrier control **1.** The modification, adjustment, or switching of a carrier wave. **2.** Adjustment of a circuit or device by means of a carrier wave.

carrier current The current component of a carrier wave, or the amplitude of that current. Compare CARRIER POWER and CARRIER VOLTAGE.

carrier-current communication See WIRED WIRELESS.

carrier-current control **1.** Control of the current component in a carrier wave. **2.** Remote control by means of wired wireless.

carrier-current receiver See WIRED-RADIO RECEIVER.

carrier-current relay A radio-frequency (RF) relay circuit, operated over a wire line by means of a transmitter.

carrier-current transmitter See WIRED-RADIO TRANSMITTER.

carrier deviation See CARRIER SWING.

carrier dispersion In a semiconductor, the spreading out of electrons and holes that leave the emitter simultaneously, but arrive at the collector at various times after following different paths.

carrier frequency The center frequency of a CARRIER WAVE.

carrier-frequency pulse A pulse that contains radio-frequency oscillation.

carrier-frequency range The band of carrier frequencies over which a transmitter or signal generator can operate.

carrier injection The apparent emission (injection) of electrons or holes into a semiconductor when a voltage is applied to the junction.

carrier leak **1.** A point at which carrier-wave energy escapes a circuit or enclosure. **2.** The residual carrier voltage present in the output of a carrier-suppressing circuit.

carrier level The amplitude of an unmodulated carrier wave.

carrier lifetime In a semiconductor, the interval before an injected current carrier (see CARRIER INJECTION) recombines with an opposite carrier and ceases to be mobile.

carrier line In carrier-current systems (see WIRED WIRELESS), the line or cable conducting the carrier-wave energy.

5059F-pC-93-162 4/9/01 4:51 PM Page 101

carrier mobility Symbol, μ. In a semiconductor material, the average drift velocity of electrons and holes per unit electrostatic field.

carrier noise Modulation of a carrier when there is no input from the modulator itself; unwanted modulation.

carrier noise level The noise signal amplitude that results from unintentional fluctuations of an unmodulated carrier.

carrier-on-light transmission A form of transmission in which many different signals are sent simultaneously by modulating a beam of light at multiple frequencies.

carrier-on-microwave transmission A form of transmission in which many different signals are sent simultaneously by modulating a microwave signal at multiple lower frequencies.

carrier-on-wire transmission A form of transmission in which many different signals are sent at the same time over a wire, by using radio-frequency carriers. Also called CARRIER-CURRENT COMMUNICATIONS or WIRED RADIO.

carrier oscillator In a single-sideband receiver, the radio-frequency (RF) oscillator that supplies the missing CARRIER WAVE.

carrier power The actual power represented by a radio-frequency (RF) carrier applied to an antenna, measured by either the direct or indirect method. The direct method involves determination of power according to the formula $P = I^2R$, where I is antenna current and R is antenna resistance at the point of current measurement. The indirect method involves determination of power according to the formula $P = EIF$, where E and I are antenna voltage and current, and F is a factor less than 1.0, whose value depends on the type of modulation used.

carrier power-output rating The power delivered by an unmodulated transmitter or generator to the normal load or its equivalent.

carrier shift In an amplitude-modulated transmitter or generator, the undesired change of average carrier voltage during modulation.

carrier-shift indicator An instrument for detecting carrier shift. It usually contains only a pickup coil, semiconductor diode, and dc milliammeter in series. Meter deflection is steady until carrier shift is detected; then, the needle fluctuates.

carrier signaling In wire telephony, the use of carrier-wave signals to operate such functions as dialing, ringing, busy signal, etc.

carrier storage In a semiconductor device, the tendency of mobile carriers to stay near a junction for a short time after the junction voltage has been removed or reversed in polarity.

carrier suppression The elimination of the carrier in an amplitude-modulated signal so that only the sideband energy remains.

carrier swing In frequency-modulated or phase-modulated transmission, the total deviation (lowest to highest instantaneous frequency) of the carrier wave.

carrier system The transmission of many signals over one circuit, accomplished by modulating various different carriers at different frequencies. Different signals can use different modulation methods.

carrier telegraphy **1.** Continuous-wave telegraphy by WIRED WIRELESS. **2.** Wired-wireless telegraphy in which a radio-frequency carrier is modulated by an audio-frequency keying wave.

carrier telephony Telephone communication by WIRED WIRELESS.

carrier terminal **1.** At each end of a carrier-current line or cable, the equipment for generating, modifying, or utilizing the carrier energy. **2.** In a balanced modulator, the point of carrier insertion.

carrier-to-noise ratio The ratio of carrier amplitude to noise-voltage amplitude.

carrier transmission Transport of information by a carrier, as by an amplitude-modulated radio wave that carries the low-frequency information as the AF modulation envelope and delivers it to the demodulator at the receiving station.

carrier-type dc amplifier A high-frequency ac amplifier, ahead of which is operated a generator and transducer. A dc voltage applied to the transducer modulates the carrier supplied by the generator; the amplifier boosts the modulated wave, and the resultant output is rectified at a level higher than that of the dc input signal.

carrier voltage The voltage component of a carrier wave; also, the amplitude of this component. Compare CARRIER CURRENT and CARRIER POWER.

carrier wave A sine wave that is modulated to convey information in wireless and cable communications systems. The lowest frequency normally used for wireless signal transmission is 9 kHz, corresponding to a wavelength of approximately 33 km. The highest frequency is less well defined; some systems make use of visible light waves, whose wavelengths are as short as approximately 4×10^{-7} m. For modulation to work effectively, the carrier must have a frequency at least 10 times the highest frequency of the modulating signal.

carry **1.** In adding a column of figures, the digit added to the column at the left when the sum exceeds one less than the radix value. **2.** In digital computers and counters, a pulse that corresponds to the arithmetic operation in which a figure is carried to the next column in addition.

carrying capacity The ability of a conductor, such as copper wire, to carry current safely (expressed in maximum amperes).

carry-complete signal In an arithmetic computation by a computer, an adder-produced signal indicating that the pertinent carries have been generated.

carry system A communications system in which several carries occupy one circuit.

5059F-pC-93-162 4/9/01 4:51 PM Page 102

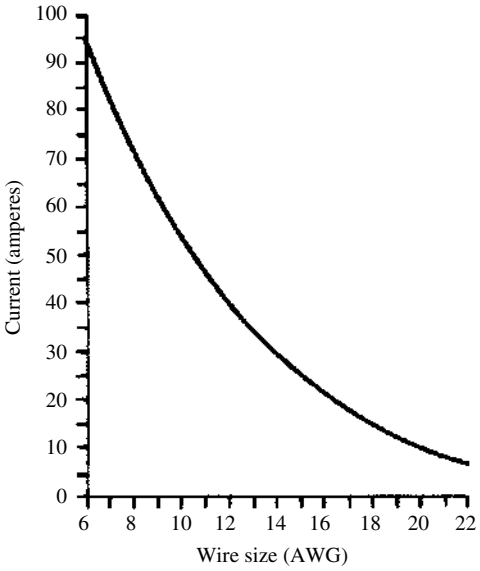

carrying capacity (of some AWG sizes of copper wire)

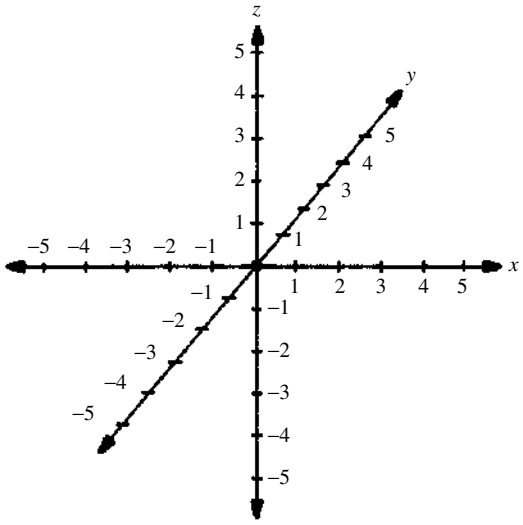

Cartesian three-space

carry time The time taken for a digital computer or counter to perform a carry operation (See CARRY, **2**).

Cartesian coordinate geometry Also called *rectangular coordinate geometry.* In robotic systems, a movement scheme in two or three dimensions. The position of the robot arm is determined by linear coordinates, relative to an origin point. These coordinates are specified along linear axes—each of which is perpendicular to the others at the origin. See CARTESIAN COORDINATES, CARTESIAN PLANE, and CARTESIAN THREE-SPACE.

Cartesian coordinates Also called *rectangular coordinates.* A mathematical system that uniquely defines the position of a point on a plane, in space, or in general, in an *n*-dimensional hyperspace when *n* is a whole number greater than 3. There are *n* axes for *n* dimensions, each axis intersects all the others at a single point, called the origin. The axes are mutually perpendicular at this origin. The axes are scaled in units with the origin having coordinate values that are all equal to zero (usually). Positive values go along the axes in one direction; negative numbers go in the opposite direction for each axis. Usually, the axes are graduated in equal-sized units. The system gets its name from the mathematician Rene Descartes.

Cartesian plane A linear, two-dimensional coordinate plane commonly used for graphing equations in one variable.

Cartesian three-space A linear, three-dimensional graph-coordinate system used for rendering equations in one or two variables.

Cartesian three-space graph A three-dimensional graph that shows an equation in one or two variables. Three-space graphs are often displayed more clearly by means of computer graphics, in which the entire display can be rotated to show the characteristics of the surface resulting from a given equation or function.

Cartesian n-space The coordinate space defined by a Cartesian system of *n* coordinates, where *n* is a whole number of 2 or greater.

cartridge **1.** The replaceable transducer assembly of a microphone. **2.** A magnetic-tape magazine. Also see TAPE CARTRIDGE. **3.** A removable computer mass-storage medium, containing a tape, magnetic diskette, or optical diskette. **4.** An insulating tube housing a fuse, semiconductor component, resistor, capacitor, or other part.

cartridge fuse A fuse consisting of a fusible wire enclosed in a cartridge, having a ferrule at each end for plug-in connection.

cascadable Capable of, or designed for, being connected in cascade with other similar or identical components.

cascade **1.** Components or stages connected and operated in sequence, as in a three-stage amplifier. The components or stages are often but not necessarily identical. **2.** To form a cascade.

cascade control **1.** In an automatic control system, a controller whose setting is varied by the output of another controller. **2.** An automatic control system in which the control units are connected in stages, so that one unit must operate before the next one can function.

cascaded amplifier A multistage amplifier in which the stages are forward-coupled in succession.

5059F-pC-93-162 4/9/01 4:51 PM Page 103

cascaded carry In digital computer practice, a system of performing the carry operation (see CARRY) in which the $n + 1$ place receives a carry pulse only when the nth place has received carry information to generate the pulse.

cascade thermoelectric device A thermoelectric component or circuit that consists of several cascaded sensors (see CASCADE, **1**).

cascade voltage doubler A voltage-doubler circuit (see VOLTAGE DOUBLER) consisting of two diode-capacitor combinations in cascade. Unlike the conventional voltage-doubler circuit with two capacitors in the output, the cascade voltage doubler has one in the input and one in the output.

cascode A high-gain, low-noise, high-input-impedance amplifier circuit, consisting of a grounded-emitter or grounded-source input stage coupled directly to a grounded-base or grounded-gate output stage.

cascode (field-effect transistor arrangement)

case temperature The temperature at a designated point on the outside surface of a component's case or housing.

Cassegrain antenna A dish antenna that uses CASSEGRAIN FEED.

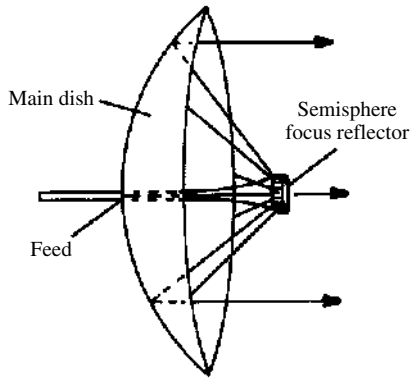

Cassegrain antenna

Cassegrain feed A dish-antenna feed system in which the feed point is located at the center of the dish itself. For transmission, the radio-frequency energy emerges from a waveguide and is directed to a small convex reflector at the focal point of the dish. The small reflector directs the signal back to the dish, spreading the energy out to cover the entire surface of the dish. The dish reflects the energy again and collimates it in the desired direction of propagation. For reception, the process is reversed; the dish focuses the energy on the small reflector, which propagates it back to the feed point.

cassette **1.** A holder (magazine) of reels of magnetic tape that is itself a mechanical subassembly, which can be easily inserted into and removed from a tape deck. **2.** A lightweight holder of photographic film or X-ray plates (before, during, and after exposure).

castor oil A viscous insulating oil extracted from castor beans. Highly refined castor oil is used as an impregnant in some oil-filled capacitors. Dielectric constant, 4.3 to 4.7. Dielectric strength, 380 V/mil.

CAT Abbreviation of COMPUTERIZED AXIAL TOMOGRAPHY.

catalysis The process whereby an agent, called a catalyst, enhances a chemical reaction without entering into the reaction. Catalysts are used in electronics, for example, to promote the setting of resins in potting and encapsulating operations.

catalytic agent A substance that accomplishes catalysis.

cataphoresis As caused by the influence of an electrostatic field, the migration toward the cathode of particles suspended in a liquid.

catastrophic failure **1.** Sudden, unexpected failure of a component or circuit. **2.** Failure that can result in the breakdown of an entire system. Also called *catastrophic breakdown.*

catcher In a Klystron, the second reentrant cavity. (See KLYSTRON.)

catcher diode A diode that is connected to regulate the voltage at the output of a power supply. The cathode is connected to a source of reference voltage. If the anode, connected to the source to be regulated, becomes more positive than the cathode, the diode conducts and prevents the regulated voltage from rising more than 0.3 volt above the reference voltage (for germanium diodes) or 0.6 volt above the reference voltage (for silicon diodes).

catcher grids In a Klystron, the grids through which the bunched electrons pass on their way from the buncher to the collector. Catcher grids absorb energy from the bunched electrons and present it to the collector circuit.

category In a computer system, a group of magnetic disk volumes containing information related by a common application.

category storage A computer-file storage section that contains a number of categories and used by an operating system.

catenation See CONCATENATION.

cathode **1.** The negative electrode of a device (i.e., the electrode from which electrons move when a

5059F-pC-93-162 4/9/01 4:51 PM Page 104

current passes through the device). **2.** In an electrochemical cell, the electrode that gains electrons. This is generally the positive electrode. **3.** In a vacuum tube, the electron-emitting electrode (filament or indirectly heated cathode sleeve).

cathode current Symbol I_K. The current flowing in the cathode circuit of a tube. Cathode current is the total of grid, plate, screen, and suppressor currents, and can have an ac and a dc component.

cathode dark current The electron emission from the photocathode of a camera tube when there is no illumination.

cathode element In a vacuum tube, an indirectly heated emitter of electrons. Also see CATHODE, **2.**

cathode emission **1.** The giving up of electrons by the cathode element of a device, such as a vacuum tube. Electrons can be emitted by either hot or cold cathodes, depending on the tube. **2.** Collectively, electrons released by a cathode.

cathode heating time The time required for the temperature of a tube cathode to increase from cold to its maximum specified operating temperature after the cathode current has been initiated. Also called cathode warmup time.

cathode luminous sensitivity For a photomultiplier tube, the cathode's sensitivity to light. This sensitivity figure is the ratio of photocathode current to incident light flux.

cathode-ray oscillograph An instrument that provides a permanent record, by photographic or other means, of the image on the screen of a cathode-ray tube.

cathode-ray oscilloscope See OSCILLOSCOPE.

cathode rays Invisible rays emanating from the cathode element of an evacuated tube operated with a high voltage between the anode and cathode. Cathode rays (electrons) cause certain substances, PHOSPHORS, to glow upon striking them.

cathode-ray scanning tube Any tube in which an electron beam is deflected horizontally and vertically to scan an area. These include oscilloscope tubes, some computer monitors, radar displays, and television camera tubes.

cathode-ray tube **1.** An evacuated tube containing an anode and cathode that generates cathode rays when operated at high voltage. **2.** An oscilloscope tube. **3.** A picture tube.

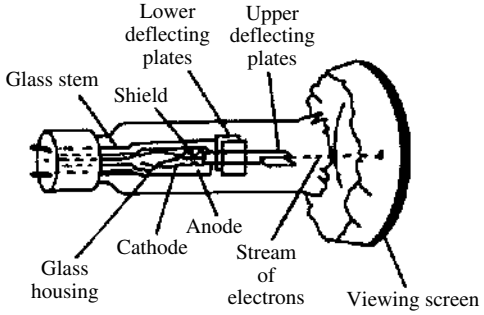

cathode-ray tube

cathode terminal **1.** In a diode (semiconductor or tube), the terminal to which a negative dc voltage must be applied for forward-biasing the diode. Compare ANODE TERMINAL. **2.** In a diode, the terminal at which a positive dc voltage appears when the diode acts as an ac rectifier. Compare ANODE TERMINAL. **3.** The terminal connected internally to the cathode element of device. **4.** In a vacuum tube, an indirectly heated electron emitter.

cathode voltage Symbol, E_K. The voltage between ground (or B-minus) and the cathode of a tube; it can have both ac and dc components.

cathodic protection A method of preventing corrosive galvanic action in underground metal pipes or the submerged hulls of ships. The part to be protected is used as the cathode of a circuit through which a direct current is passed in the direction opposite to that which caused the corrosion, thus counteracting it.

cathodofluorescence Fluorescence resulting from a material's exposure to cathode rays.

cathodoluminescence In a vacuum chamber in which a metal target is bombarded with high-velocity electrons (cathode rays), the emission of radiation of a wavelength characteristic of the metal.

cation A positive ion. Also see ION.

CAT scanner The X-ray apparatus for COMPUTERIZED AXIAL TOMOGRAPHY.

CATV Abbreviation of COMMUNITY-ANTENNA TELEVISION (usually cable television).

caustic soda electrolyte Symbol, NaOH. Sodium hydroxide solution, as used in some secondary cells and experimental devices.

cavitation The local formation of cavities in a fluid used in ultrasonic cleaning because of the reduction in pressure at those points.

cavitation noise In an ultrasonic cleaner, the noise resulting from the collapse of bubbles produced by cavitation.

cavity A metallic chamber (can) in which energy is allowed to reflect, sometimes resulting in resonance.

cavity filter A microwave (usually band rejection) filter consisting of a resonant cavity and associated coupling devices.

cavity frequency meter See CAVITY WAVEMETER.

cavity impedance The impedance across a cavity at a particular frequency. At resonance, the cavity impedance is purely resistive.

cavity laser A laser that employs a resonant cavity filled with gas, such as helium/neon or argon, and a pair of reflectors. Resonance occurs between the reflectors, one of which is totally reflective and the other of which is approximately 95 percent reflective. Output is from the partially reflective end of the device.

5059F-pC-93-162 4/9/01 4:51 PM Page 105

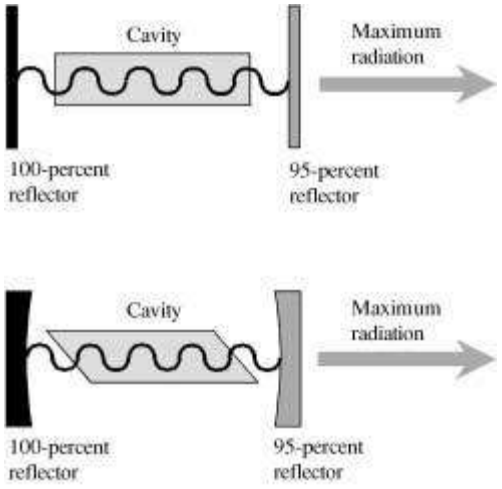

cavity laser

cavity magnetron A magnetron whose anode is a series of resonant cavities.

cavity oscillator An oscillator with a cavity-tuned circuit.

cavity radiation Energy radiated from a tiny hole in an otherwise sealed chamber. The radiation occurs at all electromagnetic wavelengths; the greater the temperature within the chamber, the greater the frequency at which the radiation has its maximum amplitude.

cavity resonance The phenomenon whereby a hollow cavity resonates; specifically, resonance in small metal cavities at microwave frequencies.

cavity resonator See RESONANT CAVITY.

cavity wavemeter An absorption wavemeter whose adjustable element is a tunable resonant cavity into which radio-frequency (RF) energy is injected through a waveguide or coaxial cable. Such an instrument is useful at microwave frequencies.

CB Abbreviation of CITIZENS BAND.

Cb Symbol for COLUMBIUM.

C_B Symbol for BASE CAPACITANCE of a transistor.

C band The band of radio frequencies between 3.9 and 6.2 GHz.

C_C Symbol for collector capacitance of a transistor.

cc **1.** Alternative abbreviation of *cubic centimeter*. The International Organization for Standardization recommends cm^3. **2.** Abbreviation of COTTON-COVERED.

CCA Abbreviation of CURRENT-CONTROLLED AMPLIFIER.

CCD Abbreviation of CHARGE-COUPLED DEVICE.

CCIS Abbreviation of COMMON-CHANNEL INTERFACE SIGNALING.

CCIR Abbreviation of *Comite Consultatif International des Radiocommunications (International Radio Consultative Committee).*

CCIT Abbreviation of *Comite Consultatif International Telegrafique (International Telegraph Consultative Committee).*

CCITT Abbreviation of *Comite Consultatif International Telegrafique et Telephonique (International Telegraph and Telephone Consultative Committee).*

CCS **1.** Abbreviation of CONTINUOUS COMMERCIAL SERVICE. **2.** Abbreviation of *common-channel signaling.*

CCTV Abbreviation of CLOSED-CIRCUIT TELEVISION.

CCTV monitor A video monitor that receives a signal from a CCTV transmitter.

CCTV signal The picture signal in a CCTV system. It can be either a modulated radio-frequency signal or a composite video signal.

ccw Abbreviation of COUNTERCLOCKWISE.

CD Abbreviation of COMPACT DISK.

Cd Symbol for CADMIUM.

cd Abbreviation of CANDELA.

CD-4 A method of obtaining quadraphonic reproduction on a phonograph disk using modulated carriers with frequencies above the human hearing range.

CDI Abbreviation of CAPACITOR-DISCHARGE IGNITION.

C display A radar display showing the target as a dot whose coordinates represent the bearing (horizontal) and angle of elevation (vertical). Compare A DISPLAY, J DISPLAY, and K DISPLAY.

cd/m^2 Candelas per square meter, the SI unit of luminance.

CD-ROM Abbreviation of COMPACT-DISK READ-ONLY MEMORY.

Ce Symbol for CERIUM.

C_e Symbol for EMITTER CAPACITANCE of a transistor.

ceiling **1.** The maximum possible power output from a transmitter. **2.** The maximum possible current or voltage that a circuit can deliver. **3.** In aviation, the level of the cloud base.

ceilometer An instrument for measuring ceiling (cloud height).

cel In animated graphics, an individual image or frame.

cell **1.** A single (basic) unit for producing dc electricity by electrochemical or photovoltaic action, as in a battery or a solar panel. Also see PRIMARY CELL, STANDARD CELL, STORAGE CELL. **2.** An addressable, one-word-capacity storage element in a computer memory. **3.** The geographic region covered by a specified repeater in a cellular communications network. See CELLULAR COMMUNICATIONS. **4.** An electrostatic charge dipole in the atmosphere, usually occurring in or near thunderstorms. **5.** A thunderstorm.

cell constant The surface area of the electrodes in a cell divided by the distance between them. The basic linear units must be the same: for example, square centimeters for surface area and centimeters for distance.

5059F-pC-93-162 4/9/01 4:51 PM Page 106

cell counter A bioelectronic instrument used to count blood cells and other minute particles.

cell reversal A condition that can occur in some rechargeable electrochemical cells and batteries, such as *nickel-cadmium batteries.* It most often results from neglecting to recharge the cell or battery when it has become fully discharged.

cell-type enclosure A room designed to prevent the entrance or escape of radio-frequency (RF) electromagnetic fields, characterized by double-walled copper-mesh shielding.

cellular coil A coil having a crisscross (usually multilayer) winding. Examples: lattice-wound coil, honeycomb coil, basket-weave coil.

cellular communications A radio, telephone, or television communications network that makes use of numerous fixed repeaters. Subscribers use mobile or portable transceivers that are always within range of at least one repeater. The most common form is known as *cellular telephone* or *cellular mobile radio telephone.*

celluloid A thermoplastic dielectric material that is a blend of cellulose nitrate and camphor. Dielectric constant, 4 to 7. Dielectric strength, 250 to 780 V/mil.

cellulose acetate A plastic dielectric material used as a substrate for magnetic tapes, photographic film, and similar applications. Dielectric constant, 6 to 8. Dielectric strength, 300 V to 1 kV/mil. Also see ACETATE.

cellulose acetate base See ACETATE BASE.

cellulose acetate butyrate A thermoplastic dielectric material that is an acetic and butyric acid ester of cellulose.

cellulose acetate tape See ACETATE TAPE.

cellulose nitrate The nitric acid ester of cellulose, a plastic insulating material.

cellulose propionate A thermoplastic molding material that is a propionic acid ester of cellulose.

Celsius scale A temperature scale in which 0 degrees is the freezing point of water, and 100 degrees the boiling point of water. Also called CENTIGRADE SCALE. Compare ABSOLUTE SCALE, and FAHRENHEIT SCALE.

cent An audio-frequency interval of 0.01 (1/100) of a half step. A half step is the frequency difference between two immediately adjacent keys on a piano.

center channel In high-fidelity stereo, a phantom sound source that appears to exist midway between the left and right speakers or earpieces. The effect is caused by identical, or nearly identical, signals in the left and right channels.

center-fed antenna An antenna in which the feeders are connected to the center of the radiator.

center feed **1.** Attaching a feeder or transmission line to the center of the radiator of an antenna. **2.** Connection of signal-input terminals to the center of a coil. **3.** Descriptive of paper tape whose feed holes are aligned with character hole centers. Compare ADVANCE FEED TAPE.

center frequency **1.** The frequency, in a communications receiver, that is midway between the lower and upper 3-dB-down amplitude points. **2.** The average frequency of a modulated carrier. **3.** The carrier frequency of a modulated signal, whether or not the carrier is suppressed.

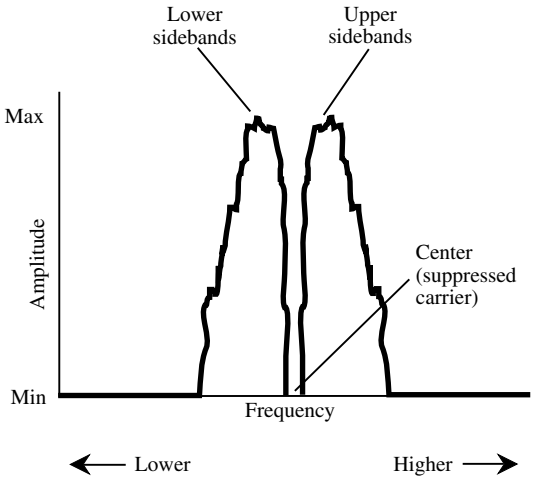

center frequency, 3.

centering control In an oscilloscope circuit, a potentiometer used to position the image on the screen (particularly in the center). Separate controls are provided for horizontal and vertical centering.

center loading In an inductively loaded antenna, placement of the loading coil(s) at or near a point or points midway between the feed point and the end(s) of the radiating element.

center of beam **1.** In a directional antenna system, the direction, denoted by a straight ray, where the signal strength or response is the greatest. **2.** In a beam of visible light, the geometric center of the spot produced when the beam strikes a surface perpendicular to the beam. **3.** In a beam of visible light, the axis within the beam where the intensity is greatest.

center of channel The frequency that is midway between the lowest and highest frequency components of a communications channel.

center of radiation The point from which the energy radiated by an object appears to arrive.

center tap A connection made to the centermost turn of a coil or to the center-value point of a resistor, filament, or capacitor pair.

center-tapped coil See CENTER-TAPPED WINDING.

center-tapped filament A tube or lamp filament that has a tap at its center.

5059F-pC-93-162 4/9/01 4:51 PM Page 107

center-tapped inductor An inductor that has a tap at half the total number of turns (the physical center of the winding).

center-tapped potentiometer A potentiometer that has a tap at half the total resistance of the resistance element.

center-tapped resistor A fixed resistor that has a tap at half the total resistance.

center-tapped transformer A transformer that has one or more center-tapped windings.

center-tapped winding A winding that has a tap at half the total number of turns (the physical center of the winding).

center-tapped winding

center tracking frequency In three-frequency alignment (tracking) of a circuit, the frequency between the upper and lower frequency limits (alignment or tracking points of the circuit).

center-zero meter A meter that has its zero point at the center of the scale (e.g., a dc galvanometer).

centi- Abbreviation, c. Prefix meaning hundredth(s) (10^{-2}).

centigrade scale See CELSIUS SCALE.

centimeter Abbreviation, cm. A unit of length equal to 10^{-2} meter, or 0.3937 inch.

centimeter-gram-second system Abbreviation, cgs. A system of units, now seldom used, in which the centimeter is the fundamental unit of length, the gram is the fundamental unit of mass, and the mean solar second is the fundamental unit of time. Electrical units in the cgs system fall into two categories: *electrostatic* and *electromagnetic.* The names of cgs electrostatic units have the prefix *stat-* (e.g., STATAMPERE, STATVOLT, etc.). Cgs electromagnetic units have the prefix *ab-* (e.g., ABAMPERE, ABVOLT, etc.).

centimetric waves See MICROWAVES.

centipoise A cgs measure of the dynamic viscosity of liquids. Equal to 10^{-2} poise.

central office In telephone systems, a switching network at which numerous circuits or subscriber lines converge.

central processing unit Abbreviation, CPU. In a digital computer, the section containing the arithmetic and logic unit (ALU), control circuits, and internal memory circuits. Also called *central processor.*

Central Radio Propagation Laboratory A government laboratory that studies radio propagation and collects, correlates, and analyzes data for predicting propagation conditions. The organization also studies methods of measuring propagation.

centrifugation potential An electric potential that occurs in a colloidal solution when the solution is centrifuged.

centrifugal switch A switch actuated by rotational motion (e.g., the automatic disconnection switch in a capacitor motor).

centripetal force The force that draws the mass of a rotating body toward the axis of rotation.

ceramal See CERMET.

ceramet seal See CERAMIC-TO-METAL SEAL.

ceramic-based microcircuit A tiny circuit printed or deposited on a ceramic substrate.

ceramic capacitor A component made with sheets of metal stacked alternately with wafers of ceramic. This material, like mica, has low loss, and therefore allows for high efficiency. For low values of capacitance, only one layer of ceramic is needed, and two metal plates can be glued to a disk of porcelain, one on each side. Alternatively, a tube or cylinder of ceramic can be employed, and metal ink applied to the inside and outside of the tube. These capacitors have values ranging from a few picofarads to about 0.5 μF. Their voltage ratings are comparable to those of paper capacitors. Compare ELECTROLYTIC CAPACITOR, MICA CAPACITOR, PAPER CAPACITOR, PLASTIC-FILM CAPACITOR, TANTALUM CAPACITOR.

ceramic dielectric **1.** A ceramic used as a dielectric in capacitors. Examples: barium titanate, barium strontium titanate, and titanium dioxide. Ceramic dielectrics provide high dielectric constant. **2.** A ceramic used as an insulator. Examples: isolantite, porcelain, and steatite.

ceramic filter A resonant filter similar to a crystal filter, but using a piezoelectric ceramic material.

ceramic magnet A permanent magnet made of a magnetic ceramic material, such as mixtures of barium oxide and iron oxide.

ceramic microphone A microphone that uses a CERAMIC PIEZOELEMENT to convert sound waves into electrical impulses.

ceramic piezoelement A component that uses a piezoelectric ceramic material. Examples: ceramic filter, ceramic microphone, ceramic phono pickup, ceramic transducer, and electrostrictive transducer. Also called PIEZOELECTRIC CERAMIC.

ceramic resistor A carborundum resistor whose value is voltage-dependent. It usually displays a negative temperature coefficient of resistance (but a positive coefficient is available) and a negative voltage coefficient of resistance.

ceramics **1.** Clay-based materials used as dielectrics and insulators in electronics. Examples: barium titanate, titanium dioxide, porcelain, isolantite, and steatite. **2.** The science and art of using and developing ceramics.

ceramic-to-metal seal A bond in which ceramic and metal bodies are joined, for example, the bonding of a metal lead to a ceramic disk, through which it passes to provide a leak-proof seal. Also called *ceramet seal.*

5059F-pC-93-162 4/9/01 4:51 PM Page 108

ceramic transducer A transducer that uses a CERAMIC PIEZOELEMENT to translate such parameters as pressure and vibration into electrical pulses.

ceramic tube A high-temperature vacuum tube that uses a ceramic material, instead of glass, as the envelope; the tube offers low losses at high frequencies.

Cerenkov radiation Light emanating from a transparent material that is traversed by charged particles, whose speed is higher than the speed of light through the material.

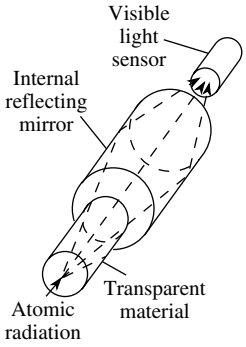

Cerenkov radiation

Cerenkov rebatron device An apparatus for generating radio-frequency energy by passing an electron beam through a piece of dielectric having a small aperture.

ceresin wax A yellow or white wax obtained by refining *ozocerite.* Used as an insulant and sealant against moisture. Dielectric constant, 2.5 to 2.6.

cerium Symbol, Ce. A metallic element of the rare-earth group. Atomic number, 58. Atomic weight, 140.13.

cerium metals A group of metals belonging to the rare-earth group: cerium, lanthanum, neodymium, praseodymium, promethium, and samarium.

cermet An alloy of a ceramic, such as titanium carbide, and nickel, a metal. A thin film of cermet is used as a resistive element in some microcircuits. Cermet is an acronym for *ceramic metal.*

certified tape A magnetic recording tape that has been thoroughly checked and found to have no flaws.

cesium Symbol, Cs. A metallic element of the alkali-metal group. Atomic number, 55. Atomic weight, 132.91. The oscillations of this element's atoms have been used as atomic time standards. The element is used in some phototubes as the light-sensitive material, and in some arc lamps.

cesium-vapor lamp A low-voltage arc lamp used as an infrared source.

Cf Symbol for CALIFORNIUM.

cgs Abbreviation of CENTIMETER-GRAM-SECOND.

chad The punched-out particle(s) constituting refuse from paper-tape punching.

chadded tape Punched paper tape in which the chad is left partially attached to the tape's punched holes.

chadless tape Punched paper tape without CHAD.

chafe **1.** An area that has been abraded by rubbing or scraping. **2.** To produce a chafe.

chaff Strips of metal foil used to create radar interference or ambiguity in locating a target by multiple reflections of the beam. Also called MIRROR.

chain broadcasting Simultaneous transmissions from a number of broadcast transmitters connected together in a network by wire line, coaxial cable, or microwave link.

chain calculation As performed by a calculator, a calculation that can be entered as it would normally be written (i.e., without the need for regrouping operands).

chain printer In the readout channel of a digital computer, a high-speed printer carrying printer's type on a revolving chain.

chain radar system A number of radar stations along a missile-flight path that are connected in a communications or control network.

chain reaction A reaction (as in nuclear fission) that is self-sustaining or self-repeating. Unless controlled from outside, such a reaction runs to destruction.

chain switch A switch that is actuated by pulling a light metal chain. Successive pulls turn the switch alternatively on and off.

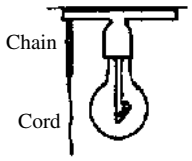

chain switch

change dump In computer operation (especially in debugging), the display of the names of locations that have changed following a specific event.

change file See TRANSACTION FILE.

change of control In a sequence of computer records being processed, a logical break that initiates a predetermined action, after which processing continues.

changer In a high-fidelity disk player, a device that allows several disks to be played, one after the other, without the need for manually exchanging the disks.

change record A computer record that changes information in a related master record. Also called *transaction record.*

5059F-pC-93-162 4/9/01 4:51 PM Page 109

change tape See TRANSACTION TAPE.

channel **1.** A frequency (or band of frequencies) assigned to a radio or television station. **2.** See KEYWAY. **3.** A subcircuit in a large system [e.g., the radio-frequency (RF) channel of a receiver, the vertical-amplifier channel of an oscilloscope, or the modulator channel of a radio transmitter]. **4.** The end-to-end electrical path through the semiconductor body in a field-effect transistor. **5.** One of the independent audio circuits in a stereo sound system (e.g., the left channel or the right channel).

channel analyzer A (usually multiband) continuously tunable instrument, similar to a tuned radio receiver, used in troubleshooting radio communications circuits by substituting a perfect channel for one that is out of order.

channel balance The state in which the apparent amplitude of two or more channels is identical.

channel bank In a transmission system, the terminal equipment used for the purpose of multiplexing the individual channels.

channel capacity The fullest extent to which a channel can accommodate the information (frequencies, bits, words, etc.) to be passed through it.

channel designator A name, number, or abbreviation given to a channel in a communications system.

channel effect The possible current flow through a high impedance between the collector and emitter in a bipolar transistor.

channel frequency The CENTER FREQUENCY of a communications channel.

channeling Multiplex transmission in which separate carriers within a sufficiently wide frequency band are used for simultaneous transmission.

channelizing The subdivision of a relatively wide frequency band into a number of separate subbands.

channel reliability **1.** The proportion of time, usually expressed as a percentage, that a communications channel is useful for its intended purpose. **2.** The relative ease with which communications can be carried out over a particular channel.

channel reversal In stereo reproduction, interchanging the left and right channels.

channel-reversing switch In a stereo system, a switch that allows channel reversal without the need for reorienting speaker cables or connectors.

channel sampling rate The rate at which individual channels are sampled. For example, in the electronic switching of an oscilloscope, the number of times per second each input-signal channel is switched to the instrument.

channel selector A switch or relay used to put any of a series of channels into functional status in a system.

channel separation **1.** The spacing between communications channels, expressed in kilohertz. **2.** In stereo reproduction, the degree to which the information on one channel is separate from the other; usually expressed in decibels.

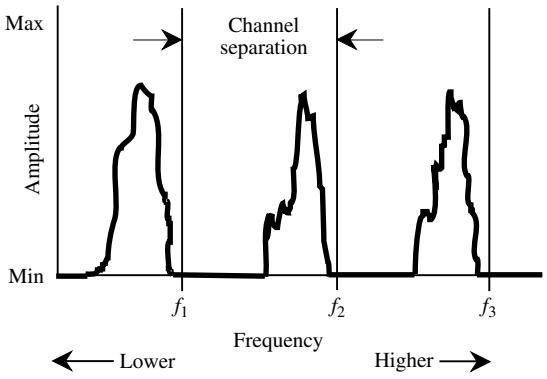

channel separation, 1.

channel slot On a carrier modulated by numerous signals, the position or frequency of a specific modulating signal.

channel shift The interchange of communications channels (e.g., the shift from a calling frequency to a working frequency).

channel strip A fixed-channel amplifier for a television receiver.

channel time slot In a frame of transmitted information, such as a television picture, a time interval designated to a channel for the transmission of a character signal or other information.

channel-to-channel connection A device, such as a channel adapter, used to transfer data rapidly between any two channels of two digital computers, at the data speed of the slower channel.

channel-utilization index An indication of the extent to which channel capacity is used. For a given channel, the index is the ratio of information rate to channel capacity, each expressed in units per second.

channel wave An acoustic wave that travels within a region or layer of a substance because of a physical difference between that layer and the surrounding material. An example of a channel wave is the propagation of sound over a still lake.

channel width In a frequency channel, the difference $f_2 - f_1$, where f_1 is the lower-frequency limit and f_2 is the upper-frequency limit of the channel.

chapter A self-contained computer program section.

character **1.** One of the symbols in a code. **2.** In computer operations, a digit, letter, or symbol used alone or in some combination to express information, data, or instructions.

character code In a communications or computer system, the combination of elements (e.g., bits) representing characters.

character crowding A reduction of the time interval between successive characters—especially those read from tape.

character density The number of characters that can be stored in a given length or surface area of

5059F-pC-93-162 4/9/01 4:51 PM Page 110

a medium. On a magnetic tape, it might be specified in characters per millimeter; on a magnetic disk, it might be specified in characters per square millimeter.

character emitter A coded-pulse generator in a digital computer.

character generator A device that converts coded information into readable alphanumeric characters.

characteristic **1.** A quantity that characterizes (typifies) the operation of a device or circuit. Examples are emitter current, output power, and frequency deviation. **2.** In floating point notation, the exponent.

characteristic curve A curve showing the relationship between an independent variable and a dependent variable, with respect to the parameter(s) for a device or circuit. Example: the collector voltage-collector current characteristic curve of a transistor.

characteristic distortion **1.** In a digital signal, pulse distortion caused by the effects of the previous pulse or pulses. **2.** Distortion in the characteristic curve of a component or device.

characteristic frequency The frequency peculiar to a given channel, service, or response.

characteristic impedance Symbol, Z_0. **1.** Theoretically, the impedance that would be simulated by a given two-conductor or coaxial line of uniform construction, if that line were of infinite length. This value is determined by the materials used for the two conductors, the dielectric used to insulate the two conductors, the diameters of the conductors, and the spacing between them. **2.** In practice, for a transmission line or waveguide terminated with a load that produces no standing waves on the line, the ratio of radio-frequency (RF) voltage to RF current. This ratio is the same at all points along the length of a perfectly matched line, and depends on the physical construction of the line. Coaxial lines typically have Z_0 between 50 and 100 ohms. Twinlead is available with 75-ohm and 300-ohm Z_0 values. Open-wire line has Z_0 between 300 and 600 ohms, depending on the spacing between the conductors, and also on the type of dielectric (insulating material) employed to keep the spacing constant between the conductors. **3.** Experimentally, the value of impedance that, if it terminates a transmission line or waveguide, results in no reflected power from the load end of line. This is always a pure resistance; that is, it contains no reactance.

characteristic overflow In floating-point arithmetic, the condition that occurs when a characteristic exceeds the upper limit specified by a program or computer.

characteristic spread The range of values over which a characteristic extends. For example, if an amplifier's output ranges from 15 W to 25 W, its characteristic spread is 10 W.

characteristic underflow In floating-point arithmetic, the condition that occurs when a characteristic exceeds the lower limit specified by a program or computer.

character modifier In address modification, a constant (compare VARIABLE) that refers to a specific character's location in memory.

character-oriented A computer in which character locations, rather than words, can be addressed.

character printer A computer output device that prints matter in the manner of a conventional typewriter.

character reader Also called an *optical scanner.* In a digital computer, an input device that can read printing and script directly.

character recognition The reading of a written or printed character by a computer, including its identification and encoding.

character sensing The detection of characters by a computer input device. This can be done galvanically, electrostatically, magnetically, or optically.

character set The set of characters in a complete language, or in a communications system.

character signal The set of elements or bits representing a character in a digital transmission system. The signal can also represent the quantizing value of a sample.

characters per minute An expression of the speed of transmission of a digital signal. The number of characters (on average) transmitted in a period of one minute. In Morse code (CW) transmission, this is generally taken as the number of times the word *paris* plus the subsequent space, multiplied by six (five letters and one space following), can be sent in one minute.

characters per second An expression of the speed of transmission of a digital signal. The number of characters (on average) transmitted in a period of one second.

character string A one-dimensional character array [i.e., a list of characters that, when printed or displayed, would appear in a row or column, but not both (as in a matrix)].

character subset A classification of characters within a set.

Charactron A cathode-ray readout tube that displays letters, numbers, and symbols on its screen. More commonly called a *monitor.*

charcoal tube In a system for producing a high vacuum, a trap containing activated charcoal, which is heated to dull red, then cooled by liquid air to absorb gases.

charge **1.** A quantity of electricity associated with a space, particle, or body. **2.** To electrify a space, particle, or body (i.e., to give an electric charge). **3.** To store electricity, as in a storage battery or capacitor. Compare DISCHARGE.

charge carrier **1.** An ELECTRON whose movement constitutes a flow of electric current. **2.** An elec-

5059F-pC-93-162 4/9/01 4:51 PM Page 111

tron deficiency (HOLE) whose movement constitutes a flow of electric current. **3.** Any particle, such as a charged atom (ION), PROTON, ALPHA PARTICLE, or BETA PARTICLE, whose movement constitutes a flow of electric current.

charge-coupled device Abbreviation, CCD. A form of analog-to-digital converter that generates a digital signal output representing an analog image input. The transfer of stored charges provides the method of operation. Used in machine vision systems and in numerous scientific applications.

charge density The degree of charge or current-carrier concentration in a region.

charged particle **1.** See CHARGE CARRIER. **2.** See ION.

charged voltage **1.** The voltage across a fully charged capacitor. **2.** The terminal voltage of a fully charged storage cell.

charge holding See CHARGE RETENTION.

charge of electron The negative electric charge carried by a single electron. Approximately equal to 1.602×10^{-19} coulombs.

charger **1.** See BATTERY CHARGER. **2.** Any device or circuit that charges a capacitor.

charge retention **1.** The holding of an electric charge by a cell or battery when no current is being drawn from it. **2.** A measure of the ability of a cell or battery to maintain an electric charge when no current is drawn from it. Often specified in terms of *shelf life.* **3.** The holding of a charge by a capacitor.

charge-storage tube A cathode-ray tube that holds a display of information on its screen until the operator removes it by pressing an erase button.

charge-to-mass The ratio of the electric charge to the mass of a subatomic particle.

charge-to-mass ratio of electron The ratio of the charge (e) of the electron to the mass (m_e) of the electron, in coulombs per kilogram (C/kg). For an electron at rest, e/m_e is approximately equal to 1.602×10^{-19} C divided by 9.11×10^{-31} kg = 1.76×10^{11} C/kg.

charge transfer **1.** The switching of an electric charge from one capacitor to another. **2.** The capture of an electron by a positive ion from a neutral atom of the same kind, resulting in the ion becoming a neutral atom, and the previously neutral atom becoming a positive ion.

charge transfer device A semiconductor in which an electric charge is moved from location to location. Applications include delay lines, video signal processing, and signal storage.

charging **1.** The process of storing electrical energy in a capacitor. **2.** The process of storing electrochemical energy in a storage cell or battery.

charging current **1.** The current flowing into a capacitor. **2.** The current flowing into a previously discharged storage cell.

charging rate **1.** The rate at which charging current flows into a storage cell or battery, expressed in amperes or milliamperes. For most cells and batteries, the rate is greatest initially, when the cell or battery is depleted or nearly depleted; the rate decreases as the cell or battery becomes charged. **2.** The instantaneous rate at which charging current flows into a capacitor or capacitance-resistance circuit, expressed in amperes, milliamperes, or microamperes.

charged voltage **1.** The voltage across a fully charged capacitor. **2.** The terminal voltage of a fully charged storage cell.

Charlie Phonetic alphabet code word for the letter C.

chassis A (usually metal) foundation on which components are mounted and wired.

chassis ground A ground connection made to the metal chassis on which the components of a circuit are mounted. When several ground connections are made to a single point on the chassis, a COMMON GROUND results.

chatter **1.** A rapidly repetitive signal, caused by interruption or variation of a current (usually interference). **2.** Extraneous vibration, as of the armature in a relay.

chatter time The interval between the instant that contacts close (for example, in a relay) and the instant at which chatter ends.

cheater cord An extension cord used to conduct power to a piece of equipment (especially a television receiver) by temporarily bypassing the safety switch or interlock. Use of such a cord presents a potentially fatal shock hazard to personnel using, or working on, the equipment.

Chebyshev filter Also spelled *Tschebyscheff* or *Tschebysheff.* A form of inductance-capacitance (LC) lowpass, highpass, bandpass, or band-rejection filter, characterized by an attenuation-versus-frequency curve with ripple in the passband.

check **1.** A test generally made to verify condition, performance, state, or calculations; specifically, in computer operations, it applies to operands or results. **2.** The usually abrupt halting of an action.

check bit A binary CHECK DIGIT.

check character In a group of characters, one whose value depends on the other characters, which it checks when the group is stored or transferred.

check digit Also called *check number.* In computer operations, a number added to a group of digits, forming a code that identifies entities in the system (including personnel) and can be used for verification. The check digit is the remainder when the number code (for example, 459) is divided by a fixed number (for example, 5); in this case, the check digit (the remainder of 459/5) is 4, and the amended code number is 4594.

check indicator An indication, made via a video display, that something has been shown to be invalid according to a check.

checking program Also called *checking routine.* For debugging purposes, a diagnostic computer

5059F-pC-93-162 4/9/01 4:51 PM Page 112

program capable of detecting errors in another program.

checkout A test routine that ascertains whether or not a circuit or system is functioning according to specifications.

checkout routine A routine used by programmers to debug programs.

checkpoint A point in a digital-computer program at which sufficient information has been stored to allow restarting the computation from that point.

checkpoint dump The process of recording details of a computer program run. This process might be necessary in the event of a system failure that requires reconstruction of a program or programs.

checkpointing The writing of a computer program in such a manner that, during a program run, information is frequently dumped as insurance against possible loss in the event of a system failure.

check problem A presolved problem used to check the operation of a digital computer or program.

check register In some digital computers, a register in which transferred information is stored so that it can be checked against the same information as it is received a second time.

check routine A special program designed to ascertain if a program or computer is operating correctly. Also see CHECK PROBLEM.

checksum Used as part of a summation check, a sum derived from the digits of a number. For example, the checksum of 23,335 is 16. Also called HASH TOTAL.

check symbol For a specific data item, a digit or digits obtained by performing an arithmetic check on the item, which it then accompanies through processing stages for the purpose of checking it.

check total See CONTROL TOTAL.

check word A check symbol in the form of a word added to, and containing data from, a block of records.

chelate Pertaining to cyclic molecular structure in which several atoms in a ring hold a central metallic ion in a COORDINATION COMPLEX.

chemical deposition The coating of a surface with a substance resulting from *chemical reduction* of a solution. In mirror making, for example, formaldehyde reduces a solution of silver nitrate, and deposits metallic silver on the surface of polished glass. Also see CHEMICALLY DEPOSITED PRINTED CIRCUIT and CHEMICAL REDUCTION.

chemical detector See ELECTROLYTIC DETECTOR.

chemical effect An alteration in the chemical makeup of a substance or solution, resulting from the passage of an electric current through it. Examples include electrolysis, electroplating, and the reduction of ores.

chemical energy Energy that is stored in the chemical bonds of a material or solution. An example is the stored energy in terms of watt hours in an electrolytic cell.

chemical load An arrangement of a chemical material or device for the passage of electricity through it. Examples: electroplater, electrolytic cell for the production of hydrogen gas, and storage battery.

chemically deposited printed circuit A printed circuit in which the pattern of metal lines and areas are chemically deposited on a substrate.

chemically pure Abbreviation, CP. Free from impurities.

chemical rectifier See ELECTROLYTIC CELL.

chemical reduction The process of making a chemical compound (usually in solution) into a metal, by removing the nonmetallic component from the compound. For example, when copper oxide is heated in the presence of hydrogen (a reducting agent), the oxygen (the nonmetallic component) is driven out, and copper (along with some water) remains.

chemical resistor See ELECTROLYTIC RESISTOR.

chemical switch See ELECTROCHEMICAL SWITCH.

CHIL Abbreviation for *current-hogging injection logic*. A form of bipolar digital logic technology.

chip **1.** An INTEGRATED CIRCUIT. **2.** A small slab, wafer, or die of dielectric or semiconductor material, on which a subminiature component or circuit is formed or deposited.

chip capacitor A subminiature capacitor formed on a chip.

chip resistor A subminiature resistor formed on a chip.

chip tray A chad receptacle located at a card or paper tape punching site.

Chireix-Mesny antenna A high-frequency (HF) beam antenna, in which each dipole section constitutes one side of a diamond. Cophased horizontal and vertical components of current flow in each of the diagonals, and radiation is broadside to the plane of the driven element.

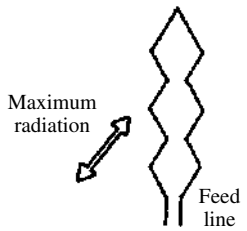

Chireix-Mesny antenna

chirp A rapid change in the frequency of a continuous-wave Morse-code signal. The chirp usually occurs at the beginning of each dot or dash, and

5059F-pC-93-162 4/9/01 4:51 PM Page 113

can go up or down in frequency. Chirp occurs because of a change in the output impedance of an oscillator as it is keyed. Modern code transmitters do not exhibit significant chirp.

chirp modulation A form of modulation in which the frequency of a signal is deliberately changed in a systematic way. Used in some radar systems.

chirp radar A radar system that uses CHIRP MODULATION.

Chladni's plates Conducting plates that are used to evaluate the nature of a vibration in a solid material. The plates are clamped to the material, and sand is sprinkled on the surface. This produces patterns that indicate the nature of the vibrations.

chlorinated diphenyl A synthetic organic substance used as an impregnant in some oil-filled capacitors.

chlorinated naphthalene See HALOWAX.

chlorine Symbol, Cl. A gaseous element of the halogen family. Atomic number, 17. Atomic weight, 35.453.

choke **1.** To restrict or curtail passage of a particular current or frequency by means of a discrete component, such as a choke coil. **2.** See CHOKE COIL.

choke air gap A fractional-inch opening in the iron core of a filter choke, usually filled with wood or plastic. The gap prevents saturation of the core when the choke coil carries maximum rated direct current.

choke coil **1.** A large-value inductor that provides a high impedance to alternating current (ac), while offering virtually no opposition to direct current (dc). **2.** In radio-frequency (RF) applications, an inductor that provides a high impedance to RF signals while showing low impedance for audio-frequency (AF) signals and direct currents (dc).

choke-coupled modulation An amplitude-modulation (AM) scheme, in which the modulator is coupled to the radio-frequency (RF) amplifier through a shared iron-core choke coil.

choke flange At the end of a waveguide, a flange in which a groove forms a CHOKE JOINT.

choke-input filter A filter whose input component is an inductor (choke). The choke-input power-supply filter is distinguished by its superior voltage regulation, compared with the CAPACITOR-INPUT FILTER.

choke joint A joint connecting two waveguide sections and permitting efficient energy transfer without requiring electrical contact with the inside wall of the waveguide.

chopped dc See INTERRUPTED DC.

chopped mode In a single-gun cathode-ray-tube (CRT) oscilloscope, a technique for sequentially displaying several signals that are not referenced to the oscilloscope sweep.

chopped signal An ac or dc signal that is periodically interrupted, as by means of a CHOPPER.

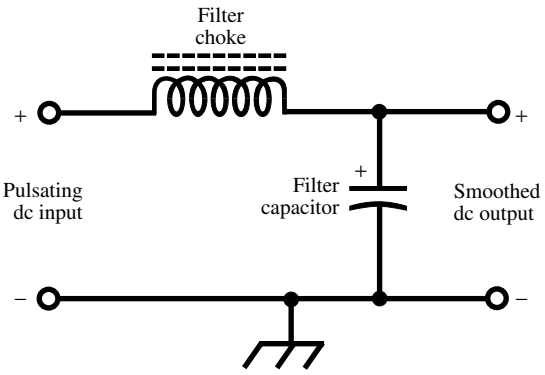

choke-input filter

chopper A device or circuit that interrupts a direct current (dc) at some predetermined rate. Ideally, such a device is characterized by distinct on and off operation.

chopper amplifier A circuit that amplifies the output of a CHOPPER. Used in conjunction with a CHOPPER CONVERTER in dc amplification.

chopper converter A device that interrupts a direct current (dc), and changes it to a pulsating, rectangular-wave current or voltage that can be handled by a stable ac amplifier and rectified to supply amplified dc.

chopper power supply Also called *power inverter.* A circuit that delivers high-voltage ac from a dc source. The input is typically 12 volts dc, and the output is usually 117 volts rms ac. These devices facilitate the use of small appliances such as computers, television sets, and communications radios in portable and mobile environments. The output of a low-cost power inverter is generally not a good sine wave. More sophisticated inverters produce good sine waves and have a frequency close to 60 Hz.

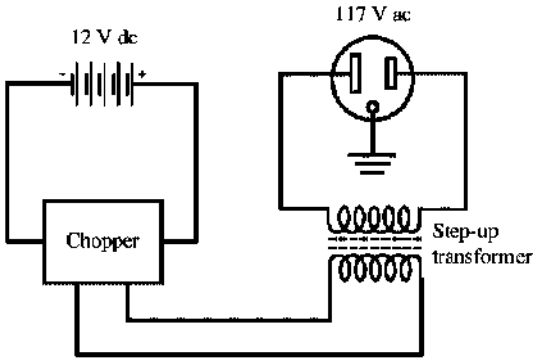

chopper power supply

5059F-pC-93-162 4/9/01 4:51 PM Page 114

chopper stabilization **1.** Stabilization of direct-current (dc) amplification by using a CHOPPER CONVERTER ahead of a stable ac amplifier, and rectifying the amplifier output. **2.** In a regulated power supply, use of a CHOPPER AMPLIFIER at the control-circuit input to improve regulation.

chopper-stabilized amplifier See CHOPPER AMPLIFIER and CHOPPER STABILIZATION, **1.**

chopper transistor A transistor that provides rapid and repeated on/off switching of direct current (dc), in the manner of an electromechanical interrupter. See CHOPPER.

chopping frequency The frequency at which a chopper interrupts a signal.

chord **1.** A harmonious mixture of musical tones of various frequencies. **2.** A straight line that joins two points on a curve (such as an arc of a circle). **3.** The width of an airfoil.

chord organ An electronic organ that will sound a musical chord when a key is pressed (see CHORD, **1**).

choreographer program A computer program similar to one originally written by Charles Lecht of Lecht Sciences, Inc. The computer operator gives commands that cause a human form, portrayed on the display screen, to make various movements. Used in animated computer graphics.

chorus Signals at very low radio frequencies (VLF), natural in origin, that sweep upward in frequency. Believed to result from lightning-generated electromagnetic fields that circulate in the magnetosphere (earth's magnetic field). The term is derived from the sound the signals make in high-gain audio-frequency (AF) amplifiers connected directly to VLF receiving antennas.

Christiansen antenna A radio-telescope antenna for obtaining high resolution. Two straight arrays are placed at an angle, intersecting approximately at their centers. The resulting interference pattern has extremely narrow lobes.

Christmas tree A tree-like pattern on the screen of a television receiver, caused by loss of horizontal synchronization.

chroma The quality of a color: *hue* and *saturation.*

chroma circuit In color television, one of several circuits whose ultimate purpose is to produce a color component on the screen.

chroma-clear raster In color television reception, the clear raster resulting from a white video signal, or from operation of the chroma circuits of the receiver (as if they were receiving a white transmission). Also called *white raster.*

chroma control In a color television receiver, a rheostat or potentiometer that permits adjustment of color saturation through variation of the chrominance-signal amplitude before demodulation.

chromatic fidelity See COLOR FIDELITY.

chromaticity **1.** The state of being chromatic (see CHROMA). **2.** A quantitative assessment of a color in terms of dominant or complementary wavelength and purity.

chromaticity coordinate For a color sample, the ratio of any one of the three tristimulus values (primary colors) to the sum of the three.

chromaticity diagram A rectangular-coordinate graph in which one of the three CHROMATICITY COORDINATES of a three-color system is plotted against another coordinate.

chromaticity flicker Flicker caused entirely by chromaticity fluctuation (see CHROMATICITY, **2**).

chromel A nickel-chromium alloy with some iron content, used in thermocouples.

chromel-alumel junction A thermocouple that uses wires of the alloys *chromel* and *alumel.*

chromel-constantan thermocouple A thermocouple consisting of a junction between wires or strips of *chromel* and *constantan.* Typical output is 6.3 mV at 100°C.

chrome plating The process of coating a metal with chromium. Generally protects against corrosion.

chrome recording tape Also called *chrome tape* or *chromium tape.* Tape that is manufactured from the compound chromium dioxide. Noted for its ability to faithfully record and reproduce music.

chrominance In color television, the difference between a reproduced color and a standard reference color of the same luminous intensity.

chrominance amplifier In a color television circuit, the amplifier separating the chrominance signal from the total video signal.

chrominance cancellation On a black-and-white picture tube screen, cancellation of the fluctuations in brightness caused by a chrominance signal.

chrominance-carrier reference In color television, a continuous signal at the frequency of the chrominance subcarrier; it is in fixed phase with the color burst and provides modulation or demodulation phase reference for carrier-chrominance signals.

chrominance channel In color television, a circuit devoted exclusively to the color function, as opposed to audio and general control channels.

chrominance component In the NTSC color television systems, either of the components (I-signal or Q-signal) of the complete chrominance signal.

chrominance demodulator In a color television receiver, a demodulator that extracts video-frequency chrominance components from the chrominance signal, and a sine wave from the chrominance subcarrier oscillator.

chrominance gain control A rheostat or potentiometer in the red, green, and blue matrix channels of a color television receiver, used to adjust the primary-signal amplitudes.

chrominance modulator In a color television transmitter, a device that generates the chrominance signal from the I and Q components and the chrominance subcarrier.

5059F-pC-93-162 4/9/01 4:51 PM Page 115

chrominance primary One of the transmission primaries (red, green, and blue) upon which the chrominance of a color depends.

chrominance signal The signal component in color television that represents the hues and saturation levels of the colors in the picture.

chrominance subcarrier In color television, the 3579.545-kHz signal that serves as a carrier for the I- and Q-signals.

chrominance-subcarrier oscillator In a color television receiver, a crystal-controlled oscillator that generates the subcarrier signal (see CHROMINANCE SUBCARRIER).

chrominance video signals Output signals from the red, green, and blue channels of a color television camera or receiver matrix.

chromium Symbol, Cr. A metallic element. Atomic number, 24. Atomic weight, 51.996. Commonly used as a plating for metals to improve resistance to corrosion.

chronistor An elapsed-time indicator in which current, flowing during a given time interval, electroplates an electrode. The duration of the interval is determined from the amount of deposit.

chronograph **1.** An instrument that provides an accurate time base along the horizontal axis of its permanent record. **2.** Stopwatch.

chronometer A precision clock. Electronic chronometers often use a highly accurate and stable crystal oscillator, followed by a string of multivibrators to reduce the crystal frequency to an audio frequency (such as 1 kHz) that drives the clock motor.

chronoscope An instrument for precisely measuring small time intervals.

CHU Call letters of the Canadian time-signal station whose primary frequency is 7.335 MHz.

Ci Symbol for INPUT CAPACITANCE.

CIE Abbreviation for *International Commission on Illumination.*

cinching In a reel of magnetic tape, the slipping of tape as force is applied.

cinematograph See KINEMATOGRAPH.

cipher A code used for the purpose of preventing interception of a message by third parties.

circ **1.** Abbreviation of *circuit.* **2.** Abbreviation of *circular.*

circle graph Also called a *pie graph.* A representational device consisting of a disk subdivided into various triangular areas (radiating from the center of the circle), which are proportional to represented quantities.

circle of confusion A circular image of a point source of light, resulting from an aberration in an optical system.

circle of declination The graduated circular scale of a *declinometer.*

circlotron amplifier A high-powered microwave amplifier of the one-port, cross-field, nonlinear type using a magnetron.

circuit **1.** A closed path through which current flows from a generator, through various components, and back to the generator. (An electronic circuit is often a combination of interconnected subcircuits.) **2.** The wiring diagram of an electronic device or system.

circuit analysis The careful determination of the nature and behavior of a circuit and its various parts. It can be theoretical, practical, or both. Compare CIRCUIT SYNTHESIS.

circuit analyzer See CIRCUIT TESTER.

circuit board A panel, plate, or card on which electronic components are mounted and interconnected to provide a functional unit.

circuit breaker A resettable fuse-like device that is designed to protect a circuit against overloading. In a typical circuit breaker, the winding of an electromagnet is connected in series with the load circuit and with the switch contact points. Excessive current through the magnet winding causes the switch to be opened.

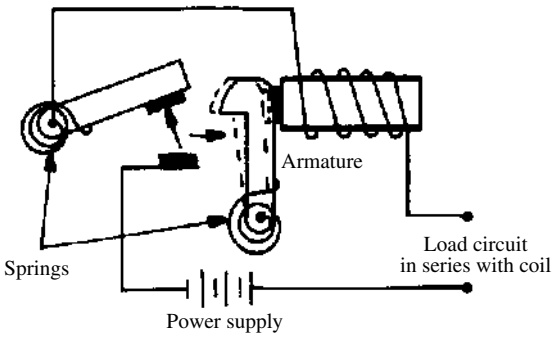

circuit breaker

circuit capacitance The total capacitance (lumped, distributed, and stray) present in a circuit.

circuit capacity **1.** The ability of a circuit to handle a quantity (such as current, voltage, frequency, power, etc.) safely and efficiently. **2.** The maximum value of some parameter at which a circuit can function safely and efficiently (e.g., a circuit capacity of 50 A). **3.** The number of channels that can be accommodated simultaneously by a circuit.

circuit component **1.** Any of the electronic devices or parts (capacitors, resistors, transistors, etc.) that are connected through wiring to form a circuit. **2.** An electrical quantity required for, or arising from, circuit operation. Examples: input voltage, feedback current, stray capacitance, and circuit noise.

circuit diagram A drawing in which symbols and lines represent the components and wiring of an electronic circuit. Also called CIRCUIT

5059F-pC-93-162 4/9/01 4:51 PM Page 116

SCHEMATIC, SCHEMATIC DIAGRAM, and WIRING DIAGRAM.

circuit dropout A momentary interruption of circuit operation, often caused by a break in the circuit.

circuit efficiency A quantitative measure of the effectiveness of circuit operation, customarily expressed as the ratio of the useful output power to the total input power.

circuit element See CIRCUIT COMPONENT, **1.**

circuit engineer An electronics engineer who specializes in circuit analysis, circuit synthesis, or both.

circuit fault **1.** Malfunction of a circuit. **2.** An error in circuit wiring.

circuit hole A perforation within the conductive area of a printed-circuit board, for the insertion and connection of a pigtail, terminal, etc., or for connecting the conductors on one side of the board with those on the other.

circuit loading Intentionally or unintentionally drawing power from a circuit.

circuit noise **1.** Electrical noise generated by a circuit in the absence of an applied signal. **2.** In wire telephony, electrical noise as opposed to acoustic noise.

circuit noise level The ratio of circuit-noise amplitude to reference-noise amplitude, expressed in decibels above the reference amplitude.

circuit-noise meter A meter that measures the intensity of the noise generated within a circuit.

circuit parameter See CIRCUIT COMPONENT, **2.**

circuit protection Automatic safeguarding of a circuit from damage from overload, excessive drive, heat, vibration, etc. Protection is afforded by various devices and subcircuits, ranging from the common fuse to sophisticated limiters and breakers.

circuit reliability A quantitative indication of the ability of a circuit to provide dependable operation as specified. See MEAN TIME BEFORE FAILURE and MEAN TIME BETWEEN FAILURES.

circuitry **1.** Collectively, electronic and electrical circuits. **2.** A detailed plan of a circuit and its subcircuits. **3.** Collectively, the components of a circuit.

circuit schematic See CIRCUIT DIAGRAM.

circuit simplification **1.** In circuit analysis, the reduction of a complex circuit to its simplest representation to minimize labor and to promote clarity. Thus, through application of Kirchhoff's laws, a complicated circuit could theoretically be reduced to a single generator in series with a single impedance. **2.** In circuit synthesis, the arrangement of a circuit so as to provide desired performance with the fewest components and least-complex wiring.

circuit switching In telephony, a method of connection in which a single circuit is maintained between two subscribers for the entire duration of the call. The signal path does not change. The connection is maintained even during periods of silence (no data transmitted by either subscriber). Compare PACKET SWITCHING.

circuit synthesis The development of a circuit under the guidance of theoretical or practical knowledge of basic electronics principles and component parameters. Compare CIRCUIT ANALYSIS.

circuit tester An instrument for checking the performance of electronic circuits. Often consists of a specialized continuity tester, but occasionally it includes a dynamic performance tester.

circuit tracking The alignment and/or pretuning of circuits for identical or optimum response. It applies especially to cascaded circuits, whose variable elements, such as tuned inductance-capacitance (LC) networks, must follow each other in step when ganged together.

circular angle The angle described by a radius vector as it rotates counterclockwise around a circle.

circular antenna A half-wave horizontally polarized antenna, whose driven element is a rigid conductor bent into a circle with a break opposite the feed point. Also called *halo antenna.* Used primarily at very-high frequencies (VHF).

circular electric wave An electromagnetic wave with circular electric lines of flux. An example is the field in the immediate vicinity of a CIRCULAR ANTENNA.

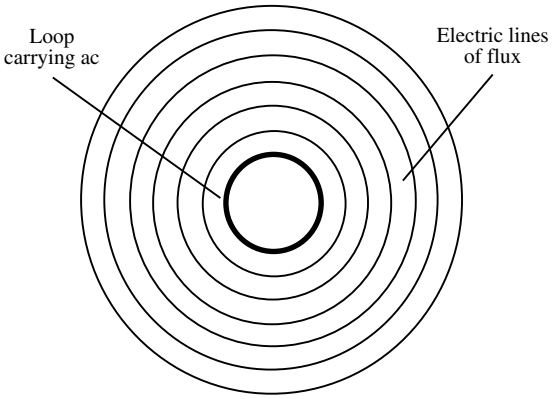

circular electric wave

circular functions Trigonometric functions of the angle described by a vector rotating counterclockwise around a circle. Also see COSINE, COSECANT, COTANGENT, SECANT, SINE, and TANGENT.

circular magnet See RING MAGNET.

circular magnetic wave An electromagnetic wave in which the magnetic lines of flux are circular. An example is the field in the immediate vicinity of a straight-conductor antenna.

5059F-pC-93-162 4/9/01 4:51 PM Page 117

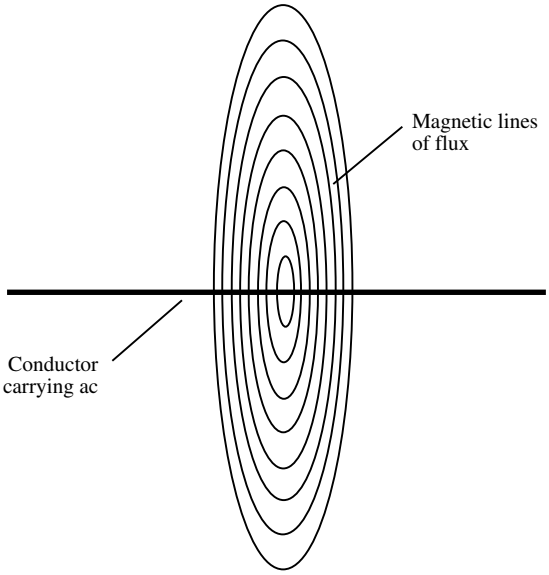

circular magnetic wave

circular mil A unit of cross-sectional area equivalent to 0.785 millionths of a square inch, or the area of a circle having a diameter of 0.001 inch. Generally, the circular mil is used to specify the cross-sectional area of a conductor, such as wire.

circular mil foot A unit of volume in which the length is 1 foot and the cross-sectional area is 1 circular mil.

circular polarization A form of electromagnetic-wave polarization in which the orientation of the electric flux rotates continuously and uniformly as the wave propagates through space. Circular polarization can occur in either a clockwise or counterclockwise sense.

circular radian The angle enclosed by two radii of a unit circle and subtended by a unit arc. Equal to about 57.296 angular degrees.

circular scan A radar scan in which the electron-beam spot describes a circle centered around the transmitting antenna.

circular sweep In an oscilloscope, a sweep obtained when the horizontal and vertical sinusoidal deflecting voltages have the same amplitude and frequency, but are out of phase by 90 degrees (1/4 cycle).

circular trace An oscilloscope pattern consisting of a circle obtained with a circular sweep of the electron beam.

circular waveguide A waveguide with a circular cross section.

circulating register In a digital computer, a register in which digits are taken from locations at one end and returned to those at the other end.

circulating tank current The alternating current that oscillates between the capacitor and inductor within a tank circuit.

circulator A multi-terminal coupler in which microwave energy is transmitted in a particular direction from one terminal to the next.

circumvention In a security or alarm system, the evasion of detection. Can be done by physically avoiding regions of coverage, or by defeating the system electronically.

cis A prefix meaning "on this side of." For example, the *cislunar field* is the field on this side of the moon.

Citizen Band Abbreviation, CB. A band of radio frequencies allocated for two-way communication between private citizens (apart from amateur and commercial services).

Citizens Radio Service Two-way radio communication in a CITIZEN BAND. In the United States, the FCC licenses users of this service without requiring them to take an examination.

C/kg Abbreviation of *coulombs per kilogram,* the unit for electron charge-to-mass ratio.

C/kmol Abbreviation of *coulombs per kilomole,* the unit for the Faraday constant.

ckt Abbreviation of CIRCUIT.

Cl Symbol for CHLORINE.

cl Abbreviation of CENTILITER.

cladding The bonding of one metal to another to minimize or prevent corrosion. A common example is copper-clad steel wire, ideal for use in radio-frequency antenna systems. The copper provides excellent conduction, and the steel provides high tensile strength with a minimum of wire stretching.

clamper A device that restricts a wave to a predetermined dc level. Also called DC RESTORER.

clamping **1.** Fixing the operation of a device at a definite dc level. Also see CLAMPER. **2.** In television, establishing a fixed level for the picture signal at the start of each scanning line.

clamping circuit See CLAMPER.

clamping diode A diode used to fix the voltage level of a signal at a particular reference point.

clapper In a bell, the ball or hammer that strikes the bell; in an electric bell, it is affixed to the vibrating armature.

Clapp-Gouriet oscillator A *Colpitts oscillator* in which a capacitor is connected in series with the inductor. The circuit offers high frequency stability in the presence of input and output capacitance variations.

Clapp oscillator A series-tuned hybrid *Colpitts oscillator,* having a tuning capacitor in series with the inductor, rather than in parallel with the inductor. The circuit allows the use of a smaller tuning capacitor, resulting in improved stability.

Clark cell See ZINC STANDARD CELL.

class-A amplifier An amplifier whose bias is set at approximately the midpoint of the characteristic curve. Output electrode current flows during the

5059F-pC-93-162 4/9/01 4:51 PM Page 118

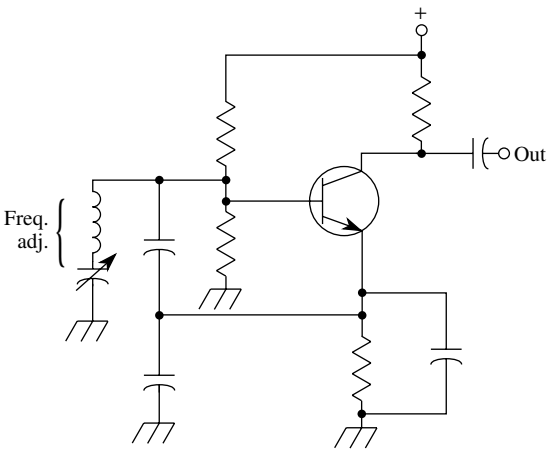

Clapp oscillator

complete ac driving-voltage cycle. The input signal never drives the device into the nonlinear portion of the characteristic curve.

class-AB amplifier Either a CLASS-AB_1 AMPLIFIER or a CLASS-AB_2 AMPLIFIER.

class-AB_1 amplifier An amplifier whose bias is adjusted to a level between that of a class-A amplifier and that of a class-AB_2 amplifier. Output electrode current flows during the entire ac driving-voltage cycle. The input signal drives the device into the nonlinear portion of the characteristic curve during part of the cycle.

class-AB_2 amplifier An amplifier whose bias is adjusted to a level between that of a class-AB_1 amplifier and that of a class-B amplifier. Output electrode current flows during more than 50 percent, but less than 100 percent, of the input signal cycle.

class-AB modulator A modulator whose output stage is a class-AB_1 or class-AB_2 amplifier.

class-A modulator A circuit for obtaining amplitude-modulated signals; essentially a class-A amplifier with two inputs, one for the carrier and the other for the modulating signal.

class-A operation The operation of a transistor, field-effect transistor, or vacuum tube, in which the collector, drain, or plate current flows during the entire signal cycle.

class-B amplifier An amplifier whose bias is adjusted to operate at the cutoff point in the characteristic curve. Output current flows during approximately 50 percent of the input signal cycle. Efficiency is higher than that of a class-A amplifier.

class-B modulator A push-pull modulator whose output stage is a class-B amplifier.

class-B operation The operation of a transistor, field-effect transistor, or vacuum tube, in which the collector, drain, or plate current flows for approximately half the signal cycle.

class-C amplifier An amplifier whose input-electrode bias is adjusted for operation at a point considerably beyond cutoff. Output current flows during less than half of the input signal cycle. Such an amplifier requires comparatively high driving power, but is capable of excellent efficiency. Commonly used in continuous-wave (CW), amplitude-modulated (AM), and frequency-modulated (FM) radio transmitters.

class-C operation The operation of a transistor, field-effect transistor, or vacuum tube, in which the collector, drain, or plate current flows for significantly less than half the signal cycle.

class-D telephone A telephone restricted to use by emergency services, such as fire departments and guard alarm installations.

classical electron radius Abbreviated r_e. The quantity expressed as $e^2/(m_e c^2)$, where e is the electron's charge in electrostatic units, m_e is its rest mass, and c is the speed of light. The value r_e is equal to approximately 2.82×10^{-13} cm or 2.82×10^{-15} m.

clean room A room for the assembly or testing of critical electronic equipment. The term is derived from the extraordinary steps taken to remove dust and other contaminating agents. The personnel wear carefully cleaned garments (or disposable clothing), gloves, caps, and masks; in some situations, they are required to walk between ceiling and floor ducts of a vacuum system upon entering the room.

cleanup process In the process of electron tube evacuation, a technique used to remove residual and occluded gases from the vacuum apparatus and from the device being evacuated.

clear **1.** In computer operations, to restore a switching element (e.g., a flip-flop) or a memory element to its standard (e.g., zero) state. **2.** In computer practice, an asynchronous input.

clearance The distance between two live terminals, or between one live terminal and ground.

clear band In optical character recognition, the part of a document that must remain unprinted.

clear channel **1.** A channel in the standard amplitude-modulation (AM) broadcast band that is designated to only one station within the area covered by the signal from that station. **2.** In television broadcasting, a channel for which there are no restrictions on the nature of the programming.

clear memory A function in a calculator or small computer that erases the contents of the memory.

clear raster The raster on the screen of a television picture tube in the absence of a signal, noise, or faulty beam deflection.

cleavage In a crystalline substance, the quality of splitting along definite planes. Also, a fragment resulting from such a cleft.

click filter See KEY-CLICK FILTER.

click method An emergency technique for rendering an electric current audibly detectable, by

5059F-pC-93-162 4/9/01 4:51 PM Page 119

making and breaking the circuit carrying the current to a headset or earphone. A single click results from each make and each break. Also see TIKKER.

click suppressor See KEY-CLICK FILTER.

climate chamber A test chamber that provides accurately controlled temperature, humidity, and/or barometric pressure, for evaluating the performance of electronic components and circuits. Also called ENVIRONMENTAL TEST CHAMBER.

climatometer An instrument incorporating a hygrometer and bimetallic thermometer, whose dial pointers intersect to indicate comfort zones (best temperature-to-humidity ratio).

clinometer An electromechanical device that measures the steepness of a slope. When the device is level (horizontal), the output voltage is zero. If the device is tipped in one direction, a negative voltage is produced; if it is tipped in the other direction, a positive voltage is produced. The output voltage is proportional to the angle at which the device is tipped. Used in mobile robots.

clip A pinch-type connector whose jaws are normally held closed by a spring.

clip

clipped-noise modulation Modulation of a jamming signal through clipping action to increase the sideband energy and resulting interference.

clipper A circuit whose output voltage is fixed at a value for all input voltages higher than a predetermined value. Clippers can flat-top the positive, negative, or both positive and negative peaks of an input voltage.

clipper amplifier An amplifier operated so that the positive, negative, or both positive and negative peaks are clipped in the output signal. The clipping action results from feeding a regular symmetric waveform into an amplifier so that on negative excursion extremes, the stage is cut off; on positive excursion extremes, the amplifier is driven into saturation.

clipper limiter A device that delivers an output signal whose amplitude range corresponds to input-signal voltages between two predetermined limits. It can be used as a *noise limiter* with an element or elements that clip all pulses whose amplitudes are greater than the signal being processed.

clipping **1.** Leveling off (flat-topping) a signal peak at a predetermined level. Also see CLIPPER. **2.** In audio practice, the loss of syllables or words because of cutoff periods in the operation of the circuit (usually caused by overdriving a stage).

clock In a digital computer or controller, the device or circuit that supplies timing pulses to pace the operation of the system.

clocked flip-flops A master-slave arrangement of direct-coupled flip-flops. Information entered into the master unit when the input-trigger pulse amplitude is high is transferred to the slave unit when the amplitude is low.

clock frequency In a digital computer or control, the reciprocal of the period of a single cycle, expressed in terms of the number of cycles occurring in one second of time (hertz, kilohertz, or megahertz).

clock generator A test-signal generator that supplies a chain of pulses identical to those supplied by the clock of a digital computer.

clock module A complete plug-in or wire-in digital unit whose readout indicates time of day or elapsed time. Connected to a suitable power supply, it serves as either a clock or timer.

clock pulse A time-base pulse supplied by the clock of a digital computer, expressed as a period whose reciprocal is frequency.

clock rate See CLOCK FREQUENCY.

clock track On a magnetic tape or disk for data storage, a track containing read or write control (clock) pulses.

clockwise Abbreviation, cw. Rotation in a right-hand direction around a circle, starting at the top. Compare COUNTERCLOCKWISE.

clockwise-polarized wave An elliptically polarized electromagnetic wave whose electric-intensity vector rotates clockwise, as observed from the point of propagation. Compare COUNTERCLOCKWISE-POLARIZED WAVE.

clone A machine manufactured by a relatively unknown company that performs all the same functions, in basically the same way, as another machine manufactured by a well-known, major corporation. The term is used especially in reference to computers and computer peripherals. If a device is compatible with a certain computer, then clones of that device are generally compatible with that computer. Also, the device is likely to be compatible with all clones of the computer.

close coupling Also called *tight coupling.* In a transformer, the placement of the primary and secondary coils as close together as possible for maximum energy transfer. Compare LOOSE COUPLING.

closed capacitance The value of a variable capacitor whose rotor plates are completely meshed with the stator plates. Compare OPEN CAPACITANCE.

closed circuit A continuous unbroken circuit (i.e., one in which current can flow without interruption). Compare OPEN CIRCUIT.

closed-circuit cell A primary cell, such as the early gravity cell, designed for heavy and polarization-free service.

closed-circuit communication Communication between units only within a defined, hard-wired system, not extending to other units or systems.

closed-circuit security system An electronic security or alarm system, consisting of subsystems

5059F-pC-93-162 4/9/01 4:51 PM Page 120

interconnected so that a disturbance anywhere in the circuit will result in an alarm signal pinpointing the location of the disturbance.

closed-circuit signaling Signaling accomplished by raising or lowering the level of a signaling current flowing continuously in a circuit.

closed-circuit television Abbreviation, CCTV. A usually in-plant television system, in which a transmitter feeds one or more receivers through a cable.

closed core A magnetic core generally constructed in an "O" or "D" configuration to confine the magnetic path to the core material. Compare OPEN CORE.

closed-core choke A choke coil wound on a CLOSED CORE. Also called CLOSED-CORE INDUCTOR.

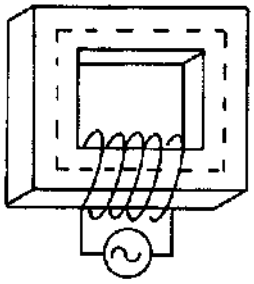

closed-core choke

closed-core transformer A transformer wound on a CLOSED CORE.

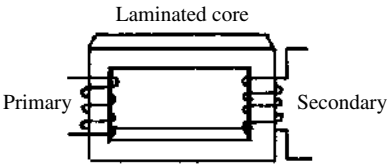

closed-core transformer

closed loop **1.** The feedback path in a self-regulating control system. An oscillator, for example, is a closed-loop amplifier. **2.** A loop within a program that would continue indefinitely, except for an external exit command.

closed-loop bandwidth The frequency at which the gain of a closed-loop circuit (see CLOSED LOOP, **1**) drops 3 decibels from the direct-current or midband value.

closed-loop control system A control system in which self regulation is obtained by means of a feedback path (see CLOSED LOOP). An example is a voltage regulator, in which a rise in output voltage is fed back to the input. This changes the input voltage and reduces the output voltage to its correct value. Compare OPEN-LOOP CONTROL SYSTEM.

closed-loop input impedance The input impedance of an amplifier that has feedback.

closed-loop output impedance The output impedance of an amplifier that has feedback.

closed-loop voltage gain The voltage gain of an amplifier that has feedback.

closed magnetic circuit A magnetic circuit in which the flux is uninterrupted, as in a ferromagnetic core, which has no air gap. Also see CLOSED CORE.

closed subroutine In a digital computer program, a subroutine that can be accessed and left by branch instructions, such as GOSUB and RETURN in the high-level language BASIC.

close-spaced array A beam antenna in which the elements (radiator, director, and reflector) are spaced less than a quarter-wavelength apart.

close-talk microphone A microphone that must be placed close to the mouth. Such a microphone is less susceptible to background noises than an ordinary microphone, and is useful in environments where the ambient noise level is high.

closing rating A specification for closure conditions in a relay, including duty cycle and contact life (total guaranteed closures before contact failure).

closure **1.** The act of closing or being closed (e.g., *switch closure* or *relay closure*). **2.** Circuit completion (i.e., the elimination of all discontinuities).

cloud The mass of electrons constituting the space charge in a vacuum tube.

cloverleaf antenna An omnidirectional transmitting antenna in which numerous horizontal, four-element radiators (stacked vertically, a quarter-wavelength apart) are arranged in the shape of a four-leaf clover.

C/L ratio See LC RATIO.

clutter Extraneous echoes that interfere with the image on a radar display.

clutter gating In radar operations, a switching process that causes the normal video to be displayed in regions free of clutter, and the video indicating target movement to be displayed only in cluttered areas.

Cm Symbol for CURIUM.

cm Abbreviation of CENTIMETER.

c.m. Abbreviation of CIRCULAR MIL.

cm^2 Abbreviation of *square centimeter.*

cm^3 Abbreviation of *cubic centimeter.*

C_{max} Abbreviation of *maximum capacitance.*

C meter See CAPACITANCE METER.

C_{min} Abbreviation of *minimum capacitance.*

CML Abbreviation of CURRENT-MODE LOGIC.

CMOS Abbreviation of COMPLEMENTARY METAL-OXIDE SEMICONDUCTOR.

CMR See COMMON-MODE REJECTION.

5059F-pC-93-162 4/9/01 4:51 PM Page 121

CMRR See COMMON-MODE REJECTION RATIO.

CMV See COMMON-MODE VOLTAGE.

C network A circuit with three impedances connected in series, the free leads being connected to a pair of terminals and the two internal junctions, to another pair of terminals.

Co Symbol for COBALT.

C_o Symbol for OUTPUT CAPACITANCE.

coalesce In computer operations, to create one file from several.

coarse adjustment Adjustment of a quantity in large increments. Compare FINE ADJUSTMENT.

coarse-chrominance primary See Q SIGNAL.

coastal bending A change in the horizontal direction of a line-of-sight radio wave when it crosses a coastline.

coast station In the Maritime Mobile Radio Service, a land station that communicates with shipboard stations.

coating **1.** The application of a substance to another substance by means of electroplating, electrophoresis, or similar process, for the purpose of protecting the material, isolating it from the environment, or improving the conductivity of an electrical connection to some other object. **2.** The magnetic material on a recording tape. **3.** In a computer system, the magnetic material on a magnetic diskette or hard disk.

coating thickness On magnetic tape or magnetic disks, the depth of the magnetic coating applied to the base.

coax Abbreviation of COAXIAL CABLE or COAXIAL LINE.

coaxial antenna A half-wave vertical antenna that is center-fed by coaxial cable. The cable runs upward through a 1/4-wave section of tubing that composes the lower half of the antenna. The outer conductor of the cable is connected to this tubing through a shorting disk at the top. The inner conductor of the cable is connected to a 1/4-wave vertical radiator that is insulated from, and that extends upward from the top of, the lower section.

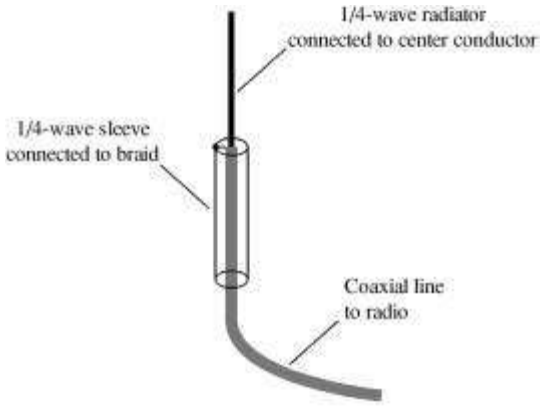

coaxial antenna

coaxial cable An unbalanced cable consisting of two concentric conductors: an inner wire and an outer, braided sleeve. The inner and outer conductors are separated by a dielectric, usually solid or foamed polyethylene. The outer conductor is generally grounded while the inner conductor carries the signals. This cable is used in community-antenna television (CATV) networks, and as a transmission line connecting antennas to radio transmitters, receivers, and transceivers at low, medium, high, and very-high frequencies. It is also used in some high-fidelity sound systems—especially to connect microphones, compact-disc players, tape players, tuners, and speakers to audio amplifiers.

coaxial cable
(From left to right: insulating jacket, woven outer conductor, low-loss insulating sleeve, inner conductor.)

Characteristics of prefabricated coaxial transmission lines.

Type	*Characteristic impedance, (ohms)*	*Velocity factor*	*Outside dia. (in.)*	*Picofarads per foot*
RG-8/U	52	0.66	0.41	29.5
RG-9/U	51	0.66	0.42	30.0
RG-11/U	75	0.66	0.41	20.6
RG-17/U	52	0.66	0.87	29.5
RG-58/U	54	0.66	0.20	28.5
RG-59/U	73	0.66	0.24	21.0
RG-174/U	50	0.66	0.10	30.8
hard line	50	0.81	0.50	25.0
($^1/_2$-inch)	75	0.81	0.50	16.7
hard line	50	0.81	0.75	25.0
($^3/_4$-inch)	75	0.81	0.75	16.7

coaxial capacitor **1.** A somewhat uncommon, but highly effective, capacitor that uses two telescoping sections of tubing. It works because there is a certain effective surface area between the inner and the outer tubing sections. A sleeve of plastic dielectric is placed between the sections of tubing. This allows the capacitance to be adjusted by sliding the inner section in or out of the outer section. Coaxial capacitors are especially useful in antenna systems for tuning and/or impedance matching. Their values are generally from a few

5059F-pC-93-162 4/9/01 4:51 PM Page 122

picofarads up to about 100 pF. **2.** A short length of coaxial cable that is used as a capacitor rather than a transmission line because of the inherent capacitance between its center conductor and braid. See COAXIAL CABLE.

coaxial cavity A cavity consisting of a cylindrical metal chamber housing a central rod. The cavity can be tuned to resonance by means of a piston.

coaxial connector A device used to splice coaxial line or to connect a coaxial line to a transmitter, receiver, or other piece of apparatus.

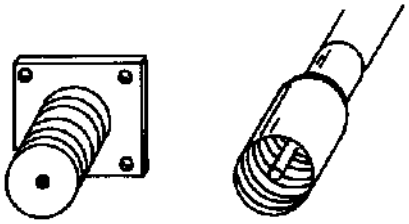

coaxial connector

coaxial diode A semiconductor diode housed in a cylindrical metal shell acting as one contact, and provided with a recessed, concentrically mounted end pin, which serves as the other contact.

coaxial driver See COAXIAL SPEAKER.

coaxial filter **1.** A filter that uses a coaxial cable as a tuned circuit. **2.** A filter designed to be used in a coaxial transmission line.

coaxial jack A female receptacle or connector, whose concentric terminals have the same spacing as a male coaxial-cable connector designed to fit it.

coaxial line A signal transmission line consisting of COAXIAL CABLE.

coaxial-line frequency meter A microwave absorption wavemeter (see WAVEMETER) with input and output receptacles for insertion into a coaxial line.

coaxial-line oscillator See CONCENTRIC-LINE OSCILLATOR.

coaxial loudspeaker See COAXIAL SPEAKER.

coaxial plug A male connector whose concentric terminals have the same spacing as a female coaxial cable connector designed to fit it.

coaxial receptacle A coaxial connector, such as a coaxial jack or plug. Receptacles are installed in equipment, whereas plugs are usually attached to the end of coaxial cables.

coaxial relay A relay designed to connect and disconnect, or to interchange, coaxial cables in a transmission line without disturbing the characteristic impedance of the line.

coaxial speaker Also called *coaxial driver* and *coaxial loudspeaker.* A large low-frequency speaker and a small high-frequency speaker mounted concentrically, the smaller within the larger. When used with a crossover network, this arrangement provides fairly good wide-range audio-frequency response, and saves physical space, compared with the use of separate speakers.

coaxial stub **1.** A length of coaxial cable acting as a branch to another coaxial cable. Commonly used for impedance matching. **2.** A length of coaxial cable, usually cut to 1/4 or 1/2 wavelength, and connected across a coaxial transmission line to act as a WAVETRAP. Commonly used to reject strong interfering signals.

coaxial switch A switch designed to connect and disconnect, or to interchange, coaxial cables in a transmission line without disturbing the characteristic impedance of the line.

coaxial tank A tank circuit consisting of a rod within a cylinder. The tank is usually tuned by a small variable capacitor connected between the rod and cylinder at one end of the combination. Generally used at ultra-high frequencies (UHF).

coaxial-tank oscillator A stable, self-excited oscillator that uses a COAXIAL TANK. Also see CONCENTRIC-LINE OSCILLATOR.

coaxial transistor A transistor in which a semiconductor wafer is mounted centrally in a metal cylinder (the base connection) and is contacted on opposite faces by the emitter and collector whiskers, which are axially mounted.

coaxial transmission line A transmission line that is a COAXIAL CABLE.

coaxial wavemeter A type of absorption wavemeter in which the tunable element is a section of coaxial line (i.e., a metal cylinder surrounding a metal rod). An internal short-circuiting disk is moved along the cylinder to connect its inner wall to selected points along the rod's length, thereby varying the resonant frequency. The instrument is useful at microwave frequencies.

cobalt Symbol, Co. A metallic element. Atomic number, 27. Atomic weight, 58.94.

cochannel interference Interference between similar signals transmitted on the same channel.

Cockcroft-Walton accelerator A proton accelerator in which nuclei of hydrogen atoms are given high velocity through a straight tube by a high dc voltage.

codan Any of several muting (SQUELCH) systems. In particular, a squelch circuit that suppresses noise in a sensitive receiver equipped with automatic gain control (AGC). The receiver is quiet until a carrier of predetermined strength is received. The name is an acronym for *carrier-operated device antinoise.*

codan lamp A lamp that alerts a radio operator that a signal of satisfactory strength is being received. Also see CODAN.

code **1.** A set of symbols for communications (e.g., the Morse code of radiotelegraphy and wire telegraphy in which dots and dashes correspond to

5059F-pC-93-162 4/9/01 4:51 PM Page 123

letters, numbers, and marks of punctuation). **2.** In a computer program, symbolically represented instructions. **3.** ENCODE.

codec In encoding and decoding equipment, a *coder/decoder*, usually in a single package and operating at 8 kHz for an input signal with a passband of 3100 Hz (300 to 3400 Hz).

code character **1.** The representation of character in a particular code form. **2.** A sequence of dots and dashes in the Morse code.

code conversion The translation of a coded signal from one form of code to another.

coded decimal digit A number expressed in binary form (computer code), that is, in terms of zeros and ones only.

code-directing characters Characters added to a message to indicate how and where it is going.

coded program See PROGRAM.

coded signal **1.** A wire- or radiotelegraph signal in which secrecy is achieved by using letters in cipher groups, instead of straight language. **2.** SCRAMBLED SIGNAL.

coded stop See PROGRAMMED HALT.

code elements The smallest identifiable parts that compose a digital code. For example, in computer code, the elements are ones and zeroes (*high* and *low* logic states); in Morse code, they are *dots* and *dashes.*

code holes In a punched card or tape, holes representing data.

code line A written computer program instruction.

code machine Any one of several devices for recording or reproducing code signals.

code position The part of a data medium (e.g., card row) reserved for data.

code-practice oscillator A simple keyed audio oscillator intended for practicing Morse code.

coder **1.** In computer operations, a person who prepares instructions from flow charts and procedures devised by a programmer. **2.** A device that delivers coded signals.

code receiver A radiotelegraph receiver.

code ringing A method of ringing a telephone subscriber in a predetermined manner to convey a certain message.

code segment The instruction part of computer storage associated with a process. Compare DATA SEGMENT and DUMP SEGMENT.

code set The collection of codes representing all of the characters in a language.

code speed See KEYING SPEED.

code transmitter **1.** A radiotelegraph transmitter. **2.** A tape-operated keyer for wire telegraphy or radiotelegraphy.

code word See PHONETIC ALPHABET CODE WORD.

coding **1.** Performing the service of a CODER. **2.** Writing instructions for a digital computer; a part of programming.

coding check A pencil-and-paper verification of a routine's validity.

coding sheet A form on which program instructions are written prior to input.

codiphase radar A radar system that uses beam forming, signal processing, and a phased-array antenna.

codistor A voltage-regulating semiconductor device.

coefficient **1.** A factor in an indicated product. Thus, in $4y$, 4 is the coefficient of y. **2.** A parameter that indicates a specific characteristic of some component or device (e.g., COEFFICIENT OF COUPLING or COEFFICIENT OF REFLECTION).

coefficient of coupling Symbol k. The ratio of MUTUAL INDUCTANCE between two inductors to the maximum possible (theoretical) value of mutual inductance. This ratio is always greater than or equal to 0 (no coupling between inductors), and less than or equal to 1 (perfect coupling between inductors).

coefficient of current detection See CURRENT-DETECTION COEFFICIENT.

coefficient of reflection A measure of the amount of electromagnetic field reflected in a transmission line from the load feed point. The coefficient of reflection is equal to the square root of the reflected power divided by the forward power.

coercive force The demagnetizing force required to remove residual magnetism from a material.

coercivity See COERCIVE FORCE.

cogging Nonuniform rotation of a motor armature. The velocity increases as an armature coil enters the magnetic field and decreases as it leaves the field.

coherence In electromagnetic radiation, a condition in which all the wavefronts are in phase. This results in high energy concentration, and makes possible the long-distance transmission of infrared, visible light, and ultraviolet, because the rays are almost perfectly parallel. It also makes possible the extreme radiation intensity characteristic of some LASER devices.

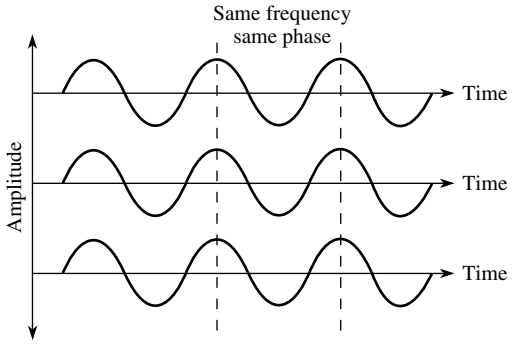

coherence

5059F-pC-93-162 4/9/01 4:51 PM Page 124

coherent bundle A bundle of optical fibers, such that the individual fibers are in the same relative positions at either end of the bundle.

coherent carrier A carrier that agrees in frequency and phase with a reference signal.

coherent electroluminescent device See LASER DIODE.

coherent light Visible light in which the phase relationship between successive waves is such that the beam consists of parallel rays that provide a high concentration of energy. Also see LASER.

coherent-light radar See COLIDAR.

coherent oscillator In a radar system, an oscillator that provides a COHERENT REFERENCE.

coherent-pulse operation Pulse operation characterized by a fixed phase relationship between pulses.

coherent radiation Radiation characterized by COHERENCE.

coherent reference A stable reference frequency with which other signals are phase locked for coherence.

coherent transponder A transponder in which the frequency and phase of the input and output signals have a fixed relationship.

coil A long conductor or group of conductors wound into a tight helical package, often in several layers on a cylindrical form. This takes advantage of the resulting concentration of magnetic flux, maximizing the inductance that can be obtained in a component of limited physical size. Further increases in inductance can be realized by the use of ferromagnetic core materials. See also INDUCTOR.

coil antenna See LOOP ANTENNA.

coil checker An alternating-current (ac) meter or simple bridge for checking inductors. Such instruments usually only indicate inductance values, but some list readings of resistance or approximate inductor *Q* factor.

coil dissipation The power wasted in a coil as heat. Generally, this dissipation or loss is proportional to the resistance of the coil, and to the square of the current passing through the coil.

coil form The insulating support around which an air-core coil is wound.

coil loading The insertion of one or more inductors into a transmission line or antenna element, for the purpose of impedance matching, alteration of the resonant frequency, or both.

coil magnification factor The *Q* factor of an inductor. Generally given by the ratio X_L/R_L, where X_L is the inductive reactance of the coil in ohms, and R_L is the resistance of the coil in ohms.

coil neutralization See INDUCTIVE NEUTRALIZATION.

coil resistance The resistance of a coil (inductor), as distinct from its reactance. It is almost entirely the result of ohmic loss in the wire from which the coil is manufactured.

coilshield A metal can designed to provide efficient electrostatic and electromagnetic shielding of a coil, preventing unwanted inductive coupling to other components.

coincidence The simultaneous occurrence of two or more signals. Compare ANTICOINCIDENCE.

coincidence amplifier An amplifier that delivers an output signal only when two or more input signals occur simultaneously.

coincidence circuit See AND CIRCUIT.

coincidence counter A circuit or device, such as a gate, that delivers an output pulse only when two or more input pulses occur simultaneously; the output pulses go to a device that counts them.

coincidence detector See AND CIRCUIT.

coincidence gate See AND GATE.

coincident-current selection Selection of a magnetic core (in a core memory or similar device) by applying two or more currents simultaneously.

coin shooting Searching for coins and similar small, buried metallic objects using a METAL LOCATOR.

coke A porous material obtained from the destructive distillation of coal. It is valued for the production of carbon components for electronics, such as dry-cell electrodes and motor brushes.

cold **1.** Pertaining to an electrical circuit, component, or terminal that is at ground potential. **2.** A term denoting a bad solder joint. **3.** Pertaining to an unheated electrode or element. See COLD CATHODE.

cold alignment The alignment of a tracking system (especially of its tuned circuits) when the system is not in operation, as when transistor power is off. Also called QUIET ALIGNMENT.

cold cathode **1.** In an electron tube, a cathode that emits electrons without being heated. **2.** A cathode electrode operated at a temperature below ambient temperature.

cold chamber An enclosure in which electronic equipment can be tested at selected, precise low temperatures. Compare OVEN.

cold flow The (usually gradual) change in the dimensions of a material, such as plastic in a molded part.

cold junction In a thermocouple system, an auxiliary thermocouple connected in series with the hot thermocouple, and immersed in ice or operated at ambient temperature.

cold light Light produced without significant heat, as from the ionization of a gas by a high voltage (as in neon bulbs and fluorescent lamps), or by electroluminescence, bioluminescence, cathodoluminescence, or a similar phenomenon.

cold pressure welding Welding sometimes used in the fabrication of electronic equipment, in which the metal parts to be joined are pressed together tightly to the point of deformation, whereupon they become welded.

cold resistance The resistance of an unheated electronic component. Compare HOT RESISTANCE.

5059F-pC-93-162 4/9/01 4:51 PM Page 125

cold rolling A method of manufacturing an inductor core so that the magnetic grains are all arranged lengthwise.

cold solder joint A solder joint in which insufficient heat has been applied, resulting in a bad connection.

cold spot **1.** An area of a circuit or component whose temperature is ordinarily lower than that of the surrounding area. **2.** A node of current or voltage. Compare HOT SPOT.

cold weld A welded joint produced by means of COLD PRESSURE WELDING.

colidar An optical radar system using unmodulated, coherent (laser-produced) light. The term is an acronym for *coherent light detection and ranging.*

collate In data processing, to produce an ordered set from two or more similarly ordered sets (as punched cards).

collator In a punched-card system, a device that collates (see COLLATE) punched cards.

collector **1.** In a bipolar transistor, the electrode toward which emitted current carriers travel. **2.** In a Klystron, the final electrode toward which electrons migrate after passing through the buncher and catcher. **3.** In an iconoscope, a cylindrical electrode around the circumference of the tube, which gathers and conducts away the electrons released by the mosaic. **4.** The final (target) electrode in a backward-wave or traveling-wave tube. **5.** A computer program segment that collates compiled segments so that they can be loaded into the computer.

collector capacitance **1.** Symbol, C_C. The capacitance of the collector junction in a bipolar transistor. **2.** The capacitance of the collector electrode in a Klystron, iconoscope, backward-wave tube, or traveling-wave tube.

collector current **1.** Symbol, I_C. The current flowing in the collector circuit of a bipolar transistor. Also see AC COLLECTOR CURRENT and DC COLLECTOR CURRENT. **2.** Current flowing in the collector circuit of a Klystron, iconoscope, backward-wave tube, or traveling-wave tube.

collector-current cutoff See COLLECTOR CUTOFF.

collector cutoff In a bipolar transistor, the condition in which the collector current is cut off (i.e., reduced to the residual value). Also see CUTOFF CURRENT.

collector cutoff current See CUTOFF CURRENT.

collector-diffusion isolation A method of making integrated circuits that contain bipolar transistors. Provides electrical separation of the transistors in a semiconductor integrated circuit.

collector dissipation Symbol, P_C. In a bipolar transistor, the power dissipation of the collector electrode. The collector dc power dissipation is the product of collector current and collector voltage: $P_C = V_C I_C$.

collector efficiency In a bipolar transistor circuit, the ratio of ac power output to dc collector-power input.

collector family For a bipolar transistor, a group of collector current versus collector voltage curves. Each is plotted for a particular value of base current (common-emitter circuit) or emitter current (common-base circuit).

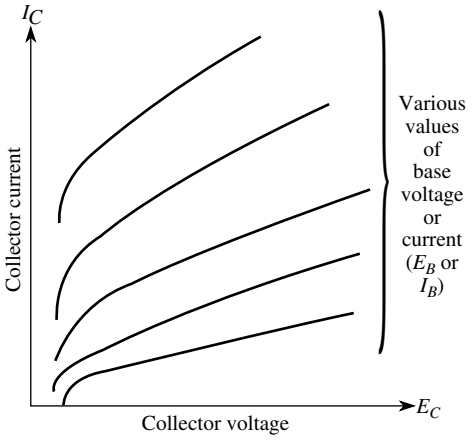

collector family

collector junction In a bipolar transistor, the junction between collector and base layers.

collector mesh In a cathode-ray storage tube, a flat, fine wire screen that attracts and conducts away the secondary electrons knocked out of the storage mesh by the electron beam.

collector multiplication In a bipolar transistor, an increase in the number of electrons at the collector electrode, caused by a momentary alteration of the charge density of the collector junction by injected carriers reaching the junction.

collector resistance In a bipolar transistor, the internal resistance of the collector junction. See AC COLLECTOR RESISTANCE and DC COLLECTOR RESISTANCE.

collector ring **1.** A rotating, brush-contacted ring electrode connected to one end of a coil in an ac generator. **2.** A similar ring which, with a brush, serves as a connection to a rotating element, as in a signal-gathering system. **3.** The collector electrode in an iconoscope.

collector transition capacitance The capacitance between the collector and base of a bipolar transistor under normal operating conditions. This capacitance has a limiting effect on the operating frequency of a bipolar device.

collector voltage Symbol, V_C. In a bipolar transistor, the voltage on the collector electrode. See AC

5059F-pC-93-162 4/9/01 4:51 PM Page 126

COLLECTOR VOLTAGE and DC COLLECTOR VOLTAGE.

collimated rays Electromagnetic waves made parallel or nearly parallel. This can be done by means of a reflector, a lens, or a laser.

collimation **1.** The process of rendering electromagnetic rays parallel. **2.** Adjustment of the line of sight of an instrument, such as a level or transit.

collimation equipment Optical-alignment equipment.

collimator A device for producing parallel rays of light or other radiation. In electronics, the most common example is a *dish antenna.*

collinear antenna A broadside directional antenna consisting of two or more half-wave radiators; the current is kept in phase in each section by quarter-wave stubs between each radiating section. The radiators are stacked end to end horizontally or vertically. Also called FRANKLIN ANTENNA.

Collins coupler A single-section, pi-filter circuit, used to match a radio transmitter to a wide range of antenna impedances. Also called *pi coupler* and *Collins network.*

collodion A viscous solution of pyroxylin and a solvent (such as acetone, alcohol, or ether) sometimes used as a binding agent for coils and other components.

cologarithm Abbreviation, colog. The logarithm of the reciprocal of a number; colog $x = \log (1/x) = \log x^{-1} = -\log x$.

color A perceived characteristic, and a direct function, of visible-light wavelength. Seen by the human eye as a spectrum of hues, ranging from red at the longest visible wavelengths, through orange, yellow, green, blue, indigo, and finally violet at the shortest visible wavelengths. See HUE.

coloration In audio applications, a blending of sounds as a result of mixing among components at different frequencies. Sometimes this is done deliberately; in other instances, it is undesirable.

color balance In a color television receiver, adjustment of the beam intensities of the individual guns of a three-gun picture tube. Compensates for the difference in light emissivity of the red, green, and blue phosphors on the tube screen.

color bar-dot generator A radio-frequency (RF) signal generator that produces a bar or dot pattern on the screen of a color television picture tube. Used for testing and alignment.

color-bar pattern A color television test pattern of vertical bars—each of a different color.

color breakup A transient separation of a color television picture into its red, green, and blue components, as a result of a sudden disturbance of viewing conditions (blinking of eyes, moving of head, intermittent blocking of screen, etc.).

color burst As a phase reference for the 3.579545-MHz oscillator in a color television receiver, approximately nine cycles of the chrominance subcarrier added to the back porch of the horizontal blanking pedestal in the composite color signal.

color carrier See CHROMINANCE SUBCARRIER.

colorcast A color television broadcast.

color code **1.** A system that uses colored stripes or dots to mark the nominal values and other characteristics on capacitors, resistors, and other components. **2.** A code that represents the various frequencies being used by radio-control modelers in competition, and used on flags attached to transmitters, for example, as a safeguard against jamming.

color coder See COLOR ENCODER.

color contamination In a color television system, faulty color reproduction resulting from incomplete separation of the red, green, and blue channels.

color-coordinate transformation In a color television system, the computation (performed electrically in the system) of the tristimulus (primary) values with reference to one set of primaries, from the same colors derived from another set of primaries.

color depth An expression for the extent to which an image can accurately render color. Generally expressed in bits or in number of colors. Some systems can reproduce millions of different colors.

color-difference signal Designated B-Y, G-Y, and R-Y. The signal resulting from reducing the amplitude of a color signal by an amount equal to the luminance-signal amplitude. Also see B-Y SIGNAL, G-Y SIGNAL, and R-Y SIGNAL.

color dot **1.** A phosphor spot on the screen of a color television picture tube. **2.** One of the spots stamped on a capacitor, indicating the capacitance, voltage, and tolerance (see COLOR CODE, **1**). **3.** A spot stamped on a resistor, indicating the number of zeros to be added to the value indicated by the color bands.

color edging In a color television picture, an aberration consisting of false color at the boundaries between areas of different color.

color encoder In a color television transmitter, the circuit or channel in which the camera signals and the chrominance subcarrier are combined into the color-picture signal.

color equation A mathematical means of determining the resultant color obtained by adding primary colors in various proportions.

color fidelity The faithfulness with which a color television system, lens, or film reproduces the colors of a scene.

color filter A transparent plate or film that transmits light of a desired color, and eliminates or attenuates all other colors.

color flicker In a color television system, image instability that occurs when the luminance and chromaticity both fluctuate.

color fringing In a color television picture, false color around objects, sometimes causing them to appear separated into different colors.

5059F-pC-93-162 4/9/01 4:51 PM Page 127

color generator A special radio-frequency (RF) signal generator to adjust or troubleshoot a color television receiver. The color signals it delivers are identical to those produced by a broadcast station.

color graphics Computer graphics displayed in color on a cathode-ray tube (CRT) or liquid-crystal display (LCD).

colorimeter A device used to quantitatively measure the color intensity of a sample relative to a standard.

colorimetric A characteristic of visible light, representing the wavelength concentration. Refers to the perceived color of a light beam.

colorimetry The science and art of color measurement.

color killer In a color television receiver, a circuit that, in the absence of a color signal, delivers a negative bias to cut off the bandpass amplifier.

color match In photometry, the condition in which color agreement exists between the halves of an area. Also see COLOR MATCHING.

color matching The art of selecting colors that are identical in hue, saturation, and brilliance. This can be done with the unaided eye or with the help of an instrument.

color media Substances that transmit essentially one color of visible light while blocking other colors.

color meter A photoelectric instrument for measuring color values, and comparing and matching colors.

color mixture An additive combination of two or more colors. Thus, red + yellow = orange, blue + red = violet, red + blue + green = white, etc.

color oscillator The oscillator in a color television receiver that coordinates the color response. This oscillator is operated at 3.579545 MHz, to within plus or minus 10 Hz.

color palette In a color video image, the total number of possible colors that can be displayed.

color phase In color television, the phase difference between an I or Q chrominance primary signal and the chrominance carrier reference.

color-phase diagram In color television, a quadrant diagram showing (for each of the three primary and complementary colors) the difference in phase between the color-burst signal and the chrominance signal, as well as the peak amplitude of the chrominance signal. Also shown are the peak amplitude and polarity of both in-phase and quadrature components required for the chrominance signals. For color TV receiver adjustment, the color-phase diagram is displayed, in effect, by a VECTORSCOPE when a suitable signal from a color generator is applied to the receiver.

color picture signal **1.** In color television and/or computer graphics, an electrical signal containing components corresponding to the hue, saturation, and brilliance of a fixed or changing visual image. **2.** In color television, the combination of chrominance and luminance signals minus blanking and sync signals.

color picture tube A specialized type of cathode-ray tube (CRT), used in color television receivers and computer displays. Three different images are produced: one in red, one in blue, and one in green. The three monochrome images are combined to form a complete color image.

color primaries **1.** Also called *additive primaries* or *primary colors.* In color television, the hues red (R), green (G), and blue (B). When these colors are mixed in various ratios, any visual color can result. **2.** Also called *subtractive primaries* or *primary pigments.* In color printing, the hues magenta (M), cyan (C), and yellow (Y). These roughly correspond to red (R), blue (B) and yellow (Y). Sometimes black (K) is also included. When these pigments are mixed in various ratios, any visual pigment can result.

color purity The ratio of wanted to unwanted components in a color. In a pure color, there are no components other than those required to produce the color. Color, in this context, includes white, black, and all shades of gray.

color-purity magnet A permanent magnet on the neck of a color television picture tube, used to help ensure color purity by maintaining proper displacement of the electron beam.

color registration In color television reception, the precise superimposition of red, green, and blue so that the composite is free from COLOR EDGING.

color rendering index A mathematical expression defining the effect of the color of a light source on an object. For example, in red light, a blue object appears nearly black.

color sampling rate The number of times per second that each primary color is sampled in a color television receiver.

color saturation A measure of the purity of a hue. The extent to which a hue is without a white component; 100% saturation indicates a complete absence of white.

color sensing In machine vision systems, the ability to distinguish between light of different wavelengths. Usually done with red, green and blue color filters and three separate cameras.

color sensitivity **1.** The degree of which a photosensitive device, such as a photocell or camera tube, responds to various colors of light. **2.** The degree to which photographic film responds to various colors of light.

color signal See COLOR PICTURE SIGNAL.

color spectrum The band of electromagnetic energy containing visible light; it extends from red (at the longest wavelengths) to violet (at the shortest). Commonly measured in *nanometers (nm)*, where 1 nm = 10^{-9} m. Also expressed in *Angstroms*, where 1 Angstrom = 10^{-10} m = 0.1 nm. In order of decreasing wavelength, the colors are red at 750 to 700 nm (7500 to 7000

5059F-pC-93-162 4/9/01 4:51 PM Page 128

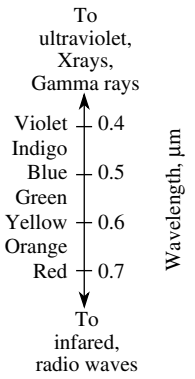

color spectrum

Angstroms), orange, yellow, green, blue, indigo, and violet at 410 to 390 nm (4100 to 3900 Angstroms).

color subcarrier A modulated monochrome signal whose sidebands convey color information.

color-sync signal See COLOR BURST.

color system Also called *RGB color model.* A means of representing a color in terms of mathematical coordinates. This can be done in three dimensions because there are three COLOR PRIMARIES. Each color primary is represented by an axis. Any COMPOSITE COLOR can be represented by a unique vector. The relative amount of each color primary is given by the length of the composite-color vector components along each axis.

color television Television in which the picture approximates natural color. It operates on the basis of mixing three primary colors (red, blue, and green) of phosphors on the picture tube screen.

color television receiver A television receiver designed to reproduce color pictures.

color television signal The signal transmitted by a color television transmitter, containing all of the information needed to reproduce a complete, full-color, moving image.

color transmission The television transmission of a picture in color.

color triad On the screen of a color picture tube, one of the color cells, each of which contains one of the three phosphor dots: red, green, and blue.

color triangle A triangle that can be inscribed on a chromaticity diagram to reveal the chromaticity range resulting from adding the three color primaries.

color TV signal The complete signal (video, color, and sync components) required for transmitting a picture in color.

color weather radar A computer-enhanced radar rendition of weather patterns, usually showing various intensities of precipitation as different colors. Commonly, areas of precipitation show up as violet, blue, green, yellow, orange, and red, in order of increasing intensity.

Colpitts oscillator A radio-frequency (RF) oscillator that uses a single, untapped inductor. A combination of two fixed capacitors in series is connected in parallel with the inductor. The feedback is controlled by the ratio of capacitances. A permeability-tuned coil or a roller inductor can be used to obtain variable-frequency operation. Stability is enhanced when the output of the oscillator is taken from the emitter or source portion of the circuit. To prevent the output signal from being short-circuited to ground, an RF choke is connected in series with the emitter or source. Compare HARTLEY OSCILLATOR.

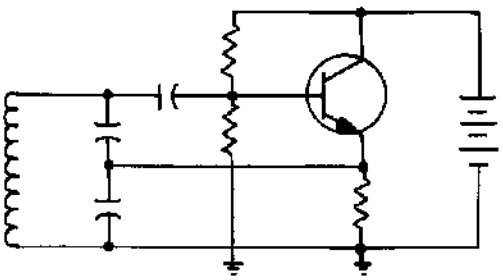

Colpitts oscillator

columbium Symbol, Cb. The former name of the metallic element *niobium.* Atomic number, 41. Atomic weight, 92.9064.

column See CARD COLUMN.

columnar graph A graphical presentation of data, in which the ordinates are represented by vertical columns whose height depends on the value. Commonly used in *presentation graphics*, but less common in *analytical graphics.*

column binary Binary number representation on punched cards, wherein consecutive digits correspond to consecutive column punching positions.

column speaker An acoustic speaker with a long cabinet, so that a large column of air is used for resonating or reinforcing purposes. This type of speaker radiates over a wide azimuth angle, while providing a narrow beam in the elevation plane.

column split On a punched card machine, the device for reading, as two separate characters or codes, two parts of a single column.

COM 1. Abbreviation for *communications port.* **2.** Abbreviation for *computer output on microfilm.*

coma An aberration that causes the beam spot on the screen of a cathode-ray tube to resemble a comet.

coma lobes An aberration in the radiation or response pattern of a dish antenna that occurs when the radiating element is not exactly at the focal point of the reflector. When the directional

5059F-pC-93-162 4/9/01 4:51 PM Page 129

pattern is altered by moving the driven element, rather than turning the entire antenna, these lobes appear.

comb amplifier An arrangement of several sharply tuned bandpass amplifiers whose inputs are connected in parallel and whose outputs are separate; the amplifiers separate various frequencies from a multifrequency input signal. The name is derived from the comb-like appearance of the response pattern of various output peaks displayed along a frequency-base axis.

comb filter A selective device that passes several narrow bands of frequencies within a larger band, while rejecting frequencies in between the narrow bands. So called because its frequency-response curve resembles the teeth of a comb when observed on a spectrum analyzer. Also see COMB AMPLIFIER.

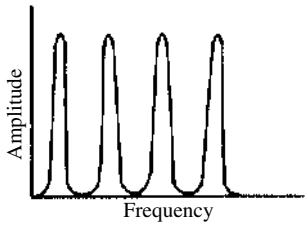

comb filter response

comb generator **1.** A signal generator that provides outputs at evenly spaced frequencies. So called because, on a spectrum analyzer, its output looks like the teeth of a comb. **2.** A transmitter with many spurious signals at its output.

combination **1.** A functional, usually stationary, installation consisting of two or more pieces of equipment. Examples: transmitter/receiver combination, motor/generator combination, and tuner/amplifier combination. **2.** In mathematics, a selection of several factors from a group, without regard to order. Thus, from the group ABC, the three possible combinations are AB, AC, and BC. Compare PERMUTATION.

combinational circuit Two or more basic logic circuits, combined in such a way that the output state depends entirely on the input states.

combination bridge A bridge that affords two or more classes of measurement, usually selectable by means of a function switch. Examples: capacitance-inductance bridge, and capacitance-resistance bridge.

combination cable A cable that has conductors grouped in pairs, threes, quads, or similar arrangements.

combination feedback See CURRENT-VOLTAGE FEEDBACK.

combination microphone Two or more microphones combined into one unit.

combination speaker Two or more loudspeakers combined into one (e.g., a COAXIAL SPEAKER).

combination tone An acoustic tone resulting from the combination of two other acoustic tones. If the original tones have frequencies f_1 and f_2 (where f_1 is higher than f_2), then the first-order combination frequencies are $f_1 + f_2$ and $f_1 - f_2$. Higher-order combination tones can result from mixing among the original tones and the first-order combination tones.

combinatorial logic A form of digital logic, in which the output states depend on the input states, but on no other factor.

combined head See READ-WRITE HEAD.

combined reactance The net reactance (X) in a circuit, obtained by vectorially adding the inductive reactance (X_L) and the capacitive reactance (X_C).

combiner A circuit or device for mixing various signals to form a new signal. Also see MIXER.

combiner circuit In a color television camera, the circuit that combines the chroma and luminance with the sync.

comeback A spurious response in a bandpass or band-rejection filter, at a frequency well above or below the passband or stopband.

command **1.** In computer operations, the group of selected pulses or other signals that cause the computer to execute a step in its program. **2.** Instruction.

command chain Part of a computer operation carried out independently as a series of input/output instructions.

command control In automation, electronic control, and computer operations, the performance of functions in response to a transmitted signal.

command destruct signal A signal for instigating the destruction of a missile in flight.

command guidance system A system in which a guided missile and its target are both tracked by radar.

command language A computer language made up of command operators.

command link In a command guidance system, the section that transmits missile-steering commands.

command network A radio communications network in which the chain of command is rigorously defined and followed.

command reference The current or voltage to which a feedback signal is referenced in a control system or servomechanism.

comment A statement written into a computer program for a documentation, rather than implementation (e.g., to describe the purpose of a step or subroutine).

comment field A record or file in which instructions or explanations are given.

commercial data processing A commercial (rather than industrial, scientific, or personal) application of data processing.

5059F-pC-93-162 4/9/01 4:51 PM Page 130

commercial-level security See LEVEL-2 SECURITY.

commercial killer A usually remote-controlled, electronic relay for disabling a radio or television receiver during advertisements.

commercial language A computer programming language for commercial applications (payroll, for example).

common **1.** Grounded. **2.** Pertaining to a connection shared by several different points in a circuit or system. **3.** See COMMON GROUND.

common area A computer storage area usable by several programs or segments within a program.

common-base circuit A bipolar transistor circuit in which the transistor base is the common (or grounded) electrode. Also called *grounded-base circuit.*

common battery **1.** A battery shared by two or more different circuits or pieces of equipment. **2.** In wire telephony, a central office battery that supplies the entire system.

common-battery office In wire telephony, a central office that provides a common battery.

common business-oriented language See COBOL.

common-capacitor coupling The process of coupling one tuned circuit to another by means of a capacitor that is common to both circuits.

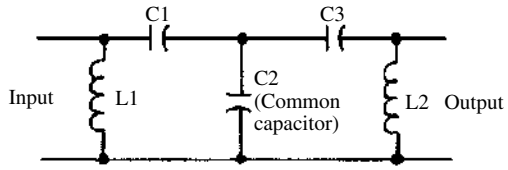

common-capacitor coupling

common-carrier fixed station A fixed radio station that provides public service.

common-cathode circuit A tube circuit in which the cathode is the common (or grounded) electrode. Also called *grounded-cathode circuit.*

common-channel interference Radio interference resulting from two stations transmitting on the same channel. It is characterized principally by beat-note (heterodyne whistle) generation, and suppression or capture of the weaker signal by the stronger one.

common-collector circuit A bipolar-transistor circuit in which the collector is the common (or grounded) electrode. Also called *grounded-collector circuit* and EMITTER FOLLOWER.

common communications carrier A communications company authorized by the licensing agency to furnish public communications.

common-component coupling See COMMON-CAPACITOR COUPLING, COMMON-INDUCTOR COUPLING, and COMMON-RESISTOR COUPLING.

common-drain circuit A field-effect transistor circuit in which the drain terminal is the common (or grounded) electrode. Also called *grounded-drain circuit* and SOURCE FOLLOWER.

common-emitter circuit A bipolar transistor circuit in which the emitter is the common (or grounded) electrode. Also called *grounded-emitter circuit.*

common-gate circuit A field-effect transistor circuit in which the gate is the common (or grounded) electrode. Also called *grounded-gate circuit.*

common-grid circuit A tube circuit in which the control grid is the common (or grounded) electrode. Also called *grounded-grid circuit.*

common ground A single ground-point connection shared by several portions of a circuit.

common impedance A single impedance shared by parts of a circuit. Because currents from the various parts flow through this impedance simultaneously, coupling (desired or undesired) can occur between them.

common-impedance coupling See COMMON-CAPACITOR COUPLING, COMMON-INDUCTOR COUPLING, and COMMON-RESISTOR COUPLING.

common-inductor coupling The process of coupling one tuned circuit to another by means of an inductor that is common to both circuits.

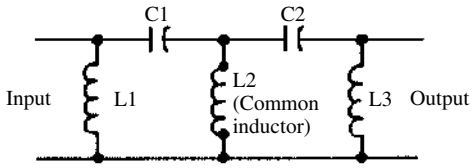

common-inductor coupling

common language A language recognized by all the equipment in a data processing system.

common logarithm Abbreviation, $\log_{10}$. Also called *base-10 logarithm.* A logarithm in which the base number is 10. Also see LOGARITHM.

common mode Pertaining to signals or signal components that are identical in amplitude and duration.

common-mode characteristics In an operational amplifier, characteristics denoting amplifier performance when a common signal is applied to inverting and noninverting inputs.

common-mode gain The voltage gain of a differential amplifier with a common-mode input.

common-mode impedance input The impedance between ground and one of the inputs of a differential amplifier. Compare COMMON-MODE INPUT IMPEDANCE.

common-mode input capacitance In a differential amplifier, the internal capacitance of the common-mode input circuit.

5059F-pC-93-162 4/9/01 4:51 PM Page 131

common-mode input circuit In a differential amplifier, the input circuit between ground and the inputs connected together.

common-mode input impedance In a differential amplifier, the open-loop impedance between ground and the inputs connected together. Compare COMMON-MODE IMPEDANCE INPUT.

common-mode input signal A signal applied to the common-mode input circuit of a differential amplifier (i.e., to both inputs connected together). Compare COMMON-MODE SIGNAL.

common-mode input voltage In a differential amplifier, the maximum voltage that can be applied safely between ground and the inputs connected together.

common-mode interference A form of interference that occurs across the terminals of a grounded system.

common-mode rejection The extent to which a differential amplifier will reject a signal presented simultaneously to both inputs in phase, or of two signals identical in amplitude, frequency, and phase applied separately to the two inputs. Also see COMMON-MODE REJECTION RATIO.

common-mode rejection ratio In a differential amplifier, the extent to which the amplifier cancels undesired signals. It is the ratio of the differential gain to the common-mode gain. Also see COMMON-MODE REJECTION.

common-mode signal The algebraic average of two signals applied simultaneously to the two ends of a balanced circuit, such as a differential amplifier. Compare COMMON-MODE INPUT SIGNAL.

common-mode voltage The part of the input that is common to both inputs of a differential amplifier circuit. It is quantitatively defined as the arithmetic mean of the voltages at the inputs.

common-mode voltage gain See COMMON-MODE GAIN.

common-mode voltage range The range limited by the maximum nonsaturating input voltage that can be applied to both inputs of an operational amplifier.

common pool An assigned memory store, utilized by two or more circuits or systems.

common-resistor coupling The process of coupling one circuit to another by means of a resistor that is common to both circuits.

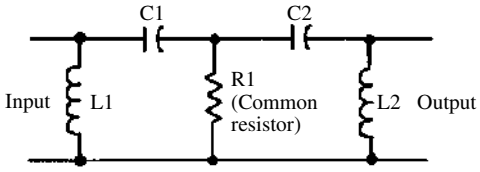

common-resistor coupling

common-source circuit A field-effect transistor circuit in which the source terminal is the common (or grounded) electrode. Also called *grounded-source circuit.*

common-user channels Communication channels open to all licensees in a particular service.

communication band A band of frequencies whose use is authorized expressly for communications, rather than for other services (such as broadcasting, education, remote control, etc.).

communication channel **1.** In radio or wire service, a (usually auxiliary) channel for direct exchange of information between units of the service (e.g., a "talking circuit" between a broadcast studio and the transmitter house). **2.** A data transmission channel between two points (e.g., a remote terminal and a central computer system).

communication link **1.** Collectively, the equipment providing a communication channel between two transmitters. **2.** Data terminal equipment.

communication protocol The specifications of a digital signal, including the speed in bits per second (bps) or bauds, the code type, the bit duration, the mark-to-space ratio, etc.

communications The science and art of using and developing electronic equipment and processes for the transmission and reception of information.

communications common carrier An organization licensed to provide public communication services.

communications network An organization of transmitting and receiving stations for the reliable exchange of intelligence. Also called *net.*

communications receiver A general-coverage or multiband radio receiver, designed primarily for listening to amateur, weather, or other nonbroadcast stations. Compare BROADCAST RECEIVER.

communications satellites Satellites in earth orbit that provide propagation paths (e.g., by reflection or retransmission) for radio waves between terrestrial transmitters and receivers. Also see ACTIVE COMMUNICATIONS SATELLITE and PASSIVE COMMUNICATIONS SATELLITE.

community-antenna television Abbreviation, CATV. A system in which an advantageously located receiving station receives television signals, amplifies them if necessary, and distributes them in the community served by the system. Commonly called *cable TV.*

commutating capacitor **1.** In a flip-flop circuit, a capacitor connected in parallel with the cross-coupling resistor to accelerate the transition from one stable state to the other. Also called *speedup capacitor.* **2.** A capacitor connected in parallel between silicon-controlled rectifier (SCR) stages to momentarily reverse the current going through the SCR, thereby causing the SCR to go into the cutoff condition.

5059F-pC-93-162 4/9/01 4:51 PM Page 132

commutation **1.** In a direct-current (dc) generator, periodic reversal of the current in the armature coils as the coils alternately pass the north and south poles of the magnetic field. When the ends of each coil are connected to opposite bars of the commutator, the electrical polarity at the commutator brushes remains constant. **2.** In a thyratron or silicon-controlled rectifier (SCR) circuit, momentarily reversing the polarity to cut the device off.

commutator **1.** In a direct-current (dc) motor, generator, or rotating selector, an arrangement of parallel metal bars or strips on a rotating drum. As the drum turns, the bars contact one or more brushes that are in sliding contact with the commutator. **2.** An electronic circuit that switches a single input sequentially to a series of output terminals, or switches a number of inputs sequentially to a single pair of output terminals.

commutator ripple The pulsating voltage superimposed on the direct-current (dc) voltage delivered by an unfiltered dc generator.

compact disc Abbreviation, CD. A digital, high-density optical disc, used in high-fidelity stereo sound systems. Also used to store computer data. The information is encoded as tiny pits on the surface of the disc, and is recovered by a laser, a sensor and a digital-to-analog (D/A) converter. These disks have largely superseded magnetic tapes, and have rendered long-playing vinyl disks and turntables obsolete. See also COMPACT-DISK READ-ONLY MEMORY.

compact-disk read-only memory Abbreviation, CD-ROM. A digital COMPACT DISC used for the long-term storage of computer data and/or software programs. Usually the same size as a high-fidelity stereo disk, it can hold over 600 megabytes of data. Although data can be read from the disk, it cannot be overwritten.

compander Term for *compressor/expander.* In the transmission and reception of audio-frequency (AF) intelligence, a system that uses an amplitude compressor at the transmitter and an amplitude expander at the receiver. The compressor reduces the dynamic range before transmission, and the expander restores it after reception. Provides improved signal-to-noise ratio under marginal communications conditions. Also increases the ratio of average power to peak power. See COMPANDING.

companding A process in which a signal is compressed at the transmitting end of a circuit and expanded at the receiving end, yielding a signal like the original at the receiver output. Signals are more efficiently transmitted when they are compressed because the average power increases, relative to the peak power. This improves the average signal-to-noise ratio for weak signals. See COMPANDER.

companding law The mathematical function used for companding. It is an output-amplitude versus input-amplitude function for the compression at the transmitter, and the inverse of this function for the expansion at the receiver.

companion keyboard An auxiliary keyboard connected to a regular keyboard and operated remotely.

companionship machine A computer or robot with sufficient machine intelligence to provide entertainment and mental stimulation for humans.

comparator **1.** An integrated circuit (IC) with two inputs, called A and B. The device compares the voltages that appear at these inputs. If the input voltage at A is significantly greater than the input voltage at B, the output is about +5 V. If the input voltage at A is not greater than the input voltage at B, the output voltage is about +2 V. These ICs are used to actuate, or trigger, other devices such as relays and electronic switching circuits. **2.** In general, any circuit that compares some characteristic of two input signals and produces an output that depends on the relationship between the inputs. **3.** An instrument for checking the condition of a component by comparing it directly with an identical component of known quality has a scale reading in percentage deviation, or simply "GO/NO-GO." Examples: capacitor comparator, resistor comparator, coil comparator.

compare In computer operations, a relational test performed on two quantities to determine their relative magnitude, including an indication of the test result and, sometimes, the taking of action. Example: the process and acton resulting from execution of the statement "IF A > B THEN GO TO LINE 250."

comparison **1.** An expression of the relationship between two voltages, currents, phase angles, component values, or other quantities in an electrical or electronic circuit or system. **2.** An examination of different data bits or items, which results in a conclusion about some aspect of their relationship.

comparison bridge A bridge designed especially for the quick comparison of components (e.g., the comparison of resistors with a standard resistor, inductors with a standard inductor, and capacitors with a standard capacitor).

comparison measurement A measurement in which a quantity or component is compared with a known, similar quantity or component value, rather than having the measurement displayed directly by a meter. Examples: bridge measurements, potentiometric measurements, and frequency matching.

compass **1.** Any of several instruments for determining direction on the earth's surface [e.g., magnetic (mariner's) compass and gyrocompass]. **2.** A radio direction finder. **3.** An instrument for drawing circles.

5059F-pC-93-162 4/9/01 4:51 PM Page 133

compatibility **1.** A desirable condition in which devices or systems can function efficiently together, without any modification of equipment. **2.** In computer operations, a desirable condition in which different computers can run the same software, without any modification of hardware or software.

compatible color television A color-television system whose transmissions can be received in black and white by any ordinary monochromatic receiver.

compatible integrated circuit A hybrid integrated circuit (IC) that has an active element inside the integrated structure and a passive element deposited on its insulated outer surface.

compensated amplifier A wideband amplifier whose frequency range is extended by special components and circuit modifications. Also see COMPENSATING CAPACITOR and COMPENSATING COIL.

compensated diode detector A diode detector in which a positive dc voltage from the automatic-gain-control (AGC) rectifier is applied to the diode anode. The voltage is always proportional to the signal carrier. The arrangement allows the diode to handle a heavily modulated AM signal without producing excessive distortion.

compensated-impurity resistor A resistor consisting of a diffused semiconductor material to which are added controlled amounts of n- or p-type dopants (impurities).

compensated-loop direction finder A direction finder whose loop antenna is complemented by another antenna for polarization-error compensation.

compensated semiconductor A doped semiconductor material in which the acceptor impurity cancels the effects of the donor impurity.

compensated volume control A combination volume-tone control that provides bass boost at low volume levels to compensate for the ear's deficiency at low frequencies.

compensating capacitor **1.** A capacitor that has a temperature coefficient of capacitance numerically equal to, but having the opposite sign from, that of another capacitor in a tank or other circuit. When the capacitors are connected in parallel, a temperature-induced value change in the main capacitor is balanced by an equal and opposite change in the compensating capacitor; the net capacitance of the circuit does not change. This greatly reduces frequency drift. **2.** In a video amplifier, a large capacitance connected between ground and a tap on the collector or drain resistor to boost low-frequency response. Compare COMPENSATION COIL. **3.** A usually low-capacitance capacitor of known temperature coefficient, operated in combination with a main capacitor to reduce capacitance/temperature drift of the latter to zero or to some desired positive or negative value.

compensating diode A junction diode used to temperature-stabilize a transistor circuit. It is usually forward-biased in the base-bias network of the transistor.

compensating filter **1.** A selective filter used for the purpose of eliminating some irregularity in the frequency distribution of received energy. **2.** A filter used to change the wavelength distribution of electromagnetic energy.

compensating resistor **1.** A low-value resistor of known temperature coefficient, connected in series with a main resistor to reduce the resistance/temperature drift to zero, or to some desired positive or negative value. **2.** See TRIMMER RESISTOR.

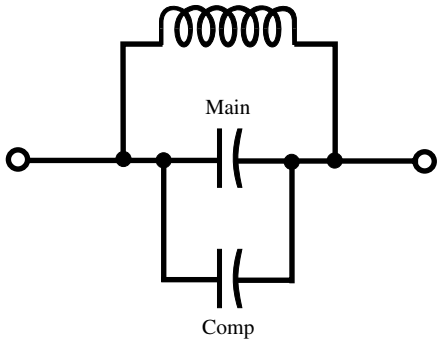

compensating capacitor, 1.

compensating resistor, 1.

compensation Adjusting a quantity, manually or automatically, to obtain precise values, or to counteract undesired variations. Example: temperature compensation of electronic components. For illustration, see COMPENSATING CAPACITOR, **1**.

compensation coil In a video amplifier, an inductor connected in series with the collector or drain resistor, or in the coupling path between stages, or both, to boost high-frequency response.

compensation filter See COMPENSATING CAPACITOR, **2**.

compensation signal A signal recorded on a tape track containing computer data, to ensure that the tape plays back at exactly the correct speed at all times.

compensation theorem An impedance (Z) in a network can be replaced by a generator having

5059F-pC-93-162 4/9/01 4:51 PM Page 134

zero internal impedance, and whose generated voltage equals the instantaneous potential difference produced across *Z* by the current flowing through it. Compare MAXIMUM POWER TRANSFER THEOREM, NORTON'S THEOREM, RECIPROCITY THEOREM, SUPERPOSITION THEOREM, and THEVENIN'S THEOREM.

compensator A device or circuit that facilitates the adjustment of a quantity, manually or automatically, to obtain precise values, or to counteract undesired variations.

compilation time The period during which a program is compiled, as distinct from RUN TIME.

compile **1.** To unify computer subroutines into an all-encompassing program. **2.** To gather information or data together into a single file or file set.

compiler In computer operations, a program that changes a HIGH-LEVEL LANGUAGE, such as BASIC, C, C++, COBOL, or FORTRAN, into MACHINE LANGUAGE. A compiler must be written especially for the high-level language being used.

compiler language Any computer language that serves as an interface between the operator and the computer.

compiler program A program that converts compiler language into machine language.

compiling routine In digital computer operation, a routine permitting the computer itself to construct a program to solve a problem.

complement **1.** The difference between a number and the radix (modulus or base) of the number system. For example, the complement of 7 is equal to 3 (because 10 – 7 = 3) in the decimal (radix-10) number system. **2.** Also called *ones complement.* In computer operations, a representation of the negative value of a binary number. All the available digits are set to 1, and then the number in question is subtracted. For example, the complement of 101 is equal to 010 (because 111 – 101 – 010); the complement of 1001 is equal to 0110 (because 1111 – 1001 = 0110).

complementary A Boolean operation whose result is the same as that of another operation, but with the opposite sign; thus, OR and NOR operations are complementary.

complementary colors **1.** In the additive color system, two colors that produce light gray or white when combined. **2.** In the subtractive color system, two pigments that produce dark gray or black when combined. **3.** Colors or pigments that are opposite each other on the color wheel.

complementary constant-current logic A form of bipolar logic with high operating speed and high component density.

complementary metal-oxide semiconductor Also sometimes called *complementary metal-oxide silicon.* Acronym, CMOS (pronounced "seamoss"). A digital integrated-circuit (IC) technology, in which logic gates are formed by n-channel/p-channel pairs of metal-oxide-semiconductor field-effect transistors (MOSFETs) fabricated on a substrate. Noted for high speed and low current drain.

complementary operator The logical negation (NOT) operation.

complementary pushpull circuit See COMPLEMENTARY-SYMMETRY CIRCUIT.

complementary rectifier In the output circuit of a magnetic amplifier, nonsaturating half-wave rectifier elements.

complementary silicon-controlled rectifier A silicon-controlled rectifier that has polarity opposite from the usual silicon-controlled rectifier.

complementary-symmetry circuit A bipolar-transistor circuit that uses an npn and pnp transistor. The transistors conduct during opposite half-cycles of the input signal, the result being that push-pull output is provided with a single-ended input; no phase-splitting input circuit is required. The complementary-symmetry circuit offers very low output impedance, permitting a loudspeaker voice coil (or other low-impedance load) to be operated directly without a coupling transformer.

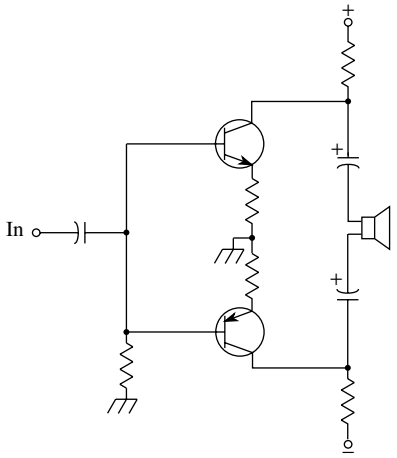

complementary-symmetry circuit

complementary tracking A control system in which several secondary (slave) devices are controlled by a primary (master) device.

complementary transistors A transistor pair of opposite polarity operated in a complementary-symmetry circuit or its equivalent.

complementary wave An electromagnetic wave in a transmission line that occurs as a result of reflection. Any impedance discontinuity will result in complementary waves.

5059F-pC-93-162 4/9/01 4:51 PM Page 135

complementer A logic circuit that provides an output pulse when there is no input pulse, and vice versa. Also called INVERTER and NOT CIRCUIT.

complement number In a base-*n* number system, for a given positive integer *p* less than *n*, the positive integer *m* such that $m + p = n$. For example, in the decimal (base-10) system, the complement of 4 is 6, the complement of 7 is 3, and the complement of 9 is 1. In the hexadecimal (base-16) number system, the complement of 4 is 12, the complement of 7 is 9, and the complement of 9 is 7.

complement-number handling A computer system in which the operations are carried out via the complements of the input numbers.

complement-setting technique A process of determining the number of pulses required to complete the switching of a counter circuit when it is started at some state higher than full zero. The number of pulses required for completion is equal to the number that represents the starting state's complement.

complete carry In digital computer operation, a system permitting all carries to generate carries.

complete circuit See CONTINUOUS CIRCUIT.

complete modulation Modulation to the maximum extent possible while maintaining acceptable circuit or system operation.

complete operation In computer operations, the condition in which the machine rigorously follows program instructions.

complete routine A vendor-supplied computer program that is usable without modification.

complex function **1.** A mathematical function of a complex-number variable. **2.** An integrated circuit (IC) containing two or more subcircuits that perform an operation more complicated that of any one of the circuits alone.

complex notation Notation taking into consideration both the real-number and imaginary-number components of a quantity. Thus, impedance (Z) is a complex quantity that includes a resistive (real) component (R) and a reactive (imaginary) component (jX). See COMPLEX NUMBER and COMPLEX OPERATOR.

complex number A number expressed in complex notation (e.g., $a + jb$, where a and b are real numbers and j is the COMPLEX OPERATOR). Can also be expressed as a point or a vector in an ARGAND DIAGRAM.

complex operator The unit imaginary number, represented as j by engineers and as i by mathematicians. This number is defined mathematically as the positive square root of –1.

complex parallel permeability An expression of the permeability of an inductor core under actual operating conditions, assuming zero loss in the conductors of the coil winding. A parallel combination of reactance and resistance.

complex periodic wave A periodic wave composed of a sine-wave fundamental and certain harmonics in specific proportions.

complex permeability An expression of inductor-core permeability, obtained from the mathematical ratio of the magnitudes of the vectors representing the induction and electromagnetic field strength within the core.

complex plane A Cartesian coordinate system with real numbers on the horizontal axis and imaginary numbers on the vertical axis. Used for vectorial representation of complex numbers. See ARGAND DIAGRAM.

complex quantity A quantity containing both real and imaginary components. Example: Impedance (Z) is a complex combination of resistance R (a real component) and reactance jX (an imaginary component): $Z = R + jX$.

complex radar target A radar target that is large enough in theory to be detected by radar, but, because of its geometry, cannot be detected. This effect is the result of phase combinations of signal components reflected from various surfaces on the target.

complex series permeability An expression of complex permeability of an inductor core under actual operating conditions, assuming zero loss in the conductors of the coil winding. A series combination of reactance and resistance.

complex steady-state vibration Periodic vibration with more than one sine-wave component.

complex tone An audio tone made up of more than one sine-wave component.

complex variable A variable having real and imaginary parts.

complex waveform The shape of a COMPLEX PERIODIC WAVE. It is the resultant of the individual sine-wave components (i.e., of the fundamental and the harmonics).

complex-wave generator A signal generator whose output signal is any of several selectable waveforms and frequencies (or repetition rates). Also see FUNCTION GENERATOR.

compliance **1.** The ease with which a material can be flexed or bent, an important characteristic of transducers (such as loudspeakers). Expressed in cm/dyne, compliance is the reciprocal of stiffness, and is the acoustical or mechanical equivalent of capacitance. **2.** A measure of the output impedance of a switched-current signal source. Generally given as maximum current for a certain change in the voltage.

compliance range The voltage range required to maintain a constant current throughout a load-resistance range.

compliance voltage The range over which the output voltage of a constant-current power supply must swing in order to maintain a steady current in a varying load.

compliance-voltage range The output voltage range of a constant-current power supply.

component **1.** A device or part used in a circuit to obtain some desired electrical action [e.g., a resistor (passive component) or an integrated circuit

5059F-pC-93-162 4/9/01 4:51 PM Page 136

(active component)]. Also see ACTIVE COMPONENT and PASSIVE COMPONENT. **2.** An attribute inherent in a device, circuit, or performance (e.g., the REACTIVE COMPONENT of an inductor). **3.** A specified quantity or term (e.g., the WATTLESS COMPONENT of ac power). **4.** A piece of equipment in a high-fidelity sound system.

component density The number of components (see COMPONENT, **1**) in an electronic assembly of a given physical volume.

component failure rate **1.** The percentage of components, out of a specified group, that can be expected to fail within a specified length of time. **2.** The frequency with which a given component, in a certain application, can be expected to fail.

component layout The mechanical arrangement of components (see COMPONENT, **1**) in an electronic assembly.

component stress The electrical or mechanical strain to which a component is subjected. In general, the greater the stress, the higher the component failure rate.

composite cable A cable containing other cables of different types.

composite circuit A circuit handling telegraphy and telephony simultaneously without causing mutual interference.

composite color A color that is not one of the COLOR PRIMARIES, but instead, consists of a combination of the three color primaries.

composite color signal The complete color television signal, including all picture, color, and control components.

composite conductor A set of wires connected in parallel. The wires are often, but not necessarily, of identical size and constitution.

composite current A current having both alternating-current (ac) and direct-current (dc) components; an alternating current superimposed on a direct current. Also called *fluctuating current.*

composite curve A curve or pair of curves showing two modes of operation, as of biased and unbiased conditions.

composite filter A filter consisting of more than one section. The sections might be, but often are not, identical.

composite video signal The television picture signal containing picture information and sync pulses.

composite-video-signal distortion Distortion of the composite video signal as evidenced by overshooting, ringing, and sync-pulse shortening.

composite voltage A voltage having both alternating-current (ac) and direct-current (dc) components; an ac voltage superimposed on a dc voltage. Also called *fluctuating voltage.*

composite wave filter Two or more wave filters (not necessarily of the same type) operated in cascade.

composition resistor A resistor made from a mixture of materials, usually finely powdered carbon and a binder.

compound A substance in which the atoms of two or more elements have united chemically to form a molecule. For example, an atom of cadmium (Cd) and one of sulfur (S) combine to form a molecule of cadmium sulfide (CdS).

compound connection A direct connection of two transistors, the amplified output of the first being further amplified by the second. The connection provides extremely high current gain. Also called DARLINGTON PAIR.

compound generator A generator that has both series and shunt fields. Also called *compound-wound generator.*

compound horn A horn reflector used for transmission of microwave energy. The faces of the horn approach four geometric plane surfaces as the distance from the center increases.

compound modulation A system of successive modulation, the modulated wave from one step becoming the modulating wave in the next. Also called *multiple modulation.*

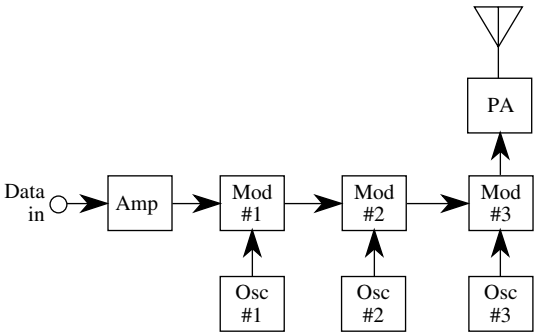

compound modulation

compound motor An electric motor having both series and shunt fields. Also called *compound-wound motor.*

compound transistor Two or more transistors directly coupled in the same envelope for increased amplification. Also see COMPOUND CONNECTION.

compound-wound generator See COMPOUND GENERATOR.

compound-wound motor See COMPOUND MOTOR.

compress **1.** In communications, to reduce or minimize the bandwidth of a signal. **2.** In communications, the processing of a signal to increase low-level components and thereby raise the average power level relative to the peak power level. **3.** In computer operations, to reduce or minimize the number of bits in a digital signal or file, while

5059F-pC-93-162 4/9/01 4:51 PM Page 137

still retaining all the essential information. Compare EXPAND.

compressed-air capacitor A high voltage air-dielectric capacitor enclosed in a case in which the air pressure is held at several atmospheres. The device exploits the dielectric strength of compressed air, which is higher than that of air at normal pressure.

compressed-air speaker A speaker that uses an airtight chamber to enhance the acoustic reproduction at certain frequencies.

compression **1.** In communications, the reduction or minimization of signal bandwidth. **2.** In communications, the processing of a signal to increase low-level components and thereby raise the average power level relative to the peak power level. Usually, a logarithmic function. **3.** In computer operations, the reduction or minimization of the number of bits in a digital signal or file, while still retaining all the essential information. Compare EXPANSION.

compression ratio In a system using COMPRESSION, the ratio A_1/A_2, where A_1 is the gain (or transmission) at a reference-signal level and A_2 is the gain (or transmission) at a specified higher signal level.

compression wave A wave disturbance that travels via longitudinal motion of particles in a medium. Sound waves through air are the most common example.

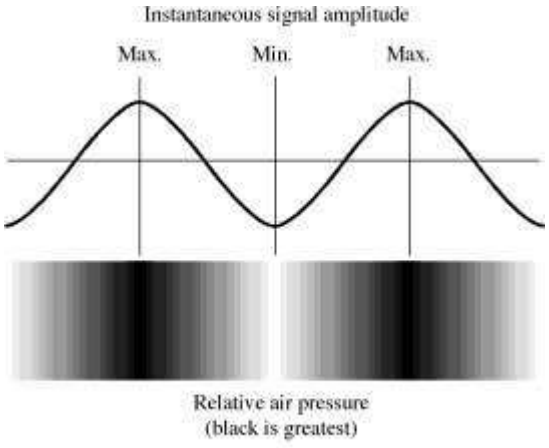

compression wave

compressor A circuit or device that limits the amplitude of its output signal to a predetermined value, despite wide variations in input signal amplitude.

compressor driver unit A loudspeaker that works into an air space connected by a throat to a horn, rather than by driving a diaphragm.

Compton diffusion An effect that occurs when a photon and electron collide. Some of the energy from the photon is transferred to the electron. On a large scale, such collisions result in diffusion of electromagnetic waves.

Compton effect The increase in wavelength (decrease in frequency) of X-rays scattered by the electrons of lighter atoms bombarded with the X-rays.

Compton shift See COMPTON EFFECT.

compute To perform a mathematical operation by means of a relatively simple process. Thus, a digital computer solves intricate problems using simple arithmetic steps. Compare CALCULATE.

computer A device or machine for performing mathematical operations on data, and producing the results as information or control signals. There are numerous types, the most common being the *digital computer.*

computer-aided design Abbreviation, CAD. The use of computers in conceiving, developing, and perfecting new products.

computer-aided manufacturing Abbreviation, CAM. The use of automated manufacturing systems, such as assembly lines, that are partially or totally controlled by computers.

computer antibody Also called *vaccine.* A small subprogram designed to eliminate viruses from computer systems.

computer-assisted instruction Abbreviation, CAI. The use of computers as teaching and training aids.

computer code See MACHINE LANGUAGE.

computer consciousness The degree to which a machine can be considered aware of its own existence. Until recently, this idea was considered ridiculous. But as microprocessor power continues to grow, some researchers now consider it worth thinking about.

computer-controlled catalytic converter A microprocessor-controlled system for automatically supervising gaseous emissions exhausted by a motor vehicle. An oxygen sensor monitors the exhaust stream, and the associated electronic system adjusts the air-to-fuel ratio of the carburetor to reduce smog-producing pollutants in the exhaust.

computer diode A semiconductor diode having low capacitance and fast RECOVERY TIME, thus suiting it to rapid switching in computer circuits and to very-high-frequency applications.

computer engineer A person skilled in the theory and application of computers, related equipment, and associated mathematics.

computer file See FILE.

computer game See VIDEO GAME.

computer graphics **1.** The use of computers to assist in drawing and drafting, and in the processing of video images such as photographs. **2.** Broadly, any computer-generated or computer-processed image.

5059F-pC-93-162 4/9/01 4:51 PM Page 138

computer instruction See INSTRUCTION.

computer interfacing apparatus The equipment used to connect a computer to other systems, and to peripherals.

computerized axial tomography Abbreviation, CAT. A multiple X-ray system that enables the observer to obtain cross-sectional images of the internal organs of the body.

computer map A blueprint, used in conjunction with machine vision, sonar, radar or beacons, that a mobile robot can use as a navigational aid. One or more such blueprints are stored in the robot controller's main memory.

computer music **1.** Music that is composed by a computer. **2.** See MUSICAL INSTRUMENT DIGITAL INTERFACE.

computer program See PROGRAM.

computer programmer A person skilled in devising and/or writing the routines that a digital computer uses to solve problems or process data.

computer storage tube A cathode-ray tube in which the electron beam scans and stores information in thousands of memory cells on a target. A cell "remembers" by acquiring and holding an electrostatic charge when it is struck by the beam from the writing gun. Information taken is read out of a cell by a second beam from the reading gun.

computer system A central processor and its associated online and offline peripherals, such as a monitor, modem, printer, optical scanner, magnetic disk drives, CD-ROM drive, and tape backup.

computer technician A professional skilled in building, repairing, and maintaining computers, and who, occasionally, designs them. Usually works under the supervision of a computer engineer.

computer terminal **1.** A teleprinter or video display unit and keyboard, used by human operator(s) of a computer. **2.** An interface between a computer and its human operator(s).

computer/TV interface A device or circuit for delivering the output of a digital computer to a standard television receiver so that the latter can serve as a GRAPHIC TERMINAL.

computer virus A deliberately created and disseminated subprogram or piece of programming code, that electronically spreads through computer systems and hinders operation. Usually diverts the computer(s) from intended functions; sometimes causes a catastrophic malfunction. Often exists undetected, being transferred from one computer to another by means of diskettes or software.

computer word See WORD.

computing amplifier See OPERATIONAL AMPLIFIER.

computing machine See COMPUTER.

concatenation **1.** A method of speed control for a 3-phase motor in which two induction motors are operated with their shafts coupled together. The stator of the first motor is connected to the 3-phase supply, and the slip rings of this motor are connected to the field of the second motor. The slip rings of the second motor are connected to the three ganged sections of a Y-rheostat used for adjusting the speed. **2.** Arrangement of a set into a series.

concentrated-arc lamp A brilliant low-voltage lamp, containing nonvaporizing electrodes in an inert-gas atmosphere. An arc across the electrodes creates the light source.

concentrated winding A coil winding that has a large number of turns in a small space.

concentration cell An electrolytic cell in which two electrodes are immersed in solutions of the same compound but having different combinations. The voltage is usually very small, 0.1 volt or less.

concentration gradient Between points in a semiconductor, the difference in electron or hole concentration.

concentric cable See COAXIAL CABLE.

concentric capacitor A fixed or variable capacitor whose plates are concentric cylinders. Also called *concentric-plate capacitor.*

concentric jack See COAXIAL JACK.

concentric line See COAXIAL LINE.

concentric-line oscillator A stable, self-excited oscillator whose frequency-determining tank consists principally of a section of concentric (coaxial) line. Used primarily at ultra-high frequencies (UHF).

concentric plug See COAXIAL PLUG.

concentric receptacle See COAXIAL RECEPTACLE.

concentric tank See COAXIAL TANK.

concentric-wound coil A combination of two or more coils wound on top of, and insulated from, each other.

conceptual modeling A technique for solving problems by devising a mathematical model based on the results of an experiment; experiments performed on the model are used to verify its validity.

concurrent conversion In computer operations, running conversion and conventional programs together. Also see CONVERSION PROGRAM.

concurrent processing See MULTIPROGRAMMING.

condenser **1.** An obsolete term for CAPACITOR. **2.** A mirror or lens for concentrating light (on an object, for example). **3.** Something that condenses a gas or vapor. **4.** See CONDENSER MICROPHONE.

condenser antenna A two-wire horizontal antenna system in which the radiator is a wire situated above a counterpoise.

condenser microphone Also called *capacitor microphone.* A microphone in which a tightly stretched metal diaphragm forms one plate of an

5059F-pC-93-162 4/9/01 4:51 PM Page 139

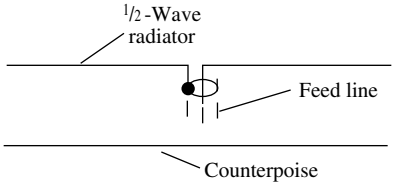

condenser antenna

air capacitor, and a closely situated metal plug forms the other plate. A dc bias voltage is applied to the arrangement. Impinging sound waves cause the diaphragm to vibrate, varying the capacitance and causing the output current to fluctuate accordingly.

condensing routine In computer operations, a program that compresses data. See COMPRESSION, **3**.

condensite A plastic insulating material whose base is phenol formaldehyde resin.

conditional Pertaining to a quantity or phenomenon that depends on some external factor, and is therefore subject to change.

conditional branch A point in a computer program where a relational test is performed, and the statement line in which the test is made is left so that an out-of-sequence instruction can be implemented. Such a branch might be made, for example, following a statement, such as "IF Z = Y THEN GO TO LINE 380."

conditional branch instruction The instruction in a computer program that causes a CONDITIONAL BRANCH.

conditional implication operation A Boolean operation in which the result of operand values X and Y are such that the output is high only if input X is high and input Y is low. Also called *inclusion* or *if-then operation.*

conditional jump See CONDITIONAL BRANCH.

conditional stop instruction In a computer program, an instruction that can cause a halt in the run, as dictated by some specified condition.

conditional transfer See CONDITIONAL BRANCH.

condition code A set of constraints for a computer program; sets limits on what can be done with the computer under certain circumstances.

conditioning **1.** The process of making equipment compatible for use with other equipment. Generally involves some design or installation changes. **2.** Interfacing.

Condor A continuous-wave navigational system that produces a cathode-ray-tube display for automatically determining the bearing and distance from a ground station.

conductance Symbol, *G*. Unit, siemens. The ability of a circuit, conductor, or device to conduct electricity. Conductance in siemens is the reciprocal of resistance: $G = 1/R$, where R is the resistance in ohms.

conducted heat Heat transferred by conduction through a material substance, as opposed to *convection* and *radiation.* A heatsink conducts dissipated energy away from a transistor, whereupon convection and radiation allow heat to escape from the sink.

conduction **1.** The propagation of energy through a medium, depending on the medium for its travel. **2.** The transfer of electrons through a wire. **3.** The transfer of holes through a P-type semiconductor material. **4.** Heat transfer through a material object (see CONDUCTED HEAT).

conduction angle See ANGLE OF CONDUCTION.

conduction band In the arrangement of energy levels within an atom, the band in which a free electron can exist; it is above the *valence band* in which electrons are bound to the atom. In a metallic atom, conduction and valence bands overlap; but in semiconductors and insulators, they are separated by an energy gap.

conduction current **1.** The electromagnetic-field flow that occurs in the direction of propagation. A measure of the ease with which the field is propagated. **2.** Current in a wire or other conductor.

conduction-current modulation In a microwave tube, cyclic variations in the conduction current; also, the method of producing such modulation.

conduction electron See FREE ELECTRON.

conduction error In a temperature-acutated transducer, error caused by conduction of heat between the sensor and the mounting.

conduction field An energy field that exists in the vicinity of an electric current.

conductive coating A conducting layer applied to the glass envelope of a cathode-ray tube, such as an oscilloscope tube or picture tube.

conductive coupling See DIRECT COUPLING.

conductive material See CONDUCTOR.

conductive pattern The pattern of conductive lines and areas in a printed circuit.

conductivity Unit, S/m (siemens per meter). An expression of conductance per unit length of a material; the reciprocal of *resistivity.*

conductivity meter A device for measuring electrical conductivity. Generally, such a device is calibrated in siemens.

conductivity modulation In a semiconductor, the variation in conductivity that results from a variation of charge-carrier density.

conductivity-modulation transistor A transistor in which the bulk resistivity of the semiconductor material is modulated by minority carriers.

conductor **1.** A material that allows charge carriers (usually electrons) to move with ease among atoms. Examples are metals, electrolytes, and ionized gases. Substances vary widely in their suitability as conductors; the conductivity of commercial copper, for example, is almost twice that of aluminum. Compare INSULATOR. **2.** An individual conducting wire in a cable, insulated or uninsulated.

5059F-pC-93-162 4/9/01 4:51 PM Page 140

conduit A hollow tube, made of plastic or metal, through which wires, cables, and other transmission media are fed.

cone The conical diaphragm of a (usually dynamic) loudspeaker.

cone antenna An antenna in which the radiator is a sheet-metal cone or a conical arrangement of rods or wires.

Conelrad An early amplitude-modulation (AM) broadcast protocol, intended for use in the event of a nuclear war. Now replaced by the EMERGENCY BROADCAST SYSTEM.

cone marker A UHF marker beacon whose conical energy lobe radiates vertically from a radio-range beacon station. Aircraft in flight use such markers to accurately locate the beacon station.

cone of protection The zone surrounding a lightning rod, in which the chances of a lightning strike are greatly reduced. The cone has an apex angle of 45°, relative to the rod. Objects entirely within this cone are unlikely to be struck (although it is still possible).

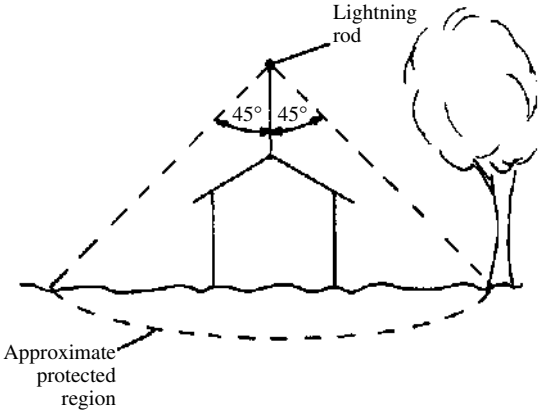

cone of protection

cone of silence A small zero-signal zone directly over a low-frequency radio-range beacon. The zone is the product of the combined directive properties of the beacon transmitting antenna and the antenna on an aircraft.

cone speaker A loudspeaker having a sound-producing cone (diaphragm) made of specially treated paper or other material, as opposed to a loudspeaker having a flat diaphragm.

confetti On a color TV screen, color spots caused by chrominance-amplifier noise.

confidence The probability that a predicted result will occur.

confidence factor Confidence, expressed either as a fraction (between 0 and 1) or as a percentage.

confidence interval The range over which a parameter can vary so that a given confidence factor is maintained.

confidence level See CONFIDENCE FACTOR.

confidence limitations The maximum and minimum points of a confidence interval. Outside the confidence-limitation points, the confidence factor drops below the required minimum.

configuration **1.** The characteristic arrangement of components in an electronic assembly, or of the equipment symbols in the corresponding circuit diagram. **2.** Computer system.

configuration state In a computer system, an expression of the availability status of a device for a given application. A *configured-in* device is available; a *configured-out* device is available, but is restricted to certain users; a *configured-off* device is unavailable.

configuration table Within a computer's operating system, a table that provides the configuration state for various system units.

configured-in See CONFIGURATION STATE.

configured-off See CONFIGURATION STATE.

configured-out See CONFIGURATION STATE.

conformance The degree to which a quantity or variable corresponds to a standard or to expectations.

conformance error The extent (usually expressed as a percentage) to which conformance is lacking.

conical antenna See CONE ANTENNA.

conical horn A horn (antenna, loudspeaker, or sound pickup) having the general shape of a cone: the cross-sectional area varies directly as the square of the horn's axial length.

conical monopole antenna An unbalanced broadband antenna that derives its name from its shape. It is usually constructed from wire and must be operated against a good radio-frequency (RF) ground.

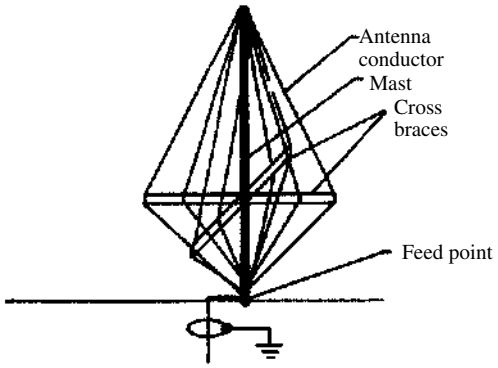

conical monopole antenna

conical scanning In radar transmission, a method of scanning in which the beam describes a cone, at the apex of which is the antenna.

conic sections The geometric plane figures that result from the intersection of a cone with a

5059F-pC-93-162 4/9/01 4:51 PM Page 141

plane. These figures are the *circle*, the *ellipse*, the *parabola*, and the *hyperbola.*

conjugate For a given complex number $A + jB$, the quantity $A - jB$. When complex conjugates are multiplied together, the result is $A^2 + B^2$.

conjugate branches In a network, two branches of such a nature that a signal in one has no effect on the other.

conjugate bridge A bridge in which the detector and generator occupy positions opposite to those in a conventional bridge of the same general type.

conjugate impedance For a given complex impedance, $R + jX$, where R is the resistive component and jX is the reactive component, the impedance: $R - jX$. The resistance is identical; the reactance is of equal magnitude, but opposite sign (capacitive as opposed to inductive, or vice versa).

conjunction The logical AND operation.

connect To provide an electrical path between two points.

connection The point at which two conductors are physically joined.

connective An operation symbol written between operands.

connector **1.** A device that provides electrical connection. **2.** A fixture (either male or female) attached to a cable or chassis for quickly making and breaking one or more circuits. **3.** A symbol that connects points on a flowchart.

conoscope A device that uses focused polarized light to examine crystals (as in checking the optical axis of a quartz crystal).

consequent poles The poles of an equivalent single magnet that is formed when two magnets are aligned with their two identical poles together. Thus, when the two north poles are placed together, the consequent poles are a south pole at each end and a north pole at the center.

conservation of energy **1.** The preservation of the potential for work by a given quantity of energy—even when it undergoes a change in form within a system. **2.** The *law of conservation of energy*, which states that energy can be neither created nor destroyed, but only changed in form.

console **1.** The main station or position for the control of electronic and/or computer equipment. **2.** The equipment at a fixed location. **3.** An equipment-containing cabinet that stands on the floor. **4.** Equipment permitting communication with a computer. Also called *dumb terminal.*

consonance **1.** Harmony between audio tones. **2.** Acoustical or electrical resonance between bodies or circuits that are not physically connected.

constant **1.** A quantity whose value remains fixed, such as the speed of light in a vacuum. Compare VARIABLE. **2.** The value of a component specified for use in a particular electronic circuit. **3.** An electronic component, particularly a capacitance or inductance. **4.** In a computer program, data items that remain unchanged for each run.

constant-amplitude recording In sound recording, the technique of holding the maximum amplitude of the signal steady as the frequency changes.

constantan An alloy of copper and nickel used in some thermocouples and standard resistors.

constantan-platinum thermocouple A thermocouple that uses the junction between constantan and platinum wires, which is contained in thermocouple-type meters.

constant area As allocated by a computer program, an area of memory that holds constants.

constant bandwidth In a broadband tuned circuit, bandwidth that does not change with frequency.

constant current A current that undergoes no change in value as it flows through a changing resistance. Compare CONSTANT VOLTAGE.

constant-current characteristic A condition in which the current through a circuit remains constant—even if the voltage across the circuit increases or decreases.

constant-current curve A graph in which the dependent variable is an electric current that levels off at, or approaches, a specific maximum. An example is the collector-current versus collector-voltage curve for a bipolar transistor.

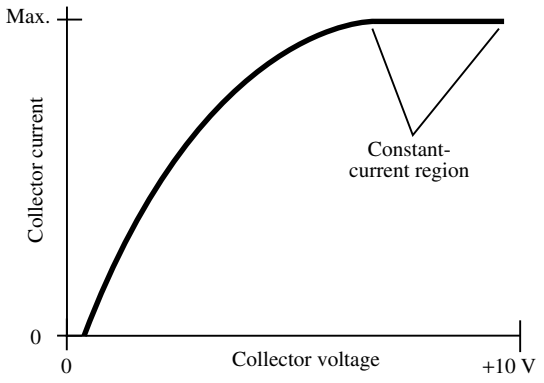

constant-current curve

constant-current drive Driving power obtained from a constant-current source.

constant-current modulation See CHOKE-COUPLED MODULATION.

constant-current power supply See CONSTANT-CURRENT SOURCE.

constant-current sink See CURRENT SINK.

constant-current source A power supply whose current remains steady during variations in load resistance. Also called *constant-current supply* and *current-regulated supply.* Compare CONSTANT-VOLTAGE SOURCE.

5059F-pC-93-162 4/9/01 4:51 PM Page 142

constant-current supply See CONSTANT-CURRENT SOURCE.

constant-current transformer A transformer supplied from a constant-voltage source that automatically delivers a constant current to a varying secondary load.

constant-k filter Also called a *Zobel filter.* A filter section in which Z_1Z_2 equals k^2 at all frequencies, where Z_1 is the impedance of the series element and Z_2 is the impedance of the shunt element.

constant-power dissipation line A line connecting points on a family of current-voltage characteristic curves, the points corresponding to the maximum power that can safely be dissipated by the device to which the curves apply.

constant-resistance network A circuit of resistors that, when terminated in a resistance load, presents a constant resistance to a driving source under various conditions of operation.

constant-speed motor **1.** Also called a *shunt motor.* A motor whose speed varies little, or not at all, with variations in the armature current. **2.** A motor that runs at an unvarying speed through the action of associated automatic electronic control circuitry.

constant voltage A voltage that does not change as the load resistance varies. Compare CONSTANT CURRENT.

constant-voltage, constant-current supply A combination current-regulated and voltage-regulated power supply; delivers constant current to low load resistances and constant voltage to high load resistances.

constant-voltage drive Driving power obtained from a CONSTANT-VOLTAGE SOURCE.

constant-voltage source A power supply whose output voltage remains steady during variations in load current. Also called *constant-voltage supply* and *voltage-regulated supply.*

constant-voltage transformer A special transformer used to reduce variations in power-line voltage. A capacitor in the device causes a winding to resonate at the line frequency (e.g., 60 Hz). This tends to maintain a more constant current than would be the case in an ordinary transformer.

construct A source (user's) computer program statement that, when implemented, produces a predetermined effect.

consumer reliability risk **1.** The chance a consumer takes when buying a component or piece of equipment that has not been subjected to quality-assurance/quality-control (QA/QC) testing. **2.** An expression of the failure rate for a consumer item.

contact **1.** A conducting body (such as a button, disk, or blade) that serves to close an electric circuit when pressed against another conductor. Example: switch contact and spring contact. **2.** The state of being touched together, as when two conductors are brought into contact to close a circuit.

contact arc The arc that initially occurs when current-carrying contacts are separated.

contact area **1.** The face of an electrical contact. **2.** The common area shared by two conductors in mutual contact.

contact bounce The springing apart or vibration of contacts upon making or breaking.

contact chatter The abnormal vibration of mating contacts, caused by contact bounce or by an extraneous alternating current.

contact-closure input The input circuit of a device, such as a control-system amplifier, that is actuated by the closing of switching contacts. Compare CONTACT-OPEN INPUT.

contact combination The set of contacts on a switch or electronic relay.

contact detector A rectifier or demodulator, composed of two dissimilar materials in contact with each other. Semiconductor diodes are of this general type. Some contact-detector action can be obtained with two dissimilar fine wires (such as copper and iron) by touching their tips lightly together.

contact EMF Short for *contact electromotive force*; also called *contact potential.* A low direct-current (dc) voltage that is sometimes generated by the contact of two dissimilar materials.

contact follow The tendency of relay contacts to follow the actuating signals.

contact force **1.** The force with which relay contacts close with a given amount of coil current. **2.** The force with which a pair of relay contacts are held together when current flows through the coil. **3.** In a mercury-wetted relay, the force exerted by the mercury on the contacts as the relay closes.

contact gap The distance between contacts when they are open.

contact load **1.** The power dissipated by a load that is connected to a power supply through a closed set of contacts. **2.** The current passing through a set of closed contacts.

contact microphone A microphone placed in direct contact with a vibrating surface for pickup. Actuated by the vibration of a solid, rather than by the movement of air molecules.

contact miss **1.** The improper alignment of contacts in a switch or relay. **2.** The condition of relay contacts not lining up properly.

contact modulator An electromechanical CHOPPER.

contact-open input The input circuit of a device, such as a control-system amplifier, that is actuated by the opening of switching contacts. Compare CONTACT-CLOSURE INPUT.

contactor A switch used for frequent opening or closing of a circuit. An example is a relay contactor used for keying a transmitter.

contactor noise **1.** Electrical noise that is the product of make-and-break contact action or fluctuations in conduction when the contacts are

5059F-pC-93-162 4/9/01 4:51 PM Page 143

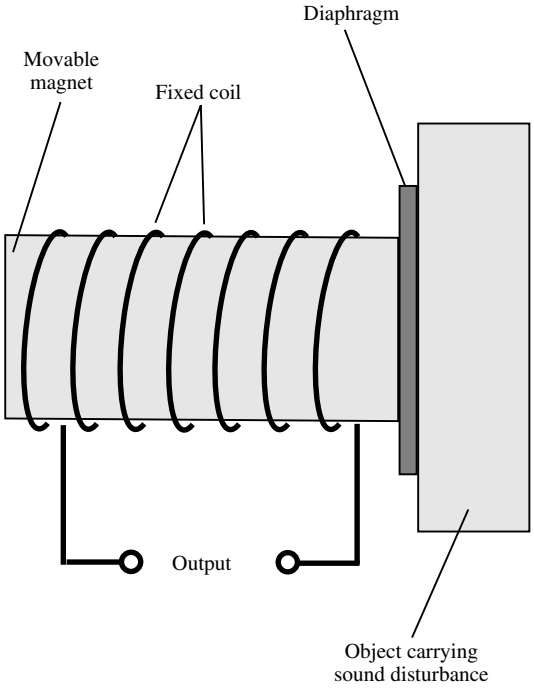

contact microphone

closed. **2.** Sounds coming directly from contacts that are opening and closing.

contact potential The small direct-current (dc) voltage that results from the bombardment of an electrode by electrons, when the electrode has no external voltage applied to it.

contact pressure The pressure that holds contacts together.

contact protector A component (such as a diode, capacitor, resistor, or combination of these) that serves to suppress contact arcing.

contact rating The maximum current, voltage, and/or power specified for a given set of contacts.

contact rectifier A rectifier consisting of two dissimilar materials in direct contact. Examples: copper and copper oxide, magnesium and copper sulfide, selenium and aluminum, and germanium and indium.

contact resistance The resistance of the closed contacts of switches, relays, and other similar devices. Normally, this is a very small resistance.

contact separation See CONTACT GAP.

contact strip See TERMINAL STRIP.

contact switch An electromechanical switch that uses contacts to make and break a circuit, as compared with an electronic switch that uses semiconductor devices.

contact travel The distance over which a relay or switch contact must move to close a circuit.

contact wetting The use of mercury (a conducting liquid) to improve the action of a relay contact or contacts.

contact wipe A sliding motion between closed contacts. Helps to establish a good connection and to keep the contact surfaces clean.

container file See CONTROLLING FILE.

contaminated material **1.** A semiconductor material containing some undesired substance. **2.** A material unintentionally made radioactive.

contamination **1.** The presence of an impurity in a substance. **2.** The addition of a radioactive material to a substance. **3.** In a coaxial cable, the tendency for the jacket material to bleed through the outer braid into the dielectric, resulting in increased loss.

content-addressed storage In a computer, memory- or data-storage locations identified by content (see CONTENTS), instead of by address. Also called *associative storage.*

contention The result of interference among more than one transmitting station on the same communications channel.

contents **1.** The data in a computer random-access memory (RAM). **2.** The data in a specific storage location, such as on a hard disk, diskette, or CD-ROM.

context **1.** The environment in which a word is used in a natural language (such as English, Spanish, or Russian). Important in speech recognition and speech synthesis. **2.** The environment in which a string of characters, composing a data unit or word, is used in a computer program.

Continental code A version of the Morse code used internationally in radiotelegraphy. Also called *International Morse code* and *general service code.* Compare AMERICAN MORSE CODE.

continuity A condition of being uninterrupted—especially pertaining to current flowing in an electrical or electronic circuit.

continuity test A test of the completeness of an electrical path. Ideally, the only concern is whether the circuit is open or closed, but sometimes circuit resistance is also of interest.

continuity tester A device (such as an ohmmeter, battery and buzzer, and battery and lamp) with which a continuity test can be made.

continuity writer The person who prepares copy for a radio or television broadcaster.

continuous carrier A medium (such as a radio-frequency wave) that will convey information (as when the carrier is modulated) with no disruption of the medium itself.

continuous circuit An uninterrupted circuit.

Continuous Commercial Service Abbreviation, CCS. A category in which safe operating parameters are listed for electronic components and communications equipment operated over long, uninterrupted periods. Compare INTERMITTENT COMMERCIAL AND AMATEUR SERVICE.

5059F-pC-93-162 4/9/01 4:51 PM Page 144

Character	*Symbol*
A	•–
B	–•••
C	–•–•
D	–••
E	•
F	••–•
G	––•
H	••••
I	••
J	•–––
K	–•–
L	•–••
M	––
N	–•
O	–––
P	•––•
Q	––•–
R	•–•
S	•••
T	–
U	••–
V	•••–
W	•––
X	–••–
Y	–•––
Z	––••
0	–––––
1	•––––
2	••–––
3	•••––
4	••••–
5	•••••
6	–••••
7	––•••
8	–––••
9	––––•
Period	•–•–•–
Comma	––••––
Query	••––••
Slash	–••–•
Dash	–••••–
Break (pause)	–•••–
Semicolon	–•–•–•
Colon	–––•••

Continental code

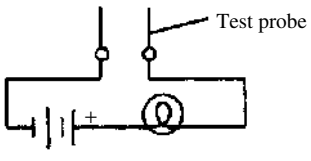

continuity tester

continuous duty The requirement of a device to sustain a 100-percent duty cycle for a prolonged period of time.

continuous-duty rating A maximum current, voltage, or power rating for equipment operated for extended periods at a 100-percent duty cycle.

continuous load A load that requires a continuous feed for a prolonged period of time.

continuous memory See NONVOLATILE MEMORY.

continuous-path motion In robotics, machine movement that occurs in a smooth fashion, rather than in discrete steps. Allows precise positioning of a mechanical arm or gripper.

continuous power The maximum sine-wave power that an amplifier can deliver for 30 seconds.

continuous recorder An instrument that provides an uninterrupted recording.

continuous recording A record made on a continuous sheet or tape, instead of on separate sheets or tapes. An example is a continuous-playing tape used for repeated public announcements.

continuous spectrum **1.** The range of all electromagnetic frequencies between a specified lower limit f_1 and a specified upper limit f_2. **2.** A range of electromagnetic frequencies that exhibits similar behavior between its lower and upper limits.

continuous stationery Also called *fanfold paper.* The pack of paper a line printer uses. It consists of sheets connected by perforated or tear-off edges, folded in accordion fashion. It usually has tear-off perforated strips along either side to facilitate feed through the printer mechanism.

continuous variable A variable that can attain any value within a specific range of values. An example is a frequency within the 75- to 80-meter amateur radio band, from 3.5 to 4.0 MHz.

continuous wave Abbreviation, CW. **1.** A periodic wave, such as a radio-frequency (RF) carrier, that is not interrupted at any point between its normal start and termination, and that is unmodulated. **2.** An RF carrier that is interrupted digitally with a keying device according to some code (such as Morse), for the purpose of conveying information.

continuous-wave laser See CW LASER.

continuous-wave radar See CW RADAR.

contour A control on an audio reproduction system that increases the base and treble amplitudes at low levels to compensate for the ear's natural losses in these ranges. Alternatively, this control can attenuate signals in the 3-kHz region, where the human ear is most sensitive.

contours of equal loudness See AUDIBILITY CURVES.

CONTRAN A computer language that requires no compiler, or translating, interface between the operator and the machine. The programming is done in a language similar to machine language.

contrast **1.** In a video image, the degree to which adjacent areas of a picture are differentiated. Insufficient contrast makes for a "flat" picture; ex-

5059F-pC-93-162 4/9/01 4:51 PM Page 145

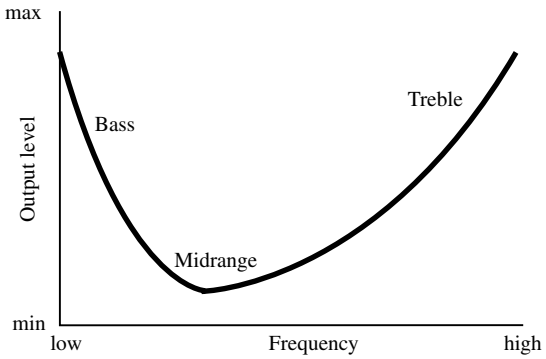

contour

cessive contrast, a "hard" picture. **2.** In optical character recognition, the degree to which a character is distinguishable from its background.

contrast control A potentiometer for adjusting the gain of the video in a television receiver or cathode-ray-tube (CRT) computer display and, accordingly, the image contrast.

contrast range In an image or pattern, the brightness range from the lightest to the darkest parts.

contrast ratio In a video image, the ratio of maximum to minimum luminance.

control **1.** An adjustable component, such as a rheostat, potentiometer, variable capacitor, or variable inductor, that allows some quantity to be varied at will. **2.** A test or experiment conducted simultaneously with another similar test conducted under conditions lacking the factor under consideration. Thus, if 100 resistors coated with a special varnish are tested at 120°F, 100 identical unvarnished resistors could be tested (as a control) under the same conditions; in this way, the effect of the varnish would be ascertainable. **3.** As a computer function, understanding and implementing instructions or carrying out tasks, according to specific conditions.

control ampere-turns The ampere-turns of the control winding in a magnetic amplifier.

control block A storage block for control information in a computer.

control bus In a digital computer, the electrical conductors linking the central-processing-unit (CPU) control register to the memory circuits.

control card A card that provides control information for a computer.

control character A character (bit group) used to start the control of a peripheral.

control characteristic A representation (such as a collector-current versus collector-voltage curve) depicting the extent to which the value of one quantity affects or controls the value of another.

control circuit **1.** A circuit in which one signal or process is made to control another signal or process. **2.** In a digital computer, a circuit that handles and interprets instructions and commands, particularly in the arithmetic and logic unit (ALU).

control computer A computer that receives signals concerning the parameters in some process, and responds with signals that control those parameters.

control counter See CONTROL REGISTER.

control data **1.** In a computer record having a key, information used to put the records in some sequence. **2.** Information affecting a routine's selection or modification.

control electrode An electrode to which an input signal can be applied to control an output signal. Common examples are the base of a bipolar transistor, the gate of a field-effect transistor, and the inputs of a logic gate.

control field **1.** In direct-current generators of the amplifying type, an auxiliary field winding used for feedback and regulation, in contrast to the self-excited field winding (which is the conventional field winding of the generator). **2.** A computer record field containing control data.

control flux In an amplidyne, magnetic flux generated by current flowing through the control winding.

control grid See GRID, **1**.

control-grid bias The negative dc voltage applied between ground and the control grid of a vacuum tube to establish the operating point.

control language Within the operating system of a computer, the command set that the operator or programmer uses to control the running of a program or the operation of peripherals. Also called *job control language* or *system control language.*

control language interpreter See CONTROL LANGUAGE and INTERPRETER.

controlled avalanche diode Also called *avalanche diode* or *Zener diode.* A diode that has a well-defined avalanche voltage. Used primarily for voltage regulation in power supplies.

controlled-carrier modulation See QUIESCENT CARRIER OPERATION.

controlled-carrier transmission See QUIESCENT CARRIER OPERATION.

controlled rectifier A rectifier whose dc output can be varied by adjusting the voltage or phase of a signal applied to the control element. See SILICON-CONTROLLED RECTIFIER.

controller **1.** The control signal of an electronic control (or servo), system. **2.** A device, such as a specialized variable resistor, used to adjust current or voltage. **3.** A computer that oversees and controls the operation of a robot or fleet of robots.

controller function The control of the movements of a servo system.

controlling file A computer storage area encompassing several complete magnetic disk cylinders; its size can be changed to accommodate a number of files.

5059F-pC-93-162 4/9/01 4:51 PM Page 146

control loop See CONTROL TAPE.

control mark See TAPE MARK.

control panel **1.** An accessible surface on which are mounted switches, buttons, potentiometers, meters, digital indicators, monitoring devices, and other apparatus essential to regulating and supervising an electronic system. **2.** The console that a computer operator or programmer uses to communicate with the central processing unit (CPU).

control plate The metallic plate or disk that serves as the antenna of a CAPACITANCE RELAY or TOUCHPLATE RELAY.

control program A program that arranges computer-operation programs in a certain order. Puts information in the computer memory for later use.

control rectifier A semiconductor diode device, used for the purpose of switching large currents. A small control signal can provide switching of high-power devices.

control register In a computer, the register that stores the address of the next instruction in the program being run.

control sequence The order in which instructions are executed in a digital computer.

control stack In a computer system, a unit of hardware having storage locations and used to perform arithmetic, assist in allocating memory to programs, and to control internal processes.

control statement In a programming language, an instruction that causes some action to be taken, as specified by a condition; it is also applicable to source program statements that affect the compiler's operation without modifying the machine code.

control tape Punched paper or plastic tape in the form of a closed loop and used to control printing devices. Also called *control loop.*

control total For a file or record group, a total derived during an operation; it is used to verify that all the records have been processed similarly.

control transfer The situation in which the control unit of a digital computer leaves the main sequence of instructions and takes its next instruction from an out-of-sequence address.

control transfer instruction See BRANCH INSTRUCTION.

control-voltage winding In a servomotor, the winding that receives a varying voltage of a phase different from that applied to the fixed-voltage windings.

control winding In a magnetic amplifier, the winding that conducts the control-signal current.

control word A word (a bit group) stored in a computer memory and used for a control function.

convection The flow of a gas or liquid that results in the transfer of heat from one location to another.

convection cooling The removal of excess heat from a component, such as a power vacuum tube or transistor, via upward movement of surrounding air that has been heated by the component.

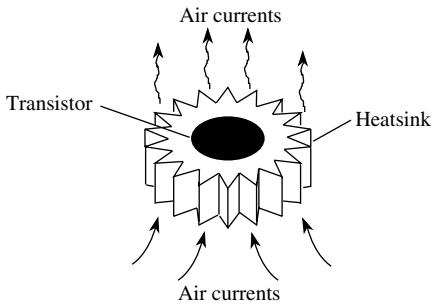

convection cooling

convection current **1.** The motion of current carriers or a charge across the surface of a conductor or dielectric. **2.** Air currents rising above a heat source or heated body.

convective discharge The continuous high-voltage current discharge across a spark gap.

convectron A device that indicates the angle, with respect to the vertical, based on convection cooling of a straight wire. The temperature difference is greatest when the angle is 0 degrees (the wire is vertical); the temperature difference decreases as the angle increases, reaching a minimum at 90 degrees (when the wire is horizontal).

convenience outlet **1.** In North America, a wall outlet providing a nominal 117 volts alternating current (ac) at 60 Hz for common household appliances. **2.** An outlet in a laboratory that provides power for a certain application.

conventional current The notion that current flows from the positive pole to the negative pole in an electric circuit. This representation is used most often by physicists. Electron flow is opposite to conventional current flow; positively charged particles, such as holes, move in the same direction as the conventional current.

convergence **1.** The eventual meeting of values or bodies at some point (sometimes at infinity, as in certain mathematical series). **2.** The intersection point of the beams from separate electron guns in a cathode-ray tube (CRT).

convergence coil One of a pair of coils used in a color television receiver to produce dynamic beam convergence (see CONVERGENCE, **2**).

convergence control In a color television receiver, a potentiometer in the high-voltage circuit for convergence adjustment (see CONVERGENCE, **2**).

convergence electrode An electrode that provides an electrostatic field for converging electron beams. Compare CONVERGENCE MAGNET.

convergence frequency The frequency of the last member of a spectrum series.

convergence magnet An assembly that provides a magnetic field to converge electron beams. Compare CONVERGENCE ELECTRODE.

5059F-pC-93-162 4/9/01 4:51 PM Page 147

convergence phase control In a three-gun color picture tube, a variable resistor or variable inductor used to adjust the phase of the dynamic convergence voltage.

convergence plane **1.** In a color picture tube, the plane in which the red, green, and blue beams all focus. **2.** In a cathode-ray tube, the plane in which the electron beam reaches its sharpest focus.

convergent series A mathematical series that approaches a specific, finite numerical value as the number of terms increases. Thus, the series 0.3 + 0.03 + 0.003 + . . . approaches a limiting value of *1/3*. Compare DIVERGENT SERIES and INFINITE SERIES.

converging lens A lens having a real focus for parallel rays; generally a *convex lens*.

conversational compiler In computer operations, a compiler that, using the CONVERSATIONAL MODE of operation, shows the programmer whether or not each statement entered into the computer is valid, and whether or not to proceed with the next instruction.

conversational mode High-level computer operation or programming, in which the computer gives responses to the operator's input.

conversion **1.** The deliberate mixing of radio-frequency (RF) signals to produce signals at the sum and/or difference frequencies. **2.** The process of changing direct current (dc) to alternating current (ac). **3.** The process of changing low-voltage dc to high-voltage dc. **4.** The changing of a computer file to another format and, possibly, transferring it to a different storage medium (e.g., from tape to internal memory). **5.** The processing of a program or file written for one computer or application into a form suitable for another computer or application.

conversion efficiency In a converter (see CONVERTER, **1**), the ratio of output-signal amplitude to input-signal amplitude. For example, in a superheterodyne converter, a large intermediate-frequency (IF) output for a low radio-frequency (RF) input indicates high conversion efficiency.

conversion equipment In a computer system, an offline device for transferring data from one medium to another [e.g., a disk-to-tape converter (tape drive)]. Also called CONVERTER.

conversion exciter An exciter for transmitters, in which an output signal of a desired frequency is obtained by beating the output of a variable-frequency self-excited oscillator with the output of a fixed-frequency oscillator (such as a crystal oscillator).

conversion gain Amplification as a byproduct of conversion. See CONVERSION EFFICIENCY.

conversion loss Conversion gain of less than 1.

conversion program In computer operations, a program for data conversion (see CONVERSION, **4** and **5**).

conversion rate Also called *sampling rate*. The number of samples per second taken by an ANALOG-TO-DIGITAL CONVERTER.

conversion time In digital computer operation, the time required for the machine to read out all the digits in a coded word.

conversion transconductance See CONVERSION EFFICIENCY.

convert **1.** To perform frequency conversion (see CONVERSION, **1**). **2.** To perform voltage conversion (see CONVERSION, **2** and **3**). **3.** In computer operations, to change information from one number base to another. **4.** To perform data conversion (see CONVERSION, **4** and **5**).

converter **1.** A heterodyne mixer in which two input signals of different frequency are mixed to yield a third (output) signal of yet a different frequency. **2.** A machine for converting direct current (dc) to alternating current (ac) (e.g., a chopper converter). **3.** A transistor circuit for converting a low-voltage dc to higher-voltage dc. **4.** Conversion equipment. **5.** A circuit or device that changes analog data to digital data or vice versa.

converter amplifier See CHOPPER AMPLIFIER.

converter stage A circuit used principally to mix two signals (such as a received signal and local-oscillator signal in a superheterodyne receiver), and deliver the resultant signal.

convexo-concave Pertaining to a lens having a convex face of greater curvature than its concave face.

coolant A liquid (often water or oil) used to remove heat from an electronic component.

Coolidge X-ray tube An X-ray tube containing a heated filament (with focusing shield) and a slanting tungsten target embedded in a heavy copper anode.

cooling Maintenance of the operating temperature of an electronic component or system at a safe level. Common devices for cooling are heatsinks, circulating or forced air, and circulating liquid.

coordinate bond A covalent bond that consists of a pair of electrons supplied by only one of the atoms joined by the bond.

Coordinated Universal Time Abbreviation, UTC. Astronomical time at the Greenwich meridian (zero degrees longitude). The UTC day begins at 0000 hours and ends at 2400 hours. Based on the mean, or average, synodic (sun-based) rotational period of the earth. The earth is slightly behind UTC near June 1, and is slightly ahead near October 1.

coordinate digitizer A device or circuit that encodes a coordinate graph into digital signals for storage or transmission.

coordinate of chromaticity See CHROMATICITY COORDINATE.

coordinates A set of axes with points that can be uniquely defined or located on a line, in a plane, or in space. See CARTESIAN COORDINATES and POLAR COORDINATES.

5059F-pC-93-162 4/9/01 4:51 PM Page 148

coordinate system A mathematical means of uniquely defining or locating a point on a line, in a plane, or in space. The most common coordinates are CARTESIAN COORDINATES (also called *rectangular coordinates*), consisting of numbered lines intersecting at right angles.

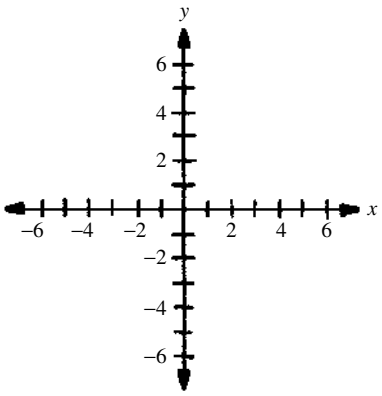

coordinate system (Cartesian)

coordination complex An ion or compound having a central (usually metallic) ion combined by coordinate bonds with a definite number of surrounding groups, ions, or molecules.

coplanar array A set of antennas that lie in the same plane, and are fed by a common transmission line.

copper Symbol, Cu. A metallic element. Atomic number, 29. Atomic weight, 63.546. An excellent conductor of electricity and heat, commonly used in the manufacture of wires and cables.

copper-clad wire Iron or steel wire plated with copper.

copper-constantan thermocouple A thermocouple consisting of a junction between wires or strips of copper and constantan. Typical output is 4.24 mV at 100°C.

copper loss Power (I^2R) loss in copper wires, cables, and/or coils.

copper-oxide diode A small diode in which the semiconductor material is copper oxide. Such diodes, widely used before the ready availability of selenium and silicon, are still occasionally found in meter-rectifier service.

copper-oxide modulator An amplitude modulator whose action is derived from the nonlinear conduction characteristic of copper-oxide diodes.

copper-oxide photocell A photoelectric cell in which the light-sensitive material is copper oxide.

copper-oxide rectifier A rectifier in which the semiconductor material is copper oxide. Rectifiers of this type are suitable for low-voltage service; they were widely used before the advent of germanium, silicon, and selenium rectifiers.

copper pyrites See CHALCOPYRITE.

copper-sulfide rectifier A rectifier in which the unilateral junction is between copper-sulfide and magnesium elements. Like the copper-oxide rectifier, the copper-sulfide unit was once widely used in low-voltage applications.

copy **1.** Also called *hard copy*. Printed or written text. **2.** In communications, a qualitative expression of the extent to which received data is intelligible (e.g., a radio operator's signal report, "You are solid (perfect) copy."). **3.** To duplicate data in a storage system, the original being in another system, or in a different location in the same system. **4.** An exact duplicate of data in any form.

copying telegraph A descriptive term for a *facsimile* system.

Corbino disk A variable resistor consisting of a semiconductor disk capable of exhibiting the CORBINO EFFECT. The disk is inserted into an adjustable magnetic field, which serves as the control medium.

Corbino effect A phenomenon similar to the HALL EFFECT, in which a current flows around a disk carrying a radial current when the disk is inserted into a magnetic field whose lines of flux are perpendicular to the disk. Compare HALL EFFECT.

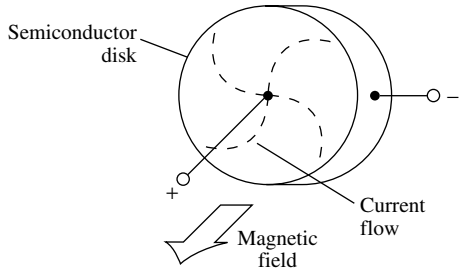

Corbino effect

cord **1.** A length of flexible, insulated cable, usually having two or three conductors. **2.** Tough, insulating string (e.g., *dial cord* or *lacing cord*).

cordless **1.** Descriptive of a plug without a flexible cord. **2.** Pertaining to radio-frequency (RF) or infrared short-range links for communications and control (e.g., a *cordless telephone* set).

cordless keyboard A computer keyboard that employs an infrared (IR), very-high frequency (VHF), or ultra-high-frequency (UHF) transmitter and receiver. Commonly used with so-called Web TV systems and in presentations using a display projection system. Operates according to the same electronic scheme as a CORDLESS MOUSE.

cordless modem See WIRELESS MODEM, 3.

5059F-pC-93-162 4/9/01 4:51 PM Page 149

cordless mouse A hand-controlled computer mouse that employs an infrared (IR), a very-high frequency (VHF), or an ultra-high-frequency (UHF) transmitter and receiver. The transmitter is inside the device, and the receiver is contained either inside the computer main unit, or in a small box attached to the computer main unit by a cord. The box can be placed somewhere out of the way; for example, at the back of the desk. Then the mouse can be moved around freely. This link is effective at distances of up to 20 or 30 feet.

cordwood A type of construction in which electronic components are sandwiched perpendicularly between layers of components. So called because it looks somewhat like stacked cordwood.

cordwood module A module containing discrete components mounted perpendicularly between two parallel printed circuits.

core **1.** The body or form on which a coil or transformer is wound. Can be made of ferromagnetic or dielectric material. The properties depend on the application. **2.** CORE MEMORY.

core dump Dumping core memory content to an output peripheral. Also see DUMP.

coreless induction heater An induction heater in which the body to be heated receives energy directly from the field of the energizing coil (there is no intervening core). Compare CORE-TYPE INDUCTION HEATER.

core loss Loss of energy in a magnetic core, caused by eddy currents and hysteresis in the core material.

core memory An older memory technology, consisting of a series of small ringshaped magnetic cores, into or out of which data can be written or read by changing the magnetization of the cores.

core plane A usually flat assembly of special magnetic cores, through which pass associated current-conducting wires to provide a CORE MEMORY.

core saturation The condition in which a core of magnetic material accommodates the maximum number of magnetic lines characteristic of that material. Increasing the magnetizing force produces no additional magnetization.

core shift register A shift register that uses special magnetic cores as bistable components. See CORE MEMORY.

core storage A high-speed magnetic core storage unit. Also see CORE MEMORY and CORE PLANE.

core transformer A transformer whose coils are wound around a ferromagnetic core.

core wrapping The placing of an insulating layer over an inductor or transformer core. This minimizes the chances of short-circuiting between the windings and the core material.

core-type induction heater An induction heater in which the body to be heated is magnetically linked, by a core, to the energizing coil. Compare CORELESS INDUCTION HEATER.

corner **1.** An abrupt turn in the axis of a waveguide. **2.** The line, and the region in the vicinity thereof, at which two intersecting plane surfaces meet (e.g., the reflector screen of a CORNER-REFLECTION ANTENNA). The plane surfaces are usually perpendicular to each other. **3.** The point, and the region in the vicinity thereof, at which three intersecting plane surfaces meet. Generally, the plane surfaces are mutually perpendicular. **4.** The passband frequency limit(s) of a bandpass, band-rejection, high-pass, or low-pass filter. **5.** A sharp bend in the attenuation-versus-frequency curve of a bandpass, band-rejection, high-pass, or low-pass filter, depicting the limit(s) of the passband.

corner diffraction **1.** The bending of sound waves around a corner. **2.** The bending of radio-frequency (RF) energy around an object, when the wavelength is great, compared with the size of the object.

corner effect A rounding off of the frequency response of a filter at the corner(s) [i.e., at the limit(s) of the passband].

corner frequency See CORNER, **4**.

corner reflection The reflection of a beam of light (or of microwave energy or other short-wavelength energy) from a corner reflector, so the beam leaves the reflector in exactly the opposite direction from which it approaches. See CORNER REFLECTOR, **2**.

corner-reflection antenna A directional antenna consisting of a dipole radiator situated at the apex formed by two nonparallel, flat reflecting sheets or a single folded sheet. See CORNER REFLECTOR, **1**.

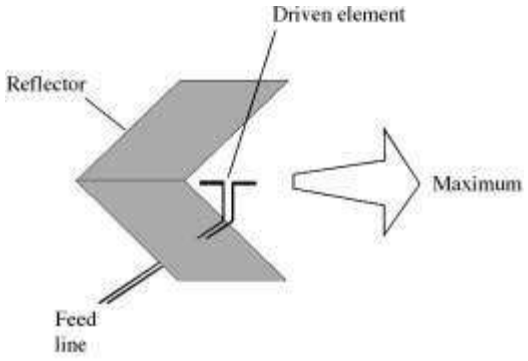

corner-reflection antenna

corner reflector **1.** An antenna with a half-wave driven element and a reflector made of wire mesh, screen, or sheet metal that resembles an open folder. The flare angle of the reflecting element is about 90 degrees. The antenna is used at ultra-

5059F-pC-93-162 4/9/01 4:51 PM Page 150

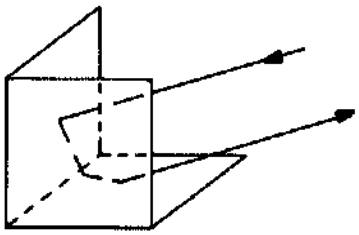

corner reflector, 2

high and microwave frequencies for television reception and satellite communications. Sometimes several half-wave dipoles are fed in phase and arranged along a common line with a single, elongated reflector. **2.** Also called *tricorner reflector*. A set of three flat metal surfaces or screens, attached together in a manner identical to the way two walls meet the floor or ceiling in a room. Such a device, if it is at least several wavelengths across, returns electromagnetic energy in exactly the same direction from which it arrives. Devices of this type are used as radar dummy targets and in optical and infrared (IR) wireless ranging systems.

corona A luminous discharge in the space surrounding a high-voltage conductor; caused by ionization of the air. The discharge constitutes a loss of energy.

corona effect The production of a luminous discharge, especially at the end of a pointed terminal, when the voltage gradient reaches a critical value.

corona failure A form of high-voltage failure, resulting from the erosion of an object (such as an electrical insulator) by corona.

corona loss Loss caused by energy dissipation through a corona. It occurs as a result of the emission of electrons from the surface of electrical conductors at high potentials, and depends on the curvature of the conductor surface, with most emission occurring from sharp points and the least from surfaces with a large radius of curvature. It is often accompanied by a blue glow and a crackling or hissing sound.

corona resistance The length of time that an insulating material can withstand a specified level of field-intensified ionization before completely breaking down.

corona shield A shield surrounding a high-voltage point to prevent corona by redistributing the electric flux.

corona starting voltage The minimum voltage between two electrodes, or on a single electrode in free space, at which corona occurs.

corona voltmeter A voltmeter used to measure the peak value of a voltage in terms of corona discharge. It consists of a metal tube in which a central wire is mounted, the parts being connected to the voltage source. The air density in the tube is varied until corona occurs.

corpuscle A tiny particle. It was the name given to the ELECTRON by some early experimenters and theorists.

correction **1.** The addition of a factor that provides greater accuracy in a measurement. **2.** A change in the calibration of an instrument to increase the accuracy.

correction factor A percentage, or numerical factor, added to or subtracted from a reading to provide a greater degree of accuracy. Often used with instruments known to be inaccurate by a certain amount.

corrective feedback Feedback that is used to correct (bring to a prescribed level) a quantity constituting the input to a system.

corrective maintenance The repair of a circuit or system after it has malfunctioned or broken down.

corrective network A network that improves the performance of the circuit into which it is inserted.

corrective stub A combination tuning-matching stub used in some antenna systems. It matches the resistive component of the antenna impedance to the characteristic impedance of a feed line, and also eliminates any reactance that might be present at the antenna feed point.

correed relay A sealed reed relay used as a high-speed switching device in communications equipment.

correlation A statistical expression or measure of the degree to which two sets of data are related. Can be given qualitatively (high-positive, low-positive, zero, low-negative, or high-negative) or quantitatively (as a number between –1 and 1). Does not necessarily imply causation.

correlation detector A detector that compares a signal of interest with a standard signal at every point, delivering an output that is proportional to the correspondence between the two signals.

correlation distance The smallest distance between two antennas that results in fading of signals under conditions of tropospheric propagation. It is used at very-high frequencies (VHF) and above, to determine the maximum range over which communications can be carried out reliably.

correlation tracking A method of target tracking in which phase relationships are used to determine positions.

correspondence The ability of a binocular machine vision system to tell when both of its optical sensors are processing an image from the same object; also, the ability of the system to keep both sensors tracking the same object.

corrosion-resistant Pertaining to materials that are treated to be immune to corrosion by the elements. Such substances are preferable for use in marine or tropical environments, where corrosion is especially severe.

5059F-pC-93-162 4/9/01 4:51 PM Page 151

corruption The altering of data or a code as a result of a program error or machine fault.

COS Abbreviation of COMPLEMENTARY-SYMMETRY CIRCUIT.

cosecant Abbreviation, csc. A trigonometric function; csc $q = c/a$, where c is the hypotenuse of a right triangle and a is the side opposite q. The cosecant is the reciprocal of sine: csc $q = 1/\sin q$.

cosecant-squared antenna A radar antenna that radiates a COSECANT-SQUARED BEAM.

cosecant-squared beam A radar beam whose intensity varies directly with the square of the cosecant of the angle of elevation.

cosech Abbreviation of HYPERBOLIC COSECANT. Also abbreviated as csch.

cosh Abbreviation of HYPERBOLIC COSINE.

cosine Abbreviation, cos. A trigonometric function; cos $q = b/c$, where b is the side adjacent to q and c is the hypotenuse of the right triangle.

cosine law The brightness in any direction from a perfectly diffusing surface is proportional to the cosine of the angle between the direction vector and a vector perpendicular to the surface.

cosine wave A periodic wave that follows the cosine of the phase angle. It has a shape identical with a SINE WAVE, but differs by 90 degrees of phase.

cosine yoke A magnetic-deflection yoke that has nonuniform windings for improved focus at the edges of a television picture. Also called *anastigmatic yoke* and *full-focus yoke.*

cosmic noise Radio noise produced by signals from extraterrestrial space.

cosmic rays Extremely penetrating rays consisting of streams of atomic nuclei entering the earth's atmosphere from outer space.

COS/MOS IC An integrated circuit (IC), such as an operational amplifier, utilizing metal-oxide-semiconductor (MOS) field-effect transistors in a complementary-symmetry (COS) arrangement.

cost analysis In a commercial or industrial organization, ascertaining the expense associated with a service, process, or job.

cot Abbreviation of COTANGENT.

cotangent Abbreviation, cot. A trigonometric function; cot $q = b/a$, where a is the side adjacent to q and b is the side opposite q (in a right triangle). Cotangent is the reciprocal of tangent: cot $q = 1/\tan q$.

coth Abbreviation of HYPERBOLIC COTANGENT.

Cotton-Mouton effect See KERR MAGNETO-OPTICAL EFFECT.

Cottrell process Dust precipitated by high voltage. Dust in the air is made to flow through a grounded metal chamber that contains a wire maintained at high voltage. The dust particles become charged and adhere to the chamber walls, from which they are later collected.

coul-cell A coulometer of the electrolytic-cell type.

coulomb (Charles Augustin Coulomb, 1736–1806). Abbreviation, C. The unit of electrical charge quantity, equal to the charge contained in 6.24×10^{18} electrons. A current of one ampere (1 A) represents 1 coulomb per second (C/s).

Coulomb's law The force between two electrically charged objects is directly proportional to the product of the charge quantities in coulombs, and inversely proportional to the square of the distance between the charge centers. This force is an attraction for opposite charges, and a repulsion for similar charges.

coulometer An instrument that measures electrical charge quantity in coulombs. A typical version keeps a cumulative count of coulombs (ampere-seconds) by integrating current, with respect to time. Also called *coulombmeter.*

Coulter counter See CELL COUNTER.

count **1.** The number of pulses tallied by a counting system in a given period of time. **2.** A single response by a radioactivity counter. **3.** A record of the number of times an instruction or subroutine in a computer program is executed (by increasing the value of a variable by one, as stated in a FOR-NEXT loop, for example).

countdown A decreasing count of time units remaining before an event or operation occurs showing time elapsed and time remaining.

counter **1.** A circuit, such as a cascade of flip-flops, that tracks the number of pulses applied to it and usually displays the total number of pulses. **2.** A mechanism, such as an electromechanical indicator, that tracks the number of impulses applied to it and displays the total. **3.** An electronic switching circuit, such as a flip-flop or stepping circuit, that responds to sequential input pulses applied to it, giving one output pulse after receiving a certain number of input pulses.

counter- Prefix meaning "opposite to" or "contrary to." Examples: *counter EMF, counterclockwise.*

counterclockwise Abbreviation, ccw. Pertaining to rotational motion in a sense opposite that of a typical analog clock. Movement is to the left at the top of the rotational circle, and to the right at the bottom of the circle. Compare CLOCKWISE.

counterclockwise-polarized wave An elliptically polarized electromagnetic wave whose electric-intensity vector rotates counterclockwise as observed from the point of propagation. Compare CLOCKWISE-POLARIZED WAVE.

counter efficiency The sensitivity of a radiation counter or scintillation counter to incident X-rays or gamma rays.

counterelectromotive cell A cell used to counteract a direct-current voltage.

counter EMF See BACK VOLTAGE and KICK-BACK.

counter-meter A radioactivity instrument, such as a Geiger counter, that indicates the number of radioactive particles per unit time.

counterpoise A means of obtaining a radio-frequency (RF) ground by using a grid of wires or tubing in a plane parallel to the earth's surface or

5059F-pC-93-162 4/9/01 4:51 PM Page 152

to average terrain. The radius of the grid is usually at least 0.25 wavelength, but might be smaller if the feed-point impedance of the antenna is very high.

counterpoise ground system A counterpoise with a radius such that resonance is obtained with a quarter-wavelength antenna operated at a height of more than 0.25 wavelength above actual ground. Usually such a system consists of three or four radials measuring 0.25 wavelength each, and extending outward from the base of the antenna nearly parallel to the average terrain.

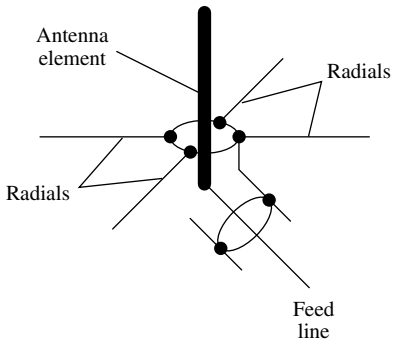

counterpoise ground system

counter tube A tube, such as the Geiger-Meuller tube, in which a penetrating radioactive particle ionizes a gas and produces an output pulse.

counter voltage See BACK VOLTAGE and KICKBACK.

counting-type frequency meter A direct-reading analog or digital frequency meter that indicates the number of pulses (or cycles) per second applied to it.

count-remaining technique See COMPLEMENT-SETTING TECHNIQUE.

couple Two dissimilar metals in contact with each other or immersed in an electrolyte.

coupled circuits Circuits between which energy is transferred electrostatically, electromagnetically, by some combination of the two, or by direct connection.

coupled impedance The impedance that a circuit "sees" when it is coupled to another circuit. Thus, when the secondary of a transformer is terminated with an impedance, the primary "sees" a combination of that impedance and its own.

coupler A device for transferring energy between two circuits and using capacitive coupling, direct coupling, inductive coupling, or some combination of these.

coupling **1.** Also called *electrostatic coupling* or *capacitive coupling.* The linking of two circuits or devices by electric flux. **2.** Also called *magnetic coupling* or *inductive coupling.* The linking of two circuits or devices by magnetic flux. **3.** Also called *direct coupling.* The linking of two circuits or devices by direct connection. **4.** Also called *resistive coupling.* The linking of two circuits or devices through a resistance. **5.** Also called *optical coupling.* The linking of two circuits or devices through an optoisolator.

coupling aperture A hole in a waveguide that is used to transmit energy to the waveguide, or receiving energy from outside the waveguide.

coupling capacitor A capacitor used to conduct ac energy from one circuit to another. Also see CAPACITIVE COUPLING.

coupling coefficient See COEFFICIENT OF COUPLING.

coupling diode A semiconductor diode connected between the stages of a direct-coupled amplifier. When the diode is connected in the correct polarity, it acts as a high resistance between stages when there is no signal, and does not pass the high dc operating voltage from one stage to the next. When a signal is present, the diode resistance decreases, and the signal gets through.

coupling efficiency A measure of the effectiveness of a coupling system (i.e., the degree to which it delivers an undistorted signal of correct amplitude and phase).

coupling loop **1.** A single turn of a coupling transformer. **2.** A small loop inserted into a waveguide to introduce microwave energy.

coupling probe A usually short, straight wire or pin protruding into a waveguide to electrostatically introduce microwave energy into the waveguide. It acts like a miniature whip antenna.

coupling transformer A transformer used primarily to transfer alternating-current (ac) energy electromagnetically into or out of a circuit.

covalent binding forces In a crystal, the binding forces resulting from the sharing of valence electrons by neighboring atoms.

covalent bonding The binding together of the atoms of a material as a result of shared electrons or holes.

coverage **1.** The area within which a broadcast or communication station can be reliably heard. **2.** The shielding effectiveness of a coaxial cable.

coversed sine Abbreviation, covers. The trigonometric functional equivalent of the *versed sine* of the complement of an angle [i.e., the difference between the sine of an angle and unity (1)]. Thus, covers $q = 1 - \sin q$.

CP Abbreviation of *chemically pure.*

cp **1.** Abbreviation of CANDLE POWER. **2.** Abbreviation of *central processor.*

cps **1.** Abbreviation of CYCLES PER SECOND. Cycles per second, to denote ac frequency, has been supplanted by HERTZ. **2.** Abbreviation of *characters per second.*

CPU Abbreviation of CENTRAL PROCESSING UNIT.

5059F-pC-93-162 4/9/01 4:51 PM Page 153

CQ A general call signal used in radio communication, especially by amateur stations, to invite a response from any station that hears it.

Cr Symbol for CHROMIUM.

cracked-carbon resistor A high-stability resistor in which the resistance material is particulate carbon.

cracker A hacker with malicious intent (also see HACKER). Such a person attempts to gain access to computer systems or databases in order to steal something or inflict damage. Examples include theft, erasure, or mutilation of data; fraudulent debiting of bank accounts; alteration of credit information; and identity theft.

cradle guard See GUARD WIRE.

cradlephone A telephone set in which the microphone and earphone are mounted on opposite ends of a handle. This handle, called the *receiver*, rests on the crossmember of a stand connected to a base containing the dial and ringing circuits. Also called *French phone, French telephone*, and *handset.*

crash **1.** A condition in which a computer or network server becomes inoperative because of a software or memory-management problem. **2.** In a computer hard disk or diskette drive, contact of the read/write head with the surface of a disk or platter. Usually, it is the result of excessive physical vibration or shock.

crate A foundation unit into which modules are plugged to establish a circuit.

crawl **1.** See CREEPING COMPONENT. **2.** The credits (names of staff and their contribution to content) superimposed and moving on a television picture at the end of a program.

crazing The formation of tiny cracks in materials, particularly in such dielectrics as plastic and ceramic.

creep See COLD FLOW.

creepage Current leakage across the surface of a dielectric.

creeping component A quantity, such as current, voltage, or frequency, that slowly changes in value with time.

crest factor See AMPLITUDE FACTOR.

crest value The maximum amplitude of a composite current or voltage.

crest voltmeter A peak-reading (or sometimes peak-responsive) voltmeter.

crippled mode The mode of operation for a computer or other hardware in which some of the components are inoperable. Compare GRACEFUL DEGRADATION.

crisscross neutralization See CROSS-CONNECTED NEUTRALIZATION.

crisscross rectifier circuit A conventional bridge rectifier circuit configured in such a way that two of the diodes are connected in crisscross fashion between the input and output terminals.

critical angle **1.** In radio communications, an angle of departure that a transmitted electromagnetic field subtends, with respect to the horizon at the transmitting (TX) point, below which the ionosphere will reliably return the signal to the earth, and above which the ionosphere will not reliably return the signal. This angle (shown by the double arc marked *X* in the drawing) depends on the frequency of the transmitted electromagnetic wave, and also on ionospheric conditions. **2.** For an electromagnetic wave or ray approaching a boundary at which the index of refraction abruptly decreases, the minimum angle of incidence (relative to a line perpendicular to a plane tangent to the boundary) at which the energy is totally reflected.

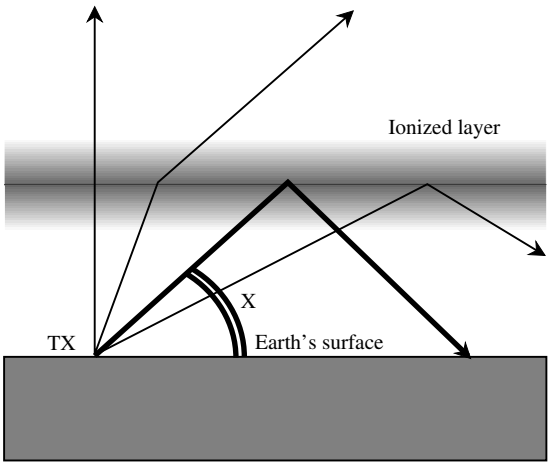

critical angle, 1

critical characteristic A parameter that has a disproportionate effect on other variables. A small change in this characteristic can result in a large change in the operating conditions of a circuit or system.

critical component A component or part that is especially important in the operation of a circuit or system.

critical coupling The value of coupling at which maximum power transfer occurs. Increasing the extent of coupling beyond the critical value decreases power transfer.

critical damping The value of damping that yields the fastest transient response without overshoot.

critical dimension The cross-sectional size of a waveguide that determines its minimum usable frequency.

critical failure A component or circuit failure that results in shutdown of a system, or a malfunction that results in improper operation.

critical field The smallest magnetic-field intensity in a magnetron that keeps an electron, emitted from the cathode, from reaching the anode.

5059F-pC-93-162 4/9/01 4:51 PM Page 154

critical frequency For a particular layer of the ionosphere, the high frequency at which a vertically propagated wave is no longer reflected back to the earth.

critical inductance In a choke-input power-supply filter, the minimum inductance that will maintain a steady value of average load current.

critical potential The potential difference required for an electron to excite or ionize an atom with which it collides.

critical voltage The voltage at which a gas ionizes.

critical wavelength The wavelength that corresponds to CRITICAL FREQUENCY.

CRO Abbreviation of *cathode-ray oscilloscope.*

Crookes dark space In a glow-discharge tube, the narrow dark space next to the cathode. Also see CROOKES TUBE.

Crookes tube A glow-discharge tube containing an anode, cathode, and a small amount of gas under low pressure.

cross antenna An antenna in which two (usually equal-length) horizontal radiators cross each other at right angles and are connected together to a feeder at their point of intersection. It takes its name from its horizontal-cross shape.

cross assembler A program used with one computer to translate instructions for another computer.

crossband operation **1.** Communications in which two frequency bands are used. Station X, for example, might transmit on frequency f_A in band A and receive on frequency f_B in band B; station Y would then transmit on f_B and receive on f_A. **2.** In satellite communications, the use of two frequency bands to facilitate full-duplex operation and to allow the satellite transponder to effectively function. The transponder receives signals from the earth within a specific frequency band, and converts this entire band of signals to a set of signals that occupies an equal amount of spectrum space on another frequency band. The converted signals are then retransmitted back to earth.

crossbar switch A three-dimensional array of switch contacts in which a magnetic selector chooses individual contacts, according to their coordinates in the matrix.

cross bearings A method of radionavigation, in which directional readings are taken from a receiving station (such as a ship or aircraft) for two fixed transmitting stations whose locations are known. Lines are drawn on a map from the transmitting stations, in directions 180 degrees opposite the bearings obtained from the receiving station. The intersection point of these lines is the location of the receiving station.

cross beat A spurious frequency arising from CROSS MODULATION.

cross-check To compare the result of a calculation or computer routine with the result obtained by a different method.

cross color In the chrominance channel of a color television receiver, crosstalk interference caused by monochrome signals.

cross-connected neutralization Neutralization of a push-pull amplifier by feedback through two capacitors—each connected from the output circuit of one transistor to the input circuit of the other.

cross-coupled multivibrator A multivibrator circuit in which feedback is provided by a coupling capacitor between the output of the second stage and the input of the first stage; the stages are forward-coupled by a capacitor of the same value.

cross coupling **1.** The state of being cross-coupled (see, for example, CROSS-COUPLED MULTIVIBRATOR). **2.** Undesired coupling between two circuits.

cross current A current that flows in the opposite direction from some other current.

crossed-pointer indicator **1.** Also called *crossed-needle meter.* A combination of two analog metering instruments in one case. Each needle has its own independently calibrated scale. A third scale corresponds to the intersection point of the needles. Commonly used in directional wattmeters that simultaneously show forward power, reflected power, and standing-wave ratio (SWR). **2.** A two-pointer meter used in aircraft to show the position of the aircraft, relative to the glide path.

crossed-wire thermoelement Two wires or strips of dissimilar metals joined or twisted at a point that constitutes a thermoelectric junction. In usual operation, a high-frequency current is passed through one wire, and a proportional direct-current (dc) voltage, generated by thermoelectric action, appears at the other wire.

cross flux The magnetic flux component that is perpendicular to the flux produced by field magnets.

cross-hair pattern A television test pattern consisting of a single vertical line and a single horizontal line, which form a simple cross. The pattern resembles the cross hairs of an optical instrument.

crosshatch generator A modulated radio-frequency (RF) signal generator that produces a crosshatch pattern on a picture-tube screen.

crosshatch pattern A grid of horizontal and vertical lines produced on a picture-tube screen by a cross-hatch generator. It is used in checking horizontal and vertical linearity.

cross modulation **1.** A type of radio-frequency interference (RFI) between two strong stations that are close in frequency. The desired carrier is modulated by the interfering signal. **2.** The production of signals by rectifier junctions in pipes and wiring near a radio receiver. These objects pick up waves and deliver energy at a different frequency, which finds its way into the receiver. Also called *external cross modulation.* **3.** The interaction between signals of different frequency when

5059F-pC-93-162 4/9/01 4:51 PM Page 155

they magnetize a core of nonlinear magnetic material. Also see CROSSTALK.

cross-modulation factor An expression of the amount of cross modulation (or crosstalk) present in a particular instance. It is equal to M_1/M_2, where M_1 is the modulation percentage that a modulated wave produces in a superimposed unmodulated wave, and M_2 is the modulation percentage of the modulated wave.

cross-neutralized circuit See CROSS-CONNECTED NEUTRALIZATION.

crossover **1.** In a circuit diagram, a point at which lines representing wires intersect, but are not connected. **2.** In a characteristic curve, point at which the plot crosses an axis or operating point. **3.** See CROSSOVER NETWORK.

crossover distortion Distortion of a characteristic at a crossover point (see CROSSOVER, **2**); for example, a bend in the curve where the plot of a waveform passes through zero.

crossover frequency The frequency at which a crossover network delivers equal power to the two circuits it supplies.

crossover network Following final amplification in a sound-reproduction system, an outboard filter circuit that facilitates delivery of the low and high audio frequency (AF) components to the correct speakers.

crossover point See CROSSOVER, **2**.

crossover S-curve The S-shaped image obtained on an oscilloscope screen during sweep-generator alignment of a frequency-modulation (FM) detector. In correct alignment, the exact center of the S-curve (the crossover point) coincides with the zero point on the screen.

cross product Also called *vector product.* For vectors **A** and **B** having lengths A and B, respectively, and subtending an angle θ relative to each other, the cross product $\mathbf{A} \times \mathbf{B}$ points in a direction perpendicular to the plane containing both **A** and **B**. The length of $\mathbf{A} \times \mathbf{B}$ is equal to AB sin θ.

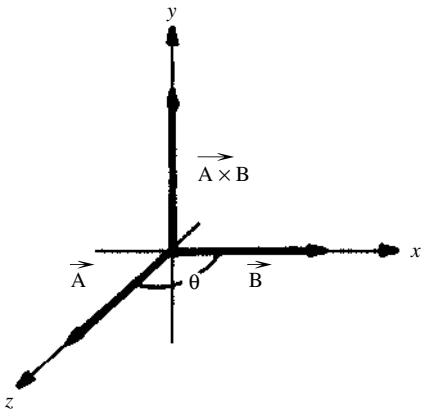

cross product

cross-sectional area **1.** The surface area of a face of a conductor after cutting through it at a right angle. Specified in square inches, square millimeters, or circular mils. **2.** The total of the cross-sectional areas of all the wires in a stranded conductor.

cross-sectional testing In quality assurance and quality control (QA/QC), a method of checking a large lot of units or components. Instead of testing every device, a fraction of the devices is tested. The sampling is taken uniformly from the group (e.g., every fifth unit).

crosstalk Undesired transfer of signals between or among telephone lines, data lines, or system components. In computer operations, this effect places a practical limit on the lengths of parallel data cables.

crosstalk coupling Undesired coupling between circuits, caused by crosstalk.

crosstalk factor See CROSS-MODULATION FACTOR.

crosstalk level The amplitude of crosstalk, usually expressed in decibels above a reference level.

crosstalk loss Loss of energy caused by crosstalk.

crowbar An action producing a high overload on a circuit protection device.

crowfoot **1.** A pattern formed by the cracking or crazing of solid plastics of solidified encapsulating compounds, so called from its resemblance to a bird's footprint. **2.** In a gravity battery cell, the zinc electrode, so called from its resemblance to a bird's foot.

CRT Abbreviation of CATHODE-RAY TUBE.

crud **1.** Broadband electrical noise, originating inside and/or outside a system. **2.** Undesired signals that interfere with a desired signal.

cryogenic device A device that exhibits unique electrical characteristics (such as superconductivity) at extremely low temperatures.

cryogenic motor A motor designed for operation at extremely low temperatures.

cryoelectronics The study of the behavior of electronic devices, circuits, and systems at extremely low temperatures.

cryogenics The branch of physics dealing with the behavior of matter at temperatures approaching absolute zero. Also concerned with methods of obtaining such temperatures in controlled environments.

cryosar A semiconductor switch utilizing low-temperature avalanche breakdown.

cryoscope An instrument used to determine freezing point.

cryostat A chamber for maintaining a very low temperature for cryogenic operations. Also see CRYOGENICS.

cryotron A switching device consisting essentially of a straight tantalum wire, around which a single-layer control coil is wound. The magnetic field generated by control current flowing through the coil causes the tantalum wire to become

5059F-pC-93-162 4/9/01 4:51 PM Page 156

superconductive at a temperature of approximately 4.4 degrees K.

cryotronics Low-temperature electronics, concerned with such phenomena as superconductivity. The term is an acronym from cryogenics and electronics. Also see CRYOGENICS.

cryptanalysis The breaking of ciphers.

crypto- A prefix added to words, that implies encoding for the purpose of changing or hiding the meaning of a message or signal.

cryptography The creating and writing of ciphers.

cryptology The art and science of creating, writing, unscrambling, and breaking ciphers.

crystal **1.** A material distinguished by the arrangement of its atoms into a redundant pattern called a *lattice* that presents, in fragments of various sizes, a characteristic polyhedral shape. Common shapes include cubes, parallelepipeds, and hexagonal prisms. **2.** A fragment of material as defined in (1). **3.** A plate or bar cut from a piece of piezoelectric material.

crystal amplifier **1.** A semiconductor diode circuit using carrier storage. Transistor action and, accordingly, pulse amplification is obtained by alternately making one electrode of the diode an emitter or collector. **2.** Archaic term for TRANSISTOR.

crystal audio receiver An audio radar receiver, consisting of a crystal detector and audio-amplifier stages.

crystal axes The imaginary lines traversing a piezoelectric crystal, along which (or perpendicular to which) plates are cut for oscillators, resonators, or transducers.

crystal calibrator A crystal oscillator used to generate harmonic checkpoints for frequency calibration. Common fundamental calibrator frequencies are 100 kHz and 1 MHz.

crystal capacitor See VARACTOR.

crystal control The control of the operating frequency of a circuit by means of a piezoelectric crystal.

crystal-controlled receiver A superheterodyne radio receiver whose local oscillator is crystal controlled.

crystal-controlled transmitter A radio transmitter whose master oscillator is crystal controlled.

crystal counter A device for counting the frequency of subatomic particles, based on their ability to change the conductivity of a crystal. The particles can be photons, electrons, protons, neutrons, or the nuclei of atoms.

crystal current Current flowing through a crystal; specifically, the radio-frequency (RF) current flowing through a quartz plate in a crystal-controlled oscillator.

crystal cuts The classification of piezoelectric plates according to the angle at which they were cut from a quartz crystal. Common cut designations are AT, BT, CT, DT, X, Y, and Z. Various cuts afford such complementary factors as frequency, temperature, and thickness. Also see CRYSTAL AXES.

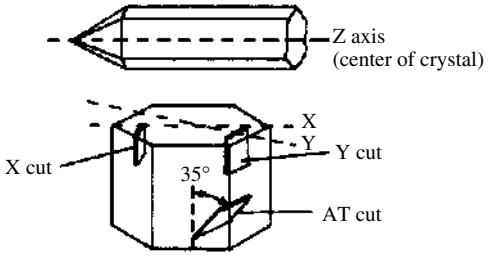

crystal cuts

crystal detector A rudimentary form of semiconductor diode consisting of a mounted lump of mineral (the crystal) in contact with a springy wire ("cat's whisker"). The point of the wire is moved to various points of contact on the crystal surface until the most-sensitive rectifying spot is found.

crystal diffraction The tendency of electromagnetic waves to be scattered when passing through a crystal material.

crystal diode Archaic term for SEMICONDUCTOR DIODE. Also see GALLIUM-ARSENIDE DIODE; GERMANIUM DIODE; JUNCTION DIODE; LASER DIODE; POINT-CONTACT DIODE; SELENIUM DIODE; SIGNAL DIODE; SILICON DIODE.

crystal earphone An earphone in which the transducer is a piezoelectric crystal. Electrical impulses applied to the crystal vary its shape and cause a vibration that is transmitted to a diaphragm; this in turn produces corresponding sound waves.

crystal filter See CRYSTAL RESONATOR.

crystal headphone See CRYSTAL EARPHONE.

crystal holder A fixture specially designed to hold a piezoelectric crystal; it ensures minimum distortion of crystal dimensions and minimum residual capacitance, inductance, and resistance.

crystal imperfection A flaw in the lattice structure of a crystal.

crystal lattice The orderly, redundant pattern of atoms and molecules within a crystalline material; it is a characteristic of a given material.

crystal-lattice filter A crystal resonator in which piezoelectric crystals are used to give a desired shape to the filter response curve.

crystalline material A material exhibiting the characteristic properties of a crystal (see CRYSTAL, **1**).

crystallogram An X-ray photograph or other record of crystal structure.

crystallography The science dealing with crystals and their properties (see CRYSTAL, **1**).

crystal loudspeaker A loudspeaker whose transducer is a piezoelectric crystal. Electrical impulses applied to the crystal vary its shape and

5059F-pC-93-162 4/9/01 4:51 PM Page 157

cause vibrations that are transmitted to a diaphragm or cone, which produces corresponding sound waves.

crystal meter A rectifier-type ac meter using a semiconductor diode in series with a dc milliammeter or microammeter.

crystal microphone A microphone whose transducer is a natural or synthetic piezoelectric crystal. Sound waves striking the crystal (directly or via a diaphragm) vary its shape, making it produce an audio-frequency (AF) output voltage.

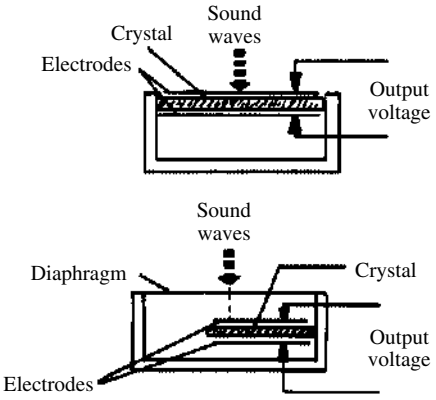

crystal microphones

crystal mixer A mixer (converter) circuit utilizing the nonlinearity of a semiconductor diode to mix signals.

crystal operation **1.** The characteristics of a piezoelectric crystal in a particular circuit. **2.** Crystal frequency control.

crystal oscillator An oscillator whose operating frequency is determined by the dimensions of an oscillating piezoelectric quartz-crystal plate. Compare SELF-EXCITED OSCILLATOR.

crystal oven A constant-temperature chamber for stabilizing the frequency of a quartz crystal by maintaining its operating temperature at a fixed point.

crystal photocell A photoelectric cell in which the light-sensitive material is a crystalline substance, such as germanium, selenium, silicon, etc.

crystal pickup A phonograph pickup whose transducer is a natural or synthetic piezoelectric crystal. The crystal is attached (either directly or through a mechanical linkage) to a stylus, whose movement in the disk groove varies the shape of the crystal. The resultant vibration generates a corresponding audio-frequency (AF) output voltage across the crystal.

crystal probe A radio-frequency (RF) probe, whose rectifying element is a semiconductor diode.

crystal pulling **1.** The extraction of a single crystal from a molten mass of crystalline material. Single crystals are used for high-quality semiconductor devices. Also see CZOCHRALSKI METHOD, SINGLE CRYSTAL, and SINGLE-CRYSTAL MATERIAL. **2.** The use of an inductor or capacitor in a crystal-controlled radio-frequency (RF) oscillator circuit to allow adjustment of the frequency over a small range.

crystal receiver See CRYSTAL SET.

crystal rectifier **1.** A semiconductor diode used for the purpose of rectifying alternating current (dc), usually in a power supply.

crystal resistor A temperature-sensitive resistor made from silicon, and exhibiting a positive temperature coefficient of resistance.

crystal resonator A highly selective resonant circuit in which the center frequency is the resonant frequency of a piezoelectric quartz-crystal plate.

crystal sensor See CRYSTAL TRANSDUCER.

crystal set A simple radio receiver that uses a tuned circuit, semiconductor-diode detector, and earphones.

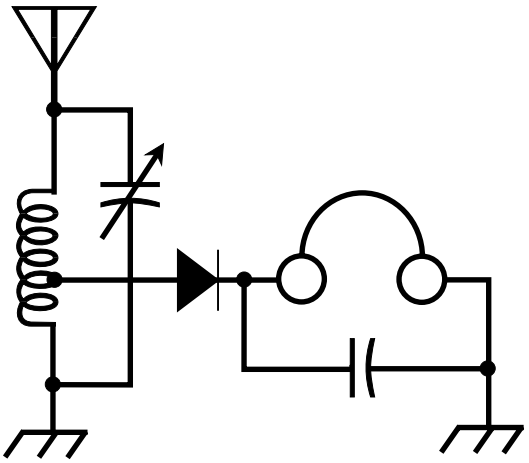

crystal set

crystal slab See QUARTZ BAR.

crystal socket **1.** A low-capacitance, low-loss socket for a piezoelectric crystal. **2.** A socket for a semiconductor diode.

crystal tester **1.** An oscillator used to check quartz crystals. Most such units check only the crystal's ability to oscillate; more elaborate ones also check crystal current, frequency, temperature coefficient, activity, filter action, etc. **2.** An instrument for checking the electrical characteristics of semiconductor diodes. **3.** An instrument for checking the performance of piezoelectric ceramics.

5059F-pC-93-162 4/9/01 4:51 PM Page 158

crystal tetrode A transistor having four elements: emitter, collector, and two bases.

crystal transducer A transducer using a piezoelectric crystal as the sensitive element. Examples: crystal earphone, crystal loudspeaker, crystal microphone, and crystal pickup.

crystal triode See TRANSISTOR.

Cs Symbol for CESIUM.

CS Abbreviation of COMPLEMENTARY SYMMETRY. Also COS.

C_S **1.** Symbol for *standard capacitance.* **2.** Symbol for *source capacitance.*

csc Abbreviation of COSECANT.

C scan See C DISPLAY.

csch Abbreviation of HYPERBOLIC COSECANT.

C scope A cathode-ray tube used in radar to provide a C DISPLAY.

CT-cut crystal A piezoelectric plate cut from a quartz crystal at an angle of rotation around the X-axis of +38°. Such a plate has a zero temperature coefficient of frequency at 25°C. Also see CRYSTAL AXES and CRYSTAL CUTS.

CTL Abbreviation of *complementary-transistor logic.*

Cu Symbol for COPPER.

cube **1.** A regular polyhedron with six identical square faces and eight vertices. At each vertex, three edges converge at mutual right angles. **2.** The third power of a number; thus the cube of n is written n^3.

cube tap An electrical adapter, in which a set of male prongs and three sets of female contacts are on the sides of a molded cube. Allows three appliances to be used with a single electrical socket.

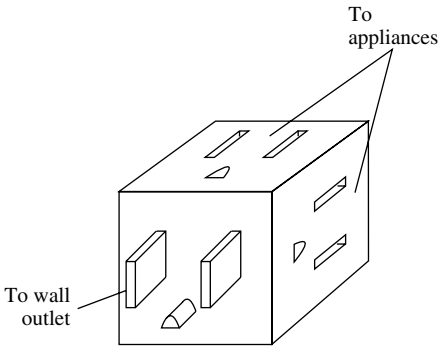

cube tap

cubical antenna An antenna in which the elements form the outline of a geometric cube or rectangular prism. The most common example is the QUAD ANTENNA.

cubical quad antenna See QUAD ANTENNA.

cubic equation A polynomial equation of the third degree. Its general form is $ax^3 + bx^2 + cx + d = 0$.

cue A condition or signal that alerts an operator, circuit or system to act in a specific manner.

cue circuit A device for transmitting cues used in program control.

cueing receiver **1.** A (usually miniature) radio receiver used to pick up cues. Example: a receiver carried by a technician, actor, or lecturer. **2.** A receiver or other pickup circuit that receives a cuing pulse, which it uses to set another circuit.

cu ft Abbreviation of *cubic foot* or *cubic feet.*

cu in Abbreviation of *cubic inch* or *cubic inches.*

cumulative error In a sum or other final value, the total error that has accumulated from the individual errors in the terms. Also called *systematic error.*

cup core A coil core that also forms a magnetic shield around the coil.

cuprous-oxide rectifier See COPPER-OXIDE RECTIFIER.

cur Abbreviation of CURRENT.

curie Abbreviation Ci. A unit of radioactivity; 1 curie is the amount of radiation from (or in equilibrium with) 1 gram of radium. Also equivalent to 3.7×10^{10} atomic breakdowns per second.

Curie point **1.** The temperature above which a ferromagnetic material loses its magnetism or becomes paramagnetic. **2.** The temperature at which the ferroelectric properties of a substance disappear.

curie temperature As a magnetized substance is heated, the lowest temperature at which magnetization is lost. It is generally measured in degrees Celsius or degrees Kelvin. For iron, this temperature is 760 degrees Celsius; for nickel, it is 356 degrees Celsius.

Curie's law For a paramagnetic substance, the ratio of the magnetization to the magnetizing force is inversely proportional to the absolute temperature.

Curie-Weiss law Above the Curie point, the susceptibility of a paramagnetic material varies inversely as the excess of temperature above the Curie point increases. This law is invalid for applications at or below the Curie point.

curium Symbol, Cm. A radioactive metallic element produced artificially. Atomic number, 96. Atomic weight, 247.

current Symbol, I or i. The movement of charge carriers, such as electrons, holes, or ions. Also see AMPERE.

current amplification **1.** An electronic process in which the instantaneous, average, or peak magnitude of a current is increased. **2.** The extent to which a current increases in a circuit; the ratio (always greater than one) of output current to input current, I_{out}/I_{in}. Also called *current gain.*

current amplifier An amplifier operated primarily to increase a signal current. Compare POWER AMPLIFIER and VOLTAGE AMPLIFIER.

current antinode See CURRENT LOOP.

5059F-pC-93-162 4/9/01 4:51 PM Page 159

current attenuation **1.** The reduction of current amplitude along a line. **2.** The extent to which a current decreases in a line or circuit; the ratio (always less than one) of output current to input current, I_{out}/I_{in}.

current balance An instrument for determining the size of the ampere. This is done by measuring the force between two current-carrying conductors.

current-balance switch A switch or relay, operated by the existence of a difference between two currents.

current-carrying capacity The maximum current (usually expressed in amperes) that a conductor or device can safely conduct.

current coil The series coil in a nonelectronic wattmeter. Compare POTENTIAL COIL.

current-controlled amplifier Abbreviation, CCA. An amplifier in which gain is controlled by means of a current applied to a control-input terminal.

current density The current (usually expressed in amperes per square centimeter) passing through a cross-sectional area of a conductor.

current drain **1.** The current supplied to a load by a generator or generator-equivalent. **2.** The current required by a device for its operation; also, the current taken by the device during standby periods.

current echo Reflected current in a transmission line that is not terminated in an impedance exactly matching its characteristic impedance.

current-fed antenna An antenna in which the transmission line is attached to the radiator at a current loop (voltage node). Compare VOLTAGE-FED ANTENNA.

current feed **1.** The delivery of power to a device or circuit at a point where current dominates. Compare VOLTAGE FEED. **2.** In an antenna, feeding it at a current maximum.

Current feed

current feedback **1.** A feedback signal consisting of current fed from the output to the input circuit of an amplifier. **2.** A system or circuit for obtaining current feedback.

current-feedback pair A two-stage, direct-coupled transistor amplifier having direct-current shunt-series feedback.

current flow Charge carriers passing through a solid, liquid, gas, or vacuum. Also see CURRENT and CURRENT DENSITY.

current gain See CURRENT AMPLIFICATION.

current hogging **1.** An undesirable condition that sometimes takes place when two or more transistors are operated in parallel. One device tends to do all the work, taking all the current. The result can be destruction of that device. **2.** The tendency of one component in a group of identical parallel-connected components to dissipate most of the power.

current-hogging injection logic Acronym, CHIL. A form of bipolar digital logic, similar to current-hogging logic but having the greater density characteristic of injection logic.

current instruction register A register in which are held instructions ready for execution by a program controller.

current lag A circuit condition in which current variations are delayed by up to 180 degrees of phase relative to voltage variations. Compare CURRENT LEAD.

current lead A circuit condition in which current variations occur earlier than voltage variations by up to 180 degrees of phase. Compare CURRENT LAG.

current limiting The controlling of current so that it does not exceed a desired value.

current-limiting resistor A series resistor inserted into a circuit to limit the current to a prescribed value.

current loop A point on a transmission line or antenna radiator at which the current reaches a local maximum. Compare CURRENT NODE.

current meter A usually direct-reading instrument, such as an ammeter, milliammeter, or microammeter, used to measure current strength. Also see ELECTRONIC CURRENT METER.

current-meter operation The operation of a voltmeter as a current meter by connecting it to respond to the voltage drop across a resistor that carries the current of interest.

current-mode logic In computer operations, transistor logic in which the transistors operate in the unsaturated mode.

current node A point on a transmission line or antenna radiator at which the current reaches a local minimum. Compare CURRENT LOOP.

current noise Electrical noise produced by current flowing through a resistor.

current probe A transformer usually having a snap-around, one-turn coil that picks up energy from a conductor and couples it into an alternating-current ammeter.

current rating **1.** A specified value of operating current. **2.** See CURRENT-CARRYING CAPACITY.

current-regulated supply See CONSTANT-CURRENT SOURCE.

current regulation The stabilization of current at a predetermined level or value.

current regulator See BARRETTER.

current relay A relay actuated by specific values of pickup and dropout current.

5059F-pC-93-162 4/9/01 4:51 PM Page 160

current saturation In the operation of a device (such as a transistor, saturable reactor, or magnetic amplifier), the leveling off of current at a value beyond which no further increase occurs—even though an input parameter is further increased.

current sense amplifier An amplifier used to increase the sensitivity of, or to decrease the loading of, a current-sensing component.

current sensing Sampling a current (e.g., when the voltage drop across a series resistor is used as a proportional indication of the current flowing through the resistor).

current-sensing resistor A low-value resistor inserted into a circuit primarily for current sensing.

current sensitivity In a current meter or galvanometer, current (in amperes or fractions thereof) per scale division.

current-sheet inductance Symbol, L_S. The low-frequency inductance of a single-layer coil, calculated with the formula $L_S = (0.10028\ a^2N^2)/s$, where L_S is in microhenrys, a is the coil radius in inches, N is the total number of turns, and s is the coil length in inches.

current shunt **1.** A resistor connected in parallel with a voltmeter to convert it into an ammeter. **2.** A resistor connected in parallel with the input of a voltage amplifier to make the response of the amplifier proportional to input-signal current.

current sink A circuit or device through which a constant current can be maintained.

current-sinking logic A form of bipolar digital logic. Current flows from one stage to the input of the stage immediately before.

current-squared meter An ammeter or milliammeter whose deflection is proportional to the square of the current.

current-stability factor In a common-base connected bipolar transistor, the ratio dI_E/dI_C, where I_E is the emitter current and I_C is the collector current.

current strength The magnitude of electric current (see CURRENT) (i.e., the number of carriers flowing past a given point per unit time, expressed in coulombs per second or in amperes).

current transformer **1.** A transformer used to increase or decrease current flow. A primary-to-secondary step-up turns ratio reduces the current; a primary-to-secondary step-down turns ratio increases the current. **2.** A particular transformer (as in 1) used to change the range of an alternating-current milliammeter or ammeter.

current vector In a vector diagram, a line with an arrowhead (vector) showing the magnitude and phase of a current. Compare VOLTAGE VECTOR.

current-voltage feedback In an amplifier or oscillator, the process of applying some of the output current and voltage to the input. This feedback might be in phase (positive) or out of phase (negative), with respect to the input.

cursor **1.** A marker that indicates the position where a character can be entered in a video alphanumeric display. Commonly used in computers and word processors. **2.** The sweeping line on a radar display. **3.** The movable marker on a slide rule.

curve trace **1.** A device that supplies a special variable test voltage to a component or circuit under test, at the same time supplying a sweep voltage to an oscilloscope. The component's output voltage is also presented to the oscilloscope. As a result, the response curve of the component appears on the oscilloscope screen. **2.** A device that produces a permanent record (photographic or graphic) of an electrical phenomenon. Also called OSCILLOGRAPH or RECORDER.

curvilinear trace A trace made on paper with curved vertical lines. The lines are curved to match the arc through which the recording pen swings.

cut-in angle In a semiconductor rectifier circuit, a phase angle slightly greater than zero degrees, at which current conduction begins. Compare CUT-OUT ANGLE.

Cutler antenna A parabolic-dish antenna, in which the driven element consists of a waveguide that has two apertures on opposite sides of a resonant cavity.

Cutler feed An aircraft antenna feed system in which radio-frequency (RF) energy is fed to the reflector by a resonant cavity at the end of a waveguide.

Cutler tone control A dual resistance-capacitance (RC) filter circuit of the general bridged-tee variety. Variation of the series leg provides adjustable treble boost; variation of the shunt leg provides adjustable bass boost.

cutoff **1.** The process of reducing some operating parameter, such as collector current, to zero by adjusting the bias at the input electrode. **2.** The point on the characteristic curve of an amplifying device, at which the output current drops to zero under no-signal conditions. **3.** The lowest frequency at which a waveguide will efficiently function. **4.** The frequency or frequencies corresponding to the point or points in a filter response, at which the attenuation is three decibels greater than the lowest attenuation within the passband. See also CUTOFF FREQUENCY.

cutoff attenuator A variable, nondissipating attenuator consisting of a variable length of waveguide used at a frequency below cutoff.

cutoff bias In a transistor or vacuum-tube circuit, the value of control-electrode bias that produces output current cutoff.

cutoff current Symbol, I_{co}. In a transistor, the small collector current that flows when the emitter current is zero (common-base circuit) or when the base current is zero (common-emitter circuit).

cutoff frequency **1.** Symbol, f_{co}. The high frequency at which the current-amplification factor

5059F-pC-93-162 4/9/01 4:51 PM Page 161

of a transistor drops to 70.7% of its 1-kHz value. **2.** In a filter, amplifier, or transmission line, the frequency point(s) at which transmission loss or filter rejection begins. It is generally specified as the half-power point(s), or the point(s) at which the attenuation is three decibels, relative to the lowest attenuation. Examples: the high-frequency cutoff of an amplifier and the upper and lower cutoff points of a bandpass filter.

cutoff limiting Output-peak clipping that results from overdrive in an amplifying device. Compare SATURATION LIMITING.

cutoff potential See CUTOFF BIAS.

cutoff voltage See CUTOFF BIAS.

cutoff wavelength **1.** The wavelength corresponding to cutoff frequency. **2.** For a waveguide, the ratio of the velocity of electromagnetic waves in free space (3×10^8 meters per second) to the cutoff frequency of the waveguide in Hz. The result is thus expressed in meters.

cutout **1.** A device, such as a circuit breaker, that automatically disconnects a circuit, usually to prevent overload, but occasionally to prevent underload. **2.** Emergency switch. **3.** Fuse.

cut-out angle In a semiconductor rectifier circuit, a phase angle slightly less than 180 degrees at which current conduction ceases. Compare CUT-IN ANGLE.

cutout base A fuse block.

cut rate **1.** The speed at which a cutter moves across the surface of a blank vinyl disk during the recording process. **2.** The number of cut lines per inch in a vinyl disk recording.

CW **1.** Abbreviation of CONTINUOUS WAVE. **2.** Abbreviation of CLOCKWISE.

CW filter In a communications receiver, a highly selective filter in the intermediate-frequency (IF) or audio-frequency (AF) stage. The bandwidth is typically 200 Hz to 500 Hz; some audio filters can be set for bandwidths as low as about 50 Hz.

CW laser A laser that emits energy in an uninterrupted stream, rather than in pulses.

CW monitor See KEYING MONITOR.

CW oscillator **1.** In a radio receiver, a variable-frequency oscillator that heterodynes a radiotelegraph signal in the intermediate-frequency (IF) amplifier chain, to make audible the continuous-wave dits and dahs. **2.** Sometimes, an external variable-frequency radio-frequency (RF) oscillator, whose output beats against the actual carrier of a continuous-wave radiotelegraph signal, making it audible as dits and dahs. **3.** An unmodulated, unkeyed oscillator.

CW radar A radar system in which radio-frequency (RF) energy is transmitted continuously.

CW reference signal A sinusoidal radio-frequency (RF) signal, used to control the conduction time of a synchronous demodulator in color television.

C_x Symbol for UNKNOWN CAPACITANCE.

cyan Blue-green, one of the three primary pigments.

cyber- A prefix that indicates relevance to, or involvement with, computers, computer systems, and electronic control systems.

cybernetics The study of control system theory in terms of the relationship between animal and machine behavior.

Cyber Sapiens An expression for a computer or robot with artificial intelligence (AI) on the forefront of current technology.

cyberspace **1.** Alternative expression for INFORMATION SUPERHIGHWAY. **2.** Alternative expression for VIRTUAL REALITY.

cyborg Acronym of the words *cybernetic* and *organism.* **1.** A human being with at least one artificial body part, such as a *prosthesis* (artificial limb). **2.** A human being who is largely composed of robotic body parts.

cycle **1.** Abbreviation, c. One complete, 360-degree revolution of the current or voltage vector in an alternating-current (ac) wave. An ac frequency of 1 cycle per second is 1 Hz (see HERTZ). **2.** A complete sequence of operations.

cycle counter A device that totals the number of cycles of a phenomenon repeated during a given period.

cycle index The number of times that a particular cycle has been, or must be, iterated in a computer program.

cycle index counter A variable that indicates how often a cycle of computer program instructions has been executed. In a program, for example, this can be accomplished by increasing, through instruction, the value of a location's content every time a loop operation is performed.

cycle life The total number of charge-discharge cycles a rechargeable cell or battery can tolerate before becoming useless.

cycle reset To change the value of a cycle count (making it zero or some other value).

cycle shift See CYCLIC SHIFT.

cycles per second Abbreviation, cps. Archaic term for HERTZ.

cycle time Pertaining to an operation, the duration of a complete cycle.

cycle timer A timer that switches a circuit or device on and off, according to a predetermined cycle. Also called *programmed timer.*

cyclic code See GRAY CODE.

cyclic memory In computer operations, a memory whose locations can only be accessed points in a cycle, as of a magnetic diskette.

cyclic shift The moving of data out of one end of a storage register and reentering it character-by-character or bit-by-bit at the other end in a closed loop (e.g., 87654 cyclically shifted one place to the right becomes 48765).

cyclic variations Periodic changes in the features of the ionosphere, occurring on a daily, seasonal, or sunspot-related basis. These changes are fairly predictable.

5059F-pC-93-162 4/9/01 4:51 PM Page 162

cycling The tendency of a parameter to oscillate back and forth between two different values.

cyclogram A method of showing the relationship between two signals on an oscilloscope. The two signals must have a fixed phase relationship.

cyclotron A type of particle accelerator. An applied electromagnetic field, acting together with an intense applied magnetic field, cause charged subatomic particles to travel with increasing velocity in a spiral path between two semicircular metal boxes called *dees.* When the particles go fast enough in the correct path, they are expelled and strike a target in their path.

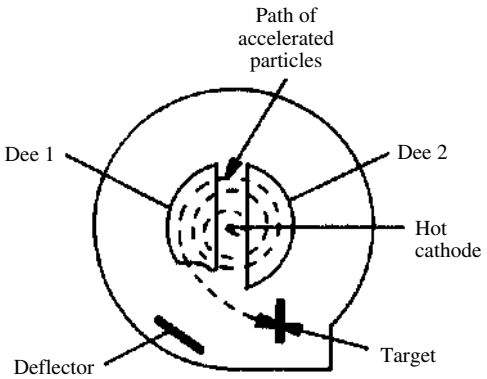

cyclotron

cyclotron frequency The angular frequency of a charged particle in a cyclotron. The cyclotron frequency depends on the number of times per second the magnetic field of the device is reversed.

cyclotron radiation An electromagnetic field produced by the circular movement of charged particles in a fluctuating magnetic field.

cylinder In computer operations, the combination of equal-radius tracks on the platters of a hard disk.

cylinder magnet A permanent magnet in the shape of a cylinder.

cylindrical capacitor See CONCENTRIC CAPACITOR.

cylindrical contour The most common curvature of the face of a magnetic tape recording head; it is a section of a cylinder having a constant radius of 0.5 inch to 1 inch.

cylindrical coordinate geometry A scheme for robot-arm movement. There are three coordinates, called *reach, angle,* and *elevation.* It allows precise positioning of a robot end effector within a region consisting of two concentric cylinders and all the volume in between.

cylindrical coordinates A method of locating a point in three-space in which height, distance, and angle are used to uniquely define points.

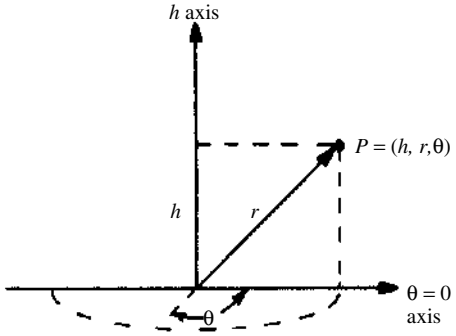

cylindrical coordinates

cylindrical magnet See CYLINDER MAGNET.

cylindrical wave An electromagnetic wave whose field surfaces are nearly perfect cylinders.

cylindrical waveguide A waveguide resembling a round pipe.

cylindrical winding A method of coil winding in which the wire is formed into a helix. There might be only one layer, or there might be several layers. The length of the coil is greater than the diameter. Also called a *linear winding.*

Czochralski method A technique for obtaining a relatively large single crystal from a substance, such as the semiconductors germanium and silicon. The method consists essentially of dipping a seed crystal into a molten mass of the same substance, then slowly withdrawing it while rotating it.

5059F-pD-163-223 4/9/01 5:22 PM Page 163

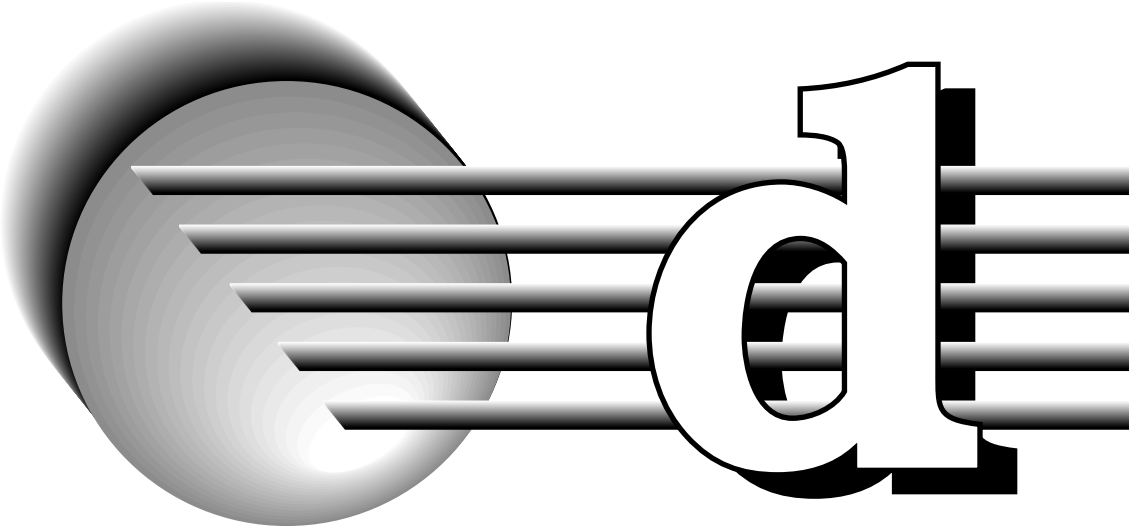

D **1.** Symbol for DEUTERIUM. **2.** Symbol for ELECTRIC DISPLACEMENT. **3.** Symbol for ELECTRIC FLUX DENSITY. **4.** Symbol for DISSIPATION FACTOR. **5.** Symbol for *drain* (see DRAIN, **3**). **6.** Abbreviation of DISSIPATION. **7.** Symbol for *determinant.* **8.** Symbol for DIFFUSION CONSTANT.

d **1.** Abbreviation of DECI. **2.** Symbol for DIFFERENTIAL. **3.** Symbol for distance. **4.** Symbol for DENSITY. **5.** Symbol for *drain* (see DRAIN, **3**). **6.** Abbreviation of DISSIPATION. **7.** Abbreviation of day. **8.** Abbreviation of DEGREE. **9.** Abbreviation of diameter. **10.** Abbreviation of DRIVE.

D/A Abbreviation of DIGITAL-TO-ANALOG. See DIGITAL-TO-ANALOG CONVERSION.

dA **1.** Symbol for DIFFERENTIAL OF AREA. **2.** Symbol for *differential of amplification.* **3.** Seldom-used abbreviation of *deciampere.*

da Abbreviation of DEKA.

DAC Abbreviation of DIGITAL-TO-ANALOG CONVERTER.

DACI Abbreviation of *direct adjacent-channel interference.*

DAGC Abbreviation of DELAYED AUTOMATIC GAIN CONTROL.

daisy chain A method of transferring a signal in a computer from one stage to the next.

daisy wheel A form of printing device consisting of a disk having several dozen radial spokes, each of which has a character molded on its face. The disk rotates to the proper position in the printing process, and a hammer strikes the spoke to press the molding against the ribbon and paper.

DAM Abbreviation of *data-addressed memory.*

Damon effect The change that the susceptibility of ferrite undergoes under the influence of high RF power.

damped galvanometer A galvanometer with a provision for overswing limiting or oscillation prevention.

damped loudspeaker A loudspeaker in which undesirable excursions are prevented by damping in the associated amplifier or speaker circuit.

damped meter **1.** A meter with a provision for overswing limiting or oscillation prevention. **2.** A meter that is protected during transport by a shorting bus between the two meter terminals.

damped natural frequency **1.** The frequency at which a damped system having one degree of freedom will oscillate after momentary application of a transient force. **2.** In the presence of damping, the rate at which a sensing element oscillates freely.

damped oscillations Oscillations in which the amplitude of each peak is lower than that of the preceding one; the oscillation eventually dies out (the amplitude becomes zero). Compare CONTINUOUS WAVE.

damped speaker See DAMPED LOUDSPEAKER.

damped wave A wave whose successive peaks decrease in amplitude (i.e., it decays), eventually reaching an amplitude of zero. Compare CONTINUOUS WAVE and UNDAMPED WAVE.

damped-wave decay See DECREMENT, **1**.

dampen To cause the amplitude of a signal to decay.

damper See DAMPING DIODE.

damper diode See DAMPING DIODE.

Copyright 2001 The McGraw-Hill Companies, Inc. Click Here for Terms of Use

5059F-pD-163-223 4/9/01 5:22 PM Page 164

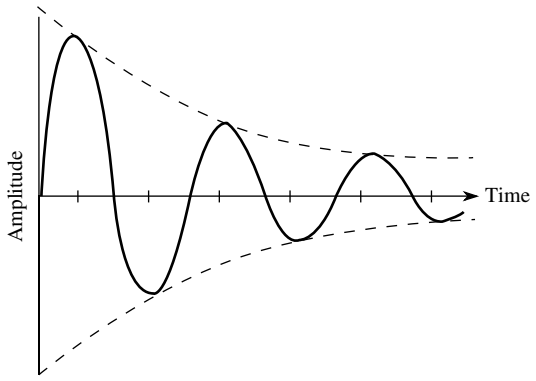

damped wave

damper winding A special short-circuited motor winding that opposes pulsation or rotation of the magnetic field.

damping **1.** See DAMPING ACTION. **2.** In a loudspeaker, sound-absorbent material used to minimize resonant effects within the enclosure.

damping action **1.** Quenching action. **2.** The prevention of overswing, dither, or flutter in a meter or loudspeaker (see DAMPED GALVANOMETER, DAMPED LOUDSPEAKER, DAMPED METER). **3.** The prevention of oscillation or ringing in a circuit. **4.** Inhibition of the vibration of an acoustic transducer to prevent ringing and other unwanted effects.

damping coefficient A figure expressing the ratio of the damping in a system to critical damping.

damping diode A diode used to prevent oscillation in an electric circuit (e.g., the diode that prevents ringing in the power supply of a television receiver). Also called *damper.*

damping factor **1.** Symbol, α. For a coil of inductance L and RF resistance R in a damped-wave circuit, the value $R/2L$, where L is in henrys and R in ohms. **2.** Abbreviation, F_o. For a torque motor, the ratio of the stall torque to the no-load rotational speed.

damping magnet A permanent magnet so situated, with respect to a moving conductor, disk, or plate, that the resulting field opposes the movement.

damping ratio See DAMPING COEFFICIENT.

damping resistance **1.** The value of shunt resistance required to prevent ringing in a coil. **2.** The value of resistance required for critical damping of a galvanometer.

damping resistor **1.** A shunt across a coil to prevent ringing. **2.** A resistor used to provide critical damping of a galvanometer.

Daniell cell A nonpolarizing primary wet cell with zinc (negative) and copper (positive) electrodes. The zinc plate is in a porous cup containing a weak zinc-sulfate solution with a little sulfuric acid; the cup is in a jar filled with a saturated copper-sulfate solution in which the copper electrode is immersed. Typical voltage for the cell is 1.1 V.

daraf The unit of ELASTANCE. Elastance in darafs is the reciprocal of capacitance in farads.

dark conduction The flow of dark current in a photoconductive or glow-discharge device.

dark current The usually tiny current flowing through a darkened photoconductive cell, phototransistor, or glow-discharge device.

dark discharge The occurrence of a discharge in a gas, without the production of visible light.

dark-spot signal A spurious signal generated by some camera tubes, arising from secondary-emission effects.

dark-trace tube An oscilloscope tube on whose white screen a long-persistence magenta image is traced by the electron beam. Illuminating the screen with bright light intensifies the image.

Darlington amplifier A high-gain amplifier that uses a COMPOUND CONNECTION of two bipolar transistors.

Darlington pair See COMPOUND CONNECTION.

D'Arsonval current A large, low-voltage, high-frequency current at one time thought to be therapeutic.

D'Arsonval meter A electromechanical analog meter, in which a coil turns on jeweled pivots between the poles of a strong magnet and against the force of spiral springs. A pointer is attached to the coil. The pointer moves over a calibrated scale.

D'Arsonval movement The mechanism of a D'Arsonval meter.

DART Abbreviation of *data analysis recording tape.*

dart leader A flow of electrons along a path traveled by a lightning stroke, preceding a second stroke. The dart leader, if any, occurs a few milliseconds after the first stroke. Several strokes could occur, each preceded by a dart leader, within less than 1 second.

dash The longer of the two characters (DOT and DASH) of the telegraph code. The duration of the dash is three times longer than that of a dot.

dashpot A delayed-action device in which the movement of a piston is slowed by air or a liquid in a closed cylinder.

dashpot relay A time-delay relay assembly in which the delay is obtained with a DASHPOT.

DAT **1.** Abbreviation of DIGITAL AUDIO TAPE. **2.** Abbreviation of *diffused-alloy transistor.*

data **1.** A collection of digital bits (binary digits) with informational content (e.g., a computer file, a digital image, or a digital sound recording). **2.** General expression for information, especially in encoded or written form.

data acquisition The reception and gathering of data (see DATA COLLECTION and DATA SYSTEM, **1**).

data-acquisition system A computer or dumb terminal used to gather data from one or more external points.

5059F-pD-163-223 4/9/01 5:22 PM Page 165

data analysis display unit A video display peripheral for online data analysis.

data area A computer memory area that holds data only (i.e., one that does not contain program instructions).

data bank A data file stored in a direct-access storage device, which can be drawn from by many system users through remote terminals.

database **1.** A computer file containing often-used information (e.g., names and addresses, or electronic part numbers). **2.** A popular form of computer software that allows users to create, maintain, and modify information.

data block A set of data bits, comprising an identifiable item.

data bus A conductor or medium over which digital data is transmitted from one place to another within a computer.

data carrier storage A medium of data storage outside of a computer (e.g., a magnetic disk).

data code A set of abbreviations or codes for data characters or words.

data collection The pickup of signals representing test data and their transmission to a computer, data processor, or recorder. Also see DATA SYSTEM, **1**.

datacom Acronym for DATA COMMUNICATION.

data communication The transmission and reception of data signals between or among points in a system.

data communication terminal A computer peripheral providing an input and output link to a central computer system, and that can be used offline for other functions.

data compression **1.** The process of reducing the size of a data file by eliminating redundancies. **2.** The process of minimizing the length of a data transmission by eliminating redundancies. **3.** The process of reducing the bandwidth of a data transmission. **4.** The process of reducing the dynamic amplitude range of a data transmission.

data control The automatic control of incoming and outgoing data in a data processing system.

data conversion The process of changing data from one form to another, e.g., from analog to digital (A/D), digital to analog (D/A), parallel to serial, or serial to parallel.

data converter **1.** A circuit or device for performing DATA CONVERSION. **2.** An analog-to-digital (A/D) converter. **3.** A digital-to-analog (D/A) converter. **4.** A parallel-to-serial converter. **5.** A serial-to-parallel converter.

data description The description of a unit of data, as included in a computer source program.

data display A device, such as a cathode-ray tube (CRT) or liquid-crystal display (LCD), that presents data for visual examination. Compare DATA PRINTOUT.

data element **1.** A component of a data signal (e.g., a number, letter, symbol, or the equivalent electrical pulses). **2.** A device or circuit for acquiring or processing data. **3.** A unit of data (e.g., a field in a file).

data-flow diagram A block diagram showing the movement of data through a data-processing system.

data format The form of data in a record or file (e.g., character format or numerical format).

data gathering See DATA COLLECTION.

data-handling capacity **1.** The amount of data that can be stored in a memory circuit. **2.** The amount of data that can be transmitted over a certain medium. **3.** The rate at which data can be transferred under certain conditions.

data-handling system A system that gathers, routes, transmits, or receives data, but does not necessarily process it.

data item A logical element (character, byte, or bit) describing a characteristic of a record used by a system for which there is a specific application.

data level Descriptive, through a programming language, of the relative weight of logical elements (data items) in a computer record. Also called *data hierarchy.*

data link The portion of a computer system that gathers data and, if necessary, converts it to a form acceptable by a computer.

data matrix Variables and their possible values stored as a series of columns and rows of values in a computer memory.

data name An operand specified in a computer source program.

data pickup **1.** A transducer that collects data signals from a source; it converts nonelectrical data into corresponding electrical signals and delivers its output to a data processing system. **2.** Data acquisition.

data playback The reproduction of data signals stored by some method of data recording.

data plotter See X-Y PLOTTER.

data printout **1.** A device that prints a record of data or the results of a computation. **2.** A permanent printed record, usually of a calculation or computation—especially the printed output of a computer peripheral device.

data processing Work performed on acquired data, as in solving problems, making comparisons, classifying material, organizing files. Usually done by a computer.

data-processing equipment A digital computer and the peripheral equipment needed to collate, store, analyze, and reduce data.

data-processing machine A computer or system used to collate, store, analyze, and reduce data, as opposed to a computer or system used primarily to solve problems or perform routine tasks. Also called *data processor.*

data-processing system An electronic system for automatic data processing. It can be based on analog and/or digital techniques.

data processor See DATA-PROCESSING MACHINE.

5059F-pD-163-223 4/9/01 5:22 PM Page 166

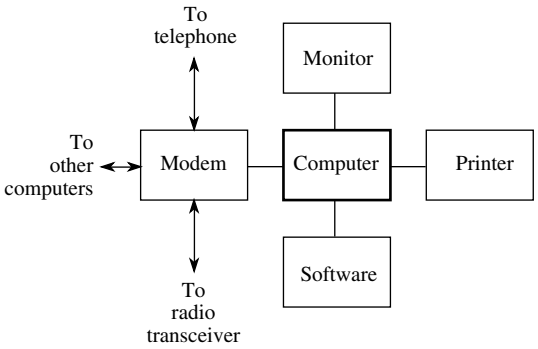

data-processing system

data receiver At a particular point in a data-processing system, a circuit or device for receiving data from a data transmitter.

data reception Receiving data signals from some point within or outside a data-processing system.

data-reception system A data receiver and its associated equipment.

data record A computer-processed record containing a data unit.

data recorder A machine for storing data acquired in the form of electrical signals (see DATA RECORDING).

data recording **1.** The preservation of data signals by some process, such as magnetic-disk encoding, optical-disk encoding, or tape recording, for future use or as a backup. **2.** A record of data signals, as on magnetic tape.

data reduction The summarization of a mass of electronically gathered data.

data-reduction system A system used to minimize the amount of data necessary to convey given information.

data representation Values and data as described by numerals, symbols, and letters (e.g., computer program instructions).

data segment As related to a particular computer process, a subunit of allocated storage containing data only.

data selector/multiplexer A digital circuit that has several or many input signals, and feeds one of them onto a common line.

data set A device that connects a data processor to a telegraph or telephone line.

data signal **1.** A signal (such as one of binary bit combinations) that can represent data as numbers, letters, or symbols. **2.** A signal current or voltage proportional to some sampled quantity, and that can be used to actuate indicating instruments during tests or measurements.

data statement A computer source program statement identifying a data item and specifying its format.

data storage The preservation of data, particularly computer files, for long periods of time in nonvolatile form (no source of power is required to ensure that the data remains intact).

data storage media Hardware that preserves data, particularly computer files, for long periods of time in nonvolatile form (no source of power is required to ensure that the data remains intact). Common media include magnetic disks, magnetic tape, and optical disks.

data synchronizer A device used to synchronize data transmission within a computing or processing system.

data system **1.** An arrangement for collecting, recording, and routing data in the form of electrical signals. **2.** An arrangement for processing data (i.e., for correlating, computing, routing, storing, etc.).

data terminal A remote input/output device connected to a central computer.

data throughput In a computer system, the amount of data per unit time (bytes, kilobytes, megabytes, gigabytes, or terabytes per second or minute) that can be transferred from one place to another.

data transducer In tests and measurements, a transducer that converts a monitored phenomenon into electrical quantities that can be used for computer analysis or calculations.

data transmission Sending data signals from a pickup point or processing stage to another point within a data-processing system; also, sending such signals to points outside the system.

data-transmission system A data transmitter and its associated equipment.

data transmission utilization measure The ratio of the useful data output of a data-transmission system to the total data input.

data transmitter A circuit or device for sending data from point to point within or outside of a data-processing system.

data unit Characters in a group that are related in a way that makes them a meaningful whole (e.g., a text word, or an object such as a circle in vector graphics).

data value A measure of the amount of information contained in a certain number of data bits. The greater the ratio of the actual information to the number of bits, the higher the data value.

data words In digital computer operations, words (bit groups) representing data, rather than program instructions.

DAVC Abbreviation of DELAYED AUTOMATIC VOLUME CONTROL.

David Phonetic alphabet code word for letter D.

daylight effect The modification of transmission paths during the day because of ionization of the upper atmosphere by solar radiation.

daylight lamp An incandescent lamp whose filament is housed in a blue glass bulb, which absorbs some red radiation and transmits most of

5059F-pD-163-223 4/9/01 5:22 PM Page 167

the green, blue, and violet. So called because the spectral output resembles that of typical daylight.

daylight range The distance over which signals from a given transmitter are consistently received during the day.

DB **1.** Abbreviation of DIFFUSED BASE of a transistor. **2.** Abbreviation of DOUBLE BREAK (relay).

dB **1.** Abbreviation of DECIBEL or *decibels.* **2.** Symbol for *differential of susceptance.*

dBa Abbreviation of ADJUSTED DECIBELS.

dBc Abbreviation of *decibels referred to the carrier.*

DBD Abbreviation of *double-base diode.*

dBd The power gain of an antenna in the direction of maximum radiation, compared to the radiation in the favored direction of a half-wave dipole in free space receiving the same amount of power. Expressed in decibels.

dBi The power gain of an antenna in the direction of maximum radiation, compared to the radiation from a theoretical isotropic antenna in free space receiving the same amount of power. Expressed in decibels.

dBj The level of an RF signal, in decibels, relative to 1 millivolt.

dBk Abbreviation of DECIBELS REFERRED TO 1 KILOWATT.

DBM Abbreviation of *database management.*

dBm Abbreviation of DECIBELS REFERRED TO 1 MILLIWATT.

dBm0 Signal level in dBm, referred to a zero-transmission level.

dBm0p Noise in dBm0, measured with set phosphometric weighting.

dB meter A usually high-impedance ac voltmeter with a scale reading directly in decibels.

dBmp The level in dBm, measured with phosphometric weighting. Generally equal to dBm –2.5, for a noise level that is flat within the communications audio range.

dBmr Decibels measured with respect to zero transmission level.

dBmV Abbreviation of DECIBELS REFERRED TO 1 MILLIVOLT.

dBrap Abbreviation of DECIBELS ABOVE REFERENCE ACOUSTIC POWER (10^{-6} W).

dBrn Abbreviation for *decibels above reference noise.* A level of 0 dBrn is defined as noise power of 10^{-9} W (1 nanowatt).

dBrnc Noise power in dBrn for a circuit with message weighting c.

dBrnc0 Noise in dBrnc measured with respect to zero transmission level.

dBV Abbreviation of DECIBELS REFERRED TO 1 VOLT.

dBW Abbreviation of DECIBELS REFERRED TO 1 WATT.

dBx Abbreviation of DECIBELS ABOVE REFERENCE COUPLING.

dC Symbol for *differential of capacitance.*

dc **1.** Abbreviation of DIRECT CURRENT. **2.** Abbreviation of *direct-coupled.*

dc-ac converter A circuit that converts a dc input voltage into an ac output voltage, with or without step-up or step-down. Also called INVERTER.

dc alpha The current amplification factor (ALPHA) of a common-base transistor stage for a dc input (emitter) signal. Compare DC BETA.

dc amplifier **1.** A *direct-coupled amplifier.* 2. An amplifier for boosting direct-current signals.

dc balance **1.** Adjustment of a circuit or device for dc stability or dc null. **2.** Adjustment of a circuit for dc stability during gain changes. **3.** A potentiometer or other variable component used to stabilize or null a dc circuit.

dc bar See DC BUS.

dc base current Symbol, $I_{B(dc)}$. The static direct current in the base element of a bipolar transistor.

dc base resistance Symbol, $R_{B(dc)}$. The static dc resistance of a bipolar transistor's base element; $R_{B(dc)} = V_B/I_B$.

dc base voltage Symbol, $V_{B(dc)}$. The static dc voltage at the base element of a bipolar transistor.

dc beta The current amplification factor (BETA) of a common-emitter-connected transistor for a dc input (base) signal. Compare DC ALPHA.

dc block A coaxial section that has a capacitance in series with the inner or outer conductor, or both, to block dc while passing RF. Compare DC SHORT.

dc bus A supply conductor carrying direct current only.

dcc Abbreviation of double cotton covered (wire).

dc cathode current Symbol, $I_{K(dc)}$. The static direct current in the cathode element of an electron tube.

dc cathode resistance Symbol, $R_{K(dc)}$. The static dc resistance of the cathode path of an electron tube.

dc cathode voltage Symbol, $V_{K(dc)}$. The static dc voltage at the cathode of an electron tube.

dc circuit breaker A circuit breaker operated by direct-current overload or underload, depending on its design and application.

dc collector current Symbol, $I_{C(dc)}$. The static direct current in the collector element of a bipolar transistor.

dc collector resistance Symbol, $R_{C(dc)}$. The static dc resistance of a bipolar transistor's collector element; $R_{C(dc)} = V_C/I_C$.

dc collector voltage Symbol, $V_{C(dc)}$. The static dc voltage at the collector element of a bipolar transistor.

dc component In a complex wave (i.e., one containing both ac and dc), the current component having an unchanging polarity. The dc component constitutes the mean (average) value around which the ac component alternates, pulsates, or fluctuates.

dc converter A dynamoelectric machine for converting low-voltage dc into higher-voltage dc. It is essentially a low-voltage dc motor coupled me-

5059F-pD-163-223 4/9/01 5:22 PM Page 168

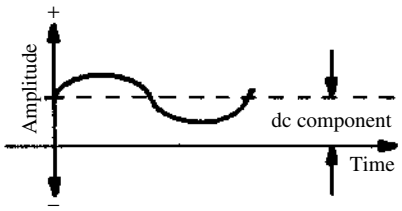

dc component

chanically to a higher-voltage dc generator. Compare DC INVERTER.

dc coupling See DIRECT COUPLING.

dc drain current Symbol, $I_{D(dc)}$. The static direct current in the drain element of a field-effect transistor.

dc drain resistance Symbol, $R_{D(dc)}$. The static dc resistance of an FET's drain element; $R_{D(dc)} = V_D/I_D$.

dc drain voltage Symbol, $V_{D(dc)}$. The static dc voltage at the drain element of a field-effect transistor.

dc dump In digital computer operation, removing dc power from a computer, which would eradicate material stored in a volatile memory.

dc emitter current Symbol, $I_{E(dc)}$. The static direct current in the emitter element of a bipolar transistor.

dc emitter resistance Symbol, $R_{E(dc)}$. The static dc resistance of a bipolar transistor's emitter element; $R_{E(dc)} = V_E/I_E$.

dc emitter voltage Symbol, $V_{E(dc)}$. The static dc voltage at the emitter element of a bipolar transistor.

dc equipment Apparatus designed expressly for operation from a dc power supply. Compare AC EQUIPMENT and AC/DC.

dc erase head In a magnetic recorder, a head supplied with a dc current for the purpose of removing data.

dc error voltage In a television receiver, the dc output of the phase detector, which is used to control the frequency of the horizontal oscillator.

dc gate current Symbol, $I_{G(dc)}$. The very small static direct current in the gate element of a field-effect transistor.

dc gate resistance Symbol, $R_{G(dc)}$. The very high, static dc resistance of an FET's gate element; $R_{G(dc)} = V_G/I_G$.

dc gate voltage Symbol, $V_{G(dc)}$. The static dc voltage at the gate element of a field-effect transistor.

dc generator **1.** A rotating machine (dynamo) for producing direct current. Also see DYNAMOELECTRIC MACHINERY. **2.** Generically, a device that produces direct current: batteries, photocells, thermocouples, etc.

dc generator amplifier A special type of generator that provides power amplification. The input signal energizes the field winding of a constant-speed machine; because the output voltage is proportional to field flux and armature speed, a high output voltage is obtained. Also see AMPLIDYNE.

dc grid bias Steady dc control-grid voltage used to set the operating point of an electron tube.

dc grid current Symbol, $I_{G(dc)}$. The static direct current in the control-grid element of an electron tube.

dc grid resistance Symbol, $R_{G(dc)}$. The static dc resistance in the control-grid element of an electron tube; $R_{G(dc)} = V_G/I_G$.

dc grid voltage Symbol, $V_{G(dc)}$. The static dc voltage at the control grid of an electron tube.

dc inserter In a television transmitter, a stage that adds the dc pedestal (blanking) level to the video signal.

dc inverter An electrical, electronic, or mechanical device that converts dc to ac. Also called INVERTER.

dcl Abbreviation of *dynamic load characteristic.*

dc leakage The unintended flow of direct current.

dc leakage current **1.** The direct current that normally passes through a correctly polarized electrolytic capacitor operated at its rated dc working voltage. **2.** The zero-signal reverse current in a semiconductor pn junction.

DCM Abbreviation of DIGITAL CAPACITANCE METER.

D/CMOS Combination of DMOS and CMOS on a monolithic chip.

dc motor A motor that operates from direct current only.

dc noise Noise heard during the playback of magnetic tape that was recorded while direct current was in the record head.

dc noise margin In a digital or switching circuit, the difference $V_o - V_i$, where V_o is the output-voltage level of a driver gate and V_i is the input threshold voltage of a driven gate.

dc operating point For a bipolar transistor, field-effect transistor, or vacuum tube, the static, zero-signal dc voltage and current levels.

dc overcurrent relay A relay or relay circuit actuated by dc coil current rising above a specified level. Compare DC UNDERCURRENT RELAY.

dc overvoltage relay A relay or relay circuit actuated as a result of the dc coil voltage rising above a specified level. Compare DC UNDERVOLTAGE RELAY.

dc patch bay A patch bay in which the dc circuits of a system are terminated.

dc picture transmission In television, transmission of the dc component of the video signal; this component corresponds to the average illumination of the scene.

dc plate current Symbol, $I_{P(dc)}$. The static direct current in the plate element of an electron tube.

dc plate resistance Symbol, $R_{P(dc)}$. The static dc resistance of the internal plate-cathode path of an electron tube; $R_{P(dc)} = V_P/I_P$.

5059F-pD-163-223 4/9/01 5:22 PM Page 169

dc plate voltage Symbol, $V_{P(dc)}$. The static dc voltage at the plate electrode of an electron tube.

dc positioning Alignment of the spot on the screen of an oscilloscope tube, by means of adjustable dc voltages applied to the horizontal and vertical deflecting plates.

dc power Symbol, P_{dc}. Unit, watt. The power in a dc circuit; $P_{dc} = EI$, where E is in volts and I is in amperes. Compare AC POWER. Also see POWER.

dc power supply A power unit that supplies direct current only. Examples: battery, transformer/rectifier/filter circuit, dc generator, and photovoltaic cell. Compare AC POWER SUPPLY.

dc relay A relay having a simple coil and core system for closure by direct current, which can be rectified ac.

dc resistance Resistance offered to direct current, as opposed to in-phase ac resistance.

dc resistivity The resistivity of a sample of material measured using a pure dc voltage under specified conditions (physical dimensions, temperature, etc.).

dc restoration The reinsertion of the dc component into a signal from which the component has been extracted through a capacitor or transformer.

dc restorer A circuit that reinserts the average dc component of a signal after the component has been lost because the signal passed through a capacitor or transformer.

DCS Abbreviation of DORSAL COLUMN STIMULATOR.

dc shift A shift in the DC OPERATING POINT.

dc short A coaxial fitting providing a dc path between the center and outer conductors, while permitting radio-frequency (RF) current to flow easily through the coaxial section. Compare DC BLOCK.

dc signaling A signaling procedure that uses direct current as the medium (e.g., simple wire telegraphy or telephony).

dc source **1.** DC GENERATOR. **2.** A live circuit point from which one or more direct currents can be taken.

dc source current Symbol, $I_{S(dc)}$. The static direct current in the source element of a field-effect transistor.

dc source resistance Symbol, $R_{S(dc)}$. The static dc resistance of an FET's source element.

dc source voltage Symbol, $V_{S(dc)}$. The static dc voltage at the source element of a field-effect transistor.

DCTL Abbreviation of DIRECT-COUPLED TRANSISTOR LOGIC.

dc-to-dc inverter See DC INVERTER.

dc transducer **1.** A transducer that depends on direct current for its operation (i.e., it has a dc power supply whose output is modulated by the sensed phenomenon). **2.** A transducer that converts a direct current into some other form of energy, such as heat, pressure, or sound.

dc transformer A dc-to-dc converter providing voltage step-up. The applied dc is usually first converted to ac, which is then stepped up by a transformer. The higher-voltage ac is then rectified to produce a high dc output voltage.

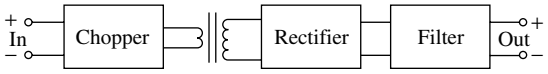

dc transformer

dc transmission **1.** Sending dc power from a generating point to a point of use. **2.** In television transmission, the retention of the dc component in the video signal.

dc tuning voltage The capacitance-varying dc voltage applied to a varactor in an inductance-capacitance (LC) tuned circuit.

dcu Abbreviation of decimal counting unit.

dc undercurrent relay A relay or relay circuit that is actuated as a result of the dc coil current dropping below a specified level. Compare DC OVERCURRENT RELAY.

dc undervoltage relay A relay or relay circuit that is actuated as a result of the dc voltage dropping below a specified level. Compare DC OVERVOLTAGE RELAY.

dcv Abbreviation of DC VOLTS or DC VOLTAGE.

dc voltage Abbreviation, dcv. A voltage that does not change in polarity, an example being the voltage delivered by a battery or dc generator. Also see VOLTAGE.

dc working voltage Abbreviation, dcwv. The rated dc voltage at which a component can be operated continuously with safety and reliability.

dc working volts Abbreviation, dcwv. The actual value, expressed in volts, of a DC WORKING VOLTAGE.

dcwv Abbreviation of DC WORKING VOLTAGE.

dD Symbol for *differential of electric displacement.*

DDA Abbreviation of *digital differential analyzer.*

DDD Abbreviation of DIRECT DISTANCE DIALING (telephone).

D display See D SCOPE.

DE Abbreviation of *decision element.*

dE Symbol for *differential of voltage.*

deac In frequency-modulation (FM) receivers, a device used for deemphasis. The name is short for *deaccentuator.*

deactuating pressure For an electrical contact, the pressure at which contact is made or broken as the pressure reaches the level of activation.

dead **1.** Unelectrified. **2.** Lacking electromagnetic signals or fields. **3.** Electrically or mechanically inoperative.

dead band **1.** A radio-frequency band on which no signals are heard. **2.** A range of values for which an applied control quantity (e.g., current or voltage) has no effect on the response of a circuit.

5059F-pD-163-223 4/9/01 5:22 PM Page 170

deadbeat The state wherein a moving body (such as the pointer of a meter or the voice coil of a loudspeaker) comes to rest without overswing or oscillation.

deadbeat galvanometer See DEADBEAT INSTRUMENT.

deadbeat instrument A meter or recorder that is highly damped to ensure that overswing or oscillation does not occur.

deadbeat meter See DEADBEAT INSTRUMENT.

dead break An unreliable contact of a relay, caused by insufficient pressure.

dead circuit A circuit that is electrically disabled.

dead end The unused end of a tapped coil (i.e., the turns between the end of the coil and the last turn used).

dead-end tower A supporting tower for an antenna or transmission line that can withstand stresses caused by loading or pulling.

dead file A computer file that is not in use, but is being kept in a record.

dead front panel A metal panel that, for safety and desensitization, is completely insulated from voltage-bearing components mounted on it; it is often grounded.

dead interval See DEAD TIME.

dead line A deenergized line or conductor.

dead period See DEAD TIME.

dead room An anechoic room in which acoustic tests and studies are made.

dead short A short circuit with extremely low (virtually no) resistance from dc into the radio-frequency spectrum.

dead space See DEAD BAND.

dead spot **1.** An area in which radio waves from a particular station are not received. **2.** On a vacuum-tube cathode (directly or indirectly heated), a spot from which no electrons are emitted.

dead stretch The tendency of insulating materials to permanently retain their approximate dimensions after having been stretched.

dead time **1.** DOWN TIME. **2.** An interval during which there is no response to an actuating signal. **3.** In a computer system, an interval between related events that is allocated to prevent interference between the events.

dead volume In a pressure transducer, the zero-stimulus volume of the pressure port cavity.

dead zone See ZONE OF SILENCE.

debatable time Computer time that cannot be placed in any other category.

debounced switch A switch in sensitive computer or control systems that has circuitry for eliminating the electrical effects of bounce (see BOUNCE, **1**).

de Broglie waves Electromagnetic waves that are believed to be associated with moving particles (such as electrons, protons, and neutrons).

debug **1.** To eliminate errors in, and maximize the efficiency of, a computer program or group of programs. **2.** To optimize the design and construction of electronic equipment.

debugging A process by which engineers eliminate the flaws in a circuit, machine, or computer program.

debugging aid routine A computer program used to test other programs.

debugging period The time interval following completion of a software design, a hardware interconnection, or the manufacture of a piece of electronic equipment, during which errors and imperfections are sought and corrected.

debunching In a velocity-modulated tube, such as a Klystron, a beamspreading space-charge effect that destroys electron bunching.

Debye length The maximum distance between an electron and a positive ion over which the electron is influenced by the field of the ion.

Debye shielding distance See DEBYE LENGTH.

deca- A prefix that indicates multiplication by 10.

decade **1.** A frequency band whose upper limit is 10 times the lower limit. Example: 20 Hz to 200 Hz. **2.** A set of 10 switched or selectable components in which the total value is 10 times that of individual values. Example: a *decade capacitor*. Also called DECADE BOX. **3.** A group, sometimes a unit of access, of 10 computer storage locations.

decade amplifier An amplifier or preamplifier whose gain can be adjusted in increments of 10 (×1, ×10, ×100, etc.).

decade box A group of components that provides values in 10 equal steps selected by a switch or jacks. For compactness, the components and the associated hardware are enclosed in a box or can. See, for example, DECADE CAPACITOR.

decade capacitor A composite capacitor whose value is variable in 10 equal steps. For example, the values might be set at 100 picofarads (pF), 200 pF, 300 pF, etc., up to 1000 pF. Compare DECADE INDUCTOR and DECADE RESISTOR.

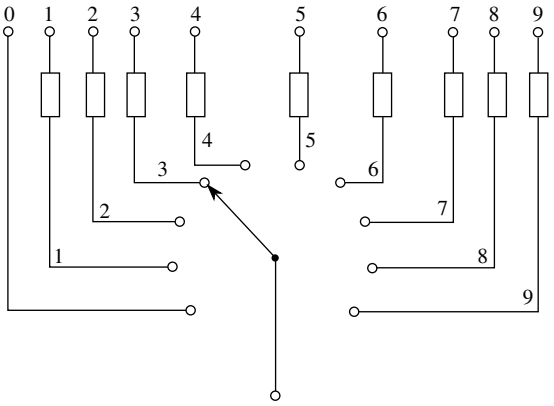

decade box

5059F-pD-163-223 4/9/01 5:22 PM Page 171

decade counter A counter (see COUNTER, **1**, **2**) in which the numeric display is divided into sections, each having a value 10 times that of the next and displaying a digit from zero to nine.

decade inductor An inductor whose value is variable in 10 equal steps. Compare DECADE CAPACITOR and DECADE RESISTOR.

decade resistor A resistor whose value is variable in 10 equal increments. Compare DECADE CAPACITOR and DECADE INDUCTOR.

decade scaler A scale-of-10 electronic counter (i.e., a circuit delivering one output pulse for each group of 10 input pulses).

decametric waves Waves in the 10- to 100-meter band (30 to 3 MHz).

decay **1.** The decrease in the value of a quantity, e.g., current decay in a resistance-capacitance circuit. **2.** The gradual, natural loss of radioactivity by a substance.

decay characteristics **1.** The decay of a parameter; usually an exponential function. **2.** The persistence time in a storage oscilloscope.

decay curve A curve, usually logarithmic, representing the function of quantity versus time for a signal decrement, the decrement of radioactivity, or other natural process.

decay rate A quantitative expression for the rapidity with which a quantity decreases. Generally listed in decibels per second (dB/s) or decibels per millisecond (dB/ms).

decay time The time required for pulse amplitude to fall from 90% to 10% of the peak value. Also called FALL TIME.

Decca A 70- to 130-kHz CW radio navigation system (British).

decelerated electron A high-speed electron that is abruptly decelerated upon striking a target, causing X-rays to be emitted.

decelerating electrode A charged electrode that slows the electrons in an electron beam.

deceleration Acceleration that results in a decrease in speed.

deceleration time **1.** The time taken by magnetic tape to stop moving after the last recording or playback has finished. **2.** The time taken by a mechanical data storage medium, such as a hard disk, to come to rest after completion of a read or write operation, or on powering-down.

decentralized data processing Data processing in which the computing equipment is distributed among managerial subgroups.

deception A method of producing misleading echoes in enemy radar.

deception device A radar device, or radar-associated device, for deception.

deci- Abbreviation, d. A prefix meaning one-tenth (10^{-1}). Examples: DECIBEL, DECIMETER.

decibel Abbreviation, dB. A practical unit of relative gain. In terms of power, the relative gain in decibels is equal to:

$$\text{Gain (dB)} = 10 \log_{10}(P_{out}/P_{in}),$$

where P_{out} is the output power and P_{in} is the input power. For voltage, if the input and output impedances are the same, the gain in decibels is given by:

$$\text{Gain (dB)} = 20 \log_{10}(V_{out}/V_{in}),$$

where V_{out} is the output voltage and V_{in} is the input voltage. For current, if the input and output impedances are the same, the gain in decibels is given by:

$$\text{Gain (dB)} = 20 \log_{10}(I_{out}/I_{in}),$$

where I_{out} is the output current and I_{in} is the input current. Losses are indicated by negative dB gain values.

decibels above reference acoustic power Abbreviation, dBrap. The ratio of a given acoustic power level to a lower reference acoustic power level, specified in decibels.

decibels above reference noise Abbreviation, dBrn. The ratio of the noise level at a selected point in a circuit to a lower reference noise level, in decibels.

decibels referred to 1 millivolt Abbreviation, dBmV. The relative voltage level of a signal when compared with a 1-mV signal measured at the same terminals.

decibels referred to 1 milliwatt Abbreviation, dBm. The ratio, in decibels, of an applied power level to the power level of 1 mW.

decibels referred to 1 volt Abbreviation, dBV. The ratio, in decibels, of a given voltage to 1 V, expressed in decibels.

decibels referred to 1 watt Abbreviation, dBW. The ratio of a given power level to the power level of 1 W, expressed in decibels.

decider See DECISION ELEMENT.

decigram A unit of mass equal to 0.1 gram.

deciliter A unit of volume equal to 0.1 liter, or 10^{-4} cubic meter.

decilog A unit equal to 0.1 times the common logarithm of a ratio.

decimal **1.** Pertaining to the base-10 number system (see DECIMAL NUMBER SYSTEM). **2.** A base-10 numerical fraction, represented by figures to the right of the radix point (decimal point), and arranged serially according to negative powers of 10. Examples: $0.12 = 1.2 \times 10^{-1}$, $0.00135 = 1.35 \times 10^{-3}$.

decimal attenuator An attenuator circuit whose resistances are chosen for attenuation in decimal steps. Thus, one section provides attenuation in steps of 0.1 times the applied voltage, another in steps of 0.01 times the applied voltage, another in steps of 0.001 times the applied voltage, etc.

decimal code A method of defining numbers, in which each place has a value of ten times that immediately to the right.

5059F-pD-163-223 4/9/01 5:22 PM Page 172

decimal-coded digit **1.** A numeral from 0 to 9. **2.** A numeral in the DECIMAL NUMBER SYSTEM. **3.** A binary representation of a decimal value from 0 to 9.

decimal digit A numeral from 0 to 9.

decimal equivalent The decimal number equal to a given fraction (e.g., the decimal equivalent of $^{21}/_{64}$ is 0.3281).

decimal fraction See DECIMAL, 2.

decimal notation See DECIMAL NUMBER SYSTEM.

decimal number system The familiar base-10 or radix-10 number system, in which the digits 0 through 9 represent values according to their position, relative to the decimal point (also called the *radix point*). Positions to the left of the point represent successive positive powers of 10, and those to the right represent successive negative powers of 10.

decimal point The radix point in a decimal number. It serves to separate the integral part from the fractional part of the number.

decimeter waves See MICROWAVES.

decimetric waves Electromagnetic waves having lengths ranging from 0.1 meter to 1 meter (3000 MHz to 300 MHz). Also known as *ultrahigh frequency (UHF)*.

decineper A natural-logarithmic unit equal to 0.1 *neper*.

decipher See DECODING, **3**.

decision **1.** A choice based on the evaluation and comparison of data, and the identification of a specified objective. **2.** In digital computer operations, the automatic selection of the next step in a sequence, on the basis of data being compared by a relational test.

decision box A block on a computer flowchart indicating the point at which a decision (see DECISION, **2**) must be made as to which of several branches the program will take.

decision elements See LOGIC CIRCUITS.

decision instruction A computer program instruction to compare the values of operands and take an appropriate action, as per the BASIC instruction "IF A = B THEN GO TO (line number)."

decision procedure In decision theory, a series of calculations made to optimize the speed or efficiency of a process, or to minimize risk, failure, cost, etc.

decision theory A statistical discipline concerned with identifying and evaluating choices and alternatives, and determining the best sequence of steps to take in reaching an objective.

decision tree In decision theory, a diagram showing alternative choices, so called from its resemblance to a tree with branches.

decision value A value that defines the boundary between two intervals in the encoding process.

deck **1.** See TAPE DECK. **2.** A pack of punched cards in a computer file.

declarative macroinstruction As part of an assembly language, instructions to the compiler to do something or record a condition without affecting the object program.

declarative statement A computer source program instruction specifying the size, format, and kind of data elements and variables in a program for a compiler.

declination **1.** The angle representing the deviation of magnetic north from true north; it is the angle subtended by a freely turning magnetic needle and the meridian. Compare INCLINATION. **2.** Celestial latitude.

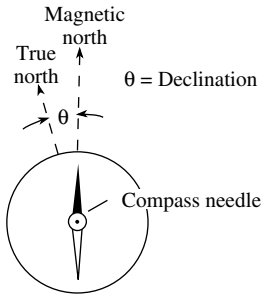

declination, 1

declinometer An instrument for measuring declination.

decode **1.** To unscramble a coded message. **2.** In digital computer operations, to deliver a specific output from character-coded inputs. **3.** In a multiplex system, the separation of the subcarrier from the main carrier.

decoder A circuit or device for performing DECODING.

decoder/demultiplexer A circuit that places an input signal on a selected output line.

decoder/driver An integrated circuit containing a decoder and driver.

decoding **1.** In computer and data-processing operations, DIGITAL-TO-ANALOG CONVERSION. **2.** The conversion to English of a message received in a code. **3.** Translating a message from a secret code (i.e., deciphering a message). **4.** The automatic conversion of a signal into the appropriate switching action (as the enabling of a transmitter or receiver by a tone in a selective calling system).

decoding circuit A circuit intended for the purpose of translating a code into ordinary language.

decollator An offline computer device for separating the parts of output continuous stationery sets. Also see CONTINUOUS STATIONERY.

decommutation The extraction of a signal component from the composite signal, resulting from commutation.

5059F-pD-163-223 4/9/01 5:22 PM Page 173

decommutator A circuit or device for performing decommutation, including demodulators, demultiplexers, and signal separators.

decoupler A device that isolates two circuits so that a minimal amount of coupling exists between them.

decoupling The elimination or effective minimization of coupling effects, as in decoupling amplifier stages to prevent interaction through a common power-supply lead.

decoupling capacitor **1.** A capacitor that provides a low-impedance path to ground to prevent undesired stray coupling among the circuits in a system. **2.** The capacitive member of a resistance-capacitance (RC) decoupling filter.

decoupling filter A resistance-capacitance (RC) filter, usually inserted into a common dc line in a multistage amplifier to prevent interstage feedback coupling through the common impedance of the line.

decoupling network One or more decoupling filters.

decoupling resistor The resistive member of a resistance-capacitance (RC) decoupling filter.

decoy In radar, an object that provides misleading reflections. Also see CHAFF.

decreasing function A function whose curve has a negative slope at all points in the domain.

decrement **1.** Also called *logarithmic decrement.* The rate at which a damped wave dies down. The decrement value is the natural (base-*e*) logarithm of the ratio of two successive peaks of the same polarity. **2.** A quantity used to lessen the value of a variable. **3.** To lower the value (of a register, for example) by a single increment.

decremeter An instrument for measuring the decrement of a radio wave.

decremeter capacitor A variable capacitor for use in a decremeter. The rotor plates are shaped so that equal angular rotations correspond to the same decrement at all settings. Thus, the percentage of capacitance change for a given angle of rotation is constant throughout the capacitance range.

decryption The conversion of an encrypted signal from a cipher into plain text, graphics, or other commonly recognizable form. Also see CIPHER. Compare ENCRYPTION.

decryption key An algorithm, or a set of algorithms, that converts an encrypted signal from a cipher into plain text, graphics, or other commonly recognizable form. Each cipher has its own unique algorithm or set of algorithms for this purpose. The signal cannot be decrypted unless all the components of the key are present.

dedicated Assigned exclusively to a certain purpose [e.g., a dedicated facsimile (fax) line].

deductive logic A form of symbolic logic used to demonstrate that a certain conclusion will always follow, given a certain set of circumstances. The logic of digital circuits is deductive. Compare INDUCTIVE LOGIC.

dee In a cyclotron, one of the D-shaped chambers in and between which particles accelerate in a spiral path to high velocity.

dee line In a cyclotron, a support for the dee, with which it forms a resonant circuit.

deemphasis In frequency modulation, the introduction of a low-pass characteristic (response falls as modulating frequency increases) to complement the rising response of preemphasis. Also called *postemphasis* or *postequalization.* Compare PREEMPHASIS.

deemphasis amplifier An amplifier used to remove the high-frequency preemphasis applied to signals prior to broadcasting, multiplexing, tape recording, or telemetering. Also see DEEMPHASIS and PREEMPHASIS.

deemphasis circuit A low-pass filter that provides deemphasis in an FM receiver.

deemphasis network See DEEMPHASIS CIRCUIT.

deenergize To take a circuit or device out of operation (i.e., to remove its power or signal excitation).

deep cycle Pertaining to a rechargeable cell or battery that can operate until it is almost completely discharged. It generally has a high ampere-hour capacity.

deep-diffused junction A pn junction made by diffusing the impurity material deep in the semiconductor wafer. Compare SHALLOW-DIFFUSED JUNCTION.

deep discharge The nearly complete discharge of a cell or battery; usually done prior to recharging.

deep-space net A radar system intended for constant monitoring of spacecraft.

defeating **1.** The disabling or circumvention of an alarm or security system, leaving the protected property vulnerable to intrusion. **2.** The dangerous, and potentially lethal, disabling of a safety device in an electrical or electronic system.

defect **1.** Absence of an electron (hence, presence of a hole) in the lattice of a semiconductor crystal. **2.** An abnormality of design, construction, or performance of an electronic circuit or device. **3.** In a computer system, a hardware or software fault that could be the eventual cause of a failure. **4.** A flaw in a crystalline substance.

defect conduction In a semiconductor material, conduction via holes.

deferred addressing Indirect addressing in which a preset counter makes several references to find a desired address.

deferred entry An entry into a computer subroutine, delayed because of a delay in the exit from a control program.

deferred exit An exit from a computer subroutine, delayed because of a particular command.

defibrillation Use of a CARDIAC STIMULATOR to halt fibrillation of the heart, as caused by electric shock.

defibrillator See CARDIAC STIMULATOR.

definite-purpose component A component designed for a specific use, rather than for a wide

5059F-pD-163-223 4/9/01 5:22 PM Page 174

range of possible applications (e.g., a video detector diode, as opposed to a general-purpose diode). Compare GENERAL-PURPOSE COMPONENT.

definition **1.** Clarity of a video image (i.e., one having good contrast and faithful tones). **2.** Good intelligibility of reproduced sounds.

deflecting coil One of a set of external coils carrying sawtooth currents, which provide electromagnetic deflection of the cathode-ray beam in picture tubes, camera tubes, radar display tubes, sonar display tubes, and some oscilloscopes. Also called *deflection coil.*

deflecting electrode An electrode, such as a deflecting plate, used to alter the direction an electron beam. Also called *deflection electrode.*

deflecting plate In a cathode-ray tube, a plate that attracts or repels the electron beam, causing the spot to move horizontally or vertically on the screen. Also called *deflection plate.*

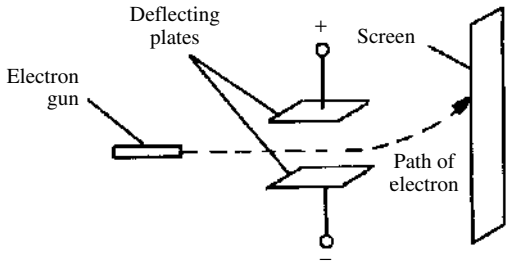

deflecting plate

deflecting torque The torque required to move the pointer of a meter, or the pen or mirror of a recorder.

deflection **1.** In a cathode-ray tube, movement of the electron beam by electric or magnetic fields. **2.** Movement of the pointer of a meter or the pen or mirror of a recorder by an applied current or voltage.

deflection factor Symbol, G. The reciprocal of DEFLECTION SENSITIVITY.

deflection plane In a cathode-ray tube, the plane perpendicular to the axis of the tube. This plane contains the electromagnetic and/or electrostatic lines of flux that result in deflection of the electron beam.

deflection coil See DEFLECTING COIL.

deflection electrode See DEFLECTING ELECTRODE.

deflection plate See DEFLECTING PLATE.

deflection polarity In a cathode-ray tube, the polarity of the voltage applied to a particular deflecting plate to move the electron beam in a particular direction.

deflection sensitivity Symbol, S. A quantitative measure of the extent to which the input voltage will displace the electron beam on the screen of an electrostatic cathode-ray tube. Expressed in volts per centimeter (V/cm) or volts per inch (V/in).

deflection voltage The potential difference between the deflection plates of an electrostatic cathode-ray tube. It is used to control the direction of the electron beam striking the phosphor screen.

deflection yoke An assembly of deflection coils in picture and camera tubes, and in some magnetically deflected oscilloscope tubes. The usual combination is two series-connected horizontal deflection coils and two series-connected vertical deflection coils.

deflector **1.** A beam-forming plate in a beam-power tube. **2.** A deflection plate in a cathode-ray tube. **3.** A deflection coil or yoke in a picture tube, camera tube, or magnetic-deflection oscilloscope tube. **4.** A mechanical attachment for improving the angle of radiation of a loudspeaker by spreading the higher-frequency waves.

defocusing Blurring of the image on the screen of a cathode-ray tube, caused by spreading of the electron beam.

deformation potential The voltage generated when a crystal lattice is subjected to pressure. An example is the voltage produced by a crystal microphone when acoustic waves strike the crystal.

defruiting The elimination of non-synchronized echoes in a radar system.

deg Abbreviation of DEGREE.

degassing During the evacuation of a vacuum tube or similar device, the removal of gas, including that which has bonded to the glass and metal parts.

degauss See DEMAGNETIZE.

degausser **1.** A circuit that performs DEGAUSSING. **2.** A device for bulk erasing magnetic tape; also called a *bulk tape eraser.*

degaussing **1.** The demagnetization of an object; in particular, the removal of all residual magnetism. **2.** The erasure of data from a magnetic or magneto-optical data-storage medium.

degaussing circuit In a color television receiver, a circuit including a thermistor, voltage-dependent resistor, and coil for automatically demagnetizing the picture tube when the receiver is switched on.

degaussing coil A coil carrying an alternating current; the resulting magnetic field demagnetizes objects that have become accidentally magnetized.

degeneracy In microwave practice, the appearance of a single resonant frequency for two or more modes in a resonator.

degenerate modes In microwave operations, a set of modes with the same resonant frequency or propagation constant.

degenerate parametric amplifier An inverting parametric amplifier, in which the two signals are of the same frequency, which is half the pump frequency.

5059F-pD-163-223 4/9/01 5:22 PM Page 175

degenerate semiconductor A semiconductor that behaves like a metal over a wide range of temperatures.

degeneration In an amplifier, the technique of feeding a portion of the output back to the input out of phase with the input signal, to improve fidelity at the expense of gain. Also called *negative feedback* or *inverse feedback.* Compare REGENERATION.

degenerative resistor An unbypassed emitter resistor in a common-emitter bipolar-transistor circuit, or an unbypassed source resistor in a common-source field-effect transistor circuit. Signal current flowing through the resistor produces negative feedback current (degeneration), which reduces the gain of the stage, but increases the linearity of the transfer characteristic.

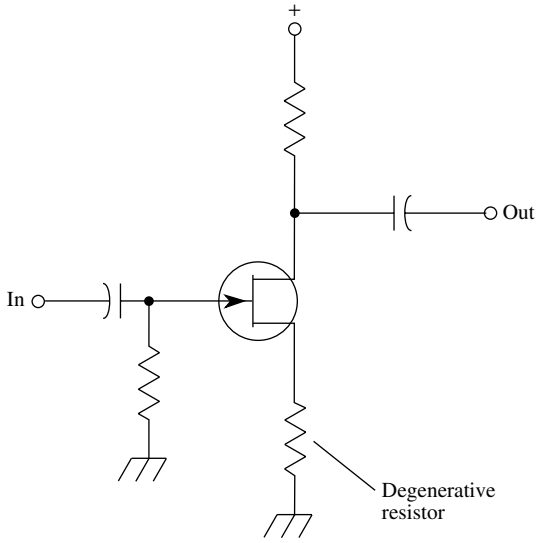

degenerative resistor

degradation **1.** Gradual deterioration in the condition or performance of a circuit or device. **2.** In a computer system, compromised performance caused by component failure.

degradation failure Failure occurring at the terminal point of degradation.

degraded operation See DEGRADATION.

degreaser See ULTRASONIC CLEANING TANK.

degree **1.** A unit of circular angular measurement equal to $\frac{1}{360}$ of the circumference of a circle. Also called GEOMETRIC DEGREE. **2.** A unit of temperature measurement. See DEGREE ABSOLUTE, DEGREE CELSIUS, DEGREE CENTIGRADE, DEGREE FAHRENHEIT, and DEGREE REAUMUR.

degree absolute Symbol, K. The unit of temperature on the absolute scale. Also see ABSOLUTE SCALE.

degree Celsius Symbol, °C. The unit of temperature on the CELSIUS SCALE.

degree centigrade Symbol, °C. The unit of temperature on the *centigrade scale* (now called CELSIUS SCALE).

degree Fahrenheit Symbol, °F. The unit of temperature on the FAHRENHEIT SCALE.

degree of current rectification For a rectifier, the ratio of the average direct output current to the root-mean-square (rms) alternating input current.

degree of voltage rectification For a rectifier, the ratio of the average direct-current (dc) output voltage to the root-mean-square (rms) alternating-current (ac) input voltage.

degree Reaumur Symbol, °R. The unit of temperature on the REAUMUR SCALE.

degrees of freedom **1.** The ways in which a point can move or a system can change. In three-dimensional space, a rigid body has six degrees of freedom: motion in three linear directions, and rotation around three linear axes extending through its center. **2.** The ways in which a robot arm can move, including linear motion and rotational motion.

degrees of rotation A measure of the extent to which a robot joint, or a set of robot joints, can be turned. Some reference axis is always used; angles are specified in degrees, relative to that axis.

degrees-to-radians conversion The conversion of angles in degrees to angles in radians. To change degrees to radians, multiply degrees by 0.01745. Compare RADIANS-TO-DEGREES CONVERSION.

deion circuit breaker A circuit breaker in which the arc occurring when the contacts open is quickly extinguished by an external magnetic device.

deionization The conversion of an ionized substance, such as a gas, to a neutral (non-ionized) state. The process changes the ions into uncharged atoms.

deionization potential The voltage at which an ionized substance becomes deionized; for example, the voltage at which a glow discharge is extinguished when the gas ions become neutral atoms at that voltage. Also called *extinction potential.*

deionization time The time required for an ionized gas to become neutral after the removal of the ionizing voltage.

deionization voltage See DEIONIZATION POTENTIAL.

deionize To restore to an electrically neutral condition (i.e., to convert ions to neutral atoms, as in the deionization of the gas when the discharge in a glow tube is extinguished).

deka- A prefix meaning ten(s) (e.g., DEKAMETER).

5059F-pD-163-223 4/9/01 5:22 PM Page 176

dekahexadecimal number system See HEXADECIMAL NUMBER SYSTEM.

delamination The splitting apart, in layers, of an insulating material, such as mica or bonded plastic film.

delay **1.** The interval between the instant at which a signal or force is applied or removed and the instant at which a circuit or device subsequently responds in a specified manner. **2.** The time required for a signal to traverse a given medium, such as air, mercury, or quartz.

delay action Response occurring some time after a stimulus has been applied or removed (e.g., the retarded opening of a delayed-dropout relay).

delay circuit **1.** A circuit, such as a resistance-capacitance (RC) or resistance-inductance (RL) combination, that introduces a time delay. **2.** See DELAY LINE.

delay coincidence circuit A coincidence circuit (see AND CIRCUIT) triggered by two pulses, one of which lags behind the other.

delay counter In a digital computer, a device that halts a program run long enough for an operation to be completed.

delay distortion **1.** Distortion resulting from variations in the phase delay of a circuit or device at different points in its frequency range. **2.** In a facsimile (fax) signal, variations in the delay of different frequency components of the signal.

delayed AGC See DELAYED AUTOMATIC GAIN CONTROL.

delayed automatic gain control An automatic gain control circuit that operates only when the signal amplitude exceeds a predetermined threshold level, thus providing maximum amplification of weaker signals.

delayed automatic volume control See DELAYED AUTOMATIC GAIN CONTROL.

delayed break In relay or switch operation, contacts separating some time after the switch has been thrown or the relay deenergized. Compare DELAYED MAKE.

delayed close See DELAYED MAKE.

delayed closure See DELAYED MAKE.

delayed contacts Contacts that open or close at a predetermined instant after their activating signal is applied or removed.

delayed drop-in See DELAYED MAKE.

delayed dropout See DELAYED BREAK.

delayed loop In security applications, a circuit or system that registers an alarm some time after intrusion is first detected. The delay can usually be selected or preadjusted.

delayed make In relay or switch operation, contacts closing some time after the switch has been thrown or the relay has been energized. Compare DELAYED BREAK.

delayed open See DELAYED BREAK.

delayed PPI Plan-position indicating radar having a delayed time base.

delayed pull-in See DELAYED MAKE.

delayed repeater A repeater that receives and stores information, and retransmits the information later, in response to a switching or interrogation signal.

delayed repeater satellite An active communications satellite that acts as a delayed repeater (i.e., it receives and records information at one time and retransmits it at a later time).

delayed sweep **1.** In an oscilloscope or radar, a sweep that starts at a selected instant after the signal under observation has started. **2.** The (usually calibrated) circuit for producing a sweep, as defined in (**1**).

delayed updating Updating a computer record or record set so that the record fields are left unchanged until all other changes attendant to the pertinent event are processed.

delay equalizer A network that corrects DELAY DISTORTION.

delay-frequency distortion Distortion caused by variation of envelope delay within a frequency band.

delay line A device (not always a line) that introduces a time lag in a signal. The lag is the time required for the signal to pass through the device, minus the time necessary for the signal to traverse the same distance through a wire, cable, optical fiber, or free space.

delay-line memory In a digital computer, a memory that uses a delay line, associated input- and output-coupling devices, and an external regenerative-feedback path. Information is kept stored by causing it to recirculate in the line by regeneration.

delay-line register In a digital computer, a register that operates in the manner of a DELAY-LINE MEMORY and has a register length (capacity) of an integral number of words.

delay-line storage See DELAY-LINE MEMORY and DELAY-LINE REGISTER.

delay multivibrator See MONOSTABLE MULTIVIBRATOR.

delay-power product Unit, watt-second. The figure of merit for an integrated circuit (IC) gate. Increasing gate power reduces propagation delay. Also called PROPAGATION DELAY-POWER PRODUCT.

delay relay A relay that opens or closes at the end of a predetermined time interval.

delay switch A switch having delayed make, delayed break, or both.

delay time **1.** The interval between the instant a voltage or current is applied and the instant a circuit or device operates. **2.** In an output pulse, the interval between the instant an ideal pulse is applied to the input of a system and the instant the output pulse reaches 10% of its maximum amplitude. **3.** The time elapsed between the presentation of a pulse to the input of a delay line and the appearance of the pulse at the output.

5059F-pD-163-223 4/9/01 5:22 PM Page 177

delay timer **1.** A timer that starts or stops an operation after a prescribed length of time. **2.** A delay relay or switch.

delay unit In a radar system, a circuit for delaying pulses.

delete **1.** To erase or blank out a signal. **2.** The elimination from a computer file of a record or record group. **3.** To remove a computer program from memory or storage.

deletion record In the master file of a digital computer, a new record that causes existing ones to be deleted.

delimiter In digital computer operations, a character limiting a sequence of characters of which it is not itself a member.

Dellinger effect The sudden disappearance of a radio signal as a result of an abrupt increase in atmospheric ionization caused by a solar eruption.

deliquescent material A material that absorbs enough moisture from the air to get wet. For example; calcium chloride, a deliquescent material, is often used to keep electronic equipment dry. Compare HYGROSCOPIC MATERIAL.

delta circuit A three-phase electrical circuit with no common ground.

delta connection A triangular connection of coils or load devices in a three-phase system, so called from its resemblance to the Greek letter delta. Compare WYE-CONNECTION.

delta-matched antenna See WYE-MATCHED IMPEDANCE ANTENNA.

delta-matched impedance antenna See WYE-MATCHED IMPEDANCE ANTENNA.

delta matching transformer In a WYE-MATCHED IMPEDANCE ANTENNA, the fanned-out (roughly delta-shaped) portion of the two-wire feeder at its point of connection to the radiator. It matches the impedance of the feeder to that of the radiator.

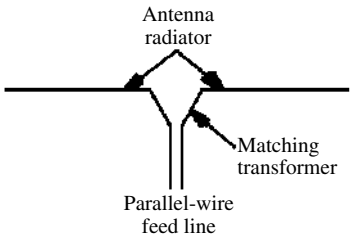

delta-matching transformer

delta modulation The conversion of an analog signal into a digital pulse train that can be decoded to yield the original analog signal.

delta network See DELTA CONNECTION.

delta pulse-code modulation In wire or radio communications, the conversion of an audio signal into a digital pulse train.

delta quantity An increment (i.e., the difference between two values of a variable).

delta rays The emission of secondary electrons as a result of radioactivity.

delta-sigma modulation A method of analog-to-digital conversion. The output is a pulse density function of the input. The input can be obtained by low-pass filtering of the output.

delta tune Also called *receiver incremental tuning (RIT).* In high-frequency (HF) communications transceivers, a control that allows the receiver frequency to be adjusted up to several kilohertz higher or lower than the transmitter frequency.

delta waves Brain waves having a frequency less than 9 Hz. Also see ELECTROENCEPHALOGRAPH and ELECTROENCEPHALOGRAM.

Deluc's pile See DRY PILE.

dem Abbreviation of DEMODULATOR.

demagnetization curve The portion of a magnetic hysteresis curve, showing reduction of demagnetization.

demagnetization effect The phenomenon in which uncompensated magnetic poles at the surface cause a reduction of the magnetic field inside a sample of a material.

demagnetize To remove magnetism from an object, either temporarily or permanently.

demagnetizer See DEGAUSSER.

demagnetizing current The half-cycle of an alternating current (or polarity of a direct current) flowing through a coil wound on a permanent magnet (as in a headphone, permanent-magnet loudspeaker, or polarized relay), that reduces the magnetic field.

demagnetizing force **1.** A magnetic force whose direction reduces the residual induction of a magnetized material. **2.** An effect that reduces the magnetism of a permanent magnet, such as high temperature or a physical blow.

demand factor In the use of electric power, the ratio of the consumer's maximum demand to the actual power consumed.

demand processing Descriptive of a system that processes data as it is available, without storing it.

demarcation strip An interface between a terminal unit and a carrier line.

Dember effect The appearance of a voltage between regions in a semiconductor when one of the regions is illuminated.

demodulation The process of retrieving the information (modulation) from a modulated carrier. In receivers and certain test instruments, this process is called DETECTION.

demodulator **1.** A circuit that recovers the information from a modulated analog or digital signal. In radio communications, such a device is usually called a DETECTOR. **2.** In computer communications, a device that performs ANALOG-TO-DIGITAL CONVERSION of incoming online signals.

5059F-pD-163-223 4/9/01 5:22 PM Page 178

demand read (write) Inputting or outputting data blocks to or from a central processor, as needed for processing.

demodulator probe A diode probe that removes the modulation envelope from an applied amplitude-modulated signal, and presents the envelope to a voltmeter or oscilloscope.

demonstrator A device used to show and teach the way in which a component, circuit, or system operates.

DeMorgan's theorem A rule of sequential or digital logic. It states that the negation of (A AND B), for any two statements A AND B, is equivalent to NOT A OR NOT B. Also, the negation of (A OR B) is equivalent, logically, to NOT A AND NOT B.

demultiplexer A circuit or device that separates the components of a multiplexed signal transmitted over a channel.

demultiplexing circuit See DEMULTIPLEXER.

denary band A band in which the highest frequency is 10 times the lowest frequency.

dendrite **1.** The branching (tree-like) structure formed by some materials, such as semiconductors, as they crystallize. **2.** The branching portion of a nerve cell; hence, the corresponding circuit element in the electronic model of such a cell.

dendritic growth **1.** Dendrite (see DENDRITE, **1**). **2.** The process of growing long, flat semiconductor crystals.

dendron See DENDRITE, **2**.

dens Abbreviation of DENSITY.

dense binary code A binary representation system, in which any possible combination of characters is assigned some correspondent.

densitometer An instrument for measuring the density of a body.

density **1.** Mass per unit volume of a material. **2.** Concentration of charge carriers or of lines of flux. **3.** The number of items per unit volume, area, distance, or time.

density modulation Modulation of the density, with respect to time, of electrons in an electron beam.

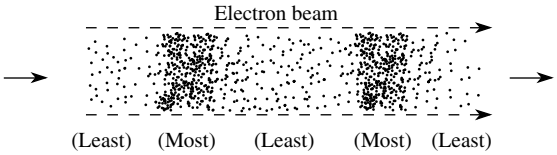

density modulation

density of electrons The concentration of electrons (i.e., the number per unit volume, area, distance, or time).

density packing A figure indicating the quantity of bits per inch or per centimeter, stored on a magnetic tape.

dependent equations Equations that are alike and have an infinite number of solutions. Compare INDEPENDENT EQUATIONS and INCONSISTENT EQUATIONS.

dependent linearity Linearity (especially in its deviation from an ideal slope) as a dependent variable.

dependent variable A changing quantity whose value at any instant is governed by the value at that instant of another changing quantity (the independent variable). Compare INDEPENDENT VARIABLE.

depletion-enhancement-mode MOSFET A metal-oxide-semiconductor field-effect transistor (MOSFET) designed for zero gate-bias voltage. An ac gate signal voltage drives the MOSFET alternately into the depletion mode (negative signal half-cycle) and enhancement mode (positive signal half-cycle). Compare DEPLETION-TYPE MOSFET and ENHANCEMENT-TYPE MOSFET.

depletion field-effect transistor A field-effect transistor whose operation is based on the control of depletion layer width.

depletion layer See BARRIER, **1**.

depletion-layer capacitance See JUNCTION CAPACITANCE.

depletion-layer rectification Rectification provided by a semiconductor junction.

depletion-layer transistor A transistor whose action depends on modulation of current carriers in a space-charge region (depletion layer).

depletion mode Operation characteristic of the DEPLETION-TYPE MOSFET.

depletion region See BARRIER, **1**.

depletion-type MOSFET A metal-oxide-semiconductor field-effect transistor (MOSFET) in which the channel directly under the gate electrode is narrowed by a negative gate voltage (in an n-channel device) or by a positive gate voltage (in a p-channel device).

depolarization **1.** In a primary cell, the removal of the agents that have caused polarization. **2.** The addition of a polarization-inhibiting substance to the electrolyte of a primary cell.

depolarizer A substance that retards polarization in an electrochemical cell. An example is the manganese dioxide used in dry cells.

depolarizing agent See DEPOLARIZER.

deposition The application of a layer of one substance (usually a metal) to the surface of another (the substrate), as in evaporation, sputtering, electroplating, silk-screening, etc.

depth finder See ACOUSTIC DEPTH FINDER.

depth indicator **1.** A sounding instrument for determining the depth of a body of water. **2.** On an ACOUSTIC DEPTH FINDER, the meter that indicates the depth of water.

depth of cut On a phonograph disk, the depth of the recorded groove.

depth of discharge Abbreviation, DOD. In a rechargeable cell or battery, a measure of the extent

5059F-pD-163-223 4/9/01 5:22 PM Page 179

to which discharging has occurred. It is generally specified as a percentage. For example, if the DOD of a 10-ampere-hour (10-AH) battery is 80 percent, then 8 AH have been used up, and 2 AH remain before recharging will be necessary.

depth of heating In dielectric heating, the depth of heat penetration in the sample when both electrodes are applied to one of its faces.

depth of modulation The degree to which a carrier wave is modulated.

depth of penetration The extent to which a skin-effect current penetrates the surface of a conductor.

depth sounder See ACOUSTIC DEPTH FINDER.

de-Q **1.** To reduce the *Q* of a component or tuned circuit. **2.** To inhibit laser action during an interval when an ion population excess is pumped up.

derating To reduce an operating parameter (e.g., current, voltage, power) as another factor (such as temperature) increases, to ensure efficient, reliable, and safe operation.

derating curve A graph that shows the extent to which a quantity (such as allowable power dissipation) must be reduced as another quantity (such as temperature) increases.

derating factor The amount by which a current, power, or voltage must be decreased to ensure safe and efficient operation of a circuit or device in a given environment (temperature, altitude, humidity, etc.). Also see DERATING and DERATING CURVE.

derivative **1.** A mathematical expression indicating the rate at which a function changes, with respect to the independent variable. See DERIVATIVE FUNCTION. **2.** The slope of a line tangent to a curve at a given point. **3.** The output signal of a DIFFERENTIATOR, relative to the input signal.

derivative action In a control system, an action producing a corrective signal proportional to the rate of change (derivative) of the controlled variable.

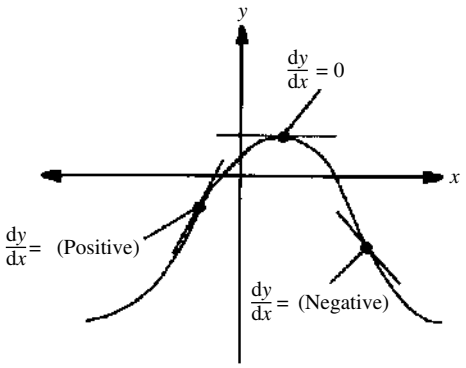

derivative

derivative control A method of automatic control, actuated according to the number of errors per second.

derivative function For a mathematical function $f(x)$, the function $f'(x) = \mathrm{d}f(x)/\mathrm{d}x$, over the domain of f. For any specific point x_0 in the domain of f, the value of $f'(x_0)$ is equal to the slope of a line tangent to f at the point $(x_0, f(x_0))$.

derived center channel The sum or difference of the left and right channels in a stereophonic system.

Dershem electrometer A variation of the *quadrant electrometer*. In the Dershem instrument, the needle (to which a small mirror is attached) rotates within slots cut in the quadrant plates and, therefore, can never accidentally touch the plates.

descending node For a satellite orbiting the earth or another planet, any point at which the groundtrack crosses the equator as it moves from the northern hemisphere into the southern hemisphere. This node generally changes for each succeeding orbit, because the earth or planet rotates underneath the orbit of the satellite. Compare ASCENDING NODE.

descending pass For a specific point on the earth's surface, the time during which an artificial communications satellite is accessible when its latitude is moving southward. The duration of accessibility depends on the altitude of the satellite and on how close its groundtrack comes to the earth-based point. Compare ASCENDING PASS.

description A data element that is part of a record and is used to identify it.

desensitization **1.** The process of making a circuit or device less responsive to small values of a quantity. **2.** Also called *desensing*. In a communications receiver, an unwanted, often intermittent reduction in front-end gain, caused by an extremely strong local signal.

desensitize **1.** To reduce the sensitivity of a receiver. **2.** To reduce the gain of an amplifier. **3.** To reduce the small-quantity response of an instrument.

desiccant A compound, such as cobalt chloride, used for the purpose of keeping enclosed items dry.

design **1.** A unique, planned arrangement of electronic components in a circuit, in accordance with good engineering practice, to achieve a desired end result. **2.** A unique layout of components or controls, in accordance with good engineering practice, esthetics, and (often) ergonomics. **3.** Invention. **4.** Plan. **5.** To produce a design, as defined in **1**, **2**, **3**, or **4**.

designation Within a computer record, coded information identifying the record so that it can be handled accordingly.

5059F-pD-163-223 4/9/01 5:22 PM Page 180

design-center rating A specified parameter that, if not exceeded, should provide acceptable average performance for the greatest number of the components so rated.

design compatibility The degree to which a transmitter and receiver are designed for the rejection of unwanted electromagnetic noise.

design engineer An engineer who is skilled in the creation of new designs and in the comparative analysis of designs.

design-maximum rating See MAXIMUM RATING.

design-proof test A performance test made on a newly completed circuit or device to determine the suitability of the design.

Desk-Fax A facsimile transceiver that can be placed on a desktop, used for wire or radio transmission and reception of still images.

desk microphone A microphone equipped with a stand that sits on a table or desktop. It allows the operator to use both hands for equipment adjustment, taking notes, etc.

desktop computer A personal computer designed for nonportable use, usually equipped with a built-in hard disk, one or more diskette drives, a CD-ROM drive, and a fax/modem. It generally uses an external cathode-ray-tube display, printer, and keyboard. The power supply is intended for use with 117-volt utility circuits.

desolder To unsolder joints, usually with a special tool that protects delicate parts and removes melted solder by suction.

destaticization A chemical process used to minimize the retention of electrostatic charges by certain substances.

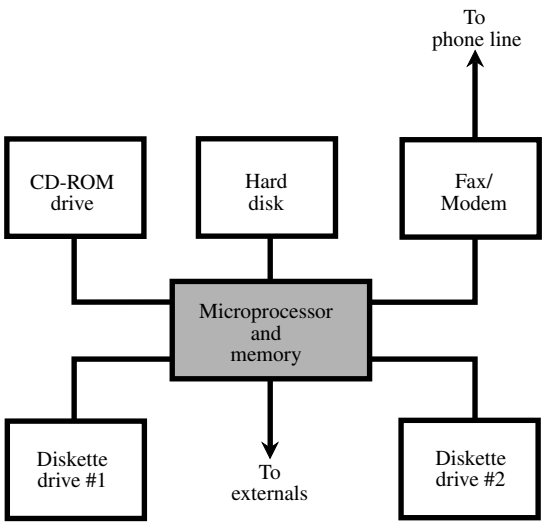

desktop computer (main unit only)

destination **1.** The point in a system to which a signal of any sort is directed. **2.** In communications, a receiving station.

destination file A computer file that receives data output during a specific program run.

destination register In a digital computer, a register into which data is entered.

Destriau effect Light emission resulting from the action of an alternating electric field on phosphors embedded in a dielectric.

destructive addition A computer logic operation in which the sum of two operands appears in the memory location occupied by one of the operands.

destructive breakdown A breakdown in which the effects are irreversible (e.g., permanent damage to a dielectric by excessive applied voltage).

destructive interference Interference resulting from the addition of two waves that have the same frequency, but opposite phase.

destructive read In a computer or calculator, the condition in which reading the answer erases the data (as from a location) used in the calculation.

destructive test A test that unavoidably destroys the test sample. Compare NONDESTRUCTIVE TEST.

DETAB A COBOL-based computer programming language permitting the programmer to present problems as decision tables.

detail constant Pertaining to a video signal, the ratio V_H/V_L, where V_H is the amplitude of high-frequency components, and V_L is the amplitude of the low-frequency reference component.

detected error In a computer system, an error that is identified, but remains uncorrected until final output is available.

detection **1.** See DEMODULATION. **2.** The sensing of a change in the operating parameters of a circuit or system.

detection range In security applications, the radius within which transducers or sensors can be expected to reliably operate. This radius varies, depending on the environment, the sensitivity of the receiving circuits and transducers, and the strength of the transmitted signal (if any).

detectophone A device for eavesdropping on a conversation. The device can use a tape recorder or a tiny radio transmitter.

detector **1.** In radio communications, a device or circuit that extracts the information from a modulated carrier. Also sometimes called a *demodulator.* **2.** A device that senses a signal or condition and indicates its presence.

detector balanced bias In a radar system, bias obtained from a controlling circuit and used to reduce or eliminate clutter.

detector bias Steady dc voltage applied to a detector to set its operating point.

detector blocking In a regenerative receiver, a phenomenon in which a strong signal tends to pull the detector oscillator into phase with itself,

5059F-pD-163-223 4/9/01 5:22 PM Page 181

thereby causing the detector to oscillate at the signal frequency.

detector circuit A demodulator circuit (i.e., one used to recover the intelligence from a modulated carrier).

detector probe See DEMODULATOR PROBE.

detector pull-in See DETECTOR BLOCKING.

detector stage In a receiver or instrument, the separate stage that contains the detector circuit. Some systems, such as a superheterodyne receiver, have more than one detector. Also see FIRST DETECTOR and SECOND DETECTOR.

detent A mechanical stop used on a rotary switch to hold the switch pole securely in each selected position.

detune **1.** To adjust a circuit to some frequency other than its resonant frequency. **2.** To set the frequency of a receiver or transmitter to some point other than the frequency normally used. **3.** To stagger-tune a receiver intermediate-frequency system.

detuning Tuning to a point above or below the frequency to which a device or system is normally (or initially) adjusted (usually the resonant frequency of the device).

detuning stub A device used for the purpose of coupling a feed line to an antenna, while choking off currents induced on the feed line as a result of the near-field radiation of the antenna.

deupdating Producing an earlier form of a computer file by substituting older records for current ones.

deuterium Symbol, D, d, H^2, or ^2H. Also called *heavy hydrogen.* The hydrogen isotope having a nucleus consisting of one proton and one neutron.

deuterium oxide Symbol, D_2O. Also called *heavy water.* This compound has wide use in nuclear reactors.

deuteron The nucleus of a deuterium atom.

deuton See DEUTERON.

deutron See DEUTERON.

deviation **1.** In a frequency-modulated (FM) radio signal, the instantaneous amount of carrier frequency shift away from the unmodulated frequency. It is usually expressed in kilohertz; directly proportional to the amplitude of the modulating signal, up to a certain maximum that depends on the bandwidth allowed. **2.** The maximum instantaneous carrier frequency shift in a FM signal. **3.** The extent or amount by which a quantity drifts from its proper value.

deviation distortion In a frequency-modulation (FM) receiver, distortion resulting chiefly from discriminator nonlinearity and restricted bandwidth.

deviation ratio In a frequency-modulated (FM) signal, the ratio between the highest modulating frequency and the maximum carrier deviation.

deviation sensitivity For a frequency-modulation (FM) receiver, the smallest deviation that will produce a specified audio output power. Expressed in kilohertz, or as a percentage of rated deviation of the receiver, measured with the receiver set for maximum gain.

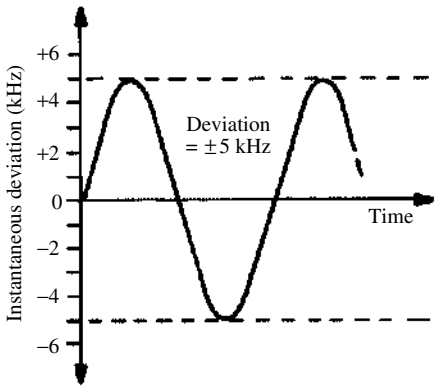

deviation

device **1.** A simple or complex discrete electronic component. **2.** A subsystem used as a unit, and regarded as a single component.

device complexity The number of components in an integrated circuit.

device independence A characteristic of a computer, that allows operation independent of the types of input/output devices used.

dew point For a gas containing water vapor (typically air), the highest temperature at which the vapor condenses as the gas is cooled. The dew point depends on the amount of vapor in the gas.

dew-point recorder An instrument for determining and recording the temperature at which water vapor in the air condenses to a liquid.

DF Abbreviation of DIRECTION FINDER.

DF antenna An antenna that is mechanically rotatable or has an electrically rotatable response pattern for use with a direction finder.

DF antenna system Two or more DF antennas arranged for maximum directivity and maneuverability, together with associated feeders and couplers.

D flip-flop A delayed flip-flop. The state of the input determines the state of the output during the following pulse, rather than during the current pulse.

dg Abbreviation of *decigram.*

dia Abbreviation of *diameter.*

diac A two-terminal, bilateral, three-layer semiconductor device that exhibits negative resistance. When the applied voltage exceeds a critical value, the device conducts.

diagnosis **1.** Determination of the cause and location of a hardware malfunction. **2.** In computer operations, determination of the cause of a system operation error.

5059F-pD-163-223 4/9/01 5:22 PM Page 182

diagnostic routine **1.** An efficient sequence of diagnostic tests for rapid, foolproof trouble-shooting of electronic hardware. **2.** A computer software package intended for debugging programs, or for finding the cause of a hardware or operating-system malfunction. Also called *diagnostic*, *diagnostic program*, or *diagnostic utility*.

diagnostic test **1.** A test made primarily to ascertain the cause of dysfunction in electronic equipment. Compare PERFORMANCE TEST. **2.** To apply a diagnostic routine to hardware faults, or to implement one to prevent such a fault.

diagnotor In digital computer operations, a troubleshooting routine combining both diagnosis and editing.

diagram A (usually line) drawing depicting a circuit, assembly, or organization. See, for example, BLOCK DIAGRAM and CIRCUIT DIAGRAM.

dial **1.** A graduated scale, arranged horizontally, vertically, in a circle, or over an arc. Used to show the distance through which a variable component (such as a potentiometer, variable capacitor, or switch) has been adjusted. A pointer can move over the scale, or the scale can be moved past a stationary pointer. **2.** The graduated face of a meter. **3.** In a telephone system, to press the keys or actuate the tones that establish contact with another subscriber.

dial cable A flexible cable or belt conveying motion on the shaft of an adjustable component (such as a potentiometer or variable capacitor) to a dial.

dial-calibrated attenuator A variable attenuator with a dial reading directly in decibels.

dial-calibrated capacitor A variable capacitor with a dial reading directly in picofarads.

dial-calibrated inductor A variable inductor with a dial reading directly in microhenrys.

dial-calibrated potentiometer A potentiometer with a dial reading directly in output volts, percentage of input voltage, number of turns (when resistance is a linear function), or other quantity.

dial-calibrated resistor A variable resistor with a dial reading directly in ohms, kilohms, or megohms.

dial-calibrated rheostat See DIAL-CALIBRATED RESISTOR.

dial cord A form of dial cable. Cord usually designates a fabric string, whereas a cable is a flexible, braided wire.

dial knob The knob used to turn a dial under a pointer, or to turn a pointer over a dial scale.

dial lamp See DIAL LIGHT.

dial light A small lamp sometimes used to illuminate a dial. Can also serve as a pilot light.

dial lock A small mechanism used to lock a dial at a particular setting to prevent further turning.

dialer See AUTOMATIC DIALING UNIT.

dialing key In a telephone system, a dial that uses keys, rather than a rotary dial.

dial jack In a telephone system, a set of jacks that facilitates interconnections between dial cords and external lines.

dial light A lamp or light-emitting diode placed in the dial mechanism of a radio receiver, transmitter, or transceiver. Allows the dial to be read in dim light or in darkness.

dialog equalizer In sound transmission and recording, a high-pass filter that reduces low-frequency response during dialog and extreme closeups.

dial pulse An interruption of the direct current in a telephone system when the dial contacts of the calling telephone open. The number of such interruptions corresponds to the digit dialed.

dial scale The graduated portion of a dial.

dial system **1.** See DIAL TELEPHONE SYSTEM. **2.** The arrangement of dials and knobs that facilitates adjustment of electronic equipment.

dial telephone A telephone set in which a numbered rotatable disk is used to produce the switch interruptions that cause generation of the transmitted multidigit telephone numbers.

dial telephone system The complete automatic circuit, including central-office facilities, for dial telephone operation.

dial tone In a telephone system, a constant hum or whine heard before dialing, indicating that the system is operational.

dial-up In a telephone system, the calling of one subscriber by another, using a dial system.

diam Abbreviation of *diameter*.

diamagnetic Pertaining to a material having magnetic permeability less than unity.

diamagnetism The state of having magnetic permeability less than unity. A material with this property reduces the flux density of a magnetic field, relative to the flux density in air or in free space.

diamond antenna Also called *rhombic antenna*. A nonresonant wideband directional antenna whose horizontal wire elements are arranged in the shape of a diamond (rhombus). The arrangement is fed at one corner, the opposite corner being terminated with a noninductive resistor.

diamond lattice The orderly internal arrangement of atoms in a redundant pattern in crystalline materials, such as germanium or silicon.

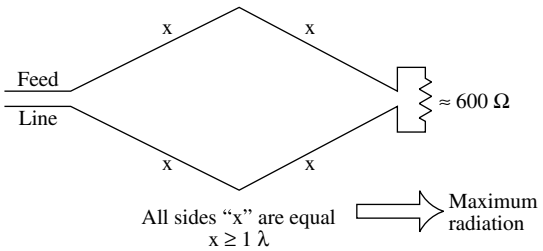

diamond antenna

5059F-pD-163-223 4/9/01 5:22 PM Page 183

diamond stylus A phonograph "needle" having as its point a small, ground diamond.

diapason **1.** Either of the two principal stops (open and closed) of an electronic organ that cover the entire range of the instrument. When one is used, a note played is automatically sounded in several octaves. **2.** Tuning fork.

diaphony See DISSONANCE.

diaphragm A usually thin metal or dielectric disk used as the vibrating member in headphones, loudspeakers, and microphones, and as the pressure-sensitive element in some sensors and barometers.

diaphragm gauge A sensitive gas pressure gauge using a thin metal diaphragm stretched flat. Increments of pressure move the diaphragm, relative to a nearby electrode, varying the capacitance between the two.

diathermic Pertaining to a substance that efficiently transfers heat or infrared energy.

diathermotherapy The use of diathermy in the treatment of various physiological disorders.

diathermy **1.** In medicine and physical therapy, the production of heat in subcutaneous (below the skin) tissues by means of high-frequency radio waves. **2.** A radio-frequency (RF) power oscillator and associated equipment used to produce heat in subcutaneous tissues.

diathermy interference Radio-frequency interference (RFI) resulting from the operation of unshielded and/or unfiltered diathermy equipment.

diathermy machine See DIATHERMY, **2**.

diatomic Having two atoms (e.g., a DIATOMIC MOLECULE).

diatomic molecule A molecule (such as that of oxygen) composed of two atoms. Compare MONATOMIC MOLECULE.

dibble A mathematical function in which a number (usually an integer) is doubled, and then one is added to the result. Thus, dibble $n = 2n + 1$.

dibit A combination of two binary digits (bits). The four possible dibits are 00, 01, 10, and 11.

dice Plural of DIE, **1**, **3**.

dichotomizing search Also called *binary search.* In digital computer operations, locating an item in a table of items that are arranged by key values in serial order. The required key is compared with a key halfway through the table; according to this relational test, half of the table is accepted and again divided for comparison, etc. until the keys match and the item is found.

dichotomy Characterized by the usually repetitive branching into two sets, groups, or factions.

dichroism Also called *dichromatism.* **1.** The property of a crystal showing different colors, depending on which axis corresponds to the line of sight. **2.** The property of a solid taking on different colors as the thickness of the transmitting layer changes. **3.** The property of a liquid changing color, according to solution concentration.

dichromate cell An electrolytic cell consisting of electrodes of carbon and zinc. The zinc electrode is immersed in a diluted solution of sulfuric acid, and the carbon electrode in a solution of potassium dichromate.

dicing The cutting of a semiconductor melt, crystal wafer, or other material into dice (see DIE).

dictionary A table of specifications for the size and format of computer file operands, and data names for field and file types.

die **1.** A small wafer of useful electrical material, such as a semiconductor or a precision resistor chip. **2.** A casting designed to mold molten metal into a specific configuration until the metal hardens. **3.** Any small object of roughly cubical proportions. **4.** To lose power or energy completely, usually unintentionally. **5.** In a computer program, to produce unpredicted and useless results following an initial run.

die bonding The bonding of dice or chips to a substrate.

die casting Making a casting by forcing molten metal (such as an aluminum alloy, lead, tin, or zinc) under high pressure into a die or mold.

dielectric A material that is a nonconductor of electricity; especially, a substance that facilitates the storage of energy in the form of an electric field. Such materials are commonly used in capacitors and transmission lines.

dielectric absorption The ability of certain dielectric materials to retain some of their electric charge—even after being momentarily short-circuited. Capacitors with this property must be shorted out continuously for a certain length of time before the dielectric has completely discharged.

dielectric amplifier A voltage amplifier circuit in which the active component is a capacitor having a nonlinear dielectric. A signal voltage applied to the capacitor varies the capacitance, thus varying the current. The modulated current flows through a load resistor, developing an output-signal voltage higher than the input-signal voltage.

dielectric antenna An antenna in which some or all of the radiating element is made of a dielectric material, such as polystyrene. Primarily used at microwave frequencies.

dielectric breakdown Sudden, destructive conduction through a dielectric when the applied voltage exceeds a critical value.

dielectric breakdown voltage The voltage at which DIELECTRIC BREAKDOWN occurs in an insulating material. Varies, depending on the particular dielectric substance.

dielectric capacity See DIELECTRIC CONSTANT.

dielectric constant Symbol, *k.* For a dielectric material, the ratio of the capacitance of a two-plate capacitor using the dielectric material, to the capacitance of the equivalent capacitor with dry air as a dielectric. Also called *inductivity* and *specific inductive capacity.*

5059F-pD-163-223 4/9/01 5:22 PM Page 184

dielectric current **1.** Current flowing over the surface of a dielectric material in response to a varying electric field. **2.** Current flowing through a dielectric as a result of its finite insulation resistance.

dielectric dissipation For a dielectric material in which an electric field exists, the ratio of the lost (dissipated) electrical energy to the recoverable electrical energy.

dielectric dissipation factor The cotangent of the dielectric phase angle, also equal to the reciprocal of the *Q* factor.

dielectric fatigue In some dielectric materials subjected to a constant voltage, the deterioration of dielectric properties with time.

dielectric guide A waveguide made from a solid dielectric, such as polystyrene.

dielectric heater A high-frequency power generator used for DIELECTRIC HEATING.

dielectric heating The heating and forming of a dielectric material, such as a plastic, by temporarily making the material the dielectric of a two-plate capacitor. This capacitor is connected to the output of a high-power radio-frequency (RF) generator. Losses in the dielectric cause its heating. Compare INDUCTION HEATING.

dielectric hysteresis See DIELECTRIC ABSORPTION.

dielectric isolation In a monolithic integrated circuit (IC), the isolation of circuit elements from each other by a dielectric film, as opposed to isolation by reverse-biased pn junctions.

dielectric lens A molded piece of dielectric material used to focus microwaves. Its operation is analogous to that of an optical lens.

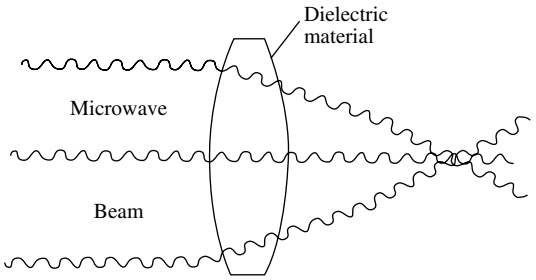

dielectric lens

dielectric loss For a dielectric material subjected to a changing electric field, the rate of transformation of electric energy into heat.

dielectric loss angle Ninety degrees minus the DIELECTRIC PHASE ANGLE.

dielectric loss factor For a dielectric material, the product of the dielectric constant and the tangent of the dielectric loss angle.

dielectric loss index See DIELECTRIC LOSS FACTOR.

dielectric matching plate A dielectric plate used in some waveguides for impedance matching.

dielectric mirror A reflector containing a number of layers of dielectric material. Its action depends on electromagnetic energy being partially reflected from the interfaces between materials having unequal indexes of refraction.

dielectric phase angle For a dielectric material, the angular phase difference between a sinusoidal voltage applied to the material and the component of the resultant current having the same period as that of the voltage.

dielectric phase difference See DIELECTRIC LOSS ANGLE.

dielectric polarization The effect characterized by the slight displacement of the positive charge in each atom of a dielectric material, with respect to the negative charge, under the influence of an electric field.

dielectric power factor The cosine of the dielectric phase angle, or the sine of the dielectric loss angle.

dielectric puncture voltage See DIELECTRIC BREAKDOWN VOLTAGE.

dielectric rating The breakdown voltage, and sometimes the power factor, of the dielectric material used in a device, such as a relay, motor, or switch.

dielectric ratings Electrical characteristics of a dielectric material: breakdown voltage, power factor, dielectric constant, etc.

dielectric resistance See INSULATION RESISTANCE.

dielectric rigidity See DIELECTRIC STRENGTH.

dielectric-rod antenna A unidirectional antenna that uses a dielectric substance to obtain power gain.

dielectric soak See DIELECTRIC ABSORPTION.

dielectric strain The distorted internal state of a dielectric, caused by the influence of an electric field. Also called DIELECTRIC STRESS.

dielectric strength The highest voltage a dielectric can withstand before DIELECTRIC BREAKDOWN occurs. Usually expressed in volts or kilovolts per mil of material thickness.

dielectric stress The distortion of electron orbits in the atoms of a dielectric material subjected to an electric field.

dielectric susceptibility For a polarized dielectric, the ratio of polarization to electric intensity.

dielectric tests Laboratory experiments performed to determine the dielectric characteristics of a substance—especially the dielectric constant and the dielectric breakdown voltage.

dielectric waveguide See DIELECTRIC GUIDE.

dielectric wedge A wedge-shaped dielectric slug placed inside a waveguide for impedance matching.

dielectric wire A small dielectric waveguide that acts as a wire to carry signals between points in a circuit.

5059F-pD-163-223 4/9/01 5:22 PM Page 185

Dietzhold network A four-terminal, shunt m-derived circuit used in some wideband amplifiers.

Dietzhold peaking In some wideband amplifiers, frequency compensation obtained with a shunt m-derived network (see DIETZHOLD NETWORK).

difference amplifier See DIFFERENTIAL AMPLIFIER.

difference channel In a stereophonic amplifier, an audio channel that handles the difference between signals in the right channel and those in the left channel.

difference detector A detector whose output is the difference between two simultaneous input signals.

difference frequency A signal frequency produced by mixing or heterodyning of signals at two other frequencies. If the lower input signal frequency is f_1 and the higher input signal frequency is f_2, then the difference frequency f_d is equal to $f_2 - f_1$.

difference of potential The absolute value of the algebraic difference of voltages at two points of different electrical potential. Thus, the difference of potential between a +5-V point and a –5-V point is +5 – (–5) V = 10 V. Also see POTENTIAL DIFFERENCE.

difference quantity See INCREMENT.

difference signal **1.** The resultant signal obtained by subtracting, at every instant for at least one full cycle, the amplitudes of two signals. **2.** The difference of the left- and right-channel outputs in a stereo system.

differential **1.** A device, consisting of a gear system, that adds or subtracts angular motions and delivers the result. **2.** A gear system in which the motion of a shaft is transferred to two other shafts aligned with each other and perpendicular to the first shaft. **3.** One of two coils arranged to produce opposite polarities at a point in a circuit. **4.** Pertaining to a difference between two signals or quantities.

differential amplifier A circuit, usually an operational amplifier, that amplifies the voltage difference between two input signals. The instantaneous output voltage is equal to some constant multiple of the difference between the instantaneous input voltages.

differential analyzer An analog computer that solves differential equations using integrators.

differential angle For a mercury switch, the angle between operation and release positions.

differential capacitor A dual variable capacitor with two identical stator sections, and a single rotor section that turns into one stator section and out of the other. The capacitance of one section decreases while that of the other increases.

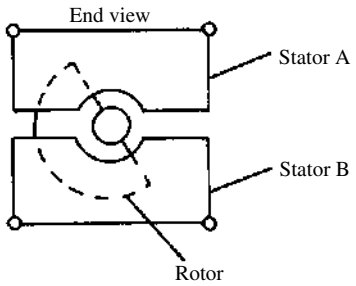

differential capacitor

differential coil See DIFFERENTIAL, **3**.

differential comparator A linear integrated circuit (IC) that delivers an output proportional to the difference between two input signals.

differential compound dc generator A compound-wound dc generator in which the magnetomotive force of the series field opposes that of the shunt (main) field.

differential compound dc motor A compound-wound dc motor in which the magnetomotive force of the series field coil opposes that of the shunt (main) field coil.

differential cooling Reducing temperature at different points on a surface at different rates.

differential delay The difference $d_{max} - d_{min}$ across a frequency band, where d_{max} is the maximum frequency delay and d_{min} is the minimum frequency delay.

differential discriminator A device that passes pulses, whose amplitudes are between two predetermined values above or below zero.

differential distortion In an automatic-gain-control circuit, distortion from effects that cause shunting of the diode load resistor.

differential flutter Fluctuations in the speed of a magnetic tape that are nonuniform in different parts of the tape.

differential gain In a differential amplifier, the average gain of the two sections of the amplifier. Compare DIFFERENTIAL UNBALANCE.

differential gain control A circuit or device for setting the gain of a radio receiver in terms of an anticipated change in signal strength, to reduce the receiver output signal differential.

differential galvanometer A galvanometer in which currents in two similar coils neutralize each other; thus, there is zero deflection when the currents are equal.

differential gap The smallest range of values that a controlled variable must take to change a three-position controller's output from on to off, or vice versa.

differential heating Increase of temperature at different points on a surface at different rates.

differential impedance See DIFFERENTIAL-INPUT IMPEDANCE.

differential induction coil An induction coil having two differentially wound primary coils.

differential input In a differential amplifier, the circuit between input terminals 1 and 2, as opposed to the circuit between input 1 or input 2 and ground.

5059F-pD-163-223 4/9/01 5:22 PM Page 186

differential-input amplifier A differential amplifier whose output is proportional to the difference between two input signals—each applied between an input terminal and common ground.

differential-input capacitance In a differential amplifier, the capacitance between the input terminals.

differential-input impedance In a differential amplifier, the impedance between the input terminals.

differential-input measurement For a differential amplifier, a floating measurement made between the input terminals.

differential-input rating In an operational amplifier, the greatest difference signal that can be placed between the inputs while allowing proper operation.

differential-input resistance In a differential amplifier, the resistance between the input terminals.

differential-input voltage In a differential amplifier, the signal voltage presented to the floating input terminals.

differential-input voltage range In a differential amplifier, the range of signal voltages that can be applied between the differential input terminals without overdriving the amplifier.

differential input-voltage rating The maximum differential-input voltage that can be applied safely to a differential amplifier.

differential instrument A galvanometer or other meter in which deflection results from the differential effect of currents flowing in opposite directions through two identical coils. Also see DIFFERENTIAL GALVANOMETER.

differential keying A system of break-in keying, in which the oscillator stage of a transmitter containing a keyed amplifier is disabled when the key is open to prevent interference with the receiver at the keying station, and is enabled when the key is closed.

differential-mode gain In an operational amplifier, the ratio, in decibels, between the output voltage and the differential input voltage.

differential-mode input In an operational amplifier in differential mode, the difference between the two input signal voltages.

differential-mode signal In a balanced three-terminal circuit, such as the input of a differential amplifier, a signal applied between the floating (ungrounded) input terminals.

differential multiplexer An analog multiplexer that selects both the high and low portion of the input signal.

differential nonlinearity Incremental error from an ideal analog output difference when the input is changed by a certain value. Generally expressed as a fraction of full-scale output.

differential permeability The derivative of normal induction, with respect to magnetizing force.

differential phase In a television system tested with a low-level, high-frequency sine-wave signal (f_1) superimposed on a low-frequency, sine-wave signal (f_2), the difference in phase shift of f_1 throughout the system for two specified levels of f_2.

differential phase-shift keying Keying of a carrier by varying the carrier phase.

differential pressure The difference in pressure between two points.

differential-pressure transducer A transducer that delivers an output proportional to the difference between two sensed actuating pressures.

differential protective relay A differential relay that operates to protect equipment or personnel when the difference between the two actuating quantities reaches a prescribed level.

differential receiver A synchro differential that receives the electrical output of two synchro transmitters. The receiver can subtract one input voltage from the other.

differential relay A relay actuated by the difference between two currents or voltages.

differential selsyn A selsyn in which the position assumed by the rotor is proportional to the sum of rotor and stator field values.

differential stage See DIFFERENTIAL AMPLIFIER.

differential synchro See DIFFERENTIAL RECEIVER and DIFFERENTIAL TRANSMITTER.

differential transducer A dual-input, single-output sensor, such as a pressure transducer, that is actuated by two sensed quantities and delivers an output proportional to their difference.

differential transformer A variable inductance transformer having a (usually cylindrical) core that is moved in and out to provide adjustable coupling between the interwound primary and secondary windings. This permits adjustment of the amplitude and phase of the transformer output voltage, with respect to the input voltage.

differential transmitter A synchro differential connected to a synchro transmitter. In a synchro receiver supplied by this combination, the change in rotor position is the algebraic difference between the transmitter-rotor position and the differential-rotor position.

differential unbalance For a differential amplifier, the average difference in gain between the two amplifier sections. Compare DIFFERENTIAL GAIN.

differential voltage **1.** The voltage difference between the input signals to a differential device. **2.** The breakdown voltage minus the operating voltage for a lamp.

differential voltage gain **1.** The ratio, in decibels, between the differential output and differential input voltages of an amplifier. **2.** The instantaneous ratio, in decibels, between the rate of change of the output signal voltage and the rate of change of the input signal voltage in an amplifier.

differential-wound field In a motor or generator, a field winding having series and shunt coils whose fields are opposing.

5059F-pD-163-223 4/9/01 5:22 PM Page 187

differentiate **1.** To produce an output signal, the instantaneous amplitude of which is proportional to the instantaneous rate of change of the input amplitude. **2.** To determine the derivative of a mathematical function.

differentiating circuit See DIFFERENTIATING NETWORK.

differentiating network A four-terminal resistance-capacitance (RC) network whose output voltage is the derivative of the input voltage, with respect to time. Compare INTEGRATING NETWORK.

differentiation **1.** The processing of an input signal to create an output signal whose voltage waveform represents the derivative, with respect to time, of the input voltage waveform. **2.** The process of computing a mathematical derivative.

differentiator **1.** See DIFFERENTIATING NETWORK. **2.** An operational amplifier whose output waveform is the mathematical derivative of the input waveform.

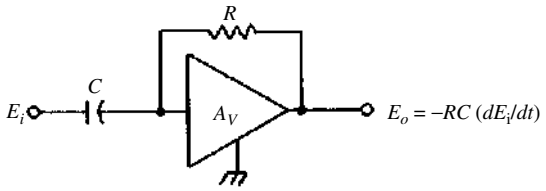

differentiator, 2

diffracted wave A wave or ray of energy undergoing DIFFRACTION.

diffraction **1.** Interference of one part of an energy beam with another part when the beam is deflected along two or more paths having different lengths. When this happens with visible light, dark and light bands or colored bands appear. This effect is responsible for the rainbow-like appearance of light reflected from the surface of a compact disc. **2.** The bending of electromagnetic waves around an object. This effect explains why radio signals can propagate around large obstructions, such as buildings and hills. The effect becomes more pronounced as the wavelength increases (the frequency decreases). **3.** The bending of acoustic waves around an object. This effect explains why sound propagates around large obstructions, such as buildings. The effect becomes more pronounced as the wavelength increases (the frequency decreases).

diffraction grating A transparent plate containing thousands of parallel lines or grooves spaced extremely close together. Light passing through the slits between the lines produces a rainbow spectrum as a result of DIFFRACTION.

diffraction spectrum **1.** The spectrum produced in visible light by a diffraction grating. **2.** The distribution of energy at various frequencies, produced by diffraction of electromagnetic waves. **3.** The distribution of energy at various frequencies, produced by diffraction of acoustic waves.

diffractometer An instrument for measuring the diffraction of radiation, such as light or X-rays.

diffuse **1.** To produce or cause DIFFUSION. **2.** Energy that is diffused.

diffused-alloy transistor See DRIFT-FIELD TRANSISTOR.

diffused-base transistor A bipolar transistor in which the base region has been diffused into the semiconductor wafer. Also see DIFFUSED JUNCTION.

diffused device A semiconductor device in which the junction is produced by diffusion (see DIFFUSION, **1**). Examples: DIFFUSED-BASE TRANSISTOR, DIFFUSED DIODE, DIFFUSED-JUNCTION RECTIFIER, and DIFFUSED-MESA TRANSISTOR.

diffused diode A semiconductor diode having a diffused junction.

diffused-emitter-and-base transistor A transistor in which n and p materials both have been diffused into the semiconductor wafer to provide emitter and base junctions. Also see DIFFUSION, **1** and DIFFUSED TRANSISTOR.

diffused junction In a semiconductor device, a pn junction formed by diffusing a gas into a semiconductor at a high temperature that is below the melting point of the semiconductor. Typically, a gas containing an n-type impurity is diffused into p-type semiconductor material. Compare ALLOY JUNCTION.

diffused-junction rectifier A semiconductor rectifier using a diffused junction.

diffused-junction transistor See DIFFUSED-BASE TRANSISTOR, DIFFUSED-MESA TRANSISTOR, and DIFFUSED TRANSISTOR.

diffused-layer resistor In an integrated circuit, a resistor produced by diffusing a suitable material into the substrate.

diffused-mesa transistor A transistor whose base is a n-type layer diffused into a p-type wafer (the remaining p-type material serving as the collector); its emitter is a small p-type area diffused into or alloyed with the n-layer. Unwanted diffused portions are etched away, leaving the transistor in a mesa shape.

diffused planar transistor A diffused transistor in which emitter, base, and collector electrodes are exposed at the face of the wafer, which has an oxide layer to forestall leakage between surface electrodes.

diffused resistor See DIFFUSED-LAYER RESISTOR.

diffused sound **1.** Sound distributed so that its energy flux is the same at all points. **2.** Sound whose source is difficult to locate or seems to shift, as that heard from out-of-phase stereo channels.

5059F-pD-163-223 4/9/01 5:22 PM Page 188

diffused transistor A transistor in which one or both electrodes are created by diffusion. See DIFFUSED JUNCTION.

diffused-junction transistor See DIFFUSED-BASE TRANSISTOR, DIFFUSED-MESA TRANSISTOR, and DIFFUSED TRANSISTOR.

diffusion **1.** In the fabrication of semiconductor devices, the slow, controlled introduction of a material into the semiconductor, for example, the high-temperature diffusion of a n-type impurity (from a gas containing it) into a p-type wafer to form a diode. **2.** The random velocity and movement of current carriers in a semiconductor, resulting from a high-density gradient. **3.** The characteristic spreading of light reflected from a rough surface or transmitted through a translucent material. **4.** The spreading-out of sound waves, for example when reflected from acoustic baffles. **5.** The migration of atoms from one substance to another, as in the spreading of one gas throughout another.

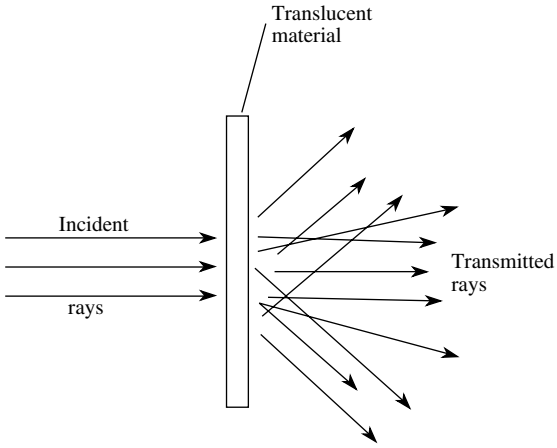

diffusion, 3

diffusion bonding A method of joining different substances by diffusing atoms of one into the other. This technique is employed in the manufacture of certain semiconductor diodes, transistors, and other devices.

diffusion capacitance The current-dependent capacitance of a forward-biased semiconductor junction.

diffusion current Current resulting from the diffusion of carriers within a substance (see DIFFUSION, **2**).

diffusion length In a semiconductor junction, the distance a current carrier travels to the junction during carrier life.

diffusion process **1.** The technique of processing semiconductor devices by diffusion (see DIFFUSION, **1**). **2.** Producing a high vacuum by means of diffusion (see DIFFUSION PUMP).

diffusion pump A pump for fast, efficient creation of a high vacuum in electron tubes and similar devices. In one form, the pump, in conjunction with a force pump, uses mercury vapor as the pumped medium. Gas molecules evacuated from the device diffuse into a chamber, where condensing mercury vapor traps and carries them off.

diffusion theory The notion that, in a homogeneous medium, current density is directly proportional to the gradient of particle flux density.

diffusion transistor A transistor whose operation is based principally on the diffusion of current carriers (see DIFFUSION, **2**).

diffusor In acoustics, a device or structure deliberately installed to spread sound waves throughout a region.

dig-in angle A stylus angle of 90 degrees, relative to the surface of a phonograph disc. Compare DRAG ANGLE.

DIGIRALT Acronym for *digital radar altimetry.* A system that utilizes digital techniques to enhance the accuracy of an altimeter using radar.

digit A single symbol in a numbering system (e.g., 0 through 9 in the decimal system, or 0 or 1 in the binary system), whose value depends on its position in a group and on the radix of the particular system used.

digital **1.** Pertaining to components, circuits, or systems that use signals having an integral number of discrete levels or values, rather than signals, whose levels or values vary over a continuous range. **2.** Pertaining to a numeric readout or display. **3.** See BINARY, **1**.

digital annunciator An annunciator that gives an alphanumeric digital display of information, as well as sounding an alarm.

digital audio tape Abbreviation, DAT. A magnetic tape intended for recording digitally encoded audio data. Used in some high-fidelity applications, and also for computer data storage.

digital barometer An electronic barometer providing a digital readout.

digital capacitance meter Abbreviation DCM. A meter with a digital readout for measuring capacitance values.

digital cellular See PERSONAL COMMUNICATIONS SERVICE.

digital circuit A circuit affording a dual-state switching operation (i.e., on or off, high or low, etc.). Also called *binary circuit.*

digital communications Radio or wire communications using a dual-state mechanism (on/off, positive/negative, or modulated/unmodulated) to represent information.

digital comparator A comparator that presents two digital values, one for each of the quantities being compared.

5059F-pD-163-223 4/9/01 5:22 PM Page 189

digital computer A high-speed, electronic machine for performing mathematical operations, file management, machine control, or other "intelligent" functions, and whose basic internal operations (data storage, comparing, and computation) are based on semiconductor devices assuming one of two states (on or off, high or low). Compare ANALOG COMPUTER.

digital data Information represented and processed in the form of combinations of digits (0 and 1, in the binary system).

digital-data cable A cable designed to conduct high-speed digital pulses with minimal distortion and loss.

digital data-handling system A system that accepts, sorts, modifies, classifies, or records digital data, displaying the final result or passing the data to a computer.

digital delay circuit A device that stores digitized audio data, and releases it after a specified delay.

digital device **1.** A digital integrated circuit (IC). **2.** Any circuit or system that operates by digital means.

digital differential analyzer Abbreviation, DDA. A digital computer that can perform integration using specialized circuitry.

digital display A presentation of information (such as the answer to a problem) in the form of actual digits, as opposed to one in the form of, for example, a meter deflection. See, for example, DIGITAL-TYPE METER.

digital divider In a computer, a device that can divide (i.e., provide a quotient and remainder using dividend and divisor signals).

digital electrometer An electrometer that has a digital current or voltage indicator.

digital electronics The branch of electronics concerned with components, circuits, and systems that use signals having an integral number of discrete levels or values, as opposed to signals whose levels or values vary over a continuous range. Compare ANALOG ELECTRONICS.

digital frequency meter A direct-reading frequency meter using high-speed electronic switching circuits and a digital readout. Such instruments read frequency from less than 1 Hz to many gigahertz.

digital HIC A hybrid integrated circuit (HIC) designed for digital applications. Also see DIGITAL INTEGRATED CIRCUIT.

digital IC See DIGITAL INTEGRATED CIRCUIT.

digital incremental plotter A device that can draw, according to signals received from a computer, graphs depicting solutions to problems.

digital information See DIGITAL DATA.

digital information display See DIGITAL DISPLAY.

digital integrated circuit An integrated circuit (IC) intended for binary operations, such as switching, gating, etc. Compare LINEAR INTEGRATED CIRCUIT.

digital integrator A device that can perform integration, in which increments in input variables, and an output variable, are represented by digital signals.

digital logic A form of Boolean algebra, consisting of negation, conjunction, and disjunction, in which the binary digit 1 has the value "true" and 0 the value "false" (in positive logic) or vice versa (in negative logic). Digital logic is the basis by which all digital devices function.

digital-logic module **1.** A circuit that performs digital operations. **2.** A logic gate.

digital meter A meter that produces a readout in discrete blocks or directly as numerals. The first, more primitive and less precise type, is known as a BAR METER. The second, more sophisticated type can resolve to several significant digits and often includes a fixed or floating radix point. This scheme eliminates the need for personnel to interpolate the reading on a scale. There is little chance for error on the part of the technician or engineer, because the readout is straightforward. Another advantage is the fact that there are no moving parts to wear out or be damaged by physical shock. Compare ANALOG METER.

digital multimeter Abbreviation, DMM. A voltohm-milliammeter producing a digital readout of measured values.

digital multiplex **1.** The combination of several or many digital signals into a single digital signal. **2.** Also called *digital demultiplex.* The reverse process from that defined in 1, in which the original signals are obtained from the combination signal. **3.** Communication using the techniques defined in 1 and 2.

digital multiplex equipment Equipment that accomplishes digital multiplexing or the reverse process, digital demultiplexing.

digital multiplier In a digital computer, a device that produces a product signal from multiplier and multiplicand signals.

digital output An output signal of digital pulses representing a number equal or proportional to the value of a corresponding input signal.

digital panel meter A numeric-readout meter whose relatively small size allows mounting on a panel.

digital phase shifter A phase shifter actuated by a digital control signal.

digital photometer An electronic photometer providing a digital readout of illumination values.

digital power meter An electronic wattmeter providing a digital readout of measured power.

digital readout An indicating device that displays a sequence of numerals that represent a measured value.

digital recording A system for tape-recording high-fidelity sound. The audio is converted from analog to binary digital form, and the binary digits (bits) are recorded on magnetic tape.

digital representation The use of digital signals to represent information as characters or numbers.

5059F-pD-163-223 4/9/01 5:22 PM Page 190

digital rotary transducer A device that delivers a digital output signal proportional to the rotation of a shaft.

Digital Satellite System Abbreviation, DSS. Trade name for a satellite television (TV) system developed by RCA. The analog signal is changed into digital pulses at the transmitting station via analog-to-digital (A/D) conversion. The digital signal is amplified and uplinked to a geostationary satellite. The satellite has a transponder that receives the signal, converts it to a different frequency, and downlinks it back to the earth. The downlink is picked up by a portable dish that can be placed on a balcony or patio, on a rooftop, or in a window. A tuner selects the channel that the subscriber wants to watch. The digital signal is amplified. If necessary, digital signal processing (DSP) can be used to improve the quality of reception under marginal conditions. The digital signal is changed back into analog form, suitable for viewing on a conventional TV set, via digital-to-analog (D/A) conversion.

digital signal A signal having an integral number of discrete levels or values, as opposed to a signal whose levels or values vary over a continuous range.

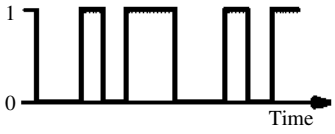

digital signal

digital signal processing Abbreviation, DSP. A method of signal enhancement that operates by eliminating confusion between digital states. This improves dynamic range and frequency response, reduces the number of errors, and virtually eliminates noise. It is used extensively in digital communication and recording, often in conjunction with analog-to-digital (A/D) and digital-to-analog (D/A) conversion to enhance the quality of analog signals and recordings.

digital sound Sound recording and reproduction accomplished with digital, rather than analog, signals. Advantages include wideband frequency response, superior dynamic range, and relative immunity to noise.

digital speech communications A system of voice communications, in which the analog voice signal is encoded into digital pulses at the transmitter, and decoded at the receiver.

digital subtractor In a computer, a device that produces an output signal whose value is equal to the difference of the values of two input signals.

digital switching Routing operations carried out on digital signals to establish communications links between specified system users.

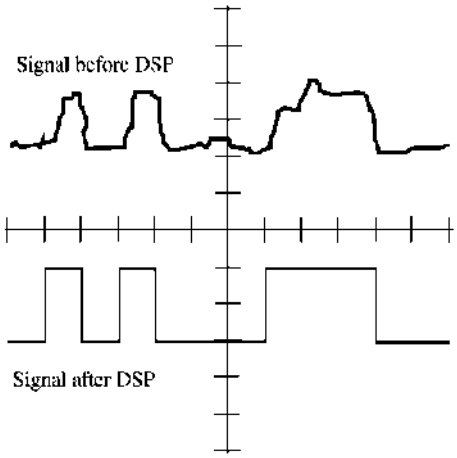

digital signal processing

digital television **1.** A television system in which the picture information is encoded into digital form at the transmitter, and decoded at the receiver. **2.** A form of television picture transmission that functions according to picture motion, rather than absolute brightness.

digital temperature indicator See DIGITAL THERMOMETER.

digital thermometer An electronic thermometer that provides a digital readout of temperature.

digital-to-analog conversion The conversion of a digital quantity into an analog representation, such as shown by a performance curve. Compare ANALOG-TO-DIGITAL CONVERSION.

digital-to-analog converter A circuit or device that performs DIGITAL-TO-ANALOG CONVERSION.

digital transmission **1.** A method of signal transmission in which the modulation occurs in defined increments, rather than over a continuous range. **2.** A message that is sent in digital form.

digital-type meter An indicating instrument in which a row of numeral indicators displays a value. Compare ANALOG-TYPE METER.

digital voltmeter Abbreviation, DVM. An electronic voltmeter having a direct numerical readout, rather than an analog display.

digital wattmeter See DIGITAL POWER METER.

digital compression In digital computer operation, the process of representing data with an economy of characters to reduce file size.

digit current In digital computer operations, the current associated with writing or reading a digit into or out of a memory cell.

digit delay element A logic element (gate) whose output signal lags the input signal by one digit period.

5059F-pD-163-223 4/9/01 5:22 PM Page 191

digit filter A device for detecting designations. See DESIGNATION.

digitize **1.** To express the results of an analog measurement in digital units. **2.** To convert an analog signal into corresponding digital pulses.

digitizer See ANALOG-TO-DIGITAL CONVERTER.

digit period In a digital circuit or system, the time interval between the start of one digital pulse and the start of the next pulse.

digit place See DIGIT POSITION.

digit plane In a matrix-type computer memory, the plane within a three-dimensional array of memory storage elements representing a DIGIT POSITION.

digit position The ordinal position of a digit in a numeral, the first position being occupied by the least-significant digit (e.g., 7 is in the third position in the numeral 756).

digit pulse A pulse that energizes magnetic core memory elements representing a digit position in several words.

digitron A display in which all of the characters lie in a single, flat plane.

digit time The duration of a digit signal in a series of signals.

digit time slot In digital communications, the interval of time assigned to one bit or one digit.

digit-transfer bus In a digital computer, a main line (of conductors) that transfers information among various registers; it does not handle control signals.

diheptal CRT base The 14-pin base of a cathode-ray tube. Also see BIDECAL, DUODECAL, and MAGNAL.

DIIC Abbreviation for *dielectric-isolated integrated circuit.* Several separate integrated-circuit wafers are contained in a single package, and kept electrically insulated by layers of dielectric.

dilatometer An instrument used to measure expansion.

dimension **1.** Any measurable quantity, such as distance, time, temperature, humidity, etc. **2.** An axis in the three-dimensional Cartesian coordinate system. **3.** An independent variable in a function of one or more variables.

dimensional analysis A mathematical procedure whereby an equation involving quantities with different units is verified as being *dimensionally correct.* The original variables are replaced with fundamental quantities, such as resistance (R), current (I), length or displacement (d), and time (t), applicable to electrical systems. The equation is dimensionally correct if it can be shown that the left and right sides of the equation are identical.

dimensional ratio In magnetism, the ratio of the longest diameter of an elongated ellipsoid of revolution to the shortest.

dimensional stability Nonvariance or little variance in the shape and size of a medium (such as film) during the processing of that material.

dimensionless quantity A quantity that is merely a real number. Example: logarithm, exponent, numerical ratio, etc. In contrast are physical quantities: 3 volts, 5000 hertz, 10 amperes, etc.

diminished radix complement See COMPLEMENT.

dimmer An electronic device used for controlling the brightness of incandescent lamps. Using amplified control, the device enables high-wattage lamp loads to be smoothly adjusted via a small rheostat or potentiometer. A photoelectric-type dimmer automatically controls lamps in accordance with the amount of daylight.

dimmer curve The function of a light-dimmer voltage output as a function of setting on a linear scale.

DIN Abbreviation for *Deutsche Industrie Normenausschuss.* A German association that sets standards for the manufacture and performance of electrical and electronic equipment, as well as other devices.

D indicator In radar operations, an indicator combining type B and C indicators (see B DISPLAY and C DISPLAY).

Dingley induction-type landing system An aircraft landing system that provides lateral and vertical guidance; instead of radio, it uses the magnetic field surrounding two horizontal cables laid on or under either side of the runway.

diode A two-element device containing an anode and a cathode, and providing unidirectional conduction. The many types are used in such devices as rectifiers, detectors, peak clippers, mixers, modulators, amplifiers, oscillators, and test instruments.

diode action **1.** The characteristic behavior of a diode (i.e., rectification and unidirectional conduction). **2.** Two-electrode rectification or unidirectional conductivity in any device other than a diode (e.g., asymmetrical conductivity between the collector and base of a transistor).

diode amplifier **1.** A parametric amplifier employing a varactor. **2.** An amplifier utilizing hole-storage effects in a semiconductor diode. **3.** A negative-resistance amplifier using a tunnel diode.

diode array A combination of several diodes in a single housing.

diode assembly See DIODE ARRAY.

diode bias A steady direct-current (dc) voltage applied to a diode to establish its operating point.

diode capacitance The capacitance existing at the p-n junction of a semiconductor diode when the junction is reverse-biased. The capacitance generally varies, depending on the reverse-bias voltage.

diode capacitor **1.** A capacitor normally operated with a diode. **2.** A voltage-variable capacitor utilizing the junction capacitance of a semiconductor diode (e.g., a varactor).

diode-capacitor memory cell A high-value capacitor in series with a high-back-resistance semi-

5059F-pD-163-223 4/9/01 5:22 PM Page 192

conductor diode. A data pulse forward-biases the diode and charges the capacitor, which remains charged, thus holding the data bit, because of the long time constant of the high capacitance and the high back resistance of the diode.

diode characteristic The current-versus-voltage curve for a diode.

diode checker An instrument for testing semiconductor diodes. There are two forms: A static checker, which measures forward and reverse current; and a dynamic checker (see DYNAMIC DIODE TESTER), which displays the entire diode response curve on an oscilloscope screen.

diode chopper A chopper using an alternately biased diode as the switching element.

diode clipper A clipper using one or more diodes. A single biased diode will limit the positive or negative peak of an applied alternating-current (ac) voltage, depending on diode polarity and bias. Two biased diodes with opposing polarity will clip both peaks. Also see LIMITER.

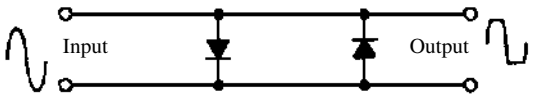

diode clipper

diode converter See DIODE MIXER.

diode current The forward or reverse current flowing through a diode.

diode current meter A direct-current (dc) milliammeter or microammeter with a semiconductor-diode rectifier that allows the measurement of alternating current (ac).

diode curve changer A diode or network of diodes used to make a linear current-voltage curve acquire some nonlinear shape.

diode demodulator See DEMODULATOR PROBE and DIODE DETECTOR.

diode detector A detector circuit in which a diode demodulates a signal. The diode, a simple device, provides linear response at high signal amplitudes, but affords no amplification.

diode feedback rectifier **1.** In a rectified-carrier, negative-feedback system for an amplitude-modulated (AM) transmitter, the diode that rectifies the modulated carrier and provides the audio envelope for use as negative-feedback voltage. This voltage is applied to the speech amplifier/modulator channel to reduce distortion, noise, and hum, at the same time providing automatic modulation control. **2.** The diode that rectifies a part of the signal at the output of an audio amplifier and provides a proportional direct-current (dc) voltage for use as bias in an automatic-gain-control (AGC) circuit.

diode field-strength meter A simple meter for measuring the intensity of a radio-frequency (RF) electromagnetic field. It consists of a short whip antenna, an inductance-capacitance (LC) tuned circuit, a diode detector, and a direct-current (dc) microammeter. The deflection of the meter is roughly proportional to the RF signal voltage.

diode gate A passive switching circuit of biased diodes. Also see AND CIRCUIT and OR CIRCUIT.

diode impedance The vector sum (resultant) of the resistive and reactive components of a diode. In a semiconductor diode, the inductive component of reactance is almost entirely the inductance of leads and electrodes, whereas the capacitive component of reactance is the shunting capacitance between leads and electrodes, plus the voltage-variable capacitance of the pn junction. The resistive component is almost entirely the voltage-variable resistance of the pn junction.

diode isolation A means of insulating an integrated-circuit chip from its substrate. The chip is surrounded by a pn junction that is reverse-biased. This prevents conduction between the chip and the substrate.

diode lamp See LASER DIODE.

diode laser See LASER DIODE.

diode light source See LASER DIODE.

diode limiter See DIODE CLIPPER.

diode load **1.** The current drawn from a diode acting as a rectifier or demodulator. **2.** The output (load) resistor into which a diode operates.

diode load resistance The required value for a diode load resistor.

diode load resistor A resistor usually connected to the output of a diode rectifier or diode detector.

diode logic Digital circuitry, such as AND and OR circuits, using diodes as the principal components.

diode matrix In some digital devices, a grid of wires, the intersections of some being interconnected through diodes, whose polarities determine circuit operation. A series of AND circuits is provided by this arrangement, which acts as a high-speed rotary switch when it is supplied with input pulses.

diode mixer A frequency converter that operates via the nonlinearity of semiconductor diodes.

diode noise limiter A noise limiter circuit having one or more biased diodes.

diode oscillator An oscillator based on the negative resistance or breakdown characteristics of certain diodes, such as high-reverse-biased germanium diodes, tunnel diodes, Gunn diodes, and four-layer diodes. It is generally used at microwave frequencies.

diode pack A device containing more than one diode. An example is the full-wave bridge-rectifier integrated circuit.

diode peak detector A diode detector whose load resistance is high at modulation frequencies; the voltage across the resistance is proportional to the peak amplitude of the modulated signal.

5059F-pD-163-223 4/9/01 5:22 PM Page 193

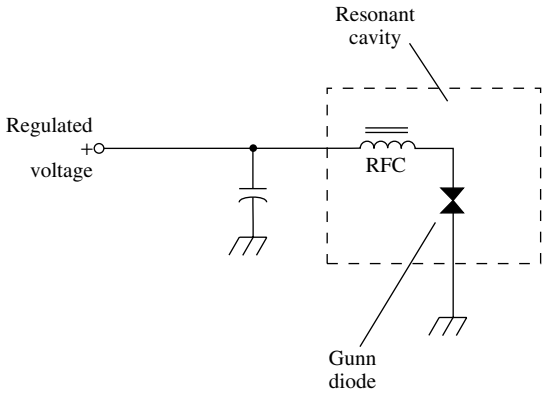

diode oscillator, 1

diode peak voltmeter A diode-type alternating-current (ac) voltmeter, in which the deflection of the direct-current (dc) milliammeter or microammeter is proportional to the peak value of the applied ac voltage.

diode probe A test probe containing a diode used as either a rectifier or demodulator.

diode recovery time The interval during which relatively high current continues to flow after the voltage across a semiconductor junction has been abruptly switched from forward to reverse. Recovery time is attributable to DIODE STORAGE.

diode rectification Conversion of alternating current (ac) to pulsating direct current (dc) by diode action.

diode rectifier **1.** A diode device that converts alternating current (ac) to pulsating direct current (dc) in a power supply. **2.** A small-signal diode device that converts ac to dc in the automatic-gain-control (AGC) circuit of a superheterodyne receiver. Also called *AGC rectifier.*

diode resistor **1.** A resistor usually operated with a diode. **2.** A voltage-variable resistor utilizing the (usually forward) resistance of a semiconductor diode.

diode storage The charge carriers (electrons and holes) remaining within a pn junction for a short time after forward bias has been either removed or switched to reverse polarity.

diode storage time See DIODE RECOVERY TIME.

diode switch See DIODE GATE.

diode sync separator A diode used in a television receiver circuit to separate and deliver the sync pulses from the composite video signal.

diode temperature stabilization **1.** Keeping the temperature of a diode at a constant level. **2.** Using the temperature-resistance characteristic of a forward-biased semiconductor diode to stabilize a circuit (such as a transistor amplifier stage) (i.e., to prevent variations caused by temperature changes).

diode tester See DIODE CHECKER.

diode transistor **1.** See UNIJUNCTION TRANSISTOR. **2.** A semiconductor diode whose operation simulates that of a transistor by means of pulsed operation that alternately makes the single junction an emitter or collector. **3.** A transistor connected to operate solely as a diode.

diode-transistor logic Abbreviation, DTL. Logic circuitry in which a diode is the logic element and a transistor acts as an inverting amplifier.

diode-type meter A rectifier-type alternating-current (ac) meter consisting of a semiconductor diode(s) and a direct-current (dc) milliammeter or microammeter. The diode rectifies the ac input, the resulting dc deflecting the meter.

diode varactor A conventional semiconductor diode or rectifier used as a makeshift varactor (voltage-variable capacitor).

diode variable resistor See DIODE VARISTOR.

diode varistor A conventional diode used as a makeshift varistor (voltage-variable resistor).

diode voltage reference See ZENER VOLTAGE REFERENCE.

diode voltage regulator See ZENER VOLTAGE REGULATOR.

DIP Abbreviation of DUAL IN-LINE PACKAGE.

dip **1.** A distinct decrease in the value of a varying quantity, followed by an increase [e.g., the sudden drop, followed by a rise, in collector current when a bipolar-transistor radio-frequency (RF) power amplifier is tuned through resonance]. **2.** Also called *magnetic inclination.* The slanting of a compass needle, resulting from the orientation of the geomagnetic lines of flux, with respect to the earth's surface. It varies, depending on magnetic latitude.

dip adapter An external accessory that allows a radio-frequency (RF) signal generator to be used as a DIP METER.

dip coating **1.** Applying a protective coat of insulating material to a conductor or component by dipping it into the liquid material, then draining and drying it. Compare SPRAY COATING. **2.** The coat applied in this way.

dip encapsulation Embedding a component or circuit in a protective block of insulating material (such as a plastic) while the material is in a liquid state, and then allowing the material to harden in ambient air or in an oven.

dip impregnation Saturating a component or material (such as absorbent film) with a substance (such as oil or wax) by dipping or vacuum forcing.

diplexer A coupler that permits two or more transmitters to operate simultaneously into a single antenna.

diplex operation **1.** Simultaneous transmission or reception of two signals using a single antenna. **2.** Simultaneous transmission or reception of two signals on a single carrier.

diplex reception The reception of signals while transmitting with the same antenna.

5059F-pD-163-223 4/9/01 5:22 PM Page 194

diplex transmission The transmission of signals while receiving with the same antenna.

dip meter A tunable radio-frequency (RF) instrument that, by means of a sharp dip of an indicating meter, indicates resonance with an external circuit under test. Specific names are derived from the active component used: *grid-dip meter*, *gate-dip meter*, etc.

dip needle See INCLINOMETER.

dipolar Also, *bipolar.* Possessing two poles (usually electric or magnetic).

dipolarization See DEPOLARIZATION.

dipole **1.** A pair of electrically opposite charge poles separated by a specific distance. **2.** A pair of magnetically opposite poles separated by a specific distance. **3.** See DIPOLE ANTENNA. **4.** See FOLDED DIPOLE.

dipole antenna Also called *dipole* and *doublet.* A half-wavelength radiator fed at the center with a two-wire or coaxial transmission line. Each "leg" of the antenna is one-quarter wavelength long. Such an antenna can be oriented horizontally or vertically, or at a slant. The radiating element is usually straight. For a straight wire radiator, properly insulated at the ends and placed well away from obstructions, the length L_{ft} (in feet) at a design frequency f (in megahertz) is approximately

$$L_{ft} = 467/f$$

The length L_m (in meters) is close to

$$L_m = 143/f$$

Because of its simplicity, this antenna is popular among shortwave listeners and radio amateurs, especially at frequencies below 10 MHz. A full-size antenna of this type has a feed-point impedance of approximately 73 ohms, purely resistive. Compare FOLDED DIPOLE.

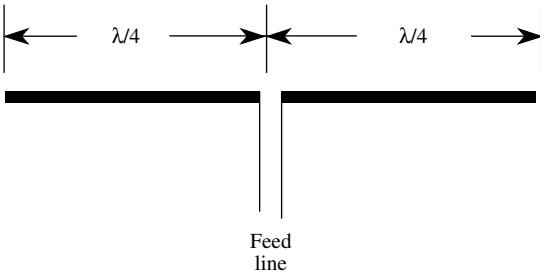

dipole antenna

dipole disk feed A method of coupling radio-frequency energy to a disk-shaped antenna. The energy is applied to a dipole located adjacent to the disk.

dipole feed A method of coupling radio-frequency energy to an antenna by means of a half-wave dipole. The dipole is directly fed by the transmission line, and the dipole radiates energy to the rest of the system.

dip oscillator The oscillator that provides the signal for a DIP METER.

dipotassium tartrate Abbreviation, DKT. An organic piezoelectric material.

dipped component A discrete electronic component that has been given a protective coating by dipping into a suitable material (such as oil, varnish, or wax) and draining off the surplus.

dipper Collective term for resonance-type instruments, such as a DIP METER or DIP ADAPTER.

dipper interrupter A cyclic switching device in which a contact pin is part of a revolving wheel partially immersed in mercury.

dipping **1.** The application of a protective coating or impregnant to a component by immersing it in a suitable material. Also see DIP COATING, DIP ENCAPSULATION, and DIP IMPREGNATION. **2.** In a resonant (tuned) amplifier circuit, the adjustment of the resonant circuit for minimum current through the amplifying device.

dipping needle See INCLINOMETER.

dip soldering **1.** Soldering leads or terminals by dipping them into molten solder and then removing excess solder. **2.** Tinning printed-circuit patterns by dipping the boards into molten solder or placing them in contact with the surface of a solder bath. **3.** Soldering leads in printed circuits by the methods defined in (2).

DIP switch A switch (or group of miniature switches) mounted in a dual-inline package (DIP) for easy insertion into an integrated-circuit socket or printed-circuit board.

direct-access storage device A computer memory in which data access time is unaffected by the data location. Also called *random-access memory device.*

direct-acting recorder See GRAPHIC RECORDER.

direct-acting recording instrument See GRAPHIC RECORDER.

direct address The actual address of a computer storage location (i.e., the one designated by machine code 0. Also called *absolute address* or *real address.*

direct capacitance The capacitance between two points in a circuit, as opposed to the capacitance between either point and other objects (including ground).

direct allocation In digital computer operations, to specify the necessary memory locations and peripherals for a particular program when it is written.

direct coding Computer programming in machine language.

direct control Control of one machine by another, for example, the control of a computerized mobile robot by a central computer system.

direct-conversion receiver A heterodyne receiver in which the incoming radio-frequency (RF) signal

5059F-pD-163-223 4/9/01 5:22 PM Page 195

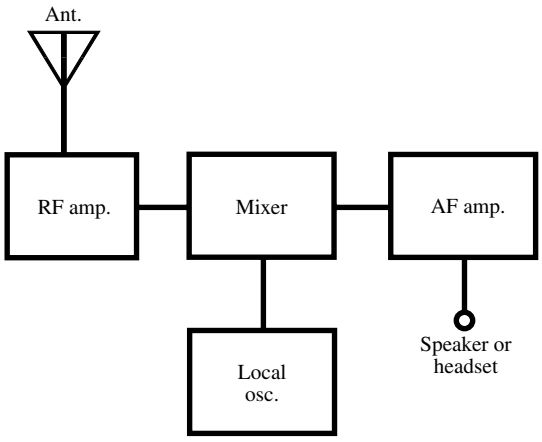

direct-conversion receiver

is amplified, then mixed with the RF output of a tunable local oscillator, producing an audio-frequency (AF) beat note. The AF is amplified; audio filtering can be added. Although the direct-conversion receiver somewhat resembles the superheterodyne type, it has no intermediate-frequency (IF) chain, and does not normally provide single-signal reception. Also see ZERO-BEAT RECEPTION.

direct-coupled amplifier An amplifier in which the output circuit of one stage is wired directly to the input circuit of the following stage (i.e., there is no intervening capacitor or transformer). Such an amplifier can handle alternating-current (ac) or direct-current (dc) signals, and has wide frequency response.

direct-coupled transistor logic Abbreviation, DCTL. In digital computer and switching circuits, a logic system using only direct-coupled transistor stages.

direct coupling Direct connection of one circuit point to another for signal transmission (i.e., without intermediate capacitors or transformers). Because coupling devices aren't used, direct coupling provides transmission of direct current (dc), as well as alternating current (ac).

direct current **1.** Abbreviation, dc. A current that always flows in the same direction (i.e., the polarity never reverses). The current might be constant, as from a battery or a regulated power supply; it might be pulsating, as from an unfiltered rectifier. **2.** Pertaining to current that always flows in the same direction. **3.** Descriptive of a voltage, resistance, or other parameter under conditions in which there is a usually constant current that always flows in the same direction.

direct-current amplifier An amplifier for boosting direct-current (dc) signals, as opposed to dc voltage signals.

direct-current bar See DC BAR.
direct-current beta See DC BETA.
direct-current block See DC BLOCK.
direct-current bus See DC BUS.
direct-current circuit breaker See DC CIRCUIT BREAKER.
direct-current component See DC COMPONENT.
direct-current converter See DC CONVERTER.
direct-current coupling See DC COUPLING.
direct-current dump See DC DUMP.
direct-current equipment See DC EQUIPMENT.
direct-current erase head See DC ERASE HEAD.
direct-current generator See DC GENERATOR.
direct-current inverter See DC INVERTER.
direct-current leakage See DC LEAKAGE.
direct-current motor See DC MOTOR.
direct-current noise See DC NOISE.
direct-current power See DC POWER.
direct-current relay See DC RELAY.
direct-current resistance See DC RESISTANCE.
direct-current shift See DC SHIFT.
direct-current short See DC SHORT.
direct-current signaling See DC SIGNALING.
direct-current source See DC SOURCE.
direct-current transducer See DC TRANSDUCER.
direct-current transformer See DC TRANSFORMER.
direct-current transmission See DC TRANSMISSION.

direct digital control In a digital computer, multiplexing or time sharing among a number of controlled loops.

direct display unit A cathode-ray-tube (CRT) peripheral that displays data recalled from memory.

direct-distance dialing A form of telephone service that allows dialing of long-distance numbers without involving a human operator.

direct drive **1.** Pertaining to electromechanical accessories for electronic equipment. **2.** The transmission of power directly from a source (such as a motor) to a driven device without intermediate gears, belts, or clutches.

direct-drive robot A robot that uses the minimum possible number of gears and other drive systems.

direct-drive torque motor In a positioning or speed-control system, a servoactuator connected directly to the driven load.

direct-drive tuning A tuning or adjusting mechanism in which the shaft of the variable component (such as a potentiometer or variable capacitor) is turned directly by a knob (i.e., without gearing, dial cable, or similar linkage).

directed number A number having direction as well as magnitude; a vector quantity.

direct electromotive force A direct-current (dc) voltage that does not fluctuate or pulsate.

direct emf See DIRECT ELECTROMOTIVE FORCE.

direct ground **1.** A ground connection made by the shortest practicable route. Compare INDIRECT GROUND. **2.** An earth ground.

5059F-pD-163-223 4/9/01 5:22 PM Page 196

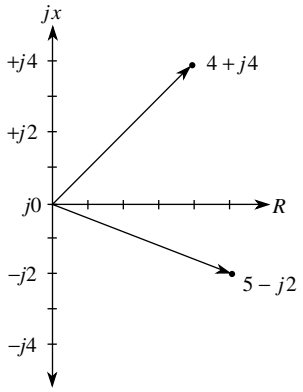

directed number

direct induced current A transient current induced in the same direction as the induction current when it is interrupted.

directing antenna See DIRECTIONAL ANTENNA.

direct-input circuit A circuit, especially an amplifier, whose input is wired directly to the input electrode of the active device (i.e., without a coupling capacitor or transformer).

direct-insert subroutine In digital computer operations, a subroutine directly inserted into a larger instruction sequence. It must be rewritten at every point it is needed.

direct instruction A computer program instruction that indicates the location of an operand in memory.

directional **1.** Depending on direction or orientation. **2.** Having a concentration in an identifiable direction. **3.** Pertaining to a transducer in which radiation, or sensitivity, is concentrated in certain directions at the expense of radiation or sensitivity in other directions.

directional antenna An antenna that transmits and receives signals more effectively in some directions than in others. Also called *beam*, *beam antenna*, and *directive antenna.*

directional array **1.** A directional antenna having a set of elements assembled in such a way that their combined action shapes the radiation into a unidirectional pattern. **2.** A group of antennas spaced and phased to produce unidirectional radiation and reception patterns.

directional beam **1.** An antenna whose radiation or reception pattern strongly favors a specific direction. **2.** The radiation or reception pattern of such an antenna.

directional characteristic The precise directional properties of an antenna or transducer.

directional CQ In amateur radio, a transmission that invites replies only from stations in a certain direction or in a particular city, state, or country.

directional coupler A microwave device that couples an external system to waves traveling through the coupler in one direction.

directional diode A high-back-resistance semiconductor diode inserted into a direct-current (dc) signal circuit or control circuit. Permits unidirectional current flow.

directional filter In carrier-current transmission, a filter that halves the frequency band, one half being for transmission in one direction, and the other half being for transmission in the opposite direction.

directional gain Symbol, k_S. The ratio of the power that would be radiated by a loudspeaker if the free-space axial sound pressure were constant over a sphere, to the actual radiated power. Usually expressed in decibels.

directional homing A scheme for locating the source of a radio signal. An effort is made to keep the bearing of the target or guiding station constant. Therefore, the search path is as direct (as nearly a straight line) as practicable.

directional horn See DIRECTIVE HORN.

directional hydrophone A hydrophone whose response pattern strongly favors one direction.

directional lobe In the spatial response pattern of a device, such as an antenna or loudspeaker, a portion showing emphasized response in a given direction.

directional microphone A microphone that strongly favors sound emanating from in front of it.

directional pattern See DIRECTIVITY PATTERN.

directional phase shifter A phase-shifting circuit in which the characteristics are different in one direction, as compared with the other direction.

directional power relay A relay that is actuated when the monitored power reaches a prescribed level in a given direction.

directional relay See POLARIZED RELAY.

directional response For any form of transducer, a radiation or sensitivity pattern that is concentrated in certain directions.

directional separation filter See DIRECTIONAL FILTER.

directional transducer A device that senses or emits some effect to an extent that depends on the direction from which the effect comes. Directional effects are often, but not always, accompanied by gain in the favored direction(s). Examples: *directional microphone*, *directional speaker*, and *directional antenna.*

directional variation of radio waves Changes in the field strength of radio waves, depending on the direction. There are various causes, including antenna directivity, ground characteristics, ionospheric factors, weather conditions, and the presence of obstructing objects.

directional wattmeter A device that can measure radio transmitter output power and can also give an indication of how well an antenna is matched

5059F-pD-163-223 4/9/01 5:22 PM Page 197

to a transmission line. Such meters fall into two categories. One type has a single scale, calibrated in watts, and sometimes also in milliwatts or kilowatts (switch selectable). The meter reads either forward power or reflected power, depending on the position of a switch or rotatable internal element. Another type has two needles in a single enclosure, with a different calibrated scale for each needle. Both of these scales are graduated in watts, and sometimes also in milliwatts or kilowatts. One needle/scale indicates forward power and the other needle/scale indicates reflected power. There is a third scale, calibrated for the point where the two needles cross. This scale indicates the standing-wave ratio (SWR). See also CROSSED-POINTER INDICATOR.

direction angle In radar operations, the angle between the center of the antenna baseline and a line going to the target.

direction finder A receiver specially adapted to show the direction from which a signal is received, thus revealing the direction of the receiver with respect to the transmitting station, and vice versa. In its simplest form, it is a receiver with a loop antenna that is rotatable over a map or compass card. For increased accuracy, checks are made with signals from two transmitting stations; the exact location of the receiver is pinpointed by triangulation.

direction finding The taking of bearings by means of a direction finder.

direction of lay In a multiconductor cable, the lateral direction of winding of the topmost conductors as they recede from the observer; called *left-hand lay* or *right-hand lay.* If the cable is viewed from either end, left-hand lay is equivalent to conductors that rotate clockwise as they recede from the viewer; right-hand lay is equivalent to conductors that rotate counterclockwise as they recede from the viewer.

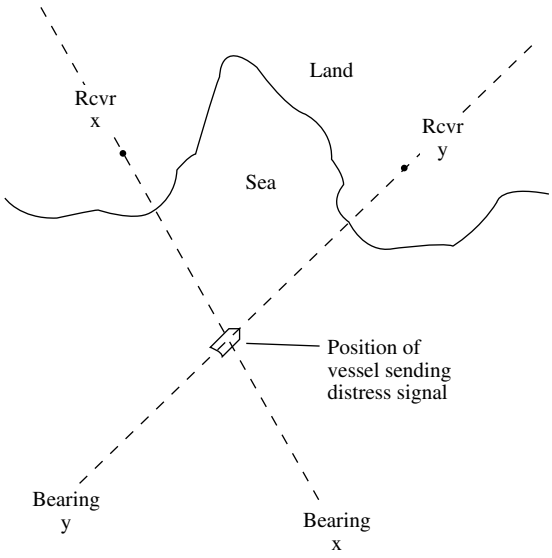

direction finding

direction of polarization The direction of the electrostatic field in a linearly polarized wave.

direction of propagation The direction in which energy moves from a transmitter, or between equivalent points in a sector of space under consideration.

direction rectifier In a control system, a rectifier whose direct-current (dc) output voltage has a magnitude and polarity dependent on the magnitude and phase of an alternating-current (ac) selsyn error voltage.

direction resolution **1.** The smallest difference in azimuth that a direction-finding device can detect. **2.** The smallest angular separation between two targets that allows a radar set to show two separate echoes rather than a single echo.

directive In a computer source program, a statement directing the compiler in translating the program into machine language without being translated itself. Also called *control statement.*

directive antenna An antenna designed for best propagation or reception in one (often steerable) horizontal direction. Also called *beam antenna* and *directional antenna.*

directive gain For a directional antenna, a rating equal to 12.566(*Pr*/*Pt*), where *Pr* is the radiated power per steradian in a given direction and *Pt* is the total radiated power.

directive horn A microwave antenna having the shape of a (usually rectangular) horn.

directivity **1.** In an antenna, a directional response. **2.** The degree to which the radiation or sensitivity of a transducer is concentrated in certain directions. **3.** The angle between the half-power points of a directive antenna in the azimuth plane. **4.** In an antenna system, the ratio, in decibels, between the power in the favored direction and the power in the exact opposite direction; also called front-to-back ratio. **5.** The forward power gain of an antenna, with respect to a dipole in free space. **6.** The forward power gain of an antenna, with respect to an isotropic radiator in free space.

directivity diagram A graph of the radiation/response pattern of a beam antenna or other directional device, usually in a horizontal or vertical plane. Also see DIRECTIVITY PATTERN.

directivity factor **1.** A measure of the directivity of an antenna or transducer. **2.** In acoustics, the ratio, in decibels, between the gain in the maximum direction and the gain in the minimum direction, for a transducer, such as a speaker or microphone.

directivity index **1.** For an acoustic-emitting transducer, the ratio, in decibels, of E_1 to E_2,

5059F-pD-163-223 4/9/01 5:22 PM Page 198

where E_1 is the average intensity over an entire sphere surrounding the transducer, and E_2 is the intensity on the acoustic axis. **2.** For an acoustic pickup transducer, the ratio, in decibels, of E_1 to E_2, where E_1 is the average response over an entire sphere surrounding the transducer, and E_2 is the response on the acoustic axis.

directivity of antenna For a beam antenna, the ratio E_{max}/E_{avg}, where E_{max} is the maximum field intensity at a selected distance from the antenna and E_{avg} is the average field intensity at the same distance.

directivity of directional coupler The ratio, in decibels, of P_1 to P_2, where P_1 is the power at the forward wave-sampling terminals (measured with a forward wave in the transmission line) and P_2 is the power at the terminals when the wave is reversed in direction.

directivity pattern The calculated or measured radiation or response pattern (transmission or reception) of an antenna, microphone, loudspeaker, or similar device, with particular attention to the directional features of the pattern.

directivity signal A spurious output signal resulting from finite directivity in a coupler.

direct light Light rays traveling directly from a source to a receptor or target without reflection.

directly grounded Connected to earth or to the lowest-potential point in a circuit, without any intervening resistance or reactance.

directly heated cathode A vacuum-tube filament. It is so called because, when heated, it becomes the cathode of the tube (i.e., the emitter of electrons).

directly heated thermistor A thermistor whose temperature changes with the surrounding temperature, and also as a result of power dissipation in the device itself. Compare INDIRECTLY HEATED THERMISTOR.

directly heated thermocouple A meter thermocouple heated directly by signal currents passing through it. Compare INDIRECTLY HEATED THERMOCOUPLE.

direct measurement Immediate measurement of a quantity, rather than determining the value of the quantity through adjustments of a measuring device (e.g., measuring capacitance with a capacitance meter, rather than with a bridge). Compare INDIRECT MEASUREMENT.

direct memory access Abbreviation, DMA. The transfer of data from a computer memory to some other location, without the intervention of the central processing unit (CPU).

direct numerical control In a computer or data system, the capability for distributing information among numerically controlled machines whenever desired.

director In a multielement directional antenna, an element that is usually mounted in front of the radiator element, and that is phased and spaced to direct the radiation forward. The director functions in conjunction with the reflector element, which is usually mounted behind the radiator.

directory See DICTIONARY.

direct pickup The broadcasting, especially in television, of events at the same time as they occur (e.g., without recording/reproduction).

direct piezoelectricity The production of a piezoelectric voltage by mechanically stressing a suitable crystal.

direct playback In audio or video recording, the reproduction of a recording without additional processing (e.g., the playing of an original recorded tape, rather than a tape that has been mass produced).

direct-point repeater A relay-operated telegraph repeater. The received signals actuate the relay, which switches the second line.

direct-radiator loudspeaker A loudspeaker whose cone or diaphragm is directly coupled to the air.

direct ray An electromagnetic ray (wave) that reaches a receiver without reflection or refraction, and without encountering obstructions.

direct recording **1.** A record produced by a graphic recorder. **2.** The technique of producing such a record.

direct-recording instrument A device, such as a graphic recorder, that directly produces a permanent record (such as an inked trace) of the variations of a quantity.

direct resistance coupling A form of coupling in which the output of the first amplifying device is connected through a resistor directly to the input of the second device. The resistance value can vary; sometimes the connection is a short circuit.

directrix A fixed line to which a curve is referred (e.g., the axis of a parabola).

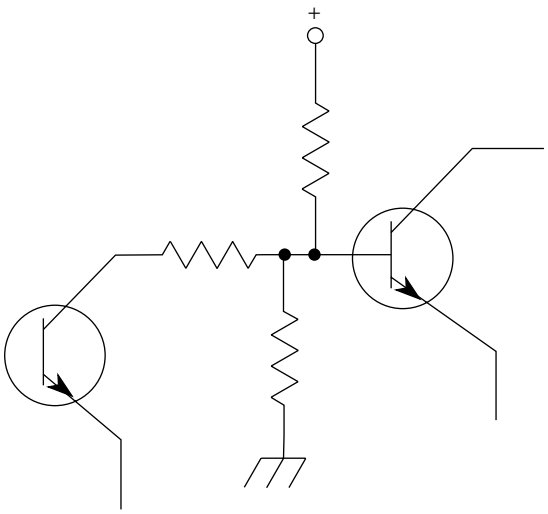

direct resistance coupling

5059F-pD-163-223 4/9/01 5:22 PM Page 199

direct scanning In television, the sequential viewing of parts of a scene by the camera—even though the entire scene is continuously illuminated.

direct serial file organization A technique of organizing files stored in a direct access device, in which a record can be chosen by number and amended where it is without altering other members of the file.

direct sound wave A sound wave arriving directly from its source—especially a wave within an enclosure that is not affected by reflection.

direct substitution **1.** An exact component replacement. **2.** Installing an exact component replacement.

direct synthesizer A device for producing random, rapidly changing frequencies for security purposes. A reference oscillator provides a comparison frequency; the output frequency is a rational-number multiple of this reference frequency.

direct voltage See DC VOLTAGE.

direct wave A wave that travels from a transmitter to a receiver without being reflected by the ionosphere or the ground. Compare SKYWAVE.

direct Wiedemann effect Twisting force (torque) in a wire carrying current in a longitudinal magnetic field. Occurs because of interaction between the longitudinal field and the circular magnetic field around the wire.

direct-wire circuit A communications or control line of wires connecting a transmitter (or control point) and a receiver (or controlled point) without an intermediary, such as a switchboard.

direct-writing recorder See GRAPHIC RECORDER.

direct-writing telegraph **1.** See PRINTING TELEGRAPH. **2.** See TELAUTOGRAPH.

dis- A prefix meaning "deprived of." For the formation of electronic terms, the prefix must be distinguished from *un-*, meaning "not." For example, a *discharged* body is one that was charged, but has been emptied of its charge. An *uncharged* body is one that ordinarily or presently is not charged.

disable **1.** To deliberately render a circuit, device, or system inoperative. **2.** In digital computer operations, to defeat a software or hardware function.

disc See DISK.

disc engraving **1.** Recording sound by cutting a groove in a record disc. **2.** The groove resulting from such a process.

discharge The emptying or draining of electricity from a source, such as a battery or capacitor. The term also denotes a sudden, heavy flow of current, as in DISRUPTIVE DISCHARGE. Compare CHARGE.

discharge current **1.** Current flowing out of a capacitor. **2.** Current flowing out of a cell—especially a storage cell. Compare CHARGING CURRENT.

discharge key See DISCHARGE SWITCH.

discharge lamp A gas-filled tube or globe in which light is produced by ionization of the gas between electrodes. Familiar examples are the neon bulb and fluorescent tube.

discharge phenomena The effects associated with electrical discharges in gases, such as luminous glow.

discharge potential See IONIZATION POTENTIAL.

discharger **1.** A short-circuiting tool for discharging capacitors. **2.** A spark gap or other device for automatically discharging an overcharged capacitor.

discharge rate **1.** The current that can be supplied by an electrochemical cell or battery reliably during its discharging cycle. Usually expressed in milliamperes or amperes. **2.** An expression of the speed with which a battery is being discharged at a specific point in time. It is usually specified in amperes or milliamperes.

discharge switch A switch for connecting a charged capacitor to a resistor or other load, through which the capacitor discharges. In some circuits, when the switch is in its resting position, it connects the capacitor to the charging source.

discharge voltage See IONIZATION POTENTIAL.

discharging **1.** The conversion of chemical energy to electrical energy by an electrochemical cell or battery. **2.** The release of stored electrical energy from a capacitor, or from a network containing capacitors.

discharging tongs See DISCHARGER, **1**.

discone antenna An antenna consisting of a horizontal metal or wire-mesh disk above a metal or wire-mesh cone. The antenna has an omnidirectional radiation pattern in the horizontal plane, and provides a good match to a coaxial transmission line over a frequency range of several octaves. Commonly used at very-high frequencies (VHF) and ultra-high frequencies (UHF).

disconnect **1.** To separate leads or connections, thereby interrupting a circuit. **2.** A type of connector whose halves can be pulled apart to open a cable or other circuit quickly. **3.** To open a switch or relay.

disconnector See DISCONNECT, **2** and DISCONNECT SWITCH.

disconnect signal A signal sent over a telephone line, ending the connection.

disconnect switch A switch whose main function is to open a circuit quickly (either manually or automatically) in the event of an overload.

discontinuity **1.** A break in a conductor. **2.** A point at which the impedance in a transmission line abruptly changes.

discontinuous wave trains See DAMPED WAVES.

discrete **1.** Complete and self-contained, as opposed to a part of something else. **2.** Composed of individual, separate members.

discrete capacitor Capacitance that is entirely self-contained, rather than being electrically dis-

5059F-pD-163-223 4/9/01 5:22 PM Page 200

tributed. Also called LUMPED CAPACITOR. Compare DISTRIBUTED CAPACITANCE.

discrete circuit A circuit comprised of discrete components, such as resistors, capacitors, diodes, and transistors, not fabricated into an integrated circuit.

discrete component A self-contained device that offers one particular electrical property in lumped form (i.e., concentrated at one place in a circuit, rather than being distributed). A discrete component is built especially to have a specific electrical property, and exists independently, not in combination with other components. Examples: disk capacitor, toroidal inductor, and carbon-composition resistor. Compare DISTRIBUTED COMPONENT.

discrete device Any component or device that operates as a self-contained unit.

discrete element A discrete device that forms part of a larger system.

discrete inductor An inductive component that is entirely self-contained, rather than being electrically spread out. Also called *lumped inductor.* Compare DISTRIBUTED INDUCTANCE.

discrete information source A source of data containing a finite number of individual elements, rather than a continuously variable parameter.

discrete part See DISCRETE COMPONENT.

discrete resistor A resistive component that is entirely self-contained, rather than being electrically spread out. Also called *lumped resistor.* Compare DISTRIBUTED RESISTANCE.

discrete sampling Sampling of individual bits or characters, one or more at a time.

discrete thin-film component A discrete component produced by the thin-film process (e.g., thin-film capacitor, thin-film potentiometer, etc.).

discretionary wiring A method of interconnecting the components and circuits on a semiconductor wafer for optimum performance. This requires a separate analysis and wiring pattern for every chip.

discrimination **1.** Sharp distinction between electrical quantities of different value. **2.** The detection of a frequency-modulated (FM) signal (i.e., the delivery of an audio signal corresponding to the frequency or phase variations in the FM carrier).

discriminator A second detector for frequency-modulated (FM) signals, in which two diodes are operated from the center-tapped secondary of a special intermediate-frequency (IF) transformer. The circuit is balanced for zero output when the instantaneous received signal frequency is at the unmodulated carrier frequency; the circuit delivers output when the instantaneous received signal frequency swings above or below the unmodulated carrier frequency. Also see FOSTER-SEELEY DISCRIMINATOR and TRAVIS DISCRIMINATOR.

discriminator transformer The special input transformer in a DISCRIMINATOR.

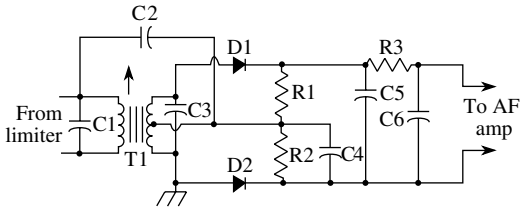

discriminator

discriminator tuner A device that tunes a discriminator to a selected subcarrier.

discriminator tuning device See DISCRIMINATOR TUNER.

dish See DISH ANTENNA.

dish antenna A transmitting and/or receiving antenna consisting of a driven element and a large reflector. The reflector has the shape of a shallow, circular section of a paraboloid or sphere. The feed point is at the focus of the reflector. This antenna, noted for its high directivity and gain, is used mainly at ultra-high and microwave frequencies for communications and satellite television. Large antennas of this type are used in some radio telescopes.

dish-type construction A type of panel-and-chassis construction in which the chassis is fastened vertically to the back of the panel.

disintegration **1.** The destructive breakdown of a material. **2.** The stripping of a vacuum-tube cathode of its emissive coating (see DISINTEGRATION VOLTAGE). **3.** The decay of a radioactive material.

disintegration voltage The anode voltage at which the cathode of a gas tube begins to be stripped of its electron-emitting material. For safety and reasonable tube life, the anode working voltage must be between the ionization and disintegration values.

disintegrator An ultrasonic device for reducing crystals or particles to fine suspensions.

disjunction The logical inclusive-OR operation.

disk **1.** A flat, circular plate (e.g., *rectifier disk*). **2.** See DISKETTE. **3.** See HARD DISK. **4.** See COMPACT DISC. **5.** See CD-ROM. **6.** A phonograph record or the equivalent unrecorded blank.

disk capacitor A fixed (usually two-plate) capacitor consisting of a disk of dielectric material on whose faces are deposited metal-film plates.

disk capacitor

5059F-pD-163-223 4/9/01 5:22 PM Page 201

disk coil See DISK WINDING.

disk dynamo A rudimentary direct-current (dc) generator, in which a copper disk rotates between the poles of a permanent magnet. The outer edge of the disk becomes positively charged; the center of the disk becomes negatively charged.

diskette A magnetic recording disk used for microcomputer data storage. Housed in a square, flat case. In personal computing, there are two sizes: 5.25 inches square and 3.5 inches square. The 5.25-inch version is flexible and is sometimes called a *floppy disk*.

disk files An information-storage system in which data are recorded on rotating magnetic disks.

disk generator **1.** See DISK DYNAMO. **2.** A disk-type electrostatic generator.

disk memory A common misnomer for DISK STORAGE.

Disk Operating System Abbreviation, DOS. Any of several command-driven operating systems commonly used in IBM-compatible personal computers.

disk pack In disk files, a set of disks that can be handled as a single unit.

disk recorder A device for recording (and usually also playing back) sound or other signals on record disks.

disk recording **1.** Recording sound or other signals on disks. **2.** A disk resulting from such a recording. See DISK.

disk rectifier A semiconductor rectifier (such as copper-oxide, selenium, magnesium-copper-sulfide, or germanium type) in which the active material is deposited on a metal disk.

disk resistor A resistor consisting of a resistive material deposited on a metal disk; or a disk of resistive material. In the latter, electrodes are plated on the faces of the disk, one or more of which are held between clips or screws for connections.

disk storage In digital computer systems, an online or offline data storage scheme, in which information is recorded on the magnetic coating of a rotating disk or set of disks. See DISKETTE, and HARD DISK.

disk system A sound-motion-picture system using audio disks synchronized with the film.

disk thermistor A thermistor having the general shape of a disk.

disk-type storage See DISK STORAGE.

disk varistor A varistor having the general shape of a disk.

disk winding An armature or coil winding that is flat, rather than cylindrical. Also called *disk coil*, *pancake coil*, and *spiral coil*.

dislocation A crystal region in which the arrangement of atoms does not have the perfect lattice structure of the crystal.

dispersion **1.** The property of a material that causes energy at different wavelengths to pass through it at different speeds. **2.** The separation of a wave into its various component frequencies (as when white light is broken up into the color spectrum by a prism). **3.** The scattering of a microwave beam when it strikes an obstruction. **4.** The scattering of sound or ultrasound as it emanates from an acoustic transducer. **5.** A suspension of finely divided particles within another substance.

dispersive medium A medium that disperses a wave passing through it.

displacement **1.** A change in the position of a point, particle, figure, or body. **2.** The vector representing a change in the position of a point, particle, figure, or body. **3.** Movement of a member through a specified distance.

displacement current **1.** An alternating current proportional to the rate of change of an electric field, and existing in addition to usual conduction current. **2.** The current flowing into a capacitor immediately after application of a voltage. This current continues to flow, although continually diminishing in value, until the capacitor becomes fully charged.

displacement of porches In a television signal, the amplitude difference between the front porch and back porch of a horizontal sync pulse.

displacement of vectors Vector rotation through a specified number of angular degrees or radians.

displacement transducer A transducer in which movement (displacement) of a rod, armature, core, reed, or other object converts mechanical energy into proportionate electrical energy.

display **1.** Visually observable presentation of information, such as data entered into a computer, an answer to a problem solved by a computer, the value of a measured quantity, or a graph of a function. **2.** The screen in a computer system or terminal that visually portrays text and graphical data. In laptop, notebook, and portable computers, this is usually a *liquid-crystal display (LCD)*; in desktop computers and terminals, it is usually a *cathode-ray tube (CRT)*. **3.** To portray information in a visual manner (e.g., as text, numerals, symbols, or graphic images).

display blanking See DISPLAY INHIBIT.

display console In a computer system, a peripheral that is used to access and display data being processed or stored; often, it is a unit with a cathode-ray tube (CRT), keyboard, and light pen.

display control An interface device between a central processor and several visual display units (terminals).

display dimming See DISPLAY INHIBIT.

display inhibit In a digital meter, the blanking or dimming of the display when the instrument is not being used. It is used to conserve battery energy.

display loss The ratio P_1/P_2, where P_1 is the minimum input-signal power that can be detected by an ideal output device at the output of a receiver, and P_2 is the minimum input-signal power value

5059F-pD-163-223 4/9/01 5:22 PM Page 202

seen by an operator using an output device with the same receiver. Also called *visibility factor.*

display mode **1.** A particular method of presenting a display. For example, a character display on a video unit might consist of bright characters on a dark background, or dark characters on a light background. **2.** An operating mode for a particular device, in which a display is used.

display module A self-contained unit with circuitry and readouts for indicating a numerical count.

display primaries Also called *primary colors.* In a color television receiver, the colors red, green, and blue. When mixed correctly, these three colors can produce any visible hue.

display-storage tube A special cathode-ray tube in which patterns and other information can be stored for later viewing. The tube has two electron guns: a writing gun and a reading (viewing) gun.

display unit A device that presents information for visual reading. Included are analog and digital meters, cathode-ray tubes, data printers, graphic recorders, etc. Also see DISPLAY CONSOLE.

display visibility The ease with which a display can be read by an operator.

display window **1.** In a panoramic display, the width of the presented frequency band in hertz. **2.** The panel opening through which the indication of a display unit appears.

displayed part That portion of a number displayed in the readout of a calculator or computer. There might be digits that are not displayed, but which the machine might take into consideration when making calculations. For example, in a 10-digit calculator display, the number 245.789378214895 would be displayed as 245.7893782. Depending on the calculator design, the machine might truncate (disregard) the undisplayed digits (14895), or take the undisplayed digits into account when making calculations.

disposable component A circuit component or machine part that is so inexpensive that it is more cost-effective to discard it than to repair it when it fails.

disruptive discharge Sudden, heavy current flow through a dielectric material when it fails completely under electric stress.

dissector A transducer that samples an illuminated image point by point.

dissector tube A camera tube using a flat photocathode, upon which the image is focused by the lens system. Electromagnetic deflection from external coils provides scanning. Electrons pass sequentially from the image cathode to a scanning tube at the opposite end of the camera tube. Also called *Farnsworth dissector tube* and *orthiconoscope.*

dissipation **1.** The consumption of power, often without contributing to a useful end, and usually accompanied by the generation of heat. **2.** In an amplifier, the difference between the collector, drain, or plate input power and the usable output power.

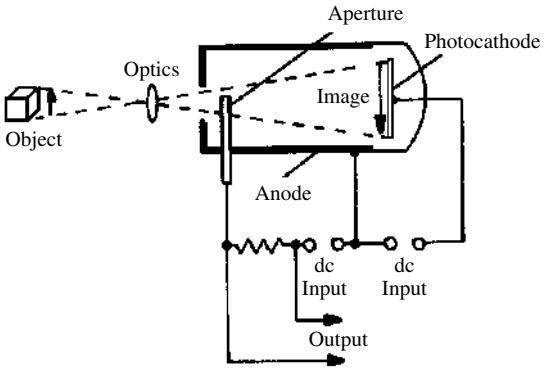

dissector tube

dissipation constant For a thermistor, the ratio of the change in power dissipation to a corresponding change in body temperature.

dissipation factor **1.** For a dielectric material, the tangent of the dielectric loss angle. Also called *loss tangent.* **2.** Symbol, *D.* For an impedance (such as a capacitor), the ratio of resistance to reactance; $D = R/X$. It is the reciprocal of the *figure of merit (Q).*

dissipation line A resistive section of transmission line, used for dissipating power at a certain impedance. Two parallel lengths of resistance wire are terminated by a large, noninductive resistor that has a value equal to the characteristic impedance of the line.

dissipator **1.** A device used primarily to consume power (i.e., a power sink). **2.** A device for removing heat generated by a device's operation (e.g., a heatsink attached to a power transistor).

dissociation The condition that characterizes electrolytes (certain acids, bases, or salts in water solution) in which the molecules of the material break up into positive and negative ions.

dissonance The unpleasant effect (especially in music) produced by nonharmonious combinations of sounds.

dissymmetrical network A network having unequal input and output image impedances.

dissymmetrical transducer A transducer having unequal input and output image impedances.

distance-double law A theoretical rule for determining the rate at which sound intensity decreases as distance increases. Under ideal conditions, when the distance from a sound source is doubled, the sound pressure is reduced to one-fourth of its original level, a reduction of 6 decibels. This is analogous to the *inverse-square law* for visible light and other radiant energy.

5059F-pD-163-223 4/9/01 5:22 PM Page 203

distance mark On a radar screen, a mark indicating the distance from the radar set to the target.

distance measurement Also called *ranging.* A method or system that allows a robot to navigate in its environment. It also allows a central computer to track the locations of robots under its control. Can use radar, sonar, visible light, or infrared.

distance-measuring equipment In radionavigation, a system that measures the distance of the interrogator to a transponder beacon in terms of the transmission time to and from the beacon.

distance protection The use of a protective device within a specified electrical distance along a circuit.

distance relay In circuit protection, a relay that operates to remove power when a fault occurs within a predetermined distance along the circuit.

distance resolution **1.** Qualitatively, the ability of a ranging system to differentiate between two objects or beacons that are almost, but not quite, the same distance away. See RANGING. **2.** Quantitatively, the minimum radial separation of objects or beacons necessary for a ranging system to tell them apart. **3.** For two targets having the same azimuth bearing, the minimum difference in range for which a radar display renders them as distinct blips.

distant control See REMOTE CONTROL.

distorted-drive multiplier A frequency multiplier whose excitation signal is a peaked wave that has been predistorted to decrease the angle of flow in the device, thus increasing its efficiency.

distorted nonsinusoidal wave A nonsinusoidal wave whose ideal shape (square, rectangular, sawtooth, etc.) has been altered.

distorted sine wave A wave that is approximately of sinusoidal shape (i.e., it is not an exact plot of a sine wave because of the presence of harmonics).

distortion **1.** Deformation of a signal waveform. **2.** The additional deformation of a signal exhibiting a less-than-ideal waveshape when it passes through a circuit. Some distortion originates within the signal generator itself; other forms result from circuits and devices transmitting the signal. **3.** Any degradation in the quality of a high-fidelity audio signal. **4.** See TOTAL HARMONIC DISTORTION.

distortionless **1.** Having no distortion. **2.** Having a propagation velocity that does not depend on frequency.

distortion meter An instrument for measuring harmonic distortion. It consists of a highly selective band-rejection filter (notch filter) that removes the fundamental frequency of the signal under test, and a sensitive voltmeter that can be switched between the filter input and the filter output. The distortion percentage is determined from the ratio between filter-output and filter-input voltages.

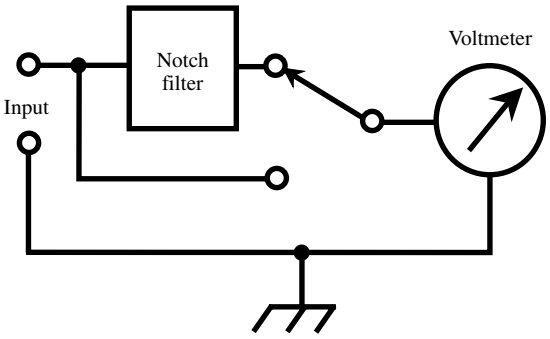

distortion meter

distortion tolerance The maximum amount of distortion that can be present in a signal without making it useless. This varies over wide limits. The maximum harmonic distortion that might be acceptable in a high-fidelity sound system could be less than 0.1% total, whereas in some applications of ac power, 10% would be acceptable.

distress frequency A radio frequency on which an emergency signal is transmitted. Ships at sea and aircraft over the sea use 500 kHz (by international agreement). In Citizen Band communications, channel 9 has been set aside for emergency use.

distress signal A signal indicating that trouble exists at the transmitting station and imploring aid from the recipient. The international radiotelegraph distress signal is the three-letter combination *SOS*; the international radiotelephone distress signal is the word *mayday*, the phonetic equivalent of the French *m'aidez* (help me).

distributed Existing over a measurable interval, area, or volume; not concentrated in a single place or places.

distributed amplifier A wideband, untuned amplifier whose active devices are spaced (distributed) along parallel, artificial delay lines consisting of coils that act in combination with the input and output capacitances of the active devices. Adding active devices to the lineup increases the gain. Commonly used as preamplifiers for television receivers.

distributed capacitance Symbol, C_d. Capacitance that is dispersed throughout a component or system, rather than being lumped in one place. An example is the distributed capacitance of a coil.

distributed component An electrical property that is spread throughout a circuit or device, rather than being concentrated at one point, as in a discrete component. For example, DISTRIBUTED CAPACITANCE and DISTRUBUTED INDUCTANCE are spread along the length of a transmission line. Another example is the DISTRIBUTED RESISTANCE of a wire coil. Distributed compo-

5059F-pD-163-223 4/9/01 5:22 PM Page 204

nents are often unintended, but they can be useful. Compare DISCRETE COMPONENT and LUMPED COMPONENT.

distributed constant See DISTRIBUTED COMPONENT.

distributed-constant delay line A delay line whose capacitance and inductance are distributed throughout the line. Compare LUMPED-CONSTANT DELAY LINE.

distributed inductance Symbol, L_d. Inductance that is dispersed throughout a system or component, rather than being lumped in one place, such as in a coil (e.g., the inductance of an antenna or capacitor).

distributed network **1.** A network in which electrical properties (such as resistance, inductance, and capacitance) are distributed over a measurable interval, area, or volume. **2.** A network whose characteristics do not depend on frequency within a given range.

distributed-parameter network A network composed of distributed components, rather than lumped components.

distributed pole In a motor or generator, a pole having a DISTRIBUTED WINDING.

distributed resistance Symbol, R_d. Resistance that is dispersed throughout a component or circuit, rather than being lumped in one place, such as in a resistor. An example is the high-frequency resistance of an antenna system.

distributed-shell transformer A transformer having two complete closed cores that are perpendicular to each other.

distributed winding In a motor or generator, a winding that is placed in several slots (rather than in one slot) under a pole piece.

distributing amplifier An amplifier having a single input and two or more outputs that are isolated from each other; it distributes signals to various points.

distributing cable **1.** In cable television, the cable connecting the receiver to the transmission cable. **2.** In power service, the cable running between a feeder and a consumer's house.

distribution **1.** The selective delivery of a quantity (e.g., *power distribution*). **2.** In statistical analysis, the number of times particular values of a variable appear. Also called *frequency distribution.*

distribution amplifier A low-output-impedance power amplifier that distributes a radio, television, or audio signal to a number of receivers or speakers.

distribution cable See DISTRIBUTING CABLE.

distribution center **1.** The central point from which a signal is routed to various points of use. **2.** In electric power operations, the point at which generation, conversion, and control equipment is operated to route power to points of use.

distribution factor For a polyphase alternator, the factor by which the total voltage V_T can be determined in terms of the coil voltage V_C and the number of coils n: $V_T = nV_C$. Distribution factor $k_d = (\sin(sd/2))/(s \times \sin(d/2))$, where s is the number of slots per phase per pole, and d is the angle between adjacent slots.

distribution function In statistical analysis, the function $F(x)$ expressing the probability that F takes on a value equal to or less than x.

distribution switchboard **1.** A switchboard through which signals can be routed to or among various points. **2.** A switchboard for routing electric power to points of use.

distribution transformer A step-down transformer used to supply low-voltage alternating-current (ac) utility power to one or more consumers from a high-voltage line.

distributor **1.** See COMMUTATOR. **2.** A switching device consisting of a rotating blade and a number of contacts arranged in a circle. Accomplishes sequential switching of a voltage to a number of points in a circuit. A common example is the distributor in the ignition system of an automotive engine.

disturbance An undesired variation in, or interference with, an electrical or physical quantity.

disturbed-one output In digital computers, the one output of a magnetic cell that has received only a partial write pulse train because it was last written into. Compare UNDISTURBED-ONE OUTPUT.

disturbed-zero output In digital computers, the zero output of a magnetic cell that has received only a partial write pulse train since it was last read from. Compare UNDISTURBED-ZERO OUTPUT.

dither **1.** Vibrate; quiver. **2.** The condition of vibration or quivering (e.g., the dither of a meter pointer). **3.** To blend pixels in a digitized image to obtain various shades and colors.

divergence **1.** The tendency of a collimated beam of energy to spread out. **2.** The extent to which a collimated beam of energy spreads out, generally measured in seconds of arc, minutes of arc, angular degrees, or angular radians.

divergence loss Loss of transmitted sound energy, resulting from spreading.

diverging lens A lens having a virtual focus for parallel rays; generally a *concave lens.*

diversity **1.** The property of consisting of two or more independent components or media. **2.** See DIVERSITY RECEPTION. **3.** See DIVERSITY TRANSMISSION.

diversity factor **1.** A measure of the degree to which a system exhibits unity among its constituents. **2.** The sum of the requirements of each constituent of a system, divided by the total requirement of the system.

diversity gain **1.** Signal gain achieved by using two or more receiving antennas. **2.** Signal gain achieved by using two or more transmitting antennas.

5059F-pD-163-223 4/9/01 5:22 PM Page 205

diversity reception Also called *dual-diversity reception.* A method of minimizing the effects of fading in ionospheric communication at high frequencies (HF). Accomplished using two receivers whose antennas are 5 to 10 wavelengths apart. Each receiver, tuned to the same signal, feeds a common audio amplifier. The timing of the fading is different at the two antennas because of phasing effects. The composite signal, therefore, fades less than either of the component signals. Some diversity systems use three or more antennas and receivers to reduce the effects of fading even further; this is sometimes called *multiple-diversity reception.*

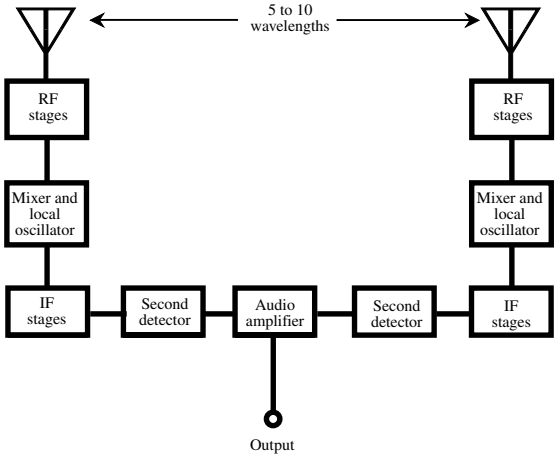

diversity reception

diversity transmission Also called *dual-diversity transmission* or *multiple-diversity transmission.* A scheme similar to DIVERSITY RECEPTION, except applied at the transmitting end of a communication circuit. The signals from two or more transmitters, at identical frequencies, are fed to antennas spaced several wavelengths apart.

diverter-pole generator A well-regulated direct-current (dc) generator, whose shunt winding is on the main field pole, the series winding being on a diverter pole whose flux opposes that of the main pole.

divide-by-seven circuit A three-stage binary circuit having feedback from stage three to stage one. Stage three is switched on by the fourth input pulse; at that time, the feedback pulse switches on stage one, simulating one input pulse and reducing the usual counting capacity from eight to seven.

divide-by-two circuit A circuit that delivers one output pulse for each two successive input pulses (i.e., a *flip-flop*).

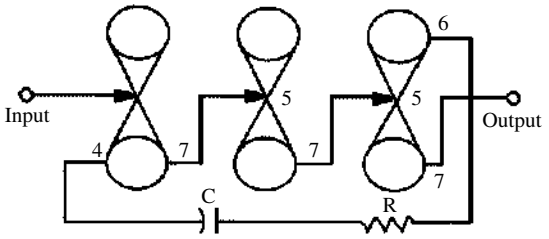

divide-by-seven circuit

divided-carrier modulation Modulation obtained by adding two identical frequency carriers that are 90 degrees out of phase.

divided circuit A *parallel circuit.*

divided equipment A system of modular electronic components interconnected with cables. A simple example is a radio receiver having an external power supply and external loudspeaker.

divider **1.** See VOLTAGE DIVIDER. **2.** See FREQUENCY DIVIDER. **3.** See PULSE-COUNT DIVIDER. **4.** A computing circuit or device for performing mathematical division.

divider probe A test probe that divides an applied signal voltage by some factor (such as 2, 5, or 10) to place it within the range of the instrument with which the probe is used.

dividing network See CROSSOVER NETWORK.

division **1.** Separating a quantity into a number of equal parts, as indicated by the divisor. **2.** Voltage division (see VOLTAGE DIVIDER). **3.** Frequency division (see FREQUENCY DIVIDER). **4.** Pulse-count division (see PULSE-COUNT DIVIDER).

division of vectors **1.** The quotient of two rectangular vectors determined by the principle of rationalization in algebra (i.e., by multiplying the numerator and denominator of the indicated division by the conjugate of the denominator, simplifying, and performing the division). **2.** To find the quotient of two polar vectors: the quotient of their moduli and the difference of their arguments.

dj Abbreviation of *diffused junction.*

DKT Abbreviation of *dipotassium tartrate.*

D layer A layer of the ionosphere that is below the E layer; its altitude is approximately 60 kilometers.

dm Abbreviation of *decimeter.*

DMA Abbreviation of DIRECT MEMORY ACCESS and *direct memory addressing.*

DME Abbreviation of DISTANCE-MEASURING EQUIPMENT.

DMM Abbreviation of DIGITAL MULTIMETER.

DMOS Abbreviation for *double-diffused metal-oxide semiconductor*, a type of field-effect transistor that exhibits extremely low capacitance and low source-drain resistance when conducting.

DNL See DIFFERENTIAL NONLINEARITY.

5059F-pD-163-223 4/9/01 5:22 PM Page 206

DNS Abbreviation of *Doppler navigation system.*

doctor To use unconventional (sometimes substandard) methods in fixing a circuit or device or in correcting a bad design.

document **1.** In digital computer operations, especially in file maintenance, a form that provides information pertinent to a transaction. Also see TRANSACTION. **2.** To perform documentation (see DOCUMENTATION, **2**). **3.** A computer text file.

documentation **1.** Paperwork explaining the scope of programs and how they can be optimized. **2.** Annotating a computer program at critical points during its writing (e.g., so that the purpose of various segments are understood). A measure of good programming, documentation becomes especially valuable for program modification or debugging.

document reader An electronic device that reads printed cards, usually for data entry into a computer.

dog **1.** A malfunctioning circuit or device. **2.** The cause of a circuit or device malfunction.

doghouse An enclosure for antenna loading inductors and other resonating components, placed at the base of a vertical broadcasting tower.

dog whistle See ULTRASONIC WHISTLE.

Doherty amplifier A highly efficient linear radio-frequency (RF) amplifier in which a *carrier tube* and a *peak tube* operate jointly, both receiving amplitude-modulated RF excitation. During unmodulated intervals, the carrier tube supplies carrier power to the load, while the peak tube, biased to cutoff, idles. On positive modulation peaks, the peak tube supplies output power that combines with that of the carrier tube, the increase in power corresponding to the condition of full modulation of the carrier. On negative modulation peaks, the peak tube does not supply power, and the output of the carrier tube is reduced to zero.

Dolby An electronic method of improving the audio reproduction quality of magnetic-tape systems. The gain is increased for low-level sounds during the recording process. During playback, the gain of the low-level sounds is reduced back to its original level.

Dolby A A Dolby system with four frequency ranges, operated independently. It is used mostly by recording professionals.

Dolby B A modified form of Dolby A, with only one band of noise-reducing circuitry. It is used primarily by hobbyists.

Dolezalek electrometer See QUADRANT ELECTROMETER.

dolly **1.** A low, wheeled frame or platform for transporting electronic equipment. **2.** A tool with which one end of a rivet is held while the head is hammered out of the other end.

DOM Abbreviation of DIGITAL OHMMETER.

domain **1.** A region of unidirectional magnetization in a magnetic material. **2.** A region of unidirectional polarization in a ferroelectric material. **3.** A region in which a variable is confined.

domestic electronics Also called *consumer electronics.* The branch of electronics concerned with appliances, automatic controls, protective devices, entertainment systems, communications devices, and other equipment for the home.

domestic induction heater A household cooking utensil heated by currents induced in it. A primary coil (connected to the power line) is imbedded in the utensil, which acts as a short-circuited secondary coil.

dome tweeter A speaker designed for high-frequency (treble), high-fidelity audio, and often functional at frequencies considerably above the limit of the human hearing. Characterized by a convex diaphragm. Usually part of an assembly including a woofer and midrange speaker.

dominant In statistical analysis, the nature of any quantity that imposes its effects even in the presence of other quantities.

dominant mode In a waveguide, the propagation mode exhibiting the lowest cutoff frequency.

dominant wave In a waveguide, the wave having the lowest cutoff frequency.

dominant wavelength For visible light of a given hue, the wavelength at which the emitted energy is the greatest.

donor An electron-rich impurity added to a semiconductor to make it into an n-type material. So called because it donates its excess electrons. Compare ACCEPTOR.

donor atom An atom having an excess electron. When a substance having such atoms is added to an intrinsic semiconductor, the extra electron is donated, making the semiconductor into an n-type material.

donor impurity A substance whose atoms have excess electrons, and that donates electrons to the atomic structure of the semiconductor crystal to which it is added. Donor elements make semiconductors into n-type materials. Also see DONOR ATOM. Compare ACCEPTOR IMPURITY.

do-nothing instruction A computer program instruction that causes no action to be taken. Can be used to provide space for future program updating, or to fill out a block of instructions, as needed by a compiler. Also called *dummy instruction.*

don't-care state In a logic function or gate, an input digit whose state (high or low) does not affect the output.

donut capacitor A flat, ring-shaped capacitor.

donut coil See TOROIDAL COIL.

donut crystal A relatively large, zero-temperature-coefficient piezoelectric quartz crystal cut in the form of a torus with the y-axis passing through the center of rotation.

donut magnet See RING MAGNET.

donut pattern The three-dimensional radio-frequency (RF) radiation/response pattern of a free-space straight antenna element measuring ½ wavelength, neglecting the effects of ground and nearby objects.

5059F-pD-163-223 4/9/01 5:22 PM Page 207

doohickey A usually unnamed device—especially one used to achieve some significant modification of circuit performance.

doorknob capacitor A high-voltage fixed capacitor, so called from its round package, which somewhat resembles a doorknob.

doorknob tube A special UHF vacuum tube, so called from its characteristic shape. The unique design provides short electron-transit time and low interelectrode capacitance. Largely replaced in recent years by semiconductor devices.

dopant An impurity added in controlled amounts to a semiconductor to make it an n-type or p-type material. Also see ACCEPTOR and DONOR.

dope To add impurities to a semiconductor material. Doping allows the manufacture of n-type or p-type semiconductors with varying degrees of conductivity. In general, the greater the extent of doping, the higher the conductivity.

doped junction In a semiconductor device, a junction produced by adding a dopant to the semiconductor melt.

doping Adding a dopant to a semiconductor to alter the way it conducts current.

doping agent See DOPANT.

doping compensation Opposite doping (i.e., adding a donor impurity to p-type semiconductor material or adding an acceptor impurity to n-type semiconductor material).

doping gas A gas diffused into a semiconductor material to dope it. For example, phosphorus pentoxide gas can be used to create an n-type region in a p-type silicon chip.

doping level The relative concentration of impurity added to a semiconductor material to obtain a certain resistivity and polarity. The greater the doping level, the lower the resistivity.

Doppler broadening In a spectrum, the spreading out or blurring of a spectral line caused by DOPPLER EFFECT, in turn resulting from motion of molecules, atoms, or other particles in the medium.

Doppler cabinet A loudspeaker enclosure with which a vibrato effect is achieved by rotating or reciprocating either the loudspeaker or a baffle board; the length of the sound path is altered cyclically.

Doppler effect A change in the frequency of a wave that occurs when the source and observer are in relative motion. The frequency of the wave increases (the wavelength shortens) as the source and observer approach each other; the frequency decreases (the wavelength becomes greater) as the source and observer recede from each other. This effect is often observed with sound waves, as when the pitch of an automobile horn seems to rise as the car approaches and to fall as the car passes. The effect is also observable in electromagnetic radiation at all wavelengths. It affects satellite communication and space communication.

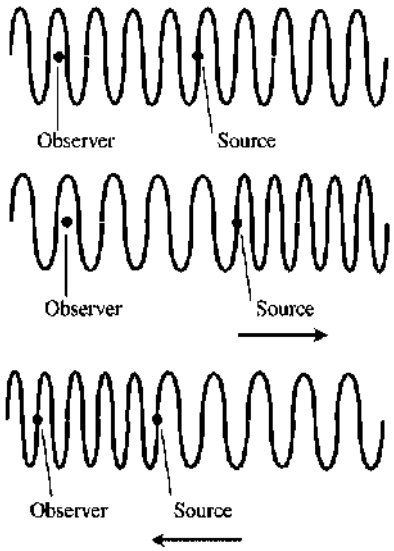

Doppler effect

Doppler enclosure See DOPPLER CABINET.

Doppler radar A radar that uses the change in carrier frequency of the signal returned by a moving target (approaching or receding) to measure its velocity. Used by law enforcement officers to determine the speed of moving vehicles. Also used by meteorologists to evaluate air circulation patterns in thunderstorms, and to determine wind speeds in hurricanes and tornadoes.

Doppler ranging See DORAN.

Doppler shift The extent to which the frequency or wavelength of a signal changes because of DOPPLER EFFECT. Can be measured in Hertz (for frequency) or in meters (for wavelength). In astronomy, the shift is also measured as displacement of absorption or emission lines in an infrared, visible, or ultraviolet spectrum.

Doppler's principle See DOPPLER EFFECT.

doran A continuous-wave trajectory-measuring system utilizing Doppler shift (see DOPPLER EFFECT). The name is a contraction of *doppler ranging.*

dorsal column stimulator Abbreviation, DCS. A machine that generates radio-frequency energy that is applied to human tissues for the temporary relief of pain.

dosage meter See DOSIMETER.

dose The total quantity of radiation received upon exposure to nuclear radiation or X-rays.

dosimeter An instrument for measuring the amount of exposure to nuclear radiation or X-rays.

dot **1.** The shorter of the two characters (dot and dash) of the telegraph code. The dot, a short sound, mark, or perforation, is one-third the

5059F-pD-163-223 4/9/01 5:22 PM Page 208

length (duration) of a dash. Compare DASH. **2.** One of the small spots of red, green, or blue phosphor on the screen of a color-television picture tube or cathode-ray-tube (CRT) computer display. **3.** A small spot of material alloyed with a semiconductor to form an alloy junction. **4.** The junction of two lines on a schematic diagram, representing a wired connection; also called *solder dot.*

dot AND Externally connected circuits or functions whose combined outputs result in an AND function. Compare DOT OR.

dot-and-dash telegraphy Telegraphy (wire or radio) by means of dot and dash characters.

dot cycle One period of an alternation between two signaling conditions, each of which is of unit duration (e.g., a unit mark followed by a unit space).

dot encapsulation A method of packaging cylindrical components by pressing them into the holes of perforated disks; interconnections are made, to complete a circuit, on each face of the disks.

dot generator A special radio-frequency (RF) signal generator used to produce a pattern of red, green, and blue dots on the screen of a color television receiver.

dot matrix A rectangular array of spaces, some of which are filled in to form alphanumeric and punctuation characters.

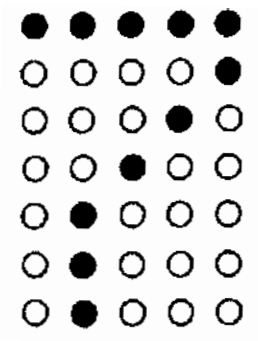

dot matrix

dot-matrix display A display that shows characters in dot-matrix form.

dot-matrix printer A computer output peripheral that prints characters and images on paper as a fine grid of dots. A print head, containing several pins, presses the ribbon against the paper as it moves laterally across each line. Can be used to print text and/or graphics.

dot movement pattern The movement of the red, green, and blue dots on the screen of a color television picture tube as the red, green, and blue magnets and the lateral magnet are adjusted for convergence of the dots at the center. The blue dots move horizontally or vertically; the red and green dots, diagonally.

dot OR Externally connected circuits or functions whose combined outputs result in an OR function. Compare DOT AND.

dot pattern In color television testing with a dot generator, dots of color (a red group, green group, and blue group) produced on the screen. With overall beam convergence, the three groups blend to produce white.

dot-sequential system The color television system in which the image is reproduced by means of primary-color dots (red, green, blue) sequentially activated on the screen of the picture tube. Compare FIELD-SEQUENTIAL SYSTEM and LINE-SEQUENTIAL SYSTEM.

double-amplitude-modulation multiplier A modulating system in which a carrier is amplitude-modulated first by one signal and then by a second signal. The resulting signal is fed to a detector, the output of which contains the product of the two modulating signals.

double-anode diode A semiconductor diode having two anodes and a common cathode.

double armature An armature (such as that of a dynamotor or a two-voltage generator) that has two separate windings on a single core, and has two separate commutators.

double-balanced mixer See BALANCED MIXER.

double-balanced modulator See BALANCED MODULATOR.

double-base diode See UNIJUNCTION TRANSISTOR.

double-base junction transistor A junction transistor having the usual emitter, base, and collector electrodes, plus two base connections, one on either side of the base region. The additional base connection acts as a fourth electrode to which a control voltage is applied. Also called *tetrode transistor.*

double-beam CRT See DUAL-BEAM OSCILLOSCOPE.

double-beam oscilloscope See DUAL-BEAM OSCILLOSCOPE.

double-bounce calibration In radar operations, a calibration technique for determining zero-beat error. Round-trip echoes are observed, the correct range being the difference between the two echoes.

double-bounce signal A signal that is received after having been reflected twice.

double-break contacts The member of a set of contacts that is normally closed on two others. Compare DOUBLE-MAKE CONTACTS.

double-break switch A switch that opens a previously closed circuit at two points simultaneously on closing. Compare DOUBLE-MAKE SWITCH.

double bridge See KELVIN DOUBLE BRIDGE.

double buffering In the input/output operation of a computer peripheral, the use of two memory areas for temporary storage.

5059F-pD-163-223 4/9/01 5:22 PM Page 209

double-button microphone A carbon microphone having two buttons mounted on each side of the center of a stretched diaphragm, and connected in push-pull. Also see BUTTON MICROPHONE.

double-channel duplex Two-way communication over two independent channels. One station transmits on one channel, and the other station transmits on the other channel. The result is conversation-mode communications, in which one operator can interrupt the other at any time; both receivers are always operational.

double-channel simplex A system of communication in which two channels are used. One station transmits on one channel, and the other station transmits on the other channel. Interruption is not possible because whenever either operator transmits, the station receiver is muted.

double-checkerboard pattern In a magnetic core memory, the maximum noise that appears when half of the half-selected cores are in the one state and the others are in the zero state. Also called *worst-case noise pattern.*

double circuit tuning A circuit whose output and input are tuned separately. Such tuning provides increased selectivity when the input and output are resonant at the same frequency, and decreased selectivity when they are tuned to different frequencies. Also see DOUBLE-TUNED AMPLIFIER.

double clocking A phenomenon that occurs in some digital circuits when the input pulse is nonuniform, and appears as two pulses to the device. The device is thus actuated at twice the desired frequency.

double-coil direction finder A radio direction finder (RDF) using an antenna that consists of two identical, perpendicular coils. The directivity of the antenna is the resultant of the directivity of the individual coils.

double conversion **1.** Two complete frequency conversions in a superheterodyne system. For example, the incoming signal might be converted to a 9-MHz first intermediate frequency (first IF); at a later stage, this signal might be converted to a 455-kHz second IF. The high first IF widely separates the signal from the image; the low second IF allows superior selectivity to be achieved at a reasonable cost. Also called *dual conversion.* **2.** Pertaining to a superheterodyne receiver with two intermediate frequencies.

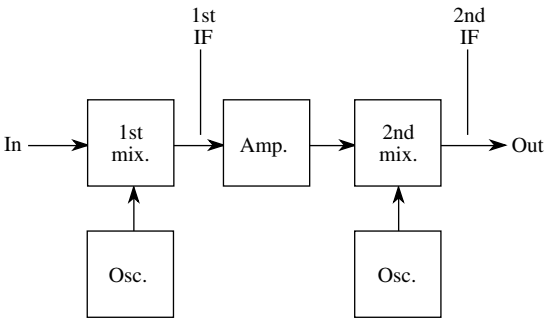

double conversion

double-conversion receiver Also called *double-conversion superheterodyne.* A superheterodyne receiver using DOUBLE CONVERSION to achieve optimum selectivity and image rejection.

double-current generator **1.** A dynamo-type generator supplying both alternating current (ac) and direct current (dc) from one armature winding. **2.** A rotary converter operating on dc and delivering ac.

double-diamond antenna A broadband antenna consisting of two rhomboid plates, one attached to each side of the feeder.

double-diffused epitaxial mesa transistor A transistor in which a thin mesa crystal is overlaid on another mesa crystal. Also called *epitaxial-growth mesa transistor.*

double-diffused transistor See DIFFUSED-EMITTER-AND-BASE TRANSISTOR.

double diode See DUODIODE.

double-diode limiter A limiter in which two diodes are connected back to back in parallel, to limit both peaks of an alternating-current (ac) signal.

double-doped transistor See GROWN-JUNCTION TRANSISTOR.

double edit In audio tape recording, to make two changes in a given span of the tape. For example, a producer might dislike the wording of a certain sentence, and re-record the sentence. Then, changing his or her mind, the producer might record the original sentence back over the re-recorded sentence. These changes increase the risk of audible irregularities appearing in the final recording.

double emitter follower See COMPOUND CONNECTION.

double-ended amplifier See PUSH-PULL AMPLIFIER and DOUBLE-ENDED CIRCUIT.

double-ended circuit A symmetrical circuit (i.e., one having identical halves, each operating on a half-cycle of the input signal). Example: a push-pull amplifier.

double-extended Zepp antenna A horizontal, collinear, center-fed antenna, in which each section measures 0.65 wavelength. This antenna gives increased gain over that of the Zepp and double Zepp (see DOUBLE ZEPP ANTENNA).

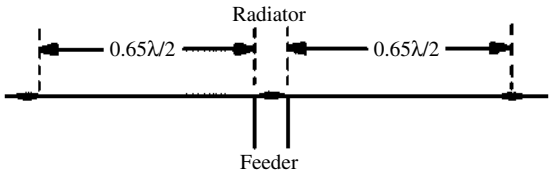

double-extended Zepp antenna

5059F-pD-163-223 4/9/01 5:22 PM Page 210

double-hump resonance curve A resonant response that is flattened by double tuning; it exhibits two resonance peaks. Also see DOUBLE-TUNED AMPLIFIER.

double-hump wave See DOUBLE-PULSE WAVE.

double image Two overlapping television pictures, one usually fainter than the other. Caused by the signal arriving over two different paths (one possibly attributable to reflection of the wave) and, hence, at different instants in time. The fainter image is called a GHOST.

double insulation The use of two layers of insulation on a conductor, made of different materials.

double ionization Ionization resulting from an electron colliding with an ion. In a gas, for example, a neutral atom might collide with an electron, which can knock an electron out of the atom. The atom then becomes a positive ion; it might in turn be bombarded by an electron, releasing still another electron.

double-junction photosensitive semiconductor See PHOTOTRANSISTOR.

double layer See HELMHOLTZ DOUBLE LAYER.

double local oscillator A mixer system in which a local oscillator generates two accurate radio-frequency (RF) signals separated by a few hundred hertz. The difference frequency is used as a reference in some applications.

double-make contacts A set of normally open contacts of which one closes against two others simultaneously. Compare DOUBLE-BREAK CONTACTS.

double-make switch A switch that closes a previously open circuit at two points simultaneously. Compare DOUBLE-BREAK SWITCH.

double moding In microwave operations, the abrupt changing of frequency at irregular intervals.

double modulation Using a modulated carrier to modulate another carrier of a different frequency.

double-play tape A thin magnetic recording tape that has approximately twice the playing time of the usual tape. Although the playing time is longer, double-play tape is more subject to jamming and stretching than standard-thickness recording tape.

double-pole Having two poles or switchable circuits (e.g., a double-pole switch).

double-pole, double-throw switch or relay Abbreviation, DPDT. A switch or relay having two contacts that can be closed simultaneously in one of two directions, to close or open two circuits.

double precision The use of two computer words to represent a single number to gain precision.

double-pole, single-throw switch or relay Abbreviation, DPST. A switch or relay having two contacts that can be closed in only one direction, to simultaneously close or open two circuits.

double precision hardware Within a computer, arithmetic units permitting the use of double-precision operands, sometimes also accommodating floating-point arithmetic.

double-precision number In digital computer operations, a number represented by two words for greater precision.

double pulse reading Pertaining to a magnetic core in a computer memory, recording bits as two states held simultaneously by one core having two areas that can be magnetized with alternate polarities. For example, positive-negative could represent zero, and negative-positive could represent one.

double-pulse wave An alternating-current (ac) wave having two successive positive peaks followed by two successive negative peaks within each cycle. The output voltage of a varistor bridge has such a waveshape for an ac input.

double-pulsing station A loran station that transmits at two pulse rates upon receiving two pairs of pulses.

double pumping A method of obtaining increased peak output power from a laser by pumping it for a comparatively long interval and then immediately pumping it for a short interval.

doubler **1.** A circuit or device for multiplying a frequency by two (see FREQUENCY DOUBLER). **2.** A circuit or device for multiplying a voltage by two (see VOLTAGE DOUBLER).

double probe A test probe that multiplies an applied signal voltage by two, so it can be handled more effectively by the instrument with which the probe is used.

double punching In perforating a punched card, putting two holes in one column; it is an error if it occurs in a field of a card that is part of a record.

double rail A form of logic system in which two lines are used, with three possible states. The output can be high, low, or undecided.

double response **1.** Two-point response, as that associated with tuning a receiver to a signal and then to its image. **2.** See DOUBLE-HUMP RESONANCE CURVE.

double screen A cathode-ray tube having a two-layer screen on which there is an additional, long-persistence coating of a different color.

double shield Two independent electromagnetic shields for a circuit enclosure or cable. The shielding structures are concentric, and can be connected together at a single point (the common point).

double sideband Abbreviation, DSB. In a modulated signal, the presence of both sidebands.

double-sideband suppressed carrier Abbreviation, DSSC. A transmission technique in which both sideband products of modulation are transmitted and the carrier is suppressed. Compare LOWER SIDEBAND, SUPPRESSED CARRIER, UPPER SIDEBAND, and SUPPRESSED CARRIER.

double-sideband system A modulation or demodulation system utilizing both sidebands, with or without the carrier.

5059F-pD-163-223 4/9/01 5:22 PM Page 211

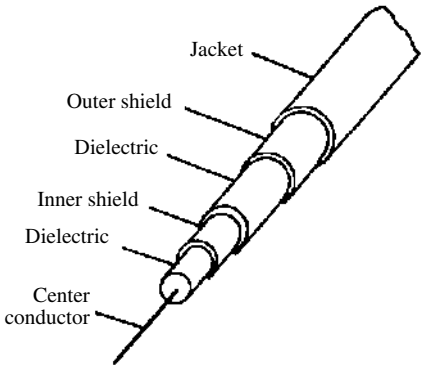

double shield

double-sideband transmitter A modulated transmitter using a double-sideband system.

double signal In reception, the property of having a signal on either side of the carrier frequency, as in a direct-conversion receiver. The two signals represent the sum and difference of the local oscillator signal and the actual received signal. Because the two signals convey identical information, the phenomenon is wasteful of received spectrum, and degrading to receiver selectivity and sensitivity.

double-signal receiver A receiver, such as a direct-conversion type, in which the signals occur in replicated form on either side of the local oscillator signal. Compare SINGLE SIGNAL.

double-spot tuning In a superheterodyne receiver, tuning in the same signal at two different places on the dial, a condition caused by image response.

double squirrel-cage induction motor A polyphase induction motor having a double squirrel-cage rotor. The rotor slots contain two bars, an upper bar having low reactance (being near the air gap) and high resistance, and a lower bar having high reactance and low resistance. This motor has low starting current, high starting torque, and a full-load slip of less than 5%.

double-stream amplifier A traveling-wave tube in which microwave amplification results from the interaction of two electron beams of different average velocity.

double-stub tuner Two stubs (see STUB) connected in parallel with a transmission line and usually spaced 0.375 wavelength (135 electrical degrees) apart; it is used as an impedance matcher.

double superheterodyne See DOUBLE-CONVERSION SUPERHETERODYNE.

double superheterodyne reception See DOUBLE-CONVERSION SUPERHETERODYNE.

double-surface transistor See COAXIAL TRANSISTOR.

doublet See DIPOLE ANTENNA.

double-throw Operating in opposite directions as selected (e.g., a double-throw relay or switch).

double-throw circuit breaker A circuit breaker that closes in both its pull-in and dropout positions.

double-throw switch or relay A switch or relay having two ganged poles.

double-trace recorder See DOUBLE-TRACK RECORDER, **2**.

double tracing Displaying two signals simultaneously on the screen of an oscilloscope through the use of an electronic switch.

double-track recorder **1.** A tape recorder whose head is positioned so that separate recordings can be made as two tracks on the tape. **2.** A graphic recorder that produces two separate parallel tracings.

doublet trigger A two-pulse, constant-spaced trigger signal used for coding.

double-tuned amplifier An amplifier whose input and output circuits are both tuned.

double-tuned circuit A circuit, such as an amplifier or filter, using separate input and output tuning. Also see DOUBLE CIRCUIT TUNING and DOUBLE-TUNED AMPLIFIER.

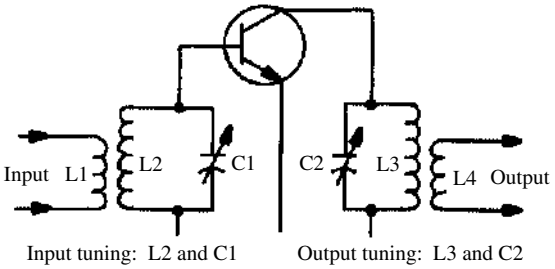

double-tuned circuit

double-tuned detector A form of frequency-modulation (FM) discriminator with two resonant circuits. One is tuned slightly higher than the channel center frequency, and the other is tuned an equal amount below the center.

double-vee antenna A broadband, modified dipole antenna resembling two vees in line. Also see VEE ANTENNA.

double-winding generator A dynamo-type generator having separate armature windings for supplying two voltages, either of which can be direct (dc voltage) or alternating (ac voltage).

double-wye rectifier A heavy-load circuit using six rectifier diodes, each conducting for 120 degrees of the cycle. An interphase winding is used. The circuit is equivalent to two three-phase, half-wave rectifiers connected in parallel.

double-Y rectifier See DOUBLE-WYE RECTIFIER.

double Zepp antenna A usually horizontal, straight, center-fed, full-wavelength antenna.

5059F-pD-163-223 4/9/01 5:22 PM Page 212

Also called *two half waves in phase.* Its name was derived because it is, in fact, two Zepp antennas forming a collinear array.

doubling **1.** Producing the second harmonic of a signal. **2.** In communication, unintentional simultaneous transmission by both operators, resulting in missed information. **3.** In a speaker, distortion resulting in large amounts of second-harmonic output.

doubly balanced modulator See BALANCED MODULATOR.

doughnut capacitor See DONUT CAPACITOR.

doughnut coil See TOROIDAL COIL.

doughnut crystal See DONUT CRYSTAL.

doughnut magnet See RING MAGNET.

down convert In superheterodyne conversion, to heterodyne a signal to an intermediate frequency lower than the signal frequency. Compare UP CONVERT.

down lead See LEAD-IN.

downlink The signal sent down from an active communications satellite to the earth, usually on a different frequency than the signal sent up. See UPLINK.

downlink beamwidth The angle subtended between the half-power points of the downlink signal from an active communications satellite.

downlink frequency The frequency of the downlink signal from an active communications satellite. Usually, the downlink signals occupy a certain band of frequencies, anywhere from several kilohertz to several megahertz wide.

downlink power **1.** The output power of the downlink transmitter in an active communications satellite. **2.** The effective radiated power (ERP) of the downlink signal from an active communications satellite.

down time A period of time during which electronic equipment is completely inoperative (for any reason).

downturn A usually sudden dip in a performance curve. Compare UPTURN.

downward modulation Modulation in which the average carrier component decreases during modulation. Example: amplitude modulation of a transmitter in which the antenna current decreases during modulation. Compare UPWARD MODULATION.

DP Abbreviation of DATA PROCESSING.

DPDT Abbreviation of *double-pole, double-throw* (switch or relay).

DPM **1.** Abbreviation of *digital power meter.* **2.** Abbreviation of DIGITAL PANEL METER. **3.** Abbreviation of *disintegrations per minute.*

DPS Abbreviaton of *disintegrations per second.*

DPST Abbreviation of *double-pole, single-throw* (switch or relay).

dr Abbreviation of *dram.*

drag **1.** A retarding force, caused by friction, acting on a moving body in contact with another moving or stationary body or medium. **2.** A retarding force introduced by an applied magnetic or electric field.

drag angle In disk recording, an angle of less than 90° between the stylus and the disk. The acute angle causes the stylus to drag instead of digging in.

drag cup A cup of nonmagnetic metal (usually copper or aluminum) that, when rotated in a magnetic field, acquires a voltage proportional to the speed of rotation. The device is often used as a brake.

drag-cup motor A servomotor whose shaft has a copper or aluminum drag cup that rotates in the field of a two-phase stator. Eddy currents set up in the cup by the field winding produce torque; braking action, direction control, and speed control are obtainable by means of associated electronics.

drag magnet In a motor-type meter, a braking magnet (i.e., one used to reduce speed through eddy-current effects). Also called *retarding magnet.*

drain **1.** The current or power drawn from a signal or power source. **2.** A load that absorbs current or power. **3.** The electrode in a field-effect transistor (FET) from which the output is usually taken; equivalent to the collector of a bipolar transistor.

drainage equipment Devices and systems for protecting circuits against transients generated by circuit breakers and similar safety devices.

drain-coupled multivibrator An oscillator that uses two field-effect transistors (FETs) in the circuit equivalent of a collector-coupled bipolar-transistor multivibrator. The drain of one stage is capacitance-coupled to the gate of the other stage.

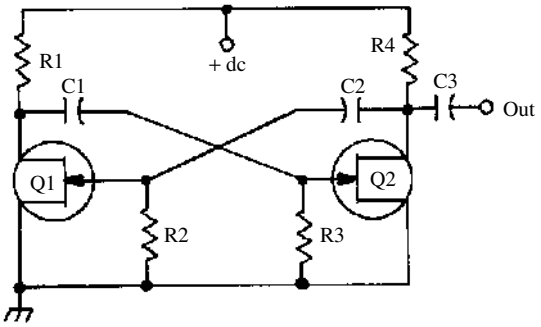

drain-coupled multivibrator

D-region A low region of the ionosphere beneath the E-region, whose ionization varies with the inclination of the sun. The greatest ionization is at midday; the layer disappears at night.

dress The (usually experimental) arrangement of leads for optimum circuit operation (minimum

5059F-pD-163-223 4/9/01 5:22 PM Page 213

capacitance, best suppression of oscillation, minimum pickup, etc.).

dressed contact A contact having a permanently attached locking spring member.

drift **1.** Within a conductor or semiconductor, the controlled, directed movement of charge carriers resulting from an applied electric field. **2.** A usually gradual and undesirable change in a quantity, such as current, as a result of a disturbing factor, such as temperature or age.

drift current In a semiconductor, the current resulting from a flow of charge carriers in the presence of an electric field. The charge carriers are electrons in n-type material and holes in p-type material.

drift field The inherent internal electric field of a DRIFT-FIELD TRANSISTOR.

drift-field transistor An alloy-junction, bipolar, radio-frequency (RF) transistor for which the impurity concentration is graded from high on the emitter side of the base wafer to low on the collector side. This creates an internal drift field that accelerates current carriers and raises the upper frequency limit of the transistor.

drift-matched components Active or passive components that have been closely matched in terms of the drift of one or more parameters, with respect to time, temperature, etc.

drift mobility For current carriers in a semiconductor, the average drift velocity per unit electric field.

drift space **1.** In a vacuum tube, a space that is nearly free of alternating-current (ac) fields from the outside, and in which the repositioning of electrons is governed by the space-charge forces and the velocity distribution of the electrons. **2.** In a Klystron, the space between buncher and catcher cavities in which there is no field.

drift speed The average velocity of charge carriers moving through a medium.

drift transistor See DRIFT-FIELD TRANSISTOR.

drift velocity The net velocity of a charged particle (electron, hole, or ion) in the direction of the field applied to the conducting medium.

drift voltage The usually gradual change in voltage resulting from such causes as internal heating. Also called voltage drift.

drip loop In a transmission line for an antenna or power service, a loop near the point of entry to the building for the purpose of allowing condensation or rain water to drip off.

drip-proof motor A motor with ventilating apertures arranged so that moisture and particles cannot enter the machine.

drip-tight enclosure A housing designed to prevent entry of rain, snow, and dust; it also prevents accidental contact with the enclosed apparatus or machinery.

drive **1.** To excite (i.e., to supply with input-signal current, power, or voltage) (see DRIVING CURRENT, DRIVING POWER, and DRIVING VOLTAGE). **2.** Input-signal excitation (see DRIVING CURRENT, DRIVING POWER, and DRIVING VOLTAGE). **3.** A device that moves a recording medium (e.g., *tape drive* and *diskette drive*). **4.** The transmission of mechanical energy from one place to another (e.g., *motor drive*).

drive array A set of two or more hard-disk drives in a computer system. They function together to minimize the possibility of data loss. Such a system can also increase the amount of fast-access data storage.

drive belt A continuous belt used to transmit mechanical energy from a driving pulley to a driven pulley.

drive circuit **1.** A circuit used to provide the excitation to a motor. **2.** An amplifier that supplies drive to a more powerful amplifier.

drive control In a television receiver, the potentiometer used to adjust the ratio of horizontal pulse amplitude to the level of the linear portion of the sawtooth scanning-current wave.

driven element In a multielement antenna, an element to which electromagnetic energy is fed directly, as opposed to a PARASITIC ELEMENT, which is excited by a nearby radiator element.

driven-element directive antenna A multielement directional antenna whose elements are driven from the feed line (i.e., no element is parasitic). Compare PARASITIC-ELEMENT DIRECTIVE ANTENNA.

driven multivibrator A multivibrator whose operation or frequency is controlled by an external synchronizing or triggering voltage. Compare FREE-RUNNING MULTIVIBRATOR.

driven single sweep A single oscilloscope sweep that is initiated by the signal under observation.

drive pattern A pattern of interference in a facsimile system that is caused by improper synchronization of the recording spot.

driven sweep An oscilloscope sweep that is initiated by the signal under observation.

drive pin A pin used to prevent a record from slipping on the rotating turntable of a recorder or reproducer. It is similar to, and located near, the center pin of the turntable.

drive pulse In digital computer operations, a pulse that magnetizes a cell in a memory bank.

driver **1.** A device that supplies a useful amount of signal energy to another device to ensure its proper operation (e.g., a current driver for a magnetic-core memory, an oscillator driving a loudspeaker). **2.** A power amplifier stage that supplies signal power to a higher-powered amplifier stage. **3.** In a digital computer, a stage that increases the output current or power of another stage (e.g., a clock driver). **4.** The cone and magnet of a dynamic speaker.

driver element In a multielement directive antenna, the element excited directly by the feeder, the other elements (directors and reflectors) being parasitic.

5059F-pD-163-223 4/9/01 5:22 PM Page 214

driver impedance **1.** The output impedance of a driver stage. **2.** The impedance "seen" from the driven stage of an amplifier, through the driver transformer, to the driver stage. It is the vector sum of driver reactance and resistance.

driver inductance In an amplifier's driver transformer, the inductance, as "seen" looking through the transformer from the driven stage into the driver stage.

driver resistance In an amplifier's driver transformer, the resistance "seen" looking through the transformer from the driven stage into the driver stage.

driver stage An amplifier stage whose chief purpose is to supply excitation (input-signal current, power, or voltage) to the next stage. Also see DRIVER.

driver transformer The transformer that couples a driver stage to a driven stage. Example: the interstage transformer inserted between the collector of a single-ended driver transistor and the two bases of a push-pull power-output stage in an audio amplifier.

driving current In a power amplifier, the input signal current required to produce a given amount of output power.

driving-point admittance The reciprocal of DRIVING-POINT IMPEDANCE.

driving-point impedance The input impedance of a network.

driving power In a power amplifier, the input signal power required to produce a given amount of output power.

drive wire The wire forming the coil around the toroidal cell in a magnetic core memory; supplies pulses that magnetize the cell.

driving-range potential In cathodic protection, the difference of potential between the anode and (protected) cathode.

driving signal **1.** Drive (see DRIVE, **2**). **2.** In television, time-scanning signals (line-frequency pulses and field-frequency pulses) at the pickup location.

driving spring In a stepping relay, the spring that moves the wiper blades.

driving voltage In a power amplifier, the input signal voltage required to produce a given amount of output power.

DRO Abbreviation of DIGITAL READOUT.

drone A pilotless radio-controlled aircraft without a human pilot.

drone cone An undriven loudspeaker cone that is mounted in a bass-reflex enclosure with other speakers. Also called PASSIVE RADIATOR.

droop **1.** A dip in the graph of a function. **2.** In a pulse train, the decrease in mean amplitude (in percent of maximum amplitude) at a given instant after attainment of maximum amplitude.

drooping radials In a ground-plane antenna, radials that slope downward to provide a transmission-line impedance match. The slope angle depends on the characteristic impedance of the line; typically, the angle is between 45 degrees and 70 degrees, relative to horizontal.

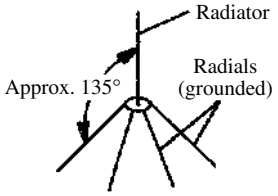

drooping radials

drop **1.** In wire communications, the line connecting a telephone cable to a subscriber's building. **2.** See VOLTAGE DROP.

drop bar A device that automatically grounds or short-circuits a capacitor when the door of a protective enclosure is opened.

drop cable See DISTRIBUTING CABLE, **1**.

drop channel In a communications system utilizing several channels, a channel that is not used.

drop-in The unintentional creation of bits when a magnetic storage device is being read from or written into. Compare DROP-OUT, **4**.

drop indicator In a signaling system, such as an annunciator, a hinged flap that drops into view when the signaling device is actuated.

drop-out **1.** The opening of a relay or circuit breaker. **2.** In digital computer operations, variation in signal level of the reproduced tape-recorded data. Such variation can result in errors in data reproduction. **3.** In the production of monolithic circuits, a special image placed at a desired point on the photomask. **4.** Digit loss during a read or write operation involving a magnetic storage device.

dropout current See DROPOUT VALUE.

dropout power See DROPOUT VALUE.

dropout value The level of current, power, or voltage at which a device, such as a circuit breaker or relay, is released.

dropout voltage See DROPOUT VALUE.

dropping resistor A series resistor providing a voltage reduction equal to the voltage drop across itself. For example, a 1000-ohm resistor in series with a 45-V battery, and carrying a current of 10 mA, will provide a voltage reduction equal to 10 V ($IR = 0.01 \times 1000 = 10$ V), thus dropping the 45 V to 35 V.

drop relay In a telephone system, a relay that is activated by the ringing signal. The relay is used to switch on a buzzer, light, or other device.

drop repeater A repeater intended for a termination of a communications circuit in a telephone system.

dropsonde A parachute-supported radiosonde dropped from a high-flying aircraft.

5059F-pD-163-223 4/9/01 5:22 PM Page 215

drop-tracks The tracks of radioactive particles made visible by moisture in an ionization chamber.

drop wire A wire that runs from a building to a pole (for line extension) or to a cable terminal (for cable extension).

drum **1.** A rotating cylinder coated with a magnetic material on which digital information can be recorded in the form of tiny magnetized spots. These spots are read as the drum rotates under pickup heads, or erased when the stored information is no longer needed. **2.** In some graphic recorders, facsimile receivers, etc., a rotating cylinder carrying the recording sheet.

drum capacitor See CONCENTRIC CAPACITOR.

drum controller The device that regulates the recording process on a drum memory.

drum mark On a track of a magnetic drum, a character that signifies the end of a character group.

drum memory In digital computers, a memory based on a magnetic drum (see DRUM, **1**). They have been largely replaced in recent years by electronic random-access memory, in the form of integrated circuits (ICs) and/or PCMCIA standard adapter cards.

drum parity The degree of accuracy in a drum recording/reproducing system.

drum programmer A device for sequencing operations. Its heart is a rotating drum, around whose surface contacts or points can be placed to actuate or terminate operations at selected times.

drum receiver A facsimile receiver using recording paper or photographic film wound around a revolving drum.

drum recorder A graphic recorder in which the record sheet is wound around a rotating drum.

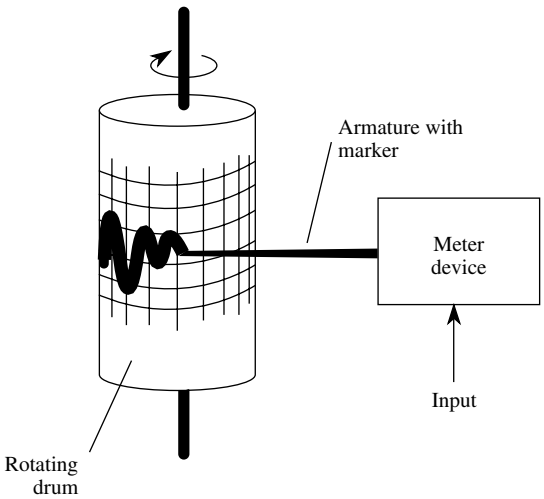

drum recorder

drum resistor A resistor consisting of a hollow cylinder of resistive material. Such a resistor can be cooled by circulating air or liquid through the cylinder.

drum speed The speed, usually measured in revolutions per minute (rpm), of the rotating drum in a graphic recorder, facsimile transmitter, or facsimile receiver.

drum storage The storage of data as magnetic impulses on a cylindrical, or drum-shaped, medium. Largely supplanted in recent years by magnetic disks, optical disks, and magnetic tapes.

drum switch A sequential switch whose contacts are pins or teeth placed at points around the outside of a revolving drum.

drum transmitter A facsimile transmitter in which the sheet bearing the material to be transmitted is wound around a revolving drum.

drum-type controller A motor-driven drum switch arranged to time various operations through sequential switching.

drum varistor A varistor that is a hollow cylinder of nonlinear resistance material. This varistor can be cooled by circulating air or liquid through it.

drum winding In a motor or generator, an armature whose conductors are on the outer face of the core, the two branches of a turn lying under adjacent poles of opposite polarity.

drunkometer An instrument for testing the extent of alcoholic intoxication. It electronically measures blood alcohol content through analysis of the subject's breath.

dry In an electric cell, a term used to describe an electrolyte that is semiliquid or solid.

dry battery A battery of dry cells.

dry cell **1.** A Leclanche primary cell in which the positive electrode is carbon, the negative electrode is zinc, and the electrolyte is a gel of ammonium chloride and additives. Also see CELL and PRIMARY CELL. **2.** A cell whose electrolyte is a gel or paste.

dry circuit A circuit in which the maximum voltage is 50 mV and the maximum current 200 mA.

dry-contact rectifier See DRY-DISK RECTIFIER.

dry contacts Contacts that neither make nor break a circuit.

dry-disk rectifier A solid-state rectifier, such as a copper-oxide, magnesium-copper-sulfide, or selenium type, that consists of a metal disk coated with a semiconductor material. The name was originally used to distinguish this rectifier from the *wet electrolytic rectifier.*

dry electrolytic capacitor An electrolytic capacitor whose electrolyte is a paste or solid. Compare WET ELECTROLYTIC CAPACITOR.

dry flashover voltage The breakdown voltage between electrodes in dry air when all insulation is clean and dry.

5059F-pD-163-223 4/9/01 5:22 PM Page 216

dry pile A voltaic pile containing numerous disks silvered or tinned on one face and covered with manganese dioxide on the other.

dry reed A metal contact, generally used as a relay or switch, that moves toward or away from another fixed contact under the influence of a magnetic field.

dry-reed relay See DRY-REED SWITCH.

dry-reed switch A switch consisting of two thin, metallic strips (reeds) hermetically sealed in a glass tube. The tube is surrounded by a coil of wire. When a current flows in the coil, a magnetic field affects the reeds. In the *normally open dry-reed switch*, the magnetic field causes the reeds to come together and close the circuit. In the *normally closed dry-reed switch*, the magnetic field causes the reeds to separate, opening the circuit. Compare MERCURY-WETTED REED RELAY.

dry run **1.** The preliminary operation of equipment for testing and appraisal. Such a procedure precedes putting the equipment into regular service. **2.** A step-by-step, paper-and-pencil "run" of a computer program before it is machine-implemented.

dry shelf life The life of a battery cell stored without its electrolyte.

dry-transfer process A method of transferring printed-circuit patterns and panel labels from sheets by rubbing them onto the substrate or panel.

dry-type forced-air-cooled transformer A DRY-TYPE TRANSFORMER that is cooled by convection of air circulated by a blower or fan. This increases the amount of power that the transformer can safely handle.

dry-type self-cooled transformer A DRY-TYPE TRANSFORMER that is cooled by natural air circulation (convection), without the use of a blower or fan.

dry-type transformer A transformer that, rather than being immersed in oil, is cooled entirely by the circulation of air.

DSB Abbreviation of DOUBLE SIDEBAND.

DSBSC Abbreviation of DOUBLE-SIDEBAND SUPPRESSED CARRIER. Also abbreviated DSSC.

dsc Abbreviation of *double silk covered* (wire).

D scope A radar whose display resembles that of a C scope, the difference being that blip height gives an approximation of the distance.

D service A Federal Aviation Agency service providing radio broadcasts of weather data, notices to aircraft personnel, and other advisory messages.

D-shell connector A multi-pin connector (either male or female) with a characteristic shape that ensures proper pin placement. Commonly used for computer ports, and for connections of peripherals to electronic equipment.

dsp Abbreviation of *double silver plated.*

DSR Abbreviation of DYNAMIC SPATIAL RECONSTRUCTOR.

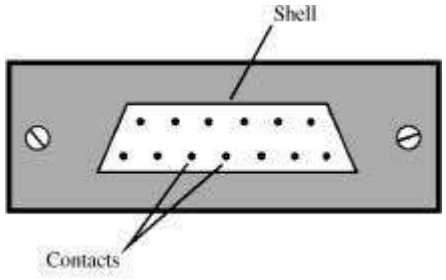

D-shell connector

DSS Abbreviation of *direct station selection* (telephone).

DSSC Abbreviation of DOUBLE-SIDEBAND SUPPRESSED CARRIER. Also abbreviated DSBSC.

DT Abbreviation of DATA TRANSMISSION.

DTA Abbreviation of *differential thermoanalysis.*

DT-cut crystal A piezoelectric plate cut from a quartz crystal at an angle of rotation about the z-axis of –53 degrees. It has a zero temperature coefficient of frequency at approximately 30 degrees Celsius. Also see CRYSTAL AXES and CRYSTAL CUTS.

DTL Abbreviation of DIODE-TRANSISTOR LOGIC.

DTn Abbreviation of DOUBLE TINNED.

DTS **1.** Abbreviation of DATA-TRANSMISSION SYSTEM. 2. Abbreviation of *digital telemetry system.*

DU Abbreviation of DUTY CYCLE.

dual **1.** Pertaining to a combination of two components such as diodes, transistors, etc., in a single housing. The components are often carefully matched. Compare QUAD. **2.** Pertaining to a device or circuit that behaves in a manner analogous to that of another operating with component and parameter counterparts. Thus, a current amplifier can be the dual of a voltage amplifier; a series-resonant circuit, the dual of a parallel-resonant circuit; or a field-effect transistor, the dual of a bipolar transistor.

dual-beam CRT A cathode-ray tube having two separate electron guns, for use in a dual-beam oscilloscope.

dual-beam oscilloscope Also called *dual-trace oscilloscope.* An oscilloscope having two electron guns and deflection systems; it can display two phenomena on the screen simultaneously for comparison.

dual capacitor **1.** Two fixed capacitors combined in a single housing, sometimes sharing a common capacitor plate. **2.** A two-section, ganged variable capacitor.

dual-channel amplifier An amplifier having two separate, independent channels (e.g., a stereo high-fidelity audio amplifier).

dual-cone speaker A speaker designed for a wide range of audio frequencies. One cone responds to the bass (low) and midrange audio frequencies, and a smaller cone responds to the treble (high) audio frequencies.

5059F-pD-163-223 4/9/01 5:22 PM Page 217

dual diode A discrete component consisting of two diodes in one package.

dual-diversity receiver A receiver or receiver system for DIVERSITY RECEPTION.

dual-diversity reception See DIVERSITY RECEPTION.

dual-emitter transistor A low-level silicon pnp chopper transistor of the planar passivated epitaxial type; it has two emitter electrodes.

dual-frequency calibrator A secondary frequency standard providing two fundamental test frequencies (e.g., 100 kHz and 1 MHz).

dual-frequency induction heater An induction heater whose work coils carry energy of two different frequencies. The coils heat the work either simultaneously or successively.

dual gate **1.** A digital integrated circuit (IC) consisting of two logic gate units. **2.** Pertaining to a field-effect transistor (FET) with two gates or gate electrode connections.

dual-gate FET A field-effect transistor with two gate (input) electrodes.

dual-gate MOSFET A metal-oxide-semiconductor field-effect transistor (MOSFET) with two gate (input) electrodes.

dual-inline package Abbreviation, DIP. A flat, molded integrated-circuit (IC) package having terminal pins along both long edges.

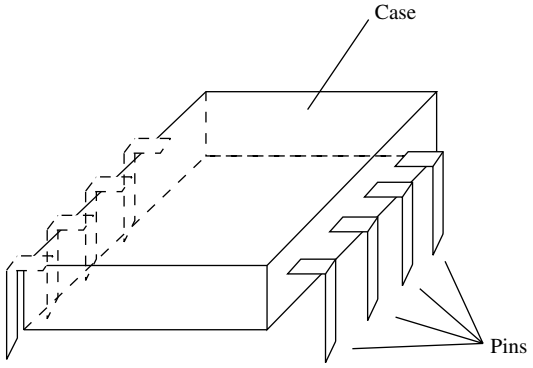

dual-inline package

duality **1.** The condition of being dual (see DUAL). This can be an aid in the design of certain circuits requiring complementary parameters, e.g., current-operated circuit analogs of voltage-operated circuits. **2.** See DUALITY OF NATURE.

duality of nature **1.** Any of various situations in which a phenomenon exhibits two distinct and different natures. A commonly cited example is the dual model of light. In some instances, visible light behaves like a barrage of particles, but in other environments it appears to be a wave effect. Another example is the dual model of electrostatic energy, behaving as point charges in some scenarios and as force fields in other situations. **2.** The tendency of a set of principles to be duplicated in sense by predictable analogies, as between inductance and capacitance, electrostatics and magnetics, etc.

dual local oscillator See DOUBLE LOCAL OSCILLATOR.

dual meter A meter having two meter movements and scales in a single case; the arrangement permits simultaneous monitoring of two quantities.

dual modulation The modulation of a single carrier or subcarrier by two different types of modulation—each carrying different information.

dual network A network that is the dual of another network having complementary parameters. For example, a common-emitter, current-sensitive, bipolar-transistor circuit is the dual of a common-source, voltage-sensitive, field-effect-transistor (FET) circuit. Also see DUALITY.

dual operation In digital logic, the operation resulting from inverting all of the digits. Every 1 is replaced with a 0, and vice versa.

dual-output power supply A power supply with two outputs. Often, one output is positive and the other is negative. In some cases, one output consists of alternating current (ac) and the other consists of direct current (dc).

dual pickup In disk reproduction, a pickup having two styli, one for large-groove records and one for fine-groove records.

dual potentiometer A ganged assembly of two potentiometers. The resistance values might or might not be the same.

dual preset counter A preset counter that will set alternately to two different numbers.

dual rail See DOUBLE RAIL.

dual resistor See DUAL POTENTIOMETER and DUAL RHEOSTAT.

dual rheostat A ganged assembly of two rheostats. The resistance values might or might not be the same.

dual stereo amplifier **1.** A two-channel audio amplifier for stereophonic audio applications. **2.** A two-channel linear integrated circuit (IC) for stereophonic audio applications.

dual-system loudspeaker See TWO-WAY SPEAKER.

dual trace In a cathode-ray oscilloscope, the use of two separate electron beams, which can show two different signals simultaneously on a single screen.

dual-trace recorder See DOUBLE-TRACK RECORDER, **2**.

dual-track recorder See DOUBLE-TRACK RECORDER.

dual recording In digital computer operations, updating two sets of master files simultaneously.

dual use The use of a communications system for two modes of data transfer at the same time.

Duant electrometer See BINANT ELECTROMETER.

5059F-pD-163-223 4/9/01 5:22 PM Page 218

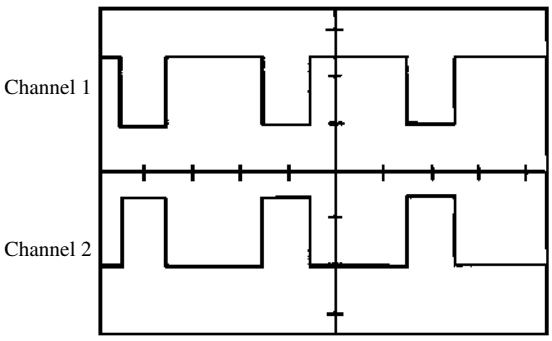

dual trace

duct **1.** A narrow propagation path, sometimes traveled by microwaves, created by unusual atmospheric conditions. **2.** A pipe or channel for cables and wires.

dubbing The adding of sound to a recorded magnetic tape, record disk, or film (e.g., replacing the sound track of a film in one language with that of another language).

dubnium Symbol, Db. Also clalled *unnilpentium* (Unp) and *hahnium* (Ha). Atomic number, 105. The most common isotope has atomic weight 262. Classified as a transition metal. It has a half-life on the order of a few seconds to a few tenths of a second (depending on the isotope), is human-made, and is not known to occur in nature.

duct **1.** A narrow propagation path, sometimes traveled by microwaves, created by unusual atmospheric conditions. **2.** A pipe or channel for cables and wires. **3.** An opening, vent, or other airway used for various purposes, such as cooling and acoustic wave transmission.

ducted port An opening in a speaker cabinet that has an airway (duct) extending several inches into the cabinet. It improves the quality of sound from a speaker system by equalizing the air pressure inside and outside the cabinet. Also provides resonant audio effects at frequencies that depend on the dimensions of the duct.

duct effect see TROPOSPHERIC DUCTING.

ductilimeter An instrument used for measuring the ductility of metals.

ducting The confinement of a radio wave to a duct (see DUCT, **1**) between two layers of the atmosphere or between an atmospheric layer and the earth.

Duddell arc A carbon copper arc circuit that produces audible continuous waves. Consists of a series inductance-capacitance (LC) circuit shunting an electric arc.

Duerdoth's multiple feedback system In an amplifier, feedback through several paths to improve response over that afforded by single-path feedback. In a simple application of multiple feedback, a single external loop is augmented with unbypassed emitter resistors in the amplifier stages.

Duerdoth's stability margin A feedback-amplifier stability margin equal to a 6-dB increase in gain at low and high frequencies over beta values between 0.3 and somewhat less than 2. For higher beta values, Duerdoth adopts an angular margin (for example, 15°); below $\beta = 0.3$, no danger of instability is present.

dummy **1.** A nonoperative model of a piece of equipment, usually assembled with dummy components (see DUMMY COMPONENT, **1**) for the purpose of developing a layout. **2.** DUMMY ANTENNA, DUMMY COMPONENT, or DUMMY LOAD. **3.** Part of a computer program that, rather than being useful for the problem at hand, only serves to satisfy some other format or logic requirement.

dummy antenna **1.** A nonradiating device that serves as a load for a transmitter (i.e., it takes the place of the regular antenna during tests and adjustments of the transmitter). **2.** A device containing a network of discrete inductive, capacitive, and resistive elements, inserted between a radio-frequency signal generator and receiver to simulate a standard antenna.

dummy component **1.** A nonoperative component used in developing a layout or package. **2.** A nonoperative component fraudulently included in a piece of equipment (e.g., an unwired transistor in a receiver circuit, a common occurrence during the early days of the transistor, when a 10-transistor radio brought more money than an 8-transistor radio, without regard to the circuit itself).

dummy instruction In a computer, a command that serves no operational purpose, other than to fill a format requirement.

dummy load **1.** A load device, usually consisting of resistance without reactance, used to terminate a power generator or power amplifier during adjustments and tests. The load resistance is equal to the output impedance of the generator or amplifier. **2.** See DUMMY ANTENNA.

dummy resistor A power-type resistor used as a dummy load.

dump **1.** In digital-computer operations, to transfer, completely or partially, the contents of memory into a peripheral. **2.** To switch off all power to a computer, deliberately or accidentally, thereby losing what is in the volatile memory.

dump and restart During a halt in a computer program run, to backtrack to the last dump point and use the data there to resume the run. Also see DUMP POINT.

dump check In digital-computer operations, the checking of all digits being transferred (see DUMP, **1**) to prevent errors when they are retransferred.

5059F-pD-163-223 4/9/01 5:22 PM Page 219

dumping To transfer the output at various stages in a computer program run to an external storage medium, so it will be available (in case of a failure) for the program's resumption from a point other than at the beginning.

dump point In writing a computer program, a point at which instructions are given to transfer data processed thus far to a storage medium that would be unaffected by a software or hardware failure. Also see DUMP AND RESTART and DUMPING.

dumping resistor **1.** See BLEEDER. **2.** A resistor having the minimum resistance permissible in a given situation. Used to discharge a capacitor, it acts to provide an alternative path to a potentially destructive short circuit.

duo Any pair of matched components, usually in a single package.

duodecal CRT base The 12-pin base of a cathode-ray tube. Also see BIDECAL, DIHEPTAL, and MAGNAL.

duodecal socket A 12-pin tube socket. Also see DUODECAL CRT BASE.

duodecimal **1.** Having 12 possibilities, states, choices, etc. **2.** Pertaining to the DUODECIMAL NUMBER SYSTEM. **3.** A number or numeral in the DUODECIMAL NUMBER SYSTEM.

duodecimal number system A system of numbering in which the radix, also called the base or modulus, is 12. The system uses the digits 0 through 9, plus two other characters (usually A and B) to represent 10 and 11. Thus, counting proceeds as 0, 1, 2, . . . , 9, A, B, 10, 11, 12, . . . , 19, 1A, 1B, 20, 21, 22, etc. At one time, some people seriously proposed that this system replace the DECIMAL NUMBER SYSTEM for general use.

duodiode See DUAL DIODE.

duolateral coil A multilayer, lattice-wound coil (see UNIVERSAL WINDING) in which the turns in successive layers are staggered slightly. Also called *honeycomb coil.*

duopole A two-pole all-pass device.

duplex **1.** A mode of communication in which two channels are used so that either operator in a conversation can interrupt the other at any time. **2.** The transmission of two messages over a single circuit, at the same time.

duplex artificial line In wire telephony, a balancing network that simulates the impedance of the actual line and the remote terminal equipment; it prevents an outgoing transmission from interfering with the local receiver.

duplex cable A cable consisting of a twisted pair of insulated stranded-wire conductors.

duplex channel A channel used for wire or radio DUPLEX OPERATION.

duplex communication See DUPLEX OPERATION.

duplex diode See DUAL DIODE.

duplexer In radar operations, a device operated by the transmitted pulse to automatically switch the antenna from the receiver to the transmitter.

duplexing assembly In a radar system, a device that automatically makes the receiver unresponsive to the outgoing transmitted signal while allowing incoming signals to reach the receiver easily. Also see TRANSMIT-RECEIVE SWITCH.

duplex computer system An installation of two computer systems, one standing by to take over in case the other fails.

duplex operation The simultaneous operation of a transmitter and receiver at a single location. This becomes possible (without mutual interference) through the use of two sufficiently separated carrier frequencies.

duplex system A system composed of two identical equipment sets—either of which will perform the intended function while the other stands by.

duplication check In digital-computer operations, the checking of an operation by doing it twice, using different methods in each case, to ensure the accuracy of results.

duplication house A professional person or company who makes high-quality copies of tape recordings (either audio or video). Charges vary, depending on the type and length of the recording.

duplicate To transfer data from one storage location to another. Compare DUMP, **1**.

dural See DURALUMIN.

duralumin An alloy of aluminum, copper, magnesium, manganese, and silicon. It offers strength with minimal weight.

duration control A potentiometer or variable capacitor for adjusting the duration of a pulse.

duration time The period during which a pulse is sustained (i.e., the interval between turn-on and turn-off time).

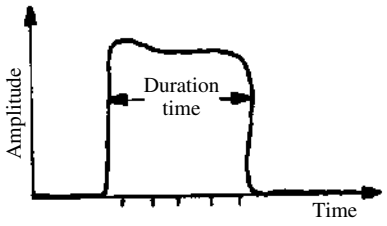

duration time

during cycle The interval during which a timer is in operation.

durometer An instrument for measuring the hardness of a material.

dust collector See DUST PRECIPITATOR.

dust core A magnetic core for radio-frequency coils consisting of very minute particles of iron or an alloy, such as Permalloy.

dust cover A removable, usually plastic cover for electronic and computer equipment, to protect hardware during periods of nonuse.

5059F-pD-163-223 4/9/01 5:22 PM Page 220

dust-ignition-proof motor A motor whose housing completely prevents the entry of dust, virtually eliminating the danger of fine dust sparking inside the machine.

dust precipitator An electrostatic device for removing dust, lint, and other particles from the air. It consists essentially of a pair of screens or wires through which the air passes; a potential of several thousand volts is maintained between them. The particles acquire a charge, then stick to the oppositely charged screen.

Dutch metal A copper-zinc alloy.

duty cycle **1.** The proportion or percentage of time during which a device, circuit, or system is operating or handling power. For example, when a radiotelegraph transmitter is keyed on and off to send Morse code, the duty cycle is approximately 50 percent; with frequency-shift keying, the duty cycle is 100 percent. **2.** The conditions under which an electrochemical cell or battery is used. In particular, the proportion or percentage of time during which current is drawn from the cell or battery for the purpose of operating an electrical or electronic circuit, device, or system.

duty cyclometer A direct-reading instrument for measuring duty cycle.

duty factor **1.** The ratio P_{avg}/P_{pk}, where P_{avg} is the average power in a system and P_{pk} is the peak power. **2.** The product of the duration and the repetition rate of regularly recurring pulses comprising a carrier.

duty ratio See DUTY FACTOR, 1.

DVM Abbreviation of DIGITAL VOLTMETER.

DVOM Abbreviation of DIGITAL VOLT-OHM-MILLIAMMETER.

dwell meter An instrument that shows the period (or angle) during which contacts remain closed.

dwell switching Switching action in which the contacts are held closed (or a circuit kept on) for specified periods, as opposed to MOMENTARY SWITCHING.

dwell tachometer A combination dwell meter/tachometer for automobile engine testing and adjustment. The dwell meter allows observation and adjustment of the ignition point cam angle; the tachometer shows the motor speed in revolutions per minute (rpm).

DX **1.** Radiotelegraph abbreviation meaning *long distance* or *foreign country.* **2.** A communication or broadcast station located far away and/or in a foreign country. **3.** Abbreviation of DUPLEX.

DXer An amateur radio operator who prefers to communicate with stations far away and/or in foreign countries.

Dy Symbol for DYSPROSIUM.

dyadic operation A binary operation (i.e., one using two operands).

dyn Abbreviation of DYNE.

dyna- A prefix (combined form) meaning *power* (e.g., dynamometer and dynatron).

dynamic acceleration Acceleration whose magnitude and direction are constantly changing.

dynamic allocation In multiprogramming, a system in which a monitor program assigns peripherals and areas of memory to a program.

dynamic analogy A mathematical similarity between or among various phenomena involving the motion of particles.

dynamic base current See AC BASE CURRENT.

dynamic base resistance See AC BASE RESISTANCE.

dynamic base voltage See AC BASE VOLTAGE.

dynamic behavior **1.** The behavior of a component, device, or system when signals are applied, as opposed to *static behavior* under no-signal conditions. **2.** The behavior of a device or system involving the motion of particles over a period of time.

dynamic braking A technique for stopping a motor quickly using a resistor (the dynamic braking resistance) connected across the spinning armature. The resistor dissipates the energy generated by the motor, producing a damping action that results in braking.

dynamic characteristic The performance characteristic of a device or circuit under alternating-current (ac) operating conditions, as opposed to the *static characteristic*, when only direct current (dc) flows.

dynamic check **1.** A test made under actual operating conditions of a device or circuit. **2.** A test made with an alternating-current (ac) applied signal, rather than with direct-current (dc) quantities.

dynamic collector current See AC COLLECTOR CURRENT.

dynamic collector resistance See AC COLLECTOR RESISTANCE.

dynamic collector voltage See AC COLLECTOR VOLTAGE.

dynamic contact resistance In relay or switch contacts, variation in the electrical resistance of the closed contacts because of variations in contact pressure.

dynamic convergence In a color picture tube, the meeting of the three beams at the aperture mask during scanning.

dynamic current amplification Abbreviation, DCA. An expression of gain in a bipolar transistor. Specified as the ratio of the difference in collector current I_C to the difference in base current I_B

$$\text{DCA} = dI_C/dI_B$$

Geometrically, the dynamic current amplification at a given bias point is the slope of a line tangent to the I_C-versus-I_B curve at that point.

dynamic curve A characteristic curve that accounts for the presence of resistance in series with the device to which the curve applies.

dynamic debugging Any debugging operation performed on a computer system during a normal-speed program run.

5059F-pD-163-223 4/9/01 5:22 PM Page 221

dynamic decay Decay resulting from such factors as ion charging in a storage tube.

dynamic demonstrator A teaching aid consisting of a board displaying an electronic circuit, behind which is mounted the actual circuit. Various circuit components (especially adjustable ones) are mounted on the front of the board, in clear view at places where their circuit symbols appear. Pin jacks at important test points in the circuit allow connection of a meter, signal generator, and oscilloscope leads for testing or demonstrating the circuit.

dynamic deviation The difference between ideal output and actual output of a circuit or device operating with a reference input that changes at a constant rate and is free of transients.

dynamic diode tester An instrument that displays the response curve (or family of curves) of a diode on a calibrated oscilloscope screen. The horizontal axis of the screen indicates voltage, the vertical axis shows current, and zeros for both quantities are at center screen. Also see DYNAMIC RECTIFIER TESTER.

dynamic drain current See AC DRAIN CURRENT.

dynamic drain resistance See AC DRAIN RESISTANCE.

dynamic drain voltage See AC DRAIN VOLTAGE.

dynamic dump A dump that occurs during a program run. See DUMPING.

dynamic electric field An electric field whose intensity is constantly changing, either periodically or in a complex way.

dynamic emitter current See AC EMITTER CURRENT.

dynamic emitter resistance See AC EMITTER RESISTANCE.

dynamic emitter voltage See AC EMITTER VOLTAGE.

dynamic equilibrium **1.** The state of balance between constantly varying quantities. **2.** The tendency of two current-carrying circuits to maintain at a maximum the magnetic flux linking them.

dynamic error In a periodic signal delivered by a transducer, an error resulting from the restricted dynamic response of the device.

dynamic flip-flop A flip-flop (bistable multivibrator) that is kept on by recirculating an alternating-current (ac) signal. The device can be switched on or off by a single pulse. Compare STATIC FLIP-FLOP.

dynamic focus Compensation for defocusing, caused by the electron beam sweeping in an arc across a flat color picture-tube screen; the method uses an alternating-current (ac) focusing-electrode voltage.

dynamic gate voltage See AC GATE VOLTAGE.

dynamic impedance The impedance of a device (such as a transistor or diode) when it is operating with an applied alternating-current (ac) signal, as opposed to its *static resistance* with only direct current (dc) applied.

dynamic limiter A limiter, such as is used in frequency-modulation (FM) receivers, that maintains the output-signal level, despite appreciable excursions of input-signal amplitude.

dynamic loudspeaker See DYNAMIC SPEAKER.

dynamic magnetic field A magnetic field whose intensity is constantly changing, either periodically or in a complex way.

dynamic memory A usually random-access data storage method in which the memory cells must be electrically refreshed periodically to avoid the loss of held data.

dynamic microphone A microphone in which a small coil attached to a vibrating diaphragm or cone moves in a uniform magnetic field to generate the output signal.

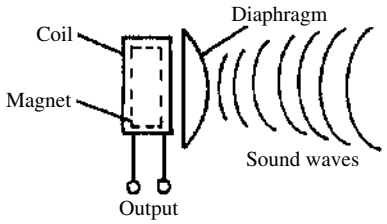

dynamic microphone

dynamic mutual conductance See DYNAMIC TRANSCONDUCTANCE.

dynamic noise suppressor A noise limiter consisting of an audio filter whose bandwidth is directly proportional to signal strength (i.e., it is varied automatically by signal amplitude).

dynamic operating line A curve displaying the control function of a device. For example, the collector-current-versus-base-current curve of a bipolar transistor is drawn between the limits of saturation and cutoff.

dynamic output impedance The output impedance of a power supply, as "seen" by the load.

dynamic pickup A phonograph pickup whose stylus causes a small coil to vibrate in the field of a permanent magnet. Works on the same principle as the DYNAMIC MICROPHONE.

dynamic printout A printout that occurs as a single function, actuated by one command, and completing itself in one operation.

dynamic problem checking A method of checking the solution obtained by an analog computer, to see that it makes sense (is not absurd).

dynamic programming A method of problem solving in which continual checks are made to ensure accuracy or conformance to a certain set of rules.

dynamic range **1.** In high-fidelity audio, the ratio of the loudest sound to the faintest sound that can be reproduced without significant distortion

5059F-pD-163-223 4/9/01 5:22 PM Page 222

or noise. It is usually expressed in decibels. **2.** In a communications receiver, a measure of the ability to receive both weak and strong signals without excessive noise, distortion, desensitization or other undesirable effects. It is expressed in various ways, typically in decibels. **3.** The ratio between the loudest and faintest sounds, or between the strongest and weakest signals, encountered in a given environment or situation. It is usually expressed in decibels.

dynamic rectifier tester An instrument that displays the response curve of a rectifier on a calibrated oscilloscope screen. During the test, the rectifier receives an alternating-current (ac) voltage with a low positive peak and high negative peak, both corresponding to the rated forward and reverse voltages (respectively) of the rectifier. The horizontal axis of the screen indicates voltage, the vertical axis indicates current, and zeros for both quantities are at center screen.

dynamic regulation In an automatically regulated system, such as a voltage-regulated power supply, the transient response of the system. Dynamic regulation is determined from maximum overshoot and recovery time when the load or line value is suddenly changed.

dynamic regulator A circuit or device providing dynamic regulation.

dynamic reproducer **1.** See DYNAMIC MICROPHONE. **2.** See DYNAMIC PICKUP. **3.** See DYNAMIC SPEAKER.

dynamic resistance See DYNAMIC IMPEDANCE.

dynamic run See DYNAMIC CHECK, **1**. See also DYNAMIC DEBUGGING.

dynamics The study of bodies, charges, fields, forces, or pulses in motion. Compare STATICS.

dynamic sequential control In digital computer operation, the computer's changing the sequence of instructions during a run.

dynamic source current See AC SOURCE CURRENT.

dynamic source resistance See AC SOURCE RESISTANCE.

dynamic source voltage See AC SOURCE VOLTAGE.

dynamic spatial reconstructor Abbreviation, DSR. An advanced x-ray machine, developed at the Mayo Clinic, that displays organs in three-dimensional views in motion, and allows them to be electronically dissected without actually operating on the patient.

dynamic speaker A loudspeaker in which a small coil (voice coil), attached to a diaphragm or cone and carrying an audio-frequency signal current, moves back and forth in a permanent magnetic field and, accordingly, causes the diaphragm or cone to vibrate (emit sound). Compare MAGNETIC SPEAKER.

dynamic stability A measure of the ability of a robot to maintain its balance while in motion.

dynamic stop As caused by a computer program instruction, a loop indicating the presence of an error.

dynamic storage See DYNAMIC MEMORY.

dynamic subroutine A form of computer subroutine that allows the derivation of other subroutines in various forms.

dynamic test See DYNAMIC CHECK.

dynamic transconductance Transconductance determined from alternating-current (ac) signal parameters, rather than from direct-current (dc) parameters.

dynamic transducer A coil-and-magnet device that converts mechanical vibration into electric currents, or vice versa. Common examples include most microphones, headphones, and loudspeakers.

dynamic transfer characteristic An input-output characteristic determined, with respect to the load of a transfer device. Also see DYNAMIC CHARACTERISTIC.

dynamic transistor tester **1.** An instrument for checking the alternating-current (ac) gain of a transistor, rather than its direct-current (dc) beta. **2.** An instrument for determining the condition of a transistor from its performance in a simple oscillator circuit. **3.** An instrument that displays a transistor response curve, or a family of such curves, on a calibrated oscilloscope screen. Also see DYNAMIC DIODE TESTER and DYNAMIC RECTIFIER TESTER.

dynamo A mechanical generator of electricity; typically a rotating machine.

dynamoelectric machinery Rotating electric machinery. Examples: amplidynes, generators, dynamotors, rotary converters.

dynamometer **1.** See ELECTRODYNAMOMETER. **2.** A device for mechanically measuring the output power of a motor.

dynamometer ammeter See ELECTRODYNAMOMETER.

dynamometer voltmeter See ELECTRODYNAMOMETER.

dynamophone A dynamometer (see DYNAMOMETER, **2**) that uses two telephone circuits to measure the twist of a shaft.

dynamostatic machine A machine driven by alternating-current (ac) or direct-current (dc) power for the generation of static electricity.

dynamotor A (usually small) self-contained motor-generator. The motor and generator portions are enclosed in a common housing, giving the machine the appearance of a simple motor.

dynaquad A pnpn four-layer semiconductor device with three terminals, similar to the silicon-controlled rectifier or thyristor.

dynatron A form of vacuum tube that displays a negative-resistance characteristic, resulting in oscillation at ultra-high and microwave frequencies.

5059F-pD-163-223 4/9/01 5:22 PM Page 223

dynatron frequency meter A heterodyne-type frequency meter using a dynatron oscillator.

dyne Abbreviation, d. A unit of force. One dyne (10^{-5} newton) is the force that will give a mass of 1 gram an acceleration of 1 centimeter per second per second. Compare NEWTON.

dyne-centimeter See ERG.

dyne-five In the Giorgi mks system, a unit of force equal to 1 newton.

dyne per square centimeter Abbreviation, d/cm^2. A unit of pressure equal to 0.1 pascal (9.869×10^{-7} atmosphere).

dyne-seven A unit of force equal to 10^7 dynes.

dynistor A semiconductor diode that continues to conduct after the forward voltage is reduced below the normal threshold point. To stop the conduction, a reverse voltage must be applied, or voltage must be entirely removed from the device. It is used in switching applications.

dynode In a photomultiplier tube, any of several slanting electrodes that receives a beam of electrons generated by the light-sensitive cathode and reflects it, along with secondary electrons. This amplifies the beam; the process is repeated several times. Thus, the emission from the cathode is greatly amplified when it reaches the plate.

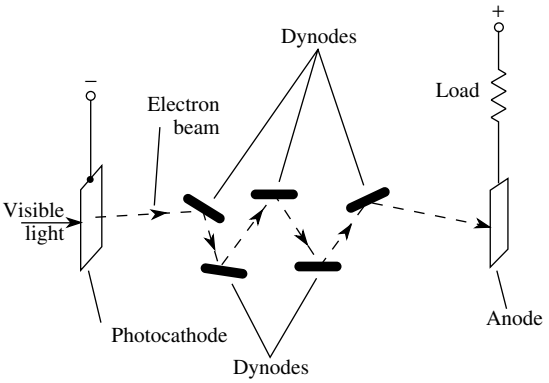

dynode

dysprosium Symbol, Dy. An element of the rare-earth group. Atomic number, 66. Atomic weight, 162.50. Dysprosium is a highly magnetic substance.

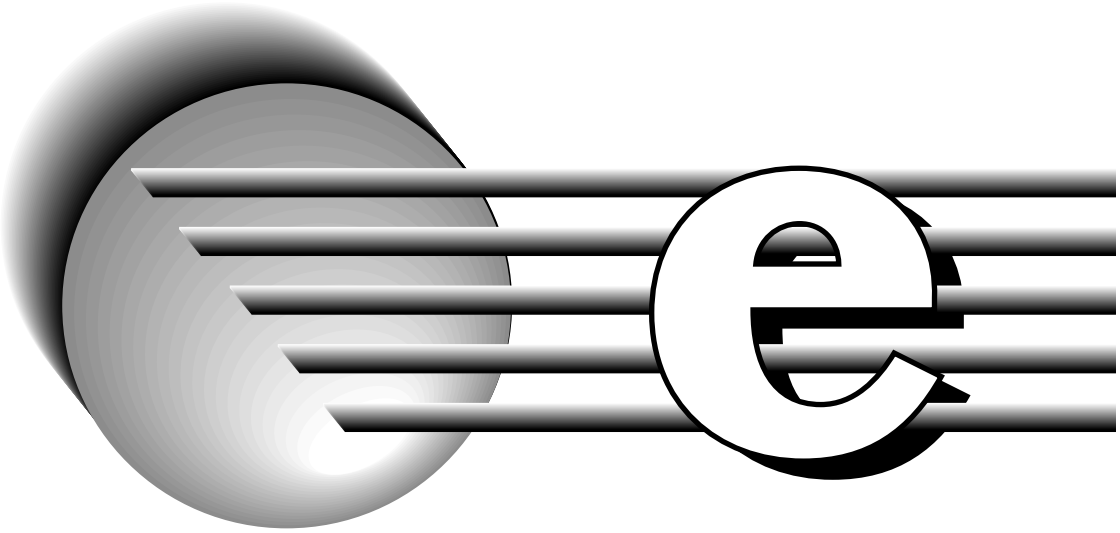

E **1.** Symbol for VOLTAGE. **2.** Symbol for ELECTRIC FIELD STRENGTH. **3.** Abbreviation of EMITTER. **4.** Symbol for prefix EXA. **5.** Symbol for ENERGY.

e **1.** Symbol for VOLTAGE. **2.** Abbreviation of EMITTER. **3.** Symbol for ELECTRON CHARGE. **4.** Symbol for the natural logarithm base (approximately equal to 2.71828). **5.** Symbol for ECCENTRICITY. **6.** Abbreviation of ERG.

EAM Abbreviation of *electronic accounting machine.*

E and M terminals The output and input leads in some signaling systems. Also called *E and M leads.*

early early sound Sound propagated through solids and/or liquids that reaches a pickup device (such as a microphone) before the sound propagated through the air. In general, sound waves travel faster as the medium becomes more dense.

early-failure period The period immediately after manufacture of a device, during which the failure rate (caused by defects in equipment or workmanship) is high.

early-warning radar Abbreviation, EWR. A radar system that produces immediate warning when enemy aircraft enter the monitored area.

earphone **1.** *Headphone* (usually a single unit). **2.** Telephone receiver. **3.** A miniature acoustic transducer that is small enough to be inserted into the ear.

earpiece See EARPHONE, **3**.

earth **1.** The ground. **2.** An electrical connection to the earth (see GROUND CONNECTION, **2**). **3.** In space communications, the planet Earth.

earth connection See GROUND CONNECTION, **2**.

earth currents **1.** Electric currents induced in the earth by current flowing through underground or underwater cables. **2.** Electric currents flowing through the earth between ground connections of electrical equipment.

earth ground **1.** A common connection to an electrode buried in the earth so that good conductivity is maintained between the common circuit point and the earth itself. **2.** A rod driven into the surface of the earth for use as a common circuit connection.

earth inductor A magnetometer consisting of a coil that is rotated in the earth's magnetic field. It delivers an alternating-current (ac) voltage proportional to the field strength. Also called *generating magnetometer.*

earth-moon-earth See MOONBOUNCE.

earth resonance A resonant effect at extremely low frequencies, caused by reflection of currents within the earth. Resonant currents have been tested as a means of communicating with submarines worldwide.

earth's magnetic field Also called *geomagnetic field.* The natural magnetic field whose lines of flux extend from north to south. The earth's magnetic poles, also called the *geomagnetic poles*, do not exactly coincide with the geographic poles. The field somewhat resembles that of a bar magnet.

Eastern Standard Time Abbreviation, EST. Local mean time at the 75th meridian west of Greenwich.

east-west effect The phenomenon in which the number of cosmic rays approaching earth near the equator from the west is greater than that from the east by 10 percent.

Copyright 2001 The McGraw-Hill Companies, Inc. Click Here for Terms of Use

5059F-pE-224-273 4/9/01 5:26 PM Page 225

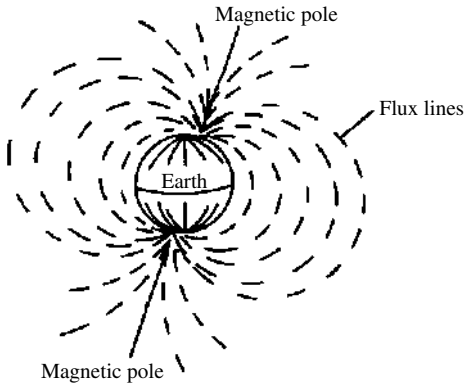

earth's magnetic field

E_{avg} Symbol for AVERAGE VOLTAGE.

E_b Symbol for BATTERY VOLTAGE.

E bend In a waveguide, a smooth change in the direction of the axis, which remains parallel to the direction of polarization.

EBI Abbreviation of EQUIVALENT BACKGROUND INPUT.

ebiconductivity Conductivity resulting from electron bombardment.

ebonite Hard rubber used as an insulant. Dielectric constant: 2.8. Dielectric strength: 30 to 110 kV/mm.

EBR Abbreviation of ELECTRON-BEAM RECORDING.

EBS Abbreviation of ELECTRON-BOMBARDED SEMICONDUCTOR.

EBS amplifier An amplifying device using an electron-bombarded semiconductor. The electron beam is modulated by the input signal, and the modulated resistance of the semiconductor target modulates a relatively heavy current to provide an amplified output. Current gains on the order of 2000 are possible.

ec Abbreviation of ENAMEL-COVERED (in reference to wire).

eccentric circle See ECCENTRIC GROOVE.

eccentric groove On a phonograph record, an off-center groove in which the stylus rides at the end of the recording, where it causes the tone arm to trip the record-changing mechanism.

eccentricity **1.** The condition of being off center, intentionally or not. It is often a consideration in the behavior of dials, potentiometers, and servomechanisms. **2.** On a phonograph record, the condition in which the spiral recording groove and the center hole of the disk are not concentric. **3.** A quantitative expression for the extent to which an ellipse is elongated.

eccentricity of orbit The extent to which the orbit or path of a satellite differs from a circle. A circular orbit has eccentricity zero. As the orbit becomes elliptical and deviates more and more from a perfect circle, the eccentricity increases. When the eccentricity reaches 1, the object takes a parabolic path through space. If the eccentricity exceeds 1, the path is a hyperbola.

ECCM Abbreviation of ELECTRONIC COUNTER-COUNTERMEASURES.

ECDC Abbreviation of *electrochemical diffused collector.*

ECG Abbreviation of electrocardiogram. (Also, EKG.)

ECG telemetry Use of a radio telemetering system to monitor the heart function of a person from a distance.

echelon **1.** A level of calibration accuracy, the highest echelon being the national standard for the particular measurement involved. **2.** A level of maintenance in which lower ordinal numbers refer to less-critical tasks, and higher ordinal numbers refer to tasks requiring progressively higher skills and technological expertise.

echelon grating A diffraction grating with extremely high resolution. Generally useful only over a small range of wavelengths.

echo **1.** A signal that is reflected back to the point of origin. **2.** A reflected or delayed signal component that arrives at a given point behind the main component. **3.** A radar blip, indicating an object or thundershower. **4.** Reflection of the signal on a telephone line, caused by improper impedance matching, or by overload of the system by too many subscribers attempting to use the system at the same time. **5.** In audio systems, a circuit that causes sounds to repeat one or more times, at intervals ranging from a fraction of a second to several seconds. **6.** The effect produced by a circuit, as defined in 5.

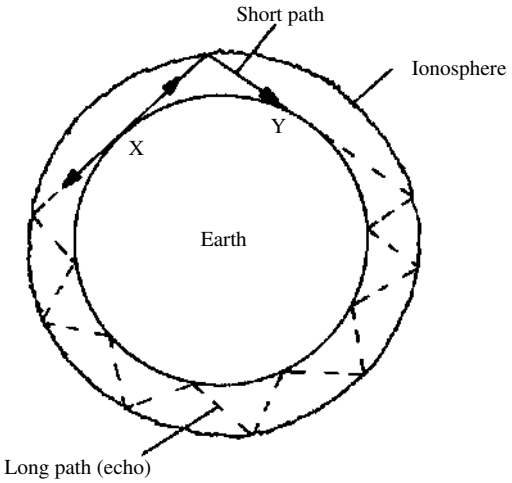

echo

5059F-pE-224-273 4/9/01 5:26 PM Page 226

echo area The area of a target that will return a radar signal as an echo.

echo attenuation In a bidirectional wire-communication circuit equipped with repeaters or multiplexers, the attenuation of echo currents set up by conventional operation.

echo box A resonant-cavity device used to test a radar set. Part of the transmitted energy enters the box, which retransmits it to the receiver. The signal reaching the receiver is a slowly decaying transient whose intensity eventually falls below the level that can be displayed on the screen; the time required to reach this level indicates radar performance.

echo chamber A reverberation chamber, electronic recording device, or room for acoustic tests or for simulating sonic delays.

echo check In data communication, a means of checking the accuracy of received data by sending it back to the transmitting station for comparison with the original data.

echo depth sounder See ACOUSTIC DEPTH SOUNDER.

echo eliminator **1.** A device that quiets a navigational instrument after receipt of a pulse, to prevent reception of a subsequent, delayed pulse. **2.** In a two-way telephone circuit, a voice-operated device that suppresses echo currents caused by conversation currents going in the opposite direction.

echoencephalograph An ultrasonic medical instrument that allows viewing of internal organs. Used for diagnostic purposes in certain situations, instead of the X-ray machine.

echogram In acoustics, a graph of the sound decrement in an enclosure. Time is plotted on the horizontal axis; signal amplitude is plotted on the vertical axis. An intense pulse is transmitted from a speaker; a microphone picks up the echoes and sends them to a pen recorder or microprocessor.

echo intensifier A device used at a radar target to boost the intensity of reflected energy.

echo interference Radio interference resulting from a reflected signal arriving slightly later than the direct signal.

echo matching In an echo-splitting radar system, the trial-and-error orientation of the antenna to find the direction from which the pulse indications are identical.

echo ranging An ultrasonic method of determining the bearing and distance of an underwater object.

echo send In an audio mixer, an output for delivering signals to external systems, such as an echo box (see ECHO, **5**). It can also provide an auxiliary output for a second set of speakers, a tape recorder, etc.

echo sounder See ACOUSTIC DEPTH SOUNDER.

echo splitting Separating a radar echo into two parts so that a double indication appears on the radar screen.

echo suppression In a telephone circuit, a device that chokes off reflected waves, thereby minimizing audible echo.

echo suppressor See ECHO ELIMINATOR.

echo talk Echo in a telephone system that results in distracting interference.

echo wave A reflected wave, such as a radio wave reflected alternately between earth's surface and the ionosphere.

ECL Abbreviation of EMITTER-COUPLED LOGIC.

eclipse effect A decrease in the critical frequency of the E and F1 layers of the ionosphere during a solar eclipse.

ecliptic orbit Any orbit that lies in the same plane as the orbit of the earth around the sun (the *ecliptic plane*). The ecliptic plane is slanted about 23.5° from the plane of the earth's equator.

ECM Abbreviation of ELECTRONIC COUNTERMEASURES.

ECO Abbreviation of ELECTRON-COUPLED OSCILLATOR.

econometer An instrument for continuously monitoring the amount of carbon dioxide in (factory) flue gases.

E core A transformer or transducer core having the shape of an E. Coils can be wound on one, two, or all three of the crosspieces.

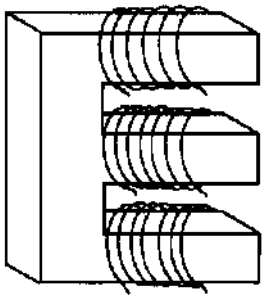

E core

ECPD Abbreviation of *Engineer's Council for Professional Development.*

ECTL Abbreviation of *emitter-coupled transistor logic.*

EDD Abbreviation of ENVELOPE-DELAY DISTORTION.

eddy current A circulating current induced in a conducting material by a varying magnetic field, often parasitic in nature. Such a current can, for example, flow in the iron core of a transformer.

eddy-current device A brake, coupling, clutch, drag cup, drive unit, or similar device whose operation is based on the generation of torque, pull, or opposition by the action of eddy currents.

eddy-current heating Heating caused by eddy-current loss in a material.

eddy-current loss Power loss resulting from eddy currents induced in nearby structures by an

5059F-pE-224-273 4/9/01 5:26 PM Page 227

electromagnetic field. Eddy currents in the core of a transformer give rise to such loss.

edge connector A terminal block with a number of contacts, attached to the edge of a printed-circuit board for easy plugging into a foundation circuit.

edge control In the manufacture of paper, a robotic system for maintaining the width of a sheet by sensing the edges and correcting the machine accordingly. Transducers that sense the passing edges deliver output signals proportional to variations from standard width.

edge detection The ability of a machine vision system to locate and follow boundaries. Used extensively in mobile robots.

edge effect The extension of electric lines of flux between the outer edges of capacitor plates. This portion of the interplate field contributes a small amount of capacitance. Because the lines of flux are not confined to the space between plates, they can cause capacitive coupling with external bodies.

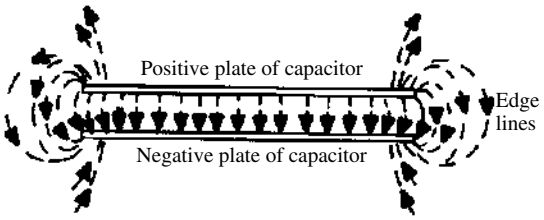

edge effect

edge-punched card In digital computer operations, a punched card whose edge is perforated in a narrow column, the center being used for written annotation.

edgewise meter A meter having a curved horizontal scale; this arrangement allows mounting the instrument edgewise in a panel.

edgewise-wound coil A coil made of a flat metal strip cut in the shape of a coil spring. The design allows the use of clips to vary the inductance, but this advantage is often offset by the coil's high distributed capacitance.

edging In a color television picture, extraneous color of a different hue than the objects around whose edges it appears.

Edison base A threaded base on light bulbs, cone-type heaters, and some pilot lamps.

Edison battery A group of Edison cells connected in series, parallel, or both, and contained in a single package with two electrodes.

Edison cell A secondary (storage) cell in which the active positive plate material consists of nickel hydroxide held in steel tubes assembled into a steel grid; the active negative plate material is powdered iron oxide mixed with cadmium; the electrolyte is potassium hydroxide. The open-circuit voltage of the cell is typically 1.2 V at full charge.

Edison distribution system A three-wire, 110- to 250-volt direct-current (dc) power-distribution system.

Edison effect Thermionic emission of negatively charged particles (electrons) from a hot filament sealed in an evacuated bulb; they are attracted by a cold, positively charged metal plate in the bulb.

E display A radar display in which the horizontal coordinate indicates distance, and the vertical coordinate indicates elevation.

edit **1.** In tape recording, the modifying of the recorded material by deleting (cutting out or erasing), adding (splicing or overrecording), or changing the sequence of the material by physically or magnetically altering the tape. **2.** In digital computer operations, to make data ready for processing.

edit decision list In the editing of a digital audio/video presentation, a record of every change (cut and paste). The list is automatically made by the computer and stored on disk for later reference if needed.

editing **1.** Alteration of a magnetic-tape recording by means of splicing. **2.** Alteration of data stored in memory, either by adding information, removing information, changing information, or (usually) a combination of these operations.

EDL Abbreviation of EDIT DECISION LIST.

EDM Abbreviation of ELECTRICAL-DISCHARGE MACHINING.

EDP Abbreviation of *electronic data processing.*

EDPC Abbreviation of ELECTRONIC DATA-PROCESSING CENTER.

EDPM Abbreviation of ELECTRONIC DATA-PROCESSING MACHINE.

EDPS Abbreviation of ELECTRONIC DATA-PROCESSING SYSTEM.

EDT **1.** Abbreviation of *ethylene diamine tartrate* (a synthetic piezoelectric material). **2.** Abbreviation of *Eastern Daylight Time.*

EDU Abbreviation of *electronic display unit.*

educational robot A robot that can be programmed for the purpose of teaching its users something. Popular as an educational toy for children.

EDVAC Acronym for *Electronic Discrete Variable Automatic Computer*, a development of the University of Pennsylvania.

EE Abbreviation of ELECTRICAL ENGINEER or ELECTRONICS ENGINEER.

$\mathbf{E_{eff}}$ Symbol for EFFECTIVE VOLTAGE.

EEG Abbreviation of ELECTROENCEPHALOGRAM.

EEPROM Abbreviation of ELECTRICALLY ERASABLE PROGRAMMABLE READ-ONLY MEMORY. See PROM and ROM.

EES Abbreviation of EARLY EARLY SOUND.

effective acoustic center The apparent point of propagation of spherically divergent sound waves radiated by an acoustic generator.

5059F-pE-224-273 4/9/01 5:26 PM Page 228

effective actuation time The total actuation time of a relay (i.e., the sum of the initial actuation time and subsequent intervals of contact chatter).

effective address The address a computer uses in implementing an instruction (i.e., one not necessarily coinciding with the address given in the instruction).

effective ampere An effective current of 1 ampere. Also see EFFECTIVE CURRENT.

effective antenna length See ELECTRICAL LENGTH.

effective antenna resistance The radiation resistance of an antenna, as measured at the input point.

effective bandwidth The bandwidth of an ideal bandpass filter, which, at a reference frequency, has the same transfer ratio as an actual bandpass filter under consideration; it also has the same current and voltage characteristics.

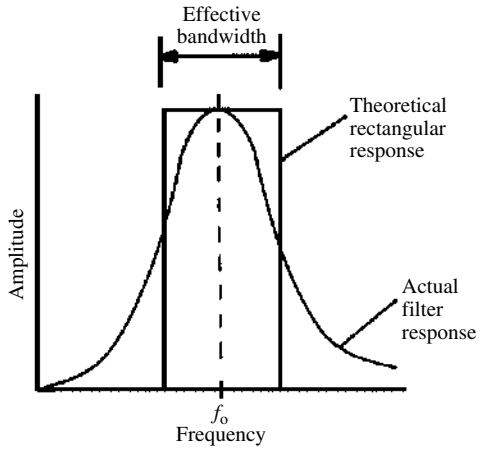

effective bandwidth

effective capacitance The actual capacitance between two points in a circuit resulting from the combination of inherent, lumped, and stray capacitances.

effective conductivity Conductivity measured between the parallel faces of a unit cube of a material.

effective confusion area In a radar system, an area in which interference makes it impossible to see whether a target is present.

effective current Symbol, I_{eff}. The root-mean-square (rms) value of alternating current (see EFFECTIVE VALUE). For a sinusoidal current, $I_{eff} = 0.707I_{max}$, where I_{max} is the maximum value of the current. Also called *rms current.*

effective cutoff See EFFECTIVE CUTOFF FREQUENCY.

effective cutoff frequency For a filter or similar device operated between specified impedances, the frequency at which insertion loss is higher than the loss at a specified reference frequency in the passband.

effective field intensity The root-mean-square (rms) value of the field-strength voltage, averaged for all points at a horizontal distance of one mile from a transmitting antenna.

effective height The height of an antenna in terms of its performance as a transmitter or receiver of electromagnetic energy.

effective input capacitance The actual operative capacitance present at the input terminals of a circuit or device, caused by the shunt capacitance of the terminals themselves and the net capacitance of the circuit connected to the terminals.

effective internal resistance In an electrochemical cell or battery, a resistance that originates within the electrolyte and electrodes. This resistance is low when the current drain is low; it rises as the current drain increases. It limits the maximum current that the cell or battery can deliver.

effective isolation The condition of components or circuits being so well isolated or shielded that no significant direct coupling, capacitive coupling, or inductive coupling exists between them.

effective instruction The machine-language version of an instruction given in a computer program, as produced by resident software.

effectively bonded The condition afforded by an extremely low-resistance union between two conducting surfaces that are solidly fastened together.

effectively grounded The condition of being connected to earth or to the low-potential end of a circuit by means of an extremely low-resistance connection.

effective parallel capacitance Inherent capacitance that manifests itself in parallel with two circuit points in combination with any lumped capacitance.

effective parallel resistance **1.** The leakage resistance that manifests itself in parallel with a dielectric (e.g., the leakage resistance of a capacitor). **2.** Parallel-resistance effects caused by stray shunt-resistance components.

effective percentage of modulation For a complex waveform, an expression of the equivalent percentage of modulation by a pure sine wave. Given a certain proportion of power in the sidebands with modulation by a complex signal, the effective percentage of modulation is that percentage which, when the modulating signal is sinusoidal, results in the same proportion of power in the sidebands.

effective phase angle In alternating-current (ac) circuits, the phase angle, with respect to waveforms for current and voltage. When both waveforms are sinusoidal, the effective phase angle is

5059F-pE-224-273 4/9/01 5:26 PM Page 229

the actual phase angle. But when harmonics are present in current or voltage, the angles differ, the difference being greater in capacitive circuits than in inductive circuits.

effective radiated power Abbreviation, ERP or P_{ER}. **1.** A measure of the performance of a wireless transmitting antenna. Suppose a test antenna, A_T, is set up and the field strength in its favored direction at a frequency f is measured at a distance d in free space. Let the field strength thus measured be F watts per square meter. Suppose A_T is replaced with an isotropic radiator, A_I, and the field strength at the same frequency f is measured at the same distance d in free space. Let the radio-frequency (RF) power at the feed point of the isotropic radiator A_I be varied until the field strength is F, the same as it was with the test antenna A_T. Let this RF power be symbolized P. Then P is defined as the effective radiated power (ERP or P_{ER}) of the test antenna, A_T. **2.** The figure defined as in (1), measured in some direction other than the favored direction of a test antenna.

effective resistance **1.** In a coupled circuit, the sum of the actual resistance of the circuit and the reflected resistance of the load. **2.** See EFFECTIVE ANTENNA RESISTANCE.

effective series inductance Inherent (distributed) inductance acting in series with other components in a circuit. The inherent inductance of the wire in a wirewound resistor, for example, manifests itself in series with the resistance of the device.

effective series resistance Inherent (distributed) resistance acting in series with other components in a circuit. Thus, the inherent resistance of the wire in a coil appears in series with the inductance of the coil. Likewise, a capacitor has an effective series resistance because of the resistance of the leads, plates, and connections.

effective shunt capacitance See EFFECTIVE PARALLEL CAPACITANCE.

effective shunt resistance See EFFECTIVE PARALLEL RESISTANCE.

effective sound pressure The root-mean-square (rms) value of instantaneous sound pressure at one point in a sound cycle.

effective speed of transmission In telegraphy (wire or radio) and in electronic data transmission, the transmission speed (characters per minute, bits per second, etc.) that can be reliably maintained for a given period.

effective thermal resistance The effective temperature rise (in degrees per watt of dissipation) of a semiconductor junction above an external reference temperature that is at equilibrium.

effective time For a computer, the time during which useful work is performed.

effective transmission speed See EFFECTIVE SPEED OF TRANSMISSION.

effective value The root-mean-square (rms) value of an alternating-current (ac) quantity. The effective value an alternating current produces in a pure resistance has the same heating effect as the equivalent direct current. See also ROOT MEAN SQUARE.

effective volt An effective potential of one root-mean-square (rms) volt. Also see EFFECTIVE VOLTAGE.

effective voltage Symbol, E_{eff}. The root-mean-square value of alternating-current (ac) voltage (see EFFECTIVE VALUE). For a sinusoidal voltage, $E_{eff} = 0.707E_{max}$, where E_{max} is the maximum value of the voltage. Also called *rms voltage.*

effective wavelength Wavelength in terms of measured frequency and effective propagation velocity.

effects processor In audio systems, a circuit that produces various sound effects via digital signal processing.

efficiency **1.** The ratio of useful power or energy output to total power or energy input to a device or system. **2.** The proportion of applied audio-frequency (AF) power that a loudspeaker converts into acoustic energy. **3.** See ELECTRICAL EFFICIENCY.

efficiency modulation A system of amplitude modulation in which the efficiency of a radio-frequency (RF) power amplifier is varied at an audio-frequency (AF) rate.

efficiency of rectification For a rectifier, the ratio of the direct-current (dc) output voltage to the peak value of alternating-current (ac) input voltage. For percent efficiency, the ratio is multiplied by 100.

efflorescence The giving up of water by a substance upon exposure to air. Some materials used in electronics exhibit this property. Common efflorescent compounds are hydrated ferrous carbonate, ferrous sulfate, and sodium carbonate.

efflorescent material A material exhibiting efflorescence. Compare DELIQUESCENT MATERIAL.

E field **1.** An electric field. **2.** the electric-field component of an electromagnetic wave.

EFL Abbreviation of *emitter-follower logic.*

E_g Symbol for GENERATOR VOLTAGE.

EHD Abbreviation of *electrohydrodynamic(s).*

EHF Abbreviation of EXTREMELY HIGH FREQUENCY.

EHP Abbreviation of *effective horsepower.*

E-H tee A waveguide junction in which E- and H-plane tee junctions intersect the main waveguide at the same point. Also see WAVEGUIDE TEE.

E-H tuner An impedance-transforming E-H tee with two arms that are terminated in tunable plungers for critical adjustments. See WAVEGUIDE PLUNGER.

EHV Abbreviation of *extra-high voltage.*

E_i Symbol for INPUT VOLTAGE.

EIA Abbreviation of *Electronics Industries Association.*

eight-level code A code, such as the *American Standard Code for Information Interchange (ASCII)*,

5059F-pE-224-273 4/9/01 5:26 PM Page 230

in which each character is represented by eight bits.

E indicator A radar elevation display, in which the horizontal scale shows range and the vertical scale shows elevation.

Einstein equation The equation depicting the interconversion of mass and energy; $E = mc^2$, where E is energy (ergs), m is mass (grams), and c is the speed of light in a vacuum (centimeters per second).

einsteinium Symbol, Es. A radioactive element produced artificially. Atomic number, 99. Atomic weight, 252.

Einstein/Dehaas effect The tendency for an iron or steel cylinder to become magnetized as it rotates.

Einstein shift The decrease in frequency and loss of energy experienced by quanta acted upon by gravitation.

Einthoven string galvanometer A simple galvanometer in which a silvered glass filament carrying current is mounted in a magnetic field set up by either a permanent magnet or an electromagnet. The current causes the filament to be deflected through a distance proportional to current strength, the deflection being observed through a microscope.

EIT Abbreviation of *engineer-in-training.*

either-or operation The logical inclusive-OR operation.

EJC Abbreviation of *Engineers' Joint Council.*

eka-aluminum See GALLIUM.

eka-silicon See GERMANIUM.

EKG Abbreviation of ELECTROCARDIOGRAM. (Also, ECG.)

EKG telemetry See ECG TELEMETRY.

EL Abbreviation of ELECTROLUMINESCENCE.

elapsed time **1.** In data-processing and computer operations, what appears to be the duration of a process, compared with actual processing time, as measured by internal clocks, for example. **2.** The accumulated time, usually expressed in hours, minutes, and seconds, that an operation takes or a machine runs.

elapsed-time meter An instrument that indicates the time an electronic device or system has been in operation. Most such meters are based on electric clockwork that runs only while the system is in operation, holding the count during shutdown periods. Also see ELECTROLYTIC ELAPSED-TIME METER.

elastance Unit, daraf. The opposition of a capacitor to being charged. It is the reciprocal of capacitance.

elastic collision A collision between two charged particles in which neither loses energy—even though they are deflected from their normal paths.

elasticity **1.** The ability of a body to return to its original shape after being deformed. See YOUNG'S MODULUS. **2.** See ELASTIVITY.

elastic limit The maximum stress that can be tolerated by a material without being permanently deformed.

elastic wave A wave in an elastic medium, such as air or water; thus, a wave that is mechanically produced.

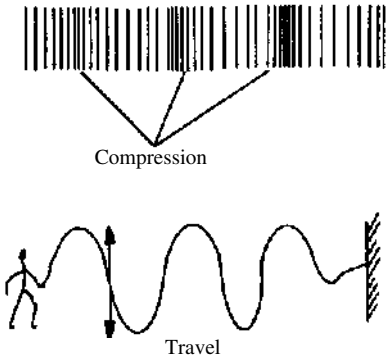

elastic waves

elastivity **1.** Specific elastance (i.e., the elastance in darafs per cubic unit of a dielectric). **2.** The ratio of electric stress to displacement.

elastomer A compressible, conducting substance used in pressure sensing. In one arrangement, an array of electrodes is connected to each side of a pad of the material. When pressure appears at some point, the material compresses, lowering the resistance in the pressure zone. A microprocessor determines the location and extent of the pressure.

E layer A layer in the ionosphere that is 50 to 90 miles above the surface of the earth, and is noted for returning radio waves at high and very-high frequencies.

elbow bend A 90-degree bend in a waveguide.

ELD Abbreviation of *edge-lighted display.*

electra A radio-navigational system in which equal-intensity signal zones (usually 24) are provided.

electralloy A nonmagnetic alloy used in the manufacture of radio hardware, such as chassis.

electre See ELECTRUM.

electrepeter A device used to change the direction of an electric current.

electret A device whose heart is a dielectric disk or slab that is permanently polarized electrically, and so possesses a permanent electric field. The electrical equivalent of the permanent magnet. Certain waxes, ceramics, and plastics acquire permanent polarization after they have been heated, then cooled slowly in an intense electric field.

electret microphone Also called *electret capacitor microphone.* A microphone in which sound waves cause an electret to vibrate and generate

5059F-pE-224-273 4/9/01 5:26 PM Page 231

audio-frequency (AF) output current. An internal power supply (such as a battery) supplies the necessary voltage.

electric **1.** Pertaining to electricity and its various manifestations. **2.** See ELECTROSTATIC.

electric absorption See DIELECTRIC ABSORPTION.

electric accounting machine A self-contained data-processing machine that is neither a computer nor a computer peripheral.

electrical-acoustical transducer A transducer, such as a headphone, sonic applicator, or buzzer, that converts electrical energy into sound energy. Compare ACOUSTICAL-ELECTRICAL TRANSDUCER.

electrical angle The angle assumed at any instant by the rotating vector representing an alternating current or voltage. A complete cycle is divided into 360 electrical degrees. Thus, for an alternating-current (ac) sine wave, the angle is 0 degrees for zero and positive-going, 90 degrees for positive maximum, 180 degrees for zero and negative-going, and 270 degrees for negative maximum.

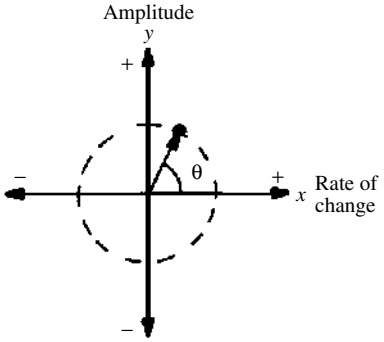

electrical angle

electrical attraction The attraction between two oppositely charged bodies or particles. Compare ELECTRICAL REPULSION.

electrical axis In a quartz crystal, the axis through opposite corners of the hexagonal cross section. The various electrical axes are *x*, *x*', and *x*" (or *x*-*x*, *x*'-*x*', and *x*"-*x*"). The electrical axis is perpendicular to the mechanical axis, which runs through the crystal's length. Also see CRYSTAL AXES and X-AXIS, **2**.

electrical bail An action in which a special switch changes contact position and locks itself in that position after a station has been actuated, at the same time releasing a previously actuated station.

electrical bandspread In a tuned circuit, bandspread obtained by changing values of inductance or capacitance, rather than by mechanical gearing.

electrical bias A current maintained in a relay coil (sometimes an auxiliary coil) to keep the relay partially closed, thus sensitizing it. Compare MECHANICAL BIAS.

electrical boresight In radar operations, the tracking axis, as determined by an electrical test, such as one involving a sharp null or sharp peak response.

electrical center The point at which an adjustable component (variable resistor, variable inductor, etc.) has exactly half its total value. This point does not always coincide with the physical center.

electrical conductance See CONDUCTANCE.

electrical conduction The flow of charge carriers through a material. The degree of conduction is indicated by the material's value of conductance.

electrical conductivity See CONDUCTIVITY.

electrical coupling The coupling of two or more circuits or elements by means of electric-field effects.

electrical degree **1.** In a periodic waveform, the length of time corresponding to $\frac{1}{360}$ of the time for completion of one cycle. **2.** In space, that distance representing $\frac{1}{360}$ of the wavelength in the medium through which electromagnetic energy travels.

electrical discharge The flow of current out of a voltage reservoir, such as a battery or capacitor.

electrical discharge in gases The phenomenon of electric conduction (current) by a gas, caused by sudden breakdown as a result of gas ionization. The discharge is often accompanied by light, as in the red glow of a neon bulb.

electrical-discharge machining A method of machining metals in which the metal is vaporized by an arc formed between an electrode and the metal workpiece (anode). In this way, metal is removed in tiny bits from the surface of the workpiece.

electrical distance Distance in terms of the time required for an electromagnetic wave to travel between two points in a particular medium.

electrical drainage The diversion of electric currents away from underground pipes to prevent corrosion by electrolysis.

electrical efficiency The ratio of the output of an electrical or electronic device to the total input. It can be expressed as a decimal or percentage. For example, for a bipolar transistor amplifier, the percent efficiency is equal to $100(P_{out}/P_{in})$, where P_{in} is the collector input in volt-amperes, and P_{out} is the output power in watts.

electrical elasticity See CAPACITANCE.

electrical element See ELEMENT, **2**.

electrical energy Energy in the form of electricity (see ELECTRICITY, **1**). The term is often used in place of ELECTRICITY.

electrical engineer Abbreviation, EE. A trained professional skilled in applying physics and mathematics to electricity, and in the theory and application of basic engineering and related subjects. Of particular interest to the EE are the generation

5059F-pE-224-273 4/9/01 5:26 PM Page 232

and distribution of electrical energy and the design and application of electromechanical devices. Compare ELECTRONICS ENGINEER.

electrical erosion In electrical contacts, the loss of metal as a result of the evaporation or transfer of metal during switching.

electrical filter A bandpass, band-rejection, high-pass, or low-pass filter that operates by electrical means. Examples: Butterworth filter and Chebyshev filter.

electrical forming See ELECTROFORM, **1**.

electrical gearing In an electromechanical system, such as a servo, the condition in which an output shaft is electrically rotated at a speed different from that of an input shaft.

electrical glass High-temperature insulating materials made from glass fibers.

electrical inertia See INDUCTANCE.

electrical initiation **1.** Starting an action (electrical or nonelectrical) by means of an electrical signal. **2.** Using an enabling pulse.

electrical instrument A device for measuring an electrical quantity (such as voltage, current, or power).

electrical interlock Also called an *interlock switch* or *door-interlock switch*. A door- or lid-operated switch connected in series with the power switch of a piece of equipment. The interlock causes power to be removed from internal circuits whenever the door is opened, the lid lifted, or the case removed. This minimizes the chance for electric shock to occur to service personnel.

electrical length The length, in wavelengths, of an antenna or transmission line. The electrical length usually differs from the actual length because of ground-capacitance effects, end effects, and the speed of electromagnetic waves in conductors and/or dielectrics.

electrical load A device connected to a source of electricity (generator, amplifier, network, etc.) for a useful purpose (heat, work, etc.).

electrically connected Connected via direct path, such as through a wire, resistance, inductance, or capacitance.

electrically erasable PROM A programmable read-only memory (PROM) that can be erased by an electrical signal, rather than by exposure to ultraviolet light. Also see PROM and ROM.

electrically variable capacitor See VOLTAGE-VARIABLE CAPACITOR.

electrically variable inductor An inductor whose value varies inversely with the amount of direct current that is caused to flow through it or through an auxiliary winding on the same core.

electrically variable resistor See VOLTAGE-DEPENDENT RESISTOR.

electrical nature of matter The general behavior of matter as a complex interplay of waves and particles. Also see ELECTRON THEORY OF MATTER, WAVE MECHANICS, and WAVE THEORY OF MATTER.

electrical network A circuit containing two or more components (including generators and loads), usually arranged in some pattern.

electrical noise Extraneous currents and/or voltages that interfere with desired electrical quantities. Compare ACOUSTIC NOISE.

electrical polarity The distinct difference observable in electrification, designated positive (or plus) and negative (or minus). Negative electrification is generally characterized by a surplus of electrons; positive electrification is characterized by a deficiency of electrons.

electrical quantity **1.** See COULOMB and QUANTITY, **3**. **2.** An electrical unit (e.g., AMPERE, OHM, VOLT, and WATT).

electrical repulsion The mutual repulsion of bodies or particles having similar electric charges. Two positively charged objects will repel each other, as will two negatively charged objects.

electrical reset An electromechanical device for resetting a relay that ordinarily remains in the position resulting from actuation.

electrical resistance The in-phase current-retarding effect that all conductors exhibit to some extent. Also see RESISTANCE.

electrical resistivity See RESISTIVITY.

electrical resolver A synchro whose rotor has two perpendicular windings in addition to another winding.

electrical scan A method of changing the orientation of the major lobe of an antenna. The antenna is kept physically stationary, but the phase/amplitude relationships of the signals applied to different driven elements are varied.

electrical sheet Sheet iron or steel used for motor laminations.

electrical system **1.** The overall configuration of electrical elements for a set of apparatus. **2.** The wiring system that supplies power to a set of devices. **3.** One of several methods of quantizing electrical properties, such as METER-KILOGRAM-SECOND (mks), CENTIMETER-GRAM-SECOND (cgs) electromagnetic, cgs electrostatic, and the INTERNATIONAL SYSTEM OF UNITS (SI).

electrical taste See GALVANIC TASTE.

electrical technology The theory and practical application of electricity. Taught as a subengineering major, usually in two-year colleges that award the degree of Associate in Arts (AA) or Associate in Science (AS).

electrical time constant For a torque motor, the ratio of armature inductance to effective armature resistance. Compare MECHANICAL TIME CONSTANT.

electrical transcription **1.** A phonograph record made electrically, as opposed to one made mechanically. **2.** A radio program in which such a record is played. **3.** Any direct mechanical or electrical recording of an audio signal.

electrical transducer **1.** A transducer that converts a nonelectrical phenomenon into a proportional

5059F-pE-224-273 4/9/01 5:26 PM Page 233

current, voltage, or frequency. **2.** A transducer that converts electricity in one form to electricity in another [e.g., a transducer actuated by direct-current (dc) voltage, delivering an alternating-current (ac) output, whose frequency is proportional to the dc input voltage].

electrical twinning A defect in which two quartz crystals intergrow in such a way that the electrical sense of their axes becomes reversed. Compare OPTICAL TWINNING.

electrical unit A standard for measuring an electrical quantity (e.g., ampere, ohm, volt, watt, siemens, etc.).

electrical wavelength The distance between one point in an electromagnetic wave cycle and the next identical point. This is usually expressed as the separation between points where the instantaneous amplitude of the electric field is zero and increasing positively. This quantity depends on the velocity factor, v, of the medium through, or along, which the field propagates. The electrical wavelength also depends on the frequency, *f*, of the energy. In a transmission line with a velocity factor v (given as a fraction rather than as a percentage), the electrical wavelength λ is given by

$$\lambda = 3.00 \times 10^8 \, v \, / \, f$$

where *s* is in meters, v is in meters per second, and *f* is in hertz. Often, this formula is modified for values of *f* expressed in megahertz (Mhz) rather than in hertz. The equation in this case becomes

$$\lambda = 300 \, v \, / \, f$$

The wavelength of a signal in a radio-frequency (RF) transmission line is always less than the wavelength of the same signal in free space.

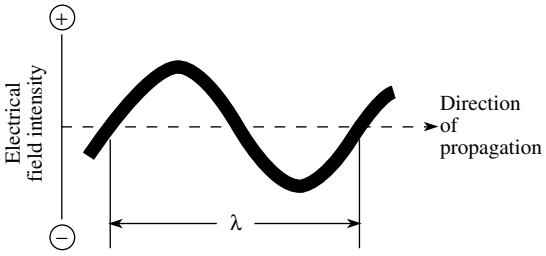

electrical wavelength

electrical zero **1.** A zero-output or minimum-output point resulting from the adjustment of a bridge or other zero-set circuit. **2.** In a meter whose pointer is mechanically set to some point above or below the zero on the scale, the zero setting obtained when the meter is deflected to scale zero by a current or voltage. **3.** For a synchro, the position at which the amplitudes and time phase of the outputs are defined.

electric and magnetic double refraction See KERR ELECTRO-OPTICAL EFFECT and KERR MAGNETO-OPTICAL EFFECT.

electric arc A sustained luminous discharge in the space between two electrodes. Compare ELECTRIC SPARK.

electric aura See ELECTRIC WIND.

electric balance See BRIDGE, **1** and **2**.

electric bell See BELL.

electric brazing A method of brazing in which electric current generates the required heat.

electric breakdown **1.** The usually sudden ionization of a gas by an electric field and the accompanying heavy current flow through the gas. **2.** The (destructive) puncture of a dielectric by the strain produced by high voltage. Also see DIELECTRIC STRENGTH. **3.** The usually nondestructive, abrupt increase in semiconductor junction current at a high reverse voltage. See, for example, AVALANCHE BREAKDOWN.

electric breakdown voltage **1.** The voltage at which avalanche effect occurs. **2.** Dielectric strength.

electric breeze See ELECTRIC WIND.

electric buzzer See BUZZER. Compare ELECTRONIC BUZZER.

electric calculator An electrically driven machine for performing mathematical operations. Its electromechanical nature distinguishes it from the electronic calculator, which features no moving parts, other than keys. Also see CALCULATOR.

electric catfish A fish native to tropical and northern Africa, capable of delivering a strong electric shock.

electric cell See CELL, **1**.

electric chair An electrode-bearing chair used in some states for administering the death penalty via high-voltage electricity. See ELECTROCUTION.

electric charge Potential energy as the electrification of a body or component. For a capacitance of *C* farads charged to a potential of *E* volts, the charge *Q*, in coulombs, is equal to the product *CE*. Also see ENERGY STORED IN CAPACITOR.

electric chronograph An instrument for accurately recording time intervals.

electric chronometer A precision electric or electronic timepiece. Also see ELECTRIC CLOCK and ELECTRONIC CLOCK.

electric circuit A network of interconnected components and devices, often including a source of electric power. Current flowing through a circuit is acted on by components, which produce specific desired effects.

electric clock A clock driven by electric current. Electric clocks fall into two categories: those driven by synchronous alternating-current (ac) motors, and those driven by stepping mechanisms that usually operate from direct current (dc).

electric column See VOLTAIC PILE.

5059F-pE-224-273 4/9/01 5:26 PM Page 234

electric conduction The flow of current carriers through a conductor.

electric constant Also called *permitivity of vacuum*. The fixed electrical permitivity of free space, the value of which is 8.8542×10^{-12} farad per meter.

electric contact See CONTACT, **1**, **2**.

electric controller An adjustable device for modifying the operating voltage or power of a component or system. Compare ELECTRONIC CONTROLLER.

electric cooling **1.** Cooling via PELTIER EFFECT. **2.** See ELECTROSTATIC COOLING. **3.** Forced-air cooling (of equipment) by electric blowers or fans.

electric current The phenomenon wherein charge carriers move in a directed manner through a material or vacuum. In most electrical conductors, current results from movement of electrons. In a semiconductor material, electric current can result from the movement of holes, as well as electrons; the proportion of holes to electrons depends on the nature of the semiconductor. In a gas or electrolyte, current consists of a flow of ions. In certain situations, electric currents can result from the movement of positrons, protons, anti-protons, alpha particles, and various atomic nuclei.

electric current density See CURRENT DENSITY.

electric delay line See DELAY LINE.

electric density See ELECTRIC SPACE DENSITY and ELECTRIC SURFACE DENSITY.

electric dipole A pair of equal charges having opposite polarity and separated by a fixed distance.

electric discharge See ELECTRICAL DISCHARGE.

electric-discharge lamp See DISCHARGE LAMP.

electric disintegration See ELECTRIC DISPERSION.

electric dispersion In a colloidal suspension, dispersion accomplished by passing an electric current through the material.

electric displacement The movement of a body or particle in response to an electric current or field.

electric double refraction See KERR ELECTRO-OPTICAL EFFECT.

electric dust precipitator See DUST PRECIPITATOR.

electric eel An eel (fish) capable of delivering a disabling shock on contact.

electric elasticity See ELASTIVITY, **1**, **2**.

electric endosmosis See ELECTRO-OSMOSIS.

electric eye A sensing device that uses a radiant energy beam to detect objects. It generally uses a laser diode as the beam source, and a photoelectric cell, phototransistor, or photovoltaic cell as the beam detector. The output is used to control some external machine or system.

electric fence A wire fence through which an electric current is passed. Anyone touching the fence will receive a shock. It is used in some prisons, and also by cattle ranchers to keep people or animals contained.

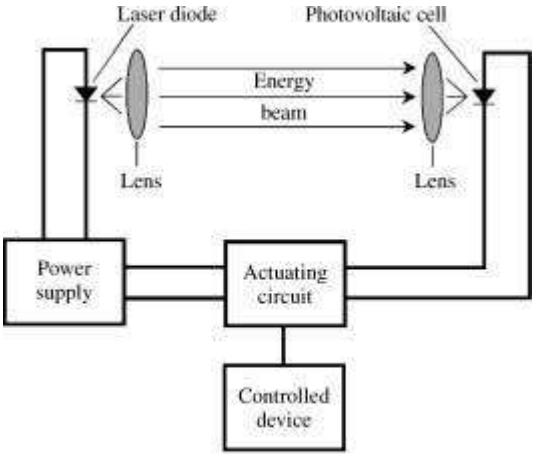

electric eye

electric fidelity The frequency response of a circuit or device.

electric field The space surrounding an electric charge or charged body, in which electric energy acts (electric lines of flux fill the space).

electric field intensity See ELECTROSTATIC FIELD INTENSITY.

electric field strength **1.** Symbol, *E*. In an electromagnetic wave, the amplitude of the electric component of the field, expressed in volts per meter. **2.** Dielectric strength.

electric-field vector See ELECTRIC-FIELD STRENGTH, **1**.

electric filter See ELECTRIC WAVE FILTER.

electric fish Fish capable of generating intense electric shocks (e.g., *electric catfish* and *electric eel*).

electric flux See ELECTROSTATIC FLUX.

electric flux density Symbol, *D*. In an electric field, the number of lines of flux per unit area, usually expressed in coulombs per square meter.

electric flux lines The direction of the electric field in the vicinity of a charged object. The field is denoted by means of "lines of flux" or "lines of force," with each line representing a designated electric field intensity. The closer together the lines, the more intense the field in a given region.

electric focusing See ELECTROSTATIC FOCUSING.

electric force The force exerted by an electrically charged particle or an electric field.

electric forces The forces exerted by electric charges or electric fields. Also see UNIT ELECTROSTATIC CHARGE.

electric furnace An electrically heated chamber (sometimes heated by an electric arc) used in ore reduction, carbide manufacture, and other high-temperature processes.

electric generator A device for producing electricity. Thus, many different devices, such as bat-

5059F-pE-224-273 4/9/01 5:26 PM Page 235

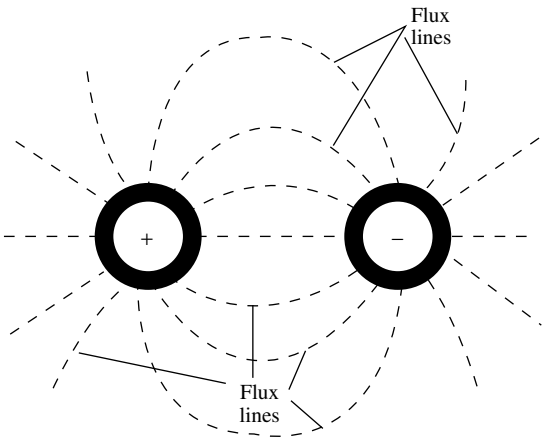

electric flux lines

teries, dynamos, oscillators, solar cells, and thermocouples, are classed as generators.

electric glow The light (usually pale blue) that occasionally accompanies an electric discharge in air.

electric guitar A guitar whose acoustic vibrations are converted by a transducer to an electrical signal for amplification.

electric hygrometer An instrument for measuring humidity in terms of the moisture-sensitive resistance of a sensor. A relatively simple direct-current (dc) circuit is used. Compare ELECTRONIC HYGROMETER.

electric hysteresis See ELECTROSTATIC HYSTERESIS.

electrician A professional person who installs and services electrical equipment and wiring.

electric image For solving certain problems involving electricity, an array of electrical points forming an image of certain other electrical points.

electricity **1.** Phenomena resulting from the existence of stationary or moving electric charge carriers, such as electrons, holes, and ions. **2.** A branch of physics concerned with phenomena resulting from the existence of stationary or moving charge carriers. **3.** Electrical energy or power. **4.** The voltage existing at utility outlets. In the North America, this is nominally an alternating-current (ac) voltage of 117 or 234 V at 60 Hz.

electric lamp An electric-powered device used primarily as a source of light. Common types are arc, incandescent, and fluorescent.

electric light **1.** Visible light produced by means of electricity. **2.** Electric lamp.

electric lines of flux Lines of flux associated with an electric charge and constituting the charge's electric field.

electric machine A mechanical device for generating static electricity. See, for example, ELECTROSTATIC GENERATOR, VAN DE GRAAFF GENERATOR, and WIMSHURST MACHINE.

electric meter **1.** An instrument such as an ammeter, voltmeter, or wattmeter, used to indicate an electrical quantity (usually directly). **2.** See KILOWATT-HOUR METER.

electric mirror See ELECTRON MIRROR.

electric moment In an electric field of unit intensity, the maximum torque exerted on an electric dipole.

electric motor A machine that converts electrical energy into mechanical work. The familiar form is a machine in which an armature rotates between the poles of a field magnet, mechanical energy being produced at the armature's revolving shaft.

electric needle A needle electrode carrying high-frequency current; it is used in surgery to cut tissue and sear it immediately to prevent bleeding.

electric network See ELECTRICAL NETWORK.

electric organ See ELECTRONIC ORGAN.

electric oscillations The alternate flow of electric charges in opposite directions, occurring at a defined frequency or frequencies.

electric osmosis See ELECTRO-OSMOSIS.

electric piano See ELECTRONIC PIANO.

electric polarization **1.** The orientation of flux lines in an electric field. **2.** The orientation of the electric field component in an electromagnetic field.

electric potential See ELECTROSTATIC POTENTIAL.

electric power Symbol, *P*. Unit, watt. The rate at which electrical energy is used. Power is energy per unit time; in the context of electricity, it is expressed as the product of current and voltage. In terms of heat losses, it is often expressed as I^2R (current in amperes squared, multiplied by resistance in ohms).

electric precipitator See DUST PRECIPITATOR.

electric probe A pin or rod inserted into an electrostatic field to sample it, or into an electromagnetic field to sample its electric component. See, for example, WAVEGUIDE PROBE. Compare MAGNETIC PROBE.

electric radiation **1.** The radiation of energy by means of electric waves. **2.** The energy so radiated.

electric recording Inkless recording on paper by direct use of an electric current. The two principal types are: (1) A current-carrying stylus burns away (in a fine line) the metallic coating of the recording paper, exposing the dark underlying layer. (2) A stylus delivers current that produces a line by means of electrolysis in a special paper (see ELECTROLYTIC RECORDER). Compare ELECTROSTATIC PRINTER.

electric reset See ELECTRICAL RESET.

electric residue A residual electric charge, such as might remain on a capacitor after it has been incompletely discharged.

5059F-pE-224-273 4/9/01 5:26 PM Page 236

electric rings Colored rings formed on a plate by the electrolytic deposition of substances, such as copper and some peroxides.
electric screen See ELECTROSTATIC SCREEN.
electric shield See ELECTROSTATIC SCREEN.
electric shock A physiological reaction caused by the passage of electric current through living tissue. When slight, it is characterized by tingling sensations and involuntary contractions of the muscles; a severe shock can cause paralysis, unconsciousness, heart fibrillation, and/or burns. If heart fibrillation occurs or if burns are severe, death can result.
electric spark A momentary, luminous discharge of electricity in the space between two electrodes. Compare ARC, **1**.
electric steel Steel that has been processed in an electric furnace.
electric strain See DIELECTRIC STRAIN.
electric strain gauge A device for detecting the strain that a certain stress produces in a body. Typically, such a gauge consists of one or more fine insulated wires cemented to the surface under test. As the surface becomes strained, the wire stretches, undergoing a change in electrical resistance that is proportional to the change in strain.
electric strength See DIELECTRIC STRENGTH.
electric stress See DIELECTRIC STRESS.
electric stroboscope See ELECTRONIC STROBOSCOPE.
electric surface density The ratio of the electric charge on a surface to the area of the surface. Compare ELECTRIC VOLUME DENSITY.
electric tachometer See ELECTRONIC TACHOMETER.
electric telemeter A device that sends metered data over a wire transmission line to a remote point for monitoring.
electric thermometer See ELECTRONIC THERMOMETER.
electric transcription See ELECTRICAL TRANSCRIPTION.
electric transducer A transducer that responds to non-electric energy, then delivers a proportional electric current or voltage to another circuit.
electric tuning A means of adjusting the frequency of a receiver, transmitter, transceiver, or oscillator, without the use of mechanical devices. An example is the use of a varactor diode, whose capacitance varies with voltage.
electric utilities The power companies that supply electric current for industrial and consumer use.
electric vane A small demonstration device consisting of a rotor having several spokes terminating in points. The rotor is mounted on a pivot bearing and, when it is connected to a source of high voltage, spins from the force of electricity escaping from the points into the surrounding air.

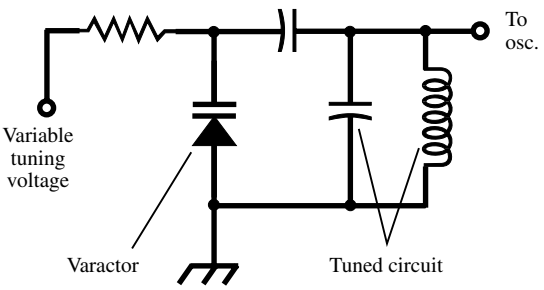

electric tuning

electric vector In an electromagnetic field, the vector representing the electric component. It is perpendicular to the magnetic vector.
electric volume density The ratio of the electric charge in a space to the volume of the space. Compare ELECTRIC SURFACE DENSITY.
electric watch A small timepiece driven by a tiny, self-contained electrochemical cell that drives an electrical escapement or other stepping mechanism. Compare ELECTRONIC WATCH.
electric wave See ELECTROMAGNETIC WAVES.
electric-wave filter A circuit or device for separating signals of one frequency from those of other frequencies.
electric whirl See ELECTRIC VANE.
electric wind **1.** Air currents set up by electrons escaping from the sharp point of a high-voltage electrode. **2.** The outward-rushing plasma (solar wind) ejected by the sun and traveling through space.
electrification **1.** Generating an electric charge in a body, as in charging a glass rod by rubbing it with a silk cloth. **2.** Providing electric service (e.g., RURAL ELECTRIFICATION). **3.** The conversion of a system from purely mechanical to electrical or electromechanical.
electroacoustic Pertaining to devices and systems that exhibit both electrical and acoustic effects. For example, speakers and microphones are electroacoustic devices.
electroacoustic device A device that transfers energy by converting it from electrical to acoustic form or vice-versa.
electroacoustic transducer A transducer that converts sound vibrations into electrical pulsations or, conversely, one that converts electricity into sound.
electroanalysis Chemical analysis performed by electrolytic methods.
electroanesthesia Anesthesia produced by an electric current going through some part of the body.
electroballistics A branch of physics concerned with the electrical or electronic measurement of the velocities and trajectories of projectiles.

5059F-pE-224-273 4/9/01 5:26 PM Page 237

electrobath A solution in which ELECTROPHORESIS or ELECTROPLATING is done.

electrobiology Biology concerned with electrical phenomena in living organisms.

electrobioscopy The examination of a body for viability by inducing muscular contractions with an electrical impulse.

electrocapillarity The production of capillary effects by means of electricity. See, for example, CAPILLARY ELECTROMETER.

electrocardiogram Abbreviation, ECG or EKG. A record made by an electrocardiograph of the changes in potential caused by the heartbeat; used as a diagnostic aid.

electrocardiograph An instrument that records changes in electrical potential caused by the heartbeat.

electrocardiophonograph A medical instrument that detects and records the impulses of the heart.

electrocatalysis Catalytic action produced by electricity (see CATALYSIS).

electrocautery **1.** In medicine, a cauterizing instrument consisting essentially of a platinum wire (at the tip of an insulated probe) that is heated by an electric current. Also see ELECTRIC NEEDLE. **2.** Cauterizing with an electrocautery.

electrochemical deterioration An electrochemical reaction that results in the permanent or temporary failure of a device.

electrochemical diffused-collector transistor A high-current pnp transistor in which metal has replaced the etched-away mass of p material, providing a built-in heatsink.

electrochemical equivalent In electrolysis or electroplating, a constant (Z) for the metal in plates. For a given metal, Z is the mass (in grams) of the metal deposited by 1 coulomb of electricity.

electrochemical junction transistor See SURFACE-BARRIER TRANSISTOR.

electrochemical measurements **1.** Measurements made on chemical substances with electrical instruments to determine such factors as conductivity, pH, dielectric strength, dielectric constant, etc. **2.** Measurements of electrical or electronic phenomena in terms of electrochemical response (e.g., current drain in terms of weight of plated metal, or voltage in terms of gas breakdown).

electrochemical polarization The disabling of a primary cell caused by gas products deposited around or on one of the electrodes.

electrochemical recording See ELECTRIC RECORDING.

electrochemical reduction Extracting a metal from a compound by means of electrolysis.

electrochemical series See ELECTROMOTIVE SERIES.

electrochemical switch A static, ionic alternating-current (ac) switch consisting of an anode, cathode, and a control electrode, all immersed in an electrolyte. A positive control-electrode voltage switches the device on, initiating ion current from anode to cathode through the liquid.

electrochemical transducer A transducer that converts chemical changes into electrical quantities, or vice versa. Examples: soil-acidity probe and electrolytic elapsed-time meter.

electrochemistry The branch of chemistry, overlapping with physics, concerned with chemical action arising from the effect of electricity on substances, and electrical effects produced by chemical action.

electrochromic display A display that operates by means of electric fields, which control the light-transmission and light-reflection characteristics in different regions of the material.

electrochronometer A precision electric or electronic clock. Also see ELECTRIC CLOCK and ELECTRONIC CLOCK.

electrocoagulation Use of a high-frequency alternating current to solidify tissue, as in arresting bleeding.

electrocorticogram See ELECTROENCEPHALOGRAM.

electroculture Acceleration or modification of plant growth through the application of electricity to plants, seeds, or soil.

electrocution **1.** Death resulting from electric shock. **2.** An electric shock inflicted for the purpose of causing death (e.g., in an ELECTRIC CHAIR).

electrode A body, point, or terminal in a device or circuit that delivers electricity, or to which electricity is applied. A positive electrode is usually an ANODE; a negative electrode is usually a CATHODE.

electrode admittance The admittance encountered by current flowing through an electrode; the property is entirely that of the electrode and is the reciprocal of ELECTRODE IMPEDANCE. Consists of a real-number component (ELECTRODE CONDUCTANCE) and an imaginary-number component that is 90 degrees out of phase (ELECTRODE SUSCEPTANCE).

electrode capacitance The capacitance between an electrode and a reference body, such as ground or another electrode.

electrode characteristic The mathematical function or graph of electrode current versus electrode voltage.

electrode conductance The conductance encountered by current flowing through an electrode; the property is entirely that of the electrode and is the reciprocal of ELECTRODE RESISTANCE.

electrode current Current entering or leaving an electrode.

electrode dark current See DARK CURRENT.

electrode dissipation The power lost in the form of heat in an electrode.

electrode drop Voltage drop resulting from ELECTRODE RESISTANCE.

electrode efficiency In an electrolytic cell, the ratio of the yield of metal deposited to the maximum

5059F-pE-224-273 4/9/01 5:26 PM Page 238

possible theoretical yield. This value ranges between 0 and 1 (0 percent and 100 percent).

electrode impedance The impedance encountered by alternating current flowing through an electrode; the property is entirely that of the electrode and is the reciprocal of ELECTRODE ADMITTANCE. Consists of a real-number component (ELECTRODE RESISTANCE) and an imaginary-number component that is 90 degrees out of phase (ELECTRODE REACTANCE).

electrodeless discharge Discharge in a gas tube that is not directly connected to a power source. A familiar example is the glow of a neon lamp held in a strong radio-frequency (RF) electromagnetic field.

electrodeposit **1.** To deposit a substance by electrical action. Also see ELECTROPHORESIS and ELECTROPLATING. **2.** A deposit that is formed on an electrode by electrophoresis or electroplating.

electrodeposition The electrical application of a layer of one material (such as a metal) on the surface of another (the substrate) (e.g., electroplating, evaporation, and sputtering).

electrode potential See ELECTRODE VOLTAGE.

electrode reactance The imaginary-number component of ELECTRODE IMPEDANCE.

electrode resistance The resistance encountered by current flowing through an electrode; the property is entirely that of the electrode and is the reciprocal of ELECTRODE CONDUCTANCE.

electrodermography A method of monitoring the functions of the human body by measuring the resistance between two electrodes placed on the surface of the skin.

electrode susceptance The imaginary-number component of ELECTRODE ADMITTANCE.

electrode voltage The voltage between an electrode and a reference point, such as ground or another electrode.

electrodiagnosis **1.** The diagnosis of a disease or disorder through the use of electromedical instruments. **2.** Troubleshooting the electrical portion of electromechanical equipment.

electrodialysis See ELECTRO-OSMOSIS.

electrodissolution Dissolving a constituent substance of an immersed electrode by means of electrolysis.

electrodynamic Pertaining to electricity in motion (i.e., current flow and its accompanying electric and magnetic fields).

electrodynamic braking Stopping a tape-deck motor quickly by applying a braking voltage. In this method, direct braking current flows through the shaded-pole alternating-current (ac) reel motor.

electrodynamic instrument See ELECTRODYNAMOMETER.

electrodynamic loudspeaker See DYNAMIC SPEAKER.

electrodynamics The branch of physics concerned with moving electric charge carriers, such as electrons, holes, and ions. Also concerned with the interaction of electrical and mechanical phenomena. Important in the design and manufacture of devices, such as motors and generators.

electrodynamic speaker See DYNAMIC SPEAKER.

electrodynamism See ELECTRODYNAMICS.

electrodynamometer An indicating meter whose movable coil rotates between two stationary coils. All three coils are connected in series, and the magnetic fields of the two stationary coils are additive. This meter produces a positive indication for alternating current (ac), as well as for direct current (dc). Can be adapted for use as an ammeter, voltmeter, or wattmeter.

electroencephalogram Abbreviation, EEG. A record made by an ELECTROENCEPHALOGRAPH, showing changes in electric potential resulting from bioelectric action in the brain. The record is used as a diagnostic aid.

electroencephalograph An instrument that produces a record of voltage changes resulting from the brain's bioelectricity.

electroencephaloscope A type of oscilloscope used to pick up, amplify, and display changes in potential caused by the brain's bioelectric action.

electroextraction Extracting a substance from a mixture (e.g., a metal from an ore) by an electrical process, such as electrolysis.

electroform **1.** To precondition a material or device (e.g., a semiconductor junction) by passing a current through it for a specified period. **2.** To form articles by electrodepositing material on a mold or core.

electrogalvanized Electroplated with zinc.

electrogastrogram A recording of the electrical impulses and other functions of the stomach, for medical diagnostic purposes.

electrograph **1.** A picture transmitting or receiving device (see FACSIMILE RECEIVER and FACSIMILE TRANSMITTER). **2.** A device used for the electrolytic etching or transfer of designs.

electrographic recording A method of producing a visible pattern or record, using electrodes to create discharge through an insulating material.

electrographite Synthetic graphite prepared by heating carbon in an electric furnace.

electrojet A region of high current concentration in the sky near bright auroral displays or along the magnetic equator.

electrokinetic energy The energy of electric charge carriers in motion; a form of kinetic energy. The current in a wire (a flow of electrons) is a common manifestation of this form of energy. Compare ELECTROSTATIC ENERGY.

electrokinetics A branch of electricity concerned with (1) the behavior of moving charged particles (such as ions and molecules) and bodies in

5059F-pE-224-273 4/9/01 5:26 PM Page 239

motion, and (2) the generation of static charges by moving liquids or solids in contact with each other.

electroless process Plating a metal from a solution of one of its salts without using electricity.

electroluminescence The ability of certain phosphors to emit light continuously when an alternating-current (ac) voltage is applied to them.

electroluminescent cell A device for generating light by electroluminescence. It consists of a luminescent-phosphor layer and two transparent metal films. An alternating-current (ac) voltage applied between the films causes the phosphor to glow through the transparent metal.

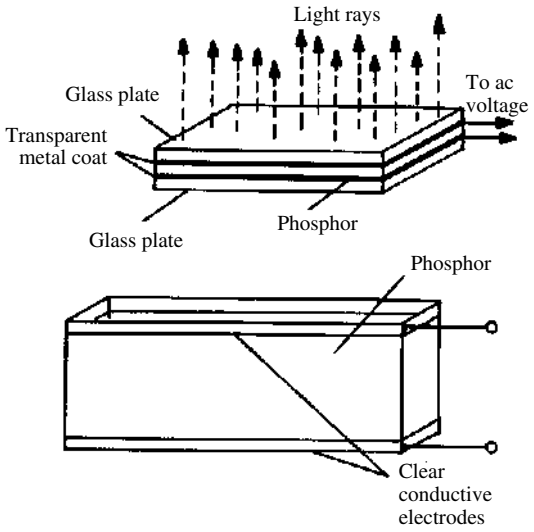

electroluminescent cell

electroluminescent lamp A lamp using one or more electroluminescent panels.

electroluminescent panel A panel that forms a complete electroluminescent cell. It delivers low-intensity visible light when an alternating-current (ac) voltage is applied to it. Available in various sizes and shapes.

electrolysis **1.** The action whereby a current passing through a conductive solution (electrolyte) produces a chemical change in the solution and the electrodes. **2.** An electrical method of destroying hair roots.

electrolyte A substance that ionizes in solution. Electrolytes conduct electricity; in batteries, they are instrumental in producing electricity by chemical action.

electrolytic **1.** Containing an electrolyte substance. **2.** See ELECTROLYTIC CAPACITOR.

electrolytic capacitor A component that is manufactured by rolling up aluminum foil strips separated by paper saturated with electrolyte. When a polarized voltage is applied, the aluminum oxidizes. The oxide layer forms the dielectric for the capacitor. The layer is extremely thin, producing high capacitance per unit volume. This type of capacitor must be connected with the proper polarity in a circuit. The component can have values up to thousands of microfarads, and some units can handle thousands of volts. They are used in audio circuits and in power supplies. Compare CERAMIC CAPACITOR, MICA CAPACITOR, PAPER CAPACITOR, PLASTIC-FILM CAPACITOR, TANTALUM CAPACITOR.

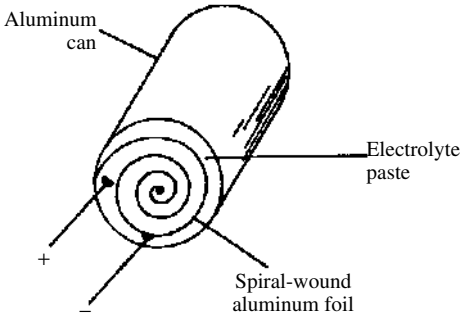

electrolytic capacitor

electrolytic cell An electrochemical device containing an electrolyte and at least two electrodes. Included in this category are voltaic cells, electrolytic capacitors, and electrolytic resistors.

electrolytic conduction Electric current flowing through an electrolyte, an action characterized by (1) positive electrolyte ions migrating to the negative electrode, where they acquire electrons; (2) negative ions migrating to the positive electrode, where they lose electrons; and (3) current flow in the external circuit, which consists of conventional electron flow (current in the electrolyte is a movement of ions).

electrolytic conductivity Conductance of an electrolyte. It is the conductance of a cube of the electrolyte, measuring one centimeter along each edge, at a specified temperature.

electrolytic corrosion Corrosion caused by an applied voltage, or that is accelerated by the voltage. Compare GALVANIC CORROSION.

electrolytic current meter See VOLTAMMETER.

electrolytic dissociation See DISSOCIATION.

electrolytic elapsed-time meter An instrument that indicates the time that equipment has been in operation in terms of the amount of metal

5059F-pE-224-273 4/9/01 5:26 PM Page 240

electroplated on the cathode of an electrolytic cell by energy consumed during the period.

electrolytic gas A gas produced by electrolysis. Examples are hydrogen (H) and oxygen (O), generated in a ratio of two to one, by the electrolysis of water (H_2O).

electrolytic iron Very pure iron obtained by electrolytic refining.

electrolytic polarization In electrolysis, the tendency for the products to recombine. In an electrolytic cell, this effect interferes with the performance of the cell, reducing the voltage.

electrolytic potential The difference of potential that appears between a metal electrode in an electrolyte and the electrolyte immediately surrounding it. Also see ELECTROMOTIVE SERIES.

electrolytic recorder A data recorder that uses a paper impregnated with a chemical that turns dark when an electric current passes through the paper from the point of a stylus.

electrolytic rectifier A rectifier consisting of an aluminum electrode and a lead or carbon electrode in a solution of borax or sodium bicarbonate, or in a solution of ammonium citrate, ammonium phosphate, and potassium citrate. Also called *chemical rectifier*.

electrolytic refining Extracting or purifying metals by electrolysis.

electrolytic resistor An emergency resistor made by immersing two wire leads in an electrolyte; the weaker the solution, the higher the resistance.

electrolytic switch See ELECTROCHEMICAL SWITCH.

electrolyze To subject something to electrolytic action.

electrolyzer A cell used in the production of various materials by electrolysis. See, for example, ELECTROCHEMICAL REDUCTION and ELECTROLYTIC REFINING.

electromagnet **1.** A coil of insulated wire wound around an iron or steel cylinder, intended for use as a magnet. When current flows through the coil, a magnetic field develops, in effect rendering the cylinder a strong bar magnet. **2.** Any device that exhibits magnetism only while an electric current flows through it.

electromagnetic Exhibiting both electric and magnetic properties (e.g., an *electromagnetic wave*).

electromagnetic attraction **1.** The attraction of iron or steel to an electromagnet. **2.** The attraction of an electromagnetic pole to the opposite pole of another electromagnet. A unit pole attracts another unit pole 1 centimeter away with a force of 1 dyne or 10^{-5} newton. Compare ELECTROMAGNETIC REPULSION.

electromagnetic communication **1.** Any form of communication using a combination of electric and magnetic phenomena. Examples include wire telegraphy, wire telephony, radiotelegraphy, radiotelephony, facsimile, and television. **2.** Electronic communication via electromagnetic fields (i.e., radio communication).

electromagnetic compatibility **1.** The ability of a set of electronic devices to work together without being adversely affected by each other's electromagnetic fields. **2.** In radio communication, the relative immunity of a device or devices to the effects of electromagnetic fields.

electromagnetic complex A system that produces electromagnetic radiation.

electromagnetic component **1.** The magnetic component of an electromagnetic wave, which is perpendicular to the electrostatic component, and can be thought of as the wave's current component. **2.** A device operated by electromagnetism, such as a coil-type relay or a current-operated field magnet.

electromagnetic consonance An effect that takes place when two antenna elements, both having identical or nearly identical resonant frequencies, are in close proximity. If one antenna is fed with energy at its resonant frequency, currents will be induced in the other antenna, and it, too, will radiate. Parasitic arrays, such as the Yagi antenna and the quad antenna, operate on this principle. See RESONANCE.

electromagnetic constant **1.** Symbol, *c*. The propagation speed of electromagnetic waves in a vacuum, approximately equal to 299,792 kilometers per second or 186,282 miles per second. Also called SPEED OF LIGHT and VELOCITY OF LIGHT. **2.** The propagation speed of electromagnetic waves in a particular medium. Equal to vc, where v is the VELOCITY FACTOR of the medium, and c is the speed of electromagnetic waves in a vacuum (299,792 kilometers per second or 186,282 miles per second).

electromagnetic coupling See INDUCTIVE COUPLING.

electromagnetic crack detector An instrument that uses electromagnetic fields to find cracks in iron or steel.

electromagnetic CRT A cathode-ray tube using electromagnetic deflection.

electromagnetic cylinder See SOLENOID.

electromagnetic deflection In a television picture tube and some oscilloscopes, deflection of the electron beam by the magnetic fields of external horizontal- and vertical-deflection coils. Compare ELECTROSTATIC DEFLECTION.

electromagnetic deflection coil See DEFLECTION COILS.

electromagnetic delay line See DELAY LINE.

electromagnetic energy Energy in the form of electric and magnetic fields. A radio wave traveling through space, for example, has electric and magnetic components, between which energy oscillates.

electromagnetic energy conversion The conversion of electrical energy into mechanical work

5059F-pE-224-273 4/9/01 5:26 PM Page 241

and vice versa, through the intermediary of an electromagnetic field.

electromagnetic environment A region in which electric and magnetic fields are present.

electromagnetic field A combination of alternating electric and magnetic fields. The electric lines of flux are perpendicular to the magnetic lines of flux at every point in space. The field propagates in a direction perpendicular to both the electric and magnetic lines of flux. The frequency of oscillation can range from a fraction of one Hz to many quadrillions of Hz. In order from longest wavelength (lowest frequency) to shortest wavelength (highest frequency), effects of this type include radio waves, infrared, visible light, ultraviolet, X rays, and gamma rays.

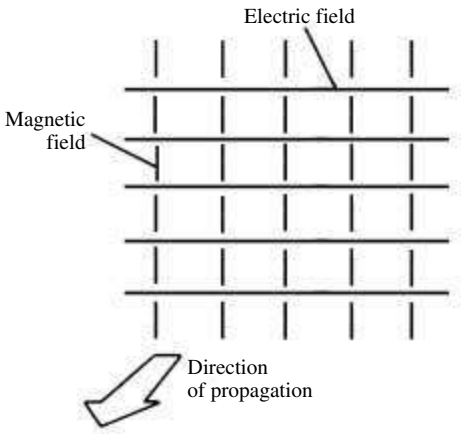

electromagnetic field

electromagnetic flux The magnetic field surrounding a coil or conductor carrying an electric current.

electromagnetic focusing In a television picture tube, electron-beam focusing obtained by varying the direct current flowing through an external focusing coil.

electromagnetic force The force that causes a conductor to be displaced from its position in a magnetic field when it conducts current.

electromagnetic frequency spectrum The frequency range of electromagnetic fields including radio waves, infrared, visible light, ultraviolet, X rays, and gamma rays. Ranges from a fraction of one Hz to many quadrillions of Hz.

electromagnetic horn radiator A horn used to radiate microwave energy. Also see HORN ANTENNA.

electromagnetic induction Inducing a voltage in a circuit or conductor by causing alternating current to flow in another nearby circuit or conductor. Compare ELECTROSTATIC INDUCTION.

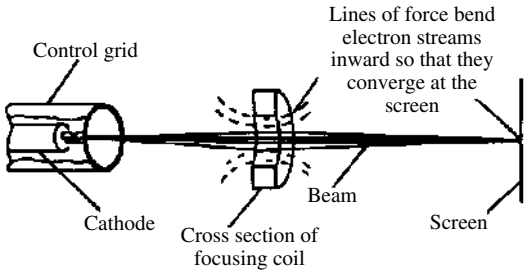

electromagnetic focusing

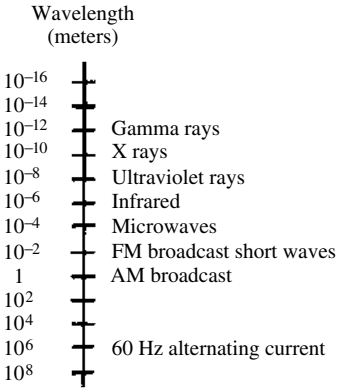

electromagnetic frequency spectrum

electromagnetic inertia The tendency for the current in a circuit to lag the voltage at high frequencies.

electromagnetic interference Abbreviation, EMI. A phenomenon in which electronic devices upset each other's operation. Computers, television receivers, telephone sets, high-fidelity sound equipment, and certain medical devices can malfunction because of strong radio-frequency fields such as those from a nearby broadcast transmitter. The EMI is usually the result of improper or ineffective shielding in the affected device or system.

electromagnetic lens A coil or coil system whose magnetic field causes an electron beam passing through it to converge or diverge as a light beam does in passing through an optical lens. Compare ELECTROSTATIC LENS. Also see ELECTROMAGNETIC FOCUSING.

electromagnetic mass The mass that a moving electric charge is thought to possess.

electromagnetic microphone A microphone in which sound energy is converted into proportionate electrical energy by electromagnetism. Common

5059F-pE-224-273 4/9/01 5:26 PM Page 242

examples are the *dynamic microphone* and *velocity microphone*.

electromagnetic mirror A reflector of electromagnetic waves (e.g., antenna elements, ionospheric layers, buildings, and hills).

electromagnetic momentum The momentum of a moving electric charge, comparable to that of matter in motion. Electromagnetic momentum is the product of electromagnetic mass and charge velocity.

electromagnetic oscillograph **1.** An electromechanical data recorder for tracing the waveform or variations of a signal. **2.** See ELECTROMECHANICAL OSCILLOSCOPE.

electromagnetic oscilloscope **1.** An oscilloscope using electromagnetic deflection. **2.** See ELECTROMECHANICAL OSCILLOSCOPE.

electromagnetic pump A device used for moving conducting or semiconducting fluids. When a current is passed through the fluid, a force is exerted on the molecules of the fluid because of the magnetic field set up by the current.

electromagnetic pulse Abbreviation, EMP. **1.** A broadband electromagnetic field emitted in a short, intense burst from a lightning stroke or nuclear explosion. This field can disrupt the operation of, and (in some cases) cause damage to, electrical and electronic apparatus. **2.** In electromagnetic induction, the displacement of an electron in a conductor by the magnetic field.

electromagnetic radiation The propagation of electromagnetic fields through space; it normally occurs at approximately 299,792 kilometers per second or 186,282 miles per second.

electromagnetic reaction The reaction between magnetic fields. Also see ELECTROMAGNETIC ATTRACTION and ELECTROMAGNETIC REPULSION.

electromagnetic reconnaissance In military applications, the use of electromagnetic apparatus to detect potential enemy activity in a certain geographic region.

electromagnetic relay See ELECTROMECHANICAL RELAY.

electromagnetic repulsion The repulsion of a pole of an electromagnet by the pole of another electromagnet (north pole opposing north pole, south opposing south). Compare ELECTROMAGNETIC ATTRACTION.

electromagnetics A branch of physics concerned with the theory and application of electromagnetism.

electromagnetic screen See ELECTROMAGNETIC SHIELD.

electromagnetic shield **1.** A partition, can, or box made of magnetic material (iron, steel, or special alloy) enclosing a magnetic component. The magnetic flux generated by the component is confined by the shield, thus preventing interference with external components. Likewise, external magnetic fields are prevented from reaching the component. **2.** A grounded partition, metal sheet, wire braid, or other barrier that prevents electromagnetic fields from passing through. Commonly used in electronic equipment to prevent ELECTROMAGNETIC INTERFERENCE. Also used in COAXIAL CABLE to confine electromagnetic fields to the transmission line.

electromagnetic shielding The use of an ELECTROMAGNETIC SHIELD to prevent undesired interaction among electrical and electronic devices and systems.

electromagnetic spectrum See ELECTROMAGNETIC FREQUENCY SPECTRUM and ELECTROMAGNETIC WAVELENGTH SPECTRUM.

electromagnetic switch **1.** A switch actuated by magnetism produced by control current flowing through a coil wound on an iron core. **2.** See ELECTROMECHANICAL RELAY.

electromagnetic theory of light The theory that light consists of electromagnetic waves that are similar to radio waves, but of shorter wavelength.

electromagnetic tube A cathode-ray tube using electromagnetic deflection (e.g., a television picture tube).

electromagnetic unit Abbreviation, emu. A unit of measure in the electromagnetic system of CENTIMETER-GRAM-SECOND (cgs) units.

electromagnetic vibrator See INTERRUPTER.

electromagnetic wavelength spectrum The wavelength range of electromagnetic fields, including radio waves, infrared, visible light, ultraviolet, X rays, and gamma rays. It ranges from many kilometers to a tiny fraction of one millimeter.

electromagnetic-wave polarization The orientation of the electric flux lines in an electromagnetic (EM) field, especially a field propagating through space. The polarization is generally parallel with the active element of a radio transmitting or receiving antenna. Thus, a vertical antenna radiates and receives fields with *vertical polarization*, and a horizontal antenna radiates and receives fields having *horizontal polarization*. Some antennas radiate and receive an EM field whose polarization continually and rapidly rotates. This is *elliptical polarization*. If the rate of rotation is constant, it is *circular polarization*.

electromagnetic waves Waves produced in a conductor or in space by the acceleration or oscillation of electric charge carriers. Such waves have an electric and a magnetic component acting at right angles to each other. The waves propagate at right angles to both the electric and magnetic flux lines.

electromagnetism **1.** Magnetism resulting from the movement of electric charge carriers (e.g., the magnetic field surrounding a coil of wire carrying an electric current). **2.** See ELECTROMAGNETICS.

electromagnetizer A magnetizer using continuous direct current (dc) as the magnetic-field source.

5059F-pE-224-273 4/9/01 5:26 PM Page 243

electromechanical Descriptive of any device that converts energy from electrical to mechanical form or vice-versa. Examples are the motor and the generator.

electromechanical amplifier An amplifier that converts an electrical input signal into mechanical motion (vibratory or rotary), which it then converts back into an electrical output signal of higher current, voltage, or power.

electromechanical chopper A vibrator-type interrupter used primarily to chop direct current, converting it into a square-wave signal, whose amplitude is proportional to current strength. Also see CHOPPER.

electromechanical counter A device that indicates the number of pulses that have been applied to it. Typically, it has a series of dials—each capable of displaying the numerals 0 to 9 in sequence, one for each decade in the count. The dials are geared together, the train being operated by the stepping action of an electromagnetic escapement. Compare ELECTRONIC COUNTER.

electromechanical energy The energy stored by an inductor or capacitor in an electromechanical device.

electromechanical filter See ULTRASONIC FILTER, **1**.

electromechanical flip-flop See BISTABLE RELAY.

electromechanical frequency meter A usually direct-reading instrument for measuring frequency in the lower and middle portions of the audio spectrum. It works via the mechanical motion resulting from the applied signal. The two varieties are the movable-iron type and the reed type.

electromechanical modulator See CHOPPER.

electromechanical oscillator An oscillator consisting of an electromechanical amplifier provided with regenerative feedback.

electromechanical oscilloscope A galvanometer-type instrument for displaying a varying or alternating current or voltage. The signal is applied to a meter movement having a movable coil, which swings or vibrates in response to the signal. A tiny mirror cemented to the coil reflects a beam of light to a rotating mirror that sweeps the beam across a translucent screen on which the image is produced.

electromechanical recorder An instrument in which a pen or stylus is moved on a sheet of paper by the varying signal current or voltage being recorded.

electromechanical rectifier A rectifier in which a moving part, such as a vibrating reed or rotating commutator-slip-ring unit, is driven by alternating current (ac) to close the circuit during positive or negative ac half-cycles, thus rectifying the ac. Compare ELECTROLYTIC RECTIFIER and ELECTRONIC RECTIFIER.

electromechanical relay An electromagnetic switch consisting of a multiturn coil wound on an iron core near an armature with a movable end contact. When control current flows through the coil, it becomes magnetized and attracts the armature, closing the movable contact against a stationary one.

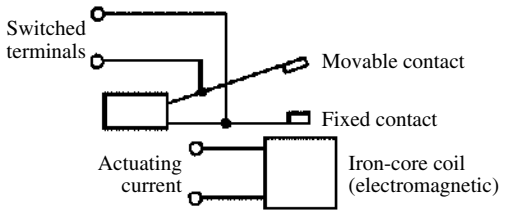

electromechanical relay

electromechanical timer A device for automatically timing a process or an observed event. Most such timers are based on an accurate clock (electric or spring driven) that opens or closes contacts at predetermined instants. Compare ELECTRONIC TIMER.

electromechanical transducer A transducer that translates mechanical signals directly into electrical ones or vice versa, without the intermediary of active devices, such as transistors or integrated circuits.

electromechanical valve A usually poppet-type valve for gases or liquids. The valve is operated by electromagnetic action and is often aided by an electronic (servo) circuit.

electromechanics The theory and application of electromechanical devices.

electromedical engineering The branch of electronics engineering concerned with the theory, design, and application of electronic equipment for medical diagnosis or treatment.

electromedical equipment Electrical or electronic equipment used in medical diagnosis or treatment.

electromerism Ionization in gases.

electrometallurgy The branch of metallurgy concerned with the use of electricity (especially in electrolysis) to separate or purify metals or to furnish heat for metallurgical processes.

electrometer A specially designed, highly sensitive electronic voltmeter used to measure extremely low voltages and, indirectly, extremely low currents. It is sometimes used as a galvanometer.

electrometer amplifier A stable low-noise amplifier for increasing the sensitivity of an electrometer.

electrometry The science of electrical measurements.

electromigration The movement of atoms in a substance from one place to another, because of interaction between electrons and ions in the presence of electric currents. This effect can cause the eventual deterioration of certain semiconductor devices.

5059F-pE-224-273 4/9/01 5:26 PM Page 244

electromotion Motion produced by electric charges or electrons.

electromotive force Abbreviation, emf. Electrical pressure, the potential that causes charge carriers to move through a substance or circuit. See VOLTAGE.

electromotive series A list of metals arranged according to the potential between the surface of the metals and an electrolyte into which they are immersed. Some metals acquire a positive potential (with respect to hydrogen, for which the potential is zero) and others, a negative potential.

electromotor A generator or motor, depending upon the context in which the term is used.

electromyogram The record produced by an ELECTROMYOGRAPH.

electromyograph An instrument for detecting, measuring, and analyzing the weak electrical currents generated by muscular activity.

electromyography The monitoring and analysis of the electrical activity of human muscles.

electron The subatomic particle that carries the unit negative charge of electricity. The electron has a mass of 9.109×10^{-31} kilogram and carries a charge of 1.602×10^{-19} coulomb.

electron acceleration See ELECTRON MOTION, **2**.

electronarcosis Loss of consciousness caused by passing a weak current through the brain. Useful in treating certain mental disorders, the process is somewhat similar to ELECTROSHOCK.

electron attachment The bonding of an electron to a neutral atom to form a negative ion. Also see ANION and ION.

electron avalanche See AVALANCHE and ELECTRON MULTIPLICATION.

electron band **1.** An emission line in the spectrum of an element or compound, caused by the movement of electrons from higher to lower energy levels within the atoms. **2.** An absorption line in the spectrum of an element or compound, caused by the movement of electrons from lower to higher energy levels within the atoms.

electron beam See ELECTRON STREAM, **1**.

electron-beam bender Any element that causes intentional deflection of the electron stream in a cathode-ray tube.

electron-beam focusing Reducing the size of the spot produced by the electron beam in a cathode-ray tube or television picture tube. This is accomplished by adjusting the direct-current (dc) bias voltage on a focusing electrode.

electron-beam generator **1.** See ELECTRON GUN. **2.** A tube, such as a Klystron, in which velocity modulation of the electron beam generates extremely high radio frequencies.

electron-beam instrument An instrument, such as an oscilloscope, based on a cathode-ray tube.

electron-beam machining Welding or shaping materials by controlled electron beams.

electron-beam magnetometer A magnetometer in which the magnetic field under measurement deflects the electron beam in a cathode-ray tube over a distance that is proportional to field intensity.

electron-beam recording In digital computer operations, a technique whereby the output of a computer is recorded on microfilm by an electron beam.

electron-beam scanning tube A tube in which an electron beam strikes a sensitized screen to produce a spot of light, which is deflected electrically or magnetically across a screen. Examples are oscilloscope tubes, storage tubes, and television picture tubes.

electron-beam tube Electron tubes (such as beam-power tubes, klystrons, oscilloscope tubes, and television picture tubes), in which an electron beam is generated and controlled.

electron-beam welding A method of welding in which an electron beam is focused on the workpiece to heat it.

electron-bombarded semiconductor A semiconductor wafer, plate, or junction that is acted on by an electron beam; it alters the resistance of the semiconductor to control the current in an external circuit.

electron-bombarded semiconductor amplifier See EBS AMPLIFIER.

electron bunching See BUNCHING.

electron charge See ELEMENTARY CHARGE.

electron cloud A mass of free electrons.

electron diffraction Diffraction that occurs when a beam of electrons passes through a crystal material. Fast-moving electrons have wavelike properties; the wavelength depends on the speed of the particles. This effect can also occur with beams of other particles, such as neutrons, protons, or alpha particles.

electron drift **1.** The movement of an electron from atom to atom in a conductor, as caused by the influence of an applied voltage. **2.** In a semiconductor, directed electron movement. Also see DRIFT, **1**.

electronegative Having negative electrification or polarity (see ELECTRICAL POLARITY). Compare ELECTROPOSITIVE.

electron emission The emission of electrons into surrounding space by a material. Depending on the material, this effect can be initiated by application of heat, light, torsion, electron impact, a high-voltage field, and other actions.

electron flow See ELECTRON DRIFT.

electron g-factor A physical constant that expresses the ratio of electron magnetic moment to the Bohr magneton, and equal to approximately 1.00116. Also called *free-electron g-factor.*

electron-gas binding forces See METALLIC BINDING FORCES.

electron-gas bonding See BONDING, **1** and METALLIC BINDING FORCES.

electron gun A composite electrode for generating an electron beam (see ELECTRON STREAM, **1**) in

5059F-pE-224-273 4/9/01 5:26 PM Page 245

a vacuum. In a cathode-ray tube, the gun comprises a heated cathode, control electrode, accelerating electrodes, and a focusing electrode.

electron-hole pair In a semiconductor, an electron and a related hole. Each electron in the conduction band has a counterpart in the valence band, a vacancy (hole) left by the electron's moving to the conduction band.

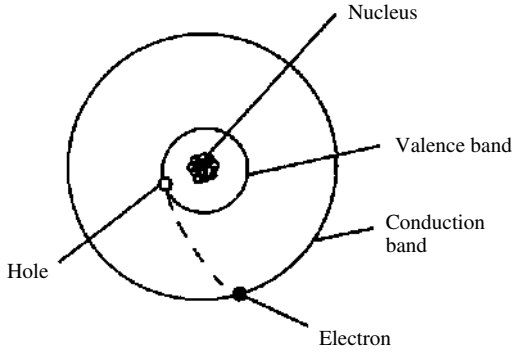

electron-hole pair

electronic **1.** Descriptive of any component, device, or system that functions, according to the principles of ELECTRONICS. **2.** Pertaining to electrons.

electronic adder A circuit (such as an operational amplifier) for performing arithmetic addition. In such a circuit, the output-signal amplitude is the sum of the input-signal amplitudes. Also see ADDER and ANALOG ADDER.

electronic aid An electronic device or circuit that contributes to the operation of a nonelectronic device or system; a pH meter, for example, is an electronic aid to chemistry.

electronics aide See ELECTRONICS TECHNICIAN.

electronic attenuator An attenuator in which the variable resistor is the output section of an active device, such as a transistor. Varying the direct-current (dc) bias of the input section varies the resistance of the output section.

electronic autopilot A servo system for detecting and automatically correcting an aircraft's flight path.

electronic balance An electronic scale, which uses a sensitive current-measuring device in conjunction with a movable tension device.

electronic brain **1.** A high-end computer. **2.** A robot controller. **3.** A system that possesses or uses artificial intelligence (AI).

electronic breadboard **1.** A thin, usually nonmetallic board or card having prepunched holes for the quick assembly of electronic circuits for test and evaluation. **2.** Any circuit prototype that is manually wired during the experimental phase of product development.

electronic bug **1.** A semiautomatic telegraph key that produces dots via an oscillating mechanical arm. The operator produces dashes manually. **2.** A telegraph keying device that automatically generates dots and dashes. Also see ELECTRONIC KEY, **1**. **3.** An undetermined source of problems or improper operation in an electronic circuit.

electronic buzzer **1.** A mechanical buzzer driven by a direct-current (dc) amplifier. **2.** An oscillator circuit that produces a sound similar to that of a mechanical buzzer.

electronic calculating punch A machine that punches on a card the result of calculations it has performed on data it has read from another punched card.

electronic calculator A fully electronic machine for performing mathematical calculations. The simplest machines perform basic arithmetic; more sophisticated ones can do operations with trigonometric, logarithmic, hyperbolic, and other scientific functions. Basic machines are available in department stores for about five dollars. It is usually powered via a small cell or battery, or by a small photovoltaic panel.

electronic camouflage The use of electronics by a target craft to minimize or prevent the reflection of radar echoes.

electronic carillon An electronic system that produces sounds resembling those of a bell carillon.

electronic chime See ELECTRONIC CARILLON.

electronic circuit An electric circuit containing active electronic components, such as transistors and integrated circuits, as opposed to a circuit containing only passive electrical components (such as resistors, switches, heating elements, etc.).

electronic clock **1.** An electric clock whose motor is driven by a constant-frequency oscillator (crystal or tuning fork type), followed by multivibrators and amplifiers. **2.** Any electronic timing circuit that produces pulses at predetermined intervals for the purpose of regulating the operation of other circuits, subsystems, or assemblies.

electronic commutator See COMMUTATOR, **2**.

electronic conduction A flow of electric current resulting from the movement of electrons among atoms in a conductor.

electronic control **1.** The science of automatically controlling machines and devices by means of electronic circuits. **2.** A circuit or device that provides automatic electronic control.

electronic controller A controller (see CONTROLLER, **2**) having no moving parts. For automatic operation, such a device often contains a circuit that senses control signals, compares them with a signal standard, and automatically adjusts the output control power accordingly.

electronic counter A fully electronic circuit that indicates the number of pulses that have been

5059F-pE-224-273 4/9/01 5:26 PM Page 246

applied to it (see COUNTER, **1**). Unlike the electromechanical counter, the electronic counter has no moving parts and is therefore capable of extremely high-speed, noiseless operation.

electronic counter-countermeasures Abbreviation, ECCM. Military procedures for interfering with a foe's electronic countermeasures.

electronic countermeasures Abbreviation, ECM. Interference with enemy radio and radar emissions by electronic means. Also see JAMMING.

electronic coupling Coupling via electronic effects or devices.

electronic crowbar A switch that prevents destructive currents from flowing through the components of a circuit.

electronic current meter A current meter that uses an amplifier ahead of an analog or digital indicator to provide increased sensitivity.

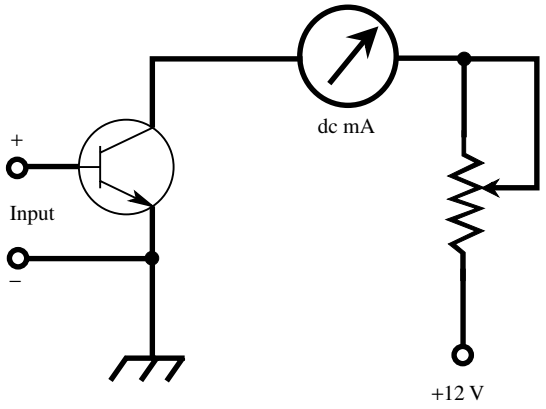

electronic current meter

electronic data processing Abbreviation, EDP. See DATA PROCESSING and ELECTRONIC INFORMATION PROCESSING.

electronic data-processing center Abbreviation, EDPC. An installation of electronic equipment and accessories for processing and storing data, usually in digital form. Also see DATA PROCESSING and ELECTRONIC INFORMATION PROCESSING.

electronic data-processing machine Abbreviation, EDPM. A device, such as an electronic computer, used in the automatic processing of data, usually in digital form.

electronic data-processing system **1.** A unique arrangement of machines for processing data. **2.** The sequence of steps in, and the underlying rationale for, the processing of data by automated equipment.

electronic deception See DECEPTION and DECEPTION DEVICE.

electronic differential analyzer See ANALOG DIFFERENTIATOR, DIGITAL DIFFERENTIAL ANALYZER, and DIFFERENTIAL ANALYZER.

electronic differentiator A circuit that performs mathematical differentiation. Also see DIFFERENTIATOR, **2**.

electronic divider **1.** An electronic device for performing arithmetic division. In a digital computer, such a divider can be a sequence of flip-flops, each of which produces a single output for every two input pulses. In an analog computer, the output signal amplitude is equal to the quotient of two input-signal amplitudes. **2.** See FREQUENCY DIVIDER. **3.** A voltage divider using active components, rather than resistors.

electronic dust precipitator See DUST PRECIPITATOR.

electronic efficiency A quantitative expression for the effectiveness of an electron beam as a medium of power transmission. The electronic efficiency, in percent, is equal to $100P_{out}/P_{in}$, where P_{out} is the (output) power delivered by the beam, and P_{in} is the (input) power supplied to the beam.

electronic equivalent of gravity In equations for the acceleration, velocity, and distance traveled for an electron, the factor equal to eF/m, where e is the electron charge, F is the potential gradient of field, and m is the electron mass. Also see ELECTRON MOTION, **2**.

electronic flash **1.** A device containing a circuit that uses an electronic flash tube as a light source for photography or other purposes. Also called *photoflash.* **2.** A bright momentary light burst produced by the equipment described in **1**, above.

electronic flash tube A tube used to produce brilliant bursts of light in photoflash units, stroboscopes, and laser exciters. A flash tube usually contains xenon gas, which is fired by a high-voltage pulse.

electronic frequency meter **1.** An instrument that gives direct readings of frequency in hertz, kilohertz, or megahertz on an analog scale or as a digital readout. **2.** Any device that indicates the operating frequency of another device, directly or indirectly, when used for such purpose.

electronic frequency synthesizer An instrument that supplies a number of selectable frequencies derived from one or more internally generated fixed frequencies.

electronic gas A collection of free electrons whose behavior resembles that of a gas.

electronic gate **1.** A logic gate that operates by electronic means. **2.** A security system, consisting of a mechanical gate controlled electronically. Similar to an electronic garage door.

electronic guitar See ELECTRIC GUITAR.

electronic heating The production of heat in an object via high-frequency energy. The two principal methods are *dielectric heating* and *induction heating.*

5059F-pE-224-273 4/9/01 5:26 PM Page 247

electronic hygrometer An electrical device for measuring relative humidity, whose sensitivity and stability have been increased by the addition of active amplifying devices.

electronician See ELECTRONICS TECHNICIAN.

electronic induction See ELECTROSTATIC INDUCTION.

Electronic Industries Association Abbreviation, EIA. An American association of electronic manufacturers and engineers. It sets standards, disseminates information, provides industry-government liaison, and maintains public relations for the industry.

electronic information processing The use of electronic equipment (especially digital computers and attendant devices) to perform mathematical operations on data entered into the system in the form of electrical signals. Also see DATA PROCESSING.

electronic instrument An instrument whose circuit uses active devices for increased sensitivity over that of the electrical counterpart, and for minimum loading of a device under test. Compare ELECTRICAL INSTRUMENT.

electronic integrator A active device (such as an operational amplifier) for performing mathematical integration. Also see INTEGRATOR, **2**.

electronic intelligence **1.** Information exchanged by electronic means. Examples: radio messages, radar information, and computer data. **2.** The faculties of reasoning and decision making, as apparently simulated by a high-level computer.

electronic interference The malfunctioning of a device because of nearby currents, voltages, or electromagnetic fields.

electronic inverter An electronic device for converting direct current (dc) to alternating current (ac). Typically, an inverter is a transistorized square-wave oscillator inductively coupled to ac output terminals. The dc to be inverted energizes the transistors, which perform the switching function at the rate determined by the components of the circuit. Also see INVERTER, **1**.

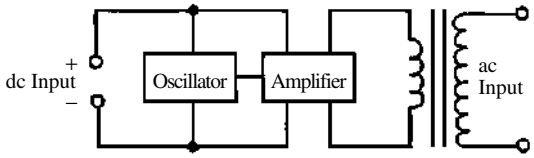

electronic inverter

electronic jamming The deliberate transmission of electromagnetic energy for the purpose of interfering with the operation of a device or devices.

electronic key **1.** For telegraphy (radio or wire), an electronic circuit that generates a continuous string of accurately spaced and timed Morse code dots or dashes, depending on its lever's position (right or left). **2.** For telegraphy (radio or wire), a keyboard that produces perfectly timed Morse code output that corresponds to the operator's typed input. **3.** An electronic device for opening an electronic lock.

electronic keyer See ELECTRONIC KEY, **1**.

electronic lock A lock that will open only after application of a special coded sequence of signals.

electronic mail Also called *e-mail.* A communications system that allows people to leave digital text messages for each other. It is popular among users of personal computers. Operates through the telephone lines using terminal emulation software and a modem. It can also be used via amateur radio packet communications.

electronic microammeter See FET CURRENT METER and TRANSISTOR CURRENT METER.

electronic microvoltmeter See MICROVOLTMETER.

electronic milliammeter See FET CURRENT METER and TRANSISTOR CURRENT METER.

electronic millivoltmeter A millivoltmeter that uses an amplifier ahead of an analog or digital indicator to provide high input impedance and increased sensitivity.

electronic multimeter A *voltohm-milliammeter* that uses active amplifying devices. Also see ELECTRONIC INSTRUMENT.

electronic multiplier A device, such as a Hall generator, whose output is equal (or proportional) to the product of two inputs (i.e., it can perform arithmetic multiplication).

electronic music **1.** Music produced by a combination of electronic oscillator, amplifier, and loudspeaker. A number of successful instruments have been developed. See, for example, ELECTRONIC CARILLON, ELECTRONIC ORGAN, ELECTRONIC PIANO, and THEREMIN. **2.** The electronically amplified sounds of conventional musical instruments.

electronic organ A musical instrument with a keyboard similar to that of a conventional organ, in which tones produced by oscillators or electrically driven reeds are processed and amplified for delivery to a system of loudspeakers.

electronic packaging See ENCAPSULATION.

electronic part A lowest replaceable unit, or component, in an electronic circuit.

electronic phase meter An electronic instrument for measuring phase difference. Direct readings, in degrees of lead or lag, are visible on an analog scale or as a digital readout.

electronic photoflash A transistorized light-intensity meter. Also see ELECTRONIC INSTRUMENT.

electronic piano A musical instrument having the keyboard of a conventional piano and provided with electronic amplification.

electronic power supply A power supply using transistors or integrated circuits for stabilization and output control.

5059F-pE-224-273 4/9/01 5:26 PM Page 248

electronic precipitator See DUST PRECIPITATOR.

electronic product Any commercially manufactured electronic device, intended for purchase by the public, by industry, or by government.

electronic profilometer An electronic instrument for measuring surface roughness.

electronic ratchet A stair-step circuit or other arrangement functioning in the manner of an equivalent electromechanical stepping switch. Also see COMMUTATOR.

electronic reconnaissance In military applications, the use of electronic systems to locate enemy installations (such as radio stations, guided-missile sites, and radar bases).

electronic rectifier A rectifier that uses active devices to change alternating current (ac) to direct current (dc).

electronic regulator A voltage regulator that uses active electronic circuits, as opposed to a reactor-type or electromechanical device. See, for example, VOLTAGE REGULATOR.

electronic relay **1.** A switching circuit that uses one or more transistors, and performs the relay function without moving parts. **2.** An electronic component designed to switch when gating signals are applied (e.g., triac, diac, or silicon-controlled rectifier).

electronic resistor **1.** The effective internal collector-emitter resistance of a common-emitter bipolar-transistor stage. **2.** The effective internal drain-source resistance of a field-effect transistor (FET) stage.

electronics The branch of physics concerned with the behavior and application of electric charge carriers in components, devices and systems that accomplish amplification, oscillation, signal processing, and/or switching.

electronics engineer A trained professional skilled in the physics and mathematics of electronics, and in the theory and application of basic engineering and related subjects. Compare ELECTRICAL ENGINEER.

electronics service person An electronics technician skilled in repairing and maintaining electronic equipment. Also called *electronics service technician.*

electronic shutter See KERR CELL.

electronics technician A professional skilled in building, testing, repairing, or maintaining electronic equipment.

electronics technology The theory and practical application of electronics. Taught as a subengineering major, usually in two-year junior colleges or technical institutes, awarding the degree of associate in arts (AA) or associate in science (AS).

electronic stethoscope A stethoscope employing a miniature microphone, amplifier, and earphones. The amplifier gain is continuously controllable, and its bandwidth often selectable for emphasizing particular heart sounds and other body noises.

electronic stimulator A device for applying controlled electrical pulses to the body to stimulate muscles or nerves during diagnosis or therapy.

electronic stroboscope A stroboscope that uses a rate-calibrated oscillator, rather than a mechanical contactor to generate pulses that strobe the lamp.

electronic subtracter An electronic circuit for performing arithmetic subtraction.

electronic surge A sudden, large increase in the current in a conductor. Can be caused by an electromagnetic pulse; can also occur when utility power is restored following a blackout.

electronic switch **1.** A nonmechanical device, such as a flip-flop or gate, whose characteristic on-off operation can be used to make and break an electric circuit. Compare CONTACT SWITCH. **2.** A device using electronic gating and sequencing circuits to present several signals alternately to the single input of an oscilloscope, allowing simultaneous viewing of the signals.

electronic tachometer An instrument for measuring angular velocity, usually in revolutions per minute (rpm). Ideally, the response is independent of sensor voltage amplitude, showing only the number of pulses per unit time reaching the meter circuit.

electronic thermal conductivity The thermal-conductivity component, resulting from the transfer of heat by electrons and holes.

electronic thermometer An instrument for measuring temperature as a result of variations in a temperature-sensitive component, such as a resistor, thermocouple, or thermistor.

electronic timer An electronic circuit or device for automatically timing a process or observed event. Most are based on the time constant of a stable resistance-capacitance (RC) circuit. Compare ELECTROMECHANICAL TIMER.

electronic tube See ELECTRON TUBE.

electronic tuning Variation of the resonant frequency of a device or circuit by changing the bias voltage or current of a controlling electronic component.

electronic voltmeter A voltmeter that uses electronic amplification ahead of the indicating meter to provide high input impedance and increased sensitivity. Also see FET VOLTMETER and TRANSISTOR VOLTMETER.

electronic voltohmmeter A voltohmmeter that uses electronic amplification ahead of the indicating meter to provide high input impedance and increased sensitivity.

electronic typewriter A typewriter with a microcomputer that provides features, such as buffering, automatic repeat, erase memory, and paragraph/page memory.

electronic warfare The use of electronic systems for military purposes, including interfering with an enemy's use of similar systems.

electronic watch **1.** A watch whose movement is a tiny, high-frequency, alternating-current (ac)

5059F-pE-224-273 4/9/01 5:26 PM Page 249

motor driven by a stable oscillator. **2.** Any miniature timepiece incorporating solid-state circuitry, but especially one using a digital readout.

electronic wattmeter A wattmeter in which an amplifier is used for increased sensitivity.

electronic waveform synthesizer A signal generator that delivers an alternating or pulsating signal whose waveform can be tailored by means of adjustable circuit components.

electron lens A device that focuses an electron beam in a manner similar to the focusing of light rays by a glass lens. Also see ELECTROSTATIC LENS, ELECTROMAGNETIC LENS, and WAVEGUIDE LENS.

electron magnetic moment The energy per unit flux density available in an electron. Approximately equal to 9.2848×10^{-24} joule per tesla.

electron mass See MASS OF ELECTRON AT REST.

electron microscope A microscope in which the source of illumination is an electron beam focused by electromagnetic lenses. It allows much greater magnification than is possible with optical microscopes.

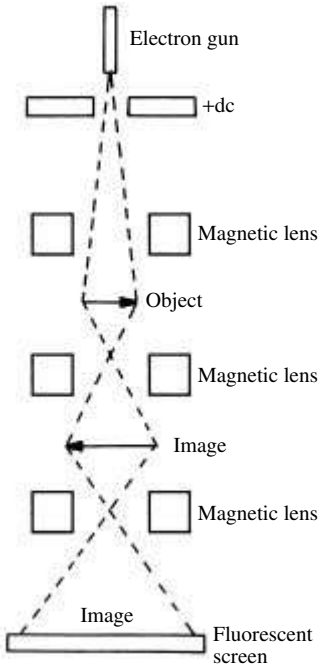

electron microscope

electron mirror A reflector of electrons—especially a dynode element in a photomultiplier tube or electron-multiplier tube.

electron motion **1.** The movement of electrons in a conductor, semiconductor, or space, as the result of electric or magnetic attraction or repulsion. **2.** The movement of an electron as a charged mass. In an electric field, this movement simulates that of a free-falling body in a gravitational field.

electron multiplication **1.** In a gas discharge, the production of additional electrons as a result of collisions between electrons, atoms, and molecules. **2.** The increased production of electrons in a semiconductor when avalanche occurs.

electron-multiplier tube **1.** A vacuum tube utilizing a sequence of secondary emissions for increased current amplification. Electrons from the cathode strike a positively biased dynode with a force that dislodges secondary electrons, which, upon joining those first emitted, are reflected to a second positive dynode that contributes more secondary electrons, reflecting the total to a third positive dynode, etc. The last dynode in the chain reflects the enhanced beam to an anode collector that passes the high current to an external circuit. **2.** See PHOTOMULTIPLIER TUBE.

electronography Printing by means of the electrostatic transfer of ink from a printing plate across a gap to an impression cylinder.

electron optics See ELECTRO-OPTICS.

electron orbits See ELECTRON SHELLS.

electron oscillator A device in which oscillation is obtained by causing electrons to move in an oscillatory path, to travel in bunches, etc. Examples: klystron, magnetron, and traveling-wave tube.

electron pair Two electrons from adjacent atoms, which sometimes share the same orbits, but always produce a bond between two adjacent atoms.

electron-pair bond The bond between an electron pair.

electron physics The physics of electronics, usually from a highly theoretical viewpoint.

electron-proton magnetic moment ratio A physical constant whose value is approximately equal to 658.211, derived from the division of the magnetic moment of the electron by that of the proton.

electron recoil The recoil of an electron from a photon it has collided with.

electron rest mass See MASS OF ELECTRON AT REST.

electron scanning Deflection of an electron beam. See, for example, ELECTROSTATIC DEFLECTION and ELECTROMAGNETIC DEFLECTION.

electron shells The spheres, concentric with the nucleus of an atom, that represent the median distances from the nucleus around which electrons migrate.

electron spin The rotation of an electron (i.e., around its axis). This motion is independent of the electron's movement around the nucleus of an atom.

electron stream **1.** The beam of electrons generated by the electron gun in a cathode-ray tube.

5059F-pE-224-273 4/9/01 5:26 PM Page 250

2. The electrons moving between the cathode and plate in an electron tube.

electron-stream instrument See ELECTRON-BEAM INSTRUMENT.

electron-stream meter An oscilloscope (or cathode-ray tube alone) used as a device for making measurements.

electron-stream transmission efficiency The ratio of the current through a positive electrode to the current impinging on it. In a tube, for example, some electrons are absorbed by the plate, and others are reflected.

electron telescope A telescope using a combination of a glass lens, photocathode, and electrostatic focusing. Light from the object is focused on the photocathode by the lens, the electrons emitted being focused electrostatically on a phosphorescent viewing screen.

electron transit time The time required for an electron to travel a given distance. For a vacuum tube, the upper frequency limit of operation is governed by the time required for an electron to reach the plate after leaving the cathode. Transit time is usually stated in fractions of a microsecond.

electron tube An evacuated or gas-filled chamber in which electrons are emitted (usually by a hot cathode) and controlled (usually by a voltage applied to a grid electrode).

electron unit See ELEMENTARY CHARGE.

electron velocity The velocity acquired by an electron that moves between two points having a given potential difference. Also see ELECTRON MOTION, **2**.

electronvolt Abbreviation, eV. The energy acquired by a unit charge moving through a potential difference of one volt; it is equal to approximately 1.6022×10^{-19} joule.

electron-wave tube A tube, such as a klystron or traveling-wave tube, in which electrons traveling at different velocities interact with each other, modulating the electron stream.

electro-oculogram A recording of the voltage that is found between the anterior and posterior parts of the eyeball.

electro-optical transistor A phototransistor or pair of phototransistors in a single package. Used in electronic circuits to sense changes in light levels.

electro-optical valve See KERR CELL.

electro-optic radar A form of radar that makes use of visual apparatus for locating a target.

electro-optics The branch of electronics dealing with related electrical and optical phenomena: photoelectricity, light generation, laser technology, light amplification, etc. It is also concerned with electronic phenomena that are analogous to optical phenomena, such as electronic focusing, reflection, refraction, diffraction, etc. Also called *electron optics* and *optoelectronics*.

electro-osmosis Causing liquids to flow by applying an electric field across the walls of a porous plug. The force exerted by the field on ions in the liquid causes it to flow.

electropad The skin-contacting electrode of an electrocardiograph.

electropathy See ELECTROTHERAPY.

electrophilic Pertaining to the tendency to seek electrons.

electrophobia An irrational fear of electricity, a psychological condition sometimes exhibited by victims of serious electric shock.

electrophonic effect Sound heard by a person when an alternating current is passed through some part of the body.

electrophoresis The movement of dielectric particles through a liquid in which they are suspended, produced by the electric field between electrodes immersed in the suspension.

electrophoresis equipment 1. Any device intended for the purpose of depositing a dielectric material onto a metal by means of electrophoresis. **2.** Any equipment in which electrophoresis occurs.

electrophoresis scanner A device that senses the movement of charged particles caused by electrophoresis effects.

electrophoretic deposition A type of deposition in which a low-voltage direct current passing through a colloidal suspension of dielectric polymer particles deposits them as a coating on a metallic body (the anode in the process). It can provide a better coating than one obtained with spray painting or dipping.

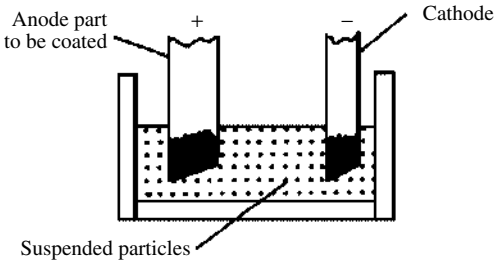

electrophoretic deposition

electrophorus A simple device used to demonstrate electrostatic generation and induction. It consists of a smooth metal plate at the end of an insulating handle and an accompanying cake of resin or hard rubber. The cake is rubbed with cat's fur, making it negatively charged. The metal plate is touched to the charged cake; by induction, it acquires a bound positive charge on the face that touched the cake and a free negative charge on the opposite face. When the plate is lifted and its top face touched momentarily with the finger or grounded, the negative charge leaks

5059F-pE-224-273 4/9/01 5:26 PM Page 251

off, often with a sharp spark, but the positive charge remains.

electrophotographic process See XEROGRAPHY.

electrophotography The production of photographs by means of electricity. See XEROGRAPHY.

electrophotometer A light-intensity meter using a photoelectric sensor and a meter, but usually not incorporating an amplifier. Compare ELECTRONIC PHOTOMETER.

electrophrenic respiration A system of inducing respiration in which one or both of the phrenic nerves (i.e., of the diaphragm) are stimulated electrically to produce contractions of the diaphragm muscles.

electrophysiology **1.** The study of electrical processes in the human body. **2.** The study of how electrical impulses affect, and are produced by, body organs.

electroplaques In electric fish, small voltage-generating cells that are connected in series-parallel networks.

electroplate **1.** To cause one metallic substance to adhere to the surface of another through the effects of electrolysis. **2.** A metal plating deposited via electrolysis.

electroplating Depositing one metal on the surface of another by electrolytic action.

electropolar Having electrical polarity (either positive or negative).

electropolishing An electrolytic method of smoothing a rough metal surface. The workpiece to be polished becomes the anode of an electrolytic cell in which electrolytic action dissolves tiny surface irregularities.

electropositive Having positive electrification or polarity. Compare ELECTRONEGATIVE.

electropotential series See ELECTROMOTIVE SERIES.

electropsychrometer An electronic instrument for humidity measurements.

electroreduction In electrolysis, reduction of the cathode electrode.

electrorefining The refining of metals by means of electrolysis.

electroretinograph An instrument used to measure the electrical response of the human retina to light.

electroretinography The process of detecting and measuring electrical impulses from the retina.

electroscope An instrument for detecting electric charges and fields. The common type uses a pair of gold-leaf strips hung from the end of a metal rod in a glass tube or jar. When the exposed end of the rod is brought near a charged object, the leaves repel each other and spread apart.

electrosection The use of an arc-generating device for making surgical incisions.

electrosensitive recording See ELECTRIC RECORDING.

electroshock **1.** The system of creating a controlled electric shock in the brain as a treatment for certain mental disorders. **2.** The electric shock used in the therapy described in **1**.

electrospinograph An instrument that senses and records electrical impulses from the spinal cord.

electrostatic Pertaining to stationary electric charges and fields, and their application.

electrostatic actuator A device for measuring the sensitivity of a microphone. Electrostatic charges produce forces on the diaphragm of the microphone, and the resulting output is recorded.

electrostatic amplifier See DIELECTRIC AMPLIFIER.

electrostatic charge See ELECTRIC CHARGE.

electrostatic component The electric component of an electromagnetic wave. It is perpendicular to the magnetic component and can be thought of as the wave's voltage component.

electrostatic constant See ELECTRIC CONSTANT.

electrostatic convergence See ELECTROSTATIC FOCUSING.

electrostatic cooling Accelerated cooling of a body through the application of an intense electrostatic field. The body must be in a free convection state, a corona discharge must be present, and the field must not be uniform.

electrostatic copier A document-copying apparatus that uses electrostatic effects to reproduce printed material.

electrostatic coupling See CAPACITANCE COUPLING.

electrostatic deflection In a cathode-ray tube, deflection of the electron beam by the electrostatic fields between pairs of internal horizontal and vertical deflecting plates. It is primarily used in laboratory oscilloscopes. Compare ELECTROMAGNETIC DEFLECTION.

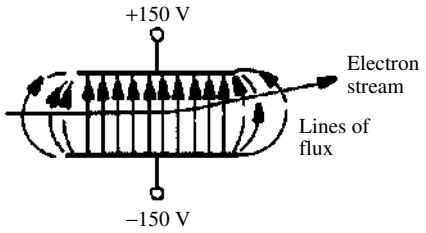

electrostatic deflection

electrostatic electrometer See KELVIN ABSOLUTE ELECTROMETER.

electrostatic electrophotography See XEROGRAPHY.

electrostatic energy The potential energy contained in an electrostatic field (e.g., the energy in a charged capacitor). Compare ELECTROKINETIC ENERGY.

electrostatic field A stationary electric field.

5059F-pE-224-273 4/9/01 5:26 PM Page 252

electrostatic field intensity An expression of the strength of an electrostatic field. Usually expressed in volts per meter, millivolts per meter, or microvolts per meter.

electrostatic flux The flux existing around an electric charge or a charged body.

electrostatic focusing In a cathode-ray tube, electron-beam focusing achieved by varying the dc bias voltage on a focusing electrode. Compare ELECTROMAGNETIC FOCUSING.

electrostatic galvanometer A galvanometer operating on the principle of the electrostatic voltmeter.

electrostatic generator A device for producing high-voltage electric charges; e.g., a *Van de Graaff generator.*

electrostatic headphone A device similar to an electrostatic speaker, but held against the head for private listening. Incoming audio signals cause attraction and repulsion among charged plates, resulting in acoustic vibration.

electrostatic hysteresis The tendency of some dielectrics (especially ferroelectric materials) to saturate and retain a portion of their polarization when an alternating electric field to which they are exposed reverses polarity. This causes the charge to lag behind the charging force.

electrostatic induction The charge acquired by a body inserted into an electric field. Compare ELECTROMAGNETIC INDUCTION.

electrostatic instrument See ELECTROSTATIC VOLTMETER.

electrostatic lens An assembly of deflecting plates or cylinders, whose electric field causes an electron beam to converge or diverge in much the same way as a visible light beam passing through an optical lens. Compare ELECTROMAGNETIC LENS.

electrostatic loudspeaker See ELECTROSTATIC SPEAKER.

electrostatic memory A memory unit in which an information bit is stored as an electric charge.

electrostatic memory tube A cathode-ray tube in which information bits are stored in capacitive cells swept by the scanning electron beam.

electrostatic microphone See CAPACITOR MICROPHONE.

electrostatic phase shifter See PHASE-SHIFTING CAPACITOR.

electrostatic potential In an electric field, the potential energy represented by the voltage between the two elements creating the field, or between any two points within the field.

electrostatic precipitator See DUST PRECIPITATOR.

electrostatic printer A computer output peripheral in which the printing medium, a fine dust, is fused by heat onto paper that has been charged according to the data being represented.

electrostatic process **1.** Any process that uses electrostatic action. **2.** A method of photography in which visual images are converted to electrostatic images.

electrostatic recording A method of recording that employs a signal-controlled electric field.

electrostatic relay A high-input-impedance relay consisting of two polarity-controlled contacts; opposite charges on the contacts close the relay, and like charges open it.

electrostatics The branch of electricity concerned with electrical charges at rest. Compare ELECTRODYNAMICS and ELECTROKINETICS.

electrostatic screen A shield against electric flux consisting of a number of straight, narrowly separated rods or wires joined at only one end. The shield has little effect on magnetic flux. Also called *Faraday shield.*

electrostatic separator A device for separating fine particles from a mixture by exposing the mixture to an intense electrostatic field.

electrostatic series A list of materials arranged in this sequence: any one of them becomes positively electrified when rubbed with another lower in the list, or negatively electrified when rubbed with another higher in the list. Compare ELECTROMOTIVE SERIES.

electrostatic shield Any metallic enclosure designed to confine an electric field.

electrostatic speaker A loudspeaker whose vibrating diaphragm is one of two plates in a large air-dielectric capacitor, the other being a closely situated metal plate (or plug). An audio voltage applied to the plates causes them to vibrate. Also called *capacitive loudspeaker* and *capacitor loudspeaker.*

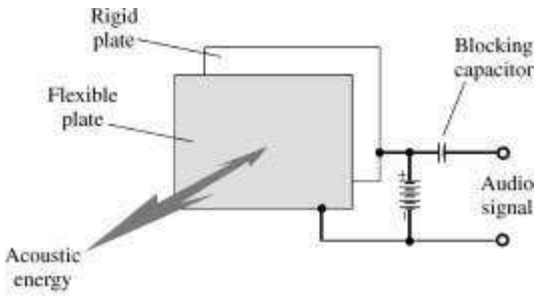

electrostatic speaker

electrostatic sprayer An equipment for spray painting in which fine droplets of paint are attracted by an electrostatic field to the surface to be coated.

electrostatic storage See ELECTROSTATIC MEMORY.

electrostatic stress **1.** Stress in the vicinity of a charged body or particle. **2.** See DIELECTRIC STRESS.

5059F-pE-224-273 4/9/01 5:26 PM Page 253

electrostatic transducer See CAPACITANCE TRANSDUCER.

electrostatic tube of flux The space between electric lines of flux going through adjacent points on the boundary of a given area in an electric field.

electrostatic tweeter A small electrostatic speaker for reproducing high-frequency sounds. Compare WOOFER.

electrostatic unit Abbreviation, esu. A unit of measure in the electrostatic system of cgs units. Also see CENTIMETER-GRAM-SECOND. Compare ELECTROMAGNETIC UNIT.

electrostatic vector See ELECTRIC VECTOR.

electrostatic voltmeter An indicating meter whose movement consists of a stationary metal plate near a rotating metal plate. A voltage applied to the plates charges them, and the attraction between them causes the movable member to rotate against the torque of a returning spring over an arc proportional to the voltage.

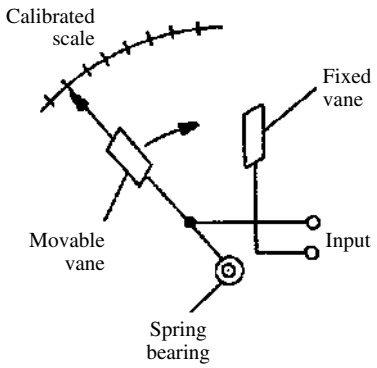

electrostatic voltmeter

electrostatography See XEROGRAPHY.

electrosteel See ELECTRIC STEEL.

electrostenolysis The deposition of certain metals from a solution in capillary tubes when an electric current passes through the solution.

electrostimulation Electrical excitation of nerves for the relief of pain.

electrostriction In certain materials, the physical contraction that occurs when a voltage is applied. Compare MAGNETOSTRICTION.

electrostrictive ceramic A ceramic exhibiting ELECTROSTRICTION when voltage is applied.

electrostrictive relay A relay in which the movable contact is carried by a bar of electrostrictive material, such as barium titanate. A control voltage deforms the material, causing the contacts to close.

electrosurgery Surgery, sometimes bloodless, achieved with diathermy-like equipment. See DIATHERMY, **2**.

electrosynthesis Chemical synthesis produced by means of electric currents or fields.

electrotape Also called *electronic tape measure.* Any device that measures distance by electronic means, such as radar or sonar.

electrotechnology See ELECTRICAL TECHNOLOGY and ELECTRONICS TECHNOLOGY.

electrotellurograph An instrument for measuring ground currents.

electrotherapeutics See ELECTROTHERAPY.

electrotherapy The treatment of disorders or diseases by electrically induced heat—especially by DIATHERMY.

electrothermal **1.** Pertaining to electrically generated heat. **2.** Pertaining to a combination of electricity and heat.

electrothermal device A device whose operation depends on the heat generated by an electric current (e.g., a bolometer, hot-wire ammeter, thermocouple, or varistor).

electrothermal expansion element A thermostatic element, such as a bimetallic strip, whose expansion is used in heat-sensitive switches.

electrothermal instrument A hot-wire or thermocouple-type meter.

electrothermal recorder See ELECTRIC RECORDING, **1** and THERMAL RECORDER.

electrothermic See ELECTROTHERMAL.

electrothermics The study and application of the heating effects of electricity in conductors and junctions.

electrotitration In chemistry, the completion of titration, as indicated by an electrical measurement, such as of the resistance of the solution being titrated.

electrotonic Pertaining to ELECTROTONUS.

electrotonus Modification of a nerve's sensitivity by passing a constant current through it.

electro-ultrafiltration In physical chemistry, filtering a colloidal suspension by electro-osmosis.

electrovalence **1.** The number of charges acquired by an atom gaining electrons. **2.** The number of charges forfeited by an atom losing electrons. **3.** Valence resulting from electron transfer between atoms and the resulting creation of ions.

electrovalency See ELECTROVALENCE.

electrovalent bond See IONIC BOND.

electrowin To recover (win) a metal from a solution of its salts by means of electrolysis.

electrum A natural alloy of gold and silver.

element **1.** See ELECTRODE. **2.** A circuit component intended for a specific purpose. **3.** A specific part of an antenna array (e.g., *driven element* or *parasitic element*). **4.** A fundamental, unique substance whose atoms are of only one kind (examples: aluminum, carbon, silicon, and sulfur). There are more than 100 elements, some man-made. Elements combine to form compounds. **5.** A circuit, such as an AND gate, that can be taken as a unit because it performs a special function. **6.** In digital computer

5059F-pE-224-273 4/9/01 5:26 PM Page 254

operations, a subunit of a category that cannot be further categorized [e.g., a *bit* (word element) or a *record* (file element)].

elemental area In a facsimile or television picture, a scanning line segment as long as the line's width.

elemental charge See ELEMENTARY CHARGE.

elemental semiconductor A semiconductor containing one undoped chemical element.

elementary charge Symbol, *e*. Also called *unit electric charge.* The electric charge of a single electron or proton. This charge is approximately equal to 1.6022×10^{-19} coulomb.

elementary particle **1.** A minute charged or uncharged particle within the atom (i.e., electron, proton, neutron, quark, etc.). **2.** In theory, a subatomic particle that cannot be broken down into smaller particles.

element error rate In communications or data transfer, the ratio n_i/n_t, where n_i is the number of elements received incorrectly and n_t is the number of elements transmitted.

element spacing **1.** The spacing between radiator, director, and reflector elements in a directional antenna. **2.** The spacing between the internal electrodes of a vacuum tube.

elevation Angular position (in degrees) of a point above the horizontal.

elevation-position indicator A type of radar display simultaneously indicating the elevation of, and the line-of-sight distance to, the target.

elevator control **1.** An electronic system for automatically stopping an elevator and opening the doors. Various safety functions are included, an example being the reopening of a closing door when a passenger steps into the car. **2.** In an aircraft, the mechanical, electronic, or electromechanical devices or circuits involved in actuation of the elevators.

ELF Abbreviation for EXTREMELY LOW FREQUENCY.

eliminator **1.** A device or circuit acting as a surrogate for an inconvenient or undesirable component (e.g., battery eliminator). **2.** A device for removing or minimizing an undesirable signal or quantity (e.g., harmonic eliminator); interference eliminator.

ell A coaxial fitting that is a right-angle line section with a coaxial connector at each end. It takes its name from its L shape.

ellipse A geometric figure having the Cartesian-plane formula $(x - x_0)^2/a^2 + (y - y_0)^2/b^2 = 1$, where a and b are constants, and x_o and y_0 represent the center point.

elliptical filter See ELLIPTIC FILTER.

elliptical function See ELLIPTIC FUNCTION.

elliptical load line For any amplifier with an output transformer, a load line in the shape of an ellipse, obtained when the load connected to the output element is reactive, rather than purely resistive.

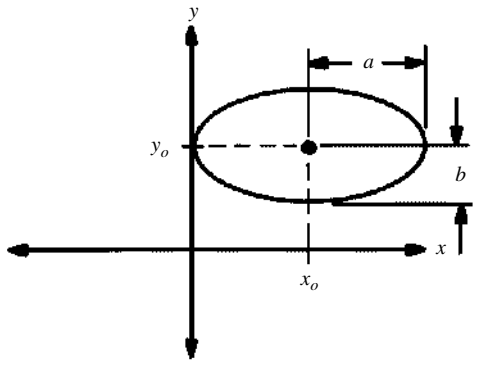

ellipse

elliptically polarized wave An electromagnetic wave in which the rotation of the electric-intensity vector at one point describes an ellipse.

elliptical orbit A satellite orbit that is not a perfect circle. In theory, all satellites deviate slightly from perfectly circular orbits. Sometimes a satellite is deliberately put into an orbit that is greatly elongated. The closer the satellite is to the earth, the faster it moves.

elliptical polarization Polarization characterized by elliptical rotation of the wave vector at a given point.

elliptical stylus In a phonograph (turntable) system, a stylus with a characteristic ellipsoidal shape.

elliptic filter A band-pass, band-stop, high-pass, or low-pass inductance-capacitance (LC) filter, designed according to an ELLIPTIC FUNCTION. Characterized by a steep attentuation-versus-frequency cutoff response with ripple in both the passband and the stopband.

elliptic function A function, similar to the Chebyshev and Butterworth functions, used in the design of certain selective filters. The elliptic function results in a better filter magnitude response than the Chebyshev or Butterworth functions in some applications. See ELLIPTIC FILTER.

elongation A form of modulation distortion resulting from multipath propagation. Some of the paths result in greater propagation delay than other paths; this causes the modulation envelope to spread out. The higher the modulating frequency, the greater the effect.

ELSE A word used in a BASIC computer program that provides an instruction based on a relational test and, in this respect, is related to IF-THEN, ON-GOTO, etc. It specifies the operation to be done if the conditions given in the same program line don't occur.

ELSIE Abbreviation of *electronic letter-sorting and indicator equipment.*

5059F-pE-224-273 4/9/01 5:26 PM Page 255

EM **1.** Abbreviation of EFFICIENCY MODULATION. **2.** Abbreviation of ELECTROMAGNETIC(S). **3.** Abbreviation of *electromagnetic iron.* **4.** Abbreviation of ELECTROMAGNETIZER. **5.** Abbreviation of ELECTRON MICROSCOPE. **6.** Abbreviation of EXPOSURE METER. **7.** Abbreviation of *electromotive.*

E_m **1.** Symbol for MAXIMUM VOLTAGE. **2.** Symbol for MAXIMUM JUNCTION FIELD.

emanation **1.** Emission of electrons. **2.** Emission of radioactive particles or ionizing radiation. **3.** Emission of electromagnetic energy.

E_{max} Symbol for MAXIMUM VOLTAGE.

embedded path A means of guiding a mobile robot along a specific route. One common scheme uses a buried, current-carrying wire that produces a magnetic field. The robot can sense and follow this field. Colored paints and tapes can also be used in conjunction with machine vision systems. Compare EDGE DETECTION.

embedded training The inclusion of training/tutorial programs in computerized equipment that assist users in the operation of the equipment.

embedding See ENCAPSULATION.

embossed-foil printed circuit A printed circuit made by pressing the pattern from metal foil into the insulating substrate and then removing the surplus foil.

embossed-groove recording **1.** A phonograph record into which grooves are embossed, rather than scribed. **2.** Recording sound by embossing grooves on record disks.

embossing stylus The rounded-tip stylus used to make an embossed-groove recording.

EMC Abbreviation of ELECTROMAGNETIC COMPATIBILITY.

EME Abbreviation of *earth-moon-earth.* See MOONBOUNCE.

e/m_e The ratio of the elementary electron charge to its mass: 1.7588×10^{11} coulombs per kilogram. Also see CHARGE-MASS RATIO.

Emergency Broadcast System In the United States, a general plan for dissemanating information via broadcast stations in the event of a national emergency.

emergency channel A communication channel allocated for emergency service.

emergency communication Radio or other electronic transmission and reception of urgent messages (e.g., distress signals, storm warnings, etc.).

emergency equipment **1.** Apparatus kept in standby status for immediate operation when regularly used equipment fails. **2.** Equipment, especially vehicular, for use in emergency situations. Examples are ambulances, fire-fighting trucks and equipment, etc.

emergency power supply An alternating-current (ac) or direct-current (dc) power unit kept in standby status for immediate use when the regular power supply fails.

emergency service A communications service devoted exclusively to emergency communication.

EMF, emf Abbreviation of ELECTROMOTIVE FORCE.

emf standard See STANDARD CELL.

EMG **1.** Abbreviation of ELECTROMYOGRAM. **2.** Abbreviation of ELECTROMYOGRAPH.

EMI Abbreviation of ELECTROMAGNETIC INTERFERENCE.

E microscope See ELECTRON MICROSCOPE.

emission **1.** The ejection of particles, especially electrons, from a material. **2.** Waves radiated from any source (as from a transmitting antenna or from an amplifier stage). **3.** The emanation of radiant, electromagnetic, acoustical, electrical, or magnetic energy.

emission code A system of abbreviating the various types of radio emission. See EMISSION MODE.

emission frequency **1.** In communications, the carrier frequency of the transmitted signal as it is radiated from the antenna or fed into a transmission line. **2.** The actual frequency or frequency range of a signal as it is transmitted or radiated. This might be the carrier frequency. **3.** The frequency of energy in an emission band or bands in a spectrum.

emission lines In a spectrum, radiation intensity peaks that appear as bright lines in a visible display. In a radio-frequency spectrum, the emission lines occur as sharp peaks in radiated energy at specific wavelengths.

emission mode Any of various official classifications of radio communication emission types. Emissions are designated according to the modulation method used (e.g., continuous waves, amplitude modulation, single-sideband with suppressed carrier, frequency modulation, pulse modulation, etc.).

emission power **1.** The rate at which energy is radiated from an object. **2.** In radio communication, the transmitter output power.

emission spectrum The radiation spectrum of a substance that emits energy (e.g., the light spectrum of an incandescent metal).

emission types See EMISSION MODE.

emission velocity The initial velocity of an electron as it leaves an emitting surface.

emission wavelength **1.** In communications, the carrier wavelength of the transmitted signal as it is radiated from the antenna or fed into a transmission line. **2.** The actual wavelength or wavelength range of a signal as it is transmitted or radiated. This might or might not be the carrier wavelength. **3.** The wavelength of energy in an emission band or bands in a spectrum.

emissive power The rate at which a surface emits energy of all wavelengths in all directions, per unit area of radiating surface, regardless of temperature.

emissivity For a radiating source, the ratio W_1/W_2, where W_1 is the energy emitted by the

5059F-pE-224-273 4/9/01 5:26 PM Page 256

source at a particular temperature, and W_2 is the energy emitted by a blackbody (i.e., a theoretically perfect radiator) at the same temperature.

emittance For an energy-radiating source, the radiated power per unit area of radiating surface.

emitted electron An electron that has left an atom of a material and has escaped into surrounding space or entered a neighboring material.

emitter **1.** A body that discharges particles or waves (see EMISSION). **2.** In a semiconductor device, the area, region, or element from which current carriers are injected into the device. In a transistor symbol, the emitter is that electrode shown with an arrowhead.

emitter-base junction In a bipolar transistor, the boundary between base and emitter regions.

emitter bias Emitter current or voltage maintained to set the operating point of a bipolar transistor.

emitter bulk resistance The portion of the resistance of the semiconductor material in a transistor that affects emitter resistance.

emitter-coupled logic A bipolar form of digital logic, abbreviated ECL.

emitter-coupled multivibrator A two-transistor multivibrator circuit in which the emitters share a common resistor.

emitter-coupled phase inverter A transistor phase inverter in which the out-of-phase component is taken from the collector and the in-phase component from the emitter resistor (of the same transistor). Another transistor is often used to amplify the in-phase component so that both outputs are equal in magnitude.

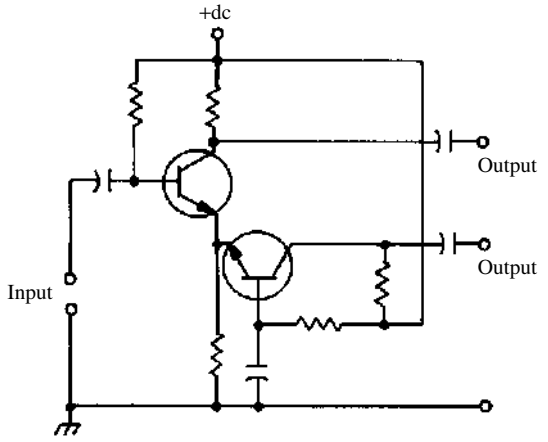

emitter-coupled phase inverter

emitter current Symbol, I_E. The current in the emitter electrode of a bipolar transistor.

emitter degeneration In a transistor amplifier, current degeneration obtained by use of an unbypassed emitter resistor. The arrangement results in virtually distortion-free amplification at a sacrifice in voltage gain.

emitter follower A transistor circuit in which the input signal is applied to the base, and the output signal is taken from the emitter resistor. Gain is always less than unity; output impedance is low.

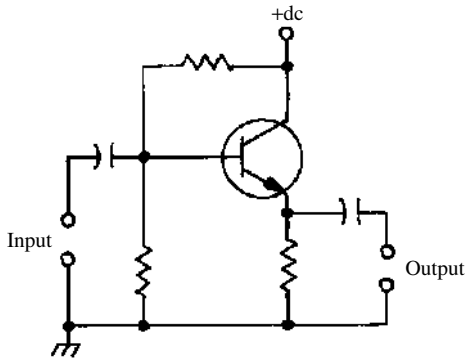

emitter follower

emitter-input circuit See COMMON-BASE CIRCUIT.

emitter junction See EMITTER-BASE JUNCTION.

emitter resistance Symbol, R_E. **1.** The resistance of the emitter electrode in a bipolar transistor. **2.** External resistance connected to a transistor's emitter terminal.

emitter stabilization In a common-emitter transistor stage, an emitter resistor that stabilizes the circuit against temperature variations.

emitter-to-base junction See EMITTER-BASE JUNCTION.

emitter voltage Symbol, V_E. The voltage at the emitter electrode of a bipolar transistor.

EMP, emp **1.** Abbreviation of ELECTROMAGNETIC PULSE. **2.** Abbreviation of *electromagnetic power.*

emphasis Modification of the amplitude-versus-frequency output or response of an audio circuit, for the purpose of optimizing signal intelligibility.

emphasizer An audio-frequency device with a specially tailored response, intended to maximize intelligibility of a voice.

Empire cloth Varnished cambric used as an insulating sheet or tape.

empirical Observable; derived from experimentation.

empirical curve A curve plotted from data acquired from observations, tests, and calculations, rather than from mathematical laws or other theory.

empirical design The design of electronic circuits by cut-and-try methods and, to some extent,

5059F-pE-224-273 4/9/01 5:26 PM Page 257

through intuition arising from experience (i.e., practical as opposed to theoretical design).

empirical probability Probability estimated from experience and observations. This method is often used in quality-control and reliability procedures.

empty medium A computer storage medium, such as a magnetic tape or disk, that is ready to accept data (i.e., rather than being completely blank, it contains the signals necessary for processing the to-be-added data).

EMU, emu Abbreviation of ELECTROMAGNETIC UNIT(S).

emulator In computer engineering, a sophisticated device that substitutes for a similar device or stage in the computer, and thereby provides a basis for experimenting and troubleshooting without disturbing the equivalent part of the computer.

E_n Symbol for *voltage remaining at null.*

enable To initiate the operation of a circuit or device by applying a pulse or trigger signal.

enable pulse **1.** A pulse that initiates the operation of a circuit or device. **2.** A binary pulse that augments a write pulse to make a magnetic core change state.

enabling gate A digital device that regulates the length of a pulse for specialized use.

enameled wire Wire that is insulated by a thin coat of baked enamel. Commonly used in coil winding because the thin enamel allows for a maximum number of turns in a given volume for a given wire gauge.

encapsulant A material, such as potting resin, used to embed (encapsulate) a component, circuit, or device.

encapsulated circuit A component, circuit, or device embedded in plastic or wax (see ENCAPSULATION).

encapsulated component An electronic part that is embedded in plastic or wax (see ENCAPSULATION).

encapsulating material See ENCAPSULANT.

encapsulation The embedding of a circuit or component in a solid mass of plastic or wax. The mold or container remains as part of the assembly after the plastic or wax has solidified. Protects against the environment, and/or against the effects of physical vibration. Compare POTTING.

encephalogram See ELECTROENCEPHALOGRAM.

encephalograph See ELECTROENCEPHALOGRAPH.

enciphered facsimile Facsimile communications that have been rearranged or scrambled at the transmitting location so that it cannot be intercepted by a third party. A deciphering device is needed at the receiver end of the circuit.

enclosure **1.** A cabinet, case, or other housing for electronic equipment, such as a receiver, transmitter, or test instrument. **2.** A specially designed housing for a loudspeaker.

encode **1.** To convert signals or data into a desired (usually digital) form. Also called CODE. **2.** To equip a transmitter with a tone-producing device (encoder). **3.** To develop and apply an encoding system to a group of transceivers or transmitters of a communications network.

encoder **1.** An analog-to-digital or digital-to-analog converter. **2.** An electromechanical device for translating the angular position of a rotating shaft into a corresponding series of digital pulses. Also see SHAFT-ANGLE ENCODER. **3.** A device for encoding data (see ENCODE). **4.** A machine with a keyboard for printing characters that can be read by optical character recognition (OCR) equipment. **5.** A tone generator used as a receiver enabler in the transmitters of a communications network.

encoding **1.** The translation, either by a machine or by a human operator, of a spoken or written language into digital code. **2.** Any function performed by an ENCODER.

encryption The conversion of a signal from plain text, graphics, or other commonly recognizable form into a cipher. See also CIPHER. Compare DECRYPTION.

end-around carry In a computer, a carry produced in the most significant position, causing a carry into the least-significant position.

end-around shift In digital-computer operations, the transfer of characters from one end of a register to the other end. Also called LOGICAL SHIFT.

end bell **1.** The part of a motor housing that supports the bearing and protects internal rotating parts. **2.** A clamping part fastened to the back of a plug or receptacle. **3.** Either of the two frames of a transformer that contains the mounting lugs.

end bracket See END BELL, **2**.

end cell A cell intended for series operation in conjunction with a storage battery. As the voltage of the battery drops, the end cell can be added into the circuit.

end effect **1.** In a tapped coil, losses because of induced currents flowing in the inductance and distributed capacitance of the unused end of the coil. **2.** EDGE EFFECT in a capacitor. **3.** An effective capacitance at the ends of an antenna, resulting from air discharge. This lowers the resonant frequency slightly below that predicted by theory. The effect is exaggerated by the proximity of objects, such as trees and buildings, or when an antenna is placed close to the earth.

end effector The device or tool connected to the end of a robot arm (e.g., a gripper, screwdriver, drill, or soldering iron).

end-fed antenna An antenna whose lead-in or feeders are attached to an end of the radiator.

end feed A method of feeding electromagnetic fields to an antenna by connecting the transmission line to the end. Ordinarily, the antenna must be a multiple of 0.5 wavelength long for end feed to be effective.

5059F-pE-224-273 4/9/01 5:26 PM Page 258

end-fire antenna See END-FIRE ARRAY.

end-fire array Also called *end-fire antenna.* A phased antenna in which the greatest radiation/response takes place off one or both ends. The array consists of two or more parallel driven elements, all of which lie in a single plane. A typical system might consist of two half-wave dipoles, fed 90 degrees out of phase and spaced one-quarter wavelength apart in free space. This produces a unidirectional directivity pattern. Two elements might be driven in phase and spaced 1 wavelength apart, producing a bidirectional pattern. These systems show some power gain, in their favored directions, compared to a single half-wave dipole. The larger the number of elements, with optimum phasing and spacing, the greater the gain.

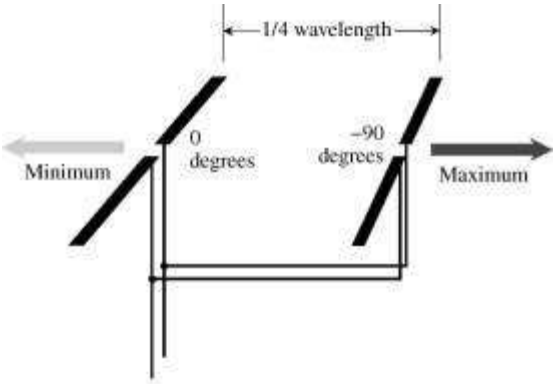

end-fire array

end-fire directivity In a directive antenna, beaming a signal along the plane of the antenna (i.e., off its ends).

end instrument A device capable of converting intelligence into electrical signals or vice versa, and that needs to be connected to only one terminal of a loop.

end item A final, completed product or component.

endless loop Also called *infinite loop.* A computer programming bug that causes the machine to go in an indefinite, and often useless, logical circle. For example, suppose that at line 180, the computer encounters the command GOTO 250, meaning "Go to line 250," but line 250 gives the command GOTO 180. Once the computer gets to line 180, it enters a loop in which nothing is accomplished, and from which the only escape is intervention by the operator (e.g., terminating the program).

end mark In digital-computer operations, a signal or code indicating the close of an information unit.

endodyne reception See ZERO-BEAT RECEPTION.

end-of-charge voltage For a rechargeable cell or battery, the voltage at full charge (i.e., just after disconnection of the charging apparatus and before use).

end-of-data mark A code or character signaling that all the data in a computer storage medium has been read or used.

end-of-discharge voltage For a rechargeable cell or battery, the voltage at the termination of a discharging cycle, immediately before the unit is taken out of use and the charging apparatus is connected.

end-of-field mark In computer operations, a "flag" code that signals when the end of a field has been reached.

end-of-file mark In computer operations, a code instruction that signals when the last record in a file has been read.

end-of-line unit The last device or circuit in a chain.

end-of-message character A character or code signaling the end of a message.

end-of-run The end of a computer program or program run, as indicated by the program.

end-of-tape mark A physical marker at the end of a magnetic tape (e.g., something that can be sensed by methods other than that used to read the tape).

end-of-tape routine A computer program that handles the processing needed after the last record on a reel of magnetic tape has been reached.

end-on armature A relay armature that moves in the direction of the core's axis.

end-on directional antenna See END-FIRE ANTENNA and END-FIRE ARRAY.

endoradiograph An X-ray picture, derived or enhanced by the introduction of substances into the body.

endoradiosonde A tiny pill-enclosed transducer and radio transmitter for sensing physiological conditions in the stomach and intestines; it transmits corresponding signals to instruments outside.

endothermic reaction A chemical reaction producing cold (i.e., one in which kinetic energy is lost). Compare EXOTHERMIC REACTION.

end-plate magnetron A magnetron whose oscillation intensity is increased by a positive and a negative end plate, the electric field between them causes the electrons to move axially while spinning.

end point **1.** For a precision potentiometer, the shaft position between the last and first positions of measurement. **2.** The point at which the useful life of a device can be considered spent. **3.** The point at which a time interval or operational sequence ends. **4.** The end-point voltage of a primary or Edison storage cell. **5.** For a

5059F-pE-224-273 4/9/01 5:26 PM Page 259

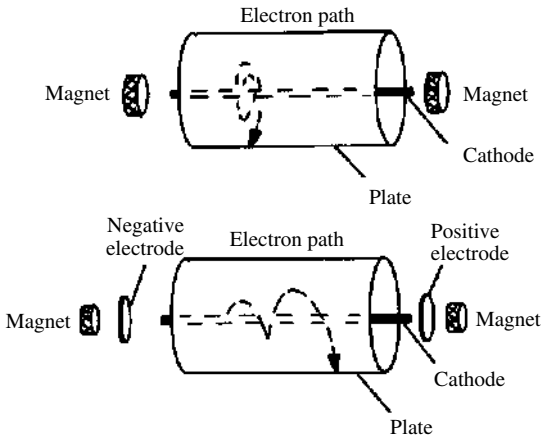

end-plate magnetron

lead-acid storage cell, the specific-gravity value of the electrolyte at which the cell is considered in need of recharging (nominally 1.150 to 1.175).

end-point control A form of quality control in which the end item is checked for defects.

end-point sensitivity A means of expressing the sensitivity of a meter or other indicating device: the ratio, in decibels, between the input signal required to produce a full-scale or maximum reading and the smallest detectable input signal.

end-point voltage The voltage of a battery or cell terminal when the device is no longer useful.

end resistance In a rheostat or potentiometer, the resistance between the wiper and the end terminal when the wiper is set to the end point of the device.

end-resistance offset In a potentiometer, the resistance between the wiper and an end terminal when they are in contact.

end-scale deflection See END-SCALE VALUE.

end-scale value For an indicating meter, the electrical quantity indicated at the last graduation on the scale.

end section Either the input or output section of a multisection filter.

end setting **1.** The fully clockwise or fully counterclockwise setting of a rotatable control. **2.** The minimum or maximum setting of a control.

end shield In a magnetron, a shield that confines the space charge to the interaction space.

end spaces The cavities at either end of the anode block in a multicavity magnetron tube; they terminate all the anode-block cavity resonators.

end use The intended application of a circuit or device.

energize To apply operating power and input signals to a circuit or device.

energized The condition of a circuit or device that is powered or excited.

energy Symbol, W. Common units: joule, watt-hour, and kilowatt-hour. **1.** The capacity for doing work. Some common forms of energy are electrical, mechanical, and chemical. Also see CONSERVATION OF ENERGY, KINETIC ENERGY, and POTENTIAL ENERGY. **2.** The work performed by electric power. The unit used by utility companies is the kilowatt-hour (kWh), equal to the product Pt, where P is power in kilowatts and t is the period (hours) during which the power is used.

energy-band diagram A diagram depicting the various energy levels within the atom of a conductor, semiconductor, or insulator.

energy barrier The natural potential gradient across a semiconductor junction. In the absence of an applied voltage, the gradient, not measurable from the outside, prevents total interaction between the n- and p-type materials.

energy cell **1.** A usually small primary or secondary cell—especially the kind used in hearing aids and electronic watches. **2.** A capacitive-type direct-current (dc) source (see ENERGY-STORAGE DEVICE, **2**).

energy consumption **1.** The conversion of energy from one form to another by a component, circuit, system, or machine, in the process of performing some useful task. **2.** The amount of energy involved in the process defined in **1**.

energy conversion The transformation of energy from one form to another. See also CONSERVATION OF ENERGY and ENERGY TRANSFORMATION.

energy-conversion device A component, circuit, system, or machine that changes energy from one form to another. See also CONSERVATION OF ENERGY.

energy density **1.** For an energy-producing cell, such as an electrochemical cell, the ratio of available energy to cell mass. It is expressed in joules per gram or in watt-hours per kilogram. **2.** For an energy-producing cell, the ratio of available energy to cell volume. Expressed in joules per cubic centimeter or in watt-hours per cubic centimeter.

energy gap In the energy-level diagram for a semiconductor or insulator, the region between valence and conduction bands representing the minimum energy required to make the electron pass from the valence to the conduction band (i.e., to become a current carrier). Also called *forbidden energy band.*

energy level A constant-energy state, such as one of the energy levels of an electron in an atom.

energy-level diagram **1.** A diagram showing the energy levels (in electronvolts) of electrons in the various shells of an atom. **2.** A diagram showing variations in power that correspond to variations in current in a channel.

5059F-pE-224-273 4/9/01 5:26 PM Page 260

energy loss In any system, the energy that is unavoidably lost (i.e., it is not converted into useful work). Also see ENTROPY and POWER LOSS.

energy of a charge The energy level of an electrostatic charge. It is $QV/2$ ergs, where Q is the quantity of electricity in coulombs, and V is the potential in volts.

energy product An expression of the effectiveness of a permanent magnet. The magnetic flux density is multiplied by the magnetic field strength to obtain the energy product, specified in gauss-oersteds.

energy redistribution A mathematical process for determining the effective duration of an irregular pulse. The instantaneous power output of the irregular pulse is integrated from the start to the end of the pulse. Then, a rectangular pulse is constructed having the same peak power and the same total energy content (area under the power curve). The length of this rectangular pulse is considered to be the effective duration of the irregular pulse.

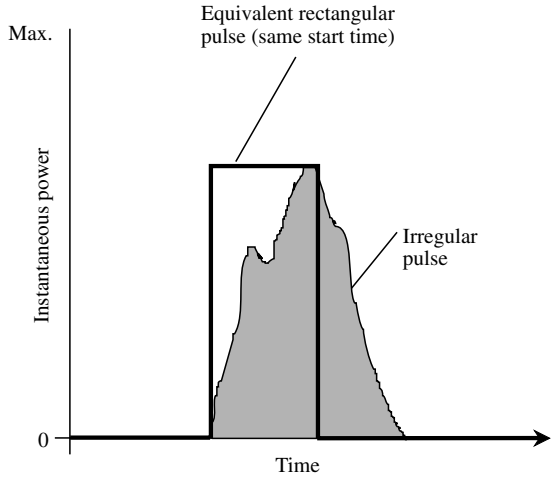

energy redistribution

energy state The condition of an electron, as expressed by its position and velocity, with respect to the position and velocity of other electrons.

energy-storage capacitor A usually high-value capacitor used primarily to store the charge used to fire a lamp (as in a photoflash unit), create a spark discharge (as in electronic ignition), or perform some similar function.

energy-storage device **1.** See CAPACITOR. **2.** A small, electrochemical component offering very high capacitance (e.g., several farads) and low leakage current (less than 1 pA). It has a number of applications, including long-interval timing, power-supply filtering, and energy-cell service. Its active ingredients are compressed powders.

energy stored in capacitor The electrical energy in the field between the plates of a charged capacitor. In this instance, energy $W = CE^2/2$, where W is the energy in joules, C is the capacitance in farads, and E is the voltage in volts.

energy stored in inductor The magnetic energy in the field surrounding an inductor carrying current. In this instance, energy $W = LI^2/2$, where W is the energy in joules, L is the inductance in henrys, and I is the current in amperes.

energy transformation The conversion of one form of energy into another, as with a transducer.

engine analyzer An instrument for checking the performance of an automobile engine. In addition to measuring voltage and resistance throughout a car's electrical system, the instrument measures engine speed, cam dwell angle, and other factors.

engineer **1.** A person who designs machines, circuits, and other devices. **2.** A person who develops methods of utilizing machines, circuits, or other devices more efficiently, or for new applications. **3.** To design or implement an apparatus.

engineering The science of applying scientific laws to technical problems and designing practical devices. Also see ELECTRICAL ENGINEER and ELECTRONICS ENGINEER.

enhanced-carrier demodulation A method of reducing distortion in the demodulation of amplitude-modulated (AM) signals. A properly phased and synchronized local carrier is added to the signal in the demodulator.

enhancement mode Operation characteristic of an ENHANCEMENT-TYPE MOSFET.

enhancement-type MOSFET A metal-oxide semiconductor field-effect transistor (MOSFET) in which the channel directly under the gate electrode is widened (enhanced) by a negative gate voltage in the n-channel unit or by a positive gate voltage in the p-channel unit. Compare DEPLETION-TYPE MOSFET.

ENIAC An electronic computer developed at the University of Pennsylvania. The name is an acronym for *Electronic Numerical Integrator And Calculator.*

ENIC Abbreviation of *voltage negative-impedance converter.*

enrichment In a mixture of different isotopes of a given element, the increase in the relative concentration of one particular isotope.

ensemble **1.** A collection of devices that functions together as a complete unit. **2.** In music recording, the ability of all the musicians to hear each other during the session. **3.** A set of random mathematical functions, all starting at the same point.

ENSI Abbreviation of EQUIVALENT-NOISE-SIDEBAND INPUT.

entladungsstrahlen Ultraviolet radiation emitted by electric arcs. At atmospheric pressure, the wavelength is approximately 40 to 90 nanometers,

5059F-pE-224-273 4/9/01 5:26 PM Page 261

depending on the arc length. The term is derived from the German word for *discharge rays.*

entrainment Providing a path for gases to escape from an electrochemical cell or battery.

entrance delay In security applications, a delay that allows authorized people time to leave the protected area after activating the alarm system, or to deactivate the system after entering the protected area. The delay is approximately 30 to 45 seconds.

entropy **1.** In all closed physical systems, the measure of energy wasted. According to the second law of thermodynamics, for example, supplied heat can never be converted entirely into work. **2.** In communications, the amount of information in a message, defined as the base-10 logarithm of the number of equivalent messages that can exist. **3.** A natural process in which the energy in the universe tends to become more uniformly distributed with the passage of time.

entropy coding A form of digital encoding that minimizes redundancy, thereby increasing the amount of data in a given amount of memory or storage space.

entry **1.** A unit of computer input or output information. **2.** A data item in a table or list. **3.** A computer source program statement. **4.** In a computer program, the address of the first instruction.

entry condition A condition that must be specified before a computer program is run (e.g., establishing operand values).

entry-level system **1.** The least-sophisticated computer that will perform the things that a user requires. **2.** A simple electronic or computer system (e.g., an amateur radio transciever or personal computer, intended for ease of operation, and from which the user expects to upgrade to a more powerful system at a later date).

entry point In a computer program, the first instruction to be implemented, or a point during the run when data can be entered.

envelope **1.** On a graph, the imaginary line joining successive signal peaks. In the graph for an amplitude-modulated signal, the line reproduces the modulating wave. **2.** The enclosure of a transistor or integrated circuit. **3.** The glass shell of a vacuum tube.

envelope delay In a tuned amplifier, time delay introduced in the envelope of a modulated signal by varying the phase of the envelope with the modulating frequency. This delay varies directly with the amount by which the sidebands shift, with respect to the carrier frequency.

enveloped file A computer file with labels permitting it to be handled by a computer of a type different from that used to make the file.

environmental conditions See ENVIRONMENTAL FACTORS.

environmental factors Aspects of the space immediately surrounding and sometimes influencing electronic equipment. Examples: altitude, dust, light, moisture, noise, pressure, shock, temperature, and vibration.

environmentally sealed Sealed against the effects of adverse environmental factors.

environmental test chamber See CLIMATE CHAMBER.

E_o **1.** Symbol for OUTPUT VOLTAGE. **2.** Symbol for *zero reference voltage.*

EOF Abbreviation of *end of file.*

EOL Abbreviation of *end of line.*

EOLM Abbreviation of *electro-optical light modulator.*

EOR Abbreviation of END OF (program) RUN.

EOS Abbreviation of *electro-optical system(s).*

EOT Abbreviation of *end of tape.*

EOTS Abbreviation of *electro-optical tracking system.*

E_P **1.** Symbol for PLATE VOLTAGE. **2.** Symbol for PEAK VOLTAGE.

EP Abbreviation for EXTENDED PLAY.

ephemeris time Time measured with respect to the orbit of the earth around the sun. Initiated in the year 1900 AD.

epipolar navigation A scheme for position sensing and navigation that uses an artificially intelligent vision system. Allows calculation of position and velocity, based on changes in the visualized direction, size, and shape of an object whose actual location, size, and shape are precisely known. It is used in some mobile robots.

episcotister A mechanical light beam modulator. The device consists of a series of rotating disks having transparent and opaque sections that alternately interrupt and pass the light beam at an audio-frequency rate.

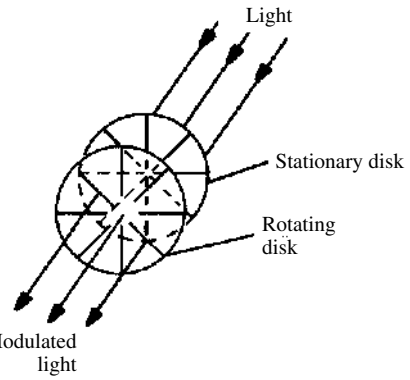

episcotister

epitaxial Pertaining to, or having the property of, EPITAXY.

epitaxial deposition The tendency of certain materials to grow on a semiconductor substrate under certain conditions.

5059F-pE-224-273 4/9/01 5:26 PM Page 262

epitaxial device A semiconductor device built by means of EPITAXIAL GROWTH.

epitaxial film A film of single-crystal semiconductor material deposited onto a single-crystal semiconductor substrate.

epitaxial growth Growing monocrystalline silicon on a silicon wafer by precipitating silicon from a gas in which the wafer is placed. Epitaxy is secured between the precipitate and the wafer.

epitaxial layer A semiconductor layer exhibiting epitaxy. Also see EPITAXIAL GROWTH.

epitaxial mesa transistor See DOUBLE-DIFFUSED EPITAXIAL MESA TRANSISTOR.

epitaxial planar transistor A planar transistor having an epitaxially grown collector on a low-resistivity substrate, and a diffused base and emitter.

epitaxial process See EPITAXIAL GROWTH PROCESS.

epitaxial transistor A transistor in which an epitaxial layer (into which a base region later is diffused and an emitter region alloyed) is grown on the face of a semiconductor wafer, which serves as the collector. Also see DOUBLE-DIFFUSED EPITAXIAL MESA TRANSISTOR.

epitaxy The condition in which atoms in a thin film of single-crystal semiconductor material grown on the surface of the same kind of wafer continue their characteristic alignment. Also see EPITAXIAL GROWTH.

E plane The plane of an antenna containing the electric field.

E plane bend See E BEND.

E-plane tee junction A waveguide junction whose structure changes in the plane of the electric field.

epoxy resin A synthetic resin used to encapsulate electronic equipment, or as a cement. Epoxy resins are based on ethylene oxide or its derivatives.

EPROM Abbreviation of *erasable programmable read-only memory.*

EPU **1.** Abbreviation of *electronic power unit.* **2.** Abbreviation of *emergency power unit.*

Eq **1.** Abbreviation of *equation.* **2.** Abbreviation of EQUALIZER or EQUALIZATION.

equal alternations Positive and negative half-cycles of a wave that have identical shape and amplitude.

equal-energy source A light source that has a constant emission rate (energy per unit wavelength).

equal-energy white The color of light emitted by a source radiating equally the wavelengths of the visible-light spectrum.

equal heterodyne In a beat-frequency system, the condition in which the outputs of the two heterodyning oscillators are identical.

equality circuit A logic circuit that, when two numbers are put into it, outputs logic 1 if the numbers are equal, and logic 0 if the numbers are not equal.

equalization **1.** The use of an EQUALIZER to make the frequency response of a line, amplifier, or other device uniform over a given frequency range. **2.** The use of an EQUALIZER to modify the frequency response of a line, amplifier, or other device.

equalizer A circuit or device, such as a compensated attenuator, that allows the user to tailor the frequency response of a line, amplifier, or other device. Sometimes used in sophisticated high-fidelity stereo amplifier systems, to obtain a desired bass/midrange/treble frequency output.

equalizer circuit breaker A form of circuit breaker that trips in the event of unbalance in an electrical system.

equalizing current A current that flows in the circuit of two compound generators connected in parallel.

equalizing network A circuit used to equalize a line.

equalizing pulses In a television signal waveform, several pulses (preceding and following the vertical sync pulse and having a repetition rate of twice the power-line frequency) that start the vertical retrace at the correct instant for good interlace.

equal-loudness curves See AUDIBILITY CURVES.

equal vectors Vectors having the same magnitude and the same direction. They do not necessarily originate at the same point. Compare IDENTICAL VECTORS.

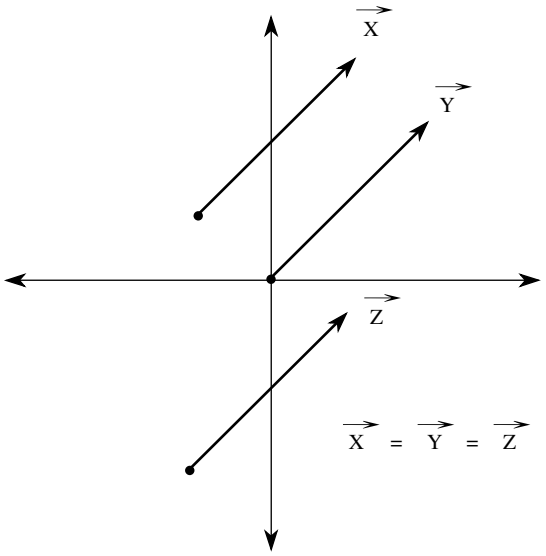

equal vectors

equation solver A (usually analog) computer for solving linear simultaneous equations or for determining the roots of polynomials.

5059F-pE-224-273 4/9/01 5:26 PM Page 263

equatorial orbit A satellite orbit that lies in the plane of the earth's equator.

equiphase surface Any surface in a wave, over which the field vectors at a particular instant have either 0° or 180° phase difference.

equiphase zone The space region in which two radionavigation signals show no phase difference.

equipment **1.** Collectively, apparatus or components designated for a specific purpose (e.g., *radio equipment*). **2.** A functional electronic unit, such as a test instrument, receiver, or memory unit.

equipment chain A system consisting of series-connected circuits or devices.

equipment ground An electrical ground connection intended to reduce the chances of electric shock. An equipment ground does not necessarily constitute a good radio-frequency ground; it serves only to eliminate potential differences among the individual units in a system.

equipment life The period during which electronic equipment functions according to specifications; it is terminated at an END POINT.

equipment test A usually preliminary, qualifying test of electronic equipment.

equipotential Having a potential difference of zero; being at the same voltage level.

equipotential line Between two charged plates, the locus (an imaginary line) of points having the same potential, with respect to the plates.

equipotential surface A surface on which all points have the same electrical potential.

equisignal Pertaining to signals having equal intensity.

equisignal localizer See TONE LOCALIZER.

equisignal radio-range beacon For aircraft guidance, a radio-range beacon that transmits two distinct signals that are received by aircraft with equal intensity only in certain directions.

equisignal surface The "surface" around a transmitting antenna formed by points of equal field intensity.

equisignal zone The region in which two radionavigation signals have identical amplitude.

equivalence The condition existing when one network can be substituted for another without disturbing currents, impedances, and voltages at the terminals.

equivalent absorbing power See EQUIVALENT STOPPING POWER.

equivalent absorption Unit, sabin. The rate at which a surface absorbs sound energy.

equivalent binary digits For a given decimal number or specific character, the corresponding binary digits (bits).

equivalent bit rate The number of binary digits (bits) that can be sent in a given unit of time, such as one second, in a digital communications system.

equivalent capacitance The value of a single lumped capacitance, that would cause the same action as the capacitance distributed throughout a circuit.

equivalent circuit A circuit that has the same overall current, impedance, phase, and voltage relationships as a more-complicated counterpart that it usually replaces for analysis.

equivalent component density For a circuit in which discrete components are not used or are not evident, the volume of that circuit divided by the number of discrete components that would be required if the circuit used them.

equivalent conductivity The conductivity of a solution that contains 1 gram equivalent of the solute in the space between electrodes 1 centimeter apart.

equivalent dark-input current For a photoelectric device, the illumination required for an output current equal to the DARK CURRENT of the device.

equivalent decrement The value of decrement in a damped wave that would result in the same amount of interference at a receiver as the interference caused by the sidebands of an amplitude-modulated signal.

equivalent delay line A comparatively simple network, such as a resistance-capacitance (RC) circuit, that will provide the attenuation and phase characteristics of an ideal delay line.

equivalent delta In a three-phase system, a delta-connected circuit that is equivalent to a given wye-connected circuit, from the standpoint of impedance and phase. Also see DELTA CONNECTION and WYE CONNECTION. Compare EQUIVALENT WYE and WYE-EQUIVALENT CIRCUIT.

equivalent differential input capacitance For a differential amplifier, the equivalent input capacitance (see EQUIVALENT CAPACITANCE) at one input (inverting or noninverting) when the opposite input is grounded.

equivalent differential input impedance For a differential amplifier, the equivalent input impedance at one input (inverting or noninverting) when the other input is grounded.

equivalent differential input resistance For a differential amplifier, the equivalent input resistance at one input (inverting or noninverting) when the other input is grounded.

equivalent equations Two equations for an unknown that have the same root.

equivalent four-wire system A two-wire line over which full-duplex operation is obtained by use of frequency division.

equivalent height See VIRTUAL HEIGHT.

equivalent impedance **1.** The value of a single lumped impedance that would cause the same action as the impedance distributed throughout a circuit. **2.** An impedance that draws current of the same strength and phase as that drawn by an impedance it replaces.

equivalent inductance The value of a single lumped inductance that would cause the same

5059F-pE-224-273 4/9/01 5:26 PM Page 264

action as the inductance distributed throughout a circuit.

equivalent input offset current For a differential amplifier, the difference between currents flowing into the inverting and noninverting inputs when the output voltage is zero.

equivalent input offset voltage For a differential amplifier, the input voltage required to reduce the output voltage to zero.

equivalent input wideband noise voltage For a differential amplifier, the ratio V_o/G_v, where V_o is the root-mean-square (rms) output-noise voltage, and G_v is the direct-current (dc) voltage gain.

equivalent length of antenna **1.** The electrical length of an antenna, as measured in degrees or wavelengths. **2.** The free-space length of an antenna. **3.** The length d (in feet) of a quarter-wave resonant antenna at a specific frequency f (in megahertz), given by the formula $d = 234/f$. **4.** The length d (in feet) of a half-wave resonant antenna at a specific frequency f (in megahertz), given by the formula $d = 468/f$.

equivalent length of electric dipole The distance, measured in a straight line, separating the points that represent the charge centers of an electric dipole.

equivalent length of feed line The electrical length of a feed line as measured in degrees or wavelengths. Generally, this is equal to $1/v$ times the line length in free-space wavelengths, where v is the VELOCITY FACTOR of the line, expressed as a fraction between 0 and 1.

equivalent length of magnet The distance separating the poles of a magnet. In a bar magnet, these poles are not exactly at the ends. The actual equivalent length is about 83% of the length of the bar magnet.

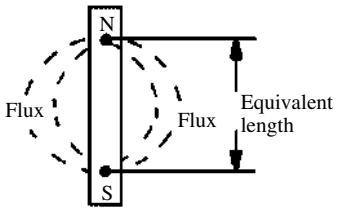

equivalent length of magnet

equivalent loudness The actual intensity, in decibels, of a given sound whose apparent loudness changes with frequency.

equivalent network A network that can replace a more-complex network for analysis purposes.

equivalent noise input The value of modulated luminous flux that, when applied to a photoelectric device, produces a root-mean-square (rms) output current equal to the device's rms noise current.

equivalent-noise-sideband input Abbreviation, **ENSI.** A specification for receiver noise characteristics. Numerically, $ENSI = 0.3E_s(P_n/P_s)^{1/2}$, where E_s is the voltage of an unmodulated radio-frequency (RF) carrier applied to the receiver, P_n is the resulting noise-output power of the receiver (measured with an rms meter), and P_s is the noise-output power measured with the RF signal 30% amplitude modulated at 400 Hz with a 400-Hz bandpass filter inserted between the receiver output terminals and the meter.

equivalent noise temperature For a component having resistance, the temperature (degrees absolute) at which a theoretically perfect resistor having the resistance of the component would generate the same noise the component generates at room temperature.

equivalent optics The analogy between certain optical lenses and prisms and the electrostatic deflection of an electron beam. Thus, when the upper deflecting plate in an electrostatic deflection system is made negative and the lower plate is positive, the beam is deflected downward, like horizontal light rays bent by a prism. When both plates are made equally negative, the beam converges to a point, as light rays do when they pass through a double convex lens. When both plates are made equally positive, the beam spreads out, as do light rays passing through a double concave lens.

equivalent permeability The permeability of a component made of certain materials, compared with that of a component having the same reluctance, shape, and size, but made of different materials.

equivalent reactance The value of a single lumped reactance that would cause the same action as the reactance distributed throughout a circuit.

equivalent resistance The value of a single lumped resistance that would cause the same action as the resistance distributed throughout a circuit.

equivalent series and parallel circuits Series and parallel circuits in which current, voltage, phase, and frequency relationships are identical. Any series circuit can be transformed into an equivalent parallel circuit.

equivalent series resistance The equivalent resistance acting in series with circuit components.

equivalent sine wave A sine wave of the same frequency and effective voltage as a given wave.

equivalent stopping power For a material in the path of radioactive particles, the thickness of the material that produces the same energy loss as that produced by one centimeter of air.

equivalent time The effective duration of some phenomenon, such as a pulse.

equivalent volt See ELECTRONVOLT.

equivalent wye In a three-phase system, a wye-connected circuit that is equivalent to a given delta-connected circuit from a standpoint of impedance and phase. Also see DELTA

5059F-pE-224-273 4/9/01 5:26 PM Page 265

CONNECTION, EQUIVALENT DELTA, WYE CONNECTION, and WYE-EQUIVALENT CIRCUIT.

equivalent Y See EQUIVALENT WYE.

equivocation A condition in which the meaning of data depends on certain parameters.

ER Abbreviation of ECHO RANGING.

Er Symbol for ERBIUM.

E_r Symbol for voltage drop across a resistance.

erasable storage In computer operations, any storage medium holding information that can be erased.

erasable PROM A programmable read-only memory (PROM) from which the data can be removed, usually by exposure to ultraviolet light. Also see PROM.

erase To obliterate or remove a signal, especially a recorded one, as in the erasure of recorded material from a magnetic tape or the data from a computer disk.

erase button A pushbutton that actuates the circuit supplying a signal that erases stored material (as the display on a storage oscilloscope).

erase current In an electromagnetic erase head, the current flowing through the coil of the head. In most instances, it is a high-frequency current (usually the regular bias current), but it can be as low as 60 Hz, as long as the speaker does not respond to what remains of it on the tape after erasure.

erase head In a tape recorder, a head used to erase recorded material from tape. It can contain a permanent magnet (see ERASE MAGNET) or an electromagnet whose coil carries erase current.

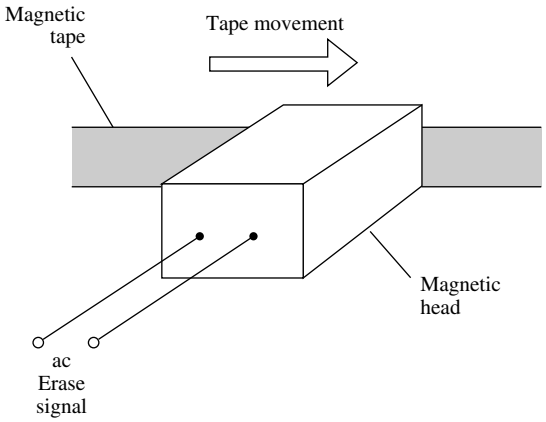

erase head

erase magnet In a tape recorder, a magnet used to erase recorded material from tape. Because the strength of the magnet is greater than that of the magnetized areas on the tape, erasure is complete (the tape left demagnetized).

erase oscillator In a tape recorder, a high-frequency (typically 30 to 80 kHz) oscillator that supplies erase current.

eraser See BULK ERASER.

erase signal A signal that causes recorded material to be erased (see ERASE and ERASE CURRENT).

erasing speed The rate at which successive storage elements are erased, as in a charge-storage tube.

erasure **1.** In tape-recording and digital-computer operations, the process of erasing a recorded signal (see ERASE). **2.** An erasure accomplished by the process described in 1, above.

erbium Symbol, Er. A metallic element of the rare-earth group. Atomic number, 68. Atomic weight, 167.26.

E region See E LAYER.

e register In a computer, a register used in double-precision calculations.

E_r-E_y signal In color television, the resultant signal that is the difference between the original full-red and E_y signals.

ERG Abbreviation of ELECTRORETINOGRAPHY.

erg Abbreviation, *e.* A unit of work. It is the work done by a force of one dyne (10^{-5} newton) acting through a distance of one centimeter.

ergograph An instrument used to measure and record work done by muscles.

ergometer An instrument for measuring energy consumed or work accomplished.

ergon See ERG.

E_{rms} Symbol for ROOT-MEAN-SQUARE VOLTAGE.

ERP Abbreviation of EFFECTIVE RADIATED POWER.

error **1.** In calculations and measurements, the difference between a true value and an observed or calculated value. **2.** In electronic circuits, especially those of automatic control systems, the difference between a required (or reference signal) level and the actual signal level. **3.** In communications, a discrepancy between the transmitted data and the received data.

error accumulation The adding-up of maximum possible error when measurements are repeatedly made. Generally, the maximum plus-or-minus error per measurement is multiplied by the number of measurements.

error amplifier An amplifier for boosting error current or voltage.

error-checking code An error-correcting or error-detecting code.

error-correcting code An error-detecting code that, in addition to the function indicated by its name, indicates the correct code.

error-correcting telegraph A digital communications system in which an improbable or incorrect character is not accepted. In the event that such a character is received, the receiver instructs the transmitter to send that character again.

error correction **1.** The restoration of mutilated, corrupted, or missing data in a digital system,

5059F-pE-224-273 4/9/01 5:26 PM Page 266

especially in magnetic data storage media, such as tapes and disks. **2.** In digital communications, any scheme in which the receiver (destination) automatically eliminates (to the greatest possible extent) errors in data from a transmitter (source). For example, the destination can instruct the source to repeat questionable characters or words.

error-correction routine In computer operations, a series of programmed instructions to detect and correct errors in files. A common example is a spell-checking program for word-processed document files.

error current An error signal that is a feedback current for automatically correcting a system.

error curve A bell-shaped curve that describes the distribution of errors in measurement around a true value.

error-detecting code In computer operations, a character-coding system that ensures that an impossible combination (forbidden characters) will be generated by an error (for error detection).

error-detecting routine A computer program that detects errors by checking the validity of data.

error detection and feedback In computer operations, a system in which an error (sensed by an error-detecting code) automatically generates a request to repeat the suspect signal.

error detector A sensor that responds to an error signal by delivering a signal proportional to the error.

error diagnostics As performed by a compiler, detecting and indicating the presence of errors in source language statements.

error interrupt A computer program halt caused by a software or hardware error and accompanied by a display of what has happened.

error list As produced by a compiler, a list of source language statement faults.

error message During a computer program run, a statement (displayed on a peripheral) of what is in error.

error of measurement The positive or negative difference between the value of an actual measurement and the true (or most probable) value.

error range For a data item, the range of values over which it will cause an error.

error rate In data transmission, the ratio of errors transmitted to the data transmitted.

error-rate damping Damping that involves adding to an error signal another signal that is proportional in rate of change.

error ratio **1.** In a received message, the number of incorrect characters divided by the total number of characters. Can be represented as a fraction between 0 and 1 or as a percentage by multiplying the fraction by 100. **2.** A measure of distortion for digital signal communications. The number of inaccurately received bits divided by the total number of received bits.

error routine A computer program segment that is input when an error is detected so that an appropriate action is taken (correct the error, repeat the process, etc.).

error-sensing circuit A circuit that samples the output current or voltage of a power supply, amplifier, or control system, compares this output with a standard value, and delivers a feedback (correction) signal whose amplitude is proportional to the difference (error).

error signal In a servo system, an output signal whose value is proportional to the difference between the actual operating quantity of the system and a standard reference quantity. The signal is fed back to the input of the system for automatic correction.

error tape In data processing, a record tape designed and used for storing errors for subsequent study.

error voltage An error signal that is a feedback voltage for automatically correcting a system.

Es Symbol for EINSTEINIUM.

Esaki diode See TUNNEL DIODE.

E scope See E DISPLAY.

escape character In computer operations, a character indicating that the next character belongs in a new group.

escapement A (usually oscillating) mechanical or electromechanical device that stores energy (often in a spiral spring) on one swing, and returns that energy on the next swing. Such a mechanism advances a shaft progressively in a clock or watch, and in some control equipment.

escape velocity **1.** The minimum velocity (about 25,000 miles per hour or seven miles per second) required for a space vehicle to completely escape the gravitational field of the earth. **2.** The minimum velocity required for a space vehicle to completely escape the gravitational field of a planet or star. **3.** The minimum velocity required for an electron to escape the electrical influence of an atomic nucleus.

escutcheon A usually decorative plate that frames an opening or covers a panel in a piece of equipment (e.g., the escutcheon of a radio tuning dial).

ESD Abbreviation of ENERGY-STORAGE DEVICE.

ESG Abbreviation of *electronic sweep generator.*

Esnault-Pelterie formula A formula for approximately calculating the inductance of a single-layer solenoidal coil:

$$L = 0.1008(a^2n^2)/(s + 0.92a)$$

where L is the coil inductance in microhenrys, a is the radius of the coil in inches, s is the length of the coil in inches, and n is the number of turns in the winding. The formula is accurate to 0.1 percent for all values of $2a/s$ between 0.2 and 1.5.

ESS Abbreviation of *electronic switching system.*

EST Abbreviation of EASTERN STANDARD TIME.

esu Abbreviation of ELECTROSTATIC UNIT(S).

ET Abbreviation of EPHEMERIS TIME.

5059F-pE-224-273 4/9/01 5:26 PM Page 267

ETC Abbreviation of *electronic temperature control.*

etchant Any substance such as cupric chloride, ferrous chloride, or hydrochloric acid, used in etching.

etched circuit A circuit produced by etching the metallic coating of a substrate to provide the required pattern of conductors and terminals to which discrete components are soldered.

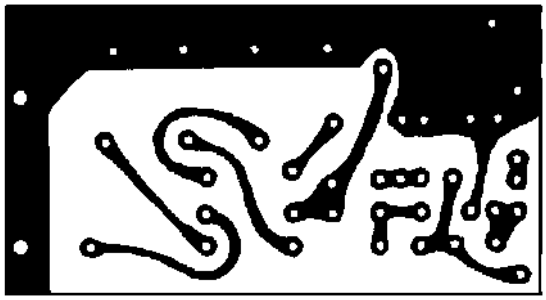

etched circuit

etch factor The ratio of the depth to the width of an etched track in an etched circuit.

etching **1.** Chemically eating away a metal to form a desired pattern, such as an etched circuit. **2.** Thinning a quartz-crystal plate by slowly eroding one or both of its faces with hydrofluoric acid to fine-tune the resonant frequency.

ET-cut crystal A piezoelectric plate cut from a quartz crystal at an angle of +66°, with respect to the z-axis. Also see CRYSTAL AXES and CRYSTAL CUTS.

ether **1.** Also called *luminiferous ether.* A nonviscous fluid once thought to fill space, convey waves (radio, light, etc.), and sustain fields. **2.** A volatile liquid occasionally used in electronics as a solvent [e.g., ethyl oxide $(C_2H_5)_2O$].

ether drift The postulated motion between a material body and the ether (see ETHER, **1**). The concept was checked by Michelson and Morley, who failed to find that the earth moves relative to the ether. This eventually led to scientific rejection of the so-called *ether theory* of the propagation of light.

ethical slave A machine, especially a smart robot, that is treated in the manner of a slave, based on the notion that a machine cannot have "feelings." Some researchers fear that the use of ethical slaves could lead to technological nightmares. For example, robots might be used as soldiers in a marauding offensive army; the commanders could rationalize that there is nothing immoral about the war because there is no loss of life on their side.

E transformer A differential transformer whose primary is wound on the center leg of an E core, the secondaries being wound on the outer legs.

Ettinghausen effect A phenomenon somewhat like the HALL EFFECT. It occurs when a metal strip, carrying current longitudinally, is placed into a magnetic field perpendicular to the plane of the strip: corresponding points on opposite edges of the strip exhibit different temperatures.

Eu Symbol for EUROPIUM.

eudiometer **1.** An instrument for measuring the amount of oxygen in the air. **2.** An instrument for analyzing gases.

eureka **1.** See CONSTANTAN. **2.** The ground transponder beacon in the British rebecca-eureka radar navigational system (see REBECCA-EUREKA SYSTEM).

europium Symbol, Eu. An element of the rare-earth group. Atomic number, 63. Atomic weight, 151.96.

eutectic **1.** A form of reaction in which mixed liquids solidify when cooled. **2.** The solid substance resulting from a reaction as defined in **1**.

eutectic alloy A metallic alloy with a specific melting point, made via eutectic process.

eutectic bond A connection between two dissimilar metals, facilitated by a third metal alloyed, via eutectic process, to the adjoining faces.

eV Symbol for ELECTRONVOLT.

evacuation The removal of air or other gases from a tube or chamber, specifically, the envelope of a vacuum tube that houses the internal elements.

evaporation **1.** A technique for electrically depositing a film of a selected metal on a metallic or nonmetallic surface. A filament of the metal to be deposited is heated by an electric current in a vacuum chamber, which makes filament particles travel to the (nearby) object to be coated, where they condense as a film. In an alternate method, a piece of the metal to be deposited is laid on or wrapped around a filament of some other metal. **2.** Electron emission by a hot cathode.

evaporation theory The theory that electrons will acquire sufficient escape velocity to leave a material when the energy acquired by (or imparted to) the electron exceeds the work function of the material. Also see WORK FUNCTION.

E vector The vector that represents the electric component of an electromagnetic wave.

even-even nucleus An atomic nucleus containing an even number of protons and an even number of neutrons. An example is the alpha particle, or helium nucleus, which contains two protons and two neutrons.

even harmonic In a complex waveform, an even-numbered multiple of the fundamental frequency. Compare ODD HARMONIC.

even line In a television picture, an even-numbered member of the 262.5 horizontal lines scanned by the spot in developing the even-line field. Compare ODD LINE.

even-line field On a television screen, the complete field obtained when the spot has traced all

5059F-pE-224-273 4/9/01 5:26 PM Page 268

the even-numbered lines. Compare ODD-LINE FIELD.

even parity check A check to verify the presence of an even number of ones or zeros in a group of bits.

event An occurrence that affects the state of a computer file.

event counter Any device that measures the number of specified events taking place within a certain interval of time.

evolution Extracting a root of a number (e.g., square root, cube root, etc.).

E wave In microwave operations, the transverse magnetic (TM) wave. Also see WAVEGUIDE MODES.

EWR Abbreviation of EARLY-WARNING RADAR.

EWS Abbreviation of *early-warning system.*

E_X **1.** Symbol for voltage drop across a reactance. **2.** Symbol for EXCITATION ENERGY.

exa- Symbol, E. A prefix meaning 10^{18} (International System of Units).

exalted-carrier reception In radio reception, overcoming the effects of selective fading by maintaining the carrier at a high amplitude. This is accomplished before demodulation by removing the carrier from an amplitude-modulated or phase-modulated signal, amplifying it, and reinserting it at a higher amplitude with the sidebands.

exc **1.** Abbreviation of EXCITER. **2.** Abbreviation of EXCITATION.

except gate A logic gate that delivers an output pulse when an input pulse is present at one or more of a set of input terminals, and absent from one or more of another set of input terminals. Also called *exclusive-OR element.*

excess charge The amount of overcharge for a storage battery.

excess conduction In a semiconductor, current conduction by excess electrons.

excess electron **1.** An electron that, when introduced into an atom, results in a negative ion. **2.** An electron resulting from the addition of a donor impurity to a semiconductor substance.

excess meter A meter that integrates the amount of power in excess of some predetermined level.

excess minority carriers The number of minority carriers in excess of the normal equilibrium number in a semiconductor material.

excess modified index of refraction Symbol, M. For waves transmitted through a refracting medium, a modified index of refraction greater than unity.

excess noise Electrical noise caused by current in a semiconductor material.

excess sound pressure Unit, dyne/cm^2. In a medium conducting sound waves, the quantity $P_t - P_s$, where P_t is total instantaneous pressure at a given point in the medium, and P_s is static pressure in the absence of the sound waves.

excess-three code A computer code derived from binary notation by adding binary three (i.e., 0011) to each four-bit group. Thus, decimal seven is 1010 in the code (it is 0111 in binary). Unlike the binary representation for zero, the excess-three representation (0011) contains two ones, a feature that distinguishes actual zero from a machine fault.

exchange **1.** To reverse the contents of two memory banks. For example, if the memory banks are called A and B, an exchange is the placing of the contents of memory A into memory B, and the placing of the contents of memory B into memory A. The original contents are removed. **2.** A two-way sequence of data transmissions. **3.** A designated location in a telephone circuit.

exchange line A telephone line.

exciplex In a laser, a method of adjusting the color by means of chemical reactions in organic dyes.

excitant The electrolyte in a voltaic cell.

excitation **1.** Supplying input-signal driving current, driving power, or driving voltage. **2.** Input-signal driving current, driving power, or driving voltage.

excitation anode In a mercury-pool tube, an auxiliary anode whose operation maintains the cathode spot when no output current is being drawn from the tube.

excitation current **1.** Input-electrode current in an excited transistor amplifier. **2.** Grid current in an excited vacuum-tube amplifier. **3.** Current flowing in the circuit of the excitation anode of a mercury-pool tube. **4.** Current flowing in the exciter circuit of an alternator. **5.** Shunt-field current in a motor.

excitation energy **1.** Symbol, E_X. In artificial transmutation, the energy of a nucleus when protons of less than maximum energy have been emitted from the atom. **2.** Electrical energy required by a transducer.

excitation purity In color television, complete saturation of a hue (i.e., there is no contamination by other colors, and the saturated hue is distributed uniformly).

excitation voltage **1.** The signal voltage that achieves, or is required for, excitation (see EXCITATION, **1**). **2.** The value of driving voltage.

excitator An electrical discharger.

excited atom An atom in which one or more electrons have been pushed out of their normal orbits into higher ones by energy applied from the outside.

excited-field speaker A dynamic speaker in which the magnetic field is provided, not by a permanent magnet, but by direct current flowing through a large coil of wire wound around the speaker core. The coil usually acts as a filter choke in the power supply of the attendant amplifier or receiver.

excited state In artificial transmutation, the state of the nucleus when protons of less-than-maximum energy have been emitted from the atom. The energy of the protons, in this instance, is greater than the ground state.

5059F-pE-224-273 4/9/01 5:26 PM Page 269

exciter **1.** An amplifier or oscillator (or a system of such units) that supplies the input (driving) signal to the output amplifier in a radio transmitter or similar device. **2.** A small direct-current (dc) generator that supplies direct current to the field winding of an alternating-current (ac) generator. **3.** See INDUCTION COIL.

exciter lamp **1.** A concentrated-filament, high-intensity incandescent lamp used in sound-on-film recording and reproduction and in some types of electromechanical television. **2.** In a facsimile transmitter, the lamp illuminating what is being scanned.

exciter relay In an electromechanical generator, the relay that activates the direct-current (dc) field excitation during machine startup.

exciter response **1.** A change in the exciter voltage of a motor when the field-circuit resistance changes. **2.** A change in the operating conditions of a radio frequency exciter, as a result of a change in the impedance at the input of the final amplifier.

exciter unit See EXCITER.

exciting current **1.** The output current produced by the exciter of a generator (see EXCITER, **2**). **2.** The field current of a dynamo-type generator. **3.** Primary current in an unloaded transformer.

exciting power **1.** The output power produced by an exciter. **2.** The input-signal power required for full output from a power amplifier. Also called DRIVING POWER.

exciting voltage **1.** Input-signal voltage. **2.** The input-signal-voltage amplitude required for full rated output from a power amplifier. Also called DRIVING VOLTAGE. **3.** The output voltage produced by an exciter.

exciton In a semiconductor or dielectric, a bound electron-hole pair.

excitron A mercury-pool rectifier whose arc is initiated mechanically (e.g., by means of a magnetic plunger in the tube).

exclusion principle The rule that only one particle of a particular kind can occupy a given quantum state at one time.

exclusive-NOR A logic function where the output is 1 if both inputs are 1 or both are 0 (same). The output is 0 if one input is 0 and the other is 1 (different). Compare EXCLUSIVE OR.

exclusive-OR A logic function in which the output is 1 when the two inputs are different, and is 0 when the two inputs are the same.

excursion **1.** A change in the value of a quantity in a given direction. **2.** In an oscillatory system, a body's moving away from the point of equilibrium or mean position.

execution A computer's performance of the operations required by an instruction.

execution time The length of time required for a computer to complete a designated operation.

executive routine In computer operations, a program that controls and processes other routines.

A	B	C
0	0	0
0	1	1
1	0	1
1	1	0

exclusive-OR

Also called *monitor program.* Compare MONITOR SYSTEM.

exhaust analyzer An instrument for examining the exhaust fumes of an internal combustion engine, to measure the presence of noxious materials and to evaluate air-to-fuel ratio and combustion efficiency.

exhaustion See EVACUATION.

exit **1.** In computer operations, the last instruction in a program or program segment, often taking a subroutine back to the main program. **2.** To leave a computer application, routine or subroutine.

exoskeleton A robot that resembles a suit of armor, and that greatly magnifies the force of physical movements. A human operator occupies the interior. Thus, for example, the operator might use the machine to throw a football 2500 yards, or to run 50 miles an hour, or to smash through walls. Primarily a tool of science fiction writers, this machine is within the scope of current robotic technology.

exosphere The extreme outer layer of the earth's atmosphere.

exothermic Pertaining to a chemical or electrochemical reaction in which heat is given off. Compare ENDOTHERMIC.

exothermic reaction In a chemical reaction, the production of positive reaction energy (i.e., kinetic energy is gained). Compare ENDOTHERMIC REACTION.

exp **1.** Symbol for EXPONENTIAL. **2.** Abbreviation of EXPERIMENT(AL).

expand **1.** In communications, to increase the bandwidth of a signal, restoring it to normal bandwidth after it has been compressed. **2.** In communications, to increase the dynamic range of a signal. **3.** In computer operations, to restore a file to full or normal size after it has been compressed. **4.** To widen the scale of a meter. **5.** To widen (or magnify a portion of) the trace of an oscilloscope beam. Compare COMPRESS.

expandable Capable of being built up into larger circuits or systems.

5059F-pE-224-273 4/9/01 5:26 PM Page 270

expandable gate In digital logic, a gate that can be provided with an unlimited number of input lines by electrical interconnection with other gates.

expanded memory In personal computer systems, memory beyond the basic 640 kilobytes (640 kb), up to one megabyte (1 MB). This memory resides in integrated circuits (ICs) in the computer, and is normally volatile (i.e., it is not retained when power is removed). Compare EXTENDED MEMORY.

expanded-scale meter A meter having a scale designed to display a narrow range of values. Such a meter used for monitoring the 117-V power line might have a scale reading 100 to 140 V, instead of a conventional scale beginning at zero.

expanded sweep **1.** In an oscilloscope, speeding up the deflection of the beam during a selected portion of the trace. **2.** The circuit for the action described in **1**.

expander A circuit for increasing the dynamic range over which a signal or quantity can vary. A typical example is the volume expander, a device that greatly increases the amplitude of strong signals while weakening, or having no effect on, signals of low amplitude.

expansion **1.** In communications, the process of increasing the bandwidth of a signal, restoring it to normal bandwidth after it has been compressed. **2.** In communications, a process in which stronger components are amplified more than weak ones, restoring a signal to its normal dynamic range after it has been compressed. **3.** In computer operations, the restoration of a file to full or normal size after it has been compressed. **4.** The widening of a meter scale. **5.** The widening or magnification of an oscilloscope trace. Compare COMPRESS.

expansion chamber A cloud chamber for viewing the paths of radioactive particles. It consists of a closed glass cylinder containing humid air and a piston. An electrostatic field is applied through the cylinder, the piston is pulled quickly, and the volume of the chamber expands. The temperature inside falls below the dew point, a cloud is formed, and droplets of water condense on ions, making their paths visible for observation or photography through the cylinder walls.

expansion ratio In communications, the inverse of COMPRESSION RATIO.

expansion time For an expansion chamber, the interval during which expansion occurs. The interval is kept short to ensure that the temperature will drop low enough for vapor condensation, and to minimize the possibility of continuing gas motion distorting the track of a particle.

expectation In probability theory, the middle value (average or mean) of a random variable.

expendable A component or system that, for economy, is best discarded instead of repaired when it fails. Also called DISPOSABLE COMPONENT.

experiment One or a series of carefully planned tests carried out under controlled conditions to obtain data or to check performance.

experimental chassis See ELECTRONIC CHASSIS.

experimental model A prototype of an electronic circuit or device, produced solely for operational tests or as a model against which theory and design can be checked.

experimental service A special, nonamateur radio service intended for on-the-air testing of new methods and equipment.

experimental station A station specially licensed to operate on specific frequencies in the experimental service.

expert system Also called *rule-based system.* A form of artificial intelligence (AI) that allows a computer or smart robot to act as a highly talented specialist in a specific field. An example is the use of a computer to help a physician diagnose a complex disease. A smart robot might be used as a surgical assistant.

exploring coil A pickup coil for sensing a signal or magnetic field. Sometimes called a *sniffer.*

exploring electrode **1.** A sampling electrode sealed in a discharge tube for measuring ionization at the point of insertion. **2.** Broadly, a test probe.

explosion-proof device A device that is housed and operated so that its sparking, heating, or production of radiant energy will not cause materials in the environment to explode.

exponent A number written as a superscript indicating the power to which another number (called the *base*) is to be raised. For example, 2^2 is the square (second power) of 2; x^3 is the cube (third power) of x.

exponential **1.** A base (such as the natural number e) modified by an exponent. **2.** Related to a change in value as determined by an exponent. Thus, using increments for x in the equation $y = e^x$ produces an exponential curve.

exponential curve A curve based on powers of a number (such as for $y = e^x$). Also see EXPONENTIAL, EXPONENTIAL DECREASE, and EXPONENTIAL INCREASE.

exponential damping Damping action described by an exponential curve.

exponential decay See EXPONENTIAL DECREASE.

exponential decrease The continuous reduction in the value of a quantity, according to the equation $y = e^{-x}$, which depicts the natural decay curve.

exponential function A function, such as $f(x) = e^x$, that varies exponentially. See, for example, EXPONENTIAL DECAY, EXPONENTIAL GROWTH, and EXPONENTIAL SERIES.

exponential horn A horn of circular or rectangular cross section, whose cross-sectional area S at any point x feet along its axis is given by the formula $S = S_0e^{mx}$, where S_0 is the cross-sectional area at the throat, e is the natural logarithm base

5059F-pE-224-273 4/9/01 5:26 PM Page 271

(approximately 2.71828), and m is the horn flaring constant.

exponential increase The continuous increase of a quantity, according to the equation $y = e^x$, which depicts the natural growth curve.

exponential line A transmission line whose characteristic impedance varies exponentially with its electrical length.

exponential quantity A quantity involving an exponential (e.g., $3e^x$).

exponential series A mathematical series based on exponential expressions. Example: $e^x = 1 + x + (x^2/2!) + (x^3/3!) + (x^4/4!) + \ldots$

exponential sweep In cathode-ray-tube (CRT) devices, such as oscilloscopes, a beam sweep that starts fast and slows exponentially.

exponential transmission line See EXPONENTIAL LINE.

exponential waveform Any waveform in which the rate of change in the amplitude is directly or inversely proportional to the instantaneous amplitude. The absolute value of the derivative of such a waveform is equal to the absolute value of the instantaneous amplitude, multiplied by a constant that depends on the amplitude units.

exposure **1.** The total amount of radiation received in a given area, or by a given sample, or by a person, over a specified length of time. **2.** The extent to which a photographic film has been darkened or otherwise modified by visible light, infrared, ultraviolet, or X rays.

exposure meter **1.** A usually simple instrument for measuring light intensity—especially for photographic purposes. A common form consists of a self-generating photocell connected to a direct-current microammeter. **2.** A device that indicates the amount of ionizing radiation that has been received over a given period of time.

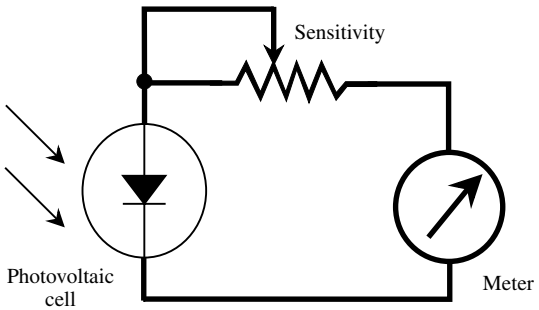

exposure meter

expression control A volume control in an electronic organ.

extended double Zepp antenna See DOUBLE-EXTENDED ZEPP ANTENNA.

extended memory In personal computer systems, memory beyond the first megabyte (1 MB). There is no limit in theory to the extent of this memory, although it is limited by current technology. Used in high-level programs—especially those involving graphical applications, artificial intelligence, or intensive calculations. Resides in integrated circuits (ICs) in the computer, and is normally volatile (i.e., it is not retained when power is removed). Compare EXPANDED MEMORY.

extended octaves Audio-frequency tones above or below the normal range of an electronic musical instrument. Special circuits must be added to make the extended octaves available.

extended play Pertaining to a recorded phonograph disc that provides a longer playing time than conventional discs of the same size and recording speed.

extender A substance added to an encapsulant to make it go further.

extensimeter See EXTENSOMETER.

extension cable A flexible, low-capacitance (usually concentric) cable for connecting part of one circuit to part of another. Extension cables are available with a variety of end connectors.

extension cord A flexible power cord having a male plug on one end and female receptacle on the other.

extension loudspeaker An auxiliary loudspeaker serving areas in which the main speakers can't be adequately heard.

extensometer An instrument used to measure small amounts of expansion, contraction, or deformation.

exterior label On a diskette or tape cartridge used for computer data storage, a written identification on the housing or cartridge, as opposed to the label, which is recorded on the diskette or tape itself.

external armature In a dynamo-type machine, an armature that rotates around the outside of the field magnets, as opposed to the usual (inside) arrangement.

external capacitor A high-value capacitor connected externally to an oscillator or sweep generator to lower its frequency.

external circuit A circuit or subcircuit connected and external to a main equipment.

external controls **1.** Control devices that are connected to, but operated away from, a main circuit. **2.** Manual or screwdriver-adjusted controls that are mounted on the panel of an equipment, as opposed to those mounted in the case or behind the panel.

external critical damping resistance The value of external resistance that must be connected to a galvanometer or other meter to produce critical damping.

external damping device A resistor or short-circuiting bar connected temporarily between the terminals of a meter to keep its movement immobile during transportation.

5059F-pE-224-273 4/9/01 5:26 PM Page 272

external feedback Negative or positive feedback through a separate path outside of and around the main circuit. Example: negative feedback through a resistance-capacitance (RC) path between the output terminals and the input terminals of an amplifier.

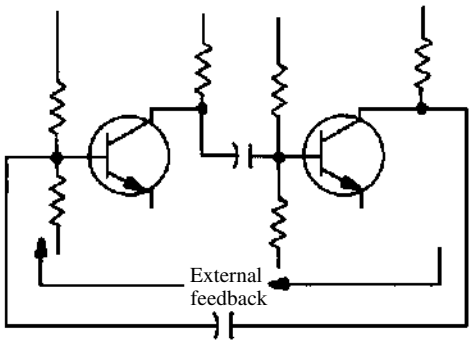

external feedback

external impedance Load impedance (i.e., an impedance connected to the output terminals of a generator or amplifier).

external load See EXTERNAL IMPEDANCE.

external loudspeaker See EXTERNAL SPEAKER.

externally caused chatter In a relay, contact chatter caused by mechanical vibration outside of the relay.

externally caused failure Failure of a circuit or component resulting from unfavorable environmental factors.

external memory In computer operations, a memory unit outside of the computer mainframe.

external power supply A power supply unit situated apart from the powered equipment. Such separation is helpful in eliminating the disturbing effects of heat, hum, and vibration associated with internal power units.

external *Q* For a microwave tube, the quantity $1/(1/Q_1 + 1/Q_2)$, where Q_1 is the loaded Q and Q_2 is the unloaded Q.

external S-meter A signal-strength meter connected to a receiver, but not installed in its panel.

external speaker A loudspeaker that doesn't share an enclosure with an amplifier, receiver, or other device that drives it. Such isolation is helpful in eliminating the undesirable effects of vibration and acoustic feedback.

external storage In computer operations, storage media (such as magnetic diskettes or tapes) that are outside of the computer.

extinction potential See DEIONIZATION POTENTIAL.

extinction voltage See DEIONIZATION POTENTIAL.

Extra-class license An amateur-radio license that conveys all available amateur operating privileges in the United States. The highest class of amateur license.

extract **1.** To remove a signal or quantity from some product containing it, or from its source. Examples: extracting a fifth harmonic from a complex signal, extracting the direct-current (dc) component from a signal containing both alternating current (ac) and dc. **2.** To derive a factor (e.g., to extract a root). **3.** To separate certain classes of information from an aggregate of information.

extract instruction In computer operations, the instruction to generate a new word by the serial arrangement of designated segments of specified words.

extractor **1.** A circuit or device for removing a signal (or a signal component) from another circuit or device. A demodulator probe, for example, extracts the modulation from a modulated signal. **2.** A device for removing used active devices from a circuit board. Such extractors can also employ heat to desolder, as well as remove the devices.

extraneous component A usually undesired inherent effect that results from the physical nature of a component or device. Examples: distributed capacitance of a coil, internal inductance of a capacitor.

extraneous emission Undesired emission from a transmitter (e.g., excessive harmonics).

extraneous response The unintended response of a circuit or device (e.g., image response in a superheterodyne communications receiver).

extraneous root In the solution of an equation derived from another equation, one or more roots that satisfy the derived equation but not the original one.

extraneous signal A superfluous and potentially interference-causing signal.

extranuclear Outside the nucleus of an atom.

extraordinary ray Of the two rays resulting from the double refraction of electromagnetic waves, the one that does not follow the usual laws of refraction. Also see X WAVE.

extraordinary wave See X WAVE.

extrapolar **1.** Outside of electrical or magnetic poles. **2.** Not between electrical or magnetic poles.

extrapolation Estimation of values beyond the range of available data. An example is the extension of a curve beyond its final plotted point to determine a value for a variable. There is always some margin for error, which increases as the process is extended further and further beyond the range of actual data values. Commonly done by computers (e.g., prediction of the probable path of a hurricane 12, 24, 36, and 48 hours in advance).

extrared See INFRARED.

extraviolet See ULTRAVIOLET.

extreme **1.** The lowest or highest value of a

5059F-pE-224-273 4/9/01 5:26 PM Page 273

quantity. **2.** The lowest or highest point of the dependent variable in the range of a function. **3.** An unusual value for a parameter (e.g., temperature extreme and pressure extreme).

extremely high frequency Abbreviation, EHF. A frequency near the upper limit of the radio-frequency spectrum—especially one in the 30- to 300-GHz band.

extremely low frequency **1.** Abbreviation, ELF. Pertaining to a signal or current within the audio-frequency (AF) range, but not used for audio applications. **2.** Electromagnetic emissions from a cathode-ray tube (CRT), resulting from the currents in the deflecting coils and/or electron beam. **3.** The 60-Hz electromagnetic field generated by utility power lines and wiring.

extrinsic base-resistance/collector-capacitance product Units: seconds, milliseconds, and microseconds. For a bipolar transistor, the product R_BC_C, where R_B is the base resistance and C_C is the collector capacitance. This product is a time constant that determines the high-frequency operating limit of the transistor.

extrinsic conductance For a material, the conductance resulting from impurities or such external factors as environmental conditions.

extrinsic properties For a semiconductor material, properties resulting from doping (e.g., altered resistivity or majority/minority carrier differentiation). Also see EXTRINSIC SEMICONDUCTOR.

extrinsic semiconductor A semiconductor material, such as germanium or silicon, to which a controlled amount of a suitable impurity material has been added to give the semiconductor a desired resistivity and polarity. Compare INTRINSIC SEMICONDUCTOR.

extrinsic transconductance Symbol, g_m. For a bipolar transistor, the first derivative of collector current, with respect to base-emitter voltage. It is the ratio of a small change in collector current (dI_C) to the small change in base-emitter voltage (dV_{BE}) that produced it, collector voltage being constant; $g_m = dI_C/dV_{BE}$.

extrusion The process of forming a material such as metal or plastic, by forcing it through dies. Many pieces of electronic hardware are mass produced in this manner. Examples are insulating rods and tubes, metal cans, and metal tubing.

eye-in-hand system In robotics, a scheme that uses a vision system, servo, and microprocessor to precisely manipulate an END EFFECTOR, such as a robot gripper ("hand"). A camera (the "eye") is contained in the end effector itself, and is designed to work at close range (i.e., approximately one meter down to a fraction of a millimeter).

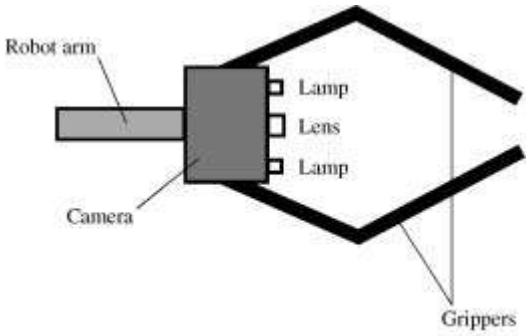

eye-in-hand system

eyelet connection A connection made by fastening conductors together with an eyelet or by soldering leads or pigtails to an eyelet.

eyepiece A small lens system for viewing an oscilloscope screen through a camera setup.

E_Z Symbol for *voltage drop across an impedance.*

E zone A portion of the earth including most of the eastern hemisphere. When propagation forecasts are made, this region is one of three longitude zones specifie

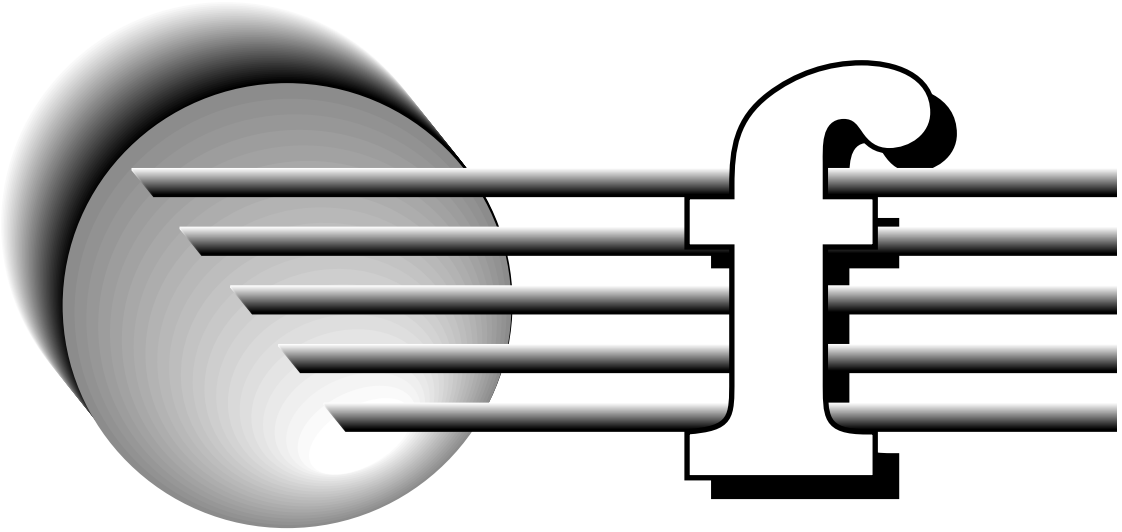

F **1.** Symbol for FORCE. **2.** Symbol for FLUORINE. **3.** Abbreviation of FAHRENHEIT. **4.** Abbreviation of FARAD. **5.** Abbreviation of FERMI. **6.** Symbol for FOCAL LENGTH. **7.** Symbol for FUSE. **8.** Symbol for FARADAY CONSTANT.

f **1.** Abbreviation of FEMTO. **2.** Symbol for FREQUENCY. **3.** Symbol for FUNCTION.

F_0 Symbol for DAMPING FACTOR.

F1 layer The lower part of the ionosphere's F REGION. Also called *F1 region.*

F2 layer The upper part of the ionosphere's F REGION. Also called *F2 region.*

fA Abbreviation of FEMTOAMPERE.

fabrication tolerance The amount of variation that can be tolerated in the manufacture of components.

Fabry-Perot interferometer A resonant cavity, often used with lasers, that has mirrors at each end; the interferometer produces the optical equivalent of standing waves.

face **1.** A flat crystal surface whose orientation can be expressed as its position relative to other faces. **2.** The viewer's side of a screen. **3.** The scale part of a meter.

face material In a tape recorder, the plastic used to coat the face of a head.

face-parallel cut See Y-CUT CRYSTAL.

face-perpendicular cut See X-CUT CRYSTAL.

face side The side of pressure-sensitive insulating tape that is coated with adhesive.

facom A radionavigation system that operates by means of phase comparison at low frequencies. Effective over long distances and under poor conditions.

facsimile Also called *fax.* The transmission and reception, through the medium of radio or by wire, of permanent pictures, writing, and other graphic material.

facsimile receiver The complete device or system that selects, amplifies, and demodulates a picture signal received up from the air, wires, or cable, and uses the elements of this signal to reproduce the picture. Also see FACSIMILE.

facsimile recorder The machine that puts a transmitted facsimile image on paper.

facsimile transmitter The complete device or system that generates signals depicting graphic material (pictures, writing, printing, etc.) and sends them to a distant point via cable, wire lines, or radio for subsequent reproduction. Also see FACSIMILE.

factor **1.** A data element that is an operand in an arithmetic operation. **2.** To find the two or more numbers whose product is the number being factored. **3.** One of two or more numbers whose product is the number being factored.

factorial Symbol, !. For an integer n, the product of all positive integers up to and including n. Thus, $5! = 1 \times 2 \times 3 \times 4 \times 5 = 120$. The term $n!$ is read "n factorial."

factor of merit See FIGURE OF MERIT.

factor of safety See SAFETY FACTOR.

fade in To gradually increase an audio or video signal—especially for recording.

fade out **1.** To gradually decrease an audio or video signal—especially for recording. **2.** The complete disappearance of a radio communications signal. See FADING.

fader **1.** In sound amplification systems, an attenuator circuit that enables the operator to fade out one signal and fade in another. Ordinarily, a fader does not provide mixing action. **2.** In an au-

Copyright 2001 The McGraw-Hill Companies, Inc. Click Here for Terms of Use

5059F-pF-274-306 4/9/01 5:31 PM Page 275

tomotive high-fidelity sound system, a control that adjusts the volume of the front speaker set and rear speaker set. Usually, this is a single knob; increasing the front volume decreases the rear volume, and vice-versa.

fading **1.** Repeated increases and decreases of radio communications signal amplitude at the reception point. Fading of a radio wave results from multiple propagation paths from transmitter to receiver, causing the received waves to arrive in constantly varying phase relationships. **2.** In a cell or battery power supply, a gradual loss of power-delivering capability that occurs during the discharge cycle.

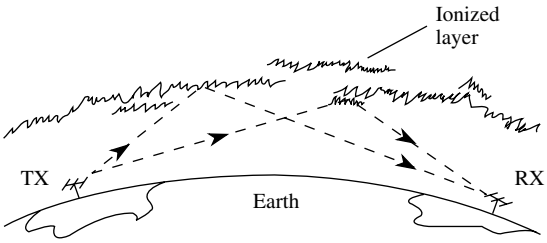

fading

factory automation The use of robotic devices, to the greatest extent possible, as laborers in manufacturing plants.

Fahnestock clip A flat, sheet-metal spring clip for holding a wire (usually in a temporary breadboard setup).

Fahrenheit scale A temperature scale on which the freezing point of water is 32 degrees, and the boiling point of water is 212 degrees. Compare ABSOLUTE SCALE and CELSIUS SCALE.

failsafe Pertaining to devices or circuits that, upon failure, cause no damage or serious malfunction.

failsoft In a computer, a system in which operation is maintained—even in the event of partial failure. Efficiency is reduced but the computer does not completely shut down.

failure The condition wherein a circuit, system, or device is not operating correctly.

failure analysis **1.** The process of determining the failure rate for a component, system, or device. **2.** The process of determining the cause of a failure.

failure mode The particular way in which a failure of equipment or a method occurs.

failure unit A unit of machine or device failure: one failure per billion (10^9) hours of operation.

fall-in The time when synchronous speed is attained in a synchronous motor.

falling characteristic A NEGATIVE RESISTANCE characteristic.

fall time **1.** Decay time. **2.** The time required for the amplitude of a pulse to decrease from 90 percent to 10 percent of its peak amplitude. Compare RISE TIME.

false add A logic add (i.e., addition without carries).

false alarm **1.** Improper operation of an electronic security system, resulting in actuation of the device when no breach of security has occurred. **2.** In radar, the presence of a false echo that causes the attendant circuits or personnel to act as though an enemy target is present.

false error A condition in which a computer system erroneously signals the existence of an error.

false precision See MISLEADING PRECISION.

false retrieval The incorrect specification of criteria for information to be selected for retrieval so that an unwanted item of data is selected. Also called *false drop.*

family Any group of components, circuits, ratings, or characteristics, classed together because of some common or analogous feature or application. Examples: IC family, family of curves, and family of equations.

family of curves A group of curves plotted on the same axes, that depict the performance of a circuit or device at several levels of a third parameter (e.g., curves showing transistor collector current vs. collector voltage for several levels of base current).

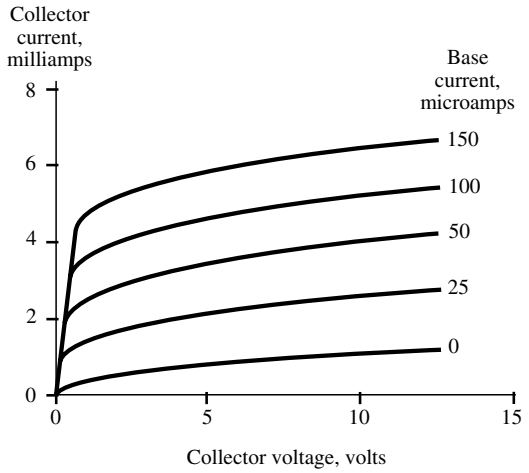

family of curves

fan antenna See DOUBLE-V ANTENNA.

fan-in **1.** A number of inputs entering a common input terminal. **2.** In digital computer operations, the number of inputs that can be accommodated by a logic circuit. Compare FAN-OUT.

fan-in circuit A circuit having a number of input lines entering a common input point. Also see FAN-IN, **1**.

fan-out **1.** One common output terminal feeding a number of output lines. **2.** In digital computer

5059F-pF-274-306 4/9/01 5:31 PM Page 276

operations, the number of outputs that can be fed by a logic circuit. Compare FAN-IN.

fan-out circuit A circuit in which a number of output lines leave a common output terminal. Also see FANOUT, **1**.

fantasy robot A robot as portrayed in science fiction or fantasy. Such robots are usually, but not always, *androids* (that is, they have humanoid form). Some fictional robot characteristics are later realized. Science fiction can even give roboticists ideas for future designs.

farad (Michael Faraday, 1791–1867) Abbreviation, F. The basic unit of capacitance. A capacitor has a capacitance of 1 F when a charge of 1 volt per second across the capacitor produces a current of 1 ampere through it.

faraday An electrical quantity approximately equal to 9.65×10^4 coulombs; it is the quantity of electricity required in electrolysis to free 1 gram atomic weight of a univalent element. The equivalent, and preferred, unit is the COULOMB. Also called *Faraday constant*.

Faraday cage See ELECTROSTATIC SCREEN.

Faraday constant See FARADAY.

Faraday cylinder A cylindrical metal shield placed around electrical equipment or circuits to prevent electromagnetic fields from affecting the equipment or circuits.

Faraday rotation **1.** A change in the polarization of an electromagnetic wave as it passes through a medium. **2.** Constant and random fluctuations in the polarization of radio signals as they pass through the earth's ionosphere. This phenomenon affects signals having linear polarization at frequencies well below 10 GHz. It has little or no effect on circularly polarized signals, or on signals at frequencies above 10 GHz. It can be a problem with some satellite communications links.

Faraday effect See MAGNETO-OPTICAL ROTATION.

Faraday's disk dynamo See DISK DYNAMO.

Faraday shield See ELECTROSTATIC SCREEN.

Faraday's law The voltage induced in a conductor moving in a magnetic field is proportional to the rate at which the conductor cuts the magnetic lines of flux.

Faraday's laws of electrolysis **1.** In electrolysis, the mass of a substance liberated from solution is proportional to the strength and duration of the current. **2.** For different substances liberated by the same current in a certain time, the masses are proportional to the electrochemical equivalents of the substances. Also see ELECTROCHEMICAL EQUIVALENT; ELECTROLYSIS, **1**; and ELECTROLYTE.

faradic current The lopsided alternating current produced by an induction coil.

faradmeter An alternate term for MICROFARAD METER.

far field **1.** The region beyond the near field of an antenna (see NEAR FIELD, **1**). **2.** The region beyond the near field of a loudspeaker (see NEAR FIELD, **2**).

far infrared Also called far IR. The lower-frequency portion of the infrared (IR) spectrum.

farming robot A robot that performs labor in an agricultural setting. Examples: fruit-picking robot, field-watering robot, cow-milking robot. Such machines are usually overseen by a central computer, via which the farmer can monitor and control the robots' actions.

far zone See FAR FIELD, **1**, **2**.

fast access storage In a computer memory, the section from which information can be most quickly accessed, depending on the relative speed of other system devices.

fast-break, fast-make relay A relay that opens and closes rapidly.

fast-break, slow-make relay A relay that opens rapidly and closes slowly.

fast charge The rapid charging of a rechargeable cell or battery, particularly of a nickel-cadmium (NICAD) or nickel-metal-hydride (NiMH) device.

fast diode See COMPUTER DIODE.

fast drift The rapid change of a quantity or setting, usually in one direction. Compare SLOW DRIFT.

fast-food robot A robot that prepares and/or serves items in a fast-food establishment. Robots have not yet gained wide acceptance in this setting, mainly because of technical difficulties and prohibitive cost. Another problem is that some customers are put off or intimidated by robots.

fast-forward Abbreviation, FF or FFWD. In a tape recorder, a mechanism for running the tape through the machine rapidly.

fast groove The informationless groove between tracks on a disk recording.

fast-make/fast-break relay A relay that closes and opens rapidly.

fast-make, slow-break relay A relay that closes rapidly and opens slowly.

fast-forward playback In a videotape recorder, the playing back of the tape at faster than real-life speed. It allows the viewer to move quickly ahead in a program, and also to watch the images so as to know when to resume normal replay.

fast-reverse playback In a videotape recorder, the playing back of the tape rapidly backwards. It allows the viewer to move quickly back in a program, and also to watch the images so as to know when to resume normal replay.

fast time constant **1.** The property of responding quickly to changes in input parameters. **2.** In radar, a method of defeating attempts at jamming by modification of the receiving circuitry.

fathometer See ACOUSTIC DEPTH FINDER.

fathom **1.** To measure the depth of a body of water, as in the use of sonar for this purpose. **2.** A unit of length (distance) equal to six feet.

fatigue **1.** The degradation of the performance of circuits or materials with time. **2.** The tendency of

5059F-pF-274-306 4/9/01 5:31 PM Page 277

bodies and materials to weaken, deform, or fracture under repeated strain.

fault **1.** A defective point or region in a circuit or device. **2.** A failure in a circuit or device.

fault current **1.** A momentary current surge. **2.** A leakage current.

fault finder A troubleshooting instrument or device (e.g., a multimeter).

fault resilience **1.** A design scheme for an electronic or computer device or system so that if a component or circuit fails, the system will continue to operate, although perhaps at reduced efficiency. The operator is notified of the problem so that it can be repaired with minimal downtime. **2.** In a computer system, the property of being as nearly sabotage-proof as possible.

fault tolerance Total redundancy in an electronic or computer system so that if a component or circuit fails, the system will continue to function at full efficiency. Every component has a backup that automatically takes over in case of failure. The operator is notified of the problem, so the defective part or circuit can be replaced while its backup keeps the circuit working continuously at 100-percent capacity.

Faure plate A storage battery plate consisting of a lead grid containing a chemical electrolytic paste.

fax Abbreviation of FACSIMILE.

fc Abbreviation of FOOT-CANDLE.

f_c Abbreviation of CARRIER FREQUENCY.

FCC See FEDERAL COMMUNICATIONS COMMISSION.

f_{co} Abbreviation of CUTOFF FREQUENCY.

F connector A type of antenna feedline connection especially common on television receivers and videocassette recorders.

F display See F SCAN.

FDM Abbreviation of *frequency-division multiplex.*

FE Abbreviation of FERROELECTRIC. See FERROELECTRICITY.

Fe Symbol for IRON.

feasibility study The procedures for evaluating the potential gains in applying a computer system to a job or to an organization's process, or in modifying or replacing an existing system.

FEB Abbreviation of FUNCTIONAL ELECTRONIC BLOCK.

Federal Communications Commission Abbreviation, FCC. Established in 1934, the U.S. Government agency that regulates electronic communications. The FCC succeeded the Federal Radio Commission (FRC), which was established in 1927; the FRC succeeded the Radio Division of the Bureau of Navigation in the Department of Commerce, whose jurisdiction over radio began in 1912.

feed **1.** To supply power or a signal to a circuit or device. **2.** The method of supplying such a signal or power. See, for example, PARALLEL FEED and SERIES FEED. **3.** To cause data to be entered into a computer for processing.

feedback **1.** The transmission of current or voltage from the output of a circuit or device back to the input, where it interacts with the input signal to modify operation of the device. Feedback is positive when it is in phase with the input, and is negative when it is out of phase. **2.** To input the result at one point in a series of operations to another point; the method allows a system to monitor its actions and make necessary corrections.

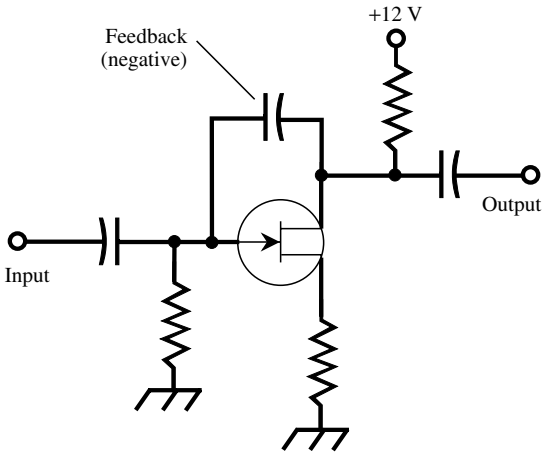

feedback, 1.

feedback amplifier **1.** An amplifier whose performance (especially frequency response) is modified by means of positive, negative or both positive and negative feedback. **2.** An amplifier placed in the feedback path of another circuit to increase the amplitude of feedback.

feedback attenuation **1.** In an operational-amplifier circuit, the attenuation in the voltage from output to input. **2.** In an audio-frequency or radio-frequency amplifier circuit, the reduction of feedback by electronic means.

feedback bridge A bridge circuit in the feedback channel of an amplifier or oscillator.

feedback capacitance **1.** A capacitance through which feedback current is coupled from the output to the input of a circuit or system. **2.** The interelectrode capacitance of a vacuum tube.

feedback control **1.** The variable component (potentiometer or variable capacitor) used to adjust the level of feedback current or voltage. **2.** The control of circuit performance by means of feedback.

feedback cutter A device used for the purpose of cutting grooves in phonograph disks. Feedback is used to provide a flat frequency response.

feedback factor For a feedback amplifier, the quantity $1 - bA$, where A is the open-loop gain of the amplifier and b is the FEEDBACK RATIO.

5059F-pF-274-306 4/9/01 5:31 PM Page 278

feedback input current In a feedback network, the current drawn by the feedback input. This current affects the design parameters of a network.

feedback loop The part of a circuit that provides controlled feedback in an operational-amplifier circuit.

feedback oscillator A circuit in which oscillation is obtained by feeding a portion of the output of an active amplifying device back to the input circuit by inductive coupling. Also called *tickler oscillator.*

feedback path A path over which feedback, either positive or negative, can occur in a circuit. The feedback can be intentionally produced, or it can be undesirable.

feedback percentage Symbol, *n*. In a feedback circuit, the percentage of output voltage that is fed back; $n = 100V_f/V_o$, where V_f is the feedback voltage and V_o is the open-loop output voltage. Compare FEEDBACK RATIO.

feedback ratio For a feedback system, the ratio V_f/V_o, where V_f is the voltage that is fed back and V_o is the open-loop output voltage of the system.

feedback rectifier See DIODE FEEDBACK RECTIFIER.

feedback regulator In a controlled-feedback circuit, the device that determines the amount of feedback.

feedback resistance **1.** The internal base resistance of a point-contact transistor. **2.** The resistance in a feedback loop.

feedback transfer function The transfer function of a feedback loop exclusively.

feedback winding A special winding on a magnetic amplifier or saturable reactor, for the introduction of feedback currents.

feeder **1.** A conductor or set of conductors that carries electric power from one point to another. **2.** The transmission line connecting a transmitter to an antenna.

feeder cable **1.** A communication cable running in a primary route from a central station (or in a secondary route from a main feeder cable) as a means of making connections to distribution cables. **2.** In a cable television system, the cable carrying transmission from the head end to the trunk amplifier. Also called TRUNK CABLE.

feeder loss Loss of energy resulting from resistance in, or radiation from, feeder lines.

feeding In character recognition, a system in which documents go into the transport of a character reader at a steady, specified rate.

feed pitch The distance between feed holes.

feed reel The tape supply reel of a tape recorder.

feedthrough **1.** The usually undesirable transmission of a signal through a circuit without being processed by the circuit, because of unavoidable capacitive coupling, for example. **2.** Contraction of FEEDTHROUGH COMPONENT.

feedthrough capacitor A capacitor whose design is like that of a feedthrough terminal; it is mounted in a hole in a chassis. The center screw or wire is the "high" terminal of the capacitor, to which connections can be made above or below the chassis. The body of the device is the "low" terminal of the capacitor; it is soldered to the chassis or secured with a nut.

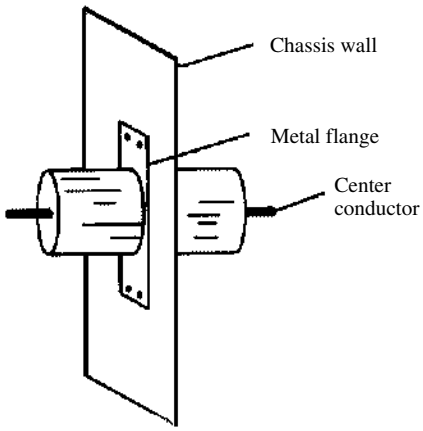

feedthrough capacitor

feedthrough component A passive device permanently installed in a panel or plate (e.g., a FEEDTHROUGH CAPACITOR or FEEDTHROUGH INSULATOR).

feedthrough insulator An insulator mounted tightly in a hole in a wall or chassis, and provided with a center hole for a lead.

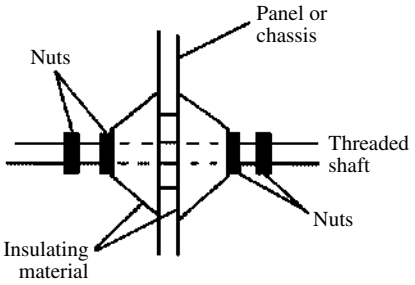

feedthrough insulator

feedthrough terminal A terminal mounted tightly in a hole in a chassis or wall; it consists of a screw going through a feedthrough insulator. Connections can be made to either end of the screw.

5059F-pF-274-306 4/9/01 5:31 PM Page 279

FE-EL Abbreviation of *ferroelectric-electroluminescent.*

feeler **1.** A wire or blade contact (e.g., a finger that senses holes in a punched card). **2.** The wire portion of a point-contact diode.

Felici mutual-inductance balance An inductive null circuit for determining mutual inductance (M_x) in terms of a standard mutual inductance (M_s). The secondary coils of two mutual-inductance circuits are connected in phase opposition. The standard mutual inductor, which is variable, is adjusted for null. At null, $M_x = M_s$.

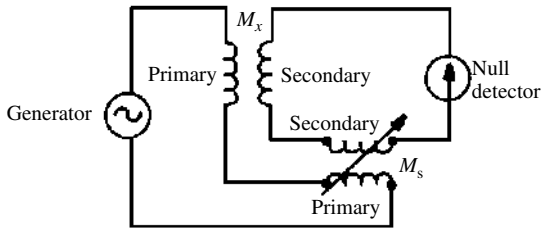

Felici mutual-inductance balance

female plug A plug whose contacts are separated by a recess into which the prongs of a mating male plug are inserted. Compare HERMAPHRODITE PLUG and MALE PLUG.

femto- Abbreviation, f. A prefix meaning quadrillionth (10^{-15}).

femtoampere Abbreviation, fA. A unit of extremely low current; 1 fA equals 10^{-15} A.

femtofarad Abbreviation, fF. A unit of extremely low capacitance; 1 fF equals 10^{-15} F.

femtovolt Abbreviation, fV. A unit of extremely low voltage; 1 fV equals 10^{-15} V.

fence A system or string of early warning radar stations.

Fermat's principle The principle that the path of a ray of radiant energy between two points in any medium is the shortest distance between those points in that medium. This path is also the path of least propagation time. This might not necessarily be a straight line. On a flat plane, the path of least time between any two points is always a straight line, assuming constant velocity of propagation. However, on a sphere, the path of least time between two points is represented by a great circle.

fermi Abbreviation, F. An extremely small unit of length and wavelength, equal to one quadrillionth (10^{-15}) of a meter.

Fermi-Dirac distribution function The probability that an electron will be in a certain quantum state under conditions of thermal equilbrium. This is determined as the probability that the electron will be in a given energy band at a particular instant of time.

fermium Symbol, Fm. A radioactive metallic element that is artificially produced. Atomic number, 100. Atomic weight, 257.

ferpic Acronym for *ferroelectric ceramic picture* device. An image-storing device containing a photoconductive film, transparent electrodes, and a ferroelectric ceramic, in layers.

ferreed A form of magnetic switching device, similar to a reed relay, that maintains its position indefinitely without the need for a continuous current.

ferret A vehicle or craft equipped for determining the locations of enemy radar transmitters.

ferri- A prefix used to denote magnetic properties.

ferric oxide Formula, Fe_2O_3. A red oxide of iron used to coat magnetic recording tape.

ferristor A high-frequency magnetic amplifier using a ferroresonant circuit.

ferrite A high-resistance magnetic material consisting principally of ferric oxide and one or more other metals. After being powdered and sintered, ferrites exhibit low eddy-current loss at high frequencies and make ideal core material for inductors and switching elements. Also used in television deflection yokes and in miniature antennas. Also see FERROSPINELS.

ferrite antenna See FERRITE-ROD ANTENNA.

ferrite bead **1.** A magnetic storage device in the form of a bead of ferrite powder fused onto the signal conductors of a memory matrix. **2.** A tiny ring of ferrite that can be slipped over a wire or cable to choke off radio-frequency (RF) currents.

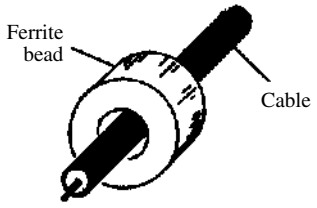

ferrite bead

ferrite core A coil or switching-element core made from a ferrite; specifically, in a core memory, a small magnetic toroid that can retain its polarity when charged by a pulse.

ferrite core memory A magnetic memory in which ferrite cores are interconnected by a network of input and output wires.

ferrite isolator A microwave device that permits energy to pass with negligible loss in one direction through a waveguide or coaxial line, while absorbing energy passing in the opposite direction.

ferrite limiter A device used in the antenna circuit or front end of a receiver, to prevent overload while maintaining a linear response. Used mostly at ultra-high and microwave frequencies.

5059F-pF-274-306 4/9/01 5:31 PM Page 280

ferrite loopstick See FERRITE-ROD ANTENNA.

ferrite memory A static memory using ferrite cores. See CORE MEMORY.

ferrite-rod antenna Also called *loopstick antenna*. A small antenna that can be used for wireless reception at frequencies below approximately 20 MHz. This antenna consists of a coil wound on a solenoidal, high-permeability, powdered-iron core, usually less than 20 centimeters (cm) long and 1 cm in diameter. A series or parallel capacitor, in conjunction with the coil forms a tuned circuit. The operating frequency is determined by the resonant frequency of the inductance-capacitance (LC) combination. Response is maximum off the sides of the coil, and a sharp null occurs off the ends. This antenna has narrow bandwidth. The null can be oriented to minimize system response to undesired local signals or humanmade noise. Compare SMALL LOOP ANTENNA.

ferrite switch A device that regulates the flow of power through a waveguide. The electric-field vector is rotated, resulting in a high degree of attenuation when actuated, but little or no attenuation when not activated.

ferroelectric **1.** Producing ferroelectricity. **2.** A ferroelectric material.

ferroelectric amplifier See DIELECTRIC AMPLIFIER.

ferroelectric capacitor A capacitor in which a ferroelectric material is the dielectric.

ferroelectric cell See FERROELECTRIC CAPACITOR.

ferroelectric crystal A crystal of ferroelectric material.

ferroelectric flip-flop A flip-flop based on the hysteresis of a ferroelectric capacitor. Compare FERRORESONANT FLIP-FLOP.

ferroelectricity Electric polarization in certain crystalline materials. The effect is analogous to the magnetization of a ferromagnetic material by a magnetic field.

ferroelectric-luminescent Pertaining to a ferroelectric cell that emits light.

ferroelectric material A nonlinear dielectric material capable of producing ferroelectricity. Examples: barium titanate, barium strontium titanate, potassium dihydrogen phosphate, guanadine aluminum sulfate hexahydrate (GASH), Rochelle salt, and triglycene sulfate.

ferromagnetic **1.** Pertaining to a substance that conducts a magnetic field with relative ease. **2.** Pertaining to a material in which a magnetic-field change causes a voltage, which in turn results in a measurable current flow.

ferromagnetic-core inductor A coil of wire designed to introduce inductive reactance into a circuit or system, wound around a core consisting of ferromagnetic material that greatly increases the inductance for a given number of turns. With proper design and choice of core material, the Q factor (selectivity attainable) can be extremely high. The core confines much of the magnetic flux within itself. When the coil current exceeds a certain level, *core saturation* occurs, and further increases in the current will not produce a corresponding increase in magnetic flux. This decreases the effective inductance, and reduces the efficiency because power is dissipated as heat in the core.

ferromagnetic material A substance that concentrates magnetic lines of flux relative to their concentration in free space. Iron, powdered iron, and ferrite are common examples.

ferromagnetic resonance The point at which the permeability of a magnetic material peaks at a microwave frequency.

ferromagnetic spinels Highly permeable and resistive ceramic-like materials. The low eddy-current losses and high permeability of these materials suit them for use as cores in radio-frequency (RF) transformers and inductors. Also see FERRITE.

ferromagnetic tape Magnetic tape used for winding closed transformer cores.

ferrometer An instrument for testing hysteresis and permeability in steel and iron.

Ferron detector See IRON-PYRITES DETECTOR.

ferroresonant circuit An inductance-capacitance (LC) circuit in which the coil is a saturable reactor. Because of coil nonlinearity, the circuit is resonant at only one value of alternating-current (ac) voltage, and exhibits both negative resistance and bistable operation.

ferroresonant counter A digital counter using ferroresonant flip-flops, rather than semiconductor devices.

ferroresonant flip-flop A flip-flop using one or two ferroresonant circuits instead of semiconductor devices. See BISTABLE MULTIVIBRATOR. Compare FERROELECTRIC FLIP-FLOP.

ferroresonant shift register A shift register using ferroresonant circuits instead of semiconductor devices.

ferrosoferric oxide See MAGNETITE.

ferrospinels See FERROMAGNETIC SPINELS.

ferrous Pertaining to a substance that contains iron and is magnetizable.

Ferroxcube A nonmetallic ferromagnetic material having high permeability and resistivity, and a Curie point near room temperature. These characteristics make the material suitable for the cores of radio-frequency (RF) inductors and transformers, and for high-frequency magnetic shields.

Fessenden oscillator In underwater communications, a transmitter of acoustic waves.

FET Abbreviation of FIELD-EFFECT TRANSISTOR.

fetch An operation in a computer run in which the location of the next instruction is taken from memory and changed if necessary; it then goes to the control register.

5059F-pF-274-306 4/9/01 5:31 PM Page 281

FET current meter An ammeter, milliammeter, or microammeter having a self-contained amplifier that uses field-effect transistors. Also see ELECTRONIC CURRENT METER.

FET op-amp **1.** An operational amplifier composed of field-effect transistors and associated components. **2.** An operational amplifier having a field-effect transistor in its input stage.

FET voltmeter A voltmeter using a field-effect transistor amplifier for high-impedance input. Also see ELECTRONIC VOLTMETER.

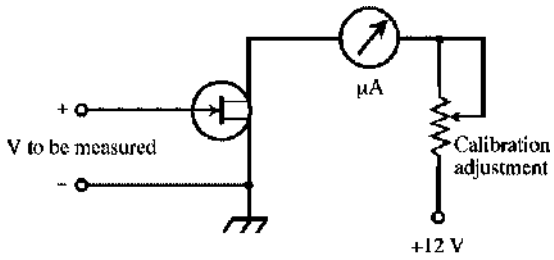

FET voltmeter

FET VOM A volt-ohm-milliammeter (VOM) using a field-effect transistor amplifier for increased sensitivity and high input impedance.

FF Abbreviation of FLIP-FLOP.

fF Abbreviation of FEMTOFARAD.

FFI Abbreviation of FUEL-FLOW INDICATOR.

fhp Abbreviation of FRACTIONAL HORSEPOWER.

fiber **1.** A tough, vulcanized insulating material. Dielectric constant, 2.5 to 5. Dielectric strength, 2 kV/mm. **2.** A thin thread of a material. **3.** Also called *optical fiber.* A light-conductive transparent filament; see FIBEROPTICS, **1**.

fiber electrometer An instrument for measuring small quantities of electricity. It consists of a thin thread, such as one of plasticized quartz, hanging freely between two knife-edged metal pieces that are charged by the electricity being measured. The charge draws the fiber away from its position of rest. The movement can be observed with a microscope. A special form of this instrument, using two fibers, is the *bifilar electrometer.*

fiber needle A soft phonograph needle made from a fiber. It produces less disk wear than other styli, but is short-lived.

fiber metallurgy A process in which metallic fibers or filaments are grown.

fiberoptic bundle A cable of optical fibers. See FIBEROPTICS, **1**.

fiberoptic coupling Also called *optical coupling.* A method of coupling in which a light-conducting fiber is placed between a light (signal) source and a photoreceptor. Also see FIBEROPTICS, **1**, **2**.

fiberoptics **1.** Also called *optical fibers.* Extruded materials, such as certain plastic filaments, that provide paths for light. **2.** The science of developing and using communications systems that use optical fibers to transfer data.

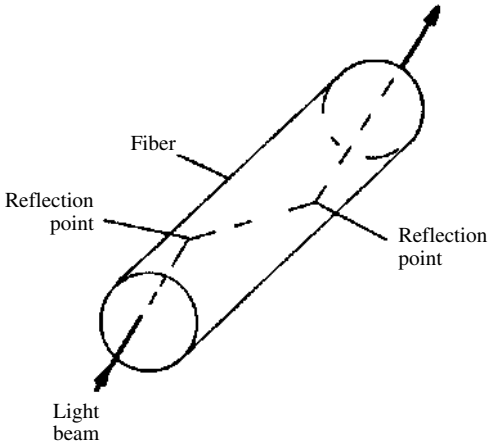

fiberoptics

fiberoptic scrambler A fiberscope in which a center section of fibers in the core is deliberately disoriented before the bundle is encapsulated; when cut, one half can decode the image encoded by the other half. See FIBERSCOPE.

fiberscope A flexible bundle of optical fibers having a lens at each end; it is used to view areas that are otherwise inaccessible to view.

fiber stylus See FIBER NEEDLE.

fibre Alternate (Brit.) spelling of FIBER.

fibrillation Dangerous, irregular beating of the heart that often follows electric shock. Also see CARDIAC STIMULATOR and DEFIBRILLATION.

fidelity The degree to which a circuit or device transmits a signal without distorting it. Pertains especially to acoustic devices and stereo audio equipment.

field **1.** A volume of space in which a force is operative. See, for example, ELECTRIC FIELD and MAGNETIC FIELD. **2.** Half of a video image, consisting either of all the even-numbered lines, or all the odd-numbered lines. **3.** A computer record subdivision containing an information unit (e.g., a bank account record might have deposits as a field).

field circuit breaker A circuit breaker designed to control the field excitation of a motor or other device.

field coil **1.** The winding on the field pole of a motor or generator. **2.** The winding on the pole of an electrodynamic speaker. **3.** The main coil of a relay. **4.** The fixed coil in an electrodynamometer.

5059F-pF-274-306 4/9/01 5:31 PM Page 282

Field Day In amateur radio, an annual contest sponsored by the American Radio Relay League (ARRL) to simulate emergency communication conditions. It occurs during the last full weekend in June.

field direction The direction in which an electric field or magnetic field exerts its force.

field effect The phenomenon in which the flow of current carriers in a solid substance is controlled by an external electric field. A useful application is the FIELD-EFFECT TRANSISTOR (FET).

field-effect tetrode Also called *dual-gate FET*. A field-effect transistor (FET) in which the gate electrode is split into two parts, each connected to a separate external lead. The reverse bias between the channel and either gate lead affects the conductivity through the device.

field-effect transistor Abbreviation, FET. A monolithic semiconductor amplifying device in which a high-impedance GATE electrode controls the flow of current carriers through a thin bar of silicon (rarely, germanium) called the CHANNEL. Ohmic connections made to the ends of the channel constitute SOURCE and DRAIN electrodes. Also see JUNCTION FIELD-EFFECT TRANSISTOR, METAL-OXIDE SEMICONDUCTOR FIELD-EFFECT TRANSISTOR, and CHANNEL JUNCTION FIELD-EFFECT TRANSISTOR.

field-effect varistor A nonlinear dual-terminal semiconductor device capable of maintaining a value of current for a range of voltages.

field-emission microscope An instrument for examining the atomic structure of high-melting-point metals; it magnifies more than 2 million times. The metal to be examined is made into a needle that is subjected to 5 to 30 kV; electrons emitted by the tip of the needle form an image on a fluorescent screen.

field forcing A method of controlling a motor by changing the magnetic field in the windings.

field frequency In television, the product of frame frequency and fields per frame (in the United States, 60 per second).

field intensity **1.** The strength of an electric or magnetic field. **2.** The strength of an electromagnetic field, usually expressed in microvolts per meter or millivolts per meter.

field-intensity meter See FIELD-STRENGTH METER.

field ionization The tendency for atoms to be ionized in a gas by a high-intensity electric field. The ionization occurs mostly near the poles of the electric field.

field-ion microscope A high-resolution field-emission microscope that uses helium ions instead of electrons. The ions are repelled by the tip of the metal needle under observation, forming an image on a fluorescent screen. Also see FIELD-EMISSION MICROSCOPE.

field length Record field size in applicable units, usually bytes, characters, or words.

field magnet **1.** The permanent magnet in a dynamic speaker. **2.** A similar magnet in an earphone, generator, microphone, motor, phono pickup, transducer, etc.

field pickup **1.** A probe or sensor for insertion into an electric or magnetic field. **2.** An on-location radio or television program (i.e., one coming from outside the studio). Also called remote or NEMO.

field resistor A resistive component consisting of an insulated form with a thin layer of conductive material.

field rheostat The rheostat whose setting determines the amount of current flow through the field coil of a motor or generator.

field scan A form of television scanning in which the lines are scanned alternately.

field-sequential system A color-television system in which the image is reproduced by means of primary color fields (red, green, and blue) flashed sequentially on the screen of the picture tube. Compare DOT-SEQUENTIAL SYSTEM and LINE-SEQUENTIAL SYSTEM.

field strength See FIELD INTENSITY.

field-strength meter An instrument for measuring the radio-frequency (RF) voltage of a signal reaching a chosen location. The instrument consists essentially of a radio detector equipped with a portable antenna and an output meter.

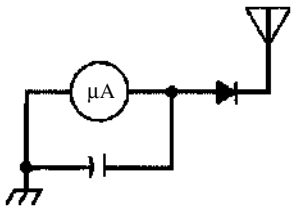

field-strength meter

field telephone A rugged, portable telephone system for outdoor use.

field test A test of equipment under actual operating conditions (i.e., outside the laboratory or factory).

field winding See FIELD COIL, **1**, **2**.

fig. Abbreviation of *figure* (usually in reference to an illustration).

figure-8 pattern **1.** A bidirectional antenna pattern whose cross section, in a specified plane, resembles the numeral 8. **2.** A Lissajous figure resembling the numeral 8.

figure of merit **1.** For a capacitor, inductor, or tuned circuit, the ratio of reactance to resistance. Also called *Q factor* or *Q*. **2.** For a magnetic amplifier, the ratio of power amplification to control time constant. **3.** For a transistor, the *gain-bandwidth factor.*

fil Abbreviation of FILAMENT.

5059F-pF-274-306 4/9/01 5:31 PM Page 283

filament In a vacuum tube or incandescent lamp, the thin wire heated by electric current; it emits electrons, light, and heat. The filament is the cathode in a filament-type tube, but serves only to heat indirectly the cathode sleeve in an indirectly heated tube.

filament battery See A BATTERY.

filament choke A radio-frequency (RF) choke operated in the filament lead of an electron tube. Such chokes are necessary in filament-type tubes in RF power amplifiers.

filament circuit The circuit carrying filament current.

filament coil See FILAMENT WINDING.

filament current Symbol, I_F. The current flowing through the filament of a vacuum tube.

filament emission Electrons emitted directly by the filament in an electron tube (thermionic emission) or the amount of such emission.

filament hum A hum signal caused by voltage induced in a circuit by the alternating-current (ac)-operated filaments (heaters) of tubes or by the filament wiring.

filament lag The time delay in the heating and cooling of an ac tube or lamp filament as filament-current changes polarity.

filament power supply A source of power, usually alternating-current, for heating the filament of a vacuum tube or tubes.

filament resistance **1.** The resistance of the filament in an electron tube or incandescent lamp. **2.** The resistance of an external dropping resistor in the filament circuit of a tube or lamp.

filament transformer A step-down transformer that supplies power exclusively to the filament (heater) of an electron tube.

filament-type bolometer A BOLOMETER in which the sensitive element is a wire filament. Examples: barretter, incandescent lamp, and wire fuse.

filament voltage Symbol, V_F. The voltage across the filament of an electron tube.

filament winding In a power transformer, the coil that supplies heating power to the filament of a vacuum tube. Also called FILAMENT COIL.

file An organized collection of records related by a common format, data source, or application.

file conversion Converting data files from one form to another, often for the purpose of making them compatible with other computers.

file gap An area of a data medium that signifies the end of a file; it can also mark the start of another file.

file identification A code that identifies a file.

file label File identification in which the first record in the file is a set of characters unique to the file; it conveys such information about (for example, a tape file as a description of content, generation number, reel number, date of writing, etc.). Also called HEADER LABEL.

file layout How the contents of a file are organized; usually defined by the system or specified by a program.

file maintenance To delete, add, or correct records in a file. Unlike updating, which is done to reflect changes in events recorded in the file, maintenance ensures that the contents of the file are accurate records of the necessary data.

file management A method of storing and recalling data from computer storage media, such as magnetic disks.

filename In a computer file label, the alphanumeric character set that identifies and describes the file. It generally consists of one to eight characters, often including an extension of one to three characters. In some computer operating systems, filenames can be much longer (e.g., up to 32 characters). See FILENAME EXTENSION.

filename extension A group of one, two, or three characters following the main body of a FILENAME, and separated from it by a period (.). It generally denotes the application or purpose of the file. The extension .BAK, for example, denotes a backup file; .TXT denotes a text file; .BMP denotes a bit-mapped graphics file.

file organization The way words, bits, or records are physically arranged in the storage medium for a file, possibly including the method of access (serial, alphabetical, random, etc.).

file-oriented programming Computer programming that uses a general file and record-control program to simplify I/O coding.

file-oriented system A system having file storage as its basis.

file print A hard copy (printout) of the contents of a file.

file processing The operations associated with making and using files.

file protection Preventing the possibility of writing over data files before they are made available for use. It is usually done by having a program check file labels.

file reconstitution Restoring a partially or completely damaged file by updating a previous generation of the file using a file of interim transactions.

file recovery Following the interruption of file processing because of system failure, the procedure for reestablishing the file's condition as necessary for the resumption of processing without losing accuracy.

file section Part of a file in certain consecutive locations on a storage medium.

file security Protective and security measures (e.g., the issuance of clearances, status markers, etc.) as they relate to computer files.

file set A collection of interrelated files stored consecutively in a magnetic disk volume (package).

fill The percentage of lines in a cable that are actually in use at a given time.

filler A nonessential data part used, for example, to bring a record to a standard size.

5059F-pF-274-306 4/9/01 5:31 PM Page 284

film See THIN-FILM MEMORY.

film capacitor A capacitor in which the electrodes are plated or deposited on the faces of a thin film of plastic or other dielectric material.

film chain A system designed for the transmission of movies over a television system. This requires synchronization of the movie frame rate with the television scanning rate.

film frame A single picture on a strip of motion picture film.

film-frame blanking interval The interval during which a film frame is blanked out as motion-picture film moves through a camera, projector, or pickup. The blanking action allows a frame to move into position without blurring the image as seen by viewers.

film integrated circuit A monolithic circuit whose elements are films formed on an insulating substrate.

film pickup A photocell, photodiode, or phototransistor circuit used to pick up recordings from the sound track of motion-picture film.

film reader A device for converting data on film into digital form for a computer.

film recorder An apparatus that records data as a sound pattern on film. Compare FILM REPRODUCER.

film reproducer An apparatus that plays back data recorded on photographic film. Compare FILM RECORDER.

film resistor Also called *carbon-film resistor* or *metal-film resistor.* An electronic component consisting of a mixture of ceramic, carbon, and/or metal, applied to a cylindrical form in a thin layer to obtain a desired value of resistance. The cylindrical form is made of an insulating substance, such as porcelain. The film can be deposited on this form by various methods, and the value tailored as desired. Metal-film units can be made to have nearly exact values. Film type resistors usually have low to medium-high resistance. A major advantage of film-type resistors is that they, like carbon-composition units, do not have much inductance or capacitance. A disadvantage, in some applications, is that they cannot handle as much power as the more massive carbon-composition units, or as wirewound types. Compare CARBON-COMPOSITION RESISTOR, WIREWOUND RESISTOR.

film scanning The conversion of a movie into a form suitable for transmission by television.

film speed **1.** The speed at which motion-picture film moves intermittently through a camera, projector, or pickup, measured in feet or frames per second. **2.** A measure of film's light sensitivity, given as an ASA (American Standards Association) or DIN (European) number; in either system, the higher the number, the greater the light sensitivity.

filter **1.** A circuit or device that passes alternating currents at some frequencies while attenuating or blocking currents at other frequencies. Examples: BANDPASS FILTER, BAND-REJECTION FILTER, HIGH-PASS FILTER, and LOW-PASS FILTER. **2.** An inductance-capacitance (LC) or resistance-capacitance (RC) circuit for removing the ripple from the output of a power-supply rectifier. **3.** A transparent disk with special optical properties placed in front of a camera lens for a special photographic effect. **4.** A character patterned to control the elimination or selection of characters in another pattern. **5.** A device or program that separates information, according to certain specifications or characteristics. **6.** A machine word that specifies the elements to be treated in another machine word; also called MASK.

filter attenuation In a selective filter, the power, current, or voltage loss, in decibels, that occurs within the passband.

filter attenuation band In a selective filter, the frequency band(s) outside the passband; that is, the frequency range over which signals are significantly attenuated.

filter bank In audio applications, a set of bandpass filters, each of which covers a specific portion of the audio-frequency (AF) spectrum. There is some (minimal) overlap between the passbands of the filters, so an AF signal of a specific frequency will always pass through at least one of the filters, but will never pass through more than two of the filters.

filter capacitor A capacitor that provides capacitive reactance in a wave filter or power-supply filter while also blocking direct current.

filter center A place where information is modified for transmission to aircraft pilots. Such information can include weather data, course changes, or other instructions.

filter choke An inductor that provides inductive reactance in a wave filter or power-supply filter while affording relatively easy conduction of direct current.

filter crystal A piezoelectric crystal used in a CRYSTAL RESONATOR.

filter cutoff The frequency or frequencies at which the transmission figure of a filter is below its maximum value by a prescribed amount, usually 3 dB, representing the half-power point(s).

filter discrimination The amount of fluctuation in the insertion loss of a bandpass, band-rejection, high-pass, or low-pass selective filter. The fluctuation is measured at various points in the filter passband.

filter inductor See FILTER CHOKE.

filter passband The frequency range over which a selective filter passes signals with minimum attenuation.

filter reactor See FILTER CHOKE.

filter slot In a waveguide, a slot that acts as a choke to suppress undesirable modes.

filter stopband See FILTER ATTENUATION BAND.

5059F-pF-274-306 4/9/01 5:31 PM Page 285

filter transmission band See FILTER PASSBAND.

fin **1.** A metal disk or plate attached to a component for the purpose of radiating heat. **2.** A projection in an irregular heatsink.

final amplifier Also called *output amplifier* or *power amplifier.* In a wireless transmitter, the amplifier that boosts the signal power to the level to be emitted over the airwaves. The input is provided by the driver; the output is connected to the system, to a transverter, or to a network cable power amplifier. In some transmitters, the output amplifier requires no tuning; in others, adjustment of the output circuitry is necessary to obtain proper coupling to the antenna system. In a single-sideband (SSB) or amplitude-modulated (AM) transmitter, all amplifiers following the modulator must be linear. In transmitters intended for use only in digital modes or for frequency modulation (FM), power amplifiers need not be linear.

final result A result displayed at the end of a data processing operation. Compare INTERMEDIATE RESULT.

finder The switch or group of relays that selects the path for a call going through a telephone switching system. Also called LINE FINDER.

fine adjustment Adjustment of a quantity in small increments or as a smooth, continuous variation. Compare COARSE ADJUSTMENT.

fine-chrominance primary See I SIGNAL.

fine frequency control A variable component, such as a potentiometer or variable capacitor, that permits a signal or response frequency to be varied over a small increment; it is often used in conjunction with a coarse frequency control.

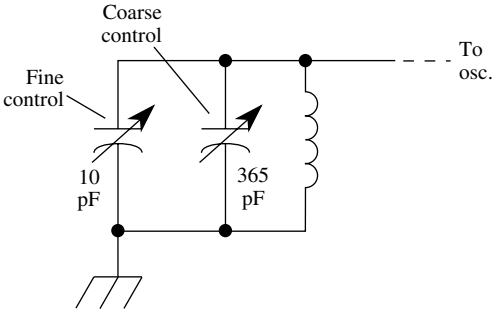

fine frequency control

fine-groove record See MICROGROOVE RECORD.

fine index In computer operations, a secondary, supplemental index used with a main, or gross, index when the latter does not adequately detail the differences between the items being indexed.

fine-motion planning The scheme used by a robotic end effector ("hand") to get in exactly the correct position. It uses machine vision, tactile sensors, pressure sensors, or high-precision displacement transducers.

finger See FEELER, **1**.

finger plethysmograph A device that senses and records the resistance through the human finger during various parts of the heart cycle.

finger rules See FLEMING'S LEFT-HAND RULE, FLEMING'S RIGHT-HAND RULE, and RIGHT-HAND RULE FOR WIRE.

finish lead The lead attached to the last turn of a coil. Also called *outside lead.* Compare START LEAD.

finished blank The end product in the crystal manufacturing process, often including electrodes.

finishing The careful handwork and testing involved in bringing a crystal blank to a condition that is acceptable as finished, according to specifications.

finishing rate The rate of charging a battery, as the battery approaches a full charge. Generally, the finishing rate is less than the normal charging rate.

finite Pertaining to that which has defined limits.

finite sample space In statistics, a sample space having definite limits.

finite series A mathematical series having a limited number of terms. Example: 1 + 0.1 + 0.01 + 0.001, a finite series containing four terms and whose sum is equal to 1.111.

finned surface The irregular surface of a heatsink. The ratio of surface area to volume is greater than with a flat surface; this increases the cooling effectiveness of the heatsink.

fins Metal vanes radiating from components that dissipate large amounts of power as heat.

FIR Abbreviation of FAR INFRARED.

fire A transition from non-conduction to conduction in an ionizing switching device.

fire control The aiming and firing of guns automatically via radar and associated electronic systems.

firefighter robot A robotic device or system intended to protect lives and property from fire. Such a robot can be simple, such as an automatic sprinkler system actuated via heat sensors and/or smoke detectors. More sophisticated systems might use autonomous or remotely controlled androids that perform the same functions as human firefighters.

Fire Underwriter's regulations See NATIONAL ELECTRIC CODE.

firing The pulse that initiates conduction in an ionization switching device.

firing angle **1.** For a magnetic amplifier, the angular distance through which the input-voltage vector rotates before the core is driven into saturation. **2.** For a silicon-controlled rectifier (SCR), the point, as an angle (in degrees or radians), along the control voltage half-cycle at which the SCR fires.

5059F-pF-274-306 4/9/01 5:31 PM Page 286

firing circuit Any circuit, such as a phase shifter, that permits adjustment of the firing angle of a silicon-controlled rectifier (SCR) or similar device, or which delivers the required pulse or other signal to initiate firing.

firmware **1.** Programs (software) in nonvolatile computer memory [e.g., in a read-only memory (ROM), that can only be changed by replacement with an alternate unit]. **2.** Unalterable internal interconnections that determine what a computing device or system can do. Also called MICROPROGRAM.

first detector In a superheterodyne circuit, the signal frequency detector. Compare SECOND DETECTOR.

first filter capacitor The input capacitor in a capacitor-input power-supply filter.

first Fresnel region A portion of a directional transmitted electromagnetic ray, shaped generally like a paraboloid with the apex at the transmitter and the axis in the direction of transmission. Any point in the first Fresnel zone is in such a position that the sum of the lengths of the paths from the point to the receiver, and the point to the transmitter, is no greater than 0.5 wavelength more than the distance from the transmitter to receiver.

first harmonic The fundamental frequency in a complex waveform from which multiples are generated.

first-in/first-out Acronym, FIFO. A read-write memory commonly used as a buffer to smooth out the flow of data bits in a digital system. The output bits are in the same order (sequence) as the input bits. If a data bit *x* goes into the FIFO before data bit *y*, then *x* will always emerge from the FIFO before *y*. Compare PUSHDOWN STACK.

first-in/last-out See PUSHDOWN STACK.

first law of thermodynamics Quantities of heat can be converted into mechanical work, and vice versa. Also see MECHANICAL EQUIVALENT OF HEAT.

first level address See ABSOLUTE ADDRESS.

first selector The selector that responds to the first-digit dial pulses when a telephone number is called.

fishbone antenna An untuned, wideband directional antenna of the general end-fire type. Consists of a number of collector antennas, each capacitively coupled to the resistor-terminated transmission line in collinear pairs. It is so called from its resemblance to the skeleton of a fish.

fishpaper A chemically treated, vulcanized-fiber paper used for electrical insulation.

fish pole A microphone boom that can be held in the hand.

fist In radiotelegraphy and wire telegraphy, an operator's manual sending style.

fitting A device intended to mechanically fasten a wire or cable in place.

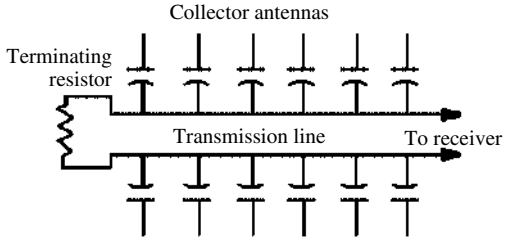

fishbone antenna

five-element code A five-impulse telegraph code that describes a character (e.g., Baudot, which also includes start and stop elements).

five-layer device A semiconductor device containing four pn junctions. Examples: diac and triac.

five-level code A teletype code that utilizes five binary elements to define a character.

fix **1.** In direction finding, the point at which two lines of direction intersect. **2.** In electronics maintenance, to repair successfully. **3.** To subject an in-process circuit board to a solution or other medium to stop a photographic action permanently. Also, the solution in which such photosensitive materials can be immersed to halt development.

fixed bias Bias voltage or current supplied from a fixed external source (such as a battery or power supply) independent of the operation of the biased device. Compare AUTOMATIC BIAS.

fixed block length Blocks of data having a fixed number of words or characters, as required because of hardware limitations or a program instruction. Compare VARIABLE BLOCK LENGTH.

fixed capacitor A nonadjustable capacitor (i.e., one having a single unalterable value).

fixed component Any component (e.g., a capacitor, inductor, or resistor that has one unalterable value).

fixed contact The stationary contact in a relay or switch. Compare MOVABLE CONTACT.

fixed-crystal detector A simple crystal detector in which the point of the contact wire is permanently placed in contact with a sensitive spot on the surface of the crystal.

fixed field Fields in records organized so that those containing similar information in each record are the same length and in the same relative position in the record. Compare VARIABLE FIELD.

fixed form coding The coding of source languages so that each part of the instruction is in a fixed field.

fixed-frequency amplifier An amplifier that is pretuned to operate on one frequency, or in a relatively narrow band of frequencies.

fixed-frequency oscillator An oscillator that is preset to operate on one frequency. Such an os-

5059F-pF-274-306 4/9/01 5:31 PM Page 287

cillator can be self-excited or controlled (crystal, fork, magnetostriction, etc.).

fixed-frequency receiver A receiver that is pretuned to receive signals of one frequency.

fixed-frequency transmitter A transmitter that is pretuned to radiate signals of one frequency. Such a transmitter can contain a self-excited or crystal-controlled oscillator.

fixed inductor A nonadjustable inductor (i.e., one having an unalterable value of inductance).

fixed-length record A record in which word or character size is constant. Compare VARIABLE LENGTH RECORD.

fixed logic Applicable to computers or peripherals whose logic can only be altered internally by changing connections.

fixed memory A nonvolatile readout computer memory that can only be altered mechanically.

fixed placement file A file that has been allocated a fixed location in storage.

fixed-point system A notation system in which a single set of digits represents a number, and the radix point (in the decimal system, the decimal point) can only be placed in one position for the value being expressed. Also see FLOATING-POINT CALCULATION.

fixed resistor A nonadjustable resistor (i.e., one having an unalterable value of resistance).

fixed-sequence robot A robot that performs one task or set of tasks, making exactly the same movements every time. The sequence is programmed in the robot controller via firmware. Many assembly robots and toy robots are of this type. Compare FLEXIBLE AUTOMATION.

fixed station A radio station operating from a stationary point; one that is not mobile.

fixed-step potentiometer A potentiometer whose output is varied in one or more discrete steps by fixed-resistor sections. Also see POTENTIOMETER.

fixed wireless 1. A cellular communications network in which some, or all, of the end users are at fixed locations. This is increasingly popular as an alternative to conventional hard-wired telephone and Internet access. 2. The use of wireless equipment, such as cell phones and wireless-modem–equipped computers, at fixed (rather than mobile or portable) locations.

fixed word length Applicable to the organization of information in storage in which each computer word stored has a fixed number of characters or bits.

fixture A piece of hardware used in equipment setups (e.g., microwave couplers, joints, sections, etc.).

fL Abbreviation of FOOT-LAMBERT.

flag **1.** A piece of information added to a data item that gives information about the data item. **2.** A bit added to a character or word to delineate a field boundary. **3.** An indication that an operation is complete and need not be done by the program. **4.** An indicator identifying the members of mixed sets. **5.** A character that signals the presence of some condition (e.g., an *error flag* indicates that a data item caused an error).

flag event A program condition that causes a flag to be set.

flag line An input pulse to a microprocessor that depends on specific external instructions. Indicates a certain condition or change of state.

flagpole antenna **1.** Any of several vertical UHF or VHF antennas consisting of a radiator mounted atop a coaxial pipe or cable (see, for example, COAXIAL ANTENNA). It takes its name from its resemblance to a flagpole. **2.** A vertical antenna formed by shunt-feeding a pole already in existence, such as a flagpole. This can be done to conceal the antenna.

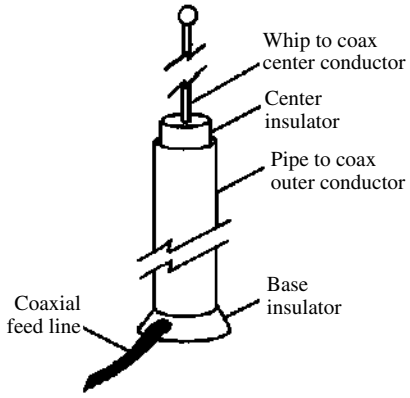

flagpole antenna, 1

flag terminal A form of terminal that does not require soldering for electrical contact. A protruding "flag" is crimped around the conductor.

flame alarm A (usually photoelectric or thermoelectric) device or circuit for detecting a flame and actuating an alarm.

flame control A (usually photoelectric or thermoelectric) device or circuit for sensing and automatically controlling the height of a flame, such as a gas pilot.

flame-failure control A FLAME CONTROL that automatically cuts off the fuel if the flame goes out.

flame microphone A microphone in which two electrodes in a flame undergo a change in electrical resistance when the flame is influenced by sound waves, thus modulating current passing between the electrodes.

flange **1.** A flat, protruding edge used for fastening a connector or plug to the chassis of a piece of equipment. **2.** In a waveguide, a coupling used for connection to another section of waveguide, or to a horn or other external device.

5059F-pF-274-306 4/9/01 5:31 PM Page 288

flange focus The focal length of a lens, based on the distance from the mounting flange to the focal plane.

flanging In sound systems, a means of obtaining special effects using a COMB FILTER. Creates an "extraterrestrial," digitized sound. Commonly used by rock music bands.

flanking Modification of the response of a selective filter, resulting from the parallel connection of two or more similar filters.

flap See DROP INDICATOR.

flap attenuator A waveguide attenuator consisting of a sheet of resistance material inserted transversely into the waveguide through a slot.

flare **1.** The hyperbolic cross section of a horn antenna or loudspeaker. **2.** A transient or stationary bright area with (usually) a central pip on the screen of an otherwise blank oscilloscope or television picture tube.

flare angle The gradual change in a waveguide's diameter over its length.

flare factor The angle at which the faces of a horn speaker are curved or turned outward.

flaring constant Symbol, *m.* A number expressing the degree of flare (see FLARE, **1**) in a horn antenna or loudspeaker. The value of m is equal to $0.6931/d$, where d is the distance along the axis required for the cross-sectional area A of the horn to double. If d is given in feet (ft), for example, then A is in units of square feet (ft^2) and m is in units of reciprocal feet (1/ft). If d is in centimeters (cm), then A is in units of square centimeters (cm^2) and m is in units of reciprocal centimeters (1/cm).

flash **1.** A photographic camera flash. **2.** To vaporize a metal (such as magnesium) in an electron tube being evacuated, to absorb gases. **3.** Flashover.

flash arc In a vacuum tube, a sudden high-current arc between cathode and plate at high plate voltages; it can short-circuit the plate power supply.

flashback voltage The maximum inverse voltage that causes the gas in a tube to ionize.

flash delay A device that automatically postpones the operation of a FLASHTUBE until a predetermined instant, such as the moment when a moving object arrives at a particular point before a camera.

flasher An electrical or electronic device or circuit that flashes a light or a series of lights sequentially.

flasher LED A light-emitting diode (LED) that, when connected to a low-voltage direct-current (dc) source, emits light that flashes at a basic rate of a few pulses per second.

flashlamp **1.** See FLASHTUBE. **2.** A small portable light operated from self-contained cells; a flashlight or lantern.

flashlight See FLASHLAMP, **2**.

flash memory High-capacity, nonvolatile random-access memory, used in some computers in place of an electromechanical hard drive. This type of memory allows a computer to store, access, and run large data files or programs much faster than is possible with a conventional hard drive. See also NONVOLATILE MEMORY, RANDOM-ACCESS MEMORY.

flashover The sudden discharge of electrical energy between electrodes or conductors, often accompanied by light; it is usually the result of excessive voltage.

flashover voltage **1.** The peak voltage at which FLASHOVER occurs. **2.** The voltage at which disruptive discharge occurs between electrodes and across the surface of an insulating material.

flash plating Electroplating in which a thin layer is deposited quickly.

flash test Insulation testing by applying a higher-than-normal voltage for a short time.

flashtube A straight or coiled glass tube filled with gas and provided with electrodes. When a high voltage is applied to the electrodes, the tube emits a brilliant flash of light.

flat cable Also called *ribbon cable.* A cable whose flexible conductors are molded side by side in a flexible, flat ribbon of plastic (such as polyethylene).

flat-compounded generator A compound-wound generator whose windings are proportioned so that the full-load and no-load voltages are identical.

flat fading Fading of a radio signal that occurs independently of frequency; all frequency components of the signal fade to the same extent at the same time.

flat file A computer file containing unfolded documents.

flat frequency response Relatively equal response to all fixed-point frequencies within a given spectrum, exhibited by an amplifier or other circuit that must transmit a band of frequencies.

flat line A transmission line in which there are no standing waves, or for which the standing-wave ratio is very low.

flat pack An integrated circuit package consisting of a square or rectangular flat housing, with pins projecting straight outward from the edges.

flat response A response characteristic in which the dependent variable is substantially constant over a specified range of values of the independent variable. For example, in amplifier operation, an output signal whose component fundamental frequencies and their harmonics are in the same proportion as those of the input signal being amplified.

flat-ribbon line A transmission line (feeder) consisting of two flexible conductors molded in a flexible, flat ribbon of plastic, such as polyethylene. Also called *twinlead.*

flattening The leveling-off or blunting of a normally peaked or curved response, often caused by signal saturation within a circuit. Sine-wave clipping is an example.

5059F-pF-274-306 4/9/01 5:31 PM Page 289

flat top **1.** The horizontal radiating portion of an antenna. **2.** See FLAT-TOP ANTENNA. **3.** Of an amplifier, to distort by clipping of the positive half-cycles.

flat-top antenna An antenna having a horizontal wire or wires at the top to lower the resonant frequency and increase the bandwidth.

flat-top beam A bidirectional, end-fire antenna consisting of two close-spaced dipoles center-fed out of phase. Also see KRAUS ANTENNA.

flat-topping The positive-peak clipping of a modulation envelope that occurs when an amplifier is overdriven or when a signal is overmodulated. This is in contrast to deliberate clipping. Flat-topping results in "splatter" and is, therefore, an undesirable characteristic in an amplitude-modulated signal.

flat-top response The ability to uniformly transmit frequencies in a given band.

flat transmission line **1.** A transmission line that is free of standing waves. Also see MATCHED TRANSMISSION LINE. **2.** See FLAT-RIBBON LINE.

flaw An irregularity in a substance that can result in problems, such as mechanical failure or poor equipment performance.

flaw detector An instrument that uses ultrasonic waves to detect internal flaws in metal. The waves are reflected by flaws.

F layer See F REGION.

fLb Abbreviation of FOOT-LAMBERT.

Fleming/Kennelly law Under conditions at or near magnetic saturation in a ferromagnetic substance, the reluctivity is directly proportional to the intensity of the magnetic field.

Fleming's generator rule See FLEMING'S RIGHT-HAND RULE.

Fleming's left-hand rule A simple way of indicating certain relationships in the behavior of electric generators and motors. If the thumb, index finger, and middle finger of the left hand are positioned so that they are at right angles to each other, the thumb will point in the direction of force or motion when the index finger is pointed in the direction of flux; the middle finger points in the direction of current flow. Compare FLEMING'S RIGHT-HAND RULE.

Fleming's motor rule See FLEMING'S LEFT-HAND RULE.

Fleming's right-hand rule A simple way of indicating certain relationships in the behavior of electric generators and motors. If the thumb, index finger, and middle finger of the right hand are positioned so that they are at right angles to each other, the middle finger points in the direction of an induced voltage, the thumb in the direction of the motion of a conductor, and the index finger in the direction of the magnetic field. Compare FLEMING'S LEFT-HAND RULE.

Fletcher-Munson curves A set of curves depicting the uneven frequency response of human hearing. Also called AUDIBILITY CURVES.

flexible automation The ability of a robot or system to do various different tasks. Changing from one task to another is simply a matter of changing software. Compare FIXED-SEQUENCE ROBOT.

flexible collodion A viscous solution of pyroxylin (cellulose nitrates) used sometimes as a binder for coils.

flexible contact A contact made from flat, metal spring stock; it is usually bent or curved. Also called *spring contact.*

flexible coupling A device for joining two shafts and conveying rotary motion from one to the other; it is elastic, so the shafts need not be exactly aligned with each other.

flexible flat cable See FLAT CABLE.

flexible manufacturing system A roboticized manufacturing plant that can turn out a variety of different products. One or more central computers oversee the operation of the facility. Such factories are commonly used in the production of electronic devices (such as printed circuits, calculators, and portable radios).

flexible resistor An insulated, wirewound resistor that can be bent, coiled, or knotted.

flexible shaft A control shaft that can be bent somewhat while still allowing easy adjustment.

flex life A measure of how much bending a conductor or other flexible object can take without breaking.

flexode A diode that is flexible in that its junction can be changed (i.e., reversed without reversing its leads, its resistance being variable from the forward- to backward-resistance value).

flicker **1.** A tendency for a video image to appear, disappear, and reappear, or to increase and decrease in intensity frequently. **2.** The effect created by such action (as in a flickering light).

flicker frequency The number of times the screen illumination flashes on and off in the projection of a motion picture. It is 48 per second (twice the frame rate) in conventional movie projectors; for each frame, the screen is blanked once when the frame is pulled into position and once again during projection of the frame.

flight control Electronic monitoring and control of an aircraft in flight.

flight path The course planned for an aircraft's flight.

flight-path computer A computer that controls the course of an aircraft in flight, from takeoff to landing.

flight-path deviation The departure of an aircraft in flight from the course in the flight plan. Also see FLIGHT PATH.

flight-path-deviation meter An instrument that provides a visual indication of the departure of an aircraft in flight from the course in the flight plan.

flight telerobotic servicer A remotely controlled robot used to maintain and repair space vehicles and satellites. The machine can be controlled by

5059F-pF-274-306 4/9/01 5:31 PM Page 290

a computer program or by a human operator. The most-sophisticated machines can use TELEOPERATION and/or TELEPRESENCE so that a human can perform dangerous work without being placed at personal risk.

flight test **1.** To test airborne electronic equipment in actual flight. **2.** Any test made as in **1**.

Flinders bar In a magnetic compass, a metal bar that corrects for the vertical component (inclination) of the earth's magnetic field. The bar must be designed differently in different geographic locations, because the inclination varies from place to place. Inclination is greatest near the geomagnetic poles, and is zero at the geomagnetic equator.

flint glass A hard, bright, lead glass. Dielectric constant, 7 to 9.9. Dielectric strength, 30 to 150 kV/mm. Also see GLASS.

flip chip A monolithic semiconductor device (such as a diode, transistor, or integrated circuit), in which bead-like terminals are provided on one face of the chip for bonding.

flip-chip bonding A scheme for making connections between a semiconductor chip and a header, in which leads are not run between chip and header. Instead, bead-like projections are electrodeposited as terminals around one face of the chip, which is then registered with the header terminals and bonded to them.

flip-flop **1.** See BISTABLE MULTIVIBRATOR. **2.** A two-position relay that locks in alternate positions upon receiving successive actuating pulses.

flip-flop key In a video display, a key that, when pressed, allows viewing of one half of the screen and then the other.

flip-flop memory A bistable computer memory that stores bits of data as flip-flop states.

flip-flop relay See BISTABLE RELAY.

float charging The constant charging of a storage battery, keeping the battery at or near the fully charged state at all times.

floated battery A storage battery connected in parallel with a generator, which supplies the load; the battery, always completely charged, helps during high-current demands.

floating **1.** To float a storage battery; see FLOAT. **2.** An ungrounded device or circuit that is not connected to a source of voltage. **3.** Not loaded or driven. **4.** Not fixed in position. **5.** A dedicated ground connection that remains isolated from the common circuit ground.

floating address See RELATIVE ADDRESS.

floating charge See TRICKLE CHARGE.

floating control **1.** A potentiometer, such as a gain control, installed with its shaft insulated from ground and, accordingly, subject to body-capacitance effects. **2.** A type of automatic control in which the rate of final control element movement depends on the amount that the controlled variable deviates from a prescribed value.

floating ground See FLOATING, **5**.

floating input An ungrounded input circuit.

floating-input measurement See DIFFERENTIAL-INPUT MEASUREMENT.

floating instrument An instrument whose signal terminals are above ground.

floating I/O port An input/output (I/O) terminal that is not loaded or being driven.

floating junction A junction (in a semiconductor device, for example), that has no net current flowing through it.

floating neutral A circuit with a variable common voltage reference.

floating paraphase inverter A dual-transistor adaptation of the paraphase inverter. The second stage receives its input signal from a tap on the load resistor of the first stage and provides the additional phase shift that is required.

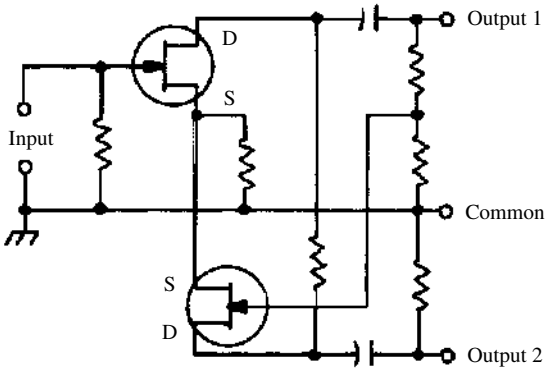

floating paraphase inverter

floating-point calculation An electronic calculation using a floating point number [i.e., a number whose value is represented by two sets of digits, a fixed-point part (see FIXED-POINT SYSTEM) and a radix (base number) with an exponent]. Important in the operation of microprocessors, especially in computer systems.

floating-point number A number expressed in the floating-point system.

floating-point package Computer-vendor software that enables that computer to perform floating-point calculations.

floating-point system A system of notation in which a number n is represented by two sets of numbers: a fixed-point part (see FIXED-POINT SYSTEM) a, the radix (base number) r, and an exponent b as follows: $n = a \times r^b$. For example, in the floating-point system, 623 can be written 6.23×10^2. Floating-point numbers can be stored economically (in terms of memory) and in magnitudes that might otherwise be beyond the capacity of the computer to operate upon with relatively consistent accuracy. Compare FIXED-POINT SYSTEM.

5059F-pF-274-306 4/9/01 5:31 PM Page 291

floating probe A test electrode (wire or plate) inserted in a discharge tube at a desired point to sample the potential gradient, but which acquires a misleading negative charge, with respect to the gas cloud, because electrons (traveling faster than the positive ions) tend to accumulate on the probe.

floating zero A control system in which the reference point is easily moved.

floating zone In a semiconductor ingot undergoing purification, a molten zone in which impurities float. The material in the zone is melted by the radio-frequency (RF) field of an external heating coil, which is passed along the ingot to move the molten zone to one end, picking up impurities along the way and concentrating them at the end that is later sawed off.

float switch A switch operated by a float, such as in a sump pump.

flocking **1.** Particulate felt used on phonograph turntables to protect disks from being scratched. **2.** To coat with flocking.

flood gun In a storage (image-holding) oscilloscope, the electron gun that sprays the storage target with low-velocity electrons and makes the image visible on the viewing screen. The gun is mounted next to one pair of deflection plates. Compare WRITING GUN.

floor stand A support for a microphone, consisting of a heavy base that rests on the floor, and an adjustable, vertical boom that allows the microphone to be set at various heights.

floppy disk A flexible magnetic disk used in recording, as in computer and data system storage. It usually refers to a 5.25-inch diskette.

flow **1.** The movement of current carriers under the influence of an electric field. **2.** See ANGLE OF CONDUCTION. **3.** A series of interrelated events in a time sequence.

flow angle See ANGLE OF CONDUCTION.

flowchart **1.** A diagram depicting the logic steps in a digital-computer program. **2.** A diagram showing the flow of material through a sequence of processes.

flow direction The method of delineating antecedent and successor events on a flowchart; usually arrows and flowlines connecting the events in the way a page is read (top to bottom, left to right).

flowed-wax disk A form of recording disk, in which wax is melted onto a plastic or metal base. The grooves are cut in the wax layer.

flowline A line showing flow direction on a flowchart.

flowmeter An instrument for measuring liquid flow rate.

flow relay A relay that is actuated by a predetermined rate of fluid flow.

fluctuating current See COMPOSITE CURRENT.

fluctuating voltage See COMPOSITE VOLTAGE.

fluid absorption See LIQUID ABSORPTION.

fluid analogy The comparison of electric current flow to the movement of a simple fluid. Also see WATER ANALOGY.

fluid capacitor See WATER CAPACITOR.

fluid computer A digital computer that uses fluid logic elements (i.e., one that contains no electronic circuits or moving parts).

fluid damping Use of a viscous fluid to damp a mechanical member's movement.

fluid-flow alarm An electronic circuit that actuates an alarm when fluid flowing through pipes or other channels changes from a predetermined rate.

fluid-flow control A servo system that automatically maintains or adjusts liquid flow through pipes or other channels.

fluid-flow gauge See FLUID-FLOW METER.

fluid-flow indicator See FLUID-FLOW METER.

fluid-flow meter An instrument that indicates fluid flow rate through pipes or other channels.

fluid-flow switch In a fluid-cooled system, a switch that actuates an alarm when the fluid slows or stops.

fluidics **1.** A form of digital logic in which circuits operate by means of fluid flow. **2.** A branch of physics concerned with the behavior of fluids; more commonly called *fluid dynamics.*

fluid-level control A servo system that automatically maintains the level of a fluid in a tank.

fluid-level gauge An electronic system that provides direct readings of the level of a fluid in a tank.

fluid-level indicator See FLUID-LEVEL GAUGE.

fluid logic Logic operations carried out by varying the flow and pressure of a gas or liquid in a circuit of channels. Also see FLUID COMPUTER.

fluid ounce (U.S.) Abbreviation, fl. oz. A unit of volume equal to 2.957×10^{-5} cubic meters, or 0.02957 liter. A quart is 32 ounces; a gallon is 128 ounces.

fluid-pressure alarm An electronic circuit that actuates an alarm when fluid pressure rises or falls beyond set limits.

fluid-pressure control A servo system that automatically maintains or adjusts fluid pressure in pipes or other channels.

fluid-pressure gauge See FLUID-PRESSURE METER.

fluid-pressure indicator See FLUID-PRESSURE METER.

fluid-pressure meter An instrument that indicates the pressure of a fluid in a pipe or other channel.

fluid valve See ELECTROMECHANICAL VALVE.

fluorescence The property of some materials to glow when excited by a stimulus, such as ultraviolet, X rays, or an electron beam. Compare PHOSPHORESCENCE.

fluorescent lamp See FLUORESCENT TUBE.

fluorescent materials Materials that glow when irradiated, but cease to glow when the source of excitation is removed. An example is the phosphor coating on the screen of a cathode-ray tube (CRT).

5059F-pF-274-306 4/9/01 5:31 PM Page 292

fluorescent screen A transparent or translucent plate (such as the end of a cathode-ray tube or fluoroscope) coated with phosphors that glow when struck by an electron beam, or by high-energy electromagnetic radiation, such as ultraviolet or X rays.

fluorescent tube A mercury-vapor glow lamp distinguished by having a glass tube whose inner wall is coated with a phosphor that emits light when excited by the ultraviolet glow discharge in the vapor.

fluorescent X rays X rays reradiated by the atoms of a material that has absorbed X radiation. During initial exposure, energy absorbed from the radiation raises the energy level of electrons in the atoms; when the electrons return to their normal energy levels, they reradiate some of the absorbed energy.

fluorine Symbol, F. A gaseous element of the halogen family. Atomic number, 9. Atomic weight, 18.998.

fluoroscope A device used for viewing the internal structures of objects. A screen coated with material that fluoresces when exposed to X rays is mounted in one end of a light-tight viewing hood. When an object is placed between the screen and an X-ray tube, an image is produced on the screen. In medical applications, this device has been supplanted by methods that do not use ionizing radiation; *nuclear magnetic resonance imaging (NMRI)* is one example.

fluoroscopy The art of using a fluoroscope in the inspection of materials and parts or in medical examinations.

flush A form of mounting in which there is little or no protrusion from the panel surface.

flutter **1.** In a high-frequency superheterodyne receiver, a rapid fluctuation in signal strength, caused by tuning and detuning of the oscillator stage. This usually results from poor direct-current (dc) power-supply regulation. **2.** Repetitive, rapid fluctuations in the output of a sound reproducer. Also see WOW. **3.** An echo effect sometimes observed in rooms or auditoriums of poor acoustic design.

flutter bridge A bridge-type instrument for measuring flutter in constant-speed machines, such as sound recording and reproducing devices.

flutter rate The frequency of flutter, in cycles per second (Hertz).

flux **1.** Theoretical lines of force that extend in all directions from an electric charge (electric flux) or from a magnetic pole (magnetic flux). **2.** A material that makes metals more amenable to being joined by soldering. **3.** The number of photons that pass through a surface for a given time.

flux density Symbol, *B*. Unit, tesla. The degree of concentration of magnetic lines of force. One tesla represents a flux density of one volt-second per square meter ($V \cdot s/m^2$).

fluxgate A device that controls the azimuth bearing of a directional system by means of interaction with the geomagnetic field.

fluxgate magnetometer A magnetic compass for robot guidance. Uses coils to sense changes in artificially generated reference fields. Output from the sensors is sent to a computer that calculates the robot's position, based on the orientation and intensity of the lines of flux in the reference fields.

flux graph A device that graphically records the intensity of a magnetic field around a permanent magnet or electromagnet, or around an inductor carrying a current.

flux leakage See MAGNETIC LEAKAGE.

flux lines The theoretical lines of force in an electric or magnetic field.

flux linkage The passage of lines of force set up by one component through another component, so as to enclose most of the penetrated component's volume.

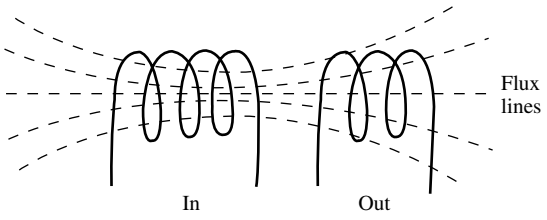

flux linkage

fluxmeter An instrument for measuring magnetic flux density. Also called *gaussmeter*.

flux refraction The tendency for magnetic lines of flux to change direction at the boundary between substances having different permeability. Flux refraction resembles refraction of electromagnetic radiation in or at a boundary between substances having different indices of refraction.

flyback **1.** The abrupt drop or reversal of a current or voltage that was previously increasing (e.g., the rapid fall of a sawtooth wave). Also see KICKBACK. **2.** The duration of the drop of a current or voltage that was previously increasing, for a sawtooth or similar wave. **3.** In an oscilloscope or picture tube, the rapid return of the beam to its starting position.

flyback checker An apparatus that senses the presence of short or open circuits in motors, transformers, and generators, by measuring the amount of flyback (kickback).

flyback power supply See KICKBACK POWER SUPPLY.

flyback time The time taken for the electron beam in an oscilloscope tube, picture tube, or camera tube to return to its starting point after it has reached the point of maximum deflection.

5059F-pF-274-306 4/9/01 5:31 PM Page 293

flyback transformer In a television receiver circuit, the horizontal output transformer. The unit supplies horizontal scanning voltage and kickback voltage, which is rectified to produce the high-voltage direct-current (dc) anode potential. Also see FLYBACK and KICKBACK POWER SUPPLY.

flying eyeball An undersea exploration robot consisting of a television camera, illumination lamps, and thrusters (such as jets or propellers). A cable, which also serves as a tether, sends data to a human operator, and allows the operator to control the movements of the robot. In some cases, the tether/cable can be replaced by an infrared or visible-light laser data link.

flying-spot tube A tube, such as a camera tube, in which a rapidly deflected spot of light scans an image on a transparent screen; the spot is projected through the picture to a photomultiplier.

fly's-eye lens A lens consisting of hundreds of much smaller lenses. Used in microelectronic circuit fabrication to produce many images of the same circuit.

flywheel effect 1. In an inductance-capacitance (LC) tank circuit, the completion of a partial input wave cycle at the resonant frequency, resulting from the storage and release of energy. This provides a nearly perfect sine-wave output for class-AB, class-B, and class-C radio-frequency (RF) power amplifiers. **2.** In an LC tank circuit, the action in which energy continues to oscillate between the capacitor and inductor after an input signal has been removed. The oscillation stops when the tank-circuit finally loses the energy absorbed. The lower the inherent resistance of the circuit, the longer the decrement (decay time).

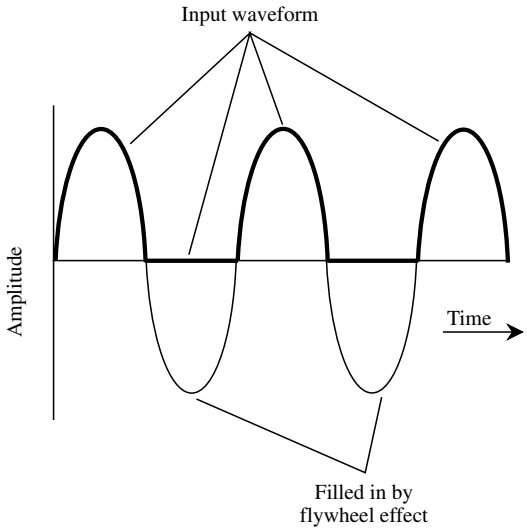

flywheel effect, 1.

flywheel synchronization A form of television scanning synchronization used when the received signal is very weak. The synchronization signals from the transmitter are sensed by the receiver, which then produces its own local pulses based on the rate of received pulses.

flywheel tuning A tuning dial mechanism in which the control shaft has a flywheel for the smoother tuning action afforded by the added momentum.

Fm Symbol for FERMIUM.

FM Abbreviation of FREQUENCY MODULATION.

f_m Abbreviation of MODULATION FREQUENCY.

FM-AM Pertaining to equipment that will operate with either amplitude-modulated or frequency-modulated signals.

FM-AM multiplier A method of frequency multiplication using both amplitude and frequency modulation of a carrier wave.

FM broadcast band The 88- to 108-MHz frequency band, within which channels spaced 200 kHz apart occupy positions from 88.1 to 107.9 MHz.

FM detector See DISCRIMINATOR, RATIO DETECTOR, and SLOPE DETECTOR.

FM-FM Frequency modulation by one or more FM subcarriers.

FM limiter In a frequency-modulation circuit, a stage which holds the amplitude of the FM signal to a constant value. The limiter can be active (e.g., an amplifier-limiter transistor) or passive (e.g., a diode clipper).

FM multiplex See MULTIPLEX ADAPTER.

FM noise Unintentional modulation of a frequency-modulated transmitter, resulting from noise in the audio-input stages.

FM-PM A system of modulation in which a carrier is phase modulated by frequency-modulated subcarriers.

FM radar A radar system in which the signal is frequency modulated; the distance to the target is measured in terms of the beat note between transmitted and reflected waves.

FM repeater A two-way radio system composed of a simultaneously operating receiver and transmitter, the latter of which retransmits (usually on a different frequency) all signals picked up by the receiver. The system is usually tower- or hilltop-mounted, and is used to extend the range of two-way units in a communications network.

FM stereo The use of multiplex methods to transmit and receive stereophonic programs in an FM channel. Also see MULTIPLEX ADAPTER.

FM tuner A compact radio receiver that handles frequency-modulated (FM) signals, and delivers its low-amplitude audio output to a high-fidelity system. Compare AM TUNER and AM-FM TUNER.

focal length Symbol, F. The distance from the center of a lens or dish antenna to the principal focus. Also see PRINCIPAL FOCUS.

5059F-pF-274-306 4/9/01 5:31 PM Page 294

focus **1.** The point at which rays converge. Also see PRINCIPAL FOCUS. **2.** To bring rays to a point of convergence.

focus coil See FOCUSING COIL.

focus control In an oscilloscope or television circuit, the potentiometer that controls the voltage on the focusing electrode of the cathode-ray tube and, accordingly, the sharpness of the image.

focus grid **1.** The focusing electrode in an electrostatic cathode-ray tube. **2.** The focusing electrode in an oscilloscope tube.

focusing Bringing a ray of particles or energy to a common point. This can be done using lenses, deflecting coils, deflecting plates, or reflecting devices. Focusing can be done with acoustic waves, electromagnetic waves, and theoretically with any kind of disturbance propagated through any medium.

focusing anode See FOCUSING ELECTRODE.

focusing coil An external coil used to focus an electron beam in a cathode-ray tube. Also see ELECTROMAGNETIC FOCUSING.

focusing electrode The internal electrode (grid or ring) used to focus the electron beam in a cathode-ray tube. Also called focus electrode. Also see ELECTROSTATIC FOCUSING and FOCUS GRID, **1**, **2**.

focusing magnet A permanent magnet assembly for focusing the electron beam in a cathode-ray tube.

foil **1.** The thin conductive strips on a printed-circuit board. **2.** Also known as *tape.* Thin metal supplied in strips, intended for use in certain security systems. It can be installed in closed loops at potential points of entry.

foil capacitor A capacitor whose plates are sheets or strips of metal foil separated by a dielectric film.

foil coil See FOIL-WOUND COIL.

foil conductor A conductor that is a strip of metal foil, rather than wire. Also see FOIL PATTERN.

foil electroscope See LEAF ELECTROSCOPE.

foil pattern The pattern of thin metal circuit paths that constitute the "wiring" of a printed circuit. Also see ETCHED CIRCUIT and PRINTED CIRCUIT.

foil-wound coil A coil wound with metal foil (usually aluminum or copper) instead of wire. Such coils substantially reduce the weight of large transformers and filter chokes.

foldback **1.** See FOLDBACK CURRENT LIMITING. **2.** In audio recording, the routing of sound (via an audio mixer) to some other destination in addition to the recording medium. Example: playing an electronic organ while singing, recording the arrangement on tape, and also listening to it (organ and voice) in a headset.

foldback current limiting In a power supply, a method of automatically reducing the output current to a safe level when the load current exceeds the maximum recommended value. This action protects both the power supply and the powered equipment.

folded dipole A half-wavelength, center-fed antenna constructed of two parallel wires with their ends connected together. It has the same length as a simple dipole antenna, but the feed-point impedance is four times that of the ordinary dipole. Instead of approximately 73 ohms, the folded dipole presents a resistive impedance of about 300 ohms. This makes the folded antenna desirable for use with high-impedance, parallel-wire transmission lines. It also can be used to obtain a good match with 75-ohm coaxial cable when four antennas are connected in phase, or with 50-ohm coaxial cable when six antennas are connected in phase. Compare DIPOLE ANTENNA.

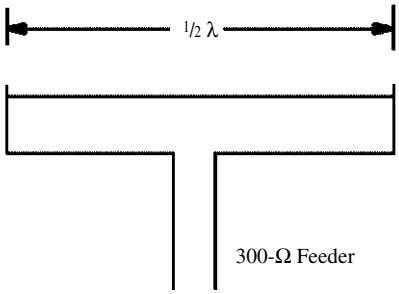

folded dipole

folded horn A loudspeaker having a horn whose flare is divided into several zigzagging chambers; that is, the horn is, in effect, folded to squeeze a required length into a small cabinet.

folded-horn enclosure See LABYRINTH SPEAKER.

folded pattern An oscilloscope image having an elongated time axis obtained by successive horizontal sweeps—each placed slightly lower on the

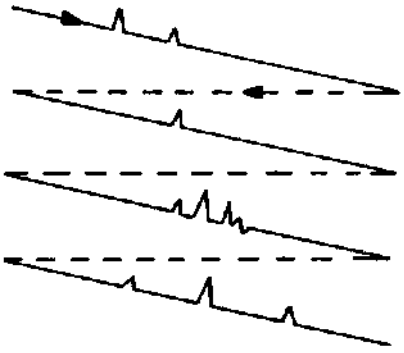

folded pattern

5059F-pF-274-306 4/9/01 5:31 PM Page 295

screen than the preceding one. The folded-pattern technique provides a time axis several times longer than the screen width.

folding frequency In a system where sampling is made at uniform frequency increments, the frequency corresponding to half the sampling rate in hertz.

foldover Distortion characterized by the horizontal or vertical overlapping of a television picture.

follower A single-stage, active circuit characterized by zero phase reversal, and voltage gain less than unity. The *emitter follower* is also called a *common-collector circuit*; the *source follower* is also known as a *common-drain circuit.* Characterized by moderate to high input impedance, and low output impedance over a wide band of frequencies.

follower drive In a servo system, the drive that mechanically follows the master drive.

following blacks In a television picture, the effect in which a moving white object has a black border following it.

following whites In a TV picture, the effect in which a moving dark object has a white border following it.

follow-up motor See SERVOMOTOR.

font The physical shape and size of the letters and numbers in an alphanumeric system.

font reticle In optical character recognition, an overlay reference pattern of lines used to check the size and configuration of an input character, the size of punctuation marks, and spacing between lines and characters.

food-service robot Any robot that is used for the purpose of packaging, preparing, and/or serving food.

foot Abbreviation, ft. A unit of linear measure in the English system equal to 0.3048 meter.

foot-candle Abbreviation, fc. A unit of illuminance; 1 fc is the amount of direct light emitted by 1 candela (see CANDLEPOWER) that falls on 1 square foot of a surface on which every point is 1 foot away from the source. In the International System of Units, the unit is *lux* (lumens per square meter). Compare METER-CANDLE.

foot-candle meter A light meter whose scale reads directly in foot-candles.

foot-lambert Abbreviation, fL. A unit of luminance; the average brightness of a surface that emits or reflects 1 lumen per square foot. The Standard International (S.I.) unit is the *candela per square meter* (cd/m^2); 1 fL = 3.426 cd/m^2.

foot-pound Abbreviation, ft-lb. In the English system, a unit of energy equal to 1 pound displaced through 1 foot in the direction of the exerting force. The Standard International (S.I.) unit is the *joule* (j); 1 ft-lb = 1.356 j.

foot-pound-second system See FPS SYSTEM OF UNITS.

foot switch A switch operated by the foot, generally used for the purpose of turning a playback or recording system on and off. Often used for taking dictation.

forbidden band See ENERGY GAP.

forbidden character code An error-finding code using forbidden characters: combinations of prohibited bits. Also called *forbidden combination.*

forbidden energy band See ENERGY GAP.

force **1.** Symbol, F. Units: newton, dyne, poundal. The agency or influence that accomplishes work. **2.** An operator interjection made during a program run that causes the computer to execute a branch instruction; it is usually necessary when a condition responsible for halting a program must be bypassed.

forced coding Programming that minimizes the time required to retrieve information from storage. Also called *minimum latency programming* or *minimum access programming.*

forced oscillations Oscillations in a circuit, such as in an inductance-capacitance (LC) tank, that result from continuously applied alternating-current (ac) excitation. Compare FREE OSCILLATIONS.

foreground job A relatively high-priority, short-running program that is carried out by interrupting a low priority, long-running program. Compare BACKGROUND JOB.

force pump In a multistage vacuum system, the first pump that reduces the pressure considerably below atmospheric pressure. Also see DIFFUSION PUMP and VACUUM PUMP.

force summing device A transducer element that is physically moved by a force being transduced.

foreshortened addressing In control computers, the mixing of available storage by using simplified addressing instructions.

fork oscillator An audio-frequency oscillator controlled by a tuning fork. The dimensions of the fork determine its vibration frequency and, accordingly, the frequency of the oscillator.

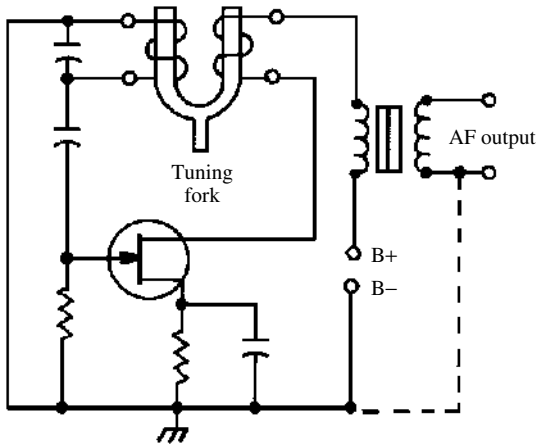

fork oscillator

5059F-pF-274-306 4/9/01 5:31 PM Page 296

form **1.** The core or frame upon which an inductor is wound. **2.** A vessel, such as a mold, used in the shaping stage of a manufacturing process.

formaldehyde Formula, HCHO. A colorless, pungent gas that is a constituent of many well-known plastic insulating materials (see PHENOLFORMALDEHYDE PLASTICS).

formant **1.** The audio-frequency range in which the sound of a spoken syllable is concentrated. **2.** Any general group of audio frequencies.

formant filter In an electronic organ, an audio filter that changes the waveshape of a tone so that the tone will have the desired characteristics.

format **1.** The form in which data is presented (e.g., the arrangement of characters, fields, words, totals, etc.). **2.** To prepare a computer disk or tape so that it will accept data.

form factor **1.** The SHAPE FACTOR for a filter or tuned circuit. **2.** For a half-cycle of an alternating-current (ac) quantity, the ratio of the root-mean-square (rms) value to the average value.

form feed **1.** A mechanical system that positions paper being supplied to a line printer. **2.** The FF character that initiates advancement of printout paper in a printer. **3.** The advancement of printout paper in a printer.

form feed character In a control loop, a character (symbol, FF) used on printing devices for controlling form feed.

forming See ELECTROFORM, **1**.

form stop An automatic device that stops a printer when the paper runs out.

FORTH A high-level computer programming language used in certain robots, automated factories, medical electronic devices, and electronic games. It was originally developed in the 1970s to facilitate computer control of equipment in astronomical observatories.

FORTRAN A high-level computer programming language developed in the 1950s, and still used in some scientific and mathematical applications. It is not especially useful for the control of electronic or mechanical devices.

fortuitous conductor A medium that creates an unwanted electrical path.

fortuitous distortion Waveform distortion that results from causes other than characteristic effects or bias effects.

forward AGC Automatic gain control provided by special transistors whose transconductance decreases with increasing emitter current, and vice versa. Compare REVERSE AGC.

forward-backward counter A counter that runs forward to perform addition and backward to perform subtraction.

forward bias Forward voltage or current in a transistor or semiconductor diode.

forward-blocking state For a silicon-controlled rectifier, the off state, during which the forward bias is so much less than the forward breakover voltage that only small off-state current flows.

forward breakover voltage **1.** For a semiconductor pn junction, the smallest forward voltage at which appreciable conduction occurs. This is about 0.3 V for germanium and 0.6 V for silicon. **2.** For a silicon-controlled rectifier, the forward voltage value at which the device abruptly switches on.

forward characteristic The current-voltage response of a semiconductor junction that is biased in the forward (high-conduction) direction. Compare REVERSE CHARACTERISTIC.

forward compatibility standards Standards developed to make programs for one computer system usable for additional or replacement equipment.

forward conduction The increased current conduction through a pn junction that is forward biased. Compare REVERSE CONDUCTION.

forward current Symbol, I_f. The increase in current flow through a pn junction that is forward biased. Compare REVERSE CURRENT.

forward current-transfer ratio The current gain of a bipolar transistor (alpha for the common-base connection and beta for the common-emitter connection).

forward power **1.** In a transmission line, the power leaving the generating source, as measured by a directional wattmeter at that location. **2.** The power arriving at the load at the terminating end of a transmission line.

forward propagation by ionospheric scatter See FORWARD SCATTER.

forward propagation by tropospheric scatter Abbreviation, FPTS. A method of transmitting part of a radio signal beyond the horizon using the scattering effect of the troposphere. Also see FORWARD SCATTER and TROPOSPHERE.

forward resistance Symbol, R_f. The resistance of a forward-biased pn junction. Also see FORWARD BIAS. Compare REVERSE RESISTANCE.

forward-reverse ratio See FRONT-TO-BACK RATIO.

forward scatter Also called *forward propagation by ionospheric scatter*. The scattering of a radio wave in the normal direction of propagation to points beyond the skip zone. The phenomenon occurs because of waves returned from regions in the ionosphere. Compare BACK SCATTER.

forward transconductance Symbol, g_{fs}. For a common-source-connected FET, the ratio of a drain-current differential to the differential of gate-to-source voltage that produces it; $g_{fs} = 1000(dI_D/dV_{GS})$, where g_{fs} is in microsiemens, I_D is the drain current in milliamperes, and V_{GS} is the gate-to-source voltage in volts.

forward voltage Symbol, E_f or V_f. Voltage whose polarity causes maximum current to flow through a pn junction. Compare REVERSE VOLTAGE.

forward voltage drop The voltage across a semiconductor junction that is biased in the forward (high-conduction) direction. Compare REVERSE VOLTAGE DROP.

5059F-pF-274-306 4/9/01 5:31 PM Page 297

FOSDIC Acronym for *film optical scanning devices for input to computer.*

Foster-Seeley discriminator A discriminator circuit in which the diodes are operated from a single-tuned, center-tapped secondary of the input transformer. The center tap is also capacitively coupled to the top of the transformer's primary coil. Compare TRAVIS DISCRIMINATOR.

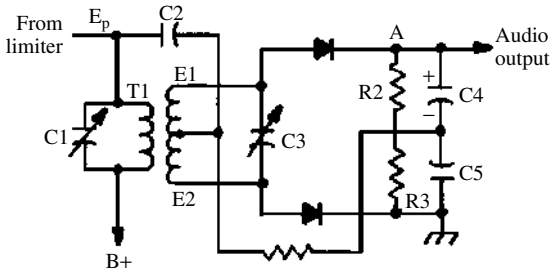

Foster-Seeley discriminator

Foucault currents See EDDY CURRENTS.

four-address instruction A computer instruction in which the address is comprised of four addresses: two for operands, one for the result of the operation, and one for the upcoming instruction.

four-channel sound system Also called *quadraphonic sound system.* A high-fidelity, stereophonic sound reproduction system, in which there are four channels, rather than the usual two. The channels are generally designated left front, left rear, right front, and right rear. The four-channel system is an enhancement of two-channel stereo.

four-dimensional continuum **1.** In relativistic theory, the space-time continuum. There are three spatial dimensions and one time dimension. A point in the continuum can be uniquely defined by three space coordinates and one time coordinate. **2.** Any continuum that requires four and only four coordinates to uniquely determine the position of a point.

Fourier analysis Use of the FOURIER SERIES to evaluate the components of a complex wave, or to define a complex wave in terms of its components.

Fourier series An infinite mathematical series that shows any periodic function to be a combination of sine terms and cosine terms. Any complex wave (e.g., a square wave) consists of fundamental and harmonic sine-wave components. In simplified form, the series is:

$f(x) = A_0/2 + A_1 \cos x + B_1 \sin x + A_2 \cos 2x + B_2 \sin 2x + A_3 \cos 3x + B_3 \sin 3x + \ldots$

In general, the more terms to which the series is calculated, the better the approximation of a complex waveform.

four-layer diode A dual-terminal npnp device that is usable as a bistable switch, sawtooth or pulse generator, memory device, etc.

four-layer transistor A transistor in which the wafer or block has four processed regions; however, the device might have only three terminals. Some examples are the silicon-controlled rectifier, silicon-controlled switch, and thyristor.

four-level laser A laser identical to the three-level laser, except for the addition of one excited state.

four-phase system A two-phase system in which the center taps of the coils are interconnected. Also called QUARTER-PHASE SYSTEM.

four-terminal network A network having two input terminals and two output terminals. One input terminal can be internally connected to one output terminal (as when a common ground is present), but this is not mandatory.

four-space **1.** A mathematical space in which four coordinates (w,x,y,z) are necessary to uniquely define a point. **2.** Three-dimensional space with the addition of time as a fourth dimension; coordinates are, for example, (x,y,z) for space and t for time.

four-space coordinates **1.** A system of coordinates for uniquely determining points in four-space. Such a system can be Euclidean or non-Euclidean, as with space of any number of dimensions. **2.** The set of numbers that defines a particular point uniquely in four-space; for example, $P = (3,-15,0,-7)$.

four-sphere The set of all points equidistant from a given point P in four-space. Formula is $w^2 + x^2 + y^2 + z^2 = r^2$, where r is the radius and the coordinates are (w,x,y,z) in the Euclidean, Cartesian system.

four-track recording A tape recording in which four channels are recorded in two adjacent tracks on the tape. Usually, tracks number 1 and 3 are in the forward direction, and tracks number 2 and 4 are in the reverse direction.

four-track tape A magnetic tape with four parallel sound paths.

four-wire wye system A three-phase system in which three wires supply the respective phases, a fourth being the neutral conductor.

F_p Symbol for POWER-LOSS FACTOR.

fp Abbreviation of FREEZING POINT.

FPC Abbreviation of *Federal Power Commission.*

FPI Abbreviation of FUEL-PRESSURE INDICATOR.

FPIS Abbreviation of *forward propagation by ionospheric scatter.* See FORWARD SCATTER.

fpm Abbreviation of *feet per minute.*

fps **1.** Abbreviation of *feet per second.* **2.** Abbreviation of *frames per second.* **3.** Abbreviation of *foot-pound-second (fps),* a chiefly British system of units.

fps system of units The British system of units of measurement that uses the foot for length, the pound for mass, and the second for time. Compare CENTIMETER-GRAM-SECOND and INTERNATIONAL SYSTEM OF UNITS.

5059F-pF-274-306 4/9/01 5:31 PM Page 298

FPTS Abbreviation of FORWARD PROPAGATION BY TROPOSPHERIC SCATTER.

Fr Symbol for FRANCIUM.

fr Abbreviation of FRANKLINE.

fractional exponent An exponent indicating that a number is to be raised to a fractional power (e.g., $10^{4/3}$). The numerator of the exponent indicates the power to which the base number must be raised; the denominator of the exponent indicates the root that must be taken of the result. Thus, na/b is equal to the bth root of na.

fractional gain Amplification less than unity. A notable example is the transfer function of a source follower or emitter follower.

fractional horsepower Any power rating lower than one horsepower (1 hp). Also see HORSEPOWER.

fractional uncertainty See RELATIVE UNCERTAINTY.

frame **1.** A single, complete video image, scanned in ⅟₃₀ second in conventional television receivers. **2.** A single motion-picture (film) image. **3.** In packet communications, a fundamental unit of data. The three types are called *information (I) frame*, *supervisory (S) frame*, and *unnumbered (U) frame*. **4.** One of a recurring cycle of pulses. **5.** In pulse-code modulation (PCM), a cyclic word group including a sync signal. **6.** A complete commutator cycle. **7.** A digital representation of a set of objects, useful in robotics and artificial intelligence (AI).

frame alignment The condition in which the receiver, or receiving apparatus, is in correct alignment with the signal to be received. In television, for example, this results in true rendition of the picture. Incorrect frame alignment (misalignment) might result in the picture being split with the top and bottom interposed. For other types of signals, misalignment would result in garbled reception.

frame-alignment signal In television, a transmitted signal that is used to ensure that frame alignment occurs in the receiver. It is a form of synchronizing pulse.

frame-alignment time slot In a transmitted television frame, an interval of time that is used for the purpose of transmitting a frame-alignment signal. There might or might not be other signal information transmitted during this time interval.

frame frequency The number of frames of a motion-picture film that come into position per unit of time in a camera, projector, or pickup.

frame of reference Geometric relationships used to describe the location of a body in space.

frame rate See FRAME FREQUENCY.

frame-repetition rate See FRAME FREQUENCY.

frame roll Momentary vertical roll in a television picture.

frame synchronizing signal **1.** In pulse amplitude modulation (PAM), a coded pulse indicating initiation of a commutation frame. **2.** In pulse-code modulation (PCM), a signal used to identify an information frame.

framing **1.** Synchronization of the vertical component of a video signal so that the top and bottom of the transmitted and received pictures line up. **2.** The process of lining up the top and bottom of a movie picture. **3.** Alignment of the characters in a digital alphanumeric transmission.

francium Symbol, Fr. A radioactive metal element of the alkali-metal group. Produced artificially through radioactive disintegration. Atomic number, 87. Atomic weight, 223.

Frankenstein scenario A theme often depicted in science fiction, in which intelligent machines seize power from their human creators. With the rapid advance of technology, especially in robotics and artificial intelligence (AI), some people, including a few educated researchers, believe this scenario is within the realm of possibility. Most scientists think it is highly improbable.

Franklin antenna A vertical collinear array that produces omnidirectional gain because of phasing among the individual components.

frankline (Benjamin Franklin, 1706–1790) Abbreviation, fr. A name that has been suggested for the unit of electric charge; 1 fr is the charge that exerts a force of 1 dyne on an equal charge at a distance of 1 centimeter in a vacuum.

Franklin oscillator A dual-terminal, audio/radio-frequency (AF/RF) oscillator circuit. Consists of a two-stage, resistance-capacitance (RC) coupled amplifier, with a tuned inductance-capacitance (LC) tank in the input gate circuit, and with capacitive feedback from the second drain to the tank.

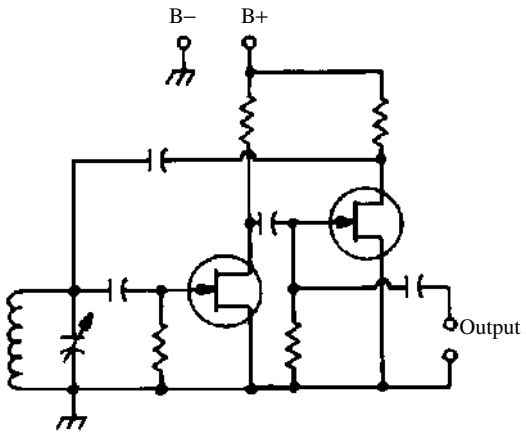

Franklin oscillator

Fraunhofer region The area surrounding a radiating antenna, throughout which the energy ap-

5059F-pF-274-306 4/9/01 5:31 PM Page 299

pears to come from a single point located near the actual antenna.

free air resonance For a speaker, the resonant frequency or frequencies exhibited when the device is not mounted in a cabinet.

free carrier A free electron or, in a semiconductor material, the equivalent hole. Also see ELECTRON and HOLE.

free charge The portion of a charge on a conductor that, being unaffected by a neighboring charge, will escape to ground when the conductor is grounded. Compare BOUND CHARGE.

free electron **1.** An electron situated in one of the outer orbits of an atom, held loosely by the nucleus. Because free electrons can easily escape the attraction of atomic nuclei, they will drift among atoms if the material is subjected to an electric potential. The result is electric current. Also see ELECTRON and BOUND ELECTRON. **2.** An electron that is not associated with any atomic nucleus.

free field Data organized in a storage medium in such a way that a data item or field can be anywhere in the medium. Compare FIXED FIELD.

free impedance For a transducer, the input impedance produced by a perfectly short-circuited load.

free magnetic pole A magnetic pole that is so well isolated from its opposing pole that it experiences little or no influence from the latter.

free magnetism A theoretical medium or fluid to which magnetic effects are conventionally given. The sum of free magnetism in any given object is always zero. Within any small part of the field, the free magnetism is thought of as flux lines. This theoretical medium can be any nonmagnetic material.

free net In radio communications, a network in which stations are free to communicate with other stations in the net without constant supervision by the net control station. Such communication is carried out on a frequency slightly above or below that of the net's formal operation.

free oscillations Oscillations in a circuit, such as an inductance-capacitance (LC) tank, that continue after excitation has been removed. Also see FLYWHEEL EFFECT. Compare FORCED OSCILLATIONS.

free path In a gas tube, the path taken by an electron as it collides with atoms. Also see MEAN FREE PATH.

free-power supply **1.** A simple tuned radio-frequency (RF) detector diode, used to rectify a radio signal and supply small amounts of direct current for the operation of low-powered transistor circuits. **2.** See SOLAR BATTERY.

free reel The supply reel of a magnetic-tape recorder.

free-running frequency The frequency at which a synchronized generator, such as a multivibrator or self-excited oscillator, will operate when the synchronizing voltage is removed.

free-running multivibrator See ASTABLE MULTIVIBRATOR and UNCONTROLLED MULTIVIBRATOR.

free space Empty space; a theoretical ideal.

free-space loss Radio transmission loss disregarding variable factors (a theoretical condition).

free-space pattern The ideal directivity pattern of an antenna that is situated many wavelengths above ground. In use, this pattern is modified by reflections from ground.

free speed The angular velocity of an unloaded motor.

free-standing display In a computer system, a remote display unit for prompting peripheral operators.

freezing point Abbreviation, fp. The temperature at which a liquid starts becoming a solid at normal pressure. Compare MELTING POINT.

F region Also called *F layer*. A region of the ionosphere with an altitude at night of approximately 175 miles. In daytime, the region splits into the lower *F1 region* and the higher *F2 region*. This layer is primarily responsible for long-distance propagation of radio waves at high frequencies (3 MHz to 30 MHz). At times it returns waves at frequencies as high as about 70 MHz.

Fremodyne detector A frequency-modulation (FM) detector that is essentially a conventional amplitude-modulation (AM) circuit detuned to one side of resonance (slope-tuned) to demodulate a frequency-modulated signal. Also see SLOPE DETECTOR.

French phone See CRADLEPHONE.

freqmeter Contraction of FREQUENCY METER.

frequency Symbol, f. The rate at which a phenomenon is repeated. The basic unit of frequency is the *Hertz (Hz)*, which represents one complete cycle per second. Common units encountered in electronics are the *kilohertz (kHz)*, *megahertz (MHz)*, and *gigahertz (GHz)*, where 1 kHz = 10^3 Hz, 1 MHz = 10^6 Hz, and 1 GHz = 10^9 Hz. Occasionally, the *terahertz (THz)* is used; 1 THz = 10^{12} Hz.

frequency-agile radar A radar system in which the transmitter frequency is shifted in a predetermined pattern for the purpose of avoiding detection. A frequency-agile radar system, with a complex frequency control program, is very difficult to jam.

frequency allocation **1.** The assignment of frequencies to radio and allied services by the licensing authority (in the United States, the Federal Communications Commission). **2.** A specific assignment of a frequency or a band of frequencies. Also see RADIO SPECTRUM.

frequency band A given range of frequencies, usually specified for some application (e.g., the band allocated for standard radio broadcast service). Also see BAND.

5059F-pF-274-306 4/9/01 5:31 PM Page 300

frequency bias An intentional change in the frequency of a transmitted signal.

frequency bridge **1.** Any alternating-current bridge, such as the *Wien bridge* or *resonance bridge*, that can be nulled at only one frequency for a given set of bridge-arm values. **2.** Any alternating-current bridge that is used to measure unknown frequencies.

frequency calibrator A device, such as a crystal oscillator, that provides a signal of precise frequency with which other signals can be compared. Also see SECONDARY FREQUENCY STANDARD.

frequency changer **1.** A superheterodyne converter (see CONVERTER). **2.** A motor-generator in which the output voltage has the same value as the input voltage, but is of a different frequency. **3.** See FREQUENCY-MULTIPLYING TRANSFORMER. **4.** See FREQUENCY MULTIPLIER.

frequency-change signaling See FREQUENCY-SHIFT KEYING.

frequency channel A relatively narrow segment of a frequency band allocated to a station in a particular service. The bandwidth of the channel depends on the type of modulation used, the type of data to be transmitted, and the speed or fidelity of the data to be transmitted.

frequency comparator A device, such as an oscilloscope or zero-beat indicator, used to check one frequency against another. Also see FREQUENCY COMPARISON.

frequency comparison The observation of a current or voltage of one frequency for similarities in that of another frequency. Comparisons (as in frequency matching) can be made by audio means, by visual means, or both. Common instruments used are oscilloscopes, beat-note detectors, and beat-note meters.

frequency-compensated attenuator An attenuator, such as one in an electronic voltmeter or wideband oscilloscope, that has been modified by the addition of capacitors or inductors to achieve reasonably flat response over a wide range of frequencies.

frequency compensation The modification of a circuit, such as an amplifier or attenuator, by the addition of capacitors or inductors to tailor its response at specified frequencies.

frequency control **1.** An adjustable component (potentiometer, variable capacitor, or variable inductor) with which the frequency or frequency response of a circuit is adjusted. **2.** A device, such as a quartz crystal or tuning fork, that automatically sets the frequency of an oscillator.

frequency conversion The process of changing a signal from one frequency to another, usually without altering the signal bandwidth. In some cases, a signal is turned "upside down" by this process [e.g., an upper-sideband (USB) signal might be changed to a lower-sideband (LSB) signal]. Generally accomplished by means of a MIXER.

frequency converter **1.** An active or passive device for changing the frequency of a signal. **2.** The mixer in a superheterodyne circuit.

frequency correction Manual or automatic resetting of a deviated frequency to its original value.

frequency counter An instrument that counts signal cycles or pulses over a standard time base (a frequency measurement). Often used to accurately measure the frequencies of radio or television signals; in this application, it is a precision FREQUENCY METER.

frequency cutoff See CUTOFF FREQUENCY.

frequency detector See FREMODYNE DETECTOR.

frequency deviation **1.** The degree to which a frequency changes from a prescribed value. Thus, if the frequency of a 1000-Hz oscillator drifts between 990 and 1010 Hz, the deviation is ±10 Hz. **2.** In a frequency-modulated (FM) signal, the amount of instantaneous frequency shift above and below the unmodulated carrier frequency.

frequency-deviation meter In frequency-modulation (FM) communications operations, a meter that gives a direct reading of frequency deviation resulting from a modulating signal. It uses either a tuned circuit or a frequency comparator.

frequency difference **1.** In a superheterodyne circuit, the difference between the signal frequency and the oscillator frequency. **2.** In any beat-frequency operation, the quantity $f_2 - f_1$, where f_2 is the higher frequency and f_1 is the lower frequency. Compare FREQUENCY SUM.

frequency discriminator See DISCRIMINATOR.

frequency distortion A form of distortion in which the amplification of some frequencies is different from that of others.

frequency distribution See DISTRIBUTION, **2**.

frequency diversity The transmission and reception of signals at two or more frequencies for the purpose of reducing the effects of fading. It is generally used in long-distance, high-frequency circuits.

frequency divider A circuit or device whose output frequency is a fraction of the input frequency. Compare FREQUENCY MULTIPLIER.

frequency-dividing network See CROSSOVER NETWORK.

frequency-division multiplex A form of multiple-signal parallel transmission in which a single carrier is modulated by two or more signals simultaneously.

frequency doubler A circuit that multiplies an input frequency by two. If a doubler's input circuit is tuned to frequency f, then its output circuit is generally tuned to $2f$. Frequency doubling is performed by various nonlinear devices, including transistors, varactors, and biased diodes.

frequency drift An undesired, usually gradual, change in the frequency of a signal from its intended frequency or channel; expressed in hertz or kilohertz.

5059F-pF-274-306 4/9/01 5:31 PM Page 301

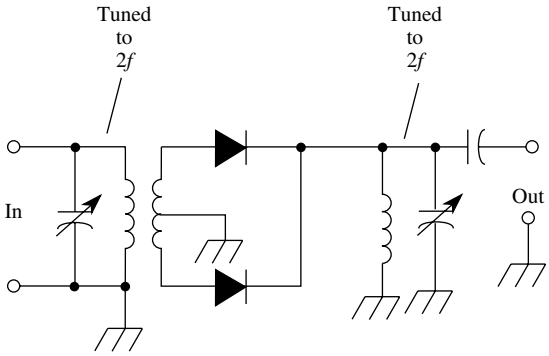

frequency doubler

frequency function See PROBABILITY DENSITY FUNCTION.

frequency indicator **1.** A device that indicates when a phase or frequency is common to two alternating currents. **2.** The display or dial that shows the operating frequency of a radio receiver or transmitter. **3.** See FREQUENCY METER.

frequency keying See FREQUENCY-SHIFT KEYING.

frequency meter An instrument for measuring the frequency of an alternating current. The several different types are used in different applications. Also see AUDIO FREQUENCY METER, FREQUENCY COUNTER, POWER-FREQUENCY METER, and WAVEMETER.

frequency-modulated radar See FM RADAR.

frequency modulation Abbreviation, FM. A method of conveying intelligence in wireless communications and broadcasting. The amplitude of the carrier remains constant, and the instantaneous frequency varies. One scheme for obtaining this type of modulation is to apply the modulating signal to a varactor in an oscillator. Another method is to modulate the phase of the oscillator signal. This causes small fluctuations in the frequency as well, because any instantaneous phase change shows up as an instantaneous frequency change (and vice versa). Also see AMPLITUDE MODULATION, PHASE MODULATION, SINGLE SIDEBAND.

frequency modulation deviation **1.** In frequency modulation (FM), the largest difference between the instantaneous signal frequency and the unmodulated carrier frequency. **2.** The maximum bandwidth of an FM signal at its audio modulation amplitude peak.

frequency modulator **1.** A circuit or device that modulates the frequency of an oscillator. **2.** The modulator section of an FM transmitter.

frequency monitor A device used (often continuously) to check the frequency of a signal (e.g., a frequency-deviation meter used in radio broadcast stations or a frequency meter used in electric-generating stations).

frequency multiplier A circuit or device whose output frequency is a multiple of the input frequency. See, for example, FREQUENCY DOUBLER.

frequency-multiplying amplifier See MULTIPLIER AMPLIFIER.

frequency-multiplying transformer A magnetic amplifier that generates harmonics of the supply frequency. The effect results from the nonlinearity of the transformer core material.

frequency offset **1.** The difference between an actual frequency and the desired frequency. **2.** In a communications transceiver, the difference between the receiver frequency and the transmitter frequency. In some modes, such as single-sideband (SSB), the offset is normally zero. In other modes, notably continuous-wave (CW) Morse code, the offset is normally several hundred Hz. **3.** See FREQUENCY SPLIT, **1**.

frequency overlap **1.** A common band of frequencies between two adjacent channels in a communications system. **2.** A common frequency region between two assigned bands. **3.** A condition in which parts of the sidebands of two signals occupy the same range of frequencies.

frequency pulling A change in the frequency of a circuit, especially of a self-excited oscillator, resulting from the detuning effects of an external circuit, device, or condition (such as body capacitance or a change in the temperature).

frequency pushing An effect in which a current change in a source oscillator causes a shift in source frequency.

frequency quadrupler See QUADRUPLER, **2**.

frequency quintupler See QUINTUPLER, **2**.

frequency range **1.** A communication system's frequency transmission limits, beyond which the power output is attenuated below a specified amount. **2.** The frequency band or bands within which a radio transmitter, receiver, or transceiver is designed to operate.

frequency ratio counter See FREQUENCY RATIO METER.

frequency ratio meter A meter that indicates the ratio between two frequencies, and is useful in the quick identification of harmonics.

frequency record A phonograph test disk containing recordings of various frequencies at specified amplitudes.

frequency rejection The elimination, usually by a filter, of a single frequency (or narrow band of frequencies) from a mixture of frequencies. Compare FREQUENCY TRANSMISSION.

frequency relay A frequency-sensitive relay (see SELECTIVE RELAY, **1**).

frequency response A performance characteristic that describes the operation of a device or circuit over a specified range of signal frequencies (e.g., the gain-versus-frequency characteristic of an amplifier).

5059F-pF-274-306 4/9/01 5:31 PM Page 302

frequency-response recorder A graphic recorder that automatically plots a frequency-response curve for a device under test.

frequency run A test, or test sequence, that determines the loss characteristics of a circuit as a function of the operating frequency.

frequency scanning **1.** A controlled fluctuation of the transmitter frequency in a frequency-agile radar or communications system. **2.** In a programmable, digital communications receiver or transceiver, a form of simultaneous digital monitoring of two or more channels. **3.** The frequency-response change in a spectrum analyzer.

frequency scaler See SCALER.

frequency-selection sensor A sensor that passes or rejects phenomena at certain frequencies while ignoring those at other frequencies.

frequency-selective relay See SELECTIVE RELAY, **1**.

frequency-sensitive bridge A bridge, such as the *Wien bridge* or *resonance bridge*, that can be balanced at only one frequency for a given set of bridge-arm values.

frequency separator In a television receiver, the circuit that separates horizontal- and vertical-scanning sync pulses.

frequency-shift keying Abbreviation, FSK. A method of digital signal transmission. The logic 1 (*high* or *mark*) pulses are sent at a specific carrier frequency, and the logic 0 (*low* or *space*) pulses are transmitted at another frequency slightly higher or lower than the logic 1 pulses. This is the most primitive form of frequency modulation (FM). The difference between the mark and space frequencies is called the *shift*, and is usually between 100 and 1000 Hz. Compare AUDIOFREQUENCY-SHIFT KEYING.

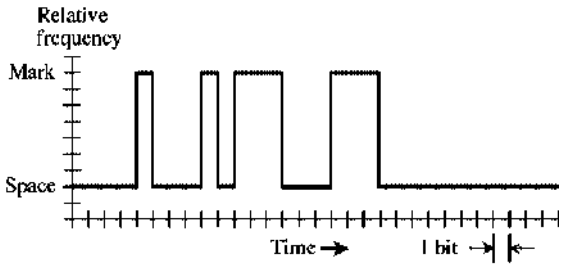

frequency-shift keying

frequency-shift radar See DOPPLER RADAR.

frequency span The difference $f_2 - f_1$, where f_1 is the lowest frequency in a given range of frequencies and f_2 is the highest frequency. Compare FREQUENCY SPREAD.

frequency spectrum All electromagnetic radiation, from longest to shortest wavelengths, within a set of specified limits.

frequency split **1.** The difference between the receiver frequency and the transmitter frequency in a communications repeater. **2.** See FREQUENCY OFFSET, **2**.

frequency spotting The setting-up of signals at reference frequencies (usually harmonics of a standard-frequency oscillator), and their use in identifying unknown frequencies. Also see FREQUENCY CALIBRATOR.

frequency spread The ratio f_2/f_1, where f_1 is the lowest frequency in a given range of frequencies and f_2 is the highest frequency. Compare FREQUENCY SPAN.

frequency stability The degree to which a frequency remains constant during variations in temperature, current, voltage, and similar factors. It is specified in Hertz (Hz), kilohertz (kHz), or megahertz (MHz), or in parts per million per unit of the variable parameter.

frequency standard A signal source of a precise frequency, against which other signal sources can be calibrated. See specifically PRIMARY FREQUENCY STANDARD and SECONDARY FREQUENCY STANDARD.

frequency sum In a beat-frequency system, the quantity $f_1 + f_2$, where f_1 is the lower frequency and f_2 is the higher frequency. Compare FREQUENCY DIFFERENCE, **2**.

frequency swing See FREQUENCY DEVIATION, **1**, **2**.

frequency synthesizer A generator of signals at a precise frequency or set of frequencies, generally adjustable in discrete frequency steps. It is used for test or communications purposes. The signals are derived from a single-frequency source, usually a crystal oscillator. Also see SIGNAL SYNTHESIZER.

frequency tolerance The acceptable amount by which a frequency can vary from its intended value. The tolerance can be specified as a percentage of the stated frequency, a certain number of parts per million, or a certain number of hertz (Hz), kilohertz (kHz), or megahertz (MHz). Example: 3.675000 MHz ±10 Hz.

frequency-to-voltage converter A device or circuit that delivers an output voltage that is proportional to the input frequency.

frequency translation **1.** The conversion of a given frequency band from one part of the electromagnetic spectrum to another, without changing the actual separation of channels or the overall width of the band. **2.** See FREQUENCY CONVERSION.

frequency transmission The passage of a frequency or band of frequencies from a mixture of frequencies through a filter or other circuit. Compare FREQUENCY REJECTION.

frequency tripler See TRIPLER, **2**.

frequency-variation method A method of determining the figure of merit (Q) of a tuned circuit by varying the frequency of the applied test voltage

5059F-pF-274-306 4/9/01 5:31 PM Page 303

from resonance (f_r) to a high point (f_2) and a low point (f_1). At the high and low points, the circuit voltage is 0.707 times the voltage at resonance. The figure of merit then is calculated from the formula $Q = f_r/(f_2 - f_1)$.

frequency-voltage converter See FREQUENCY-TO-VOLTAGE CONVERTER.

frequency-wavelength conversion See WAVELENGTH-PERIOD-FREQUENCY RELATIONSHIPS.

fresnel (A.J. Fresnel, 1788–1827) A unit of frequency equal to 10^{12} Hz. Also called *terahertz* and abbreviated THz.

fresnel lens A usually square plastic sheet with progressively thicker concentric areas; its effect is similar to that of an automotive headlight lens.

Fresnel number A measure of the relative effects of diffraction in an optical lens. The Fresnel number is equal to the radius of the lens divided by the product of the light wavelength and the lens focal length, all measured in the same units.

Fresnel region For a radio-frequency transmitting antenna, the zone between the antenna and the FRAUNHOFER REGION. The size of the Fresnel region depends on the wavelength of the radiated energy.

friction The resistance to mechanical motion when one material is rubbed against another. Friction was one of the earliest sources of human-made electricity (see FRICTIONAL ELECTRICITY and ELECTRIC MACHINE). Electrical resistance, opposing the flow of current, is analogous to friction.

frictional electricity Static electricity generated by rubbing one material against another.

frictional electric machine See ELECTRIC MACHINE.

frictional error The change in parameters of a phonograph pickup, resulting from friction with the disk surface.

frictional loss A decrease or impairment in the efficiency with which energy is converted into useful work, caused by friction between moving parts.

fringe area The region in which a signal falls to the minimum field strength necessary for satisfactory communication.

fringe howl In a regenerative detector, a howling sound that occurs when the transistor first begins to oscillate, obscuring the signal. The term is used because the circuit is operated at the fringe of oscillation.

fringing See EDGE EFFECT.

Fritch Trade name (American Telephone & Telegraph Co.) for *frequency-selective switch.*

fritting A condition in which electrical contact corrosion creates a small hole, through which molten contact material passes to form a conductive bridge.

front contact The movable contact of a relay.

front end 1. The first radio-frequency (RF) amplifier stage in a radio or television receiver. **2.** The converter portion of a superheterodyne communications receiver (i.e., the RF amplifier, first detector, and local oscillator). Compare REAR END.

front layer photocell See RECTIFIER PHOTOCELL.

front porch In a television horizontal sync pulse, the interval between the end of the sync pulse and the fall of the blanking pedestal. Compare BACK PORCH.

front projection In big-screen video, a scheme in which the images from a set of bright cathode-ray tubes (CRTs) are projected onto a reflective screen, in a manner similar to the way the film is projected in a movie theater.

front-surface mirror Also called *first-surface mirror.* A mirror that has its reflective material on the front, instead of on the back.

front-to-back ratio Abbreviation, f/b. An expression of the ability of a unidirectional antenna to concentrate its radiation or response in its favored direction. This specification is nearly always given in decibels (dB). The field strength in the favored direction is compared with the field strength exactly opposite the favored direction at the same distance from the antenna in free space, at the same frequency, and with the same power applied to the antenna feed point. Measurements can be made with a calibrated field-strength meter. Compare FRONT-TO-SIDE RATIO.

front-to-side ratio Abbreviation, f/s. An expression of the directivity of a unidirectional or bidirectional antenna system. This specification is nearly always given in decibels (dB). The field strength in the favored direction(s) is compared with the field strength at right angles to the favored direction(s) at the same distance from the antenna in free space, at the same frequency, and with the same power applied to the antenna feed point. Measurements can be made with a calibrated field-strength meter. Compare FRONT-TO-BACK RATIO.

frost alarm A device or circuit that responds to the presence of frost and actuates an alarm. Such alarms are sensitive to temperature, moisture, or both.

FRUGAL Acronym for *FORTRAN rules used as a general applications language.*

FRUSA Acronym for *flexible rolled-up solar array*, such as the type used in spacecraft and communications satellites.

F scan In radar operations, a display in which a central blip represents the target at which the antenna is pointed; horizontal and vertical displacement of the blip indicate corresponding horizontal and vertical aiming errors.

FSK Abbreviation of FREQUENCY-SHIFT KEYING.

FSM Abbreviation of FIELD-STRENGTH METER.

FS meter See FIELD-STRENGTH METER.

FSR Abbreviation of *feedback shift register.*

ft Abbreviation of *foot* or *feet.*

5059F-pF-274-306 4/9/01 5:31 PM Page 304

FT-cut crystal A piezoelectric plate cut from a quartz crystal at an angle of +57°, with respect to the z-axis. Also see CRYSTAL AXES and CRYSTAL CUTS.

ft-Lb Abbreviation of FOOT-LAMBERT.

ft-lb Abbreviation of FOOT-POUND.

Fuchs antenna A simple antenna consisting of a single-wire radiator without feeder or transmission line, connected directly to the transmitter. It is usually an odd multiple of 0.25 wavelength long. When a good radio-frequency (RF) ground is used, this antenna can be effective at high frequencies, although part of its radiated field is often inside the transmitter building.

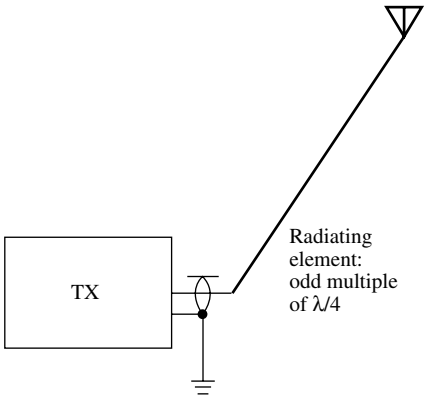

Fuchs antenna

fuel alarm A sensing circuit that actuates an alarm when the fuel in a tank or reservoir falls to a prescribed level.

fuel cell A generator that produces electricity directly from a reaction between fuel substances, such as hydrogen and oxygen.

fuel-flow alarm An electronic circuit that actuates an alarm when fuel flow changes from a prescribed value.

fuel-flow control A servo system that automatically maintains or corrects the flow rate of a fuel.

fuel-flow gauge See FUEL-FLOW METER.

fuel-flow indicator See FUEL-FLOW METER.

fuel-flow meter An instrument for measuring fuel flow rate.

fuel-flow switch A switch that is actuated by fuel flowing in pipes or other channels.

fuel gauge An instrument consisting of a transducer that senses the level of liquid fuel in a tank and delivers a proportional output current or voltage, and an electric meter whose needle is deflected in proportion to the current or voltage and, therefore, to the fuel level. Alternatively, the meter can be a direct-readout digital device, showing the number of gallons remaining in the tank, and/or the extent to which the tank is full (fraction or percentage).

fuel meter See FUEL GAUGE.

fuel-pressure indicator An instrument for measuring fuel pressure in pipes or other channels.

fuel-pressure meter See FUEL-PRESSURE INDICATOR.

full adder In a digital computer, an adder circuit that can handle the carry signal, as well as the binary elements that are to be added. Also see ADDER and CARRY. Compare HALF ADDER.

full bridge A bridge-rectifier circuit in which each of the four arms contains a diode. By comparison, the three-quarter bridge contains a resistor in one arm; the half bridge, resistors in two arms; and the quarter bridge, resistors in three arms.

full-duplex system In data communications, a system that transmits data in both directions simultaneously and continuously. Compare HALF-DUPLEX SYSTEM.

full-focus yoke See COSINE YOKE.

fullhouse A multichannel radio-control model plane system that allows the use of a realistic complement of working control surfaces.

full-load current The output current from a source when the load is maximum (that is, the load resistance is minimum).

full-load power The power drawn from a source when the load is maximum (that is, the load resistance is minimum).

full-load voltage The output voltage of a source when full power is drawn [i.e., when the load is maximum (that is, the load resistance is minimum)].

full-load wattage See FULL-LOAD POWER.

full-power frequency response The highest frequency at which a signal can fluctuate at full voltage (peak-to-peak) without causing distortion of more than a certain specified amount.

full-range speaker See MONORANGE SPEAKER.

full scale **1.** The operating range of an instrument. **2.** In an analog meter, the quantity indicated by maximum deflection of the needle (usually at the extreme right-hand end of the calibrated scale). **3.** Transducer output as a function of highest allowable input stimulus.

full-scale current Symbol, I_{FS}. In a digital-to-analog converter, the maximum current that can occur at the output.

full-scale error For an electrical indicating instrument, the rated full-scale input signal minus the actual input signal that causes a full-scale deflection. Thus, the predictable error in an instrument, expressed as a percentage of the full-scale reading.

full-scale frequency Generally expressed in Hertz (Hz) or kilohertz (kHz). The maximum frequency at which a voltage-to-frequency converter can operate while remaining within its specifications.

full-scale sensitivity The current, voltage, or power required to deflect a meter mechanism to full scale.

5059F-pF-274-306 4/9/01 5:31 PM Page 305

full-scale symmetry Expressed in microamperes (mA). The mathematical difference between the full-scale current outputs in a complementary-output digital-to-analog converter.

full track A recording track covering the full width of a magnetic tape.

full-track head A tape-recorder head having a gap that covers the full width of the tape.

full-track recording Usually applicable to quarter-inch or narrower magnetic recording tape, a one-track recording made by a head that magnetizes essentially the entire width of the tape.

full-wave bridge rectifier See BRIDGE RECTIFIER.

full-wave, center-tap rectifier A circuit in which the center-tapped secondary winding of a transformer operates two rectifier diodes, each on an alternate half-cycle of secondary voltage. The frequency of the ripple in the direct-current (dc) output is equal to twice the alternating-current (ac) input frequency. Compare BRIDGE RECTIFIER.

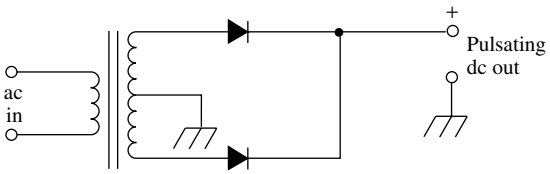

full-wave, center-tap rectifier

full-wave detector A detector circuit using two diodes in a full-wave, center-tap rectifier configuration.

full-wave doubler See FULL-WAVE VOLTAGE DOUBLER.

full wavelength Symbol, λ. The distance that corresponds to 360 degrees of phase as an electromagnetic (EM) field is propagated. In free space, it is related to the frequency by a simple equation:

$$L_{ft} = 984/f$$

where L_{ft} represents λ in feet, and f represents the frequency in megahertz. If λ is expressed in meters, then the formula is:

$$L_m = 300/f$$

Where L_m represents the displacement in meters. In general, if v is the velocity factor (expressed as a ratio) in a given medium, then:

$$L_{ft} = 984v/f$$

and

$$L_m = 300v/f$$

Compare HALF WAVELENGTH, QUARTER WAVELENGTH.

full-wave loop antenna A loop antenna with a circumference of one wavelength, fed at a break. The loop can be circular, square, triangular, or occasionally some odd shape. The most efficient configuration is the circular loop. Maximum radiation occurs perpendicular to the plane of the loop.

full-wave rectifier A rectifier that delivers a half-cycle of pulsating direct-current (dc) output voltage for each half-cycle of applied alternating-current (ac) voltage. The successive output half-cycles have the same polarity. See, specifically, BRIDGE RECTIFIER and FULL-WAVE, CENTER-TAP RECTIFIER. Compare HALF-WAVE RECTIFIER.

full-wave vibrator **1.** In a vibrator-type power supply, an interrupter that closes contacts on both ends of its swing, thus causing direct current (dc) to flow through the transformer in alternate directions. **2.** A vibrator-type rectifier that closes in both directions.

full-wave voltage doubler A voltage-doubler circuit whose direct-current (dc) output has a ripple of twice the alternating-current (ac) supply frequency. Compare HALF-WAVE VOLTAGE DOUBLER.

function **1.** A mapping between two sets of quantities or points A and B, such that: (1) For each y in B, there exists at least one corresponding x in A; and (2) For each x in A, there exists exactly one y in B. In this case y is said to be a function of x; this can be written as $y = f(x)$. The set A is called the *domain* of f; the set B is called the *range* of f. **2.** A mathematical expression, using symbols, relating variables (e.g., the expression $x - y = z$ is a function of variables x, y, and z). **3.** The behavior and application for which a device or system is designed. **4.** Part of a computer instruction specifying the operation to be done.

functional blocks Combinations of substances or components that perform specific tasks in an electronic circuit. An example is a tuned circuit, containing inductive reactance, capacitive reactance, and resistance.

functional character See CONTROL CHARACTER.

functional design Design specifications encompassing a description of how system elements will interrelate, and what their logic design will be.

functional diagram FUNCTIONAL DESIGN represented in graphic form; that is, as an illustration or set of illustrations.

functional electronic block Abbreviation, FEB. A complete integrated circuit. See INTEGRATED CIRCUIT.

functional end (FE) point In a system operating from a battery power supply, the lowest voltage at which the equipment will properly operate. As a battery discharges, the voltage decreases; when the voltage drops to the FE point, the battery must be replaced or recharged.

functional test A performance test of a device or circuit, to see that it behaves as intended in the environment in which it is to be used.

function generator **1.** A signal generator whose output is any of several selectable waveforms

5059F-pF-274-306 4/9/01 5:31 PM Page 306

(e.g., sine, square, triangular, step-pulse) and frequencies (or repetition rates). **2.** An analog computer circuit that produces a variable based on a mathematical function and one or more input variables.

function key **1.** In digital communications, a keyboard key used to control the form in which a message will be received. **2.** On a computer keyboard, any of 12 keys (usually designated F1 through F12) that activates special functions. The precise action of a given key depends on the program being run.

function polling A polling technique in which a disabled device signals its condition and specifies the remedy.

function switch In a multifunction instrument, such as a voltohm-milliammeter, the switch that permits selection of the various functions.

function table **1.** A table of mathematical function values. **2.** Hardware or software that translates one representation of information into another. **3.** A routine that allows a computer to use the values of independent variables to determine the value of a dependent variable.

fundamental Contraction of FUNDAMENTAL FREQUENCY.

fundamental component The FUNDAMENTAL FREQUENCY of a complex wave.

fundamental frequency **1.** The lowest frequency in a complex wave containing harmonic energy. **2.** In a radio or television transmitter, the intended frequency of operation. **3.** In acoustics and audio applications, the predominant pitch of a musical tone.

fundamental group A set of trunk lines in a telephone system, through which zone centers are interconnected.

fundamental mode See DOMINANT MODE.

fundamental suppression Removal of the fundamental frequency from a complex wave, leaving only the harmonics, as in the operation of a null network adjusted to the fundamental frequency.

fundamental units Base units of an absolute system of units. Example: the meter (m), the kilogram (kg), and the second (s) in the mks system.

fundamental wavelength The wavelength that corresponds to the FUNDAMENTAL FREQUENCY of a wave or signal.

fuse A safety device consisting of a wire of low-melting-point metal. When current passing through the wire exceeds a prescribed (safe) level, the resulting heat melts the wire and opens the circuit, protecting equipment from damage. See PROXIMITY FUSE.

fuse box A set of electrical fuses, usually enclosed in a metal box.

fused junction In a semiconductor, a junction produced by alloying metals to the semiconductor material.

fused junction See ALLOY JUNCTION.

fuse resistor See FUSIBLE RESISTOR.

fuse wire The low-melting-point wire used in fuses. See FUSE.

fusible resistor A low-value resistor that also serves as a fuse in certain appliances, such as television receivers.

fusing current The specified current level at which a wire of a given diameter and material composition will melt.

fusion **1.** In acoustics, pertaining to delayed or reflected waves that arrive within approximately ½₅ of a second of the direct wave. So called because the human ear/brain "fuses" (blends) sounds together when they are separated by less than about ½₅ second. If the delay is longer, the ear/brain usually perceives an echo instead. **2.** In a nuclear reaction, the uniting of two atomic nuclei, accompanied by the release of energy.

future labels In a computer system, program instruction labels that refer to locations not designated as absolute addresses by a compiler or assembler.

futurist A person who tries to anticipate or predict, based on current technology and trends, what will be accomplished in a given field in the next several years or decades.

fuzz A form of deliberate distortion in the waveform produced by an electric guitar.

fuzzbox A circuit that distorts the waveform produced by an electric guitar, for the purpose of creating various musical sound effects.

fuzz buster Slang for a specialized mobile radio receiver, used by drivers of vehicles to signal the presence of law-enforcement radar equipment.

fV Abbreviation of *femtovolt.*

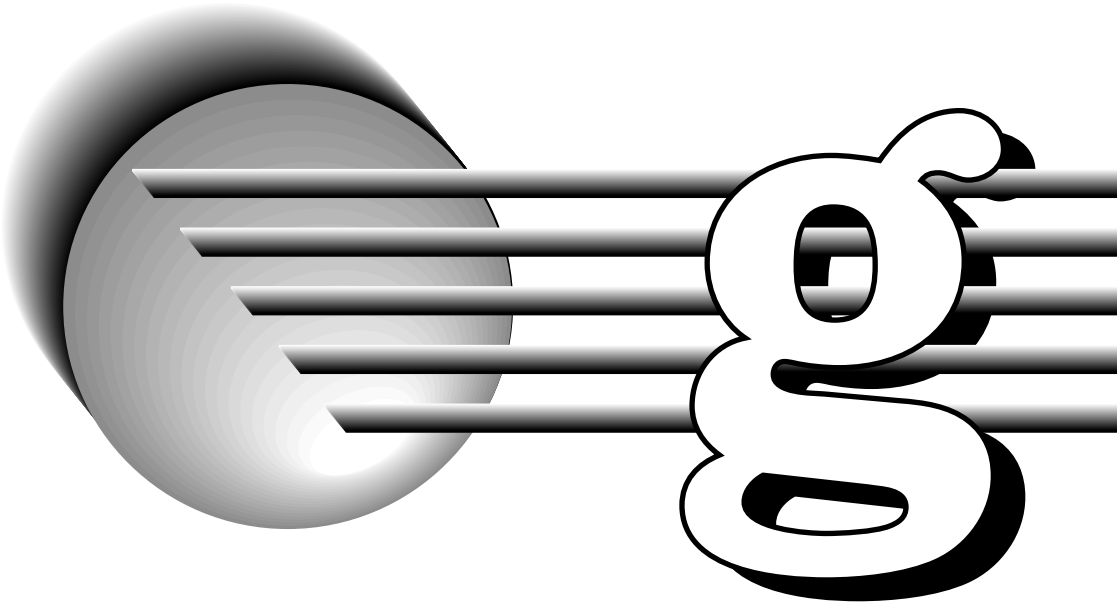

G **1.** Symbol for CONDUCTANCE. **2.** Abbreviation of GIGA-. **3.** Symbol for DEFLECTION FACTOR. **4.** Symbol for PERVEANCE. **5.** Symbol for GRAVITATIONAL CONSTANT. **6.** Symbol for GENERATOR. **7.** Symbol for GATE. **8.** Abbreviation for GAUSS.

g **1.** Symbol for CONDUCTANCE. **2.** Abbreviation of GRAM. **3.** Subscript for GATE. **4.** Subscript for GENERATOR. **5.** Symbol for GRAVITY.

GA Radiotelegraph abbreviation of "Go ahead."

G/A Abbreviation of *ground-to-air*.

Ga Symbol for GALLIUM.

GaAs **1.** Formula for *gallium arsenide*. **2.** Pertaining to semiconductor devices based on gallium arsenide.

GA coil A special form of coil, wound with extra space among the turns to reduce the distributed capacitance.

gadget **1.** A device or component. **2.** A superfluous or makeshift device.

gadolinium Symbol, Gd. A metallic element of the rare-earth group. Atomic number, 64. Atomic weight, 157.25.

gage See GAUGE.

gain The extent to which a component, circuit, device, or system increases current, voltage, or power. Applicable especially to active devices, such as transistors and integrated circuits (ICs), and to amplifiers and filters that use them. Also used to express the directional properties of some antenna systems. Usually specified in decibels (dB). See AMPLIFICATION, CURRENT AMPLIFICATION, DECIBEL, VOLTAGE AMPLIFICATION, and POWER AMPLIFICATION.

gain bandwidth product Symbol, f_T. The frequency at which the gain of a bipolar transistor is equal to 1 (no amplification or loss) in the common-emitter configuration. The f_T represents an absolute upper limit for the frequency at which a bipolar transistor will works as an amplifier. Any attempt to design an amplifier using a bipolar transistor at a frequency higher than its f_T will inevitably fail. Compare ALPHA CUTOFF FREQUENCY.

gain control **1.** To adjust the gain of an amplifier. **2.** A potentiometer used to adjust amplifier gain.

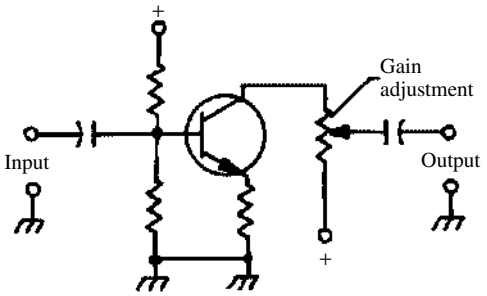

gain control

gain function A function between two currents or voltages in a circuit with gain.

gain-level linearity The quantitative measure of the extent to which the gain of a device depends on the signal level. The level is found by compar-

Copyright 2001 The McGraw-Hill Companies, Inc. Click Here for Terms of Use

5059F-pG-307-325 4/10/01 8:57 AM Page 308

ing the output to the input level over a range of input signal levels.

gain reduction The drop in gain of an amplifier at high- and low-frequency extremes.

gain sensitivity control See DIFFERENTIAL GAIN CONTROL.

gain stability The degree to which the gain of a system remains constant during changes in related factors, such as temperature, supply power, and loading.

gain temperature coefficient The extent to which the full-scale current varies over a certain temperature range, expressed in parts per million per degree Celsius (ppm/°C).

galactic noise Radio noise propagated from the plane of our galaxy, and especially from the center, located in the direction of the constellation Sagittarius. It is of significance in space communications and radio astronomy.

galena Formula, PbS. Natural lead sulfide, which in nature takes the form of bluish-gray, cubical crystals.

gallium Symbol, Ga. Atomic number, 31. Atomic weight, 69.72. One of the constituents of the semiconductor compound GALLIUM ARSENIDE.

gallium arsenide Formula, GaAs. A compound of gallium and arsenic, used as a semiconductor material. It is noted for its low-noise characteristics.

gallium-arsenide diode A diode in which the semiconductor material is processed gallium arsenide.

gallium-arsenide varactor A low-noise, microwave varactor in which the semiconductor material is gallium arsenide.

gallium-phosphide diode A light-emitting diode in which the semiconductor material is processed gallium phosphide.

galloping ghost A form of radio-control system in which the elevation and rudder can be moved to the desired extent.

Galton whistle A device for producing high-frequency acoustic waves (ultrasound), similar to a common dog whistle.

galvanic cell Generic term for any electrochemical primary voltaic cell.

galvanic corrosion Corrosion that occurs on one of two dissimilar metals when they are immersed in an electrolyte. Caused by battery action between them. Compare ELECTROLYTIC CORROSION.

galvanic couple See VOLTAIC COUPLE.

galvanic current A very small direct current such as that produced by dissimilar metals in acid or by nervous reaction in living tissue.

galvanic pile See VOLTAIC PILE.

galvanic series A list of metals and alloys arranged in order of the most to least likely to oxidize in a given environment.

galvanic skin response Abbreviation, GSR. The variations in electrical resistance of the (usually human) skin. This phenomenon is a useful indicator in physiology, psychology, and criminology.

galvanic taste A sharp, metallic taste experienced when a small electric current is passed through the tip of the tongue.

galvanism (After Luigi Galvani, 1737–1798) The production of an electric current by chemical action, as in a battery.

galvanize To coat steel with zinc to forestall corrosion.

galvanometer A sensitive, bi-directional current meter. Used in various electrical tests—especially as a null indicator in bridge operation. Also see MICROAMMETER.

galvanometer constant The number by which a galvanometer reading must be multiplied in order to obtain the current in microamperes, milliamperes, or amperes.

galvanometer recorder A graphic recorder in which a mirror in a movable-coil galvanometer reflects a beam of light to a passing strip of photographic film.

galvanometer shunt A resistor placed in parallel with a galvanometer to decrease its sensitivity. Also see SHUNT RESISTOR.

galvanometry The use of galvanometers to determine the intensity and direction of electric currents.

galvanoplastics The science of ELECTROPHORESIS and ELECTROPLATING.

galvanoscope An instrument for detecting and showing the direction of very weak electric currents.

galvanotherapy The use of electric currents to produce heat in the body of a human or animal.

gamma ferric oxide A form of coating used in formulation of magnetic recording tape.

gamma match A linear transformer for matching an unbalanced (usually coaxial) feed line to a balanced (usually half-wave) antenna. The outer conductor of the cable is connected to the center of the radiator, and an extension of the center conductor runs for a short distance parallel to the radiator, making a right-angle bend before connecting to the radiator.

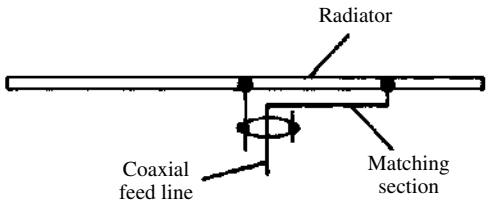

gamma match

gamma rays High-energy, ionizing radiation emitted by radioactive substances; similar to X rays, but of a shorter wavelength.

5059F-pG-307-325 4/10/01 8:57 AM Page 309

gamma section See GAMMA MATCH.

gang To mechanically couple components (pots, switches, etc.) for operation by a single knob.

gang capacitor A variable capacitor consisting of sections mounted on the same shaft for simultaneous variation. It is usually specified by the number of sections (e.g., four-gang capacitor). Compare GANGED CAPACITORS.

ganged capacitors Separate variable capacitors mechanically connected together (e.g., by belt or gear drive) for simultaneous variation. Compare GANG CAPACITOR.

ganged potentiometers Separate potentiometers mechanically connected together (e.g., by belt or gear drive) for simultaneous variation. Compare GANG POTENTIOMETER.

ganged rheostats See GANGED POTENTIOMETERS.

ganged switches Separate switches mechanically connected together for simultaneous operation. Compare MULTISWITCH.

ganged tuning Simultaneous tuning of separate circuits by means of ganged capacitors or ganged potentiometers.

gang potentiometer A potentiometer consisting of sections mounted on the same shaft for simultaneous variation. Usually specified according to the number of sections (e.g., *dual potentiometer*).

gang printer In digital computer and data processing operations, an electromechanical printer capable of printing an entire line at one time.

gang punch **1.** To punch identical or nonvarying information into the cards of a group. **2.** A machine for this operation.

gang rheostat See GANG POTENTIOMETER.

gang switch See MULTISWITCH.

Gantt chart A chart of activity versus time used in industry as an aid in making decisions regarding the allocation of resources for specific activities [e.g., as applied to PERT (project evaluation and review techniques)].

gap **1.** A space between electrodes or magnetic poles. **2.** A device consisting essentially of separated electrodes (e.g., *spark gap*). **3.** A relatively narrow space cut in iron cores to provide a break in a magnetic circuit. Also see SLOT, **1**. **4.** The opening between the opposite poles of a tape recorder or playback head.

gap arrester A lightning arrester consisting of a number of metal cylinders separated by air gaps.

gap coding A system in which silent periods are inserted, according to a specific timing code, into a transmission.

gap depth In a magnetic recording head, the depth of the gap (taken perpendicular to the face). Compare GAP WIDTH.

gap digit A digit that contributes no intelligence to the word in which it appears (e.g., a *parity bit*).

gap energy The energy represented by the forbidden gap in electron energy levels (e.g., between the M-valence band and the N-conduction band in a material).

gap filling Modification of an antenna for the purpose of eliminating nulls in the directional pattern.

gap insulation See SLOT INSULATION, **1**, **2**.

gap loss In a reproducing head, the loss that occurs because of the GAP DEPTH.

gap-type protector A spark gap used to protect equipment from high-voltage transients.

gap voltmeter See NEEDLE GAP and SPHERE GAP.

gap width In a magnetic recording head, the width of the gap (taken parallel with the face). Compare GAP DEPTH.

garbage **1.** In digital computer operations, a colloquialism for useless or incorrect data. **2.** Colloquialism for unreadable signals or severe intermodulation in a radio communications circuit. **3.** Colloquialism for an unsound theory.

garble **1.** Garbled matter. **2.** Also called *scramble*. To purposely render communications or data unintelligible to everyone, except the intended recipient(s). See SCRAMBLER CIRCUIT.

garbled matter Confused communications or data, usually resulting from distortion in a circuit or system. Also called GARBLE.

garbler See SCRAMBLER CIRCUIT.

garnet maser A maser that uses natural or synthetic garnet as the stimulated material. Also see YTTRIUM-IRON-GARNET.

gas One of the states of matter, characterized by molecules that are widely separated and are in continual, relatively rapid motion. Because it is a fluid, a gas will readily conform to a container of any shape. Gases can readily be compressed and liquefied. Compare LIQUID, PLASMA, and SOLID.

gas amplification In a radiation-counting device, the ratio, in decibels, of the charge collected to the charge produced in the gas.

gas breakdown The ionization of a gas by means of high voltage. The intensity of the electric field prevents recombination of ions. Collisions among atoms cause further ionization. Thus, the gas becomes a good conductor of current.

gas cell A cell whose operation depends on gas absorption by the electrodes.

gas cleanup Loss of pressure in a gas-filled tube, eventually leading to failure. Caused by gas ions forming compounds with metal parts or with the glass envelope.

gas detector A device for sensing presence of various gases in the air—especially toxic or explosive gases (such as chlorine, hydrogen, or methane).

gaseous conduction The conduction of an electric current through an ionized gas.

gaseous phototube A PHOTOTUBE containing a small amount of a gas suitable for ionic conduction.

gaseous voltage regulator A gas-filled diode across which the voltage drop is substantially

5059F-pG-307-325 4/10/01 8:57 AM Page 310

constant during the gas discharge and which accordingly delivers a constant output voltage.

gas-filled cable A sealed cable filled with an inert gas that serves as a low-loss dielectric and moisture barrier.

gas-filled counter tube A radiation counter tube containing a gas that ionizes when irradiated. See GEIGER-MUELLER TUBE.

gas-filled lamp **1.** An incandescent lamp filled with a gas, such as nitrogen, for improved performance. **2.** Discharge lamp.

gas-filled tube An enclosure filled with gas that is subjected to an electric potential, intended to produce specific effects, such as light emission or voltage regulation.

gas-flow alarm An electronic circuit that actuates an alarm when the flow of gas through a pipe changes from a predetermined rate.

gas-flow control A servo system for automatically maintaining or adjusting the flow of gas through pipes.

gas-flow gauge See GAS-FLOW METER.

gas-flow indicator See GAS-FLOW METER.

gas-flow meter An instrument that indicates the rate of gas flow through a pipe, in terms of volume per unit time (e.g., cubic feet per minute).

gas-flow switch In a gas-circulating system, a switch that actuates an alarm when the gas flow rate changes.

gas focusing In a cathode-ray tube, a technique by which a gas is used for the purpose of focusing an electron beam. The ionization of the gas causes the electron beam to be made more narrow.

GASH Acronym for *guanidine aluminum sulfate hexahydrate,* an organic crystalline material used as the dielectric in certain ferroelectric capacitors and ferroelectric memory elements.

gas laser A LASER that uses a gas or mixture of gases (instead of a solid rod) as the stimulated medium. Some of the gases used are argon, carbon dioxide, helium, krypton, and neon.

gas maser A MASER in which the stimulated material is a gas, such as ammonia.

gas multiplication See GAS AMPLIFICATION.

gas noise Electrical noise resulting from the undirected motion of gas molecules in a gas-filled tube.

gas-pressure alarm An electronic circuit that actuates an alarm when gas pressure rises or falls.

gas-pressure control A servo system for automatically maintaining or adjusting gas pressure in pipes or other channels.

gas-pressure gauge See GAS-PRESSURE METER.

gas-pressure indicator See GAS-PRESSURE METER.

gas-pressure meter An instrument that indicates gas pressure in a pipe or container, but provides no means for automatically correcting the pressure.

gas ratio For a gas-filled tube, the ratio I_i/E_i, where I_i is the ion current and E_i is the ionization potential.

gas sensor Any element, such as the filament in a hot-filament gas detector, that responds to the presence of a gas in the environment and activates the detector or alarm circuit.

gassing **1.** The generation of gas by a storage battery, especially while it is being charged. **2.** The generation of gas during electrolysis.

gas sniffer See GAS DETECTOR.

gaston A device intended for the purpose of modulating an aircraft signal, making the signal difficult to jam. The signal is randomly modulated by noise from the device.

gas tube See GAS-FILLED TUBE.

gas-tube lightning arrester A lightning arrester, consisting of a special gas diode. The tube has virtually infinite resistance at low voltages, but provides a low-resistance path to ground when the high voltage of a lightning stroke ionizes the gas.

gas-tube oscillator A relaxation oscillator using a two-element gas tube, such as a neon lamp, as the breakdown device.

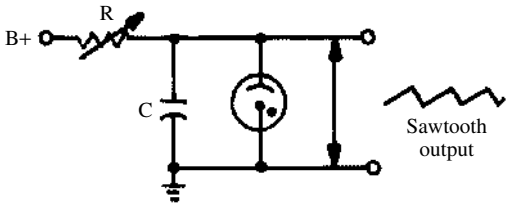

gas-tube oscillator

gas valve See ELECTROMECHANICAL VALVE.

gas X-ray tube An X-ray tube in which the positive ions of a gas bombard the cathode, which emits electrons.

gate **1.** A device or circuit that has no output until it is triggered into operation by one or more enabling signals, or until an input signal exceeds a predetermined threshold amplitude. **2.** The input (control) electrode of a field-effect transistor or thyristor device (e.g., silicon-controlled rectifier). **3.** A signal that triggers the passage of other signals through a circuit.

gate array Basic gates arranged in a pattern on a chip; the gates can be interconnected during manufacture to form a unit that performs whatever function is needed.

gate circuit **1.** An electronic switching circuit (see GATE, **1**). **2.** The circuit associated with the gate electrode of a field-effect transistor.

gate-controlled switch A device similar to a silicon-controlled rectifier or thyristor. A negative current, applied to the gate, switches the device off.

gate current Symbol, I_G. Current flowing in the gate (control) circuit of a semiconductor device. The current is finite in thyristors, but is almost zero in some types of field-effect transistors.

gated amplifier An amplifier whose input is effectively switched on and off by gating signals.

5059F-pG-307-325 4/10/01 8:57 AM Page 311

gated buffer A low-voltage, high-current driver, used for differentiation in a multivibrator circuit.

gated flip-flop A flip-flop in which it is impossible for both outputs to be low simultaneously.

gate-dip meter A dip meter using a field-effect-transistor oscillator with the indicating microammeter in the gate circuit.

gate-dip oscillator See GATE-DIP METER.

gated multivibrator A rectangular-wave generator that produces a gate voltage when triggered.

gate-drain voltage Symbol, V_{GD}. In a field-effect transistor, the maximum voltage permitted between the gate and drain electrodes.

gated sweep **1.** In radar, a sweep whose initiation and duration are closely controlled to eliminate echoes in the image. **2.** A circuit providing the action described in **1**.

gate electrode See GATE, **2**.

gate impedance **1.** The impedance of the gate electrode of a field-effect transistor with respect to the other electrode, which serves as the return. **2.** The impedance of the gate winding of a magnetic amplifier.

gate leakage current See GATE REVERSE CURRENT.

gate nontrigger voltage Symbol, V_{Gnt}. For a thyristor, the direct-current (dc) voltage applied between the gate and the cathode, above which the device fails to maintain its rated blocking voltage.

gate power dissipation Symbol, P_G. In a silicon controlled rectifier, the power consumed by the gate-cathode path.

gate-protected MOSFET A metal-oxide-semiconductor field-effect transistor in which the gate electrode is protected from accidental burnout via built-in Zener diodes, connected back-to-back.

gate pulse **1.** A pulse applied to the gate electrode to actuate a gate-controlled semiconductor device. **2.** An actuating pulse in a gate circuit.

gate recovery time Symbol, t_{Gr}. For a silicon-controlled rectifier, an extension of the reverse recovery time: the interval following application of the reverse voltage required before the forward blocking voltage can be reapplied and then blocked by the device.

gate reverse current Symbol, I_{GSS}. In a field-effect transistor, reverse current in the gate-source circuit. Also called *gate leakage current.*

gate signal **1.** The input or control signal applied to the gate electrode of a semiconductor device. **2.** An actuating signal in a gate circuit.

gate-source breakdown voltage Symbol, BV_{GSS}. The voltage at which the gate junction of a junction field-effect transistor (JFET) enters avalanche.

gate-source pinchoff voltage Symbol, V_P. In a field-effect transistor, the gate-source voltage at which the conduction channel just closes.

gate-source voltage Symbol, V_{GS}. In a field-effect transistor, the direct-current (dc) voltage between the gate and source electrodes.

gate terminal **1.** The terminal connected to the gate semiconductor in a field-effect transistor. **2.** The terminal, or terminals, connected to the input or inputs of a digital-logic network.

gate trigger current In a gate-controlled semiconductor switch, the current flowing in the gate circuit when the device is being switched on by a gate trigger voltage.

gate trigger voltage In a gate-controlled semiconductor switch, the trigger voltage required to actuate the device.

gate turn-off current In a gate-controlled semiconductor switch, the low value of gate current that flows when the device is being switched off. Turn-off current varies with collector (anode) current.

gate turn-off voltage In a gate-controlled semiconductor switch, the low value of gate voltage that causes the device to switch off.

gate voltage **1.** The voltage applied to the gate electrode of a field-effect transistor. See GATE-SOURCE VOLTAGE. **2.** The instantaneous gate-cathode voltage in a silicon-controlled rectifier. **3.** The voltage across the gate winding of a magnetic amplifier.

gate winding In a magnetic amplifier, a winding that produces gating action.

gating **1.** The process of using one signal to switch another (or part of another) on or off for a desired interval. **2.** Selecting a part of a wave for observation or for control purposes.

gauge **1.** Any device, such as a METER, used for the purpose of measuring the magnitude of a quantity. **2.** Wire data and measurements (see WIRE GAUGE, **1**, **2**, **3**). **3.** Sheet metal thickness (e.g., 10 gauge).

Gauss (Karl F. Gauss, 1777–1855) Unit of magnetic flux density, equivalent to one line of flux per square centimeter. The SI (preferred) unit of magnetic flux density is the TESLA (webers per square meter); 1 gauss equals 10^{-4} teslas (symbol, T). Also see FLUX DENSITY.

Gaussian curve See BELL-SHAPED CURVE.

Gaussian distribution In statistics, the symmetrical distribution described by a bell-shaped curve. Also called NORMAL DISTRIBUTION.

Gaussian function A mathematical function used in the design of lowpass filters. The Gaussian response is characterized by low band-edge selectivity, high transition bandwidth, negligible step response overshoot, and low step-response delay time.

Gaussian noise Electrical noise whose amplitude-versus-frequency characteristic is described by the GAUSSIAN DISTRIBUTION.

Gaussian waveform A waveform that results in minimal side lobes in a pulse-compression system.

gaussmeter See FLUXMETER.

Gauss' theorem Across any closed surface within an electric field, the total flux is approximately equal to 12.566 times the enclosed quantity of electric charge.

5059F-pG-307-325 4/10/01 8:57 AM Page 312

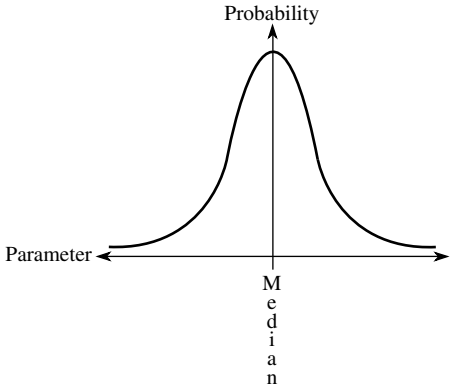

Gaussian distribution

gauze resistor See WOVEN RESISTOR.
GAVRS Abbreviation of *gyrocompass attitude vertical reference system.*
GCA Abbreviation of GROUND-CONTROLLED APPROACH.
GCI Abbreviation of GROUND-CONTROLLED INTERCEPTION.
GCM Abbreviation of *gyrocompass module.* See GYROCOMPASS.
GCT Abbreviation of GREENWICH CIVIL TIME.
Gd Symbol for GADOLINIUM.
G display See G SCAN.
GDO **1.** Abbreviation of GRID-DIP OSCILLATOR. **2.** Abbreviation of GATE-DIP OSCILLATOR.
Ge Symbol for GERMANIUM.
gear **1.** Collectively, electronic equipment. **2.** A toothed wheel commonly used in mechanical devices.
gearmotor An electric motor with a gear train for speed changing.
gear-wheel pattern A pattern produced on an oscilloscope by intensity-modulating a circular trace. A signal of unknown frequency f_x is applied to the intensity-modulation (z-axis) input. The signal produces corrugations in the trace. If there are n corrugations around the trace, and if the trace itself completes f_s revolutions per second, then the unknown frequency f_x, in Hz, is equal to nf_s. Compare SPOT-WHEEL PATTERN.

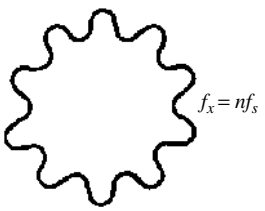

gear-wheel pattern

Geiger counter A radioactivity rate-counting instrument based on the GEIGER-MUELLER TUBE. Pulses from the tube drive a transistor, which, in turn, drives a meter or digital counter to indicate the count.

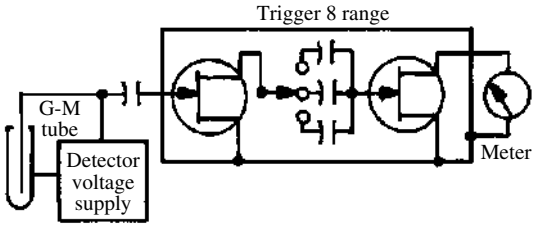

Geiger counter

Geiger-Mueller counter See GEIGER COUNTER.
Geiger-Mueller region For a GEIGER-MUELLER TUBE, the range of voltages within which the output pulse amplitude is constant, regardless of ionizing radiation intensity.
Geiger-Mueller threshold The lowest voltage in the Geiger-Mueller region.
Geiger-Mueller tube A gas-filled radiation detector/counter tube consisting of a straight wire as an anode, surrounded by a cylindrical cathode. The tube is biased by high voltage. Radiation penetrating the tube ionizes the gas; each ionizing event causes an output pulse.
Geiger point counter See POINT COUNTER.
Geiger region See GEIGER-MUELLER REGION.
Geiger threshold See GEIGER-MUELLER THRESHOLD.
Geissler tube A simple gas-filled glow-discharge tube with metal electrodes sealed in each end. When a sufficiently high voltage is applied between the electrodes, the highly rarefied gas ionizes and glows with the color associated with the particular gas used.
gel A substance equivalent to colloidal solution in the solid phase (e.g., silica gel).
gel battery A rechargeable electrochemical BATTERY designed for use with portable electronic and computer equipment. Noted for its ability to deliver high current for short periods, when necessary, and also to deliver moderate current continuously throughout its discharge cycle.
gen Abbreviation of GENERATOR.
genemotor Contraction of *generator/motor*, a (usually battery-driven) dynamotor that has separate motor and generator windings on the same armature core.
general class license An amateur-radio license that conveys some privileges in the high-frequency bands, and all operating privileges in the very-high-frequency region and above. An examination of moderate difficulty is required.

5059F-pG-307-325 4/10/01 8:57 AM Page 313

General Packet Radio Service A form of packet radio especially designed for mobile use. Subscribers pay for the volume of data they send and receive, rather than for the time they spend accessing the network. This optimizes the efficiency of the network, both from an engineering standpoint and a financial standpoint. See PACKET COMMUNICATIONS.

general-purpose bridge See UNIVERSAL BRIDGE.

general-purpose component A component designed or used for a wide range of applications. For example, a general-purpose germanium diode is useful as a detector, mixer, limiter, clipper, meter rectifier, automatic-gain-control (AGC) rectifier, and curve changer.

general-purpose computer A computer that can be used in a number of applications for which it was not specifically designed.

general-purpose diode A small-signal semiconductor diode that is useful for a variety of applications, such as detection, light-duty rectification, limiting, logic switching, etc.

general-purpose function generator A nonspecialized function generator that is capable of generating a variety of different waveforms.

general-purpose program A program for the solution of a class of problems or for a specific problem, according to certain parametric values. Also called *general routine.*

general-purpose relay Any relay that can be used in various situations, such as for switching alternating or direct currents.

general-purpose tester An instrument, such as a voltohm-milliammeter, that offers several test capabilities.

general-purpose transistor A transistor that can be used in several applications, such as audio amplification, detection, and oscillation.

general service code See CONTINENTAL CODE.

generate **1.** To produce a signal or carrier wave. **2.** To convert some non-electrical form of energy (usually mechanical) into electrical energy. **3.** To develop subroutines from parameters applied to skeletal coding. **4.** To use a program generator to produce a specialized version of a general-purpose program.

generated address An address developed by program instructions for later use by that program.

generated noise **1.** Electrical noise caused by battery action (i.e., between dissimilar metals) in a component, such as in a potentiometer. **2.** Electrical noise caused by small output variations of generating devices (rotating machines, vibrators, etc.). Also called *generator noise.*

generating magnetometer See EARTH INDUCTOR.

generating station An electric power station.

generating voltmeter An instrument based on a rapidly spinning variable capacitor. A direct-current (dc) voltage applied to the capacitor is converted into an alternating current (ac) by the varying capacitance; the ac is proportional to the voltage.

generation **1.** The production of a signal or carrier wave. **2.** The conversion of some non-electrical form of energy (usually mechanical) into electrical energy. **3.** The number of recording steps between a master recording and a copy. **4.** A copy of data in any form (e.g., tape recording, disk file, and photocopy).

generation number A number that identifies the age of a file; it is included in the file label on the disk or tape containing the file.

generator **1.** Symbol, G. Any signal source. **2.** A rotating machine for producing electricity. **3.** An electronic device for converting direct current into alternating current of a specific frequency and waveshape. **4.** In computer operation, a routine (akin to a compiler) that will produce a program to perform a specific version of some general operation by implementing skeletal coding, according to specific parameters (e.g., *sort generator*).

generator efficiency The ratio of consumed power to delivered power in a generator. It is usually expressed as a percentage.

generator noise Electrical noise caused by a rotating generator. Also see GENERATED NOISE, **2**.

generator-type microphone A microphone that produces an output voltage without the need for a supply voltage. Examples: ceramic, crystal, dynamic, electret, and velocity types.

generator-type transducer A transducer that converts mechanical motion into an electrical signal of a proportional voltage. In such a transducer, an armature or conductor moves in a magnetic field.

generic A form of software collection. Several specialized software packages can be derived from the generic collection, for use in different systems.

geodesic **1.** On a surface, the shortest path between two points. **2.** The shortest path between two geographical locations, measured over the surface of the earth. Also called *geodetic* and *great circle.*

geodesy The branch of applied mathematics concerned with the precise dimensions of the earth.

geodetic system The application of a computer to seismographic studies for the purpose of reducing drilling and mining costs.

geomagnetic field See EARTH'S MAGNETIC FIELD.

geomagnetism The earth's magnetism. Also see EARTH'S MAGNETIC FIELD.

geometric capacitance The ratio of the free charge of a capacitor to the voltage across its terminals.

geometric mean The *n*th root of the product of *n* quantities.

geometric progression A mathematical sequence in which each term after the first is obtained by multiplying the preceding one by a constant quantity (e.g., 1, 2, 4, 8, 16, 32, 64, . . .). Also called *geometric sequence.*

5059F-pG-307-325 4/10/01 8:57 AM Page 314

geometric symmetry In a bandpass or band-rejection filter, a condition in which the response is identical on either side of the center frequency. Also called *mirror-image symmetry.*

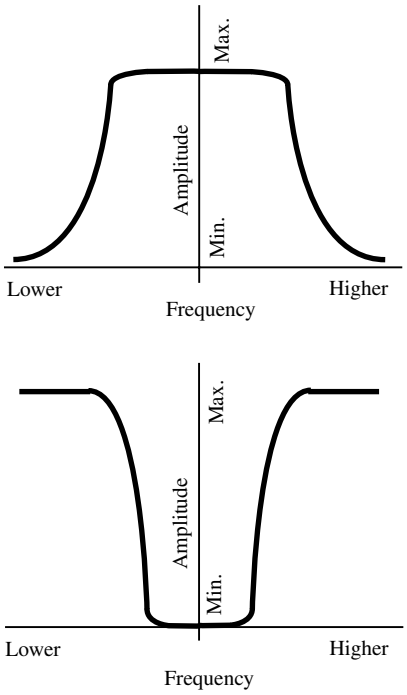

geometric symmetry

george box In an intermediate-frequency amplifier, a device used to reject jamming signals. Any jamming signal with an amplitude lower than a certain minimum is rejected.

geostationary orbit An orbit in which a satellite revolves around the earth exactly once a day, so it remains over the same place on the earth all the time. The altitude must be 22,300 miles, and the orbit must lie in the plane of the earth's equator.

geostationary satellite A satellite in GEOSTATIONARY ORBIT. It is always in the same spot in the sky from any given observing point. A geostationary satellite provides coverage over about 40 percent of the earth, and is commonly used for communications and weather-observation purposes.

germanium Symbol, Ge. A metalloidal element. Atomic number, 32. Atomic weight, 72.59. Used in semiconductor diodes, photocells, rectifiers, and transistors.

germanium diode A diode in which the semiconductor material is specially processed germanium.

germanium dioxide Formula, GeO_2. A gray or white powder obtainable from various sources; it is reduced in an atmosphere of hydrogen or helium to yield germanium, a semiconductor material.

germanium junction diode A germanium diode that contains a pn junction.

germanium photocell A photoconductive cell consisting of a reverse-biased germanium point-contact diode or germanium junction diode.

germanium point contact The contact between a pointed metal wire and a germanium wafer, as in a point-contact diode or point-contact transistor.

germanium rectifier A power rectifier that contains a germanium pn junction.

germanium transistor A transistor in which germanium is the semiconductor material. Such a transistor has lower internal resistance and greater temperature drift than a silicon transistor.

German silver A copper-nickel-zinc alloy used in some resistance wires. Also called NICKEL SILVER.

GEV Abbreviation of *ground effect vehicle.*

GeV Abbreviation of GIGAELECTRONVOLT.

gfi Abbreviation of GROUND-FAULT INTERRUPTER.

g-force See GRAVITY, **2**.

g_{FS} Symbol for FORWARD TRANSCONDUCTANCE.

G/G Abbreviation of GROUND-TO-GROUND.

ghost In television reception, a slightly displaced image appearing on the screen simultaneously with its twin (the false member of a double image).

ghost signal Any signal (such as an undesired reflection) that produces a ghost.

GHz Abbreviation of GIGAHERTZ.

G_i Symbol for INPUT CONDUCTANCE.

Gibson girl A portable radio transmitter, powered by an integral crank-operated generator, introduced during World War II for pilots forced down at sea.

giga- Abbreviation, G. **1.** A prefix meaning billion (10^9). **2.** In digital data applications, a prefix meaning 2^{30}.

gigabit A unit of digital data, equal to 2^{30} bits or 1024 megabits. Also see BIT and MEGABIT.

gigabyte A unit of digital data, equal to 2^{30} bytes or 1024 megabytes. Also see BYTE and MEGABYTE.

gigacycle See GIGAHERTZ.

gigaelectronvolt Abbreviation, GeV. A large unit of voltage; 1 GeV equals 10^9 eV. Also see BEV, ELECTRONVOLT, MEV, and MILLION ELECTRON VOLTS.

gigahertz Abbreviation, GHz. A unit of ultra-high frequency; 1 GHz equals 1,000,000,000 Hz = 10^9 Hz.

gigaohm A unit of extremely high resistance, reactance, or impedance, equal to 1,000,000,000 ohms = 10^9 ohms.

GIGO Abbreviation of *garbage in = garbage out,* an expression signifying that incorrect or improper

5059F-pG-307-325 4/10/01 8:57 AM Page 315

input to a computer will produce meaningless output.

gilbert (William Gilbert, 1540–1603) A unit of magnetomotive force, equal to 1.26 times the number of ampere-turns. The SI (preferred) unit of magnetomotive force is the ampere (symbol, A); 1 gilbert = 0.796 A.

gilbert per centimeter See OERSTED.

gimbal A suspension device whose orientation can be changed without affecting the attitude of the body being suspended.

gimmick **1.** Colloquialism for any unnamed device. Also see GADGET. **2.** Colloquialism for any tricky manipulation or design. **3.** A low-value capacitor made by twisting two short pieces of insulated wire together.

gimp Colloquialism for the tinsel and cloth conductor used in some earphone cords.

Giorgi system The *meter-kilogram-second (mks)* system of units.

GJD Abbreviation of GERMANIUM JUNCTION DIODE.

glass A hard, brittle, amorphous, and usually transparent substance that is largely silicon dioxide. Glass has a multitude of uses in electronics, and there are several kinds, each having different electrical properties. The dielectric constant ranges from about 4 to 10; the dielectric strength ranges from about 20 to 300 kilovolts per millimeter.

glass arm A stiffness of the wrist or forearm, somewhat resembling writer's cramp, sometimes experienced by radiotelegraph operators or wire telegraph operators after prolonged use of a hand key.

glass bulb The glass enclosure of electron tubes and incandescent lamps.

glass capacitor A capacitor that uses thin glass as the dielectric, and usually has plates consisting of metal electroplated or electrodeposited on opposite faces of the glass. Also see MOLDED GLASS CAPACITOR.

glass diode A semiconductor diode molded in glass.

glass electrode A probe used with a pH meter; it consists of a thin-walled glass tube containing potassium chloride and mercurous chloride. Also see CALOMEL ELECTRODE.

glass envelope See GLASS BULB.

glassivation A procedure for encapsulating semiconductor devices in glass or other dielectric material.

glass-metal seal See GLASS-TO-METAL SEAL.

glass plate capacitor See GLASS CAPACITOR.

glass shell See GLASS BULB.

glass-to-metal seal A bond between glass and metal in electronic devices, such as vacuum tubes, feedthrough terminals, and glass capacitors.

glass tube A vacuum tube whose elements are housed in an evacuated glass envelope.

glide path The guidance beam used by aircraft making instrument landings.

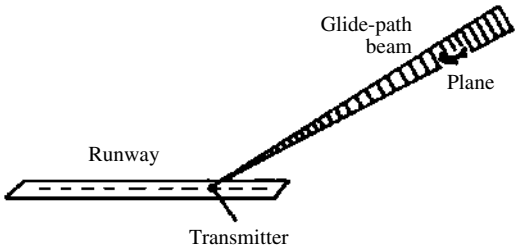

glide-path transmitter

glide-path transmitter A radio-frequency transmitter that produces a guidance beam for aircraft landing purposes. The aircraft follows the beam toward the runway.

glide slope See GLIDE PATH.

G line A microwave conductor consisting of a round wire coated with a dielectric.

glitch **1.** In a television image, a narrow, horizontal interference bar that moves vertically. **2.** A very short and unwanted high-amplitude transient that recurs irregularly in an electronic system.

glitter **1.** In radar, an echo or set of echoes that fluctuates rapidly in intensity because of motion in the target. **2.** A system in which moving devices are used to confuse enemy radar systems.

gloss factor For a reflecting surface, the ratio of reflected light in a selected direction to reflected light in all directions.

glossmeter An instrument for determining GLOSS FACTOR.

glow discharge The luminous electrical discharge resulting from the passage of current through ionized gas in a partially evacuated tube. The color of the glow is characteristic of the particular gas used.

glow-discharge microphone A device that produces audio-frequency currents from the action of sound waves in a glow-discharge tube.

glow-discharge tube A partially evacuated tube that contains two or more electrodes. The rarefied gas in the tube glows when a sufficient voltage is applied to the electrodes. See DISCHARGE LAMP, FLUORESCENT TUBE, and NEON BULB.

glow lamp See DISCHARGE LAMP.

glow modulator tube A gas tube whose luminous output can be modulated by an audio input signal.

glow potential The voltage at which glow discharge just begins in a gas-filled tube.

glow switch In fluorescent light circuits, an electron tube containing two bimetal strips that make mutual contact when heated by the glow discharge.

glow tube See DISCHARGE LAMP, FLUORESCENT TUBE, GLOW MODULATOR TUBE, NEON BULB, and STROBOTRON.

glow voltage See BREAKDOWN VOLTAGE, **2**.

glucinium See BERYLLIUM.

5059F-pG-307-325 4/10/01 8:57 AM Page 316

gluon A subatomic particle that is believed to bind quarks together (coined by Prof. Murray Gell-Mann of California Institute of Technology).

GM Abbreviation of *Geiger-Mueller* (see, for example, GEIGER-MUELLER TUBE).

gm Abbreviation of *gram.* Also abbreviated g.

g_m Symbol for TRANSCONDUCTANCE.

g-m Abbreviation of GRAM-METER.

gm-cal Abbreviation of GRAM-CALORIE.

gm-cm Abbreviation of GRAM-CENTIMETER.

G-M counter See GEIGER COUNTER.

GMT Abbreviation of GREENWICH MEAN TIME.

G/M tube See GEIGER-MUELLER TUBE.

gnd Abbreviation of GROUND.

g_o Symbol for OUTPUT CONDUCTANCE.

gold Symbol, Au. A precious metallic element. Atomic number, 79. Atomic weight, 196.967. Electrical contacts that must have low radio-frequency resistance, and that must be relatively immune to corrosion, are often plated with gold.

gold-bonded diode A germanium point-contact diode having a fine gold wire whose point is bonded to the germanium wafer. Its principal features are high forward current and almost constant, low reverse current.

gold doping The diffusion of gold into the base and collector regions of a diffused-mesa transistor; it shortens carrier storage time.

golden ratio A set of proportions used in the design of some speaker cabinets. The width (W) is ⅝ of the height (H); the depth (D) is ⅝ of the width. These correspond to a ratio $H : W : D = 1.000 : 0.625 : 0.391$. These proportions are thought by some acoustics engineers to result in the best possible sound quality.

gold-leaf electroscope See ELECTROSCOPE.

Goldschmidt alternator An early dynamo for generating radio-frequency power. The high-frequency energy was not generated directly by the machine, but by resonant circuits and frequency-multiplying interaction between components.

Golf Standard phonetic alphabet code word for the letter G.

goniometer **1.** Generically, any radio direction finder. **2.** An inductive coupler having a secondary coil rotated by a dial calibrated to read azimuth. The coupler, when used with a suitable antenna system, comprises a direction finder. **3.** A device for electrically varying the directional pattern of an antenna.

go-no test A test that indicates only acceptance or rejection of a device. No diagnosis is made.

GOTO In computers and programmable calculators, an instruction that, followed by a suitable label, directs the program to that label.

goto circuit In a digital-logic circuit, a device that senses the direction of electric current.

goto pair A pair of diodes connected in reverse series used in digital-logic circuits.

governor **1.** A device that prevents a motor or engine from running faster than a certain speed. **2.** Any device that limits a circuit parameter.

g parameters Conductance parameters obtained for the equivalent-pi model of a transistor: g_{BE}, g_{GC}, g_{CE}, and g_m.

gpc Abbreviation of GERMANIUM POINT CONTACT.

GPI Abbreviation of GROUND-POSITION INDICATOR.

GPRS Abbreviation for GENERAL PACKET RADIO SERVICE.

gr Abbreviation of *grain(s).*

graceful degradation A computer programming technique used to prevent debilitating breakdown by operating the system—even though several subsystems have malfunctioned; also known as *crippled mode.*

grad A unit of angular measurement equal to 0.9 degree.

graded-base transistor See DIFFUSED-BASE TRANSISTOR.

graded filter A power-supply filter that supplies direct-current output at various points in the filter sequence. Thus, the points in the powered equipment that can tolerate the least ripple are connected to the filter output, and those that can tolerate appreciable ripple are connected to the filter input; fairly critical points are connected to an intermediate position in the filter, such as at the junction of two chokes.

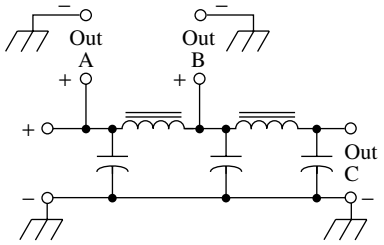

graded filter

graded-junction transistor A grown-junction transistor in which the temperature of the melt and the rate at which the crystal is pulled from it are closely controlled as the n and p layers are formed.

gradient The rate at which a variable quantity increases or decreases. See, for example, VOLTAGE GRADIENT.

gradient microphone A microphone whose output varies with sound pressure. Also see PRESSURE MICROPHONE.

Graetz bridge A full bridge rectifier (i.e., one having a diode in each arm).

Graffiti **1.** Trade name for a specialized written alphabet used for entering data into a handheld computer using a stylus. **2.** The entry of data into

5059F-pG-307-325 4/10/01 8:57 AM Page 317

a handheld computer using a stylus. See HANDHELD COMPUTER.

grain boundary In a polycrystalline solid, a boundary between single crystalline regions.

gram **1.** Abbreviation, g. A unit of mass and weight, equal to 0.001 kilogram or 0.0353 ounce. **2.** A suffix meaning something drawn (written), or recorded, as in *radiogram* or *electrocardiogram*.

gram atom See GRAM ATOMIC WEIGHT.

gram atomic weight Also called *gram-equivalent*. The quantity of an element with a mass in grams that is equal to the atomic weight of the element. For example, copper has an atomic weight of 63.546; therefore, one gram atomic weight of copper has a mass of 63.546 grams.

gram-calorie Abbreviation, gm-cal. The amount of heat required to raise the temperature of one gram of water by one degree Celsius.

gram-centimeter Abbreviation, gm-cm. The work done by a force of one gram exerted over a distance of one centimeter. Also see JOULE.

gram-equivalent See GRAM ATOMIC WEIGHT.

grammar **1.** The sequence of words and/or abbreviations in a communication or part of a communication. **2.** The sequence of codes and/or commands in a high-level computer programming language.

gramme armature See GRAMME RING.

Gramme ring A type of armature for a motor or generator, consisting of an iron ring onto which is wound a coil of wire, each turn being connected to a commutator bar.

gram-meter Abbreviation, g-m. A unit of work equal to a force of one gram exerted over a distance of one meter. Compare JOULE.

gram-molecular weight See MOL.

gram molecule See MOL.

gramophone Archaic term for *phonograph*.

grandfather cycle A backup scheme in a magnetic reproduction system. The original records are retained for a period of time so that new copies of high precision can be made in case of loss.

grandfather file An original copy of a file on a magnetic disk or tape, retained as a source for reconstruction as needed. Usually, three generations of a file (grandfather, father, and son) are kept, each identified by a generation number. Sometimes the terms *grandparent*, *parent*, and *child* are used instead. See GENERATION NUMBER.

grand synthesizer A hypothetical child with a mind perfectly attuned to artificial intelligence (AI), who grows up to revolutionize the whole industry; a "grand master of AI."

granular carbon Carbon in the form of fine granules, used in the button of a carbon microphone.

granularity **1.** In a digital device, the smallest increment that can be differentiated. **2.** The limit of detail in a reproduction system.

granule One of many narrow frequency subbands, the combination of which composes a complete signal. Each subband carries its own specific data.

graph **1.** A presentation of data, particularly a depiction of the manner in which one variable or set of variables changes, with respect to another. Can be in the form of discrete points, curves, bars, columns, pie-shaped slices, etc. **2.** A curve or set of curves in a coordinate system.

graphical analysis The solution of problems through the use of graphic devices, such as vector diagrams, load lines, Nyquist plots, topological flow diagrams, etc.

graphical harmonic analysis See SCHEDULE METHOD.

graphical user interface Acronym, GUI (pronounced "gooey"). An operating system or software that makes it easy for lay people to use a computer. Commands are given by making choices from among items displayed on the screen. Popular versions use symbols, called *icons*, along with a pointing device, such as a *mouse* or *trackball*.

graphic documentation Records of data in the form of graphs, charts, tables, diagrams, etc.

graphic equalizer A device for tailoring the amplitude-versus-frequency response of a high-fidelity audio system. Consists of a splitter, several audio filters, and a mixer. The gain of each filter is adjustable via a slide potentiometer. The potentiometers are arranged on the front panel in such a way that their relative positions show the approximate shape of the response curve.

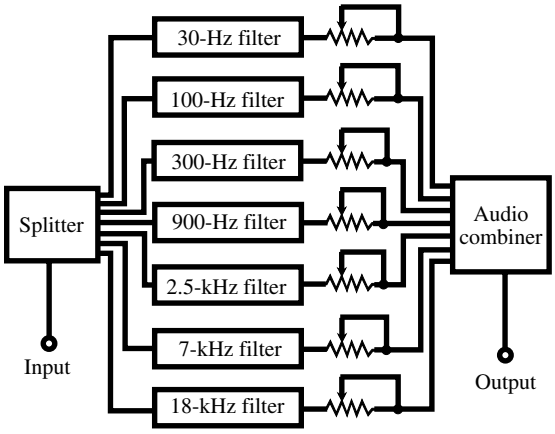

graphic equalizer

graphic instrument See GRAPHIC RECORDER.

graphic-level recorder An instrument that makes a permanent recording of signal amplitude as a function of some independent variable (such as time, frequency, or direction).

graphic panel In process control, a panel of illuminated lights or dials that display the status of a process.

5059F-pG-307-325 4/10/01 8:57 AM Page 318

graphic recorder An instrument in which a signal-driven pen or stylus makes a permanent record of a quantity on graph paper. The paper passes at a controlled speed beneath the pen.

graphics **1.** Diagrams, charts, photos, tables, or similar, often symbolic, artwork used to convey information. **2.** The video display in a computer system. **3.** Computer software designed specifically to create and edit illustrations.

graphic solution **1.** A method of depicting the solution(s) to a problem or equation by means of graphs. **2.** The process of solving problems or equations with the aid of graphs.

graphic terminal A display or plotter that provides visual output of a computer run.

graphite A soft form of carbon used in resistors, attenuators, contacts, brushes, vacuum-tube plates, cathode-ray tube coatings, etc.

graphite-line resistor An emergency, makeshift resistor consisting of a pencil line drawn on a piece of paper. The heavier the line for a given width and length, the lower its resistance.

graphophone Archaic term for *phonograph.*

grasping planning A scheme that a robot arm and gripper use to get hold of a particular object. It can use a vision system, a bar-code reader, tactile sensing, and/or proximity sensing. The robot controller (computer) must be programmed to recognize the input from these devices, and to seek out the object.

grass The background noise (noise floor) on the display of a spectrum analyzer; it also appears on certain types of radar displays.

grasshopper fuse A special type of spring-operated fuse. When it burns out, it actuates an alarm that alerts personnel of a possible circuit or system malfunction.

graticule Calibrated gridwork, as on the face of an oscilloscope or spectrum-analyzer screen.

grating A set of parallel, closely spaced, equidistant conductors or bars. When an electromagnetic field that has a wavelength comparable to the conductor spacing passes through the plane containing the conductors, diffraction occurs, producing an interference pattern. An adaptation of this device, called a DIFFRACTION GRATING, is used to separate visible light into its constituent spectral colors.

grating reflector A metal antenna reflector consisting of numerous parallel, straight, closely spaced conductors. When the conductor spacing is much smaller than the wavelength, the set behaves like a solid sheet of metal.

Gratz rectifier A form of full-wave rectifier circuit in a three-phase, alternating-current system.

gravitational constant Symbol, g. The acceleration produced by the attraction of a unit mass at unit distance; $g = 6.673 \times 10^{-11}\ \mathrm{N \cdot m^2/kg^2}$.

gravitational wave See GRAVITY WAVE.

gravity **1.** The universal force of attraction between material bodies—especially that force evidenced by the earth's drawing of bodies toward its center, causing them to have weight. **2.** Abbreviation, g. The rate at which a free-falling mass accelerates in a vacuum at the earth's surface; equal to 9.802 meters per second per second ($\mathrm{m/s^2}$). **3.** The rate at which a free-falling mass accelerates in a vacuum in the vicinity, or at the surface, of an astronomical object, such as a planet or star.

gravity cell An electrochemical cell in which the positive electrode is made of copper and the negative electrode is made of zinc. The copper electrode is placed at the bottom of a jar, and the zinc electrode is placed at the top. The jar is half filled with copper sulfate solution, and then filled with zinc sulfate solution. The solutions remain separate because copper sulfate has a higher specific gravity than zinc sulfate.

gravity wave A disturbance in a gravitational field, such as might be caused by a collapsing star. These waves might emanate from black holes or rapidly spinning neutron stars.

gray body A radiating body exhibiting constant spectral emissivity at all wavelengths. That is, the emitted energy is the same at all wavelengths and all frequencies.

Gray code A computer code in which the expressions representing sequential numbers differ in only one bit.

gray scale A reference scale for use in black-and-white television and video display images, consisting of several defined levels of brightness with neutral color.

Gray scale: hypothetical 16-shade binary codes.

Code	Relative shade	Percent brightness
0000	Black	0.00
0001		6.67
0010	Very dark gray	13.33
0011		20.00
0100	Dark gray	26.67
0101		33.33
0110	Medium-dark gray	40.00
0111		46.67
1000	Medium gray	53.33
1001		60.00
1010	Medium-light gray	66.67
1011		73.33
1100	Light gray	80.00
1101		86.67
1110	Off-white	93.33
1111	White	100.00

gray tin A form of tin that exhibits some properties of a semiconductor at temperatures below 18 degrees Celsius.

5059F-pG-307-325 4/10/01 8:57 AM Page 319

greatest lower bound The largest value of a parameter that can be obtained without changing some characteristic of a circuit, program, or system.

Greek alphabet The 24-letter alphabet of the Greek language. Virtually all of letters are used as symbols in electronics and related sciences.

Green Book A specialized format for *compact-disk read-only memory (CD-ROM)* computer data storage media, developed by Sony and Philips. Requires the use of a *Compact Disk-Interactive (CD-I)* player for data retrieval. See also CD-ROM, ORANGE BOOK, RED BOOK, and YELLOW BOOK.

green gun The electron gun in a color cathode-ray tube whose correctly adjusted beam strikes only the green phosphors on the screen.

green video voltage In a three-gun color cathode-ray-tube circuit, the green-signal voltage, which actuates the green gun.

Greenwich Civil Time Abbreviation, GCT. Mean time counted from mean midnight at Greenwich, England, the location of zero meridian.

Greenwich Mean Time Abbreviation, GMT. Mean solar time at zero degrees longitude, also called the *Greenwich meridian* because it passes through Greenwich, England. In recent years, GMT has been supplanted by COORDINATED UNIVERSAL TIME (UTC) as the basis of standard time throughout the world.

grid **1.** The prime control electrode in a vacuum tube. Usually, it is a coil or mesh, but it can have other forms. Also called *control grid.* **2.** Any electrode in a vacuum tube placed between the cathode and the anode (plate) (e.g., *screen grid* and *suppressor grid*). **3.** Two sets of straight, uniformly spaced, parallel conducting wires or rods, one set perpendicular to the other. The conductors are electrically connected at all crossing points. Used as an electrostatic or electromagnetic shield, or as a reflector of electromagnetic waves. **4.** Two sets of uniformly spaced parallel lines, one set perpendicular to the other, used as a system of coordinates or as a basis for physical measurements.

grid capacitor **1.** A capacitor in series with the grid of a vacuum tube, used for blocking purposes. **2.** A bypass capacitor in a grounded-grid tube type amplifier. **3.** The capacitor in the grid tank circuit of a tube type oscillator or amplifier.

grid-cathode capacitance Symbol, *CGK*. The internal capacitance between the control grid and cathode of an electron tube. Also called INPUT CAPACITANCE.

grid characteristic The grid-current-versus-grid-voltage performance curve for a vacuum tube.

grid circuit The external circuit associated with the control grid of a vacuum tube.

grid current Symbol, I_G. Current flowing between the control grid and cathode in a vacuum tube.

grid cylinder The metal cylinder that acts as a control grid in a cathode-ray tube.

grid-dip meter **1.** A dip meter that contains a vacuum-tube oscillator; the indicating microammeter is in the grid circuit. **2.** Loosely, any frequency-sensitive wavemeter that indicates resonance by a marked dip in input (base, grid, and gate) current.

grid-dip oscillator See GRID-DIP METER.

grid dissipation **1.** The amount of power given up as heat in the grid circuit of a vacuum-tube amplifier. **2.** The maximum amount of power that a tube can safely dissipate as heat in the grid.

grid drive See GRID EXCITATION.

grid-driving power The signal power required by the control grid of a power tube.

grid emission Electron or ion emission by the control grid of a vacuum tube.

grid excitation Signal voltage or power applied to the control grid in a vacuum-tube amplifier circuit.

grid impedance Symbol, Z_G. The internal impedance of the grid-cathode path in a vacuum tube.

grid input impedance The impedance of the grid input section of a vacuum-tube circuit. It is a complex combination of grid impedance and the impedance of input-circuit components.

gridistor A special form of field-effect transistor with several channels.

grid-limiter resistor A resistor connected in series with the grid of a tube to limit grid current during the positive half-cycle of grid-signal voltage.

grid limiting The cutting off of plate current in a vacuum tube, with consequent limiting action, by means of a high, negative grid voltage developed by overdriving the grid.

grid loading effect The tendency of the internal grid-cathode path of a vacuum tube to load a tuned circuit—especially when the grid draws current.

grid locking A vacuum-tube fault in which the grid potential has become permanently positive because of excessive grid electron emission.

grid mesh The mechanical structure of a grid (e.g., gauze or a metal screen).

grid neutralization See GRID-NEUTRALIZED AMPLIFIER.

grid-neutralized amplifier A neutralized radio-frequency power amplifier in which the neutralizing capacitor is connected from the plate of the tube to the free end of a center-tapped grid-tank coil.

grid north In the grid system of navigation, the direction most nearly corresponding to geographic north.

grid-plate capacitance See PLATE-GRID CAPACITANCE.

grid pool tube A gas-discharge tube in which the cathode is a pool of mercury.

grid power loss Driving-power loss in the grid-input circuit of a power amplifier.

grid resistor A high-value resistor connected between the control grid and ground in a vacuum-tube amplifier circuit.

5059F-pG-307-325 4/10/01 8:57 AM Page 320

grid return The circuit path through which the control grid of a vacuum tube is returned to ground or to the negative grid bias supply.

grid-separation circuit A vacuum-tube circuit in which the control grid is grounded. See COMMON-GRID CIRCUIT.

grid swing The peak-to-peak variation of a grid excitation signal.

grid tank A resonant inductance-capacitance circuit operating in the control-grid circuit of a vacuum tube. Compare PLATE TANK.

grid tank capacitance The capacitance required to tune a GRID TANK to resonance.

grid tank inductance The inductance of the coil in a GRID TANK.

grid tank voltage The alternating-current (ac) voltage developed across the grid tank of a vacuum-tube circuit.

grid tuning Tuning of a vacuum-tube circuit by varying the capacitance, inductance, or both in the GRID TANK.

grid voltage **1.** Symbol, V_G. The direct-current (dc) bias voltage applied to the control grid of a vacuum tube. **2.** Symbol, $V_{G(ac)}$. The voltage of the radio-frequency (RF) or audio-frequency (AF) signal in the grid circuit.

grille A covering for an acoustic speaker, used primarily to protect the speaker cone, but also for esthetic appeal.

grille cloth A durable fabric often used for speaker grilles in high-fidelity sound systems. It transmits sound at all audio frequencies, but protects the speaker(s) and provides an attractive physical appearance.

gripper See ROBOT GRIPPER.

grommet An elastic washer inserted through a hole in a chassis to prevent accidental grounding of a conductor or to reduce wear on a cord or cable exiting the chassis.

groove **1.** See KEYWAY. **2.** The fine, spiral line cut into a phonograph disc when it is manufactured.

groove angle On a phonograph disk, the angle between the walls of the unmodulated groove.

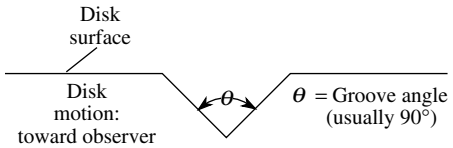

groove angle

groove speed In a phonograph recording or reproducing system, the speed of the cutter or needle, with respect to the disc. The speed is greatest near the outer edge of the disk, and least near the center.

gross content The overall amount of data contained in a message. It can be expressed in bits, bytes, words, or other units.

gross index One of a pair of indexes, used to give a reference in the *fine index*, a supplement; both indexes are used to locate computer records in storage.

gross-motion planning The method(s) that a robot uses to navigate in a general area without running into objects, knocking things over, falling down stairs, or losing its balance. It is often performed using a COMPUTER MAP of the work environment.

ground **1.** The earth in relation to electricity and magnetism. **2.** An electrical connection to the earth. **3.** The return point in a circuit. **4.** A short-circuit to the earth or to a circuit return point. **5.** A short-circuit to the metal chassis, case, or panel of a piece of equipment.

ground absorption The absorption (and resulting loss) of radio-frequency electromagnetic energy by the earth.

ground bus A conductor connected to an earth ground, and to which devices in a system are individually connected. The common ground points (e.g., chassis) of the individual devices are not directly connected to each other, so *ground loops* are avoided. This scheme minimizes the probability of ELECTROMAGNETIC INTERFERENCE to or from the system. Compare GROUND LOOP.

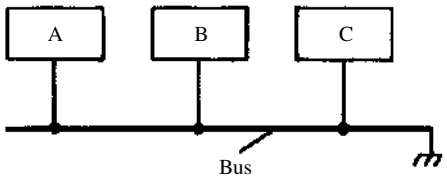

ground bus

ground clamp A device that provides a mechanical and electrical bond between a conductor and a ground rod or pipe. It is generally capable of passing a large amount of current.

ground clutter **1.** In a surface-based radar system, echoes from nearby buildings, hills, and other objects, producing blips or blobs near the center of the screen. **2.** In radar operations, an interference pattern on the screen, caused by accidental grounding in the system.

ground conductivity The ease with which the earth will carry electrical current. Saltwater has the best conductivity; dark, moist soil and fresh water (because of the mineral content) rate from fair to good. Sandy soil has the poorest ground conductivity.

ground conduit A pipe housing one or more ground leads.

5059F-pG-307-325 4/10/01 8:57 AM Page 321

ground connection **1.** A low-resistance connection to the earth. **2.** The common point, such as a chassis, to which zero-potential terminals of circuit components are connected.

ground constants The conductivity and dielectric constant of the earth for a particular kind of terrain and soil at a given location. Affects the behavior of radio antenna systems and electrical utility systems. Usually, high conductivity (low resistance) and low dielectric constant are desirable characteristics.

ground-controlled approach Abbreviation, GCA. In air navigation, a ground radar system that provides information for radio-directed aircraft approaches.

ground-controlled interception Abbreviation, GCI. A ground radar system by which an aircraft can be directed to intercept enemy aircraft.

ground current **1.** A direct electric current flowing into the earth from an electrical or electronic device, or into a device from the earth. **2.** An alternating current flowing between the earth and a device. **3.** An electric current flowing through the earth between two points. **4.** A current flowing in the normal ground (low-potential) line of a circuit.

ground detector A device that indicates whether or not a given circuit point is at direct-current ground.

grounded antenna See MARCONI ANTENNA.

grounded-base circuit See COMMON-BASE CIRCUIT.

grounded-cathode circuit See COMMON-CATHODE CIRCUIT.

grounded-collector circuit See COMMON-COLLECTOR CIRCUIT.

grounded-drain circuit See COMMON-DRAIN CIRCUIT.

grounded-emitter circuit See COMMON-EMITTER CIRCUIT.

grounded-gate circuit See COMMON-GATE CIRCUIT.

grounded-grid circuit See COMMON-GRID CIRCUIT.

grounded outlet An outlet with a receptacle having a ground contact that can be connected to equipment-grounding conductors.

grounded-source circuit See COMMON-SOURCE CIRCUIT.

grounded system A set of electrical conductors or a transmission line in which one conductor is deliberately grounded.

ground effect **1.** Modification or distortion of the ideal free-space directivity pattern of an antenna by reflections from, and absorption by, the earth. **2.** Effects of the earth on radio-wave propagation (e.g., the production of a *reflected wave* and a *surface wave*, neither of which can exist if the earth is not part of the signal path). **3.** Effects on antenna behavior, such as modification of the impedance and resonant frequency, caused by the proximity of the earth.

ground efficiency In an antenna system, the quality of the ground circuit. For some antenna systems, such as a balanced dipole at great height, this is not a consideration. Ideal ground efficiency (100%) results in zero ground loss.

ground environment **1.** See GROUND CONSTANTS. **2.** The ground characteristics in the vicinity of an unbalanced antenna working against ground. **3.** In aviation, the set of ground-based installations.

ground fault **1.** Loss of a ground connection. **2.** A short-circuit to ground.

ground-fault interrupter Abbreviation, GFI. A fast-acting electronic circuit breaker that opens the power-line circuit breaker to prevent electric shock or equipment damage when the path of current flow is through the earth.

grounding electrode A device, such as a ground plate or ground rod, that facilitates low-resistance connections to the earth.

grounding plate A metal plate connected to the earth, on which a person stands to discharge static electricity from the body.

grounding rod See GROUND ROD.

ground insulation Electrical insulation used between adjacent energized and grounded parts, such as transformer windings and metal cores.

ground level See GROUND STATE.

ground loop A closed current path resulting from improper grounding of the components in a system. A loop is formed when two devices are connected to each other, and also to separate earth grounds or to a single earth ground via conductors of appreciable length. The loops can act as antennas, increasing the likelihood of ELECTROMAGNETIC INTERFERENCE to or from the system. The use of a single GROUND BUS is preferred.

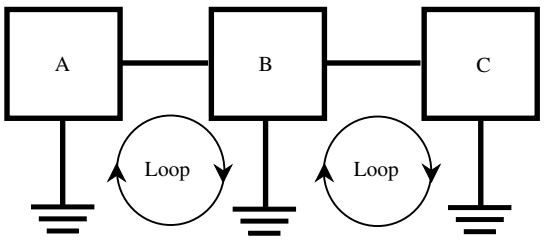

ground loop

ground mat A grid or network of conductors, connected to earth ground, for the purpose of improving the earth conductivity.

ground-mounted vertical antenna A vertical radiator mounted at the earth's surface or at the surface of a body of water, and fed with coaxial cable. The radiator can be any physical length, but it is tuned to resonance at the operating frequency.

5059F-pG-307-325 4/10/01 8:57 AM Page 322

The center conductor of the cable is connected to the base of the radiator, and the shield is connected to a ground system. Radial wires, usually buried just below the surface, minimize losses. The antenna can be made resonant on several frequencies by inserting multiple loading coils or traps in the radiator. The chief advantages of this antenna are unobtrusiveness and ease of installation. The main problems are marginal efficiency and susceptibility to human-made electromagnetic noise. See also RADIAL, 1. Compare GROUND-PLANE ANTENNA.

ground noise **1.** Electrical noise that results from a faulty ground connection. **2.** Background noise. **3.** In wire circuits, such as a telephone system, electrical noise that results from fluctuations in ground current.

ground plane **1.** A metal plate or a system of horizontal rods or wires mounted high on a mast, at the base of a vertical antenna, to provide a radio-frequency ground at a point several wavelengths above the surface of the earth. Also see GROUND-PLANE ANTENNA. **2.** In noise and interference tests, a sheet metal structure used to simulate the skin of an aircraft or missile. **3.** On a circuit board, a thin metallic sheet, usually bound to the underside, that serves as a common ground and RF shield.

ground-plane antenna A vertical radiator operated against a system of quarter-wave radials, elevated at least a quarter wavelength above the earth's surface and fed with coaxial cable. The center conductor of the cable is connected to the base of the radiator, and the shield is connected to three or four quarter-wave radials that run outward from the base of the radiator. At shorter wavelengths, a disk or cone can replace the radials. The chief advantages of this antenna are simplicity and high efficiency. The main problem is susceptibility to human-made electromagnetic noise. See also RADIAL, 1. Compare GROUND-MOUNTED VERTICAL ANTENNA.

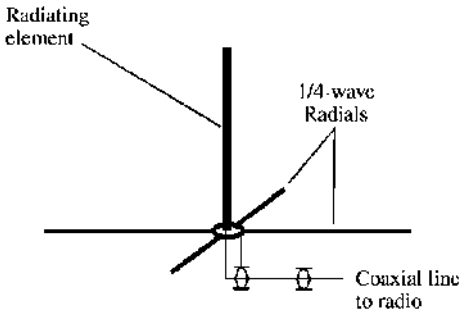

ground-plane antenna

ground plate A metal plate buried in the earth to provide a low-resistance ground connection.

ground-position indicator Abbreviation, GPI. A computer system that gives a continuous indication of an aircraft's position in terms of heading, elapsed time, and speed, with respect to the surface. This provides a more useful indication of the aircraft position than an *air-speed indicator* because it is not affected by high-altitude winds.

ground potential See ZERO POTENTIAL, **3**.

ground protection The use of a GROUND-FAULT INTERRUPTER.

ground-reflected wave A radio wave component that results from ground reflection.

ground reflection The reflection of a radio wave by the earth.

ground resistance The direct-current resistance of a connection to the earth, or the resistance between two points through the earth. The magnitude of the resistance depends on several factors: composition of the soil, amount of moisture, soil electrolytic action, and the area of contact with the earth.

ground return **1.** The point or path used to return a circuit to ground for completion. **2.** In radar, echoes returned from the earth's surface (including reflections from objects on it).

ground-return circuit A circuit, such as a single-wire telephone line, in which earth ground forms one leg of the circuit. Compare METALLIC CIRCUIT.

ground rod A strong metal rod driven deep into the earth as a point of ground connection.

ground speed The speed of an aircraft or missile, relative to the surface of the earth.

ground state The least-energy level of all possible states in a system.

ground support equipment Electronic surface-based apparatus upon which the functioning of a weapons system is dependent.

ground switch A switch for grounding an outside antenna during idle periods. Also called *lightning switch*. Ideally, antennas should be disconnected from equipment, as well as grounded, when not in use.

ground-to-air communication Radio or radar transmission from a land station to an aircraft in flight.

ground-to-ground **1.** Pertaining to communications between land-based stations. **2.** Pertaining to missiles intended for use between points on the surface of the earth.

ground-to-ground communication Communications between land-based stations.

groundtrack For an earth-orbiting satellite, the path followed by the point on the earth's surface from which the spacecraft appears directly overhead. For most satellites, this path shifts toward the west for each succeeding orbit, because the earth rotates eastward underneath the satellite. For geostationary satellites, the point never

5059F-pG-307-325 4/10/01 8:57 AM Page 323

changes position on the surface. For satellites in equatorial orbits, the track follows the equator.

ground wave In wireless communications and broadcasting, an electromagnetic (EM) wave that consists of three distinct components: the *direct wave* (also called the *line-of-sight wave*), the *reflected wave,* and the *surface wave.* The direct wave is significant only when the transmitting and receiving antennas are connected by a line through free space without obstructions. The reflected wave, after returning from the earth's surface or a human made structure, combines with the direct wave (if any) at the receiving antenna. The surface wave travels in electrical contact with the earth. This occurs only with vertically polarized EM fields at frequencies below about 15 MHz. Below about 300 kHz, the surface wave propagates for hundreds or even thousands of miles. Sometimes the surface wave is called the *ground wave.*

ground wire A conductor between an equipment and a ground connection, either for circuit completion or for safety.

group **1.** A series of computer storage locations containing a specific record or records. **2.** The data in these locations. **3.** A record set having a common key value in a sorted file.

group busy In a telephone system, an audio signal indicating that all of the lines in a group are in use.

group code In digital communications, an error-detecting code used to verify a character group transferred between terminals.

group delay In a modulated signal, a delay in the transmission of data.

grouped-frequency operation In a two-wire communications system, the grouping of directional signals into certain frequency bands.

grouped records A set of data records in which the key of one record identifies the entire set.

grouping **1.** The arrangement of data into blocks or sets. **2.** On a phonograph disc, the insertion of gaps in the arrangement of grooves. **3.** Any periodic irregularity in the spacing of a data transmission. **4.** The bunching of grooves on a disc recording. **5.** In a facsimile system, occasional spacing errors between recorded lines. **6.** A mass of data arranged into groups, according to common characteristics.

group mark **1.** In telegraphy, an indicator that signals the end of a data unit. **2.** A character indicating the end of a character group; usually, it is a logical record that is addressed and processed as a unit.

group velocity The velocity at which a group of waves or a pulse is propagated.

Grove cell A closed-circuit primary cell in which the positive electrode, platinum, is immersed in nitric acid; the negative electrode, zinc, is immersed in sulfuric acid. The nitric acid is held in a porous cup, surrounded by a larger jar of sulfuric acid.

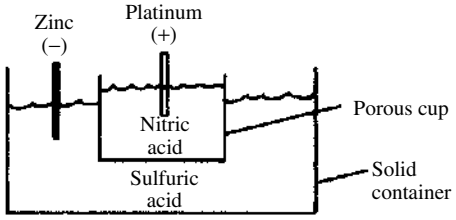

Grove cell

growler **1.** An electromechanical troubleshooting device that indicates the location of short circuits and grounds (especially in electric motors) by emitting a growling or rumbling sound. **2.** Any tester that provides an audible signal, which indicates electrical continuity.

grown-diffused transistor A transistor that is made by first growing the emitter and collector regions as a crystal, into which the base region is later diffused while the crystal is being pulled.

grown diode A semiconductor diode created by growing a layer of p-type material into n-type material (or vice versa) as the single-crystal material is being pulled from the melt.

grown junction A pn junction produced by adding impurities in various amounts to a crystal while it is being pulled from molten semiconductor material.

grown-junction diode See GROWN DIODE.

grown-junction photocell A grown-junction diode used as a photoconductive cell.

grown-junction transistor A transistor made by adding n-type and p-type impurities successively to a crystal in its molten state, then slicing the resulting npn formations from the finished crystal.

G-scan A rectangular radar display consisting of a laterally centered blip that "grows wings" as a target approaches. Horizontal and vertical displacement of the blip indicate horizontal and vertical aiming errors.

G scope See G SCAN.

GSR Abbreviation of GALVANIC SKIN RESPONSE.

G-string antenna In microwave operations, a communications path provided by a dielectric-coated wire that behaves like an extremely low-loss coaxial line with its outer conductor removed to infinity. A horn at each end matches the line to the transmitter and receiver. The term comes

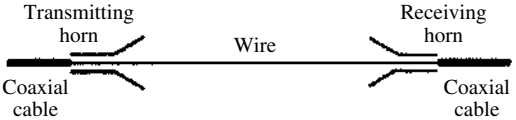

G-string antenna

5059F-pG-307-325 4/10/01 8:57 AM Page 324

from the first initial of Dr. George Groubau, inventor of the device, and the stringy appearance of the wire.

GTO Abbreviation of GOTO.

guard band A narrow unoccupied band of frequencies at the upper and lower limits of an assigned channel; its purpose is to prevent adjacent-channel interference by ensuring adequate separation between channels.

guard circle On a phonograph disk, an inner groove that prevents collision of the pickup with the spindle at the center of the disc.

guard circuit An auxiliary circuit added to an alternating-current bridge to compensate for the effects of stray capacitance in the bridge arms. One of its several forms is the WAGNER GROUND.

guarded input An input-terminal arrangement in which one terminal, maintained at the proper potential, shields the entire input-terminal combination.

guarding A method of short-circuiting a leakage current to ground. On a printed-circuit board, guarding is usually accomplished by the use of a large conducting foil surface near critical components.

guard relay A relay that ensures that only one linefinder will be connected to a line circuit when other line relays are in operation.

guard ring A metal ring (or other configuration) surrounding, but separate from, a charged body or terminal, for the purpose of evenly distributing the electric charge over the latter's surface.

guard shield A shield that encloses the input circuit of an amplifier or instrument.

guard terminal In a GUARDED INPUT, the terminal that shields the combination.

guard wire A grounded wire that is intended to catch and ground a broken high-voltage line.

Gudden-Pohl effect The tendency of an ultraviolet irradiated phosphor to glow momentarily when subjected to an electric field.

GUI Acronym for GRAPHICAL USER INTERFACE. Can be spelled out or pronounced "gooey."

guidance Electronic control of the path or course of a robot, missile, or other vehicle.

guidance system The complete electromechanical system for control of a robot, missile, or other vehicle. It consists of hardware and software. The hardware includes beacons, sensors, drive systems, rockets, etc. The software interprets data from, and transmits commands to, the hardware. The nature of the hardware and software depend on the application.

guidance tape In a guided missile, a magnetic tape containing computer instructions for steering the missile in a designated course.

guide See WAVEGUIDE.

guide connector See WAVEGUIDE CONNECTOR.

guided missile A missile whose progress to a target is controlled electronically by signals from a control station or by sensing equipment aboard the missile.

guided propagation A form of radio-wave propagation in which air masses of different temperatures or humidity levels cause refraction and/or reflection of electromagnetic waves, guiding signals over long distances with very little attenuation. Commonly observed at very-high and ultra-high frequencies.

guide elbow See WAVEGUIDE ELBOW.

guide flange See WAVEGUIDE FLANGE.

guide gasket See WAVEGUIDE GASKET.

guide junction See WAVEGUIDE JUNCTION.

guide load See WAVEGUIDE LOAD.

guide slot See KEYWAY.

guide wavelength See WAVEGUIDE WAVELENGTH.

Guillemin effect The tendency for a strip of ferromagnetic material to become straight in a strong magnetic field. This is a form of MAGNETOSTRICTION.

Guillemin line In radar operations, a special pulse-forming network for controlling modulation pulse duration.

guillotine capacitor A variable capacitor in which a sliding (instead of rotary) plate moves between two stator plates. Its name results from its resemblance to the infamous beheading apparatus.

gulp Several bytes of digital information.

gun See ELECTRON GUN.

Gunn diode A semiconductor diode that can operate as an oscillator in the ultra-high-frequency (UHF) and microwave parts of the radio spectrum. Oscillation takes place as a result of a negative-resistance effect in which, within a certain range of applied voltages, the current decreases as the voltage increases. The device is not particularly efficient. Only a small fraction of the input power results in useful signal output. The frequency and oscillation stability are sensitive to changes in temperature and bias voltage. See GUNN EFFECT, NEGATIVE RESISTANCE.

Gunn effect A semiconductor phenomenon named after J. Gunn of International Business Machines (IBM) who first observed and studied it in the 1960s. In certain types of diodes having a negative-resistance characteristic, oscillation occurs when the applied voltage is within a certain range. See GUNN DIODE, NEGATIVE RESISTANCE.

Gunn-effect circuit Any circuit exploiting the Gunn effect, especially a GUNN OSCILLATOR.

Gunn oscillator A discrete semiconductor microwave oscillator using a GUNN DIODE.

Gunnplexer A microwave transmitter consisting of a Gunn-diode oscillator connected to a horn antenna. Usually, the entire device is a compact, self-contained unit. The output power is low. When the device is placed at the focal point of a large dish antenna with the horn pointing toward the dish reflector (conventional dish feed), consid-

5059F-pG-307-325 4/10/01 8:57 AM Page 325

erable transmission range is possible. Used primarily by experimenters, and in wireless communications links. See GUNN DIODE.

gutta percha A hard, rubberlike, organic insulating material. Dielectric constant, 3.3 to 4.9. Dielectric strength, 203 to 508 kV/in.

guyed tower In radio communications or in microwave links, a structure that is supported by one or more sets of guy wires to add strength and to prevent collapse.

guying The support of a radio communications or microwave-link tower by the use of one or more sets of guy wires.

guy insulator Also called *egg insulator.* An insulator designed to electrically break a guy wire while maintaining its ability to support a structure. Such an insulator has two slots with holes placed at right angles, in such a position that the wire will not separate even if the insulator breaks. The stress exerted on the insulator is compression, and the insulating material is stronger under this type of stress than under tension (pulling).

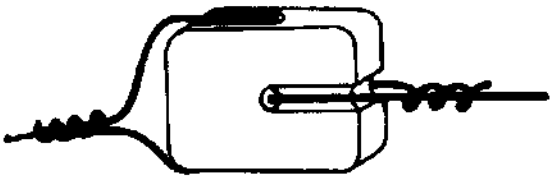

guy insulator

guy wire A bracing wire for antenna masts or towers.

gyrator An active (usually cascaded-transistor) device exhibiting nonreciprocal phase shift. It provides, among other functions, the simulation of inductance using capacitors.

gyro Contraction of GYROSCOPE.

gyro- A prefix meaning "pertaining to gyroscopes," "containing a gyroscope," or "behaving like a gyroscope."

gyrocompass A type of compass in which a spinning gyroscope, acted upon by the earth's rotation, causes the device to point to true north. Compare MAGNETIC COMPASS.

gyrofrequency The natural frequency of rotation of charged particles around the earth's magnetic lines of flux.

gyromagnetic Pertaining to the magnetic properties of rotating electric charges (e.g., the effect of electrons spinning inside an atom).

gyromagnetic effect The tendency of a rotating body to become magnetized because of the magnetic field of the earth.

gyropilot See AUTOPILOT.

gyroscope A device that consists of a spinning wheel mounted in a gimbal. The shaft of the wheel will point in one direction, despite the movement of the earth beneath it.

gyrostat See GYROSCOPE.

G-Y signal In a color-television circuit, the signal representing primary green (G) minus luminance (Y). A primary green signal is obtained when the G-Y signal is combined with the luminance (Y) signal. Compare B-Y SIGNAL and R-Y SIGNAL.

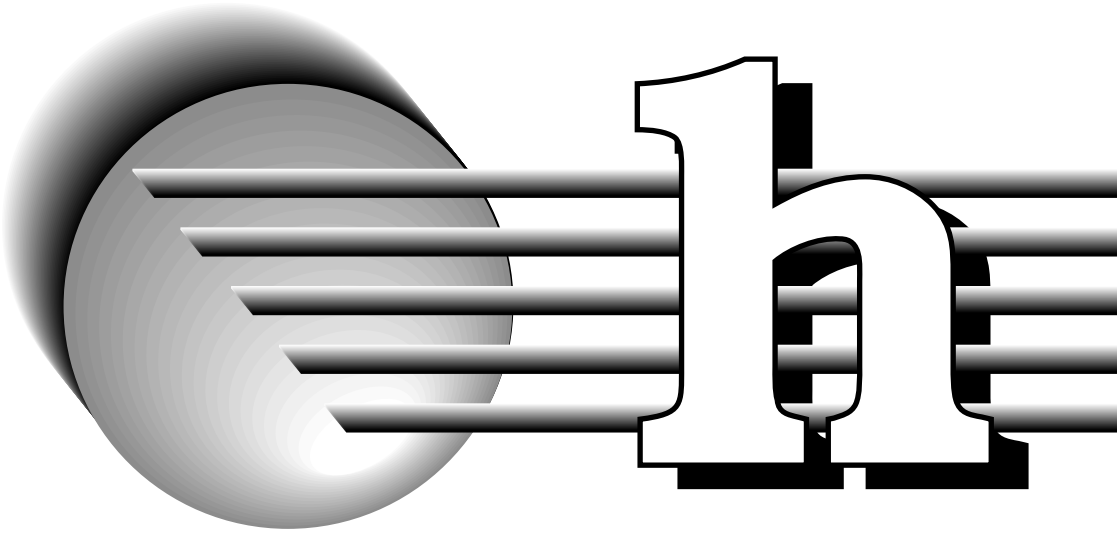

H **1.** Symbol for *magnetic field strength.* **2.** Symbol for MAGNETIZING FORCE. **3.** Symbol for HYDROGEN. **4.** Symbol for UNIT FUNCTION. **5.** Abbreviation of HORIZONTAL. (Also, hor and horiz.) **6.** Symbol for HENRY. **7.** Symbol for HARMONIC.

h **1.** Abbreviation of prefix HECTO-. **2.** Symbol for the PLANCK CONSTANT. **3.** Abbreviation of HOUR.

Haas effect See FUSION, **1**.

hack In computer networking, to access, and sometimes to change, sensitive data without authorization.

hacker A person knowledgeable in computer networking who uses his or her expertise to access, and sometimes alter, sensitive data. This is illegal and can sometimes be destructive. The intent, is rarely malicious, however, the activity is viewed as a challenge. Compare CRACKER.

HACKER program A computer program developed by Gerry Sussman as an early experiment with artificial intelligence (AI), to see how the machine would deal with complex decision-making problems.

hadron A subatomic particle consisting of quarks.

hafnium Symbol, Hf. A metallic element. Atomic number, 72. Atomic weight, 178.49. Readily emits electrons.

hahnium See DUBNIUM.

hailer **1.** A marine microphone-amplifier-speaker system for calling to other boats or persons ashore. **2.** A comparable system for land vehicles, such as police cars. Also see MEGAPHONE, **1**.

hair See HAIRLINE.

hair hygrometer A device for measuring relative humidity, in which a stretched hair is the moisture-sensitive element.

hairline A fine line used as an index or a graticule marker in a precision instrument.

hairpin coil A quarter-turn coil, so called from its resemblance to a hairpin.

hairpin coupling coil A hairpin coil used as a low-impedance primary or secondary coil for input or output coupling.

hairpin match A form of impedance-matching network used at the feed point of a half-wave dipole antenna. A short length of open-wire transmission line, short-circuited at the far end, is connected in parallel with the antenna at the feed point.

hairpin pickup A short, doubled length of wire that acts as a pickup coil at very-high and ultra-high frequencies.

hairspring A fine, usually spiral spring—especially the one in a movable-coil meter or the one connected to the balance wheel of a watch or clock.

hair-trigger Pertaining to extreme sensitivity of response, such as the tendency of a switching device to change state when excited by a weak pulse.

hair wire **1.** An extremely thin wire filament in a lamp or bolometer. **2.** Very small gauge wire (e.g., #44).

hal Abbreviation of HALOGEN.

half-add The sum of two binary digits, in which the carry operation is omitted. Thus 0 + 0 = 0, 0 + 1 = 1, 1 + 0 = 1, and 1 + 1 = 0.

half-adder In digital systems, an adder circuit that can handle the two binary bits that are to be added, but that cannot accommodate a carry signal. Compare FULL ADDER.

Copyright 2001 The McGraw-Hill Companies, Inc. Click Here for Terms of Use

5059F-pH-326-351 4/10/01 9:00 AM Page 327

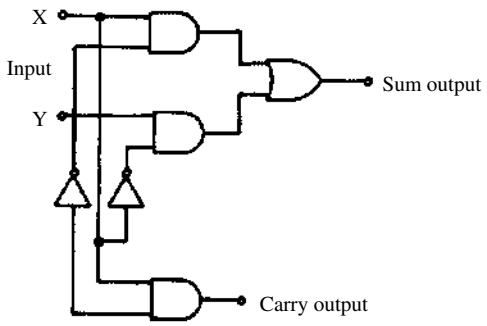

half-adder

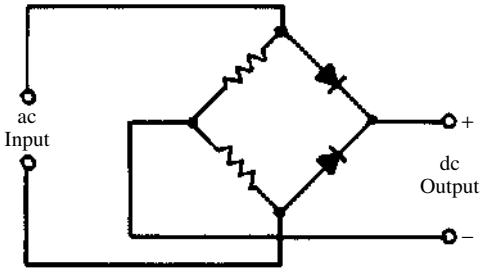

half-bridge

half-bridge A bridge rectifier that has diodes in two arms and resistors in the other two.

half-cell A voltaic cell consisting of a single electrode immersed in an electrolyte and having a definite difference of potential; it is, in effect, half of a primary cell. Also see HELMHOLTZ DOUBLE LAYER.

half-cycle Half of a complete alternation (i.e., 180 degrees of phase).

half-cycle magnetizer A magnetizer using half-cycles of rectified alternating current as the magnetic-field source.

half-duplex channel A communications channel in a HALF-DUPLEX SYSTEM.

half-duplex system In data communications, a system that transmits data in both directions, but not simultaneously. Compare FULL-DUPLEX SYSTEM.

half-lattice crystal filter A band-pass crystal-filter circuit using two piezoelectric crystals in a four-arm bridge. Also see CRYSTAL RESONATOR.

half-nut In a facsimile receiver, a device that guides the lead screw.

half-power point In a response curve or directional pattern, such as for a selective filter or a unidirectional antenna, the points on each side of maximum at which the power is 3 dB below the peak value.

half-power width In a directional antenna system, an expression of beamwidth. It is usually listed as the horizontal-plane angle, in degrees, between the half-power points in the main lobe of the directive pattern.

half-step **1.** In audio engineering, the frequency interval between two sounds, whose ratio is 1.06:1. **2.** The difference in pitch between the notes produced by two adjacent keys on a piano.

half tap A bridging circuit or device that can shunt another circuit with the least electrical disturbance.

half-track recorder A magnetic tape recorder that applies signals to both halves of a tape with a head that covers only half the tape's width in each of two directions. Also called *dual-track recorder.*

half-track tape Magnetic tape recorded by a HALF-TRACK RECORDER.

half-wave Half of a complete wave (i.e., a complete rise and fall in one direction). Its graphic representation is similar in appearance to that for a half-cycle.

half-wave antenna An antenna whose radiator measures an electrical half wavelength from end to end. Such a radiator is about 5 percent less than a free-space half-wavelength long, because of capacitive effects and the velocity factor of the conductor.

half-wave chopper A chopper that closes a circuit during only half the switching signal cycle.

half-wave dipole A center-fed antenna whose radiator measures 0.5 electrical wavelength from end to end. Also see DIPOLE ANTENNA.

half-wave doubler See HALF-WAVE VOLTAGE DOUBLER.

half-wave feeder See HALF-WAVE TRANSMISSION LINE.

half-wavelength Symbol λ/2. The distance that corresponds to 180 degrees of phase as an electromagnetic (EM) field is propagated in free space, it is related to the frequency by a simple equation:

$$L_{ft} = 492/f$$

where L_{ft} represents λ/2 in feet, and f represents the frequency in megahertz. If λ/2 is expressed in meters, then the formula is:

$$L_m = 150/f$$

where L_m represents the displacement in meters. In general, if v is the velocity factor (expressed as a ratio) in a given medium, then:

$$L_{ft} = 492v/f$$

and

$$L_m = 150v/f$$

Compare FULL WAVELENGTH, QUARTER WAVELENGTH.

5059F-pH-326-351 4/10/01 9:00 AM Page 328

half-wave loop antenna A loop antenna having a circumference of 0.5 wavelength with a break opposite the feed point. It is, in effect, a HALF-WAVE DIPOLE bent into a circle or square (although any symmetrical configuration can be used). The circle is the most efficient configuration.

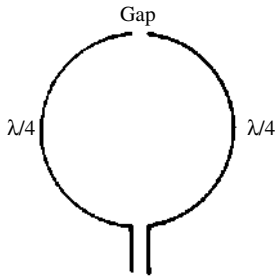

half-wave loop antenna

half-wave radiator An antenna consisting of a single, usually straight, active element that measures an electrical half wavelength from end to end. It is therefore a resonant element. A simple half-wavelength (λ/2) conductor with a high length-to-diameter ratio measures approximately 95 percent of λ/2 in free space. The element can be much shorter than free-space λ/2 yet remain λ/2-resonant if inductance is inserted in series with the radiator. The element can be much longer than free-space λ/2 yet remain λ/2-resonant if distributed capacitances are inserted in series with the radiator.

half-wave rectification The conversion of alternating current (ac) to direct current (dc) during half of each ac cycle. Also see HALF-WAVE RECTIFIER.

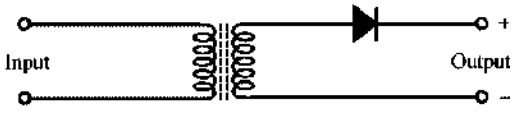

half-wave rectifier

half-wave rectifier A rectifier that delivers a half-cycle of direct-current (dc) output for every other half-cycle of applied alternating-current (ac) voltage. Because the successive dc half-cycles are 180 degrees apart, they have the same polarity. Compare FULL-WAVE RECTIFIER.

half-wave transmission line A transmission line measuring 0.5 electrical wavelength at the transmission frequency. The physical length is somewhat less than a free-space half wavelength because of the VELOCITY FACTOR of the line.

half-wave vibrator A vibrator (see INTERRUPTER) whose reed operates against only one stationary contact. Compare FULL-WAVE VIBRATOR.

half-wave voltage doubler A voltage-doubler circuit whose direct-current (dc) output has a ripple frequency equal to that of the alternating-current (ac) supply. Although its output is harder to filter than that of a full-wave doubler, this circuit has the advantage of a common ground. Compare FULL-WAVE VOLTAGE DOUBLER.

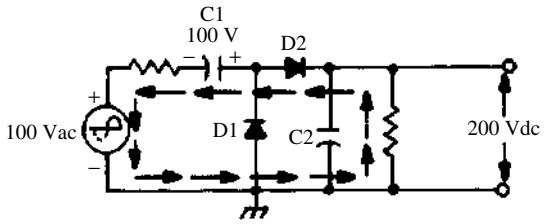

half-wave voltage doubler

halide A compound of a HALOGEN. Examples: sodium iodide, used as a scintillating crystal; ammonium chloride, used as the electrolyte in a dry cell.

halide crystal A halogen-compound crystal, such as mercuric iodide and sodium iodide, useful in detecting radioactivity.

Hall coefficient For a current-carrying conductor, the constant relationship between the Hall (transverse electric) field and the magnetic flux density.

Hall constant For a current-carrying conductor, the constant of proportionality k given by the equation $k = e/(im)$, where e is the transverse electric field (Hall field), i is the current density, and m is the magnetic field strength.

Hall effect A phenomenon observed in thin strips of metal and in some semiconductors. When a strip carrying current longitudinally is placed in a magnetic field that is perpendicular to the strip's plane, a voltage appears between opposite edges of the strip that, although feeble, will force a current through an external circuit. The voltage is positive in some metals (such as zinc) and negative in others (such as gold). Also see ETTINGHAUSEN EFFECT, NERNST EFFECT, and RIGHT-LEDUC EFFECT.

Hall-effect modulator A device that uses the HALL EFFECT to modulate a signal, or to mix two signals.

Hall-effect multiplier A device based upon the Hall generator and used in analog mathematical operations, such as multiplication and the extraction of roots.

Hall field The transverse electric field of a conductor carrying current in a magnetic field.

5059F-pH-326-351 4/10/01 9:00 AM Page 329

Hall generator A semiconductor device exhibiting the HALL EFFECT. It is a thin wafer or film of indium antimonide or indium arsenide with leads on opposite edges.

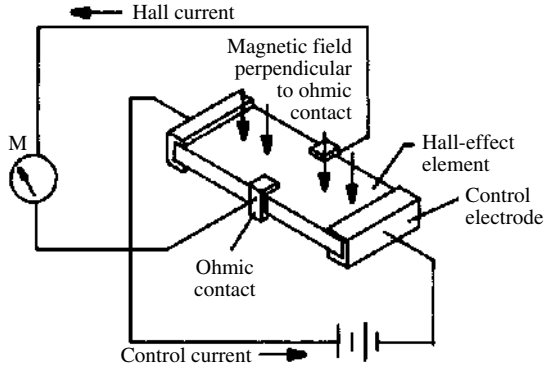

Hall generator

Hall mobility For a conductor or semiconductor, the product of conductivity and the HALL CONSTANT.

Hall network A resistance-capacitance null circuit whose general configuration is two cascaded high-pass tee-sections bridged by a high resistance. The circuit can be tuned with one potentiometer.

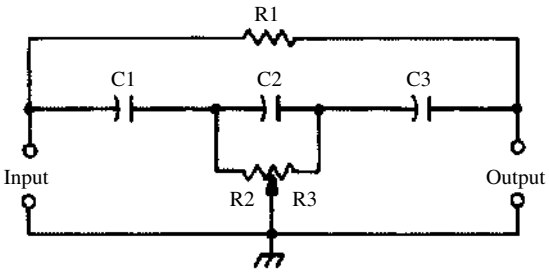

Hall network

Hallwacks effect The phenomenon (observed by Hallwacks in 1888) in which ultraviolet light falling on a polished zinc plate causes a negatively charged electroscope to which it is connected to discharge.

hallucination In complex computers and artificially intelligent systems, the generation or appearance of data for no apparent reason.

halo See AFTERGLOW and PERSISTENCE.

halo antenna A horizontally polarized antenna, consisting of a circular half-wave dipole whose ends are capacitance loaded. Commonly used at very high frequencies (VHF).

halogen Abbreviation, hal. A group of five very active nonmetallic elements whose similar chemical properties put them in group VIIA of the periodic table; they are *astatine*, *bromine*, *chlorine*, *fluorine*, and *iodine*.

Halowax A chlorinated naphthalene wax used as an impregnant for paper capacitors. Dielectric constant, 3.4 to 5.5. Resistivity, 10^{13} to 10^{14} ohm-cm.

halt A stop during the execution of a computer program run, often resulting from a HALT INSTRUCTION.

halt instruction An instruction in a computer program that causes a break in the program's execution, as by BASIC's STOP command, for example.

ham Colloquialism for AMATEUR RADIO operator.

ham radio See AMATEUR RADIO.

Hamilton's principle Also called the *principle of least action*. Motion tends to occur in such a way that the integral of the product of kinetic energy and elapsed time is minimal.

hammer **1.** The striking member in a WHEEL PRINTER. **2.** The clapper in an electric bell or gong.

hammer-and-wheel See WHEEL PRINTER.

Hamming code An error-correction code used in some digital communications circuits.

hand capacitance Also called *body capacitance*. Capacitive coupling effects between a circuit and the human body (e.g., as evidenced between an operator's hand and a device having extremely high impedance and poor grounding and/or shielding).

hand generator An electric generator operated by turning a hand crank.

handheld computer Also called *personal digital assistant (PDA)* or *palmtop computer*. The names PalmPilot and Palm are proprietary (Palm Computing, Inc.) and refer to specific families of handheld computers, although they might someday become generic and refer to handheld computers in general. A battery-powered portable computer, smaller than a notebook computer, and used for simple tasks such as note-taking and record keeping. Some units incorporate wireless modems for connection to the Internet. Others include paging, wireless fax, videoconferencing capability, remote-control capability, and other features. Many units can recognize a specialized form of handwriting so users can enter data with a penlike device called a *stylus*.

Handie-Talkie Abbreviation, HT. Tradename for a portable transceiver small enough to be held in the hand during operation.

hand key Also called *brass pounder*. An old-fashioned, hand-operated telegraph key, operated by manual downward pressure.

handoff In cellular communications networks, the changeover of reception from, and transmission

5059F-pH-326-351 4/10/01 9:00 AM Page 330

to, a mobile or portable set from one repeater to another as the subscriber moves from one cell into another. When the subscriber is moving rapidly—for example, driving along a freeway, such transfers occur relatively often. When a subscriber is moving slowly, for example, walking along a trail, such transfers occur rarely. When a subscriber is in a fixed location, such transfers do not normally occur.

hand-operated device A device manipulated directly and manually by the operator's hand(s). Also called *manual device.*

hand receiver **1.** A single earphone that must be held against the ear. **2.** A telephone receiver.

hand rules See FLEMING'S LEFT-HAND RULE, FLEMING'S RIGHT-HAND RULE, and RIGHT-HAND RULE FOR WIRE.

handset See CRADLEPHONE.

handshaking **1.** A controlled, periodic exchange of synchronizing pulses between a digital transmitter and receiver. **2.** In a digital communications system, a method of error correction. The receiver detects nonstandard or improbable character sequences, and instructs the transmitter to repeat them for double-checking.

hand-type pointer In an electric meter, a spear-like pointer (resembling the hand of a clock), as opposed to a knife-edged pointer.

hand-wired Pertaining to electronic equipment wired by hand, rather than being assembled on printed-circuit boards. This form of construction is rarely seen nowadays, except in some radio-frequency power amplifiers.

hang AGC An automatic-gain-control (AGC) circuit whose action is sustained for a brief interval after an actuating signal has passed, an advantage in some applications. Also called *fast-attack/slow-release AGC.*

hangover In sound operations, the blurring or smearing of low-frequency (bass) notes by a poorly damped or poorly mounted loudspeaker.

hangup **1.** In phonograph operation, the state in which the same material is played repetitiously (i.e., the stylus does not move toward the spindle). **2.** In digital-computer operations, an unexpected break during a program run as a result of software or hardware failure. Sometimes called UNEXPECTED HALT.

H antenna See LAZY-H ANTENNA.

hard copy **1.** In digital computer operations, a readable document (printout) of material being translated to a form understood by a computer. **2.** Generally, written or typed documents, as opposed to data on other media, such as diskettes, tapes, CD-ROM, etc.

hard disk An electromechanical data storage medium commonly used in personal computers. Consists of several rigid disks, called *platters*, coated with ferromagnetic material.

hard-drawn wire High-tensile-strength unannealed wire.

hard dump See HARDWARE DUMP.

hard magnetic material High-retentivity magnetic material. Also see RETENTIVITY.

hardness **1.** The property that causes a material to resist penetration, deformation, scratches, etc. **2.** The penetrative ability of ultraviolet rays, X rays, or other ionizing radiation. Generally, the radiation hardness increases as the wavelength decreases, and as the photon or particle energy increases.

hardness tester A device for measuring the hardness of a solid in terms of the force required to penetrate its surface. Also see HARDNESS, **1**.

hard radiation In general, any radiation with high penetrating power. Usually, this term is used in reference to short-wavelength (high-energy) ultraviolet rays or X rays.

hard solder Solder that melts at a comparatively high temperature. Compare SOFT SOLDER.

hard vacuum A nearly perfect vacuum, that is, a medium essentially devoid of atomic or subatomic particles.

hardware **1.** Collectively, electronic circuit components and associated fittings and attachments. **2.** In a computer system, the electronic and electromechanical components (e.g., integrated circuits, keyboards, and disk drives) associated with operation. Compare SOFTWARE.

hardware availability ratio A figure depicting the availability of a computer system to do productive work; as a percentage, it is given by the formula:

$$A = 100(ta - td)/ta,$$

where A is the availability ratio, ta is the operational time, and td is the downtime over a specified time period.

hardware check A check on data being transferred within a computer, as done by hardware (e.g., a parity check).

hardware cloth A finely woven wire screen sometimes used in place of a metal plate for an antenna element, an antenna reflector, or a shielded enclosure. Especially useful when free-air circulation is required.

hardware dump During a computer program run, data sent to a storage device for later evaluation; it occurs at the time of a failure. Also called AUTOMATIC HARDWARE DUMP.

hardware engineer A person who designs and perfects the actual electronic circuitry in a system. The hardware engineer is not involved with the programming of the system.

hardware recovery A computer system's ability (through software or hardware) to recover from a failure (i.e., to proceed from the point of failure).

hardware serviceability ratio See HARDWARE AVAILABILITY RATIO.

hardwire **1.** To construct a circuit for direct-current conductivity. **2.** A circuit exhibiting direct-current conductivity over a complete, closed path.

hard-wire telemetry See WIRE-LINK TELEMETRY.

5059F-pH-326-351 4/10/01 9:00 AM Page 331

hard wiring **1.** In computer systems, functions or programs built directly into the machine hardware. In order to alter such functions or programs, the system wiring and/or components must be physically changed. **2.** A system interconnected entirely by wires and cables, and using no free-space links, such as radio or infrared.

hard X rays High-frequency (shortwave) X rays. Such radiation has high penetrating power. Compare SOFT X RAYS.

harmonic **1.** Symbol, H. In a complex sound or signal wave, a component whose frequency is a multiple of the FUNDAMENTAL FREQUENCY by a whole-number factor of 2 or more. **2.** Pertaining to whole-number multiples of the FUNDAMENTAL FREQUENCY of a sound or signal, as defined in **1**.

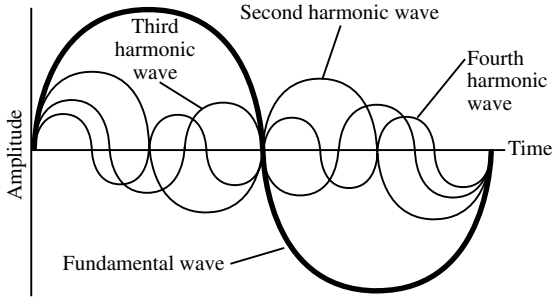

A

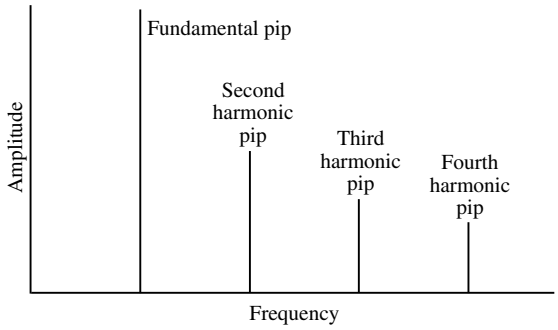

B

harmonic: waves (A) and spectrum-analyzer display (B)

harmonic accentuation Increasing the amplitude of harmonic components in a complex wave using filters, amplifiers, or special modes of operation.

harmonic accentuator A circuit or device, such as a harmonic amplifier or bandpass filter, for emphasizing signal harmonics.

harmonically related bands In communications, frequency bands arranged so that the frequencies in one band are harmonics of the frequencies in another band. An example of bands that are precisely related in this way are 4.1 to 4.3 MHz and 8.2 to 8.6 MHz. Various amateur radio bands are harmonically related to some extent, such as 40 meters (7.0 to 7.3 MHz) and 20 meters (14.0 to 14.35 MHz).

harmonic amplifier An amplifier, such as one used with a frequency standard, used to increase the amplitude of weak harmonics. Also see HARMONIC ACCENTUATION.

harmonic analysis **1.** The evaluation of the harmonic content of a complex wave. See, for example, HARMONIC WAVE ANALYZER; SCHEDULE METHOD, **2**; SPECTRUM ANALYZER; and WAVE ANALYZER. **2.** See FOURIER ANALYSIS.

harmonic analyzer See HARMONIC WAVE ANALYZER, SPECTRUM ANALYZER, and WAVE ANALYZER.

harmonic antenna An antenna operated at a harmonic of the lowest frequency at which it is resonant. For example, a half-wave dipole cut for 7.0 MHz, but used for transmitting and receiving at 21.0 MHz, is functioning at the third harmonic.

harmonic attenuation Reduction of the amplitude of harmonic components in a complex wave using filters, tuned amplifiers, or special modes of operation.

harmonic attenuator A circuit, device, or method of operation (such as a filter, tuned amplifier, special biasing, or special bypassing) for reducing the amplitude of harmonics.

harmonic component See HARMONIC.

harmonic composition See HARMONIC DISTRIBUTION.

harmonic content The amount of harmonic energy present in a complex wave. Also see HARMONIC-DISTORTION PERCENTAGE and HARMONIC RATIO.

harmonic-cut crystal Also called *overtone crystal.* A quartz crystal that, when operated in the proper circuit, oscillates at a harmonic of the (fundamental) frequency dictated by its thickness.

harmonic detector A detector tuned to respond to a harmonic of a signal.

harmonic distortion **1.** The generation of harmonics by the circuit or device by which the signal is processed. **2.** The deformation of the original signal that results from the action described in **1**. **3.** The disproportionate reproduction of a signal's harmonic components.

harmonic distortion meter See DISTORTION METER.

harmonic-distortion percentage In a signal containing harmonics, the harmonic energy as a percentage of the total signal energy (fundamental plus all harmonics). Also called *total harmonic distortion (THD).*

5059F-pH-326-351 4/10/01 9:00 AM Page 332

harmonic distribution For a given signal, the various frequencies and amplitudes of its harmonics, specified within a certain range of frequencies.

harmonic elimination The complete removal of one or more harmonics from a complex wave using a filter or special mode of operation.

harmonic eliminator A circuit or device, such as a band-suppression filter, for removing harmonics.

harmonic filter **1.** A bandpass filter for transmitting one or more harmonics of a complex input wave. **2.** A band-suppression filter for removing one or more harmonics of a complex input wave.

harmonic frequency **1.** In a complex wave, the frequency of a component that is a multiple of the FUNDAMENTAL FREQUENCY by a whole-number factor of two or more. **2.** A frequency that is a whole-number (two or more) multiple of another frequency to which it is referred. Compare NONHARMONIC FREQUENCY.

harmonic generator **1.** An oscillator operated so that it generates strong harmonics of the fundamental frequency. **2.** See FREQUENCY MULTIPLIER. **3.** See HARMONIC AMPLIFIER.

harmonic intensification See HARMONIC ACCENTUATION.

harmonic intensifier See HARMONIC ACCENTUATOR.

harmonic interference Interference resulting from the harmonics of radio or test signals.

harmonic motion Periodic motion typified by a swinging pendulum and illustrated by the plot of a sine wave.

harmonic oscillator A crystal oscillator whose output frequency is a harmonic of the crystal frequency.

harmonic percentage See HARMONIC-DISTORTION PERCENTAGE.

harmonic producer **1.** An oscillator that uses a tuning fork to establish the fundamental frequency. The output can be an odd or even harmonic of this frequency. **2.** See FREQUENCY MULTIPLIER. **3.** A nonlinear circuit used in a calibrator to generate markers at integral multiples of the fundamental frequency.

harmonic ratio **1.** In a complex wave, the ratio of harmonic energy to total signal energy (fundamental plus all harmonics). **2.** In a complex wave, the ratio of harmonic energy to fundamental-frequency energy.

harmonic reducer See HARMONIC ATTENUATOR.

harmonic reduction See HARMONIC ATTENUATION.

harmonic resonance Resonance of an antenna or a circuit at a whole multiple of the applied signal frequency.

harmonic ringing In wire telephony, the use of alternating-current signal harmonics for selective ringing.

harmonic series of tones A set of audio-frequency tones in which the frequencies can be specified by *f*, 2*f*, 3*f*, 4*f*, and so on.

harmonic suppression See HARMONIC ELIMINATION.

harmonic suppressor See HARMONIC ELIMINATOR.

harmonic tolerance The harmonic content permissible in a given system.

harmonic totalizer An instrument for measuring *total harmonic distortion.* See, for example, DISTORTION METER.

harmonizer A circuit that changes the frequency of an audio signal, or produces an output at several audio frequencies from an input having only one audio frequency. Used in sound recording for special effects.

harness A tied bundle of wires or cables for wiring electronic equipment.

harp antenna A vertical antenna consisting of a number of wires that fan out from point to point along a horizontal supporting wire.

hartley A unit of digital information equivalent to 3.32 bits. Used in certain computer applications.

Hartley oscillator A radio-frequency (RF) oscillator that uses a single inductor with a tap on the windings to provide the feedback. The amount of feedback is controlled by the position of the coil tap. A variable capacitor in parallel with the inductor determines the oscillating frequency and allows for frequency adjustment. The circuit uses about 25 percent of its output power to produce feedback. The other 75 percent of the power can be delivered to external circuits or devices. Compare COLPITTS OSCILLATOR.

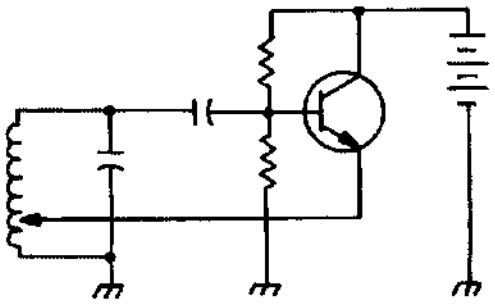

Hartley oscillator

hash **1.** Electrical noise, especially wideband noise with a characteristic hissing sound in a radio receiver. **2.** Undesirable or purposefully meaningless information, as used in a hash total (checksum).

hash filter A radio-frequency filter for eliminating HASH noise in a radio receiver.

hassium Symbol, Hs. Also called *unniloctium* (Uno). Atomic number, 108. The most common isotope has atomic weight 265. Classified as a transition metal. It is human-made and not known to occur in nature.

5059F-pH-326-351 4/10/01 9:00 AM Page 333

hat **1.** Also called *capacitance hat.* A small disk or set of wires attached to the end(s) of an antenna radiator, lowering the resonant frequency and increasing the usable bandwidth. **2.** A procedure for randomizing data.

hash total See CHECKSUM.

hatchdot pattern A television test pattern consisting of a crosshatch pattern with dots around its outer edges and one dot at its center.

hatted code A form of code in which randomization is used to maximize the difficulty of breaking the code.

Hay bridge An alternating-current bridge for measuring the inductance and Q of an inductor in terms of resistance, frequency, and a standard capacitance.

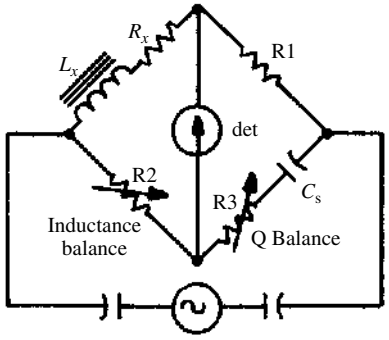

Hay bridge

haywire Loose, disorderly, or apparently careless wiring.

haz Abbreviation of HAZARD.

hazard Abbreviation, haz. A dangerous or potentially dangerous circuit, device, material, method, situation, or system (e.g., *electric-shock hazard*).

H beacon A form of homing beacon with an omnidirectional radiation pattern and a radio-frequency output of between 50 W and 2 kW.

H bend See H-PLANE BEND.

HCD Abbreviation of *hard-copy device.*

HCM Abbreviation of HALF-CYCLE MAGNETIZER.

HDB-3 code Abbreviation of HIGH-DENSITY BIPOLAR-3 CODE.

HDF Abbreviation of HIGH-FREQUENCY DIRECTION FINDER.

HDTV Abbreviation of HIGH-DEFINITION TELEVISION.

H-display See H-SCAN.

He Symbol for HELIUM.

head **1.** The top or operating portion of a device (e.g., microphone head or dynamic-speaker head). **2.** In magnetic recording and reproduction, the magnetic device (transducer) that delivers or picks up recorded impulses. **3.** In a hard disk or diskette drive, a transducer that delivers and picks up recorded data.

head alignment **1.** Positioning the cone of a dynamic speaker so that the voice coil moves freely (i.e., without rubbing against the core). **2.** Positioning a magnetic-recorder head so that a proper relationship to the moving tape is maintained.

head amplifier A self-contained amplifier or preamplifier in the head of a microphone or sound-on-film pickup.

head degausser A device used for the purpose of demagnetizing the head of a tape recorder. Unwanted magnetization can build up because of direct-current components in the driving signal.

head demagnetizer See HEAD DEGAUSSER.

head end In a television network or system, the location from which signals are sent to subscribers.

header **1.** A (usually glass) disk or wafer through which one or more leads pass and to which they are fully sealed. Can be used as the terminal base of an enclosed plug-in unit, such as a miniature coil, filter, or similar components. Also see GLASS-TO-METAL SEAL. **2.** A data set placed before other sets as a means of identifying them and, possibly, including control data pertinent to the sets so identified.

header capacitance Capacitance between or among the leads in a header (see HEADER, **1**).

header label A header recorded on a magnetic tape file (see HEADER, **2**).

head gap **1.** In computer disk or tape drives, the distance between the head and the magnetic medium. **2.** In audio operations, the spacing between tape-unit head electrodes; also called *gap width.*

heading The direction taken by a vehicle with reference to some point (such as a radio beacon, true north, or magnetic north).

headlight In radar operations, a small rotating antenna.

headphone A small acoustic transducer worn against the ear for listening to music without disturbing others, or for monitoring live or recorded material without being disturbed by noise in the environment. Also see RECEIVER, **2**.

headphone amplifier An audio-frequency amplifier designed and operated primarily to supply a signal to headphones.

headphone receiver A portable radio receiver, usually for AM and/or FM broadcast, consisting of a pair of headphones or a headset with the radio built into it.

head room **1.** In a high-fidelity sound system, the extent, measured in decibels, to which an amplifier can be operated beyond the zero point on its volume-unit (VU) meter without causing objectionable distortion on sound peaks. **2.** In tape recording, the region between the maximum recording level specified by the manufacturer of the equipment, and the amplitude at which tape overload occurs. It is specified in decibels.

5059F-pH-326-351 4/10/01 9:00 AM Page 334

headset An assembly consisting of one or two earphones, a headband, and a flexible cord. Also see HEADPHONE and RECEIVER, **2**.

head stack In magnetic recording, an assembly of two or more heads for multitrack service. Also see HEAD, **2**.

head station See BASE STATION.

head-to-tape contact In magnetic-tape recording or playback, physical contact between the tape and the head.

hearing aid A miniature audio-frequency device that amplifies sound for people with impaired hearing. It consists of a microphone, a high-gain amplifier, and an earphone or bone-conduction transducer.

hearing-aid battery A physically small battery designed for use with hearing aids. Such a battery is usually of the lithium type, or some other type that has long life under conditions of low current drain.

hearing loss A measure of hearing impairment. Generally expressed as the ratio, in decibels, of an individual's threshold of hearing to the normal threshold of hearing. Also see AUDIOLOGIST, AUDIOMETER, and AUDIOMETRIST.

heart fibrillation A condition in which the heart muscle twitches at random, rather than pumping blood normally. This can be caused by an electric shock through the heart of 100 mA to 300 mA. If normal heart function is not restored, death will follow.

heart pattern See CARDIOID PATTERN.

heart telemetry See ECG TELEMETRY.

heat A form of energy transferred by conduction, convection, or radiation between two bodies having different temperatures. The amount of heat is expressed in degrees, British thermal units, calories, joules, or kelvins.

heat aging **1.** The degeneration of a substance, aggravated by high temperatures. **2.** A test that indicates the immunity of a substance to degeneration because of high temperatures.

heat coil A device that disconnects a circuit when the temperature reaches a certain minimum level.

heat detector A sensor of heat. See, for example, BOLOMETER, INFRARED DETECTOR, MICRORADIOMETER, RADIOMETER, THERMISTOR, THERMOCOUPLE, and THERMOPILE.

heated-pen recorder See THERMAL RECORDER.

heated-stylus recorder See THERMAL RECORDER.

heated-wire flowmeter See HOT-WIRE FLOWMETER.

heated-wire sensor A hot wire used to discriminate between substances, according to how they affect its heating. See, for example, GAS DETECTOR (also usable as a vacuum gauge), HOT-WIRE ANEMOMETER, and HOT-WIRE MICROPHONE.

heat engine A machine that converts heat energy into mechanical energy.

heater **1.** The filament of an indirectly heated vacuum tube. **2.** The filament in an indirectly heated thermistor.

heater-voltage coefficient The amount of frequency change per volt of fluctuation in the filament voltage of a Klystron.

heat exchanger A device or system that removes heat from a hot body and transfers it to another body or to the surrounding air.

heat-eye tube An infrared-sensitive device used for the purpose of locating objects in visible darkness. The tube consists of a cathode-ray device that is sensitive to infrared radiation.

heat gradient The temperature difference between two points on a body, divided by the distance between the two points.

heating depth See DEPTH OF HEATING.

heating effect The production of heat (power loss) by electric current flowing in a conductor.

heating element **1.** See HEATER. **2.** The resistance element (such as a strip or coil) that generates heat in an electric-heating device.

heat loss **1.** Heat emitted by conduction, convection, or radiation from a body at a relatively high temperature. **2.** Power loss as a result of the heating effect of an electric current.

heat of fusion The amount of heat required to melt a unit mass of a solid that has reached its melting point.

heat of radioactivity Heat generated during the process of radioactive disintegration.

heat of reaction In a chemical or electrochemical reaction, the heat (in calories) absorbed or released.

heat of vaporization The amount of heat required to convert 1 gram of a liquid to a vapor without raising its temperature.

heat radiator See HEATSINK.

heat rays See INFRARED RAYS.

heat remover **1.** See HEATSINK. **2.** A forced-air or forced-liquid cooling system.

heat-resistant glass See PYREX.

heat-sensitive resistor See THERMISTOR.

heat-sensitive switch A make-and-break device, such as a thermostat, that is actuated by a change in temperature.

heat-shrink tubing An insulated flexible sleeving made from a plastic that shrinks permanently for a tight fit when heated; it is commonly used at the joint between a cable and connector.

heatsink A heat exchanger in the form of a heavy, metallic mounting base or a set of radiating fins. It conducts heat away from such devices as power transistors, heavy-duty resistors, or power tubes, and dissipates the heat into the surrounding environment via convection and radiation.

heatsink resistance The opposition offered by a heatsink to the flow of heat.

heat therapy **1.** The use of radio-frequency heating for therapeutic purposes. Also see DIATHERMY. **2.** The use of infrared rays for therapeutic purposes.

5059F-pH-326-351 4/10/01 9:00 AM Page 335

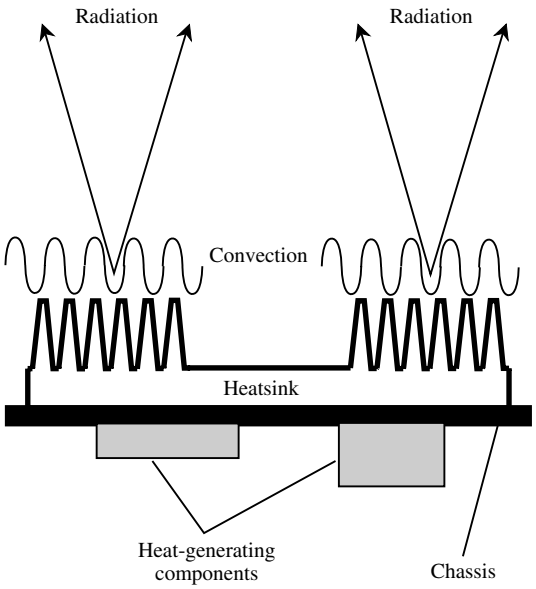

heatsink

heat transfer The movement of heat from one point to another by absorption, conduction, convection, or radiation.

heatronic Pertaining to the heating of a dielectric material subjected to a high voltage.

heat unit **1.** See BRITISH THERMAL UNIT. **2.** See CALORIE. **3.** See KELVIN.

heat waves See INFRARED RAYS.

heat writer See THERMAL RECORDER.

Heaviside-Campbell bridge A form of mutual-inductance bridge. Mutual inductance is determined without regard to the operating frequency.

Heaviside layer See KENNELLY-HEAVISIDE LAYER.

heavy hydrogen An isotope of hydrogen. The term is applied to *deuterium*, whose nucleus consists of one proton and one neutron, and also to *tritium*, whose nucleus consists of one proton and two neutrons.

heavy metal A metal having a specific gravity of 5.0 or higher. Examples: iron (7.85 to 7.88), lead (11.3), nickel (8.6 to 8.9), mercury (13.6), platinum (21.4).

heavy water Formula, D_2O. Water in which deuterium (HEAVY HYDROGEN), rather than ordinary hydrogen has combined with oxygen.

hecto- Abbreviation, h. A prefix meaning hundred(s), (i.e., 10^2).

hectometric wave An electromagnetic field whose wavelength is on the order of hundreds of meters (i.e., at least 100 meters, but less than 1000 meters). The frequency ranges from 300 kHz to 3 MHz.

hectowatt Abbreviation, hW. A unit of power equal to 100 watts. Seldom used; power in this range is usually expressed in terms of the WATT or the KILOWATT.

heelpiece A part of an electronic relay that provides mechanical support for the armature.

Hefner candle A unit of luminous intensity equal to 0.9 candela; the standard (German) is the HEFNER LAMP.

Hefner lamp A standard light source whose luminous intensity is 0.9 candela. It burns amyl acetate (banana oil) and its flame has been the standard of the HEFNER CANDLE, a unit of luminous intensity devised in Germany. Also see CANDLE POWER and LUMINOUS INTENSITY.

height control In a television receiver circuit, the potentiometer or rheostat that controls the vertical dimension of the picture by varying the amplitude of vertical scanning pulses.

height finder An altitude-measuring radar system.

height-position indicator Abbreviation, HPI. A radar displaying the height of a target, its angular elevation, and the slant range.

Heil oscillator An oscillator based on a special tube consisting of a heated cathode, first anode, metal cylinder, and second anode. Electrons emitted by the cathode pass through a hole in the first anode and become a beam, which passes through the cylinder and strikes the second anode (collector). Electron bunching in the cylinder causes energy to be transferred to a tank circuit between the cylinder and anodes.

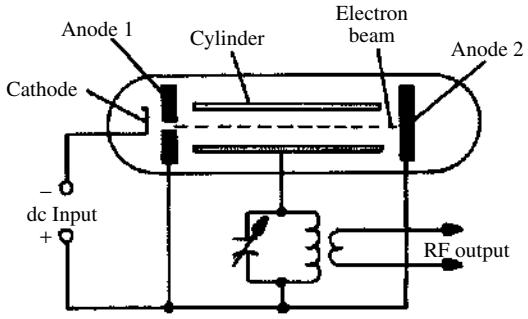

Heil oscillator

Heisenberg uncertainty principle See UNCERTAINTY PRINCIPLE.

hekto- See HECTO-.

heliacal cycle See SUNSPOT CYCLE.

helical antenna A spring-shaped antenna mounted perpendicular to a flat metal-plate reflector, an arrangement that produces circularly polarized waves in a narrow beam. It is used primarily at ultra-high and microwave radio frequencies.

5059F-pH-326-351 4/10/01 9:00 AM Page 336

helical-beam antenna See HELICAL ANTENNA.

helical line The helix in a backward-wave oscillator or traveling-wave tube.

helical potentiometer A potentiometer whose resistance element is a wire wound into a coil of several turns. The slider moves over the wire (or the larger coil) from one end to the other as the slider or coil is turned through several complete revolutions. Also called MULTITURN POTENTIOMETER.

helical scanning Radar scanning by an antenna that moves vertically as it moves horizontally, producing a spiral motion to the radiated beam.

helical sweep See SPIRAL SWEEP, **1**, **2**.

helical transmission line See HELICAL LINE.

helicone An antenna used at ultra-high and microwave frequencies, consisting of a helical radiator within a cone-shaped reflector.

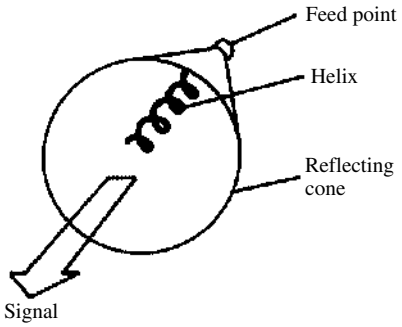

helicone

helionics The science of converting solar heat into electrical energy. The term is an acronym from *helio-* (pertaining to the sun) and *electronics.*

heliostat **1.** A servo-controlled motor-driven device that drives a mirror to keep sunlight trained upon a specific target. **2.** By extension, any similar device to keep a solar cell pointed to the sun.

helitron A form of oscillator used at ultra-high and microwave frequencies. The output frequency is variable over a wide range.

helium Symbol, He. A gaseous element. Atomic number, **2**. Atomic weight, 4.0026.

helium group The six inert gases in group 0 of the periodic table: *argon*, *helium*, *krypton*, *neon*, *xenon*, and *radon.*

helium-neon laser A laser in which the lasing substance is a mixture of helium and neon. Produces a characteristic brilliant red visible output. Also see HELIUM and NEON.

helix **1.** A single-layer coil. **2.** That which is coil-shaped (i.e., spiral in configuration). **3.** See HELICAL ANTENNA. **4.** See HELICAL LINE.

helix line See HELICAL LINE.

helix recorder An information recorder using a spiral method of scanning. The recording medium is usually drum-shaped.

Helmholtz coil A device consisting of two crossed-field primary windings in which an inductively coupled secondary winding rotates. The primary windings carry currents that differ in phase by 90 degrees. Rotating the secondary coil provides 360 degrees of continuously variable phase shift.

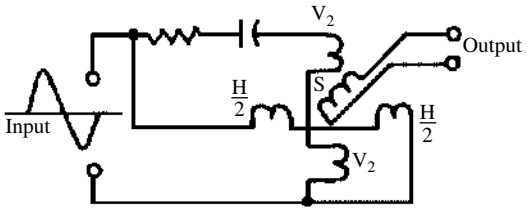

Helmholtz coil

Helmholtz double layer An intermolecular layer between a metal and an electrolyte in which it is immersed. It is formed when the adhesive force between the metal and electrolyte decreases the surface tension of the metal, causing positive ions to migrate from the metal into the liquid. The metal, charged negatively, and the electrolyte, charged positively, form a capacitor whose dielectric is the Helmholtz layer.

Helmholtz resonator An acoustic (sound) chamber whose geometry, in combination with the size of a small opening, results in resonance at a specific frequency.

HEM Abbreviation of *hybrid electromagnetic* (see, for example, HYBRID ELECTROMAGNETIC WAVE).

hemimorphic Pertaining to an object with ends that have unlike faces.

He-Ne laser See HELIUM-NEON LASER.

henry Symbol, H. The standard unit of inductance. It is the inductance exhibited by a closed circuit in which one volt is produced by a current changing uniformly at one ampere per second. This is a large unit of inductance; more common units are the MILLIHENRY and the MICROHENRY.

hermaphroditic plug A plug that has the prongs of a male plug and the recessed contacts of a female plug. Compare FEMALE PLUG and MALE PLUG.

hermetically sealed Constructed in manufacture so as to be permanently closed against the entry of air or other gases, dust, and moisture.

hermetic seal A permanent, air-tight seal that effectively prevents corrosion from elements in the outside environment.

herringbone pattern A pattern of interference in a television picture, so named because of its resemblance to the skeleton of a fish.

Herschel-Quincke tube An acoustic device that demonstrates sound interference. The device has

5059F-pH-326-351 4/10/01 9:00 AM Page 337

two hollow cylinders, one of which can be adjusted in length. At the far end of the apparatus, the cylinders are joined together. The resultant amplitude depends on the difference in length between the cylinders. Sound wavelengths can be measured using this apparatus.

hertz Abbreviation, Hz. The standard unit of frequency (of periodic phenomena, such as alternating or pulsating currents); 1 Hz = 1 cycle per second. One Hz is an extremely small unit of frequency; more common units are the KILOHERTZ, the MEGAHERTZ, and the GIGAHERTZ.

Hertz antenna An ungrounded halfwave antenna fed by a transmission line attached to one end or to the center of the radiator. See, for example, CENTER-FED ANTENNA and END-FED ANTENNA. Compare MARCONI ANTENNA.

Hertz effect Ionization of a gas, produced by intense ultraviolet radiation.

Hertzian antenna See HERTZ ANTENNA.

Hertzian oscillator See HERTZ OSCILLATOR.

Hertzian radiation Radiation of electromagnetic (radio) waves.

Hertzian waves Electromagnetic waves in the radio spectrum, with wavelengths longer than those of infrared, visible light, ultraviolet, X rays, or gamma rays.

Hertz oscillator A damped-wave generator of oscillations, used by Hertz in his demonstration of radio waves in 1888 (verifying the earlier prediction by James Clerk Maxwell). The oscillator contains a spark gap supplied by an induction coil, attendant coils, capacitors (in the prototype, Leyden jars), and two large metal plates.

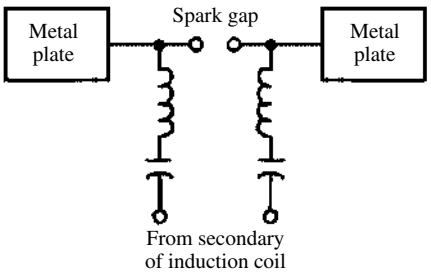

Hertz oscillator

Hertz vector A single vector that specifies the electromagnetic field (electric and magnetic components) of a radio wave.

hesitation As distinct from a halt, a brief break in a computer program run during which internal operations are occurring, such as data transfer to a peripheral.

heterochromatic Consisting of different frequencies, wavelengths, or colors. Compare MONOCHROMATIC.

heterodyne **1.** To beat one alternating-current signal against another to produce one or more beat-frequency signals. Also see BEAT FREQUENCY and BEAT NOTE. **2.** The whistle produced when two signals very close in frequency are mixed in a radio receiver. **3.** To combine radio signals in a mixer, the purpose of which is to produce a sum or difference signal for further processing.

heterodyne detection **1.** Signal detection by beating the incoming signal against one produced by a local oscillator. In this way, an unmodulated signal is made audible (the beat note is an audio frequency). **2.** Signal detection by a superheterodyne circuit.

heterodyne detector **1.** A detector that makes a radio-frequency (RF) signal audible by beating it against the RF signal of a local oscillator, the product being an audio-frequency (AF) beat note. **2.** The FIRST DETECTOR or SECOND DETECTOR in a SUPERHETERODYNE CIRCUIT. **3.** A combination linear detector and local RF oscillator used to detect and measure the frequency of test signals. Also see HETERODYNE FREQUENCY METER.

heterodyne eliminator See WHISTLE FILTER.

heterodyne filter See WHISTLE FILTER.

heterodyne frequency The frequency of the signal obtained by beating one signal against another.

heterodyne frequency meter A frequency-measuring device that contains a variable-frequency oscillator (VFO), a mixer, and an indicator such as an analog meter. The oscillator frequency is adjusted until zero beat is reached with the signal source. This condition is shown by a dip in the meter indication. An audio amplifier can be coupled to the output of the device instead of a meter; in this case the heterodyne appears as an audible tone whose frequency drops to zero when the oscillator frequency is equal to the signal frequency being measured.

heterodyne method See HETERODYNE, **1**.

heterodyne oscillator A signal generator whose output is the beat product of outputs from two internal oscillators. The output frequency can be either the sum or the difference of the oscillator frequencies, as selected by output filtering or tuning. See BEAT-FREQUENCY OSCILLATOR.

heterodyne reception Radio reception (especially in telegraphy) by means of the beat-note process. Also see HETERODYNE DETECTION, **1** and HETERODYNE DETECTOR, **1**.

heterodyne repeater A REPEATER in which the received signals are converted to another frequency before transmission.

heterodyne-type frequency meter See HETERODYNE FREQUENCY METER.

heterodyne wave analyzer A type of audio-frequency (AF) wave analyzer. The input signal is heterodyned in a balanced modulator with the signal from an internal tunable oscillator. One of the resulting sidebands is passed through a

5059F-pH-326-351 4/10/01 9:00 AM Page 338

sharp bandpass filter, whose output actuates an alternating-current (ac) voltmeter. The internal oscillator is tuned slowly so that different components of the balanced-modulator output sideband pass successively through the filter. The amplitude-versus-frequency function of the input signal is determined by noting the meter readings as the internal oscillator is tuned.

heterodyne wavemeter See HETERODYNE FREQUENCY METER.

heterodyne whistle See HETERODYNE, **2**.

heterogeneous Pertaining to a group of objects or devices that have differing characteristics.

heterogeneous radiation Any broadband form of radiation. In particular, broadbanded radio waves, infrared radiation, visible light, ultraviolet, X rays, or gamma rays.

heterolysis The HYDROLYSIS of a compound into two oppositely charged ions.

heteropolar generator An electric generator in which the active conductors move through magnetic fields, first in one direction, then in the other direction. This is done by means of rotation in a nonuniform magnetic field. Most generators in common use are of this kind.

heuristic knowledge In artificial intelligence (AI), a form of machine knowledge in which a computer learns from its mistakes. As a complex program is repeatedly run over a period of time, the number of errors per run approaches zero.

heuristic program In artificial intelligence (AI), a program with which the computer solves a problem by trial and error, often learning in the process so that mistakes will not be repeated on subsequent runs.

Heusler's alloys Ferromagnetic alloys that contain one or more non-magnetic metals (such as aluminum, copper, or manganese).

hexadecimal number system An alphanumeric, base-16 system of number notation used in some computers. The system uses the usual digits plus the letters A through F to represent the numbers 10 through 15 (each place can only hold one symbol).

hex inverter A collection of six digital inverters, or NOT gates, contained within one package, usually an integrated circuit.

Hf Symbol for HAFNIUM.

HF Abbreviation of HIGH FREQUENCY.

Hg Symbol for MERCURY.

HH beacon In radionavigation, a nondirectional homing beacon.

hi **1.** Contraction of HIGH. **2.** Radiotelegraph symbol for a laugh, often verbalized by radio amateurs.

HIC Abbreviation of HYBRID INTEGRATED CIRCUIT.

HIDM Abbreviation of HIGH-INFORMATION DELTA MODULATION.

hierarchical password protection Also called *multilevel password protection*. A security feature that prevents unauthorized use of a computer, network, or database. The password levels allow users various degrees of control over the host machine.

hi-fi **1.** Contraction of HIGH-FIDELITY. **2.** In video recording, the addition of sound having high fidelity.

high **1.** Pertaining to a circuit point or condition at some potential above ground. **2.** The logical digit 1. **3.** The condition of having relatively large magnitude (e.g., HIGH FREQUENCY and HIGH VOLTAGE). **4.** Pertaining to the upper portion of a range, as in HIGH BAND or HIGH FREQUENCY. **5.** Characterized by greater-than-normal response or performance, as in HIGH *Q* or HIGH FIDELITY.

high band **1.** The higher or highest frequency band used in communications, testing, or processing, when several bands are available. **2.** The very-high-frequency (VHF) television channels 7 through 13. **3.** The communications frequency range from about 144 MHz to about 170 MHz.

high boost In sound recording and reproduction, the emphasis of high frequencies in an operating spectrum. Also called HIGH-FREQUENCY COMPENSATION.

high-C circuit A tuned circuit having high capacitance and low inductance at a given frequency. Such a circuit is characterized by high selectivity and low voltage. Compare HIGH-L CIRCUIT. Also see LC RATIO.

high contrast In an image, a limited range of gray values between black and white, or a similar condition in a color image (overbright whites, little shadow detail). Also see CONTRAST.

high definition In facsimile or television, a condition of minute detail so that the original scene is faithfully reproduced.

high-definition television Abbreviation, HDTV. A method of getting enhanced detail into a television (TV) picture and for obtaining better audio quality, compared with standard analog TV. There are several different schemes. The most noticeable feature is the crispness of the picture. This is vividly apparent in big-screen installations, which have traditionally suffered from image blurring. A standard TV picture has 525 lines per frame, but HDTV systems can have more than twice that number. Another important difference is that HDTV is digital; this minimizes susceptibility to interference. Interlacing is used in some systems.

high-density bipolar-3 code A communications or digital code in which two logic highs (ones) can occur in sequence, without the need for an intervening logic low (zero) to separate them.

high-efficiency linear amplifier A LINEAR AMPLIFIER with higher operating efficiency than is obtainable with conventional class-B linear amplifiers. Efficiencies on the order of 60% at 100% modulation are possible.

5059F-pH-326-351 4/10/01 9:00 AM Page 339

high-energy materials See HARD MAGNETIC MATERIALS.

high-energy particle **1.** A SUBATOMIC PARTICLE that has been given high velocity by a particle accelerator. **2.** High-speed subatomic particles emitted by the sun during a solar flare, or arriving from outer space.

high-energy physics The discipline dealing with the characteristics, properties, and applications of HIGH-ENERGY PARTICLES.

higher-order language See HIGH-LEVEL LANGUAGE.

high fidelity Abbreviation, hi-fi. Pertaining to an audio-frequency system that is very faithful to the signal it is processing (i.e., one characterized by extremely low distortion and wide frequency response).

high frequency Abbreviation, HF. Pertaining to frequencies in the 3- to 30-MHz band (wavelengths from 10 to 100 meters). Also see RADIO SPECTRUM.

high-frequency alternator A dynamo for generating radio-frequency energy.

high-frequency bias In a tape recorder, a high-frequency sinusoidal signal superimposed on the signal being recorded, for improving linearity and dynamic range.

high-frequency compensation See HIGH BOOST.

high-frequency converter See SHORTWAVE CONVERTER.

high-frequency crystal See HARMONIC CRYSTAL.

high-frequency direction finder Abbreviation, HDF. A direction finder operated at high radio frequencies (i.e., between about 3 MHz and 30 MHz).

high-frequency heating Electronic heating of materials by high-frequency energy. See, for example, DIELECTRIC HEATING and INDUCTION HEATING.

high-frequency resistance See RADIO-FREQUENCY RESISTANCE.

high-frequency speaker See TWEETER.

high-frequency trimmer **1.** In older high-frequency communications receivers, a low-value variable capacitor operated in parallel with a usually front-panel tuning capacitor to set the high-frequency end of the tuning range. See, for example, OSCILLATOR TRIMMER. **2.** A small variable capacitor used in conjunction with a larger tuning capacitor, the function of which is to permit precision tuning of the larger device.

high-impedance-state output current Pertaining to tests that ensure that an integrated circuit will not overload a bus line.

high-impedance voltmeter A voltmeter having an input impedance of at least several megohms.

high-information delta modulation A companded form of delta modulation, operating at comparatively low sample rate.

high-L circuit A tuned circuit having high inductance and low capacitance at a given frequency. Such a circuit is characterized by low selectivity and high voltage. Compare HIGH-C CIRCUIT. Also see LC RATIO.

high-level audio signal An audio-frequency signal that has been preamplified (e.g., the output of a compact-disc player). Compare LOW-LEVEL AUDIO SIGNAL.

high-level input current **1.** Pertaining to the testing of intertransistor leakage in an integrated circuit (IC) having multiple emitter inputs. **2.** The current into an IC input at minimum high-level voltage.

high-level language Also called *higher-order language*. A computer programming language in which the operator is easily able to communicate with the machine. It generally serves as an interface between a human programmer and the MACHINE LANGUAGE. Examples are BASIC, C, C++, COBOL, and FORTRAN.

high-level modulation In an amplitude-modulated transmitter, introduction of the audio at the final stage of radio-frequency amplification, permitting 100% modulation of the full-power signal.

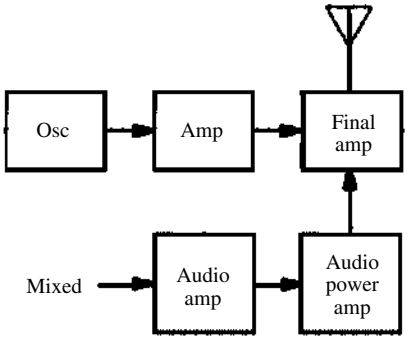

high-level modulation

high-level output current **1.** Pertaining to the testing of drive capability and fanout of an integrated circuit (IC). **2.** The current flowing from an IC output when in the high state.

high-level recovery Hardware recovery using data not involved in the failure, such as that on a magnetic storage medium. Also see HARDWARE RECOVERY.

highlight **1.** A bright area in a television picture. **2.** In computer data processing, the defining or setting-off of a block of data (such as text), with the intention of relocating, editing, or deleting it.

high-noise-immunity logic Abbreviation, HNIL. A form of bipolar digital logic designed for minimal sensitivity to noise. Also known as *high-threshold logic (HTL)*.

high order Descriptive of the relationship between bits or digits in a word or number. Of two digits,

5059F-pH-326-351 4/10/01 9:00 AM Page 340

the one holding the higher place value is the high-order digit (e.g., 2 is the high-order digit in 25).

high-pass filter A combination of capacitance, inductance, and/or resistance, intended to produce large amounts of attenuation below a certain frequency and little or no attenuation above that frequency. The frequency at which the transition occurs is called *cutoff*. At cutoff, the power attenuation is 3 dB with respect to the minimum attenuation. At frequencies above cutoff, the power attenuation is less than 3 dB. At frequencies below cutoff, the power attenuation is more than 3 dB. The simplest circuit consists of a parallel inductor or a series capacitor. The inductance-capacitance (LC) circuit has a combination of parallel inductors and series capacitors. In the resistance-capacitance (RC) circuit, resistors are substituted for the inductors. Compare BAND-PASS FILTER, BAND-REJECTION FILTER, LOW-PASS FILTER.

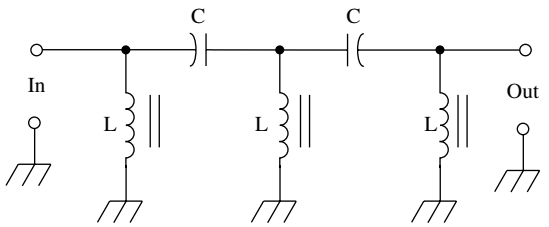

high-pass filter

high-pass-filter method A method of measuring the total harmonic distortion (THD) percentage using a high-pass filter to separate the harmonics from the fundamental. The output voltage V_o of the filter is compared with the input voltage V_i; then THD = $100V_o/V_i$.

high-performance Pertaining to apparatus designed for continuous operation with maximum reliability.

high-performance navigation system Acronym HIPERNAS. An electromechanical guidance system that is purely inertial and self-compensating.

high-potential test A high-voltage test of insulation, in which the applied voltage is continuously increased until the breakdown point of the dielectric is reached.

high-power rectifier A rectifier designed for high-voltage, high-current operation.

high Q For a component or circuit, a high value for the ratio X/R (reactance to resistance). This is a relative term because a particular numerical value of Q, considered high in one situation, might be regarded as low under other circumstances. Also see FIGURE OF MERIT.

high-resistance joint In the wiring of electronic equipment, a joint or connection between conductors that is poorly made, thereby introducing a high resistance between the parts.

high-resistance voltmeter A voltmeter having an input resistance of at least several megohms.

high-speed carry In computer operation, a carry into a column causing a carry out, circumventing the usual intermediate adding circuit.

high-speed diode See COMPUTER DIODE.

high-speed flip-flop A flip-flop having short switch-on and switch-off time.

high-speed oscilloscope An oscilloscope with excellent high-frequency and unit-function response. It can reproduce high-speed pulses faithfully.

high-speed relay A relay with a short make or short break interval.

high-speed transistor See SWITCHING TRANSISTOR.

high tension Pertaining to utility power-transmission lines on which there are very high voltages, typically 100 kilovolts (100 kV) or more.

high-tension line A power-transmission line carrying a very high voltage. It is generally used for the transfer of electric power over long distances.

high-threshold logic See HIGH-NOISE-IMMUNITY LOGIC.

high voltage **1.** A voltage considerably higher than those ordinarily encountered in a particular application. The term is comparative; a few hundred volts might be considered high in one situation, but low in another. **2.** In a cathode-ray tube, the voltage that accelerates the beam electrons. **3.** In a television receiver, the picture-tube anode voltage. **4.** In a vacuum-tube power amplifier, the plate supply voltage.

high-voltage probe A very-high-resistance probe for measuring high voltages with a low-range voltmeter.

highway A path over which multiple signals are propagated using time-division multiplexing.

HILAC Acronym for *heavy-ion linear accelerator*.

hill-and-dale recording See VERTICAL RECORDING.

hinged-iron instrument An alternating-current meter whose input transformer core is hinged in two parts. By means of a thumb trigger, the core can be opened, then closed around the current-carrying conductor that induces magnetism in the core; a secondary coil delivers current to the meter. Also called *clamp ammeter* or *clamp voltmeter*.

HIPERNAS Acronym for HIGH-PERFORMANCE NAVIGATION SYSTEM.

hipernick A high-permeability alloy of iron and nickel.

hipot Contraction of *high potential*. See HIGH-POTENTIAL TEST.

hiss **1.** A high-pitched sound rich in sibilants (*s*, *sh*, and *z* sounds) produced by random high-frequency fluctuations in current. **2.** The characteristic, high-pitched background noise (as in 1) accompanying super-regeneration. **3.** Internally generated noise in a communications receiver, amplified by the audio-frequency stages and appearing at the speaker or headphones.

5059F-pH-326-351 4/10/01 9:00 AM Page 341

hiss filter See HASH FILTER.

hit **1.** The occurrence of a lightning stroke at a specific point on the ground. Also called *direct hit.* **2.** The coincidence of two pulses.

H lines Magnetic lines of flux.

HLL Abbreviation of HIGH-LEVEL LANGUAGE.

H network A network of five impedances: two connected in series between the upper input and output terminals, two between the lower input and output terminals, and one shunted between the junctions of the series-connected impedances. Also called *H pad*, *balanced tee network*, and *balanced tee pad.*

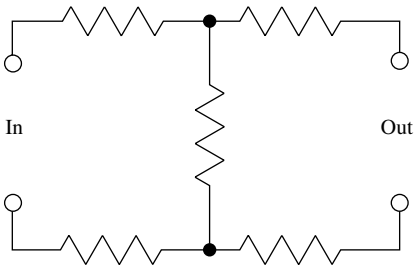

H network

Ho Symbol for HOLMIUM.

hobby robot A robot intended for amusement and, sometimes, for education. Such robots often take humanoid form. Some are programmable, and can give demonstrations, play musical instruments, and do other complex routines.

hockey-stick lead On a capacitor, resistor, or other component, a pigtail lead that is given a single crimp for easy insertion into a printed-circuit board.

hodoscope An instrument consisting essentially of closely spaced ion counters, for studying the path of an ionizing particle.

Hoffmann electrometer See BINANT ELECTROMETER.

hog horn A form of horn antenna used in microwave applications. It is generally used in the feed system of a dish antenna. The horn opening points in the direction of the feed waveguide.

hold **1.** To retain data in a storage device after the data has been duplicated in another location or device. **2.** A momentary halt of an operation or process. **3.** In a television receiver, a control that stabilizes the vertical or horizontal synchronization.

hold circuit **1.** See HOLDING CIRCUIT. **2.** In a television receiver, the circuit associated with the hold control(s). Also see HORIZONTAL-HOLD CONTROL and VERTICAL-HOLD CONTROL.

hold control See HORIZONTAL-HOLD CONTROL and VERTICAL-HOLD CONTROL.

hold current Symbol, I_h. The minimum current that will keep a normally open relay closed or a normally closed relay open.

hold electrode In a mercury switch, the electrode that is in permanent contact with the mercury.

holding beam In an electrostatic cathode-ray storage tube, the electron beam that generates replacement charges for those that were stored on the dielectric surface and then lost.

holding circuit In an electromechanical relay, a separate circuit that, when energized, keeps the relay actuated.

holding coil In an electromechanical relay, the extra coil that is associated with the holding circuit.

holding current **1.** Current in the holding coil of a relay. **2.** In a gas tube, the minimum current required to maintain ionization.

holding gun In an electrostatic cathode-ray storage tube, the electron gun that generates the holding beam.

hold mode A condition in which the output state of a digital-logic circuit remains unchanged while the input signals are removed.

hold-off voltage The highest voltage that can be applied to a flashtube without causing it to fire.

holdover The flow of current through the ionized path created by an electric arc.

hold time **1.** The time permitted for a weld to harden in resistance welding. **2.** In digital communications, the time for which a signal is maintained at a certain input after changing state at another specified input.

hole **1.** In a semiconductor atom, the vacancy resulting from the loss of an electron. When an electron is lost, so is its negative charge, leaving an equivalent net positive charge. This charge, like that of an electron, can move as a current carrier. **2.** The punched-out portion of a chassis or panel, through which wires can be passed or components mounted.

hole conduction In a semiconductor material, electrical conduction as a result of HOLE CURRENT.

hole current In a semiconductor material, the electrical current resulting from the movement of positive charge carriers (holes). Also see HOLE.

hole density The degree of concentration of holes in a semiconductor. Also see HOLE.

hole-electron pair In a semiconductor, a hole and a related electron. Each electron in the conduction band has a counterpart in the valence band, a vacancy (HOLE) left by the movement of the electron to the conduction band.

hole injection The creation of mobile holes in a semiconductor by applying an electric charge. Also see HOLE.

hole injector **1.** The emitter electrode of a bipolar pnp transistor. **2.** The metal whisker of a point-contact diode having an n-type wafer. **3.** The player of a forward-biased junction diode.

5059F-pH-326-351 4/10/01 9:00 AM Page 342

hole mobility The ease with which a hole moves within a semiconductor. Also see CARRIER MOBILITY.

hole storage See CARRIER STORAGE.

hole storage factor In a bipolar transistor biased to saturation, the amount of storage charge caused by excess base current.

hole trap In a semiconductor, an impurity that can cancel holes by releasing electrons to fill them.

hollow coil A coreless inductor.

hollow conductor Tubing used as a low-loss conductor at radio frequencies.

hollow core A core that is not solid throughout—especially one that has a central mounting hole.

holmium Symbol, Ho. A metallic element of the rare-earth group. Atomic number, 67. Atomic weight, 164.93. Forms highly magnetic compounds.

holocamera A camera for making holograms. Also see HOLOGRAM, **1** and HOLOGRAPHY.

hologram **1.** A wavefront recording made on photographic film by the process of HOLOGRAPHY. By changing the frequency of the light transmitted, various magnifications of the image can be obtained. Produces a true three-dimensional image. **2.** A visible, three-dimensional display projected in the air or underwater by means of lasers. They are often used at outdoor music concerts and other events.

holography A method of producing a wavefront recording of an object illuminated by laser light. The result, an interference pattern, appears meaningless when viewed in ordinary diffuse light. But when a point source of illumination is used, especially a laser, an image appears that is convincingly three-dimensional.

homeostasis The condition of being in static equilibrium.

home station See BASE STATION.

homing **1.** Guidance by means of an electronic beacon. The vehicle maintains a course toward the beacon. **2.** Guidance by means of some form of emission from a target object. The emission can be acoustic or electromagnetic energy.

homing antenna A direction-finding antenna—especially one on a mobile vehicle.

homing beacon A station radiating a beam for use in direction finding by mobile vehicles.

homing device A receiving device mounted on a mobile vehicle, and that continuously indicates the direction of a selected transmitting station that is the vehicle's destination.

homing relay A stepping relay that returns to its starting position after each switching sequence. Also see STEPPING SWITCH.

homing station See HOMING BEACON.

homodyne reception See ZERO-BEAT RECEPTION.

homogeneous **1.** Uniform in structure; similar at all points or locations. **2.** Consisting of many identical elements.

homogous field A field whose lines of flux in one plane pass through a single point.

homolysis The decomposition of a compound into a pair of neutral atoms or radicals.

homomorphism A one-to-one correspondence between the elements of two sets.

homopolar Pertaining to the union of atoms of the same polarity; nonionic.

homopolar generator A direct-current (dc) generator whose poles have the same polarity, with respect to the armature. Thus, no commutator is necessary.

homopolar magnet A magnet whose pole pieces are concentric.

homunculus In artificial intelligence (AI), a computer or robot that exhibits characteristics of a living being; especially, an ANDROID.

honeycomb coil A multilayer coil having a UNIVERSAL WINDING.

honeycomb winding See UNIVERSAL WINDING.

honker Also called *midrange speaker.* A loudspeaker that favors the middle audio frequencies. Compare TWEETER and WOOFER.

hood A light shield for a cathode-ray tube; it allows the screen to be viewed with a minimum of interference from room light.

Hooke's law Strain is proportional to the stress that produces it, as long as the ELASTIC LIMIT is not exceeded.

hook switch A switch that closes a circuit when a headset or handset is lifted from the resting position. The common telephone receiver uses such a switch.

hook transistor A four-layer pnpn semiconductor device, in which the outer p and n layers serve as emitter and collector, the inner n layer being the base. This places a p layer between the base and collector, resulting in a transistor that provides high alpha as a result of carrier multiplication by the additional junction in the collector layer.

hookup See SCHEMATIC DIAGRAM.

hookup wire Flexible, insulated wire used in the wiring of some electrical and electronic devices.

hoop antenna See CAGE ANTENNA.

hoot stop During a computer program run, a loop made evident by a sound signal.

hop In long-distance radio communications, the transmission of a wave and its subsequent return to the earth from the ionosphere; it is of importance mainly at low, medium, and high frequencies.

hor Abbreviation of HORIZONTAL. (Also, *H* and *horiz.*)

horiz Occasional abbreviation of HORIZONTAL. The usual form is *hor*; another alternate is *H.*

horizon **1.** For a specific location, the circle on the celestial sphere midway between the zenith (the point directly overhead) and the nadir (the point directly underfoot). **2.** Also called *visual horizon.* The set of points, as viewed from a particular

5059F-pH-326-351 4/10/01 9:00 AM Page 343

location, where the sky and the earth appear to meet (i.e., the last visible part of the earth's surface from a given observation point). **3.** Also called *radio horizon.* The set of points, from a particular location at a given radio frequency, representing the maximum communications range via the ground wave under normal conditions. Also see ARTIFICIAL HORIZON.

horizontal **1.** Pertaining to objects or effects in a plane perpendicular to a line connecting the zenith (the point directly overhead) and the nadir (the point directly underfoot). **2.** Pertaining to that which is parallel to an assumed flat surface. **3.** Pertaining to width deflection on a cathode-ray tube.

horizontal AFC In a television receiver circuit, *automatic frequency control (AFC)* of the horizontal sweep. It keeps the receiver's horizontal scanning in step with that of the camera at the transmitting station.

horizontal amplification Gain provided by the horizontal channel of a device, such as an oscilloscope, cathode-ray electrocardiograph, or television receiver. Compare VERTICAL AMPLIFICATION.

horizontal amplifier A circuit or device that provides HORIZONTAL AMPLIFICATION. Compare VERTICAL AMPLIFIER.

horizontal angle of radiation For an antenna, the direction of maximum radiation in the horizontal plane (see HORIZONTAL, **1**), provided as an azimuth angle measured clockwise from geographic north.

horizontal angle of deviation In a communications circuit, the angular difference, in degrees, between the compass direction from which a received signal arrives, and the great-circle path connecting the receiving station with the transmitting station.

horizontal axis The axis that is parallel to an assumed horizontal surface (of the earth, for example) or the one so represented in a diagram. Also see X-AXIS.

horizontal beamwidth In a directional antenna system, the angle, measured in the horizontal plane, between the half-power points in the major lobe.

horizontal blanking See HORIZONTAL RETRACE BLANKING.

horizontal-blanking pulse In a television signal, the rectangular pedestal-shaped pulse that occurs between the active horizontal lines to achieve horizontal retrace blanking. Compare VERTICAL-BLANKING PULSE.

horizontal centering control See CENTERING CONTROL.

horizontal channel The system of amplifiers, controls, and terminations that constitute the path of the horizontal signal in an equipment, such as an oscilloscope or graphic recorder. Compare VERTICAL CHANNEL.

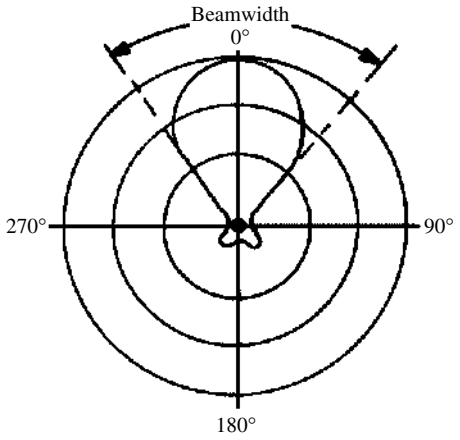

horizontal beamwidth

horizontal-convergence control In a color television receiver, the variable component for adjusting the horizontal dynamic convergence voltage.

horizontal coordinates See CARTESIAN COORDINATES.

horizontal deflection In a cathode-ray tube, the lateral movement of the electron beam on the screen. Compare VERTICAL DEFLECTION.

horizontal deflection coils The pair of coils that produces the magnetic field to horizontally deflect the electron beam in an electromagnetic cathode-ray tube. Also see DEFLECTION COIL.

horizontal-deflection electrodes See HORIZONTAL DEFLECTION COILS and HORIZONTAL DEFLECTION PLATES.

horizontal deflection plates In an electrostatic cathode-ray tube (typical of laboratory oscilloscopes and some early television picture tubes), a pair of plates that produces an electric field to horizontally deflect the electron beam. Compare VERTICAL DEFLECTION PLATES.

horizontal directivity The radiation or reception pattern of a directional antenna in the horizontal plane.

horizontal-drive control See DRIVE CONTROL.

horizontal dynamic convergence During the scanning of a horizontal line in a color picture tube, convergence of the electron beams at the aperture mask. Compare VERTICAL DYNAMIC CONVERGENCE.

horizontal field strength The field strength of signals passing through an antenna in a horizontal plane. Compare VERTICAL FIELD STRENGTH.

horizontal-field-strength diagram A plot of horizontal field strength, usually in polar form. Compare VERTICAL-FIELD-STRENGTH DIAGRAM.

horizontal flowcharting Flowcharting the movement of documents or files, rather than the data bits themselves, through a digital system.

5059F-pH-326-351 4/10/01 9:00 AM Page 344

horizontal frequency In television circuits, the horizontal scanning frequency [i.e., the frequency at which the horizontal lines are traced (generally 15.750 kHz)].

horizontal frequency response The gain-vs-frequency characteristic of the horizontal channel of an oscilloscope or graphic recorder. Compare VERTICAL FREQUENCY RESPONSE.

horizontal gain At a specified frequency, the overall amplification of the horizontal channel of an oscilloscope or graphic recorder. Compare VERTICAL GAIN.

horizontal-gain control A control, such as a potentiometer, for adjusting horizontal gain. Compare VERTICAL-GAIN CONTROL.

horizontal-hold control In a television receiver, the control for adjusting the horizontal oscillator frequency to prevent horizontal tearing of the picture. Compare VERTICAL-HOLD CONTROL.

horizontal hum bars Dark, horizontal interferential bars in a television picture, caused by HUM interference.

horizontal linearity The precision of gain and deflection in the horizontal channel of an oscilloscope, graphic recorder, or television receiver. A linear picture is a faithful (undistorted) reproduction of the original image. Compare VERTICAL LINEARITY.

horizontal-linearity control In an oscilloscope or television receiver, the control with which horizontal linearity is adjusted. Compare VERTICAL-LINEARITY CONTROL.

horizontal line frequency See HORIZONTAL FREQUENCY.

horizontal lock See HORIZONTAL-HOLD CONTROL.

horizontally polarized wave An electromagnetic wave whose electric lines of flux are parallel to the plane of the horizon. Compare VERTICALLY POLARIZED WAVE.

horizontal multivibrator In a television receiver, a 15.750-kHz multivibrator that generates the horizontal sweep signal.

horizontal oscillator In a TV receiver, the oscillator (usually a multivibrator) that generates the horizontal sweep signal. Compare VERTICAL OSCILLATOR.

horizontal output stage In a television receiver, an output amplifier following the horizontal oscillator. Compare VERTICAL OUTPUT STAGE.

horizontal output transformer In a television receiver, the output transformer in the horizontal-oscillator-output amplifier section. Also called FLYBACK TRANSFORMER.

horizontal polarization Pertaining to an electromagnetic wave whose electric lines of flux are horizontal. In general, when the radiating element of an antenna is horizontal, the electric lines of flux in the transmitted waves are horizontal, and the antenna is most sensitive to incoming signals whose electric lines of flux are horizontal. Compare VERTICAL POLARIZATION.

horizontal positioning control See CENTERING CONTROL.

horizontal quantity The quantity measured along the X-axis of a graph represented by the horizontal deflection of an oscilloscope beam. Compare VERTICAL QUANTITY.

horizontal recording See LATERAL RECORDING.

horizontal repetition rate See HORIZONTAL FREQUENCY.

horizontal resolution In a television picture, the number of picture elements (*pixels*) that can be discerned in a horizontal scanning line. Compare VERTICAL RESOLUTION.

horizontal retrace In a cathode-ray device, such as an oscilloscope or television receiver, the rapid return of the electron beam to its starting point after completing a horizontal sweep of the screen. Compare VERTICAL RETRACE.

horizontal retrace blanking In oscilloscopes and television receivers, the automatic cutoff of the electron beam during a horizontal retrace period, preventing an extraneous line on the screen during the period. Compare VERTICAL RETRACE BLANKING.

horizontal scanning **1.** The lateral sweeping of the electron beam in a cathode-ray tube. **2.** The sampling of x-axis values in a repetitive or nonrepetitive sweep of that axis.

horizontal scanning frequency See HORIZONTAL FREQUENCY.

horizontal sensitivity The signal voltage required at the input of a horizontal channel for full horizontal deflection. Also see HORIZONTAL GAIN. Compare VERTICAL SENSITIVITY.

horizontal signal A signal serving as a horizontal quantity. Compare VERTICAL SIGNAL.

horizontal sweep **1.** In a cathode-ray tube, the horizontal movement of the spot on the screen; in particular, the movement from left to right, during which a line of the image is formed on the screen. **2.** The circuit that produces horizontal sweep.

horizontal sweep frequency The frequency at which horizontal sweep occurs; in a television receiver, it is generally 15.750 kHz. Also called *horizontal sweep rate.* Compare VERTICAL SWEEP FREQUENCY.

horizontal sweep rate See HORIZONTAL SWEEP FREQUENCY.

horizontal-sync discriminator In a television receiver, a circuit that compares horizontal sync-pulse phase with the phase of the signal from the horizontal sweep oscillator.

horizontal synchronization In a television receiver, synchronization of the horizontal component of scanning with that of the transmitting camera. Also see HORIZONTAL SYNC PULSE. Compare VERTICAL SYNCHRONIZATION.

5059F-pH-326-351 4/10/01 9:00 AM Page 345

horizontal sync pulse In a video signal, the pulse that synchronizes the horizontal scanning component in a television receiver with that of the camera; it also triggers horizontal retrace and blanking. Also see BACK PORCH. Compare VERTICAL SYNC PULSE.

horizontal wave See HORIZONTALLY POLARIZED WAVE.

horizontal-width control See WIDTH CONTROL, **1**, **2**.

horn A radiating device that is essentially a cylindrical or rectangular pipe, whose surface flares from a narrow entry to a wide exit. See, for example, HORN ANTENNA, HORN SPEAKER, and MEGAPHONE.

horn antenna An antenna used for transmission and reception of signals at microwave frequencies. There are several configurations; most have a square or rectangular cross section. The antenna provides a unidirectional radiation and response pattern, with the favored direction coincident with the opening of the horn. The feed line consists of a waveguide that joins the antenna at the narrowest point (throat) of the horn. This type of device is used alone in microwave transmitters known as *Gunnplexers*. The device works well in the feed systems of large dish antennas; the horn is pointed toward the center of the dish, in the opposite direction from the favored direction of the dish. See also DISH ANTENNA, GUNNPLEXER.

horn cutoff frequency The lowest frequency at which an exponential horn will function properly.

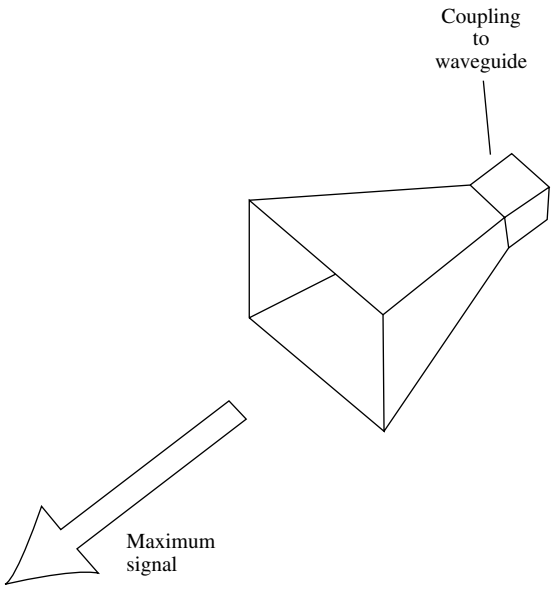

horn antenna

horn loading In a sound-transmission system, a form of propagation that makes use of a horn-shaped speaker.

horn mouth The wider (radiating) end of a horn antenna or speaker. Compare HORN THROAT.

horn radiator See HORN ANTENNA.

horn speaker A loudspeaker using a horn in conjunction with an acoustic transducer. It generally produces sound of low fidelity, and is intended for use in marginal environments, such as outdoor public-address (PA) systems.

horn throat The narrower (input) end of a horn antenna or speaker. Compare HORN MOUTH.

horsepower Abbreviation, hp. A unit of power equal to 746 watts. It is generally used to express mechanical power delivered by engines and electric motors.

horsepower-hour Abbreviation, hp-hr. A unit of energy or work represented by the equivalent of one horsepower delivered for a period of one hour; equal to 746 watt-hours.

horseshoe coil See HAIRPIN COIL and HAIRPIN COUPLING COIL.

horseshoe magnet A (usually permanent) magnet having the shape of a horseshoe or a U and a rectangular cross section.

host A programmable computer that gathers and stores the information from all of the data-entry terminals in a system.

HOT **1.** Abbreviation of HORIZONTAL OUTPUT TRANSFORMER. **2.** Abbreviation of HORIZONTAL OUTPUT TUBE.

hot **1.** Pertaining to an object from which heat energy is transferred to the environment by radiation, convection, and/or conduction. **2.** Charged to an electrical potential, either positive or negative, with respect to common ground. **3.** Pertaining to a conductor that carries a high radio-frequency (RF) current or voltage.

hot carrier In a semiconductor, a charge carrier (electron or hole) whose energy is higher than that of majority carriers normally encountered in the same material.

hot-carrier diode A semiconductor diode having a metal base that receives HOT CARRIERS from a semiconductor layer. The unit has a fast switching speed because there are virtually no minority carriers—either injected or stored.

Hotel Phonetic alphabet code word for the letter H.

hot-filament gas detector A gas detector in which the sensor is a heated filament acting as one arm of a Wheatstone bridge circuit. The bridge, previously balanced, becomes unbalanced when gas impinges upon the filament and changes its resistance.

hot junction The heated junction in a two-junction thermocouple circuit. Compare COLD JUNCTION.

hot line **1.** An energized wire, transmission line, or busbar. **2.** A private communications channel (wire or radio) kept in constant readiness for instant use between persons of high authority.

5059F-pH-326-351 4/10/01 9:00 AM Page 346

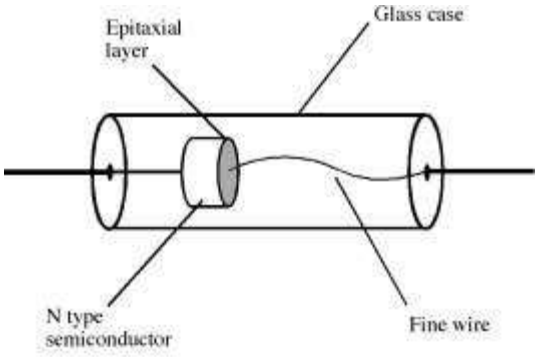

hot carrier diode

hot-pen recorder See THERMAL RECORDER.

hot plate A metal device, usually heated by means of electricity, used for the purpose of conducting certain experiments.

hot resistance The resistance of a component during its operation (i.e., after it has been heated by ambient temperature or internal power dissipation). Compare COLD RESISTANCE.

hot spark A brilliant flash seen when a capacitor discharges through a spark gap in a vacuum.

hot spot **1.** In a circuit or component, an area whose temperature is ordinarily higher than that of the surrounding area. **2.** A local current or voltage maximum on an antenna or transmission line. **3.** In communications operations, a geographic location in which reception is markedly better than in other nearby places or from which the transmitted signal appears to be stronger.

hot-strip ammeter A current meter similar to the hot-wire meter, except that it has a heated metallic strip instead of a heated wire.

hot-stylus recorder See THERMAL RECORDER.

hot-tip writing The use of a heated-tip stylus in graphic recording. Also see THERMAL RECORDER.

hot-wire ammeter See HOT-WIRE METER.

hot-wire anemometer An electrical anemometer whose indication is based on the cooling effect of the wind on a heated filament.

hot-wire flowmeter An instrument for determining the rate of flow of a gas in a pipe or other channel. The circuit is similar to that of the gas detector and hot-wire anemometer.

hot-wire gasmeter See GAS DETECTOR.

hot-wire instrument See HOT-WIRE METER.

hot-wire meter A meter in which current heats a wire, stretching it so that it moves a pointer across a scale over a distance proportional to the magnitude of the current.

hot-wire microphone A microphone in which sound waves vary the temperature of a heated wire and, accordingly, its electrical resistance.

hot-wire relay A time-delay relay in which actuating current heats a wire, causing it to expand, eventually opening or closing the contacts. Also see DELAY RELAY.

hot-wire sensor See HEATED-WIRE SENSOR.

hot-wire transducer See HOT-WIRE MICROPHONE.

hour Abbreviation, h; (sometimes, hr). A unit of time measure equal to 60 minutes or 3600 seconds. Compare MINUTE, **1** and SECOND, **1**. Also see TIME.

housekeeping In digital-computer operations, the part of a program that attends to chores (e.g., setting variables to zero), rather than being involved in making computations for a solution.

howl A discordant sound produced in headphones or a loudspeaker, usually as a result of acoustic or electrical feedback.

howler **1.** An audio-frequency alarm device. **2.** A sound-emitting test device (see GROWLER, **1**, **2**).

howl repeater A form of electric feedback in which a hum or howl occurs because of oscillation. The term is used to describe an oscillating conduction in a wire-communications-system repeater.

hp Abbreviation of HORSEPOWER.

h-p Abbreviation of HIGH PRESSURE.

H pad See H NETWORK.

***h* parameters** Parameters of the four-terminal network equivalent of a transistor. They are *hybrid parameters* (thus, *h*) because of their appearance in mesh and nodal equations. The basic *h* parameters are h_{11}, input resistance with output short-circuited; h_{12}, reverse voltage ratio with input open-circuited; h_{21}, forward current gain with output short-circuited; and h_{22}, output conductance with input open-circuited.

h particle A positive hydrogen ion or proton obtained by bombarding a hydrogen atom with alpha particles or high-velocity positive ions.

HPF Abbreviation of *highest probable frequency.*

hp-hr Abbreviation of HORSEPOWER-HOUR.

HPI Abbreviation of HEIGHT-POSITION INDICATOR.

H plane The plane of the magnetic field of an antenna, or the magnetic component of an electromagnetic field. Compare E PLANE.

H-plane bend In a waveguide, a smooth change in the direction of the axis perpendicular to the direction of polarization.

H-plane tee junction A waveguide tee junction, whose structure changes in the magnetic-field plane. Also see WAVEGUIDE JUNCTION and WAVEGUIDE TEE.

hr Abbreviation of HOUR. (Also, h.)

H scan A radar display in which the target is represented by two close blips, approximating a line, whose shape is proportional to the sine of the target's angle of elevation.

H scope See H SCAN.

5059F-pH-326-351 4/10/01 9:00 AM Page 347

HSM Abbreviation of *high-speed memory.*

HTL Abbreviation of HIGH-THRESHOLD LOGIC.

hub The hole in the center of a magnetic tape reel.

hue The quality of having a particular visible color; an attribute that depends on the wavelength(s) of light emitted or reflected. Thus, electromagnetic energy at a wavelength of 700 nanometers (nm) has a red hue; energy at a wavelength of 400 nm has a violet hue. Compare SATURATION, **2**.

hue control Also called *tint control.* In a color television receiver, a control that allows adjustment of the color wavelength, but does not affect the saturation (intensity).

hum **1.** Alternating current having a frequency of 60 Hz. **2.** Residual ripple in the output of a power supply, having a frequency of 60 Hz or 120 Hz, depending on the type of rectifier circuit used. **3.** An electromagnetic field of long wavelength, usually originating from utility lines and having a primary frequency of 60 Hz. **4.** The effects of low-frequency electromagnetic fields or currents, such as moving horizontal bars on a television screen. **5.** An acoustic disturbance of long wavelength (low pitch).

human engineering **1.** Also called *user-friendliness.* The extent to which an electronic or electromechanical device or system is easy to operate. **2.** The branch of engineering devoted to interfacing human beings with the machines and instruments they operate. Both a science and an art, the discipline is concerned with the safest and most efficient design, arrangement, and operation of equipment.

human interface The interface between a sophisticated electronic device and a human operator.

human-made interference Also called *artificial interference.* Electromagnetic interference to radio and television receiving systems or to data terminals, originating from artificial sources (such as radio transmitters, certain electrical appliances, and internal-combustion engines). Of the numerous different forms, some affect only a narrow band of frequencies or set of frequencies, and others affect a wide band of frequencies.

humanoid robot A robot that bears structural resemblance to a human being (e.g., has arms, a head, and perhaps legs). In its most advanced form, such a robot is an ANDROID.

hum-balance potentiometer A potentiometer connected across an alternating-current power supply, with its slider grounded. At a certain setting, hum interference is nulled.

hum bars See HORIZONTAL HUM BARS.

hum bucking The reduction of hum interference by introducing an alternating-current voltage of the same frequency and amplitude as the hum, but opposite in phase.

hum-bucking coil An auxiliary coil used in conjunction with the field and voice coils of an electrodynamic speaker. Reduces hum interference via HUM BUCKING.

hum field The magnetic field surrounding a conductor carrying hum-frequency alternating current.

humidity The amount of moisture in the air. Also see ABSOLUTE HUMIDITY and RELATIVE HUMIDITY.

humidity meter See ELECTRIC HYGROMETER and ELECTRONIC HYGROMETER.

humidity sensor A pickup whose resistance or capacitance varies proportionally with ambient humidity.

hum interference Electrical interference resulting from HUM in any of its various electrical forms (see HUM, **1–4**).

hum loop A ground loop that results in undesired hum in the output of an amplifier.

hummer A nonelectronic audio oscillator similar to the fork oscillator, but using a thick, metal reed, instead of a tuning fork. A carbon microphone button attached to the reed provides the feedback path necessary for sustained oscillation.

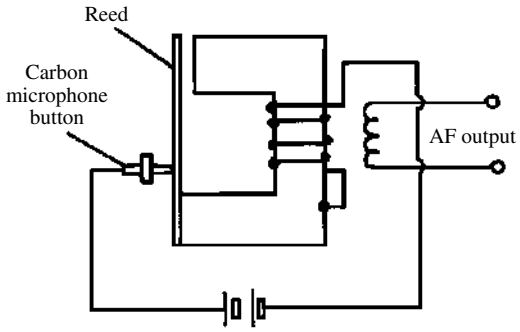

hummer

hum modulation Undesirable modulation of a radio signal or audio amplifier output signal by HUM interference.

hump **1.** Either the positive or the negative half-cycle of a sine wave; that is, either the portion from 0 degrees to 180 degrees, or the portion from 180 degrees to 360 degrees. **2.** A curve whose graph is a multiple of the sine function, and whose domain is restricted to a half-cycle (0 to 180 degrees or 180 to 360 degrees). See, for example, DOUBLE-HUMP RESONANCE CURVE and DOUBLE-HUMP WAVE.

hunting An undesirable condition in which an electrical or electromechanical system oscillates back and forth, relative to some mean mode of operation ("hunts" for the mode), sometimes eventually settling down at the mode. It can occur in a servo system because of overcompensation, lack of hysteresis, or both.

Huygens' principle The observation that an advancing wave is the resultant of secondary waves

5059F-pH-326-351 4/10/01 9:00 AM Page 348

that arise from points in the medium that have already been passed.

HV Abbreviation of HIGH VOLTAGE.

H vector A vector representing the magnetic field of an electromagnetic wave. Compare E VECTOR.

hW Abbreviation of HECTOWATT.

H-wave mode In a waveguide, a mode of transmission in which the electric lines of flux are at right angles to the direction of the waveguide. Also called *transverse-electric (TE) mode*.

hy Occasional abbreviation of HENRY. The SI abbreviation and symbol, H, is preferred.

hybrid Descriptive of a device that is an offspring of other devices or a product of dissimilar technologies (but using elements of each). See, for example, HYBRID JUNCTION and HYBRID COIL.

hybrid active circuit An active circuit (such as an amplifier, oscillator, or switch) using a combination of two dissimilar active devices (e.g., transistors and vacuum tubes).

hybrid coil A special type of bridging transformer used in wire telephony to prevent self-oscillation in a repeater amplifier that operates in both directions.

hybrid computer A computer system incorporating more than one major computer technology. Examples: analog/digital and digital/neural-network.

hybrid electromagnetic wave Abbreviation, HEM wave. An electromagnetic wave whose electric-field and magnetic-field vectors are both in the direction of propagation.

hybrid IC See HYBRID INTEGRATED CIRCUIT.

hybrid integrated circuit Abbreviation, HIC. An integrated circuit embodying both integrated and microminiature discrete components (i.e., one combining both monolithic and thin-film construction).

hybrid junction **1.** See MAGIC TEE. **2.** A four-terminal device, such as a resistor circuit, special transformer, or waveguide assembly, in which a signal applied to one pair of terminals divides and appears at only the two adjacent terminals.

hybrid microcircuit A microcircuit containing diffused or thin-film elements interconnected with separate chip elements.

hybrid parameters See H PARAMETERS.

hybrid ring A hybrid waveguide junction (see HYBRID JUNCTION, **2**) consisting essentially of a reentrant line with four side arms. Used as an equal power divider.

hybrid-tee See HYBRID JUNCTION, **1**.

hybrid thin-film circuit A microcircuit in which semiconductor devices and discrete components are attached to passive components and conductors that have been electrodeposited on a substrate.

hybrid transformer See HYBRID COIL.

hydroacoustic Pertaining to the sound of fluids, especially water, under pressure.

hydroacoustic transducer A transducer that converts energy from the high-pressure flow of a fluid into acoustic energy.

hydrodynamic pressure The pressure of a fluid in motion. Compare HYDROSTATIC PRESSURE.

hydroelectric Pertaining to the production of electricity by water power, as by a generator turned by water turbines.

hydroelectric machine A device for generating electricity from high-pressure steam escaping from a series of jets.

hydroelectric power See WATER POWER.

hydrogen Symbol, H. A gaseous element. Atomic number, **1**. Atomic weight, 1.00794. Used in making semiconductor materials, it is the lightest and most abundant element in the universe. Compare DEUTERIUM and TRITIUM.

hydrogen atmosphere The nonoxidizing atmosphere in which semiconductor materials are melted and processed, and in which semiconductor crystals are grown. Occasionally, helium is used instead of hydrogen.

hydrogen atom A single atom of the element hydrogen, consisting of one electron and one proton.

hydrogen-ion concentration See pH.

hydrogen lamp A glow-discharge lamp that produces light by means of the ionization of rarefied hydrogen gas. Visible light is emitted at discrete wavelengths.

hydrokinetic Pertaining to fluids in motion or the forces behind such motion.

hydrolysis The process whereby chemical substances become ionized in water solution, producing electrolytes.

hydromagnetics See MAGNETOHYDRODYNAMICS.

hydromagnetic wave In a fluid, a wave in which the energy is propagated via magnetic and dynamic modes.

hydrometer An instrument for measuring the specific gravity of liquids.

hydrophone An underwater sound-to-electricity transducer (microphone).

hydropower See WATER POWER.

hydrostatic pressure The pressure of a fluid at rest. Compare HYDRODYNAMIC PRESSURE.

hygristor A resistor, the resistance of which depends on humidity. A common application is in the measurement of relative atmospheric humidity.

hygrogram A graphic rendition of atmospheric humidity versus time, made by a HYGROGRAPH.

hygrograph A device that produces a graphic recording of atmospheric humidity as a function of time. Consists essentially of a HYGROMETER connected to a permanent data-storage device, such as a computer or pen recorder.

hygrometer An instrument for measuring humidity. Also see ELECTRIC HYGROMETER, ELECTRONIC HYGROMETER, and HAIR HYGROMETER.

5059F-pH-326-351 4/10/01 9:00 AM Page 349

hygroscopic material A material that absorbs moisture from the air, but not enough to get wet (e.g., lime and silk). Compare DELIQUESCENT MATERIAL.

hygrostat A humidity-sensitive relay or switching circuit.

hygrothermograph A graphic recorder indicating humidity and temperature on the same chart, both as functions of time.

hyperacoustical zone In the upper atmosphere, a region in which the distance between air molecules is comparable to the wavelengths of audible sound. As the altitude increases within this zone, the upper-frequency limit of effective sound propagation decreases. At altitudes above this zone, no audible sound can be propagated.

hyperbola A conic-section curve satisfying the equation:

$$(x - x_0)^2/a^2 - (y - y_0)^2/b^2 = 1$$

where x and y are the independent and dependent variables, x_0 and y_0 are the coordinates of the center, a is half the length of the major axis, and b is half the length of the minor axis.

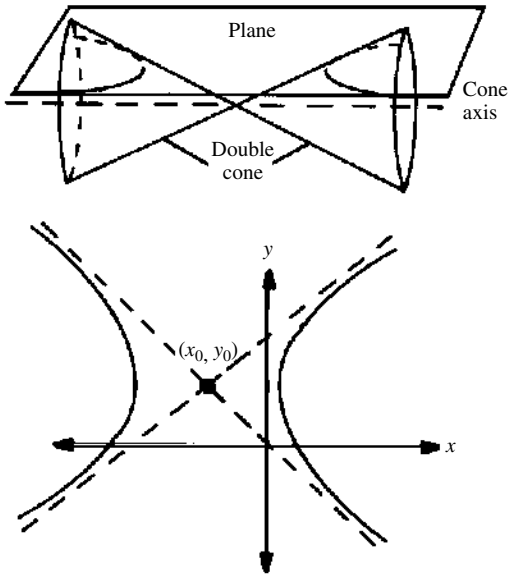

hyperbola

hyperbolic angle An angle subtended by a sector of a hyperbola in a manner analogous to that in which a circular angle is subtended by an arc of a circle.

hyperbolic-cosine horn See CATENOIDAL HORN.

hyperbolic error **1.** In an interferometer, a miscalculation in the direction of arrival of a signal. The signal from one antenna in the system can be assumed to be in phase with the signal from another antenna, when actually the two components differ by an integral number of whole wavelengths. **2.** The angular error, in degrees, minutes, or seconds of arc, resulting from a miscalculation of phase in an interferometer.

hyperbolic face contour See HYPERBOLIC GRIND.

hyperbolic functions The nonperiodic functions of a hyperbolic angle. Hyperbolic functions are related to the hyperbola in the same manner that common trigonometric functions are related to the circle. Hyperbolic functions are useful in calculations involving traveling waves on transmission lines, attenuator design, and wave-filter design.

hyperbolic grind The shape (approximately hyperbolic) to which the face of a magnetic recording head is ground. It provides optimum contact with the tape and ensures good high-frequency response.

hyperbolic horn A horn antenna whose cross-sectional area is a hyperbolic function of the distance along the axis.

hyperbolic logarithm See NAPIERIAN LOGARITHM.

hyperbolic navigation A radionavigation system in which the operator of an aircraft or boat determines position by comparison of two received signals. The two transmitters radiate signals from known positions and with known timing characteristics. The time delay from each transmitter is determined, resulting in two hyperbolic curves on a map. The point of intersection of the curves is the location of the aircraft or ship.

hyperbolic radian A unit of measure derived from a hyperbolic angle. A hyperbolic radian is the hyperbolic angle that encloses an area of 0.5 when the distance along the x-axis to the hyperbola is unity. Also see HYPERBOLIC ANGLE. Compare CIRCULAR RADIAN.

hyperbolic trigonometry The branch of mathematics dealing with the theory and application of hyperbolic angles and their functions.

hypercardioid microphone A unidirectional microphone with exceptional sensitivity in front, and minimal responsiveness from the sides and rear.

hypercardioid pattern A directional CARDIOID PATTERN with accentuated responsiveness or emission in the favored direction (front), and greatly suppressed responsiveness or emission in other directions (sides and rear).

hyperfocal distance The shortest distance to which a lens can be focused without degrading definition at infinity.

hyperfrequency waves See MICROWAVES.

hypernik See HIPERNICK.

hyperon Any one of various particles having a mass greater than that of a neutron or proton.

hyperpolarization The production of an increased voltage across a biological membrane.

5059F-pH-326-351 4/10/01 9:00 AM Page 350

hypersonic Pertaining to speeds of at least five times that of sound. In air at normal atmospheric pressure, such speeds are more than approximately 1700 meters, or 5600 feet, per second.

hypersonic speed Any speed greater than five times the speed of sound in a given medium.

hypersyn motor A high-efficiency, high-power-factor synchronous motor combining the advantages of the *direct-current-excited synchronous motor* (stiffness), the *hysteresis motor* (synchronizing torque), and the *induction motor* (high starting torque).

hypervelocity Velocity in excess of 3 kilometers per second.

hypotenuse The side of a right triangle opposite to the right angle.

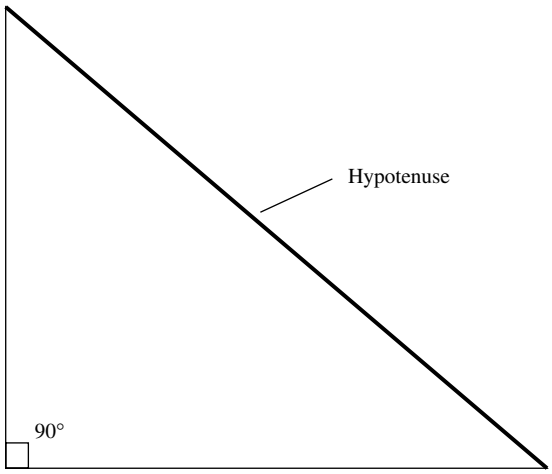

Hypotenuse

hypothesis An idea, concept, or system that seems true or workable, but must be subjected to logical analysis and/or practical testing to prove its validity.

hypsometer An altimeter in which a thermistor (connected to a battery and current meter) is immersed in a boiling liquid. Because the liquid's boiling point is proportional to altitude, it affects the resistance of the thermistor and, hence, the deflection of the meter.

hysteresigram The hysteresis-curve record produced by a HYSTERESIGRAPH.

hysteresigraph A graphic recorder that displays or records the hysteresis curve for a material. Also see HYSTERESISCOPE.

hysteresimeter See HYSTERESIS METER.

hysteresis **1.** The tendency of a magnetic material to saturate and retain some of its magnetism after the alternating magnetic field to which it is subjected reverses polarity, thus causing magnetization to lag behind the magnetizing force. **2.** A similar electrostatic action in a ferroelectric dielectric material. **3.** In a servo system, the condition in which a variable quantity lags the effect or stimulus that causes it to change. The plot for this is a double-line HYSTERESIS CURVE.

hysteresis brake A brake whose retarding action comes from hysteresis in a permanent-magnet motor.

hysteresis clutch A magnetic clutch whose output torque (for synchronous drive or continuous slip) comes from hysteresis in a permanent-magnet motor.

hysteresis coefficient In a sample of iron whose volume is one cubic centimeter, the energy in ergs dissipated during one cycle of magnetization. Also called *coefficient of hysteresis.*

hysteresiscope An oscilloscope that is specially designed to display the hysteresis curve of a material. Compare HYSTERESIGRAPH.

hysteresis curve A response curve depicting hysteresis in a magnetic material, a dielectric, or a servo system. A graph of the extent to which a variable quantity lags the effect or stimulus that causes it to change (e.g., a curve showing the effect of response delay in a thermostatically controlled heating/cooling system).

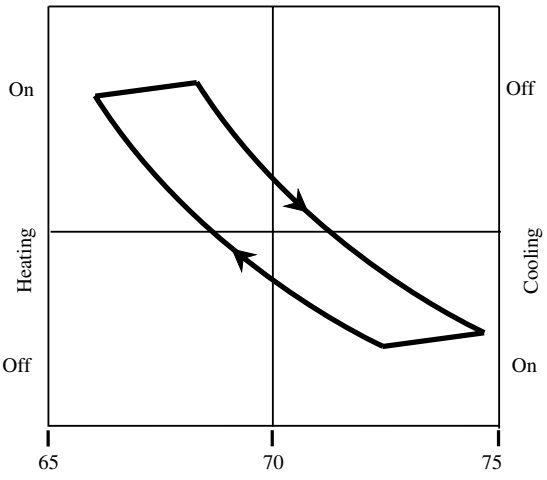

hysteresis curve

hysteresis cycle A complete hysteresis curve.

hysteresis distortion Signal distortion in iron-core components, such as coupling transformers, resulting from hysteresis in the iron.

hysteresis error In a meter, a difference in indications for increasing and decreasing current, an effect caused by hysteresis in iron meter parts.

5059F-pH-326-351 4/10/01 9:00 AM Page 351

hysteresis heater An induction heater in which heating results from hysteresis loss in the load.

hysteresis loop See HYSTERESIS CURVE.

hysteresis loss Power loss caused by hysteresis in a magnetic material exposed to an alternating magnetic field, or in a dielectric material exposed to an alternating electric field. It is characterized by the generation of heat.

hysteresis meter An instrument that determines the hysteresis loss in a ferromagnetic material in terms of the torque produced when the material is rotated in a magnetic field, or vice versa.

hysteresis motor A synchronous motor that does not require direct-current excitation, and does not have salient poles. It is started by means of hysteresis losses that the rotating magnetic field causes in the secondary.

hysteretic constant For a ferromagnetic material, hysteresis loss in ergs per cubic centimeter of material per cycle of magnetization.

hysteretic loss See HYSTERESIS LOSS.

hystoroscope A device used to determine the magnetic characteristics of a material.

Hz Abbreviation of HERTZ.

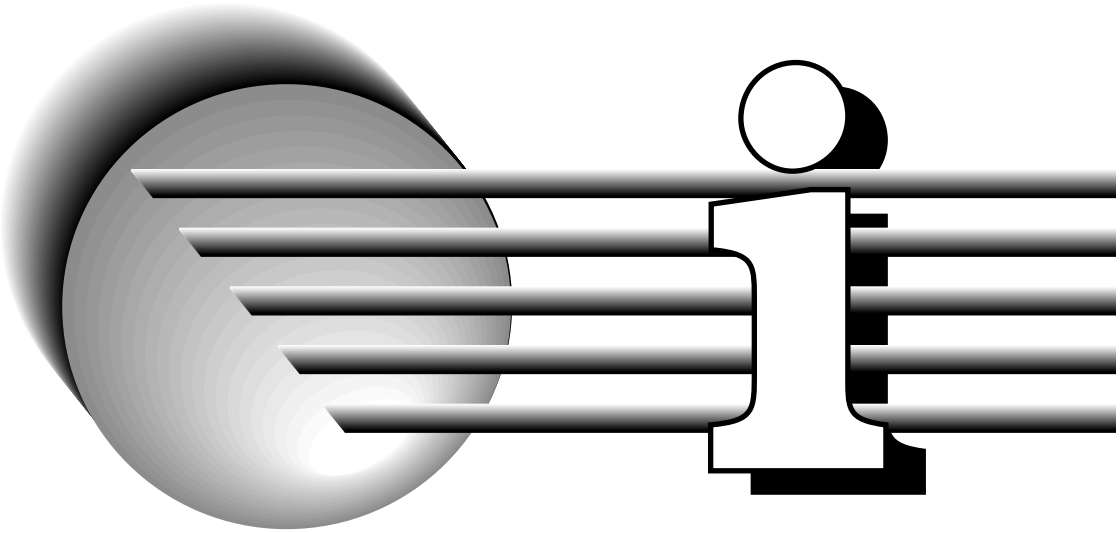

I **1.** Symbol for CURRENT. **2.** Symbol for INTRINSIC SEMICONDUCTOR. **3.** Symbol for LUMINOUS INTENSITY. **4.** Symbol for IODINE.

i **1.** Symbol for the unit imaginary number, the square root of -1. (Also, *j*.) **2.** Subscript for INSTANTANEOUS VALUE. **3.** Symbol for INTRINSIC SEMICONDUCTOR. **4.** Symbol for ANGLE OF INCIDENCE. **5.** Symbol for INSTANTANEOUS CURRENT. (Also, I_i.) **6.** Symbol for a unit vector parallel to the x-axis. **7.** Symbol for INCIDENT RAY.

I_{ac} Symbol for the ac component of a COMPOSITE CURRENT.

I_{AF} Symbol for AUDIO-FREQUENCY CURRENT.

IAGC Abbreviation of INSTANTANEOUS AUTOMATIC GAIN CONTROL.

IAVC Abbreviation of INSTANTANEOUS AUTOMATIC VOLUME CONTROL.

I_B **1.** Symbol for *plate power-supply current*. **2.** Occasional symbol for *plate current* (usually, I_P).

IBM Abbreviation for *International Business Machines* Corporation.

IC **1.** Abbreviation of INTEGRATED CIRCUIT. **2.** Abbreviation of INTERNAL CONNECTION.

I_C **1.** Symbol for transistor COLLECTOR CURRENT. **2.** Occasional symbol for *grid current* (usually, I_G).

ICAD Abbreviation of *integrated control and display.*

ICAS Abbreviation of INTERMITTENT COMMERCIAL AND AMATEUR SERVICE.

I_{CBO} Symbol for the static reverse collector (leakage) current in a common-base connected transistor with an open-circuited emitter.

ICBS Abbreviation of *interconnected business system.*

I_{CEO} Symbol for the static reverse collector (leakage) current in a common-emitter-connected transistor with an open-circuited base.

ice loading **1.** In an antenna, power-line system, or other structure, the additional stress caused by accumulation of ice. **2.** The weight or thickness of ice a structure can safely withstand.

ice-removal circuit A high-voltage, low-frequency power supply used to heat certain antennas to melt ice that accumulates on them.

ICET Abbreviation of *Institute for the Certification of Engineering Technicians* (National Society of Professional Engineers).

ICME Abbreviation of *International Conference on Medical Electronics.*

I_{co} Symbol for the collector cutoff current (static leakage current) of a bipolar transistor (see CUTOFF CURRENT).

icon In a graphical computer interface, a symbol that aids the user in recognizing a selection that can be made.

iconoscope A camera tube in which an electron beam scans a photomosaic on which the image is focused. The light-sensitive droplets of the mosaic form tiny capacitors with the insulated, metallic backplate of the mosaic, each capacitor becoming charged by the light of the picture. As the electron beam scans the mosaic, each capacitor discharges as the beam strikes it, delivering an output pulse proportional to the light intensity at that spot in the picture.

IC tester An instrument for checking the operation of an integrated circuit.

ICW Abbreviation of INTERRUPTED CONTINUOUS WAVE.

Copyright 2001 The McGraw-Hill Companies, Inc. Click Here for Terms of Use

5059F-pI_352-384 4/10/01 9:03 AM Page 353

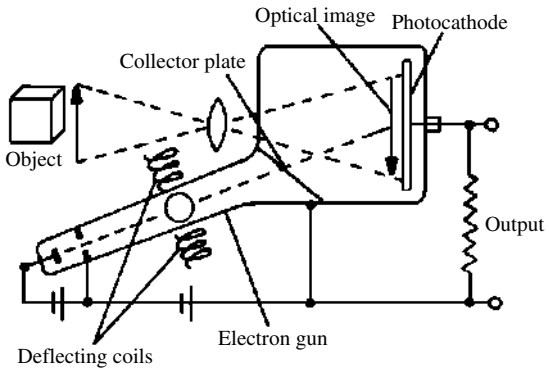

iconoscope

ID Abbreviation of INSIDE DIAMETER.

IDA Abbreviation of *integrodifferential analyzer.*

I_{dc} Symbol for the dc component of a COMPOSITE CURRENT.

ideal Pertaining to a circuit, device, material, or manner of operation that is assumed to conform to the theoretical best-case example; it is not usually realized in real life. Thus, an ideal reactance has no inherent resistance.

ideal capacitor A capacitor having zero dielectric loss and a constant value of capacitance at all alternating-current frequencies.

ideal component A theoretical component that is assumed to be 100-percent efficient and to have no extraneous properties. Compare PRACTICAL COMPONENT.

ideal crystal A piezoelectric crystal that acts as a theoretically perfect tuned circuit, that is, an ideal capacitor and inductor.

ideal inductor An inductor having zero loss and a constant value of inductance at all alternating-current frequencies.

I demodulator In a color-television receiver circuit, a demodulator that receives the chrominance and 3.58-MHz oscillator signals and delivers a video output corresponding to color in the picture.

identical vectors Equal vectors that have the same initial point or point of application.

identification **1.** In radar operations, the (often automatic) determination of the target's identity. See, for example, IDENTIFICATION, FRIEND OR FOE. **2.** In digital computer operations, a symbol or set of symbols within a label identifying a unit of data or its location.

identification beacon **1.** A beacon used for the determination of a particular geographic location. **2.** An automatically transmitted station-identification signal or code, usually superimposed on the regular transmission in the form of a subcarrier or subaudible signal.

identification division The division (one of four) in a COBOL program that describes and identifies the program being compiled.

identification, friend or foe Abbreviation, IFF. A technique in which a radar station transmits an interrogating signal and the station questioned replies automatically with a suitable pulse or other signal if it is aboard a friendly aircraft or vessel. If it is aboard an enemy vehicle, the station gives no reply or sends an unsatisfactory one.

identifier A data file identification label in an input/output device, or a label that identifies a specific storage location.

identity element A logic element that, upon receipt of two input signals, provides an output that is logic 1 (high) only if the input signals are both logic 1 (high) or logic 0 (low).

idiochromatic Possessing the photoelectric properties of a true crystal.

I display See I SCAN.

idle channel noise A measurement of wideband noise. The total energy at an output of an integrated circuit or other communications stage with that output grounded (idle).

idle character A digital character that conveys no information, but helps maintain synchronization between the transmitter and receiver. Sometimes called a *blank.*

idler wheel In a phonograph or magnetic tape recorder, an auxiliary, rubber-coated wheel that transfers rotary motion from the motor pulley to the platter or the rim of the capstan flywheel.

idle time The period during which data processing equipment, although operable, is not in use.

idling Standby equipment operation, as when vacuum-tube filaments in a radio-frequency power amplifier are kept hot—even when the amplifier is not actually being used to transmit a signal.

idling current The current flowing in a device during a standby period, as opposed to operating current. Also called STANDBY CURRENT.

idling frequency In a parametric amplifier, the difference between the signal frequency and pump frequency.

idling power See STANDBY POWER.

idling voltage The voltage required by or measured in a device that is in standby mode.

$I_{D(off)}$ Symbol for drain cutoff current in a field-effect transistor.

IDOT Abbreviation of *instrumentation online transcriber.*

IDP **1.** Abbreviation of INDUSTRIAL DATA PROCESSING. **2.** Abbreviation of INTEGRATED DATA PROCESSING. **3.** Abbreviation of INTERMODULATION-DISTORTION PERCENTAGE.

I_{DSS} Symbol for DRAIN CURRENT AT ZERO GATE VOLTAGE in a field-effect transistor.

I_E Symbol for EMITTER CURRENT.

IEC Abbreviation of *integrated electronic component.*

5059F-pI_352-384 4/10/01 9:03 AM Page 354

IEE Abbreviation of *Institution of Electrical Engineers* (British).

IEEE Abbreviation of *Institute of Electrical and Electronics Engineers.*

IES Abbreviation of *Illuminating Engineering Society.*

IF Abbreviation of INTERMEDIATE FREQUENCY.

IF amplifier See INTERMEDIATE-FREQUENCY AMPLIFIER.

I_{FB} In an integrated circuit, current limit feedback or feedback current.

IF channel See INTERMEDIATE-FREQUENCY CHANNEL.

IF converter The converter (first detector-oscillator) section of a superheterodyne radio receiver.

IFF Abbreviation of IDENTIFICATION, FRIEND OR FOE.

IF gain **1.** The amplification provided by the intermediate-frequency (IF) channel of a superheterodyne receiver, usually specified in decibels. **2.** A control that allows adjustment of the amplification in the IF channel of a superheterodyne radio receiver.

IF interference See INTERMEDIATE-FREQUENCY INTERFERENCE.

IFIPS Abbreviation of *International Federation of Information Processing Societies.*

IF selectivity See INTERMEDIATE-FREQUENCY SELECTIVITY.

IF strip A (sometimes removable) circuit section containing a complete intermediate-frequency channel.

IF/THEN/ELSE In computer systems and artificial intelligence, a two-way choice that is made during the execution of a program. For example, in finding the absolute value of a number, the logic proceeds as follows: "IF $x < 0$, THEN multiply x by -1; otherwise (ELSE) leave it alone."

IF transformer See INTERMEDIATE-FREQUENCY TRANSFORMER.

I_G Symbol for GATE CURRENT.

I_G Symbol for GRID CURRENT.

IGFET Abbreviation of INSULATED-GATE FIELD-EFFECT TRANSISTOR.

ignition coil A small open-core transformer having a high step-up turns ratio for converting 6- or 12-volt battery potential to the high voltage needed in an automotive ignition system.

ignition interference Electrical noise generated by the ignition system of an internal combustion engine.

ignition potential **1.** The minimum voltage needed to cause electrical discharge in an internal combustion engine. **2.** See BREAKDOWN VOLTAGE, **1**, **2**.

ignition reserve The extra voltage provided by the starter, as compared with the voltage actually needed for ignition of an internal-combustion engine.

ignition system An electrical or electronic system that supplies the high voltage in an automotive engine. See, for example, CAPACITOR-DISCHARGE IGNITION SYSTEM.

ignition voltage See IGNITION POTENTIAL.

ignitron A form of rectifier tube that contains ionized mercury. It is used with some extremely high-voltage power supplies.

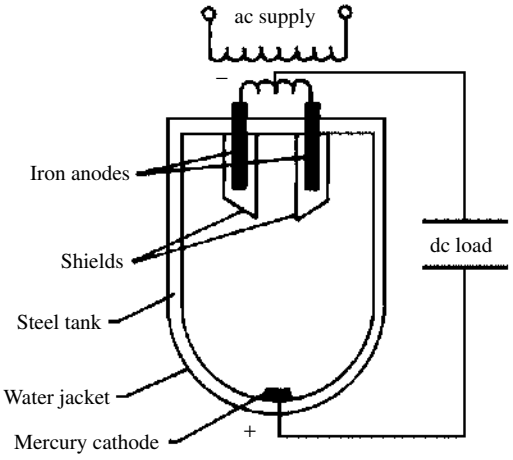

ignitron

ignore character **1.** A character used as a signal to inhibit an action. **2.** A digital character that is ignored by the system.

I_{GSS} Symbol for GATE REVERSE CURRENT in a field-effect transistor.

IGY Abbreviation for INTERNATIONAL GEOPHYSICAL YEAR.

I_H **1.** Symbol for HOLD CURRENT. **2.** Symbol for HOLDING CURRENT.

IHF Abbreviation of INHIBIT FLIP-FLOP.

IHFM Abbreviation for *Institute of High Fidelity Manufacturers.*

ihp Abbreviation of INDICATED HORSEPOWER.

ihp-hr Abbreviation of INDICATED HORSEPOWER-HOURS.

I_i **1.** Symbol for INPUT CURRENT. **2.** Symbol for INSTANTANEOUS CURRENT (also, i).

I_K Symbol for CATHODE CURRENT.

I_L Symbol for current in an inductor.

I^2L Abbreviation of INTEGRATED INJECTION LOGIC. (Also IIL.)

illegal character **1.** A character or bit group that is, according to some standard, invalid. **2.** A bit group that represents a symbol in a character set.

illuminance The amount of luminous flux received per unit surface area, measured in lux (lumens per square meter).

illuminant-C In color television, the reference white that closely resembles average daylight.

illuminated pushbutton See LIGHTED PUSHBUTTON.

5059F-pI_352-384 4/10/01 9:03 AM Page 355

illuminated switch See LIGHTED SWITCH.

illumination **1.** Visible light. **2.** The condition of being irradiated by visible light. **3.** The intensity of visible light irradiating an object or region.

illumination control A photoelectric circuit that automatically regulates electric lights, according to the amount of daylight.

illuminometer A device for measuring the intensity of visible light, or, less often, infrared or ultraviolet. In its simplest form, the meter consists of a photovoltaic cell, a potentiometer for adjusting the sensitivity, and a microammeter. More sophisticated devices include direct-current amplification.

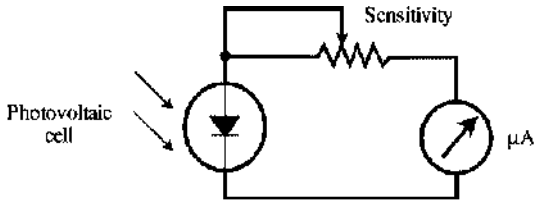

illuminometer

ILS Abbreviation of INSTRUMENT LANDING SYSTEM.

IM Abbreviation of INTERMODULATION.

I_m **1.** Abbreviation of *maximum current.* (Also, I_{max}). **2.** Abbreviation of *meter current.*

image **1.** In a superheterodyne circuit, a spurious response whose frequency differs from that of the desired signal by twice the intermediate frequency. **2.** A picture on the screen of a television receiver or computer display. **3.** A pattern on the screen of an oscilloscope tube. **4.** A picture on the mosaic of a television camera tube. **5.** A duplicate of a computer storage area that is in another part of storage or on another medium.

image admittance The reciprocal of IMAGE IMPEDANCE.

image antenna An imaginary "mirror" antenna below the effective radio-frequency (RF) ground surface, at a depth equal to the height of the true radiating antenna above effective RF ground.

image attenuation constant The real-number part of the IMAGE TRANSFER CONSTANT. Also see IMAGE PHASE CONSTANT.

image compression Any of various methods by which the number of bytes in a digital image can be reduced, without significant degradation of image quality. The two most common methods are *JPEG (Joint Photographic Experts Group) image compression* and *fractal image compression.* Other schemes include *MPEG (Moving Picture Experts Group) image compression* and *Indeo*, developed by Intel Corporation. Fractal image compression can provide a compression factor of as much as 100:1 without significant degradation of image quality.

image converter **1.** A device that changes an invisible image into a visible image. Examples include the *snooperscope*, an infrared-to-visible converter, and photographic apparatus for infrared, ultraviolet, and X-ray wavelengths. **2.** A tube that operates as an image converter.

image dissector See DISSECTOR TUBE.

image effect The effect of reflection of electromagnetic waves from the ground. An IMAGE ANTENNA appears to radiate from a point beneath the effective RF ground plane. The depth of the image antenna below the effective RF ground plane is equal to the height of the actual antenna above the effective RF ground plane.

image frequency The frequency of the image response in a superheterodyne radio receiver. See IMAGE, **1**.

image impedance The property of a network in which the load impedance is "seen," looking into the output terminals with the generator connected to the opposite end, and the generator impedance is "seen," looking into the input terminals with a load connected to the opposite end.

image intensification An increase of the brightness of the display on a cathode-ray tube.

image intensifier A device that increases the brightness of the spot produced when a beam of electrons or X rays hits a fluorescent screen.

image interference A type of interference that can occur in superheterodyne circuits. It occurs when there is a sufficiently strong signal on the IMAGE FREQUENCY.

image orthicon See ORTHICON.

image phase constant The imaginary-number part of the IMAGE TRANSFER CONSTANT. Also see IMAGE ATTENUATION CONSTANT.

image potential The potential energy of a charged particle at a given distance from a metal surface. The metal surface acts in a way similar to a mirror; a reflected image of the object, having equal charge but opposite polarity, is formed on the other side of the surface.

image ratio See SIGNAL-TO-IMAGE RATIO.

image rejection In a superheterodyne radio receiver, the suppression or elimination of IMAGE INTERFERENCE by means of a selective circuit, such as a radio-frequency preamplifier.

image response In a superheterodyne receiver, an undesired response to signals removed from the desired frequency by twice the intermediate frequency.

image transfer constant A number depicting the transfer of power by an impedance network. It has the same value, regardless of the direction of transmission through the network. Also see IMAGE ATTENUATION CONSTANT and IMAGE PHASE CONSTANT.

5059F-pI_352-384 4/10/01 9:03 AM Page 356

imaginary axis In a vector diagram of complex impedance, the axis of the imaginary-number component (*jX*).

imaginary number A real-number multiple of the positive square root of -1. Engineers depict the positive square root of -1 by the lowercase letter *j*; mathematicians use the lowercase letter *i*. Engineers write imaginary numbers in the form *jX*, and mathematicians write *Xi*, where *X* is a real number.

imaginary-number component The imaginary-number part of a COMPLEX NUMBER.

I_{max} Abbreviation of *maximum current.*

IM distortion meter INTERMODULATION METER.

IM distortion percentage See INTERMODULATION-DISTORTION PERCENTAGE.

I_{min} Abbreviation of *minimum current.*

imitation The transmission of false signals for purposes of deception. For example, during wartime, the signals from an enemy station might be recorded and retransmitted.

immediate access **1.** The ability of a computer to store and retrieve data in a minimal amount of time. **2.** Computer storage that can be accessed in a minimal amount of time.

immediate address An instruction address that is used as data by that instruction.

IM meter See INTERMODULATION METER.

immitance Impedance or admittance; a contraction of IMPEDANCE and ADMITTANCE. Example: a *negative-immitance circuit.*

immortal knowledge Knowledge that can be kept indefinitely in the form of detailed computer data files. Some scientists and sociologists believe that this will eventually have a profound effect on the way that future generations view history.

impact excitation See SHOCK EXCITATION.

impact strength **1.** The ability of a component or material to withstand mechanical shock loading. **2.** The work required to fracture the material under shock loading.

IMPATT diode Acronym for *impact avalanche transit time* diode. A microwave semiconductor (silicon or gallium arsenide) diode exhibiting negative resistance resulting from the combined effects of charge-carrier transit time and impact avalanche breakdown. It is used as an oscillator or amplifier.

IMPATT oscillator A microwave oscillator that uses an IMPATT DIODE.

impedance Symbol, *Z.* Unit, ohm. The total opposition offered by a circuit or device to the flow of alternating current. It is the vector sum of RESISTANCE and REACTANCE. This is a COMPLEX NUMBER whose real-number component is resistance *R*, and whose imaginary-number component is reactance *jX*; mathematically, $Z = R + jX$.

impedance angle The angle between the resistance and impedance vectors in an IMPEDANCE TRIANGLE.

impedance arm The network branch that contains one or more impedances, as opposed to an arm that contains only resistance or (predominantly, reactance). Also called *impedance leg.*

impedance branch See IMPEDANCE ARM.

impedance bridge **1.** An alternating-current (ac) bridge (commonly operated at 1 kHz) used to measure resistance, inductance, capacitance, and resistive components associated with inductors and capacitors, from which impedance can be calculated. **2.** Sometimes, an ac half-bridge circuit in which an unknown impedance is compared with a known resistance. **3.** A radio-frequency bridge circuit whose balancing element reads impedance directly in ohms.

impedance bump A discontinuity in the characteristic impedance of a radio-frequency transmission line. It is often caused by the use of improper splicing techniques.

impedance coil See CHOKE COIL.

impedance converter See IMPEDANCE TRANSFORMER.

impedance-coupled amplifier An amplifier using capacitor/coil combinations for interstage and output load coupling.

impedance drop In an alternating-current circuit, the complex sum of the resistance drop and reactance drop.

impedance ground A ground connection in which the impedance at the operating frequency is determined by a network of resistors, capacitors, and/or inductors.

impedance leg See IMPEDANCE ARM.

impedance magnetometer A device that is used for measuring small local variations in the intensity of the earth's magnetic field. A small change in the intensity of the magnetic field will cause a change in impedance of a nickel-iron wire having high permeability.

impedance match The condition (for maximum power transfer) when the transmitting impedance equals the receiving impedance, or when a suitable transformer is inserted between different impedances for matching purposes. Also see IMPEDANCE MATCHING.

impedance matching **1.** The adjustment or modification of two impedances so that they are identical, that is, the two resistive components are equal, and the two reactive components are equal. **2.** The insertion of a suitable transformer or network between circuits having different impedances, for the purpose of optimizing power transfer.

impedance-matching network A network of discrete components, often adjustable, that is used to match a circuit having a certain impedance to a circuit having a different impedance. An example is the inductive-capacitive (LC) coupler, also called a *transmatch*, commonly used to match a radio transmitter to an antenna system.

5059F-pI_352-384 4/10/01 9:03 AM Page 357

impedance-matching transformer See IMPEDANCE TRANSFORMER.

impedance meter See Z METER.

impedance plethysmograph An electronic device used to measure changes in the chemical content of body cells.

impedance poles See POLES OF IMPEDANCE.

impedance ratio The quotient of two impedances that are related in some situation, such as impedance match or impedance mismatch. The impedance ratio of a transformer is equal to the square of the turns ratio.

impedance transformer **1.** A transformer for converting an impedance to a different value. The turns ratio is equal to the square root of the impedance ratio. **2.** An emitter follower or source follower circuit, used primarily to match a high impedance to a lower impedance. **3.** A short-circuited transmission-line section used to match or convert impedances at radio frequencies.

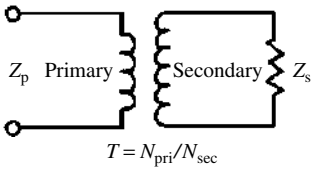

impedance transformer

impedance triangle A triangular vector diagram in which the impedance vector is the hypotenuse, and the reactance and resistance vectors are the perpendicular sides.

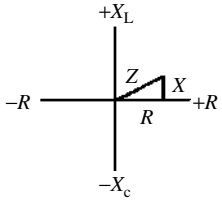

impedance triangle

impedance vector In a vector diagram, the resultant (vector) representing the combined reactance and resistance vectors. Also see IMPEDANCE TRIANGLE.

impedance zeros See ZEROS OF IMPEDANCE.

imperative macroinstruction A MACROINSTRUCTION used to create object (machine language) program instructions.

imperative statement A source language program instruction that is converted into object program (machine language) instructions.

imperfection A fault in the lattice of a crystal. Also see CRYSTAL LATTICE.

implementation **1.** Putting a system into operation and evaluating its performance. **2.** Doing all that is necessary to install a device or system.

implosion The inward collapse of an evacuated chamber, such as the envelope of a cathode-ray tube. It is the opposite of explosion, an outward bursting.

impregnant A substance for the IMPREGNATION of electronic components. Examples: waxes, oils, liquid plastics, and varnish.

impregnation The process of filling the spaces within a material or structure with an insulating compound. Various electronic components, such as capacitors, inductors, transformers, transistors, and diodes, are impregnated for protection and stability.

impressed voltage The voltage applied or presented to a circuit or device.

impulse **1.** A signal of extremely short duration (e.g., a noise burst). **2.** A brief, unidirectional surge in voltage (usually) or current.

impulse excitation Driving a tank circuit with a single pulse, then allowing it to oscillate at its own frequency until another driving pulse arrives.

impulse frequency In a digital telephone, the number of pulse periods per second, corresponding to a dialed digit, generated by the pulse springs.

impulse generator See MARX GENERATOR.

impulse noise Electrical noise from short-duration pulses, such as those produced by an automotive ignition system.

impulse ratio The ratio V_p/V_s, where V_p is the breakdown (or flashover or sparkover) voltage caused by an impulse, and V_s is the corresponding voltage at the crest of the power-frequency cycle.

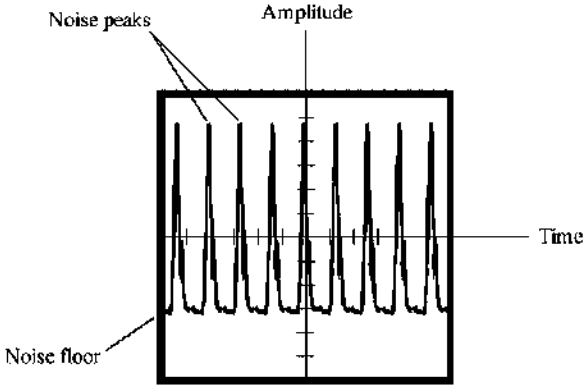

impulse noise

5059F-pI_352-384 4/10/01 9:03 AM Page 358

impulse relay A relay that is able to close or open completely when driven by a short pulse.

impulse speed The switching rate of a telephone dialing device as it transmits pulses.

impulse timer A synchronous-motor-driven timer whose cams can control many circuits; it can advance by a number of specified increments, as controlled by an integral stepping mechanism.

impulse transmission A method of transmission in which defined impulses are used to denote changes in signal content or format.

impurity A substance added to an intrinsic semiconductor to alter its electrical properties.

impurity atom In a processed semiconductor material, an atom of an IMPURITY material that produces either n- or p-type properties to the intrinsic semiconductor.

impurity density In the manufacturing process of a semiconductor material, the amount of impurity added to the original semiconductor.

impurity ion In a crystal, an ion in a space between atoms, or one taking the place of an atom.

impurity level **1.** The energy existing in a semiconductor material as a result of doping (the addition of an impurity). **2.** See IMPURITY DENSITY.

impurity material See IMPURITY.

IN Abbreviation for INTELLIGENT NETWORK.

In Symbol for INDIUM.

I_n Symbol for the *n*th value of current in a series of values.

in **1.** Abbreviation of INPUT. **2.** Abbreviation of INCH.

inaccuracy **1.** The state or condition of instrument error. **2.** The difference between the actual value of a parameter and the value indicated by an instrument. **3.** The percentage of instrument error.

inactive leg Within a transducer, an electrical component whose characteristic remains unchanged when the stimulus (quantity being transduced) is applied; specifically, a Wheatstone bridge element in a transducer.

inactive lines In a conventional television picture, blanked lines that do not contribute to the visible part of the image. Approximately half of these lines are at the top of the screen; the other half are at the bottom.

inactive time The period during which a radioactivity counter is insensitive to ionizing agents.

incandescence The state of glowing from intense heat, as when a metal becomes white hot from an electric current flowing through it.

incandescent lamp A filament-type lamp. The filament becomes so hot when an electric current passes through it that it glows brilliantly.

inch Abbreviation, in. A unit of linear measure in the English system; 1 in. = 2.54 centimeters = 0.0254 meter.

inching See JOGGING.

inch-pound Abbreviation, in-lb. A unit of work equal to a force of 1 pound exerted over a distance of 1 inch. Compare FOOT-POUND.

incident **1.** A failure in a computer system requiring the intervention of an operator in removing or revising the job involved. **2.** Pertaining to a ray or rays of energy striking a surface or boundary, or encountering a device (such as an antenna or photovoltaic cell).

incidental AM Undesired amplitude modulation in a frequency-modulated signal. Compare INCIDENTAL FM.

incident field intensity The field strength of an electromagnetic field as it arrives at a receiving antenna.

incidental FM Undesired frequency modulation in an amplitude-modulated signal. Compare INCIDENTAL AM.

incidental time Computer time devoted to other than program runs or program development.

incident light The light that strikes or enters an altering device or medium. See INCIDENT RAY.

incident power In a transmission line, the power that reaches the end of the line. Compare REFLECTED POWER.

incident ray The ray that strikes the surface of a reflecting, refracting, or absorbing body. Compare REFLECTED RAY and REFRACTED RAY.

incident wave **1.** A wave propagated to the ionosphere. Compare REFLECTED WAVE and REFRACTED WAVE. Also see IONOSPHERE and IONOSPHERIC PROPAGATION. **2.** A wave that encounters a change (in density, for example) in a propagation medium or the transition point between media.

in-circuit tester An instrument that permits the checking of components (especially transistors) without removing them from the circuit in which they are wired.

inclination **1.** At a given geographic location, the angle between the earth's magnetic lines of flux and the horizon. This angle ranges from 0 degrees at the geomagnetic equator to 90 degrees at the geomagnetic poles. Compare DECLINATION, 1. **2.** The angle between the plane of a satellite orbit and the plane containing the equator of the earth, planet, or star around which the satellite revolves. Generally measured as the angle at which the satellite crosses the equator while passing from the southern hemisphere to the northern hemisphere. This angle is between 0 and 90 degrees for satellites in non-retrograde orbits, and between 90 and 180 degrees for satellites in retrograde orbits.

inclinometer An instrument for measuring INCLINATION. One form consists of a magnetic needle mounted so that it can swing inside a vertically mounted circular scale.

inclusive-OR Also called *OR operation.* A logical operation between two operands, the result of which depends on rules for combining bits in

5059F-pI_352-384 4/10/01 9:03 AM Page 359

each position within the operands: an output of 1 results if one or both of the bits have a value of 1; zero only if both are zero. Compare EXCLUSIVE-OR.

incoherent light Electromagnetic radiation in the visible spectrum in which the waves are not aligned (not in phase) and can be of more than one wavelength.

incoherent radiation Electromagnetic radiation in which the waves are not aligned (not in phase) and can be of more than one frequency or wavelength.

incoming inspection The examination of equipment and materials as they enter a factory or laboratory, for the purpose of identifying damaged or faulty units.

incoming line A line that enters a device, facility, or stage. Compare OUTGOING LINE.

Incompleteness Theorem A mathematical theorem of significance in artificial intelligence. For any consistent set of axioms (postulates), there are always more true statements than provable statements.

incomplete program Also called *incomplete routine.* A computer program of generalized steps that must be augmented with specific requirements to be implemented for a given operation.

inconsistency Contradictory computer statements, as detected by the program.

inconsistent equations A set of equations that have no common solution.

Increductor A specialized radio-frequency magnetic amplifier or saturable reactor.

increment **1.** The difference between two successive values of a variable. **2.** A small change in a quantity, such as mass, distance, or time. **3.** A quantity to be added to another quantity. **4.** The difference in value between adjacent hash marks on a meter scale.

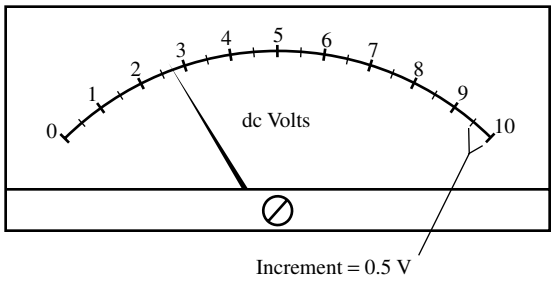

increment, 4

incremental computer A computer that operates on changes in variables. Example: differential analyzer.

incremental digital recorder A magnetic tape recorder that moves the tape across the record head in increments.

incremental display A device that converts digital data into a form for display (characters; graphs).

incremental inductance The inductance exhibited by an inductor, such as an iron-core choke, carrying a direct current.

incremental permeability The permeability exhibited by a material when an alternating-current magnetizing force is superimposed upon a direct current.

incremental plotter A device that, by direction of a computer program, provides the results of a program run in the form of curves or points on a curve, along with annotational characters.

incremental representation For incremental computers, a method of representing variables in terms of changes in the variables.

incremental sensitivity The smallest change in a quantity under measurement that can be detected by the instrument used.

ind **1.** Abbreviation of *indicator.* **2.** Abbreviation of INDUCTANCE (more commonly, *L*). **3.** Abbreviation of INDUCTOR (More commonly, *L*).

indefinite integral See INTEGRAL, **1**.

Indeo Also called *Digital Video Interactive (DVI).* A method of IMAGE COMPRESSION developed by Intel Corporation.

independent equations A set of equations having one common solution.

independent events In probability and statistics, the case where the occurrence of one event has no effect on the occurrence of another.

independent failure A circuit failure whose direct cause is not related to malfunctions elsewhere in the system.

independent mode In tracking supplies, an optional method of operation in which the separate units are adjustable independently of each other. Compare TRACKING MODE.

independent variable A changing quantity whose value at any instant is not governed by the value of any other quantity. Compare DEPENDENT VARIABLE.

index **1.** A reference line, hair, or point (e.g., a *file index*). **2.** In mathematics, an exponent. **3.** A ratio of one quantity to another, as *index of refraction.* **4.** In a computer memory, a table of references in a key sequence; it can be addressed to find the addresses of other data items. **5.** A number that is used to select a specific item within an array of items in memory.

index counter Also called *tape counter.* In a magnetic tape recorder, a (usually electromechanical) counting device that the operator can refer to in order to find material on the tape.

indexed address During or preceding the execution of a computer program instruction, an address that is modified by the content of an index register.

indexing **1.** An information retrieval technique used with files on a direct-access storage medium or on tables in memory. **2.** To modify an instruction using an index word.

5059F-pI_352-384 4/10/01 9:03 AM Page 360

index of modulation In frequency modulation, the ratio of carrier frequency deviation to modulating frequency.

index of refraction Symbol, *n*. The ratio v_1/v_2, where v_1 is the speed of energy propagation in the first medium through which the energy passes, and v_2 is the speed in the second medium.

index register Abbreviation, XR. In digital computer operations, a register holding a modifier that allows data to be directly addressed (each program refers to an index register when addressing storage locations). Also called MODIFIER REGISTER.

index word A word (bit group) containing a modifier that will be added to a basic instruction when it is executed during a program run.

India mica High-grade mica mined in India. Its excellent dielectric properties make it useful for capacitor stacks, high-*Q* radio-frequency circuits, and other critical applications.

indicated horsepower Abbreviation, ihp. Horsepower calculated from data or ratings, as opposed to measured horsepower.

indicated horsepower-hours Abbreviation, ihp-hr. Horsepower-hours based on calculation of indicated horsepower.

indicating fuse A fuse that provides some signal (such as a protruding pin) to show that it has blown.

indicating instrument An instrument, such as a meter, that provides direct readings of a measured quantity, as opposed to an instrument, such as a bridge, that must be manipulated and whose operation must often be followed by calculations.

indicating lamp A lamp that is marked or coded so that when it is on or off it conveys information.

indicator **1.** Meter (see METER, **1**). **2.** See MONITOR. **3.** See ANNUNCIATOR. **4.** In a computer, a device that can be set by a specific condition (e.g., by a negative result or error indicator).

indicator probe A test probe having a built-in meter.

indicial response Symbol, I(T). The sum of the transient and steady-state responses to a unit function.

indirect addressing In computer programming, a technique in which the address in an instruction refers to a different location containing another address, that can specify yet another address or an operand. Also called *multilevel addressing.*

indirect coupling Collectively, capacitive and inductive coupling, as opposed to direct coupling.

indirect ground An unintentional ground connection (e.g., accidental grounding of part of a circuit) or one obtained through a roundabout path. Compare DIRECT GROUND.

indirect light Light that has been reflected from one or more surfaces. Compare DIRECT LIGHT.

indirectly controlled Influenced by a directly controlled parameter, but not itself directly controlled.

indirectly grounded Connected to earth or to the lowest-potential point in a system inadvertently or through a roundabout path (e.g., by means of an indirect ground). Compare DIRECTLY GROUNDED.

indirectly heated cathode An electron-tube cathode consisting of a cylindrical or rectangular sleeve coated with a substance that is a rich emitter of electrons; it is heated by a filament inside the cylinder.

indirectly heated thermistor A thermistor whose temperature is changed by a built-in heater (filament) operated by the control current.

indirectly heated thermocouple A meter thermocouple heated by a small heater (filament) through which the signal current passes.

indirect material A semiconductor substance in which electrons move from the conduction band to the valence band in discrete jumps or steps.

indirect measurement The measurement of a quantity by comparing it with a similar quantity, using an instrument that requires adjustment or manipulation (rather than a simple meter). For example, resistance can be measured with a bridge, instead of an ohmmeter. Compare DIRECT MEASUREMENT.

indirect piezoelectricity In a piezoelectric crystal, the application of a voltage for the purpose of producing a strain on the crystal. A piezoelectric buzzer operates on this principle.

indirect scanning A method of video scanning, in which a fast-moving spot of light scans the film or an object and is passed through the film (or reflected by the object) to a photocell.

indirect wave **1.** In communications, a wave that arrives at a receiver after having traveled via refraction, reflection, or both. **2.** A radio wave propagated via the ionosphere. **3.** A wave reflected from some object, such as the moon or a meteor trail. **4.** A wave received from a satellite, originating from a distant earth station.

indium Symbol, In. A metallic element. Atomic number, 49. Atomic weight, 114.82. Used as a dopant in semiconductor processing.

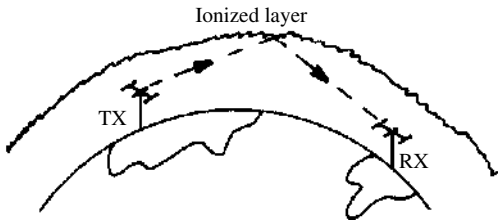

indirect wave

5059F-pI_352-384 4/10/01 9:03 AM Page 361

indoor antenna An antenna erected and operated in a building, but kept away from other objects as much as possible.

indoor radiation Electromagnetic radiation from the part of an antenna feeder or lead-in that is inside the transmitter building.

indoor transformer A power service transformer that, for protection against the elements, is installed inside the building it serves.

induced Brought about by the influence of a magnetic or electric field.

induced charge An electric charge produced in a body by the electric field surrounding another charge.

induced current An alternating current established in one circuit by the alternating magnetic field of another circuit. Also see INDUCTION.

induced EMF See INDUCED VOLTAGE.

induced failure A form of component failure that occurs because of operation beyond the normal specifications.

induced voltage An alternating voltage set up across one circuit (especially a coil) by the alternating magnetic field of another circuit. Also see INDUCTION.

inductance Symbol, *L*. Unit, henry. In a conductor, device, or circuit, the inertial property (caused by an induced reverse voltage) that opposes the flow of current when a voltage is applied; it opposes a change in current that has been established. Also see HENRY, INDUCTION, and MUTUAL INDUCTANCE.

inductance bridge An alternating-current bridge for measuring inductance in terms of a standard inductance or a standard capacitance. See, for example, HAY BRIDGE, MAXWELL BRIDGE, and OWEN BRIDGE.

inductance-capacitance Abbreviation, *LC*. **1.** A combination of inductance and capacitance in a circuit, such as a filter, a parallel-resonant circuit, or a series-resonant circuit. **2.** Pertaining to a device for measuring inductance and capacitance (e.g., *LC bridge* and *LC meter*).

inductance-capacitance bridge An alternating-current bridge for measuring inductance and capacitance only.

inductance-capacitance filter A filter composed of inductors and capacitors. Also called *LC filter*.

inductance-capacitance meter A direct-reading meter for measuring inductance and capacitance.

inductance-capacitance-resistance Abbreviation, *LCR*. **1.** A combination of inductance, capacitance, and resistance in a circuit, such as a basic tuned circuit. The resistive component represents loss in the inductor and capacitor. **2.** Pertaining to a device for measuring inductance, capacitance, and resistance (e.g., *LCR bridge* and *LCR meter*).

inductance-capacitance-resistance bridge See IMPEDANCE BRIDGE.

inductance coil See INDUCTOR.

inductance filter A filter using only an inductor, usually a coil of wire.

inductance-resistance time constant The time constant t (see ELECTRICAL TIME CONSTANT) of a circuit containing, ideally, only inductance and resistance. Mathematically, $t = LR$, where t is in seconds, L is the inductance in henrys, and R is the resistance in ohms. Also called *LR time constant*.

inductance standard A highly accurate, stable inductor used in precision measurements. Also see PRIMARY STANDARD and SECONDARY STANDARD.

induction **1.** The ability of an alternating, pulsating, or otherwise changing current flowing in one circuit to set up a current in a nearby circuit. The circuits need not be physically connected, but need only be linked by magnetic lines of flux. Also see SELF-INDUCTION. **2.** The phenomenon whereby a body becomes electrically charged by the field surrounding a nearby charged body. Also see ELECTRIC CHARGE.

induction coil A special high-voltage step-up transformer having an open core and a vibrator-interrupter in series with the primary winding, which carries direct current from a battery. The current is broken up into short pulses by the interrupter, and a high alternating-current voltage is generated in the secondary winding.

induction compass A compass whose indications depend on current induced in a coil revolving in the earth's magnetic field. Compare GYROCOMPASS and MAGNETIC COMPASS.

induction factor The ratio of total current to nonproductive current in an alternating-current circuit.

induction field The portion of an electromagnetic field that returns to a radiator, such as a coil, as opposed to the RADIATION FIELD.

induction frequency converter A mechanical device used for converting a signal at a fixed frequency to a signal at another fixed frequency.

induction furnace A furnace in which high-frequency magnetic fields induce currents in metal ores, causing the ore to become hot enough to melt.

induction heater A high-power, radio-frequency generator designed especially for induction heating.

induction heating The heating of metallic work samples by placing them in (but insulated from) a WORK COIL carrying current from a high-power radio-frequency generator. The workpiece is heated by radio-frequency currents induced in it as a result of the intense alternating magnetic field within the coil. Compare DIELECTRIC HEATING.

induction loss Loss of energy from a current-carrying conductor because of inductive coupling to a nearby conductor.

induction modulator See ELECTROMECHANICAL MODULATOR.

5059F-pI_352-384 4/10/01 9:03 AM Page 362

induction motor An electric motor in which the stator's rotating magnetic field makes the rotor revolve.

induction speaker An acoustic loudspeaker in which an audio-frequency current is passed through a diaphragm or coil located in a constant magnetic field. This results in movement of the diaphragm or coil.

induction transducer See INDUCTIVE TRANSDUCER.

induction-type landing system See DINGLEY INDUCTION-TYPE LANDING SYSTEM.

induction welding Welding in which the heating current flowing in the workpieces is induced by an electromagnetic field.

inductive capacitor A wound capacitor in which the inductance of the roll is controlled and specified. Such a capacitor is useful in compact filters and in single-frequency bypassing, where the reactive components are supplied by the capacitor. Compare NONINDUCTIVE CAPACITOR.

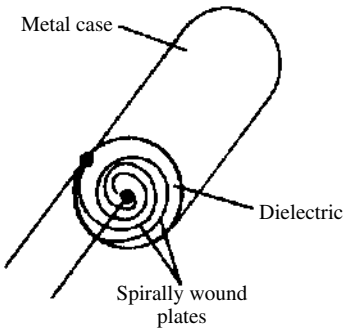

inductive capacitor

inductive circuit **1.** A circuit in which inductance predominates. **2.** A (theoretical) circuit containing inductance only.

inductive coupling The transfer of energy between two inductors (or inductive devices) by a linking electromagnetic field. Also see COEFFICIENT OF COUPLING, COUPLING, INDUCTION, and MUTUAL INDUCTANCE.

inductive feedback See MAGNETIC FEEDBACK.

inductive heater See INDUCTION HEATER.

inductive heating See INDUCTION HEATING.

inductive kick See BACK VOLTAGE and KICKBACK.

inductive load A load device that approaches a pure inductive reactance (e.g., loudspeaker and electric motor).

inductive loading In an antenna, the addition of inductance in series with the element(s). This reduces the resonant frequency for a radiator having a given physical length. It can also serve to reduce the physical length required for a radiator having a specified resonant frequency. Compare CAPACITIVE LOADING.

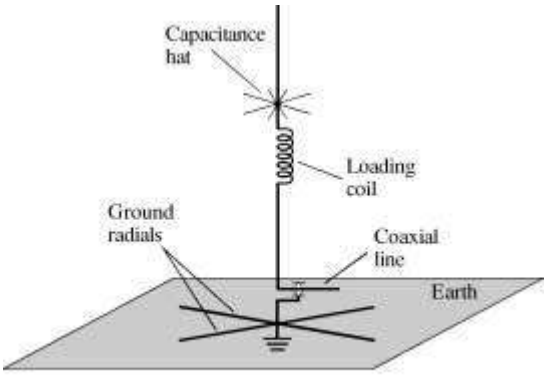

inductive loading

inductive logic A form of reasoning that demonstrates that a certain conclusion is highly probable, given a certain set of circumstances. This is of interest to researchers in artificial intelligence (AI). Compare DEDUCTIVE LOGIC.

inductive microphone A microphone in which sound waves vibrate a conductor or coil in a strong magnetic field, producing a corresponding alternating-current output by the resulting induction. Example: *dynamic microphone.*

induction neutralization Neutralization of a vacuum-tube radio-frequency power amplifier, via negative feedback from the output to the input through coupling coils.

inductive reactance Symbol, X_L Unit, ohm. The reactance exhibited by an ideal inductor, considered as a positive imaginary-number quantity; $X_L = j6.28fL$, where X_L is in ohms, f is the frequency in Hertz, L is the inductance in henrys, and j is the unit imaginary number (the square root of –1). Alternatively, f can be specified in megahertz, and L in microhenries. In a pure inductive reactance, current lags 90 degrees behind voltage. Also see INDUCTANCE, INDUCTION, INDUCTOR, and REACTANCE.

inductive switching Switching operations in a circuit containing an inductor. Switching time is influenced by the INDUCTANCE-RESISTANCE TIME CONSTANT of the inductor; overall operation is affected by the back voltage generated by the inductor.

inductive transducer A transducer in which the sensed phenomenon causes a change in inductance (or reluctance), which, in turn, causes a proportional change in output current, voltage, frequency, or bridge balance. Compare CAPACITIVE TRANSDUCER, CRYSTAL TRANSDUCER, MAGNETIC TRANSDUCER, and RESISTIVE TRANSDUCER.

5059F-pI_352-384 4/10/01 9:03 AM Page 363

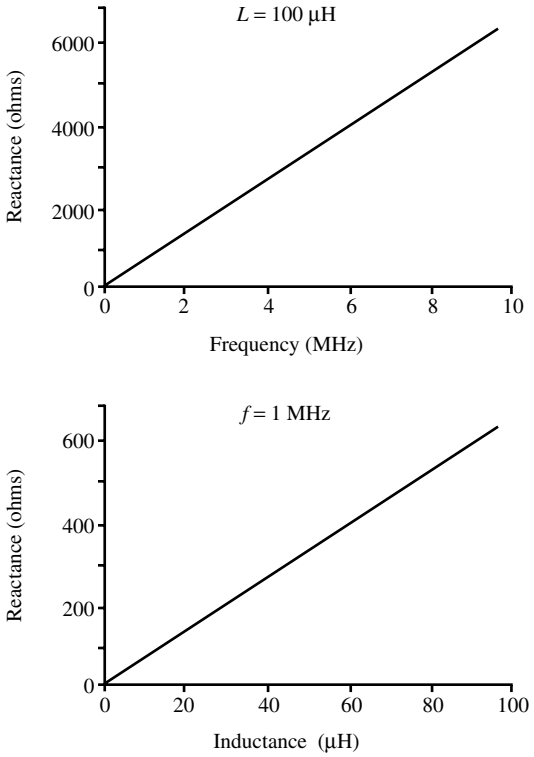

inductive reactance

inductive trimmer See TRIMMER INDUCTOR.

inductive tuning Also called *permeability tuning.* In a radio receiver, transmitter or transceiver, the adjustment of frequency by changing the inductance of a coil having a movable core.

inductivity See DIELECTRIC CONSTANT.

inductometer An instrument for measuring inductance in terms of the resonant frequency of an INDUCTANCE-CAPACITANCE (*LC*) circuit, in which *L* is the unknown inductance and *C* is calibration capacitance.

inductor A coil of wire wound according to various designs, with or without a core of ferromagnetic material, to concentrate the magnetic flux resulting from current flowing in the wire. The coiling of the wire and/or the addition of a ferromagnetic core increases the self-inductance compared with that of a straight wire having the same length. Also see INDUCTANCE; INDUCTION, **1**; and SELF-INDUCTANCE, **1**.

inductor alternator See ALTERNATOR.

inductor amplifier See MAGNETIC AMPLIFIER.

inductor decade See DECADE INDUCTOR.

inductor microphone See INDUCTIVE MICROPHONE.

inductors in parallel See PARALLEL INDUCTORS.

inductors in parallel-series See PARALLEL-SERIES INDUCTORS.

inductors in series See SERIES INDUCTORS.

inductors in series-parallel See SERIES-PARALLEL INDUCTORS.

inductor substitution box An enclosed assortment of common-value inductors that can be switched, one at a time, to a pair of terminals. In troubleshooting and circuit development, any of several useful fixed inductances can be thus obtained.

industrial data processing Abbreviation, IDP. The application of digital computers and associated equipment to industrial problems, through the classification, sorting, storing, and manipulation of information.

industrial electronics The branch of electronics concerned with manufacturing processes and their control, and with the operation and safeguarding of factories.

industrial instrumentation **1.** Supplementing an industrial process with electrical and electronic measuring instruments. **2.** The instruments used for the purpose defined in **1**.

industrial television Abbreviation, ITV. A usually closed-circuit television (CCTV) system, used as an adjunct to a manufacturing process, or as a means of communication or surveillance within an industrial plant.

industrial robot A robotic device used in industrial applications (e.g., mining, construction, manufacturing, or laboratory work).

industrial tube An (often heavy-duty) highly reliable vacuum tube designed expressly for industrial service, such as high-power radio or television broadcasting.

ineffective time The period during which an otherwise operational computer is not being used effectively because of delays or idle time.

inelastic collision A collision between charged particles in which one gains energy and the other loses energy.

inert gas A gas that does not readily react with other elements. Inert gases include *argon*, *helium*, *krypton*, *neon*, and *xenon.* Such gases are often used in hermetically sealed devices to retard corrosion.

inertance See ACOUSTIC INDUCTANCE.

inertia The tendency of a body at rest to remain at rest unless acted on by an outside force. Also, the tendency for a body in motion to maintain that motion unless acted on by an outside force. Compare MOMENTUM.

inertia in electric circuit The condition in a circuit containing inductance, in which a current change lags behind a voltage change (analogous to mechanical inertia; see INERTIA).

inertial guidance A system that automatically guides missiles and satellites in a desired trajectory without the need for continuous control by signals from a station.

5059F-pI_352-384 4/10/01 9:03 AM Page 364

inertia relay A time-delay relay whose operation is slowed by the addition of weights or other attachments.

inertia switch A switch that can sense a disturbance of its inertia.

inference engine A circuit that gives instructions to a computer or robot, by applying programmed rules to commands issued by a human operator. Comprises the functional portion of an EXPERT SYSTEM.

infinite Pertaining to a quantity or region that has no defined limits.

infinite baffle A loudspeaker baffle having no openings for the passage of sound from the front to the back of the speaker cone.

infinite-impedance detector A detector that offers the very high input impedance of a gate-source circuit and the large-signal capabilities of a diode detector. Audio-frequency output is taken across the source resistor, which is bypassed for radio-frequency signals. There is no drain resistor. Drain current increases with the input signal from a very low value at zero signal level.

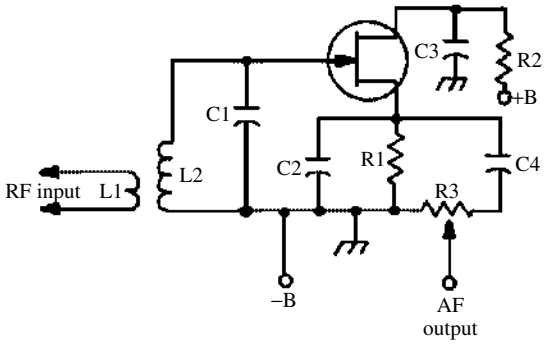

infinite-impedance detector

infinite line See INFINITE TRANSMISSION LINE.

infinite regress A reasoning pattern (either human or machine-based) that is fallacious because it defines or explains something in terms of itself.

infinite sample space In statistics, a sample space having no definite limits.

infinite series A mathematical series in which the number of terms is limitless. For example, ⅛ = 0.1 + 0.06 + 0.006 + 0.0006 + . . .

infinitesimal **1.** A quantity, such as a differential, that approaches zero as the limit. **2.** Pertaining to a quantity whose magnitude is extremely small or negligible. **3.** Pertaining to an extremely small change in a quantity or measured value.

infinite transmission line A theoretical transmission line with normal characteristics, but extending away from the signal generator or receiver for a limitless distance.

infinity Symbol, ∞. A quantity that is unlimited in duration or dimension. A quantity that increases without limit is sometimes said to "approach infinity."

infix notation A system of logical operation notation wherein operands are separated by operators, thus, A & B, where the ampersand means AND. Compare PREFIX NOTATION.

Infobahn See INFORMATION SUPERHIGHWAY.

infobond On a printed circuit board, a form of wiring on the side opposite the components. The wiring is used in place of the foil normally on such a circuit board.

information **1.** Collectively, data or communications, excluding the symbols or signals used to describe, present, or store them. **2.** The result of data processing (i.e., that which is derived from the compilation, analysis, and distillation of data).

information bits In an encoded signal, data characters or digits that can be treated to give information (excluding control characters).

information center A storage bank designed for use by many different subscribers, via computer.

information channel A channel through which data and associated signals are transmitted and received.

information feedback system In message transmission, a control system in which intelligence received at a terminal is returned to the sending unit for automatic verification.

information gate A device or circuit that opens and closes an information channel.

"information processor" species Anything that uses data to derive conclusions, to produce other data, or to take specific actions, and whose functioning can be explained entirely on the basis of data-processing operations. This includes computers and smart robots. Many (but not all) scientists believe that animals are also included; some believe that human beings qualify as well.

information retrieval In digital computer and data-processing operations, the categorizing and storage of information and the automatic recall of specific file items. Also see ACCESS TIME.

information separator An indicator that separates items of information or fields in a (usually variable-length) record.

information storage In digital computer and data processing operations, holding information in memory pending retrieval.

information superhighway **1.** General expression for a worldwide network consisting of computers (personal, educational, industrial, and government) interconnected by telephone lines. **2.** See INTERNET. **3.** A massive, evolving, somewhat controversial data communication network linking computers, television, and telephone systems. It uses high-speed, high-volume data links. Communication technologies include fiberoptics, radio-frequency repeaters, microwaves, geosta-

5059F-pI_352-384 4/10/01 9:03 AM Page 365

tionary satellites, and low-earth-orbit (LEO) satellite systems.

information word A character group representing stored information and managed, as a unit, by hardware or software.

infra- Prefix meaning *below* or *lower than* (e.g., INFRARED).

infrablack region In a composite video signal, the blacker-than-black region (see BLACKER THAN BLACK).

infradyne receiver A superheterodyne receiver in which the intermediate frequency is the sum of the signal and oscillator frequencies, rather than their (usual) difference.

infrared Pertaining to electromagnetic energy in a band whose wavelength is longer than that of visible light, but shorter than that of microwave energy.

infrared communication Communication by keying or modulating infrared rays.

infrared counter-countermeasure A military tactic in which action is taken against an enemy infrared countermeasure.

infrared countermeasure A military tactic using countermeasure methods to cripple enemy infrared equipment.

infrared detector A device that senses the presence of infrared energy. Some such detectors are bolometers, radiometers, radiomicrometers, and photocells.

infrared-emitting diode Abbreviation, IRED. A semiconductor diode, such as the gallium-arsenide type, that emits infrared rays when a current passes through the p-n junction in the forward direction.

infrared guidance A navigation and reconnaissance system using infrared rays.

infrared homing The method whereby a guided missile uses infrared rays to guide it to its target.

infrared light See INFRARED RAYS.

infrared motion detector See MOTION DETECTOR and INFRARED.

infrared photography Photography in which the scene is illuminated with infrared light or emits infrared rays, and the film is infrared sensitive.

infrared radiation See INFRARED RAYS.

infrared rays Radiation at frequencies in the INFRARED region. Also (somewhat mistakenly) called *heat rays.*

infrared remote control **1.** The use of an infrared link, usually over short line-of-sight distances, for the purpose of controlling the operation of electronic equipment. A common example is the local remote control of a television receiver or high-fidelity system. **2.** A small box, containing buttons, a transmitter and an infrared-emitting diode (IRED), used for local remote control of devices, such as television receivers and high-fidelity sound systems.

infrared spectrum The region of the electromagnetic spectrum in which INFRARED radiation is found. This band lies between the microwave radio spectrum and the visible-light spectrum.

infrared therapy The use of infrared rays by physicians and other practitioners to treat certain disorders.

infrared waves Electromagnetic waves whose lengths are greater than those of visible light waves, but less than those of microwaves.

infrared window Any portion of the infrared spectrum in which energy is easily transmitted through the lower atmosphere of the earth.

infrasonic Pertaining to acoustic disturbances whose frequencies are below the range of human hearing (less than about 20 Hz).

infrasonic intrusion detector A system that detects the presence of extremely low-frequency acoustic disturbances, and sends a signal to an alarm. Such INFRASONIC waves can be caused by various actions such as walking on a wooden floor, opening or closing a door, etc.

infrasonics The branch of physics dealing with INFRASONIC phenomena.

infrasound Acoustic disturbances in the air, whose frequencies are lower than about 20 Hz, and whose wavelengths are longer than about 55 feet (17 meters).

inharmonic distortion Distortion in which the frequencies of extraneous components are not harmonically related to the fundamental frequency. It is sometimes experienced when a tone-burst signal is applied to a loudspeaker.

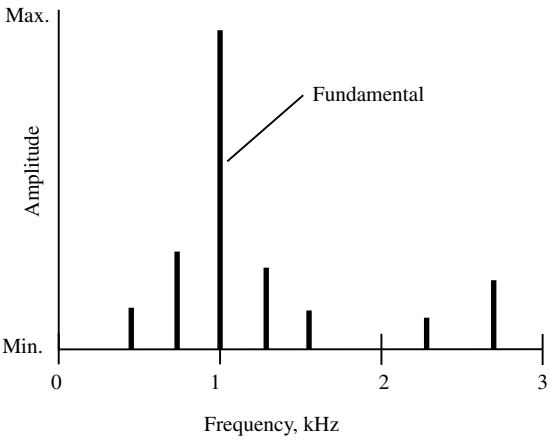

inharmonic distortion

inherent component A (usually extraneous) property possessed by a device because of its internal peculiarities. Thus, an inductor has inherent capacitance; a capacitor has inherent inductance.

inherited error In an extended calculation, an error carried through from one of the earlier steps.

5059F-pI_352-384 4/10/01 9:03 AM Page 366

inhibit **1.** In digital computer and logic operations, to prevent an action or block the input of data by means of a pulse. **2.** To delay an action or process.

inhibit gate A pulse-actuated gate circuit that acts as an INHIBITOR.

inhibitor **1.** A device or circuit that produces a pulse or signal that prevents an action, or that blocks data input. **2.** An additive, such as an organic liquid, that delays the hardening of a mixture, such as an encapsulating compound.

inhibit pulse In a computer, a drive pulse that prevents other pulses from changing the direction of magnetization in the cells of a magnetic core memory.

inhibit signal In digital computer and logic operations, the signal that causes an INHIBIT action.

initial drain **1.** The current supplied by a battery or cell at its rated voltage. **2.** The current delivered by a rechargeable battery or cell when it is put to use immediately after receiving a full charge.

initial failure The first failure occurring in the operation of a circuit or device.

initial instructions A resident computer routine used to aid program loading. Also called *initial order.*

initial ionizing event In the operation of a radioactivity counter, the first event that starts the chain of similar events constituting the count.

initialization A computer program instruction that sets the value of a variable to zero.

initial permeability Permeability in the low magnetization region of a material.

initial time delay Abbreviation, ITD. In acoustics, the elapsed time between the instant the direct sound wave is first heard, and the instant the first echoes (reflected sound waves) arrive.

initiate See TRIGGER.

injection **1.** Introducing a signal into a circuit or device. **2.** Introducing charge carriers (electrons or holes) into a semiconductor.

injector **1.** An element or electrode for INJECTION. **2.** A device or circuit that injects a signal into another device or circuit.

injector electrode See INJECTOR, **1**.

ink bleed In the printing of matter for optical character recognition, ink flow around the characters, often making them unrecognizable to the reader.

inkjet galvanometer A galvanometer whose movement controls the pressure of a jet of ink for making a recording on a paper chart. Also see LIQUID-JET OSCILLOGRAPH.

inkjet printer A printer commonly used with personal computers, in which images are created by jets of ink sprayed directly onto the paper. Noted for low operating noise level, high image resolution, and excellent color-reproduction capability.

ink-mist recorder A graphic recorder in which the line is traced by a mist of ink.

ink recorder A graphic recorder using a pen-and-ink stylus.

ink squeeze-out In the printing of matter for optical character recognition, the squeezing of ink from a character's center.

ink-vapor recorder See INK-MIST RECORDER.

in-lb Abbreviation of INCH-POUND.

inlead The part of an electrode that passes through the external shell or case of a component.

inline procedure The main portion of a COBOL computer program, responsible for the primary operations.

inline processing The action peculiar to a system that processes data almost immediately upon receipt (i.e., one that need not be capable of storing a lot of unprocessed data).

inline readout In digital computer operations, a readout device that displays digits side-by-side horizontally.

inline subroutine A subroutine that must be written each time it is needed, as compared with one that can be accessed by a program branch.

inline tuning Tuning of all the stages of a channel, such as an intermediate-frequency amplifier, to the same frequency.

inner conductor The inner wire or rod of a coaxial cable or coaxial tank. It generally carries the signal, and is isolated from the surrounding environment by the grounded OUTER CONDUCTOR.

inorganic Consisting of materials other than carbon compounds; therefore, it is not related to living things.

inorganic electrolyte Any electrolyte that is completely inorganic: containing no compounds of carbon.

in phase The condition in which alternating or pulsating waves or wave phenomena are in step with each other at all points. Compare OUT-OF-PHASE.

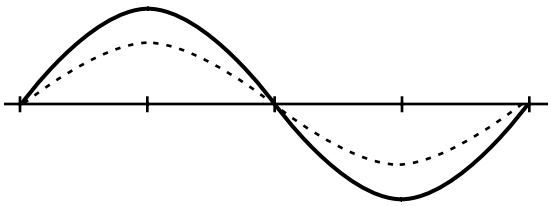

in phase

in-phase carrier See I-PHASE CARRIER.

in-phase current Resistive current in an ac circuit (i.e., current in phase with voltage). Compare QUADRATURE CURRENT.

in-phase feedback Feedback in phase with a main signal. Also called POSITIVE FEEDBACK and REGENERATION.

in-phase voltage A voltage that is in phase with another (reference) voltage.

in-plant system An automatic data communications system within a specific building or complex.

5059F-pI_352-384 4/10/01 9:03 AM Page 367

input **1.** Energy or information delivered or transferred to a circuit or device. **2.** The terminals of a device or circuit to which energy or information is applied. **3.** To deliver or transfer energy or information to a circuit or device (as to input data from a computer peripheral to memory).

input admittance Symbol, Y_i. The internal admittance of a circuit or device, as "seen" from the input terminals; the reciprocal of input impedance. Compare OUTPUT ADMITTANCE.

input area In a computer memory, an area set aside for data input from a source other than a program.

input bias current The input bias required by an operational amplifier.

input capacitance Symbol, C_i. **1.** The internal capacitance of a circuit or device, as "seen" from the input terminals. Compare OUTPUT CAPACITANCE. **2.** The grid-cathode capacitance of a vacuum tube.

input capacitor **1.** In a capacitance-coupled circuit, the input coupling capacitor. Compare OUTPUT CAPACITOR. **2.** The first capacitor in a capacitor-input filter (i.e., that capacitor electrically nearest the rectifier output electrode).

input choke The first choke in a choke-input filter (i.e., that choke electrically nearest the rectifier output electrode, when no preceding capacitor is used).

input circuit The circuit or subcircuit constituting the input section of a network or device. Compare OUTPUT CIRCUIT.

input clamp current The current from an input when the input is in a state below ground potential. A test for the input clamp diode.

input conductance Symbol, G_i. The internal conductance of a circuit or device, as "seen" from the input terminals; it is the reciprocal of INPUT RESISTANCE. Compare OUTPUT CONDUCTANCE.

input coupling capacitor See INPUT CAPACITOR, **1**.

input coupling transformer See INPUT TRANSFORMER.

input current Symbol, I_i. **1.** The current delivered to a circuit or device. **2.** Current flowing in the input leg or electrode of a circuit or device.

input device **1.** A device, such as an input transformer, that couples energy or information to a circuit or device. Compare OUTPUT DEVICE. **2.** A device through which another device receives data.

input equipment Collectively, input devices used with a computer.

input error voltage In an operational amplifier, the error voltage at the input terminals when a feedback loop operates around the amplifier.

input extender A diode network that provides increased fan-in for a logic circuit. Also see FAN-IN, **1**.

input gap In a velocity-modulated tube, the gap in which the electron stream is initially modulated.

input guarding A method of eliminating stray coupling among inputs in an integrated circuit. A shield is provided at the input; it is driven to follow along with the input voltage. This ensures low loss and minimum errors resulting from unwanted coupling.

input impedance Symbol, Z_i. The internal impedance of a circuit or device, as "seen" from the input terminals. Compare OUTPUT IMPEDANCE.

input limited The processing time limitation imposed by an input unit on the speed of a program run.

input noise current At the input of an integrated circuit, the root-mean-square (rms) or peak-to-peak (pk-pk) noise current existing within a specified range of frequencies.

input noise current density The noise current, usually expressed as a root-mean-square (rms) value, in a band 1 Hz wide around a given frequency.

input noise voltage At the input of an integrated circuit, the root-mean-square (rms) or peak-to-peak (pk-pk) noise voltage existing within a specified range of frequencies.

input noise voltage density The noise voltage, usually expressed as a root-mean-square (rms) value, in a band 1 Hz wide around a given frequency.

input offset current In an operational amplifier, the difference between the currents going to the input terminals when the output is zero.

input offset voltage In an operational amplifier, the potential that has to be applied between the input terminals for a zero output voltage.

input/output Abbreviation, I/O. **1.** Data transmitted to, or received from, a computer. **2.** A terminal through which data is transmitted to, or received from, a device.

input/output bound A condition affecting a system in which the time consumed by input and output operations is greater than that required for other processes.

input/output buffer A computer memory area specifically reserved for the receipt of data coming from or going to a peripheral.

input/output control The part of a computer system that coordinates activity between a central processor and peripherals.

input/output equipment **1.** In digital computer operations, devices for entering information into the computer or for reading information from it. Examples: keyboard, mouse, display, and optical scanner. **2.** In robotics and artificial intelligence, a data link between a controller and one or more robots, and/or between or among two or more controllers.

input/output isolation Arrangement or operation of a circuit or device so that there is no direct path between input and output terminals around the circuit or device. Also see ISOLATION.

input/output module See INPUT/OUTPUT EQUIPMENT.

5059F-pI_352-384 4/10/01 9:03 AM Page 368

input/output routine A routine for simplifying the programming of standard input/output equipment operations.

input/output switching The allocation of more than one channel to peripherals for communications with a central processor.

input/output voltage differential At a given load current, the potential difference that is necessary for an integrated circuit to operate according to its output voltage specifications.

input power Symbol, P_i. **1.** The power presented to the input terminals of a circuit or device. Also called POWER INPUT. Compare OUTPUT POWER. **2.** The operating power of a circuit or device (i.e., the power-supply requirement).

input protection In an integrated circuit, a means of preventing damage to the device from excessive voltage at the input, such as transient spikes or the result of malfunctioning of some other circuit.

input record **1.** A computer record of immediate interest that is ready for processing. **2.** During a computer program run, a record read into memory from an input device.

input recorder A device that makes a permanent record of the signals or data input to a circuit or system.

input register In a computer, a register that receives data from a peripheral relatively slowly and then passes it on to a central processor at a faster speed as a sequence of informational units. Also see REGISTER.

input resistance Symbol, R_i. The internal resistance of a circuit or device, as "seen" from the input terminals. Compare OUTPUT RESISTANCE.

input resonator In a velocity/modulated tube, the resonator in which electron bunching occurs.

input routine A computer program section that manages data transferal between an external storage medium and a memory input area.

input section **1.** See INPUT ROUTINE. **2.** See INPUT AREA.

input sensitivity **1.** The level of input-signal amplitude that will result in a certain signal-to-noise ratio at the output of a device. The specified signal-to-noise ratio is usually 10 or 20 dB. **2.** The level of input signal in a frequency-modulated device, required to produce a specified amount of noise quieting. The specified level of noise quieting is usually 20 dB. Alternatively, 12-dB SINAD (ratio of signal to the level of noise and distortion) can be specified. **3.** The minimum level of input voltage required to actuate a logic gate.

input signal The signal (current, voltage, and power) presented to the input terminals of a circuit or device for processing.

input tank In a double-tuned stage of a transmitter or power generator, the tank circuit in which the input signal is resonated. This is generally the base or gate circuit. Compare OUTPUT TANK.

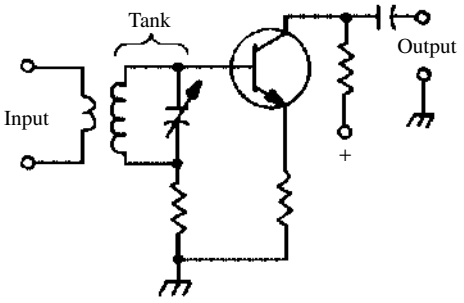

input tank

input terminals Terminals (usually a pair) associated with the input section of a circuit or device. Compare OUTPUT TERMINALS.

input transformer The transformer that delivers signal voltage or power to the input circuit of a network or device. Compare OUTPUT TRANSFORMER.

input uncertainty The combination of all parameters that result in adverse behavior in an operational amplifier.

input unit In a digital computer, the device or circuit that receives information from peripherals.

input voltage **1.** Symbol, E_i or V_i. The voltage presented to a circuit or device. Compare OUTPUT VOLTAGE, **1**. **2.** The voltage across the input leg or electrode of a circuit or device. Compare OUTPUT VOLTAGE, **2**.

input-voltage drift For an integrated circuit (IC), the time- and temperature-dependent change in output voltage divided by the IC's open-loop voltage gain.

input-voltage offset For a differential amplifier, the input signal voltage at the differential input that results in zero output voltage.

input-voltage range The range, in volts, over which the input voltage can fluctuate in an integrated circuit so that the common-mode rejection ratio (CMRR) specifications are not exceeded.

input winding The signal winding of a magnetic amplifier.

inquiry A programmed request for information from storage in a computer.

inquiry display terminal A video display/keyboard terminal used to make an inquiry to a computer system, and display the response.

inquiry station A terminal from which an inquiry can be sent to a central computer.

inrush The initial surge of current that occurs when voltage is first applied to the primary winding of a transformer with no load connected.

inscribe To convert data to a form on a document that is readable by a character-recognition device, as through the use of magnetic ink, for example.

insect robot A member of a fleet of robots, all of which are under the control of a single computer.

5059F-pI_352-384 4/10/01 9:03 AM Page 369

The term arises because the system functions like an anthill or beehive, in which the individual machines are "stupid," but the system as a whole is "smart." Such robots often have six legs, like insects. Compare AUTONOMOUS ROBOT.

insert A (usually metallic) bushing that can be molded into a plastic part (or pressed into it after molding is completed) to provide a bearing sleeve or threaded hole.

insert core A ferromagnetic core whose position can be adjusted to vary the inductance of the coil surrounding it.

insert edit **1.** In magnetic tape recording, a section of tape on which new audio is recorded over existing audio. **2.** The process of recording new audio over existing audio in a defined interval on a magnetic tape.

insertion gain In a circuit or system, the gain resulting from the amplifier inserted into the system; it is usually expressed in decibels. Compare INSERTION LOSS.

insertion loss Loss of energy or gain by placing certain devices or subcircuits (filters, impedance matchers, etc.) in a circuit. It is usually expressed in decibels. Also see INSERTION RESISTANCE.

insertion phase shift The difference in phase produced by a circuit installed in an electrical transmission line.

insertion resistance The resistance of a component or instrument that is introduced into a circuit. Thus, the internal resistance of a microammeter becomes an insertion resistance in the circuit in which the meter is connected for current measurement.

inside antenna See INDOOR ANTENNA.

inside diameter Abbreviation, ID. The innermost diameter of a body or figure having two concentric diameters. Compare OUTSIDE DIAMETER.

inside lead See START LEAD.

inside radiation See INDOOR RADIATION.

inside spider A voice-coil centering device within a loudspeaker.

inst **1.** Abbreviation of INSTRUMENT or INSTRUMENTATION. **2.** Abbreviation of INSTANT.

instability Inconsistency in the operation of a circuit or device, in the parameters of a device, or in an electrical quantity. It can be attributed to a number of causes, including temperature, loading, age, humidity, negative resistance, and radioactivity.

installation tape number An identification number given to a reel of magnetic tape by the processing facility.

instant Abbreviation, inst. The point in time at which an event occurs, or at which a quantity reaches a particular value.

instantaneous Occurring at a specified moment, or instant, of time.

instantaneous amplitude The amplitude, specified in amperes, volts, or watts, of a signal, specified at a particular moment in time.

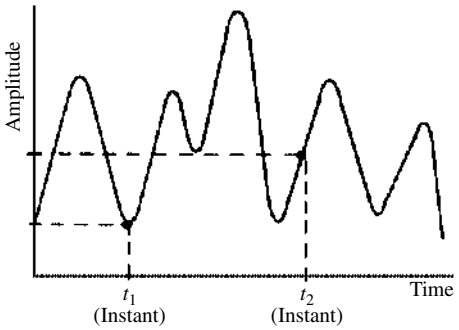

instantaneous amplitude

instantaneous automatic gain control Abbreviation, IAGC. An automatic gain control whose operation almost immediately follows a change in signal amplitude.

instantaneous automatic volume control Abbreviation, IAVC. An instantaneous automatic gain control system for the immediate control of volume in receivers and audio-frequency amplifiers.

instantaneous companding A form of companding that operates according to the instantaneous amplitude of the input signal.

instantaneous contacts Timer contacts that open or close almost immediately upon application of the control signal.

instantaneous current Symbol, i or I_i. The value of an alternating or fluctuating current at a particular instant in the cycle.

instantaneous disc A phonograph disc that can be played back immediately after being recorded.

instantaneous frequency The frequency of a signal at a particular moment in time. The instantaneous frequency changes in frequency-modulated or phase-modulated signals.

instantaneous power **1.** In a single-sideband, suppressed-carrier signal, the power at a specified instant in time. It varies between zero and the peak envelope power (PEP). **2.** The output power of an audio amplifier at a specified instant in time.

instantaneous power output The rate of power delivery to a load at a given instant.

instantaneous relay A relay, such as a fully electronic type (having no moving parts), that shows virtually no delay in its operation.

instantaneous sample A measurement obtained by INSTANTANEOUS SAMPLING.

instantaneous sampling The measurement of wave or signal amplitude at a specific moment in time. See, for example, INSTANTANEOUS CURRENT and INSTANTANEOUS VOLTAGE.

instantaneous speech power In the output of an audio amplifier, the instantaneous value of power in a speech wave, as opposed to that in a sine wave. Also see INSTANTANEOUS VALUE and SPEECH POWER, **1**.

5059F-pI_352-384 4/10/01 9:03 AM Page 370

instantaneous value The magnitude of a fluctuating value at a selected instant in time. See, for example, INSTANTANEOUS CURRENT, INSTANTANEOUS POWER, INSTANTANEOUS SPEECH POWER, and INSTANTANEOUS VOLTAGE. Compare AVERAGE VALUE, and EFFECTIVE VALUE.

instantaneous voltage Symbol, e or E_i. The value of an alternating or fluctuating voltage at a particular instant in the cycle.

instant loop In electronic security applications, a circuit that actuates an alarm without delay when an intrusion is detected.

instruction In digital computer operations, a set of bits defining an operation. Consists of an operation code specifying the operation to be performed, one or more operands or their addresses, and one or more modifiers or their addresses (to modify the operand or its address).

instruction address In a computer memory, the address of a location containing an instruction.

instruction address register Also called *program counter.* A register that holds instruction addresses so that the retrieval of the instructions from memory can be controlled during a program run.

instruction code Also called INSTRUCTION SET. The symbols and characters that compose the syntax of a computer programming language.

instruction format In a computer's basic machine code, the part that specifies how characters or digits are used to represent the codes within the machine's instruction set.

instruction modification In a computer instruction, a change in the instruction code that makes the computer do a different operation when the routine containing the code is encountered again.

instruction register A register in a computer containing the address of the current instruction. Also called CONTROL REGISTER (abbreviation, CR).

instruction set **1.** The range of commands that form a programming language. **2.** See INSTRUCTION CODE.

instruction storage A memory circuit that stores computer instructions or programs.

instruction time The time required for a control unit to analyze and implement a computer program instruction.

instruction word In digital computer programming, a word containing the instruction code (type of operation to be performed) and the address part (location of the associated data in storage).

instrument A device for measuring electrical quantities or the performance of electronic equipment. A *meter* provides a direct indication; other devices, such as a *bridge*, must be adjusted, the measured quantities being determined from one or more adjustments (sometimes augmented with calculations).

instrumental error See INSTRUMENT ERROR.

instrument amplifier Also called INSTRUMENTATION AMPLIFIER. A high-gain, wideband amplifier that increases the sensitivity of an instrument (such as an oscilloscope, meter, or graphic recorder).

instrument-approach system See INSTRUMENT LANDING SYSTEM.

instrumentation Planning and providing instruments and instrument systems for the collection and, sometimes, storage and analysis of data.

instrumentation amplifier **1.** A form of integrated-circuit voltage amplifier designed for high linearity, high input impedance, and high common-mode rejection. It is intended for use with electronic instruments. **2.** See INSTRUMENT AMPLIFIER.

instrument chopper A refined chopper for converting a direct-current (dc) signal to alternating current (ac) for an ac instrument, such as a voltmeter or recorder.

instrument error Discrepancy in measured quantities resulting from inaccuracy of the instrument used, insertion resistance, environmental factors, operator error, etc.

instrument flight Also called *blind flight.* Aircraft flight guided by navigational instruments and signals alone. Required when visibility is extremely poor.

instrument fuse A fast-acting, low-current fuse used to protect a sensitive instrument, such as a galvanometer, milliammeter, and/or microammeter.

instrument lamp A light or lamp that illuminates the face of an instrument to facilitate viewing in the dark.

instrument landing Also called *blind landing.* Aircraft landing guided entirely by instruments. Required when visibility is poor and when landing is imperative at a given location at a given time.

instrument landing station The radio or radar station in a blind-landing system (see INSTRUMENT LANDING SYSTEM).

instrument landing system Abbreviation, ILS. The complete instrument and signal system (on the ground or in aircraft) required for an INSTRUMENT LANDING.

instrument multiplier See MULTIPLIER PROBE, **1**.

instrument preamplifier An external, sensitive amplifier for an instrument that has an internal input amplifier. Also see INSTRUMENT AMPLIFIER.

instrument relay See METER RELAY.

instrument resistance See METER RESISTANCE.

instrument shunt A resistance connected in parallel with a current-measuring instrument, used to increase the range of currents that can be measured.

instrument transformer A transformer used to change the range of an alternating-current meter.

5059F-pI_352-384 4/10/01 9:03 AM Page 371

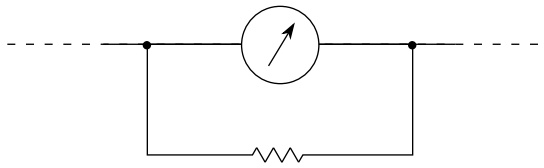

instrument shunt

For ammeters, it is called a *current transformer*; for voltmeters, it is called a *potential transformer*.

insulant A nonconducting material, used to prevent the flow of electric current between or among points. See INSULATOR, **1**.

insulated Isolated from conductors by an INSULANT.

insulated-gate field-effect transistor Abbreviation, IGFET. See METAL-OXIDE SILICON FET.

insulated resistor A resistor around which is molded a nonconducting material, such as vitreous enamel or a plastic.

insulating tape Electrical insulation in the form of a thin, usually adhesive, strip of fabric, paper, or plastic.

insulation **1.** A coating of dielectric material that prevents a short circuit between a conductor and the surrounding environment. **2.** The application of a dielectric coating to an electrical conductor. **3.** Electrical separation between or among different components, circuits, or systems.

insulation breakdown Current leakage through, and rupture of, an insulating material because of high-voltage stress.

insulation ratings Collectively, the dielectric constant, dielectric strength, power factor, and resistivity of an insulating material. Sometimes included are such physical properties as rupture strength, melting point, etc.

insulation resistance The very high resistance exhibited by a good insulating material. It is expressed in megohms (or higher units of resistance) for a sample of material of stated volume or area.

insulation system Collectively, the materials needed to insulate a given electronic device.

insulator **1.** A material that, ideally, conducts no electricity; it can, therefore, be used for isolation and protection of energized circuits and components (also see DIELECTRIC). Actually, no insulator is perfectly nonconductive (see, for example, INSULATION RESISTANCE). **2.** A molded piece of solid insulating material, used to electrically isolate conductors—especially in antenna systems and power transmission lines. **3.** Any body made from an insulating material.

insulator arcover A sudden arc, or flow of current, over the surface of an insulator, because of excessive voltage.

integer A positive or negative whole number, as opposed to a fraction or mixed number.

integral **1.** Also called *indefinite integral* and *antiderivative*. For given mathematical function f, function g, whose derivative is equal to f. **2.** Also called *definite integral*. The area under a curve of a function, between two vertical lines defined by two specific points in the domain of the function. **3.** The part of a number to the left of the radix point. **4.** Pertaining to integers (positive or negative whole numbers) or quantities that can be represented by integers.

integral action In automatic control operations, a control action delivering a corrective signal proportional to the time that the controlled quantity has differed from a desired value.

integral contact In a relay or switch, a contact that carries current to be switched.

integral-horsepower motor A motor rated at one horsepower.

integral multiple A whole multiple of a number. Thus, a harmonic is an integral multiple of fundamental frequency f: $2f$, $3f$, $4f$, etc.

integral number See INTEGER.

integrate **1.** To perform the function of mathematical or electrical INTEGRATION. **2.** To construct a circuit on a piece of semiconductor material.

integrated Constructed on a single piece of material, such as a semiconductor wafer.

integrated amplifier An audio-frequency (AF) amplifier having a preamplifier, intermediate amplifier, and output amplifier on a single chassis.

integrated capacitor In an integrated circuit, a fixed capacitor in which one plate is a layer of material diffused into the substrate, the dielectric is a thin-oxide film grown on top of the first layer, and the other plate is a metal layer deposited on top of the oxide film.

integrated circuit Abbreviation, IC. A circuit whose components and connecting "wires" are made by processing distinct areas of a chip of semiconductor material, such as silicon. Classified according to construction (e.g., *monolithic IC*, *thin-film IC*, *hybrid IC*).

integrated data processing Abbreviation, IDP. The detailed electronic classification, sorting, storage, and mathematical processing of data within a coordinated system of equipment, usually at one location.

integrated electronics The branch of electronics that is concerned with the design and fabrication of integrated circuits.

integrated resistor See DIFFUSED-LAYER RESISTOR.

Integrated Services Digital Network Abbreviation, ISDN. A communications network or connection intended primarily for Internet access via telephone lines. Allows significantly higher data speed than is possible with a conventional analog connection. In addition, it is possible to use a digital system, such as a computer, online simultaneously with an analog voice conversation.

5059F-pI_352-384 4/10/01 9:03 AM Page 372

integrating circuit See INTEGRATING NETWORK.

integrating galvanometer A device for measuring the change in electric flux produced in a coil in an electric field. Even very slow changes can be measured.

integrating meter An instrument whose indication is a summation (usually) of an electrical quantity that is time-dependent (e.g., *ampere-hour meter* and *watt-hour meter*).

integrating motor An electric motor that follows the integral of the input signal. The angle of rotation of the motor shaft is equal to the integral of the input waveform.

integrating network A four-terminal network whose output voltage is proportional to the time integral of the input voltage. It can be a passive resistance-capacitance (RC) circuit or it can use an operational amplifier. Compare DIFFERENTIATING NETWORK.

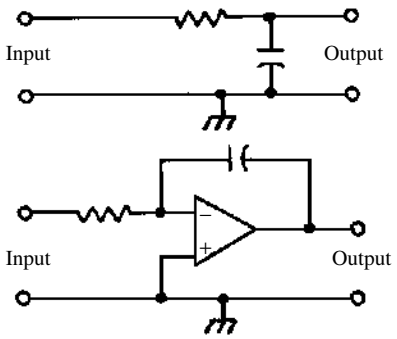

integrating networks

integrating photometer A photometer whose reading is the average candlepower at all angles in one plane.

integration **1.** The process of determining a mathematical function when its derivative is given. **2.** The processing of a signal by an INTEGRATOR circuit. **3.** Collectively, the processes by which an INTEGRATED CIRCUIT is manufactured.

integrator **1.** See INTEGRATING NETWORK. **2.** A device having an output variable whose value is proportional to the integral of one variable, with respect to another, or is proportional to the integral of an input variable, with respect to elapsed time.

intelligence **1.** Meaningful data that modulates a carrier [e.g., the voice or music in a frequency-modulated (FM) radio signal, or the image in a television signal]. **2.** Also called *machine intelligence.* The quality of a system or device, especially a computer, that allows it to "learn" (i.e., to better its capability by repeatedly operating on a given problem).

intelligence bandwidth **1.** The bandwidth necessary to convey a specified amount of data within a certain period of time. **2.** The total bandwidth of one complete signal channel in a communications or broadcast system.

intelligence signal **1.** A signal that conveys data or information. **2.** The modulating waveform in a communications or broadcast transmission.

intelligent network Abbreviation, IN. **1.** In general, any advanced and sophisticated communications network, particularly a broadband digital network. **2.** A network designed to readily accommodate new technologies and services, such as videoconferencing, interactive television, or remote control.

intelligent terminal A computer terminal (e.g., an input/output video display/keyboard unit) that through its circuitry (i.e., by use of a microprocessor) has some data-processing ability.

intelligibility tests Tests that measure the coherence of electronically reproduced speech.

intensification of image See IMAGE INTENSIFICATION.

intensifying ring In some electrostatic cathode-ray tubes, an internal metal ring serving as an extra anode to accelerate the beam and, thus, brighten the image.

intensity The degree or extent of a phenomenon (such as amplitude, brightness, loudness, power, force, etc.).

intensity control In an oscilloscope circuit, the potentiometer that adjusts the direct-current voltage on the control electrode of the cathode-ray tube and, accordingly, the brightness of the image. Also called BRIGHTNESS CONTROL and BRILLIANCE CONTROL.

intensity level **1.** A measure of sound magnitude, expressed in decibels, with respect to a value of one microwatt per square centimeter (10^{-6} W/cm^2) at sea level in the atmosphere. **2.** The setting of the brightness control in a cathode-ray-tube device.

intensity modulation **1.** Modulation of electron-beam intensity in a cathode-ray tube. Also called *z-axis modulation.* **2.** Sometimes, the video-signal modulation in a television image.

intensity-modulation amplifier The z-axis amplifier in an oscilloscope. Also see INTENSITY MODULATION.

interaction The (sometimes mutual) influence of one circuit or device on the behavior of another, as in induction.

interactive display A computer display device with which its operator can supply data to the computer in response to what is displayed. Example: *touch screen.*

interactive graphics A computer graphics system using a cathode-ray tube to draw or modify three-dimensional representations.

interactive photovoltaic system A solar-power plant that operates in conjunction with the utility

5059F-pI_352-384 4/10/01 9:03 AM Page 373

companies. Energy is sold to the companies during times of daylight and minimum usage, and is bought back from the companies at night or during times of heavy usage. The principal advantage of this system is that the user can keep using electricity (by buying it all from the utilities) if the solar-energy system breaks down. But such a system does not provide the independence from utility companies that some users desire. Compare STAND-ALONE PHOTOVOLTAIC SYSTEM.

interactive program A computer program in which the machine and its operator engage in two-way communication. Most personal computing software is of this type, in contrast to programs that carry out all their functions without operator intervention (other than initialization).

interactive television Television provided to consumers, in which viewers can transmit data, as well as receive it. For example, a survey might be conducted in which viewers are polled and send in their responses. Another example: products might be ordered while viewing an advertisement.

interactive mode See CONVERSATIONAL MODE.

interbase resistance The internal resistance between the bases of a unijunction transistor.

interblock A part of a computer program or a hardware device that will prevent interference between parts of a computer system.

interblock space **1.** On a magnetic tape, the space between recordings, caused by starting and stopping the tape. **2.** On magnetic tape used as a computer storage medium, the interval between recorded blocks.

intercarrier receiver A television (TV) receiver circuit in which video, sound, and sync components of the composite TV signal are amplified together in the radio-frequency (RF), intermediate-frequency (IF), and video IF stages; then they are separated in the video detector and video amplifier stages. Compare SPLIT-SOUND RECEIVER.

intercept receiver In military service, a search receiver tuned over a wide band of frequencies to locate and evaluate enemy signals.

interchangeability The ability of one component to substitute directly for another component of the same kind. Example: capacitor interchangeability, transistor interchangeability. Also see REPLACEMENT.

intercharacter space The three-unit interval between letter symbols in telegraphy. Compare INTERWORD SPACE.

intercom A comparatively simple two-way telephone or low-power radio system for use on the premises of a home or business.

intercommunicator See INTERCOM.

interconnection **1.** A mutual connection of separate circuits. **2.** The interconnection of two or more separate power-generating systems.

interdigital contacts A pair of contacts with "fingers" that are plated, printed, or deposited on the surface of a resistor material or semiconductor substrate. The fingers of each contact are interconnected at one end, the fingers of one contact being interleaved with those of the other.

interdigital tube A magnetron having a cathode surrounded by anode segments that are alternately interconnected at opposite ends in the manner of INTERDIGITAL CONTACTS.

interelectrode capacitance Capacitance between or among electrodes—especially between the plate and control grid of a vacuum tube.

interelement capacitance Internal pn-junction capacitance in a semiconductor device, such as a diode or transistor.

interface **1.** The circuitry that interconnects and provides compatibility between a central processor and peripherals in a computer system. **2.** Collectively, the hardware and software that allows a computer to interact with its operator. **3.** To provide an efficient pathway for data between two devices or systems. **4.** The meeting of surfaces or regions in a material. **5.** The surface of a body that mates with another body similar or identical to it.

interface resistance See CATHODE INTERFACE.

interface routine A computer program routine that links one system to another.

interfacial connection A connection that runs through a printed-circuit board and joins circuit joints on opposite faces of the board.

interference **1.** In communications, degradation of reception caused by noise or undesired signals. **2.** The interaction of acoustic or electromagnetic waves from more than one source, especially when they are of the same frequency, producing a characteristic INTERFERENCE PATTERN of high-amplitude and low-amplitude regions.

interference attenuator A device or mode of operation that reduces the amplitude of interference.

interference eliminator A filter, wavetrap, or similar device that removes interfering signals or noise. Also see INTERFERENCE.

interference filter See INTERFERENCE ELIMINATOR.

interference pattern A regular pattern of high-amplitude and low-amplitude regions, lobes, or bands, produced when waves of identical frequency from two or more sources combine in varying phase. Such patterns can be observed with sound, radio waves, infrared, visible light, ultraviolet, X rays, and gamma rays. The phenomenon is of interest in acoustic engineering, the design of radio antenna systems, and in physics (particularly optics).

interference stub A length of twin-lead feeder cut to appropriate length, connected to the antenna-input terminals of a television receiver, and short-circuited at the opposite end. A stub of the correct length resonates at the frequency of an interfering signal and, acting as a wavetrap, keeps it out of the receiver. Also see STUB.

5059F-pI_352-384 4/10/01 9:03 AM Page 374

interference trap A wavetrap that suppresses interfering signals at the rejection frequency of the trap.

interferometer **1.** A radio telescope having two antennas spaced at a distance of many wavelengths, providing much greater resolution than a single antenna. Pioneered by M. Ryle of England and J.L. Pawsey of Australia. **2.** Any device that displays an INTERFERENCE PATTERN for testing or experimental purposes.

interfix A method used in information-retrieval systems that eliminates ambiguity in the responses to inquiries by describing the relationship between keywords in a record.

Interframe A method of digital IMAGE COMPRESSION developed by *MPEG (Moving Picture Experts Group).* It operates by eliminating redundant data from between image frames. Compare INTRAFRAME.

interharmonic beats Beat notes produced by various combinations of the harmonics of a signal.

interim storage See TEMPORARY STORAGE.

interior label On a magnetic tape used as a computer-storage medium, a label recorded at the beginning of the tape. Compare EXTERIOR LABEL.

interior protection **1.** In electronic security applications, a set of sensors contained entirely within the region to be protected. **2.** The installation and operation of a security system whose sensors are all within the region to be protected.

interlace A form of data storage in which portions of the data are stored in alternate locations in the tape or disk.

interlaced field A video image field produced by INTERLACED SCANNING.

interlaced scanning In the display of a video image, the alternate presentation of the even- and odd-line fields. This process increases the obtainable image resolution for a given refresh rate, but can result in "jerkiness" of the image when rapid motion is portrayed.

interlace factor A number expressing the extent to which two fields are interlaced. Also see INTERLACED SCANNING.

interleaving In multiprogramming, the inclusion in a program of segments of another program so that both can be effectively executed simultaneously.

interlock switch See ELECTRICAL INTERLOCK.

intermediate amplifier See BUFFER.

intermediate frequency Abbreviation, IF. In a superheterodyne circuit, the frequency of the signal that results from beating the incoming signal with the signal produced by the local oscillator.

intermediate-frequency amplifier In a superheterodyne circuit, the fixed-frequency amplifier that boosts the intermediate-frequency signal. Also see INTERMEDIATE FREQUENCY.

intermediate-frequency channel Usually, the intermediate-frequency amplifier in a superheterodyne circuit, but sometimes including the second detector, automatic gain control (AGC), and oscillator stages.

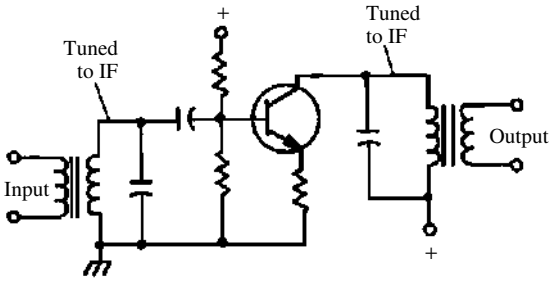

intermediate-frequency amplifier

intermediate-frequency converter See IF CONVERTER.

intermediate-frequency interference Interference from signals at the intermediate frequency of a receiver or instrument.

intermediate-frequency selectivity The selectivity of an intermediate-frequency (IF) channel alone, usually determined by the characteristics of the bandpass filter(s) in the IF channel.

intermediate-frequency transformer A coupling transformer designed for use in an intermediate-frequency amplifier.

intermediate-puck drive In a tape recorder, a speed-reducing drive system in which an intermediate wheel conveys motion from the motor shaft to the rim of the flywheel.

intermediate puck wheel See IDLER WHEEL.

intermediate repeater In wire telephony, a repeater inserted into a line or trunk at some point other than the end.

intermediate result Obtained during a program run or the execution of a subroutine, a result that is used again as an operand in deriving the final result.

intermediate section Any of the internal sections of a multisection filter. Thus, the middle section of a three-section filter.

intermediate storage In a computer system, a storage medium for temporarily holding totals or working figures. Also called WORK AREA.

intermediate subcarrier A modulated or unmodulated subcarrier that modulates either a carrier or another intermediate subcarrier.

intermittent **1.** Pertaining to a circuit fault, such as an open or short circuit, that occurs some of the time, but not all the time. **2.** See INTERMITTENT CONDITION. **3.** Pertaining to a phenomenon that is observed some of the time, but not all the time; sporadic. **4.** Pertaining to a DUTY CYCLE greater than zero, but less than 100 percent; usually between 25 and 50 percent.

intermittent commercial and amateur service Abbreviation, ICAS. Operation of equipment, such as radio transmitters, for short, irregular

5059F-pI_352-384 4/10/01 9:03 AM Page 375

periods, as in amateur (hobbyist) activity or infrequent commercial service. ICAS ratings are higher than continuous commercial service (CCS) ratings. Compare CONTINUOUS COMMERCIAL SERVICE.

intermittent condition A defect in a circuit or device that causes erratic and unreliable operation. The cause of such a problem is often difficult to determine.

intermittent dc See INTERMITTENT DIRECT CURRENT.

intermittent direct current A regularly pulsed unidirectional current. Also called PULSATING DIRECT CURRENT.

intermittent duty A DUTY CYCLE of less than 100 percent, but greater than zero. Generally, an operating duty cycle of 25 to 50 percent.

intermittent-duty rating The dissipation or power rating of a component, circuit, or system, under conditions of intermittent use, usually a 25-percent to 50-percent DUTY CYCLE.

intermittent operation Operation characterized by often long nonoperating intervals. Intermittent operation is often random, whereas on-off operation tends to be regular.

intermittent signal An interrupted signal resulting from the intermittent operation of a circuit or device.

intermodulation Abbreviation, IM. **1.** The (usually undesired) modulation of one signal by another, caused by nonlinear processing of the signals. **2.** The heterodyning of components in the sidebands produced by an amplitude-modulated (AM) or single-sideband (SSB) transmitter.

intermodulation distortion Abbreviation, IMD. **1.** Distortion products in the output of an amplitude-modulated (AM) or single-sideband (SSB) transmitter, caused by heterodyning of components in the sidebands. **2.** Distortion products in the output of an audio amplifier, caused by heterodyning of the fundamental components. **3.** The extent to which distortion as defined in 1 occurs. See INTERMODULATION-DISTORTION PERCENTAGE.

intermodulation-distortion meter See INTERMODULATION METER.

intermodulation-distortion percentage Abbreviation, IDP. The degree to which a low-frequency test signal modulates a higher-frequency test signal when both are applied simultaneously (in a prescribed amplitude ratio) to a device under test; $IDP = 100(b - a)/a$, where a is the peak-to-peak amplitude of the unmodulated high-frequency wave and b is the peak-to-peak amplitude of the modulated high-frequency wave.

intermodulation meter An instrument for measuring percentage of intermodulation distortion (IMD). The instrument combines a dual-frequency signal generator, filter circuits, and percent-of-modulation meter. Also see INTERMODULATION-DISTORTION PERCENTAGE.

intermodulation noise Electrical noise produced in one channel by signals in another; it is caused by INTERMODULATION.

internal absorptance The ratio of flux absorbed in a substance to the flux leaving at the entry surface of the substance. It does not include energy reflected at the entry surface.

internal amplification In a radioactivity counter tube, current enhancement resulting from cumulative ionization initiated by an ionizing particle.

internal arithmetic In a digital computer, arithmetic operations performed in the computer, as opposed to those performed by peripherals.

internal impedance The impedance in a device, as opposed to that added from the outside. Compare INTERNAL RESISTANCE.

internal input impedance The impedance in a circuit or device, as "seen" from the input terminals. Compare INTERNAL OUTPUT IMPEDANCE.

internal input resistance The resistance in a circuit or device, as "seen" from the input terminals. Compare INTERNAL OUTPUT RESISTANCE.

internal noise Electrical noise generated within a circuit, as opposed to that picked up from outside. Such noise comes from transistors, diodes, integrated circuits, resistors, and any other component through which current flows.

internal output impedance The impedance in a circuit or device, as "seen" from the output terminals. Compare INTERNAL INPUT IMPEDANCE.

internal output resistance The resistance in a circuit or device, as "seen" from the output terminals. Compare INTERNAL INPUT RESISTANCE.

internal resistance **1.** The resistance of a device, as opposed to added resistance. See, for example, METER RESISTANCE. **2.** In a cell or battery, the equivalent resistance, resulting from imperfect conductivity of the electrolyte and electrodes, which limits the maximum deliverable current.

internal thermal shutdown In an integrated circuit, the junction temperature at which thermal shutdown occurs. It is generally indicated in degrees Celsius (°C).

internal transmittance The ratio of flux reaching the exit surface of a material to the flux leaving the entry surface. Reflection is not taken into account. The sum of internal transmittance and INTERNAL ABSORPTANCE is always equal to 1.

international broadcast station A shortwave broadcast station transmitting programs for international reception between 6 and 26.6 MHz.

international callsign The call letters of a station, assigned within a country, according to the method of arrangement (identifying letters, or letters and numerals) prescribed by the International Telecommunication Union.

international candle See CANDLE.

international coulomb A unit of electrical quantity, equal to 0.99985 absolute coulomb.

international farad A unit of capacitance, equal to 0.99952 absolute farad.

5059F-pI_352-384 4/10/01 9:03 AM Page 376

international henry A unit of inductance, equal to 1.00018 absolute henry.

international joule A unit of energy, equal to 1.00018 absolute joule.

International Morse Code See CONTINENTAL CODE.

international ohm A unit of electrical resistance, equal to 1.000495 absolute ohm. The other international units are derived from this value.

International Radio Consultative Committee Abbreviation, CCIR (*Comite Consultatif International Radiodiffusion*). An international organization reporting to the International Telecommunication Union, and studying technical operations and tariffs of radio and television.

International Steam Table calorie A unit of heat energy equal to 4.1868 joules.

International System of Units Abbreviation, SI (*Systeme International d'Unites*). The system of units of measurement established in 1960 under the Treaty of the Meter. The base units are as follows.

–METER (m), length: 1,650,763.73 times the wavelength of the light emitted in a vacuum of krypton 86

–KILOGRAM (kg), mass: the mass of the protype kilogram kept at Sevres, France

–SECOND (s), time: the duration of 9,192,631,770 periods of the radiation that corresponds to the transition between the two hyperfine levels of the ground state of cesium 133

–KELVIN (K), thermodynamic temperature: $\frac{1}{273.16}$ the thermodynamic temperature of the triple point of water

–AMPERE (A), electric current: the current that, flowing through two infinitely long parallel wires in a vacuum and separated by 1 meter, produces a force of 2×10^{-7} newton per meter of length between the wires

–CANDELA (cd), luminous intensity: the luminous intensity of $\frac{1}{600,000}$ square meter of perfectly radiating surface at the temperature of freezing platinum

International Telecommunication Union Abbreviation, ITU. An international, nongovernmental organization devoted to standardizing worldwide communications practices and procedures.

International Telegraph and Telephone Consultative Committee See CCITT.

International Telegraph Consultative Committee See CCIT.

international units A system of electrical units, based on the resistance through a specified quantity and configuration of the element mercury. The INTERNATIONAL OHM forms the basis for the international system of units.

international volt A unit of electrical potential, equal to 1.00033 absolute volt.

international watt A unit of power, equal to 1.00018 absolute watt.

Internet A worldwide, interconnected system of computer networks. Originated in the late 1960s as *ARPAnet* (Advanced Research Projects Agency network). Still used extensively by educators and scientists, but gaining popularity among personal-computer users. Sometimes called the INFORMATION SUPERHIGHWAY.

interphone An intercom aboard a mobile vehicle.

interpolation Finding a value that falls between two values listed in a table, indicated by a dial, plotted on a graph, derived by estimate, or given by intermediate calculation. For example, if a linear variable capacitor has a value of 100 pF when its dial is set to 10, and 140 pF when the dial is set to 20, then the capacitance when the dial reads 15 (midway between 10 and 20) can be assumed to be 120 pF (midway between 100 pF and 140 pF). When functions are not linear, interpolation is usually not exact.

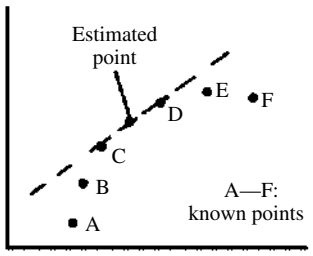

interpolation

interpolation meter See INTERPOLATION-TYPE INSTRUMENT.

interpolation oscillator A frequency-measuring signal generator with a built-in crystal oscillator, whose harmonics provide calibration points on the tuning dial. The dial provides a continuous indication of generator frequencies between crystal-harmonic points. Also see INTERPOLATION-TYPE INSTRUMENT.

interpolation-type instrument An instrument, such as a meter or signal generator, that is used to transfer an accurate quantity point from a standard to another instrument and to provide a range of values between such points. A secondary standard is sometimes used as an interpolation-type instrument (see, for example, INTERPOLATION OSCILLATOR).

interpole motor A direct-current motor with small auxiliary poles (*interpoles*) between its main field poles. The interpoles reduce sparking at the commutator.

interpreter A computer program that can convert instructions given in a high-level language (BASIC, for example) into the machine language that

5059F-pI_352-384 4/10/01 9:03 AM Page 377

a computer uses; if it is not resident in the computer's nonvolatile memory, it must be loaded each time the machine is activated.

interrecord gap See INTERBLOCK SPACE.

interrupt A break in a computer program, as when a background job is interrupted so that a foreground job can be run. Also see BACKGROUND JOB and FOREGROUND JOB.

interrupted commercial and amateur service See INTERMITTENT COMMERCIAL AND AMATEUR SERVICE.

interrupted continuous wave Abbreviation, ICW. A continuous wave that is interrupted at regular intervals, as in the chopping of a wave at a regular rate. Compare CONTINUOUS WAVE (CW) and MODULATED CONTINUOUS WAVE (MCW).

interrupted dc A direct current or voltage that is periodically started and stopped by switching or chopping.

interrupter contacts Auxiliary contacts operated directly by the armature of a stepping switch.

interruption frequency See QUENCHING FREQUENCY.

interruption-frequency oscillator See QUENCH OSCILLATOR.

interrupt signal The signal that causes a break (INTERRUPT) in a computer program.

intersatellite communication **1.** Communication between or among satellites. **2.** Communication between two earth-based stations, using two or more satellites. **3.** Communication between an earth-based station and a satellite-based station, using at least one intermediate relaying satellite.

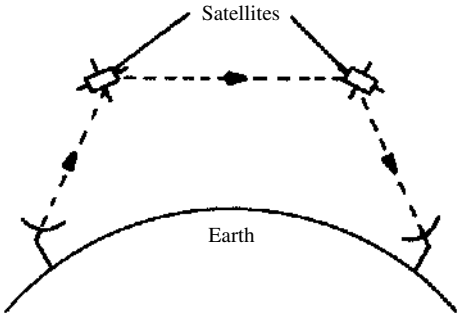

intersatellite communication

intersecting storage ring A device for producing great amounts of energy. It is similar to a vacuum tube. High-speed subatomic particles are fed to a ring-shaped evacuated structure in opposite directions. The two particle beams collide at various points, yielding high energy.

intersection The logical AND operation.

interstage capacitor A coupling capacitor used between two circuit stages.

interstage coupling The transfer of a signal between two circuit stages, such as those of an amplifier. Common forms of interstage coupling include *direct coupling*, *capacitive coupling*, *transformer coupling*, *diode coupling*, and *optoisolator coupling*.

interstage diode A semiconductor coupling diode used between two circuit stages.

interstage transformer A coupling transformer used between two circuit stages. It provides direct-current isolation, and also can match purely resistive impedances.

intersymbol interference In a digital communications signal, a condition in which a given symbol overlaps with one or more other symbols (either immediately preceding it or immediately following it), upsetting the ability of the receiver to decipher signals in certain time intervals. The phenomenon is sometimes a problem in time-division multiplexing—especially at data speeds near the maximum for the system.

intersystem A power-generating network of interconnected separate systems.

intersystem communications Communications between computer systems, either through direct linking of central processors, or by mutual use of peripherals and input/output channels.

intertie See INTERCONNECTION, **2**.

interval **1.** The amount of separation between successive points, events, or quantities. **2.** The continuous range of values between two defined points. **3.** A specific period of time, with defined beginning and ending points.

intervalometer A timing device for operating equipment over a precisely defined time interval.

interval timer A device that provides power to an equipment for a precise interval upon application of a simple initiating signal or action. See also INTERVALOMETER.

interword space The seven-unit interval between words or code groups in telegraphy. Compare INTERCHARACTER SPACE.

intoxication tester See DRUNKOMETER.

intracoding The coding of data using only data that it contains.

Intrafax Western Union's private facsimile system.

Intraframe A method of digital IMAGE COMPRESSION developed by *MPEG (Moving Picture Experts Group)* and *JPEG (Joint Photographic Experts Group)*. It operates by eliminating redundant data within image frames. Compare INTERFRAME.

intrinsic-barrier diode See PIN DIODE.

intrinsic-barrier transistor A bipolar transistor with a layer of intrinsic semiconductor between one of its pn junctions.

intrinsic concentration The number of minority carriers exceeding the normal equilibrium number in a semiconductor.

intrinsic conduction The flow of electron/hole pairs in an intrinsic semiconductor subjected to an electric field.

5059F-pI_352-384 4/10/01 9:03 AM Page 378

intrinsic flux A quantity equal to the product of the intrinsic flux density and the cross-sectional area in a magnet.

intrinsic flux density The increased flux density of a magnet in its actual environment, as compared with the flux density resulting from the same magnetizing force in a perfect vacuum.

intrinsic mobility Electron mobility in an intrinsic semiconductor. Also see CARRIER MOBILITY and MOBILITY.

intrinsic *Q* The value of the *Q*, also known as the FIGURE OF MERIT, for an unloaded circuit. This value is generally higher than the value when a load is connected to the circuit.

intrinsic semiconductor A semiconductor whose characteristics are identical to those of a pure crystal of the material. In this condition, the semiconductor is nearly an insulator. Example: highly purified germanium or silicon before n- or p-type impurities have been added. Compare EXTRINSIC SEMICONDUCTOR.

intrusion alarm A set of electronic sensors and associated circuitry composing a system that detects and warns of the presence of unauthorized personnel within a specific region.

intrusion sensor A sensitive pickup (such as a photocell, ultrasonic detector, or capacitive transducer) that responds to a nearby body by delivering an actuating signal to an intrusion alarm.

INV Abbreviation of INVERTER.

inv Abbreviation of INVERSE.

Invar A nickel-steel alloy (36% nickel) having a low temperature coefficient of linear expansion (1 ppm/°C). Invar is used in electronic equipment where mechanical distortion resulting from temperature changes must be negligible, and in magnetostrictive circuits (see MAGNETOSTRICTION).

inverse **1.** Opposite in nature (e.g., an INVERSE CHARACTERISTIC). **2.** Of opposite sign (e.g., a negative current or voltage). **3.** An operation of opposite kind; thus, subtraction is the inverse of addition, and division is the inverse of multiplication.

inverse beta The beta of a transistor operated with the emitter and collector interchanged.

inverse bias See REVERSE BIAS.

inverse characteristics The characteristics of a bipolar transistor when operated with the emitter and collector reversed.

inverse conduction See REVERSE CONDUCTION.

inverse cube law A principle relating the intensity of an effect to the reciprocal of the cube of the distance from the source. The magnetic field around a solenoidal coil of wire obeys this principle.

inverse current See REVERSE CURRENT.

inverse-distance law The inverse-square law applied to the propagation of radio waves, assuming that the waves do not encounter obstacles.

inverse feedback See DEGENERATION.

inverse fourth-power law A rule of propagation for certain complex forms of energy: $I = k/d^4$, where I is the intensity of the field, d is the distance from the source, and k is a constant.

inverse impedances Impedances (Z_1 and Z_2) that are the reciprocal of another impedance (Z_3), satisfying the relationship $Z_1Z_2 = (Z_3)^2$. Also called RECIPROCAL IMPEDANCES.

inverse leakage The flow of a small static reverse current in semiconductor devices.

inverse-parallel circuit See BACK-TO-BACK CIRCUIT and BACK-TO-BACK CONNECTION.

inverse peak voltage See PEAK INVERSE VOLTAGE.

inverse piezoelectric effect Mechanical movement in a piezoelectric material, caused by application of voltage.

inverse resistance See REVERSE RESISTANCE.

inverse resonance See PARALLEL RESONANCE.

inverse-square law The energy or power intensity of a phenomenon is inversely proportional to the square of the distance from the source. This is often applied to quantitative reasoning about radiant energy, electromagnetic energy, and acoustic energy. Thus, if the distance doubles, the energy or power drops to ¼ its previous value.

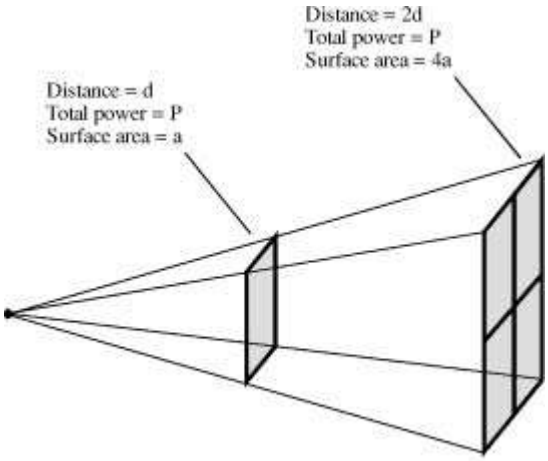

inverse-square law

inverse trigonometric function An angle expressed in terms of a given trigonometric function, followed by the exponent -1 or preceded by "arc" (sin^{-1} is the equivalent of *arcsin*).

inverse voltage **1.** The negative voltage at the anode of a rectifier during the negative half-cycle of alternating-current (ac) input. **2.** The voltage across a power-supply filter capacitor during the

5059F-pI_352-384 4/10/01 9:03 AM Page 379

negative half-cycle of ac input. **3.** Semiconductor-junction reverse voltage.

inverse Wiedeman effect See DIRECT WIEDEMAN EFFECT.

inversion **1.** A reversal of the normal vertical temperature gradient of the atmosphere, often resulting in long-distance tropospheric radio-wave propagation. **2.** Speech scrambling (see SCRAMBLER CIRCUIT). **3.** Phase inversion (see PHASE INVERTER). **4.** Changing direct current into alternating current, often increasing the voltage (see INVERTER, **1**).

inverted amplifier A push-pull, grounded-gate, field-effect-transistor (FET) amplifier.

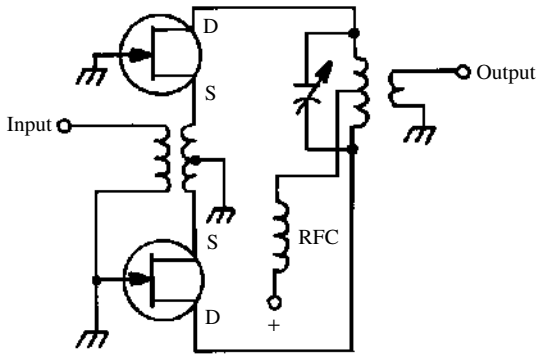

inverted amplifier

inverted-L antenna An antenna having a horizontal radiator and a vertical feeder or lead-in attached to one end of the radiator. The entire arrangement resembles an upside-down L. The overall length is generally ¼ to ½ wavelength.

inverted speech See SCRAMBLED SPEECH.

inverter **1.** Also called *power inverter.* A device that converts direct current (dc) into alternating current (ac), often of a much higher voltage (e.g., 12 Vdc into 117 Vac). **2.** A logic circuit that provides an output pulse that is a negation of the input pulse. Also called a COMPLEMENTER or a NOT CIRCUIT. **3.** See PHASE INVERTER.

inverting adder An analog adder circuit that is provided with an amplifier for a 180° phase shift.

inverting amplifier An amplifier providing a 180° phase shift between input and output.

inverting connection Connection to the inverting input terminals of a differential amplifier or operational amplifier. Also see INVERTING INPUT. Compare NONINVERTING INPUT.

inverting input In a differential amplifier or operational amplifier, the input circuit that produces a phase reversal between the input and output. Compare NONINVERTING INPUT.

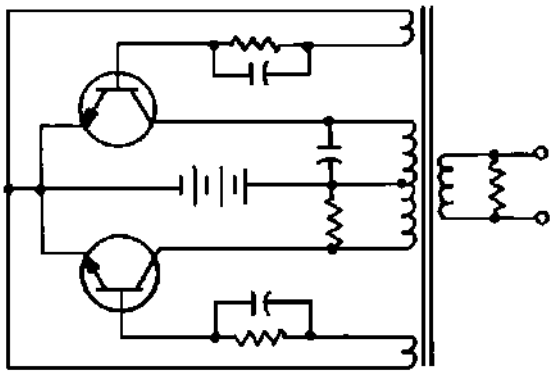

inverter, 1

In	Out
0	1
1	0

inverter, 2

inverting transponder In a communications satellite, a transponder in which the downlink band is "upside-down" in frequency relative to the uplink band. That is, the highest downlink frequency corresponds to the lowest uplink frequency, and the lowest downlink frequency corresponds to the highest uplink frequency. Compare NONINVERTING TRANSPONDER. See also DOWNLINK, TRANSPONDER, UPLINK.

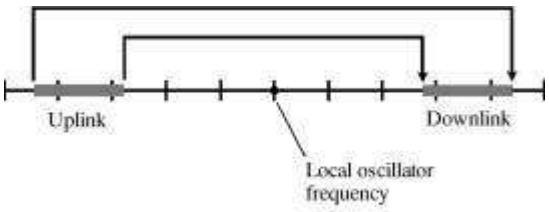

inverting transponder

invisible failure In a computer system, a hardware or software failure whose effect on the system is unnoticeable in a given application. A failure that is invisible in one application might be vividly apparent in some other application.

invister A unipolar semiconductor material, capable of operation at very high frequencies.

5059F-pI_352-384 4/10/01 9:03 AM Page 380

involution Raising a number to a power: squaring, cubing, etc. Compare EVOLUTION.

inward-outward dialing Also called *direct dialing.* In a telephone system, a method of dialing in which calls can be made to and from branch exchanges, without operator assistance.

I/O Abbreviation of *input/output* (see INPUT/OUTPUT EQUIPMENT).

Io Symbol for OUTPUT CURRENT.

iodine Symbol, I. A nonmetallic element of the halogen family. Atomic number, 53. Atomic weight, 126.905. Also see HALOGEN.

ion A charged atom [i.e., one that has gained one or more electrons (a negative ion, or *anion*) or lost one or more electrons (a positive ion, or *cation*)].

ion burn A spot burned on the screen of a cathode-ray tube by negative ions from the cathode striking a single point on the faceplate with high intensity for long periods.

ion concentration **1.** The number of ions, expressed as a percentage or as a number per unit volume, in a substance. **2.** Ionization density in the atmosphere.

ion exchange resins Granular resins that contain acid or base groups, and that trade ions with salts in solutions. The resins play a part in the purification of water for various industrial processes.

ionic binding forces In a crystal, the binding forces that occur when valence electrons of one atom are joined to those of a neighboring atom whose outer shell they fill.

ionic bond In a solid, a bond between atoms, formed as a result of the attraction between oppositely charged atoms (ions).

ionic conduction Conduction, as in a gas or electrolyte, by ion migration (positive to the cathode, negative to the anode).

ionic crystal A crystal whose lattice is held together by the electric forces between ions. Also see IONIC BINDING FORCES and IONIC BOND.

ionic current Current caused by ion movement in a gas or liquid. Also see ION, IONIZATION, and IONIC CONDUCTION.

ionic semiconductor A semiconductor in which the carrier is an ion, as opposed to an electron or hole.

ionic switch See ELECTROCHEMICAL SWITCH.

ionization **1.** The loss or gain of one or more electrons by an atom. Also see ANION, CATION, and ION. **2.** The formation or existence of significant numbers of ions in a gas, liquid, or solid (e.g., ionization of the upper atmosphere).

ionization arc The electrical discharge resulting from the ionization of a material because of high voltage.

ionization chamber An enclosure containing a gas and a pair of electrodes between which a high voltage is applied. Radiation, such as X rays or radioactive particles, passing through the walls of the chamber ionize the gas, creating an ionization current that is proportional to the intensity of the radiation.

ionization current **1.** Current in an ionized gas (such as air). **2.** Current flowing in an electrolyte. **3.** Current in an ionization chamber, Geiger-Mueller tube, or similar gaseous device. **4.** In a gas tube, current flowing after the ignition potential has been reached. **5.** Negative grid current resulting from gassiness in a vacuum tube.

ionization density The extent to which ionization exists in an ionized layer of the atmosphere. The higher the ionization density, the greater the effect on radio waves—especially at frequencies below about 150 MHz.

ionization gauge A form of vacuum tube that can be used to measure the hardness of a vacuum. It consists of a cathode, an anode (plate), and a positively charged grid. Plate current flows as a result of ionization of the atoms within the tube. The more nearly perfect the vacuum, the lower the plate current.

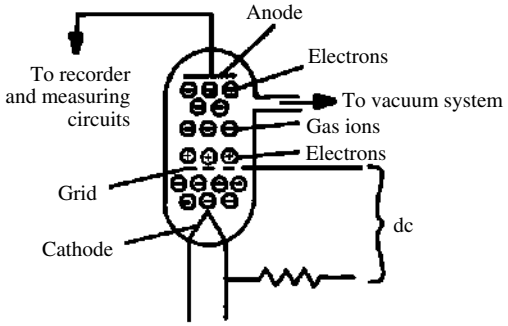

ionization gauge

ionization potential The voltage at which a substance (especially a gas) ionizes. Also called (for a gas) *ignition potential* (see BREAKDOWN VOLTAGE).

ionization pressure In an ionized gas, the pressure increase resulting from the ionization, as compared with the same volume and mass of gas when not ionized.

ionization resistance See CORONA RESISTANCE.

ionization smoke detector A device that senses the presence of smoke or other particles as a result of changes in the IONIZATION CURRENT through the air. When the ionization current suddenly changes, a signal is sent to an alarm circuit.

ionization time The interval, usually measured in microseconds or milliseconds, between the instant that an ionizing potential is applied to a gas, and the instant at which the gas begins to ionize. Compare DEIONIZATION TIME.

5059F-pI_352-384 4/10/01 9:03 AM Page 381

ionization trail The ionized path of a meteor as it passes through the upper atmosphere.

ionize To cause the electrons in a substance, particularly a gas, to move freely from atom to atom.

ionized gas A gas whose atoms, under the influence of a strong electric field or IONIZING RADIATION, have become positive or negative ions.

ionized layer See KENNELLY-HEAVISIDE LAYER.

ionized liquid See ELECTROLYTE.

ionizing radiation **1.** Any high-energy electromagnetic radiation that causes ionization in a gas through which the field passes. Examples: ultraviolet, X rays, and gamma rays. **2.** High-speed atomic nuclei (e.g., protons or alpha particles).

ion migration The movement of ions through a solid, liquid, or gas because of the influence of an electric field.

ionosphere **1.** Any of several ionized regions at specific altitudes above the earth's surface. These layers cause absorption and refraction of electromagnetic (EM) fields at some radio frequencies. The D layer exists at an altitude of about 30 miles (50 km) and is ordinarily present only on the daylight side of the planet. This layer does not contribute to, and in fact sometimes hinders, wireless communications. The E layer, about 50 miles (80 km) above the surface, also exists mainly during the day, but nighttime ionization is sometimes observed. The E layer can facilitate medium-range radio communication at certain frequencies. The uppermost regions are the F1 and F2 layers. The F1 layer, normally present only on the daylight side of the earth, forms at about 125 miles (200 km) altitude; the F2 layer exists at about 180 miles (300 km) more or less around the clock. Sometimes the distinction between the F1 and F2 layers is ignored, and they are spoken of together as the F layer.

ionospheric disturbance See IONOSPHERIC STORM.

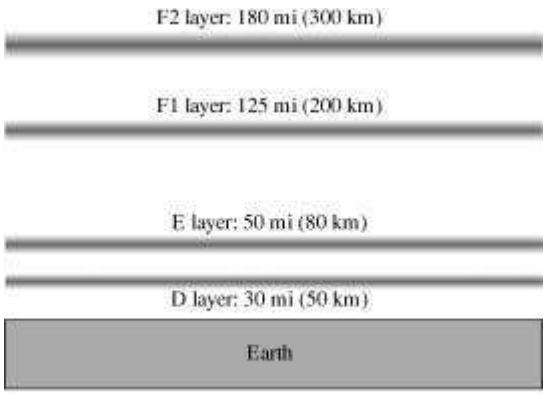

ionosphere

ionospheric forecasting Predicting ionospheric conditions. Radio propagation data is derived from such predictions.

ionospheric layers The respective layers of the ionosphere: *D layer* (at an altitude of about 30 mi or 50 km), *E layer* (at an altitude of about 50 mi or 80 km), the *F1 layer* (at an altitude of about 125 mi or 200 km), and the *F2 layer* (at an altitude of about 180 mi or 300 km). The F1 layer is generally present only in the daytime.

ionospheric propagation Propagation of radio waves by means of reflection or refraction by the ionosphere. Also see HOP; INCIDENT WAVE; IONOSPHERE; MULTIHOP PROPAGATION; REFLECTED WAVE, **1**; REFRACTED WAVE; and SKYWAVE.

ionospheric storm Turbulence in the ionosphere, usually accompanied by a magnetic storm and caused by high-speed particles emitted from an eruption on the sun.

ion sensor A device whose operation is based on the detection of ions and the delivery of a proportionate voltage. Examples are the *Geiger counter*, *halogen gas leak detector*, *mass spectrometer*, and *vacuum gauge.*

ion spot See ION BURN.

ion trap See BENT-GUN CRT.

ion-trap magnet An external (usually double) magnet used with a television picture tube to deflect the ion beam away from the screen. This prevents ION BURN.

I/O port That part of a computer providing, via a connector, a point through which data can enter from, or exit to, peripheral equipment.

I_P **1.** Abbreviation of PLATE CURRENT. **2.** Abbreviation of PEAK CURRENT.

I-phase carrier In color television, a carrier separated by 57 degrees from the color subcarrier.

I-picture A video image that is coded using only data that it contains.

ipm Abbreviation of INCHES PER MINUTE.

ips Abbreviation of INCHES PER SECOND.

IR **1.** The product of current and resistance (see, for example, IR DROP). **2.** Abbreviation of INSULATION RESISTANCE. **3.** Abbreviation of INFRARED.

I_r Symbol for IRIDIUM.

I_r Symbol for CURRENT in a resistor.

IRAC Abbreviation for *Interdepartment Radio Advisory Committee* (a federal government group in the United States).

IR diode See INFRARED DIODE.

IR drop The voltage drop (E) across a resistance (R) when there is a current (I) through the resistor; according to Ohm's law, $E = IR$.

IRE Abbreviation for *Institute of Radio Engineers*, the predecessor of the IEEE (*Institute of Electrical and Electronics Engineers*).

IRED Abbreviation for INFRARED-EMITTING DIODE.

I_{RF} Symbol for RADIO-FREQUENCY CURRENT.

5059F-pI_352-384 4/10/01 9:03 AM Page 382

iridescence A sparkling, colorful appearance in a material, resulting from refraction, internal reflection, and interference in light waves passing through the substance. It is especially noticeable in quartz and certain gems.

iridium Symbol, Ir. A metallic element of the platinum group. Atomic number, 77. Atomic weight, 192.22.

iron Symbol, Fe. A ferromagnetic, metallic element. Atomic number, 26. Atomic weight, 55.847. Iron (and its special form, steel) is widely used in magnetic circuits.

iron/constantan thermocouple A thermocouple consisting of a junction between wires or strips of IRON and CONSTANTAN.

iron core A transformer or choke core made from iron or steel. The core is usually laminated to reduce eddy-current loss.

iron-core coil An inductor having an iron or steel core, usually laminated to reduce eddy-current loss.

iron-core IF transformer An intermediate-frequency transformer having a core of powdered iron, a form of iron that has the advantage of high permeability while greatly minimizing eddy currents.

iron-core transformer A transformer whose coils are wound on a core of laminated iron or steel.

iron loss Power lost in the iron cores of transformers, inductors, and electrical machinery as a result of eddy currents and hysteresis.

iron magnet A permanent magnet consisting of magnetized iron or a mixture of iron and nickel.

iron oxide A compound of iron and oxygen, whose most familiar form is common rust. The several variants have characteristics that depend on the number of iron and oxygen atoms in the iron-oxide molecule. See, for example, MAGNETITE and RED OXIDE OF IRON.

iron pyrites Formula, FeS_2. Natural iron sulfide that occurs as bright yellow crystals in its natural state.

iron-vane meter An alternating-current meter whose movable element, a soft iron vane, carries the pointer and pivots near a similar, stationary vane. The vanes are mounted in a multiturn coil of wire. The current flows through the coil, the resulting magnetic field magnetizing the vanes. Because the magnetic poles of the vanes are identical, they repel each other; the movable vane is deflected (against the torque of returning springs) over an arc proportional to the current, carrying the pointer over the scale.

irradiance The amount of radiant flux impinging on a unit surface area; it is generally specified in watts per square meter (W/m^2).

irradiation **1.** Exposure of a device to radioactivity or X rays. **2.** The total radiant power density that is incident upon a receiving surface.

irrational number A number that cannot be expressed as the quotient of two integers. Its decimal expansion is nonterminating and nonrepeating.

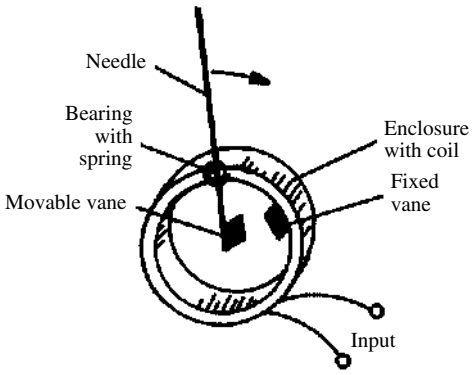

iron-vane meter

irregularity **1.** The condition of being nonuniform, or rapidly fluctuating, rather than constant. **2.** A departure from normal operating conditions. **3.** Nonuniformity in a surface. **4.** Nonuniform distribution of matter. **5.** Nonuniform distribution of data.

irregular wave A wave disturbance, or the plot of such a disturbance versus time, that has a complex, periodic, repeating nature.

IR viewer A device that allows observation of images at infrared wavelengths. See SNIPERSCOPE and SNOOPERSCOPE.

I_s **1.** Symbol for source current in a field-effect transistor. **2.** Symbol for *screen current* in a vacuum tube.

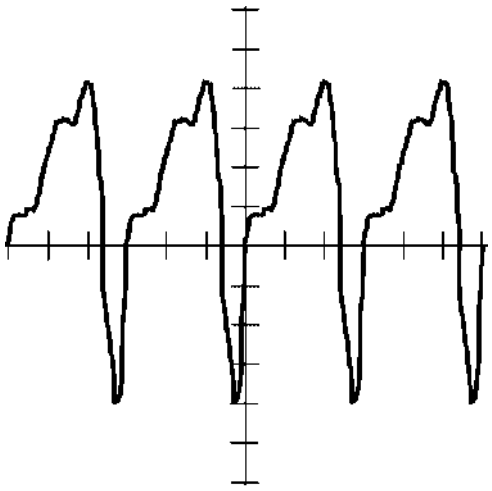

irregular wave

5059F-pI_352-384 4/10/01 9:03 AM Page 383

ISDN Abbreviation for INTEGRATED SERVICES DIGITAL NETWORK.

ISCAN Abbreviation of *inertialess steerable communications antenna.*

I-scan A radar display in which the target is shown as a complete circle, whose radius is proportional to the distance to the target.

I-signal With the Z-signal, one of the two signals that modulates the chrominance subcarrier in color television. The I-signal results from mixing a B-Y signal (with -0.27 polarity) and an R-Y signal (with +0.74 polarity).

Isinglass Thinly laminated mica.

ISO Abbreviation for *International Standards Organization.*

ISO 9660 A standard format for producing CD-ROM (COMPACT DISK READ-ONLY MEMORY) mass storage media for use with computers. It is a part of the YELLOW BOOK scheme.

isobar **1.** An atom whose nucleus has the same weight as that of another atom but differs in atomic number. **2.** On a weather map, a line connecting points of equal pressure. Also see BAR, **1**.

isochromal phenomena **1.** Effects occurring at regular time intervals. **2.** Effects of equal duration.

isochromatic Also *orthochromatic.* **1.** The quality of having or producing natural visible-light hues. **2.** Color sensitivity excluding a response to red.

isochronal See ISOCHRONE.

isochrone On a map, a line connecting points of constant time difference in radio-signal reception. It is useful in radiolocation and radionavigation.

isochronous Having identical resonant frequencies or wavelengths.

isoclinic line See ACLINIC LINE.

isodose Pertaining to points receiving identical dosage of radiation.

isodynamic line On a map of the geomagnetic field (the earth's magnetic field), a line connecting points of equal flux density.

isoelectric Having a potential difference of zero.

isoelectronic Having the same number of electrons.

isogonal **1.** See ISOGONIC LINE. **2.** Having uniform magnetic declination at all points.

isogonic line On a map of the geomagnetic field (the earth's magnetic field), a line connecting points of equal magnetic declination.

isolantite An insulating ceramic. Dielectric constant, 6.1.

isolated **1.** Electrically insulated. **2.** Separated in such a way that interaction does not take place.

isolated input **1.** An ungrounded input. **2.** An input circuit with a blocking capacitor to prevent the passage of direct current.

isolated location In a computer, a storage location that is hardware-protected from being addressed by a user's program.

isolating amplifier See BUFFER, **1**.

isolating capacitor A series capacitor inserted in a circuit to pass an alternating-current signal while blocking direct current. Also called a BLOCKING CAPACITOR.

isolating diode A diode used (because of its unidirectional conduction) to pass signals in one direction, but block them in the other direction.

isolating resistor A high-value resistor connected in series with the input circuit of a voltmeter or oscilloscope to protect the instrument from stray pickup. In most voltmeters, this resistor is built into the probe.

isolating transformer A power transformer, usually having a 1:1 turns ratio, for isolating equipment from direct connection to the power line.

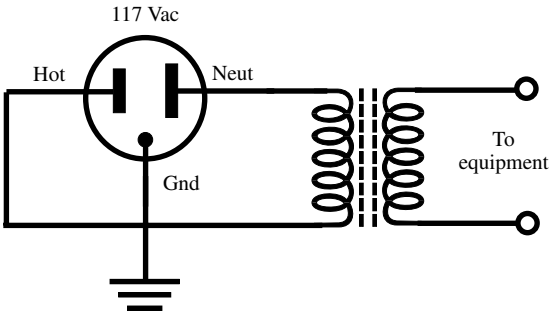

isolating transformer

isolation The arrangement or operation of a circuit so that signals in one portion are not transferred to (nor affect) another portion.

isolation amplifier See ISOLATING AMPLIFIER.

isolation capacitor See ISOLATING CAPACITOR.

isolation diode **1.** In an integrated circuit, a reverse-biased diode that is formed in the substrate to prevent cross-coupling and grounds. **2.** See ISOLATING DIODE.

isolation resistor See ISOLATING RESISTOR.

isolation transformer See ISOLATING TRANSFORMER.

isolator See OPTOELECTRONIC COUPLER.

isolith A form of monolithic integrated circuit, in which the semiconductor is removed in certain places for the purpose of isolating different parts of the circuit.

isomagnetic Having equal magnetic intensity.

isomer A material that has the same atomic number or chemical formula as some other substance, but, because of a difference in the atomic structure, is an entirely different substance. An example is carbon; it can be either *graphite* (by far the more common form) or *diamond.*

isophote On a graph of visible-light intensity, a curve joining points of equal brightness.

isoplanar An integrated-circuit configuration in which insulating barriers or metal oxides are fabricated among the bipolar elements.

5059F-pI_352-384 4/10/01 9:03 AM Page 384

isothermal process A physical or chemical process in which there is no temperature change as other factors vary. Compare ENDOTHERMIC REACTION and EXOTHERMIC REACTION.

isotope An atom having the same number of protons as another atom, thereby composing the same chemical element, but having a different number of neutrons. Thus, *deuterium* is an isotope of *hydrogen.* Some isotopes are radioactive [e.g., *carbon 14* (an isotope of the more-common *carbon 12*)]. The two extra neutrons in carbon 14 make it less stable than carbon 12.

isotropic antenna A theoretically ideal antenna that transmits and/or receives electromagnetic fields equally well, and with 100-percent efficiency, in all directions in three-dimensional free space.

isotropic radiator A theoretically ideal radiating element that transmits electromagnetic fields equally well, and with 100-percent efficiency, in all directions in three-dimensional free space.

I_{sup} Symbol for *suppressor current.*

I(t) Symbol for INDICIAL RESPONSE.

ITD Abbreviation for INITIAL TIME DELAY.

item **1.** Component. **2.** Any one of a number of similar or identical components, circuits, or systems.

iteration Repeating a series of arithmetic operations to arrive at a solution to a problem. Computers are commonly programmed to do this thousands, millions, or billions of times. Such a program must include a statement of acceptable accuracy so that it knows when to leave the iteration loop.

iterative impedance In a network consisting of identical, cascaded sections, the input impedance of a section to which the output impedance of the preceding section is made equal.

iterative routine A program or subroutine that provides a solution to a problem by iteration.

iterative transfer constant Symbol, *P.* A property of ITERATIVE IMPEDANCE networks. If I_i is the network input current and I_o is the network output current, then $P = \log_e(I_o/I_i)$.

ITU Abbreviation for *International Telecommunication Union.*

ITV **1.** Abbreviation of INDUSTRIAL TELEVISION. **2.** Abbreviation for INTERACTIVE TELEVISION.

I-type semiconductor See INTRINSIC SEMICONDUCTOR.

I_X Symbol for *current in a reactance.*

I_Y Symbol for *current in an admittance.*

I_Z Symbol for *current in an impedance.*

-ize A suffix used, with some liberty, to form verbs from nouns. In electronics, this commonly refers to procedures or processes (e.g., to ANODIZE, ELECTROCIZE, PLASTICIZE, or TRANSISTORIZE).

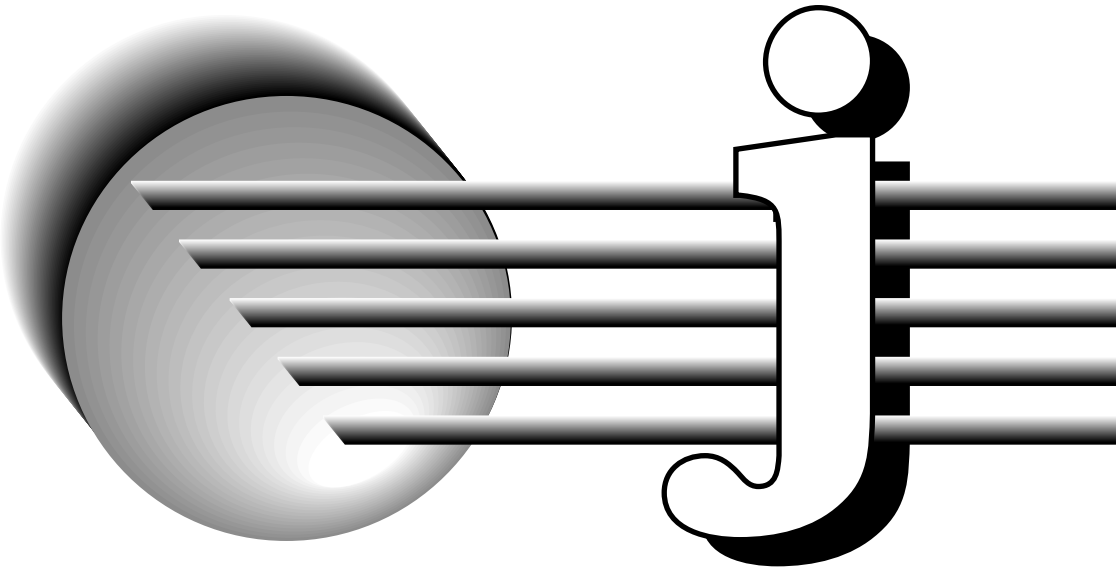

J **1.** Abbreviation for JOULE. **2.** Symbol for JACK or CONNECTOR. **3.** Symbol for EMISSIVE POWER.

***j* (*j* operator)** The square root of –1; an imaginary number (usually denoted *i* in mathematics). Assigned to reactance values depicted on the vertical axis of the resistance-reactance (RX) plane in impedance vector diagrams, and whose currents are 90 degrees out of phase with the current in the resistive part of an alternating-current circuit.

jack A receptacle for a plug. A plug (a male connector) is inserted into a jack (a female connector) to complete a circuit or removed from it to break a circuit.

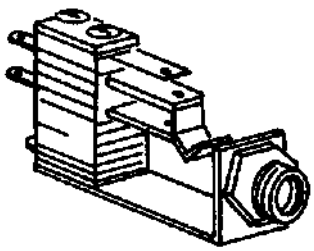

jack

jack box A (usually metallic) box or can used to hold, shield, or protect a jack or group of jacks.

jacket **1.** The outer covering on a cable, as opposed to the insulation or dielectric separating the individual conductors within the cable. **2.** An insulating outer case or wrapper on a component, such as a capacitor. **3.** A shield can or shield box. **4.** A heat-radiating or water-conducting enclosure used in cooling a power vacuum tube.

jack panel A (usually metallic) panel in which a number of jacks are mounted, usually in some order or sequence as denoted by labels.

jack panel

jackscrew In a two-piece connector, a screw for mating or separating the halves of the connector.

Jacob's law A principle concerning the behavior of motors. An electric motor develops maximum power when $E_i = 2E_{bk}$, where E_i is the applied voltage and E_{bk} is the back voltage.

JAES Abbreviation for *Journal of the Audio Engineering Society.*

jaff Colloquial term for radar jamming that combines electronic and chaff techniques.

jag Distortion caused by temporary loss of synchronization between the scanner and recorder in a facsimile system.

jam input **1.** A means of setting a logic line to the desired condition by directly applying the desired high or low voltage. **2.** A voltage applied to a logic line to force it high or low.

jammer **1.** A radio transmitter or station used for the purpose of JAMMING communications be-

Copyright 2001 The McGraw-Hill Companies, Inc. Click Here for Terms of Use

5059F-pJ-385-388 4/10/01 9:06 AM Page 386

tween or among other stations. **2.** A radio operator who engages in the practice of deliberately JAMMING communications between or among other stations.

jamming The deliberate use of countermeasures, such as malicious transmission of interfering signals, to obstruct communications.

jamming effectiveness The extent to which JAMMING is able to disrupt a service. It can be expressed quantitatively as the ratio of jamming signal voltage to jammed signal voltage. It can also be determined according to the percentage of data that is effectively obliterated.

JAN Abbreviation of JOINT ARMY-NAVY.

janet A system for point-to-point communication via meteor-trail forward scatter. It is generally used at very high frequencies (VHF).

Jansky noise Wideband, high-frequency electromagnetic noise generated by objects in interstellar and intergalactic space.

J antenna An end-fed half-wave antenna having a quarter-wave, parallel-wire matching section. The entire antenna, when oriented vertically, resembles the letter J.

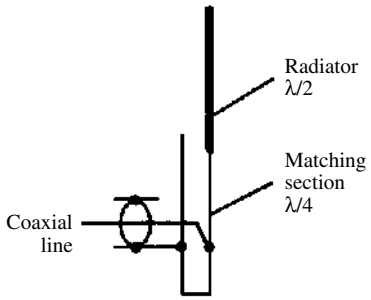

J antenna

Janus antenna array (from *Janus*, an ancient Roman god.) A Doppler-navigation antenna array radiating forward and backward beams.

jar **1.** (From *Leyden jar*) An obsolete unit of capacitance equal to 1/900 microfarad. **2.** The container for the elements of a storage cell.

JASA Abbreviation for *Journal of the Acoustical Society of America.*

J-carrier system In carrier-current (wired/wireless) telephony, a broadband system that provides 12 telephone channels at frequencies up to 140 kHz.

JCET Abbreviation of *Joint Council on Educational Television.*

JCL Abbreviation of *job control language.*

J-display A radar display having a circular time base. The transmitted pulse and reflected (target) pulse are spaced around the circumference; distances can be measured circumferentially between them.

JEDEC Acronym for *Joint Electron Device Engineering Council.*

jerk The rate of change of acceleration; the third derivative of displacement.

JETEC Acronym for *Joint Electron Tube Engineering Council.*

jewel bearing A low-friction bearing used in electric meters and other sensitive devices. It takes its name from a jewel pivot (such as a sapphire) in the groove of which rides the pointed end of a rotating shaft. Also called *jeweled bearing* or *jewel.*

jezebel A passive sonobuoy used in military applications. It detects enemy submarine noises, and transmits them by radio to a monitoring station.

JFET Abbreviation of *junction field-effect transistor.*

JHG Abbreviation of JOULE HEAT GRADIENT.

jig A device constructed especially for the purpose of holding an equipment or circuit board during its repair.

jitter A (usually small and rapid) fluctuation in a phenomenon, such as a quantity or wave, because of noise, mechanical vibration, interfering signals, or similar internal or external disturbances. It is used especially in reference to cathode-ray-tube (CRT) displays.

J/K Abbreviation for *joule(s) per Kelvin*, the SI unit of entropy; also the unit for the Boltzmann constant.

J-K flip-flop A transistor-resistor flip-flop stage producing an output signal even when both inputs are in the logic 1 state (high). It is so called because its input terminals are labeled J and K.

J/(kg·K) Abbreviation for *joule(s) per kilogram Kelvin*, the SI unit of specific heat capacity.

job A unit of computer work, usually consisting of several program runs.

job control language An operating system language used to describe the control requirements for jobs within the system.

job control program A program that uses control language statements and implements them as instructions controlling a job in an operating system.

job control, stacked See SEQUENTIAL-STACKED JOB CONTROL.

job flow control To control the order of jobs being processed by a computer to make the most efficient use of peripherals and central processor time—either manually or by an operating system.

job library A series of related sets of data that will be loaded for a given job.

job-oriented terminal A terminal that produces data in computer-ready form.

job statement A control statement identifying the beginning of a series of job control statements for a job.

job step The execution of a computer program according to a job control statement; several job steps can be specified by a job.

job stream In a processing system, a group of consecutively run jobs.

5059F-pJ-385-388 4/10/01 9:06 AM Page 387

jogging Rapid, repetitive switching of power to a motor to advance its shaft by small amounts. Also called *inching.*

Johnson counter See RING COUNTER.

Johnson curve A spectral curve (important in appraising solar cell performance) for air mass zero (i.e., for conditions beyond the earth's atmosphere).

Johnson-Lark-Horowitz effect The resistivity gained by a metal or degenerate semiconductor (one in which conduction is nearly equal to that of a simple metal) because of electron scattering by impurity atoms.

Johnson noise See THERMAL NOISE.

Johnson-*Q* feed system See *Q*-ANTENNA.

join Also called *disjunction.* The logical inclusive-OR operation.

joined actuator A form of multiple circuit breaker in which the opening of one circuit results in the opening of all circuits.

joint See JUNCTION, **1**.

joint circuit A communications circuit shared by two or more services.

joint communications Communication facilities being used by more than one service of the same country.

joint denial The logical NOR (NOT-OR) operation.

joint-force sensor A feedback servo device that prevents a robot joint from exerting excessive force. It works by detecting the mechanical resistance the robot arm encounters. If the resistance becomes too great, the joint force is reduced or removed.

jolt **1.** Colloquialism for KILOVOLT. **2.** Colloquialism for ELECTRIC SHOCK. **3.** Colloquialism for TRANSIENT. **4.** Colloquialism for a lightning discharge.

Joly transformer A frequency-tripling transformer whose frequency-multiplying action depends on the nonlinearity of the magnetic induction curve of the core material.

Jones plug A special form of polarized receptacle having numerous contacts.

Jones plug

***j* operator** See *J.*

Josephson effect The phenomenon, predicted by Brian Josephson, wherein a current flows across the gap between the tips of two superconductors brought close together; a high-frequency wave is generated.

Joshi effect The phenomenon whereby current in a gas changes as the result of irradiation by light.

joule Abbreviation, J. The SI unit of work. One joule is the work performed when the point of application of one newton is moved one meter in the direction of the applied force. Also see NEWTON.

Joule calorimeter A heat-measuring device that operates electrically.

Joule constant See MECHANICAL EQUIVALENT OF HEAT.

Joule effect **1.** The heat resulting from current flowing through a resistance. **2.** See MAGNETOSTRICTION.

joule heat See JOULE EFFECT, **1**.

joule heat gradient The rate of change in the temperature of a resistive object through which a current flows.

joule meter An integrating wattmeter producing readings in joules.

Joule's law The rate at which heat is produced by current flowing in a constant-resistance circuit is proportional to the square of the current.

journal A file of messages within an operating system, providing information for restarts and historical analysis of system functioning.

joystick A two- or three-dimensional potentiometer with a movable lever, allowing control of a parameter, according to the position of the lever in the up/down and left/right directions. It is often used in computer games for the purpose of manipulating images on a screen. In some such devices, the lever can be rotated clockwise or counterclockwise to obtain additional functions.

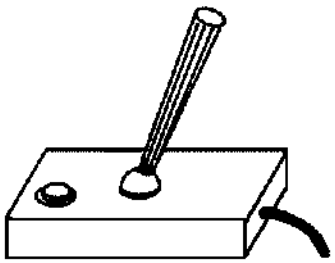

joystick

JPEG Abbreviation of *Joint Photographic Experts Group.*

JPEG image compression An image-compression scheme that eliminates redundancies, greatly reducing the necessary digital storage space. The process is fast enough to allow animated graphics at moderate speed.

JPL Abbreviation of *Jet Propulsion Laboratory.*

J-pole antenna See J ANTENNA.

J rule During transitions of orbital electrons from higher to lower energy states (accompanied by the emission of photons), changes in the inner quantum number can only be by a factor of 0 or +1, or −1.

5059F-pJ-385-388 4/10/01 9:06 AM Page 388

J scan See J DISPLAY.

J scope A radar device that produces a J DISPLAY.

JSR Abbreviation of *jump to subroutine.*

JTAC Abbreviation of *Joint Technical Advisory Committee.*

judder In facsimile transmission, distortion caused by movements of the transmission or reception equipment.

juice Colloquialism for electric voltage or current.

jukebox An automatic phonograph (usually found in public places) that contains a large assortment of records.

Juliet Phonetic representation for the letter J, used in voice communications.

jump **1.** To purposely provide a short circuit around some component or circuit. **2.** Also called *branch.* In digital computer operations, a programming instruction specifying the memory location of the next instruction and directing the computer to it.

jump, conditional See CONDITIONAL BRANCH.

jump, unconditional See UNCONDITIONAL BRANCH INSTRUCTION.

jumper A short piece of wire (usually flexible, insulated, and equipped with clips) for jumping a component or circuit. See JUMP, **1**.

jump instruction See BRANCH INSTRUCTION.

junction **1.** A joint (connection) between two conductors. **2.** The region of contact between semiconductor materials of opposite type (e.g., *pn junction*). **3.** A waveguide fitting used to attach a branch waveguide to a main waveguide at an angle.

junction barrier See DEPLETION REGION.

junction battery A nuclear battery in which a silicon pn junction is irradiated by strontium 90.

junction box A (usually metal) protective box or can into which several conductors are brought together and connected.

junction capacitance In a semiconductor pn junction, the internal capacitance across the junction; it is of special interest when the junction is reverse-biased. Also called *barrier capacitance.*

junction capacitor See VOLTAGE-VARIABLE CAPACITOR.

junction diode A semiconductor diode created by joining an n-type region and p-type region as a wafer of semiconductor material, such as germanium or silicon.

junction field-effect transistor Abbreviation, JFET. A field-effect transistor in which the gate electrode consists of a pn junction.

junction filter A combination of separate low- and high-pass filters having a common input, but separate outputs. The filter is used to separate two frequency bands and transmit them to different circuits.

junction laser See LASER DIODE.

junction light source See LIGHT-EMITTING DIODE.

junction loss **1.** The loss that occurs in a telephone circuit at connecting points. **2.** Loss in a semiconductor pn junction. **3.** Loss occurring at an electrical connection because of poor bonding.

junction photocell A photoconductive or photovoltaic cell that is essentially a light-sensitive JUNCTION DIODE.

junction point **1.** A point at which two or more conductors, components, or circuits join in an electrical connection. **2.** The point in a computer routine at which one of several choices is made.

junction rectifier A semiconductor rectifier that is, in effect, a heavy-duty junction diode, or the equivalent of several heavy-duty junction diodes in combination.

junction station A microwave relay station joining one or more microwave radio legs to the main route or through route.

junction transistor A transistor in which the emitter and collector consists of junctions (see JUNCTION, **2**) between p and n semiconductor regions. Compare POINT-CONTACT TRANSISTOR.

junctor In a crossbar system, a circuit that bridges frames of a switching unit and terminates in a switching device on each frame.

Jungian-world theory The theory that societies keep repeating the same mistakes, generation after generation. Of interest to some researchers in artificial intelligence. It has been suggested that supercomputers might help find solutions to recurring social problems.

justification **1.** The alignment of text along the left margin, the right margin, or both margins. **2.** A method of altering the speed of a digital signal so that it can be received by equipment designed for a different data speed. The rate of speed is lower after this process is applied. Also called *pulse stuffing.*

justify **1.** To adjust the printing of words for aligned left and/or right margins. **2.** In computer operations, to shift an item in a register so that the most- or least-significant digit is at the corresponding end of the register.

just-operate value The current or voltage level at which a relay or similar device just closes. Also called *just-close value.*

just-release value The current or voltage level at which a relay or similar device just opens. Also called *just-open value.*

just scale A musical scale of three consecutive triads, the highest note of each being the lowest note of the next. Each triad has the ratio 4:5:6 or 10:12:15.

jute Tar-saturated fiber, such as hemp, used as a protective covering for cable.

jute-protected cable A cable whose outer covering is a wrapping of JUTE or similar material.

juxtaposed elements Components placed or mounted side by side.

juxtaposed images Images (e.g., those on the screen of a dual-beam cathode-ray tube) that are close to each other for simultaneous viewing, but do not overlap at any point.

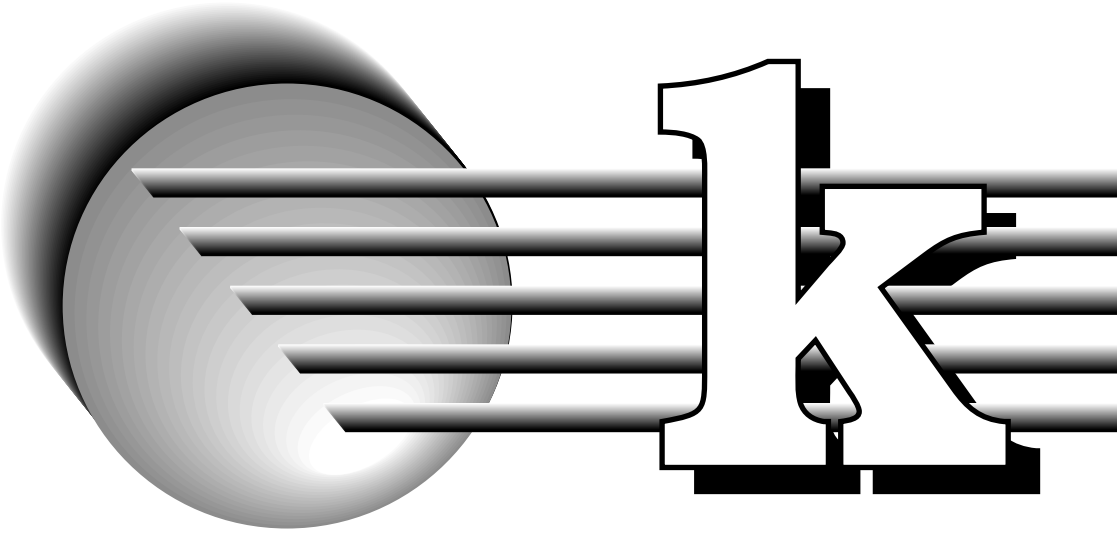

K **1.** General symbol for CONSTANT. **2.** Symbol for POTASSIUM. **3.** Symbol for KELVIN. **4.** Radiotelegraph symbol for *go ahead* or *over.* **5.** Symbol for CATHODE. **6.** Symbol for KILOBYTE. **7.** Abbreviation of KILOHM (k is preferred). **8.** Abbreviation of KILO-.

k **1.** Abbreviation of KILO-. **2.** Symbol for the BOLTZMANN CONSTANT. **3.** General symbol for a mathematical constant. **4.** Symbol for DIELECTRIC CONSTANT. **5.** Abbreviation for KILOHM.

kA Abbreviation of KILOAMPERE.

Karnaugh map A logic chart showing switching-function relationships and used in computer logic analysis to determine quickly the simplest form of logic circuit for a given function. The Karnaugh map is sometimes regarded as a tabular form of the Venn diagram.

Kansas City standard A frequency-shift modulation standard for a computer/tape-recorder interface. Also called *byte standard.*

KB **1.** Abbreviation of KEYBOARD. **2.** Abbreviation of KILOBYTE.

K band The 18- to 27-GHz band of frequencies, pertaining to their use in radar applications.

kcal Abbreviation of KILOCALORIE.

K carrier system A four-wire carrier-current telephone system using frequencies up to 60 kHz and providing 12 channels.

kCi Abbreviation of KILOCURIE.

kcs Abbreviation of *kilocharacter per second* (1000 characters per second).

K display See K SCAN.

KDP Abbreviation of POTASSIUM DIHYDROGEN PHOSPHATE, a ferrolelectric material.

keeper A small iron bar placed across the poles of a permanent magnet to forestall demagnetization.

K electron In certain atoms, one of the electrons whose orbit is nearest the nucleus.

Kel-f Abbreviation of *polymonochlorotrifluorethylene,* a high-temperature insulating material.

Kellie bond **1.** The junction of two mated electrically conductive surfaces that are held together by an adhesive that exhibits negligible resistance thermally and electrically when set. **2.** To make a thermally conductive joint, as from a heatsink to a chassis or component.

kelvin (Lord Kelvin, 1824–1907) Symbol, K. The SI unit of thermodynamic temperature; 1 K = 1/273.16, the thermodynamic temperature of the triple point of water.

Kelvin absolute electrometer An electrostatic voltmeter consisting of a movable metal plate (or plates) and a stationary metal plate (or plates)

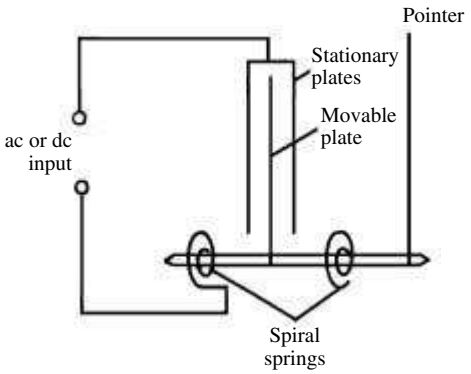

Kelvin absolute electrometer

Copyright 2001 The McGraw-Hill Companies, Inc. Click Here for Terms of Use

5059F-pK-389-395 4/10/01 9:11 AM Page 390

between which voltage is applied. The movable plate(s) is displaced over a distance that is proportional to the potential, against the torque of a return spring.

Kelvin balance An apparatus for measuring current in terms of magnetic pull. A coil is attached to each end of the beam of a balance, and coils ride directly above two stationary coils. Current flows through all coils, making one pair attractive and the other repellent, thus unbalancing the beam. Balance is restored by sliding a weight whose position along a graduated scale indicates the current strength.

Kelvin contacts Electrical contacts designed to eliminate the effect of lead resistance on the accuracy of measurement. Two leads run to each test point, one lead carrying the test signal and the other leading directly to the measuring instrument.

Kelvin double bridge A special bridge for measuring very low resistance (0.1 ohm or less). The arrangement of the bridge reduces the effects of contact resistance that causes significant error when such low resistances are connected to conventional resistance bridges.

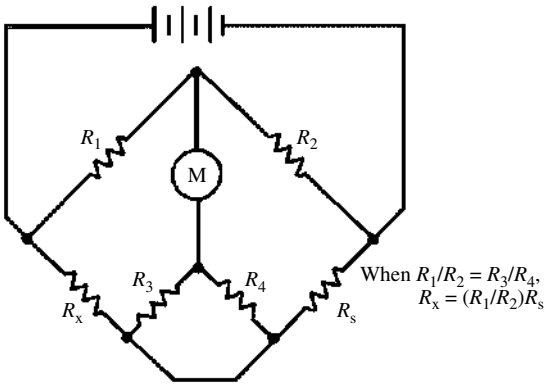

Kelvin double bridge

Kelvin replenisher A static generator consisting of two pairs of concentric, rotating semicircular conductors connected to brushes. The machine can be regarded as a rotating electric doubler.

Kelvin scale See ABSOLUTE SCALE.

Kelvin temperature scale See ABSOLUTE SCALE.

Kelvin voltmeter An electrostatic voltmeter in which an assembly of figure-8-shaped metal plates rotates between the plates of a stationary assembly when a voltage is applied between the assemblies. The length of the arc of rotation is proportional to the electrostatic attraction and, thus, to the applied voltage.

Kendall effect Distortion in a facsimile record caused by unwanted modulation produced by a carrier signal.

Kennelly-Heaviside layer (A.E. Kennelly, 1861–1939; Oliver Heaviside, 1850–1925) An early name for ionized regions in the upper atmosphere. These regions reflect and refract radio waves at certain frequencies. There are several layers at various altitudes. Also see IONOSPHERE and IONOSPHERIC LAYERS.

keraunograph A meteorological instrument for detecting distant electrical storms. In its simplest form, it consists of a galvanometer connected in series with an antenna and ground.

keraunophone A radio-receiving KERAUNOGRAPH.

kernel Inside an electrical conductor, a line along which the magnetic field strength is zero. Generally, this line is near the center of the conductor.

Kerr cell A nitrobenzene-filled cell that makes use of the KERR ELECTRO-OPTICAL EFFECT. It can function as an electric light shutter or control.

Kerr electro-optical effect The tendency of certain dielectric materials to become double-refracting in an electric field.

Kerr magneto-optical effect The tendency of glass and some other solids and liquids to become double-refracting in a magnetic field.

Kerst induction accelerator See BETATRON.

keV Abbreviation of KILOELECTRONVOLT.

Kew magnetometer A special magnetometer used to measure the intensity of the earth's magnetic field, and also the magnetic declination at a given point on the earth's surface. The device is designed for very high accuracy, using magnifying lenses.

key **1.** See DECRYPTION KEY. **2.** A projection or pin that guides the insertion of a plug-in component into a holder or socket. **3.** A digit or digits used to locate or identify a computer record (but not necessarily part of the record). **4.** A specialized hand-operated switch, used to make and break a circuit repetitively to form the dot and dash signals of Morse code telegraphy. Primarily of historical interest. Used by some amateur radio operators for hobby purposes. **5.** Slang for *principal* or *main.*

keyboard An array of lettered or numbered, low-torque push buttons, used to enter information into a computer, telegraph, teletypewriter, or automatic control system.

keyboard computer A digital computer in which the input device is an electrical keyboard of the typewriter or calculator type.

keyboard entry The operation of a keyboard to enter information into a computer for processing.

keyboard keyer A device for automatically sending Morse code using a typewriter-like keyboard, rather than a paddle or straight key. Each key on the keyboard, when pressed, produces the complete character and a space following it. Most keyboard keyers have buffers to allow typing well ahead of the code being sent, with insertion of all the correct spaces. The speed range is usually

5059F-pK-389-395 4/10/01 9:11 AM Page 391

from about 5 words per minute (wpm) to 60 or 70 wpm, although some keyboard keyers are programmed for speeds over 100 wpm.

keyboard lockout A keyboard interlock in a data transmission circuit that prevents data from being transmitted while the transmitter of another station on the same circuit is operating.

keyboard send-receive unit A teletypewriter lacking an automatic input device.

key cabinet In a telephone system, a facility that shows a subscriber which lines are busy and which lines are open.

key chirp A chirping sound in a received signal, resulting from slight frequency shift when a radiotelegraph transmitter is keyed. It does not occur with a well-designed transmitter.

key-click filter An inductance-capacitance (LC) or resistance-capacitance (RC) filter for smoothing a keying wave to eliminate KEY CLICKS. It functions by optimizing the rise and decay times of the keyed waveform.

key clicks Excessive bandwidth of a radiotelegraph signal that can result when a keyed signal has rise and decay times that are too rapid. Produces characteristic clicking or popping sounds, with resulting interference, in receivers tuned to frequencies near that of the transmitted signal. A KEY-CLICK FILTER can eliminate this.

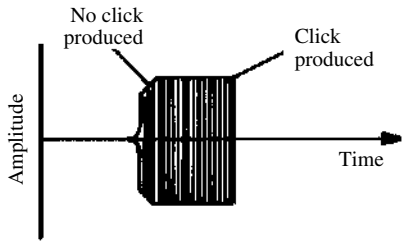

key clicks

keyed AGC A controlled automatic gain control (AGC) system in a television receiver circuit. The AGC acts when the horizontal sync pulse appears; it is inactive between pulses. This prevents unwanted actuation of the AGC by noise transients and picture-signal elements.

keyed clamp A clamping circuit that uses a control signal to determine the clamping time.

keyed interval In a transmission system that is keyed periodically, an interval beginning with a change in state and having a duration of the shortest time between changes in state.

keyed rainbow generator For testing of color-television receivers, a signal generator that produces a rainbow color pattern on the screen (i.e., a set of 10 vertical color bars representing the spectrum, with blank bars in between). The pattern results from gating the 3.56-MHz oscillator in the receiver at a frequency of 189 kHz.

keyer An automatic device for keying a radiotelegraph transmitter or wire telegraph circuit. The keyer can operate from perforated tape, an embossed disk, magnetic tape, or other similar recording.

keyer adaptor A modulated-signal detector that produces a direct-current signal having an amplitude sympathetic with the modulation; it provides the keying signal for a frequency-shift exciter in radio facsimile transmission.

key escrow A controversial system in which the government is provided with certain components of decryption keys to all communications ciphers, according to laws that would allow the government to eavesdrop on private communications or transactions after getting a court order. The key components are held in a secure place, that is, in "escrow," unless and until the necessary court order is obtained. See DECRYPTION KEY.

keying **1.** The modulation of a carrier by switching it on and off. It is commonly used in radiotelegraphy. **2.** The modulation of a carrier by switching its frequency between two defined values. It is also called FREQUENCY-SHIFT KEYING (FSK) and it is used in data transmission. **3.** The modulation of a carrier with an audio tone that is switched on and off. The carrier can be modulated via amplitude modulation (AM), frequency modulation (FM), pulse modulation, or any other form that will convey the audio tone. It is occasionally used in radiotelegraphy at very-high frequencies (VHF) and above. Also called *audio keying*. **4.** The modulation of a carrier with an audio tone whose frequency is switched between two defined values. The carrier can be modulated via amplitude modulation (AM), frequency modulation (FM), pulse modulation, or any other form that will convey the audio tone. It is commonly used in data transmission at VHF and above. Also called AUDIO FREQUENCY-SHIFT KEYING (AFSK).

keying chirp A rapid change in the frequency of a continuous-wave signal, occurring at the beginning of each code element. In the receiver, the resulting sound is a chirp.

keying error rate In data transmission, the ratio of incorrectly keyed signals to the total number of signals keyed.

keying filter See KEY-CLICK FILTER.

keying frequency **1.** In audio-keyed radiotelegraphy, the audio frequency (tone) of the dot and dash signals (as opposed to the carrier frequency). **2.** In radiotelegraphy, the transmission speed (see KEYING SPEED). **3.** The number of times per second that a black-line signal occurs while an object is scanned in a facsimile system.

keying monitor A simple detector used by an operator to listen to the keying of a radiotelegraph transmitter.

keying speed The speed (in words per minute) of a telegraph or radio-telegraph transmission.

5059F-pK-389-395 4/10/01 9:11 AM Page 392

keying transients **1.** Transients arising from the keying of a radiotelegraph transmitter or wire telegraph circuit. **2.** Transients that arise from the repetitive making and breaking of any circuit.

keyless ringing In a telephone system, ringing that begins as soon as the calling plug is put in the appropriate jack on the jack panel.

key pulse In telephone operations, a signaling system in which the desired numbers are entered by pressing corresponding pushbuttons or keys.

key punch A keyboard-operated machine for recording information by perforating a tape or cards.

keyshelf A shelf that supports manually operated telephone switchboard keys.

key station The master (control) station in a communications or control network.

keystoning A form of video image distortion in which the top of the picture is wider than the bottom, or vice versa. Thus, the image area is shaped like a trapezoid, rather than a rectangle.

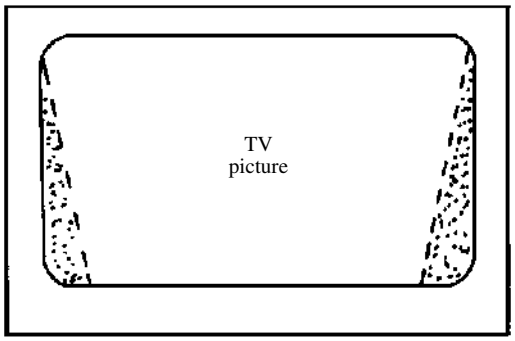

keystoning

key switch **1.** A lockable switch that is operated by inserting and turning a key in it. **2.** A switch having a long handle that transmits motion to the mechanism through a cam. **3.** See KEY, **1**. **4.** The separate short-circuiting switch sometimes mounted on the base of a telegraph key (see KEY, **1**). **5.** A switch that actuates the keys of an electronic organ.

key-to-disk unit A keyboard-to-magnetic-disk data-processing unit.

keyway A groove or slot into which a mating key slides to position a plug-in component (see KEY, **2**).

keyword In information retrieval systems, the significant word in the title describing a document (e.g., in the title "A Primer on French Cuisine," the word *cuisine* would be the keyword, the others having no singular significance).

kg Abbreviation of KILOGRAM.

kgC Abbreviation of KILOGRAM-CALORIE.

kgm Abbreviation of KILOGRAM-METER.

kg/m^3 Symbol for KILOGRAMS PER CUBIC METER, the SI unit of density.

K-H layer See KENNELLY-HEAVISIDE LAYER.

kHz Abbreviation of KILOHERTZ.

kick **1.** To place into sudden operation, as by the quick, forcible closure of a switch or the rapid application of an enabling pulse. **2.** See TRIGGER. **3.** Colloquialism for an abrupt, momentary electric shock.

kickback **1.** The counter EMF that appears across an inductor when current is interrupted. **2.** See FLYBACK.

kickback power supply A high-voltage power supply using the flyback principle. See FLYBACK.

kidney joint A waveguide coupling used in radar. The joint is flexible, or can consist of an air gap, to allow rotation of the antenna.

Kikuchi lines A characteristic spectral pattern produced by the electrons scattered when an electron beam strikes a crystal.

killer **1.** A pulse or other signal used to disable a circuit temporarily (e.g., a blanking pulse). **2.** In personal computing, an application of such importance that it alone serves as the motivation for someone to purchase or upgrade a system. Common examples are word processing and online communications.

killer circuit **1.** A circuit that disables some function of a system, such as the audio in a television receiver. **2.** The blanking circuit in a radar receiver. **3.** A circuit that prevents responses to side-lobe signals in a repeater or transponder.

Kilo Pronunciation, *KEY-low.* Phonetic alphabet code word for the letter K.

kilo- Abbreviation, K or k. **1.** A prefix meaning thousand(s). **2.** In digital data applications, a prefix meaning 2^{10} (1024).

kiloampere Abbreviation, kA. A unit of current equal to 1000 amperes.

kilobit A unit of digital data equal to 2^{10} (1024) bits. Also see BIT.

kilobyte Abbreviation, K or KB. A unit of digital data equal to 2^{10} (1024) bytes. Also see BYTE.

kilocalorie Abbreviation, kcal. A large unit of heat; 1 kcal equals 1000 calories. See CALORIE.

kilocurie Abbreviation, kCi. A large unit of radioactivity equal to 3.71×10^{13} disintegrations per second; 1 kCi equals 1000 curies. Also see CURIE, MEGACURIE, MICROCURIE, and MILLICURIE.

kilocycle See KILOHERTZ.

kiloelectronvolt Abbreviation, keV. A large unit of electrical energy equal to 1000 electronvolts. See ELECTRONVOLT.

kilogauss A large unit of magnetic flux density; 1 kilogauss equals 1000 gauss or 0.1 tesla.

kilogram Abbreviation, kg. The SI base unit of mass; it is equal to 1000 grams.

kilogram-calorie The heat required to raise 1 kilogram of water 1°C.

5059F-pK-389-395 4/10/01 9:11 AM Page 393

kilogram-meter Abbreviation, kgm. A unit of mechanical energy (work); 1 kgm is the energy required to raise a mass of 1 kilogram vertically by a distance of 1 meter (equal to 7.2334 foot-pounds). Also see JOULE.

kilohertz Abbreviation, kHz. A unit of frequency; 1 kHz equals 1000 Hz.

kilohm Symbol, kΩ. A unit of high resistance, reactance, or impedance; 1 kΩ equals 1000 ohms.

kilojoule Abbreviation, kJ. A unit of energy or work; 1 kJ equals 1000 joules. See JOULE.

kilolumen Abbreviation, klm. A unit of luminous flux equal to 1000 lumens. See LUMEN.

kilomega- See GIGA-.

kilomegahertz See GIGAHERTZ.

kilometer Abbreviation, km. A large metric unit of linear measure; 1 km equals 1000 meters (3280.8 feet).

kilo-oersted Abbreviation, kOe. A unit of magnetic field strength; 1 kOe equals 1000 oersteds. See OERSTED.

kiloroentgen Abbreviation, kr. A large unit of radioactive radiation; 1 kr equals 1000 roentgens. See ROENTGEN.

kilorutherford Abbreviation, krd. A large unit of radioactivity equal to 10^9 disintegrations per second.

kilovar A compound term coined from *kilo-* and *VAR* (the abbreviation of *volt-amperes reactive*). It is equal to a reactive power of 1000 watts.

kilovar-hour A large unit of reactive electrical energy, equivalent to 1000 reactive watts manifested for a period of one hour.

kilovolt Abbreviation, kV. A unit of high voltage; 1 kV equals 1000 V.

kilovolt-ampere Abbreviation, kVA. A unit of high power that gives the TRUE POWER in a direct-current circuit and the APPARENT POWER in an alternating-current circuit; 1 kVA equals 1000 W. Also see DC POWER.

kilovolt-ampere reactive See KILOVAR.

kilovoltmeter A voltmeter designed to measure thousands of volts (kilovolts).

kilowatt Abbreviation, kW. A unit of high power; 1 kW equals 1000 watts. Also see WATT.

kilowatt-hour Abbreviation, kWh. A common unit of electrical energy; 1 kWh equals 1000 watt hours, or the equivalent of 1000 watts dissipated for a period of one hour. Also see ENERGY, KILOWATT-HOUR, POWER, WATT-HOUR, and WATT-SECOND.

kilowatt-hour meter A motorized meter for recording (electrical) power consumption in kilowatt-hours. Also see KILOWATT-HOUR.

kinematograph A motion picture camera. Also called CINEMATOGRAPH and KINETOGRAPH.

kine **1.** See KINESCOPE, **1**. **2.** See KINESCOPE RECORDING.

kinescope **1.** The picture tube in a television receiver. **2.** See KINESCOPE RECORDING.

kinescope recorder A film or tape apparatus for recording television pictures.

kinescope recording A motion-picture or videotape made from the screen (or taken from the circuit) of a television picture tube.

kinetic energy The energy associated with particles, bodies, or electric charge carriers in motion.

kinetograph See KINEMATOGRAPH.

kinetoscope A motion-picture projector.

kiosk A computer and peripherals set up for the purpose of multimedia use by the general public. It generally uses a touch screen for inputting data and must be ruggedly constructed to tolerate rough treatment.

Kirchhoff's first law The sum of the currents flowing out of a point in a direct-current circuit equals the sum of the currents flowing into that point.

Kirchhoff's laws (Gustav Robert Kirchhoff, 1824–1887) Two laws of electric circuits that account for the behavior of certain networks. See KIRCHHOFF'S FIRST LAW and KIRCHHOFF'S SECOND LAW.

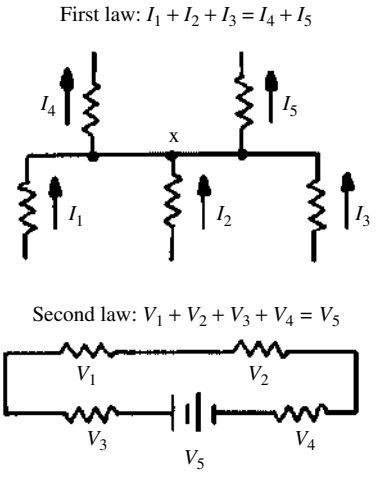

Kirchhoff's laws

Kirchhoff's second law The algebraic sum of all the voltage drops around a direct-current circuit (including supply voltages) is always equal to zero.

kit A selection of components, associated equipment, supplies (such as wire and hardware), and instructions for constructing a piece of electronic equipment.

kite-supported antenna A longwire antenna that uses a kite as a support for the far (nonstation) end. A tether is used to reduce the chance that the kite will fly away with wire attached. It was used by Marconi in early experiments with radio. Radio amateurs and shortwave listeners sometimes use this scheme at low and medium

5059F-pK-389-395 4/10/01 9:11 AM Page 394

frequencies. It is a dangerous antenna because of electrostatic buildup, a tendency to attract lightning, the possibility of its breaking loose, and the risk that it might contact utility lines.

kJ Abbreviation of KILOJOULE.

k-line programming A method by which an artificially intelligent robot can learn as it does a job, so it will have an easier time doing the same job in the future. The robot controller actually learns from the robot's mistakes.

Klipsch horn A loudspeaker that includes a folded low-frequency horn housed in a corner enclosure.

klm Abbreviation of KILOLUMEN.

kludge **1.** A crude, useless, or grossly inefficient machine or process. **2.** A hastily contrived prototype of a circuit or device, put together for the purpose of testing a concept, but not intended as a representative of a production unit.

klydonograph A device that photographically records the voltage gradient in the presence of an electric field.

klystron A microwave tube whose operation is based on the velocity modulation of an electron beam by buncher and cavity reentrant cavities.

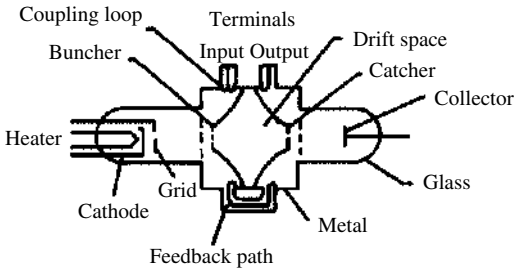

klystron

klystron amplifier A microwave amplifier using a klystron.

klystron harmonic generator A frequency-multiplying power amplifier using a klystron. It is used at microwave radio frequencies.

klystron oscillator A klystron operated as a self-excited microwave oscillator.

klystron repeater A microwave amplifier in which a klystron inserted in a waveguide boosts the amplitude of an incoming signal.

km Abbreviation of KILOMETER.

knee **1.** A sharp bend in a response curve for a device, usually indicating the onset of conduction, saturation, cutoff, pinchoff, or limiting action. It applies especially to semiconductor diodes and transistors. **2.** The characteristics of a device when it is operated at a point in the vicinity of a sharp bend in its response curve.

knee noise Electrical noise generated by rapidly repeating current fluctuations at the knee in a Zener diode.

knife-edge diffraction The lessening of atmospheric signal attenuation when the signal passes over a sharp obstacle and is diffracted.

knife switch A switch composed of one or more flat blades roughly resembling knife blades, which are slid firmly between the jaws of pinching contacts to close a circuit.

knob **1.** A (usually round and insulated) finger dial for adjusting a variable electronic component, such as a potentiometer, variable capacitor, or rotary switch. **2.** A solid round insulator usually having a low diameter to height ratio. **3.** A small ball- or rod-shaped electrode or protuberance.

knocker A fire-control radar subassembly of synchronizing and triggering circuits.

knockout An area in a metal box or chassis that is easily removed by tapping or knocking to provide an opening.

knot A unit of speed, corresponding to 1 nautical mile per hour. A speed of 1 knot is about 1.15 statute miles per hour; a speed of 1 statute mile per hour is about 0.868 knots. It is used by mariners for specifying speeds at sea, and also occasionally by meteorologists in specifying wind speeds.

knowledge The data in a computer and in mass-storage media, accumulated over time and capable of being put to practical use.

kOe Abbreviation of KILO-OERSTED.

Kolster decremeter An absorption wavemeter with a movable scale; it permits measurement of the decrement of a radio wave.

Kooman antenna A unidirectional antenna consisting of stacked, full-wave, center-fed driven elements, and a reflecting screen.

Korner Killer Trade name for an acoustically absorbent object that reduces sound echoes that can occur in enclosed rooms. The name results because the device works best when placed in a corner (where two walls meet).

Kovar An alloy of cobalt, iron, and nickel. It is used mostly in glass-to-metal seals because it has characteristics of both kinds of material.

Kozanowski oscillator A positive-grid vacuum-tube UHF oscillator circuit using two tubes having cylindrical elements, and a pair of parallel-wire tanks.

Kr Symbol for KRYPTON.

kr Abbreviation of KILOROENTGEN.

K radiation X rays emitted from an atom when an electron becomes a K electron.

kraft paper Strong brown paper used for insulation and as the dielectric of paper capacitors.

Kramer system A system of three-phase motor control providing constant horsepower, and having a direct-current (dc) motor coupled to the shaft of a wound-rotor three-phase induction motor. The dc supply for the motor also supplies a rotary converter. The speed-control rheostat is connected in series with the field of the motor and the dc power supply.

5059F-pK-389-395 4/10/01 9:11 AM Page 395

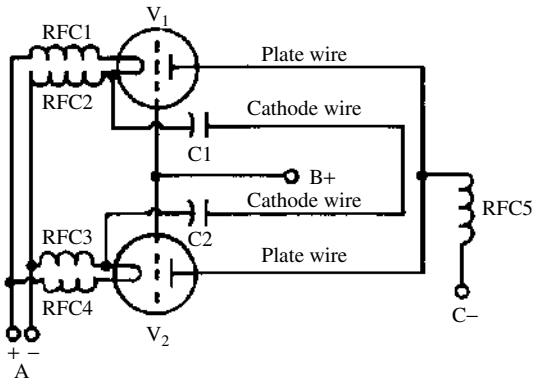

Kozanowski oscillator

Kraus antenna A bidirectional, flat-top beam antenna consisting of a pair of closely spaced dipoles. Several such sections can be connected in series by crisscrossing the wires at voltage loops.

krd Abbreviation of KILORUTHERFORD.

Kryptol A mixture of clay, graphite, and silicon carbide. It is used in electric heater elements because of its low resistance and high melting point.

krypton Symbol, Kr. An inert, gaseous element. Atomic number, 36. Atomic weight, 83.80. Krypton is present in trace amounts in the earth's atmosphere.

K scan In radar operations, a modified A-scan used in aiming antennas in which two pips are displayed; their relative amplitudes indicate the antenna-aiming error.

K series A series of spectral lines for the shortest wavelengths of radiation from the innermost electron shell of a radiating atom.

KSR Abbreviation of *keyboard send-receive* unit.

Ku band A band of microwave frequencies between approximately 12 and 18 GHz.

Kundt's law The index of refraction of a medium does not change continuously with wavelength in the absorption bands.

Kundt tube A device used to measure the speed of sound in gases under various conditions. Suspended particles in the gas form standing waves that can be easily seen. Knowing the frequency of the disturbance and the distance between nodes of the standing waves, the speed can be determined. The pressure and density of the gas, as well as temperature and humidity, affect the speed.

kurchatovium See RUTHERFORDIUM.

kV Abbreviation of KILOVOLT.

kVA Abbreviation of KILOVOLT-AMPERE.

kVAR Abbreviation of REACTIVE KILOVOLT-AMPERE.

kVARh Abbreviation of KILOVAR-HOUR.

kW Abbreviation of KILOWATT.

kWh Abbreviation of KILOWATT-HOUR.

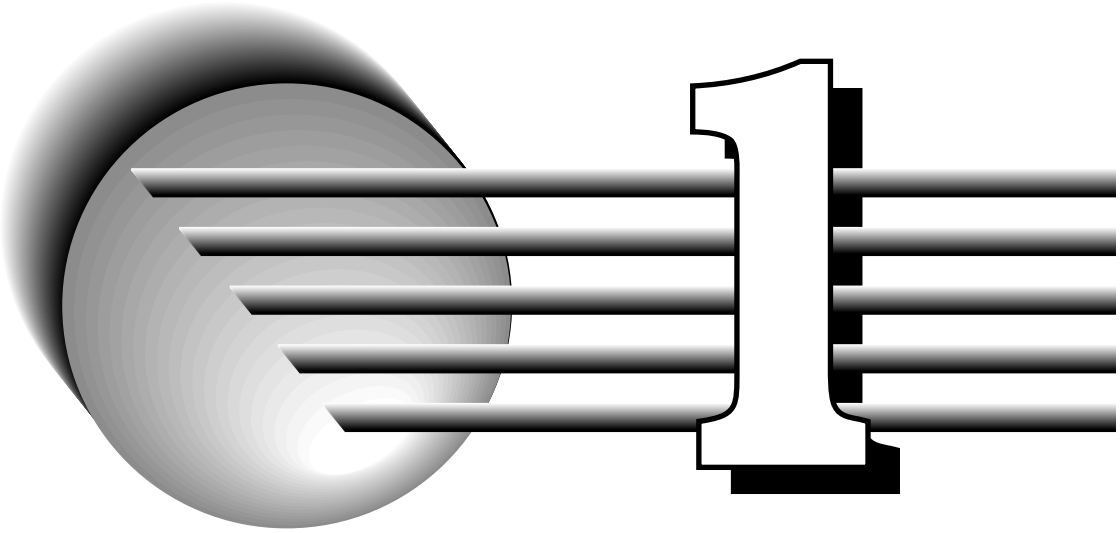

L **1.** Symbol for INDUCTANCE. **2.** Symbol for MEAN LIFE. **3.** Abbreviation of LOW. **4.** Resembling the capital letter L in physical shape. **5.** Symbol for LAPLACE TRANSFORM.

l **1.** Symbol for LENGTH. **2.** Abbreviation of LITER. **3.** Subscript for LOW. **4.** Abbreviation of LUMEN; also abbreviated *lm* (preferred) and *lum.*

La Symbol for LANTHANUM.

label **1.** A symbolic group of characters that identifies an area of memory, an item of data, a file, or a record. **2.** A name assigned to a source program instruction step to identify the step as a coding entry point, or to make the step usable as a reference point for entry to the routine or subroutine in which it appears.

label group A collection of labels, usually of the same type, held in an operating system.

label identifier Within a label, a character set used to name the kind of item labeled.

label record A record identifying a file recorded on a magnetic storage medium (e.g., magnetic tape).

label set A collection of labels having a common label identifier.

labile oscillator A frequency-controlled local oscillator.

laboratory conditions The environmental, mechanical, and electrical parameters characteristic of controlled conditions. Actual operating conditions can be much different.

laboratory-grade instrument An instrument having the high accuracy and stability that suit it to precision measurements in a laboratory. Also called PRECISION INSTRUMENT. Compare SERVICE-TYPE INSTRUMENT.

laboratory power supply A regulated direct-current source whose adjustable output is less than 10 kV at no more than 500 W.

laboratory standard See PRIMARY STANDARD and SECONDARY STANDARD.

labyrinth speaker A loudspeaker whose enclosure (a wooden cubicle) includes a folded pipe or acoustic transmission line (behind the speaker); the inner walls are lined with a sound-absorbent material. When the pipe, which is open-ended, is half as long as the wavelength of the frequency being reproduced, the sound emerging from the open end is in phase with that radiated by the front of the speaker and, therefore, reinforces it.

laced wiring Circuit wiring in which wires or cables run parallel in bundles that are tied together with LACING CORD.

lacing cord Strong, sometimes waxed cord used to tie together wires running parallel in a bundle. Also see LACED WIRING.

lacquer disk See CELLULOSE-NITRATE DISK.

lacquer-film capacitor A fixed capacitor with a plastic film dielectric; the film is applied as liquid lacquer to the metal foil.

lacquer master A master recording made on a CELLULOSE-NITRATE DISK.

lacquer original See LACQUER MASTER.

ladar Abbreviation of LASER DOPPLER RADAR. Also abbreviated *lopplar.*

ladder attenuator See LADDER-TYPE ATTENUATOR.

ladder filter A form of delay line or filter. It generally consists of series and parallel impedances, either in a balanced or unbalanced form.

ladder line See AIR-INSULATED LINE.

Copyright 2001 The McGraw-Hill Companies, Inc. Click Here for Terms of Use

5059F-pL-396-423 4/10/01 9:14 AM Page 397

ladder network A network consisting of several L sections in cascade. See L SECTION, **1**, **2**, **3**.

ladder-type attenuator An attenuator consisting of a ladder network equipped with a switching circuit for selecting the output at various sections.

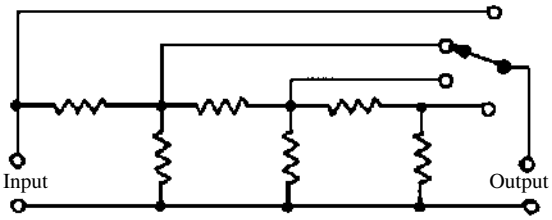

ladder-type attenuator

LAFOT Coded weather broadcasts aired every six hours by the U.S. Weather Bureau through marine radiotelephone broadcasting stations for the Great Lakes region.

lag In computations relating the phase of alternating-current signals, the extent to which one quantity follows another in time (e.g., the current lags the voltage by 90 degrees in a pure inductive reactance). Compare LEAD.

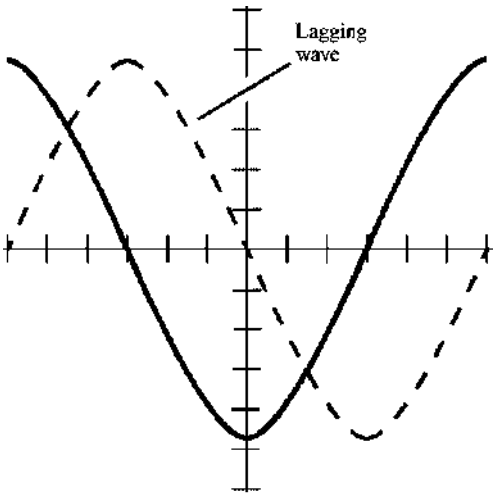

lag

lagged-demand meter A meter with a built-in time delay.

lagging current Current that follows voltage (in time). Also see LAG.

lagging load A load in which current lags behind voltage (i.e., an inductive load). Compare LEADING LOAD.

lag network A phase-shifting circuit containing series-resistance and shunt-capacitance arms. It produces a lagging phase shift. Compare LEAD NETWORK.

lambda wave An electromagnetic disturbance that travels along the surface of an object. An example is the surface wave characteristic of low-frequency propagation.

lambert Symbol, L. The centimeter-gram-second (cgs) unit of luminance, equal to the brightness of an ideal diffusing surface that radiates or reflects light at 1 lumen per square centimeter. The SI (preferred) unit of luminance is the candela per square meter (cd/m^2); 1 lambert equals 10^4 cd/m^2. Also see CANDELA.

Lambert's law of illumination The illumination of a surface by a point light source is inversely proportional to the square of the distance between the surface and the source. If the surface is not perpendicular to the rays, the illumination is proportional to the cosine of the angle of incidence.

laminated armature An armature for a motor or generator, made of stacked laminations.

laminated contact A switch contact consisting of a number of laminations—each contacting a conducting counterpart.

laminated core A core for a transformer, choke, relay, or similar device, made of stacked laminations.

laminated disk A layered recording disk.

laminated pole A pole within a motor, generator, relay, electromagnet, or similar device, made of stacked laminations.

lamination **1.** A relatively thin sheet of metal cut to a required shape to be stacked with other similar sheets to form a laminated core or pole. **2.** A relatively thin sheet of plastic that is bonded together and heat-formed with other similar sheets to produce a sheet or piece of desired thickness and strength.

lamp A device for converting electrical energy into visible light. The term includes a number of devices (e.g., arc lamp, fluorescent tube, incandescent lamp, mercury-vapor lamp, and neon bulb).

lamp-bank resistor A makeshift heavy-duty resistor consisting of several incandescent lamps arranged so that they can be switched in various series, parallel, and series-parallel combinations to vary the resistance provided by the filaments.

lampblack Carbon obtained from soot deposited by a smoky flame. The substance is used as the basic material for some resistors.

lamp cord A two-wire insulated cord, used with low-wattage alternating-current appliances at 117 volts. The wire is usually stranded copper equivalent to American Wire Gauge (AWG) #16.

lamp dimmer See DIMMER.

lamp driver A usually single-stage circuit for amplifying a small pulse to drive an indicator lamp.

5059F-pL-396-423 4/10/01 9:14 AM Page 398

lamp extractor A special tool used to insert or extract miniature lamps for electronic equipment.

lamp jack A receptacle with a spring release that holds a small incandescent bulb. The bulb is removed and replaced by pushing and twisting.

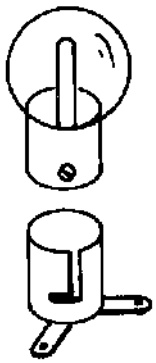

lamp jack

lamp-type expander A volume expander in which the tungsten filament in an incandescent lamp serves as the nonlinear resistor.

lamp-type readout For counters, calculators, and digital meters, a readout device in which each digit is indicated by a lamp.

LAN Abbreviation of LOCAL AREA NETWORK.

land **1.** The flat, reflective surface between pits on a compact disc (CD). Compare PIT, **1**. **2.** The thin vinyl wall between grooves on a phonograph record. **3.** A bonding point in a microcircuit. **4.** Pertaining to earthbound communications stations.

Land camera See POLAROID CAMERA.

landing beacon The aircraft landing-beam transmitter. Also see LANDING BEAM.

landing beam A highly directional airport radio signal beamed upward to guide aircraft landing during conditions of poor visibility.

landline A telephone or telegraph circuit completed with wires.

landmark beacon Any beacon that is not an airway or airport beacon.

land mobile service Two-way radio service between a base station and mobile land vehicles, or among mobile land vehicles.

land mobile station A radio station aboard a mobile, earthbound vehicle.

land return Ground reflection of radar signals back to the transmitter.

land station A fixed ground station.

Langevin ion An electrically charged particle, such as a grain of dust or droplet of water, resulting from the accumulation of ions.

Langmuir dark space In a luminous gas discharge, the dark region around a negatively charged probe inserted into the positive column. Compare CROOKES' DARK SPACE.

Langmuir's law See CHILD'S LAW.

language In digital-computer operations, any one of the detailed systems for representing data, instructions, and procedures through the use of symbols and symbol sequences. See MACHINE LANGUAGE, ASSEMBLY LANGUAGE, COBOL, FORTRAN, and BASIC.

language laboratory An electronic contribution to the teaching and learning of languages. It consists of recordings in a language being studied and all the equipment associated with recording, playback, and monitoring. Students listen to the speech of experts in the language record, listen to, and later erase their own utterances in the language.

language translation **1.** The conversion of statements in one computer language to equivalent statements in another. **2.** The conversion of one written natural language into another (e.g., French to Russian) by means of a computer program.

language translator **1.** An assembly program, compiler, or other routine used for translation between computer languages. **2.** A high-level program that allows a computer to translate one written natural language into another (e.g., Chinese to Italian).

L antenna See INVERTED-L ANTENNA.

lantern battery A moderate-sized electrochemical battery usually rated at 6 volts. Derives its name from its original use as a power source for portable lamps. One type has spring contacts on the top. Another type has thumbscrew terminals. The nonrechargeable battery consists of 4 zinc–carbon or alkaline cells in series. Some varieties are rechargeable, consisting of nickel–cadmium (NiCd) or nickel–metal-hydride (NiMH) cells. This type of battery can provide enough energy to operate a low-power radio transceiver. Two units connected in series, or four units in series-parallel, make a 12-volt battery that can power a small portable Citizen Band (CB) or amateur radio station.

lanthanum Symbol, La. An elemental metal of the rare-earth group. Atomic number, 57. Atomic weight, 138.906.

lanyard A wire or cable used to quickly pull apart the halves of a quick-disconnect connector.

lap A device used for grinding piezoelectric crystals for resonance at a desired frequency.

lap dissolve The simultaneous fading out of one televised scene while another is fading in so that one is apparently dissolving into the next. It is also applicable to motion pictures.

lapel microphone A small microphone that is clipped to a lapel of a user's jacket or coat.

lap joint An overlapping splice of two conductors.

Laplace transform Symbol, *L*. An operator that reduces the work of solving certain differential equations by permitting them to be handled by simpler algebraic methods.

5059F-pL-396-423 4/10/01 9:14 AM Page 399

lapping Fine-tuning quartz crystal plates by moving them over a flat plate coated with a liquid abrasive.

laptop computer See NOTEBOOK COMPUTER.

lap winding In a motor or generator armature, a winding in which the opposite ends of each coil are connected to the adjoining segments of the commutator.

lap wrap **1.** A form of asbestos cloth wire insulation. **2.** A method of wrapping with electrical tape, in which there is considerable overlap among the turns of the tape.

large calorie See KILOGRAM-CALORIE.

large loop antenna A single-turn open or closed loop, usually having a circumference of 0.5 wavelength or 1 wavelength. With a half-wavelength open or closed loop, maximum radiation occurs in the plane of the loop. A full-wavelength closed loop exhibits maximum radiation and response along the axis. This type of antenna can be used for wireless transmitting and receiving applications. Either the open or the closed half-wavelength loop exhibits a slight power loss relative to a dipole, but the full-wavelength loop shows a small gain over a dipole in its favored directions. Compare SMALL LOOP ANTENNA.

large-scale integration Abbreviation, LSI. The inclusion of more than 100 transistors, performing various individual, but interrelated circuit functions, on a single integrated-circuit chip.

large signal A relatively high-amplitude signal that traverses so large a part of the operating characteristic of a device that nonlinear portions of the characteristic are usually encountered. Compare SMALL SIGNAL.

large-signal analysis The rigorous study of circuits and devices that process large signals.

large-signal component **1.** A coefficient or parameter such as amplification, transconductance, or dynamic resistance, measured under conditions of large-signal operation. Also see LARGE SIGNAL and LARGE-SIGNAL EQUIVALENT CIRCUIT. **2.** A device designed for operation at high signal levels.

large-signal equivalent circuit For a given transistor circuit, the equivalent circuit at high signal levels (i.e., at amplitudes approaching saturation and cutoff levels). Also see EQUIVALENT CIRCUIT.

large-signal operation The use of a circuit or device at signal levels sufficiently high so that nonlinear portions of the characteristic are usually encountered. Compare SMALL-SIGNAL OPERATION.

large-signal transistor See POWER TRANSISTOR.

large-signal voltage gain In an integrated-circuit amplifier, the voltage gain under open-loop conditions, determined as the difference in the output voltage divided by the difference in the input voltage. It is usually specified in volts per millivolt or volts per microvolt.

Larmor orbit The path followed by a charged particle in a constant magnetic field. Because of interaction between the external field and the field generated by the particle, the charged particle travels in a circular path.

laryngaphone See THROAT MICROPHONE.

LASCR Abbreviation of LIGHT-ACTIVATED SILICON-CONTROLLED RECTIFIER.

LASCS Abbreviation of LIGHT-ACTIVATED SILICON-CONTROLLED SWITCH.

lase To emit coherent electromagnetic energy in the visible-light spectrum. See LASER.

laser Acronym for *light amplification by stimulated emission of radiation.* A device that produces coherent radiation in the visible-light range, that is, between 750 and 390 nanometers (one nanometer is 10^{-9} meter). Some devices that produce coherent radiation in the infrared, ultraviolet, or X-ray parts of the spectrum are also referred to as lasers. Lasers can be either continuous or pulsed, and are characterized by coherent, monochromatic emissions. The peak intensity ranges from a few microwatts to many megawatts.

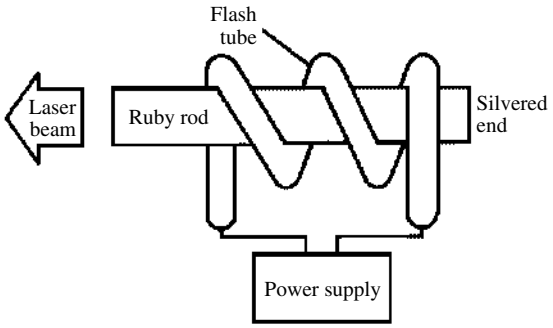

laser

laser beam The radiation from a laser—especially if the divergence is very low, that is, the rays are almost perfectly parallel, resulting in minimal divergence.

laser-beam communication A form of coherent infrared or optical communication in which a laser beam is the link between transmitting and receiving stations. Also see LASER, LASER DIODE, and LIGHT-BEAM COMMUNICATION.

laser capacitor An energy-storage capacitor used to discharge-fire the exciter lamp of a laser. Also see LASER.

laser cavity An optical-resonant cavity that results in the emission of coherent light.

laser cutting A method of using a laser for severing materials.

laser diode A special form of semiconductor light-emitting diode (LED), usually of the gallium-arsenide type, that emits coherent light when a voltage is applied to its terminals. Also see LASER.

5059F-pL-396-423 4/10/01 9:14 AM Page 400

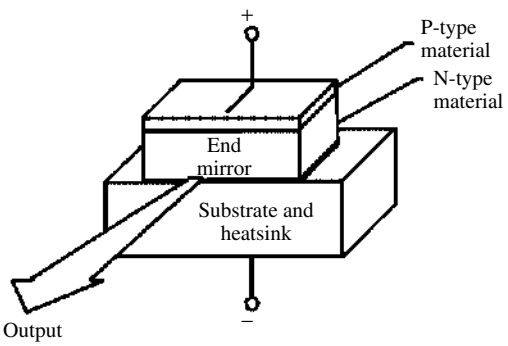

laser diode

laser disk A method of reproducing sound in which a laser is used to recover the sound from a compact disk.

laser Doppler radar Acronyms, *ladar* or *lopplar.* A form of Doppler radar using the light beam of a laser instead of radio waves.

laser eye surgery A method of repairing the retina of the eye without cutting the eyeball, using laser beams to push loose retina tissue back into place.

laser gun A colloquial term for a weapon that makes use of a laser as a device of destruction.

laser optical videodisc system A system in which a low-powered laser reads audio and video information from a videodisc and delivers it to a television receiver.

laser ranger A radar-like device using intense light (instead of microwaves).

laser show A three-dimensional, midair display having motion, made by using lasers in various combinations.

laser surgery The application of a laser in medicine for the purpose of assisting in, or actually performing, operations on human subjects.

laser welding Welding (especially of tiny pieces) with the heat produced by a laser beam.

lasing The emission of coherent electromagnetic energy in the visible-light spectrum. See LASER.

lat Abbreviation of LATITUDE.

latch **1.** A feedback loop in a symmetrical digital circuit, such as a flip-flop, used to maintain a given state. **2.** A simple logic-circuit storage element that consists of two gates as a unit. **3.** To maintain a closed (energized) state in a pair of relay contacts after initial energization from a single electrical pulse. See LATCHING RELAY.

latching current In a thyristor, the minimum value of anode current (slightly higher than the holding current) that will sustain conduction immediately after switch-on.

latching relay An electromechanical or fully electronic relay that locks into whichever mode it is energized for (on or off).

latch-on relay See LOCKING RELAY.

latchup In a transistor switching circuit, the abnormal condition in which the collector voltage remains at its switched-on level after the transistor is switched to cutoff from saturation.

latch voltage The input voltage at which a flip-flop changes states.

late contacts Relay contacts that are operated following the movement of other contacts during the relay's operation.

latency **1.** The time taken by a digital computer to deliver information from its memory. **2.** In a serial storage system, the access time less the word time.

latent image **1.** In a storage tube, a stored image that is not yet visible. **2.** An image stored in the mosaic of an iconoscope. **3.** The image that will appear when photographic film or paper is developed.

lateral chromatic aberration An aberration affecting the sharpness of off-axis color television images.

lateral compliance In phonograph reproduction, the ease with which the stylus can move laterally as it follows the groove. Also see COMPLIANCE and LATERAL RECORDING.

lateral-correction magnet In a color picture tube, a magnet operated with a set of pole pieces attached to the focus element of the blue gun; it controls horizontal positioning of the blue beam for convergence.

lateral magnet See LATERAL-CORRECTION MAGNET.

lateral recording A disc recording in which the groove undulates from side to side. Compare VERTICAL RECORDING.

latitude Abbreviation, lat. Angular distance measured around the earth's circumference to the north and south from the equator. Compare LONGITUDE.

latitude effect The tendency of the earth's magnetic field to decrease the number of charged subatomic particles that reach the surface of the earth near the equator, as compared with the number reaching the surface at other latitudes.

Latour alternator See BETHENOD ALTERNATOR.

lattice **1.** The orderly internal pattern (matrix) of atoms in a crystal. Also see CRYSTAL LATTICE. **2.** A symmetrical arrangement of components in a network (such as an attenuator, a filter, or a bridge circuit).

lattice filter A lattice network having reactance in its arms that makes it a selective circuit.

lattice network See LATTICE, **2**.

lattice section See LATTICE, **2**.

lattice structure See LATTICE, **1**.

lattice winding See UNIVERSAL WINDING.

laue diagram A pattern of spots on a photographic plate produced by the scattering of high energy radiation as it falls on a thin crystal. This pattern is used to determine the nature of the crystal material.

5059F-pL-396-423 4/10/01 9:14 AM Page 401

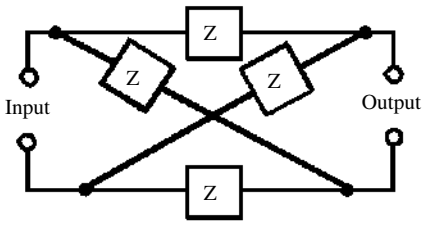

lattice filter

launching The energy transference from a cable into a waveguide.

lavalier microphone A small microphone that can be hung from the user's neck on a cord or chain.

law **1.** A general, verifiable statement that describes the behavior of entities or the relationships between phenomena or concepts. The product of inductive reasoning that follows many observations and controlled experiments (e.g., *first law of thermodynamics*, *inverse-square law*, *Kirchhoff's laws*, and *Ohm's law*. **2.** The nature of the change of a dependent variable, particularly as depicted by a response curve (e.g., *square law*).

LAWEB Civilian weather bulletins issued every six hours from ship and shore positions along the Great Lakes during the sailing season.

lawn mower **1.** A facsimile term for a helix recording mechanism. **2.** A radar receiver preamplifier.

law of a curve See LAW, **2**.

law of averages In probability and statistics, a principle stating that for a large sampling of events, the numerical probability value will be more closely approached than when the sampling is small. Compare LAW OF LARGE NUMBERS.

law of charges Different electric charges attract each other, and similar charges repel each other.

law of electric charges See LAW OF CHARGES.

law of electromagnetic induction See LENZ'S LAW.

law of electrostatic attraction See COULOMB'S LAWS.

law of electrostatic repulsion See COULOMB'S LAWS.

law of first wavefront In acoustics, a rule stating that the perceived direction from which a sound arrives is determined by the first wavefront that reaches the listener's ears.

law of induction See FARADAY'S LAW.

law of inverse squares See INVERSE-SQUARE LAW.

law of large numbers In probability and statistics, a principle stating that with a large sample, the sample average will approximate the population average. It is often erroneously called LAW OF AVERAGES.

law of magnetism Different magnetic poles attract each other, and similar magnetic poles repel each other.

law of natural decay See EXPONENTIAL DECREASE.

law of natural growth See EXPONENTIAL INCREASE.

law of normal distribution Gauss' law of the frequency distribution of a repetitive function, describing the probability of deviations from the mean.

law of octals Chemical activity occurs between two atoms lacking eight valence electrons, and continues until the requirement of eight electrons is satisfied for all but the first orbit, where only two electrons are required. Of interest in the study of semiconductors.

law of radiation See QUANTUM THEORY.

law of reflection For a ray of energy striking a smooth reflective surface, the angle of reflection is equal to the angle of incidence, with respect to a plane tangent to the surface at the point of incidence.

Lawrence accelerator See CYCLOTRON.

lawrencium Symbol, Lr (occasionally Lw). A short-lived radioactive element produced artificially from californium. Atomic number, 103. Atomic weight, about 260.

lay See DIRECTION OF LAY.

layer **1.** A complete coil winding consisting of turns laid side by side (not on top of each other). **2.** In a semiconductor device, a region having unique electrical properties (e.g., *n layer*). **3.** A region of the ionosphere. See IONOSPHERIC LAYERS. **4.** The tape on a reel or in a cassette, encompassing one complete turn (rotation). **5.** In general, a single stratum of a stratified medium.

layer-to-layer transfer In a roll of magnetic tape, unwanted transfer of data between adjacent turns on the reel. If severe, this transfer can cause drop-in or drop-out in a computer. In audio applications, it can sometimes be heard as a delayed echo or a faint sound occurring just prior to the actual recorded sound.

layer winding A coil winding in which the turns are arranged in two or more concentric layers.

layerwound coil An inductor wound in layers, one on top of the other. Also see LAYER, **1**. Compare SINGLE-LAYER COIL.

layout The arrangement of components on a chassis, printed circuit board, or panel.

lazy-H antenna An antenna consisting of two vertically stacked collinear elements, producing both horizontal and vertical directivity.

Lb Abbreviation of LAMBERT; also, *L* (preferred).

lb Abbreviation of POUND.

L band A radio-frequency band extending from 390 MHz to 1.55 GHz. For subdivisions of this band, see L_C BAND, L_F BAND, L_K BAND, L_L BAND, L_P BAND, L_S BAND, L_T BAND, L_X BAND, L_Y BAND, and L_Z BAND.

LC **1.** Abbreviation of LIQUID CRYSTAL; also abbreviated *lix*. **2.** Abbreviation of INDUCTANCE-CAPACITANCE. **3.** Symbol for LC CONSTANT.

5059F-pL-396-423 4/10/01 9:14 AM Page 402

L carrier In a telephone system, a carrier having a frequency between approximately 68 kHz and 10 MHz. It can be used in wire-transmission or radio links.

L_C band A section of the L BAND extending from 465 MHz to 510 MHz.

LC bridge See INDUCTANCE-CAPACITANCE BRIDGE.

LC constant Abbreviation, LC. The product of the inductance and capacitance required for resonance at a given frequency.

LCD Abbreviation of LIQUID-CRYSTAL DISPLAY.

LC filter See INDUCTANCE-CAPACITANCE FILTER.

L circuit See L NETWORK.

LC meter See INDUCTANCE-CAPACITANCE METER.

LCR See INDUCTANCE-CAPACITANCE-RESISTANCE.

LC ratio In a tuned circuit, the ratio of inductance to capacitance.

LCR bridge See IMPEDANCE BRIDGE, **1**.

L_d Symbol for DISTRIBUTED INDUCTANCE.

LDF See LOW-FREQUENCY DIRECTION FINDER.

L display Also called *L scan.* A radar display in which the target appears as two horizontal traces, one extending from a vertical timebase to the right, the other to the left.

lead Pronunciation, *leed.* **1.** A conductor (usually a wire) leading to or emerging from a terminal or electrode. **2.** In computations relating phase, the extent to which one quantity precedes another (e.g., current leads voltage by 90 degrees in a pure capacitance). Compare LAG.

lead Pronunciation, *led.* Symbol, Pb. A heavy metallic element. Atomic number, 82. Atomic weight, 207.2. It can be used as a shield against atomic radiation, and has various applications in electronics (e.g., as electrodes in batteries and as a component of solder). See LEAD-ACID BATTERY, FUSE, and SOLDER.

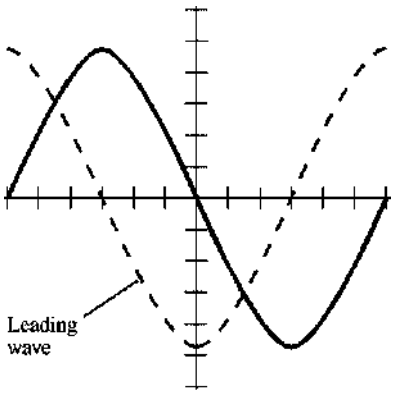

lead, 2.

lead–acid battery A set of two or more lead–acid cells connected in series, usually housed in a common enclosure. Some batteries of this type, notably automotive batteries, are made from sets of lead–acid cells having a free-flowing liquid acid. Other cells have a semisolid "paste" electrolyte. These batteries are popular in consumer electronic devices that require a moderate amount of current. They are also used in uninterruptible power supplies (UPSs) for personal computers. See LEAD–ACID CELL.

lead–acid cell A rechargeable electrochemical cell having an electrolyte of sulfuric acid. The electrodes are lead (negative) and lead dioxide (positive). Produces about 1.5 volts under no-load conditions when fully charged. A large cell of this type can store several tens of ampere-hours. Smaller units have less capacity but more versatility. Their main advantage is reasonable cost, considering that they can be charged and discharged many times.

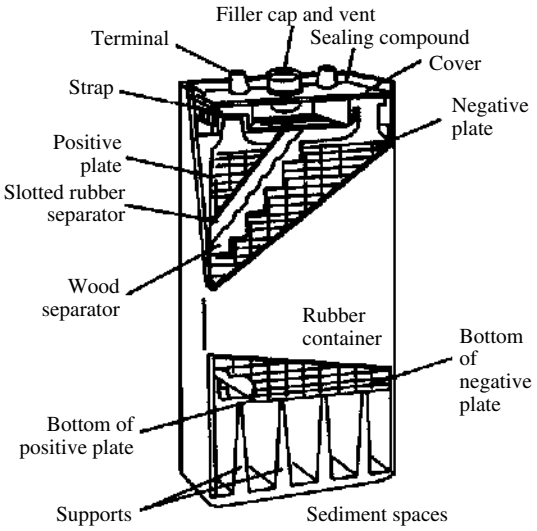

lead-acid cell

lead cell **1.** A lead-acid cell. **2.** A lead-sulfide photocell; see LEAD SULFIDE, **1**.

lead dress See DRESS.

leader **1.** The blank section at the beginning of a magnetic tape. It is usually made of plastic. **2.** A record, preceding a group of records, that identifies the group and provides other data pertinent to the group. **3.** In a lightning stroke, the initial movement of electrons or positive ions, creating the ionized path that allows discharge.

lead frame The metal frame holding the leads of a circuit package (DIP) in place before encapsulation.

5059F-pL-396-423 4/10/01 9:14 AM Page 403

lead-in The wire connecting an antenna to a receiver or transmitter.

leading current Current that precedes voltage in time. Also see LEAD.

leading edge The rising edge of a pulse; compare TRAILING EDGE.

leading ghost A twin television image to the left of the original on the screen.

leading load A load in which current leads voltage (i.e., a capacitive load).

lead-in groove Around the outer edge of a phonograph record, a blank spiral groove that leads the stylus into the first groove of the recording. Compare LEAD-OUT GROOVE.

leading whites In a television picture, an abnormal condition in which the leading (left) edge of a black object has a white border.

leading-zero suppression In a digital meter, the blanking out of all zeros to the left of the decimal point.

lead-in spiral See LEAD-IN GROOVE.

lead-in tube A tube of insulating material, such as plastic or ceramic, used to conduct an antenna lead-in through a wall.

lead-in wire **1.** A single wire, used as a feed line for a shortwave receiving antenna. **2.** The feed line for a television receiving antenna. **3.** A feed line for a transmitting antenna.

lead network A phase-shift circuit containing series capacitance and shunt resistance; it produces a leading phase shift. Compare LAG NETWORK.

lead-out groove Around the inner edge of a phonograph record, a blank spiral groove leading into the eccentric or locked groove.

lead-over groove On a phonograph record containing several recorded tracks, a blank groove that conducts the stylus from the end of one recording to the beginning of the next.

lead screw **1.** A threaded rod that guides the cutter across the surface of a disc during its recording. **2.** In facsimile transmission, a threaded shaft that moves the drum or scanning mechanism lengthwise.

lead sulfate Formula, $PbSO_4$. An insulating compound formed in a LEAD-ACID CELL by the chemical action between the lead in the plates and the sulfuric-acid electrolyte. If the sulfate is not broken down during charging of the cell, it will eventually ruin the cell.

lead sulfide Formula, PbS. A compound of lead and sulfur used as the light-sensitive material in some photoconductive cells.

lead zirconate titanate A synthetic piezoelectric material.

leaf electroscope An electroscope using a pair of gold leaves or a single gold leaf and a solid strip of metal.

leak **1.** The loss of energy through a stray path not intended for conduction. **2.** A point from which energy is lost through a stray path not intended for conduction.

leakage **1.** The small current that flows through an electrical insulator. **2.** The electromagnetic field that is radiated or received by a feed line that should theoretically have 100-percent shielding.

leakage current The zero-signal current flowing across a reverse-biased semiconductor junction.

leakage flux Collectively, magnetic lines of flux around a transformer that do not link the primary and secondary coils.

leakage inductance Self-inductance caused by LEAKAGE FLUX. Leakage inductance is effectively in series with the primary or secondary winding of a transformer.

leakage resistance **1.** In an imperfect insulator, the ohmic resistance, calculated by dividing the voltage across the insulator by the current flowing through the insulator. **2.** The quotient of voltage and current in a reverse-biased semiconductor junction.

leakage radiation Radiation from parts of a system, as compared with that from the true radiator.

leakage reactance Inductive reactance caused by leakage inductance in the primary or secondary circuit of a transformer.

leakance The conductance of an insulating material, measured in siemens. It is equal to the reciprocal of the leakage resistance in ohms.

leaky **1.** Descriptive of a capacitor in which the dielectric material is not a perfect insulator. **2.** Descriptive of imperfect shielding in a coaxial transmission line. **3.** Descriptive of a waveguide with imperfect shielding.

leaky dielectric See LEAKY INSULATOR.

leaky insulator An insulator that conducts significant current at a specified (test) voltage.

leaky waveguide A waveguide that has imperfect shielding, allowing some electromagnetic field to escape.

leapfrogging In radar, a phasing process that eliminates false echoes resulting from the signals of other radar sets.

leapfrog test A test performed on different locations by a computer program in memory; it moves to another memory area to continue tests on other locations.

learning The ability of an artificially intelligent machine to improve or expand its knowledge with time. This can occur as a result of accumulation of information; it can also occur in systems that track their errors to avoid repeating them.

leased line A communications circuit reserved exclusively for a specific user.

least-significant bit Abbreviation, LSB. The digit with the lowest place value in a binary number.

least-significant character Abbreviation, LSC. In positional notation, the extreme right-hand character in a group of significant characters. See POSITIONAL NOTATION.

least-significant digit Abbreviation, LSD. The digit in a number that is at the extreme right (i.e., the one having the lowest place value).

5059F-pL-396-423 4/10/01 9:14 AM Page 404

least upper bound The smallest value of a parameter that can be obtained without changing some characteristic of a circuit, program or system.

Lecher frame A sturdy assemblage of LECHER WIRES.

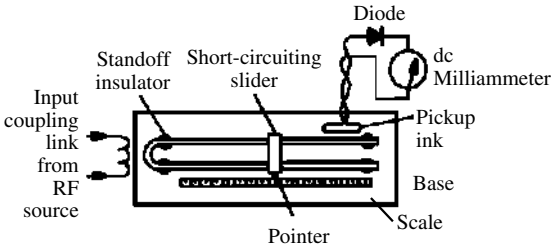

Lecher frame

Lecher lines See LECHER WIRES.

Lecher oscillator A self-excited radio-frequency oscillator using Lecher wires in place of an inductance-capacitance (LC) tank circuit. Also see LINE-TYPE OSCILLATOR.

Lecher wires A circuit segment consisting of two parallel wires or rods joined by a coupling loop on one end, the other end being open. A short-circuiting bar is moved along the wires to vary the effective length of the circuit. Radio-frequency energy is inductively coupled into the system through the loop, and the bar is slid along to various response points, as indicated by a meter or lamp coupled to the wires. The frequency can be determined by measuring the distance between adjacent response points. It is used at very-high frequencies (VHF), ultra-high frequencies (UHF), and microwave frequencies. Also called *Lecher frame* and *Lecher lines*.

Leclanche cell See DRY CELL, **1**.

LED See LIGHT-EMITTING DIODE.

LED phototransistor isolator An optoelectronic isolator in which the light source is a light-emitting diode and the light-sensitive component is a phototransistor.

LEDE Abbreviation for LIVE END/DEAD END.

LEF See LIGHT-EMITTING FILM.

left-hand lay See DIRECTION OF LAY.

left-hand motor rule See FLEMING'S LEFT-HAND RULE.

left-hand polarized wave See COUNTERCLOCKWISE-POLARIZED WAVE.

left-hand taper Potentiometer or rheostat taper in which most of the resistance is in the counterclockwise half of rotation as viewed from the front. Compare RIGHT-HAND TAPER.

left justified An item of data that occupies consecutive locations in storage, starting at the left-hand end of its area; empty locations might appear consecutively at the right-hand end if the item needs fewer positions than have been provided.

left shift A shift operation in which the digits of a word are displaced to the left; the effect is multiplication in an arithmetic shift.

leg **1.** Any one of the distinct branches of a circuit or network; also called ARM or BRANCH. **2.** In a computer program, a path in a routine or subroutine.

L electron In certain atoms, an electron whose orbit is outside of, and nearest to, the orbit of the K electrons.

Lenard rays See CATHODE RAYS.

length **1.** The number of bits or characters in a record, word, or other data unit. **2.** The end-to-end dimension of a device, circuit, line, etc. **3.** The start-to-finish duration of a time interval.

length to fault In cable or line measurements from the home station, the distance (i.e., the cable or line length) to the point at which a fault, such as a short circuit or ground, is located.

lens **1.** A usually circular piece of transparent material with one or both surfaces curved in cross section, used (through its refractive properties) to focus or spread rays that pass through it. Lenses for visible light must be transparent, but those for other radiation, such as radio waves, need not transmit light. Also see ANTENNA LENS. **2.** In a cathode-ray tube, one or more high-voltage electrodes for focusing an electron beam to a fine point on the screen.

lens antenna See ANTENNA LENS.

lens disk A NIPKOW DISK having a lens in each hole.

lens speed The light-transmitting ability of a lens, given as an f-stop number: the lens' focal length divided by its diameter.

lens turret A multiple-lens mount on a camera that can be rotated for quick lens interchange.

LEO Acronym for LOW EARTH ORBIT.

LEO satellite system A set of several dozen low earth orbit (LEO) satellites in polar orbits spaced strategically around the globe such that, for any point on the earth, there is always at least one satellite in range. The satellites can relay messages throughout the fleet. Any two points on the surface are always able to make contact through the satellites.

Lepel discharger See QUENCHED SPARK GAP.

letter-identification word See PHONETIC ALPHABET CODE WORD.

letters patent See PATENT.

letters shift In a text communications terminal, a control character that causes all of the following characters to occur in the lower case. This can be an automatic or a manual control character.

let-through current The current conducted by a circuit breaker during a short-circuit.

level-0 security In communications, the complete lack of security measures. Anyone can listen in on a conversation at any time, provided they are

5059F-pL-396-423 4/10/01 9:14 AM Page 405

willing to spend the money and/or time to obtain the necessary equipment. Examples are amateur ("ham") radio and Citizens' Band (CB) voice communications.

level-1 security Also called *wire-equivalent security.* In communications, the implementation of security measures such that the circuit is protected to the extent of a typical hard-wired link. The encryption is anticipated to be unbreakable for at least 12 months, and preferably for 24 months or more. The technology is updated at least every 12 months, and preferably every 6 months.

level-2 security Also called *commercial-level security.* In communications, the implementation of security measures such that the circuit is deemed safe for ordinary commercial transactions. The encryption is anticipated to be of such a nature that engineers believe it would take a hacker at least 10 years, and preferably 20 years or more, to break the cipher. The technology should be updated at least every 10 years, but preferably every 3 to 5 years, and more often if possible.

level-3 security Also called *mil-spec security.* In communications, the implementation of security involving the most sophisticated forms of encryption and personnel restriction that a government can muster.

level **1.** The amplitude at which a device is functioning or at which a phenomenon occurs (e.g., collector-current level, or received signal level). **2.** The minimum amplitude at which a phenomenon occurs; also called *threshold amplitude.* **3.** A functional plateau or echelon.

level clipper See CLIPPER.

level compensator **1.** An automatic gain control (AGC) that effectively reduces amplitude variations in a received signal. **2.** An automatic gain control in telegraph receiving equipment.

level control **1.** The adjustment of amplitude or threshold. **2.** A potentiometer or other variable component for adjusting the amplitude or threshold of a quantity.

level indicator See VOLUME INDICATOR.

level translator Any circuit or device that alters the voltage levels of input signals. An example is a converter that changes positive-logic signals to negative-logic signals.

level-triggered flip-flop A flip-flop that responds to voltage level, rather than to the frequency of an input signal.

lever switch **1.** A switch designed for rapid making and breaking of a circuit. **2.** A radiotelegraph key.

Lewis antenna A form of antenna used at ultrahigh and microwave frequencies. It resembles a horn antenna.

Leyden bottle See LEYDEN JAR.

Leyden jar [Leyden, Holland (also Leiden), site of the invention in 1745 by Peiter van Musschenbroek, 1692–1761.] The first practical capacitor. In modern form, it is a glass jar covered inside and out with metal foil and has a rod topped by a metal ball that touches the inner foil. It is still used occasionally in classrooms for demonstrating static electricity. The Leyden jar was coinvented by van Musschenbroek and invented independently by E. G. von Kleist of Pomerania, among others.

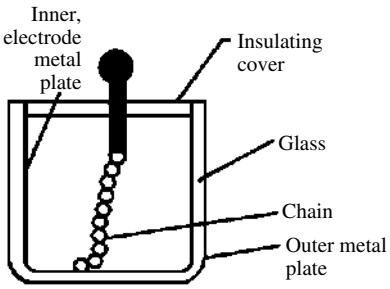

Leyden jar

Leyden phial See LEYDEN JAR.

Leyden vial See LEYDEN JAR.

LF Abbreviation of LOW FREQUENCY.

L_F band A section of the L BAND extending from 1.35 to 1.45 GHz.

L fitting See ELL.

LHD Abbreviation of LOAD/HAUL/DUMP.

Li Symbol for LITHIUM.

librarian program A computer program controlling a LIBRARY.

library In digital-computer and data-processing operations, the permanent storage of data or instructions. Also called *permanent mass storage.*

libration fading In earth-moon-earth (EME) communications, also known as *moonbounce,* rapid and deep fading, accompanied by phase modulation, that takes place because the moon does not always show the earth exactly the same portion of its surface. The moon "wobbles" slightly back and forth on its axis. This causes changes in the relative phases of signals reflected from the topographic features (mountains, in particular) on the lunar surface.

licrystal An acronym from *liquid* and *crystal.* See LIQUID CRYSTAL.

lidar See LIGHT DETECTION AND RANGING.

lie detector See POLYGRAPH.

life **1.** The duration of useful service (or of operation before failure) of electronic equipment. **2.** For a non-rechargeable cell or battery, the length of time it will last in a given application before it must be discarded and replaced. **3.** In robotics and artificial intelligence (AI), a general term that refers to qualitative similarities between machines and animate creatures, including human beings.

5059F-pL-396-423 4/10/01 9:14 AM Page 406

life test An assessment of the life of electronic equipment—either by means of full-time test runs or accelerated time tests.

lifetime See CARRIER LIFETIME.

lifter A device in a magnetic tape recorder that removes the tape from the recording and playback heads under fast-forward and rewind conditions.

light Visible electromagnetic radiation occurring in the wavelength band of about 750 nanometers (red light) to 390 nanometers (violet light). Included sometimes in the category of light are infrared and ultraviolet rays.

light-activated silicon-controlled rectifier Abbreviation, LASCR. A silicon-controlled rectifier that functions both as a photosensor and a heavy-duty bistable electronic switch, allowing high currents to be switched by means of a light beam.

light-activated silicon-controlled switch Abbreviation, LASCS. A pnpn device that acts simultaneously as photocell and electronic switch.

light adaption **1.** The process whereby the eye adjusts itself to an increase or decrease in illumination. **2.** Similar action in photoelectric devices. **3.** The length of time required for the eye to adjust itself to an increase or decrease in illumination.

light amplifier A solid-state amplifier using an input electroluminescent cell and an output photocell, or some similar pair of components. The device is essentially an optoelectronic coupler with gain.

light-beam communication A system of communication in which a beam of light between transmitting and receiving stations is modulated or interrupted to convey intelligence. A laser is commonly used because it has minimal beam divergence, allowing maximum communication range.

light-beam meter An electric meter using a LIGHT-BEAM POINTER.

light-beam pointer A slender beam of light that replaces the pointer in a moving-coil meter. The light comes from a small incandescent lamp and is reflected by a mirror attached to the coil; when the coil moves, a spot of light moves over the scale of the meter.

light-beam receiver The receiver in a LIGHT-BEAM COMMUNICATION system.

light-beam recorder A graphic recorder using a light-beam pointer. In this device, a small spot of light traces a pattern on moving photographic film, which is subsequently developed to produce a permanent record.

light-beam transmitter The transmitter in a LIGHT-BEAM COMMUNICATION system.

light cable A cable, consisting of numerous thin optical fibers, through which light can be transmitted for communication or control purposes. See, for example, LIGHT-WAVE TELEPHONY.

light chopper A device that modulates a light beam by interrupting it repetitively.

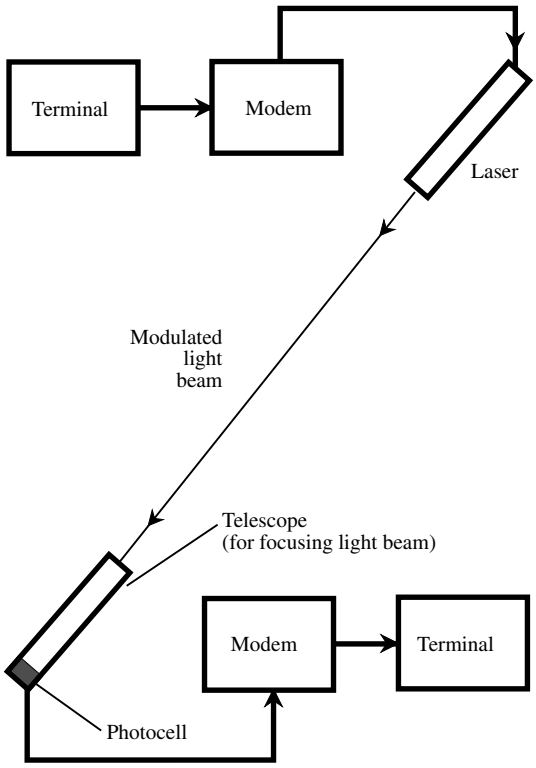

light-beam communication

light detection and ranging Acronym, lidar. A navigation and surveillance system in which laser light scans in a manner similar to that of RADAR.

light dimmer See DIMMER.

lighted pushbutton See LIGHTED SWITCH.

lighted switch A pushbutton switch containing a pilot light that glows to show when the switch is on. Also called *illuminated switch*.

light-emitting diode Abbreviation, LED. A semiconductor device that emits visible light when forward biased. Also see LASER DIODE.

light-emitting film A thin phosphor film that becomes luminescent when a high-frequency voltage is applied across its surface. Also see ELECTROLUMINESCENCE and ELECTROLUMINESCENT CELL.

light flasher An electronic circuit or simple automatic flasher switch for flashing a lamp at regular intervals.

light flicker See LOAD FLICKER.

light flux See LUMINOUS FLUX.

light hood See HOOD.

light-induced electricity See PHOTOELECTRICITY.

5059F-pL-396-423 4/10/01 9:14 AM Page 407

light load A load that is a fraction of the usual value for a given application. That is, its resistance or impedance is several times higher than normal.

light meter An electronic instrument for measuring the intensity of light. It generally consists of a photodiode, a battery, and a direct-current microammeter connected in series. A direct-current amplifier can be used to increase the sensitivity.

light microsecond A unit of electrical distance; the distance that light, or any electromagnetic disturbance, travels in free space in 1 microsecond. Approximately equal to 300 meters.

light modulation Variation of the instantaneous brightness of a visible light beam in synchronization with the instantaneous amplitude of a modulating signal. Also see LIGHT MODULATOR.

light modulator A device with which a beam of light can be modulated by an electrical signal.

light negative Pertaining to negative photoconductivity, the decrease in conductivity of a photosensitive material under illumination. Compare LIGHT POSITIVE.

lightning The discharge that occurs between positive and negative poles in the atmosphere. Common in and near areas where heavy rainfall is occurring. It also can occur in snow storms, in sand storms, and over erupting volcanoes. Generally, the negative pole is in a cloud and the positive pole is at the surface of the earth, resulting in a flow of electrons from cloud to ground. Some lightning occurs as a flow of electrons from ground to cloud, or between two clouds. Such discharges sometimes attain current levels of more than 1,000,000 amperes.

lightning arrester A device that bypasses high-voltage pulses from most nearby lightning discharges to the earth, helping to protect electronic equipment connected to an outdoor antenna or power line. Is not a total guarantee of protection, however.

lightning conductor **1.** A system for protecting buildings from lightning strikes. A common system includes a lightning rod, heavy conductor, and ground rod. The ground rod is placed at least six feet from the base of a building and is at least eight feet long. **2.** The conductor between the lightning rod and ground rod in a system, as defined in **1**.

lightning detector See KERAUNOGRAPH and KERAUNOPHONE.

lightning rod A protective device mounted on the outside of structures, consisting of a pointed, grounded metal rod that will conduct a lightning discharge to earth.

lightning strike A direct hit of an object by a lightning stroke. It usually causes extensive damage to electrical and electronic equipment through which the discharge passes.

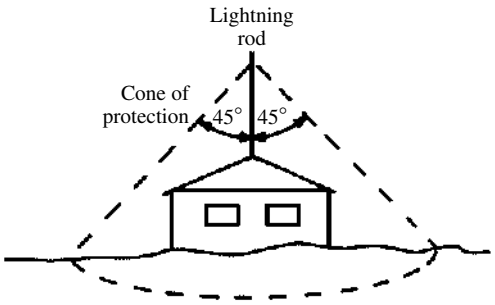

lightning rod

lightning stroke The discharge that occurs with lightning. The peak current is typically several tens of thousands of amperes, but in some cases can exceed 1,000,000 amperes. A stroke can consist of one discharge or several individual discharges in rapid succession.

lightning switch See GROUND SWITCH.

light-operated relay See PHOTOELECTRIC RELAY.

light-operated switch A PHOTOELECTRIC RELAY, or a switch operated by such a relay.

light pen A probe containing a tiny photosensor in its tip. The tip of the light pen is touched to the screen of a cathode-ray tube to sense the beam when it passes the spot of contact. It is used as an input device in some computers and terminals.

light pipe **1.** An OPTICAL FIBER. **2.** A cable consisting of numerous optical fibers in a bundle. See FIBEROPTICS, **1**.

light positive Pertaining to positive photoconductivity, when the conductivity of a photosensitive material increases under illumination. Compare LIGHT NEGATIVE.

light quantum See PHOTON.

light ray A thin beam of light. Theoretically, a ray emerges from a point source (i.e., it has no width).

light receiver See LIGHT-BEAM RECEIVER.

light relay A photoelectric device that operates a relay, according to fluctuations in the intensity of a light beam.

light-sensitive cathode Also called *photocathode.* A cathode that emits electrons when exposed to light.

light-sensitive diode A semiconductor diode usable as a photoconductive cell. Such diodes are available as both junction and point-contact types.

light-sensitive material A photoconductive or photoemissive substance.

light-sensitive resistor See PHOTOCONDUCTIVE CELL.

light sensor **1.** A light-sensitive device, such as a photocell, photodiode, phototransistor, or

5059F-pL-396-423 4/10/01 9:14 AM Page 408

phototube. **2.** A light-sensitive substance, such as cesium, selenium, silicon, cadmium selenide, or lead sulfide.

light source Any generator of light. Under some conditions, the source is regarded as a point.

light spectrum See ELECTROMAGNETIC THEORY OF LIGHT.

light-spot scanner Also called *flying-spot scanner.* A television camera using (as a source of illumination) a spot of light that scans what is to be televised.

light transmitter See LIGHT-BEAM TRANSMITTER.

light valve **1.** An electromechanical device for varying the intensity of light passing through its adjustable aperture. **2.** See KERR CELL.

light-wave telephony Telephone communication by means of modulated-light transmission, usually through an OPTICAL FIBER.

light-year Abbreviation, lt-yr. Pertaining to astronomy, a unit of distance equal to the distance traveled by light in one year in a vacuum: $9.460\ 55 \times 10^{15}$ meters (5.878×10^{12} miles).

likelihood In probability and statistics, the chance that an event will occur or that an outcome will be realized. Also see PROBABILITY, **1**, **2**.

lim Abbreviation of LIMIT.

Lima Pronunciation, *LEE-ma.* Phonetic alphabet word for the letter L.

limen A unit that has been proposed as the minimum audible change in frequency that can be detected by at least half of a group of listeners.

limit **1.** The lowest or highest frequency in a band. **2.** In mathematics, a fixed value that a variable approaches. **3.** The upper and lower extremes in any performance range or value range.

limit bridge A bridge used to check a component (e.g., resistance, capacitance, or inductance) in terms of the tolerance limits, rather than the nominal (named) value, of that component. Also see BRIDGE, **2**.

limited integrator A circuit that integrates two input signals until the corresponding output signal exceeds a certain limit.

limited stability A characteristic of a circuit or system, allowing proper operation only if the input signal and applied voltages are within certain maximum and minimum limits.

limiter A device or circuit whose output-signal amplitude remains at some predetermined level, despite wide variations in input-signal amplitude.

limiting The restriction of the maximum peak amplitude of a signal to a designated level.

limiting amplifier An amplifier that automatically holds the output-signal level to a prescribed value.

limiting current In electrolysis, the highest current that conducts under certain conditions of ion concentration. This current depends on the electrolyte material, the concentration of the electrolyte in solution, the electrode substance, and the size of the electrolytic cell.

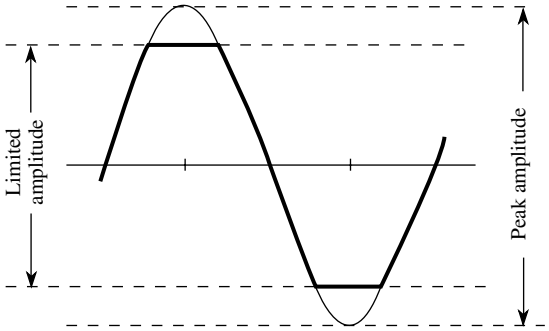

limiting

limiting error The anticipated maximum value of the absolute error in a computation.

limiting resistor See CURRENT-LIMITING RESISTOR.

limiting resolution As a measure of video image resolution, the maximum number of lines for picture height that can be discriminated on a test chart.

limit switch A switch that is actuated when a monitored quantity (e.g., current, voltage, or illumination) reaches the limit of its range.

line **1.** A wire, cable, or waveguide, along which electrical or electromagnetic energy travels from one defined place to another. **2.** One lengthwise path in which a force, such as electricity or magnetism, is evidenced. Such a *line of flux* has theoretically zero width.

line advance **1.** The physical separation between the centers of adjacent scanning lines in a television system. **2.** Line feed in a text data transmission system.

line amplifier An amplifier in a telephone line or similar channel, or one feeding such a line from the input end.

linear **1.** In a straight line. **2.** In the manner of a straight line. Thus, linear response is indicated when one quantity varies directly with another; the graph of this response is a straight line (i.e., one of constant slope). **3.** The characteristic of a signal that is a replica of another (e.g., an amplifier output signal of the same waveform as that of the input signal).

linear absorption coefficient A number expressing the extent to which the intensity of an X-ray beam is reduced per centimeter of the material through which it passes.

linear accelerator A device in which subatomic particles are accelerated in a straight line through a long tube. This action is in contrast with that occurring in a circular accelerator, such as a CYCLOTRON.

linear algebra A branch of mathematics that deals with the solving of linear equations or sets of linear equations.

5059F-pL-396-423 4/10/01 9:14 AM Page 409

linear amplifier **1.** An amplifier for which a linear relationship exists between input and output parameters (e.g., a high-fidelity audio amplifier). **2.** A class-AB radio-frequency power amplifier that does not distort the envelope of an amplitude-modulated (AM) or single-sideband (SSB) signal. It is commonly used by amateur radio operators.

linear array A directional antenna having equally spaced, in-line elements.

linear circuit **1.** A circuit whose output is a faithful reproduction of the input. See LINEAR AMPLIFIER, **1** and LINEAR DETECTOR. **2.** A circuit whose performance is linear. See LINEAR RESPONSE, **1**.

linear decrement In a damped wave, a constant decrease in amplitude with time, as opposed to a decrease that is a logarithmic or otherwise nonlinear function of time. Compare DECREMENT.

linear detector A detector whose output/input relationship is linear. Also see LINEAR, **2**, **3**; LINEAR CIRCUIT, **1**; and LINEAR RESPONSE, **1**, **2**, **3**.

linear differential transformer A device that converts the physical position of an object into an output voltage or current. The voltage or current is directly proportional to the displacement.

linear distortion Amplitude distortion in which the output and input signal envelopes are disproportionate (in the absence of spurious frequencies).

linear equation See FIRST-DEGREE EQUATION.

linear function **1.** In Cartesian two-space, a function of the form $y = mx + b$, where the coordinates are (x,y), the slope is m (any real number) and b is the point on the y axis at which the graph crosses the axis. **2.** Any function in any number of dimensions whose graph appears as a straight line in the Cartesian system of coordinates.

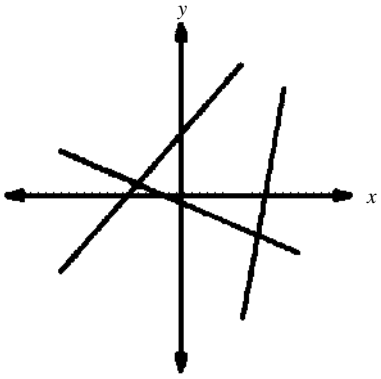

linear function

linear IC See LINEAR INTEGRATED CIRCUIT.

linear integrated circuit An integrated circuit designed for analog operations (such as signal amplification, oscillation, nondigital regulation, analog instrumentation, and similar applications). Compare DIGITAL INTEGRATED CIRCUIT.

linearity **1.** The degree to which performance or response approaches the condition of being linear, expressed in percent or parts per million. Also see LINEAR AMPLIFIER, **1**; LINEAR CIRCUIT, **1**, **2**; LINEAR OSCILLATOR, **1**; LINEAR RESPONSE, **1**, **2**, **3**; and LINEAR TAPER. **2.** In a cathode-ray-tube image, absence of compression or stretching of any portion of the image; that is, an undistorted reproduction.

linearity control In a cathode-ray-tube display, the potentiometer used to correct image linearity. See LINEARITY, **2**.

linearity error **1.** The difference between a theoretically linear function and the actual function, as observed under experimental conditions. **2.** The degree of nonlinearity in an amplifier that is supposed to be linear.

linear modulation **1.** Modulation in which the instantaneous amplitude of the input signal is directly proportional to the instantaneous amplitude of the output signal. **2.** Modulation in which the instantaneous amplitude of the input signal is inversely proportional to the instantaneous amplitude of the output signal. **3.** Modulation in which the instantaneous amplitude of the input signal is directly proportional to the frequency or phase deviation of the output signal.

linear motor A motor in which the stator and rotor are parallel and straight.

linear oscillator **1.** An oscillator whose alternating-current output amplitude varies linearly with its direct-current input. **2.** A line-type oscillator.

linear programming A method of determining the optimum value for a certain set of linear equations. Generally, this is done by finding the point on a plane in space closest to some point not on the plane.

linear quantizing A method of quantizing in which all of the intervals are of equal size or duration. An example is a linear analog-to-digital converter circuit.

linear reflex detector See INFINITE-IMPEDANCE DETECTOR.

linear response **1.** A response in which the value of the dependent variable is equal or directly proportional to the value of the independent variable. Thus, the graph of the response function is a straight line over the range of normal operating values. Compare LOGARITHMIC RESPONSE, **1** and SQUARE-LAW RESPONSE. **2.** A type of response in which a quantity (such as current) varies directly with another quantity (such as voltage). Compare LOGARITHMIC RESPONSE, **2**. **3.** Low-distortion response. Also see HIGH FIDELITY.

linear scale A scale in which all of the divisions represent the same differential and are equally spaced. On a linear scale, a given difference

5059F-pL-396-423 4/10/01 9:14 AM Page 410

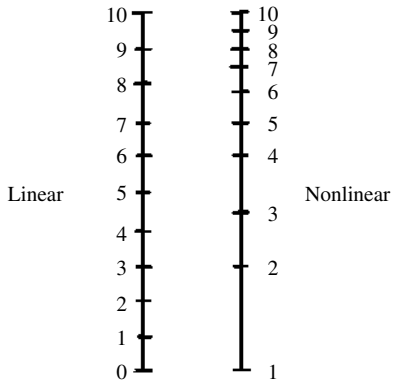

linear scale

always has the same physical length, no matter where on the scale it appears. For example, the interval between 3 and 4 on a linear scale is the same as any interval between x and $x + 1$, where x is any real value on the scale.

linear sweep In a television or oscilloscope circuit, the scanning of the electron beam across the screen at a constant speed. Also see LINEAR, **1**; LINEAR RESPONSE, **1**; and LINEARITY, **2**.

linear taper In a potentiometer or rheostat, resistance variation that is directly proportional to shaft rotation. Thus, half the total resistance corresponds to movement of the shaft over half the arc of full rotation. Compare LOG TAPER. Also see TAPER.

linear time base For an oscilloscope, the base provided by sweeping the electron beam horizontally at a uniform rate. Also see LINEAR SWEEP.

linear track On a video tape, the track that contains audio information that accompanies the video data. It was so named because it is a single, straight track, in contrast to the video tracks, which are angled.

linear tracking In a turntable system, a design scheme in which the lateral movement of the stylus, as the disc is played, occurs in a straight line, rather than in an arc.

linear transformer A radio-frequency transformer consisting of a section of transmission line.

linear variable differential transformer Abbreviation, LVDT. A differential transformer exhibiting linear response. Also see LINEAR RESPONSE, **1**, **2**.

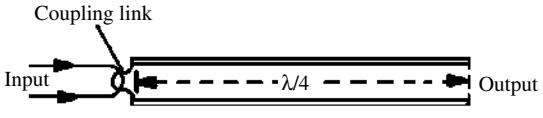

linear transformer

line balance The degree of electrical similarity between transmission line conductors, or between a conductor and ground.

line-balance converter A device used to isolate the outer conductor at the end of a coaxial line from ground.

line characteristic distortion Fluctuations in the duration of received signal impulses in text data communications, caused by changing current transitions in the wire circuit.

line circuit The telephone system relay equipment associated with stations connected to a switchboard.

line code A code between the digits in processing equipment and the pulses representing the digits in a line transmission.

line conditioning In data communications, the modification of private or leased lines by adding compensating reactances to reduce amplitude variations or phase delays over a band of frequencies.

line contact stylus A needle used to reproduce stereo high-fidelity sound from vinyl discs. It has a characteristic oblate ellipsoidal shape.

line coordinate A symbol identifying a specific row of cells in a matrix; a specific cell can be located with an additional column coordinate.

line cord A flexible two- or three-wire insulated cable connecting equipment to the power line by means of a plug that mates to a standard electrical outlet.

line current **1.** Current flowing from a power line into equipment. **2.** Current flowing in a transmission line. **3.** Current flowing into a parallel-resonant circuit.

line diffuser A circuit that creates minor vertical oscillations of the spot on a television screen, making the individual scanning lines less noticeable.

line driver An integrated circuit capable of transmitting logic signals through long lines.

line drop The voltage drop along a line supplying power to a device.

line equalizer See EQUALIZER.

line fault A discontinuity in a transmission line, resulting in signal loss at the receiving end of a circuit.

line feed In a text data transmission system, the movement of the paper, platen, or cursor to allow for printing or displaying an additional line of text.

line filter **1.** A circuit that can be inserted in the utility power cord of an appliance, device, or system for transient suppression and the minimization of electromagnetic interference (EMI). The filter employs series inductors, parallel capacitors, and in some cases, a clamping device. Installed between a radio transmitter and the utility lines, such a filter can choke off radio-frequency (RF) current and help keep utility wiring from acting as an antenna. Installed in the

5059F-pL-396-423 4/10/01 9:14 AM Page 411

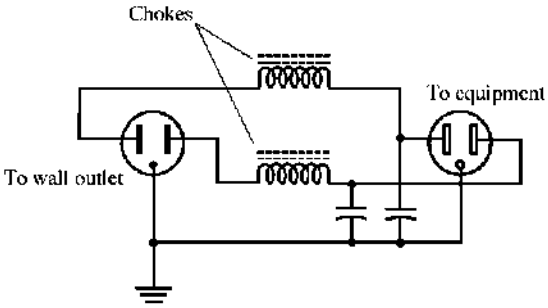

line filter

power cords of home entertainment equipment, such as stereo audio amplifiers, line filters can keep RF from entering the apparatus through the power supply. **2.** A circuit containing parallel capacitors and/or series inductors, installed in a twisted-pair telephone line to reduce or eliminate the effects of EMI and transients in a telephone set.

linefinder A switching device that finds one of a group of calling telephone lines and connects it to a trunk, connector, or selector.

line frequency **1.** The frequency of power-line voltage in the United States, 60 Hz. **2.** The rate at which the horizontal lines are traced in a video image. Also see HORIZONTAL FREQUENCY.

line group **1.** A group of signals sent by wire transmission. **2.** The frequency spectrum occupied by a group of signals sent by wireless transmission.

line leakage Resistance between insulators of two wires in a telephone line loop.

line loss The sum of energy losses in a transmission line.

lineman A technician who works mainly with telephone or telegraph lines.

line matching transformer A device that provides an impedance match in an audio circuit, and also can adapt balanced to unbalanced audio transmission lines (or vice versa).

line noise **1.** Electrical noise (as received by a radio) arising from fluctuations of current or voltage in a power line. **2.** Noise in a data transmission line.

line of flux **1.** A line (usually curved) depicting the points of equal-intensity field strength in the vicinity of an electric charge or a charged body. Also see FLUX. **2.** A line depicting the points of equal-intensity field strength in the vicinity of a magnetic pole or a magnetized body. Also see FLUX.

line-of-sight communication Radio communications between points located so that a straight line between them does not pass through the earth, or through any major obstructions. Also see LINE-OF-SIGHT DISTANCE.

line-of-sight distance The maximum distance over which an ultra-high-frequency (UHF) or microwave signal can be directly transmitted along the surface of the earth. It is slightly more than the maximum optical line-of-sight distance.

line oscillator See LINE-TYPE OSCILLATOR.

line plug The plug terminating a line cord. Also see MALE PLUG.

line printer A machine that prints the results of a computer run, line by line.

line radio See WIRED RADIO.

line regulation Automatic stabilization of power-line voltage.

line-sequential system The color television system in which the image is reproduced by means of primary color lines (red, green, and blue) sequentially beamed across the screen of the picture tube. Compare DOT-SEQUENTIAL SYSTEM and FIELD-SEQUENTIAL SYSTEM.

lines of cleavage See CLEAVAGE.

lines oscillator See LINE-TYPE OSCILLATOR.

line supervision In electronic security systems, a method of monitoring circuit characteristics to detect possible tampering.

line switch **1.** The main power-line switch to a system. **2.** Within a piece of electronic equipment, the switch that opens and closes the circuit to the incoming power line.

line-type amplifier A radio-frequency amplifier in which the tuned circuits are transmission lines consisting of parallel wires, rods, or tubing, or of coaxial cable sections.

line-type oscillator A radio-frequency oscillator in which the tuned circuits are transmission lines consisting of parallel wires, rods, or tubing, or of coaxial cable sections.

line unit In a wire data transmission system, the terminal unit, or device that converts the text signals into electrical impulses and vice versa.

line voltage **1.** The voltage between the conductors in a power line. **2.** The voltage between the conductors of a transmission line.

line-voltage drop See LINE DROP.

line-voltage monitor See POWER-LINE MONITOR.

linguistics The study of languages, including structure, symbology, and phonetics.

link **1.** The small coupling coil used in link coupling. **2.** A communication path between two radio facilities for the purpose of extending the range of one, as between a remote pickup point and a broadcast transmitter. **3.** A data connection between two different computers. **4.** The act or process of creating a signal path or data connection, as defined in **1**, **2**, or **3**. **5.** In a digital computer, a branch instruction, or an address in such an instruction, used to leave a subroutine to return to some point in the main program.

linkage Coupling between separated conductors or devices through the medium of electric or magnetic lines of flux.

5059F-pL-396-423 4/10/01 9:14 AM Page 412

link circuit A closed-loop coupling circuit having two coils of a few turns of wire; each coil is placed near one of the circuits to be coupled.

link coupling Low-impedance coupling via a small (usually one-turn) input or output coil fed by a twisted pair or a coaxial line.

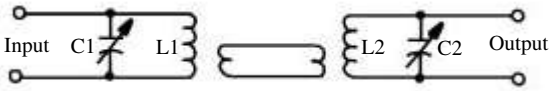

link coupling

linked subroutine A subroutine, entered by a branch instruction from a main routine, that executes a branch instruction returning control to the main routine.

link fuse A fuse consisting of an exposed length of fuse wire.

link neutralization Neutralization achieved by out-of-phase current fed back via link coupling from the output to the input of an amplifier. Also called INDUCTIVE NEUTRALIZATION.

lin-log receiver A radar receiver whose amplitude response is linear for small signals, but logarithmic for large ones.

lip microphone A small microphone operated close to or in contact with the lips.

liquid A state of matter characterized by a level of molecular motion intermediate between that of gases and solids; liquids have the ability (like gases) to take the shape of a container and are only slightly compressible. Compare GAS, PLASMA, and SOLID. Also see STATE OF MATTER.

liquid absorption For a solid material, such as dielectric, the ratio of the weight of liquid absorbed by the material to the weight of the material.

liquid capacitor See WATER CAPACITOR.

liquid cell See ELECTROLYTIC CELL.

liquid conductor See ELECTROLYTE.

liquid cooling Use of circulating water, oil, or other fluid to remove heat from components or equipment, such as microprocessors or power amplifiers.

liquid crystal A liquid exhibiting some of the characteristics of a crystal. Also see NEMATIC CRYSTAL and SMECTIC CRYSTAL.

liquid-crystal display Abbreviation, LCD. A flat-panel display noted for its thin profile, light weight, and low power consumption. The simplest devices are used in calculators, meters, wristwatches, and radios. More sophisticated displays are used in computers and portable video units. This type of display can operate at a much lower voltage than a cathode-ray tube (CRT). This makes it ideal for portable electronic systems in which batteries are used. Older displays of this type can be difficult to read from certain viewing angles. This situation has improved in recent years with the advent of *active-matrix,* also known as *thin-film-transistor* (TFT), displays.

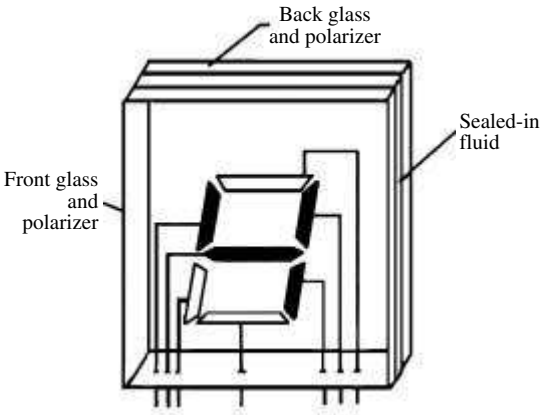

liquid-crystal display

liquid-filled transformer A transformer filled with a protective liquid insulator, such as oil.

liquid-flow alarm An electronic circuit that actuates an alarm when the flow of a liquid through pipes or other channels changes from a desired rate.

liquid-flow control A servo system that automatically maintains or corrects the rate of liquid flow through pipes or other channels.

liquid-flow gauge See LIQUID-FLOW METER.

liquid-flow indicator See LIQUID-FLOW METER.

liquid-flow meter An instrument that indicates the rate at which a liquid moves through pipes or other channels.

liquid-flow switch In a liquid-cooled system, a switch that actuates an alarm when the liquid slows or stops.

liquid-jet oscillograph A graphic recorder using an ink-jet galvanometer to trace the pattern on a paper chart.

liquid laser A laser in which the active material is a liquid.

liquid-level alarm An electronic device that actuates visual or audio signal devices when the surface of a liquid inside a tank rises or falls to a predetermined level.

liquid-level control A servo system that automatically maintains the liquid in a tank at a predetermined level.

liquid-level gauge An electronic system that provides direct readings of the level of a liquid in a tank.

liquid-level indicator See LIQUID-LEVEL GAUGE.

liquid-level meter See LIQUID-LEVEL GAUGE.

liquid load See WATER LOAD.

liquid-pressure alarm An electronic circuit that actuates an alarm when the pressure of a liquid changes.

5059F-pL-396-423 4/10/01 9:14 AM Page 413

liquid-pressure control A servo system that automatically maintains or corrects liquid pressure in pipes or other channels.

liquid-pressure gauge See LIQUID-PRESSURE METER.

liquid-pressure indicator See LIQUID-PRESSURE METER.

liquid-pressure meter An instrument that provides direct readings of liquid pressure in a pipe or other channel.

liquid-pressure switch A switch that actuates an external circuit or device when the pressure of a liquid changes.

liquid rheostat See WATER RHEOSTAT.

liquid valve See ELECTROMECHANICAL VALVE.

liser An oscillator that produces an extremely pure microwave carrier signal.

LISP A digital-computer language written in the form of lists. A program can be directly interpreted as data, and vice versa. The entire language is derived from a few basic functions. Programs are easy to debug. It is used in artificial intelligence (AI) research. Also see LANGUAGE.

Lissajous figure Any one of several curves resulting from the combination of two harmonically related sine waves. These figures are familiar in electronics; they are obtained when signals are applied simultaneously to both axes of an oscilloscope. It is also called *Lissajous pattern.*

list **1.** To print serially the records in a file or in memory. **2.** To print (instruct a computer to display) every item of input data in a program. **3.** A one-dimensional array of numbers.

listener fatigue Physiological symptoms, such as headaches, caused by prolonged listening to certain sounds (e.g., a pure sine wave or poorly reproduced music).

listening angle In stereo sound reproduction, the angle between the speakers, with respect to the listener. This angle can vary from zero to 180 degrees. Larger angles result in increased apparent channel separation.

listening test The subjective evaluation of audio equipment by listeners.

liter Abbreviation, l. A metric unit of volume equal to 1.0567 U.S. liquid quarts or 0.908 U.S. dry quart. A liter is the volume of 1 kilogram of water at 4°C and under a pressure of 1 pascal.

literal operands It is usually applicable to source language instructions, operands that specify the value of a constant, rather than an address of a location in which the constant is stored.

lithium Symbol, Li. An element of the alkali-metal group, and the lightest elemental metal. Atomic number, 3. Atomic weight, 6.941.

lithium battery See LITHIUM CELL.

lithium cell A type of electrochemical cell with exceptional energy-to-mass ratio and long shelf life. There are several variations in the chemical makeup; they all contain lithium, a light, highly reactive metal. These units can be manufactured to supply 1.5 to 3.5 volts, depending on the particular chemistry used. These cells can last for years in very-low-current applications such as memory backup.

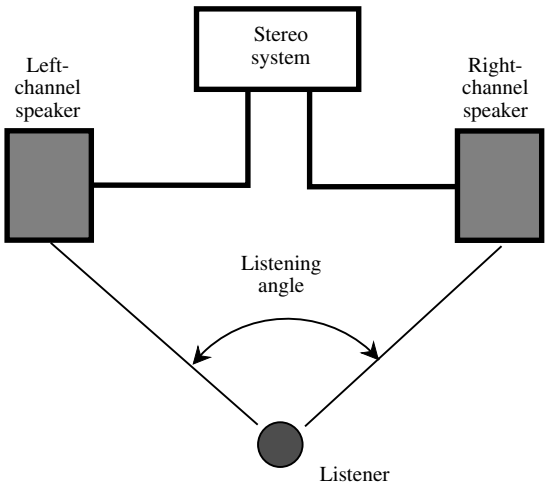

listening angle

Litzendraht wire See LITZ WIRE.

Litz wire A woven wire having a number of copper strands, each separately enameled to insulate it from the others. The wire is woven so that inner strands come to the surface at regular intervals. It is noted for its low losses at radio frequencies.

live **1.** Electrically activated (i.e., sustaining voltage or current). **2.** Being broadcast as it occurs. **3.** Acoustically reflective, as in a LIVE ROOM (contrasted with one that is acoustically absorbent).

live end **1.** In a recording or broadcasting studio, the part of the room in which the acoustic concentration is greatest. **2.** In a utility circuit, the wire or terminal that carries 117 volts alternating current (the ungrounded end).

live end/dead end Pertaining to a room that is acoustically reflective (live) at one end, and acoustically absorbent (dead) at the other end.

live room A room with little or no acoustically absorbent material in its ceiling, walls, and floor, with the result that echoes and reverberation are pronounced. Compare DEAD ROOM.

lix Abbreviation of LIQUID CRYSTAL.

L_K band A section of the L BAND that extends from 1.150 to 1.350 GHz.

L_L band A section of the L BAND that extends from 510 to 725 MHz.

LLL Abbreviation of LOW-LEVEL LOGIC.

lm Preferred abbreviation of LUMEN.

lm/ft² Abbreviation of *lumens per square foot.* Also see LUMEN.

lm-hr Abbreviation of LUMEN-HOUR.

5059F-pL-396-423 4/10/01 9:14 AM Page 414

lm/m² Abbreviation of *lumens per square meter*. Also see LUMEN and LUX.

lm/W Abbreviation of *lumens per watt*, a unit of luminosity. Also see LUMEN.

ln Representation of the natural (base-*e*) logarithm function (see NAPIERIAN LOGARITHM). Also written *loge*.

L network An impedance-matching circuit, filter, or attenuator whose schematic representation resembles an inverted letter L.

LO Abbreviation of LOCAL OSCILLATOR.

lo Abbreviation of *low*, usually as a prefix or subscript. Also abbreviated L.

load **1.** Also called *electrical load*. A device or circuit that is operated by the electrical power output of another device or circuit. Examples: speaker, light bulb, power amplifier, antenna system. **2.** Also called *mechanical load*. The mechanical power output demanded of a machine—especially a motor. **3.** To fill an internal computer storage with information from an external storage [e.g., from a magnetic disk to a computer's random access memory (RAM)]. **4.** To add inductors and/or capacitors to an antenna system to alter the characteristics of the system—especially the resonant frequency. **5.** To adjust the output circuit of a radio-frequency power amplifier for optimum energy transfer to the antenna system.

load-and-go Automatic coding in which a user's (source) program is translated automatically into machine language and stored.

load capacitance **1.** The capacitance present in an electrical load (see LOAD, **1**). **2.** A capacitance used as an electrical load.

load capacity **1.** In pulse-code modulation, the level at which a sine-wave signal has peaks coinciding with the plus/minus virtual decision values of the encoder. **2.** The maximum number of signals that a medium or line can carry without serious degradation of reception.

load circuit **1.** The circuit that forms the load, or power-consuming portion, of a system. **2.** A circuit that facilitates transfer of power to a load.

load coil See WORK COIL.

load current The current flowing in a load. See LOAD.

load division A method of connecting two or more power sources to a single load, for optimum power transfer.

loaded antenna An antenna incorporating a LOADING COIL and/or LOADING DISK to increase its electrical (effective) length. See LOADING COIL and LOADING DISK.

loaded line A transmission line in which inductors or capacitors are inserted at appropriate points to alter the characteristics of the line.

load end The end of a transmission line to which a radiator or receiver is connected.

load flicker Fluctuations in the brightness of lamps, caused by intermittent loading of the power line by other devices.

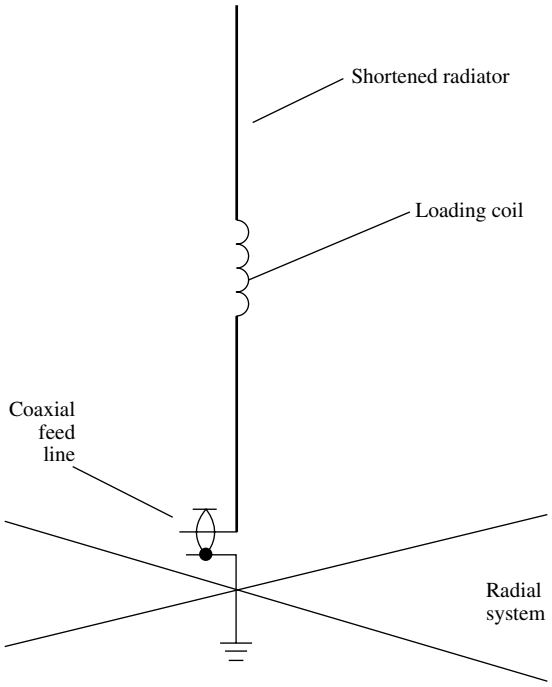

loaded antenna

load/haul/dump Abbreviation, LHD. A remote-controlled or computer-controlled robot used in mining and construction work. Under the direction of a human operator or a computer, it loads, hauls, and dumps materials (hence its name). It can use various navigation methods, including beacons, computer maps, position sensors, and vision systems.

load impedance Symbol, Z_L. The impedance presented by a load connected to a generator or other source.

loading **1.** The matching of source impedance to load impedance, usually by means of the introduction of an inductance or capacitance into the load itself. **2.** Any form of impedance matching. **3.** The addition of inductance and/or capacitance to an antenna system to alter the characteristics of the system—especially the resonant frequency. **4.** The modification of the acoustic impedance of a loudspeaker.

loading coil An inductor inserted in a circuit to increase its total inductance or to provide some special effect, such as canceling capacitive reactance. See LOADED ANTENNA and PUPIN COIL.

loading disk Also called *capacitance hat*. A metal disk mounted atop a vertical antenna to increase its effective length and thereby lower its resonant frequency. It also increases the bandwidth of the system.

5059F-pL-396-423 4/10/01 9:14 AM Page 415

loading factor The ratio of source impedance to load impedance before the introduction of loading circuits.

loading inductance **1.** The inductance present in a load. **2.** An inductance used as a load.

loading routine Also called *loading program.* A routine permanently in memory; it allows a program to be loaded into memory from an external storage medium.

load life The longevity of a device in terms of the number of hours it can withstand its full power rating.

load line In a group of voltage-current (*EI*) curves, a line connecting points of equal resistance (*E*/*I*) that are equal to a particular value of load resistance (impedance).

load power The power dissipated in a load.

load regulation Automatic stabilization of load resistance (impedance) at a constant value.

load resistance **1.** The resistance present in a load. **2.** A resistance used as load.

load stabilizer A device for holding load current or load voltage to a constant value.

loadstone Alternate spelling of LODESTONE.

load termination The load connected to the output of a circuit or device as the terminal element in a circuit or system.

load voltage The voltage developed across a load.

load-voltage stabilization Automatic regulation of load voltage.

load wattage See LOAD POWER.

lobe In the directivity pattern of a transducer, a figure, such as a circle or ellipse enclosing an area of intensified response. Applicable especially to antennas.

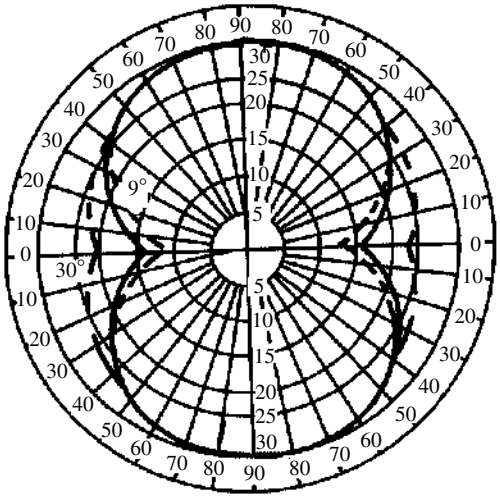

lobe (pattern of horizontal half-wave antenna)

lobing **1.** In a transmitting or receiving antenna, the effect of ground reflection, resulting in phase reinforcement (lobes) at some elevation angles and phase opposition (nulls) at other angles. **2.** The pattern of secondary maxima in the radiation response of a directional antenna.

local action Electrolysis between separate areas of a single electrode immersed in an electrolyte. The action is caused by impurities at different spots in the electrode metal, causing one spot to act as an anode and the other as a cathode, thereby creating a small battery cell.

local alarm In security applications, a visible and/or audible alarm that can be seen and/or heard easily throughout the protected zone.

local area network Abbreviation, LAN. A group of computers and/or terminals that are linked together within a relatively small geographic area, such as a college campus. Interconnections are usually made via cable. There are several different configurations, called *topologies.*

local battery In wire telephony, a battery installed on the subscriber's premises.

local broadcast station A standard broadcast station licensed in the local service. See LOCAL CHANNEL and LOCAL STATION.

local channel A channel in the standard amplitude-modulation (AM) broadcast band, intended to serve only the area near the station. Transmitter power and operating time are restricted to prevent long-distance propagation.

local control The control of a radio transmitter from the site (in contrast to remote control).

local feature focus In robotic systems, the use of only a small portion of the available image data to perform a function. The robot computer recognizes and acts on the data it needs, disregarding the rest.

local feedback Feedback within a circuit stage.

localizer A radionavigation transmitter whose signal guides aircraft to the centerline of a runway.

local oscillator Abbreviation, LO. In a wireless transmitter, one of the oscillators that contributes to the signal that is ultimately modulated and transmitted. The LO output is mixed with the output of a variable-frequency oscillator (VFO). The LO frequency can be switchable at increments of several hundred kilohertz (500 kHz and 1000 kHz are typical), facilitating band changes when mixed with the VFO output. In some transmitters, the LO can operate at a single, fixed frequency if the VFO tunes over an exceptionally wide range.

local program A program that originates at the same single broadcast station from which it is transmitted.

local reception The reception of signals from local stations. Compare LONG-DISTANCE COMMUNICATIONS.

local side The group of circuits and components associated with a communications terminal at a given location.

5059F-pL-396-423 4/10/01 9:14 AM Page 416

local station A station situated within the same general area as the receiver, as opposed to a distant station.

local system library A computer program library containing standard software associated with a specific system.

local transmission The sending of signals to receivers in the same general locality as the transmitter, as opposed to long-distance transmission.

local trunk In a telephone system, the interconnecting line between local and long-distance lines.

location In digital computer operation, a memory position (often a register) specified by an address and usually described in terms of the basic storage unit a particular system uses (e.g., a character is a location in a character-oriented machine).

location counter A register in the control section of a computer containing the address of the instruction being executed.

locked groove A continuous blank groove around the inside of a phonograph record. When the disc is done playing, this groove keeps the stylus from running into the label or sliding across the disc.

locked oscillator **1.** A fixed-frequency oscillator, such as a crystal-controlled oscillator. **2.** See BRADLEY DETECTOR.

lock-in A state of synchronism, as when a self-excited oscillator is synchronized (locked-in) with a standard-frequency generator.

lock-in amplifier A detector that makes use of a balanced amplifier. The output is the difference between the collector or drain currents of the two devices.

locking circuit See HOLDING CIRCUIT.

locking relay See LATCHING RELAY.

lock-in relay See LATCHING RELAY.

lock-out **1.** To prevent a hardware unit or routine from being activated (e.g., when there would be a conflict between operations using the same areas of memory). **2.** A safeguard against an attempt to refer to a routine in use.

lock-up relay An electromagnetic relay that can be locked in the actuated state nonmechanically (i.e., by means of an electromagnet or permanent magnet).

locus The set of all points located by stated conditions (e.g., the locus of secondary points that are all equidistant from a primary point is a sphere).

lodestone A natural magnet; a form of the mineral magnetite. Also spelled *loadstone.*

log **1.** Abbreviation of LOGARITHM. **2.** A continuous record of communications kept by a station, or a record of the operation of an equipment.

$\log_{10}$ Abbreviation of *common logarithm* (base-10 logarithm). Also called *Briggsian logarithm.*

logarithm Abbreviation, log. The power y to which a fixed number a, called the *base,* must be raised to equal a given number x. Suppose $x = a^y$, where a, x, and y are real numbers. Then, $\log_a x = y$. The most common logarithmic bases are 10 and the transcendental number e, approximately equal to 2.71828. See COMMON LOGARITHM and NAPIERIAN LOGARITHM.

logarithmic amplifier An amplifier whose output-signal amplitude is proportional to the logarithm of the input-signal amplitude.

logarithmic curve A graphical representation of a logarithmic function, having the form $y = k \log_a x$, where k is a nonzero real-number constant, and a is a positive real number (the logarithmic base).

logarithmic decrement See DECREMENT.

logarithmic graph Also called *log-log graph.* A graph in which the x and y axes are both incremented logarithmically. Compare SEMILOGARITHMIC GRAPH.

logarithmic horn A horn whose diameter varies directly, according to the logarithm of the displacement along the axis. See HORN.

logarithmic mean See GEOMETRIC MEAN.

logarithmic meter A current meter or voltmeter whose deflection is proportional to the logarithm of the quantity under measurement. The increments on the scale of such an instrument are closer together in the upper portion.

logarithmic rate of decay See EXPONENTIAL DECREASE.

logarithmic rate of growth See EXPONENTIAL INCREASE.

logarithmic response **1.** Response in which the value of a dependent variable is at every point proportional to the logarithm of the independent variable. **2.** A type of response in which a quantity (such as current) varies directly with the logarithm of another quantity (such as voltage).

logarithmic scale A graduated scale in which the coordinates are positioned, according to the logarithm of the actual distance from the origin.

logarithmic voltmeter See LOGARITHMIC METER.

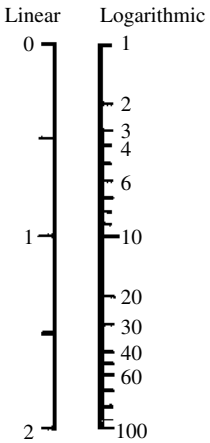

logarithmic scale

5059F-pL-396-423 4/10/01 9:14 AM Page 417

$\log_e$ Abbreviation of *logarithm to the base e* (the NAPIERIAN LOGARITHM). Also written *ln*.

logic **1.** In digital circuits, the mathematics dealing with the truth or falsity of statements (represented by variables) and their combinations. Also see SYMBOLIC LOGIC. Generally, "truth" is represented by the binary digit 1, and "falsity" is represented by the binary digit 0. **2.** Collectively, the switching circuits and associated hardware for implementing digital functions (see 1), such as AND, NAND, NOR, OR, etc.

logical decision During a computer program run, a choice between alternatives based on specified conditions. For example, one alternative path in a routine might be selected because an intermediate result was negative.

logical diagram A schematic diagram showing the interconnection between gates of a logic circuit.

logical equivalence The condition in which two logical statements have identical truth value for all possible combinations of truth value of their constituents.

logical file A data set composing one or several logical records.

logical implication For logical statements *x* and *y*, the condition that *y* is true whenever *x* is true: If *x*, then *y*.

logical operation **1.** An operation using logical operators: AND, NOR, OR, and NAND. **2.** A processing operation in which arithmetic is not involved (e.g., a shift).

logical operator A word or symbol representing a logic function operating on one or more operands. Examples: NOT, OR, AND, NOR, and NAND.

logical shift A shift operation in which digits in a word are moved to the left or right in circular fashion; digits displaced at one end of the word are returned at the other. Also called CYCLIC SHIFT.

logic array In logic circuits, a redundant arrangement of identical components in a single package.

logic circuit In digital systems, a gating or switching circuit that performs such logical operations as AND, NAND, NOR, OR, and XOR. It can use diodes, transistors, charge-coupled devices, tunnel diodes, thyristors, ferroelectric elements, magnetic-core elements, or a combination of these. It usually consists of diodes and transistors fabricated onto an integrated-circuit (IC) chip.

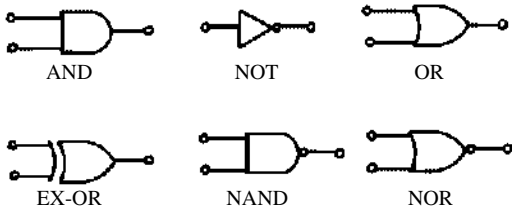

logic circuits (or gates)

logic comparison An operation in which two operands are compared for equal value.

logic connectives Words connecting operands in a logic statement; the truth or falsity of the statements can be determined from their content and the connectives' meanings.

logic diagram **1.** A graphic representation of a logic function (e.g., AND, NAND, NOR, OR, and XOR). **2.** The design of a device or system represented by graphic symbols for logic elements and their relationships.

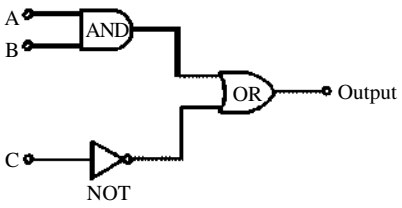

A	B	C	$AB + \overline{C}$
0	0	0	1
0	0	1	0
0	1	0	1
0	1	1	0
1	0	0	1
1	0	1	0
1	1	0	1
1	1	1	1

logic diagram and truth table

logic diode See COMPUTER DIODE.

logic flowchart The logical steps in a program or subroutine represented by a set of symbols.

logic function An expression for an operation involving one or a combination of logic operators.

logic gate See LOGIC CIRCUIT.

logic input current In an integrated circuit, the input current to the logic gate at a certain voltage value.

logic input levels The range of voltages over which the logic trip level occurs, from low to high or high to low. It is usually expressed in volts for the low state and the high state; for example, low is –1 to +2 volts, high is +4 to +6 volts.

logic instruction A command to execute a logical function.

logic level **1.** One of the two logic states 0 or 1 (on or off, high or low). **2.** Of the two logic states, that which represents the "true" condition. **3.** The voltage amplitude of digital signals in a logic system.

logic probe A test probe with a built-in amplifier and (usually) indicating LEDs; its tip is touched to various test nodes in a digital logic circuit to trace logic levels and pulses.

5059F-pL-396-423 4/10/01 9:14 AM Page 418

logic relay See BISTABLE RELAY.

logic swing In a logic circuit, the difference between the voltage corresponding to the high state and the voltage corresponding to the low state.

logic symbol **1.** A symbol used to represent a logic element in a circuit diagram. **2.** A symbol used to represent a logic connective.

log-log graph See LOGARITHMIC GRAPH.

LOGO A high-level computer programming language used for robot control and as an education aid. It is especially useful for teaching children how to operate computers and computerized robots. Statements are simple enough so that elementary-school children can learn to write short programs.

log-periodic antenna Also called *log-periodic dipole array (LPDA).* A broad-spectrum, multiband directional antenna in which the lengths and spacing of the radiator and elements increase logarithmically from one end of the antenna to the other.

log polar navigation A computerized navigation system in which polar-coordinate data is converted into rectangular-coordinate data. In the transformation process, the logarithm of the radius (range) is taken. This results in improved image resolution at close range, although it sacrifices resolution at greater ranges.

log taper In a potentiometer or rheostat, resistance variations that correspond to the logarithm of shaft rotation, or vice versa. Compare LINEAR TAPER. Also see TAPER.

long Abbreviation of LONGITUDE.

long-distance communication **1.** Radio communication between stations separated by distances too great for ground-wave propagation to be effective. **2.** In telephone service, communications that require the dialing of an area code in addition to the local exchange number.

long-distance loop A direct telephone line connecting a subscriber's station to a long distance switchboard.

long-distance reception Reception of radio signals from stations beyond the range of ground-wave propagation. See also LONG-DISTANCE COMMUNICATION, **1**.

long-distance transmission Transmission of radio signals to points beyond the range of ground-wave propagation. See also LONG-DISTANCE COMMUNICATION, **1**.

longitude Abbreviation, long. Angular displacement, measured in degrees around the earth's circumference, to the east and west of the prime meridian that passes through Greenwich, England. Compare LATITUDE. Also see MERIDIAN.

longitude effect The variation (caused by the earth's rotation and magnetic field) of the strength of cosmic rays arriving at different longitudes on the surface of the earth.

longitudinal current Current flowing in the same direction in the parallel wires of a pair (the return circuit is via ground).

longitudinal parity Parity associated with bits recorded on one track of a magnetic storage medium to indicate whether the number of bits is even or odd.

longitudinal redundancy A computer condition, generally affecting magnetic tape records, in which the bits in each track of a record do not meet the required parity, as determined by a LONGITUDINAL REDUNDANCY CHECK.

longitudinal redundancy check A parity check performed on a block of characters or bits (for example, on a track of a magnetic disk). A parity character is generated and transmitted as the last character of the block; thus, each longitudinal block has either even or odd parity.

longitudinal wave A wave in which the movement of particles in a medium is parallel with the direction of propagation.

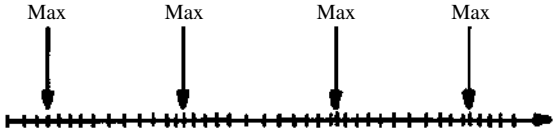

longitudinal wave

long line **1.** A single-wire antenna whose length is greater than the length of the wave fed to it for propagation. Also see LONG-WIRE ANTENNA. **2.** In wire telegraphy, an electrical line that has great physical length. **3.** In electronics theory, a transmission line of indeterminate length, but whose characteristics remain stable and predictable to infinity.

long-persistence screen A cathode-ray-tube screen on which the image remains for a time after the electron beam has passed.

long-play Abbreviation, LP. Descriptive of phonograph discs designed to play at 33.3 revolutions per minute (rpm). Also see MICROGROOVE RECORD.

long-play record See MICROGROOVE RECORD.

long-range navigation See LORAN.

long-range radar Radar that can detect targets at distances of 200 miles or more.

long skip Ionospheric radio-wave propagation, usually via the F layer, between or among stations separated by large geographic distances. The wave angles of departure (from transmitting stations) and arrival (at receiving stations) are very small relative to the horizon. Compare SHORT SKIP.

long-term drift Gradual change in the value of a quantity, such as voltage or frequency, observed over a long period, in contrast to that noted for a brief interval. Compare SHORT-TERM DRIFT.

long-term input offset voltage stability Expressed in microvolts per month. The extent to

5059F-pL-396-423 4/10/01 9:14 AM Page 419

which the input offset voltage in an integrated circuit stays stable over long periods of time.

long-term stability Stability reckoned over a period of weeks, months or years, as contrasted to that noted for brief intervals of time (minutes or hours).

long throw A speaker design term that describes a woofer moving through long excursions; the objective is to provide good low-frequency response with low distortion.

long waves Low-frequency radio waves, particularly those in the frequency range of 30 kHz to 300 kHz (10 km to 1 km).

long-wire antenna A horizontal or sloping wire antenna measuring a full wavelength or more and fed at a high-current point or at one end. As the wire is made longer, the main radiation/response lobes get more nearly in line with the antenna, and their amplitudes increase. As the wire is made shorter, the main lobes get farther from the axis of the antenna, and their amplitudes decrease. This antenna can produce high gain and excellent low-angle radiation, provided it is straight, is at least several wavelengths long, and is clear of obstructions. However, it cannot be rotated conveniently to change the direction in which maximum gain occurs. Also, a great deal of real estate is needed at medium and high frequencies.

lookup A computer programming technique in which a data item identified by a key is selected from an array.

loop **1.** An electrical circuit consisting of elements connected in series. **2.** In a standing-wave system, a maximum-response point (e.g., *current loop* and *voltage loop*). Compare NODE, **2**. **3.** See LOOP ANTENNA. **4.** A signal path (e.g., *feedback loop*). **5.** A one- or two-turn coil for low-impedance coupling. Also see LINK, **1**. **6.** In a computer program run, the repetitious execution of a series of instructions that terminates when some specified condition is satisfied by a relational test, at which point the next instruction in the main program is obeyed.

loop antenna **1.** A small portable receiving antenna in the form of a wire coil. **2.** A half-wave conductor bent into a circle or square. The conductor is broken at the point opposite the feed point. It can be used for transmitting and receiving. **3.** A full-wavelength, continuous conductor bent into a circle or square. It can be used for transmitting and receiving.

loop checking A method of checking the accuracy of data transmitted over a data link by returning signals received at one terminal to the transmitting terminal for comparison with the original data.

looped amplification See FEEDBACK FACTOR.

looping plug A double phone-plug unit for simultaneously plugging into two phone jacks. Completes (loops) the circuit between the two jacks.

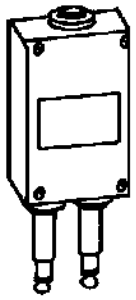

looping plug

loop-input signal A signal introduced into a feedback control loop.

loop pulsing The regular, intermittent breaking of the direct-current path at the transmitting end of a transmission line; also called DIAL PULSING.

loop resistance The resistance of the electrical path around a complete loop (see LOOP, **1**).

loop response time In a security system, the length of time between the first sensing of an abnormal condition (e.g., an intrusion) and the recognition of that condition by the controller.

loopstick antenna See FERRITE-ROD ANTENNA.

loop test A means of locating a discontinuity in a circuit by creating a closed loop, including the suspected fault point.

loose coupling Coupling that transfers only small amounts of energy, as when a primary and secondary coil are spaced so far apart that the coefficient of coupling is small. Compare CLOSE COUPLING.

loosely coupled twin In computer operations, a system in which two processors, each having its own operating system, are used with switches so that they can use common peripherals. Also see SWITCH.

lopplar Acronym for *laser Doppler radar.* Also abbreviated as ladar.

lorac A radio-navigation system that operates by means of phase comparison. Similar to LORAN. Trade name of Seismograph Service Corporation.

loran A long-range radionavigation system in which two pairs of ground stations transmit pulsed signals that are used by aircraft and ships to determine their positions. The name is an acronym for *long-range navigation.*

loran C A radionavigation system that operates at a frequency of 100 kHz. It operates on the hyperbolic principle.

loran D A radionavigation system similar to loran C. It is used by aircraft, operates independent of ground stations, and prevents unwanted enemy detection of aircraft position.

Lorentz force For a charge Q moving with velocity v in a magnetic field B and an electric field E, the force $F = Q(E + (v \times B))$.

5059F-pL-396-423 4/10/01 9:14 AM Page 420

loss Energy that is dissipated without doing useful work in a circuit or system. See POWER LOSS.

loss angle For an insulating material, 90 degrees minus the PHASE ANGLE.

loss index For an insulating material, the product of the POWER FACTOR and the DIELECTRIC CONSTANT.

lossless data compression A process in which the number of bits in a data file is reduced by eliminating redundancies, without sacrificing any of the precision or detail in the file. Compression of text and programs must usually be lossless. Image compression need not generally be lossless. Compare LOSSY DATA COMPRESSION.

lossless line A perfect transmission line (i.e., one having no resistance loss, no dielectric loss, and no radiation loss). It is not realizable in practice, but useful in some theoretical calculations.

loss tangent See DISSIPATION FACTOR, **1**.

lossy data compression A process in which the number of bits in a data file (especially a digital image) is reduced by eliminating redundancies, with some sacrifice of precision or detail. In image compression, some loss can usually be tolerated, allowing larger compression ratios than would be possible if zero loss were mandatory. Lossy compression is not generally acceptable for text files and programs. Compare LOSSLESS DATA COMPRESSION.

lossy line A line or cable having comparatively high or excessive attenuation per unit length.

loudness The amplitude of sound, especially in audio reproduction equipment, such as a high-fidelity stereo amplifier. Also called VOLUME.

loudness control See COMPENSATED VOLUME CONTROL.

loudness curves See AUDIBILITY CURVES.

loudness switch/button In a high-fidelity audio amplifier, a switch or button that can be actuated when music is played at low loudness. Increases the volume of the bass relative to the midrange and treble.

loudspeaker A transducer that converts electrical impulses into sound waves of sufficient volume to be heard easily by a number of listeners situated at some distance from the device. Also called *speaker*.

loudspeaker damping See DAMPED LOUDSPEAKER.

loudspeaker dividing network See CROSSOVER NETWORK.

low **1.** The logical digit 0. **2.** Of relatively small magnitude (e.g., LOW VOLTAGE and LOW-FREQUENCY). **3.** In a rechargeable cell or battery, the condition of being near the end of the discharge cycle.

low band **1.** The low or lowest frequency band used in communications, testing, or processing in a given situation. **2.** Television channels 2 to 6 (54 to 88 MHz). **3.** In two-way radio operations, those radio channels between 30 MHz and about 70 MHz.

low battery **1.** The condition of a battery needing replacement or recharging. **2.** An indicating device that shows when a battery needs to be replaced or recharged.

low-battery bias current The current into a designated pin of an integrated circuit required for proper operation of the LOW-BATTERY INDICATOR.

low-battery indicator A device, such as a light-emitting diode (LED) and associated circuitry, that gives a visible indication of the condition of LOW BATTERY.

low-capacitance probe A test probe in which capacitance has been minimized to reduce loading and detuning of the circuit under test.

low earth orbit Acronym, LEO. An artificial satellite orbit that is comparatively low in altitude, resulting in a short orbital period (in some cases less than 2 hours). See also LEO SATELLITE SYSTEM.

low-energy criterion See VON HIPPEL BREAKDOWN THEORY.

lower sideband Abbreviation, LSB. In an amplitude-modulated wave, the lower band of frequencies equal to the difference between the carrier frequency and the modulating frequency. Compare UPPER SIDEBAND.

lower sideband suppressed carrier Abbreviation, LSSC. A single-sideband transmission technique in which the lower sideband is transmitted, but the upper sideband and carrier are suppressed. Compare DOUBLE SIDEBAND SUPPRESSED CARRIER and UPPER SIDEBAND SUPPRESSED CARRIER.

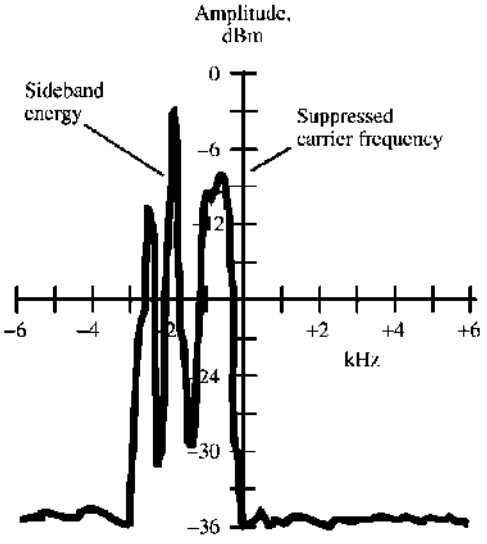

lower sideband

5059F-pL-396-423 4/10/01 9:15 AM Page 421

lowest usable frequency Abbreviation, LUF. The lowest frequency that can be used successfully at a given time for communication via the ionosphere. Compare MAXIMUM USABLE FREQUENCY.

low filter A highpass filter that removes low-frequency audio noise from the modulating waveform of a broadcast station. The result is a lower level of transmitted hum and rumble.

low-frequency Abbreviation, LF. **1.** Pertaining to radio frequencies in the band from 30 kHz to 300 kHz (wavelengths from 10 kilometers to 1 kilometer). Also see RADIO SPECTRUM. **2.** Pertaining to audio frequencies below 500 Hz.

low-frequency compensation **1.** In video-amplifier design, special measures, such as use of high coupling and bypass capacitances, to boost low-frequency gain. **2.** Use of special circuits to increase the low-frequency response of an audio amplifier. Also see BASS BOOST, **1**, **2**.

low-frequency direction finder Abbreviation, LDF. A direction finder operated in or below the standard amplitude-modulation (AM) broadcast band, that is, below 1.605 MHz.

low-frequency padder See OSCILLATOR PADDER.

low-frequency parasitics Parasitic oscillations of a frequency lower than that being processed by the amplifier or generated by the oscillator in which they occur.

low-level **1.** A logic term for the more negative of the two (binary) logic levels. **2.** Having an amplitude that is below that normally available in comparable circuits or systems. **3.** In computer operations, pertaining to programming languages (such as assembly language or machine language) that control the machine, but do not directly interface with the operator.

low-level audio signal In audio operations, a signal that has not been amplified by any means (e.g., the output of a dynamic microphone). Compare HIGH-LEVEL AUDIO SIGNAL.

low-level contact A switch or relay contact intended for use with low values of current and voltage.

low-level input current **1.** A test used to check an input pull-up resistor in an integrated circuit to ensure that the fan-in is as specified. **2.** The current flowing from an input when the highest low-level output voltage specified is applied to the input of the device.

low-level language A computer programming language in which each instruction has only one equivalent machine code. Examples are *machine language* and *assembly language*. Compare HIGH-LEVEL LANGUAGE.

low-level logic Abbreviation, LLL. In digital-computer operations, any logic system that operates at low voltage or current levels.

low-level modulation Modulation of a radio or television transmitter at a stage preceding the final radio-frequency (RF) power amplifier.

low-level output current **1.** A test to ascertain that the fan-out and current-sinking capability of an integrated circuit are as specified. **2.** The current flowing into an output with input conditions that cause the output to be at logic low.

low-level signal **1.** A signal with small amplitude. **2.** A signal with peak-to-peak voltage so low that it does not drive an amplifier circuit out of the linear range of operation.

low-loss material A material, particularly a dielectric, having low electrical loss at a given frequency. Also see LOSS.

low-noise Pertaining to circuits, especially weak-signal communications receiving amplifiers and converters, designed to generate the smallest possible amount of internal noise.

low-noise down converter In a satellite television receiving system, a circuit that converts the signals from the dish antenna to frequencies that correspond to the channels on a conventional television set.

low order The lesser-value place(s) of characters or digits in the hierarchy of a group (number or word). For example, 5 and 6 are low-order digits in the number 123,456.

low-order position The extreme right-hand (least significant) position in a number or word.

low-pass filter A combination of capacitance, inductance, and/or resistance, intended to produce large amounts of attenuation above a certain frequency and little or no attenuation below that frequency. The frequency at which the transition occurs is called *cutoff*. At cutoff, the power attenuation is 3 dB with respect to the minimum attenuation. At frequencies below cutoff, the power attenuation is less than 3 dB. At frequencies above cutoff, the power attenuation is more than 3 dB. The simplest circuit consists of a series inductor or a parallel capacitor. The inductance-capacitance (LC) circuit has a combination of series inductors and parallel capacitors. In the resistance-capacitance (RC) circuit, resistors are substituted for the inductors. Compare BAND-PASS FILTER, BAND-REJECTION FILTER, HIGH-PASS FILTER.

low power Abbreviation, LP. Power considerably lower than that ordinarily encountered in a

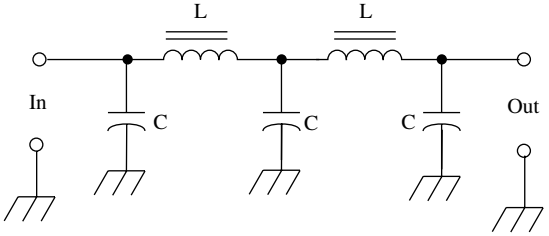

low-pass filter

5059F-pL-396-423 4/10/01 9:15 AM Page 422

particular application. The term is arbitrary; several hundred watts might be regarded as low power in one situation, whereas a fraction of a watt would be implied in another.

low-print recording tape Magnetic tape that is less susceptible to print-through than conventional tape.

low *Q* For a component or circuit, a low quotient for the ratio of reactance to resistance (*X*/*R*). This is a relative term because a particular *Q* value considered low in one situation might be high in other circumstances. Also see FIGURE OF MERIT, **1**.

low tension See LOW VOLTAGE.

low voltage **1.** A voltage considerably lower than that ordinarily encountered in a particular application. The term is arbitrary; several hundred volts might be regarded as low in one situation, and a fraction of a volt would be implied in another. **2.** In a television receiver, the supply voltage applied to all points other than the high-voltage circuit or the picture tube.

low-voltage rectifier In a television receiver, the rectifier that supplies power for the low-voltage stages. See LOW VOLTAGE, **2**.

LP **1.** Abbreviation of LOW POWER. **2.** Abbreviation of LONG PLAY. **3.** Abbreviation of *low pressure.*

L pad An attenuator consisting of one series arm and one shunt arm, arranged in such a way that the schematic representation of the circuit resembles an inverted capital letter L. It is noted for its constant input resistance or impedance as the amount of attenuation is varied.

LPB Abbreviation of LIGHTED PUSHBUTTON.

L_P band A section of the L BAND extending from 390 to 465 MHz.

lpm Abbreviation of *lines per minute*: the output speed of a line printer.

lpW Abbreviation of *lumens per watt*; lm/W is preferred.

Lr Symbol for LAWRENCIUM.

L + R, L – R The sum and difference of the left (L) and right (R) channel signals in a stereo high-fidelity sound system. The L + R signal is the in-phase combination of the two channels; the L – R signal is the out-of-phase combination.

L regulator See L-TYPE VOLTAGE REGULATOR.

LRR Abbreviation of LONG-RANGE RADAR.

LR time constant See INDUCTANCE-RESISTANCE TIME CONSTANT.

LSA diode Abbreviation for *limited-space-charge-accumulation diode.* A solid-state diode that acts as a microwave oscillator.

LSB **1.** Abbreviation of LOWER SIDEBAND. **2.** Abbreviation of LEAST-SIGNIFICANT BIT.

L_S band A section of the L band that extends from 900 to 950 MHz.

LSC Abbreviation of LEAST-SIGNIFICANT CHARACTER.

LSD Abbreviation of LEAST-SIGNIFICANT DIGIT.

L section **1.** A filter section whose schematic representation has the general shape of an inverted capital letter L. **2.** An attenuator circuit whose schematic representation has the general shape of an inverted capital letter L. **3.** A network section consisting of a series (input) impedance arm and a shunt (output) impedance arm. See L PAD. **4.** A right-angle bend in coaxial cable (see ELL).

LSI See LARGE-SCALE INTEGRATION.

LSSC Abbreviation of LOWER SIDEBAND SUPPRESSED CARRIER.

L_T band A section of the L BAND extending from 780 to 900 MHz.

LTROM Abbreviation of LINEAR-TRANSFORMER READ-ONLY MEMORY.

L-type antenna See INVERTED-L ANTENNA.

L-type voltage regulator A simple voltage regulator containing a series current-limiting resistor and shunt regulator (zener diode, VR tube, voltage-dependent resistor, etc.). The schematic representation resembles an inverted capital letter L.

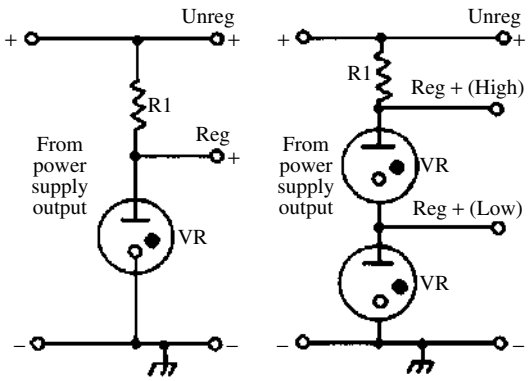

L-type voltage regulator

lt-yr Abbreviation of LIGHT-YEAR.

Lu Symbol for LUTETIUM.

Lucalox General Electric's translucent ceramic; its chief constituent is polycrystalline alumina. The material has many applications in electro-optics.

Lucite Trade name for METHYL METHACRYLATE RESIN.

Luddites During the Industrial Revolution, people who sabotaged automated factory equipment because they believed the machines would put them out of work. The word comes from the name of Ned Ludd, their supposed leader. The term is sometimes applied nowadays to people who fear computers, robots, and other technological innovations because of real or imagined threats to personal job security.

LUF Abbreviation of LOWEST USABLE FREQUENCY.

lug **1.** A contact attached to the end of a wire lead to facilitate connection to a binding post. **2.** A

5059F-pL-396-423 4/10/01 9:15 AM Page 423

contact attached to a terminal strip, to which wire leads are soldered.

lum Abbreviation of LUMEN. The preferred (SI) form is lm.

lumen Abbreviation, lm, and sometimes l or lum. The SI unit of luminous flux; it is equal to the light that is emitted in one steradian (the unit solid angle) by a uniform point source of one candela. Also see CANDLE POWER, ILLUMINANCE, LUMINOUS INTENSITY, SOLID ANGLE, and STERADIAN.

lumen-hour Abbreviation, lm-hr. The amount of light that a source having a luminous flux of one LUMEN delivers in a time period of one hour.

luminaire A complete and self-contained lighting system, for television-studio use or photographic use. The kit includes all of the needed parts and accessories.

luminance The amount of light emitted or scattered by a surface. This property is expressed in *candelas per square meter* (cd/m^2).

luminance channel In a color television circuit, the channel that processes the Y SIGNAL.

luminance signal See Y SIGNAL.

luminescence The production of visible light, but not heat, by a material stimulated by radiation or electron bombardment. See ELECTROLUMINESCENT CELL and LUMINESCENT SCREEN.

luminescent cell See ELECTROLUMINESCENT CELL.

luminescent screen A cathode-ray tube whose screen is coated with a material that glows under the influence of ionizing radiation, X rays, or electron beams.

luminiferous ether See ETHER, **1**.

luminosity The luminous efficiency of radiant energy, as given by the ratio of luminous flux to radiant flux (lumens per watt) for a specific wavelength.

luminosity factor Abbreviated K, and expressed in lumens per watt. The luminous intensity divided by the actual radiant intensity at a given wavelength of visible light.

luminous energy The energy in visible electromagnetic radiation.

luminous flux The rate of transfer or flow of luminous energy.

luminous intensity Luminous flux through a unit solid angle, expressed in candelas. Also see CANDELA.

lumistor An amplifier or coupling device in which the input signal varies the brilliance of a lamp, electroluminescent cell, or light-emitting diode, and a photocell (or other light-sensitive device) picks up the fluctuating light and uses it to modulate an output current. In a compact lumistor, the light-emitting and light-sensing components are separate layers in a wafer or block of material. Compare LIGHT AMPLIFIER.

lumped Pertaining to a property that is concentrated at or around a single point, rather than being distributed through a circuit (e.g., *lumped capacitance* and *lumped inductance*).

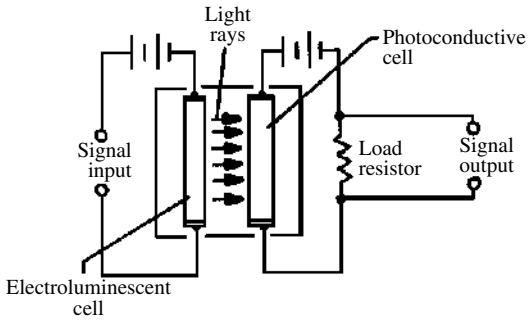

lumistor

lumped capacitor See DISCRETE CAPACITOR.

lumped component A discrete component (i.e., one that is self-contained). Compare DISTRIBUTED COMPONENT.

lumped constant The total value of any single electrical property in an electrical or electronic component.

lumped-constant delay line A delay line having discrete capacitance and inductance components. Compare DISTRIBUTED-CONSTANT DELAY LINE.

lumped impedance A reactance and/or resistance manifested in a definite location. Examples are ordinary components, such as capacitors, inductors, and resistors.

lumped inductor See DISCRETE INDUCTOR.

lumped parameter Any circuit parameter that can be considered as a discrete parameter—even if it is not made up of a single component.

lumped resistor See DISCRETE RESISTOR.

lutetium Symbol, Lu. A metallic element of the rare-earth group. Atomic number, 71. Atomic weight, 174.967.

lux The unit of illuminance, equivalent to one LUMEN per square meter.

Luxemberg effect The generation of interference by cross-modulation of two or more signals whose paths intersect in the same region of the ionosphere.

luxmeter A device for measuring visible illuminance.

LV Abbreviation of LOW VOLTAGE.

LVDT Abbreviation of LINEAR VARIABLE DIFFERENTIAL TRANSFORMER.

Lw Symbol for LAWRENCIUM; more commonly *Lr.*

lx Abbreviation of LUX.

L_X band A section of the L BAND that extends from 950 MHz to 1.15 GHz.

L_Y band A section of the L BAND that extends from 725 to 780 MHz.

L_Z band A section of the L BAND that extends from 1.450 to 1.550 GHz.

LZT Abbreviation of LEAD ZIRCONATE-TITANATE, a ceramic used in electronics.

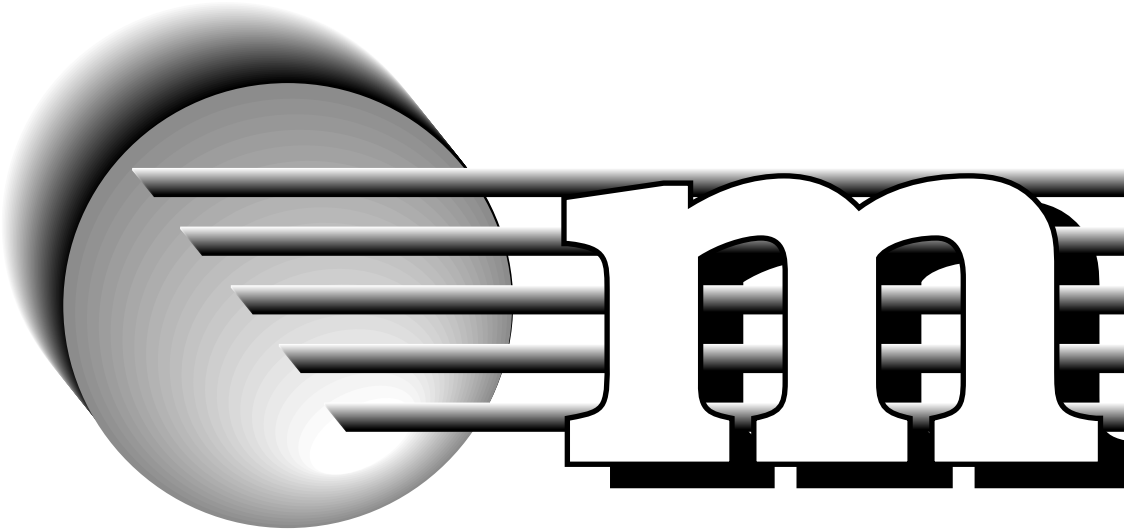

M **1.** Abbreviation of prefix MEGA-. **2.** Symbol for MUTUAL INDUCTANCE. **3.** Symbol for MODIFIED INDEX OF REFRACTION.

m **1.** Abbreviation of prefix MILLI-. **2.** Symbol for MASS. **3.** Abbreviation of METER. **4.** Abbreviation of MILE. (Also, mi.) **5.** Symbol for MODULATION COEFFICIENT.

m^2 Abbreviation of *square meter*, the SI unit of area.

m^3 Abbreviation of *cubic meter*, the SI unit of volume.

MA **1.** Abbreviation of MAGNETIC AMPLIFIER. (Also, *magamp.*) **2.** Abbreviation of MEGAMPERE.

mA Abbreviation of MILLIAMPERE.

Mache unit A unit of radioactivity equivalent to 13.47 disintegrations per second (3.64×10^{-10} curie) per liter. It represents the concentration of radon gas per liter (when all radiation is absorbed) that will result in a saturation current of 10^{-3} esu (not to be confused with MACH NUMBER).

machine address See ABSOLUTE ADDRESS.

machine code See MACHINE LANGUAGE.

machine cycle In a machine whose operation is periodic, a complete sequence constituting a period of operation.

machine error In a computer or data-processing system, an error attributable to a hardware failure, rather than to a software fault.

machine instruction A computer program instruction written in MACHINE LANGUAGE.

machine knowledge General term for data stored in an artificially intelligent computer system, and the ability of the computer to use that data in meaningful ways.

machine language Computer program instructions and data represented in binary form. In the hierarchy of programming languages, it is the lowest; the computer works directly with it. All high-level languages are translated to machine language by an assembler, compiler, interpreter, or monitor system.

machine learning In artificial intelligence, a computer's ability to learn through repeated calculations for particular problems.

machine logic **1.** The way that a computer's functional parts are interrelated. **2.** The facility whereby a computer solves problems.

machine operation The performance by a computer of a built-in function (e.g., subtraction).

machine operator A person participating in implementing and overseeing the processing of computer programs.

machine word In computer operations, the address of a memory location composed of the full number of bits normally handled by each register of the machine.

machining In industrial robotics, the mechanical modification of parts during assembly. Examples: drilling, welding, sanding, polishing, and painting.

Mach number For a medium such as air, the ratio of the speed of a body in motion to the speed of sound in the medium. (Not to be confused with MACHE UNIT.)

macro **1.** A control shortcut, in which a function requiring the actuation of several switches is abbreviated, via a microcomputer, so that it can be executed by actuating only one or two switches. **2.** Abbreviation of MACROINSTRUCTION.

Copyright 2001 The McGraw-Hill Companies, Inc. Click Here for Terms of Use

5059F-pM-424-465 4/10/01 9:19 AM Page 425

macro- Prefix denoting extremely large. Compare MICRO-.

macro assembly program An assembly program whose source statements are translated to several machine-language instructions.

macroinstruction A source program instruction that becomes several machine-language instructions when operated on by a compiler.

macroknowledge In artificial intelligence, knowledge in the large sense (i.e., knowledge about information). Example: a set of definitions in an expert system. Compare MICROKNOWLEDGE.

macroprogram A computer program consisting of macroinstructions.

macrosonics The theory and applications of high-amplitude sound waves.

madistor A component that produces changes in current by means of magnetic-field effects. It is used as an oscillator or amplifier.

MADT Abbreviation of MICROALLOY DIFFUSED TRANSISTOR.

MAG Abbreviation of MAXIMUM AVAILABLE GAIN.

magamp Acronym for MAGNETIC AMPLIFIER.

magazine A tape or film cartridge.

magenta One of the primary pigments used in color printers. It has a pinkish-red hue.

magnal CRT base An 11-pin base typical of many cathode-ray tubes.

magnesium Symbol, Mg. A metallic element. Atomic number, 12. Atomic weight, 24.305.

magnesium fluoride phosphor A substance used as a phosphor coating on the screen of a very-long-persistence cathode-ray tube. The fluorescence and phosphorescence are orange.

magnesium silicate phosphor A substance used as a phosphor coating on the screen of a cathode-ray tube. The fluorescence is orange-red.

magnesium tungstate phosphor A substance used as a phosphor coating on the screen of a cathode-ray tube. The fluorescence is very light blue.

magnet A device or body of material that has the ability to attract to itself pieces of iron and other magnetic metals, and the ability to attract or repel other magnets. Also see ELECTROMAGNET, PERMANENT MAGNET, and TEMPORARY MAGNET.

magnet armature See KEEPER.

magnet battery A group of several magnets placed together in parallel (i.e., with similar poles touching or resting nearby) to act as a single magnet.

magnet charger A device that produces an intense magnetic field for restoring weakened magnets or for making new magnets.

magnetic **1.** Pertaining to MAGNETISM. **2.** Possessing MAGNETISM. **3.** Capable of being magnetized. **2.** See MAGNETIC MATERIAL.

magnetic air-gap A space between two magnetic poles, either the same (in which case the force is repulsive) or opposite (in which case the force is attractive).

magnetic amplifier An iron-core device that uses the principle of the saturable reactor to obtain amplification. In its simplest form, it consists of input and output coils wound on a core of square-loop magnetic metal. The input coil consists of two identical windings connected in series-opposition so that currents in the output winding cannot induce voltage in the input winding. The output coil is connected in series with a load and an alternating-current (ac) supply. A small ac signal applied to the input winding causes a large change in the impedance of the output winding and, therefore, a large change in the voltage across the load.

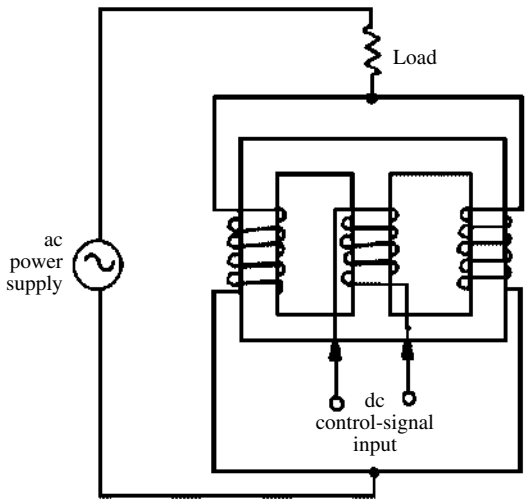

magnetic amplifier

magnetic analysis See MASS SPECTROMETER.

magnetic attraction **1.** The force that causes a magnetic pole to draw to itself an opposite magnetic pole. Thus, a north pole attracts a south pole, and a south pole attracts a north pole. Compare MAGNETIC REPULSION. **2.** The force that causes a magnetic pole to draw to itself a piece of magnetic material, such as iron or steel.

magnetic axis A straight line joining the poles of a magnet.

magnetic bearing The azimuth, or compass direction, measured with respect to magnetic north (the direction of the north geomagnetic pole). It is usually expressed in degrees and can be read directly from a compass.

magnetic azimuth An azimuth bearing relative to magnetic north (the direction of the north geomagnetic pole).

magnetic balance An instrument for measuring the force, either attractive or repulsive, between two objects that are magnetized, or between a

5059F-pM-424-465 4/10/01 9:19 AM Page 426

magnet and a magnetic substance. The device can also be used for measuring the intensity of a magnetic field, either from a permanent magnet, an electromagnet, or from the earth.

magnetic bias A steady magnetic force applied to another magnetic field to set the latter's quiescent point (e.g., sensitizing a relay by using a permanent magnet to lower the relay draw-in point).

magnetic blowout **1.** The extinction of an electric arc by a strong magnetic field. **2.** The apparatus for accomplishing the action described in **1**.

magnetic bottle A container envisioned for atomic fusion reactions, and that would consist of a magnetic field. Conventional containers cannot withstand the extremely high temperatures involved in atomic fusion.

magnetic braking See ELECTROMAGNETIC BRAKING.

magnetic bridge An instrument comparable to the WHEATSTONE BRIDGE, used to measure magnetic permeability.

magnetic bubble memory See BUBBLE MEMORY.

magnetic capacity The maximum magnetization a given material can receive.

magnetic card A computer storage medium in the form of a card that can be selectively magnetized or imprinted with magnetic ink to represent data.

magnetic cartridge A variable-reluctance phonograph pickup. As the stylus moves in the groove, the vibrations are translated into electric currents by a magnet and coil.

magnetic centering Centering the beam in a television picture tube by means of an electromagnetic focusing coil, a permanent magnet, or both.

magnetic character A letter, numeral, or other symbol written or printed in (visible) magnetic ink for its automatic sensing or reading in computing and signaling operations.

magnetic circuit The closed path determined by a line of magnetic flux or by a set of lines of flux.

magnetic clutch A clutch in which the magnetism of one rotating member causes a second member to lock in and rotate. There need not be physical contact between the two.

magnetic coil The winding in an electromagnet or similar device.

magnetic compass A direction-indicating device using a horizontally suspended magnetic needle as the indicator. The needle tends to point in the direction of the north geomagnetic pole. Compare GYROCOMPASS.

magnetic component See ELECTROMAGNETIC COMPONENT.

magnetic conductivity See PERMEABILITY.

magnetic constant The absolute permeability of free space. It is approximately 1.26×10^{-6} H/m.

magnetic controller A controller that uses electromagnets for some of its functions.

magnetic core The iron core of an electromagnet, choke, transformer, relay, or similar device.

magnetic coupling See INDUCTIVE COUPLING.

magnetic course In navigation, a course referenced to geomagnetic north, rather than geographic north.

magnetic crack detector See ELECTROMAGNETIC CRACK DETECTOR.

magnetic creeping A gradual increase in the magnetization of a material under the influence of a steady magnetizing force.

magnetic cycle **1.** For a material in an alternating magnetic field, the change in magnetic flux as a function of time. **2.** The change in the magnetic-field polarity of the earth. This polarity reverses every few thousand years.

magnetic damping The production of a damping effect or drag in a machine or meter by means of magnetic action on a moving member, in accordance with LENZ'S LAW.

magnetic declination See DECLINATION.

magnetic deflection See ELECTROMAGNETIC DEFLECTION.

magnetic density The concentration of magnetic flux in a region, expressed as the number of lines per unit area of cross section.

magnetic dip At a particular location on the earth's surface, the angle between the terrestrial magnetic field and a horizontal line.

magnetic dipole **1.** A molecule or particle with a north and south magnetic pole. **2.** Any pair of adjacent north and south magnetic poles.

magnetic direction finder Abbreviation, MDF. A type of compass operated by an electric signal delivered by a gyrostabilized magnetic-compass movement.

magnetic disk A rotating disk coated with a layer of magnetic material for the recording, storage and retrieval of information. They are available in various sizes, configurations, and storage capacities. Commonly used with personal computers. Also see DISKETTE and HARD DISK.

magnetic doublet See DOUBLET, **2**.

magnetic drive A device in which mechanical movement is conveyed from one moving part to another by means of a magnetic clutch.

magnetic drum See DRUM.

magnetic effect of electric current The presence of a magnetic field around a conductor carrying electric current.

magnetic equator Also called *geomagnetic equator.* An imaginary circle around the earth, along which a magnetic needle shows no dip. It is near, but slightly displaced from, the geographic equator, and is midway between the geomagnetic poles.

magnetic feedback Feedback by means of inductive coupling between the output and input circuits of a system. It can be positive or negative.

magnetic field The space around a magnetic pole or magnetized body in which magnetic energy acts.

magnetic field intensity See MAGNETIC INTENSITY.

5059F-pM-424-465 4/10/01 9:19 AM Page 427

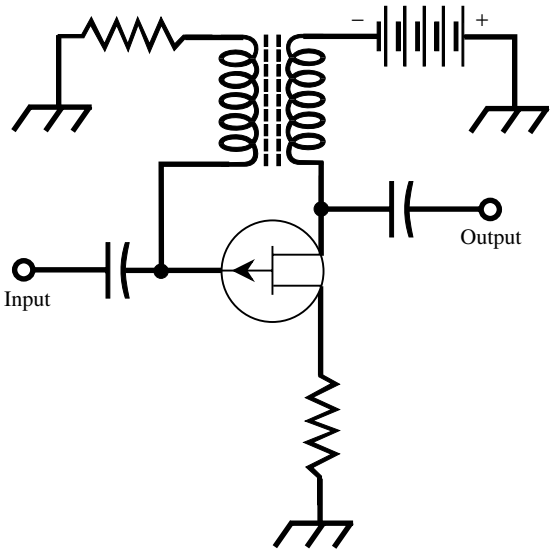

magnetic feedback

magnetic field strength See MAGNETIC INTENSITY.

magnetic-field viewer A device for visually examining a magnetic field. It consists of a clear plastic watchcase filled with iron-oxide particles in liquid suspension. When it is placed within a magnetic field, the particles align themselves in the direction of the magnetic lines of flux.

magnetic-film memory A magnetic memory in which memory cells consist of a thin film (thick film in some instances) of a magnetic material deposited on a substrate. Information is written into and read out of the cell through coils. Also called *thin-film memory.*

magnetic flip-flop A bistable multivibrator using magnetic amplifiers or square-loop cores in place of transistors.

magnetic flux The intensity of a magnetic field through a given area. The unit of magnetic flux is the weber, and the symbol is F. It can loosely be expressed as the number of lines passing through a region of a certain area or of a unit area, such as one square meter. See FLUX.

magnetic flux density See FLUX DENSITY.

magnetic flux linkage The passage of magnetic lines of flux through separate materials or circuits, thereby coupling them magnetically.

magnetic focusing See ELECTROMAGNETIC FOCUSING.

magnetic force The force exerted by a magnet on a body of magnetic material, or on another magnet, within its field.

magnetic friction **1.** See HYSTERESIS, **1**. **2.** The resistance experienced by a magnetic material moving in a magnetic field.

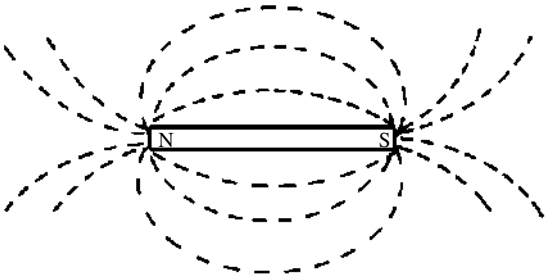

magnetic flux

magnetic gap A space separating the materials in a magnetic circuit. This break is either an air space or one filled with a comparatively thin piece of nonmagnetic material (e.g., the gap in a choke-coil core).

magnetic head See MAGNETIC PICKUP HEAD and MAGNETIC RECORDING HEAD.

magnetic hysteresis See HYSTERESIS, **1**.

magnetic inclination See MAGNETIC DIP.

magnetic induction **1.** The magnetization of a magnetic material, such as iron or steel, when it is placed in a magnetic field. **2.** The induction of an alternating voltage in a conductor by a nearby alternating magnetic field. Also see ELECTROMAGNETIC INDUCTION.

magnetic ink Writing or printing ink that is a suspension of finely divided particles of magnetic material. Also see MAGNETIC CHARACTER.

magnetic instability **1.** The tendency of a magnetic recording medium to deteriorate with time. **2.** Any fluctuation in the intensity of a magnetic field.

magnetic intensity The free-space strength of a magnetic field at a particular point. Specifically, the force (in dynes) that the magnetic field would exert on a unit magnetic pole placed at that point.

magnetic iron oxide See MAGNETITE.

magnetic leakage The usually undesired extension of magnetic flux beyond the confines of a magnetic body, such as the core of a choke.

magnetic lens See ELECTROMAGNETIC LENS.

magnetic line of flux See LINE OF FLUX, **2**.

magnetic load An electromagnetic device operating on the output of an electrical source. Such devices include actuators, alarms, electromagnets, magnetic tapes and disks, relays, and loudspeakers.

magnetic loudspeaker See MAGNETIC SPEAKER, **1**, **2**.

magnetic material **1.** A material, such as magnetite, that exhibits natural magnetism. **2.** A material, such as iron or steel, that is capable of being magnetized.

magnetic media Any medium that stores data as tiny magnetic fields; in particular, MAGNETIC DISK or MAGNETIC TAPE.

5059F-pM-424-465 4/10/01 9:19 AM Page 428

magnetic memory **1.** See RETENTIVITY. **2.** A digital memory circuit using magnetic fields to store data bits. Example: BUBBLE MEMORY.

magnetic meridian The circle of the celestial sphere that passes through the zenith and earth's magnetic poles.

magnetic mine A naval mine detonated by a magnetic switch that is closed by the proximity of the steel hull of a ship.

magnetic modulator A core-type device that is somewhat similar to a magnetic amplifier used for amplitude modulation. Modulating current passes through the control winding, and the carrier current through the output winding.

magnetic moment Unit, joule per tesla. For a magnet, the product of pole strength and the distance between poles.

magnetic needle The pivoted magnetic pointer in a magnetic compass.

magnetic north See NORTH MAGNETIC POLE.

magnetic oxide Iron oxide used as the sensitive coating of magnetic recording tape.

magnetic pickup **1.** A phonograph pickup of the variable-reluctance type (see VARIABLE-RELUCTANCE PICKUP). **2.** A magnetic transducer (such as a phono cartridge, tape recording head, or similar input element).

magnetic-pickup head In a tape recorder, the transducer that receives up magnetic impulses from the passing tape and converts them into alternating currents. These currents are amplified to obtain the original sound. Compare MAGNETIC RECORDING HEAD.

magnetic-plate wire Wire in which a magnetic metal has been plated on top of a nonmagnetic metal.

magnetic poles **1.** The points in a MAGNET at which the magnetic lines of flux converge. **2.** The points on the earth at which the geomagnetic lines of flux converge. See NORTH MAGNETIC POLE and SOUTH MAGNETIC POLE.

magnetic pressure See MAGNETOMOTIVE FORCE.

magnetic printing **1.** Also called *magnetic print-through.* In a recording material, such as magnetic tape, the transfer of information from one part of the material to another part (or from one medium to another) by the magnetic field of the recorded material. This phenomenon, which is also called PRINT-THROUGH, sometimes occurs in recording tape on a reel. **2.** Conventional lithography, letterpress, or other reproduction process in which MAGNETIC INK is used.

magnetic print-through See MAGNETIC PRINTING, **1**.

magnetic probe A loop or coil inserted in an electromagnetic field to sample the magnetic component. See, for example, WAVEGUIDE PROBE. Compare ELECTRIC PROBE.

magnetic recording **1.** The recording of sounds or data by varying the magnetization of a medium, such as a magnetic disk or tape. **2.** A magnetic medium on which data has been recorded.

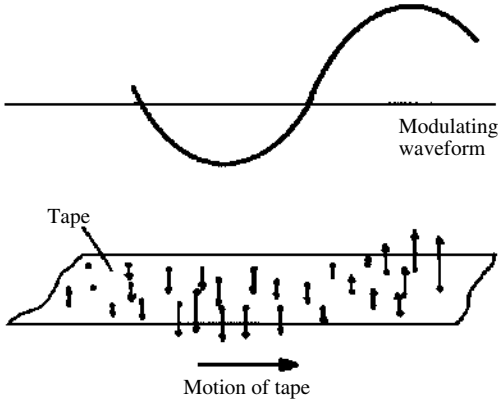

magnetic recording

magnetic recording head In a tape recorder, the transducer that receives current impulses (analogs of the original sound vibrations) from an amplifier and converts them into magnetic impulses that magnetize spaces on the passing tape. Compare MAGNETIC PICKUP HEAD.

magnetic recording medium **1.** A magnetic cylinder, disk, drum, tape, or wire used in the recording of sound or data. **2.** The sensitive material with which any of these is coated.

magnetic relay A relay having a permanent magnet in whose field a coil, bar, or reed moves to open or close a pair of contacts.

magnetic remanence See RESIDUAL MAGNETISM.

magnetic repulsion The force that causes a magnetic pole to push away a similar magnetic pole, although they are not in mutual contact. Thus, two north poles repel each other, and so do two south poles. Compare MAGNETIC ATTRACTION.

magnetic-resonance accelerator See CYCLOTRON.

magnetics **1.** Collectively, magnetic components and equipment. **2.** Collectively, magnetic materials. **3.** A branch of physics dealing with magnets and magnetism.

magnetic saturation The condition in which a magnetic material passes all of the magnetic lines of flux that its permeability allows. Increasing the intensity of the magnetizing force will produce no increase in magnetization.

magnetic scan See ELECTROMAGNETIC DEFLECTION.

magnetic screen See ELECTROMAGNETIC SHIELD.

magnetic shield See ELECTROMAGNETIC SHIELD and MAGNETIC SHIELDING.

magnetic shielding **1.** Enclosing a magnetic field to confine its flux, thus preventing interaction

5059F-pM-424-465 4/10/01 9:19 AM Page 429

with outside bodies. **2.** Devices (such as boxes, cans, or shells of iron, steel, or a magnetic alloy) used for the purpose described in **1**.

magnetic shift register A shift register using magnetic flip-flops.

magnetic shunt A device that allows the useful magnetic flux of an instrument's magnet to be controlled. The device consists of a piece of magnetic material near the magnet in an electrical measuring instrument.

magnetic south See MAGNETIC SOUTH POLE.

magnetic speaker **1.** A loudspeaker that is essentially an enlarged earphone with a horn that conveys and intensifies the sound from the vibrating diaphragm. **2.** A loudspeaker in which the vibration of a diaphragm or reed in the field of a permanent magnet is conveyed by a pin to a paper or composition cone. Compare DYNAMIC SPEAKER.

magnetic storage **1.** A data bank or memory that stores information in the form of magnetic fields. **2.** The data on a magnetic tape or disk.

magnetic storm A disturbance in the earth's magnetic field that typically follows a solar flare. Often causes interference to radio communications at low, medium and high frequencies.

magnetic strip A strip of powdered iron or ferrite on the back of an identification card, bank cash card, or credit card, that carries a code to identify the account number and verify that the secret entry code (if any) is correct, or that the credit is good.

magnetic susceptibility See SUSCEPTIBILITY.

magnetic switch **1.** In security systems, a switch kept open by the presence of a magnet attached to a door, window, or other movable object. When the object is moved, the magnet moves away from the switch, closing the switch and actuating an alarm. **2.** A REED SWITCH operated by a magnetic field.

magnetic tape Plastic tape coated with a film of magnetic material; it can be magnetized along its length to record sounds, video signals, and computer information.

magnetic-tape core A strip of magnetic metal wound spirally to create a toroid (donut) shape. Such construction is sometimes used in choke or transformer cores. Also see TOROID.

magnetic tape deck See TAPE DECK.

magnetic tape drive See TAPE TRANSPORT.

magnetic tape head See MAGNETIC PICKUP HEAD and MAGNETIC RECORDING HEAD.

magnetic tape library In a computer installation, the place where magnetic tape files are kept, or magnetic tape files and the records needed to utilize them.

magnetic tape parity As a safeguard against losing information bits during the transfer of information between magnetic tape and a memory device, a technique in which an extra bit is generated and added to characters under certain conditions, to make the output uniform temporarily. Lack of uniformity in output then serves as an error indicator. The original quantity is recovered by dropping the extra bit following a parity check.

magnetic tape reader A tape deck for playing back data on magnetic tape.

magnetic tape recorder A recorder-reproducer using magnetic tape.

magnetic test coil See SEARCH COIL.

magnetic thick film A film of magnetic material at least 10^{-6} meter in thickness, deposited on a substrate. Compare MAGNETIC THIN FILM.

magnetic thin film A film of magnetic material, less than 10^{-6} meter in thickness, deposited on a substrate. Compare MAGNETIC THICK FILM.

magnetic transducer A transducer that uses a coil, magnet, or both, to convert displacement into variable magnetic fields or electric currents. Common varieties are the inductance type, transformer type, and generator type. Compare CAPACITIVE TRANSDUCER, CRYSTAL TRANSDUCER, and INDUCTIVE TRANSDUCER.

magnetic tuning In a microwave oscillator, a means of tuning in which a ferrite rod in the cavity resonator is made to have adjustable magnetization so that the resonant frequency of the cavity varies and the frequency of the oscillator is thus adjustable. It is also used at ultra-high frequencies (UHF) and occasionally at very-high frequencies (VHF).

magnetic-vane meter See IRON-VANE METER.

magnetic vector In an electromagnetic field, the vector representing the magnetic component. It is perpendicular to the electric vector.

magnetic viscosity A property of certain materials, described in terms of the time required to magnetize a given substance to a specified level.

magnetic whirl One of the circular magnetic lines of flux around a straight conductor that carries electric current.

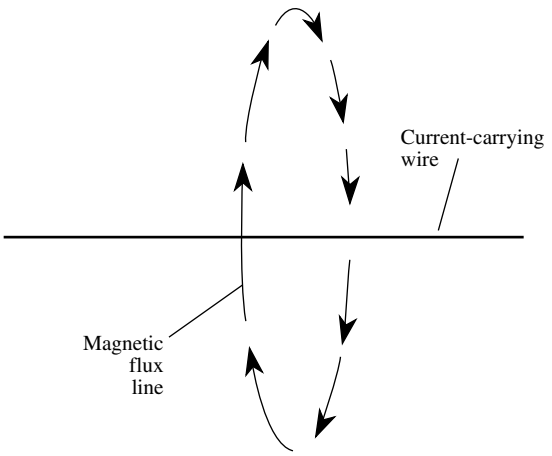

magnetic whirl

5059F-pM-424-465 4/10/01 9:19 AM Page 430

magnetic wire The thin wire used in wire recording and playback. See WIRE RECORDER.

magnetism The property of having or causing a magnetic field. It occurs when magnetic dipoles are aligned and when electric charge carriers are in motion.

magnetite A natural magnetic oxide of iron. Also called LODESTONE.

magnetization curve A curve depicting the magnetization of a material versus the applied magnetizing force. See, for example, HYSTERESIS CURVE.

magnetizer A device for magnetizing magnetic materials, as in the making of permanent magnets. Also see MAGNET CHARGER. Compare DEMAGNETIZER.

magnetizing current **1.** A current that sets up a magnetic field of useful intensity. **2.** The half-cycle of an alternating current or the polarity of a direct current flowing through a coil wound on a permanent magnet (as in a headphone, permanent-magnet loudspeaker, or polarized relay) that increases magnetic field strength. Compare DEMAGNETIZING CURRENT. **3.** The field current of a dynamo.

magnetizing force **1.** Magnetomotive force (in gilberts) divided by spatial distance (in meters). **2.** The intensity of a magnetic field that causes a material to become magnetized.

magnet keeper See KEEPER.

magnet meter See MAGNET TESTER.

magnet motor See PERMANENT-MAGNET MOTOR.

magneto See PERMANENT-MAGNET GENERATOR.

magnetocardiogram Abbreviation, MCG. A record, made by a MAGNETOCARDIOGRAPH, of the pulsating magnetic field of the heart. It is used as a diagnostic aid.

magnetocardiograph An instrument that produces a record of the pulsating magnetic field generated around the torso by natural ion currents in the heart.

magnetoelectric generator See MAGNETOGENERATOR.

magnetofluid mechanics See MAGNETOHYDRODYNAMICS.

magnetofluidynamics See MAGNETOHYDRODYNAMICS.

magnetogasdynamics See MAGNETOHYDRODYNAMICS.

magnetoionic duct A propagation path for radio waves between two points that have the same geomagnetic longitude on the surface of the earth. The radio waves tend to travel with the geomagnetic lines of flux at some frequencies under certain conditions.

magnetoionics The study of the effects of the geomagnetic field on the propagation of radio waves.

magnetogenerator See PERMANENT-MAGNET GENERATOR.

magnetograph An instrument for automatically recording a magnetic field.

magnetohydrodynamic generator A device using magnetohydrodynamic principles to generate electric power directly from gases. In the generator, a hot gas is passed through an intense magnetic field; a pair of collector plates picks up electrons from the ionized gas.

magnetohydrodynamic gyroscope A gyroscope whose spin is obtained by a rotating magnetic field circulating a conducting fluid, such as mercury, around a closed loop. Also see MAGNETOHYDRODYNAMICS.

magnetohydrodynamic power generator See MAGNETOHYDRODYNAMIC GENERATOR.

magnetohydrodynamics Abbreviation, MHD. The theory and application of phenomena produced by electrically conductive fluids and gases in electric and magnetic fields.

magnetometer An instrument for measuring the strength and direction of magnetic fields.

magnetomotive force Abbreviation, mmf. Unit, ampere. The phenomenon that is sometimes descriptively called *magnetic pressure.* It is analogous to electromotive force (and to water pressure) and is the agent that produces a magnetic field.

magneton See BOHR MAGNETON.

magneto-optical rotation The tendency of a magnetic field to rotate the plane of polarization of light passing through a substance. Also see KERR MAGNETO-OPTICAL EFFECT.

magneto-optical technology A computer data-storage technology that uses lasers to guide the read/write head in a magnetic disk drive. This greatly increases the amount of data that can be effectively stored on, and retrieved from, a magnetic disk.

magneto-optical valve See KERR MAGNETO-OPTICAL EFFECT.

magnetopause The high-altitude limit of the MAGNETOSPHERE.

magnetoplasmadynamics See MAGNETOHYDRODYNAMICS.

magnetoresistance The phenomenon whereby the resistance of a material, such as a semiconductor, changes when it is exposed to a magnetic field. Also see MAGNETORESISTOR.

magnetoresistor A material (such as bismuth wire, indium antimonide, or indium arsenide) whose resistance varies with the strength of a magnetic field in which it is placed.

magnetosphere In the upper atmosphere, a region extending thousands of kilometers from the earth, in which charged particles are trapped by the earth's magnetic field.

magnetostatic field A stationary magnetic field, such as that produced by a permanent magnet.

magnetostriction The expansion or contraction of a bar or rod of magnetic material (such as Invar, Monel metal, Nichrome, nickel, or Stoic metal) in proportion to the strength of an applied magnetic field. Magnetostrictive vibration in such a rod is

5059F-pM-424-465 4/10/01 9:19 AM Page 431

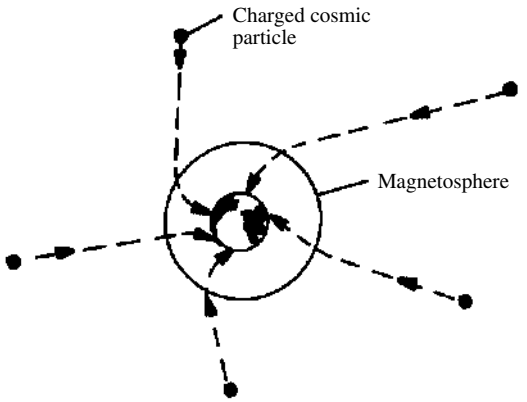

magnetosphere

comparable to piezoelectric vibration in a quartz crystal.

magnetostriction filter See ULTRASONIC FILTER, **1**.

magnetostriction oscillator An oscillator whose frequency is controlled by a magnetostrictive rod (see MAGNETOSTRICTION). The dimensions of the rod and the type of metal it contains determine its vibration frequency and, accordingly, the operating frequency of the oscillator.

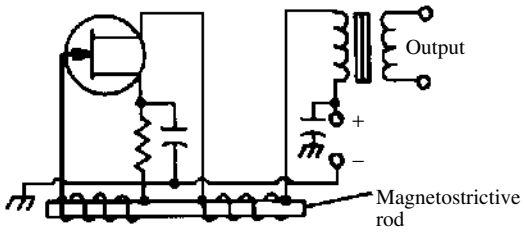

magnetostriction oscillator

magnetostrictive delay line A delay line in which the signal is propagated through a magnetostrictive rod. Also see MAGNETOSTRICTION.

magnetostrictive microphone A microphone in which sound vibrations produce changes in a magnetostrictive element, which, in turn, are converted into output-voltage changes. Also see MAGNETOSTRICTION.

magnetostrictive transducer A transducer in which some phenomenon, such as vibration or pressure, produces changes in a magnetostriction element, which in turn are converted into output-voltage changes. Also see MAGNETOSTRICTION.

magnet protector See KEEPER.

magnetrode The trademark of a radio-frequency device for externally producing hyperthermia (elevated temperature) inside the body, as in heating a cancerous tumor for therapeutic purposes.

magnetron A microwave vacuum tube consisting of a diode (with a cylindrical anode) through which the field of a powerful external permanent magnet passes. The magnetic field causes electrons leaving the cathode to travel in spiral paths between the electrodes. This action gives the tube a negative-resistance characteristic, resulting in oscillation when the tube is connected in an appropriate circuit. Some magnetrons have a built-in resonant cavity.

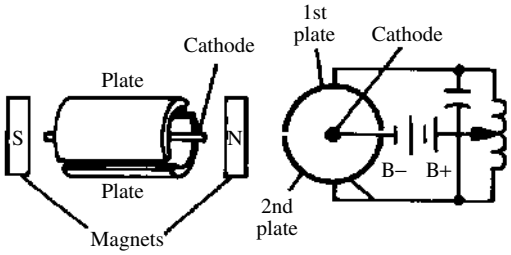

magnetron

magnet steel A high-retentivity alloy of chromium, cobalt, manganese, steel, and tungsten, used in the manufacture of permanent magnets.

magnet tester An instrument used to measure the flux of a magnet. Also see FLUXMETER.

magnet wire Insulated wire (usually solid copper) of 14 to 40 gauge, so called because of its original major use in winding the coils of electromagnets.

magnitude **1.** General expression for degree, size, or extent. **2.** Signal strength (amplitude). **3.** For a number or vector quantity, the absolute value or length. **4.** A measure of the relative or absolute brightness of celestial objects.

mAh Abbreviation of *milliampere-hour*.

main British expression for the alternating-current (ac) utility power available in a house or building.

main bang **1.** In a radar display, the pip or pulse resulting from the actual transmitted signal. This pulse is blanked out. **2.** In a spectrum analyzer, the pip corresponding to a frequency of zero, and caused by the local oscillator.

mainframe **1.** The chassis containing the central processor and arithmetic and logic circuits for a large computer. **2.** The general term for a large, powerful computer.

main lobe Also called *major lobe*. In a directional antenna system, the portion of the directivity pattern representing the greatest transmitted signal gain and/or the greatest received signal response. Also see MINOR LOBE, SIDE LOBE.

main memory The principal (immediate process) memory unit in a digital computer or data-processing system.

5059F-pM-424-465 4/10/01 9:19 AM Page 432

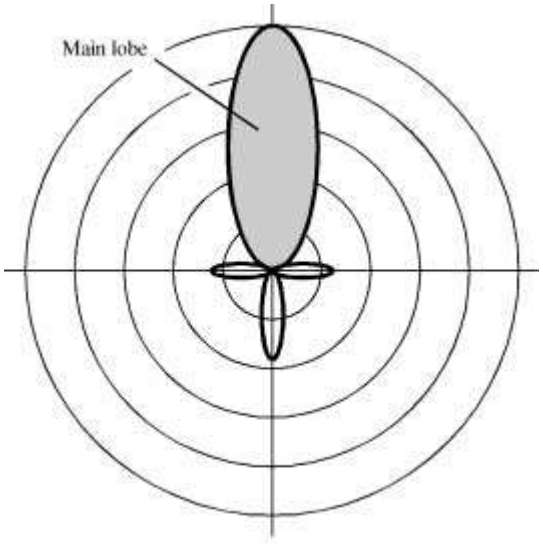

main lobe

main path In a computer program, the sequence of instruction execution disregarding the execution of subroutines.

main program The part of a computer program other than a subroutine.

main routine See MAIN PROGRAM.

mains **1.** In a power-distribution center, the lines that supply the entire system. An example is the set of lines leading into a house. **2.** The utility wires and associated outlets in a house or building.

maintenance The process of keeping a system, circuit, or component in operating condition, with minimal down time.

maintenance routine A computer program used by computer service personnel for diagnosis during a regular service interval.

major beats The principal beats produced in a beat-note system; they are usually the sum and/or difference of two fundamental frequencies. Compare MINOR BEATS.

major face In a hexagonal quartz crystal, one of the three larger faces. Compare MINOR FACE.

majority carrier The predominant charge carrier in processed semiconductor material. Electrons are the majority carriers in n-type material; holes are the majority carriers in p-type material. Compare MINORITY CARRIER.

majority logic A logic gate in which the output is high whenever the majority of its inputs is high, regardless of which inputs are high. Thus, in a five-input gate of this type, the output is high when any three or more of the inputs are high.

major lobe See MAIN LOBE.

major loop The principal path for the circulation of information or control signals in an electronic system (e.g., *major feedback loop*). Compare MINOR LOOP.

make **1.** The closing of a pair or set of contacts. **2.** To close a pair or set of contacts.

make-before-break contacts A pair of contacts in which the movable arm closes with the next contact before breaking with the previous one. Compare BREAK-BEFORE-MAKE CONTACTS.

make time The time required for a relay to latch completely, or for a switch (either mechanical or electronic) to close completely. Compare BREAK TIME.

male plug A plug having one or more protruding contacts in the form of pins, blades, or prongs. Compare FEMALE PLUG and HERMAPHRODITIC PLUG.

male plug

Malter effect The tendency for a layer of semiconductor having a high secondary emission ratio to become positively charged when bombarded by electrons. This occurs when a thin insulator separates the semiconductor from a metal plate. The insulator must be very thin (on the order of 10^{-7} meters). This results in a potential difference of up to about 100 volts.

manganese Symbol, Mn. A metallic element. Atomic number, 25. Atomic weight, 54.938.

manganese-dioxide depolarizer In a dry cell, manganese dioxide mixed with powdered carbon, the mixture being a depolarizing agent. Also see DEPOLARIZER.

manganin A low-temperature-coefficient alloy used in making wire for precision resistors. A typical composition is: copper (84 percent), manganese (12 percent), and nickel (4 percent).

manipulator A robot arm and end effector, as used in mechanical processes.

man-made interference See HUMAN-MADE INTERFERENCE.

man-made static See HUMAN-MADE INTERFERENCE.

manometer An instrument for measuring gas or vapor pressure—especially at low levels.

manpack A portable radio transceiver that can be used while walking.

mantissa **1.** The portion of a logarithm to the right of the decimal point. Thus, in 3.952502 ($\log_{10}$ 8964), the mantissa is 0.952502. **2.** The fixed point part of a number in scientific notation; thus, in 4×10^3, the mantissa is 4.

manual **1.** Actuated or operated directly by mechanical means, rather than automatically. **2.** A

5059F-pM-424-465 4/10/01 9:19 AM Page 433

book, or a set of online information files, detailing the operation and maintenance procedures for a device or system.

manual input Use of a keyboard, mouse, trackball, or other electromechanical input device to enter data into a computer program or system.

manual operation In data processing, an operation in which automatic machines are not involved.

manual telegraphy Telegraphy that consists signals transmitted by a hand-operated key and recorded by hand (pen, pencil, or typewriter).

manual tuning Tuning performed entirely by adjusting variable circuit components by hand.

manual word generator A device by which an operator can originate information words for input into computer memory.

manufacturing automation protocol In a factory using computer-controlled robots, the set of standards for data communication between the robots and the controller and/or between individual robots. It keeps the factory operating smoothly.

MAR Abbreviation of MEMORY-ADDRESS REGISTER.

Marconi antenna A quarter-wave radio transmitting or receiving antenna operated against an earth ground.

Marconi effect The undesired tendency of an entire receiving antenna system, including lead-in or feeders, to act as a MARCONI ANTENNA.

margin **1.** A gap or space between two objects, such as adjacent plates of a capacitor. **2.** Clearance. **3.** The maximum error that can be tolerated without risk of improper or abnormal operation. **4.** In a teletypewriter, the range of adjustments in which the error frequency is acceptable.

marginal relay A relay having a small difference between its on and off currents or voltages.

marginal test As performed on equipment in a computer installation, a test to either determine the cause of an intermittent malfunction, or verify an equipment's operating tolerances.

marine broadcast station A coastal station that broadcasts information of interest to shipping: time, weather, ocean currents, etc.

marine radio Radio communications between seagoing vessels or between vessels and shore stations.

marine radiobeacon station A land-based radionavigation station whose transmitted signals are used for taking bearings.

mariner's compass See MAGNETIC COMPASS.

mark **1.** In telegraphy, the dot or dash portion of a character, as opposed to the dead space between such portions. **2.** The intelligence part of a similar signal (such as sound, light, etc.). **3.** The high (logic 1) state represented by a binary bit, as opposed to the low (logic 0) state. **4.** A character identifying the end of a data set. Also called MARKER (see MARKER, **2**).

marker **1.** A pip that indicates a particular frequency on a response curve displayed on an oscilloscope screen. **2.** A character that identifies the end of a data set. Also called MARK (see MARK, **4**).

marker beacons Individual coded-signal transmitters placed along a radio range and indicating features of the course marked by them.

marker frequency **1.** A known frequency that can be used to identify a spot-frequency harmonic of a frequency-standard signal. **2.** A known accurate signal used to identify the limit of a radio band. **3.** The frequency at some point on a response curve as identified by a marker pip (see MARKER).

marker generator An oscillator that supplies a marker pip (see MARKER).

mark hold In telegraphy, an unmodulated signal meaning information is not being sent.

mark reading The reading by an optical scanning device of marks made in specific areas of a document; the process also includes the marks' conversion to digital signals for input to a computer.

mark scanning See MARK READING.

mark sensing A process similar to MARK READING, except that the marks are sensed electrically.

marker trap A wave trap that supplies a dip-type marker pip when used in conjunction with a radio-frequency test oscillator (see MARKER).

market scanner Also called *bar-code reader.* A device that scans a black-bar binary label printed on a carton or other package (or magazine), and indicates the price of the merchandise on the readout of the checkout register.

mark-to-space ratio In radiotelegraphy, the ratio of the duration (mark) of a dot to the interval (space) between successive dots.

Marx generator An impulse-type high-voltage direct-current generator circuit in which several capacitors are charged in parallel through a high-resistance network. When the capacitor voltage reaches a critical high value, discharge occurs in series through spark gaps, producing a high-voltage pulse for each discharge.

maser A low-noise microwave amplifying device in which a microwave input signal causes high-energy-state molecules of ammonia or ruby to fall to the low-energy state and, as a result, to emit large amounts of energy as an output signal. The name is an acronym for *microwave amplification by stimulated emission of radiation.*

Marx generator

5059F-pM-424-465 4/10/01 9:19 AM Page 434

mask **1.** A kind of stencil through which plating, electrodeposition, or diffusion can be done. **2.** The viewing screen, or GRATICULE, of an oscilloscope. **3.** To obliterate a signal with a stronger one. **4.** A bit or character pattern used to change or extract bit positions in another pattern.

masking **1.** The use of a MASK of any type. **2.** The tendency of one effect or phenomenon to obscure another. It applies especially in audio systems, where certain sounds impair the ability of a listener to hear other sounds that occur at the same time. **3.** The extent to which one effect or phenomenon obscures another.

Masonite Masonite Corporation's tough fiberboard used for panels and bases of some electronic equipment.

mass The quantity of matter in a body. Like weight, mass is expressed in kilograms in the metric (SI) system and in pounds in the English system. For a given piece of material, mass can be determined by dividing the weight by the acceleration of gravity.

mass data Data in excess of the maximum amount that can be stored in the main (internal) storage unit of a digital computer (i.e., that which can only be accommodated by external media such as magnetic disks or tapes).

mass-energy equation Energy (E) is the product of a given mass (m) and the square of the speed of light (c^2): $E = mc^2$. It is also called the *Einstein equation.*

mass number **1.** Symbol, A. A number representing the total of neutrons and protons in the nucleus of an atom. The approximate mass of an atom is equal to $A \times m_p$, where m_p is the total proton (rest) mass. **2.** The number indicating the sum of nuclear protons and neutrons in an atom. It is usually written following the symbol for the atom: thus, U238 is uranium having 238 nucleons. An isotope of an element will have a different mass number than that of the normal atom.

mass of electron at rest Symbol, m_e. The amount of matter in an electron; $m_e = 9.1093897 \times 10^{-31}$ kg.

mass of neutron at rest Symbol, m_n. The mass of a neutron in the nucleus of an atom; $m_n = 1.6749286 \times 10^{-27}$ kg.

mass of proton at rest Symbol, m_p. The mass of a proton in the nucleus of an atom; $m_p = 1.6726231 \times 10^{-27}$ kg.

mass resistivity **1.** The resistance of a wire one meter long having a mass of one gram. It varies, depending on the composition of the wire. **2.** The resistance of a wire one mile long having a weight of one pound. It varies, depending on the composition of the wire.

mass spectograph An instrument used to analyze chemical compounds and mixtures in terms of their distinctive mass spectra, exhibited by ionized samples of the materials in a magnetic field.

mass spectrometer Abbreviation, MS. An instrument that permits rapid analysis of chemical compounds via the MASS SPECTRUM.

mass spectrum An electron spectrum that can be used to identify a chemical element. Different elements have nuclei with different charge-to-mass ratios. This results in each element having a unique mass spectrum.

mass storage In a computer system, a magnetic or optical storage medium capable of holding large amounts of data. Examples: magnetic diskette, magneto-optical diskette, external hard disk, compact-disk read-only memory (CD-ROM), and magnetic tape.

mass unit See ATOMIC MASS UNIT.

master **1.** The primary or main element or device in a system. **2.** A primary data medium or recording from which copies are made. **3.** A primary reference standard. See the following several definitions.

master clock **1.** In a digital computer, the primary generator of timing pulses. **2.** A standard time clock that drives other (slave) clocks, or to which clocks of lesser accuracy can be referred.

master console In a computer system, an equipment with panel instruments and controls, which permits operations to be governed, monitored, and controlled by a human operator.

master control **1.** The main control circuit in a system. **2.** A point from which signals or programs are distributed in a communications or broadcast system.

master data Also called *archives.* In a computer record, data elements that remain unaltered for a long time, and from which copies are made.

master file A computer file of data used routinely and remaining unchanged for a long time.

master gain control The principal gain control in an audio amplifier or mixer [i.e., the one used to adjust the gain (volume) of the entire system].

master instruction tape Magnetic tape on which various related computer programs are recorded.

master library tape See MASTER PROGRAM FILE.

master oscillator Abbreviation, MO. The main oscillator in an electronic system (e.g., the oscillator stage in an oscillator-amplifier type of radio transmitter). This oscillator can be either self-excited or crystal-controlled.

master oscillator-power amplifier Abbreviation, MOPA. A type of transmitter or signal generator in which a frequency-determining oscillator drives a power amplifier, which in turn delivers an output signal. Because the oscillator is isolated from the output load, this arrangement has greater stability than one in which the oscillator alone supplies power to the load.

master pattern The etching pattern used for manufacture of a batch of identical printed-circuit boards.

master program file A reel of magnetic tape on which is recorded the programs regularly used in

5059F-pM-424-465 4/10/01 9:19 AM Page 435

a data-processing installation. It is also called *master library tape.*

master record In a data-processing system, the current record (usually stored on a disk or tape) that will be used for the next computer run.

master relay A relay that operates other (slave) relays. Compare SLAVE RELAY.

master station See KEY STATION.

master switch A switch that can actuate or deactuate an entire installation or system.

master tape **1.** In sound recording and reproduction, a magnetic tape that contains material from which other tapes and discs can be made. **2.** In automation, a magnetic tape on which is recorded the basic signal sequence for controlling a process and other recorders. **3.** In data processing, a magnetic tape that must not be erased.

master volume control See MASTER GAIN CONTROL.

masurium See TECHNETIUM.

MAT Abbreviation of MICROALLOY TRANSISTOR.

match **1.** To mate devices, signals, impedances, etc. for optimum compatibility in terms of signal transfer, equipment interfacing, and other optimizing qualities. **2.** The condition of being compatibly mated, physically or electrically.

matched components Circuit components (capacitors, coils, diodes, resistors, transistors, etc.) that are carefully selected for similar or particularly compatible operating characteristics.

matched filter **1.** A filter with input and output impedances matched to the input line and output load, respectively. **2.** A filter designed for separating a signal with a particular waveform from other signals and noise.

matched impedance A usually non-reactive impedance that has the same value as that of another impedance with which it is operated. Maximum power is transferred between impedances that are matched.

matched load A purely resistive load, the impedance of which is the same as the characteristic impedance of the feed line. This results in optimum power transfer from the line to the load.

matched pair A pair of matched components offered in a single package.

matched transmission line A transmission line terminated in a purely resistive impedance whose value is identical to the characteristic impedance of the line. Such a line transfers all of its energy to its load without reflection; no standing waves are on the line.

matching pad An inductance-capacitance (LC) network for matching the impedance of a load to the output impedance of a signal generator.

matching stub See STUB.

matching transformer An audio-frequency (AF) or radio-frequency (RF) transformer used to match one purely resistive impedance to another.

matchtone A transistorized, single-frequency audio oscillator that can be used to monitor transmitted radiotelegraph signals. The carrier wave from the transmitter is rectified by a small semiconductor diode, whose direct-current output powers the oscillator.

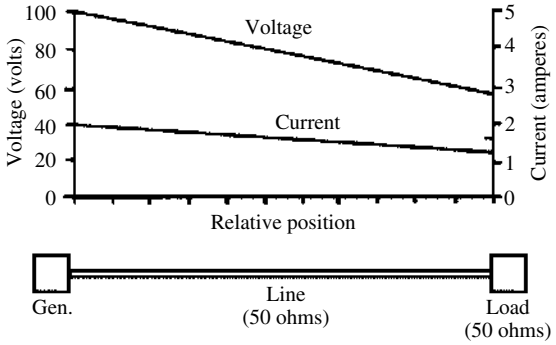

matched transmission line

Mateucci effect The generation of a potential difference in a helically wound, ferromagnetic wire when its magnetization fluctuates.

mathematical check A test of the validity of the result of an arithmetic process (by using alternate methods, for example).

mathematical logic **1.** A branch of mathematics that involves the theoretical behavior of various systems of reasoning. **2.** See BOOLEAN ALGEBRA. **3.** See DIGITAL LOGIC.

mathematical model See MODEL, **2**.

mathematical subroutine Within a computer program, a subroutine serving as an arithmetic function (i.e., one for performing an operation not integral to the monitor program).

matrix **1.** A high-speed switching or memory array used in counters and computers. **2.** Generally, any two-dimensional array of objects. **3.** A device for solving linear simultaneous equations, consisting of a rectangular array of coefficients.

matrix printer See WIRE PRINTER.

mat switch A form of PRESSURE SENSOR used in some security systems. When weight appears on the mat, switches close, actuating an alarm.

matter The building material of the universe that occupies space and has mass that can be measured. See, for illustration, ATOMIC THEORY and STATES OF MATTER.

matter waves See DE BROGLIE WAVES.

max Abbreviation of MAXIMUM.

maxima Points along a curve at which a function reaches a local maximum value. Also see MAXIMA AND MINIMA.

maxima and minima **1.** The loops and nodes of current or voltage on an antenna or transmission line. **2.** The lobes and nulls in a directivity pattern. **3.** The bright and dark bands in a visible-light interference pattern. **4.** In radar reflections, regions of localized maximum and minimum

5059F-pM-424-465 4/10/01 9:19 AM Page 436

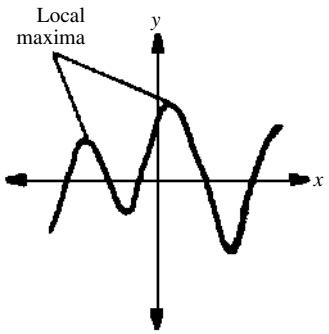

maxima

intensity. **5.** The study and solution of maximum, minimum, and inflection points on the curve of a function.

maximal flatness For an amplifier or network, the condition in which peaks are not present in the normal passband response.

maximum Abbreviation, max. The highest value in a range or set. Also see MAXIMA AND MINIMA and PEAK.

maximum available gain Abbreviation, MAG. The amplification provided by a circuit or device whose input and output impedances are correctly matched to source and load.

maximum current **1.** Symbol, I_m or I_{max}. The highest value reached by an alternating-current half-cycle or by a pulse current. Also called PEAK CURRENT. **2.** The highest value of current in a series of current values.

maximum power **1.** Symbol, P_m or P_{max}. The highest value of power that an equipment can be called upon to supply. **2.** The highest value of power in a series of measurements or calculations.

maximum-power discharge current For a cell or battery, the current at which the greatest amount of power is delivered.

maximum power output See MAXIMUM POWER, **1**.

maximum power transfer The condition in which the largest amount of power is delivered by a source to a load.

maximum power transfer theorem Maximum power is transferred from a generator to a load when the impedance of the load equals the internal impedance of the generator. Compare COMPENSATION THEOREM, NORTON'S THEOREM, RECIPROCITY THEOREM, SUPERPOSITION THEOREM, and THEVENIN'S THEOREM.

maximum rating **1.** The highest value of a quantity (e.g., current, voltage, or power) that can safely be used with a given device. **2.** The highest value of a quantity afforded by a given device (e.g., *maximum capacitance* of a variable capacitor).

maximum record level **1.** In a magnetic tape, magnetic disk, or phonograph disc, the highest amplitude of input signal that can be recorded with an acceptable amount of distortion. **2.** The recording-head current or power that results in third-harmonic distortion of three percent.

maximum signal level **1.** In an amplitude-modulated signal, the peak power. **2.** In an amplitude-modulated facsimile or television system, the amplitude that results in a black or white picture (depending on whether the highest amplitude produces black or white).

maximum undistorted power output Abbreviation, MUPO. The highest power that an active amplifying device will deliver before significant distortion occurs.

maximum usable frequency Abbreviation, MUF. The highest frequency that can be used successfully at a given time, between two specific geographic locations, for communication via the ionosphere.

maximum voltage **1.** Abbreviation, E_m, E_{max}, V_m, or V_{max}. The peak value reached by an alternating-current voltage half-cycle, or by a voltage pulse. **2.** The highest value of voltage in a series of voltage measurements or calculations.

maximum wattage See MAXIMUM POWER.

maxterm form In mathematical calculations, the factored form of a function, expressed as a product of sums. For example, the maxterm form of $f(x) = x^2 + 5x + 6$ is $f(x) = (x + 2)(x + 3)$.

maxwell Symbol, Mx. The cgs unit of magnetic flux, equivalent to one line of flux or 10^{-8} weber.

Maxwell bridge A four-arm alternating-current bridge for measuring inductance against a standard capacitance.

Maxwell's equations A set of four equations developed by James Clerk Maxwell in 1864 and 1873, describing vector quantities pertaining to points in space subjected to varying electric and magnetic forces. Through his classic presentation, Maxwell

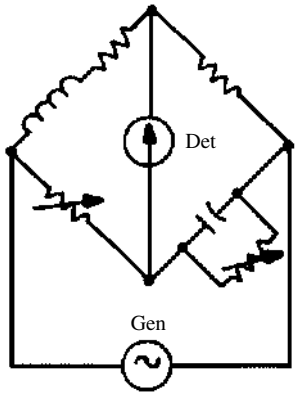

Maxwell bridge

5059F-pM-424-465 4/10/01 9:19 AM Page 437

predicted the existence of electromagnetic waves, whose later discovery made radio possible.

Maxwell's law Also called *Maxwell's rule.* Every part of an electric circuit is acted upon by a force tending to move it in the direction that results in the maximum magnetic flux being enclosed.

maxwell-turn A unit of magnetic coupling (linkage) equal to 1 maxwell per turn of wire in a coil linked by magnetic flux. Also see MAXWELL.

mayday In radiotelephony, a word spoken as an international distress signal equivalent to SOS in radiotelegraphy. The word is the phonetic equivalent of the French *m'aidez* (help me).

MB Abbreviation of MIDBAND.

Mb Abbreviation of MEGABAR.

MBB Abbreviation of MAKE BEFORE BREAK.

MBM Abbreviation of *magnetic bubble memory.*

MBO Abbreviation of MONOSTABLE BLOCKING OSCILLATOR.

MBS Abbreviation of *magnetron beam switching.*

mc **1.** Symbol for MILLICURIE (mCi is preferred). **2.** Symbol for METER-CANDLE.

Mc **1.** Symbol for MEGACURIE (MCi is preferred). **2.** Obsolete abbreviation of *megacycle(s)*, a term superseded by MEGAHERTZ.

MCG Abbreviation of MAGNETOCARDIOGRAM.

McLeod gauge An instrument for measuring gas under low pressure. A measured volume of the gas under test is first compressed (to a lower known volume) to a pressure more easily measured via a mercury manometer and the application of Boyle's law.

MCM Abbreviation of MONTE CARLO METHOD.

McProud test A simple test for checking the tracking efficiency of a phonograph pickup and arm for microgroove discs.

Mc/s Obsolete abbreviation of *megacycle(s) per second*, a term superseded by MEGAHERTZ.

MCS **1.** Abbreviation of *Master of Computer Science.* **2.** Abbreviation of *missile control system.*

MCW Abbreviation of MODULATED CONTINUOUS WAVE.

Md Symbol for MENDELEVIUM.

MDAS Abbreviation of *medical data acquisition system.*

m-derived filter A filter whose inductance (L) and capacitance (C) values are derived by multiplying those of a constant-k filter by a factor m between zero and 1. This factor is a function of the ratio f_i/f_c, where f_i is the frequency of infinite attenuation, and f_c is the cutoff frequency. This type of filter exhibits sharper response than the equivalent constant-k filter.

MDI Abbreviation of MAGNETIC DIRECTION INDICATOR.

M-display See M-SCAN.

MDS Abbreviation of MINIMUM DISCERNIBLE SIGNAL.

m_e Symbol for MASS OF ELECTRON AT REST.

Meacham oscillator A highly stable radio-frequency oscillator consisting of an amplifier provided with a feedback circuit containing a four-arm bridge, one arm of which is a quartz crystal, and another, a tungsten-filament lamp acting as a nonlinear resistor. Also called *bridge-stabilized oscillator.*

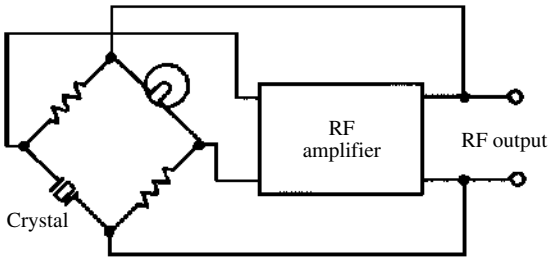

Meacham oscillator

mean **1.** A general term meaning *average.* **2.** See ARITHMETIC MEAN. **3.** See GEOMETRIC MEAN.

mean charge **1.** In an object that is nonuniformly charged, the average charge per unit distance, area, or volume. **2.** In a capacitor carrying a fluctuating current, the average amount of charge held by the plates.

mean free path **1.** In acoustics, the average distance that sound waves travel before striking a barrier or reflecting surface. **2.** The average distance that sound waves travel between reflections (echoes) in a chamber. **3.** In a gas tube, the average of all the free paths of electrons at a specified temperature.

mean life **1.** Symbol, *L.* The average life of a radioactive substance [i.e., the time taken for $1/e$ (e = base of natural logarithms) of the substance to disintegrate]. **2.** The time required for excess carriers injected into a semiconductor to recombine with carriers of opposite sign. Also called *average life.*

mean proportional See GEOMETRIC MEAN.

mean time before failure Abbreviation, MTBF. The average length of time that a component or system will perform before the first failure occurs. It is generally specified in hours.

mean time between failures Abbreviation, MTBF. The average length of time that a component or system will perform before failure occurs—either initially or after repair or replacement. It is generally specified in hours.

measured A quantity that is presented to an instrument for measurement.

measured service Any service in which charges are assessed per unit-time usage block. Online computer services are a common example. In some cases, other factors, such as distance, affect the cost per unit time; most long-distance telephone services fall into this category.

measurand Any quantity that is measured with an instrument.

5059F-pM-424-465 4/10/01 9:19 AM Page 438

measurement **1.** The process by which the magnitude, extent, or duration of a parameter is found. **2.** The value of a parameter, as obtained, according to **1**.

measurement error The difference between the measured value of a quantity and its true value. Also see NEGATIVE ERROR OF MEASUREMENT and POSITIVE ERROR OF MEASUREMENT.

measurement range In a measuring device, the range within which the error is smaller than a specified value.

mechanical analogs Familiar mechanical devices, systems, or effects with which certain electrical counterparts can be compared for ease in teaching or understanding (e.g., inductance compared with mass, capacitance with elasticity, voltage with pressure, and current with velocity).

mechanical axis In a quartz crystal, the axis perpendicular to the faces of the hexagon. Also see Y-AXIS, **2**.

mechanical bandspread Bandspread tuning obtained by reduction-ratio gearing of the tuning mechanism. Compare ELECTRICAL BANDSPREAD.

mechanical bias **1.** A steady pull applied by a spring to the armature of a relay to sensitize it by decreasing the distance that the armature must move to close the contacts. **2.** Bending of a relay frame to position the armature closer to the magnet for the purpose defined in **1**.

mechanical damping Damping action obtained entirely by mechanical devices (such as weights, dashpots, etc.).

mechanical equivalent of heat The amount of mechanical work required to produce a unit quantity of heat. For example, 4.183 joules can be converted into 1 calorie of heat.

mechanical equivalent of light The expression of luminous energy in equivalent power units. In practical measurements, this is taken as the total power output of a lamp minus the power absorbed by a transparent jacket used to remove the infrared and ultraviolet rays.

mechanical filter See ULTRASONIC FILTER, **1**.

mechanical joint A union of electrical conductors consisting exclusively of a junction or splice made without brazing, soldering, or welding.

mechanical load An electromechanical device that uses the output of an electrical source. Such devices include actuators, brakes, clutches, meters, motors, and relays.

mechanical rectifier A vibrator or commutator used to change an alternating current into a direct current by selecting and passing only positive or negative half-cycles. Also see ELECTROMECHANICAL RECTIFIER.

mechanical scanner **1.** A mechanical device for scanning an object or scene and breaking it into horizontal lines that are converted to signals. **2.** A device that scans the reproducer lamp in a mechanical television receiver. See, for example, NIPKOW DISK.

mechanical switch A switch actuated by moving or sliding a lever, pressing a button, or otherwise applying mechanical pressure.

mechanical time constant For a torque motor, the ratio of moment of inertia to damping factor. Compare ELECTRICAL TIME CONSTANT.

mechanical wave filter See ULTRASONIC FILTER, **1**.

mechanics The branch of physics concerned with forces and motion and the laws of gases and liquids. It is subdivided into *kinematics* and *kinetics*.

mechatronics Combination of the words *mechanics* and *electronics*, referring to the use of electromechanical devices (especially robots) in manufacturing. The term was originally coined in Japan.

median **1.** The middle value in a sequence of numbers. For example, in the series: 1, 2, 3, 4, 5, 6, 7, the median is 4. Compare ARITHMETIC MEAN and GEOMETRIC MEAN. **2.** In a statistical distribution, the value *s* in the domain so that the area under the curve for all values less than *s* is equal to the area under the curve for all values greater than *s*.

medical electronics See ELECTROMEDICAL ENGINEERING.

medical robot **1.** A robot used in a doctor's office, or in a hospital to assist doctors and nurses. There are various applications, some of which have provoked controversy (e.g., *robotic surgical assistant*). It generally performs simple, noncritical tasks. It has been suggested as a means of entertaining hospital patients—especially children. **2.** See BIOMECHANISM.

medium In a computer system, that storage device onto or into which data is recorded for input into memory (e.g., magnetic disk, magnetic tape, optical disk, etc.).

medium-frequency Abbreviation, MF. Pertaining to frequencies in the range 300 kHz to 3 MHz, representing wavelengths from 1000 meters to 100 meters.

medium of propagation The substance (or vacuum) through which electromagnetic energy is transmitted (e.g., outer space, the atmosphere, or a dielectric material).

medium-scale integration A method of manufacturing integrated circuits, in which there are at least 10, but less than 100, individual gates on each chip. Abbreviated MSI.

medium-scan television A television (TV) communications medium in which the scanning rate is slowed down compared to regular (fast-scan) TV, but is faster than the commonly used slow-scan TV. It provides some conception of motion, although not as realistic as fast-scan TV.

5059F-pM-424-465 4/10/01 9:19 AM Page 439

medium tension Medium voltage. A relative term, but generally referring to common alternating-current utility voltage (e.g., 117 volts or 234 volts).

medium wave Abbreviation, MW. Pertaining to wavelengths corresponding to medium frequencies (see MEDIUM-FREQUENCY) (i.e., those in the 100- to 1000-meter range).

meg **1.** Colloquialism for MEGOHM(s). **2.** Colloquialism for MEGABYTE(s).

mega- Abbreviation, M. **1.** A prefix meaning *million(s)*, (i.e., 10^6 or 1,000,000). **2.** In digital data applications, a prefix meaning 2^{20} or 1,048,576.

megabar Abbreviation, Mb. A cgs unit of high pressure. 1 Mb = 10^6 bars = 10^{11} pascals. Also see BAR, **1**.

megabit A unit of digital data equal to 2^{20} (1,048,576) bits. Also see BIT.

megabyte Abbreviation, M or MB. A unit of digital data equal to 2^{20} (1,048,576) bytes. Also see BYTE.

megacurie Abbreviation, MCi. A large unit of radioactivity equal to 3.71×10^6 disintegrations per second; 1 MCi = 10^6 curies. Also see CURIE.

megacycle See MEGAHERTZ.

megaelectronvolt Abbreviation, MeV. A large unit of electrical energy; 1 MeV = 10^6 eV. Also see ELECTRONVOLT.

megahertz Abbreviation, MHz. A unit of frequency; 1 MHz = 10^6 Hz = 1,000,000 Hz.

megampere Abbreviation, MA. A unit of high current; 1 MA = 10^6 A = 1,000,000 A.

megaphone **1.** A hand-held microphone/amplifier/loudspeaker used to amplify the voice of a person who must be heard over an appreciable area. **2.** A simple horn for amplifying the voice.

megarutherford Abbreviation, Mrd. A large unit of radioactivity equal to 1 trillion (10^{12}) disintegrations per second; 1 Mrd = 10^6 rd = 1,000,000 rd. Also see RUTHERFORD.

megavolt Abbreviation, MV. A unit of extremely high voltage; 1 MV = 10^6 V = 1,000,000 V.

megavolt-ampere Abbreviation, MVA. A unit of extremely high reactive power; 1 MVA = 10^6 VA = 1,000,000 VA. Also see VOLT-AMPERE.

megawatt Abbreviation, MW. A unit of high power; 1 MW = 10^6 W = 1,000,000 W. Also see WATT.

megawatt-hour Abbreviation, MWh. A large unit of electrical energy or of work; 1 MWh = 10^6 Wh = 1,000,000 Wh = 3.6×10^9 joules. Also see WATT-HOUR.

megger An instrument containing an internal high-voltage direct-current power supply, used for measuring high values of resistance. Compare MEGOHMMETER.

meg-mike **1.** Colloquialism for MEGOHM-MICROFARAD(s). **2.** Colloquialism for MEGOHM-FARAD(s).

megohm Symbol, M. A unit of high resistance, reactance, or impedance; 1 M = 10^6 ohms = 1,000,000 ohms.

megohm-farads For a large capacitor, the product of leakage resistance (megohms) and capacitance (farads). Also see MEGOHM-MICROFARADS.

megohmmeter A special ohmmeter for measuring resistances in the megohm range.

megohm-microfarads For a capacitor, the product of leakage resistance (megohms) and capacitance (microfarads). The figure is an expression for the relative insulation resistance of a capacitor.

Meissner circuit An oscillator tuned by means of LECHER WIRES (parallel-conductor resonant circuits). It is used primarily at ultra-high frequencies (UHF).

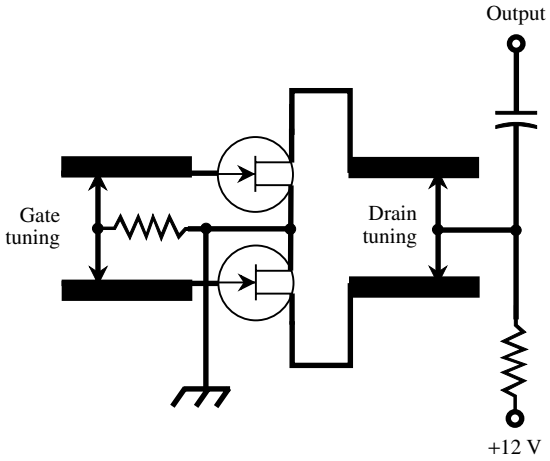

Meissner circuit

Meissner effect In a superconductive material, the abrupt loss of magnetism when the temperature of the material is reduced to a value below that required for superconductivity.

Meissner oscillator See MEISSNER CIRCUIT.

meitnerium Symbol, Mt. Also called *unnilenium* (Une). Atomic number, 109. The most common isotope has atomic weight 266. Classified as a transition metal. It is human-made and not known to occur in nature.

mel An expression of apparent or perceived sound pitch. A tone of 1 kHz, at a level of 40 dB, with respect to the threshold of hearing, represents 1 mel. The perceived pitch depends, to some extent, on the intensity of the sound, as well as on the actual frequency.

M electron In certain atoms, one of the electrons whose orbits are outside of and nearest to those of the L electrons.

meltback process The technique of remelting a doped semiconductor material and allowing it to refreeze to form a grown junction.

meltback transistor A grown-junction transistor produced by the MELTBACK PROCESS.

5059F-pM-424-465 4/10/01 9:19 AM Page 440

melting point Abbreviation, mp. The temperature at which a solid starts becoming liquid at a pressure of one atmosphere. Compare FREEZING POINT and MIXTURE MELTING POINT.

memory **1.** The section of a digital computer that records and holds data until it is necessary. In personal computers, the term generally refers to RANDOM-ACCESS MEMORY and READ-ONLY MEMORY, contained in integrated circuits (ICs). Compare STORAGE. **2.** See MEMORY DRAIN.

memory address register In computer storage, a register in which is stored the address of operands in other locations.

memory area A portion of computer memory reserved for a specific type of data. Also called *area.*

memory capacity As a function of the number of memory locations available, the number of bytes that can be stored. It is usually specified in kilobytes, megabytes, or gigabytes. Also see GIGABYTE, KILOBYTE, and MEGABYTE.

memory cycle **1.** The period of execution of a sequence of operations. **2.** The complete operational cycle for inputting data to memory or retrieving it.

memory dialing In a telephone set, a feature that allows rapid dialing of stored digits. The simplest version is the "redial" feature, in which the most recently dialed number is rapidly dialed at the touch of a button. Some sets can store several different numbers, usually including area codes, and sometimes country codes as well.

memory drain Also called *battery memory.* A phenomenon occasionally exhibited by nickel–cadmium cells and batteries, in which the useful ampere-hour capacity is reduced even though the unit is not physically damaged. The depth of the charge cycle decreases to a fraction of its rated value. The problem can usually be overcome by discharging the cell or battery fully, then recharging fully, and repeating the process several times. See also NICKEL–CADMIUM.

memory dump In computer operations, to either print out what is stored in some of or all of the memory locations or transfer the data from a bank of memory cells to some external storage medium.

memory effect See MEMORY DRAIN.

memory guard In a computer, hardware or software that keeps certain memory locations from being addressed by a program being run.

memory location In a computer memory, a place where an information unit (word or character) can be stored; the stored information can be retrieved by appropriate addressing instructions.

memory organization packets In artificial intelligence (AI) and expert systems, a method of arranging computer memory into general rules or statements. The statements are used by software to derive models, forecasts, diagnoses, etc.

memory power Computer memory efficiency in terms of data processing (cycle) speed.

memory protection A hardware device in a multiple programming computer that prevents programs from being altered by other operating programs in the installation.

memory register In a digital computer, a register used in all instruction and data transfers between the memory and other sections of the machine.

memory unit See MEMORY.

mendelevium Symbol, Md. A radioactive element produced artificially. Atomic number, 101. Atomic weight, 258 (approx.).

menu In computer operations, a list of commands for using various functions of the system.

MEP Abbreviation of *mean effective pressure.*

mercuric iodide Formula, HgI_2. A compound whose crystals are useful at room temperature as detectors in high-resolution gamma-ray spectroscopy.

mercury Symbol, Hg. A metallic element. Atomic number, 80. Atomic weight, 200.59. The only metal that is liquid at room temperature. It is used extensively in switches, certain high-voltage rectifiers, high-vacuum pumps, and thermometers.

mercury arc The arc discharge occurring in mercury vapor between solid or liquid (mercury) electrodes. The discharge emits ultraviolet radiation.

mercury-arc rectifier A heavy-duty rectifier tube utilizing ionized mercury vapor. The two general types are MERCURY-VAPOR RECTIFIER and MERCURY-POOL RECTIFIER.

mercury battery Also called *mercuric-oxide battery.* A set of two or more mercury cells stacked one atop the other, electrically connected in series. The resulting battery has a cylindrical shape. A set of four cells provides approximately 5.4 volts under no-load conditions; a battery of seven cells provides 9.5 volts; a battery of nine cells provides 12 volts. See MERCURY CELL.

mercury cadmium telluride Formula HgCdTe. An alloy used as a semiconductor in certain transistors, integrated circuits, and infrared detectors.

mercury cell Also called *mercuric-oxide cell.* An electrochemical cell having a button-like shape, small enough to fit inside a wristwatch. The unit is housed in a steel container and has a mercuric-oxide cathode, amalgamated-zinc anode, and potassium hydroxide and zinc-oxide electrolyte. The potential difference under no-load conditions is 1.35 volts, with a high ratio of stored energy per unit mass. The cell has a flat discharge curve; the voltage remains essentially constant until the charge is almost depleted, and then the voltage drops rapidly. There has been a decrease in the use of mercury cells and batteries in recent years, because mercury is toxic. Unless these cells are discarded in a special way, the mercury from them can cause dangerous contamination of soil and water.

5059F-pM-424-465 4/10/01 9:19 AM Page 441

mercury delay line A delay line in which delay is obtained by propagating the signal through a pipe of mercury.

mercury diffusion pump A vacuum diffusion pump using mercury vapor.

mercury displacement relay A form of switching relay in which the electrical contact is made by moving mercury.

mercury-jet switch A multipoint switch using a jet of mercury instead of the conventional wiper arm, for high-speed operation and reduced wear.

mercury memory A recirculating memory using a mercury delay line. Also see DELAY LINE and DELAY-LINE MEMORY.

mercury-pool cathode In certain industrial electron tubes, such as the ignitron, a cathode electrode consisting of a pool of mercury.

mercury-pool rectifier A type of mercury-arc rectifier whose cathode is a pool of mercury. In one type, the arc is initiated by tilting the tube momentarily to bring the mercury into contact with a third electrode, thus causing a starting current to flow through the pool. In another type, the *ignitron*, a starter electrode is in continual contact with the mercury.

mercury pump See MERCURY DIFFUSION PUMP.

mercury rectifier See MERCURY-POOL RECTIFIER and MERCURY-VAPOR RECTIFIER.

mercury relay A relay in which at least one of the contacts is mercury.

mercury storage See MERCURY MEMORY.

mercury switch A switch consisting essentially of two or more stiff wire electrodes and a drop of mercury hermetically sealed in a glass tube. Tilting the tube causes the mercury to flow toward one end, where it immerses the electrodes, providing a conductive path between them.

mercury-vapor lamp A glow lamp emitting blue-green light that causes ionization of mercury vapor by an electric current.

mercury-vapor rectifier A tube-type high-voltage diode rectifier containing a small amount of mercury that vaporizes and ionizes during tube operation.

mercury-vapor tube **1.** See MERCURY-VAPOR LAMP. **2.** See MERCURY-VAPOR RECTIFIER.

mercury-wetted reed relay A reed relay in which the reeds are wetted with mercury in a pool by capillary action. The film of mercury forms a tiny bridge when the reeds open; when this bridge separates, a clean, high-speed break occurs without contact bounce. Compare DRY-REED SWITCH.

merge **1.** In computer operations, to make a single set or file from two or more record sets. **2.** In word processing, to create a corrected master recording from two input media: the original master recording and the recording that contains the corrections.

meridian **1.** A great circle passing through earth's geographic poles and a given point on the surface of the earth. **2.** A line of longitude on a map or globe. Also see TIME ZONE, ZERO MERIDIAN, and ZONE TIME.

mesa A flat-topped, protruding region in a semiconductor wafer. The mesa is produced by etching the surrounding part of the material. Some bipolar transistors are manufactured in this way.

mesa diffusion A method of manufacturing bipolar transistors. The different semiconductor materials are first diffused together. Then part of the resulting wafer is etched away, resulting in a mesa shape.

mesa transistor A diffused planar transistor in which the silicon area around the base has been etched away to reduce collector-to-base capacitance; the base-emitter region remains elevated like a high plateau (mesa).

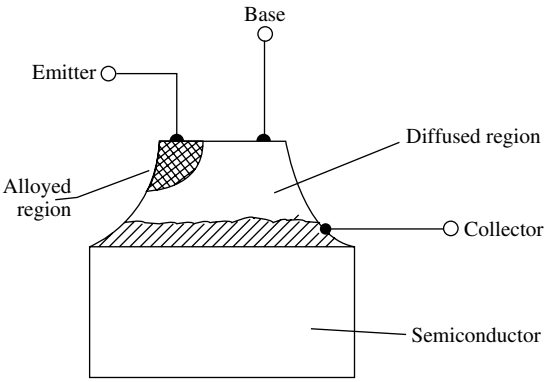

mesa transistor

MESFET A form of field-effect transistor combining depletion-mode and enhancement-mode properties. A Schottky barrier forms the gate electrode.

mesh **1.** A combination of the elements that form a closed path in a network. **2.** The closed figure (such as the delta or star) obtained by connecting polyphase windings together. **3.** A grid, screen, or similar structure in a vacuum tube.

mesh equations Equations describing fully the current and voltage relations in a network of meshes (see MESH, **1**).

Mesny circuit A push-pull ultra-high-frequency (UHF) oscillator whose gate or base tank is a pair of parallel wires short-circuited by a slider; the drain or collector tank is a similar pair of wires. The frequency is varied by moving the sliders along the wires.

mesochronous A condition for signals in which significant instants pass at identical average speeds, such as bits per second.

meson An unstable nuclear particle first observed in cosmic rays. A meson can be electrically positive, negative, or neutral. Its mass lies between that of the electron and proton.

5059F-pM-424-465 4/10/01 9:19 AM Page 442

mesotron See MESON.

message **1.** In communications, a body of information sent from a source (transmitter) to a destination (receiver). **2.** Data entered into a transaction-processing system.

message exchange In a digital communications channel, a hardware unit that carries out certain switching functions that would otherwise have to be done by a computer.

message switching system A data communications system having a central computer that receives messages from remote terminals, stores them, and transfers them to other terminals as needed.

metadyne See DC GENERATOR AMPLIFIER.

metal An elemental material that exhibits several familiar properties (such as luster, ductility, malleability, good electrical and heat conductivity, relatively high density, and the ability to emit electrons). Common examples are aluminum, copper, gold, lead, and silver. Compare METALLOID and NONMETAL.

metal-base transistor A bipolar transistor in which the base is a metal film, and the emitter and collector are films of n-type semiconductor material.

metal-ceramic construction The building of certain electronic components by bonding ceramic parts to metal parts. Also see CERMET.

metal-film resistor A fixed or variable resistor in which the resistance element is a film of a metal alloy deposited on a substrate such as a plastic or ceramic.

metal finder See METAL LOCATOR.

metallic binding forces In a crystal, the binding electrostatic force between cations and electrons. Also called *electron-gas binding forces.*

metallic bonding See BONDING, **1** and METALLIC BINDING FORCES.

metallic circuit A circuit, such as a two-wire telephone line, in which earth ground is not a part of the circuit. Compare GROUND-RETURN CIRCUIT.

metallic crystal A crystal substance in which positive ions and free electrons exist; it is, therefore, a good electrical conductor.

metallic insulator A short-circuited quarter-wave section of transmission line that acts as an insulator at the quarter-wavelength frequency.

metallicize To make a circuit fully metallic, as when two wires are used instead of one wire and a ground connection. (Not to be confused with METALLIZE.)

metallic rectifier A dry rectifier using a metal disk or plate coated with a material (such as selenium, an oxide, or a sulfide).

metallic tape Recording tape made from metal, rather than from plastic. Noted for its excellent audio-reproduction characteristics.

metallize To treat, coat, or plate with a metal. (Not to be confused with METALLICIZE.)

metallized capacitor A capacitor in which each face of a dielectric film is metallized to form conductive plates.

metallized-paper capacitor A paper-dielectric capacitor whose plates are metal areas electrodeposited on each side of a paper film.

metallized-polycarbonate capacitor A fixed capacitor in which the dielectric is a polycarbonate plastic film, and the plates are metal areas electrodeposited on each face of the film.

metallized resistor See METAL-FILM RESISTOR.

metal locator An electronic device for locating metal deposits, pipes, or wires underground, in walls, or under floors. It operates via the disturbance that these objects cause to a radio-frequency or magnetic field.

metalloid An element that has some of the properties of a metal. Examples of metalloidal elements widely used in electronics are antimony, arsenic, germanium, silicon, and tin.

metal master See ORIGINAL MASTER.

metal negative See ORIGINAL MASTER.

metal-oxide resistor A resistor in which the resistance material is a film of tin oxide deposited on a substrate.

metal-oxide semiconductor field-effect transistor Abbreviation, MOSFET. A field-effect transistor in which the gate electrode is not a pn junction (as in the junction field-effect transistor), but a thin metal film insulated from the semiconductor channel by a thin oxide film. Gate-control action is entirely electrostatic. Also called *insulated-gate field-effect transistor.* Also see DEPLETION-TYPE MOSFET, DEPLETION-ENHANCEMENT-TYPE MOSFET, and ENHANCEMENT-TYPE MOSFET.

metal-oxide varistor A VOLTAGE-DEPENDENT RESISTOR in which the resistance material is a metallic oxide, such as zinc oxide.

metal-plate rectifier See METALLIC RECTIFIER.

metal tube A vacuum tube housed in a metal envelope for self-shielding and mechanical ruggedness.

metamer A visible-light beam that is identical in color (hue), but different in concentration (saturation), with respect to a reference color.

meteor-burst signals Momentary signals, or increases in signal strength, resulting from reflection of electromagnetic energy from meteor ionization trails. See METEOR SCATTER, **1**.

meteor ionization trail A cloud of ions left in the upper atmosphere as a meteor passes. This cloud tends to reflect radio signals at certain frequencies for a short period of time. During a meteor shower, there could be a sufficient number of such trails to allow continuous over-the-horizon communication when other over-the-horizon modes are unusable.

meteorograph An instrument for the simultaneous measurement of various meteorological phenomena such as temperature, humidity, etc.

5059F-pM-424-465 4/10/01 9:19 AM Page 443

meteorology The science of the atmosphere, especially the study of weather and climate. (Not to be confused with METROLOGY.)

meteor-scatter propagation The reflection of radio signals from the ionized trails produced by meteors as they pass through the upper atmosphere. This can result in over-the-horizon radio communication or reception. A meteor produces a trail that persists for a few tenths of a second up to several seconds, depending on the size of the meteor, its speed, and the angle at which it enters the atmosphere. This is not sufficient time for the transmission of very much information, but during a meteor shower, ionization can be almost continuous. Meteor-scatter propagation has been observed at frequencies considerably above 30 MHz.

meteor-trail reflections Momentary reflection of signals by the ionized trails of meteors passing through a signal path.

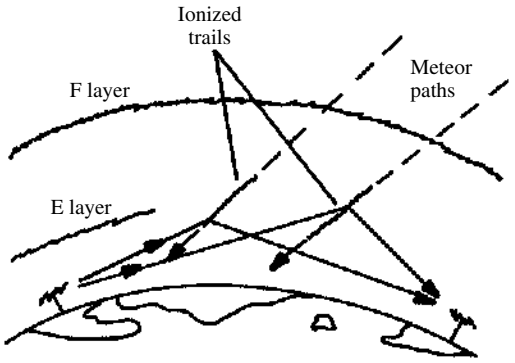

meteor-trail reflections

meter **1.** An instrument for measuring and indicating the value of a particular quantity. See, for example, CURRENT METER and VOLTMETER. **2.** Abbreviation, m. A unit of linear measure and of electrical wavelength, equivalent to 1.65076373×10^6 wavelengths (in a vacuum) of the radiation corresponding to the transition between the two levels of the krypton-86 atom, and approximately equal to 39.37 inches. **3.** To supply in specific increments or by a governed amount.

meter alignment See VISUAL ALIGNMENT.

meter-ampere A unit of transmitted radio signal intensity. Determined by multiplying the antenna current (in amperes) by the height (in meters) of the antenna above ground.

meter-candle Abbreviation, mc. A metric unit of illuminance, equivalent to the illumination on a surface 1 meter from a light source of 1 candle power. Compare FOOT-CANDLE and LUX.

meter equivalent The number of meters equal to a given English measure of length (e.g., the meter equivalent of 3 feet is approximately 0.9144).

meter-kilogram-second Abbreviation, mks. The system of units in which the meter is the standard unit of length, the kilogram is the standard unit of mass, and the second is the standard unit of time. Compare CENTIMETER-GRAM-SECOND and INTERNATIONAL SYSTEM OF UNITS.

meter multiplier See MULTIPLIER RESISTOR.

meter protector A nonlinear resistor, such as a varistor or semiconductor diode, used to prevent overswing in an electric meter by limiting the current flowing through it.

meter rating The maximum reading on a meter, at or below which the accuracy is within a specified limit, but above which the error might exceed that limit.

meter rectifier A light-duty semiconductor diode or bridge circuit, used to change alternating current (ac) to direct current (dc) for deflection of a D'Arsonval-type dc milliammeter or microammeter.

meter relay A sensitive relay that is essentially a moving-coil meter, whose pointer closes against a stationary contact mounted at some point along the scale.

meter resistance Symbol, R_m. The internal resistance of an electric meter. In a simple D'Arsonval meter, it is the resistance of the movable coil. In more-complicated meter circuits, it is the resistance of the parallel combination of the coil and METER SHUNT.

meter scale factor See SCALE FACTOR, **1**.

meter sensitivity See VOLTMETER SENSITIVITY.

meter shunt A resistor connected in parallel with an ammeter, milliammeter, or microammeter to increase the range of currents that the device can measure.

meter torque See DEFLECTING TORQUE.

meter-type relay See METER RELAY.

methyl methacrylate resin Also known by the trade name *Lucite*. A plastic insulating material. Dielectric constant, 2.8 to 3.3. Dielectric strength, 20 kV/mm.

metre Abbreviation, m. Alternate spelling of *meter* when used to specify displacement or wavelength. See METER, **2**.

metric system The decimal system of weights and measures based on the meter, kilogram, and second. Also see CENTIMETER-GRAM-SECOND, METER-KILOGRAM-SECOND, and INTERNATIONAL SYSTEM OF UNITS.

metric ton Abbreviation, MT. A metric unit of weight equal to 1000 kilograms or 1.1023 English tons.

metric waves British designation for electromagnetic energy having wavelengths ranging from 10 meters down to 1 meter, corresponding to frequencies from 30 MHz up to 300 MHz.

metrology The science of weights and measures, including electrical standards and electronic instruments and measurements. (Not to be confused with METEOROLOGY.)

5059F-pM-424-465 4/10/01 9:19 AM Page 444

metronome A mechanical or electronic device that produces audible beats (ticks). It is commonly used in setting the tempo for music, and for audibly timing certain processes.

MeV Abbreviation of MEGAELECTRONVOLT(s).

MEW Abbreviation of MICROWAVE EARLY WARNING.

mF Abbreviation of MILLIFARAD.

MF **1.** Abbreviation of MEDIUM FREQUENCY. **2.** Abbreviation of MIDFREQUENCY.

MFD Abbreviation of MAGNETOFLUID DYNAMICS (see MAGNETOHYDRODYNAMICS).

MFSK Abbreviation of MULTIPLE FREQUENCY-SHIFT KEYING.

Mg Symbol for MAGNESIUM.

mg Abbreviation of MILLIGRAM.

MGD Abbreviation of MAGNETOGASDYNAMICS (see MAGNETOHYDRODYNAMICS).

MHD Abbreviation of MAGNETOHYDRODYNAMICS.

MHD generator See MAGNETOHYDRODYNAMIC GENERATOR.

MHD gyroscope See MAGNETOHYDRODYNAMIC GYROSCOPE.

MHD power generation See MAGNETOHYDRODYNAMIC GENERATOR.

mho Obsolete term for the standard unit of electrical conductance. See SIEMENS.

mhp Abbreviation of MILLIHORSEPOWER.

MHz Abbreviation of MEGAHERTZ.

mi Abbreviation of MILE. (Also, m.)

MIC Abbreviation of MICROWAVE INTEGRATED CIRCUIT.

mic Abbreviation of MICROPHONE.

mica A dielectric mineral of complex silicate composition, easily separated into numerous thin, transparent sheets. It is widely used as a capacitor dielectric and high-temperature electrical insulator. Dielectric constant, 2.5 to 7. Dielectric strength, 50 to 220 kV/mm. Also see MUSCOVITE.

mica capacitor A component that is made by alternately stacking metal sheets and layers of mica, or by applying silver ink to sheets of mica. The metal sheets are wired together into two meshed sets, forming the two terminals of the capacitor. This type of capacitor is noted for low loss. Voltage ratings can be up to several thousand volts if thick sheets of mica are used. But these capacitors are physically bulky in proportion to their capacitance. The main application is in radio receivers and transmitters. Compare CERAMIC CAPACITOR, ELECTROLYTIC CAPACITOR, PAPER CAPACITOR, PLASTIC-FILM CAPACITOR, TANTALUM CAPACITOR.

MICR Abbreviation of MAGNETIC INK CHARACTER RECOGNITION.

micro- **1.** A prefix meaning MILLIONTH(S) (i.e., 10^{-6}). **2.** A prefix meaning extremely small (as in microstructure). Compare MACRO-.

microalloy diffused transistor Abbreviation, MADT. A MICROALLOY TRANSISTOR having a uniform base region that is diffused into the wafer before the emitter and collector electrodes are produced by alloying.

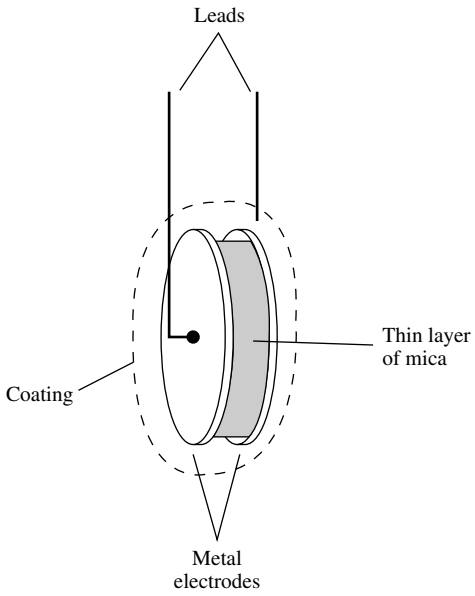

mica capacitor

microalloy transistor Abbreviation, MAT. A transistor having tiny emitter and collector electrodes that are formed by alloying a thin film of impurity material with a collector pit and emitter pit facing each other on opposite surfaces of the semiconductor wafer. Also see SURFACE-BARRIER TRANSISTOR.

microammeter A usually direct-reading instrument used to measure current in the microampere range. Also see CURRENT METER.

microampere A small unit of current, equal to 10^{-6} (0.000001) A.

microbalance A sensitive electronic weighing device. One type uses one or more servo amplifiers for the balancing operation.

microbar A cgs unit of low pressure, equal to 10^{-6} b or 0.1 pascal. Also see BAR, **1** and MILLIBAR.

microbarograph A barograph that is sensitive to small changes in pressure.

microbeam An energy beam (ray) having extremely small cross section.

microcircuit An extremely small circuit fabricated upon and within a substrate, such as a semiconductor chip. Also see INTEGRATED CIRCUIT.

microcode **1.** See MICROINSTRUCTION. **2.** A code for MICROPROGRAMMING.

microcomponent A tiny component in an electronic circuit. Examples are the resistors, capacitors, diodes, and transistors fabricated onto an integrated-circuit chip.

5059F-pM-424-465 4/10/01 9:19 AM Page 445

microcomputer **1.** A computer contained within a single integrated circuit (IC). The simplest such devices perform elementary functions and are available for a few dollars. More sophisticated devices control radio receivers and transmitters, television sets, automobiles, aircraft, and robots. The most advanced devices can be programmed to provide electrical impulses to control erratically functioning body organs, move the muscles of paralyzed persons, and transcribe speech to writing or vice versa. Compare MICROPROCESSOR. **2.** In general, any small computer.

microcrystal A crystal that is invisible to the naked eye.

microcurie A small unit of radioactivity equal to 3.71×10^4 disintegrations per second or 10^{-6} curie. Also see CURIE.

microelectrode **1.** An electrode used in MICROELECTROLYSIS. **2.** A tiny electrode, especially one of those used in integrated circuits and in certain biological applications.

microelectrolysis Electrolysis of tiny amounts of material. Also see ELECTROLYSIS, **1**.

microelectronic circuit **1.** A tiny electronic circuit other than an INTEGRATED CIRCUIT (i.e., one assembled in a small space with small discrete or integrated components). **2.** See MICROCIRCUIT.

microelectronic device See MICROELECTRONIC CIRCUIT.

microelectronics The branch of electronics dealing with extremely small components and circuits fabricated on substrates. Also see INTEGRATED CIRCUIT.

microelectrophoresis Electrophoresis of single particles.

microelectroscope A very sensitive electroscope used to detect minute quantities of electricity.

microelement A tiny component (capacitor, resistor, coil, semiconductor device, or transformer) mounted on a wafer and used in a MICROCIRCUIT.

microelement wafer A microwafer on which a microelement is mounted or deposited.

microfarad Abbreviation, μF. A unit of capacitance equal to 10^{-6} (0.000001) F.

microfarad meter **1.** A dynamometer-type meter that indicates the value of a capacitor directly in microfarads. Such instruments operate from an alternating-current power line. **2.** A direct-reading capacitance meter.

microfiche A method of storing printed information on small film cards. The pages are reduced and arranged in order from left to right and top to bottom. The card is inserted into a projecting machine to allow retrieval of the information. The photographic method is similar to that used in MICROFILM.

microfilm A method of storing printed or photographic information. The pages are reduced and arranged sequentially on a strip of film, usually 35-mm size. The film is inserted into a projecting device for retrieval of the information.

microgalvanometer A highly sensitive GALVANOMETER.

microgauss A magnetic unit equal to 10^{-6} (0.000001) gauss.

microgram A metric unit of weight or mass equal to 10^{-6} (0.000001) gram.

microgroove record A phonograph disc with a very fine groove (200 to 300 per inch), designed for playback at 33⅓ revolutions per minute (rpm).

microhenry Symbol, μH. A unit of inductance, equal to 10^{-6} (0.000001) H.

microhm Symbol, μΩ. A unit of low resistance, reactance, or impedance, equivalent to 10^{-6} (0.000001) ohm.

microhm-centimeter A unit of low resistivity, equal to 10^{-6} (0.000001) ohm-cm. See OHM-CENTIMETER and RESISTIVITY.

microhmmeter An instrument for measuring ultra-low resistance. Such an instrument must have a special provision for canceling the effects of contact and lead resistance.

microinch A unit of linear measure equal to 10^{-6} (0.000001) inch.

microinstruction A machine-code instruction that controls the operation of a computer directly (i.e., it is a "wired-in" instruction, or one set by DIP switches, independent of programs loaded into the machine).

microknowledge In artificial intelligence (AI), detailed machine knowledge. It includes logic rules, computer programs, and data in memory. Compare MACROKNOWLEDGE.

microliter A unit of volume, equal to 10^{-6} (0.000001) liter.

microlock A special form of phase-locked-loop system, used especially with radar to improve the signal-to-noise ratio.

micromanipulator A machine that permits handling tiny parts in very small areas. An example of its use is in placing connections close together in microcircuits.

micrometer **1.** An instrument for measuring very small thicknesses, diameters, etc. **2.** Also called *micron.* The SI unit of length, equal to 10^{-6} (0.000001) meter, or 10^{-3} (0.001) millimeter.

micromho See MICROSIEMENS.

micromicro- See PICO-.

micromicrofarad See PICOFARAD.

micromicrohenry See PICOHENRY.

micromicron A unit of linear measure equal to 10^{-12} meter, or 10^{-6} (0.000001) micrometer.

micromillimeter See NANOMETER.

microminiature Pertaining to an extremely small body, component, or circuit; the last adjective in the sequence of those describing size: *standard*, *small*, *midget*, *miniature*, *subminiature*, and *microminiature.*

micromodule A small, encapsulated circuit, consisting of smaller components. The components

5059F-pM-424-465 4/10/01 9:19 AM Page 446

can be discrete, can consist of integrated circuits, or can be a combination of both. The module is easily removed and replaced by means of a plug-in socket.

micron See MICROMETER.

microphone A transducer that converts sound waves, especially speech and music, into electrical voltage analogs.

microphone amplifier A sensitive, low-distortion, low-noise amplifier used in voice wireless transmitters and public address systems. Most amplifiers of this type have a tailored frequency response, passing audio between about 300 Hz nd 3000 Hz, and attenuating audio outside this a range. The range 300 Hz to 3000 Hz is sufficient to convey intelligible voice signals, and also allows for audio-frequency-shift keying (AFSK) and slow-scan television (SSTV) audio input.

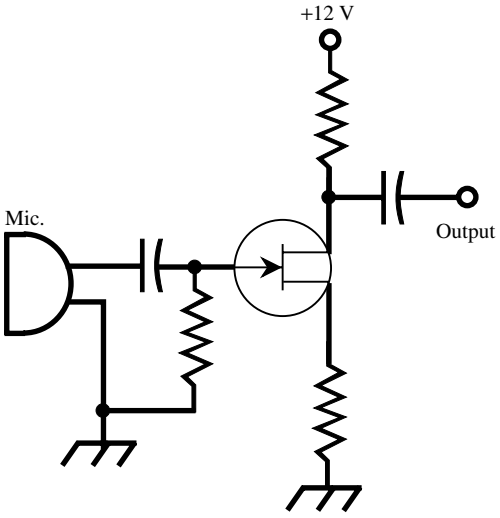

microphone amplifier

microphone boom A device used to hang a microphone, with the base out of the way. It is often used in radio broadcasting.

microphone hummer See HUMMER.

microphone input In an audio amplifier, a jack or other receptacle provided for connection to an external microphone. It can also be used with other low-level audio apparatus. The jack is connected to a MICROPHONE AMPLIFIER that provides high gain with minimum internal noise.

microphone oscillator See HUMMER.

microphonics Ringing (electrical noises) set up by the vibration of a component having loose or movable elements. For example, ringing noises are generated in some circuit boards when they receive a physical blow.

microphonograph A recorder of very low-intensity sound.

microphonoscope An electronic stethoscope, using amplification to enhance the response.

microphotograph An extremely small photograph, often of a pattern or mask used in producing transistors and integrated circuits. Not to be confused with *photomicrograph*, a photograph taken through a microscope.

microphotometer A sensitive instrument for measuring small-area light intensity.

microphysics The branch of physics concerned with atoms, molecules, and subatomic particles.

micropower Extremely small amounts of power—especially the very low direct-current supply power required by some transistors.

microprocessor The integrated circuit (IC), also known as a *chip,* that coordinates the actions of a computer and does the calculations. It is located on the motherboard (sometimes called the *logic board*). These devices get more powerful every year. Physically, this translates to an increasing number of digital switching transistors per chip. The number of digital switches that can be fabricated onto a semiconductor chip of a particular size is ultimately limited by the structure of matter. Compare MICROCOMPUTER.

microprogram **1.** In computer operations, a routine of microinstructions that provides a computer a specific function, independent of those established by programs being run or by the monitor program. Also see MICROINSTRUCTION. **2.** In the direction of a computer, use of a routine that is stored specifically in the memory, instead of elsewhere.

microprogramming In the direction of a computer, the use of a routine that is stored specifically in the memory, instead of elsewhere.

micropulsation Also called *micropulse.* A pulse of extremely short duration.

microradiometer A sensitive detector of heat and infrared radiation, consisting essentially of a thermopile carried by the moving coil of a galvanometer.

microrutherford A unit of radioactivity equal to one disintegration per second or 10^{-6} (0.000001) rutherford. Also see RUTHERFORD.

microsecond A unit of time measure equal to 10^{-6} (0.000001) second.

microsiemens A unit of conductance equal to 10^{-6} (0.000001) siemens.

microspectrophotometer An extremely sensitive spectrophotometer for examining light from tiny areas.

microstrip A microwave component that is, in effect, a single-wire transmission line operating above ground.

microsyn A device that translates rotational position into an electrical signal. Similar to a SELSYN. It is used for such purposes as rotator-direction reading.

5059F-pM-424-465 4/10/01 9:19 AM Page 447

microsystems electronics The technology of electronic systems using tiny electronic components. Also see INTEGRATED CIRCUIT, MICROELECTRONIC CIRCUIT, MICROELEMENT, MICROELEMENT WAFER, and MICROWAFER.

microvolt A unit of low voltage, equal to 10^{-6} (0.000001) volt.

microvolter An accurate, external attenuator (usually for an audio signal generator) providing stepped and continuously variable output in microvolts and millivolts.

microvoltmeter A usually direct-reading instrument used to measure voltages in the microvolt range. An input amplifier boosts the test voltage sufficiently to deflect the indicating meter.

microvolts per meter A unit of radio-frequency (RF) field strength. It refers to the RF voltage (in microvolts) between an antenna and ground, divided by the height of the antenna (in meters) above ground. Compare MILLIVOLTS PER METER.

microvolts per meter per mile A means of expressing absolute radio-frequency (RF) field strength. Generally, the numerical value is based on the field strength, in MICROVOLTS PER METER, at a distance of 1 statute mile (5280 feet) from the source.

microwafer A wafer of insulating material, such as a ceramic, on which one or more microelements are mounted and terminals deposited or plated.

microwatt A unit of low power, especially electrical power, equal to 10^{-6} (0.000001) watt.

microwattage See MICROPOWER.

microwattmeter An instrument for measuring power in the microwatt range. Such an instrument obtains its sensitivity from a built-in input amplifier.

microwave See MICROWAVES.

microwave security system A circuit using microwave radio-frequency energy to detect intruders. When an object moves within the field, the intensity of the field changes at one or more pickup sensors, triggering an alarm.

microwave acoustics See ACOUSTOELECTRONICS and ACOUSTIC DELAY LINE.

microwave dish A dish antenna for use at microwave frequencies.

microwave early warning Abbreviation, MEW. A high-power early warning radar system that affords large traffic-handling capacity and long range.

microwave filter A bandpass filter built into a waveguide for use at microwave frequencies.

microwave frequencies The general expression for radio frequencies above the ultra-high range, that is, 3 GHz or more, but below the frequencies of infrared energy. This corresponds to radio wavelengths of 10 centimeters or less.

microwave integrated circuit Abbreviation, MIC. An integrated circuit designed for use at microwave frequencies.

microwave lens See WAVEGUIDE LENS.

microwave mirror A reflector of microwaves.

microwave oven A device consisting essentially of a radio-frequency heater using a magnetron oscillator. It produces microwave energy that causes heating of certain substances via excitation of the molecules.

microwave plumbing Collectively, the waveguides, tees, elbows, and similar fixtures and connections used in microwave setups.

microwave radio relay The use of microwaves to relay radio, television, and control signals from point to point.

microwave refractometer An instrument using microwaves (around 10 GHz) to measure the refractive index of the atmosphere.

microwave region See MICROWAVE FREQUENCIES and MICROWAVES.

microwave relay See MICROWAVE RADIO RELAY.

microwave relay system A series of microwave transmitter-receiver stations for relaying communications in several line-of-sight hops.

microwaves Radio-frequency electromagnetic energy at wavelengths shorter than about 10 centimeters, but longer than the wavelengths of infrared energy. See also MICROWAVE FREQUENCIES.

microwave spectrum See MICROWAVE FREQUENCIES and MICROWAVES.

microwave transistor A transistor whose semiconductor properties and special fabrication enable it to operate at microwave frequencies.

microwave tube A KLYSTRON, MAGNETRON, or similar tube, used to generate or amplify microwave radio-frequency signals.

midband Abbreviation, MB. The region whose limits are immediately above and below a MIDFREQUENCY; the limits are usually specified for a particular case.

midband frequency See MIDFREQUENCY.

midfrequency The center frequency in a specified band of frequencies.

midget Of reduced size (smaller than *small* and larger than *miniature*).

MIDI Acronym for MUSICAL INSTRUMENT DIGITAL INTERFACE.

midpoint voltage The voltage at the terminals of a cell or battery when it has been discharged halfway (i.e., when the amount of energy used up is equal to the amount of energy remaining).

midrange Pertaining to audio frequencies in the middle of the human hearing range, where the ear is the most sensitive. These frequencies lie between the BASS and TREBLE.

midrange horn A MIDRANGE SPEAKER equipped with a flared horn to give the device a unidirectional sound-emission pattern. It is used primarily in high-power systems and by popular music bands or high-end audio enthusiasts.

midrange speaker A loudspeaker operating most efficiently at frequencies in the middle of the

5059F-pM-424-465 4/10/01 9:19 AM Page 448

audio spectrum. Such a speaker is intermediate in performance between a WOOFER and a TWEETER.

midsection The center section of a multisection filter having an odd number of sections; thus, the second section of a three-section filter.

migration See ION MIGRATION.

mike **1.** See MICROPHONE. **2.** See MICROFARAD. **3.** See MICROMETER.

MIL Abbreviation of *military.*

mil **1.** A small unit of linear measure; 1 mil = 10^{-3} (0.001) inch = 0.0254 mm. **2.** Thousand, as in *n* parts per mil.

mile Abbreviation, m or mi. A large unit of linear measure, 1 mi = 1.609 km = 5280 feet.

military robot A robot designed and used for the purpose of executing some task in warfare. The two general types are: human-operated and computer-controlled. An example of a human-operated military robot is an aircraft that is flown by remote control by a ground-based pilot. The same robot, or a whole fleet of them, might be flown by a computer using sophisticated EXPERT SYSTEMS.

mill A telegraph operator's typewriter.

Miller oscillator A crystal oscillator circuit in which the crystal is connected between the control electrode and ground. The tuned tank is connected in the output circuit. The internal capacitance of the active device provides feedback coupling. Sometimes called *conventional crystal oscillator.*

milli- Abbreviation, m. A prefix meaning thousandth(s): 10^{-3} (0.001).

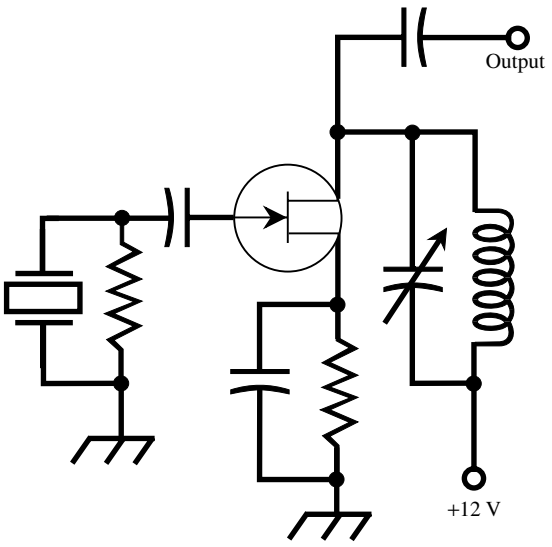

Miller oscillator

milliammeter A usually direct-reading instrument for measuring current in the milliampere range. Also see CURRENT METER.

milliampere Abbreviation, mA. A unit of current equal to 10^{-3} (0.001) ampere.

milliampere-hour Abbreviation, mAh. A unit of low current drain or charging rate, equal to 10^{-3} (0.001) ampere-hour. Also see AMPERE-HOUR and BATTERY CAPACITY.

millibar Abbreviation, mb. A unit of low pressure equal to 10^{-3} (0.001) bar or = 100 pascals.

millicurie Abbreviation, mCi. A small unit of radioactivity equal to 3.71×10^{7} disintegrations per second, or 10^{-3} (0.001) curie. Also see CURIE.

millifarad Abbreviation, mF. A seldom-used unit of capacitance, equal to 10^{-3} (0.001) farad or 1000 microfarads.

milligram Abbreviation, mg. A metric unit of weight equal to 10^{-3} (0.001) gram.

millihenry Abbreviation, mH. A unit of inductance, equal to 10^{-3} (0.001) henry.

millihorsepower Abbreviation, mhp. A unit of power equal to 10^{-3} (0.001) horsepower or 0.746 watt. Also see HORSEPOWER.

millilambert Abbreviation, mL. A small unit of brightness equal to 10^{-3} (0.001) lambert.

milliliter Abbreviation, ml. A metric unit of volume equal to 10^{-3} (0.001) liter.

millimaxwell Abbreviation, mMx. A small unit of magnetic flux equal to 10^{-3} (0.001) maxwell or 10^{-11} weber.

millimeter Abbreviation, mm. A metric unit of linear measure equal to 10^{-3} (0.001) meter or 0.03937 inch.

millimeter equivalent The number of millimeters equal to a given English measure fraction (e.g., the millimeter equivalent of $\frac{5}{16}$ inch is 7.937).

millimeter waves Wavelengths between 0.6 and 10 mm (frequencies from 30 to 500 GHz).

millimicro See NANO-.

millimicrofarad See NANOFARAD.

millimicrohenry See NANOHENRY.

millimicron Abbreviation, mm. A unit of wavelength equal to 10^{-3} micron or one nanometer (10^{-9} meter).

millimilliampere See MICROAMPERE.

millimole Abbreviation, mmol. A unit in chemistry equal to 10^{-3} (0.001) mole.

milliohm A small unit of resistance, reactance, or impedance, equal to 10^{-3} (0.001) ohm.

milliohmmeter An ohmmeter for measuring resistances in the milliohm range.

million electronvolt(s) See MEGAELECTRONVOLT.

milliphot A unit of illumination equal to 10^{-3} (0.001) phot.

millipuffer See PUFFER.

milliradian Abbreviation, mrad. A unit of angular measure equal to 10^{-3} (0.001) radian.

milliroentgen Abbreviation, mr. A small unit of radioactive dosage; 1 mr = 10^{-3} (0.001) roentgen = 2.57976×10^{-7} Ci/kg.

5059F-pM-424-465 4/10/01 9:19 AM Page 449

millirutherford Abbreviation, mrd. A small unit of radioactivity equal to 1000 disintegrations per second; 1 mrd = 10^{-3} (0.001) rutherford.

millisecond Abbreviation, ms or msec. A small unit of time equal to 10^{-3} (0.001) second.

millitorr Abbreviation, mT. An obsolete unit of low pressure equal to 10^{-3} (0.001) torr, or 0.133322 pascal. Also see TORRICELLI.

millivolt Abbreviation, mV. A unit of voltage equal to 10^{-3} (0.001) volt.

millivoltmeter A usually direct-reading instrument for measuring low electric potential. Its sensitivity is provided by a high-gain amplifier operated ahead of the indicating meter.

millivolt potentiometer Abbreviation, MVP. A potentiometer-type null instrument for accurately measuring small direct-current voltages, such as those delivered by a thermocouple. Also see POTENTIOMETRIC VOLTMETER.

millivolts per meter Abbreviation, mV/m. A unit of radio-frequency (RF) field strength. It refers to the RF voltage (in millivolts) developed between an antenna and ground, divided by the height (in meters) of the antenna above ground. Compare MICROVOLTS PER METER.

milliwatt Abbreviation, mW. A unit of power equal to 10^{-3} (0.001) watt.

milliwattmeter An instrument for measuring power in milliwatts. Such instruments usually obtain their sensitivity from a built-in preamplifier.

Mills cross A radio-telescope antenna, consisting of two collinear or phased arrays with a common intersecting lobe. The result is high resolution.

mil-spec security See LEVEL-3 SECURITY.

min **1.** Abbreviation of MINIMUM. **2.** Abbreviation of MINUTE.

mineral An element or compound that occurs naturally in the earth's crust. Most minerals are crystalline and many of these have found use in electronics. Some have been produced artificially.

mineral oil A natural liquid insulant derived from petroleum. Dielectric constant, 2.7 to 8.0. Power factor, 0.08 to 0.2 percent at 1 kHz.

mineral-oil capacitor An oil capacitor whose paper dielectric has been impregnated with mineral oil, which is also the filler.

miniature Very small (smaller than midget and larger than subminiature).

miniature cell An electrochemical cell of very small size (e.g., a *button cell* of the kind used in cameras and watches).

miniaturization The technology of minimizing the physical size of a circuit or system, while maintaining its ability to accomplish a given task.

minicalculator A pocket-size electronic calculator.

minicomputer General term for a computer that is more sophisticated than a MICROCOMPUTER, but less powerful than a MAINFRAME.

mini connector A jack or plug having two or three conductors, and measuring ⅛ (0.125) inch in diameter. It is commonly used with audio equipment.

minifloppy A smaller than standard flexible magnetic disk (floppy).

minima Points along a curve at which a function reaches a local minimum value. Also see MAXIMA AND MINIMA.

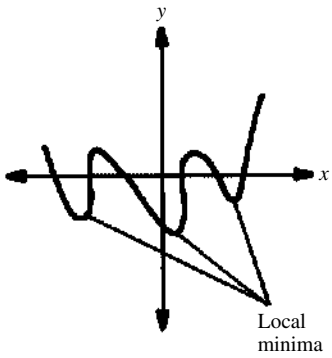

minima

minimum Abbreviation, min. The smallest value in a range or set. Also see MAXIMA AND MINIMA.

minimum detectable signal A signal whose intensity is just higher than the threshold of detection.

minimum discernible signal Abbreviation, MDS. The lowest input-signal amplitude that will produce a discernible output signal in a radio receiver.

miniscope A very-small-sized, lightweight oscilloscope.

minitrack A system used to track an earth satellite, using signals transmitted to the satellite by a line of ground radio stations.

minometer A radioactivity-measuring instrument composed of an ionization chamber and a string galvanometer.

minor beats Secondary or extraneous beats produced in a beat-note system, caused by various sum and difference frequency byproducts of the heterodyne process. Compare MAJOR BEATS.

minor bend A bend in a rectangular waveguide, made without twisting.

minor cycle See WORD TIME.

minor face In a hexagonal quartz crystal, one of the three smaller faces. Compare MAJOR FACE.

minority carrier The type of charge carrier present in relatively small numbers in a processed semiconductor material. Electrons are minority carriers in p-type material; holes are minority carriers in n-type material. Compare MAJORITY CARRIER.

minor lobe In a directional antenna system, any lobe other than the main lobe(s). Such a lobe represents reduced sensitivity and/or power gain

5059F-pM-424-465 4/10/01 9:19 AM Page 450

relative to the main lobe. Also see MAIN LOBE, SIDE LOBE.

minor loop A subordinate path for the circulation of information or control signals in an electronic system (e.g., *minor feedback loop*). Compare MAJOR LOOP.

minute **1.** Abbreviation, min. A unit of measure of time equal to 60 seconds or ⅙₀ hour. **2.** Also called *minute of arc.* Symbol (′). A unit of arc measure equal to ⅙₀ angular degree or 60 seconds. **3.** General term meaning "extremely small."

MIR Abbreviation of *memory-information register.*

mirror **1.** A device consisting chiefly of a highly polished or silvered surface that reflects a large part of the radiation (such as light) striking it. **2.** Radar-interference material (see CHAFF). **3.** To reflect, as by a mirror.

mirror galvanometer A galvanometer in which a mirror is moved by the coil. The mirror either reflects a spot of light along an external scale, or it reflects the scale, which is then read through a small telescope.

mirror-galvanometer oscillograph See ELECTROMECHANICAL OSCILLOSCOPE.

mirror image **1.** An image or curve that is exactly reversed relative to a straight line or flat plane, compared to a reference image or curve. Compare BILATERAL SYMMETRY. **2.** For a quarter-wave Marconi antenna, the extra quarter-wave element supplied by the earth. **3.** For an antenna at a distance d above a ground plane, an effective antenna at an equal distance d below the ground plane.

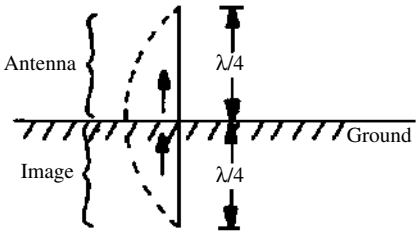

mirror image, 2

mirror-reflection echo A false radar echo or set of echoes, caused by reflection of the radar beam from a plane surface prior to its encountering the target or targets. The beam can also be reflected from one target to another.

mirror-type meter A meter whose movable coil carries a small mirror (rather than a pointer) that reflects a beam of light to produce a spot on a translucent scale.

misaligned head In a tape recorder, a record or a pickup head that is incorrectly oriented, with respect to the passing tape.

misfire Failure of a gas tube or mercury-arc tube to ignite at the correct instant.

misleading precision In electronic calculations and data recording, greater precision than the instruments or conditions justify. Also see SIGNIFICANT FIGURES.

mismatch The condition resulting from joining two circuits, or connecting a line to a circuit, in which the impedances are substantially different.

mismatched impedances Impedances that are unequal, and thus do not satisfy the conditions for maximum power transfer.

mismatch factor For a load not perfectly matched to a driving circuit, the ratio of current flowing in the load to the current that would flow in the load if its impedance were perfectly matched to the output impedance of the driving circuit.

mismatch loss For a load that is mismatched to a source, the ratio P_1/P_2, where P_1 is the power a matched load would absorb from the source, and P_2 is the power actually absorbed by the mismatched load.

mistor A variable-resistance device, used to detect the presence of a magnetic field and to measure magnetic-field strength.

MIT Abbreviation of MASTER INSTRUCTION TAPE.

mix **1.** To produce a beat signal (either the sum or the difference frequency) from two input signals. **2.** The proportion of powdered iron and other inert substances in a ferromagnetic transformer core. Different mixes result in different operating characteristics.

mixdown A method of combining recorded sound from two or more audio tracks, and recording the result onto an audio tape or disc. It is used to create special audio effects.

mixed-base notation A number system in which the base (radix) alternates between two digit positions. Also called *mixed radix notation.*

mixed calculation A mathematical calculation or expression in which more than one operation is used.

mixed modulation Modulation of several kinds coexisting in a system. Thus, a small amount of undesired frequency modulation might accompany amplitude modulation, or vice versa.

mixed number A number having integral (whole) and fractional parts (e.g., 3.14159).

mixer **1.** A device, such as a transistor or semiconductor diode, used to mix two input signals and deliver an output equal to their difference and/or sum (see MIXING). **2.** See AUDIO MIXER. **3.** Any device that combines two or more signals, yielding one output signal whose nature is determined by the characteristics of the circuit.

mixer noise Electrical noise that occurs in a MIXER.

mixing Combining several signals so that some desired mixture of the original signals is obtained. Compare MODULATION.

mixture **1.** A combination of two or more signals that retain their characteristics—even when they interact to produce beat-frequency products. **2.** A

5059F-pM-424-465 4/10/01 9:19 AM Page 451

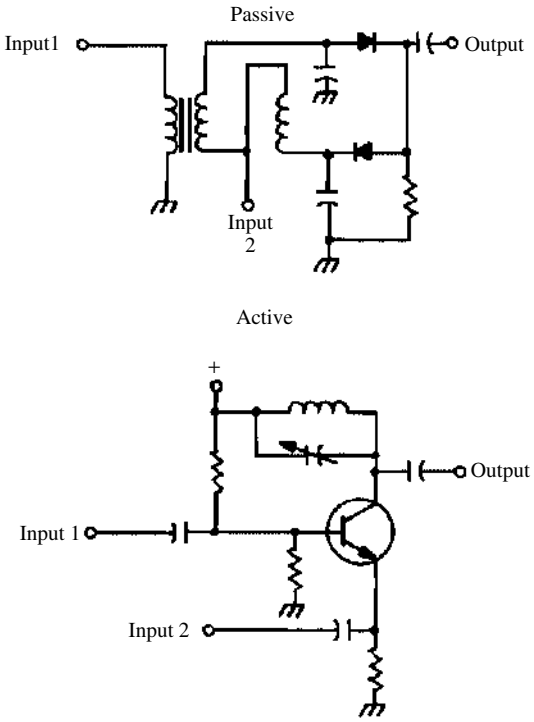

mixer

diffusion of one substance throughout another, without a solution or a chemical reaction resulting.

mixture melting point Abbreviation, mmp. The temperature at which a mixture of solid substances starts turning into a liquid at 1 atmosphere of pressure. This melting point depends upon the melting points of the substances and their relative concentration in the mixture. Also see MELTING POINT and MIXTURE.

mks Abbreviation of METER-KILOGRAM-SECOND.

mL Abbreviation of MILLILAMBERT.

ml Abbreviation of MILLILITER.

mm Abbreviation of MILLIMETER.

mmf Abbreviation of MAGNETOMOTIVE FORCE.

mmol Abbreviation of MILLIMOLE.

mmp Abbreviation of MIXTURE MELTING POINT.

mmv Abbreviation of MONOSTABLE MULTIVIBRATOR.

Mn Symbol for MANGANESE.

m_n Symbol for MASS OF NEUTRON AT REST.

mnemonic **1.** Pertaining to MEMORY or to memory systems. **2.** A memory code or device.

mnemonic code In computer operations, a programming code, such as assembly language, that, although easily remembered by the programmer, requires subsequent conversion to machine language.

mntr Abbreviation of MONITOR. (Also, mon.)

MO Abbreviation of MASTER OSCILLATOR.

Mo Symbol for MOLYBDENUM.

mobile communications **1.** Radio communications between or among stations on board moving or stationary land, waterborne, or airborne vehicles. **2.** Radio communications between at least one fixed station and one or more moving or stationary land, waterborne, or airborne stations.

mobile radio service See MOBILE COMMUNICATIONS.

mobile receiver A radio, television, or other receiver aboard a moving or stationary land, waterborne, or airborne vehicle.

mobile-relay station A fixed station that receives a signal from a MOBILE STATION and retransmits it to one or more other mobile stations.

mobile station A station installed and operated aboard a moving or stationary vehicle. The vehicle might be on land, under water, or in the air. Compare PORTABLE STATION.

mobile transmitter A radio, television, or other transmitter aboard a moving or stationary vehicle. The vehicle might be on land, under water, or in the air.

mobility See CARRIER MOBILITY.

mockup See DUMMY, **1**.

mod **1.** Abbreviation of MODULATOR. **2.** Abbreviation of MODULUS. **3.** Abbreviation of MODIFICATION.

mode **1.** One of the ways a given resonant system can oscillate. **2.** One of the ways that electromagnetic energy can be propagated through a device or system. See MODES OF PROPAGATION. **3.** The method via which intelligence is conveyed in a communications or broadcast signal. See EMISSION MODE. **4.** Resonance of sound waves within an acoustic chamber.

mode coupling The exchange or interaction of energy between identical modes (see MODE, **1**, **2**).

mode filter A waveguide filter that separates waves of different propagation mode, but of the same frequency (see MODES OF PROPAGATION).

model **1.** A working or mockup version of a circuit, system, or device, illustrative of the final version. **2.** A mathematical representation of a process, device, circuit, or system. Example: the Rutherford model of the atom.

modeling The creation of an object in three-dimensional computer graphics.

modem See MODULATOR-DEMODULATOR.

mode purity In a modulated radio-frequency signal, the condition in which no undesirable types of modulation exist. For example, a frequency-modulated signal in which there is zero amplitude modulation.

moderator A substance, such as graphite or heavy water, used to slow neutrons in an atomic reactor. Also see ACCELERATOR, **1** and REACTOR, **2**.

5059F-pM-424-465 4/10/01 9:19 AM Page 452

modes of propagation The configurations in which microwave energy can be transmitted through a WAVEGUIDE.

modes of resonance In a microwave cavity, the configurations in which resonant oscillation can exist, depending on the way the cavity is excited.

modification **1.** Changing the configuration of a circuit, device, or system, usually to a minor extent, to tailor its characteristics for a specific purpose. **2.** Changing some aspect of a signal for a specific purpose (e.g., reducing the emission bandwidth to allow more signals to fit within a given band of frequencies). **3.** In computer operations, changing program addresses and instructions by performing logic and arithmetic on them, as if they were data. Also see PROGRAM MODIFICATION.

modified alternate mark inversion A signal that is similar to alternate mark inversion (AMI), but contains certain differences that are specified by a rigorous set of standards for the particular signal.

modifier A data item used to change a computer program instruction so that it can be used to implement different successive operations. Also see PROGRAM MODIFICATION.

modifier register See INDEX REGISTER.

modify To perform a MODIFICATION to a circuit, device, system, signal, program address, etc.

moding A fault characterized by oscillation of a MAGNETRON in undesirable modes.

modular technique See BUILDING-BLOCK TECHNIQUE.

modulated amplifier A usually high-frequency amplifier whose output is varied in some way for the purpose of conveying intelligence. Compare MODULATED OSCILLATOR. In the amplitude modulation of an amplifier, there is little or no disturbance of the carrier frequency. Also see MODULATION.

modulated beam **1.** An electron beam (as in a cathode-ray tube), whose intensity is varied by a desired signal. **2.** A light beam whose intensity is varied for communications or control purposes.

modulated carrier A carrier wave whose amplitude, frequency, or phase is varied to convey intelligence.

modulated continuous wave Abbreviation, mcw. A high-frequency carrier wave modulated by a continuous, lower-frequency wave, as in MCW telegraphy.

modulated CW See MODULATED CONTINUOUS WAVE.

modulated electron beam See MODULATED BEAM, **1**.

modulated light beam See MODULATED BEAM, **2**.

modulated oscillator A usually high-frequency oscillator whose output is varied in some way to convey intelligence. Compare MODULATED AMPLIFIER. Also see MODULATION.

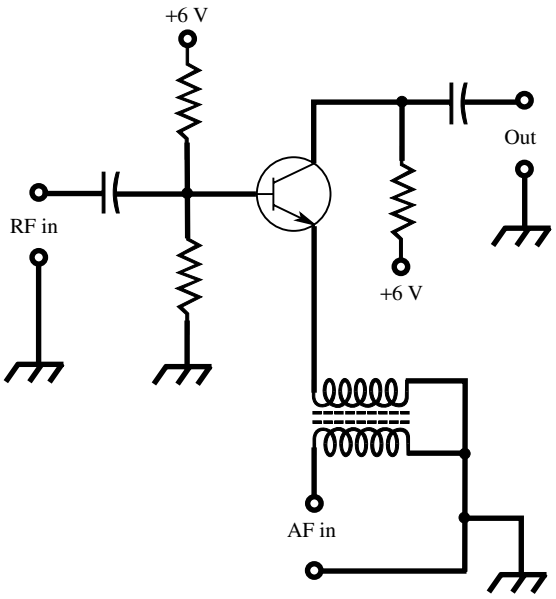

modulated amplifier

modulated-ring pattern See GEAR-WHEEL PATTERN and SPOT-WHEEL PATTERN.

modulated stage A transmitter, amplifier, or oscillator in which the signal information is impressed on the carrier.

modulated wave See MODULATED CARRIER.

modulatee A stage or circuit upon which modulation is impressed (e.g., a MODULATED AMPLIFIER or a MODULATED OSCILLATOR).

modulating electrode **1.** In an oscilloscope, an electrode (usually the intensity electrode) to which a signal can be applied to intensity-modulate the electron beam. **2.** In a cathode-ray tube, the electrode to which the video signal is applied.

modulating signal Intelligence that modulates a carrier (e.g., binary data in radioteletype, or music in broadcasting).

modulation Combining two signals with the result that some aspect of one signal (the carrier) is varied by and in sympathy with the other (the modulating signal). Usually, the carrier has a frequency considerably higher than that of the modulating signal.

modulation bars A form of television interference in which an amplitude-modulated signal causes horizontal bars, alternating light and dark, to appear on the picture screen. The higher the modulating frequency, the closer together the bars appear. In severe cases, the bars completely obliterate the picture.

modulation capability The maximum percentage of modulation a transmitter will permit before

5059F-pM-424-465 4/10/01 9:19 AM Page 453

modulation bars

nonlinearity occurs. Also see MODULATION LINEARITY.

modulation characteristic For an amplitude-modulated wave, the ratio of the instantaneous amplitude of the modulated signal to the instantaneous modulating voltage.

modulation code In a modulated transmitter, a system of modulation in which certain signal variations or pulses represent particular characters. Examples are ASCII, BAUDOT CODE, and MORSE CODE.

modulation coefficient Symbol, *m*. A figure expressing the depth (extent) to which a signal is amplitude-modulated. For a signal in which the upward modulation is equal to the downward modulation, $m = (E_m - E_c)/E_c$, where E_c is the peak-to-peak voltage of the unmodulated signal, and E_m is the peak-to-peak voltage of the modulated signal. For full (100%) modulation, $m = 1$.

modulation depth See DEPTH OF MODULATION.

modulation distortion **1.** In a modulated signal, envelope distortion introduced by the modulation process or by the receiver circuit. **2.** External cross modulation (see CROSS MODULATION, **1**).

modulation envelope See ENVELOPE, **1**.

modulation-envelope distortion Undesirable distortion in the ENVELOPE of the modulating intelligence in an amplitude-modulated or single-sideband signal at the output of a radio transmitter.

modulation factor See MODULATION COEFFICIENT.

modulation frequency Abbreviation, f_m. The frequency of a modulating signal.

modulation linearity In a modulated signal, the degree to which the instantaneous signal amplitude or frequency follows the instantaneous amplitude of the modulating signal.

modulation meter See PERCENTAGE-MODULATION METER.

modulation monitor **1.** A linear detector with a pickup coil (or antenna) and headphones for listening to an amplitude-modulated signal. **2.** See PERCENTAGE-MODULATION METER. **3.** A device that displays the modulation characteristics of a signal (e.g., the envelope for amplitude modulation and single sideband or the frequency-vs. time function for frequency modulation).

modulation noise See NOISE BEHIND THE SIGNAL.

modulation percentage A measure of the extent to which a signal is amplitude modulated. It is expressed as the MODULATION COEFFICIENT multiplied by 100.

modulation ratio For a modulated signal, the quotient M_r/M_i, where M_r is the percentage of radiated-signal modulation, and M_i is the percentage of current modulation.

modulator A device or circuit for modulating a carrier.

modulator cell See KERR CELL.

modulator crystal A transparent piezoelectric crystal to which a signal voltage can be applied to modulate a beam of polarized light passing through it.

modulator-demodulator Also called *modem*. **1.** A device that converts binary data to audio-frequency-shift-keyed (AFSK) analog signals, and vice-versa. It is commonly used to interface computers and terminals with telephone lines and radio transceivers. **2.** A circuit or device, such as a

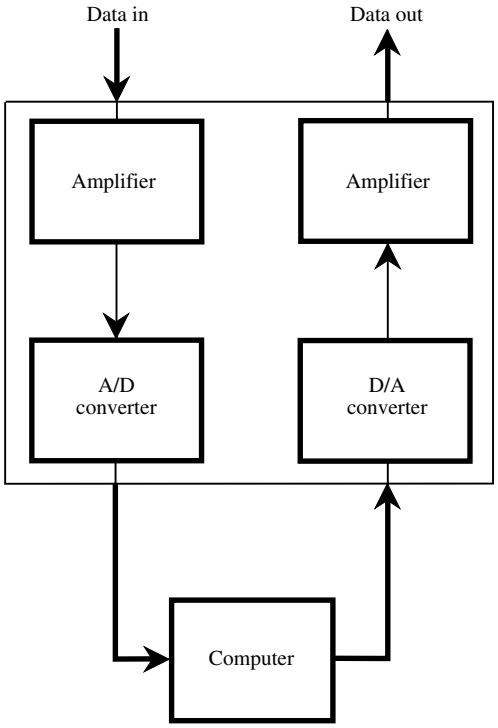

modulator-demodulator

5059F-pM-424-465 4/10/01 9:19 AM Page 454

biased diode or diode bridge, that can perform either modulation or demodulation.

modulator driver An amplifier stage that delivers excitation current, voltage, or power to a modulator stage.

module An assembly containing a complete self-contained circuit (or subcircuit), often miniaturized and made for plug-in operation.

modulometer Any instrument, such as a percentage-modulation meter, used to measure the degree of modulation of a signal. Often, it can also measure other signal characteristics (e.g., carrier shift, extraneous amplitude modulation, and extraneous frequency modulation).

modulo n check In computer operations, a technique for verifying the validity of a number used as an operand. The number being so checked is divided by another number to provide a remainder (check digit) that goes with the number. After the number is, for example, transmitted through some part of a computer system, it is again divided by the original divisor, and if the remainder is the check digit, the data has retained its integrity.

modulus **1.** Absolute magnitude. Also see ABSOLUTE VALUE and IMPEDANCE. **2.** Abbreviation, mod. In computer operations, a whole number that indicates the number of states a counter sequences through in each cycle. **3.** Abbreviation, mod. A number (constant or coefficient) expressing the degree to which some property is possessed by a material or body (e.g., *modulus of elasticity*, *shear modulus*, and *bulk modulus*). **4.** A constant by which a logarithm to one base must be multiplied to obtain a logarithm of the same number to another base.

modulus of elasticity The stress-to-strain ratio in a material under elastic deformation.

moire In a television or facsimile picture, an effect produced by the convergence of straight lines. When the lines are nearly parallel to the scanning lines, the converging lines appear irregular.

moisture meter See ELECTRIC HYGROMETER and ELECTRONIC HYGROMETER.

mol Abbreviation of MOLE.

molar conductance See MOLECULAR CONDUCTANCE.

molar polarization Any molecule in an electric field undergoes a small displacement of the positive and negative electrical centers. This results in an electric dipole.

molar solution A solution, such as an electrolyte, containing 1 mol of solute per liter of solvent. Compare NORMAL SOLUTION.

mold **1.** To form matter into a desired shape, as by pouring liquefied material into a container or liquefying the material in the container, then allowing the liquid material to solidify. In *hot molding*, the material is melted in the container and then cooled to hardness; in *cold molding*, the material is shaped without heat and it solidifies with time. **2.** The hollow container used to shape a material, as in **1**.

molded capacitor A capacitor that is molded into a protective body of insulating material. Also see MOLD, **1**, **2** and MOLDED COMPONENT.

molded ceramic capacitor A ceramic-dielectric capacitor enclosed in a molded housing. Also see MOLD, **1**, **2**; MOLDED CAPACITOR; and MOLDED COMPONENT.

molded coil See MOLDED INDUCTOR.

molded component A part (such as a capacitor, coil, or resistor) that is completely enclosed in a protective material (such as a plastic) that is molded around it. Also see MOLD, **1**, **2**.

molded electrolytic capacitor A solid-dielectric electrolytic capacitor enclosed in a molded housing. Also see MOLD, **1**, **2**; MOLDED CAPACITOR; MOLDED COMPONENT; and SOLID-ELECTROLYTIC CAPACITOR.

molded glass capacitor A glassplate-dielectric capacitor enclosed in a molded glass housing. Also see GLASS CAPACITOR; MOLD, **1**, **2**; MOLDED CAPACITOR; and MOLDED COMPONENT.

molded inductor An inductor that is molded into a protective housing of insulating material. Also see MOLD, **1**, **2** and MOLDED COMPONENT.

molded mica capacitor A mica-dielectric capacitor enclosed in a molded housing. Also see MICA CAPACITOR; MOLD, **1**, **2**; MOLDED CAPACITOR; and MOLDED COMPONENT.

molded mud A molding compound that has inferior electrical characteristics. Also see MOLD, **1**, **2** and MOLDED COMPONENT.

molded paper capacitor A paper-dielectric capacitor enclosed in a molded housing. Also see MOLD, **1**, **2**; MOLDED CAPACITOR; MOLDED COMPONENT; and PAPER CAPACITOR.

molded porcelain capacitor A capacitor enclosed in a body of molded porcelain. Also see MOLD, **1**, **2**; MOLDED CAPACITOR; MOLDED COMPONENT; and PORCELAIN.

molded resistor A resistor that is molded in a protective housing of insulating material. Also see MOLD, **1**, **2** and MOLDED COMPONENT.

molded transistor A transistor that is encapsulated in a protective molding compound, such as epoxy resin. Also see MOLD, **1**, **2** and MOLDED COMPONENT.

mole Abbreviation, mol. **1.** The amount of substance in a system containing as many specified entities (atoms, molecules, ions, subatomic particles, or groups of such particles) as there are atoms in 12 grams of carbon 12. **2.** It is also called the *Avogadro constant.* A unit of quantity in chemistry, equal to approximately 6.022×10^{23}.

molectronics See MOLECULAR ELECTRONICS.

molecular circuit See MONOLITHIC INTEGRATED CIRCUIT.

molecular conductance For a solution, such as an electrolyte, the product of specific conductivity

5059F-pM-424-465 4/10/01 9:19 AM Page 455

and the volume (in liters) of a solution that contains 1 gram molecule of the solute. Also see SOLUTE; SOLUTION, **1**; and SOLVENT, **1**, **2**.

molecular conductivity See MOLECULAR CONDUCTANCE.

molecular electronics The technique of processing a single block of material so that separate areas perform the functions of different electronic components. The entire block constitutes a circuit (e.g., a MONOLITHIC INTEGRATED CIRCUIT).

molecular magnets According to the molecular theory of magnetism, the elemental magnets formed by individual molecules.

molecular theory of magnetism Each molecule in a piece of magnetic metal is itself a magnet (possessing a north and a south pole). These tiny magnets are thought to be normally oriented at random, but when the material is magnetized by an external force, they align themselves with each other.

molecular weight Abbreviation, mol wt. In a molecule of a substance, the sum of the atomic weights of the constituent atoms.

molecule The basic particle of a compound; each molecule usually contains two or more atoms. For example, the formula $AgNO_3$ represents silver nitrate, each molecule of which contains one atom of silver (Ag), one atom of nitrogen (N), and three atoms of oxygen (O).

moletronics See MOLECULAR ELECTRONICS.

mol wt Abbreviation of MOLECULAR WEIGHT.

molybdenum Symbol, Mo. A metallic element. Atomic number, 42. Atomic weight, 95.94. It is used in the grids and plates of certain vacuum tubes.

moment The tendency to produce motion around a point, as by torque, or the product of a quantity and the distance to a point. The moment of force is expressed as the product Fd, where F is force and d is distance.

momentary-contact switch A switch that maintains contact only while it is held down. Such a device is usually a *pushbutton switch*, although it might be a *toggle switch*, a *slide switch*, or a *lever switch.*

momentary switching Switching of short duration, often characterized by a quick make and break immediately following activation of the switch. Compare DWELL SWITCHING.

moment of inertia For a torque motor, the inertia of the armature around the axis of rotation. Also see MOMENT.

mon **1.** Abbreviation of MONITOR. **2.** Abbreviation of MONAURAL.

monatomic **1.** Pertaining to a molecule with only one atom. **2.** Pertaining to a molecule with only one replaceable atom or radical.

monatomic molecule A molecule having a single atom (e.g., argon, helium, and neon). Compare DIATOMIC MOLECULE.

monaural **1.** Pertaining to an audio system having one channel. **2.** Pertaining to hearing with one ear, as opposed to BINAURAL.

monaural recorder A single-track recorder, as opposed to a stereophonic recorder.

Monel metal An alloy of nickel (67%), copper (28%), iron, manganese, and other metals (5%). Its resistivity is approximately 42 microhm-centimeters at 20°C.

monimatch An amateur version of the reflected-power meter and SWR meter.

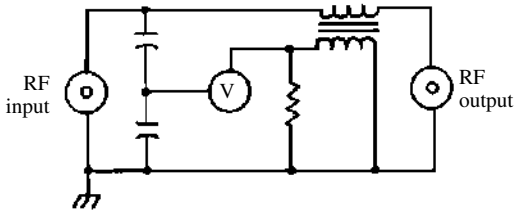

monimatch

moniscope A special cathode-ray tube that produces a stationary picture for testing television equipment. Its name is a contraction of monitor and scope.

monitor **1.** A device that allows the sampling of a signal or quantity. Examples: *line-voltage monitor*, *television monitor*, and *modulation monitor.* **2.** A cathode-ray-tube (CRT) computer display.

monitor head A separate playback head included in some tape recorders for listening to the tape as it is being recorded.

monitoring The act, process, or technique of observing an action while it is in progress or checking a quantity while it is varying. Examples: *carrier monitoring*, *modulation monitoring*, and *line-voltage monitoring.*

monitoring amplifier An auxiliary amplifier used in monitoring an audio-frequency system.

monitoring antenna A usually small pickup antenna used with a signal monitor or monitoring receiver.

monitoring key In a telephone system, a device used to listen to a two-way conversation.

monitoring receiver A radio or television receiver used specifically to monitor a transmission directly.

monitoring station In a security system, a central control location from which personnel can observe the input from sensors, cameras, and other devices at remote locations throughout the secured area.

monitor system A computer program usually stored in the read-only memory (ROM) supplied by the hardware vendor. It controls the implementation of programs written by the user, and the operation of peripherals associated with

5059F-pM-424-465 4/10/01 9:19 AM Page 456

program runs and inputting or outputting data to or from memory. Also called *executive program.*

monkey chatter The characteristic sound of a single-sideband (SSB) signal when the receiver is mistuned, or when the receiver is set for the wrong sideband.

monk's cloth A coarse drapery fabric sometimes used to soundproof the walls and ceiling of a radio studio or recording booth.

mono See MONAURAL.

mono- Prefix meaning *single.*

monobrid circuit An integrated circuit in which either several monolithic IC chips are interconnected to form a larger, single-package circuit, or monolithic IC chips are interwired with thin-film components into a single-package circuit. The name is a contraction of *monolithic hybrid.*

monochromatic **1.** Being of one color (hue) in nature. **2.** Being of a single wavelength in nature (pertaining to radiation of any kind). **3.** Pertaining to black-and-white television.

monochromaticity Consisting of one color of visible light. The brightness can vary from black to maximum.

monochromatic power density At a given temperature, the energy radiated per square centimeter of blackbody surface per second per unit wavelength range. Also see BLACKBODY and BLACKBODY RADIATION.

monochromatic sensitivity Sensitivity to light of one color only.

monochrome television Black-and-white television.

monoclinic crystal A crystal having three axes of unequal length; two of them intersect obliquely and are perpendicular to the third [e.g., the type of crystal found in one form of sulfur (monoclinic sulfur)].

monocrystalline material See SINGLE-CRYSTAL MATERIAL.

monode A one-element device, such as a filament-type lamp, thermistor, voltage-dependent resistor, barretter, etc.

monogroove stereo A method of making a stereophonic phonograph disc in which both channels are recorded as a single groove.

monolayer A thin film having a thickness of one molecule.

monolithic integrated circuit An integrated circuit (IC) formed in a single block or wafer of semiconductor material. The name is derived from the Greek monolithos ("one stone"). Compare HYBRID INTEGRATED CIRCUIT and THIN-FILM INTEGRATED CIRCUIT.

monometallic Containing or using only one metal.

monomolecular film See MONOLAYER.

monophonic recorder See SINGLETRACK RECORDER.

monophonic system A single-channel sound system. Compare STEREO SYSTEM.

monopole antenna See QUARTER-WAVE MONOPOLE.

monopulse In radar and electronic-navigation operations, using one pulse to determine azimuth and elevation simultaneously.

monorange speaker A loudspeaker that reproduces most of the full audio range. Also called *extended range speaker.* Compare TWEETER and WOOFER.

monostable Having one stable state.

monostable blocking oscillator Abbreviation, MBO. A blocking oscillator that behaves somewhat like a one-shot multivibrator. The oscillator delivers a single output pulse each time it receives an input (trigger) pulse.

monostable multivibrator A multivibrator that delivers one output pulse for each input (trigger) pulse. Also called *one-shot circuit* and *single-shot multivibrator.* Compare ASTABLE MULTIVIBRATOR and BISTABLE MULTIVIBRATOR.

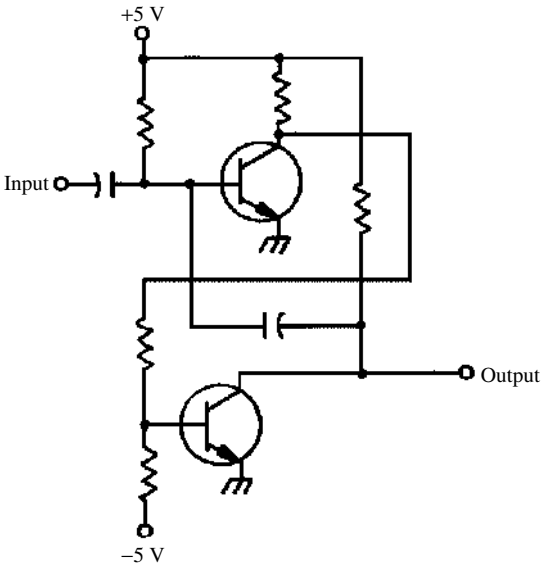

monostable multivibrator

monostatic reflectivity The property whereby, for certain reflectors (such as a tricorner reflector), all incident rays are reflected in exactly the opposite direction from which they arrive.

monotone A sound or series of sounds having a single, constant pitch (frequency).

monotonicity In a digital-to-analog converter, a condition where the output either remains the same or increases for any single increase in the input code.

monovalent See UNIVALENT.

5059F-pM-424-465 4/10/01 9:19 AM Page 457

Monte Carlo method **1.** The use of statistical sampling in the approximate solution of an engineering problem. **2.** In computer operations, the construction of mathematical models from randomly selected components taken from representative statistical populations.

Moog synthesizer An electronic device that can be made to simulate virtually any sound, including that of musical instruments and the human voice, through the use of several audio oscillators, whose output can be controlled to produce tones of various harmonic content, duration, attack, and decay periods.

moonbounce Also called *earth-moon-earth (EME).* Radio communication, usually at very-high frequencies (VHF) or ultra-high frequencies (UHF), in which the moon is used as a passive reflector. This is a popular mode among some amateur radio operators.

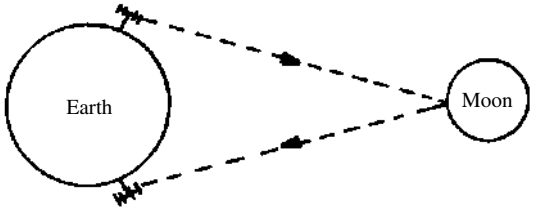

moon bounce

MOPA Abbreviation of MASTER OSCILLATOR/POWER AMPLIFIER.

morphological electronics See MOLECULAR ELECTRONICS.

Morse **1.** See MORSE CODE. **2.** Telegraphy (wire or radio). **3.** To signal by means of the Morse code.

Morse code Either of two similar binary codes used in radio and wire telegraphy. It uses short pulses (dots or dits) and long pulses (dashes or dahs) to represent letters of the alphabet, numerals, and punctuation marks. It usually refers to the CONTINENTAL CODE, but occasionally it refers to the AMERICAN MORSE CODE.

MOS Abbreviation of *metal-oxide-semiconductor.*

mosaic **1.** See PHOTOMOSAIC. **2.** The pattern of tiny photoelectric particles in a television camera tube that convert the image into electric charges.

mosaic crystal A form of imperfect crystal. The defects have certain properties, one of which is to cause additional energy levels in semiconductor materials manufactured from such crystals.

MOS capacitor A capacitor using metal-oxide-semiconductor (MOS) technology. It is used in MOS integrated circuits. A silicon substrate forms one electrode (generally p-type material). An oxide layer forms the dielectric. An electrode forms the other plate of the capacitor. The capacitance might be variable by changing the applied voltage at the metal gate electrode.

MOSFET Abbreviation of METAL-OXIDE-SEMICONDUCTOR FIELD-EFFECT TRANSISTOR.

MOSROM Abbreviation of *metal-oxide-semiconductor read-only memory* (see READ-ONLY MEMORY).

MOST Abbreviation of *metal-oxide-semiconductor transistor.*

most significant character Abbreviation, MSC. In positional number representation, the leftmost character in a significant group, such as a word.

most significant digit Abbreviation, MSD. In a number, the leftmost digit that is not zero (zero being insignificant in this context).

mother **1.** A term or prefix referring to a component that supports (or appears to support) other similar components (e.g., MOTHERBOARD). **2.** A term referring to the source from which samples or components are derived (e.g., MOTHER CRYSTAL). **3.** A mold that has been electroformed from a master phonograph disc.

motherboard In a computer or data-processing device, the circuit board on which most of the main circuitry is mounted.

mother crystal A natural quartz crystal from which is produced the piezoelectric plates and other components used in electronics.

motion detector A device for sensing the movement or stopping of a body, such as a rotating shaft. Various sensors are used in different detectors: magnetic, photoelectric, capacitive, etc.

motion frequency The natural frequency (especially that of oscillation) of a servo.

Motion Picture Experts Group Abbreviation, MPEG. A data-compression standard used for animated digital video. It is useful in computer videoconferencing and telecommuting, and for the development of multimedia presentations.

motion-picture pickup In television operations, a camera (and the technique for using it) for picking up scenes directly from motion-picture film.

motion sensor In security systems, a set of devices that produces an output signal whenever anything moves within a certain area. Such equipment might use infrared, ultrasound, microwaves, capacitive effects, thermal sensors, air-current detectors, sound detectors, video cameras, or a combination of these.

motor **1.** A machine for converting electrical energy into mechanical energy. **2.** The driving mechanism of a loudspeaker.

motorboard The basic mechanism of a tape recorder, embodying motor, flywheel, capstan, rollers, etc., assembled on a board or panel.

motorboating A repetitive, low-frequency popping or puffing noise sometimes observed in malfunctioning audio circuits. It was so named because of its resemblance to the sound of a motorboat.

motorboating filter In an audio amplifier circuit, a simple filter installed to prevent

5059F-pM-424-465 4/10/01 9:19 AM Page 458

MOTORBOATING caused by unwanted positive feedback. Also see DECOUPLING FILTER.

motor capacitor See MOTOR-RUN CAPACITOR and MOTOR-START CAPACITOR.

motor constant The ability, expressed numerically, of a torque motor to convert electric input power into torque.

motor converter An electromechanical device for converting alternating current to direct current.

motor-driven relay An electromechanical relay whose contacts are opened and closed by a rotating motor.

motor effect Magnetic force between adjacent current-carrying conductors.

motor-generator A combination of motor and generator in a single machine assembly. A common arrangement is a low-voltage motor turning a high-voltage generator. The machine shafts can be coupled, or the motor can turn the generator through a belt, chain, or gear train.

motor meter A meter in which the movable element is essentially a continuously rotating motor. See, for example, KILOWATT-HOUR METER.

motor-run capacitor A power-factor-boosting capacitor connected (together with its auxiliary winding) in parallel with the main winding in an induction motor. Also see CAPACITOR MOTOR.

motor-speed control A method of controlling the speed of a motor by varying the magnitude and/or phase of its current. Electronic devices usually use diode, diac, or triac circuits.

motor-start capacitor A capacitor that, with an auxiliary winding, is switched into a motor circuit during the starting period, and is automatically disconnected (with the winding) after the motor reaches normal running speed. Also see CAPACITOR MOTOR.

motor starter See STARTING BOX.

mould See MOLD.

mount **1.** A mechanical device with which a component is attached to a circuit board or chassis. **2.** The attachment of a circuit board to a chassis. **3.** The hardware with which an antenna is attached to a mast. **4.** The hardware with which a microphone is attached to a boom or other support. **5.** In general, any attaching hardware.

Mountain standard time Abbreviation, MST. Local mean time at the 105th meridian west of Greenwich. Also see GREENWICH MEAN TIME, STANDARD TIME, TIME ZONE, and COORDINATED UNIVERSAL TIME.

mounting flange The portion of a speaker frame, usually made of metal, that is equipped with holes for attachment to a cabinet or panel.

mouse A pointing device commonly used with personal computers. It is about the size of a candy bar. The computer operator moves the display pointer or cursor by sliding the mouse on a flat surface. Functions and commands are executed by pressing a button (clicking) on the device.

mouth The radiating end of a horn (antenna, loudspeaker, etc.).

MOV Abbreviation of METAL-OXIDE VARISTOR.

movable-coil meter See D'ARSONVAL METER.

movable-coil modulator See ELECTROMECHANICAL MODULATOR.

movable contact The traveling contact in a relay or switch. Compare FIXED CONTACT.

movable-iron meter See IRON-VANE METER.

movies on demand In television, a system that makes it possible for subscribers to choose the programs they want to see, and also to choose the viewing times for the programs.

moving-coil galvanometer A galvanometer whose movable element is a coil of fine wire suspended or pivoted between the poles of a magnet.

moving-coil microphone See DYNAMIC MICROPHONE.

moving-coil motor The driving mechanism of a moving-coil DYNAMIC SPEAKER.

moving-coil pickup See DYNAMIC PICKUP.

moving-coil speaker See DYNAMIC SPEAKER.

moving-conductor microphone See VELOCITY MICROPHONE.

moving-diaphragm meter A headphone used as a sensitive indicator in alternating-current bridge measurements.

moving element In an electromechanical device, the portion that moves physically under variable operating conditions.

moving-film camera An oscilloscope camera in which the film is drawn past the lens continuously at a constant speed, rather than being advanced frame by frame, as in a motion-picture camera.

moving-iron meter See IRON-VANE METER.

moving-vane meter See IRON-VANE METER.

mp Abbreviation of MELTING POINT.

m_p Symbol for MASS OF PROTON AT REST.

MPEG Abbreviation for MOTION PICTURE EXPERTS GROUP.

MPG Abbreviation of *microwave pulse generator.*

mph Abbreviation of *miles per hour.* Also, mi/h.

MPO Abbreviation of *maximum power output.*

mps **1.** Abbreviation of *meters per second.* Also, m/s. **2.** Abbreviation of *miles per second.* Also, mi/s.

MPT Abbreviation of MAXIMUM POWER TRANSFER.

MPX Abbreviation of MULTIPLEX.

MR Abbreviation of MEMORY REGISTER.

mrad Abbreviation of MILLIRADIAN.

MRIA Abbreviation of *Magnetic Recording Industry Association.*

mrm Abbreviation of *milliroentgens per minute.*

MS Abbreviation of MASS SPECTROMETER.

m^2/s Abbreviation of *meters squared per second.* The unit of kinematic viscosity.

M scan In radar operations, a modified A-scan display in which a pedestal signal is moved along the base line to a point where it coincides with the

5059F-pM-424-465 4/10/01 9:19 AM Page 459

base line of the reflected signal to determine the distance to the target.

msec Abbreviation of MILLISECOND. Also, ms.

msg Abbreviation of MESSAGE.

MSI Abbreviation of MEDIUM SCALE INTEGRATION.

MST Abbreviation of MOUNTAIN STANDARD TIME.

MT Abbreviation of METRIC TON.

MTR Abbreviation of MAGNETIC TAPE RECORDER.

mtr Alternate abbreviation of METER.

MTS Abbreviation for MULTICHANNEL TELEVISION SOUND.

M-type backward-wave oscillator A broadband, voltage-tuned oscillator in which the electrons interact with a backward traveling radio-frequency wave. Compare O-TYPE BACKWARD-WAVE OSCILLATOR.

mu Symbol, μ. **1.** Abbreviation of the prefix MICRO-. **2.** Expression for AMPLIFICATION FACTOR. **3.** Expression for PERMEABILITY. **4.** Expression for MICRON. **5.** Expression for ELECTRIC MOMENT. **6.** Expression for INDUCTIVITY. **7.** Expression for MAGNETIC MOMENT. **8.** Expression for MOLECULAR CONDUCTIVITY.

μ **1.** Symbol for MU.

μ**A** Abbreviation of MICROAMPERE.

μ_B Symbol for BOHR MAGNETON.

μ**b** Abbreviation of MICROBAR.

μ**Ci** Abbreviation of MICROCURIE.

μ_e Symbol for ELECTRON MAGNETIC MOMENT.

μ**F** Abbreviation of MICROFARAD.

μ**g** Abbreviation of MICROGRAM.

μ**H** Abbreviation of MICROHENRY.

μ**in** Abbreviation of MICROINCH.

μ**l** Abbreviation of MICROLITER.

μ**mm** Abbreviation of *micromillimeter* (see NANOMETER).

μ_n Symbol for NUCLEAR MAGNETON.

μ_o Symbol for FREE-SPACE PERMEABILITY CONSTANT.

μ_p Symbol for PROTON MAGNETIC MOMENT.

μ**P** Abbreviation of MICROPROCESSOR.

μ**rd** Abbreviation of MICRORUTHERFORD.

μ**S** Abbreviation of MICROSIEMENS.

μ**s** Abbreviation of MICROSECOND. (Also, μsec.)

μ**V** Abbreviation of MICROVOLT.

μ**V/m** Abbreviation of MICROVOLTS PER METER.

μ**W** Abbreviation of MICROWATT.

MUF Abbreviation of MAXIMUM USABLE FREQUENCY.

mu factor See MU, **2**.

mu law In communications, a companding standard generally used in the United States and Canada.

Muller tube A tube that conducts by means of ionization of an internal gas. It is used for radiation detection.

multiaddress In a computer, a multiple memory location.

multiband amplifier A radio-frequency power amplifier capable of operation on more than one frequency band. The bands are often (but not always) harmonically related. Compare WIDEBAND AMPLIFIER.

multiband antenna A single antenna, such as one used in amateur radio and television reception, operated in several frequency bands or channels. The bands are often (but not always) harmonically related.

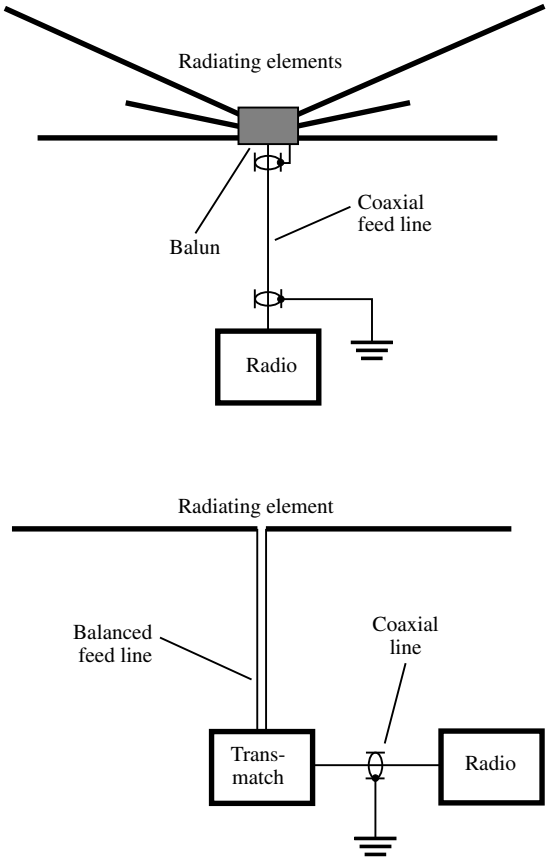

multiband antenna

multiband device A device (such as a tuner, receiver, transmitter, or test instrument) that operates in several selectable frequency bands.

multiband oscilloscope See WIDEBAND OSCILLOSCOPE.

multiband receiver A communications receiver capable of operation on more than one frequency band. Such a receiver might, but does not necessarily, provide continuous coverage over a wide

5059F-pM-424-465 4/10/01 9:19 AM Page 460

range of frequencies. Compare WIDEBAND RECEIVER.

multicasting The use of two frequency-modulation (FM) broadcast stations, or one FM station and one television station, to broadcast separately the two channels of a stereo program. The program is picked up simultaneously with two receivers.

multicavity magnetron A magnetron whose anode block has two or more cavities.

multicellular horn A loudspeaker in front of which are placed rectangular cells through which the sound passes.

multichannel Pertaining to a radio-communication system that operates on more than one channel at the same time. The individual channels might contain identical information, or they might contain different signals.

multichannel analyzer A test instrument, such as a spectrum analyzer, that splits an input into several channels for testing.

multichannel television sound Abbreviation, MTS. In television broadcasting, audio transmitted on more than one channel to provide stereo sound to subscribers.

multichip circuit A MICROCIRCUIT composed of interconnected active and passive chip-type components.

multichip integrated circuit An INTEGRATED CIRCUIT composed of circuit elements on separate, interconnected chips.

multicontact switch A switch having more than two contacting positions.

multicoupler An impedance-matching device used to couple several receivers to a single antenna.

multielement antenna A directive antenna having more than one element. Such antennas include phased arrays and parasitic arrays. Common examples are the LOG-PERIODIC ANTENNA, the QUAD ANTENNA, and the YAGI ANTENNA.

multiemitter transistor **1.** A bipolar transistor having more than one emitter. **2.** A bipolar power transistor having several emitters connected in parallel in the transistor structure.

multiframe A set of frames in a signal that are adjacent to each other in time (consecutive) and positioned according to an alignment signal.

multigun CRT A cathode-ray tube (CRT) having more than one electron gun.

multihop propagation Propagation of a radio wave by several successive reflections between the ionosphere and the surface of the earth.

multilayer circuit A circuit consisting of several sections printed or deposited on separate layers, which are subsequently stacked in a sandwich-like manner.

multilayer coil A coil in which the turns of wire are wound in several complete layers, one on top of the other. Compare SINGLE-LAYER COIL.

multilevel password protection See HIERARCHICAL PASSWORD PROTECTION.

multimedia **1.** In computing, the use of video, voice, music, electromechanical control, and/or data transfer at the same time. Useful in education, entertainment, business, and gaming applications. **2.** The use of voice, images, data, and/or video in a communications system or network, and, in particular, in wireless applications. An example is videoconferencing between a corporate office and the user of a handheld computer equipped with a wireless modem.

multimedia computer A personal computer designed especially for multimedia use. It includes a sound board, speakers, a microphone, and a CD-ROM (compact-disk read-only memory) drive. It often has a large-screen, high-resolution monitor (17 inches or greater diagonal measure).

multimeter A meter that allows measurement of different quantities (e.g., current, voltage, and resistance); the functions are usually made available through a selector switch.

multimode operation **1.** In radio communication, the use of two or more transmitters simultaneously, operating in different modes [e.g., one using single-sideband (SSB) and another using frequency modulation (FM)]. **2.** The transmission of visible light or infrared energy through an optical fiber in more than one mode at the same time. **3.** The operation of any device in more than one of its modes simultaneously.

multipactor A microwave switching tube capable of operating at high power levels. Characterized by high operating speed.

multipath cancellation A phenomenon sometimes observed in radio-wave propagation. Separate signal components arrive at the receiver in equal amplitude, but opposite phase. Also see MULTIPATH FADING and MULTIPATH RECEPTION.

multipath delay In MULTIPATH RECEPTION, the lag between signal components arriving over different paths.

multipath effect At a receiver, the difference in arrival time of multipath signals. Also see MULTIPATH DELAY.

multipath fading In radio communication, variations in the received signal that result from phasing various components of the transmitted signal that are propagated over different paths. At low, medium, and high frequencies, this effect is usually the result of ionospheric fluctuation. At very-high and ultra-high frequencies, it could occur as a result of changes in the state of the intervening atmosphere or, occasionally, reflection from objects, such as aircraft.

multipath reception Reception of a signal over more than one path. This often results in fading (see MULTIPATH FADING) and other undesirable effects, such as ghosting in television reception.

multipath transmission **1.** Transmission of a signal over two or more paths. Also see MULTIPATH RECEPTION. **2.** See MULTIHOP PROPAGATION.

5059F-pM-424-465 4/10/01 9:19 AM Page 461

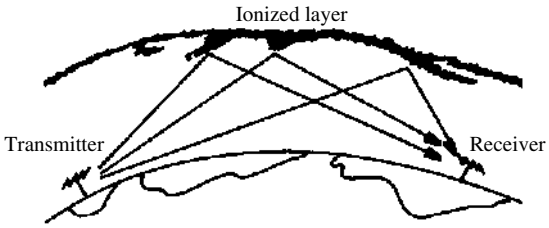

multipath reception

multiphase system See POLYPHASE SYSTEM.

multiple access system A timesharing data processing system that can be used by a number of people at remote locations, usually through peripherals other than conventional terminals (e.g., cash registers linked to a computer system for inventory control).

multiple-address code In computer operations, an instruction code that requires the user to specify the address of more than one operand per instruction.

multiple address instruction A computer program instruction specifying the address of more than one operand.

multiple break **1.** Interruption of a circuit at several points. **2.** Contact bounce.

multiple-chip circuit See HYBRID INTEGRATED CIRCUIT.

multiple connector In a flowchart, a symbol showing the merging of several flowlines.

multiple ionization Successive ionization, as when an ion repeatedly collides with electrons. Also see DOUBLE IONIZATION.

multiple-length number In computer operations, a number occupying more than one register.

multiple-loop feedback system A feedback system using more than one feedback loop. An example is a tunable audio amplifier (see PARALLEL-TEE AMPLIFIER) in which a negative-feedback path provides tuning, while a positive-feedback path sharpens selectivity.

multiple modulation See COMPOUND MODULATION.

multiple precision arithmetic An arithmetic process using several words (bit groups) for an operand to ensure accuracy.

multiple programming **1.** Computer operation in which several programs in memory share peripherals and processor time. **2.** Programming a computer so that several logic or arithmetic operations can be carried out at the same time.

multiple-purpose meter See MULTIMETER.

multiple-purpose tester A multimeter sometimes combined with some other instrument, such as a test oscillator.

multiple reel file In a data-processing system, a magnetic tape data file of more than one reel.

multiple speakers A group of more than two loudspeakers, usually operated from a single amplifier system.

multiple-stacked broadside array A stacked array in which a number of collinear elements are stacked above and below each other. Also see BROADSIDE ARRAY and COLLINEAR ANTENNA.

multiple station Descriptive of a communications network in which more than one terminal is used.

multiple-unit steerable antenna A shortwave antenna system intended to prevent or minimize the effects of fading in received signals. It consists principally of a number of rhombic antennas feeding the receiver. The system utilizes the various waves arriving at different angles. An electric steering system causes the antennas to be selected automatically in the best combination and with their outputs in the proper phase. Also see DIVERSITY RECEPTION.

multiple winding See DRUM WINDING.

multiplex Pertaining to a communications or broadcasting system in which *multiplexing* is used. See MULTIPLEXING, **1**, **2**, **3**.

multiplex adapter A special circuit (or auxiliary unit) used in frequency-modulated radio receivers for stereophonic reception from a station transmitting a multiplex broadcast. Also see MULTIPLEXING, **1** and MULTIPLEX STEREO.

multiplex code The transmission of multiple signals over a single medium, using a code (such as Morse, Baudot, or ASCII). See MULTIPLEXING, **2**, **3**.

multiplex data terminal A computer terminal acting as a modem by virtue of its accepting and transferring signals between its input/output devices and a data channel.

multiplexer A device that allows two or more signals to be transmitted simultaneously on a single carrier wave, communications channel, or data channel. See MULTIPLEXING, **2**, **3**.

multiplexing **1.** A process in which a comparatively low-frequency carrier is modulated, then mixed with a signal that has a higher frequency. Also see SUBCARRIER and SUBSIDIARY COMMUNICATION AUTHORIZATION. **2.** The simultaneous transmission of numerous relatively low-frequency signals on a single carrier having a higher frequency. Also called *frequency-division multiplexing.* **3.** The transmission of numerous signals on a single channel by breaking each signal into timed fragments (intervals) and transmitting the fragments in a rotating sequence. Also called *time-division multiplexing.* **4.** In certain digital light-emitting-diode (LED) displays, the lighting of various parts of the display in a rapidly rotating sequence.

multiplex stereo The use of *multiplexing* to broadcast both channels of a stereophonic program on a single carrier wave. See MULTIPLEXING, **1**, **2**.

5059F-pM-424-465 4/10/01 9:19 AM Page 462

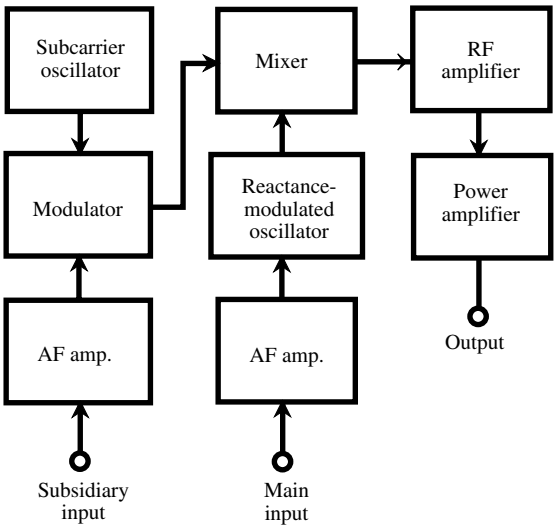

multiplexing, 1.

multiplex telegraphy **1.** A system of wire telegraphy in which two or more messages are sent simultaneously in one or both directions. **2.** A system of radiotelegraphy in which two or more messages can be sent simultaneously on the same carrier wave.

multiplex telephony **1.** A system of wire telephony in which two or more messages can be sent simultaneously in one or both directions over the same line. **2.** A system of radiotelephony in which two or more messages can be sent simultaneously on the same carrier wave.

multiplication **1.** The arithmetic process whereby a certain factor is added to itself the number of times indicated by another factor (the multiplier). **2.** A method of increasing a quantity, magnitude, or rate by some desired factor. See, for example, FREQUENCY MULTIPLIER and VOLTAGE MULTIPLIER.

multiplier **1.** See FREQUENCY MULTIPLIER. **2.** See VOLTAGE MULTIPLIER. **3.** A circuit or device for performing arithmetic multiplication. **4.** See VOLTMETER MULTIPLIER.

multiplier amplifier A frequency-multiplying amplifier (such as a doubler, tripler, or quadrupler), whose output circuit is tuned to an integral multiple of the input frequency. Compare STRAIGHT-THROUGH AMPLIFIER.

multiplier phototube See PHOTOMULTIPLIER TUBE.

multiplier prefix A prefix that, when affixed to the name of a quantity (e.g., Hertz and byte) indicates the amount, usually a power of 10 or a power of 2, by which that quantity is to be multiplied. Also called *prefix* and *prefix multiplier.* See PREFIXES table in Appendix B. Also see, for example, GIGA-, KILO-, MEGA-, MICRO-, MILLI-, NANO-, and PICO-.

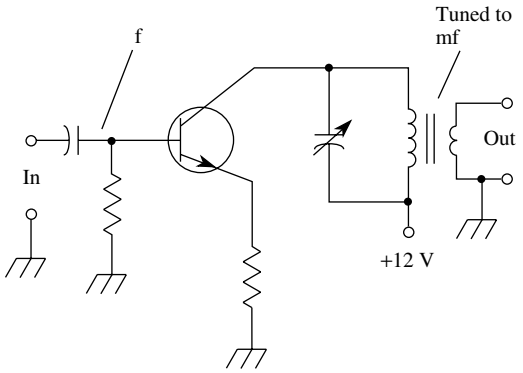

multiplier amplifier

multiplier probe **1.** A resistor-type test probe for a voltmeter, which increases the range of the meter and, therefore, acts as a voltmeter multiplier. **2.** A voltage-multiplier type of test probe for a voltmeter, which multiplies the test voltage before it is applied to the instrument (e.g., voltage-doubler probe).

multiplier register In a computer, a register that retains a number during a multiplication operation.

multiplier resistor A resistor connected in series with a current meter (usually a milliammeter or microammeter) to make it a voltmeter. Also called VOLTMETER MULTIPLER.

multiplier tube See PHOTOMULTIPLIER TUBE.

multipoint circuit A transmission circuit or system, in which information can be entered or retrieved at two or more locations.

multipoint distribution service In radio broadcasting, the transmission of programs via microwave links from a central facility to various local stations.

multipolar Pertaining to the presence of more than two magnetic poles.

multipolar machine A motor or generator having a number of poles in its armature and field.

multiposition relay A relay having more than two positions of closure. See, for example, SELECTOR RELAY.

multiposition switch A switch having more than two contacting positions. See, for example, SELECTOR SWITCH and STEPPING SWITCH.

multiprocessing **1.** In a computer system, the running of more than one program at once. **2.** The use of more than one microprocessor simultaneously in a single computer. Also called *parallel processing.* **3.** See TIME SHARING.

multiprogramming Also called *multitasking.* In a computer system, a technique that allows two or more programs to be executed at the same time.

5059F-pM-424-465 4/10/01 9:19 AM Page 463

multipurpose meter An electric meter that performs several functions, usually available through a function selector. Examples: VOLTAMMETER, VOLT-OHMMETER, and VOLT-OHM-MILLIAMMETER.

multirange instrument An instrument provided with several separate ranges, usually selectable by range switching (e.g., five-range voltmeter, two-scale ammeter, and four-band oscillator).

multisection filter A filter having two or more selective sections connected in cascade.

multisegment magnetron See MULTICAVITY MAGNETRON.

multiskip propagation See MULTIHOP PROPAGATION.

multistage device A device having several stages operating in cascade or otherwise coordinated with each other (e.g., a five-stage amplifier).

multistage feedback Feedback (positive or negative) between several stages in a system, as opposed to feedback between the output and input of a single stage.

multistage oscillation Oscillation resulting from positive feedback between or among two or more stages of an amplifier chain, as opposed to oscillation occurring between the output and input of a single amplifier stage.

multistage X-ray tube An X-ray tube providing electron acceleration by means of successive ring-shaped anodes—each biased to a higher voltage than the preceding one.

multiswitch A switch having a number of poles and contacts.

multitester An instrument, such as a multimeter or a combined signal generator and oscilloscope, that performs a number of different test functions.

multitrack recording **1.** A recording on two or more tracks (e.g., *multitrack disk* and *multitrack tape*). **2.** Making a recording on a tape or disc with two or more tracks.

multiturn loop antenna A small loop antenna (whose diameter measures less than approximately 10 degrees of phase in free space) that has two or more turns of wire or tubing. The loop has significant inductance. A capacitor, connected in parallel or in series with the loop, can produce a narrowband frequency response.

multiturn potentiometer A potentiometer whose shaft must be rotated through several complete revolutions to cover the full resistance range.

multivalent Having a valence greater than 2. Compare UNIVALENT.

multivibrator A circuit usually containing two transistors in a resistance-capacitance (RC) coupled amplifier, whose output is capacitance-coupled to the input. The two stages switch each other alternately in and out of conduction at a frequency determined by the *R* and *C* values. Also see ASTABLE MULTIVIBRATOR, BISTABLE MULTIVIBRATOR, and MONOSTA-BLE MULTIVIBRATOR.

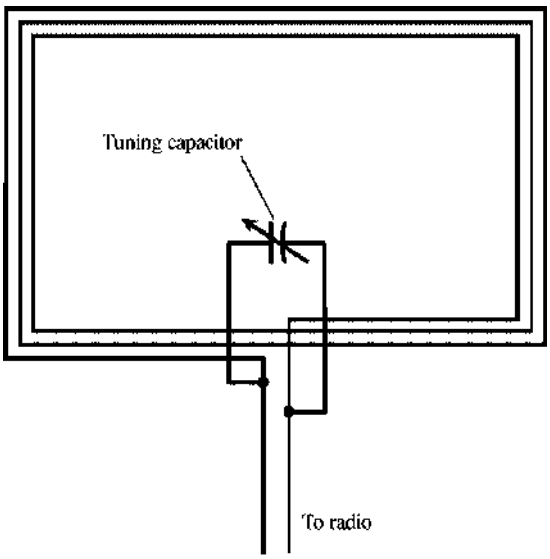

multiturn loop antenna

multiwire antenna An antenna having more than one wire in the radiating section. In early flat-top antennas, such wires were usually connected together at one end.

multiwire doublet antenna A doublet antenna having more than one wire in its radiator. A common form is the *folded dipole*, in effect two closely spaced dipole radiators connected together at both ends, one being center-fed.

Mumetal A high-permeability alloy of iron and nickel, valued especially for use as a magnetic shield for cathode-ray tubes.

Munsell color system A system for specifying colors in terms of hue, saturation, and brilliance, according to charts. Also see COLOR MATCHING.

Muntz metal See YELLOW METAL.

MUPO Abbreviation of MAXIMUM UNDISTORTED POWER OUTPUT.

Murray-loop bridge A specialized form of Wheatstone bridge in which two of the resistance arms are supplied by a two-wire line (such as a telephone line). By means of resistance measurements made with the bridge, the distance from an office or station to a ground fault on the line can be determined.

MUSA Abbreviation of *multiple-unit steerable antenna.*

muscovite Formula, $KH_2Al_2(SiO_4)_3$. A high-grade variety of mica having low dielectric loss.

Musical Instrument Digital Interface Acronym, MIDI. A computer language used in electronic music. It "tells" the computer when to play a note, how long to play it, and how loud to play it. It also sets the tempo of the music, based on how long a

5059F-pM-424-465 4/10/01 9:19 AM Page 464

quarter-note lasts. It controls the operation of a music synthesizer, and allows two or more synthesizers to communicate.

musical quality See TIMBRE.

musical scale A series of tones between a given tone and its second harmonic, scaled in intervals of ⅛ octave. The most common example can be found on a piano. Variations exist (e.g., *13-note scale*, *six-note scale*, and *five-note scale*).

music chip An integrated circuit for producing various musical effects (such as tones, percussion, etc.).

music power For a power amplifier, the short-term output power obtained in the reproduction of music waveforms, in contrast to root-mean-square (rms) or effective power output.

music synthesizer A set of oscillators, usually operated with a computer, used to create or playing electronic music. Also see MOOG SYNTHESIZER and MUSIC INSTRUMENT DIGITAL INTERFACE.

music under Pertaining to low-volume, continuous, background music, often added to presentations, radio and television advertisements, educational programs, etc.

muting **1.** Disabling a receiver or amplifier under no-signal or weak-signal conditions. **2.** Softening or muffling a sound.

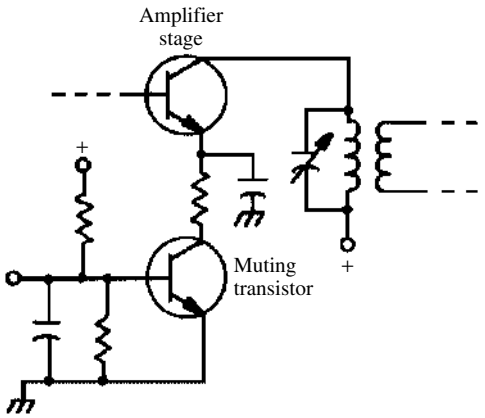

muting

muting circuit **1.** An interference-preventing device that automatically shuts off a radio receiver during the operation of a transmitter, and vice versa. **2.** A squelch circuit. **3.** In a stereo receiver, an electronic element that cuts off all audio when no signal is present or when the receiver is being tuned between carriers.

muting switch A switch or relay that cuts off a receiver during periods of transmission, or when reception is not desired. Generally, a cutoff voltage is applied to one of the intermediate-frequency stages to accomplish muting. In some cases, the audio-frequency circuit is disabled.

mutual antenna coupling Electromagnetic coupling between or among antennas when they are placed too close together. Usually, it is an undesirable phenomenon.

mutual capacitance Inherent capacitance between two conductors.

mutual-capacitance attenuator An attenuator that, in its simplest form, is essentially a shielded, two-plate variable capacitor.

mutual conductance See TRANSCONDUCTANCE.

mutual impedance An impedance shared by two or more branches of a circuit.

mutual inductance Symbol, *M*. Unit, henry. The property shared by neighboring inductors or inductive devices that enables induction to occur. A mutual inductance of 1 henry is present when a current change of 1 ampere per second in one inductor induces 1 volt across another inductor. Also see INDUCTANCE.

mutual-inductance attenuator An attenuator consisting essentially of two coupled coils (input and output), whose spacing can be gradually changed.

mutual-inductance bridge See CAREY-FOSTER MUTUAL-INDUCTANCE BRIDGE.

mutual induction The action whereby the magnetic field produced by alternating current in one conductor produces a voltage in another isolated conductor.

mutual interference **1.** See ADJACENT-CHANNEL INTERFERENCE. **2.** Any kind of interference between or among radio-frequency communications circuits.

mutually exclusive events Two or more events (or data points) so that the occurrence of one prevents the occurrence of the other(s). That is, two events cannot take place simultaneously.

MV **1.** Abbreviation of MEGAVOLT. **2.** Abbreviation of MULTIVIBRATOR.

mV Abbreviation of MILLIVOLT.

MV Abbreviation of MEDIUM VOLTAGE.

MVA Abbreviation of MEGAVOLT-AMPERE.

mV/m Abbreviation of millivolts per meter.

mVP Abbreviation of MILLIVOLT POTENTIOMETER.

MW Symbol for MEGAWATT.

mW Symbol for MILLIWATT.

mw Abbreviation of MEDIUM WAVE.

MWH Abbreviation of MEGAWATT-HOUR.

mW RTL Abbreviation of *milliwatt resistor-transistor logic* or *low-power resistor-transistor logic*.

Mx Abbreviation of MAXWELL.

Mycalex Trade name for an insulating material consisting of mica bonded with glass. Dielectric constant, 6 to 8. Resistivity, 10^{13} ohm-cm.

Mylar A DuPont registered trademark. A tough, plastic insulating material commonly used as a magnetic tape base. Dielectric constant, 2.8 to 3.7. Dielectric strength, 7000 V/mil.

5059F-pM-424-465 4/10/01 9:19 AM Page 465

Mylar capacitor A capacitor in which the dielectric film is Mylar.

Mylar tape Magnetic recording tape using a Mylar film as the substrate.

mym Abbreviation of MYRIAMETER.

myoelectricity 1. Bioelectric pulses of 10- to 1000-mV amplitude produced by muscular activity and detectable by electrodes attached to the skin. Also see ELECTROMYOGRAM, ELECTROMYOGRAPH, and ELECTROMYOGRAPHY. **2.** The study of phenomena, as defined in **1**.

myogram See ELECTROMYOGRAM.

myograph See ELECTROMYOGRAPH.

myography See ELECTROMYOGRAPHY.

myriameter Abbreviation, mym. A metric unit of linear measure equal to 10 kilometers (10^4 meters).

myriametric waves British designation for electromagnetic energy having wavelengths from 100 kilometers down to 10 kilometers, corresponding to frequencies from 3 kHz up to 30 kHz.

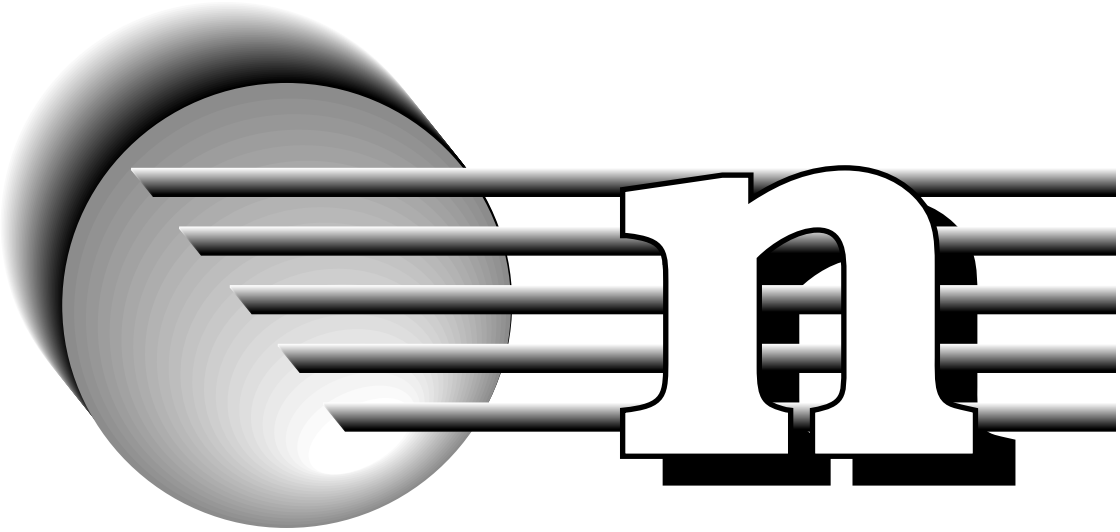

N **1.** Symbol for NUMBER. **2.** Symbol for NITROGEN. **3.** Abbreviation for NEWTON. **4.** Abbreviation of NUMBER (also, No.). **5.** Symbol for the set of natural (counting) numbers (0, 1, 2, 3, . . .).

n **1.** Abbreviation of prefix NANO-. **2.** Symbol for NUMBER. **3.** Symbol for a term (e.g., a multiplier) having an assigned value. **4.** Symbol for part of an expression or operator (as in $2n$, $n - 1$, n^2, etc.). **5.** Symbol for INDEX OF REFRACTION. **6.** Symbol for amount of substance (unit, mole).

NA **1.** Abbreviation of *not available* (as on a specifications sheet). **2.** Abbreviation of *not applicable.*

N_A Symbol for AVOGADRO'S CONSTANT.

Na Symbol for SODIUM.

nA Abbreviation of NANOAMPERE.

NAB Abbreviation of NATIONAL ASSOCIATION OF BROADCASTERS.

NAB curve In audio-frequency operations, the standard magnetic tape playback equalization curve developed by the National Association of Broadcasters (NAB).

NAE Abbreviation of *National Academy of Engineering.*

NAND circuit Also called *NOT-AND circuit.* A binary digital circuit whose output is high (logic 1) if any of the input signals are low (logic 0); the output is low only when all the inputs are high. The performance of the NAND circuit is the inverse of that of the AND circuit.

NAND gate A gate that performs the function of a NAND circuit.

nano- Abbreviation, n. A prefix meaning billionth(s) (i.e., 10^{-9}).

nanoampere Abbreviation, nA. A unit of current; 1 nA equals 10^{-9} ampere.

A	B	C
0	0	1
0	1	1
1	0	1
1	1	0

NAND circuit

nanofarad Abbreviation, nF. A unit of capacitance; 1 nF equals 10^{-9} farad.

nanohenry Abbreviation, nH. A unit of low inductance; 1 nH equals 10^{-9} henry.

nanometer Abbreviation, nm. A unit of short wavelength or displacement; 1 nm equals 10^{-9} meter.

nanosecond Abbreviation, ns. A time interval of 10^{-9} second.

nanotechnology The design and construction of superminiature electronic and electromechanical devices. For example, microscopic, computer-controlled robots might someday be used as programmable antibodies to fight infectious diseases, or to build integrated circuits, atom by atom.

nanovolt Abbreviation, nV. A unit of low voltage; 1 nV equals 10^{-9} volt.

nanovoltmeter A sensitive voltmeter for measuring potential in the nanovolt range.

Copyright 2001 The McGraw-Hill Companies, Inc. Click Here for Terms of Use

5059F-pN-466-487 4/10/01 9:21 AM Page 467

nanowatt Abbreviation, nW. A unit of low power; 1 nW equals 10^{-9} watt.

nanowattmeter A meter for measuring power in the nanowatt range.

NAP Abbreviation of *nuclear auxiliary power.*

napier See NEPER.

Napierian base Symbol, *e.* An irrational number, equal to approximately 2.718282, and used as the NAPIERIAN LOGARITHM base.

Napierian logarithm Abbreviation, ln or $\log_e$. A logarithm to the base *e* (see NAPIERIAN BASE). Also called NATURAL LOGARITHM. Compare COMMON LOGARITHM.

NAPU Abbreviation of *nuclear auxiliary power unit.*

narrative A computer program statement that, rather then being an instruction, merely describes the purpose of what follows (usually the steps in a routine or a block of instructions) as a debugging or program modification aid. In a program written in BASIC, such a statement is preceded by the abbreviation REM, for remark. Also called COMMENT.

narrowband **1.** A frequency band in which the difference between upper and lower limits is small compared with bandwidths typical of the service specified. **2.** Pertaining to a radio-frequency emission whose bandwidth is limited or restricted. **3.** Pertaining to a circuit or device that operates over a comparatively small range of frequencies. **4.** In a digital network, a channel having a bandwidth of 64 kbps or less.

narrowband amplifier An amplifier whose passband is restricted to a fraction of the frequency spread common to the amplifier's application.

narrowband FM See NARROWBAND FREQUENCY MODULATION.

narrowband frequency modulation Abbreviation, NBFM or NFM. Frequency modulation in which the maximum instantaneous frequency deviation is no greater than the highest modulating frequency.

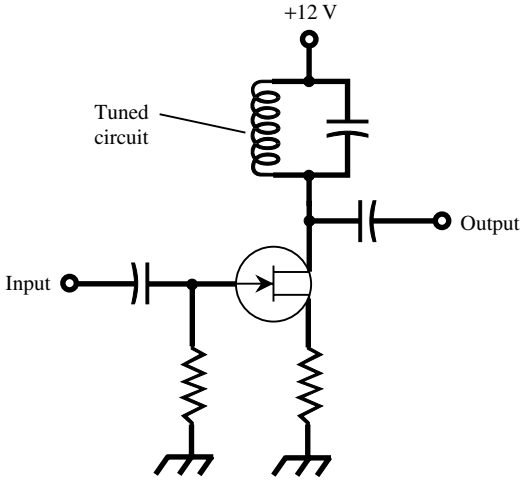

narrowband amplifier

narrowband interference Signal interference whose bandwidth is narrow, compared with that of the circuit affected.

narrowband voice modulation Abbreviation, NBVM. A scheme via which an analog voice signal is compressed into a band of frequencies narrower than that normally required for effective communication.

narrow bandwidth Pertaining to a radio-frequency emission whose bandwidth is comparatively narrow (e.g., a small fraction of the available spectrum space in the frequency band being used).

narrow-sector recorder A directional radio receiver for locating sources of atmospheric noise.

NARTB Abbreviation of *National Association of Radio and Television Broadcasters.*

NAS Abbreviation of *National Academy of Sciences.*

National Association of Broadcasters Abbreviation, NAB. A countrywide organization of radio and television broadcasters.

National Bureau of Standards Abbreviation, NBS. An agency in the U.S. that maintains values for physical constants in the Standard International (SI) System of Units. It also maintains radio broadcast stations that transmit standard time and frequency signals.

National Electrical Manufacturers Association Abbreviation, NEMA. A countrywide organization of manufacturers of electrical and electronic equipment and supplies.

National Electric Code Abbreviation, NEC. Safety regulations and procedures issued by the National Fire Protection Association for the installation of electrical wiring and equipment in the United States. Although the code is advisory from the Association's standpoint, it is enforced to various degrees by local authorities.

National Television Standards Committee Abbreviation, NTSC. A U.S. organization of television companies and other interested organizations. It developed the original black-and-white and color television standards that were approved by the Federal Communications Commission.

natural-decay curve See EXPONENTIAL DECREASE.

natural antenna frequency The fundamental resonant frequency of an electromagnetic antenna.

natural disintegration **1.** The decay of a radioactive substance as a result of the continuous emission of particles and rays. **2.** Also called *half life.* The time required for half of a quantity of a radioactive substance to decay into a different isotope or element.

natural electricity **1.** Atmospheric electricity. **2.** The electricity in living organisms, that is, BIOELECTRICITY.

natural frequency See NATURAL RESONANT FREQUENCY.

5059F-pN-466-487 4/10/01 9:21 AM Page 468

natural-growth curve See EXPONENTIAL INCREASE.

natural interference Interference from atmospheric and celestial sources, as opposed to human-made interference.

natural language A spoken or written human language (such as French or Japanese), as opposed to a computer language (such as machine language, C++, or LISP). Translation between natural language and machine language is important in optical character recognition, speech recognition, and speech synthesis.

natural logarithm See NAPIERIAN LOGARITHM.

natural magnet A material, such as magnetite (lodestone), found in nature and exhibiting permanent magnetism.

natural magnetism Magnetism found in some natural materials (see NATURAL MAGNET) and in the earth itself.

natural number **1.** Any nonnegative whole number, that is, a member of the set $N = (0, 1, 2, 3, \ldots)$. **2.** See NAPIERIAN BASE.

natural period The time required for one complete wave cycle to occur in a device at its NATURAL RESONANT FREQUENCY.

natural radiation Noise in the form of radiation emitted by natural radioactive substances, cosmic rays, etc. Also called BACKGROUND RADIATION.

natural resonance Resonance resulting from the unique physical constants of a body, circuit, or system. Also see NATURAL RESONANT FREQUENCY.

natural resonant frequency **1.** The frequency at which a circuit or device responds with maximum amplitude to applied signals. **2.** The frequency at which a circuit or device generates maximum energy. **3.** The frequency at which an object vibrates at maximum amplitude.

natural wavelength The wavelength corresponding to the NATURAL RESONANT FREQUENCY of a circuit, device, or object.

nautical mile A nautical unit of linear measure equal to 1.852 kilometers (1.1508 statute miles).

nav **1.** Abbreviation of *navigation.* **2.** Abbreviation of *navigational.*

Navaglobe A radionavigation system used at very-low or low frequencies over long distances.

NAVAIDS Abbreviation of NAVIGATIONAL AIDS.

navar A radar system in which a ground radar scans the immediate vicinity of an airport, observes the flight activity, and transmits such observations to aircraft in flight. The name is a contraction of the term *navigation and ranging.*

navigation aid An electronic device or system, such as radar or radio direction finding, that assists in the navigation of vehicles on land, at sea, or in the air.

navigation beacon A beam that provides aircraft and ships with navigational aid.

NAWAS Abbreviation of *National Attack Warning System.*

Nb Symbol for NIOBIUM.

nb Abbreviation of NARROWBAND.

NBFM Abbreviation of NARROWBAND FREQUENCY MODULATION. Also abbreviated NFM.

NBS Abbreviation for NATIONAL BUREAU OF STANDARDS.

NBTDR Abbreviation of *narrowband time-domain reflectometry.*

nbw Abbreviation of NOISE BANDWIDTH.

NC **1.** Abbreviation of NORMALLY CLOSED. **2.** On drawings, abbreviation of *no connection.* **3.** Abbreviation of NUMERICAL CONTROL.

N/C Abbreviation of NUMERICAL CONTROL.

nc Abbreviation of *no connection.*

n-channel junction field-effect transistor Abbreviation, NFET. A junction field-effect transistor in which the gate junction is formed on a bar or die of n-type semiconductor material.

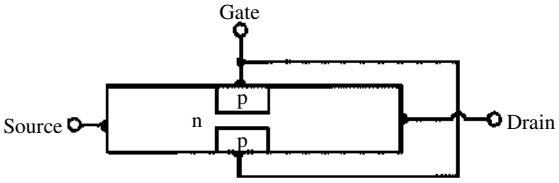

n-channel junction field-effect transistor

n-channel MOSFET A metal-oxide-semiconductor (MOS) field-effect transistor in which the channel is n-type material.

NCMT Abbreviation of NUMERICALLY CONTROLLED MACHINE TOOL.

NCS Abbreviation of *net control station(s).*

N curve A negative-resistance voltage-current curve having a shape roughly resembling an uppercase letter N. Compare S CURVE.

Nd Symbol for NEODYMIUM.

N display A radar display in which the target is represented by a pair of vertical blips, whose amplitude indicates target direction and whose position along the horizontal base line (as determined by lining up a pedestal signal with the blips) is read from the pedestal-adjustment calibration.

n-doped zinc-oxide ceramic A nonlinear-resistance material used in the manufacture of some voltage-dependent resistors.

NDR Abbreviation of NONDESTRUCTIVE READ.

NDT Abbreviation of NONDESTRUCTIVE TEST.

Ne Symbol for NEON.

near-end crosstalk Crosstalk originating at, or near, the telephone subscriber line in which the interference is noticed.

near field **1.** The radiation field within a radius of 1 wavelength from a transmitting antenna. **2.** The sound field near a loudspeaker or other reproducer.

near infrared Pertaining to electromagnetic radiation of 3 to 30 micrometers in wavelength.

5059F-pN-466-487 4/10/01 9:21 AM Page 469

near ultraviolet That part of the ultraviolet spectrum nearest the visible light wavelengths. These are the least-penetrating ultraviolet rays. They are also called *soft ultraviolet.*

near video on demand In television, a local service in which various programs/videos are broadcast at specified times.

near zone See NEAR FIELD, **1**.

NEB Abbreviation of *noise equivalent bandwidth.*

NEC Abbreviation of NATIONAL ELECTRIC CODE.

necessary bandwidth The minimum bandwidth needed (with a given emission) to transmit information at a required rate and of a required quality. In general, as data speed increases (as measured in bits per second, baud, or words per minute), the minimum required bandwidth increases. For slow-speed Morse code signals, it can be as small as a few Hertz; for fast-scan television, it is several megahertz.

neck The straight portion of a cathode-ray-tube (CRT) envelope (i.e., the part between the base and the flared portion).

NEDA Abbreviation of *National Electronic Distributors' Association.*

needle **1.** The stylus of a phonograph cartridge. **2.** The pointer of an indicating meter. **3.** One of the electrodes in a voltage-measuring spark gap (see NEEDLE GAP). **4.** The slender, pointed metal tip of a test probe.

needle chatter See NEEDLE TALK.

needle drag In disc recording and reproduction, friction between the needle (stylus) and disc. Also called *stylus drag.*

needle electrode See NEEDLE, **3**, **4**.

needle gap A spark gap composed of two needles having an adjustable air gap between their points. An unknown high voltage is measured in terms of the gap width necessary for sparking.

needle memory A computer memory in which the dual-state elements are thin magnetic needles.

needle pointer The pointer of a meter or compass.

needle pressure See VERTICAL STYLUS FORCE.

needle probe See NEEDLE-TIP PROBE.

needle scratch In disc recording and reproduction, noise resulting from vibration of the needle (stylus) because of an irregular groove surface. Also called *surface noise.*

needle talk Direct radiation of sound by the stylus of a phonograph pickup. Also called *needle chatter.*

needle telegraph A telegraph in which the Morse code characters are converted into magnetic needle deflections.

needle test point See NEEDLE, **4**.

needle-tip probe A test probe that terminates in a sharp point. Also see NEEDLE, **4**.

needle voltmeter See NEEDLE GAP.

neg Abbreviation of NEGATIVE.

negate **1.** To insert the NOT operation in front of a digital expression. **2.** To change logic 1 to logic 0 (high to low) or vice versa.

negation The logical NOT operation (see NOT) in digital systems. Also see NAND CIRCUIT, NOR CIRCUIT, NOR GATE, NOT CIRCUIT, and NOT-OR CIRCUIT.

negation element In a computer system, a device that can give the reverse of a condition, event, or signal.

negative **1.** Possessing NEGATIVE ELECTRIFICATION. **2.** In voice communications, a word often used for "no," especially when interference is present or signals are weak. **3.** Pertaining to a real number less than zero. **4.** An image whose shadings are opposite to those in the scene.

negative acceleration A decrease in speed or velocity; also called *deceleration.*

negative acknowledgment character In a handshaking or forward-error-correction (FEC) system, a response by the receiving station that indicates a missed bit or bits.

negative angle **1.** An angle in the third or fourth quadrant in a system of rectangular coordinates. **2.** An angle measured clockwise from the positive *x*-axis in a rectangular coordinate system. Compare POSITIVE ANGLE.

negative bias A steady, negative direct-current voltage or current applied continuously to an electrode of a device, such as a transistor to establish the operating point. Compare POSITIVE BIAS.

negative bus See NEGATIVE CONDUCTOR.

negative charge An electric charge consisting of a quantity of NEGATIVE ELECTRIFICATION. Also see CHARGE, **1**; ELECTRIC CHARGE; and UNIT ELECTROSTATIC CHARGE. Compare POSITIVE CHARGE.

negative conductor The conductor or wire connected to the negative terminal of a current, power, or voltage source. Compare POSITIVE CONDUCTOR.

negative electricity See NEGATIVE CHARGE and NEGATIVE ELECTRIFICATION.

negative electrification Electrification characterized by an excess of electrons. For example, when a glass rod is rubbed with a silk cloth, the cloth becomes negatively charged because electrons are transferred from the glass to the cloth. Similarly, when a neutral atom acquires an extra electron, the atom becomes negatively charged because it has an excess of electrons. Compare POSITIVE ELECTRIFICATION.

negative electrode **1.** An electrode connected to the negative terminal of a current, power, or voltage source. **2.** The negative output terminal of a current, power, or voltage source, such as a battery or generator.

negative error of measurement An error of measurement in which the difference between a measured value and the true or most probable value is negative. Compare POSITIVE ERROR OF MEASUREMENT.

negative exponent In mathematical notation, an exponent indicating that a number is to be raised

5059F-pN-466-487 4/10/01 9:21 AM Page 470

to a negative power. Raising a number x to a negative power $-n$ means taking the reciprocal of the number raised to the power n. That is, $x^{-n} = 1/x^n$; for example, $10^{-2} = 1/10^2 = 1/100 = 0.01$.

negative feedback Feedback that is out of phase with the input signal. Also called INVERSE FEEDBACK, DEGENERATION, and DEGENERATIVE FEEDBACK. Compare POSITIVE FEEDBACK.

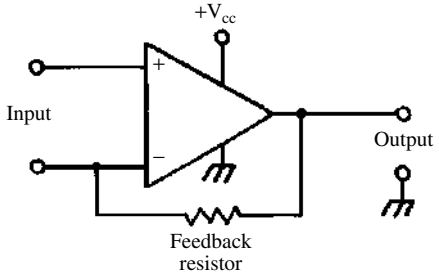

negative feedback

negative-feedback amplifier An amplifier in which negative feedback is used to improve performance or modify response.

negative function A trigonometric function having the negative sign. In a rectangular coordinate system, the sine function is negative in the third and fourth quadrants, the cosine in the second and third, and the tangent in the second and fourth. Compare POSITIVE FUNCTION.

negative gain A misnomer for FRACTIONAL GAIN, arising because fractional gain can be expressed in negative decibels.

negative ghost In a television picture, a ghost with negative (see NEGATIVE, **4**) shading.

negative ground In a direct-current power system, the connection of the negative pole to common ground.

negative image **1.** A picture in which the blacks, whites, and shades in between are the reverse of those in the scene (see NEGATIVE, **4**). **2.** An abnormal image that has the reverse shading described in **1**.

negative impedance An impedance that displays the same behavior as that of NEGATIVE RESISTANCE.

negative ion An atom with an excess of electrons and, consequently, a net negative charge. Also called ANION. Compare POSITIVE ION.

negative-ion generator A device for generating negative ions and circulating them into the surrounding air. This is believed by some people to be beneficial to health.

negative lead See NEGATIVE CONDUCTOR.

negative-lead filtering Power-supply filtering in which the choke coils and capacitors are in the negative direct-current lead, rather than in the positive lead (the usual position). One advantage of this arrangement is the lower insulation requirement of the choke.

negative light modulation In television image transmission, the condition in which transmitted power is increased by a decrease in the initial intensity of light. Compare POSITIVE LIGHT MODULATION.

negative line See NEGATIVE CONDUCTOR.

negative logic **1.** Binary logic in which a high negative state represents logic 1, and a low negative state represents logic 0. **2.** Binary logic in which a low positive state represents logic 1, and a high positive state represents logic 0. Compare POSITIVE LOGIC.

negative measurement error See NEGATIVE ERROR OF MEASUREMENT.

negative modulation Amplitude-modulated television transmission in which the transmitted power decreases as image brightness increases. Compare POSITIVE MODULATION.

negative modulation factor For an amplitude-modulated wave having unequal positive and negative modulation peaks, a ratio expressing the maximum negative deviation from the average for the envelope. Compare POSITIVE MODULATION FACTOR.

negative number A real number less than zero (i.e., one to which the minus sign is assigned).

negative peak The maximum negative instantaneous current or voltage in an alternating-current waveform.

negative-peak voltmeter An electronic meter for measuring the NEGATIVE PEAK voltage of an alternating-current waveform.

negative phase-sequence relay A relay that responds to the negative phase sequence in a polyphase circuit. Compare POSITIVE PHASE-SEQUENCE RELAY.

negative picture modulation See NEGATIVE MODULATION.

negative picture phase In a television signal, the picture-signal voltage swing from zero to negative, in response to an increase in brightness. Compare POSITIVE PICTURE PHASE.

negative plate The negative member of a battery cell; electron flow is from the plate through the external circuit.

negative pole See NEGATIVE ELECTRODE, **1**, **2**.

negative positive zero Abbreviation, NP0. Pertaining to temperature-compensating capacitors having a temperature coefficient of capacitance that changes sign within a specified temperature range.

negative potential **1.** The potential measured at a negative electrode, with respect to the positive electrode or to ground. **2.** Potential less than that of the earth as a reference.

negative resistance **1.** A decrease in voltage across a device as the current through it increases, and an increase in voltage as the current decreases. **2.** A decrease in current through a device as the

5059F-pN-466-487 4/10/01 9:21 AM Page 471

voltage across it increases, and an increase in current as the voltage decreases. This is opposite to the behavior of an ohmic (positive) resistance. Also see N-CURVE, NEGATIVE-RESISTANCE REGION, NEGATIVE RESISTOR, and S CURVE.

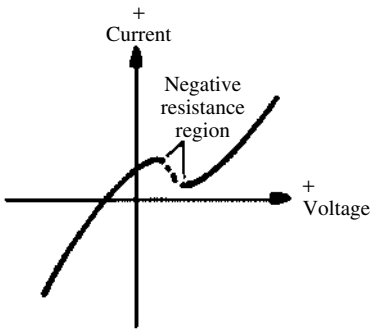

negative resistance

negative-resistance amplifier A simple circuit in which a negative-resistance device, such as a TUNNEL DIODE, cancels the positive resistance of the circuit, causing amplification or oscillation.

negative-resistance device See NEGATIVE RESISTOR.

negative-resistance diode **1.** See TUNNEL DIODE. **2.** A reverse-biased germanium diode (and occasionally a silicon diode) that exhibits NEGATIVE RESISTANCE. **3.** A special diode tube that, when operated at ultrahigh frequencies, exhibits negative resistance because of transit-time effects.

negative-resistance magnetron A split-anode magnetron operated at a combination of anode voltage and magnetic field strength corresponding to cutoff; it exhibits negative resistance to voltage applied symmetrically between the anode halves. The frequency of oscillation is determined by an external tank circuit.

negative-resistance oscillator An oscillator that consists of a negative-resistance device connected across a tuned circuit. The arrangement oscillates because the negative resistance cancels the positive resistance (losses) of the tuned circuit. See, for example, NEGATIVE-RESISTANCE MAGNETRON and TUNNEL-DIODE OSCILLATOR.

negative-resistance region In certain devices, a portion of the voltage-versus-current curve having negative slope (i.e., the current decreases as the voltage increases, or vice versa). Also see N CURVE, NEGATIVE RESISTANCE, and S CURVE.

negative-resistance repeater A repeater that produces gain by means of NEGATIVE RESISTANCE effects.

negative resistor Any device exhibiting NEGATIVE RESISTANCE.

negative space charge The cloud of electrons (negative particles) in the region surrounding an emitter, such as the hot cathode of a vacuum tube.

negative temperature coefficient Abbreviation, NTC. A number expressing the amount by which a quantity (such as the rating of a component) decreases when the temperature is raised. The coefficient is stated as a percentage, or as a certain number of parts per million (ppm) per degree temperature rise. Compare POSITIVE TEMPERATURE COEFFICIENT and ZERO TEMPERATURE COEFFICIENT.

negative terminal See NEGATIVE ELECTRODE, **2**.

negative torque In an electric motor, a torque that acts against the operating torque.

negative transmission In a television or facsimile system, the condition in which brighter light corresponds to lower transmitted power, and dimmer light corresponds to higher transmitted power.

negative valence The valence of a negative ion. Also see VALENCE.

negator A logical NOT element [i.e., one that outputs the complement of an input bit (1 for 0 and vice-versa)].

negatron The term that specifically differentiates the familiar ELECTRON from a POSITRON (positive electron).

NEI Abbreviation of *noise equivalent input.*

neighborhood node A local site at which a fiberoptic television (video) signal is converted to a cable signal.

NEL Abbreviation of *National Electronics Laboratory.*

NELA Abbreviation of *National Electric Light Association.*

N electron In certain atoms, an electron whose orbit is outside of, and nearest to, those of the M electrons.

NEMA Abbreviation of *National Electrical Manufacturers' Association.*

nematic crystal A normally transparent liquid crystal that becomes opaque when an electric field is applied to it, and becomes transparent again when the field is removed. The crystal material is cut in the form of a letter or numeral and provided with a reflecting backplate for display readouts in calculators, watches, and various electronic devices.

nematic-crystal display A device in which an electrically controlled film of nematic-crystal material is used to transmit and interrupt light from a lamp or from a reflecting mirror, in this way displaying characters in whose shape the film has been formed.

nematic liquid In a liquid-crystal display (LCD), a normally clear liquid that becomes opaque in the presence of an electric field.

nemo A radio or television program that is picked up from a location outside the studio. Also called *field pickup* or *remote.*

5059F-pN-466-487 4/10/01 9:21 AM Page 472

neodymium Symbol, Nd. A metallic element of the rare-earth group. Atomic number, 60. Atomic weight, 144.24.

neodymium-YAG laser A laser that uses neodymium and yttrium-aluminum-garnet (YAG) crystal. It is used in medical applications, such as surgery and various other jobs where high precision is required. Generally, it is a low-to-medium-power laser.

neomatachograph An instrument used in psychology to measure complex reaction time. Compare NEOMATACHOMETER.

neomatachometer An instrument used in psychology to measure simple reaction time. Compare NEOMATACHOGRAPH.

neon Symbol, Ne. An inert-gas element. Atomic number, 10. Atomic weight, 20.179. Neon, present in trace amounts in the earth's atmosphere, is used in some glow tubes, readout devices, and indicator lamps.

neon bulb A (usually small) neon-filled gas diode. It has a characteristic pink glow and is ignited by a firing voltage for the particular unit. Also called *neon glow lamp* and *neon tube.*

neon-bulb flip-flop A flip-flop circuit (bistable multivibrator) using two neon bulbs as the bistable components.

neon-bulb gate A gate circuit containing a neon bulb biased below the firing point. A trigger voltage added to the bias voltage raises the applied voltage and fires the bulb, producing an output pulse.

neon-bulb logic Logic circuits composed of neon-bulb gates.

neon-bulb memory See NEON-BULB STORAGE.

neon-bulb multivibrator A multivibrator using two neon bulbs as the switching components.

neon-bulb oscillator A simple relaxation oscillator consisting essentially of a neon bulb, capacitor, resistor, and direct-current supply. The frequency of the sawtooth-wave output depends principally on the capacitance and resistance values. The maximum operating frequency is limited to about 5 kHz by the deionization time of the gas.

neon-bulb overmodulation indicator The application of a neon-bulb overvoltage indicator as a monitor for amplitude-modulated radio-frequency signals. The bulb flashes each time the modulation percentage exceeds a predetermined value. Also called *neon-bulb modulation alarm.*

neon-bulb overvoltage indicator A relatively simple circuit in which a neon bulb flashes each time a voltage monitored by the circuit exceeds a predetermined value. The flash shows that the portion of the voltage presented to the bulb has exceeded the firing potential.

neon-bulb peak indicator See NEON-BULB OVERVOLTAGE INDICATOR.

neon-bulb ring counter A ring counter composed of neon-bulb flip-flops. The maximum counting speed is limited by the deionization time of the neon bulbs to approximately 300 events per second.

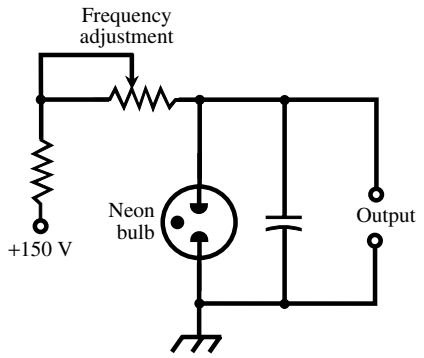

neon-bulb oscillator

neon-bulb sawtooth generator A relatively simple relaxation oscillator using a neon bulb, capacitor, and resistor. The output is a sawtooth wave, whose frequency is determined principally by the capacitance and resistance values.

neon-bulb scale-of-two circuit A scale-of-two circuit (frequency halver) using neon bulbs as the bistable elements.

neon-bulb storage A storage (memory) device composed of neon bulbs. A fired bulb (representing a bit of stored information) remains fired until turned off by an erase signal.

neon-bulb stroboscope A stroboscope in which a neon bulb supplies the light flashes. The circuit is essentially that of the neon-bulb oscillator, the flash rate being continuously variable by an adjustable frequency control.

neon-bulb voltage regulator A simple circuit utilizing the constant voltage drop across a fired neon bulb as a regulated voltage. The usual circuit configuration is a neon bulb and current-limiting resistor in series with a power supply.

neon-bulb volume indicator A neon-bulb overvoltage indicator used in some tape recorders to show when the volume exceeds a predetermined level—especially when the volume is high enough to cause an unacceptable amount of distortion.

neon glow lamp See NEON BULB.

neon lamp See NEON BULB.

neon pilot lamp A neon bulb used as a pilot lamp operated from the power-line circuit of an electronic equipment. Also called *neon pilot light.*

neon tube See NEON BULB.

NEP Abbreviation of NOISE EQUIVALENT POWER.

NEPD Abbreviation of *noise equivalent power density.*

neper Abbreviation, Np. A Napierian-logarithmic unit expressing a ratio of power levels; $Np = \log_e (P_1/P_2)^{1/2}$, where P_1 and P_2 are the power values being compared and e is the Napierian logarithm base, equal to approximately 2.71828. The neper is related to the decibel (dB), a similar unit based

5059F-pN-466-487 4/10/01 9:21 AM Page 473

on common logarithms, in the following manner: 1 Np = 8.686 dB; 1 dB = 0.1151 Np.

neptunium Symbol, Np. A radioactive metallic element produced artificially. Atomic number, 93. Atomic weight, 237.05.

Nernst effect The appearance of a voltage between the opposite edges of a metal strip that is conducting heat longitudinally when the strip is placed in a magnetic field perpendicular to the plane of the strip.

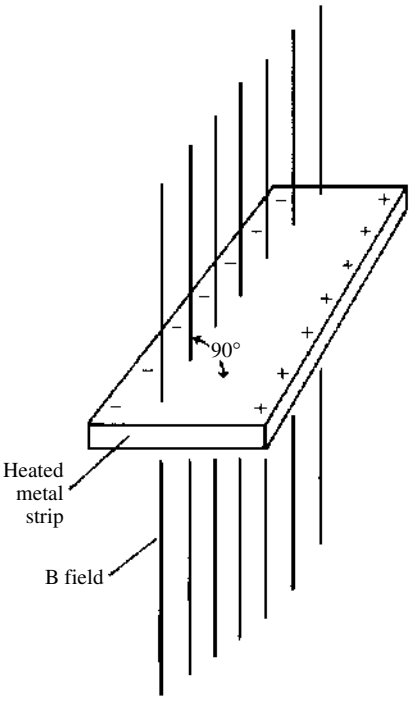

Nernst effect

Nernst-Ettinghausen effect In a piezoelectric crystal, the tendency for a temperature gradient to exist as a result of applied electromagnetic fields.

Nernst lamp An incandescent lamp in which the filament material is a mixture of magnesia and certain rare oxides (such as yttria). A surrounding current-carrying coil heats the filament, lowering its resistance and causing it to glow, after which it continues to operate on a low current.

nerve center The most essential part of a control system or communication network.

nerve current In an animal organism, the small electrical current that flows along nerve fibers.

nervous breakdown The upset of a function in a digital computer (which becomes disabled as a result).

NESC Abbreviation of *National Electrical Safety Code.*

nested loops See NESTING.

nesting In digital computers and data processing, the inclusion of one or more loops or subroutines inside a larger loop or subroutine. Nested loops, for example, can be used to assign values to double-subscripted variables.

NET Abbreviation of *noise equivalent temperature.*

net **1.** An effective, useful, or resultant quantity (e.g., NET CAPACITANCE). **2.** Colloquialism for *communications network.* See NETWORK, **2**.

net authentification A password or other special identification used in a radio network.

net capacitance The resultant capacitance in a circuit in which capacitances act in combination with each other.

net component The total value of two or more passive components of the same sort. See, for example, NET CAPACITANCE, NET CURRENT, NET IMPEDANCE, NET INDUCTANCE, NET POWER, NET REACTANCE, NET RESISTANCE, and NET VOLTAGE.

net current The current flowing in a circuit in which currents aid or oppose each other.

net gain For an amplifier, the amount of gain remaining after all losses in the device have been subtracted.

net impedance The impedance of a circuit in which impedances act in combination with each other.

net inductance The inductance of a circuit in which inductances act in combination with each other.

net loss For an amplifier or other system, the algebraic sum of gains and losses between two points in the system.

net power The resultant power observed when power signals aid or oppose each other in a single circuit or system.

net radiometer A device for measuring the difference in intensity between radiation entering the earth's surface and radiation leaving it. This is generally visible light or infrared radiation from the sun.

net reactance Symbol, X_t. The combined inductive reactance (X_L) and capacitive reactance (X_C) in a circuit or device.

net resistance The resistance of a circuit in which resistances act in combination with each other.

net voltage The resultant voltage at a point where voltages aid or oppose each other.

network **1.** A circuit arrangement of electronic components, sometimes redundant in its design [e.g., resistance-capacitance (RC) network]. **2.** A group of interconnected computers, communications stations, or other facilities, often organized for simultaneous operation and data transfer. **3.** To conduct research or gather information using a group of interconnected computers, communications stations, or other facilities.

network analog A circuit or circuits representing variables and used to express and solve a mathematical relationship between the variables.

5059F-pN-466-487 4/10/01 9:21 AM Page 474

network analysis The rigorous examination of a network to determine its properties and performance. Compare NETWORK SYNTHESIS.

network analyzer An analog or digital circuit for simulating and analyzing a network (see NETWORK, **1**) by means of measurements and calculations from the model so obtained.

network assurance The construction and operation of a network in such a manner that failures can be quickly and easily located and corrected.

network calculator An analog or digital device for determining the component values and performance of a given network (see NETWORK, **1**).

network constant The value of a passive component (capacitance, inductance, resistance, etc.) used in a network (see NETWORK, **1**).

network filter A transducer that passes or rejects signals, depending on their frequency.

network interface unit Abbreviation, NIU. A device, provided to each subscriber, that connects telephones, television sets, and personal computers to an electrical or fiberoptic cable. Envisioned as an integral component of the multimedia INFORMATION SUPERHIGHWAY.

network provisioning The control of a network by means of computer software, rather than via manual rearrangement of system devices.

network relay **1.** A relay that provides protection of the circuits in a network (see NETWORK, **1**); a circuit breaker. **2.** In a communications network (see NETWORK, **2**), the reception and retransmission of a message by a human operator.

network synthesis The design and fabrication of a network (see NETWORK, **1**) by rigorous engineering methods to achieve a prescribed performance.

network theorems See COMPENSATION THEOREM, MAXIMUM POWER TRANSFER THEOREM, NORTON'S THEOREM, RECIPROCITY THEOREM, SUPERPOSITION THEOREM, and THEVENIN'S THEOREM.

network topology The analysis of networks (see NETWORK, **1**) with signal-flow diagrams. Components of the diagram represent signal paths, open loops, closed loops, and node points.

network transfer function A function describing the overall processing of energy by a network (see NETWORK, **1**); it is equal to V_o/V_i, where V_i is the input voltage and V_o is the output voltage of the network.

Neuman's law A property of mutual inductances. For a given orientation and environment for two inductors, the value of the mutual inductance does not change, regardless of the magnitude, frequency, or phase of the currents in the coils. That is, mutual inductance is subject only to the physical environment surrounding the coils.

neuristor A two-terminal semiconductor device that simulates the behavior of a neuron (nerve cell) and allows machines to duplicate some of the neurological phenomena observed in the human body.

neuroelectricity Low-voltage electricity in the nervous system of a human being or animal.

neuron A nerve cell in a living organism.

neurosurgery assistance robot An electromechanical device, controlled by a human operator and assisted by computers, that helps to perform simple neurosurgical operations requiring extreme precision and steadiness. One procedure for which a robot has been used is the drilling of holes in the skull prior to brain surgery.

neutral **1.** Having no electric charge; thus, an atom is normally neutral because its internal positive charges neutralize its internal negative charges. **2.** Devoid of voltage (e.g., a neutral line). **3.** Pertaining to a chemical, especially a solution, that is neither acidic nor alkaline.

neutral bus See NEUTRAL WIRE.

neutral circuit **1.** A deenergized circuit (i.e., a "dead" one). **2.** In a teletypewriter system, a circuit in which current flows in one direction.

neutral conductor See NEUTRAL WIRE.

neutral ground A ground connection to a neutral wire or to the neutral point of a circuit.

neutralization The process of balancing out positive feedback in an amplifier to prevent self-oscillation. Also see NEUTRALIZING CAPACITOR and NEUTRALIZING COIL.

neutralization indicator A neon bulb or radio-frequency meter used during neutralization of an amplifier. When the amplifier is properly neutralized, the bulb or meter will show zero signal with no input to the amplifier, indicating that the circuit is not oscillating.

neutralize To eliminate positive feedback in a radio-frequency amplifier.

neutralized amplifier An amplifier in which neutralization has been performed to prevent self-oscillation.

neutralizing capacitor In a capacitively neutralized circuit, a small capacitor that serves as a coupler of signal energy from the output back to the input in reverse phase, to cancel self-oscillation of the circuit.

neutralizing circuit Any component or set of components that is used to neutralize a radio-frequency amplifier.

neutralizing coil In an inductively neutralized circuit, a small coupling coil that picks up signal energy from the output and applies it in reverse phase to the input, to cancel circuit self-oscillation.

neutralizing tool A nonconducting screwdriver-like device for adjusting a neutralizing capacitor or coil. It is usually made of fiber or plastic.

neutralizing voltage The feedback voltage that cancels self-oscillation in the process of neutralization.

neutralizing wand See NEUTRALIZING TOOL.

neutral line See NEUTRAL WIRE.

neutral relay See UNPOLARIZED RELAY.

neutral wire In a polyphase power-transmission system, the line (wire) that does not carry current until the system is unbalanced.

5059F-pN-466-487 4/10/01 9:21 AM Page 475

neutrodon See NEUTRODYNE.

neutrodyne A radio-frequency amplifier that is neutralized by feeding energy through a small capacitor from a tap on the secondary coil of the collector or drain output transformer back to the base or gate.

neutron An uncharged atomic particle having a mass approximately equal to that of the proton. The neutron is present in the nucleus of every atom, except that of hydrogen.

neutron age 16.7% of the mean square displacement of a neutron as it moves through a specified energy range.

neutron rest mass See MASS OF NEUTRON AT REST.

new candle See CANDELA.

newton (Sir Isaac Newton.) Symbol N. The SI unit of force. A force of 1 newton imparts an acceleration of 1 meter per second per second to a mass of 1 kilogram. The newton is equal to 10^5 dynes.

Newton's laws of motion Three natural laws discovered in 1686 by Sir Isaac Newton. First law: A body at rest or in motion tends to remain in that state, unless it is acted upon by some force. Second law: A body tends to accelerate or decelerate when it is acted upon by a force, the acceleration or deceleration being directly proportional to the force and inversely proportional to the mass of the body. Third law: For every action or acting force, there is an equal and opposite reaction or reacting force.

nexus An interconnection point in a system.

NF Abbreviation of NOISE FIGURE.

nF Abbreviation of NANOFARAD.

NFET Abbreviation of N-CHANNEL JUNCTION FIELD-EFFECT TRANSISTOR.

NFM Abbreviation of NARROWBAND FREQUENCY MODULATION. Also abbreviated NBFM.

NFM reception Reception of a signal having NARROWBAND FREQUENCY MODULATION. Standard discriminators and ratio detectors can be used. Slope detection can be achieved with an amplitude-modulation (AM) receiver by tuning slightly to one side of the center frequency of the FM signal.

NFM transmission Transmission of a signal via NARROWBAND FREQUENCY MODULATION. A simple method consists of frequency modulating the master oscillator of the transmitter at the modulation frequency. Phase modulation can also be used.

NFPA Abbreviation of *National Fire Protection Association* (see NATIONAL ELECTRIC CODE).

NFQ Abbreviation of *night frequency.*

NG **1.** Abbreviation of NEGATIVE GLOW. **2.** Abbreviation of *no good*, used for marking inoperative or malfunctioning components.

nH Abbreviation of NANOHENRY.

nhp Abbreviation of NOMINAL HORSEPOWER.

Ni Symbol for NICKEL.

nibble In computer operations, a four-bit word.

NICAD Acronym for NICKEL–CADMIUM.

NiCd Chemical symbol for NICKEL–CADMIUM.

Nichrome A nickel-chromium alloy used in the form of a wire or strip for resistors and heater elements.

nickel Symbol, Ni. A metallic element. Atomic number, 28. Atomic weight, 58.69. Nickel is familiar as an alloying metal in some resistance wires and as the material used in some electron-tube elements.

nickel–cadmium Acronym, NICAD. Chemical symbol, NiCd. A mixture used in certain rechargeable electrochemical cells and batteries. In recent years, these cells and batteries have been largely replaced by nickel–metal-hydride (NiMH) and lithium-based units. These batteries must be disposed of in a special way because of the toxic cadmium they contain. Compare NICKEL–METAL-HYDRIDE.

nickel–cadmium battery **1.** A battery of nickel–cadmium cells. **2.** Loosely, a nickel–cadmium cell. See also NICKEL–CADMIUM.

nickel-cadmium cell A small, rechargeable, electrochemical cell. The anode is cadmium, the cathode is nickel hydroxide, and the electrolyte is potassium hydroxide. See also NICKEL–CADMIUM.

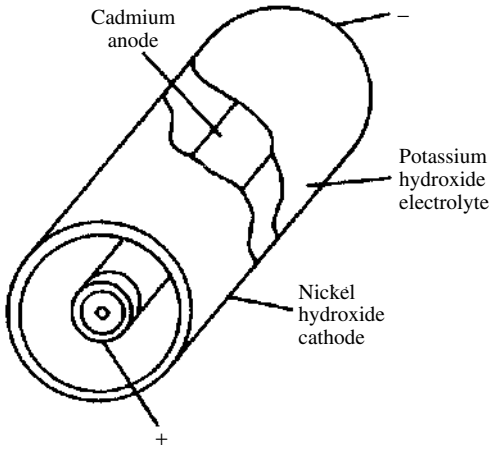

nickel-cadmium cell

nickel hydroxide Chemical symbol, NiOH. A compound used in certain rechargeable electrochemical power supplies. Examples are nickel–cadmium (NiCd or NICAD) and nickel–metal-hydride (NiMH) batteries, used in older notebook computers.

nickel–iron Chemical symbol, NiFe. A mixture used for a specialized rechargeable electrochemical cell in which the active positive plate material consists of nickel hydroxide. The active negative plate material is powdered iron oxide mixed with cadmium, and the electrolyte is potassium hydroxide.

5059F-pN-466-487 4/10/01 9:21 AM Page 476

nickel-iron battery See EDISON BATTERY.

nickel-metal–hydride Chemical symbol, NiMH. A mixture used in certain rechargeable electrochemical cells and batteries. This type of cell or battery is less likely than nickel–cadmium units to develop *battery memory* or *memory drain,* in which the ampere-hour capacity is reduced because of repeated partial discharging. In addition, the chemicals in NiMH cells and batteries are less toxic than those in NICADs. Compare NICKEL–CADMIUM.

nickel–metal-hydride battery **1.** A small, rechargeable, nickel-based electrochemical battery, similar to the nickel–cadmium (NICAD) type. **2.** Loosely, a nickel–metal-hydride cell. See NICKEL–METAL-HYDRIDE.

nickel–metal-hydride cell A small, rechargeable, nickel-based electrochemical cell, similar to the nickel–cadmium type. See also NICKEL–METAL-HYDRIDE.

nickel-oxide diode A diode fabricated from nickel-oxide semiconductor material.

nickel silver An alloy of copper, nickel, and zinc, sometimes used for making resistance wire. Also called GERMAN SILVER.

Nicol prism An optical component for producing or analyzing plane-polarized light. It consists of two prisms of Iceland spar cemented together. Light entering the device strikes the interface, where the ordinary ray is totally reflected and the extraordinary ray passes through, both rays being plane-polarized perpendicular to each other.

NIDA Abbreviation of *numerically integrating differential analyzer.*

NIF Abbreviation of NOISE IMPROVEMENT FACTOR.

NiFe Chemical symbol for NICKEL–IRON.

night effect A phenomenon sometimes observed at frequencies below approximately 500 kHz. Direction-finding signals received between sunset and the following sunrise appear to come from a transmitter that moves slowly back and forth.

night-effect errors In radio direction-finding, inaccurate or uncertain readings resulting from the NIGHT EFFECT.

night range The distance over which signals from a given transmitter are consistently received after sunset.

ni junction In a semiconductor device, the junction between an n-type layer and an intrinsic layer.

nil **1.** Colloquialism for *negligible.* **2.** British expression for *zero.* Also, *nought.* **3.** Colloquialism for *nothing.*

NiMH Chemical symbol for NICKEL–METAL-HYDRIDE.

niobium Symbol, Nb. A metallic element chemically resembling tantalum. Atomic number, 41. Atomic weight, 92.91.

NIPO Abbreviation of *negative input/positive output.*

NIR Abbreviation of NEAR INFRARED.

nit In digital-computer operations, a unit of data equal to 1.44 bits.

nitrocellulose See CELLULOSE NITRATE.

nitrogen Symbol, N. A gaseous element. Atomic number, 7. Atomic weight, 14.007. Nitrogen is the most-abundant component (about 78%) of the Earth's atmosphere.

NIU Abbreviation of NETWORK INTERFACE UNIT.

Nixonite A trade name for cellulose acetate, a plastic.

Nixonoid A trade name for cellulose nitrate, a plastic.

NJCC Abbreviation of *National Joint Computer Conference.*

n layer A semiconductor layer doped to provide current carriers that are predominantly electrons. Compare P LAYER.

n-level logic **1.** A multilevel form of logic, with *n* different possible states. **2.** In a computer, the connection of up to *n* logic gates.

NLR **1.** Abbreviation of *nonlinear resistance.* **2.** Abbreviation of NONLINEAR RESISTOR.

NLS Abbreviation of NO-LOAD SPEED.

N/m² Abbreviation of *newtons per meter squared* (pascals).

Nm²/kg Newton meters squared per kilogram, the SI unit of the *gravitational constant.*

NMAA Abbreviation of *National Machine Accountants Association.*

NMOS A metal-oxide semiconductor device made on a p-type substrate whose active carriers, electrons, migrate between n-type source and drain contacts.

NMR **1.** Abbreviation of NUCLEAR MAGNETIC RESONANCE. **2.** Abbreviation of NORMAL-MODE REJECTION.

n-n junction In a semiconductor device, especially an integrated circuit, the junction between two n-type regions having somewhat different properties (sometimes designated n_1 and n_2).

NO Abbreviation of NORMALLY OPEN.

No Symbol for NOBELIUM.

No. Abbreviation of NUMBER.

no-address instruction In digital computer operations, an instruction requiring no reference to storage or memory for its execution.

nobelium Symbol, No. A radioactive element produced artificially. Atomic number, 102. Atomic weight, approximately 259 (varies with isotope).

Nobili's rings See ELECTRIC RINGS.

noble Chemically inert or inactive. For example, *noble metals* oxidize less rapidly than *base metals.*

noble gas An inert rare gas (such as argon, helium, krypton, neon, or xenon). It is used in electronic glow devices.

noble metal A comparatively nonreactive metal (such as gold, silver, or platinum).

noctovision A television transmission system using infrared rays instead of visible light to scan the object. This makes it possible to televise images in complete visual darkness (hence, the prefix *nocto-*, meaning "night").

5059F-pN-466-487 4/10/01 9:21 AM Page 477

no-charge machine fault time Unproductive computer time resulting from errors or a malfunction.

nodal point See NODE.

node **1.** The terminal point at which two or more branches of a circuit meet, or a point that is common to two circuits. **2.** In a standing-wave system, a zero point or minimum point, e.g., current node. Compare LOOP, **1. 3.** A database management system expression defining the location of information about a record, user, field, etc. **4.** A point at which a satellite crosses the equator. See also ASCENDING NODE, DESCENDING NODE.

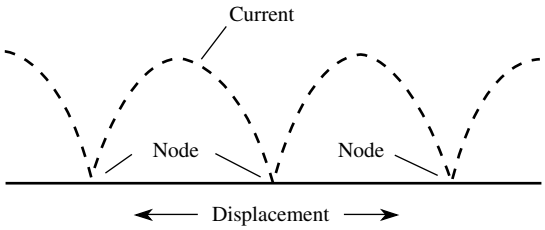

node, 2

nodules **1.** Oxide particles that protrude above the surface of magnetic tape. **2.** In a planar pattern describing radiation or pickup characteristics (as for antennas, microphones, loudspeakers), a small peak aligned in a direction other than that of the main lobe.

no-field release In the starting box for a shunt motor, the electromagnet that normally holds the arm in full-running position; it is connected in series with the field winding. When the field current is lost, the arm is released, disconnecting the armature for safety. Compare NO-VOLTAGE RELEASE.

noise **1.** A random-frequency current or voltage signal extending over a considerable frequency spectrum and having no useful purpose, unless it is intentionally generated for test purposes. **2.** Dissonant, interferential sound; unlike harmonious sound, it is disagreeable. **3.** In audio operations, unwanted hiss and/or hum. **4.** Extra bits or bytes that must be removed from digital data before it can be useful.

noise abatement The elimination or reduction of noise intensity—especially a measure in a program concerned with noise pollution in the environment.

noise analysis The measurement of the amplitude and spectral distribution of noise and the determination of its character.

noise analyzer An instrument for evaluating the nature of noise in a communications system. See, for example, NOISE METER. Noise analyzers are sometimes adapted for vibration analysis.

noise-balancing system A bridge circuit inserted between a receiver and antenna for balancing out interferential signals resulting from nearby power-line leaks or similar causes.

noise bandwidth Abbreviation, NBW. A figure obtained by dividing the area under the power-output-vs.-frequency curve of a device by the power amplitude at the noise frequency of interest.

noise behind the signal Noise caused by, but exclusive of, a signal.

noise blanker A device that cuts off one of the intermediate-frequency stages of a radio receiver during a noise pulse. The noise blanker is effective against high-amplitude impulses of short duration.

noise-canceling antenna A specialized receiving antenna system that uses two elements, one intended for receiving primarily the desired signal(s) and the other intended for receiving primarily local human-made noise. The outputs from the two elements are combined so that the noise impulses appear out of phase, but of equal amplitude. Because one element is located in a favorable position for reception of desired signals while the other element is not, the desired signals do not cancel at the receiver input. As a result, the signal-to-noise ratio is greatly improved, compared with the use of the signal antenna alone.

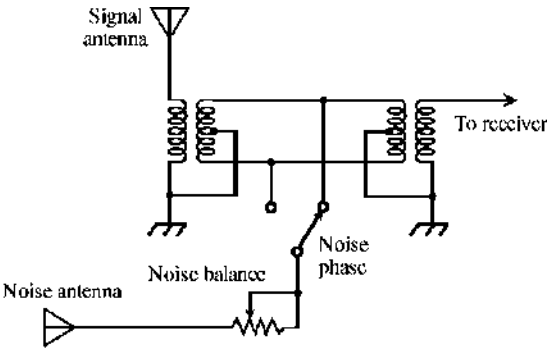

noise-canceling antenna

noise-canceling microphone A microphone that discriminates against background sounds. It is usually directional and relatively insensitive, requiring the user to talk directly into it at close range.

noise clipper A biased-diode circuit used as an automatic noise limiter. The device cuts off all signals above a predetermined amplitude on the theory that noise peaks are high-level transients in an otherwise uniform signal. Noise is reduced at the sacrifice of system reproduction fidelity.

noise criteria An expression for the level of ambient acoustic noise.

noise current Noise-generated current.

5059F-pN-466-487 4/10/01 9:21 AM Page 478

noise-current generator A noise generator that supplies a useful current. Compare NOISE-VOLTAGE GENERATOR.

noise digit A digit (usually zero) generated during normalization of a floating-point number. See NORMALIZE.

noise diode A reverse-biased semiconductor diode that produces a standard noise voltage.

noise elimination The nearly complete removal of noise effects from a system. Noise can never be eliminated altogether because the movement of electrons and atoms generates some electrical and thermal noise. However, in some digital systems, the effects of noise can be almost totally overcome. Compare NOISE SUPPRESSION.

noise equivalent power Abbreviation, NEP. The power that produces an rms signal-to-noise ratio of 1 in a detector.

noise factor For a circuit, especially a communications receiver or weak-signal amplifier, the ratio R_1/R_2, where R_1 is the signal-to-noise power ratio of an ideal circuit, and R_2 is the signal-to-noise ratio of the circuit under test. Compare NOISE FIGURE.

noise figure The NOISE FACTOR of a circuit, expressed in decibels. If N is the noise factor expressed as a ratio, then noise figure N_{dB} can be determined by $N_{dB} = 10 \log_{10} N$.

noise filter A filter designed to suppress noise that would otherwise enter an electronic circuit (e.g., a power-line noise filter).

noise floor **1.** In a receiver, the level of noise in microvolts that determines the weakest signal that can be heard or accurately received. **2.** In a spectrum analyzer, the level of noise that determines the weakest signal that will be visibly displayed.

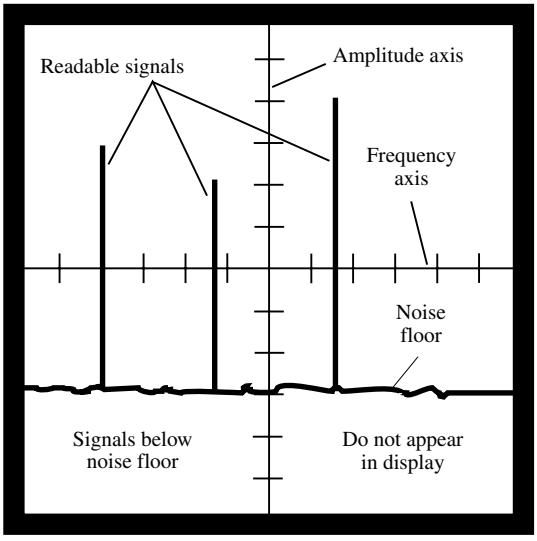

noise floor, 2.

noise generator A device for generating precise amounts of noise voltage for test purposes.

noise grade **1.** The relative level of radio-frequency background noise, over all electromagnetic frequencies, in a particular geographic location. The noise grade is generally lowest near the poles and highest near the equator. **2.** The mathematical function of relative electromagnetic noise intensity versus latitude and longitude.

noise immunity The degree to which a circuit or device is insensitive to extraneous energy—especially noise signals.

noise-improvement factor Abbreviation, NIF. For a radio receiver, the ratio SN_i/SN_o, where SN_i is the input signal-to-noise ratio and SNo is the output signal-to-noise ratio.

noise killer **1.** See AUTOMATIC NOISE LIMITER. **2.** See NOISE FILTER. **3.** See NOISE BLANKER.

noiseless alignment See VISUAL ALIGNMENT.

noise level **1.** The amplitude of ambient electrical noise generated outside an electronic system of interest. **2.** The amplitude of electrical noise generated in an electronic system of interest. **3.** The intensity of ambient acoustic noise.

noise limiter See AUTOMATIC NOISE LIMITER.

noise margin In a binary logic circuit, the difference between operating and threshold voltages.

noise-measuring set See NOISE METER.

noise meter An instrument for measuring acoustic noise level. It consists essentially of a sensitive, multirange voltmeter provided with a microphone, amplifier, and attenuators. The meter scale reads noise level directly in decibels.

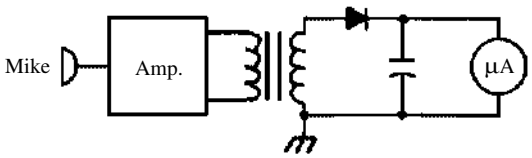

noise meter

noise power The power component of a noise signal.

noise power ratio The ratio of noise power at the output of a circuit (such as a receiver) to the noise power at the input.

noise pulse A random short-duration noise burst whose amplitude exceeds the average peak noise level.

noise quieting In a radio receiver, the reduction (in decibels) of background noise, with respect to a signal of interest.

noise ratio See NOISE POWER RATIO.

noise-reducing antenna A receiving antenna having a balanced transmission line and usually some form of noise-balancing system for reducing electrical noise picked up by the antenna.

5059F-pN-466-487 4/10/01 9:21 AM Page 479

noise reduction See NOISE SUPPRESSION.

noise residue The residual output (see NULL VOLTAGE, **1**) of a balanced bridge, caused entirely by noise.

noise silencer A noise-limiting circuit that removes noise-pulse transients with little or no effect on the signal from which the noise is removed. Compare NOISE CLIPPER.

noise source See NOISE GENERATOR.

noise spike See NOISE PULSE.

noise suppression **1.** In communications, the reduction of noise amplitude to a level that is noncompetitive with desired signals. **2.** In audio recording and reproduction, reduction of unwanted noise (e.g., hiss) to the greatest extent possible without degrading the fidelity of the desired audio. Compare NOISE ELIMINATION.

noise suppressor A device for eliminating electrical noise or reducing its amplitude. See, for example, AUTOMATIC NOISE LIMITER and NOISE BLANKER.

noise temperature At a given frequency, the temperature of a passive system that has the same noise power per unit bandwidth as that observed at the terminals of a device under test.

noise voltage The voltage component of an electrical noise signal.

noise-voltage generator A signal generator that supplies an alternating-current waveform containing random-frequency pulses of relatively uniform distribution over a given frequency spectrum. Compare NOISE-CURRENT GENERATOR.

noisy mode During normalization of a floating-point number, the generation of digits, excluding zero, as part of the fixed-point part (see NORMALIZE).

NOL **1.** Abbreviation of *National Ordnance Laboratory.* **2.** Abbreviation of *Naval Ordnance Laboratory.*

no-load current **1.** Output-electrode current (e.g., drain, plate, or collector current) when a device is not delivering output to an external load. **2.** Current flowing in the primary winding of an unloaded transformer.

no-load losses Losses in an unloaded transformer (see NO-LOAD CURRENT, **2**).

no-load speed The rotational speed of an unloaded motor.

no-load voltage The open-circuit output voltage of a power supply, amplifier, generator, or network.

nominal **1.** Named, rated, or specified. The nominal value of a speaker, for example, might be 8 ohms, even though the actual impedance value depends on the frequency of the applied signal. **2.** Approximate, and specified as a typical example only, for the purpose of identifying the operating or value range. For example, an automotive circuit might have a nominal rating of 12 volts—even though it can be operated at 10 volts to 14.6 volts.

nominal band In a facsimile signal, the waveband extending between zero and the maximum frequency of modulation.

nominal bandwidth **1.** For a filter, the difference $f_{c2} - f_{c1}$, where f_{c1} is the nominal lower cutoff frequency and f_{c2} is the nominal upper cutoff frequency. **2.** For an allocated communication channel, the total bandwidth, including upper and lower guard frequencies. **3.** The intended and specified bandwidth of a given channel, regardless of the bandwidth of the signal on that frequency at any given time.

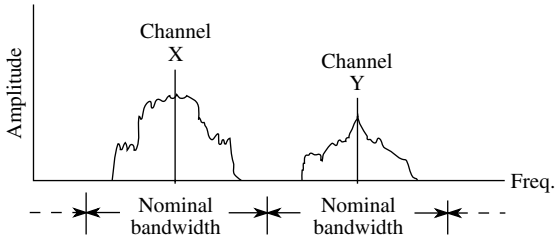

nominal bandwidth, 2

nominal capacitance The rated ("label") value of a capacitor. Also see NOMINAL VALUE.

nominal current The rated ("nameplate") value of required current or of current output. Also see NOMINAL VALUE.

nominal horsepower The rated ("nameplate") horsepower of a machine, such as a motor. Also see NOMINAL VALUE.

nominal impedance The rated impedance of a circuit or device. Also see NOMINAL VALUE.

nominal inductance The rated ("label") value of a coil's inductance. Also see NOMINAL VALUE.

nominal line pitch In a television raster, the average center-to-center separation between adjacent lines.

nominal line width **1.** For a television raster, the factor $1/n$, where n is the number of lines per unit width for the direction in which the lines progress. **2.** In facsimile, the average center-to-center separation of scanning or recording lines.

nominal power factor The rated ("nameplate") value of power factor of a device. Also see NOMINAL VALUE.

nominal power rating The rated ("nameplate") value of power output, power drain, or power dissipation. Also see NOMINAL VALUE.

nominal *Q* The rated ("nameplate") value of Q of a capacitor, inductor, transformer winding, or tank circuit. Also see NOMINAL VALUE.

nominal rating See NOMINAL, **1**, **2**.

nominal resistance The rated ("label") value of a resistor or similar device. Also see NOMINAL VALUE.

nominal speed The highest speed of a data-processing unit or system, disregarding slowdowns because of factors other than computational operations.

nominal value A named, specified, rated, or labeled value, given without reference to tolerance.

5059F-pN-466-487 4/10/01 9:21 AM Page 480

This can differ significantly from the actual value. For example, the nominal value of a capacitor might be 100 pF; but if the tolerance is ±10 percent, the actual capacitance might be any value between 90 pF and 110 pF.

nominal voltage **1.** The rated ("nameplate") value of required voltage or of voltage output. Also see NOMINAL VALUE. **2.** In a cell or battery, the MIDPOINT VOLTAGE.

nomogram See ALIGNMENT CHART.

nomograph See ALIGNMENT CHART.

nomography The geometric representation of a mathematical function or relation by means of alignment charts.

nonaccountable time The period during which a computer system is unavailable to the user (because of a power outage, for example).

nonarithmetic shift See LOGICAL SHIFT.

nonblinking meter A digital meter that does not alternate, or oscillate, between two different values when the measured parameter is between two discrete values. Instead, the display is rounded off to the nearest value, and the display remains at that value continuously.

nonblocking system In a telephone communications network, a system that ensures a circuit will be completed when necessary. That is, at no time is it impossible for a connection to be made. Under conditions of extremely heavy usage, the quality of communications might be degraded, but the connection will not be cut off.

nonbridging contact In a switch or relay, a movable contact that leaves one stationary contact before contacting another.

nonchargeable battery A primary battery (i.e., one that cannot ordinarily be recharged). An example is a battery of common zinc-carbon or alkaline cells.

noncoherent Pertaining to electromagnetic radiation in which the wave disturbances are not all precisely aligned in frequency and phase.

nonconductor See DIELECTRIC.

noncontact temperature measurement The use of infrared or optical electronic equipment to measure the temperature of bodies without touching them.

noncorrosive flux A solder flux that does not corrode the metals to which solder is applied.

noncrystalline Pertaining to materials that possess none of the characteristics of crystals. Compare CRYSTALLINE MATERIAL.

nondestructive read In digital computer and counter operation, the process of reading data without erasing it as a result. The name is also applied to the readout device.

nondestructive test Abbreviation, NDT. A test that does little or no irreversible harm to the test sample. Compare DESTRUCTIVE TEST.

nondeviated absorption Absorption that slows waves by a negligible amount; also, normal skywave absorption.

nondirectional antenna An antenna that displays equally intense radiation or equally sensitive reception in all directions within a specified plane. An example is a vertical dipole antenna, which is nondirectional in the horizontal plane.

nondirectional microphone A microphone that responds equally well to sound from any direction; an omnidirectional microphone.

nondissipative load A purely reactive load. In such a load, the only power consumed is that which is dissipated in the inherent resistance (losses) of the load.

nondissipative stub A stub that exhibits only slight losses; it consumes no power, except that dissipated in small, inherent losses. Also see STUB.

nonelectrical Not electrical in nature. The term is commonly used to designate the mechanical parts of electromechanical systems, such as robots and servomechanisms.

nonelectrolyte A substance that does not ionize in water solution. Compare ELECTROLYTE.

nonelectronic meter A meter that uses no electronic devices (such as transistors, liquid crystals, light-emitting diodes, or integrated circuits). Also called *conventional meter.*

nonequivalence operation See EXCLUSIVE-OR OPERATION.

nonerasable storage In digital-computer and data-processing operations, storage media that cannot be erased under ordinary circumstances. A common example is CD-ROM (compact-disk read-only memory).

nonferrous metal A metal or alloy that does not contain iron, and is not related to iron in the sense that it is not attracted to magnets.

nonflammable Pertaining to a material that is resistant to burning.

nonharmonic frequency A frequency that has no integral numerical relationship to another frequency of interest. Compare HARMONIC FREQUENCY.

nonharmonic oscillations Parasitic oscillations that do not occur at the fundamental frequency nor at any harmonic frequency of an oscillator or amplifier in which they appear.

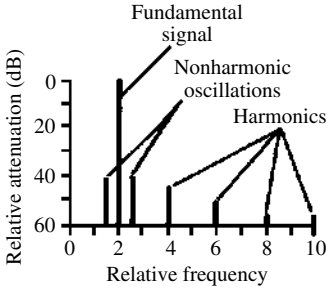

nonharmonic oscillations

5059F-pN-466-487 4/10/01 9:21 AM Page 481

nonillion The number 10^{30}, so called because when written out, the number contains nine groups of three zeros (following the first 1000).

noninductive capacitor A wound capacitor in which the edges of one of the spiral windings are connected together to minimize the inductance of the roll. Compare INDUCTIVE CAPACITOR.

noninductive resistor A wirewound resistor constructed so that the magnetic field of the coil is self-canceling. Therefore, the inductance is practically eliminated.

noninterlaced scanning In the display of a video image, the presentation of all the raster lines in a single scan. It is commonly used in cathode-ray-tube (CRT) computer monitors. This process minimizes "jerkiness" in rapidly moving images.

noninverting connection Connection to the noninverting input of a differential or operational amplifier. Also see NONINVERTING INPUT. Compare INVERTING CONNECTION.

noninverting input In a differential or operational amplifier, the input that provides an output signal in phase with the input. Compare INVERTING INPUT.

noninverting transponder In a communications satellite, a transponder in which the downlink band is "rightside-up" in frequency relative to the uplink band. That is, the highest downlink frequency corresponds to the highest uplink frequency, and the lowest downlink frequency corresponds to the lowest uplink frequency. Compare INVERTING TRANSPONDER. Also see DOWNLINK, TRANSPONDER, UPLINK.

nonionic **1.** Possessing none of the properties of ions. **2.** Electrically neutral.

nonionizing radiation Electromagnetic radiation that does not cause ionization of gases under a given set of conditions. Examples: radio signals, television signals, and visible light.

nonlinear **1.** Pertaining to components, circuits, or devices in which the instantaneous output signal amplitude is not directly proportional to the instantaneous input signal amplitude. The graph of instantaneous output versus instantaneous input is a curve, not a straight line. Example: CLASS-C AMPLIFIER. **2.** Pertaining to components, circuits, or devices in which a specified value is not directly proportional to some other specified value. Example: NONLINEAR CAPACITOR.

nonlinear bridge See VOLTAGE-SENSITIVE BRIDGE.

nonlinear capacitor A capacitor whose value varies nonlinearly with applied voltage. Also see VOLTAGE-VARIABLE CAPACITOR, **1**, **2**.

nonlinear coil See SATURABLE REACTOR.

nonlinear dielectric A material (such as processed barium-strontium titanate) whose dielectric constant varies with applied voltage.

nonlinear distortion Distortion caused by nonlinear response of an amplifier or component. This causes different parts of the signal to be amplified or transmitted by different amounts; therefore, the amplitude variations in the output signal differ from those in the input signal.

nonlinear inductor See SATURABLE REACTOR.

nonlinearity **1.** The condition of being NONLINEAR. In an amplifier, this means that the output signal is not a faithful reproduction of the input signal, and distortion occurs. **2.** A measure of the extent to which a circuit is nonlinear. Expressed as a percentage of peak-to-peak full-scale output, the maximum extent to which the output differs from a perfect reproduction of the input.

nonlinearity error An error in received signals resulting from nonlinearity in one or more of the stages in the communications circuit.

nonlinear mixing The mixing of signals as a result of the nonlinear response of a device (such as a semiconductor diode operated in its square-law region) through which they are passed simultaneously. Also see MIXER and MIXING.

nonlinear network A circuit that produces distortion in an input waveform; the output and input waves are not related by a linear function.

nonlinear quantizing A method of signal quantizing in which the intervals are not all the same size or duration.

nonlinear resistor A resistor whose value varies with applied voltage. Also see VOLTAGE-DEPENDENT RESISTOR.

nonlinear response Any response for which the corresponding plot is not a straight line; doubling the independent variable, for example, does not double the dependent variable.

nonloaded *Q* See UNLOADED *Q*.

nonmagnetic **1.** Possessing no magnetism. **2.** Incapable of being magnetized.

nonmathematical Pertaining to materials and methods that rely upon physical description and qualitative procedures instead of mathematical development, prediction, and quantitative procedures.

nonmetal An elemental material devoid of the properties exhibited by metals (e.g., luster, good ductility, electrical conductivity, heat conductivity, and malleability). Examples: carbon, phosphorus, sulfur. Compare METAL and METALLOID.

nonmetallic conduction Collectively, ionic conduction in liquids and gases, conduction in dielectrics by small leakage currents, and thermionic conduction in a vacuum.

nonmicrophonic Without microphonic properties, e.g., a nonmicrophonic integrated circuit does not produce electrical ringing when physically struck.

nonnumeric character A character that is not a numeral, i.e., a symbol or letter.

nonohmic response **1.** Nonlinear resistance or reactance. Compare OHMIC RESPONSE. **2.** See NEGATIVE RESISTANCE.

nonoscillating detector A detector devoid of positive feedback action and, therefore, unable to

5059F-pN-466-487 4/10/01 9:21 AM Page 482

generate a signal on its own. Compare OSCILLATING DETECTOR.

nonplanar **1.** Existing in three spatial dimensions. **2.** Pertaining to a circuit that cannot be fabricated on a two-dimensional board without the use of jumper wires.

nonpolar **1.** Having no pole(s). **2.** Pertaining to atoms that share electrons to complete their outer shells. **3.** Not polarized nor requiring polarization. Example: a 100-pF disk ceramic capacitor is nonpolar because it can be used in circuits without consideration of voltage polarity.

nonpolar crystal A crystal in which lattice points are identical.

nonpolarized electrolytic capacitor An electrolytic capacitor that has no definite negative and positive terminals and, consequently, can be used in alternating-current circuits, as well as in direct-current circuits. See also NONPOLAR, **3**.

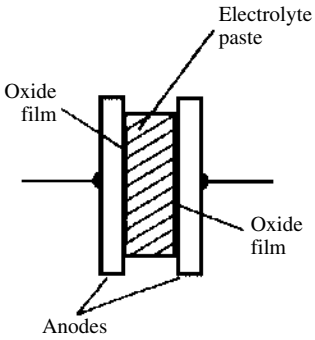

nonpolarized electrolytic capacitor

nonpolarized reactor A saturable reactor in which the lines of flux produced in the three-leg core by the coils on the two outer legs oppose each other in the center leg. When direct current (dc) is passed through the coil on the center leg to saturate the core, operation remains the same for either dc polarity. Compare POLARIZED REACTOR.

nonpolarized relay See UNPOLARIZED RELAY.

nonprint code In telegraphy, a code used to start teleprinter functions excluding printing.

nonreactive circuit A circuit containing pure resistance only.

nonrechargeable battery See NONCHARGEABLE BATTERY.

nonrecurrent Pertaining to phenomena that do not repeat periodically. Thus, a single sweep in an oscilloscope is nonrecurrent.

nonrecurrent sweep See NONREPETITIVE SWEEP.

nonregenerative detector A detector having no regenerative feedback. Such a detector is stable, but relatively insensitive. Compare REGENERATIVE DETECTOR.

nonregenerative receiver A radio receiver in which no local signal whatever is generated.

nonrepetitive phenomena See NONRECURRENT.

nonrepetitive sweep In an oscilloscope, a single horizontal sweep of the electron beam, initiated either by the operator or by the signal under observation. Also called SINGLE SWEEP. Compare RECURRENT SWEEP.

nonreset timer A timer that must be reset manually.

nonresident routine A computer routine not permanently stored in memory. Compare RESIDENT ROUTINE.

nonresonant **1.** Pertaining to a resonant circuit or device operated at some frequency other than one of its resonant frequencies. Thus, reactance is present at the operating frequency. See RESONANCE. **2.** Pertaining to a circuit or device that exhibits pure resistance (without reactance) over a wide range of frequencies.

nonresonant lines Transmission lines so dimensioned and operated that they do not resonate at the operating frequency.

nonresonant load An alternating-current load that is either purely resistive or is detuned from the fundamental and harmonic frequencies of the source from which it is operated.

nonreturn to zero In the magnetic recording of digital data, the system in which the current flowing in the write-head coil is sustained (i.e., does not return to zero) after the write pulse.

nonsalient pole A nonprojecting (often flush) pole. Compare SALIENT POLE.

nonsaturated color **1.** Visible light that consists of energy at more than one wavelength. **2.** A color that contains some white, in addition to the pure color.

nonsaturated logic A logic circuit in which transistors are prevented from saturating. This results in higher operating speed than SATURATED LOGIC using the same transistors.

nonshorting switch A multiple-throw switch that disconnects one circuit before completing another; that is, no two poles are ever connected simultaneously.

nonsinusoidal waveform A waveform whose curve cannot be represented by the equation $y = c \sin a(x + b)$, where a, b, and c are constants, y is the dependent variable (usually instantaneous amplitude or frequency), and x is the independent variable (usually time), for any real-number values of a, b, and c. Examples: BACK-TO-BACK SAWTOOTH, SAWTOOTH, and SQUARE WAVE. The COSINE WAVE is sinusoidal, being a SINE WAVE shifted in phase by 90 degrees.

nonsymmetrical wave See ASYMMETRIC WAVE.

nonsynchronous Unrelated in cyclic quality to other such qualities in the system.

nonsynchronous network A communications network in which the clocks are not all synchronized.

nonsynchronous vibrator A power-supply vibrator that is essentially a single-pole, double-throw switch providing no mechanical rectification. A separate rectifier must be used. Compare

5059F-pN-466-487 4/10/01 9:21 AM Page 483

VIBRATOR-TYPE RECTIFIER. Also see VIBRATOR-TYPE POWER SUPPLY.

nontechnical Pertaining to circuits, devices, systems, or phenomena described in lay terms, using concise graphics and little or no mathematics. An example is the simplified explanation of the operation of a spread-spectrum radio transmitter.

nontonal components See NOISE, **3**.

nontrigger voltage For a thyristor, the maximum gate-to-cathode voltage that can be applied without triggering the device. The amplitude of interferential signals, including noise, must be below this level to prevent accidental triggering.

nonuniform field An electric or magnetic field whose intensity is not the same at all points.

nonvolatile memory Memory whose data is retained even when power is removed for extended periods. This type of memory requires no backup power source. The main advantage of this type of memory is the fact that the data is not lost in case of a power interruption. Memory should not be confused with storage. Magnetic, magneto-optical, or optical disks (including hard drives) are storage media, not memory. Memory data can be stored and retrieved much faster than storage data, because memory uses no mechanical parts. Also see RANDOM-ACCESS MEMORY, READ-ONLY MEMORY. Compare VOLATILE MEMORY.

nonvolatile storage A computer storage medium in which the data does not require a source of power to be retained. Examples: MAGNETIC DISK, MAGNETIC TAPE, and COMPACT-DISK READ-ONLY MEMORY.

no-op instruction An instruction that commands a computer to perform no operation, other than to proceed to the following instruction.

NOR circuit Also called NOT-OR CIRCUIT. In computer and control operations, a circuit that delivers a zero output signal, except when two or more input signals are zero. The NOR circuit function is the inverse of that of the OR circuit.

NOR gate A gate that performs the functions of a NOR circuit.

norm The average or ambient condition.

A	B	C
0	0	1
0	1	0
1	0	0
1	1	0

NOR circuit

normal **1.** Pertaining to the most commonly observed set of conditions or parameters. **2.** Standard. **3.** Perpendicular; oriented at right angles. **4.** Pertaining to a NORMAL DISTRIBUTION. **5.** Pertaining to a NORMAL SOLUTION. **6.** Pertaining to an atom at its lowest energy state. See NORMAL STATE OF ATOM.

normal curve See BELL-SHAPED CURVE.

normal distribution In a statistical evaluation, a probability distribution represented by the so-called bell-shaped curve. The maximum probability occurs at the 50-percent value.

normal-distribution curve See BELL-SHAPED CURVE.

normal electrode A standard electrode used in electrode-potential measurements.

normal fault An unintended path between the hot terminal of a load and ground.

normal fault plus grounded neutral fault A combination of NORMAL FAULT and GROUNDED NEUTRAL FAULT.

normal glow discharge In a glow-discharge tube, the discharge region between the Townsend discharge and the abnormal glow in which current increases sharply, but a constant voltage drop is maintained across the tube.

normal impedance A transducer's input impedance when the load impedance is zero.

normal induction curve A saturation curve for a magnetic material. Also see BOX-SHAPED LOOP and SATURABLE REACTOR.

normalize In computer programming, to use floating-point numbers to modify the fixed-point part of a number so that it is within a desired range.

normalized admittance The quantity $1/Z_n$, where Z_n is NORMALIZED IMPEDANCE.

normalized frequency The unitless number represented by the ratio f/f_r, where f_r is a reference frequency and f is a frequency of interest. Response plots are sometimes conveniently drawn on the basis of normalized frequency, the reference (or resonant) frequency being indicated as **1**, twice the reference frequency as **2**, etc.

normalized impedance A value of impedance divided by the characteristic impedance of a waveguide.

normally closed Abbreviation, NC. Pertaining to a switch or relay whose contacts are closed when the device is at rest. Compare NORMALLY OPEN.

normally open Abbreviation, NO. Pertaining to a switch or relay whose contacts are open when the device is at rest. Compare NORMALLY CLOSED.

normal mode Pertaining to a device or system operated in its usual or most common manner.

normal mode A state of acoustic resonance in an enclosure, such as a speaker cabinet or a room.

normal-mode rejection Abbreviation, NMR. In a digital direct-current voltmeter, the level of noise on the applied voltage that will be rejected by the instrument. Compare COMMON-MODE REJECTION.

5059F-pN-466-487 4/10/01 9:21 AM Page 484

normal position In a switch or relay, the state of the contacts when the device is at rest.

normal solution A solution, such as an electrolyte, in which the amount of dissolved material is chemically equivalent to 1 gram-atomic weight of hydrogen per liter of the solution. Compare MOLAR SOLUTION.

normal state of atom The condition in which an atom is at its lowest energy level. For the hydrogen atom, for example, the state in which the electron is in the lowest-energy orbit.

normal-through A feature in an audio PATCH BAY or PATCH PANEL that connects two sockets by default. The top socket and the one immediately below it are connected, even when a patch cord is not plugged into either of them.

northern lights See AURORA.

north magnetic pole The north pole of the equivalent bar magnet constituted by the EARTH'S MAGNETIC FIELD. The north magnetic pole lies close to the geographic north pole. Compare SOUTH MAGNETIC POLE.

north pole 1. See NORTH MAGNETIC POLE. **2.** The earth's geographic north pole. **3.** See NORTH-SEEKING POLE.

north-seeking pole Symbol, N. The so-called north pole of a magnet. When the magnet is suspended horizontally, this pole points in the direction of the earth's north magnetic pole. Compare SOUTH-SEEKING POLE.

Norton's equivalent An equivalent circuit based on NORTON'S THEOREM, replacing a Thevenin equivalent for a current-actuated device, such as a bipolar transistor. Also see THEVENIN'S THEOREM.

Norton's theorem With reference to a particular set of terminals, any network containing any number of generators and any number of constant impedances can be simplified to one constant-current generator and one impedance. The equivalent circuit will deliver to a given load the same current that would flow if the output terminals of the original circuit where short-circuited. Compare COMPENSATION THEOREM, MAXIMUM POWER TRANSFER THEOREM, RECIPROCITY THEOREM, SUPERPOSITION THEOREM, and THEVENIN'S THEOREM.

NOT In binary logic, an operation that changes high to low and vice versa. Also see NAND CIRCUIT, NOR CIRCUIT, NOR GATE, NOT CIRCUIT, and NOT-OR CIRCUIT.

NOT-AND circuit See NAND CIRCUIT.

notation The way that numbers, quantities, or formulas are represented (e.g., *binary notation*, *Polish notation*, and *scientific notation*).

notch A dip in frequency response, typical of a band-suppression (band-elimination) filter or other frequency-rejection circuit. Compare PEAK, **3**.

notch amplifier An amplifier containing a notch filter or other arrangement that permits it to reject one frequency or a given band of frequencies while passing all higher and lower frequencies.

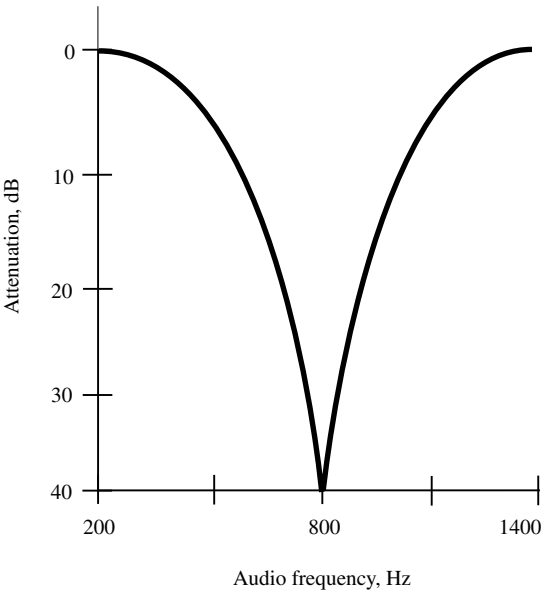

notch

notch antenna An antenna with a slot in the radiating surface, for the purpose of obtaining a directional response.

notcher See NOTCH FILTER.

notcher-peaker A circuit or device that can be set to perform either as a NOTCH FILTER or PEAK FILTER.

notch filter A circuit that exhibits high attenuation at and near a single frequency and little or no attenuation at all other frequencies. This type of device is used in some radio communications receivers, and can reduce interference caused by strong, unmodulated carriers within the passband. The notch frequency is adjustable, so that the deep null can be tuned to any frequency within the receiver passband. A properly designed circuit can produce attenuation in excess of 40 dB in the center of the notch. Some sophisticated types, especially audio designs, can provide more than 60 dB of attenuation at the notch frequency. Audio notch filters employ operational amplifiers with resistance-capacitance (RC) circuits. In some audio notch filters, the notch width (sharpness) and frequency are both adjustable. Compare BAND-REJECTION FILTER.

notch gate In radar, a gate that determines the minimum and maximum range.

notch sweep An oscilloscope sweep that expands only a small portion (notch) of the pattern on the screen, leaving the portions on either side of the notch untouched. Thus, the first dozen or so

5059F-pN-466-487 4/10/01 9:21 AM Page 485

cycles might appear at the normal sweep speed, the next two cycles expanded, and the remaining two or three at normal sweep speed.

NOT circuit A logic circuit that provides an output pulse when there is no input pulse, and vice versa. Also called COMPLEMENTER, NEGATOR, and INVERTER.

note See BEAT NOTE.

notebook computer A portable personal computer, also called a *laptop computer.* It is about the size of a typical three-ring notebook, and generally contains a DISKETTE DRIVE, a HARD DISK, a MODEM, and attachments for peripherals, such as printers. It uses rechargeable batteries and can be operated for approximately two to six hours between battery charges.

NOT gate A digital circuit that inverts a logical condition—either from high (logic 1) to low (logic 0) or vice versa. Also called an *inverter.*

NOT-OR circuit A logical OR CIRCUIT combined with a NOT CIRCUIT.

novelty calculator See SPECIAL-PURPOSE CALCULATOR.

November Phonetic alphabet code word for the letter N.

novice **1.** A beginner class of amateur radio license. **2.** Any beginner or inexperienced practitioner.

no-voltage release In the starting box for a shunt motor, the electromagnet that normally holds the arm in full-running position. It is connected directly across the power line to disconnect the motor in the event of power failure. When the arm is released, it falls to its off position, thereby preventing burnout that would result if the motor were left connected to the line in the full-running position when power resumed. Compare NO-FIELD RELEASE.

noys scale A scale of apparent acoustic noise, based on a linear function instead of the more common logarithmic function.

Np **1.** Symbol for NEPTUNIUM. **2.** Abbreviation of NEPER.

N_p Symbol for number of primary turns in a transformer.

n-phase system A polyphase system having n phases.

npin transistor A junction transistor having an intrinsic layer between a p-type base and an n-type collector. The emitter is a second n-type layer on the other side of the base.

N plant See NUCLEAR POWER PLANT.

n-plus-one address instruction A computer program instruction containing two addresses, one of which specifies the location of an upcoming instruction to be executed.

NPM Symbol for *counts per minute.*

npnp device A semiconductor switching device having three junctions. Examples: FOUR-LAYER DIODE, and SILICON-CONTROLLED RECTIFIER. Also called *pnpn device.*

npn transistor A bipolar transistor in which the emitter and collector layers are n-type semiconductor material, and the base layer is p-type semiconductor material. Compare PNP TRANSISTOR.

NP0 Abbreviation of NEGATIVE POSITIVE ZERO.

NP0 capacitor A fixed capacitor exhibiting temperature-compensating ability over a wide temperature range, in which the coefficient has negative, positive, and zero values.

NPS Symbol for *counts per second.*

N radiation X rays emitted as a result of an electron becoming an N electron.

NRD Abbreviation of NEGATIVE-RESISTANCE DIODE.

N region See N LAYER.

NRZ Abbreviation of NONRETURN TO ZERO.

N_s Symbol for number of secondary turns in a transformer.

ns Abbreviation of NANOSECOND.

N scan See N DISPLAY.

N scope Colloquialism for a radar set using an N DISPLAY.

nsec Alternate abbreviation of NANOSECOND.

Ns/m² Newton-seconds per meter squared, the unit of dynamic viscosity.

n-space A coordinate system in n variables. It is generally of mathematical interest. The coordinates are written $(x_1, x_2, x_3, \ldots, x_n)$ and are called *ordered n-tuples.*

NSPE Abbreviation of *National Society of Professional Engineers.*

NTC Abbreviation of NEGATIVE TEMPERATURE COEFFICIENT.

nth harmonic An unspecified harmonic, having a frequency of n times the fundamental frequency, where n is some positive integer. Also see HARMONIC and HARMONIC FREQUENCY.

nth term An unspecified term in a mathematical sequence or series.

NTP Abbreviation of NORMAL TEMPERATURE AND PRESSURE.

NTSC Abbreviation of *National Television Standards Committee.*

NTSC color signal The color-television signal specified by the National Television Systems Committee. In the signal, the phase of a 3.58-MHz signal varies with the instantaneous hue of the transmitted color, and the amplitude varies with the instantaneous saturation of the color.

NTSC triangle On a chromaticity diagram, a triangle whose sides encompass the range of colors obtainable from the additive primaries.

NTSC-type generator A special radio-frequency signal generator for color-television tests. It provides separate, individually selected color bars that are fully saturated. The signals are strictly in accordance with NTSC standards.

n-type conduction In a semiconductor, current flow consisting of electron movement. Compare P-TYPE CONDUCTION.

5059F-pN-466-487 4/10/01 9:21 AM Page 486

n-type material Semiconductor material that has been doped with a donor-type impurity and, consequently, conducts a current via electrons. Germanium, for example, when doped with arsenic, becomes n-type. Compare P-TYPE MATERIAL.

n-type semiconductor See N-TYPE MATERIAL.

nuclear battery See ATOMIC BATTERY.

nuclear bombardment In nucleonics, the bombarding of the nucleus of an atom with subatomic particles, usually neutrons.

nuclear charge The net positive charge of the nucleus of an atom.

nuclear clock A chronometer based on the rate of disintegration of a radioactive material.

nuclear energy Energy resulting from the splitting of the nucleus of an atom or from the fusion of nuclei. Also see ATOMIC ENERGY, ATOMIC POWER, NUCLEAR FISSION, NUCLEAR FUSION, NUCLEAR REACTOR, and NUCLEUS.

nuclear fission A nuclear reaction resulting from the bombardment of nuclei in the atoms of certain radioactive materials. The bombardment with neutrons creates two new nuclei (by splitting) and several new neutrons that split several other nuclei, producing still more nuclei and neutrons, etc. The result is a *chain reaction* that can lead to a violent explosion if not checked. Compare NUCLEAR FUSION.

nuclear force A strong attraction that holds together pairs of nucleons in an atomic nucleus. This prevents an electric charge of protons from driving the nucleus apart. Nuclear force acts only over very minute distances. At greater distances, electrostatic repulsion is stronger.

nuclear fusion A nuclear reaction resulting from the violent collision of the nuclei of the atoms of a hydrogen isotope (such as deuterium) at extremely high temperature. The process produces more energy than does NUCLEAR FISSION, and leaves no hazardous radioactive waste.

nuclear magnetic resonance An atomic phenomenon in which a particle, such as a proton, in a steady magnetic field "flips over" when an alternating magnetic field is applied perpendicular to the steady field.

nuclear magnetic resonance imaging Abbreviation, NMRI. The use of NUCLEAR MAGNETIC RESONANCE effects to produce a picture of internal body organs. Using computers, three-dimensional renditions can be generated. It is useful in medicine as a diagnostic aid.

nuclear medicine A branch of medicine involving the use of radioactive isotopes in diagnosing and treating disease. A radioactive isotope is put inside the body and it tends to accumulate in certain areas. Abnormal concentration of radioisotopes might indicate abnormal body activity in a certain area.

nuclear pile See NUCLEAR REACTOR.

nuclear power plant A power-generating plant using a NUCLEAR REACTOR.

nuclear reaction **1.** A reaction in which a heavy atomic nucleus is split into two or more lighter nuclei, with an accompanying release of radiant energy. Also called NUCLEAR FISSION. **2.** A reaction in which two or more light nuclei combine to form a heavier nucleus, accompanied by the release of radiant energy. Also called NUCLEAR FUSION.

nuclear reactor **1.** A device in which nuclear fission can be initiated and controlled. At the center of the reactor is a core of nuclear fuel, such as a fissionable isotope of uranium. The core is surrounded by a graphite moderator jacket that is, in turn, surrounded by a coolant jacket; the whole is surrounded by a thick concrete shield. Neutron-absorbing rods are inserted through various walls to different depths in the fuel to control the reaction. Also called *atomic pile.* **2.** A controlled nuclear fusion device, not yet perfected, but under development. It would provide all the benefits of an atomic pile (fission reactor), but would be more efficient and would not produce hazardous radioactive waste.

nuclear recoil An observable vibration of an atomic nucleus when it disintegrates.

nuclear resonance The condition wherein a nucleus absorbs a gamma ray emitted by an identical nucleus.

nuclear service robot A remotely controlled (teleoperated) robot used for general work in environments where the level of radioactivity is too high for humans (e.g., the maintenance of a nuclear reactor). It could also be used, if necessary, for such tasks as disarming nuclear warheads and cleaning up after a nuclear accident.

nucleon A proton or neutron in the nucleus of an atom.

nucleonics The branch of physics concerned with nucleons and nuclear phenomena. The name is an acronym for *nuclear electronics.*

nucleon number See MASS NUMBER.

nucleus The center or core of an atom. Contains neutrons, protons, and other particles. The net electric charge of the nucleus is positive, and is equal to the sum of the negative charges of the orbital electrons of the atom.

null **1.** The condition of zero output current or voltage resulting from adjusting or balancing a circuit, such as a bridge. **2.** A local minimum in an interference pattern or directivity pattern.

null balance In potentiometric-measuring circuits for comparing one voltage to another, the balance condition in which no current flows through the galvanometer.

null current In potentiometric-measuring circuits for comparing one voltage to another, the galvanometer current remaining at null when the null point is not fully zero.

null detection Direction finding by means of an antenna with a bidirectional or unidirectional null response.

null detector See BRIDGE DETECTOR.

5059F-pN-466-487 4/10/01 9:21 AM Page 487

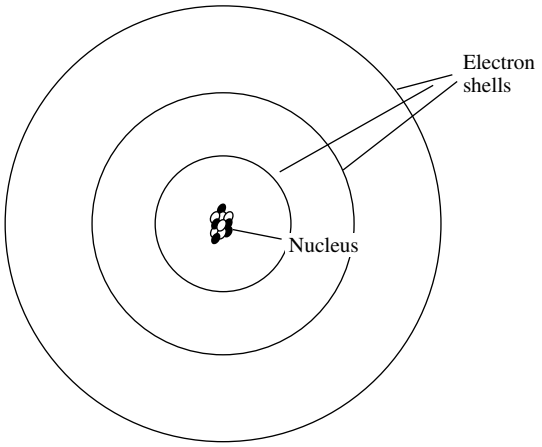

nucleus

null frequency The frequency at which a frequency-sensitive circuit, such as a Wien bridge or twin-tee network, can be balanced.

null meter See BRIDGE DETECTOR.

null method See ZERO METHOD.

null point In a balanced circuit, such as a bridge or potentiometer, the point of zero output voltage (or current) or minimum output voltage (or current).

null potentiometer **1.** The variable resistor that constitutes one arm of a four-arm bridge and is used to balance the bridge. **2.** A potentiometric circuit using the null method to compare one voltage with another. Also see POTENTIOMETER, **2**.

null setting **1.** The setting of a bridge circuit or other null device that balances the circuit. **2.** The electrical zero setting of an electronic voltmeter.

null voltage **1.** In a conventional bridge, the output voltage remaining when the bridge is set for its best null. **2.** For a voltage-sensitive bridge, the input voltage that will produce zero output voltage.

number The mathematical representation of a quantity. It is generally used in electronics to denote coefficients, magnitudes, component values, frequencies, etc.

number cruncher A computer with great computational power, but one not necessarily able to process large amounts of data (such as payroll information).

number system A systematic sequence of numbers based on a radix and a logical arrangement. See, for example, BINARY NUMBER SYSTEM and DECIMAL NUMBER SYSTEM.

numeral A member of a digit set in a number system.

numerical analysis A mathematical approach to solving problems numerically, including finding the limits of error in the results.

numerical code A code having a character set restricted to digits.

numerical control A method of programming computer-controlled mechanical devices, used in some early robots. An automated system in which number sequences fed to a digital computer cause it to control machines or processes in a manufacturing operation.

nV Abbreviation of NANOVOLT.

nW Abbreviation of NANOWATT.

nybble A piece of digital information that is larger than a bit and smaller than a byte. Compare GULP.

Nylon The trade name for a synthetic fiber-forming polyamide, useful for electrical insulation.

Nyquist criterion of stability With reference to a NYQUIST DIAGRAM for a feedback amplifier, the amplifier is stable if the polar plot of loop amplification for all frequencies from zero to infinity is a closed curve that neither passes through nor encloses the point $1 + j0$.

Nyquist diagram A graph of the performance of a reactive feedback system (such as a degenerative amplifier) that depicts the variation of amplitude and phase of the feedback factor with frequency. The plot is polar and accounts for the real and imaginary components.

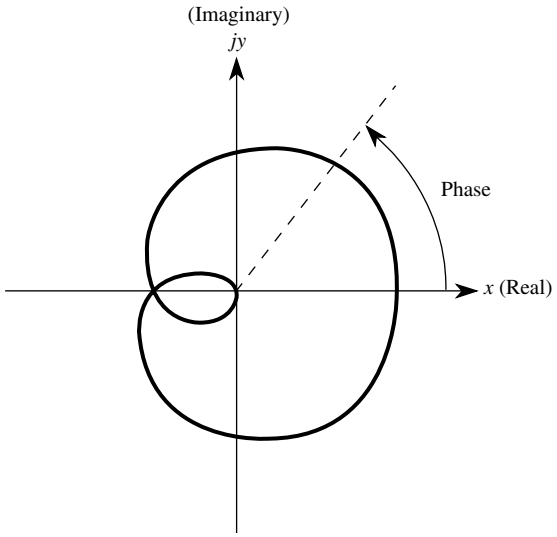

Nyquist diagram

Nyquist noise rule The power dissipated in a resistor because of thermal noise at a given frequency. The derivative of frequency, with respect to power, is equal to the absolute temperature times the Boltzmann constant.

N zone See N LAYER.

5059F-pO-488-509 4/10/01 9:24 AM Page 488

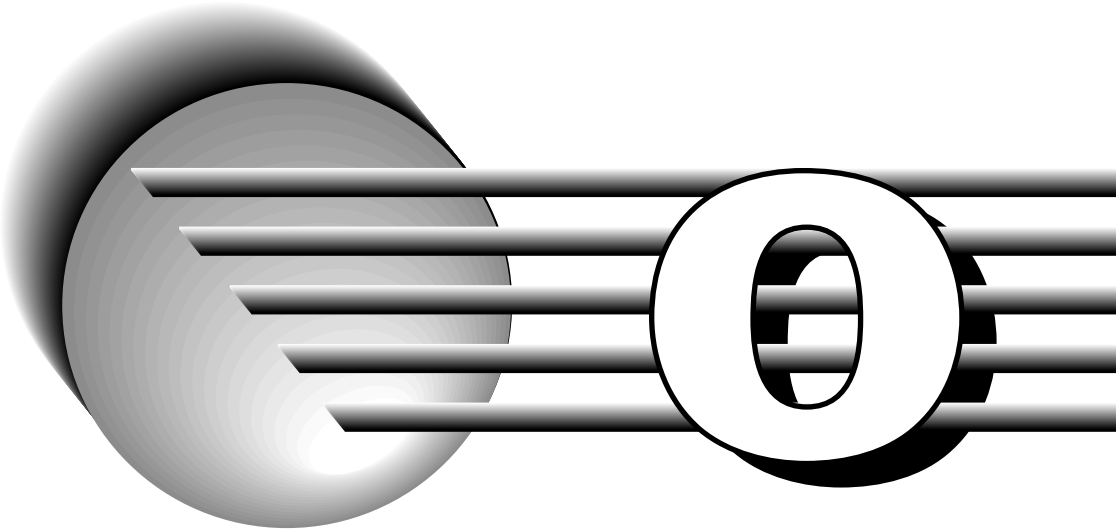

O **1.** Symbol for OXYGEN. **2.** Abbreviation of OUTPUT.

o **1.** Symbol for OUTPUT. (Also, OUT; both are used as subscripts.) **2.** Symbol for ORIGIN.

O_2 Symbol for OXYGEN.

O_3 Symbol for OZONE.

OAT Abbreviation of OPERATING AMBIENT TEMPERATURE.

object code **1.** In a computer system, the machine-language output of the compiler, directed to the computer. **2.** In a computer, the high-level output of the compiler, directed to the operator. **3.** The assembly language, directed to the compiler for translation between machine language and high-level language and vice versa.

object language The computer language that a compiler derives from a high-level (source) language (such as C++, LISP, etc.); it is usually machine language, but it can be an intermediate code that requires further conversion.

object-oriented graphics Also called *vector graphics.* In computer graphics, the use of equations to represent curves in a coordinate plane to define shapes, rather than defining the shapes pixel-by-pixel.

object-oriented language A computer program that uses on-screen objects, called icons, to represent commands. A movable device, such as a mouse or trackball, is used to move an arrow or other pointer to the icon; then a button is pressed to carry out the function indicated by the icon.

object-oriented programming Abbreviation, OOP. A computer programming language that builds sophisticated programs from basic programs called modules.

object program A machine or high-level language version of a user's computer program, as produced by a compiler.

object recognition In robotic systems, any method used to identify specific objects, according to characteristics, such as shape, texture, weight, etc. Common schemes use bar-code labels and machine vision. More-complex methods make use of pattern-recognition programs.

oblique-incidence transmission Transmission of radio signals via ionospheric reflection.

oblique mode In acoustics, a resonance within a room that involves all four walls, the floor, and the ceiling.

oboe A system of radar navigation in which a pair of ground stations measures the distance to an airborne transponder beacon and then transmits the information to the aircraft.

obsolescence-free Pertaining to a design or process that is not likely to become obsolete in the near future. Compare OBSOLESCENCE-PRONE.

obsolescence-prone Pertaining to a design or process subject to being soon outdated. Compare OBSOLESCENCE-FREE.

OBWO Abbreviation of O-TYPE BACKWARD-WAVE OSCILLATOR.

o/c Abbreviation of OPEN CIRCUIT.

occluded gas Gas that has been absorbed or adsorbed by solid material, such as glass or metals, and that must be eliminated during the evacuation of an electronic device, such as a vacuum tube. Also see OUTGASSING.

occultation **1.** The passage of the moon or other planetary body in front of a more distant celestial object, resulting in the cutting off of electromag-

Copyright 2001 The McGraw-Hill Companies, Inc. Click Here for Terms of Use

5059F-pO-488-509 4/10/01 9:24 AM Page 489

netic radiation from that object. **2.** The eclipsing of one object by another.

occupied band A frequency band used by at least one transmitting station regularly.

occupied bandwidth For a given emission, the continuous band of frequencies ($f_2 - f_1$) for which the mean (average) radiated power above f_2 and below f_1 is 0.5 percent of the total mean radiated power.

occupied orbit In an atom, an orbit in which an electron is present.

Ocean Phonetic alphabet code word for the letter O.

OCR Abbreviation of OPTICAL CHARACTER RECOGNITION.

oct Abbreviation of OCTAL.

octal Abbreviation, oct. Based on the number eight. See, for example, OCTAL NUMBER SYSTEM.

octal digit One of the figures in the group 0 through 7 used in the OCTAL NUMBER SYSTEM.

octal notation See OCTAL NUMBER SYSTEM.

octal number system The base-eight system of number notation. It uses digits 0 through 7. Compare BINARY NUMBER SYSTEM and DECIMAL NUMBER SYSTEM. The octal system is often used as shorthand for otherwise-cumbersome binary numbers. The binary number is separated into groups of three digits from right to left; each such group is then converted into its decimal equivalent, with the result being the octal form of the binary number [e.g., binary 111 001 011 = octal 713 (111 = decimal 7; 001 = decimal 1; and 011 = decimal 3)].

Decimal	*Octal*
0	0
1	1
2	2
3	3
4	4
5	5
6	6
7	7
8	10
9	11
10	12
11	13
12	14
13	15
14	16
15	17
16	20

octal number system

octal-to-decimal conversion Conversion of numbers in the octal number system to numbers in the more-familiar decimal number system. This is done by expressing the octal number serially in powers of eight. Thus, octal 12 = $(1 \times 8^1) + (2 \times 8^0) = 8 + 2$ = decimal 10.

octant One-eighth of a circle; therefore, 45 degrees, or 0.5 quadrant.

octave **1.** The range of frequencies between a given frequency (f) and twice that frequency ($2f$). **2.** The range of frequencies between a given frequency (f) and half that frequency ($f/2$).

octave band A band of frequencies one octave wide (see OCTAVE).

octave-band noise analyzer A noise analyzer having bandpass-filter channels whose center frequencies are one octave apart.

octave-band pressure level Sound pressure level within an OCTAVE BAND.

octave pressure level See OCTAVE-BAND PRESSURE LEVEL.

OCTL Abbreviation of OPEN-CIRCUITED TRANSMISSION LINE.

octonary signal An eight-level signaling code.

octonary system See OCTAL NUMBER SYSTEM.

OD Abbreviation of OUTSIDE DIAMETER.

odd-even check A method of checking the integrity of data transferred in a computer system, in which each word carries an extra digit to show whether the sum of ones in the word is odd or even.

odd harmonic In a complex waveform, a harmonic that is an odd-numbered multiple of the fundamental frequency (e.g., third harmonic, fifth harmonic, etc.). Compare EVEN HARMONIC.

odd-harmonic intensification In a complex waveform, emphasis of the amplitude of odd harmonics, with respect to that of even harmonics, a property of some multivibrators and nonsinusoidal waves.

odd line In a conventional television picture, one of the 262.5 odd-numbered horizontal lines scanned by the electron beam in developing the odd-line field. Compare EVEN LINE.

odd-line field On a conventional television screen, the complete field obtained when the electron beam has traced all the odd-numbered lines. Compare EVEN-LINE FIELD.

odd-line interlace See ODD-LINE FIELD.

odd parity check A computer check for an odd number of ones or zeros in digital data.

Odex Trade name for a series of autonomous robots developed by Odetics, Inc. They use legs for locomotion. Noted for their ability to maneuver in places that most robots cannot reach.

odograph An electromechanical or electronic plotter that traces the path of a vehicle on a map, or on the image of a map as portrayed on a display screen.

odometer An electromechanical device that indicates the speed of, and distance covered by, a moving vehicle or robot. Some such devices give a constant position indication, via mathematical integration of the measured velocity (speed and direction), relative to time. It can function in one, two, or three dimensions.

odometry A method of speed, velocity, and/or position sensing. It is commonly used in mobile

5059F-pO-488-509 4/10/01 9:24 AM Page 490

vehicles and mobile robots. The most-sophisticated systems give a constant indication of position on the basis of a starting point (origin) and mathematical integration of the velocity (speed and direction), with respect to time. It can function in one, two, or three dimensions.

Oe Symbol for OERSTED.

oersted Symbol, Oe. The cgs unit of magnetic field intensity; 1 Oe = 79.58 A/m. Formerly the unit of reluctance.

off-air alarm A device that gives a visible or audible indication when the carrier of a transmitter is lost. In its most rudimentary form, the device consists of a radio-frequency relay that actuates a bell, buzzer, horn, or lamp.

off-center display A radar display whose center point does not correspond to the location of the antenna.

off-center-fed antenna An antenna in which a feeder is attached to one side of the center point of the radiator. See, for example, WINDOM ANTENNA.

off-center feed The connection of a feed line to an antenna radiator at some point other than the physical center of the radiator.

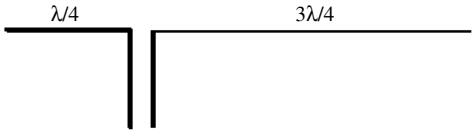

off-center feed

off delay The interval during which a circuit remains on after the control signal has been switched off. Compare ON DELAY.

off-ground **1.** An above- or below-ground operating voltage. **2.** The ground return for a voltage, as defined in **1**, not common with the system ground.

offhook In a telephone system, the condition in which the receiver is removed from its receptacle, or in which the line is otherwise engaged (e.g., a fax machine or modem is in use).

off isolation A measure of the extent to which an open switch isolates the output from the input, specified as the output voltage divided by the input voltage. For percentage, multiply this quantity by 100. The ideal value is zero (or zero percent).

off-limit In a stepping relay, a condition in which the armature has gone past the limit of its travel.

offline **1.** In a computer installation, equipment that is not controlled by the central processor. **2.** In computers and data processing, operations that are not under the direct real-time control of a central processor. **3.** A computer memory facility or device not connected to a central processor. **4.** In personal computing, the use of a computer by itself (i.e., not connected in a network). Compare ONLINE.

offline editing In video production, a process in which copies are made of the original recording; these copies are edited in a trial-and-error scheme to develop the final presentation. Compare ONLINE EDITING.

offloading The use of computers and/or robots to perform repetitive, mundane tasks, leaving people free to do more interesting things. Example: a personal robot that mows the lawn.

off-on operation See ON-OFF OPERATION.

off period **1.** The interval during which an on-off circuit or device is off. **2.** The time during which an equipment is shut down.

offset An imbalance between the halves of a normally symmetrical circuit, such as that of a differential amplifier. Also see OFFSET CURRENT and OFFSET VOLTAGE.

offset adjustment range The change in offset voltage, in millivolts or in microvolts, that can be affected by means of the external offset adjustment circuit(s).

offset current For an operational amplifier, the input current when the offset voltage is zero.

offset voltage For an operational amplifier, the particular value of direct-current bias voltage required at the input to produce zero output voltage.

off state **1.** The condition of an on-off circuit or device, such as a flip-flop, that is off. Compare ON STATE, **1**. **2.** The condition in which a circuit or device is shut down. Compare ON STATE, **2**.

off-state voltage The voltage drop across a semiconductor device, such as a diode, rectifier, or thyristor, when the device is in its normal off (nonconducting) state. Compare ON-STATE VOLTAGE.

off-target jamming In radio or radar jamming, the use of a remote jamming transmitter that will not betray the location of the base station.

off time The period during which no useful work is being performed, as of equipment when it is not functioning because of a circuit breakdown.

OGL Abbreviation of OUTGOING LINE.

OGO Abbreviation of *orbiting geophysical observatory.*

ohm Symbol, Ω. The basic unit of resistance, reactance, or impedance. A resistance of 1 ohm passes a current of 1 ampere in response to an applied emf of 1 volt.

ohmage Electrical resistance or resistivity expressed in ohms.

ohm-centimeter A unit of volume resistivity (see RESISTIVITY): the resistance of a centimeter cube of the material under measurement. Also see MICROHM-CENTIMETER.

ohmic component A resistive or reactive circuit or device exhibiting an OHMIC RESPONSE.

ohmic contact A usually very-low-resistance connection between two materials that provides

5059F-pO-488-509 4/10/01 9:24 AM Page 491

bilateral linear conduction. It exhibits none of the properties of a rectifying junction or a nonlinear resistance.

ohmic heating **1.** Heating caused by current passing through a resistive material (i.e., I^2R losses in the material). **2.** In an electric field, heat generated by charged particles when they collide with other particles.

ohmic loss Loss resulting from the direct-current resistance in a circuit or transmission line.

ohmic region The portion of the response curve of a negative-resistance device that exhibits positive (ohmic) resistance. The *E-I* curve of a tunnel diode, for example, has two such positive-slope regions with a negative-slope (negative-resistance) region between them.

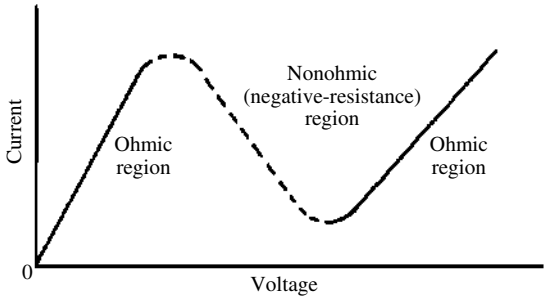

ohmic region

ohmic resistance A resistance exhibiting OHMIC RESPONSE.

ohmic response Response that follows OHM'S LAW: $I = E/R$. In strictly ohmic devices, neither resistance nor reactance changes with current or voltage. Compare NONOHMIC RESPONSE.

ohmic value Electrical resistance expressed in ohms, or in multiples or fractions of ohms (kilohms, megohms, milliohms, etc.)

ohmmeter An instrument for the direct measurement of electrical resistance. It usually consists of a milliammeter or microammeter, a battery, and several switchable resistors having very close tolerances. The scale is calibrated in ohms; the switch selects multiplier factors (e.g., ×100, ×10,000, ×1,000,000). The scale is usually reversed (i.e., 0 is at the extreme right and "infinity" is at the extreme left).

ohmmeter zero **1.** The condition of proper adjustment of an ohmmeter, indicating zero resistance for a direct short circuit. **2.** The potentiometer, or other control, used for adjusting an ohmmeter to obtain a reading of zero with a short circuit.

ohm-mile A rating meaning 1 mile of wire having a resistance of 1 ohm.

ohms adjust The rheostat or potentiometer used to set the pointer of an ohmmeter before it is used to take resistance readings.

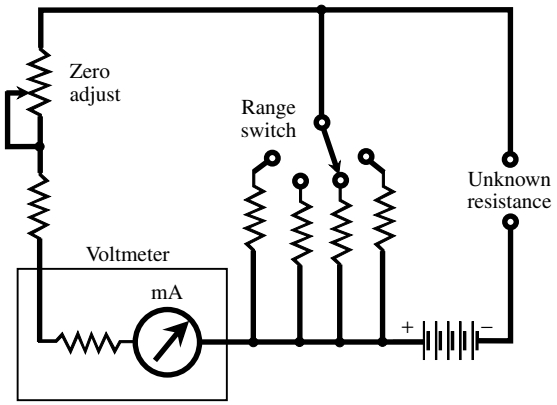

ohmmeter

Ohm's law The statement of the relationship among current, voltage, and resistance. In a direct-current circuit, current varies directly with voltage and inversely with resistance: $I = E/R$, where I is the current in amperes, E is the voltage in volts, and R is the resistance in ohms. For alternating current, Ohm's law states that $I = E/X = E/Z$, where X is reactance and Z is impedance.

ohms per square The resistance (in ohms) between two parallel edges of a square of thin-film resistance material.

ohms-per-volt A specification that indicates the sensitivity and impedance of a voltmeter. In general, the higher the rating, the better. When measuring voltage in high-impedance circuits, the rating should be as high as possible. Field-effect-transistor (FET) voltmeters and vacuum-tube voltmeters have the highest ratings.

oil-burner control An electronic system for starting and stopping the operation of an oil burner to prevent puffback and to interrupt the supply when the flame becomes erratic.

oil calorimeter A calorimeter used to measure power in terms of the rise in temperature of oil heated by the electrical energy of interest.

oil capacitor A capacitor impregnated or filled with oil, such as high-grade castor or mineral oil. Also see OIL DIELECTRIC.

oil circuit breaker A circuit breaker filled with a high-grade insulating oil for cooling and arc elimination.

oil-cooled transformer A heavy-duty transformer, through which oil is circulated for heat removal and arc prevention.

oil dielectric A highly refined oil used as an electrical insulating material (e.g., between the plates of a capacitor). Familiar examples are *castor oil*, *mineral oil*, and the synthetic oil *chlorinated diphenyl*.

oil diffusion pump See OIL PUMP.

5059F-pO-488-509 4/10/01 9:24 AM Page 492

oiled paper Insulating paper impregnated with oil for waterproofing and to increase its dielectric strength.

oil-filled cable A cable whose insulation is impregnated with oil that can be maintained at a constant pressure.

oil-filled capacitor See OIL CAPACITOR.

oil-filled circuit breaker See OIL CIRCUIT BREAKER.

oil-filled transformer A transformer whose case is filled with an insulating oil.

oil fuse cutout A fuse cutout that is filled with an insulating oil. Compare OPEN-FUSE CUTOUT.

oil-immersed transformer See OIL-FILLED TRANSFORMER.

oil-impregnated capacitor See OIL CAPACITOR.

oil pump A vacuum diffusion pump using oil instead of mercury. Also see DIFFUSION PUMP.

oil switch A switch enveloped by insulating oil.

OLRT Abbreviation of *online real time* (operation).

OM Amateur radio jargon for OLD MAN: chief (male) operator, or husband of female operator.

omega A phase-dependent radionavigation system using single-frequency, time-shared, ICW transmissions from two or more locations.

omnibearing A navigational bearing obtained by means of OMNIRANGE.

omnibearing converter An electromechanical device in which an OMNIRANGE signal and vehicle heading information are combined, the output being a signal that is fed to a meter.

omnibearing indicator Abbreviation, OBI. An omnibearing converter with a dial and pointer.

omnibearing line In an OMNIRANGE system, one of the imaginary lines extending from the geographic center of the omnirange.

omnibearing selector A device that can be set manually to a selected omnibearing.

omniconstant calculator A calculator that adds or multiplies numbers in succession in such a manner as to arithmetically or geometrically increase the exponent as a single button is repeatedly pressed.

omnidirectional **1.** Pertaining to a device that responds equally well to acoustic or electromagnetic energy from any direction in three dimensions. **2.** Pertaining to a device that radiates acoustic or electromagnetic energy equally well in any direction in three dimensions. **3.** Also, NONDIRECTIONAL. Pertaining to an antenna that intercepts or radiates equally well in any azimuth (horizontal) direction.

omnidirectional antenna See NONDIRECTIONAL ANTENNA.

omnidirectional hydrophone A hydrophone that picks up underwater sounds coming from any direction.

omnidirectional microphone A microphone that picks up sounds coming from any direction.

omnidirectional radio range See OMNIRANGE.

omnidirectional range See OMNIRANGE.

omnidirectional range station Abbreviation, ORS. A radionavigation station for OMNIRANGE service.

omnigraph A Morse-code generator that operates via marked or perforated paper tape.

omnirange A radionavigation system in which each station in a chain broadcasts a beam in all directions. It usually operates at very-high frequencies (VHF) or ultra-high frequencies (UHF). Pilots of aircraft home on a particular station by tuning it in and noting its bearings.

OMR Abbreviation for OPTICAL MARK RECOGNITION.

on air See ON THE AIR.

on-call channel An assigned radio channel of which exclusive, full time use is not demanded.

on-course curvature In navigation, the rate at which the course of a vehicle deviates with reference to the distance along the true course.

on-course signal A single-tone-modulated signal indicating to an aircraft pilot following a radio beam that the flight is substantially on course.

on current See ON-STATE CURRENT.

on delay An interval during which a circuit remains off after an actuating signal has been supplied. Compare OFF DELAY.

on-demand system A system, especially in computer and data-processing operations, that delivers information or service immediately upon request.

ondograph An electromechanical device that graphically draws alternating-current waveforms on paper.

ondoscope A radio-frequency (RF) energy detector that consists of a neon bulb attached to the end of an insulating rod. When a bulb is held in an intense RF field, the field energy ionizes the gas in the bulb, causing it to glow without direct connection to the RF circuit.

one-address code In computer programming, a code in which the address in an instruction refers to only one memory location.

one condition See ONE STATE.

one-digit adder See HALF ADDER.

one-element rotary antenna A directional antenna consisting of a radiator only (no directors or reflectors) that can be rotated. A straight, rigid, half-wave rotatable dipole is the most common configuration.

one-for-one compiler A compiler that generates one machine language instruction from one source language instruction.

one-input terminal In a flip-flop, the input terminal that must be energized to switch the circuit to its logic 1 output.

one-level address See ABSOLUTE ADDRESS.

one-level subroutine In a computer program, a subroutine in which no reference is made to other subroutines.

one-lunger Colloquialism for a radio transmitter consisting entirely of a one-transistor oscillator.

5059F-pO-488-509 4/10/01 9:24 AM Page 493

one output See ONE STATE.

one-output signal The signal that results from reading a computer memory unit that is in the logic 1 state.

one-output terminal In a flip-flop, the output terminal that is energized when the circuit is in its logic 1 state.

one-plus-one address A method of computer programming in which instructions contain two addresses and an operation, the addresses referring to the location of the next instruction and the location of the data to be used.

ones complement Binary notation in the *radix-minus-one-complement form.*

one shot See MONOSTABLE MULTIVIBRATOR.

one-shot circuit See MONOSTABLE MULTIVIBRATOR.

one-shot multivibrator See MONOSTABLE MULTIVIBRATOR.

one-sided wave A waveform consisting of only negative or positive half-cycles. Example: a rectified alternating-current signal.

one state Also, *logic 1 state.* The high, on, or true logic state of a bistable device, such as a flip-flop. Compare ZERO STATE. In binary notation, the one state is represented by the digit 1.

one-third-octave band A frequency band that is ⅓ octave wide; that is, the difference between the upper-frequency limit (f_2) and the lower-frequency limit (f_1) is one-third of an octave. Also see OCTAVE BAND.

one-to-one assembler An assembler computer program that produces a machine language instruction as a result of translating a source-language statement.

one-to-one correspondence A mapping between two sets *A* and *B* so that every element in set *A* has exactly one correspondent in *B*, and every element in *B* has exactly one correspondent in *A.*

O network A four-impedance network containing two series (upper and lower) arms and two shunt (input and output) arms.

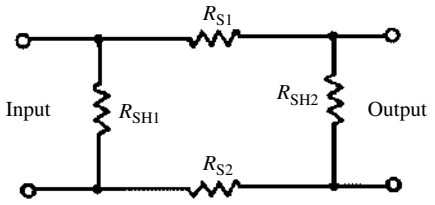

O network

one-way communication **1.** The transmission of a message to one or more stations that receive only. Compare TWO-WAY COMMUNICATION. **2.** See BROADCASTING.

one-way conduction See UNILATERAL CONDUCTIVITY.

one-way radio See ONE-WAY COMMUNICATION.

one-way repeater In wire telephony, a device that amplifies and retransmits a signal in the direction the signal was traveling when it arrived at the repeater. Compare TWO-WAY REPEATER.

one-way valve A diode or rectifier (British variation).

on interval See ON TIME.

online **1.** Descriptive of equipment under the control of a central processor. **2.** Pertaining to operations being controlled by a central processor. **3.** Relating to a computer storage device independent of a central processor. **4.** In personal computing, the use of a computer in a network (e.g., with a modem for operation on the Internet). Compare OFFLINE.

online data reduction Processing data as it enters a computer system.

online editing In video production, the final phase of editing. The original recording (not copies) is used to prepare the presentation, based on the trials that were performed using the copies. Compare OFFLINE EDITING.

online service A computer network accessible via telephone lines, television cable systems, and/or radio. It is generally available to owners of personal computers. It provides such services as electronic mail, special-interest forums, news, weather, sports, shopping, and general information.

on-off keying Keying, as in radiotelegraphy and wire telegraphy, by switching a signal source on and off to form dots and dashes or a binary code, rather than alternately changing the amplitude or frequency of the signal.

on-off operation A switching operation, especially that performed by nonmechanical (fully electronic) circuits.

on-off ratio **1.** For a circuit or device, the ratio of off time to on time. **2.** For a pulse, the ratio of pulse duration to the dead space between pulses.

on-off switch **1.** In electronic equipment, the switch by which the equipment can be started or stopped. It can be, but is not necessarily, the power-line or B-plus switch. **2.** An electronic circuit or stage that is designed to operate as a conventional switching element when triggered by an appropriate signal.

on period See ON TIME.

ONR Abbreviation of *Office of Naval Research.*

on resistance See ON-STATE RESISTANCE.

on state **1.** For a switch or switching device (such as a flip-flop), the condition of the device when it conducts current or delivers an output voltage. Compare OFF STATE, **1**. **2.** The condition of a circuit or device that is activated for operation. Compare OFF STATE, **2**.

on-state current The current flowing through a semiconductor device (such as a diode, rectifier, or thyristor) when it is conducting. Also see ON-STATE VOLTAGE.

5059F-pO-488-509 4/10/01 9:24 AM Page 494

on-state resistance The resistance of a voltage-dependent resistor that is conducting current.

on-state voltage The voltage drop across a semiconductor device (such as a diode, rectifier, or thyristor) when the device is conducting current. Also see ON-STATE CURRENT.

on the air **1.** The state of a radio station that is transmitting. **2.** In broadcasting, the condition in which the transmitter is operational and the sound and/or video from the studio is being disseminated.

on time The length of time a switch or switching device (such as a flip-flop) remains on.

on voltage See ON-STATE VOLTAGE.

OOP Abbreviation of OBJECT-ORIENTED PROGRAMMING.

op **1.** Abbreviation of OPERATE. **2.** Abbreviation of *operator* (see OPERATOR, **1**). **3.** Abbreviation of OPERATION. **4.** Abbreviation of *operational.*

opacimeter **1.** An instrument for measuring the extent to which a material blocks light. **2.** An instrument, such as a field-strength meter, used to measure the effectiveness of an electrical shielding material in blocking radio waves, X rays, or other radiation.

opacity The condition of being opaque. This applies to all forms of radiation. For example, a material can be opaque to light rays, but be transparent to radio waves, or it can be transparent to gamma rays while being opaque to alpha particles.

op amp See OPERATIONAL AMPLIFIER.

op code Abbreviation of OPERATION CODE.

open-air line See OPEN-WIRE LINE.

open-back cabinet A loudspeaker enclosure in which the space behind the speaker is open to the room.

open capacitance The value of a variable capacitor whose rotor plates have been rotated completely out of mesh with the stator plates. Compare CLOSED CAPACITANCE.

open-center display A radar display in which a ring around the center indicates zero range.

open-chassis construction A method of assembling electronic equipment by mounting components and wiring them on an unenclosed chassis, often without a front panel. Similar to breadboard construction.

open circuit **1.** A discontinuous circuit (i.e., one that is broken at one or more points and, consequently, cannot conduct current nor present a voltage at its extremities). Compare CLOSED CIRCUIT. **2.** Pertaining to no-load conditions, for example, the open-circuit voltage of a battery. **3.** For a bipolar transistor, the operating characteristics under independent input and output conditions.

open circuit breaker A circuit breaker whose contacts are open.

open-circuit current Current flowing in the primary winding of an unloaded transformer.

open-circuited line See OPEN-CIRCUITED TRANSMISSION LINE.

open-circuited transmission line Abbreviation, OCTL. An unterminated transmission line in which the conductors at the far end are not connected together.

open-circuit impedance For a transmission line or a four-terminal network, the input or driving-point impedance when the output end of the line or network is open-circuited.

open-circuit jack A telephone jack that introduces a break in a circuit until a plug connected to a closed external circuit is inserted.

open-circuit plug See OPEN PLUG.

open-circuit resistance For a four-terminal network, the input or driving-point resistance when the output end of the network is unterminated.

open-circuit signaling A system of signaling in which no current flows until the signal circuit is in active operation. In a simple telegraph circuit, for example, current flows only when the key is pressed (to form a dot or dash).

open-circuit alarm system A security system in which all the actuating sensors are normally open and connected in parallel. When one of the sensors is actuated, it closes, causing a short circuit that triggers the alarm.

open-circuit voltage See NO-LOAD VOLTAGE.

open-collector configuration In an integrated circuit, an output scheme utilizing no internal pull-up resistor. Wired-OR outputs can thus have opposite states without risk of damage to the device.

open component An open-circuit component (e.g., an open diode, coil, resistor, etc.).

open core A magnetic core having a cylindrical shape. A disadvantage of this core configuration, in some applications, is that much of the magnetic flux extends outside the core. Compare CLOSED CORE.

open-core choke A choke coil wound on an open core. Also called OPEN-CORE INDUCTOR. Compare CLOSED-CORE CHOKE.

open-core transformer A transformer wound on an open core. Compare CLOSED-CORE TRANSFORMER.

open-delta connection See VEE-CONNECTION OF TRANSFORMERS.

open-ended Pertaining to a circuit or device that can be built upon without modifying its original configuration.

open-end stub A stub that is neither short-circuited nor terminated at its far end.

open-end stub tuning Adjustment of an OPEN-END STUB, by pruning its length, for optimum operation at a given frequency.

open-entry contact In a connector, an unprotected, opening contact of the female type.

open feeder See OPEN-WIRE LINE.

open-frame machine See OPEN GENERATOR and OPEN MOTOR.

5059F-pO-488-509 4/10/01 9:24 AM Page 495

open-fuse cutout A type of enclosed-fuse cutout having an exposed fuse holder and support. Compare OIL FUSE CUTOUT.

open generator An unsealed generator (i.e., one that has openings in its housing for air circulation).

open line **1.** See OPEN-WIRE LINE. **2.** See OPEN-CIRCUITED TRANSMISSION LINE.

open loop **1.** In a control system, a feedthrough path having no feedback and that is not self-regulating. **2.** In an operational amplifier, the configuration in which there is no feedback, and in which the device operates at maximum gain. **3.** A loop within a program from which the computer automatically exits after a specific number of iterations.

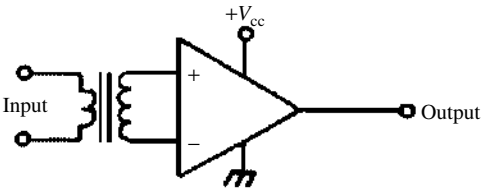

open loop, 2.

open-loop bandwidth The bandwidth of an open-loop device, such as an amplifier, without feedback. Also see OPEN LOOP.

open-loop control system A control system having no feedback and that is not self-regulating. An example is a fluid-level gauge that indicates the height of fluid in a tank, but that cannot correct the level automatically. Compare CLOSED-LOOP CONTROL SYSTEM.

open-loop differential voltage gain For a differential amplifier, the overall voltage gain (when either input is used) when the amplifier has no feedback.

open-loop gain The overall gain (ratio of output to input) of an open-loop device, such as an amplifier without feedback. Also see OPEN LOOP.

open-loop input impedance The input impedance of an open-loop device, such as an amplifier without feedback. Also see OPEN LOOP.

open-loop output impedance The output impedance of an open-loop device, such as an amplifier without feedback. Also see OPEN LOOP.

open-loop output resistance The output resistance of an open-loop device, such as an amplifier without feedback. Also see OPEN LOOP and OPEN-LOOP IMPEDANCE.

open-loop system **1.** A circuit in which the input and output currents are independent. **2.** A robot that does not use a servo system. It depends entirely on alignment and precision for positioning accuracy. **3.** An electromechanical device that does not use corrective feedback.

open-loop voltage gain The overall voltage gain of an open-loop amplifier (i.e., one having no feedback). Also see OPEN LOOP.

open magnetic circuit A magnetic circuit in which a complete path is not provided for magnetic flux. See, for example, OPEN CORE. Compare CLOSED MAGNETIC CIRCUIT.

open motor An unsealed motor (i.e., one that has openings in its housing for air circulation).

open-phase protection Use of an automatic device, such as an open-phase relay, to interrupt the power to a polyphase system when one or more phases are open-circulated.

open-phase relay In a polyphase system, a protective relay that opens when one or more phases are open-circuited. Also see OPEN-PHASE PROTECTION.

open plug A phone plug to which no external connections are made; it is used to hold the blades of a jack as if they were plugged in.

open-reel A tape-recording system in which the tape, during record or playback condition, is wound into a take-up reel that is physically separate from the tape reel. Also called *reel-to-reel arrangement.*

open relay **1.** A relay in its open-contact state. **2.** A relay having an open-circuited coil. **3.** An unenclosed relay.

open routine In computer operations, a routine that can be inserted directly into a larger routine and requires no link to the main program.

open subroutine In computer operations, a subroutine that can be inserted into a larger instructional sequence and must be recopied whenever it is required. Also called *direct-insert subroutine.*

Open Systems Interconnection Reference Model Abbreviation, OSI-RM. A standard set of protocols for computer network communication. It consists of seven levels, also called layers: *physical layer*, *link layer*, *network layer*, *transport layer*, *session layer*, *presentation layer*, and *application layer.*

open temperature pickup A temperature transducer that must be placed directly in contact with the monitored medium.

open volume Pertaining to the maximum-gain operation of a sound-reproducing system (i.e., operation at full volume).

open wire **1.** An unterminated wire. **2.** A wire supported above the surface of the earth and often ungrounded. **3.** See OPEN-WIRE LINE.

open-wire feeder See OPEN-WIRE LINE.

open-wire line A transmission line or feeder usually consisting of two straight, parallel wires held apart by bars of low-loss insulating material at regular intervals along the line.

open-wire loop A branch line connected to a main open-wire line.

open-wire transmission line See OPEN-WIRE LINE.

5059F-pO-488-509 4/10/01 9:24 AM Page 496

open-wire wavemeter See LECHER WIRES.

operand In computer operations, a quantity that enters into or results from an operation.

operate **1.** To manipulate according to an established procedure (e.g., to operate an instrument). **2.** To perform according to specifications, in the sense that an electronic circuit functions.

operate current A signal current or trigger current required to actuate a device. Compare OPERATE VOLTAGE.

operate delay See OPERATE TIME, **1**.

operate interval See OPERATE TIME, **2**.

operate time **1.** The interval starting after the application of an operate current or voltage to a device, and ending when the device operates. **2.** The period during which an electronic equipment is in operation. Also see OPERATING TIME, **1**.

operate voltage The signal voltage or trigger voltage required to actuate a device. Compare OPERATE CURRENT.

operating ambient temperature Abbreviation, OAT. The maximum or recommended temperature in the space immediately surrounding an equipment in operation.

operating angle In an amplifier circuit, the excitation-signal cycle, in degrees, during which drain, collector, or plate current flows. Class-A amplifiers operate for 360 degrees of the input signal cycle; class-AB amplifiers operate for more than 180 degrees, but less than 360 degrees of the input signal cycle; class-B amplifiers operate for 180 degrees of the input signal cycle; class-C amplifiers operate for less than 180 degrees of the input signal cycle.

operating bias In a circuit containing transistors, diodes, or vacuum tubes, the value(s) of direct-current bias required for normal operation.

operating code The code used by the operator in a computer or data-processing system.

operating conditions The environment in which a circuit or system functions in normal use.

operating current The current required by a device during its operation. Compare IDLING CURRENT.

operating cycle The sequence of events in the operation of a device. For example, the repetitive operation of a neon-bulb relaxation oscillator is a sequence of three events: (1) slow charge of capacitor, (2) firing of bulb, and (3) abrupt discharge of capacitor.

operating frequency **1.** The fundamental frequency at which a circuit or device is operated. **2.** The frequency of the current, voltage, or power delivered by a generator.

operating frequency range **1.** The range of operating frequencies, expressed as a minimum and maximum, for a communications receiver, transmitter, or transceiver. **2.** For an integrated-circuit oscillator, the minimum and maximum frequency, and all frequencies in between, at which the device is guaranteed to operate.

operating life The maximum period (from seconds to years) over which a device will operate before failure (from which it usually cannot recover). Compare SHELF LIFE.

operating line A line drawn across a family of curves depicting the performance of a device. It intersects each curve at a single point and graphically displays the performance of the device for a given condition. Thus, an operating line on a family of output curves for a transistor might depict operation with a given load resistor.

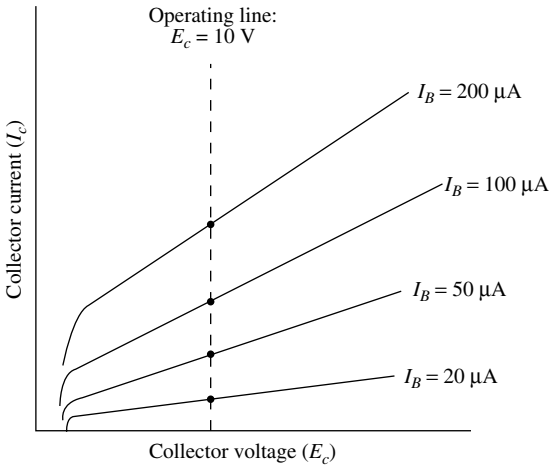

operating line

operating overload The extent and/or duration of overload to which an equipment can be exposed during customary operation, and still continue to properly function.

operating point On the response curve for a device, the point indicating the quiescent level of operation (such as determined by a fixed bias voltage or current). An alternating-current signal applied at this point oscillates above and below the point as a mean.

operating-point shift A movement of an operating point due to faulty operation of a circuit or device, or to a value change in some critical component.

operating position **1.** The control point in a system, [i.e., the place where an operator (see OPERATOR, **1**) normally functions]. **2.** The actual or recommended physical orientation of a device during its operation (e.g., a vertical operating position for a power vacuum tube).

operating power **1.** The power actually used by a device during its operation. **2.** The antenna power of a radio station.

operating ratio For a given period, the ratio t_o/t, where t_o is the time during which an equipment is operating correctly, and t is the duration of the period.

5059F-pO-488-509 4/10/01 9:24 AM Page 497

operating station In a computer installation, one or more consoles for the control of a data-processing system by an operator.

operating system Abbreviation, OS. In a computer, a set of programs that oversee the functioning of the hardware and application software. It works with the basic input/output system (BIOS).

operating temperature The actual or recommended temperature of a device during its operation.

operating-temperature range For a given device, the spread between maximum and minimum values of operating temperature.

operating time **1.** The interval during which an equipment is in operation. **2.** The period corresponding to OPERATING ANGLE.

operating-time characteristic For a coil-type relay, the relationship between operating time and operating power.

operating voltage The voltage required by a device, or measured at the device, during its operation. Compare IDLING VOLTAGE.

operation **1.** The working of a circuit or device (i.e., its performance). **2.** A process usually involving a sequence of steps (e.g., a mathematical operation).

operational amplifier Also called an *op amp*. A specialized linear integrated circuit (IC) that consists of several transistors, resistors, diodes, and capacitors, interconnected to produce gain over a wide range of frequencies. A single amplifier can comprise an entire IC, or an IC can contain several amplifiers. The *dual op amp* and the *quad op amp* are common variants. Some ICs contain one or more amplifiers in addition to other circuits. The devices can be used with resistance-capacitance (RC) network combinations to build active filters for use at audio frequencies.

operational differential amplifier An OPERATIONAL AMPLIFIER preceded by a DIFFERENTIAL AMPLIFIER.

operational readiness In statistical analysis, the probability that a system will, at a certain time, be correctly operating or ready to operate.

operational reliability Reliability determined empirically from a study of the actual operation of a device or system under controlled conditions. Also called ACHIEVED RELIABILITY.

operational transconductance amplifier Abbreviation, OTA. An integrated-circuit amplifier that differs from the conventional operational amplifier in that its output current is proportional to its input-signal voltage.

operation code In computer operations, the part of an instruction that specifies an operation.

operation decoder In a digital computer, the circuit that reads an OPERATION CODE and directs other circuitry in the execution of the code.

operation envelope See WORK ENVELOPE.

operation number In computer programming, a number that indicates the position in the program of a particular operation or subroutine.

operation part In a computer program, the part of an instruction containing the OPERATION CODE.

operation register In a digital computer, the register that stores the operation code of an instruction.

operations research A branch of computer engineering, devoted to the solution and/or optimization of functions of many variables.

operation time The interval between the instant of application of all voltages to a circuit, and the instant when the current reaches a specified percentage of its final steady value.

operator **1.** A person who performs an operation (see OPERATE, **1**). **2.** In mathematics, a symbol indicating an operation (e.g., *j*, +, –, ×, etc.).

operator j See J OPERATOR.

opposition **1.** The state of two quantities that are 180 degrees out of phase with each other. **2.** A state in which two effects or quantities operate against each other in some manner (e.g., physically, mathematically, electrically, etc.).

opt Abbreviation of OPTICAL.

Optacon An electronic aid for the blind. It has a camera that scans printed matter and a device that forms corresponding raised letters that can be read, as would Braille, with the fingertips. The name is a contraction of *optical to tactile converter.*

optical **1.** Generating or sensing visible light. **2.** Visible electromagnetic radiation in the range of approximately 390 to 750 nanometers wavelength.

optical ammeter A type of OPTICAL PYROMETER that measures the current flowing through the filament of an incandescent lamp.

optical antenna A photosensitive device intended for the reception of modulated-light or modulated-infrared signals. Usually consists of a convex lens or a concave reflector and a semiconductor photodetector.

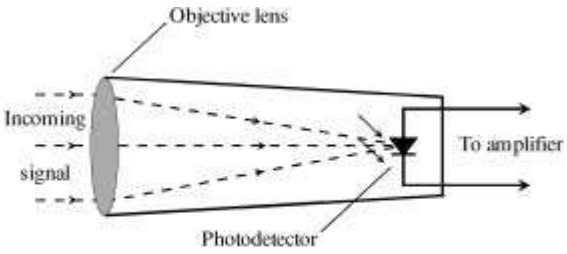

optical antenna

optical axis The z-axis of a quartz crystal (see Z-AXIS, **4**).

optical character reader A device that uses OPTICAL CHARACTER RECOGNITION to discern printed characters.

5059F-pO-488-509 4/10/01 9:24 AM Page 498

optical character recognition Abbreviation, OCR. In computer and data-processing operations, the reading of alphabetical, numerical, and other characters from hard copy (usually printed matter) by photoelectric methods. It converts the characters into digital data that can be stored in computer memory, on disks and tapes, and transmitted via digital communications networks. It can also allow a computer or robot to read signs, maps, etc.

optical communications One-way or two-way communications via modulated visible light. It can be conducted through optical fibers, the atmosphere, water, or any other transparent medium.

optical coupler A coupling device consisting essentially of a light source (actuated by an input signal) mounted in an opaque housing with a light-sensitive device (that delivers the output signal). In its simplest form, the arrangement consists of a light-emitting diode (LED) and a photodiode.

optical coupler

optical detector An integrated-circuit (IC) that provides light-to-voltage conversion. Its direct-current output voltage is proportional to the intensity of light impinging on its sensor.

optical encoder An electronic device that measures the extent to which a mechanical shaft has rotated. It can also measure the rate of rotation (angular speed). It consists of a light-emitting diode (LED), a photodetector, and a disk with alternate light and dark bands (chopping wheel). It is commonly used in digital controls and jointed robot arms.

optical fiber A glass or plastic medium through which light is propagated for optical-communications purposes. The refractive characteristics of the fiber keep the visible light inside.

optical lever A device for amplifying the effect of a small rotation. The rotating member carries a small mirror that reflects a light beam over a curved scale, the distance through which the light spot travels on the scale being proportional to the distance between the scale and the rotating mirror. In this way, the deflection on the scale is several times the length of the arc described by the mirror, the rotation being thus amplified.

optical link See OPTICAL COUPLER.

optical mark recognition A method of data transfer that involves the use of optical techniques.

optical maser See LASER.

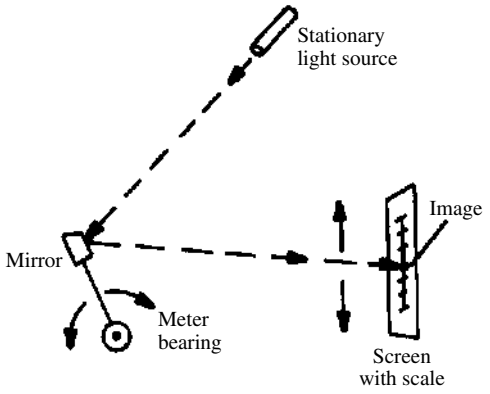

optical lever

optical mode The vibration mode that produces an oscillating dipole in a crystal lattice.

optical pattern A Christmas-tree-like pattern produced by parallel rays of light striking a phono disk. Also see DIFFRACTION.

optical playback See OPTICAL SOUND REPRODUCER.

optical pyrometer A pyrometer for measuring the temperature of a hot body in terms of the intensity and color of light it emits.

optical scanner An electronic device that converts hard-copy text and graphics into digital form suitable for processing and storage in a computer. There are several types; the most common resembles a small photocopy machine and is known as a *flatbed scanner*. See OPTICAL SCANNING.

optical scanning An electronic process that converts hard-copy text and graphics into digital form suitable for processing and storage in a computer. Text scanners work in conjunction with specialized software. The optical scanner and software together form the equivalent of audio speech recognition and sound interpretation. Usually, scanners are employed to convert printed matter to digital data. However, scanning technology can also be used at a distance, for example, by a robot for the purpose of reading road signs.

optical sound recorder A photoelectric machine for recording sound on photographic film. Also see OPTICAL SOUND RECORDING.

optical sound recording A system for recording sound on photographic film, as in sound motion pictures. The sound is picked up by a microphone and amplified to vary the intensity of a light source. The film passing this modulated beam becomes exposed to a variable-width or variable-density track corresponding to the modulation (see VARIABLE-DENSITY SOUND RECORD and VARIABLE-WIDTH SOUND RECORD). When de-

5059F-pO-488-509 4/10/01 9:24 AM Page 499

veloped film is played back, its sound track modulates a light beam in the reproducer by actuating a photocell or phototube to produce the audio signal, which is then amplified.

optical sound reproducer A photoelectric machine for reproducing sound on film. A light beam in the device is modulated by the passing sound track, and it, in turn, modulates photocell or phototube current, which is amplified to drive a loudspeaker. Also see OPTICAL SOUND RECORDING.

optical system Collectively, the functional arrangement of lenses, mirrors, prisms, and related devices in optoelectronic apparatus.

optical tachometer An optoelectronic instrument for measuring (by means of reflected-light variations) the speed of a body, such as a rotating shaft, without electrical or mechanical attachments to the latter.

optical thermometer See OPTICAL PYROMETER.

optical twinning A kind of defect in which two types of quartz occur in the same crystal. Compare ELECTRICAL TWINNING.

optical type font A special type (printing) style designed for use with OPTICAL CHARACTER RECOGNITION equipment.

optical wand A pencil-like optical probe, used to read bar codes from a printed page and translate the codes into information that is then loaded into a computer or calculator.

optic axis See OPTICAL AXIS.

optic flow See EPIPOLAR NAVIGATION.

optics **1.** The science of light, its measurement, application, and control. **2.** A system of lenses, prisms, filters, or mirrors used in electronics to direct, control, or otherwise modify light rays.

optimization The adjustment or manipulation of the elements of a process or system for the best operation or end result.

optimize **1.** To manipulate a set of variables or parameters for the best possible performance of a circuit or system. **2.** To maximize the value of a multivariable function.

optimum angle of radiation For a given altitude of the ionosphere, the angle, with respect to the horizon, at which a radio signal should be transmitted from a specific geographic location to provide optimum reception at some other specific location. This angle varies, depending on the altitude of the ionospheric layer from which signals are returned, the distance between the transmitting and receiving stations, and the number of hops taken by the signal between the earth and the ionosphere.

optimum bunching In a velocity-modulated tube, such as a klystron, the bunching associated with maximum output.

optimum collector load The ideal load impedance (see OPTIMUM LOAD) for a particular transistor operated in a specified manner.

optimum coupling The degree of coupling between two circuits tuned to the same frequency that results in maximum energy transfer. Also called CRITICAL COUPLING.

optimum current The value of current that produces the most-effective performance of a circuit or device.

optimum frequency See OPTIMUM WORKING FREQUENCY.

optimum load The value of load impedance that produces maximum transfer of power from a generator or amplifier.

optimum plate load The ideal load impedance (see OPTIMUM LOAD) for a particular electron tube operated in a specified manner.

optimum *Q* The most effective figure of merit for a capacitor, inductor, or tuned circuit at a specified frequency.

optimum reliability The value of reliability that ensures minimum project cost.

optimum voltage The value of voltage that results in the most effective performance of a circuit or device.

optimum working frequency In radio transmission involving reflection from the ionosphere, the frequency of use that results in the most reliable communication between two points.

optoelectronic coupler An assembly consisting of an LED and a phototransistor. An input signal causes the diode to glow, and the light activates the transistor, which in turn delivers an output signal of higher amplitude than that of the input signal.

optoisolator A light-emitting diode (LED) or infrared-emitting diode (IRED) and a photodiode combined in a single package with a transparent gap between them. The LED or IRED converts an electrical signal to visible light or IR; the photodiode changes the visible light or IR back into an electrical signal. This device eliminates interstage impedance reflections that can plague systems that employ electronic coupling. Even the most drastic changes in load impedance have no effect on the impedance "seen" by the signal source. The devices can also protect expensive equipment against electrical transients; for example, in telephone-line modems used with personal computers.

optoelectronics A branch of electronics that involves the use of visible light for communications or data-transfer purposes.

optoelectronic transistor A transistor having an electroluminescent emitter, transparent base, and photoelectric collector.

optophone A photoelectric device for converting light into sounds of proportionate pitch to enable blind persons to "see" by ear.

Orange Book Trade name (Sony and Philips) for a specialized format for *compact-disc recordable (CD-R)* computer data storage media. It allows recording of data onto, as well as retrieval of data from, an optical compact disc. See also GREEN BOOK, RED BOOK, and YELLOW BOOK.

5059F-pO-488-509 4/10/01 9:24 AM Page 500

orange peel On a phonograph disc, a mottled surface that produces high background noise; so called from its resemblance to an orange peel.

orbit **1.** Also called *shell.* The median path of an electron around the nucleus of an atom. **2.** The circular or elliptical path of an artificial satellite (e.g., a communications satellite) around the earth. **3.** The elliptical path of the moon around the earth. **4.** The elliptical path of the earth or another planet around the sun. **5.** Any closed, usually circular or elliptical path, that an object follows around another object.

orbital-beam multiplier tube An electron-multiplying UHF oscillator or amplifier tube in which a positively charged electrode focuses electrons in a circular path.

orbital electron An electron in orbit around the nucleus of an atom.

orbital period The length of time required by a satellite to go around a celestial body, usually the earth. It can vary from about 90 minutes for very low orbits to months or even years for orbits beyond that of the moon. The moon's period is about a month.

OR circuit Also called *inclusive-OR circuit.* In digital systems and other switching circuits, a logic gate whose output is high (logic 1) when any of the input signals is high. The output is low (logic 0) only when all of the inputs are low. Compare AND CIRCUIT.

A	B	C
0	0	0
0	1	1
1	0	1
1	1	1

2-input OR circuit

order **1.** An instruction to a digital computer. **2.** Sequence.

OR element See OR CIRCUIT.

ordered pair A set of two variables or numbers that can be mapped one-to-one onto a set of points in a plane. The most familiar example is (*x,y*), used to depict the Cartesian (rectangular) coordinate system on which characteristic curves and other functions are plotted.

order of interference The position of an interference fringe that depends on whether the interference arises from one, two, three, or more wavelength differences. Generally, the first fringe results from a difference of one wavelength, the second fringe from a difference of two wavelengths, etc. The center fringe indicates that the two signals are exactly in phase; that is, the difference is zero wavelengths.

order of logic **1.** A mathematical expression for the complexity of a system of logic. **2.** The relative speed with which logical information is processed in a system.

order tone A warning signal to receiving operators in the form of a tone transmitted over a trunk preceding the transmission of an order.

ordinary ray As a result of the double refraction of electromagnetic waves, the member of a pair of rays that follows the usual laws of refraction. Also see O WAVE. Compare EXTRAORDINARY RAY.

ordinary wave See O WAVE.

ordinate In the rectangular coordinate system, a point located on the vertical axis.

organ **1.** A computer subsystem. **2.** An electronic device used for the purpose of generating music.

organic decay See EXPONENTIAL DECREASE.

organic electricity Electricity in the living tissues of animals and plants.

organic growth See EXPONENTIAL INCREASE.

organic semiconductor A semiconductor material consisting of, or combined with, some compound of carbon.

OR gate See OR CIRCUIT.

orientation **1.** The direction or position of an object in space, expressed in terms of coordinate values. **2.** In a teleprinter, the calibration or alignment that determines the speed of response to a received character.

orientation of quartz plates See CRYSTAL AXES and CRYSTAL CUTS.

orifice An opening or window, such as that in a loudspeaker enclosure or waveguide, through which energy is transmitted.

origin **1.** The starting point in a coordinate system. **2.** Relative to address modification in computer operations, an address to which a modifier is added to derive a variable operand address.

original lacquer In disc-recording operations, an original recording made on a lacquer-surfaced disc that is subsequently used to make a master.

original master In disk recording, the master disc produced from a wax or lacquer disc (see ORIGINAL LACQUER) by means of electroforming.

origin distortion The change in the shape of a wave as it swings through zero (polarity).

OR operation See OR CIRCUIT.

ORS Abbreviation of OMNIDIRECTIONAL RANGE STATION.

orthicon A television camera tube somewhat similar to the iconoscope, but which provides internal amplification of light and, accordingly, can be used in dimmer places than the iconoscope. Light amplification is provided by an arrangement similar to that of a photomultiplier tube.

orthiconoscope See ORTHICON.

5059F-pO-488-509 4/10/01 9:24 AM Page 501

orthoacoustic recording **1.** A system of disc recording in which the inherent differences between high-frequency recording and low-frequency recording are compensated to provide reproduction that more closely resembles the actual sound. **2.** A disc made by the method defined in **1**.

orthogonal axes Perpendicular axes [e.g., those in a Cartesian (rectangular) coordinate system].

Os Symbol for OSMIUM.

OS Abbreviation of OPERATING SYSTEM.

osc Abbreviation of OSCILLATOR.

OSCAR Abbreviation for *Orbiting Satellite Carrying Amateur Radio.* A satellite with a transponder that has an uplink in one amateur band and a downlink in another amateur band.

osciducer See OSCILLATING TRANSDUCER.

oscillate **1.** To fluctuate in amplitude in a uniform manner. **2.** To vary above and below a specified value at a constant rate.

oscillating arc A small arc, especially one produced by slow-opening relay contacts, that generates high-frequency oscillations.

oscillating circuit A closed circuit containing inductance, capacitance, and inherent resistance, in which energy passes back and forth between inductor and capacitor at a frequency determined by the inductance (*L*) and capacitance (*C*) values.

oscillating crystal **1.** A piezoelectric plate maintained in a state of oscillation in a circuit. See, for example, CRYSTAL OSCILLATOR and QUARTZ CRYSTAL. **2.** An oscillating semiconductor diode (see NEGATIVE-RESISTANCE DIODE, **1**, **2**).

oscillating current See OSCILLATORY CURRENT.

oscillating detector A detector provided with positive feedback; therefore, it is capable of generating a signal of its own. Compare NON-OSCILLATING DETECTOR.

oscillating diode **1.** A semiconductor diode biased into its negative-resistance region so that it oscillates in a suitable circuit. **2.** An oscillating tunnel diode. **3.** Any of several microwave diodes, such as the IMPATT diode, which will oscillate in a suitable system. **4.** See MAGNETRON. Also see DIODE OSCILLATOR.

oscillating field An alternating electric or magnetic field.

oscillating rod A rod of magnetostrictive metal maintained in a state of oscillation in a circuit. See, for example, MAGNETOSTRICTION and MAGNETOSTRICTION OSCILLATOR.

oscillating transducer A transducer in which an input quantity varies a frequency proportionately from its center value.

oscillating wire A wire of magnetostrictive metal maintained in a state of oscillation in a circuit. See, for example, MAGNETOSTRICTION and MAGNETOSTRICTION OSCILLATOR.

oscillation The periodic change of a body or quantity in amplitude or position (e.g., oscillation of a pendulum, voltage, or crystal plate).

oscillation constant For an oscillating inductance-capacitance (LC) circuit, the expression $(LC)^{1/2}$, where L is the inductance in henrys and C is the capacitance in farads. The reciprocal of the OSCILLATION NUMBER.

oscillation control A manual or automatic device for adjusting the frequency or amplitude of the signal generated by an oscillator.

oscillation efficiency The ratio, as a percentage, of the alternating-current (signal) power output of an oscillator (P_{out}) to the corresponding direct-current power input (P_{in}). $Efficiency = 100P_{out}/P_{in}$.

oscillation number For an oscillating circuit, the number of complete oscillation cycles that occur in 6.28 (2 pi) seconds.

oscillation test **1.** A test of an oscillator to determine if a signal is being generated. **2.** A test for transistors wherein the transistor is used as an oscillator to give a rough indication of its condition in terms of oscillation amplitude.

oscillation transformer A tank coil of a radio transformer—especially one that includes an output coupling coil.

oscillator A device that produces an alternating or pulsating current or voltage electronically. The term is sometimes used to describe any alternating-current-producing device other than an electromechanical generator.

oscillator circuit The specific manner in which the components of an OSCILLATOR are interconnected. The three general types are: positive-feedback, negative-resistance, and relaxation.

oscillator coil A tapped coil that provides the input and output windings required for an oscillator circuit. Such coils are used in signal generators, oscillators, and superheterodyne receivers.

oscillator-doubler A circuit consisting of an oscillator and a frequency doubler (e.g., a crystal oscillator whose output frequency is twice the crystal frequency).

oscillator drift A usually gradual change in frequency of an oscillator caused by such factors as warmup time, voltage variations, capacitance change, inductance change, or change in transistor characteristics.

oscillator frequency The fundamental frequency at which an oscillator operates. It can be determined by a tuned circuit, crystal, cavity, section of waveguide or transmission line, or by a resistance-capacitance circuit.

oscillator harmonic interference In a superheterodyne receiver, interference that is the beat product of local oscillator harmonics and received signals.

oscillator interference Radio-frequency interference caused by signals from the high-frequency oscillator of a receiver.

oscillator keying Keying by making and breaking the signal output, direct-current (dc) power, or dc bias of the oscillator stage of a radiotelegraph transmitter.

5059F-pO-488-509 4/10/01 9:24 AM Page 502

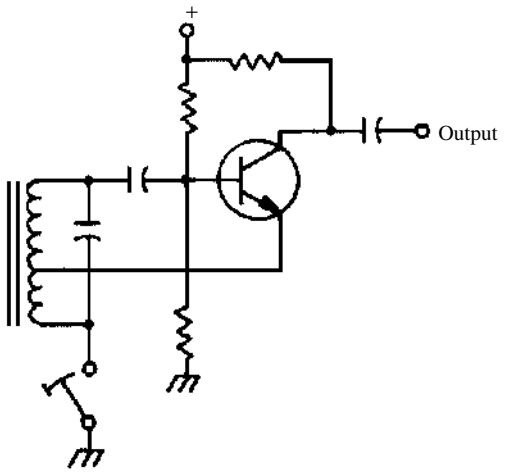

oscillator keying

oscillator-mixer **1.** A combination stage in which a transistor functions as a local oscillator and mixer in a receiver or test instrument. **2.** A device designed specifically to function as a local oscillator and mixer.

oscillator-mixer-detector **1.** In a superheterodyne receiver, a stage in which the functions of high-frequency oscillator, mixer, and first detector are performed by a single transistor. **2.** A device designed specifically to function as a local oscillator, mixer, and detector.

oscillator-multiplier A single circuit that serves simultaneously as an oscillator and frequency multiplier. See, for example, OSCILLATOR-DOUBLER.

oscillator padder In a superheterodyne receiver, a small, limited-range variable capacitor connected in series with the oscillator coil for tracking oscillator tuning at the low end of a band. Compare OSCILLATOR TRIMMER.

oscillator power supply **1.** The direct-current or alternating-current power supply for an oscillator. **2.** See OSCILLATOR-TYPE POWER SUPPLY.

oscillator radiation The emission of radio-frequency energy by the oscillator stage of a superheterodyne receiver. Also see OSCILLATOR INTERFERENCE.

oscillator-radiation voltage The radio-frequency voltage at the antenna terminals of a superheterodyne receiver that results from signal emission by the oscillator stage.

oscillator stabilization **1.** The automatic compensation of an oscillator circuit for the frequency drift resulting from changes in temperature, current, voltage, or component parameters. **2.** The automatic stabilization of the operating point of an oscillator circuit against variations resulting from changes in temperature, supply current or voltage, or component parameters.

oscillator synchronization The locking of an oscillator in step with another signal source, such as a frequency-standard generator.

oscillator tracking In a superheterodyne receiver, the constant separation of the oscillator frequency from the signal frequency by an amount equal to the intermediate frequency at all settings of the tuning control.

oscillator transmitter A radio transmitter consisting only of a radio-frequency oscillator and its power supply. The oscillator can be modulated in various ways [e.g., on-off keying, frequency-shift keying, voice amplitude modulation (AM), voice frequency modulation (FM)].

oscillator trimmer In a superheterodyne receiver, a small, limited-range capacitor connected in parallel with the oscillator coil for tracking oscillator tuning at the high end of a band. Compare OSCILLATOR PADDER.

oscillator tuning The separate, often ganged, tuning of the oscillator stage in a circuit.

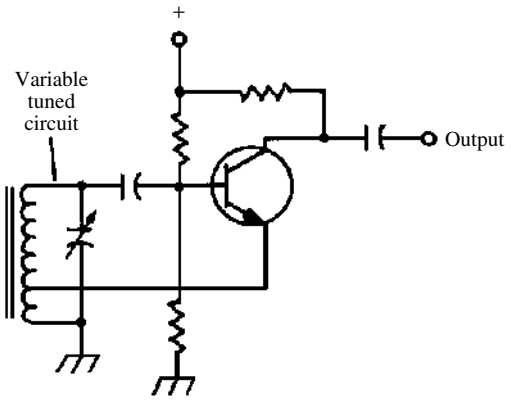

oscillator tuning

oscillator-type power supply A high-voltage, direct-current (dc) power supply in which a radio-frequency (RF) oscillator generates a low-voltage alternating current (ac). This ac voltage is stepped up by an RF transformer, and is finally rectified to obtain high-voltage dc.

oscillator-type transmitter See OSCILLATOR TRANSMITTER.

oscillator wavelength The fundamental wavelength at which an oscillator operates. It is usually expressed in meters, centimeters, or millimeters. It can be determined by a tuned circuit, crystal, cavity, section of waveguide or transmission line, or by a resistance-capacitance circuit.

oscillatory current A current that alternates periodically, particularly the current in an inductance-capacitance (LC) tank circuit that results

5059F-pO-488-509 4/10/01 9:24 AM Page 503

from the oscillation of energy back and forth between the inductor and capacitor.

oscillatory discharge An electrical discharge, such as that of a capacitor, that sets up an OSCILLATORY CURRENT.

oscillatory surge A current or voltage surge that includes both positive and negative excursions.

oscillatory transient See OSCILLATORY SURGE.

oscillistor A device consisting essentially of a bar of semiconductor material positioned in a magnetic field; it will produce oscillations under certain conditions.

oscillogram **1.** The image produced on the screen of an oscilloscope. **2.** A permanent, usually photographic, record made from the screen of an oscilloscope.

oscillograph **1.** An instrument that makes a permanent record (photograph or pen recording) of a rapidly varying electrical quantity. Also called *recorder* (see RECORDER, **2**). Compare OSCILLOSCOPE. **2.** An obsolete term for OSCILLOSCOPE.

oscillograph recorder A direct-writing recorder (see RECORDER, **2**).

oscillography The use of a graphic oscillation recorder (OSCILLOGRAPH).

oscillometer A device used for determining the peak amplitude of an oscillation.

oscilloscope An instrument that presents for visual inspection the pattern representing variations in an electrical quantity. Also see CATHODE-RAY OSCILLOSCOPE. Compare OSCILLOGRAPH.

oscilloscope camera A special high-speed, short-focus camera with fixtures for attachment to an oscilloscope to record images from the screen. Standard and instant-film types are available.

oscilloscope differential amplifier An amplifier that processes the difference between two signals, for the purpose of displaying on an oscilloscope or oscillograph.

oscilloscope tube A cathode-ray tube for use in an oscilloscope. It contains an electron gun, accelerating electrode, horizontal and vertical deflecting plates, and a fluorescent screen.

Os-Ir Symbol for OSMIRIDIUM.

OSI-RM Abbreviation of OPEN SYSTEMS INTERCONNECTION REFERENCE MODEL.

OSL Abbreviation of *orbiting space laboratory.*

osmiridium Symbol, Os-Ir. A natural alloy of osmium and iridium.

osmium Symbol, Os. A metallic element of the platinum group. Atomic number, 76. Atomic weight, 190.2.

osmotic pressure The force that causes the positive ions to pass out of a solution toward a metal body immersed in an electrolyte. Also see HELMHOLTZ DOUBLE LAYER.

OSO Abbreviation of *orbiting solar observatory.*

osteophone A bone-conduction hearing aid.

OTA Abbreviation of OPERATIONAL TRANSCONDUCTANCE AMPLIFIER.

OTL Abbreviation of OUTPUT-TRANSFORMER-LESS.

O-type backward-wave oscillator Abbreviation, OBWO. A backward-wave oscillator using harmonics having opposing phases.

ounce Abbreviation, oz. A unit of weight equal to $\frac{1}{16}$ pound or 28.35 grams.

ounce-inch Abbreviation, oz-in. A unit of torque equal to the product of a force of 1 ounce and a moment arm of 1 inch. Compare POUND-FOOT.

outage **1.** Loss of power to a system. **2.** Loss of a received signal.

outboard components **1.** Discrete components (capacitors, coils, resistors, or transformers) connected externally to an integrated circuit. **2.** Discrete components connected externally to any existing electronic device.

outcome In statistical analysis, the result of an experiment or test. An outcome can be numerical or nonnumerical.

outdoor antenna An antenna erected outside, usually high above the surface of the earth clear of obstacles. It generally provides superior performance compared with an INDOOR ANTENNA. Also reduces the probability of radio-frequency interference (RFI) when used for transmitting.

outdoor booster A signal preamplifier mounted on an outdoor television receiving antenna for improved reception.

outdoor transformer A weatherproof distribution transformer installed outside the building it services.

outer conductor The outer metal cylinder or jacket of a coaxial cable or coaxial tank. Compare INNER CONDUCTOR.

outgassing **1.** In the evacuation of electronic devices, such as vacuum tubes, the removal of occluded gases from glass, ceramic, and metal by means of slow baking and by flashing an internal metal getter (such as one of magnesium). **2.** The production of gases in certain electrochemical cells and batteries during the final stage of charging.

outgoing line A power or signal line that leaves a device, facility, or stage. Compare INCOMING LINE.

outlet A female receptacle that delivers a signal or operating power to equipment plugged into it.

outline flowchart In computer operations, a preliminary flowchart showing how a program will be divided into routines and segments, input and output functions, program entry points, etc.

out-of-line coding Instructions for a computer program routine stored in an area of memory other than that in which the routine's program is stored.

out of phase Pertaining to the condition in which the alternations or pulsations of two or more separate waves or wave phenomena, having identical frequencies, are out of step with each other. Compare IN PHASE.

5059F-pO-488-509 4/10/01 9:24 AM Page 504

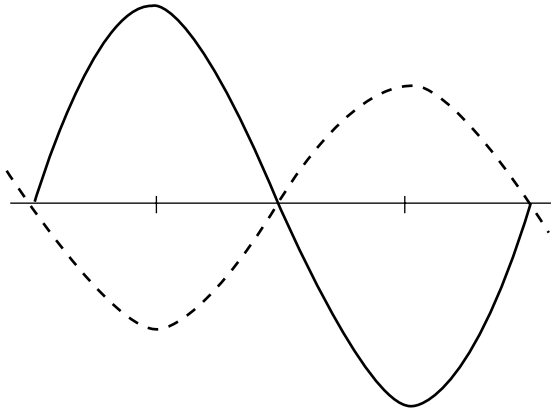

out of phase

out-of-phase current Reactive current in an alternating-current circuit (i.e., current that is out of phase with voltage. Also see QUADRATURE CURRENT).

out-of-phase voltage Voltage across a reactance; so called because it is out of phase with the current.

outphaser A device that converts a sawtooth wave to a square wave. It is used in electronic organs and synthesizers.

outphasing modulation A system of modulation in which the sideband frequencies are shifted 90 degrees from the phase position in an amplitude-modulated wave. The resulting constant-envelope wave is then amplified with high efficiency and low distortion by a class-C stage; then the signal is reconverted to an amplitude-modulated one by phase shifting the carrier, with respect to the sidebands.

out-plant system A data-processing system in which a central computer receives data from remote terminals.

output **1.** Energy or information delivered by a circuit, device, or system. Compare INPUT, **1**. **2.** The terminals at which energy or information is taken from a circuit, device, or system. Compare INPUT, **2**.

output admittance Symbol, Y_o. The internal admittance of a circuit or device, as "seen" at the output terminals; the reciprocal of OUTPUT IMPEDANCE. Compare INPUT ADMITTANCE.

output amplifier See FINAL AMPLIFIER.

output area In a computer system, the portion of storage holding information for delivery to an output device. Also called *output block*.

output axis For a gyroscope that has received an input signal, the axis around which the spinning wheel precesses.

output block See OUTPUT AREA.

output buffer **1.** A circuit that follows an oscillator and reduces the effects of variable load impedance on the oscillator frequency or signal amplitude. **2.** An amplifier, usually with a voltage gain of 6 dB, that follows a video multiplexer. The amplifier drives a coaxial transmission line.

output bus driver In a computer, a device that amplifies output signals sufficiently to provide signals to other devices without undue loading of the supply line (bus).

output capability The maximum power or voltage output that a circuit can deliver without distortion or other improper operating conditions.

output capacitance Symbol, C_o. The internal capacitance of a circuit or device, as seen at the output terminals. Compare INPUT CAPACITANCE.

output capacitive loading For an operational amplifier at unity gain, the maximum capacitance that can be connected to the output of the amplifier before phase shift increases to the point of oscillation.

output capacitor **1.** In a capacitance-coupled circuit, the output coupling capacitor. Compare INPUT CAPACITOR. **2.** The last capacitor in a power-supply filter circuit.

output capacity The maximum output capability of a device or system expressed in appropriate units, such as current, voltage, power, torque, horsepower, etc.

output choke The last choke (inductor) in a power-supply filter circuit.

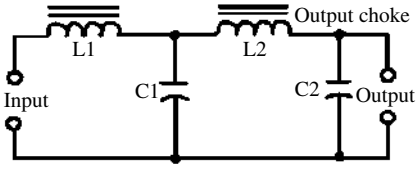

output choke

output circuit The circuit or subcircuit that constitutes the output portion of a network or device. Also see OUTPUT and OUTPUT TERMINALS. Compare INPUT CIRCUIT.

output-circuit distortion Distortion in the output portion of a circuit or device (such as a transistor or transformer), usually caused by an overload or nonlinear response.

output conductance Symbol, G_o. The internal conductance of a circuit or device, as "seen" at the output terminals. It is the reciprocal of OUTPUT RESISTANCE. Compare INPUT CONDUCTANCE.

output control **1.** The gain control of an amplifier. **2.** The level control of a variable power supply.

output coupling capacitor See OUTPUT CAPACITOR.

output coupling transformer See OUTPUT TRANSFORMER.

5059F-pO-488-509 4/10/01 9:24 AM Page 505

output current **1.** Symbol, I_o. The current delivered by a source, such as a battery, generator, or amplifier. Compare INPUT CURRENT, **1**. **2.** Symbol, I_o. Current flowing in the output leg or electrode of a circuit or device. Compare INPUT CURRENT, **2**.

output device **1.** A load device, such as a resistor, loudspeaker, lamp, relay, motor, etc., that utilizes the output energy delivered by a generator, amplifier, or network. **2.** A device, such as an output transformer, that serves to transfer energy or information from a circuit or device. Compare INPUT DEVICE. **3.** In computer operations, a device that presents the results of computer operation in a comprehensible form. Examples: printer, monitor, disk drive, tape drive, modem, etc.

output efficiency The efficiency of a device, such as a generator or amplifier, in delivering an output signal. For an amplifier, the efficiency ($Eff_{\%}$) is given as a percentage by the formula $Eff_{\%} = 100P_o/P_i$, where P_i is the direct-current power input, and P_o is the alternating-current (signal) power output.

output equipment See OUTPUT DEVICE, **3**.

output filter The direct-current filter of a power supply operating from alternating current. Also see CAPACITOR-INPUT FILTER and CHOKE-INPUT FILTER.

output gap A device via which current or power is intercepted from an electron beam in a beam-power tube.

output impedance Symbol, Z_o. The impedance "looking" into the output terminals of an amplifier, generator, or network. Compare INPUT IMPEDANCE.

output indicator A device, such as an analog meter, digital meter, or bar-graph meter, that provides a visual indication of the output-signal amplitude of an equipment.

output leakage current In an open-collector integrated circuit, the current from collector to emitter with the output in the "off" condition and a certain specified voltage applied to the device. It can be expressed in milliamperes or microamperes.

output limiting A process for automatically maintaining the amplitude of the signal delivered by a generator or amplifier. See, for example, AUTOMATIC GAIN CONTROL, AUTOMATIC MODULATION CONTROL, VOLUME COMPRESSION, and VOLUME LIMITER.

output load See OUTPUT DEVICE, **1**.

output load current **1.** The current through the output load of an amplifier. Generally, this current is expressed in root-mean-square (rms) form. **2.** The highest rms current that an amplifier can deliver to a load of a specified impedance.

output meter A meter that gives a quantitative or qualitative indication of the output of an amplifier or generator. See, for example, OUTPUT-POWER METER.

output offset In an integrated circuit, the voltage at the output when the inputs are grounded.

output port The output terminal of a logic device.

output power Symbol, P_o. The power deliverable by an amplifier, generator, or circuit. Also called *power output*. Compare INPUT POWER.

output-power meter A type of direct-reading wattmeter for measuring the power output of an amplifier or generator.

output regulator A circuit or device that automatically maintains the output of a power supply or signal source at a constant amplitude.

output resistance Symbol, R_o. The internal resistance of a circuit or device, as "seen" at the output terminals. Compare INPUT RESISTANCE.

output routine In computer operations, a routine (program segment) that performs the work involved in moving data to an output device, often including intermediate transferals and modifying the data as necessary.

output section See OUTPUT AREA.

output sink current In an integrated circuit, for a specified set of conditions at the input and output, current into the output as measured in milliamperes or microamperes.

output source current In an integrated circuit, for a specified set of conditions at the input and output, the current out of the output, as measured in milliamperes or microamperes.

output stage The last stage of an amplifier. Delivers the signal to the load.

output terminals Terminals (usually a pair) associated with the output of a circuit or device (see OUTPUT, **1**, **2**). Compare INPUT TERMINALS.

output tank In a transmitter or power generator, a parallel-tuned combination of inductance and capacitance in the collector, drain, or plate circuit, that is generally tuned to resonance at the operating frequency. IT optimizes efficiency and couples the signal to the load. Compare INPUT TANK.

output transformer The output-coupling transformer that delivers signal voltage or power from an amplifier, generator, or network to a load or to another circuit. Compare INPUT TRANSFORMER.

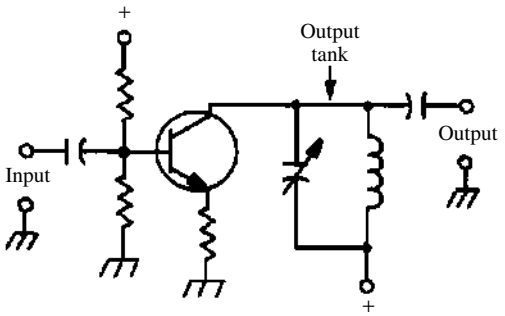

output tank

5059F-pO-488-509 4/10/01 9:24 AM Page 506

output-transformerless Abbreviation, OTL. Pertaining to an oscillator, amplifier, or generator that requires no output coupling transformer.

output transistor A transistor in the final stage of an amplifier or generator; usually, it is a power transistor.

output tube A vacuum tube in the final stage of an amplifier or generator; usually, it is a power tube.

output unit See OUTPUT DEVICE.

output voltage **1.** Symbol, E_o or V_o. The voltage delivered by a source, such as a battery, generator, or amplifier. Compare INPUT VOLTAGE, **2**. **2.** Symbol, E_o or V_o. The voltage across the output leg or electrode of a circuit or device. Compare INPUT VOLTAGE, **2**.

output voltage compliance In an integrated circuit, the voltage range over which the output can be made to swing, while keeping the operation of the circuit within a certain maximum allowable nonlinearity limit. It is measured in volts or millivolts.

output voltage noise In an integrated circuit, the output noise over a given range of frequencies, as measured in peak-to-peak millivolts or microvolts. It can also be measured as the root-mean-square (rms) value.

output voltage swing In an integrated circuit with a specified load, the output-voltage change measured as a difference between maximum and minimum in volts or millivolts.

output voltage tracking For an integrated-circuit dual regulator, the difference between the absolute values of the output voltages of a dual regulator. It can be expressed as a specific voltage or as a percentage of the specified output voltage of the device.

output winding The secondary coil of an output transformer.

outside antenna See OUTDOOR ANTENNA.

outside booster See OUTDOOR BOOSTER.

outside diameter Abbreviation, OD. The outermost diameter of a body or figure having two concentric diameters (e.g., tubing or conduit). Compare INSIDE DIAMETER.

outside lead See FINISH LEAD.

outside transformer **1.** See OUTDOOR TRANSFORMER. **2.** A transformer mounted outside of an equipment in whose circuit it is included. External mounting can eliminate hum in the equipment circuit, and can help to prevent overheating.

oven **1.** Also called *crystal oven.* A chamber providing a closely controlled operating temperature for an electronic component, such as a quartz crystal. **2.** An enclosure in which electronic equipment can be tested at selected, precise high temperatures. Compare COLD CHAMBER.

overall feedback Positive or negative feedback around an entire system (such as a public-address system), as opposed to feedback confined to one stage or a few stages within the system.

overall gain The total gain of an entire system (such as a multistage amplifier), as opposed to that of one or several stages.

overall loudness The apparent intensity of an acoustic disturbance, generally measured with respect to the threshold of hearing, and expressed in decibels, relative to the threshold level.

overbiased unit A component, such as a transistor or vacuum tube, whose bias current or voltage is higher than the correct value for a given mode of operation. Compare UNDERBIASED UNIT.

overbunching In a velocity-modulated tube, such as a Klystron, the condition in which the buncher voltage exceeds the value required for optimum bunching.

overcharging In a secondary cell or battery, the application of charging current longer than necessary to obtain full charge. This can sometimes cause problems, such as cell heating.

overcompounded generator A dynamo-type generator having a compound field winding in which the series-field winding increases the field intensity beyond the point needed to maintain the output voltage. Compare UNDERCOMPOUNDED GENERATOR.

overcompounding A characteristic of electromechanical motors, resulting in increased running speed with decreasing load resistance.

overcoupled transformer A transformer having greater than critical coupling between its primary and secondary windings. In tuned circuits, such as intermediate-frequency (IF) transformers, this produces a double-peak response.

overcoupling Extremely close coupling (see CLOSE COUPLING).

overcurrent A current greater than the specified, nominal, or desired level. Compare UNDERCURRENT.

overcurrent circuit breaker A circuit breaker that opens when current exceeds a predetermined value.

overcurrent protection The use of a circuit breaker, relay, or other device to protect a circuit or system from damage resulting from an excessive flow of current.

overcurrent relay A protective relay that opens a circuit when current exceeds a predetermined value. Compare UNDERCURRENT RELAY.

overcutting In disc recording, the condition in which an excessively high amplitude signal causes the stylus to cut through the wall between adjacent grooves. Compare UNDERCUTTING.

overdamping Damping greater than the critical value (see DAMPING ACTION, **2**). Compare UNDERDAMPING.

overdesign Also called *overengineering.* **1.** To use an unnecessarily high safety factor in the design of equipment. **2.** To design equipment for performance superior to that which is required in the intended application. **3.** A design that results from operations defined in **1** and **2**.

5059F-pO-488-509 4/10/01 9:24 AM Page 507

overdrive In an analog amplifier, an undesirable operating condition that occurs with the application of excessive input signal voltage or power. This results in increased distortion, nonlinearity, excessive harmonic generation, and excessive output signal bandwidth. In a high-fidelity audio system, such a condition grossly degrades the quality of the sound. The amplifying device (transistor or vacuum tube) is in or near saturation during part of the signal cycle. This reduces the efficiency of the circuit, can cause excessive collector, drain, or plate current, and can overheat the base–collector (B-C) junction of a bipolar transistor. In the worst case, it can destroy the component.

overdriven amplifier See OVERDRIVEN UNIT.

overdriven unit An amplifier, oscillator, or transducer whose driving signal (current, voltage, power, or other quantity) is higher than that which the device can properly or efficiently handle for correct or intended operational performance.

overdub In audio recording, a method of combining two or more signals onto a single tape track. For example, a live voice can be recorded on a tape containing pre-recorded music.

overexcited Receiving higher than normal excitation, as in radio-frequency amplifiers or alternating-current generators.

overflow **1.** In computer or calculator operation, the condition in which an arithmetic operation yields a result exceeding the capacity of the location or display for a result. **2.** The carry digit that results from the condition described in (1).

overflow indicator **1.** In a digital calculator, a display that indicates that a numerical value is too large or too small to be shown with the available number of decimal places. **2.** In data processing, a display that indicates the presence of too many bits or characters for the available storage capacity.

overflow position In a digital computer, an auxiliary register position for developing the overflow digit (see OVERFLOW, **1**, **2**).

overflow record In data processing, a record that will not fit the storage area allotted for it, and that must be kept where it can be retrieved, according to some reference stored in its place.

overflow storage In a calculator or computer, extra storage space, allowing a small amount of overflow without loss of accuracy.

overhanging turns The turns in the unused portion(s) of a tapped coil.

overhead line A power or transmission line suspended above the ground between poles or towers.

over-horizon radar A form of radar used at high frequencies, in which pulses are transmitted and received. The signals are returned to earth via the ionosphere, both in the forward and reflected directions, making it possible to detect such things as missile launchings from thousands of miles away.

over-horizon transmission See FORWARD SCATTER.

overinsulation Use of excessive insulation for a particular application. Compare UNDERINSULATION.

over insulation The insulation (usually a strip of tape) laid over a wire brought up from the center of a coil. Compare UNDER INSULATION.

overlap **1.** The time during which two successive operations are performed simultaneously. **2.** In a facsimile or television system, a condition in which the scanning line is wider than the center-to-center separation between adjacent scanning lines.

overlap radar A long-range radar situated in one sector and covering part of another sector.

overlay **1.** A sheet of transparent or translucent material laid over a schematic diagram for the purpose of tracing connections that have been made in wiring an equipment from the diagram. **2.** In computer operations, a method whereby the same internal storage locations are used for different parts of a program during a program run. It is used when the total storage requirements for instructions exceed the available main storage capacity.

overlay transistor A double-diffused epitaxial transistor having separate emitters connected together by means of diffusion and metallizing to increase the edge-to-area ratio of the emitters. This design raises the current-handling ability of the transistor. Also see DIFFUSED TRANSISTOR and EPITAXIAL TRANSISTOR.

overload **1.** Current or power drain in excess of the rated output of a circuit or device. **2.** An excessive driving signal.

overload circuit breaker See CIRCUIT BREAKER.

overloaded amplifier A power amplifier delivering excessive output power. Compare UNDERLOADED AMPLIFIER, **2**.

overloaded oscillator An oscillator from which excessive power is drawn, causing instability, frequency shift, lowered output voltage, and overheating.

overload indication Any attention-catching method, such as an audible or visual alarm, for warning that a prescribed signal or power level has been exceeded.

overload level The amount of overload that can safely be applied to an equipment (see OVERLOAD, **1**).

overload protection The use of circuit breakers, relays, automatic limiters, and similar devices to protect equipment from overload damage by reducing current or voltage, disconnecting the power supply, or both.

overload recovery time Following an overdrive at the input of an integrated-circuit device, the time required for the output to resume its normal characteristics.

5059F-pO-488-509 4/10/01 9:24 AM Page 508

overload relay A relay actuated when circuit current exceeds a predetermined value. Compare UNDERLOAD RELAY.

overload time The maximum length of time that an equipment can safely be subjected to an overload level of current.

overmodulation Modulation in excess of a prescribed level—especially amplitude modulation greater than 100%. Compare COMPLETE MODULATION and UNDERMODULATION.

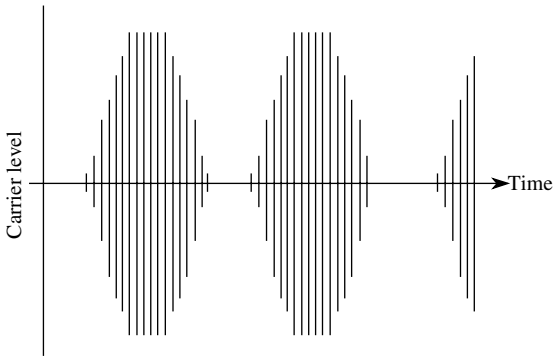

overmodulation

overmodulation alarm See OVERMODULATION INDICATOR.

overmodulation indicator A device, such as a neon bulb, incandescent lamp, light-emitting diode, analog meter, or digital meter, adapted to give an alarm when the modulation percentage of a signal exceeds a predetermined value.

overpotential See OVERVOLTAGE.

overpower relay A relay actuated by a rise in power above a predetermined level. Compare UNDERPOWER RELAY.

overpressure For a pressure transducer, pressure in excess of the maximum rating of the device.

override **1.** To intentionally circumvent an automatic control system. **2.** To bridge a functional stage of a system.

overscanning The deflection of the beam of a cathode-ray tube beyond the edges of the screen.

overshoot **1.** The momentary increase of a quantity beyond its normal maximum value (e.g., the spike sometimes seen on a square wave because of the overswing of a rising voltage). **2.** Momentary overtravel of the pointer of an analog meter.

overswing See OVERSHOOT, **2**.

overtemperature protection The use of an automatic device, such as a thermal relay or thermostat, to disconnect a device from the power supply when the device's temperature becomes excessive.

overthrow See OVERSHOOT, **2**.

overtone See HARMONIC.

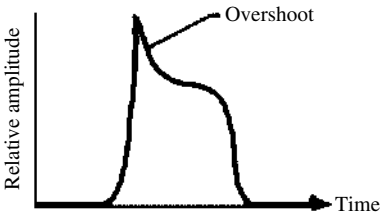

overshoot

overtone crystal A piezoelectric quartz crystal that oscillates at odd multiples of the frequency for which it was cut. This allows crystal operation at frequencies otherwise obtainable only from a fundamental-frequency crystal ground so thin as to be prohibitively fragile.

overtone oscillator A crystal oscillator using an OVERTONE CRYSTAL.

overtravel See OVERSHOOT, **2**.

overvoltage A voltage higher than a specified or rated value. Compare UNDERVOLTAGE.

overvoltage circuit breaker A circuit breaker that opens when voltage exceeds a predetermined value.

overvoltage protection The use of a special circuit or device to protect equipment from excessive voltage. When voltage increases beyond the overvoltage limit, the protective circuit causes shutdown.

overvoltage relay A relay actuated when voltage rises above a predetermined value. Compare UNDERVOLTAGE RELAY.

overwrite In computer operations, to record new data over existing data (e.g., to update the files on a magnetic disk or tape).

Ovshinsky effect In thin-film solid-state devices, the tendency for switches to have the same characteristics for currents in either direction.

O wave One (the ordinary) of the pair of components into which an ionospheric radio wave is divided by Earth's magnetic field. Compare X WAVE.

Owen bridge A wide-range four-arm bridge that measures inductance in terms of a standard capacitance and bridge-arm resistances.

own coding Additional program steps added to vendor-supplied software so that it can be modified to fit special needs.

ox Abbreviation of OXYGEN.

oxidation **1.** The combination of a substance with oxygen. Generally a slow process, such as the corrosion of iron or aluminum in the atmosphere. The process is accelerated by the presence of moisture and/or high temperatures. **2.** The loss of electrons from a cell or battery during discharge.

oxidation-reduction potential The potential at which oxidation occurs at the anode of an electrolytic cell, and at which reduction occurs at the cathode.

5059F-pO-488-509 4/10/01 9:24 AM Page 509

oxide-coated cathode See OXIDE-COATED EMITTER.

oxide-coated emitter An electron-tube cathode or filament coated with a material, such as thorium oxide, for increased electron emission at low emitter temperatures.

oxide-coated filament See OXIDE-COATED EMITTER.

oxide film **1.** The thin film of iron oxide that constitutes the recording surface of a magnetic disk or tape. **2.** The layer of copper oxide formed on the copper plate of a copper-oxide rectifier.

oxide-film capacitor An electrolytic capacitor, so called because the dielectric is a thin oxide film.

oxide rectifier A solid-state rectifier using a junction between copper and copper oxide. Also called COPPER-OXIDE RECTIFIER.

oximeter A photoelectric instrument for measuring the oxygen content of the blood. It operates by passing visible light through the earlobe, and analyzing the color and intensity of the emerging beam. Also called ANOXEMIA TOXIMETER.

oxygen Symbol, O. Abbreviation, O_2. A gaseous element. Atomic number, 8. Atomic weight, 15.999. Constitutes 21% of Earth's atmosphere. It readily combines with various elements to form compounds (see OXIDATION).

oxygen analyzer An electronic gas analyzer designed especially to measure oxygen content. The operation of this instrument is based on the paramagnetic properties of oxygen.

oxygen recombination In nickel-cadmium (NICAD) cells and batteries, a process in which oxygen is generated in the vicinity of the positive electrode, and is reduced with water in the vicinity of the negative electrode. This produces battery heating.

oz **1.** Abbreviation of OUNCE. **2.** Abbreviation of OZONE.

oz-in Abbreviation of OUNCE-INCH.

ozocerite An insulating mineral wax. Dielectric constant, 2.2. Dielectric strength, 4 to 6 kV/mm. Also spelled OZOKERITE.

ozone Symbol, O_3. An allotropic form of oxygen. Its formula indicates that each molecule has three atoms. Produced by the action of ultraviolet rays (or electrical discharge) on oxygen, its characteristic odor (somewhat like weak chlorine) can often be detected around sparking contacts or in the air after a thunderstorm.

ozone layer In the earth's atmosphere, a layer of ozone gas in the upper troposphere and lower stratosphere. It is produced by ultraviolet radiation from space, mainly from the sun. The ozone layer tends to block ultraviolet radiation, reducing the amount that reaches the surface of the earth.

ozone monitor An instrument for measuring the concentration of ozone in the atmosphere. One version measures the extent to which ultraviolet radiation is absorbed by a sample of air; the greater the absorption, the higher the ozone concentration in the sample.

5059F-pP-510-565 4/10/01 9:32 AM Page 510

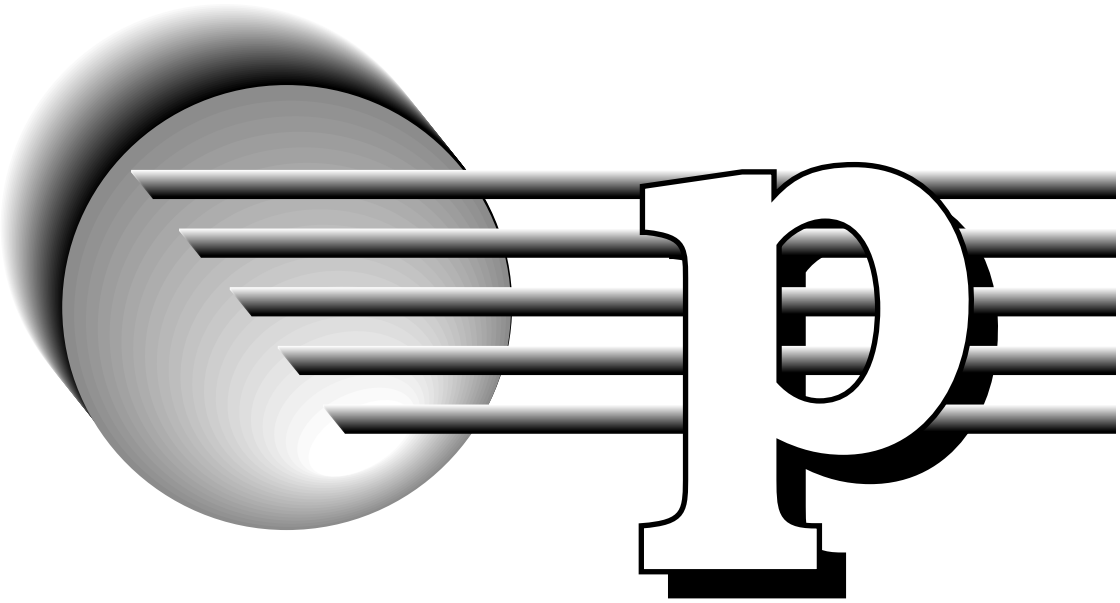

P **1.** Symbol for POWER. **2.** Symbol for PLATE (of a vacuum tube). **3.** Symbol for PHOSPHORUS. **4.** Abbreviation of PRESSURE. **5.** Symbol for PRIMARY. **6.** Abbreviation for prefix PETA-. **7.** Symbol for PERMEANCE. **8.** Abbreviation of POINT.

p **1.** Abbreviation of prefix PICO-. **2.** Subscript for PEAK. **3.** Abbreviation of POUND. **4.** Abbreviation of POINT (often capitalized). **5.** Subscript for PRIMARY. **6.** Subscript for PLATE (of a vacuum tube). **7.** Abbreviation of PITCH. **8.** Abbreviation of PER.

PA **1.** Abbreviation of POWER AMPLIFIER. **2.** Abbreviation of PULSE AMPLIFIER. **3.** Abbreviation of *particular average.* **4.** Abbreviation of *pilotless aircraft.* (Also, P/A.) **5.** Abbreviation of PUBLIC ADDRESS (as in PA system).

Pa **1.** Symbol for PROTACTINIUM. **2.** Symbol for PASCAL.

pA Abbreviation of PICOAMPERE.

pacemaker See CARDIAC STIMULATOR.

pacer See CARDIAC STIMULATOR.

Pacific Standard Time Abbreviation, PST. Local mean time at the 120th meridian west of Greenwich. Also see GREENWICH MEAN TIME, STANDARD TIME, TIME ZONE, and COORDINATED UNIVERSAL TIME.

pack A technique for maximizing a computer memory device's storage capacity, wherein more than one information item is stored in a single storage unit. Also called *crowd.*

package **1.** The enclosure for an electronic device or system. This includes a wide range of housings, from the simple encapsulation of miniature transistors to forced-air-cooled enclosures for heavy power units. **2.** To assemble and house an electronic equipment, or to design a housing for it, in accordance with good engineering techniques. **3.** A computer program of general use for an application (e.g., *payroll package*).

package count The number of discrete packaged circuits in a system.

packaging density **1.** See VOLUMETRIC EFFICIENCY. **2.** Computer storage capacity in terms of the number of information units that can be contained on a given segment of a magnetic medium. Also called PACKING DENSITY. **3.** Within a given integrated circuit, the capacity in terms of the number of active devices that can be contained on a single silicon chip.

packet **1.** A unit of digital information in PACKET COMMUNICATIONS. It consists of a header followed by a certain number of data bits or bytes. **2.** See WAVE PACKET. **3.** See PACKET COMMUNICATIONS. **4.** See PACKET RADIO.

packet communications A method via which data is exchanged through a network between or among people or computers. Information is sent and received in blocks of information called *packets.* Each packet is routed individually through the network according to the most efficient possible path at the time of its transit. At the destination, the packets are reassembled into the original signal. This scheme makes more efficient use of network resources than continuous-connection or single-path methods. However, when network usage is heavy, there can be a delay in the arrival of a sufficient number of packets to produce an intelligible received signal.

packet radio The transmission and reception of PACKET COMMUNICATIONS data via radio.

Copyright 2001 The McGraw-Hill Companies, Inc. Click Here for Terms of Use

5059F-pP-510-565 4/10/01 9:32 AM Page 511

packet switching In telephony, a method of connection in which data is exchanged between subscribers by splitting the data into units (packets). Each packet is sent over the optimum path at the time of transmission. The signal path can, and usually does, vary from packet to packet. At the destination, the packets are reassembled into the original singal. The connection is in effect nonexistent during periods of silence (no data transmitted by either subscriber). Compare CIRCUIT SWITCHING.

packing In the button of a carbon microphone, bunching and cohesion between the carbon granules.

packing density The number of discrete package circuits within a given surface area or volume.

packing factor **1.** See VOLUMETRIC EFFICIENCY. **2.** In computer operations, the number of bits that can be recorded in a given length of magnetic memory surface. Also called PACKING DENSITY.

pack transmitter A portable transmitter that can be strapped to the operator's back.

pack unit A portable transceiver that can be strapped to the operator's back or carried on an animal's back.

PACM Abbreviation of *pulse-amplitude code modulation.*

pad **1.** An attenuator network (usually a combination of resistors) that reduces the amplitude of a signal by a desired amount while maintaining constant input and output impedance. **2.** In computer operations, to make a record a fixed size by adding blanks or dummy characters to it. **3.** To lower the frequency of an inductance-capacitance (LC) circuit by adding capacitance to an already capacitively tuned network.

padder See OSCILLATOR PADDER.

padding capacitor See OSCILLATOR PADDER.

padding character In a digital communications system, a character that is inserted solely for the purpose of consuming time while no meaningful characters are sent. The insertion of such characters maintains the synchronization of the system.

paddle-handle switch A toggle switch the lever of which is a flattened rod. Compare BAT-HANDLE SWITCH, ROCKER SWITCH, and SLIDE SWITCH.

PADT Abbreviation of POST-ALLOY-DIFFUSED TRANSISTOR.

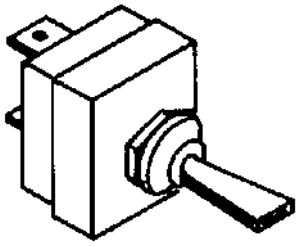

paddle-handle switch

page A display of text data on a computer display that completely fills the screen.

page printer A computer peripheral that prints a message in lines on a page, according to an established format, rather than in a single line.

pager **1.** A public-address system used for summoning purposes. **2.** See BEEPER, **2**.

page turning The successive display of pages (see PAGE).

pair **1.** Two wires, especially two insulated conductors in a cable. **2.** A set of two particles or charge carriers (e.g., *electron-hole pair*). **3.** A set of two transistors or vacuum tubes, operating together in push-pull or parallel in a power amplifier.

paired cable A cable consisting of separate twisted pairs of conducting wires.

paleomagnetism The study of certain rocks and minerals to determine the nature of the earth's magnetic field at the time the rocks were formed. When the age of the rock is determined by means of radioactive dating, and numerous rock samples are found covering many different eras, the nature of the earth's magnetic field can be graphed over time.

palladium Symbol, Pd. A metallic element of the platinum group. Atomic number, 46. Atomic weight, 106.42.

palletizing In industrial robots, the automatic placing of objects in a tray according to a computer program.

Palm See HANDHELD COMPUTER.

Palmer scan In radar, a method of simultaneously scanning the azimuth and the elevation.

PalmPilot See HANDHELD COMPUTER.

palmtop computer See HANDHELD COMPUTER.

PAM Abbreviation of PULSE-AMPLITUDE MODULATION.

Pan In radiotelephony, a spoken word indicating that an urgent message is to follow. It is equivalent to the XXX of radiotelegraphy.

pan **1.** To make a panoramic sweep [e.g., to sweep a wide area with a beam (as from an antenna), or to sweep a wide band of frequencies with a suitable tuning circuit]. **2.** A panoramic sweep made as defined in **1**. **3.** In audio engineering, to gradually shift from one audio channel to another or from one reproducer to another.

pan and tilt **1.** An azimuth-elevation mounting for a television camera. **2.** The simultaneous movement of a television camera in the vertical and horizontal directions.

pancake coil See DISK WINDING.

panel A flat surface on which are mounted the controls and indicators of an equipment, for easy access to the operator.

panel lamp **1.** See ELECTROLUMINESCENT PANEL. **2.** See PANEL LIGHT.

panel light A pilot light for illuminating the front panel of a piece of equipment.

panel meter A usually small meter for mounting on, or through an opening in, a panel.

5059F-pP-510-565 4/10/01 9:32 AM Page 512

panic button In a security system, a button or switch that immediately triggers an alarm when it is closed.

panoramic adapter An external device that can be connected to a receiver to sweep a frequency band and indicate carriers on the air as pips on a screen at the corresponding frequency points. Also called *pan adapter*.

panoramic display **1.** A wide-angle display. **2.** A spectrum-analyzer display that shows a wide range of frequencies, from zero to well above the maximum frequency in the monitored system.

panoramic radar An omnidirectional radar (i.e., one that transmits wide-beam signals in all directions without scanning).

panoramic receiver A receiver that displays pips on a screen to show carriers on the air in a given frequency band. All frequencies in the band are presented along the horizontal axis of the screen.

panpot A potentiometer with which panning can be achieved (see PAN, **3**).

pan-range A form of radar display in which target motion can be ascertained.

pantography The transmission of radar information to a distant location for observation or recording.

Papa Phonetic alphabet code word for the letter P.

paper advance mechanism In a data-processing system, the part of a printer that moves (sometimes by computer control) the paper through the printer.

paper capacitor A component that is made by placing paper, soaked with mineral oil, between two strips of foil. The assembly is rolled up, and wire leads are attached to the two pieces of foil. Finally, the rolled-up foil and paper are enclosed in a cylindrical case. These components are sometimes found in radio-frequency (RF) electronic equipment. They have values ranging from about 0.001 microfarads (μF) to 0.1 μF, and can handle low to moderate voltages, usually up to about 1000 volts. Compare CERAMIC CAPACITOR, ELECTROLYTIC CAPACITOR, MICA CAPACITOR, PLASTIC-FILM CAPACITOR, TANTALUM CAPACITOR.

PAR Abbreviation of PRECISION APPROACH RADAR.

par Abbreviation of PARALLEL.

parabola A plane curve that is the locus of points that are equidistant from a fixed point (the focus) and a fixed straight line (the directrix). In the Cartesian *xy*-plane, the general equation is $y = ax2 + b$, where a and b are constants.

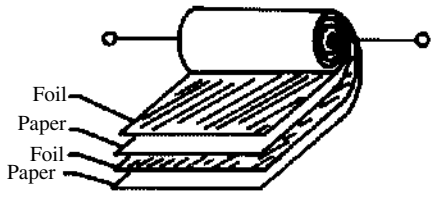

paper capacitor

parabola control See VERTICAL-AMPLITUDE CONTROL, **2**.

parabola generator A circuit for generating a parabolic-waveform signal.

parabolic microphone A directional microphone mounted at the principal focus of a parabolic sound reflector; the front of the microphone faces the inside of the parabola. It is useful for detecting sounds from great distances.

parabolic reflector Also called *paraboloidal reflector*. A reflector having the shape of a paraboloid. It is particularly useful for focusing or directing radiation. For example, if a radiator, such as an antenna rod, is placed at the focus of the paraboloid, a beam of parallel rays will be emitted by the reflector.

paraboloid The surface generated by a PARABOLA rotated about its axis of symmetry.

paraffin A relatively inexpensive, easily available, solid, white petroleum wax. At one time, it was used to impregnate capacitors and coils and to waterproof paper used for insulating purposes.

parallax The apparent shift in the position of a relatively nearby object when the observer moves or alternately blinks either eye. Thus, a pointer-type meter will seem to give different readings when viewed from different angles. Some meters have mirrored scales to eliminate this effect.

parallel **1.** Pertaining to the type of operation in a computer when all elements in an information item (e.g., bits in a word) are acted upon simultaneously, rather than serially (one at a time). **2.** The condition in which two comparably sized objects or figures are equidistant at all facing points. **3.** Pertaining to the shunt connection of components or circuits.

parallel access In computer operations, inputting or outputting data to or from storage in whole elements of information items (a word, rather than a bit at a time, for example).

parallel adder In a computer or calculator, an adder in which corresponding digits in multibit numbers are added simultaneously. Also see PARALLEL, **1**.

parallel antenna tuning Antenna-feeder tuning in which the tuning capacitor is connected in parallel with the two feeder wires. Compare SERIES ANTENNA TUNING.

parallel arithmetic unit See PARALLEL ADDER.

parallel capacitance **1.** A capacitance connected in parallel (shunt) with some other component. **2.** The capacitance between the turns of a coil. Also see DISTRIBUTED CAPACITANCE.

parallel capacitors Two or more capacitors connected in parallel (shunt) with each other. The total capacitance is equal to the sum of the individual capacitances. Also see PARALLEL CIRCUIT.

5059F-pP-510-565 4/10/01 9:32 AM Page 513

parallel circuit A circuit in which the components are connected across each other (i.e., so that the circuit segment could be drawn showing component leads bridging common conductors as rungs would across a ladder). Compare SERIES CIRCUIT.

parallel-component amplifier An amplifier stage in which the active devices (transistors or vacuum tubes) are connected in parallel with each other for increased power output. Also see PARALLEL CIRCUIT.

parallel-component oscillator An oscillator stage in which transistors are connected in parallel with each other for increased power output. Also see PARALLEL CIRCUIT.

parallel computer A computer equipped to handle more than one program at a time, but not through the use of multiple programming or time-sharing.

parallel-cut crystal See Y-CUT CRYSTAL.

parallel-diode half-wave rectifier See PARALLEL LIMITER.

parallel-fed amplifier An amplifier circuit in which the direct-current operating voltage is applied in parallel with the alternating-current output voltage. Also see PARALLEL FEED.

parallel-fed oscillator An oscillator circuit in which the direct-current operating voltage is applied in parallel with the alternating-current output voltage. Also see PARALLEL FEED.

parallel feed **1.** The presentation of parallel alternating-current (ac) and direct-current (dc) voltages to a device. **2.** The presentation of a dc operating voltage in parallel with the ac output voltage of a device (as in a parallel-fed amplifier or oscillator). Also see SHUNT FEED.

parallel gap welding A welding technique using two electrodes separated by a gap.

parallel gate circuit **1.** A gate circuit using two bipolar transistors with parallel-connected collectors and emitters, and a common collector resistor. The input signal is applied to one base, and the control signal to the other. **2.** A gate circuit using two field-effect transistors with parallel-connected drains and sources, and a common drain resistor. The input signal is applied to one gate, and the control signal to the other.

parallel inductance An inductance connected in parallel (shunt) with some other component.

parallel inductors Inductors connected in parallel and separated or oriented to minimize the effects of mutual inductance. Also see PARALLEL CIRCUIT.

parallel inverse feedback In a single-ended audio amplifier circuit, a simple system for obtaining negative feedback: A high resistance is connected from the output-transistor collector or drain to the driver-transistor collector or drain.

parallel limiter A limiter (clipper) circuit in which the diode is in parallel with the signal. Compare SERIES LIMITER.

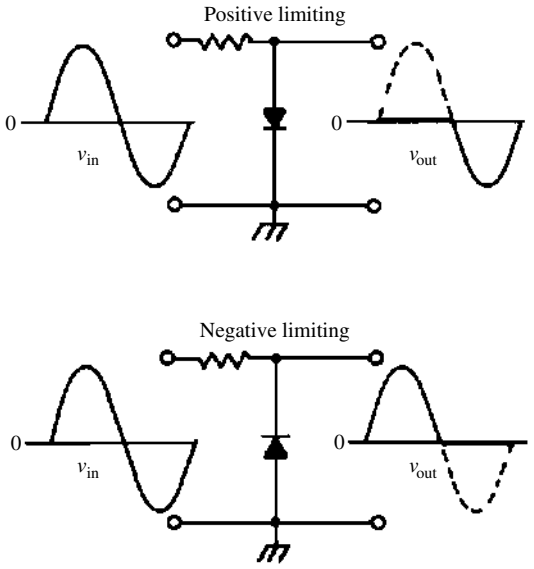

parallel limiter

parallel-line tuning At ultra-high frequencies (UHF) and microwave frequencies, the use of two parallel wires or rods for tuning. A straight short-circuiting bar is slid along the wires to accomplish tuning.

parallelogram A two-dimensional geometric figure that has four sides. Opposite pairs of sides are parallel. Opposite interior angles have equal measure.

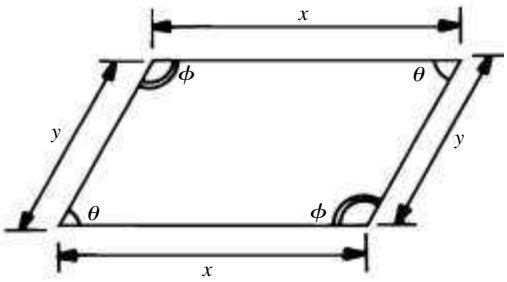

parallelogram

parallelogram of vectors A graphic device for finding the sum of two vectors. A parallelogram is constructed for which the two vectors are adjacent sides. The sum of the vectors is represented by the diagonal of the parallelogram.

parallel operation In computer operations, the simultaneous transmission of all bits in a multibit word over individual lines, as compared with the serial transmission of a word bit by bit.

5059F-pP-510-565 4/10/01 9:32 AM Page 514

parallel output A digital output consisting of two or more lines, all of which carry data at the same time.

parallel processing In computer operations, the simultaneous processing of several different programs through separate channels. Compare SERIAL PROCESSING.

parallel *Q* Symbol, Q_p. The figure of merit of a parallel circuit of inductance, capacitance, and resistance.

parallel resistance **1.** A resistance connected in parallel (shunt) with some other component. **2.** The resistance between the plates of a capacitor. **3.** The resistance across a coil.

parallel resistors Resistors connected in parallel. If the individual resistances are represented by R_1, R_2, R_3, . . ., Rn, then total resistance R_t is equal to $1/(1/R_1 + 1/R_2 + 1/R_3 + \ldots + 1/R_n)$. Also see PARALLEL CIRCUIT.

parallel resonance Resonance in a circuit consisting of a capacitor, inductor, and alternating-current source connected in parallel. At the resonant frequency, the inductive reactance is equal in magnitude, but opposite in effect, to the capacitive reactance. The capacitor current and inductor current are maximum, the line current is minimum, and the circuit impedance is maximum. Compare SERIES RESONANCE.

parallel-resonant circuit A resonant circuit in which the capacitor, inductor, and alternating-current source are connected in parallel. Compare SERIES-RESONANT CIRCUIT.

parallel-resonant trap A wavetrap consisting of a parallel-resonant inductance-capacitance (LC) circuit. Compare SERIES-RESONANT TRAP.

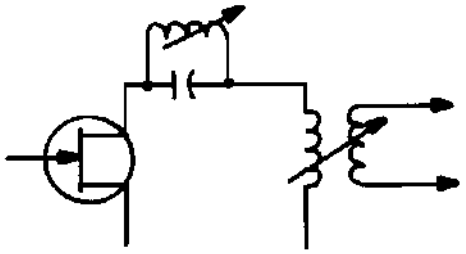

parallel-resonant trap

parallel-resonant wavetrap See PARALLEL-RESONANT TRAP.

parallel-rod oscillator An ultra-high-frequency (UHF) oscillator tuned by means of two straight, parallel quarter- or half-wave rods, one rod connected to the base or gate of a transistor, and the other rod connected to the collector or drain.

parallel-rod tuning Adjustment of the resonant frequency of a section of open-wire transmission line. A movable shorting bar allows quarter-wave resonance. The impedance at resonance is very high.

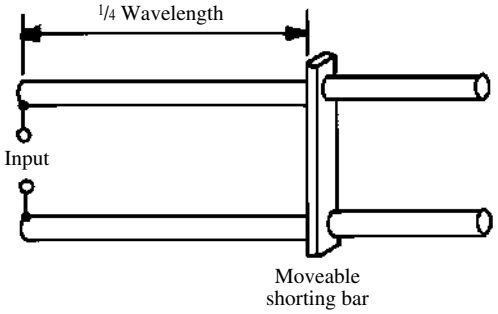

parallel-rod tuning

parallel-series Also called *series-parallel.* Pertaining to an arrangement of components, usually similar (e.g., resistances), consisting of parallel circuits connected in series with each other, or of series circuits connected in parallel with each other. Usually, the component values or ratings are all identical, so currents and/or voltages are equally shared among them. Also see PARALLEL CIRCUIT and SERIES CIRCUIT.

parallel-series capacitors Capacitors connected in PARALLEL-SERIES, usually to obtain higher voltage and/or current ratings than an individual capacitor can provide.

parallel-series inductors Inductors connected in PARALLEL-SERIES and separated or oriented to minimize the effects of mutual inductance.

parallel-series resistors Resistors connected in PARALLEL-SERIES, usually to obtain a higher power rating than an individual resistor can provide.

parallel storage In a computer, storage in which all information items can be made available in the same amount of time.

parallel-tee amplifier A bandpass amplifier having a parallel-tee network in its negative-feedback path. The null frequency of the network determines the pass frequency of the amplifier.

parallel-tee measuring circuit A parallel-tee network used for measuring circuit constants. Also called TWIN-TEE MEASURING CIRCUIT.

parallel-tee network A resistance-capacitance (RC) network containing two tee sections (with R and C elements opposite in the tees) connected in parallel. The network produces a null at one frequency. Also called TWIN-T NETWORK.

parallel-tee oscillator A resistance-capacitance tuned oscillator having a parallel-tee network in its negative-feedback path. The null frequency of the network determines the oscillator frequency.

parallel transfer A form of digital information transfer, consisting of two or more lines that carry data at the same time.

parallel-wire line A transmission line consisting of two parallel wires whose separation is kept

5059F-pP-510-565 4/10/01 9:32 AM Page 515

constant by dielectric rods (open-wire line) or a solid dielectric web (ribbon line).

parallel-wire tank In an ultra-high-frequency (UHF) amplifier or oscillator, a resonant circuit consisting of two separate parallel wires connected to the transistor(s) or tube(s) at one end, and short-circuited or tuned at the other end.

paramagnet A paramagnetic substance (see PARAMAGNETISM). Compare DIAMAGNET.

paramagnetic Possessing PARAMAGNETISM. Compare DIAMAGNETISM.

paramagnetism The state of having a magnetic permeability slightly greater than **1**. Compare DIAMAGNETISM.

parameter **1.** An operating value, constant, or coefficient that can be either a dependent or an independent variable (e.g., a transistor-electrode current or voltage). **2.** The ratio of one coefficient to another, where both are either fixed or variable (e.g., transconductance of a vacuum tube).

parameter word In a computer memory, a place having a capacity of a word (bit group) in which is stored a parameter for a program.

parametric amplifier A radio-frequency power amplifier based on the action of a voltage-variable capacitor in a tuned circuit.

parametric amplifier diode See VARACTOR.

parametric converter A frequency converter in which a parametric device, such as a varactor, is used to change a signal of one frequency to a signal of another frequency. Also see PARAMETRIC DOWN-CONVERTER and PARAMETRIC UP-CONVERTER.

parametric diode A variable-capacitance diode (see VOLTAGE-VARIABLE CAPACITOR, **1**).

parametric down-converter A parametric converter in which the output signal is of a lower frequency than the input signal. Compare PARAMETRIC UP-CONVERTER.

parametric equalizer A set of audio filters similar to a GRAPHIC EQUALIZER, except that the center frequencies are adjustable, rather than fixed. The center frequencies are selected by the operator; then the attenuation level (in decibels) is set for each frequency. It is used in audio recording studios.

parametric modulation Modulation in which either the inductance or capacitance of a tank circuit or coupling device is varied at the modulation frequency.

parametric oscillator An oscillator that generates visible light energy by means of a parametric amplifier and a tunable cavity.

parametric up-converter A parametric converter in which the output signal is of a higher frequency than the input signal. Compare PARAMETRIC DOWN-CONVERTER.

parametron See PHASE-LOCKED OSCILLATOR.

paramistor A device consisting of several digital circuit elements that use parametric oscillators.

paramp Abbreviation of PARAMETRIC AMPLIFIER.

paraphase inverter A single-transistor phase inverter in which the two out-of-phase output signals are obtained by taking one output from the collector or drain, and the other output from the emitter or source. Thus, the 180-degree phase difference between collector/drain and emitter/source is exploited.

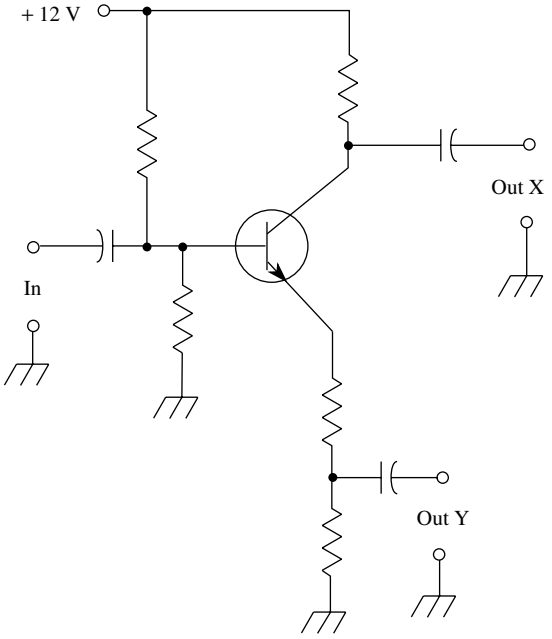

paraphase inverter

parasitic See PARASITIC OSCILLATION.

parasitic antenna See PARASITIC ARRAY, PARASITIC ELEMENT.

parasitic array Any of several types of directional antenna employing parasitic elements, sometimes in combination with phasing, to obtain directivity and gain. Common examples include the Yagi and quad. Arrays with numerous parasitic elements (usually directors) can produce upwards of 15 dBd forward gain. When several high-gain arrays are phased, the realizable gain becomes greater still. Two-element, three-element, and four-element arrays are common below 30 MHz. At very-high and ultra-high frequencies, especially above 100 MHz, bays of antennas of this type are used in satellite communications and radio astronomy. See PARASITIC ELEMENT, QUAD ANTENNA, YAGI ANTENNA.

parasitic capacitance Stray capacitance. It can be internal or external to a circuit and can introduce undesirable coupling or bypassing.

5059F-pP-510-565 4/10/01 9:32 AM Page 516

parasitic choke A small radio-frequency choke coil (with or without a shunting resistor) that suppresses or eliminates parasitic oscillation in a power amplifier.

parasitic director In a multielement directional antenna, a parasitic element acting as a director; usually, it is a few percent shorter than the driven element.

parasitic element An electrical conductor that comprises an important part of an antenna system, but that is not directly connected to the feed line. Such elements are used for the purpose of obtaining directivity and power gain. They operate via electromagnetic coupling to the driven element(s). The principle of operation was first discovered by the Japanese engineers Yagi and Uda, who observed that antenna elements parallel to a driven element but not connected to anything, at a specific distance from the driven element, and having a certain length, cause the radiation pattern to show gain in one direction and loss in the opposite direction. See DRIVEN ELEMENT, PARASITIC ARRAY, PARASITIC DIRECTOR, PARASITIC REFLECTOR.

parasitic-element directive antenna See PARASITIC ARRAY.

parasitic eliminator See PARASITIC SUPPRESSOR.

parasitic excitation Excitation of a beam-antenna element without a direct connection to the transmitter. Thus, a director or reflector element can be excited by the field of the radiator element.

parasitic inductance Stray inductance (e.g., the internal inductance of a wirewound resistor).

parasitic oscillation Extraneous, useless oscillation present as a fault in an electronic circuit, particularly a radio-frequency power amplifier.

parasitic reflector In a multielement beam antenna, a parasitic element acting as a reflector; usually, it is a few percent longer than the driven element.

parasitic resistance Stray resistance (e.g., the inherent, internal resistance of a multilayer coil).

parasitic suppressor A small resistor, coil, or parallel combination of the two, connected in series with the plate or collector of a vacuum tube or transistor to eliminate parasitic oscillations in a radio-frequency power amplifier.

PARD Abbreviation of PERIODIC AND RANDOM DEVIATION.

parity **1.** At par (with respect to the even-or-odd state of the characters in a group). **2.** Having the quality that the number of bits (or the number of similar bits) are even or odd, as intended.

parity bit **1.** In computer operations, a logic 1 added to a group of bits so that the number of 1s in the group is, according to specification, even or odd. **2.** In computer operations, a check bit that can be a logic 1 or 0, depending on the parity (see PARITY, **1**) of the total of 1s in the bit group being checked.

parity check A check of the integrity of data being transferred by adding the bits in, for example, a word, and then determining the parity bit needed and comparing that with the transmitted parity bit.

parity error An error disclosed by a parity check.

parity tree A digital device used to check parity.

parsec Abbreviation, pc. The distance at which the mean radius of the earth's orbit around the sun subtends an angle of 1 second of arc; 1 pc = 3.0857×10^{13} kilometers or 3.2616 light years.

part See CIRCUIT COMPONENT, **1**.

part failure The usually destructive breakdown of a circuit component.

partial One of the frequencies in a complex musical tone. It might be a harmonic of the fundamental frequency, although this is not always the case.

partial carry The temporary storage of some or all of the carry information in a digital calculation.

particle **1.** A tiny, discrete bit of matter. **2.** A unit of matter smaller and lighter than an atom. See, for example, ANTIPARTICLE, ELECTRON, MESON, NEUTRETTO, NEUTRINO, NEUTRON, NUCLEON, POSITRON, and PROTON.

particle accelerator See ACCELERATOR, **1**.

particle theory of radiation In physics, a model that explains the nature of electromagnetic radiation (radio waves, infrared, visible light, ultraviolet, X rays, and gamma rays) in terms of discrete particles. Each particle, called a PHOTON, carries a certain amount of energy that depends on the wavelength of the radiation.

particle velocity **1.** The speed and direction of the particles from a source of atomic radiation. **2.** The speed and direction of the molecules in the medium of an acoustic disturbance.

partitioning In computer operations, breaking down a large block of data into smaller blocks that can be better handled by the machine.

parton model A model for atomic nuclei, in which protons and neutrons are made up of smaller particles called *partons*. Subparticles have been found, commonly called *quarks*.

Pascal A high-level computer programming language, similar to BASIC or FORTRAN in structure. It is used in some schools to teach computer programming.

pascal Symbol, Pa. The SI (derived) unit of pressure; 1 $Pa = 1\ N/m^2 = 1.4503 \times 10^{-4}\ lb/in^2$.

Paschen-Back effect See ZEEMAN EFFECT.

Paschen's law For a two-element, parallel-plate, gas-discharge tube, the plate-to-plate sparking potential is proportional to Pd, where P is the gas pressure, and d is the distance between plates.

pass amplifier A tuned amplifier having the response of a bandpass filter. Like the filter, the amplifier passes one frequency (or a narrow band of frequencies) readily while rejecting or attenuating others. Compare REJECT AMPLIFIER.

5059F-pP-510-565 4/10/01 9:32 AM Page 517

passband The continuous spectrum of frequencies transmitted by a filter, amplifier, or similar device. Compare STOPBAND.

passband ripple Multiple low-amplitude attenuation variations within the passband of a filter or tuner, resulting in a ripple pattern on the nose of the response curve.

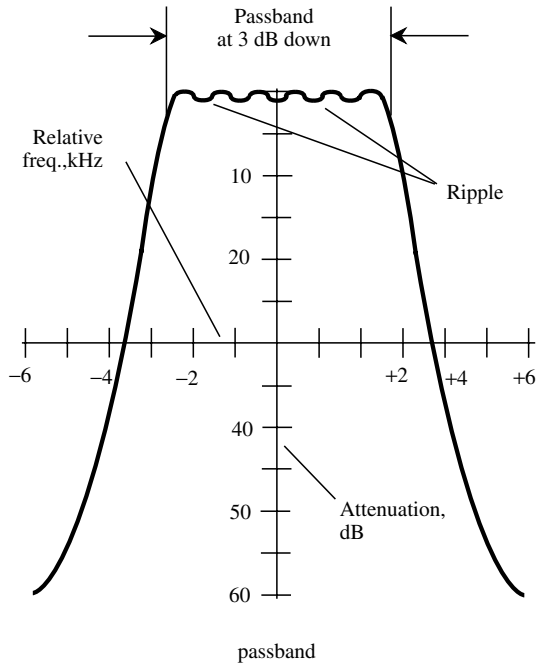

passband ripple

passivation The process of growing a thin oxide film on the surface of a planar semiconductor device to protect the exposed junction(s) from contamination and short circuits. See, for example, PLANAR EPITAXIAL PASSIVATED TRANSISTOR and PLANAR TRANSISTOR.

passive absorber A substance that reflects minimal sound energy. Examples include acoustical ceiling tile and thick carpeting.

passive circuit A circuit consisting entirely of nonamplifying components, such as capacitors, resistors, inductors, and diodes.

passive communications satellite A communications satellite that reflects electromagnetic waves, but does not contain a transponder; that is, it does not receive and retransmit the signals. Also called *passive comsat*. Compare ACTIVE COMMUNICATIONS SATELLITE.

passive component A device that is basically static in operation (i.e., it is ordinarily incapable of amplification or oscillation and usually requires no power for its characteristic operation). Examples: conventional resistor, capacitor, inductor, diode, rectifier, and fuse. Compare ACTIVE COMPONENT, **1**.

passive comsat See PASSIVE COMMUNICATIONS SATELLITE.

passive decoder A decoder that responds to only one signal code, rejecting all others.

passive detection In reconnaissance, detecting a target without betraying the location of the detector.

passive electric network See PASSIVE NETWORK.

passive frequency multiplier A frequency multiplier that does not require a power supply, but operates only from the input signal energy. Usually consists of one or more semiconductor diodes, sometimes in conjunction with inductors and/or capacitors. The output signals appear at integral multiples of the input frequency.

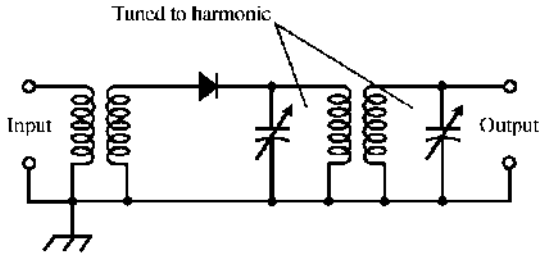

passive frequency multiplier

passive infrared sensor A device that detects infrared directly, such as that given off by humans because of their body heat. It does not generate energy of any kind. It is used in some intrusion detection systems.

passive mixer A signal mixer using only passive components (diodes, nonlinear resistors, and nonlinear reactances) (i.e., one without active components, such as transistors). Passive mixers introduce some loss. Compare ACTIVE MIXER.

passive modulator A modulator using only passive components (diodes, nonlinear resistors, and nonlinear reactances) (i.e., one without active components, such as transistors). Passive modulators introduce some loss. Compare ACTIVE MODULATOR.

passive network A network composed entirely of passive components (i.e., one containing no generators and providing no amplification).

passive radiator See DRONE CONE.

passive reflector A metal surface used to reflect electromagnetic energy at ultra-high and microwave frequencies.

5059F-pP-510-565 4/10/01 9:32 AM Page 518

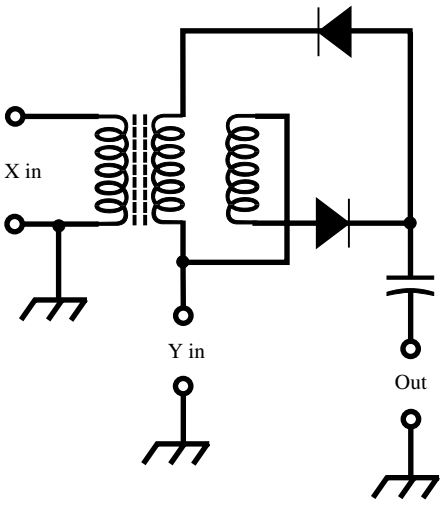

passive mixer

passive transponder A device that allows a machine, such as a computer or robot, to identify an object. A bar-code reader is a common example. Magnetic labels, such as those on credit cards and bank cash cards, are another example. It is so named because it does not transmit data; it requires a sensor for data detection.

password As a security device in computer operations, a group of characters upon whose presentation to the system via a terminal the user is allowed access to memory or control of information.

password retry limitation A security feature that prevents hackers from making repeated guesses at passwords in an attempt to break into a computer, network, or database. If more than three unsuccessful entries are made in succession, for example, the system will not accept further access attempts for a certain preprogrammed length of time, say 1 hour.

paste In "dry" batteries and electrolytic capacitors, a gelatinous electrolyte.

patch **1.** A temporary signal path, as between a radio receiver and a telephone or, conversely, between a telephone line and a radio transmitter. **2.** To make quick, usually temporary connections, as with a patch cord. **3.** Instructions entered by an unconditional branch to a computer program for the purpose of correction.

patch bay **1.** See PATCH PANEL. **2.** A set of patch panels.

patch cord A flexible line of one or more conductors with a jack or connector at each end, used to interconnect (patch) circuit points exposed for the purpose on a panel or breadboard.

Patchett tone control A dual tone-control circuit using a variable series resistance-capacitance (RC) filter for treble boost, and a variable shunt RC filter for bass boost. The input signal is applied in parallel to both filters. The outputs are combined in an audio mixer.

patching The interconnection of two or more signal media or lines.

patch panel A panel on which the terminals of a system are accessible for interconnection, tests, etc. It is used especially in high-fidelity audio recording systems. It was once commonly used in manual telephone-switching applications.

patch up **1.** To replace faulty or damaged parts in an electronic system with roughly appropriate surrogates to restore operation quickly (usually under emergency conditions). Also see DOCTOR. **2.** To wire a circuit quickly using patch cords for preliminary test and evaluation.

patent **1.** A document awarded by a government body, giving to an inventor the exclusive right to exploit an invention for a specified number of years. Formally called *letters patent.* **2.** The monopoly granted by a document, as defined in **1**.

path **1.** The route over which current flows. **2.** In radio and navigation, the imaginary line extending directly between transmitter and receiver (or target). **3.** In a computer program, the logical order of instructions.

pathometer A form of lie detector that indicates changes in the electrical resistance of the human body.

pattern **1.** An established sequence of steps in a process. **2.** An arrangement of terms in a matrix. **3.** The graphical representation of a varying quantity (e.g., an alternating-current wave pattern). **4.** The image on the screen of an oscilloscope, or the record traced by an oscillograph. **5.** The graphic polar representation of the radiation field of an antenna. **6.** The arrangement of bits in a word or field.

pattern recognition In machine-vision systems, a method of identifying an object or decoding data according to geometric shape. Optical character recognition (OCR) is an example. The machine recognizes combinations of shapes, and deduces their meanings via a computer program.

pause editing In the editing of audio tape recordings, the use of a "pause" switch to temporarily stop the tape when necessary.

PAV Abbreviation of PHASE-ANGLE VOLTMETER.

pawl In a mechanical stepping device, as in a nonelectric clock, a device made to engage the sloping sprockets on a wheel to ensure shaft rotation in one direction only.

PAX Abbreviation of PRIVATE AUTOMATIC EXCHANGE.

pay-per-view Abbreviation, PPV. Television service in which each subscriber pays only for individually selected programs.

pay TV See SUBSCRIPTION TV.

Pb Symbol for LEAD.

5059F-pP-510-565 4/10/01 9:32 AM Page 519

P band A radio-frequency band extending from 225 to 390 MHz.

PBX Abbreviation of PRIVATE BRANCH EXCHANGE.

PC **1.** Abbreviation of PERSONAL COMPUTER. **2.** Abbreviation of PRINTED CIRCUIT. **3.** Abbreviation of PHOTOCELL. **4.** Abbreviation of POSITIVE COLUMN. **5.** Abbreviation of POINT-CONTACT. **6.** Abbreviation of PERCENT (also, pct.). **7.** Abbreviation of PROGRAM COUNTER.

pc **1.** Abbreviation of PICOCOULOMB. Also, pC (preferred). **2.** Abbreviation of PICOCURIE. Also, pCi (preferred). **3.** Abbreviation of PARSEC.

pC Abbreviation for PICOCOULOMB.

PCB Abbreviation of PRINTED-CIRCUIT BOARD.

PC board See PRINTED-CIRCUIT BOARD.

PC diode See POINT-CONTACT DIODE.

p-channel JFET See P-CHANNEL JUNCTION FIELD-EFFECT TRANSISTOR.

p-channel junction field-effect transistor Abbreviation, PFET. A junction-type FET in which the gate junction has been formed on a bar or die of p-type semiconductor material. Compare N-CHANNEL JUNCTION FIELD-EFFECT TRANSISTOR.

p-channel MOSFET A metal-oxide semiconductor field-effect transistor in which the channel is composed of p-type silicon. Also see DEPLETION-TYPE MOSFET, DEPLETION-ENHANCEMENT-TYPE MOSFET, and ENHANCEMENT-TYPE MOSFET.

pCi Symbol for PICOCURIE.

PCL Abbreviation of PRINTED-CIRCUIT LAMP.

PCM Abbreviation of PULSE-CODE MODULATION.

PCM-FM Pertaining to a carrier that is frequency modulated by information that is pulse-code modulated. Also see FREQUENCY MODULATION and PULSE-CODE MODULATION.

PCM-FM-FM Pertaining to a carrier that is frequency modulated by one or more subcarriers that are frequency modulated by information that is pulse-code modulated. Also see FREQUENCY MODULATION and PULSE-CODE MODULATION.

PCM level In a pulse-code-modulated signal, one of several different possible signal conditions.

PCM-PM Pulse-code modulation that is accomplished by varying the phase of the carrier wave.

PC relay See PRINTED-CIRCUIT RELAY.

PCS Abbreviation for PERSONAL COMMUNICATION SERVICE.

PC transistor See POINT-CONTACT TRANSISTOR.

PD **1.** Abbreviation of PLATE DISSIPATION. **2.** Abbreviation of PULSE DURATION. **3.** Abbreviation of PROXIMITY DETECTOR. **4.** Abbreviation of POTENTIAL DIFFERENCE.

Pd Symbol for PALLADIUM.

PDA Abbreviation for *personal digital assistant.* See HANDHELD COMPUTER.

PDAS Abbreviation of *programmable data acquisition system.*

P display See PLAN POSITION INDICATOR.

PDM Abbreviation of PULSE-DURATION MODULATION.

PDM-FM Pertaining to a carrier that is frequency modulated by one or more subcarriers that are frequency modulated by pulses that are pulse-duration modulated. Also see FREQUENCY MODULATION and PULSE-DURATION MODULATION.

PDM-FM-FM Pertaining to a carrier that is frequency modulated by one or more subcarriers that are frequency modulated by pulses that are pulse-duration modulated. Also see FREQUENCY MODULATION and PULSE-DURATION MODULATION.

PDM-PM Pertaining to a carrier that is phase modulated by pulse-duration-modulated information. Also see PHASE MODULATION and PULSE-DURATION MODULATION.

PDT Abbreviation of PACIFIC DAYLIGHT TIME.

PDVM Abbreviation of PRINTING DIGITAL VOLTMETER.

PE **1.** Abbreviation of POTENTIAL ENERGY. **2.** Abbreviation of PROFESSIONAL ENGINEER. **3.** Abbreviation of PROBABLE ERROR.

peak **1.** The maximum value of a quantity. **2.** In an alternating-current cycle, the maximum positive or negative current or voltage point. **3.** The frequency at which the transmission by a bandpass circuit or device is maximum (attenuation is minimum), evidenced by a maximum in the frequency-response curve.

peak amplitude **1.** The maximum positive or negative current or voltage of a wave. **2.** The maximum instantaneous power of a signal.

peak anode (plate) current The maximum instantaneous current flowing in the anode (plate) circuit of a vacuum tube.

peak anode (plate) voltage The maximum instantaneous voltage applied to the anode (plate) of a vacuum tube.

peak chopper See PEAK CLIPPER.

peak current Abbreviation, I_p. The highest value reached by an alternating-current half-cycle or a current pulse. Also called MAXIMUM CURRENT.

peak detector See PEAK PROBE.

peak distortion **1.** The maximum instantaneous distortion in a signal, generally expressed as a percentage. **2.** Distortion of a modulated signal at envelope peaks.

peaked sawtooth A wave composed of a sawtooth and peaking-pulse components. The deflection voltage of a magnetic-deflection cathode-ray tube requires this waveform to produce a current sawtooth in the deflecting coils.

peaked waveform An alternating-current waveform having nearly pointed positive and negative half-cycles. Such a wave contains appreciable third-harmonic energy.

peak envelope power Abbreviation, PEP. For a linear radio-frequency (RF) power amplifier handling a modulated signal, the average RF output

5059F-pP-510-565 4/10/01 9:32 AM Page 520

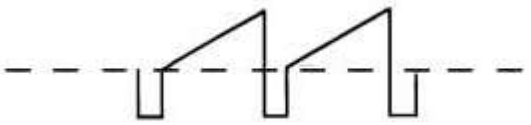

peaked sawtooth

power during a single RF cycle at the highest peak of the modulation envelope.

peaker **1.** See PEAK FILTER. **2.** See PEAKING TRANSFORMER.

peaker-notcher See NOTCHER-PEAKER.

peak factor For an alternating-current wave, the ratio E_m/E_{rms} or I_m/I_{rms}, where E_m is the maximum voltage, E_{rms} is the effective (root-mean-square) voltage, I_m is the maximum current, and I_{rms} is the effective current.

peak filter A frequency-selective circuit, such as a bandpass filter, for producing a peak response (see PEAK, **3**).

peak inductor current In a switching regulator, the maximum instantaneous current through the inductor when the device is switching at its fully rated duty cycle.

peaking The adjustment of a control or device for maximum indication on a meter or other display.

peaking coil A small inductor used to compensate the frequency response of a circuit, such as a video amplifier or video detector. Both series and shunt peaking coils are used.

peaking transformer A transformer whose output waveform is sharply peaked (of short duration, with respect to a cycle). The effect is obtained by means of a special core that, because it contains little iron, saturates easily.

peak inverse voltage Abbreviation, PIV. Often used interchangeably with the term PEAK REVERSE VOLTAGE. **1.** The peak value of the voltage applied to a rectifier diode in the reverse direction. **2.** The maximum value of reverse voltage that a rectifier diode will tolerate according to its specifications.

peak level lamp In audio recording and reproduction, a bulb or light-emitting diode (LED) that illuminates when sound peaks exceed a predetermined amplitude.

peak limiting **1.** A method of limiting the maximum amplitude of a signal. When the instantaneous peak amplitude, either positive or negative, exceeds a certain value, the output is clipped at that value. **2.** In pulse-code modulation, the effect resulting from the application of an input signal in excess of the virtual decision value.

peak modulated power In an amplitude-modulated wave, the maximum instantaneous signal power (including the carrier and sidebands). In 100-percent sinusoidal modulation, the peak modulated power is four times the unmodulated carrier power.

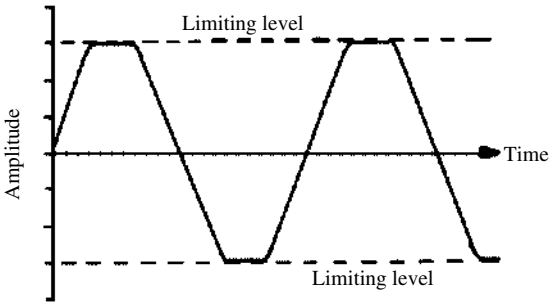

peak limiting

peak point The highest current point in the current-voltage response curve of a tunnel diode. Immediately beyond this point, the current decreases as the applied voltage is increased, indicating a negative-resistance region. Compare VALLEY POINT.

peak power **1.** Symbol, P_p. Unit, watt. Alternating-current power that is the product of the peak voltage (E_p) and the peak current (I_p). For E_p in volts and I_p in amperes, the peak power in watts is given by $P_p = E_pI_p$. **2.** The highest output power that an amplifier or device can produce without excessive distortion. **3.** The maximum instantaneous power that a speaker can handle without risk of damage.

peak probe A voltmeter test probe containing a diode circuit whose direct-current output voltage is close to the peak value of the applied alternating-current test voltage.

peak recurrent forward current For a semiconductor diode, the maximum repetitive instantaneous forward current as measured under specified conditions of operation.

peak reverse voltage Abbreviation, PRV. In semiconductor operations, the peak value of the voltage applied in reverse polarity across the junction. It is often used interchangeably with the term PEAK INVERSE VOLTAGE.

peak signal level The maximum instantaneous signal power or voltage specified for particular operating conditions.

peak-to-peak Abbreviations, p-p or pk-pk. For an alternating-current waveform, pertaining to the arithmetic difference between the positive peak and negative peak values of current or voltage.

peak-to-peak probe A voltmeter test probe containing a diode circuit whose direct-current output voltage is close to the peak-to-peak value of the applied alternating-current test voltage.

peak-to-peak voltage The arithmetic sum of positive and negative peak voltages in an alternating-current (ac) wave. Thus, a symmetrical sine-wave ac voltage of 115.0 V rms has a peak value of 162.63 V and a peak-to-peak value of 325.3 V. Also see PEAK VOLTAGE.

5059F-pP-510-565 4/10/01 9:32 AM Page 521

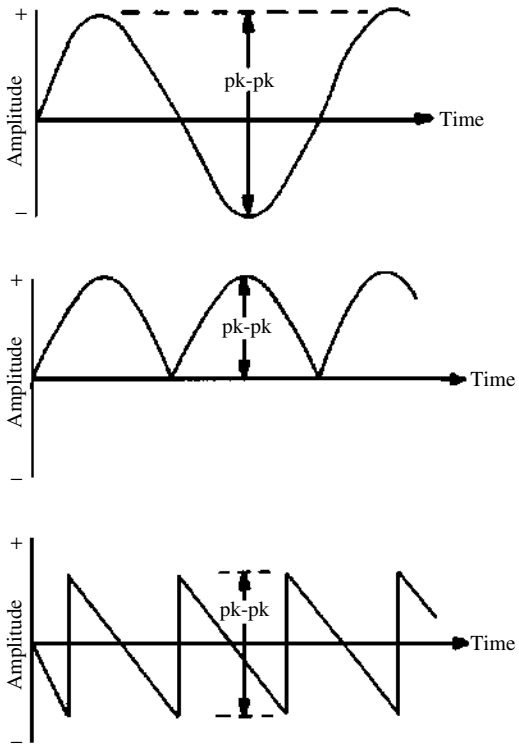

peak-to-peak voltage

peak torque Symbol, T_p. For a torque motor, the maximum useful torque at maximum recommended input current.

peak voltage Abbreviation, E_p. The highest value reached by an alternating-current voltage half cycle, or by a voltage pulse. Also called MAXIMUM VOLTAGE.

peak voltmeter **1.** An alternating-current (ac) voltmeter that responds to the peak value of the applied voltage. **2.** An ac voltmeter that responds to the average value of the applied voltage—even though its scale reads in peak volts.

pea lamp A miniature incandescent bulb, sometimes used as a control-panel or meter light.

PEC Abbreviation of PHOTOELECTRIC CELL.

pedestal See BLANKING PEDESTAL.

pedestal level See BLANKING LEVEL.

pel See PIXEL.

Peltier effect A drop below ambient temperature at the junction between two dissimilar metals when an electric current is passed through the junction.

PEM Abbreviation of *photoelectromagnetic.*

pen-and-ink recorder A graphic recorder in which a fountain-pen-type stylus inscribes an ink line on a paper chart. Also called *pen recorder.*

pencil **1.** A beam of electrons or other particles or rays that either converges to, or diverges from, a specific point. **2.** A pair of geometric entities sharing a property (e.g., lines intersecting at a single point).

pendulum switch A device that closes a circuit when subjected to physical shock. One type consists of a dangling element resembling a pendulum, with one or more nearby contacts.

penetrating frequency For a particular layer of the ionosphere, the lowest high frequency at which a vertically propagated wave penetrates the layer (i.e., it is not reflected back to earth). Also called CRITICAL FREQUENCY.

penetrating radiation Ionizing radiation that passes through otherwise opaque materials. A relative term; low-energy X rays are less penetrating than high-energy X rays, which, in turn, are less penetrating than gamma rays.

penetrating rays See COSMIC RAYS.

penetration depth See DEPTH OF PENETRATION.

pent Abbreviation of PENTODE.

pentavalent element An element whose atoms have five valence electrons (e.g., antimony or arsenic).

pentode A five-electrode vacuum tube in which the electrodes are an anode, cathode, control grid, screen grid, and suppressor grid.

pentode field-effect transistor A field-effect transistor with three separate gates.

pentode transistor A bipolar transistor with three emitters.

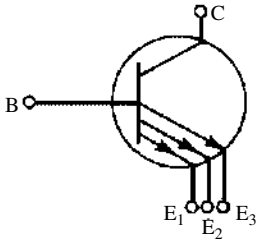

pentode transistor

penumbra **1.** That part of a shadow in which the light source is not fully obscured by the eclipsing object. **2.** In a sunspot, the outer part of the spot; it is less dark than the inner portion.

PEP **1.** Abbreviation of PLANAR EPITAXIAL PASSIVATED. **2.** Abbreviation of PEAK ENVELOPE POWER.

PEP diode See PLANAR EPITAXIAL PASSIVATED DIODE.

PEP reading wattmeter A wattmeter that shows the peak envelope power output of a transmitter.

PEP transistor See PLANAR EXPITAXIAL PASSIVATED TRANSISTOR.

5059F-pP-510-565 4/10/01 9:32 AM Page 522

perceived level The level of a disturbance, particularly sound, as sensed by a person. It is generally expressed in decibels, with respect to a certain threshold value. The threshold is assigned an intensity of 0 dB.

percent An expression of a fraction, in terms of hundredths. A quantity of x percent indicates a fraction of $x/100$. Percent is usually abbreviated by the symbol %.

percentage error The amount by which a measured value differs from the true value, expressed as a percentage (the number of parts per 100 that the measurement is in error).

percentage-modulation meter An instrument that provides direct readings of the modulation percentage of an amplitude-modulated signal. The meter scale or dial is graduated in increments from 0 to somewhat more than 100 percent.

percentage uncertainty The maximum possible error in a measurement, expressed as a percentage of the measured value. Also see UNCERTAINTY IN MEASUREMENT.

percent distortion Symbol, *%D*. In the determination of harmonic distortion, the total harmonic voltage expressed as a percentage of the fundamental voltage, plus total harmonic voltage; $\%D = 100E_h/E_t$, where E_h is the total voltage of the harmonic components, and E_t is the total signal voltage (fundamental plus harmonics).

percent modulation See MODULATION PERCENTAGE.

percent modulation meter See PERCENTAGE-MODULATION METER.

percent ripple The amount of ripple voltage in the direct-current (dc) output of a rectifier or generator, expressed as a percentage of the nominal dc output voltage.

perfect crystal A crystal without defects or impurities. The atoms are arranged in a regular pattern with no faults.

perforated board A plastic panel provided with a number of small holes in orderly columns and rows for the insertion of the pigtails of components, or of push-in terminals to facilitate quick assembly of prototype circuits. Also called *perfboard*.

performance curve A curve depicting the behavior of a component or circuit under specified conditions of operation. Such a curve, for example, might display the variation of output power with input power, the variation of frequency with voltage, etc. Compare CHARACTERISTIC CURVE.

performance test A test made primarily to ascertain how a system behaves. The test is concerned with normal operation, whereas a diagnostic test is a troubleshooting procedure. Compare TROUBLESHOOTING TEST.

perigee **1.** The point at which an earth-orbiting satellite attains its lowest altitude. It occurs once for every complete orbit. At this point, the satellite travels faster than at any other point in the orbit. **2.** The altitude, measured from the earth's surface or the earth's center, of an earth-orbiting satellite at its closest approach.

perihelion **1.** The point at which a solar-orbiting satellite attains its lowest altitude. It occurs once for every complete orbit. At this point, the satellite travels faster than at any other point in the orbit. **2.** The altitude, measured from the sun's surface or the sun's center, of a solar-orbiting satellite at its closest approach.

perimeter protection The use of a security system to restrict or prevent access to a designated area, using sensors and/or barriers around the boundaries of the area.

period Symbol, *T*. Unit, second. The duration of a complete alternating-current cycle or of any cyclic event; $T = 1/f$, where f is the frequency in Hertz. Also see CYCLE, FREQUENCY, and HERTZ.

periodic and random deviation Abbreviation, PARD. In the direct-current output of a rectifier, the combined PERIODIC DEVIATION, including ripple, noise, hum, and transient spikes.

periodic curve A curve that repeats its shape in each period (e.g., a sine curve).

periodic deviation Repetitive deviation of a quantity from its normal value (e.g., ripple in the direct-current output of a rectifier).

periodic function A mathematical function that is represented by a periodic curve (e.g., the sine function $y = \sin x$).

periodicity In a transmission line, the tendency for power to be reflected at a point or points where the diameter of the line changes.

periodic law The observation that when the chemical elements (see ELEMENT, **3**) are arranged in increasing order of atomic number, their physical and chemical properties recur periodically. Also see PERIODIC TABLE.

periodic table A table in which the chemical elements (see ELEMENT, **3**) are arranged according to the periodic law. The vertical columns in the table, labeled groups, contain elements possessing related properties (e.g., silicon and germanium in group IV). The rows, labeled periods, depict the periodic shift in the properties of the elements.

peripheral **1.** Pertaining to equipment accessory to a central system (e.g., peripheral input/output devices online or offline to computers, data recorders, and indicators). Also see ANCILLARY EQUIPMENT. **2.** Peripheral equipment in a computer system (e.g., printers, modems, external disk drives, tape drives, etc.).

peripheral buffer As part of a peripheral in a computer system, a storage unit in which data temporarily resides on its way to or from the central processing unit. Also called INPUT/OUTPUT BUFFER.

peripheral electron See VALENCE ELECTRON.

5059F-pP-510-565 4/10/01 9:32 AM Page 523

peripheral equipment See PERIPHERAL, **1**, **2**.

peripheral interface adapter Abbreviation, PIA. An integrated circuit that acts as an input/output port to interface a microprocessor with peripheral devices.

peripheral transfer In a computer system, the transfer of a unit of data between peripherals, or between a peripheral and the central processing unit.

Permalloy A high-permeability alloy of iron and nickel.

permamagnetic speaker See PERMANENT-MAGNET SPEAKER.

permanent magnet A body that is always magnetized (i.e., without the application of electricity and without requiring the presence of another magnet). Compare TEMPORARY MAGNET.

permanent-magnet erase Erasure of magnetic tape by the field of a permanent magnet. Typically, it is a two-step process: a magnet erases what it can of the signal, leaving any residual magnetization for erasure by a second magnet.

permanent-magnet focusing In a cathode-ray tube, the focusing of the electron beam by means of permanent magnets.

permanent-magnet generator An electromechanical generator in which the field (either stationary or rotating) is provided by a multipole permanent magnet. Also called *magneto.*

permanent-magnet loudspeaker See PERMANENT-MAGNET SPEAKER.

permanent-magnet magnetizer A magnetizer using a permanent magnet as the magnetic-field source.

permanent-magnet meter An indicating meter in which a movable coil rotates between the poles of a permanent magnet. Compare ELECTRODYNAMOMETER and IRON-VANE METER.

permanent-magnet motor A motor having a permanent-magnet field.

permanent-magnet relay A polarized relay using a permanent magnet.

permanent-magnet speaker An acoustic loudspeaker in which the core is a strong permanent magnet (as opposed to a direct-current electromagnet). Also see MAGNETIC SPEAKER.

permanent storage See NONVOLATILE MEMORY.

permeability Unit, H/m. A quantitative indicator of the extent to which a material concentrates magnetic flux: for a given constant magnetic-field intensity, the ratio of magnetic flux density in the material to the magnetic flux density in air.

permeability curve See B-H CURVE.

permeability-tuned oscillator A radio-frequency oscillator in which the frequency is varied or adjusted by moving a ferromagnetic core in and out of the coil of an inductance-capacitance (LC) tuned circuit.

permeability tuning Variation of the resonant frequency of an inductance-capacitance LC circuit by changing the position of a magnetic core within the inductor. This type of tuning is used in amplifiers, oscillators, filters, and wavetraps.

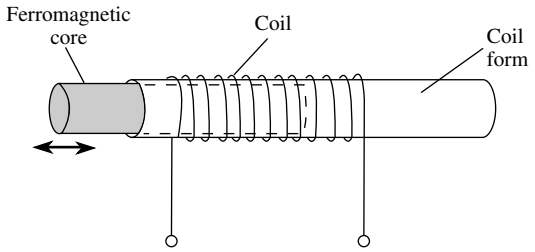

permeability tuning

permeameter An instrument for measuring permeability.

permeance Unit, Wb/A. In a magnetic circuit, the ease with which a magnetic field is established. The reciprocal of RELUCTANCE.

Permendur A high-permeability magnetic alloy containing equal parts of iron and cobalt. At saturation, the flux density of this material can be 2 teslas (20,000 gauss).

Perminvar A high-permeability magnetic alloy of cobalt, iron, and nickel. At saturation, the flux density of this material can approach 1.2 teslas (12,000 gauss).

permittivity See DIELECTRIC CONSTANT.

permutation A selection of several factors or objects from a group, in a specific ordered sequence. For example, one of the permutations of the elements of the set (1, 2, 3, 4, and 5) is the ordered sequence 4, 1, 3, 5, 2.

permutation modulation A method of modulation accomplished by varying the sequence of digital bits.

peroxide of lead In a lead-acid cell or battery, a compound of lead and oxygen that composes the positive electrode or electrodes.

persistence **1.** The effect whereby the retina of the eye continues to register a projected scene for approximately 0.05 second after the scene disappears. This allows perception of a sequence of video frames as a continuous moving image. **2.** The tendency of certain phosphors to glow after the excitation has been removed. Thus, after the electron beam in a cathode-ray tube has passed over the screen, the phosphor might continue to glow for a certain time along the path traced by the beam. Some phosphors, such as those used in high-speed oscilloscopes, have virtually no persistence, whereas others have long persistence.

persistent oscillations Successive oscillations of constant amplitude. Also called CONTINUOUS WAVE.

persistor A device used at low temperatures for temporary memory storage that operates between superconducting and normal conditions.

5059F-pP-510-565 4/10/01 9:32 AM Page 524

personal communications service Abbreviation, PCS. Also called *digital cellular.* An enhanced wireless network using digital modulation, cellular repeaters, and facilitating telephone and Internet connections. Emphasis is on maximizing user mobility and portability, and minimizing blind zones. Compare CELLULAR COMMUNICATIONS.

personal computer A small computer equipped with a keyboard, display, hard disk, diskette drive(s), a modem or fax/modem, one or more serial data ports, and one or more parallel data ports. They are used extensively by individuals and businesses for record keeping, data processing, communications, word processing, graphics, etc.; they are also used in schools as an educational aid.

personal digital assistant Abbreviation, PDA. See HANDHELD COMPUTER.

personal equation The value of systematic error for a person observing specific phenomena or making measurements.

personality Characteristics that make an intelligent computer or robot human-like. In general, the more powerful the computer, the more personality it can have, depending on the installed software. In some cases, certain malfunctions in a computer can produce personality quirks.

personal robot A usually autonomous robot intended for use by individuals. The most common examples are robot toys, programmable with a PERSONAL COMPUTER, intended for the education and entertainment of children. More sophisticated devices can perform domestic tasks, such as cleaning floors and mowing lawns.

peta- Abbreviation, P. A prefix meaning 10^{15}.

petagram Abbreviation, Pg. A large unit of mass or force, equal to 10^{15} grams or 10^{12} kilograms.

petameter Abbreviation, Pm. A large unit of (astronomical) distance, equal to 10^{15} meters or 10^{12} kilometers.

pF Abbreviation of PICOFARAD.

pf Symbol for POWER FACTOR.

PFET Abbreviation of P-CHANNEL JUNCTION FIELD-EFFECT TRANSISTOR.

PFM Abbreviation of PULSE-FREQUENCY MODULATION.

PG Abbreviation of POWER GAIN.

Pg Abbreviation of PETAGRAM.

pH **1.** Symbol for *hydrogen-ion concentration.* Numerically, pH is the negative logarithm of the effective hydrogen-ion concentration in gram equivalents per liter. The scale runs from zero to 14, on which 7 denotes neutrality relative to acidity vs. alkalinity; values between zero and 7 denote acidity, and values between 7 and 14 denote alkalinity. **2.** Abbreviation of PICOHENRY.

phantom Radio interference in the form of a beat note (heterodyne), resulting from interference between two strong carriers, often from local radio stations. When the phantom frequency lies within the tuning range of a receiver, the phantom can be tuned in as a separate signal. But when the phantom corresponds to the intermediate frequency (IF) of the receiver, it will ride into the IF amplifier and be present as an untunable interferential signal.

phantom channel In a properly phased high-fidelity stereo sound system, the apparent sound source centered between the left- and right-channel loudspeakers.

phantom circuit In wire telephony, a third circuit that has no wires; it results from a method (using repeating coils) of making two other circuits do the work of (this third) one.

phantom signal Also called *bogey.* In a radar system, a signal that does not correspond to an actual target. The origin of the phantom signal or echo cannot be readily determined.

phantom target See ECHO BOX.

phase angle Unit, degree or radian. In an alternating-current (ac) circuit, the lag or lead between the instant that one alternating quantity reaches its maximum value and the instant that another alternating quantity reaches its maximum value. It is usually given in degrees (a complete cycle being 360 degrees) along the horizontal axis of the time-versus-magnitude graph of the ac quantity.

phase-angle voltmeter An instrument that indicates both the magnitude and phase of a voltage.

phase coincidence For signals having the same frequency, the condition of their coinciding in terms of instantaneous amplitudes, so positive peaks of the first signal correspond to positive peaks of the second signal, and negative peaks of the first signal correspond to negative peaks of the second signal. For periodic waves that do not change their characteristics with time, this is the same thing as being shifted by an integral multiple of 360 degrees in phase. Compare PHASE OPPOSITION.

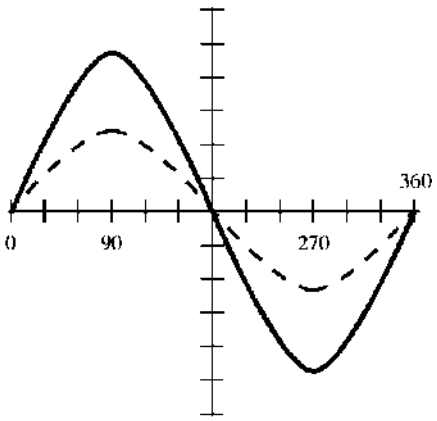

phase coincidence

5059F-pP-510-565 4/10/01 9:32 AM Page 525

phase compensation In an operational amplifier, compensation for excessive phase shift in the feedback.

phase compressor A push-pull phase-inverter circuit in which a capacitor is connected between each collector or drain and the opposite output terminal to attenuate in-phase components, such as even-numbered harmonics.

phase constant A figure providing the rate (in degrees of phase per unit length) at which the phase lag of the current or voltage field component in a traveling wave increases linearly in the propagation direction.

phase corrector A circuit that returns a signal to a certain phase after the signal has passed through a circuit or medium that has caused phase distortion.

phased antenna See PHASED ARRAY.

phased array Also called *phased antenna.* An antenna system having two or more driven elements fed with a certain relative phase, and spaced at a certain distance, resulting in a directivity pattern that exhibits gain in some directions and little or no radiation/response in other directions. Such an array can have two elements, producing a unidirectional cardioid or bidirectional figure-eight pattern. More complex arrays have several elements, usually vertical antennas, strategically positioned and fed with signals of specified phase to produce a highly tailored pattern. The most sophisticated systems have rotatable or steerable radiation/response patterns.

phase-delay equalizer See DELAY EQUALIZER.

phase detector See PHASE-SENSITIVE DETECTOR.

phase diagram A graphical representation of waves having equal frequency, but differing in phase. The phase difference for two identical waveforms is greater than or equal to zero degrees, but less than 360 degrees.

phase difference **1.** The difference (in time, angle, or fractional cycle) between the instants at which two alternating quantities reach a given value. **2.** For a dielectric, the complement of PHASE ANGLE; that is, 90 degrees minus the phase angle in degrees.

phase discriminator See DISCRIMINATOR, FOSTER-SEELEY DISCRIMINATOR, RATIO DETECTOR, and TRAVIS DISCRIMINATOR.

phase distortion Distortion characterized by input/output phase shift between various components of a signal passed by a circuit or device.

phase inverter A resistance-capacitance-coupled amplifier with a single-ended input and a push-pull output. This circuit enables a push-pull amplifier to be driven without an input transformer.

phase-locked loop Abbreviation, PLL. An oscillator that combines the flexibility of a conventional variable-frequency oscillator (VFO) with the stability of a crystal oscillator. The oscillator output is passed through a programmable divider that divides the frequency by a specific integral value *n* chosen by the operator. The output frequency of the divider is locked, by means of a phase comparator, to the signal from a crystal-controlled reference oscillator. As long as the output from the divider is exactly at the reference-oscillator frequency, the two signals are in phase, and the output of the phase comparator is zero volts dc. If the VCO frequency changes, the phase also changes, and the phase comparator produces a dc error voltage. The error voltage is applied to the VCO, causing the VCO frequency to correct itself. This maintains the VCO frequency at precisely *n* times the reference-oscillator frequency.

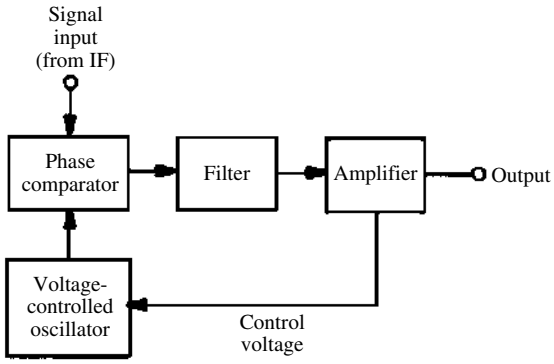

phase-locked loop

phase-locked oscillator An oscillator in which the inductance or the capacitance is varied periodically at half the driving frequency.

phase margin In an integrated-circuit amplifier, the extent to which the device shifts the phase of a signal more or less than one-half cycle (180 degrees) for a certain signal voltage.

phase modulation Abbreviation, PM. A method of modulation in which the phase of the carrier current is varied in accordance with the instantaneous modulating-signal voltage. The result is similar to FREQUENCY MODULATION.

phase modulator A circuit or stage that produces PHASE MODULATION.

phase multiplier A circuit used for the purpose of phase comparison between signals. The frequency of the measured signal is multiplied, resulting in multiplication of the phase difference. This improves the sensitivity of the measuring apparatus.

phase opposition For signals having the same frequency, the condition of their being inverted relative to each other in terms of instantaneous amplitudes, so positive peaks of the first signal correspond to negative peaks of the second signal, and negative peaks of the first signal correspond to positive peaks of the second signal. This is not the same thing as being shifted by an odd

5059F-pP-510-565 4/10/01 9:32 AM Page 526

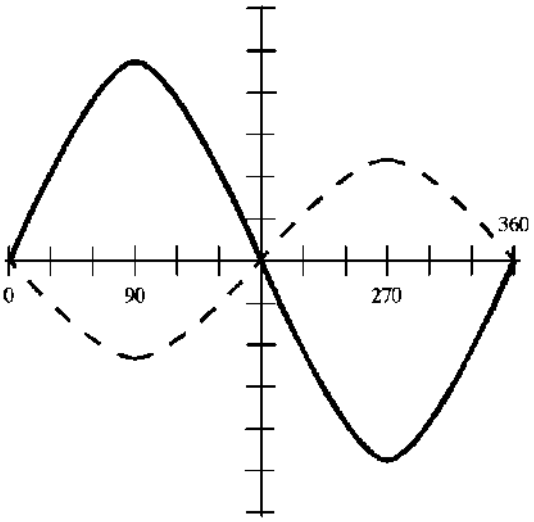

phase opposition

integral multiple of 180 degrees in phase, although in practice, with sine waves and square waves, the effect is the same. Compare PHASE COINCIDENCE.

phase resonance See VELOCITY RESONANCE.

phase reversal **1.** The inversion of an alternating-current (ac) signal. The instantaneous amplitude (current or voltage) is multiplied by a negative constant. Thus, the positive half-cycles become negative, and the negative half-cycles become positive. **2.** A phase shift of ±180 degrees (±½ cycle) in an ac signal.

phase-rotation relay See PHASE-SEQUENCE RELAY.

phase-rotation system A system for producing single-sideband signals without using selective filters. In one such system, two balanced modulators are used. One of these receives carrier and modulating voltages that are 90 degrees out of phase with voltages that are fed to the other balanced modulator.

phase-sensitive detector Abbreviation, PSD. A detector for frequency modulation (FM) and phase modulation (PM). It delivers a direct-current output voltage whose value is proportional to the difference in phase between a reference signal and the signal from a local oscillator.

phase-sequence relay In a polyphase system, a relay or relay circuit that is actuated by voltages reaching maximum positive amplitude in a predetermined phase sequence. Also called PHASE-ROTATION RELAY.

phase shift **1.** A change in the displacement, as a function of time, of a periodic disturbance having constant frequency. **2.** The magnitude of a

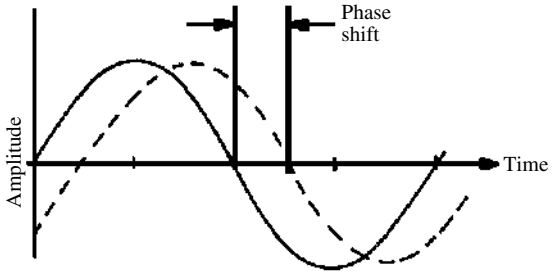

phase shift

change, as defined in **1**, measured in fractions of a wavelength or in electrical degrees.

phase-shift bridge A four-arm-bridge circuit for shifting the phase of an alternating-current signal. Such a circuit is often used (with one arm variable) to shift the phase of the firing voltage for a thyratron.

phase-shift discriminator See FOSTER-SEELEY DISCRIMINATOR.

phase shifter A circuit, such as an inductance-capacitance (LC) or resistance-capacitance (RC) network, or a device, such as a Helmholtz coil or phase-shifting capacitor, that introduces a phase shift between input and output signals.

phase-shifting capacitor A special four-stator, one-rotor variable capacitor that, with a transformer-coupled resistance-capacitance (RC) circuit, provides 360 degrees of continuously variable phase shift for one rotation of the rotor. The rotor plate turns like a cam under the stators because of the off-center insertion of the rotor shaft.

phase-shift oscillator A single-stage oscillator in which the required 180-degree phase shift in the signal (fed back from output to input) is obtained by passing the output through a phase-shifting network.

phase-shift-type distortion meter A distortion meter in which the output signal of a device under test is compared with a distortion-free input test signal. The output signal phase is shifted 180 degrees, with respect to the input, and the two amplitudes are made equal. If there is no distortion, the signals cancel each other, and the result is zero. Any remaining signal is proportional to the total harmonic distortion (THD).

phase-splitting circuit A circuit that produces, from a single input signal, two output signals differing in phase.

phase-splitting driver A PHASE INVERTER used as the driver of a push-pull amplifier.

phase velocity The velocity of a wave, provided by the product of the frequency and the wavelength.

phase windings In an alternating-current generator, windings that deliver voltages that differ in phase.

5059F-pP-510-565 4/10/01 9:32 AM Page 527

phasing capacitor In a crystal filter, a small variable capacitor that constitutes one arm of a four-arm bridge in which the crystal is another arm. Adjustment of this capacitor balances the bridge, thus preventing the undesirable passage of a signal through the capacitance of the crystal holder.

phenol-formaldehyde plastics A family of plastic insulating materials made with phenolic resin, and occasionally used as dielectrics and air-core coil forms. Some of the trade names for these materials include *Bakelite*, *Catalin*, *Durez*, *Durite*, *Formica*, and *Micarta*.

phenolic insulants See PHENOL-FORMALDEHYDE PLASTICS.

phenolic resin A synthetic resin made by condensing phenol (carbolic acid) with formaldehyde.

phenomenon An event or circumstance that can be verified by the senses, as opposed to one subject to theory or speculation (e.g., the phenomenon of magnetic attraction).

Phillips gate A device that allows measurement of the gas pressure in a confined chamber. A current is passed through the gas. The magnitude of the current, for a given gas, is a function of the gas pressure and temperature.

Phillips screw A screw with a pair of slots in its head. The slots are arranged like an x. Phillips screws are available in many different sizes, as are ordinary screws. The x-shaped pair of slots reduces the tendency for the screwdriver to slip out of the screw head as the screw is rotated.

Phi phenomenon The illusion of motion resulting from the rapid presentation to the eye of pictures showing objects in a succession of different positions. Television and motion pictures exploit this illusion. Also see PERSISTENCE.

pH meter An instrument used to measure the acidity or alkalinity of solutions. Also see PH, **1**.

phon A unit of apparent change in loudness discerned by a listener. Unlike the decibel, the phon includes compensation for the ear's nonlinear response to attendant frequency changes. At a frequency of 1 kHz, a change in loudness of 1 phon is the equivalent of 1 decibel.

phone **1.** Telephone (wire or radio). **2.** To establish communication via telephone. **3.** Colloquialism for voice communication (radiotelephone), particularly via amateur-radio single sideband on the high-frequency bands (160 through 10 meters). **4.** A minimal, unique speech sound. Also called SOUND UNIT.

phoneme An individual sound or syllable in the human voice, with a characteristic amplitude-vs. frequency spectral pattern. It is important in speech recognition and speech synthesis. Computers can be programmed to identify and transcribe these sounds; computers can also be programmed to generate the sounds from text data.

phone jack The female mating device for a PHONE PLUG.

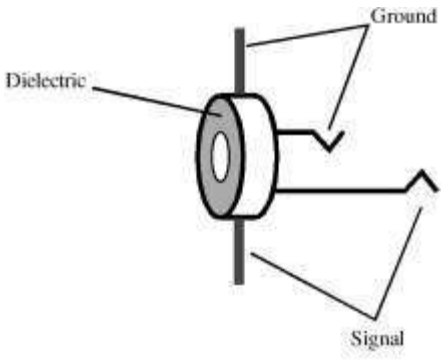

phone jack

phone monitor A simple device for listening to amplitude-modulated radio transmissions to test their quality. In its most rudimentary form, it consists of a pickup antenna, semiconductor-diode detector, and high-resistance headphones.

phone patch A device for establishing a connection (patch) between radio and wire-telephone facilities. Also see PATCH.

phone plug A type of plug originally designed for patching telephone circuits, now widely used in electronics and instrumentation. In its conventional form, it has a rod-shaped neck that serves as one contact, and a ball on the tip of the neck, but insulated from it, that serves as the other contact. Typical diameters are ⅛ inch and ¼ inch.

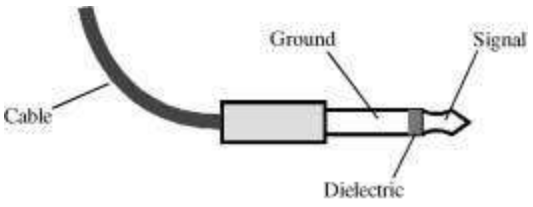

phone plug

phone test set An instrument for checking the performance of a radiotelephone transmitter. The set combines the functions of field-strength meter, modulation indicator, and aural monitor. Sometimes it includes a volt-ohm-milliammeter for troubleshooting the transmitter.

phonetic alphabet Words whose initial letters are used to identify the letters of the alphabet for

5059F-pP-510-565 4/10/01 9:32 AM Page 528

which they stand. These words are spoken in radiotelephony to identify letters that, if spoken by themselves, might not be clearly heard.

Phonetic alphabet

Letter	Phonetic (Capitals indicate emphasis)
A	AL-fa
B	BRAH-vo
C	CHAR-lie
D	DEL-ta
E	ECK-o
F	FOX-trot
G	GOLF
H	ho-TEL
I	IN-dia
J	Ju-li-ETTE
K	KEE-low
L	LEE-ma
M	Mike
N	No-VEM-ber
O	OS-car
P	pa-PA
Q	Que-BECK
R	ROW-me-oh
S	see-AIR-ah
T	TANG-go
U	YOU-ni-form
V	VIC-tor
W	WHIS-key
X	X-ray
Y	YANK-key
Z	ZOO-loo

phonetic alphabet code word In radio and wire telephony, a word chosen for its easy recognition by ear to identify the letter of the alphabet with which it begins. For example: *Golf* for G, *Juliet* for J, *X-ray* for X.

phonics See ACOUSTICS, **1**.

phonocardiogram The record made by a PHONOCARDIOGRAPH.

phonocardiograph An instrument that makes a graphic record of heart sounds.

phono cartridge The vibration-to-electricity transducer (pickup) of a phonograph; it is actuated by the stylus (needle). Common types are ceramic, variable-inductance, and variable-reluctance. See PHONOGRAPH and PHONOGRAPH DISC.

phonocatheter A microphone that can be inserted into the body for the purpose of listening to the functions of internal organs.

phonograph A device for reproducing sound recorded on disc. It consists of a turntable, an amplifier, and one or more speakers.

phonograph cartridge See PHONO CARTRIDGE.

phonograph disc A thin, lightweight disc, usually made of vinyl or similar plastic, on which audio-frequency signals are recorded as irregularities in a spiral groove. In reproduction, these irregularities cause vibration in a PHONO CARTRIDGE as the turntable rotates.

phonograph oscillator See PHONO OSCILLATOR.

phono jack Also called *RCA jack.* A jack similar to a PHONE JACK, designed especially for the quick connection and disconnection of coaxial cables used with audio and low-frequency devices.

phonon A unit of energy resulting from vibration, as of a piezoelectric crystal.

phono oscillator A small radio-frequency (RF) oscillator modulated by the audio-frequency (AF) voltage from a phonograph. The modulated RF signal is picked up by a remote radio receiver (usually in the same room), and the sound is reproduced through a loudspeaker connected to the receiver.

phono plug Also called *RCA plug.* A plug similar to a PHONE PLUG, designed especially for the quick connection and disconnection of coaxial cables used with audio and low-frequency devices.

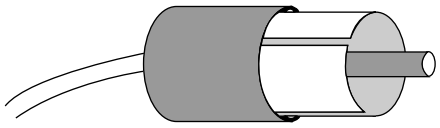

phono plug

phonoreception The hearing of high-frequency sounds.

phonorecord A PHONOGRAPH disc.

phonoselectroscope A special type of stethoscope, in which the main heartbeat is attenuated. This makes abnormal sounds more audible. The device can be adjusted in various ways to listen for abnormalities characteristic of various heart diseases.

phosphor A substance that glows when an electron beam strikes it. Such a substance is used as a coating on the screens of cathode-ray tubes. See also BEAT ZINC SILICATE; CADMIUM BORATE, SILICATE, and TUNGSTATE; CALCIUM PHOSPHATE, SILICATE, and TUNGSTATE; MAGNESIUM FLUORIDE, SILICATE, and TUNGSTATE; ZINC ALUMINATE; ZINC BERYLLIUM SILICATE; ZINC BERYLLIUM ZIRCONIUM SILICATE; ZINC BORATE; ZINC CADMIUM SULFIDE; ZINC GERMANATE; ZINC MAGNESIUM FLUORIDE; ZINC ORTHOSILICATE; ZINC OXIDE; ZINC SILICATE; and ZINC SULFIDE.

phosphor bronze A form of bronze whose elasticity, hardness, and toughness have been greatly improved by the addition of phosphorus. The metal is used for brushes, springs, switch blades, and contacts.

phosphor copper An alloy of copper and phosphorus used in the manufacture of PHOSPHOR BRONZE.

5059F-pP-510-565 4/10/01 9:32 AM Page 529

phosphorescence The property of some materials that ordinarily fluoresce to continue to glow after the stimulus (light or an electron beam) has been removed. Compare FLUORESCENCE.

phosphorescent screen A viewing screen coated with a phosphor (e.g., oscilloscope screen).

phosphorous Exhibiting the properties of phosphor (e.g., glowing after stimulation with light). Not to be confused with PHOSPHORUS.

phosphorus Symbol, P. A nonmetallic element of the nitrogen family. Atomic number, 15. Atomic weight, 30.974. It is used as a dopant in semiconductor processing.

phot The cgs unit of illumination: The direct illumination produced upon a one-centimeter-distant surface by a uniform point source of one international foot-candle. Equivalent to one lumen per square centimeter.

photocathode **1.** The photomosaic of a video camera tube. **2.** The light-sensitive cathode in a phototube.

PhotoCD Trade name for an image-recording system developed by Kodak, in which photographs can be stored on compact discs. Viewing is accomplished using personal computers.

photocell See PHOTOELECTRIC CELL.

photocell amplifier An amplifier used to boost the output of a photocell. With respect to the nature of the input signal, it can be an alternating-current (ac) or direct-current (dc) amplifier, depending on whether the output of the photocell is modulated dc or pure dc.

photochemical effect The phenomenon whereby certain substances undergo chemical change when exposed to light or other radiant energy. An example of such a substance is the silver bromide, silver chloride, or silver iodide on photographic film.

photoconductive cell A photoelectric cell, such as the cadmium-sulfide type, whose resistance is proportional to the intensity of light impinging upon it. The photoconductive cell acts as a light-sensitive variable resistor in a current path. Also see PHOTOCONDUCTIVE MATERIAL.

photoconductive effect The tendency for the electrical resistance of a substance to change when infrared radiation, visible light, or ultraviolet radiation strikes it. Different substances exhibit different degrees of this effect.

photoconductive material A substance that exhibits decreased electrical resistance when exposed to infrared rays, visible light, or ultraviolet. Some photoconductive substances are cadmium selenide, cadmium sulfide, germanium, lead sulfide, selenium, silicon, and thallous sulfide. Also see ACTINOELECTRIC EFFECT.

photoconductivity The phenomenon whereby the electrical resistance of certain materials (such as cadmium sulfide, cadmium selenide, germanium, selenium, and silicon) is lowered upon exposure to infrared rays, visible light, or ultraviolet. Also see PHOTOCONDUCTIVE MATERIAL.

photoconductor **1.** See PHOTOCONDUCTIVE MATERIAL. **2.** See PHOTOCONDUCTIVE CELL.

photocurrent See PHOTOELECTRIC CURRENT.

photo-Darlington Also, *photodarlington*. **1.** A phototransistor fabricated as a Darlington amplifier for high output current. **2.** A combination of photodiode (see LIGHT-SENSITIVE DIODE) and Darlington amplifier.

photodecomposition Chemical breakdown by the action of radiant energy. Also called *photolysis*.

photodetachment The removal of an electron from an atom or ion, resulting from the impact of a PHOTON.

photodetector **1.** An illumination meter that uses a PHOTOCELL. **2.** See OPTOELECTRONIC COUPLER.

photodielectric effect The tendency for the dielectric constant of a substance to change when infrared radiation, visible light, or ultraviolet radiation strikes it. Different substances exhibit different degrees of this effect.

photodiffusion effect See DEMBER EFFECT.

photodiode See LIGHT-SENSITIVE DIODE.

photodisintegration In the nucleus of an atom, disintegration resulting from PHOTON bombardment.

photoelasticity The tendency for the light-transmission characteristics of a substance to change with externally applied forces.

photoelectric alarm An alarm actuated when a light beam impinging on a photocell is interrupted.

photoelectric amplifier **1.** An amplifier for boosting the output of a photosensitive device. **2.** An OPTOELECTRONIC COUPLER possessing gain.

photoelectric cell A device that converts infrared, visible-light, or ultraviolet energy into electricity or electrical effects. It can function by producing a voltage (see PHOTOVOLTAIC CELL, SELENIUM CELL, SILICON CELL, SOLAR CELL, and SUN BATTERY) or by acting as a light-sensitive resistor (see LIGHT-SENSITIVE DIODE, PHOTOCONDUCTIVE CELL, and SELENIUM CELL).

photoelectric constant The quantity h/e, where h is Planck's constant and e is the unit electron charge.

photoelectric counter A counting device (electromechanical or fully electronic) that counts objects as they interrupt a light beam impinging upon a photocell.

photoelectric disintegration See PHOTODISINTEGRATION.

photoelectric effect The phenomenon whereby temporary changes occur in the atoms of certain substances under the influence of infrared, visible light, or ultraviolet radiation. Some of these materials undergo a change in their electrical resistance, whereas others generate electric current (see, for comparison, PHOTOCONDUCTIVE MATERIAL and PHOTOVOLTAIC MATERIAL).

photoelectric efficiency See QUANTUM YIELD.

5059F-pP-510-565 4/10/01 9:32 AM Page 530

photoelectric field-effect transistor See PHOTOFET.

photoelectricity Electricity produced by the action of light on certain materials, such as cesium, selenium, and silicon. Also see PHOTOEMISSION and PHOTOVOLTAIC CELL.

photoelectric material See PHOTOCONDUCTIVE MATERIAL and PHOTOEMISSIVE MATERIAL.

photoelectric multiplier A device that internally amplifies the current resulting from bombardment by infrared, visible light, or ultraviolet radiation. A PHOTOMULTIPLIER TUBE is an example of such a device.

photoelectric photometer An instrument that uses a photoelectric device for the purpose of measuring the intensity of infrared radiation, visible light, or ultraviolet radiation.

photoelectric proximity sensor A device that uses a light-beam generator, a photodetector, an amplifier, and a microprocessor to detect the presence of nearby objects. It is useful in robot guidance systems.

photoelectric pyrometer An optical pyrometer in which a photocell and appropriate filters act instead of the human eye.

photoelectric relay A relay actuated directly by a photocell or a photocell and amplifier. This type of relay is the basis of some PHOTOELECTRIC ALARM devices.

photoelectric sensor 1. See ELECTRIC EYE. **2.** See PHOTOELECTRIC PROXIMITY SENSOR. **3.** See PHOTOELECTRIC CELL.

photoelectric smoke alarm An alarm that is tripped by a PHOTOELECTRIC SMOKE DETECTOR when the density of smoke exceeds a safe level.

photoelectric smoke control A system for making automatic adjustments to a burning process when the smoke density exceeds a prescribed level. The initial element in the system is a PHOTOELECTRIC SMOKE DETECTOR.

photoelectric smoke detector A smoke detector in which a photocell, photodiode, phototransistor, or phototube is excited by a light beam passing through the air. The cell output current decreases when smoke fills the air. This current change trips an alarm or deflects an indicating meter when the density of the smoke exceeds a prescribed level.

photoelectric tape reader A punched-tape reader using a photocell, photodiode, phototransistor, or phototube to sense light passing through the holes.

photoelectric transducer A photocell, photodiode, phototransistor, or phototube used as a sensor.

photoelectric tube See PHOTOTUBE.

photoelectric wattmeter A power-measuring instrument useful for the approximate measurement of radio-frequency power. It consists of an incandescent lamp sharing an opaque enclosure with a photovoltaic cell. The power to be measured is applied to the lamp, which glows proportionately. The light excites the cell, causing it to deliver a direct current proportional to the power. This current deflects a milliammeter or microammeter. The meter can be calibrated to read directly in watts.

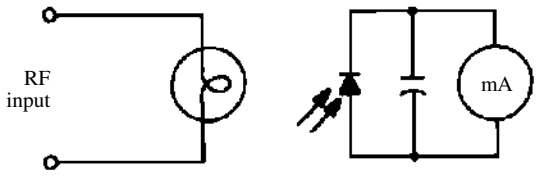

photoelectric wattmeter

photoelectromotive force The electromotive force (voltage) produced by a photovoltaic cell.

photoelectron An electron displaced within, or ejected from, an atom, as the result of infrared, visible light, or ultraviolet radiation striking the atom.

photo-emf See PHOTOELECTROMOTIVE FORCE.

photoemission The ejection of electrons from certain materials, such as cesium, when these materials are exposed to infrared, visible light, or ultraviolet radiation. Also see PHOTOEMISSIVE MATERIAL.

photoemissive material A substance that emits electrons when exposed to infrared, visible light, or ultraviolet radiation. A typical use of such a material is in the coating of the light-sensitive cathode of a phototube. The metals cesium, potassium, rubidium, and sodium are photoemissive.

photofabrication 1. A method of circuit-board manufacturing. The etching pattern is placed over the circuit-board material, the board is placed in a special solution, then the assembly is exposed to visible light. The light interacts with the solution to dissolve the metal in areas exposed to the light, but not in areas covered by the etching pattern. **2.** The technique in **1**, applied to the manufacture of integrated circuits.

photoFET A FIELD-EFFECT TRANSISTOR that exhibits properties similar to those of a bipolar PHOTOTRANSISTOR.

photoflash See ELECTRONIC FLASH, **1**.

photoglow tube See DISCHARGE LAMP.

photogram The permanent shadow produced by an object placed between a light source and photographic paper.

photographic exposure meter See EXPOSURE METER, **1**.

photographic recorder A graphic recorder that uses a light beam, deflected by galvanometer movement, that moves across photographic film or paper to produce a trace representing a varying quantity.

photographic sound recording See OPTICAL SOUND RECORDING.

5059F-pP-510-565 4/10/01 9:32 AM Page 531

photograph reception **1.** The use of FACSIMILE to print photographs transmitted in analog form via wire or radio. **2.** The use of a computer, equipped with a modem and graphics software, to display and/or store photographs transmitted in digital form via wire or radio.

photograph transmission **1.** The use of FACSIMILE to scan and send photographs in analog form via wire or radio. **2.** The use of a computer, equipped with a modem and video camera or optical scanner, to digitize and send photographs via wire or radio.

photoionization The ejection of electrons from atoms or molecules by the action of infrared, visible light, or ultraviolet radiation.

photoisolator See OPTOELECTRONIC COUPLER.

photojunction cell A photocell consisting of a semiconductor pn junction. The cell is useful mainly for its photoconductivity, although infrared, visible light, or ultraviolet energy striking the junction produces a small amount of photovoltaic action.

photokinesis Light-induced motion, as in a RADIOMETER.

photolithographic process A method of producing integrated circuits and printed circuits by photographing (often at considerable reduction) an enlarged pattern of the circuit on a suitable light-sensitized surface of metal or semiconductor, and chemically etching away unwanted portions of the surface.

photolysis See PHOTODECOMPOSITION.

photomagnetic effect Light-sensitive magnetic susceptibility in some materials.

photomap A photo taken of terrain from a high altitude and usually overlaid with a reference grid.

photomask In PHOTOFABRICATION, the transparent film or template on which the etching pattern is drawn.

photometer An instrument used to compare the luminous intensity of two light sources.

photometric measurement of power See PHOTOELECTRIC WATTMETER.

photometry The science of visible-light measurement. The response of the human eye is used as the basis for preferred sensors (those used with photometric instruments, which have spectral sensitivity curves resembling those of the eye). Compare RADIOMETRY.

photomosaic In a television camera tube, the flat photocathode screen on which the image is projected by the lens system and scanning electron beam. The surface of the screen is covered with tiny light-sensitive droplets. Also see DISSECTOR TUBE, ICONOSCOPE, and ORTHICON.

photomultiplier tube A type of PHOTOTUBE that delivers high output current for a given light intensity by utilizing the secondary emission of electrons. The initial light-sensitive cathode emits electrons; these strike a specially placed metal plate with a force that dislodges more electrons. These electrons, together with the initial emission, are reflected to a second plate, where they dislodge still more electrons. This process continues from deflection plate to deflection plate through the tube. The final plate deflects the accumulated electrons to the anode (collector electrode).

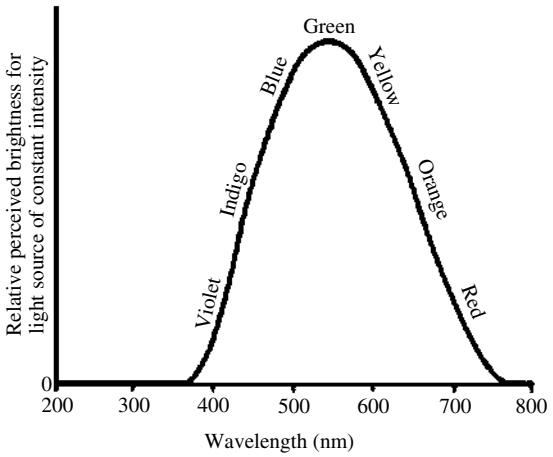

photometry

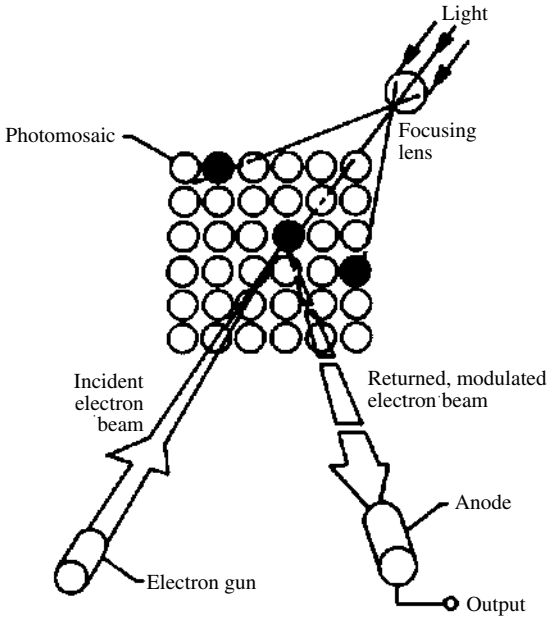

photomosaic

photon A quantum of radiant energy whose energy constant W (in joules) is equal to hf, where h is the PLANCK CONSTANT and f is the frequency in Hertz.

5059F-pP-510-565 4/10/01 9:32 AM Page 532

photoneutron A neutron released by PHOTODISINTEGRATION.

photophone **1.** A telephone-type communication system using a modulated light beam transmitted between stations. **2.** A process for recording sound on motion-picture film (see OPTICAL SOUND RECORDING).

photorelay See PHOTOELECTRIC RELAY.

photoresistive cell See PHOTOCONDUCTIVE CELL.

photoresistive material See PHOTOCONDUCTIVE MATERIAL.

photoresistivity See PHOTOCONDUCTIVITY.

photoresistor See PHOTOCONDUCTOR, **1**, **2**.

photosensitive device A light-sensitive electronic device. See, for example, PHOTOCONDUCTIVE CELL, PHOTODIODE, PHOTOFET, PHOTOMULTIPLIER TUBE, PHOTOTRANSISTOR, PHOTOTUBE, and PHOTOVOLTAIC CELL.

photosphere The luminous layer at the surface of a star.

photoswitch A light-activated switch. Some photoswitches contain an electromechanical relay; others, such as the light-activated silicon-controlled switch, have no moving parts.

phototimer An electronic timer for timing photographic processes.

phototransistor A transistor in which current carriers emitted as a result of illumination constitute an input-signal current. This current is amplified by the transistor. The output signal delivered by the transistor, accordingly, is larger than the output of an equivalent photodiode.

phototube An electron tube that converts light energy into electrical energy by acting as a light-sensitive resistor. Characteristically, the tube contains an illuminated cathode coated with a photoemissive material, and an anode wire situated nearby. Light energy causes electrons to be emitted from the cathode in amounts proportional to light intensity; the electrons are attracted by the anode, which is connected externally to a positive direct-current voltage.

photovoltaic cell Also called *solar cell*. A semiconductor diode, usually made from silicon, that converts visible light, infrared, and/or ultraviolet directly into electric current. The device consists of a flat P-N junction; the assembly is transparent so that radiant energy can fall directly on the P-type silicon. Metal ribbing, forming the positive electrode, is interconnected with tiny wires. The negative electrode is a metal backing, placed in contact with the N-type material. The component produces about 0.5 to 0.6 volts in direct sunlight under no-load conditions.

photovoltaic material A substance that generates a voltage when exposed to light. The principal substances exhibiting this effect are silicon, selenium, and germanium. Also see ACTINOELECTRIC EFFECT.

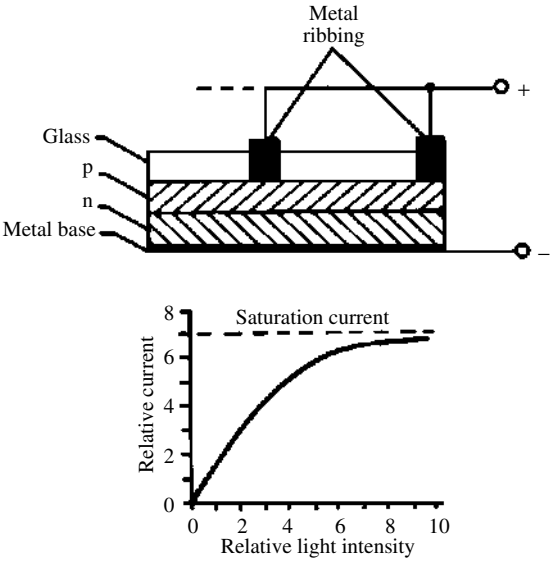

photovoltaic cell

photran A light-sensitive, four-layer semiconductor device, used for switching purposes.

physical properties The distinguishing characteristics of matter, apart from its chemical properties. Included are *boiling point*, *density*, *ductility*, *elasticity*, *electrical conductivity*, *hardness*, *heat conductivity*, *index of refraction*, *malleability*, *melting point*, *specific heat*, and *state* (solid, liquid, gaseous, or plasma).

physical quantity A quantity expressing the actual number of physical units under consideration, as compared with a dimensionless number. Examples: 50 volts, 39 kilometers, and 30 picofarads. Compare DIMENSIONLESS QUANTITY.

physics The science of energy and matter and their interactions. Physics is subdivided into several fields, including *mechanics*, *thermodynamics*, *acoustics*, *optics*, and *electricity/magnetism*. Many subdivisions are within the traditional fields.

P_i Symbol for INPUT POWER.

picket fencing An effect often observed at very-high frequencies (VHF) and ultra-high frequencies (UHF), in which movement of the transmitting station antenna, the receiving station antenna, or both antennas causes rapid fading. The fading is the result of phase effects between the direct wave and indirect wave(s). These effects are most pronounced with vertically polarized antennas.

PIA Abbreviation of PERIPHERAL INTERFACE ADAPTER.

pickoff **1.** To monitor a voltage, current, or other characteristic in an active circuit, without dis-

5059F-pP-510-565 4/10/01 9:32 AM Page 533

turbing the operation of the circuit. **2.** A device for electronically monitoring linear or angular displacement.

pickup **1.** A device that serves as a sensor of a signal or quantity. This covers a wide variety of items, including *temperature sensors*, *vibration detectors*, *microphones*, *phonograph pickups*, etc. **2.** Collectively, energy or information that is received (e.g., *sound pickup*).

pickup arm The pivoted arm that holds the cartridge and stylus of a phonograph.

pickup cartridge See PHONO CARTRIDGE.

pickup current **1.** The current required to close a relay. **2.** Current flowing through, or generated by, a pickup.

pickup pattern The directional pattern of a microphone or other transducer that converts acoustic energy into electrical signals.

pickup voltage **1.** The voltage required to close a relay or circuit breaker. **2.** The voltage delivered by a pickup.

pico- **1.** Abbreviation, p. A prefix meaning 10^{-12}. **2.** A prefix meaning extremely small.

picoammeter A usually direct-reading instrument used to measure current in the picoampere range. Also see CURRENT METER.

picoampere Abbreviation, pA. A small unit of current equal to 10^{-12} ampere.

picocoulomb Abbreviation, pC. A small unit of electrical quantity equal to 10^{-12} coulomb.

picocurie Abbreviation, pCi. A small unit of radioactivity equal to 10^{-12} curie.

picofarad Abbreviation, pF. A small unit of capacitance equal to 10^{-12} farad.

picohenry Abbreviation, pH. A small unit of inductance equal to 10^{-12} henry.

picosecond Abbreviation, ps or psec. A small unit of time equal to 10^{-12} second.

pi coupler See COLLINS COUPLER.

picovolt Abbreviation, pV. A small unit of voltage equal to 10^{-12} volt.

picovoltmeter A usually direct-reading electronic instrument used to measure electromotive force in the picovolt range.

picowatt Abbreviation, pW. A small unit of power equal to 10^{-12} watt.

pictorial See PICTORIAL WIRING DIAGRAM.

pictorial diagram See PICTORIAL WIRING DIAGRAM.

pictorial wiring diagram A wiring diagram in the form of a drawing or photograph of the components, as opposed to one of circuit symbols. The components are shown in their positions in the finished equipment, and the wiring as lines running between them.

picture black In facsimile or television, the signal condition resulting from the scanning of a black portion of the image.

picture detector See VIDEO DETECTOR.

picture diagram See PICTORIAL WIRING DIAGRAM.

picture element See PIXEL.

picture information In a television signal, the variable-amplitude component (i.e., the one carrying energy corresponding to the picture elements) that fills the space between blanking pulses.

picture-in-picture Abbreviation, PIP. In some television receivers, a feature that allows simultaneous viewing of two programs. One program occupies the full screen, and another program appears in a small portion of the screen.

picture reception **1.** See PHOTOGRAPH RECEPTION. **2.** The reception of television signals.

picture transmission **1.** See PHOTOGRAPH TRANSMISSION. **2.** The transmission or broadcasting of television signals.

picture tube The cathode-ray tube used in a television receiver to display the image. Also called KINESCOPE.

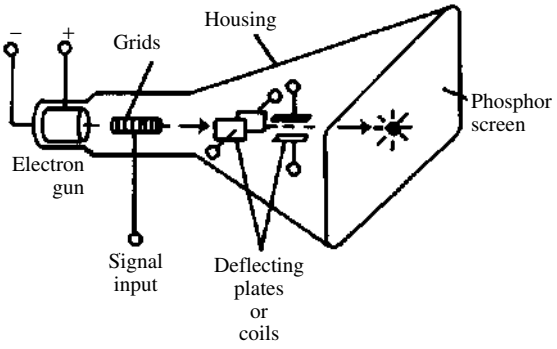

picture tube

pie chart See CIRCLE GRAPH.

Pierce oscillator A simple crystal oscillator in which the crystal is connected directly between the input and output terminals of the active device (usually a bipolar or field-effect transistor). A tuned inductance-capacitance (LC) circuit might be included, but is not required.

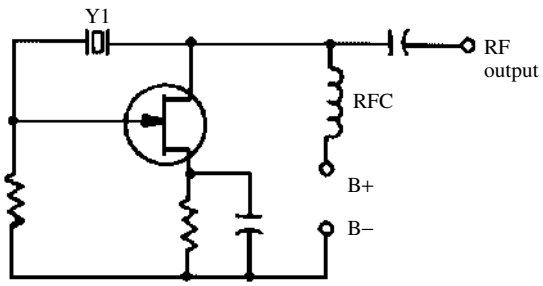

Pierce oscillator

5059F-pP-510-565 4/10/01 9:32 AM Page 534

pie winding A method of coil winding in which two or more separate, multilayer coils are connected in series and placed along a common axis. It is sometimes used in radio-frequency chokes to minimize capacitance among the windings.

piezo- A prefix meaning *pressure* (see PRESSURE, **2**).

piezodielectric A substance that, when stretched or compressed, exhibits a change in dielectric constant.

piezoelectric accelerometer An accelerometer using a piezoelectric crystal, whose voltage output is proportional to acceleration.

piezoelectric ceramic A ceramic material that delivers a voltage when deformed, or that changes in shape when a voltage is applied to it.

piezoelectric crystal A crystal (such as quartz, Rochelle salt, tourmaline, or various synthetics) that delivers a voltage when mechanical force is applied between its faces, or that changes its shape when a voltage is applied between its faces.

piezoelectric earphone See CRYSTAL EARPHONE.

piezoelectric filter See CRYSTAL FILTER and CRYSTAL RESONATOR.

piezoelectricity Electricity produced by deforming (squeezing, stretching, bending, or twisting) certain crystals, such as those of quartz, Rochelle salt, or tourmaline.

piezoelectric loudspeaker See CRYSTAL LOUDSPEAKER.

piezoelectric microphone See CERAMIC MICROPHONE and CRYSTAL MICROPHONE.

piezoelectric oscillator See CRYSTAL OSCILLATOR.

piezoelectric pickup See CRYSTAL PICKUP.

piezoelectric resonator See CRYSTAL FILTER and CRYSTAL RESONATOR.

piezoelectric sensor See CRYSTAL TRANSDUCER.

piezoelectric transducer See CRYSTAL TRANSDUCER.

piezoid A complete piezoelectric crystal device.

piezoresistance In certain substances, the tendency of the resistance to change with stretching or compression.

piezo tweeter A tweeter of the piezoelectric type (see CRYSTAL LOUDSPEAKER).

pi filter An unbalanced filter section having one series arm and two shunt arms; its schematic representation has the general shape of the uppercase Greek letter pi.

piggyback component See OUTBOARD COMPONENT.

piggyback control See CASCADE CONTROL.

piggyback tuner A separate ultra-high-frequency (UHF) television tuner operated in conjunction with the very-high-frequency (VHF) tuner of the receiver.

pigtail **1.** A usually long and sometimes flexible lead, such as the pigtail of a fixed capacitor.

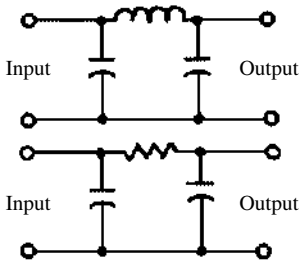

pi filters

2. Descriptive of a device containing a long lead or leads, and usually mounted by such leads.

pile **1.** See VOLTAIC PILE. **2.** See NUCLEAR REACTOR. **3.** A battery of electrochemical cells. **4.** Any packed group of particles or granules.

pillow speaker A small, flat loudspeaker intended for use under a pillow.

PILOT Acronym for *programmed inquiry learning or teaching.* A straightforward high-level computer programming language, used in computer-assisted instruction (CAI).

pilot lamp See PILOT LIGHT.

pilot light A usually small, incandescent or neon lamp. When glowing, it serves as a signal that a piece of equipment is in operation.

pilot model A preliminary model of a circuit or device constructed primarily to test the efficacy of a production process. The pilot model usually follows the PROTOTYPE.

pilot production The often small-scale production of a device in a special assembly line apart from the main line in a factory.

pilot regulator A variable-gain circuit that maintains a constant output—even if the input amplitude changes.

PIM Abbreviation of PULSE-INTERVAL MODULATION.

pi mode In a vane-anode magnetron, the mode of operation in which adjacent vanes have radio-frequency voltages of opposite polarity.

pin **1.** A semiconductor junction consisting of a layer of instrinsic semiconductor material situated between n and p layers. **2.** A slender, straight, stiff prong used as a terminal or locking device (see, for example, BASE PIN and BAYONET BASE).

pinchoff In a junction field-effect transistor, the condition in which the gate voltage causes the two depletion regions to meet and close the channel to obstruct drain-current flow.

pinchoff voltage In a junction field-effect transistor, the lowest value of gate voltage that will produce pinchoff.

pinch roller In a tape recorder, a rubber-tired, rotating cylinder that helps to pull the tape past the recording and/or playback heads.

5059F-pP-510-565 4/10/01 9:32 AM Page 535

pincushion A type of television picture distortion in which each side of the raster sags toward center screen. Also see ANTIPINCUSHIONING MAGNETS.

pincushion-correction generator A circuit for generating a deflection signal to correct pincushion distortion (see PINCUSHION). One form consists of a parabola generator and op-amp-type differentiator.

pin diode A silicon junction diode having a lightly doped intrinsic layer serving as a dielectric barrier between p and n layers.

pi network See COLLINS COUPLER.

ping An acoustic pulse; it can be audible sound or ultrasound.

pinhole **1.** A tiny hole present as a defect in a film of dielectric, semiconductor, or metal. **2.** A tiny aperture that acts as a universal lens by permitting the passage of a very small bundle of light rays. The smaller the aperture, the greater the depth of field.

pinhole detector An electronic device for finding pinholes in materials. Also see PINHOLE, **1**.

pin jack A jack into which a pin plug is inserted for quick connection.

pink noise Acoustical noise whose amplitude is inversely proportional to the frequency within a limited frequency spectrum. In the extreme, it creates a hissing sound. Compare WHITE NOISE.

pinout A diagram of an integrated circuit depicting the locations of the pins for various functions. It generally takes the form of a rectangle for the circuit itself, and short lines for the pins with designators printed next to the lines.

pin plug A plug consisting of a slender metal pin inserted between the blades of a PIN JACK for a quick connection. The plug usually has a small insulated back for convenient handling.

pin straightener A device for straightening the pins of a transistor, integrated circuit, or other electronic component.

pin switch A switch that changes state when a small pin is pushed or pulled.

pin-usage factor For an integrated circuit, the number of gate equivalents per package pin. Also see GATE EQUIVALENT.

PIO Abbreviation of *parallel input/output.*

pion A subatomic particle consisting of one quark and one antiquark.

PIP Abbreviation of PICTURE-IN-PICTURE.

pip See BLIP.

pi pad A resistance-type attenuator having a series arm, a shunt input arm, and shunt output arm; its name is derived from its resemblance to the Greek letter pi. Also see PAD.

pipe radiator A waveguide having an open end from which microwave energy is radiated.

Pirani gauge A type of vacuum gauge in which a heated filament, composing one arm of a four-arm resistance bridge, is sealed into the vacuum system. The bridge is balanced before evacuation starts. As evacuation progresses, the heat removed from the filament becomes proportional to the pressure in the system, and the resistance of the filament changes accordingly. The bridge is then rebalanced, and the difference between initial and subsequent null conditions indicate the extent of the vacuum when the bridge has been appropriately calibrated.

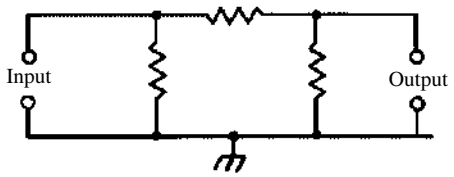

pi pad

pi section An unbalanced filter or tuner section whose schematic representation has the general shape of the uppercase Greek letter pi.

pi-section coupling Use of a PI SECTION for coupling a radio transmitter to an antenna. Also see COLLINS COUPLER and PI-SECTION TANK.

pi-section filter A pi section used as either a low-pass or high-pass filter, depending on the position of the capacitors in the circuit.

pi-section tank A pi section used as the collector, drain, or plate tank circuit of a radio-frequency power amplifier, and also serving as an antenna coupler.

piston **1.** The movable element (cone) of a loudspeaker. **2.** The movable, solid plunger of a trimmer capacitor that consists of a plug within a cylinder.

piston directivity Directivity of sound emitted by the piston of a loudspeaker (see PISTON, **1**). As the frequency of the audio signal increases, radiation from a loudspeaker tends to be concentrated along the axis of the piston.

pit **1.** A microscopic depression in a compact disc; scatters and/or absorbs light from the laser, rather than reflecting it. Compare LAND, **1**. **2.** In a printed-circuit board, a pockmark in a component or foil run. **3.** A pockmark in a metallic substance, resulting from corrosion.

pitch **1.** The frequency of a sound, either in general terms (e.g., low, midrange, and high) or as a specific quantity (e.g., 2450 Hz). **2.** The distance between the peaks of adjacent grooves on a phonograph disc. **3.** The distance between adjacent threads of a screw. **4.** The distance between centers of turns in a coil (see PITCH OF WINDING) **5.** The number of teeth or threads per unit length. **6.** The distance along its axis a propeller moves in a revolution. **7.** Up-and-down motion of a robot end effector or other electromechanical device. **8.** The extent or range of movement, as defined in **7**.

5059F-pP-510-565 4/10/01 9:32 AM Page 536

pitch of winding In a coil, the distance from the center of one turn to the center of the adjacent turn in a single layer of winding.

PIV Abbreviation of PEAK INVERSE VOLTAGE.

pivot The sometimes jeweled, stationary member of the bearing in an analog meter movement.

pi-wound choke A choke coil consisting of several series-connected sections, mounted on a single core and separated to reduce internal capacitance.

pix Abbreviation of PICTURE.

pixel Contraction of *picture element*. The smallest bit of data in a video image. Also called *pel*. The smaller the size of the pixels in an image, the greater the resolution for a given image area.

pixel aspect ratio In a video image, the ratio of PIXEL height to pixel width.

pix tube See PICTURE TUBE.

PL Abbreviation for PRIVATE LINE.

place effect An apparent change in the perceived pitch of a sound, caused by variations in the way the waves interact inside the human ear.

planar diffusion In the production of a semiconductor device, the diffusion of all the elements into one face of a wafer. Consequently, connections to the elements all lie in one plane. Also see EPITAXIAL PLANAR TRANSISTOR and PLANAR TRANSISTOR.

planar diode A semiconductor diode, having a pn junction that lies entirely within a single plane.

planar epitaxial passivated diode A junction diode that, like the planar epitaxial transistor, has been manufactured by planar diffusion, then passivated to protect the junction. Also see EPITAXIAL GROWTH, EPITAXY, PASSIVATION, and PLANAR DIFFUSION.

PL/1 A computer programming language that is a hybrid of scientific and commercial types (like ALGOL and COBOL), the combined features being powerful problem-solving and mass-data-handling abilities.

planar epitaxial passivated transistor A planar epitaxial transistor that has been passivated to protect the exposed junctions. Also see EPITAXIAL PLANAR TRANSISTOR, PLANAR TRANSISTOR, EPITAXIAL TRANSISTOR, PASSIVATION, and PLANAR TRANSISTOR.

planar transistor A transistor in which the emitter, base, and collector elements terminate on the same face (plane) of the silicon wafer. A thin film of silicon dioxide is grown on top of the wafer to insulate the exposed junctions after the leads have been attached (i.e., the transistor is passivated).

Planck constant Symbol, *h*. Unit, joule-second. The constant of proportionality in the fundamental law of the quantum theory, stating that radiant energy is composed of quanta proportional to the frequency of the radiation; $h = q/f = 6.62608 \times 10^{-34}$ J•s, where q is the value of the quantum and f is the frequency in Hz.

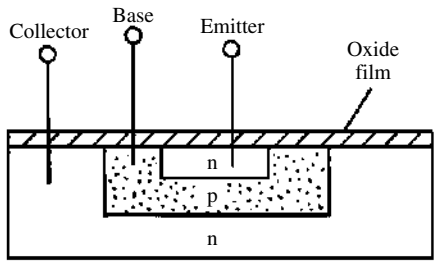

planar transistor

plane of polarization The plane containing the direction of propagation and the electric field vector of a plane-polarized wave (see POLARIZATION, **3** and POLARIZED LIGHT).

plane-polarized light See POLARIZATION, **3** and POLARIZED LIGHT.

plane-reflector antenna A directive antenna in which the reflector is a sheet of metal or a metal screen. In a corner-reflector antenna, the reflector is a folded sheet, or two sheets joined along one edge.

planetary electron See ORBITAL ELECTRON.

planimeter A mechanical instrument for measuring the area of a closed figure. The outline of the figure is traced with the pointer of the device, and the area is read from a pair of dials. In this application, the planimeter does the work of integral calculus.

PLANNER A high-level computer programming language sometimes used in artificial intelligence. It is a "goal-oriented" language in that it seeks a solution to a problem using various schemes, as necessary.

plan position indicator Abbreviation, PPI. A radar display on whose screen small spots of light reconstruct the scanned vicinity, revealing objects, such as buildings, boats, aircraft, etc. The distance from the center of the screen to a spot depicts the range of an object, and the radial angle reveals its bearing.

plant In computer operations, to put the result of an operation specified by a routine in a storage location from which it will be taken for implementation of an instruction further on in the program.

plaque resistor A flat, noninductive, power resistor, often used as a dummy load during high-frequency power measurements.

plasma A usually high-temperature gas that is so highly ionized that it is electrically conductive and susceptible to magnetic fields; it is recognized as one of the states of matter. Also see PHYSICAL PROPERTIES.

plasma diode A diode in which a plasma substance produces conduction in one direction, but not in the other.

5059F-pP-510-565 4/10/01 9:32 AM Page 537

plasma length See DEBYE LENGTH.

plasma oscillation In a plasma, a form of electric-field oscillation of the rapidly moving electrons.

plasma torch A torch, used for such high-heat applications as melting metal, in which a gas is heated by electricity to the high temperature at which it becomes a plasma.

plasmatron A form of amplifier tube sometimes used at ultra-high and microwave frequencies. It is similar to a thyratron. An inert gas is excited until it becomes a plasma, producing amplification under certain operating conditions.

Plastacele See CELLULOSE ACETATE.

plastic A synthetic material usually made from various organic compounds through polymerization (see POLYMERIZE). Plastics can be molded into solid shapes and are available as films. Examples: *celluloid*, *cellulose acetate*, *cellulose nitrate*, *polyethylene*, and *polystyrene.* Also see THERMOPLASTIC MATERIAL and THERMOSETTING MATERIAL.

plastic-film capacitor A capacitor made using polyester, polyethylene, or polystyrene. The method of manufacture is similar to that for paper capacitors when the plastic is flexible. Stacking methods can be used if the plastic is more rigid. The geometries can vary, and these capacitors are therefore found in several different shapes. Capacitance values for plastic-film units range from about 50 pF to several tens of microfarads. Most often they are in the range of 0.001 μF to 10 μF. Plastic-film capacitors are employed in audio equipment, and also in wireless transmitters and receivers. The efficiency is good, although not as high as that for mica-dielectric units. Compare CERAMIC CAPACITOR, ELECTROLYTIC CAPACITOR, MICA CAPACITOR, PAPER CAPACITOR, TANTALUM CAPACITOR.

plasticizer A substance added to a plastic to make it softer or more flexible.

plastic-leaded chip carrier Abbreviated PLCC. A surface-mounted package for an integrated circuit. It is small in size and has high electrical and mechanical reliability.

plate **1.** The anode of an electron tube. **2.** One of the electrodes of a primary or secondary battery cell. **3.** One of the electrodes of a capacitor.

plateau In a response curve, a region in which an increase in the independent variable produces no further change in the dependent variable. Example: the saturation region in a common-base transistor collector-current curve.

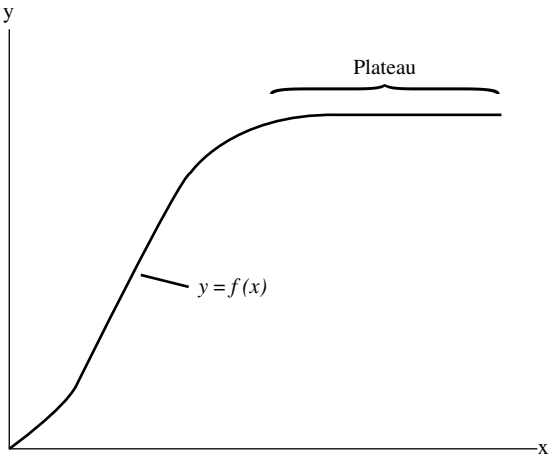

plateau

plate blocking capacitor A capacitor connected between the plate of an electron tube and the plate tank. It allows the direct-current supply voltage to be applied directly to the plate without it passing through the tank coil, while at the same time preventing the tank coil from short-circuiting the plate power supply. The capacitor freely transmits alternating-current signal energy to the tank.

plate capacitance See PLATE-CATHODE CAPACITANCE.

plate-cathode capacitance Symbol, C_{PK}. Unit, pF. The internal capacitance between the plate and cathode of an electron tube. Also called OUTPUT CAPACITANCE.

plate characteristic For an electron tube, the family of plate current-vs-plate voltage curves for various grid-bias voltages.

plate circuit The external circuit associated with the plate of an electron tube.

plate-circuit relay A direct-current relay operated in series with the plate of an electron tube.

plate conductance Symbol, g_P. Unit, siemens. Conductance of the internal plate circuit of an electron tube. The value of static g_P is equal to the plate current divided by the plate voltage (I_P/E_P). The value of dynamic g_P is equal to the derivative of the static g_P: d_{IP}/d_{EP}. Plate conductance is the reciprocal of PLATE RESISTANCE.

plate current Symbol, I_P. Direct current flowing in the plate circuit of an electron tube.

plate-current shift A change in the plate current of a radio-frequency power amplifier during amplitude modulation. The action discloses faulty operation because the average plate current should remain constant during modulation.

plate dissipation Abbreviation, *PD.* Unit, watt. Power expended in the plate of an electron tube. For an unloaded tube, PD = $E_P I_P$, where E_P is the direct-current (dc) plate voltage in volts, and I_P is the dc plate current in amperes. For a loaded tube, $PD = P_o - P_i$, where P_o is the alternating-current (ac) power output of an amplifier or oscillator in which the tube operates, and P_i is the dc plate power input.

plated magnetic wire A wire with a ferromagnetic outer coating on a core that is not magnetic.

5059F-pP-510-565 4/10/01 9:32 AM Page 538

plated-wire memory See WIRE MEMORY.

plate-grid capacitance Symbol, C_{PG} or C_{GP}. Unit, pF. The internal capacitance between the plate and control grid of an electron tube. Also called INTERELECTRODE CAPACITANCE and FEEDBACK CAPACITANCE.

plate load The power-consuming load into which the plate circuit of an electron tube operates. In an intermediate stage of a multistage amplifier, this load is the grid circuit of the following tube.

plate load impedance Symbol, Z_{LP}. Unit, ohm. In a tube circuit, the (output) impedance that is ac-connected between the plate and ground, or dc-connected between the plate electrode and dc plate power supply.

plate meter A direct-current ammeter or milliammeter that indicates the plate current of an electron tube.

plate modulation A method of AMPLITUDE MODULATION in which a modulating voltage is superimposed on the direct-current plate voltage of a higher-frequency amplifier or oscillator.

platen The "roller" in a teletypewriter or impact printer. It supports the paper against impact by the print head; it also helps to move the paper through the machine.

plate-neutralized amplifier A vacuum-tube radio-frequency power amplifier in which a neutralizing capacitor is connected between the control grid and the free end of a center-tapped plate-tank coil.

plate power Symbol, P_P. Unit, watt. Power in the plate circuit of an electron tube; $P_P = E_P I_P$, where E_P is the plate voltage in volts and I_P is the plate current in amperes.

plate power input See PLATE POWER.

plate power output The output signal power delivered by the plate circuit of an electron tube. Compare PLATE POWER INPUT.

plate power supply The (usually direct current) power supply that furnishes energy to the plate of an electron tube.

plate pulse modulation A method of obtaining pulse modulation by injecting high-voltage pulses into the plate circuit of a vacuum-tube amplifier.

plate relay A relay operated in series with the plate of an electron tube.

plate resistance Symbol, r_P. Unit, ohm. Resistance of the internal plate circuit of an electron tube. The static value of r_P is equal to E_P/I_P, where E_P is the plate voltage in volts, and I_P is the plate current in amperes. The dynamic value is dE_P/dI_P.

plate saturation In an electron tube, the point at which, while plate voltage is increasing, the plate attracts all the electrons emitted by the cathode (i.e., the point beyond which no further significant increase in plate current results from a further increase in plate voltage).

plate-screen capacitance Symbol, C_{PS}. Unit, pF. The internal capacitance between the plate and screen grid of an electron tube.

plate-screen modulation A method of AMPLITUDE MODULATION in which the modulating voltage is superimposed simultaneously on the direct-current plate and screen voltages of a higher-frequency amplifier or oscillator.

plate series compensation In an audio amplifier, the use of a plate decoupling circuit to obtain a fixed amount of bass boost.

plate shunt compensation The addition of a network to the plate-output circuit of a tube to boost the bass response of an amplifier.

plate spacing **1.** The distance between plates in a fixed capacitor. This dimension is usually the same as dielectric thickness. **2.** The distance between plates in a variable capacitor. Also called *capacitor air gap.*

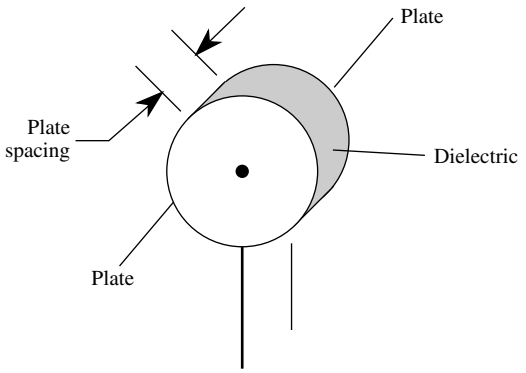

plate spacing, 1

plate supply voltage Symbol, E_{BB}. The output voltage of a plate power supply.

plate tank A resonant inductance-capacitance (LC) circuit operated from the plate of an electron tube.

plate tank capacitance The capacitance required to tune a PLATE TANK to resonance.

plate tank inductance The inductance of the coil in a PLATE TANK.

plate tank *Q* Figure of merit (see *Q*) of a plate tank, a function of the load resistance and the tank inductance-to-capacitance (L/C) ratio.

plate tank voltage The audio-frequency or radio-frequency voltage developed across the plate tank of an electron-tube circuit.

plate tuning Tuning an electron-tube circuit by varying the capacitance, inductance, or both in the plate tank.

plate tuning capacitance See PLATE TANK CAPACITANCE.

plate tuning inductance See PLATE TANK INDUCTANCE.

plate-type capacitor A capacitor having flat metal plates, rather than concentric cylinders, a cylinder and rod, etc.

5059F-pP-510-565 4/10/01 9:32 AM Page 539

plate voltage Symbol, E_P. The direct-current voltage applied to the plate of an electron tube.

plate winding **1.** An inductor connected in series between the plate of a vacuum tube and the positive power-supply voltage. **2.** The primary winding of a plate-circuit output transformer.

platiniridium A natural alloy of PLATINUM and IRIDIUM.

platinotron A form of traveling-wave vacuum tube used as an amplifier at ultra-high and microwave frequencies. There are two output connections.

platinum Symbol, Pt. A precious metallic element. Atomic number, 78. Atomic weight, 195.08. It is sometimes used for plating of relay and switch contacts, and for certain parts of vacuum tubes.

platinum metals The rare metals IRIDIUM, OSMIUM, PALLADIUM, PLATINUM, RHODIUM, and RUTHENIUM. They do not react readily with other elements.

platinum-tellurium thermocouple A thermocouple using the junction between platinum and tellurium wires; it is used in thermocouple-type meters.

platter **1.** One of the individual disks in a computer HARD DISK drive. **2.** The rotating turntable in a PHONOGRAPH.

playback The reproduction of recorded material in audio-tape, audio-disc, video-tape, or video-disc systems.

playback computer system A personal computer and associated peripherals, equipped for reproducing multimedia that has been recorded on CD-ROM.

playback head In a magnetic recorder/reproducer, the head that picks up the signal from the tape or disc for reproduction. Also called *read head* and *play head.*

playback loss In disc recording, the difference (at a particular point on the disc) between the recorded level and the reproduced level.

player A semiconductor layer that is doped to provide current carriers that are predominantly holes. Compare N LAYER.

player A device or system that reproduces (plays back) data from a tape or disc, but cannot be used to record data onto the tape or disc.

play head See PLAYBACK HEAD.

playthrough The condition in which an amplifier delivers a small output signal when the gain control is set to zero.

PLC Abbreviation of POWER-LINE COMMUNICATION.

PLCC Abbreviation of PLASTIC-LEADED CHIP CARRIER.

plethysmograph A medical-electronic device that allows the monitoring of the amount of blood in different parts of the body.

PLL Abbreviation of PHASE-LOCKED LOOP.

PLM Abbreviation of *pulse-length modulation* (see PULSE-DURATION MODULATION).

PLO Abbreviation of PHASE-LOCKED OSCILLATOR.

plot **1.** A curve depicting the variations of one quantity, with respect to another. **2.** To generate, print, or display a curve of the type defined in **1**.

plotter A machine that plots (see PLOT, **2**) automatically, often by the direction of a computer.

PL tone encoder An audio oscillator and modulator that cause a subaudible-tone modulation of a signal for use in restricted communications systems.

plug A usually male quick-connect device that can be inserted into a JACK to make a circuit connection, or be pulled out of the jack to break the connection. See, for example, MALE PLUG, PHONE PLUG, POWER PLUG, and POLARIZED POWER PLUG.

plug-and-jack connection A connection made by inserting a PLUG into a JACK.

plug fuse A fuse provided with an Edison base for screwing into a socket.

pluggable Capable of being completely removed from the rest of the system without the need for removing any wiring. Pluggable components and circuit boards simplify the servicing of electronic equipment.

plug-in See PLUG-IN COMPONENT and PLUG-IN UNIT.

plug-in capacitor A capacitor with pins or ferrules that can be quickly inserted into, or removed from, a socket.

plug-in coil A coil wound on a form having pins that can be quickly inserted into, or removed from, a socket.

plug-in coil form An insulating form with base pins that mate with socket terminals so that a coil wound on the form can be quickly inserted into, or removed from, a circuit.

plug-in component A component or module, such as a transistor, capacitor, coil, lamp, etc., provided with pins, clips, or contacts for easy insertion into, or removal from, a circuit. See, for example, PLUG-IN CAPACITOR, PLUG-IN COIL, PLUG-IN FUSE, PLUG-IN LAMP, PLUG-IN METER, PLUG-IN RESISTOR, PLUG-IN TRANSFORMER, and PLUG-IN UNIT.

plug-in fuse A cartridge fuse having a metal ferrule on each end for insertion into a matching clip for easy installation and removal.

plug-in fuse

plug-in lamp A lamp with base pins for quick insertion into, or removal from, a socket.

plug-in meter A meter with pins or banana plugs for quick insertion into, or removal from, a circuit.

5059F-pP-510-565 4/10/01 9:32 AM Page 540

plug-in resistor A resistor with pins or ferrules for quick insertion into, or removal from, a socket.

plug-in transformer A small transformer with pins for quick insertion into, or removal from, a socket.

plug-in unit A unit, such as a tuned circuit, amplifier, or meter, that has pins or contacts for easy insertion into, or removal from, a larger piece of equipment.

plumber's delight An antenna whose construction, including that of the mast, is entirely of metal rods or tubing, with no insulating parts. Short circuits and grounds are prevented by making all attachments and joints at points that are at zero voltage, with respect to the standing-wave pattern.

Plumbicon A television camera tube, similar to the VIDICON, with a lead-oxide target. It is noted for high sensitivity. The image lag time is shorter than in the conventional vidicon.

plumbing Collectively, the waveguides, tees, elbows, and similar pipelike devices and fixtures used in microwave setups.

plunger-type meter A meter in which an iron or steel plunger is pulled into a coil by the magnetism produced by a current flowing in the coil. The plunger is attached to a pointer that moves over the scale.

plutonium Symbol, Pu. A radioactive metallic element that is artificially produced. Atomic number, 94. Atomic weight, approximately 244.

PM **1.** Abbreviation of PERMANENT MAGNET. **2.** Abbreviation of PULSE(D) MODULATOR. **3.** Abbreviation of *post meridian.* **4.** Abbreviation of PHASE MODULATION.

Pm **1.** Symbol for PROMETHIUM. **2.** Abbreviation of PETAMETER.

Pm Symbol for MAXIMUM POWER.

PME Abbreviation of *photomagnetoelectric.*

PMG Abbreviation of PERMANENT-MAGNET GENERATOR.

PMM Abbreviation of PERMANENT-MAGNET MAGNETIZER.

PMOS Abbreviation of P-CHANNEL METAL-OXIDE SEMICONDUCTOR.

PMU Abbreviation of *portable memory unit.*

PN **1.** Abbreviation of POLISH NOTATION. **2.** Abbreviation of POSITIVE-NEGATIVE (often lowercase).

pn Abbreviation of POSITIVE-NEGATIVE.

pn boundary See PN JUNCTION.

pnip transistor A junction transistor having an intrinsic layer between an n-type semiconductor base and one of the p-type semiconductor layers.

pneumatic computer A computer that uses fluid logic [i.e., one in which information is stored and transferred by the flow of a fluid (gas or liquid) and pressure variations therein].

pn junction The boundary between p-type and n-type semiconductor materials in a single block or wafer of the materials. The junction cannot be duplicated by merely touching two pieces of material (one n-type and one p-type) together, however smooth their mating faces.

pn-junction diode A diode consisting of the junction between p-type and n-type regions in the same wafer of semiconductor material.

PNM Abbreviation of PULSE-NUMBERS MODULATION.

pnpn device See NPNP DEVICE.

pnp transistor A bipolar junction transistor in which the emitter and collector layers are p-type semiconductor material, and the base layer is n-type semiconductor material. Compare NPN TRANSISTOR.

Po Symbol for POLONIUM.

Po Symbol for OUTPUT POWER or POWER OUTPUT.

POGO Abbreviation of *polar orbiting geophysical observatory.*

point **1.** A dot indicating the place of separation between the integral and fractional parts of a number (e.g., *decimal point*). Also called RADIX POINT. **2.** A precisely defined location in three-dimensional space that has theoretically zero length, zero width, and zero depth (e.g., *focal point*). **3.** The place on a graph in any number of dimensions, at which two or more curves or coordinates intersect. **4.** A set of operating conditions for a component, device, or system (e.g., *cutoff point, operating point*). **5.** A defined condition at which some specific physical phenomenon occurs (e.g., *melting point*).

point charge An electric charge imagined to occupy a single point in space; thus, it has neither area nor volume.

point contact The point at which the sharply pointed tip of a wire or rod conductor touches a second conductor (e.g., the contact between a "cat whisker" and a semiconductor wafer).

point-contact diode A semiconductor diode having a fine wire ("cat whisker"), whose point is in permanent contact with the surface of a wafer of semiconductor material, such as germanium or silicon.

point-contact junction The pn junction electroformed under the point at which the "cat whisker" touches the semiconductor wafer in a point-contact diode or transistor.

point-contact transistor A transistor having two fine wires ("cat whiskers") that serve as the emitter and collector electrodes. The pointed tips of the wires are nearly in contact with (a few mils apart from) the surface of a wafer of semiconductor material, such as germanium. The semiconductor serves as the base electrode. This device was a predecessor of the JUNCTION TRANSISTOR.

point counter A Geiger counter tube in which the central electrode is a pointed, fine wire. Also see PROPORTIONAL COUNTER.

point defect **1.** In a semiconductor substance or piezoelectric crystal, the absence of an atom from

5059F-pP-510-565 4/10/01 9:32 AM Page 541

its place in the lattice structure. **2.** The presence of an extra atom in the lattice structure.

point effect The tendency of an electrical discharge to occur more readily at a sharp point than at a blunt surface (as of an electrode).

pointer A pointed blade, stiff wire, or inscribed line on a transparent blade; it moves over a scale to indicate a setting or the value of a quantity. Also called NEEDLE.

pointer-type meter An analog meter in which a pointer moves over a calibrated scale.

point impedance **1.** The impedance observed at a given point in a circuit. **2.** In a transmission line, the intensity of the electric field divided by the intensity of the magnetic field at a given point.

points of saturation For a magnetic core, saturation as evidenced by a leveling-off of the positive and negative halves of the magnetization curve.

point source A source from which electromagnetic radiation emanates, and that appears as a geometric point from a great distance.

point mode Descriptive of cathode-ray-tube display operation (in a computer system), in which data is portrayed as plotted dots.

point-to-point communication Communication between two stations whose location can be precisely specified.

point-to-point motion A method of robot arm movement in which the device can attain only certain positions. The coordinates of each stopping point are stored in the robot controller (computer) memory.

point-to-point station A radio station that provides POINT-TO-POINT COMMUNICATION.

point-to-point wiring A method of wiring an electronic circuit in which wires are run directly between the terminals or components, usually by the shortest practicable route. It is used mainly in high-voltage circuits, such as power amplifiers. Compare CABLED WIRING.

poise The cgs unit of absolute viscosity; 1 poise is the absolute viscosity of a fluid that requires a shearing force of 1 dyne to move a 1-sq-cm area of one of two parallel layers of the fluid (1 cm apart) with a velocity of 1 cm per second, with respect to the other layer. The comparable SI unit is the *newton-second per meter squared* ($N \cdot s/m^2$); 1 poise = 0.1 $N \cdot s/m^2$.

polar axis **1.** In a crystal, the axis of rotation not perpendicular to a reflection plane. **2.** The straight line connecting epicenters of electric, magnetic, or gravitational poles in a system. **3.** The axis about which the earth or another planet rotates.

polar coordinate conversion See POLAR COORDINATE TRANSFORMATION.

polar-coordinate geometry A two-dimensional system for movement of industrial-robot arms. It is based on a system of POLAR COORDINATES, in which a radius and a direction angle are assigned to each point in the working plane.

polar coordinates The magnitude and direction of a vector in a defined plane, listed as a radius (magnitude) in combination with an angle (direction) between the vector and the polar axis.

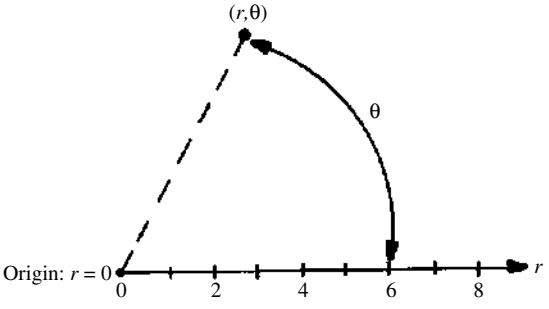

polar coordinates

polarimeter An instrument for measuring the amount of polarized light in a ray that is only partially polarized.

polariscope An instrument used in the observation or testing of materials under POLARIZED LIGHT.

polarity **1.** The condition of being electrically positive or negative. **2.** The condition of being magnetically north or south. **3.** The orientation of the positive and negative poles in a battery or power supply relative to a circuit. **4.** The orientation of a magnetic field, relative to the surrounding environment.

polarity blanking See POLARITY INHIBIT.

polarity inhibit In some instruments, especially those having automatic polarity, the automatic blanking of the polarity sign.

polarity-sensitive relay A direct-current relay actuated only when coil current flows in one direction. One of the simplest versions is a relay having a semiconductor diode connected in series with its coil.

polarity shifter A potentiometer connected to two direct-current sources so that a pair of output terminals has plus and minus polarities at one extreme of potentiometer adjustment, and minus and plus at the other extreme. At the center of the range, the output voltage is zero.

polarity switch A double-pole, double-throw switch connected between a pair of direct-current input terminals so that the polarity of a pair of output terminals can be interchanged.

polarization **1.** In a radio wave, the orientation of the electric lines of flux, with respect to the surrounding environment (e.g., *horizontal polarization* and *vertical polarization*). **2.** The disabling of a battery cell by the formation of insulating gas on one of the plates. **3.** The condition in which transverse waves of light are confined to a specific (e.g., horizontal or vertical) plane.

5059F-pP-510-565 4/10/01 9:32 AM Page 542

polarization diversity A form of reception in which two separate receivers, tuned to the same signal, are connected to independent antennas. One antenna is vertically polarized and the other is horizontally polarized. The result is a reduction in fading caused by ionospheric effects on the polarization of the incoming signal.

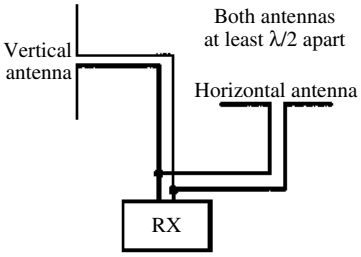

polarization diversity

polarization error In the operation of a loop antenna (e.g., that of a direction finder), null error caused by waves arriving with polarization opposite that of the loop (thus, vertically polarized waves at a horizontal-plane loop, and vice versa).

polarization fading In radio reception, a form of fading that results from changes in the polarization of the arriving signal with respect to the receiving antenna. When the polarization of the arriving signal coincides with that of the receiving antenna, the received signal strength is maximum. When the received-signal polarization is at right angles to the receiving antenna, the signal strength is minimum.

polarization modulation A method of impressing information on a signal by changing the polarization of the radiated electromagnetic field.

polarization selectivity For a photoemissive surface, the condition in which the ratio of photocurrents for two different angles of plane polarization of the light incident to the surface differs from the ratio of the corresponding amounts of light absorbed by the surface. Also see PHOTOEMISSION; PHOTOEMISSIVE MATERIAL; and POLARIZATION, **3**.

polarized capacitor A conventional electrolytic capacitor, so called because one particular terminal must be connected to the more positive of the two connection points. Compare NONPOLARIZED ELECTROLYTIC CAPACITOR.

polarized light Visible light waves whose electric lines of flux are confined more or less to a single plane. This effect can be obtained via filtering; it also occurs naturally under certain conditions. Scattered sunlight is polarized to some extent by the atmosphere. Light is polarized to some extent when it reflects from a plane surface. Also see POLARIZING FILTER.

polarized plug A plug that can be inserted into a socket or receptacle in only one way to ensure safe and foolproof operation.

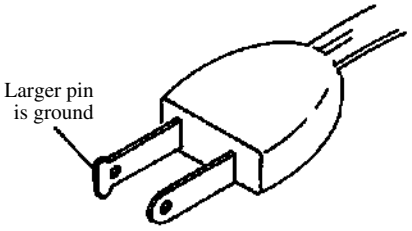

polarized plug

polarized power plug A polarized plug for connection of equipment to an alternating-current utility power source.

polarized reactor A saturable reactor in which the lines of flux produced in the three-leg core by the coils on the two outer legs are added in the center leg. Consequently, the flux can reinforce or oppose the controlling current in the coil on the center leg, depending on the direction of the current. Compare NONPOLARIZED REACTOR.

polarized receptacle A receptacle constructed so that it can receive a plug in only one way, thus preventing incorrect connections.

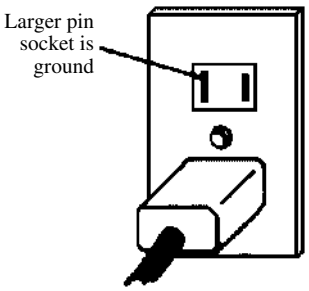

polarized receptacle

polarized relay A relay actuated by one polarity of direct current, or by one particular phase of alternating current. Such a relay sometimes contains an armature-centering permanent magnet.

polarized socket See POLARIZED RECEPTACLE.

polarized X rays X-ray waves whose electric lines of flux are more or less oriented in a specific plane, as when they are scattered by carbon blocks. See, for illustration, POLARIZATION, **3** and POLARIZED LIGHT.

polarizing filter A light filter that consists essentially of microscopic heraphathite plastic plate. The plate can be rotated to cause light passing

5059F-pP-510-565 4/10/01 9:32 AM Page 543

through it to be polarized in any particular plane between horizontal and vertical, depending on the degree of rotation. Also see POLARIZED LIGHT.

polarography In chemistry, a form of qualitative or quantitative analysis utilizing IE curves obtained when the voltage is gradually increased across a solution in ELECTROLYSIS.

polar orbit An orbit that carries a satellite over the geographic polar regions of the earth. This type of orbit is oriented at, or nearly at, 90 degrees with respect to the equator, and can have a period ranging from about 90 minutes to several weeks or even months. Low-earth-orbit (LEO) satellites generally have such orbits.

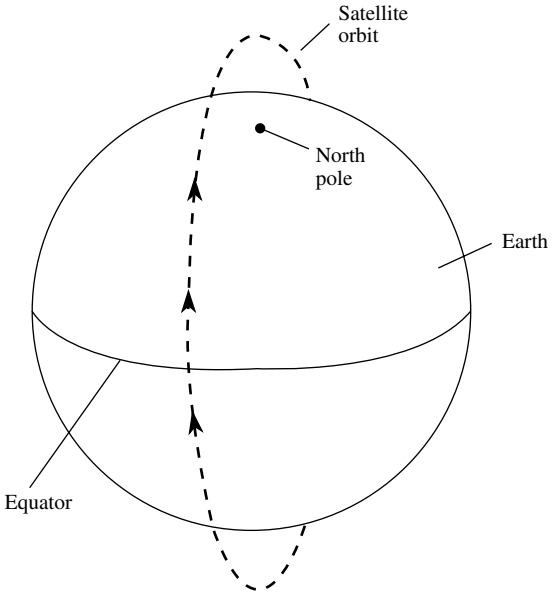

polar orbit

polar-orbiting satellite Any satellite in a POLAR ORBIT.

polar planimeter See PLANIMETER.

polar relay See POLARIZED RELAY.

polar response The horizontal-plane directional response of an antenna or other transducer.

pole **1.** An extremity or terminus that possesses POLARITY. Examples: *magnetic pole* and *electric pole*. **2.** The movable member of a switch. **3.** One of the frequencies at which a transfer function becomes infinite.

pole face The smooth end surface of a pole piece.

pole piece **1.** A section of specially shaped iron or steel that is attached to a magnetic core. **2.** Half of a two-piece magnetic core that terminates in a pole.

pole shoe In an electric motor, the section of the field pole nearest the armature.

poles of impedance For a reactive network, the frequencies at which the impedance is infinite. Compare ZEROS OF IMPEDANCE.

poles of network function The values at which a network function is infinite. Compare ZEROS OF NETWORK FUNCTION.

poles of transfer function The frequencies at which a transfer function becomes infinite. Compare ZEROS OF TRANSFER FUNCTION.

police robot A proposed robotic machine, either autonomous or remotely controlled (teleoperated), that would be used to assist in law enforcement, particularly in dangerous operations.

poling The deliberate adjustment of electromagnetic-field polarity.

Polish notation In Boolean algebra, a form of notation wherein the variables in a statement are preceded by the operators.

polling In data transmission, a technique in which channels being shared by more than one terminal are tested to find one over which data is coming in, or to ascertain which is free for transmission.

polonium Symbol, Po. A radioactive metallic element. Atomic number, 84. Atomic weight, approximately 209.

polychromatic radiation **1.** Visible-light radiation having more than one wavelength; in particular, covering a broad range of wavelengths. **2.** Electromagnetic radiation over a broad band of wavelengths.

polycrystalline material A substance, such as a semiconductor, of which even a very small sample consists of a number of separate crystals bound tightly together. Compare SINGLE-CRYSTAL MATERIAL.

polydirectional microphone See OMNIDIRECTIONAL MICROPHONE.

polyelectrolyte An ELECTROLYTE having high molecular weight.

polyester A resin made by reacting a dihydroxy alcohol with a dibasic acid.

polyester backing A polyester tape on the surface of which iron oxide is deposited to yield a magnetic recording tape.

polyethylene A plastic insulating material. Dielectric constant, 2.2. Dielectric strength, 585 V/mil.

polyethylene disc A phonograph disc made of polyethylene.

polygonal coil A coil wound on a form having a polygonal, rather than circular cross section. Some polygonal forms have as many as 12 sides in cross section.

polygraph An instrument for measuring and recording electrical signals proportional to blood pressure, skin resistance, breathing rate, and other reactions that vary under emotional stress. Also called LIE DETECTOR. Compare PATHOMETER.

5059F-pP-510-565 4/10/01 9:33 AM Page 544

polymer A compound that is the product of *polymerization*, resulting from the chemical union of monomers. Also see POLYMERIZE.

polymerize To unite monomers or polymers of the same kind to form a molecule having a higher molecular weight.

polyphase In alternating-current circuits, pertaining to the existence or generation of two or more specific electrical phases. Compare SINGLE PHASE.

polyphase antenna An antenna consisting of two dipole radiators mounted perpendicular to each other at their midpoint and excited 90 degrees out of phase. The radiation pattern is approximately circular in the plane of the elements. Also called TURNSTILE ANTENNA.

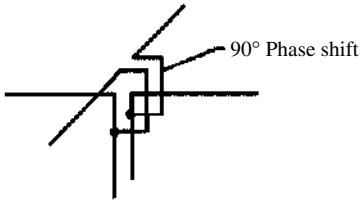

polyphase antenna

polyphase generator **1.** A dynamo-type generator of polyphase power (two-phase, three-phase, etc.). **2.** See POLYPHASE OSCILLATOR.

polyphase oscillator An oscillator circuit that generates polyphase alternating current. The circuit contains separate oscillators for each phase. A three-phase circuit, for example, has three symmetrical oscillators with matched inductance and capacitance values.

polyphase power **1.** The total dissipated power in a polyphase alternating-current circuit. **2.** Polyphase alternating current provided for utility purposes.

polyphase rectifier A rectifier of polyphase alternating current generally obtained from a three-phase power line through a transformer. The several common circuits usually contain a diode for each phase. Such rectifiers offer the advantage of higher ripple frequency than is obtainable by single-phase operation. For a three-phase rectifier, for example, the ripple frequency is three times the line frequency; for a six-phase rectifier, it is six times the line frequency.

polyphase system An alternating-current circuit in which voltages or currents are normally out of phase with each other by some fixed amount. Familiar types are two-phase and three-phase.

polyphase transformer An alternating-current transformer specifically designed for use in circuits that have two or more simultaneous current phases.

polypropylene A plastic material commonly used as an electrical insulator. Dielectric constant, 2.0. Dielectric strength, 600 V/mil.

polyrod antenna A tapered dielectric antenna, usually made of polystyrene, for directional microwave transmission.

polysilicon A polycrystalline form of silicon (see POLYCRYSTALLINE MATERIAL).

polystyrene A clear, colorless thermosetting-type plastic. It is widely used as an insulating material in radio-frequency circuits and, to some extent, as a dielectric film in fixed capacitors. Dielectric constant, 2.4 to 2.9. Dielectric strength, 20 to 28 kV/mm.

polystyrene capacitor A high-Q capacitor in which the dielectric film is polystyrene.

polyvinyl chloride Abbreviation, PVC. A plastic insulating material. Dielectric constant, 3.6 to 4.0. Dielectric strength, 800 V/mil.

pool cathode In an industrial electron tube, a cathode consisting of a pool of mercury.

pool-cathode tube An industrial electron tube using a pool cathode. Examples: excitron, ignitron, and mercury-arc rectifier.

popcorn noise A temperature-dependent, random-shot electrical noise. In a radio receiver or audio circuit, this noise resembles the sound of popping corn. It occurs in some operational amplifiers.

population In statistical analysis, the total group of items, quantities, or values under consideration. Sometimes called *universe.*

porcelain A hard, white, usually glazed ceramic used as a dielectric and insulant. Dielectric constant, 6 to 7.5. Dielectric strength, 40 to 100 V/mil. Also called *china.*

porcelain capacitor A ceramic-dielectric capacitor in which the dielectric is composed of porcelain or a related substance.

porcelain insulator An electric insulator fabricated from porcelain.

porch See BACK PORCH and FRONT PORCH.

port **1.** In a circuit, device, or system, a point at which energy or signals can be introduced or extracted in a particular manner (e.g., *two-port circulator* and *I/O port*). **2.** An aperture in a loudspeaker enclosure.

portable-mobile station See MOBILE STATION.

portable station A communications station that can be carried from one location to another. A portable station differs from a mobile station in that a portable station does not usually operate while in motion, whereas a mobile station does.

ported reflex enclosure A loudspeaker cabinet with openings that facilitate bass (low-frequency) sound reproduction.

pos **1.** Abbreviation of POSITIVE. **2.** Abbreviation of POSITION.

position **1.** The location of a point or object with respect to one or more (usually fixed) references. **2.** The setting of an adjustable device, such as a potentiometer, rotary switch, or variable capacitor.

5059F-pP-510-565 4/10/01 9:33 AM Page 545

positional notation A method of representing numbers in which the number is indicated by the positions and value of the component digits. The decimal number system belongs in this category (e.g., the decimal number 1284.67 is equal to $1 \times 10^3 + 2 \times 10^2 + 8 \times 10^1 + 4 \times 10^0 + 6 \times 10^{-1} + 7 \times 10^{-2}$).

positional number system See POSITIONAL NOTATION.

positional representation See POSITIONAL NOTATION.

position-control potentiometers In an oscilloscope, potentiometers used to control the voltage applied to the horizontal and vertical deflecting plates to position the spot on the screen. Also see CENTERING CONTROL.

position controls See POSITION-CONTROL POTENTIOMETERS.

position feedback In a servo or other control system, feedback current, or voltage that is proportional to the position assumed by a member.

position fixing The determination of a position from the intersection on a map of two lines derived from the direction-finding pickups of two transmitting stations. Also see DIRECTION FINDER.

position indicator In a tape recorder, a counter whose numbered wheels revolve when the reels do, thus aiding in locating a desired spot on the tape. Also called *tape counter*.

positioning circuit The circuit associated with a horizontal or vertical centering control (see CENTERING CONTROL).

position sensing **1.** In robotics and navigation systems, a method of determining location, relative to the surrounding environment. **2.** Any method via which a robot can accurately determine the location(s) of its end effector(s).

position sensor An electronic circuit that detects physical displacement, and transmits a signal proportional to the displacement.

positioning control See CENTERING CONTROL.

positive **1.** Possessing positive (plus) direct-current electrical polarity. **2.** Pertaining to real numbers greater than zero. **3.** A photographic image whose shadings are the same as those in the scene.

positive angle **1.** In a system of rectangular coordinates, an angle in the first or second quadrant. **2.** In rectangular coordinates, an angle measured counterclockwise from the positive *x*-axis. Compare NEGATIVE ANGLE.

positive bias A positive voltage or current applied continuously to an electrode of a device (as to a transistor base) to maintain the device's operating point. Compare NEGATIVE BIAS.

positive bus See POSITIVE CONDUCTOR.

positive charge An electrical charge characterized by having relatively fewer electrons than a negative charge. Also see CHARGE, **1**; ELECTRIC CHARGE; and UNIT ELECTROSTATIC CHARGE. Compare NEGATIVE CHARGE.

positive conductor The conductor or line connected to the positive terminal of a current, voltage, or power source. Compare NEGATIVE CONDUCTOR.

positive electricity See POSITIVE CHARGE and POSITIVE ELECTRIFICATION.

positive electrification Electrification characterized by a deficiency of electrons. For example, when a glass rod is rubbed with a silk cloth, the rod becomes positively charged because electrons are rubbed off the glass onto the silk. Similarly, when an atom loses an electron, it becomes electrified positively because it has a deficiency of electrons. Compare NEGATIVE ELECTRIFICATION.

positive electrode **1.** An electrode connected to the positive terminal of a current, voltage, or power source. **2.** The positive terminal of a current, voltage, or power source, such as a battery or generator.

positive electron See POSITRON.

positive element See POSITIVE ELECTRODE, **1**.

positive error of measurement An error of measurement in which the difference between a measured value and the true or most probable value is positive. Compare NEGATIVE ERROR OF MEASUREMENT.

positive exponent A positive superscript indicating that a number (x) is to be raised to the positive nth power. Thus, in the expression x^n, the value of n is greater than zero. Compare NEGATIVE EXPONENT.

positive feedback Feedback that is in phase with an input signal. Also called REGENERATION and REGENERATIVE FEEDBACK. Compare NEGATIVE FEEDBACK.

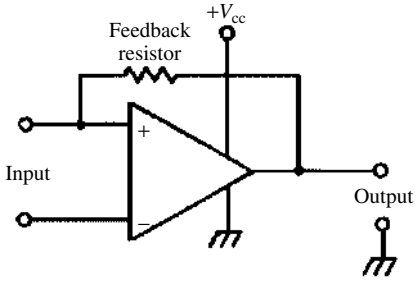

positive feedback

positive function A function having the positive sign. In the rectangular coordinate system, the trigonometric sine function is positive in the first and second quadrants, the cosine in the first and fourth, and the tangent in the first and third. Compare NEGATIVE FUNCTION.

positive ghost In a television picture, a ghost with positive shading (see POSITIVE, **3**). Also see GHOST.

5059F-pP-510-565 4/10/01 9:33 AM Page 546

positive-going Pertaining to a signal whose value is changing in a positive direction. This is not restricted to signals of actual positive polarity; a decreasing negative voltage, for example, is positive-going as it falls in the direction of zero—even if it never crosses the zero line.

positive grid In an electron tube, a control grid whose bias or signal voltage is positive, with respect to the cathode.

positive-grid oscillator A microwave oscillator circuit in which the control grid of a triode tube is operated at a positive direct-current potential, and the plate at a negative potential. Electrons move back and forth between cathode and plate, through the grid, and thus give rise to an oscillating current.

positive ground A direct-current electrical system in which the positive power-supply terminal is connected to the common ground. It is not generally used in North America.

positive half-alternation See POSITIVE HALF-CYCLE.

positive half-cycle That half of an alternating-current cycle in which the current or voltage increases from zero to maximum positive and returns to zero.

positive image **1.** A picture in which the blacks, whites, and grays correspond to those in the actual scene (see POSITIVE, **3**). **2.** A normal television picture (i.e., one that has the shading described in **1**).

positive ion An atom that has a deficiency of electrons and, consequently, exhibits a net positive charge. Also called CATION.

positive lead See POSITIVE CONDUCTOR.

positive light modulation In television transmission, the condition in which transmitted power increases as the light intensity increases. Compare NEGATIVE LIGHT MODULATION.

positive line See POSITIVE CONDUCTOR.

positive logic **1.** Binary logic in which a low positive state represents logic 0, and a high positive state represents logic 1. **2.** Binary logic in which a high negative state represents logic 0, and a low negative state represents logic 1. Compare NEGATIVE LOGIC.

positive magnetostriction A form of MAGNETOSTRICTION in which the physical size of a substance is directly proportional to the intensity of the surrounding magnetic field.

positive measurement error See POSITIVE ERROR OF MEASUREMENT.

positive modulation In amplitude-modulated television transmission, the increase in transmitted power when the brightness of the scene increases. Compare NEGATIVE MODULATION.

positive modulation factor For an amplitude-modulated wave having unequal positive and negative peaks, a ratio expressing the maximum positive deviation (increase) from the average value of the envelope. Compare NEGATIVE MODULATION FACTOR.

positive number A real number, whose value is greater than zero. Compare NEGATIVE NUMBER.

positive peak The maximum amplitude of a positive half-cycle or positive pulse.

positive-peak clipper A peak clipper that levels off the positive half-cycle of an alternating-current wave to a predetermined level.

positive-peak modulation Amplitude modulation of the positive peaks of a carrier wave.

positive-peak voltmeter An electronic voltmeter for measuring the amplitude of the positive peak of an alternating-current (ac) wave. In its simplest form, it consists essentially of a direct-current (dc) microammeter with a diode oriented to pass the positive half-cycle. A series capacitor in the circuit is charged to approximately the peak value of the applied ac voltage. Compare NEGATIVE-PEAK VOLTMETER.

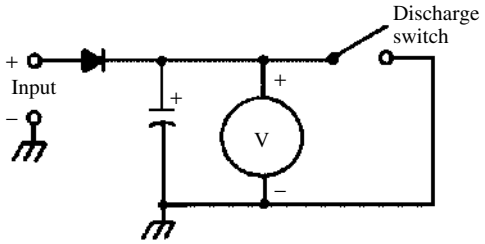

positive-peak voltmeter

positive phase-sequence relay A phase-sequence relay that responds to the positive phase sequence in a polyphase circuit. Compare NEGATIVE PHASE-SEQUENCE RELAY.

positive picture modulation See POSITIVE MODULATION.

positive picture phase In a television signal, the swinging of the picture-signal voltage from zero to positive, in response to an increase in brightness in the scene. Compare NEGATIVE PICTURE PHASE.

positive plate **1.** The positive member of an electrochemical cell or battery. Electrons flow to this plate from the negative plate, through the external circuit. **2.** A vacuum-tube plate that is biased positively, as in a conventional tube circuit.

positive pole See POSITIVE ELECTRODE, **1**, **2**.

positive potential **1.** The voltage at a positive electrode (with respect to the negative electrode). **2.** Voltage greater than that at ground as a reference.

positive power See POSITIVE EXPONENT.

positive resistance Ohmic resistance (see OHMIC RESPONSE). Compare NEGATIVE RESISTANCE.

positive resistor A resistor whose value does not change with current or voltage changes. Compare NEGATIVE RESISTOR.

5059F-pP-510-565 4/10/01 9:33 AM Page 547

positive temperature coefficient Abbreviation, PTC. A number expressing the amount by which a quantity (such as the value of a component) increases when temperature is increased. The coefficient is stated as a percentage of the rated value per degree, or in parts per million per degree. Compare NEGATIVE TEMPERATURE COEFFICIENT and ZERO TEMPERATURE COEFFICIENT.

positive transmission In facsimile or television, a form of amplitude modulation in which the picture brightness is directly proportional to the signal strength at any given instant of time.

positive valence The valence of a positive ion.

positron A positively charged particle having the same mass as that of the electron, and the same magnitude of electric charge, but positive (instead of negative). Sometimes called *positive electron.*

post See BINDING POST.

post- Prefix meaning "following," "subsequent to," or "behind."

post-accelerating electrode In a cathode-ray tube, the high-voltage electrode that produces POST-DEFLECTION ACCELERATION of the electron beam. Also called INTENSIFIER ELECTRODE.

postacceleration See POST-DEFLECTION ACCELERATION.

post-alloy-diffused transistor Abbreviation, PADT. A transistor in which electrodes are diffused into the semiconductor wafer after other electrodes have been alloyed.

post-conversion bandwidth The bandwidth of a signal after it has been converted from one frequency to another.

post-deflection accelerating electrode See POST-ACCELERATING ELECTRODE.

post-deflection acceleration In a cathode-ray tube, the intensification of the electron beam following beam deflection. Also see POST-DEFLECTION CRT.

post-deflection CRT An oscilloscope tube provided with a high-voltage intensifier electrode in the form of a ring encircling the inside flare of the tube, between the deflecting plates and the screen. The deflected electron beam is accelerated by this electrode. This arrangement allows the beam to be deflected at low velocity and high sensitivity, then to be accelerated for a brighter image.

post edit The editing of data in a computer output.

postemphasis See DEEMPHASIS.

post-equalization **1.** In sound recording and reproduction, equalization during playback. Compare PREEQUALIZATION. **2.** See DEEMPHASIS.

postmortem An investigation into the cause of failure of a circuit, device, or system.

postmortem dump At the end of a computer program run, a dump to supply information for debugging purposes.

post office box A type of wheatstone bridge that contains resistance coils in a special box. The coils are connected so that they can be replaced by shorting connectors.

pot **1.** See POTENTIOMETER. **2.** See DASHPOT. **3.** Abbreviation of POTENTIAL. **4.** To encapsulate a circuit in a potting compound, such as epoxy resin.

potassium Symbol, K. A metallic element of the alkali-metal group. Atomic number, 19. Atomic weight, 39.098.

potassium chloride Formula, KCl. A compound used as a phosphor coating on the screen of a nearly permanent-persistence cathode-ray tube. The fluorescence is magenta or white, as is the phosphorescence.

potassium cyanide Formula, KCN. A highly toxic salt that is an electrolyte in some forms of electroplating.

potassium dihydrogen phosphate Abbreviation, KDP. An inorganic ferroelectric material.

pot core A magnetic core for a coil, made of ferrite or of powdered iron, consisting of a central rod, a surrounding potlike enclosure, and a lid. The rod passes through the center of the coil, and the pot and lid completely enclose the coil. This arrangement provides a completely closed magnetic circuit and coil shield.

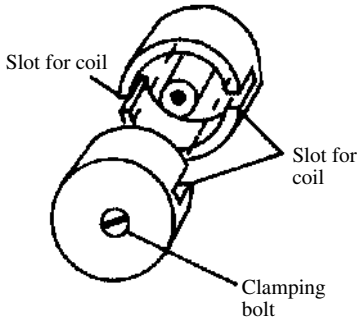

pot core

potential See ELECTROMOTIVE FORCE.

potential barrier The electric field produced on each side of a semiconductor junction by minority carriers (i.e., by holes in the n-layer and electrons in the p-layer) that face each other across the junction, but cannot diffuse across the junction and recombine.

potential coil The shunt coil in a conventional wattmeter.

potential difference See ELECTROMOTIVE FORCE and VOLTAGE.

potential divider See VOLTAGE DIVIDER.

potential drop **1.** A voltage difference between two points in a circuit. **2.** The voltage across a resistor in a direct-current circuit.

potential energy Energy resulting from the position of a body or particle (e.g., the energy stored

5059F-pP-510-565 4/10/01 9:33 AM Page 548

in something lifted against gravity and held in its new position) or from the position of charges (e.g., the energy stored in a charged capacitor). Compare KINETIC ENERGY.

potential gradient See VOLTAGE GRADIENT.

potential profile A rectangular-coordinate display of the VOLTAGE GRADIENT across a body (e.g., the cross section of a transistor).

potential transformer A small step-up transformer for increasing the range of an alternating-current voltmeter.

potentiometer **1.** A variable resistor used as a voltage divider. The input voltage is applied across the entire resistance element and the output voltage is taken from the wiper, relative to one end of the element. One end is usually grounded (at zero potential). **2.** A null device whose operation is based on a variable resistor, and is used for precise voltage measurements. The unknown voltage is applied to the input of a variable resistor whose settings are known with great accuracy; the resistance is adjusted for an output voltage that exactly equals the voltage of a standard cell (as indicated by a null between the two voltages). The unknown voltage is then determined from the resistance and the standard-cell voltage.

potentiometer noise In a current-carrying potentiometer, electrical noise generated when the wiper blade rubs against the resistance element, or by contact between the blade and element.

potentiometric recorder A type of graphic recorder. It consists essentially of a resistance-calibrated potentiometer, a standard cell, and a galvanometer. When an unknown voltage (E_x) is applied to the input terminals of the potentiometer and the potentiometer is set for null, $E_x = E_s (R_2/R_1)$, where *Es* is the voltage of the standard cell, *R1* is the input resistance of the potentiometer, and *R2* is the output resistance of the potentiometer.

Potier diagram An illustration of the phase relationship between current and voltage in an alternating-current circuit that contains reactance.

POTS Acronym for *plain old telephone service*, meaning basic service without optional features (such as call waiting, conference calling, call forwarding, etc.).

potted circuit A circuit embedded in plastic or wax to protect it against the environment, and/or to minimize the effects of physical vibration (see POTTING).

potted component An electronic part embedded in a suitable plastic or wax to protect it against the environment, and/or to minimize the effects of physical vibration (see POTTING).

potting A process of embedding a component or circuit in a solid mass of plastic or wax held in a container. The process is similar to encapsulation, except that in potting, the container (envelope) remains as part of the assembly. Compare ENCAPSULATION.

potting material A substance, such as a resin or wax, used for potting electronic gear. Also called *potting compound.*

pound **1.** Abbreviations, lb, p. A unit of weight equal to 16 avoirdupois ounces. **2.** Abbreviation, lbf. A unit of force approximately equal to 4.448 newtons. **3.** Abbreviation, lbm. A unit of mass approximately equal to 0.4536 kilogram.

poundal A unit of force equal to approximately 13825.5 dynes or 0.138255 newton. One poundal is the force that, when acting for one second, will impart a speed of one foot per second to a one-pound mass.

pound-foot Abbreviation, lb-ft. A unit of torque equal to the product of a force of one pound and a moment arm of one foot. Compare OUNCE-INCH.

pounds per square inch absolute Abbreviation, psia. Absolute pressure (i.e., the sum of atmospheric pressure and the pressure indicated by a gauge). Compare POUNDS PER SQUARE INCH GAUGE.

pounds per square inch gauge Abbreviation, PSIG. The value of pressure indicated by a gauge, without correction for atmospheric pressure. Compare POUNDS PER SQUARE INCH ABSOLUTE.

powdered-iron core A magnetic core consisting of minute particles of iron, each coated with a film to insulate it from others, molded into a solid mass. Because of its low eddy-current loss, this type of core is usable in radio-frequency transformers and coils, where it increases the inductance of the winding.

power **1.** Symbol, *P.* Unit, watt. The rate of doing work, or producing or transmitting energy. In direct-current circuits, and in alternating-current circuits containing no reactance, power is the product of the root-mean-square current and voltage. See, for example, AC POWER, APPARENT POWER, DC POWER, KILOVOLT-AMPERE, POWER FACTOR, REACTIVE KILOVOLT-AMPERE, REACTIVE VOLT-AMPERE, TRUE POWER, VOLT-AMPERE, WATT, and WATTLESS POWER. **2.** The product obtained by multiplying a quantity x by itself n times, written x^n. For example, $2^4 = 2 \times 2 \times 2 \times 2 = 8$; here, 8 is the *fourth power* of 2. Compare ROOT, **1**. **3.** The exponent in an expression, as defined in **2**.

power amplification **1.** The amplification of a signal having a certain power (wattage) to produce a signal having greater power. **2.** The signal power increase, expressed as a ratio or as a figure in decibels, resulting from the process defined in **1**. Also called POWER GAIN.

power amplification ratio See POWER AMPLIFICATION, **2** and POWER GAIN.

power amplifier An amplifier that delivers useful amounts of power to a load, such as one or more speakers. Compare CURRENT AMPLIFIER and VOLTAGE AMPLIFIER.

5059F-pP-510-565 4/10/01 9:33 AM Page 549

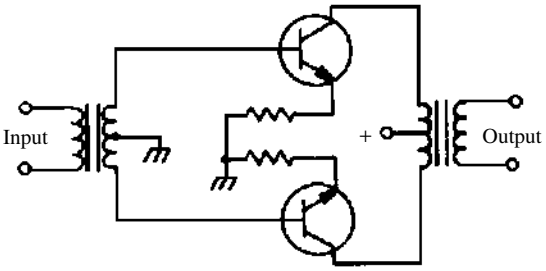

power amplifier

power-amplifier device A high-current tube or transistor designed especially for high power output. Such a device does not always provide significant voltage amplification, but always provides power amplification. Compare VOLTAGE-AMPLIFIER DEVICE.

power at peak torque Symbol, *Pp*. For a torque motor, the input power in watts needed for peak torque at stall at a winding temperature of 25 degrees Celsius.

power attenuation **1.** A reduction of power level. **2.** See POWER LOSS.

power bandwidth For a high-fidelity audio amplifier, the difference between the maximum and minimum frequencies at which the amplifier can produce at least 50 percent of its maximum power output, with less than a certain amount of total harmonic distortion (usually 10 percent).

power blackout A situation in which all electric power is lost to utility subscribers in a defined region.

power consumption **1.** For a direct-current device, the normal operating voltage multiplied by the normal drawn current. **2.** For an alternating-current circuit, the root-mean-square voltage multiplied by the root-mean-square current.

power control The adjustment of the output voltage of a power supply, usually by means of a variable autotransformer, silicon-controlled rectifier, thyratron, or similar device.

power cutoff frequency Symbol, f_{co}. The frequency at which the power gain of a transistor drops 3 dB below its low-frequency value.

power derating For a temperature higher than the specified ambient temperature, a deliberate reduction of the power dissipated by a component or device. This is done to prevent failure of the component or device. Also see DERATING, DERATING CURVE, and DERATING FACTOR.

power difference An expression of the power lost in a circuit when power is absorbed by a dielectric material.

power diode A heavy-duty diode that is usually used in power-supply service. Also called *rectifier diode.*

power dissipation Abbreviation, PD. The power consumed by a device during normal operation. This power is not available in the electrical output of the device. An example is the direct-current power dissipated in the collector circuit of a high-fidelity audio amplifier.

power divider A circuit that distributes power, in a predetermined manner, among various loads.

power drain The amount of power drawn by a device. It can be operating power or standby power.

power dump See DUMP, **2**.

power equations Variations of the basic power equation: $P = EI = E^2/R = I^2R$, where P is the power in watts, E is the voltage in volts, I is the current in amperes, and R is the resistance in ohms.

power factor Abbreviation, PF. In an alternating-current circuit, the ratio (expressed either as a decimal or a percentage) of true power (power actually consumed) to apparent power (simple product of voltage and current). The power factor is equal to the cosine of the phase angle. Also see AC POWER.

power-factor balance In a capacitance bridge, a separate null adjustment for the internal resistance component of a capacitor under measurement. The dial of the variable component for this adjustment reads directly in percent power factor in some bridges.

power-factor correction To raise the power factor of an inductive circuit by inserting a parallel capacitance. In power circuits, this affords improved economy of operation because the current drain is brought more in line with that of a resistive circuit.

power-factor meter An instrument that gives direct readings of power factor (lead or lag). One such meter uses a dynamometer-type movement (see ELECTRODYNAMOMETER) in which the rotating element consists of two coils fastened together at right angles.

power-factor regulator A device that regulates the power factor of an alternating-current line.

power-factor relay An alternating-current relay actuated by a rise or fall in power factor, with respect to a predetermined value.

power frequency **1.** See POWER-LINE FREQUENCY. **2.** The frequency of an alternating-current generator. **3.** The output frequency of a power inverter (see INVERTER, **1**).

power-frequency meter An instrument for measuring power-line frequency. It can use electromechanical devices, or can directly count the number of alternations per second.

power gain Abbreviations, *PG* or PG_{dB}. The extent to which power is increased by a power amplifier. It can be expressed as the ratio of power output to power input as $PG = P_o/P_i$, or in decibels as $PG_{dB} = 10 \log_{10}(P_o/P_i)$.

power grid An aggregation of power-generating stations, transmission lines, and associated

5059F-pP-510-565 4/10/01 9:33 AM Page 550

equipment, usually extending over hundreds of miles and embracing several communities, so operated that individual members can deliver power to the system or draw power from it, according to local demand.

power ground The power-supply ground for a circuit or system.

power-handling capacity **1.** The amount of power that a device can dissipate, either continuously or intermittently, without suffering damage. **2.** The maximum input power that can be tolerated by an amplifier transistor or tube without overheating.

power hyperbola For a semiconductor device or vacuum tube, a curve plotted from the device's current and voltage values, which provide the power value when multiplied (e.g., a 2-watt curve for the direct-current collector input of a power transistor).

power input See INPUT POWER.

power-input control The adjustment of the output of a power supply by varying the alternating-current input to the power transformer. Usually, a variable autotransformer is operated ahead of the power transformer. See, for example, VARIABLE TRANSFORMER and VARIAC.

power inverter See CHOPPER POWER SUPPLY.

power-level indicator **1.** See DB METER. **2.** See OUTPUT POWER METER.

power line The line through which electrical energy is received by a subscriber.

power-line communication Abbreviation, PLC. Carrier-current telephony or telegraphy over power lines that are common to transmitting and receiving stations. Also see WIRED WIRELESS.

power-line filter **1.** A heavy-duty radio-frequency (RF) filter inserted in the power line close to a device that generates RF energy, such as a radio transmitter. It prevents transmission of RF energy via the power line. **2.** An RF filter inserted in the power line, where it enters the power supply of a sensitive electronic device, such as a computer or high-fidelity audio amplifier. It prevents RF energy on the power line from entering the device via the power supply.

power-line frequency The frequency of the alternating current and voltage available over commercial power lines. In the United States, it is 60 Hz; in some countries, it is 50 Hz.

power-line monitor An expanded-scale alternating-current voltmeter for the continuous monitoring of power-line voltage.

power-line pickup The interception of radio-frequency energy by utility power lines acting as receiving antennas. This energy can enter a sensitive electronic device, such as a computer or a high-fidelity audio amplifier, via the power supply.

power loss The power dissipated in a component. It generates heat while doing no useful work. Represents energy loss, except when the generation of heat is the end purpose.

power-loss factor Symbol, F_p. In interstage coupling, the ratio of available power (with the coupling network in place) to the available power when the network is disconnected.

power meter See WATTMETER.

power modulation factor In amplitude modulation, the ratio of the peak power to the average power.

power oscillator A heavy-duty oscillator delivering useful power output.

power output See OUTPUT POWER.

power-output meter See OUTPUT POWER METER.

power pack An external power-line-operated unit supplying alternating or direct current for the operation of electronic equipment.

power pentode A heavy-duty pentode vacuum tube designed to deliver relatively high output power.

power plug A plug for insertion into a power-line outlet.

power programmer A device that adjusts radar output power, in accordance with the target distance.

power rating **1.** The specified power required by an equipment for normal operation. **2.** The specified power output of a generator or amplifier.

power reactive See REACTIVE VOLT-AMPERE.

power rectifier A heavy-duty semiconductor diode used to rectify alternating current for power-supply purposes.

power relay A heavy-duty relay designed to switch significant amounts of power. The heavy contacts and armature require high actuating current; this necessitates a larger coil than is used in lighter-duty relays.

power resistor A heavy-duty resistor (i.e., one designed to carry large currents without overheating).

power stack A selenium rectifier consisting of a number of rectifier plates stacked in series for higher voltage handling.

power supply **1.** A device, such as a generator or a transformer-rectifier-filter arrangement, that produces the power needed to operate an electronic equipment. **2.** A reserve of available power (e.g., the power line, an installation of batteries, etc.).

power-supply filter A low-pass filter that is used to remove the ripple from the output of a power-supply rectifier. See, for example, BRUTE-FORCE FILTER.

power-supply rejection ratio The ratio of the output-voltage change for an amplifier, oscillator, or other circuit, to the change in power-supply voltage. It is determined on an instantaneous basis.

power-supply sensitivity In an operational amplifier, sensitivity of the offset to variations in the power-supply voltage.

power surge **1.** A momentary increase in the voltage on a utility line. **2.** An abnormally high voltage that sometimes exists for the first several milliseconds after utility power is restored following a blackout.

5059F-pP-510-565 4/10/01 9:33 AM Page 551

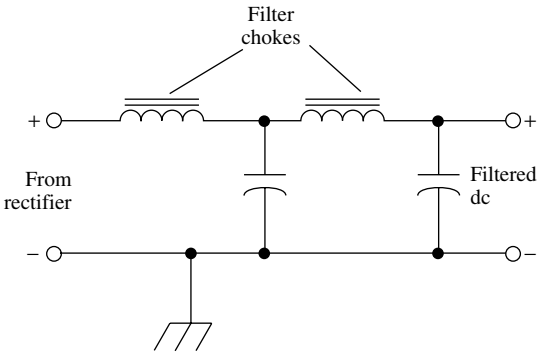

power-supply filter

power switch The switch for controlling power to a piece of equipment. Also see ON-OFF SWITCH.

power switching Switching operating power on and off. There are two principal methods: One involves making and breaking the connections between equipment and the power line; the other involves making and breaking the output of a line-operated or battery-type power supply.

power tetrode A heavy-duty tetrode vacuum tube designed to deliver relatively high output power.

power-to-decibel conversion Abbreviation, P_{dB}. Power expressed in decibels, with respect to a reference power level. Determined by the formula $P_{dB} = 10 \log_{10}(P_x/P_{ref})$, where P_x is the given power level and P_{ref} is the reference power level.

power transfer **1.** The passage of power from a generator to a load. **2.** The passage of power from one circuit to another.

power transfer theorem See MAXIMUM POWER TRANSFER THEOREM.

power transformer A transformer designed solely to supply operating power to electronic equipment—either directly or through a rectifier-filter circuit. Because a power transformer is used at low (power-line) frequencies, its core does not require the high-grade iron used in audio transformers, nor are special winding techniques needed to reduce the leakage inductance and interwinding capacitance.

power transistor A heavy-duty transistor designed for power-amplifier and power-control service.

power triode A heavy-duty triode vacuum tube designed to deliver relatively high output power.

power tube A heavy-duty electron tube designed to deliver useful amounts of power. See, for example, POWER PENTODE, POWER TETRODE, and POWER TRIODE.

power unit **1.** A power supply (see POWER SUPPLY, **1**). **2.** A unit of power measurement. See, for example, KILOWATT, MEGAWATT, MICROWATT, MILLIWATT, PICOWATT, and WATT.

power user In personal or business computing, a serious user who has extensive, up-to-date knowledge of hardware and software.

power winding In a magnetic amplifier or saturable reactor, the output winding (i.e., the winding through which the controlled current flows).

Poynting vector In an electromagnetic wave, the vector product of instantaneous electric intensity and magnetic intensity.

PP Abbreviation of *peripheral processor.*

PP **1.** Symbol for PLATE POWER. **2.** Symbol for PEAK POWER.

ppb Abbreviation of *parts per billion.*

PPI Abbreviation of PLAN POSITION INDICATOR.

pp junction In a semiconductor wafer, the boundary between two p-type regions that have somewhat different properties.

PPM Abbreviation of PULSE-POSITION MODULATION.

ppm **1.** Abbreviation of *parts per million.* **2.** Abbreviation of *pulses per minute.*

pps Abbreviation of *pulses per second.*

ppt Abbreviation of *parts per thousand.*

PPV Abbreviation of PAY PER VIEW.

Pr Symbol for PRASEODYMIUM.

practical component A circuit component considered in proper combination with the stray components inherent in it. Thus, a resistor has residual inductance and capacitance, an inductor has residual capacitance and resistance. Compare IDEAL COMPONENT.

practical units A set of physical/electrical units especially suited to a particular application. For example, in direct-current electrical applications, practical units are the AMPERE, OHM, VOLT, and WATT.

praetersonics See ACOUSTOELECTRONICS; ACOUSTIC DELAY LINE; SURFACE-WAVE AMPLIFIER; SURFACE-WAVE FILTER.

pragilbert The unit of MAGNETOMOTIVE FORCE in the absolute mks (Giorgi) system.

pragilbert per weber The unit of RELUCTANCE in the absolute mks (Giorgi) system.

praoersted The unit of MAGNETIZING FORCE in the absolute mks (Giorgi) system.

praseodymium Symbol, Pr. A metallic element of the rare-earth group. Atomic number, 59. Atomic weight, 140.908.

preaccelerating electrode In the electron gun of a cathode-ray tube, the high-voltage electrode that provides initial acceleration to the electron beam.

pre-alarm signal An audio and/or visual indicator that an alarm will sound if an area is not cleared within a short time. An example is a voice recording in a car alarm system (e.g., "Stand back!").

preamplifier **1.** A high-sensitivity, low-noise amplifier that usually uses a high-gain field-effect transistor (FET) and is used to enhance the sensitivity of a radio communications receiver. They are especially used at frequencies above

5059F-pP-510-565 4/10/01 9:33 AM Page 552

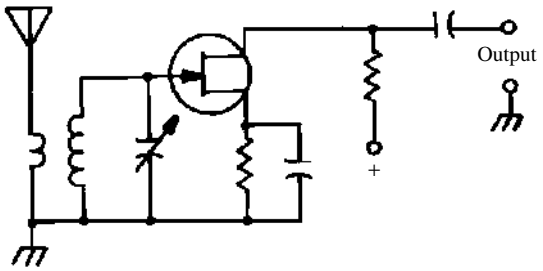

preamplifier

approximately 15 MHz, where most of the noise comes from the receiver, rather than from outside sources. **2.** A low-noise amplifier used for boosting weak signals for television reception. **3.** A low-noise, low-level amplifier used for boosting signal levels from transducers, such as microphones or photocells.

prebiased relay A relay through which is maintained a steady current that is just lower than that needed to close the relay. The actuating signal, then, need only be a small amount of additional current.

precedence effect See FUSION, **1**.

precipitation **1.** Water falling from the atmosphere in some form (rain, snow, hail, or sleet). See PRECIPITATION STATIC. **2.** The amount of precipitation occurring in a given period of time at a specific location. **3.** Separation of a solid material from a solution, as a result of a chemical or physical action.

precipitation static **1.** Radio noise that sometimes occurs when it rains or snows. It can be mistaken for artificially generated noise. **2.** Radio noise caused by atmospheric electricity arising from rain, snow, ice crystals, hail, or dust clouds, through which an aircraft carrying the radio flies.

precipitator See DUST PRECIPITATOR.

precipitron See DUST PRECIPITATOR.

precision **1.** Pertaining to electronic hardware, especially test instruments and measuring devices, designed and built to function with a high degree of accuracy. **2.** The relative accuracy of a meter or other indicating device. **3.** The accuracy of the results of an experiment, test, or measurement.

precision approach radar A radar aimed along the approach path to guide an aircraft during approach.

precision instrument An instrument possessing high accuracy and stability (i.e., one capable of reproducing readings or settings for various trials under set circumstances).

precision potentiometer **1.** A POTENTIOMETER possessing highly accurate resistance calibration, linearity, and repeatability of settings. **2.** A potentiometer-type voltage-measuring instrument.

preconduction current **1.** The cutoff current in a transistor. **2.** In a thyratron, the small (anode) current flowing before the tube is fired.

predetermined counter A counter programmed to count to a desired number and stop.

predistortion See PREEMPHASIS.

pre-Dolby **1.** To record a tape with DOLBY compression. **2.** A tape that has been recorded with Dolby compression.

preemphasis In frequency modulation, the introduction of a rising-response characteristic (response rises as modulation frequency increases). Compare DEEMPHASIS.

preequalization **1.** In sound recording and reproduction, equalization during recording. **2.** See PREEMPHASIS.

preferred values of components A number system used by the Electronics Industries Association (EIA) for establishing the values of composition resistors and small fixed capacitors.

prefix multiplier See MULTIPLIER PREFIX.

prefix notation As used with complex expressions involving many operators and operands, a type of notation in which the expressions, rather than containing brackets, are given a value, according to the relative positions of operators and operands.

preform **1.** A small wafer, usually dry-pressed from powdered plastic, from which the body of a component, such as a capacitor or resistor, is heat-molded. Also called a *pill* or *biscuit.* **2.** The preformed slab used in molding a phonograph disc. **3.** To shape a moldable circuit before fixing the final configuration or package.

preliminary information For manufactured electronic components, data that is released prior to the actual availability of the device. Subject to change when units are produced.

premix A molding compound of reinforced plastic.

prerecorded disc A phonograph disc on which a recording has been made (i.e., a recorded disc).

prerecorded tape Magnetic tape on which a program or data has been recorded. Also called RECORDED TAPE.

p region See P LAYER.

prescaler A device operated ahead of a counter to establish a new, usually higher-frequency, range over which frequency measurements can be made.

preselector A tuned or untuned radio-frequency amplifier operated ahead of a radio or television receiver to boost the sensitivity of the receiver.

presence **1.** In sound reproduction, the quality of being true to life. **2.** The effect of boosted upper-midrange frequencies in music.

preset counter A pulse counter that delivers one output pulse for a number of successive input pulses, determined by the settings of counter-circuit controls. Thus, a preset counter might give an output pulse for each train of 125 input pulses.

5059F-pP-510-565 4/10/01 9:33 AM Page 553

preset element In automation and control, an element that can be preset to a given level or value, and to which other elements can then be referred.

preset switch In the circuit of a PRESET COUNTER, a multiposition rotary switch that can be set to determine the number of input pulses that must be received for the circuit to deliver one output pulse.

preshoot A downward-moving transient pip that sometimes precedes the rise of a pulse.

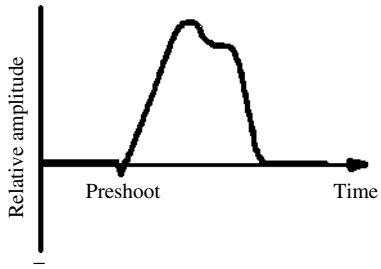

preshoot

preshoot amplitude The peak voltage of a PRESHOOT, measured from the zero line to the valley of the preshoot.

preshoot time The width of a PRESHOOT, measured along the horizontal base line (time axis).

pressing **1.** A process by which phonographic discs are fabricated from plastic. **2.** A disc pressed from plastic.

press-to-talk microphone A microphone that uses a PRESS-TO-TALK SWITCH for actuation.

press-to-talk switch A switch in a microphone or on the end of a control cord. It is used to actuate a transmitter, telephone, or recorder when the operator wishes to speak.

pressure Abbreviation, P or p. **1.** Force per unit area. It can be expressed in any appropriate units of force and area (e.g., newtons per square meter, pounds per square inch, grams per square centimeter, etc.). **2.** The application of force over part or all of a surface. **3.** Compression. **4.** See TENSION, **1**.

pressure amplitude The pressure caused by an acoustic disturbance. It is usually measured in dynes per square centimeter.

pressure capacitor An enclosed fixed or variable capacitor, whose breakdown voltage increases when the air pressure rises inside the container.

pressure contact **1.** Electrical contact made by pressing two conducting surfaces together (to complete a circuit). **2.** A contact for obtaining the condition described in **1**.

pressure-gradient microphone See PRESSURE MICROPHONE.

pressure microphone A microphone that receives sound waves at only one side of its diaphragm. This one-sided exposure results in the displacement of the diaphragm by an amount proportional to the instantaneous pressure of the sound waves.

pressure pad In a tape recorder, a small pad that holds the tape against one of the heads.

pressure pickup See PRESSURE TRANSDUCER.

pressure roller In a tape recorder, a rubber-tired roller that presses the tape against the capstan.

pressure sensor A device that detects the presence of, and/or measures, physical force within a specific area. One simple device uses two metal plates separated by electrically resistive foam. Pressure compresses the foam and reduces the resistance between the plates. This resistance change can be detected and measured.

pressure switch A switch that is opened or closed by a change in pressure within a system.

pressure transducer A sensor for converting pressure into proportionate current or voltage. Some use strain gauges; others use piezoelectric crystals, potentiometers, and other variable elements.

pressure zone A region of high air pressure that is immediately adjacent to a surface reflecting an acoustic (sound) wave.

pressure-zone microphone A microphone equipped with a deflector that helps to guide acoustic energy toward the diaphragm.

prestore To place data in memory before it is intended for use.

pretuned stage A stage, such as one in an intermediate-frequency amplifier or single-frequency receiver, that is preset to a frequency, rather than being continuously tuned.

prf Abbreviation of PULSE REPETITION FREQUENCY.

pri Abbreviation of PRIMARY.

primaries See PRIMARY COLORS.

primary **1.** See PRIMARY WINDING. **2.** See PRIMARY STANDARD.

primary battery A battery composed of primary cells.

primary block A fundamental group of channels in pulse-code modulation, combined by means of time-division multiplexing.

primary capacitance **1.** The distributed capacitance of the primary winding of a transformer whose secondary winding is unloaded. Compare SECONDARY CAPACITANCE, **1**. **2.** A series or shunt capacitance used to tune the primary coil of a radio-frequency transformer. Compare SECONDARY CAPACITANCE, **2**.

primary cell An electrochemical cell that does not require, and generally will not accept, an electrical charge in order to function. Once it has been discharged, the cell must usually be thrown away. Compare STORAGE CELL. Also see CELL, DRY CELL, and STANDARD CELL.

primary circuit **1.** The circuit associated with the primary winding of a transformer. **2.** The circuitry associated with the input to a device or system.

primary coil See PRIMARY WINDING.

5059F-pP-510-565 4/10/01 9:33 AM Page 554

primary colors See COLOR PRIMARY.

primary current The current flowing in the primary winding of a transformer. Also called TRANSFORMER INPUT CURRENT. Compare SECONDARY CURRENT.

primary electron The electron possessing the greater energy after a collision between two electrons. Compare SECONDARY ELECTRON.

primary emission Emission arising directly from a source, such as the cathode of an electron tube. Compare SECONDARY EMISSION.

primary frequency standard A device that generates unmodulated signals at precise frequencies. It generally uses a highly stable crystal oscillator that can be referred to a time standard and periodically corrected. A string of multivibrators, together with harmonic amplifiers and buffers, divide, and multiply the fundamental crystal frequency. The resulting signals provide markers for calibrating receivers and test equipment. Compare SECONDARY FREQUENCY STANDARD. Also see PRIMARY STANDARD.

primary impedance **1.** The impedance of the primary winding of a transformer whose secondary winding is unloaded. Compare SECONDARY IMPEDANCE, **1**. **2.** An external impedance presented to the primary winding of a transformer. Compare SECONDARY IMPEDANCE, **2**.

primary inductance The inductance of the primary winding of a transformer whose secondary winding is unloaded. Compare SECONDARY INDUCTANCE.

primary kVA The kilovolt-amperes in the primary circuit of a transformer. Compare SECONDARY KVA.

primary measuring element A detector, sensor, or transducer that performs the initial conversion in a measurement or control system. Such an element converts a phenomenon into a signal that can be transmitted to appropriate instruments for translation and evaluation.

primary power Power in the primary circuit of a transformer. Also see PRIMARY KVA and PRIMARY VA. Compare SECONDARY POWER.

primary radiator **1.** The driven element of a directive antenna system that incorporates parasitic elements. **2.** The driven element of a directive antenna that uses a reflector, such as a screen or dish.

primary resistance The direct-current resistance of the primary winding of a transformer. Compare SECONDARY RESISTANCE.

primary standard A usually stationary source of a quantity (e.g., capacitance, frequency, time, inductance, resistance, etc.). This source is so precise, and is maintained with such care, that it can be used as a universal reference. Compare SECONDARY STANDARD.

primary turns Symbol, N_p. The number of turns in the primary winding of a transformer. Compare SECONDARY TURNS.

primary utilization factor Abbreviation, UF_p. For a transformer in a rectifier circuit, the ratio of direct-current power output to primary volt-amperes. Numerically, the primary utilization factor is higher than the secondary utilization factor, but is less than 1. Also see SECONDARY UTILIZATION FACTOR and UTILITY FACTOR.

primary VA The volt-amperes in the input circuit of a transformer. Compare SECONDARY VA.

primary voltage The voltage across the primary winding of a transformer. Also called *transformer input voltage*. Compare SECONDARY VOLTAGE.

primary winding The normal or usual input winding of a transformer. Also called *primary coil*. Compare SECONDARY WINDING.

prime meridian See ZERO MERIDIAN.

prime mover A machine, such as a gas engine, steam engine, or water turbine, that converts a natural force or material into mechanical power.

primitive oscillation period In a complex oscillation waveform, the shortest period for which a definite repetition occurs; the highest fundamental frequency.

principal axis The line passing through the center of the spherical part of a lens, mirror, or dish reflector.

principal focus The focal point of rays arriving parallel to the principal axis of a lens, mirror, or dish reflector.

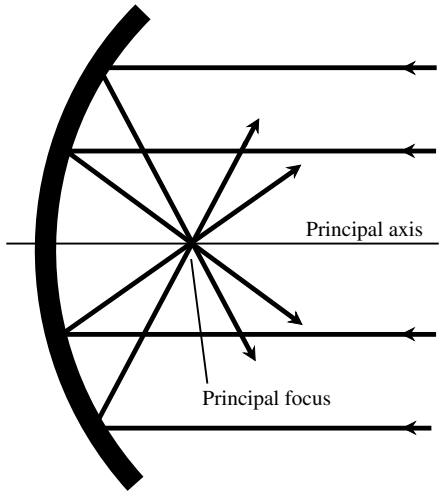

principal focus

principal mode See DOMINANT MODE.

principal ray The path described by an electron entering an electron lens parallel to the lens' axis, or by an electron leaving this lens parallel to the axis.

print **1.** The material transferred from a typewriter onto paper. **2.** The command, in a computer sys-

5059F-pP-510-565 4/10/01 9:33 AM Page 555

tem, that causes data to be placed on paper or onto the output screen. **3.** The alphanumeric output of a computer or data terminal.

printed capacitor A two-plate capacitor formed on a printed circuit.

printed circuit A pattern of conductors (corresponding to the wiring of an electronic circuit) formed on a board of insulating material, such as a phenolic, by photo-etching, silk-screening of metallic paint, or by the use of pressure-sensitive preforms. The leads or pins of discrete components are soldered to the printed metal lines at the proper places in the circuit, or the components can be formed along with the conductors. Also see ETCHED CIRCUIT.

printed-circuit board A usually copper-clad plastic board used to make a printed circuit.

printed-circuit lamp A baseless lamp having flexible leads for easy soldering or welding to a printed circuit.

printed-circuit relay A usually small relay provided with pins or lugs for easy solder connection to a printed circuit.

printed-circuit switch A rotary switch whose contacts and contact leads are printed on a substrate.

printed-circuit template Also called *etching pattern.* A drawing for the purpose of making printed-circuit boards by photographic means.

printed coil A flat, spiral coil formed on a printed circuit.

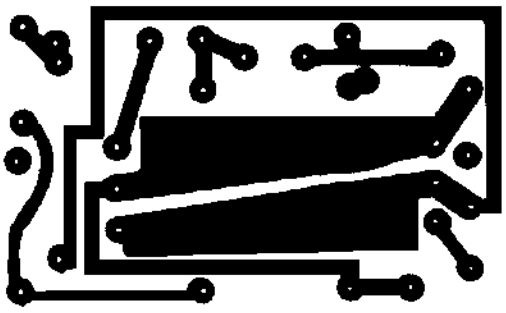

printed-circuit template

printed component A component formed on the substrate of a printed circuit. See, for example, PRINTED CAPACITOR, PRINTED COIL, and PRINTED RESISTOR.

printed display See DATA PRINTOUT, **2**.

printed element See PRINTED COMPONENT.

printed inductor See PRINTED COIL.

printed resistor A resistor printed or painted on a printed circuit.

printed wiring The printed or etched metal lines that serve as the conductors in a printed circuit.

printer In computer and calculator operations and in measurement procedures, a readout device that prints a permanent record of output data. There are several types, including the *dot-matrix printer*, the *daisy-wheel printer*, the *inkjet printer*, and the *laser printer.* Some printers, such as the daisy-wheel type, can render only text data; others, such as the laser type, can print high-resolution graphic images, sometimes in color.

printing calculator **1.** An electronic calculator that supplies a printed record of the results of a calculation. **2.** For a programmable calculator, the results, a record of program steps, and plots of curves.

printing digital voltmeter Abbreviation, PDVM. A digital voltmeter that delivers a printed record of a voltage reading, in addition to the usual digital readout of the voltage.

printing telegraph **1.** A telegraph that prints the received message on a tape or page. **2.** See TELETYPEWRITER.

printing wheel See PRINT WHEEL.

print format The form of data transmitted by a computer program to a printer (e.g., plain text, graphics, color graphics, etc.).

printout See DATA PRINTOUT, **1**, **2**.

print-through In prerecorded magnetic tape on a reel or cassette, the transfer of magnetism between layers of the rolled-up tape.

print wheel In a daisy-wheel printer, the rotatable wheel on whose rim the letters, numbers, and other symbols are inscribed in relief.

priority indicator In data transmission, a code that specifies the order of importance of a message in a group of messages to be sent.

priority processing In multiple programming operations, a system for ascertaining the order of processing for different programs.

privacy code **1.** A subaudible tone used in cordless telephone systems to reduce the chances of interference between phones operating on the same channel in close proximity. **2.** A subaudible tone used in radio transmissions, especially in conjunction with repeaters, to allow only those stations with the proper code to be received. **3.** A tone-burst sequence at the beginning of a transmission that actuates a receiver, allowing only those stations with the proper code to be received.

privacy equipment Devices, such as speech scramblers and digital encryption programs, that provide some measure of secrecy in communications.

privacy switch In a telephone amplifier, a switch (usually a pushbutton) for muting outgoing messages.

private automatic exchange Abbreviation, PAX. A dial telephone system for use within an organization and having no connection to the central office. Compare PRIVATE BRANCH EXCHANGE.

private branch exchange Abbreviation, PBX. A telephone system, complete with a private manually operated switchboard and individual telephone sets, installed and operated on private

5059F-pP-510-565 4/10/01 9:33 AM Page 556

premises but having trunk-line connection to the central office. Compare PRIVATE AUTOMATIC EXCHANGE.

private line **1.** A communication circuit in which the use is limited, by electronic means, to certain subscribers. **2.** A subaudible-tone system used to restrict access to a communications system. The tone frequency is predetermined. For access to the system, a transmitted signal must contain the tone of the appropriate subaudible frequency, in addition to the voice or other information.

probability **1.** The branch of mathematics concerned with the likelihood of an event's occurrence. It has many applications in quality control and physics. **2.** The mathematical likelihood that an event will occur.

probable error Abbreviation, PE. The value of error above and below which all other error values are equally likely to occur.

probe **1.** A usually slender pencil-like implement with a pointed metal tip and a flexible, insulated lead. It is used to contact live points in a circuit under test (e.g., *voltmeter probe* and *oscilloscope probe*). **2.** A device used to sample a radio-frequency voltage or current at a desired point (e.g., WAVEGUIDE PROBE). **3.** A pickup device shaped like a probe for insertion into close quarters (e.g., PROBE THERMISTOR).

probe meter See PROBE-TYPE VOLTMETER.

probe thermistor A thermistor of slender construction for insertion into an area in which the temperature is to be monitored or controlled.

probe thermocouple A thermocouple in the form of a slender probe for insertion into close quarters for temperature sensing or temperature control.

probe tip See PROD.

probe-type voltmeter A voltmeter installed in a long probe or wand. Kilovoltmeters are sometimes constructed in this fashion, with a long multiplier resistor housed in the probe.

probing A process for locating, or determining the existence of, external artificial interference (e.g., power-line noise) in a radio communications circuit.

problem-oriented language Any high-level computer programming language that allows the user to write programs as statements in terms applicable to the field of interest (e.g., COBOL's statements in English for problems relating to business).

problem reduction In artificial intelligence, a process in which problems are made easier by breaking them down into smaller logical parts.

process control The control of a process, such as one of manufacturing, by means of computers.

processor **1.** A circuit or device used to modify a signal in response to certain requirements (e.g., *clipper* and *waveshaper*). **2.** See DATA-PROCESSING MACHINE. **3.** See CENTRAL PROCESSING UNIT. **4.** See MICROPROCESSOR.

prod The metal tip of a probe (see PROBE, **1**).

product **1.** The result of mixing or heterodyning of two or more signals. **2.** The result of modulating one signal with another. **3.** The result of combining or processing a signal or signals in a specified manner. **4.** The saleable end result of a manufacturing process. **5.** The result obtained when two or more quantities are multiplied by each other.

product detector A detector circuit whose output is the product of two signals applied simultaneously to the circuit. In a single-sideband receiver, for example, one of the signals is the incoming signal; the other, the signal from the local beat-frequency oscillator.

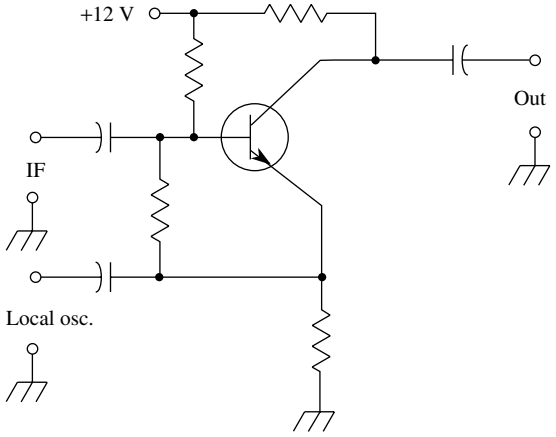

product detector

production lot A manufactured set of components, circuits, or systems, intended for sale. All of the units in the lot are identical. The finished product is suitable (presumably) for consumer use.

production unit One unit in a production lot; a finished unit, ready for use by a consumer.

product modulator A modulator whose output is equal or proportional to the product of carrier voltage and modulating voltage.

product of sine waves The result of multiplying one sine wave by another with attention being paid to the power factor. In the case of a resistive circuit, where the power factor is equal to 1, all voltage-current (*EI*) products are positive, and are equal to the true power. A product wave has negative half-cycles when the circuit contains reactance.

professional engineer A person licensed by a state board of examiners to work independently as an engineering. Also see PE and REGISTERED PROFESSIONAL ENGINEER.

program **1.** In computer operations, a detailed sequence of instructions representing an algorithm

5059F-pP-510-565 4/10/01 9:33 AM Page 557

(the necessary steps in solving a problem) that can be implemented by a computer. **2.** The content of a radio or television broadcast during a specified period of time. **3.** In audio recording, the composite output from the mixer, used to make the master tape or disc.

program address counter See INSTRUCTION REGISTER.

program amplifier A broadcast preamplifier used at the studio or a remote location.

programatics The study of computer programming.

program circuit In wire telephony, a circuit capable of handling music and other audio data that covers a wide band of frequencies.

program compatibility The condition in which a program written for one computer can be used with another computer having a different architecture.

program controller In a central processor, a unit that controls the sequence and execution of program instructions.

program counter See CONTROL REGISTER.

program file A flexible reference system for software library maintenance.

program flowchart A representation of a computer program in the form of a flowchart. Each function and transition point is indicated by a box in the chart. A user can follow the flowchart and determine the outcome of the program for any given set of input parameters.

program library A collection of computer or programmable-calculator programs. Usually, it means the collection of programs used in a given computer system, often a software package supplied by the hardware vendor. It might also be a catalog of programs with instructions for their use.

programmable calculator A calculator that can be programmed to perform a chain of operations in a given order repetitively.

programmable read-only memory In a computer, a read-only memory (ROM) that can store a program.

program maintenance The ongoing correcting, updating, and modification of computer programs belonging to a system.

programmed dump A dump that occurs during a program run, according to a program instruction.

programmed halt During a computer program run, a temporary cessation resulting from an interrupt or halt instruction.

programmed instruction See MACRO INSTRUCTION.

programmed timer See CYCLE TIMER.

programmer A person who writes computer programs.

program modification **1.** In computer programming operations, a change in the effect of instructions and addresses during a program run by performing arithmetic and logical operations on them. **2.** Rewriting, or adding a patch to, a computer program. Also see PATCH, **3**.

program register See CONTROL REGISTER.

program segment A unit within a computer program that is stored with others in memory at the time of the program's execution, or sometimes, as overlays loaded individually when the entire program exceeds memory capacity.

program specification A description of the steps involved in the solution of a problem, from which a programmer devises a computer program.

program step An instruction in a computer program.

program tape In computer operations, a magnetic or paper tape that contains programs for a system or application.

program timer **1.** A programmed timer (see CYCLE TIMER). **2.** A timing unit that controls the duration of a program.

progressive scanning Non-interlaced television raster scanning, in which the lines are traced from top to bottom in succession. Conventional television broadcasting uses INTERLACED SCANNING.

progressive wave A wave disturbance that travels through a theoretically perfect homogeneous medium. This can be a compression (longitudinal) wave, a transverse wave, or an electromagnetic wave.

projected cutoff For an amplifier circuit, the operating point at which crossover distortion vanishes. The direct-current bias voltage (grid or gate) required for projected cutoff is somewhat lower than the value corresponding to conventional cutoff of plate or drain current.

project engineering A field of engineering dealing with the coordination of a complete project.

projection television Large-screen television for viewing by a relatively large group, usually accomplished via a projection tube and optical system.

projection tube A cathode-ray tube, especially a television picture tube, capable of producing a bright image that can be projected onto a large screen by means of a lens system.

projector **1.** A device that transmits a visible image onto a surface for reproduction. **2.** In general, any device that transmits a signal into space.

PROLOG Acronym for *programming in logic.* A high-level computer programming language, similar to LISP, used in artificial intelligence. The operator inputs facts and rules; the computer, in effect, derives theorems from the facts by following the logical rules.

PROM Abbreviation of PROGRAMMABLE READ-ONLY MEMORY.

promethium Symbol, Pm. A metallic element of the rare-earth group, produced artificially. Atomic number, 61. Atomic weight, approximately 145. Formerly called *illinium.*

promethium cell A radioactive battery cell using an isotope of promethium. Radioactive particles from this substance strike a phosphor, causing it

5059F-pP-510-565 4/10/01 9:33 AM Page 558

to glow. Self-generating photocells then convert this light into electricity.

PROM programmer An electronic device that can store a computer program in a PROGRAMMABLE READ-ONLY MEMORY (PROM). It uses a built-in keyboard.

prompt In computer operations, a message received by an operator from an operating system or an individual program. For example, in disk operating system (DOS), it could be the statement "Bad command or file name."

prompting In computer or programmed-calculator operations, the entry of a special, required variable when the machine halts and awaits such entry.

prong See PIN.

prony brake An arrangement for measuring the mechanical power output of a rotating machine. It is a special form of friction brake consisting of a band passed around a pulley on the rotating shaft of the machine under test and held at each end by a spring balance.

propagation 1. The extension of energy into and through space. Thus, radiant energy is *propagated* from and by its source. **2.** A phenomenon resulting from the extension of energy into and through space. Thus, radio waves can be spoken of as a *propagation.*

propagation constant For waves transmitted along a line, a number showing the effect the line has on the wave. This is a complex figure [i.e., one containing a real-number component (the attenuation constant) and an imaginary-number component (the phase constant)].

propagation delay 1. Symbol, t_{pd}. In an integrated-circuit logic gate, the time taken for a logic signal to be propagated across the gate. **2.** In digital-circuit operation, the time required for a logic-level change to be transmitted through one or more elements.

propagation delay-power product See DELAY-POWER PRODUCT.

propagation factor The ratio E/E_o, where E is the complex electric-field strength at a point to which a wave has been propagated, and E_o is the complex electric-field strength at the point of origin. Also called *propagation ratio.*

propagation loss The path loss of an electromagnetic disturbance between the transmitting and receiving antennas.

propagation mode See WAVEGUIDE MODE.

propagation ratio See PROPAGATION FACTOR.

propagation time In digital-circuit operation, the time required for a binary bit to be transferred from one point to another in the system.

propagation velocity See VELOCITY OF PROPAGATION.

proportional action An action, such as amplification or conversion, that produces an output signal proportional to the input signal.

proportional amplifier An amplifier in which the instantaneous output amplitude is proportional to the instantaneous input amplitude.

proportional control A voltage-regulation system in which the feedback correction voltage is proportional to the output-voltage error.

proportional counter A Geiger tube having a pointed-wire (or ball-tipped-wire) anode. The voltage developed across the load resistor is proportional to the number of ions created by the radioactive particles entering the tube.

proprioceptor A set of transducers and associated circuitry that allows a computerized robot to constantly sense the positions of its end effectors, and use this data in carrying out programmed tasks.

prosodic features Variations in voice tone and emphasis that lend meaning and implication to spoken statements. It is important in advanced computer speech recognition and speech synthesis systems. Two sentences with identical wording can have greatly different meanings, depending on these factors (e.g., "*You* are!" versus "You *are?*").

prosthesis An electromechanical artificial human limb or body part. Examples: artificial legs, artificial hands, and artificial respirators. Some such devices are computer-controlled; others can be manipulated by nerve impulses.

protactinium Symbol, Pa. A relatively short-lived radioactive metallic element. Atomic number, 91. Atomic weight, 231.04 Formerly called *protoactinium.*

protected area A region to which access is restricted, and that is secured by an alarm system, surveillance cameras, or other intrusion-prevention systems.

protected location In computer storage, a location whose contents are protected from mutilation or erasure by making the location usable only by following a special procedure (e.g., using a password).

protection In a multiple processing computer system, preventing interference between data or programs.

protective bias In the final power amplifier of a radio transmitter, external direct-current bias applied to the base, gate, or grid. Prevents runaway in collector, drain, or plate current when the bias caused by the driving signal is lost.

protective capacitor A power-line bypass capacitor.

protective device 1. A component that breaks a circuit in the event of excessive voltage or current from the power supply. **2.** A device that prevents excessive power from being delivered to a load by a driving circuit.

protective gap 1. A spark gap connected in parallel with a component, or between a line and ground as protection against high-voltage transients and surges. **2.** A spark-gap-type lightning arrester.

5059F-pP-510-565 4/10/01 9:33 AM Page 559

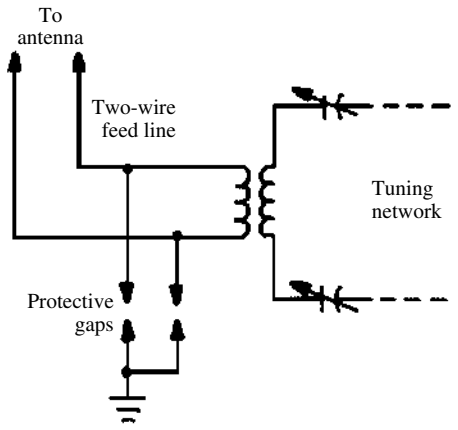

protective gap

protective resistor **1.** A bleeder resistor connected in parallel with a filter capacitor in a high-voltage direct-current power supply to discharge the capacitor automatically, thus preventing electric shock. **2.** A series resistor that limits the current going through a device.

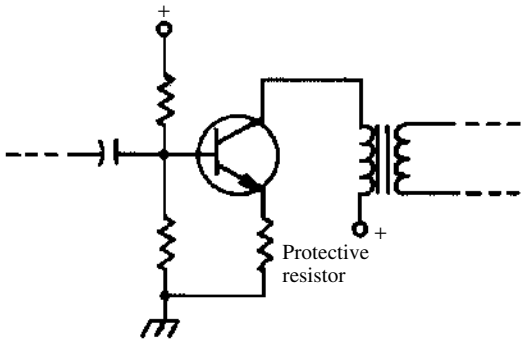

protective resistor, 2.

protector **1.** A fast-acting power-disconnect device, such as a circuit breaker or fuse, that acts to protect electronic equipment. **2.** A device or connection, such as a safety ground or ground-fault interrupter, that protects an operator from electric shock. **3.** See CONTACT PROTECTOR.

protium The light isotope of hydrogen, having an atomic mass of 1.

protoactinium See PROTACTINIUM.

protocol **1.** A set of parameters for a digital communications signal. **2.** The method by which a procedure is followed; a uniform set of governing regulations. It ensures proper operation of a system or network.

proton A positively charged particle in the nucleus of an atom. The mass of a proton is approximately 1840 times the mass of an electron.

proton rest mass See MASS OF PROTON AT REST.

proton-synchrotron A synchrotron that uses frequency modulation of the radio-frequency accelerating voltage. It can accelerate protons to energies of several billion electronvolts.

prototype The preliminary design or model of a device or system. It is often modified numerous times before the final design is attained. Compare PILOT MODEL.

proustite Crystalline silver arsenide trisulfide. Artificial crystals of this compound are used in tunable infrared-ray instruments.

proximity alarm A capacitance relay used to actuate an alerting-signal device when an area is intruded upon or a person is too close to a protected object. Also called INTRUSION ALARM.

proximity detector See PROXIMITY SENSOR.

proximity effect **1.** The influence of high-frequency current flowing in one conductor on the distribution of current flowing in an adjacent conductor. **2.** In an audio system, the result of placing a microphone too close to a person's mouth. Under these conditions, some spoken consonants (e.g., B, F, P, and T) produce clapping or booming sounds.

proximity fuse An electronic device situated in the nose of a missile. When the missile is near the target, the fuse transmits a signal that is reflected back from the target; this reflected signal detonates the missile.

proximity relay See CAPACITANCE RELAY.

proximity sensing The ability of a machine, especially a robot, to detect when an object is near. This is an aid in robot navigation because it prevents collisions. Some devices can measure the distance from a robot, or from a robotic end effector, to a nearby object.

proximity sensor A device that indicates the presence of a nearby body. Such a device uses some form of circuit, such as that of a CAPACITANCE RELAY, that changes its operating characteristics when an object enters its field.

proximity switch See CAPACITANCE RELAY.

PRR Abbreviation of PULSE REPETITION RATE.

PRV Abbreviation of PEAK REVERSE VOLTAGE.

PS Abbreviation of POWER SUPPLY.

ps Abbreviation of PICOSECOND. (Also, psec.)

PSD Abbreviation of PHASE-SENSITIVE DETECTOR.

psec Abbreviation of PICOSECOND. (Also, ps.)

pseudocode In a computer system, an instruction or code symbol that affects the operation of the programming in an indirect manner.

pseudo-instruction In computer programming operations, data representing an instruction and requiring translation by a compiler or assembler.

5059F-pP-510-565 4/10/01 9:33 AM Page 560

pseudo-offlining During input/output operations in a computer system, maximizing hardware by disconnecting slow devices from the process in question.

pseudo-operation In computer operations, an operation that, rather than being performed by hardware, is carried out by special software or by macroinstruction.

pseudo-random numbers Numbers that, although produced by a computer operating on an algorithm for their generation, are useful for an application requiring random numbers.

pseudo-stereophonic effect A somewhat heightened binaural effect obtained when two loudspeakers are situated, relative to the listener, so that a transit-time difference of 1 to 30 milliseconds results.

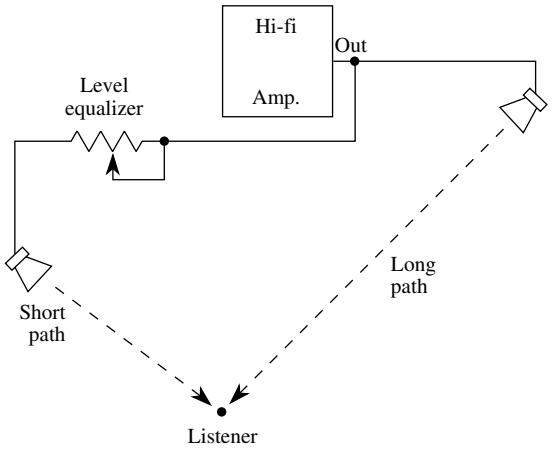

pseudo-stereophonic effect

psf Abbreviation of *pounds per square foot.* (Also, lb per sq ft, lb/ft^2.)

psi **1.** Abbreviation of *pounds per square inch.* (Also, lb per sq in, lb/in^2.)

psia Abbreviation of POUNDS PER SQUARE INCH ABSOLUTE.

psig Abbreviation of POUNDS PER SQUARE INCH GAUGE.

psi particle A massive elementary particle that represents a resonance in an electron-positron interaction.

PSK Abbreviation of PHASE-SHIFT KEYING.

PSM Abbreviation of *pulse-spacing modulation,* more commonly called PULSE-INTERVAL MODULATION.

psophometer A device used to measure noise in a wire communications system. It provides quantitative readings based on typical human observations.

psvm Abbreviation of *phase-sensitive voltmeter.*

PSWR Abbreviation of *power standing-wave ratio.*

psychoacoustics A field of acoustics, overlapping with psychology, concerned with the effects of sounds on human beings.

PT Abbreviation of *Pacific Time.*

Pt Symbol for PLATINUM.

PTC Abbreviation of POSITIVE TEMPERATURE COEFFICIENT.

PtIr Symbol for PLATINIRIDIUM.

PTM Abbreviation of PULSE-TIME MODULATION.

PTO Abbreviation of PERMEABILITY-TUNED OSCILLATOR.

PTT Abbreviation for *press-to-talk.* See PRESS-TO-TALK MICROPHONE; PRESS-TO-TALK SWITCH.

PTV Abbreviation of *public television.*

p-type conduction In a semiconductor, current flow consisting of the movement of holes. Compare N-TYPE CONDUCTION.

p-type material Semiconductor material that has been doped with an acceptor-type impurity and, consequently, conducts current mainly via hole migration. Germanium, for example, when doped with indium, becomes p-type. Compare N-TYPE MATERIAL.

p-type semiconductor An acceptor-type semiconductor (i.e., one containing an excess of holes in its crystal lattice).

PU Abbreviation of PICKUP.

Pu Symbol for PLUTONIUM.

public-address amplifier A high-gain, high-power audio amplifier designed especially for the reproduction of speech and music at large gatherings.

public-address system A system of sound reproduction especially designed for use at large gatherings indoors or outdoors. The system includes microphones, a public-address amplifier, loudspeakers, and sometimes recorders and playback devices. Also called *PA system.*

puck drive In a tape recorder, a speed-reduction system for driving the flywheel from the shaft of the (high-speed) motor. In some machines, a rubber tire mounted on the flywheel is driven, through friction, by the motor shaft. In others, an intermediate rubber-tired wheel is placed between the motor shaft and the rim of the flywheel.

puffer A meter or bridge for measuring small values of capacitance. The name comes from the spoken sound of *pF,* the abbreviation of PICOFARAD.

pulldown Descriptive of a circuit, device, or individual component used to lower the value (e.g., impedance) of a circuit to which it is connected.

pull-in current The current required to close a relay.

pulling **1.** The abnormal tendency of one circuit to cause another to slip into tune with it. This often results from coupling (intended or accidental) that is too tight. Thus, when two oscillators feed a common circuit, such as a mixer, one might pull the other into tune with itself. **2.** Lowering of a crystal frequency by an external reactance.

5059F-pP-510-565 4/10/01 9:33 AM Page 561

pull-in voltage The voltage required to close a relay.

pull switch A mechanical switch actuated by a pulling action.

pullup Descriptive of a circuit or component used to raise the value (e.g., impedance) of a circuit to which it is connected.

pulsar An extremely dense, rapidly rotating collapsed star that produces radio signals at regular intervals. The pulse frequency varies from less than one hertz to several tens or hundreds of hertz.

pulsating direct current A direct current that periodically rises and falls between zero and a maximum value (or between two positive or negative values) without changing polarity. Thus, it is possible to have either a pulsating positive current or a pulsating negative current. Also see DIRECT CURRENT.

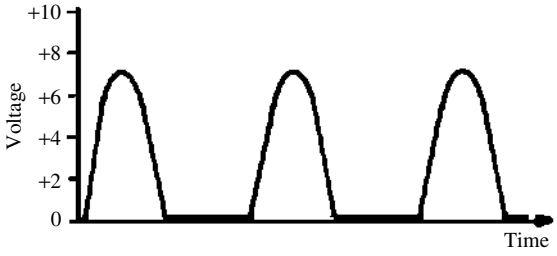

pulsating direct current

pulsating wave See PULSATING DIRECT CURRENT.

pulse A transient signal that is usually of short duration, constant amplitude, and one polarity. A typical example is a narrow positive or negative spike.

pulse amplifier An amplifier having wide frequency response and low distortion, used for amplifying steep-sided pulses of short duration.

pulse-amplitude modulation Abbreviation, PAM. A method of conveying information in wireless communications. A train of pulses is transmitted. The strength of each individual pulse varies according to the modulating waveform. Normally, the pulse amplitude increases as the instantaneous modulating-signal level increases (positive modulation). However, this can be reversed so that higher audio levels cause the pulse amplitude to go down (negative modulation).

pulse bandwidth For an amplitude pulse, the minimum bandwidth occupied. The faster the rise and/or decay times of a pulse, the greater the bandwidth. The greater the pulse frequency, the greater the bandwidth.

pulse code A code in which groups of pulses represent digits.

pulse-code modulation Abbreviation, PCM. A method of conveying information in wireless communications. A train of pulses is transmitted. The intelligence-carrying signal is sampled periodically and the amplitude is converted into binary code. The code might allow for eight levels (000 to 111), 16 levels (0000 to 1111), 32 levels (00000 to 11111), or 64 levels (000000 to 111111).

pulse-code-modulation binary code A pulse code used in communications not in the form of line transmission. Individual values are denoted by binary numbers.

pulse-code modulation multiplex equipment A multiplexer/demultiplexer for signal conversion between a single signal and multiple-channel signals. It uses both pulse-code modulation and time-division multiplexing.

pulse-count divider A circuit or device that receives an input of a certain number of pulses (or pulses per second) and delivers an output that is a function of that quantity. See, for example, DIVIDE-BY-SEVEN CIRCUIT and DIVIDE-BY-TWO CIRCUIT.

pulse counter A circuit or device that indicates the number of pulses presented to it in a given time interval.

pulse counting Counting pulses in a sequence. At low speed (pulse repetition rate), this can be done with an electromechanical dial-type counter. At high speed, a fully electronic circuit is required.

pulse delay circuit A monostable multivibrator adapted to deliver its single output pulse a predetermined time after the input pulse has been applied.

pulse dialing A form of telephone dialing in which each digit is formed by a series of pulses, usually at 10 to 20 Hz. The pulses are the equivalent of disconnecting the line for a few milliseconds. Each digit has the corresponding number of pulses, except digit 0, which is formed by 10 pulses.

pulse droop Distortion observable as a downward-sloping top on the oscilloscope trace of a pulse. It can be quantified in volts, millivolts, microvolts, amperes, milliamperes, or microamperes.

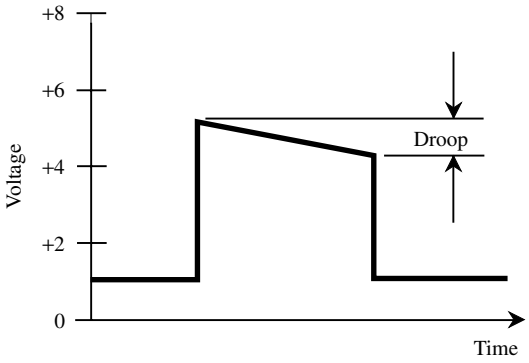

pulse droop

5059F-pP-510-565 4/10/01 9:33 AM Page 562

pulsed laser A laser in which flashes (pulses) of high-intensity light excite the lasing medium.

pulse duration The time period during which a pulse exists (i.e., its width on an oscilloscope display).

pulse-duration modulation Abbreviation, PDM. See PULSE WIDTH MODULATION.

pulse equalizer A MONOSTABLE MULTIVIBRATOR adapted to deliver pulses of equal amplitude, shape, and width—even when it receives trigger pulses of different kinds.

pulse fall time The time required for the trailing edge of a pulse to fall from 90 to 10 percent of its peak amplitude. Compare PULSE RISE TIME.

pulse-forming line A circuit used in radar for producing high-intensity pulses. Inductances and capacitances are combined in a long string, and the effect is to generate high-amplitude radio-frequency pulses.

pulse-frequency modulation Abbreviation, PFM. See PULSE-INTERVAL MODULATION.

pulse generator A signal generator that produces pulses. A general-purpose generator of this sort will produce pulses of adjustable amplitude, duration, shape, and repetition rate.

pulse-height discriminator A circuit or device that passes only pulses whose amplitudes exceed a predetermined level.

pulse interval The interval between successive pulses.

pulse-interval modulation Abbreviation, PIM. Also called *pulse-frequency modulation* (PFM) or *pulse-numbers modulation* (PNM). A method of conveying information in wireless communications. A train of pulses is transmitted. Every pulse has the same amplitude and the same duration, but their rate fluctuates with the modulating waveform. When there is no modulation, the pulses are evenly spaced with respect to time. An increase in the instantaneous data amplitude might cause pulses to be sent more often (positive modulation) or less often (negative modulation).

pulse inverter A single-stage, wideband, low-distortion, common-emitter, or common-source amplifier. The output-pulse waveforms are therefore inverted, with respect to the input-pulse waveforms.

pulse jitter In a pulse train, a disturbance characterized by random changes in the spacing between pulses.

pulse-length modulation See PULSE-DURATION MODULATION.

pulse load The load impedance for a pulse generator.

pulse mode See PULSE MODULATION.

pulse modulation See PULSE-AMPLITUDE MODULATION, PULSE-CODE MODULATION, PULSE-INTERVAL MODULATION, PULSE-POSITION MODULATION, PULSE-WIDTH MODULATION.

pulse modulator **1.** A modulator that delivers power or voltage pulses for modulating a carrier. **2.** A device that modulates pulses (see PULSE MODULATION, **2**).

pulse narrower A circuit or device that reduces the duration (width) of a pulse.

pulse-numbers modulation Abbreviation, PNM. See PULSE-INTERVAL MODULATION.

pulse operation Intermittent operation of a circuit, in the form of discrete pulses.

pulse oscillator Any oscillator with an output that consists of a series of pulses.

pulse-position modulation Abbreviation, PPM. A method of conveying information in wireless communications. A train of pulses is transmitted. The timing of each individual pulse varies according to the modulating waveform. The pulses occur earlier or later than the nominal (zero-modulation) time, depending on the instantaneous amplitude of the modulating signal.

pulse rate See PULSE REPETITION RATE.

pulse ratio The ratio of pulse height (amplitude) to pulse width (duration).

pulse regeneration Restoration of the original waveform and frequency to a pulse. It eliminates distortion caused by circuits or propagation conditions.

pulse repetition frequency Abbreviation, PRF. See PULSE-REPETITION RATE.

pulse-repetition rate Abbreviation, PRR. The number of pulses per unit time; usually pulses per second (pps).

pulse rise time The time required for the leading edge of a pulse to rise from 10 to 90 percent of its maximum amplitude. Compare PULSE FALL TIME.

pulse scaler A circuit actuated by the reception of a definite, predetermined number of input pulses.

pulse-shaping circuit **1.** A circuit for producing a pulse from a wave of some other shape (e.g., sine wave). **2.** A circuit for tailoring a pulse to desired shape, amplitude, and duration.

pulse spacing The interval between successive pulses.

pulse-spacing modulation Abbreviation, PSM. See PULSE-INTERVAL MODULATION.

pulse-steering diode In a flip-flop circuit, a diode through which the trigger pulse must pass to switch the circuit. Because of the unidirectional conductivity of a diode, pulses of only one polarity are passed.

pulse stretcher **1.** A shaping circuit that widens a pulse (i.e., increases its duration). **2.** A circuit, such as a special monostable multivibrator, that generates a pulse that is wider than the trigger pulse.

pulse stuffing See JUSTIFICATION, **2**.

pulse tilt The sloping of the normally flat top of a pulse either up or down. Also see PULSE DROOP.

pulse time See PULSE DURATION.

pulse-time modulation See PULSE-POSITION MODULATION.

5059F-pP-510-565 4/10/01 9:33 AM Page 563

pulse train A series of successive pulses of usually one kind.

pulse transformer A transformer designed to accommodate the fast rise and fall times of pulses and similar nonsinusoidal waveforms. Such transformers often use special core materials and are made using special winding techniques.

pulse transmitter **1.** A device that transmits a series of pulses. **2.** A pulse-modulated transmitter. **3.** See PULSE MODULATOR.

pulse waveform The general shape of a pulse as it appears on an oscilloscope display. The various forms range from positive or negative half-sinusoids, through rectangles, to thin-line spikes.

pulse width The horizontal dimension of a pulse (i.e., its duration).

pulse-width modulation Abbreviation, PWM. Also called *pulse-duration modulation* (PDM). A method of conveying information in wireless communications. A train of pulses is transmitted. The width (duration) of each individual pulse varies according to the modulating waveform. Normally, the pulse width increases as the instantaneous modulating-signal level increases (positive modulation). However, this can be reversed so that higher audio levels cause the pulse width to decrease (negative modulation).

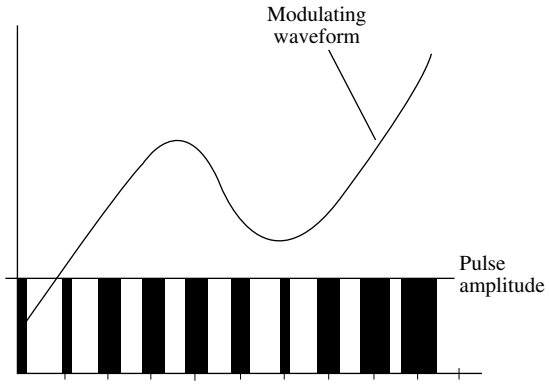

pulse-width modulation

pump **1.** In a parametric amplifier, the oscillator that supplies the signal that periodically varies the reactance of the varactor. **2.** The pumping signal in **1**. **3.** To perform the operation (pumping) described in **1**. **4.** To increase the energy level of an atom or molecule (by exposing it to electromagnetic radiation) to such an extent that oscillation or amplification occurs. A ruby laser, for example, produces its intense, coherent beam as a result of pumping. **5.** The radiation used to pump an atom or molecule. **6.** The device producing the radiation required to pump an atom or molecule.

pump frequency The frequency of a PUMP voltage.

pumping A method of laser actuation. A series of pulses, at the resonant frequency of the lasing material, is injected to cause laser output.

pump oscillator An oscillator for producing a pump voltage.

pump voltage The voltage of a pumping signal. Also see PARAMETRIC AMPLIFIER and PUMP, **1**, **2**.

punch **1.** A tool for cutting holes in metal chassis, panels, and boxes for electronic equipment. **2.** High signal strength.

punch-in editing In audio recording, a feature that allows convenient insertion of new material on a tape. The tape recorder can be switched instantly from Play to Record, and back again, whenever the operator wants to add material.

punchthrough In a bipolar transistor, the potentially damaging condition resulting when the reverse bias of the collector is increased to a voltage high enough to spread the depletion layer entirely through the base. This tends to effectively connect the emitter to the collector.

punchthrough region The conduction region associated with higher-than-punchthrough voltage, in which bipolar-transistor current is excessive. Also see PUNCHTHROUGH.

punchthrough voltage The voltage that causes PUNCHTHROUGH in a given bipolar transistor.

puncture voltage See BREAKDOWN VOLTAGE, **1**.

Pupin coil One of several loading coils that can be inserted at intervals in series with a telephone line to cancel line-capacitance effects and, thus, improve the clarity of speech.

pure tone An audio-frequency (AF) tone having essentially no harmonic content; a sine-wave AF tone.

pure wave A wave containing no distortion products.

purging The removal of an undesired gas or other substance from a system by introducing a material to displace it.

purifier A power-line operated alternating-current electromagnet that can be manually rotated in front of a color-television picture tube to demagnetize the tube. Also called a DEGAUSSER.

purity **1.** In color television, complete saturation of a hue. **2.** In a waveform, complete freedom from distortion. **3.** The extent to which spurious signals are attenuated in the output of a radio or television transmitter. Also called *spectral purity*.

purity adjustment In a color-television picture tube, adjustment of each purity control for pure color.

purity coil A variable-current coil around the neck of a color-television picture tube that is used to adjust color purity.

purity control For a purity coil, the variable resistor that controls the current for color correction.

5059F-pP-510-565 4/10/01 9:33 AM Page 564

purity magnet A ring-magnet collar around the neck of a color-television picture tube to adjust, by rotation, color purity.

purple plague Corrosion that occurs when aluminum and gold are placed in contact.

pushbutton tuner A radio or television tuner utilizing pushbutton tuning.

pushbutton tuning The tuning of a circuit to various frequencies in single steps by means of pushbutton switches.

pushdown list In data processing, a method of amending a list. A new item entered at the top moves each existing item one position down.

pushdown stack Also called *first-in/last-out.* A digital read-write memory in which data bits emerge in reverse sequence from the order they go in. If data bit *x* enters the pushdown stack before data bit *y*, then *x* will come out after *y*. Compare FIRST-IN/FIRST-OUT.

push-in terminal A circuit contact or tie point, usually of thin, springy material, that can be inserted into a hole in a perforated board.

push-pull Pertaining to a circuit in which two active devices are used, with the inputs and outputs both placed in phase opposition. In the output circuit, even harmonics are canceled, and odd harmonics are reinforced.

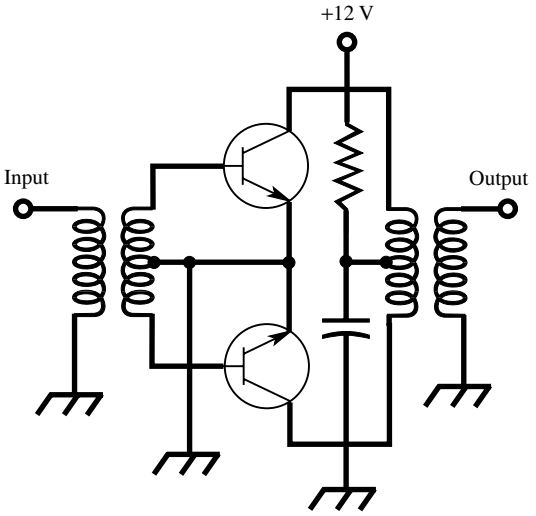

push-pull

push-pull amplifier An amplifier stage in which, for increased power output, two active devices are operated 180 degrees out of phase with each other in opposite halves of a symmetrical circuit. Also see PUSH-PULL CIRCUIT.

push-pull circuit A symmetrical circuit in which two active devices operate on separate halves of the input-signal cycle and deliver a combined output signal.

push-pull deflection In an oscilloscope, the application of deflection voltage to a pair of deflecting plates 180 degrees out of phase with each other. For this purpose, the output amplifier in the horizontal or vertical deflection channel is a push-pull stage.

push-pull doubler See PUSH-PULL MULTIPLIER.

push-pull microphone A set of two microphones, in which the audio-frequency outputs are in phase opposition.

push-pull multiplier A push-pull amplifier with its output circuit tuned to an odd-numbered multiple of the input frequency. This circuit is unsuitable for even-harmonic operation, but has some merit as an odd-harmonic multiplier (e.g., a *tripler* or *quintupler*). Also see PUSH-PUSH MULTIPLIER.

push-pull oscillator An oscillator stage in which, for increased power output, two active devices are operated 180 degrees out of phase with each other in opposite halves of a symmetrical circuit. Also see PUSH-PULL CIRCUIT.

push-pull/parallel amplifier An amplifier stage in which tubes or transistors are connected in push-pull/parallel for increased power output. Also see PARALLEL-COMPONENT AMPLIFIER, PUSH-PULL AMPLIFIER, and PUSH-PULL/PARALLEL CIRCUIT.

push-pull/parallel circuit A push-pull circuit in which two or more active devices are connected in parallel on each side of the circuit. This arrangement gives increased power output over that of the conventional push-pull circuit. See, for example, PUSH-PULL/PARALLEL AMPLIFIER and PUSH-PULL/PARALLEL OSCILLATOR.

push-pull/parallel oscillator An oscillator stage in which active devices are connected in push-pull/parallel for increased power output. Also see PARALLEL-COMPONENT OSCILLATOR, PUSH-PULL OSCILLATOR, and PUSH-PULL/PARALLEL CIRCUIT.

push-pull recording A type of film sound track consisting of two side-by-side images 180 degrees out of phase with each other.

push-pull transformer A transformer having a center-tapped winding for operation in a push-pull circuit.

push-push Pertaining to a circuit in which two active devices are used, with the inputs connected in phase opposition, and the outputs connected in parallel. The result is reinforcement of the even harmonics, and cancellation of the fundamental frequency and all odd harmonics.

push-push circuit See PUSH-PUSH MULTIPLIER.

push-push multiplier An amplifier circuit containing two active devices with their inputs connected in phase opposition and their outputs connected in parallel. This circuit is unsuitable for fundamental-frequency and odd-harmonic operation,

5059F-pP-510-565 4/10/01 9:33 AM Page 565

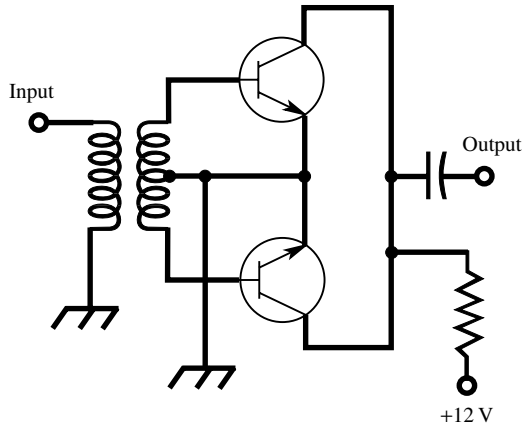

push-push

but has some merit as an even-harmonic multiplier (e.g., a *doubler* or *quadrupler*). Also see PUSH-PULL MULTIPLIER.

push-to-talk switch See PRESS-TO-TALK SWITCH.

pushup list In data processing, a method of amending a list, whereby new items are added at the end of the list; all other items retain their original positions. Compare PUSHDOWN LIST.

pV Abbreviation of PICOVOLT.

PVC Abbreviation of POLYVINYL CHLORIDE.

pW Abbreviation of PICOWATT.

PWM **1.** Abbreviation of PULSE-WIDTH MODULATION. **2.** Abbreviation of PLATED-WIRE MEMORY.

pwr Abbreviation of POWER.

Pyralin See CELLULOSE NITRATE.

pyramidal horn antenna A rectangular horn antenna that is flared in two dimensions. The horn width and height both increase linearly with increasing distance (in the direction of maximum radiation/response) from the feed point.

pyramidal wave See BACK-TO-BACK SAWTOOTH.

Pyrex A heat-resistant glass having numerous applications in electronics and chemistry.

pyrheliometer An instrument used to measure infrared radiation.

pyroelectricity In certain crystals, electricity generated by temperature change, and in particular, by the application of heat.

pyroelectric lamp See NERNST LAMP.

pyroelectric material A crystalline material that generates an output voltage when it is heated.

pyrolysis The process whereby heat changes a substance into one of several different substances by rearranging its atoms.

pyromagnetic effect In a material or circuit, the combined effect of heat and magnetism.

pyrometer An instrument, other than a thermometer, used for the measurement of temperature. See, for example, OPTICAL PYROMETER.

Pythagorean scale A sound scale defining a specific type of relationship among audio tones. If x and y are related by the Pythagorean scale and are adjacent in frequency, then a specific frequency (f) exists, so $x = f^2$ and $y = f^3$.

Pythagorean theorem A theorem of plane geometry. For a right triangle, with sides of lengths a, b, and c, where c is the side opposite the right angle, it is always true that $a^2 + b^2 = c^2$.

p-zone See P LAYER.

PZM Abbreviation of PRESSURE-ZONE MICROPHONE.

PZT Abbreviation of LEAD ZIRCONATE TITANATE.

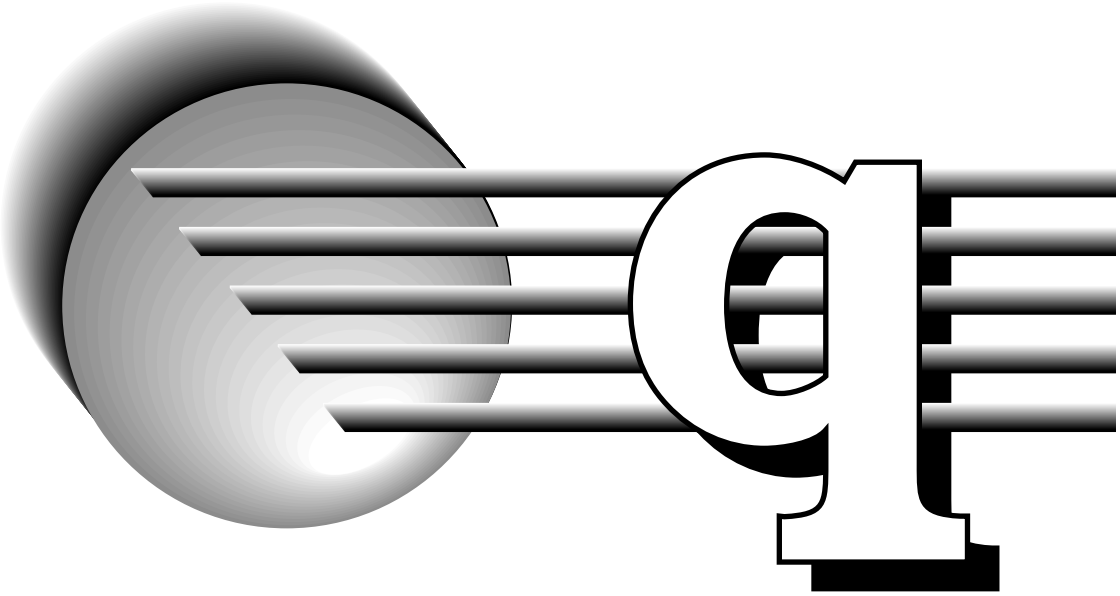

Q **1.** The figure of merit of a capacitor, inductor, or inductance-capacitance (LC) circuit, equal to the reactance divided by the resistance. **2.** Symbol for electrical charge. **3.** Occasional symbol for SELECTIVITY. **4.** See Q BAND. **5.** See *Q* OUTPUT.

q **1.** Symbol for quantity of electricity (in coulombs). **2.** Symbol for the charge carried by an electron (the charge carried by a hole is represented by –q). **3.** Symbol for the value of a quantum.

QA Abbreviation of QUALITY ASSURANCE.

Q **adjustment** The separate null adjustment for the *Q* value of a component being tested in an impedance bridge having separate resistive and reactive balances.

Q**-antenna** An antenna in which the transmission line (feeder) is matched in impedance to the center of the radiator by means of a *Q*-matching section.

QAVC Abbreviation of QUIET AUTOMATIC VOLUME CONTROL.

Q band The radio-frequency band 36 to 46 GHz. It is subdivided as follows: Q_a, 36 to 38 GHz; Q_b, 38 to 40 GHz; Q_c, 40 to 42 GHz, Q_d, 42 to 44 GHz; and Q_e, 44 to 46 GHz.

Q **bar** One of the parallel metal tubes in a *Q*-matching section. Also see *Q* ANTENNA.

Q **booster** See *Q* MULTIPLIER.

Q **bridge** An alternating-current bridge used principally to determine the *Q* of capacitors and inductors. Bridges are usually used for audio-frequency *Q* determinations; resonant-type *Q* meters are generally used for measurement of radio-frequency *Q*.

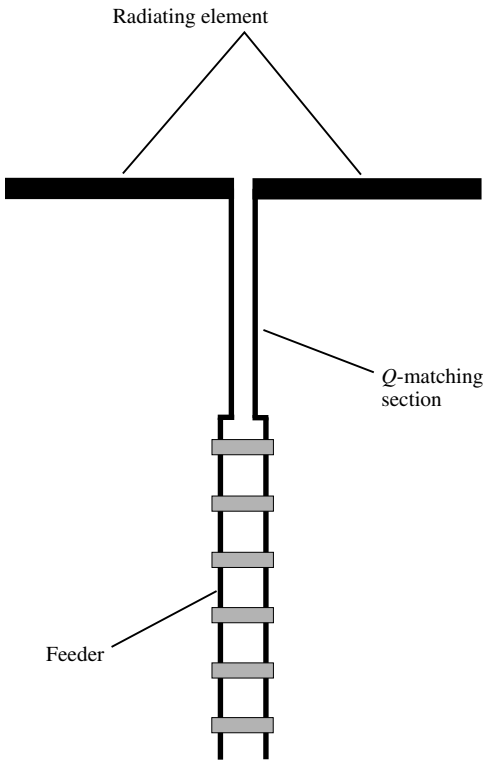

Q**-antenna**

Copyright 2001 The McGraw-Hill Companies, Inc. Click Here for Terms of Use

5059F-pQ-566-573 4/10/01 9:35 AM Page 567

QC Abbreviation of QUALITY CONTROL.

QCE Abbreviation of QUALITY-CONTROL ENGINEERING or QUALITY-CONTROL ENGINEER.

Q channel In American (NTSC) color television, the 508-kHz-wide green-magenta color information transmission band.

QCT Abbreviation of QUALITY-CONTROL TECHNICIAN.

QCW In the local oscillator and associated circuitry of a color television receiver, a 3.85-MHz CW signal of Q PHASE.

QCW signal In a color television receiver, the component of the chrominance signal that is 90 degrees out of phase with the in-phase component.

Q demodulator In a color television receiver, the demodulator that combines the chrominance signal and the color-burst oscillator signal to recover the Q signal (see Q SIGNAL, **2**).

QED **1.** Abbreviation of QUANTUM ELECTRODYNAMICS. **2.** Abbreviation of *quod erat demonstrandum*, Latin for "which was to be demonstrated." Also, Q.E.D. Often written at the conclusions of valid logical proofs and derivations.

***Q* factor** See *Q*.

QFM Abbreviation of QUADRATURE MODULATION.

QM Abbreviation of QUADRATURE MODULATION.

***Q*-matching section** A linear radio-frequency impedance-matching transformer consisting of two straight, rigid, parallel metal conductors that are used to match a feeder to an antenna. The section is ¼ wavelength long at the operating frequency. The diameters and center-to-center spacing of the conductors are such that the characteristic impedance of the matching section is equal to the geometric mean of the feeder characteristic impedance and the radiation resistance of the radiator. Also see *Q* ANTENNA and QUARTER-WAVELENGTH MATCHING STUB.

***Q* meter** A usually direct-reading instrument for determining the *Q* of a capacitor, inductor, or inductance-capacitance (LC) circuit. Most *Q* meters are operated at radio frequencies, but audio-frequency instruments are available.

***Q* modulation** Amplitude modulation obtained by varying the effective *Q* of a radio-frequency tank circuit in step with a modulating component. See ABSORPTION MODULATION.

QMQB Abbreviation of *quick make/quick break.*

***Q* multiplier** A positive-feedback (regenerative) amplifier that increases the effective *Q* of a tuned circuit, and thereby sharpens its response, when its input is connected across the tuned circuit.

Q output The reference output of a flip-flop.

Q phase A color-television carrier signal that is 147 degrees out of phase with the color subcarrier.

Q point The point or points at which a load line intersects a device characteristic (such as the collector curve of a transistor or plate curve of a tube) and that identifies the quiescent operating point.

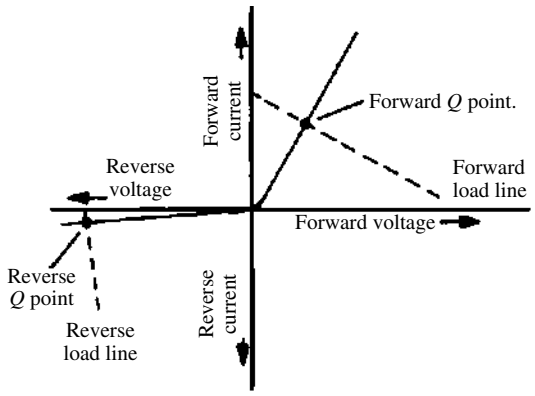

***Q* points on diode characteristic**

QRD Abbreviation of QUADRATIC RESIDUE DIFFUSOR.

***Q*-section transformer** See *Q*-MATCHING SECTION.

Q signal In color television, the quadrature component of the chrominance signal, equal to +0.48(R-Y) and to +0.41(B-Y), where B is the blue camera signal, R is the red camera signal, and Y is the luminance signal.

Q signals A set of three-letter groups, each beginning with the letter Q, used for simplified telegraph and radiotelegraph communication, and sometimes rapid voice communication (in radiotelephony). Each signal represents a commonly used phrase or message.

QSL card A card verifying communication with, or the reception of signals from, the station sending the card. Such verification is common in the amateur radio service and with some shortwave broadcast and CB stations.

QSO Amateur radiotelegraph abbreviation for TWO-WAY COMMUNICATION.

Q spoiler A device or circuit that produces Q SPOILING in a laser.

Q spoiling The technique of inhibiting laser action during an interval when an ion population excess is pumped up. When the laser is subsequently triggered by Q switching, a more powerful pulse of light results than would be otherwise obtained.

Q switching A laser-switching action obtainable with Kerr cells or rotating reflecting prisms, which consists of holding the Q of the laser cavity to a low value during an ion-population buildup, then abruptly switching the Q to a higher value.

***Q* transformer** See *Q*-MATCHING SECTION.

qty Abbreviation of QUANTITY.

quad **1.** A combination of four components, such as diodes, transistors, etc., in a single housing. The components are usually carefully matched. **2.** In a cable, a combination of four separately insulated conductors (sometimes, two twisted pairs) twisted

5059F-pQ-566-573 4/10/01 9:36 AM Page 568

together. **3.** Abbreviation of QUADRANT. **4.** See QUAD ANTENNA. **5.** See QUADROPHONIC.

quad antenna A directional antenna similar to the Yagi, except that full-wavelength loops are used instead of straight elements. A two-element array can consist of a driven element and a reflector, or it can have a driven element and a director. A three-element system has one driven element, one director, and one reflector. The director has a perimeter of about 0.97 electrical wavelength, the driven element measures exactly 1 electrical wavelength around, and the reflector has a perimeter of about 1.03 electrical wavelength. Additional director elements can be added to the basic three-element quad design to form arrays having any desired numbers of elements. The gain and directivity increase as the number of elements increases. Compare YAGI ANTENNA.

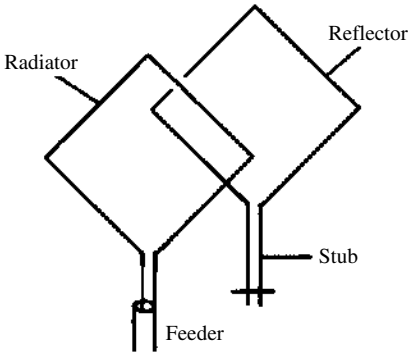

quad antenna

quadded cable See QUAD, **2**.

quadding Redundancy obtained by connecting components in series-parallel for enhanced reliability and/or increased power-handling capacity.

quad latch A set of four interconnected flip-flops that is used for digital data storage.

quadrant **1.** A specific 90-degree arc of a circle. **2.** One of the four parts formed on a plane surface by rectangular coordinates and designated I, II, III, and IV in a counterclockwise direction, starting with the upper-right quadrant. **3.** An altitude-measuring instrument.

quadrantal deviation The part of magnetic-compass deviation caused by the induction of transient magnetism into the horizontal soft iron of a vessel by the horizontal component of terrestrial magnetism.

quadrantal error See QUADRANTAL DEVIATION.

quadrant electrometer An electrometer whose principal parts are quadrants (a pillbox-shaped brass chamber split into four parts) and a needle (a flat, bowtie-shaped aluminum vane) suspended by a platinized quartz fiber between the quadrants.

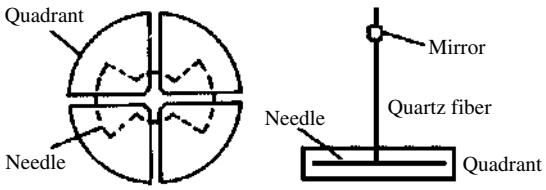

quadrant electrometer

quadraphonic sound Sound recording and reproduction involving four channels.

quadraphony Music recording or playback in which four distinct information channels are used. Also called *four-channel stereo.*

quadratic equation A second-degree equation [i.e., one in which the highest exponent is 2 (the square of an unknown) (e.g., $ax2 + bx + c = 0$)].

quadratic residue diffusor Abbreviation, QRD. In acoustics, a sound-reflection grating that scatters (diffuses) sound waves almost uniformly in all directions. The depths of the indentations in the grating are determined according to a QUADRATIC EQUATION.

quadrature The state of (cyclic events or points) being 90 degrees out of phase.

quadrature amplifier An amplifier circuit that introduces a 90-degree phase shift. Such amplifiers are used in control devices, test instruments, transmitters, and color television receivers.

quadrature axes The vertical axes in the complex-number plane (i.e., the $+j$ and $-j$ axes).

quadrature carrier See Q PHASE.

quadrature component **1.** The reactive component of an alternating current or voltage. **2.** A vector perpendicular to a reference vector. **3.** The imaginary-number component in a complex-number expression.

quadrature current Reactive current in an alternating-current circuit.

quadrature modulation In-phase modulation of two carrier components having a 90-degree phase difference.

quadrature number See IMAGINARY NUMBER.

quadrature-phase subcarrier signal See QCW SIGNAL.

quadrature portion In color television, the portion of the chrominance signal having the same (or opposite) phase as that of the Q-signal-modulated subcarrier, and that is 90 degrees out of phase with the in-phase portion.

quadrature sensitivity The sensitivity of a transducer to motions in a direction that is perpendicular to the normal axis of response.

quadrature voltage A voltage 90 degrees out of phase with another (reference) voltage.

quadrilateral **1.** Pertaining to an object having four sides. **2.** A four-sided plane polygon.

quadrillion The number 1,000,000,000,000,000 (10^{15}).

5059F-pQ-566-573 4/10/01 9:36 AM Page 569

quadripartite Having four parts.

quadripole network A four-terminal network, usually with input- and output-terminal pairs.

quadrivalent Having a valence of 4. Tin, for example, is quadrivalent. Also called TETRAVALENT.

quadruped robot A robot with four legs that can move independently. It offers better stability than three-legged designs. Functions well in mobile machines that must navigate irregular terrain.

quadrupler **1.** A rectifier circuit that delivers a direct-current output voltage approximately equal to four times the peak value of the alternating-current input voltage. **2.** An amplifier or other circuit that delivers an output signal of four times the frequency of the input signal.

quadruplex circuit A data circuit in which two messages are carried in each direction simultaneously.

quadrupole **1.** A combination of two dipoles, producing a force that varies inversely with the fourth power of distance. **2.** A four-pole magnet used in some synchrotrons and linear accelerators to focus and bend a particle beam. **3.** A system consisting of two dipoles of equal and opposite direct moment.

qualification The quality-control or quality-assurance scheme used in the production of components, circuits, or systems. Certain minimum requirements must be met for a device to obtain qualification.

qualitative test A test performed to determine the general mode of operation or the presence of certain factors, without regard to numerical values. Compare QUANTITATIVE TEST.

quality **1.** In audio-frequency applications, fidelity of transmission or reproduction. **2.** The degree of conformity of a product to specifications.

quality assurance The outcome of measures taken to bring performance into conformity with specifications. See QUALITY, **2**.

quality control The surveillance of selection, manufacturing, and testing operations to ensure conformity of a product to specifications.

quality-control engineering The branch of engineering concerned principally with the technical methods of quality control and statistical methods of assessing quality (see QUALITY, **2**).

quality-control technician A technician whose principal duty is the performance of operations in the areas of incoming inspection, manufacturing support, and product testing. Sometimes statistical evaluations are required.

quality engineering A field of engineering that deals with quality assurance and quality control in the production of components, circuits, and systems.

quality factor See *Q*.

quality-factor bridge See *Q* BRIDGE.

quality-factor meter See *Q* METER.

quanta Plural of QUANTUM.

quantimeter An instrument used to measure the quantity of X rays to which a body has been exposed.

quantitative test A test performed to determine the numerical values (and their relationships) connected with observable phenomena. Compare QUALITATIVE TEST.

quantity **1.** A parameter (e.g., collector current, grid voltage, etc.). **2.** In calculations, a positive or negative real number. **3.** Electrical charge, usually specified or measured in coulombs (see COULOMB). Also called *electrical quantity.*

quantization The conversion of a quantity having infinitely many possible values or levels (such as an analog signal) into one that can attain only a finite number of defined values or levels (such as a digital signal). The number of levels is usually some integral power of 2 (i.e., 2, 4, 8, 16, 32, etc.). This allows the levels to be represented as binary numbers.

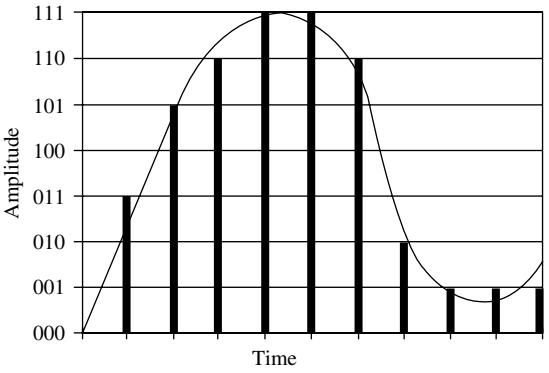

quantization

quantization distortion Distortion introduced by the process of QUANTIZATION in a communications or broadcast signal.

quantization distortion power The level of the distortion in a signal resulting from QUANTIZATION. It is expressed in microwatts, milliwatts, or watts. It can also be expressed as a percentage, or as a level in decibels, relative to the power level of the input signal.

quantization error The difference between the actual values of quantities and their quantized values.

quantization noise Noise introduced by the process of QUANTIZATION in a communications or broadcast signal.

quantize **1.** To perform the process of QUANTIZATION. **2.** To split a quantitative commodity, such as energy into its smallest measurable incremental units.

quantized pulse modulation Pulse modulation involving QUANTIZATION. Examples are PULSE-CODE MODULATION and PULSE-NUMBERS MODULATION.

5059F-pQ-566-573 4/10/01 9:36 AM Page 570

quantizer A circuit or device that selects the digital subdivision into which an analog quantity is placed (e.g., an analog-to-digital converter).

quantizing See QUANTIZATION.

quantometer An instrument for measuring magnetic flux.

quantum **1.** Abbreviation, Q. Plural, *quanta.* In physics, the elemental unit or particle of electromagnetic energy. The energy contained in one such particle is directly proportional to the frequency, and inversely proportional to the wavelength. **2.** See PHOTON. **3.** Any discrete unit derived by QUANTIZATION.

quantum chromodynamics A term coined by Professor Murray Gell-Mann for the theory of *quarks* and *gluons.*

quantum counter A radiation-counter tube with a window for the admission of light to the cathode.

quantum efficiency See QUANTUM YIELD.

quantum electrodynamics A branch of quantum mechanics that involves the motions of electrons, photons, and muons caused by electromagnetic action. Quantum electrodynamics takes relativistic effects into account.

quantum electronics The branch of electronics concerned with energy states in matter.

quantum equivalence The principle that one electron is emitted for each photon absorbed by a material (when the photon has the necessary energy).

quantum jump The abrupt movement of a particle from one discrete energy state to another.

quantum level The orbit or ring occupied by an electron in an atom.

quantum mechanics A branch of physics concerned with the behavior of matter and energy, on the basis of observable data.

quantum noise A noise signal arising from random variations in the average rate at which quanta impinge upon a detector.

quantum number A number that describes the energy level, or change in energy level, for a particle.

quantum statistics A branch of QUANTUM MECHANICS concerned with the distribution of elementary particles through various quantized energy levels.

quantum theory The theory that the emission or absorption of energy by atoms or molecules occurs in discrete packages or units, rather than continuously. Each unit is the emission or absorption of an energy packet called a QUANTUM. Thus, radiant energy is thought to be divided into *quanta.*

quantum transition The movement of an electron from one energy level to another within an atom.

quantum yield The photoelectric efficiency of a light-sensitive surface in terms of the number of electrons emitted for each absorbed quantum of light.

quark A hypothetical particle having a fractional electrical charge; quarks are thought to be constituents of other subatomic particles.

quarter-deflection method A method of measuring high-frequency resistance, involving the use of a sine-wave signal source, a standard noninductive variable resistor, and a square-law radio-frequency ammeter.

quarter-phase See TWO-PHASE.

quarter wave **1.** The length of time corresponding to 90 electrical degrees in a wave disturbance. **2.** The distance in space, or along a wire or feed line that corresponds to 90 electrical degrees in a wave disturbance.

quarter-wave antenna An antenna in which the radiator is an electrical quarter-wavelength long at the operating frequency.

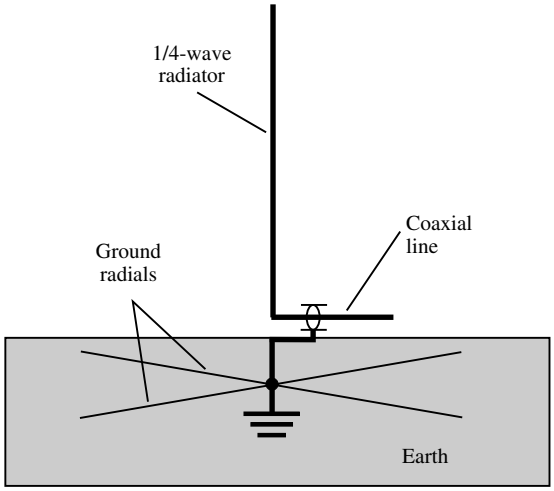

quarter-wave antenna

quarter-wave attenuator In a transmission line or waveguide, two energy-absorbing structures separated by an odd number of quarter wavelengths so that the reflection from one structure is canceled by that from the other.

quarter-wave balun A balun using quarter-wave elements. One form of this device consists of a grounded quarter-wavelength-long cylinder closed at one end and open at the other, for matching an unbalanced low-impedance line to a balanced high-impedance line.

quarter wavelength Symbol, λ/4. The distance that corresponds to 90 degrees of phase as an electromagnetic (EM) field is propagated. In free space, it is related to the frequency by a simple equation

$$L_{ft} = 246/f$$

where L_{ft} represents λ/4 in feet, and f represents the frequency in megahertz. If λ/4 is expressed in meters, then the formula is

$$L_{m} = 75/f$$

5059F-pQ-566-573 4/10/01 9:36 AM Page 571

where L_m represents the displacement in meters. In general, if v is the velocity factor (expressed as a ratio) in a given medium, then:

$$L_{ft} = 246v/f$$

and

$$L_m = 75v/f$$

Compare FULL WAVELENGTH, HALF WAVELENGTH.

quarter-wavelength line A transmission line or feeder that is a quarter-wavelength long at the operating frequency. Also called *quarter-wave line.*

quarter-wavelength matching stub An arrangement consisting of a quarter-wavelength-long parallel-wire section of transmission line, used for matching the impedance of a nonresonant feeder to that of an antenna. It is similar to a Q-MATCHING SECTION, except that flexible transmission line (e.g., ladder line) is used, rather than rigid metal rods or tubing.

quarter-wave monopole A nondirectional UHF vertical antenna requiring no ground. The radiator is ¼ wavelength long, and is an enlarged-diameter outer sleeve connected to the outer conductor of the coaxial feeder. The two sections simulate a half-wave antenna.

quarter-wave plate A plate of double-refracting crystalline material whose thickness allows the introduction of a quarter-cycle phase difference between the ordinary and extraordinary components of light transmitted by it.

quarter-wave radiator An antenna consisting of a single, usually straight, active element that measures an electrical quarter wavelength from end to end. When operated against electrical ground, the element exhibits resonance. A simple quarter-wavelength (λ/4) conductor with a high length-to-diameter ratio measures approximately 95 percent of λ/4 in free space. The element can be much shorter than free-space λ/4 yet remain resonant when operated against electrical ground if inductance is inserted in series with the radiator. The element can be much longer than free-space λ/4 yet remain resonant when operated against electrical ground if distributed capacitances are inserted in series with the radiator.

quarter-wave resonance Resonance at the operating frequency in a quarter-wave antenna.

quarter-wave resonant line A section of transmission line (such as open-wire line or coaxial cable) that is a quarter-wavelength long at the operating frequency. Such a section is useful in impedance matching and in various radio-frequency tests and measurements.

quarter-wave stub See QUARTER-WAVE TRANSFORMER.

quarter-wave support In a coaxial line, a quarter-wave metal stub that can be used, instead of an insulator, to separate the inner and outer conductors.

quarter-wave termination In a waveguide, a set of two metal barriers separated by 90 electrical degrees. One barrier totally reflects the energy striking it. The other barrier allows some energy to pass through. Resonance occurs in the space between the barriers.

quarter-wave transformer A quarter-wave resonant line short-circuited at one end by an adjustable slider. This arrangement is useful for radio-frequency impedance matching.

quarter-wave transmission line See QUARTER-WAVE LINE.

quartic equation A fourth-degree equation of the form $ax^4 + bx^3 + cx^2 + dx + e = 0$, where a, b, c, d, and e are constants. Also called BIQUADRATIC EQUATION.

quartz A mineral that is a variety of natural silicon dioxide, or an artificially grown material of the same sort. In the natural state, quartz occurs in hexagonal crystals having pyramidal ends. It has various uses in electronics; one of the most common is the manufacture of piezoelectric crystals.

quartz bar A comparatively large, thick piezoelectric quartz plate used in standard-frequency oscillators and in sharply tuned low-frequency filters. Common resonant frequencies are 50 kHz, 100 kHz, and 1000 kHz.

quartz crystal A natural or artificial piece of quartz cut to specific dimensions, usually self-contained in a solder-in or plug-in enclosure. The device acts as a highly stable selective circuit. It exhibits a sharp resonance at the frequency for which it is cut, and at harmonics of this frequency. It is used as the frequency-determining element in precision oscillators.

quartz-crystal oscillator See CRYSTAL OSCILLATOR.

quartz-crystal resonator See CRYSTAL RESONATOR.

quartz delay line An acoustic delay line using quartz to transmit the sound waves.

quartz-fiber electroscope An electroscope using a gold-plated quartz fiber, instead of gold leaves.

quartz-halogen lamp An incandescent, usually low-voltage lamp used in automotive headlights, and in some home and office lighting appliances. It provides greater efficiency than conventional incandescent lamps.

quartz lamp A mercury-vapor lamp with a transparent quartz (instead of glass) envelope. Unlike glass, quartz readily passes the ultraviolet rays generated by the mercury discharge.

quartz lock A circuit that uses a CRYSTAL OSCILLATOR to regulate frequency, timing, or speed. It is used in electronic clocks and watches, television receivers, synthesized radio receivers, transmitters, transceivers, high-fidelity turntables, etc.

quartz oscillator See CRYSTAL OSCILLATOR.

quartz plate A piezoelectric plate cut from a quartz crystal. The plate is itself often called a *crystal.* Also see CRYSTAL AXES and CRYSTAL CUTS.

5059F-pQ-566-573 4/10/01 9:36 AM Page 572

quartz resonator See CRYSTAL RESONATOR.

quartz timepiece A watch or clock having as its control element a time-determining quartz crystal.

quasi- A prefix meaning "to some extent" or "similar to," as in *quasi-optical radio wave* (a radio wave that behaves like a light ray).

quasi-bistable circuit A trigger-operated multivibrator. It operates as a flip-flop when the trigger frequency is sufficiently high.

quasi-instruction In a computer program, a data item appearing as an encoded instruction, but that is not acted upon.

quasi-linear feedback system A system in which the feedback elements are nearly linear, but not entirely linear.

quasi-negative Pertaining to a voltage that is negative, with respect to some other voltage, but whose absolute polarity is positive. For example, +0.5 volt is quasi-negative, with respect to +5.5 volts.

quasi-optical Behaving like light. The term is used to describe certain extremely short radio waves or other radiations that, like light rays, follow line-of-sight paths and can be directed, reflected, refracted, or diffused.

quasi-optical path A line-of-sight path followed by very short radio waves, such as microwaves.

quasi-positive Pertaining to a voltage that is positive, with respect to some other voltage, but whose absolute polarity is negative. For example, –0.5 volt is quasi-positive, with respect to –5.5 volts.

quasi-random A set of numbers considered to be random, but chosen according to an algorithm.

quasi-rectangular wave A wave whose shape approaches that of a rectangular wave, but that possesses a small amount of tilt and/or curvature.

quasi-scientific A term that is sometimes applied to the design of electronic systems or to the appraisal of circuit behavior, using an intuitive, rather than analytical approach.

quasi-sine wave A waveform that is not a perfect sine curve, but is close enough to be considered sinusoidal, for all practical purposes.

quasi-single sideband A modulated waveform that somewhat resembles single sideband, in which parts of both sidebands are present.

quasi-square wave A waveform that is not a perfect square, but is close enough to be considered square for all practical purposes. It is sometimes applied to a rectangular wave when a square wave is desired.

quasi-technical A term sometimes applied to qualitative tests, as opposed to quantitative tests.

quaternary **1.** Pertaining to a base-4 number system. **2.** Of an atom, joined to carbon atoms for four bonds. **3.** The fourth member of a 4-unit set.

Quebec Phonetic alphabet code word for the letter Q.

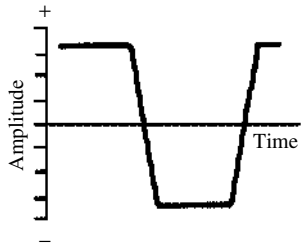

quasi square wave

quench **1.** To suddenly bring to an end (e.g., to quench an oscillation). **2.** To cool quickly, as in the quenching of a heated metal object. **3.** To extinguish the discharge in a gas tube.

quench capacitor A capacitor that prevents a spark from arcing across an inductor when current flow abruptly stops.

quench frequency See QUENCHING FREQUENCY.

quenching action Typical operation of a superregenerative circuit, in which regeneration is increased to nearly the point of oscillation and then reduced; this action is repeated at an ultrasonic frequency and results in very high sensitivity. Also see QUENCHING FREQUENCY, QUENCH OSCILLATOR, and SUPERREGENERATIVE CIRCUIT.

quenching frequency The frequency at which regeneration in a superregenerative circuit is increased and decreased.

quench oscillator In some superregenerative circuits, the separate ultrasonic oscillator that produces the required quenching action.

quench resistor A resistor in a quenching network that prevents a spark from occurring across an inductor when current flow stops.

queue A list of data, steps in a process, or commands awaiting execution in a specific order.

queuing theory A branch of mathematical electronics, dealing with the optimum order in which steps should be executed to obtain a particular end result.

quibinary code In computer operations, a binary-coded decimal system in which each decimal digit is represented by seven bits occupying places whose values are 8, 6, 4, 2, 0, 1, and 0.

quibinary decade circuit A decade counter consisting of a ring-of-5, followed by a single binary stage.

quick break An operating characteristic of a switch, relay, or circuit breaker whereby the contacts open rapidly—even when the actuating current or mechanical force is slow-acting.

quick-break fuse A fuse in which the wire melts and breaks almost instantly when the current rating is exceeded. Also called *quick-blow fuse.* Compare SLOW-BLOW FUSE.

5059F-pQ-566-573 4/10/01 9:36 AM Page 573

quick-break switch A switch that opens rapidly—even if its handle or lever is moved slowly by the operator. This action minimizes arcing and prevents chatter. Compare QUICK-MAKE SWITCH.

quick charge The process of charging a battery, such as a nickel-cadmium (NICAD) or nickel-metal-hydride (NiMH) type, at a relatively rapid rate, at high charging current. It is sometimes used to charge a battery from a state of almost total discharge. Compare TRICKLE CHARGE.

quick-disconnect The characteristic of a connector that enables its mating halves to be separated quickly and simply, to break the circuit in which it is situated.

quickening liquid A solution of mercuric cyanide or mercuric nitrate, into which objects can be dipped prior to electroplating with silver. The process ensures good adhesion of the silver to the object.

quick make An operating characteristic of a switch, relay, or circuit breaker, whereby the contacts close rapidly—even when the actuating current or mechanical force is slow acting.

quick-make switch A switch that closes rapidly—even if its handle or lever is moved slowly by the operator. Compare QUICK-BREAK SWITCH.

quick printer A high-speed printer, used with a data terminal or computer. A relative term, depending on the user and the application.

quicksilver See MERCURY.

quick-stop control A control on tape recorders and some dictating machines that allows the operator to stop the tape, but keep the machine in the play or record mode. Also called *pause control.*

QuickTime Trade name (Apple Computer, Inc.) for system software commonly used in MULTIMEDIA applications with personal computers.

QUICKTRAN For multiaccess computer systems, a computer programming language based on FORTRAN and offering facilities, through the use of remote terminals, for running, testing, debugging, and compiling programs.

quiescent carrier operation A modulation system in which the carrier is present only during modulation (i.e., it is suppressed at all other times). Also called *controlled-carrier transmission.*

quiescent-carrier telephony A carrier-current (wired-wireless) telephone system in which the carrier is suppressed when there is no voice or alerting signal.

quiescent component In an electronic device, a component that is momentarily nonfunctional.

quiescent current Operating current (usually a direct current) flowing in a circuit or component during zero-signal or no-drain intervals. Also called IDLING CURRENT.

quiescent operation Zero-signal operation of a device, such as a transistor, diode, magnetic amplifier, or similar component.

quiescent period The no-signal interval during which equipment is not operating—even though it is energized.

quiescent point The point on the characteristic curve of a transistor, diode, or similar device, denoting the zero-signal operating conditions.

quiescent push-pull Denoting a push-pull stage, especially an audio power-output amplifier, in which the direct-current signal is essentially zero.

quiescent state The inactive, or resting, state of an active component, such as a transistor or vacuum tube.

quiescent value The zero-signal value of current or voltage for any component supplied with operating power.

quiet AGC See DELAYED AUTOMATIC GAIN CONTROL.

quiet automatic gain control See DELAYED AUTOMATIC GAIN CONTROL.

quiet automatic volume control See DELAYED AUTOMATIC GAIN CONTROL.

quiet AVC See DELAYED AUTOMATIC GAIN CONTROL.

quiet battery A direct-current source specially designed and filtered to minimize noise components in its output.

quieting Noise-voltage reduction in the output of a frequency-modulation (FM) receiver when an unmodulated carrier is received. Also called *noise quieting.*

quieting level In a frequency-modulation (FM) receiver, the limiter threshold point.

quieting sensitivity In a frequency-modulation (FM) receiver, the lowest input-signal amplitude at which the output signal-to-noise ratio is below the specified limit.

quiet tuning A system of tuning in which the output of a receiver is muted until a station is tuned in properly.

quinary code See BIQUINARY CODE.

quinary counter A decade counter consisting of a five-stage ring.

quinhydrone electrode A pH meter electrode consisting of a platinum wire in a solution of quinhydrone ($C_{12}H_{10}O_4$). Also see PH METER.

quintillion The number 1,000,000,000,000,000,000 (10^{18}).

quintupler **1.** A rectifier circuit that delivers a direct-current output voltage equal to about five times the peak value of the alternating-current input voltage. **2.** A circuit that delivers an output signal at the fifth harmonic of the input signal.

QWERTY The standard typewriter and computer keyboard layout. The name is derived from the first several letters in the top letter row: Q, W, E, R, T, and Y.

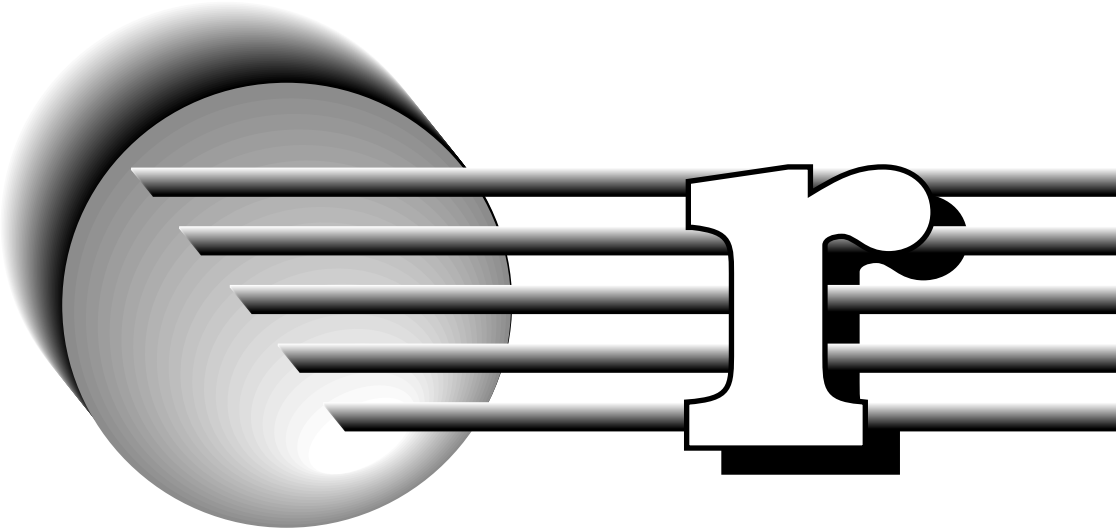

R **1.** Symbol for RESISTANCE. (Also, r.) **2.** Radiotelegraph abbreviation for ROGER. **3.** Symbol for RELUCTANCE. **4.** Abbreviation of RADIUS.

r **1.** Symbol for ROENTGEN. **2.** Symbol for *correlation coefficient.* **3.** Abbreviation of RADIUS. (Also, abbreviated R.)

r_e Symbol for CLASSICAL ELECTRON RADIUS.

RA **1.** Abbreviation of *right ascension.* **2.** Abbreviation of RANDOM ACCESS.

rabbit ears An indoor antenna, sometimes used with a television receiver, consisting of two vertical whips (usually telescoping), the angle between which is adjustable.

RAC Abbreviation of RECTIFIED ALTERNATING CURRENT.

R_{ac} Symbol for AC RESISTANCE. (Also, r_{ac}.)

race Incorrect interpretation of the clock pulses by a digital circuit. Also called *racing.* The circuit improperly attempts to do many operations during one clock pulse, rather than a single operation.

RACES Abbreviation of *Radio Amateur Civil Emergency System.*

raceway See WIRE DUCT and WIREWAYS.

rack An upright frame for holding equipment of RACK-AND-PANEL CONSTRUCTION.

rack-and-panel construction A method of building electronic equipment on a chassis attached horizontally or vertically to a vertical panel. After completion of a unit, the panel is fastened in place on a RACK. Several such panels fill the rack.

rack and pinion A device used for mechanical adjustment of a control, such as the tuning control in a radio receiver. A gear engages a serrated rod. As the gear is turned, the rod moves lengthwise.

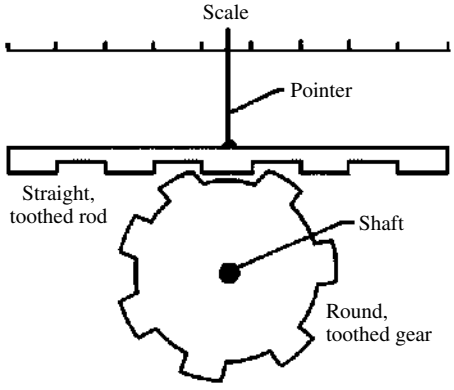

rack and pinion

rack up In computer operations, a way of displaying data, in which a new line added to the already completely occupied screen bumps up what has forgone, thus eliminating the top line.

racon Acronym for *radar beacon.*

rad **1.** A unit of ionizing radiation received by a body (dose) equal to 0.001 J/kg. **2.** Abbreviation of RADIAC. **3.** Abbreviation of RADIAN. **4.** Abbreviation of RADIO. **5.** Abbreviation of RADIX.

radar **1.** A microwave system for detecting objects and determining their distance, direction, heading, speed, and other characteristics. Signals from the transmitter are reflected back to the transmitter site by the object, and the reflection (sometimes along with the transmission) is displayed on a cathode-ray screen. The name is an

Copyright 2001 The McGraw-Hill Companies, Inc. Click Here for Terms of Use

5059F-pR-574-606 4/10/01 9:42 AM Page 575

acronym for *radio detection and ranging.* **2.** The theory and application of radio detection and ranging systems as defined in **1**.

radar altitude The distance of an aircraft above the surface of the earth, as determined by radar. This value varies with the terrain over which the aircraft passes.

radar antenna Any antenna used for transmitting and/or receiving radar signals.

radar astronomy The use of radar equipment to observe and map planets, moons, and asteroids, and to measure their distance from the earth or from a spacecraft.

radar beacon A radar transceiver that, on receipt of radar signals, transmits encoded signals from which the operator can take a bearing.

radar beam The cone-shaped main lobe of energy emitted by a radar antenna. The narrower the beam, the greater the resolution of the radar system.

radar clutter Visual interference on a radar screen caused by reflections from ground or sea.

radar countermeasures Abbreviations, RCM and rad CM. In wartime, any method of interfering with enemy radar, such as jamming or use of decoys.

radar detector **1.** A device used in automobiles and trucks to detect the proximity of police or highway-patrol radar. **2.** A device used in military applications, especially aviation, to indicate the presence of radar.

radar display The scheme via which a radar set portrays the relative positions of the objects that produce echoes. The most common is the azimuth/range display, showing compass bearings (usually in degrees clockwise from geographic north) and radius from the transmitter (usually in miles or kilometers). Altitude above mean sea level can be displayed for individual echoes.

radar homing A method of missile homing in which radar is used to track a target.

radar speed trap A radar system used by traffic police to spot speeding vehicles.

radar telescope The transmission and reception unit used in radar astronomy. Compare RADIO TELESCOPE.

RadCM Abbreviation of RADAR COUNTERMEASURES. (Also, RCM.)

radial **1.** One of several conductors used to enhance the performance of an unbalanced, vertical antenna. These can be constructed from wire or metal tubing, and generally measure one-quarter wavelength or more. When a vertical antenna is mounted at the earth's surface, the ground conductivity is improved by these conductors, which run outward from the base of the radiator, and are connected to the shield of a coaxial feed line. The greater the number of radials of a given length, the more the ground loss is reduced. Also, the longer the radials for a given number, the better. If a vertical radiator is mounted with its base more than one-quarter wavelength above the earth's surface, there need only be three or four conductors measuring exactly one-quarter wavelength. See GROUND-MOUNTED VERTICAL ANTENNA, GROUND-PLANE ANTENNA. **2.** Pertaining to the distance from the center of a circle to its periphery. **3.** Pertaining to the distance from the center of a sphere to its surface. **4.** Extending or emanating outward in a straight line from a defined point.

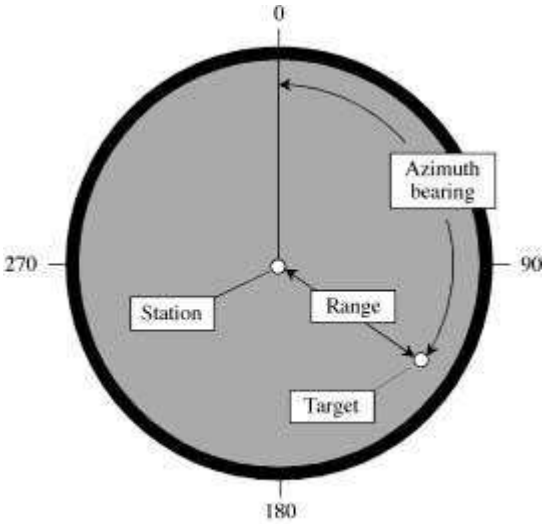

radar display

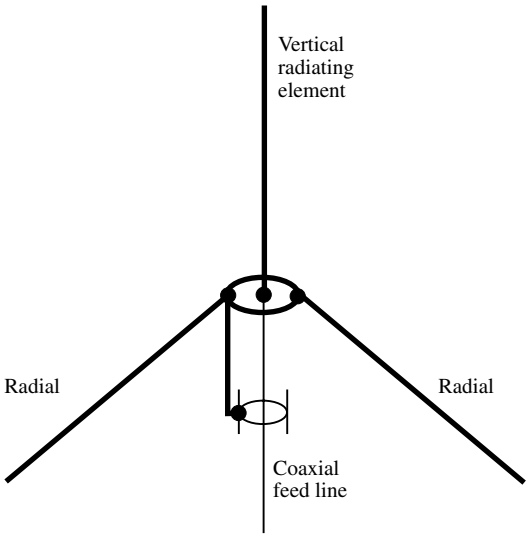

radials

5059F-pR-574-606 4/10/01 9:42 AM Page 576

radial ground An earth connection composed of radials buried in the ground.

radial lead A lead (pigtail) attached perpendicular to the axis of a component, such as a resistor or capacitor.

radian Abbreviation, rad. The angle at the center of a circle subtended by an arc whose length is equal to the radius. Equal to approximately 57.2958 degrees.

radiance The radiant flux emitted by an object. Radiance is measured in terms of the amount of energy contained in a unit solid angle (steradian) with the source at the apex.

radians-to-degrees conversion The conversion of radian angular measure into degrees. To change radians to degrees, multiply the number of degrees by 57.2958. Thus, 0.7854 radian = 45 degrees. Compare DEGREES-TO-RADIANS CONVERSION.

radiant efficiency The ratio of the radiant energy emitted by a source to the energy consumed by the source. The radiant energy is generally specified within a certain range of wavelengths. An example is the incandescent light bulb, which has relatively low radiant efficiency in the visible spectrum between about 750 and 390 nanometers.

radiant energy **1.** Any form of energy emitted by a source and propagated through space as an electromagnetic disturbance. Included are radio waves, infrared, visible light, ultraviolet, X rays, and gamma rays. **2.** Electromagnetic disturbances at infrared and shorter wavelengths.

radiant flux The rate at which radiant energy is emitted.

radiation **1.** The emission of energy or particles (e.g., waves from an antenna, X rays from an X-ray tube, energy from a radioactive material, heat from a body, etc.). **2.** Radio waves, infrared, visible light, ultraviolet, X rays, or gamma rays. **3.** Ionizing emissions from radioactive substances (e.g., alpha particles, beta particles, neutrons, gamma rays, etc.).

radiation angle The horizontal or vertical angle at which electromagnetic waves are radiated from an antenna. Measured between the central axis of the main lobe and the horizon, or between the central axis of the main lobe and geographic north.

radiation belts See VAN ALLEN RADIATION BELTS.

radiation counter An instrument used for determining the intensity of atomic-particle radiation, X rays, or gamma rays. It operates by means of ionization of a gas in a sealed tube.

radiation field The portion of the electromagnetic field that is propagated by a radiator, as opposed to the induction field.

radiation intensity For a directional radio transmitting antenna, the radiated power per steradian in a given direction.

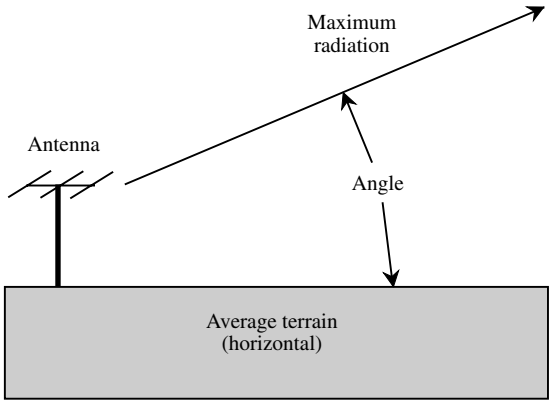

radiation angle

radiation loss Loss of energy through radiation from a conductor. Also see LOSS.

radiation pattern A graphical representation of the intensity of the electromagnetic field in various directions from a radiator, such as a transmitting antenna. It is usually shown in either the horizontal plane or a specific vertical plane containing the antenna. Also see LOBE.

radiation physics The study of radiation and its effects on matter. Radiation physics is especially concerned with ionizing radiation, but it can involve any kind of particle or electromagnetic energy.

radiation pressure Pressure exerted on a surface by impinging electromagnetic radiation.

radiation resistance The inherent resistance at the feed point of a resonant radio antenna.

radiation sickness General physiological symptoms resulting from a short-term overdose of X rays, gamma rays, or atomic-particle radiation.

radiator **1.** The element of an antenna from which radio energy is directly radiated, as opposed to the transmission line, lead-in, reflector, or director. **2.** See LOUDSPEAKER.

radio **1.** Wireless electrical communication, i.e., by means of electromagnetic waves. **2.** See RADIO RECEIVER. **3.** See RADIO TRANSCEIVER. **4.** See RADIO TRANSMITTER. **5.** To communicate by radio.

radio- **1.** A prefix meaning "pertaining to wireless electrical communication." Examples: *radiotelephone* and *radiotelegraph.* **2.** A prefix meaning "using radio waves." Examples: *radiosonde*, *radiolocator*, and *radiothermics.* **3.** A prefix meaning "pertaining to using or possessing radioactivity," or "pertaining to X rays." Examples: *radiograph*, *radioisotope*, and *radiologist.*

radioactive Having the property of emitting alpha, beta, and (sometimes) gamma rays as the result of nuclear disintegration. Also see HALF-LIFE.

5059F-pR-574-606 4/10/01 9:42 AM Page 577

radioactive element A chemical element that is RADIOACTIVE (e.g., uranium). Also called *radioelement.*

radioactive isotope See RADIOISOTOPE.

radioactive tracer A quantity of radioactive material put into a system so that its path can be monitored by means of a radiation detector. An example is the introduction of radioactive barium into the large intestine. The flow and concentration of the barium gives an indication of the functioning of the lower intestine.

radioactive transducer A pickup device for detecting and measuring radioactivity (e.g., *Geiger-Mueller tube*).

radioactivity counter See GEIGER COUNTER and SCINTILLATION COUNTER.

radio altitude See RADAR ALTITUDE.

radio amateur An electronics hobbyist licensed to operate two-way wireless communications stations in various assigned frequency bands, without receiving payment for services rendered.

Radio Amateur Civil Emergency System Abbreviation, RACES. A civil-defense organization of licensed amateur radio stations. Also see RADIO AMATEUR.

radio astronomy The observation, study, and analysis of radio-frequency electromagnetic emissions from bodies or points in space, and the study of these bodies through their radiations.

radioautograph See AUTORADIOGRAPH.

radio beacon **1.** A radio transmitter of direction-finding or guidance signals. **2.** Also called *radio beam.* The signals transmitted by a radio beacon, as defined in **1**.

radio beam **1.** Antenna radiation focused in one direction. **2.** See RADIO BEACON, **2**.

radiobiology A field of biology concerned with the influence of radiant energy or radioactivity on living organisms.

radio broadcast A radio transmission directed to numerous, nonspecific receivers—especially by a station in the *broadcast service.* Also called RADIOCAST. Also see BROADCAST SERVICE, **1**, **2**.

radio car An automobile equipped with a two-way radio.

radio carbon Radioactive carbon (i.e., carbon 14).

radiocast See RADIO BROADCAST.

radio channel A single, usually narrow radio-frequency band within a larger band, in which stations are authorized to transmit signals of a specified type. Also see CHANNEL, **1**; CHANNEL SEPARATION; and CHANNEL WIDTH.

radiochemistry The chemistry of radioactive substances.

radio communication Wireless communication carried on by means of radio-frequency electromagnetic waves.

radio compass See DIRECTION FINDER.

radioconductor A substance or body whose electrical conductivity is affected by radio waves, and that can be used as a sensor of such waves.

radio control See REMOTE CONTROL.

radio direction finder See DIRECTION FINDER.

radio Doppler **1.** A change in the frequency of a radio signal emitted by a source having radial motion, with respect to the receiver. **2.** An electronic device used to measure radial speed by means of the Doppler effect at radio frequencies.

radio-electronics The branch of electronics specifically involved with wireless communications.

radioelement See RADIOACTIVE ELEMENT.

radio engineer A trained professional skilled in the physics and mathematics of radio communications, and in the theory and application of basic electronics engineering and related subjects. Also see RADIO ENGINEERING.

radio engineering The branch of electronics engineering devoted to the theory and operations of radio communication.

radio field strength The intensity of radio waves at a given point. Also see FIELD INTENSITY, **2** and RADIO MAP.

radio frequency Abbreviation, RF. **1.** Consisting of, or pertaining to, alternating currents at frequencies above about 9 kHz (the lowest allocated radio communications frequency). **2.** Consisting of, or pertaining to, electromagnetic fields whose wavelengths are longer than those of infrared, but shorter than about 33 kilometers (corresponding to a frequency of 9 kHz). Also see RADIO SPECTRUM.

radio-frequency amplifier **1.** In a superheterodyne circuit, the channel in which the incoming signal is amplified. Compare INTERMEDIATE-FREQUENCY AMPLIFIER. **2.** Broadly, an amplifier of radio-frequency signals.

radio-frequency choke Abbreviation, RFC. A low-inductance coil used to block radio-frequency (RF) alternating currents. Many RF chokes have air cores; some have cores of ferrite or powdered iron.

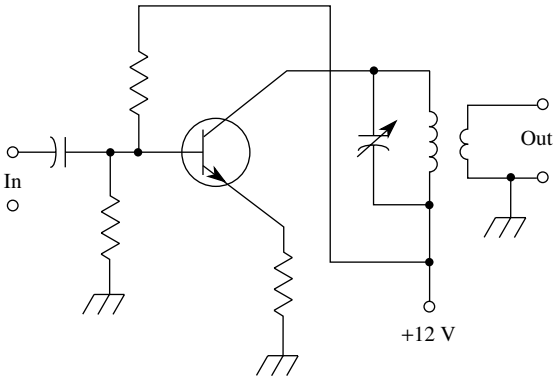

(General bipolar circuit)

radio-frequency amplifier, 2

5059F-pR-574-606 4/10/01 9:42 AM Page 578

radio-frequency current Symbol, I_{RF}. **2.** The intensity of a generated radio-frequency (RF) signal, usually expressed in microamperes. **2.** Loosely, any measurable RF signal.

radio-frequency heating The generation of heat in an object by an intense radio-frequency electromagnetic field. See, for example, DIATHERMY, **1**; DIELECTRIC HEATING; and INDUCTION HEATING.

radio-frequency interference Abbreviation, RFI. **1.** Annoying electrical noise in radio-frequency (RF) amplifiers, detectors, and instruments. **2.** Undesired RF signals that compete with desired ones in amplifiers, receivers, and instruments. **3.** The unwanted interception and demodulation of a strong RF signal by an audio-frequency (AF) device, such as a telephone set or high-fidelity stereo amplifier.

radio-frequency meter An instrument for measuring signals of RADIO FREQUENCY (9 kHz and above).

radio-frequency oscillator Abbreviation, RFO. An oscillator (self-excited or crystal-controlled) for operation at radio frequencies. In such an oscillator, stray components, efficiency, and general losses are of primary concern. Also see RADIO FREQUENCY.

radio-frequency power Symbol, P_{RF}. Alternating-current power at radio frequencies.

radio-frequency resistance The total in-phase resistance exhibited by a conductor at radio frequencies. This opposition to current includes direct-current resistance and the in-phase components caused by skin effect, shielding, and the presence of dielectrics.

radio-frequency selectivity The selectivity of a radio-frequency (RF) channel, such as the RF amplifier and first detector of a superheterodyne circuit.

radio-frequency transformer Abbreviation, RF transformer. A device used for the purpose of impedance matching, antenna tuning, or interstage coupling at frequencies above the range of human hearing (approximately 20 kHz and up). The device might consist of solenoidal windings with an air core, solenoidal windings with a powdered-iron or ferrite core, or toroidal windings with a powdered-iron or ferrite core. The windings are designed to minimize distributed capacitance and direct-current resistance. When no reactance is present, the impedance-transfer ratio is equal to the square of the turns ratio. Compare AUDIO-FREQUENCY TRANSFORMER.

radio-frequency transistor **1.** A transistor capable of providing significant amplification at radio frequencies. **2.** A transistor operable at frequencies above 100 kHz.

radiogenic Produced by radioactivity.

radiogoniometer A radio compass (see DIRECTION FINDER and GONIOMETER, **1**).

radiogram A (usually printed out) message transmitted and received via radiotelegraphy or radioteletype. The term is an acronym for *radio telegram.*

radiograph **1.** To contact by sending a RADIOGRAM. **2.** An X-ray photograph.

radio homing **1.** A method of homing that uses the tracking of a target on the basis of a radio signal emitted by that target. **2.** A method of keeping a missile on track via radio remote control.

radio interference **1.** Interference to radio communication, from whatever cause. **2.** See RADIO-FREQUENCY INTERFERENCE.

radioisotope A radioactive isotope (natural or artificial) of a normally nonradioactive chemical element (e.g., radioactive carbon). Also see ISOTOPE.

radio jamming See JAMMING.

radio knife A surgical instrument consisting essentially of a needle that forms a high-frequency arc. The arc simultaneously cuts and cauterizes tissue.

radiolocation A process whereby the position of a vehicle, aircraft, or ocean-going vessel is determined. The simplest method is the directional method. Two or three fixed receiving stations are used. Radio direction-finding (RDF) equipment is employed at each station, in conjunction with a transmitter aboard the vessel, to establish the bearings of the vessel with respect to each station. Radar can also be used to locate vessels. In wartime, enemy craft can sometimes be located by visual or infrared apparatus. Satellites can locate enemy ships and missiles, in some cases with an error smaller than the length of the vessel itself. Compare RADIONAVIGATION.

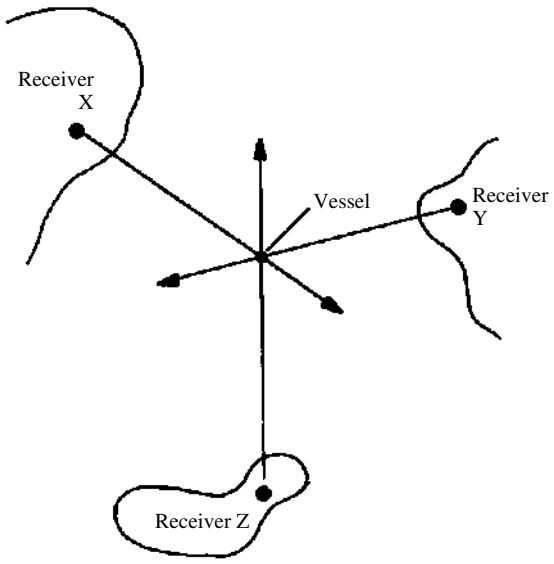

radiolocation

5059F-pR-574-606 4/10/01 9:42 AM Page 579

radiolocator See RADAR.

radiological system See X-RAY THERAPY SYSTEM.

radiologist A specialist skilled in RADIOLOGY.

radiology The science embracing the theory and use of X rays and radioactive substances in the diagnosis and treatment of diseases and ailments.

radiolucency **1.** The property of a material that allows ionizing radiation to pass through it with little or no absorption. **2.** The extent to which a material transmits ionizing radiation.

radioluminescence Visible light emitted from a radioactive material. A good example is radium; it was once used on wristwatch dials so that they could be seen in the dark.

radiolysis Chemical decomposition brought about by radiation.

radioman A radio technician or operator.

radio map A map of a geographic area, on which lines are drawn connecting measured points of equal field strength for signals from a radio station at the approximate center of the area.

radiometeorograph See RADIOSONDE.

radiometer A device for detecting and measuring the strength of radiant energy. One form consists of a set of vanes blackened on one side and mounted on pivots in a partially evacuated glass bulb. Visible light or infrared causes the vane assembly to rotate, the speed being proportional to the intensity of the light.

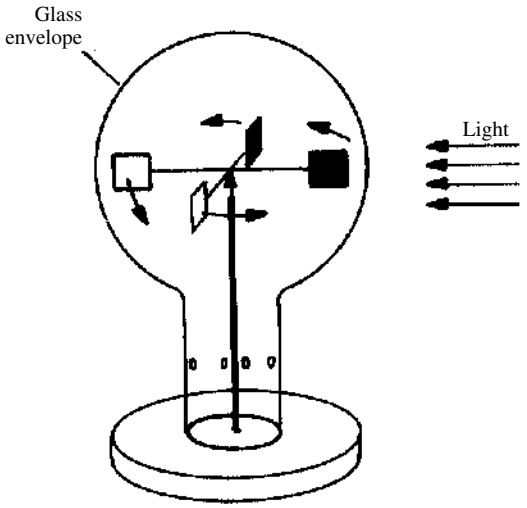

radiometer

radiometry The science and art of measuring radiation in the infrared, visible, and ultraviolet regions of the electromagnetic frequency spectrum. Compare PHOTOMETRY.

radio micrometer See MICRORADIOMETER.

radionavigation The use of radio apparatus, usually in conjunction with computers, by personnel aboard moving vessels, for the purpose of plotting, correcting, and maintaining a course. The intersecting-line method is simplest. Two or three land-based transmitters are needed. Their locations must be accurately known. A direction-finding device on the vessel is used to determine the bearings of each of the transmitters. Aircraft radionavigation can be performed with the aid of radar. The most sophisticated radionavigation techniques employ the Global Positioning System (GPS). Computers are used to project the course of a craft based on its current position, its speed, and the direction of its movement. Course corrections are made by choosing the desired course and having the computer calculate speed and/or direction changes. Compare RADIOLOCATION.

radio net A group of radio stations operating together in an organization, often on or near the same frequency.

radio network See RADIO NET.

radio operator A technician licensed to operate a transmitter in the radio, television, or radar services.

radiopaque Opaque to X rays or other ionizing radiation. Compare RADIOPARENT.

radioparent Transparent to X rays or other ionizing radiation. Compare RADIOPAQUE.

radiophone See RADIOTELEPHONE.

radiophoto A photograph transmitted and received by radio. Also see FACSIMILE.

radio pill See ENDORADIOSONDE.

radio prospecting The use of radio-frequency devices to locate underground or underwater metals and mineral deposits. Also see METAL LOCATOR.

radio range A radio station providing navigational aid to airplanes.

radio receiver The complete apparatus that selects, amplifies, demodulates, and reproduces a radio signal for purposes of communication, as distinct from *facsimile receiver*, *remote-control receiver*, *telemetry receiver*, *television receiver*, etc.

radiosensitivity **1.** The property of being sensitive to ionizing radiation. Most photographic films have this property. **2.** The extent to which a substance or device is sensitive to ionizing radiation.

radio service technician An electronics technician skilled in the repair and maintenance of radio equipment—especially receivers.

radiosonde A balloon-carried combination of radio transmitter and transducers, for sending to a ground monitoring station signals revealing such atmospheric conditions as temperature, humidity, and pressure. It is used mainly for gathering meteorological data at high altitudes.

radiosonobuoy See SONOBUOY.

radio spectroscope A device used by radio astronomers to obtain the radio-frequency profile of a distant star or galaxy. It generally consists of a

5059F-pR-574-606 4/10/01 9:42 AM Page 580

graph, obtained by scanning the radio spectrum and plotting signal intensity as a function of frequency or wavelength.

radio spectrum The continuum of frequencies useful for radio communication and control. Classified in the following manner: *Very low frequency (VLF)*, 9 to 30 kHz; *low frequency (LF)*, 30 to 300 kHz; *medium frequency (MF)*, 300 to 3000 kHz; *high frequency (HF)*, 3 to 30 MHz; *very high frequency (VHF)*, 30 to 300 MHz; *ultrahigh frequency (UHF)*, 300 to 3000 MHz; *super high frequency (SHF)*, 3 to 30 GHz; *extremely high frequency (EHF)*, 30 to 300 GHz.

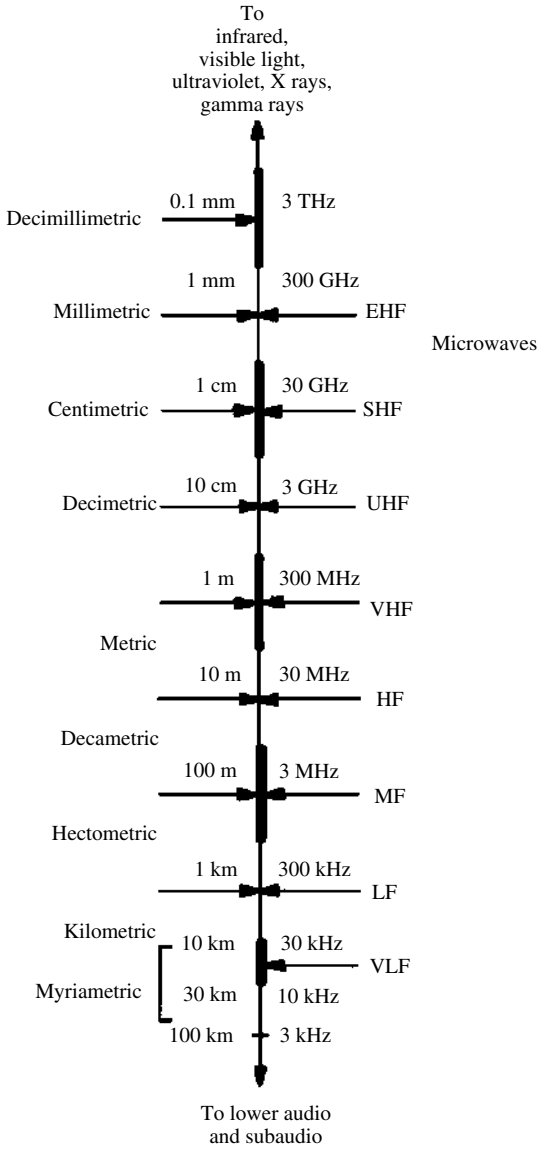

radio spectrum

radiostat See CRYSTAL FILTER.

radio station **1.** The location at which a radio transmitter and/or receiver is/are installed. **2.** The complete set of equipment for a radio receiving and/or transmitting installation, including the studio, linking apparatus, and antennas. **3.** A standard broadcast station.

radio technician A professional skilled in the construction, testing, repair, and maintenance of radio equipment, and sometimes in its design, and who usually works under the supervision of a radio engineer. Also see RADIO SERVICE TECHNICIAN.

radiotelegram See RADIOGRAM.

radiotelegraph **1.** Pertaining to the theory and application of, and the equipment for, Morse code transmission and/or reception via radio. **2.** An installation for Morse code transmission and/or reception via radio. **3.** The transmission and/or reception of Morse code signals via radio.

radiotelegraph code See CONTINENTAL CODE.

radiotelegraph distress signal See SOS.

radiotelegraph monitor See KEYING MONITOR.

radiotelegraphy The transmission and/or reception of telegraphic communications, usually Morse code, by means of radio.

radiotelephone **1.** Pertaining to the theory and application of, and the equipment for, voice transmission and/or reception via radio. **2.** An installation for voice transmission and/or reception via radio. **3.** The transmission and/or reception of voice signals via radio.

radiotelephone distress signal See MAYDAY.

radio/telephone patch See PHONE PATCH.

radiotelephony The transmission and/or reception of audio signals, usually human voices, by means of radio.

radio telescope A directional antenna and associated equipment for receiving and evaluating the radio-frequency electromagnetic radiation from space—especially from celestial objects (such as the sun, planets, stars, nebulae, galaxies, quasars, etc.). See RADIO ASTRONOMY.

radioteletype **1.** Pertaining to the theory and application of, and the equipment for, text data transmission and/or reception via radio. **2.** An installation for text data transmission and/or reception via radio. **3.** The transmission and/or reception of text data signals via radio.

radioteletypewriter A teletypewriter adapted to radio, rather than wire service; it is used in some RADIOTELETYPE installations. In recent years, personal computers and terminals have largely replaced adapted teletypewriters for this purpose.

radiotherapy The use of X rays and/or radioactive substances in the treatment of disease and disorders.

radiothermics The science of the generation of heat by means of radio-frequency current.

5059F-pR-574-606 4/10/01 9:42 AM Page 581

radiothermy See DIATHERMY.
radio thorium Radioactive THORIUM.
radiotracer See TRACER.
radio transceiver A RADIO RECEIVER and RADIO TRANSMITTER built into a single unit, and generally intended for use in two-way communication.
radio transmitter The complete apparatus that generates radio-frequency power, modifies it with the data needed for communication, and delivers the product to an antenna for radiation into space. Here, the radio transmitter is distinguished from similar equipment: *facsimile transmitter*, *remote-control transmitter*, *telemetry transmitter*, *television transmitter*, etc.
radio-transparent material 1. A substance through which radio waves pass with little or no attenuation. **2.** A substance through which X rays, gamma rays, or high-speed subatomic particles can pass with little or no attenuation.
radiotrician Acronym for *radio electrician*. See RADIO SERVICE TECHNICIAN.
radio tube 1. A VACUUM TUBE used at radio frequencies. **2.** A vacuum tube used as an amplifier, local oscillator, detector, or mixer in an early radio receiver.
radiovision See TELEVISION.
radio watch See WATCH.
radio waves Electromagnetic waves in the RADIO SPECTRUM.
radio window That portion of the radio-frequency electromagnetic spectrum that passes through the atmosphere, rather than being refracted or absorbed. The wavelength range is about 20 meters to 5 millimeters, or 15 MHz to 60 GHz. The lower limit of this range is affected by ionospheric conditions. The upper frequency limit depends on various factors, including relative humidity and dust content of the air.
radium Symbol, Ra. A rare radioactive metallic element. Atomic number, 88. Atomic weight, 226.025.
radius The straight-line distance from the center of a circle or sphere to its periphery.
radius vector In spherical or polar coordinates, a line segment drawn from the pole, or origin, and representing the vector magnitude.
radix The number indicating the number of symbols in a system of numerical notation, and the powers of which give the place values of the system. Thus, 10 is the radix of the decimal system, and 2 is the radix of the binary system. Also called BASE.
radix point In a number, the point (dot or period) separating the integral and fractional digits. Its specific name depends on the system of notation involved: *binary point*, *decimal point*, etc.
radome A plastic shell housing a radar antenna—especially aboard an aircraft.
radon Symbol Rn. A gaseous radioactive element that results from the disintegration of radium. Atomic number, 86. Atomic weight, 222.
rad/s Abbreviation of *radians per second*, the SI unit of angular velocity.
rad/s² Abbreviation of *radians per second squared*, the SI unit of angular acceleration.
radux A continuous-wave, low-frequency radionavigation system. Position is determined by comparing the phase of two signals sent from different locations.
RAID Acronym for REDUNDANT ARRAY OF INDEPENDENT DISKS.
rainbow generator A test-signal generator that produces a full color spectrum, a pattern resembling the successive coloration of a rainbow, on the screen of a color-television receiver. Also see RAINBOW PATTERN.
rainbow pattern A test pattern for servicing a color-television receiver. It consists of a full color spectrum, thus taking its name from its resemblance to a rainbow. Also see RAINBOW GENERATOR.
RAM Abbreviation of RANDOM-ACCESS MEMORY.
ramp A sawtooth wave with a linear rise and a practically instantaneous decay; its name was derived from its resemblance to an incline.

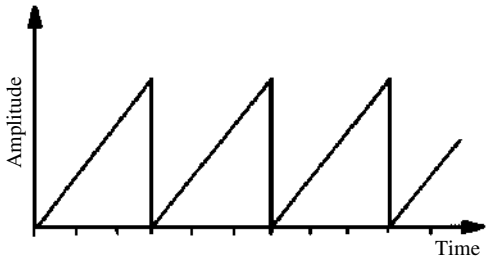

ramp

ramp generator A test-signal generator that produces sawtooth-wave signals. Also see RAMP.
R and D Abbreviation of research and development or research and design. (Also, R&D.)
random access Abbreviation, RA. In computer and data-processing operations, pertaining to storage or memory in which data can be recovered in any order.
random-access memory In computer and data-processing systems, a memory providing access time that is independent of the address.
random deviation Irregular RIPPLE.
random-fed antenna An antenna that uses RANDOM FEED.
random feed A method of connecting a transmission line to an antenna, wherein the feed point is not necessarily at the center and not necessarily at a current loop or voltage loop. This technique is rarely used; it generally results in some radiation from the feed line.

5059F-pR-574-606 4/10/01 9:42 AM Page 582

random noise Electrical noise in which the pulses or fluctuations have no discernible pattern of occurrence (i.e., they are haphazard in frequency and amplitude).

random number A number derived by chance. It is used in statistical analysis for various purposes.

random number generator Hardware or software that provides a sequence of numbers or digits that are random for the purpose of a given statistical application.

random occurrence See CHANCE OCCURRENCE.

random variable In statistics, a variable that can have a number of values, each of the same probability.

random winding A coil winding in which the turns are wound haphazardly to reduce distributed capacitance.

range **1.** The limits within which a circuit or device operates (i.e., the territory defined by such limits). Examples: *current range*, *frequency range*, and *voltage range.* **2.** The difference between the upper and lower limits of deflection of a meter. **3.** The distance over which a transmitter operates reliably. **4.** A clear area for testing antennas. **5.** The distance between a radar station and a target. **6.** The possible values for a quantity or function that lie between given limits.

range capacitor See TRIMMER CAPACITOR.

range-height indicator Abbreviation, RHI. A radar display in which the horizontal axis shows distance to the target, and the vertical axis shows elevation of the target.

range mark See DISTANCE MARK.

range plotting The creation of a graph of the distance (range) to objects, as a function of direction or orientation in two or three dimensions. Commonly used in robot guidance systems.

range resistor See TRIMMER RESISTOR.

range sensing The measurement of distances to objects via electronic methods such as radar, sonar, vision systems, etc. Commonly used in robot guidance systems.

ranging **1.** Any means of determining the distance from a station or vehicle to an object or objects. **2.** Any of several methods for a vehicle, vessel, aircraft, spacecraft, or robot to navigate in its environment by measuring, and keeping track of changes in, the distance between itself and one or more objects or beacons.

rank **1.** To arrange in a specific sequence according to significance. **2.** A place in such a sequence.

Rankine scale A temperature scale on which the freezing point of water is 491.69 degrees, and the boiling point 671.69 degrees. Absolute zero is represented by 0 degrees. For conversion to kelvins, multiply degrees Rankine by 5/9.

rapid drift A fast change of a quantity or setting (usually in one direction) with time.

rapid printer See QUICK PRINTER.

raser A device that produces coherent electromagnetic waves at radio frequencies; the radio-frequency equivalent of a LASER.

raster The rectangle of light (composed of unmodulated lines) seen on the screen of a television picture tube when no signal is present.

ratchet circuit See COMMUTATOR, **2** and ELECTRONIC RATCHET.

rate action See DERIVATIVE ACTION.

rate effect In a four-layer semiconductor device, the tendency for the switch to conduct undesirably as a result of a transient spike.

rate-grown transistor See GRADED-JUNCTION TRANSISTOR.

rate gyro A special gyroscope for measuring angular rates.

rate of change **1.** The extent to which the value of a dependent variable changes in accordance with a specified change in an independent variable (usually time). **2.** A quantitative expression of the speed with which a dependent variable changes, with respect to an independent variable (usually time).

rate signal A signal whose amplitude is proportional to the derivative of a variable, with respect to time.

rate time In automatic-control operations, the time over which the addition of DERIVATIVE ACTION advances PROPORTIONAL ACTION.

ratio-arm bridge A simple four-arm bridge in which the balancing potentiometer supplies the two arms, one on each side of the slider at all settings.

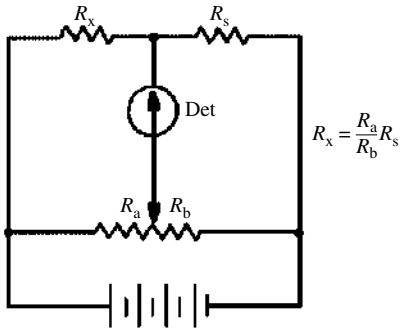

ratio-arm bridge

ratio arms Two impedance arms serving to establish the numerical ratio of a bridge circuit.

ratio control In automatic-control operations, a system in which the controlled variable is in a prescribed ratio to another variable.

ratio detector A frequency-modulation (FM) second detector resembling the FOSTER-SEELEY DISCRIMINATOR, except that one of the two

5059F-pR-574-606 4/10/01 9:42 AM Page 583

diodes is reversed and the junction point of the load resistors is grounded. In an FM circuit using a ratio detector, no limiter is required. The ratio of the direct-current outputs is proportional to the ratio of the instantaneous signal voltages applied to the two diodes.

ratio meter An instrument that compares two different signals (and indirectly their sources) and delivers a reading of their ratio.

rational number A number that can be expressed in the form a/b, where a and b are integers and b is not equal to zero.

rational operation Any of the conventional arithmetic operations: multiplication, division, addition, or subtraction.

ratio of geometric progression In a geometric progression, the ratio of one value to the next.

ratio of similitude The ratio of the lengths of corresponding sides in similar geometric figures.

rat race See HYBRID RING.

raven red A variety of red oxide of iron, a commercial red paint used as the magnetic coating of early recording tapes.

raw ac Unrectified alternating current (ac) or voltage.

raw data Data that has not been processed in any way.

rawinsonde A RADIOSONDE tracked by a radio direction finder to determine wind velocity. The name is an acronym from *radar wind radiosonde.*

raw tape See BLANK TAPE.

ray **1.** A line of radiant energy. Such a line (e.g., the path of a single photon of visible light) is imagined to arise from a point source and have zero width. **2.** A thin beam of radiant energy (e.g., the beam of electrons in a cathode-ray tube). **3.** A quantity of radiant energy or ionizing radiation (e.g, *gamma ray*). **4.** One of numerous lines converging toward, or emanating from, a specific point. **5.** A vector representing the direction in which an electromagnetic field or acoustic disturbance travels. **6.** Also called *half line.* The set of points on a line consisting of a defined origin and all the points on one side of the origin. Example: the positive reactance axis in an ARGAND DIAGRAM.

Raydist A continuous-wave, medium-frequency radionavigation system. The position is determined according to the phase difference between two signals transmitted from different locations.

Rayleigh-Carson theorem An expression of the reciprocal relationship between the transmitting and receiving properties of an antenna. If voltage E applied to antenna A causes current I to flow at a given point in antenna B, then the same voltage (E) applied at that point in antenna B will produce identical current I (same magnitude and phase) at the point in antenna A, where voltage E originally was applied. Also see RECIPROCITY THEOREM.

Rayleigh distribution A probability-density function, used to describe the behavior of sky-wave electromagnetic signals.

Rayleigh's law The hysteresis loss in a magnetic material varies in proportion to the cube of the magnetic induction.

Rb Symbol for RUBIDIUM.

$\boldsymbol{R_B}$ Symbol for BASE RESISTANCE. (Also, r_B.)

RC **1.** Abbreviation of RESISTANCE-CAPACITANCE. **2.** Abbreviation of RADIO-CONTROLLED. **3.** Abbreviation of REMOTE CONTROL.

$\boldsymbol{R_c}$ **1.** Symbol for COLLECTOR RESISTANCE. (Also, r_C.) **2.** Symbol for COLD RESISTANCE.

RCA jack See PHONO JACK.

RCA plug See PHONO PLUG.

RC circuit See RESISTANCE-CAPACITANCE CIRCUIT.

RC-coupled amplifier See RESISTANCE-CAPACITANCE-COUPLED AMPLIFIER.

RC coupling See RESISTANCE-CAPACITANCE COUPLING.

RC filter See RESISTANCE-CAPACITANCE FILTER.

RCL **1.** Abbreviation of RECALL. **2.** Abbreviation of RESISTANCE-CAPACITANCE-INDUCTANCE.

RCM Abbreviation of RADAR COUNTERMEASURES. (Also, radCM.)

RC phase shifter See RESISTANCE-CAPACITANCE PHASE SHIFTER.

RC time constant See RESISTANCE-CAPACITANCE TIME CONSTANT.

RCTL Abbreviation of RESISTOR-CAPACITOR-TRANSISTOR LOGIC.

RC tuning See RESISTANCE-CAPACITANCE TUNING.

RCV Abbreviation for *receive.* (Also, rcv.)

RCVR Abbreviation for RECEIVER. (Also, rcvr, rx.)

rd Abbreviation for *rutherford.*

R & D See R AND D.

$\boldsymbol{R_D}$ Symbol for DRAIN RESISTANCE.

$\boldsymbol{R_d}$ **1.** Symbol for DIODE RESISTANCE. (Also, r_d.) **2.** Symbol for DISTRIBUTED RESISTANCE.

R-DAT Abbreviation of ROTARY DIGITAL AUDIO TAPE.

$\boldsymbol{R_{dc}}$ Symbol for DC RESISTANCE. (Also, r_{dc}.)

RDF Abbreviation of RADIO DIRECTION FINDER.

Re Symbol for RHENIUM.

$\boldsymbol{R_e}$ Symbol for EMITTER RESISTANCE. (Also, r_E.)

REA Abbreviation of *Rural Electrification Administration.*

reachthrough See PUNCHTHROUGH.

reachthrough region See PUNCHTHROUGH REGION.

reachthrough voltage See PUNCHTHROUGH VOLTAGE.

reactance Symbol, X. Unit, ohm. The opposition offered to the flow of alternating current by pure capacitance, pure inductance, or a combination of the two. Reactance introduces phase shift. Also see CAPACITIVE REACTANCE and INDUCTIVE REACTANCE. Compare RESISTANCE.

5059F-pR-574-606 4/10/01 9:42 AM Page 584

reactance chart A nomograph for capacitance, inductance, and frequency.

reactance factor The ratio of the alternating-current resistance of a conductor to the direct-current resistance. The reactance factor generally increases as the frequency increases because of skin effect and because the length of the conductor might be a sizable part of the wavelength of the transmitted energy.

reactance modulator A frequency modulator using a variable reactance, usually a varactor diode in the oscillator.

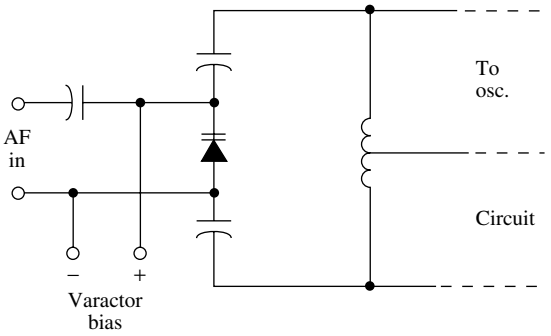

reactance modulator

reactance transistor A transistor used as a REACTANCE MODULATOR.

reaction-time meter See NEOMATACHOGRAPH and NEOMATACHOMETER.

reactive absorber In acoustics, a device that dissipates impinging sound waves by means of reflection, resonance, and other effects, besides dissipation in the form of heat.

reactive attenuator An attenuator that functions by means of reactance, rather than by means of resistance.

reactive current The component of alternating current that is not in phase with the voltage. Compare RESISTIVE CURRENT.

reactive kilovolt-ampere Abbreviation, kVAR. A unit of high apparent power; it is the product of kilovolts and amperes in a reactive component of a circuit. Also see APPARENT POWER, KILOVOLT-AMPERE, REACTIVE VOLT-AMPERE, and VOLT-AMPERE.

reactive load **1.** A load device that is capacitive or inductive, rather than resistive. **2.** A load device that contains reactance as well as resistance.

reactive power See REACTIVE KILOVOLTAMPERE and REACTIVE VOLT-AMPERE.

reactive volt-ampere Abbreviation, VAR. A unit of apparent power; it is the product of volts and amperes in a reactive component of a circuit. Also see APPARENT POWER, KILOVOLT-AMPERE, REACTIVE KILOVOLT-AMPERE, and VOLT-AMPERE.

reactor **1.** An inductor, especially one having very low internal resistance, used principally for its inductive reactance. **2.** A chamber in which the nuclei of atoms are split to provide atomic energy. Also see NUCLEAR REACTOR. **3.** In industrial chemistry, a vat in which reactions take place.

read **1.** In computer operations, to extract data from memory or a storage medium and (usually) transfer it to another area of memory or other medium. Compare WRITE. **2.** In digital communications, to transcribe data into printed form. **3.** In radiotelegraphy, to listen to Morse-code signals and comprehend the text without necessarily writing it down. **4.** To observe and note the indication of an instrument, such as a meter.

readability In electronic communications, the degree to which a desired signal can be recognized and interpreted in a given context.

readback In a multiplexer, a feature that facilitates inspection of the contents of the control latch.

reader A device that transcribes digital signals or markings into meaningful data. Examples: *Morse-code reader* and *bar-code reader.*

read head In a magnetic memory or in a tape recorder or wire recorder used for data recording, the head that picks up the magnetic pulses from the drum, tape, disk, or wire. Compare WRITE HEAD.

reading rate The number of input characters per second that a computer or other data-processing device handles.

read-only memory Abbreviation, ROM. In a computer or calculator, a memory unit in which instructions or data are permanently stored for use by the machine or for reference by the user. The stored information is read out nondestructively.

readout lamp An electron tube containing several cathodes, filled with a gas (such as neon), and used as a numeric or alphanumeric display device. Each cathode is connected to a separate pin on the base. A single anode is common to all cathodes. The cathode(s) to which a voltage is applied glow(s), showing the shape of a numeral, letter of the alphabet, or other symbol. In recent years, this type of display has been replaced by light-emitting diodes (LEDs) and liquid-crystal displays (LCDs).

readout pulse In a random-access memory (RAM), a pulse applied to the word line, facilitating readout of the information in a certain storage slot.

read pulse In computer operations, a pulse that activates the read function (see READ). Compare WRITE PULSE.

read rate The number of data units an input read device can transcribe per unit of time [e.g., *bits per second (bps)* and *words per minute (wpm)*].

readthrough **1.** The reception of signals between transmitted pulses at the same frequency. **2.** The continuous monitoring of a signal being jammed. Any change in the frequency, modulation, or other characteristics of the signal can

5059F-pR-574-606 4/10/01 9:42 AM Page 585

then be detected, and the jamming signal adjusted accordingly.

read time The period during which data is being transferred from a computer storage unit.

read-write channel In computer operations, a channel over which activity between a central processing unit and a specific peripheral occurs.

read-write head An electromagnetic transducer used for both reading and writing data. See READ and WRITE.

read-write memory **1.** A small data storage bank for short-term use. The contents of the memory are easily changed. **2.** See RANDOM ACCESS MEMORY.

real address See ABSOLUTE ADDRESS.

real axis The axis of the real-number component of a COMPLEX NUMBER (i.e., the horizontal axis in an ARGAND DIAGRAM).

real component The real-number part of a COMPLEX NUMBER.

real image The image formed on a screen when rays from the object converge on passing through a lens. Compare VIRTUAL IMAGE.

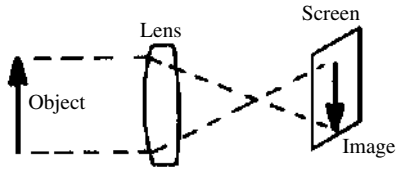

real image

real number A number in the category that includes zero, all rational numbers, and all irrational numbers. Also see COMPLEX NUMBER, IMAGINARY NUMBER, IRRATIONAL NUMBER, and RATIONAL NUMBER.

real power The apparent power multiplied by the power factor in an alternating-current circuit containing reactance. Real power is the difference between the apparent power and the reactive power. Actual radiated or dissipated power cannot exceed the real power.

real time Pertaining to the operation of a computer, communications, or data processing system in which events are represented or acted on as they occur. Data is processed as it becomes available, usually through the use of time-sharing, direct-access storage devices, and remote terminals.

real-time clock A device that produces periodic signals that reflect the interval between events. It is sometimes used to indicate time of day.

rear end The low-frequency portion of a superheterodyne receiver (i.e., the intermediate-frequency amplifier, second detector, and audio-frequency amplifier). Compare FRONT END.

rear projection A method of big-screen television picture reproduction. The image is focused onto a translucent, flat surface. The viewer is positioned on the side of the screen opposite to the projecting beam.

Reaumur scale A thermometer scale on which zero is the freezing point of water and 80 degrees is the boiling point of water. Compare ABSOLUTE SCALE, CELSIUS SCALE, FAHRENHEIT SCALE, and RANKINE SCALE.

rebecca The airborne interrogator in the British REBECCA-EUREKA SYSTEM.

rebecca-eureka system A British 90-mile-hovering radar navigation system that consists of an airborne interrogator (rebecca) and a ground transponder beacon (eureka).

rebroadcast The retransmission of a radio broadcast simultaneously by a station other than the originator. Also see AUTOMATIC RELAY STATION.

rebroadcast station See AUTOMATIC RELAY STATION.

recalescence During the cooling of a metal, the sudden release of heat. Also see RECALESCENT POINT. Compare DECALESCENCE.

recalescent point In a metal whose temperature is being lowered from a higher value, the temperature at which heat is suddenly released. Compare DECALESCENT POINT.

recall Abbreviation, RCL. In computers and calculators, an instruction that brings material from the memory for examination or use. The opposite instruction is STORE.

receiver **1.** A device or system operated at the destination end of a communication link; it accepts a signal and processes or converts it for local use. Also see specific entries for various types of receiver. **2.** The earpiece of a telephone. **3.** A radio broadcast-band tuner integrated with a general-purpose preamplifier and power amplifier, and containing standard jacks for input and output of audio signals to and from peripheral equipment.

receiver detector In a wireless communications or broadcast receiver, a circuit that extracts the information from the signal. The design depends on the type of emission to be received. See also DISCRIMINATOR, ENVELOPE DETECTOR, PHASE-LOCKED LOOP, PRODUCT DETECTOR, RATIO DETECTOR.

receiver dynamic range A quantitative measure of the ability of a wireless receiver to maintain a fairly constant output, and yet to maintain its rated sensitivity, in the presence of signals ranging from very weak to extremely strong. This figure is specified in decibels. It is typically 100 dB or more in a well-engineered communications receiver.

receiver front end The portion of a wireless communications or broadcast receiver consisting of the first radio-frequency (RF) amplifier, and often also including bandpass filters between this amplifier and the antenna. The dynamic range and sensitivity of a receiver are determined by the performance of this stage. These two characteristics are among the most important for any receiver.

5059F-pR-574-606 4/10/01 9:42 AM Page 586

Low-noise, high-gain amplifiers are the rule. Field-effect transistors are commonly used.

receiver IF chain In a wireless communications or broadcast receiver, the series of radio-frequency (RF) amplifier stages in which most of the gain takes place. These stages are also where the best possible RF selectivity is obtained. The intermediate frequency (IF) on which the amplifiers works is a constant frequency. This simplifies the design of the amplifiers to produce optimum gain and selectivity. Crystal-lattice filters or mechanical filters are commonly used in these stages to obtain the desired bandwidth and response.

receiver mixer In a superheterodyne wireless communications or broadcast receiver, a stage that converts the variable input signal frequency to a constant intermediate frequency (IF), or a stage that converts the first IF to a second IF usually having a lower frequency. This type of circuit is nonlinear, and combines the signal with a carrier from a local oscillator (LO). The output is either the sum or the difference of the signal frequency and the LO frequency.

receiver muting See MUTING, **1**.

receiver noise figure A quantitative measure of the ability of a wireless receiver to respond to desired signals while rejecting unwanted noise. This can be quantified in various ways. In general, the lower the noise figure, the better the sensitivity. Gallium–arsenide field-effect transistors (GaAsFETs) are well known for the low levels of noise they generate, even at quite high frequencies. Other types of FETs can be used at lower frequencies. Bipolar transistors tend to be noisy. See also NOISE FACTOR, NOISE FIGURE.

receiver post-detector stages In a wireless communications or broadcast receiver, one or more stages of amplification and/or filtering employed to refine the detector output to a form suitable for feeding a speaker, headset, printer, fax machine, slow-scan television picture tube, computer, electromechanical device, or other peripheral equipment.

receiver primaries See DISPLAY PRIMARIES.

receiver selectivity A quantitative measure of the ability of a wireless receiver to respond to a desired signal, but not to undesired ones. The frequency window is established by a preselector in the early RF amplification stages, and is honed to precision by bandpass filters in later amplifier stages. The preselector passes energy within a range of about plus-or-minus 10 percent of the signal frequency; other frequencies are attenuated. This reduces the chance for strong, out-of-band signals to impair the performance of the receiver. The narrowband filter in the final intermediate-frequency (IF) stage responds only to energy within the actual signal band. This minimizes adjacent-channel interference. In some receivers, yet another bandpass filter is used in the audio-amplifier stages.

receiver sensitivity A quantitative measure of the ability of a wireless receiver to recover weak signals and process them into readable data. The most common expression is the number of signal microvolts that must exist at the antenna terminals to produce a certain signal-to-noise ratio (S/N). Sometimes, the signal-plus-noise-to-noise ratio (abbreviated S+N/N) is given. The front end, or first RF amplifier stage, of a receiver is the most important stage with regard to sensitivity. Sensitivity is directly related to the gain of this stage, but the amount of noise the stage generates is even more significant. A good front end should produce the best possible S/N or S+N/N ratio at its output. All subsequent stages amplify the front-end noise output as well as the front-end signal output.

receiving set RADIO RECEIVER.

receiving station A station that ordinarily only receives signals (i.e., it makes no type of transmission). Compare TRANSMITTING STATION.

receptacle **1.** See SOCKET. **2.** The half of a connector that is mounted on a support, such as a panel, and that is therefore stationary.

recharge In certain cells and batteries, the restoration of chemical energy following use so that the device is ready to deliver its full rated electric current. Also see RECHARGEABLE.

rechargeable Pertaining to a secondary cell or battery that can accept a restoration of chemical energy following use, and thus can be completely charged and discharged numerous times. Examples: *nickel-metal-hydride (NiMH) battery* and *lead-acid battery*.

reciprocal impedances See INVERSE IMPEDANCES.

reciprocal ohm See SIEMENS and MHO.

reciprocation **1.** The determination of a mathematical reciprocal value from a given value. **2.** The transmission of a message in response to a received message.

reciprocity in antennas See RAYLEIGH-CARSON THEOREM.

reciprocity theorem When a voltage E across branch A of a network causes a current I to flow in branch B of the network, the voltage can be applied across branch B to cause the same value of current to flow in branch A. Compare COMPENSATION THEOREM, MAXIMUM POWER TRANSFER THEOREM, NORTON'S THEOREM, SUPERPOSITION THEOREM, and THEVENIN'S THEOREM.

recombination The refilling of holes by electrons in a semiconductor.

recombination current In a transistor circuit, base current resulting from recombination.

recombination rate In a semiconductor material, the speed at which the electrons and holes recombine. It can be expressed as the time required for a certain proportion of charge carriers to recombine.

5059F-pR-574-606 4/10/01 9:42 AM Page 587

recompile In computer operations, to COMPILE again, usually according to program amendments following debugging, or to create a different form of a program so that it will be compatible with other hardware.

record **1.** See PHONOGRAPH DISC. **2.** A chart delivered by a graphic recorder. **3.** To make one of the foregoing. **4.** In data processing, a constituent of a file. **5.** In data processing, a data unit portraying a specific transaction.

record blocking In data processing operations, making data blocks from groups of records so that the blocks can, in a single operation, be transferred to a nonvolatile storage medium, such as diskette or tape.

record count A usually running total of a file's records.

recorded disc A phonograph disc on which a recording has been made. Also called PRERECORDED DISC.

recorded tape Magnetic tape containing recorded material. Also called PRERECORDED TAPE. Compare BLANK TAPE.

recorder **1.** A machine for preserving sound, video, or data signals in the sequence in which they occur (e.g., DISC RECORDER, TAPE RECORDER, and WIRE RECORDER). **2.** A machine for making a permanent visual record (photographically or by stylus) of an electrical phenomenon. Examples: DRUM RECORDER and OSCILLOGRAPH.

record head See RECORDING HEAD.

recording density In a magnetic storage medium, the number of information units (bits, bytes, etc.) represented by magnetized areas, per unit area or length.

recording disc A phonograph record on which material has not been recorded, or from which recorded material has been removed. Compare PRERECORDED DISC.

recording head In a magnetic recorder/reproducer, the head that magnetizes the medium in accordance with sounds or other signals. Also called RECORD HEAD and WRITE HEAD. Compare PLAYBACK HEAD.

Recording Industry Association of America Abbreviation, RIAA. An organization that sets standards for audio recording and reproduction in the United States.

recording instrument A measuring instrument, such as a voltmeter or ammeter, that makes a permanent record of its deflections. Also see RECORDER, **2**.

recording loss **1.** Loss of data during a recording process. **2.** Loss resulting from recording efficiency of less than 100 percent; audio power loss.

recording tape Magnetic tape on which nothing has been recorded, or from which all data has been erased. Compare PRERECORDED TAPE.

recovery time **1.** Symbol, t_r. The time required for a semiconductor pn junction to attain its high-resistance state when the bias voltage is suddenly switched from forward to reverse. **2.** The time required for a circuit to recover from momentary overdrive. **3.** The time required for a computer system to stabilize following a degenerative operation. **4.** The time required for switching a memory from the write to the read mode. It is measured as the length of time from switching out of the write mode until meaningful signals occur at the output. **5.** In a transceiver, the time required from the completion of a transmitted signal until the receiver is activated.

rect Abbreviation of RECTIFIER.

rectangular coordinates See CARTESIAN COORDINATES.

rectangular scan **1.** A method of beam scanning in a cathode-ray tube, in which the beam moves sequentially in parallel lines to cover a rectangular region. Used in television. **2.** In radar, a two-dimensional scan, covering a specific rectangular region.

rectangular wave An alternating or pulsating current or voltage whose rise and decay times are essentially zero, and whose maxima and minima are essentially flat, but not necessarily of equal duration. The SQUARE WAVE is a special type of rectangular wave.

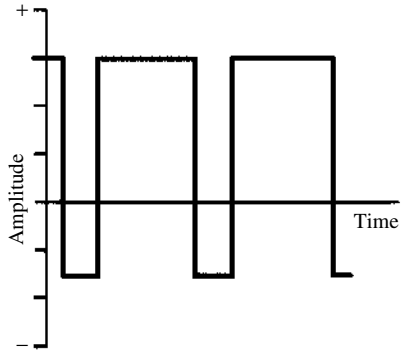

rectangular wave

rectangular waveguide A waveguide having a rectangular cross section.

rectification The conversion of alternating current into pulsating direct current by any means other than the use of a motor-generator. Also see RECTIFIER.

rectification efficiency The ratio (expressed as a percentage) of the direct-current output voltage to the peak alternating-current input voltage of a rectifier.

rectified alternating current The unfiltered, pulsating direct-current output of a rectifier. It consists of the unidirectional half-cycles passed by the rectifier (one per cycle for half-wave rectification, and two per cycle for full-wave rectification).

5059F-pR-574-606 4/10/01 9:42 AM Page 588

rectifier Abbreviation, rect. An electronic or electromechanical device that converts alternating current into pulsating direct current.

rectifier diode A heavy-duty tube or semiconductor diode designed primarily to change alternating current to pulsating direct current in power supplies.

rectifier filter A circuit containing parallel capacitance, sometimes in combination with series inductance, intended for smoothing out the ripple in the output of a power-supply rectifier.

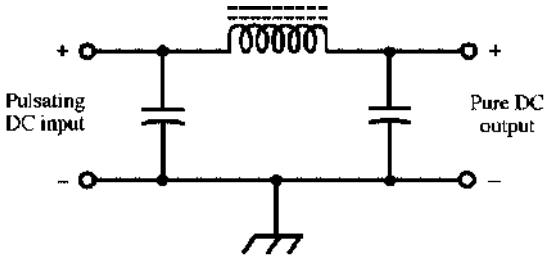

rectifier filter

rectifier-filter system The rectifier plus power-supply-filter combination for converting alternating current into direct current.

rectifier photocell A photovoltaic cell consisting of two layers of material with a semiconductor junction between them. The device produces direct current when exposed to visible light, infrared, or ultraviolet radiation.

rectifier probe A diode-type probe used with a direct-current (dc) voltmeter to measure radio-frequency (RF) voltage. The diode rectifies the RF signal and presents to the meter a dc voltage proportional to the peak RF voltage.

rectifier stack An assembly of separate rectifier disks or plates in series on a central bolt, as in most selenium rectifiers.

rectifier tube A two-element electron tube, once commonly used for converting alternating current into pulsating direct current in high-voltage, high-current power supplies.

rectifier-type meter See DIODE-TYPE METER.

rectilinear chart A graphic-recorder chart in which the crossing coordinates are arcs, rather than straight lines, to correspond to the swing of the pen. Also see STRIP CHART.

rectilinear scan See RECTANGULAR SCAN, **1**.

recurrent network A circuit in which several sections of identical configuration (e.g., L sections) are cascaded.

recurrent phenomenon A phenomenon that repeats itself periodically.

recurrent sweep In an oscilloscope, a repetitive horizontal sweep of the beam occurring at a frequency determined by the settings of the sweep controls. Also called REPETITIVE SWEEP. Compare NONREPETITIVE SWEEP.

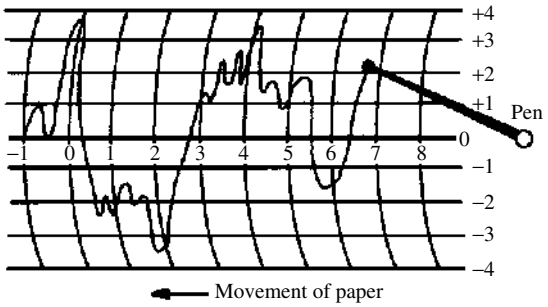

rectilinear chart

recursion **1.** Generating a complete sequence of functions or numbers by applying an algorithm to initial values in the sequence. **2.** In computer programming and artificial intelligence, a logical process containing loops in calculation or reasoning.

recursive Relating to a procedure or set of steps that repeat endlessly.

Red Book The first format developed for compact-disc data storage media, developed by Sony and Philips. It is commonly used in digital audio systems. See also CD-ROM, GREEN BOOK, ORANGE BOOK, and YELLOW BOOK.

red-green-blue Abbreviation, RGB. In video applications, the three primary colors from which all other colors are derived. Also see COLOR TELEVISION.

red gun In a three-gun color-television picture tube, the electron gun whose (correctly adjusted) beam strikes only the red phosphor dots on the screen.

red oxide of iron An iron oxide of the general formula Fe_2O_3, used as the magnetic coating of recording tape. Also see IRON OXIDE.

red oxide of zinc See ZINCITE.

red-tape operation An operation or function needed for organizational purposes, but that does not directly contribute to the completion of the task at hand.

reduced instruction set computer Abbreviation, RISC. A computer architecture in which program instructions are simplified to obtain enhanced processing speed. It is useful especially in complex graphics, animation, multimedia, and scientific work requiring many calculations.

reductio ad absurdum A method of obtaining a conclusion by proving that its negation results in a contradiction. It is sometimes used in computer programming involving mathematical proofs.

reduction In an electrochemical cell or battery, a transfer of electrons to the active chemical.

reductionism The theory that all human thought processes, including emotion and intuition, can

5059F-pR-574-606 4/10/01 9:42 AM Page 589

be reduced to digital logic, and thus can be duplicated by a sufficiently powerful computer. It is of interest to researchers in artificial intelligence.

reductionist A person who subscribes to the theory of REDUCTIONISM.

redundancy **1.** The repetition of components in a circuit (e.g., series or parallel connection of them) so that one will be available for circuit operation if the other fails. **2.** Having available more than one method for performing a function. **3.** Having on hand several copies of data as a safeguard against data loss.

redundancy check A check for the integrity of digitized data to which extra bits have been added for the purpose (e.g., *parity check*).

redundant **1.** Pertaining to any two units of data that resemble each other in such a manner that if either unit is removed, no information is lost from the system. **2.** A unit of data that contains information already present in the system.

redundant array of independent disks Acronym, RAID. A set of data storage media used to store video programs.

red video voltage In a three-gun color-television circuit, the red-signal voltage that actuates the red gun.

reed A usually thin metal blade, leaf, or strip used in vibrators, reed-type relays, reed-type oscillators, and similar devices.

reed oscillator See REED-TYPE OSCILLATOR.

reed relay See DRY-REED SWITCH and MERCURY-WETTED REED RELAY.

reed-relay logic Logic circuits using reed relays. Also see RELAY LOGIC.

reed switch **1.** A frequency-sensitive switch in which the movable contact is mounted on the tip of a thin, metal strip (reed). The reed is actuated by an alternating-current (ac) coil. The reed closes the contacts when the ac excitation is at its natural frequency. **2.** See DRY-REED SWITCH.

reed-type oscillator An electromechanical audio-frequency oscillator whose frequency is controlled by a vibrating metal strip (reed) instead of a tuning fork. Also see HUMMER.

reed-type switch See REED SWITCH.

reel **1.** The spool around which a magnetic tape or video film is wound. **2.** A spool containing magnetic tape or video film.

reentrant cavity A resonant cavity in which one or more sections are directed inward to confine the electric field to a small volume.

reentrant winding A winding of wire that returns to its starting point—especially in a motor armature.

ref Abbreviation of REFERENCE.

reference address As a point of reference, an address for instructions having relative addresses.

reference amplifier A voltage-regulation device consisting of a transistor and Zener diode in the same envelope.

reference angle In radar, the angle of incidence of the beam against a target surface, measured with respect to the normal (perpendicular) line at the surface.

reference antenna A standard antenna, such as an isotropic radiator or a half-wave dipole, used to establish a reference for determining the relative gain of another antenna.

reference bias current In a reference amplifier, the input current that subtracts from the reference current. It is generally measured in microamperes.

reference current range In a digital-to-analog converter, the difference between the maximum and minimum reference current for which the device is within specifications for resolution.

reference diode A Zener diode whose constant voltage drop is used as a direct-current reference potential in calibrator circuits and voltage regulators.

reference dipole See REFERENCE ANTENNA.

reference electrode For use with a pH meter, an electrode that provides a reference potential.

reference input slew rate In a digital-to-analog converter, the average rate of change in output for a given change in the reference input. It is expressed in milliamperes or microamperes per microsecond.

reference level A specific value of a quantity (e.g., current, frequency, power, or voltage) to which other values of the same quantity are referred.

reference time The point at which a trigger pulse attains 10 percent of its maximum amplitude.

reference tone A standard audible tone of known frequency [e.g., 440 Hz (representing A below middle C)]. Sometimes the intensity as well, as the frequency, is specified.

reference white level The television picture signal value representing the uppermost limit for peak white signals.

R_{eff} Symbol for EFFECTIVE RESISTANCE.

reflectance **1.** See MISMATCH FACTOR. **2.** The reflected part of the radiant flux striking a surface. It is expressed as a fraction of the total incident radiation.

reflected binary code See CYCLIC CODE.

reflected electromagnetic field In a transmission line, the electromagnetic energy not absorbed by the load when an impedance mismatch exists between the load and the line. See INCIDENT POWER and REFLECTED POWER.

reflected impedance In a coupled circuit, the impedance in the secondary that appears in the primary circuit, or vice-versa, as if it were reflected through the coupling transformer.

reflected power In a transmission line not perfectly matched to a load at the feed point, an expression of the amount of electromagnetic field reflected from the feed point, rather than absorbed by the load. In general, this can be expressed in watts or as a percentage of the incident power. It is not a true indicator of the

5059F-pR-574-606 4/10/01 9:42 AM Page 590

loss caused by the mismatch because the reflected field is usually all returned again when it arrives back at the transmitter.

reflected-power meter A radio-frequency instrument, connected between a source and a load, that can measure INCIDENT POWER and REFLECTED POWER.

reflected ray The ray that is reflected by the surface of a body or region it strikes. Compare INCIDENT RAY and REFRACTED RAY.

reflected resistance **1.** In a transformer, the effective resistance across the primary winding when a resistive load is connected to the secondary. **2.** In a transmission line, the resistance at the input end when a load is connected to the output end.

reflected wave **1.** An electromagnetic wave reflected by the ionosphere or by the surface of the earth. Compare INCIDENT WAVE and REFRACTED WAVE. Also see IONOSPHERE and IONOSPHERIC PROPAGATION. **2.** A wave that is bounced off an obstruction, such as a building or mountain.

reflecting galvanometer A galvanometer having a light-beam pointer.

reflecting shell See IONOSPHERE.

reflection **1.** The turning back of a ray by a surface it strikes. Examples of reflecting media are the surface of the earth, the polished surface of a material, and a layer of the ionosphere. Compare REFRACTION. **2.** The return of energy to the source by the mismatched end of a transmission line or by the end of a radiator.

reflection error In a radar, radionavigation, or radiolocation system, an error in the reading caused by reflections of the signal from objects other than the intended signal source or object.

reflection factor See MISMATCH FACTOR.

reflection law When a ray strikes a smooth reflecting surface, the angle of incidence is equal to the angle of reflection.

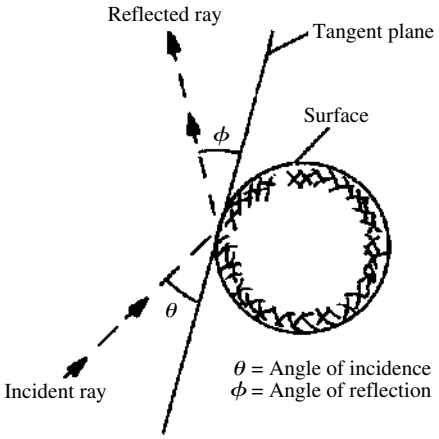

reflection law

reflection loss **1.** Loss caused by the reflection of an electromagnetic field at a discontinuity in a transmission line. **2.** Loss that occurs when an electromagnetic wave is reflected from a surface or object.

reflection phase grating A device that diffuses sound waves by diffraction effects. The acoustic equivalent of an electromagnetic-wave DIFFRACTION GRATING.

reflective code See GRAY CODE.

reflectivity **1.** See MISMATCH FACTOR. **2.** The degree to which a point, plane, or surface reflects the radiation (light, for example) that strikes it.

reflectometer **1.** See REFLECTED-POWER METER. **2.** A type of photometer used to measure reflection.

reflector **1.** A smooth, metal surface or wire screen for reflecting radio waves. See, for example, PARABOLIC REFLECTOR. **2.** A length of wire, rod, or tubing used in a parasitic antenna to reflect radio waves. Compare DIRECTOR and RADIATOR. **3.** A polished surface for reflecting visible light or infrared rays (i.e., a mirror). **4.** See REPELLER.

reflector element See REFLECTOR, **2**.

reflector satellite A satellite whose skin reflects radio waves.

reflector voltage In a reflex Klystron, the reflector-to-cathode voltage.

reflex baffle A loudspeaker BAFFLE constructed so that some of the sound radiated to the rear of the diaphragm is transmitted forward (after phase shift) to boost acoustic radiation at some frequencies.

reflex bunching In a Klystron, electron bunching following direct-current-field-induced reversal of the velocity-modulated electrons. Also see REFLEX KLYSTRON.

reflex circuit A radio receiver circuit in which a single transistor is used successively for different functions. For example, one active device can act as a mixer and as a radio-frequency amplifier.

reflex Klystron A Klystron having only one cavity. This cavity serves first as the buncher and then, as the electrons are turned around and caused to pass through again, as the catcher.

refracted ray The ray that is refracted by a body or region through which it passes. Compare INCIDENT RAY and REFLECTED RAY.

refracted wave An electromagnetic wave that is refracted by the ionosphere. Compare INCIDENT WAVE and REFLECTED WAVE. Also see IONOSPHERE and IONOSPHERIC PROPAGATION.

refraction The bending of an energy ray as it passes through media that cause a change in the speed of propagation. It can occur with radio waves, infrared, visible light, ultraviolet, X rays, gamma rays, and sound waves.

refractive index See INDEX OF REFRACTION.

refractivity The extent of the ability to refract, given as the quantity $(v_1/v_2) - 1$, where v_1 is the phase

5059F-pR-574-606 4/10/01 9:42 AM Page 591

velocity in free space, and v_2 is the phase velocity in the medium through which a wave passes.

refractory A heat-resistant, nonmetallic ceramic material.

refrigerator A chamber used to maintain a circuit or component at a constant temperature that is lower than the ambient temperature. This device is analogous to the oven, which maintains a higher temperature than the surrounding medium. A refrigerator can be used to maintain precise frequency for a reference oscillator.

regeneration **1.** The processing of a distorted signal so that it has its original characteristics. **2.** Positive feedback generally used for the purpose of causing oscillation, or for detection in a regenerative receiver. See POSITIVE FEEDBACK.

regeneration period The period during which the electron beam scans a cathode-ray tube screen to restore changes to the screen surface.

regenerative amplifier An amplifier that uses regeneration to increase its gain and/or selectivity.

regenerative detector A detector provided with regenerative feedback. Although such a detector is sensitive, it can be unstable. Compare NONREGENERATIVE DETECTOR.

regenerative feedback Feedback producing regeneration (i.e., positive feedback). Compare DEGENERATIVE FEEDBACK.

regenerative IF amplifier An intermediate-frequency amplifier in which regeneration is introduced to boost sensitivity and, sometimes, selectivity.

regenerative reading A method of reading data (see READ) so that it is automatically restored, by writing, to locations from which it came.

register In computer systems, an arrangement of several storage devices, such as flip-flops, for storing a certain number of digits (a two-bit register, for example, requires two flip-flops).

register capacity The range of values for quantities that can be handled by a register.

registered professional engineer A title granted by a state board of examiners to a person licensed to work as an engineer.

register length The number of characters or bits that can be held in a register, according to its capacity.

registration The accurate alignment of terminals or other points on different components or on opposite sides of a board so that when the surfaces containing those points are overlaid, all points mate precisely.

regulated power supply A power supply whose output is held automatically to a constant level or within a narrow range, regardless of loading variations.

regulating transformer See VOLTAGE-REGULATING TRANSFORMER.

regulation **1.** In general, the adjustment or control of a component, device, or system. **2.** Automatic control. See, for example, SELF-REGULATION.

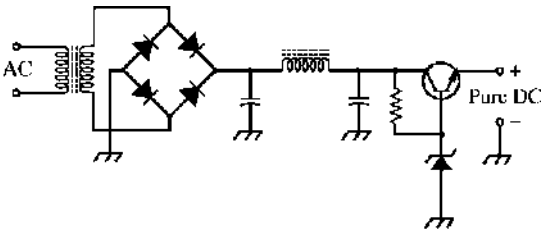

regulated power supply

3. See CURRENT REGULATION. **4.** See VOLTAGE REGULATION.

regulator **1.** A device that automatically holds a quantity to a constant value (e.g., a voltage regulator). **2.** A device via which a quantity can be varied (e.g., *potentiometer*, *rheostat*, and *variable autotransformer*).

regulator diode A semiconductor diode—especially a Zener diode used as a two-terminal voltage regulator.

reinitialization The setting of all lines in a microcomputer or microprocessor to logic zero automatically when power is removed, then reapplied.

reject amplifier A tuned amplifier having the response of a band-suppression filter. Like the filter, the amplifier rejects or severely attenuates one frequency (or band of frequencies) while readily passing lower and higher frequencies. Compare PASS AMPLIFIER.

reject filter See REJECTION FILTER.

rejection circuit A circuit performing the function of a REJECTION FILTER.

rejection filter A filter that suppresses one frequency (or band of frequencies) while passing all other frequencies.

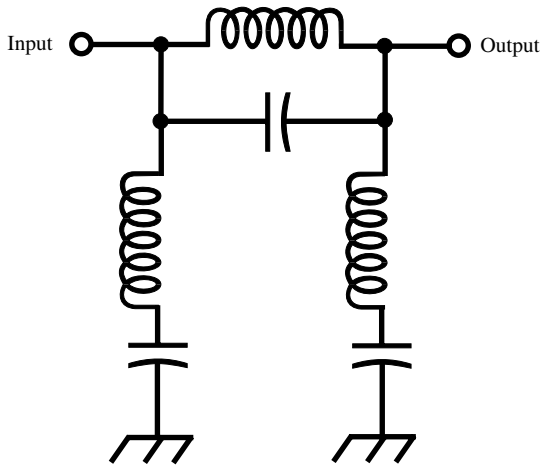

rejection filter

5059F-pR-574-606 4/10/01 9:42 AM Page 592

rejection notch A sharp dip in the transmission characteristic of a crystal filter. It provides rejection-filter action at the notch frequency. Also see CRYSTAL RESONATOR and REJECTION FILTER.

rejectivity The degree to which a selective circuit rejects an unwanted signal. Compare TRANSMITTIVITY.

rejuvenation See REACTIVATION.

rel Symbol, R. The cgs unit of reluctance, equivalent to gilberts per maxwell.

relative accuracy In a measuring instrument, the error determined as a percentage of the actual value; the difference between the actual and measured values, divided by the actual value, then multiplied by 100.

relative address In the address part of a computer program instruction, a number specifying a location relative to a BASE ADDRESS. When the base address is added to the relative address, it yields the ABSOLUTE ADDRESS.

relative error The ratio of the absolute error to the exact value of a quantity.

relative gain The current, voltage, or power gain, measured, with respect to a reference standard.

relative humidity Abbreviation, rh. The ratio, as a percentage, of the amount of moisture in the air to the amount the air could contain at a given temperature. Compare ABSOLUTE HUMIDITY.

relative luminosity Luminosity measured with respect to a reference level.

relative permeability The ratio of the permeability of a given material to the permeability of another material (or of the same material under different conditions).

relative power Power level specified with respect to another (often reference) power level.

relative uncertainty The uncertainty of a measurement divided by the measured value. The maximum value that this quotient can have is 1. Also see UNCERTAINTY IN MEASUREMENT.

relative visibility Response of the human eye to light. This is relative because the eye does not see equally well throughout the visible spectrum. The peak response of the human eye is around 5.4×10^{14} Hz; this represents yellow-green light. Photoelectric devices have peak responses that can differ considerably from this value.

relativity theory See EINSTEIN'S THEORY.

relaxation A delayed change in circuit conditions, as a result of change in the input.

relaxation inverter An inverter circuit in which the direct-to-alternating-current conversion device is a RELAXATION OSCILLATOR.

relaxation oscillator An oscillator whose operation results from the buildup of a charge in a capacitor, followed by sudden discharge of the capacitor, the sequence being repeated periodically. In one circuit, a capacitor is connected in series with a resistor and a direct-current power supply, and a neon bulb is connected in parallel with the capacitor. The output is a sawtooth wave.

relaxation time **1.** The time required for an exponentially decreasing variable to fall to $1/e$ (approximately 36.8 percent) of its initial value, where e is the natural-logarithm base (approximately 2.71828). **2.** For a gas, the time required for it to return to its original state after having been disturbed.

relay **1.** A signal-actuated switching device. In most instances, a relatively weak current or voltage is used to make the relay switch a higher current or voltage. A relay can be electromechanical or fully electronic (no moving parts). See, for example, ELECTROMECHANICAL RELAY and ELECTRONIC RELAY. **2.** A repeater station. **3.** In communications, to receive a message and retransmit it en route from a source to a destination.

relay amplifier See RELAY DRIVER.

relay booster See RELAY DRIVER.

relay driver A direct-current amplifier (usually one stage) used to actuate an electromechanical relay in response to a low-powered signal.

relay flip-flop See BISTABLE RELAY.

relay logic Abbreviation, RL. In computer and industrial-control operations, a logic system using electromechanical relays as flip-flops (see BISTABLE RELAY).

relay transmitter See AUTOMATIC REPEATER STATION.

release time **1.** The interval between the instant power is removed from a relay and the instant the armature is released sufficiently to operate the contacts. **2.** The time between one control input becoming inactive and another becoming active. **3.** The time required for reception to resume in a transceiver, once transmission has stopped. **4.** An expression for the rapidity with which an automatic gain control reverts to maximum sensitivity following the reception of a strong signal.

reliability **1.** The dependability of operation of a device or circuit under specified conditions. **2.** The proportion of units that still work after a set of units has been in use for a specified length of time.

reliability engineering The branch of engineering devoted to the theory and application of reliability; based on fundamental engineering and advanced statistical concepts.

reluctance Symbol, R. SI unit, A/Wb; cgs unit, rel. In a magnetic circuit, the opposition to the establishment of a magnetic field; it is analogous to resistance in electric circuits.

reluctance motor An electric motor having a squirrel-cage rotor with some of its teeth ground down, and a shaded-pole or split-phase type of stator that supplies a rotating magnetic field. When starting, this motor comes up to speed like an induction motor, but the protruding teeth of the rotor then follow the field in the manner of the poles of a hysteresis motor.

5059F-pR-574-606 4/10/01 9:42 AM Page 593

reluctivity Specific reluctance (i.e., the reluctance of a sample of magnetic material one centimeter long and one square centimeter in cross section). Reluctivity is the reciprocal of permeability.

rem Acronym for *roentgen equivalent man*, an amount of ionizing radiation having the same effect on the body as a one-roentgen dose of gamma or X radiation.

remagnetizer A magnetizer used principally to restore weakened permanent magnets.

remainder **1.** The result of subtracting one quantity (the subtrahend) from another (the minuend). Also called DIFFERENCE. **2.** In division, the numerical value left over after the integral part of the quotient has been determined; it becomes the fractional part when divided by the divisor. For example, in 25/3, the remainder is 1.

remanence See RESIDUAL MAGNETISM.

remanent flux density See REMANENCE.

remodulator Any device that changes the modulation of a signal from one form to another, such as from frequency modulation to amplitude modulation, without loss of intelligence.

remote alarm In security systems, an alarm that occurs at a location different from where an intrusion occurs (e.g., at the headquarters of a security company).

remote control Control of distant devices by mechanical means or by radio-frequency signals sent from a transmitter especially designed for the purpose; in the latter case, it is sometimes called *radio control.*

remote-control receiver The complete device that selects, amplifies, and demodulates or rectifies a radio signal for control of a circuit or mechanism at a distance from the transmitter of the control signal. Some receivers have self-contained antennas.

remote-control transmitter The complete device that generates radio-frequency power, adds to it the signals needed for remote control, and radiates the modified power.

remote-control system The complete set of hardware units and software programs facilitating the operation of a computer or robot from a distance.

remote data terminal In a computer system, a terminal connected to the central processor by a telephone line or radio link. It is used for the transfer of data without providing control of the system. Also called *remote data station.*

remote error sensing A method of regulation used in some power supplies. The voltage across the load, or the current through the load, is determined by remote control. The power-supply output is adjusted to compensate for losses in the system.

remote job entry In computer operations, the keying-in of input data at a site physically distant from the central processor.

remote tuning The electrical or radio tuning of a circuit or device from a distance.

rendering In three-dimensional computer animation, the software process in which all the aspects of the model are combined to obtain the presentation.

rep **1.** Acronym for *roentgen equivalent physical*, an amount of ionizing radiation that, upon absorption by body tissue, will develop the energy of a one-roentgen dose of gamma or X radiation. **2.** Colloquial abbreviation for *repetition*, as in *rep rate.* **3.** Colloquial abbreviation for *representative*, as in *service representative.*

repeatability The ability of an instrument, system, or method to give identical performance or results in successive instances.

repeater A receiver/transmitter device that retransmits a signal it receives from another source, often simultaneously. In this way, a signal can be transmitted on several frequencies, or the service area of the original station can be extended. Also see ONE-WAY REPEATER and TWO-WAY REPEATER.

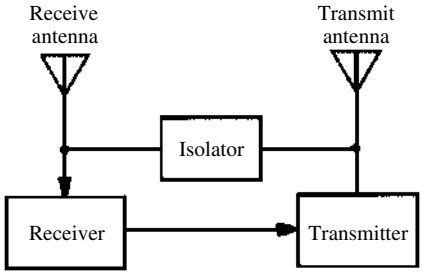

repeater

repeater station See AUTOMATIC REPEATER STATION and REPEATER.

repeating decimal A decimal fraction in which groups of digits recur endlessly (e.g., 25/99 = 0.252525. . .).

repeller An electrode, especially in a velocity-modulated tube, for reversing the direction of an electron beam.

repertoire The instruction set for a particular object or source computer programming language.

repetition instruction In a loop in a computer program, an instruction that causes the repetitive implementation of one or more instructions.

repetitive phenomenon See RECURRENT PHENOMENON.

repetitive sweep See RECURRENT SWEEP.

replication In an electronic system, especially in a computer, the redundancy of hardware units to provide standby facilities in case of failure.

replacement A component or circuit that can be substituted directly for another; it fits exactly into place and functions exactly like the component it replaces, without modification to the equipment.

5059F-pR-574-606 4/10/01 9:42 AM Page 594

report **1.** The results of testing and evaluation of a device, organized into a written document. **2.** The output of a computer, printed on paper for permanent reference.

report program generator Abbreviation, RPG. A computer programming language with which programs can be produced for the generation of business reports.

reproduce head See PLAYBACK HEAD.

reproducing stylus A stylus for the playback of material from a phonograph disc.

reproduction **1.** The recovery of data from storage, and its presentation in original form. **2.** Data obtained by the process defined in **1**. **3.** See PLAYBACK.

reproduction loss See PLAYBACK LOSS.

repulsion A force that pushes objects away from each other, as between similar electric charges or similar magnetic poles. Compare ATTRACTION. Also see LAW OF REPULSION.

repulsion-induction motor An alternating-current motor arranged to start as a REPULSION MOTOR and run as an INDUCTION MOTOR, but with better regulation than that of the latter.

repulsion motor An alternating-current motor having an armature and commutator similar to those of a direct-current motor, and a stator similar to that of a split-phase motor, without the auxiliary starting winding. Repulsion caused by the negative half-cycle of torque is utilized to drive the armature, by placing the brushes in such a way that they close the coils only when the latter are in position to receive this repulsive action.

repulsion-start motor An alternating-current motor that starts as a REPLUSION MOTOR but at approximately 75 percent of full speed. Its commutator is automatically short-circuited and the motor runs as an INDUCTION MOTOR. Also see REPULSION INDUCTION MOTOR.

request slip In computer operations, peripheral and memory needs for a program given in a written statement.

reradiation Radiation of energy by a body that has been exposed to radiation, as when a receiving antenna retransmits a signal.

rerecording A recording of played-back material.

reroute **1.** In computer operations, to establish new channels between peripherals and main memory. **2.** To establish new circuit paths, physically (as by changing conductor orientation) or electronically (as by selecting an alternate signal bus).

rerun See ROLLBACK.

res **1.** Abbreviation of RESISTANCE or RESISTOR. (Also, R and r.) **2.** Abbreviation of RESEARCH. **3.** Abbreviation of RESOLUTION.

reset **1.** The clearing of a flip-flop of data in storage (i.e., the setting of the flip-flop to its zero state). **2.** In a computer program, an instruction to initialize the value of a variable. **3.** In a security system, a function that terminates an alarm signal following an intrusion, and renders the system operational again so that it can detect subsequent intrusions should they occur.

reset action **1.** The return of a circuit or device to its normal operating condition. **2.** A method of adjusting a circuit to compensate for the severity of an abnormal condition. The extent of readjustment is determined by the extent of the departure from normal conditions.

reset generator A circuit or device that generates a pulse for resetting a flip-flop or counter. Also see RESET and RESET TERMINAL.

reset pulse A pulse that resets (see RESET, **1**) a storage cell in a computer memory.

reset terminal In a flip-flop, the zero-input terminal. Compare SET TERMINAL.

reset time The elapsed time between a malfunction and the completion of the reset action.

reset timer A device that returns a circuit or device to its initial state after a specified time delay.

reserve In multiple programming computer operations, to allocate memory areas and peripherals for a program.

reserve battery A battery in which the electrolyte is in a special standby chamber outside of the interelectrode section while the battery is on the shelf. When the battery is readied for service, the electrolyte is caused to flow into position between the electrodes, either by heating the battery, shocking it mechanically, or inverting it.

residual amplitude modulation See INCIDENTAL AM.

residual charge The electric charge remaining in a capacitor after it has been initially discharged. It results from dielectric absorption.

residual current A current that continues to flow in a circuit after removing power. The duration is measured in nanoseconds or microseconds.

residual frequency modulation **1.** See INCIDENTAL FM. **2.** Frequency modulation of the fundamental frequency of a Klystron by noise or alternating-current heater voltage.

residual gas Minute quantities of gas remaining in a vacuum tube after evacuation.

residual magnetism Magnetism remaining in a material, such as iron, after the magnetizing force has been removed.

residual modulation **1.** Modulation of a signal by hum or noise. **2.** See INCIDENTAL AM. **3.** See INCIDENTAL FM.

residual voltage In the output of a null device, such as a bridge, a usually small voltage still present at null and preventing zero balance.

residue check In computer operations, the verification of the result of an arithmetic operation using the remainders generated when each operand is divided by a special number; the remainder is transmitted along with the operand as a check digit.

resilience Also called *fault resilience.* The ability of an electronic device or system, especially a computer, to keep functioning after part of it has failed.

5059F-pR-574-606 4/10/01 9:42 AM Page 595

resin A natural or synthetic organic substance that is polymeric in structure and largely amorphous. Various plastics are made from synthetic resins.

resistance **1.** Symbol, *R* or *r*. Unit, ohm. In a device, component, or circuit, the simple opposition to current flow. Resistance by itself causes no phase shift. In a purely resistive circuit, $R = E/I$, where R is the resistance in ohms, E is the voltage in volts, and I is the current in amperes. **2.** A property of circuits, devices, or substances that causes impinging energy to be dissipated by conversion to heat. Compare REACTANCE.

resistance

Per kilometer of solid copper wire for American Wire Gauge (AWG) 1 through 40.

AWG	*ohms/km*	*AWG*	*ohms/km*
1	0.42	21	43
2	0.52	22	54
3	0.66	23	68
4	0.83	24	86
5	1.0	25	110
6	1.3	26	140
7	1.7	27	170
8	2.1	28	220
9	2.7	29	270
10	3.3	30	350
11	4.2	31	440
12	5.3	32	550
13	6.7	33	690
14	8.4	34	870
15	11	35	1100
16	13	36	1400
17	17	37	1700
18	21	38	2200
19	27	39	2800
20	34	40	3500

resistance alloys Metallic alloys used in the manufacture of resistance wire and resistance elements. Such alloys include CONSTANTAN, GERMAN SILVER, MANGANIN, MONEL METAL, and NICHROME.

resistance balance A device used to balance a circuit, by means of the insertion of resistances.

resistance brazing A method of brazing in which metal is heated by passing a current through it. The I^2R loss, or dissipated power, occurs in the form of heat.

resistance bridge A bridge (see BRIDGE, **2**) for measuring resistance only.

resistance-capacitance Abbreviation, *RC*. Pertaining to a combination of resistance and capacitance (e.g., RESISTANCE-CAPACITANCE CIRCUIT).

resistance-capacitance bridge **1.** A four-arm null circuit containing only resistors and capacitors. Also see BRIDGE, **1**. **2.** An alternating-current bridge (see BRIDGE, **2**) for measuring resistance and capacitance.

resistance-capacitance circuit A circuit containing only resistors and capacitors. There are no inductors.

resistance-capacitance-coupled amplifier A multistage amplifier circuit in which RESISTANCE-CAPACITANCE COUPLING is used between stages and at the input and output points of the circuit.

resistance-capacitance coupling Coupling, especially between stages in a circuit, using blocking capacitors and supply-path resistors.

resistance-capacitance filter A power-supply filter or wave filter containing only resistors and capacitors. The resistors are in the positions occupied by inductors in inductance-capacitance filters.

resistance-capacitance-inductance Abbreviation, *RCL*. Pertaining to a combination of resistance, capacitance, and inductance.

resistance-capacitance phase shifter A phase shifter containing only resistors and capacitors to obtain the desired shift.

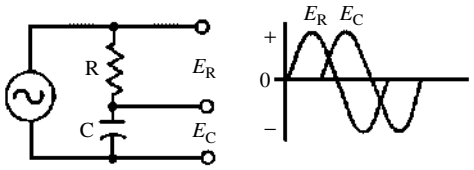

resistance-capacitance phase shifter

resistance-capacitance time constant Symbol, *t*. The time constant (see ELECTRICAL TIME CONSTANT) of a circuit containing (ideally) only resistance and capacitance; $t = RC$, where t is in seconds, R is in ohms, and C is in farads. Compare RESISTANCE-INDUCTANCE TIME CONSTANT.

resistance-capacitance tuning Tuning of a circuit, such as that of an amplifier or oscillator, by means of a variable resistor or ganged units of this type. See, for example, PARALLEL-TEE AMPLIFIER, PARALLEL-TEE OSCILLATOR, and WIEN-BRIDGE OSCILLATOR.

resistance-coupled amplifier See RESISTANCE-CAPACITANCE-COUPLED AMPLIFIER.

resistance drop The voltage drop across a resistor, or across the inherent resistance of a device.

resistance-inductance Abbreviation, *RL*. Pertaining to a combination of resistance and inductance (e.g., RESISTANCE-INDUCTANCE CIRCUIT).

resistance-inductance bridge **1.** A four-arm null circuit containing only resistors and inductors. Also see BRIDGE, **1**. **2.** An alternating-current bridge (see BRIDGE, **2**) for measuring resistance and inductance only.

resistance-inductance circuit A circuit containing only resistors and inductors. There are no capacitors.

5059F-pR-574-606 4/10/01 9:42 AM Page 596

resistance-inductance phase shifter A phase shifter containing only resistors and inductors to obtain the desired phase shift.

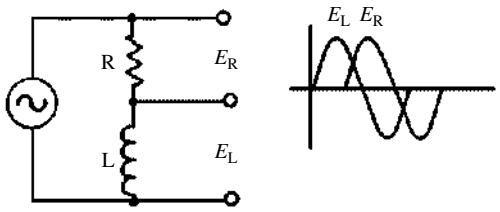

resistance-inductance phase shifter

resistance lamp An incandescent bulb inserted in series with a circuit to provide a dropping resistance. Such a lamp is capable of dissipating a large amount of power, shows very little reactance at low frequencies, and is inexpensive.

resistance magnetometer A magnetometer whose operation is based upon the change of electrical resistance of a material (such as bismuth wire) placed in the magnetic field under test.

resistance material A substance, such as carbon or German silver, whose resistivity is high enough to enable its use as a lumped resistor. See, for example, RESISTANCE ALLOYS and RESISTANCE METAL.

resistance metal A metal, such as iron, whose resistivity is high enough to enable its use as a lumped resistor. Also see RESISTANCE ALLOYS.

resistance pad An attenuator composed of noninductive resistors.

resistance standard A highly accurate and stable resistor used in precision measurements of resistance. Also see PRIMARY STANDARD and SECONDARY STANDARD.

resistance strain gauge An electrical strain gauge in which the stressed element is a thin resistance wire.

resistance strip A strip of metallic or nonmetallic resistance material. Also see RESISTANCE ALLOYS and RESISTANCE METAL.

resistance temperature detector A transducer consisting of a specially made resistor whose resistance varies linearly with temperature.

resistance thermometer An electronic thermometer whose operation is based on the change of resistance of a wire as it is heated or cooled.

resistance transducer See RESISTIVE TRANSDUCER.

resistance tuning See VARIABLE-RESISTANCE TUNING.

resistance welding An electrical or electronic welding process in which the workpieces are heated by current flowing through the inherent resistance of their junction.

resistance wire Wire made of a metal or alloy that exhibits significant resistivity. See, for example, RESISTANCE ALLOYS and RESISTANCE METAL.

resistance-wire sensor A specific length of resistance wire, properly mounted, whose resistance is proportional to a sensed phenomenon (such as strain, temperature, presence of gas, pressure, etc.). See, for example, ELECTRICAL STRAIN GAUGE, GAS DETECTOR, and PRESSURE TRANSDUCER.

resistive current The component of alternating current that is in phase with voltage. Also called WATT CURRENT. Compare REACTIVE CURRENT.

resistive cutoff frequency Symbol, f_{rco}. The frequency beyond which a tunnel diode ceases to exhibit negative resistance.

resistive load A load device that is essentially a pure resistance.

resistive losses Losses resulting from the resistance of a circuit or device, and usually appearing as heat.

resistive transducer A transducer in which the sensed phenomenon causes a change in resistance, which in turn produces a corresponding change in output current or voltage. Compare CAPACITIVE TRANSDUCER, CRYSTAL TRANSDUCER, INDUCTIVE TRANSDUCER, MAGNETIC TRANSDUCER, and PHOTOELECTRIC TRANSDUCER.

resistive trimmer See TRIMMER RESISTOR.

resistive voltage The voltage across the resistance component in a circuit. In an alternating-current circuit, the resistive voltage is in phase with the current.

resistivity Symbol, *r*. Resistance per unit volume or per unit area. It can be expressed in terms of ohms per cubic meter or ohms per square meter. Also see MICROHM-CENTIMETER and OHM-CENTIMETER.

resistor A device having resistance concentrated in lumped form. Also see RESISTANCE and RESISTIVITY.

resistor-capacitor-transistor logic Abbreviation, RCTL. A form of RESISTOR-TRANSISTOR LOGIC in which capacitors are used to enhance switching speed.

resistor color code See COLOR CODE.

resistor core A form around which a resistance wire can be wound for the purpose of constructing a high-power resistor.

resistor decade See DECADE RESISTOR.

resistor diode A usually forward-biased semiconductor diode that acts as a VOLTAGE-DEPENDENT RESISTOR.

resistor FET See ELECTRONIC RESISTOR.

resistor fuse See FUSIBLE RESISTOR.

resistors in parallel See PARALLEL RESISTORS.

resistors in parallel-series See PARALLEL-SERIES RESISTORS.

resistors in series See SERIES RESISTORS.

resistors in series-parallel See SERIES-PARALLEL RESISTORS.

5059F-pR-574-606 4/10/01 9:42 AM Page 597

resistor substitution box A self-contained assortment of common-value resistors arranged to be switched one at a time to a pair of terminals. In troubleshooting and circuit development, any of several useful fixed resistance values can thus be obtained.

resistor transistor See ELECTRONIC RESISTOR.

resistor-transistor logic Abbreviation, RTL. A circuit in which the logic function is performed by resistors, and an inverted output is provided by transistors.

resnatron A form of vacuum tube that is used as an oscillator and amplifier at ultra-high and microwave frequencies. It is essentially a cavity resonator.

resolution **1.** The degree to which closely adjacent parts of an image can be differentiated. **2.** The reduction of a problem by means of logical analysis. **3.** The ability of a vision or ranging system to distinguish between objects that are close together in terms of radial distance, direction, or absolute separation.

resolution ratio In a television image, the ratio of horizontal resolution to vertical resolution.

resonance **1.** The state in which the natural response frequency of a circuit coincides with the frequency of an applied signal, or vice versa, yielding intensified response. **2.** The state in which the natural vibration frequency of a body coincides with an applied vibration force, or vice versa, yielding reinforced vibration of the body.

resonance bridge An alternating-current bridge (see BRIDGE, **2**) in which one or two arms are series-resonant or parallel-resonant, the other arms being resistances. Also see SERIES-TYPE RESONANCE BRIDGE and SHUNT-TYPE RESONANCE BRIDGE.

resonance curve A graph of the insertion gain or loss of a component, device, circuit, or system to variations in the frequency of an applied sound or signal. Such curves are almost always plotted in rectangular coordinates with frequency as the independent variable on the horizontal axis. The dependent variable, plotted on the vertical axis, can be any characteristic that displays a peak or dip at the resonant frequency or frequencies. In radio-frequency circuits, such parameters include current, voltage, attenuation, gain, and impedance.

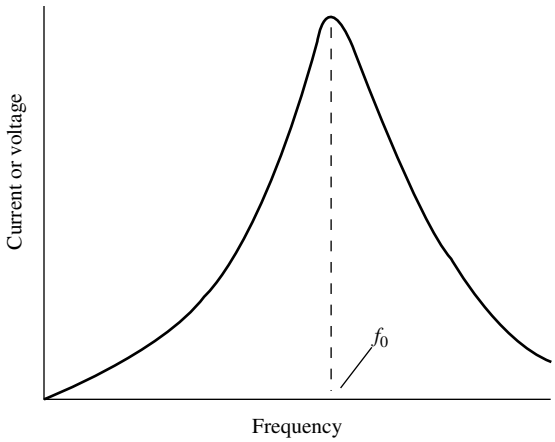

resonance curve

resonance theory of hearing The theory that sound waves pass down the *auditory canal* and cause the *eardrum* to vibrate. Behind the eardrum is a system of three bones leading to the *cochlea.* The cochlea consists of fibers that resonate. Therefore, they vary in length and tension. Various groups of fibers are activated by different sounds, and the vibrations are transmitted to nerves leading to the brain.

resonance radiation Electromagnetic radiation from an energized substance, resulting from movement of electrons from a higher to lower energy level. When an electron moves from a higher to a lower orbit, a photon, having a definite wavelength, is emitted.

resonant cavity A chamber whose size reinforces energy injected into it at a natural frequency, which is determined by the chamber's dimensions. Such cavities can be used with acoustic or electromagnetic waves.

resonant circuit A circuit whose constants are chosen for maximum circuit response at a given frequency. Examples: *parallel-resonant circuit* and *series-resonant circuit.* Also see RESONANCE and RESONANT FREQUENCY.

resonant current Current flowing in a tuned circuit at resonance.

resonant feeder An antenna feeder that is resonant at the operating frequency.

resonant filter A filter containing at least one series- or parallel-resonant arm for sharp response. Thus, a power-supply filter of this kind might have a parallel-resonant arm acting as a wave-trap at the ripple frequency.

resonant frequency Symbol, f_r or f_o. The natural frequency at which a circuit oscillates or a device vibrates. In an inductance-capacitance circuit (series-resonant or parallel-resonant), the reactances cancel at the resonant frequency, leaving only resistance.

resonant-gate transistor A transistor embodying a tiny tuning fork for resonance at low frequencies, thus eliminating bulky coils and capacitors.

resonant line A transmission line that is resonant at the operating frequency.

resonant-line amplifier See LINE-TYPE AMPLIFIER.

resonant-line circuit A circuit using resonant lines as a tank. See, for example, LINE-TYPE AMPLIFIER and LINE-TYPE OSCILLATOR.

resonant-line oscillator See LINE-TYPE OSCILLATOR.

5059F-pR-574-606 4/10/01 9:42 AM Page 598

resonant-line wavemeter See LECHER WIRES.
resonant rise See VOLTAGE RISE.
resonant-slope amplifier See DIELECTRIC AMPLIFIER.
resonant-slope detector See SLOPE DETECTOR.
resonant suckout The drawing of radio-frequency energy out of the energized part of a coil or transmission line by the part not intended to be energized, when the latter resonates at the same frequency.
resonant-voltage rise See VOLTAGE RISE.
resonant-voltage stepup See VOLTAGE RISE.
resonate **1.** To exhibit RESONANCE—either electrically or acoustically. **2.** To adjust a variable-frequency electrical or acoustical device so that it exhibits RESONANCE at a specific frequency.
resonator A device that produces or undergoes resonance. See, for example, HELMHOLTZ RESONATOR and RESONANT CAVITY.
resource A part of a computer system that can be used for a specific application as a unit (e.g., printer, PCMCIA standard adapter card, tape drive, etc.).
responder The transmitting section of a transponder.
response The behavior of a circuit or device (especially in terms of its dependent variables), in accordance with an applied signal (e.g., *frequency response* and *current-vs.-voltage response*).
response curve A graph depicting the performance of a circuit or device. Examples: *attenuation-vs.-frequency curve* and *current-vs.-voltage curve.*
response time The interval between the instant a signal is applied to or removed from a circuit or device and the instant that the circuit acts accordingly.
restart Following a malfunction or error occurring during a computer program run, to go back to an earlier point in the program.
resting state See QUIESCENT STATE.
restore See RESET.
resultant **1.** The vector that results from the addition of two or more vectors. **2.** A quantity that results from mathematical operations performed on other quantities.
retarding magnet See DRAG MAGNET.
retentivity **1.** The property whereby a material retains magnetism imparted to it. **2.** A quantitative measure of the extent to which a material retains magnetism imparted to it.
retention period In computer operations, the time during which the data on a magnetic medium (disk or tape) must be kept intact.
retrace **1.** In a cathode-ray tube, the return of the scanning beam to its starting point. **2.** In a cathode-ray tube, a line traced on the screen by the scanning beam as it returns to its starting point, if RETRACE BLANKING is not used.
retrace blanking Obliteration of the RETRACE of the electron beam in a cathode-ray tube. It renders the retrace line invisible on the screen so that it will not interfere with the display.
retrace line See RETRACE, **2**.
retrace ratio For the swept beam in a cathode-ray tube, the ratio of the scanning velocity in the trace direction to the scanning velocity in the RETRACE direction.
retrace time In a cathode-ray tube, the amount of time required for the scanning beam to move from the end of one trace or line to the beginning of the next.
retrofit To supply something with specially designed or adapted parts that were not available when it was made.
retrograde orbit For an artificial earth satellite, an orbit whose direction is east-to-west, relative to the earth's surface.
return **1.** See RETRACE. **2.** See RETURN CIRCUIT. **3.** See RETURN POINT. **4.** In an electronic circuit, the electrical ground and ground current path.
return circuit The circuit through which current returns to a generator.
return instruction In a computer program, an instruction in a subroutine directing operation back to a specific point in the main program.
return interval See RETRACE TIME.
return line See RETRACE, **2**.
return point **1.** The point to which circuits are returned (e.g., a common ground point). **2.** The terminal point of a return circuit.
return ratio See FEEDBACK FACTOR.
return time See RETRACE TIME.
return to zero **1.** Abbreviation RZ or RTZ. In the magnetic recording of data, a method in which the write current returns to zero following the write pulse. Compare NONRETURN-TO-ZERO. **2.** A logic system in which the zero and one states are represented by zero voltage and a discrete voltage.
return trace See RETRACE, **1**, **2**.
REV **1.** Abbreviation of REENTRY VEHICLE. **2.** Abbreviation of REVERSE.
rev **1.** Abbreviation of REVOLUTION. **2.** To quickly and substantially increase the angular velocity of a motor.
reverberation **1.** Multiple reflections of sound waves from the inside surfaces of an enclosed chamber. **2.** The dying-out of sound waves in an enclosed chamber as the waves reflect repeatedly from the inside surfaces. **3.** In sound recording and/or reproduction, an electronically produced echo. It is used for special effects—especially in electronic music systems. **4.** See RESONANCE, **2**.
reverberation chamber A room in which the walls, floor, and ceiling absorb very little sound, resulting in echoes. To avoid standing waves, the room is designed so that no two surfaces are exactly parallel.
reverberation system A system of devices operated with an electronic organ to simulate the effect of reverberation in a large room, such as a church auditorium.

5059F-pR-574-606 4/10/01 9:42 AM Page 599

reverberation time In an enclosed chamber, the time required for a sound to die down to a specified level (usually -60 dB) after the disturbance has stopped.

reverberation unit A device for producing artificial echoes—especially in the operation of electronic music systems.

reverse **1.** To alter the direction of a current or process or motion of an object so that the new direction is exactly opposite the previous direction. **2.** In a directional wattmeter, the reflected-power indication or switch position.

reverse AGC Automatic gain control in which a signal-dependent voltage is fed back to an earlier stage to adjust its gain automatically. Compare FORWARD AGC.

reverse bias Reverse voltage or current in a transistor or a semiconductor diode. Compare FORWARD BIAS.

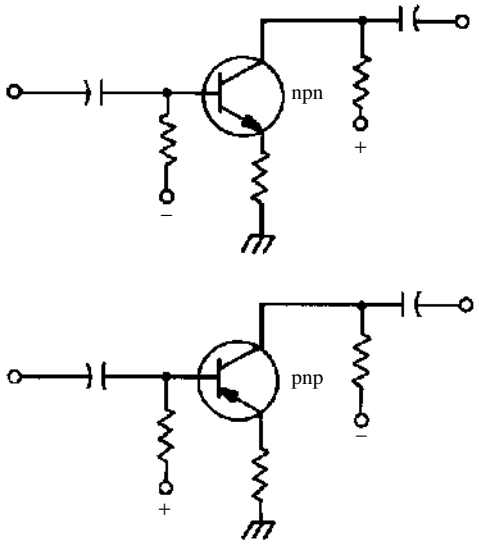

reverse bias

reverse breakdown See AVALANCHE.

reverse breakdown voltage See AVALANCHE VOLTAGE.

reverse characteristic The current-vs.-voltage response of a semiconductor junction that is biased in the reverse (low-conduction) direction. Compare FORWARD CHARACTERISTIC.

reverse conduction The very small current conduction through a pn junction when it is reverse-biased. Compare FORWARD CONDUCTION.

reverse current Symbol, I_r. The current that flows through a pn junction when it is reverse-biased. Also called *back current.* Compare FORWARD CURRENT.

reverse engineering A design process in which a specific device or system is copied functionally, but not literally.

reverse Polish notation Abbreviation, RPN. A system of notation for expressing mathematical operations in which the operators follow the operands being manipulated. It is a mode of entry for some calculators (e.g., the operation 7×2 might be entered by pressing keys in this order: 7, ENTER, 2, ×).

reverse recovery time See RECOVERY TIME, **1**.

reverse resistance Symbol, R_r. The resistance of a reverse-biased pn junction. Also called BACK RESISTANCE. Compare FORWARD RESISTANCE.

reverse voltage Symbol, E_r or V_r. Direct-current voltage applied to a pn junction so that the p-type material is electrically more negative than the n-type material. Also called BACK VOLTAGE. Compare VOLTAGE.

reverse-voltage capacitance The internal capacitance of a reverse-biased semiconductor pn junction.

reverse voltage drop The voltage drop across a semiconductor pn junction that is biased in the reverse (low-conduction) direction.

reversible counter A counter that, by a control signal, can have the value it is holding either increased or decreased.

reversible permeability The permeability of a ferromagnetic substance when the magnitude of the alternating-current field is arbitrarily small.

reversing switch **1.** A switch that reverses the polarity of a direct-current voltage. **2.** A switch that reverses the direction of motor rotation.

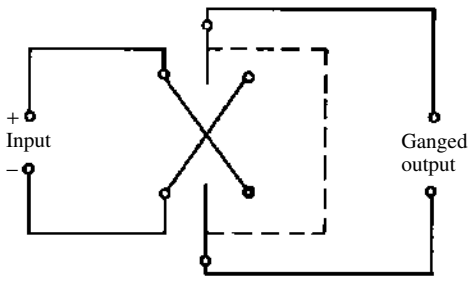

reversing switch

revolute geometry A method by which a robot arm can move freely in three dimensions. The entire assembly rotates from the base in a horizontal plane through a complete circle (360 degrees). An elevation joint at the base moves the arm from horizontal to vertical (90 degrees). A joint in the middle of the arm can bend through about 180 degrees.

revolution Abbreviation, r or rev. One complete rotation (i.e., 360 degrees of circular travel).

5059F-pR-574-606 4/10/01 9:42 AM Page 600

revolving field See ROTATING FIELD.

rewind To run a magnetic tape on a transport at a high speed, in the direction opposite to that associated with the play mode.

rewrite In computer operations, to return information read from a storage location to that location by recording.

R_F Symbol for FILAMENT RESISTANCE.

RF Abbreviation of RADIO FREQUENCY.

RF amplifier See RADIO-FREQUENCY AMPLIFIER.

RFC Abbreviation of RADIO-FREQUENCY CHOKE.

RF heating See RADIO-FREQUENCY HEATING.

RFI Abbreviation of RADIO-FREQUENCY INTERFERENCE.

RF inverse feedback A negative-feedback system for radiophone transmitters, in which a portion of the modulated radio-frequency (RF) signal is rectified, and the resulting direct-current voltage is filtered and applied as bias to one of the audio stages in the proper polarity for degeneration.

RF lamp A lighting lamp, used with radio-frequency (RF) alternating current, rather than the conventional 60-Hz utility current. This results in better efficiency, and allows much more light to be generated with a given filament lamp, as compared with 60-Hz current.

RF motion detector In security systems, an intrusion detection and alarm system that senses Doppler-effect-induced changes in the frequency or phase of a radio-frequency (RF) electromagnetic field. The Doppler effect results from motion of objects in the secured area.

RFO Abbreviation of *radio-frequency oscillator.*

RF power supply See OSCILLATOR-TYPE POWER SUPPLY.

RF preamplifier A sensitive, radio-frequency amplifier circuit intended for improving the signal-to-noise (S/N) ratio in a wireless receiver. Generally placed between the receiver and the antenna or feed line. Some such devices are tunable; others are broadbanded. See also PREAMPLIFIER.

RF probe See RECTIFIER PROBE.

RF resistance See RADIO-FREQUENCY RESISTANCE.

RF selectivity See RADIO-FREQUENCY SELECTIVITY.

RF transformer See RADIO-FREQUENCY TRANSFORMER.

RF transistor See RADIO-FREQUENCY TRANSISTOR.

R_g Symbol for GRID RESISTANCE.

R_G Symbol for GATE RESISTANCE.

RGB Abbreviation of RED-GREEN-BLUE.

RGT Abbreviation of RESONANT-GATE TRANSISTOR.

Rh Symbol for RHODIUM.

R/h Abbreviation of ROENTGENS PER HOUR.

R_H **1.** Symbol for HEATER RESISTANCE. **2.** Symbol for HOT RESISTANCE.

rh Abbreviation of RELATIVE HUMIDITY.

rhenium Symbol, Re. A metallic element. Atomic number, 75. Atomic weight, 186.207. It is used in some thermocouples.

rheostat A wirewound variable dropping resistor of the rotary type or slider type.

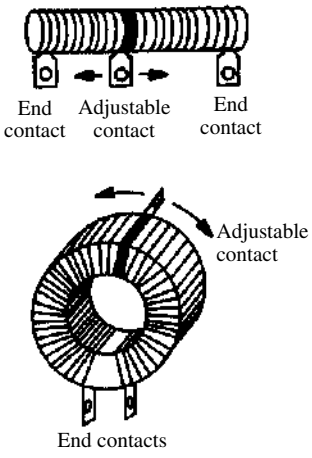

rheostat

R_{HF} Symbol for *high-frequency resistance* (see RADIO-FREQUENCY RESISTANCE).

RHI Abbreviation of RANGE-HEIGHT INDICATOR.

rhodium Symbol, Rh. A metallic element. Atomic number, 45. Atomic weight, 102.906.

rhombus A four-sided geometric plane figure, in which all four sides have equal length, and opposite angles have equal measure.

rhombic antenna See DIAMOND ANTENNA.

rho-theta A radio-navigation system in which a single transmitting station is used, and the position is determined, according to polar coordinates (distance and direction).

rhumbatron A RESONANT CAVITY—especially one in a KLYSTRON.

RI Abbreviation of RADIO INTERFERENCE.

R_i Symbol for INPUT RESISTANCE. (Also, R_{in}.)

RIAA Abbreviation of RECORDING INDUSTRY ASSOCIATION OF AMERICA.

RIAA curve The amplitude-versus-frequency function used in recording and reproduction of long-playing (33.3 rpm) phonograph discs, and specified by the Recording Industry Association of America (RIAA). The RIAA curve takes advantage of the sensitivity of the human ear at various frequencies to reduce the level of audible noise.

ribbon microphone See VELOCITY MICROPHONE.

ride gain In broadcasting, the operations of constantly adjusting the audio modulation of the transmitter for optimum operation.

Rieke chart A visual aid, similar to the SMITH CHART, used with traveling-wave tubes in the

5059F-pR-574-606 4/10/01 9:42 AM Page 601

ultra-high-frequency (UHF) and microwave frequency bands for determining the optimum load impedance.

rig Colloquialism for a radio communications installation—especially a transmitter or transceiver. It is commonly used among amateur radio operators.

right-angle line section See ELL.

right-hand lay See DIRECTION OF LAY.

right-hand polarized wave See CLOCKWISE-POLARIZED WAVE.

right-hand rule for induced emf See FLEMING'S RIGHT-HAND RULE.

right-hand rule for wire A simple rule for indicating the direction of the magnetic field surrounding a straight wire that carries current. When the wire is grasped in the right hand with the thumb pointing in the direction of current flow, the fingers curl in the direction of the magnetic field.

right-hand taper Potentiometer or rheostat taper in which most of the resistance is in the clockwise half of rotation, as viewed from the front. Compare LEFT-HAND TAPER.

right justified In a computer memory location, a data item that takes up consecutive bit positions, from right to left.

Right-Leduc effect A phenomenon somewhat analogous to the Hall effect. When a metal strip conducting heat is placed in a magnetic field perpendicular to the plane of the strip, a temperature difference develops across the strip.

right shift In computer operation, a shift whereby word bits are displayed to the right; the effect is division in a right arithmetic shift.

rim drive **1.** In a tape recorder, a driving method in which the motor shaft is provided with a smooth pulley that transfers motion directly to the rubber-tired rim of the flywheel. **2.** A driving method for a phonograph turntable in which a rotating wheel contacts the outer edge of the platter.

R_{in} Symbol for INPUT RESISTANCE. (Also, R_i.)

ring **1.** The core of a toroidal coil. **2.** See HYBRID RING. **3.** See RING MODULATOR. **4.** See RING INDUCTOR. **5.** See RING MAGNET. **6.** See RINGING.

ring armature A motor or generator armature having a ring winding.

ringback In a telephone system, the signal sent from the receiving (destination) telephone set back to the sending (source) set, indicating that the signal is being received. This consists of a tone, interrupted by pulses at intervals of about 0.05 second. The signal stops when the destination set is taken off the hook. Also see RINGDOWN.

ring circuit **1.** See RING MODULATOR. **2.** A waveguide hybrid-tee resembling a ring having radial branches. **3.** In amateur radio operations, a circuit connected to a telephone line and radio transmitter. The radio transmitter is energized and modulated with an identifiable signal each time the telephone rings, so the telephone can be answered via remote control.

ring counter An electronic counter in which successive cascaded stages form a ring (i.e., the last stage in the chain is connected to the first stage so that the counter advances through the cycle, stage by stage, repetitively).

ringdown In a telephone system, the signal sent from the transmitting (source) set to the receiving (destination) set, causing the destination set to ring. Also see RINGBACK.

ring head In tape recorders, a recording and playback head that consists essentially of a metal ring with a gap at one point, and on which the coils are wound.

ring inductor **1.** An inductor consisting of a single turn of wire, or of a conductor bent into a loop. **2.** See SHADING COIL.

ringing Self oscillation in a pulsed inductance-capacitance circuit, sustained by the circuit's flywheel action (hysteresis), and usually producing a damped wave.

ringing coil In the horizontal oscillator in a television circuit, a small, adjustable coil (shunted by a capacitor) used to produce a sharp rise in input-signal voltage.

ringing current In wire telephony, an alternating current superimposed on the direct operating current. Produces RINGDOWN.

ringing time See RING TIME, **1**.

ring magnet A permanent magnet in the shape of a ring or donut.

ring main An electric power main that is closed to form a ring. This results in two independent electrical paths between any two points in the circuit. If one path is interrupted, power can still be transmitted to any other point in the circuit from a power station.

ring modulator A double-balanced diode-type modulator circuit; its name is derived from the ring-like arrangement of the four diodes.

ring oscillator A self-excited oscillator in which two sets of two transistors are operated in push-pull/parallel.

ring shift In computer operation, the cyclic shifting of digits from one end of a register to the other.

ring time **1.** The period of a damped oscillation—especially one set up in an inductance-capacitance circuit by a pulse. **2.** The time required for an ECHO BOX signal to decay below the display level.

ring winding A winding in which the turns of the coil are laid on the outside of a ring-shaped core and passed through its center, resulting in a donut coil with a core.

ripple **1.** A small alternating-current component in the output of a direct-current power supply with inadequate filtering. **2.** In computer and data-processing operations, the serial transmission of data.

5059F-pR-574-606 4/10/01 9:42 AM Page 602

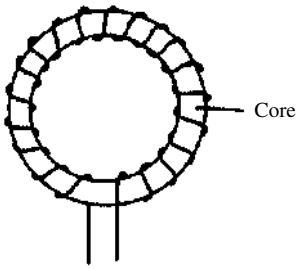

ring winding

ripple amplitude The peak or peak-to-peak value of ripple in a power supply (see RIPPLE, **1**).

ripple counter A binary counter consisting of flip-flops cascaded in series. A pulse must pass sequentially from the input, through each stage, to the output of the chain.

ripple current Current flowing in a circuit as the result of ripple voltage (see RIPPLE AMPLITUDE).

ripple factor The ratio of the RIPPLE AMPLITUDE to the direct-current voltage output of a power supply.

ripple frequency The frequency of a ripple component (see RIPPLE, **1**). In power supplies using half-wave rectification, this frequency is normally 60 Hz (the line frequency); in full-wave supplies, it is normally 120 Hz (twice the line frequency).

ripple percentage See PERCENT RIPPLE.

ripple torque Symbol, T_R. In a torque motor, the small fluctuation in torque resulting from commutator switching action.

ripple voltage See RIPPLE AMPLITUDE.

RISC Abbreviation of REDUCED INSTRUCTION SET COMPUTER.

rise **1.** See VOLTAGE RISE. **2.** See RISE TIME. **3.** An increase in the amplitude of a pulse or wave.

rise cable **1.** A vertical feeder cable. **2.** A vertical section of a feeder cable.

rise time The time required for a pulse to rise from 10 percent to 90 percent of its peak amplitude. Compare FALL TIME.

RJE Abbreviation of REMOTE JOB ENTRY.

R_k Symbol for cathode resistance.

RL **1.** Abbreviation of RESISTANCE-INDUCTANCE. **2.** Abbreviation of RELAY LOGIC.

R_L Abbreviation of LOAD RESISTANCE.

RL bridge See RESISTANCE-INDUCTANCE BRIDGE.

RL circuit See RESISTANCE-INDUCTANCE CIRCUIT.

R_{LF} Symbol for low-frequency resistance.

RL phase shifter See RESISTANCE-INDUCTANCE PHASE SHIFTER.

R_m Symbol for METER RESISTANCE.

r_m Symbol for *emitter-collector transresistance* of a bipolar transistor.

rms Abbreviation of ROOT MEAN SQUARE.

rms converter See ROOT-MEAN-SQUARE CONVERTER.

rms current See EFFECTIVE CURRENT.

rms meter A current meter or voltmeter whose deflection is proportional to the root-mean-square (rms) value of current or voltage. In most meters, the deflection is proportional to either the peak value or the average value, but the scale of an rms unit is graduated on the basis of sine-wave input.

rms value See EFFECTIVE VALUE.

rms voltage See EFFECTIVE VOLTAGE.

Rn Symbol for RADON.

R_n **1.** Symbol for NEGATIVE RESISTANCE. (Also, –R.) **2.** Symbol for *null resistance.*

R_o Symbol for OUTPUT RESISTANCE. (Also, R_{out}.)

roaming **1.** In cellular communications, an ideal condition in which the user of a mobile or portable wireless telephone set can travel throughout a specified geographic region with no "dead zones" or interruption in service. **2.** For a mobile or portable cellular telephone subscriber, the act of traveling throughout a large geographic region and, in particular, among different states or countries.

robot **1.** An electromechanical device or system capable of reliably performing complex and/or repetitive tasks. It can be controlled by a human operator or by a computer. **2.** A usually autonomous device, as defined in **1**, built to physically resemble a human being, with a head, two arms, and some form of locomotion.

robot generations Agreed-on milestones or criteria in the evolution of robots and smart machines. *First generation:* Before 1980. Mainly mechanical, stationary, physically rugged, no external sensors, no artificial intelligence. *Second generation:* 1980–1990. Tactile sensors, vision systems, position sensors, pressure sensors, microcomputer control, programmable. *Third generation:* After 1990. Mobile, autonomy or group control, artificial intelligence, speech recognition/synthesis, teleoperation, navigation systems. *Fourth generation:* In conceptual stages. Highly intelligent, capable of building other robots, capable of doing many human tasks.

robot gripper A robotic END EFFECTOR designed specifically to grasp objects. The two basic designs are: hand-like and specialized. Hand-like grippers are engineered according to the notion that the human hand has evolved to near perfection, and should be mimicked in robots. Specialized grippers are built by trial-and-error methods and often bear little resemblance to human hands.

robotics The science and art of robot design, construction, operation, and maintenance.

Rochelle salt Sodium potassium tartrate, a substance whose crystals are piezoelectric. Such crystals are used in some microphones, loudspeakers, and transducers. Also called SEIGNETE SALT.

5059F-pR-574-606 4/10/01 9:42 AM Page 603

rock Slang for QUARTZ CRYSTAL.

rockbound Pertaining to an oscillator or radio transmitter whose frequency is determined by a quartz crystal, and is, therefore, not variable over a significant range.

rocker switch A toggle switch whose lever is a specially shaped bar. The bar is rocked back and forth to operate the switch. Compare BAT-HANDLE SWITCH, PADDLE SWITCH, and SLIDE SWITCH.

rocker switch

rod **1.** A unit of length or distance; 1 rod = 5.029 meters. **2.** A bar of material with special properties.

rod antenna See FERRITE-ROD ANTENNA.

rod magnet A permanent magnet in the shape of a rod with circular or elliptical cross section.

roentgen Abbreviation, r. A unit of ionizing radiation; 1 r is the quantity of radiation that produces 1 esu of electricity (positive or negative) per cubic centimeter of air at standard temperature and pressure. In average tissue, 1 r produces ionization equivalent to an energy concentration of 2.58×10^{-4} C/kg (93 ergs per gram). Also see MILLIROENTGEN.

roentgen equivalent man See REM.

roentgen equivalent physical See REP.

roentgen ray See X RAY.

roger A communications signal meaning "Acknowledged."

Roget spiral A spring-like wire device that contracts in proportion to the magnitude of the current flowing through it.

role indicator In computer operations, a code classifying a keyword as a part of the speech (e.g., noun).

roll **1.** In a display terminal having a line length of less than the standard 80 characters, an operating feature that allows the operator to follow the text along. The cursor remains fixed near the center of the displayed line, while the text moves from right to left. **2.** Vertical movement of a television picture, resulting from lack of vertical synchronization.

rollback In computer operations, the running again of a computer program or portion of the program. Also called RERUN.

roller inductor A variable inductor, usually of the air-core type, with a shaft attached that allows the whole assembly to be rotated; a wheel contact provides a movable tap. Such an indicator is continuously variable and is often used in such devices as antenna-tuning networks.

rolling In television, the apparent continuous upward or downward movement of the picture, resulting from lack of vertical synchronization between the transmitter and receiver.

rolloff **1.** The rate at which a dependent variable (e.g., output amplitude) diminishes above or below a certain critical value of the independent variable (e.g., frequency). It pertains especially to frequency response in audio devices and systems. **2.** Attenuation of the bass and/or treble response or output in an audio system.

ROM Abbreviation of READ-ONLY MEMORY.

Romeo Phonetic alphabet code word for the letter R.

Romex cable A form of wire cable with a covering that is highly resistant to the environment.

roof mount A metal bracket for fastening an antenna mast to a roof.

room noise Ambient acoustic noise in a room.

room resonance Acoustic resonance caused by the geometry and contents of a room.

room temperature Abbreviation, RT. **1.** The temperature of the chamber in which a test or fabrication is carried out. It is commonly used to distinguish between operations that can be performed at the ambient temperature and those that require an oven or a cold chamber. **2.** A temperature typical of an indoor environment, approximately 21 degrees Celsius (70 degrees Fahrenheit).

room tone A qualitative expression for the suitability or behavior of an enclosed area for a given acoustic application. It affected by factors (such as resonances or lack thereof, echoes or lack thereof, overall room size and proportions, and background noise).

root mean square Abbreviation, rms. The square root of the arithmetic mean (average) of the squares of a set of values.

root-mean-square converter A device that converts an input signal of any waveform into a direct-current signal of the same value as the EFFECTIVE VALUE of the input signal.

root-mean-square current See EFFECTIVE CURRENT.

root-mean-square value See EFFECTIVE VALUE.

root-mean-square voltage See EFFECTIVE VOLTAGE.

ROP Abbreviation of *record of production.*

rosin A substance derived chemically from an extract of pine wood, and used in some solders.

rotameter A fluid flow gauge consisting of a float within a glass tube having incremental markings.

rotary amplifier See AMPLIDYNE.

rotary antenna See ROTATABLE ANTENNA.

rotary beam A beam antenna, such as a Yagi, that can be rotated in a (usually horizontal) plane to

5059F-pR-574-606 4/10/01 9:42 AM Page 604

allow transmission and/or reception in various directions. Also see ROTATABLE ANTENNA.

rotary-beam antenna See ROTARY BEAM.

rotary converter A dynamo (electric machine) having a direct-current armature connected to a commutator on one end of the shaft and to slip rings on the other end. When the machine is operated as a direct-current motor, it delivers an alternating-current output, and vice versa. Also called DOUBLE-CURRENT GENERATOR.

rotary dialing An older style of telephone dialing in which a rotary pulse generator is used to dial the digits.

rotary digital audio tape Digital audio tape used with a recording/playback system that uses a rotating head or heads.

rotary encoder An optical analog-to-digital (A/D) converter that operates by passing a light beam through a rotating disk. The amplitude of the analog input signal at any moment causes a certain angular rotation of the disk, cutting off the light beam, according to the nature of the pattern on the disk. The resulting modulated light beam has digital characteristics and can be detected using photocells.

rotary inverter A motor-generator used to change a direct-current input voltage into an alternating-current output voltage.

rotary-motion sensor A transducer that delivers an output voltage proportional to the arc over which its shaft has been turned.

rotary power amplifier See DC GENERATOR AMPLIFIER.

rotary relay An electromechanical relay in which a pivoted armature rotates to open or close the contacts. The *meter relay* is an example.

rotary selector switch See ROTARY SWITCH.

rotary stepping relay See STEPPING SWITCH.

rotary stepping switch See STEPPING SWITCH.

rotary switch A switch in which a blade moves in a circle or in arcs over the contacts.

rotary transformer A motor-generator used to change an input voltage into a lower or higher output voltage.

rotatable antenna An antenna that can be turned to change the orientation of its main lobe (direction of greatest forward gain) in a specific plane (usually horizontal).

rotating amplifier See DC GENERATOR AMPLIFIER.

rotating antenna An antenna that constantly turns to scan a given area (e.g., a RADAR ANTENNA).

rotating-capacitor modulator A frequency modulator consisting of a motor-driven variable capacitor. Also see WOBBULATOR.

rotating field An alternating-current electric or magnetic field, such as that generated by the stators of some motors, that revolves between poles.

rotating interrupter A commutator (see COMMUTATOR, **1**).

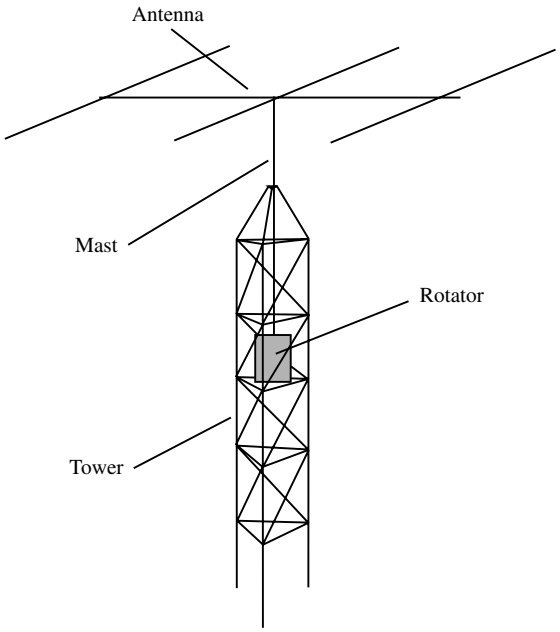

rotatable antenna

rotating machines Electromechanical devices (such as motors, generators, amplidynes, rotary converters, etc.) that utilize magnetic flux to convert angular motion or displacement into electrical energy, or vice-versa.

rotating memory See DISK MEMORY and DRUM MEMORY.

rotating voltmeter See GENERATING VOLTMETER.

rotator A motor-driven, remotely controlled mechanism for turning a directional antenna in a specific plane.

rotor **1.** A rotatable coil—especially in a motor or generator. Compare STATOR, **1**. **2.** The rotating member of a motor or generator. Compare STATOR, **2**. **3.** The rotating-plate assembly of a variable capacitor. Compare STATOR, **3**.

rotor blade The wiper arm of a rheostat or potentiometer.

rotor coil See ROTOR, **1**.

rotor plate The rotating plate(s) of a variable capacitor. Compare STATOR PLATE.

roulette pattern A circular pattern for frequency identification with an oscilloscope, consisting of loops around the screen's circumference. Compare GEAR-WHEEL PATTERN, LISSAJOUS FIGURE, and SPOT-WHEEL PATTERN.

rounding **1.** A method of approximating a quantity by reducing the number of significant digits. For example, rounding 3.44 to two significant digits yields 3.4; rounding 3.46 to two significant digits

5059F-pR-574-606 4/10/01 9:42 AM Page 605

yields 3.5. Compare TRUNCATION. **2.** The approximation of a value to a specified number of decimal places or significant digits. **3.** Smoothing of the corners of a square wave or sawtooth wave, resulting in lengthening of the transition time from one state to another.

rounding error The error resulting from the rounding of a number (see ROUNDING, **1**, **2**).

round off To shorten an otherwise lengthy number by replacing numerical digits with zeros and increasing the final nonreplaced digit by 1 if the leftmost replaced digit is 5 or greater. Thus, 3.141592653 can be rounded off to 3.1416 or 3.14.

round-up A form of numerical approximation, in which a number with a value of *n*.5 or greater is assigned the value *n* + 1. This is a feature of many calculators using scientific notation or a fixed number of decimal places.

***R*$_{out}$** Symbol for OUTPUT RESISTANCE. (Also, R_o.)

route **1.** To physically position wires or conducting circuit paths by planning and deliberation. **2.** The path over which conductors are positioned. **3.** A path over which signals or information can be carried.

routine **1.** In computer operations, the complete sequence of instructions for performing an operation (i.e., a program or program segment). **2.** A test or measurement procedure. **3.** An assembly or manufacturing procedure. **4.** A standard troubleshooting procedure.

row In a matrix, a horizontal arrangement or set of values.

***R*$_P$** **1.** Symbol for PLATE RESISTANCE. (Also, r_P.) **2.** Symbol for POSITIVE RESISTANCE. **3.** Symbol for PARALLEL RESISTANCE. (Also, R_{par}.) **4.** Symbol for PRIMARY RESISTANCE. (Also, R_{pri}.)

***R*$_{par}$** Symbol for PARALLEL RESISTANCE. (Also, R_P.)

r parameters **1.** Device or network parameters expressed as resistances. **2.** Transistor parameters in terms of resistance values in the equivalent tee network. Compare G PARAMETERS and H PARAMETERS.

RPG Abbreviation of REPORT PROGRAM GENERATOR.

rpm Abbreviation of *revolutions per minute.*

rpm meter See ELECTRONIC TACHOMETER and STROBOSCOPE.

RPN Abbreviation of REVERSE POLISH NOTATION.

***R*$_{pri}$** Symbol for PRIMARY RESISTANCE. (Also, R_P.)

rps Abbreviation of *revolutions per second.*

RPT Radiotelegraphic abbreviation of *repeat.*

***R*$_{req}$** **1.** Symbol for REQUIRED RESISTANCE. **2.** Symbol for SCREEN RESISTANCE.

***R*$_{RF}$** Symbol for RADIO-FREQUENCY RESISTANCE.

***R*$_S$** Symbol for SOURCE RESISTANCE in a field-effect transistor.

***R*$_s$** **1.** Symbol for SERIES RESISTANCE. (Also, R_{ser}.) **2.** Symbol for SECONDARY RESISTANCE. (Also, R_{sec}.)

***R*$_{sec}$** Symbol for SECONDARY RESISTANCE. (Also, R_s.)

***R*$_{ser}$** Symbol for SERIES RESISTANCE. (Also, R_s.)

RST flip-flop A conventional flip-flop subject to the operations of reset, set, and trigger.

RST system In the amateur radio service, a method of reporting signal quality in terms of *readability*, *strength*, and *tone.*

R sweep In an oscilloscope or spectrum analyzer, an expanded portion of the trace produced by a long triggered sweep. It permits detailed analysis of a small portion of a displayed waveform or frequency band.

RT **1.** Abbreviation of RADIOTELEPHONE. **2.** Abbreviation of ROOM TEMPERATURE.

rt Abbreviation of RIGHT.

***R*$_T$** **1.** Symbol for THERMAL RESISTANCE. **2.** Symbol for *total resistance.* (Also, R_t.)

***R*$_t$** Symbol for *total resistance.*

RTD Abbreviation of RESISTANCE TEMPERATURE DETECTOR.

RTL Abbreviation of RESISTOR-TRANSISTOR LOGIC.

RTTY Abbreviation of RADIOTELETYPE.

RTZ Abbreviation of RETURN TO ZERO. (Also, RZ.)

Ru Symbol for RUTHENIUM.

rubber A natural insulating material; an elastomer exhibiting rapid elastic recovery. Dielectric constant, 2 to 3.5. Dielectric strength, 16 to 50 kV/mm. Also called *India rubber.* Compare HARD RUBBER.

rubber-covered wire Wire insulated with a jacket of rubber.

rubidium Symbol, Rb. A metallic element. Atomic number, 37. Atomic weight, 85.468.

ruby laser A laser using a ruby rod as the resonant element.

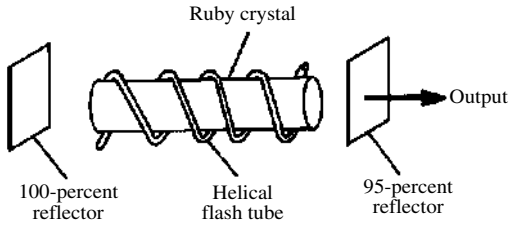

ruby laser

ruby maser A maser in which the resonant material is ruby.

Ruhmkorff coil See INDUCTION COIL.

rumble **1.** Low-frequency acoustical noise of a frequency below about 50 Hz. **2.** Low-frequency electrical noise in an audio circuit of a frequency

5059F-pR-574-606 4/10/01 9:42 AM Page 606

below about 50 Hz. **3.** Vibrations that can occur in a poorly designed or malfunctioning phonograph turntable.

rumble filter An audio high-pass filter having sharp cutoff below 50 Hz, for eliminating rumble arising from irregularities in the rotation of a phonograph turntable. Also see RUMBLE, **3**.

run **1.** The execution of a computer routine or program. **2.** To execute a routine or program. **3.** To cause a routine or program to be executed. **4.** A command that causes a routine or program to be executed.

runaway In a current-carrying circuit or device, especially a semiconductor, a rapid increase in current that causes the temperature to rise, in turn resulting in a further increase in current. Unless preventive measures are taken, this will ultimately damage or destroy the component.

run chart In computer operations, a flowchart showing the organization and order of pertinent programs to be run.

running accumulator A computer storage unit having registers linked so that data is transferred unidirectionally from one to the other, and in which only one register is accessible from the outside.

running open **1.** The condition of a mechanical teleprinter running continuously in the absence of a signal. The teleprinter operates, but nothing is printed; this keeps the machine in synchronization. **2.** Operation of a transmitter at the maximum rated level of input or output power.

running-time meter See ELAPSED-TIME METER.

run time **1.** The period of time during which a computer program is executed. **2.** The length of time required for a computer program to be executed.

rupture **1.** The usually rapid and violent tearing apart, or breaking through, of an insulating material subjected to excessive voltage. **2.** The clean opening of relay, circuit-breaker, or switch contacts to interrupt a current-carrying circuit.

rush Broadband audio background noise, such as that arising from superheterodyne receivers and high-gain amplifiers. Its name is derived from resemblance to the gentle rushing of wind. Compare HISS, **1**, **2**.

ruthenium Symbol, Ru. A rare metallic element. Atomic number, 44. Atomic weight, 101.07.

rutherford Abbreviation, rd. A unit of radioactivity equal to 10^6 disintegrations per second (2.7×10^{-5} curie). Also see KILORUTHERFORD, MEGARUTHERFORD, MICRORUTHERFORD, and MILLIRUTHERFORD.

Rutherford atom An early concept of the nature of the atom, proposed by Rutherford in 1912. In this model, negatively charged electrons orbit a central, positively charged nucleus in a manner similar to the way planets orbit the sun. Compare BOHR ATOM.

rutherfordium Symbol, Rf. Also called *unnilquadium* (Unq) and *kurchatovium* (Ku). Atomic number, 104. The most common isotope has atomic weight 261. Classified as a transition metal. It has a half-life on the order of a few seconds to a few tenths of a second (depending on the isotope), is human-made, and is not known to occur in nature.

RW Abbreviation of *radiological warfare.*

R_x Symbol for unknown resistance.

RY Abbreviation of RELAY.

ryotron A form of inductive semiconductor switch, operated at cold temperatures to maximize conductivity.

R-Y signal In a color-television circuit, the signal representing primary red (R) minus luminance (Y). A primary red signal is obtained when the R-Y signal is combined with the luminance (Y) signal. Compare B-Y SIGNAL and G-Y SIGNAL.

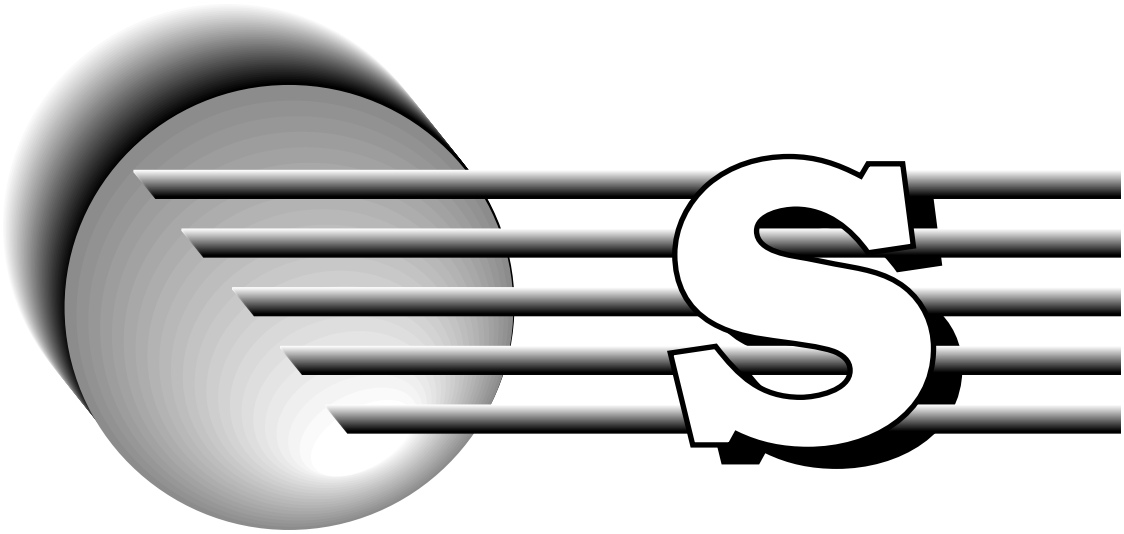

S **1.** Symbol for SCREEN GRID of a vacuum tube. **2.** Symbol for SHELL of a tube or semiconductor device. **3.** Symbol for SULFUR. **4.** Symbol for DEFLECTION SENSITIVITY. **5.** Symbol for SWITCH. **6.** Symbol for ELASTANCE. **7.** Abbreviation of SYNC. **8.** Symbol for SECONDARY. **9.** Abbreviation for SIEMENS. **10.** Abbreviation of SINE. **11.** Symbol for ENTROPY.

s **1.** Symbol for distance or DISPLACEMENT. **2.** Symbol for SCREEN GRID of a vacuum tube. **3.** Symbol for STANDARD DEVIATION. **4.** Abbreviation for SECOND.

SA Abbreviation of SUBJECT TO APPROVAL.

S_A band A section of the S band, extending from 3100 to 3400 MHz.

sabin A unit of sound absorption; 1 sabin represents a surface that can absorb sound at the same rate as 1 square foot of a perfectly absorbent surface.

SADT Abbreviation of *surface alloy diffused-base transistor.*

SAE **1.** Abbreviation of SHAFT-ANGLE ENCODER. **2.** Abbreviation of *Society of Automotive Engineers.*

safe noise level A level of acoustic intensity equal to 85 dB above the threshold of hearing. At sound levels higher than this, eardrum damage is possible.

safety factor A figure denoting the extent of overload that a device can withstand before breaking down.

safety ground A connection made between equipment (usually the metal chassis, panel, case, or B-minus circuit) and the earth as a protective measure against fire and electric shock.

safety switch See ELECTRICAL INTERLOCK.

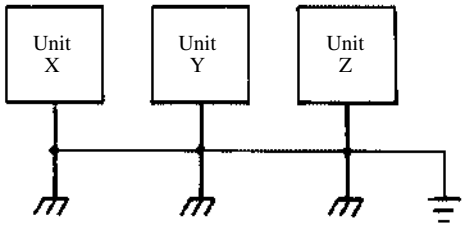

safety ground

sal ammoniac Formula, NH_4Cl. Ammonium chloride, the principal ingredient in the gelatinous electrolyte of some dry cells and batteries.

salient pole A pole, such as the polepiece of a motor or generator, that projects from the rest of the structure (rotor assembly or motor frame).

Salisbury chamber A radio-frequency test chamber in which the walls are non-reflective at various frequencies, thus simulating free space.

salt-spray test A test to assess the life and performance of electronic equipment in a marine environment. The equipment is sprayed, usually with a saltwater mist, and various electrical parameters are measured at prescribed time intervals.

samarium Symbol, Sm. A metallic element of the rare-earth group. Atomic number, 62. Atomic weight, 150.36.

sample **1.** A selection of quantities, events, or objects, taken at a specific time or time interval for analysis or testing. **2.** To take a sample, as defined in **1**. **3.** To test a quantity (current, voltage, temperature, pressure, etc.) or a material

Copyright 2001 The McGraw-Hill Companies, Inc. Click Here for Terms of Use

5059F-pS-607-670 4/10/01 9:47 AM Page 608

(electrolyte, insulant, corrosion, rust, etc.) taken from a larger group or body.

sample and hold A method of storing a variable signal for detailed examination.

sampled data system A system that can be either analog or digital, and that works from samples of the input signals.

sampler In audio systems, a device that digitizes and stores sound for a brief interval of time.

sample size In statistics, the number of items in the sample space chosen for analysis.

sample space In statistics, the set of events, numbers, or other items chosen for analysis.

sampling **1.** Observation of a signal at various points in a circuit, without affecting the operation of the circuit. **2.** The conversion of analog signals to binary signals—especially for use in digital communications systems and in computers. **3.** In statistics and probability, a set of function values corresponding to specifically chosen points in the domain.

sampling rate The frequency with which samples are taken [e.g., 1/hr (one sample per hour) or 10/min (10 samples per minute)].

sampling window See WINDOW, **2**.

sand load A microwave power dissipator in which the absorptive material is a mixture of sand and carbon.

sapphire needle See SAPPHIRE STYLUS.

sapphire stylus A jewel-tipped stylus for disc recording and playback. It is noted for durability.

sat **1.** Abbreviation of *saturate.* **2.** Abbreviation of SATURATION. **3.** Abbreviation of SATELLITE.

satd Abbreviation of *saturated.*

satellite An artificial object sent into orbit around the earth or another planet. See, for example, ACTIVE COMMUNICATIONS SATELLITE and PASSIVE COMMUNICATIONS SATELLITE.

satellite communication Communication via one or more satellite transponders. Usually both stations are on the ground, although sometimes one or both stations are airborne or in space.

satellite processor **1.** In a computer, a microprocessor that is subsidiary to the central processing unit (CPU). **2.** In a data-processing system, a CPU used to handle the running of programs of secondary importance to the system's main application.

satellite television The broadcasting and reception of television (TV) signals via earth-orbiting satellite. Usually, the satellite is in a geostationary orbit. The receiving station employs a dish antenna, a tuner, a digital-to-analog (D/A) converter (if the signals are digital), and a TV receiver.

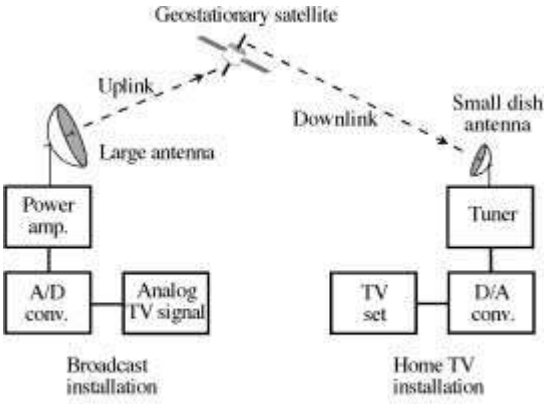

satellite television

satisfy To make a statement of inequality or an equation true (e.g., $x = 2$ satisfies the equation $2x = x^2$).

saturable capacitor A voltage-variable ceramic or semiconductor capacitor in which variations in capacitance stabilize at a reasonably constant value after a particular voltage level is reached.

saturable-core magnetometer A MAGNETOMETER in which the sensor is a saturable magnetic core with a winding. The readout is proportional to the change in permeability of the core produced by the magnetic field under test.

saturable reactor An inductor consisting essentially of a coil wound on a core of magnetic material whose magnetic flux can easily reach saturation level. The inductance and, accordingly, the reactance of the device can be varied by passing a direct current through the coil simultaneously with the alternating current to be controlled.

saturable transformer A transformer having a saturable core that permits automatic regulation of an alternating-current voltage.

saturated color A visible color whose energy is concentrated at a single wavelength or in a narrow band of wavelengths. Also called *pure color.*

saturated logic Any form of digital-logic circuit in which the transistors are either completely cut off or completely saturated. It is characterized by relative immunity to noise, high speed, and high input-level requirements.

saturated operation **1.** The operation of a magnetic core at or beyond its saturation point (i.e., in the region where an increase in coil current produces no change in core magnetization). **2.** The operation of a transistor or vacuum tube beyond its saturation point (i.e., in the region where an increase in voltage produces no change in current, or vice versa). Compare UNSATURATED OPERATION.

saturated solution A solution, such as an electrolyte, that contains all of the solute that it ordinarily will hold at a given temperature and pressure. Compare SUPERSATURATED SOLUTION. Also see SOLUTE; SOLUTION, **1** and SOLVENT, **2**.

saturating current See SATURATION CURRENT.

saturation **1.** See SATURATION POINT. **2.** The state of purity of a color. In general, the greater

5059F-pS-607-670 4/10/01 9:47 AM Page 609

the saturation, the narrower the bandwidth of the electromagnetic energy. The highest possible saturation is represented by energy at a single wavelength [e.g., light of 700 nanometers (nm) appears as highly saturated red, and light of 400 nm appears as highly saturated violet]. Compare HUE. **3.** The condition of a ferromagnetic material in which it can accommodate no additional magnetic flux. **4.** The condition of a dielectric material in which it can accommodate no additional electric flux.

saturation current In a device, the current flowing at and beyond the SATURATION POINT.

saturation flux **1.** The magnetic flux density that will saturate a given sample of magnetic material. **2.** The electric flux density that will saturate a given sample of dielectric material.

saturation flux density See SATURATION INDUCTION.

saturation induction For a magnetic material, the maximum possible flux density.

saturation limiting Output peak clipping that occurs when a transistor or vacuum tube is driven into saturation during part of the input cycle. Compare CUTOFF LIMITING.

saturation point On a voltage-current conduction curve, the point beyond which a further increase in voltage produces no appreciable increase in current.

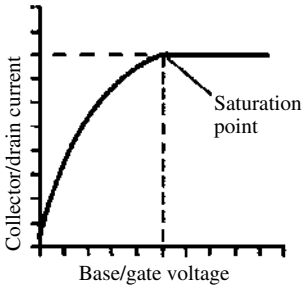

saturation point

saturation resistance The voltage-to-current ratio for a saturated semiconductor.

saturation switching The on/off switching operation in which a transistor is in its saturated state when conducting.

saturation value **1.** In a transistor, field-effect transistor, or vacuum tube, the lowest level of the input current, voltage, or power that results in saturation. **2.** The maximum obtainable output level for a given circuit. **3.** In a magnetic material, the smallest level of magnetizing force that results in the maximum possible flux density.

saturation voltage The (usually direct-current output) voltage appearing across a device operating in its saturation region (e.g., the collector voltage of a switching transistor in its switched-on state).

SAVOR Abbreviation of SIGNAL-ACTUATED VOICE RECORDER.

sawtooth An alternating or pulsating wave of current or voltage that is characterized by a gradual rise in amplitude followed by a rapid fall, or vice versa; its name is derived from its graphic resemblance to the teeth of a saw.

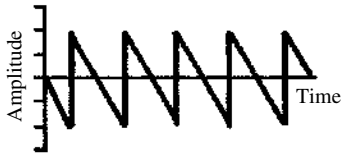

sawtooth

SB **1.** Abbreviation of SIDEBAND. **2.** Abbreviation of SIMULTANEOUS BROADCAST.

Sb Symbol for ANTIMONY.

S band A radio-frequency band extending from 1550 to 5200 MHz. For subdivisions of this band, see S_A BAND, S_C BAND, S_D BAND, S_F BAND, S_G BAND, S_H BAND, S_Q BAND, S_S BAND, S_T BAND, S_W BAND, S_Y BAND, and S_Z BAND.

SBC Abbreviation of SINGLE-BOARD COMPUTER.

SBDT Abbreviation of SURFACE-BARRIER DIFFUSED TRANSISTOR.

SBT Abbreviation of SURFACE-BARRIER TRANSISTOR.

SC **1.** Abbreviation of SUPPRESSED CARRIER. **2.** Abbreviation of SHORT CIRCUIT. **3.** On drawings, the abbreviation for *silk-covered.*

Sc Symbol for SCANDIUM.

sc **1.** Abbreviation of SINGLE CRYSTAL. **2.** Abbreviation of SCALE. **3.** Abbreviation of *sine-cosine.* **4.** Abbreviation of *science.*

SCA Abbreviation of SUBSIDIARY COMMUNICATION AUTHORIZATION.

SCA adapter An auxiliary tuner unit for separating the SCA subcarrier from a main frequency-modulated signal on which it is superimposed. Also see SCA SUBCARRIER and SUBSIDIARY COMMUNICATIONS AUTHORIZATION.

scalar quantity A quantity having magnitude, but for which direction is not specified. Compare VECTOR QUANTITY.

scale **1.** A graduated line or curve for indicating values of a quantity. **2.** An ordered set of values. **3.** An ordered series of quantities, such as tones, frequencies, voltages, etc. (e.g., *musical scale*).

scale division The space between consecutive graduations on a scale (see SCALE, **1**).

scale down In computer operations, to adjust a group of quantities according to a fixed factor so that it can be accommodated by hardware or software.

5059F-pS-607-670 4/10/01 9:47 AM Page 610

scale expansion Spreading out the divisions in part of a scale (see SCALE, **1**).

scale factor **1.** A figure by which the readings from a particular scale must be multiplied or divided to give the true values of measured quantities. **2.** A figure via which values in one system of notation are converted to those in another system. **3.** In scaling down (see SCALE DOWN), the factor by which a group of quantities is adjusted. **4.** The ratio of output frequency to input voltage for a voltage-to-frequency converter.

scale-factor adjustment In some meters, an adjustment that allows full-scale deflection to be set at any desired value (within certain limits) of applied-signal amplitude.

scale-factor error The absolute value of the difference between the actual scale factor and the ideal scale factor for a multiplier circuit.

scale-factor tolerance The extent to which a measured value for the scale factor differs from the computed value. It is generally given as a percentage.

scale length The end-to-end dimension of a scale (see SCALE, **1**), in inches, centimeters, geometric degrees, or number of divisions.

scale multiplier See SCALE FACTOR, **1**.

scale-of-two counter A circuit that delivers one output pulse for two successive input pulses.

scale-of-10 counter A circuit that delivers one output pulse for 10 successive input pulses.

scale-of-ten scaler See SCALE-OF-10 COUNTER.

scaler A circuit or device for extending the frequency range of another device (e.g., a circuit that extends the range of a 1-MHz counter to 100 MHz).

scale range The difference between the lowest and highest values on a scale.

scale span See SCALE RANGE.

scaling The fact, and the implications of the fact, that the mechanical strength of a structure increases in proportion to the square of linear dimension while the weight increases, according to the cube of linear dimension. Thus, weight increases more rapidly than strength as a structure, composed of a given material, is made larger. It is important in the design of large antennas and support structures.

scaling adder An inverting OPERATIONAL AMPLIFIER used to weight and sum multiple voltages.

scaling circuit A circuit, such as one or more flip-flops, that will deliver one output pulse after a predetermined number of input pulses have been received; therefore, it will provide pulse or frequency division. See, for example, SCALE-OF-TWO COUNTER.

scaling factor For a scaler, the number of input pulses required for one output pulse.

scaling ratio See SCALING FACTOR.

scan **1.** To traverse a range, field, or dimension. **2.** The amount of traversal in **1**. **3.** See SWEEP. **4.** To sample or reproduce an image in a single-line element, as in facsimile or television. **5.** A single line resulting from 4. **6.** In information retrieval operations, to inspect each record in a file or constituent of a list. **7.** To check communications or data channels for availability.

scan conversion In television reception, the scanning of each line twice to convert a conventional image into one that can be displayed on a high-definition picture tube.

scan-converter tube A face-to-face assembly of a cathode-ray tube and a vidicon in one envelope.

scandium Symbol, Sc. A metallic element. Atomic number, 21. Atomic weight, 44.956.

scan frequency See SCANNING FREQUENCY.

scanner A device, especially a radio receiver, equipped with a circuit that searches communications or data channels for signals.

scanner amplifier An amplifier for boosting a scanning signal. Also see SCAN, **1**, **3**, **4**.

scanning **1.** In a cathode-ray tube or camera tube, the synchronized movement of the electron beam (or other marker) from right to left and/or from top to bottom. **2.** The intermittent, but repetitive, monitoring of two or more communications channels in rotating sequence. **3.** The movement of a radar beam for the purpose of obtaining coverage over a specified area.

scanning antenna A transmitting or receiving antenna (such as a rotating one) that covers a generally circular region.

scanning beam The deflected electron beam in a cathode-ray tube. Also see SCAN, **1**, **2**, **3**, **4**, **5**.

scanning circuit A circuit for producing a scan (see SCAN, **2**, **4**).

scanning frequency The number of scans per unit time, usually expressed in lines, sweeps, or channels per second or per minute. Also called SCANNING RATE.

scanning line A single line sampled or produced by a scanning process, as in facsimile, television, and graphic recording.

scanning line frequency See SCANNING FREQUENCY.

scanning linearity Uniformity of scanning rate. In a linear scan, for example, scan speed is the same at all points along a line.

scanning loss The effective reduction in radar sensitivity that occurs as the beam scans a given area, rather than remaining in a fixed orientation.

scanning rate See SCANNING FREQUENCY.

scanning receiver A receiver whose tuning is automatically and continuously swept through a frequency band to detect all signals in the band.

scanning sonar A form of distance-measuring or depth-finding sonar, in which the receiving transducer scans to find the direction of the echo or echoes.

scanning speed The rate at which a line, region, or quantity is scanned or at which samples are taken.

scanning yoke See YOKE, **2**.

5059F-pS-607-670 4/10/01 9:47 AM Page 611

scan rate **1.** The rate at which a controlled quantity is checked periodically by a control computer. **2.** See SCANNING FREQUENCY.

scan tuning Repetitive, automatic sweeping of a frequency band by a tuned circuit containing a varactor, whose capacitance is periodically varied by a sawtooth voltage.

SCARA Abbreviation of SELECTIVE COMPLIANCE ASSEMBLY ROBOT ARM.

SCA subcarrier An auxiliary carrier (commonly 67 kHz) superimposed on a main frequency-modulated carrier to convey subsidiary communications, such as music without commercials. Also see SUBSIDIARY COMMUNICATION AUTHORIZATION.

scatter To disperse or diffuse transmitted electromagnetic radiation.

scattering **1.** The tendency of a concentrated beam of energy to be spread out when it passes through a given medium or substance. **2.** The spreading out of radio waves as they pass through the ionosphere or troposphere.

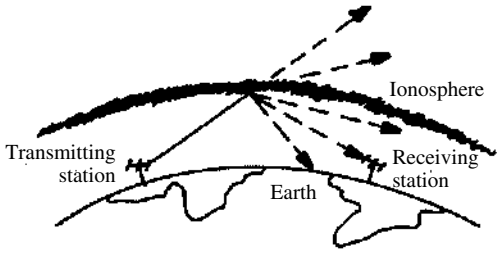

scattering

scatter read In data processing, to distribute data from an input record to several storage areas.

scatter transmission See BACK SCATTER and FORWARD SCATTER.

S_C band A section of the S BAND extending from 2000 to 2400 MHz.

scc Abbreviation of SINGLE-COTTON-COVERED (WIRE).

SCDSB Abbreviation of SUPPRESSED CARRIER DOUBLE-SIDEBAND (see DOUBLE-SIDEBAND SUPPRESSED CARRIER).

SCE Abbreviation of *saturated calomel electrode.*

sce Abbreviation of SINGLE-COTTON-ENAMELED (WIRE).

SCEPTRON Acronym for SPECTRAL COMPARATIVE PATTERN RECOGNIZER.

schedule In computer operations, to establish the order of importance of jobs to be run, and assign the necessary resources for those jobs.

schedule method A method of waveform analysis involving the evaluation of instantaneous amplitudes at numerous points in time. The values are obtained at specific intervals from the image of one complete wave cycle, as displayed on an oscilloscope or plotted on a graph.

schematic diagram An electronic circuit diagram. Also called WIRING DIAGRAM and *schematic.*

schematic symbol A graphic symbol used to represent electronic components in a circuit diagram.

Schering bridge A four-arm capacitance bridge in which the unknown capacitance is compared with a standard capacitance. This bridge is frequently used in testing electrolytic capacitors, to which a direct-current polarizing voltage is applied during the measurement.

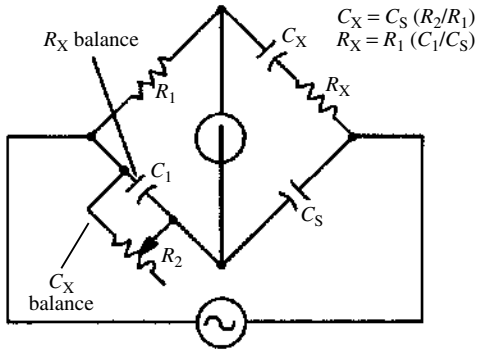

Schering bridge

Schmidt optical system In projection television, a lens system used between the bright-image picture tube and the screen.

Schmitt limiter See SCHMITT TRIGGER.

Schmitt trigger A multivibrator that produces uniform-amplitude output pulses from a variable-amplitude input signal. This circuit has many applications, one being the conversion of a sine wave into a square wave.

Schottky diode A solid-state diode in which a metal and a semiconductor form the pn junction. Electrons injected into the metal have a higher energy level than the charge carriers in a semiconductor, and energy storage at the junction is low because current flow is not accompanied by hole movement. Also known as HOT-CARRIER DIODE.

Schottky logic A form of integrated-injection logic with enhanced operating speed.

Schottky noise The random noise resulting from the emission of charged particles, usually electrons or holes, from an electrode in an amplifying device. This noise is usually of a wideband nature.

scientific language Any computer programming language used primarily for mathematical or scientific applications.

scientific notation The expression of very large and very small numbers as a fixed-point part (mantissa) and a power of the radix (usually 10).

5059F-pS-607-670 4/10/01 9:47 AM Page 612

Generally, the mantissa is greater than or equal to 1, but less than 10; the power of 10 is adjusted accordingly. Thus, for example, 203,700 = 2.037×10^5; 0.000533 = 5.33×10^{-4}. See also SIGNIFICANT FIGURES.

scintillating crystal A crystal, such as one of sodium iodide, that sparkles or flashes when exposed to radioactive particles or rays.

scintillation **1.** In radar operations, the apparent rapid displacement of a target from its mean position. **2.** A momentary flash of light produced in a phosphor or scintillating crystal when a high-velocity particle strikes it. **3.** A small fluctuation in radio field intensity at a receiving point.

scintillation counter A radiation counter consisting essentially of a scintillating crystal in combination with a photomultiplier tube. Flashes from the excited crystal cause the tube to deliver output pulses that are totaled and indicated.

scintillator material A substance, such as crystalline sodium iodide, that scintillates under certain stimuli.

scissoring A method of interrupting the electron beam in a cathode-ray tube when the beam would not land on the phosphor screen.

SCLC Abbreviation of SPACE-CHARGE-LIMITED CURRENT.

sco Abbreviation of SUBCARRIER OSCILLATOR.

scope Colloquialism for OSCILLOSCOPE.

Scott oscillator See PARALLEL-TEE OSCILLATOR.

scp Abbreviation of SPHERICAL CANDLEPOWER.

SCR Abbreviation of SILICON-CONTROLLED RECTIFIER.

scrambled signal Any signal in which (for secrecy or exclusivity) the elements are disarranged according to an encryption algorithm. Thus, intelligent reception is possible only if the signal is processed via a suitable decryption algorithm. Example: SCRAMBLED SPEECH.

scrambled speech Voice transmission in which the frequencies have been inverted to prevent eavesdropping. It is automatically unscrambled (by reinversion) at the receiver to restore intelligibility.

scrambler circuit A circuit containing filters and frequency inverters for scrambling speech.

scratch filter An audio-frequency low-pass filter that suppresses high-frequency noise caused by friction between a phonograph disc and the needle.

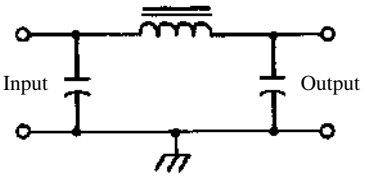

scratch filter

scratchpad memory In computers, a low-capacity memory that stores an intermediate result of a calculation.

scratch tape Magnetic data tape that can be overwritten for any purpose.

screen **1.** See SCREEN GRID. **2.** See SHIELD. **3.** The front surface of a cathode-ray tube. **4.** The surface of a computer or terminal display.

screen angle In radar, the angular difference between the actual horizon and the plane perpendicular to the line connecting the radar set with the center of the earth.

screen current Symbol, I_S or I_{SG}. The current flowing in the screen circuit of an electron tube.

screen grid In a vacuum tube, a grid element between the control grid and plate. It reduces the internal grid-plate capacitance, and consequently prevents self-oscillation when the tube is used in a straight-through amplifier.

screen-grid neutralization Neutralization of an amplifier that uses a tetrode vacuum tube. Such circuits require smaller neutralizing capacitances than those used in triode amplifiers because of the lower interelectrode capacitance of the screen-grid tube.

screen illumination Edge lighting of the transparent screen of an oscilloscope, to make the lines of the graticule more clearly visible.

screen material See PHOSPHOR.

screen resistance Symbol, R_S or R_{SG}. The internal resistance presented by the screen-grid/cathode path of an electron tube.

screen room See CAGE.

screen voltage Symbol, E_S or E_{SG}. The voltage at the screen grid of an electron tube.

scribing The etching of a semiconductor wafer to facilitate breaking the wafer into smaller pieces.

ScriptX A high-level programming language used in the writing of software for personal computers—especially in multimedia. Developed by Kaleida Laboratories.

SCS Abbreviation of SILICON-CONTROLLED SWITCH.

SCT Abbreviation of SURFACE-CHARGE TRANSISTOR.

S curve **1.** The voltage-versus-current curve for a negative-resistance device. Compare N CURVE. **2.** The response curve for a frequency-modulation discriminator or ratio detector.

SD Abbreviation of STANDARD DEVIATION.

S_D band A section of the S BAND extending from 4200 to 5200 MHz.

SDF Abbreviation of static direction finder.

SDR See SOFTWARE-DEFINED RADIO.

Se Symbol for SELENIUM.

seaborgium Symbol, Sg. Also called *unnilhexium* (Unh). Atomic number, 106. The most common isotope has atomic weight 263. Classified as a transition metal. It has a half-life on the order of 1 second or less, is human-made, and is not known to occur in nature.

5059F-pS-607-670 4/10/01 9:47 AM Page 613

sea clutter Collectively, the radar echoes that the sea reflects.

seal **1.** The point at which a lead or electrode enters or leaves and is secured to an envelope, case, or housing. Such a point is often tightly closed against the passage of air in or out of the envelope. **2.** To close off a circuit or component from tampering.

sealed dry battery A set of electrochemical dry cells that can be installed without concern for orientation or position. Example: 9-volt "transistor battery."

sealed meter **1.** A meter that is tightly closed against the entry of moisture and foreign materials. **2.** A meter that is locked or otherwise protected against tampering.

sealing compound A substance (such as wax, pitch, or plastic) used to enclose and protect electronic devices.

search **1.** To scan or sweep through a range of quantities or through a region of interest. **2.** To examine (usually in some prescribed order) items of information in a computer memory to find those satisfying a given criterion.

search coil An inductive probe (exploring coil) used to sample magnetic fields.

search oscillator A variable-frequency oscillator used to locate and identify signals by the heterodyne method.

search probe **1.** See SEARCH COIL. **2.** A capacitive probe used to sample electric fields.

search radar A radar that displays a target almost immediately after that target enters a scanned area.

search time The time needed to test items during a search (see SEARCH, **2**).

sea return See SEA CLUTTER.

seasonal effects In ionospheric propagation, the changes produced as a result of the revolution of the earth around the sun. The path of the sun across the sky, and the length of the day, are primarily responsible for such effects.

seasonal static Atmospheric electrical interference, most prevalent during the summer.

S_E band A section of the S BAND extending from 1550 to 1650 MHz.

sec **1.** Abbreviation of SECOND. **2.** Abbreviation of SECTION. (Also, sect.) **3.** Abbreviation of SECONDARY. **4.** Abbreviation of SECANT.

secant Abbreviation, sec. The trigonometric function representing the ratio of the hypotenuse of a right triangle to the adjacent side (c/b). The secant is the reciprocal of the cosine; $\sec x = 1/\cos x$.

second **1.** Abbreviation, s and sec. A unit of time. The mean solar second is 1/86,400 of a mean solar day, and is 1/60 minute or 1/3600 hour. **2.** Symbol ("). A unit of arc measure. 1" = 1/3600 geometric degree.

secondaries See SECONDARY COLORS.

secondary **1.** See SECONDARY WINDING. **2.** See SECONDARY STANDARD.

secondary battery See STORAGE BATTERY.

secondary calibration The calibration of an instrument, based on a reference instrument calibrated against an absolute source.

secondary capacitance **1.** The distributed capacitance of the secondary winding of a transformer whose primary winding is unloaded. Compare PRIMARY CAPACITANCE, **1**. **2.** A series or shunt capacitance used to tune the secondary coil of a radio-frequency transformer. Compare PRIMARY CAPACITANCE, **2**.

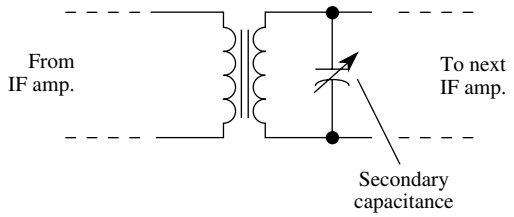

secondary capacitance, 2

secondary cell See STORAGE CELL.

secondary circuit **1.** The circuit associated with the secondary winding of a transformer. **2.** See OUTPUT CIRCUIT.

secondary coil See SECONDARY WINDING.

secondary color **1.** A color prepared by mixing two primary colors. **2.** In television operations, any displayed color composed of two or more color primaries.

secondary current The current flowing in the secondary winding of a transformer. Also called TRANSFORMER OUTPUT CURRENT. Compare PRIMARY CURRENT.

secondary electron **1.** The electron possessing the lesser energy after a collision between two electrons. Compare PRIMARY ELECTRON. **2.** An electron ejected by secondary emission.

secondary emission The action whereby electrons in the atoms at the surface of a target are ejected as a result of bombardment by a beam of (primary) electrons. Thus, in an electron tube, electrons from the cathode strike the plate with a force that drives secondary electrons out of the plate, into the surrounding space.

secondary emitter A source of secondary electrons (e.g., the plate of an electron tube or a dynode in a photomultiplier tube).

secondary failure The failure of a component or circuit, resulting from the failure of some other component. For example, the pass transistor in a power supply might burn out, causing the output voltage to increase; this increased voltage can damage equipment connected to the supply.

secondary frequency standard A device for generating signals of accurate frequency, but that does

5059F-pS-607-670 4/10/01 9:47 AM Page 614

not possess the very high stability and extreme accuracy of a primary frequency standard. The secondary standard is periodically checked against a PRIMARY FREQUENCY STANDARD and appropriately corrected.

secondary impedance **1.** The impedance of the secondary winding of a transformer whose primary winding is unloaded. Compare PRIMARY IMPEDANCE, **1**. **2.** An external impedance presented to the secondary winding of a transformer. Compare PRIMARY IMPEDANCE, **2**.

secondary inductance The inductance of the secondary winding of a transformer whose primary winding is unloaded. Compare PRIMARY INDUCTANCE.

secondary kVA The kilovolt-amperes in the secondary circuit of an operating transformer. Compare PRIMARY KVA.

secondary power The power in the secondary circuit of a transformer. Also see SECONDARY KVA and SECONDARY VA. Compare PRIMARY POWER.

secondary radiation **1.** The (sometimes random) reradiation of electromagnetic waves, as from a receiving antenna. **2.** Rays emitted by atoms or molecules when the latter are struck by other radiation.

secondary rays Rays emitted by atoms or molecules that have been bombarded by other rays of the same general nature. Examples: *secondary X rays* and *secondary beta rays.*

secondary resistance The direct-current resistance of the secondary winding of a transformer. Compare PRIMARY RESISTANCE.

secondary standard An accurate source of a quantity (capacitance, frequency, inductance, resistance, etc.), that is referred periodically to a primary standard for correction.

secondary storage In computer and data-processing operations, storage that is auxiliary to the main storage. Also called *backing storage.*

secondary turns The number of turns in the secondary winding of a transformer. Compare PRIMARY TURNS.

secondary utilization factor For a transformer in a rectifier circuit, the utility factor of the secondary winding (ratio of direct-current power output to secondary volt-amperes).

secondary VA The volt-amperes in the secondary circuit of a transformer. Compare PRIMARY VA.

secondary voltage The voltage across the secondary winding of a transformer. Also called TRANSFORMER OUTPUT VOLTAGE. Compare PRIMARY VOLTAGE.

secondary winding The normal output winding of a transformer. Also called SECONDARY COIL. Compare PRIMARY WINDING.

second breakdown In a large-area power transistor, a destructive breakdown caused by thermal runaway.

second-breakdown voltage The collector voltage at which second breakdown occurs in a transistor.

second-channel attenuation See SELECTANCE, **2**.

second-channel interference In a given channel, interference arising from authorized signals two channels removed.

second detector In a superheterodyne receiver, the intermediate-frequency detector. Compare FIRST DETECTOR.

second-level address In a computer program instruction, an address giving the location of the address of a required operand. Also called *indirect address.*

sect Abbreviation of SECTION. (Also, sec.)

section **1.** A subcircuit or stage of a larger circuit (e.g., the *oscillator section* of a receiver). **2.** The smaller unit described in **1**, when self-contained and operated independently (e.g., *filter section*). **3.** See PROGRAM SEGMENT.

sectionalized antenna A set of collinear radiating elements, placed end-to-end with reactances between them, for the purpose of modifying the radiation pattern.

sectionalized winding **1.** A method of winding a coil in complete, multilayer sections that are stacked side by side or top to bottom, a technique that reduces distributed capacitance. **2.** A coil wound, as defined in **1**.

sector On a magnetic disk, a specific portion of a track.

sectoral horn antenna An (usually sheetmetal) antenna with the shape of a horn of rectangular cross section. It is flared in one dimension only.

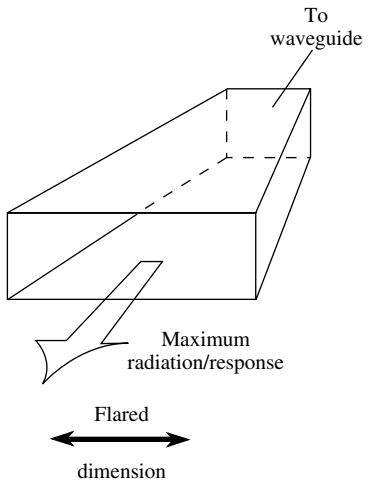

sectoral horn antenna

sector display In a radar, a display that allows the continuous observation of a portion of the scanned area.

secular equilibrium The state in which a radioactive substance changing into another substance

5059F-pS-607-670 4/10/01 9:47 AM Page 615

is decaying as fast as the second substance is being formed.

secular variation A slow change in the intensity of the terrestrial magnetic field.

secure mode In a security system, the condition of being fully activated.

securite In radiotelephony, a spoken word (pronounced say-kyoor-ee-tay) identifying a transmission concerning safety. Equivalent to TT in radiotelegraphy.

security code **1.** A set of alphanumeric characters (letters and/or numbers) or switch settings that activates or deactivates a security system. **2.** See PASSWORD.

security robot In a smart home, a robot that assists in protection of a home or business, and its occupants, from intrusion, burglary, or attack. If an intruder enters the property, the security robot might drive the offender away or detain the offender until police arrive. The robot might employ iris-print detection or facial feature detection to identify an intruder from a distance. The robot would be linked to the home computer via a broad-bandwidth, high-speed wireless system. Compare SENTRY ROBOT. Also see SMART HOME OR BUSINESS.

security system A set of electronic (and sometimes also electromechanical) devices designed to do one or more of the following: restrict access to a premises or computer system, detect abnormal conditions, detect unauthorized entry, alert human operators of abnormal conditions, alert owners and/or authorities of unauthorized entry to a premises, and (in some cases) provide physical protection of property.

Seebeck effect The development of an electromotive force in a junction of two dissimilar metals (a thermocouple) when the temperature of the junction is different from that of the rest of the metal.

Seebeck emf The electromotive force resulting from the Seebeck effect.

seed crystal A small single crystal from which a larger single crystal (e.g., germanium or silicon) is grown. Also see CZOCHRALSKI METHOD.

seeing-eye robot A robot that serves in the capacity of a seeing-eye dog, to help visually impaired people in their daily activities.

seek See SEARCH.

seek area An area of direct-access storage to which are assigned specific records and from which the records can be accessed quickly.

segment **1.** The portion of a line or curve lying between two points. **2.** See PROGRAM SEGMENT.

segmental meter An expanded-scale meter (see SCALE EXPANSION).

segmented encoding law An approximation of a smooth encoding law, done by means of linear partitions or segments. The greater the number of segments, the more accurate the approximation.

segmenting See PARTITIONING.

segment mark A character indicating the division between tape file sections.

segue (Pronounced SEG-way.) A smooth transition from one sound or channel to another (e.g., between musical selections in a radio broadcast). The first selection decreases in volume as the second selection increases. There is some overlap.

Seignette salt See ROCHELLE SALT.

seismic detector A vibration sensor used in some types of intrusion-detection systems.

seismogram A record produced by a SEISMOGRAPH.

seismograph An instrument for detecting and recording earth tremors. Indicates the direction, magnitude, and time of a quake.

seismometer See SEISMOGRAPH.

seismoscope An instrument that shows the occurrence and time of an earthquake. Compare SEISMOGRAPH.

select To accept or separate a unit, quantity, or course of action from all those available (in a group, mixture, or series).

selectance **1.** For a resonant circuit, the ratio *Er*/*Ex*, where *Er* is the voltage at resonance, and *Ex* is the voltage at a specified nonresonant frequency. **2.** For a receiver, the figure *S2*/*S1*, where *S1* is the sensitivity of the receiver in a given frequency channel, and *S2* is the sensitivity in another specified channel.

selected mode In an encoder, a mode in which one output is read and the others are ignored.

selective Pertaining to a device or system, such as a radio receiver, with a high degree of SELECTIVITY.

selective absorption The attenuation or absorption of some frequencies or bands of frequencies, with little or no attenuation at other frequencies or bands of frequencies.

selective amplifier An amplifier that can be tuned, with the desired degree of sharpness, to a single frequency or band of frequencies. Radio-frequency amplifiers are generally tuned by means of inductance-capacitance (LC) circuits; audio-frequency amplifiers are usually tuned by means of resistance-capacitance (RC) circuits.

selective calling The calling, alerting, or alarming of a desired station without interfering with other stations.

selective compliance assembly robot arm Abbreviation, SCARA. An electromechanical device designed especially for use in assembly lines. It uses cylindrical coordinate geometry to allow precise, programmable movements in three dimensions.

selective dump In computer operations, a dump (see DUMP) affecting a small, specific memory area.

selective fading Fading caused by propagation conditions, whose effects differ at slightly different frequencies. In an amplitude-modulated signal, this effect causes the sidebands and carrier

5059F-pS-607-670 4/10/01 9:47 AM Page 616

to arrive in various phase relationships, with resulting distortion in the received signal.

selective interference Interference confined to a narrow band of frequencies.

selective polarization See POLARIZATION SELECTIVITY.

selective reflection In the reflection of electrons directed into a crystal by means of an electron gun, the tendency of the electrons to be reflected more readily when they strike the crystal at certain speeds.

selective relay **1.** A relay or relay circuit tuned to open or close at one signal frequency. **2.** A relay or relay circuit adjusted to open or close at one value of current or voltage.

selective trace In computer operations, a diagnostic program used to analyze certain areas of memory or specific kinds of program instructions, for debugging purposes.

selectivity **1.** The ability of a circuit or device to pass signals of one frequency and reject signals at other frequencies. **2.** The degree to which a circuit or device passes signals of one frequency and rejects signals at other frequencies.

selectivity control In some equipment (such as receivers, crystal filters, wave analyzers, and vibration meters) an adjustment that permits variation of selectivity.

Selectoject A fully electronic, continuously tunable, notcher-peaker that is resistance-capacitance tuned. The name is an acronym for *select or reject.*

selector **1.** A channel switch in a radio or television receiver. **2.** See SELECTOR SWITCH.

selector channel In data-processing and computer systems, a data transmission channel controlling the information flow between peripherals and a central processing unit.

selector pulse In digital communications, an identifying pulse that represents a certain group of bits or data.

selector relay A device, such as a stepping switch, that actuates one of a number of available circuits on receipt of a predetermined number of pulses.

selector switch A (usually rotary) multiposition switch that allows an operator to select from among several options (such as frequency channels, frequency bands, or selective filters).

selenium Symbol, Se. A nonmetallic element. Atomic number, 34. Atomic weight, 78.96. It is used in the manufacture of some diodes, rectifiers, and photocells.

selenium cell A photoelectric cell that uses specially processed selenium as the light-sensitive material. It can be operated as a photoconductive cell or a photovoltaic cell.

selenium diode A junction diode in which the semiconductor material is specially processed selenium. Also see JUNCTION DIODE.

selenium photocell See SELENIUM CELL.

selenium rectifier A disk- or plate-type power rectifier utilizing the junction between selenium and aluminum or selenium and iron.

self-bias For a transistor or vacuum tube, input-electrode bias voltage resulting from the flow of output-electrode current through a resistor common to both circuits. Also called AUTOMATIC BIAS.

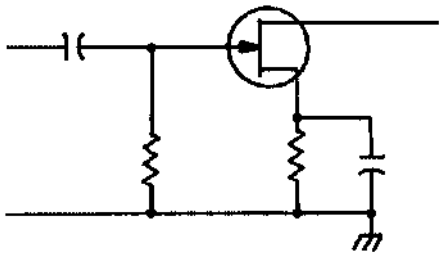

self-bias

self-capacitance The inherent internal capacitance of a device other than a capacitor.

self-checking number A number whose digits have a value that determines the check digit attached to it; thus, it can be verified following its transfer between storage locations or peripherals.

self-cleaning contacts Switch or relay contacts that clean themselves automatically by means of wiping action.

self-contained device A device containing all parts and sections (e.g., main circuit, power supply, meter, loudspeaker, etc.) needed for full operation (i.e., no auxiliary equipment is needed).

self-controlled oscillator See SELF-EXCITED OSCILLATOR.

self discharge The tendency of an electrochemical cell or battery to gradually lose stored energy when not in use.

self-discharge rate A quantitative expression of the speed with which SELF DISCHARGE occurs in an electrochemical cell or battery when it is stored without being used.

self-energy Symbol, *E.* The energy mc^2, in joules, of a particle traveling at the speed of light c (2.9979×10^8 meters per second) and whose mass is m kilograms.

self erasing In a magnetic tape, the unwanted erasing of data near a highly magnetized region.

self-excited generator An alternating-current generator in which the field coils are supplied with direct current produced by the machine itself. Compare SEPARATELY EXCITED GENERATOR.

self-excited oscillator An oscillator consisting of an amplifier that supplies its own input signal through positive feedback, and whose oscillation frequency depends entirely on circuit constants,

5059F-pS-607-670 4/10/01 9:47 AM Page 617

such as the capacitance and inductance in a tank circuit. Compare CRYSTAL OSCILLATOR, FORK OSCILLATOR, HUMMER, and MAGNETOSTRICTION OSCILLATOR.

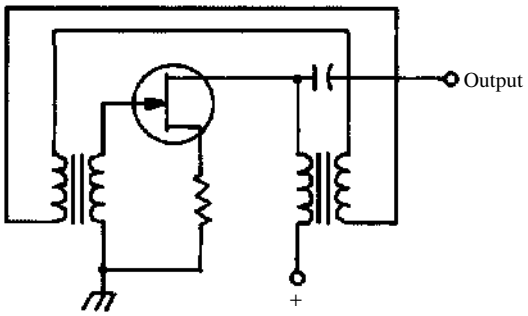

self-excited oscillator

self-focus picture tube A television picture tube in which the electron gun has an automatic, electrostatic focusing arrangement.

self-generating photocell See PHOTOVOLTAIC CELL.

self-generating transducer A voltage-producing transducer, such as a piezoelectric pickup or dynamic microphone.

self-healing capacitor A capacitor, such as a wet electrolytic unit, in which the dielectric is restored to its normal condition after a high-voltage breakdown.

self-heated thermocouple A thermocouple in which the passage of an applied current produces the heat necessary for the activation of the thermocouple.

self-heating thermistor A thermistor heated to above ambient temperature by the current passing through it. Also called DIRECTLY HEATED THERMISTOR. Compare INDIRECTLY HEATED THERMISTOR.

self impedance The effective or measured impedance at a circuit point.

self-inductance **1.** The inductance of an inductor. **2.** The inherent internal inductance of a device other than an inductor.

self-induction Induction that occurs in a single circuit. An instance is the generation of an opposing voltage across a coil by an alternating current flowing through it. Compare INDUCTION. Also see INDUCTANCE.

self-latching relay A relay that remains in the state that it has been switched (i.e., locked open or closed) until a subsequent signal is received.

self-modulated oscillator A circuit, such as a blocking oscillator, in which oscillation occurs simultaneously at two frequencies, one modulating the other.

self-organizing Pertaining to a computer or system that can change the arrangement of data files for particular purposes.

self-powered device A device that requires no external source of power (i.e., it is equipped with a self-contained battery or a generator).

self-pulsing blocking oscillator A blocking oscillator that produces a train of radio-frequency pulses. Compare SINGLE-SWING BLOCKING OSCILLATOR.

self-quenching detector A super-regenerative detector (see SUPER-REGENERATIVE CIRCUIT) in which the low-frequency quenching voltage is supplied by the regenerative detector itself. Also see QUENCHING ACTION and QUENCH OSCILLATOR. Compare SEPARATELY QUENCHED DETECTOR.

self-quenching oscillator A circuit, such as a blocking oscillator, in which oscillation is periodically switched off automatically, resulting in a self-interrupted wave train.

self-rectifying vibrator A vibrator-type power supply in which one vibrator reed chops the direct-current input to the primary winding of the transformer, and a second vibrator reed rectifies the alternating-current output delivered by the secondary winding. Also see VIBRATOR RECTIFIER.

self-rectifying X-ray tube An X-ray tube operated with alternating-current anode voltage.

self-regulation The ability of a circuit or device to control its output automatically, according to some predetermined plan, by using output error to correct operation or to vary the input.

self reset **1.** The action of a circuit breaker to reapply power after a certain elapsed time. **2.** The action of any device, returning a circuit or system to normal automatically.

self-resetting loop In a computer program, a loop in which instructions cause locations used in the loop to assume their condition prior to the loop's execution.

self-resistance The inherent internal resistance of a device other than a resistor.

self-resonant frequency The frequency at which a device will resonate naturally (without external tuning). Thus, an inductor will self-resonate with its distributed capacitance; similarly, a capacitor will resonate with its stray inductance.

self-saturation In a magnetic amplifier, saturation resulting from rectification of the saturable-reactor output current.

self-starting motor An alternating-current motor that starts running as soon as voltage is applied (i.e., no external mechanical force is needed). Also see SHADING COIL.

self-sustained oscillations Oscillations maintained by means of positive feedback (inductive or capacitive) from the output to the input of a circuit. See, for example, SELF-EXCITED OSCILLATOR.

5059F-pS-607-670 4/10/01 9:47 AM Page 618

self-test Any arrangement whereby a device or system determines, without the aid of an external operator, whether or not it is operating correctly.

self-ventilated motor See OPEN MOTOR.

self-wiping contacts See SELF-CLEANING CONTACTS.

selsyn See AUTOSYN and SYNCHRO.

SEM **1.** Abbreviation of SINGLE-ELECTRON MEMORY. **2.** Abbreviation of SCANNING ELECTRON MICROSCOPE.

semantic network A reasoning scheme sometimes used in artificial intelligence. Logical state-ments or sentences are broken down into nodes (generally nouns) and relationships (generally verbs and modifiers). This allows statements to be mapped in a way that is easy for computers to store and modify.

semiautomatic key Also called *bug*. A telegraph key that mechanically produces a string of Morse-code dots (short pulses) when its lever is pressed to one side (usually toward the right), and continuous circuit closure when the lever is pressed to the opposite side (usually toward the left). Dashes are manually sent by the operator.

semiconductor A material whose natural resistivity lies between that of conductors and insulators (e.g., GERMANIUM, SILICON, SELENIUM, and GALLIUM ARSENIDE).

semiconductor capacitor A miniaturized component that takes advantage of reverse biasing in a semiconductor P-N junction. When a voltage source is connected across a diode so that it does not conduct, the diode acts as a capacitor. The capacitance varies depending on how much reverse voltage is applied to the diode. The greater the reverse voltage, the smaller the capacitance. Some diodes are especially manufactured to serve this function. This phenomenon can be useful in the fabrication of integrated circuits (ICs). See also INTEGRATED CIRCUIT, VARACTOR.

semiconductor counter A device for measuring the intensity of ionizing radiation (such as alpha particles, beta particles, or gamma rays) using a photodiode and sensing circuit.

semiconductor device A component (such as a diode, photocell, rectifier, or transistor) that exploits the properties of a semiconductor.

semiconductor diode A solid-state diode, as opposed to a vacuum-tube diode or gas-tube diode. Examples: *germanium diode*, *selenium diode*, and *silicon diode*.

semiconductor junction Within a body of semiconductor material, the area of physical contact between two regions (usually n and p) having opposite electrical properties.

semiconductor laser See LASER DIODE.

semiconductor material See SEMICONDUCTOR.

semiconductor-metal junction The area of physical contact between a metal and a semiconductor.

semiconductor photosensor A semiconductor photodiode or phototransistor, as opposed to a phototube.

semiconductor rectifier A heavy-duty semiconductor diode (or assembly of such diodes) designed primarily to change alternating current to direct current in power-supply units. Rectifiers commonly are made from copper oxide, germanium, magnesium-copper sulfide, selenium, or silicon. Also see JUNCTION DIODE and METER RECTIFIER.

semiconductor resistor A tiny resistor manufactured from semiconductor material, especially one that is etched onto the chip of an integrated circuit (IC). The thickness, and the types and concentrations of impurities added, determine the resistance of the component. Such resistors can handle only a tiny amount of power because of their small size. But because IC circuits are designed to consume minimal power, this is not a problem. The small signals produced by ICs can be amplified, using circuits made from discrete components, if it is necessary to obtain higher signal power. See also INTEGRATED CIRCUIT.

semidirectional Pertaining to a transducer that exhibits different directional characteristics at different frequencies.

semiduplex operation A two-frequency communication system that operates in duplex at one end of the link, and in simplex at the other end. Also see DUPLEX OPERATION and SIMPLEX TELEGRAPHY.

semilogarithmic graph Also called *semilog graph*. A graph in which one axis is logarithmic and the other axis is linear.

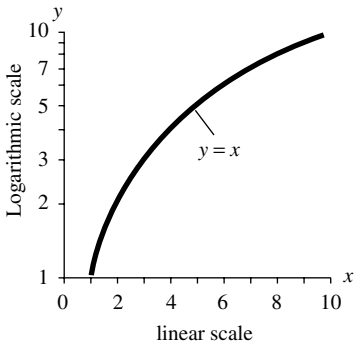

semilogarithmic graph

semimetal An elemental substance that exhibits some, but not all, of the properties of a metal (e.g., antimony and arsenic). Also called METALLOID.

semiresonant line An open-wire transmission line cut approximately to resonant length at the frequency of operation.

5059F-pS-607-670 4/10/01 9:47 AM Page 619

semitone See HALF STEP.

sender See TRANSMITTER, **1**, **3**.

sending-end impedance See DRIVING-POINT IMPEDANCE.

sending set **1.** See RADIO TRANSMITTER. **2.** An equipment for transmitting electromagnetic waves. Also see TRANSMITTER, **1**.

sensation level The level of sound that produces a tingling or noticeable sensation in the ear.

sense **1.** To check the condition of a switching device, such as a gate. **2.** See READ.

sense amplifier A device that produces a control signal when some characteristic of the input signal changes.

sense determination In a direction finder that provides an ambiguous indication (two readings 180 degrees apart), the process of deducing, or the ability of the apparatus to deduce, the true direction from which the signal is coming.

sense resistor A (usually low-value) resistor used to sense current in a circuit without introducing a significant loss. The voltage drop across this resistor is proportional to the current and can be applied to a voltmeter, oscilloscope, or other instrument for measurement or observation.

sensing circuit **1.** A circuit that samples a quantity. **2.** In a voltage regulator, the circuit that monitors the output voltage and delivers a control voltage proportional to the output-voltage error.

sensing window See WINDOW, **2**.

sensitive communications Two-way communications of an emergency or priority nature, or involving the security of government operations.

sensitive device A device that responds to a signal of low amplitude.

sensitivity **1.** The ability of a circuit or device to respond to a low-level applied stimulus. **2.** For a receiver, the input-signal (in microvolts or millivolts) required for a specified output level. **3.** For a galvanometer, microamperes or milliamperes per scale division. **4.** The ohms-per-volt rating of a voltmeter. Also see VOLTMETER SENSITIVITY.

sensitivity adjustment **1.** An input gain control in an amplifier circuit. **2.** The radio-frequency gain control of a receiver. **3.** A control or switch that is used to select the range or threshold of a piece of test equipment.

sensitivity control A manual or automatic device for adjusting the sensitivity of a circuit or device.

sensitometer An instrument used to measure the sensitivity of certain materials to light.

sensor **1.** A device that samples a phenomenon, and delivers a proportionate current or voltage in terms of which the intensity of the phenomenon can be measured, or with which control action can be initiated. **2.** An electronic device that detects abnormal conditions (e.g., smoke and heat) and delivers a warning signal to human operators and/or computers. **3.** An electronic device that detects intrusion to a premises and delivers a warning signal to human operators and/or computers.

sentry robot In a smart home or business, a robot that alerts the owner to abnormal conditions. It can detect fire, burglars, or water in places it should not be. It might also detect abnormal temperature, barometric pressure, wind speed, humidity, or air pollution. A wireless link alerts the owner via a device similar to a common beeper. Compare SECURITY ROBOT. Also see SMART HOME OR BUSINESS.

separately excited generator An alternating-current generator whose field coils are supplied with direct current from another generator or from a battery. Compare SELF-EXCITED GENERATOR.

separately quenched detector A superregenerative detector (see SUPERREGENERATIVE CIRCUIT) in which the quenching voltage is supplied by a separate low-frequency oscillator. Also see QUENCHING ACTION and QUENCH OSCILLATOR. Compare SELF-QUENCHED OSCILLATOR.

separation See CHANNEL SEPARATION.

separation energy The energy required to remove a proton or neutron from the nucleus of an atom. The separation energy depends on the atomic number.

separator **1.** See FILTER, **1**. **2.** A perforated or porous plate of insulating material (usually plastic or wood) for holding active plates apart in a storage cell. **3.** In computer operations, a character marking the division between logical data units. Also called *data delimiter.*

septate cavity A coaxial cavity containing a SEPTUM between the inner and outer conductors.

septate waveguide A waveguide containing one or more septa (see SEPTUM) to control power transmission.

septum A thin metal vane used as a reflector in a waveguide or cavity.

sequence **1.** A succession of objects, parameters, or numbers. **2.** An ordered set of numbers—each of which is related to its predecessor by a specific mathematical function.

sequence checking routine In computer operations, a routine that verifies the order of items of data.

sequence control register In a computer memory, a register whose contents determine the instruction to be implemented next.

sequence programmer A timing device that can be preset to start or stop various operations at predetermined times.

sequencer A device that initiates or terminates events in a desired sequence.

sequence relay A relay whose several contacts close in a predetermined order.

sequence timer A timer in which separate delay circuits are actuated in a predetermined sequence.

sequential In computer operations, a term denoting operations on data items in which the items

5059F-pS-607-670 4/10/01 9:47 AM Page 620

(e.g., records in a file) are taken in an order determined by key values, rather than in the order in which the items are physically arranged.

sequential access memory Any semiconductor memory in which data can be recalled or addressed only in a certain specified order.

sequential analysis In statistics, using an unspecified number of observations as samples from which a result is derived. Each observation is accepted or rejected, or another observation is made.

sequential color television The successive transmission of the three primary colors in a television system, and their reproduction at the receiver in the same order. Also see DOT-SEQUENTIAL SYSTEM, FIELD-SEQUENTIAL SYSTEM, and LINE-SEQUENTIAL SYSTEM.

sequential control Computer operation in which the order of instruction implementation is the same as the order of instruction storage.

sequential relay See SEQUENCE RELAY.

sequential scanning Rectilinear television scanning in which the center-to-center distance between successive lines is the same as the nominal line width.

sequential switch **1.** A switch that provides selection of two or more ports in a rotating succession. **2.** In a television system, a switch that allows the monitoring technician to select any of the cameras for viewing.

sequential timer See SEQUENCE TIMER.

ser **1.** Abbreviation of SERIES. **2.** Abbreviation of SERIAL.

serial **1.** Pertaining to the performance of steps, or the occurrence of elements (such as data items on magnetic tape), in succession. **2.** An order, row, or sequence in which one item follows another (as opposed to parallel).

serial access Access to data file records in their order in a storage medium.

serial adder See SERIAL ARITHMETIC UNIT.

serial arithmetic unit In computer operations, an arithmetic unit in which digits are handled in order. Compare PARALLEL ADDER.

serial bit Data in which the bits of each byte or word are sent or received one at a time.

serial memory A register in which the input and output data is stored and retrieved one bit at a time.

serial-parallel **1.** Pertaining to data transfer that is serial in one sense and parallel in another sense. For example, entire words might be serially transmitted within a system, but the constituent bits of each word might be transferred in parallel. **2.** See PARALLEL-SERIES.

serial processing In computer operations, the sequential processing of several different programs through a single channel. Compare PARALLEL PROCESSING.

serial storage In computer operation, storage in which elements are entered in order and are available only in the same order. Compare PARALLEL STORAGE.

serial transfer The propagation of information along a single path, in which data bits are sent one after the other.

series **1.** The sum of a mathematical sequence (see SEQUENCE, **2**). **2.** Pertaining to the connection of elements or components end-to-end (see SERIES CIRCUIT).

series addition See SERIES-AIDING.

series-aiding The condition in which two series voltages or magnetic fields are added together. Compare SERIES-BUCKING.

series antenna tuning Antenna-feeder tuning in which a separate tuning capacitor is connected in series with each wire. Compare PARALLEL ANTENNA TUNING.

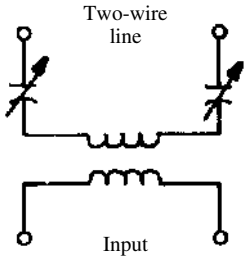

series antenna tuning

series bucking The condition in which two series voltages or magnetic fields oppose each other. Compare SERIES-AIDING.

series capacitance Capacitance acting, or connected, in series with another capacitance or other quantity.

series capacitors Capacitors connected in series. If the individual capacitors have values $C1$, $C2$, . . . , Cn, then the total capacitance Ct is equal to $1/(1/C1 + 1/C2 + \ldots + 1/Cn)$. Also see SERIES CIRCUIT.

series circuit A circuit whose components are, in effect, connected in a string (i.e., end-to-end). Compare PARALLEL CIRCUIT.

series-diode half-wave rectifier See SERIES-DIODE RECTIFIER.

series-diode rectifier A rectifier circuit in which the diode is connected in series with the source and load. Compare SHUNT-DIODE RECTIFIER.

series dropping resistor See DROPPING RESISTOR.

series equivalent impedance A series impedance that will draw the same current (magnitude and phase) drawn by a given parallel circuit connected across the same single-phase source.

series equivalent of parallel circuit See SERIES EQUIVALENT IMPEDANCE.

5059F-pS-607-670 4/10/01 9:47 AM Page 621

series-fed amplifier An amplifier circuit in which the operating voltages are applied in series with the alternating-current signal voltages. Also see SERIES FEED.

series-fed oscillator An oscillator circuit in which the direct-current operating voltage is applied in series with the alternating-current output voltage. Also see SERIES FEED.

series feed The application of alternating-current (ac) and direct-current (dc) voltages in series to a device. Example: the presentation of the dc operating voltages for an amplifier in series with the ac signal voltages (see SERIES-FED AMPLIFIER).

series feedback A feedback system in which the feedback signal is presented to the input point in series with the input signal. Compare SHUNT FEEDBACK.

series field A magnetic field produced by a series winding in a motor or generator.

series generator An electric generator in which the armature and field windings are connected in series. Compare SHUNT GENERATOR.

series inductance **1.** Inductance acting, effectively, in series with some other quantity (e.g., the inherent inductance of a wirewound resistor). **2.** An inductance connected in series with other inductances, or with some other quantity (e.g., capacitance and resistance).

series inductors Inductors connected in series, and separated or oriented in a way that minimizes the effects of mutual inductance. Assuming zero mutual inductance, if the individual inductors have values *L1*, *L2*, . . . , *Ln*, then the total inductance *Lt* is equal to *L1* + *L2* + . . . + *Ln*. Also see SERIES CIRCUIT.

series limiter A limiter (clipper) circuit in which the diode is essentially in series with the signal. Compare PARALLEL LIMITER.

series loading The series insertion of reactances in a circuit for the purpose of impedance matching.

series magnetic circuits A combination of several magnetic paths in line so that flux extends through each path in sequence; this is analogous to the passage of electric current successively through series-connected resistors.

series motor An electric motor whose armature and field windings are connected in series. Compare SHUNT MOTOR.

series operation The operation of units in succession, necessitating sequential current flow through each. Also see SERIES CIRCUIT.

series opposition See SERIES BUCKING.

series-parallel See PARALLEL-SERIES.

series-parallel capacitors See PARALLEL-SERIES CAPACITORS.

series-parallel inductors See PARALLEL-SERIES INDUCTORS.

series-parallel resistors See PARALLEL-SERIES RESISTORS.

series regulator A voltage regulator circuit in which the controlled device is in series with the load. Compare SHUNT REGULATOR.

series resistance **1.** Resistance acting in series with another resistance or with another quantity (e.g., capacitance and inductance). **2.** The inherent resistance that acts effectively in series with the plates of a capacitor. **3.** The resistance of the wire in a coil, acting effectively in series with the inductance.

series resistors Resistors connected in series with each other. If the individual resistors have values *R1*, *R2*, . . . , *Rn*, then the total resistance *Rt* is equal to *R1* + *R2* + . . . + *Rn*. Also see SERIES CIRCUIT.

series resonance Resonance in a circuit consisting of a capacitor, inductor, and an alternating-current generator in series. At the resonant frequency, the inductive reactance and the capacitive reactance cancel, so the net reactance is zero. The capacitor current and inductor current are maximum and equal, and the circuit impedance is minimum. Compare PARALLEL RESONANCE.

series-resonant circuit A resonant circuit in which the capacitor, inductor, and generator are connected in series. Also see SERIES RESONANCE. Compare PARALLEL-RESONANT CIRCUIT.

series-resonant trap A wavetrap consisting of a series-resonant inductance-capacitance (LC) circuit. Compare PARALLEL-RESONANT TRAP.

series-resonant wavetrap See SERIES-RESONANT TRAP.

series-shunt circuit See PARALLEL-SERIES.

series tee junction See E-PLANE TEE JUNCTION.

series tracking capacitor See OSCILLATOR PADDER.

series-type frequency multiplier A varactor frequency-multiplier circuit in which the varactor is in series with the input and output. Compare SHUNT-TYPE FREQUENCY MULTIPLIER.

series-type resonance bridge A resonance bridge in which the impedance arm is a series-resonant circuit. Compare SHUNT-TYPE RESONANCE BRIDGE.

series winding **1.** In a motor or generator, a winding connected in series with the armature. **2.** A method of motor or generator construction in which the field winding is connected in series with the armature.

series-wound generator See SERIES GENERATOR.

series-wound motor See SERIES MOTOR.

serrated pulse A pulse having a notched or slotted top. An example is the vertical sync pulse in television.

serrated rotor plate In a variable capacitor, an external rotor plate that is slotted radially. This alters the capacitance-variation curve of the capacitor to allow alignment of sensitive apparatus

5059F-pS-607-670 4/10/01 9:47 AM Page 622

(e.g., the tracking of radio-frequency tuned circuits in a radio receiver).

serrated vertical sync pulse In television, the vertical sync pulse notched at twice the horizontal sweep frequency.

service **1.** To maintain or repair electronic equipment. **2.** To provide maintenance or repair of electronic equipment.

serviceability ratio For a device or system, the ratio $ts/(ts + td)$, where *ts* is serviceable (operational) time, and *td* is downtime (non-operational time).

serviceable time The cumulative time during which an operator-monitored (but not necessarily operated) device or system is capable of normal operation.

service area For a broadcast or communications station, the useful coverage area.

service band **1.** For a communications system, the band of frequencies in which operation is normally carried out. **2.** A band of frequencies specifically assigned, by government regulation, to a certain communications service or services.

service channel The band of frequencies that a particular broadcast or communications station occupies, when the carrier frequency is held constant.

service charge The amount charged by a technician for installation, maintenance, or repair of equipment. It is often performed on a per-hour basis.

service maintenance For a cell or battery, the relative amount of energy capacity (percentage of full-charge capacity) available at a given time, or after a certain length of time in normal use.

service meter **1.** An energy ("power") meter. Also see KILOWATT-HOUR METER. **2.** A rugged multimeter used by a service technician.

service oscillator A signal generator designed expressly for troubleshooting and repair service.

service switch **1.** The main switch controlling the electric service to a building or other place of installation. **2.** In television repair, a switch on the rear of a chassis. The switch facilitates adjustment of screen controls by removing vertical deflection temporarily.

service-type instrument An instrument having reasonable accuracy and a degree of ruggedness so that it is suitable for field or shop use. Examples: SERVICE METER and SERVICE OSCILLATOR. Compare LABORATORY-GRADE INSTRUMENT.

servo amplifier A highly stable amplifier designed expressly for use in a SERVOMECHANISM.

servo loop In a control system (particularly a servo amplifier), the output-to-input feedback loop, through which automatic control is performed.

servomechanism Also called *servo.* A self-correcting, closed-loop control system. It usually uses an electromechanical device, such as a motor, that controls some electronic device. Error signals, supplied by the controlled electronic device, cause the motor to run in such a way as to optimize or stabilize the system.

servomotor A motor operated by the output signal of a servo amplifier. Depending on the end application of the servo system, the motor signal might or might not be corrected.

servo oscillation In a servo system, a back-and-forth movement or fluctuation, relative to the optimum setting or position. It Results from improper system adjustment. Sometimes the system stabilizes at the optimum after a short period of oscillation; in some cases, the oscillation continues indefinitely.

servo robot A (usually industrial) robot whose motion sequence is programmed into a computer. The robot follows the instructions given by the computer, and makes precise, timed movements on that basis. Different computer programs allow different motion sequences, so a single robot can be used for various tasks.

servo system An automatic control system using one or more servomechanisms.

set **1.** A piece of equipment or a system (e.g., *radio set*). **2.** In a flip-flop circuit, an input that is not controlled by the clock. **3.** To adjust a circuit or device, such as a flip-flop, to a desired operating point or condition. **4.** A class of numbers, things, or events. **5.** In computer programming, to initialize a variable (i.e., to assign a label to a location).

set analyzer A combination test instrument designed originally for troubleshooting radio receivers. It consists of a multimeter and transistor tester or vacuum-tube tester.

set noise Electrical noise arising inside a radio or television receiver, as opposed to that picked up from the outside.

set pulse A pulse used to adjust a device to a certain state (see SET, **3**).

set terminal In a flip-flop, the one-input terminal. Compare RESET TERMINAL.

setting The position or value to which an adjustable device is set for a particular purpose.

settling time **1.** In a digital voltmeter, the time required between the application of a test voltage and the final display of an accurate readout. **2.** In a digital-to-analog converter, the time between half of the level change over all inputs and the arrival of the output to a level within a certain tolerance of its specified final level. It is defined for either full-scale to zero or zero to full-scale.

set up To arrange and prepare equipment for operation.

setup See SET, **1**.

set-up time **1.** The time required to install and test an electronic system, and to ready the system for operation. **2.** In a digital gate, the length of time that a pulse must be held to produce a change of state.

sexadecimal number system See HEXADECIMAL NUMBER SYSTEM.

5059F-pS-607-670 4/10/01 9:47 AM Page 623

sexagesimal number system A number system whose radix is 60.

SF **1.** Abbreviation of SAFETY FACTOR. **2.** Abbreviation of SINGLE FREQUENCY. **3.** Abbreviation of STANDARD FREQUENCY. **4.** Abbreviation of STABILITY FACTOR.

SFA Abbreviation of SINGLE-FREQUENCY AMPLIFIER.

S_F band A section of the S BAND extending from 1650 to 1850 MHz.

sferics In wireless broadcast or communications reception, random electromagnetic noise generated by the earth's atmosphere. Some of this noise is thermal in origin; some originates in thunderstorms. Sometimes this noise is called *static.*

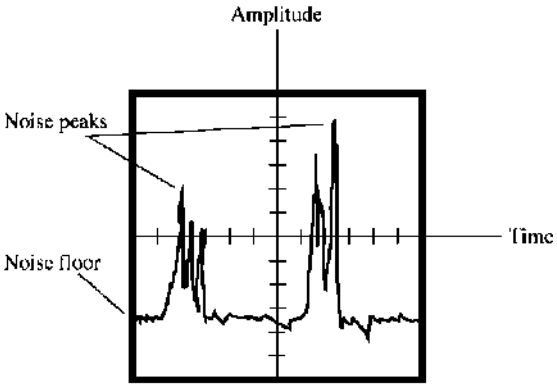

sferics

SFO **1.** Abbreviation of SINGLE-FREQUENCY OSCILLATOR. **2.** Abbreviation of STANDARD-FREQUENCY OSCILLATOR.

SFR Abbreviation of SINGLE-FREQUENCY RECEIVER.

SFR-Chireix-Mesny antenna See CHIREIX-MESNY ANTENNA.

SG Abbreviation of SCREEN GRID.

S_G band A section of the S BAND extending from 2700 to 2900 MHz.

SGCS Abbreviation of *silicon gate-controlled switch* (see SILICON-CONTROLLED SWITCH).

shaded-pole motor An induction-type alternating-current motor using shading coils on the field poles for self-starting with a single-phase supply.

shading Electronic enhancement of a television picture, resulting in a different brightness over various portions of the background, as compared with the actual situation. It can be used, for example, to make certain subjects stand out from the background.

shading coil **1.** A single, short-circuited turn (copper ring) encircling the tip of the core of a coil that carries alternating current (ac), such as the field pole of a motor. Current induced in the coil causes a momentary flux shift that approximates a rotating field that self-starts a simple single-phase induction motor. **2.** A coil used in a simple ac relay to prevent chatter.

shading ring See SHADING COIL.

shading signal In a television camera, a signal that increases the gain of the amplifier while the beam scans a dark part of the image.

shadow area A region in which signal attenuation or the absence of a signal results from the SHADOW EFFECT.

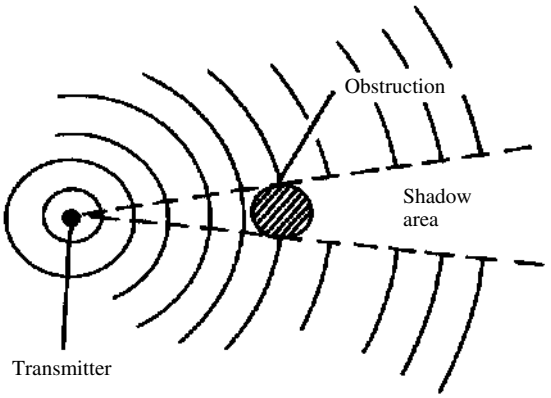

shadow area

shadow attenuation **1.** The attenuation of electromagnetic energy caused by an obstacle. It is generally measured in decibels. **2.** The attenuation of electromagnetic energy produced by the curvature of the earth.

shadow effect The obstruction of radio waves by objects in their path.

shadow mask See APERTURE MASK.

shadow meter See SHADOW TUNING INDICATOR.

shadow region See SHADOW AREA.

shadow tuning indicator A tuning meter in which the indicating medium is a shadow whose width is proportional to meter current.

shaft The rodlike part of an adjustable component (such as a potentiometer or variable capacitor) to which a rotating (or turning) member is attached.

shaft-angle encoder An electronic system for converting shaft rotation into direct binary or decimal readings.

shaft lock A device for fastening the shaft of an adjustable component (such as a potentiometer, rotary switch, or variable capacitor) in position at a particular setting.

shaft-position encoder See SHAFT-ANGLE ENCODER.

shaft-position indicator A device that delivers an analog or digital output signal proportional to the arc of rotation of a shaft.

5059F-pS-607-670 4/10/01 9:47 AM Page 624

shaker See VIBRATOR, **2**.

shake table A platform, actuated by a vibrator, on which components can be mounted for a vibration test.

shallow-diffused junction A pn junction made by diffusing the impurity material for a short distance into the semiconductor wafer. Compare DEEP-DIFFUSED JUNCTION.

shape factor **1.** For a tuned circuit, the ratio of the 60-dB bandwidth to the 6-dB bandwidth. **2.** For a filter, the ratio of bandwidth at high attenuation to that at low attenuation.

shaping network A combination of components for changing the natural response of a circuit to a desired response (i.e., a curve-changing circuit).

shared file A data file that is available for use by more than one system simultaneously.

shared files system A data-processing system having one direct-access storage device from which information can be accessed by more than one computer.

sharpener **1.** A circuit or device for increasing the selectivity of another circuit or device. **2.** A circuit or device for decreasing the rise or fall time of a pulse or square wave. **3.** A circuit or device for steepening the response of a filter.

sharpness See SELECTIVITY.

sharp pulse A pulse having extremely fast rise and fall times and narrow width (i.e., a spike).

shaving The physical modification of a phonograph disc, or other permanent recording surface, in preparation for rerecording.

S_H band A section of the S BAND extending from 3700 to 3900 MHz.

sheath See POSITIVE-ION SHEATH.

shelf corrosion In a dry cell in storage, deterioration of the negative electrode because of local action in the zinc.

shelf life **1.** The longest period of time that electronic equipment can be continuously kept in storage before deterioration of materials or degradation of performance occurs. **2.** The longest period of time that a battery can be stored without use before it must be discarded or recharged.

shell **1.** An electronic orbit (imaginary shell) in an atom. **2.** The envelope of a component (e.g., the outer casing of a power transistor or the housing of a plug). **3.** The rigid case in an audio or video tape cassette.

shell-type choke See SHELL-TYPE INDUCTOR.

shell-type core A core that completely surrounds the coil(s) of a choke or transformer.

shell-type inductor An inductor in which the core completely surrounds the coil.

shell-type transformer A transformer in which the core completely surrounds the coils.

shf Abbreviation of SUPERHIGH FREQUENCY.

shield A metallic partition or box for confining an electric or magnetic field.

shield baffle A sheet-type shield. Also see BAFFLE, **2** and SHIELD PARTITION.

shield box A shield having a general box shape, and which is usually enclosed on all sides.

shield braid Tubing woven from wire, through which an insulated wire is passed and thus shielded.

shield can A cylindrical shield, usually enclosed on all sides.

shield disk A flat shield having a disk shape. Also see BAFFLE, **2**; SHIELD BAFFLE; and SHIELD PARTITION.

shielded cable Cable completely enclosed within a metal sheath that is either flexible or rigid.

shielded wire A single strand of insulated wire completely enclosed in a flexible or rigid shield.

shield partition A wall-type shield usually consisting of a single, flat sheet of metal, sometimes bent into an angle. Also called BAFFLE SHIELD (see BAFFLE, **2**).

shield plate See BAFFLE, **2**; SHIELD BAFFLE; SHIELD DISK; and SHIELD PARTITION.

shield room See CAGE.

shield wire A (usually grounded) wire, near and parallel to another wire that it shields.

shift **1.** To move from one operating point to another in a characteristic curve, or in the operation of an equipment. **2.** To transfer data from one point to another in a system, or move it left or right in a register.

shift flip-flop circuit A flip-flop designed especially as a stage in a shift register.

shift pulse In a shift register, a drive pulse that initiates the shifting of characters.

shift register In computers, calculators, and storage systems, a circuit (usually composed of flip-flops in cascade) in which pulses can be shifted from stage to stage and finally out of the circuit.

shingle-type photocell A device in which several separate photocells are series connected by slightly overlapping the ends of adjacent cells.

ship station A radio or radar station installed aboard a ship that is not in port.

ship-to-shore communication Radio communication between a ship at sea and a land-based station.

shock **1.** See ELECTRIC SHOCK. **2.** A signal applied momentarily to a circuit, as in the *shock excitation* of a tank. **3.** A sudden, dramatic change in an environmental variable (such as temperature). **4.** Physical blows or vibration.

shock absorber Any object or device intended for reducing physical vibration of a component, set of components, circuit, or system.

shock device **1.** A device for administering shock therapy (see ELECTROSHOCK, **1**). **2.** An induction coil and associated primary supply for applying high voltage to a wire fence.

shock excitation Driving an inductance-capacitance (LC) tuned circuit into damped oscillation by momentarily applying a pulse.

shock-excited oscillator A type of self-excited oscillator in which the transistor is suddenly cut off

5059F-pS-607-670 4/10/01 9:47 AM Page 625

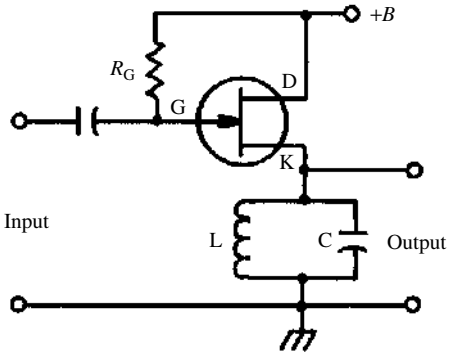

shock-excited oscillator

by applying a cutoff voltage to the gate or base electrode. This abrupt interruption of steady drain or collector current shocks the tank into damped oscillations.

shock hazard **1.** Any situation that presents the danger of electric shock to attendant personnel. **2.** The existence of a potential difference that will cause a current of at least 5 mA to flow through a resistance of 500 ohms or more, for a prolonged period of time.

Shockley diode See FOUR-LAYER DIODE.

shock mount A structure that secures a microphone while minimizing the pickup of vibrations through the table, floor, or other surface on which the microphone is placed.

shock therapy See ELECTROSHOCK, **1**.

shoran Contraction of SHORT-RANGE NAVIGATION.

shore effect The tendency of radio waves traveling along a shore to be bent either toward or away from the shore. It can occur because of differences in surface conductivity and/or atmospheric temperature over land, as compared with water.

shore station A fixed, land-based radio station that communicates with ships at sea.

shore-to-ship communication See SHIP-TO-SHORE COMMUNICATION.

short circuit An often unintended low-resistance path through which current bypasses a component or circuit.

short-circuit current In a power supply, the current that flows when the output is directly shorted. Many power supplies have shutdown devices that cause the current to stop flowing when the output terminals are short-circuited; other supplies effectively insert resistance in series with the load, if necessary, to limit the current.

short-circuiting switch A rotary selector switch in which unused contacts are automatically short-circuited.

short-circuit parameter A parameter for which zero resistance is assumed in the part of the circuit under consideration. The current amplification factor (alpha) of a common-base-connected transistor is such a parameter because its collector load resistance is assumed to be zero.

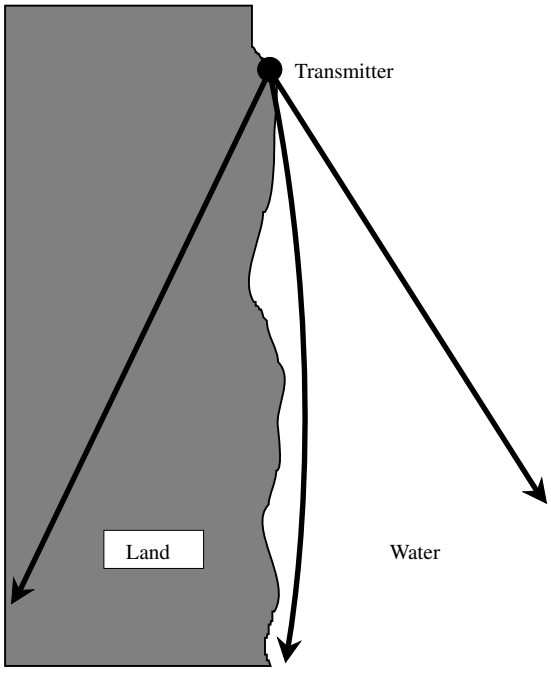

shore effect

shorted-stub tuning Tuning a stub to match a feeder to an antenna by sliding a short-circuiting bar along the two wires of the feeder.

shorting bar A thick, metal strap for short-circuiting two binding posts.

shorting link A sheet-metal strip for connecting together two binding posts.

shorting loop In a telephone system, a device that short-circuits two specified points for the purpose of testing or line fault location.

shorting stick A metal rod with an insulating handle, used to short-circuit a charged capacitor to remove the shock hazard.

shorting switch See SHORT-CIRCUITING SWITCH.

short-line tuning Use of a parallel capacitance to tune a transmission line that is less than a quarter-wave long.

short-range navigation Contraction, shoran. Navigation by means of SHORT-RANGE RADAR.

short-range radar A radar having a 50- to 150-mile maximum line-of-sight range for a 1-square-meter reflecting target that is perpendicular to the radar beam.

short skip Skip of only a few hundred miles range. Also see SHORT-SKIP COMMUNICATION.

5059F-pS-607-670 4/10/01 9:47 AM Page 626

short-skip communication Radio communication via the ionosphere over relatively short distances (400 to 1300 miles). See, for example, SPORADIC-E SKIP.

short-term drift The gradual change in the value of a quantity, such as frequency or voltage, observed over a comparatively brief interval, as opposed to change occurring over a long period. Compare LONG-TERM DRIFT.

short-term effect The variation of any electrical parameter over a relatively brief time interval. Example: frequency drift over a short time period. Also called *short-time effect.*

short-term stability Stability reckoned over a comparatively brief time interval, as opposed to stability for a long period. Compare LONG-TERM STABILITY.

short-time effect See SHORT-TERM EFFECT.

shortwave **1.** Pertaining to wavelengths shorter than 200 meters (i.e., frequencies higher than 1.50 MHz). **2.** Pertaining to the frequencies above the standard amplitude-modulation broadcast band (above 1.605 MHz), but below 30 MHz.

shortwave converter A superheterodyne converter for adapting a longwave receiver (such as a broadcast receiver) for shortwave reception.

shortwave listener Abbreviation, SWL. A radio hobbyist who receives, but does not transmit, shortwave signals.

shortwave receiver Any radio receiver capable of intercepting and demodulating signals in the range 1.705 MHz to 30 MHz.

shortwave transmitter Any radio transmitter capable of producing energy in the range 1.705 MHz to 30 MHz.

shot-effect noise Electrical noise caused by random fluctuations in a current, as in a diode or transistor. Also see EQUIVALENT NOISE RESISTANCE. Compare THERMAL NOISE.

shotgun microphone A highly directional microphone sensitive only to sounds coming from a specific direction; the response pattern has a narrow main lobe. It name results from its long, cylindrical configuration.

shot noise Electrical noise arising from intermittent impulses, such as those produced by spark discharges, make-and-break contacts, etc. Its name results from its resemblance to pistol shots.

shrink The amount by which a material being measured with an electronic instrument decreases in surface dimension. Compare STRETCH.

shrink tubing Plastic sleeving placed over a conductor or at a conductor/connector joint, and made to shrink tightly with the application of heat.

shunt Synonym, *parallel.* **1.** Pertaining to the connection of one component across (in parallel with) another (e.g., *shunt resistor*). **2.** Pertaining to connection of components in such a manner that they each (or all) are subjected to identical voltages. **3.** A deliberately produced short circuit between two specific points in a device or system. **4.** To deliberately bypass some part of a system by means of a short circuit.

shunt circuit See PARALLEL CIRCUIT.

shunt-diode rectifier A rectifier circuit in which the diode is connected in parallel with the source and load. Compare SERIES-DIODE RECTIFIER.

shunt-fed **1.** Pertaining to a circuit or device in which the direct-current operating voltage and alternating-current signal voltage are applied in parallel to an electrode. **2.** Pertaining to a base-grounded vertical antenna excited at some point above ground.

shunt feed See PARALLEL FEED.

shunt feedback A feedback system in which the fed-back signal is presented to the input of the network in parallel with the input signal. Compare SERIES FEEDBACK.

shunt generator An electric generator in which the armature and field windings are connected in parallel. Compare SERIES GENERATOR.

shunting effect The condition in which a quantity, such as stray capacitance or resistance, acts in parallel with another quantity. Example: the shunting (parallel) resistance of an electrolytic capacitor.

shunt leads Interconnecting wires used for the purpose of attaching a shunting component to a test instrument.

shunt limiter See PARALLEL LIMITER.

shunt loading The parallel insertion of reactance in a circuit, for the purpose of impedance matching.

shunt motor An electric motor whose armature and field windings are connected in parallel. Compare SERIES MOTOR.

shunt regulator A voltage-regulator circuit in which the controlled transistor or vacuum tube is in parallel with the output (load) terminals. Compare SERIES REGULATOR.

shunt resistor **1.** A resistor connected in parallel with a meter or recorder to increase its current range. **2.** A resistor connected in parallel with a voltmeter to convert it into a current meter. Compare MULTIPLIER RESISTOR.

shunt-series circuit See PARALLEL-SERIES CIRCUIT.

shunt tee junction A waveguide H-PLANE TEE JUNCTION.

shunt-type frequency multiplier A varactor frequency multiplier circuit in which the varactor is in parallel with the input and output. Compare SERIES-TYPE FREQUENCY MULTIPLIER.

shunt-type resonance bridge A resonance bridge in which the impedance arm is a parallel-resonant circuit. Compare SERIES-TYPE RESONANCE BRIDGE.

shunt-wound generator See SHUNT GENERATOR.

shunt-wound motor See SHUNT MOTOR.

SI Abbreviation of (Standard) INTERNATIONAL SYSTEM OF UNITS.

5059F-pS-607-670 4/10/01 9:47 AM Page 627

S/I Abbreviation of *signal-to-intermodulation ratio.*

Si Symbol for SILICON.

sibilants **1.** High-frequency (hissing) components of speech. **2.** High-frequency sounds or audio signals.

SIC Abbreviation of *specific inductive capacity* (see DIELECTRIC CONSTANT).

SiC Formula for SILICON CARBIDE.

sideband **1.** With respect to a carrier, one of the additional frequencies generated by the modulation process. In simple amplitude modulation, the two sidebands are *fc* + *fm* and *fc* – *fm*, where *fc* is the carrier frequency, and *fm* is the modulation frequency. **2.** Pertaining to sidebands as defined in **1**.

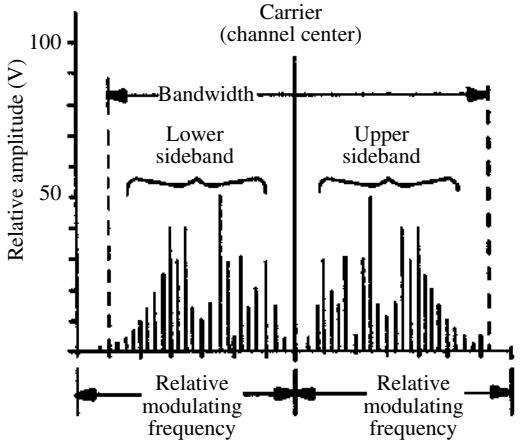

sideband

sideband attenuation See SIDEBAND CUTTING.

sideband cutting Elimination or attenuation of the sidebands of a modulated signal by a circuit having insufficient bandwidth.

sideband frequency The frequency of the modulation-generated signal accompanying a carrier. One sideband frequency is that of the carrier minus that of the modulating signal; another is the sum of the carrier and the modulation frequency. See also SIDEBAND, **1**.

sideband interference **1.** Interference arising from one or both of the normal sidebands of a modulated signal. **2.** Interference caused by spurious sidebands, resulting from overmodulation.

sideband power The power contained in the sideband(s) of a signal.

sideband slicing See SIDEBAND CUTTING.

sideband splatter In an amplitude-modulated or single-sideband signal, the emission of sideband energy at frequencies other than within the designated channel. Also simply called splatter.

sideband technique A method of using, for communications or other purposes, one or both of the sidebands of a modulated signal without the carrier.

side-chain amplifier An auxiliary amplifier that is external to a main amplifier. Such an amplifier might be used, for example, in a feedback channel or in a volume-compression or volume-expansion channel.

side frequency See SIDEBAND.

side lobe In certain directional antenna systems, a minor lobe in the horizontal-plane directivity pattern that appears at right angles, or nearly at right angles, to the main lobe. Such a lobe represents reduced sensitivity and/or power gain relative to the main lobe. Also see MAIN LOBE, MINOR LOBE.

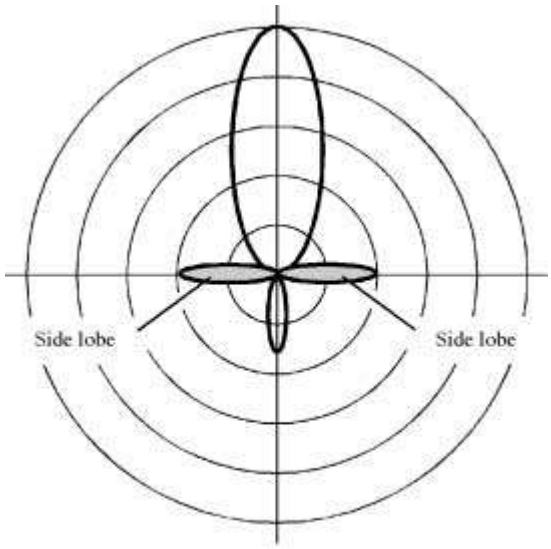

side lobe

sidelobe suppression Elimination of the sidelobe(s) from the radiation pattern of an antenna.

sidestacked antennas Antennas mounted in a horizontal line, parallel to each other, and connected by a common coupler to a transmitter or receiver.

sideswiper A manual telegraph key operated by moving the lever sideways, rather than up and down.

sidetone **1.** In wire telephony, the reproduction by the receiver of sounds picked up by the transmitter of the same telephone. **2.** In radiotelegraphy, an audible tone actuated when the carrier is transmitted. It allows the sending operator to hear Morse code elements as they are sent.

5059F-pS-607-670 4/10/01 9:47 AM Page 628

sidetone telephone A telephone set with no provision for canceling the sidetone.

siemens Symbol, S. The SI unit of conductance. The conductance of a component or medium in siemens is equal to the reciprocal of the resistance in ohms.

Siemen's electrodynamometer A spring-tension meter that operates by means of torque, with zero current through the device representing zero torque. It can be used for measurements of current, voltage, or power.

Sierra Phonetic alphabet code word for the letter S.

sig Abbreviation of SIGNAL.

sign **1.** Any indicator denoting whether a value is positive or negative. **2.** A graphic device indicating an operation. Examples: + (addition), × (multiplication). **3.** Any symbol. An ampersand, for example, is an "and" sign. **4.** A characteristic symptom of malfunction or improper operation (e.g., a high standing-wave ratio in an antenna system is a sign of an impedance mismatch).

signal An electrical quantity, such as a current or voltage, that can be used to convey information for communication, control, calculation, etc.

signal-actuated voice recorder Abbreviation, SAVOR. A recorder that goes into operation automatically when the speaker starts talking and stops when the speaker finishes.

signal amplitude The intensity of a signal quantity (see SIGNAL).

signal booster See PREAMPLIFIER.

signal channel In a system, a channel through which only signals flow, control and modifying impulses being accommodated by other channels.

signal circuit A circuit handling signal currents and voltages to the exclusion of control and operating currents and voltages.

signal conditioner Any accessory device (such as a peak probe, demodulator probe, current shunt, etc.) used to modify or change the function of a basic instrument (such as an electronic voltmeter).

signal converter See CONVERTER, **1**.

signal current The current component of a signal, as opposed to operating current in a system.

signal diode A diode designed primarily for light-duty signal applications (detection, demodulation, modulation, curve changing), as opposed to the heavy-duty applications of power diodes and rectifiers.

signal distance In two words (bit groups) of the same length, the number of corresponding bit positions whose states differ. For example, the signal distance between 01001 and 10011 is 3.

signal-flow analysis A graphic method of analyzing circuits, particularly those using feedback, through the use of diagrams in which straight arrows represent transmission paths, dots represent nodes, and curved arrows represent feedback paths.

signal-flow diagram The transmission-path diagram used in SIGNAL-FLOW ANALYSIS.

signal gain The gain of an amplifier circuit—especially if used in small-signal applications. See also AMPLIFICATION, and GAIN.

signal generator An instrument that produces signals of precise frequency and amplitude, usually over a wide range.

signal ground **1.** Any circuit point that remains at zero signal potential. **2.** A connection to a point that is deliberately maintained at zero signal potential.

signal/image ratio See SIGNAL-TO-IMAGE RATIO.

signaling In a communications system, the exchange of data in electrical form, either analog or digital.

signaling rate In data communications, the speed at which data is transmitted. It is commonly expressed in bits per second (bps). Also, it is sometimes expressed in baud or in words per minute (wpm).

signaling time slot In a communications signal, a specified interval of time, starting at a certain instant in each signal frame. This interval is used exclusively for the purpose of signaling.

signal injection **1.** The introduction of a signal into a circuit. **2.** A method of troubleshooting in communications receivers. A signal generator is used to introduce a test signal into each stage, starting with the output and proceeding stage-by-stage toward the input, until the defective stage or component is located.

signal injector A simple (usually single-frequency) signal generator used in troubleshooting to introduce a test signal at selected points in a circuit, to locate malfunctioning stages or components. Also see SIGNAL INJECTION, **2**.

signal intensity See SIGNAL STRENGTH.

signal inversion Phase reversal of a signal passing through a circuit, device or medium.

signal level At a given point in a circuit, the strength of a signal, with respect to a reference amplitude.

signal loss **1.** A reduction in the amplitude of a signal as it passes through a system. **2.** The complete disappearance of a signal. **3.** See FRACTIONAL GAIN.

signal mixer See MIXER.

signal/noise ratio See SIGNAL-TO-NOISE RATIO.

signal notcher See NOTCH FILTER.

signal peaker See PEAK FILTER.

signal power The amplitude of a signal expressed in watts, milliwatts, or microwatts, as opposed to amplitude expressed as a current or voltage.

signal processor Any device, (e.g., preamplifier, expander, amplitude limiter, delay network) inserted into or added onto a system to modify an input or output signal.

signal rectification The conversion of an alternating-current signal into a proportionate direct-current signal, usually by means of a diode circuit.

5059F-pS-607-670 4/10/01 9:47 AM Page 629

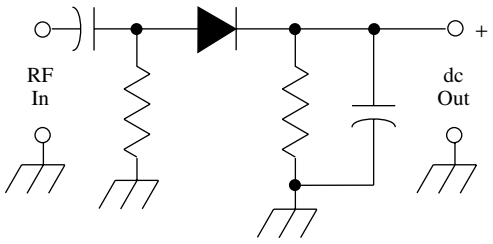

signal rectification

signal rectifier See SIGNAL DIODE.

signal regeneration See SIGNAL RESHAPING.

signal reshaping **1.** The processing of a signal so that it acquires its original waveform. Also called *signal regeneration.* **2.** Passing a digital signal of any type through a circuit that delivers a uniform output pulse on a real-time one-to-one basis.

signal shifter **1.** A device used for quickly changing the frequency of a transmitted signal. **2.** A device that automatically causes a transmitted signal to be sent on a frequency that differs from the receiver frequency by a known and predetermined amount. **3.** See MIXER, **1**. **4.** See CONVERTER, **1**.

signal squirter See SIGNAL INJECTOR.

signal strength The amplitude of a signal, usually in terms of voltage. Current or power is specified in some applications.

signal-strength meter **1.** See FIELD-STRENGTH METER. **2.** See S-METER.

signal synthesizer A special signal generator delivering signals whose frequency, amplitude, and waveshape can be adjusted at will.

signal time delay The time required for an element of a signal to be transmitted through a circuit or network. This delay results in phase shift in an amplifier.

signal-to-distortion ratio In a receiver, the ratio of the desired signal to the level of distortion other than the specified signal. Usually expressed in decibels (dB).

signal-to-image ratio Abbreviation, S/I. In a receiver, the ratio of signal amplitude to image amplitude, both being measured in the same units. It is usually expressed in decibels (dB).

signal-to-noise-plus-noise ratio Abbreviation, (S+N)/N. In a receiver, the ratio of the combined signal and noise amplitude to the amplitude of the noise alone. It is usually expressed in decibels (dB). Peak voltages are used to determine this ratio in the case of pulse noise; root-mean-square (rms) voltages are used in the case of random noise.

signal-to-noise ratio Abbreviations: S/N, SNR. In a receiver, the ratio of signal amplitude to noise amplitude. It is usually expressed in decibels (dB). Peak voltages are used to determine this ratio in the case of pulse noise; root-mean-square (rms) voltages are used in the case of random noise.

signal-to-noise-and-distortion ratio Abbreviation, SINAD. In a receiver, the ratio of the desired signal to the level of noise and distortion, other than the specified signal. It is usually expressed in decibels (dB).

signal tracer A tuned or untuned detector/amplifier having an input probe and an output indicator (meter, loudspeaker, or both), for following a test signal through a circuit.

signal voltage The voltage component of a signal, as opposed to the operating voltage of the circuit generating or passing the signal.

signal wave **1.** Any electromagnetic disturbance of a periodic nature that is modulated to convey information. **2.** The visual illustration or rendition of an electromagnetic disturbance that is modulated to convey information.

signal winding In a magnetic amplifier or saturable reactor, the coil that receives the control current.

signal window See WINDOW, **2**.

signal wobbulator A frequency modulator used with an unmodulated signal generator to provide sweep signals for visual alignment. Also see WOBBULATOR.

sign bit A one-bit SIGN DIGIT.

sign digit A character indicating the sign (positive or negative) of the value of the field or word to which it is attached (usually at the end).

signed field In a computer record, a field having a number whose sign is indicated by a SIGN DIGIT.

significant digits See SIGNIFICANT FIGURES.

significant figures In a numerical quantity, especially one expressed in scientific (power of 10) notation, those figures (digits) that depict a quantity to a required, relevant, or justifiable degree of precision. For example, 173,201 expressed to three significant figures is 1.73×10^5; 0.00477583 expressed to four significant figures is 4.776×10^{-3}. See also SCIENTIFIC NOTATION.

silencer See AUTOMATIC NOISE LIMITER.

silent alarm In security systems, the transmission of a warning signal to attendant human operators and/or computers, without producing an audible or visible warning to intruders.

silent alignment See VISUAL ALIGNMENT.

silent piano See ELECTRONIC PIANO.

silica pencil A rod of silicon dioxide heated to emit infrared rays.

silicon Symbol, Si. A metalloidal element. Atomic number, 14. Atomic weight, 28.086. Silicon is abundant in the earth's crust. It is used in many semiconductor devices, including integrated circuits, diodes, photocells, rectifiers, and transistors.

silicon capacitor See VOLTAGE-VARIABLE CAPACITOR.

5059F-pS-607-670 4/10/01 9:47 AM Page 630

silicon carbide Formula, SiC. A compound of silicon and carbon valued as a semiconductor, an abrasive material, and a refractory substance. The commercial product is made by heating carbon and sand to a high temperature in an electric resistance furnace. Also called CARBORUNDUM.

silicon cell A type of photovoltaic cell using specially processed silicon as the light-sensitive material. This cell has a comparatively high voltage output.

silicon-controlled rectifier Abbreviation, SCR. A four-layer semiconductor device commonly used in power control applications (e.g., light dimmers and motor-speed controls). The electrodes are called the anode, the cathode, and the gate. The control signal is applied to the gate.

silicon-controlled switch Abbreviation, SCS. A four-terminal semiconductor switching device similar to the SILICON-CONTROLLED RECTIFIER. It is used for light-duty switching.

silicon crystal detector **1.** See SILICON JUNCTION DIODE. **2.** See SILICON POINT-CONTACT DIODE. **3.** A point-contact diode in which a lump of silicon is contacted by either a fine wire (cat whisker) or a blunt-tipped steel screw under pressure.

silicon detector See SILICON CRYSTAL DETECTOR.

silicon-diffused transistor A silicon bipolar transistor fabricated by diffusion techniques. It is characterized by high power-dissipation tolerance.

silicon diode A semiconductor diode in which the semiconductor material is specially processed silicon. Also see SILICON JUNCTION DIODE and SILICON POINT-CONTACT DIODE.

silicon dioxide Formula, SiO_2. A compound of silicon and oxygen. In the passivation of transistors and integrated circuits, a thin layer of silicon dioxide is grown on the surface of the wafer to protect the otherwise exposed junctions.

silicone A polymeric material characterized by a recurring chemical group containing oxygen and silicon atoms in the main chain as links. Various silicone compounds have numerous uses in electronics.

silicon junction diode A semiconductor diode using a pn junction in a silicon wafer. Compare SILICON POINT-CONTACT DIODE.

silicon on sapphire Abbreviation, SOS. Pertaining to integrated-circuit fabrication in which a silicon epitaxial layer is grown on a sapphire substrate.

silicon oxide A compound containing both silicon monoxide and silicon dioxide, and having dielectric properties. It is used in the manufacture of metal-oxide-semiconductor (MOS) devices.

silicon photocell A photocell using a silicon pn junction as the light-sensitive medium.

silicon photodiode A silicon diode constructed so that radiant energy can strike the barrier between the P- and N-type materials. A reverse bias is applied. When light falls on the P-N junction, current flows. The current is proportional to the intensity of the impinging energy, within certain limits. The greatest sensitivity is in the near infrared (IR). When energy of variable brightness falls on the P-N junction under conditions of reverse bias, the output current follows the intensity variations. This makes the device useful in fiberoptic communications systems.

silicon point contact The contact between a pointed metal wire (cat whisker) and a silicon wafer.

silicon point-contact diode A diode in which a tungsten wire (cat whisker) contacts a wafer of single-crystal silicon. It is useful at ultra high frequencies (UHF). Compare SILICON JUNCTION DIODE.

silicon rectifier A semiconductor rectifier consisting essentially of a junction between n- and p-type silicon inside a specially processed wafer or plate of single-crystal silicon.

silicon resistor See CRYSTAL RESISTOR.

silicon solar cell A relatively heavy-duty photovoltaic cell using specially processed silicon as the light-sensitive material.

silicon steel A high-permeability, high-resistance steel containing 2 to 3 percent silicon. It is used as core material in transformers and other electromagnetic devices.

silicon transistor A transistor in which the semiconductor material is single-crystal silicon.

silk-enameled wire Wire whose insulation is a layer of silk on top of an enamel coating.

silver Symbol, Ag. A precious metallic element. Atomic number, 47. Atomic weight, 107.87. It is used in circuits where low resistance and high Q are mandatory.

silver arsenide trisulfide See PROUSTITE.

silver-dollar construction Printed-circuit assembly on a disk-shaped board, about the size of a U.S. silver dollar.

silver-mica capacitor A fixed capacitor made by painting or depositing a silver layer (capacitor plate) on both faces of a thin mica film (dielectric separator).

silver migration The undesirable tendency of silver to be removed from one location and deposited in another under adverse environmental conditions.

silver-oxide battery A set of two or more silver-oxide cells stacked one atop the other, electrically connected in series. The resulting battery has a cylindrical shape. A set of four cells provides approximately 6 volts under no-load conditions; a battery of six cells provides 9 volts; a battery of eight cells provides 12 volts. See also SILVER-OXIDE CELL.

silver-oxide cell An electrochemical cell having a button-like shape, small enough to fit inside a wristwatch. There are several available sizes and thicknesses, all with similar appearance. The

5059F-pS-607-670 4/10/01 9:47 AM Page 631

generated potential difference under no-load conditions is 1.5 volts, with a high ratio of stored energy per unit mass. The cell has a flat discharge curve; the voltage remains essentially constant until the charge is almost depleted, and then the voltage drops rapidly.

silver solder A solder consisting of an alloy of silver, copper, and zinc. It has a comparatively high melting temperature. Also see HARD SOLDER.

silverstat A multiconductor device used to adjust the balance of a resistance or reactance bridge.

similar decimals Two or more decimal numbers that have the same number of digits to the right of the radix point (e.g., 3.14 and 6.39, or 1.234 and 1.000).

simple quad A combination of two parallel paths—each containing two elements in series.

simple tone A pure sine-wave tone (i.e., one having negligible harmonic content).

simplex channel An information channel for unidirectional transmission.

simplex system **1.** In data communications, a system that transmits data in only one direction. Compare FULL DUPLEX SYSTEM and HALF DUPLEX SYSTEM. **2.** In voice communications via radio, a direct path over a single channel, used alternately for transmitting and receiving at each station.

simplex telegraphy Wire telegraphy in which only one message at a time can be sent over a line.

simplification of circuits See CIRCUIT SIMPLIFICATION.

simulation **1.** Imitation of the performance of a process, device, or system. **2.** The use of a mathematical model to represent a physical process, device, or system. **3.** The use of a computer, sometimes with virtual reality hardware and software, to mimic a real-life situation.

simulator **1.** A software or hardware system capable of simulation (see SIMULATION, **2**). **2.** A computer program whose implementation allows programs written for one computer to be compatible with another computer. **3.** A system of equipment for simulation (see SIMULATION, **1**).

simulcast **1.** To broadcast a program over two or more different channels at the same time. **2.** To broadcast a program over two or more different types of mode, for example, television and radio, at the same time. **3.** A program broadcast over two or more channels or modes at the same time.

simultaneous access See PARALLEL ACCESS.

simultaneous broadcasting See SIMULTANEOUS TRANSMISSION.

simultaneous computer See PARALLEL COMPUTER.

simultaneous transmission The transmission of the same information in two or more channels, or by means of two or more processes, at the same time.

sin Abbreviation of SINE.

$\sin^{-1}$ Symbols for the inverse of the sine function, also called the *arc sine.*

sine Abbreviation, sin. The trigonometric function a/c, the ratio of the opposite side of a right triangle to the hypotenuse.

SINAD See SIGNAL-TO-NOISE-AND-DISTORTION RATIO.

sine galvanometer A galvanometer in which the sine of the angle of deflection is proportional to the current. Compare TANGENT GALVANOMETER.

sine law The variation in radiation intensity in any direction from a linear source is proportional to the sine of the angle between the axis of the source and the direction of interest.

sine potentiometer A POTENTIOMETER whose output is proportional to the sine of the angle through which the shaft has rotated.

sine wave A periodic wave that can be represented by a sine curve (i.e., its amplitude is directly proportional to the sine of a linear quantity, such as displacement or time). Compare COSINE WAVE.

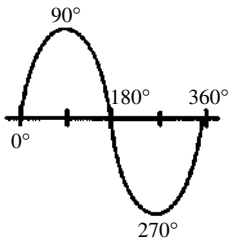

sine wave

singing Audible oscillation in a circuit or device, such as the low-level buzz emanating from the filament of a lamp dimmed with a phase-control circuit.

single-address coding In computer programming, the use of instruction words that contain the address for the location of the data to be operated on, and no other addresses.

single-board computer Abbreviation, SBC. A computer built entirely on one circuit board.

single-button microphone A carbon microphone having only one button attached to the diaphragm. Also see BUTTON MICROPHONE.

single-channel codec A form of CODEC intended for operation on a single signal source, rather than in a multiplexed system.

single-chip codec An integrated circuit contained entirely on one chip and in one package that can accomplish all CODEC functions. It can be a single-channel device or multiplexed.

single-cotton-covered wire Wire insulated with one layer of cotton.

single cotton enameled wire Wire insulated with one layer of cotton on top of an enamel coating.

5059F-pS-607-670 4/10/01 9:47 AM Page 632

single-crystal Pertaining to the internal structure of a crystalline material, in which the characteristic lattice is continuous throughout any size piece of the material. Also called MONOCRYSTALLINE.

single-crystal material A substance, such as a semiconductor, of which a sample, regardless of size, consists of only one crystal (i.e., there are no grain boundaries). Also see SINGLE-CRYSTAL. Compare POLYCRYSTALLINE MATERIAL.

single-crystal pulling See CZOCHRALSKI METHOD.

single-dial control Adjustment of a multistage system via one rotatable, calibrated control attached to a ganged arrangement that tunes all stages simultaneously.

single-diffused transistor A transistor in which only one diffusion of an impurity substance is made. Thus, in a diffused-base transistor, a single diffusion provides the base region and at the same time creates the emitter-base and collector-base junctions. Compare DOUBLE-DIFFUSED TRANSISTOR.

single-electron memory Abbreviation, SEM. A computer memory in which the movement of one electron can change a logic bit from 1 (high) to 0 (low) or vice versa.

single-element rotary antenna See ONE-ELEMENT ROTARY ANTENNA.

single-ended circuit A circuit that has one end grounded, as opposed to a double-ended circuit and push-pull circuit.

single-ended deflection In an oscilloscope or similar device, horizontal or vertical deflection provided by a single-ended deflection channel. Compare PUSH-PULL DEFLECTION.

single-ended input An input circuit with one terminal grounded (or the equivalent ungrounded input circuit). Also called *unbalanced input.* Compare BALANCED INPUT.

single-ended multiplexer A group of analog switches that selects from several analog signals.

single-ended output An output circuit with one terminal grounded (or the equivalent ungrounded output). Also called *unbalanced output.* Compare BALANCED OUTPUT.

single-ended push-pull circuit An arrangement, such as a complementary symmetry circuit, that provides push-pull output with single-ended input, but does not require transformers.

single-frequency Also called *fixed-frequency.* Pertaining to circuits or devices that normally operate at one frequency only (e.g., *single-frequency oscillator*).

single-frequency amplifier An amplifier that normally operates at only one frequency (or within a very narrow band of frequencies) (e.g., an intermediate-frequency amplifier, or a selective audio-frequency amplifier used for harmonic analysis or bridge balancing).

single-frequency duplex Two-way communications over one medium or frequency. Voice-actuated (VOX) or break-in devices are used at both ends of the circuit.

single-frequency oscillator An oscillator that normally delivers a signal at only one frequency until it is switched to another frequency (e.g., *crystal-controlled oscillator*).

single-frequency receiver A radio or television receiver that normally operates at one carrier frequency, rather than being tunable. Such receivers are used in monitoring specific programs, picking up standard-frequency signals, and in similar applications.

single-gun color picture tube A color-television picture tube in which the image is produced by a single beam that scans the red, green, and blue color-phosphor dots sequentially.

single-hop propagation Long-distance radio-wave propagation involving only one encounter with the ionosphere, and involving no intermediate reflections from the earth's surface.

single-hop return distance The return distance, as a function of the angle of departure from a radio transmission, from a layer of the ionosphere. The illustration shows the maximum possible distance under average conditions and assuming an angle of departure of zero degrees.

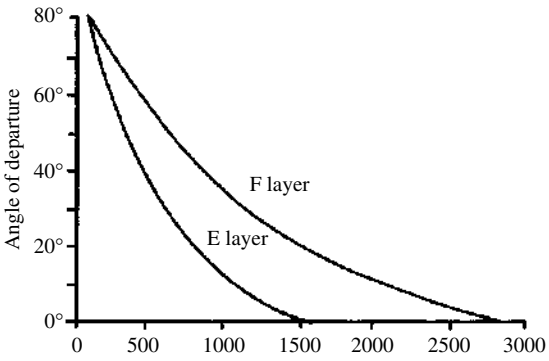

single-hop return distance (miles)

single-image response In an oscilloscope presentation, a single pattern, as opposed to a double-trace pattern.

single-inline package Abbreviation, SIP. A flat, molded component package having terminal pins along one edge. All the pins lie along a common line.

single-junction transistor See UNIJUNCTION TRANSISTOR.

single-layer coil A coil whose turns are wound side by side in one layer.

single-layer solenoid See SINGLE-LAYER COIL.

5059F-pS-607-670 4/10/01 9:47 AM Page 633

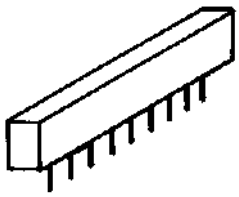

single-inline package

single-line tap In a telephone system, a connection that provides or designates a separate line (e.g., to serve a single household).

single-loop feedback Feedback through only one path.

single phase Pertaining to the presence or generation of one alternating-current phase only. Compare POLYPHASE.

single-phase full-wave Pertaining to a rectifier operated from a single-phase alternating-current (ac) power line, and rectifying both half-cycles of ac voltage. Compare SINGLE-PHASE/HALF WAVE.

single-phase/full-wave bridge A bridge rectifier operated from a single-phase alternating-current supply, usually from the untapped secondary winding of a transformer. Compare SINGLE-PHASE/FULL-WAVE CIRCUIT and SINGLE-PHASE/HALF-WAVE CIRCUIT.

single-phase/full-wave circuit A rectifier circuit in which each half-cycle of single-phase alternating current is rectified by a separate diode supplied from the ends of a center-tapped winding of a transformer. Compare SINGLE-PHASE/FULL-WAVE BRIDGE and SINGLE-PHASE/HALF-WAVE CIRCUIT.

single-phase/half-wave Pertaining to a rectifier operated from a single-phase alternating-current (ac) power line, and rectifying only one half-cycle of ac voltage.

single-phase/half-wave circuit A rectifier circuit in which a diode, output load, and single-phase alternating-current supply are connected in series, only one half-cycle of the cycle being passed by the diode. Compare SINGLE-PHASE/FULL-WAVE CIRCUIT and SINGLE-PHASE/FULL-WAVE BRIDGE.

single-phase rectifier See SINGLE-PHASE/FULL-WAVE BRIDGE, SINGLE-PHASE/FULL-WAVE CIRCUIT, and SINGLE-PHASE/HALF-WAVE CIRCUIT.

single-point ground One ground connection to which all channels of a circuit are returned. Such a common connection eliminates or greatly minimizes the common coupling often encountered when separate ground points are used.

single-pole double-throw Abbreviation, SPDT. Descriptive of an electrical, electronic, or mechanical switch with a pole that can be connected to either of two adjacent poles, but not to both.

single-pole single-throw Abbreviation, SPST. Descriptive of an electrical, electronic, or mechanical switch with a pole that can be connected to an adjacent pole (or disconnected from it) at will. It is used to provide the make and break function in a single circuit.

single rail **1.** A one-conductor communications medium with a ground return. **2.** A one-conductor data line, with a ground return.

single shot Also called *one shot*. Pertaining to circuit operation in which a single input pulse applied to a switching device (such as a multivibrator) causes it to deliver a single output pulse, rather than switch to a stable "on" state. A MONOSTABLE MULTIVIBRATOR operates in this mode.

single-shot multivibrator See MONOSTABLE MULTIVIBRATOR.

single sideband Abbreviation, SSB. Pertaining to a system of modulation in which one of the sidebands from an amplitude-modulated signal is attenuated or canceled out, leaving only one sideband. The carrier is generally suppressed also.

single-sideband suppressed-carrier Abbreviation, SSSC or SSBSC. Pertaining to a system of modulation in which the carrier and one sideband from an amplitude-modulated signal are suppressed; only the remaining sideband is transmitted. Sometimes this mode is simply called SINGLE SIDEBAND.

single signal Pertaining to a mode of reception in which signals appear on only one side of zero beat, enhancing selectivity and reducing interference among received signals. Most superheterodyne receivers have this feature; most direct-conversion receivers do not.

single-signal receiver A superheterodyne receiver that achieves high selectivity via a selective filter in the intermediate-frequency amplifier chain. Signals appear on only one side of zero beat, in a band whose width can be adjusted or selected for various values from about 200 Hz to 3 kHz.

single silk-covered wire Wire insulated with one layer of silk.

single-skip propagation See SINGLE-HOP PROPAGATION.

single-step operation See STEP-THROUGH OPERATION.

single sweep In an oscilloscope, a single time-axis deflection of the electron beam. Also see SWEEP, **1**, **2**. Compare RECURRENT SWEEP.

single-sweep blocking oscillator A blocking oscillator that cuts off after generating a single cycle or pulse.

single-throw switch A single-action switch with two or more poles.

single-tone keying Modulated continuous-wave keying. A single audio-frequency tone is used to amplitude-modulate or frequency-modulate the carrier.

single-track recorder A recorder, such as a magnetic-tape recorder or a graphic recorder, that permits recording along only one track.

5059F-pS-607-670 4/10/01 9:47 AM Page 634

single-trip multivibrator See MONOSTABLE MULTIVIBRATOR.

single-tuned circuit A circuit tuned by varying only one of its components [e.g., an intermediate-frequency transformer in which only the secondary coil (rather than both primary and secondary) is tuned].

single-turn coil **1.** A coil consisting of a single turn of wire, tubing, or strip. **2.** See RING INDUCTOR. **3.** See SHADING COIL.

single-turn potentiometer A potentiometer that can be adjusted through its entire resistance range by no more than one full rotation of the shaft. Usually, the turning range is somewhat less than a full circle (e.g., 300 degrees).

single-wire-fed antenna See WINDOM ANTENNA.

single-wire line **1.** See SINGLE-WIRE TRANSMISSION LINE. **2.** A single wire used for communication or control purposes. The earth furnishes the return path.

single-wire transmission line An antenna transmission line or feeder consisting of one wire only (see, for example, WINDOM ANTENNA).

sink **1.** A device or circuit into which current drains. **2.** See HEATSINK.

sink circuit The circuit associated with a load or other sink. Compare SOURCE CIRCUIT, **2**.

sinker A piece of semiconductor material used to reduce the base-collector junction resistance in a bipolar transistor.

sintering A process in which various solid bodies are formed from fusible powders at temperatures below their melting points. Example: *sintered magnetic core.*

sinusoidal Having the shape and properties of a SINE WAVE.

SIO Abbreviation of *serial input/output.*

SIP Abbreviation of SINGLE-INLINE PACKAGE.

six-phase rectifier A polyphase rectifier circuit operated from a three-phase supply. The output ripple frequency is six times the supply frequency.

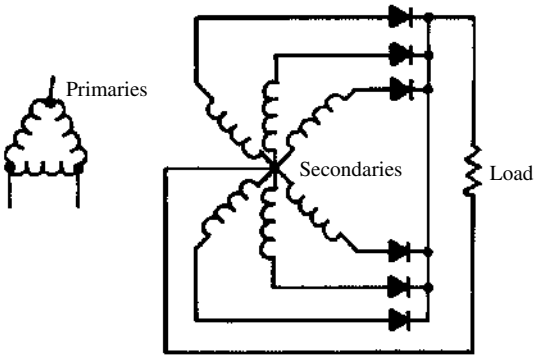

six-phase rectifier

SJD Abbreviation of SILICON JUNCTION DIODE.

skating In a phonograph turntable, the tendency of the tone arm to swing toward the spindle during record play, independent of the action produced by the stylus following the groove.

skeletal code A generalized computer routine needing only certain parameters to be usable for a specific application.

skeleton bridge A bridge consisting of an adjustable arm (potentiometer) and a pair of binding posts for each of the other three arms. Suitable resistors, capacitors, or inductors are connected to the binding posts to set up the bridge circuit desired.

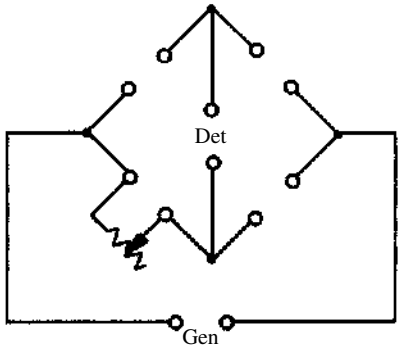

skeleton bridge

skeleton-type assembly **1.** A method of electronic-equipment construction in which a minimum of supporting members is used. An example is the use of an open framework, instead of a chassis, to support components. **2.** An assembly of electronic equipment, consisting essentially of a foundation unit (containing the basic circuitry) and plug-in units for setting up various complete equipments.

skew **1.** A condition resulting from failure of the horizontal synchronization in facsimile or television. The picture appears distorted, and appears as a non-rectangular parallelogram. **2.** In a print display, nonalignment of columns resulting from an incorrect number of line spaces in each line. **3.** In a probability function, an accumulation of values toward either side of center.

skewing **1.** The bending of a curve away from its normal shape. **2.** In a differential amplifier, the offset between two signals. Also see OFFSET.

Skiatron A special form of cathode-ray tube, with the fluorescent coating replaced by a screen of halide crystals that darken, instead of glow, when exposed to the electron stream.

skin depth The depth to which current penetrates below the surface of a conductor, as a result of the SKIN EFFECT.

5059F-pS-607-670 4/10/01 9:47 AM Page 635

skin effect The tendency of high-frequency alternating current to travel along the surface of a conductor; the high-frequency reactance is lower along the outside than at the center of a conductor. This tends to increase the resistivity of solid conductors at high alternating-current frequencies, as compared with low frequencies and direct current.

skip **1.** Ionosphere-reflected radio transmissions. **2.** In a computer program, an instruction whose sole function is that of causing a jump to the next instruction.

skip distance For a signal propagated via the ionosphere, the distance from the transmitter to the point at which the returned skywave strikes the earth.

skip fading For a signal propagated via the ionosphere, changes in signal strength caused by fluctuations in the altitude and/or contour of the ionized layer(s).

skip zone See ZONE OF SILENCE.

skirt selectivity **1.** The bandwidth between points of high attenuation (usually 30 dB or 60 dB) on the selectivity curve in a communications receiver. **2.** The relative steepness of the attenuation-vs.-frequency curve in a communications receiver.

SKM Abbreviation of *sine-cosine multiplier.*

skyhook **1.** Colloquialism for ANTENNA. **2.** A wire antenna supported by a captive balloon or kite.

sky noise Radio noise originating in outer space.

skywave A radio wave propagated by ionospheric reflections and/or refractions. Compare GROUND WAVE.

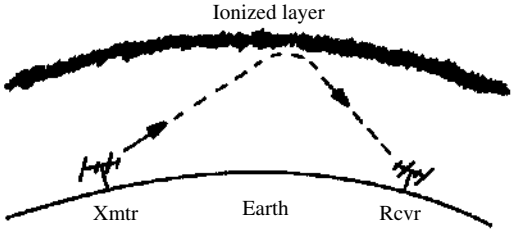

skywave

skywave correction A factor applied to long-range radionavigation signals to account for the time delay resulting from ionospheric propagation.

skywire See OUTSIDE ANTENNA.

slab **1.** A relatively thick body of quartz, ceramic, semiconductor, or dielectric. **2.** See SUBSTRATE.

slap back The return of sounds by an acoustically reflective object or surface a short distance away, resulting in almost immediate echoes.

slashed-field-gun CRT A straight-gun television picture tube (see STRAIGHT-GUN CRT). Because the gap between the anodes in this tube is slanted, the electrostatic field is diagonal, causing the electron and ion beams to be diverted at an angle.

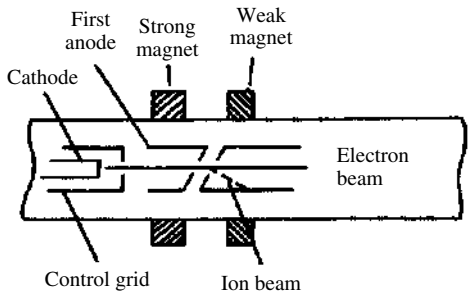

slashed-field-gun CRT

slave flash A photoflash operated by the light flash from another such unit.

slave relay A relay operated by, and whose action follows, a MASTER RELAY.

SLC Abbreviation of STRAIGHT-LINE CAPACITANCE.

sleeping sickness A gradual increase in transistor leakage current.

sleep machine An electronic device sometimes used as an aid for relaxation or sleeping. It consists of a wideband audio-frequency noise generator that produces low-level sounds similar to the noise of waves on a beach or a light wind through trees.

sleeve antenna A vertical antenna in which the upper half is a quarter-wave rod connected to the inner conductor of a coaxial feeder, and the lower half is a quarter-wave metal sleeve connected to the outer conductor of the feeder. Also called COAXIAL ANTENNA.

sleeving A material in tubular form that can be slipped over another material [e.g., insulating sleeving for wires (spaghetti)].

slew rate In an operational amplifier, the rate at which the output can be driven between its limits.

SLF Abbreviation of STRAIGHT-LINE FREQUENCY.

slice A semiconductor wafer cut from a single-crystal ingot.

slicer See CLIPPER-LIMITER.

slide-back meter An electronic voltmeter in which an unknown alternating-current signal voltage applied to the input of an amplifier stage is bucked by an internal, adjustable, accurately known signal voltage. The internal voltage is adjusted until a null occurs, indicating that its magnitude is equal to that of the unknown voltage.

slider A flat-spring contact that slides along the turns of a resistance or inductance coil to vary the coil's resistance or inductance. Also called a WIPER.

5059F-pS-607-670 4/10/01 9:47 AM Page 636

slide-rule dial A dial mechanism having a straight scale that resembles a slide rule.

slide switch A switch actuated by sliding a block-shaped button. Compare BAT-HANDLE SWITCH, PADDLE SWITCH, and ROCKER SWITCH.

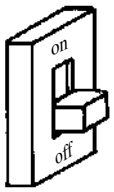

slide switch

slide wire A simple potentiometer consisting of a single, straight piece of resistance wire with a sliding contact. Also see SLIDE-WIRE RESISTOR.

slide-wire bridge A simple four-arm bridge in which the adjustable element is a single, straight resistance wire along which a clip or slider is moved, and that supplies two arms of the bridge (one on each side of the slider).

slide-wire resistor A variable resistor consisting of a single wire (straight or coiled) along whose length a slider is moved to vary the resistance.

sliding contact A contact that mates with another contact, or moves along a contacted surface, with a sliding motion. Also called SELF-CLEANING CONTACT and WIPING CONTACT.

slip **1.** In an eddy-current brake, coupling, or drive, the difference in speed between the field magnets and the iron eddy-current ring. **2.** In a synchronous motor, the difference between rotor speed and stator speed.

slip clutch In a gear or rack-and-pinion drive system, a device that releases the load if the torque becomes excessive. The gears then slip instead of being damaged.

slip ring See COLLECTOR RING, **1**.

slip speed See SLIP, **2**.

slope **1.** The slant of a line (graph) in rectangular coordinates, depicted as the ratio of the change in the dependent variable y to the change in the independent variable x. If (x_1,y_1) and (x_2,y_2) are two points on the line, then slope m is determined by $m = (y_2 - y_1)/(x_2 - x_1)$. **2.** The slant of a line in rectangular coordinates as defined in **1**, when the line is tangent to a curve (graph) at a specified point. **3.** The skirt(s) of a selectivity curve, particularly in a communications receiver, where a small change in frequency results in a significant change in gain or attenuation. **4.** The ratio of the extent of change in a quantity to the extent of change in some other quantity, when a causal relation exists between the magnitudes of the quantities. Example: See SLOPE RESISTANCE.

slope detector An amplitude-modulation (AM) receiving circuit detuned to one side of resonance (i.e., to a point along the skirt of the selectivity curve) to detect a frequency-modulated (FM) signal. The FM swing occurs along the slope of the resonance curve. Slope detection is useful in narrowband FM when conventional FM circuitry is not available.

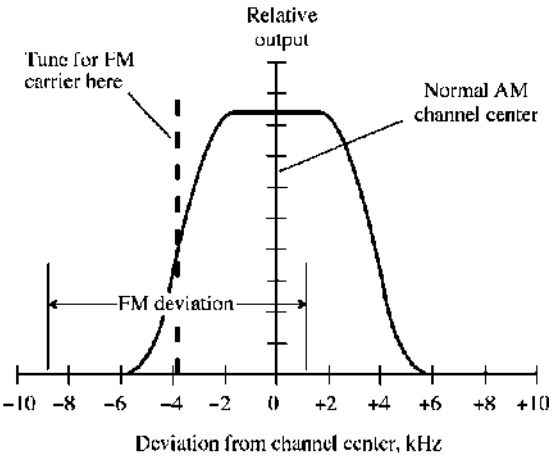

slope detector

slope resistance The ratio of a small change in voltage to a small change in current at an electrode or in a component.

slop-jar capacitor See WATER CAPACITOR.

slop-jar rectifier See ELECTROLYTIC RECTIFIER.

slot **1.** In the armature of a motor or generator, a groove in which the windings are laid. **2.** The notch in the response curve of a crystal filter.

slot antenna A microwave antenna that radiates energy through a slot cut in a surface, such as the metal skin of an aircraft.

slot cell A reinforcing, dielectric material (such as plastic) placed in the slot of a ferromagnetic core.

slot coupling Coupling microwave energy between a waveguide and a coaxial cable by means of two slots, one in the waveguide and the other in the outer conductor of the cable.

slot-discharge resistance See CORONA RESISTANCE.

slot insulation **1.** Insulation of wires in the slots of the armature of a motor or generator (see SLOT, **1**). **2.** A material in the form of tape or sheets, used for the purpose defined in **1**.

slot radiator See SLOT ANTENNA.

slotted line A device consisting of a section of air-dielectric coaxial line arranged for microwave measurements. The outer conductor is a metal cylinder, and the inner conductor is a concentric metal rod. The cylinder is provided

5059F-pS-607-670 4/10/01 9:47 AM Page 637

with a lengthwise slot through which a small pickup probe extends for sampling the electromagnetic field inside the device. The probe is attached to a carriage that slides along a graduated scale on the outside of the cylinder. Radio-frequency energy is injected into one end of the line through a coaxial cable; as the probe moves along, response points are indicated by an external detector connected to the probe. The scale is read at these points to determine frequency, standing-wave ratio, impedance, and power. An alternate form of slotted line uses a section of slotted waveguide, instead of a section of coaxial line.

slotted rotor See SERRATED ROTOR PLATE.

slotted section See SLOTTED LINE.

slotted waveguide See SLOTTED LINE.

slot width **1.** The width of a slot in the armature of a motor or generator (see SLOT, **1**). **2.** The bandwidth of the notch in the response curve of a band-suppression filter of any kind. See, for example, NOTCH FILTER.

slow-acting relay Any relay designed to operate at some finite period following the application of the actuation voltage.

slow-blow fuse A fuse in which the melting wire breaks apart slowly. The time delay allows the fuse to withstand momentary current surges that do not damage the protected equipment, but that would cause a fast-blow fuse to break the circuit needlessly.

slow-break, fast-make relay A relay that opens slowly and closes rapidly.

slow-break, slow-make relay A relay that opens slowly and closes slowly.

slow charge Storage-battery charging in which a low current is passed through the battery over a long period of time. It ensures that the rated ampere-hour capacity will be restored to the battery.

slow death **1.** The gradual deterioration of transistor performance. **2.** The gradual deterioration in the performance of a component, circuit, device, or system.

slow drift The gradual change of a quantity or setting (usually in one direction). Compare FAST DRIFT.

slow-make, fast-break relay A relay that closes slowly and opens rapidly.

slow-make, slow-break relay A relay that closes slowly and opens slowly.

slow-operate, fast-release relay See SLOW-MAKE-FAST-BREAK RELAY.

slow-operate, slow-release relay See SLOW-MAKE-SLOW-BREAK RELAY.

slow-release, fast-operate relay See SLOW-BREAK-FAST-MAKE RELAY.

slow-release, slow-operate relay See SLOW-BREAK-SLOW-MAKE RELAY.

slow storage A form of memory with long storage and recovery time.

slow time scale An extended time scale, i.e., one larger than the time unit of the system under consideration.

SLS Abbreviation of SIDELOBE SUPPRESSION.

slug **1.** A movable core of ferromagnetic material, used to tune (varying the inductance of) coil by changing its position along the axis of the coil. Also see SLUG-TUNED COIL. **2.** A copper ring attached to the core of a relay for time-delay purposes (see SLUG-TYPE DELAY RELAY).

slug-tuned coil A coil whose inductance is varied by means of a ferromagnetic slug that slides in and out of the coil.

slug tuner A tuner for a radio or television receiver or test instrument, using slug-tuned coils.

slug-type delay relay A delayed-response relay that achieves time delay through the action of a heavy copper slug on the core. The slug forms a low-resistance, short-circuited single turn in which a current is induced by the magnetic flux, resulting from energizing the relay. The resulting flux of the slug opposes the buildup of relay-coil flux.

slumber switch An alarm-reset switch on an electronic clock radio. If the alarm activates, the slumber switch (usually a pushbutton device) can be pressed to turn off the alarm for a predetermined length of time. Also called *snooze button.*

SLW Abbreviation of STRAIGHT-LINE WAVELENGTH.

Sm Symbol for SAMARIUM.

small-current amplifier **1.** A direct-current (dc) amplifier for low-level input currents (i.e., currents of 1 milliampere or less). **2.** An amplifier (such as a silicon-transistor unit) requiring very low dc operating current.

small-scale frequency response For an analog circuit, the output frequency at which the level is –3 dB, relative to the maximum level, with a small signal at the input, normally 1 volt peak-to-peak.

small loop antenna A closed loop antenna with one to several turns and a circumference less than 0.1 wavelength at the highest operating frequency. This antenna is suitable for wireless reception, but generally not for transmission because the radiation resistance is extremely low. The antenna is least responsive along its axis, and is most responsive in the plane defined by its turn(s). The null along the axis is sharp and deep. A capacitor can be connected in series or parallel with the loop to provide a resonant response. This type of antenna can reduce interference caused by human-made noise or strong local signals. It is also useful for radio direction finding (RDF) at frequencies up to approximately 20 MHz. Compare FERRITE-ROD ANTENNA, LARGE LOOP ANTENNA.

small signal A low-amplitude signal. Such a signal covers so small a part of the operating characteristic of a device that operation is essentially linear. Compare LARGE SIGNAL.

5059F-pS-607-670 4/10/01 9:47 AM Page 638

small-signal analysis Analysis of circuit or component operation in which it is assumed that the signals deviate from (fluctuate to either side of) the steady bias levels by only a small amount. Also see SMALL SIGNAL.

small-signal bandwidth The frequency at which the output signal of an analog circuit decreases to –3 dB, relative to the value for direct current. The output voltage is generally set at 0.1 volt peak-to-peak for testing this value so that the circuit is not overdriven.

small-signal component **1.** A coefficient or parameter (such as amplification, transconductance, dynamic resistance, etc.) calculated or measured under conditions of small-signal operation. Also see SMALL SIGNAL and SMALL-SIGNAL EQUIVALENT CIRCUIT. **2.** A device designed for operation at low signal levels.

small-signal diode See SIGNAL DIODE.

small-signal equivalent circuit For a given transistor circuit, the equivalent circuit for low signal levels (i.e., at amplitudes lower than saturation and cutoff levels). Also see EQUIVALENT CIRCUIT.

small-signal operation Operation at low signal amplitudes (i.e., at signal levels that do not extend into the saturation or cutoff levels of a transistor, diode, or other component).

small-signal transistor A transistor designed for low-level applications, such as the amplification of small voltages and currents and low-voltage switching. Compare POWER TRANSISTOR.

SmallTalk A high-level computer programming language that uses a graphical user interface (GUI). It is used in complex design and research, and in robotics.

smart home or business An electronically controlled home or business, in which computers and robots take care of cooking, dish washing, floor scrubbing, waste removal, laundry, yard maintenance, snow removal, and other mundane chores. Intrusion detection and fire prevention are constantly maintained. In some cases, intruders can actually be identified or detained; fires can be extinguished by controlled sprinkler systems or remotely controlled robots. Some tasks can be monitored and controlled directly by the owner from remote locations, via telephone lines or wireless.

smartness The ability of an electronic system, especially a computer or control system, to perform a complete series of operations, substituting alternative steps, where necessary—all with a minimum of instructions from, and supervision by, human operators.

smearing In television or facsimile, a form of picture distortion caused by an excessively narrow receiving bandpass. The image appears fattened and horizontally blurred. Contrast might also be lost.

smectic crystal A liquid crystal in which the molecules are arranged in parallel layers and cannot slide past each other.

S meter In a radio communications receiver, a meter graduated in S units and/or decibels to indicate the strength of a received signal.

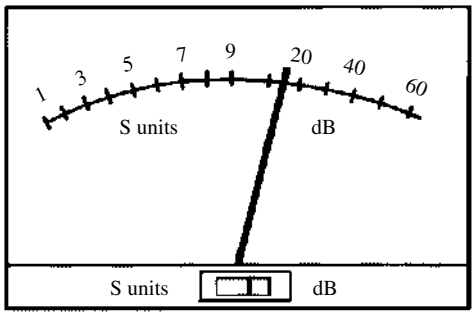

S meter

Smith chart A curvilinear graph on which complex-number impedance values can be plotted. It is useful in evaluating the behavior of radio-frequency circuits, transmission lines, and antenna systems—especially with regard to impedance mismatches and standing-wave ratio.

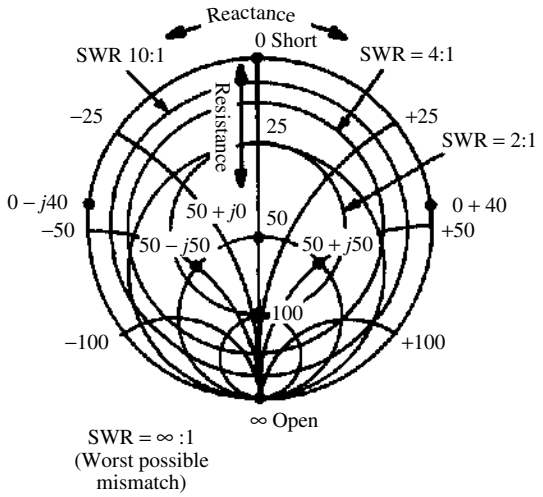

Smith chart

smoke alarm A device that produces audible and/or visible signals in the presence of smoke or unusual gases in the air. Also see PHOTOELECTRIC SMOKE ALARM.

smoke control See PHOTOELECTRIC SMOKE CONTROL.

smoke detector Any circuit or device used to sense the presence of smoke or noxious gases.

5059F-pS-607-670 4/10/01 9:47 AM Page 639

Some types detect changes in the ionization potential of the air; others sense changes in the dielectric constant of the air. Also see PHOTOELECTRIC SMOKE DETECTOR.

smoke sensor See SMOKE DETECTOR.

smooth **1.** Relatively free from surface irregularity. **2.** To reduce or eliminate irregularities in the voltage or current from a direct-current power source. **3.** To reduce or eliminate irregularities in data or signal amplitude.

smoothing choke A power-supply filter choke having a core with an air gap that prevents saturation at maximum rated direct current. Compare SWINGING CHOKE.

smoothing factor For a power-supply filter, a quantity approximately equal to $6.28fRC$, where f is the alternating-current frequency in Hertz, R is the filter resistance (in an RC filter) or the series reactance of the choke (in an LC filter) in ohms, and C is the filter capacitance in farads.

smoothing filter **1.** A filter for smoothing the alternating-current ripple component of a direct-current power supply following rectification. It can consist of one or more parallel capacitors of large value, and one or more series chokes of large inductance. **2.** A low-pass filter used at the output of a digital-to-analog (D/A) converter for eliminating high-frequency components generated by sampling.

SMPTE Abbreviation of SOCIETY OF MOTION PICTURE AND TELEVISION ENGINEERS.

smudge See SQUEEZEOUT.

SN Abbreviation of semiconductor network.

S/N Abbreviation of SIGNAL-TO-NOISE RATIO.

Sn Symbol for TIN.

snake **1.** A long, strong, flexible wire or strip used to pull other wires through electrical conduits. **2.** To route wires or cables through a group of circuits, components, or boards.

snap-action switch A switch that snaps quickly into the on or off position to prevent arcing and consequent premature contact deterioration.

snap diode A semiconductor diode in which switch-off time after carrier storage is extremely short (e.g., under 1 nanosecond).

snap magnet A magnet that reduces the tendency for arcing in relay-control instruments, thereby minimizing electromagnetic interference and prolonging contact life.

snap-on connector An electrical connector that locks in place, reducing the chance that it will detach unless it is deliberately removed.

snapshot dump During a computer program run, a dump, for debugging purposes, of certain storage areas.

snap switch See SNAP-ACTION SWITCH.

sneak current Unintended current flow through a path that is auxiliary to a main circuit.

sneak path A path through which current is accidentally detoured; it is usually a leakage path.

Snell's law A rule of physics that applies to visible light passing from air (or a vacuum) to some medium with an index of refraction c. If the light ray strikes the medium at an angle u, relative to a line normal (perpendicular) to the surface, and passes into the medium at angle v relative to the normal, then $(\sin u)/(\sin v) = c$.

sniffer See EXPLORING COIL.

sniperscope A telescope, snooperscope, or starlight scope for a carbine or rifle.

(S+N)/N Abbreviation of SIGNAL-PLUS-NOISE-TO-NOISE RATIO.

SNOBOL Acronym for *string-oriented symbolic language*, a computer-programming language for manipulating character strings.

snooperscope **1.** An infrared-sensitive device that permits viewing objects and surroundings in total darkness. It presents the image on a fluorescent screen. **2.** A rifle-mounted starlight scope.

snow A type of television picture interference that typically occurs when the signal-to-noise ratio is low (the reception is marginal or poor). Characterized by countless tiny out-of-focus light spots, whose rapid, random motion mimics the appearance of falling snow.

SNR Abbreviation of SIGNAL-TO-NOISE-RATIO.

soak value The smallest value of current that will cause saturation of a relay core.

Society of Motion Picture and Television Engineers Abbreviation, SMPTE. A group that decides on various procedures in video recording and reproduction, both on magnetic media (tape or disk) and on film.

socket A (usually female) fixture into which a plug, integrated circuit, or other component is inserted for easy installation in, or removal from, a circuit.

socket punch See PUNCH, **2**.

sodium Symbol, Na. A metallic element of the alkali-metal group. Atomic number, 11. Atomic weight, 22.9898.

sodium silicate See WATER GLASS.

sodium-vapor lamp A gas-discharge lamp containing neon and a small amount of sodium. After the filaments of the lamp are lighted for a short time, the heat vaporizes the sodium, and the filaments are disconnected by an automatic switch. Under the influence of the voltage across the lamp, the sodium vapor glows with a characteristic yellow light.

sofar A system for pinpointing the source of underwater sounds (coming from as far away as 2000 miles) through triangulation. The name is an acronym for *sound fixing and ranging.*

soft-drawn wire Wire that is highly malleable, and is therefore easily bent and unbent. Compare HARD-DRAWN WIRE.

soft iron A grade of iron, used in some cores, that is easily demagnetized.

soft solder A low-melting-point solder.

software **1.** Vendor-supplied or user-generated programs or groups of programs for a computer

5059F-pS-607-670 4/10/01 9:47 AM Page 640

or computer system. **2.** The detailed instructions for performing a particular operation with a calculator or a computer.

software-defined radio Abbreviation, SDR. **1.** Wireless communications in which the modulation waveforms and protocols are generated and decoded by computer software. This allows a single, microcomputer-controlled radio receiver, transmitter, or transceiver to operate in a variety of services that use different protocols. Changing the modulation waveform or protocol requires only a change in the program run by a microcomputer that controls the radio. **2.** A receiver, transmitter, or transceiver that employs the technology defined in (1). **3.** The use of wireless equipment that employs the technology defined in (1).

soft X rays Low-frequency (long-wavelength) X rays. Such radiation has relatively poor penetrating power. Compare HARD X RAYS.

sol **1.** Abbreviation of SOLUTION. **2.** Abbreviation of SOLUBLE.

solar access For a specific property or location, the availability of direct exposure to the sun's rays as a source of energy.

solar absorption index A quantitative measure of the effect of the sun on the ionospheric absorption of radio waves.

solar activity See SOLAR RADIATION and SUNSPOT cycle.

solar battery A battery composed of solar cells connected in series and/or parallel for increased output.

solar cell A photovoltaic power transducer that converts visible light to electricity. It is called a cell because its output is a low direct-current voltage. Such cells can be connected in series and/or parallel to provide useful electric power output.

solar cycle See SUNSPOT CYCLE.

solar energy **1.** The total energy arriving from the sun, over a given period of time and within a specific surface area, at a given location on the surface of the earth. **2.** Any energy derived entirely from the sun.

solar-energy conversion Any process that changes solar radiant energy into another useful form.

solar flare A violent storm on the surface of the sun. These events tend to occur near the peak of the 11-year sunspot cycle. They cause an increase in the level of radio noise that comes from the sun, and they emit high-speed subatomic particles that reach earth a few hours after the first appearance of the flare. Because the particles are electrically charged, they are accelerated by the geomagnetic field. Sometimes a geomagnetic storm results, producing aurora near the poles and deterioration of ionospheric radio-propagation conditions.

solar flux An indicator of general solar activity. The solar noise level is measured at a particular frequency, such as 2800 MHz. The solar flux tends to be highest during periods of the greatest sunspot activity and immediately following a solar flare.

solar laser See SUNLIGHT-POWERED LASER.

solar noise Broadband electromagnetic noise generated by the sun. In particular, noise that occurs at radio frequencies and affects satellite, moonbounce, and space communications. This noise varies in intensity with the 11-year sunspot cycle, being generally higher at and near sunspot maxima. A solar flare can cause a sudden and dramatic increase in the noise at all wavelengths. See SOLAR FLARE.

solar panel An array consisting of a number of series-connected or series-parallel-connected solar cells mounted on a flat plate.

solar power Useful amounts of electricity obtained from suitable arrays of solar cells.

solar radiation Electromagnetic energy of various wavelengths originating in the sun. Such radiation, after passing through the earth's atmosphere, consists mostly of infrared rays and visible light. Some ultraviolet rays also reach the earth's surface.

solar relay See SUN SWITCH.

solar switch See SUN SWITCH.

solar wind Continuous emission of high-speed subatomic particles by the sun. It causes distortion of the lines of flux in the earth's magnetic field. It becomes more intense following a solar flare.

solder **1.** A metal alloy (usually of tin and lead) that is melted to electrically and mechanically join pieces of other metals. Also see HARD SOLDER and SOFT SOLDER. **2.** To join metals with solder.

solder

Solder type	*Melting point (°F/°C)*	*Principal uses*
Tin-lead 50 : 50, rosin-core	430/220	Electronic circuits
Tin-lead 60 : 40, rosin-core	370/190	Electronic circuits, low-heat
Tin-lead 63 : 37, rosin-core	360/180	Electronic circuits, low-heat
Tin-lead 50 : 50, acid-core	430/220	Non-electronic metal bonding
Silver	600/320	High-current, high-heat

soldering Joining (usually nonferrous) metal parts with solder, a lead-alloy substance. Compare BRAZING.

soldering gun An electric soldering iron having the general shape of a handgun. The element heats and cools more rapidly than the element in a

5059F-pS-607-670 4/10/01 9:47 AM Page 641

typical soldering iron. The element is heated by pressing a device similar to the trigger on a pistol.

soldering iron An electric or nonelectric tool having a heated tip for melting solder.

solderless breadboard A foundation (see BREADBOARD, **1**) on which a circuit can be assembled by plugging components into tiny jacks without the use of solder.

solderless connection A connection between leads, or between leads and terminals, accomplished entirely through crimping, pinching, splicing, or wire wrapping. Solder is not used. Also see WIRE-WRAP CONNECTION.

solderless terminal A terminal to which a solderless connection can be made. Also see WRAP POST.

solenoid **1.** A coil of wire having a single layer, wound on a cylindrical form. **2.** A multilayer coil used as an electromagnet, and usually having a straight, iron core.

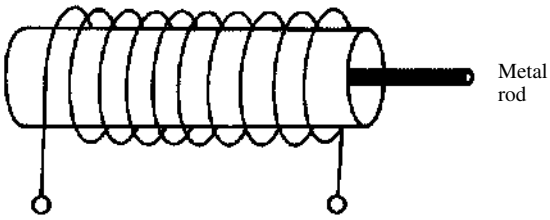

solenoid

solenoid switch A switch consisting of a solenoid coil (see SOLENOID, **2**) into which a core is pulled by the magnetic field to close a pair of contacts.

solid **1.** One of the states of matter. It is characterized by a definite shape and volume, and by atoms that maintain a fixed position, relative to each other. Compare GAS, LIQUID, and PLASMA. **2.** An enclosed, defined volume of three-dimensional space. **3.** In communications, descriptive of error-free reception of a series of coded signals. **4.** In printing and data transmission, a large print area whose entire surface is of equal and maximum intensity (of ink, light, or darkness).

solid angle Unit, steradian. The angle within the apex of a cone formed by all line segments between the center of a sphere and a defined circle on the surface of the sphere.

solid circuit Any circuit consisting of a single piece of hardware that is not normally separated into smaller parts.

solid conductor See SOLID WIRE.

solid electrolyte A solid substance affording ionic action similar to that in a liquid electrolyte.

solid electrolytic capacitor A capacitor using a solid electrolyte.

solid ground See DIRECT GROUND.

solid-state Pertaining to devices and circuits in which the flow of charge carriers (electrons and holes) is controlled in specially prepared blocks, wafers, rods, or disks of solid materials. Semiconductor devices, such as transistors and integrated circuits, are solid-state components.

solid-state battery An atomic battery consisting essentially of a photovoltaic cell in combination with a quantity of radioactive material, whose radiation causes the cell to generate electricity.

solid-state camera A video camera device that makes use of solid-state technology. The target is a matrix of charge-coupled devices (CCDs). When light strikes these devices, charge carriers are separated in a manner similar to that in a photovoltaic cell. The matrix is scanned according to a particular scheme, and the voltages developed in each CCD combine to produce the video signal output.

solid-state capacitor See SOLID ELECTROLYTIC CAPACITOR.

solid-state chronometer Any semiconductor device to indicate or measure time.

solid-state circuit See MONOLITHIC INTEGRATED CIRCUIT.

solid-state lamp **1.** See LIGHT-EMITTING DIODE. **2.** See LASER DIODE. **3.** See ELECTROLUMINESCENT CELL.

solid-state maser A device, such as the ruby maser, in which the stimulated medium is a solid material.

solid-state photosensor A semiconductor photodiode or phototransistor, as opposed to a phototube.

solid-state physics The branch of physics concerned with the nature and applications of such solids as electronic semiconductors.

solid-state relay **1.** A sensitive relay consisting of a conventional electromagnetic relay preceded by a transistorized amplifier. **2.** A completely electronic relay (i.e., one without moving parts) in which switching transistors provide the on and off states. **3.** See THYRISTOR.

solid-state thermometer An electronic thermometer utilizing one or more solid-state components, such as transistors, integrated circuits, or thermistors.

solid-state thyratron See SILICON-CONTROL-LED RECTIFIER and SILICON-CONTROLLED SWITCH.

solid-state tube A semiconductor device (diode, rectifier, transistor, SCR, etc.) whose housing and base allow it to replace directly an electron tube.

solid tantalum capacitor A capacitor using tantalum as a solid electrolyte.

solid wire Wire consisting of a single strand of metal. Compare STRANDED WIRE.

solute A substance that is dissolved in some other substance. Also see SOLUTION, **1**.

solution **1.** A well-diffused mixture of two or more substances. It can consist of a gas in a liquid, a gas in a solid, a gas in a gas, a liquid in a solid, or

5059F-pS-607-670 4/10/01 9:47 AM Page 642

a solid in a solid. A solution, typically, is molecular (i.e., there is no chemical reaction between its constituents). Also see SATURATED SOLUTION; SOLUTE; SOLVENT, **1**; and SUPERSATURATED SOLUTION. **2.** The result of solving a problem or making a calculation. Also called *answer* or *result.*

solution conductivity The electrical conductivity of a solution, such as an electrolyte. The conductivity (and conversely, the resistance) depends on the number and mobility of ions in the solution.

solution-conductivity bridge A direct-current bridge specially designed and calibrated to measure the conductivity of chemical solutions.

solution pressure In an electrolyte into which a metal body is immersed, the force that causes the metal to tend to pass into solution as positive ions and to form a Helmholtz double layer.

solvent **1.** A fluid that dissolves other materials. **2.** The constituent of a solution that dissolves one or more other constituents. Thus, in a saltwater solution, water is the solvent and salt the solute. Also see SOLUTION, **1**.

SOM Abbreviation of *start of message.*

Sonalert Tradename for a small, but loud, sound reproducer used with solid-state circuits for alarm purposes.

sonar A system of detection and ranging by means of sonic and ultrasonic signals. In this system of echo ranging, the distance to an underwater object is determined from the time it takes a sound signal to reach the object and be reflected back to the transmitter. The name is an acronym for *sound navigation and ranging.*

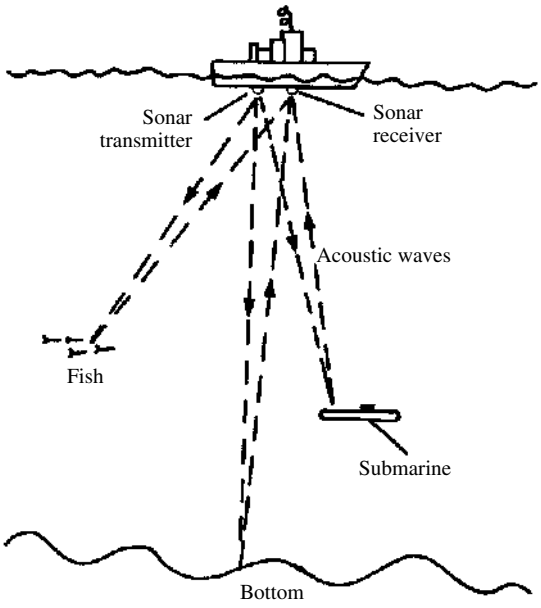

sonar

sonde A device for automatically gathering meterological data at high altitudes. An example is the *radiosonde.*

sone A unit of loudness for an individual listener. The level of 1 sone is the loudness of a 1000-Hz tone that is 40 dB above the particular listener's threshold of hearing.

sonic altimeter An altimeter (see ABSOLUTE ALTIMETER) using sound waves. The time required for a transmitted wave to reach a target and be reflected back to the transmitter is proportional to the distance between the transmitter and the target.

sonic boom An explosive sound occurring when the shock wave produced by an aircraft flying at supersonic speed strikes the earth.

sonic delay line A delay line using electroacoustic transducers and an intervening medium through which a sound wave is transmitted.

sonic depth finder See ACOUSTIC DEPTH FINDER.

sonic thermocouple A thermocouple whose heat-absorbing properties are enhanced by subjecting it to acoustic vibrations.

sonobuoy A buoy equipped with an acoustic receiver and radio transmitter. The device is parachuted into the water, where it receives submarine sounds and transmits them to a monitoring station. Several sonobuoys communicating with a computer will track the path of a submarine.

sonovox An electronic device used to produce special sound effects when it is held against the throat of the operator. The special sounds are formed into words by the operator's mouth.

SOP Abbreviation of *standard operating procedure.*

sophisticated electronics Advanced electronics theory and operations, usually dealing with complex devices or systems and requiring rigorous analysis to describe their operation and devise applications. Compare UNSOPHISTICATED ELECTRONICS.

sorption processes Processes whereby certain substances (e.g., activated charcoal) occlude and retain gases and vapors. A chamber containing such a substance is often useful in the production of a vacuum. Sorption includes both absorption and adsorption.

sort **1.** To group information items using their keys. Also see KEY. **2.** To group information items according to some system of classification, as to print an alphabetical list of words stored in a random sequence.

sorting routine A computer program for sequencing data items according to key words (values in specific fields) of the different records.

SOS **1.** The international radiotelegraph distress signal; equivalent to *mayday* in radiotelephony. It consists of three dits ("dots"), followed by three dahs ("dashes"), followed by three more dits. **2.** Abbreviation of SILICON ON SAPPHIRE.

5059F-pS-607-670 4/10/01 9:47 AM Page 643

sound The vibratory or wave phenomenon to which the sense of hearing is responsive. Conducted by waves in solids, liquids, and gases; not propagated through a vacuum.

sound absorption The nonreflection and nontransmission of acoustic energy by a body or medium, and the attendant conversion of the acoustic energy into another form of energy (usually heat).

sound absorption coefficient A quantitative expression of the extent to which a surface absorbs acoustic energy (as opposed to reflecting, transmitting, diffusing, or scattering it).

sound amplifier **1.** An audio amplifier—especially the sound channel of a television system. **2.** A device, such as a horn or reflector, that directly boosts the intensity of sound at a given listening point.

sound analyzer An instrument, often a wave analyzer equipped with a microphone, for measuring such characteristics of sound as amplitude, frequency (pitch), and harmonic content (timbre).

sound articulation See ARTICULATION.

sound bars In a television picture, horizontal bars resulting from interference between the audio and video channels of the receiver.

sound carrier In a television signal, the frequency-modulated carrier that transmits the audio part of the program. Compare VIDEO CARRIER.

sound chamber An air enclosure, usually a box or can, for modifying the acoustic qualities of sound or of an audio signal.

sound detector The discriminator or ratio detector that demodulates the sound signal in a television receiver circuit.

sound-energy density Sound energy per unit volume, expressed in joules per cubic meter or ergs per cubic centimeter.

sound-energy flux The average rate of flow of sound energy through a specified area, as expressed in ergs or joules per second.

sound field A volume of space or material containing sound waves.

sound film Motion-picture film on which a sound track is recorded. Also see OPTICAL SOUND RECORDING.

sound flux The rate of flow of sound energy, usually expressed in terms of sound pressure at a point or over a unit area normal to the direction of sound propagation.

sound gate An optical device used to convert the sound track of a movie film into electrical impulses.

sound generator Any combination of oscillator, amplifier, and transducer (loudspeaker or headphones) for producing sound waves.

sound-hazard integrator An instrument used to measure cumulative noise exposure received by persons in noisy environments. One such instrument provides direct readings in percent of permissible exposure.

sound IF amplifier In a television receiver circuit, the separate amplifier for the sound intermediate frequency. See, for illustration, INTERCARRIER RECEIVER and SPLIT-SOUND RECEIVER.

sound-level meter See SOUND SURVEY METER.

sound marker A marker indicating the sound-carrier point on a television alignment curve displayed on an oscilloscope screen.

sound-marker generator A special radio-frequency signal generator (or a special circuit in a television-alignment generator) for the production of a sound marker.

sound mirage See ACOUSTIC MIRAGE.

sound mix In sound recording or reproduction, the composite output from an audio mixer circuit.

sound-on-film recording See OPTICAL SOUND RECORDING.

sound-on-sound recording The simultaneous recording (on a single track on magnetic tape) of new material with previously recorded material. The old recording is not erased.

sound-operated relay **1.** A relay operated indirectly from sound, through the medium of a pickup microphone and amplifier. **2.** A relay having a delicately poised armature that operates directly from sound vibrations.

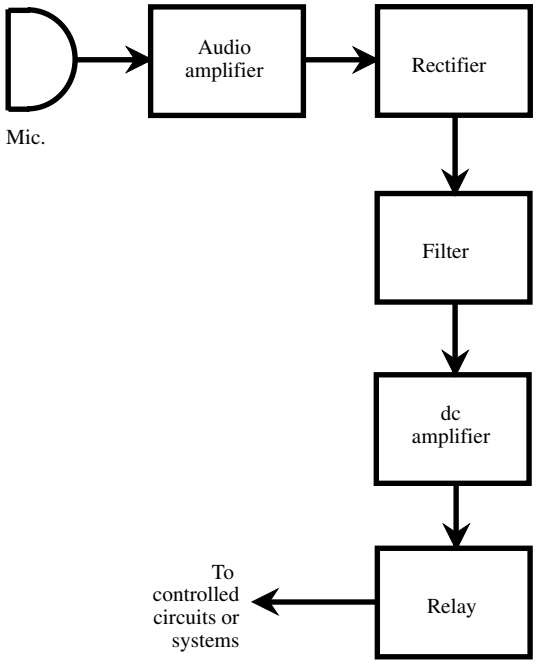

sound-operated relay

sound power The total sound energy per unit time produced by a sound source, as expressed in ergs per second or in watts.

sound power level The extent, in decibels, by which SOUND POWER exceeds one picowatt (10^{-12} watt).

5059F-pS-607-670 4/10/01 9:47 AM Page 644

sound pressure **1.** The force exerted by sound waves on a surface area, expressed in dynes per square centimeter (as an rms value over 1 cycle). The sound pressure is proportional to the square root of sound-energy density. **2.** The instantaneous difference between actual air pressure and average air pressure at a given point.

sound pressure level The extent, in decibels, via which SOUND PRESSURE exceeds 20 micropascals (2.0×10^{-5} pascal).

sound probe A transducer used to receive acoustic vibrations for detection or measurement purposes.

sound recording The electrical recording of sound, using cylinder, disc, tape, wire, or other comparable storage medium.

sound-recording system A complete, integrated array of equipment for recording sound, including such components as microphones, amplifiers, pickups, filters and other shaping networks, attenuators, level indicators, and recording mechanisms. Compare SOUND-REPRODUCTION SYSTEM.

sound reinforcement Intensification of sound by horns, resonant chambers, or other acoustical devices.

sound relay See SOUND-OPERATED RELAY.

sound reproduction The electrical reproduction of sound from recordings on vinyl discs, magnetic tapes, magnetic discs, compact optical disbs, etc.

sound-reproduction system A complete, integrated array of equipment for the playback of recorded sound, including such components as tape or record players, amplifiers, filters and other shaping networks, attenuators, level indicators, loudspeakers, and headphones. Compare SOUND-RECORDING SYSTEM.

sound spectrograph A device that produces a display of sound amplitude vs. frequency. Similar to a SPECTRUM ANALYZER, except that it operates at audio frequencies (about 20 Hz to 20 kHz) and is actuated by acoustic disturbances, rather than by electromagnetic signals.

sound spectrum The continuous band of frequencies (about 20 Hz to 20 kHz) constituting audible sounds, and sometimes the immediately adjacent (subaudible and superaudible) frequencies.

sound stage The apparent dimensions of a sound source.

sound survey meter A portable instrument for measuring the intensity and other characteristics of sound.

sound sweetening In audio recording or reproduction, the modification of the sound to achieve some desired effect.

sound system A sound-recording system, sound-reproduction system, or a combination of the two.

sound takeoff In a television receiver circuit, the point at which the frequency-modulated sound signal is extracted from the complex signal.

sound track The variable-density or variable-width recording on one side of the film in sound-on-film recording and reproduction. Also see OPTICAL SOUND RECORDING.

sound transducer See ACOUSTIC TRANSDUCER.

sound-transmission coefficient See ACOUSTICAL TRANSMITTIVITY.

sound trap In a television receiver circuit, a wave-trap that prevents the sound signal from entering the picture channels.

sound unit See PHONE, **2**.

sound wave The vibratory phenomenon produced in a medium by acoustic energy. A sound wave in air consists of alternate compressions and rarefactions of the air. Also see ACOUSTIC WAVE.

source **1.** The origin of a signal or electrical energy (e.g., a transmitting station). **2.** In a field-effect transistor, the electrode that is equivalent to the emitter of a common-emitter-connected bipolar transistor, or the cathode of a vacuum tube. **3.** That which is being transcribed to magnetic tape. **4.** Manufacturer, wholesaler, or retailer.

source circuit **1.** The circuit associated with the source electrode of a field-effect transistor. **2.** A generator circuit. Compare SINK CIRCUIT.

source code See SOURCE LANGUAGE.

source computer A computer for compiling a source program.

source-coupled multivibrator A multivibrator circuit using field-effect transistors, in which feedback coupling is achieved with a common source resistor for the two FETs. This circuit is equivalent to the emitter-coupled bipolar-transistor-type multivibrator.

source data automation A means of storing a master data file for easy duplication, whenever necessary.

source deck An audio or video tape player that reproduces original recordings in the editing process.

source follower A field-effect-transistor circuit in which the output is taken across a resistor between source and ground. This circuit is equivalent to the emitter follower, and is a unity-gain stage whose impedance-transformation characteristics make it ideal in signal conditioning, buffering, and impedance-matching applications.

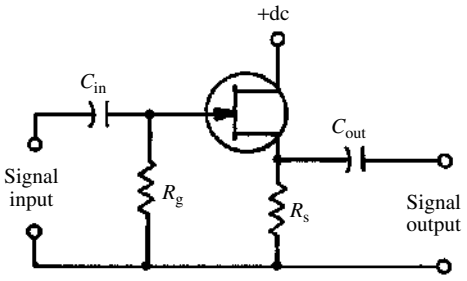

source follower

5059F-pS-607-670 4/10/01 9:47 AM Page 645

source impedance **1.** The impedance of a generator in a circuit. **2.** The impedance of the source electrode of a field-effect transistor.

source language A computer programming language from which is derived (by a compiler) the machine (object) language on which the computer operates.

source program A computer program written in a source language.

south magnetic pole The south pole of the equivalent bar magnet constituted by earth's magnetic field (see EARTH'S MAGNETIC FIELD). The south magnetic pole lies close to the geographic south pole. Compare NORTH MAGNETIC POLE.

south-seeking pole Symbol, S. The so-called south pole of a magnet. When a bar magnet is suspended horizontally, this pole points to earth's south magnetic pole. Compare NORTH-SEEKING POLE.

SP Abbreviation of STACK POINTER.

sp **1.** Abbreviation of *single pole.* **2.** Abbreviation of *special.*

space-charge field **1.** The electric field existing within a group of charged particles. **2.** The electric field existing in a plasma.

space diversity See DIVERSITY RECEPTION.

space-diversity reception See DIVERSITY RECEPTION.

space division A method of data transfer in which different paths are used for the transmission of different signals.

space-division switch A switch having two or more ports and different paths connecting the ports.

space lattice The three-dimensional, redundant pattern formed by atoms and molecules in a crystal and having a shape that is characteristic of a particular crystalline material.

spacer An insulating rod or bar that serves to hold apart the conductors of a two-wire, four-wire, or coaxial air-dielectric transmission line.

space suppression Following the printing of a line by a printer, the prevention of normal paper travel.

space-time-space switch Abbreviated STS switch or STSS. A large switching array with two space switch blocks and a time switch block between them.

space wave One of the components of an electromagnetic ground wave. The space wave, unlike the *surface wave*, is not earth-guided. It has two components: the *direct wave* and the *ground-reflected wave.*

spaghetti Slender, varnished-cambric tubing used as slipover insulation for wires and busbars.

span On an instrument scale, the difference between the highest value and the lowest value.

spark See ELECTRIC SPARK.

spark absorber **1.** See SPARK SUPPRESSOR. **2.** See KEY-CLICK FILTER.

spark coil A small induction coil. Its name is derived from its initial purpose of supplying the high voltage for spark plugs in gas engines.

spark energy The energy dissipated by an electric arc or spark.

spark gap A device consisting essentially of two metal points, tips, or balls that are separated by a small air gap. A high voltage applied to the electrodes causes a spark to jump across the gap.

sparking distance The maximum separation of the electrodes of a spark gap at which a given voltage will produce a spark.

sparking voltage The lowest voltage that will cause a spark to jump across a gap of a given width.

spark killer See SPARK SUPPRESSOR.

sparkover A discharge in air, a vacuum, or a dielectric. It is characterized by sparking between electrodes in the medium.

spark plate In some automobile radios, a noise-interference-eliminating bypass capacitor in which the chassis is one plate.

spark-plug suppressor A small resistive device connected in series with a spark plug to suppress electrical noise arising from the ignition in an internal combustion engine.

spark quencher See SPARK SUPPRESSOR.

spark suppressor A resistor, capacitor, and/or diode used to eliminate or minimize sparking between make-and-break contacts.

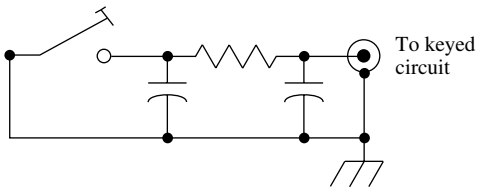

spark suppressor

spark-suppressor diode See SUPPRESSOR DIODE.

spatial distribution The three-dimensional directional pattern of a transducer (such as an antenna, microphone, or speaker).

spc **1.** Abbreviation of *silicon point contact.* **2.** Abbreviation of *silver-plated copper.*

SPDT Abbreviation of SINGLE-POLE/DOUBLE-THROW (switch or relay).

speaker See LOUDSPEAKER.

speaker damping See DAMPED LOUDSPEAKER.

speaker-level audio In a sound reproduction system, radio receiver, or other audio circuit, an audio-frequency signal of sufficient amplitude to drive a speaker or speaker system directly, without the need for additional amplification.

speaking arc A method of modulated-light transmission. An electric arc is modulated by audio-frequency signals.

special character A printed, displayed, or encoded character other than a numeral or letter, such as

5059F-pS-607-670 4/10/01 9:47 AM Page 646

an ampersand (&) or a pound sign (#). Also called SYMBOL.

special effects Various techniques used in filmmaking, computer animation, and videotape recording for achieving certain visual scenes or images.

special-purpose computer A computer designed to handle problems or be suitable for applications of a specific category; a dedicated computer.

special-purpose calculator An electronic calculator intended for essentially "nonmathematical" purposes, such as biorhythm data, astrological information, metric conversions, musical composing, etc.

specific address See ABSOLUTE ADDRESS.

specification **1.** For an electronic device, a statement of performance over specific parameters. Example: for a high-fidelity stereo amplifier, 50 watts per channel over a frequency range of 10 Hz to 30 kHz, with less than 1 percent total harmonic distortion. **2.** A precise listing of requirements or expectations.

specific conductivity Conductance per unit volume. In SI units, this is expressed in siemens per cubic centimeter (S/cm^3).

specific dielectric strength For an insulant, the dielectric strength per millimeter of thickness.

specific gravity Abbreviation, sp gr. The ratio of the density of a material to the density of a substance accepted as a standard (usually water at 4 degrees Celsius or 39.2 degrees Fahrenheit).

specific inductive capacity See DIELECTRIC CONSTANT.

specific resistance See RESISTIVITY.

specific sound-energy flux See SOUND INTENSITY.

spectral comparative pattern recognizer Acronym, SCEPTRON. Equipment used to classify automatically complex signals obtained from information that has been converted into electrical signals.

spectral density For a complex signal, the amount of energy contained within a given band of frequencies.

spectral energy distribution The occurrence of different amounts of energy in different areas of a spectrum (as in a visible-light spectrum, sound spectrum, or radio-frequency spectrum).

spectral response The characteristic of a device, such as a photocell or the human eye, that describes the device's sensitivity to radiations of various frequencies in a given spectrum.

spectral sensitivity The color response of a light-sensitive device.

spectrograph A recording SPECTROMETER.

spectrometer **1.** An instrument used to measure spectral wavelengths. **2.** An instrument used to measure the index of refraction. **3.** See MASS SPECTROMETER.

spectrophotometer A photoelectric instrument for chemical analysis. In the device, light passing through the material under analysis is broken up into a spectrum that is examined with a photoelectric circuit, which, in turn, plots a spectrogram.

spectroscope An instrument that resolves a radiation into its various frequency components and permits measurement of each.

spectrum A band of frequencies or wavelengths (e.g., *radio spectrum*, *visible-light spectrum*, and *sound spectrum*).

spectrum analyzer **1.** An automatic wave analyzer with a visual display (oscilloscope). **2.** A scanning receiver with a screen that shows a plot of signals and their bandwidths over a specific frequency band.

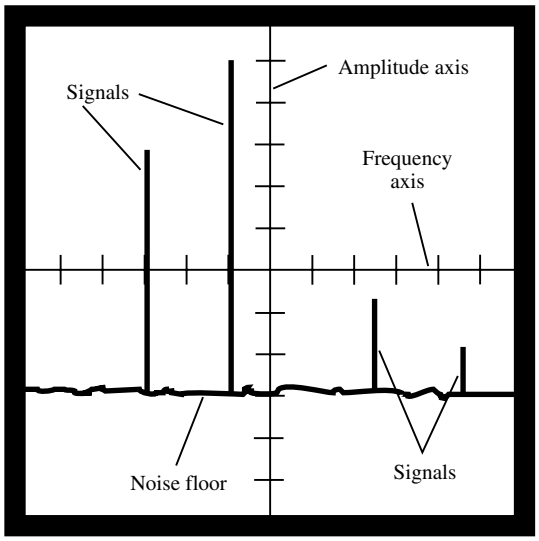

spectrum analyzer, 2.

specularity A qualitative or experimentally derived expression of the efficiency with which a DIFFRACTION GRATING works.

specular reflection Reflection in which the reflected ray is in the same plane as the incident ray, as in reflection from an extremely smooth surface.

speech amplifier A (usually low-level) audio amplifier designed especially for speech frequencies. It is generally used to amplify the signals from a microphone.

speech clipper A device, such as a biased diode, (see POSITIVE PEAK CLIPPER) for holding speech signals to a constant amplitude. Compare SPEECH COMPRESSOR. Also see SPEECH CLIPPING.

speech clipping The use of a limiting circuit to maintain the output-signal amplitude of a speech amplifier against fluctuations in the intensity of

5059F-pS-607-670 4/10/01 9:47 AM Page 647

speech input. The resulting signal requires filtering to remove harmonics generated by the process. Compare SPEECH COMPRESSION.

speech compression Automatic regulation of the gain of a speech amplifier to maintain its output-signal amplitude against speech-input fluctuations. Compare SPEECH CLIPPING.

speech compressor A circuit or device, such as an automatic-gain-control (agc) system, for performing speech compression. Compare SPEECH CLIPPER.

speech digit signaling A method of digital signaling, where time slots generally used for encoded audio or video are used alternately for signaling.

speech frequencies See VOICE FREQUENCIES.

speech intelligibility The quality of reproduced speech that makes it easily understood by a reasonably proficient user of the language. For good speech intelligibility, a circuit should transmit frequencies between 300 Hz and 3000 Hz with minimal distortion. Increased bandwidth improves fidelity, but does not provide a significant increase in intelligibility for normal speech.

speech inverter See SCRAMBLER CIRCUIT.

speech power **1.** The alternating-current power in an electric wave corresponding to speech, as opposed to that in a sine wave. **2.** Sound power in a speech transmission.

speech recognition The ability of a device to translate audible spoken words, phrases, or sentences into binary digital signals that can be used by machines, such as computers and robots.

speech recognizer An electronic device that translates audible spoken words, phrases, or sentences into binary digital signals that can be used by machines, such as computers and robots.

speech scrambler See SCRAMBLER CIRCUIT.

speech synthesis The ability of a device to translate binary digital signals from a machine, such as a computer or robot, into audible, coherent spoken words, phrases, or sentences.

speech synthesizer An electronic device that translates binary digital signals from a machine, such as a computer or robot, into audible, coherent spoken words, phrases, or sentences.

speed key **1.** A semiautomatic key for manual generation of Morse code characters. **2.** A similar, fully automatic key used especially for high-speed telegraphy.

speed of light Symbol, *c*. The speed at which electromagnetic waves propagate in a vacuum; approximately 299,792 kilometers per second (186,282 miles per second).

speed of sound The speed at which acoustic waves propagate. It depends on the nature of the medium. In air, at ordinary temperatures, it is approximately 344 meters (1129 feet) per second. In fresh water, it is approximately 1463 meters (4800 feet) per second.

speed of transmission The amount of data sent in a given unit of time. It is generally measured in

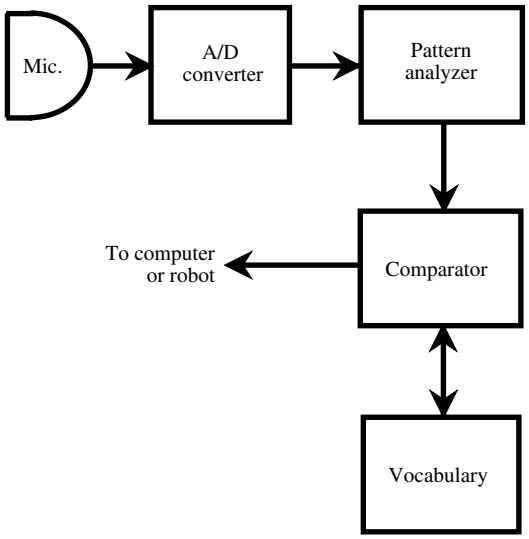

speech recognizer

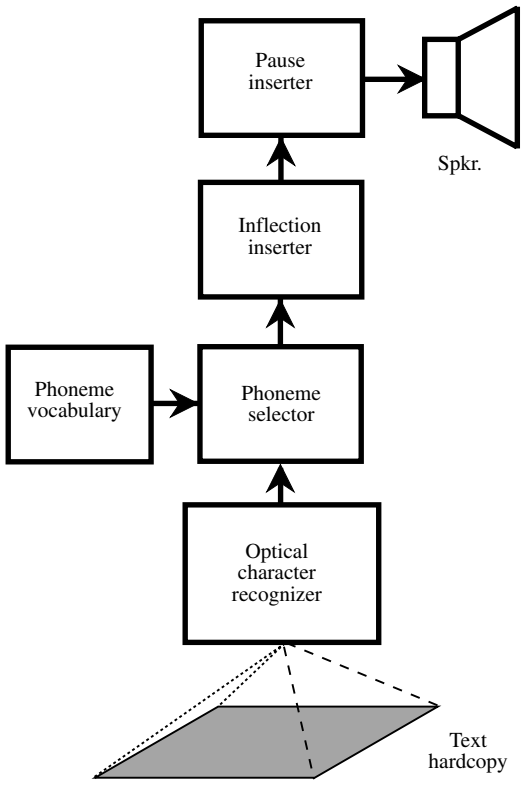

speech synthesizer

5059F-pS-607-670 4/10/01 9:47 AM Page 648

bits per second (bps), characters per second (cps), characters per minute (cpm), or words per minute (wpm). It is used primarily for digital codes.

speedup capacitor See COMMUTATING CAPACITOR.

SPFW Abbreviation of SINGLE-PHASE FULL-WAVE.

sp gr Abbreviation of SPECIFIC GRAVITY.

sphere **1.** A closed surface in three-dimensional space, represented by the set of all points equidistant from a specified center point. **2.** A solid in three-dimensional space, represented by the set of all points on or within a closed surface, as defined in **1**.

sphere gap A spark gap in which the spark passes between two polished metal spheres. When the air gap is adjustable, unknown high voltages can be measured in terms of the largest gap width at which sparking occurs. Compare NEEDLE GAP.

sphere-gap voltmeter See SPHERE VOLTMETER.

sphere voltmeter A gap voltmeter using a SPHERE GAP.

spherical aberration In a spherical lens, mirror, or reflecting dish, distortion as a result of the spherical (as opposed to paraboloidal) shape of the surface. This causes the focus to be elongated into a short line segment along the principal axis.

spherical angle An angle formed by the intersection of two arcs on the surface of a sphere.

spherical coordinate geometry A scheme for guiding a robot arm in three dimensions via SPHERICAL COORDINATES. The length (radius) of the arm can be varied, as can the elevation (latitude) and azimuth (longitude).

spherical coordinates A method of defining a point (P) in three-space using two angles (latitude and longitude) and a radial distance (r) from the origin.

spherical degree A unit equal to $\frac{1}{720}$ of the surface area of a sphere.

spherical distance The length of the shortest arc (lying on a great circle) connecting two specified points on a sphere.

spherical divergence The manner in which energy normally propagates from a fixed point source in three dimensions. Wavefronts expand from the source in the form of spheres, whose centers are at the point source.

spherical reflector A microwave reflector (dish) whose contour is that of a sphere, rather than that of a paraboloid.

spherical wave A wave characterized by wavefronts that are concentric spheres.

spheroidal antenna A sheetmetal or wire-mesh antenna having the cross section of a sphere that is flattened at the ends of one axis.

SPHW Abbreviation of SINGLE-PHASE HALF-WAVE.

spider **1.** The flat, round, springy part that holds the apex of the vibrating cone of a dynamic speaker. **2.** A quickly assembled, chassisless hookup in which the pigtails of components form the wiring and the mechanical support for a circuit.

spiderweb antenna A set of dipole antennas for different frequencies, arranged in a common (usually horizontal) plane. The result is a broadband antenna.

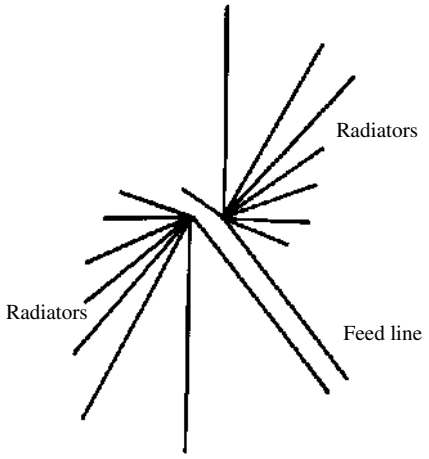

spiderweb antenna

spiderweb coil A flat, single-layer coil in which a strand of wire is woven over and under the spokes of a wheel-like form, and having the general appearance of a spiderweb. The criss-cross winding reduces distributed capacitance by breaking up the parallelism of adjacent turns.

spike **1.** A current or voltage pulse of extremely short duration. **2.** A sharp transient, such as an overshoot on a pulse or square wave.

spike suppressor A clipper or similar device for removing a spike from a signal voltage.

spin A quantity of angular momentum possessed by a subatomic particle. It can be positive, negative, or zero, but it always exists in integral multiples of ½.

spindle **1.** The pivoted shaft that carries the movable element and rotates between the pivots in a meter movement. **2.** The rotor of an alternator—especially when the rotor is a permanent magnet. **3.** The rotating shaft in a motor, generator, or similar electric machine.

spinning electron An electron having nonzero angular momentum.

spinthariscope An optical device for observing the effect of alpha particles emitted by a radioactive substance, from the scintillations they produce upon striking a small, fluorescent screen.

spiral coil See DISK WINDING.

spiral distortion A form of television camera-tube distortion caused by spiraling of the electrons as they are emitted from the photocathode. The result is a twisted image.

5059F-pS-607-670 4/10/01 9:47 AM Page 649

spiral-rod oscillator A parallel-line-type oscillator in which the lines are rods that are rolled up into spirals to conserve space. Also see LINE-TYPE OSCILLATOR.

spiral sweep **1.** A means of sweeping the electron beam in a cathode-ray tube to produce a spiral trace on the screen. **2.** The circuit for producing such a sweep.

spiral trace See SPIRAL SWEEP.

spiral winding See DISK WINDING.

spkr Abbreviation of *speaker* (see LOUDSPEAKER).

splatter See SIDEBAND SPLATTER.

splatter-suppression filter In an amplitude-modulated (AM) or single-sideband (SSB) radio transmitter, a low-pass filter inserted between the output of the audio amplifier and the audio input of the modulator. It suppresses high-frequency audio components that would otherwise cause sideband splatter.

splaying The construction of a room or auditorium so that the walls do not meet at right angles. It is useful in optimizing the acoustic characteristics of the enclosure because it tends to reduce acoustic resonant effects.

splice **1.** A physical or electrical connection between two wires, made by tightly winding the ends together. Solder is often applied for additional mechanical strength and electrical continuity. **2.** A physical connection between two lengths of magnetic tape, made in such a way as to cause minimal disturbance in reproduced audio, video, or data. **3.** To prepare a joint, as defined in **1** or **2**.

splicer A device for making a SPLICE.

splicing block A device specifically designed to facilitate easy splicing of audio, video, or digital magnetic tape.

splicing tape A durable, flexible adhesive designed to hold a magnetic-tape splice together.

spline-based modeling In video animation and advanced computer graphics, a scheme that uses curve-generating formulas (e.g., Bezier curves) to create lifelike images.

split-anode magnetron A magnetron in which the plate (anode) consists of two semicylinders with the cathode at their axis.

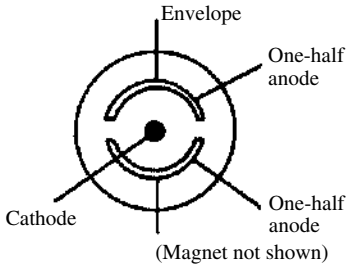

split-anode magnetron

split-load phase inverter See PARAPHASE INVERTER.

split-phase motor A fractional-horsepower, alternating-current motor that starts like a two-phase motor and runs like a single-phase motor. After the machine approaches approximately 75 percent of full speed, a centrifugal switch cuts out the starting winding.

split projector An acoustic transmission device with several independently operated transducers.

split-reed vibrator See SELF-RECTIFYING VIBRATOR.

split-rotor plate See SERRATED ROTOR PLATE.

split-stator capacitor A variable capacitor having two separate stator sections and a common rotor section.

split-sound receiver A television receiver circuit in which the sound signal is separated from the composite signal shortly after pickup by the antenna, and is amplified separately from the video signal. Compare INTERCARRIER RECEIVER.

splitter A device used to couple two or more television receivers to a single antenna.

spool See REEL.

sporadic-E layer ionization Occasional, scattered ionization in the E-layer of the ionosphere.

sporadic-E propagation At certain radio frequencies, the long-distance propagation of electromagnetic (EM) waves via the E layer of the ionosphere. This layer exists at an altitude of approximately 50 miles (80 km) above sea level. This mode of propagation tends to be intermittent, and conditions can change rapidly. It is most likely to occur between 20 MHz and 150 MHz. Occasionally, it is observed at frequencies as high as 200 MHz. The propagation range is normally several hundred miles, but occasionally can occur over distances of 1,000 to 1,500 miles. The standard frequency modulation (FM) broadcast band is sometimes affected by this propagation. The same is true of the lowest television (TV) broadcast channels, especially channels **2** and **3.** See IONOSPHERE.

SPOT Abbreviation of *satellite position and tracking.*

spot brightness In a cathode-ray tube, the relative brilliance of the glowing dot or trace produced on the screen by the electron beam.

spot check **1.** To take a random sample or to make a random test by arbitrarily selecting a single item from a run of similar items and subjecting it to analysis, examination, performance, or parametric evaluation, etc. **2.** A random sample or test.

spot frequency **1.** A single frequency or signal to which other frequencies can be referred. **2.** A frequency or signal that acts as a limit marker (e.g., to define the edges of an allocated frequency band).

spot jamming Deliberate interference to a radio signal at some frequency and at some specific time.

spot modulation In a cathode-ray tube, modulation of the brightness of the spot (and, accordingly, of the image) produced on the screen by the

5059F-pS-607-670 4/10/01 9:47 AM Page 650

electron beam. Also see INTENSITY MODULATION.

spot welding A method of electrical welding in which the parts to be joined are held together, overlapping, between the points of two electrodes, between which a current is passed to heat the parts at the spot of contact.

spot-wheel pattern A frequency-identifying wheel pattern produced on an oscilloscope screen by intensity-modulating a circular trace. The circular trace is produced by applying a standard-frequency signal to the horizontal and vertical input terminals 90 degrees out of phase. A square-wave signal of unknown frequency is applied to the intensity-modulation (*z*-axis) input terminals. The square wave chops the circle into a number of bright sectors or spots. The unknown frequency (*fx*) equals *Nfs*, where *N* is the number of spots in the circle, and *fs* is the standard frequency. Compare GEAR-WHEEL PATTERN.

sprat Acronym for *small portable radar torch.* A portable radar unit that uses a Gunn diode to generate microwave energy. The range is about 500 meters (⅓ mile).

spray coating **1.** Applying a protective coat of insulating material to a conductor or component by spraying it with a liquid substance and allowing it to dry. Compare DIP COATING. **2.** The coat applied, as defined in **1**.

spreader **1.** An insulator used to separate the wires of an air-spaced transmission line. **2.** Any of the rods composing the supporting structure in a cubical quad antenna.

spreading current In a semiconductor, current caused by the movement of charge carriers by circuitous routes, that is, in paths that deviate significantly from straight lines.

spreading loss Energy lost during the transmission of radiation.

spreading resistance In a semiconductor device, the resistance that is a consequence of electrical paths through material that is not along straight lines between electrodes.

spread spectrum **1.** A method of transmission in which the occupied bandwidth of the signal is deliberately increased, or spread out, over a much wider range than it would normally occupy with conventional modulation. **2.** A signal transmitted, as defined in **1**.

spring coil See SOLENOID, **1**.

spring contact See FLEXIBLE CONTACT.

sprite In video and animated computer graphics, a brief insert, such as a little insect that scurries across the screen, or a face that pops in and smiles. It is used primarily for effect.

SPST Abbreviation of SINGLE-POLE/SINGLE-THROW (switch or relay).

spurious emission From a radio or television transmitter, an unintended and unwanted output signal on a frequency other than the fundamental signal frequency. It can be generated by faulty modulation, amplification, and/or oscillation.

spurious oscillation **1.** Oscillation in a normally nonoscillatory circuit. **2.** In an oscillator, simultaneous oscillation at a frequency other than the normal one.

spurious response In a communications receiver, a signal that appears to be on a certain frequency, when, in fact, the received signal is not on that frequency. It often results from inadequate image rejection.

spurious-response ratio The ratio of the transmission (or gain) of a circuit of a desired signal to its transmission (or gain) for a spurious signal at the same setting of the circuit (e.g., *signal-to-image ratio*).

spurious sidebands In an amplitude-modulated (AM) or single-sideband (SSB) radio signal, sideband energy at frequencies outside the nominal signal band, usually resulting from improper modulation, inadequate filtering, improper envelope clipping, or nonlinear amplification.

Sputnik The first orbiting artificial earth satellite. It was launched by Russia (then known as the Union of Soviet Socialist Republics) in 1957.

sputter **1.** A layer of material obtained by sputtering (see SPUTTERING, **1**). **2.** To carry out the process of sputtering (see SPUTTERING, **1**).

sputtering **1.** A technique for electrically depositing a film of metal on a metallic or nonmetallic surface. In a vacuum chamber, the piece of metal to be deposited is made the cathode of a high-voltage circuit, with respect to a nearby anode plate. The high voltage causes atoms to be ejected from the surface of the cathode and strike the surface of an object placed in their path, becoming deposited on it as a film of cathode metal. Compare EVAPORATION, **1**. **2.** The disintegration of a vacuum-tube cathode through ejection of surface atoms from the cathode by impinging positive ions.

sq Abbreviation of SQUARE.

S_q band A section of the S BAND, from 2400 to 2600 MHz.

SQC Abbreviation of STATISTICAL QUALITY CONTROL.

SQR **1.** Abbreviation of SQUARE ROOTER. **2.** In the BASIC computer-programming language, a function that computes the square root of a positive number.

S quad See SIMPLE QUAD.

square-law demodulator See SQUARE-LAW DETECTOR.

square-law detector A detector whose output is proportional to the square of the root-mean-square (rms) value of the input. Also called WEAK-SIGNAL DETECTOR.

square-law meter **1.** A meter whose deflection is proportional to the square of the quantity applied to it. Also see CURRENT-SQUARED METER. **2.** A high-impedance electronic voltmeter, whose

5059F-pS-607-670 4/10/01 9:47 AM Page 651

deflection is proportional to the square of the applied voltage.

square-law modulator A circuit or device that accomplishes amplitude modulation of one signal current by another, by simultaneously passing the two currents through a component, such as a nonlinear resistor, having a square-law response.

square-law response Circuit or component operation that results in an output signal, proportional to the square of the input.

square rooter An analog or digital device used to extract the square root of a number.

square wave An alternating or pulsating current or voltage whose rise and decay times are essentially zero, and whose maxima and minima are essentially flat. The duration of the maxima is equal to the duration of the minima. A special form of RECTANGULAR WAVE.

square-wave amplifier An amplifier designed to operate with square waves.

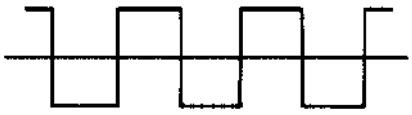

square wave

square-wave converter See SQUARING CIRCUIT.

square-wave generator A signal generator delivering an output signal that has a square waveform. Compare SQUARING CIRCUIT, **1**.

square-wave testing Testing the response of a circuit or device, such as an amplifier, by observing the extent to which it distorts a square-wave signal passing through it (a measure of high-frequency response).

squaring circuit **1.** A circuit (such as a twin-diode clipper, overdriven amplifier, or Schmitt trigger) that converts a sine wave or pulse into a square wave. **2.** A circuit whose instantaneous output-signal amplitude is equal to the square of the instantaneous input-signal amplitude.

squarish wave **1.** A signal whose oscilloscope trace is nearly, but not exactly, the same as that of a square wave. **2.** A rectangular wave that is not a square wave; that is, whose maxima and minima are not of the same duration. See RECTANGULAR WAVE and SQUARE WAVE.

squawker **1.** In a three-way speaker system, the midrange speaker. **2.** Any slave station in a multistation intercom network.

squeal A high-pitched interferential sound, such as that encountered in spuriously oscillating systems.

squeezeout In optical character recognition (OCR), a condition in which errors occur because the printed characters have excessive ink at the edges. Also called *smudge.*

squegging A choking-type cutoff action in a circuit caused by an excessively strong signal.

squegging oscillator An oscillator that starts and stops oscillating intermittently as a result of SQUEGGING.

squelch See SQUELCH CIRCUIT.

squelch amplifier An amplifier that can be controlled by a squelch signal. Also see SQUELCH CIRCUIT.

squelch circuit One of several circuits that automatically disable a receiver or amplifier, except when incoming signals exceed a predetermined threshold amplitude. This action mutes the equipment, eliminating annoying background noise and unwanted signals. Also called MUTING CIRCUIT.

squelch signal The activating or deactivating signal delivered by a SQUELCH CIRCUIT.

squiggle See BLIP, **2**.

squint **1.** The angular resolution of a radar antenna. **2.** The angular difference between the antenna axis and the major lobe of a radar transmitter.

squirrel-cage induction motor See SQUIRREL-CAGE MOTOR.

squirrel-cage motor An induction-type alternating-current motor using a squirrel-cage rotor.

squirrel-cage rotor In an alternating-current motor, a rotor composed of straight copper bars embedded in a laminated soft-iron core and short-circuited at the ends by rings. Its name is derived from its resemblance to a revolving squirrel cage.

squirter See SIGNAL INJECTOR.

SR **1.** Abbreviation of SILICON RECTIFIER. **2.** Abbreviation of *silicone rubber* (see SILICONE). **3**. Abbreviation of SHIFT REGISTER.

S-R Abbreviation of SEND-RECEIVE.

Sr Symbol for STRONTIUM.

sr Abbreviation of STERADIAN.

SRAM Abbreviation of *static random-access memory.*

S-rays See SECONDARY RAYS.

SRF Abbreviation of SELF-RESONANT FREQUENCY.

S-RF meter A dual-function meter in a radio transceiver. In the receiving mode, the meter indicates S units. In the transmit mode, the meter indicates relative output power.

SRR Abbreviation of SHORT-RANGE RADAR.

SS **1.** Abbreviation of SOLID STATE. **2.** Abbreviation of SINGLE SHOT. **3.** Abbreviation of *small signal.* **4.** Abbreviation of SINGLE SIGNAL. **5.** Abbreviation of *same size.* **6.** Abbreviation of *stainless steel.*

SSB Abbreviation of SINGLE SIDEBAND.

S_S band A section of the S BAND extending from 2900 to 3100 MHz.

SSBSC Abbreviation of SINGLE-SIDEBAND SUPPRESSED CARRIER.

ssc Abbreviation of *single-silk-covered* (wire).

5059F-pS-607-670 4/10/01 9:47 AM Page 652

S scale A scale of numbers used in radio communications, and especially in amateur radio, to report the approximate strength of signals: S1, faint signals; S2, very weak signals; S3, weak signals; S4, fair signals; S5, fairly good signals; S6, good signals; S7, moderately strong signals; S8, strong signals; S9, extremely strong signals. Also see S METER.

sse Abbreviation of *single-silk-enameled* (wire).

SSI Abbreviation of SMALL-SCALE INTEGRATION.

SSL Abbreviation of SOLID-STATE LAMP.

SSSC Abbreviation of SINGLE-SIDEBAND SUPPRESSED CARRIER. (Also, SSBSC.)

ST Abbreviation of SINGLE THROW.

sta **1.** Abbreviation of STATION. (Also *stn.*) **2.** Abbreviation of STATIONARY.

stab Abbreviated form of stabilizer (see STABILIZER, 4).

stability **1.** The condition in which an equipment or device is able to maintain a particular mode of operation without deviation. **2.** The condition in which the setting or adjustment of a device remains at a particular point without movement. **3.** The condition in which a quantity remains constant, with respect to time, temperature, or another variable. **4.** The ability of inks used in optical character recognition to retain their color after exposure to light or heat.

stability factor Abbreviation, SF. For a bipolar transistor, the derivative dI_c/dI_{co}, where I_c is the steady-state collector current and I_{co} is the collector cutoff current.

stabilized platform See STABLE PLATFORM.

stabilizer **1.** See DAMPING DIODE. **2.** See DAMPING RESISTOR. **3.** A device or circuit for the self-regulation of current or voltage. **4.** A chemical used to control or arrest a reaction.

stabilizing windings Auxiliary field windings used to prevent speed runaway in shunt motors.

Stabistor Trade name for a type of voltage-regulating semiconductor diode.

stable device A device whose characteristics and performance remain substantially unchanged with time or variations in temperature, applied power, or other quantities.

stable element **1.** A component that maintains its value or ratings, despite widely variable environmental conditions. **2.** A navigational instrument that maintains its orientation at all times.

stable platform A gyro-type device used to stabilize objects in space, and to provide accurate information regarding attitude (pitch, roll, and yaw).

stable state A stable condition, such as the high and low states of a flip-flop. The flip-flop has two stable states and will remain in one until it is switched to the other, whereupon it will then remain in that latter state until switched back to the former. Compare UNSTABLE STATE.

stack **1.** A piled assembly of capacitor plates and separating dielectric films. **2.** An assembly of selenium rectifier plates (see POWER STACK). **3.** To assemble a stacked array. **4.** A temporary storage area consisting of a small group of registers in a computer memory.

stacked array An antenna system in which two or more identical antennas, such as dipoles, Yagis, or halos, are placed one above the other or side-by-side. It provides additional forward gain, and, in some cases, enhances the front-to-back ratio and/or front-to-side ratio.

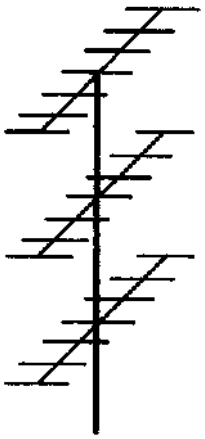

stacked array

stacked-dipole antenna A stacked array of half-wave dipole antennas.

stacking The combination of two or more identical antennas, such as dipoles, Yagis, or halos, in a STACKED ARRAY to provide enhanced forward gain. It can also enhance the front-to-back ratio and/or front-to-side ratio. Stacking can be done vertically or horizontally.

stack pointer Abbreviation, SP. A register indicating the last data item to be entered in a stack (see STACK, 4).

stage A complete functional unit of a system (e.g., *amplifier stage*, *oscillator stage*, *modulator stage*, etc.).

stage-by-stage elimination See SIGNAL INJECTION.

stage gain The amplification provided by a single stage in a system.

stage loss The loss introduced by a single stage in a system.

stagger **1.** An error in facsimile reception, occurring as a constant discrepancy in the position of the received dot. **2.** To deliberately tune a set of resonant circuits, especially in a bandpass filter, to one side or the other of the center frequency.

staggered tuning The tuning of the input and output circuits of a single stage, or the tuning of

5059F-pS-607-670 4/10/01 9:47 AM Page 653

successive stages to slightly different frequencies to obtain flat-top response.

stagger tuning See STAGGERED TUNING.

stagger-wound coil See BASKET-WEAVE COIL and SPIDERWEB COIL.

staircase circuit See STAIR-STEP CIRCUIT.

staircase generator A circuit or device for generating a STAIR-STEP WAVE.

staircase wave See STAIR-STEP WAVE.

stair-step circuit A circuit that converts a series of equal-amplitude pulses into a stair-step wave.

stair-step wave A nonsinusoidal wave characterized by a multistep rise and a steep fall. It is so called from its resemblance to the cross section of a staircase.

stair-step wave

stall torque The torque produced when a motor shaft is prevented from turning.

stalo Acronym for *stabilized oscillator.*

stand-alone photovoltaic system A solar-power plant that uses large banks of rechargeable electrochemical batteries, such as the lead–acid type, to store electric energy as it is supplied by photovoltaics during hours of bright sunshine. The energy is released by the batteries at night or in gloomy daytime weather. This system does not depend on the electric utility companies. Although this scheme offers independence from the utility companies, a blackout will occur if the system goes down. Compare INTERACTIVE PHOTOVOLTAIC SYSTEM.

standard **1.** A precise specification governing the dimensions and characteristics of a device or system (e.g., *military standard*). **2.** A highly accurate physical or electrical quantity to which similar quantities can be compared (e.g., *standard frequency*). **3.** The device or system that produces a standard quantity as defined in **2** (e.g., *frequency standard*). **4.** Having conventional and widely accepted characteristics.

standard atmosphere Abbreviation, atm. Air pressure at sea level (1.013 Pascals, or about 14.7 pounds per square inch). Also called ATMOSPHERE.

standard broadcast band Any of numerous frequency bands allocated to conventional broadcast stations. In the United States, the amplitude-modulation (AM) radio broadcast band extends from 535 to 1705 kHz, and the frequency-modulation (FM) radio broadcast band extends from 88 to 108 MHz. The television (TV) broadcast bands range from 54 MHz to 806 MHz in several sections, designated in channels from 2 through 69. Also see BROADCAST SERVICE, **1**.

standard candle See CANDELA.

standard cell A highly refined primary cell used to supply a precise direct-current voltage for electronic measurements. The *Weston standard cell* contains a mercury positive electrode, cadmium amalgam negative electrode, and cadmium sulfate electrolyte, and delivers 1.0183 volts at 20 degrees Celsius. Also see ZINC STANDARD CELL.

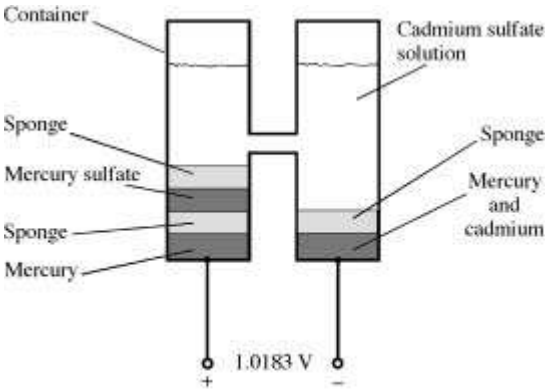

standard cell

standard deviation In statistical analysis, the square root of the mean of squares of deviation from the mean.

standard frequency A highly precise frequency to which other frequencies can be compared for identification or measurement.

standard-frequency oscillator A stable, precise oscillator that delivers a standard frequency. Also see PRIMARY FREQUENCY STANDARD and SECONDARY FREQUENCY STANDARD.

standard-frequency signal A calibration and reference signal that is broadcast on a standard frequency, such as those transmitted on 2.5, 5, 10, and 15 MHz by the National Bureau of Standards.

standard pitch The tone corresponding to the frequency 440 Hz (in music, the note A above middle C).

standard signal generator A (usually continuously variable) high-grade generator of modulated and unmodulated radio-frequency test signals. A general-purpose instrument of this type usually covers a wide range (e.g., 15 kHz to 100 MHz) in several tuning bands. For calibration, a standard signal generator is referred to a primary frequency standard or secondary frequency standard.

5059F-pS-607-670 4/10/01 9:47 AM Page 654

standard subroutine A usually vendor-supplied computer program segment applicable to more than one program and used as needed as a subroutine.

standard temperature and pressure The condition where the temperature is zero degrees Celsius and the pressure is one atmosphere. Abbreviated STP.

standard time Official civil time in a particular region. See TIME ZONE.

standby **1.** The state in which equipment is out of operation, but can be immediately activated. Also called IDLING. **2.** A state of readiness on the part of personnel, equipment, or systems.

standby battery An emergency power source for a battery-powered installation.

standby current The CURRENT DRAIN of a circuit, device, or system when in the standby condition.

standby equipment See EMERGENCY EQUIPMENT.

standby operation Keep-alive operation during a standby interval (see STANDBY).

standby power The power drawn by an equipment connected to the power supply, but out of operation.

standby power supply A circuit containing a battery, an automatic switch, and sometimes a power inverter. When utility power fails, the switch actuates the supply, and the battery supplies power to essential devices or systems. Similar to an UNINTERRUPTIBLE POWER SUPPLY.

standing wave A stationary distribution of current or voltage along a line because of the interactions between a wave transmitted down the line and a wave reflected back; it is characterized by maximum-amplitude points (loops) and minimum-amplitude or zero points (nodes).

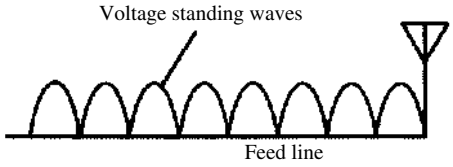

standing wave

standing-wave distortion Distortion of current or voltage caused by standing waves on a transmission line terminated in an impedance that contains reactance, and/or that differs from the characteristic impedance of the line.

standing-wave indicator **1.** A device, such as a lamp or meter, used to detect standing waves. **2.** Standing-wave meter (see SWR BRIDGE).

standing-wave loss The additional loss, over the matched-line loss, that occurs in a transmission line when the standing-wave ratio (SWR) is not 1.

standing-wave meter See SWR BRIDGE.

standing-wave ratio Abbreviation, SWR. **1.** The ratio between the maximum and minimum voltage along a transmission line. This quantity is sometimes specifically called *voltage standing-wave ratio (VSWR).* **2.** The ratio between the maximum and minimum current along a transmission line. **3.** The ratio of load impedance to feed-line characteristic impedance or vice versa, whichever is greater than or equal to 1. Ideally, the SWR is equal to 1 or 1:1, representing a load impedance that is purely resistive and has the same value as the characteristic impedance of the feed line. A high standing-wave ratio causes increased loss in the line and can also result in excessive conductor heating or dielectric breakdown.

standoff insulator An insulator (usually of the post type) that is used to hold a wire or component away from a chassis or base.

star **1.** In a gravity-battery cell, the copper electrode. The name is derived from its star shape. **2.** A star-shaped circuit of three-phase components. Also see WYE CONNECTION.

star connection See WYE CONNECTION.

Stark effect The influence of a strong transverse electric field on the spectrum lines of a gas.

starlight scope A device capable of viewing in apparent total darkness. Its operation depends on its ability to provide high amplification of extremely low light levels, such as that of objects reflecting the light from a moonless, but starlit, sky.

star rectifier See WYE RECTIFIER.

starter **1.** An ignitor electrode in an ignitron (see IGNITOR). **2.** See STARTING BOX.

starting box A special rheostat for starting a motor gradually in steps. The device is provided with an electromagnet for holding the arm in the maximum-speed position and releasing it when power is interrupted.

starting rod An ignitor electrode in an ignitron (see IGNITOR).

starting voltage **1.** For a gas tube, the minimum voltage that will initiate the glow discharge. **2.** In appropriate solid-state devices (e.g., a diac), the voltage at which conduction between electrodes occurs.

start lead The lead attached to the first turn of a coil. Also called *inside lead.* Compare FINISH LEAD.

start/stop multivibrator See MONOSTABLE MULTIVIBRATOR.

stat- A prefix denoting ELECTROSTATIC.

statampere The cgs electrostatic unit of current; 1 statampere = 3.335640×10^{-10} ampere.

statcoulomb The cgs electrostatic unit of charge; 1 statcoulomb = 3.335640×10^{-10} coulomb.

state **1.** The present condition (i.e., on or off, true or false, 1 or 0, high or low) of a bistable device, such as a flip-flop. **2.** The physical or electrial condition or status of a component, device, circuit, or system.

5059F-pS-607-670 4/10/01 9:47 AM Page 655

statement The contents of a line in a source-language computer program.

state of charge The amount of charge, measured in coulombs or ampere hours, in a storage cell or battery at a given time. A measure of the available remaining energy in the cell or battery.

statfarad The cgs electrostatic unit of capacitance; 1 statfarad = 1.112650×10^{-12} farad.

stathenry The cgs electrostatic unit of inductance; 1 stathenry = 8.987554×10^{11} henry.

static **1.** Pertaining to that which is constant in quantity (e.g., *static collector current* of a transistor). **2.** Pertaining to that which is at rest (e.g., *static electricity*). **3.** The radio noise (sferics) produced by electric discharges in the atmosphere, usually lightning. **4.** Pertaining to a test-and-measurement mode for a unit or device, without subjecting the unit or device to regular operation. Compare DYNAMIC.

static base current See DC BASE CURRENT.

static base resistance See DC BASE RESISTANCE.

static base voltage See DC BASE VOLTAGE.

static cathode current See DC CATHODE CURRENT.

static cathode resistance See DC CATHODE RESISTANCE.

static cathode voltage See DC CATHODE VOLTAGE.

static characteristic An operating characteristic determined from constant, rather than alternating or fluctuating, values of independent and dependent variables. Examples: the direct-current (dc) characteristics of diodes, transistors, and integrated circuits. Compare DYNAMIC CHARACTERISTIC.

static charge Energy stored in a stationary electric field; electricity at rest.

static collector A device that grounds the rotating wheels of a motor vehicle, thereby removing the static electricity generated by the friction of the tires on the roadway.

static collector current See DC COLLECTOR CURRENT.

static collector resistance See DC COLLECTOR RESISTANCE.

static collector voltage See DC COLLECTOR VOLTAGE.

static convergence In a color-television picture tube, the convergence of the three undeflected electron beams at the center of the aperture mask.

static device A device with no moving parts.

static discharge resistor A fixed resistor connected between the earth and the high side of the power line in a television receiver to drain off atmospheric electric charge.

static drain current See DC DRAIN CURRENT.

static drain resistance See DC DRAIN RESISTANCE.

static drain voltage See DC DRAIN VOLTAGE.

static dump In computer operations, a dump occurring at a predetermined point in a program run or at the end of the run.

static electricity Energy in the form of a stationary electric charge, such as that stored in capacitors or produced by friction or induction.

static emitter current See DC EMITTER CURRENT.

static emitter resistance See DC EMITTER RESISTANCE.

static emitter voltage See DC EMITTER VOLTAGE.

static flip-flop A flip-flop (see BISTABLE MULTIVIBRATOR) using direct-current operating voltages. A single pulse switches the unit from on to off, and vice versa. Compare DYNAMIC FLIP-FLOP.

static forward current transfer ratio Symbol, H_{FE}. An expression of gain in a bipolar transistor. It can range from a factor of just a few times up to hundreds of times. Mathematically,

$$H_{FE} = I_C / I_B$$

where I_C is the collector current and I_B is the base current. The H_{FE} rating is important because it gives engineers an indication of the greatest current amplification that can be obtained with a particular transistor.

static frequency multiplier A magnetic-core device, similar to a magnetic amplifier or peaking transformer, that provides harmonics by distorting a sine-wave signal.

static gate current See DC GATE CURRENT.

static gate resistance See DC GATE RESISTANCE.

static gate voltage See DC GATE VOLTAGE.

static grid current See DC GRID CURRENT.

static grid voltage See DC GRID VOLTAGE.

static hysteresis The condition in which the magnetization of a material (when it has the same intensity as the magnetizing force) is different when the force is increasing than when the force is decreasing, regardless of the time lag. Compare VISCOUS HYSTERESIS.

static induction See ELECTROSTATIC INDUCTION.

static machine See ELECTROSTATIC GENERATOR.

static memory Also called *nonvolatile memory*. In a computer, a data memory medium (such as programmable read-only memory, or PROM) in which information is stored until it is altered or erased. It does not require a source of power to maintain the integrity of the data. Compare VOLATILE MEMORY.

static mutual conductance See STATIC TRANSCONDUCTANCE.

static plate current See DC PLATE CURRENT.

static plate resistance See DC PLATE RESISTANCE.

static plate voltage See DC PLATE VOLTAGE.

statics The study of forces, bodies, poles, charges, or fields at rest or in equilibrium. Compare DYNAMICS.

5059F-pS-607-670 4/10/01 9:47 AM Page 656

static skew In magnetic tape recording or playback, the amount of lead or lag time of one track, with respect to another. Ideally, the static skew should be zero or practically zero.

static source current See DC SOURCE CURRENT.

static source resistance See DC SOURCE RESISTANCE.

static source voltage See DC SOURCE VOLTAGE.

static storage Also called *nonvolatile storage.* In a computer, a data storage medium (such as magnetic or optical disk) in which information is stored until it is altered or erased. It does not require a source of power to maintain the integrity of the data. Virtually all data storage media are of this type, as contrasted with memory, which is often volatile (see STATIC MEMORY and VOLATILE MEMORY).

static stability The ability of a robot to maintain its balance while standing still. A robot with two legs is generally poor in this respect. This is one of the reasons why humanoid robots (androids) are difficult to engineer. A minimum of three legs is necessary for good static stability.

static subroutine In computer programming, a subroutine that always serves the same purpose [i.e., it does not need to be tailored (according to parameters) for a specific application].

station **1.** An installation consisting of a transmitter, receiver, or both. **2.** A test-equipment installation or position. **3.** A computer installation including peripherals.

stationary battery A (usually wet storage) battery not normally moved when in use.

stationary state A particular energy state for an atom represented by its electrons being in shells at specific energy levels.

stationary wave See STANDING WAVE.

station authorization The legal privilege assigned to a broadcast or communications station, allowing that station to be used for the purpose of transmitting electromagnetic signals.

station license See STATION AUTHORIZATION.

statistical quality control Quality control based upon the techniques of probability and statistics in analyzing findings, making predictions, and formulating procedures for sampling.

statmho The cgs electrostatic unit of direct-current conductance; 1 statmho = 1.112650×10^{-12} siemens.

statoersted The cgs electrostatic unit of magnetizing force; 1 statoersted = 265.458 A/m (3.33585×10^{-11} oersted).

statohm The cgs electrostatic unit of direct-current resistance; 1 statohm = 8.987554×10^{11} ohm.

stator **1.** A stationary coil. Compare ROTOR, **1**. **2.** The stationary member of a motor or generator. Compare ROTOR, **2**. **3.** The stationary-plate section of a variable capacitor. Compare ROTOR, **3**.

stator coil A stationary coil (see STATOR, **1**, **2**).

stator plate(s) The stationary plate(s) of a variable capacitor. Compare ROTOR PLATE.

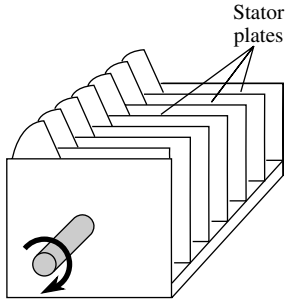

stator plate

stator section See STATOR, **3**.

statoscope An aircraft altimeter that shows small changes in altitude.

statvolt The cgs electrostatic unit of electromotive force; 1 statvolt = 299.7925 volts.

statweber The cgs electrostatic unit of magnetic flux; 1 statweber = 299.7925 webers (2.997925×10^{10} maxwells).

S_T band A section of the S BAND, extending from 1850 to 2000 MHz.

std Abbreviation of STANDARD.

steady-state component A quantity whose value remains constant during normal operation of a circuit or device, as opposed to an alternating, fluctuating, or transient component.

steerable antenna A directional antenna having a rotatable major lobe.

steering diode See DIRECTIONAL DIODE.

Stefan-Boltzmann constant Value, 5.67051×10^{-8} $Wm^{-2}K^{-4}$.

Stefan-Boltzmann law The thermal-radiation law that shows the total emissive power of a blackbody to be proportional to the fourth power of the absolute temperature of the body.

stenode See CRYSTAL FILTER.

step **1.** A computer program instruction. **2.** A single action in the operation, maintenance, or troubleshooting of equipment. **3.** A specific increment in a quantity (such as frequency, voltage, current, etc.). **4.** A sharp or rapid change in the value of a quantity.

step-by-step operation See STEPTHROUGH OPERATION.

step change A single-increment change in a value.

step circuit A circuit that produces a step (sharp change of slope) in the response curve of an amplifier.

step counter **1.** A stair-step circuit arranged to count input pulses. The output capacitor of the circuit discharges when a predetermined number of input pulses has raised the capacitor voltage to the level required to trigger a counter. **2.** In a computer or calculator, a circuit or device that counts the steps in an operation (such as division, multiplication, or shifting) called for by an instruction.

5059F-pS-607-670 4/10/01 9:47 AM Page 657

step-down ratio In a circuit or device, such as a step-down transformer or cathode follower, the ratio of the low output voltage to the high input voltage. Compare STEP-UP RATIO.

step-down transformer A transformer delivering an output voltage that is lower than the input voltage. In such a transformer, the secondary (output) winding contains fewer turns than the primary (input) winding. Compare STEP-UP TRANSFORMER.

step function See UNIT FUNCTION.

step generator **1.** A signal generator that delivers a step function (see UNIT FUNCTION). **2.** A circuit or device that generates a STAIR-STEP WAVE.

stepped leader The probing flow of electrons through the atmosphere preceding a lightning stroke. Once the path has been established, the discharge takes occurs along the ionized path determined by the stepped leader. It is so called because the electrons move in hesitations, jumping several meters with each advance or step.

stepper motor A motor in which the shaft advances in uniform angular steps, instead of rotating continuously. These motors are extensively used in robotic devices. When such a motor is stopped and its coils are carrying current, the shaft resists turning.

stepping relay See STEPPING SWITCH.

stepping switch A multiposition rotary switch in which an electromechanical ratchet mechanism advances to the next contact position each time that a pulse of current is received.

step-through operation A way of operating a computer, usually during a debugging operation, in which program instructions are executed one at a time by direction of the user. Also called *single-step operation* and *step-by-step operation.*

step-up ratio In a circuit or device, such as a step-up transformer or voltage amplifier, the ratio of the high output voltage to the low input voltage. Compare STEP-DOWN RATIO.

step-up transformer A transformer delivering an output voltage that is higher than the input voltage. In such a transformer, the secondary (output) winding contains more turns than the primary (input) winding. Compare STEP-DOWN TRANSFORMER.

steradian A unit of solid-angle measure. A cone-shaped solid angle that has a vertex at the center of a sphere (of radius r), that cuts off a portion of the sphere's surface whose outer perimeter is a circle, and that has an area (as measured on the sphere's surface) of r^2. Also see SOLID ANGLE.

Sterba array See BARRAGE ARRAY.

Sterba curtain See BARRAGE ARRAY.

stereo **1.** Contraction of STEREOPHONIC. **2.** General term for a two-channel high-fidelity audio reproduction system.

stereo-adaptable Pertaining to a television receiver or videocassette recorder (VCR) that requires a special circuit to obtain stereo sound from Multichannel Television Sound signals. Compare STEREO-READY.

stereo amplifier A two-channel amplifier for binaural reproduction (see BINAURAL).

stereophonic Pertaining to equipment or techniques for producing a (somewhat) three-dimensional perspective of sound reproduction.

stereophonic sound system See STEREO SYSTEM.

stereo-irrelevant Pertaining to sound components in a stereo system that are of equal magnitude in both (or all) channels. Thus, these components sound the same whether the system is reproducing stereophonic sound or monaural sound.

stereo phono cartridge A phono cartridge capable of reproducing sound from stereo discs.

stereo-ready Pertaining to a television receiver or videocassette recorder (VCR) that can deliver stereo sound from Multichannel Television Sound signals without the need for a decoding circuit. Compare STEREO-ADAPTABLE.

stereo recording A method of recording in which two independent sound channels are transferred to some medium simultaneously, with the intention that the two channels be reproduced at the same time.

stereoscopic television Television in which the reproduced image appears three-dimensional.

stereo system A multichannel, high-fidelity sound reproduction system including an amplifier and various other components, such as a radio receiver, compact-disc (CD) player, tape player, turntable, and speakers.

stereotape Magnetic tape bearing more than one channel (usually two channels) for the recording and reproduction of stereophonic sound.

sterilizer Any electronic device, such as an ultraviolet generator, used to kill germs.

stethoscope An electronic or nonelectronic instrument used by physicians to listen to the heartbeat and other body sounds, and by technicians to listen to mechanical sounds.

still **1.** A stationary picture on television. **2.** A picture transmitted or received by means of facsimile. **3.** A print on photographic paper of a negative.

still television See FACSIMILE.

stinger A brief, loud sound burst, such as a musical chord, sometimes used for effect in recorded audio or audio-visual presentations.

stn Abbreviation of STATION. (Also, sta.)

STO Abbreviation of STORAGE FUNCTION.

stochastic The condition in which, at any instant, a given variable can assume a state dependent on previous states, as well as chance elements (e.g., words uttered extemporaneously by a speaker are random in that they cannot be predicted), while also being dependent, by the application of grammar, on previously spoken words (i.e., previous states).

stop amplifier See REJECT AMPLIFIER.

5059F-pS-607-670 4/10/01 9:47 AM Page 658

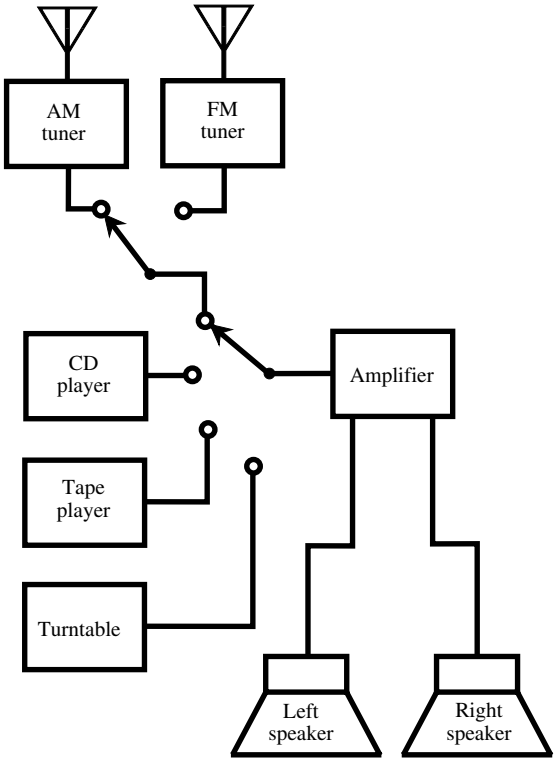

stereo system

stopband The continuous spectrum of frequencies rejected by a filter, selective amplifier, or other band-suppression device.

stopband ripple Single or multiple attenuation peaks within the stopband of an elliptic filter, where the frequency of the attenuation peak(s) is/are associated with the resonant circuit(s) in the filter.

stop code See HALT INSTRUCTION.

stop element In digital transmission, a bit or set of bits indicating the end of a character, and serving to inform the receiving device of the end of the character.

stop filter See BAND-SUPPRESSION FILTER.

stopper resistor See STOPPING RESISTOR.

stopping capacitor See BLOCKING CAPACITOR.

stopping coil See CHOKE COIL.

stopping resistor A parasitic-suppressing resistor, usually inserted in series with the input and/or output of a power amplifying device. Also called *stopper resistor.*

storage **1.** In computer operations, a medium on which data can be kept for an extended period of time. Examples: magnetic disk, magnetic tape, optical disk. **2.** The transferring of data from memory to a more permanent medium. Compare MEMORY. **3.** The retention of data of any kind, such as an oscilloscope image or video display, for use at a later time. **4.** The retention of electric energy or charge, as in a capacitor or electrochemical cell. **5.** The retention of energy in the form of a magnetic field, as in an inductor. **6.** The retention of potential energy in any form.

storage allocation The assignment of computer memory areas to certain kinds of information, as outlined in a source program and implemented by a compiler.

storage battery A rechargeable battery; the technical term is *secondary battery.* Also see STORAGE CELL.

storage capacity **1.** The amount of data that can be stored in a specific medium, such as a hard disk, diskette, or tape. Generally measured in bytes, kilobytes, megabytes, gigabytes, or terabytes. **2.** The energy-delivering capability of a storage battery in terms of ampere-hours, milliampere-hours, or other current-time units for a specific rated voltage.

storage cell **1.** An electrochemical cell whose potential can be restored by charging it with electricity. Compare PRIMARY CELL. Also see CELL. **2.** The smallest part of a computer storage medium. **3.** In computer data storage, the part that can hold a data unit (e.g., a bit).

storage CRT See STORAGE TUBE.

storage cycle In computer operation, the period during which a location of a cyclic storage device cannot be accessed.

storage density The number of data units (e.g., bytes, kilobytes, or megabytes) that can be stored in a given length or area of a storage medium.

storage device A medium into which data can be placed and kept for later use. Examples: magnetic disk, magneto-optical disk, optical disk, and magnetic tape.

storage dump See DUMP.

storage function Abbreviation, STO. The so-called "memory" function of a microcomputer chip. It causes data to be inserted into memory or storage for later use. It is commonly used in programmable calculators, automatic-dialing telephones, and radio receivers. Also called *memory function.*

storage laser A laser that stores intense energy before flashing.

storage life See SHELF LIFE.

storage mesh In the cathode-ray tube (CRT) of a storage oscilloscope, a fine metal mesh electrode that serves as the target on which the image is electrostatically stored. Also see STORAGE TUBE.

storage oscilloscope An oscilloscope that retains a displayed image until the display is erased. Also see STORAGE TUBE.

storage register In computers and calculators, a storage unit composed of flip-flops. In computers, it is independent of the central processing unit (CPU).

5059F-pS-607-670 4/10/01 9:47 AM Page 659

storage temperature **1.** The recommended temperature for storing specified electronic components. **2.** The particular temperature at which electronic components have been stored.

storage time **1.** The interval during which carriers remain in a semiconductor-junction device after the bias has been removed. Also see DIODE RECOVERY TIME. **2.** For a switching semiconductor device, the time required for the amplitude of the output pulse to fall from maximum to 90% of maximum after the input pulse has fallen to zero. **3.** In a computer, the time required for data to be transferred from random-access memory (RAM) to nonvolatile storage (e.g., hard disk).

storage tube A cathode-ray tube that retains information in the form of images on a special electrode until erased by a signal.

store **1.** To place data in a nonvolatile medium (such as a hard disk, diskette, optical disk, magnetic tape, etc.). **2.** To place in the memory of a calculator or computer. **3.** In computing, a command that causes data to be placed in a nonvolatile medium. In some applications, this is called *save.* **4.** A nonvolatile medium on which data has been placed for future use or for archival purposes.

stored base charge The carriers that remain in the base layer of a bipolar transistor immediately after the forward bias has been interrupted. This charge maintains collector current momentarily.

stored-energy welding A method of electric welding in which electrical energy is stored slowly, then released at the rate required for the welding.

STP See STANDARD TEMPERATURE AND PRESSURE.

straight adapter An inline coaxial fitting for joining two fixture-terminated coaxial lines in series.

straight angle An angle measuring 180 degrees.

straight dipole A (usually center-fed) dipole antenna having only one radiator. Also see DIPOLE ANTENNA.

straightforward Pertaining to data transmission in one direction only.

straight-gun CRT A cathode-ray tube (CRT) in which the electron gun projects the beam in a straight line through the deflecting elements to the screen. Compare BENT-GUN CRT.

straight-line capacitance Abbreviation, SLC. Pertaining to a variable capacitor for which the setting-vs.-capacitance curve is a straight line; the capacitance variation is linear. Compare STRAIGHT-LINE FREQUENCY and STRAIGHT-LINE WAVELENGTH.

straight-line coding See STRAIGHT-LINE PROGRAMMING.

straight-line frequency Abbreviation, SLF. Pertaining to a variable capacitor in a tuned circuit for which the setting-vs.-frequency curve is a straight line; the frequency variation is linear. Compare STRAIGHT-LINE CAPACITANCE and STRAIGHT-LINE WAVELENGTH.

straight-line programming During the writing of a computer program, avoiding the creation of loops by repeating a series of instructions to reduce execution time.

straight-line tracking In a phonograph turntable, linear lateral stylus movement (as opposed to motion along an arc) as the disc is played. This ensures that the stylus is always at the optimum angle in the disc groove. The result is improved sound reproduction, and longer disc and stylus life because of minimal friction between the stylus and groove.

straight-line wavelength Abbreviation, SLW. Pertaining to a variable capacitor in a tuned circuit for which the setting-vs.-wavelength curve is a straight line; the wavelength variation is linear. Compare STRAIGHTLINE CAPACITANCE and STRAIGHT-LINE FREQUENCY.

straight-through amplifier An amplifier in which the input and output circuits are tuned to the same frequency. Compare MULTIPLIER AMPLIFIER.

strain A force that compresses or squeezes a body. Compare TENSION, **1**.

strain gauge See ELECTRIC STRAIN GAUGE.

strain-gauge bridge A four-arm resistance bridge in which an ELECTRIC STRAIN GAUGE forms one arm. The resistance of the gauge changes because of strain. The amount of strain can be determined by balancing the bridge.

strain-gauge transducer A transducer, other than a strain sensor, that uses strain gauges to convert values of pressure into their electrical analogs (e.g., *pressure transducer* and *strain-gauge phonograph pickup*).

strain pickup A phonograph pickup using a strain gauge to convert sound vibrations into a varying electric current.

strand A single solid conductor in a STRANDED WIRE.

stranded wire A conductor composed of several non-insulated wires twisted together to provide mechanical flexibility. Compare SOLID WIRE.

stratosphere The portion of earth's upper atmosphere beginning at a height of approximately 10 miles and extending to the ionosphere.

stray capacitance Inherent capacitance in a place where it can be detrimental, such as that between the turns of a coil or between adjacent areas in a circuit. Also see STRAY COMPONENT.

stray component An electrical property that exists as an inherent, and usually undesirable, side effect in a circuit or device. Thus, for example, STRAY CAPACITANCE unavoidably exists between parallel conductors, and STRAY INDUCTANCE is present in all wiring.

stray field The portion of an electric or magnetic field that extends beyond the immediate vicinity of the circuit with which it is associated, and which is, therefore, capable of interfering with other circuits or devices.

5059F-pS-607-670 4/10/01 9:47 AM Page 660

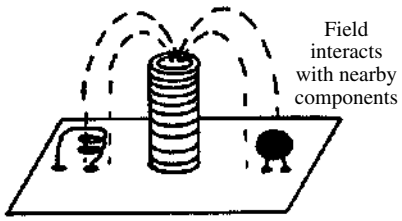

stray field

stray inductance Inherent inductance in a place where it can be detrimental (e.g., inductance in the coil of a wirewound resistor). Also see STRAY COMPONENT.

stray resistance Inherent resistance in a place where it can be detrimental, such as leakage resistance in a dielectric, and wire resistance in an inductor.

streaking In television or facsimile, a form of distortion in which the image appears enlarged in the horizontal, but not the vertical.

stress **1.** See STRAIN. **2.** See TENSION, **1**. **3.** The force per unit area that produces STRAIN or TENSION on a body.

stretch The amount by which a material being measured with an electronic device increases in surface dimensions. Compare SHRINK.

stretched string A long, thin wire or string that vibrates at a certain frequency, causing standing waves. It generally exhibits a specific fundamental frequency and integral harmonics of this frequency. As the wavelength is cut in half, the frequency doubles.

strike To initiate a discharge, as in striking a gas tube.

striking voltage See STARTING VOLTAGE.

string **1.** In computer operations, a set of items in a sequence determined by the order of keys. **2.** In a computer memory, a sequence of bits or characters. **3.** Any group of series-connected components or circuits.

string electrometer See BIFILAR ELECTROMETER.

string variable A string of characters, usually forming a word or phrase, represented by a variable name and character string symbol (BASIC's $, for example) in a computer program.

strip chart A longitudinal, as opposed to circular, chart for graphic recording. In a rectilinear chart, both coordinates are straight; in a curvilinear chart, the crosswise coordinates are arcs.

strip core A ferromagnetic core material made from a strip of the substance. The method of manufacture results in superior ferromagnetic qualities, but also imparts a polarization to the material.

strip fuse A fuse in which the fusible element is a flat strip of low-melting-point metal. Compare WIRE FUSE.

strobe **1.** See ELECTRONIC FLASH, **1**. **2.** See STROBOSCOPE.

strobe light **1.** See ELECTRONIC FLASH, **1**. **2.** See STROBOSCOPE.

Strobolume Trade name for a type of high-output stroboscope.

stroboscope **1.** An instrument that emits bright, adjustable-rate flashes of light. When this light illuminates an object that is rotating or vibrating at a fixed period, and the flash rate is made to match that period, the object seems to stand still and can be examined for flaws or faulty operation (and its speed can be measured). **2.** A rotatable, slotted disk for producing the effect defined in **1**.

stroboscopic disk A rotatable disk with alternating white and black radial regions, used in conjunction with a strobe light for precise measurement of the speed of a phonograph turntable.

strobotron A gas tetrode tube used as the flashing light source in a stroboscope.

stroke speed See SCANNING FREQUENCY.

strong coupling See CLOSE COUPLING.

strontium Symbol, Sr. A metallic element of the alkaline-earth group. Atomic number, 38. Atomic weight, 87.62. It is used in some ceramic dielectrics, such as *barium-strontium titanate.*

Strowger exchange A telephone system incorporating Strowger switches.

Strowger switch A switch with one input and 100 individually selectable outputs. It is used with telephone switching networks. The telephone dial code causes a contact to move vertically and horizontally in such a way that a particular output is connected to the input. Each output has a unique dial code and each dial code has a unique output.

structured programming Computer programming using a limited number of procedural sets, while minimizing branches to make the program as forward-going as possible. This allows it to be easily modified or debugged.

STS switch See SPACE-TIME-SPACE SWITCH.

stub A (usually short) section of transmission line that is patched onto a longer line for tuning or impedance matching.

Stubs gauge See BIRMINGHAM WIRE GAUGE.

stub tuner A tuning unit consisting of a stub with a short circuit that can be moved along the stub.

stub trap See INTERFERENCE STUB.

stub-type wavetrap See INTERFERENCE STUB.

stuffing bits In a digital communications system, extra bits inserted into some words so that all the words are the same length.

styli Plural of STYLUS.

stylus **1.** The "needle" that conveys vibrations to or from the disk in phonograph-disc recording or playback. **2.** One of the pins in the print head of a dot-matrix printer.

stylus drag See NEEDLE DRAG.

stylus friction Rubbing of the stylus against the record groove in phonograph-disc playback.

5059F-pS-607-670 4/10/01 9:47 AM Page 661

stylus pressure See VERTICAL STYLUS FORCE.

stylus printer See WIRE PRINTER.

stylus scratch See NEEDLE SCRATCH.

sub Abbreviation of *subtract*.

sub- Prefix denoting *under*, *below*, *less than*, or *lower than*, with respect to size, value, or rank. Compare SUPER-.

subassembly A completely fabricated unit that forms part of a larger unit into which it easily fits.

subatomic particle **1.** Any of various particles that comprise atoms of matter. **2.** A particle smaller than an atom. See, for example, ANTI-PARTICLE, ELECTRON, MESON, NEUTRETTO, NEUTRINO, NEUTRON, NUCLEON, POSITRON, and PROTON.

subaudible **1.** Pertaining to any frequency falling below the limit of human hearing, that is, less than about 20 Hz. **2.** Any sound that is too low in amplitude to be heard.

subaudible tone A signal, usually a steady, sine-wave tone, sent along with a radio signal. The tone frequency varies from about 20 Hz to 200 Hz, below the audio cutoff frequency of most voice communications systems. Subaudible tones are used mainly for privacy. The receiver is programmed to receive only signals having the correct subaudible tone frequency.

suballocation A portion of a radio-frequency broadcast or communications band that is legally set aside for specific purposes or users, e.g., the Extra-class segment of the 40-meter amateur-radio band.

subband **1.** A portion of a frequency band with specific characteristics. **2.** A portion of a radio-frequency broadcast or communications band that is set aside, legally or by convention, for specific purposes [e.g., the single-sideband (SSB) portion of the 20-meter amateur-radio band].

subcarrier A modulated carrier wave that composes the modulating signal for another carrier wave.

subcarrier band The band of frequencies in which a subcarrier signal is transmitted.

subcarrier frequency modulation In a system in which a carrier frequency is obtained by beating a low-frequency radio-frequency (RF) signal with a high-frequency RF signal, the application of frequency modulation to the low-frequency component. The technique is sometimes used in sweep-frequency signal generators.

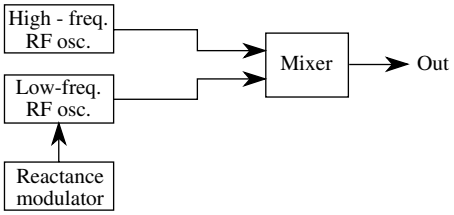

subcarrier frequency modulation

subcarrier oscillator In a color-television receiver, the oscillator operating at the burst (chrominance-subcarrier) frequency of 3.579545 MHz.

subchassis An auxiliary chassis on which one section of a larger piece of equipment is completely assembled and wired.

subfrequency See SUBHARMONIC.

subharmonic An integral submultiple of a fundamental frequency. Thus, for example, the 10th subharmonic of 15 MHz is 1.5 MHz.

submarine cable An underwater cable designed to withstand continuous immersion.

submarine robot A robot designed for underwater operation. It can be operated via telepresence or by simple remote control, usually using a conventional or fiberoptic cable. Some underwater robots have manipulators attached; others are equipped only with cameras, lights, and propulsion devices.

subminiature jack A female connector with an inside diameter of 3/32 inch.

subminiature plug A male connector with an outside diameter of 3/32 inch.

submultiple A fractional multiple, usually in reference to a frequency. For example, 7.2 MHz is a submultiple of 14.4 MHz. See SUBHARMONIC.

subpanel The front panel of a removable unit or module that forms a part of a larger unit.

subroutine In a computer program, a sequence of instructions for carrying out a section of the program's function. It is usually entered (led to) by a conditional branch (jump) instruction in the main program.

subscriber An individual user of a communications network or service.

subscript A small number or letter written to the lower right (and occasionally to the lower left) of another number or letter to identify the latter from others of the same designation (e.g., a_5, S_n). Compare SUPERSCRIPT.

subscription TV A television (TV) service paid for by subscribing viewers. The signals are scrambled so as to be useless to nonsubscribers, and legitimate subscribers are provided with a decoder to unscramble the telecasts.

subset **1.** In statistics and set theory, a set whose members are all contained in a larger set. **2.** A telephone handset or deskset (subscriber's set). **3.** A modulator/demodulator for making business machines compatible with telephone circuits.

subsidiary communication authorization Abbreviation, SCA. An authorization provided by the Federal Communications Commission (FCC) for a frequency-modulation (FM) broadcast station to transmit, in addition to its main program, a second program within the assigned bandwidth usually consisting of commercial-free background music on a subcarrier that can be detected only with a special receiver or with a special adapter attached to a standard FM receiver.

5059F-pS-607-670 4/10/01 9:47 AM Page 662

subsidiary feedback Feedback other than the main feedback in a system.

subsonic frequencies Frequencies below the range of hearing, that is, less than about 20 Hz. Also called ULTRALOW FREQUENCIES and SUBAUDIBLE FREQUENCIES.

substation An intermediate electricity-distributing location from which electrical energy is transformed and transmitted to users within a given geographical area.

substitution capacitor A capacitor used temporarily in place of another of usually the same value, as in troubleshooting. Also see CAPACITOR SUBSTITUTION BOX.

substitution inductor An inductor used temporarily in place of another of usually the same value, as in troubleshooting. Also see INDUCTOR SUBSTITUTION BOX.

substitution method **1.** A method of measuring a quantity (such as capacitance, inductance, or resistance) in which the value of the unknown quantity is determined in terms of the amount of a standard quantity that must be removed to restore the test circuit to its original state of balance. **2.** A method of troubleshooting in which good components are substituted for bad ones in a circuit (see, for example, SUBSTITUTION CAPACITOR, SUBSTITUTION INDUCTOR, SUBSTITUTION RESISTOR, SUBSTITUTION SPEAKER, and SUBSTITUTION TRANSFORMER).

substitution resistor A resistor used temporarily in place of another of usually the same value, as in troubleshooting. Also see RESISTOR SUBSTITUTION BOX.

substitution speaker A loudspeaker used temporarily in place of another, as in troubleshooting.

substitution transformer A transformer used temporarily in place of another having the same characteristics, as in troubleshooting.

substrate A plate, wafer, panel, or disk of suitable material on (or in) which the components of a unit, such as an integrated or printed circuit, are deposited or formed.

subterranean **1.** Pertaining to components, systems, or devices installed underground. It is applicable especially to cables. **2.** Pertaining to a phenomenon, such as the propagation of electric currents or acoustical waves, that occurs underground.

subterranean acoustical communication A method of communication that uses low-frequency sound waves, such as SONAR, to communicate via conduction through earth or water.

subtracter See ELECTRONIC SUBTRACTER.

subtractive color A color formed by mixing subtractive primary pigments.

subtractive primaries Broad-spectrum pigments used in printing to produce a wide variety of colors through filtering. These primaries are cyan (blue-green), magenta (pink-red), yellow, and sometimes black. They are used to print images that have been filtered through additive-primary lenses.

subtrahend In the process of subtraction, the quantity that is subtracted from another (the minuend) to produce the remainder or difference.

subwoofer A speaker designed to effectively reproduce extremely low audio frequencies, in some cases, subaudible (below 20 Hz).

successive derivatives Successive repetition of the operation of differentiating a function, which yields the first derivative, second derivative, and so on to the *n*th derivative.

successive integration The operation of double or triple integration.

Suhl effect A reduction in hole life that occurs in a semiconductor material in the presence of a magnetic field.

suite **1.** A group of computer programs run successively as a job. **2.** A bundled, high-end software package used especially in business computing.

sulfate Contraction of lead sulfate.

sulfation In a lead-acid storage cell, the formation of disabling lead sulfate during discharge of the cell.

sulfur Symbol, S. A nonmetallic element. Atomic number, 16. Atomic weight 32.06.

sulfur hexafluoride A gas used as a coolant and insulant in some power transformers.

sulfuric acid Formula, H_2SO_4. An acid used in dilute solution as the electrolyte of a lead-acid battery. This highly corrosive fluid also has many industrial uses.

sum The result obtained by adding two or more terms. Compare SUMMATION.

sumcheck See SUMMATION CHECK.

sum frequency **1.** In an amplitude-modulated carrier, the upper sideband frequency (i.e., the sideband equal to the carrier frequency plus the modulating frequency). Compare DIFFERENCE FREQUENCY. **2.** In superheterodyne operation, an intermediate frequency equal to the signal frequency plus the local-oscillator frequency.

summation **1.** The sum of a finite number of terms. Thus, the total resistance of *n* resistors connected in series is the summation of all *R* (resistance) terms. **2.** A frequency equal to the sum of two other frequencies.

summation check In computer operations, a check carried out on a group of digits. The result of adding the digits, and disregarding any overflow, is a check digit that can be compared with a standard value for the operation to verify the integrity of data.

summer **1.** See ADDER. **2.** See SUMMING AMPLIFIER.

summing amplifier An operational amplifier whose output is the sum, or is proportional to the sum, of several inputs.

sun battery A set of photovoltaic cells connected in series, parallel, or series-parallel to produce useful output voltages and currents.

5059F-pS-607-670 4/10/01 9:47 AM Page 663

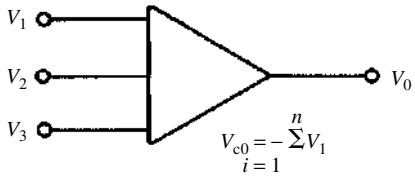

summing amplifier

S units In radio (especially amateur radio), gradations reflecting the strength of received signals. Typically, a value of S9 (9 s-units), representing "extremely strong signals," is equal to a strength of 50 microvolts. The next lower S unit (S8) is 6 dB lower in voltage (i.e., 25 microvolts); S7 is 12 dB below S9 (i.e., 12.5 microvolts), etc.

sun lamp An incandescent or fluorescent lamp with high ultraviolet output, used in medicine for the treatment of certain skin disorders. It can also be used for skin tanning; most physicians discourage habitual use of the lamps for this purpose.

sunlight lamp A lamp that produces visible light whose spectral distribution is similar to that of typical daylight. It generally produces more blue and violet light than a conventional lamp. It is sometimes used for indoor lighting in winter at high latitudes, and/or to enhance plant growth.

sunlight-powered laser A laser whose action is stimulated by sunlight collected by a system of mirrors and lenses. The life of the device is long, compared with that of conventional lasers.

sun-pumped laser See SUNLIGHT-POWERED LASER.

sun relay See SUN SWITCH.

sunspot An area on the sun's surface that is visible as a dark, irregular region of variable size, generally several thousand miles across. Sunspots are believed to be comparatively cool regions associated with solar magnetic disturbances. The number of sunspots is correlated with the frequency and intensity of solar flares (see SOLAR FLARE).

sunspot cycle Regular periodic variation of sunspot activity. The time between peaks in activity is approximately 11 years.

sun switch A photoelectric switch or relay actuated by sunlight and used for various domestic and industrial purposes, such as switching lights, operating window shades, etc.

sup Abbreviation of SUPPRESSOR.

super Contraction of *supersonic.*

super- Prefix denoting *over*, *above*, *greater than*, or *higher than*, with respect to size, value, or rank. Compare SUB-.

superaudible frequency See ULTRASONIC FREQUENCY.

superbeta transistor A transistor or transistor combination, such as a Darlington pair (see COMPOUND CONNECTION), that provides a very high current amplification factor (beta).

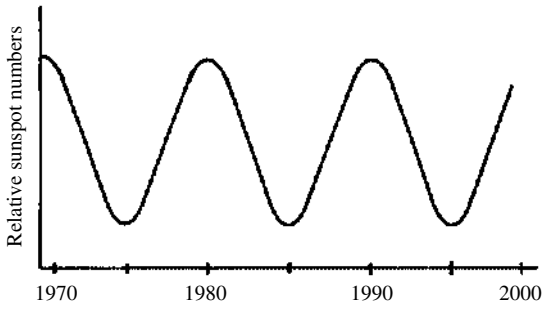

sunspot cycle

supercardioid microphone A microphone that is highly sensitive in one direction and insensitive in all other directions. The directional pattern is similar to a CARDIOID PATTERN, but is exaggerated along the axis of optimum response.

superconducting cable A cable in which superconductivity is achieved by surrounding the cable with liquid helium to lower its temperature to near absolute zero.

superconductivity The virtual disappearance of resistance in some metals cooled to temperatures in the vicinity of absolute zero. Also see CRYOGENICS, CRYOSTAT, and CRYOTRON.

superconductor A material or device that displays superconductivity.

super flatpack An integrated-circuit package of the flatpack type having considerably more components and leads than those in the conventional flatpack.

superhet Contraction of *superheterodyne.*

superheterodyne circuit A circuit in which the incoming signal in a first detector (or mixer) beats with the signal of a local oscillator, resulting in a lower (intermediate) frequency, which then is amplified by an intermediate-frequency (IF) amplifier. This IF signal is detected by a second detector whose output is amplified by an audio-frequency (AF) amplifier. Because the IF amplifier operates at a single (fixed) frequency, it can be adjusted for optimum selectivity and gain. Also called *superhet circuit.*

superheterodyne receiver A radio or television receiver using a SUPERHETERODYNE CIRCUIT.

superhigh frequency See RADIO SPECTRUM.

Supermalloy An alloy having a maximum permeability of 10^6.

supermodulation A type of amplitude modulation (AM) in which one radio-frequency (RF) power stage continuously generates the carrier, and a second (usually identical) RF power stage is gated into full operation at the proper instant by the audio modulation to add additional RF power (corresponding to 100% modulation) to the signal. At the same time, the carrier amplitude is decreased by the proper amount to fulfill the conditions of a

5059F-pS-607-670 4/10/01 9:47 AM Page 664

signal amplitude swing between zero and twice maximum for 100% modulation.

superposition In a complex wave, the manner in which the constituent waves combine. The instantaneous value of the complex wave is equal to the vector sum of the instantaneous values of all the constituent waves.

superposition theorem In a network of linear elements, if a voltage E_1 in branch A causes a current I_1 to flow through branch C, and if a voltage E_2 in branch B (which might be identical with branch A) causes a current I_2 to flow through branch C, then E_1 in branch A and E_2 in branch B applied simultaneously will cause a current equal to $I_1 + I_2$ to flow through branch C. Compare COMPENSATION THEOREM, MAXIMUM POWER TRANSFER THEOREM, NORTON'S THEOREM, RECIPROCITY THEOREM, and THEVENIN'S THEOREM.

superpower An arbitrary term denoting very high power. In the rating of standard broadcast stations, it has come to signify 1,000,000 watts (one megawatt) radio-frequency (RF) power output.

superradiance In a laser, a rapid increase in intensity of fluorescent-line emission with increasing excitation power.

superregenerative circuit A regenerative detector circuit in which regeneration is periodically increased almost to the point of oscillation, then decreased. This quenching action takes place at a supersonic rate (typically at 50 or 100 kHz) so that the quenching is inaudible. The result is that much more regeneration is afforded, without the detector going into oscillation, than is possible by simply increasing the regeneration manually. An extremely sensitive detector is the result.

supersaturated solution A solution that contains more solute than it normally would hold. Supersaturated solutions are obtained through special techniques and are extremely unstable. Compare SATURATED SOLUTION. Also see SOLUTE; SOLUTION, **1**; and SOLVENT, **2**.

superscript A small number or letter written to the upper right of another number or letter, the BASE, to indicate the power to which the base must be raised. Example: 10^5, e^x, y^2. Also called EXPONENT. Compare SUBSCRIPT.

supersensitive relay A relay that operates with a current of less than one milliampere, or with a voltage of less than one millivolt.

supersonic flow In a gas or liquid, movement of the medium at a speed greater than the speed of sound in that medium. Supersonic flow results in a greatly increased resistance or drag because of shock waves that form in the medium.

supersonic frequency See ULTRASONIC FREQUENCY.

supersonics See ULTRASONICS.

supervised line In a security system, a wire or foil strip that carries electrical current. If the current changes in such a line, an alarm is actuated.

supervisor **1.** In a computer, a set of routines that oversees the operation of the system. The supervisor routines are coordinated by the central processing unit. **2.** The execution of such a set of routines. **3.** A microcomputer that oversees the operation of a security system.

supervisory circuit In a security system, a link between a sensor and the central computer or control device. This link can be via electric current through a wire or cable, but other methods can be used, such as fiberoptics, line-of-sight optics, infrared, ultrasonic, or radio.

supply **1.** See CURRENT SUPPLY. **2.** See POWER SUPPLY. **3.** See VOLTAGE SUPPLY.

supply current Alternating or direct current available for operating a circuit, device, or system.

supply frequency The frequency of an alternating-current power supply.

supply power The maximum power that can be reliably delivered by an alternating-current or direct-current power supply.

supply reel In a reel-to-reel tape recorder or player, the reel that is initially full, and that gradually empties as the tape moves through the machine.

supply voltage The voltage of an alternating-current or direct-current power supply.

suppressed carrier A carrier that has been canceled or filtered out of a carrier/sideband combination.

suppressed-carrier double sideband See DOUBLE-SIDEBAND and SUPPRESSED CARRIER.

suppressed-zero instrument A meter or graphic recorder in which the zero point is off-scale or upscale, but has been brought to scale-zero by means of mechanical adjustment or use of a bucking voltage.

suppressor **1.** A filter used to suppress radio interference. **2.** See AUTOMATIC NOISE LIMITER. **3.** See SPARK SUPPRESSOR. **4.** In a pentode vacuum tube, a gridlike element between the screen grid and the plate, used to suppress secondary emission. Also see GRID, **2** and PENTODE.

suppressor circuit The circuit associated with the suppressor electrode of a vacuum tube.

suppressor diode A semiconductor diode used to prevent inductive kickback in circuits, to eliminate or reduce transients, or to prevent arcing between make-and-break contacts.

suppressor grid See SUPPRESSOR, **4**.

suppressor modulation A method of modulation in which a modulating voltage is superimposed on the suppressor voltage of a pentode radio-frequency power amplifier tube.

suppressor pulse A pulse that prevents electron flow.

surface analyzer A device designed for the measurement of surface flatness or uniformity.

surface-barrier diffused transistor See MICRO-ALLOY DIFFUSED TRANSISTOR.

surface-barrier transistor Abbreviation, SBT. A pnp transistor made by means of electrolysis and electroplating: Two fine streams of indium sulfate

5059F-pS-607-670 4/10/01 9:47 AM Page 665

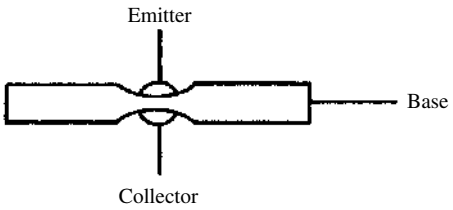

surface-barrier transistor

solution are placed on axially opposite points on the faces of an n-type wafer. At the same time, a direct current is passed through the wafer and solution in such a direction as to remove semiconductor material electrolytically from the faces; the tiny sprayed areas are etched away. When the desired wafer thickness is reached at the points of impact, the etching process is arrested by reversing the direction of current flow. This reversal causes an indium dot to be plated on each opposite face in the etched-out pit. Leads are attached to the collector and emitter dots and to the wafer (base).

surface-charge transistor A semiconductor device consisting essentially of two narrowly separated plates (source electrode and receiver electrode) deposited on the film-insulated surface of a silicon chip, and a third, overlapping electrode (the transfer gate) deposited on, but insulated from, the other electrodes. An input signal stores a charge in the capacitor formed by the source electrode and chip. A subsequent trigger signal applied to the transfer gate transfers the charge to the receiver electrode, where it becomes an output signal (often amplified, with respect to the input signal).

surface effect An effect (such as current, resistance, or resistivity) observed on the surface of a sample of material, rather than throughout the body of the material. Compare BULK EFFECT.

surface insulation A coating applied to the surfaces of core laminations to prevent the passage of currents between laminations.

surface leakage Leakage of current over the surface of a dielectric material, as opposed to leakage through the interior of the material.

surface noise See NEEDLE SCRATCH.

surface recombination rate For a semiconductor, the rate at which electrons and holes recombine at the surface. Compare VOLUME RECOMBINATION RATE.

surface resistivity The resistance of a unit area of a material, measured between opposite edges. Compare VOLUME RESISTIVITY. Also see RESISTIVITY.

surface tension The tendency of the surface of a liquid to "shrink." This property varies with different liquids and is caused by a net molecular force directed inward from the surface.

surface wave **1.** The earth-guided component of a ground wave. (The other component is the SPACE WAVE.) **2.** An acoustic wave traveling along the surface of a plate in a surface-wave amplifier or surface-wave filter.

surface-wave amplifier An amplifying device consisting essentially of a surface-wave filter to which has been added a direct-current-biased n-type silicon electrode, which is separated from the crystal substrate of the filter by a very thin oxide layer. Amplification is produced by interaction between the electron current in the silicon and the piezoelectric field of the filter. Also see ACOUSTOELECTRONICS.

surface-wave filter An acoustoelectronic device consisting essentially of a crystal plate having electrodes at each end. An alternating-current (ac) input signal applied to one electrode sets up acoustic waves that travel along the surface of the plate to the other electrode, where they generate an ac output voltage by piezoelectric action. The resonant frequency of the device is governed by the dimensions of the crystal plate. Also see ACOUSTOELECTRONICS.

surge A sudden rise or flow of current or voltage.

surge absorber See SURGE SUPPRESSOR.

surge arrester See SURGE SUPPRESSOR.

surge current A heavy current that flows initially into a capacitor when a charging voltage is applied.

surge impedance Symbol, Z_o. The impedance seen by a pulse applied to a transmission line; $Z_o = L/C$ (approximately), where L and C are the inductance and capacitance, in microhenrys and microfarads, per unit length of the line. Also called CHARACTERISTIC IMPEDANCE.

surge protector Misnomer for SURGE SUPPRESSOR.

surge suppressor A semiconductor device used to absorb potentially destructive transients or overvoltages on a utility power line. It has a three-wire cord for plugging into a 117-volt outlet, a power switch, and several three-wire outlets for connection to sensitive electronic equipment (such as personal computers, videocassette recorders, television sets, hi-fi amplifiers, etc.).

surround See SUSPENSION, **1**.

Surround Sound The trade name for a multichannel sound system for use with television receivers and videocassette players. Some televised movies, especially on cable and satellite networks, deliver multichannel sound through receiving/recording systems equipped with special decoders.

surveillance **1.** A method of monitoring a specific area or volume for intrusion or other disturbance. **2.** A means of monitoring a specified portion of the electromagnetic spectrum for unauthorized signals.

surveillance radar An air-traffic-control radar that supplies continuous information regarding the azimuth and distance of aircraft inside a selected radius around an airport.

5059F-pS-607-670 4/10/01 9:47 AM Page 666

susceptance Symbol, *B*. Unit, siemens. The reactive component of admittance, as distinguished from conductance.

susceptibility The capacity of a substance to become magnetized, expressed as the ratio of magnetization to the strength of the magnetizing force.

suspension **1.** In a speaker, the flexible, circular or elliptical structure via which the cone is attached to the frame. **2.** The wire or metallized fiber supporting the movable coil of a galvanometer. **3.** Particles of a substance and the liquid in which it is mixed, but not dissolved. **4.** The substance, as defined in **3**.

suspension galvanometer A meter with a light-beam apparatus for lengthening the arc through which the pointer travels. When the beam of light is cast a long distance, a tiny movement of the coil will cause considerable movement of the image.

sustained oscillations Oscillations that continue as long as power is supplied to the oscillation generator. Also see CONTINUOUS WAVE. Compare DAMPED OSCILLATIONS.

sustaining voltage The voltage at which second-collector breakdown occurs in a transistor (see SECOND BREAKDOWN).

S video In animation, a scheme that separates brightness and color. It can enhance the video in some applications.

SW Abbreviation of SHORTWAVE.

sw Abbreviation of SWITCH. (Also, S or s.)

swamping resistor **1.** A noninductive resistor connected in parallel with the input circuit of a class-B linear amplifier for automatic regulation of the excitation. **2.** A resistor connected in series with the emitter of a bipolar transistor to minimize the effects of temperature-induced variations in junction resistance.

swarf The string of material that threads off a disc during sound recording.

S_W band A section of the S BAND, extending from 3400 to 3700 MHz.

sweep **1.** To deflect the electron beam in a cathode-ray tube, usually horizontally, to provide a time base. **2.** The circuit for achieving the particular deflection described in **1**.

sweep circuit A circuit, such as a deflection generator (e.g., a sawtooth oscillator), for producing a sweep signal. Also see SWEEP.

sweep delay In an oscilloscope, the process of initiating the sweep of the electron beam at some selected instant after the signal has started.

sweep-delay circuit In an oscilloscope or radar, the circuit for delaying the sweep until the start of the signal. Also see DELAYED SWEEP.

sweeper **1.** See SWEEP GENERATOR. **2**. See SWEEP-SIGNAL GENERATOR.

sweep frequency **1.** The frequency at which the electron beam in a cathode-ray tube is deflected along the reference axis. **2.** The frequency at which the carrier frequency is increased and decreased by a sweep-signal generator. **3.** In an oscilloscope, the number of times that the trace moves across the screen in one second. It is equal to the reciprocal of the SWEEP PERIOD.

sweep generator **1.** A device that causes the electron beam in a cathode-ray tube to scan at a known speed. **2.** An oscillator that generates a signal that rapidly varies in frequency. It is used for the testing and adjustment of bandpass filters and other selective circuits.

sweeping receiver See SCANNING RECEIVER.

sweep magnification In an oscilloscope, increasing or multiplying the sweep frequency, thus reducing the time per horizontal division. This increases the maximum frequency of waveforms that can be analyzed, and allows closer inspection of high-frequency signal components.

sweep magnifier In an oscilloscope, a circuit for achieving sweep magnification.

sweep oscillator See SWEEP GENERATOR.

sweep period The duration, in seconds, of one complete cycle of sweep signal in an oscilloscope. It is equal to the reciprocal of the SWEEP FREQUENCY.

sweep signal The (usually linear, sawtooth) signal used to sweep the beam of an oscilloscope tube. Also see SWEEP, **1**, **2**.

sweep-signal generator A signal generator that supplies a signal whose frequency varies automatically and periodically throughout a given band.

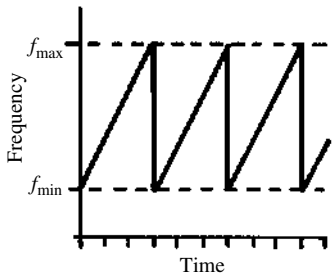

sweep-signal generator

sweep test A method of testing the attenuation-vs.-frequency characteristics of a selective circuit, using a radio-frequency sweep generator.

sweep time The actual time required for a single sweep by a deflecting signal; $t = 1/f$, where t is sweep time in seconds, and f is sweep frequency in hertz.

sweep voltage The peak voltage amplitude of the sweep signal.

SWG Abbreviation of *standard wire gauge.*

swing The maximum change exhibited by a varying quantity (e.g., *amplitude swing* and *frequency swing*).

5059F-pS-607-670 4/10/01 9:47 AM Page 667

swinging choke A filter choke that exhibits relatively high inductance when low current flows through it, and lower inductance when high current flows through it. This inductance, which swings under conditions of varying load current, permits the use of a high-resistance bleeder resistor. Compare SMOOTHING CHOKE.

Swiss-cheese packaging A method of packaging an electronic circuit, in which components are inserted into the assembly through holes drilled or punched in parallel, stacked printed-circuit boards.

switch **1.** A circuit or device (electronic, electromechanical, or mechanical) for opening and closing a circuit or for connecting a line to one of several different lines (e.g., *rotary selector switch*). **2.** To change the logic state of a circuit or device. **3.** In a computer program, a branch instruction directing the program to a line number dependent on the value of a variable or result (e.g., BASIC's GOTO). **4.** To cause an electrical circuit to change state, as from low to high or vice versa.

switch current **1.** The current flowing through a switch. **2.** The current flowing through a switching diode or transistor. **3.** The minimum current necessary to produce switching of a transistor, specified in milliamperes or microamperes.

switchgear Collectively, devices and systems for making and breaking circuits—either automatically or manually.

switchhook In a telephone set, the spring-and-switch device that engages the line when the receiver is lifted.

switching characteristics Technical data describing the performance and capabilities of switching devices and circuits.

switching circuit An on-off type of circuit containing electronic or mechanical switches.

switching diode See COMPUTER DIODE.

switching frequency The frequency at which a repetitive switch operates. Also see SWITCHING RATE.

switching mode Operation in which a device, such as a transistor or diode functions as a binary digital device, rather than as an analog device. The current is generally either zero (cutoff or pinchoff) or some value that depends on the bias and on the applied voltage.

switching rate The rate (e.g., closures per second) at which a repetitive switch operates. Also see SWITCHING FREQUENCY.

switching speed The time required for a switch to open or close or for a switching device to change states (as from cutoff to saturation). Also see SWITCHING TIME.

switching time The time required, after the application of a pulse, for an electronic switch to change state. Also see SWITCHING SPEED.

switching transistor A transistor designed especially for on-off operation. Such units exhibit short recovery time and low capacitance.

switching voltage The largest voltage that a switching device can handle without malfunctioning.

switch leakage current **1.** The current flowing through a switching device when it is supposed to be nonconducting. **2.** In a switching transistor, for a given voltage, the leakage current between the emitter and collector when the device is supposed to be nonconducting.

SWL Abbreviation of SHORTWAVE LISTENER.

SWR Abbreviation of STANDING-WAVE RATI0.

SWR bridge A four-arm resistance bridge for measuring voltage standing-wave ratio. This radio-frequency bridge has noninductive resistors in three of its arms and the device under test in the fourth arm. The bridge is balanced first with an equivalent noninductive resistor that replaces the device, and the output voltage is noted. Then the device is substituted for the test resistor, and the change in voltage is noted. The standing-wave ratio is determined from the voltage ratio.

SWR meter See SWR BRIDGE.

S_Y band A section of the S BAND, extending from 2600 to 2700 MHz.

syllable compandor A device that compresses or expands the amplitude of an audio signal. The time constant is fast enough to allow response to individual syllables. Compression is generally used at the transmitting station, and expansion at the receiving station.

sym **1.** Abbreviation of *symmetrical.* **2.** Abbreviation of SYMBOL.

symbol **1.** A letter or graphic device representing a quantity or term [e.g., *I* (current), *f* (frequency), etc.]. **2.** A conventional device denoting a mathematical operation (e.g., +, /). **3.** In a circuit diagram, a pictorial device representing a component.

symbolic address An address in a source-language computer program (i.e., the arbitrary label used by the programmer).

symbolic language See SOURCE LANGUAGE.

symbolic logic A system for representing logical relationships, such as those acted upon by computer and switching circuits, by means of symbols that are usually nonnumerical. Also see BOOLEAN ALGEBRA.

symmetrical circuit A circuit having identical configurations on each side of a dividing line, such as the ground bus. A push-pull circuit is an example.

symmetrical communications **1.** Two-way communications in which the volume of transmitted data is the same, or nearly the same, in both directions. **2.** Two-way communications in which the speed of transmitted data is the same, or nearly the same, in both directions. Compare ASYMMETRICAL COMMUNICATIONS.

symmetrical conductivity Identical conductivity for both positive and negative electricity. Compare ASYMMETRICAL CONDUCTIVITY.

5059F-pS-607-670 4/10/01 9:47 AM Page 668

symmetrical FET See SYMMETRICAL FIELD-EFFECT TRANSISTOR.

symmetrical field-effect transistor A field-effect transistor whose source and drain terminals can be interchanged without affecting circuit operation. Also called BIDIRECTIONAL TRANSISTOR. Compare UNILATERAL FIELD-EFFECT TRANSISTOR.

symmetrical input See BALANCED INPUT.

symmetrical output See BALANCED OUTPUT.

symmetrical transistor See BIDIRECTIONAL TRANSISTOR.

symmetrical wave A wave whose positive and negative half-cycles are identical in shape and peak amplitude.

symmetry **1.** The condition of having the same shape on each side of an axis. **2.** The condition of conducting positive and negative currents equally well. **3.** The condition in which a circuit is identical on both sides of a reference line, such as the ground line.

sympathetic vibration Resonant vibration of one body in response to the vibration of another body.

sync **1.** Contraction of SYNCHRONIZATION. **2.** Contraction of SYNCHRONISM.

sync amplifier In a television circuit, the amplifier used to increase the amplitude of the sync pulses after they are separated from the composite video signal.

sync generator A circuit that produces the synchronization pulses in a television transmitter.

synchro A dynamo-electric-control device that, when connected to a similar device and the alternating-current power line, permits remote control. Thus, when the rotor of one synchro is turned to a certain position, the rotor of the other assumes the same position. Also see AUTOSYN and SELSYN.

synchrocyclotron A type of cyclotron in which the variation in mass, because of increased velocity, of the charged particles is compensated, resulting in higher energy for the particles.

synchro differential A synchro that receives two input signals and delivers a single output signal. The inputs can be two electrical signals, or one electrical signal and one mechanical signal.

synchrodyne receiver A direct-conversion receiver in which the local oscillator frequency or phase is locked into synchronism with the incoming signal carrier frequency or phase.

synchroflash A flash that is synchronized with the shutter of a camera.

synchro generator The transmitting member of a synchro system.

synchro motor The receiving member of a synchro system.

synchronism **1.** The condition of being in step, as when two motors are running in synchronism with each other and the power frequency, or when two relays open and close in step. **2.** The condition of being in phase, as when two pulses occur simultaneously.

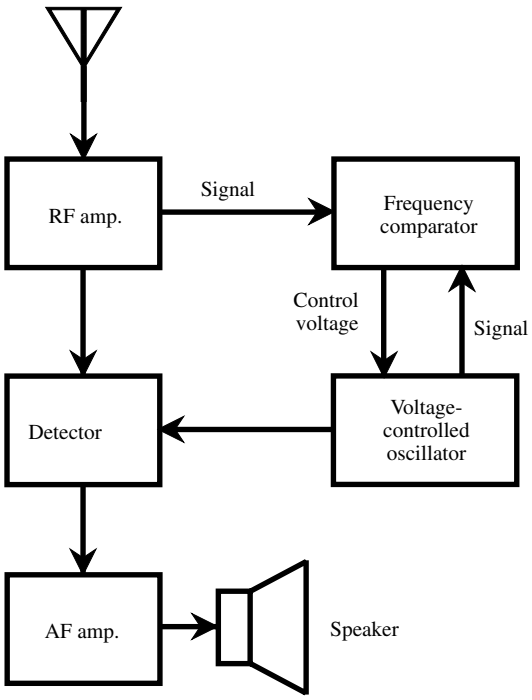

synchrodyne receiver

synchronization The coincidence of one process or operation with another, as in the synchronization of an oscillator frequency by means of an applied standard-frequency voltage, in which case the oscillator frequency becomes that of the standard signal.

synchronized clamping A type of clamping in which an output voltage is maintained at a predetermined fixed value until a synchronizing pulse is applied, whereupon the output follows the input.

synchronized multivibrator See DRIVEN MULTIVIBRATOR.

synchronizer A computer storage device used between two devices transmitting data at different speeds, to counteract this differential (as a buffer).

synchronizing signal A signal used to synchronize another signal, usually in frequency.

synchronous The condition of operating in step (phase) with some reference signal.

synchronous clock **1.** An alternating-current clock driven by a synchronous motor. Although 60-Hz models are common, such clocks are not restricted to low-frequency ac operation; 1-kHz types, for example, are used in some primary frequency standards. **2.** The timing source in a synchronous computer.

5059F-pS-607-670 4/10/01 9:47 AM Page 669

synchronous computer A computer whose operations are timed by single-frequency clock signals.

synchronous contacts The rectifying contacts of a synchronous vibrator (see VIBRATOR-TYPE RECTIFIER).

synchronous converter A synchronous machine that can run on alternating current and generate direct current, or vice versa. Also called ROTARY CONVERTER.

synchronous gate A gate whose output is synchronized, according to the input signal.

synchronous generator An alternator operating in synchronism with one or more other alternators. Also see SYNCHROSCOPE, **2**.

synchronous induction motor An alternating-current motor that is intermediate between the fractional-horsepower reluctance motor and the multiple-horsepower three-phase, synchronous motor. The synchronous induction machine starts like an induction motor and runs like a synchronous motor.

synchronous inputs In a computer flip-flop, inputs that accept pulses only at the command of the clock.

synchronous machine See SYNCHRONOUS INDUCTION MOTOR.

synchronous motor See SYNCHRONOUS INDUCTION MOTOR.

synchronous network A communications network in which all clocks are set so that they run at the same rate, their increments are identical in duration, and transitions occur simultaneously or with a specified phase difference. Such a system allows for greatly enhanced signal-to-noise ratio for a given amount of transmitter power, and also reduces the bandwidth necessary for a single signal so that many more signals can be placed in a given frequency band.

synchronous orbit See GEOSTATIONARY ORBIT.

synchronous satellite See GEOSTATIONARY SATELLITE.

synchronous speed For an alternating-current (ac) machine, the speed corresponding to the ac frequency.

synchronous transmission A method of signal transmission in which individual symbols are sent at a specified rate, according to a clock that also governs the receiver.

synchronous vibrator See VIBRATOR-TYPE RECTIFIER.

synchroscope **1.** An oscilloscope having a high-speed sweep triggered by a synchronizing signal. Such an instrument is valuable for viewing high-speed pulses. **2.** A pointer-type instrument used to indicate the synchronism between two power alternators.

synchro system A circuit or system using synchros for the transmission and reception of positioning signals. Also see SYNCHRO.

synchrotron A particle accelerator that uses a high-frequency electrostatic field and a low-frequency magnetic field to impart very high velocity to the particles.

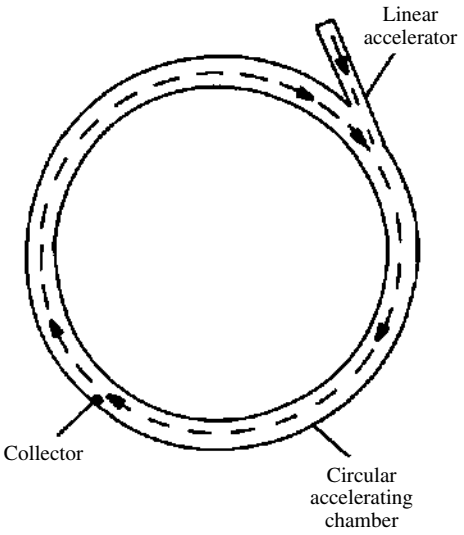

synchrotron

sync pulse **1.** A pulse used to control the frequency or repetition rate of an oscillator or other generator. **2.** In a television system, a pulse transmitted as part of the composite video signal to control scanning. Also see HORIZONTAL SYNC PULSE and VERTICAL SYNC PULSE.

sync separator In a television receiver circuit, a stage used to separate and deliver the sync pulses from the composite video signal. See, for example, DIODE SYNC SEPARATOR.

sync signal See SYNCHRONIZING SIGNAL.

sync takeoff The point in the video amplifier circuit of a television receiver at which the composite video signal is sampled to extract the sync pulses.

syntax **1.** The rules by which computer program statements are structured. **2.** The way that a written or spoken sentence is constructed. It is important in speech recognition and speech synthesis.

synthesis The rigorous (usually mathematical) design of an electronic circuit or device and the accurate prediction of its performance. Compare ANALYSIS.

synthesizer **1.** See SIGNAL SYNTHESIZER. **2.** A circuit synthesizer (i.e., a device that allows a wide variety of circuits to be set up temporarily or simulated, for testing and evaluating). Sometimes, a specially programmed computer serves this purpose. **3.** A keyboard on which music can be played, and whose output can be adjusted to simulate the sounds of various musical instruments. **4.** See MOOG SYNTHESIZER.

5059F-pS-607-670 4/10/01 9:47 AM Page 670

synthetic bass An apparent accentuation of bass notes resulting from intermodulation distortion in an amplifier.

synthetic crystal An artificially produced crystal, such as synthetic quartz.

synthetic resin An artificially produced resin. Also see THERMOPLASTIC MATERIAL and THERMOSETTING MATERIAL.

syntony See RESONANCE.

syst Abbreviation of SYSTEM.

system **1.** An integrated assemblage of hardware and/or software elements operating together to accomplish a prescribed end purpose (e.g., *servo system*, *operating system*, and *communications system*). **2.** A methodology incorporating fixed and ordered procedures for accomplishing an end purpose. **3.** A self-contained computer workstation.

systematic error See CUMULATIVE ERROR.

system engineering See SYSTEMS ENGINEERING.

system of units A set of fundamental units for defining the magnitudes of all physical variables. The most common system of units is the standard international (SI) system.

systems analysis In computer system operation, analyzing the way something is done and devising a better alternative by isolating the problem area, scrutinizing the system as it stands, studying what is thereby disclosed, devising the alternate application of software and/or hardware, disseminating the revised operational procedure, and overseeing the implementation of the new method.

systems engineering The branch of engineering devoted to the design, development, and application of complete systems. The approach takes into consideration all elements in a system or process and their integration.

systems flowchart A flowchart showing the interrelationship of activities in a system.

S_Z band A section of the S BAND, extending from 3900 to 4200 MHz.

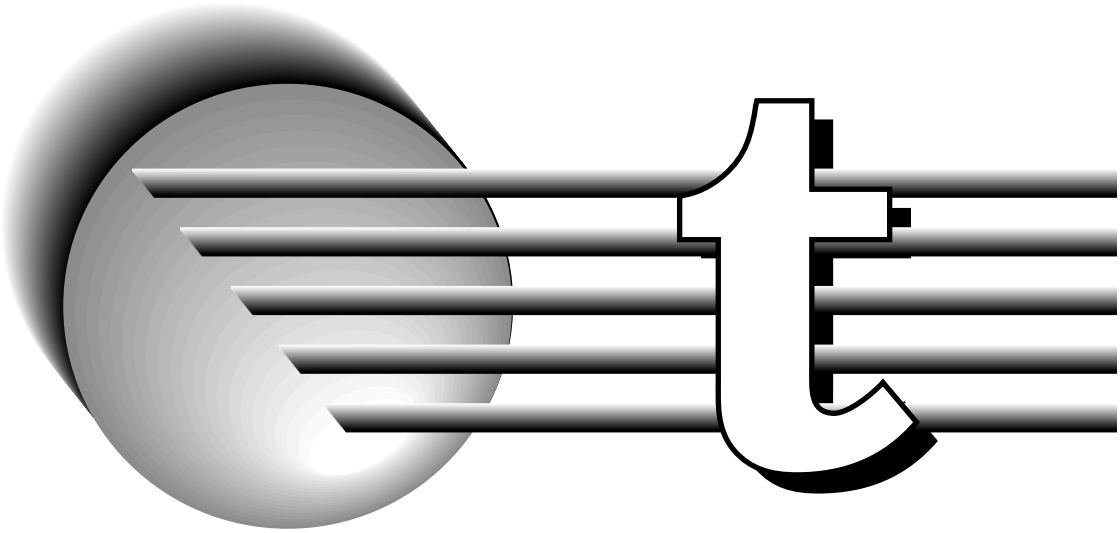

T **1.** Symbol for TRANSFORMER. **2.** Abbreviation of prefix TERA-. **3.** Symbol for *thermodynamic temperature.* **4.** Symbol for TRITIUM. **5.** Abbreviation of TON. (Also, t and tn.) **6.** Abbreviation of TESLA. **7.** Symbol for KINETIC ENERGY. **8.** Symbol for PERIOD. **9.** Symbol for *true.*

t **1.** Symbol for TIME. **2.** Abbreviation of TON. (Also, T and tn.) **3.** Symbol for CELSIUS TEMPERATURE. (Also, T.) **4.** Abbreviation of TARGET. **5.** Abbreviation of *technical.* **6.** Abbreviation of TENSION.

Ta Symbol for TANTALUM.

tab On the keyboard for a computer, typewriter, terminal, or word-processing system, a key that moves the cursor a specified number of spaces toward the right. It also performs various other functions in menu-driven or graphical computer interfaces.

table In an internal or external computer memory, an array (i.e., a list or matrix) of data that can be recalled using keys (e.g., single- or double-subscripted variables).

table look-at Abbreviation, TLA. In computer operations, finding the position of a data item in a table by implementing an algorithm.

table look-up Abbreviation, TLU. In computer operations, locating items in a table by inspecting what is in the table, key by key.

tabulate In data processing, to combine the totals for data item groups having the same key.

tabulation **1.** The printout of what has been tabulated (see TABULATE). **2.** The computer-program-directed movement of the cursor on a cathode-ray-tube display, or of a typewriter carriage, to certain positions in a line.

tabulator See TAB.

tacan A pulse-type UHF air navigation system in which a station is interrogated by signals from an aircraft to provide bearing and range information. The name is an acronym for *tactical air navigation.*

tach Abbreviated form of *tachometer.*

tachometer See ELECTRONIC TACHOMETER.

tachometer generator A small, dynamo-type electric generator that delivers a voltage proportional to the rotational speed of a shaft to which it is attached.

tachyon A high-speed subatomic particle thought to move faster than the speed of light.

tactical air navigation See TACAN.

tactical radar A radar system used in military operations.

tactile sensor A device that provides an intelligent machine with a sense of "touch": temperature, pressure, force, texture, and torque. It is important in robotics, and also in some computer applications, such as virtual reality (VR).

T-adapter See TEE-JUNCTION.

tag **1.** In data-processing and computer operations, the identification of digits or characters forming part of a record. **2.** An encoded price tag (i.e., a passive transponder or barcode strip). It is commonly used in retail stores.

tag converter A device that senses the information on tags (see TAG, **2**) and transfers it to a computer system.

tail **1.** The decay of a waveform from maximum amplitude to zero amplitude. **2.** Any pulse that follows a main pulse as a result of the main pulse.

Copyright 2001 The McGraw-Hill Companies, Inc. Click Here for Terms of Use

5059F-pT-671-699 4/10/01 9:51 AM Page 672

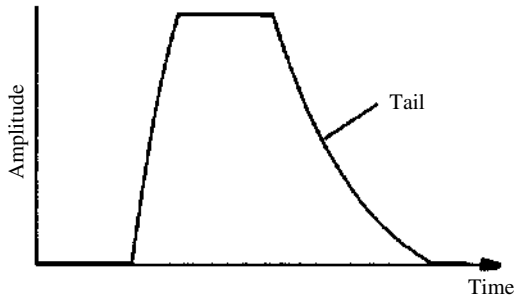

tail

taillight monitor An electronic device for warning a motorist of taillight failure.

tail pulse **1.** A pulse with a fast rise time, but a slow decay time. **2.** See TAIL, **2**.

takedown In computer operations, the process of clearing output peripherals for upcoming program runs.

take-down time The duration of the TAKEDOWN process.

take-up reel In a reel-to-reel tape recorder/reproducer, the reel on which the tape accumulates during recording or reproduction.

talk-back circuit See INTERPHONE.

talk-listen switch A transmit-receive switch in an intercommunication system (see INTERCOM).

talk power See SPEECH POWER.

tally **1.** To obtain a sum or total. **2.** The rows of operands, subtotals, and totals that an adding machine prints.

tally reader A device that, via optical character recognition (OCR), can read the digits and symbols on a tally (see TALLY, **2**).

tamper switch A device that closes a circuit or actuates an alarm when a certain set of conditions is altered.

tan Abbreviation of TANGENT.

$\tan^{-1}$ Arc tan (inverse tangent function).

tandem transistor An assembly of two series-connected transistors in the same envelope.

tangent **1.** Abbreviation, tan. The ratio of the side opposite to the side adjacent to an acute angle in a right triangle. **2.** A line that intersects a curve at a single point without crossing the curve. **3.** A plane that intersects a curved surface at a single point.

tangent galvanometer A galvanometer in which the current is proportional to the tangent of the angle of deflection. Compare SINE GALVANOMETER.

tangential mode In acoustics, the reflection of sound waves from four surfaces in a room having six interior surfaces.

tanh Abbreviation of HYPERBOLIC TANGENT.

tank **1.** A parallel-resonant inductance-capacitance circuit in the output of a radio-frequency amplifier. **2.** A circuit in which is stored electrical energy of frequencies in a range whose midpoint is resonance for the circuit. **3.** See MERCURY DELAY LINE.

tantalum Symbol, Ta. A metallic element of the vanadium family. Atomic number, 73. Atomic weight, 180.95. Tantalum is used in the elements of some electron tubes and in some electrolytic capacitors.

tantalum capacitor A type of electrolytic capacitor that uses tantalum rather than aluminum. The tantalum can be foil, as is the aluminum in a conventional electrolytic capacitor. It might also take the form of a porous pellet, the irregular surface of which provides a large area in a small volume. An extremely thin oxide layer forms on the tantalum. These capacitors have high reliability and excellent efficiency, and are used in military applications because they have a low failure rate. They can be used in audio and digital circuits in place of aluminum electrolytic capacitors. The main disadvantage of tantalum capacitors is that they are comparatively expensive. Compare CERAMIC CAPACITOR, ELECTROLYTIC CAPACITOR, MICA CAPACITOR, PAPER CAPACITOR, PLASTIC-FILM CAPACITOR.

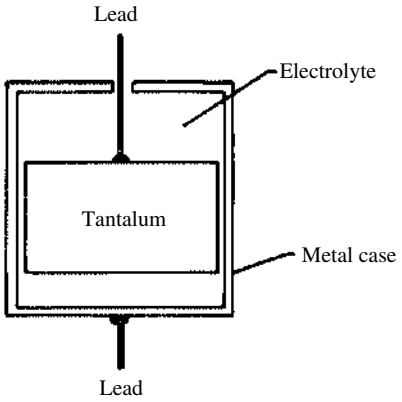

tantalum capacitor

tantalum detector A radio-frequency contact detector consisting essentially of a fine tantalum wire whose point lightly touches the surface of a small pool of mercury.

tantalum-nitride resistor A resistor consisting of a thin film of tantalum nitride deposited on a substrate. Also see THIN FILM.

T-antenna See TEE-ANTENNA.

tap A connection made to an intermediate point on a coil, resistor, or other device. See, for example, CENTER TAP and TAPPED COMPONENT.

tap changer A device that facilitates adjustment of the turns ratio of a transformer by changing the

5059F-pT-671-699 4/10/01 9:51 AM Page 673

tap on the primary winding, the secondary winding, or both. It also facilitates the adjustment of the impedance-transfer ratio. It can be used for power supplies or audio- or radio-frequency transformers.

tape **1.** Magnetic tape. **2.** Insulating tape. **3.** To make a magnetic tape recording (audio, video, and/or digital data).

tape cable **1.** A form of cable in which all of the conductor centers lie in the same plane. **2.** A flat cable, commonly used in situations, where repeated flexing occurs.

tape cartridge A holder and the reel of blank or prerecorded magnetic (⅛-inch audio or wider video) tape it contains, which can be inserted into a recorder/reproducer without having to thread or otherwise handle the tape for either playing or rewinding.

tape comparator In a data-processing or computer system, a machine that compares tapes generated from the same input, for differences in the data thereon; it is a character-by-character process.

tape core A ring-type magnetic core made by tightly winding metal tape in several layers for the desired thickness.

tape counter See POSITION INDICATOR.

tape deck In a tape recorder/reproducer, the complete tape-transport mechanism (drive, heads, equalization circuitry, and preamplifiers).

tape drive **1.** See TAPE TRANSPORT. **2.** See TAPE DECK. **3.** A tape recorder/reproducer for computer data, used for backup and/or archiving.

tape file A data file recorded on magnetic tape.

tape group An assembly of two or more tape decks.

tape label On a reel or cassette of magnetic tape containing a data file, a record at the beginning or end that contains information about the file.

tape loop An endless loop of magnetic tape.

tape magazine See TAPE CARTRIDGE.

tape mark **1.** A character that subdivides the magnetic tape file on which it is recorded. Also called CONTROL MARK. **2.** A character marking the end of a length of magnetic tape on a reel. Also called END-OF-TAPE MARK.

tape plotting system In computer operations, a system for operating a digital incremental plotter using the information on magnetic tape.

taper In a potentiometer or rheostat, the rate of change in resistance during uniform rotation of the shaft. See, for example, LINEAR TAPER and LOG TAPER.

tape recorder A machine for recording audio, video, or data signals on magnetic tape; it can usually also play back the recorded material.

tapered potentiometer A potentiometer having a tapered resistance winding (see TAPERED WINDING).

tapered winding A resistance winding (in a rheostat or potentiometer) in which the resistance change per unit length of winding is nonuniform (see, for example, LOG TAPER). However, a winding having uniform resistance change is often called LINEAR TAPER.

tape skew A condition in which a magnetic tape passes between the recording or playback heads in an irregular way. The result is that the various channels, or tracks, are not always perfectly aligned.

tape sort The (computer) operation of sorting data in a magnetic tape file into a record-key-determined sequence.

tape splicer A mechanism that aligns and secures the overlapping ends of broken magnetic tape so that they can be cut (often with an integral cutter) to form butted ends, and taped into a splice.

tape station See TAPE DECK.

tape-to-head contact See HEAD-TO-TAPE CONTACT.

tape transmitter A transmitter that receives its signal input from a recorded tape.

tape transport In a tape deck or reproducer, the device that moves the tape past the heads.

tape unit **1.** See TAPE DECK. **2.** See TAPE GROUP.

tape verifier In computer operations, a device that checks the integrity of data on paper tape through comparison with an original document.

tape width In magnetic tape, the dimension perpendicular to tape travel; in general, the greater the tape width, the more tracks the tape can contain.

tape-wound core See TAPE CORE.

tapped coil An inductor to which one or more intermediate connections (taps) are made at appropriate turns to provide intermediate values of inductance.

tapped component A coil, transformer, choke, resistor, or other component in which an intermediate connection is made. See, for example TAPPED COIL.

tapped inductor See TAPPED COIL.

tapped resistor A resistor in which one or more intermediate connections (taps) are made to appropriate parts of the resistance element to provide steps of resistance.

tapped transformer A transformer having one or more tapped windings.

tapped winding A transformer or choke winding with one or more taps. Also see TAP and TAPPED COIL.

tap switch A multiposition switch used to connect an external circuit to various taps on a component. Also see SELECTOR SWITCH and TAP.

target **1.** The bombarded electrode in an X-ray tube. **2.** The scanned storage element in a television camera tube. **3.** In radar operations, the scanned object. **4.** An object intended for nuclear-particle bombardment. **5.** A goal—especially in a production process (deadline, desired number of units, etc.).

target acquisition **1.** The moment at which a target comes within the range of a radar system. **2.** The observation of a new target on a radar screen.

5059F-pT-671-699 4/10/01 9:51 AM Page 674

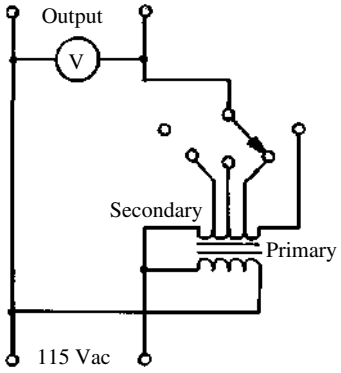

tapped transformer

target discrimination The extent to which a radar system can distinguish between two targets that are close together. Also called *target resolution.* It is specified in linear units (such as meters, kilometers, or miles).

target identification Any method by which the identity of a radar target is determined.

target voltage In a television camera tube, the backplate-to-cathode voltage.

task environment The characteristics of the space in which an autonomous robot works. It depends on such factors as the intended application(s), the required speed at which the robot(s) must work, and the human/robotic or computer/robotic interface.

task-level programming In robotics, the writing of programs to perform sequences of actions. A complex process, it is a primitive level of artificial intelligence (AI). An example is a program that directs a robot to prepare and serve a meal.

taut-band meter A movable-coil meter in which the conventional spiral springs of the coil are replaced by two tightly stretched, thin, straight metal ribbons, whose twist provides torque that returns the pointer to zero after a deflection.

Tb Symbol for TERBIUM.

BS Abbreviation of *talk between ships.*

Tc Symbol for TECHNETIUM.

TCCO Abbreviation of TEMPERATURE-CONTROLLED CRYSTAL OSCILLATOR.

T circuit See TEE NETWORK.

T circuit parameters See R PARAMETERS.

T circulator See TEE CIRCULATOR.

TCL Abbreviation of TRANSISTOR-COUPLED LOGIC.

TCM Abbreviation of *thermocouple meter* (see THERMOCOUPLE-TYPE METER).

TDM Abbreviation of TIME-DIVISION MULTIPLEX.

TDR **1.** Abbreviation of TIME-DELAY RELAY (see DELAY RELAY). **2.** Abbreviation of TIME-DOMAIN REFLECTOMETRY.

TDS Abbreviation of TIME-DELAY SPECTROMETRY.

TE Abbreviation of *transverse electric* (see, for example, TRANSVERSE ELECTRIC MODE).

Te Symbol for TELLURIUM.

teach box A robot-control device via which an operator can program the machine to carry out specific movements. The operator manipulates controls, and the robot's computer stores the data. When the data is accessed, the robot reproduces the motions.

tearing In a television picture, the abnormal condition in which poor synchronization causes the horizontal lines to be irregularly displaced. The effect resembles cloth being torn.

technetium Symbol, Tc. A metallic element produced artificially. Atomic number, 43. Atomic weight, 98. Formerly called *masurium.*

technician **1.** A person who repairs faulty electronic equipment. **2.** A person who assists with the design and debugging of a system prototype. **3.** A person who operates an electronic system.

technocentrism Overdependence on, and/or obsession with, the products of technology, particularly computers.

tee Pertaining to a network, connection, or configuration whose geometric shape or schematic representation resembles an uppercase letter T.

tee adapter See TEE JUNCTION.

tee antenna An antenna consisting of a horizontal radiator with a vertical lead-in or feeder connected to its center point.

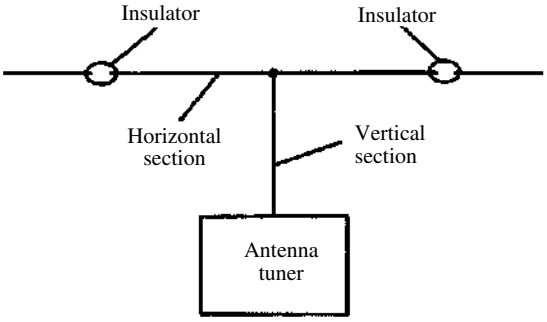

tee antenna

tee circuit See TEE NETWORK.

tee circulator In microwave systems, a tee-shaped junction of three waveguides with a ferrite post at the junction.

tee-equivalent circuit An equivalent circuit in which the components are arranged in the form of a tee. See, for example, TEE NETWORK and R PARAMETERS.

5059F-pT-671-699 4/10/01 9:51 AM Page 675

tee junction **1.** A tee-shaped splice between two wires. **2.** A tee-shaped fixture for splicing one coaxial line perpendicularly to another. **3.** A tee-shaped section for joining one waveguide perpendicularly to another. Also called WAVE GUIDE TEE.

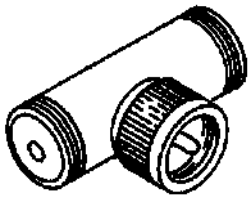

tee junction

tee network A three-terminal network resembling a tee.

tee pad A three-resistor pad in which two series resistors and a shunt resistor are arranged to form a tee.

tee switch A combination of three switches arranged to form a tee; two switches are in series with a shunt switch in between. If the series switches are open and the shunt switch is closed, isolation is greatly improved, compared to a single series switch.

Teflon FEP A plastic insulating material. Dielectric constant, 2.1. Dielectric strength, 2800 V/mil.

Teflon TFE A plastic insulating material. Dielectric constant, 2.2. Dielectric strength, 600 V/mil.

tel **1.** Abbreviation of TELEPHONE. **2.** Abbreviation of TELEGRAPH. **3.** Abbreviation of TELEGRAM.

telautograph A device that transmits and receives handwriting, drawings, and similar material. At the receiver, a pen follows the movements of a similar pen at the transmitter.

teleammeter A TELEMETER for measuring current generated at a remote point.

telecamera See TELEVISION CAMERA.

telecast A television program for general reception. The term a contraction of *television broadcast.*

telechir A remotely controlled, autonomous robot. See TELEOPERATION and TELEPRESENCE.

telecommunication Communication, usually between widely separated points, by electrical or electronic means.

telecontrol See REMOTE CONTROL and TELEOPERATION.

telefacsimile See FACSIMILE.

telegram Abbreviation, tel. A (usually printed-out) message transmitted and received via telegraph or teletypewriter. Compare CABLEGRAM and RADIOGRAM.

telegraph Abbreviation, tel. An instrument for transmitting and receiving messages by means of telegraphy. In its simplest form, it consists of a key and a sounder powered by a battery. Also see PRINTING TELEGRAPH, **1**, **2**.

telegraph channel **1.** The frequency band assigned to a particular telegraph station. **2.** The frequency band occupied by a telegraph signal.

telegraph code Broadly, Morse code. Wire telegraphy often uses a special version, such as the American Morse code.

telegraph key See KEY, **1**.

telegraph sounder See SOUNDER.

telegraph system A complete, integrated, coordinated arrangement of equipment for communication by means of telegraphy. Included are telegraph keys or keyers, sounders or printers, relays, switchboards, wire lines and cables, and power supplies.

telegraphy The branch of electrical communications that deals with the transmission and reception of messages by means of prearranged codes—especially over wires. Also see MORSE, **1**, **2**, **3**; MORSE CODE; and WIRE TELEGRAPHY.

telemeter **1.** An indicating instrument that measures the value of a quantity generated at a distant point or measures and transmits the value. **2.** The action afforded by the device in **1**.

telemetering See TELEMETRY.

telemeter receiver See TELEMETRIC RECEIVER.

telemeter transmitter See TELEMETRIC TRANSMITTER.

telemetric receiver A system that selects, amplifies, and demodulates or rectifies a radio signal, and actuates indicating instruments, recorders, or data processors.

telemetric transmitter A specialized transmitter that generates radio-frequency (RF) power, adds to it signals delivered by data transducers, and delivers the modulated power to an antenna for transmission to a distant telemetric receiver.

telemetry The transmission of data signals over a distance, either by radio or wire, and the reception and application of the signals to indicating instruments, recorders, etc.

teleoperation The remote control of autonomous robots. A human operator can control the speed, direction, and other movements of a robot from some distance away. See also TELEPRESENCE.

telephone Abbreviation, tel. An instrument for transmitting and receiving messages by means of telephony. In its simplest form, it consists of a microphone, earphone, switching and ringing devices, wire line or cable, and power supply. Also see HANDSET.

telephone accessories Devices (such as answering machines, speaker phones, facsimile machines, etc.) used in conjunction with a telephone set.

telephone amplifier A small audio amplifier, usually with a self-contained loudspeaker, for increasing the sound volume of a telephone output. Some amplifiers of this kind are connected to the

5059F-pT-671-699 4/10/01 9:51 AM Page 676

telephone line, and others receive sound from the telephone receiver.

telephone-answering machine See ANSWERING MACHINE.

telephone bypass capacitors A set of fixed capacitors installed between each wire in a telephone line and an electrical ground to bypass radio-frequency energy. It can reduce or prevent radio-frequency interference (RFI) to telephone sets and data terminals.

telephone data set A device that converts signals from a data terminal for passage over a telephone circuit to a data-processing center.

telephone dialer In a security system, a circuit that automatically dials one or more telephone numbers, alerting the recipient(s) that an emergency exists at a given location.

telephone induction coil A small telephone-to-line impedance-matching transformer used in telephone systems.

telephone patch See PHONE PATCH.

telephone pickup A device for receiving conversations from a telephone to which it isn't directly connected.

telephone plug See PHONE PLUG.

telephone-radio patch See PHONE PATCH.

telephone receiver The handheld part of a telephone set, containing the microphone and earphone, and, in some cases, the dialing keypad.

telephone repeater An amplifier and associated equipment used to boost the amplitude of a telephone signal at an appropriate point along the line.

telephone service entrance The point at which the telephone wiring in a house or building connects to the outside telephone line.

telephone silencer A device for muting a telephone or its bell.

telephone system A complete, integrated, and coordinated arrangement of equipment for communication by means of telephony. Included are telephones, switchboards and associated equipment, wire lines and cables, and power supplies. Also see DIAL TELEPHONE SYSTEM, HANDSET, PRIVATE AUTOMATIC EXCHANGE (PAX), PRIVATE BRANCH EXCHANGE (PBX), and TELEPHONE.

telephone test set See PHONE TEST SET.

telephone transmitter The sound pickup unit (microphone) of a telephone. Also see TRANSMITTER, **2**.

telephony The branch of electrical communication dealing with the transmission and reception of sounds—especially over wires. Also see WIRE TELEPHONY.

Telephoto **1.** The transmission and/or reception of photographs by means of FACSIMILE. **2.** A photograph transmitted and/or received by means of FACSIMILE.

telephoto lens A camera lens providing a telescopic effect.

Telephoto receiver See FACSIMILE RECEIVER.

Telephoto transmitter See FACSIMILE TRANSMITTER.

telepresence An advanced form of robotic TELEOPERATION, in which a human operator has the impression of being at the robot's location. It includes vision systems, pressure sensors, sound sensors, tactile sensors, and electromechanical control devices. The operator uses, or wears, equipment similar to that used for VIRTUAL REALITY (VR).

teleprinter A terminal telegraph printing machine. Also see PRINTING TELEGRAPH, **1**, **2**.

TelePrompTer A device that presents a running display on a screen before a television announcer, performer, or speaker, of dialogue.

teleran A ground-to-air communications system. Ground-based radar pictures are transmitted, via television, to aircraft.

telescoping antenna A vertical antenna consisting of separate lengths of metal tubing of progressively smaller diameter so that one can slide into another. The antenna can be pulled out to full length or compressed to the length of the largest-diameter section.

telescoping antenna

teletext A method of communication in which a video image is sent of a page of printed material.

telethermoscope A device for measuring the temperature of distant objects.

Teletorque See AUTOSYN and SYNCHRO.

Teletype **1.** The transmission and/or reception of text messages in digital form, displayed or printed at a distant location. **2.** See TELETYPEWRITER.

teletype grade A term descriptive of a circuit having the quality necessary for communication via telegraphy.

Teletypesetter An electronic system for operating a distant Linotype.

teletypewriter A variety of printing telegraph using electric typewriters and associated equipment. The message is typed on the keyboard at the transmitting station and is typed out in corresponding letters at the receiving station. The same typewriter is able to send and receive messages. Also see RADIOTELETYPEWRITER.

teletypewriter exchange Abbreviation, TWX. A center for switching and routing teletypewriter communications. Also see TELETYPEWRITER.

televiewer To observe a scene or program via television.

televise **1.** To convert a scene into a television signal. **2.** To broadcast a scene or program via television.

5059F-pT-671-699 4/10/01 9:51 AM Page 677

television **1.** Abbreviation, TV. The transmission and/or reception, via electromagnetic fields, wire cable, and/or fiberoptic cable, of images, usually with sound. **2.** A system for receiving signals, as defined in **1**. **3.** Video programs or data, with or without sound, transmitted via electromagnetic fields, wire cable, and/or fiberoptic cable.

television band See UHF TELEVISION CHANNELS and VHF TELEVISION CHANNELS.

television camera The pickup device that scans a scene and delivers a series of electrical signals that can be used to reconstruct the image on the screen of a picture tube.

television-camera tube See CAMERA TUBE, ICONOSCOPE, and ORTHICON.

television channel A radio-frequency band allocated exclusively for the transmission of a television signal. In conventional broadcasting, this band is usually 6 MHz wide. See, specifically, UHF TELEVISION CHANNELS and VHF TELEVISION CHANNELS.

television engineer A trained professional skilled in video electronics engineering, as well as in basic engineering and associated subjects.

television engineering The branch of electronics engineering devoted to the theory and application of television.

television interference Abbreviation, TVI. Interference to the reception of television signals, usually occasioned by signals from radio services or computers, or by electrical noise.

televisor **1.** A television transmitter or receiver. **2.** A person or entity responsible for the broadcast of television programs or signals.

televoltmeter A TELEMETER for measuring voltage generated at a remote point.

telewriter See TELAUTOGRAPH.

Telex **1.** A teleprinter system that operates via the telephone lines, and was once commonly used by businesses for sending and receiving short messages. It has largely been supplanted by computerized data communications systems. **2.** A hard-copy message sent or received by such a system.

telluric currents Also called *terrestrial currents.* A flow of electrical charge carriers, primarily electrons, in the earth.

tellurium Symbol, Te. A rare, metalloidal element related to selenium. Atomic number, 52. Atomic weight, 127.60.

TE mode See TRANSVERSE ELECTRIC MODE.

temp **1.** Abbreviation of *temperature.* (Also, T.) **2.** Abbreviation of *temporary.* **3.** Abbreviation of TEMPLATE.

temperament The tuning of a keyboard-type musical instrument to produce a nearly perfect diatonic scale.

temperature Symbol, T. A quantitative measure of the heat exhibited by an object or phenomenon. Also see THERMOMETER SCALE.

temperature coefficient A figure that states the extent to which a quantity drifts or varies under the influence of changing temperature. It is generally expressed in percent per degree (%/°C) or in parts per million per degree (ppm/°C).

temperature-compensated crystal oscillation Oscillation in a crystal oscillator, in which the crystal and/or circuit is automatically compensated against frequency drift caused by temperature change.

temperature-compensating component A circuit component, such as a capacitor or resistor, whose temperature coefficient is equal in magnitude and opposite in sign to that of a conventional component to which it is connected to cancel temperature-induced variation in the latter's value.

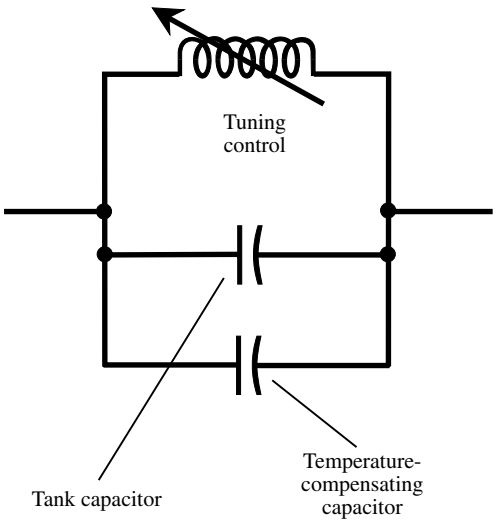

temperature-compensating component

temperature compensation The use of a device, such as a temperature-compensating component, to correct a temperature-induced deviation in the value of a conventional component.

temperature control **1.** The adjustment of temperature. **2.** The automatic maintenance of temperature at a desired level, as in a temperature-controlled oven. **3.** A device for controlling temperature, as defined in **1** or **2**.

temperature-controlled crystal oscillator Abbreviation, TCCO. A high-precision crystal oscillator in which the crystal plate (and sometimes the circuitry, as well) is held at constant temperature.

temperature degree See DEGREE, **2** and THERMOMETER SCALE.

temperature derating Deliberate reduction of operating current and/or voltage of a device to a specific temperature to ensure proper operation. Also see DERATING, DERATING CURVE, and DERATING FACTOR.

5059F-pT-671-699 4/10/01 9:51 AM Page 678

temperature gradient A range of temperature variation, such as the rate of change of temperature, with respect to change of power dissipation, or the rate of change of temperature with spatial displacement.

temperature inversion See INVERSION, **1**.

temperature meter An indicator (usually a direct-current voltmeter or millivoltmeter) whose scale reads directly in degrees.

temperature scale See THERMOMETER SCALE.

temperature-sensitive resistor See THERMISTOR.

temperature shock See THERMAL SHOCK.

temperature-to-voltage converter A circuit or device, such as a thermocouple, that delivers an output voltage proportional to an applied temperature.

template **1.** A diagram, usually drawn on paper, to show the locations at which components should be placed or tasks should be performed. It is taped or cemented temporarily to the work, and the points are transferred to the latter by prick-punching. **2.** A stencil-like plate with alphanumeric and circuit symbols, used as a drafting aid. Sometimes called "drafting stencil."

temporary magnet **1.** A body that exhibits magnetism only briefly after it has been exposed to another magnet. Compare PERMANENT MAGNET. **2.** See ELECTROMAGNET.

temporary storage **1.** In computer and data-processing operations, the storage of data or instructions only until they are needed. Also called INTERIM STORAGE. **2.** Locations in a computer memory set aside during a program run for holding intermediate results of operations.

TEM wave See TRANSVERSE ELECTROMAGNETIC WAVE.

ten code A set of abbreviations used by two-way radio operators. Each "ten signal" represents a specific statement or query.

tension **1.** A force that tends to stretch, pull tight, or pull apart. Compare STRAIN. **2.** A term referring to VOLTAGE—especially in a utility power transmission line.

ten-turn potentiometer A precision potentiometer whose shaft must be turned through 10 complete revolutions to cover the entire resistance range. Also see HELICAL POTENTIOMETER and MULTITURN POTENTIOMETER.

T-equivalent circuit See TEE-EQUIVALENT CIRCUIT.

tera- Abbreviation, T. **1.** A prefix meaning trillion(s), (i.e., 10^{12}). **2.** A prefix meaning 2^{40}.

tera-electronvolt Abbreviation, TeV. A large unit of energy; 1 TeV = 10^{12} electronvolts. Also see ELECTRONVOLT.

terahertz Abbreviation, THz. A unit of extremely high frequency equal to 10^{12} Hz. Also called *Fresnel.*

teraohm A unit of high resistance, reactance, or impedance equal to 10^{12} ohms.

terawatt Abbreviation, TW. A large unit of power; 1 TW = 10^{12} W.

terbium Symbol, Tb. A metallic element of the rare-earth group. Atomic number, 65. Atomic weight, 158.93.

terbium metals A group of rare-earth metals, including *europium*, *gadolinium*, *terbium*, and occasionally *dysprosium.*

term In an algebraic expression, constants, variables, or combinations of these, separated by operation signs (e.g., the expression $4xy + z$ has two terms).

terminal **1.** A connection point at the input, output, or an intermediate point of a device, or a point at which a voltage is to be applied. **2.** A metal tab or lug attached to the end of a lead for connection purposes. **3.** Pertaining to the end of a series of events, etc. (e.g., terminal tests). **4.** In a data-communications system, a point of data input or output. Also called *data terminal.* If it does not have computing capability of its own, it is often called a *dumb terminal.*

terminal block A group of several terminals, intended for interconnection of circuits, mounted on a solid insulating block.

terminal board An insulating board carrying several lugs, tabs, or screws as terminals (see TERMINAL, **2**). Also see TERMINAL STRIP.

terminal guidance The navigation of a missile or aircraft to help it reach its target or destination.

terminal impedance The internal impedance of a device measured at the input or output terminals.

terminal point of degradation The point at which degradation of a circuit or component is complete. Also see DEGRADATION FAILURE.

terminal repeater A telephone repeater operated at the end of a line.

terminal strip A strip of insulating material, such as plastic or ceramic, on which are mounted one or more screws, lugs, or other terminals. Also see TERMINAL, **2**.

terminal strip (lug-type)

terminal voltage The voltage at the output terminals of an unloaded battery or generator.

ternary code See TRINARY NUMBER SYSTEM.

ternary fission The splitting of an atomic nucleus into three nuclear pieces. Also see FISSION.

ternary number system See TRINARY NUMBER SYSTEM.

terrain echoes Radar images caused by reflections from hills, mountains, and other natural terrestrial surface features. Also see GROUND CLUTTER.

5059F-pT-671-699 4/10/01 9:51 AM Page 679

terrestrial magnetism See EARTH'S MAGNETIC FIELD.

tertiary coil A third winding (see TERTIARY WINDING).

tertiary winding A third winding on a transformer or magnetic amplifier.

tesla Symbol, T. A unit of magnetic flux density; 1 T = 1 weber per square meter = 10^4 gauss.

Tesla coil A special type of air-core step-up transformer for developing high voltage at radio frequencies. It consists essentially of a low-turn primary coil, through which radio-frequency (RF) current flows, and a multiturn secondary coil, across which the high voltage, is developed.

test A procedure consisting of one or several steps, in which (1) the mode of operation of a circuit or device is established, (2) the value of a component is ascertained, or (3) the behavior of a circuit or device is observed.

test bench An equipment installation intended for the testing, repair, or debugging of electronic devices by a technician.

test data Data used to test a computer program, including samples within limits that might be encountered during the program's implementation.

tester **1.** See TEST INSTRUMENT. **2.** A technician who primarily makes tests and measurements.

testing window See WINDOW, **2**.

test instrument A device for checking the operation of a circuit or the value of a component. This class of instrument is usually less accurate than measurement instruments. Also see TEST SET.

test lead The flexible, insulated wire attached to a test prod.

test pattern A picture-and-line display on the screen of a television picture tube, used to check such features as aspect ratio, linearity, contrast, etc.

test point A terminal intended for connection of test equipment in the repair or debugging of a circuit. Often, test points are labeled by the letters TP followed by numerals (such as TP1, TP2, etc.).

test probe See PROBE, **1**.

test prod A stick-type probe (see PROBE, **1**) with a flexible, insulated lead terminating in a plug or lug for attachment to an instrument.

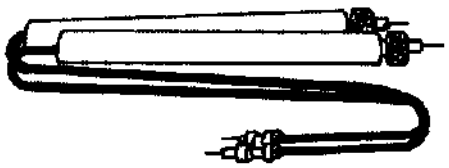

test prods

test program In computer operations, a program devised to check the functioning of hardware. Also called *utility* and *test routine.*

test run In computer operations, using test data to check the operation of a program, by comparing the results obtained thereby with what should ideally result.

test set A combination of instruments assembled on a single panel, and usually enclosed in a carrying case, for convenience in making tests.

test signal **1.** A signal used for conducting a test of a component, circuit, or system. **2.** In radiotelegraphy, a special signal signifying that the transmitting station is testing equipment. Also see VEE SIGNAL.

test-signal generator A device, such as an oscillator, for producing a signal for testing equipment (see TEST SIGNAL, **1**).

test tape A magnetic tape containing signals for testing equalization, frequency response, head adjustment, stereo balance, etc. in an audiotape recorder, high-fidelity sound system, computer tape drive, or videocassette recorder.

tetravalent See QUADRIVALENT.

tetrode An electron tube in which the principal electrodes are cathode, control grid, screen, and plate.

tetrode transistor **1.** A bipolar transistor with two emitters. **2.** A dual-gate field-effect transistor.

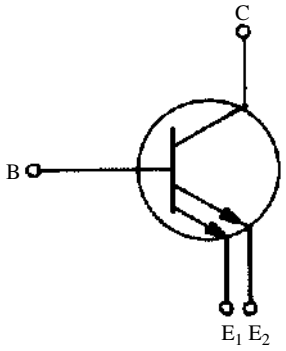

tetrode transistor

TeV Abbreviation of TERA-ELECTRONVOLT.

T_e value The temperature at which a centimeter cube of glass or ceramic exhibits 1 megohm of resistance.

TE wave See TRANSVERSE ELECTRIC MODE.

text editor A computer program for finding and changing data in a file.

texture map In computer graphics, the topographical qualities of the surface of a three-dimensional rendition. For example, the image of an orange would have a "bumpy" texture map; the image of a peach would have a "fuzzy" texture map.

texture sensing The ability of a robotic end effector to determine the relative smoothness or

5059F-pT-671-699 4/10/01 9:51 AM Page 680

roughness of a surface. One common scheme uses reflected light or infrared. Scattered reflections indicate a rough or matte surface.

tgt Abbreviation of TARGET.

TH Abbreviation of *true heading.*

Th Symbol for THEORIUM.

TH Symbol for *heater temperature.*

thallium Symbol, Tl. A metallic element. Atomic number, 81. Atomic weight, 204.38.

thalofide cell An evacuated photoconductive cell using thallium oxysulfide as the light-sensitive material.

THD Abbreviation of TOTAL HARMONIC DISTORTION.

theory A reasonable proposition put forth to account for the behavior of, or the relationships between, bodies and forces, or to explain concepts and their relations. When a theory has stood up under exhaustive tests, it might reveal a scientific law.

therm A gas heating unit. 1 therm = 100,000 British thermal units (10^5 Btu).

thermal agitation Random movement of particles (such as electrons) in a substance, because of heat.

thermal-agitation noise See THERMAL NOISE.

thermal ammeter See HOT-WIRE AMMETER.

thermal anemometer See HOT-WIRE ANEMOMETER.

thermal conductivity The heat-conducting ability of a material. Compare electrical conductivity (see CONDUCTIVITY).

thermal conductivity

Element	*Thermal conductivity (mW/m/°C)*
Aluminum	22.0
Carbon	2.4
Chrominum	6.9
Cooper	39.0
Gold	30.0
Iron	7.9
Lead	3.5
Magnesium	16.0
Mercury	0.8
Nickel	8.9
Platinum	6.9
Silicon	8.4
Silver	41.0
Thorium	4.1
Tin	6.4
Tungsten	20.0
Zinc	11.0

thermal-conductivity device An instrument or control unit using a heated filament whose temperature and, accordingly, conductivity is varied by some sensed phenomenon. See, for example, GAS DETECTOR, HEATED-WIRE SENSOR, HOT-WIRE ANEMOMETER, HOT-WIRE FLOW-METER, and HOT-WIRE MICROPHONE.

thermal-conductivity gasmeter See GAS DETECTOR.

thermal detector **1.** See BOLOMETER. **2.** In a security or fire-protection system, a device that closes a circuit or actuates an alarm if the temperature rises to a specific level.

thermal emf See SEEBECK EFFECT.

thermal gasmeter See GAS DETECTOR.

thermal imaging See THERMOGRAPHY.

thermal instrument See HOT-WIRE METER and THERMOCOUPLE-TYPE METER.

thermally sensitive resistor See THERMISTOR.

thermal meter See HOT-WIRE METER and THERMOCOUPLE-TYPE METER.

thermal neutron A neutron that is essentially in thermal equilibrium with the surrounding medium or environment.

thermal noise Frequency-independent electrical noise caused by the agitation of particles (e.g., atoms and electrons) in a material by heat. Thermal noise is proportional to bandwidth, resistance, and absolute temperature.

thermal radiation See HEAT.

thermal recorder A graphic recorder in which a strip of paper coated with a thin layer of opaque wax is drawn between a knife-edge platen and a heated writing stylus that melts the wax beneath its point, exposing the underlying black paper as a fine line.

thermal resistance Symbol, *RT*. For a semiconductor device, the rate of change of junction temperature, with respect to power dissipation; $RT = dT/dP$, where *RT* is in degrees Celsius per milliwatt, *T* is the temperature in degrees Celsius, and *P* is the power in milliwatts.

thermal resistor A resistor that is sufficiently temperature-sensitive to be used as a heat sensor. Examples: thermistor and germanium diode.

thermal response time For a power-dissipating component, the elapsed time between the initial change in power dissipation and the moment at which the temperature has changed by a specified percentage (usually 90%) of the total value.

thermal runaway A destructive process resulting from cumulative temperature effects. In bipolar transistors, this can occur if the collector current increases as the temperature rises. As the unit gets hotter, the collector-base junction dissipation increases, generating still more heat. The ultimate result, if the process continues unchecked, is destruction of the component. The process can also occur in certain batteries when they are charged too rapidly or at excessively high temperatures.

thermal shock The effect of applying heat or cold to a device so rapidly that abnormal reactions occur, such as rapid (often catastrophic) expansions and contractions.

5059F-pT-671-699 4/10/01 9:51 AM Page 681

thermal switch A switch actuated by a temperature change. Types vary from the simple thermostat to complex servosystem switches with a temperature-transducer input.

thermal time-delay relay A delay relay utilizing the slow-heating and slow-cooling property of one of its components.

thermion An ion or electron emitted by a hot body, such as the heated cathode of a vacuum tube.

thermionic Pertaining to thermions and their applications.

thermionic cathode A heated cathode, in contrast to a cold cathode, used as an emitter of electrons or ions. Also see THERMION.

thermionic current Current caused by thermionic emission—especially in an electron tube.

thermionic detector A vacuum-tube detector. Also see THERMION and THERMIONIC EMISSION.

thermionic diode A hot-cathode diode tube.

thermionic emission The emission of electrons by a hot body, such as the filament or cathode of a vacuum tube. Also see THERMION and HOT CATHODE.

thermionics The study of electron emission from objects or materials at high temperature.

thermionic tube An electron tube (i.e., one in which electrons or ions are emitted by a heated cathode). Also see THERMION, THERMIONIC CURRENT, and THERMIONIC EMISSION.

thermionic work function The energy required to force an electron from inside a heated cathode into the surrounding space (in thermionic emission). Also see WORK FUNCTION.

thermistor A temperature-sensitive resistor, usually made from specially processed oxides of cobalt, magnesium, manganese, nickel, uranium, or mixtures of such substances. Thermistors are available with either a positive or negative temperature coefficient of resistance. The name is a contraction of *thermally sensitive resistor.*

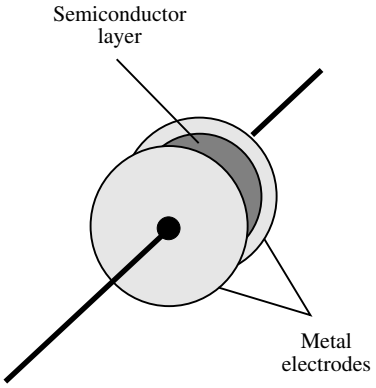

thermistor

thermistor bridge A four-arm bridge (see BRIDGE, **1**) in which one arm is a thermistor and, therefore, is temperature sensitive.

thermistor power meter A radio-frequency power-measuring instrument based on a thermistor bridge.

thermistor probe A temperature probe containing a thermistor as the sensing element.

thermistor thermometer An electronic thermometer in which the temperature-sensitive element is a thermistor.

thermoammeter See THERMOCOUPLE-TYPE METER.

thermocouple A device consisting essentially of a bond between two wires or strips of dissimilar metals (such as antimony and bismuth). When the bond is heated, a direct-current voltage appears across it.

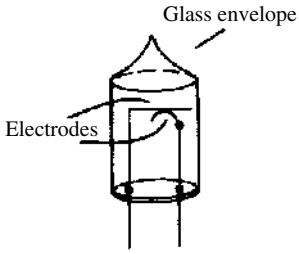

thermocouple

thermocouple bridge A four-arm bridge (see BRIDGE, **1**) in which one arm is a thermocouple; therefore, it is temperature sensitive, as well as being voltage-productive.

thermocouple meter See THERMOCOUPLE-TYPE METER.

thermocouple-type meter A radio-frequency (RF) meter consisting of a thermocouple and direct-current (dc) ammeter, milliammeter, or microammeter, connected in series. The thermocouple is heated, directly or indirectly, by an applied RF current, and the resulting dc output deflects the meter pointer.

thermodynamics The science dealing with the relationships between heat and mechanical energy and their interconversion. Also see CARNOT THEOREM, FIRST LAW OF THERMODYNAMICS, SECOND LAW OF THERMODYNAMICS, and THIRD LAW OF THERMODYNAMICS.

thermoelectric cooler A cooling device based on the Peltier effect.

thermoelectric effect The production of thermoelectricity by certain materials.

thermoelectricity Heat-produced electricity, as in thermocouple operation.

thermoelectric junction A junction between two conductors that exhibits variable characteristics under conditions of changing temperature.

5059F-pT-671-699 4/10/01 9:51 AM Page 682

thermoelectric series A series of conducting metals, sequenced so that if a thermocouple is made from two of the metals, current flows at the hot junction from the metal occurring earlier in the series.

thermoelectron An electron emitted by a hot cathode. Also see THERMION and THERMIONIC EMISSION.

thermoelement A thermocouple, especially a miniature one, used in a THERMOCOUPLE-TYPE METER.

thermogalvanometer See THERMOCOUPLE TYPE METER.

thermography A means of locating or mapping by detecting infrared images. It can be in the form of live video, similar to television, or in the form of photographs, using infrared film. Many common cameras can be used with infrared film to make infrared photographs (thermographs).

thermojunction The junction of the two metals in a thermocouple. A voltage appears when the dissimilar metals are heated.

thermoluminescence Luminescence resulting from the moderate heating of certain materials.

thermomagnetic effect The effects of temperature on the magnetism of a body, or vice versa.

thermometer A (usually direct reading) device for measuring temperature. Also see ELECTRONIC THERMOMETER and THERMOMETER SCALE.

thermometer scale The scale on a thermometer, graduated in degrees, from which temperature is read. For a description of different scales, see ABSOLUTE SCALE, CENTIGRADE SCALE, FAHRENHEIT SCALE, REAUMUR SCALE, and RANKINE SCALE. The Kelvin scale is the same as the absolute scale, and the Celsius scale is the same as the centigrade scale.

thermonuclear reaction A nuclear reaction in which energy is released when lighter atoms are converted into heavier atoms at temperatures in the millions of degrees Celsius. Also see FISSION, FUSION, and NUCLEAR REACTOR.

thermopile A device consisting of two or more thermocouples connected in series for increased voltage output.

thermoplastic material A plastic that can be resoftened by applying heat after having been molded into a desired shape. Example: polystyrene. Compare THERMOSETTING MATERIAL.

thermorelay See THERMOSTAT.

thermosensitivity Sensitivity of a circuit or device to heat.

thermosetting material A plastic that cures chemically (will not ordinarily soften again when heat is applied) after having been heat-molded into a desired shape. Example: Bakelite. Compare THERMOPLASTIC MATERIAL.

thermostat A temperature-sensitive switch. In one common form, a movable contact is carried by a strip of bimetal and the stationary contact is mounted nearby.

thermostatic switch See THERMOSTAT.

thermoswitch See THERMOSTAT.

theta wave A form of brain wave that occurs at extremely low frequencies, and is associated with sleep or mental incoherence.

Thevenin's theorem The proposition that, with reference to a particular set of terminals, a network containing a number of generators and constant impedances can be simplified to a single generator in series with a single impedance. The equivalent circuit will deliver to a given load, the same current, voltage, and power delivered by the original network. Compare COMPENSATION THEOREM, MAXIMUM POWER TRANSFER THEOREM, NORTON'S THEOREM, RECIPROCITY THEOREM, and SUPERPOSITION THEOREM.

thick film A film of selected material (conductive, resistive, dielectric, etc.) applied to a substrate by painting, photography, or similar process. See, for example, PRINTED CIRCUIT. Compare THIN FILM. Typically, thick films are 1 mil or more in thickness.

thick-film component A unit, such as a capacitor or resistor, fabricated by thick-film techniques. See, for example, PRINTED COMPONENT. Also see THICK FILM. Compare THIN-FILM COMPONENT.

thick-film resistor A resistor fabricated by thick-film techniques. See, for example, PRINTED RESISTOR. Also see THICK FILM. Compare THIN-FILM COMPONENT.

thick magnetic film See MAGNETIC THICK FILM.

thin film An extremely thin layer (less than 1 mil) of a selected material (conductive, resistive, semiconductive, dielectric, etc.) electrodeposited or grown on a substrate. Compare THICK FILM.

thin-film capacitor A capacitor made by electrodepositing a thin film of metal on each side of a grown layer of oxide, as in an integrated circuit. Also see THIN FILM.

thin-film component A unit (such as a capacitor, resistor, diode, or transistor), fabricated by thin-film techniques. Also see THIN FILM. Compare THICK-FILM COMPONENT.

thin-film integrated circuit An integrated circuit in which the components and "wiring" are produced by depositing (or growing) and processing materials on a semiconductor slab or wafer (the substrate). Compare HYBRID INTEGRATED CIRCUIT and MONOLITHIC INTEGRATED CIRCUIT.

thin-film memory In a computer, a storage meium that is a magnetic thin film (see THIN FILM) on a nonmagnetic substrate (often glass) and that can be magnetized to represent digital data.

thin-film microelectronic circuit An integrated circuit that occupies (essentially) two dimensions; that is, a very thin integrated circuit.

thin-film resistor A resistor fabricated by thin-film techniques (see THIN FILM) (e.g., TANTALUM-NITRIDE RESISTOR). Compare THICK-FILM RESISTOR.

5059F-pT-671-699 4/10/01 9:51 AM Page 683

thin-film semiconductor A very shallow layer of semiconductor material, such as single-crystal silicon, electrodeposited on a substrate. Also see THIN FILM.

thin-film transistor A transistor fabricated by thin-film techniques. Also see THIN FILM and THIN-FILM COMPONENT.

thin magnetic film See MAGNETIC THIN FILM.

third-generation computer A computer in which the active discrete components are integrated circuits.

Third Law of Thermodynamics As the temperature of absolute zero is approached in an isothermal process involving a solid or liquid, the change in entropy approaches zero; and the entropy of a substance is zero at absolute zero.

third-octave band See ONE-THIRD-OCTAVE BAND.

thirty-channel multiplex A form of pulse-code-modulated (PCM) multiplex using eight digits and the A-law. There are 30 speech channels and two utility channels.

Thomson bridge See KELVIN BRIDGE.

Thomson effect The liberation or absorption of heat (depending on the material of interest) when an electric current flows from a warmer to a cooler part of a conductor.

Thomson heat The amount of thermal energy transferred because of Thomson effect.

Thomson voltage The voltage drop between two points on a conductor that are at different temperatures.

thoriated-tungsten filament In a vacuum tube, a filament made of tungsten to which thorium oxide has been added to increase the emission of electrons. Also see THERMION and THERMIONIC EMISSION.

thorium Symbol, Th. A radioactive metallic element. Atomic number, 90. Atomic weight, 232.04. Thorium, when heated, is a copious emitter of electrons, so the filaments or cathode cylinders of some electron tubes are coated with one of its compounds.

thoron Symbol, Tn. A radioactive isotope of RADON.

three-address instruction A computer program instruction having three addresses, two for operands and one for the result (of the operation called for).

three-channel stereo A form of stereophonic sound recording and reproduction in which three distinct channels are used; these are usually designated the left, right, and center channels.

three-coil meter See ELECTRODYNAMOMETER.

three-conductor jack A female connector in which two separate conductors are provided, in addition to the ground conductor.

three-conductor plug A male connector in which two separate conductors are provided, in addition to the ground conductor.

three-dimensional television See STEREOSCOPIC TELEVISION.

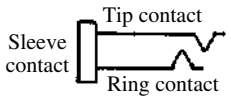

three-conductor jack

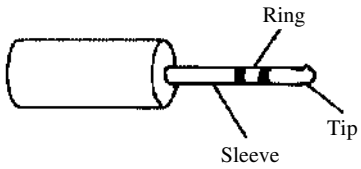

three-conductor plug

three-electrode tube See TRIODE.

three-element tube See TRIODE.

three-gun picture tube A color-television picture tube having a separate gun for each primary color (red, green, and blue).

three-halves-power law See CHILD'S LAW.

three-junction transistor A pnpn or npnp transistor. Also see NPNP DEVICE.

three-phase bridge rectifier A bridge-rectifier circuit for three-phase alternating current. Two diodes are provided for each phase. The ripple frequency is six times the line frequency. Also see BRIDGE RECTIFIER, POLYPHASE RECTIFIER, and THREE-PHASE CIRCUIT.

three-phase circuit The circuit of a three-phase system. See THREE-PHASE SYSTEM and, specifically, DELTA CONNECTION and WYE CONNECTION.

three-phase current Current in a three-phase circuit. The currents in the three legs differ in phase by 120°.

three-phase four-wire system See FOUR-WIRE WYE SYSTEM.

three-phase generator A (usually dynamo-type) generator of three-phase current or voltage. See THREE-PHASE SYSTEM.

three-phase half-wave rectifier A half-wave rectifier circuit for three-phase alternating current. One diode is provided for each phase. The ripple frequency is three times the line frequency. Also see HALF-WAVE RECTIFIER, POLYPHASE RECTIFIER, and THREE-PHASE CIRCUIT. Compare THREE-PHASE BRIDGE RECTIFIER.

three-phase motor An alternating-current motor operating on three-phase power. Above fractional-horsepower size, the three-phase motor is smoother running and more simply structured than the single-phase counterpart.

three-phase power The total power dissipated or delivered in a three-phase alternating-current circuit.

three-phase rectifier A rectifier for three-phase alternating current. At least one diode is included

5059F-pT-671-699 4/10/01 9:51 AM Page 684

for each phase. Also see POLYPHASE RECTIFIER, THREE-PHASE BRIDGE RECTIFIER, THREE-PHASE CIRCUIT, and THREE-PHASE HALF-WAVE RECTIFIER.

three-phase system An alternating-current electrical system in which three currents or voltages exist simultaneously. They are of equal amplitude, but are 120° out of phase with each other.

three-phase, three-wire system An electrical system having three conductors, with an alternating-current phase difference of 120° between conductor pairs.

three-phase-to-single-phase transformer An alternating-current transformer with three-phase input and single-phase output (one terminal is grounded).

three-phase-to-two-phase transformer An alternating-current transformer with three-phase input and two-phase output, the output currents are 180° out of phase with each other.

three-phase voltage Voltage in a three-phase alternating-current circuit. The voltages across the three legs differ by 120°.

three-quarter bridge A bridge rectifier having diodes in three arms and a resistor in the fourth.

three-space A mathematical continuum in which each point is uniquely defined by three variables in an ordered triple, such as (*x*,*y*,*z*), and each ordered triple corresponds to exactly one point in the space. A common coordinate system is the Cartesian system consisting of three axes, *x*, *y*, and *z*—each mutually perpendicular and intersecting at the origin (0,0,0).

three-space coordinates Any set of coordinates used for locating points or plotting graphs in three dimensions.

three-state logic See TRI-STATE LOGIC.

three-way speaker A set of three individual speakers contained in a single cabinet: a woofer (low-frequency speaker), a midrange speaker, and a tweeter (high-frequency speaker). It is common in high-fidelity music reproduction systems. Compare TRIAXIAL SPEAKER.

three-wire system **1.** An electric-power feed system using three wires, the center one (neutral) being at a potential midway between the potential across the other (outer) two. **2.** See THREE-PHASE and THREE-WIRE SYSTEM. **3.** See TWO-PHASE and THREE-WIRE CIRCUIT.

threshold **1.** The initial (observable) point of an effect (e.g., *threshold of hearing*). **2.** A predetermined point, such as of minimum current or voltage, for the start of operation of a circuit or device.

threshold component A value of current, voltage, sound intensity, etc., selected as the minimum level at which a circuit or device is to operate in some prescribed manner, or beyond which a certain condition will prevail. Also see THRESHOLD, **1**, **2**.

threshold current **1.** The minimum value of current at which a certain effect takes place. **2.** The smallest amount of forward current that flows through a diode. **3.** In a gas, the smallest level of current for which a discharge will maintain itself under variable conditions.

threshold detector A device that prevents a signal from passing until its peak amplitude reaches a certain value.

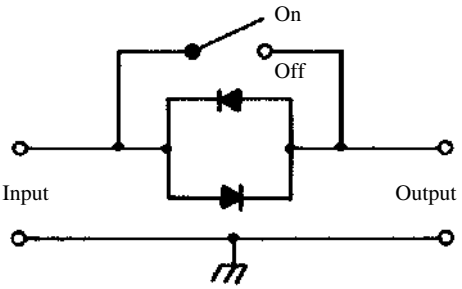

threshold detector

threshold frequency **1.** The cutoff frequency or frequencies in a band-pass, band-rejection, low-pass, or high-pass filter. **2.** The lowest frequency for a metal or semiconductor junction at which incident radiation gives rise to the photoelectric effect.

threshold of hearing The minimum intensity level at which sounds are audible in an environment containing essentially no background acoustic noise.

threshold of pain The intensity level at which hearing a sound causes physical discomfort. This is approximately 120 dB above the THRESHOLD OF HEARING for most people.

threshold signal The weakest signal that can be detected in a receiving system.

throat See HORN THROAT.

throat microphone A small microphone operated in contact with the user's throat.

throttle The feedback control device in a regenerative detector or amplifier.

throughput In computer operations, an overall quantitative indicator of processing power, expressed in terms of the amount of data processed in a given period of time.

throw-out spiral On a phonograph disc, a lead-out groove.

thulium Symbol, Tm. A metallic element of the rare-earth group. Atomic number, 69. Atomic weight, 168.93.

thumbwheel potentiometer A potentiometer operated by means of a knurled knob (usually protruding perpendicularly through a panel) that is turned with the thumb or with a finger.

thumbwheel switch A switch operated by means of a knurled knob (usually protruding perpendicularly through a panel) that is turned with the thumb or with a finger.

5059F-pT-671-699 4/10/01 9:51 AM Page 685

thy Abbreviation of THYRATRON.

thyratron A gas triode or gas tetrode used principally for switching and control purposes. Thyratron action differs from that of the vacuum tube in the unique behavior of the thyratron control electrode (grid): Anode current starts to flow abruptly when grid voltage reaches a particular value, at which point the grid provides no further control; anode current continues to flow until the anode voltage is either interrupted or reversed.

thyratron inverter An inverter circuit (see INVERTER, **1**) using thyratrons as the switching devices. Also see THYRATRON.

Thyrector A silicon diode exhibiting very high resistance (approaching that of an insulator) up to a certain voltage, beyond which the unit switches to a low-resistance conducting state.

thyristor **1.** A pnpn-type bistable semiconductor device having anode, cathode, and gate terminals that is used as an electronic switch. **2.** The generic term for all thyratronlike solid-state devices, such as the silicon-controlled rectifier.

Thyrite Ceramic silicon carbide, a nonlinear resistance material, or a resistor made of this material. The resistance of Thyrite decreases sharply as the applied voltage is increased. Thyrite resistors are used in voltage regulators, equipment protectors, lightning arresters, curve changers, and similar devices.

THz Abbreviation of TERAHERTZ.

Ti Symbol for TITANIUM.

tickler A (usually small) coil, through which energy is inductively fed back from the output to the input of a circuit to induce oscillation.

tickler coil See TICKLER.

tickler-coil regeneration Positive feedback obtained via inductive coupling between a small coil (tickler) in the output circuit of an amplifier, and a (usually larger) coil in the input circuit. Also see TICKLER.

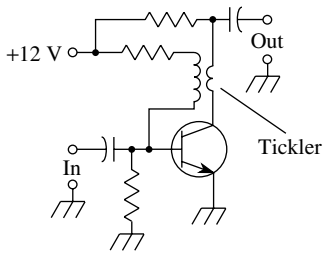

tickler-coil regeneration

tickler oscillator An oscillator circuit in which positive feedback is obtained through inductive coupling between an output (tickler) coil and an input coil.

tie A bracket, clamp, clip, ring, or strip for holding several wires tightly as a cable or bundle.

tie cable **1.** A cable that connects two distributing points in a telephone system. **2.** Any cable that interconnects two circuits.

tie point A lug, screw, or other terminal to which wires are connected at a junction.

tie-point strip A terminal strip with lugs to which conductors can be soldered.

tight coupling See CLOSE COUPLING.

tilt switch A device, such as a mercury switch, that is actuated by tilting it to a certain angle.

timbre The quality that distinguishes the sound of one voice or instrument from that of another, largely because of harmonic content.

time Symbol, *t*. **1.** The instant at which an event occurs. **2.** The instant at which a time-base variable reaches a given value. **3.** The interval between two instants, commonly called *duration* or *length of time*. Also see STANDARD TIME, TIME BASE, TIME ZONE, and ZERO TIME.

time base Time as the independent variable in a physical relation or function. It appears in expressions such as *pulses per second*, *feet per minute*, *watts per hour*, etc.

time compressor In audio recording and reproduction, a device that speeds up or slows down the tempo without changing the audio frequencies. It is used for special effects.

time constant See ELECTRICAL TIME CONSTANT and MECHANICAL TIME CONSTANT.

time delay See DELAY, **1**, **2**.

time-delay relay See DELAY RELAY.

time-delay spectrometry In acoustics, a method of simulating an echo-free environment within an enclosure that is actually not echo-free.

time-division multiplexing Abbreviation, TDM. In data and computer communications, a time-sharing technique in which several terminals use the same channel by transmitting data at regular, staggered intervals (i.e., one is active while the others are idle). This gives the appearance of simultaneous real-time operation.

time-division-multiplex switch A switch with multiple ports—each port corresponding to a certain time slot in a time-division-multiplex scheme. The input and output (send and receive) ports are connected by selecting the same TIME SLOT for each.

time-domain reflectometry Abbreviation, TDR. Measuring the reflective characteristics of a device or system by superimposing the direct and reflected components of a step-formed test signal on a time-calibrated oscilloscope screen.

time duration See TIME, **3**.

time-duration modulation See PULSE-DURATION MODULATION.

time factor The ratio *ta*/*tr*, where *ta* is analog time (the relativistic duration of an event as simulated by a computer), and *tr* is real time (the actual duration of the event). Also called TIME SCALE.

time-interval mode In computer operations, operation that allows a number of events to be counted between two points on a waveform.

5059F-pT-671-699 4/10/01 9:51 AM Page 686

time modulation Any form of modulation in which the instantaneous characteristics of a signal are varied.

timeout The expiration of an allotted time period for a given operation.

timer **1.** A device for automatically controlling the duration of an operation. See ELECTRONIC TIMER. **2.** A device for measuring the duration of an operation.

time sharing In computer operations, a method for interlaced (i.e., nearly simultaneous) use of a machine or facility by two or more persons or agencies. As the cost of computers diminishes, so does the need for time sharing. Also see TIME-DIVISION MULTIPLEXING.

time-sharing dynamic allocator In computer storage, a program that allocates memory areas and peripherals to programs being entered into a time-sharing system; it also controls program execution.

timeshift **1.** To receive a message at a significantly later time than when it was sent. **2.** To use a videocassette or videodisc recorder to view a television program at a later time than when it was transmitted.

time-shifting communications Any form of communications in which the recipient reads or views the message(s) at a significantly later time than the message is sent from the source. A common example is electronic mail (e-mail) using online computer networks.

time signals Special radio transmissions made under the auspices of the National Bureau of Standards, for indicating Coordinated Universal Time (UTC).

time slot A specifically defined time interval in a data signal. It is of importance primarily in digital communications, where a given time interval can be high or low or at some discrete value.

time-space-time switch A large switch consisting of a space block between two time blocks.

time zone One of the 24 zones into which the global map is divided for the purpose of standardizing time. Within these zones, mean solar time is determined in terms of distance east or west of the zero meridian at Greenwich (near London, England). Each zone is equal to 15 degrees of longitude, or 1 hour. Four zones fall within the continental United States: Eastern Standard Time (zone of the 75th meridian), Central Standard Time (zone of the 90th meridian), Mountain Standard Time (zone of the 105th meridian), and Pacific Standard Time (zone of the 120th meridian). Also see MERIDIAN, ZERO MERIDIAN, and ZONE TIME.

timing extraction The retrieval of a timing signal from incoming data.

timing pin current Measured in microamperes. The current that generates a timing waveform in an integrated-circuit voltage regulator.

timing signal A repeating signal sent along with data to control the synchronization of transmitter and receiver.

tin **1.** Symbol, Sn. A metallic element. Atomic number, 50. Atomic weight, 118.71. Tin is widely used in electronics as a structural material, a constituent of solder, and (in foil form) as the plates of some fixed capacitors. **2.** To prepare the tip of a soldering gun or iron, or the stripped end of a wire or cable, by applying a coat of solder.

tin-oxide resistor See METAL-OXIDE RESISTOR.

tinsel Metal film strips interwoven with fabric threads to provide a flexible cord, particularly for headphones.

tint control In a color-television receiver, the control for changing color hue.

tip jack The mating connector for a tip plug.

tip plug **1.** A prod terminating in a phone tip. **2.** A plug-type connector terminating in a phone tip.

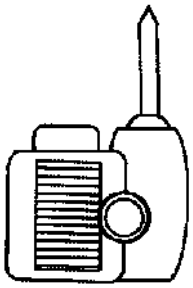

tip plug, 2

titanium Symbol, Ti. A metallic element. Atomic number, 22. Atomic weight, 47.88. Titanium enters into some dielectric compounds (e.g., titanium dioxide).

titanium dioxide Formula, TiO_2. A ceramic dielectric material. Dielectric constant, 90 to 170. Dielectric strength, 100 to 210 V/mil.

T junction See TEE JUNCTION.

Tl Symbol for THALLIUM.

T^2L Abbreviation of TRANSISTOR-TRANSISTOR LOGIC. (Also, TTL.)

TLA Abbreviation of TABLE LOOK-AT.

TLC Abbreviation of *thin-layer chromatography.*

TLU Abbreviation of TABLE LOOK-UP.

TM **1.** Abbreviation of TRANSVERSE MAGNETIC. **2.** Abbreviation of *technical manual.*

Tm Symbol for THULIUM.

TM mode See TRANSVERSE MAGNETIC MODE.

TM wave See TRANSVERSE MAGNETIC MODE.

T network See TEE NETWORK.

TNS Abbreviation of TRANSCUTANEOUS NERVE STIMULATOR.

toggle A bistable device.

toggle switch A switch having a mechanism that snaps into the on or off position at the opposite extremes to which a lever is moved.

tolerance The amount by which error is allowed in a value, rating, dimension, etc. It is usually

5059F-pT-671-699 4/10/01 9:51 AM Page 687

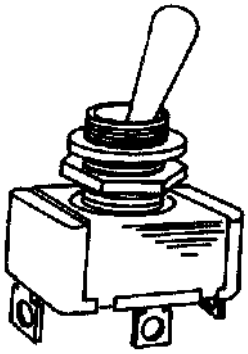

toggle switch

expressed as a percent of nominal value, plus and minus so many units of measurement (or parts per million).

toll call In a telephone system, a call that is charged on a per-minute or per-second basis.

ton Abbreviation, T, t, or tn. A unit of avoirdupois weight; in the United States, it is usually taken to mean *short ton,* a unit equal to 907.20 kilograms (2000 lb). Compare METRIC TON.

tone **1.** The pitch (frequency) and timbre (relative harmonic content) of a sound other than noise. **2.** A sound consisting of a periodic waveform having constant frequency; also called *note.*

tone arm See PICKUP ARM.

tone burst A test signal consisting of a single-frequency sine wave sustained for a brief period of time, usually having a rectangular envelope (rapid rise and decay).

tone-burst entry In repeater systems, a technique whereby a short tone signal is used at the start of a transmission to trigger a particular repeater so that all repeaters in the system will not go into operation simultaneously.

tone-burst generator An oscillator and associated circuitry for producing a tone burst.

tone control An adjustable device or circuit for modifying the frequency response of an amplifier (i.e., for emphasizing bass, treble, or midrange pitches).

tone dialing A method of telephone dialing that uses standard tone pairs actuated via a keypad with 12 keys representing digits 0 through 9 and symbols # and *. Some keypads have four additional keys: A, B, C, and D.

tone generator An oscillator for producing simple audio-frequency signals for communications, control, or testing.

tone keying In wire and radio telegraphy, the representation of code characters by audio-frequency tones. Also see MODULATED CONTINUOUS WAVE.

tone localizer A localizer that provides lateral guidance for an aircraft by comparing the amplitudes of two modulating frequencies.

tone modulation **1.** The transmission of Morse, Baudot, or ASCII signals by audio-frequency modulation of a radio-frequency carrier. **2.** Any rapid variation of the amplitude or frequency of an audio tone.

top cap A small metal cap on top of some electron tubes, serving as a direct, low-capacitance connection to one of the internal elements—usually the control grid, but sometimes the plate.

top loading A method of feeding a vertical antenna at or near the top.

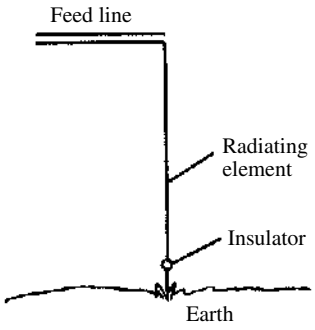

top loading

topology **1.** A branch of mathematics concerned with the properties of surfaces and spaces. **2.** The details of layout of an integrated circuit. **3.** The characteristics of a surface.

toroid See TOROIDAL COIL.

toroidal coil A coil wound on a form that is shaped like a donut. The form is made of powdered-iron or ferrite. Toroidal coils have certain advantages over solenoidal coils: greater inductance for a given physical size, better isolation properties, and higher Q factor. A disadvantage is that an air core is not practical.

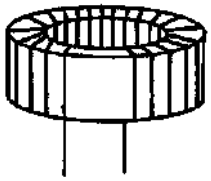

toroidal coil

torque **1.** The force that tends to produce a rotating motion. **2.** Rotation of the plane of polarization of light by some crystals.

torque amplifier A device having rotating input and output shafts and that delivers greater torque at the output shaft than that required to turn the input shaft.

5059F-pT-671-699 4/10/01 9:51 AM Page 688

torque sensitivity Symbol, *KT*. For a torque motor, torque output per ampere of input current.

torr A unit of pressure equal to the pressure required to support a column of mercury 1 millimeter high at 0°C and standard gravity; 1 torr = 133.322 Pa (1333.2 microbars).

torsion The effect on an object by torque applied to one end while the other is being held fast or torqued in the opposite direction.

torsion delay line A delay line in which the delay is manifested in a material that is torqued by mechanical vibrations.

torsion waves Waves that travel by means of torque, instead of displacement or compression. The velocity of propagation depends on the modulus of rigidity and the density of the propagating medium.

tot **1.** Abbreviation of *total*. **2.** To derive a sum or total.

total breakaway torque For a torque motor, the sum of magnetic retarding torque and brush-commutator friction.

total harmonic distortion Abbreviation, THD. The distortion caused by the combined action of all the harmonics present in a complex waveform. An important specification in high-fidelity audio amplifiers.

total distortion See TOTAL HARMONIC DISTORTION.

total internal reflection **1.** The reflection of visible light from a boundary between two substances having different indices of refraction. When the angle of incidence, relative to the tangent to the boundary, is smaller than a certain value, as light travels through the more dense medium total reflection occurs at the boundary. **2.** Reflection of electromagnetic waves from an ionized layer in the atmosphere. This occurs at angles smaller than a certain angle, relative to the tangent of the plane of the ionizing layer. In some cases, total internal reflection does not occur. Actually, most ionospheric reflection is really refraction; the electromagnetic waves are bent by the ionized layer rather than reflected.

total reflection Full return of a ray by a reflector, none of the energy being transmitted by or absorbed in the reflecting material.

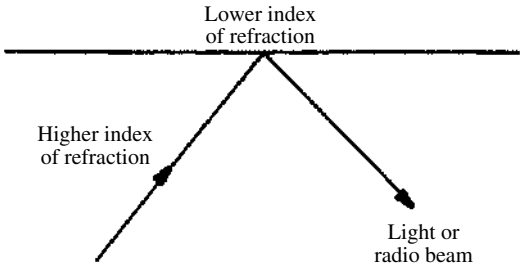

total internal reflection

touchplate relay A capacitance relay in which the pickup element is a small, metal plate that actuates the relay when it is touched.

tough dog A malfunctioning circuit that seemingly defies all attempts to diagnose and correct its trouble. Also see DOG.

tourmaline crystal A piezoelectric and pyroelectric crystal; a transparent plate of tourmaline has the ability to polarize light passing through it. Also see POLARIZATION, **3**; POLARIZED LIGHT; and POLARIZER.

tower **1.** A usually tall and self-supporting open-work structure used to support an antenna, and usually having three or four sides. **2.** A metal structure, as defined in **1**, used as a vertical antenna.

Townsend discharge In a glow-discharge tube, the discharge that begins after the applied voltage reaches a given level. It is a low-current, non-self-sustaining discharge. Compare ABNORMAL GLOW and NORMAL GLOW DISCHARGE.

touch screen A special cathode-ray tube (CRT) or video display unit that allows input of data via physical contact with the screen surface. Items are selected by simply touching the appropriate spot ("button" or icon) on the screen.

TP Abbreviation of TRANSACTION PROCESSING.

T pad See TEE PAD.

TR Abbreviation of transmit-receive.

tr **1.** Symbol for RECOVERY TIME. **2.** Symbol for RISE TIME.

trace **1.** A tiny or insignificant quantity. **2.** The movement of the electron beam across the face of a cathode-ray tube. **3.** A routine used for testing of, or for locating a fault in, a circuit or computer program. **4.** The process of implementing such a routine.

trace element See MICROELEMENT.

tracer A suitable substance or object introduced into the human body and whose progress through the body can be followed (or its state monitored) by means of electronic equipment. Tracers are sometimes used also in nonbiological systems, such as pipelines.

track **1.** A discrete information band on a magnetic disk or tape. **2.** To follow, as by a stylus, a phono disc groove. **3.** To follow, as by radar, a target.

trackability An expression of the accuracy with which a phonograph stylus follows the irregularities in a disc.

trackball A device for guiding the cursor or pointer in a computer. It is often used in laptop (notebook) computers. It resembles a ball bearing; the operator moves the cursor or pointer by pushing on the bearing with a finger.

track-drive locomotion A method of robotic locomotion using two or more wheels that drive a belt (track). It uses the same principle as a military tank.

tracking Following in step, as when ganged circuits resonate at the same frequency (or some

5059F-pT-671-699 4/10/01 9:51 AM Page 689

frequency difference) at all settings, or when a missile closely follows its guiding signal.

tracking force See VERTICAL STYLUS FORCE.

track label On a magnetic storage medium, a record that identifies a track.

tracking mode In tracking supplies, the usual manner of operation in which the output of each of the separate supplies automatically follows that of the one being adjusted. Compare INDEPENDENT MODE.

tracking supplies Adjustable power supplies, packaged two or more to the unit, in which the output of each will automatically follow adjustment made to one of them.

track pitch The distance between tracks (see TRACK, **2**).

traffic **1.** Collectively, messages handled by a communications station. **2.** Collectively, data and instructions handled by a computer system in continual use.

trailer label At the end of a magnetic-tape or floppy-disk file, a record signaling the end of the file and often giving such information as the number of records in the file.

trailer record At the end of a group of computer records, a record containing information relevant to the group's processing.

trailing edge The falling edge of a pulse. Compare LEADING EDGE.

trans Abbreviation of TRANSVERSE.

transaction The exchange of activity that occurs between a computer, via a terminal, and the user, including any processing required (e.g., that involved in adding records to, or deleting them from, a file).

transaction file In data processing, a group of records used to update a master file.

transaction processing In computer operations, the use of a central processor for handling, modifying, or otherwise acting on information by transactions.

transaction tape Magnetic tape on which a transaction file has been recorded.

transadmittance For an active device, the ratio d*I2*/d*E1*, where *I2* is the alternating-current (ac) component of the current in a second electrode (such as the drain), and *E1* is the ac component of voltage on a first electrode (such as the gate), with constant direct-current operating voltages.

transceiver **1.** A combination transmitter and receiver, housed in a single enclosure, with frequency control and some ancillary stages common to both units. This design is economical because it eliminates redundancy. Such a system is more easily tuned than a separate transmitter and receiver if the operating frequency must be changed often, but it can be difficult to carry out split-frequency or split-band communication on two frequencies that differ greatly. Compare TRANSMITTER–RECEIVER. **2.** In computer practice, a read/write data terminal capable of transmitting and receiving information to and from a channel.

transcendental functions Nonalgebraic functions. These include logarithmic functions, exponential functions, trigonometric functions, and inverse trigonometric functions.

transconductance **1.** Symbol, *gm*. Unit, micromho. In an electron tube, the extent to which plate current (*IP*) changes in response to a change in grid voltage (*EG*); *gm* = d*IP*/d*EG*. **2.** Symbol, *gfs*. Unit, micromho. In a field-effect transistor, the extent to which drain current (*ID*) changes in response to a change in gate-to-source voltage (*VGS*); *gfs* = d*ID*/d*VGS*.

transconductance amplifier An amplifier in which the output current is a linear function of the input voltage.

transcribe **1.** To record material, such as a radio program, for future transmission. **2.** In computer operations, the intermedia transfer of data, as from tape to disk.

transcriber A device used for intermedia data transfer (e.g., one that can move the data on magnetic tape to magnetic or optical disc).

transcription A recording of material, such as a record or tape of a radio program, for later use in a transmitter. See ELECTRICAL TRANSCRIPTION.

transcutaneous nerve stimulator Abbreviation, TNS. An electronic device for the temporary relief of pain. In its use, electrodes taped to the skin over the painful area are connected to a portable generator of suitable pulse energy.

transducer A device that converts one quantity into another quantity, specifically when one of the quantities is electrical. Thus, a loudspeaker converts electrical impulses into sound, a microphone converts sound into electrical impulses, a photocell converts light into electricity, a thermocouple converts heat into electricity, etc.

transducer amplifier An amplifier used expressly to boost the output of a transducer.

transducer efficiency For a transducer, the ratio of the output power to the input power.

transductor See MAGNETIC AMPLIFIER.

transfer **1.** To move a signal from one point to another—especially through a modifying circuit or device. **2.** To transmit information or data from one point or device to another, inside or outside a system.

transfer characteristic A figure or plot expressing the output-input signal relationship in a circuit or device. Also see TRANSFER, **1**.

transfer efficiency In a charge-coupled device, the proportion of charge that is transferred under given conditions.

transfer function **1.** See TRANSFER CHARACTERISTIC. **2.** An expression that mathematically shows how two entities or events occurring in different places or at different times are related.

5059F-pT-671-699 4/10/01 9:51 AM Page 690

transfer rate The speed at which data can be moved between a computer's internal memory and a peripheral.

transferred charge In a circuit containing a capacitor, the net electric charge that moves around the external circuit from one plate of the capacitor to the other.

transform **1.** See LAPLACE TRANSFORM. **2.** To change the voltage or nature of an electrical parameter (e.g., high to low voltage and alternating to direct current). **3.** To change the form, but not the content, of data.

transformation constant See DISINTEGRATION CONSTANT.

transformer **1.** A device using electromagnetic induction to transfer electrical energy from one circuit to another (i.e., without direct connection between them). In its simplest form, a transformer consists of separate primary and secondary coils wound on a common core of ferromagnetic material, such as iron. When an alternating current flows through the primary coil, the resulting magnetic flux in the core induces an alternating voltage across the secondary coil; the induced voltage can cause a current to flow in an external circuit. Also see AIR-CORE TRANSFORMER, INDUCTION, INDUCTIVE COUPLING, IRON-CORE TRANSFORMER, and TURNS RATIO. **2.** A section of radio-frequency (RF) transmission line used to match impedances. Also see LINEAR TRANSFORMER.

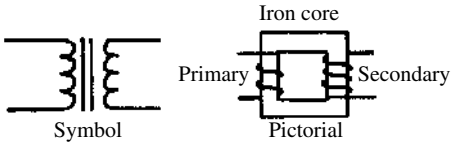

transformer, 1

transformer-coupled amplifier An amplifier using coupling transformers between its stages or at its input and output points. Compare RESISTANCE-CAPACITANCE-COUPLED AMPLIFIER.

transformer coupling The inductive coupling of circuits through a transformer. Also see COEFFICIENT OF COUPLING; INDUCTIVE COUPLING; MUTUAL INDUCTANCE; and TRANSFORMER, **1**.

transformer equivalent circuit An equivalent circuit depicting the various parameters of a transformer (such as primary and secondary resistances, primary and secondary reactances, core losses, etc.) and their relationship to each other.

transformer feedback Inductively coupled feedback (positive or negative) through a transformer.

transformer input current See PRIMARY CURRENT.

transformer input voltage See PRIMARY VOLTAGE.

transformer iron See SILICON STEEL.

transformer loss The expression (in decibels) 10 $\log_{10}$ (*P1*/*P2*), where *P1* is the calculated power that a given transformer should deliver to a particular load impedance, and *P2* is the actual power delivered.

transformer oil A petroleum product in which high-voltage, high-current transformers are sometimes immersed. The oil protects the windings from environmental damage.

transformer output current See SECONDARY CURRENT.

transformer output voltage See SECONDARY VOLTAGE.

transformer-type voltage regulator See VOLTAGE-REGULATING TRANSFORMER.

transformer utilization factor See UTILITY FACTOR.

transient **1.** A sudden, high-voltage spike in an alternating-current system, caused by arcing or lightning. **2.** A spurious signal in a hardcopy-receiving system. **3.** Any short pulse attributable to external causes. **4.** Existing for a short period of time, or intermittently for short periods of time.

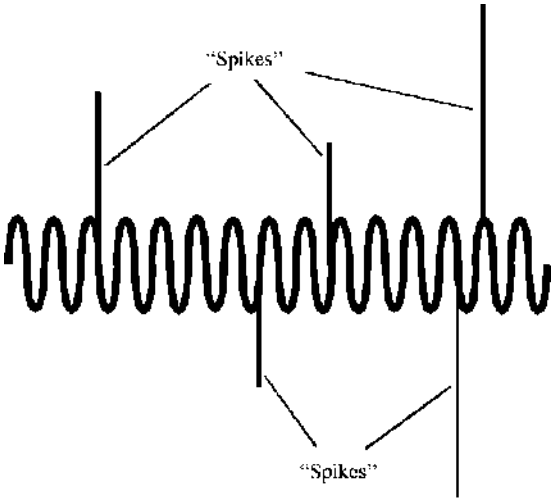

transient, 1.

transient absorber See SURGE ARRESTER.

transient arrester See SURGE ARRESTER.

transient-based amplifier See CRYSTAL AMPLIFIER, **2**.

transient current A momentary pulse of current. Also see TRANSIENT.

transient response The response of a circuit to a transient, as opposed to its steady-state response, usually evaluated in terms of its ability to reproduce a square wave.

5059F-pT-671-699 4/10/01 9:51 AM Page 691

transient suppressor See SURGE ARRESTOR.

transient voltage A momentary pulse of voltage. Also see TRANSIENT.

transient voltmeter An instrument that indicates the voltage of momentary signals. Usually, a peak-reading meter in the instrument displays the highest positive or negative value the transient attains (sometimes holding the deflection for reading later) and can respond to pulses of 1 microsecond in duration.

transistor An active (commonly three-terminal) semiconductor device capable of amplification, oscillation, and switching action. The name is a contraction of *transfer resistor.* Also see ALLOY-DIFFUSED TRANSISTOR, ALLOY TRANSISTOR, BIPOLAR TRANSISTOR, DIFFUSED-BASE TRANSISTOR, DIFFUSED EMITTER-AND-BASE TRANSISTOR, DIFFUSED-JUNCTION TRANSISTOR, DIFFUSED MESA TRANSISTOR, DIFFUSED PLANAR TRANSISTOR, DIFFUSED TRANSISTOR, DIFFUSION TRANSISTOR, DOUBLE-BASE JUNCTION TRANSISTOR, FIELD-EFFECT TRANSISTOR, FIELDISTOR, GERMANIUM TRANSISTOR, GROWN-DIFFUSED TRANSISTOR, GROWN-JUNCTION TRANSISTOR, JUNCTION TRANSISTOR, MESA TRANSISTOR, METAL-OXIDE-SEMICONDUCTOR FIELD-EFFECT TRANSISTOR, MICROALLOY DIFFUSED TRANSISTOR, MICROALLOY TRANSISTOR, PHOTOTRANSISTOR, PLANAR EPITAXIAL PASSIVATED TRANSISTOR, PLANAR TRANSISTOR, POINT-CONTACT TRANSISTOR, POWER TRANSISTOR, SILICON TRANSISTOR, SURFACE-BARRIER TRANSISTOR, SURFACE-CHARGE TRANSISTOR, TANDEM TRANSISTOR, THIN-FILM TRANSISTOR, THREE-JUNCTION TRANSISTOR, and UNIJUNCTION TRANSISTOR.

transistor amplifier An amplifier containing only transistors as the active components. Also called *transistorized amplifier.*

transistor analyzer An instrument for measuring the electrical characteristics of transistors. Compare TRANSISTOR TESTER.

transistor battery A 9-volt electrochemical battery consisting of six tiny zinc–carbon or alkaline cells in series. Each of the six cells supplies 1.5 volts. The ampere-hour capacity is small. The battery has a characteristic box shape with adjacent clip-on terminals at one end. These batteries are used in low-current electronic devices such as remote-control garage-door openers, television channel changers, remote videocassette recorder (VCR) controls, electronic calculators, and smoke detectors.

transistor-coupled logic Abbreviation, TCL. In computer and automatic-control operations, logic circuitry and systems using multi-emitter-coupled transistors. Also see RESISTOR-TRANSISTOR LOGIC and TRANSISTOR-TRANSISTOR LOGIC.

transistor current meter An ammeter, milliammeter, or microammeter circuit containing an amplifier using only transistors. Also see ELECTRONIC CURRENT METER.

transistorized voltmeter See TRANSISTOR VOLTMETER.

transistorized voltohmmeter An electronic voltmeter-ohmmeter combination using a transistorized circuit similar to that of a vacuum-tube voltohmmeter.

transistor keyer A power transistor acting as a keying device.

transistor oscillator An oscillator using only transistors as the active components. Also called *transistorized oscillator.*

transistor power supply A high-current, well-filtered, direct-current power supply for operating transistor circuits.

transistor radio Any small, portable, battery-powered radio receiver whose active components are transistors and/or other semiconductor devices.

transistor-resistor logic See RESISTOR-TRANSISTOR LOGIC.

transistor tester An instrument for checking the condition of transistors (i.e., whether good or bad). Compare TRANSISTOR ANALYZER.

transistor tetrode See DOUBLE-BASE JUNCTION TRANSISTOR.

transistor thyratron See SOLID-STATE THYRATRON.

transistor-transistor logic Abbreviation, TTL or T^2L. In computer operations, a circuit in which the multiple-diode cluster of the diode-transistor logic circuit has been replaced by a multiple-emitter transistor.

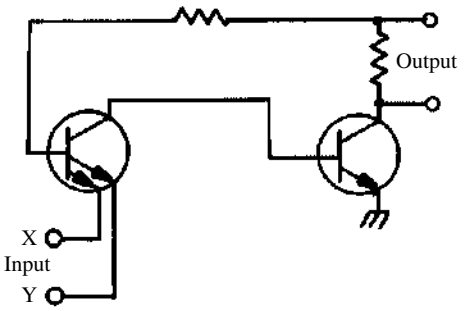

transistor-transistor logic

transistor voltmeter Abbreviation, TVM. A voltmeter containing an amplifier that uses only bipolar transistors. Also called *transistorized voltmeter.* Also see ELECTRONIC VOLTMETER. Compare FET VOLTMETER and VACUUM-TUBE VOLTMETER.

transistor VOM See TRANSISTORIZED VOLT-OHMMETER.

5059F-pT-671-699 4/10/01 9:51 AM Page 692

transit angle For an electron, the angular frequency multiplied by the time required to travel from one point to another.

transit time The time taken by an electron to travel from one electrode to another—especially from the cathode to the plate in a vacuum tube.

transistor element A metallic element whose atoms have valence electrons in two shells. Examples: chromium, iron, and nickel.

transition factor See MISMATCH FACTOR.

transition region See BARRIER, **1**.

translation loss See PLAYBACK LOSS.

translator **1.** See COMPILER. **2.** See ASSEMBLER.

transliteration **1.** To change the characters in one alphabet or code system to the characters in a different system. **2.** The function that maps the characters in one alphabet or code system to those in another.

translucence **1.** The transmission of radiation, especially visible light, through a material. **2.** The extent to which a substance can transmit radiation—especially visible light. **3.** Pertaining to a material that partially or totally transmits radiation—especially visible light.

transmission gain Current amplification, power amplification, or voltage amplification.

transmission line **1.** A single conductor or group of conductors for carrying electrical energy from one point to another. **2.** A correctly dimensioned conductor or pair of conductors for carrying radio-frequency energy from a transmitter to an antenna or coupling device.

transmission mode **1.** In a transceiver, the condition in which the transmitter is enabled and the receiver is disabled. **2.** In a waveguide, propagation via transverse waves.

transmission speed The number of information elements (words, code groups, data symbols, bits, and bytes) that can be generated or received per unit time (second or minute) by a system or operator.

transmission wavemeter A (usually simple) inductance-capacitance-tuned wavemeter that provides peak response when tuned to the frequency of a signal passing through it; also, the comparable microwave device. Compare ABSORPTION WAVEMETER.

transmit-receive switch A manually or electrically operated switch for transferring a single antenna between a transmitter and receiver.

transmittancy The relative ability of a substance to transmit radiation. Transmittancy depends on the frequency of the radiation, as well as the substance.

transmitter **1.** An equipment for producing and sending signals or data. **2.** See MICROPHONE. **3.** One who originates signals or data.

transmitter–receiver A transmitter and receiver usually contained in a single enclosure, but with separate and independent oscillators, mixers, and amplifiers. The main asset of this scheme is the fact that it is possible to conduct split-frequency communication on bands whose wavelengths differ greatly. Another asset is the ability of the system, with proper design, to operate in full-duplex mode. Installations of this type are often used in satellite communications. Compare TRANSCEIVER, **1.**

transmitting antenna An antenna designed expressly for the efficient radiation of electromagnetic energy into space.

transmitting station A station that only transmits signals (i.e., it engages in no official form of reception). Compare RECEIVING STATION.

transmittivity The degree to which a selective circuit transmits a desired signal. Compare REJECTIVITY.

transmultiplexer A device that changes a signal from one multiplexed form to another while maintaining all of the information contained in the signal. For example, a transmultiplexer might convert time-division-multiplex data to frequency-division multiplex or vice-versa.

transonic Equal to, or approximating, the speed of sound in air (approximately 1100 feet per second).

transparence The practically unimpeded transmission of radiation, such as light, through a material. Compare OPACITY and TRANSLUCENCE.

transponder An acronym for transmitter and responder. **1.** A combination transmitter–receiver that automatically transmits an identification signal whenever it receives an interrogating signal. **2.** In a communications satellite, a broadband repeater that receives signals sent up from the earth, converts them to another frequency, and retransmits them back to the earth. Some satellites have units that employ multiplexing, data storage and retrieval systems, and other schemes to maximize the amount and variety of data they can handle.

transponder overload A condition that occurs when a satellite transponder is heavily used or when an excessively strong uplink signal is received. During heavy usage, all downlink signals are consistently weaker than they are when the transponder is not dealing with many signals. If an overly powerful uplink signal is received, all downlink signals are attenuated intermittently; the greater the instantaneous power of the offending uplink signal, the greater the instantaneous attenuation of all the downlink signals. See TRANSPONDER, **2.**

transport See TAPE TRANSPORT.

transportable equipment Portable electronic equipment. See, for example, PORTABLE TRANSMITTER.

transuranium An element whose atomic number is higher than that of uranium.

transverse Occurring in a direction or directions perpendicular to the direction of propagation.

5059F-pT-671-699 4/10/01 9:51 AM Page 693

transverse electric mode In a waveguide, the condition in which the electric lines of flux are perpendicular to the direction of propagation. Compare TRANSVERSE MAGNETIC MODE. Also see WAVEGUIDE MODE.

transverse electromagnetic wave An electromagnetic wave having electric-field vectors and magnetic-field vectors perpendicular to the direction of propagation.

transverse magnetic mode In a waveguide, the condition in which the magnetic lines of flux are perpendicular to the direction of propagation. Compare TRANSVERSE ELECTRIC MODE. Also see WAVEGUIDE MODE.

trap **1.** See WAVETRAP. **2.** In a semiconductor crystal, an imperfection capable of trapping current carriers.

trapezoid **1.** A polygon having four sides, of which only two are parallel. **2.** See TRAPEZOIDAL PATTERN. **3.** See TRAPEZOIDAL WAVE.

trapezoidal distortion In television or facsimile, a form of distortion in which the frame is wider at the top than at the bottom, or vice versa.

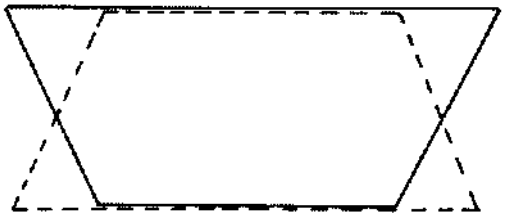

trapezoidal distortion

trapezoidal pattern An oscilloscope pattern used to check the percentage of modulation of an amplitude-modulated wave. Its name is derived from its trapezoidal shape.

trapezoidal wave A nonsinusoidal wave that is a combination of a rectangular component and a sawtooth component. It is the required waveform of the voltage applied to a magnetic deflecting coil (oscilloscope or television) to ensure a sawtooth wave of current in the coil.

traveling-wave amplifier Abbreviation, TWA. An amplifier based on the unique operation of the traveling-wave tube.

traveling-wave tube Abbreviation, TWT. A microwave tube containing an electron gun, helical transmission line, collector, and input and output couplers. A microwave signal is coupled into the helix, through which it travels while the gun projects an electron beam through the helix. When wave and electron velocities are equal, a power gain is obtained in the signal coupled out of the helix. Also see BACKWARD-WAVE OSCILLATOR.

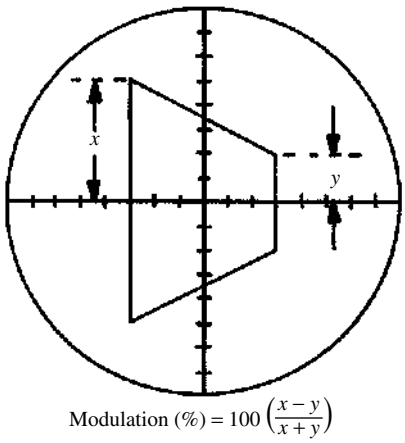

trapezoidal pattern

Travis discriminator A discriminator circuit in which the diodes are operated from separately tuned halves of the secondary winding of the input transformer. Compare FOSTER-SEELEY DISCRIMINATOR.

treasure locator See METAL LOCATOR.

treble The higher portion of the sound spectrum—especially the upper end of the musical scale (middle C and above). Compare BASS.

treble boost **1.** Amplification of high audio frequencies (the treble notes) in an audio system—especially in high-fidelity music reproduction. **2.** The extent of amplification of high audio frequencies in audio applications—especially in music reproduction. **3.** A control that allows adjustment of the relative treble gain in an audio system.

treble control See TREBLE BOOST, **3**.

tree **1.** A cause-and-effect chain with two or more independent branches. **2.** A circuit with two or more branches but no meshes.

TRF Abbreviation of *tuned radio frequency.*

TRF amplifier See TUNED RADIO-FREQUENCY AMPLIFIER.

TRF receiver See TUNED RADIO-FREQUENCY RECEIVER.

triac A three-terminal, gate-controlled, semiconductor switching device. Compare DIAC.

triangular wave See BACK-TO-BACK SAWTOOTH.

triangulation A method of radiolocation in which directional bearings are obtained for the signals from two transmitters whose positions are accurately known. The position of the receiver is indicated by the intersection of two lines on a

5059F-pT-671-699 4/10/01 9:51 AM Page 694

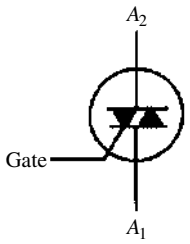

triac

map, drawn emanating from the transmitter locations 180 degrees opposite their respective bearings.

Triax A double-shielded coaxial cable. A center conductor is surrounded by two concentric, independent shield conductors.

triaxial connector A male or female connector having three concentric contacting surfaces. By contrast, the coaxial jack and coaxial plug have only two such surfaces.

triaxial speaker A dynamic loudspeaker containing three coils and three cones, for high-, low-, and middle-frequency ranges. It is, in effect, three speakers in one. It is commonly used in high-fidelity music reproduction systems. Also called *triaxial driver*. Compare THREE-WAY SPEAKER.

triboelectric Pertaining to frictional electricity.

triboelectric series See ELECTROSTATIC SERIES.

triboluminescence Luminescence produced by means of friction.

trickle charge A continuous slow charge of a storage battery, in which the charging rate is just sufficient to compensate for internal losses or normal discharge.

trickle charger A light-duty unit for charging a battery gradually at low current.

tricorner reflector A device that reflects a ray of incident energy at a 180-degree angle, regardless of the direction from which the ray approaches. Thus, the ray will return to its source, unless some obstruction intervenes. It consists of three mutually perpendicular reflecting plane surfaces that intersect in a common point. The geometry is identical to that in a typical room, where the ceiling meets two walls. It is useful at microwave, infrared, visible, and ultraviolet wavelengths.

triethanolamine An amino alcohol that precipitates metallic silver from a silver-nitrate solution in the deposition of a silver surface on a substrate, such as glass or a ceramic.

trig Abbreviation of TRIGONOMETRY.

trigatron A form of electrically operated switch. The circuit is closed by the breakdown of an electrical gap.

trigger **1.** A pulse used to start or stop the operation of a circuit or device, such as a flip-flop. **2.** To place a circuit or device into or out of operation with a start or stop pulse, as defined in **1**.

trigger diode See DIAC and FOUR-LAYER DIODE.

triggered multivibrator See DRIVEN MULTIVIBRATOR.

triggered sweep In an oscilloscope or similar device, a driven sweep.

triggering point The voltage level at which the action of an electronic switching device is initiated. Also see BREAKOVER POINT.

trigistor A three-junction semiconductor device that exhibits two-state operation, and is useful as a flip-flop or switch. Also see NPNP DEVICE.

trigonometric functions See CIRCULAR FUNCTIONS and HYPERBOLIC FUNCTIONS.

trigonometry The branch of mathematics devoted to the application of CIRCULAR FUNCTIONS in a plane. It is useful in electronics for determining impedance and phase.

trim To make a fine adjustment, as of a tuning control, balance control, output adjustment, etc.

trimmer A low-valued variable capacitor, inductor, or resistor operated in conjunction with a main unit (usually of the same sort) for vernier adjustment or range setting. See, for example, HIGH-FREQUENCY TRIMMER and OSCILLATOR TRIMMER.

trimmer capacitor A variable capacitor used as a trimmer.

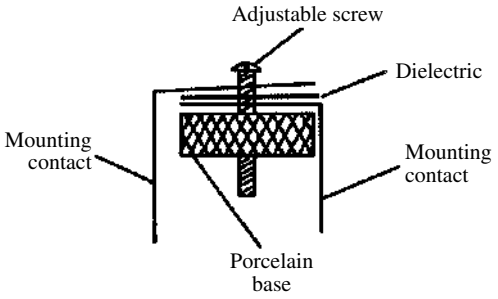

trimmer capacitor

trimmer coil See TRIMMER INDUCTOR.

trimmer inductor A variable inductor used as a trimmer.

trimmer resistor A variable resistor used as a trimmer.

trinary number system The base-3 system of notation. This system uses the digits 0, 1, and 2, the positional values being successive powers of 3 (e.g., decimal 14 equals trinary 112). Also called *ternary number system*.

Trinitron **1.** A single-gun color-television picture tube developed by Sony. **2.** A television set using

5059F-pT-671-699 4/10/01 9:51 AM Page 695

this tube. The gun has three cathodes that modulate the three color beams (red, green, and blue). The beams are accelerated by common grids and are focused at different angles by convergence plates.

Trinoscope See TRINITRON.

triode A three-electrode tube or transistor, embodying an anode, cathode, and a control electrode as the principal elements.

triple-diffused transistor A diffused transistor in which the base and emitter are diffused into the top face of the chip, and the collector into the bottom face.

triple diode An assembly of three (often closely matched) semiconductor diodes in a single housing.

tripler **1.** A rectifier that delivers a direct-current output voltage at approximately triple the peak value of the alternating-current input voltage. **2.** An amplifier or other circuit that delivers an output signal at triple the frequency of the input signal.

triplexer In radar, a device that facilitates the use of two receivers at the same time.

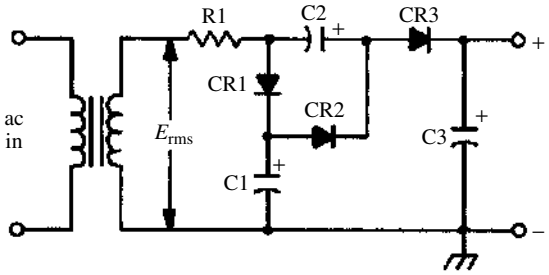

tripler, 1

Tri-state logic Digital logic in which there are three possible states, rather than the usual two. The conditions are defined as 0, 1, and undecided. Trade name of National Semiconductor.

tritium Symbol, T or H_3. An isotope of hydrogen whose nucleus contains two neutrons and one proton. Compare DEUTERIUM.

TRL Abbreviation of *transistor-resistor logic* (see RESISTOR-TRANSISTOR LOGIC).

Trojan horse A program written with the malicious intent of sabotaging the operating system and/or files in a computer. It is somewhat similar to a VIRUS; it is occasionally spread via software whose origin is questionable or unknown.

troposcatter See TROPOSPHERIC-SCATTER PROPAGATION.

troposphere The portion of the atmosphere in which virtually all weather phenomena occur. It extends from the surface to an altitude of 8 to 12 miles above sea level.

tropospheric bending A common type of radio-wave propagation that takes place when radio waves are refracted in the lower atmosphere. This effect is most dramatic near weather fronts, where warm, relatively light air lies above cool, heavy air. The cooler air has a higher index of refraction than the warm air, causing radio-frequency electromagnetic fields to be bent downward at a considerable distance from the transmitter. It is often responsible for anomalies in reception of FM and TV broadcast signals. Compare TROPOSPHERIC DUCTING, TROPOSPHERIC-SCATTER PROPAGATION.

tropospheric ducting Also called *duct effect*. A form of tropospheric propagation that occurs close to the earth's surface at very-high frequencies (VHF) and ultra-high frequencies (UHF). A duct forms when a layer of cool air becomes sandwiched between two layers of warmer air. Total internal reflection of the electromagnetic (EM) field takes place inside the duct. For this phenomenon to provide communications, both the transmitting and receiving antennas must be located within the same duct, and this duct must be unbroken and unobstructed between the two locations. A duct might measure only a few feet from top to bottom, but cover thousands of square miles parallel to the surface. Compare TROPOSPHERIC BENDING, TROPOSPHERIC-SCATTER PROPAGATION.

tropospheric propagation Also called *tropo*. Over-the-horizon propagation of radio-frequency electromagnetic waves that occurs as a result of reflection, scattering, and/or refraction in the troposphere, the lowest 10 or 12 miles of the earth's atmosphere. At wavelengths shorter than about 15 m (frequencies above 20 MHz), refraction and reflection can take place within and between air masses of different density. The air also produces some scattering of EM energy at wavelengths shorter than about 3 m (frequencies above 100 MHz). "Tropo" can often allow

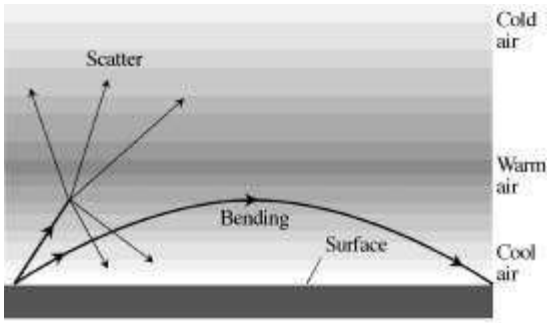

tropospheric propagation

5059F-pT-671-699 4/10/01 9:51 AM Page 696

communications over distances of several hundred miles. Also see TROPOSPHERIC BENDING, TROPOSPHERIC DUCTING, and TROPOSPHERIC-SCATTER PROPAGATION.

troposperic-scatter propagation Also called *troposcatter*. A form of tropospheric propagation that occurs at frequencies above about 100 MHz, where the atmosphere has a scattering effect on radio waves. Dust in the air increases the scattering effect, but some troposcatter occurs regardless of the weather. Troposcatter takes place mostly at low altitudes where the air is the most dense. This mode can provide reliable communication over distances of several hundred miles when the appropriate equipment is used. Communication via troposcatter requires the use of high-gain antennas. Scatter is often observed along with other modes of tropospheric propagation. Compare TROPOSPHERIC BENDING, TROPOSPHERIC DUCTING.

troubleshoot **1.** To look for the cause of equipment failure. **2.** To look for flaws in computer software or to debug a program.

troubleshooting test A test that is part of the procedure for finding the cause of faulty electronic equipment operation. Also see DIAGNOSTIC TEST. Compare PERFORMANCE TEST.

trough value The minimum amplitude of a composite current or voltage.

true complement See RADIX COMPLEMENT.

true ground The earth, as opposed to an artificial ground, such as that provided by the radials of a ground-plane antenna or an equipment chassis.

true power In an alternating-current (ac) circuit, the power actually dissipated in the resistive component; the reactive component consumes no power. In ac circuits containing reactance, the true power is less than the product of the voltage and current. Also see AC POWER and POWER FACTOR.

truncation A method of approximating a quantity by cutting off its digits beyond a certain point. For example, 3.44 and 3.46, when truncated to two significant digits, both become 3.4. Compare ROUNDING.

trunk **1.** A communications link between two points, one usually being external. **2.** The interface between a central processing unit and a peripheral device.

trunk link In computer systems, an interface permitting access to main storage via a peripheral.

truth table In logic analysis and logic circuit design, a table in which are listed all combinations of input values and the corresponding output values for a given logic function.

truth table

$(x + y)' + xz$

x	y	z	$x + y$	$(x + y)'$	xz	$(x + y)' + xz$
0	0	0	0	1	0	1
0	0	1	0	1	0	1
0	1	0	1	0	0	0
0	1	1	1	0	0	0
1	0	0	1	0	0	0
1	0	1	1	0	1	1
1	1	0	1	0	0	0
1	1	1	1	0	1	1

ts Abbreviation of tensile strength.

Tschebyscheff filter See CHEBYSHEV FILTER.

TSS Abbreviation of TIME-SHARING SYSTEM.

T switch See TEE SWITCH.

TST switch See TIME-SPACE-TIME SWITCH.

TTL Abbreviation of TRANSISTOR-TRANSISTOR LOGIC. (Also, T^2L.)

TTT In radiotelegraphy, a signal indicating that a message concerning safety is to follow (equivalent to *securite* in radiotelephony).

TTY Abbreviation of TELETYPE.

T-type antenna See TEE ANTENNA.

T-type attenuator See TEE PAD.

tube **1.** Generic term for any electron tube (e.g., vacuum tube, gas tube, cathode-ray tube, X-ray tube, etc.). **2.** Glow lamp: argon bulb, neon bulb, mercury-vapor lamp, etc.

tube capacitances The internal capacitances between the elements of an electron tube.

tube diode A two-element (cathode and anode) electron tube for current rectification. Also see DIODE.

tube of flux A group of flux lines within a circular cross section. It can vary in diameter as the density of the flux lines changes.

tube parameters Operating coefficients of electron tubes (e.g., plate current, grid voltage, screen current, transconductance, amplification factor, etc.).

tube tester An instrument for checking one or more of the parameters of an electron tube.

tubular capacitor A fixed capacitor consisting of a wound section enclosed in a cylindrical can.

tune **1.** To adjust a selective circuit to accept or reject a signal. **2.** To correct the natural frequency of vibration of a body. **3.** To adjust a radio transmitter for optimum output. **4.** To adjust the frequency of an oscillator—especially in a radio transmitter or receiver. **5.** To adjust the resonant frequency of an antenna, antenna coupler, or antenna system.

tuned AF amplifier **1.** An audio amplifier that is continuously tunable over a band of frequencies. **2.** An audio oscillator that is set to a fixed, precise frequency. See, for example, PARALLEL-TEE AMPLIFIER.

tuned-base oscillator A self-excited, common-emitter connected, bipolar-transistor oscillator in which the tuned tank is in the base circuit.

tuned circuit A (usually series-resonant or parallel-resonant) circuit adjusted to accept or reject a signal. Also see RESONANCE.

5059F-pT-671-699 4/10/01 9:51 AM Page 697

tuned-collector oscillator A self-excited, common-emitter connected, bipolar-transistor oscillator in which the tuned tank is in the collector circuit.

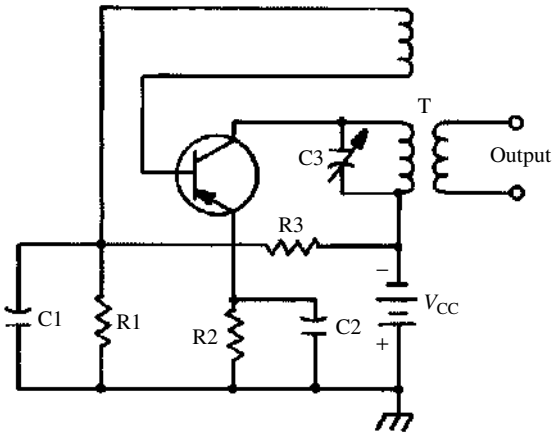

tuned-collector oscillator

tuned coupler An antenna coupler (transmatch) that can be adjusted independently of the transmitter or receiver with which it is used.

tuned dipole A half-wave, center-fed, resonant antenna.

tuned feeders An antenna feed line that is adjusted or trimmed so that the entire system (feeders and radiating element) is resonant at the transmitted-signal frequency.

tuned headphones Headphones used in radio-telegraphy that are fix-tuned to a single audio frequency (e.g., 1 kHz) by means of a small parallel capacitor.

tuned line An antenna wire or transmission line that provides a resistive load at a specific resonant frequency.

tuned pickup A pickup circuit or device (such as a radio-frequency sampling coil) that is tuned to the signal frequency.

tuned radio-frequency amplifier An amplifier circuit that is continuously tunable over a specific band of radio frequencies.

tuned radio-frequency receiver A radio receiver consisting only of a tuned-radio-frequency amplifier, detector, and audio amplifier. Compare SUPERHETERODYNE RECEIVER.

tuned reed A vibrating reed whose length, width, and/or thickness have been adjusted so that it vibrates naturally at a desired frequency.

tuned-reed frequency meter An audio frequency meter using tuned metal reeds as the indicators. Also see POWER FREQUENCY METER, **2**.

tuned relay An electronic or electromechanical relay that closes at one frequency. See, for example, REED SWITCH, **1**.

tuned signal tracer A signal tracer that can be tuned sharply to the frequency of the test signal being traced.

tuned transformer An audio-frequency or radio-frequency transformer tuned via a capacitor in parallel with its primary winding and/or a capacitor in parallel with it secondary winding.

tuner A circuit or device that can be set to select one signal from a number of signals in a frequency band.

tungsten Symbol, W. A metallic element. Atomic number, 74. Atomic weight, 183.85. Also called *wolfram.* It is used in switch and relay contacts, in the elements of some electron tubes, and in incandescent-lamp filaments.

tuning **1.** Adjustment of the frequency of a receiver to intercept a signal on a given frequency. **2.** Adjustment of a transmitter oscillator to a desired frequency. **3.** Adjustment of an inductance-capacitance circuit for resonance on a desired frequency. **4.** Adjustment of an antenna or antenna system to a desired frequency. **5.** Adjustment of a radio-frequency amplifier for optimum performance. **6.** Alignment of a musical instrument for correct tone frequency.

tuning capacitor A variable capacitor used to tune an inductance-capacitance circuit (series-resonant or parallel-resonant).

tuning coil A variable inductor used to tune an inductance-capacitance circuit (series-resonant or parallel-resonant).

tuning core See TUNING SLUG.

tuning diode See VOLTAGE-VARIABLE CAPACITOR, **1**.

tuning fork A metal device that vibrates at a precise audio frequency when struck physically. It usually has two prongs and looks something like a fork.

tuning-fork oscillator See FORK OSCILLATOR.

tuning indicator **1.** A meter or display that indicates when a receiver is properly tuned to the frequency of an incoming signal. **2.** Sometimes, a bridge null detector.

tuning meter A meter-type resonance indicator.

tuning potentiometer A single or ganged potentiometer (depending on the circuit in which it is used) used to vary the frequency response of a resistance-capacitance-tuned circuit, such as the bridge-tee, parallel-tee or Wien-bridge circuit.

tuning slug A powdered-iron core that slides or screws in and out of a coil to vary the inductance.

tuning voltage An adjustable direct-current voltage used to vary the capacitance of a varactor diode (serving as the capacitor in a tuned circuit).

tuning wand See NEUTRALIZING TOOL.

tunnel diode A specially processed junction diode whose forward conduction characteristic displays negative resistance.

tunnel-diode amplifier A circuit that uses the negative-resistance properties of a tunnel diode

5059F-pT-671-699 4/10/01 9:51 AM Page 698

to produce gain. It is used primarily at ultra-high and microwave frequencies.

tunnel-diode oscillator A circuit that uses the negative-resistance properties of a tunnel diode to produce oscillation at a specific frequency. It is used primarily at ultra-high and microwave frequencies.

turbidimeter A device used to measure the turbidity (relative opaqueness) of liquids.

turbidity meter See TURBIDIMETER.

Turing machine A hypothetical model, conceived by Alan Turing in the 1930s, devised as an exercise in problem solving. In effect, it was a computer programming language with a limited instruction set, operating in a computer with infinite memory and storage capacity.

Turing test A scheme devised by Alan Turing, designed to test computers for artificial intelligence (AI). If the machine can fool a person into thinking it is another person most of the time, then the machine in effect "passes" the test, indicating that it has some AI.

turn One complete loop of a coil.

turnaround time **1.** The length of time required for a repair to be performed. **2.** The length of time required for a computer program to be completed. **3.** The time required for a trans-ceiver to switch from the full-transmit to the full-receive condition.

turn factor For a given inductor core, the number of turns (in a standard configuration) that results in an inductance of 1 H.

turn-off time The time required for the operation of a circuit or device to cease completely after a signal or operating power has been removed. Compare TURN-ON TIME.

turn-on time The time required for a circuit or device to come up to full (normal) operation after application of a trigger or operating power. Compare TURN-OFF TIME.

turnover pickup See DUAL PICKUP.

turns ratio For a transformer, the ratio of the number of turns in the primary winding to the number of turns in the secondary winding.

turnstile antenna A polyphase antenna that resembles a turnstile gate.

turntable **1.** The motor-driven, rotating platter on which a phonograph disc rests during recording or reproduction. **2.** In a high-fidelity phonograph system, the assembly containing the platter, as defined in **1**.

turret tuner A television front-end tuner having a separate tuned-circuit section for each channel. Turning a knob rotates a desired section into position against switch contacts. Also called DETENT TUNER.

TV **1.** Abbreviation of TELEVISION. **2.** Abbreviation of *terminal velocity*.

T/V Abbreviation of *temperature to voltage*.

TV decoder A device for unscrambling a television broadcast that has been intentionally encrypted to prevent its use by unauthorized viewers. See SUBSCRIPTION TV.

TV ghost See GHOST.

TVI Abbreviation of TELEVISION INTERFERENCE.

TVL Amateur radio abbreviation of *television listener* (looker).

TVM Abbreviation of TRANSISTORIZED VOLTMETER.

TVO Abbreviation of TRANSISTORIZED VOLT-OHMMETER. (Also, TVOM.)

TVOM Abbreviation of TRANSISTORIZED VOLT-OHMMETER. (Also, TVO.)

TV projector A combination electronic and optical device for projecting television images on a large screen.

TV sound marker See SOUND MARKER.

TVT Abbreviation of *television terminal* (computer peripheral).

TW Abbreviation of TERAWATT.

TWA Abbreviation of TRAVELING-WAVE AMPLIFIER.

tweeter A loudspeaker that favors the extreme treble (high) audio frequencies, ranging from 4000 or 5000 Hz to more than 20,000 Hz. Compare WOOFER.

twin diode See DUAL DIODE.

twinlead See FLAT-RIBBON LINE.

twin line See FLAT-RIBBON LINE.

twin meter See DUAL METER.

twin-T measuring circuit See PARALLEL-TEE MEASURING CIRCUIT.

twin-T network See PARALLEL-TEE NETWORK.

twisted pair A simple wire line used for communications. It consists of two wires twisted together to form a helix.

twister A piezoelectric crystal, such as one of Rochelle salt, that generates a voltage when torqued.

twistor A magnetic-memory element consisting of a winding of magnetic wire on a length of nonmagnetic wire.

two-channel amplifier See DUAL-CHANNEL AMPLIFIER.

two-channel recorder See DOUBLE-CHANNEL RECORDER.

two-electrode amplifier See DIODE AMPLIFIER.

two-electrode tube See TUBE DIODE.

two-element amplifier See DIODE AMPLIFIER.

two-element beam A Yagi antenna consisting of a driven element and one parasitic element. The parasitic element can be either a reflector, about 5% longer than the resonant half wavelength at the operating frequency, or it can be a director, about 5% shorter than a half wavelength at the operating frequency.

two-element tube An electron tube having two principal electrodes (i.e., a tube diode).

two-five code See BIQUINARY CODE.

two-phase Pertaining to circuits or devices in which two components (two voltages, two

5059F-pT-671-699 4/10/01 9:51 AM Page 699

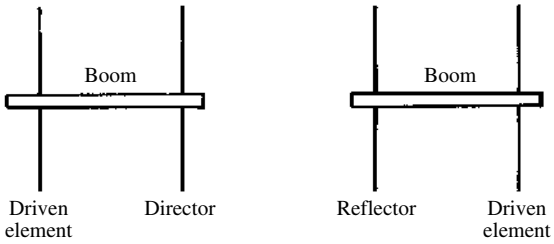

two-element beam

currents, or a current and a voltage) are 90° out of phase with each other.

two-phase system See QUARTER-PHASE SYSTEM.

two-phase, three-wire circuit A circuit using three conductors, one of which (the common return) is 90° out of phase with the other (outer) two.

two-pincher gripper A simple robotic end effector using two tongs, and resembling large tweezers or needle-nosed pliers. It grasps objects by "pinching" them.

two-point tuning See DOUBLE-SPOT TUNING.

two-space A two-dimensional mathematical continuum in which each point is uniquely defined by two variables in an ordered pair, such as (x,y), and each ordered pair corresponds to exactly one point in the continuum. A common scheme is the Cartesian coordinate system; another scheme is the polar coordinate system. See CARTESIAN COORDINATES and POLAR COORDINATES.

two-space coordinates A coordinate system for defining points in two-space. See CARTESIAN COORDINATES and POLAR COORDINATES.

two-state device A device having two stable states (e.g., a flip-flop).

two-state logic Digital logic in which there are two possible conditions (called high and low, true and false, or 1 and 0).

two-tone keying See FREQUENCY-SHIFT KEYING.

two-track recording Recording on two adjacent tracks on magnetic tape. The separate recordings can be in the same direction (as in stereo) or in opposite directions.

two-way amplifier An amplifier whose input and output terminals can be used interchangeably.

two-way communication The exchange of messages between two or more stations that transmit as well as receive. Compare ONE-WAY COMMUNICATION, **1**.

two-way radio **1.** Any form of TWO-WAY COMMUNICATION using electromagnetic waves. **2.** A radio transceiver—especially one used for voice communication at very-high or ultra-high frequencies.

two-way repeater In telephony, a device that amplifies and retransmits a signal in either direction. Also see TWO-WAY AMPLIFIER.

two-way speaker A woofer/midrange speaker and a tweeter occupying the same enclosure, and interconnected by a crossover network for wideband frequency response.

TWT Abbreviation of TRAVELING-WAVE TUBE.

TWX Abbreviation of TELETYPEWRITER EXCHANGE.

Twystron A form of microwave-oscillator tube, similar to the Klystron.

Type A telephone line A telephone line serving one subscriber (as opposed to a party line).

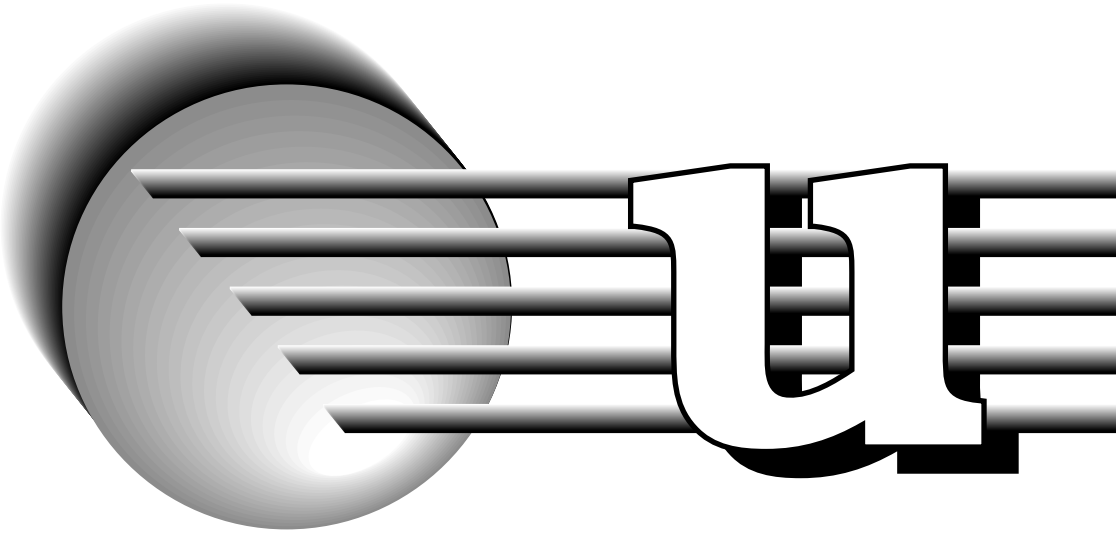

U **1.** Symbol for URANIUM. **2.** Abbreviation of UNIT.

u Symbol (ital.) for UNIFIED ATOMIC MASS UNIT.

Ua Abbreviation of *unit of activity* (electroencephalography).

UAM Abbreviation of *underwater-to-air missile.*

ubiquitous carrier A current carrier (especially an electron) whose velocity is so high, or mechanism of transfer so subtle, that it appears to be in two places simultaneously. Thus, in the tunnel diode, during the interval of tunneling a single electron, appears to be on both sides of the barrier at the same time.

Ubitron A tube in which a periodic magnetic field causes an electron beam to undulate. Through its transverse velocity component, the beam interacts with a radio-frequency wave, and its kinetic energy is converted into radio-frequency energy. The ubitron can be used as an amplifier or oscillator.

UCT Abbreviation of UNIVERSAL COORDINATED TIME.

UDC Abbreviation of *universal decimal classification.*

UDOP Abbreviation of *ultra-high-frequency Doppler.* A 440-MHz phase-coherent tracking system used to determine the velocity and position of missiles and space vehicles.

UEP Abbreviation of *underwater electric potential.*

UFET Abbreviation of unipolar field-effect transistor. (Also, UNIFET.) See UNIPOLAR TRANSISTOR.

UFO See UNIDENTIFIED FLYING OBJECT.

UG Abbreviation of underground.

UHF Abbreviation of ULTRAHIGH FREQUENCY.

UHF adaptor See UHF CONVERTER, **1**.

UHF capacitor A button-type capacitor. Because of its unique design, it is an efficient bypass capacitor at ultrahigh frequencies.

UHF converter **1.** A circuit, usually consisting of a radio-frequency amplifier and mixer, for converting ultra-high-frequency (UHF) signals to a lower band of frequencies. **2.** A circuit for converting UHF television signals to very-high-frequency (VHF) signals so that they can be accommodated by an older (VHF only) television receiver. See UHF TELEVISION CHANNELS and VHF TELEVISION CHANNELS.

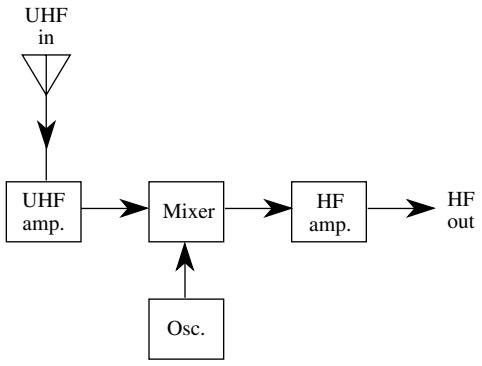

UHF converter, 1

UHF diode A semiconductor diode whose rectification efficiency is good at ultra-high frequencies.

Copyright 2001 The McGraw-Hill Companies, Inc. Click Here for Terms of Use

5059F-pU-700-715 4/10/01 9:53 AM Page 701

UHF generator **1.** An oscillating device (such as a transistor, tunnel diode, Klystron, or magnetron) used to produce radio-frequency energy at ultra-high frequencies (UHF). **2.** The equipment in which such a device is used. **3.** An ultra-high-frequency test-signal generator.

UHF loop A (usually single-turn) loop antenna with a toroidal radiation pattern perpendicular to the loop; the antenna has a natural wavelength in the ultra-high-frequency (UHF) range.

UHF receiver A receiver tunable to frequencies in any band in the range 300 MHz to 3000 MHz.

UHF television channels Television channels 14 through 69, whose frequencies lie in the ultra-high range.

UHF transistor A transistor specially designed and fabricated for ultra-high-frequency (UHF) operation. It is characterized by extended beta cutoff frequency, low junction capacitance, and fast recovery time.

UHF translator A television broadcast translator station transmitting in an ultra-high-frequency (UHF) channel.

UHF transmitter A transmitter that is specially designed for operation at ultra-high frequencies. In such a transmitter, stray parameters are minimized and special tubes or transistors are required.

UHF tube A vacuum tube specially designed for ultra-high-frequency operation. It is characterized by low interelectrode capacitance, low input and output capacitances, short electron transit time, and low lead inductance.

UHF tuner **1.** A superheterodyne receiver front end tunable in the ultra-high-frequency (UHF) range. It is usually arranged to deliver the mixer output to a lower-frequency receiver. **2.** A television receiver front end tunable to the UHF channels.

UHR Abbreviation of ULTRA-HIGH RESISTANCE.

U index The difference between consecutive daily mean values of the horizontal component of the geomagnetic field.

UJT Abbreviation of UNIJUNCTION TRANSISTOR.

UL **1.** Abbreviation of UNDERWRITERS LABORATORIES. **2.** Abbreviation of ULTRALINEAR.

ULD Abbreviation of ULTRA-LOW DISTORTION.

ULF Abbreviation of ULTRA-LOW FREQUENCY.

U-line section A short section of coaxial cable or hardline having the shape of a squared U.

ULSI See ULTRA-LARGE-SCALE INTEGRATION.

ultimate attenuation The maximum attenuation in a circuit or device when it is operated outside its passband, or within its stopband.

ultimately controlled variable In an automated system, the quantity or operation (e.g., liquid level, temperature, pressure, precision drilling, etc.), whose control is the end purpose of the system.

ultimate-range ballistic missile A ballistic missile whose range is greater than half the earth's circumference (approximately 12,000 miles).

ultimate ratio The limiting value of a ratio (i.e., the value approached by a ratio).

ultimate sensitivity **1.** In an instrument or system, the maximum degree of perception of, or response to, a quantity or condition. **2.** In a graphic recorder, half the deadband.

ultimate threshold See ULTIMATE SENSITIVITY, **2**.

ultimate trip current For a specified set of environmental conditions, the lowest value of current that will trip a circuit breaker.

ultimate trip limits For a circuit breaker, the maximum and minimum current at which the breaker trips and drops out.

ultor anode The second anode of a television picture tube or oscilloscope tube.

ultor element In a television picture tube, the element that receives the highest direct-current voltage. Also called *ultor electrode.* Also see ULTOR ANODE.

ultor voltage The high direct-current voltage applied to the second anode of an oscilloscope tube or television picture tube. Also see ULTOR ANODE.

ultra- A prefix meaning *above*, *larger than*, *greater than*, or *higher than.* See the following several definitions for examples.

ultra-atomic Pertaining to particles smaller than atoms (i.e., SUBATOMIC).

ultra-audible frequency A frequency higher than the highest audible frequency. Also called ULTRASONIC FREQUENCY and *supersonic frequency.*

ultra-audion oscillator See ULTRAUDION OSCILLATOR.

ultracentrifuge A centrifuge that spins at a very high speed.

ultrafast switch An electronic switch capable of microsecond operation.

Ultrafax A system for high-speed transmission of printed matter by facsimile, radio, or television.

ultra-high frequency A radio frequency in the range 300 MHz to 3000 MHz, corresponding to free-space wavelengths between 1 meter and 10 centimeters.

ultra-high-frequency band See UHF BAND.

ultra-high resistance Resistance of 100 megohms or higher.

ultra-large-scale integration An integrated-circuit process that goes several orders of magnitude beyond VERY-LARGE-SCALE INTEGRATION. More than 4×10^6 transistors could be on a single chip.

ultra-linear Pertaining to the most linear operation obtainable with state-of-the-art electronic equipment.

ultra-linear amplifier A high-fidelity audio-frequency power amplifier having wide frequency response and very low distortion.

ultra-low distortion Total harmonic distortion (THD) of less than 0.1 percent.

ultra-low frequencies **1.** Radio frequencies between 300 Hz and 3 kHz, pertaining to

5059F-pU-700-715 4/10/01 9:53 AM Page 702

wavelengths between 1000 kilometers and 100 kilometers. **2.** Audio frequencies lower than those in the human hearing range.

ultramicrometer An electronic instrument for extremely small linear measurements.

ultramicroscope An optical microscope using refracted light to illuminate minute particles.

ultramicrowave Pertaining to wavelengths in the range 10^{-3} to 10^{-6} meter (300 GHz to 300 THz).

ultraminiature See SUBMINIATURE.

ultraphotic rays Collectively, infrared and ultraviolet rays.

ultrared rays See INFRARED RAYS.

ultra-short waves Waves whose length correspond to ultra-high frequencies (i.e., wavelengths between 0.1 and 1 meter).

ultrasonic Of higher frequency than those that are audible (supersonic). See, for example, ULTRASONIC FREQUENCY.

ultrasonic bonding A method of bonding metal by means of physical vibration at frequencies above the human hearing range.

ultrasonic brazing Forming a nonporous bond between metal parts through the use of ultrasonic energy and a second, different metal (or alloy) having a lower melting point.

ultrasonic cleaning A method of cleaning delicate or intricately structured items (such as dentures, contact lenses, or jewelry) in which the soiled items are immersed in a fluid that is agitated by ultrasonic transducers; the foreign particles are shaken away.

ultrasonic cleaning tank A thick-walled stainless-steel tank with ultrasonic transducers mounted within its walls and used for ultrasonic cleaning.

ultrasonic coagulation The coagulation of a substance through ultrasonic agitation.

ultrasonic communication Underwater telegraphic communication between ships and/or submarines by keying the echo-ranging sonar equipment.

ultrasonic delay line A delay line, such as the mercury type, through which an ultrasonic signal is propagated. The delay results from the relatively slow propagation of the ultrasonic wave through the substance in the line.

ultrasonic densitometer A density-measuring apparatus whose operation is based on the time required for an ultrasonic signal to penetrate the material under test, or for the signal to penetrate the material and be reflected back to the transmitter.

ultrasonic depth finder See ACOUSTIC DEPTH FINDER.

ultrasonic detector A device that responds to ultrasonic waves by indicating their presence, intensity, and/or frequency.

ultrasonic diagnosis The medical determination of the condition of tissues or structures within the body, in terms of reflection of ultrasonic waves by those tissues or structures. The technique is useful in situations where other techniques, such as radiology or the use of catheter probes, are risky. Also see ULTRASOUND.

ultrasonic disintegrator In biology and related fields, a device that uses ultrasonic energy to rupture or shatter cells, tissues, or foreign bodies, such as kidney stones.

ultrasonic drill A drill running at speeds corresponding to ultrasonic frequencies. The tool is valuable in drilling hard or brittle materials and in dentistry.

ultrasonic filter **1.** A bandpass filter whose operation is based on the natural (ultrasonic) vibration frequency of small disks or rods of magnetostrictive metal. See MAGNETOSTRICTION. Also called *mechanical filter*. **2.** Generally, a filter operating at ultrasonic frequencies.

ultrasonic flaw detector A system analogous to radar, in which an ultrasonic wave is transmitted through a solid material and is reflected back to a detector and display device to reveal flaws, cracks, and strain in the material.

ultrasonic frequency For an acoustic disturbance, any frequency above the limit of human hearing (higher than 20 kHz).

ultrasonic generator **1.** An oscillator that operates at frequencies above the range of human hearing, and the output of which is intended for coupling to an electroacoustic transducer. **2.** Any device that produces ultrasonic waves.

ultrasonic grating constant For a sound wave producing a diffraction spectrum, a figure indicating the distance between diffracting centers of the wave.

ultrasonic heating The production of heat in a specimen by means of ultrasonic energy directed into or through it.

ultrasonic image converter A device that makes visible acoustic field patterns.

ultrasonic inspection The use of ultrasonic waves to detect internal flaws in solid materials, such as metals. It is valued particularly because it is nondestructive. Also see ULTRASONIC FLAW DETECTOR.

ultrasonic intrusion alarm A security system activated when an intruder disturbs a pattern of ultrasonic waves in the protected area; a sensitive relay closes, setting off an alarm.

ultrasonic level detector A level-monitoring system in which an ultrasonic transmitter and detector are mounted together on one wall of a tank or chamber. When the tank is empty, the transmitted signal is reflected by the opposite wall back to the detector. When the liquid rises, the reflection time is reduced; this change is used to operate a device that indicates that the tank has been filled to a desired level.

ultrasonic light diffraction Diffraction resulting from the periodic variation of light refraction when a beam of light passes through a longitudinal sound-wave field.

5059F-pU-700-715 4/10/01 9:53 AM Page 703

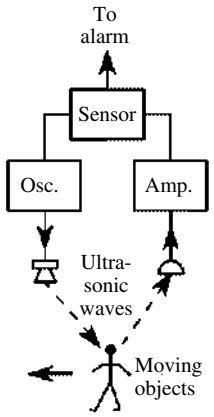

ultrasonic intrusion alarm

ultrasonic light modulator A device that modulates a light beam passing transversely through a fluid agitated by sound waves.

ultrasonic material dispersion The use of the agitative action of high-intensity ultrasonic waves to disperse or emulsify one substance in another.

ultrasonic plating The use of ultrasonic energy to deposit or bond one material onto the surface of another.

ultrasonic probe A rodlike director of ultrasonic energy.

ultrasonic relay An electronic relay actuated by ultrasound.

ultrasonics **1.** The use of high-frequency acoustic energy in industry, medicine, research, and the home. See ULTRASONIC FREQUENCY. **2.** The use of high-frequency acoustic energy for medical diagnosis and treatment. **3.** The branch of physics dealing with the effects and behavior of acoustic disturbances at frequencies above the range of human hearing.

ultrasonic soldering See ULTRASONIC BRAZING.

ultrasonic sounding Determining the depth of a body of water in terms of the time taken for a transmitted ultrasonic signal to be reflected back to a transmitting point on the surface of the water.

ultrasonic space grating A periodic variation in the index of refraction when acoustic waves are present in a light-transmitting medium. Also see ULTRASONIC LIGHT DIFFRACTION.

ultrasonic storage cell See ULTRASONIC DELAY LINE.

ultrasonic stroboscope A stroboscope that uses an ultrasonically modulated beam of light.

ultrasonic switch An electronic switch actuated by ultrasound.

ultrasonic therapy The use of ultrasonic energy in medicine for treatment of certain disorders.

ultrasonic thickness gauge An instrument that determines the thickness of a specimen in terms of the propagation time (or echo time) of ultrasonic waves through the specimen.

ultrasonic transducer A transducer that converts electrical energy into ultrasonic energy, or vice-versa. Common types are the quartz crystal, ceramic crystal, and magnetostrictive disk.

ultrasonic waves Acoustic waves whose length corresponds to ultrasonic frequencies (i.e., frequencies above 20 kHz).

ultrasonic welding A below-melting-point technique of joining two metallic bodies by clamping them tightly together and applying ultrasonic energy, rather than heat, in the plane of the desired weld. Compare ULTRASONIC BRAZING.

ultrasonic whistle A whistle whose pitch is beyond the range of human hearing. Although some are of the simile (blown) type, others are (usually miniature) electronic sound generators. These devices can be used for the remote control of television receivers, garage-door openers, and other equipment.

ultrasonography A method of examining human tissues or organs by transmitting ultrasonic waves into the body and receiving the echoes.

ultrasound **1.** Acoustic disturbances at frequencies above 20 kHz. **2.** See ULTRASONIC FREQUENCY. **3.** See ULTRASONOGRAPHY.

ultraviolet **1.** Electromagnetic radiation at wavelengths somewhat shorter than those of visible light. Longwave or *near ultraviolet* extends from approximately 390 nanometers (nm) down to 50 nm. Shortwave or *far ultraviolet* extends from 50 nm down to 4 nm. **2.** Pertaining to the behavior and effects of electromagnetic radiation in the range of approximately 390 nm to 4 nm.

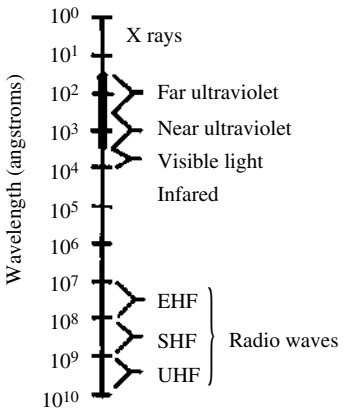

ultraviolet

ultraviolet altimeter An altimeter that uses ultraviolet rays instead of radio waves to determine the altitude of an aircraft or spacecraft.

5059F-pU-700-715 4/10/01 9:53 AM Page 704

ultraviolet lamp A lamp that delivers ultraviolet rays. Common types are arc lamps and mercury-vapor lamps.

ultraviolet light See ULTRAVIOLET RAYS.

ultraviolet power The power (in watts) of ultraviolet radiation.

ultraviolet rays Radiation at frequencies in the ultraviolet region (i.e., between the highest visible-light frequencies and the lowest X-ray frequencies).

ultraviolet therapy The use of ultraviolet rays by physicians and other health personnel in the treatment of certain disorders.

ultraviolet wavelength The wavelength range of ultraviolet radiation [e.g., 390 nanometers (nm) to 4 nm].

ultraviolet waves See ULTRAVIOLET RAYS.

umbilical cord **1.** A cord through which missiles and rockets are controlled and powered until they are launched. **2.** A cord connecting an astronaut to his space vehicle during extravehicular activity (e.g., during a space "walk").

umbilical tower The vertical tower supporting the umbilical cords extending to a rocket in the launch position.

umbra **1.** The region of total (conical) shadow behind an object situated in the path of a radiation. **2.** The comparatively dark central region in a sunspot.

umbrella antenna An antenna consisting of a number of wires, extending from the top of a vertical mast to points on a circle below, at the center of which the mast is mounted. The wires are usually fed in parallel from the top.

Umklapp process A process responsible for thermal resistance in nonconducting materials. It results from collision between phonons, or phonons and electrons.

UMW Abbreviation of ULTRAMICROWAVE.

unabsorbed field strength The field strength with no absorption between transmitter and detector. The unabsorbed field strength is an ideal quantity; the actual field strength over a given distance is always less. It is expressed in volts per meter.

unamplified back bias A negative-feedback voltage developed across a fast-time-constant circuit within a single amplifier stage.

unamplified feedback A positive or negative current or voltage taken from the output of a system and presented to the input without being boosted through auxiliary amplification.

unamplified ALC Automatic level control (ALC) in which the control-signal voltage is taken from a point in the circuit and fed to the controlled point without being boosted by an auxiliary amplifier. Compare AMPLIFIED ALC.

unattended operation Operation, as of an electronically programmed machine, with minimal (or no) human supervision.

unattended time The period, excluding down time for repair or checkout, during which a computer is unpowered.

unattenuated Not reduced in intensity of amplitude. Thus, an unattenuated signal is one that has retained its original strength during its transmission through a system.

unavailable energy The difference between the quantity of heat energy supplied to a system and the available energy of the system.

unbalance **1.** Lack of balance or symmetry in a circuit, line, or system. **2.** The condition in which a bridge (or the equivalent) is not nulled.

unbalanced circuit See SINGLE-ENDED CIRCUIT.

unbalanced delta system A three-phase circuit in which the elements are connected in a triangular (delta) configuration, but are of unequal impedance. In an unbalanced delta system, no definite relationship exists between line and phase currents. Compare BALANCED DELTA SYSTEM.

unbalanced input See SINGLE-ENDED INPUT.

unbalanced line **1.** A transmission line in which one side (conductor) is grounded (e.g., a coaxial line). **2.** A normally balanced transmission line in which the currents in the two halves are out of balance (i.e., they are not equal in amplitude and opposite in phase).

unbalanced multivibrator A multivibrator in which the time constant of one base or gate circuit differs from that of the other base or gate circuit. The asymmetry results in short-duration output pulses separated by long time periods.

unbalanced output See SINGLE-ENDED OUTPUT.

unbalanced two-phase system A two-phase circuit in which the load elements are of unequal impedance.

unbalanced wire circuit A wire line whose (two) sides are dissimilar.

unbalanced-wye system A three-phase circuit in which the elements are connected in the familiar wye, or star, configuration, but are of unequal impedance.

unbalanced-Y system See UNBALANCED-WYE SYSTEM.

unbalance-to-balance transformer A transformer for matching an unbalanced transmission line to a balanced line (e.g., a coaxial line to a parallel-wire line).

unbiased limiting Peak limiting that results from overdriving an unbiased active device.

unbiased unit A device or circuit operated without bias [e.g., a transistor without base bias (common emitter and emitter follower) or emitter bias (common base)].

unblanking Removal of the blanking pulse in a cathode-ray-tube circuit (i.e., turning on the beam).

unblanking generator A (usually pulse-type) signal source for turning on the beam of a blanked cathode-ray tube.

unblanking interval The period during which the beam of a cathode-ray tube is turned on. Compare BLANKING INTERVAL.

5059F-pU-700-715 4/10/01 9:53 AM Page 705

unblanking pulse A pulse that turns on the beam of a blanked cathode-ray tube. Compare BLANKING PULSE.

unblanking time **1.** See UNBLANKING INTERVAL. **2.** The instant at which unblanking begins.

unbonded strain gauge A strain gauge that is not directly attached (by cement, for example) to the strained surface.

unbound electron A free electron (i.e., an electron not confined to a shell within an atom).

unbuffered output An output (signal, power, etc.) that is delivered directly from the generating device without the benefit of an isolating stage, such as a buffer amplifier. Compare BUFFERED OUTPUT.

unbypassed emitter resistor In a common-emitter transistor circuit, an emitter resistor without a bypass capacitor. The flow of output-signal current through the resistor produces negative feedback within a single stage.

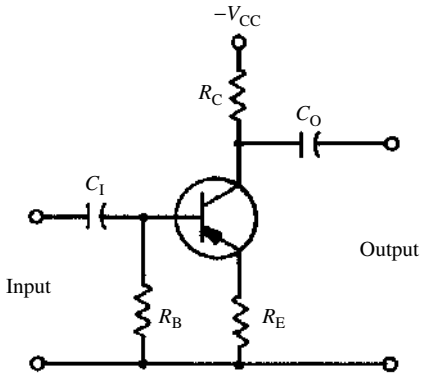

unbypassed emitter resistor (R_E)

unbypassed source resistor In a common-source field-effect transistor circuit, a source resistor without a bypass capacitor. The flow of output-signal current through the resistor produces negative feedback within a single stage.

uncage In a displacement gyroscope system, to disconnect the erection circuit.

uncalibrated unit A component, circuit, or instrument that has never been calibrated or has not recently been calibrated and, hence, is of questionable accuracy.

uncanny valley According to a theory put forth by certain Japanese roboticists, a phenomenon that can occur among people as technology advances. As machines rapidly get more sophisticated, a point is reached at which their human users become unnerved, partially offsetting the advantages the technology has to offer.

uncased choke See UNSHIELDED CHOKE.

uncased transformer See UNSHIELDED TRANSFORMER.

uncertainty in computation The degree of doubt concerning the exactness of computations. This uncertainty is always greater than that of the roughest measurement used in obtaining data for the computation. Uncertainty is closely related to the tolerance of the instruments and formulas used.

uncertainty in measurement The estimated maximum amount whereby the numerical value of a measured quantity can differ from the true value.

uncertainty principle The observation that high precision in the location of an electron is obtainable only at a sacrifice in the accuracy with which the momentum of the electron can be determined, and vice versa.

uncharged Without an electric charge, as opposed to discharged (depleted of a charge).

unclamp To switch off clamping action in a circuit. See CLAMPER and CLAMPING.

uncoated filament **1.** A plain filament (i.e., one without a coating of electron-increasing material). **2.** A stripped filament (i.e., one from which the electron-increasing coating has been burned off).

uncompensated Not modified to produce a desired type of performance, such as increased bandwidth or reduced temperature sensitivity. Example: an uncompensated amplifier put into service in the (wide) video band. Compare COMPENSATED AMPLIFIER, COMPENSATED CAPACITOR, and COMPENSATED DIODE DETECTOR.

uncompensated amplifier An amplifier without a provision for the automatic or manual modification or correction of its response. Compare COMPENSATED AMPLIFIER.

uncompensated capacitor A fixed or variable capacitor without a provision for the automatic or manual correction or modification of its capacitance or range or the improvement of its temperature coefficient. Compare COMPENSATED CAPACITOR.

uncompensated inductor A fixed or variable inductor without a provision for the automatic or manual correction or modification of its inductance or range or the improvement of its temperature coefficient.

uncompensated resistor A fixed or variable resistor without a provision for the automatic or manual correction or modification of its resistance or range or the improvement of its temperature coefficient.

unconditional branch See UNCONDITIONAL JUMP.

unconditional jump In computer operations, a program instruction that interrupts, without a relational test being made, the normal, ordered sequence of instructions and gives the address of (usually) the first instruction in a subroutine [e.g., BASIC's GOTO (line number)]. Also called *unconditional branch.* Compare CONDITIONAL JUMP.

5059F-pU-700-715 4/10/01 9:53 AM Page 706

unconditional stability Stability of a system at all frequencies and ages. Also called *absolute stability.*

unconditional transfer See UNCONDITIONAL JUMP.

uncontrolled multivibrator A multivibrator that is not synchronized with a signal source. Also called ASTABLE MULTIVIBRATOR and FREE-RUNNING MULTIVIBRATOR.

uncontrolled oscillator See SELF-EXCITED OSCILLATOR.

uncorrected power In an alternating-current circuit, a power value calculated without regard for power factor (i.e., the volt-ampere product).

uncorrected time Local standard time that has not been corrected in terms of the distance of the locality from the nearest standard-time meridian.

uncorrected tube A television picture tube operated without antipincushioning magnets.

uncoupled mode A mode of vibration existing in a system concurrent with (but independent of) other modes.

undamped galvanometer A galvanometer for which no provision has been made to limit overswing or prevent oscillation.

undamped meter **1.** A meter for which no provision has been made to limit overswing or prevent oscillation. **2.** A meter that is unprotected by a short circuit for limiting vibratory movement of the pointer during transport.

undamped natural frequency In the absence of damping, the oscillation frequency of a system having one degree of freedom when a transient force displaces the system momentarily from its position of rest.

undamped oscillation Continuous-wave oscillation. Also see CONTINUOUS WAVE.

undamped output circuit An audio power-amplifier output circuit that has not been designed so that overswing of the loudspeaker cone is prevented.

undamped speaker enclosure A loudspeaker cabinet for which provision has not been made to deaden resonances and other undesired vibration.

undamped wave See CONTINUOUS WAVE.

undeflected beam A cathode-ray beam or a light beam in its normal position of rest (quiescence).

underbiased unit A component, such as a transistor or vacuum tube, whose bias voltage or current is lower than the prescribed value. Compare OVERBIASED UNIT.

underbunching Less-than-optimum bunching of electrons in a velocity-modulated tube because of lowered buncher voltage.

undercompounded generator A generator in which the output voltage varies inversely with load resistance.

undercoupling Loose coupling, usually of an amount insufficient for optimum signal transfer.

undercurrent A current of lower than specified strength. Compare OVERCURRENT.

undercurrent relay A relay that is actuated when coil current falls below a predetermined level.

undercut The removal of the metal under the edge of the resist in a printed circuit by the etchant; thus the cross section of the conductor is reduced.

undercutting A phonograph-disc groove that is cut too shallow or with reduced internal movement of the recording stylus.

underdamping Insufficient damping of a system (i.e., not enough to prevent output oscillation following application of a transient force).

underdriven unit An amplifier, oscillator, or transducer whose driving signal (current, voltage, power, or other quantity) is lower than the prescribed value. Compare OVERDRIVEN UNIT.

underexcited Receiving lower-than-normal excitation, as in an underdriven final amplifier of a radio transmitter. Compare OVEREXCITED.

underflow In computer operations, the condition in which a quantity entered into storage is shorter than the space provided for it (e.g., a 12-digit quantity in a 16-position register).

underground antenna A transmitting or receiving antenna installed and operated below ground. Included are buried antennas and antennas on equipment operated in tunnels, cellars, and similar areas.

underground cable A cable that is buried in the earth.

underground communication Communication between a transmitter and receiver, both below the surface of the earth.

underground image The below-ground mirror image of an antenna; it combines with the actual antenna to form the complete radiation pattern.

underground line A power line laid below the surface of the earth.

underground receiver **1.** A receiver situated completely below the surface of the earth. **2.** A clandestine receiver.

underground reception Reception of an above-ground station's transmissions by an underground receiver. Compare UNDERGROUND COMMUNICATION.

underground transmitter **1.** A transmitter situated completely below the surface of the earth. **2.** A clandestine transmitter.

under insulation The insulation (usually a strip of tape) laid under a wire brought up from the center of a coil.

underinsulation Inadequate or insufficient insulation.

underlap In a facsimile or television picture, a crowding of the scanned lines.

underload circuit breaker See CIRCUIT BREAKER.

underloaded amplifier **1.** An amplifier whose load resistance (impedance) is less than the prescribed value. **2.** A power amplifier delivering less than its rated output power. Compare OVERLOADED AMPLIFIER.

5059F-pU-700-715 4/10/01 9:53 AM Page 707

underload relay A relay actuated when circuit current drops below a predetermined value. Compare OVERLOAD RELAY.

undermodulation Incomplete modulation of a carrier wave. Compare COMPLETE MODULATION and OVERMODULATION.

underpass The crossing of two conductors on a semiconductor wafer, without an electrical connection.

underpower relay A relay actuated when power drops below a predetermined level. Compare OVERPOWER RELAY.

underrate To assign a rating (e.g., current or power) lower than the quantity of the rating an equipment can handle, or tolerate. For safety or reliability, apparatus sometimes is deliberately underrated—especially in power output and maximum current or voltage.

undershoot On an oscilloscope screen or graph, a momentary swing of a current or voltage below the reference axis. Compare OVERSHOOT.

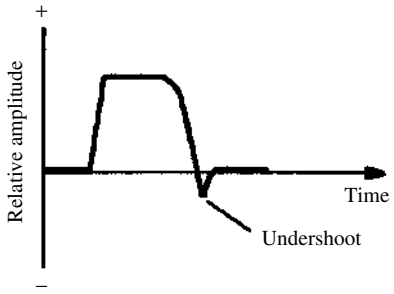

undershoot

undershoot distortion Distortion caused by reduction of the maximum amplitude of a signal wavefront below the steady-state amplitude that would be reached by a prolonged signal wave.

understudy See BACKUP.

underthrow A form of signal distortion that occurs when the modulating-waveform frequency is too high in proportion to the frequency of the wave itself.

undervoltage A voltage of lower than specified value. Compare OVERVOLTAGE.

undervoltage protection The automatic disconnection of a load device from its driving source when the driving voltage falls below a predetermined (threshold) level. This action is sometimes accomplished with a Zener diode (whose breakdown voltage is equal to the threshold voltage) in series with a disconnect relay.

undervoltage relay A relay actuated when voltage drops below a predetermined level. Compare OVERVOLTAGE RELAY.

underwater antenna A transmitting or receiving antenna normally operated in a body of water. It is usually associated with a submarine.

underwater sound projector A hydroacoustic transducer that converts audio-frequency power into sound waves, which it radiates through a body of water to a receiver.

Underwriters Code The advisory National Electrical Code adopted by the National Fire Protection Association; it is often enforced by courts of law and inspection agencies.

Underwriters Laboratories Abbreviation, UL. A private corporation that issues standards of safety for electrical components and equipment, and for their operation.

undistorted power output For active amplifier devices, a specified maximum audio power output level at which the total distortion does not exceed a specified low value (i.e., at which operation is practically distortionless).

undistorted wave **1.** A sine wave that contains essentially no harmonic energy. **2.** A nonsinusoidal wave whose shape corresponds exactly to the equation for the wave.

undisturbed-one output In digital-memory operations, the one-output of a magnetic cell or other memory unit that has received a full, rather than partial, read pulse. Compare UNDISTURBED OUTPUT SIGNAL.

undisturbed output signal In digital-memory operations, the output of a magnetic cell or other memory unit previously set to one or zero, and that has received a full, rather than partial, read pulse. Also called *undisturbed response voltage.*

undisturbed response voltage See UNDISTURBED OUTPUT SIGNAL.

undisturbed-zero output In digital-memory operations, the zero-output of a magnetic cell or other memory unit that has received a full, rather than partial, read pulse. Compare UNDISTURBED OUTPUT SIGNAL.

Universal Truth Machine (UTM) A hypothetical computer capable of proving any logically true statement. According to the Incompleteness Theorem proved in 1930, such a machine cannot exist for a first-order logical system.

undoped Pertaining to a pure semiconductor material (i.e., one containing no lattice-altering additives).

undulating current A current, such as an alternating or composite current, whose value oscillates in the manner of a wave.

undulation A wavelike alternation.

undulatory theory The theory that light is transmitted by means of an undulating (wavelike) movement between the luminous object and the eye.

unequal alternation In an alternating-current waveform, a form of asymmetry in which the positive and negative half-cycles are not exact mirror images; they might vary in peak amplitude, duration, shape, etc.

5059F-pU-700-715 4/10/01 9:53 AM Page 708

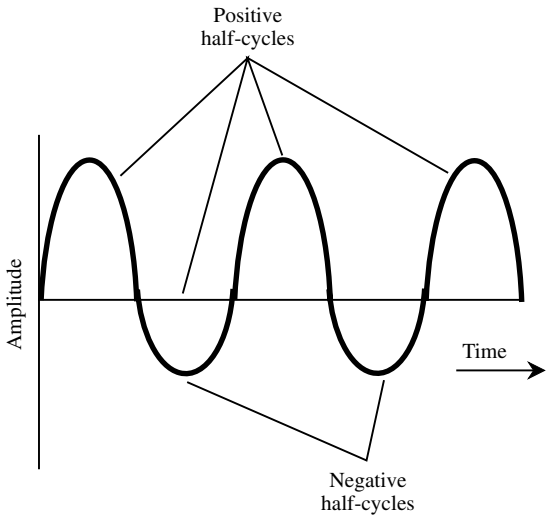

unequal alternation

unexpected halt During a computer program run, an undirected (unplanned) halt (e.g., one caused by a machine fault or program bug).

unfiltered Not having been subjected to filtering action. An example is the pulsating-direct-current output of an alternating-current-operated rectifier circuit.

unfocused light source In a photoelectric system, a light source that delivers diffused light.

unformed rectifier A newly fabricated semiconductor rectifier (especially selenium) or an electrolytic rectifier before it has been electroformed for improved characteristics.

unfurlable antenna An antenna that can be unrolled to increase its length, thereby lowering its fundamental resonant frequency; it can also be rolled up to decrease its length and increase its fundamental resonant frequency.

ungrounded item A component, circuit, or circuit point having no connection to ground, except an inadvertent one through common impedances or leakage paths.

ungrounded system A system operated entirely above ground, any path to ground being accidental.

unguided Without electronic guidance (pertaining to missiles, rockets, satellites, etc.).

uni- A prefix (combining form) meaning *one* or *single* and appearing in a number of electronic terms. See the following several definitions for examples.

uniaxial **1.** Having one axis. **2.** Referred to one axis.

uniaxial crystal A crystal having one optical axis.

unibivalent electrolyte An electrolyte, such as sodium carbonate (Na_2CO_3), that dissociates into two univalent ions and one bivalent ion.

Unicode Trade name for a 16- or 32-bit binary digital code that allows for the representation of characters and glyphs in all the written languages of the world. The 16-bit code contains 65,536 code points; the 32-bit version contains more than 1 million code points.

uniconductor cable A cable having a single conductor, usually of braided or twisted wires.

uniconductor waveguide A waveguide consisting of a metal sheath deposited on a solid dielectric of cylindrical or rectangular cross section.

unidentified flying object Abbreviation, UFO. An object claimed to have been seen in flight, but not identified by reliable authorities as any known type of vehicle.

unidirect To commutate (see COMMUTATOR).

unidirectional **1.** Flowing or acting in one direction only. **2.** Having a radiation or response sensitivity that is maximum in primarily one direction in space.

unidirectional antenna See UNIDIRECTIONAL ARRAY.

unidirectional array A beam antenna that radiates in one direction only, or principally in one direction, unless rotated.

unidirectional conductivity Electrical conductivity in only one direction; it characterizes an ideal diode.

unidirectional coupler A directional coupler sampling only one direction of transmission.

unidirectional current A current that flows always in the same direction, although it might fluctuate in intensity.

unidirectional elements Circuit elements, such as diodes or transistors, that transmit energy in only (or best in) one direction.

unidirectional field-effect transistor See UNILATERAL FIELD-EFFECT TRANSISTOR.

unidirectional hydrophone An underwater unidirectional microphone.

unidirectional loudspeaker A loudspeaker that radiates sound substantially in one direction.

unidirectional microphone A microphone that receives sound waves from one direction, usually from the front, minimum response usually being from the sides and back.

unidirectional network A network that transmits signals in only one direction (i.e., the input and output terminals are not interchangeable).

unidirectional pattern For a transducer (such as an antenna, speaker, or microphone), a radiation or response pattern that shows a pronounced maximum in one direction only.

unidirectional pulse A single-polarity pulse.

unidirectional pulse train A series of unidirectional pulses.

unidirectional response For a receiving transducer, such as an antenna or microphone, a response pattern that shows a pronounced maximum in one direction only.

5059F-pU-700-715 4/10/01 9:53 AM Page 709

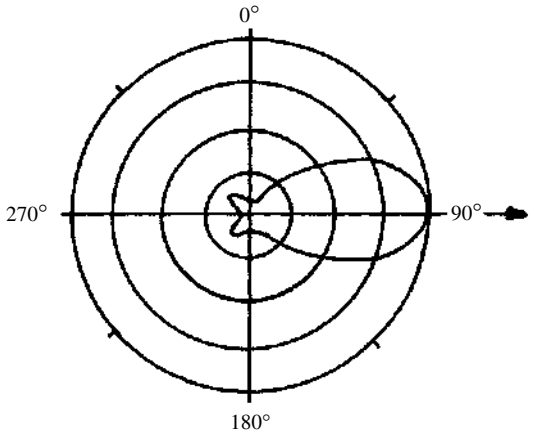

unidirectional pattern

unidirectional speaker See UNIDIRECTIONAL LOUDSPEAKER.

unidirectional transducer A transducer that operates in one direction only (i.e., its input and output cannot be interchanged).

unidirectional voltage A voltage that never changes polarity, although it might fluctuate in value.

UNIFET Abbreviation of UNIPOLAR FIELD-EFFECT TRANSISTOR. (Also, UFET.)

unified-field theory A theory, as yet unproved, that all forces in nature are interrelated and are controlled by the same causes and factors. Albert Einstein worked on this theory after he successfully developed the theories of relativity.

unifilar Having (or wound as) one fiber, wire, filament, or thread.

unifilar magnetometer A magnetometer in which a bar is suspended at its center of gravity by a single thread.

unifilar suspension A method of meter construction in which the moving part is suspended by a single filament. The torque might be provided by this filament or by a spring or other resisting device; the greater the displacement, the greater the torque.

uniform circular motion Motion at a uniform rate and describing a circle (e.g., a motor armature rotating at a constant speed).

uniform electric field An electric field in which all the lines of flux are straight and parallel, and in which the electrostatic force has the same value at all points (e.g., the field between two oppositely charged, flat, parallel plates).

uniform field See UNIFORM ELECTRIC FIELD and UNIFORM MAGNETIC FIELD.

uniform frequency response Frequency response that is flat throughout a specified range. Such response is characterized by the transmission of a signal with no introduced amplitude or phase distortion.

uniform line A transmission line having identical electrical properties over its entire length.

uniform magnetic field A magnetic field in which all the lines of flux are straight and parallel, and in which the magnetic force has the same value at all points.

uniform plane wave A free-space plane wave at an infinite distance from the generator, having constant-amplitude electric and magnetic field vectors over the equiphase surfaces.

uniform precession In regions of the uniform magnetic field of a sample of material, the state in which the magnetic moments of all atoms are parallel and precess in phase around the magnetic field.

uniform waveguide A waveguide having constant electrical and physical characteristics along its axis.

uniground **1.** The grounding of a circuit at one point to reduce susceptibility to hum and noise. **2.** The point at which such a connection is made.

unijunction transistor A semiconductor device consisting of a thin silicon bar on which a single pn junction acting as an emitter is formed near one end. Two bases are provided—each an ohmic connection made to one end of the bar. Also called *double-base diode.*

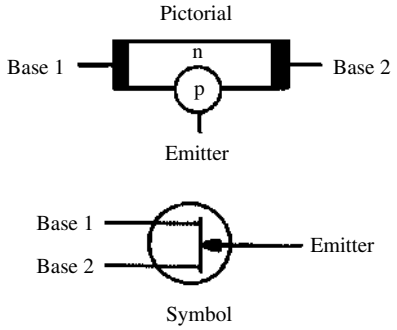

unijunction transistor

unilateral area track A film sound track having modulation on only one edge of the opaque area.

unilateral bearing In radio direction finding, a bearing obtained with a finder that produces unilateral response and thereby eliminates 180-degree error.

unilateral conductivity See UNIDIRECTIONAL CONDUCTIVITY.

unilateral element See UNIDIRECTIONAL ELEMENTS.

unilateral field-effect transistor A field-effect transistor whose source and drain terminals cannot be interchanged. Also called ASYMMETRICAL FIELD-EFFECT TRANSISTOR. Compare SYMMETRICAL FIELD-EFFECT TRANSISTOR.

5059F-pU-700-715 4/10/01 9:53 AM Page 710

unilateralization A system of neutralization used in transistor amplifiers at very-high and ultra-high frequencies, in which the internal capacitive and resistive components are compensated by the neutralization feedback.

unilateralized amplifier A transistor amplifier in which both the internal resistive and capacitive components are compensated by the neutralizing circuit. Also see UNILATERALIZATION.

unilateral network See UNIDIRECTIONAL NETWORK.

unilateral transducer See UNIDIRECTIONAL TRANSDUCER.

uninterruptible power supply Abbreviation, UPS. A device that provides a continuous utility current to electronic devices in the event of a utility power dip or blackout. It contains a battery and a power inverter. These devices are used extensively in personal computing to prevent loss of data that could otherwise result from a utility power failure.

union **1.** The logical inclusive-OR operation. **2.** See BOND, **1**.

union catalog In computer operations, the compiled list of the contents of two or more tape or disk libraries.

unionic material A material having no ions (i.e., one in which all atoms are neutral).

uniphase antenna See COLLINEAR ANTENNA.

UNIPOL Acronym for *universal problem-oriented language,* a high-level computer-programming language.

unipolar **1.** Having or using a single pole or polarity. **2.** Operating with one class of current carrier.

unipolar armature An electric-motor armature that maintains its polarity throughout a complete revolution.

unipolar field-effect transistor See UNIPOLAR TRANSISTOR.

unipolar induction Induction by only one pole of a magnet.

unipolar input The input circuit of an instrument or device designed for input signals of one polarity only.

unipolar pulse A pulse in which the current flows in only one direction, or in which the voltage occurs with only one polarity.

unipolar transistor A field-effect transistor (FET). It utilizes only one kind of carrier (electrons in the n-channel FET, holes in the p-channel FET). Compare BIPOLAR TRANSISTOR.

unipolar winding The winding of a UNIPOLAR ARMATURE.

unipole **1.** An all-pass filter having one pole and for which there is one zero. Also see ALL-PASS FILTER, POLES OF IMPEDANCE, and ZEROS OF IMPEDANCE. **2.** A hypothetical, omnidirectional antenna.

unipotential cathode An indirectly heated tube cathode. Also called *equipotential cathode.* See INDIRECTLY HEATED CATHODE.

unit **1.** A named, single magnitude adopted as a standard by physical measurement. Thus, the unit of current is the ampere, the unit of frequency is the hertz, the unit of capacitance is the farad, etc. Also see ABSOLUTE SYSTEM OF UNITS, INTERNATIONAL SYSTEM OF UNITS, and CENTIMETER-GRAM-SECOND. **2.** A single piece or assemblage of equipment, such as amplifier, converter, power supply, etc. **3.** A quantity of 1 implied when unit is the adjective describing a quantity (e.g., *unit length* means a distance of 1 meter, 1 foot, etc.).

unitary code In computer operations, a code based on one digit. The number of times the digit is repeated indicates a given number.

unit cell In crystals, the simplest polyhedron exhibiting all the structural features and which is repeated to form the crystal lattice.

unit charge See UNIT ELECTROSTATIC CHARGE.

unit electric charge See UNIT ELECTROSTATIC CHARGE.

unit electrostatic charge An electrostatic point charge that will attract or repel a point charge of equal strength 1 centimeter away in a vacuum, with a force of 1 dyne (10^{-5} newton).

unit function Symbol, *H* or *1.* A time-dependent quantity that is zero before the start of a period (when time t is zero) and 1 for all values of t greater than zero. It is approximated by a square wave, and is useful in solving problems involving transients.

unit length **1.** A fundamental unit of distance or time, used for reference in a measuring system. For example, in the mks (meter-kilogram-second) system, the distance unit length is the meter, and the time unit length is the second. **2.** The duration of a fundamental element, or bit, in a binary-code transmission system.

unitized construction The fabrication of an electronic equipment in subassemblies (such as modules) that can be tested separately, and that can be easily replaced (plugged in) in the event of individual failure.

unit line A line of electric or magnetic flux.

unit magnetic pole See UNIT POLE.

unit matrix A matrix whose main diagonal terms (all) are all at unity, the other terms being zero.

unitooth Pertaining to the use in electrical machinery of one slot per pole per phase.

unitor See OR GATE.

unit pole The strength (magnetic flux) of a (hypothetical) magnetic pole that will attract or repel a pole of equal strength 1 centimeter away in a vacuum, with a force of 1 dyne; 1 unit pole = 1.257×10^{-7} weber.

unit-ramp function A function whose value is zero before time t, and becomes equal to the time measured from t at all other instants. The integral of the UNIT FUNCTION.

unit record In computer operations, a complete record consisting of many data elements and

5059F-pU-700-715 4/10/01 9:53 AM Page 711

contained within one storage medium, such as a magnetic disk.

unitrivalent electrolyte An electrolyte, such as sodium phosphate (Na_3PO_4), that dissociates into three univalent ions and one trivalent ion.

units position In a numbering system, the rightmost position in a multidigit whole number; or, if the number contains a radix point, the digit immediately to the left of the radix point.

unit-step function See UNIT FUNCTION.

unitunnel diode A special form of semiconductor diode, used as an oscillator at ultra-high and microwave frequencies.

unit vector A vector that is 1 unit long in terms of the scale representing a factor of interest, and has the same direction as the vector of interest. For example, if u is a unit vector, then $5u$ represents a vector having the same direction and five times the magnitude of u.

unity **1.** The figure 1 implied. **2.** A ratio of 1:1. **3.** A gain of 0 dB.

unity coupling Tight coupling between two coils, the turns ratio often being 1 to 1 and the coils always being closely interwound.

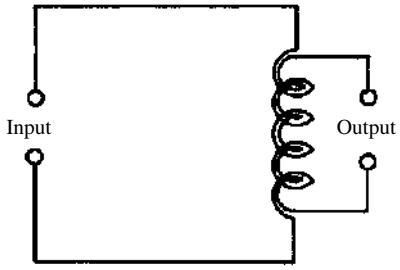

unity coupling

unity gain The condition in which the output amplitude is the same as the input amplitude; that is, a gain factor of 1, or 0 dB.

unity-gain bandwidth **1.** For an active filter, the bandwidth between the frequencies at which the gain is 0 dB. **2.** For an operational amplifier having a rolloff of 6 dB per octave, the frequency at which the open-loop gain is 0 dB.

uni-univalent electrolyte An electrolyte that dissociates into two univalent ions [e.g., sodium chloride (NaCl)].

univ Abbreviation of *universal.*

UNIVAC The name given to a family of digital computers and data-processing systems. The name is an acronym for *Universal Automatic Computer.*

univalent Having a valence of 1. For example, in the compound sodium chloride (NaCl), the sodium ion (Na+) and the chlorine ion (Cl–) are univalent.

universal bridge A bridge for the measurement of capacitance (*C*), inductance (*L*), and resistance (*R*). Such a bridge often is a skeletal foundation circuit with a provision for plugging L, C, or R standards in the various arms, as required. Also called *general-purpose bridge.*

universal coordinated time Abbreviation, UTC. Greenwich mean time coordinated by the International Time Bureau for broadcast as signals (on WWV, for example).

universal coupler **1.** An arrangement of one or more inductors and variable capacitors for matching a transmitter to virtually any antenna. One such device is the Collins coupler. **2.** A device for matching numerous generator output impedances to numerous load impedances.

universal filter An active filter that is continuously tunable over a wide frequency range and that offers low-pass, high-pass, bandpass, and band-suppression functions.

universal frequency counter A digital frequency meter usable at radio and audio frequencies.

universal motor A small series-wound motor that runs on direct current or single-phase alternating current. This type of motor is used in many household appliances and in motor-driven tools, such as portable electric drills, polishers, etc.

universal output transformer An output transformer having a number of taps on its primary and secondary windings for use with a wide variety of impedances.

universal product code Abbreviation, UPC. The variable-width-bar code appearing on price tags or product labels, and yielding such information as cost, size, and color when read by supermarket (or other retailer) optical character-recognition equipment. Also called *universal vendor marking (UVM).*

universal receiver A radio receiver that can be operated either from alternating current or direct current (i.e., from utility power or battery power).

universal shunt See AYRTON-MATHER GALVANOMETER SHUNT.

universal time See GREENWICH MEAN TIME.

universal transformer See UNIVERSAL OUTPUT TRANSFORMER.

universal transmitter A radio transmitter that can be operated either from alternating current or direct current (i.e., from utility power or battery power).

universal Turing machine In computer theory, a TURING MACHINE capable of simulating other Turing machines.

universal vendor marking See UNIVERSAL PRODUCT CODE.

universal winding A zigzag winding used to reduce the distributed capacitance of multilayer coils. Also called *lattice winding* and *honeycomb winding.*

universal-wound coil A coil using a universal winding. Such coils are common in intermediate-frequency (IF) transformers and in radio-frequency (RF) chokes.

5059F-pU-700-715 4/10/01 9:53 AM Page 712

univibrator See MONOSTABLE MULTIVIBRATOR.

unknown quantity Any variable quantity sought in calculations; it is usually represented by lowercase italic letters from the second half of the alphabet (e.g., *x*, *y*, *z*).

unlike charges Dissimilar electric charges (i.e., positive and negative).

unlike poles Dissimilar poles, such as the north and south poles of a magnet.

unload **1.** To remove data from a file. **2.** To disconnect the load from a circuit.

unloaded amplifier See UNTERMINATED AMPLIFIER.

unloaded antenna An antenna operated without added inductance or capacitance.

unloaded-applicator impedance In dielectric-heating operations, the unloaded impedance of applicator electrodes placed in their normal working position without the dielectric-material load in place.

unloaded battery **1.** A battery in the standby condition. **2.** A battery tested for open-circuit terminal voltage (i.e., with no load, except the voltmeter).

unloaded generator See UNTERMINATED GENERATOR.

unloaded line See UNTERMINATED LINE.

unloaded potentiometer A potentiometer or voltage divider with an open-circuited output.

unloaded *Q* The *Q* factor (degree of selectivity) of a coil or tuned circuit that is activated by a signal, but that delivers no output to a load.

unloaded transmitter A transmitter operated under open-circuit conditions (i.e., without an external load, such as an antenna or dummy resistor).

unmanned factory A manufacturing plant run largely by robots and computers. There must generally be at least one human being, whose job(s) is/are to oversee and maintain the operation of the machines.

unmatched elements **1.** Components (such as resistors, capacitors, semiconductors, etc.) having different values. **2.** Mating elements or devices not having the same impedance. Also called MISMATCH.

unmodulated carrier See CONTINUOUS WAVE.

unmodulated current A current whose characteristics (amplitude, phase, or frequency) are not varied by a signal or by noise.

unmodulated voltage A voltage whose characteristics (amplitude, phase, or frequency) are not varied by a signal or by noise.

unmodulated wave See CONTINUOUS WAVE.

unnilennium See MEITNERIUM.

unnilhexium See SEABORGIUM.

unniloctium See HASSIUM.

unnilpentium See DUBNIUM.

unnilquadium See RUTHERFORDIUM.

unnilseptium See BOHRIUM.

unode See MONODE.

unpack In computer operations, to remove data from a storage location into which, with other data, it has been packed (as a memory-conservation measure).

unpolarized light Light in which the wave orientation is random around the axis of the beam.

unpolarized plug A plug that can be inserted into a socket in two or more different ways, thus increasing the likelihood of a wrong connection. Compare POLARIZED PLUG.

unpolarized receptacle A receptacle into which a plug can be inserted in two or more different ways, thus increasing the likelihood of a wrong connection. Also called UNPOLARIZED SOCKET. Compare POLARIZED RECEPTACLE.

unpolarized relay A relay that always closes in the same direction, regardless of the direction of current in its coil. Also called *nonpolarized relay.*

unpolarized socket A socket into which a component or plug can be inserted in two or more different ways, thus increasing the likelihood of wrong connections. Also called UNPOLARIZED RECEPTACLE.

unprotected antenna An outside antenna operated without a lightning arrester or grounding switch. Increases the risk of damage to equipment, such as radio receivers and transmitters, connected to the antenna. It also increases the danger to personnel using the equipment.

unrationalized systems of units Collectively, the absolute centimeter-gram-second (cgs) electrostatic system of units, the absolute cgs electromagnetic system of units, and the absolute meter-kilogram-second (mks) system of units.

unreflected ray See UNREFLECTED WAVE.

unreflected wave **1.** See DIRECT WAVE. **2.** See GROUND WAVE. **3.** An electromagnetic wave that penetrates the ionosphere and passes into space.

unregulated Not held to a constant value. For example, an unregulated voltage is free to fluctuate in value.

unregulated power supply A power supply whose output current or voltage is not automatically held to a constant value. Compare CONSTANT-CURRENT SOURCE and CONSTANT-VOLTAGE SOURCE.

uns Abbreviation of UNSYMMETRICAL.

unsaturated core A magnetic core operated below the point of saturation (i.e., below the point at which an increase in coil current produces no further increase in magnetization of the core).

unsaturated logic A digital-logic scheme in which the switching devices operate between the saturated and cut-off conditions during either or both of the high and low states.

unsaturated operation Operation of a device at a point below saturation [i.e., below the point at which (1) an increase in voltage produces no further increase in current, or vice versa, or (2) an increase in coil current produces no further increase in magnetization of a core]. Compare SATURATED OPERATION.

5059F-pU-700-715 4/10/01 9:53 AM Page 713

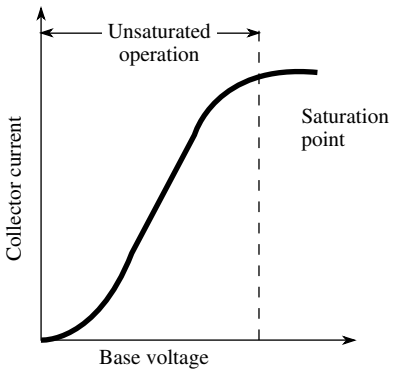

unsaturated operation

unsaturated standard cell See STANDARD CELL.

unshielded cable A cable, such as a twisted pair or a multiwire twist, lacking a shielding jacket. Unless special precautions are taken, such as transposing conductors, such a cable is susceptible to stray pickup and is capable of radiation.

unshielded choke An uncased choke (i.e., one without a protective and shielding metal housing).

unshielded coil An inductor without a field-confining enclosure.

unshielded probe An instrument probe that has no shielding enclosure. Such a probe is desirable for some tests, but it is subject to antenna-pickup effect, body capacitance, and stray-field pickup.

unshielded stage In electronic equipment, a stage operating entirely in the open (i.e., without electrostatic or magnetic shielding enclosures). It is, therefore, susceptible to stray pickup and is capable of radiation.

unshielded transformer **1.** An uncased transformer (i.e., one without a protective and shielding metal housing). **2.** A transformer having no electrostatic shield between its windings.

unshift The mechanical action in a teletypewriter when the carriage moves from the figures position to the letters position.

unshunted current meter A single-range D'Arsonval milliammeter or microammeter that has no shunt resistor. The resistance of the instrument is, therefore, equal to the resistance of the movable coil.

unsolder To separate wires, contacts, or fastenings by melting the solder that holds them together. Also called DESOLDER.

unsophisticated electronics Electronics theory and operations of the simplest kind, involving little or no mathematics. It is generally intended for a hobbyist audience. Compare SOPHISTICATED ELECTRONICS.

unstable oscillation **1.** Relaxation oscillation. **2.** The periodically interrupted oscillation characteristic of a blocking oscillation.

unstable region The negative-resistance portion of an N- or S-shaped response curve.

unstable servo A servo having unlimited output drift.

unstable state A condition, such as a negative-resistance region, that is difficult to maintain and often results in oscillation. The negative-resistance region of the tunnel diode forward-conduction curve is evidence of such a state. Compare STABLE STATE.

untapped winding A winding having two terminals, one at either end, and no intermediate terminals or connections. Also called *untapped coil.*

unterminated amplifier An amplifier operated without a load device (i.e., under open-circuit output conditions).

unterminated generator A generator operated without a load device (i.e., under open-circuit output conditions).

unterminated line A transmission line that is not terminated with an impedance (i.e., an open-ended line).

untriggered flip-flop A flip-flop that, at a particular instant, receives no actuating pulse, and that, therefore, does not change state.

untuned amplifier A radio-frequency amplifier that is not tuned to a single frequency, but has useful gain over a wide band of frequencies. Examples are the *distributed amplifier* and the *video amplifier.*

untuned filter See ALL-PASS FILTER.

untuned line An aperiodic transmission line (i.e., one that is only tuned to a particular frequency by its own distributed characteristics).

untuned transformer A transformer having simple primary and secondary windings and no tuning devices (such as capacitors in series or parallel with the windings), and designed so that its natural resonant frequency (because of distributed capacitance) lies outside the specified range of operation.

ununbium Symbol, Uub. Atomic number, 112. The most common isotope has atomic weight 277. Classified as a transition metal. It is human-made and not known to occur in nature.

ununhexium Symbol, Uuh. Atomic number, 116. The most common isotope has atomic weight 289. First reported in January 1999. It is a decomposition product of ununoctium, and it in turn decomposes into ununquadium. It is not known to occur in nature.

ununnilium Symbol, Uun. Atomic number, 110. The most common isotope has atomic weight 269. Classified as a transition metal. It is human-made and not known to occur in nature.

ununoctium Symbol, Uuo. Atomic number, 118. The most common isotope has atomic weight 293. It is the result of the fusion of krypton and lead, and decomposes into ununhexium. It is not known to occur in nature.

5059F-pU-700-715 4/10/01 9:53 AM Page 714

ununquadium Symbol, Uuq. Atomic number, 114. The most common isotope has atomic weight 285. First reported in January 1999. It is human-made, and not known to occur in nature.

ununnunium Symbol, Uuu. Atomic number, 111. The most common isotope has atomic weight 272. Classified as a transition metal. It is human-made, and not known to occur in nature.

unused time See UNATTENDED TIME.

unweighted average In the statistical analysis of data, an average calculated from terms not weighted by a factor. Compare WEIGHTED AVERAGE. Also see UNWEIGHTED TERM.

unweighted term In the statistical analysis of data, a term not operated upon by a weighting factor. Therefore, it has no extraordinary influence on a final result, such as an average. Compare WEIGHTED TERM.

unwind To eliminate all redundant or unnecessary operations in a computer system.

up-and-downer amplifier In broadcasting and sound amplification, an auxiliary amplifier that allows the level of sound effects and background music to be controlled automatically without disturbing the dialogue levels.

UPC Abbreviation of UNIVERSAL PRODUCT CODE.

upconv Abbreviation of UP CONVERTER.

up convert In superheterodyne conversion, to heterodyne a signal to an intermediate frequency higher than the signal frequency. Compare DOWN CONVERT.

update In data-processing operations, to make a file reflect the current status of pertinent information by using transactions for its modification.

up-down counter See BIDIRECTIONAL COUNTER.

uplink **1.** The signal sent up to a satellite transponder. **2.** The frequency of the signal sent up to a satellite transponder.

uplink frequency **1.** The specific frequency of a given signal sent up to a satellite transponder. **2.** The band of frequencies sent up to a satellite transponder. There can be many signals in an uplink; there can also be many different stations sending uplink signals within the band.

uplink power **1.** The power output of the transmitter sending the signal up to a satellite transponder. **2.** The effective radiated power of the station sending the uplink signal.

uplink station Any station that transmits a signal, or group of signals, up to a satellite transponder.

upper atmosphere See IONOSPHERE, STRATOSPHERE, and TROPOSPHERE.

upper sideband Abbreviation, USB. In an amplitude-modulated wave, the component whose frequency is the sum of the carrier frequency and the modulation frequency. Compare LOW-ER SIDEBAND.

upper sideband, suppressed carrier Abbreviation, USSC. A single-sideband transmission technique in which the upper sideband is transmitted, the lower sideband is suppressed, and the carrier is suppressed. Compare DOUBLE SIDEBAND, SUPPRESSED CARRIER, LOWER SIDEBAND, and SUPPRESSED CARRIER.

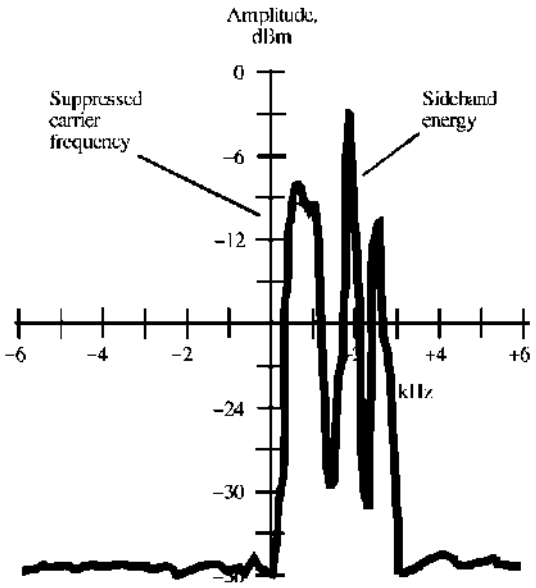

upper sideband

UPS Abbreviation for UNINTERRUPTIBLE POWER SUPPLY.

upside down **1.** In radioteletype, a signal in which the MARK and SPACE signals are reversed in frequency. **2.** In single sideband, reception of a signal on the wrong sideband, resulting in "monkey chatter."

up time See SERVICEABLE TIME.

upturn A usually sudden rise in a performance curve. Compare DOWNTURN.

upward modulation Modulation in which the output current of the modulated circuit increases during modulation. Compare DOWNWARD MODULATION.

UR Abbreviation of ULTRARED.

uranium Symbol, U. A radioactive metallic element. Atomic number, 92. Atomic weight, 238.03.

uranium 235 Symbol, U-235. An isotope of uranium of mass number 235, used in atomic bombs and atomic power plants.

uranium 238 Symbol, U-238. An isotope of uranium of mass number 238, which, under fast-neutron bombardment, decays to become neptunium and then plutonium (of mass number 239).

uranium metals The group of heavy, radioactive elements of atomic numbers 89 through 103. Also called the *actinide series.*

uranium rays The ionizing radiation emitted by uranium. In 1896, Antoine Henri Becquerel

5059F-pU-700-715 4/10/01 9:53 AM Page 715

observed that uranium salts emit rays (later identified as alpha, beta, and gamma) that can pass through bodies opaque to light and are capable of exposing a photographic plate. Also called *Becquerel rays.*

urea formaldehyde resin A thermosetting, synthetic resin used in the manufacture of a number of plastic dielectric bodies and formed by the reaction of urea with formaldehyde.

urea plastic Any of several thermosetting plastics having a urea base and used as a dielectric and as a molding material in electronics (e.g., *urea formaldehyde resin*).

URSI Abbreviation of *Union Radio Scientifique Internationale (International Radio Scientific Union).*

ursigram A broadcast message giving information on sunspots, radio propagation, terrestrial magnetism, and related subjects. Also see URSI.

usable frequency **1.** Any frequency at which communications can be maintained between two points via ionospheric propagation. **2.** Any frequency at which a communications system is operational.

usable sample **1.** The portion of an oscilloscope or monitor display that is visible on the screen. **2.** In statistics, a sample that is considered valid for calculation purposes.

USB Abbreviation of UPPER SIDEBAND.

user friendliness **1.** For electronic equipment and systems, the quality of being easy for people to operate. **2.** The relative ease with which a machine, especially a computer, can be operated by people.

useful life The elapsed time between the installation of an expendable component, circuit, or system, and the time it must be replaced.

useful line In television, the portion of a scanning line that can be used for picture signals. Also called AVAILABLE LINE.

user group A group of hobbyists or company representatives having in common the ownership and/or use of a specific brand of computer, and who meet or otherwise interact to share their expertise with, or programs, for, the machine. Also applicable to similar groups of programmable-calculator owners.

user's library A compilation of programs supplied to (by the vendor) or generated by a user group.

USM Abbreviation of *underwater-to-surface missile.*

USSC Abbreviation of UPPER SIDEBAND, SUPPRESSED CARRIER.

UTC Abbreviation of UNIVERSAL COORDINATED TIME.

utility **1.** An organization providing a public service, such as electric power or electronic communications. **2.** In computer operations, a program or set of programs intended for diagnosing and/or correcting hardware and software problems.

utility box A general-purpose aluminum or steel box, supplied in various convenient sizes (painted or unpainted), used as a housing or shield for electronic equipment.

utility factor For a transformer used in a direct-current (dc) power supply, the ratio of dc output to required kilovolt-ampere (kVA) capacity.

utilization factor See UTILITY FACTOR.

UTL Abbreviation of *unit transmission loss.*

UUM Abbreviation of *underwater-to-underwater missile.*

UV **1.** Abbreviation of ULTRAVIOLET. **2.** Abbreviation of UNDERVOLTAGE.

Uvicon A television camera tube in which a conventional vidicon scanning section is preceded by an ultraviolet-sensitive photocathode, an electron-accelerating section, and a special target.

Uviol lamp An ultraviolet lamp using uviol glass—a special glass that is transparent to ultraviolet rays.

UVM Abbreviation of UNIVERSAL VENDOR MARKING.

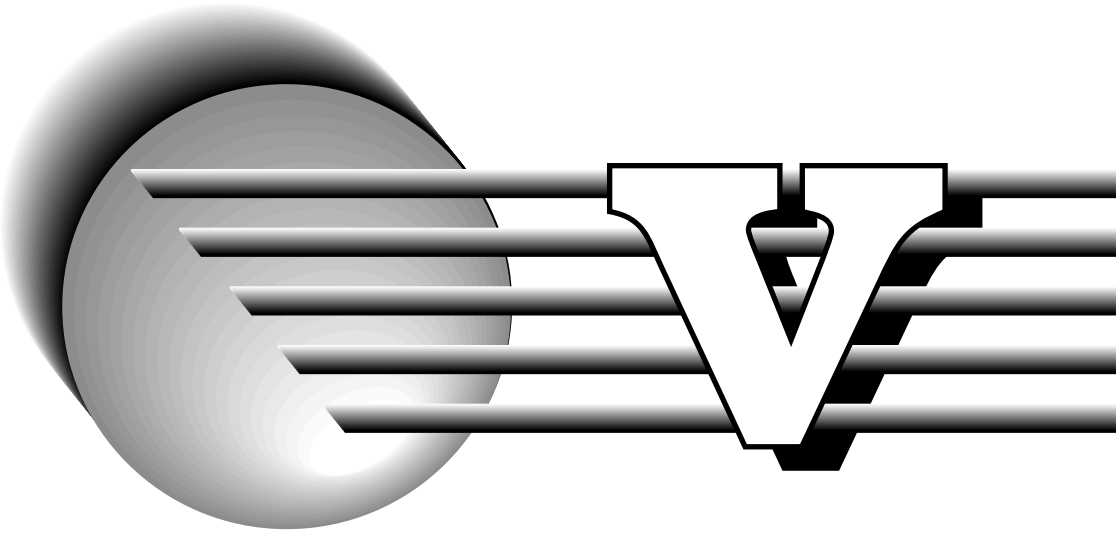

V **1.** Abbreviation of VOLT. **2.** Symbol (ital) for VOLTAGE or POTENTIAL. **3.** Symbol for VANADIUM. **4.** Symbol for VOLUME. **5.** Symbol (ital) for RELUCTIVITY. **6.** Abbreviation of VERTICAL. (Also, vert.)

v **1.** Abbreviation of VELOCITY. **2.** Abbreviation of VECTOR.

VA Abbreviation of VOLT-AMPERE.

V/A Abbreviation of *volts per ampere* (ohms).

VAC Abbreviation of *vector analog computer.*

vac Abbreviation of VACUUM.

V_{ac} Symbol for AC VOLTS. (Also, Vac.)

vacancy In a crystal lattice, a position not occupied by a nucleus.

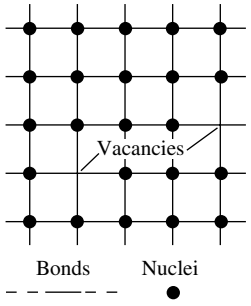

vacancy

vacuum A space from which all air and other gases have been removed to the greatest practicable extent. Some electronic parts, such as the elements of an electron tube, are housed in an evacuated space to protect them from the deterioration that would result from open-air operation.

vacuum capacitor A plate- or concentric-cylinder-type capacitor sealed in an evacuated glass tube or bulb. The vacuum acts as the dielectric and provides a dielectric constant of 1 and very high voltage breakdown.

vacuum deposition The electrical application of a layer of one material (such as a metal) to the surface of another (the substrate), carried out in a vacuum chamber (e.g., evaporation and sputtering). Also see DEPOSITION and EVAPORATION, **1**.

vacuum envelope The shell or tube of an electron tube, X-ray tube, or other electron device that requires a vacuum.

vacuum evaporation A method of manufacturing thin-film circuits by vaporizing a substance, and letting it accumulate or condense on a base.

vacuum gauge An instrument for measuring the vacuum in a device being evacuated. One of the several varieties of this gauge uses the elements of a triode, which are sealed in part of the vacuum system, some characteristic of the tube being continuously monitored as the vacuum pumping progresses. Another uses a thermistor sealed in part of the system; the resistance of the thermistor changes proportionately during the vacuum pumping.

vacuum impregnation The impregnation of a device (such as a capacitor, transformer, or choke coil) in a vacuum chamber. The process causes the pores in the device and its insulating materials to be completely filled with the impregnant.

Copyright 2001 The McGraw-Hill Companies, Inc. Click Here for Terms of Use

5059F-pV-716-737 4/10/01 9:56 AM Page 717

vacuum level **1.** The pressure, in millimeters of mercury (mm/Hg). Normal atmospheric pressure is 760 mm/Hg. A perfect vacuum would be represented by 0 mm/Hg. **2.** The proportion, or percentage, of normal atmospheric pressure in a given environment.

vacuum phototube A phototube enclosed in an evacuated envelope, as opposed to one that is gas-filled.

vacuum pump A pump for removing air and gases from electron tubes, X-ray tubes, lamp bulbs, etc. Such pumps include mechanical types, diffusion types, and combinations of these. Also see DIFFUSION PUMP.

vacuum range The range of a communications system if propagation takes place through a perfect-vacuum (theoretical) medium.

vacuum seal An airtight seal between adjoining parts in an evacuation system.

vacuum switch A switch that is enclosed in a vacuum bulb or tube to reduce contact sparking.

vacuum thermocouple A thermocouple enclosed in a vacuum bulb with a small heater element. Radio-frequency current passed through the heater raises its temperature and causes the thermocouple to generate a proportional direct-current voltage.

vacuum tube An electron tube from which virtually all air and gases are removed. Also see ELECTRON TUBE.

vacuum-tube amplifier An amplifier using one or more vacuum tubes, rather than semiconductor devices.

vacuum-tube bridge A special bridge for determining vacuum-tube characteristics by null methods.

vacuum-tube characteristics The operating parameters of a vacuum tube, such as plate current, grid voltage, input resistance, interelectrode capacitances, amplification factor, transconductance, etc., that describe tube performance.

vacuum-tube coefficients See VACUUM-TUBE CHARACTERISTICS.

vacuum-tube current meter An ammeter, milliammeter, microammeter, or nanoammeter embodying an amplifier that uses one or more vacuum tubes. Also see ELECTRONIC CURRENT METER.

vacuum-tube modulator A circuit using one or more vacuum tubes to impress a modulating signal on a carrier.

vacuum-tube rectifier **1.** An alternating-to-direct-current converter circuit using one or more vacuum tubes, rather than gas tubes or semiconductor devices. **2.** A rectifier tube.

vacuum-tube sweep A sweep oscillator using a vacuum tube, rather than a gas tube. Also called HARD-TUBE SWEEP.

vacuum-tube voltmeter Abbreviation, vtvm. A voltmeter using a tube-type amplifier. Also see ELECTRONIC VOLTMETER.

val Abbreviation of VALUE.

valence A unit showing the degree to which elements or radicals (replaceable atoms or groups of atoms) will combine to form compounds.

valence band In the energy diagram for a semiconductor, the band of lowest energy. This band lies below the forbidden band (energy gap), which is below the conduction band. Also see ENERGY BAND DIAGRAM.

valence bond In a semiconductor material, an interatomic path over which shared electrons travel.

valence electrons Electrons in the outermost orbits of an atom. These electrons determine the chemical and physical properties of a material. Also see FREE ELECTRON.

valence shells See ELECTRON SHELLS.

validate To check data for correctness.

validity **1.** Correctness or accuracy of data. **2.** The logical truth of a derivation or statement, based on a given set of propositions.

valley A dip between adjacent peaks in a curve or wave.

valley current In a tunnel diode, the current at the valley point.

valley point The lowest point of finite current on the current-voltage response curve of a tunnel diode. Immediately before this point, current decreases with increasing applied voltage (an indication of negative resistance). Beyond this point, however, the current again increases with increasing voltage. Compare PEAK POINT.

valley voltage In a tunnel diode, the voltage at the valley point.

value **1.** The level or magnitude of a quantity (e.g., voltage value). **2.** The worth of a system, procedure, device, etc., in terms of goal fulfillment or other criterion.

valve Variation (Brit.) of ELECTRON TUBE. The term was applied to the first tube, a diode (the Fleming valve), and is descriptive of the action of a tube (a controller of electric current), rather than its appearance.

vanadium Symbol, V. A metallic element. Atomic number, 23. Atomic weight, 50.94.

Van Allen radiation belts Two high-altitude zones that surround the earth and consist of high-energy subatomic particles. These belts were once thought to preclude space travel by humans beyond the immediate vicinity of the earth.

Van de Graaff generator See BELT GENERATOR.

vane-anode magnetron A magnetron having plane parallel walls between adjacent cavities.

vane attenuator A waveguide attenuator consisting essentially of a slab (vane) of resistive material that slides laterally through the waveguide.

vane instrument See IRON-VANE METER.

vane-type magnetron See VANE-ANODE MAGNETRON.

vane-type meter See IRON-VANE METER.

V antenna See VEE ANTENNA.

5059F-pV-716-737 4/10/01 9:56 AM Page 718

vapor lamp A discharge lamp consisting essentially of a glass tube filled with a small amount of gas under low pressure and some element, such as mercury or sodium. A high voltage is applied between electrodes sealed into each end of the tube. The voltage causes the element to vaporize. This, in turn, ionizes the gas, causing it to glow.

vapor pressure In a confined medium, the pressure of a gas, measured in atmospheres, pounds per square inch, or millimeters of mercury.

VAR Abbreviation of VOLT-AMPERES REACTIVE.

var Abbreviation of VARIABLE.

varactor A semiconductor-type voltage-variable capacitor. Sometimes called a *varactor diode.*

varactor amplifier A dielectric amplifier using a varactor as the voltage-variable capacitor.

varactor flip-flop A bistable multivibrator based on the nonlinear performance of one or two varactors.

varactor frequency multiplier A frequency multiplier (doubler, tripler, etc.) in which multiples of a fundamental frequency result from the nonlinear action of a varactor.

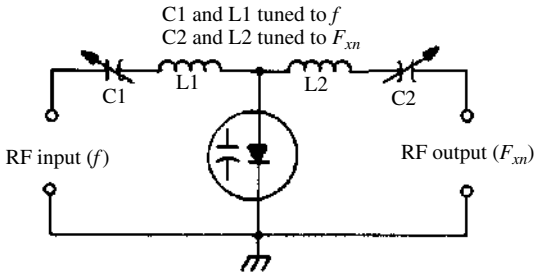

varactor frequency multiplier

varactor tuning A method of tuning a circuit or adjusting the frequency of an oscillator, using an inductor and a varactor to obtain the desired frequency. The varactor acts as a variable capacitor.

VAR-hour Abbreviation, VARh. Short for *volt-ampere-reactive-hour*, a unit of reactive energy; 1 VARh can be represented by 1 VAR for 1 hour, 2 VAR for 0.5 hour, 0.5 VAR for 2 hours, etc.

VAR-hour meter An instrument that measures reactive energy.

variable Abbreviation, var. A quantity whose value changes at some stated or calculable rate, and is given names in expressions or equations, such as *x*, *y*, or *z*. Compare CONSTANT. Also see DEPENDENT VARIABLE and INDEPENDENT VARIABLE.

variable-area sound track See VARIABLE-WIDTH SOUND RECORD.

variable block In computer operations, a unit of data, such as a group of records, whose size is dependent on data requirements (i.e., it is not fixed).

variable-capacitance diode See VARACTOR.

variable-capacitance transducer See CAPACITIVE TRANSDUCER.

variable capacitor A capacitor that can be adjusted from a low value (practically zero) to some maximum value. A step-type unit contains a number of fixed capacitors that can be switched in parallel with each other until, at the last step, all are in parallel. A continuously variable unit has a provision for moving one plate or set of plates, relative to another plate or set of plates; or one plate might be moved, with respect to another, so that the distance between them is changed. In a voltage-variable capacitor (such as a varactor), capacitance varies in accordance with an applied direct-current voltage.

variable-carrier modulation See QUIESCENT-CARRIER OPERATION.

variable connector In a flowchart, a path leading from a box in which a decision is made, to a number of other points on the diagram.

variable coupling Coupling that is adjustable. In an inductively coupled circuit, the distance or angle between the coils is usually the adjustable factor. In a capacitively coupled circuit, a variable capacitor is generally used.

variable-density sound record In photographic sound-on-film recording, a sound track made by varying, in sympathy with the sound frequency, the amount of light reaching the film. Compare VARIABLE-WIDTH SOUND RECORD.

variable-depth sonar A sonar device that can be placed far below the surface, for the purpose of detecting objects or terrain at greater depths than would be possible with a surface-located sonar device.

variable-efficiency modulation See EFFICIENCY MODULATION.

variable-erase recording In magnetic-tape operations, recording a signal by selectively erasing a previously recorded signal.

variable field **1.** Any field with an intensity that changes with time. An electromagnetic field is a common example. **2.** In a computer record, a field that is a variable block with a terminal symbol at the end.

variable-frequency oscillator Abbreviation, VFO. An oscillator (usually self-excited) whose frequency is continuously variable.

variable-inductance pickup A phonograph pickup in which vibration of the stylus causes the inductance of a small coil to vary in sympathy with the sound frequency.

variable-inductance transducer A transducer in which a monitored quantity causes the inductance of a coil to vary proportionately. The coil thereby offers a varying impedance to an alternating-current supply voltage.

variable inductor An inductor whose value can be adjusted from zero to a certain maximum. The variability might be in steps, provided by taps on the inductor, or a sliding contact can be used.

5059F-pV-716-737 4/10/01 9:56 AM Page 719

Several different inductors can be connected in series and parallel combinations, with switches to facilitate variability. One type of variable inductor uses a roller contact to allow continuous adjustment. See ROLLER INDUCTOR. Another method of varying inductance is to change the permeability of the core, such as by moving a rod of ferrite or powdered iron in and out of the coil. See VARICOUPLER and VARIOMETER.

variable-pitch indication An audible signal used in lieu of, or in conjunction with, a meter to indicate voltage, current, logic state, etc. The higher the value of the measured quantity, the higher the pitch.

variable-reluctance microphone A microphone in which the impinging sound waves cause corresponding variations in the reluctance of an internal magnetic circuit.

variable-reluctance pickup A phonograph pickup in which the stylus causes an armature to vibrate in a magnetic field, and consequently the reluctance of the magnetic circuit varies in sympathy with the audio frequency.

variable-reluctance transducer A transducer in which the monitored quantity causes the reluctance of an internal magnetic circuit to vary proportionately.

variable-resistance pickup A phonograph pickup in which the vibration of the stylus causes the resistance of an internal resistive element to vary in sympathy with the sound frequency.

variable-resistance transducer A transducer in which a monitored quantity causes the resistance of an internal resistive element to vary proportionately.

variable-resistance tuning Tuning of a selective resistance-capacitance (RC) circuit, such as a Wien bridge or parallel-tee network, by varying one or more of its resistance arms.

variable resistor A resistor whose value can be varied either continuously or in steps. Also see POTENTIOMETER and RHEOSTAT.

variable selectivity In a circuit or device, selectivity that is adjustable. Example: a variable-selectivity intermediate-frequency (IF) amplifier.

variable-speed motor Any motor whose speed is adjustable, smoothly or in steps, under load.

variable transformer A transformer (often an autotransformer) whose output voltage is adjustable from zero (or some minimum value) to maximum. For this purpose, one winding (usually the secondary in a two-winding transformer) can have a number of taps. Smooth variation can be provided by a wiper arm that slides over the turns of the winding.

variable-width wound record In photographic sound-on-film recording, a sound track made by varying the width of the track in sympathy with the sound variations. Compare VARIABLE-DENSITY SOUND RECORD.

Variac See VARIABLE TRANSFORMER.

Varicap A voltage-variable capacitor of the semiconductor-diode type. Also see VOLTAGE-VARIABLE CAPACITOR.

varicoupler An adjustable radio-frequency transformer consisting of a primary coil (usually the rotor) and a secondary coil (usually the stator), the former being rotatable to vary the coupling between the coils. The inductance of the stator is varied via a set of taps.

varindor A coil having a special core and whose inductance varies with the amount of direct current flowing through the winding. Also see SATURABLE REACTOR.

variocoupler A radio-frequency transformer in which one winding is rotatable, for the purpose of adjusting the mutual inductance between the primary and secondary. It is used in certain antenna-coupling applications.

variolosser A variable attenuator.

variometer A continuously variable inductor consisting of two coils connected in series or parallel and mounted concentrically—one rotating inside the other. Inductance is maximum when the coils are perpendicular to each other, and minimum when they are parallel.

varioplex A time-sharing method of transmitting and receiving wire telegraph signals. It allows the optimum usage of available lines.

varistor See VOLTAGE-DEPENDENT RESISTOR.

Varley-loop bridge A four-arm, direct-current bridge circuit in which one of the arms, a two-wire line, is accidentally grounded at a distant point. By adjustment of the bridge, the resulting resistance indicates the distance to the fault.

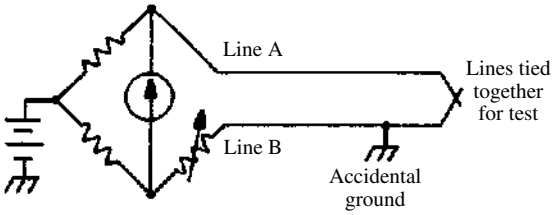

Varley loop bridge

VAR meter An instrument for measuring the apparent (VAR) power in a reactive circuit.

varnished cambric Cotton or linen fabric in sheets, tape or tubes, that has been varnish-impregnated and baked. A common form of this insulating material, the slender tubing known as *spaghetti*, has largely been replaced by plastic tubing.

varnished-cambric tubing Slender tubes of varnished cambric slipped over bare wires and busbars to insulate them. Also called *spaghetti.*

VATE Abbreviation of VERSATILE AUTOMATIC TEST EQUIPMENT.

5059F-pV-716-737 4/10/01 9:56 AM Page 720

V_B Symbol for BASE VOLTAGE of a bipolar transistor.

V_{BB} Symbol for *base-voltage supply* for a bipolar transistor.

V beam system See VEE BEAM SYSTEM.

V_C Symbol for COLLECTOR VOLTAGE of a bipolar transistor.

VCA Abbreviation of VOLTAGE-CONTROLLED AMPLIFIER.

V_{CC} Symbol for *collector-voltage supply* of a bipolar transistor.

VCCO Abbreviation of VOLTAGE-CONTROLLED CRYSTAL OSCILLATOR. (Also, lowercase.)

VCD Abbreviation of VARIABLE-CAPACITANCE DIODE.

VCG Abbreviation of VOLTAGE-CONTROLLED GENERATOR.

VCO Abbreviation of VOLTAGE-CONTROLLED OSCILLATOR.

V connection of transformers See VEE CONNECTION OF TRANSFORMERS.

VCR Abbreviation of VIDEO CASSETTE RECORDER.

VCSR Abbreviation of *voltage-controlled shift register.*

V-cut crystal See VEE-CUT CRYSTAL.

VCXO Abbreviation of VOLTAGE-CONTROLLED CRYSTAL OSCILLATOR. (Also, lowercase.)

VD **1.** Abbreviation of VOLTAGE DROP. **2.** Abbreviation of *vapor density.*

V_D Symbol for drain voltage of a field-effect transistor.

Vdc Symbol for DC VOLTS.

VDU Abbreviation of VISUAL DISPLAY UNIT.

vdcw Symbol for DC WORKING VOLTAGE. (Also, dcwv.)

VDIG Abbreviation of VIDEO DIGITIZER.

VDR **1.** Abbreviation of VOLTAGE-DEPENDENT RESISTOR. **2.** Abbreviation of VIDEODISC RECORDER.

V_{drive} Abbreviation for DRIVING VOLTAGE or OUTPUT VOLTAGE.

VE Abbreviation of value engineering.

V_E Symbol for EMITTER VOLTAGE of a bipolar transistor.

vectograph A graphic three-dimensional representation of a scene composed of superimposed images photographed through polarizing filters of different orientation, and reconstructed by a similar viewing technique.

vector **1.** A quantity having direction (in two or three dimensions) and magnitude. **2.** A graphical representation of a quantity, as defined in **1**. It consists of a straight arrow indicating the direction, and whose length is proportional to the magnitude.

vector addition The summation of two vectors, determined by adding their corresponding component values. In two dimensions, for example, suppose $\mathbf{A} = (x_1,y_1)$ and $\mathbf{B} = (x_2,y_2)$. Then $\mathbf{A} + \mathbf{B} = [(x_1 + x_2),(y_1 + y_2)]$. The sum can be found geometrically by constructing a parallelogram from the vectors, corresponding to the two known sides, as determined by the vectors. The sum is the vector originating at the point where the two vectors originate, and extending the diagonal of the parallelogram.

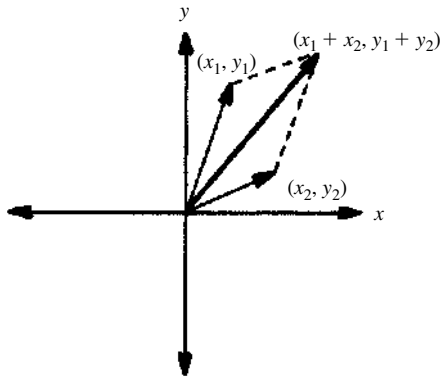

vector addition

vector admittance The reciprocal of VECTOR IMPEDANCE.

vector cardiograph An electrocardiograph that indicates the magnitude and the direction of a heart signal.

vector components **1.** The Cartesian coordinates of a vector, or its component angle and radius (polar coordinates). **2.** Quantities that can be represented by means of vectors (e.g., impedance and velocity).

vector diagram A graphical representation of vector quantities.

vector function A function having both magnitude and direction. Also see VECTOR; VECTOR COMPONENTS, **2**; and VECTOR QUANTITY.

vector generator A device that graphically illustrates vectors.

vectorial angle **1.** The angle between a vector and the horizontal axis. **2.** The angle between two vectors.

vector impedance Complex impedance (i.e., an impedance of the form $R + jX$, where R is resistance, X is reactance, and j is an operator indicating that the reactance is 90 degrees out of phase, relative to the resistance).

vector-mode display On a cathode-ray-tube display, the data representation in which points on the screen are connected by straight lines.

vector power The vector quantity $(P_a^2 + P_x^2)^{1/2}$, where P_a is the active power and Px is the reactive power.

vector power factor The ratio $P_a/(P_a^2 + P_x^2)^{1/2}$, where P_a is the active power and Px is the reactive power. In sine-wave situations, this ratio (of

5059F-pV-716-737 4/10/01 9:56 AM Page 721

active power to vector power) produces a figure identical to the conventional power factor.

vector quantity A quantity having both magnitude and direction, and that can, therefore, be represented by a vector.

vectorscope A special oscilloscope for visual adjustment of a color-television receiver by means of a color-phase diagram.

vector sum The resultant of two nonparallel vectors; therefore, the resultant of the forces or quantities represented by them. For example, reactance and resistance can be represented by two perpendicular vectors.

vector voltmeter A voltmeter that indicates the phase as well as the amplitude of an alternating-current voltage.

V_{EE} Symbol for *emitter-voltage supply* of a bipolar transistor.

vee antenna A center-fed antenna in which the two halves of the radiator form an angle considerably less than 180 degrees.

vee-beam system An elevation-measuring radar system in which fan-shaped vertical and inclined beams, intersecting at ground and rotating continuously around the vertical axis, are radiated by one antenna. Target elevation is determined from the interval between successive echoes from the target.

vee connection of transformers In a three-phase system, a method of connecting two transformers so that the line current and voltage equal the phase current and voltage. Also called *open-delta connection.*

vee-cut crystal A piezoelectric plate cut from a quartz crystal so that its faces are not parallel to the *x*, *y*, or *z* axis of the crystal. Also see CRYSTAL AXES and CRYSTAL CUTS.

vee particle A short-lived elementary particle that results when high-energy neutrons or protons collide with nuclei. The particle can be positive, negative, or neutral, and gets its name from its cloud-chamber track.

vee signal In radiotelegraphy, the letter V (di-di-di-dah) transmitted as a test signal, usually three times in rapid succession. It is used during on-the-air transmitter tests, followed by the station's call letters.

vehicle An inert substance, usually a liquid, that acts as a solvent, carrier, or binder for some other, more active substance. Thus, shellac can be the vehicle for the metallic powder in a silver paint used in silk-screening electronic circuits.

vehicle smog-control device See COMPUTER-CONTROLLED CATALYTIC CONVERTER and EXHAUST ANALYZER.

vel Abbreviation of VELOCITY.

velocimeter **1.** An instrument for measuring the velocity of sound in various materials. **2.** An electronic velocity meter—especially a radial-velocity meter using Doppler radar. **3.** An electronic flow meter.

velocity Symbol, *v*. Abbreviation, vel. Unit, distance per unit time [e.g., meters per second (m/s)]. **1.** The change in the position of a body over a specified period of time. **2.** The derivative of displacement with respect to time. Compare ACCELERATION.

velocity constant See VELOCITY FACTOR.

velocity error For a servomechanism in which the input and output shafts rotate at the same speed, the angular displacement between them.

velocity factor Abbreviation, *v*. For a transmission line, the ratio of the speed of electromagnetic wave propagation in the line to the speed of electromagnetic waves in a vacuum (299,792 kilometers per second). It can be expressed as a number between 0 and 1, or as a percentage between 0 and 100. In practical feed lines, *v* ranges from about 0.66 (for coaxial line with a solid polyethylene dielectric) to about 0.95 (for open-wire line with widely separated spacers).

velocity hydrophone A hydrophone whose output, like that of the velocity microphone, is proportional to the instantaneous particle velocity in the sound wave impinging on the device.

velocity-lag error A lag (proportional to the input-variation rate) between the input and output of a device, such as a servomechanism.

velocity level For a sound, the ratio v_0, expressed in decibels:

$$v_0 = 20 \log_{10}(v_s/v_r)$$

where v_s is the particle velocity of the sound, and v_r is a reference particle velocity.

velocity microphone A microphone in which the vibratory element is a thin, aluminum or Duralumin ribbon suspended loosely between the poles of a strong permanent magnet. Vibration of the corrugated ribbon in the magnetic field causes an audio-frequency voltage to be induced across the ribbon. The microphone is so called because its output is proportional to the instantaneous particle velocity in the sound wave impinging on the ribbon. Also called *ribbon microphone.*

velocity-modulated amplifier A circuit in which radio-frequency amplification is obtained by velocity modulation.

velocity-modulated oscillator A vacuum-tube device in which an electron stream is velocity-modulated (see VELOCITY MODULATION) as it passes through a resonant cavity (the buncher); the subsequent energy, of a higher intensity, is extracted from the bunched stream as it passes through another resonant cavity (the catcher). Feedback from catcher to buncher sustains oscillations. See, for example, KLYSTRON OSCILLATOR.

velocity-modulated tube A vacuum tube utilizing velocity modulation. See, for example, KLYSTRON.

velocity modulation The process in which the input signal of a vacuum tube varies the velocity of the electrons in a constant-current electron beam in sympathy with the input signal.

5059F-pV-716-737 4/10/01 9:56 AM Page 722

velocity resonance A state of resonance in which a 90-degree phase difference is between the fundamental frequency of oscillation of a system and the fundamental frequency of the applied signal.

velocity sorting Selecting and separating electrons, according to their velocity.

velocity spectrograph A device that uses electric or magnetic deflection to separate charged particles into various streams, according to their velocity.

velocity variation See VELOCITY MODULATION.

velocity-variation amplifier See VELOCITY-MODULATED AMPLIFIER.

velocity-variation oscillator See VELOCITY-MODULATED OSCILLATOR.

velometer An instrument used to measure the velocity of air (e.g., to determine wind speed).

venetian-blind effect A television-display malfunction in which the picture seems to appear through horizontal slits.

Venn diagram A method of illustrating the relationship among various subsets within a specified universal set. The subsets are shown as geometric figures, usually circles.

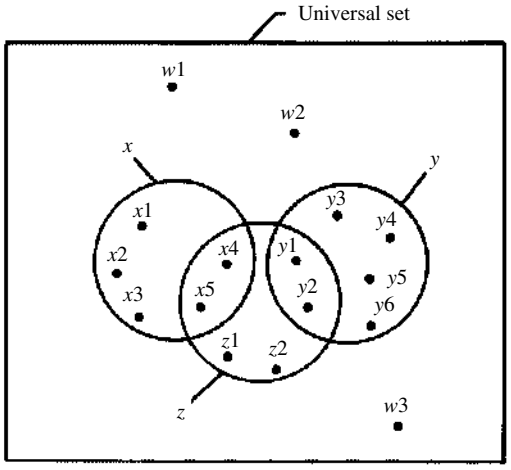

Venn diagram

vent **1.** An opening in an equipment enclosure for the entry of cool air or the escape of warm air. **2.** In an electrolytic capacitor, a lightly covered blowout hole for the relief of gas pressure in the event of severe overload. **3.** A small opening for relieving gas pressure in an automobile battery. **4.** In a loudspeaker enclosure, such as the bass-reflex type, an auxiliary opening that extends the low-frequency range of the speaker.

vented baffle A loudspeaker enclosure having the proper auxiliary opening(s) for coupling the speaker to the surrounding air.

vented-baffle loudspeaker See ACOUSTICAL PHASE INVERTER and BASS-REFLEX LOUDSPEAKER.

vent mount A metal bracket for fastening an antenna mast to a (plumbing) vent pipe on a roof.

ventricular fibrillation See FIBRILLATION.

verification **1.** The process of ensuring that two sets of data are identical. **2.** The process of validating (see VALIDATE).

vernier **1.** An auxiliary scale along which a regular, linear scale (such as that of a tuning dial) slides. The vernier scale is graduated so that when the main scale is set to an unmarked point between two of its graduations, and the "0" point on the vernier scale is used as the index, "1" on the vernier scale will exactly coincide with "1" on the main scale. The corresponding number on the vernier scale indicates the exact number of subdivisions between two points on the main scale. Vernier arrangements are provided with the dials of some precision analog instruments. **2.** See VERNIER CAPACITOR. **3.** See VERNIER DIAL. **4.** See VERNIER RESISTOR.

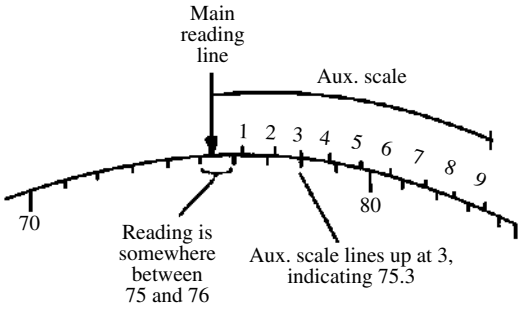

vernier, 1

vernier capacitor A low-capacitance variable capacitor connected in parallel with a higher-capacitance fixed or variable capacitor for precise adjustment of the total capacitance.

vernier dial **1.** A slow moving dial for fine tuning an adjustable device. The required reduction ratio is obtained with gears, friction wheels, or a belt-and-pulley combination. **2.** A dial provided with an accessory vernier scale.

vernier resistor A low-resistance variable resistor connected in series with a higher-resistance fixed or variable resistor to precisely adjust the total resistance.

vernier rheostat See VERNIER RESISTOR.

vers Abbreviation of VERSED SINE.

versatile automatic test equipment Abbreviation, VATE. For troubleshooting the electronic systems of missiles, a computer-controlled tester that isolates faults through logical operations.

5059F-pV-716-737 4/10/01 9:56 AM Page 723

versed sine Abbreviation, vers. A trigonometric function equal to the difference between the cosine of an angle and one; vers $x = 1 - \cos x$.

vert Abbreviation of VERTICAL.

vertex **1.** The terminal point at which two or more branches of a network meet. Also see NODE, **1**. **2.** The point of intersection of two lines that form an angle.

vertex plate In the reflector of a microwave antenna, a matching plate mounted at the vertex.

vertical **1.** The direction indicated by a line perpendicular to the plane of the horizon (e.g., a vertical axis). **2.** In the 45-45 recording process, the signal resulting from sound that arrives simultaneously and 180 degrees out of phase at the two microphones and causes up-and-down movement of the cutting stylus.

vertical amplification Gain provided by the vertical channel of a device, such as an oscilloscope, cathode-ray electrocardiograph, or television receiver. Compare HORIZONTAL AMPLIFICATION.

vertical amplifier The circuit or device that provides gain in the vertical channel of a device. Compare HORIZONTAL AMPLIFIER.

vertical-amplitude control **1.** See VERTICAL-GAIN CONTROL. **2.** In a color television receiver, one of the three controls by which the amplitude of the parabolic voltages applied to the coils of the magnetic-convergence assembly are adjusted.

vertical angle of radiation The angle, with respect to the plane of the horizon, at which radio-frequency energy is propagated from a transmitting antenna.

vertical antenna **1.** An antenna that consists essentially of a single, straight, vertical conductor. **2.** An antenna that is mounted vertically, instead of horizontally.

vertical blanking See VERTICAL RETRACE BLANKING.

vertical-blanking pulse In a television signal, the pulse at the end of each field that accomplishes vertical retrace blanking. Compare HORIZONTAL-BLANKING PULSE.

vertical-centering control See CENTERING CONTROL.

vertical channel The system of amplifiers, controls, and terminations that constitutes the path of the vertical signal applied to a device, such as an oscilloscope. Compare HORIZONTAL CHANNEL.

vertical compliance In disc sound reproduction, the ease with which the stylus can move vertically while it is in position on the disc.

vertical coordinates See CARTESIAN COORDINATES.

vertical deflection **1.** In an oscilloscope or television receiver, the movement of the spot up and down on the screen. Compare HORIZONTAL DEFLECTION. **2.** In a direct-writing recorder, up or down deflection of the pen.

vertical deflection coils In a cathode-ray tube, the pair of coils in a deflection yoke that provides the electromagnetic field for the vertical deflection of the electron beam. Compare HORIZONTAL DEFLECTION COILS.

vertical deflection electrodes See VERTICAL DEFLECTION COILS and VERTICAL DEFLECTION PLATES.

vertical deflection plates In an oscilloscope (and in some early television picture tubes), a pair of plates that provides the electrostatic field for vertical deflection. Compare HORIZONTAL DEFLECTION PLATES.

vertical dipole An antenna consisting of a straight, center-fed, half-wave conductor oriented vertically.

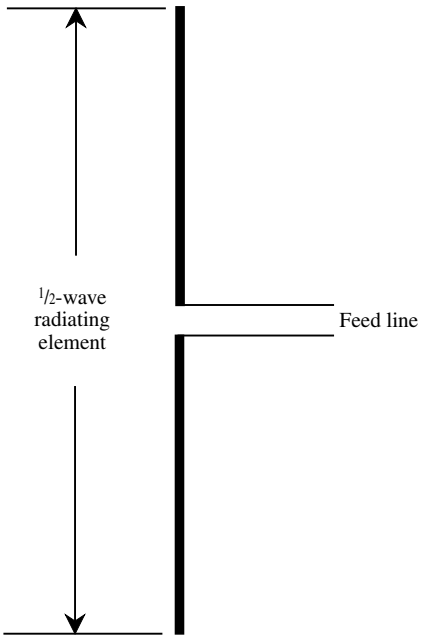

vertical dipole

vertical dynamic convergence During the scanning of points along a vertical line through the center of a color-television picture tube, the convergence of the electron beams at the aperture mask. Compare HORIZONTAL DYNAMIC CONVERGENCE.

vertical field strength The field strength of signals in a vertical plane passing through an antenna. Compare HORIZONTAL FIELD STRENGTH.

vertical-field-strength diagram A plot of vertical field strength.

vertical frequency response The gain-frequency characteristic of the vertical channel of an instrument, such as an oscilloscope. Compare HORIZONTAL FREQUENCY RESPONSE.

5059F-pV-716-737 4/10/01 9:56 AM Page 724

vertical gain The overall amplification (gain) provided by the vertical channel of an instrument, such as an oscilloscope, graphical recorder, or television receiver. Compare HORIZONTAL GAIN.

vertical-gain control A control, such as a potentiometer, for adjusting vertical amplification. Compare HORIZONTAL-GAIN CONTROL.

vertical-hold control In a television receiver, the control for adjusting the frequency of the vertical oscillator so that the picture can be locked to prevent vertical roll. Compare HORIZONTAL-HOLD CONTROL.

vertical-incidence transmission Transmission of a wave vertically to the ionosphere and the subsequent reflection of the wave to the earth.

vertical-lateral recording In stereophonic disc recording, the recording of one signal vertically (see VERTICAL RECORDING) and the other laterally (see LATERAL RECORDING).

vertical linearity Linearity of response (gain and deflection) of the vertical channel of an oscilloscope or television receiver. A linear picture is neither contracted nor expanded vertically in any part of the screen. Compare HORIZONTAL LINEARITY.

vertical-linearity control In an oscilloscope or television receiver, the control whereby vertical linearity is adjusted. Compare HORIZONTAL-LINEARITY CONTROL.

vertically polarized wave An electromagnetic wave whose electric lines of flux are perpendicular to the plane of the horizon. Compare HORIZONTALLY POLARIZED WAVE.

vertical-metal-oxide semiconductor field-effect transistor Abbreviation, VMOSFET. A metal-oxide semiconductor field-effect transistor fabricated so that the current flow within the device is vertical, instead of the usual horizontal, affording several advantages over the conventional MOSFET.

vertical oscillator In a television receiver, the oscillator that generates the vertical sweep signal. Compare HORIZONTAL OSCILLATOR.

vertical-output regulator In a television receiver, a voltage-dependent resistor used to stabilize the sweep voltage across the horizontal deflection coils—especially during warmup.

vertical output stage In a television receiver, an output amplifier following the vertical oscillator. Compare HORIZONTAL OUTPUT STAGE.

vertical polarization Pertaining to an electromagnetic wave whose electric lines of flux are perpendicular to the plane of the horizon. In general, when the radiating element of an antenna is vertical, the electric lines of flux in the transmitted waves are vertical, and the antenna is most sensitive to incoming signals whose electric lines of flux are vertical. Compare HORIZONTAL POLARIZATION.

vertical positioning control See CENTERING CONTROL.

vertical quantity The quantity measured along the *y*-axis of a graph, or represented by the vertical deflection of an electron beam. Compare HORIZONTAL QUANTITY.

vertical radiator See VERTICAL ANTENNA.

vertical recording Disc recording in which the depth of the groove is varied in sympathy with the sound. Also called HILL-AND-DALE RECORDING. Compare LATERAL RECORDING.

vertical redundance In computer operation, the error state when a character has an odd number of bits in an even-parity system, or vice versa.

vertical resolution The number of horizontal wedge-lines that can be easily seen in a television test pattern before they blend. Compare HORIZONTAL RESOLUTION.

vertical retrace In a cathode-ray device, such as an oscilloscope or television receiver, the rapid return of the beam to its starting point at the top of the screen after completely traversing the screen from top to bottom. Compare HORIZONTAL RETRACE.

vertical retrace blanking In a television receiver, the automatic shutoff of the electron beam during a vertical retrace period, to prevent an extraneous line being traced on the screen during this period. Also see BLACKOUT, **2**; BLANKING INTERVAL, **1**, **2**; BLANKING PEDESTAL; BLANKING TIME; VERTICAL RETRACE; and VERTICAL RETRACE PERIOD. Compare HORIZONTAL RETRACE BLANKING.

vertical retrace period In a television receiver, the interval during which the spot returns from the bottom to the top of the screen after having traced all horizontal lines from top to bottom. Compare HORIZONTAL RETRACE PERIOD.

vertical sensitivity The signal voltage required at the input of a vertical channel to produce full vertical deflection. Also see VERTICAL GAIN. Compare HORIZONTAL SENSITIVITY.

vertical signal A signal serving as a vertical quantity (e.g., one that deflects the beam in a cathode-ray tube upward and/or downward). Compare HORIZONTAL SIGNAL.

vertical-speed transducer A transducer whose electrical output is proportional to the vertical speed of an aircraft or missile carrying the transducer.

vertical stylus force In disc sound reproduction, the downward force (in grams or ounces) that the stylus exerts on the disc.

vertical sweep **1.** In a cathode-ray tube, especially a television picture tube, the movement of the spot up or down on the screen. Compare HORIZONTAL SWEEP. **2.** The circuit that produces this sweep.

vertical sweep frequency The frequency at which vertical sweep occurs. In a television receiver, it is 60 Hz. Also called *vertical sweep rate*. Compare HORIZONTAL SWEEP FREQUENCY.

vertical sweep rate See VERTICAL SWEEP FREQUENCY.

5059F-pV-716-737 4/10/01 9:56 AM Page 725

vertical synchronization In a television receiver, synchronization of the vertical component of scanning with that of the camera. Also see VERTICAL SYNC PULSE. Compare HORIZONTAL SYNCHRONIZATION.

vertical sync pulse In a video signal, the pulse that synchronizes the vertical component of scanning in a television receiver with that of the camera, and that triggers vertical retrace and blanking. Compare HORIZONTAL SYNC PULSE.

vertical wave See VERTICALLY POLARIZED WAVE.

vertical width control See WIDTH CONTROL, **1**, **2**.

very high frequency Abbreviation, VHF. Radio frequencies in the range 30 MHz to 300 MHz, corresponding to free-space wavelengths of 10 meters to 1 meter. It is sometimes divided into *VHF low band* (30 MHz to 50 MHz) and *VHF high band* (50 MHz to 300 MHz). Also see RADIO SPECTRUM, **1**.

very high resistance Abbreviation, VHR. Large values of resistance; usually expressed in megohms, gigohms, or teraohms.

very-high-resistance voltmeter Abbreviation, VHRVM. A voltmeter using a low-range microammeter or picoammeter and a very high value of multiplier resistance (see VOLTMETER MULTIPLIER).

very-high-speed integrated circuit An integrated circuit used for switching or other digital functions at thousands, millions, or billions of changes of state per second.

very-large-scale integration Abbreviation, VLSI. The inclusion of several complete systems, such as computers, on a single integrated-circuit chip. This can extend several orders of magnitude beyond large-scale integration (LSI).

very long range Abbreviation, VLR. Pertaining to ground radar sets having a maximum slant range of over 250 miles. Compare VERY SHORT RANGE.

very low frequency Abbreviation VLF. A radio frequency in the range 10 kHz to 30 kHz, corresponding to wavelengths between 30 kilometers and 10 kilometers. Also see RADIO SPECTRUM, **1**.

very low resistance Abbreviation, VLR. Values of resistance less than 1 ohm, usually expressed in milliohms or microhms.

very short range Abbreviation, VSR. Pertaining to ground radar sets having a maximum slant range of less than 25 miles. Compare VERY LONG RANGE.

vestigial **1.** An effect that remains as a by-product, but that serves no directly applicable purpose. See, for example, VESTIGIAL SIDEBAND. **2.** Unnecessary; extraneous.

vestigial sideband **1.** A portion of one sideband in an amplitude-modulated signal, remaining after passage through a selective filter. **2.** An amplitude-modulated signal in which one sideband has been partially or largely suppressed. **3.** The small amount of energy emitted in the unused sideband in a single-sideband transmitter.

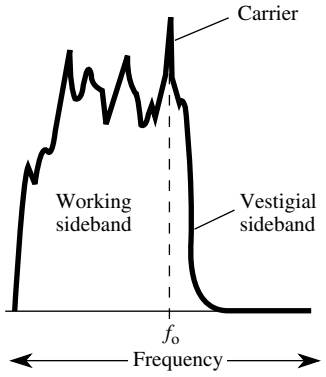

vestigial sideband, 2

vestigial-sideband filter A filter operated between an amplitude-modulated transmitter and an antenna to obtain a vestigial-sideband signal.

vestigial-sideband signal An amplitude-modulated signal in which one of the sidebands has been partially suppressed.

vestigial-sideband transmission Transmission of a signal containing a vestigial sideband. In television, for example, the upper sideband is transmitted fully, while the lower sideband is almost completely suppressed. The lower sideband is, therefore, a vestigial sideband.

vestigial-sideband transmitter An amplitude-modulated transmitter equipped with the filters or other subcircuits necessary for emitting a vestigial-sideband signal.

VF Abbreviation of VIDEO FREQUENCY.

V_{FB} Abbreviation for *feedback voltage* in an integrated circuit device. The term applies especially to operational amplifiers.

VFO Abbreviation of VARIABLE-FREQUENCY OSCILLATOR.

V_g Abbreviation of GENERATOR VOLTAGE. (Also, *Eg*.)

VGA Abbreviation of VARIABLE-GAIN AMPLIFIER.

V_{GD} Symbol for GATE-DRAIN VOLTAGE of a field-effect transistor.

V_{GS} Symbol for GATE-SOURCE VOLTAGE of a field-effect transistor.

VHF Abbreviation of VERY HIGH FREQUENCY.

VHF high band See VERY HIGH FREQUENCY.

VHF low band See VERY HIGH FREQUENCY.

VHF omnirange Abbreviation, VOR. A very-high-frequency radionavigation system that provides radial lines of position.

VHF oscillator A radio-frequency oscillator specially designed to operate in the range 30 MHz to 300 MHz.

5059F-pV-716-737 4/10/01 9:56 AM Page 726

VHF receiver **1.** A radio receiver specially designed to operate in the range of 30 MHz to 300 MHz. **2.** A television receiver for the VHF channels (see VHF TELEVISION CHANNELS).

VHF television channels Twelve 6-MHz-wide channels (television channels 2 through 13) between 54 and 216 MHz.

Channel	*Frequency (MHz)*
2	54.0 – 60.0
3	60.0 – 66.0
4	66.0 – 72.0
5	76.0 – 82.0
6	82.0 – 88.0
7	174 – 180
8	180 – 186
9	186 – 192
10	192 – 198
11	198 – 204
12	204 – 210
13	210 – 216

VHF television channels (United States)

VHF transmitter A radio or television transmitter specially designed to operate in the range 30 MHz to 300 MHz.

VHR Abbreviation of VERY HIGH RESISTANCE.

VHRVM Abbreviation of VERY-HIGH-RESISTANCE VOLTMETER.

VHS videocassette recorder A popular scheme for videocassette recording, used in millions of households in the United States alone. Typical VHS cassette play times range from about two hours to more than eight hours.

VHSIC Abbreviation for VERY HIGH SPEED INTEGRATED CIRCUIT.

VI **1.** Abbreviation of VOLUME INDICATOR. **2.** Abbreviation of VISCOSITY INDEX.

V_i Symbol for INPUT VOLTAGE. (Also, V_{in}.)

vibrating bell A bell with a striking mechanism that oscillates, causing a continuous ringing sound.

vibrating-reed frequency meter See POWER-FREQUENCY METER, **2**.

vibrating-reed oscillator An audio-frequency oscillator in which an iron, steel, or alloy reed vibrating in a magnetic field acts like a tuning fork to control the oscillation frequency.

vibrating-reed relay An electromechanical relay in which the movable contact is carried by the end of a thin, metal strip (reed) of iron or magnetic alloy. The strip is supported within the magnetic field of a coil carrying an alternating control current; when the frequency of this current corresponds to the natural (resonant) frequency of the reed, it vibrates vigorously enough to close the contacts. Such a relay, consequently, is frequency selective.

vibrating-wire oscillator An oscillator similar to the vibrating-reed oscillator, but using a wire, instead of a reed.

vibrating-wire transducer A transducer in which the fluctuating tension of a thin wire suspended in a magnetic field frequency-modulates the operating voltage.

vibration **1.** The changing of the position or dimensions of a body back and forth, usually at a rapid rate, an action seen in the repetitive movement of a musical string, headphone diaphragm, loudspeaker cone, loose machine, etc. **2.** See OSCILLATION.

vibration analyzer See VIBRATION METER.

vibration calibrator A device that generates a standard vibration, usually at a fixed frequency, for calibrating vibration meters, pickups, transducers, etc.

vibration galvanometer A type of alternating-current galvanometer. The natural frequency of the movable element of the instrument is made equal to that of the alternating current under test, to obtain a reading.

vibration isolator In an electronic-equipment assembly, a cushioning support that protects the equipment from vibration.

vibration machine See VIBRATOR, **2**.

vibration meter An instrument for measuring the amplitude and frequency of vibration (see VIBRATION, **1**). It consists essentially of a vibration pickup followed by a selective amplifier and an indicating voltmeter graduated in vibration units.

vibration pickup A transducer that senses mechanical vibration and converts it into a proportionate output voltage, or changes resistance in sympathy with the vibration.

vibrato In electronic musical instruments, a circuit or device that modulates a note by varying its frequency, amplitude, or both, at an extremely low frequency (a few hertz).

vibrator **1.** See INTERRUPTER. **2.** See VIBRATING-REED RELAY. **3.** A device for shaking something under test at selected frequencies and amplitudes.

vibrator-type power supply A battery-operated, high-voltage power supply in which one vibrator (see INTERRUPTER) makes and breaks direct current flowing from the battery into the primary winding of a step-up transformer, and another vibrator rectifies the high voltage delivered by the secondary winding.

vibrator-type rectifier A vibrator (see INTERRUPTER) that connects one terminal of the secondary winding of a transformer to an output terminal each time that terminal is positive. When the negative half-cycle appears at the transformer terminal, the vibrator is open. In this way, the alternating-current output of the transformer is rectified.

vibrocardiography A method of monitoring and recording the movement of the chest cavity as a result of the beating of the heart.

5059F-pV-716-737 4/10/01 9:56 AM Page 727

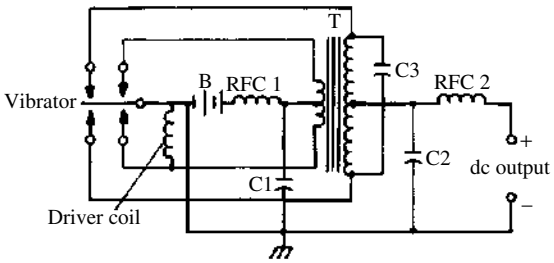

vibrator-type power supply

vibrograph A device for observing and recording vibration.

vibrometer See VIBRATION METER.

vibroscope An instrument for observing (and sometimes recording) vibration.

Victor Phonetic alphabet communications code word for the letter V.

Victron A brand of polystyrene, a low-loss plastic insulant that is especially useful at high radio frequencies.

video **1.** Pertaining to television—especially to its picture circuitry or to circuits and devices related to television, but used for other purposes. **2.** The picture portion of a television broadcast, as opposed to the sound (audio) portion. **3.** Sometimes, a cathode-ray-tube terminal or display. **4.** Generally, television in adjective sense (e.g., *video play*). **5.** The images on a computer display or monitor.

video amplifier **1.** In television, the wideband stage (or stages) that amplifies the picture signal and presents it to the picture tube. **2.** A similar wideband amplifier, such as an instrument amplifier or preamplifier having at least a 4-MHz bandwidth.

video animation Movement of graphic images on a cathode-ray-tube display by the use of computer-manipulation through special software, under the direction of an operator using a keyboard, joystick, or digitizer.

video buffer A unity-gain circuit that minimizes loading effects caused by having several video multiplexer inputs connected to the same signal source.

video carrier The television carrier amplitude-modulated by the picture information, synchronization pulses, and blanking pulses.

videocassette recorder Abbreviation, VCR. A machine for recording television programs on magnetic-tape cassettes (see CASSETTE, **1**).

videocast **1.** Television broadcast. Also called TELECAST. **2.** To make a television broadcast.

videocaster See TELECASTER.

video CD-ROM A digital optical VIDEODISC, resembling an audio or computer compact disc. A typical disc can store more than an hour's worth of conventional television programming.

video correlator A device used with radar to locate and identify a target with high precision.

video detector In a television receiver, the demodulator for the video signal. This detector follows the video intermediate-frequency amplifier and precedes the video amplifier. It usually embodies a relatively simple, wideband diode circuit.

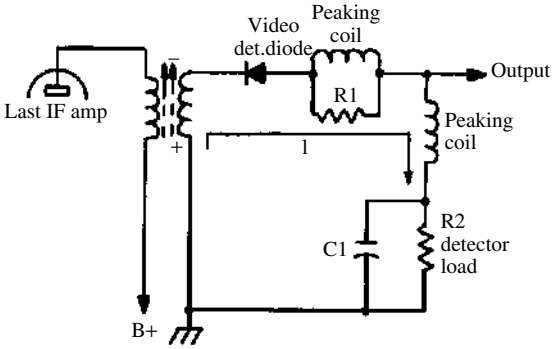

video detector

Video Digitizer Abbreviation, VDIG. A program developed for multimedia video in personal computer systems.

videodisc A flat magnetic or optical disc on which audio-visual programs are recorded, and from which they can be played back into a television receiver or multimedia personal computer.

videodisc recorder Abbreviation, VDR. A machine for recording television programs on discs comparable to those used for sound or data recording.

video discrimination In radar, the use of a circuit or device to decrease the width of the video-amplifier passband.

video frequency **1.** Pertaining to signals in the wide passband of a video amplifier: 30 Hz to 4 MHz. **2.** Pertaining to a device capable of operating over the wide passband of a video amplifier (e.g., a video-frequency alternating-current voltmeter).

video-frequency amplifier An amplifier capable of handling signals of a wide frequency range (e.g., direct current to 4 MHz). Also see VIDEO FREQUENCY, **1**.

video gain control In a television receiver, a gain control for adjusting the video signal amplitude. In a color-television receiver, a pair of these controls permits adjustment of the three color signals to the proper amplitude ratio.

video game A game, such as football, basketball, slot machine, tic-tac-toe, etc., played on the screen of a television receiver or on a computer.

videogenic Suitable for television.

video IF amplifier In a television receiver, the broadband intermediate-frequency (IF) amplifier of the video signal. In modern receivers, this IF amplifier also handles the sound signal.

5059F-pV-716-737 4/10/01 9:56 AM Page 728

video mapping A system of surveillance or mapping in which, for reference, the outlines of the area being surveyed are superimposed electronically on the radar display of the area.

video masking A form of radar signal processing in which ground clutter and other unwanted echoes are removed, making the desired targets more readily visible.

video mixer A circuit or device for mixing the signals from two or more television cameras.

video modulation In television transmission, amplitude modulation of the carrier wave with pulses and waves corresponding to the picture elements.

video on demand Television service in which subscribers can choose the programs they want to watch, and also the specific times for viewing.

video random-access memory Abbreviation, VRAM. In computer systems, RANDOM-ACCESS MEMORY used primarily for enhancing the performance of the display.

video recording **1.** Recording wideband material (such as a video signal) on a tape or disc. **2.** The recording made of a telecast. Also see VIDEOTAPE RECORDER.

video signal **1.** In television, the amplitude-modulated signal containing picture information and pulses. Also see VIDEO, **2** and VIDEO MODULATION. **2.** Broadly, a telecast signal, including sound.

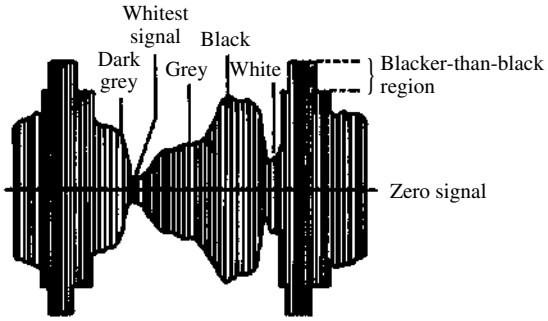

video signal

video stretching In some electronic navigation systems, increasing the duration of a video pulse.

video synthesizer A computerized device that produces graphical renditions of objects or circuits in three dimensions.

videotape **1.** A special magnetic tape for video recording (see VIDEO RECORDING, **2**). **2.** To make a video recording.

videotape recorder Abbreviation, VTR. A wideband, magnetic-tape recorder for producing video recordings with a camera, or for making a record of television programs, for subsequent reproduction (playback).

videotape recording **1.** Abbreviation, VTR. The technique of recording video signals on magnetic tape. Also see VIDEO RECORDING, **1**, **2** and VIDEOTAPE. **2.** A tape on which a video signal has been recorded.

videotext A system that allows television viewers to dial up special material, such as stock market quotations, weather data, sports scores, etc.

vidicon A television camera tube in which the electron beam scans a charged-density pattern that has been formed and stored on the surface of the photoconductor. It is commonly used in camcorders, closed-circuit television systems, and robot vision systems. Its assets include compactness and sensitivity.

viewfinder An accessory or integral device in which an image (formed optically or electronically) corresponds to the image viewed by the camera with which it is used.

viewing mesh In a cathode-ray storage tube, the mesh on which the image is presented for viewing by the operator. Also see CHARGE-STORAGE TUBE.

viewing mirror In an oscilloscope-camera assembly, a flat, slant-mounted mirror that reflects the image on the oscilloscope screen to the viewer's eye.

viewing screen In a cathode-ray device, such as an oscilloscope tube or television picture tube, the face on which the image appears.

viewing time In a storage type cathode-ray tube, the length of time for which the image persists.

viewing window See WINDOW, **2**.

Villard circuit **1.** A voltage-doubler circuit using only one diode and two capacitors. The open-circuit direct-current output voltage is approximately twice the peak value of the alternating-current input voltage. Also see VOLTAGE DOUBLER. **2.** See SELECTOJECT.

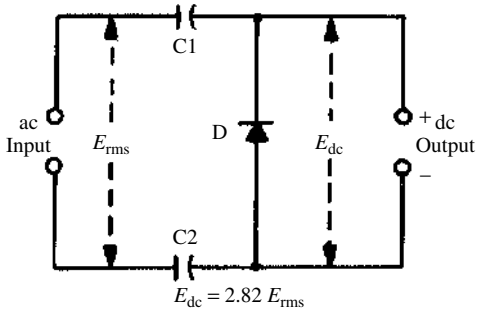

Villard circuit, 1

Villari effect In certain magnetostrictive materials, the change in magnetic induction that accompanies the application of a mechanical stress in a given direction. Also see MAGNETOSTRICTION.

vinyl A general name for *vinyl copolymer resins.*

5059F-pV-716-737 4/10/01 9:56 AM Page 729

vinylidene chloride A plastic insulant. Dielectric constant, 3 to 5. Dielectric strength, 20 kV/mm.

Vinylite-A A brand of the plastic *polyvinyl acetate.*

Vinylite-Q A brand of the plastic *polyvinyl chloride.*

vinyl resin A synthetic resin resulting from the polymerization of compounds that contain the group $CH_2 = CH–$.

violation In a security system, a condition that results in the actuation of an alarm. Example: an intruder breaks the light beam in an electric eye.

virgin magnetic material Core or shield material that has never been magnetized. When virgin material is first subjected to magnetization, the hysteresis loop starts at zero, but never returns to zero (see BOX-SHAPED LOOP).

virgin neutron Any neutron that has not been involved in a collision with another particle subsequent to its initial generation.

virgin record See BLANK RECORD.

virgin tape See BLANK TAPE.

virtual address In computer operations, an address that must be modified to refer to a location in main memory.

virtual decision value In quantizing or encoding, a method of expressing the maximum input amplitude. Two values are extrapolated from actual decision values—one at either end of the working range used.

virtual height The altitude that a vertically propagated electromagnetic wave would reach before reflection if its path in the ionosphere were a straight line. The actual distance at which the wave penetrates the ionosphere before reflection is less than the virtual height.

virtual image The image formed when rays from a scene diverge after passing beyond the focal point of a convex lens. The scene appears inverted to an observer. Compare REAL IMAGE.

virtual memory **1.** In a computer system, a means of using two or more memory stores simultaneously. **2.** Auxiliary memory used in conjunction with the main, or core, memory.

virtual ppi reflectoscope A device used to superimpose a virtual image of a chart or map onto a plan-position indicator (ppi) radar display. Also see VIDEO MAPPING.

virtual reality Abbreviation, VR. A general term for any of various high-level computer simulation or remote-control programs. The user often wears a head-mounted display that provides vivid, three-dimensional imagery and binaural sound. It can be used in robotic telepresence systems for precision remote control.

virus See COMPUTER VIRUS.

vis **1.** Abbreviation of *visibility.* **2.** Abbreviation of *visual.*

viscometer An instrument for measuring viscosity. There are several electronic versions of this device. In one, a steel ball falls through a material (such as an oil) under test and distorts the magnetic field of a pickup coil, causing the deflection of a meter by an amount proportional to the speed of the ball and, consequently, to the viscosity of the fluid.

viscosimeter See VISCOMETER.

viscosity The resistance offered by a fluid (liquid or gas) to objects passing through it. The viscosity of pure water is low; that of heavy oil is high. Expressed in newton-seconds per meter squared.

viscosity index Abbreviation, VI. A number indicating how well an oil retains its viscosity with temperature changes; larger indexes are assigned to oils that are little influenced by variations in temperature.

viscous-damped arm A phonograph pickup arm with an oil dashpot to prevent arm resonance and to slow the descent of the arm to the disc.

viscous damping The use of a viscous fluid in the dashpot of a device (such as a relay, timer, or pickup arm) to provide damping. See, for example, DASHPOT RELAY.

viscous hysteresis A slow, slight increase in the magnetization of a material when the magnetizing field is constant. Compare STATIC HYSTERESIS.

visibility factor See DISPLAY LOSS.

visible radiation Electromagnetic radiation that is perceptible to the eye. Also see VISIBLE SPECTRUM.

visible spectrum The band of electromagnetic wavelengths that the human eye perceives as visible light. For most people, this band extends from approximately 750 nanometers (nm), representing red light, down to 390 nm, representing violet light. The visibility curve peaks in the yellow-green region at about 560 nm; 1 nm = 0.000

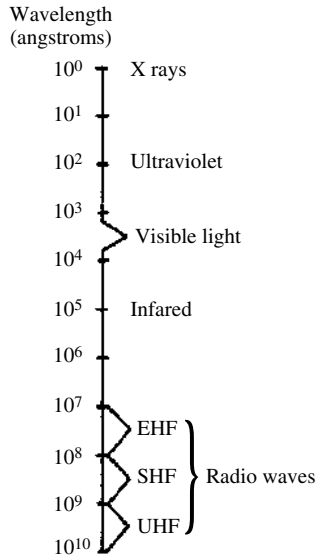

visible spectrum

5059F-pV-716-737 4/10/01 9:56 AM Page 730

000 001 meter = 10^{-9} m. Also see ELECTROMAGNETIC THEORY OF LIGHT.

vision system A set of devices that allows a machine (computer or robot) to observe and respond to visual stimuli. Typically, it includes a camera [such as a vidicon or charge-coupled device (CCD)], a cable, electromagnetic or fiberoptic link, a receiver, and software for interpreting the images.

visual alignment Optimization of a circuit (such as a radio receiver) with the aid of meter deflections, rather than with audible indications. Also called *silent alignment.*

visual-aural radio range A radio aid to air navigation (characterized by an audible signal, meter deflection, or both) used by the pilot of an aircraft to determine if the course is being followed.

visual-aural range See VISUAL-AURAL RADIO RANGE.

visual-aural signal tracer A troubleshooting instrument for following a signal through a circuit by sensing it at successive points in the circuit. The signal strength is indicated by a meter and a loudspeaker.

visual carrier frequency See VIDEO CARRIER and VIDEO-FREQUENCY, **1**.

visual communication **1.** Transmission and reception of signals by visible-light means, such as modulated beams of flashing lights. **2.** Transmission and reception of messages by direct visual observation, such as signal lights.

visual display unit Abbreviation, VDU. **1.** A computer peripheral consisting of a cathode-ray tube, a keyboard, and often a pointing device. **2.** A dumb terminal for operation of a computer from a remote site.

visual horizon **1.** The distance from a given point to the farthest visible point on the surface of the earth in a particular direction. **2.** The enclosed geometric plane figure on the surface of the earth, representing the set of farthest-visible points for a particular location.

visual telegraphy Telegraphy in which the received signals are read from a visual device, such as a blinking light, meter, or swinging pen.

visual transmitter The equipment used to transmit the picture portion of a television broadcast.

visual transmitter power The peak power output of a visual transmitter during normal operation.

vitreous Pertaining to a material or surface resembling, or related to, glass (e.g., the *vitreous enamel* on certain types of resistors).

VLF Abbreviation of VERY LOW FREQUENCY.

VLR **1.** Abbreviation of VERY LOW RESISTANCE. **2.** Abbreviation of VERY LONG RANGE.

VLSI Abbreviation of VERY-LARGE-SCALE INTEGRATION.

V/m Abbreviation of VOLTS PER METER (a unit of electric field strength).

VMOS Abbreviation of *vertical-metal-oxide semiconductor.*

VMOSFET Abbreviation of VERTICAL-METAL-OXIDE SEMICONDUCTOR FIELD-EFFECT TRANSISTOR.

V_o Symbol for OUTPUT VOLTAGE. Also, V_{out}.

VOA Abbreviation of VOLT-OHM-AMMETER.

vocabulary In computer-programming operations, a list of available operating codes and instructions for the computer. Also called INSTRUCTION SET.

Vocoder A device for reducing speech to frequencies low enough for efficient transmission through a limited-bandwidth channel. The term is a contraction of *voice coder.*

Voda In a telephone system that utilizes a radio link (using the same frequency for transmission in both directions) and land-line links, an automatic, voice-operated switching system for enabling the transmitter and disabling the receiver, and vice versa. The name is an acronym for *voice-operated device, anti-sing.*

Vodacom Contraction of *voice data communications.*

Voder An electronic device that synthesizes speech. The term is an acronym for *voice operation demonstrator.*

vogad A type of automatic gain control for audio amplifiers and modulators. In a radio transmitter, it maintains 100% modulation of the carrier—even when the speaker's voice level varies widely. The name is an acronym for *voice-operated gain adjusting device.*

voice actuation See VOICE-OPERATED CONTROL.

voice analyzer A circuit that evaluates the characteristics of human voices, such as the amplitude-vs.-frequency function or the amplitude-vs.-time function.

voice band See VOICE FREQUENCIES.

voice coil The moving coil of a dynamic microphone or dynamic speaker.

voice-controlled break-in A type of break-in operation for radiotelephony, in which the transmitter automatically switches on and the receiver switches off immediately when the operator starts talking; the transmitter switches off and the receiver switches on a moment after the operator stops talking.

voice-controlled relay An electronic relay that is actuated by the human voice.

voice filter **1.** A filter for passing, suppressing, or modifying voice frequencies. **2.** A parallel-resonant circuit inserted into a line that feeds several loudspeakers, to trap certain frequencies and thereby improve the sound of the reproduced voice.

voice frequencies **1.** The audio-frequency range of human speech, from about 60 Hz to 8000 Hz. **2.** The frequencies within the audio passband of a typical single-sideband voice transmitter or receiver. The lower limit is generally 200 Hz to 300 Hz; the upper limit is about 2500 Hz to 3000 Hz.

5059F-pV-716-737 4/10/01 9:56 AM Page 731

voice-frequency carrier telegraphy A type of carrier-current telegraphy (see WIRED WIRELESS) in which the modulated carrier can be transmitted over a telephone line having a voice-frequency bandwidth.

voice-frequency dialing A system of telephone dialing involving the conversion of direct-current pulses into voice-frequency alternating-current pulses.

voice-frequency telephony Wire telephone communication in which the frequencies of the electric waves are identical to the frequencies of the sound waves (or very nearly so).

voice grade Pertaining to a communications system having a bandpass capable of transferring a human voice with reasonable intelligibility. See VOICE FREQUENCIES, **2**.

voice-grade channel **1.** A telephone line and attendant equipment suitable for the transmission of speech and certain other information, such as control signals, digital data, etc. **2.** In a radiotelephone transmitter, a speech amplifier-modulator channel suitable only for voice frequencies.

voice-operated control Abbreviation, vox. Pertaining to a device (such as a relay, automatic modulation control, transmit-receive switch, etc.) that is actuated when the operator speaks into a microphone.

voice-operated device, anti-sing See VODA.

voice-operated gain-adjusting device See VOGAD.

voice-operated loss control and suppressor In wire telephony, a device that switches the loss from the transmitting line to the receiving line when the subscriber speaks, and vice versa.

voice-over The simultaneous recording of a human voice (such as that of a narrator) along with other sounds (such as music, children playing, wind in trees, ocean waves, chirping birds, etc.). The voice is generally louder than the other sounds.

voice print A graphic recording of the speech frequencies produced by an individual and used as a means of identifying that individual.

voice-recognition device See SPEECH RECOGNIZER.

voice security In voice communications system, the use of encryption and decryption, usually in the form of digital algorithms, to "scramble" speech at the source and "unscramble" it at the destination.

voice-stress analyzer Abbreviation, VSA. An instrument that samples the spoken voice and produces a display from which the relative amount of stress experienced by the speaker can be determined, and from which, in turn, probable truth or falsity of statements or answers can be inferred.

voice synthesis device See SPEECH SYNTHESIZER.

void space See VACUUM.

vol Abbreviation of VOLUME.

volatile **1.** Capable of evaporating (e.g., *volatile solvents* used in the encapsulation of electronic equipment). **2.** Explosive (noun and verb). **3.** Pertaining to a state which is difficult to maintain (e.g., a VOLATILE MEMORY).

volatile memory Memory, usually of the random-access type, whose data vanishes when power is removed unless some provision is made for memory backup. The most common means of memory backup is the use of an electrochemical cell or battery. Modern memory chips need so little current to store their data that a backup battery lasts almost as long in the circuit as it would on the shelf. The main advantage of this type of memory is the fact that it can easily be erased if desired. Compare NONVOLATILE MEMORY.

volatile storage See VOLATILE MEMORY.

volatile store See VOLATILE MEMORY.

Voldicon A form of semiconductor logic device used for analysis of analog signals. Trade name of Adage, Inc.

volt Abbreviation, V. The basic practical unit of difference of potential (i.e., of electrical pressure); 1 volt is the difference of potential produced across a resistance of 1 ohm by a current of 1 ampere. Also see KILOVOLT, MEGAVOLT, MICROVOLT, MILLIVOLT, NANOVOLT, and PICOVOLT.

Volta effect See VOLTA'S PRINCIPLE.

voltage Symbols, E, e, V, v. Electromotive force, or difference of potential; $E = IR$, where I is current and R is resistance. Also see VOLT.

voltage-actuated device An electronic device, such as a field-effect transistor, that amplifies a voltage signal or is controlled by a voltage, and draws virtually no signal current or control current. The opposite is a current-actuated device, such as a bipolar transistor.

voltage amplification **1.** Abbreviation, A_v. Amplification of an input-signal voltage to provide a higher output-signal voltage. **2.** Abbreviation, A_v. The signal increase (V_{out}/V_{in}) resulting from this process. Also called *voltage gain.*

voltage-amplification device A low-current device designed especially for voltage amplification. It provides little or no power amplification.

voltage amplifier An amplifier operated primarily to increase a signal voltage. Compare CURRENT AMPLIFIER and POWER AMPLIFIER.

voltage at peak torque Symbol, V_p. For a torque motor operated at 25°C, the voltage required to produce peak torque at standstill.

voltage attenuation **1.** The reduction in voltage at a given point in a circuit. **2.** For a device, the ratio of input voltage to output voltage when the output voltage is the lower quantity.

voltage-balance relay A relay actuated by a voltage differential.

voltage breakdown See BREAKDOWN VOLTAGE.

voltage-breakdown test **1.** A test in which the measured voltage applied to an insulating material is continuously increased until the

5059F-pV-716-737 4/10/01 9:56 AM Page 732

breakdown point is reached. **2.** A test in which the measured reverse voltage applied to a semiconductor junction is continuously increased until the reverse breakdown point is reached (see AVALANCHE BREAKDOWN).

voltage burden The voltage drop across a CURRENT SHUNT.

voltage calibrator A device used to calibrate, in terms of voltage, a meter scale, oscilloscope screen, graphic-recorder chart, etc.

voltage-capacitance curve A plot depicting the variation of capacitance with applied voltage for a voltage-variable capacitor. For a varactor (variable-capacitance diode), capacitance varies inversely with reverse direct-current voltage.

voltage coefficient A figure that shows the extent to which a quantity drifts under the influence of voltage. It is generally expressed in percent per volt or in parts per million per volt (ppm/V).

voltage coefficient of capacitance For a voltage-dependent capacitor, the capacitance change per unit change in applied voltage.

voltage coefficient of resistance For a voltage-dependent resistor, the resistance change per unit change in applied voltage.

voltage coil See POTENTIAL COIL.

voltage comparator A device for comparing (usually only two) voltages. The various types range from simple, manually balanced potentiometers to analog or digital devices that automatically compare the applied voltages and provide a direct readout of either their difference or the percent of unbalance.

voltage control **1.** A component or circuit that allows the adjustment of the output voltage of a power supply within a given range. **2.** The adjustment of the output voltage of a power supply to optimize the performance of a circuit connected to the supply. **3.** Any form of circuit control that is accomplished by the adjustment of the voltage at a given circuit point.

voltage-controlled amplifier Abbreviation, VCA. An amplifier in which gain is controlled by means of a voltage applied to a control terminal.

voltage-controlled attenuator An attenuator circuit in which a transistor serves as a voltage-variable resistor. The output resistance of the transistor varies inversely with the direct-current bias voltage applied to the input electrode (base, emitter, or gate).

voltage-controlled capacitor See VOLTAGE-DEPENDENT CAPACITOR.

voltage-controlled crystal oscillator Abbreviation, VCCO or VCXO. A voltage-controlled oscillator of the crystal-stabilized type.

voltage-controlled generator Abbreviation, VCG. Any signal-generating device whose output frequency is varied by changing one of the direct-current operating voltages of the device.

voltage-controlled oscillator Abbreviation, VCO. An oscillator of the inductance-capacitance (LC) type that employs a varactor diode in the capacitive portion of the tuned circuit. The varactor is placed in series or parallel with the tuning capacitor and is isolated for direct current by blocking capacitors. The frequency can be adjusted, within certain limits, by nonmechanical means. The signal can also be frequency modulated by applying the modulating voltage across the varactor.

voltage-controlled resistor See VOLTAGE-DEPENDENT RESISTOR.

voltage corrector See VOLTAGE REGULATOR.

voltage crest See VOLTAGE PEAK.

voltage-current characteristic See VOLTAGE-CURRENT CURVE.

voltage-current crossover The point at which a voltage-regulated supply becomes a current-regulated supply.

voltage-current curve For a circuit or device, the plot of the interrelationship of current and voltage, with voltage as the independent variable.

voltage-current feedback See CURRENT-VOLTAGE FEEDBACK.

voltage decay The exponential decrease of voltage across a discharging capacitor. Also see EXPONENTIAL DECREASE.

voltage-dependent capacitor A capacitor (such as a varactor) whose capacitance varies with applied voltage.

voltage-dependent resistor A nonlinear resistor whose value varies inversely with the voltage drop across it. Also called *varistor.*

voltage detector A circuit or device that delivers an output voltage only when the input voltage is of a prescribed value. Compare VOLTAGE DISCRIMINATOR.

voltage-determined property A property (capacitance, current, frequency, or resistance) whose magnitude depends on the value of an applied voltage. See, for example, VOLTAGE-DEPENDENT CAPACITOR, VOLTAGE-DEPENDENT RESISTOR, and VOLTAGE-CONTROLLED OSCILLATOR.

voltage differential Symbol, dE or dV. An infinitesimal change in voltage. Compare VOLTAGE INCREMENT.

voltage-directional relay **1.** A relay that is actuated when voltage exceeds a certain value in a given direction. **2.** A relay that closes only when the applied voltage is in a specific direction.

voltage discriminator A circuit or device whose output voltage is zero when the input voltage is of a prescribed value. When the input voltage is greater than this value, the output is positive; when it is less, the output is negative.

voltage distribution **1.** The delivery of operating voltage throughout a circuit (e.g., high and low direct-current voltages in the various stages of a control circuit). **2.** Sometimes, the distribution of electrical energy ("power" distribution).

voltage divider A resistive or capacitive potentiometer or network used to divide an applied voltage by a desired amount.

5059F-pV-716-737 4/10/01 9:56 AM Page 733

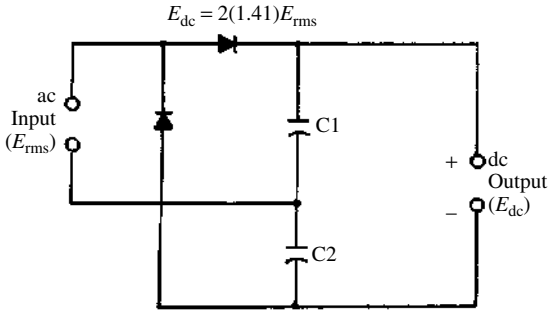

voltage doubler

voltage doubler A power-supply circuit that supplies a direct-current output voltage of about twice the peak value of the alternating-current input voltage.

voltage drift See DRIFT VOLTAGE.

voltage drop Abbreviation, VD. The voltage (*E*) set up across a resistance (*R*) carrying a current (*I*); *E* = *IR*. For alternating current, reactance *X* and impedance *Z* can be substituted for resistance, where applicable.

voltage-equalizing resistors In a power-supply filter, resistors connected across each capacitor in a string of electrolytics connected in series to withstand a high voltage. The resistors protect the capacitors by equalizing the voltage across them.

voltage-fed antenna An antenna in which the feeder is attached to the radiator at a voltage loop (current node). Compare CURRENT-FED ANTENNA.

voltage feed The delivery of voltage to a device or circuit at a point where voltage, rather than current, is dominant. Compare CURRENT FEED.

voltage feedback A feedback signal consisting of voltage fed from the output to the input circuit of an amplifier or other device. Compare CURRENT FEEDBACK and CURRENT-VOLTAGE FEEDBACK.

voltage-frequency transducer **1.** A device whose output voltage is a function of the frequency of a signal at the input. **2.** A device whose output frequency is a function of the voltage at the input.

voltage gain See VOLTAGE AMPLIFICATION.

voltage generator See VOLTAGE SUPPLY.

voltage gradient The voltage per unit length along a defined path.

voltage increment A change in voltage represented by $E_2 - E_1$, where E_2 and E_1 are the voltages at two defined points on a curve, and the difference is finite (nonzero). Compare VOLTAGE DIFFERENTIAL.

voltage input encoder An analog-to-digital encoder for which the input is an analog voltage. See, for example, VOLTAGE-TO-SHAFT-POSITION ENCODER.

voltage inverter A circuit or device whose voltage output has the sign opposite that of the input voltage. The device might or might not provide amplification.

voltage jump **1.** An upward transient in voltage. **2.** In a glow-discharge tube, a sudden break or increase in voltage drop across the tube.

voltage lag The condition in which voltage changes occur after corresponding current changes. Compare CURRENT LAG and VOLTAGE LEAD.

voltage lead The condition in which voltage changes precede corresponding current changes. Compare CURRENT LEAD and VOLTAGE LAG.

voltage level **1.** A prescribed reference value of voltage (e.g., the black level in a television picture signal). **2.** The discrete value of a steady voltage, or the average value of a fluctuating voltage, as observed or measured in a circuit.

voltage limit The maximum or minimum level in a voltage range.

voltage loop In a standing-wave system, such as an antenna or transmission line, a maximum-voltage point. Compare VOLTAGE NODE.

voltage loss **1.** Reduction of a voltage across a load, occurring because of a series resistance. **2.** The ratio, in decibels, between the input voltage to a transmission line and the output voltage at the load end of the line, assuming that the impedance is the same at both points.

voltage maximum See VOLTAGE PEAK.

voltage minimum See VOLTAGE TROUGH.

voltage-mode switching circuit A resistor-transistor-logic (RTL) NAND or NOR circuit in which (in the off state) the transistor is cut off by the V_{BB} bias voltage. The output is then approximately equal to the collector supply voltage, V_{CC}. The proper combination of input pulses overrides the cutoff bias, and the transistor switches on. The output then drops to a level equal to V_{CC} minus the voltage drop across the external collector resistor.

voltage multiplier A special type of rectifier circuit that delivers a direct-current output voltage that is a multiple of the peak value of the alternating-current input voltage, thus affording voltage step-up without a transformer. See, for example, VOLTAGE DOUBLER; VOLTAGE QUADRUPLER; QUINTUPLER, **1**; and VOLTAGE TRIPLER.

voltage node In a standing-wave system, such as an antenna or transmission line, a minimum-voltage point. Compare VOLTAGE LOOP.

voltage of self-induction The voltage drop across an inductor, resulting from the flow of alternating current through the inductor; it is caused by self-induction.

voltage peak The highest value attained by a voltage during an excursion. Also called *voltage crest* or *voltage maximum*. Compare VOLTAGE TROUGH.

5059F-pV-716-737 4/10/01 9:56 AM Page 734

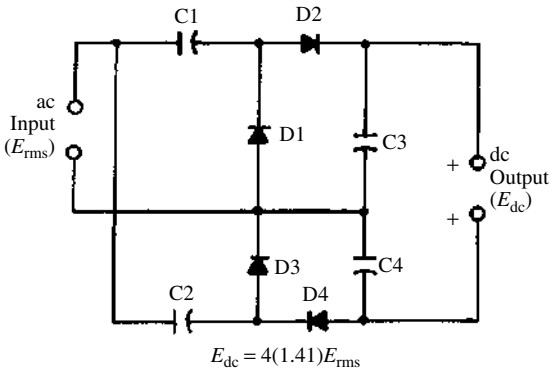

voltage quadrupler

voltage-power directional relay A relay system in which two circuits are connected when their voltage difference exceeds a predetermined value in one direction, and are disconnected when the voltage in the opposite direction exceeds a predetermined level.

voltage quadrupler A special rectifier circuit that supplies a direct-current output voltage of approximately four times the peak alternating-current input voltage.

voltage quintupler See QUINTUPLER, **1**.

voltage-range multiplier **1.** A multiplier resistor (see VOLTMETER MULTIPLIER) connected in series with a voltmeter that has an internal multiplier, to increase the range of the instrument. **2.** For an alternating-current voltmeter, an input amplifier used to increase the sensitivity of the instrument.

voltage rating **1.** For a circuit or device, the recommended maximum voltage that can be applied, or the recommended working voltage, as specified. **2.** For a generator, the specified output voltage.

voltage ratio The quotient of the voltages, E_1/E_2, at two specific points in a circuit, device, or system. Examples: ratio of input voltage to output voltage and ratio of primary voltage to secondary voltage.

voltage-ratio box See VOLT BOX.

voltage reference See STANDARD CELL and ZENER-DIODE VOLTAGE REFERENCE.

voltage-reference cell See STANDARD CELL.

voltage-reference diode A Zener diode biased into its Zener region. The voltage drop across the diode is comparatively constant. Under proper conditions, it can be used for reference purposes. Also see ZENER-DIODE VOLTAGE REFERENCE.

voltage reflection coefficient In a reflected-wave situation, the ratio E_r/E_i, where E_i is the field-strength voltage of the incident wave, and Er is the field-strength voltage of the reflected wave.

voltage-regulated supply See CONSTANT-VOLTAGE SOURCE.

voltage-regulating transformer A special transformer in which a resonant circuit and core saturation (see SATURATED OPERATION, **1**) are used to provide a constant output voltage.

voltage regulation The stabilization of a voltage against fluctuations in source or load.

voltage-regulation constant Symbol, K_v. For a voltage-regulated power supply, the ratio dE_L/dE_i, where dE_i is a change in input voltage, and dE_L is the corresponding change in load voltage.

voltage regulator A circuit or device that holds an output voltage constant during variations in the output load or input voltage.

voltage-regulator diode See ZENER-DIODE VOLTAGE REGULATOR.

voltage-regulator transformer See VOLTAGE-REGULATING TRANSFORMER.

voltage relay A relay or relay circuit that is actuated by a discrete voltage, rather than by current or power.

voltage-responsive device See VOLTAGE-ACTUATED DEVICE.

voltage rise The normal condition in a series-resonant circuit, in which the voltage across the coil or capacitor is higher than the voltage applied to the circuit.

voltage saturation In a current-actuated device, such as a bipolar transistor, the situation in which an increase in current provides no increase in voltage drop beyond a certain point (the saturation point).

voltage-sensitive bridge A bridge having a nonlinear element (such as a voltage-dependent resistor) as one of the arms. Because of this element, the bridge can be balanced (with a given set of other arms) at only one value of applied voltage. At lower voltages, the bridge becomes unbalanced in one direction; at higher voltage, in the opposite direction.

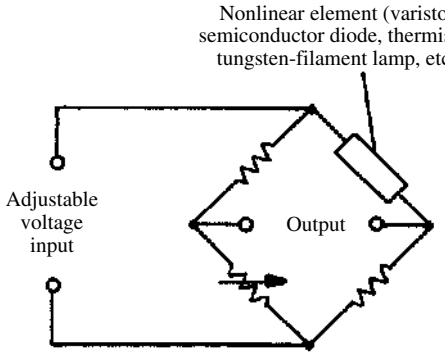

voltage-sensitive bridge

5059F-pV-716-737 4/10/01 9:56 AM Page 735

voltage-sensitive capacitor See VOLTAGE-DEPENDENT CAPACITOR.

voltage-sensitive resistor See VOLTAGE-DEPENDENT RESISTOR.

voltage sensitivity **1.** Particular responsiveness of a circuit or device to voltage, rather than current or power. See, for example, VOLTAGE-DEPENDENT CAPACITOR, VOLTAGE-DEPENDENT RESISTOR, and VOLTAGE RELAY. **2.** See VOLTMETER SENSITIVITY.

voltage-spectrum function The voltage-vs.-frequency curve at the output of a circuit or transducer.

voltage-stabilized supply See CONSTANT-VOLTAGE SOURCE.

voltage stabilizer See VOLTAGE REGULATOR.

voltage-stabilizing diode See ZENER-DIODE VOLTAGE REGULATOR.

voltage standard A device that delivers a voltage of accuracy and stability so that it can be used to calibrate other voltage generators and test instruments. See, for example, STANDARD CELL and ZENER-DIODE VOLTAGE REFERENCE.

voltage standing-wave ratio Abbreviation, VSWR. In a standing-wave system, the ratio of the maximum voltage to the minimum voltage.

voltage supply A power supply whose usable output is voltage, rather than current or power. When such a supply is not voltage-regulated, it can only be used reliably with a very light load.

voltage to chassis In electronic equipment mounted on a metal chassis, the voltage between the chassis and a given point in the circuit.

voltage-to-frequency converter A device or circuit that delivers an output frequency proportional to an input voltage (usually direct current). Compare FREQUENCY-TO-VOLTAGE CONVERTER.

voltage to ground **1.** In a circuit, the voltage measured between a given point and the ground point. **2.** The voltage measured between the earth and a line or piece of equipment.

voltage to panel In electronic equipment mounted on a metal panel, the voltage between the panel and a given point in the circuit.

voltage-to-shaft-position encoder An encoder for which the output is the rotation of a motor shaft over an arc proportional to an input voltage.

voltage transformer **1.** A transformer used primarily to supply voltage with little or no current. **2.** A small step-up transformer for increasing the sensitivity of an alternating-current voltmeter. Also called POTENTIAL TRANSFORMER.

voltage tripler A rectifier circuit that, without a transformer, supplies a direct-current output voltage of approximately three times the peak value of the alternating-current input voltage.

voltage trough The lowest value reached by a voltage during an excursion. Compare VOLTAGE PEAK.

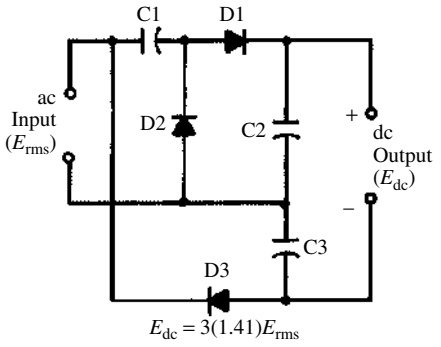

voltage tripler

voltage tuning A method of adjusting the frequency of an oscillator or resonant circuit by means of a variable, direct-current voltage.

voltage-tunable magnetron A magnetron oscillator in which the output frequency is varied by adjusting the direct-current voltage on the tube.

voltage-tunable oscillator See VOLTAGE-CONTROLLED OSCILLATOR.

voltage-turns ratio The turns ratio of a transformer, indicated by the ratio of primary voltage to secondary voltage, or vice-versa.

voltage-type telemetry Telemetry based upon the variation of a single voltage in sympathy with the changes in a sensed phenomenon.

voltage-variable capacitor **1.** A specially processed semiconductor diode of which the voltage-variable capacitance of the junction is utilized. Also called VARACTOR. **2.** A capacitor having a specially processed nonlinear dielectric, such as barium strontium titanate, whose capacitance varies inversely with the applied direct-current bias voltage.

voltage-variable resistor See VOLTAGE-DEPENDENT RESISTOR.

voltage vector In a vector diagram, a vector showing the magnitude and phase of a voltage. Compare CURRENT VECTOR.

voltaic Pertaining to chemically produced direct current. Sometimes interchangeable with *galvanic*.

voltaic cell For the generation of a direct-current voltage, a primary cell consisting of two electrodes made of different metals and immersed in an electrolyte. Also called GALVANIC CELL. Also see CELL, ELECTROMOTIVE SERIES, and PRIMARY CELL.

voltaic couple A pair of dissimilar metals (or other substances) that generate a direct-current voltage when they contact an electrolyte.

voltaic pile A rudimentary primary battery consisting of a series of disks made of two different metals, stacked alternately with electrolyte-soaked cloth or paper disks.

5059F-pV-716-737 4/10/01 9:56 AM Page 736

voltaic series See ELECTROMOTIVE SERIES.

voltameter An electrolytic cell for determining the value of an unknown current, or of an unknown quantity of electricity, from the weight of metal deposited out of an electrolyte onto the cathode by the passage of current over an accurately timed interval.

volt-ammeter A combination meter for measuring electrical voltages and currents.

volt-ampere Symbol, VA. Unit, watt. The simple product of voltage and current in volts and amperes, yielding the true power in a direct-current circuit and the apparent power in an alternating-current circuit. Also see APPARENT POWER and TRUE POWER.

volt-ampere-hour meter See VAR-HOUR METER.

volt-ampere meter See VAR METER.

volt-amperes reactive Abbreviation, VAR. The product of volts and amperes for a purely reactive circuit. This product does not produce the true power because the power factor is neglected; it produces only the apparent power. A true reactance absorbs power during one half-cycle of alternating current, and returns it to the generator during the next half-cycle.

Volta's law See VOLTA'S PRINCIPLE.

Volta's pile See VOLTAIC PILE.

Volta's principle Two dissimilar metals brought into contact (even in air) will generate a difference of potential whose value is characteristic of the metals. Also see ELECTROMOTIVE SERIES.

volt box A precision, potentiometer-type voltage divider used in the calibration of meters and other instruments. The device is usually provided with a set of terminal posts for selecting various ratios of output voltage to input voltage.

volt-electron See ELECTRONVOLT.

voltmeter A usually direct-reading instrument used to measure voltage. Also see ELECTRONIC VOLTMETER, FET VOLTMETER, TRANSISTOR VOLTMETER, and VACUUM-TUBE VOLTMETER.

voltmeter-ammeter See VOLT-AMMETER.

voltmeter amplifier A wideband, flat-frequency-response, low-distortion preamplifier used to boost the sensitivity of an alternating-current voltmeter.

voltmeter-millivoltmeter A voltmeter that provides several low ranges, as well as several high ones. A familiar example is an alternating-current voltmeter, which has various full-scale ranges from about 1 millivolt to about 1000 volts.

voltmeter multiplier A resistor connected in series with a current meter (usually a milliammeter or microammeter) to convert it into a voltmeter.

voltmeter sensitivity Unit, ohm per volt. For a voltmeter, the total resistance of the instrument (multiplier resistance plus the resistance of the meter movement) divided by the full-scale deflection of the meter. Thus, a 0-to-10 direct-current voltmeter with an input resistance of 100 kilohms has a sensitivity of 10,000 ohms per volt.

volt-milliammeter A combination meter for measuring volts and milliamperes.

volt-ohm-ammeter A multimeter for measuring voltage, resistance, and current (in amperes).

volt-ohmmeter A combination meter for measuring voltage and resistance.

volt-ohm-milliammeter Abbreviation VOM. A multimeter for measuring voltage, resistance, and current (in milliamperes and microamperes).

voltsensor See VOLTAGE DETECTOR.

volts per meter Abbreviation, V/m or Vpm. The unit of electric field strength.

volume **1.** Intensity of sound. Also called LOUDNESS. **2.** A circumscribed portion of space, either imaginary or actually occupied, and described by three dimensions (e.g., sphere, ellipsoid, cube, pyramid, etc.). **3.** In a computer system, a unit of magnetic storage medium (e.g., a diskette).

volume compression The automatic reduction of the gain of an audio amplifier. The process differs from clipping (which "slices off" the tops of waves) in that compression (ideally) reduces the amplitude while preserving the waveform. Compare VOLUME EXPANSION.

volume compressor A circuit or device (such as an automatic-gain-control amplifier) for achieving volume compression. Compare VOLUME EXPANDER.

volume conductivity The reciprocal of VOLUME RESISTIVITY.

volume control A variable resistor (usually a potentiometer) or a network of resistors (such as a pad) for adjusting the gain, and, consequently, the output-signal loudness, of an amplifier.

volume equivalent In wire telephony, speech loudness throughout the system, expressed in terms of the trunk loss in a reference system and adjusted for equal loudness.

volume expander A circuit or device for automatically boosting the volume of an audio-frequency signal. Also see EXPANDER. Compare VOLUME COMPRESSOR.

volume expansion The technique of automatically increasing the gain, and consequently the output-signal volume, of an audio amplifier. Also see VOLUME EXPANDER. Compare VOLUME COMPRESSION.

volume indicator A fast-acting alternating-current meter used to monitor the volume level in an audio channel in which the signal level is fluctuating. The scale is graduated in VOLUME UNITS. Also called *VU meter.*

volume lifetime In a homogeneous semiconductor, the interval between minority-carrier generation and recombination.

volume limiter A circuit or device that automatically holds the volume level of an audio channel to a predetermined maximum. Also see VOLUME COMPRESSION and VOLUME COMPRESSOR.

volume-limiting amplifier An amplifier that functions as a volume limiter through the action of volume-limiting subcircuits.

5059F-pV-716-737 4/10/01 9:56 AM Page 737

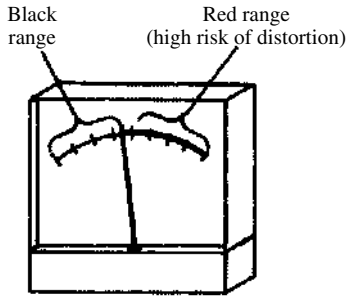

volume indicator

volume magnetostriction **1.** The decrease in the total volume of certain ferromagnetic substances under the influence of a magnetic field. **2.** The increase in the total volume of certain ferromagnetic substances under the influence of a magnetic field.

volume range Unit, decibel (dB). The difference between the maximum and minimum volume levels that a device or system can accommodate.

volume recombination rate Within the volume of a semiconductor, the rate at which electrons and holes recombine.

volume resistance The effective resistance, through a given medium, between two electrodes placed within that medium.

volume resistivity The resistance of a specific volume of a material (e.g., the resistance between opposite faces of a 1-centimeter cube of the material). Also see MICROHM-CENTIMETER; OHM-CENTIMETER; RESISTIVITY.

volumetric efficiency In an electronic assembly, the ratio of the volume of parts to the total volume of the assembly.

volumetric radar A radar providing a three-dimensional display.

volumetric sensor In security systems, a device that detects effects in a specifically defined three-dimensional region, such as an entire room (from floor to ceiling).

volume unit Abbreviation, VU. The unit of measurement of fluctuating alternating-current power, such as that of speech or music. Zero VU corresponds to a reference power of 2.51 milliwatts, or +4 dBm (four decibels above 1 milliwatt). Volume units are measured with a VOLUME INDICATOR.

volume-unit indicator See VOLUME INDICATOR.

volunteer examiner In amateur radio, a person who works with the Federal Communications Commission (FCC) to administer license examinations. Such a person is not actually an employee of the FCC, but serves on an independent, volunteer basis.

VOM Abbreviation of VOLT-OHM-MILLIAMMETER.

von Hippel breakdown theory The theory that, assuming no electron-energy distribution, breakdown occurs at field intensities for which the recombination rate of electrons and holes is lower than the rate of ionization by collision.

von Neumann architecture In computer systems, a design scheme in which the bits are transmitted serially (one by one) along a single line or bus.

VOR Abbreviation of *very-high-frequency omnirange* (see VHF OMNIRANGE).

voter See MAJORITY LOGIC.

vox Abbreviated form of VOICE-OPERATED CONTROL.

V_P **1.** Symbol for GATE-SOURCE PINCHOFF VOLTAGE of a field-effect transistor. **2.** Symbol for PLATE VOLTAGE.

V_p Symbol for VOLTAGE AT PEAK TORQUE.

V particle See VEE PARTICLE.

Vpm Abbreviation of VOLTS PER METER. (Also, V/m.)

VR **1.** Abbreviation of VIRTUAL REALITY. **2.** Abbreviation of VOLTAGE REGULATOR.

VRAM Abbreviation of VIDEO RANDOM-ACCESS MEMORY.

V_{ref} Abbreviation of *reference voltage.*

vrr Abbreviation of *visual radio range.*

V•s Abbreviation of *volt-seconds* (webers).

V•s/A Abbreviation of *volt-seconds per ampere* (henrys).

VSA Abbreviation of VOICE-STRESS ANALYZER.

VSB Abbreviation of VESTIGIAL SIDEBAND.

VSF Abbreviation of VESTIGIAL-SIDEBAND FILTER.

V signal See VEE SIGNAL.

vsr Abbreviation of VERY SHORT RANGE.

VSWR Abbreviation of VOLTAGE STANDING-WAVE RATIO.

vt **1.** Abbreviation of VACUUM TUBE. **2.** Abbreviation of *variable time.*

VT fuse See PROXIMITY FUSE.

VTL Abbreviation of VARIABLE-THRESHOLD LOGIC.

vtm Abbreviation of VOLTAGE-TUNABLE MAGNETRON.

VTO Abbreviation of VOLTAGE-TUNABLE OSCILLATOR.

VTR Abbreviation of VIDEOTAPE RECORDER or VIDEOTAPE RECORDING.

VTVM Abbreviation of VACUUM-TUBE VOLTMETER.

vt voltmeter See VACUUM-TUBE VOLTMETER.

VU Abbreviation of VOLUME UNIT.

vulcanized fiber A tough insulating material derived from cellulose. Dielectric constant, 5 to 8.

VU meter See VOLUME INDICATOR.

VVCD Abbreviation of *voltage-variable capacitor diode* (see VOLTAGE-VARIABLE CAPACITOR, **1**).

VVV signal See VEE SIGNAL.

VW Abbreviation of *volts working* (see WORKING VOLTAGE).

vy Abbreviation for *very.*

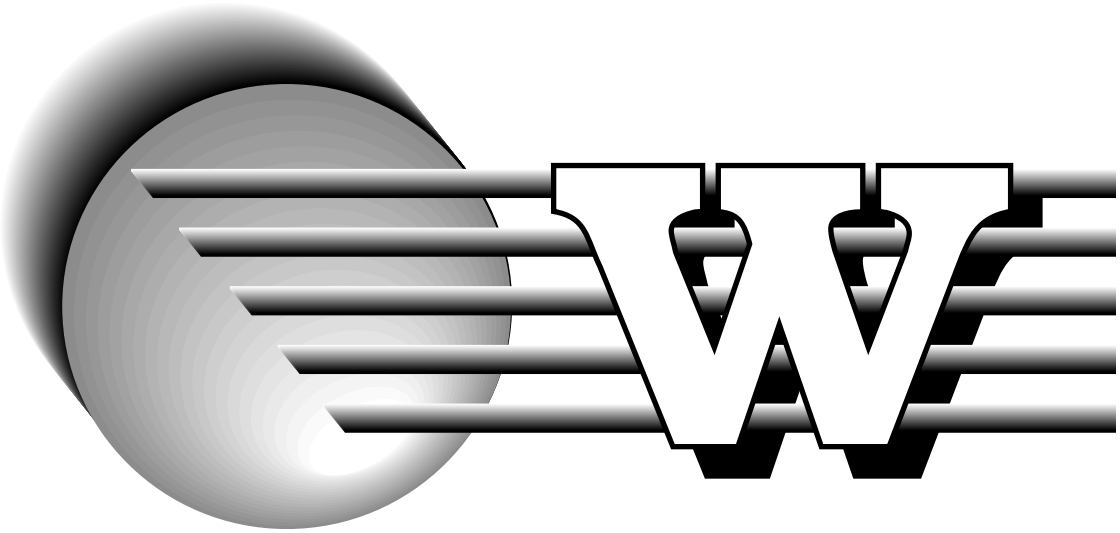

W **1.** Symbol for WORK. **2.** Abbreviation of WATT. **3.** Symbol for TUNGSTEN. **4.** Symbol for ENERGY. **5.** Abbreviation of *west.* **6.** Abbreviation of WIDTH.

w **1.** Abbreviation of WEIGHT. (Also, wt.) **2.** Abbreviation of *week.*

WAC Amateur radio abbreviation of *Worked All Continents,* an award given to operators who have engaged in verified two-way communication with stations on all continents.

wafer **1.** Semiconductor die. **2.** A thin, flat disk, ring, or plate around which the contacts of a rotary switch are spaced. **3.** A thin square or rectangle of dielectric material used as the dielectric member in a fixed capacitor. **4.** A plate cut from a crystal (e.g., a quartz wafer).

wafer fabrication The various processes used in the manufacture of semiconductor integrated circuits.

wafer slicing Cutting plates from a mother crystal, as when piezoelectric plates are cut from a quartz crystal.

wafer socket A component socket consisting of a plastic or ceramic wafer with spring-type contacts for gripping the pins.

wafer switch A rotary switch whose contacts are arranged around the periphery of a plastic or ceramic wafer.

Wagner ground A circuit (often a single potentiometer) that facilitates cancellation of stray reactance in an alternating-current bridge. The bridge is balanced alternately with the bridge-balance control and the Wagner control, until there is no further shift of null point when changing from one to the other.

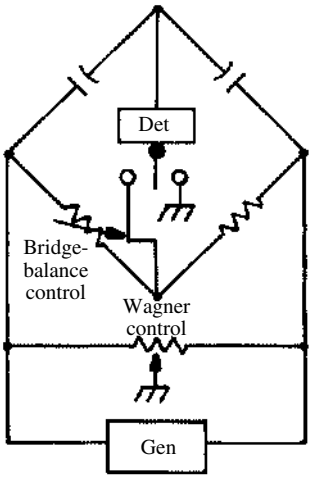

Wagner ground (with capacitance bridge)

waiting time **1.** See WARMUP TIME. **2.** The delay between the time a data transfer to or from a computer memory is called for and the actual transfer of the data. Also called LATENCY.

walkie-lookie A portable combination camera and transmitter for remote television pickup. At sports events and other gatherings, the unit is strapped to the shoulder of the camera operator.

walkie-talkie A portable, compact transceiver (or transmitter-receiver).

Copyright 2001 The McGraw-Hill Companies, Inc. Click Here for Terms of Use

5059F-pW-738-758 4/10/01 10:09 AM Page 739

wall absorption Diminished radioactive emission (especially of beta and gamma rays) because of absorption by the radiating substance.

wall box A wall-mounted (usually metal) box enclosing circuit breakers, fuses, switches, etc.

wall effect In an ionization chamber, the rise in ionization because of electrons being released by the walls of the chamber.

wall energy In a ferromagnetic substance, the energy per unit area stored in a domain wall between two regions of opposite magnetization.

Wallman amplifier A cascode amplifier (see CASCODE).

wall mount A metal bracket for fastening an antenna to a wall.

wall outlet A plug or socket, usually mounted in a protective box or can and recessed in a wall that can be accessed from the front. It is commonly used for supplying alternating-current power to appliances at 117 volts or 234 volts. It is also used in telephone and cable-television systems.

wall plaque A loudspeaker so thin that, mounted in a frame (sometimes behind grill cloth), it can be hung on a wall.

wall plate A (usually rectangular) plate of metal or plastic for holding a wall outlet or wall switch.

wall plug A male or female plug usually mounted in a protective box or can and recessed in a wall. Such a device can provide easy access to an antenna, telephone line, or load; or it can deliver alternating-current, direct-current, or radio-frequency power.

walls The sides of the groove cut into a record disc.

wall socket A male or female socket usually mounted in a protective box or can and recessed in a wall. Such a device can provide easy access to an antenna, telephone line, or load; or it can deliver alternating-current, direct-current, or radio-frequency power.

wall speaker See WALL PLAQUE.

wall switch A switch usually mounted in a protective box or can and recessed in a wall.

wall telephone A wall-mounted telephone set. It generally fits over the jack, so the only cord is between the main unit and the receiver.

wall-through tube See LEAD-IN TUBE.

Walmsley antenna A phased array consisting of several full-wavelength loops.

wamoscope A radar display tube that performs several microwave-receiver functions (detection, oscillation, amplification, etc.) as well as displaying an image. The name is an acronym for *wave-modulation oscilloscope.*

wander See SCINTILLATION, **1**.

WAP Acronym for WIRELESS ACCESS PROTOCOL.

warble **1.** A periodic rise and fall in the pitch of a musical tone or combination of tones. **2.** To rise and fall in pitch with a definite period.

warble-tone generator An audio-frequency oscillator whose frequency is varied at a subaudible rate over a fixed frequency range.

warm junction The heated junction in a two-junction thermocouple circuit. Also called HOT JUNCTION. Compare COLD JUNCTION.

warmup The process of stabilizing an electronic equipment by allowing its temperature to rise to the optimum level.

warmup time The time required for an electronic circuit to become fully operational, or to stabilize, after the power has been switched on.

warning bell (buzzer) A bell (or buzzer) used as an audible alarm in a WARNING DEVICE.

warning device A device, such as an electronic signaler, for alerting a person to an emergency (intrusion on premises, danger to life and safety, etc.) or to the existence of an intrusion into a secured area.

warning lamp See WARNING LIGHT.

warning light A lamp used as a visual alarm in a warning device.

warpage Distortion of the normally straight sides of a triangular wave.

warping In multimedia computer graphics, a change in the shape of an object that occurs smoothly over a period of time.

WAS Amateur radio abbreviation of *Worked All States,* an award given to operators who have engaged in verified two-way communication with stations in all states of the United States.

washer capacitor A very thin donut capacitor.

washer resistor A resistor made in the general shape of a washer or ring and having a center hole for a mounting screw or stacking rod.

washer thermistor A thermistor made in the general shape of a washer and having a center hole for a mounting screw or stacking rod.

washer varistor A varistor made in the general shape of a washer and having a center hole for a mounting screw or stacking rod.

washout process A method of fabricating bipolar transistors. The contact metal is deposited in the diffusion hole.

waste instruction In a computer program, an instruction not meant to be acted upon (e.g., one used to take up space in the listing for some reason). Also called *null instruction* and *dummy instruction.*

watch A work shift, as of electronic personnel (e.g., radio station operators).

watchcase receiver An earphone enclosed in a small, round case with a screw-on cap. It is derived from its resemblance to a large pocket watch.

water absorption For a solid material, such as a dielectric, the ratio of the weight of water absorbed by the material to the weight of the material.

water-activated battery A battery that contains all the ingredients of its electrolyte, except water, which must be added when the battery is put into service.

water adsorption The formation of a thin layer of water molecules on the surface of normally dry

5059F-pW-738-758 4/10/01 10:09 AM Page 740

material, but not by absorption. Also see ADSORPTION.

water analogy The useful, but not wholly accurate, teaching device of comparing an electric current with the flow of water. In such a comparison, voltage is shown equivalent to water pressure, and current to the quantity (e.g., gallons) of water flowing in unit time.

water battery A primary battery or cell using water as the electrolyte.

water calorimeter A calorimeter used to measure power in terms of the increase in temperature of water heated by the electrical energy.

water capacitor An emergency capacitor made by setting one glass of water in another larger jar of water so that the two bodies of water are separated by the walls of the smaller jar. The bodies of water, in which an electrolyte has been dissolved, form the "plates" of the capacitor, and the wall of the smaller jar serves as the dielectric between them.

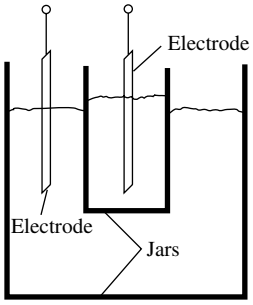

water capacitor

water-cooled tube A power tube, such as a large radio transmitting tube, cooled by the circulation of water in the space between the outside of the tube envelope and a surrounding jacket.

water cooling A method of cooling components by pumping water through pipes surrounding them.

water-flow alarm An electronic circuit that actuates an alarm when the flow of water through pipes or other channels changes from a predetermined rate.

water-flow control A servo system for automatically maintaining or adjusting the flow of water through pipes or other channels.

water-flow gauge See WATER-FLOW METER.

water-flow indicator See WATER-FLOW METER.

water-flow meter An instrument used to monitor the flow of water through pipes or other channels, sometimes showing its direction as well as its rate.

water-flow switch In water-cooled systems (e.g., water-cooled tubes), a switch that actuates an alarm when the water slows or stops.

water glass Sodium silicate, a substance used as a fireproofing agent and protective coating.

water ground An earth connection made by dropping a weighted wire into a body of water.

water jacket In a water-cooled device, the outer jacket that, along with the outer wall of the cooled component, forms a space through which the cooling water flows.

water-level control A servo system that automatically maintains or adjusts the level of water inside a tank or other container.

water-level gauge An electronic system that gives direct water level readings inside a tank or other container.

water-level indicator See WATER-LEVEL GAUGE.

water load **1.** A makeshift, power-dissipating resistive load (see DUMMY LOAD) consisting of a container of tap water or saltwater into which two wires are immersed. **2.** A waveguide termination containing water heated by the microwave energy. It is usable as a water calorimeter.

water monitor A sensitive electronic instrument for checking radioactivity in a water supply.

water-pipe ground An earth connection made by running a wire to the nearest cold-water pipe. This scheme works only with metal pipes devoid of insulating joints or splices.

water power Hydroelectric power (i.e., electrical energy produced by generators driven by water).

water-pressure alarm An electronic circuit that actuates an alarm when water in pipes or other channels changes from a predetermined level.

water-pressure control A servo system for automatically maintaining or adjusting water pressure in pipes or other channels.

water-pressure gauge See WATER-PRESSURE METER.

water-pressure indicator See WATER-PRESSURE METER.

water-pressure meter An instrument that directly indicates water pressure in a pipe or tank.

water-pressure switch A switch that actuates an alarm when water pressure rises or falls.

water pump In a water-cooled electronic system, the (usually rotary) pump that circulates the water.

water resistor An electrolytic resistor in which the electrolyte is tap water or diluted saltwater.

water rheostat A variable water resistor. Usually, the resistance is varied by moving the immersed electrodes closer together or farther apart.

water tester An instrument for checking pH, electrical resistance, and other properties of water.

water witching Locating underground water by electronic methods.

WATS Acronym for *Wide Area Telephone Service.* A form of long-distance telephone service. Rates are charged on a different basis than normal long-distance service. The system is especially favored by businesses because it saves money for subscribers making a large number of calls in each billing period.

5059F-pW-738-758 4/10/01 10:09 AM Page 741

watt Abbreviation, W. The practical unit of electric and other power. One watt is dissipated by a resistance of 1 ohm through which a current of 1 ampere flows. See also KILOWATT, MEGAWATT, MICROWATT, and MILLIWATT.

wattage Electrical power, especially when expressed in watts.

wattage rating **1.** The recommended output power of a device. **2.** The recommended power dissipation of a device.

watt current The component of alternating current that is in phase with voltage. Also called RESISTIVE CURRENT. Compare REACTIVE CURRENT.

watt-decibel conversion The conversion of a power level, such as the power output of an amplifier, in watts to the corresponding power level in decibels, with respect to a reference level. Thus, n dB = 10 $\log_{10}(P/P_{ref})$, where P is the power of interest (watts), and P_{ref} is the reference level (e.g., one milliwatt).

watt-hour Abbreviation, WH. The unit of electrical energy or work; 1 WH = 3600 joules = 10^{-3} kWH. Also see ENERGY, KILOWATT-HOURS, POWER, and WATT-SECOND.

watt-hour capacity The number of watt-hours that a storage battery can deliver reliably and safely under specified operating conditions.

watt-hour-demand meter A combination watt-hour meter and demand meter.

watt-hour efficiency For a storage battery, the ratio of watt-hours output to watt-hours of recharge.

watt-hour constant In an electric-energy meter, the number of watt-hours in one revolution of the indicating disk.

watt-hour meter An instrument for measuring electrical energy in watt-hours. One well-known type consists essentially of a small motor geared to a row of four dial indicators. An eddy-current disk keeps the motor speed proportional to the watt-hours consumed by a load, a value which is the sum of the readings of the dials. Also called SERVICE METER and KILOWATT-HOUR METER.

wattless current The component of alternating current that is out of phase with voltage. Also called REACTIVE CURRENT. Compare RESISTIVE CURRENT.

wattless power The apparent power in a reactive circuit, indicated by the product of volts and amperes. There is no actual power consumption because the power taken by a reactance during a half-cycle is returned to the generator during the next half-cycle. Also see AC POWER, APPARENT POWER, REACTIVE KILOVOLT-AMPERES, and REACTIVE VOLT-AMPERES.

wattless volt-amperes See WATTLESS POWER.

wattless watts See WATTLESS POWER.

wattmeter Abbreviation, WM. An instrument used to measure electrical power. The scale usually reads directly in watts, kilowatts, milliwatts, or microwatts. Also see ELECTRONIC WATTMETER.

watt-second Abbreviation, Ws. A small unit of electrical energy or work; 1 watt-second = 1 joule = 1/3600 watt-hour. Also see ENERGY and POWER.

watt-second constant In an electric-energy meter, the number of watt seconds in one revolution of the indicating disk.

wave **1.** A single oscillation of some property of matter or space, such as density, displacement, or field strength. It moves outward from a point of disturbance and grows weaker as it travels farther. Wave motion is associated with mechanical vibration, sound, radio, heat, light, X rays, gamma rays, and cosmic rays. See SOUND and WAVELENGTH. **2.** A single cycle of alternating or pulsating current or voltage. Also see AC VOLTAGE, ALTERNATING CURRENT, PULSATING DC VOLTAGE, and PULSATING DIRECT CURRENT.

wave absorption The removal of energy from electromagnetic waves as they pass through certain media, such as solid bodies, water, and the atmosphere. Compare POLARIZATION, WAVE REFLECTION, and WAVE REFRACTION.

wave amplitude The peak value of a wave. Also see WAVE CREST and WAVE TROUGH.

wave analyzer An instrument consisting essentially of a continuously tunable bandpass filter and an electronic alternating-current voltmeter. As the filter is tuned successively to the fundamental frequency of a complex wave and to its various harmonics, the voltmeter shows the amplitude of each of the components. Also see HETERODYNE WAVE ANALYZER.

wave angle The angle, measured with respect to the horizon, at which a radio wave is transmitted or received.

wave antenna See BEVERAGE ANTENNA.

wave attenuation The reduction of wave amplitude, with respect to distance from the source.

waveband A band of radio frequencies. Also called FREQUENCY BAND.

waveband switch See BANDSWITCH.

wave beam Unidirectional radiation from a directive antenna.

wave bounce See WAVE REFLECTION.

wave clutter Radar interference caused by waves on a body of water, particularly large swells on the ocean.

wave converter A waveguide part, such as a baffle-plate or grating, that changes a wave pattern from one type to another.

wave crest The maximum value of a wave envelope. Compare WAVE TROUGH.

wave cycle A complete single alternation of a wave.

wave direction The direction in which an electromagnetic wave travels. It is perpendicular to the wave front and depends (whether it is forward or backward) upon the direction of the electric and

5059F-pW-738-758 4/10/01 10:09 AM Page 742

magnetic components. If either is reversed, wave direction reverses; if both are reversed, the direction remains unchanged.

wave duct **1.** See DUCT, **1**. **2.** A tubular waveguide in which wave propagation is concentrated.

wave envelope The outline described by the various amplitude peaks of the cycles in an amplitude-modulated wave. The envelope frequency is equal to the modulating frequency.

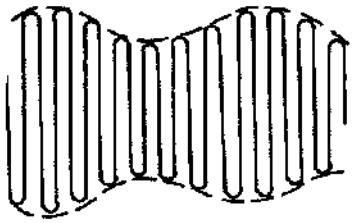

wave envelope

wave equation A second-degree partial differential equation whose solution describes wave phenomena.

wave filter A circuit or device that offers different amounts of attenuation to signals of different frequencies. See BANDPASS FILTER, BAND-SUPPRESSION FILTER, HIGH-PASS FILTER, and LOW-PASS FILTER.

waveform The shape of a wave described in terms of its resemblance to some well-known figure or to its conformity to the curve of the applicable wave equation (e.g., sinusoidal, square, sawtooth, cosine, rectangular, and triangular).

waveform-amplitude distortion See AMPLITUDE DISTORTION.

waveform analyzer See WAVE ANALYZER.

waveform converter A circuit or device for changing a signal of one waveform (such as a sine wave) into one of another waveform (such as a pulse or square wave).

waveform distortion The malfunction evidenced by a change of the waveshape of a signal passing through a circuit.

waveform error In a quantity displayed by an alternating-current test instrument, an error caused by the waveform of the measured signal. Thus, a voltmeter calibrated with a sine-wave voltage is subject to error when a measured signal is nonsinusoidal. Also called *waveform effect.*

waveform generator See FUNCTION GENERATOR.

waveform influence See WAVEFORM ERROR.

waveform monitor In television operations, an oscilloscope that continuously displays the video waveform.

waveform synthesizer A variable-frequency signal generator that allows the tailoring of waveshape to suit individual applications. A *function generator* (see FUNCTION GENERATOR, **1**) is such an instrument, but it usually provides only a choice of common waveshapes.

wave front For a radio wave, the plane that is parallel to the perpendicular electric and magnetic lines of flux. The wave propagates at right angles to this plane.

wave function A point function in a wave equation, specifying wave amplitude.

wave group The resultant of several different-frequency waves traveling over a common path.

waveguide A transmission line used at ultra-high and microwave radio frequencies. It is a hollow metal pipe with a rectangular or circular cross section. A rectangular waveguide must have sides measuring at least 0.5 wavelength and preferably more than 0.7 wavelength. A circular waveguide should be at least 0.6 wavelength in diameter, and preferably 0.7 wavelength or more. The characteristic impedance (Z_0) varies with frequency. In this sense, it differs from coaxial or parallel-wire lines, whose Z_0 values are independent of frequency.

waveguide apparatus See WAVEGUIDE COMPONENTS.

waveguide attenuator A device, such as an interposed energy-absorbing plate, for signal attenuation in a waveguide.

waveguide choke flange A waveguide flange that presents no impedance to the signal, and which need not be metallic for continuity.

waveguide component A device adapted for connection to, or insertion into, a waveguide system. Such components include waveguide parts and accessories (e.g., splicing hardware, attenuators, loads, wavemeters, etc.).

waveguide connector A fitting for joining waveguides for the efficient propagation of a signal.

waveguide coupling See WAVEGUIDE CONNECTOR.

waveguide critical dimension The cross-sectional dimension that determines the cutoff frequency for a waveguide.

waveguide cutoff In a waveguide, the highest or lowest frequency that can be propagated with less than a specified amount of attenuation per unit length.

waveguide directional coupler A directional coupler made of two parallel waveguides with a common wall. Two slots cut in the wall allow part of the microwave energy propagated in one direction in the main waveguide to be extracted, and energy traveling in the opposite direction to be rejected.

waveguide dummy load A waveguide section that dissipates the microwave energy entering it.

waveguide elbow **1.** A curved bend in a waveguide. **2.** A waveguide connector with a bend.

waveguide flange A flat, liplike fitting at the end of the pipe of a waveguide. It fastens waveguide sections together or attaches a waveguide

5059F-pW-738-758 4/10/01 10:09 AM Page 743

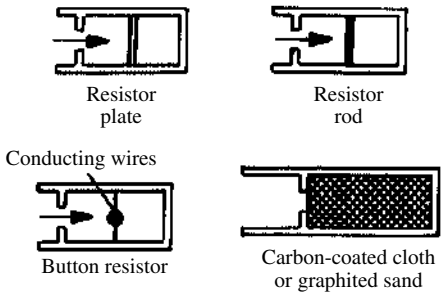

waveguide dummy load

waveguide elbow

component, equipped with an identical flange, to the end of a waveguide.

waveguide frequency meter See WAVEGUIDE WAVEMETER.

waveguide gasket A gasket that provides electrical continuity between mating waveguide sections.

waveguide grating An array of wires mounted inside a waveguide, and that passes signals at some frequencies while obstructing others.

waveguide impedance Where the power P is known, and voltage E and current I are defined, with respect to a type of wave and waveguide, the value is either E^2/P or P/I^2.

waveguide junction A fitting that allows one waveguide section to be joined at an angle to another section. See, for example, WAVEGUIDE TEE and WAVEGUIDE WYE.

waveguide lens A microwave lens consisting of waveguide sections that provide the required phase shifts.

waveguide load See WAVEGUIDE DUMMY LOAD.

waveguide mode The form of propagation indicated by the field pattern in a plane transverse to the direction in which energy is propagated through a waveguide. Common modes are TRANSVERSE ELECTRIC MODE, also called *TE mode*, and TRANSVERSE MAGNETIC MODE, also called *TM mode.*

waveguide mode suppressor A filter that suppresses undesired propagation modes in a waveguide.

waveguide phase shifter A shifter for adjusting the phase of waveguide output energy, with respect to input energy.

waveguide plunger A plunger-like device that reflects incident microwave energy in a waveguide.

waveguide post A transverse rod inside a waveguide that acts as a parallel susceptance.

waveguide probe A pickup probe (tip or loop, as required) for sampling the field inside a waveguide, or a similar injection probe for introducing energy into a waveguide. Also see WAVEGUIDE SLOTTED LINE.

waveguide propagation **1.** The transmission of microwave energy through a waveguide by successive reflections between the inner walls. **2.** Propagation of very-high-frequency (VHF), ultra-high-frequency (UHF), or microwave electromagnetic fields through an atmospheric duct (see DUCT, **1**), as if through a waveguide. **3.** Propagation of very-low-frequency (VLF) electromagnetic fields through a waveguide-like duct between the ionosphere and the earth's surface.

waveguide radiator An antenna consisting of an open-ended waveguide with or without a horn. It radiates microwave energy into space or to a reflector.

waveguide resonator A waveguide section used as a cavity resonator (see RESONANT CAVITY).

waveguide seal A protective cover for the end of a waveguide. The seal introduces very little microwave attenuation, while preventing entry of moisture and debris.

waveguide shim A thin, pliable metal sheet inserted between mating waveguide components for electrical continuity. Also see WAVEGUIDE GASKET.

waveguide shutter An adjustable mechanical barrier, such as a rotatable vane, inserted into a waveguide to block or divert microwave energy.

waveguide slotted line A section of waveguide having a slot that accommodates a movable probe or coupling element.

waveguide slug tuner A quarter-wave dielectric slug inserted into a waveguide so that its amount of penetration and position can be adjusted for tuning purposes.

waveguide stub A stub consisting of a waveguide section joined to a main waveguide at an angle and provided with a nondissipative termination.

waveguide stub tuner An adjustable piston in a waveguide stub for tuning purposes.

waveguide switch A switch consisting of a movable section of waveguide that can be positioned for coupling to one of several other waveguide sections; it thus passes the energy it receives to any of the other sections.

waveguide system Microwave "plumbing" consisting of waveguides, their fittings and accessories, and associated components (such as attenuators, loads, wavemeters, etc.).

waveguide taper A connector that is flared to allow coupling between two waveguide sections having different cross-sectional sizes.

waveguide tee In a waveguide assembly, a tee-shaped junction used to connect a section of waveguide in series or parallel with another section.

5059F-pW-738-758 4/10/01 10:09 AM Page 744

waveguide transformer A waveguide component that functions as an impedance transformer.

waveguide tuner In a waveguide system, an adjustable tuner providing impedance transformation.

waveguide twist A length of waveguide whose cross section is rotated around the longitudinal axis (e.g., from vertical to horizontal).

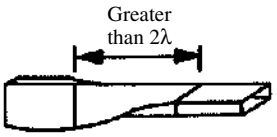

waveguide twist

waveguide wavelength In a uniform waveguide operating at a given frequency and in a particular mode, the distance between similar points for 360° phase shift.

waveguide wavemeter A waveguide component that acts as an absorption wavemeter or transmission wavemeter for identifying microwave frequencies.

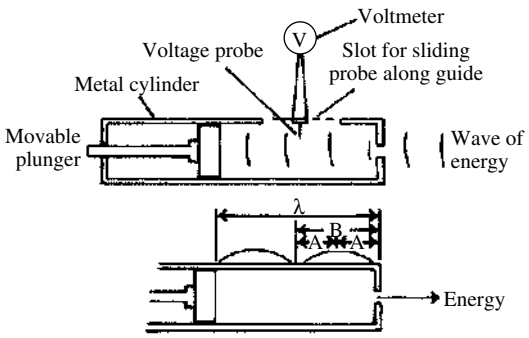

waveguide wavemeter

waveguide wedge See WEDGE, **1**.

waveguide window A thin metal opening mounted transversely inside a waveguide for impedance-matching purposes. The edges of the slit in a capacitive window are perpendicular to the electric field; in an inductive window, they are parallel to the electric field.

waveguide wye In a waveguide assembly, a wye-shaped junction for joining three waveguide sections.

wave heating Heating a material by energy absorbed from traveling electromagnetic waves.

wave interference Interaction between two or more waves, resulting in reinforcements and cancellations of energy.

wavelength Unit, meter. The displacement in one complete wave of an alternating or vibrating phenomenon, generally measured from crest to crest or from trough to trough of successive waves. For electromagnetic waves in free space, the wavelength in meters is equal to 3×10^8 divided by the frequency in Hertz. Also see WAVELENGTH-PERIOD-FREQUENCY RELATIONSHIPS.

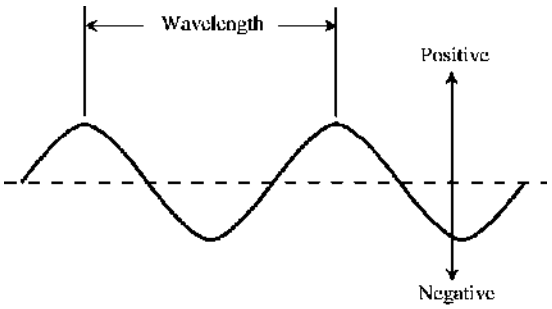

wavelength

wavelength constant The imaginary-number component of the propagation constant.

wavelength shifter **1.** A frequency shifter whose performance is indicated in units of wavelength, rather than in units of frequency. **2.** In certain photosensitive cells and tubes, a photofluorescent substance that raises the efficiency of the device by absorbing photons and then releasing ones of longer wavelength.

wave mechanics A theory of matter that views subatomic particles as complex wave patterns, and attempts to account for all physical processes in terms of wave phenomena.

wavemeter An instrument for measuring the wavelength or frequency of radio waves. One form consists of a series-resonant circuit containing an inductor, variable capacitor, and diode-type meter. The dial of the capacitor is calibrated to read in MHz. The inductor picks up energy from the radio-frequency source of unknown frequency, the capacitor is tuned for peak deflection of the meter, and the unknown frequency is read from the dial. This instrument is often called an *absorption wavemeter* because it absorbs a certain amount of power from the signal source under test. See also CAVITY WAVEMETER, COAXIAL WAVEMETER, LECHER WIRES, and SLOTTED LINE.

wave motion Undulating motion (e.g., up and down, and side to side). An electromagnetic wave has undulating electric and magnetic components that are both in phase and perpendicular to each other and to the direction of propagation of the wave.

wave normal **1.** The direction of propagation of an electromagnetic wave. **2.** A unit vector directed at

5059F-pW-738-758 4/10/01 10:09 AM Page 745

a right angle to both the electric and magnetic lines of flux in an electromagnetic wave.

wave number The reciprocal of wavelength. This number denotes the number of waves per unit distance.

wave packet A short pulse composed of waves.

wave packets Radiant energy resulting from a number of wave trains of different wavelength.

wave path The line along which a WAVE TRAIN is propagated.

wave polarization The direction (horizontal or vertical) of wave undulations (i.e., the plane of the undulations, with respect to the direction of propagation). In general, a vertical antenna radiates a vertically polarized wave, and a horizontal antenna radiates a horizontally polarized wave.

wave propagation The movement of waves through space or through some medium. Electromagnetic waves travel through space at the speed of light (approximately 3×10^8 meters, or 186,000 miles, per second) and, like light, can be reflected and refracted.

wave reflection The reflection of electromagnetic waves by an obstruction, such as a solid body or a layer of the ionosphere. Compare WAVE ABSORPTION, WAVE POLARIZATION, and WAVE REFRACTION.

wave refraction Bending of the line of propagation of electromagnetic waves as they pass through various media, such as the troposphere or the ionosphere. Compare WAVE ABSORPTION, WAVE POLARIZATION, and WAVE REFLECTION.

waveshape The overall contour of a wave—especially as revealed by a curve plotted for the particular wave equation. Also see WAVEFORM.

waveshaping circuit A circuit that receives an input signal having a certain waveshape, and delivers an output signal having a different waveshape. For example, a squaring circuit converts a sine wave into a square wave at the same frequency.

wave surface See WAVE FRONT.

wave tail In a decaying pulse or signal envelope, the interval between the beginning of the decay and the point at which the amplitude reaches zero.

wave telegraphy See RADIOTELEGRAPHY.

wave telephony See RADIOTELEPHONY.

wave theory of matter A physical theory that the charge of an electron is distributed in space, rather than being focused at a point. Also see WAVE MECHANICS.

wave tilt A slight forward tilt of the electric flux lines in a radio wave radiated at the surface of the earth by a vertical antenna.

wave train A series of identical electromagnetic wave cycles propagated at equal intervals; an electromagnetic energy burst lasting at least several cycles.

wavetrap A resonant circuit consisting of an inductor and capacitor, either or both of which can be adjustable for tuning, used to remove (trap) a signal at the resonant frequency from a signal mixture.

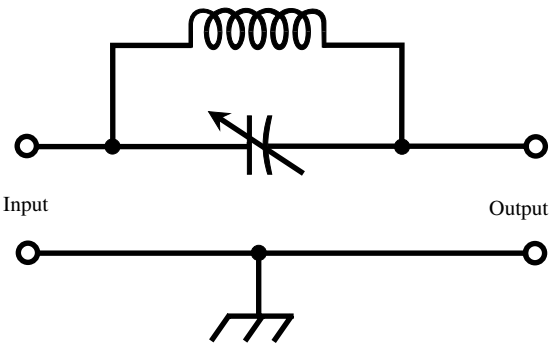

wavetrap

wave trough The minimum value of a wave envelope. Compare WAVE CREST.

wave velocity The distance per unit time traversed by a wave passing through a given medium.

wave winding See DRUM WINDING.

wa-wa pedal A foot-operated device used with an electronic musical instrument to produce a "wah-wah" sound fluctuation.

wax **1.** Any of a series of organic materials having important uses as dielectrics, impregnants, sealers, and lubricants in electronics. They are usually solid or semisolid, waterproof, and easily melted. **2.** In certain phonograph record discs, a blend of wax (see **1**, above) and metallic soaps. Also see WAX MASTER, **2**.

wax cake See WAX MASTER, **1**, **2**.

wax capacitor A fixed capacitor that has been dipped in or impregnated with a wax, such as halowax.

wax-dipped capacitor A fixed capacitor that has been dipped in a wax for sealing against moisture.

waxed paper See WAX PAPER.

wax-filled capacitor A fixed capacitor impregnated with a wax for enhancing the properties of its dielectric (usually paper) and sealing the capacitor unit.

wax master **1.** In disc-recording operations, the original recording made on a wax-surface disc. **2.** To make an original recording on a wax-surface disc.

wax original See WAX MASTER.

wax paper Wax-saturated paper used as a dielectric film in fixed capacitors and as an insulator.

way-operated circuit A single or duplex circuit shared by three or more party stations.

way point An important point selected on a radionavigational course line.

way station A station consisting of a teletypewriter connected at an intermediate point in a line (i.e., between, and in series with, other teletypewriter stations).

5059F-pW-738-758 4/10/01 10:09 AM Page 746

WAZ Amateur radio abbreviation of *Worked All Zones*, an award given to operators who have carried on verified two-way communication with stations in all communications zones of the world.

WB Abbreviation of *weather bureau.*

W_B Abbreviation of *base-region width* (in a transistor).

Wb Symbol for WEBER.

Wb/m^2 Abbreviation of *Webers per square meter* (see TESLA).

W_C Abbreviation of *collector-region width* (in a transistor).

WCEMA Abbreviation of *West Coast Electronic Manufacturers' Association.*

W/cm^2 Abbreviation of *watts per square centimeter.*

WE Abbreviation of *write enable.*

W_E Abbreviation of *emitter-region width* (in a transistor).

weak battery **1.** A battery that has been depleted to the point that its output (no-load or full-load) is too low to be useful. **2.** A battery specially designed for low-voltage output.

weak color Lack of color vividness or poor contrast between colors in a color-television picture. The condition is often caused by some malfunction in the chroma demodulator(s).

weak contrast In a television picture, poor differentiation of adjacent tonal areas.

weak coupling See LOOSE COUPLING.

weak current An extremely small electric current. The term is relative; generally, it refers to currents of a few microamperes or less.

weak magnet **1.** A magnet whose power has deteriorated considerably below a prescribed level. **2.** A body that normally is only slightly magnetic.

weak signal A signal whose amplitude is very low compared with that of signals considered satisfactory in a given application. Although the term is relative, it usually implies a signal that is noncompetitive with other signals in a given environment.

weak-signal detector A detector in which, at low input-signal amplitudes (weak-signal levels), the direct-current output is proportional to the square of the root-mean-square (rms) value of the input-signal voltage.

wearout The complete deterioration of a component or system (i.e., beyond restoration to useful service).

wearout failure Failure because of wearout, which can be predicted on the basis of known lifetime and the deterioration characteristics of components and equipment.

wearout point The instant of wearout, in terms of power output, watt-hour capacity, or some other specification.

weather antenna An antenna dimensioned for reception exclusively in the 162.4- to 162.55-MHz weather band. See WEATHER TRANSMISSION.

weathering Deterioration of electronic equipment as a result of exposure to outdoor heat, cold, moisture, wind, and similar conditions.

weather-protected machine A machine (usually a generator or motor) whose vent holes are designed to prevent entry of dust, water, and debris.

weather protection The coating, sealing, or treating of electronic equipment for protection against corrosion, humidity, and temperature changes in outdoor use.

weather satellite A satellite designed to photograph weather systems in infrared and/or visible light, and relay the pictures to earth via facsimile or television.

weather sonde See RADIOSONDE.

weather transmission The radio transmission of meteorological reports. Sometimes the transmissions are combined with guidance transmissions, from which they can be separated by means of a filter in the receiver.

weber Abbreviation, Wb. The SI unit of magnetic flux and of the magnetic flux quantum; 1 Wb = 10^8 maxwells = 1.257×10^{-7} unit pole.

Weber-Fechner law The law expressing the relationship between a stimulus and the physiological reaction it produces: The sensation is proportional to the logarithm of the stimulus.

weber per square meter Symbol, Wb/m^2. See TESLA.

weber turn A unit of magnetic flux linkage equal to 10^8 maxwell turns.

wedge **1.** In a waveguide, a termination consisting of a tapered block or plate of carbon (or other dissipative material). **2.** In a television test pattern, convergent, equally spaced lines for checking resolution.

wedge bonding In integrated-circuit fabrication, a method of bonding in which a thermocompression bond (see COLD-COMPRESSION WELDING) is obtained through pressure from a wedge-shaped tool.

Wehnelt cathode An oxide-coated cathode in an electron tube.

Wehnelt cylinder In a cathode-ray tube, the cathode-enclosing cylinder that concentrates the electrons emitted by the cathode.

weight **1.** The amount of gravitational pull on a body or particle. **2.** Extra significance given to a term or value. See, for example, WEIGHTED TERM. **3.** The dot-to-space ratio in a Morse-code signal.

weight-density Symbol, *d.* Unit, kg/m^3. The weight per unit volume of a liquid, such as an electrolyte or insulating oil; also called *density.*

weighted distortion factor In the measurement of harmonic distortion, a factor whose use allows the harmonics in the complex waveform to be weighted in proportion to their relationship.

weighted noise level Unit, dBm. The noise level weighted with respect to the 70-dB equal-loudness contour of hearing.

5059F-pW-738-758 4/10/01 10:09 AM Page 747

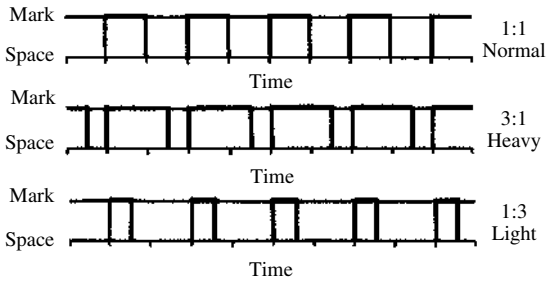

weight, 3

weighting **1.** Adjustment of a parameter to compensate for some imbalance in a system. **2.** Adjustment of the dot-to-space ratio in a Morse code signal. **3.** Adjustment of the mark-to-space ratio in a digital communications signal.

weighting filter A filter used in a communications network to represent the characteristics of the transmission passband.

weighting network A network that weighs differently (in a prescribed ratio) the frequency components appearing in an output signal by offering unequal attenuation to those frequencies.

weightlessness switch See ZERO-GRAVITY SWITCH.

Weir circuit In frequency-modulated signal transmission, a circuit used to stabilize the carrier wave. It compares the average carrier frequency with the frequency of a standard crystal oscillator, obtaining a direct-current compensating voltage (proportional to frequency deviation) that is applied to the frequency modulator. Also called *Weir stabilization circuit.*

Weiss constant In paramagnetism, a constant also known as *paramagnetic Curie temperature.* It can be positive or negative, depending on the particular paramagnetic material. It is important in defining the behavior of certain paramagnetic substances.

weld A strong bond of materials (usually metals) obtained by applying heat to areas to be joined while they are held or pressed together. No foreign metal is used, as is the case in brazing and soldering. The required heat is sometimes obtained by passing a high electric current through the materials.

welder **1.** An electrical device, often electronically controlled, for welding materials. **2.** A person who operates a device, as defined in **1**.

weldgate pulse In a welding device, the pulse that affects the arc current; therefore, it also affects the intensity of the heat produced by the device.

welding control An electronic system for controlling the interval during which current is passed through a workpiece in spot welding or seam welding. In this system, an electronic timer circuit determines the conduction time of thyratrons, ignitrons, or silicon-controlled rectifiers in the welding circuit. The control system can also regulate the welding current.

welding current The high electric current passed through a workpiece to produce the heat required for welding.

welding cycle The required sequence of steps (and the time required) in making a weld electronically.

welding time See WELD TIME.

welding transformer For electronic welding, a special very-high-current step-down transformer.

weld junction See WELD.

weld polarity The polarity of welding current. Some materials require a certain direction of current flow for a good weld.

weld time The interval during which welding current flows through the bodies to be bonded together.

well counter A radiation-counter setup in which a radioactive sample and detector are enclosed together in a thick-walled (usually lead) cylinder to minimize background count.

well-structured language An advanced form of high-level computer programming language. It is used in graphical and control applications.

Wenner element An adjustable, dual-slidewire balancing resistor used in constant-current, laboratory potentiometers to eliminate the necessity for sliding contacts in the measuring circuit.

Wenner winding A low-capacitance, low-inductance winding for high-frequency wirewound resistors in which the direction of the wire is reversed by looping alternate turns along the form.

Wertheim effect The tendency for a potential difference to develop between opposite ends of a length of wire, when the wire is placed parallel to magnetic lines of flux and rotated.

Western Union joint A strong splice of two wires made by tightly twisting a short portion of the tip of each wire along the body of the other. For increased ruggedness, the joint is often soldered. Also called *Western Union splice.*

Weston cell See STANDARD CELL.

Westrex system A system of sound recording in which signals from two separate microphone channels are recorded on opposite walls of a groove on a disc.

wet battery A battery of cells having a liquid electrolyte.

wet Liquid, especially pertaining to the electrolyte material in an electrochemical cell.

wet cell A battery cell having a liquid electrolyte. Compare DRY CELL.

wet-charged stand The length of time that a fully charged, wet storage cell can stand idle before its capacity drops by a specified amount.

wet electrolytic capacitor An electrolytic capacitor in which the electrolyte is a liquid. The leakage current in this type is higher than in the dry

5059F-pW-738-758 4/10/01 10:09 AM Page 748

electrolytic, but it is self-healing after momentary voltage breakdown. Compare DRY ELECTROLYTIC CAPACITOR.

wet grab The adherence of a pressure-sensitive tape or sheet to a surface when very little pressure is used.

wet rectifier See ELECTROLYTIC RECTIFIER.

wet shelf life The specified shelf life of a discharged, wet storage cell. Compare DRY SHELF LIFE.

wetted-contact relay See MERCURY-WETTED REED RELAY.

wetting Applying a mercury coating to a contact surface.

wetting agent A substance (such as an alcohol or ester) that promotes the spreading and adhesion of a liquid or its absorption by a porous material.

WG Abbreviation of WIRE GAUGE.

WH Abbreviation of WATT-HOUR.

wh Abbreviation of WHITE.

Wheatstone bridge A four-arm balancing circuit (see BRIDGE), having resistors in each arm and used to measure an unknown resistance in terms of a standard resistance. The bridge supply is usually direct current, but alternating current can be used if all four resistances are nonreactive.

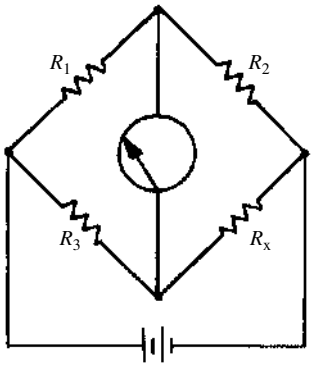

$R_x = R_3(R_2/R_1)$

Wheatstone bridge

wheel-drive locomotion The use of wheels for moving mobile apparatus such as robots. Offers simplicity and low cost. The main disadvantage is the inability to negotiate irregular terrain.

Wheeler's formula A formula for calculating the inductance of a multilayer air-core coil:

$$L = (0.8a^2n^2)/(6a + 9l + 10b)$$

where L is in microhenrys, a is the mean radius (inches) of the winding (axis to center of cross section), b is the depth of winding (inches), l is the length of winding (inches), and n is the number of turns.

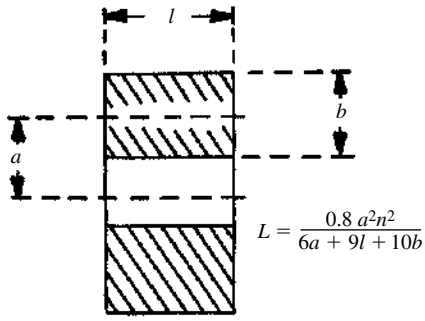

Wheeler's formula (dimensions illustrated)

wheel pattern A frequency test pattern produced on an oscilloscope screen by *z*-axis modulation of a circular trace. A sinusoidal axis signal produces a *gear-wheel pattern*, and a square-wave or pulse *z*-axis signal produces a *spot-wheel pattern.*

wheel printer A printout device for computers and calculators. It consists essentially of a rotating metal wheel around whose rim letters and numbers stand in relief. When the desired character comes into position, a hammer strikes it through the recording paper and carbon paper, printing the character on the recording paper. Also called *daisy-wheel printer.*

wheel static Static electricity (and the resulting radio interference) generated by friction between automobile tires and the road.

whiffletree switch In computer operations, a multiposition electronic switching circuit, so called from its circuit configuration, which resembles the contrivance used between a wagon and the horse team pulling it.

whip antenna A small-diameter, vertical rod (often telescoping) used as an antenna—especially in mobile communications, portable radio and television receivers, field-strength meters, etc.

whirl One of the circular, magnetic lines of flux around a straight wire carrying current.

whisker **1.** The pointer-wire electrode of a point-contact diode, point-contact transistor, or crystal detector. **2.** A slender filament of metal or ceramic, having high purity and high tensile strength.

whisker resistance In a semiconductor material, the resistance of a whisker component (see WHISKER, **1**).

Whiskey Phonetic alphabet code word for the letter W.

whistle A high-pitched tone (e.g., a beat note or acoustic feedback).

whistle filter A notch filter used to eliminate a whistle in an amplifier or other audio-frequency circuit. This filter can be of several versions, ranging from a simple resistance-capacitance

5059F-pW-738-758 4/10/01 10:09 AM Page 749

(RC) null circuit tuned to remove the offending frequency to a feedback-type band-suppression amplifier.

whistle interference The appearance of extraneous whistles in audio-frequency circuits. In some equipment, whistles result from oscillating amplifiers; in radio receivers, they are usually audible beat notes (heterodynes) produced by interfering carriers.

whistler A type of very-low-frequency (VLF) radio noise. They are thought to be caused by electromagnetic fields from distant lightning strokes, circulating in the earth's magnetic field. The name is derived from the peculiar sound the noise makes in a VLF radio receiver.

whistler mode propagation Radio transmission from the northern hemisphere to the southern hemisphere along the flux lines of earth's magnetic field.

whistlestop See WHISTLE FILTER.

whistling atmospheric See WHISTLER.

white The color that results from mixing all the additive primary colors: red, green, and blue.

white acid Hydrofluoric acid. Formula, HF. Used as an etchant, especially of glass.

white brass Brass that is more than 49% zinc.

white compression In television transmission, reduction of gain at highlight levels in the picture.

white-dot pattern In color-television tests with a dot generator, the one-white-dot pattern obtained when beam convergence has been secured.

white lamp See DAYLIGHT LAMP.

white level The lower-voltage point in a video signal, corresponding to full brilliance of the line on the screen (i.e., to the condition of whiteness in the picture).

white light See WHITE RADIATION, **2**.

white noise Random noise (acoustic or electric) equally distributed over a given frequency band, an example being the noise resulting from the random motion of free electrons in conductors and semiconductors.

white-noise generator A test device that generates electrical noise over a wide frequency spectrum. A simple type uses a reverse-biased silicon diode, the output of which is useful for testing audio amplifiers and radio receivers.

white-noise record A phonograph record containing recorded bands of white noise, each accompanied by voice announcements (e.g., instructions), and used to test the frequency response of a sound system.

white object A body that reflects and diffuses light of all wavelengths equally well.

white peak In a television picture signal, the maximum excursion in the white direction.

white radiation **1.** See WHITE NOISE. **2.** Visible light radiated with more or less equal intensity throughout the visible spectrum; seen as gray or white.

white raster See CHROMA-CLEAR RASTER.

white recording **1.** In amplitude modulation, recording characterized by a correspondence of maximum received power to minimum recording-medium density. **2.** In frequency modulation, recording characterized by a correspondence of lowest received frequency to minimum recording-medium density.

white room See CLEAN ROOM.

white saturation See WHITE COMPRESSION.

white signal The facsimile signal (see FACSIMILE) corresponding to scanning the copy area having maximum density.

white-to-black amplitude range **1.** At a point in a positive amplitude-modulated (AM) facsimile system (see FACSIMILE), the ratio (in dB) of signal current or voltage corresponding to white in the picture to that for black in the picture. **2.** At a point in a negative AM facsimile system, the ratio (in dB) of signal current or voltage corresponding to black in the picture to that for white in the picture.

white-to-black frequency swing At a point in a frequency-modulated facsimile system, the frequency difference $fw - fb$, where fb is the frequency corresponding to black in the picture, and fw is the frequency corresponding to white.

white transmission A system of picture or facsimile transmission in which the maximum copy darkness corresponds to the smallest amplitude (in an amplitude-modulated transmitter) or the highest instantaneous frequency (in a frequency-modulated transmitter). The opposite of BLACK TRANSMISSION.

white X radiation X rays of the continuous, or general, type.

whizzer An attachment that can improve the high-frequency reproduction in some audio loudspeakers.

whole-number division Arithmetic division (as in the division of binary numbers) in which the quotient is a whole number (i.e., division in which the divisor is contained in the dividend an integral number of times).

whorl See WHIRL.

WHP Abbreviation of *water horsepower.*

wick action **1.** The absorption of a liquid by, and its flow through, a cloth or thread, such as a lamp wick or lubricating wick. **2.** The flow of molten solder along and under the insulation of a wire.

wicking See WICK ACTION.

wide-angle diffusion A form of diffusion characterized by the wide-angle scattering of light; causes the source to have the same brightness at all viewing angles.

wide-area network A group of computers linked together, but separated by large geographic distances. Links can be made via telephone lines or radio.

wide-area service A teletype network that operates over long-distance wire lines.

Wide Area Telephone Service See WATS.

5059F-pW-738-758 4/10/01 10:09 AM Page 750

wideband **1.** Having a bandwidth greater than the minimum necessary to transmit a signal with acceptable intelligibility. **2.** For a voice signal, having a bandwidth greater than 6 kHz. **3.** Having the capability to operate, without adjustment, over a broad and continuous range of frequencies or wavelengths. **4.** In a digital network, a channel having a bandwidth of more than 64 kbps but less than 2 Mbps.

wideband amplifier An amplifier that exhibits reasonably flat response to a broad band of frequencies. The term is relative, depending on the application.

wideband antenna An antenna that transmits or receives signals over a broad frequency range, usually without the need for tuning.

wideband axis In a color-television signal, the direction of the fine chrominance primary phasor.

wideband communications **1.** Communications carried out over a band of frequencies wider than the minimum necessary for effective transfer of the information. **2.** A method of transmitting and receiving signals by deliberately varying the channel frequency over a wide range. Also called *spread-spectrum communications.*

wideband generator A signal generator covering a wide frequency range. Typical coverage in a laboratory-type instrument is 10 kHz to 1000 MHz.

wideband oscilloscope An oscilloscope whose horizontal, vertical, and sweep channels operate over a wide band of frequencies. Although the term wideband is relative, a wideband oscilloscope is usually assumed to be capable of displaying both radio and audio frequencies.

wideband ratio The ratio *B1*/*B2*, where *B1* is frequency bandwidth and *B2* is intelligence bandwidth.

wideband receiver A radio receiver that can tune in signals over a broad range of frequencies. An example is a communications receiver that can cover 10 kHz to 30 MHz continuously.

wideband repeater A repeater capable of operating over a wide range of input and output frequencies. Such repeaters are used in active communications satellites handling many different channels at the same time.

wideband signal generator See WIDEBAND GENERATOR.

wideband sweep **1.** In the operation of an oscilloscope, a repetitive sweep of the electron beam, the frequency of which is adjustable to any desired point within a wide range. The basic sweep rate in simple oscilloscopes is restricted to the audio-frequency spectrum (up to about 20 kHz), but a wideband sweep extends to much higher frequencies, typically several tens of MHz. **2.** A sweep circuit that produces the wideband sweep action described in **1**.

wideband test meter An alternating-current (ac) meter that can measure quantities over a wide frequency range in its basic form (i.e., without special external probes or converters). An example is an electronic ac voltmeter with a range extending from 10 Hz to 2.5 MHz.

wide-base diode A junction diode in which the p region is considerably wider than the n region.

wide-open **1.** Pertaining to wideband, untuned response. **2.** Pertaining to maximum-gain operation (e.g., a wide-open amplifier or receiver).

wide-range ammeter An ammeter that employs one or more shunt resistances to increase the full-scale deflection, usually by a power of 10 (10, 100, 1000, etc.). The resistor must be capable of carrying the current without burning out. Shunts are used when it is necessary to measure very large currents, such as hundreds of amperes. Shunts also allow a microammeter or milliammeter to be used as a multimeter with many current ranges.

wide-range reproduction High-fidelity audio-frequency reproduction.

width **1.** The horizontal dimension of a pulse, usually corresponding to its effective duration; also called PULSE DURATION. **2.** The horizontal dimension of an image, such as a television picture.

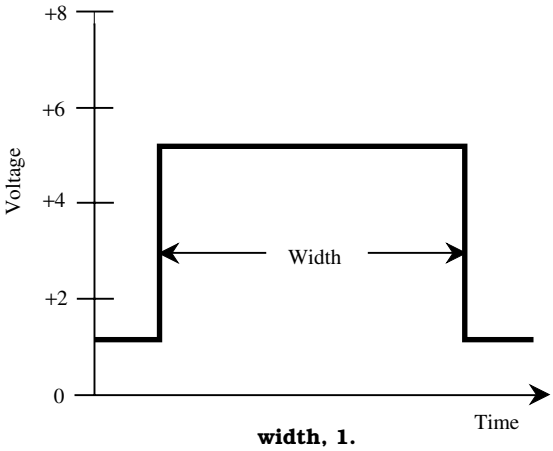

width, 1.

width coding The modification of pulse duration according to a code.

width coil See WIDTH CONTROL, **1**.

width control **1.** In a television receiver, the variable component for adjusting the swing of the horizontal deflection voltage and, therefore, the width of the picture. It is often a slug-tuned coil connected in parallel with a portion of the secondary winding of the horizontal output transformer. **2.** Sometimes, the horizontal gain control in an oscilloscope.

width mode In electronic-counter operations, a time-interval mode in which the signal is measured.

5059F-pW-738-758 4/10/01 10:09 AM Page 751

width modulation Modulation of the interval during which a gate circuit is open.

Wiedemann effect See DIRECT WIEDEMANN EFFECT.

Wiedemann-Franz law For metals that are good electrical conductors, the ratio of thermal conductivity to electrical conductivity is nearly constant, and is proportional to the absolute temperature.

Wien bridge A frequency-sensitive bridge in which two adjacent arms are resistances and the other two adjacent arms are resistance-capacitance (RC) combinations. One of the latter contains resistance and capacitance in series; the other contains resistance and capacitance in parallel. Because the bridge can be balanced at only one frequency at a time, it is useful as a simple audio frequency meter (see BRIDGE-TYPE AF METER). It is used also for capacitance and resistance measurements. When inductors are substituted for the capacitors, the Wien bridge can be used for inductance measurements (see WIEN INDUCTANCE BRIDGE).

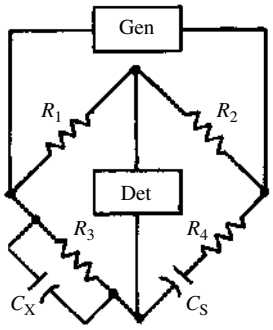

Wien bridge

Wien-bridge audio frequency meter See WIEN-BRIDGE FREQUENCY METER.

Wien-bridge distortion meter A distortion meter in which a Wien bridge circuit is used to remove the fundamental frequency from the complex waveform. The bridge is inserted between amplifier stages, and its notch response is sharpened by means of overall negative feedback.

Wien-bridge equivalent A resistance-capacitance null circuit, such as the parallel-tee (twin-tee) network, which has the same balance equation as the Wien bridge.

Wien-bridge filter A Wien bridge used as a band-suppression filter (notch circuit).

Wien-bridge frequency meter A bridge-type audio frequency meter in which the continuously variable frequency-selective circuit is a Wien bridge. Also see BRIDGE-TYPE AF METER.

Wien-bridge heterodyne eliminator A notch filter composed of a continuously variable Wien-bridge circuit (see WIEN BRIDGE). The device is connected in the audio-frequency channel of a radio receiver, and is tuned to remove a troublesome heterodyne whistle.

Wien-bridge oscillator An oscillator in which the frequency-selective feedback network is a Wien-bridge circuit (see WIEN BRIDGE). Also see BRIDGE-TYPE OSCILLATOR.

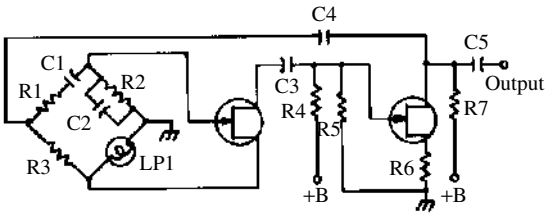

Wien-bridge oscillator

Wien capacitance bridge A Wien bridge arranged for the measurement of unknown capacitance.

Wien effect For an electrolytic substance, an increase in conductivity (decrease in resistivity) that occurs when a very large voltage is placed across the material. This voltage must be greater than approximately 1 megavolt per 50 cm.

Wien inductance bridge A Wien bridge containing inductors in place of capacitors and used for the measurement of unknown inductance.

Wien's displacement law The wavelength of maximum radiation of a black body is inversely proportional to the absolute temperature.

Wien's first law See WIEN'S DISPLACEMENT LAW.

Wien's laws See WIEN'S FIRST LAW, WIEN'S SECOND LAW, and WIEN'S THIRD LAW.

Wien's radiation law See WIEN'S SECOND LAW.

Wien's second law The emissive power of a black body is proportional to the fifth power of the absolute temperature.

Wien's third law An empirical law for the spectral distribution of energy radiated from a black body at a specified temperature. The distribution is a curve with a peak (maximum) at a wavelength that depends on the temperature. The higher the temperature, the shorter the wavelength at which maximum radiation occurs.

willemite See ZINC ORTHOSILICATE PHOSPHOR and ZINC SILICATE PHOSPHOR.

Williams tube A type of electrostatic cathode-ray storage tube.

Wilson chamber See WILSON CLOUD CHAMBER.

Wilson cloud chamber An airtight chamber containing water vapor or alcohol vapor at low pressure, and provided with a viewing window.

5059F-pW-738-758 4/10/01 10:09 AM Page 752

Radioactive particles penetrating the chamber are made visible as droplets form trails when the vapor condenses on them.

Wilson effect Electric polarization of a dielectric material being moved in a magnetic field.

Wilson electroscope A leaf-type electroscope (see ELECTROSCOPE) using a single leaf hanging vertically.

Wilson experiment An experiment demonstrating the WILSON EFFECT. It consists of rotating about its axis a hollow dielectric cylinder (whose inner and outer surfaces are metallized) in a magnetic field parallel to the axis. The result: An alternating voltage appears between the metallized surfaces.

Wimshurst machine A rotating machine used to produce high-voltage static electricity. The machine contains two glass disks, each having separate sectors of metal foil spaced around its face. The disks rotate in opposite directions, and the foil sectors passing each other form variable capacitors. Metal brushes pick up charges from the sectors passing under them and deliver this energy to one or more Leyden jars for storage.

wind charger A wind-driven generator used specifically to supply direct current for charging storage batteries.

wind-driven generator A dynamo-type generator, either stationary or mobile, powered by a windmill-like device.

wind gauge See ANEMOMETER.

winding **1.** A coil in an inductor or transformer (e.g., *primary winding*, *secondary winding*, *output winding*, etc.). **2.** A coil in a motor or generator.

winding arc The winding length of a coil, expressed in degrees.

winding cross section The cross section of a multilayer coil.

winding depth The depth of a multilayer coil, measured from the outermost layer to the innermost layer.

winding factor For a transformer or choke coil (or for a toroidal coil), the ratio of the total area of wire in the window to the window area.

winding length The length of a coil from the first turn to the last in a single-layer coil, or from the first turn to the last in one layer of a multilayer coil when all layers are identical.

winding space The window area of the core of a transformer or choke (see WINDOW, **3**).

wind loading **1.** The total wind pressure on an antenna system, generally measured in pounds or kilograms. The greater the wind speed, the greater the wind loading for a given antenna. The greater the exposed surface of the antenna, the greater the wind loading for a given wind speed. **2.** The highest wind speed, in miles per hour or meters per second, that an antenna system can safely withstand, assuming no accumulation of ice on the antenna structure.

Windom antenna **1.** A multiband antenna in which a single-wire feeder is attached to a horizontal half-wave radiator wire somewhat off center, at a point about ⅛ wavelength from one end of the radiator. The antenna operates with reasonable efficiency at the first several harmonics of the frequency at which it measures ½ wavelength. **2.** A similar antenna using a parallel-wire feeder.

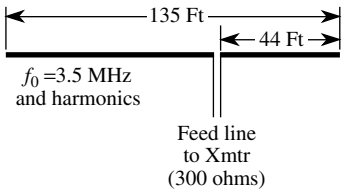

Windom antenna, 2

window **1.** Radar-interference material (see CHAFF). **2.** An interval during which a circuit is gated open to permit signal sampling. During this interval, a window is figuratively open to the signal. **3.** The open spaces between the legs of an iron core for a transformer or choke coil. **4.** An electromagnetic frequency band easily transmitted by earth's atmosphere. **5.** The period during which conditions are ideal for a complex operation, such as a rocket or spacecraft launch. **6.** An application space in a computer program that uses a graphical interface.

window area See WINDOW, **3**.

window comparator A comparator that detects voltage levels within a certain range of values, rather than simply indicating whether a voltage is more or less than a certain specified value.

window corridor An area where window (see WINDOW, **1**) has been dispersed.

window jamming The disturbance of electronic communications, especially radar, by dumping reflective material, such as metal foil, from an aircraft. Also see CHAFF; JAMMING; and WINDOW, **1**.

Windows Trade name (Microsoft) for a personal-computer interface scheme. The several versions all use selectable icons and menus.

window strip An insulated, flat, metal strip for bringing an antenna lead-in through a window. The window can be closed on the strip.

wind screen A foam covering that can minimize the roar caused by wind blowing against or across a microphone.

wind shield A radio-transparent cover placed over a radar antenna to protect it against damage from high winds. It is used especially in radar systems aboard aircraft.

wing In an antenna or other radiator, a (usually flat) member attached to, and sticking out from,

5059F-pW-738-758 4/10/01 10:09 AM Page 753

another member. Its name is derived from its characteristic shape.

winterization The protective treatment and preparation of electronic equipment for winter storage or for operation in frigid regions.

wipeout Severe interference that obliterates all desired signals.

wipeout area An area in which WIPEOUT occurs.

wiper **1.** A thin metal blade or strip in sliding contact with a coil or other element over which it is turned to vary some quantity (such as resistance, inductance, voltage, current, etc.). **2.** A brush in a motor or generator.

wiper arm See WIPER, **1**.

wiper blade See WIPER, **1**.

wiping action The movement of contacts against each other when they slide as they mate or withdraw.

wiping contact A contact that makes and breaks with a sliding motion.

wire **1.** A metal strand or thread serving as a conductor of electricity. **2.** To connect wires between points in a circuit. **3.** See TELEGRAM. **4.** To send a TELEGRAM.

wire bonding **1.** The interconnection of components within a discrete package, by means of fine wire conductors welded to the individual components. **2.** A method of temporarily splicing the outer conductors of two coaxial cables. **3.** In general, any solderless method of splicing between two conductors.

wire broadcasting Broadcasting by means of carrier-current communication (see WIRED RADIO).

wire cloth A net of fine wire, used as an electrical shield when air circulation is necessary.

wire communication Communication carried on by means of signals transmitted over wire lines, as opposed to wireless (radio) communication.

wire control The control of remote devices by means of signals transmitted over wire lines, as opposed to radio control.

wire core A magnetic core consisting of a bundle of iron (or magnetic alloy) wires.

wired AND See DOT AND.

wired-in component A component to which wires are permanently connected in a circuit, as opposed to a plug-in component.

wired OR See DOT OR.

wired-program computer A computer in which instructions are wired-in by making appropriate connections to a panel with patch cords.

wired radio The transmission and reception of voice and other sounds, telegraph signals, pictures, control signals, telemetry signals, and the like by means of radio-frequency energy conducted by wire lines. Usually, the lines are used primarily for some other purpose (e.g., power lines or telephone lines).

wired-radio receiver The complete device or system that selects, amplifies, and demodulates or rectifies a radio signal picked up from wires that conduct it from a transmitting station.

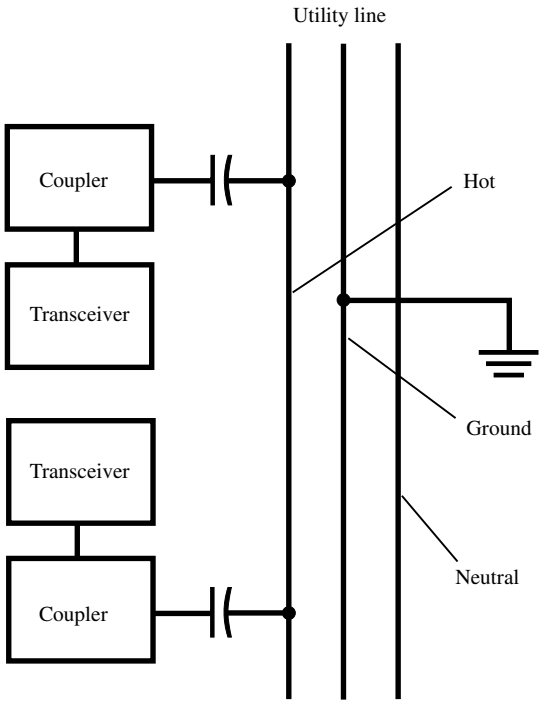

wired radio

wired-radio transmitter The complete device or system that generates radio-frequency power, adds signals (for communication, remote control, telemetry, etc.), and delivers the power to wires or to a cable for reception at a distant point.

wire drawing In the manufacture of wire, pulling metal through special dies to form wire of selected diameter.

wire dress The careful arrangement of wires in a chassis to ensure optimum performance. Also called *lead dress* (see DRESS).

wire duct A conduit through which wires are run. Such ducts have several shapes, but generally are rectangular.

wired wireless See WIRED RADIO.

wire-equivalent security See LEVEL-1 SECURITY.

wire fuse A fuse in which the fusible element is a wire of low-melting-point metal. Compare STRIP FUSE.

wire gauge **1.** A system for specifying the characteristics of wire. See AMERICAN WIRE GAUGE and BIRMINGHAM WIRE GAUGE. **2.** A wire number governed by diameter (e.g., 18-gauge wire for #18 wire). **3.** A tool or instrument for measuring wire diameter or for determining wire number.

5059F-pW-738-758 4/10/01 10:09 AM Page 754

wire gauze A fine screen of thin wires.

wire grating See WAVEGUIDE GRATING.

wire-guided Pertaining to guiding a machine, such as a robot, by means of signals sent by wire from the control point.

wire leads Leads that are (usually thin, flexible) wires, rather than pins, bars, strips, etc. An example is the wire leads of some transistors (as opposed to terminal pins).

wireless **1.** Pertaining to data communications and control systems that operate without wires (e.g., an infrared link between a notebook computer and a desktop computer). **2.** An early name for radio; it is still used in some countries. Sometimes for specificity, radio is referred to as *wireless telegraphy* or *wireless telephony*. See RADIOTELEPHONY.

wireless access protocol Acronym, WAP. A communications standard used on a worldwide basis with portable cellular telephone sets incorporating electronic mail, online service access, and/or Internet access.

wireless broadcaster See WIRELESS MICROPHONE.

wireless compass A radio compass (see DIRECTION FINDER).

wireless device A device that operates over a distance, without the use of interconnecting wires.

wireless e-mail **1.** The use of electronic mail (e-mail) in conjunction with a wireless Internet service. **2.** The use of a specialized portable wireless communications device, resembling a stripped-down computer or an enhanced cell phone, to send and receive e-mail messages.

wireless intercom An intercom using wired-radio for transmission and reception over the power line from which it is operated. Also see WIRED RADIO.

wireless Internet **1.** The use of a personal computer, usually a notebook or portable, in conjunction with a wireless modem connected to the Internet. Services of this type are provided with high-end cellular telephone subscriptions. Assets and limitations are similar to those associated with cell phone services. **2.** The use of a specialized portable or mobile wireless communications device, resembling a stripped-down computer or an enhanced cell phone, for basic Internet communications and information retrieval.

wireless microphone A device consisting of a small radio-frequency oscillator modulated by the microphone to which it is attached, and provided with a tiny antenna. The modulated signal is picked up and reproduced by a radio receiver.

wireless modem **1.** A modem that facilitates connection of a computer to the Internet using a cell phone set. **2.** A wireless transceiver that facilitates connection of a computer to the Internet. A cellular telephone connection can be included as an option. **3.** Also called *cordless modem*. A pair of short-range (on the order of a few feet) radio or infrared transceivers. One unit connects to a telephone jack or cable port, and the other unit connects to a computer. Can protect a portable computer against damage by lightning, assuming the computer uses batteries and is not connected to utility mains.

wireless tap A method of eavesdropping on communications in which a portion of the circuit makes use of a radio-frequency wireless link. An eavesdropping receiver can be positioned within range of the wireless transmitting antenna, and the signals intercepted. The existence of such a tap causes no change in the electronic characteristics of any equipment in the system, so its deployment is difficult to detect even if eavesdropping is anticipated.

wireless telegraphy See RADIOTELEGRAPHY.

wireless telephone **1.** A radio transceiver interconnected with the telephone lines. **2.** A telephone in which a short-range radio link replaces the cord between the receiver and the base unit. It normally has a range of several hundred feet.

wireless telephony See RADIOTELEPHONY.

wire line One or more wires or cables conducting currents for communication, control, or measuring purposes.

wire link A line for wire communication or wire control.

wire-link telemetry Telemetry carried on over a wire link.

wireman **1.** An electrician who specializes in the installation and servicing of electrical wiring. **2.** See LINEMAN.

wire mile A unit of measure equal to the product *ns*, where *n* is the number of separate, equal-length conductors in a line, and *s* is the length of a conductor in miles.

Wirephoto **1.** A system for transmitting and receiving photographs over wire lines. Also called *Telephoto*. See FACSIMILE. **2.** A photograph transmitted and/or received, as defined in **1**. **3.** A trademark for a photograph transmitted and received over telephone lines.

wire printer A printout device consisting of a wire array in which each wire is activated by an electromagnet. When a wire is selected (electrically), it is pushed against, and makes a dot on the recording paper. The letters and figures, then, are dot patterns. Compare WHEEL PRINTER.

wire radio See WIRED RADIO.

wire recorder In audio applications and data recording, a machine that records sounds or data pulses in the form of magnetized spots on a thin wire.

wiresonde A system for transmitting weather information data through a cable that holds a captive balloon. Compare RADIOSONDE.

wire splice A strong, low-resistance joint between (usually two) wires. See, for example, WESTERN UNION JOINT.

5059F-pW-738-758 4/10/01 10:09 AM Page 755

wire stripper A hand tool or power machine for cutting the insulating jacket on a wire and removing it without cutting or nicking the wire.

wiretap **1.** An instance of wiretapping. **2.** A wiretapping device.

wiretapper **1.** A device for wiretapping. **2.** A person who practices wiretapping.

wiretapping The act of making direct or indirect connections to a communications line to overhear or record a conversation.

wire telegraphy Telegraphic communication carried on by means of signals transmitted over wire lines, as opposed to wireless (radio) telegraphy.

wire telephony Voice communication carried on by means of signals transmitted over wire lines, as opposed to wireless (radio) telephony.

wire tie See TIE.

wire wave communication See WIRED RADIO.

wireways Hinged-cover metal troughs for containing and protecting wires and cables. Also see WIRE DUCT.

wirewound potentiometer A potentiometer in which the resistance element is a coil of resistance wire wound on a cord bent into a cylinder, or on a rigid, circular core.

wirewound resistor A resistor made from a coil of wire that is a poor conductor. The wire is usually wound around a cylindrical form; some components use toroidal forms. The resistance is determined by how well the wire metal conducts, by its diameter (gauge), and by its length. This type of resistor can be manufactured to precision tolerance. If the wire gauge is heavy, it can dissipate large amounts of power. The component has inductive reactance, making it unsuitable for use at radio frequencies. Compare CARBON-COMPOSITION RESISTOR, FILM RESISTOR.

wirewound rheostat A rheostat in which the resistance element is a coil of resistance wire wound on a card bent into a cylinder, or on a rigid, circular core.

wire wrap A method of circuit-board wiring in which components are interconnected by individual wire conductors, the ends of which are wrapped around terminal posts using a special tool.

wire-wrap connection An electrical connection made by tightly wrapping a bare wire around a special terminal.

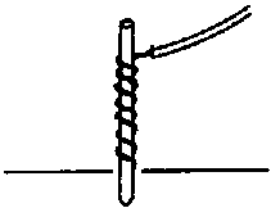

wire wrap

wire-wrapping tool A device used to make a wire-wrap connection.

wiring **1.** The system of wires or similar conductors connected between circuit components. **2.** Connecting and dressing such wires, as in wiring a circuit. **3.** Collectively, the connections (either actual wire or printed metal lines or processed semiconductor paths) between terminals and components in an electronic circuit. **4.** The process of installing or making such connections.

wiring board The control panel of a computer (i.e., a plugboard).

wiring capacitance Unavoidable capacitance between wires in a circuit, or between the wires and nearby metal bodies.

wiring connector A small (usually metal) fitting used to tie wires together.

wiring diagram See CIRCUIT DIAGRAM.

wiring impedance Unavoidable impedance in the wires in a circuit, and in associated terminals and hardware conducting alternating current. This impedance is the vector sum of WIRING REACTANCE and WIRING RESISTANCE.

wiring inductance Unavoidable inductance in the wires in a circuit, and in associated terminals and other hardware, through which alternating currents flow.

wiring reactance Unavoidable reactance in the wires in a circuit, and in associated terminals and other hardware, conducting alternating current. This reactance is caused by WIRING CAPACITANCE and/or WIRING INDUCTANCE.

wiring resistance Unavoidable resistance in the wires in a circuit and in associated terminals and other hardware.

Witka circuit A voltage-tripler circuit using only two diodes and two capacitors. Its no-load direct-current output voltage is approximately three times the peak value of the alternating-current input voltage. Also see VOLTAGE TRIPLER.

wk **1.** Abbreviation of WORK. **2.** Abbreviation of *week.*

WL **1.** Abbreviation of WAVELENGTH. **2.** Abbreviation of *waterline.*

WM Abbreviation of WATTMETER.

Wm^2 Symbol for *watt square meter* (unit of the first radiation constant).

W/(MK) Symbol for *watts per meter kelvin* (unit of thermal conductivity).

WMO Abbreviation of *World Meteorological Organization.*

wobbulator A device that sweeps the frequency of an oscillator. There are several types, from a motor-driven, rotating, tank capacitor to sophisticated, fully electronic variable capacitors or variable inductors.

wolfram See TUNGSTEN.

Wolf's equation A sunspot-number equation used to forecast maximum usable frequency: $R = k(10G + N)$, where R is relative sunspot number, k is a constant for the telescope used, G is the

5059F-pW-738-758 4/10/01 10:09 AM Page 756

number of sunspot groups observed, and *N* is the total number of sunspots.

Wollaston wire An extremely fine wire made by coating platinum with silver, drawing it thinner, and dissolving the silver coat.

womp A sudden surge in amplitude that causes a flare up of brightness in a television picture.

woodpecker A slang term used to describe the sound of the signal from over-the-horizon radar. Operating in the high-frequency part of the spectrum and changing in wavelength, roughly following the maximum usable frequency, the signal consists of repeated "spikes" that can interfere with routine communications.

woodpecker filter A special type of blanking filter used to quiet a shortwave receiver during strong, brief "spikes." It is similar to a noise blanker, but is designed to filter out the longer peaks characteristic of the over-the-horizon radar, known as the WOODPECKER.

Wood's alloy See WOOD'S METAL.

Wood's metal A low-melting-point (159.8°F) alloy containing bismuth (50%), cadmium (12.5%), lead (25%), and tin (12.5%). The alloy looks like lead and is used to mount rectifying crystals (such as galena) whose electrical sensitivity would be destroyed by the high temperatures required to melt most soft metals.

woofer A large loudspeaker, often a foot or more in diameter, designed specifically to reproduce very low (bass) audio frequencies. It is commonly used in high-fidelity stereo sound systems. Compare TWEETER.

word **1.** In computer operations, a group of bits or characters treated as a unit. **2.** In telegraphy, a data unit consisting of five characters plus one space.

word-address format A method of addressing a word by means of a single character, such as the first letter of the word.

word code **1.** A cipher in which word meanings are interchanged, rather than letter symbols. **2.** A word having an altered meaning in a cipher system, as defined in **1**. For example, "word" might mean "code."

word format The specific sequence of characters that forms a word of data.

word generator A special signal generator that delivers pulses in selected combinations corresponding to digital words (see WORD, **1**). It is used in testing computers and digital systems.

word length **1.** In computer operations, the number of bits in a word. **2.** In telegraphic communications (radio or wire), the average number of letters in a word.

word pattern The shortest meaningful word (see WORD, **1**, **2**) that can be recognized by a machine.

word processor **1.** An electronic device, similar to a typewriter, used for writing. Words, phrases, sentences, or paragraphs can be changed, replaced, or deleted prior to the final printout. **2.** A computer used for writing, as defined in **1**. **3.** Software that allows a computer to be used for writing, as defined in **1**.

word rate In a communications or computer system, the number of words per unit time (e.g., WORDS PER MINUTE).

word size See WORD LENGTH.

words per minute In telegraphy, a measure of data speed. It is approximately equal to the number of characters (including spaces) per minute divided by 6.

word time In computer operations, the time required to process one word that is in storage.

work **1.** Symbol, *W*. Units: joule, erg, foot-pound, kilogram-meter. That which is accomplished by the transfer of energy from one body to another, as when an exerted force causes a displacement. The amount of work performed is equal to force times distance: $W = Fd$. **2.** An amateur radio term meaning to engage in two-way communication with another station.

work area In computer operations, a temporary area of memory for data items being processed. Also called INTERMEDIATE STORAGE, WORKING MEMORY, and WORKING STORAGE.

work coil The alternating-current-carrying coil that induces energy in the workpiece in induction heating.

work envelope The range of motion over which a robot arm can move. It can be two-dimensional or three-dimensional.

work function Unit, eV. The energy required to bring an internal particle to the surface of a material and out into space, as when an electron is emitted by the hot cathode of a vacuum tube. The work function is the voltage required to extract 1 electrostatic unit of electricity from the material.

working data file A temporary accumulation of data sets that is erased or otherwise discarded after its transferal to another medium.

working life The expected or guaranteed lifetime of a material, device, or system in actual operation or use. Compare SHELF LIFE.

working memory See WORK AREA.

working point The operating point of an active device (i.e., the point along one of the characteristic curves around which operation is fixed).

working *Q* The *Q* of a loaded circuit or device (e.g., tank-circuit *Q* of a radio transmitter loaded with an antenna or dummy load).

working range **1.** The usable maximum distance between a transmitter and receiver in a wireless communications circuit. **2.** The allowed range over which specified parameters can vary in a particular system while facilitating normal operation, or operation within rated specifications.

working storage See WORK AREA.

working voltage The (usually maximum) voltage at which a circuit or device can be operated continuously with safety and reliability.

5059F-pW-738-758 4/10/01 10:09 AM Page 757

workout **1.** A dry run; a test. Example: checking a computer's processing power using a set of benchmark programs. **2.** An exacting test of equipment; a burn-in procedure.

workpiece The object heated by an induction or dielectric heater.

worm A cylindrical gear whose spiral "teeth" resemble a screw thread.

worm drive A mechanism for transferring motion from a tuning-knob shaft through a right angle to the shaft of an adjustable component, such as a potentiometer or variable capacitor. The knob turns a threaded shaft that mates with a gear wheel.

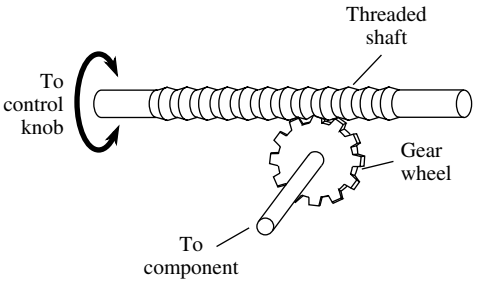

worm drive

worst-case circuit analysis Analysis that seeks the worst possible effects of variations in circuit parameters on circuit performance—especially variations in component characteristics.

worst-case noise pattern See DOUBLE-CHECKERBOARD PATTERN.

worst-case design The design of electronic equipment in such a way that normal operation is obtained—even though the characteristics of circuit components might vary widely.

woven resistor A resistance element made of strands of resistance material woven in the form of gauze.

wow Slow, periodic variations in the pitch of reproduced sound because of variations in the speed of the drive mechanism. Its name is derived from its characteristic sound. Compare FLUTTER.

wow meter An instrument that indicates the amount of wow produced by a turntable or other moving part.

Wpc Abbreviation of *watts per candle.*

wpm Abbreviation of *words per minute.*

wrap See WIRE-WRAP CONNECTION.

wrap-around **1.** The extent of curvature in magnetic tape passing over the heads during recording or playback. **2.** An enclosure that resembles a sheet (wrapped around a piece of electronic equipment). **3.** In computer and data-processing operations, a technique in which the display is cleared of data once it is filled (all available lines are occupied) and additional data is traced from top to bottom.

wrap joint See WIRE-WRAP CONNECTION.

wrapper A paper or tape wound around a component, such as a coil or capacitor, for insulation and protection.

wrapping **1.** See WRAPPER. **2.** Insulating a wire or other conductor by wrapping insulating tape around it.

wrap post A terminal post, tip, pin, or lug used in a wire-wrap connection.

wrap-up The (usually successful) completion of a design, fabrication, test, or investigation.

Wratten filter A light filter for separating colors. It is available in transparent sheets of various colors and is useful in photography and in several phases of electronics, including the operation of color meters and color matchers.

wrinkle finish A pattern of fine wrinkles created by special paint when it dries on a surface, such as that of a metal cabinet for a piece of electronic equipment.

wrist-force sensor In robotics, a set of strain gauges that detects the various forces in the joint connecting an end effector to an arm, and sends signals back to the robot controller. The controller can use the signals to direct the movements of the arm and end effector.

write **1.** In computer operations, to transfer data from one form of memory or storage to another form. Example: To transfer data in a computer from random-access memory (RAM) to the hard disk. Compare READ. **2.** To produce an image on the storage mesh in the cathode-ray tube of a storage oscilloscope.

write enable ring See WRITE PERMIT RING.

write gun See WRITING GUN.

write head In a magnetic memory or in a tape recorder or wire recorder used for recording data, the head that magnetizes the drum, tape, disk, or wire. Compare READ HEAD.

write pulse In computer operation, the pulse that causes information to be recorded in a magnetic cell, or sets it to the one-state. Compare READ PULSE.

write time The time taken to write data to a storage device.

writing gun In a storage oscilloscope, the electron gun that produces the image electronically on the storage mesh. It is mounted in the rear of the cathode-ray tube. Compare FLOOD GUN.

writing head See WRITE HEAD.

writing rate In photographing the image on a cathode-ray tube screen, the highest spot speed at which an acceptable picture can be made.

writing speed See WRITING RATE.

writing telegraph See TELAUTOGRAPH.

wrong color The instance of an undesired color (e.g., purple instead of red) in a color-television picture. The condition is often caused by a malfunction of the chroma demodulator(s).

5059F-pW-738-758 4/10/01 10:09 AM Page 758

W/(sr•m²) Abbreviation of *watts per steradian square meter.*

WT **1.** Abbreviation of wireless telegraphy. **2.** Abbreviation of WATERTIGHT.

wt Abbreviation of WEIGHT.

WUI Abbreviation of *Western Union International.*

Wulf electrometer See BIFILAR ELECTROMETER.

Wullenweber antenna An electronically steerable antenna composed of two concentric circular arrays of masts connected to the steering circuitry.

WUX Abbreviation of *Western Union telegram.*

WVdc Abbreviation of *direct-current working voltage:* the maximum continuous direct-current voltage that can safely be placed across a component.

ww Abbreviation of *wirewound.*

W/sr Abbreviation of *watts per steradian* (unit of radiant intensity).

WWV The call letters of a standard-frequency/standard-time broadcasting station operated by the National Bureau of Standards and located in the continental United States. Also see WWVH.

WWVH The call letters of a standard-frequency/standard-time broadcasting station operated by the National Bureau of Standards and located in Hawaii. Also see WWV.

wx Radiotelegraph abbreviation of weather.

WXD International Telecommunications Union symbol for *meteorological radar station.*

WXR International Telecommunications Union symbol for *radiosonde station.*

wye adapter A connector that provides two outputs for a single input, or vice versa. It is commonly used in audio applications.

wye box In a three-phase power-measuring setup, a special arrangement of two impedances, each of which is equal to the impedance of the potential element of the wattmeter used in the setup. The box permits a single wattmeter to be used, which indicates one-third the total power. Without the box, three wattmeters would be needed.

wye connection A method of connecting three windings in a three-phase system so that one terminal of each winding is connected to the neutral point. It is shaped like the letter Y. Also called *star connection.*

wye current Current through one of the branches of a three-phase star (wye) connection.

wye delta starter A starter circuit for a three-phase squirrel-cage induction motor. When the starter switch is thrown in one direction, the stator of the motor is wye-connected for starting; thrown in the opposite direction, the stator is delta-connected for continued operation.

wye equivalent circuit A wye-connected three-phase circuit equivalent to a delta-connected circuit when the impedance of any pair of corresponding lines for both wye and delta are the same; the third line is unconnected.

wye junction See WAVEGUIDE WYE.

wye-matched-impedance antenna An antenna in which the impedance of a nonresonant open-wire feed line is matched to that of the center of the radiator by spreading the end of the feeder wires out into a Y-shaped or delta-shaped matching section. Also called DELTA-MATCHED-IMPEDANCE ANTENNA.

wye point The star point in a three-phase system. Also see WYE CONNECTION.

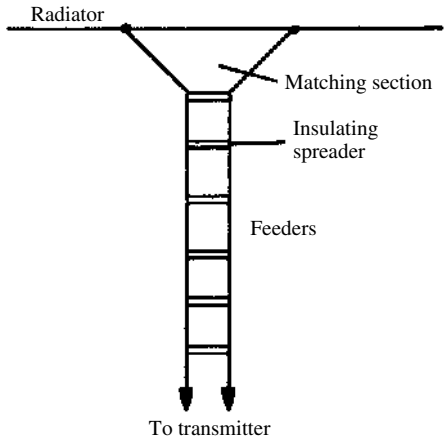

wye-matched-impedance antenna

wye potential In a three-phase armature, the voltage between a terminal and the neutral point.

wye rectifier A three-phase rectifier circuit in which the transformer or generator windings are arranged in a wye connection.

wye-wye circuit A circuit consisting a wye-connected generator and a wye-connected load.

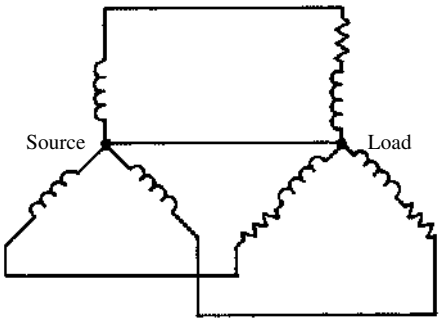

wye-wye circuit

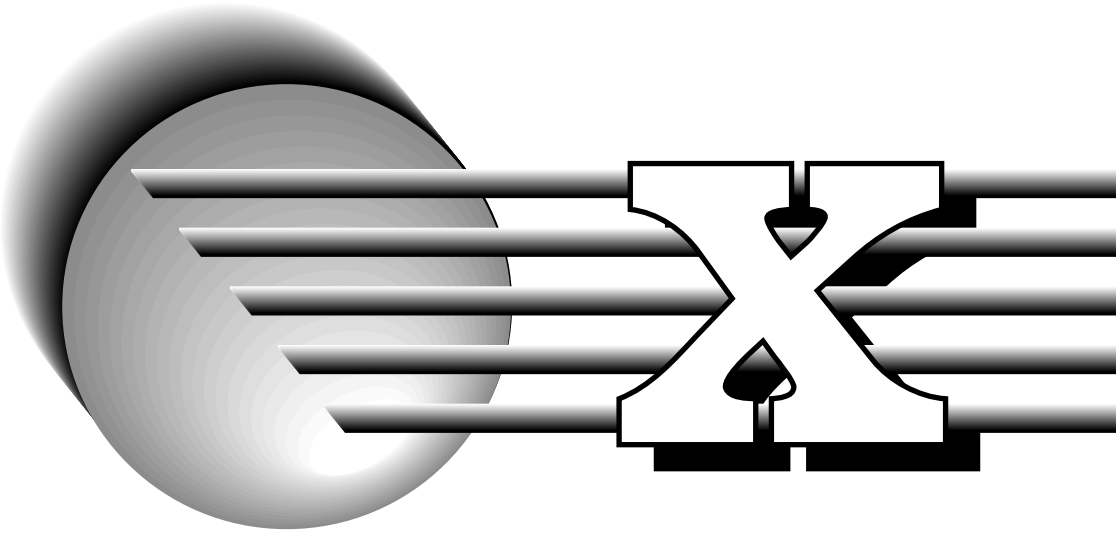

X **1.** Symbol for REACTANCE. **2.** Symbol for *no connection.* (Also, NC.) **3.** Symbol for the HORIZONTAL AXIS of a graph or screen in the rectangular (Cartesian) coordinate system. **4.** Symbol for an unknown quantity.

x **1.** Symbol for number of carriers drawn from collector to base of a transistor, for each carrier collected. **2.** Symbol for an unknown quantity. **3.** Symbol for the HORIZONTAL AXIS of a graph or screen in the rectangular (Cartesian) coordinate system.

x amplifier The horizontal amplifier of an oscilloscope or recorder. Compare Y AMPLIFIER and Z AMPLIFIER.

X and Z demodulation Color television demodulation based on the 60-degree difference between the two reinserted 3.58-MHz subcarrier signals. The R-Y, B-Y, and G-Y voltages derived from the demodulated signals control the three guns of the picture tube. Compare Q MODULATION.

x-axis **1.** The horizontal axis of a chart, graph, or screen in the rectangular (Cartesian) coordinate system. **2.** In a quartz crystal, the axis drawn through the corners of the hexagon.

x-axis amplifier See X AMPLIFIER.

XB Abbreviation of *crossbar.*

X balance The reactance balance (either the variable component or the adjustment of it) in an impedance bridge in which separate resistance (*R*) and reactance (*X*) balancing is provided.

X band The frequency band extending from 5.2 to 11 GHz.

X bar A rectangular, piezoelectric quartz bar cut from a Z-section, whose faces are parallel to the X-axis and whose edges are parallel to the X-, Y-, and Z-axes. See CRYSTAL CUTS.

X bridge An alternating-current bridge for measuring reactance.

X_C Symbol for CAPACITIVE REACTANCE.

X channel The horizontal channel of an oscilloscope or recorder. Compare Y CHANNEL and Z CHANNEL.

X-channel gain See X GAIN.

X component In a complex impedance, the reactive component (either inductive or capacitive).

x coordinate See ABSCISSA.

X-cut crystal A piezoelectric plate cut with its faces perpendicular to the X-axis of a quartz crystal. See CRYSTAL CUTS.

xcvr Abbreviation of TRANSCEIVER. Often capitalized.

X deflection Horizontal deflection of the spot on the screen of a cathode-ray tube. Compare Y DEFLECTION.

X diode The decoding diode in each of the X lines of a memory matrix. Compare Y DIODE.

X direction The horizontal direction in deflections and in graphical presentations of data.

X drive The driving source or energy for the X lines of a computer memory matrix.

xducer Abbreviation of TRANSDUCER.

Xe Symbol for XENON.

xenon Symbol, Xe. An inert gaseous element. Atomic number, 54. Atomic weight, 131.29. Xenon is present in trace amounts in the earth's atmosphere and is used in some thyratrons, electric lamps, and lasers.

xenon tube A flash tube filled with xenon.

xerography A system for the reproduction of printed matter, drawings, and other graphic matter. It is an electrostatic process in which a charged photoconductive surface is exposed to an

Copyright 2001 The McGraw-Hill Companies, Inc. Click Here for Terms of Use

5059F-pX-759-761 4/10/01 10:11 AM Page 760

image of the material to be copied. A latent image is formed on the surface and is developed (by dusting with black powder attracted to the charged image) to make the image visible.

xeroradiography Xerography using X RAYS.

xerothermic A condition characterized by both heat and dryness.

Xerox **1.** Name of a company that manufactures a wide variety of office and computer equipment. **2.** Trade name for a XEROGRAPHY machine. **3.** The reproduction obtained by means of XEROGRAPHY (generic term). **4.** To make a xerographic reproduction (generic term).

X factor **1.** An unknown or unidentifiable quantity or parameter. **2.** See X COMPONENT.

xformer Abbreviation of TRANSFORMER.

X gain The gain (or gain control) of the horizontal channel of an oscilloscope or X-Y recorder. Compare Y GAIN and Z GAIN.

X-H array See LAZY-H ANTENNA.

XHV Abbreviation of EXTREMELY HIGH VACUUM.

x intercept The *x* coordinate of the point at which a line or plane intersects the X-AXIS.

x irradiate To expose to X RAYS.

xistor Abbreviation of TRANSISTOR.

X_L Symbol for INDUCTIVE REACTANCE.

X line A horizontal line in a memory matrix. Compare Y LINE.

XLR connector A microphone connector with a locking device to prevent unintentional disconnection. It has three pins and is commonly used with balanced audio systems.

X meter **1.** An instrument for measuring reactance and phase angle. **2.** A form of simple capacitance meter whose dial is direct-reading in microfarads, although the deflection is actually proportional to the reactance of the capacitor under measurement.

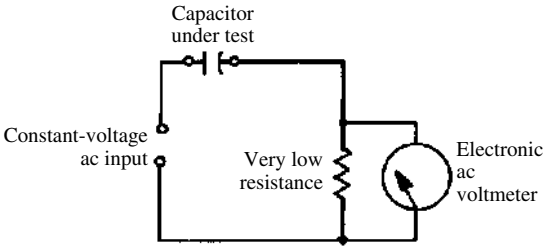

X meter, 2

xmission Abbreviation of *transmission.*

xmit Abbreviation of *transmit.* Also, xmt.

xmitter Abbreviation of TRANSMITTER. Also, xmtr.

XMODEM In data transmission, an error-correcting mode in which data is sent in blocks of 128 kilobytes (128K), or 131,072 bytes. The source and destination tally up the bytes in each block. If they agree, the next data block is sent. If they do not agree, the current data block is retransmitted. Compare YMODEM and ZMODEM.

xmt Abbreviation of *transmit.* Also, xmit.

xmtr Abbreviation of TRANSMITTER. Also, xmitter.

XOR Abbreviation of EXCLUSIVE-OR.

xover Abbreviation of CROSSOVER.

X particle See MESON.

xponder Abbreviation of TRANSPONDER.

X position **1.** The alignment of a cathode-ray beam along the horizontal axis of an oscilloscope screen. **2.** The position of a point, with respect to the horizontal axis of a graph in the rectangular (Cartesian) coordinate system.

XR Abbreviation of INDEX REGISTER.

X radiation Electromagnetic energy in the form of X rays.

X-ray **1.** Phonetic alphabet communications code word for the letter X. **2.** Pertaining to, or consisting of, X rays.

X-ray astronomy The science of observing celestial objects and the sky in the X-ray band of wavelengths. Generally, this must be done from above the earth's atmosphere because the atmosphere absorbs X rays.

X-ray crystallography The science of observing atomic patterns in a crystal by means of X rays.

X-ray detecting device **1.** An X-ray instrument for spotting flaws in solid bodies. **2.** A device, such as a fluoroscope, for showing the presence of X rays.

X-ray diagnosis The use of X rays in the diagnosis of disease and in the observation of internal parts of the body.

X-ray diffraction The diffraction of X rays by a material into or onto which they are directed. Also see X-RAY DIFFRACTION CAMERA and X-RAY DIFFRACTION PATTERN.

X-ray diffraction camera A special camera that furnishes a photograph of the pattern created by X rays diffracted by a material. See X-RAY DIFFRACTION and X-RAY DIFFRACTION PATTERN.

X-ray diffraction pattern The pattern produced on film exposed to X rays diffracted by a material. Also see X-RAY DIFFRACTION and X-RAY DIFFRACTION CAMERA.

X-ray goniometer An instrument used to find the position of the axes of a quartz crystal. It uses X rays reflected from the atomic planes of the crystal.

X-ray inspection The use of X rays in the examination and study of the internal features of materials and devices.

X-ray laser A laser designed to emit coherent X rays in a narrow beam.

X-ray load **1.** An X-ray tube that is the terminal member of an electronic system. **2.** A body, mass, or material exposed to X rays.

X-ray machine A device that generates X rays for a specific purpose, such as medical diagnosis.

X-ray photograph A photograph made by exposure to X rays, especially an *X-ray shadowgram,*

5059F-pX-759-761 4/10/01 10:11 AM Page 761

a picture made without a camera by interposing an object (such as a part of the human body) between an X-ray tube and photographic film.

X-ray radiation See X RADIATION.

X rays Invisible, electromagnetic radiation having wavelengths ranging from approximately 0.01 nanometer (10^{-11} meter) to 0.15 nanometer (1.5×10^{-10} meter). These waves are shorter than ultraviolet, but longer than gamma rays. They can be produced by bombarding a target of heavy metal (such as tungsten) with a stream of high-speed electrons in a vacuum tube. X rays have high penetrating power, can expose photographic film, and cause some substances to fluoresce. Also see X-RAY DIAGNOSIS, X-RAY INSPECTION, and X-RAY THERAPY.

X-ray spectra The continuous band of ionizing electromagnetic radiation having wavelengths ranging from approximately 0.01 nanometers to 0.15 nanometers.

X-ray spectrograph A spectrograph used to disperse and measure the wavelength of X rays.

X-ray spectrometer A spectrometer with which the diffraction angle of X rays reflected from the surface of a crystal can be measured. The device allows the characteristics and composition of almost any material to be studied.

X-ray star A collapsed star that emits high-intensity energy concentrated mainly in the X-ray region of the electromagnetic spectrum.

X-ray system Collectively, an X-ray tube and the associated equipment required for a specific application, such as crystallography, irradiation, or medical therapy.

X-ray technician **1.** A professional skilled in the operation and maintenance of X-ray systems, who usually works under the supervision of an engineer. **2.** A professional skilled in the medical use of X rays, who works under the supervision of a medical doctor.

X-ray therapy The use of X rays in the treatment of certain physiological diseases.

X-ray therapy system An X-ray system designed for X-ray therapy.

X-ray thickness gauge An instrument used to measure the thickness of metal, such as a continuously moving sheet of steel. The measurement is in terms of the amount of absorption of an applied X-ray beam by the metal.

X-ray tube A specialized, very-high-voltage diode in which a high-speed electron beam bombards an anode (target) of heavy metal, such as tungsten, causing it to emit X rays. The target is tilted to reflect the X rays through the glass wall of the tube.

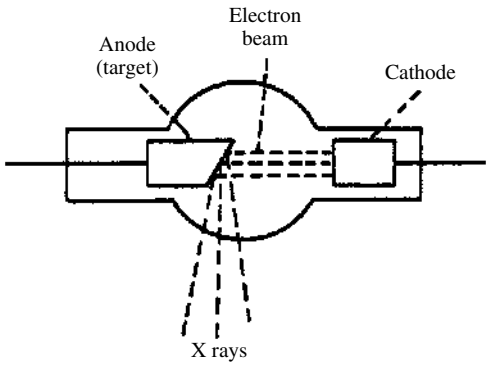

X-ray tube

X section Abbreviation of *cross section.*

X sink The circuit or device into which the X lines of a memory matrix feed. Compare Y SINK.

X_T Symbol for total reactance.

xtal Abbreviation of CRYSTAL.

xtalk Abbreviation of CROSSTALK.

x unit A small unit of length, equal to approximately 10^{-13} meter or 10^{-4} nanometer. Now seldom used, the x unit was once often used in the expression of ultraviolet and X-ray wavelengths.

X wave One (the extraordinary) of the pair of components into which an ionospheric radio wave is divided by the earth's magnetic field. Compare O-WAVE.

XXX In radiotelegraphy, a signal meaning *urgent.*

X-Y counting A technique used with electronic counters to determine the ratio of one frequency (X) to another (Y). When X is the higher frequency, the counter readout shows the number of pulses of X producing one cycle of Y.

XY-cut crystal A piezoelectric plate cut from a quartz crystal at such an angle that its electrical characteristics fall between those of the X-cut and Y-cut crystal.

x-y plotter An output device similar to the x-y recorder. It allows a digital computer to plot graphs. Also called *data plotter.*

x-y recorder An instrument that produces a permanent record (photographic print or directly inked paper) of a variable quantity on a chart having Cartesian (rectangular) coordinates.

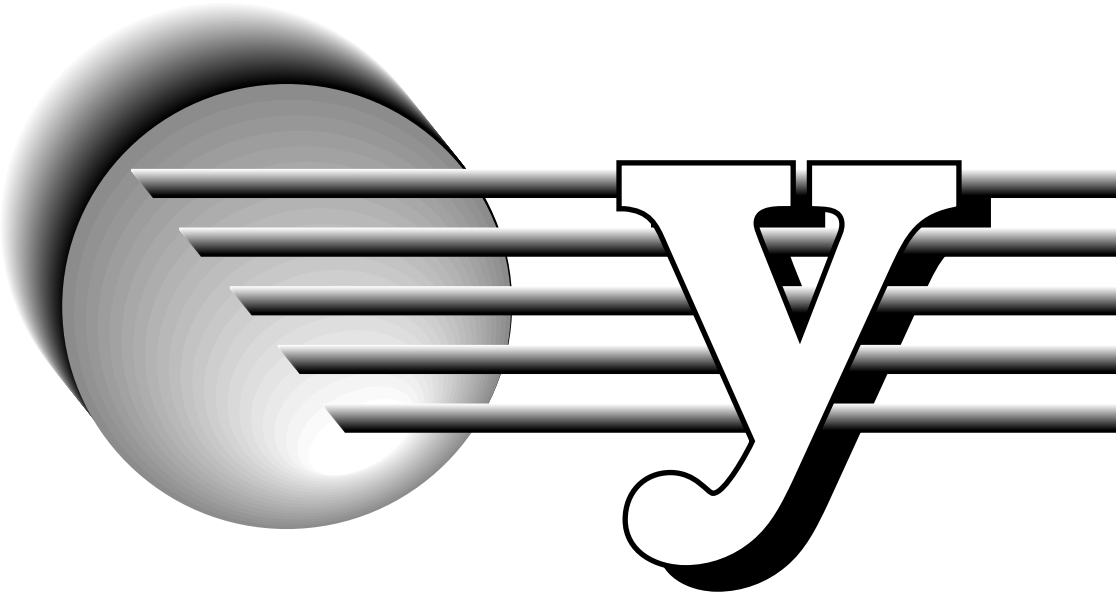

Y **1.** Symbol for ADMITTANCE. **2.** Symbol for YTTRIUM. **3.** Symbol for YOUNG'S MODULUS.

y **1.** Abbreviation of YEAR. (Also, yr.) **2.** Abbreviation of YARD. (Also, yd.) **3.** Symbol for the vertical axis of a graph or screen in the rectangular (Cartesian) coordinate system.

Y adapter See WYE ADAPTER.

YAG Abbreviation of *yttrium-aluminum-garnet*, the stimulated substance in some lasers.

Yagi antenna Also called *Yagi-Uda array* or *beam*. An antenna consisting of two or more parallel, straight elements, including at least one parasitic element and at least one driven element. The elements all lie in the same plane. Each driven element is connected to the feed line, half-wave resonant, and center-fed. A two-element array can be formed by adding a director or a reflector alongside a single driven element. An array with one director and one reflector, along with the driven element, increases the gain and directivity compared with a two-element system. The gain and directivity increase further as elements are added. This is usually done by placing additional directors in front of a three-element array. Compare QUAD ANTENNA.

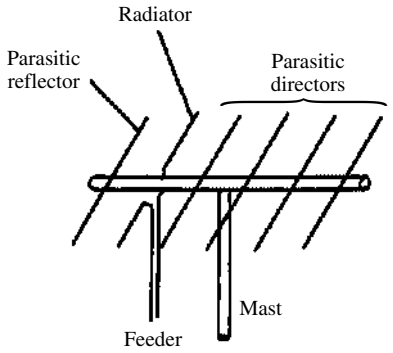

yagi antenna

y amplifier The vertical amplifier of an oscilloscope or recorder. Compare X AMPLIFIER and **Z** AMPLIFIER.

Yankee Phonetic alphabet communications code word for the letter Y.

yard Abbreviation, yd. A unit of linear measure in the English system. 1 yd = 3 ft = 36 inches = 0.9144 meter.

yaw Side-to-side movement in a vehicle or robotic end effector. Essentially horizontal displacement about the vertical axis.

yaw amplifier In an aircraft servo system, the unit that amplifies the yaw signal (the signal proportional to the deviation of the aircraft from the line of flight).

yaw meter An instrument for measuring the angle of yaw of an aircraft.

y-axis **1.** The vertical axis of a chart, graph, or screen in the rectangular coordinate system.

Copyright 2001 The McGraw-Hill Companies, Inc. Click Here for Terms of Use

5059F-pY-762-764 4/10/01 10:12 AM Page 763

2. In a quartz crystal, the axis drawn perpendicular to the faces of the hexagon.

y-axis amplifier See Y AMPLIFIER.

Yb Symbol for YTTERBIUM.

Y box See WYE BOX.

Y channel See Y AMPLIFIER.

Y-channel gain See Y GAIN.

Y circulator An interconnection among three waveguides. When power is applied to the junction through one waveguide, the wave is transferred to the adjacent waveguide immediately to the right or left.

Y connection See WYE CONNECTION.

y coordinate See ORDINATE.

Y current See WYE CURRENT.

Y-cut crystal A piezoelectric plate cut from a quartz crystal in such a way that the plane of the plate is perpendicular to the Y-axis of the crystal. See CRYSTAL AXES and Y-AXIS, **2**.

yd Abbreviation of YARD.

Y deflection Vertical deflection of the spot on the screen of a cathode-ray tube. Compare X DEFLECTION.

Y diode The decoding diode in each of the Y lines of a memory matrix. Compare X DIODE.

y direction The vertical direction in deflections and in graphical presentations of data.

Y drive The driving source or energy for the y lines of a computer memory matrix. Compare X DRIVE.

year Abbreviation, y or yr. The period of the earth's revolution around the sun, with respect to distant stars: approximately 365.25 days or 3.15576×10^7 seconds.

Yellow Book A specialized format for *compact-disk read-only memory (CD-ROM)* computer data storage media, developed by Sony and Philips. It is similar to RED BOOK, but it includes superior error correction and storage capacity. See also CD-ROM, GREEN BOOK, ORANGE BOOK, and RED BOOK.

yellow copper ore See CHALCOPYRITE.

yellow metal A copper-zinc alloy that is 60% copper.

yellow pyrites See CHALCOPYRITE.

Y-equivalent circuit See WYE-EQUIVALENT CIRCUIT.

Y gain The gain (or gain control) of the vertical channel of an oscilloscope or x-y recorder. Compare X GAIN and Z GAIN.

yield In a phototube or photocell, the photoelectric current per unit intensity of light.

yield map A diagram of an integrated circuit showing the locations of faulty components.

yield strength The lowest stress for plastic deformation of a material, below which the material is elastic and above which it is viscous.

yield value The amount of physical stress that causes a substance to become stretched permanently out of shape.

YIG Abbreviation of *yttrium-iron-garnet*, a crystalline material used in certain types of acoustic delay lines, parametric amplifiers, and filters.

YIG crystal A crystal of yttrium-iron-garnet. See YIG.

YIG filter A filter using a YIG crystal and tuned electromagnetically.

YIG-tuned parametric amplifier A parametric amplifier in which tuning is accomplished by continuously varying direct current through the solenoid of a YIG filter.

y intercept The *y* coordinate of the point at which a line or plane intersects the *y*-axis.

ylem The material from which the primordial fireball is thought to have been made, and from which the entire known universe is believed to have originated approximately 10 billion (10^{10}) years ago.

Y line A vertical line of a memory matrix. Compare X LINE.

Y-matched-impedance antenna See WYE-MATCHED-IMPEDANCE ANTENNA.

YMODEM In data transmission, an error-correcting mode in which data is sent in blocks of one megabyte (1MB), or 1,048,576 bytes. The source and destination tally up the bytes in each block. If they agree, the next data block is sent. If they do not agree, the current data block is retransmitted. Compare XMODEM and ZMODEM.

yoke **1.** The ferromagnetic ring or cylinder that holds the pole pieces of a dynamo-type generator and acts as part of the magnetic circuit. **2.** The system of coils used for magnetic deflection of the electron beam in cathode-ray tubes.

yoke method A method of measuring the permeability of a sample of magnetic material. It involves completing the magnetic circuit with a heavy yoke of soft iron.

Young's modulus Symbol, Y. The ratio of tensile stress to tensile strain.

Y parameters The admittance parameters of a four-terminal network or device.

Y point See WYE POINT.

Y position **1.** On a cathode-ray screen, the vertical position of the beam spot. **2.** On a graph, the position of a point along the vertical axis.

Y potential See WYE POTENTIAL.

yr Abbreviation of YEAR. Also, y.

Y rectifier See WYE RECTIFIER.

Y signal In color television, the monochromatic signal conveying brightness information.

Y sink The circuit or device into which the Y lines of a memory matrix feed. Compare X SINK.

ytterbium Symbol, Yb. A metallic element of the rare-earth group. Atomic number, 70. Atomic weight, 173.04.

ytterbium metals The rare-earth metals dysprosium, erbium, lutetium, holmium, thulium, and ytterbium.

5059F-pY-762-764 4/10/01 10:12 AM Page 764

Yttralox A transparent polycrystalline ceramic composed primarily of yttrium oxide, which has many applications in electro-optics.

yttria Formula, Y_2O_3. Yttrium oxide, a white powder used in Nernst lamps.

yttrium Symbol, Y. A metallic element of the rare-earth-metals group. Atomic number, 39. Atomic weight, 88.906.

yttrium-iron-garnet See YIG.

yttrium metal Any of the group of metals, including yttrium, erbium, holmium, lutetium, thulium, ytterbium, and sometimes dysprosium, gadolinium, and terbium.

Yukon Standard Time Standard time of the ninth time zone west of Greenwich, embracing the Yukon Territory and a portion of southern Alaska.

Y winding See WYE CONNECTION.

Y-Y circuit See WYE-WYE CIRCUIT.

Z **1.** Symbol for IMPEDANCE. **2.** Symbol for ATOMIC NUMBER. **3.** Symbol for *zenith distance* (astronomy).

z **1.** Abbreviation of ZERO. **2.** Symbol for ELECTROCHEMICAL EQUIVALENT. **3.** Abbreviation of ZONE. **4.** Symbol for the vertical axis of a three-dimensional Cartesian graph.

zag The short, straight deflection of a point or particle, or of waves along a jagged path in a direction opposite that of a ZIG; one of the components of ZIGZAG DEFLECTION.

Zamboni pile A high-voltage electrochemical cell consisting of an aluminum anode, a manganese-dioxide cathode, and an aluminum-chloride electrolyte.

Z amplifier The intensity-modulation amplifier in an oscilloscope. Compare X AMPLIFIER and Y AMPLIFIER.

Z-angle meter An instrument, commonly of the null-balance type, that indicates the impedance and phase angle of capacitors, inductors, and sometimes of inductance-capacitance-resistance (ICR) combinations.

z-axis **1.** The intensity-modulation input of an oscilloscope, including the associated circuit. **2.** The video-signal input of a television picture tube, including the associated circuit. **3.** The third axis in a three-dimensional coordinate system. **4.** The lengthwise axis of a quartz crystal.

z-axis amplifier See Z AMPLIFIER.

z-axis modulation See INTENSITY MODULATION.

Z bar See Z-CUT CRYSTAL.

z channel See Z AMPLIFIER.

z-channel gain See Z GAIN.

Z-cut crystal A plate cut from a quartz crystal so that the plane of the plate is perpendicular to the Z-axis of the crystal and parallel to the X-axis. See CRYSTAL AXES.

ZD Abbreviation of *zero defects.*

Z deflection Deflection of a cathode-ray beam beyond the (ordinarily defined) deflection area on the tube screen.

Zeeman effect The splitting of a spectral line of a gas into closely spaced, polarized frequency components by an applied magnetic field.

Zenely electroscope A sensitive alpha-ray electroscope (see ELECTROSCOPE) whose leaf is attracted by a metal plate biased at 50 to 200 volts. On touching the plate, the leaf becomes charged and is repelled. But the gas ions around the leaf neutralize the charge, and the leaf returns to the plate to repeat the action. This sequence causes the leaf to oscillate, the number of oscillations per second being proportional to the strength of the ionizing source.

Zener See ZENER DIODE.

Zener breakdown See AVALANCHE BREAKDOWN.

Zener current See AVALANCHE CURRENT.

Zener diode Also sometimes called *avalanche diode* or *Zener.* A semiconductor diode (usually silicon) specially fabricated to take advantage of the effects of avalanche breakdown. It is available in a wide variety of configurations and ratings; it is commonly used as a voltage regulating device in low-voltage power supplies.

Zener-diode clipper A signal-amplitude clipper that does not require direct-current bias because it uses a Zener diode. Clipping takes place at the avalanche voltage. Zener diodes can be connected back to back for alternating-current clipping.

Copyright 2001 The McGraw-Hill Companies, Inc. Click Here for Terms of Use

5059F-pZ-765-772 4/10/01 10:16 AM Page 766

Zener-diode coupling element A Zener diode used as a direct coupling element between amplifier stages in an electronic system. When no signal is present, the resistance of the diode is extremely high because the direct-current voltages of the diode-coupled amplifier stages reverse-bias the diode to below the avalanche point, and no current flows from one stage to the next. The signal raises the voltage enough to cause avalanche breakdown; the signal is thus readily transmitted from one stage to the following one.

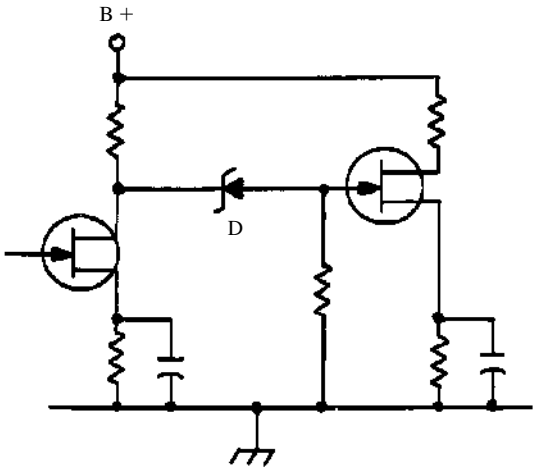

zener-diode coupling element

Zener-diode voltage reference A device that utilizes the constant voltage drop across a Zener diode operated in its breakdown region, to provide a standard voltage for reference purposes. It consists essentially of a direct-current (dc) voltage source, limiting resistor, and Zener diode. For an alternating-current (ac) reference voltage, an ac voltage source, limiting resistor, and two Zener diodes (connected in parallel, back to back) are required. Zener diodes can be connected in series to supply a higher reference voltage than can be delivered by a single diode.

Zener-diode voltage regulator A simple voltage regulator whose output is the constant voltage drop developed across a Zener diode conducting in the reverse breakdown region. The simple regulator circuit consists of a Zener diode and an appropriate limiting resistor connected in series across the output terminals of an unregulated direct-current power supply. For alternating-current voltage regulation, two Zener diodes can be connected in parallel, back to back. Zener diodes can be connected in series to regulate a higher voltage than can be accommodated by a single diode.

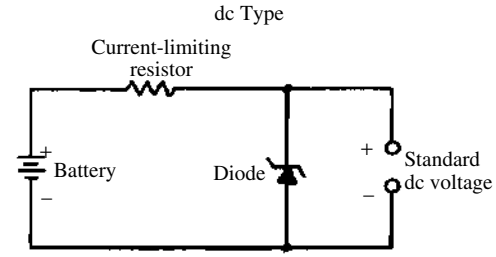

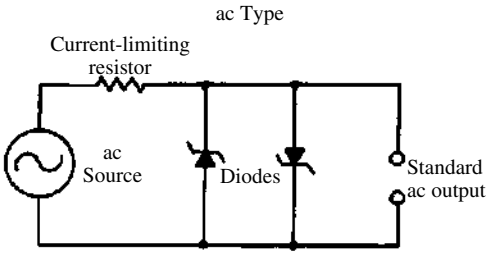

zener-diode voltage reference

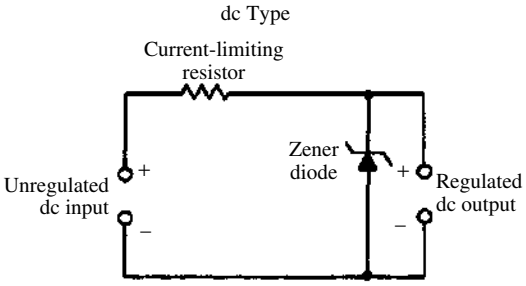

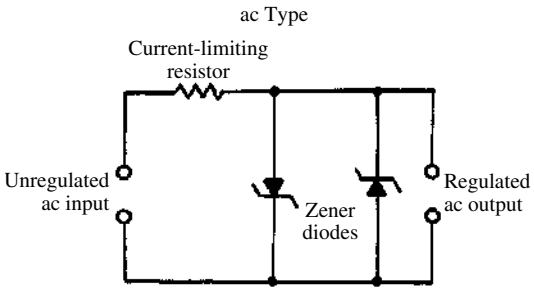

zener-diode voltage regulator

Zener effect See AVALANCHE BREAKDOWN.

Zener knee In the response of a reverse-biased Zener diode, the point of abrupt transition from low current (high resistance) to high current (low resistance). For voltage regulation and voltage

5059F-pZ-765-772 4/10/01 10:16 AM Page 767

standardization, the knee should be as sharp as possible.

Zener knee current In a Zener diode, the current that flows when the reverse bias reaches the avalanche voltage.

Zener-protected MOSFET See GATE-PROTECTED MOSFET.

Zener voltage The particular value of reverse voltage at which a Zener diode or other reverse-biased pn junction abruptly exhibits the avalanche effect. Depending on the Zener diode, this potential can be less than 10 volts, or as much as several hundred volts.

zenith In the sky, the point directly overhead, exactly 180 degrees opposite the direction of the earth's center.

Zeolite process A method using certain artificial Zeolites (hydrous silicates) to soften water used in some electronic manufacturing and testing operations.

zeppelin antenna Also called *zepp*. **1.** A half-wavelength radiator, fed at one end with a quarter-wavelength section of open-wire line. The feed line can come away from the radiator at any angle, usually 90 degrees or more. The antenna was originally used aboard zeppelins; the entire system was dangled in flight and the feed line was collinear with the radiating element. The impedance at the feed point is high; the impedance at the transmitter end of the feed line is low. The antenna will operate satisfactorily at all harmonics of the design frequency. **2.** A radiator that is an integral multiple of a half wavelength, fed with open-wire line of any length. A transmatch is employed at the transmitter and of the feed line. This arrangement is popular among radio amateurs. The primary advantage of this antenna is ease of installation; the main drawback is the fact that the feed line radiates to some extent because the system is not perfectly balanced.

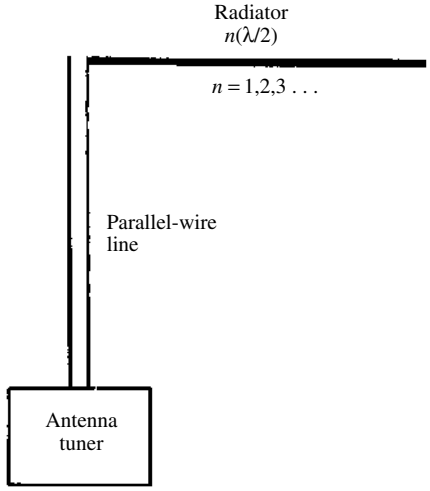

zeppelin antenna

zero **1.** The number represented by the cipher symbol (0). **2.** To set a meter or other instrument to its zero reading or condition. **3.** To align one element of a system precisely with another. **4.** In computer operations, to set a register to zero. **5.** In computer operations, using zero pulses to replace what is in a storage area.

zero-access memory See ZERO-ACCESS STORAGE.

zero-access storage Computer storage requiring negligible waiting time (latency).

zero-address instruction A computer instruction requiring no address; the operation specified by the instruction defines the locations of the operands. Also called *addressless instruction.*

zero adjust In an analog metering device, a mechanical or electrical control that allows precise setting of the reading to zero, when the parameter to be measured is actually zero.

zero adjustment **1.** The act of setting an instrument or circuit to its zero reading or zero-operating condition. **2.** A device or subcircuit used to set a meter to its zero reading. Also see ZERO SET, **1**, **2**.

zero-angle cut An alternate term for *X cut*, as applied to quartz crystal plates. Also see CRYSTAL CUTS.

zero axis In a plot of a variable quantity, the (usually horizontal) reference line that indicates the zero value of the quantity.

zero-axis symmetry The condition in which a waveshape is symmetrical about a zero axis.

zero beat Complete absence of a beat note (i.e., silence), a condition occurring when the frequencies of the beating signals (or their harmonics) are equal. See BEAT NOTE.

zero-beat detector A device or circuit used to sense and indicate the condition of zero beat.

zero-beat indicator See ZERO-BEAT DETECTOR.

zero-beat method A means of adjusting the frequency of one signal exactly to that of another (usually standard) signal by setting the first signal frequency to zero beat with the second signal frequency.

zero-beat reception A system of reception entailing zero beating an incoming signal with the signal from a local oscillator. Also called *homodyne reception.*

zero-bias operation Operation of a transistor or vacuum tube without direct-current base, gate, or grid bias.

zero-bias tube A vacuum tube designed for operation (particularly in a class-B power amplifier) without direct-current grid bias. In such a tube, the zero-signal plate current is very low because of the large amplification factor.

zero capacitance **1.** Absence of capacitance (a theoretically ideal condition). **2.** In some circuits,

5059F-pZ-765-772 4/10/01 10:16 AM Page 768

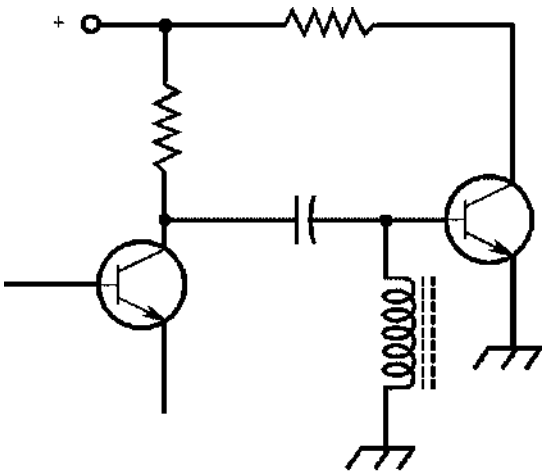

zero-bias operation

the lowest capacitance point, to which all other capacitances are referred.

zero compensation The elimination or minimizing of the zero-signal output of a transducer or similar device.

zero compression See ZERO SUPPRESSION, **1**.

zero condition See ZERO STATE.

zero current **1.** Absence of movement of electrical charge carriers. **2.** In some circuits, the lowest current level, to which all other currents are referred.

zero-cut crystal A piezoelectric plate cut from a quartz crystal in such a way that the frequency-temperature coefficient is zero.

zero-dB reference level An agreed-upon zero level for decibel ratings (which are by nature relative). Zero dBm, for example, corresponds to 1 milliwatt. Compare VOLUME UNIT.

zero drift **1.** The (usually gradual) drift of a zero point, such as the zero setting of an electronic voltmeter. **2.** The condition of no change in the value of a quantity.

zero elimination See ZERO SUPPRESSION, **1**.

zero energy The condition in which energy is neither generated, consumed, nor dissipated.

zero error **1.** In instruments and measurements, an error so small that it can be considered inconsequential. **2.** In a radar system, the inherent delay in the transmitter and receiver circuits.

zero field emission Thermionic emission from a cathode or hot conductor within a uniform electrostatic field.

zero fill See ZERO, **5**.

zero gravity The condition of weightlessness (i.e., the state in which gravitational pull by a celestial body is completely absent or has been nullified).

zero-gravity switch A switch actuated automatically when the condition of zero gravity is reached.

zero impedance **1.** Absence of impedance (a theoretically ideal condition). **2.** In some circuits, the lowest impedance level, to which all other impedances are referred.

zero inductance **1.** Absence of inductance (a theoretically ideal condition). **2.** In some circuits, the lowest inductance level, to which all other inductances are referred.

zero input **1.** Complete absence of input (signal or noise). **2.** Absence of operating voltage or power to a system. **3.** In a flip-flop, the input terminal that is not receiving a trigger signal.

zero-input terminal In a flip-flop, the input-signal terminal at which a trigger signal will switch the flip-flop output to zero. Also called *zero terminal* and RESET TERMINAL.

zero instant See ZERO TIME.

zero level The reference level for the comparison of quantities. For example, it might be a voltage or current level; in audio measurements, it is the zero-dB reference level.

zero-line stability In an analog metering device, the ability of the instrument to maintain proper zero adjustment over a period of time.

zero magnet A permanent magnet used to set the pointer of a meter to zero.

zero magnitude **1.** For a quantity, the state of being valueless (i.e., a complete absence of the quantity). **2.** In some tests, measurements, or calculations, the lowest value of a quantity, to which all other values are referred.

zero meridian The meridian at Greenwich (near London), England, from which longitude and standard time are reckoned. Also see TIME ZONE and ZONE TIME.

zero method A method of measurement entailing adjustment of a circuit or device (such as a bridge, tee network, or potentiometer) for zero response of the detector. Also called *null method.*

zero modulation The momentary lack of modulation in a communications or broadcast system, as during a pause in speech.

zero-modulation noise Noise produced by previously erased tape that is run under specified operating conditions.

zero output **1.** Complete absence of output signal or output power, sometimes disregarding noise output. **2.** In a flip-flop, the normal condition of no signal pulse at a particular output terminal.

zero-output terminal In a flip-flop, the output terminal that is not delivering an output pulse.

zero phase In an alternating-current circuit, the condition in which the current and voltage are in step. That is, the current peaks occur at exactly the same times as the voltage peaks; the phase difference between the current and voltage is zero degrees.

zero pole In a multiconductor line, the common or reference conductor.

5059F-pZ-765-772 4/10/01 10:16 AM Page 769

zero potential **1.** Complete absence of voltage. **2.** In some circuits, the lowest voltage, to which all other voltages are referred. **3.** The potential of the earth as a reference point.

zero power **1.** Complete absence of dissipated power. **2.** In some circuits and systems, the lowest power level, to which all other power values are referred.

zero-power resistance In a thermistor, the resistance at which power dissipation is zero.

zero-power resistance-temperature characteristic For a thermistor, a figure that reveals the extent to which zero-power resistance varies with the temperature of the thermistor body.

zero-power temperature coefficient of resistance A temperature coefficient that reveals the extent to which the temperature of the thermistor body causes the zero-power resistance to change (expressed in ohms per ohm per degree Celsius).

zero reactance **1.** Absence of reactance (a theoretically ideal condition in alternating-current circuits). **2.** In some circuits, the lowest reactance, to which all other reactances are referred.

zero resistance **1.** Absence of resistance (a theoretically ideal condition). **2.** In some circuits, the lowest resistance, to which all other resistances are referred.

zero scale current In a digital-to-analog (D/A) converter, the current into the output when all logic inputs are low (off) and the output is at a certain predetermined value, in microamperes or milliamperes.

zero screw The mechanical zero adjuster of a meter.

zero set **1.** A (usually screwdriver-adjusted) mechanism for setting the pointer of a meter to zero. **2.** An electrical circuit consisting of a resistance bridge or adjustable bucking voltage for setting a meter to read zero under specific conditions.

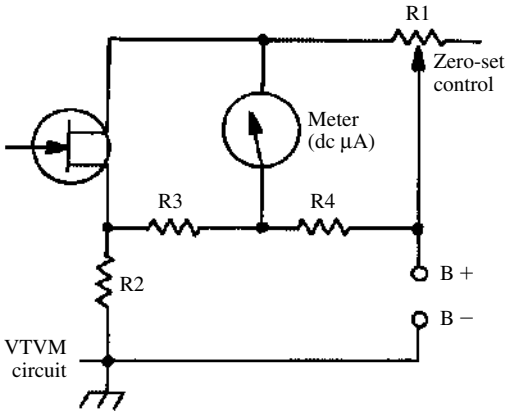

zero set, 2

zero shift See ZERO DRIFT.

zero signal **1.** The condition of complete absence of signal. **2.** A finite signal level used as a reference point against which all other signal levels are measured.

zeros of impedance For an alternating-current network, the frequencies at which the impedance is zero. Also called *zeros.*

zeros of network function The real or complex values at which the network function is zero. Compare POLES OF NETWORK FUNCTION.

zeros of transfer function The frequencies at which a transfer function becomes zero. Compare POLES OF TRANSFER FUNCTION.

zero stability Constancy of the zero condition in an instrument or system (i.e., absence of zero drift).

zero state The low, zero, off, or false logic state of a bistable device, such as a flip-flop or magnetic cell. It might be actual zero output or a low-voltage output. Compare ONE STATE. In binary notation and calculation, the zero state is represented by a cipher.

zero suppression **1.** In computer operation, automatic nonsignificant leading-zero cancellation. **2.** Absence or removal of a restraining medium, such as a noise-suppression voltage. **3.** In an audio recording system, the introduction of a voltage to cancel the steady-state component of the input signal.

zero temperature **1.** The point from which temperatures are reckoned on a thermometer scale. On the Celsius (centigrade) scale, zero degrees corresponds to the freezing point of pure water at standard atmospheric pressure. On the Fahrenheit scale, zero degrees is 32 degrees colder than the freezing point of pure water at standard atmospheric pressure. On the Kelvin or Rankine scales, zero degrees corresponds to the complete absence of thermal energy; it is the coldest possible temperature. **2.** A temperature point relative to which all other temperatures are reckoned.

zero temperature coefficient A temperature coefficient having the value zero (i.e., one that indicates there is no temperature-dependent drift of a given quantity).

zero terminal See ZERO-INPUT TERMINAL and ZERO-OUTPUT TERMINAL.

zero time **1.** In some measurements, the first instant of time, to which all other instants are referred. **2.** See ZERO PHASE.

zero time reference During one cycle of radar operation, the time reference of the schedule of events.

zero vector A vector whose magnitude is zero.

zero voltage See ZERO POTENTIAL.

zero voltage coefficient A voltage coefficient having the value of zero (i.e., one that indicates there is no voltage-dependent drift of a given quantity).

zero-zero The atmospheric condition in which the ceiling and visibility both are zero (i.e., extremely dense fog).

5059F-pZ-765-772 4/10/01 10:16 AM Page 770

Z gain The gain (or gain control) of the intensity channel of an oscilloscope. Compare X GAIN and Y GAIN.

zig The short, straight deflection of a point or particle, or of a wave along a jagged path in a direction opposite that of ZAG; a component of ZIGZAG DEFLECTION.

zigzag deflection Deflection of a particle, point, or object in a path that contains side-to-side motion, as well as forward motion. Also see ZAG and ZIG.

zigzag rectifier A special version of the three-phase star (three-phase, half-wave) rectifier circuit. Direct-current (dc) saturation of the transformer secondary is avoided by winding half the turns of each secondary on a separate core (i.e., each core carries two half-windings). The opposing flux resulting from different phases in the half-windings causes cancellation of the dc component of flux in each core.

zigzag reflections Multihop reflections of waves along a zigzag path, resulting from repeated reflections within the ionosphere.

zinc Symbol, Zn. A metallic element. Atomic number, 30. Atomic weight, 65.39. It is used as the negative-electrode material in dry cells and as a protective coating for some metals used in electronics.

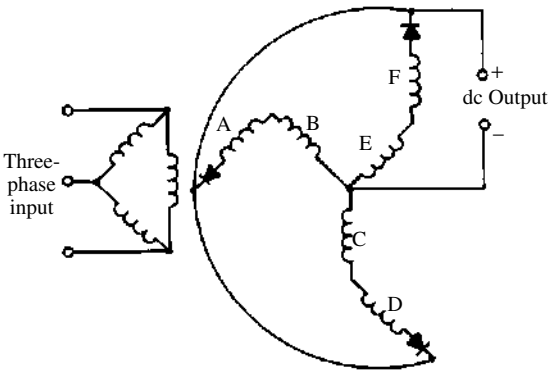

zigzag rectifier

zinc aluminate phosphor Either of two similar substances used as a phosphor coating for cathode-ray tube screens. One form glows blue; the other form glows red.

zinc beryllium silicate phosphor A substance used as a phosphor coating for cathode-ray-tube screens. It glows yellow.

zinc beryllium zirconium silicate phosphor A substance used as a phosphor coating for cathode-ray-tube screens. It glows white.

zinc borate phosphor A substance used as a phosphor coating for cathode-ray-tube screens. It glows yellow-orange.

zinc cadmium sulfide phosphor Either of two similar substances used as a phosphor coating for cathode-ray-tube screens. One form glows blue; the other form glows red.

zinc–carbon cell A common non-rechargeable electrochemical cell. Produces approximately 1.5 volts under no-load conditions. Zinc forms the outer case or shell, and is the negative electrode. A carbon rod serves as the positive electrode. The electrolyte is a paste of manganese dioxide and carbon. The cell is inexpensive, and is commercially available in various sizes. The shelf life is fairly long. Cells of this type work well at moderate temperatures, and in applications where the current drain is moderate to high. They function poorly at low temperatures. Compare ALKALINE CELL.

zinc germanate phosphor A substance used as a phosphor coating for cathode-ray-tube screens. It glows yellow-green.

zinc magnesium fluoride phosphor A substance used as a phosphor coating for cathode-ray-tube screens. It glows orange.

zincolysis Electrolysis in a cell having a zinc anode.

zinc orthoscilicate phosphor Also called *Willemite.* A substance used as a phosphor coating for cathode-ray-tube screens. It glows yellow-green.

zinc oxide A substance used as a phosphor coating for cathode-ray-tube screens. It glows blue-green. It is also used in the manufacture of certain electronic components, such as resistors.

zinc-oxide resistor A voltage-dependent resistor whose active ingredient is zinc oxide.

zinc silicate phosphor A substance used as a phosphor coating for cathode-ray-tube screens. It glows blue.

zinc standard cell A standard cell using zinc and mercury electrodes, and a mercurous sulfate excitant and depolarizer. Produces 1.4322 volts at 15°C. Also called *Clark cell.* Compare WESTON CELL.

zinc sulfide phosphor A substance used as a phosphor coating for cathode-ray-tube screens. Glows blue-green or yellow-green.

ZIP Abbreviation of *zinc-impurity photodetector.*

zip cord A simple two-conductor, flexible power cord.

zirconia Preparations of zirconium (especially ZrO_2), valued for their high-temperature dielectric properties.

zirconium Symbol, Zr. A metallic element. Atomic number, 40. Atomic weight, 91.22.

Z marker A vertically radiating marker beacon defining the zone above a radio-range station.

Z meter A device for measuring impedances. Instruments of this kind take four principal forms: **(1)** a direct-reading meter resembling an ohmmeter; **(2)** an adjustable circuit manipulated somewhat like a bridge and that compares an unknown impedance with a standard resistance;

5059F-pZ-765-772 4/10/01 10:16 AM Page 771

(3) an impedance bridge for evaluating the reactive and resistive components of an unknown impedance; **(4)** a section of transmission line used with a signal source and voltmeter for measuring impedance in terms of a standard resistor and/or standing waves.

ZMODEM In data communications, an error-correction mode similar to XMODEM, except that when an error is found during transmission of a block of data, the source retransmits only that portion of the block following the error. This improves data transmission speed because, when an error occurs, the number of bytes retransmitted is generally fewer than the 128K block size standard in XMODEM. Compare XMODEM and YMODEM.

Zn **1.** Symbol for ZINC. **2.** Symbol for AZIMUTH.

Z_0 Symbol for CHARACTERISTIC IMPEDANCE.

zone **1.** On a magnetic disk, a group of tracks whose associated transfer rate is not the same as that for the rest of the disk. **2.** In computer operations, the area of a storage medium containing digits. **3.** In a computer system, a main memory area set aside for a particular purpose. **4.** In a security system, a specified area or region under surveillance.

zone blanking In a radar system, a method of extinguishing the cathode-ray-tube beam during a portion of the antenna sweep.

zone candle power In a given zone, the luminous flux per steradian, emitted by a light source under test.

zoned circuit In a security system, a circuit in which some areas are protected at all times, while the protection in other areas can be temporarily disabled for entry or exit.

zone leveling See ZONE REFINING.

zone marker See Z MARKER.

zone melting See ZONE REFINING.

zone of silence The region between alternate reflections of a radio wave, in which no signal is detectable. Also called *skip zone.*

zone plate antenna A rapid-scan radar antenna having a reflector composed of confocal parabolas arranged in a circle.

zone-position indicator A radar that reveals the position of an object to a second radar having a restricted field.

zone purification See ZONE REFINING.

zone refining A method of purifying semiconductor materials (such as germanium and silicon) in which a molten zone in an ingot of the material moves along the length of the ingot, dissolving impurities as it travels, eventually depositing them at the end of the ingot, which is sawed off. This concentrated and segregated melting is accomplished by means of radio-frequency heating.

zone time In a given time zone, standard time in terms of the number of hours that must be added to local time to equal the time at the zero (Greenwich) meridian.

zoning **1.** A method of fabricating a microwave reflector in concentric, flat regions, producing the same practical results as a continuous paraboloid. **2.** In a communications system, the division of the coverage area into different geographic regions for a specific purpose.

zoom **1.** To rapidly change the focal length of a television or motion-picture camera lens so that the object seems to advance toward or recede from the viewer, remaining in focus as it does so. **2.** See ZOOM LENS. **3.** To magnify the image in a computer graphical user interface. A user can enlarge a specific portion of the display, at the expense of other portions. It is generally measured in percent (e.g., 200% zoom represents a magnification factor of 2).

zoom lens A continuously adjustable lens system that allows zoom effects to be obtained with a television or motion-picture camera, or a similar arrangement for still cameras that obviates the need for lens interchange when different focal lengths are needed. The lens system, which can be operated electronically, allows either narrow- or wide-angle views to be obtained without losing focus at any time.

Z parameters Device or network parameters expressed as impedances.

ZPI Abbreviation of ZONE-POSITION INDICATOR.

Z-plunger In a waveguide, a combination choke and bucket plunger for radiation leakage reduction.

Zr Symbol for ZIRCONIUM.

Z signals A collection of letter groups, each starting with the letter Z, used for simplified telegraphy and radiotelegraphy by the military services.

Zulu Phonetic alphabet communications code word for the letter Z.

Zulu time Greenwich mean time. Also see ZEBRA TIME.

zwitterion An ion that carries both a positive and a negative charge.

This page intentionally left blank.

Appendix A
Schematic symbols

Ammeter 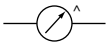

Amplifier general 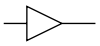

Amplifier, inverting 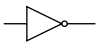

Amplifier, operational 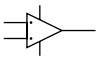

AND gate

Antenna, balanced

Antenna, general

Antenna, loop

Antenna, loop, multiturn

Battery

Capacitor, feedthrough

Capacitor, fixed

Capacitor, variable

Capacitor, variable, split-rotor

Capacitor, variable, split-stator

Copyright 2001 The McGraw-Hill Companies, Inc. Click Here for Terms of Use

Appendix A 4/10/01 10:38 AM Page 774

Cathode, electron-tube, cold

Cathode, electron-tube, directly heated

Cathode, electron-tube indirectly heated

Cavity resonator

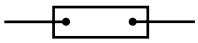

Cell, electrochemical

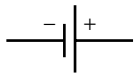

Circuit breaker

Coaxial cable

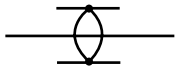

Crystal, piezoelectric

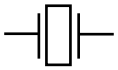

Delay line

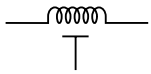

Diac

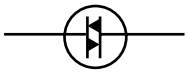

Diode, field-effect

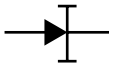

Diode, general

Diode, Gunn

Diode, light-emitting

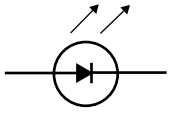

Diode, photosensitive

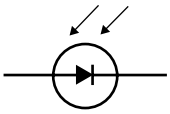

Appendix A 4/10/01 10:38 AM Page 775

Diode, PIN

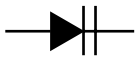

Diode, Schottky

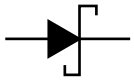

Diode, tunnel

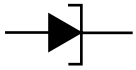

Diode, varactor

Diode, zener

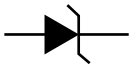

Directional coupler

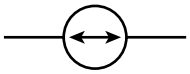

Directional wattmeter

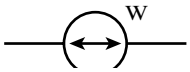

Exclusive-OR gate

Female contact, general

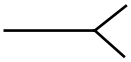

Ferrite bead

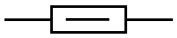

Filament, electron-tube

Fuse

Galvanometer

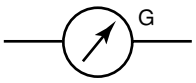

Grid, electron-tube

Ground, chassis

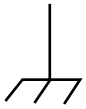

Appendix A 4/10/01 10:38 AM Page 776

Ground, earth

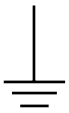

Headset

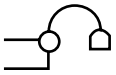

Handset, double

Headset, single

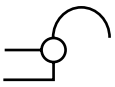

Headset, stereo

Inductor, air core

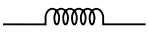

Inductor, air core, bifilar

Inductor, air core, tapped

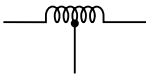

Inductor, air core, variable

Inductor, iron core

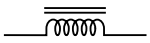

Inductor, iron core, bifilar

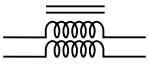

Inductor, iron core, tapped

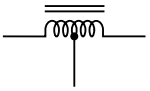

Inductor iron core, variable

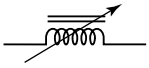

Inductor, powdered-iron core

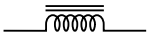

Inductor, powdered-iron core, bifilar

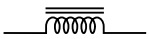

Appendix A 4/10/01 10:38 AM Page 777

Inductor, powdered-iron core, tapped

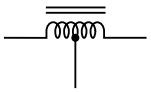

Inductor, powdered-iron core, variable

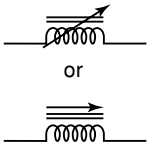

Integrated circuit, general

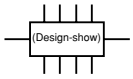

Jack, coaxial or phono

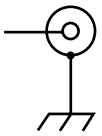

Jack, phone, two-conductor

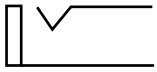

Jack, phone, three-conductor

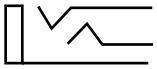

Key, telegraph

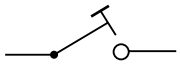

Lamp, incandescent

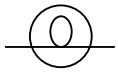

Lamp, neon

Male contact, general

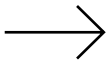

Meter, general

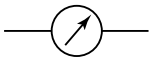

Microammeter

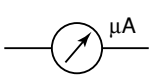

Microphone

Appendix A 4/10/01 10:39 AM Page 778

Microphone, directional

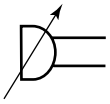

Milliammeter

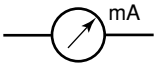

NAND gate

Negative voltage connection

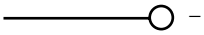

NOR gate

NOT gate

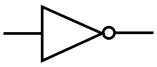

Optoisolator

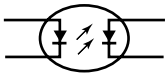

OR gate

Outlet, two-wire, nonpolarized

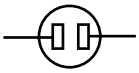

Outlet, two-wire, polarized

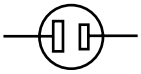

Outlet, three-wire

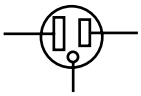

Outlet, 234-V

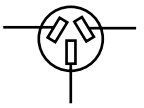

Plate, electron-tube

Plug, two-wire, nonpolarized

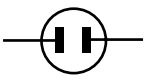

Appendix A 4/10/01 10:39 AM Page 779

Plug, two-wire, polarized

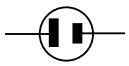

Plug, three-wire

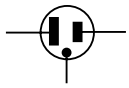

Plug, 234-V

Plug, coaxial or phono

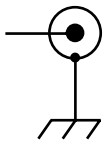

Plug, phone, two-conductor

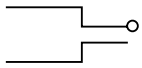

Plug, phone, three-conductor

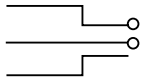

Positive voltage connection

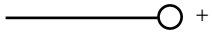

Potentiometer

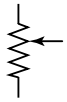

Probe, radio-frequency

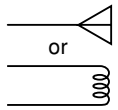

Rectifier, gas-filled

Rectifier, high-vacuum

Rectifier, semiconductor

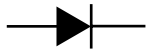

Rectifier, silicon-controlled

Appendix A 4/10/01 10:39 AM Page 780

Relay, double-pole, double-throw

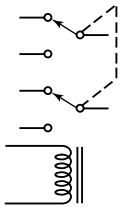

Relay, double-pole, single-throw

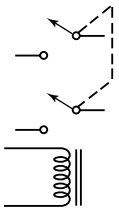

Relay, single-pole, double-throw

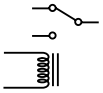

Relay, single-pole, single-throw

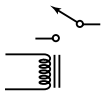

Resistor, fixed

Resistor, preset

Resistor, tapped

Resonator

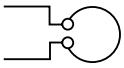

Rheostat

Saturable reactor

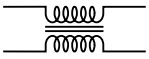

Signal generator

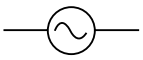

Solar battery

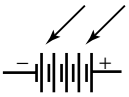

Appendix A 4/10/01 10:39 AM Page 781

Solar cell

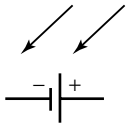

Source, constant-current

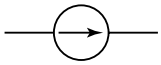

Source, constant-voltage

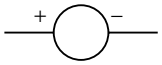

Speaker

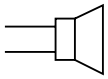

Switch, double-pole, double-throw

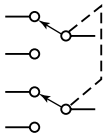

Switch, double-pole, rotary

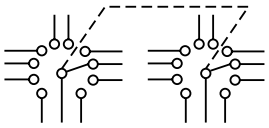

Switch, double-pole, single-throw

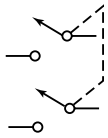

Switch, momentary-contact

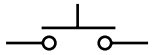

Switch, silicon-controlled

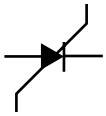

Switch, single-pole, rotary

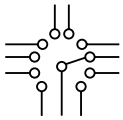

Switch, single-pole, double-throw

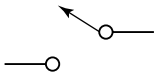

Switch, single-pole, single-throw

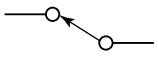

Appendix A 4/10/01 10:39 AM Page 782

Terminals, general, balanced

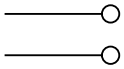

Terminals, general, unbalanced

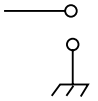

Test point

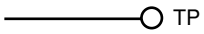

Thermocouple

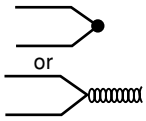

Transformer, air core

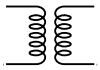

Transformer, air core, step-down

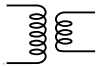

Transformer, air core, step-up

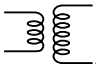

Transformer, air core, tapped primary

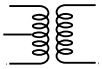

Transformer, air core, tapped secondary

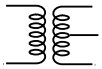

Transformer, iron core

Transformer, iron core, step-down

Transformer, iron core, step-up

Transformer, iron core, tapped primary

Transformer, iron core, tapped secondary

Appendix A 4/10/01 10:39 AM Page 783

Transformer, powdered-iron core

Transformer, powdered-iron core, step-down

Transformer, powdered-iron core, step-up

Transformer, powdered-iron core, tapped primary

Transformer, powdered-iron core,
tapped secondary

Transistor, bipolar, *NPN*

Transistor, bipolar, *PNP*

Transistor, field-effect, *N*-channel

Transistor, field-effect, *P*-channel

Transistor, MOS field-effect, *N*-channel

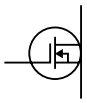

Transistor, MOS field-effect, *P*-channel

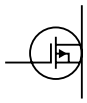

Transistor, photosensitive, *NPN*

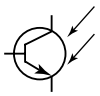

Transistor, photosensitive, *PNP*

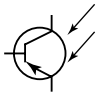

Appendix A 4/10/01 10:39 AM Page 784

Transistor, photosensitive, field-effect, *N*-channel

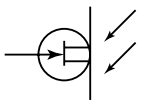

Transistor, photosensitive, field-effect, *P*-channel

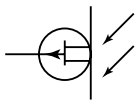

Transistor, unijunction

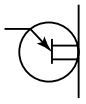

Triac

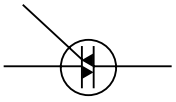

Tube, diode

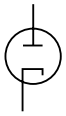

Tube, heptode

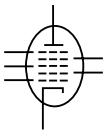

Tube, hexode

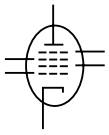

Tube, pentode

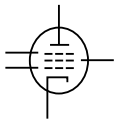

Tube, photosensitive

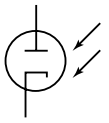

Tube, tetrode

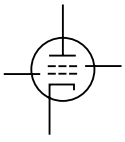

Appendix A 4/10/01 10:39 AM Page 785

Tube, triode

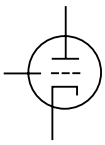

Voltmeter

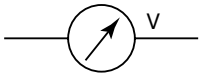

Wattmeter

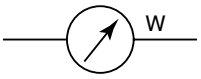

Waveguide, circular

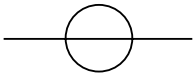

Waveguide, flexible

Waveguide, rectangular

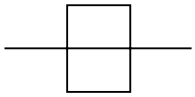

Waveguide, twisted

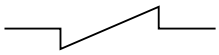

Wires, crossing, connected

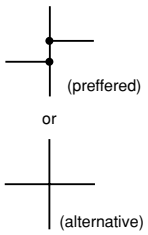

Wires, crossing, not connected

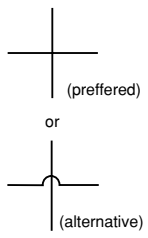

Appendix B
Tables and data

Conversion between Electrical Systems

Property	mks	System: cgs electromagnetic	System: cgs electrostatic
Capacitance	1 farad	10^{-9} abfarad	9×10^{11} statfarad
	10^{9} F	1 abF	9×10^{20} statF
	$10^{-11}/9$ F	$10^{-20}/9$ abF	1 statF
Charge	1 coulomb	0.1 abcoulomb	3×10^{9} statC
	10 C	1 abC	3×10^{10} statC
	$10^{-9}/3$ C	$10^{-10}/3$aC	1 statC
Charge density	1 coulomb/m^3	10^{-7} abcoulomb/cm^3	3×10^{3} statcoulomb/cm^3
	10^{7} C/m^3	1 abC/cm^3	3×10^{10} statCcm^3
	$10^{-3}/3$ C/m^3	$10^{-10}/3$ aC/cm^3	1 statC/cm^3
Conductivity	1 siemens/m	10^{-11} absiemens/cm	9×10^{9} statSiemens/cm
	10^{11} S/m	1 abS/cm	9×10^{20} statS/cm
	$10^{-9}/9$ S/m	$10^{-20}/9$ abS/cm	1 statS/cm
Current	1 ampere	10^{-1} abampere	3×10^{9} statampere
	10 a	1 abA	3×10^{10} statA
	$10^{-9}/3$ a	$10^{-10}/3$ abA	1 statA
Current density	1 ampere/m^2	10^{-5} abampere/cm^2	3×10^{5} statampere/cm^2
	10^{5} A/m^2	1 abA/cm^2	3×10^{10} statA/cm^2
	$10^{-5}/3$ A/m^2	$10^{-10}/3$ aA/cm^2	1 statA/cm^2
Electric field intensity	1 volt/m	10^{6} abvolt/cm	$10^{-4}/3$ statvolt/cm
	10^{-6} V/m	1 abV/cm	$10^{-10}/3$ statV/cm
	3×10^{4} V/m	3×10^{10} aV/cm	1 statV/cm
Electric potential	1 volt	10^{8} abvolt	$10^{-2}/3$ statvolt
	10^{-8} V	1 abV	$10^{-10}/3$ statV
	3×10^{2} V	3×10^{10} aV	1 statV
Electric dipole moment	1 coulomb-m	10 abC-cm	3×10^{11} statC-cm
	0.1 C-m	1 abC-cm	3×10^{10} statC-cm
	$10^{-11}/3$ C-m	$10^{-10}/3$ abC-cm	1 statC-cm

Copyright 2001 The McGraw-Hill Companies, Inc. Click Here for Terms of Use

Appendix B 4/10/01 10:42 AM Page 788

Property	System		
	mks	cgs electromagnetic	cgs electrostatic
Energy	1 joule	10^7 erg	10^7 erg
	10^{-7} J	1 e	1 e
	10^{-7} J	1 e	1 e
Force	1 newton	10^5 dyne	10^5 dyne
	10^{-5} N	1 d	1 d
	10^{-5} N	1 d	1 d
Flux density	1 Weber/m^2	10^4 gauss (or abtesla)	10^{-6}/3 electrostatic unit
	10^{-4} Wb/m^2	1 G	10^{-10}/3 esu
	3×10^6 Wb/m^2	3×10^{10} G	1 esu
Inductance	1 henry	10^9 abhenry	10^{-11}/9 stathenry
	10^{-9} H	1 abH	10^{-20}/9 statH
	9×10^{11} H	9×10^{20} abH	1 statH
Inductive capacity	1 farad/m	10^{-11} abfarad/cm	9×10^9 statfarad/cm
	10^{11} F/m	1 abF/cm	9×10^{20} statF/cm
	10^{-9}/9 F/m	10^{-20}/9 abF/cm	1 statF/cm
Magnetic flux	1 weber	10^8 Maxwell	10^{-2}/3 electrostatic unit
	10^{-8} W	1 Mx	10^{-10}/3 esu
	3×10^2 W	3×10^{10} Mx	1 esu
Magnetic dipole moment	1 ampere-m^2	10^3 abampere-cm^2	3×10^{13} statampere-cm^2
	10^{-3} A-m^2	1 abA-cm^2	3×10^{10} statA-cm^2
	10^{-13}/3 A-m^2	10^{-10}/3 abA-cm^2	1 statA-cm^2
Permeability	1 henry/m	10^7 abhenry/cm	10^{-13}/9 stathenry/cm
	10^{-7} H/m	1 abH/cm	10^{-20}/9 statH/cm
	9×10^{13} H/m	9×10^{20} abH/cm	1 statH/cm
Power	1 watt	10^7 erg/s	10^7 erg/s
	10^{-7} W	1 e/s	1e/s
	10^{-7} W	1 e/s	1e/s
Resistance	1 ohm	10^9 abohm	10^{-11}/9 statohm
	10^{-9} ohm	1 abohm	10^{-20}/9 statohm
	9×10^{11} ohm	9×10^{20} abohm	1 statohm

Appendix B 4/10/01 10:42 AM Page 789

GREEK ALPHABET

Capital	Lowercase	Name
A	α	alpha
B	β	beta
Γ	γ	gamma
Δ	δ or ∂	delta
E	ε	epsilon
Z	ζ	zeta
H	η	eta
Θ	θ or ϑ	theta
I	ι	iota
K	κ	kappa
Λ	λ	lambda
M	μ	mu
N	ν	nu
Ξ	ξ	xi
O	o	omicron
Π	π	pi
P	ρ	rho
Σ	σ or ζ	sigma
T	τ	tau
Υ	υ	upsilon
Φ	ϕ or φ	phi
X	χ	chi
Ψ	ψ	psi
Ω	ω	omega

Mathematical Functions

Signs and symbols

·	radix (base) point	≠	not equal to
•	multiplication symbol; logic AND function	~	similar to
∞	infinity	<	less than
+	plus; positive; logic OR function	≮	not less than
−	minus; negative	<<	much less than
±	plus or minus; positive or negative	>	greater than
∓	minus or plus; negative or positive	≯	not greater than
×	times	>>	much greater than
÷	divided by	≤	equal to or less than
/	divided by (expressive of a ratio)	≥	equal to or greater than
=	equal to	∝	proportional to; varies directly as
≡	identical to; is defined by	≐ or →	approaches
≃ or ≅	approximately equal to, congruent to	:	is to; proportional to
≈	approximately equal to	∴	therefore

Appendix B 4/10/01 10:42 AM Page 790

@	at the rate of; at cost of
e	natural number = 2.71828
π	pi ≈ 3.14159 . . .
( )	parentheses (use to enclose a group of terms)
[ ]	brackets (use to enclose a group of terms that includes one or more groups in parentheses)
{ }	braces (use to enclose a group of terms that includes one or more groups in brackets.
∠	angle
°	degrees (arc or temperature)
′	minutes; prime
″	seconds; double prime
||	parallel to
⊥	perpendicular to
. . .	and beyond
∇	(del or nabla) vector differential operator

Operations

$x + y$	x added to y; x OR y
$x - y$	y subtracted from x
$x \cdot y$, $x \times y$, or xy	multiplied by y; x AND y
$x \div y$	x divided by y
x/y or $\frac{x}{y}$	x divided by y
$1/x$	reciprocal of x
x^n	x raised to the indicated power of n
$\sqrt[n]{x}$	indicated root n of x
$x : y$	x is to y
$\|x\|$	absolute value of x, magnitude of x
$\bar{X}$, $\vec{X}$, or X	vector X

$\bar{x}$	average value of x; x not
f(x) or F(x)	function of x
i	$\sqrt{-1}$
j	operator, equal to $\sqrt{-1}$
Δx	increment of x
dx	differential of x
∂x	partial differential of x
$\frac{\Delta x}{\Delta y}$	change in x with respect to y
$\frac{dx}{dy}$	derivative of x with respect to y
$\frac{d}{dy}(x)$	derivative of x with respect to y
$d_y x$	derivative of x with respect to y
$\frac{\partial x}{\partial y}$	partial derivative of x with respect to y
$\sum_a$	summation
$\sum_b^a$	summation between limits (from a to b)
Π	product
$\prod_b^a$	product between limits (from a to b)
$\int$	integral
$\int_a^b$	integral between limits (from a to b)
$\int x\,dy$	integral of x with respect to y
$\|a$	evaluated at a
$\|_a^b$	evaluated between limits (from a to b)
$n!$	factorial of n

Appendix B 4/10/01 10:42 AM Page 791

Prefixes

Prefix	Quantity	Symbol
atto-	10^{-18}	a
femto-	10^{-15}	f
pico-	10^{-12}	p
nano-	10^{-9}	n
micro-	10^{-6}	μ
milli-	10^{-3}	m
centi-	10^{-2}	c
deci-	10^{-1}	d
deka-	10	da
hecto-	10^{2}	h
kilo-	10^{3}	k
mega-	10^{6}	M
giga-	10^{9}	G
tera-	10^{12}	T
peta-	10^{15}	P
exa-	10^{18}	E

RESISTOR COLOR CODE

The first three color bands supply the total resistance. The fourth color (if any) gives the tolerance. Example: A 5,600-ohm resistor would have green (first color, 5), blue (second color, 6) and red

1			2			3			4
black	=	0	black	=	0	black	=		gold ± 5%
brown	=	1	brown	=	1	brown	=	0	silver ± 10%
red	=	2	red	=	2	red	=	00	no band ± 20%
orange	=	3	orange	=	3	orange	=	000	
yellow	=	4	yellow	=	4	yellow	=	0000	
green	=	5	green	=	5	green	=	00000	
blue	=	6	blue	=	6	blue	=	000000	
violet	=	7	violet	=	7	gold	=	multiply by 0.1	
gray	=	8	gray	=	8	silver	=	multiply by 0.01	
white	=	9	white	=	9				

This page intentionally left blank.

Author 4/10/01 10:44 AM Page 795

About the author

Stan Gibilisco has authored or coauthored dozens of nonfiction books about electronics and science. He first attracted attention with *Understanding Einstein's Theories of Relativity* (TAB Books, 1983). His *Encyclopedia of Electronics* (TAB Professional and Reference Books, 1985) and *Encyclopedia of Personal Computing* (McGraw-Hill, 1996) were annotated by the American Library Association as among the best reference volumes published in those years. Stan's work has gained reading audiences in the Far East, Europe, and South America.

Copyright 2001 The McGraw-Hill Companies, Inc. Click Here for Terms of Use

This page intentionally left blank.

SOFTWARE AND INFORMATION LICENSE

The software and information on this diskette (collectively referred to as the "Product") are the property of The McGraw-Hill Companies, Inc. ("McGraw-Hill") and are protected by both United States copyright law and international copyright treaty provision. You must treat this Product just like a book, except that you may copy it into a computer to be used and you may make archival copies of the Products for the sole purpose of backing up our software and protecting your investment from loss.

By saying "just like a book," McGraw-Hill means, for example, that the Product may be used by any number of people and may be freely moved from one computer location to another, so long as there is no possibility of the Product (or any part of the Product) being used at one location or on one computer while it is being used at another. Just as a book cannot be read by two different people in two different places at the same time, neither can the Product be used by two different people in two different places at the same time (unless, of course, McGraw-Hill's rights are being violated).

McGraw-Hill reserves the right to alter or modify the contents of the Product at any time.

This agreement is effective until terminated. The Agreement will terminate automatically without notice if you fail to comply with any provisions of this Agreement. In the event of termination by reason of your breach, you will destroy or erase all copies of the Product installed on any computer system or made for backup purposes and shall expunge the Product from your data storage facilities.

LIMITED WARRANTY

McGraw-Hill warrants the physical diskette(s) enclosed herein to be free of defects in materials and workmanship for a period of sixty days from the purchase date. If McGraw-Hill receives written notification within the warranty period of defects in materials or workmanship, and such notification is determined by McGraw-Hill to be correct, McGraw-Hill will replace the defective diskette(s). Send request to:

Customer Service
McGraw-Hill
Gahanna Industrial Park
860 Taylor Station Road
Blacklick, OH 43004-9615

The entire and exclusive liability and remedy for breach of this Limited Warranty shall be limited to replacement of defective diskette(s) and shall not include or extend to any claim for or right to cover any other damages, including but not limited to, loss of profit, data, or use of the software, or special, incidental, or consequential damages or other similar claims, even if McGraw-Hill has been specifically advised as to the possibility of such damages. In no event will McGraw-Hill's liability for any damages to you or any other person ever exceed the lower of suggested list price or actual price paid for the license to use the Product, regardless of any form of the claim.

THE McGRAW-HILL COMPANIES, INC. SPECIFICALLY DISCLAIMS ALL OTHER WARRANTIES, EXPRESS OR IMPLIED, INCLUDING BUT NOT LIMITED TO, ANY IMPLIED WARRANTY OF MERCHANTABILITY OR FITNESS FOR A PARTICULAR PURPOSE. Specifically, McGraw-Hill makes no representation or warranty that the Product is fit for any particular purpose and any implied warranty of merchantability is limited to the sixty day duration of the Limited Warranty covering the physical diskette(s) only (and not the software or in-formation) and is otherwise expressly and specifically disclaimed.

This Limited Warranty gives you specific legal rights; you may have others which may vary from state to state. Some states do not allow the exclusion of incidental or consequential damages, or the limitation on how long an implied warranty lasts, so some of the above may not apply to you.

This Agreement constitutes the entire agreement between the parties relating to use of the Product. The terms of any purchase order shall have no effect on the terms of this Agreement. Failure of McGraw-Hill to insist at any time on strict compliance with this Agreement shall not constitute a waiver of any rights under this Agreement. This Agreement shall be construed and governed in accordance with the laws of New York. If any provision of this Agreement is held to be contrary to law, that provision will be enforced to the maximum extent permissible and the remaining provisions will remain in force and effect.

Copyright 2001 The McGraw-Hill Companies, Inc. Click Here for Terms of Use

Suggested additional references

Crowhurst, N. and Gibilisco, S., *Mastering Technical Mathematics—2nd Edition.* New York: McGraw-Hill, 1999.
Dorf, R., *Electrical Engineering Handbook—2nd Edition.* Boca Raton, FL: CRC Press, 1997.
Gibilisco, S., *Electronics Portable Handbook.* New York: McGraw-Hill, 1999.
Gibilisco, S., *Electronics Formulas Pocket Reference.* New York: McGraw-Hill, 1999
Gibilisco, S., *Mathematical and Physical Data, Equations, and Rules of Thumb.* New York: McGraw-Hill, 2001.
Van Valkenburg, M., *Reference Data for Engineers: Radio, Electronics, Computer and Communications.* Indianapolis: Howard W. Sams & Co., 1998.
Veley, V., *The Benchtop Electronics Reference Manual.* New York: McGraw-Hill, 1994.

Copyright 2001 The McGraw-Hill Companies, Inc. Click Here for Terms of Use

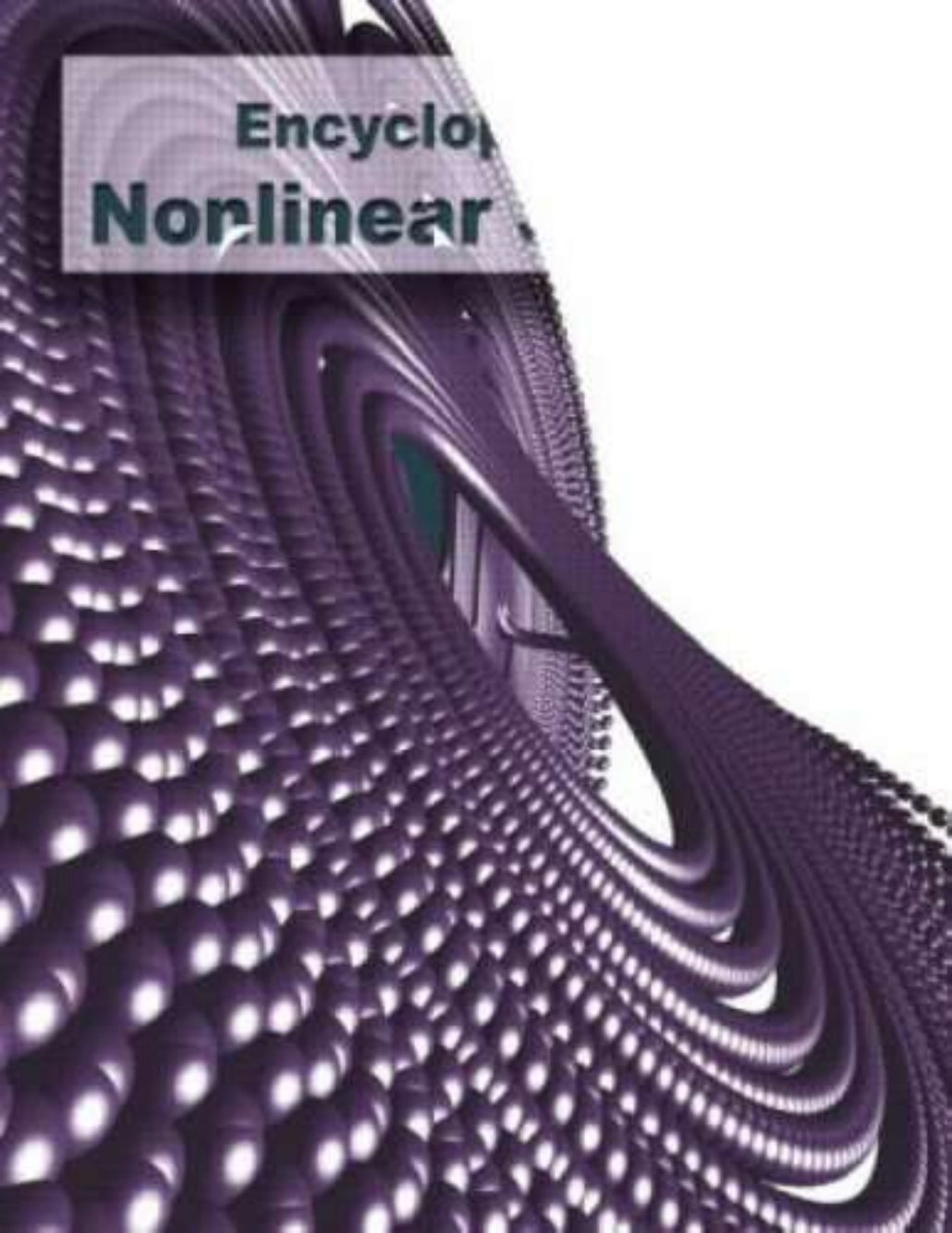
Encyclo
Nonlinear

List of Entries

Ablowitz–Kaup–Newell–Segur system
Adiabatic invariants
Alfvén waves
Algorithmic complexity
Anderson localization
Anosov and Axiom-A systems
Arnol'd diffusion
Artificial intelligence
Artificial life
Atmospheric and ocean sciences
Attractor neural network
Attractors
Aubry–Mather theory
Avalanche breakdown
Avalanches
Averaging methods

Bäcklund transformations
Ball lightning
Belousov–Zhabotinsky reaction
Bernoulli's equation
Berry's phase
Bethe ansatz
Bifurcations
Bilayer lipid membranes
Billiards
Binding energy
Biological evolution
Biomolecular solitons
Bjerrum defects
Black holes
Born–Infeld equations
Bose–Einstein condensation
Boundary layers
Boundary value problems
Branching laws
Breathers
Brownian motion
Brusselator
Burgers equation
Butterfly effect

Candle
Cardiac arrhythmias and the electrocardiogram
Cardiac muscle models
Cat map
Catalytic hypercycle
Catastrophe theory
Causality
Celestial mechanics
Cell assemblies
Cellular automata
Cellular nonlinear networks
Center manifold reduction
Chaos vs. turbulence
Chaotic advection
Chaotic dynamics
Characteristics
Charge density waves
Chemical kinetics
Cherenkov radiation
Chua's circuit
Clear air turbulence
Cluster coagulation
Coherence phenomena
Collective coordinates
Collisions
Color centers
Commensurate-incommensurate transition
Compartmental models
Complex Ginzburg–Landau equation
Conley index
Constants of motion and conservation laws
Continuum approximations
Contour dynamics

Controlling chaos
Cosmological models
Coupled map lattice
Coupled oscillators
Coupled systems of partial differential equations
Critical phenomena

Damped-driven anharmonic oscillator
Darboux transformation
Davydov soliton
Delay-differential equations
Denjoy theory
Derrick–Hobart theorem
Detailed balance
Determinism
Deterministic walks in random environments
Development of singularities
Differential geometry
Diffusion
Dimensional analysis
Dimensions
Diodes
Discrete breathers
Discrete nonlinear Schrödinger equations
Discrete self-trapping system
Dislocations in crystals
Dispersion management
Dispersion relations
Distributed oscillators
DNA premelting
DNA solitons
Domain walls
Doppler shift
Dressing method
Dripping faucet
Drude model
Duffing equation
Dune formation
Dynamical systems
Dynamos, homogeneous

Economic system dynamics
Effective mass
Einstein equations
Electroencephalogram at large scales
Electroencephalogram at mesoscopic scales
Electron beam microwave devices
Elliptic functions
Embedding methods
Emergence
Energy analysis
Entropy
Ephaptic coupling
Epidemiology
Equations, nonlinear
Equilibrium
Equipartition of energy
Ergodic theory
Euler–Lagrange equations
Evans function
Evaporation wave
Excitability
Excitons
Explosions
Extremum principles

Fairy rings of mushrooms
Feedback
Fermi acceleration and Fermi map
Fermi–Pasta–Ulam oscillator chain
Ferromagnetism and ferroelectricity
Fibonacci series
Filamentation
Fitness landscape
FitzHugh–Nagumo equation
Flame front
Flip-flop circuit
Fluctuation-dissipation theorem
Fluid dynamics
Fokker–Planck equation
Forecasting
Forest fires
Fractals
Framed space curves
Franck–Condon factor
Fredholm theorem
Free energy
Free probability theory
Frenkel–Kontorova model
Frequency doubling
Fröhlich theory
Frustration
Function spaces
Functional analysis

Galaxies
Game of life
Game theory
Gel'fand–Levitan theory
General circulation models of the atmosphere
General relativity
Generalized functions
Geometrical optics, nonlinear
Geomorphology and tectonics
Gestalt phenomena
Glacial flow
Global warming
Gradient system
Granular materials
Gravitational waves
Group velocity
Growth patterns

Hamiltonian systems
Harmonic generation
Hartree approximation
Heat conduction
Hele-Shaw cell
Helicity
Hénon map
Hénon–Heiles system
Hierarchies of nonlinear systems
Higgs boson
Hirota's method
Hodgkin–Huxley equations
Hodograph transform
Hole burning
Holons
Hopf bifurcation
Horseshoes and hyperbolicity in dynamical systems
Hurricanes and tornadoes
Huygens principle
Hydrogen bond
Hydrothermal waves
Hysteresis

Idempotent analysis
Incoherent solitons
Inertial manifolds
Information theory
Inhibition
Instantons
Integrability
Integrable cellular automata
Integrable lattices
Integral transforms
Integrate and fire neuron
Intermittency
Invariant manifolds and sets
Inverse problems
Inverse scattering method or transform
Ising model

Josephson junction arrays
Josephson junctions
Jump phenomena
Jupiter's Great Red Spot

Kadomtsev–Petviashvili equation
Kelvin–Helmholtz instability
Kerr effect
Kicked rotor
Kirchhoff's laws
Knot theory
Kolmogorov cascade
Kolmogorov–Arnol'd–Moser theorem
Korteweg–de Vries equation
Kuramoto–Sivashinsky equation

Laboratory models of nonlinear waves
Landau–Lifshitz equation
Langmuir–Blodgett films
Lasers
Lattice gas methods
Lévy flights
Lie algebras and Lie groups
Lifetime
Linearization
Liquid crystals
Local modes in molecular crystals
Local modes in molecules
Long Josephson junctions
Lorentz gas
Lorenz equations
Lyapunov exponents

Magnetohydrodynamics
Manley–Rowe relations
Maps
Maps in the complex plane
Markin–Chizmadzhev model
Markov partitions
Martingales
Matter, nonlinear theory of
Maxwell–Bloch equations
McCulloch–Pitts network
Measures
Mechanics of solids
Mel'nikov method
Mixing
Modulated waves
Molecular dynamics
Monodromy preserving deformations
Monte Carlo methods
Morphogenesis, biological
Multidimensional solitons
Multifractal analysis
Multiple scale analysis
Multiplex neuron
Multiplicative processes
Multisoliton perturbation theory
Myelinated nerves

Navier–Stokes equation
N-body problem
Nephron dynamics
Nerve impulses
Neural network models
Neuristor
Neurons
Newton's laws of motion
Nonequilibrium statistical mechanics
Nonlinear acoustics
Nonlinear electronics
Nonlinear optics
Nonlinear plasma waves

Nonlinear Schrödinger equations
Nonlinear signal processing
Nonlinear toys
Nonlinearity, definition of
Nontwist maps
Normal forms theory
N-soliton formulas
Numerical methods
N-wave interactions

One-dimensional maps
Optical fiber communications
Order from chaos
Order parameters
Ordinary differential equations, nonlinear
Overtones

Painlevé analysis
Parametric amplification
Partial differential equations, nonlinear
Particle accelerators
Particles and antiparticles
Pattern formation
Peierls barrier
Pendulum
Perceptron
Percolation theory
Period doubling
Periodic bursting
Periodic orbit theory
Periodic spectral theory
Perturbation theory
Phase dynamics
Phase plane
Phase space
Phase-space diffusion and correlations
Phase transitions
Photonic crystals
Plasma soliton experiments
Plume dynamics
Poincaré theorems
Poisson brackets
Polaritons
Polarons
Polymerization
Population dynamics
Power balance
Protein dynamics
Protein structure
Pump-probe measurements

Quantum chaos
Quantum field theory
Quantum inverse scattering method
Quantum nonlinearity
Quantum theory

Quasilinear analysis
Quasiperiodicity

Random matrix theory I: Origins and physical applications
Random matrix theory II: Algebraic developments
Random matrix theory III: Combinatorics
Random matrix theory IV: Analytic methods
Random walks
Ratchets
Rayleigh and Raman scattering and IR absorption
Rayleigh–Taylor instability
Reaction-diffusion systems
Recurrence
Regular and chaotic dynamics in atomic physics
Relaxation oscillators
Renormalization groups
Rheology
Riccati equations
Riemann–Hilbert problem
Rössler systems
Rotating rigid bodies
Rotating-wave approximation
Routes to chaos

Salerno equation
Sandpile model
Scheibe aggregates
Scroll waves
Semiconductor laser
Semiconductor oscillators
Separation of variables
Shear flow
Shock waves
Sinai–Ruelle–Bowen measures
Sine-Gordon equation
Singularity theory
Skyrmions
Solar system
Solitons
Solitons, a brief history
Solitons, types of
Spatiotemporal chaos
Spectral analysis
Spin systems
Spiral waves
Stability
Standard map
State diagrams
Stereoscopic vision and binocular rivalry
Stochastic analysis of neural systems
Stochastic processes
String theory
Structural complexity
Superconducting quantum interference device

Superconductivity
Superfluidity
Superlattices
Surface waves
Symbolic dynamics
Symmetry groups
Symmetry: equations vs. solutions
Symplectic maps
Synchronization
Synergetics

Tachyons and superluminal motion
Tacoma Narrows Bridge collapse
Taylor–Couette flow
Tensors
Tessellation
Thermal convection
Thermo-diffusion effects
Theta functions
Threshold phenomena
Time series analysis
Toda lattice
Topological defects
Topology
Traffic flow
Turbulence
Turbulence, ideal
Turing patterns
Twistor theory

Universality

Van der Pol equation
Virial theorem
Visiometrics
Volterra series and operators
Vortex dynamics in excitable media
Vortex dynamics of fluids

Water waves
Wave of translation
Wave packets, linear and nonlinear
Wave propagation in disordered media
Wave stability and instability
Wavelets
Winding numbers

Yang–Mills theory

Zeldovich–Frank-Kamenetsky equation
Zero-dispersion limits

Thematic List of Entries

General

HISTORY OF NONLINEAR SCIENCE

Bernoulli's equation, Butterfly effect, Candle, Celestial mechanics, Davydov soliton, Determinism, Feedback, Fermi–Pasta–Ulam oscillator chain, Fibonacci series, Hodgkin–Huxley equations, Introduction, Integrability, Lorenz equations, Manley–Rowe relations, Markin–Chizmadzhev model, Martingales, Matter, nonlinear theory of, Poincaré theorems, Solar system, Solitons, a brief history, Tacoma Narrows Bridge collapse, Van der Pol equation, Zeldovich–Frank-Kamenetsky equation

COMMON EXAMPLES OF NONLINEAR PHENOMENA

Avalanches, Ball lightning, Brownian motion, Butterfly effect, Candle, Clear air turbulence, Diffusion, Dripping faucet, Dune formation, Explosions, Fairy rings of mushrooms, Filamentation, Flame front, Fluid dynamics, Forest fires, Glacial flow, Global warming, Hurricanes and tornadoes, Jupiter's Great Red Spot, Nonlinear toys, Order from chaos, Pendulum, Phase transitions, Plume dynamics, Solar system, Tacoma Narrows Bridge collapse, Traffic flow, Water waves

Methods and Models

ANALYTICAL METHODS

Bäcklund transformations, Bethe ansatz, Center-manifold reduction, Characteristics, Collective coordinates, Continuum approximations, Dimensional analysis, Dispersion relations, Dressing method, Elliptic functions, Energy analysis, Evans function, Fredholm theorem, Gel'fand–Levitan theory, Generalized functions, Hamiltonian systems, Hirota's method, Hodograph transform, Idempotent analysis, Integral transforms, Inverse scattering method or transform, Kirchhoff's laws, Multiple scale analysis, Multisoliton perturbation theory, Non-equilibrium statistical mechanics, Normal forms theory, N-soliton formulas, Painlevé analysis, Periodic spectral theory, Perturbation theory, Phase dynamics, Phase plane, Poisson brackets, Power balance, Quantum inverse scattering method, Quasi-linear analysis, Riccati equations, Rotating-wave approximation, Separation of variables, Spectral analysis, Stability, State diagrams, Synergetics, Tensors, Theta functions, Time series analysis, Volterra series, Wavelets, Zero-dispersion limits

COMPUTATIONAL METHODS

Averaging methods, Cellular automata, Cellular nonlinear networks, Characteristics, Compartmen-

tal models, Contour dynamics, Embedding methods, Extremum principles, Fitness landscape, Forecasting, Framed space curves, Hartree approximation, Integrability, Inverse problems, Lattice gas methods, Linearization, Maps, Martingales, Monte–Carlo methods, Numerical methods, Recurrence, Theta functions, Time series analysis, Visiometrics, Volterra series and operators, Wavelets

TOPOLOGICAL METHODS

Bäcklund transformations, Cat map, Conley index, Darboux transformation, Denjoy theory, Derrick–Hobart theorem, Differential geometry, Extremum principles, Functional analysis, Horseshoes and hyperbolicity in dynamical systems, Huygens principle, Inertial manifolds, Invariant manifolds and sets, Knot theory, Kolmogorov–Arnol'd–Moser theorem, Lie algebras and Lie groups, Maps, Measures, Monodromy-preserving deformations, Multifractal analysis, Nontwist maps, One-dimensional maps, Periodic orbit theory, Phase plane, Phase space, Renormalization groups, Riemann–Hilbert problem, Singularity theory, Symbolic dynamics, Symmetry groups, Topology, Virial theorem, Winding numbers

CHAOS, NOISE AND TURBULENCE

Attractors, Aubry–Mather theory, Butterfly effect, Chaos vs. turbulence, Chaotic advection, Chaotic dynamics, Clear air turbulence, Dimensions, Entropy, Ergodic theory, Fluctuation-dissipation theorem, Fokker–Planck equation, Free probability theory, Frustration, Hele-Shaw cell, Horseshoes and hyperbolicity in dynamical systems, Lévy flights, Lyapunov exponents, Martingales, Mel'nikov method, Order from chaos, Percolation theory, Phase space, Quantum chaos, Random matrix theory, Random walks, Routes to chaos, Spatiotemporal chaos, Stochastic processes, Turbulence, Turbulence, ideal

COHERENT STRUCTURES

Biomolecular solitons, Black holes, Breathers, Cell assemblies, Davydov soliton, Discrete breathers, Dislocations in crystals, DNA solitons, Domain walls, Dune formation, Emergence, Fairy rings of mushrooms, Flame front, Higgs boson, Holons, Hurricanes and tornadoes, Instantons, Jupiter's Great Red Spot, Local modes in molecular crystals, Local modes in molecules, Multidimensional solitons, Nerve impulses, Polaritons, Polarons, Shock waves, Skyrmions, Solitons, types of, Spiral waves, Tachyons and superluminal motion, Turbulence, Turing patterns, Wave of translation

DYNAMICAL SYSTEMS

Anosov and axiom-A systems, Arnol'd diffusion, Attractors, Aubry–Mather theory, Bifurcations, Billiards, Butterfly effect, Cat map, Catastrophe theory, Center manifold reduction, Chaotic dynamics, Coupled map lattice, Deterministic walks in random environments, Development of singularities, Dynamical systems, Equilibrium, Ergodic theory, Fitness landscape, Framed space curves, Function spaces, Gradient system, Hamiltonian systems, Hénon map, Hopf bifurcation, Horseshoes and hyperbolicity in dynamical systems, Inertial manifolds, Intermittency, Kicked rotor, Kolmogorov–Arnol'd–Moser theorem, Lyapunov exponents, Maps, Measures, Mel'nikov method, One-dimensional maps, Pattern formation, Periodic orbit theory, Phase plane, Phase space, Phase-space diffusion and correlations, Poincaré theorems, Reaction-diffusion systems, Rössler systems, Rotating rigid bodies, Routes to chaos, Sinai–Ruelle–Bowen measures, Standard map, Stochastic processes, Symbolic dynamics, Synergetics, Universality, Visiometrics, Winding numbers

GENERAL PHENOMENA

Adiabatic invariants, Algorithmic complexity, Anderson localization, Arnol'd diffusion, Attractors, Berry's phase, Bifurcations, Binding energy, Boundary layers, Branching laws, Breathers, Brownian motion, Butterfly effect, Causality, Chaotic dynamics, Characteristics, Cluster coagulation, Coherence phenomena, Collisions, Critical phenomena, Detailed balance, Determinism, Diffusion, Domain walls, Doppler shift, Effective mass, Emergence, Entropy, Equilibrium, Equipartition of energy, Excitability, Explosions, Feedback,

Filamentation, Fractals, Free energy, Frequency doubling, Frustration, Gestalt phenomena, Group velocity, Harmonic generation, Helicity, Hopf bifurcation, Huygens' principle, Hysteresis, Incoherent solitons, Inhibition, Integrability, Intermittency, Jump phenomena, Kolmogorov cascade, Lévy flights, Lifetime, Mixing, Modulated waves, Multiplicative processes, Nonlinearity, definition of, N-wave interactions, Order from chaos, Order parameters, Overtones, Pattern formation, Period doubling, Periodic bursting, Power balance, Quantum chaos, Quantum nonlinearity, Quasiperiodicity, Recurrence, Routes to chaos, Scroll waves, Shear flow, Solitons, Spiral waves, Structural complexity, Symmetry: equations vs. solutions, Synergetics, Tachyons and superluminal motion, Tessellation, Thermal convection, Threshold phenomena, Turbulence, Universality, Wave packets, linear and nonlinear, Wave propagation in disordered media, Wave stability and instability

MAPS

Aubry–Mather theory, Bäcklund transformations, Cat map, Coupled map lattice, Darboux transformation, Denjoy theory, Embedding methods, Fermi acceleration and Fermi map, Hénon map, Maps, Maps in the complex plane, Monodromy preserving deformations, Nontwist maps, One-dimensional maps, Periodic orbit theory, Recurrence, Renormalization groups, Singularity theory, Standard map, Symplectic maps

MATHEMATICAL MODELS

Ablowitz–Kaup–Newell–Segur system, Attractor neural network, Billiards, Boundary value problems, Brusselator, Burger's equation, Cat map, Cellular automata, Compartmental models, Complex Ginzburg–Landau equation, Continuum approximations, Coupled map lattice, Coupled systems of partial differential equations, Delay-differential equations, Discrete nonlinear Schrödinger equations, Discrete self-trapping system, Duffing equation, Equations, nonlinear, Euler–Lagrange equations, Fitzhugh–Nagumo equation, Fokker–Planck equation, Frenkel–Kontorova model, Game of life, General circulation models of the atmosphere, Hénon–Heiles system, Integrable cellular automata, Integrable lattices, Ising model, Kadomtsev–Petviashvili equation, Knot theory, Korteweg–de Vries equation, Kuramoto–Sivashinsky equation, Landau–Lifshitz equation, Lattice gas methods, Lie algebras and Lie groups, Lorenz equations, Markov partitions, Martingales, Maxwell–Bloch equation, McCulloch–Pitts network, Navier–Stokes equation, Neural network models, Newton's laws of motion, Nonlinear Schrödinger equations, One-dimensional maps, Ordinary differential equations, nonlinear, Partial differential equations, nonlinear, Random walks, Riccati equations, Salerno equation, Sandpile model, Sine-Gordon equation, Spin systems, Stochastic processes, Structural complexity, Symbolic dynamics, Synergetics, Toda lattice, Van der Pol equation, Zeldovich–Frank-Kamenetsky equation

STABILITY

Attractors, Bifurcations, Butterfly effect, Catastrophe theory, Controlling chaos, Development of singularities, Dispersion management, Dispersion relations, Emergence, Equilibrium, Excitability, Feedback, Growth patterns, Hopf bifurcation, Lyapunov exponents, Nonequilibrium statistical mechanics, Stability

Disciplines

ASTRONOMY AND ASTROPHYSICS

Alfvèn waves, Black holes, Celestial mechanics, Cosmological models, Einstein equations, Galaxies, Gravitational waves, Hénon–Heiles system, Jupiter's Great Red Spot, N-body problem, Solar system

BIOLOGY

Artificial life, Bilayer lipid membranes, Biological evolution, Biomolecular solitons, Cardiac arrhythmias and electro cardiogram, Cardiac muscle models, Catalytic hypercycle, Compartmental models, Davydov soliton, DNA premelting, DNA solitons,

Epidemiology, Excitability, Fairy rings of mushrooms, Fibonacci series, Fitness landscape, Fröhlich theory, Game of life, Growth patterns, Morphogenesis, biological, Nephron dynamics, Protein dynamics, Protein structure, Scroll waves, Turing patterns

CHEMISTRY

Belousov–Zhabotinsky reaction, Biomolecular solitons, Brusselator, Candle, Catalytic hypercycle, Chemical kinetics, Cluster coagulation, Flame front, Franck–Condon factor, Hydrogen bond, Langmuir–Blodgett films, Molecular dynamics, Polymerization, Protein structure, Reaction-diffusion systems, Scheibe aggregates, Turing patterns, Vortex dynamics in excitable media

CONDENSED MATTER AND SOLID-STATE PHYSICS

Anderson localization, Avalanche breakdown, Bjerrum defects, Bose–Einstein condensation, Charge density waves, Cherenkov radiation, Color centers, Commensurate-incommensurate transition, Discrete breathers, Dislocations in crystals, Domain walls, Drude model, Effective mass, Excitons, ferromagnetism and Ferroelectricity, Franck–Condon factor, Frenkel–Kontorova model, Frustration, Heat conduction, Hydrogen bond, Ising model, Langmuir–Blodgett films, Liquid crystals, Local modes in molecular crystals, Mechanics of solids, Nonlinear acoustics, Peierls barrier, Percolation theory, Regular and chaotic dynamics in atomic physics, Scheibe aggregates, Semiconductor oscillators, Spin systems, Superconductivity, Superfluidity, Surface waves

EARTH SCIENCE

Alfvén waves, Atmospheric and ocean sciences, Avalanches, Ball lightning, Butterfly effect, Clear air turbulence, Dune formation, Dynamos, homogeneous, Fairy rings of mushrooms, Forest fires, General circulation models of the atmosphere, Geomorphology and tectonics, Glacial flow, Global warming, Hurricanes and tornadoes, Kelvin–Helmholtz instability, Sandpile model, Water waves

ENGINEERING

Artificial intelligence, Cellular automata, Cellular nonlinear networks, Chaotic advection, Chua's circuit, Controlling chaos, Coupled oscillators, Diodes, Dispersion management, Dynamos, homogeneous, Electron beam microwave devices, Explosions, Feedback, Flip-flop circuit, Frequency doubling, Hele-Shaw cell, Hysteresis, Information theory, Josephson junction arrays, Josephson junctions, Langmuir–Blodgett films, Lasers, Long Josephson junctions, Manley–Rowe relations, Neuristor, Nonlinear electronics, Nonlinear optics, Nonlinear signal processing, Optical fiber communications, Parametric amplification, Particle accelerators, Ratchets, Relaxation oscillators, Semiconductor laser, Semiconductor oscillators, Superconducting quantum interference device, Synchronization, Tacoma Narrows Bridge collapse

FLUIDS

Alfvén waves, Atmospheric and ocean sciences, Bernoulli's equation, Chaos vs. turbulence, Chaotic advection, Clear air turbulence, Contour dynamics, Electron beam microwave devices, Evaporation wave, Fluid dynamics, Forecasting, General circulation models of the atmosphere, Glacial flow, Hele-Shaw cell, Hurricanes and tornadoes, Hydrothermal waves, Jump phenomena, Jupiter's Great Red Spot, Kelvin–Helmholtz instability, Laboratory models of nonlinear waves, Lattice gas methods, Liquid crystals, Lorentz gas, Magnetohydrodynamics, Navier–Stokes equation, Nonlinear plasma waves, Plasma soliton experiments, Plume dynamics, Rayleigh–Taylor instability, Shear flow, Shock waves, Superfluidity, Surface waves, Taylor–Couette flow, Thermal convection, Thermo-diffusion effects, Traffic flow, Turbulence, Turbulence, ideal, Visiometrics, Vortex dynamics of fluids, Water waves

NEUROSCIENCE

Artificial intelligence, Attractor neural network, Cell assemblies, Compartmental models, Electroencephalogram at large scales, Electroencephalogram at mesoscopic scales, Ephaptic coupling, Evans function, FitzHugh–Nagumo equation, Gestalt

phenomena, Hodgkin–Huxley equations, Inhibition, Integrate and fire neuron, Multiplex neuron, Myelinated nerves, Nerve impulses, Neural network models, Neurons, Pattern formation, Perceptron, Stereoscopic vision and binocular rivalry, Stochastic analyses of neural systems, Synergetics

NONLINEAR OPTICS

Cherenkov radiation, Color centers, Damped-driven anharmonic oscillator, Dispersion management, Distributed oscillators, Excitons, Filamentation, Geometrical optics, nonlinear, Harmonic generation, Hole burning, Kerr effect, Lasers, Liquid crystals, Maxwell–Bloch equations, Nonlinear optics, Optical fiber communications, Photonic crystals, Polaritons, Polarons, Pump-probe measurements, Rayleigh and Raman scattering and IR absorption, Semiconductor laser, Tachyons and superluminal motion

PLASMA PHYSICS

Alfvén waves, Ball lightning, Charge density waves, Drude model, Dynamos, homogeneous, Electron beam microwave devices, Magnetohydrodynamics, Nonlinear plasma waves, Particle accelerators, Plasma soliton experiments

SOCIAL SCIENCE

Economic system dynamics, Epidemiology, Game theory, Hierarchies of nonlinear systems, Population dynamics, Synergetics, Traffic flow

SOLID MECHANICS AND NONLINEAR VIBRATIONS

Avalanche breakdown, Bilayer lipid membranes, Bjerrum defects, Charge density waves, Cluster coagulation, Color centers, Detailed balance, Dislocations in crystals, Domain walls, Frustration, Glacial flow, Granular materials, Growth patterns, Heat conduction, Hydrogen bond, Ising model, Kerr effect, Langmuir–Blodgett films, Liquid crystals, Local modes in molecular crystals, Mechanics of solids, Molecular dynamics, Nonlinear acoustics, Protein dynamics, Ratchets, Rheology, Sandpile model, Scheibe aggregates, Shock waves, Spin systems, Superlattices, Surface waves, Tessellation, Topological defects

THEORETICAL PHYSICS

Berry's phase, Black holes, Born–Infeld equations, Celestial mechanics, Cherenkov radiation, Cluster coagulation, Constants of motion and conservation laws, Cosmological models, Critical phenomena, Derrick–Hobart theorem, Detailed balance, Einstein equations, Entropy, Equipartition of energy, Fluctuation-dissipation theorem, Fokker–Planck equation, Free energy, Galaxies, General relativity, Gravitational waves, Hamiltonian systems, Higgs boson, Holons, Instantons, Matter, nonlinear theory of, N-body problem, Newton's laws of motion, Particles and antiparticles, Quantum field theory, Quantum theory, Regular and chaotic dynamics in atomic physics, Rotating rigid bodies, Skyrmions, String theory, Tachyons and superluminal motion, Twistor theory, Virial theorem, Yang–Mills theory

A

AB INITIO CALCULATIONS

See **Molecular dynamics**

ABLOWITZ–KAUP–NEWELL–SEGUR SYSTEM

In 1967, Gardner, Greene, Kruskal, and Miura (or GGKM) (Gardner et al., 1967) showed that the Kortegweg–de Vries (KdV) equation

$$q_t + 6qq_x + q_{xxx} = 0, \tag{1}$$

with rapidly decaying initial data on $-\infty < x < \infty$, can be linearized using direct and inverse scattering methods associated with the linear Schrödinger equation

$$v_{xx} + [k^2 + q(x,t)]v = 0. \tag{2}$$

The KdV equation is of practical interest, having been first derived in the study of long water waves (Korteweg & de Vries, 1895) and subsequently in several other areas of applied science.

In the method proposed by Gardner et al., the solitary wave (soliton) solution to the KdV equation (1)

$$q = 2\kappa^2 \operatorname{sech}^2 \kappa(x - 4\kappa^2 t - x_0)$$

and multisoliton solutions are associated with the discrete spectrum of Equation (2). The discrete eigenvalues were shown to be invariants of the KdV motion; for example, the above soliton solution is associated with the discrete eigenvalue of Equation (2) at $k = \mathrm{i}\kappa$.

At that time, it was not clear whether the method could be applied to other physically significant equations. In 1972, however, Zakharov and Shabat (1972) used an operator formalism developed by Lax (1968) to show that the nonlinear Schrödinger (NLS) equation

$$\mathrm{i}q_t + q_{xx} + \sigma|q|^2 q = 0, \tag{3}$$

with rapidly decaying initial data on $-\infty < x < \infty$, could also be linearized by direct and inverse scattering methods.

The NLS equation was known to arise in many physical contexts (Benney & Newell, 1967) and in 1973 Hasegawa and Tappert showed that the NLS equation describes the long-distance dynamics of nonlinear pulses in optical fibers (Hasegawa & Tappert, 1973). Motivated by these developments and indications that other equations fit into this category, David Kaup, Alan Newell, Harvey Segur, and the present author (Ablowitz et al., 1973, 1974) studied the following modification of the Zakharov–Shabat system:

$$\begin{aligned} v_{1x} &= -\mathrm{i}\zeta v_1 + q v_2, \\ v_{2x} &= \mathrm{i}\zeta v_2 + r v_1, \end{aligned} \tag{4}$$

$$\begin{aligned} v_{1t} &= A v_1 + B v_2, \\ v_{2t} &= C v_1 + D v_2. \end{aligned} \tag{5}$$

In Equations (4) and (5), v_1 and v_2 are auxiliary functions obeying the postulated linear systems; Equation (4) play the same role as Equation (2), whereas Equation (5) determine the temporal evolution of the functions v_1 and v_2. (The evolution equation associated with the auxiliary function v for the KdV equation was not given above.) The method establishes that the functions $q = q(x,t)$ and $r = r(x,t)$ satisfy nonlinear equations when the (yet to be determined) functions A, B, C, and D are properly chosen.

The key to this approach is to make Equations (4) and (5) compatible, that is, set the x-derivative of v_{it} equal to the t-derivative of v_{ix}. In other words, we set the x-derivative of the right-hand side of Equations (5) equal to the t-derivative of the right-hand side of Equations (4). The result of this calculation yields the following equations for A, B, C, and D:

$$\begin{aligned} A_x &= qC - rB, \\ B_x + 2\mathrm{i}\zeta B &= q_t - 2Aq, \\ C_x - 2\mathrm{i}\zeta C &= r_t + 2Ar, \\ D &= -A. \end{aligned} \tag{6}$$

In Ablowitz et al. (1973, 1974; see also Ablowitz & Segur, 1981), methods to solve these equations are described. The simplest procedure is to look for finite

power series expansions such as $A = \sum_{i=0}^{N} \zeta^i A_i$ and similarly for B and C.

For example, with $N = 2$, we find with $r = \mp q^*$ that the nonlinear Schrödinger equation (3) with $\sigma = \pm 1$ is a necessary condition. In this case there are 11 equations for the nine unknowns $\{A_i, B_i, C_i\}$, $i = 0, 1, 2$, and the remaining two equations determine the nonlinear evolution equations for q and r (in this case NLS when $q = \mp r^*$).

With $N = 3$ and $r = -1$, we find that q must satisfy the KdV equation. Also, with $r = \mp q$, the modifed KdV equation

$$q_t \pm 6q^2 q_x + q_{xxx} = 0 \tag{7}$$

results.

If we look for expansions containing inverse powers of ζ, additional interesting equations can be obtained. For example, postulating $A = a/\zeta$, $B = b/\zeta$, $C = c/\zeta$ results in the sine-Gordon and sinh-Gordon equations

$$u_{xt} = \sin u, \tag{8}$$

$$u_{xt} = \sinh u, \tag{9}$$

where $q = -r = -u_x/2$ in Equation (8) and $q = r = u_x/2$ in Equation (9). The sine-Gordon equation has been known to be an important equation in the study of differential geometry since the 19th century (cf. Bianchi, 1902), and it has found applications in the 20th century as models for dislocation propagation in crystals, domain walls in ferromagnetic and ferroelectric materials, short-pulse propagation in resonant optical media, and magnetic flux propagation in long Josephson junctions, among others.

Thus, a number of physically interesting nonlinear wave equations are obtained from the above formalism. In Ablowitz et al. (1973, 1974; see also Ablowitz & Segur, 1981), it was further shown as to how this approach could be generalized to a class of nonlinear equations described in terms of certain nonlinear evolution operators that were subsequently referred to in the literature as recursion operators.

Further, the whole class of nonlinear equations with rapidly decaying initial data on $-\infty < x < \infty$ was shown to be linearized via direct and inverse scattering methods. Special soliton solutions are associated with the discrete spectrum of the linear operator (4), and via (5) the discrete eigenvalues were shown to be invariants of the motion. In subsequent years, asymptotic analysis of the integral equations yielded the long-time behavior of the continuous spectrum, which in turn showed the ubiquitous role that the Painlevé equations play in integrable systems (cf. Ablowitz & Segur, 1981).

Because this formulation is analogous to the method of Fourier transforms, the method was termed the inverse scattering transform or simply the IST.

MARK J. ABLOWITZ

See also **Integrability; Inverse scattering method or transform; Korteweg–de Vries equation; Nonlinear Schrödinger equations; Solitons**

Further Reading

Ablowitz, M.J., Kaup, D.J., Newell, A.C. & Segur, H. 1973. Nonlinear equations of physical significance. *Physical Review Letters*, 31: 125–127

Ablowitz, M.J., Kaup, D.J., Newell, A.C. & Segur, H. 1974. The inverse scattering transform–Fourier analysis for nonlinear problems. *Studies in Applied Mathematics*, 53: 249–315

Ablowitz, M.J. & Segur, H. 1981. *Solitons and the Inverse Scattering Transform*, Philadelphia, PA: Society for Industrial and Applied Mathematics

Benney, D.J. & Newell, A.C. 1967. The propagation of nonlinear envelopes. *Journal of Mathematics and Physics* (Name changed to: *Studies in Applied Mathematics*), 46: 133–139

Bianchi, L. 1902. *Lezioni de Geometria Differenziale*, 3 vols, Pisa: Spoerri

Gardner, C.S, Greene, J.M., Kruskal, M.D. & Miura, R.M. 1967. Method for solving the Korteweg–deVries equation. *Physical Review Letters*, 19: 1095–1097

Hasegawa, A. & Tappert, F. 1973. Transmission of stationary nonlinear optical pulses in dispersive dielectrical fibers. I. Anamolous dispersion. *Applied Physics Letters*, 23: 142–144

Korteweg, D.J. & de Vries, F. 1895. On the change of form of long waves advancing in a rectangular canal, and on a new type of long stationary waves. *Philosophical Magazine*, 39: 422–443

Lax, P.D. 1968. Integrals of nonlinear equations of evolution and solitary waves. *Communications in Pure and Applied Mathematics*, 21: 467–490

Zakharov, V.E. & Shabat A.B. 1972. Exact theory of two-dimensional self-focusing and one-dimensional self-modulation of waves in nonlinear media. *Soviet Physics, JETP*, 34: 62–69

ABLOWITZ–LADIK EQUATION

See **Discrete nonlinear Schrödinger equations**

ACOUSTIC SOLITONS

See **Nonlinear acoustics**

ACTION POTENTIAL

See **Nerve impulses**

ACTION-ANGLE VARIABLES

See **Hamiltonian systems**

ACTIVATOR-INHIBITOR SYSTEM

See **Reaction-diffusion systems**

ADIABATIC APPROXIMATION

See **Davydov soliton**

ADIABATIC INVARIANTS

Adiabatic invariants, denoted by I, are approximate constants of motion of a given dynamical system (not necessarily Hamiltonian), which are approximately preserved during a process of slow change of the system's parameters (denoted by λ). This change is on a time scale T, which is supposed to be much larger than any typical dynamical time scale such as traversal time or the period of the shortest periodic orbits.

This is an asymptotic statement, in the sense that the adiabatic invariants are better preserved, the slower the driving of the system. In other words, the switching function $\lambda = \lambda(t)$ varies more slowly on the typical evolutionary time scale T, and the preservation is perfect in the limit $T \to \infty$.

The important point is that while the system's parameters $\lambda(t)$ and their dynamical quantities such as the total energy and angular momentum can change by arbitrarily large amounts, their combination involved in the adiabatic invariant I is preserved to a very high degree of accuracy, and this allows us to calculate changes of important quantities in dynamical systems. Examples arise in celestial mechanics, in other Hamiltonian systems, and in the motion of charged particles in magnetic and electric fields.

The accuracy of preservation can be calculated in systems with one degree of freedom and is exponentially good with T if the switching function $\lambda(t)$ is analytic (of class $\mathcal{C}^\infty$); that is to say, the change of the adiabatic invariant ΔI is of the form

$$\Delta I = \alpha \exp(-\beta T), \tag{1}$$

where α and β are known constants. If, however, the switching function $\lambda(t)$ is only of class $\mathcal{C}^m$ (m-times continuously differentiable), then the change of the adiabatic invariant ΔI during an adiabatic change over a time period of length T is algebraic only, namely

$$\Delta I = \alpha T^{-(m+1)}. \tag{2}$$

In both cases, $\Delta I \to 0$ as $T \to \infty$.

The fact that the evolutionary time scale T is large compared to the typical shortest dynamical time scales (average return time, etc.) suggests the averaging method or the so-called averaging principle. Here the long-term evolution (adiabatic evolution) of the system can be calculated by replacing the actual dynamical system with its averaged correspondent, obtained by averaging over the shortest dynamical time scales (the fast variables). Such a procedure is well known, for example, in celestial mechanics where the secular effects of the third-body perturbations of a planet are obtained by averaging the perturbations over one revolutionary period of the perturbers. This was done by Carl Friedrich Gauss in 1801 in the context of studying the dynamics of planets.

The adiabatic invariants can be easily calculated in one-dimensional systems and in completely integrable systems with N degrees of freedom. Something is known about the ergodic Hamiltonian systems, while little is known about adiabatic invariants in mixed-type Hamiltonian systems (with divided phase space), where for some initial conditions in the classical phase space, we have regular motion on invariant tori and irregular (chaotic) motion for other (complementary) initial conditions.

One elementary example is the simple (mathematical) pendulum, of point mass m and of length l with the declination angle φ, described by the Hamiltonian

$$H = \frac{p_\varphi^2}{2ml^2} - mgl\,\cos\varphi, \tag{3}$$

where $p_\varphi = ml^2\dot{\varphi}$ is the angular momentum. For small oscillations $\varphi \ll 1$, around the stable equilibrium $\varphi = 0$. It is described by the harmonic Hamiltonian

$$H' = \frac{p_\varphi^2}{2ml^2} + \frac{mgl}{2}\varphi^2. \tag{4}$$

Here the angular oscillation frequency is $\omega = 2\pi\nu = \sqrt{g/l}$, where ν is the frequency and g is the gravitational acceleration. We denote the total energy of the Hamiltonian H' by E. Paul Ehrenfest discovered that the quantity $I = E/\omega$ is the adiabatic invariant of the system, so the change of $E(t)$ on large time scales $T \gg 1/\nu$ is such that $I = E(t)/\omega(t)$ remains constant. Therefore, if for example the length of the pendulum $l = l(t)$ is slowly, adiabatically changing, then the energy of the system will change according to the law

$$E = E_0\sqrt{\frac{l_0}{l}}, \tag{5}$$

where E_0 and l_0 are the initial values and E and l the final values of the two variables. One can easily show that the oscillation amplitude φ_0 changes as $l^{-3/4}$ as the length l changes. This is an elementary example of a dynamically driven system in which the change of energy E can be very large, as is the change of ω, but $I = E/\omega$ is a well-preserved adiabatic invariant; in fact, it is exponentially well preserved if the switching function $\lambda(t)$ is analytic.

More generally, for Hamiltonian systems $H(q, p, \lambda)$ with one degree of freedom, whose state is described by the coordinate q and canonically conjugate momentum p in the phase space (q, p), and $\lambda = \lambda(t)$ is the system's parameter (slowly changing on time scale T), one can show that the action integral

$$I(E, \lambda) = I(E(t), \lambda(t)) = \frac{1}{2\pi}\oint p\,\mathrm{d}q \tag{6}$$

is the adiabatic invariant of the system, where the contour integral is taken at a fixed total energy E and a fixed value of λ. In this case, $2\pi I$ is interpreted as the area inside the curve $E = \text{const.}$ in the phase plane (q, p). The accuracy is exponentially good if $\lambda(t)$ is an analytic function and algebraic if it is of class C^m. Moreover, the theorem holds true only if the frequency ω is nonzero.

This implies that a passage through a separatrix (in the phase space of a one-dimensional system) is excluded because $\omega = 0$; thus a different approach is necessary with a highly nontrivial result. When crossing a separatrix of a one-dimensional double potential well from outside in an adiabatic way going inside, a bifurcation takes place, and the capture of the trajectory in either of the two wells is possible with some probabilities. These probabilities can be calculated quite easily, and the spread of the adiabatic invariant ΔI after such a passage can also be calculated, but this is more difficult. Important applications are found in celestial mechanics, where an adiabatic capture of a small body near a resonance with a planet can take place; in plasma physics; and in quantum mechanics of states close to the separatrix (in the semiclassical limit).

This is an interesting result, because I is precisely that quantity which according to the "old quantum mechanics" of Bohr and Sommerfeld has to be quantized, that is, made equal to an integer multiple of Planck's constant $\hbar$. Of course, the old quantum mechanics is generally wrong, but it can be a good approximation to the solution of the Schrödinger equation. Even then, strictly speaking, the quantization condition in the sense of EBK or Maslov quantization, must be written in the form

$$I = \frac{1}{2\pi} \oint p \, \mathrm{d}q = \left(n + \frac{\alpha}{4}\right) \hbar, \tag{7}$$

where $n = 0, 1, 2, \ldots$ is the quantum number and α is the Maslov index, that is, the number of caustics (projection singularities) round the cycle $E = \text{const.}$ in the phase plane. For smooth systems with quadratic kinetic energy, it is typically $\alpha = 2$. Thus, at this semiclassical level, we have the semiclassical adiabatic invariant, stating that in one-dimensional systems under an adiabatic change, the quantum number (and thus the eigenstate) is preserved. This agrees with the exact result in the theory of the Schrödinger equation in quantum mechanics. Round a closed loop in a parameter space, a quantum system returns to its original state, except for the phase. (This closed-loop phase change is essentially the so-called Berry's phase.)

The method of averaging can also be used in N-dimensional Hamiltonians $H = H(\boldsymbol{q}, \boldsymbol{p})$, where $\boldsymbol{q}$ and $\boldsymbol{p}$ are N-dimensional vectors, but it works only in two extreme cases: the integrable case and the ergodic case.

In a classical integrable Hamiltonian system we have N analytic, global, and functionally independent constants of motion $A_i = A_i(\boldsymbol{q}, \boldsymbol{p})$, $i = 1, 2, \ldots, N$, pairwise in involution; that is, all Poisson brackets $\{A_i, A_j\}$ vanish identically everywhere in phase space. The orbits in phase space are then confined to an invariant N-dimensional surface, and according to the Liouville–Arnol'd theorem the topology of these surfaces must be the topology of an N-dimensional torus. Then an action integral $I = (1/2\pi) \oint \boldsymbol{p} \cdot \mathrm{d}\boldsymbol{q}$ along a closed loop on a torus will be zero if the loop can be continuously shrunk to a point on the torus. But there are loops that cannot be shrunk to a point due to the topology of the torus. Then the integral I is different from zero, otherwise its value does not depend on the particular loop, so in a sense it is a topological invariant of the torus. On an N-dimensional torus, there are N such independent elementary closed loops C_i, $i = 1, 2, \ldots, N$. The integrals that we call simply actions or action variables

$$I_i = \frac{1}{2\pi} \oint_{C_i} \boldsymbol{p} \cdot \mathrm{d}\boldsymbol{q} \tag{8}$$

are then the most natural momentum variables on the torus, whilst angle variables $\boldsymbol{\Theta}$ specifying the position on the torus labeled by $\boldsymbol{I}$ can be generated from the transformation

$$\boldsymbol{\Theta} = \frac{\partial S(\boldsymbol{I}, \boldsymbol{q})}{\partial \boldsymbol{I}}, \tag{9}$$

where $S = \int \mathbf{p} \cdot \mathrm{d}\boldsymbol{q}$ is an action integral on the torus.

Applying the averaging principle (the method of averaging), one readily shows that for an integrable system the actions $\boldsymbol{I}$ are N adiabatic invariants, provided the system is nondegenerate, which means that the frequencies

$$\boldsymbol{\omega} = \frac{\partial H}{\partial \boldsymbol{I}} \tag{10}$$

on the given torus are not rationally connected; that is to say, there is no integer vector $\boldsymbol{k}$ such that $\boldsymbol{\omega} \cdot \boldsymbol{k} = 0$. The problem is that during an adiabatic process the frequencies $\boldsymbol{\omega}$ will change, and therefore, strictly speaking, there will be infinitely many points of $\lambda = \lambda(t)$, where $\boldsymbol{\omega} \cdot \boldsymbol{k} = 0$, which will, strictly speaking, invalidate the theorem. However, it is thought that if the degree of resonances or rationality conditions $\boldsymbol{\omega} \cdot \boldsymbol{k} = 0$ is of a very high order, meaning that all components of $\boldsymbol{k}$ are very large, then the adiabatic invariants I_i will be quite well preserved. But low-order resonances (rationality conditions) must be excluded. The details of such a process call for further investigation.

When the N actions I_i of an integrable system are quantized in the sense of Maslov, as explained above in the one-dimensional case, we again find agreement, at this semiclassical level, with quantum mechanics: in a family of integrable systems, all N quantum numbers and the corresponding eigenstates are preserved under an adiabatic change.

Another extreme of classically ergodic and thus fully chaotic systems has been considered already by Hertz. He found that in such ergodic Hamiltonian systems the phase space volume enclosed by the energy surface $H(\boldsymbol{q}, \boldsymbol{p}) = E =$ constant is the adiabatic invariant, denoted by

$$\Omega(E) = \int_{H(\boldsymbol{q},\boldsymbol{p})\leq E} \mathrm{d}^N\boldsymbol{q}\,\mathrm{d}^N\boldsymbol{p}. \qquad (11)$$

Of course, here it is required that while the system's parameter $\lambda(t)$ is slowly changing, the system itself must be ergodic for all $\lambda(t)$. Sometimes, this condition is difficult to satisfy, but sometimes it is easily fulfilled. Examples are the stadium of Bunimovich with varying length of the straight line between the two semicircles, or the Sinai billiard with varying radius of the circle inside a square. For an ergodic two-dimensional billiard of area $\mathcal{A}$ and point mass m, we have

$$\Omega(E) = 2\pi m\mathcal{A}E. \qquad (12)$$

Therefore, when $\mathcal{A}$ is adiabatically changing, the energy E of the billiard particle is changing reciprocally with $\mathcal{A}$. Diminishing $\mathcal{A}$ implies increasing E, and this can be interpreted as work being done against the "pressure" of only one particle, if we define the pressure as the time average of the momentum transfer at collisions with the boundary of our ergodic billiard. There is a formalism to proceed with this analysis close to the thermodynamic formalism, as derived from statistical mechanics, except that here we are talking about time averages rather than phase averages of classical variables.

Again, this general result for ergodic systems is interesting from the quantum point of view because $\mathcal{N} = \Omega(E)/(2\pi\hbar)^N$ is precisely the number of energy levels below the energy E in the semiclassical limit of very large $\mathcal{N}$, which is known as the Thomas–Fermi rule. It is the number of elementary quantum Planck cells inside the volume element $H(\boldsymbol{q}, \boldsymbol{p}) \leq E$. Indeed, quantum mechanically, the eigenstate and the (energy counting sequential) main quantum number $\mathcal{N}$ are preserved under an adiabatic change.

In case of a mixed-type Hamiltonian system, which is a typical case in nature, adiabatic theory is in its infancy. Moreover, in three or higher degrees of freedom, we have universal diffusion on the Arnol'd web, which is dense on the energy surface, even for KAM-type Hamiltonian systems that are very close to integrability, like our solar planetary system. On the Arnol'd web we have diffusional chaotic motion, and there is a rigorous theory by Nekhoroshev giving a rigorous upper bound to the diffusion rate in such a case. However, when compared with numerical calculations, it is found that the diffusion rate is many orders of magnitude smaller than the Nekhoroshev limit. In other words, the actual diffusion time is much longer than estimated by Nekhoroshev, implying that there we have some approximate adiabatic invariant for long times, but not very long times.

MARKO ROBNIK

See also **Averaging methods; Berry's phase; Billiards; Phase space; Quantum theory; Quasilinear analysis**

Further Reading

Arnol'd, V.I. 1989. *Mathematical Methods of Classical Mechanics*, 2nd edition, New York and Heidelberg: Springer

Cary, J.R. & Rusu, P. 1992. Separatrix eigenfunctions. *Physical Review* A, 45: 8501–8512

Cary, J.R. & Rusu, P. 1993. Quantum dynamics near a classical separatrix. *Physical Review A*, 47: 2496–2505

Landau, L.D. & Lifshitz, E.M. 1996. *Mechanics—Course of Theoretical Physics*, vol. 1, 3rd edition, Oxford: Butterworth-Heinemann

Landau, L.D. & Lifshitz, E.M. 1997. *Quantum Mechanics: Non-Relativistic Theory—Course of Theoretical Physics*, vol. 3, 3rd edition, Oxford: Butterworth-Heinemann

Lichtenberg, A.J. & Lieberman, M.A. 1992. *Regular and Chaotic Dynamics*, 2nd edition, New York and Heidelberg: Springer

Lochak, P. & Meunier, C. 1988. *Multiphase Averaging for Classical Systems*, New York and Heidelberg: Springer

Reinhardt, W.P. 1994. Regular and irregular correspondences. *Progress of Theoretical Physics Supplement*, 116: 179–205

ALFVÉN WAVES

The essence of Hannes Alfvén's contributions to cosmic and laboratory plasmas is his idea of combining electromagnetics and hydrodynamics (Alfvén, 1942), thus introducing the new concept of magnetohydrodynamics (MHD). Electromagnetic waves associated with the motion of conducting liquids in magnetic fields, now known as Alfvén waves, were first observed experimentally (Lundquist, 1949; Lehnert, 1954). Later on, waves of this nature have turned out to be fundamental constituents of numerous phenomena in all parts of the universe (Fälthammar, 1995; Wilhelmsson, 2000). In the pioneering experiments, liquid mercury was used by Lundquist, and liquid sodium by Lehnert, who achieved higher electrical conductivity and lower density, leading to a higher Lundquist number (lower damping). Alfvén used his early results to give a possible explanation for sunspots and the solar cycle (periodicity in the Sun's activity) (Alfvén, 1942). Alfvén noticed that the Sun has a general magnetic field and that solar matter is a good conductor, thus fulfilling idealized requirements for the notion of an electromagnetic wave in a gaseous conductor or plasma.

At a very early age, Alfvén was given a copy of a popular astronomy book by Camille Flammarion, which greatly stimulated his lifelong interest in astronomy and astrophysics. His early experiences building radio receivers at the school radio club were also important for his later activities. Interestingly, another great scientist, Albert Einstein, received a small compass as a present when he was five years old, which

entirely absorbed his interest. He asked everybody around him what a magnetic field was and what gravity was, and later on in his life he admitted that this early experience might have influenced his lifelong scientific activities. Other similarities between the two scientists were that in their professional work both Einstein and Alfvén were very creative individualists, striving for simplicity of their solutions, and being skilled in many areas, they often looked at problems with fresh eyes. Both received Nobel Prizes in physics: Einstein in 1922, Alfvén in 1970.

The simplest form of an Alfvén wave, a propagation of an electromagnetic wave in a highly conducting plasma, was first rejected by critics on the grounds that it could not be correct, otherwise it would already have been discovered by Maxwell. Furthermore, experiments had been performed with magnetic fields and conductive media by Ampère and others long ago. Nevertheless, "The Alfvén wave, in fact, is the very foundation on which the entire structure of magnetohydrodynamics (MHD) is erected. Beginning from a majestic original simplicity, it has acquired a rich and variegated character, and has ended up dictating most of the low-frequency dynamics of magnetized plasmas" (Mahajan, 1995).

To visualize the interaction between the magnetic field and the motion of the conductive fluid, one may use an analogy with the theory of stretched strings to obtain a wave along the magnetic lines of force with a velocity v_A, where

$$v_A{}^2 = \frac{B^2}{\mu_0 \rho} \tag{1}$$

and ρ is the mass density of the fluid, μ_0 is the permittivity, and B is the magnetic field.

The variations in velocity and current are mutually perpendicular and the magnetic field variations are in the direction of the fluid velocity variations, all variations being perpendicular to the direction of propagation. One may say that the variations of the magnetic field lines are frozen to those of the fluid motion, as can be deduced from electromagnetic equations, together with the hydrodynamic equation for the case of an incompressible fluid of infinite conductivity. The Alfvén wave is a low-frequency wave ($\omega < \omega_{ci}$, ω_{ci} being the ion cyclotron frequency) for which the displacement current is negligible. In fact, there are two types of Alfvén waves, for which

$$\omega / k_\parallel = v_A \text{ (torsional or shearwave)} \tag{2}$$

and

$$\omega / k = v_A \text{ (compressional wave)} \tag{3}$$

where ω is the frequency, $k^2 = k_\parallel^2 + k_\perp^2$, with $k_\parallel$ and $k_\perp$ being the wave numbers along and perpendicular to the magnetic field. For the shear wave, the frequency depends only on $k_\parallel$ and not on $k_\perp$, which has profound consequences and leads to a continuous spectrum (Mahajan, 1995).

For determining plasma stability and in selecting schemes for plasma heating and current drive in fusion plasma devices, the understanding of Alfvén wave dynamics is of great importance and has led to a vast literature. Nonlinear effects are of relevance to large-amplitude disturbances frequently observed in laboratory and space plasmas (Wilhelmsson, 1976). The formation and propagation of Alfvén vortices with geocosmophysical and pulsar (electron-positron plasma) applications are just two examples. Alfvén waves have also found interesting applications in solid-state plasmas in semiconductors as well as in metals and semimetals. Such studies have resulted in refined methods of measuring magnetic fields.

It is often said that the universe consists 99% of plasma. Alfvén used to say that it seems as if only the crust of the Earth is not plasma. In the mid-1960s, this author gave a talk at the Royal Institute of Technology in Stockholm about plasmas in solids (electrons and holes), which Hannes Alfvén himself attended. Among other things, the talk described recent observations of Alfvén waves in such plasmas, and Alfvén said: "Ah, they are here also. How interesting, I did not know that."

It was not until the middle of the 20th century that more intensive investigations on Alfvén waves in space and laboratory plasmas began. The slow development of the field of space plasmas was possibly because many physicists were not acquainted with the fact that electric currents can be distributed in large volumes and magnetic fields in such volumes can be present. Since then, the gigantic laboratory of the universe from the aurora originating in the Earth's magnetosphere to quasars at the rim of the universe has attracted immense interest with regard to Alfvén waves.

When propagating in inhomogeneous plasmas, for example, in the magnetosphere, the Alfvén wave experiences many interesting phenomena, including mode coupling, resonant mode conversion, and resonant absorption. We now know that shear Alfvén waves lie behind the phenomena of micropulsations in the geomagnetic field and also acceleration of particles. Micropulsations were detected a hundred years ago with simple magnetometers on the ground. It took more than 50 years before it was understood that they were related to the magnetosphere. Solar physics is another fascinating field where Alfvén waves occur, giving rise to sunspots (Alfvén, 1942). The vast amount of energy exhibited in eruptions of particles on the solar surface, originating in the interior of the Sun, is probably transported by Alfvén waves. These also play a role in heating the solar corona. Alfvén waves were first identified in the solar wind by means of spacecraft measurements by the end of the 1960s. They also occur in the exosphere of comets. A new and promising area of research

is laboratory astrophysics using high-intensity particle and photon beams that may shed light on superstrong fields in plasmas.

For applications to confinement and heating of fusion plasmas, for example, in Tokamak devices, shear Alfvén waves have been studied in toroidal plasmas, accounting for nonuniform plasmas in axisymmetric situations. It is believed that the remaining exciting challenges lie in the area of nonlinear physics of shear Alfvén waves and associated particle dynamics and anomalous losses of α particles in a deuterium-tritium plasma. Collective modes in inhomogeneous plasmas as well as energy and particle transport in plasmas with transport barriers are of paramount importance for the design of a future Tokamak power plant (Parail, 2002).

Nonlinear transport processes in laboratory and cosmic plasmas have much in common (Wilhelmsson, 2000; Wilhelmsson & Lazzaro, 2001). Similarities (and discrepancies) could be highly indicative and beneficial for an improved understanding of specific phenomena as well as for plasma dynamics in general—possibly even for describing the evolution of the universe (Wilhelmsson, 2002).

HANS WILHELMSSON

See also **Magnetohydrodynamics; Nonlinear plasma waves; Plasma soliton experiments**

Further Reading

Alfvén, H. 1942. Existence of electromagnetic-hydrodynamic waves. *Nature*, 150: 405–406

Fälthammar, C.-G. 1995. Hannes Alfvén. In *Alfvén Waves in Cosmic and Laboratory Plasmas*, edited by A.C.-L. Chian, A.S. de Assis, C.A. de Azevedo, P.K. Shukla & L. Stenflo, Proceedings of the International Workshop on Alfvén Waves, *Physica Scripta*, T60: 7

Lehnert, B. 1954. Magnetohydrodynamic waves in liquid sodium. *Physical Review*, 94: 815

Lundquist, S. 1949. Experimental demonstration of magnetohydrodynamic waves. *Nature*, 164: 145

Mahajan, S.M. 1995. Spectrum of Alfvén waves, a brief review. *Physica Scripta*, T60: 160–170

Marston, E.H. & Kao Y.H. 1969. Damped Alfvén waves in bismuth. A determination of charge-carrier relaxation times. *Physical Review*, 182: 504

Parail, V.V. 2002. Energy and particle transport in plasmas with transport barriers. *Plasma Physics and Controlled Fusion*, 44: A63–85

Wilhelmsson, H. (editor). 1982. The physics of hot plasmas. Proceedings of the International Conference on Plasma Physics, Göteborg, May 1982, *Physica Scripta*, T2 (1 and 2)

Wilhelmsson, H. (editor). 1976. *Plasma Physics: Nonlinear Theory and Experiments*, New York and London: Plenum Press

Wilhelmsson, H. 2000. *Fusion: A Voyage through the Plasma Universe*, Bristol and Philadelphia: Institute of Physics Publishing

Wilhelmsson, H. 2002. Gravitational contraction and plasma fusion burn; universal expansion and the Hubble Law. *Physica Scripta*, 66: 395

Wilhelmsson, H. & Lazzaro, E. 2001. *Reaction-Diffusion Problems in the Physics of Hot Plasmas*, Bristol and Philadelphia: Institute of Physics Publishing

ALGORITHMIC COMPLEXITY

The notion of complexity as an object of scientific interest is relatively new. Prior to the 20th century, the main concern was that of simplicity, with complexity being the denigrated opposite. This idea of simplicity has had a long history enshrined in the dictum of the 14th-century Franciscan philosopher, William of Occam, that "pluritas non est ponenda sine necessitate" [being is not multiplied without necessity], and passed on simply as "Occam's razor," or more prosaically, "keep it simple" (Thorburn, 1918).

Indeed, the razor has been invoked by such notables as Isaac Newton and, in modern times, Albert Einstein and Stephen Hawking to justify parsimony in the adoption of physical principles. Although the dictum has proved its usefulness as a support for many scientific theories, the last century witnessed a gradual concern for simplicity's complement. Implicit was a recognition that beyond logical partitions was a need to quantify the simple/complex continuum. Perhaps the first milestone on the road to quantifying complexity came with Claude Shannon's famous information entropy in the late 1940s. Although it was not specifically developed as a complexity measure, the information connection made by Warren Weaver soon provided an impetus for sustained interest in information as a unifying concept for complexity (Weaver, 1948).

Shannon approached information as a statistical measure of receiving a message (Shannon, 1948): if $p_1, p_2, \ldots, p_N$ are the probabilities of receiving messages $m_1, m_2, \ldots, m_N$, then the information carried is defined by

$$I = -\sum_{i}^{N} p_i \log_2 p_i. \qquad (1)$$

Information is typically referred to as a measure of surprise; that is, the more unlikely a message, the more information it contains. To some degree, information is related to the notion of randomness in that the more regular (less complex, less random) something is, the less surprise is available. A simple calculation of this entropy demonstrates that the maximum of the function is achieved when all probabilities are equal. Shannon had a measure of capacities of a communication channel as his goal and did not concern himself with individual objects of the messages. Nonetheless, the quantification in terms of probabilities provided a basis for viewing complexity.

This theme was soon independently taken up by Ray Solomonoff (1964), Andrey Kolmogorov (1965),

and Gregory Chaitin (1966). In a sense, Somolonoff was looking for a way to measure the effect of Occam's razor; that is, how can one measure objectively the simplicity of a scientific theory? Kolmogorov and Chaitin, on the other hand, were interested in a measure of complexity of individual objects, as opposed to Shannon's average. This Kolmogorov–Chaitin complexity has come to be known variously as algorithmic complexity, algorithmic entropy, and algorithmic randomness, among other designations. Both Kolmogorov and Chaitin were interested in binary number strings as objects and the ability to define the complexity of a string in terms of the shortest algorithm that prints out the string. Again, regularity and randomness is involved (Gammarman & Vovk, 1999). Consider, for example, the simple bit string, 101010101010, . . .; the minimal program to write the string requires only the pattern 10, the length of the string, and the "repeat, write" instructions, or

$$K(s) = \min\{|p| : s = C_T(p)\}, \qquad (2)$$

where $K(s)$ is the Kolmogorov complexity of the string, $|p|$ is the program length in bits, and $C_T(p)$ is the result of running program p on a universal Turing machine T.

Clearly, the recognition that patterns play an important role in defining complexity re-emphasized their importance in terms of data compression. In the early 1950s, David Huffman recognized their importance, and algorithmic complexity reaffirmed their utility with the ascendancy of computers and their demand for storage space (Huffman, 1952). Thus, numerous coding schemes were developed to take advantage of the fact that a simple algorithm can compress long data streams based upon the idea that recurrent patterns exist.

The efforts of Somonoloff, Kolmogorov, and Chaitin spawned numerous alternative measures of complexity, often seeking to address identified deficiencies in the definitions (Shalizi & Crutchfield, 2001). Among the deficiencies pointed out were the following: (i) Complexity is defined in terms of randomness—it is maximized by random strings. Is this what is really sought? (ii) Complexity is uncomputable, since there is no algorithm to compute it on a universal computing machine. (iii) Complexity does not provide information regarding structural patterns or organizations that have the same amount of disorder.

These questions were compounded by the expanding field of nonlinear dynamics. Kolmogorov's earlier entropy (1958)—developed to determine the rate of information creation—were among the invariants used to distinguish chaotic systems and an inferred complexity. Moreover, the description of physical dynamical systems became an additional issue (Zurek, 1989). Physical processes were typically described along the continuum of two extremes: periodic or random. However, both such systems are simply described, one by a recurrent pattern and the other by a statistical description. While information is high in a random system, it is low in a periodic process. Amalgams of two such processes might require considerable computational effort, yet no metric sufficiently expressed this. Certainly, such combined processes (random and periodic) may exhibit moderate information but the most concise description may be quite complex.

Some of these difficulties have been addressed with varying degrees of acceptance (Wakerberger et al., 1994). Increasingly, however, it appears that the question is evolving along two different lines: a formal approach (rules) with its main ramifications redounding to mathematics and computer science and a physical approach (equations) dealing with the characterization of systems.

Both approaches have in common the emphasis on the reconstruction (prediction) of an observed system and on the need to give the most parsimonious recipe for generating the studied entity. The metrics of complexity is thus expressed in terms of program lines for the mathematics-oriented option and in dimensionality for the physics-oriented definition, but there is the same basic notion of complexity as the inverse of compressibility of a given object (Boffetta et al., 2002).

This notion of compressibility has an immediate translation in terms of both multidimensional statistics and technology. In multidimensional statistics, the compressibility of a given data set corresponds to the percentage of explained variance by the optimal (generally in a least-squares sense) model of the data. More generally, something can be compressed if there exists some sort of correlation structure linking the different portions of a system, the existence of such correlations implying that the information about one part of the system is implicit in another part. Thus, all the information is not needed to reconstruct the entire system. It is evident how this concept corresponds to the cognate concept of redundancy, bringing us back to the notion of entropy (Giuliani et al., 2001).

Clearly, the diverse algorithms designed to measure complexity suggest a commonality. The question remains as to whether one metric is sufficient for its characterization.

Joseph P. Zbilut and Alessandro Giuliani

See also **Entropy; Information theory; Structural complexity**

Further Reading

Boffetta, G., Cencini, M., Falcioni, M. & Vulpiani, A. 2002. Predictability: a way to characterize complexity. *Physics Reports*, 356: 367–474

Chaitin, G.J. 1966. On the length of programs for computing finite binary sequences. *Journal of the Association for Computing Machinery*, 13: 547–569

Gammerman, A. & Vovk, V. 1999. Kolmogorov complexity: sources, theory and applications. *The Computer Journal*, 42: 252–255

Gell-Mann, M. & Lloyd, S. 1999. Information measures, effective complexity, and total information. *Complexity*, 2: 44–52

Giuliani, A., Colafranceschi, M., Webber Jr., C.L. & Zbilut, J.P. 2001. A complexity score derived from principal components analysis of nonlinear order measures. *Physica* A, 301: 567–588

Huffman, D.A. 1952. A method for the construction of minimum redundancy codes. *Proceedings IRE*, 40: 1098–1101

Kolmogorov, A.N. 1958. A new metric invariant of transitive dynamical systems and automorphism in Lebesgue spaces. *Doklady Akademii Nauk SSSR [Proceedings of the Academy of Sciences of the USSR]*, 119: 861–864

Kolmogorov, A.N. 1965. Tri podkhoda k opredeleniiu poniatiia "kolichestvo informatsii". [Three approaches to the quantitative definition of information.] *Problemy Peredachy Informatsii [Problems Information Transmission]*, 1: 3–11

Lempel, A. & Ziv, J. 1976. On the complexity of finite sequences. *IEEE Transactions on Information Theory*, 22: 75–81

Li, M. & Vitányi, P. 1997. *An Introduction to Kolmogorov Complexity and Its Applications*, 2nd edition, New York: Springer

Salomon, D. 1998. *Data Compression, the Complete Reference*, New York: Springer

Shalizi, C.R. & Chrutchfield, J.P. 2001. Computational mechanics: pattern and prediction, structure and simplicity. *Journal of Statistical Physics* 104: 819–881

Shannon, C.E. 1948. A mathematical theory of communication. *Bell System Technical Journal*, 27: 379–423

Solomonoff, R.J. 1964. The formal theory of inductive inference, parts 1 and 2. *Information and Control*, 7: 1–22, 224–254

Thorburn, W.M. 1918. The myth of Occam's razor. *Mind*, 27: 345–353

Wackerberger, R., Witt, A., Atmanspacher, H., Kurths, J. & Scheingraber, H. 1994. A comparative classification of complexity measures. *Chaos, Solitons & Fractals*, 4: 133–173

Weaver, W. 1948. Science and complexity. *American Scientist*, 36: 536–544

Zurek, W. 1989. Thermodynamic cost of computation, algorithmic complexity, and the information metric. *Nature*, 341: 119–124

ALL-OR-NOTHING RESPONSE

See **Nerve impulses**

ALMOST PERIODIC FUNCTIONS

See **Quasiperiodicity**

AMBIGUOUS FIGURES

See **Cell assemblies**

ANDERSON LOCALIZATION

Anderson localization is a phenomenon associated with the interference of waves in random media. Although Philip Anderson's original publication (Anderson, 1958) was actually motivated by experiments on the propagation of spin-waves in random magnets, the greatest application of the concept has been the study of electrical transport phenomena in metals and semiconductors. Over the past 10 years, more attention has been focused on other wave phenomena in random media, particularly optical phenomena.

Our current understanding of electronic transport in metals and semiconductors is based on the Schrödinger equation for the wave function of conduction electrons of the form

$$-\frac{\hbar^2}{2m^*}\nabla^2\psi(\boldsymbol{r}) + [U(\boldsymbol{r}) + V(\boldsymbol{r})]\,\psi(\boldsymbol{r}) = E\psi(\boldsymbol{r}),$$

where $U(\boldsymbol{r})$ is a periodic potential representing the regular lattice in the solid and $V(\boldsymbol{r})$ is a random function of position, which represents the presence of impurities in the system. In the absence of the random potential, the allowed energies of such an electron fall within a series of bands separated by energy gaps. The eigenfunctions in the absence of the random potential are all of the form $e^{i\boldsymbol{k}\cdot\boldsymbol{r}}u_{j,\boldsymbol{k}}(\boldsymbol{r})$ where the wavevector $\boldsymbol{k}$ lies within the first Brillouin zone, j labels the energy bands and the Bloch function, $u_{j,\boldsymbol{k}}(\boldsymbol{r})$, has the periodicity of the regular potential, U. Such states are *extended* in the sense that their support covers the entire system and hence they can contribute to electrical conduction.

The eigenstates of an electron subject to a random potential may be of two types. Some are extended, although there may be strong local modulations in the amplitude. These states can contribute to electrical conduction through the material, even at zero temperature, as they connect the two ends of a sample. Other states, however, are localized in that their amplitude vanishes exponentially outside a specific finite region. These states are referred to as *Anderson localized* and can only contribute to conduction via thermal activation.

One can understand the existence of localized states by considering the low-energy states of an electron moving in a very rough, random potential, $V(\boldsymbol{r})$ (Lee & Ramakrishnan, 1985). The lowest energy states will be those bound to very deep troughs in the potential function. The mixing between states localized in different wells will be very weak because states with significant spatial overlap will have very different energies, while states with similar energies are spatially well separated so that the wave function overlaps are exponentially small.

The scale on which the wave functions of localized states decay to zero defines the localization length ξ, which depends on the energy of the state and the strength of the disorder. The balance between extended and localized states depends on the strength of the disorder and the spatial dimensionality of the

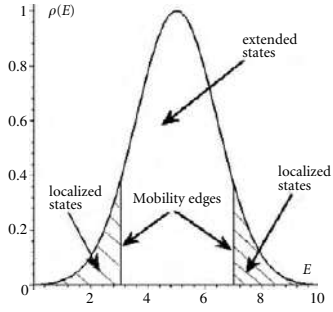

Figure 1. A schematic plot of the density of states showing a single disorder broadened band for a 3-d system. The states in the band center are extended while those in the tails are localized (shaded regions); the mobility edges between the two types of state are marked.

system. In a one-dimensional (1-d) system, all of the electronic eigenstates are strongly localized by any amount of disorder. In two dimensions, it is believed that all states are actually localized, but that the localization length can be very long in the center of a band. The application of a strong magnetic field to a disordered 2-d electron system, such as may be formed at a semiconductor heterojunction at low temperature, causes the conduction band to break up into a sequence of disorder broadened Landau bands, each with an extended state at its center—an essential feature of the quantum Hall effect. In three dimensions, the eigenstates at the center of a band are truly extended while those in the low- and high-energy tails are localized. It is believed that there are two well-defined critical energies within the band at which the nature of the states changes so that localized and extended states do not co-exist at a given energy.

The critical energies are usually referred to as mobility edges because the zero-temperature conductance of the system will be zero when the Fermi energy lies in the regime of localized states but nonzero in the extended regime (see Figure 1). The location of the mobility edges depends on the strength of the disorder —in very clean systems, only the states in the tails of a band will be localized while in a very dirty system the mobility edges may meet in the band center so that all states are localized. The behavior at the mobility edge has been studied by performing experiments on a series of devices with increasing amounts of disorder. The transition between metallic (conducting) and insulating behavior is closely analogous to other phase transitions. Mott (1973) supposed that this metal-insulator transition was first order, with the conductivity jumping from a fixed finite value, $\sigma_{\min}$, to zero. In 1979, a renormalization group analysis was carried out by the so-called "gang of four," based on earlier scaling arguments by Thouless and co-workers (Thouless, 1974), which favored a continuous metal-insulator transition for 3-d systems (Abrahams et al., 1979). The discussion of the change in nature of the states from extended to localized in terms of a zero-temperature quantum phase transition has been very fruitful. In this description, the localization length, ξ, plays the same role as the correlation length for fluctuations in a thermal transition. It is supposed that ξ diverges at the mobility edges according to a universal power law

$$\xi \sim |E - E_c|^{-\nu} .$$

Numerical evidence indicates that the value of the exponent is indeed universal and has the value $\nu \sim 1.6$.

Although the underlying physics of Anderson localization is that of linear waves in random media, the discussion can be recast in terms of nonlinear models without disorder, which are in the same family of statistical field theories used to describe thermal phase transitions, specifically nonlinear sigma models (Efetov, 1997). This has led to the notion that the spatial variation of the wave functions of states at the mobility edge displays a multifractal character.

The application of these ideas to other wave phenomena in random media has been slower. It is much harder to observe strong localization in bosonic and classical wave systems, but recently much experimental work has been carried out on optical and acoustic localization (see John (1990) for a good introduction). This work shows that Anderson localization is not an essentially quantum mechanical effect but is ubiquitous for wave propagation in random media. Similarly, the interplay between the physics of randomly disordered systems and quantum chaos is also proving very rich and fruitful (Altshuler & Simons, 1994).

There are a number of other mechanisms whereby wave excitations may become spatially localized. The propagation of excitations within macromolecules, for example, may become localized both because of interference effects associated with "random" changes in structure and also because of self-trapping effects associated with nonlinearity in the wave equation for these modes. In the case of electrons in solids, electronic excitations may become localized both by random variations in potential and by interaction effects that give rise to the so-called Mott transition. Such interaction effects are responsible for the phenomenon of Coulomb blockade observed in semiconductor nanostructures.

KEITH BENEDICT

See also **Discrete self-trapping system; Local modes in molecular crystals**

Further Reading

Abrahams, E., Anderson, P.W., Licciardello, D.C. & Ramakrishnan, T.V. 1979. Scaling theory of localization: Absence

of quantum diffusion in two dimensions. *Physical Review Letters*, 42: 673
Altshuler, B. & Simons, B.D. 1994. Universalities: from Anderson localization to quantum chaos. In *Mesoscopic Quantum Physics, Proceedings of the 61st Les Houches Summer School,* edited by E. Akkermans, G. Montambaux, J.-L. Pichard & J. Zinn-Justin, Amsterdam: North-Holland
Anderson, P.W. 1958. The absence of diffusion in certain random lattices. *Physical Review*, 109: 1492
Efetov, K. 1997. *Supersymmetry in Disorder and Chaos*. Cambridge and New York: Cambridge University Press
John, S. 1990. The localization of waves in disordered media. In *Scattering and Localization of Classical Waves in Random Media,* edited by P. Sheng. Singapore: World Scientific, pp. 1–96
Lee, P.A. & Ramakrishnan, T.V. 1985. Disordered electronic systems. *Reviews of Modern Physics*, 57: 287
Mott, N.F. 1973. In *Electronic and Structural Properties of Amorphous Semiconductors*, edited by P.G. LeComber & J. Mort, London: Academic Press, p. 1
Thouless, D.J. 1974. Electrons in disordered systems and the theory of localization. *Physics Reports*, 13: 93

ANNIHILATION (KINK-ANTIKINK)

See **Sine-Gordon equation**

ANOSOV AND AXIOM-A SYSTEMS

Two classes of dynamical systems exhibiting chaotic behavior were axiomatically defined and systematically studied for the first time in the 1960s. Previous studies had concentrated on more specific situations. Axiom-A systems were introduced by Stephen Smale in his seminal paper (Smale, 1967). Anosov systems, which are a special case of Axiom-A systems, were studied independently in Moscow around the same period. Today, Anosov and Axiom-A systems are valued as idealized models of chaos: while the conditions defining Axiom A are too stringent to include many real-life examples, it is recognized that they have features shared in various forms by most chaotic systems.

Definitions

First, we give the definitions in the discrete-time case.

Let f be a smooth invertible map (for basic notions, *See* **Phase space**). A compact invariant set of f is said to be *hyperbolic* if at every point in this set, the tangent space splits into a direct sum of two subspaces E^{u} and E^{s} with the property that these subspaces are invariant under the differential $\mathrm{d}f$, that is, $\mathrm{d}f(x)E^{\mathrm{u}}(x) = E^{\mathrm{u}}(f(x))$, $\mathrm{d}f(x)E^{\mathrm{s}}(x) = E^{\mathrm{u}}(f(x))$, and that $\mathrm{d}f$ expands vectors in E^{u} and contracts vectors in E^{s}.

If $E^{\mathrm{u}} = \{0\}$ in the definition above, then the invariant set is made up of attracting fixed points or periodic orbits. Similarly, if $E^{\mathrm{s}} = \{0\}$, then the orbits are repelling. If neither subspace is trivial, then the behavior is locally "saddle-like," that is to say, relative to the orbit of a point x, most nearby orbits diverge exponentially fast both in forward and in backward time. This is why hyperbolicity is a mathematical notion of chaos.

An *Anosov diffeomorphism* is a smooth invertible map of a compact manifold with the property that the entire space is a hyperbolic set.

Axiom A, which is a larger class, focuses on the part of the system that is not transient. More precisely, a point x in the phase space is said to be nonwandering if every neighborhood U of x contains an orbit that returns to U. A map is said to satisfy Axiom A if its nonwandering set is hyperbolic and contains a dense set of periodic points.

Definitions in the continuous-time case are analogous: f above is replaced by the time-t-maps of the flow, and the tangent spaces now decompose into $E^{\mathrm{u}} \oplus E^0 \oplus E^{\mathrm{s}}$ where E^0, which is 1-d, represents the direction of the flow lines.

Phase Space Structures and Properties

Anosov and Axiom-A systems are defined by the behavior of the differential. Corresponding to the linear structures left invariant by $\mathrm{d}f$ are nonlinear structures, namely stable manifolds tangent to E^{s} and unstable manifolds tangent to E^{u}.

Thus, two families of invariant manifolds are associated with an Anosov map and each one of these fills up the entire phase space; they are sometimes called the *stable* and *unstable foliations*. The leaves of these foliations are transverse at each point, forming a kind of (topological) coordinate system. The map f expands distances along the leaves of one of these foliations and contracts distances along the leaves of the other. For Axiom-A systems, one has a similar local product structure or "coordinate system" at each point in the nonwandering set, but the picture is local, and there are gaps: the stable and unstable leaves do not necessarily fill out open sets in the phase space.

In addition to these local structures, Axiom-A systems have a global structure theorem known as *spectral decomposition*. It says that the nonwandering set of every Axiom-A map can be written as $X_1 \cup \cdots \cup X_r$ where the X_i are disjoint closed invariant sets on which f is topologically transitive. The X_i are called basic sets. Each X_i can be decomposed further into a finite union $\bigcup X_{i,j}$, where each $X_{i,j}$ is invariant and topologically mixing under some iterate of f. (Topological transitivity and mixing are irreducibility conditions; *See* **Phase space**.) This decomposition is reminiscent of the corresponding result for finite-state Markov chains.

One of the reasons why hyperbolic sets are important is their robustness: they cannot be perturbed away. More precisely, let f be a map with a hyperbolic set Λ that is locally maximal, that is, it is the largest invariant set in some neighborhood U. Then for every map g that is C^1 near f, the largest invariant set Λ' of g in

U is again hyperbolic; moreover, f restricted to Λ is *topologically conjugate* to g restricted to Λ'. This is mathematical shorthand for saying that not only are the two sets Λ and Λ' topologically indistinguishable, but the orbit structure of f on Λ is indistinguishable from that of g on Λ'.

The above phenomenon brings us to the idea of *structural stability*. A map f is said to be *structurally stable* if every map g, that is C^1 near f is topologically conjugate to f (on the entire phase space). It turns out that a map is structurally stable if and only if it satisfies Axiom A and an additional condition called strong transversality.

Next, we discuss the idea of pseudo-orbits versus real orbits. Letting $d(\cdot, \cdot)$ be the metric, a sequence of points $x_0, x_1, x_2, \ldots$ in the phase space is called an *ε-pseudo-orbit* of f if $d(f(x_i), x_{i+1}) < \varepsilon$ for every i. Computer-generated orbits, for example, are pseudo-orbits due to round-off errors. A fact of consequence to people performing numerical experiments is that in hyperbolic systems, small errors at each step get magnified exponentially fast. For example, if the expansion rate is ≥ 3, then an ε-error made at one step is tripled at each subsequent step, that is, after only $O(|\log \varepsilon|)$ iterates, the error is $O(1)$, and the pseudo-orbit bears no relation to the real one. There is, however, a theorem that states that every pseudo-orbit is shadowed by a real one. More precisely, given a hyperbolic set, there is a constant C such that if $x_0, x_1, x_2, \ldots$ is an ε-pseudo-orbit, then there is a phase point z such that $d(x_i, f^i(z)) < C\varepsilon$ for all i. Thus, paradoxical as it may first seem, this result asserts that on hyperbolic sets, each pseudo-orbit approximates a real orbit, even though it may deviate considerably from the one with the same initial condition.

The shadowing orbit corresponding to a bi-infinite pseudo-orbit is, in fact, unique. From this, one deduces the following Closing Lemma: for any hyperbolic set, there is a constant C such that the following holds: every finite orbit segment $x, f(x), \ldots, f^{n-1}(x)$ that nearly closes up, that is, $d(x, f^{n-1}(x)) < \varepsilon$ for some small ε, lies within $< C\varepsilon$ of a genuine periodic orbit of period n. Thus, hyperbolic sets contain many periodic points.

Examples

A large class of Anosov diffeomorphisms comes from linear toral automorphisms, that is, maps of the n-dimensional torus induced by $n \times n$ matrices with integer entries, $\det = \pm 1$, and no eigenvalues of modulus one. (*See* **Cat map** for a detailed example of this). We remark that due to their structural stability (nonlinear), perturbations of linear toral automorphisms continue to have the Anosov property. This remark also applies to all of the examples below. In fact, all known Anosov diffeomorphisms are topologically identical to a linear toral automorphism (or a slight generalization of these).

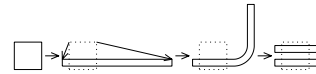

Figure 1. The horseshoe.

Figure 2. The solenoid.

Geodesic flows describe free motions of points on manifolds. Let M be a manifold. Given $x \in M$ and a unit vector v at x, there is a unique geodesic starting from x in the direction v. The geodesic flow φ^t is given by $\varphi^t(x, v) = (x', v')$, where x' is the point t units down the geodesic and v' is the direction at x'. Geodesic flows on manifolds of strictly negative curvature are the main examples of Anosov flows. They were studied by Jacques Hadamard (ca. 1900) and Gustav Hedlund and Eberhard Hopf (in the 1930s) considerably before Anosov theory was developed.

Smale's *horseshoe* is the prototypical example of a hyperbolic invariant set. This map, so called because it bends a rectangle B into the shape of a horseshoe and puts it back on top of B, is shown in Figure 1. The set $\{x: f^n(x) \in B \text{ for all } n = 0, \pm 1, \pm 2, \ldots\}$ is hyperbolic (*See* **Horseshoes and hyperbolicity in dynamical systems; Phase space**).

Finally, we mention the *solenoid* (see Figure 2, and also in the color plate section as the Smale solenoid), which is an example of an Axiom-A attractor. Here, the map f is defined on a solid torus $M = S^1 \times D_2$, where D_2 is a 2-d disk. It is easiest to describe it in two steps: first it maps M into a long thin solid torus, which is then placed inside M winding around the S^1 direction twice. The attractor is given by $\Lambda = \bigcap_{n \geq 0} f^n(M)$.

Symbolic Coding of Orbits and Ergodic Theory

An important tool for studying the orbit structure of Axiom-A systems is the *Markov partition*, constructed for Anosov systems by Sinai and extended to Axiom-A basic sets by Bowen. Given a partition $\{R_1, \ldots, R_k\}$ of the phase space, there is a natural way to attach

to each point x in the phase space a sequence of symbols, namely $(\ldots, a_{-1}, a_0, a_1, a_2, \ldots)$ where $a_i \in \{1, 2, \ldots, k\}$ is the name of the partition element containing $f^i(x)$, that is, $f^i(x) \in R_{a_i}$ for each i. In general, not all sequences are realized by orbits of f. Markov partitions are designed so that the set of symbol sequences that correspond to real orbits has Markovian properties; it is called a shift of finite type (*See* **Symbolic dynamics**).

The ergodic theory of Axiom-A systems has its origins in statistical mechanics. In a 1-d lattice model in statistical mechanics, one has an infinite array of sites indexed by the integers; at each site, the system can be in any one of a finite number of states. Thus, the configuration space for a 1-d lattice model is the set of bi-infinite sequences on a finite alphabet. Identifying this symbol space with the one from Markov partitions, Sinai and Ruelle were able to transport some of the basic ideas from statistical mechanics, including the notions of Gibbs states and equilibrium states, to the ergodic theory of Axiom-A systems.

The notion of *equilibrium states*, which is equivalent to Gibbs states for Axiom-A systems, has the following meaning in dynamical systems in general: given a potential function φ, an invariant measure is said to be an equilibrium state if it maximizes the quantity

$$h_\mu(f) - \int \varphi \, \mathrm{d}\mu,$$

where $h_\mu(f)$ denotes the Kolmogorov–Sinai entropy of f and the supremum is taken over all f-invariant probability measures μ. In particular, when $\varphi = 0$, this measure is the measure that maximizes entropy; and when $\varphi = \log|\det(\mathrm{d}f|_{E^u})|$, it is the Sinai–Ruelle–Bowen (SRB) measure. From a physical or observational point of view, SRB measures are the most important invariant measures for dissipative dynamical systems (*See* **Sinai–Ruelle–Bowen measures**).

Periodic Points and Their Growth Properties

We discuss briefly some further results related to the abundance of periodic points in Axiom-A systems.

For an Axiom-A diffeomorphism f, if $P(n)$ is the number of periodic points of period $\leq n$, then $P(n) \sim \mathrm{e}^{hn}$ where h is the topological entropy of f. That is to say, the dynamical complexity of f is reflected in its periodic behavior. An analogous result holds for Axiom-A flows.

Finally, we mention the dynamical zeta function, which sums up the periodic information of a system. In the discrete-time case, $\zeta(z) := \exp\sum_{n=1}^{\infty} P(n)z^n/n$ has been shown to be a rational function analytic on $|z| < \mathrm{e}^{-h}$. In the continuous-time case, the zeta function is given by $\zeta(z) := \prod_\gamma (1 - \exp(-z\,l(\gamma)))^{-1}$, where the product is taken over all (nonstationary) periodic orbits γ and $l(\gamma)$ is the smallest positive period of γ. This function is known to be meromorphic on a certain domain, but the locations of its poles, which are intimately related to correlation decay properties of the system, remain one of the yet unresolved issues in Axiom-A theory.

BORIS HASSELBLATT AND LAI-SANG YOUNG

See also **Cat map; Horseshoes and hyperbolicity in dynamical systems; Phase space; Sinai–Ruelle–Bowen measures; Symbolic dynamics**

Further Reading

Bowen, R. 1975. *Equilibrium States and the Ergodic Theory of Anosov Diffeomorphisms*, Berlin and New York: Springer

Branner, B. & Hjorth, P. (editors). 1995. *Real and Complex Dynamical Systems. Proceedings of the NATO Advanced Study Institute held in Hillerød, June 20–July 2, 1993*, Dordrecht and Boston: Kluwer

Fielder, B. (editor). 2002. *Handbook of Dynamical Systems*, Vol. 2, Amsterdam and New York: Elsevier

Hasselblatt, B. & Katok, A. (editors). 2002. *Handbook of Dynamical Systems*, Vol. 1A, Amsterdam and New York: Elsevier

Hasselblatt, B. & Katok, A. 2003. *Dynamics: A First Course*, Cambridge and New York: Cambridge University Press

Katok, A. & Hasselblatt, B. 1995. *Introduction to the Modern Theory of Dynamical Systems*, Cambridge and New York: Cambridge University Press

Smale, S. 1967. Differentiable dynamical systems. *Bulletin of the American Mathematical Society*, 73: 747–817

ANTISOLITONS

See **Solitons, types of**

ANTI-STOKES SCATTERING

See **Rayleigh and Raman scattering and IR absorption**

ARNOL'D CAT MAP

See **Cat map**

ARNOL'D DIFFUSION

For near-integrable Hamiltonian systems with more than two degrees of freedom, stochastic and regular trajectories are intimately co-mingled in the $2N$-dimensional phase space. Stochastic layers in phase space exist near resonances of the motion. The thickness of the layers expands with increasing perturbation, leading to primary resonance overlap, motion across the layers, and the appearance of strong stochasticity in the motion. In the limit of weak perturbation, however, primary resonance overlap does not occur. A new physical behavior of the motion then makes its appearance: motion along the resonance layers called Arnol'd diffusion (AD). For two degrees of freedom, with a weak perturbation, two-dimensional

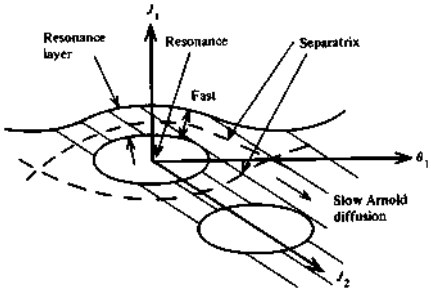

Figure 1. Illustration of the directions of the fast diffusion across a resonance layer and the slow diffusion along the resonance layer.

Kolmogorov–Arnol'd–Moser (KAM) surfaces divide the three-dimensional energy "volume" in phase space into a set of closed volumes each bounded by KAM surfaces, much as lines isolate regions of a plane. For $N > 2$ degrees of freedom, the N-dimensional KAM surfaces do not divide the $(2N-1)$-dimensional energy volume into distinct regions. Thus, for $N > 2$, in the generic case, all stochastic layers of the energy surface in phase space are connected into a single complex network—the Arnol'd web. The web permeates the entire phase space, intersecting or lying infinitesimally close to every point. For an initial condition within the web, the subsequent stochastic motion will eventually intersect every finite region of the energy surface in phase space, even in the limit as the perturbation strength approaches zero.

The merging of stochastic trajectories into a single web was proved (Arnol'd, 1964) for a specific nonlinear Hamiltonian. A general proof of the existence of a single web has not been given, but many computational examples support the conjecture. From a practical point of view, there are two major questions with respect to AD in a particular system: what is the relative measure of stochastic trajectories (fraction of the phase space that is stochastic) in the region of interest? And for a given initial condition, how fast will system points diffuse along the thin threads of the Arnol'd web?

We illustrate the motion along the resonance layer in Figure 1. A projection of the motion onto the J_1, θ_1 plane is shown, illustrating a resonance with a stochastic layer. At right angles to this plane, the action of the other coordinate J_2 is shown. If there are only two degrees of freedom in a conservative system, the fact that the motion is constrained to lie on a constant energy surface restricts the change in J_2 for J_1 constrained to the stochastic layer. However, if there is another degree of freedom, or if the Hamiltonian is time dependent, then this restriction is lifted, and motion along the stochastic layer in the J_2 direction can occur.

The diffusion rate (D) along a layer has been calculated by Chirikov (1979) for the important case of three resonances, and by Tennyson et al. (1979) for an equivalent mapping model, which they called a stochastic pump. These models predict, for a single action I corresponding to J_2 in Figure 1,

$$D = (\Delta I)^2/t \propto \mathrm{e}^{-A/\varepsilon^{1/2}}, \tag{1}$$

where t is the time, ε is a perturbation parameter, and $A \approx 1$. For coupling among many resonances, a rigorous upper bound on the diffusion rate (Nekhoroshev, 1977) generally overestimates the rate by orders of magnitude. Using a similar formalism with a somewhat more restrictive class of Hamiltonians, but still encompassing most physical problems, the upper bound can be improved (Benettin et al., 1985; Lochak & Neistadt, 1992) to give what they considered to be an optimal upper bound:

$$D \propto \mathrm{e}^{-A/\varepsilon^{\gamma}}, \ \gamma \approx N^{-1}. \tag{2}$$

If N is large, such an exponentially small diffusion could only hold for very small ε (specified within the theory), otherwise the exponential factor could be essentially unity. Also, an upper bound must be related to the fastest local diffusion. This may be much more rapid than an average global diffusion, which would be controlled by the portions of the phase space where the diffusion is slowest. For upper bound calculations, consult the original papers of Nekhoroshev (1977), Benettin et al. (1985), and Lochak & Neistadt (1992).

The simplest way to calculate local AD is to couple two standard maps together with a weak coupling term $\mu \sin(\theta_n + \phi_n)$, where θ_n and ϕ_n are the map phases and $\mu \ll 1$. Using the stochastic pump model, with a regular orbit (in the absence of coupling) in the (I, θ) map being driven by stochasticity in the (J, ϕ) map, the Hamiltonian of the mapping is approximated as $H \approx H_i + H_j$, with

$$\begin{aligned} H_i &= I^2/2 + K_i \cos\theta + 2\mu \cos(\theta + \phi), \\ H_j &= J^2/2 + K_j \cos\phi + 2K_j \cos\phi \cos 2\pi n, \end{aligned} \tag{3}$$

where n is the time normalized to mapping periods. We have retained only the lowest Fourier term from the mapping frequency in the H_j equation of (3), and considered that the stochasticity in H_i is driven by the coupling. To calculate the changes in H_i per iteration due to kicks delivered by (J, ϕ), we take the derivative

$$\begin{aligned} \frac{\partial H_i}{\partial n} &= \frac{\mathrm{d}H_i}{\mathrm{d}n} \\ &= \frac{\mathrm{d}}{\mathrm{d}n}[2\mu \cos(\theta + \phi)] \\ &\quad + 2\mu \frac{\mathrm{d}\theta}{\mathrm{d}n} \sin[\theta + \phi(n)]. \end{aligned} \tag{4}$$

For rotational orbits $\theta = w_i n + \theta_0$, scaling the time variable to revolutions of the map ($s = \omega_j n$), and defining the ratio of frequencies ($Q_0 = \omega_i/\omega_j = \omega_i/K_j^{1/2}$), Equation (4) is integrated to obtain

$$\Delta H_i = 2\mu Q_0 \left(\cos\theta_0 \int_{-\infty}^{\infty} \sin[Q_0 s + \phi(s)]\mathrm{d}s + \sin\theta_0 \int_{-\infty}^{\infty} \cos[Q_0 s + \phi(s)]\mathrm{d}s \right). \quad (5)$$

The first of the integrals in (5) integrates to zero; the second is a Mel'nikov–Arnol'd integral (Chirikov, 1979, Appendix A), which can be evaluated to give the change in ΔH_i over one characteristic half-period of the (J, ϕ) map. Squaring ΔH_i and averaging over θ_0 gives

$$\langle (\Delta H_i)^2 \rangle = 32\pi^2 Q_0^4 \mu^2 \frac{\sinh^2(\pi Q_0/2)}{\sinh^2(\pi Q_0)}. \quad (6)$$

To determine the diffusion constant D, divide $\langle (\Delta H_i)^2 \rangle$ by twice the average number of iterations in this half-period

$$\overline{T}_j = \frac{1}{\omega_j} \ln \left| \frac{32\mathrm{e}}{w_1} \right|, \quad (7)$$

where $w_1 = \Delta H / H_{\text{separatrix}}$ is the relative energy of the edge of the stochastic region, $w_1 = 8\pi(2\pi/K_j^{1/2})^3 \times \mathrm{e}^{-\pi^2/K_j^{1/2}}$, and e is the base of natural logarithms. Combining (6) and (7), and using $\Delta H_i = I \Delta I$, the diffusion constant in action space can be approximated in a form that exhibits the main Q_0 scaling:

$$D \approx 16\mu^2 n Q_0^2 \mathrm{e}^{-\pi Q_0}, \quad (8)$$

where we have assumed that $I \approx \omega_i$. Comparing (8) to (1) with $Q_0 = \omega_i/K_j^{1/2}$, we observe that $K_j \propto \varepsilon$, the perturbation parameter. The numerical results agreed well with (8) (see Lichtenberg & Aswani (1998) and references therein).

Chirikov et al. (1979) found, numerically, that one could distinguish the diffusion in a range where ε was sufficiently large and a single resonance was dominant, such that a three-resonance model scaling as in (1) holds, from a range of smaller values of ε with many overlapping weak resonances, where the scaling in (2) applies. The results of their numerical investigation demonstrated the transition between the two regimes. In another approach, the diffusion through a large number of weakly coupled standard mappings was determined numerically, with the strength of the coupling controlled in a manner such that the three-resonance model could be applied in a statistical manner to determine the diffusion rate (Lichtenberg & Aswani, 1998).

These studies indicate that the basic models can be used to determine Arnol'd diffusion in multidimensional systems if the system parameters can be sufficiently controlled. For more information on these and related topics, the reader is referred to Chirikov (1979) and to Lichtenberg & Lieberman (1991, Chapter 6).

ALLAN J. LICHTENBERG

See also **Kolmogorov–Arnol'd–Moser theorem; Phase space diffusion and correlations; Standard map**

Further Reading

Arnol'd, V.I. 1964. Instability of dynamical systems with several degrees of freedom. *Russian Mathematical Surveys*, 18: 85

Benettin, G., Galgani, L. & Giorgilli, A. 1985. A proof of Nekoroshev's theorem for the stability times of nearly integrable Hamiltonian systems. *Celestial Mechanics*, 37: 1–25

Chirikov, B.V. 1979. A universal instability of many-dimensional oscillator systems. *Physics Reports*, 52: 265–379

Chirikov, B.V., Ford, J. & Vivaldi, F. 1979. Some numerical studies of AD in a simple model. In *Nonlinear Dynamics and the Beam-Beam Interaction*, edited by M. Month & J.C. Herrera, New York: American Institute of Physics

Lichtenberg, A.J. & Aswani, A.M. 1998. Arnold diffusion in many weakly coupled mappings. *Physical Review* E, 57: 5325–5331

Lichtenberg, A.J. & Lieberman, M.A. 1991. *Regular and Chaotic Dynamics*, 2nd edition, New York: Springer

Lochak, P. & Neistadt, A.I. 1992. Estimates in the theorem of N.N. Nekhoroshev for systems with quasi-convex Hamiltonian. *Chaos*, 2: 495–499

Nekhoroshev, N.N. 1977. An exponential estimate of the time of stability of nearly itegrable Hamiltonian systems. *Russian Mathematical Surveys*, 32: 1–65

Tennyson, J.L., Lieberman, M.A. & Lichtenberg, A.J. 1979. Diffusion in near-integrable Hamiltonian systems with three degrees of freedom. In *Nonlinear Dynamics and the Beam-Beam Interaction*, edited by M. Month & J.C. Herrera, New York: American Institute of Physics

ARNOL'D TONGUES

See **Coupled oscillators**

ARTIFICIAL INTELLIGENCE

Artificial intelligence (AI) is a field of research in computer science reproducing intelligent reasoning. AI programs are mainly based on logic-oriented symbolic languages such as, for example, Prolog (Programming in Logic) or LISP (List Programming). Historically, AI was inspired by Alan Turing's question: "Can machines think?" According to the Turing test for AI, a machine is intelligent if a human user cannot distinguish whether he or she is interacting and communicating with a machine or a human being. Thus, before starting with AI, a general concept of computer and computabilty must be defined in computer science.

In 1936, Turing and Emil Post independently suggested the following definition of computability.

A "Turing machine" consists of: (a) a control box in which a finite program is placed, (b) a potentially infinite tape, divided lengthwise into squares, and (c) a device for scanning, or printing on one square of the tape at a time, and for moving along the tape or stopping, all under the command of the control box.

If the symbols used by a Turing machine are restricted to a stroke / and a blank *, then every natural number x can be represented by a sequence of x strokes (e.g., 3 by ///), each stroke on a square of the Turing tape. The blank is used to denote that the square is empty (or the corresponding number is zero). In particular, a blank is necessary to separate sequences of strokes representing numbers. Thus, a Turing machine computes a numerical function f with arguments $x_1, \ldots, x_n$ if the machine program starts with the input tape $\ldots * x_1 * x_2 * \ldots * x_n * \ldots$ and stops after finite steps with an output $\ldots * x_1 * x_2 * \ldots * x_n * f(x_1, \ldots, x_n) * \ldots$ on the tape. From a logical point of view, John von Neumann's general-purpose computer is a technical realization of a universal Turing machine that can simulate any kind of Turing program.

Besides Turing machines, there are many other mathematically equivalent procedures for defining computability (e.g., register machines, recursive functions) that are mathematically equivalent. According to Alonzo Church's thesis, the informal intuitive notion of an algorithm is identical to one of these equivalent mathematical concepts, for example, the program of a Turing machine.

With respect to AI, the paradigm of effective computabilty implies that the mind is represented by program-controlled machines, and mental structures refer to symbolic data structures, while mental processes implement algorithms. Historically, the hard core of AI was established during the Dartmouth Conference in 1956 when leading researchers, such as John McCarthy, Alan Newell, Herbert Simon, and others from different disciplines, formed the new scientific community of AI. If human thinking can be represented by an algorithm, then according to Church's thesis, it can be represented by a Turing program that can be computed by a universal Turing machine. Thus, human thinking could be simulated by a general-purpose computer and, in this sense, Turing's question ("Can machines think?") must be answered with a "yes." The premise that human thinking can be codified and represented by recursive procedures is, of course, doubtful. Even processes of mathematical thinking can be more complex than recursive functions.

The first period of AI was dominated by questions of heuristic programming, which means the automated search for human problem solutions in trees of possible derivations, controlled and evaluated by heuristics. In 1962, these simulative procedures were generalized and enlarged for the so-called General Problem Solver (GPS), which was assumed to be the heuristic framework of human problem solving. But GPS could only solve some insignificant problems in a formalized microworld. Thus, AI researchers tried to construct specialized systems of problem solving that use the specialized knowledge of human experts.

The architecture of an "expert system" consists of the following components: knowledge base, problem-solving component (interference system), explanation component, knowledge acquisition, and dialogue component. Knowledge is the key factor in the performance of an expert system. The knowledge is of two types. The first type is the facts of the domain that are written in textbooks and journals in the field. Equally important to the practice of a field is the second type of knowledge, called heuristic knowledge, which is the knowledge of good practice and judgment in a field. It is experimental knowledge, that art of good guessing, that a human expert acquires over years of work.

Expert systems are computational models of problem-solving procedures that need symbolic representation of knowledge. Unlike program-controlled serial computers, the human brain and mind are characterized by learning processes without symbolic representations. With respect to the architecture of von Neumann computers, an essential limitation derives from the sequential and centralized control, but complex dynamical systems like the brain are intrinsically parallel and self-organized.

In their famous paper "A Logical Calculus of the Ideas Immanent in Nervous Activity" in 1943, Warren McCulloch and Walter Pitts offered a complex model of neurons as threshold logic units with excitatory and inhibitory synapses. Their "McCulloch–Pitts neuron" fires an impulse along its axon at time $t + 1$ if the weighted sum of its inputs and weights at time t exceeds the threshold of the neuron. The weights are numbers corresponding to the neurochemical interactions of the neuron with other neurons. But, in a McCulloch–Pitts network, the function of an artificial neuron is fixed for all time. McCulloch and Pitts succeeded in demonstrating that a network of formal neurons of their type could compute any finite logical expression.

In order to make a neural computer capable of complex tasks, it is necessary to find procedures of learning. A learning procedure is nothing else than an adjustment of the many weights so that the desired output vector (e.g., a perception) is achieved. The first learning neural computer was Frank Rosenblatt's "Perceptron" (1957). Rosenblatt's neural computer is a feedforward network with binary threshold units and three layers. The first layer is a sensory surface called a "retina" that consists of stimulus cells (S-units). The S-units are connected with the intermediate layer by fixed weights that do not change during the learning process. The elements of the intermediate layer are

called associator cells (A-units). Each A-unit has a fixed weighted input of some S-units. In other words, some S-units project their output onto an A-unit. An S-unit may also project its output onto several A-units. The intermediate layer is completely connected with the output layer, the elements of which are called response cells (R-units). The weights between the intermediate layer and the output layer are variable and thus able to learn.

The Perceptron was viewed as a neural computer that can classify a perceived pattern in one of several possible groups. In 1969, Marvin Minsky and Seymour Papert proved that Perceptrons cannot recognize and distinguish the connectivity of patterns, in general. The Perceptron's failure is overcome by more flexible networks with supervised and unsupervised learning algorithms (e.g., Hopfield systems, Chua's cellular neural networks, Kohonen's self-organizing maps).

In the age of globalization, communication networks such as the Internet are a tremendous challenge to AI. From a technical point of view, we need intelligent programs distributed in the nets. There are already more or less intelligent virtual organisms (agents), learning, self-organizing, and adapting to our individual preferences of information, to select our e-mails, to prepare economic transactions, or to defend against attacks of hostile computer viruses, like the immune system of our body. Although the capability to manage the complexity of modern societies depends decisively on progress in AI, we need computational ecologies with distributed AI to support human life and not human-like robots to replace it.

KLAUS MAINZER

See also **Artificial life; Cell assemblies; Game of life; McCulloch–Pitts network; Neural network models; Perceptron**

Further Reading

Lenat, D.B. & Guha, R.V. 1990. *Building Large Knowledge-Based Systems*, Reading, MA: Addison-Wesley

Mainzer, K. 2003. *Thinking in Complexity. The Computational Dynamics of Matter, Mind, and Mankind*, 4th edition, Berlin and New York: Springer

Minsky, M. & Papert, S.A. 1969. *Perceptrons*, Cambridge, MA MIT Press

Minski, M. 1985. *The Society of Mind*, New York: Simon & Schuster

Nilson, N.J. 1982. *Principles of Artificial Intelligence*, Berlin and New York: Springer

Palm, G. (editor). 1984. *Neural Assemblies. An Alternative Approach to Artificial Intelligence*, Berlin and New York Springer

ARTIFICIAL LIFE

The term *artificial life* (AL) was coined in 1987 by Christopher Langton, who organized a workshop by that name in frustration with the lack of a forum for discussing work on the computer simulation of biological systems. In Langton's characterization, AL seeks to "contribute to theoretical biology by locating life-as-we-know-it within the larger picture of life-as-it-could-be" (Langton, 1989). In other words, AL aims to use computer simulation to synthesize alternative life-like systems and, thus, find out which characteristics and principles are essential and which are merely contingent on how life happened to evolve on this planet. While other branches of biology may use simulation to understand specific mechanisms, AL is broader, more abstract, and highly interdisciplinary, in addition to implying certain ideological convictions. Chief among these is the assumption that life is a process, rather than a metaphysical substance or an atomic property of matter, which emerges in a bottom-up fashion from local interactions among suitably arranged populations of individually lifeless components.

Opinions differ on whether such artificial systems may be logically equivalent to their natural counterparts and therefore really alive, or whether they are simply life-like simulacra. The former view is called the strong AL hypothesis, to associate it with a similarly functionalist standpoint known as Strong Artificial intelligence. However, the strong position in AL is considerably more tenable than its AI analog, which fails to distinguish between emergent and explicitly predetermined sources of behavior. Related to this "strong versus weak" argument is the unresolved question of whether life is an absolute category in nature at all or simply a useful way of grouping certain phenomena.

Early History

Attempts to construct living or life-like artifacts from mechanical parts date back at least to the ancient Greeks, and we can presume that many of these experiments were motivated by questions similar to those posed today. Nevertheless, these early systems tended to employ the "if it quacks like a duck it is a duck" principle, and so were only superficially lifelike, rather than in the deeper sense presently hoped for. One of the most ingenious of these early automata was indeed a duck (or at least something that moved, ate, defecated, and quacked like one), built by Jacques de Vaucanson around 1730.

Mary Shelley's *Frankenstein* explores similar issues in a fictional context. Contrary to popular belief, Shelley's monster was apparently not made from human body parts but from raw materials (cadavers are only mentioned with regard to Frankenstein's research). These components were then imbued with the "spark of life" (which Shelley associates with electricity) in order to animate them. Her viewpoint was still partially vitalistic, but there is a link between Shelley and her

contemporary Charles Babbage, whose interpretation of intelligence (if not life itself) was more formalized, abstract, and mechanical. The mechanization of the mind continued with George Boole's logical algebra and then the work of Alan Turing and John von Neumann on automating thought processes, which led directly to the invention of the digital computer and the beginnings of artificial intelligence. It was a similar inquiry into the abstract nature of life, as distinct from mind, that prompted von Neumann's investigations into self-replicating machinery and Turing's work on embryogenesis and "unorganized machines" (related to neural networks).

Formal Methods

While complexity theory is concerned with the manner in which complex behavior arises from simple systems, AL is interested in how systems generate continually increasing levels of complexity. The most striking feature of living systems is their ability to self-organize and self-maintain—a property that Humberto Maturana and Francisco Varela have termed "autopoiesis" (Maturana & Varela, 1980). Evolution, embryogenesis, learning, and the development of social organizations are therefore the mechanisms of primary interest to AL researchers.

The key features of AL models are the use of populations of semi-autonomous entities, the coupling of these through simple local interactions (no centralized control and little or no globally accessible information), and the consequent emergence of collective, persistent phenomena that require a higher level of description than that used to describe their substrate. Conventional mathematical notation is not usually appropriate for such distributed and labile systems, and the individual computer programs are often their own best description. There are, however, a number of frequently used abstract structures and formal grammars, including the following:

Cellular automata, in which the populations are arrays of finite state machines and interactions occur between neighboring cells according to simple rules. Under the right conditions, emergent entities (such as the glider in John Conway's Game of Life) arise and persist on the surface of the matrix, interacting with other entities in computationally interesting ways.

Genetic algorithms, in which the populations are genomes in a gene pool and interactions occur between their phenotypes and some form of stressful environment. Natural selection (or sometimes human choice) drives the population to adapt and grow ever fitter, perhaps solving real practical problems in the process.

L-systems, or *Lindenmayer systems*, which provide a grammar for defining the growth of branching (often plant-like) physical structures, as insights into morphology and embryology.

Autonomous agents, which are composite code and data objects, representing mobile physical entities (robots, ants, stock market traders) embedded in a real or simulated environment. They interact locally by sensing their environment and receiving messages from other agents, giving rise to emergent phenomena of many kinds including cooperative social structures, nest-building, and collective problem-solving.

Autocatalytic networks, in which the populations are of simulated enzymes and the interactions are equivalent to catalysis. Such networks are capable of self-generation and a growth in complexity, mimicking the bootstrapping process that presumably gave rise to life on Earth.

Current Status

Like most new fields, AL has undergone cycles of hubris and doubt, innovation and stasis, and differentiation and consolidation. The listing of topics for the latest in the series of workshops started by Langton in 1987 is as broad as ever, although probably the bulk of AL work today (2004) is focused on artificial evolution. Most research concentrates on fine details, while the basic philosophical questions remain largely unanswered. Nevertheless, AL remains one of relatively few fields where one can ask direct questions about one's own existence in a practical way.

STEVE GRAND

See also **Catalytic hypercycle; Cellular automata; Emergence; Game of life; Hierarchies of nonlinear systems; Turing patterns**

Further Reading

Adami, C. 1998. *Introduction to Artificial Life*, New York: Springer

Boden, M.A. (editor). 1996. *The Philosophy of Artificial Life*, Oxford and New York: Oxford University Press

Langton, C.G. (editor). 1989. *Artificial Life*, Redwood City, CA: Addison-Wesley

Levy, S. 1992. *Artificial Life: The Quest for a New Creation*, New York: Pantheon

Maturana, H.R. & Varela, F.J. 1980. *Autopoiesis and Cognition: The Realization of the Living*, Dordrecht and Boston: Reidel

ASSEMBLY OF NEURONS

See **Cell assemblies**

ATMOSPHERIC AND OCEAN SCIENCES

Earliest works on the study of the atmosphere and ocean date back to Aristotle and his student Theophrastus in 350 BC and further progressed through Torricelli's invention of the barometer in 1643, Boyle's law in 1657, and Celsius's invention of the thermometer in 1742 (due to Galileo in 1607). The first rigorous theoretical model for the study of the atmosphere was proposed by

Vilhelm Bjerknes in 1904, following which many scientists began to apply fundamental physics to the atmosphere and ocean. The advent of these theoretical approaches and the invention of efficient communication technologies in the mid-20th century made numerical weather prediction feasible and was in particular encouraged by Lewis Fry Richardson and John von Neumann in 1946, using the differential equations proposed by Bjerknes. Today, advanced numerical modeling and observational techniques exist, which are constantly being developed further in order to understand and study the complex nonlinear dynamics of the atmosphere and ocean.

This overview article summarizes the governing equations used in atmospheric and ocean sciences, features of atmosphere-ocean interaction, and processes for an idealized geometry and structure with reference to a one-dimensional vertical scale (Figure 1), a two-dimensional vertically averaged scale (Figures 3(a) and 4(a)), a two-dimensional zonally averaged meridional scale (Figures 3(b) and 4(b)), and a three-dimensional scale (Figure 2), and regimes of interacting systems (such as El Niño and Southern Oscillation and North Atlantic Oscillation) (Figures 5–7). The entry serves as an introduction to the many nonlinear processes taking place (for example, chaos, turbulence) and provides a few illustrative examples of self-organizing coherent structures of the nonlinear dynamics of the atmosphere and ocean.

Governing Equations

The combined atmosphere and ocean system can be regarded as a huge volume of fluid resting on a rotating oblate spheroid with varying surface topography moving through space, with an interface (which in general is discontinuous) between two fluid masses of differing densities. This coupled atmosphere-ocean system is driven by energy input through solar radiation (see Figure 1), gravity (for example, through interaction with other stellar bodies such as the Sun and Moon, i.e., tides), and inertia. The entire fluid is described by equations for conserved quantities such as momentum, mass (of air, water vapor, water, salt), and energy together with equations of state for air and water (*See* **Fluid dynamics; Navier–Stokes equation**). The movement of large water or air masses in a rotating reference frame adds to the complexity of motions, due to the presence of Coriolis forces, introduced by Coriolis in 1835.

Atmosphere-ocean interactions can be defined as an exchange of momentum, heat, and water (vapor and its partial masses: salts, carbon, oxygen, nitrogen, etc.) between air and water masses. The governing equations in the Euler formulation and a cartesian coordinate system are given by:

(i) The conservation of momentum

$$\frac{\mathrm{d}\boldsymbol{u}}{\mathrm{d}t} + 2\Omega \times \boldsymbol{u} = -\frac{1}{\rho}\nabla p - \boldsymbol{g} + \boldsymbol{F}_{\mathrm{ext}} + \boldsymbol{F}_{\mathrm{fric}}, \quad (1)$$

where the second term $2\Omega \times \boldsymbol{u}$ is the term due to the Coriolis force (Ω is the angular velocity of the Earth; $|\Omega| = 7.29 \times 10^{-5}\ \mathrm{s}^{-1}$), and forces due to a pressure gradient ∇p, gravity ($|\boldsymbol{g}| = 9.81\ \mathrm{m\,s}^{-2}$) and external ($\boldsymbol{F}_{\mathrm{ext}}$) as well as frictional ($\boldsymbol{F}_{\mathrm{fric}}$) forces are included. Note that the operator $\mathrm{d}/\mathrm{d}t$ is defined by

$$\frac{\mathrm{d}\boldsymbol{v}}{\mathrm{d}t} = \left(\frac{\partial}{\partial t} + \boldsymbol{v}\cdot\nabla\right)\boldsymbol{v}.$$

(ii) The conservation of mass (or continuity equation)

$$\frac{1}{\rho}\frac{\mathrm{d}\rho}{\mathrm{d}t} + \nabla\cdot\boldsymbol{u} = 0. \quad (2)$$

Note that there are alternative formulations such as the Lagrangian and impulse-flux form for these equations, and cartesian coordinate systems can be mapped to different geometries such as spherical coordinates by appropriate transformations.

(iii) The conservation of energy (First Law of Thermodynamics) and Gibbs's equation (Second Law of Thermodynamics)

$$\frac{\mathrm{d}Q}{\mathrm{d}t} = \frac{\mathrm{d}\varepsilon}{\mathrm{d}t} + p\frac{\mathrm{d}\alpha}{\mathrm{d}t},$$
$$\frac{\mathrm{d}\eta}{\mathrm{d}t} = \frac{1}{T}\frac{\mathrm{d}\varepsilon}{\mathrm{d}t} + \frac{p}{T}\frac{\mathrm{d}\alpha}{\mathrm{d}t} - \sum\frac{\mu_i}{T}\frac{\mathrm{d}\gamma_i}{\mathrm{d}t}, \quad (3)$$

where Q is the heat supply (sensible, latent, and radiative heat fluxes; see Figure 1), T is the temperature, ε the internal energy and α the specific volume ($\alpha = 1/\rho$), η the entropy, μ_i the chemical potentials, and γ_i the partial masses. The conservation of energy states in brief that the change in heat is balanced by a change in internal energy and mechanical work performed, and Gibbs's equation determines the direction of an irreversible process, relating entropy to a change in internal energy, volume, and partial masses.

(iv) The conservation of partial masses of water and air, that is, salinity for water, where all constituents are represented as salts and water vapor for air, yield equations similar to (2)

$$\frac{1}{\rho_{\mathrm{v}}}\frac{\mathrm{d}\rho_{\mathrm{v}}}{\mathrm{d}t} + \nabla\cdot\boldsymbol{u} = W_v$$

and

$$\frac{\mathrm{d}\rho s}{\mathrm{d}t} + \rho s\nabla\cdot\boldsymbol{u} = W_{\mathrm{s}}, \quad (4)$$

where ρ_{v} is the density of water vapor, s the specific salinity (gram salts per gram water), and W_v, W_s

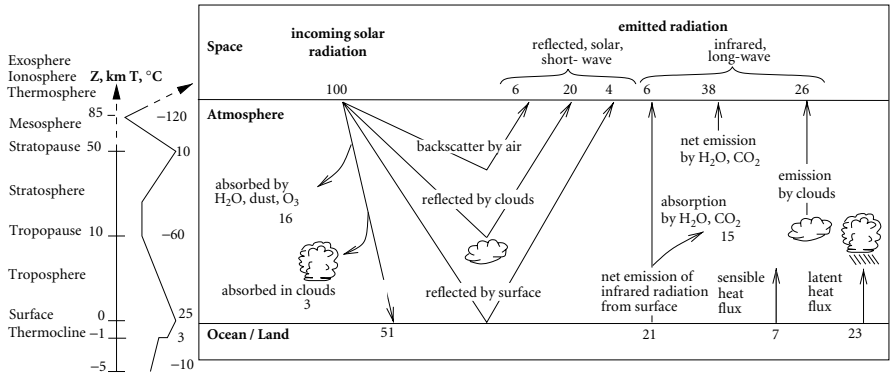

Figure 1. Sketch of the vertical structure of the atmosphere–ocean system and radiation balance and processes in the global climate system. Adapted from National Academy of Sciences (1975). Note that lengths are not to scale and and temperatures indicate only global averages.

contain possible source and sink terms as well as the effect of molecular diffusion in terms of the concentration flux density $\boldsymbol{S}$ ($-\nabla\cdot\boldsymbol{S}$) and possible phase changes.

(v) The equation of state for a mixture of salts and gases for air and water, whose constituent concentrations are virtually constant in the atmosphere and ocean is

$$p \approx \rho R T\,(1 + 0.6078\,q)\,, \tag{5}$$

where R is the gas constant for dry air ($R = 287.04\,\mathrm{J\,kg^{-1}\,K^{-1}}$) and $q = \rho_v/\rho$ is the specific humidity. Similarly, the equation of state for near incompressible water is

$$\rho \approx \rho_0[1 - \alpha(T - T_0) + \beta(S - S_0)], \tag{6}$$

where ρ_0, T_0, and S_0 are reference values for density, temperature, and salinity ($\rho_0 = 1028\,\mathrm{kg\,m^{-3}}$, $T_0 = 283\,\mathrm{K} (= 10°\mathrm{C})$, $S_0 = 35‰$), and α and β are the coefficients of thermal expansion and saline contraction ($\alpha = 1.7 \times 10^{-4}\,\mathrm{K^{-1}}$, $\beta = 7.6 \times 10^{-4}$), see Krauss (1973); Cushman-Roisin (1993).

Equations detailed in (i)–(v) form a set of hydrothermodynamic equations for the atmosphere-ocean system to which various approximations and scaling limits can be applied. Among them are the shallow-water equations, primitive equations, the Boussinesq and anelastic approximation, quasigeostrophic, and semigeostrophic equations and variants or mixtures of these. These equations have to be solved with appropriate boundary conditions and conditions at the air-sea interface; for details refer to Krauss (1973), Gill (1982) and Kraus & Businger (1994). For studies of the upper atmosphere, further equations for the geomagnetic field can also be taken into account (Maxwell's equations).

Atmospheric Structure and Circulation

In the vertical dimension, several atmospheric layers can be differentiated (see Figure 1). Figure 2 gives the length and time scales of typical atmospheric processes.

From sea level up to about 2 km is the atmospheric boundary layer, characterized by momentum, heat, moisture, and water transfer between the atmosphere and its underlying surface. Above the boundary layer is the troposphere (Greek, *tropos* meaning *turn, change*) that constitutes most of the total mass of the atmosphere (about 10 km height) and is largely in hydrostatic balance characterized by a decrease in temperature. Above the troposphere and stratosphere, which contains the ozone layer, temperatures rise throughout. The mesosphere, which is bounded by the stratopause (about 50 km height) below and mesopause (about 85 km height) above, is a layer of very thin air where temperatures drop to extreme lows. Above the mesopause, temperatures increase again throughout the thermosphere (from about 85 km to 700 km), the largest layer of the atmosphere, where the ionosphere is located (between about 100 km and 300 km). The ionosphere contains ionized atoms and free electrons and permits the reflection of electromagnetic waves. Above the thermosphere is the exosphere, which is the outermost layer of the atmosphere and the transition region between the atmosphere and outer space, the magnetosphere in particular, where atoms can escape into space beyond the so-called escape velocity and where the Van Allen belt is situated.

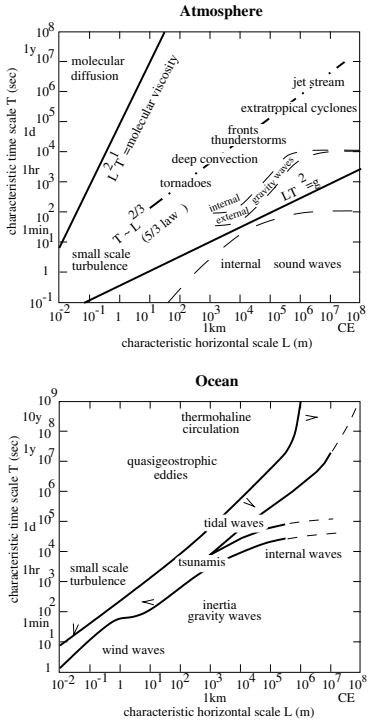

Figure 2. Schematic logarithmic time and horizontal length scales of typical atmospheric and oceanic phenomena. Note that Richardson's $L \propto T^{3/2}$ relation and CE stands for circumference of the Earth. Modified from Lettau (1952), Smagorinsky (1974), and World Meteorological Organization (1975).

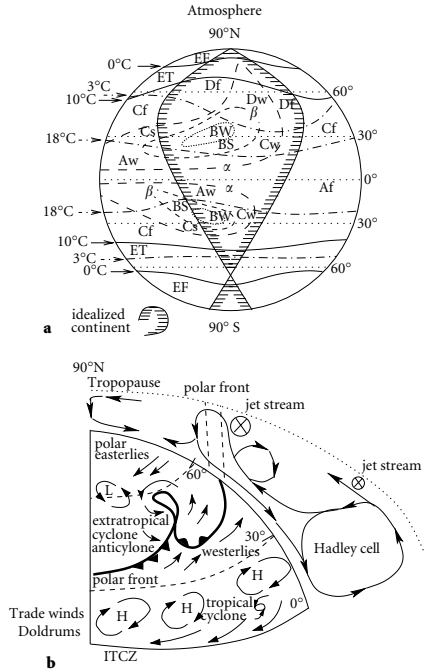

Figure 3. Sketch of the near-surface climate and atmospheric circulation of the Earth with an idealized continent. (a) Averaged isothermals of the coldest month (dashed-dot, −3°C, 18°C) and the warmest month (solid, 0°C, 10°C) and periodical dry season boundaries α and dry climate β. The following climate regions are indicated: wet equatorial climate (Af), tropical wet/dry climate (Aw), desert climate (BW), steppe climate (BS), sinic climate (Cw), Mediterranean climate (Cs), humid subtropical climate (Cf), humid continental climate (Df), continental subarctic climate (Dw), tundra climate (ET) and snow and ice climate (EF). Modified from Köppen (1923). (b) The zonal mean jet streams (primary circulation) and mass overturning (secondary circulation) in a meridional height section, the subtropical highs (H) and subpolar lows (L), polar easterlies, westerlies, polar front, trade winds, and intertropical convergence zone (ITCZ). ▲ denotes a cold front and ◗ a warm front. Adapted from Palmen (1951), Defant and Defant (1958), and Hantel in Bergmann & Schäfer (2001).

A low (high) in meteorology refers to a system of low (high) pressure, a closed area of minimum (maximum) atmospheric pressure (closed isobars, or contours of constant pressure) on a constant height chart. A low (high) is always associated with (anti)cyclonic circulation, thus also called a cyclone (anticyclone). Anticyclonic means clockwise in the Northern Hemisphere (and counterclockwise in the Southern Hemisphere). Cyclonic means counterclockwise in the Northern Hemisphere (and clockwise in the Southern Hemisphere). At zeroth order, a balance of pressure gradient forces and Coriolis forces, that is, geostrophic balance, occurs, leading to the flow of air along isobars instead of across (in the direction of the pressure gradient). A front is a discontinuous interface or a region of strong gradients between two air masses of differing densities or temperatures, thus encouraging conversion of potential into kinetic energy (examples are polar front, arctic front, cold front, and warm front).

Hurricanes and typhoons (local names for tropical cyclones) transport large amounts of heat from low to mid and high latitudes and develop over oceans. Little is known about the initial stages of their formation, although they are triggered by small low-pressure systems in the Intertropical Convergence Zone (*See* **Hurricanes and tornadoes**). Because of their strong winds, cyclones are particularly active in inducing

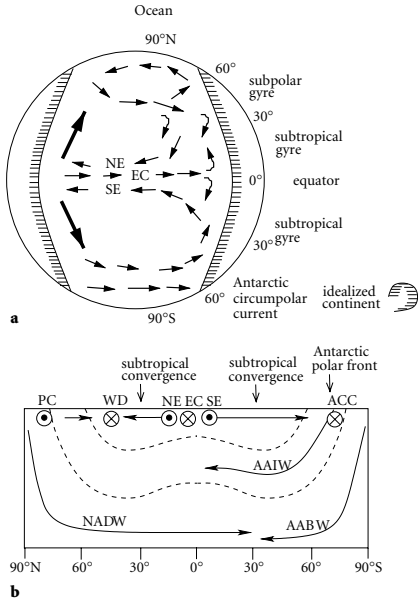

Figure 4. Sketch of the oceanic circulation of an idealized basin (a) the global wind-induced distribution of ocean currents (primary circulation) and (b) the zonal mean thermohaline circulation (secondary circulation) in a meridional depth section showing upper, intermediate, deep and bottom water masses. NE denotes the north equatorial, EC the equatorial and SE the south equatorial current. PC stands for polar current, ACC for Antarctic circumpolar current, WD for west drift, AAIW for Antarctic intermediate waters, NADW for North Atlantic deep water, and AABW for Antarctic bottom water. Adapted from Hasse and Dobson (1986).

upwelling and wind-driven surface water transport. Extratropical cyclones are frontal cyclones of mid to high latitudes (see Figures 2 and 3).

Meteorology and oceanography are concerned with understanding, predicting, and modeling the weather, climate, and oceans due to their fundamental socio-economic and environmental impact. In meteorology, one distinguishes between short (1–3 days) and medium-range (4–10 days) numerical weather prediction models (NWPs) for the atmosphere and general circulation models (GCMs, *See* **General circulation models of the atmosphere**). While NWPs for local and regional weather prediction are usually not coupled to ocean models, GCMs are global three-dimensional complex coupled atmosphere-ocean models (which even include the influence of land masses), used to study global climate change, modeling radiation, photochemistry, transfer of heat, water vapor, momentum, greenhouse gases, clouds, ocean temperatures, and ice boundaries. The atmosphere-ocean interface couples the "fast" processes of the atmosphere with the comparably "slow" processes of the ocean through evaporation, precipitation, and momentum interaction. GCMs are validated using statistical techniques and correlated to the actual climate evolution. Additionally, the application of GCMs to different planetary atmospheres, for example, on Mars and Jupiter, leads to a greater understanding of the planet's history and environment.

The complexity of the dynamics of the atmosphere and ocean is largely due to the intrinsic coupling between these two large masses at the air-sea interface.

Ocean

Ocean circulation is forced by tidal forces (also known to force atmospheric tides), due to gravitational attraction, wind stress, applied shear forces acting on the interface, and external, mainly solar, radiation, penetrating into the sea surface and affecting the heat budget and water mass due to evaporation. Primary sources of tidal forcing, earliest work on which was undertaken by Pierre-Simon Laplace in 1778, are the Moon and the Sun. One discerns between diurnal, semidiurnal, and mixed-type tides.

In the ocean, one distinguishes between two types of ocean currents: surface (wind-driven) and deep circulation (thermohaline circulation). Separating the surface and deep circulation is the thermocline, a small layer of strong gradient of temperature, salinity, and density, acting as an interface between the two types of circulations.

Surface circulation ranging up to 400 m in depth is forced by the prominent westerly winds in the mid-latitudes and trade winds in the tropical regions (see Figures 3 and 4), which are both forced by solar heating and Coriolis forces leading to expansion of water near the equator and decreased density, but increased salinity due to evaporation. An example of the latter is the Gulf Stream in the North Atlantic. The surface wind stress, solar heating, Coriolis forces, and gravity lead to the creation of large gyres in all ocean basins with clockwise (anticyclonic) circulation in the northern hemisphere and counterclockwise circulation in the southern hemisphere. The North Atlantic Gyre, for example, consists of four currents: the north equatorial current, the Gulf Stream, the North Atlantic current, and the Canary current.

Ekman transport, the combination of wind stress and Coriolis forces, leads to a convergence of water masses in the center of such gyres, which increases the sea surface elevation. The layer of Ekman transport can be 100–150 m in depth and also leads to upwelling due to conservation of mass on the western (eastern) coasts for winds from the north (south) in the Northern (Southern) Hemisphere. As a consequence, nutrient-rich

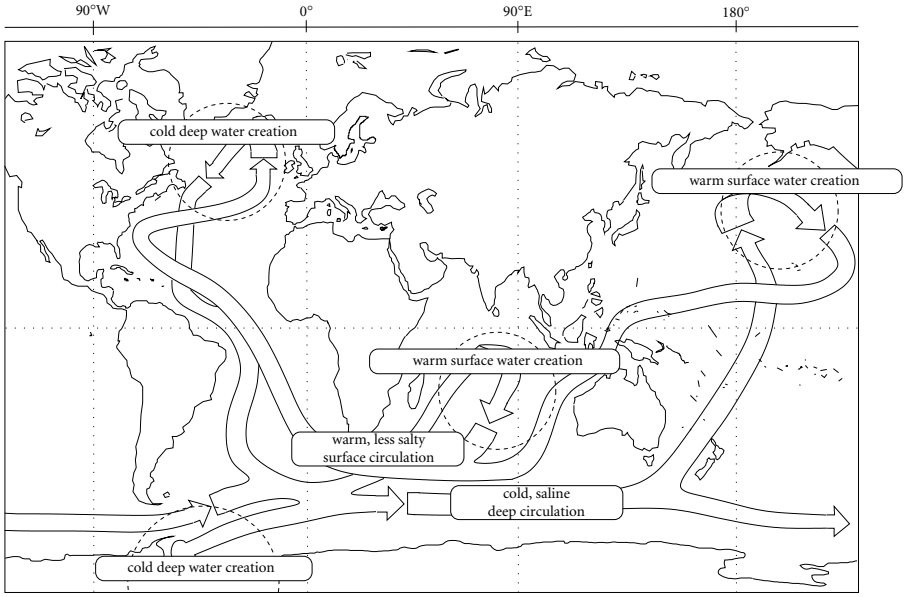

Figure 5. Sketch of the global conveyor belt through all oceans, showing the cold saline deep circulation, the warm, less salty surface circulation, and the primary regions of their creation. Note that this circulation is only characteristic of the actual global circulation. Adapted from Broecker (1987).

deep water is brought to the surface. With the opposite wind direction, Ekman transport acts to induce downwelling.

Another important combination of forces is the balance of Coriolis forces and gravity (pressure gradient forces), which is called geostrophic balance, leading to the movement of mass along isobars instead of across (geostrophic current), similar to the atmosphere. The boundary currents along the eastern and western coastlines are the major geostrophic currents in a gyre. The western side of the gyre is stronger than the eastern due to the Earth's rotation, called western intensification.

Deep circulation makes up 90% of the total water mass and is driven by density forces and gravity, which in turn is a function of temperature and salinity. High-density deep water originates in the case of extreme cooling of the sea surface in the polar regions, sinking to large depths as a density current, a strongly nonlinear phenomenon. When the warm Gulf Stream waters, which have increased salinity due to excessive evaporation in the tropics, move north due to the North Atlantic Gyre, they are cooled by Arctic winds from the north and sink to great depths forming the high-density Atlantic deep waters (see Figure 5). The downward transport of water is balanced by upward transport in low- and mid-latitude regions.

The most prominent example of the interaction between atmospheric and ocean dynamics is the global conveyor belt, which links the surface (wind-driven) and deep (thermohaline) circulation to the atmospheric circulation. The global conveyor belt is a global circulatory system of distinguishable and recognizable water masses traversing all oceans (see Figure 5). The water masses of this global conveyor belt transport heat and moisture, contributing to the climate globally. In Earth's history, the global conveyor belt has experienced flow reversals and perturbations leading to changes in the global circulatory system. The rather recent anthropogenic impact on climate and oceans through greenhouse gas emissions has the potential to create instability in this large-scale dynamical system, which could alter Earth's climate and have devastating environmental and agricultural effects.

ENSO and NAO

Another example of atmosphere-ocean coupling is the combination of the El Niño and Southern Oscillation (ENSO). The El Niño ocean current (and associated

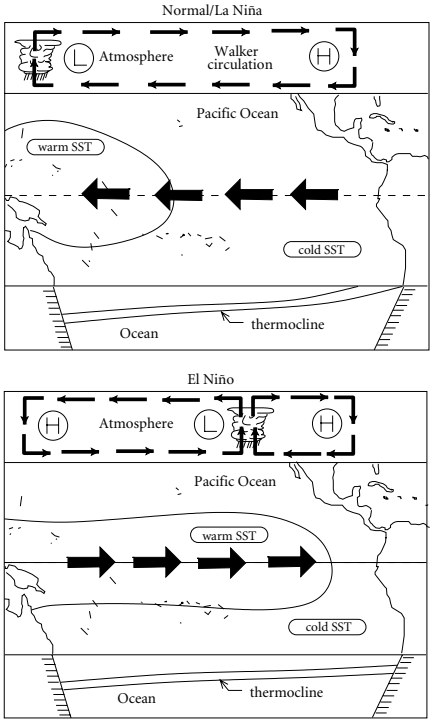

Figure 6. Sketch of the El Niño in the tropical Pacific, showing a reversal in (trade) wind direction from easterlies to westerlies during an El Niño period bringing warmer water (warm corresponds to a positive sea-surface temperature [SST]) close to the South American coast, displacing the equatorial thermocline downwards. Note the change in atmospheric tropical convection and associated heavy rainfall. After McPhaden, NOAA/TAO (2002) and Holton (1992).

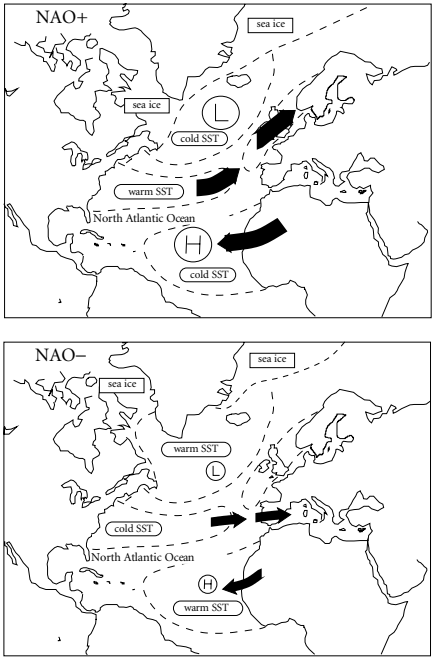

Figure 7. Sketch of the North Atlantic Oscillation (NAO) during the northern hemisphere winter season. Positive NAO (NAO+) showing an above-usual strong subtropical high-pressure center and subpolar low, resulting in increased wind strengths and storms crossing the Atlantic towards northern Europe. NAO+ is associated with a warm wet winter in Europe and cold dry winter in North America. Central America experiences mild wet winter conditions. Negative NAO (NAO−) shows a weaker subtropical high and subpolar low, resulting in lower wind speeds and weaker storms crossing the Atlantic toward southern Europe and receded sea ice masses around Greenland. NAO− is associated with cold weather in northern Europe and moist air in the Mediterranean. Central America experiences colder climates and more snow. Adapted from Wanner (2000).

wind and rain change) is named from the Spanish for Christ Child, due to its annual occurrence off the South American coast around Christmas, and may also be sensitive to anthropogenic influence (see Figure 6). The Southern Oscillation occurs as a 2–5-year periodic reversal in the east-west pressure gradient associated with the present equatorial wind circulation, called Walker circulation, across the Pacific leading to a reversal in wind direction and changes in temperature and precipitation. The easterly wind in the West Pacific becomes a westerly. As a consequence, the strong trade winds are weakened, affecting climate globally (e.g., crop failures in Australia, flooding in the USA, and the monsoon in India). The Southern Oscillation in turn leads to large-scale oceanic fluctuations in the circulation of the Pacific Ocean and sea-surface temperatures, which is called El Niño. The interannual variability, though, is not yet fully understood; consideration of a wider range of tropical and extratropical influences is needed. A counterpart to the ENSO in the Pacific is the North Atlantic Oscillation (NAO), which is essentially an oscillation in the pressure difference across the North Atlantic and is described further in Figure 7.

Monsoons

The monsoons (derived from Arabic, *mauism*, meaning season or shift in wind) are seasonally reversing

winds and one of the most pertinent features of the global atmospheric circulation. The best-known examples are the monsoons over the Indian Ocean and, to some extent, the western Pacific Ocean (tropical region of Australia), the western coast of Africa, and the Carribbean. Monsoons are characteristic for wet summer and dry winter seasons, associated with strong winds and cyclone formation. They occur due to differing thermal characteristics of the land and sea surfaces. Land, having a much smaller heat capacity than the ocean, emits heat from solar radiation more easily, leading to upward heat (cumulus) convection. In the summer season, this leads to a pressure gradient and thus wind from the land to the ocean in the upper layers of the atmosphere and subsequent conserving flow of moisture-rich air from the sea back inland at lower levels. This leads to monsoonal rains, increased latent heat release, and intensified monsoon circulation. During the monsoons of the winter season, the opposite of the summer season monsoon takes place, although less pronounced, since the thermal gradient between the land and sea is reversed. The winter monsoons thus lead to precipitation over the sea and cool dry land surfaces.

ANDREAS A. AIGNER AND KLAUS FRAEDRICH

See also **Fluid dynamics; General circulation models of the atmosphere; Hurricanes and tornadoes; Lorenz equations; Navier–Stokes equation**

Further Reading

Apel, J. 1989. *Principles of Ocean Physics*, London: Academic Press

Barry, R.G., Chorley, R.J. & Chase, T. 2003. *Atmosphere, Weather and Climate*, 8th edition, London and New York: Routledge

Bergmann, K., Schaefer C. & von Raith, W. 2001. *Lehrbuch der Experimentalphysik, Band 7, Erde und Planeten*, Berlin: de Gruyter

Cushman-Roisin, B. 1993. *Introduction to Geophysical Fluid Dynamics*, Englewood Cliffs, NJ: Prentice–Hall

Defant, A. & Defant, Fr. 1958. *Physikalische Dynamik der Atmosphäre*, Frankfurt: Akademische Verlagsgesellschaft

Gill, A. 1982. *Atmosphere–Ocean Dynamics*, New York: Academic Press

Hasse, L. & Dobson, F. 1986. *Introductory Physics of the Atmosphere and Ocean*, Dordrecht and Boston: Reidel

Holton, J.R. 1992. *An Introduction to Dynamic Meteorology*, 3rd edition, New York: Academic Press

Kraus, E.B. & Businger, J.A. 1994. *Atmosphere–Ocean Interaction*, New York: Oxford University Press, and Oxford: Clarendon Press

Krauss, W. 1973. *Dynamics of the Homogeneous and Quasi-homogeneous Ocean*, vol I, Berlin: Bornträger

LeBlond, P.H. & Mysak, L.A. 1978. *Waves in the Ocean*, Amsterdan: Elsevier

Lindzen, R.S. 1990. *Dynamics in Atmospheric Physics*, Cambridge and New York: Cambridge University Press

Pedlosky, J. 1986. *Geophysical Fluid Dynamics*, New York: Springer

Philander, S.G. 1990. *El Niño, La Niña, and the Southern Oscillation*, New York: Academic Press

ATTRACTOR NEURAL NETWORKS

Neural networks with feedback can have complex dynamics; their outputs are not related in a simple way to their inputs. Nevertheless, they can perform computations by converging to attractors of their dynamics. Here, we analyze how this is done for a simple example problem: associative memory, following the treatment by Hopfield (1984) (see also Hertz, et al., 1991, Chapters 2 and 3).

Let us assume that input data are fed into the network by setting the initial values of the units that make it up (or a subset of them). The network dynamics then lead to successive changes in these values. Eventually, the network will settle down into an attractor, after which the values of the units (or some subset of them) give the output of the computation. The associative memory problem can be described in the following way: there is a set of p patterns to be stored. Given, as input, a pattern that is a corrupted version of one of these, the attractor should be a fixed point as close as possible to the corresponding uncorrupted pattern.

We focus on networks described by systems of differential equations such as

$$\tau_i \frac{\mathrm{d}u_i}{\mathrm{d}t} + u_i(t) = \sum_{j \neq i} w_{ij} g[u_j(t)]. \qquad (1)$$

Here, $u_i(t)$ is the net input to unit i at time t and $g(\,)$ is a sigmoidal activation function ($g' > 0$), so that $V_i = g(u_i)$ is the value (output) of unit i. The connection weight to unit i from unit j is denoted w_{ij}, and τ_i is the relaxation time. We can also consider discrete-time systems governed by

$$V_i(t+1) = g\left[\sum_j w_{ij} V_j(t)\right]. \qquad (2)$$

Here, it is understood that all units are updated simultaneously. In either case, the "program" of such a network is its connection weights w_{ij}.

In general, three kinds of attractors are possible: fixed point, limit cycle, and strange attractor. There are conditions under which the attractors will always be fixed points. For nets described by the continuous dynamics of Equation (1), a sufficient (but not necessary) condition is that the connection weights be symmetric: $w_{ij} = w_{ji}$. General results about the stability of recurrent nets were proved by Cohen & Grossberg (1983). They showed, for dynamics (1), that there is a Lyapunov function, that is, a function of the state variables u_i, which always decreases under the dynamics, except for special values of the u_i at which it does not change. These values are fixed points. For values of the u_i close to such a point, the system will evolve either toward it (an attractor) or away

from it (a repellor). For almost all starting states, the dynamics will end at one of the attractor's fixed points. Furthermore, these are the only attractors.

We treat the case $g(u) = \tanh(\beta u)$ and consider the *ansatz*

$$w_{ij} = \frac{1}{N} \sum_{\mu=1}^{p} \xi_i^\mu \xi_j^\mu. \tag{3}$$

That is, for each pattern, there is a contribution to the connection weight proportional to the product of sending (ξ_j^μ) and receiving (ξ_i^μ) unit activities when the network is in a stationary state $V_i = \xi_i^\mu$. This is just the form of synaptic strength proposed by Hebb (1949) as the basis of animal memory, so this *ansatz* is sometimes called a Hebbian storage prescription.

To see how well the network performs this computation, we examine the fixed points of (1) or (2), which solve

$$V_i = \tanh\left(\beta \sum_j w_{ij} V_j\right). \tag{4}$$

The quality of retrieval of a particular stored pattern ξ_i^μ is measured by the quantity $m_\mu = N^{-1} \sum_i \xi_i^\mu V_i$. Using (4), with the weight formula (3), we look for solutions in which the configuration of the network is correlated with only one of the stored patterns, that is, just one of the m_μ's is not zero. If the number of stored patterns $p \ll N$, we find a simple equation for m_μ:

$$m_\mu = \tanh(\beta m_\mu). \tag{5}$$

This equation has nontrivial solutions whenever the gain $\beta > 1$ and for β large, $m_\mu \to 1$, indicating perfect retrieval. If the gain is high enough, there are other attractors in addition to the ones we have tried to program into the network with the choice (3), but by keeping the gain between 1 and 2.17 we can limit the attractor set to the desired states.

When p is of the same order as N, the analysis is more involved. We define a parameter $\alpha = p/N$. For small α, the overlaps m_μ between the stored patterns and the fixed points are less than, but still close to, 1. However, there is a critical value of α, $\alpha_c(\beta)$, above which there are no longer fixed points close to the patterns to be stored and the memory breaks down catastrophically. One finds $\alpha_c(1) = 0$ and, in the limit $\beta \to \infty$, $\alpha_c(\beta) \to 0.14$.

Thus, attractor computation works in this system over a wide range of the model parameters α and β. It can be shown to be robust with respect to many other variations, including dilution (random removal of connections), asymmetry (making some of the $w_{ij} \neq w_{ji}$), and quantization or clipping of the weight values. Its breakdown at the boundary $\alpha_c(\beta)$ is a collective effect like a phase transition in a physical system.

The weight formula (3) was only an educated guess. It is possible to obtain better weights, which reduce the crosstalk and increase α_c, by employing systematic learning algorithms.

It is also possible to extend the above-described model to store pattern sequences by including suitable delays in the discrete-time dynamics (2).

It appears that attractor networks play a role in computations in the brain. One example of current interest is working memory: some neurons in the prefrontal cortex that are selectively sensitive to a particular visual stimulus exhibit continuing activity after the stimulus is turned off, even though the animal sees other stimuli. Thus, they seem to be involved in the temporary storage of visual patterns. Computational network models based on the simple concepts described above (Renart et al., 2001) are able to reproduce the main features seen in recordings from these neurons.

JOHN HERTZ

See also **Cellular nonlinear networks; McCulloch–Pitts network; Neural network models**

Further Reading

Amit, D.J. 1989. *Modeling Brain Function*, Cambridge and New York: Cambridge University Press

Cohen, M. & Grossberg, S. 1983. Absolute stability of global pattern formation and parallel memory storage by competitive neural networks. *IEEE Transactions on Systems, Man and Cybernetics*, 13: 815–826 etc.

Hebb, D.O. 1949. *The Organization of Behavior*, New York: Wiley

Hertz, J.A., Krogh, A.S., & Palmer, R.G. 1991. *Introduction to the Theory of Neural Computation*, Redwood City, CA: Addison-Wesley

Hopfield, J.J. 1984. Neurons with graded responses have collective computational properties like those of two-state neurons. *Proceedings of the National Academy of Sciences USA*, 79: 3088–3092

Renart, A., Moreno, R., de la Rocha, J., Parga, N. & Rolls, E.T. 2001. A model of the IT-PF network in object working memory which includes balanced persistent activity and tuned inhibition. *Neurocomputing*, 38–40: 1525–1531

ATTRACTORS

A wide variety of problems arising in physics, chemistry, and biology can be recast within the framework of dynamical systems. A dynamical system is made up of two parts: the phase space, which consists of all possible configurations of the physical system, and the "dynamics," a rule describing how the state of the system changes over time. The fundamental insight of the theory is that some problems, which initially appear extremely complicated, can be greatly simplified if we are prepared to concentrate on their long-term behavior, that is, what happens eventually.

This idea finds mathematical expression in the concept of an attractor.

The simplest possibility is that the system settles down to a constant state (e.g., a pendulum damped by air resistance will end up hanging vertically downward). In the phase space, this corresponds to an attractor that is a single "fixed point" for the dynamics. If the system settles down to a repeated oscillation, then this corresponds to a "periodic orbit," a closed curve in the phase space. For two coupled ordinary differential equations (ODEs), it is a consequence of the Poincaré–Bendixson Theorem that these fixed points and periodic orbits are essentially the only two kinds of attractors that are possible (see Hirsch & Smale, 1974 for a more exact statement). In higher dimensions, it is possible for the limiting behavior to be quasi-periodic with k different frequencies, corresponding to a k-torus in the phase space (cf. Landau's picture of turbulence as in Landau & Lifschitz, 1987).

However, with three or more coupled ODEs (or in one-dimensional maps), the attractor can be an extremely complicated object. The famous "Lorenz attractor" was perhaps the first explicit example of an attractor that is not just a fixed point or (quasi) periodic orbit. Edward Lorenz highlighted this in the title of his 1963 paper, "Deterministic Nonperiodic Flow." The phrase "strange attractor" was coined by Ruelle & Takens (1971) for such complicated attracting sets. These attractors, and the chaotic dynamics associated with them, have been the focus of much attention, particularly in relation with the theory of turbulence (the subject of Ruelle & Takens' paper; see also Ruelle, 1989). There is no fixed definition of a "strange attractor"; some authors use the phrase as a signature of chaotic dynamics, while others use it to denote a fractal attractor (e.g., Grebogi et al. (1984) discuss "strange nonchaotic attractors").

Over the years, various authors have given precise (but different) definitions of an attractor: Milnor (1985) discusses many of these (and proposes a new one of his own). Most definitions require that an attractor attract a "large set of initial conditions and satisfy some kind of minimality property" (without this, the whole phase space could be called an attractor).

We refer to the set of all those points in the phase space whose trajectories are attracted to some set A as the basin of attraction of A and write this $B(A)$. There are essentially two choices of what it means to attract a large set of initial conditions: the more common one is that $B(A)$ contains an open neighborhood of A, while Milnor (1985) suggested that a more realistic requirement is that $B(A)$ has positive Lebesgue measure.

Exactly what type of minimality assumption we require depends on what we want our attractor to say about the dynamics. At the very least, there should be no smaller (closed) set with the same basin of

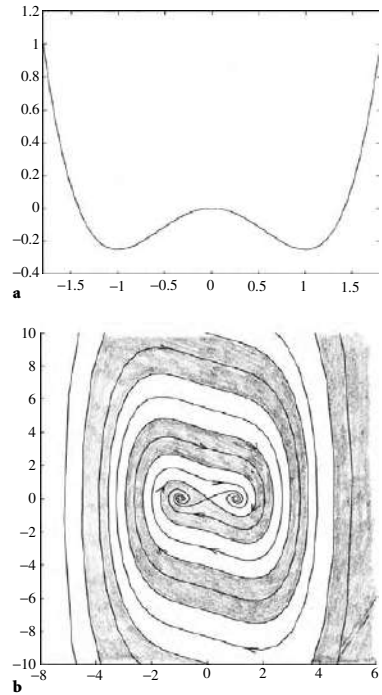

Figure 1. (a) A symmetric double-well potential. (b) Phase portrait of a particle moving in the potential of (a) with friction.

attraction: this excludes any "unnecessary" points from the attractor. A consequence of this minimality property is that the attractor is invariant: if A is the attractor of a map f, this means that $f(A) = A$ (there is, of course, a similar property for the attractor of a flow). In particular, this means that it is possible to talk about the "dynamics on the attractor."

If we want one attractor to describe the possible asymptotic dynamics of *every* initial condition, then there is no need to impose any further minimality assumption. Figure 1(b) shows the phase portrait for a particle moving with friction in the symmetric double-well potential of Figure 1(a); the basin of attraction of the fixed point corresponding to the bottom of the left-hand well is shaded. (The equations of motion are $\dot{x} = y$ and $\dot{y} = -\frac{y}{2} + x - x^3$.) We could say that the attractor consists of the three points $\{(-1, 0), (1, 0), (0, 0)\}$, but this discards much of the information contained in the phase portrait. This motivates the further requirement that an attractor be "indecomposable": it should not be possible to split it into two disjoint invariant subsets. (Some definitions require there to be a dense orbit in

the attractor: essentially, this means that one trajectory "covers" the entire attractor, so in particular the attractor cannot be split into two pieces.) This gives us two possible attractors: $(-1, 0)$ and $(1, 0)$ (the origin does not attract a neighborhood of itself, nor any set of positive measure).

In this example, the boundary between the basins of attraction of the two competing attractors is a smooth curve. However, in many examples this boundary is a fractal set. This was first noticed by McDonald et al. (1985), who observed that near a fractal boundary, it is harder to predict the asymptotic behavior of imprecisely known initial conditions. An extreme version of this occurs with the phenomenon of "riddled basins," first observed by Alexander et al. (1992): arbitrarily close to a point attracted to one attractor; there can be a point attracted to another. In this case, an arbitrarily small change in the initial condition can lead to completely different asymptotic behavior. (In addition to treating some analytically tractable examples, Alexander et al. (1992) give an impressive array of pictures from their numerical simulations.)

Attractors can also be meaningfully defined for the infinite-dimensional dynamical systems arising from partial and functional differential equations (e.g., Hale, 1988; Robinson, 2001; Temam 1988/1996), and for random and nonautonomous systems (Crauel et al. (1997) adopt an approach that includes both these cases).

JAMES C. ROBINSON

See also **Chaos vs. turbulence; Dynamical systems; Fractals; Phase space; Turbulence**

Further Reading

Alexander, J.C., Yorke, J.A., You, Z. & Kan, I. 1992. Riddled basins. *International Journal of Bifurcation and Chaos*, 2: 795–813

Crauel, H., Debussche, A. & Flandoli, F. 1997. Random attractors. *Journal of Dynamics and Differential Equations*, 9: 307–341

Grebogi, C., Ott, E., Pelikan, S. & Yorke, J.A. 1984. Strange attractors that are not chaotic. *Physica* D, 13: 261–268

Hale, J.K. 1988. *Asymptotic Behavior of Dissipative Systems*, Providence, RI: American Mathematical Society

Hirsch, M.W. & Smale, S. 1974. *Differential Equations, Dynamical Systems and Linear Algebra*. New York: Academic Press

Landau, L.D. & Lifschitz, E.M. 1987. *Fluid Mechanics*, 2nd edition, Oxford: Pergamon Press

Lorenz, E.N. 1963. Determininstic non-periodic flow. *Journal of Atmospheric Science*, 20: 130–141

Milnor, J. 1985. On the concept of attractor. *Communications in Mathematical Physics*, 99: 177–195

Robinson, J.C. 2001. *Infinite-Dimensional Dynamical Systems*, Cambridge and New York: Cambridge University Press

Ruelle, D. 1989. *Chaotic Evolution and Strange Attractors*, Cambridge and New York: Cambridge University Press

Ruelle, D. & Takens, F. 1971. On the nature of turbulence. *Communications in Mathematical Physics*, 20: 167–192

Temam, R. 1996. *Infinite-dimensional Dynamical Systems in Mechanics and Physics*, 2nd edition, Berlin and New York: Springer

AUBRY–MATHER THEORY

Named after Serge Aubry and John Mather, who independently shaped the seminal ideas, the Aubry–Mather theory addresses one of the central problems of modern dynamics: the characterization, of nonintegrable Hamiltonian time evolution beyond the realm of perturbation theory. In general terms, when a Hamiltonian system is near-integrable, perturbation theory provides a rigorous generic description of the invariant sets of motion (closed sets containing trajectories) as smooth surfaces (KAM tori), each one parametrized by the rotation number ω of the angle variable (angle-action coordinates): all the trajectories born and living inside the invariant torus share this common value of ω. An invariant set has an associated natural invariant measure, which describes the measure-theoretical (or statistical) properties of the trajectories inside the invariant set. The invariant measure on a torus is a continuous measure, so that the distribution function of the angle variable is continuous. In this near-integrable regime of the dynamics, perturbative schemes converge adequately and future evolution is—to a desired arbitrary degree—predictable for arbitrary initial conditions on each torus.

Far from integrable Hamiltonian dynamics, what is the fate of these invariant natural measures, or invariant sets of motion, beyond the borders of validity of perturbation theory? The answer is that each torus breaks down and its remaining pieces form an invariant fractal set, called by Percival a cantorus (or Aubry–Mather set) characterized by the rotation number value common to all trajectories in the cantorus. The statistical properties of the trajectories on the invariant cantorus are now described by a purely discrete measure or Cantor distribution function (see Figure 1).

Basic Theorems

The formal setting of Aubry–Mather theory for the transition from regular motion on invariant tori to orbits on hierarchically structured nowhere dense cantori is the class of maps of a cylindrical surface $\mathcal{C} = S^1 \times \mathcal{R}$ (cylindrical coordinates (u, p)) (see Figure 2) onto itself,

$$f : \mathcal{C} \to \mathcal{C}, \tag{1}$$

characterized by preservation of areas (symplectic) and the "twist" property, meaning that the torsion produced by an iteration of the map on a vertical segment of the cylindrical surface converts it into a part of the graph

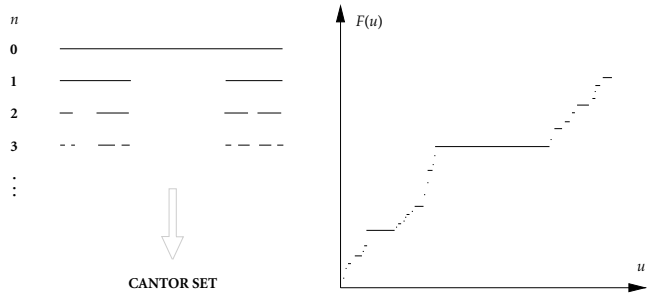

Figure 1. Left: Construction of a Cantor set from the unit real interval (or circle S^1) as a limiting process. At each step n, a whole piece is cut out from each remaining full segment. Right: The distribution function $F(u)$ of the projection onto the angular component u_n of a cantorus orbit. $F(u)$ is the limiting proportion of the values of $u_n < u$, $-\infty < n < +\infty$.

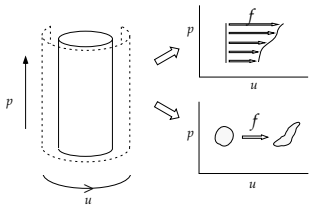

Figure 2. Schematic illustration on the unfolded cylindrical surface $\mathcal{C} = S^1 \times \mathcal{R}$ of the twist (upper right) and area-preserving (lower right) properties of the map $F : \mathcal{C} \to \mathcal{C}$. In the upper right area the curve is a single-valued function $\varphi(u)$ of the angular variable.

of some function $\varphi(u)$ of the angular coordinate. More explicitly, if we denote by $(u', p') = f(u = 0, p)$ the image of the vertical segment, then u' is a monotone function of p, so that (u', p') is the graph of a single-valued function.

An area-preserving twist map has associated an action-generating function related to the map via a variational (extremal action) principle:

- An action-generating function, $H(x, x')$, of a twist map is a two-variable function that is strictly convex:

$$\frac{\partial^2 H}{\partial u \partial u'} \leq K < 0. \tag{2}$$

- If u_0 is a critical point of $\mathcal{L}(x) = H(u_{-1}, x) + H(x, u_1)$, then a certain sequence (u_{-1}, p_{-1}), (u_0, p_0), (u_1, p_1) is a segment of a cylinder orbit of f.

(Given a sequence $\{u_j\}_{j=0}^{n}$ with fixed ends $(u_0 = a, u_n = b)$, the associated action functional $\mathcal{L}$ is the sum $\sum_{j=0}^{n-1} H(u_j, u_{j+1})$.

A cylinder orbit is called ordered when it projects onto an angular sequence ordered in the same way as a uniform rotation of angle ω. An invariant set is a minimal invariant set if it does not include proper invariant subsets and is called ordered if it contains only ordered orbits. The proper definition of an Aubry–Mather set is a minimal invariant ordered set that projects one-to-one on a nowhere dense Cantor set of the circle S^1.

The following points comprise the main core (Golé, 2001; Katok & Hasselblatt, 1995) of the Aubry–Mather theory:

- For each rational value $\omega = p/q$ of the rotation number, there exist (Poincaré–Birkhoff theorem) at least two ordered periodic orbits (Birkhoff periodic orbits of type (p, q)), which are obtained by, respectively, minimizing and maximizing the action over the appropriate set of angular sequences.

  In general, periodic orbits of rational rotation number $\omega = p/q$ do not form an invariant circle, in which case there are nonperiodic orbits approaching two different periodic orbits as $n \to -\infty$ and as $n \to +\infty$, called heteroclinic orbits (or homoclinic in some contexts). These orbits connect two Birkhoff periodic orbits through a minimal action path. Usually, the number of map iterations needed for such action-minimizing orbits to pass over the action barriers is exponentially small.
- For each irrational value of ω, there exists either an invariant torus or an Aubry–Mather set. There are also homoclinic trajectories connecting orbits on the Aubry–Mather set.

The hierarchical structure of gaps that break up the torus has its origins in the path-dependent action barriers. Note also that heteroclinics to nearby periodic orbits (of rational rotation number) pass over nearly the same action barriers, leading to a

somewhat metaphorical view of nearby resonances biting the tori and leaving gaps. Certainly, the action barriers fractalize the invariant measure according to the proximity of the irrational rotation number ω to rationals.

The explanatory power of the extremal action principle in the fractalization of invariant sets of motion suggests one of the immediate physical applications of this theory. Indeed, Aubry's work was originally motivated by the equilibrium problem of a discrete field (u_n) $n \in \mathcal{Z}$, under some energy functional, whose extremalization defines equilibrium field configurations. Under some conditions on the energy-generating function $H(u, u')$, both are equivalent mathematical physics problems, and a one-to-one correspondence between orbits (u_n, p_n) and equilibrium field configurations (u_n) does exist (Aubry, 1985).

Application to the Generalized Frenkel–Kontorova Model

From this perspective, the Aubry–Mather theory gives rigorous variational answers in the description of equilibrium discrete nonlinear fields such as the generalized Frenkel–Kontorova (FK) model with convex interactions. Although the terminology changes, every aspect of cylinder dynamics has a counterpart in the equilibrium problem of this interacting nonlinear many-body model.

- Commensurate (periodic) field configurations correspond to Birkhoff periodic orbits, and as such they are connected by the field configurations associated to heteroclinics, which are here called discrete (sine-Gordon) solitons or elementary discommensurations.
- Incommensurate (quasiperiodic) field configurations can correspond either to tori trajectories or to Aubry–Mather trajectories. The macroscopic physical properties (formally represented by averages on the invariant measure) of the field configuration experience drastic changes when passing from one case (tori) to the other (Aubry–Mather sets). This transition (called breaking of analiticity by Aubry) has been characterized as a critical phenomenon using renormalization group methods by (MacKay, 1993).

The Aubry–Mather theory puts on a firm basis what is known as discommensuration theory, which is the description of a generic incommensurate or (higher-order) commensurate field configuration as an array of discrete field solitons, strongly interacting when tori subsist, but almost noninteracting and deeply pinned when only Cantor invariant measures remain. Aubry's work provided a satisfactory understanding of the complexity of the phase diagrams and the singular character of the equations of state of the generalized FK model (Griffiths, 1990).

LUIS MARIO FLORÍA

See also **Commensurate–incommensurate transition; Frenkel–Kontorova model; Hamiltonian systems; Kolmogorov–Arnol'd–Moser theorem; Phase transitions; Standard map; Symplectic maps**

Further Reading

Aubry, S. 1985. *Structures incommensurables et brisure de la symmetrie de translation I* [Incommensurate structures and the breaking of traslation symmetry I]. In *Structures et Instabilités*, edited by C. Godréche, Les Ulis: Editions de Physique, pp. 73–194

Golé, C. 2001. *Symplectic Twist Maps. Global Variational Techniques*, Singapore: World Scientific

Griffiths, R.B. 1990. Frenkel–Kontorova models of commensurate-incommensurate phase transitions. In *Fundamental Problems in Statistical Mechanics VII*, edited by H. van Beijeren, Amsterdam: North-Holland, pp. 69–110

Katok, A. & Hasselblatt, B. 1995. *Introduction to the Modern Theory of Dynamical Systems*. Cambridge and New York: Cambridge University Press

MacKay, R.S. 1993. *Renormalisation in Area-preserving Maps*, Singapore: World Scientific

AUTO-BÄCKLUND TRANSFORMATION

See **Bäcklund transformations**

AUTOCATALYTIC SYSTEM

See **Reaction-diffusion systems**

AUTOCORRELATION FUNCTION

See **Coherence phenomena**

AUTONOMOUS SYSTEM

See **Phase space**

AUTO-OSCILLATIONS

See **Phase plane**

AVALANCHE BREAKDOWN

Charge transport in condensed matter is simply described by the current density j as a function of the local electric field E. For bulk materials, the current density per unit area is given by $j(E) = -env$, where $e > 0$ is the electron charge, n is the conduction electron density per unit volume, and v is the drift velocity. In the simplest case, v is a linear function of the field: $v = -\mu E$, with mobility μ.

Thus, the conductivity $\sigma = j/E = en\mu$ is proportional to the number of conduction electrons. In metals, n is given by the number of valence electrons, which is temperature independent. In semiconductors, however, the concentration of electrons in the conduction

band varies greatly and is determined by generation-recombination (GR) processes that induce transitions between valence band, conduction band, and impurity levels (donors and acceptors). Charge carrier concentration depends not only upon temperature but also upon the electric field, which explains why the conductivity can change over many orders of magnitude. A GR process that depends particularly strongly on the field is impact ionization, the inverse of the Auger effect. It is a process in which a charge carrier with high kinetic energy collides with a second charge carrier, transferring its kinetic energy to the latter, which is thereby lifted to a higher energy level. The kinetic energy is increased by the local electric field, which heats up the carriers. As a certain minimum energy is necessary to overcome the difference in the energy levels of the second carrier, the impact ionization probability depends in a threshold-like manner on the applied voltage.

Impact ionization processes may be classified as band-band processes or band-trap processes depending on whether the second carrier is initially in the valence band and makes a transition from the valence band to the conduction band, or whether it is initially at a localized level (impurity, donor, acceptor), and makes a transition to a band state. Further, impact ionization processes are classified as electron or hole processes according to whether the ionizing hot carrier is a conduction band electron or a hole in the valence band.

Schematically, impact ionization may be written as one of the following reaction equations, in analogy with chemical kinetics:

$$\mathrm{e} \longrightarrow 2\mathrm{e} + \mathrm{h}, \tag{1}$$

$$\mathrm{e} + \mathrm{e_t} \longrightarrow 2\mathrm{e} + \mathrm{h_t}, \tag{2}$$

$$\mathrm{h} \longrightarrow 2\mathrm{h} + \mathrm{e}, \tag{3}$$

$$\mathrm{h} + \mathrm{h_t} \longrightarrow 2\mathrm{h} + \mathrm{e_t}, \tag{4}$$

where e and h denote band electrons and holes, respectively, and $\mathrm{e_t}$ and $\mathrm{h_t}$ stand for electrons and holes trapped at impurities (donors, acceptors, or deep levels). The result of the process is carrier multiplication (avalanching), which may induce electrical instabilities at sufficiently high electric fields. Impact ionization from shallow donors or acceptors is responsible for impurity breakdown at low temperatures. Being an autocatalytic process (i.e., each carrier ionizes secondary carriers that might, in turn, impact ionize other carriers), it induces a nonequilibrium phase transition between a low- and high-conductivity state and may lead to a variety of spatiotemporal instabilities, including current filamentation, self-sustained oscillations, and chaos. The conductivity saturates when all impurities are ionized. Band-to-band impact ionization eventually induces avalanche breakdown, limiting the bias voltage that can be safely applied to a device. The conductivity increases much more strongly than during impurity breakdown because of the large number of valence band electrons available for ionization.

Impurity impact-ionization breakdown at helium temperatures (ca. 5 K) in p-Ge, n-GaAs, and other semiconductor materials has been thoroughly studied both experimentally and theoretically as a model system for nonlinear dynamics in semiconductors. It displays S-shaped current–voltage characteristics because the GR kinetics incorporating impact ionization from at least two impurity levels (ground state and excited state) allows for three different values of the carrier density $n(E)$ in a certain range of fields E. As a result of the negative differential conductivity, a variety of temporal and spatiotemporal instabilities occur, ranging from stationary and breathing current filaments and traveling charge density waves to various chaotic scenarios.

Band-to-band impact ionization of a reverse biased p–n junction is the basis of a variety of electronic devices. A number of these devices depend on a combination of impact ionization of hot electrons and transit time effects. The IMPATT (impact ionization avalanche transit time) diodes can generate the highest continuous power output at frequencies $> 30\,\mathrm{GHz}$. The originally proposed device (Read diode) involves a reverse biased $\mathrm{n^+}$–p–i–$\mathrm{p^+}$ multilayer structure, where $\mathrm{n^+}$ and $\mathrm{p^+}$ denote strongly n- or p-doped semiconductor regions, and i denotes an intrinsic (undoped) region. In the $\mathrm{n^+}$–p region (avalanche region), carriers are generated by impact ionization across the bandgap; the generated holes are swept through the i region (drift region) and collected at the $\mathrm{p^+}$ contact. When a periodic (ac) voltage is superimposed on the time-independent (dc) reverse bias, a π phase lag of the ac current behind the voltage can arise. This phase lag is due to the finite buildup time of the avalanche current and the finite time carriers take to cross the drift region (transit-time delay). If the sum of these delay times is approximately one-half cycle of the operating frequency, negative conductance is observed; in other words, the carrier flow drifts opposite to the ac electric field. This can be achieved by properly matching the length of the drift region with the drift velocity and the frequency. Other devices using the avalanche breakdown effect are the TRAPATT (trapped plasma avalanche triggered transit) diode and the avalanche transistor. The Zener diode is a p–n junction that exhibits a sharp increase in the magnitude of the current at a certain reverse voltage where avalanche breakdown sets in. It is used to stabilize and limit the dc voltage in circuits (overload and transient suppressor) since the current can vary over a large range at the avalanche breakdown threshold without a noticeable change in the voltage. The original Zener effect, on the other hand, is due to quantum mechanical tunneling across the bandgap at high fields, and is effective in highly doped (resulting in

narrow depletion layers) Zener diodes at lower breakdown voltages.

ECKEHARD SCHÖLL

See also **Diodes; Drude model; Nonlinear electronics; Semiconductor oscillators**

Further Reading

Landsberg, P.T. 1991. *Recombination in Semiconductors*, Cambridge and New York: Cambridge University Press

Schöll, E. 1987. *Nonequilibrium Phase Transitions in Semiconductors*, Berlin: Springer

Schöll, E. 2001. *Nonlinear Spatio-temporal Dynamics and Chaos in Semiconductors*, Cambridge and New York: Cambridge University Press

Schöll, E., Niedernostheide, F.-J., Parisi, J., Prettl, W. & Purwins, H. 1998. Formation of spatio-temporal structures in semiconductors. In *Evolution of Spontaneous Structures in Dissipative Continuous Systems*, edited by F.H. Busse & S.C. Müller, Berlin: Springer, pp. 446–494

Shaw, M.P., Mitin, V.V., Schöll, E. & Grubin, H.L. 1992. *The Physics of Instabilities in Solid State Electron Devices*, New York: Plenum Press

AVALANCHES

An avalanche is a downhill slide of a large mass, usually of snow, ice, or rock debris prompted by a small initial disturbance. Avalanches, along with landslides, are one of the major natural disasters that still present significant danger for people in the mountains. On average, 25 people die in avalanches every winter in Switzerland alone. Dozens of people were killed on September 23, 2002, in a gigantic avalanche in Northern Ossetia, Russia, when a 150 m thick chunk of the Kolka Glacier broke off and triggered an avalanche of ice and debris that slid some 25 km along Karmadon gorge. In 1999, some 3000 avalanches occurred in the Swiss Alps.

Avalanches vary widely in size, from minor slides to large movements of snow reaching a volume of $10^5\,\mathrm{m}^3$ and a weight of 30,000 tons. The speed of the downhill snow movement can reach 100 m/s. There are two main types of avalanches-loose avalanche and slab avalanche: depending on the physical properties of snow. Soft dry snow typically produces loose avalanches that form a wedge downward from the starting point, mainly determined by the physical properties of the granular material. In wet or icy conditions, on the other hand, a whole slab of solid dense snow may slide down. The initiation of the second type occurs as a fracture line at the top of the slab. The study of real avalanches and landslides is mostly an empirical science that is traditionally a part of geophysics and draws from the physics of snow, ice, and soil. Semi-empirical computer codes have been developed for prediction of avalanches dependent on the weather conditions (snowfall, wind, temperature profiles) and topography.

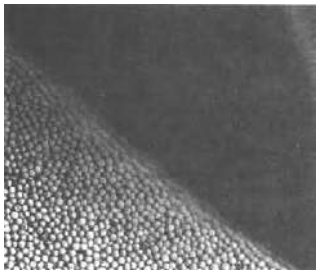

Figure 1. Only several layers of mustard seeds are involved in the rolling motion inside the avalanche: moving grains are smeared out in this long-exposure photograph. Reproduced with permission from Jaeger et al. (1998).

More fundamental aspects of avalanche dynamics have been studied in controlled laboratory experiments with dry or wet granular piles, or sandpiles. Granular slope can be characterized by two *angles of repose*—the *static* angle of repose θ_s which is the maximum angle at which the granular slope can remain static, and the *dynamic* angle of repose θ_d, or a minimum angle at which the granular flow down the slope can persist. Typically, in dry granular media, the difference between static and dynamic angles of repose is about 2–5°, for smooth glass beads $\theta_s \approx 25°$, $\theta_d \approx 23°$. Avalanches may occur in the bistable regime when the slope angle satisfies $\theta_d < \theta < \theta_s$. The bistability is explained by the need to *dilate* the granular material for it to enter flowing regime (*Bagnold's dilatancy*).

An avalanche can be initiated by a small localized fluctuation from which the fluidized region expands downhill and sometimes also uphill, while the sand always slides downhill. An avalanche in a deep sandpile usually involves a narrow layer near the surface (see Figure 1). Avalanches have also been studied in finite-depth granular layers on inclined planes. The two-dimensional structure of a developing avalanche depends on the thickness of the granular layer and the slope angle. For thin layers and small angles, wedge-shaped avalanches are formed similar to the loose snow avalanches (Figure 2a). In thicker layers and at higher inclination angles, avalanches have a balloon-type shape that expands both down- and uphill (Figure 2b).

The kinematics of the fluidized layer in one dimension can be described by a set of hydraulic equations for the local thickness $R(x,t)$ of the layer of rolling particles flowing over a sandpile of immobile particles with variable profile $h(x,t)$ (BCRE model, after Bouchaud et al., (1994)),

$$\partial_t R = -v\partial_x R + \Gamma(R,h) + (\text{diffusive terms}), \quad (1)$$

$$\partial_t h = -\Gamma(R,h) + (\text{diffusive terms}), \quad (2)$$

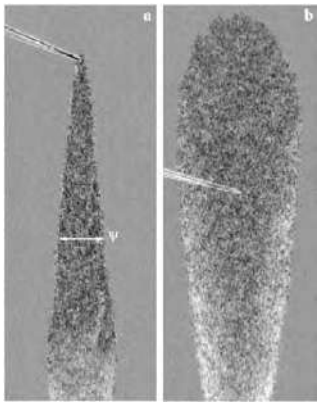

Figure 2. Structure of the avalanche in a thin (4 grain diameters) layer of glass beads: (a) wedge-shaped avalanche for $\theta = 31.5°$; (b) balloon-shaped avalanche propagating both up- and downhill for $\theta = 32.5°$. Reprinted by permission from *Nature* (Daerr & Douady, 1999).Copyright (1999) Macmillan Publishers Ltd.

where Γ is the entrainment flux of immobile particles into the rolling layer and the downhill transport velocity v is assumed constant. Γ becomes positive when the local slope becomes steeper than the static repose angle θ_s, and in the simplest case, $\Gamma = \gamma R(\partial_x h - \tan\theta_s)$. This model allows for a complete analytical treatment.

A more sophisticated continuum theory of granular avalanches is based on the fluid dynamics (Navier–Stokes) equations coupled with a phenomenological description of the first-order phase transition from a static to a fluidized state driven by the local shear stress (Aranson & Tsimring, 2001). The local phase state is described by the local order parameter ρ that is controlled by a Ginzburg–Landau-type equation with bistable free energy $F(\rho, \delta)$:

$$\partial_t \rho = D\nabla^2 \rho - \partial_\rho F(\rho, \delta) \qquad (3)$$

The control parameter δ in this equation depends on the ratio of shear to normal stress. This theory can describe a variety of "partially fluidized" granular flows, including avalanches in sandpiles. In a "shallow-water" approximation, it yields the BCRE-type equations for the local slope and the thickness of the rolling layer.

The wide distribution of scales in real avalanches led Bak et al. (1988) to propose a "sandpile cellular automaton" (*See* **Sandpile model**) as a paradigm model for *self-organized criticality* (SOC), the phenomenon that occurs in slowly driven nonequilibrium spatially extended systems when they asymptotically reach a critical state characterized by a power-law distribution of event sizes. The BTW model is remarkably simple, yet it exhibits a highly nontrivial behavior. The sandpile is formed on a lattice by dropping "grains" on a random site from above, one at a time. "Grains" form stacks of integer height at each lattice site. After each grain dropping the sandpile is allowed to relax. Relaxation occurs when the slope (a difference in heights of two adjacent stacks) reaches a critical value ("angle of repose") and the grain hops to a lower stack. This may prompt a series of subsequent hops and so trigger an avalanche. The size of the avalanche is determined by the number of grains set into motion by adding a single grain to a sandpile. In the asymptotic regime in a large system, the avalanche size distribution becomes scale-invariant, $P(s) \propto s^{-\alpha}$ with $\alpha \approx 1.5$.

The relevance of this model and its generalizations to real avalanches is still a matter of debate. The sandpile model is defined via a single repose angle, and so its asymptotic behavior has the properties of the critical state for a second-order phase transition. Real sandpiles are characterized by two angles of repose and thus exhibit features of the first-order phase transition. Experiments with avalanches in slowly rotating drums do not confirm the scale-invariant distribution of avalanches. However, in such experiments, the internal structures of the sandpile (the force chains) are constantly changing in the process of rotation. In other experiments with large monodispersed glass beads dropped on a conical sandpile, SOC with $\alpha \approx 1.5$ was observed. The characteristics of the size distribution depend on the geometry of the sandpile and the physical and geometrical properties of grains. SOC was also observed in the avalanche statistics in a three-dimensional pile of long rice; however, a smaller scaling exponent $\alpha \approx 1.2$ was measured for the avalanche size distribution.

An avalanche in a pile of sand has been used as a metaphor in many other physical phenomena including the avalanche diodes, vortices in type-II superconductors, Barkhausen effect in ferro-magnetics, $1/f$ noise, and.

LEV TSIMRING

See also **Granular materials; Sandpile model**

Further Reading

Aranson, I.S. & Tsimring, L.S. 2001. Continuum description of avalanches in granular media. *Physical Review E*, 64: 020301

Bak, P., Tang, C. & Wiesenfeld, K. 1988. Self-organized criticality. *Physical Review A*, 38: 364–374

Bouchaud, J.-P., Cates, M.E., Ravi Prakash, J. & Edwards, S.F. 1994. A model for the dynamics of sandpile surfaces. *Journal de Physique I*, 4: 1383–1410

Daerr, A. & Douady, S. 1999. Two types of avalanche behaviour in granular media. *Nature*, 399: 241–243

Duran, J. 1999. *Sands, Powders, and Grains: An Introduction to the Physics of Granular Materials*, Berlin and New York: Springer

Jaeger, H.M., Nagel, S.R. & Behringer, R.P. 1996. Granular solids, liquids, and gases. *Reviews of Modern Physics*, 68: 1259–1273

Jensen, H.J. 1998. *Self-Organized Criticality*, Cambridge: Cambridge University Press

Nagel, S.R. 1992. Instabilities in a sandpile. *Reviews of Modern Physics*, 64(1): 321–325

Rajchenbach, J. 2000. Granular flows. *Advances in Physics*, 49(2): 229–256

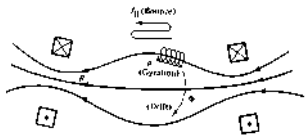

Figure 1. A hierarchy of adiabatic invariants for the charged particle gyrating in a nonaxisymmetric, magnetic mirror field. The three adiabatic invariants are the magnetic moment μ, the longitudinal invariant $J_{||}$, and the guiding center flux invariant Φ.

AVERAGING METHODS

Averaging methods are generally used for dynamical systems of two or more degrees of freedom when time scales or space scales are well separated. An average over the rapidly varying coordinates of one degree of freedom, considering the coordinates of the second degree of freedom to be constant during the average, can, with appropriate variables, retain a time-invariant quantity that enters into the solution of the slower motion. This solution, in turn, supplies a parameter to the rapid motion, which can then be solved in a lower-dimensional space. The averaging method is closely related to the calculation of *adiabatic invariants*, which are the approximately constant integrals of the motion that are obtained by averaging over the fast angle variables.

The lowest-order calculation is generally straightforwardly performed in canonical coordinates. A transformation from momentum and position coordinates (p, q), for the fast oscillation, to action-angle form (J, θ) gives a constant of the motion J, if all other variables are held constant. The action J is then the constant parameter in the equation for the slower motion. It is not always convenient to transform to action-angle form directly, but the underlying constants are related to the action variables.

The formal expansion procedure that is employed is to develop the solution in an asymptotic series. The mathematical method applied to ordinary differential equations was developed by Nikolai Bogoliubov (Bogoliubov & Mitropolsky, 1961) and in a somewhat different form by Martin Kruskal (1962). The expansion techniques can be formally extended to all orders in the perturbation parameter but are actually divergent. For multiple periodic systems, higher-order local nonlinear resonances between the degrees of freedom may destroy the ordering in their neighborhood. We will return to this problem below.

Averaging over the fastest oscillation of an N-degree-of-freedom system reduces the number of freedoms to $N-1$. A second average over the next fastest motion then produces a second adiabatic invariant to reduce the freedoms to $N-2$. This process may be continued to obtain a hierarchy of adiabatic invariants, until the system is reduced to one degree of freedom, which can be integrated to obtain a final integrable equation. The process is well known in plasma physics where, for a charged particle gyrating in a magnetic mirror field, we first find the magnetic moment invariant μ associated with the fast gyration, then find the longitudinal invariant $J_{||}$ associated with the slower bounce motion, and finally find the flux invariant Φ associated with the drift motion. The three degrees of freedom are shown in Figure 1. The small parameters in this case are ε_1, the ratio of bounce frequency to gyration frequency; ε_2, the ratio of guiding center drift frequency to bounce frequency; and ε_3, the ratio of the frequency of the time-varying magnetic field to the drift frequency. This example motivated the development of averaging methods. The derivations of these invariants are given in detail in Northrop (1963) or in other plasma physics texts.

Although the asymptotic expansions are formally good to all orders in a small dimensionless parameter of the form $\varepsilon = |\dot{\omega}/\omega^2|$, where ω is the frequency of the fast oscillation that is slowly changing in time and $\dot{\omega} \equiv \mathrm{d}\omega/\mathrm{d}t$, the series generally diverge. The physical reason is that resonances or near-resonances between degrees of freedom lead to small denominators in the coefficients of terms. For nonlinear coupled oscillatory systems, exact resonances for certain values of the action locally change the structure of the phase-space orbits so that they do not follow the values obtained by averaging. This led to the development of the secular perturbation theory (Born, 1927), in which a local transformation of the coordinates around the resonance can be made. The frequency of the oscillatory motion in the neighborhood of the exact resonance is then slow compared with the other frequencies in the transformed coordinates, and averaging can then be applied locally. A review of the various methods, their limitations, practical examples, and reference to original sources can be found in Lichtenberg (1969) and Lichtenberg & Lieberman (1991).

The above discussion is related to the study of finite-dimensional systems governed by ordinary

differential equations. The methods are usually applied to relatively low-dimensional systems, for example, the motion of a magnetically confined charged particle as described above. However, averaging methods are also applied to systems governed by partial differential equations, such as nonlinear wave propagation problems and wave instabilities. For example, waves on discrete oscillator chains can be obtained by first averaging over the discreteness using a Taylor expansion.

ALLAN J. LICHTENBERG

See also **Adiabatic invariants; Breathers; Collective coordinates; Modulated waves; Solitons**

Further Reading

Bogoliubov, N.N. & Mitropolsky, Y.A. 1961. *Assymptotic Methods in the Theory of Nonlinear Oscillators*, New York: Gordon & Beach

Born, M. 1927. *The Mechanics of the Atom*, London: Bell

Kruskal, M.D. 1962. Asymptotic theory of Hamiltonian systems with all solutions nearly periodic. *Journal of Mathematical Physics*, 3: 806–828

Lichtenberg, A.J. 1969. *Phase Space Dynamics of Particles*, New York: Wiley

Lichtenberg, A.J. & Lieberman M.A. 1991. *Regular and Chaotic Dynamics*, 2nd edition, New York: Springer

Northrop, T.G. 1963. *The Adiabatic Motion of Charged Particles*, New York: Wiley

B

BÄCKLUND TRANSFORMATIONS

Bäcklund transformations (BTs) originated in investigations conducted in the late 19th century into invariance properties of pseudospherical surfaces, namely surfaces of constant negative Gaussian curvature. In 1862, it was Edmond Bour who derived the well-known sine-Gordon equation

$$\omega_{uv} = \frac{1}{\rho^2}\sin\omega \tag{1}$$

via the Gauss–Mainardi–Codazzi system for pseudospherical surfaces with total curvature $\mathcal{K} = -1/\rho^2$, parametrized in asymptotic coordinates. In 1883, Albert Bäcklund published his now classical result whereby pseudo-spherical surfaces may be generated in an iterative manner. Thus, if $\boldsymbol{r}$ is the position vector of a pseudospherical surface Σ corresponding to a seed solution ω of Equation (1) and ω' denotes the Bäcklund transformation of ω via the BT

$$\begin{aligned} \omega'_u - \omega_u &= \frac{2\beta}{\rho}\sin\left(\frac{\omega'+\omega}{2}\right), \\ \omega'_v + \omega_v &= \frac{2}{\beta\rho}\sin\left(\frac{\omega'-\omega}{2}\right), \end{aligned} \qquad \mathbb{B}_\beta \tag{2}$$

then the position vector $\boldsymbol{r}'$ of the one-parameter class of surfaces Σ' corresponding to ω' is given by (Bäcklund, 1883)

$$\boldsymbol{r}' = \boldsymbol{r} + \frac{\mathrm{L}}{\sin\omega} \times \left[\sin\left(\frac{\omega-\omega'}{2}\right)\boldsymbol{r}_u + \sin\left(\frac{\omega+\omega'}{2}\right)\boldsymbol{r}_v\right], \tag{3}$$

where $L = \rho\sin\zeta$ and $\beta = \tan(\zeta/2)$, ζ being the constant angle between the normals to Σ and Σ' and β being termed the Bäcklund parameter. Sophus Lie subsequently observed that $\mathbb{B}_\beta$ may be decomposed according to $\mathbb{B}_\beta = \mathbb{L}_\beta^{-1}\mathbb{B}_{\beta=1}\mathbb{L}_\beta$, where $\mathbb{L}_\beta$ and $\mathbb{L}_\beta^{-1}$ are Lie invariances. Thus, Lie transformations play a crucial role in intruding the Bäcklund parameter β into the parameter-independent "Bianchi" transformation $\mathbb{B}_{\beta=1}$ to produce $\mathbb{B}_\beta$.

It was in 1892 that Luigi Bianchi in his masterly paper *Sulla Trasformazione di Bäcklund per le Superficie Pseudosferiche* established that the BT $\mathbb{B}_\beta$ admits a commutation property $\mathbb{B}_{\beta_2}\mathbb{B}_{\beta_1} = \mathbb{B}_{\beta_1}\mathbb{B}_{\beta_2}$, a consequence of which is a nonlinear superposition principle embodied in what is termed a "permutability theorem."

Bianchi's Permutability Theorem

If ω is a seed solution of the sine-Gordon equation (1), let ω_1, ω_2 denote the BT of ω via $\mathbb{B}_{\beta_1}$ and $\mathbb{B}_{\beta_2}$, that is, $\omega_1 = \mathbb{B}_{\beta_1}(\omega)$ and $\omega_2 = \mathbb{B}_{\beta_2}(\omega)$. Let $\omega_{12} = \mathbb{B}_{\beta_2}(\omega_1)$ and $\omega_{21} = \mathbb{B}_{\beta_1}(\omega_2)$. Then, imposition of the commutativity requirement $\omega_{12} = \omega_{21}$ yields a new solution of (1), namely

$$\begin{aligned} \Omega &= \omega_{12} = \omega_{21} \\ &= \omega + 4\tan^{-1}\left[\frac{\beta_2+\beta_1}{\beta_2-\beta_1}\tan\left(\frac{\omega_2-\omega_1}{4}\right)\right]. \end{aligned} \tag{4}$$

This result is commonly encapsulated in what is termed a "Lamb diagram" as shown in Figure 1. This solution-generation procedure may be iterated via what is sometimes termed a Bianchi lattice. At each iteration, a new Bäcklund parameter β_i is introduced.

The discovery of the BT for the iterative construction of pseudospherical surfaces along with its concomitant permutability theorem led to an intensive search by geometers at the turn of the 20th century for other classes of privileged surfaces that possess Bäcklund-type transformations. In this connection, Luther Eisenhart, in the preface to his monograph *Transformations of Surfaces* published in 1922, asserted that: "During the past twenty-five years many of the advances in differential geometry of surfaces in Euclidean space have had to do with transformations of surfaces of a given type into surfaces of the same type." Thus,

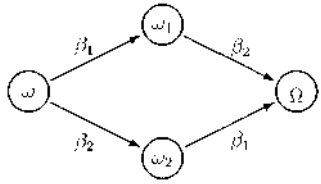

Figure 1. The Lamb diagram.

distinguished geometers such as Bianchi, Calapso, Darboux, Demoulin, Guichard, Jonas, Tzitzeica, and Weingarten all conducted extensive investigations into various classes of surfaces that admit BTs.

The particular Lamé system descriptive of triply orthogonal systems in the case when one of the constituent coordinate surfaces is pseudospherical was shown by Bianchi (1885) to admit an auto-BT, that is, a BT that renders the system invariant. Bianchi followed this in 1890 with the construction of a BT for the Gauss–Mainardi–Codazzi system associated with the class of hyperbolic surfaces with Gaussian curvature $\mathcal{K} = -1/\rho^2$ subject to the constraint

$$\rho_{uv} = 0, \tag{5}$$

where u, v are asymptotic coordinates. In 1899, Gaston Darboux constructed a BT for the nonlinear system

$$\begin{aligned} \theta_{xx} + \theta_{yy} + \kappa_1\kappa_2 \mathrm{e}^{2\theta} &= 0, \\ \kappa_{1,y} + (\kappa_1 - \kappa_2)\theta_y &= 0, \\ \kappa_{2,x} + (\kappa_2 - \kappa_1)\theta_x &= 0 \end{aligned} \tag{6}$$

descriptive of isothermic surfaces with fundamental forms

$$\mathrm{I} = \mathrm{e}^{2\theta}(\mathrm{d}x^2 + \mathrm{d}y^2), \quad \mathrm{II} = \mathrm{e}^{2\theta}(\kappa_1 \mathrm{d}x^2 + \kappa_2 \mathrm{d}y^2), \tag{7}$$

where κ_1, κ_2 are principal curvatures and x, y are conjugate coordinates. The classical BT for system (6) has been set in a modern solitonic context by Cieśliński (1997).

In the first decade of the 20th century, the Romanian geometer Gheorghe Tzitzeica embarked upon an investigation of an important class of surfaces for which, in asymptotic coordinates, the Gauss–Mainardi–Codazzi system reduces to the nonlinear hyperbolic equation

$$(\ln h)_{uv} = h - h^{-2} \tag{8}$$

to be rediscovered some 70 years later in a soliton context. Tzitzeica (1910) not only constructed a BT for (8) but also set down what, in modern terms, is a linear representation containing a spectral parameter. Tzitzeica surfaces may be subsumed in the more general class of projective minimal surfaces for which BTs can be established (Rogers & Schief, 2002). In particular, this class contains the Demoulin system (1933)

$$(\ln h)_{uv} = h - \frac{1}{hk}, \quad (\ln k)_{uv} = k - \frac{1}{hk}. \tag{9}$$

The application of BTs in physics began with the work of Seeger et al. (1953) on crystal dislocation theory. Therein, within the context of Frenkel and Kontorova's dislocation theory, the superposition of so-called "eigenmotions" was obtained via the permutability relation (4). The interaction of what are today called breathers with kink-type dislocations was both described analytically and displayed graphically. The typical solitonic features to be subsequently discovered for the Korteweg–de Vries (KdV) equation

$$u_t + 6uu_x + u_{xxx} = 0, \tag{10}$$

(namely, preservation of velocity and shape following interaction as well as the concomitant phase shift) were all recorded. Bianchi's permutability theorem was subsequently employed in an investigation of the propagation of ultrashort optical pulses in a resonant medium by Lamb (1971).

A BT for the Korteweg–de Vries equation (10), namely

$$\begin{aligned} (\Lambda + \Lambda')_x &= \beta - \tfrac{1}{2}(\Lambda - \Lambda')^2, \\ (\Lambda' + \Lambda')_t &= (u - u')(u_{xx} - u'_{xx}) \\ &\quad -2(u_x^2 + u_x u'_x + u_x'^2), \end{aligned} \tag{11}$$

where

$$\Lambda = \int_\infty^x u(\sigma, t)\mathrm{d}\sigma \tag{12}$$

was established by Wahlquist and Estabrook (1973). The spatial part of the BT was used to construct a permutability theorem, whereby multi-soliton solutions may be generated. This permutability theorem makes a remarkable appearance in numerical analysis as the so-called ε-algorithm.

A BT for the celebrated nonlinear Schrödinger (NLS) equation

$$\mathrm{i}q_t + q_{xx} + 2|q|^2 q = 0 \tag{13}$$

was established by Lamb (1974) employing a direct method due to Clairin (1902) and by Chen (1974) via the inverse scattering transform (IST) formalism. The BT adopts the form

$$\begin{aligned} q_x + q'_x &= (q - q')(4\beta^2 - |q + q'|^2)^{1/2}, \\ q_t + q'_t &= \mathrm{i}(q_x - q'_x)(4\beta^2 - |q + q'|^2)^{1/2} \\ &\quad + \frac{\mathrm{i}}{2}(q + q')(|q + q'|^2 + |q - q'|^2), \end{aligned} \tag{14}$$

the spatial part of which may be used to construct a permutability theorem (Rogers & Shadwick, 1982).

Crum's theorem may be adduced to show that, at the level of the linear representation of soliton equations, the action of the BT is to add a discrete eigenvalue to the spectrum. The role of BTs in the context of the IST and their action on reflection coefficients is treated in detail by Calogero and Degasperis (1982).

That the Toda lattice equation

$$\ddot{y}_n = \exp[-(y_n - y_{n-1})] - \exp[-(y_{n+1} - y_n)] \quad (15)$$

admits a BT, namely

$$\begin{aligned} \dot{y}_n - \dot{y}'_{n-1} &= \beta\,[\exp\{-(y'_n - y_n)\} \\ &\quad - \exp\{(y'_{n-1} - y_{n-1})\}], \\ \dot{y}'_n - \dot{y}_n &= \beta^{-1}[\exp\{-(y_{n+1} - y'_n)\} \\ &\quad - \exp\{-(y_n - y'_{n-1})\}] \end{aligned} \quad (16)$$

was established by Wadati and Toda (1975). BTs for a range of integrable differential-difference as well as integro-differential equations may be conveniently derived via Hirota's bilinear operator approach (see Rogers & Shadwick, 1982).

BTs have by now been constructed for the gamut of known solitonic equations as well as their Painlevé reductions (Gromak, 1999). The importance of BTs in soliton theory with regard to such aspects as multi-soliton generation, geometric connections, and integrable discretization is well established. Moreover, BTs also have extensive applications in continuum mechanics (Rogers & Shadwick, 1982). Important connections between infinitesimal BTs as originally introduced in a gas dynamics context (Loewner, 1952) and the construction of $2 + 1$ dimensional solitonic systems have also been uncovered.

COLIN ROGERS

See also **Hirota's method; Inverse scattering method or transform; *N*-soliton formulas; Sine-Gordon equation; Solitons**

Further Reading

Bäcklund, A.V. 1883. Om ytor med konstant negativ krökning. *Lunds Universitets Årsskrift*, 19: 1–48

Bianchi, L. 1885. Sopra i sistemi tripli ortogonali di Weingarten. *Annali di Matematica*, 13: 177–234

Bianchi, L. 1890. Sopra alcone nuove classi di superficie e di sistemi tripli ortogonali. *Annali di Matematica*, 18:301–358

Bianchi, L. 1892. Sulla traformazione di Bäcklund per le superficie pseudosferiche. *Rendiconti Lincei*, 5: 3–12

Calogero, F. & Degasperis, A. 1982. *Spectral Transform and Solitons*, Amsterdam and New York: North-Holland

Chen, H.H. 1974. General derivation of Bäcklund transformations from inverse scattering problems. *Physical Review Letters*, 33: 925–928

Cieśliński, J. 1997. The Darboux–Bianchi transformation for isothermic surfaces. Classical results versus the soliton approach. *Differential Geometry and Its Applications*, 7: 1–28

Clairin, J. 1902. Sur les transformations de Bäcklund. *Annales de l'Ecole Normale Supérieure*, 27: 451–489

Darboux, G. 1899. Sur les surfaces isothermiques. *Comptes Rendus*, 128: 1299–1305

Demoulin, A. 1933. Sur deux transformations des surfaces dont les quadriques de Lie n'ont que deux ou trois points charactéristiques. *Bulletin de l'Académie Belgique*, 19: 479–501, 579–592, 1352–1363

Gromak, V. 1999. Bäcklund transformations of Painlevé equations and their applications. In *The Painlevé Property: One Century Later*, edited by R. Conte, New York: Springer

Konopelchenko, B.G & Rogers, C. 1993. On generalised Loewner systems: novel integrable equations in 2+1-dimensions. *Journal of Mathematical Physics*, 34: 214–242

Lamb, G.L. Jr. 1971. Analytical descriptions of ultra short optical pulse propagation in a resonant medium. *Reviews of Modern Physics*, 43: 99–124

Lamb, G.L. Jr. 1974. Bäcklund transformations for certain nonlinear evolution equations. *Journal of Mathematical Physics*, 15: 2157–2165

Loewner, C. 1952. Generation of solutions of systems of partial differential equations by composition of infinitesimal Bäcklund transformations. *Journal d'Analyse Mathématique*, 2: 219–242

Rogers, C. & Schief, W.K. 2002. *Bäcklund and Darboux Transformations: Geometry and Modern Applications in Soliton Theory*, Cambridge and New York: Cambridge University Press

Rogers, C. & Shadwick, W.F. 1982. *Bäcklund Transformations and Their Applications*, New York: Academic Press

Seeger, A., Donth, H. & Kochendörfer, A. 1953. Theorie der Versetzungen in Eindimensionalen Atomreihen III. Versetzungen, Eigenbewegungen und ihre Wechselwirkung, *Zeitschrift für Physik*, 134: 173–193

Tzitzeica, G. 1910. Sur une nouvelle classe de surfaces. *Comptes Rendus*, 150: 955–956

Wadati, M. & Toda, M. 1975. Bäcklund transformation for the exponential lattice. *Journal of the Physical Society of Japan*, 39: 1196–1203

Wahlquist, H.D. & Estabrook, F.B. 1973, Bäcklund transformations for solutions of the Korteweg–de Vries equation. *Physical Review Letters*, 31: 1386–1390

BAKER MAP

See **Maps**

BAKER–AKHIEZER FUNCTION

See **Integrable lattices**

BALL LIGHTNING

Properties

Ball lightning is an impressive natural phenomenon for which there is yet no accepted scientific explanation. It consists of flaming balls or fireballs, usually bright white, red, orange, or yellow, which appear unexpectedly sometimes near the ground, following the discharge of a lightning flash, or in midair coming from a cloud.

Most observations of ball lightning are associated with thunderstorms, and they exhibit the following more detailed properties: (i) Their shape is usually spherical or spheroidal with diameters between 10 and

50 cm. (ii) They tend to move horizontally. (iii) The observed distribution of lifetimes has a most probable value between 2 and 5 s and an average value of about 10 s or higher (some cases of more than 1 min having been reported). (iv) Ball lightning is bright enough to be clearly seen in daylight, the visible output being in the range 10–150 W (similar to that of a home electric light bulb). (v) Some balls have appeared within aircraft, traveling inside the fuselage along the aisle from front to rear. (vi) There are reports of odors, similar to those of ozone, burning sulfur, or nitric oxide, and of sounds, mainly hisses, buzzes, or flutters. (vii) Most balls decay silently, but some expire with an explosion. (viii) Ball lightning has killed or injured people and animals and damaged trees, buildings, cars, and electric equipment. (ix) Fires have been started showing that there is something hot inside. In such events, the released energy has been estimated to be between 10 kJ and more than 1 MJ. (x) Ball lightning has never been produced in laboratories, in spite of many attempts and some interesting results, including anode spots and luminous objects that decay very quickly. Consequently, the properties of ball lightning are derived from reports by witnesses, who are often excited by the phenomenon and have no scientific training.

A possibly related phenomenon has been observed in submarines, after a short circuit of the batteries. Balls of plasma that float in air for several seconds have appeared at the electrodes. On these occasions, the current was about 150 kA and the energy was estimated to be between 200 and 400 kJ.

Classification of the Models

Three main characteristics must be accounted for by a successful model but seem very difficult to explain: the tendency toward horizontal motion (hot air or plasma in air tends to rise), relatively long lifetimes, and contradictions among witnesses. For example, some report that balls are cold since they did not feel any warmth when one passed nearby, while others were burned and needed medical care.

The many different models proposed to explain the phenomenon can be classified into two groups, according to whether the energy source is internal or external. In the first group, some are based on plasmoids (equilibrium configurations of plasmas), high-density plasmas with quantum mechanical properties, closed loops of currents confined by their own magnetic field (in some cases, the linking of the currents playing an important role), vortex structures as whirlwinds or rotating spheres, bubbles containing microwave radiation, chemical reactions or combustion, fractal structures, aerosols, filaments of silicon, carbon nanotubes, nuclear processes, or new physics, and even primordial mini black holes. In the second group, some assume that the balls are powered by electrical discharges or by high-frequency microwave focused from thunderclouds. None of them is generally accepted.

Chemical and Electromagnetic Models

The association of ball lightning with electrical discharges suggests strongly that they have an electromagnetic nature. However, Michael Faraday argued that ball lightning cannot be an electric phenomenon as it would decay almost instantaneously, in contrast to its observed lifetime of at least several seconds. Finkelstein & Rubinstein (1964) used the time-independent magnetic virial theorem to place a stringent upper limit to the energy of a fireball. This limit has been viewed as a compelling argument against electromagnetic models, stimulating non-electromagnetic chemical approaches.

Recently, aerosol models have received considerable attention. In one model (Abrahamson & Dinniss, 2000), a lightning discharge vaporizes silicon dioxide in the soil that—after interacting with carbon compounds—is transformed into pure silicon droplets of nanometer scale. These droplets become coated with an insulating coat of oxides and are polarized, after which they become aligned with electric fields and form networks of filaments, in loose structures called "fluff balls." In another model (Bychkov, 2002), the discharges pick up organic material from the soil and transform it into a kind of "spongy ball" that can hold electric charges. Models of this type fail to explain that some balls appear in mid air, where there is neither silicon nor organic nor any other similar material.

Electromagnetic models that include chemical effects are promising candidates for an explanation of ball lightning. Indeed, there are now counterarguments to the three main objections that express Faraday's argument in modern language. These are based on the radiated output, the pinch effect, and magnetic pressure.

The first objection is that the power emitted by a plasma of the size of a ball lightning is too high (one liter of air plasma at 15,000 K emits about 5 MW, several orders of magnitude too much). This may be, however, an indication that most of the ball is at ambient temperature, only a small fraction being hot, concentrated in filamentary structures (as hot current streamers). If this fraction is of the order of 1 ppm, the radiated output would be of the order of 10–100 W, in agreement with reports.

But the solution to the first problem raises another one. Any plasma current channel inside the ball would be necked and cut in a very short time by the pinch effect (the Lorentz force); thus, a ball structured by such currents could not last long enough. However, in 1958, Chandrasekhar and Woltjer showed in an astrophysical context that plasmas relax to minimum energy states, verifying the condition that the electric current and

the magnetic field are parallel so $\nabla \times \boldsymbol{B} = \lambda \boldsymbol{B}$, in which there can be no pinch effect since the Lorentz force vanishes. They concluded that such states, known as force-free fields, can confine large amounts of magnetic energy. Although the minimum energy of an uncontained plasma (as in ball lightning) is zero and corresponds to an infinitely expanded magnetic field, an almost force-free condition could be attained first in a very short time at a finite radius, a slow expansion continuing afterward with negligible pinch effect. This could take several seconds.

The third objection is based on the magnetic virial theorem, which states that a system of charges in electromagnetic interactions has no equilibrium state in the absence of external forces, because the large magnetic pressure must produce an explosion with no other force to compensate it. But it is not certain that the fireballs are in equilibrium; they could be just in metastable states with slow evolution, the streamers, moreover, clearly not being in equilibrium themselves. Still more important, the force-free condition annihilates the magnetic pressure or at least reduces it to a much smaller value if the field is almost force-free. Furthermore, the problem needs a much more complex analysis than has been offered up to now. For instance, one must include the thermochemical and quantum effects on the transport processes in the plasma as well as other nonlinear effects.

Faddeev and Niemi (2000) have proposed compelling arguments that challenge certain widely held views on plasmas, showing that the virial theorem does allow nontrivial equilibrium states of streamers and electromagnetic fields inside a background of plasma, which are "topologically stable solitons that describe knotted and linked flux tubes of helical magnetic fields." This kind of configuration was proposed in 1998 by Rañada et al. (2000) in the context of ball lightning. Therefore, it seems that the virial theorem does not necessarily support Faraday's view.

That ball lightning may contain force-free magnetic configurations of plasmas seems plausible. Because electric conduction in air proceeds through thin channels called streamers—as happens in ordinary lightning—it can be imagined that plasma inside the fireball consists of a self-organized set of metastable, highly conductive, wire-like or filamentary currents. Furthermore, unusually long-lived filaments (even closed loops) in high-density structures have been theoretically predicted and experimentally observed in many plasma systems within a great range of length scales, for instance, in astrophysics, tokamaks, and ordinary discharges in air. Thus, filamentary structures are currently receiving considerable attention.

The strongly nonlinear behavior of a plasma is enhanced when filamentary structures appear, leading to a complex non-isotropic system, which should be studied within a more general theory than ideal magnetohydrodynamics (MHD). Still, the main features of such systems can be described in the framework of resistive MHD. The important dissipative effects depend on the transport coefficients, such as thermal and electrical conductivities, which are highly nonlinear functions of the electromagnetic fields and the temperature, as well as of the chemical and quantum properties.

From the point of view of the MHD approximation, the dimensionless parameters of the plasma inside ball lightning may be quite similar to those found in other plasma scenarios, implying stable or metastable currents along a set of closed loops in filamentary structures. An interesting and unexplored possibility is the establishment, inside the streamers, of a quasicollision-free highly conductive regime in the direction of the magnetic field, which is strong and parallel to the streamers axis. In such a regime, both the electric and the thermal conductivities would become highly anisotropic. The first would be considerably enhanced along the axis of the streamer. On the other hand, both conductivities would be greatly reduced in the transverse directions, behaving as $1/B^2$ according to classical predictions. In this way, the dissipation and the spreading in the streamers would be much smaller than in ordinary regimes and should produce a long-lived strongly magnetized global plasma structure within an intricate stabilizing topology of filamentary currents.

In summary, even though the phenomenon of ball lightning has been known for many years, there is still no accepted theory to explain it—the alternatives currently most favored being the chemical and the electromagnetic models. The latter seem promising now, after recent results showed that some classical objections are not always applicable. As an example, a number of filamentary plasma structures have generated considerable interest, which are similar to stable plasma scenarios observed in nature, for instance, in astrophysics. These kinds of models could possibly embody chemical and electromagnetic elements.

ANTONIO F. RAÑADA, JOSÉ L. TRUEBA, AND JOSÉ M. DONOSO

See also **Helicity; Magnetohydrodynamics; Nonlinear plasma waves**

Further reading

Abrahamson, J. & Dinniss, J. 2000. Ball lightning caused by oxidation of nanoparticle networks from normal lightning strikes on soil. *Nature*, 403: 519–521

Barry, J.D. 1980. *Ball Lightning and Bead Lightning. Extreme Forms of Atmospheric Electricity*, New York: Plenum Press

Bychkov, V.L. 2002. Polymer-composite ball lightning. *Philosophical Transactions of the Royal Society* A, 360: 37–60

Faddeev, L. & Niemi, A.J. 2000. Magnetic geometry and the confinement of electrically conducting plasmas. *Physical Review Letters*, 85: 3416–3419

Finkelstein, D. & Rubinstein, J. 1964. Ball lightning. *Physical Review* A, 135: 390
Ohtsuki, Y.-H. (editor). 1988. *Science of Ball Lightning (Fire Ball)*, Singapore: World Scientific
Rañada, A.F., Soler, M. & Trueba, J.L. 2000. Ball lightning as a force-free magnetic knot. *Physical Review* E, 62: 7181–7190
Singer, S. 1971. *The Nature of Ball Lightning*, New York and London: Plenum Press
Smirnov, B.M. 1993. Physics of ball lightning. *Physics Reports*, 224: 151–236
Stenhoff, M. 1999. *Ball Lightning: An Unsolved Problem in Atmospheric Physics*, Dordrecht and New York: Kluwer
Trubnikov, B.A. 2002. Current filaments in plasmas. *Plasma Physics Reports*, 28: 312–326

BANACH SPACE

See **Function spaces**

BASIN OF ATTRACTION

See **Phase space**

BAXTER'S Q-OPERATOR

See **Bethe ansatz**

BELOUSOV–ZHABOTINSKY REACTION

In 1950, Boris Pavlovich Belousov worked at the Institute of Biophysics of the Ministry of Public Health of the USSR when he observed that the reaction between citric acid, bromate ions, and ceric ions (as catalyst) produced a regular periodic and reproducible change of color between an oxidized state and a reduced state. A temporal oscillating reaction appeared like a chemical clock. His 1951 paper on this study was largely rejected by the science community because it seemed to violate the Second Law of thermodynamics.

In 1961, Anatol Zhabotinsky, a Russian postgraduate student guided by his professor, Simon Shnoll, modified the previous reaction by replacing citric acid with malonic acid and adding ferroin sulfate as an indicator. As the oxidized state of ferroin is blue and the reduced one is red, he was able to observe an oscillating temporal reaction with larger oscillating amplitudes. This reaction

$$3CH_2(CO_2H)_2 + 4BrO_3^- = 4Br^- + 9CO_2 + 6H_2O \qquad (1)$$

was named the Belousov–Zhabotinsky (BZ) reaction. The first publications in English, recognizing the works of Belousov and Zhabotinsky, were done in 1967 by the Danish scientist Hans Degn. However, Zhabotinsky was unable to propose a complete mechanism for the system. Experimentally, the periodic evolution of the potential of the reacting solution can be followed by a potentiometric method, as shown in Figure 1.

Figure 1. A photograph showing the periodic potential obtained between a platinum electrode and a reference electrode immersed in a BZ solution.

In 1972, Richard Field, Endre Körös, and Richard Noyes, at the University of Oregon, studied this mechanism using a bromide-selective electrode to follow the reaction. They proposed 18 steps involving 21 chemical species, using the same principles of chemical kinetics and thermodynamics that govern ordinary chemical reactions—this was the FKN mechanism. In 1974, the same scientists proposed a simplified mechanism with penetrating chemical insight: the "Oregonator" (in honor of the University of Oregon).

Compound:	BrO_3^-	Organic species	HBrO
Notation:	A	B	P

Compound:	$HBrO_2$	Br^-	Ce^{4+}
Notation:	X	Y	Z

With these notations, the FKN mechanism is

- $A + Y \rightarrow X + P$,
- $A + X \rightarrow 2X + 2Z$,
- $X + Y \rightarrow 2P$,
- $2X \rightarrow A + P$,
- $B + Z \rightarrow (f/2)Y +$ other products.

The second step is fundamental for the observation of oscillations; it is an autocatalytic reaction or retroaction loop. In the fifth step, B represents all oxidizable organic species present, and f is a stoichiometric factor. The kinetic differential equations are:

$$\frac{d[X]}{dt} = k_1[A]\cdot[Y] + k_2[A]\cdot[X] - k_3[X]\cdot[Y] - 2k_4[X]^2, \qquad (2)$$

$$\frac{d[Y]}{dt} = -k_1[A]\cdot[Y] - k_3[X]\cdot[Y] + 2k_5\frac{f}{2}[B]\cdot[X], \qquad (3)$$

$$\frac{d[Z]}{dt} = 2k_2[A]\cdot[X] - k_5[B][Z]. \qquad (4)$$

The rate constants are:

Rate constants:	k_1	k_2	k_3	k_4	k_5
Value (l/mol s):	1.28	2.4×10^6	33.6	3×10^3	1

This system is clearly nonlinear. Solutions can be obtained by numerical methods, and for $0.5 \leq f \leq 2.4$, some oscillating temporal solutions are observed, whose solutions depend on the initial conditions. According to the Second Law of thermodynamics, all spontaneous chemical changes in a homogeneous and closed system involve a decrease in free enthalpy of this system. If a fluctuation disrupts the system close to equilibrium, the system will return irrevocably to this stable state, making oscillations impossible. Nonetheless, it is possible to observe oscillations when the system is far from equilibrium. One of the striking properties of nonlinear systems is the effect of fluctuations (of the concentrations of intermediates), which can transform an unstable system into new states that are more organized than the initial state. Ilya Prigogine (who was awarded the 1977 Nobel Prize in chemistry for his work on thermodynamics) gave the name "dissipative structures" to such systems to emphasize the importance of irreversible phenomena far from equilibrium.

Continuing to work on oscillating reactions, in 1970, Zhabotinsky published, with Zaikin, a paper that announced the existence of two-dimensional waves in the BZ reaction; also in 1972, Arthur Winfree observed spiral wave patterns in a BZ reaction (see Figure 2). This reaction took place without stirring in a thin (approximately 2 mm thick) layer of reactants poured into a Petri dish. Blue concentric circles (called targets) radiated across the dish on a red background and self-generating spirals appeared. Soon afterward, scientists reported that a blue target center can produce waves of oxidation propagating through the reduced medium, and as the waves advance toward the interior of the center, they transform from red to blue. The period of oscillation is variable, but the speed of propagation is roughly constant. Thus, the BZ reaction proves to be a stationary spatiotemporal oscillating reaction.

With the aid of the FKN mechanism, Field and Noyes showed how to understand the development of such target waves. The diffusion is the transport of species from the areas of high concentrations to those of low concentrations. When there is a coupling between a chemical reaction with an autocatalytic step (or feedback-retroaction loop) as in the BZ reaction with the diffusion of species, spatial organization phenomena can occur; thus these are called "reaction-diffusion systems." In such systems, molecules react chemically with each other when they collide, and as the concentrations of components change, a chemical wave propagates.

Figure 2. Spiral waves in a BZ reaction (Courtesy of A.T. Winfree). See text for details.

In 1984, Oleg Mornev (at the Institute of Theoretical and Experimental Biophysics of the Russian Academy of Sciences) showed that in an infinite plane stationary system of reaction-diffusion oscillations, Snell's sine law of refraction was verified. Thus the simple rule

$$\frac{\sin \psi_1}{\sin \psi_2} = \frac{v_1}{v_2} \tag{5}$$

dictates the angles ψ_1 and ψ_2 when waves hit an interface separating two regions with different speeds (v_1 and v_2) of wave propagation. This result was surprising because reaction-diffusion systems are nonlinear; thus, the medium is an active and an integral part of the wave. In fact, ψ_1 cannot be set arbitrarily but is slaved with ψ_2 due to the nature of the two regions.

In 1993, Zhabotinsky (at the Department of Chemistry, Brandeis University) demonstrated Snell's law experimentally. In 1998, Rui Dilaö and Joaquim Sainhas (at the Instituto Superio Tecnico, Lisbon Portugal) showed the following constraint in a reaction-diffusion system: after the reaction, the medium must be chemically identical to its initial form. In other words, while the waves are propagating and reactions are taking place, the medium has different properties, but these waves transform the medium back to the original species. By solving reaction-diffusion equations under this constraint, Dilaö and Sainhas showed (using computer simulations) that their formulation agrees with experiments, and mathematically chemical waves obey Snell's sine law. Continuing to work on the phenomenon of refraction, Mornev is developing formulations that hold both in infinite and finite media.

There are other examples of reaction-diffusion systems. In 1983, Patrick de Kepper (a French chemist in Toulouse) highlighted Turing structures

in a ClO_2^-, I^-, malonic acid reaction (CIMA reaction). In Turing structures, stationary zones of varying concentrations appear in space. For these observations, the reaction must have steps with retroaction loops containing activators and other steps with inhibitors, and the activators must diffuse more slowly than the inhibitors.

Although the intense study of oscillating chemical reactions and nonlinear dynamics in chemistry is only about 30 years old, its progress has been impressive. Depending on the initial conditions, the BZ reactions can have unpredictable behaviors, even though they are described by deterministic laws. Thus, the BZ reaction belongs to the group of physical or chemical systems that exhibits deterministic chaos.

GÉRARD DUPUIS AND NICOLE BERLAND

See also **Brusselator; Chemical kinetics; Fairy rings of mushrooms; Reaction-diffusion systems; Turing patterns; Vortex dynamics in excitable media**

Further Reading

Dilao, R. & Sainhas, J. 1998. Wave optics in reaction-diffusion systems. *Physical Review Letters*, 80: 5216

Epsein, I.R. & Pojman, J.A. 1998. *An Introduction to Nonlinear Chemical Dynamics: Oscillations, Waves, Patterns and Chaos*, Oxford and New York: Oxford University Press

Field, R.J., Körös, E. & Noyes, R.M. 1972. *Journal of American Chemical Society*, 94: 8649

Gray, P. & Scott, S.K. 1990. *Chemical Oscillations and Instabilities, Nonlinear Chemical Kinetics*, Oxford: Clarendon Press and New York: Oxford University Press

Mornev, O.A. 1984. Elements of the "optics" of autowaves. In *Self-Organization of Autowaves and Structures Far from Equilibrium*, edited by V.I. Krinsky, Berlin: Springer, pp. 111–118

Zaikin, A.N. & Zhabotinsky, A.M. 1970. Concentration wave propagation in two dimensional liquid phase self oscillating system. *Nature*, 225: 535–537

Zhabotinsky, A.M. 1964. *Biofizika*, 9, 306.

Zhabotinsky, A.M., Eager, M.D. & Epstein, I.R. 1993. Refraction and reflection of chemical waves. *Physical Review Letters*, 71: 1526–1529

BENJAMIN–BONA–MAHONY EQUATION

See **Water waves**

BENJAMIN–FEIR INSTABILITY

See **Wave stability and instability**

BENJAMIN–ONO EQUATION

See **Solitons, types of**

BERNOULLI SHIFT

See **Maps**

BERNOULLI'S EQUATION

Bernoulli's equation is possibly the best-known result in fluid mechanics—and the most frequently abused. Bernoulli's equation may be viewed as an energy-conservation budget for a fluid particle as it travels up and down the "hills" of potential energy, due to the fields of gravity and the pressure within the fluid, acquiring and relinquishing kinetic energy. In its simplest form, it states that

$$V^2/2 + p/\rho + gz = C, \qquad (1)$$

where p is the pressure in the fluid of density ρ, V is the flow speed, and z is the vertical coordinate. (The flow takes place in a uniform gravitational field of acceleration g.) The sum on the left-hand side of Equation (1) is a constant, C. The first term is the kinetic energy of the fluid per unit mass, the second and third terms are the potential energy (again per unit mass) in the combined energy "landscape" of pressure and gravity.

The result is credited to Daniel Bernoulli (1700–1782), son of Johann Bernoulli (1667–1748), and to his monograph *Hydrodynamica*, initiated in 1729 and ultimately published in 1738. The history of the equation is, however, much richer than this simple sequence of events would suggest. Hunter Rouse puts the issues this way in a book containing English translations of the writings of both the son and the father:

> Why [these] works should have been singled out for translation seems at first sight rather obvious, if only because of the frequency with which the name Bernoulli is on the hydraulician's lips. But it is only Daniel to whom one is making reference, and the word is gradually spreading that the theorem bearing his name is nowhere to be found in his habitually cited *Hydrodynamica*. Not until the last few years has mention of either the work *Hydraulica* or its author Johann Bernoulli appeared in the fluids literature with any frequency, and this almost exclusively in the writings of C. Truesdell. It is Truesdell's thesis that, whereas Daniel has received too much credit for the formulation of the Bernoulli theorem, Johann has received too little. (Carmody et al., 1968).

A complicated set of circumstances ensued in which both father (Johann) and son (Daniel) sent their manuscripts to Leonhard Euler for comment and this led to Johann's manuscript, which appears to have been composed later than Daniel's, being published in the Memoirs of the Imperial Academy of Science in St. Petersburg in 1737 and 1738 (although these were not printed until a decade later). Indeed, Johann's treatise first appeared in his collected works published in Switzerland in 1743. While Daniel's treatise has the gist of what we today call Bernoulli's equation, Johann's treatment is more mature and complete.

In the form stated in Equation (1), Bernoulli's equation applies only to steady, constant-density, irrotational flow, that is, to a flow pattern that is unchanging in time and that has no vorticity.

More refined versions may be derived. Thus, in a steady, constant-density flow with vorticity, Equation (1) still holds along each streamline, but the "constant" on the right-hand side may vary from streamline to streamline. Indeed, the gradient of this changing "Bernoulli constant," ∇C, equals the Lamb vector, the vector product of flow velocity and vorticity,

$$\boldsymbol{V} \times \boldsymbol{\omega} = \nabla C.$$

If the flow is irrotational but unsteady, a version of Bernoulli's equation again holds, but the constant on the right-hand side of (1) is replaced by (minus) the time derivative of the velocity potential. (In an irrotational flow, the velocity field is the gradient of a scalar known as the velocity potential.) With $V = -\nabla\phi$, where ϕ is the velocity potential, we obtain Bernoulli's equation in the form

$$(\nabla\phi)^2/2 + p/\rho + gz = -\frac{\partial\phi}{\partial t}, \qquad (2)$$

which, coupled with the condition of irrotational flow,

$$\Delta\phi = 0, \qquad (3)$$

gives a system of two partial differential equations for the fields p and ϕ.

Bernoulli's equation in the simplistic form "high flow speed implies low pressure and vice versa" is often applied as a first, crude explanation of many flow phenomena from the ability to balance a ball atop a plume of air to the lift on an airfoil in flight. Some of these explanations are too simplistic, not to say incorrect. Nevertheless, Bernoulli's equation, when properly applied under the assumptions that ensure its validity, can be an extremely useful and powerful tool of fluid flow analysis.

It is remarkable—and important to note—that Bernoulli's equation (1) is not invariant to a Galilean transformation, ordinarily a prerequisite for a physical law to be useful. Thus, if one wants to use Bernoulli's equation (1) to calculate the pressure distribution for flow around an object, assuming the velocity field is known, it is essential to do so in a frame of reference in which the flow satisfies the necessary assumptions, in particular, that the flow is steady. The correct result is obtained by carrying out such a calculation in a frame of reference moving with the body. If the calculation is attempted in the "laboratory frame" through which the object is moving, one has to tackle the much more complex version of Bernoulli's equation given in (2). If the version in Equation (1) is applied, one obtains an incorrect result.

HASSAN AREF

See also **Fluid dynamics**

Further Reading

Batchelor, G.K. 1967. *An Introduction to Fluid Dynamics*, Cambridge: Cambridge University Press

Carmody, T., Kobus, H. & Rouse, H. 1968. *Hydrodynamica by Daniel Bernoulli and Hydraulica by Johann Bernoulli*, translated from the Latin, with a preface by Hunter Rouse, New York: Dover

Lamb, H. 1932. *Hydrodynamics*, 6th edition, Cambridge: Cambridge University Press

BERRY'S PHASE

Consider the parallel transport of an orthonormal frame along a line of constant latitude on the surface of a sphere. In going once around the sphere, the frame undergoes a rotation through an angle $\Delta\theta = 2\pi\cos\alpha$, where α is the colatitude. This may be shown using the geometry of Figure 1. As is also evident from the figure, this phase shift is purely geometric in character—it is independent of the time it takes to traverse the closed loop.

This construction underlies the well-known phase shift exhibited by the Foucault pendulum as the Earth rotates through one full period. Although arising through a dynamical process involving two widely separated time scales (the period of the Earth's rotation and the oscillation period of the pendulum), the phase shift in this and other examples is now understood in a more unified way. *Holonomic* effects such as these arise in a host of applications ranging from problems in superconductivity theory, fiber optic design, magnetic resonance imaging (MRI), amoeba propulsion and robotic locomotion and control, micromoter design, molecular dynamics, rigid-body motion, vortex dynamics in incompressible fluid flows (Newton, 2001), and satellite orientation control. For a survey and further references on the use of phases in locomotion problems, see Marsden & Ostrowski (1998).

That the falling cat learns quickly to re-orient itself optimally in mid-flight while maintaining zero angular momentum is a manifestation of the fact that controlling and manipulating a system's internal or shape variables can lead to phase changes in the external, or group variables, a process that can be exploited and has deeper connections to problems related to the dynamics of Yang–Mills particles moving in their associated gauge field, a link that is the *falling cat theorem* of Montgomery (1991a) (see further discussion and references in Marsden (1992) and Marsden & Ratiu (1999)). One can read many of the original articles leading to our current understanding of the geometric phase in the collection edited by Shapere & Wilczek (1989).

Problems of this type have a long and complex history dating back to work on the circular polarization of light in an inhomogeneous medium by Vladimirskii and Rytov in the 1930s and by Pancharatnam in the 1950s, who studied interference patterns produced by plates of

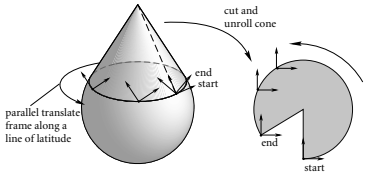

Figure 1. Parallel transport of a frame around a line of latitude.

an anisotropic crystal. Much of this early history is described in the articles by Michael Berry (Berry, 1988, 1990). The more recent literature was initiated by his earlier articles (Berry, 1984, 1985), which investigated the evolution of quantum systems whose Hamiltonian depends on external parameters that are slowly varied around a closed loop. The adiabatic theorem of quantum mechanics states that for infinitely slow changes of the parameters, the evolution of the complex wave function, governed by the time-dependent Schrödinger equation, is instantaneously in an eigenstate of the *frozen* Hamiltonian. At the end of one cycle, when the parameters recur, the wave function returns to its original eigenstate, but with a phase change that is related to the geometric properties of the closed loop. This phase change now goes by the name *Berry's phase*. Geometric developments started with the work of Simon (1983), and Marsden et al. (1989). One can introduce a bundle of eigenstates of the slowly varying Hamiltonian, as well as a natural *connection* on it; the Berry phase is then the bundle holonomy associated with this connection, while the curvature of the connection, when integrated over a closed two-dimensional (2-d) surface in parameter space gives rise to the first Chern class characterizing the topological twisting of this bundle.

The classical counterpart to Berry's phase was originally developed by Hannay (1985) (hence the terminology *Hannay's angle*) and is most naturally described by considering slowly varying integrable Hamiltonian systems in action-angle form. If we let $(I_1, \ldots, I_n; \theta_1, \ldots \theta_n)$ represent the action-angle variables of a given integrable system, then the governing Hamiltonian can be expressed as $\mathcal{H}(I_1, \ldots, I_n; R(t))$, where $R(t)$ is a slowly varying parameter that cycles through a closed loop in time period T, that is, $R(t+T) = R(t)$, $\dot{R}(t) \sim \varepsilon R$, $\varepsilon \ll 1$. The configuration space for the system is an n-dimensional torus $\mathbb{T}^n$ and we seek a formula for the angle variables as the parameter or parameters slowly evolve around the closed loop $\mathcal{C}$ in parameter space. The time-dependent system is governed by

$$\dot{\mathbf{I}} = \dot{R}(t) \cdot \frac{\partial \mathbf{I}}{\partial R}, \tag{1}$$

$$\dot{\boldsymbol{\theta}} = \boldsymbol{\omega}(\mathbf{I}) + \dot{R}(t) \cdot \frac{\partial \boldsymbol{\theta}}{\partial R}, \tag{2}$$

where

$$\omega(\mathbf{I}) \equiv \frac{\partial \mathcal{H}}{\partial \mathbf{I}}.$$

Since R is slowly varying, we can average the system around level curves of the frozen (i.e., $\varepsilon = 0$) Hamiltonian. If we let $\langle \quad \rangle$ denote this phase-space average, then the averaged canonical system becomes

$$\dot{\mathbf{I}} = \dot{R}(t) \cdot \left\langle \frac{\partial \mathbf{I}}{\partial R} \right\rangle \tag{3}$$

$$\dot{\boldsymbol{\theta}} = \boldsymbol{\omega}(\mathbf{I}) + \dot{R}(t) \cdot \left\langle \frac{\partial \boldsymbol{\theta}}{\partial R} \right\rangle. \tag{4}$$

The well-known adiabatic theorem of quantum mechanics guarantees that the action variable is nearly constant due to its adiabatic invariance, whereas the angle variables can be integrated over period T

$$\theta_T^i = \int_0^T \omega^i(\mathbf{I}) \mathrm{d}t + \int_0^T \dot{R}(t) \cdot \left\langle \frac{\partial \theta^i}{\partial R} \right\rangle \mathrm{d}t \tag{5}$$

$$= \theta_\mathrm{d} + \theta_\mathrm{g}. \tag{6}$$

The first term, θ_d, called the dynamic phase is due to the frozen system, while the second term, θ_g, arises from the time variation. This geometric phase can be rewritten in a revealing manner as

$$\theta_\mathrm{g} = \int_0^T \dot{R}(t) \cdot \left\langle \frac{\partial \theta^i}{\partial R} \right\rangle \mathrm{d}t \tag{7}$$

$$= \oint \left\langle \frac{\partial \theta^i}{\partial R} \right\rangle \mathrm{d}R. \tag{8}$$

The contour integral is taken over the closed loop $\mathcal{C}$ in parameter space. Although arising through a dynamical process, it is ultimately a purely geometric quantity that results from a delicate balance of two compensating effects in the limit $\varepsilon \to 0$. On the one hand, $T \to \infty$ in (7), while on the other, $\dot{R}(t) \to 0$. Their rates exactly balance so that the integral leaves a residual term in the limit $\varepsilon = 0$, as given in (8).

A nice example developed in Hannay (1985) is the *bead-on-hoop* problem in which a frictionless bead is constrained to slide along a closed planar wire hoop that encloses area $\mathcal{A}$ and has perimeter length $\mathcal{L}$. As the bead slides around the hoop, the hoop is slowly rotated about its vertical axis (which is aligned with the gravitational vector) through one full revolution. We are interested in the angular position of the bead with respect to a fixed point on the hoop after one full revolution of the hoop. When compared with its angular position had the hoop been held fixed (the frozen problem), this angle difference would represent the geometric phase and is given by

$$\Delta\theta = -8\pi^2 \mathcal{A}/\mathcal{L}^2. \tag{9}$$

Montgomery (1991b) shows that modulo 2π, we have the following *rigid-body phase formula*:

$$\Delta\theta = -\Lambda + 2ET/R. \tag{10}$$

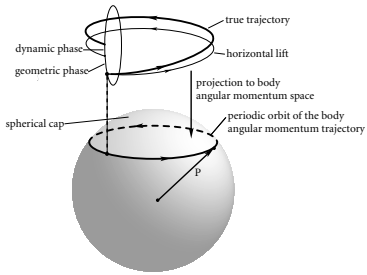

Figure 2. The geometry of the rigid-body phase formula.

Let us explain the notation in this remarkable formula. When a rigid body is freely spinning about its center of mass, one learns in mechanics that this dynamics can be described by the Euler equations, which are equations for the body angular momentum $\boldsymbol{\Pi}$. This vector in $\mathbb{R}^3$ moves on a sphere (of radius $R = \|\boldsymbol{\Pi}\|$) and describes periodic orbits (or exceptionally, heteroclinic orbits). This orbit is schematically depicted by the closed curve on the sphere shown in Figure 2. However, the full dynamics includes the dynamics of the rotation matrix for describing the attitude of the rigid body as well as its conjugate momentum. There is a projection from the full dynamic phase space (which is 6-d) to the body angular momentum space (which is 3-d). After one period of the motion on the sphere, the actual rigid-body motion was not periodic, but it had rotated about the spatial angular momentum vector by an angle $\Delta\theta$, the left-hand side of the above formula. The quantity Λ is the spherical angle subtended by the cap shown in the figure, E is the energy of the trajectory, and T is the period of the closed orbit on the sphere. A detailed history of this formula is given in Marsden & Ratiu (1999).

PAUL K. NEWTON AND JERROLD E. MARSDEN

See also **Adiabatic invariants; Averaging methods; Hamiltonian systems; Integrability; Phase space**

Further Reading

Berry, M.V. 1984. Quantal phase factors accompanying adiabatic changes. *Proceedings of the Royal Society, London* A, 392: 45–57

Berry, M.V. 1985. Classical adiabatic angles and quantal adiabatic phase. *Journal of Physics* A, 18: 15–27

Berry, M.V. 1988. The geometric phase. *Scientific American*, December, 46–52

Berry, M.V. 1990. Anticipations of the geometric phase. *Physics Today*, 43(12), 34–40

Hannay, J.H. 1985. Angle variable holonomy in adiabatic excursion of an integrable Hamiltonian. *Journal of Physics* A, 18: 221–230

Marsden, J.E. 1992. *Lectures on Mechanics*, Cambridge and New York: Cambridge University Press

Marsden, J.E., Montgomery, R. & Ratiu, T. 1989. Cartan–Hannay–Berry phases and symmetry. *Contemporary Mathematics*, 97: 279–295

Marsden, J.E. & Ostrowski, J. 1998. Symmetries in motion: geometric foundations of motion control, *Nonlinear Science Today*. (http://link.springer-ny.com)

Marsden, J.E. & Ratiu, T. 1999. *Introduction to Mechanics and Symmetry*, 2nd edition, New York: Springer

Montgomery, R. 1991a. Optimal control of deformable bodies and its relation to gauge theory. In *The Geometry of Hamiltonian Systems*, edited by T. Ratiu, New York: Springer, pp. 403–438

Montgomery, R. 1991b. How much does a rigid body rotate? A Berry's phase from the 18th century, *American Journal of Physics*, 59: 394–398

Newton, P.K. 2001. *The N-Vortex Problem: Analytical Techniques*, New York: Springer, Chapter 5

Shapere, A. & Wilczek, F. (editors). 1989. *Geometric Phases in Physics*, Singapore: World Scientific

Simon, B. 1983. Holonomy, the quantum adiabatic theorem, and Berry's phase. *Physical Review Letters*, 51(24): 2167–2170

BETHE ANSATZ

The Bethe ansatz is the name given to a method for exactly solving quantum many-body systems in one spatial dimension (1-d) or classical statistical lattice models (vertex models) in two spatial dimensions (Baxter, 1982; Korepin et al., 1993). The method was developed by Hans Bethe in 1931 (Bethe, 1931) in order to diagonalize the Hamiltonian of a chain of N spins with isotropic exchange interactions, introduced by Werner Heisenberg some years before as the simplest model for a 1-d magnet. This result was achieved by assuming the wave function to be of the form

$$f(x_1, x_2, ..., x_M) = \sum_P A_P \, \mathrm{e}^{\mathrm{i} \sum_{j=1}^{M} k_{P_j} x_j} \qquad (1)$$

with the sum performed on all possible permutations P of M distinct wave numbers $\{k_1, ..., k_M\}$, corresponding to down spins in the system (Bethe ansatz). By imposing invariance under the physical symmetries of the system (discrete translations and total spin rotations), Bethe obtained conditions on the coefficients A_P, which were satisfied if a set of M nonlinear equations (Bethe equations) in N complex parameters (Bethe numbers) were fulfilled. Surprisingly, the wave functions thus constructed were simultaneous eigenfunctions not only of the translation operator, the total spin $\boldsymbol{S}$, and its projection S_z along the z-direction but also of the isotropic Heisenberg Hamiltonian

$$H = \sum_{i=1}^{N} \left(\boldsymbol{S}_i \cdot \boldsymbol{S}_{i+1} - \frac{1}{4} \right). \qquad (2)$$

The energy and the crystal momentum were expressed as symmetric functions of the Bethe numbers; thus, the eigenvalue problem for H was reduced to the solution of an algebraic problem—solution of the Bethe equations.

This remarkable result was possible because of the existence of additional symmetries of the Heisenberg Hamiltonian, which emerged thanks to the ansatz made by Bethe on the wave function. In this original formulation, the method is known as the coordinate Bethe ansatz.

Progress in clarifying the role of symmetries in the Bethe ansatz, the link with integrable systems, and the algebraic aspect of the method was achieved by the Saint Petersburg (formerly Leningrad) School in the course of developing the quantum inverse scattering method (QISM) (Faddeev, 1984; Sklyanin & Faddeev, 1978; Korepin et al., 1993), after the work of Baxter on the integrability of vertex models (Baxter, 1982). In this approach, a key role is played by the monodromy operator defined as $\tau(\lambda) = L_N(\lambda)L_{N-1}, ..., L_1(\lambda)$, with λ being a complex number (spectral parameter) and $L_n(\lambda)$ being the quantum local Lax operator defined for the isotropic Heisenberg model as

$$L_n(\lambda) = \begin{pmatrix} \lambda + \mathrm{i}S_n^z & \mathrm{i}S_n^- \\ \mathrm{i}S_n^+ & \lambda - \mathrm{i}S_n^z \end{pmatrix} \tag{3}$$

with S^+, S^- raising and lowering spin-$\frac{1}{2}$ operators. Note that L_n can be viewed as an operator acting on the space $h_n \otimes V$, where h_n ($\equiv C^2$) is the physical Hilbert at site n (the space of couples of complex numbers), and V is an auxiliary space related to the matrix representation of L_n (for the present case, V is also identified with C^2). The product of Lax operators, taken in the auxiliary space, coincides with the usual matrix multiplication, so that the monodromy matrix can be rewritten as

$$\tau(\lambda) = \begin{pmatrix} A(\lambda) & B(\lambda) \\ C(\lambda) & D(\lambda) \end{pmatrix}, \tag{4}$$

with A, B, C, D operators acting on the full physical Hilbert space: $H = \prod \otimes h_i$. As is known from QISM (Korepin et al., 1993; Sklyanin & Faddeev, 1978; Faddeev, 1984), the commutation relations between elements of the monodromy matrix can be written in a compact form as

$$R(\lambda - \mu)\,(\tau(\lambda) \otimes \tau(\mu)) = (\tau(\mu) \otimes \tau(\lambda))\,R(\lambda - \mu), \tag{5}$$

where R is a 4×4 matrix (quantum R-matrix) satisfying the Yang–Baxter equation. From Equation (5), it follows that the trace of the monodromy operator (also known as the transfer matrix) $T(\lambda) \equiv \mathrm{tr}(\tau(\lambda)) = A(\lambda) + D(\lambda)$ gives rise, for different values of the spectral parameter, to an abelian algebra of operators

$$[T(\lambda), T(\mu)] = 0. \tag{6}$$

One can prove that the Hamiltonian is also an element of this algebra so that, for a system of N sites, there are N quantum integrals of motion in involution, corresponding to Liouville integrability in the classical limit. The diagonalization of the Hamiltonian and the other integrals of motion is thus reduced to the solution of the eigenvalue problem for the transfer matrix T. This problem can be solved by the so-called algebraic Bethe ansatz, a procedure that resembles the algebraic diagonalization of the harmonic oscillator by means of creation and annihilation operators. It relies on the existence of a vector $|\Omega\rangle$ (pseudovacuum) in the Hilbert space, which is annihilated by the operator C of the monodromy matrix

$$C(\lambda)|\Omega\rangle = 0. \tag{7}$$

For the Heisenberg chain, $|\Omega\rangle$ can be chosen as $|\Omega\rangle = \prod_{i=1}^{N} \otimes |\uparrow\rangle_i$ with $|\uparrow\rangle_i$ denoting the spin up state at site i. From Equation (3) it is clear that L_n acts on the state $|\uparrow\rangle_n$ as a triangular matrix, and the same is true for $\tau(\lambda)$ acting on $|\Omega\rangle$; thus, Equation (7) is automatically satisfied (C plays the role of an annihilation operator). From Equations (3) and (4), it is also evident that $A(\lambda)|\Omega\rangle = (\lambda + \mathrm{i}/2)^N|\Omega\rangle$, $D(\lambda)|\Omega\rangle = (\lambda - \mathrm{i}/2)^N|\Omega\rangle$. Moreover, one can show that the operator B in Equation (4) can be used as a creation operator.

By taking N different values of the spectral parameter $\lambda_1, \lambda_2, ..., \lambda_N$, one constructs a trial wave function as

$$|\Psi(\lambda_1, ..., \lambda_N)\rangle = \prod_{i=1}^{N} B(\lambda_i)|\Omega\rangle. \tag{8}$$

A direct calculation shows that

$$T(\lambda)|\Psi(\lambda_1, ..., \lambda_N)\rangle = \Lambda(\lambda)|\Psi(\lambda_1, ..., \lambda_N)\rangle + \text{unwanted terms}, \tag{9}$$

where the unwanted terms can be calculated using the commutation relations of A and D with B, obtained from Equation (5). The unwanted terms, however, are eliminated if the λ_i are taken as solutions of the Bethe equations that, for the isotropic Heisenberg chain, are of the form

$$\left(\frac{\lambda_\alpha - \mathrm{i}/2}{\lambda_\alpha + \mathrm{i}/2}\right)^N = -\prod_{\beta=1}^{M} \frac{\lambda_\alpha - \lambda_\beta - \mathrm{i}}{\lambda_\alpha - \lambda_\beta + \mathrm{i}}, \quad \alpha = 1, 2, ..., M. \tag{10}$$

The set of states obtained from Equation (8) in correspondence of the solutions of this system of nonlinear equations can be shown to be complete. The diagonalization of $T(\lambda)$, and hence of the Hamiltonian and all the quantum integrals of motion, is thus reduced to the problem of solving the Bethe equations. For finite size systems, this is a difficult problem to solve due to the nonlinearity of the equations, and one usually resorts to numerical tools. In the thermodynamical

limit, however, it is possible to obtain exact solutions of the energy spectrum by deriving linear integral equation for the density distribution of the Bethe solutions in a complex plane (however, this requires an assumption on the nature of the solution known as the string hypothesis).

The algebraic Bethe ansatz has been successfully applied to a large class of many-body problems, including anisotropic generalizations of the Heisenberg chain, the Hubbard model, and the Kondo model, and has stimulated a variety of related approaches including Baxter's q-operator method (Baxter, 1982) and the notion of quantum groups. Recent progress in the computation of correlation functions of quantum-integrable many-body problems have also been made using the Bethe ansatz (Korepin et al., 1993).

MARIO SALERNO

See also **Quantum inverse scattering method; Salerno equation**

Further Reading

Baxter, R.J. 1982. *Exactly Solved Model of Statistical Mechanics*, New York: Academic Press

Bethe, H. 1931. Zur Theorie der Metalle I. Eigenwerte and Eigenfunktionen der Linearen Atomkette. *Zeitschrift für Physik*, 71: 205–226

Faddeev, L.D. 1984. Integrable models in 1+1 dimensional quantum field theory. In *Recent Advances in Field Theory and Statistical Mechanics*, Les Houches 1982, edited by J.B. Zuber & R. Stora, Amsterdam: North-Holland

Korepin, V.E., Bogoliubov, N.M. & Izergin, A.G. 1993. *Quantum Inverse Scattering Method and Correlation Functions*, Cambridge and New York: Cambridge University Press, and references therein

Sklyanin, E.K. & Faddeev, L.D. 1978. Quantum mechanical approach to completely integrable field theory models. *Soviet Physics Doklady*, 23: 902

BIFURCATIONS

Bifurcations are critical events that arise in systems when an external control parameter is varied (Arnol'd et al., 1994). For small values of the parameter the system will be linear and a unique fixed point will exist. As the parameter is changed to ranges, where nonlinearity becomes important, instabilities in the form of new fixed points or solutions with qualitatively different dynamical behavior may arise at bifurcations. These critical events are of mathematical and practical interest since their analysis can be performed, and they form organizing centers for observed dynamics (Guckenheimer & Holmes, 1986).

As an example, consider the simple physical system of a plastic ruler that is compressed lengthwise between your hands. This was first considered by Leonhard Euler in 1744 and is often referred to as the Euler strut problem (Acheson, 1997). At small forces, the ruler is approximately straight and supports the applied load. This is called the trivial state of the system. However, as the load increases, buckling takes place so that the ruler is deflected up or down. The straight trivial state becomes unstable and is replaced by a pair of solutions where each corresponds to one of the buckled states. If the ruler and the application of the load were both perfect, this would provide a physical example of a symmetry-breaking supercritical pitchfork bifurcation of the type shown in the bifurcation diagram of Figure 1(a).

The symbol X represents the deflection of the center of the ruler, which is used as the measure of the state of the system shown plotted as a function of the applied load λ. The symmetry that is broken is the mirror-plane symmetry of the straight ruler. The bifurcation is called supercritical because the nontrivial branches have the same stability as the trivial state, and it is termed pitchfork due to its shape.

When the bifurcating solutions have a stability opposite to the trivial, the bifurcation is called subcritical. A sketch of such a bifurcation is given in Figure 1(b) where an increase in the parameter λ would involve a jump to a large X state when λ is increased beyond the critical value λ_c. In order to regain the trivial state, λ would then have to be reduced to reach the folded part of the solution branches, and a sudden change back to the trivial state would occur. Hence, hysteresis takes place between the two transitions, and such a path is labeled C in Figure 1(b). The pair of folds in Figure 1(b) are called saddle-node bifurcations (Iooss & Joseph, 1990). A physical example of this is provided by the buckling of an elastic wire such as the outer portion of a bicycle brake cable. When a short length is held vertically, it will stand upright. If you push the remaining length upward through your hand, it will eventually become long enough so that gravity will cause it to fall over through a large angle of deflection. Now pull it back downward through your hand and you will find that the deflected state remains over a range of lengths before flipping back to the vertical. This is an example of a hysteresis loop.

The two models in Figures 1(a) and (b) contain a reflection symmetry. If this is not present, the bifurcation is transcritical and an example of such a bifurcation is given in Figure 1(c). In the physical example of the buckling of the ruler, this type of bifurcation would be observed if a constant side load

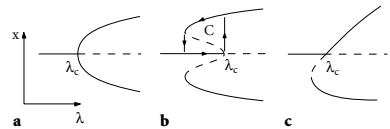

Figure 1. Sketches of (a) supercritical pitchfork, (b) subcritical pitchfork and (c) transcritical bifurcations. Solid lines indicate stable solutions and dashed lines indicate unstable.

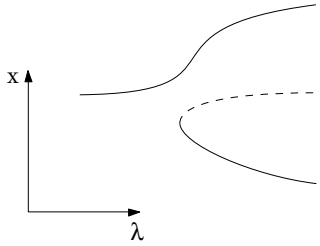

Figure 2. Imperfect pitchfork bifurcation.

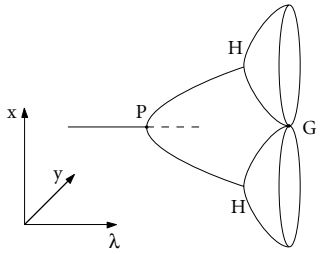

Figure 3. Schematic of a gluing bifurcation sequence.

was applied in addition to the end load in the example of the ruler. In this case, the mid-plane symmetry is automatically broken.

Of course, in any real system, physical imperfections will be present. These can be taken into account using the imperfect bifurcation theory (Golubitsky & Schaeffer, 1985). The effect of an imperfection is to disconnect the supercritical pitchfork bifurcation as shown in Figure 2. It can be seen that there is one state that evolves smoothly with an increase in parameter λ and another disconnected branch. In the example of the ruler, imperfections could arise from irregularities in the shape of the ruler or a slight imbalance in the applied load. The lower limit of the disconnected branch is defined by another type of bifurcation, a saddle node. The disconnected state can be attained, either by variation of two parameters (e.g., variation of side load for the Euler strut), or by a discontinuous or sudden jump in the parameter λ. In the latter case, there is a finite chance that the system will land on the disconnected solution. Examples of observations of such behavior in fluid flows are provided by Taylor–Couette flow (Pfister et al., 1988), a flow through a sudden expansion (Fearn et al., 1990), and convection (Arroya & Saviron, 1992).

Another very important bifurcation is a Hopf where a simply periodic cycle arises from a fixed point as a parameter is changed. As in the case of pitchforks, Hopf bifurcations may also be super- or subcritical, with hysteresis present in the latter case. An interesting feature of supercritical Hopf bifurcations is that the system takes more and more time to reach the equilibrium state as the bifurcation point nears. The observed long-term dynamics are analogous to critical slowing down (Landau & Lifshitz, 1980) in phase transitions and have been found in a fluid flow (Pfister & Gerdts, 1981), for example.

Further interesting global bifurcations (Glendinning, 1994) may occur when pitchfork and Hopf bifurcations occur sequentially. An example of this is shown schematically in Figure 3, where the pair of asymmetric states that arise at the pitchfork P then undergo a pair of Hopf bifurcations at the points labeled H. The cycles that arise at H then join together at a gluing bifurcation (Coullet et al., 1984) when λ is increased. This point is marked G in Figure 3, and it is an example of a homoclinic bifurcation. In this case, a single large orbit is formed from the pair of cycles as λ is increased beyond G with the period going to infinity exactly at G. Interesting dynamical behavior including chaos can be observed near such points in experiments when physical imperfections are taken into account (Glendinning et al., 2001).

TOM MULLIN

See also **Catastrophe theory; Critical phenomena; Equilibrium; Hopf bifurcation; Phase transitions**

Further Reading

Acheson, D. 1997. *From Calculus to Chaos*, Oxford and New York: Oxford University Press

Arnol'd, V.I., Afrajmovich, V.S., Il'yashenko, Yu.S. & Shil'nikov, L.P. 1994. *Bifurcation Theory and Catastrophe Theory*, Berlin and New York: Springer

Arroyo, M.P. & Saviron, J.M. 1992. Rayleigh Bénard convection in a small box-spatial features and thermal-dependence of the velocity field. *Journal of Fluid Mechanics*, 235: 325–348

Coullet, P., Gambaudo, J.M. & Tresser, C. 1984. Une nouvelle bifurcation de codimension 2: le collage de cycles. *Comptes Rendu de l'Academie des Sciences de Paris, Ser. I–Mathematische* 299: 253–256

Fearn, R.M., Mullin, T. & Cliffe, K.A. 1990. Nonlinear flow phenomena in a symmetric sudden-expansion. *Journal of Fluid Mechanics*, 211: 595–608

Glendinning, P. 1994. *Stability, Instability and Chaos: An Introduction to the Theory of Nonlinear Differential Equations*, Cambridge and New York: Cambridge University Press

Glendinning, P., Abshagen, J. & Mullin, T. 2001. Imperfect homoclinic bifurcations. *Physical Review* E, 64: 036208

Golubitsky, M. & Schaeffer, D.G. 1985. *Singularities and Groups in Bifurcation Theory I*, Berlin and New York: Springer

Guckenheimer, J. & Holmes, P.J. 1986. *Nonlinear Oscillations, Dynamical Systems, and Bifurcations of Vector Fields*, 2nd edition, Berlin and New York: Springer

Iooss, G. & Joseph, D.D. 1990. *Elementary Stability and Bifurcation Theory*, 2nd edition, Berlin and New York: Springer

Landau, L.D. & Lifshitz, E.M. 1980. *Statistical Physics*, part 1, 3rd edition, London: Pergamon
Pfister, G. & Gerdts, U. 1981. The dynamics of Taylor wavy vortex flow. *Physics Letters A*, 83: 23–27
Pfister, G., Schmidt, H. Cliffe, K.A. & Mullin, T. 1988. Bifurcation phenomena in Taylor–Couette flow in a very short annulus. *Journal of Fluid Mechanics*, 191: 1–18

BI-HAMILTONIAN STRUCTURE

See **Integrable lattices**

BILAYER LIPID MEMBRANES

When a group of unknown researchers reported the artificial assembly of a bimolecular lipid membrane in vitro (at a 1961 symposium on the plasma membrane sponsored by the American and New York Heart Association), it was initially met with skepticism. The research group led by Donald O. Rudin began their report with a description of mundane soap bubbles, followed by "black holes" in soap films, ending with an invisible "black" lipid membrane made from extracts of cows' brains. The reconstituted structure (7.5 nm thick) was created just like a cell membrane separating two aqueous solutions. The speaker then said:

> upon adding one, as yet unidentified, heat-stable compound. . .from fermented egg white. . . to one side of the bathing solutions. . .lowers the resistance. . .by 5 orders of magnitude to a new steady state. . .which changes with applied potential. . .Recovery is prompt. . . the phenomenon is indistinguishable. . . from the excitable alga *Valonia*. . ., and similar to the frog nerve action potential (Ottova & Tien, 2002).

The first report was published a year later (Mueller et al., 1962). In reaction to that report, the subsequent inventor of liposomes (artificial spherical bilayer lipid membranes) wrote recently in an article entitled "Surrogate cells or Trojan horses" (Bangham, 1995):

> . . .a preprint of a paper was lent to me by Richard Keynes, then Head of the Department of Physiology [Cambridge University], and my boss. This paper was a bombshell . . .They [Mueller, Rudin, Tien, and Wescott] described methods for preparing a membrane . . . not too dissimilar to that of a node of Ranvier. . .The physiologists went mad over the model, referred to as a "BLM", an acronym for Bilayer or by some for Black Lipid Membrane. They were as irresistible to play with as soap bubbles.

Indeed, the Rudin group was playing with soap bubbles using equipment purchased from a local toy shop. But scientific experimentation with soap bubbles began with the observations of Robert Hooke (who coined the word "cell" in 1665 to describe the structure of a thin slice of cork tissue observed through a microscope he had constructed), with his observation of "black spots" in soap bubbles and films. Years later, Isaac Newton estimated the blackest soap film (when light waves reflecting from one layer of soap molecules destructively interfere with light waves reflecting from the second layer of soap molecule) to be about $3–8\times10^{-6}$ in. thick. (Modern measurements give thicknesses between 5 and 9 nm, depending on the soap solution used.)

Origins of the Lipid Bilayer Concept

The recognition of the lipid bilayer as a model for biomembranes dates back to the work of Hugo Fricke, in the 1920s and 1930s, who calculated the thickness of red blood cell (RBC) membranes to be between 3.3 and 11 nm, based on frequency-dependent measurements of the impedance of cell suspensions. Modern measurements on experimental bilayer lipid membranes (BLMs) and biomembranes confirm Fricke's estimation of the thickness of the plasma membrane (Tien & Ottova, 2000).

In his 1917 studies of the molecular organization of fatty acids at the air-water interface, Irving Langmuir had demonstrated that a simple trough apparatus could provide the data to estimate the dimensions of a molecule. Evert Gorter and F. Grendel (respectively, a pediatrician and a chemist) used Langmuir's trough to determine the area occupied by lipids extracted from red blood cell (from human, pig, or rat sources) "ghosts" (empty membrane sacs) and found that there was enough lipid to form a layer two molecules thick over the whole cell surface. In other words

$$\frac{\text{surface area occupied (from monolayer experiment)}}{\text{surface area of red blood cell}} \cong 2. \tag{1}$$

Thus, Gorter and Grendel suggested that the plasma membrane of red blood cells may be thought of as a lipid bilayer, with the polar (hydrophilic) head groups oriented outward.

Experimental Realization

The structure of black soap films led to the realization by Rudin and his co-workers in 1960 that a soap film in its final stages of thinning has a structure composed of two fatty acid monolayers sandwiching an aqueous solution as follows:

air | monolayer | soap solution | monolayer | air.

With the above background in mind, Rudin et al. simply proceeded to make a BLM under an aqueous solution, which may be represented as follows:

aqueous solution | BLM | aqueous solution.

Their effort was successful (Tien & Ottova, 2001, p. 86). Rudin and his colleagues showed that a

BLM formed from brain extracts and separating two aqueous solutions was self-sealing to punctures, with many physical and chemical properties similar to those of biomembranes. Upon modification with a certain compound called excitability-inducing molecule (EIM), this otherwise electrically inert structure became excitable, displaying characteristic features similar to those of action potentials of the nerve membrane.

By the end of the early 1970s, it had been determined that an unmodified bilayer lipid membrane separating two similar aqueous solutions is about 5 nm thick and is in a liquid-crystalline state with the following electrical properties: membrane potential ($E_m \simeq 0$), membrane resistivity ($R_m \simeq 10^9\,\Omega\,\text{cm}$), membrane capacitance ($C_m \simeq$ 0.5–1$\mu\text{F}\,\text{cm}^{-2}$), and dielectric breakdown ($V_b > 250{,}000\,\text{V/cm}$). In spite of its very low dielectric constant ($\varepsilon \simeq$ 2–7), this liquid-crystallline BLM is surprisingly permeable to water (8–24 μm/s) (Tien & Ottova, 2000).

The Lipid Bilayer Principle

In spite of their variable compositions, the fundamental structural element of all biomembranes is a liquid-crystalline phospholipid bilayer. Thus, the lipid bilayer principle of cell or biological membranes may be summarily stated as follows: all living organisms are made of cells, and every cell is enclosed by a plasma membrane, the indispensable component of which is a lipid bilayer. The key property of lipid bilayer-based cells is that they are separated from the environment by a permeability barrier that allows them to preserve their identity, take up nutrients, and remove waste. This 5 nm thick liquid-crystalline lipid bilayer serves not only as a physical barrier but also as a conduit for transport, a reactor for energy conversion, a transducer for signal processing, a bipolar electrode for redox reactions, or a site for molecular recognition.

The liquid-crystalline lipid bilayer of biomembranes not only provides the physical barrier separating the cytoplasm from its extracellular surroundings, it also separates organelles inside the cell to protect important processes and events. More specifically, the lipid bilayer of cell membrane must prevent its molecules of life (genetic materials and many proteins) from diffusing away. At the same time, the lipid bilayer must keep out foreign molecules that are harmful to the cells. To be viable, the cell must also communicate with the environment to continuously monitor the external conditions and adapt to them. Further, the cell needs to pump in nutrients and release toxic products of its metabolism. How does the cell carry out all of these multi-faceted activities?

A brief answer is that the cell depends on its lipid-proteins-carbohydrate complexes (i.e., glycoproteins, proteolipids, glycolipids, etc.) embedded in the lipid bilayer to gather information about the environment in various ways. Examples include communication with hundreds of other cells about a variety of vital tasks such as growth, differentiation, and death (apoptosis). Glycoproteins are responsible for regulating the traffic of material to and from the cytoplasmic space. Paradoxically, the intrinsic structure of cell membranes creates a bumpy obstacle to these vital processes of intercellular communication. The cell shields itself behind its lipid bilayer, which is virtually impermeable to all ions (e.g., Na^+, K^+, Cl^-) and most polar molecules (except H_2O). This barrier must be overcome, however, for a cell to inform itself of what is happening in the world outside, as well as to carry out vital functions. Thus, over millions and millions of years of evolution, the liquid-crystalline lipid bilayer—besides acting as a physical restraint—has been modified to serve as a conduit for material transport, as a reactor for energy conversion, as a bipolar electrode for redox reactions, as a site for molecular recognition, and other diverse functions such as apoptosis and signal transduction.

Insofar as membrane transport is concerned, cells make use of three approaches: simple diffusion, facilitated diffusion, and active transport. Although simple diffusion is an effective transport mechanism for some substances such as water, the cell must make use of other mechanisms for moving substances in and out of the cell. Facilitated diffusion utilizes membrane channels to allow charged molecules, which otherwise could not diffuse across the lipid bilayer. These channels are especially useful with small ions such as K^+, Na^+, and Cl^-. The number of protein channels available limits the rate of facilitated transport, whereas the speed of simple diffusion is controlled by the concentration gradient. Under active transport, the expenditure of energy is necessary to translocate the molecule from one side of the lipid bilayer to the other, in contrast to the concentration gradient. Similar to facilitated diffusion, active transport is limited by either the capacity of membrane channels or the number of carriers present.

Today, ion channels are found ubiquitously. To name a few, they are in the plasma membrane of sperm, bacteria, and higher plants; the sarcoplasmic retculum of skeletal muscle, nerve membrane, synaptic vesicle membranes of rat cerebral cortex, and the skin of carps. As a weapon of attack, many toxins released by living organisms such as dermonecrotic toxin, hemolysin, brevetoxin, and bee venom are polypeptide-based ion-channel formers. For example, functioning of membrane proteins, in particular, ionic channels, can be modulated by alteration of their arrangement in membranes (e.g., electroporation, Tien & Ottova, 2003).

At the membrane level, most cellular activities involve some kind of lipid bilayer-based

receptor-ligand contact interactions. Outstanding examples among these are ion-sensing, molecular recognition (e.g., antigen-antibody binding and enzyme-substrate interaction), light conversion and detection, gated channels, and active transport. The development of self-assembled bilayer lipid membranes (BLMs and liposomes) has made it possible to investigate directly the electrical properties and transport phenomena across a 5 nm thick biomembrane element separating two aqueous phases. A modified or reconstituted BLM is viewed as a dynamic structure that changes in response to environmental stimuli as a function of time, as described by the so-called dynamic membrane hypothesis. Under this hypothesis, each type of receptor interacts specifically with its own ligand. That is, the so-called G-receptor is usually coupled to a guanosine nucleotide-binding protein that in turn stimulates or inhibits an intracellular, lipid bilayer-bound enzyme. G-protein-linked receptors mediate the cellular responses to a vast variety of signaling molecules, including local mediators, hormones, and neurotransmitters, which are as varied in structure as they are in function. G-protein-linked receptors usually consist of a single polypeptide chain, which threads back and forth across the lipid bilayer up to seven times. The members of this receptor family have a similar amino acid sequence and functional relationship. The binding sites for G-proteins have been reported to be the second and third intracellular loops and the carboxy-terminal tail. The endogenous ligands, such as hormones, neurotransmitters, and exogenous stimulants such as odorants, belonging to this class are important target analytes for biosensor technology Tien & Ottova (2003).

H. Ti. Tien and Angelica Ottova-Lueitmannova

See also **Langmuir–Blodgett films; Nerve impulses; Neurons**

Further Reading

Bangham, A.D. 1995. Surrogate cells or Trojan horses. *BioEssays*, 17: 1081–1088

Mueller, P., Rudin, D.O., Tien H.T. & Wescott, W.C. 1962. Reconstitution of cell membrane structure in vitro and its transformation into an excitable system. *Nature*, 194: 979–980

Ottova A. & Tien, H.T. 2002. The 40th anniversary of bilayer lipid membrane research. *Bioelectrochemistry*, 56: 171–173

Ottova, A., Tvarozek, V. & Tien, H.T. 2003. Supported BLMs. In *Planar Lipid Bilayers (BLMs) and Their Applications*, edited by H.T. Tien & A. Ottova-Leitmannova, Amsterdam: Elsevier

Tien, H.T. 1974. *Bilayer Lipid Membranes (BLM): Theory and Practice*, New York: Marcel Dekker

Tien, H.T. & Ottova, A.L. 2000. *Membrane Biophysics: As Viewed from Experimental Bilayer Lipid Membranes (Planar Lipid Bilayers and Spherical Liposomes)*, Amsterdam and New York: Elsevier Science

Tien, H.T. & Ottova, A. 2001. The lipid bilayer concept and its experimental realization: from soap bubbles, the kitchen sink, to bilayer lipid membranes. *Journal of Membrane Science*, 189: 83–117

Tien, H.T. & Ottova, A. 2003. The bilayer lipid membrane (BLM) under electrical fields. *IEEE Transactions on Dielectrics and Electrical Insulation*, 10(5): 717–727

BILLIARDS

In mathematical physics, the singular noun "billiards" denotes a dynamical system corresponding to the inertial motion of a point mass within a region that has a piecewise smooth boundary. The reflections from the boundary are taken to be elastic; that is, the angle of reflection equals the angle of incidence. This model arises naturally in optics, acoustics, and classical and statistical mechanics. In fact, two fundamental models in statistical mechanics, gas of hard spheres (Boltzmann gas) and the Lorentz gas, are billiards. The billiards concept occupies a central position in nonlinear physics because it provides ideal visible models for analysis of dynamical properties leading to classical chaos and an ideal testing ground for the semiclassical analysis of quantum systems.

Billiards models are Hamiltonian systems. Hence, the phase volume is preserved under the dynamics, and the system can be studied in the framework of ergodic theory. In particular, the boundary of the billiard region is supposed to be only piecewise smooth; that is, it consists of smooth components. Therefore, the dynamics of billiards is not defined for orbits that hit singular points of the boundary. However, the phase volume of such orbits equals zero. The dynamics of billiards is completely defined by the shape of its boundary. A smooth component of the boundary is called dispersing, focusing, or neutral if it is convex inward, outward the billiard region, or if it is flat (has zero curvature), respectively. Any billiard orbit is a broken line in its configuration space.

The classical examples of integrable billiards are provided by circular and elliptical boundaries. Configuration spaces of these billiards are foliated by caustics, which are smooth curves (surfaces γ) such that if one link of the billiard orbit is tangent to γ, then every other link of this orbit is tangent to γ. Billiards in a circle has one family of caustics formed by (smaller) concentric circles, while billiards in an ellipse has two families of caustics (confocal ellipses and confocal hyperbolas), which are separated by orbits such that each link intersects a focus of the ellipse. Birkhoff's conjecture (Birkhoff, 1927) claims that among all billiards inside smooth convex curves, only billiards in ellipses are integrable. Berger (1990) has shown that in three dimensions (d), only billiards in ellipsoids produce foliations of a billiard region by smooth convex caustics. However, it does not imply that only billiards in ellipsoids are integrable because if a billiard in $d > 2$ has an invariant hypersurface then this hypersurface does not necessarily consist of

rays tangent to some hypersurface in the configuration space. Using KAM theory, Lazutkin has shown that if a billiards boundary is strictly convex, with a sufficiently smooth curve and its curvature never vanishes; then there exists an uncountable number of smooth caustics in the vicinity of the boundary, and moreover, the phase volume of the orbits tangent to these caustics is positive (Lazutkin, 1991).

An opposite situation occurs when a boundary is everywhere dispersing. Such models were introduced by Sinai (1970), in his seminal paper and they are called Sinai (or dispersing) billiards (Figure 1(a)). Sinai billiards have the strongest chaotic properties; that is, they are ergodic, mixing, have a positive metric entropy, and are Bernoulli systems. If a (narrow) parallel beam of rays is made to fall onto a dispersing boundary, then after reflection it becomes divergent and, therefore, the distance between the rays in this beam increases with time. It is the mechanism of dispersing that generates sensitive dependence on initial conditions (hyperbolicity) and is responsible for strong chaotic properties of dispersing billiards.

On the other hand, focusing boundaries produce the opposite effect. Indeed, a narrow parallel beam of rays after reflection from the focusing boundary becomes convergent; that is, the distance between rays in such a beam decreases with time. Therefore, it has been the general understanding that a dispersing boundary always produces chaotization of the dynamics, while a focusing boundary produces stabilization of the dynamics. However, there exists another mechanism of chaos in billiards (and, in general, in Hamiltonian systems), which is called defocusing (Bunimovich, 1974, 1979). The point is that a narrow parallel beam of rays, after focusing because of reflection from a focusing boundary, may become divergent provided that a free path between two consecutive reflections from the boundary is long enough. Assuming that the time of divergence exceeds (averaged over all orbits) the time of convergence, one obtains chaotic billiards. One of the first, and the most famous, example of such billiards is called a stadium (Figure 1(b)). One obtains a stadium by cutting a circle into two semi-circles and connecting them by two common tangent segments. The length of these segments could be arbitrarily small, which demonstrates that the mechanism of defocusing can work under small deformations of even the integrable (a circle) billiards. Focusing billiards can have as strong chaotic properties as Sinai's billiards do (Bunimovich, 2000).

Figure 1. (a) Sinai billiard. (b) Stadium. (c) Mushroom.

There are no other mechanisms of chaos in billiards. Indeed, billiards in polygons and polyhedrons have zero metric entropy (Boldrighini et al., 1978). Nevertheless, a typical billiard in a polygon is ergodic (Kerckhoff et al., 1986). Because focusing components can form parts of the boundary of integrable as well as chaotic billiards, a natural question is whether there are some restrictions. Two classes of focusing components admissible in chaotic billiards were found (Wojtkowski, 1986; Markarian, 1988). The most general class of such focusing components is formed by absolutely focusing mirrors (AFM) (Bunimovich, 1992). AFMs form a new notion in geometric optics. A mirror γ (or a smooth component of a billiards' boundary) is called absolutely focusing if any narrow parallel beam of rays that falls on γ becomes focused after its last reflection in a series of consecutive reflections from γ. Observe that a mirror is focusing if any parallel beam of rays becomes focused just after the first reflection from this mirror. AFMs can also be characterized in terms of their local properties (Donnay, 1991; Bunimovich, 1992).

Generic Hamiltonian systems are neither integrable nor chaotic. Instead, their phase spaces get divided into KAM-islands and chaotic sea(s). The only clear and clean example of this phenomenon is a billiard in a mushroom (Bunimovich, 2001). The mushroom consists of a semicircular hat sitting on a foot (Figure 1(c)). A mushroom becomes a stadium when the width of the foot equals the width of the hat.

Clearly, the mechanism of dispersing works is higher than two dimensions as well (Sinai, 1970). It is not obvious at all for the mechanism of defocusing because of astigmatism. However, chaotic focusing billiards also do exist in dimension $d \geq 3$ (Bunimovich & Rehacek, 1998). But one pays a price of astigmatism by not allowing the focusing component to be as large as it can be in $d = 2$.

Many properties of classical dynamics of billiards are closely related to the properties of the corresponding quantum problem. Consider the Schrödinger equation with a potential equal to zero inside the billiard region and equal to infinity on the boundary. The eigenfunctions become uniformly distributed over the regions of ergodic billiards for high wave numbers (Shnirelman, 1991). On the contrary, there exist infinite series of eigenfunctions localized in the vicinity of convex caustics of billiards (Lazutkin, 1991).

LEONID BUNIMOVICH

See also **Ergodic theory; Horseshoes and hyperbolicity in dynamical systems; Lorentz gas**

Further Reading

Berger, M. 1990. Sur les caustiques de surfaces en dimension 3. *Comptes Rendu de l'Academie de Sciences*, 311: 333–336

Birkhoff, G. 1927. *Dynamical Systems*. New York, American Mathematical Society

Boldrighini, C., Keane, M. & Marchetti, F. 1978. Billiards in polygons. *Annals of Probability*, 6: 532–540
Bunimovich, L.A. 1974. On billiards close to dispersing. *Mathematical USSR Sbornik*, 95: 49–73 (originally published in Russian)
Bunimovich, L.A. 1979. On the ergodic properties of nowhere dispersing billiards. *Communications in Mathematical Physics*, 65: 295–312
Bunimovich, L.A. 1992. On absolutely focusing mirrors. In *Ergodic Theory and Related Topics*, edited by U. Krengel, et al., Berlin and New York: Springer, pp. 62–82
Bunimovich, L.A. 2000. Billiards and other hyperbolic systems with singularities. In *Dynamical Systems, Ergodic Theory and Applications*, edited by Ya. G. Sinai, Berlin: Springer
Bunimovich, L.A. 2001. Mushrooms and other billiards with divided phase space. *Chaos*, 11: 802–808
Bunimovich, L.A. & Rehacek, J. 1998. How many dimensional stadia look like. *Communications in Mathematical Physics*, 197: 277–301
Donnay, V. 1991. Using integrability to produce chaos: billiards with positive entropy. *Communications in Mathematical Physics*, 141: 225–257
Kerckhoff, S., Mazur, H. & Smillie, J. 1986. Ergodicity of billiard flows and quadratic differentials. *Annals of Mathematics*, 124: 293–311
Lazutkin, V. F. 1991. *The KAM Theory and Asymptotics of Spectrum of Elliptic Operators*. Berlin and New York: Springer
Markarian, R. 1988. Billiards with Pesin region of measure one. *Communications in Mathematical Physics*, 118: 87–97
Shnirelman, A. I. 1991. On the asymptotic properties of eigenfunctions in the regions of chaotic motion. Addendum in *The KAM Theory and Asymptotics of Spectrum of Elliptic Operators* by V. F. Lazutkin. Berlin and New York: Springer
Sinai, Ya. G. 1970. Dynamical systems with elastic reflections. Ergodic properties of dispersing billiards. *Russian Mathematical Surveys*, 25: 137–189 (originally published in Russian 1970)
Wojtkowski, M. 1986. Principles for the design of billiards with nonvanishing Lyapunov exponents. *Communications in Mathematical Physics*, 105: 391–414

BINDING ENERGY

When two particles form a bound state under a certain kind of physical interaction, the resulting state has an energy smaller than the sum of the rest energies of the constituent elements of such a bound state. That is why, by definition (or one could say by construction), bound states are ones in which work has to be done to separate the constituents.

The energy that one has to provide (equivalently the work) in order to separate a bound state into its elements is called the binding energy, E_b, and from the above, it can be directly inferred that $E_b > 0$. The equivalent mass to this energy (under the Einstein relation) also bears a name and is called the "mass defect," $\Delta m = E_b/c^2$, where c is the speed of light.

Examples of binding energy can be easily found among the fundamental forces in nature, such as the gravitational force, the electromagnetic force, and the nuclear force.

Considering an approximately circular (in reality, elliptical) motion of the Earth around the Sun, equating the gravitational force $F_g = GM_sM_e/R^2$ (where G is the gravitational constant, the subscripts s and e denote Sun and Earth, respectively, and R is their relative distance) with the centripetal force $F_c = M_e v^2/R$, one obtains $v = \sqrt{GM_s/R}$, leading to a kinetic energy $E_k = GM_eM_s/(2R)$, which combined with the potential energy of $E_p = -GM_eM_s/R$, results in a binding energy for the solar system of the form

$$E_b = G\frac{M_eM_s}{2R}. \quad (1)$$

Using the relevant masses for the Earth and Sun and their separation, this quantity can be approximately calculated as $E_b \approx 2.6 \times 10^{33}$ J ($\Delta m \approx 2.9 \times 10^{16}$ kg). However, what actually matters in terms of physical "observability" is the ratio of mass defect to the bound state mass (the closer this ratio is to 1, the greater the possibility of observing the mass defect). In the case of the gravitational system $\Delta M/M_b \approx 1.5 \times 10^{-14}$; hence, the mass defect for the gravitational force will not be observable.

Similar calculations can be performed classically for the hydrogen atom (following the same path, but substituting $G \to 1/(4\pi\varepsilon_0)$, $M_s \to |q_e|$, and $M_e \to q_e$, where ε_0 is the dielectric constant in a vacuum and q_e is the charge of the electron). In this case, for the electrostatic force,

$$E_b = \frac{1}{2}\frac{q_e^2}{4\pi\varepsilon_0 R}. \quad (2)$$

In this case, however, $R \approx 0.53 \times 10^{-10}$ m (while in the previous example, it was $\approx 1.5 \times 10^{11}$ m!). In the case of the hydrogen atom, $E_b \approx 13.6$ eV and $\Delta m \approx 2.5 \times 10^{-35}$ kg. The ratio $\Delta M/M_b \approx 1.5 \times 10^{-8}$, indicating that in this case also it is not possible to observe the mass defect.

In the case of the nuclear force, however, the ratio of $\Delta M/M_b$ is of order 10^{-3}, and hence it is possible to observe the mass defect. For example, the mass of an α particle consisting of two protons and two neutrons is 6.6447×10^{-27} kg, while the individual masses of these particles add up to 6.6951×10^{-27} kg, resulting in a binding energy of 28.3 MeV and $\Delta M/M_b \approx 0.0075$. In fact, a very common diagram in nuclear physics is the so-called nuclear binding energy curve (see, e.g., http://hyperphysics.phy-astr.gsu.edu/hbase/nucene/nucbin.html), which shows the binding energy of various elements as a function of their mass number. In this graph, the larger the E_b, the more stable the element; iron (with atomic number $A = 56$ and binding energy 8.8 MeV/nucleon) is the most stable element. Lighter elements can yield energy by fission, while heavier elements can yield energy by means of fusion, emitting energies in the MeV range.

Binding Energy in Nonlinear Systems

Naturally, bound states of multiple waves can be formed in nonlinear systems. To fix ideas, we will examine such bound states and their corresponding binding energies in the specific context of the well-known sine-Gordon equation. For a detailed exposition of the features and applications of this equation, see Dodd et al. (1982). The sine-Gordon equation in (1 + 1) dimensions is

$$u_{tt} = u_{xx} - \sin(u). \tag{3}$$

Perhaps, the best-known nonlinear wave solution of this equation consists of the topological soliton (kink), which is of the form (in the static case)

$$u(x) = 4\tan^{-1}(e^{sx}), \tag{4}$$

$s \in \{-1, 1\}$, where the case of $s = 1$ corresponds to a kink, while $s = -1$ corresponds to an antikink. The energy of such a static kink solution

$$E = \int_{-\infty}^{\infty} dx \left[\frac{1}{2}(u_t^2 + u_x^2) + 1 - \cos(u)\right] \tag{5}$$

can be calculated as $E = 8$.

Another elemental solution of the equation is the breather-like solution of the form

$$u(x,t) = 4\tan^{-1}\left[\frac{(1-\omega^2)^{1/2}}{\omega}\frac{\sin(\omega t)}{\cosh\left((1-\omega^2)^{1/2}x\right)}\right]. \tag{6}$$

This exponentially localized in space, periodic in time solution can be considered as a result of a merger of a kink and an antikink. Hence, this is perhaps the simplest example of a bound state in this nonlinear system.

The bound state character of this solution can also be revealed by the expression for its energy. Using expression (6) in Equation (5), we obtain

$$E_{\text{breather}} = 16(1-\omega^2)^{1/2}. \tag{7}$$

Hence, this energy, for any $\omega \in (0, 1)$ (ω is the frequency of the internal breathing oscillation), is less than the sum of the kink and antikink energies, verifying that the binding energy of such a state is

$$E_b = 16\left[1 - (1-\omega^2)^{1/2}\right]. \tag{8}$$

It is also worthwhile to note that the energy of such a breather excitation varies in the interval (0, 16) depending on its frequency. Hence, there is no threshold for the excitation of such a wave, but even for small amounts of energy, such waveforms will be excited (large frequency/small period ones for small excitation energy).

One can generalize the solution of the form (6) in a periodic breather lattice solution of the sine-Gordon equation in the form (see, e.g., McLachlan, 1994)

$$u(x,t) = 4\tan^{-1}[a\,\mathrm{sn}(bt, k^2)\mathrm{dn}(cx, 1-m^2)], \tag{9}$$

where $\mathrm{sn}(x,k)$ and $\mathrm{dn}(x,k)$ are the Jacobi elliptic functions with modulus k. Here

$$a = \sqrt{\frac{k}{m}},\ b = \sqrt{\frac{m}{(m+k)(1+mk)}} \text{ and}$$
$$c = \sqrt{\frac{k}{(m+k)(1+mk)}}.$$

One can then evaluate the energy (per breather) of this infinite periodic breather lattice configuration (for details of the calculation, the interested reader is directed to Kevrekidis et al., 2001) to be

$$E = 16\sqrt{\frac{k}{(k+m)(1+km)}}E(1-m^2), \tag{10}$$

where $E(1-m^2)$ is the complete elliptic integral of the second kind.

Depending on the values of the elliptic moduli, k and m, the expression of Equation (9) represents a lattice of different entities. For $m, k \to 0$, it corresponds to genuine sine-Gordon breathers. For $k, m \to 1$, the limit gives the "pseudosphere" solution $u = 4\tan^{-1}(\tanh\frac{t}{2})$, which resembles a π-kink but in time rather than space (see McLachlan, 1994). On the other hand, the $k \to$ finite, $m \to 0$ limit gives the kink-antikink pair solution $4\tan^{-1}(t\ \mathrm{sech}\ x)$. This solution has the character of a kink-antikink pair "breathing" in time.

The above different limits illustrate why Equation (10) is an important result, since it can be used (see below) to obtain the asymptotic interaction between entities such as breathers, pseudospheres, or kink-antikink pairs. When taking the appropriate above limits of expression (10), the leading-order term will be the energy of a single such entity. However, the correction to that will be the (per particle) binding energy in a configuration of multiple such entities (or, as it is often referred to, the energy of interaction between two such entities).

To calculate the breather-breather interaction (their binding energy), we take the limit $m, k \to 0$, with $k/m = (1-\omega^2)/\omega^2$, where ω is the breather frequency (see McLachlan, 1994), to obtain

$$E = \left[16\sqrt{1-\omega^2} - 8m^2\frac{(1-\omega^2)^{3/2}}{\omega^2} + 6m^4\frac{(1-\omega^2)^{5/2}}{\omega^4}\right]E(1-m^2). \tag{11}$$

Hence, the corrections to the (single) breather energy in Equation (11) correspond to the binding energy of the formed breather bound states. Similar expressions can be found for the pseudosphere:

$$E = 4\pi - \frac{\pi}{2}(k-1)^2 + \frac{\pi}{4}(m-1)^2 + \frac{3\pi}{32}(m-1)^2(k-1)^2 \tag{12}$$

(again, 4π is the energy of a single pseudosphere) and for kink-antikink pairs

$$E = \left[16 - 8\left(k + \frac{1}{k}\right) + 2m^2\left(2 + 3k^2 + \frac{3}{k^2}\right)\right] \times E(1 - m^2). \quad (13)$$

Similar examples of breather lattices also exist for other equations, such as the well-known Korteweg–de Vries (KdV) equation, and one can again infer breather-breather state binding energies in a similar manner.

In general, one can say that the concept of a bound state for nonlinear evolutionary partial differential equations supporting soliton (or solitary wave) solutions persists in a form very similar to the way it manifests itself for fundamental physical forces and their particle carriers. In the present case, the elements of the bound states are the nonlinear waves proper (a feature reminiscent of the particle-like character of such waves, manifest evidently also in their interactions). In a number of (most often integrable) cases, where the form of the bound state solutions is analytically tractable, the calculation of the bound state energy and of the energy of its constituent elements again provides information, through the difference between the two, for the binding energy (or energy of interaction) of such waves.

P.G. KEVREKIDIS

See also **Breathers; Partial differential equations, nonlinear; Sine-Gordon equation; Solitons**

Further Reading

Dodd, R.K., Eilbeck, J.C., Gibbon, J.D. & Morris, H.C. 1982. *Solitons and Nonlinear Wave Equations*, London: Academic Press

Kevrekidis, P.G., Saxena, A. & Bishop, A.R. 2001. *Physical Review* E, 64: 026613

McLachlan, R. 1994. *Math. Intelligencer*, 16: 31

BIOLOGICAL EVOLUTION

The term *evolution* defines a process that is driven by internal and/or external forces. In quantum mechanics, an evolution operator conducts change in time. Cosmic evolution in the standard model aims at a consistent description of the process from the "big bang" to the present universe. "Prebiotic evolution" deals with chemical precursors of present-day life and is determined by the conditions at the early Earth, be it in the primordial atmosphere, in the surrounding of volcanic hot springs at the sea floor, or at some other location. "Biological evolution" follows the prebiotic scenario, and it shaped and is still shaping the biosphere on Earth. A temporal change in the biosphere manifests itself as the appearance, alteration, and extinction of biological species. This view was not generally accepted before Charles Darwin. Influenced by the geologist Charles Lyell and his concept of uniformitarianism, Darwin and the proponents of the theory of evolution suggested that changes in the biosphere occur gradually, continuously, or at least, in small steps. In this aspect, which is not essential for the mechanism of evolution, Darwin's theory contrasted the view held by the majority of his contemporaries, who assumed constancy of biological species and change exclusively through catastrophic events leading to mass extinction (Ruse, 1979). The opponents of evolutionary thinking, Louis Agassiz, Georges Cuvier, and others, considered species as invariant entities. The remnants of extinct species in the fossil record were interpreted by them as witnesses from earlier worlds destroyed by punctual events, the great deluge, and other catastrophes that wiped out major parts of the organismic world. In society, the concept of evolution was heavily attacked by representatives of the Christian Churches because it was seen to be in conflict with the *Genesis* report in the Bible (Ruse, 2001). During the 20th century, European religious thought has reconciled religious belief and the idea of an evolving biosphere. In North America, the strong opposition of some groups of religious fanatics led to the peculiar development of Creationism, whose claim of being an alternative to the theory of evolution is rejected by the established scientific community (NAS, 1999).

The current theory of biological evolution originated from two epochal contributions by Charles Darwin and Gregor Mendel. Darwin conceived a mechanism for evolutionary change of the biosphere based on variation and selection, and he gathered empirical data providing evidence for the action of natural and artificial selection, the latter exercised in animal breeding and nursery gardens. Darwin's principle (published in *On The Origin of Species by Natural Selection* in 1859) has two consequences: species adapt to their environments and are related to their ancestors in terms of phylogenies, or branches of an ancestral tree of species. In 1866, Gregor Mendel introduced quantitative statistics into the evaluation of data in biology and performed the first precisely controlled fertilization experiments with plants. He discovered and interpreted correctly the action of genes in determining the properties of organisms. Mendel's work was considered irrelevant by the evolutionists of the second half of the 19th century and was "rediscovered" around 1900. Only in 1930 were the Darwinian concept of selection and Mendel's rules of inheritance combined to a common mathematical formalism by the population geneticists Ronald Fisher, John Haldane, and Sewall Wright (for a recent text in population genetics, see Hartl & Clark, 1997). In the 1940s, finally, Darwinian evolution and Mendelian genetics were united in the *Synthetic* or *Neo-Darwinian Theory of Evolution* by the works of the experimental biologists Theodosius

Dobzhansky, Julian Huxley, Ernst Mayr, and others (Mayr, 1997). In the second half of the 20th century, molecular biology put evolutionary theory on firm fundamentals, chemistry and physics. Comparison of genes and, more recently of whole genomes, allows for reconstruction of phylogenies on the basis of nucleotide sequence divergence through mutation (Judson, 1979); the exploration of molecular structures provides insights into the chemistry of present day life; and knowledge of biomolecular properties eventually led to the construction of laboratory systems that allow for observation of evolution of molecules in the test tube (Spiegelman, 1971; Watts & Schwarz, 1997).

Darwinian evolution results from the interplay of variation and selection, both being consequences of reproduction in populations. Variation operates on genomes or genotypes, which are polynucleotide sequences carrying the genetic information, and occurs in two fundamentally different ways: (i) mutation causes local changes in genomic sequences, whereas (ii) recombination exchanges corresponding segments between two genotypes. Selection is based on differences in *fitness* being a property of the phenotype. The phenotype is defined as the union of all, structural as well as dynamic, properties of an individual organism. Unfolding of the phenotype is programmed by the genome; but, at the same time, requires a highly specific environment. In addition, it is influenced by epigenetic factors (epigenetic refers to every nonenvironmental factor that interferes with the development of the organism, except those encoded in the nucleotide sequence of DNA; many epigenetic factors are already understood at the molecular level, and involve specific modifications of genomic DNA). Fitness, in essence, counts the number of fertile descendants reaching the reproductive age. It has two major components: (i) the probability of survival to reproduction, and (ii) the number of viable and fertile offspring.

To illustrate selection in a population of n asexually reproducing phenotypes, we consider a continuous-time model that describes change by a differential equation

$$\frac{\mathrm{d}x_i}{\mathrm{d}t} = x_i(f_i - \Phi), \quad i = 1, \ldots, n$$
$$\text{with } \Phi(t) = \sum_{j=1}^{n} f_j x_j = \overline{f}. \tag{1}$$

The variables denote the frequencies of reproducing variants: $x_i(t) = N_i(t)/\sum_{j=1}^{n} N_j(t)$, with $N_i(t)$ counting the number of individuals with phenotype S_i or genotype I_i at time t. (For several genotypes giving rise to the same phenotype, see *neutrality* below.) Fitness values f_i when averaged over the entire population yield the mean fitness expressed by a time-dependent flux $\Phi(t)$. Frequencies of variants with fitness values above average, $f_i > \Phi$, increase with time, those of below-average variants, $f_i < \Phi$, decrease and as a consequence, the mean fitness increases. The flux $\Phi(t)$ is a nondecreasing function of time and selection continues until all variants, except the fittest, have died out (*See also* **Fitness landscape**). For two variants, I_0 and I_1, the solution boils down to

$$\left[\frac{x_1}{x_0}\right](t) = \left[\frac{x_1}{x_0}\right](0) \cdot \exp(mt)$$

or

$$\left[\frac{X_1}{X_0}\right]_t = \left[\frac{X_1}{X_0}\right]_0 w^t,$$

where the upper equation refers to continuously varying $x(t)$ and the lower equation refers to population to discrete time variables X_t with synchronized reproduction. The *Malthusian* fitness difference $m = f_1 - f_0$ is related to the *Darwinian* relative fitness $w = (1 + f_1)/(1 + f_2)$ by $m \approx \ln w$ (see Hartl & Clark (1997)). The conditions for selection are $m > 0$ or $w > 1$, respectively. An example is shown in Figure 1.

Sexual reproduction of diploid organisms involves Mendelian genetics (see Figure 2). Every gene (A) comes in two copies, identical or different, which are chosen from a reservoir of variants A_i called alleles. Recombination occurs in the process of reproduction when the two copies are separated and reassembled in pieces through random combination. The differential equation (1) is extended to describe selection in the diploid case in the form of Fisher's selection equation:

$$\frac{\mathrm{d}x_i}{\mathrm{d}t} = x_i \cdot \left(\sum_{j=1}^{n} a_{ij} x_j - \Phi\right)$$
$$= x_i\,(\overline{a_i} - \Phi), \quad i = 1, \ldots, n \tag{2}$$

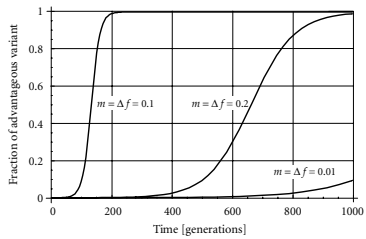

Figure 1. Illustration of selection in populations. The plotted curves represent the frequencies of advantageous mutants I_1 in a population of individuals I_0 with a Malthusian fitness difference of $m = \Delta f = f_1 - f_0 = 0.1$, 0.02, and 0.01. The population size is $N = 10{,}000$, and the mutants were initially present in a single copy: $N_1(0) = 1$ or $x_1(0) = 0.0001$.

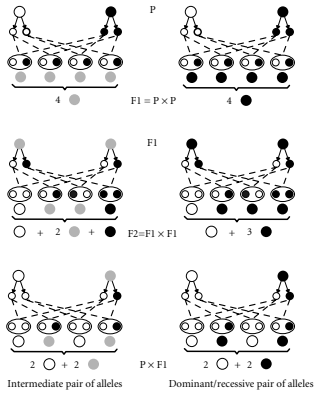

Figure 2. Mendelian genetics. In sexual reproduction, the two parental genomes are split into pieces and recombined randomly, which means each of the four alleles has a 50 % chance to be incorporated in the genome of an offspring. Mendel's laws are of a statistical nature and hold as mean values in the limit of large numbers of observations. Two cases are shown: (i) the heterozygote unfolds into a phenotype with intermediate properties (gray through blending of black and white), and (ii) the property of one allele (black) is dominant. In the latter case, the other allele (white) is called recessive. Interbreeding of two homozygous individuals (parent generation P) leads to a first offspring generation (F1) of identical heterozygous individuals; the phenotypes in the next (F2) generation show a distribution of 1:2:1 in the intermediate and 1:3 in the dominant/recessive case. Crossing of the (recessive) parent genotype with an F1-individual yields a 1:1 ratio of phenotypes.

with

$$\overline{a_i} = \sum_{j=1}^{n} a_{ij} x_j ,$$

$$\Phi(t) = \overline{a} = \sum_{i=1}^{n} \overline{a_i} x_i = \sum_{i=1}^{n} \sum_{j=1}^{n} a_{ij} x_i x_j .$$

The variables refer to alleles A_j rather than to whole genomes, and the rate coefficient a_{ij} represents the individual fitness values for the combination $A_i A_j$. Fitness is assumed to be independent of the positioning of alleles, $A_i A_j$ or $A_j A_i$, and hence, $a_{ij} = a_{ji}$ holds. The term $\overline{a_i}$ is the population-averaged mean fitness of the allele combinations carrying A_i at least once: $A_i A_j$, $j = 1, \ldots, n$. Fisher's fundamental theorem states that the flux $\Phi(t) = \sum_{i=1}^{n} \overline{a_i} x_i = \overline{a}$ is a nondecreasing function of time, but the outcome of selection need not be unique as optimization might end in a local optimum of Φ (*See also* **Fitness landscape**). For example, in the two-allele case, inferiority of the *heterozygote* $A_1 A_2$, $a_{12} < \min\{a_{11}, a_{22}\}$, results in bistability since homogenous populations of either *homozygote*, $A_1 A_1$ or $A_2 A_2$, represent stable equilibrium points. Then, the initial conditions determine the outcome of selection.

The optimization principle is not universally valid: when mutation is included or when more complex cases of recombination are considered, optimization of mean fitness is restricted to certain ranges of initial conditions, whereas different behavior is observed for other starting values. Still, optimization remains an important heuristic in evolution as it is frequently observed.

Innovation is introduced into genes by mutation consisting of a local change in the sequence of nucleotides resulting from an imperfect replication of genetic information or externally caused damage. Two scenarios are distinguished: (i) rare mutation treated by conventional population genetics and typically occurring with multicellular organisms and most bacteria, and (ii) frequent mutation handled by quasispecies theory (Eigen, 1971; Eigen & Schuster, 1977) and determining evolution of viruses. Higher mutation rates are often advantageous because they allow for adaptation, but there exists an error threshold of replication beyond which inheritance breaks down because too many mutations destroy the genetic message. RNA viruses are under a strong selection constraint by the host and their mutation rates are close to the error threshold.

The idea that genotypes and phenotypes are related one-to-one turned out to be wrong. Molecular genetics revealed a high degree of *neutrality* (Kimura, 1983): many different genotypes give rise to the same phenotype. Advantageous mutations are rare; deleterious mutations are eliminated by selection thus leaving a majority of observed changes in the genomes to result from neutral mutations. Neutrality gives rise to random drift of populations in genotype space, which was also found to be important for the mechanism of evolution since it allows populations to escape from minor local fitness optima or evolutionary traps (Schuster, 1996) and Schuster in Crutchfield & Schuster, 2003). Random drift leads to an almost constant mutation rate per year and nucleotide independent of the species being tantamount to a *molecular clock of evolution*. This clock is used for dating in the reconstruction of phylogenies from comparison of present-day genome sequences. Molecular clock dates yield substantially longer time spans compared with those from the fossil record. The discrepancy seems to be reconcilable because paleontological datings are too young and molecular clock datings are too old by systematic errors (Benton & Ayala, 2003).

The Darwinian mechanism is powerful because it makes no reference to the specific nature of the reproducing entities. Therefore, it is likewise valid for molecules, viruses, bacteria, or higher organisms. Selection based on the Darwinian principle is observed in many disciplines outside biology, for example, in

physics and chemistry, in economics, and in the social sciences.

Since its introduction, the theory of evolution has undergone changes and modifications. The rejection of catastrophic events as an important source of change in the history of life on Earth was a political issue rather than one based on scientific data. Geological evidence for fallings of large meteorites as well as major floods is now available, and such events wiped out substantial parts of the biosphere. The paleontological record reflects the interplay between continuous evolution and external influences, which resulted in epochs of gradual development interrupted by punctuated events. Interestingly, evolution of bacteria or molecules under constant conditions also showed punctuation without external triggers: populations "wait" during quasistationary periods for rare mutations that initiate fast periods of change.

Still, there are open problems in current evolutionary theory. Recent sequence data challenge the idea of a tree of life. Although animal phylogeny appears to be on a firm basis, there are problems with the reconstruction of a tree-like history of plant species. Prokaryote evolution cannot be cast into a tree: archebacteria and eubacteria exchange genetic information across species and kingdoms. Such horizontal gene transfer occurs frequently and obscures the descendance of species. Darwinian evolution, although successful in describing the mechanisms of optimization and adaptations of species, is unable to provide explanations for the major evolutionary transitions that lead from one hierarchical level of life to the next higher forms (Maynard Smith & Szathmáry, 1995; Schuster , 1996). Examples of such transitions are the origin of the genetic code; the transition from the prokaryotic to the eukaryotic cell; the transition from unicellular organisms to multicellular plants, fungi, and animals; the transition from solitary animals to animal societies; and eventually the transition to man and human societies. Common to all these transitions is the integration of individual competitors as cooperating elements into a novel functional unit. Simple model mechanisms have been proposed that can explain cooperation of competitors (see, e.g., the hypercycle Eigen & Schuster, 1978), but no real solution to the problem has been found yet.

PETER SCHUSTER

See also **Catalytic hypercycle; Fitness landscape**

Further Reading

Benton, M.J. & Ayala, F.J. 2003. Dating the tree of life. *Science*, 300: 1698–1700

Crutchfield, J.P. & Schuster, P. (editors). 2003. *Evolutionary Dynamics: Exploring the Interplay of Selection, Accident, Neutrality, and Function*, Oxford and New York: Oxford University Press

Eigen, M. 1971. Selforganization of matter and the evolution of biological macromolecules. *Naturwissenschaften*, 58: 465–523

Eigen, M. & Schuster, P. 1977. The hypercycle. A principle of natural self-organization. Part A: Emergence of the hypercycle. *Naturwissenschaften*, 64: 541–565

Eigen, M. & Schuster, P. 1978. The hypercycle. A principle of natural self-organization. Part B: The abstract hypercycle. *Naturwissenschaften*, 65: 7–41

Hartl, D.L. & Clark, A.G. 1997. *Principles of Population Genetics*, 3rd edition, Sunderland, MA: Sinauer Associates

Judson, H.F. 1979. *The Eighth Day of Creation. The Makers of the Revolution in Biology*, London: Jonathan Cape and New York: Simon and Schuster

Kimura, M. 1983. *The Neutral Theory of Molecular Evolution*, Cambridge and New York: Cambridge University Press.

Maynard Smith, J. & Szathmáry, E. 1995. *The Major Transitions in Evolution*, Oxford and New York: Freeman

Mayr, E. 1997. The establishment of evolutionary biology as a discrete biological discipline. *BioEssays*, 19: 263–266

National Academy of Sciences (NAS). 1999. *Science and Creationism. A View from the National Academy of Sciences*, 2nd edition, Washington, DC: National Academy Press

Ruse, M. 1979. *The Darwinian Revolution*, Chicago, IL: University of Chicago Press

Ruse, M. 2001. *Can a Darwinian Be a Christian? The Relationship Between Science and Religion*, Cambridge and New York: Cambridge University Press

Schuster, P. 1996. How does complexity arise in evolution? *Complexity*, 2(1): 22–30

Spiegelman, S. 1971. An approach to the experimental analysis of precellular evolution. *Quarterly Reviews of Biophysics*, 4: 213–253

Watts, A. & Schwarz, G. (editors). 1997. *Evolutionary Biotechnology—From Theory to Experiment. Biophyscial Chemistry*, vol. 66, nos. 2–3, Amsterdam: Elsevier, pp. 67–284

BIOMOLECULAR SOLITONS

Biological molecules are complex systems that evolve in an ever-changing environment and nevertheless exhibit a remarkable stability of their functions. This feature, which is reminiscent of the exceptional stability of solitons in the presence of perturbations, is perhaps what led to suggestions that solitons could have a role in some biological functions. Beyond this analogy, there are more solid arguments to consider the role of nonlinearity in biological molecules. They are very large atomic assemblies performing their function through large conformational changes, which have a cooperative character because they involve many atoms moving in a coherent manner, and are highly nonlinear due to their amplitude of motion, which is much larger than the standard thermal motions observed in small molecules. Additional nonlinearities can originate from the coupling of different degrees of freedom, as proposed for proteins. Dispersion, necessary to balance the effect of nonlinearity in order to obtain soliton-like excitations, is introduced by the discreteness of the molecular lattice, which behaves in a manner different from a continuous medium.

Besides conformational changes involved in many biological functions, issues important for biological

molecules are energy transport and storage, and charge transport. Nonlinear excitations have been proposed as possible contributors to these phenomena, in the two main classes of biological molecules: nucleic acids and proteins (Peyrard, 1995).

Following Erwin Schrödinger in his prophetic book *What Is Life?* (Schrödinger, 1944), the nucleic acid DNA can be viewed as an "aperiodic crystal." The static structure of DNA is a fairly regular pile of flat base pairs, linked by hydrogen bonds and connected by sugar–phosphate strands that form a double helix (Calladine & Drew, 1997). The lack of periodicity occurs because the base pairs can be either $A-T$ (adenine–thymine) or $G-C$ (guanine–cytosine), their sequence defining the genetic code. The static picture that emerges from crystallographic data has little to do with actual DNA in a living cell. The genetic code, buried in the double helix, would not be accessible if DNA were not a highly dynamical structure. Biologists have observed the "breathing of DNA," which is a fluctuational opening in which one or a few base pairs open temporarily. These motions are probed experimentally by monitoring deuterium-hydrogen exchange, based on the assumption that the imino-protons that bind the bases can only be exchanged for open base pairs. DNA double helix is also opened by enzymes during the transcription of a gene, that is, the reading of the genetic code.

This phenomenon is complex, but there are related experimental observations that are more amenable to physical analysis, on the thermal denaturation of DNA. When the double helix is heated, one first observes local openings over a few to a few tens of base pairs. These grow and invade the whole molecule, leading to a thermal separation of the two strands, which can be monitored by measuring the UV absorbance of the molecule, which is highly sensitive to the disturbance of the base stacking. This "DNA melting"—which appears as a phase transition in one dimension—poses challenging questions because, in order to cause the local openings, one has to break many hydrogen bonds between the bases, which requires the localization of a large amount of thermal energy in a small region of the molecule. Nonlinear effects could be at the origin of this phenomenon.

All these observations led to many investigations and models of the nonlinear dynamics of the DNA molecule. A description at the scale of the individual atoms is not necessary to analyze base-pair openings, so the bases are generally described as rigid objects in these models. The earliest attempt to describe DNA opening in terms of solitons is due to Englander et al. (1980), who viewed it as a cooperative motion involving 10 or more base pairs and propagating as a localized defect along the molecule. This idea was further formalized by Yomosa (1984), and Takeno & Homma (1983), who introduced a coupled base rotator model for the structure and dynamics of DNA. The

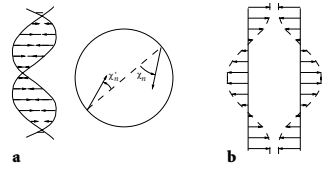

Figure 1. (a) Schematic view of the plane base rotator model for DNA. (b) A symmetric open state of the model.

general ideas behind this approach are schematized in Figure 1(a).

Only rotational degrees of freedom of the bases are introduced (denoted by angles χ_n and χ'_n in Figure 1). The pairing of the bases is described by an on-site potential $V(\chi_n, \chi'_n)$, which, in its simplest form is $V(\chi_n, \chi'_n) = A(1 - \cos\chi_n) + A(1 - \cos\chi'_n) + B(1 - \cos\chi_n \cos\chi'_n)$, and the stacking along the molecule is represented by a potential $W(\chi_n, \chi'_n, \chi_{n-1}, \chi'_{n-1} = S[1 - \cos(\chi_n - \chi_{n-1})] + S[1 - \cos(\chi'_n - \chi'_{n-1})]$, where A, B, S are constants. Adding the kinetic energy of the bases $\frac{1}{2}I(\dot{\chi}_n^2 + \dot{\chi}_n'^2)$, where I is the moment of inertia of the bases around their rotation axis, and summing over n, one obtains the Hamiltonian of the model. Various nonlinear excitations are possible depending on the symmetries of the motion (such as $\chi_n = \chi'_n, \chi_n = -\chi'_n$) and the values of the constants. If the stacking interaction is strong enough, a continuum approximation can be made. This approximation replaces the discrete variables $\chi_n(t)$ by the function $\chi(x, t)$ and finite differences such as $\chi_n - \chi_{n-1}$ by derivatives $a(\partial\chi/\partial x)$, where a is the spacing between the bases and x denotes the continuous coordinate along the helix axis. When $A = 0$, in its simplest form, the model leads to a sine-Gordon equation

$$I\frac{\partial^2\chi}{\partial t^2} - Sa^2\frac{\partial^2\chi}{\partial x^2} + B\sin\chi = 0, \qquad (1)$$

which has topological solutions such as the one schematized in Figure 1(b), where the bases undergo a 2π rotation, generating an open state that may slide along the chain.

Models for the rotation of the base pairs have been further refined by Yakushevich (1998) and are discussed in the entry on **DNA solitons**.

Another point of view was chosen later by Dauxois et al. (1993), who were interested in the statistical physics of DNA thermal denaturation. This problem had been studied by Ising models, which simply use a two-state variable equal to 0 or 1 to specify whether a base pair is closed (0) or open (1). Such models cannot describe the intermediate states, but they can be generalized by introducing a real variable $y_n(t)$ that measures the stretching of the hydrogen bonds

in a base pair that is equal to 0 in the equilibrium structure and grows to infinity when the two strands are fully separated. With such a variable, a natural shape of the on-site potential is the Morse potential $V(y_n) = D[\exp(-\alpha y_n) - 1]^2$ (D and α are constants), which has a minimum corresponding to the binding of the two bases in their equilibrium state by the hydrogen bonds, and a plateau at large y_n, which is associated to the vanishing of the pairing force $\partial V/\partial y_n$ when the bases are far apart.

Such a model does not have topological solitons, but its nonlinear dynamics leads to localized oscillatory modes, called breathers, which are approximately described by solitons of the nonlinear Schrödinger equation in the continuum limit and turn into permanently open states at a high temperature (*See* **Breathers**). These studies have focused attention on the importance of discreteness for nonlinear energy localization. In DNA, the stacking interactions are not very strong, and this is why imino-proton exchange experiments can detect the exchange on one base pair while the neighboring base pairs are not affected. As a result a continuum approximation is very crude. What could appear as a problem because it complicates analytical studies of the nonlinear dynamics turns out to have a far-reaching consequence because it has been shown that discreteness is *crucial* for the existence and formation of nonlinear localized modes (Sievers & Takeno, 1988; MacKay & Aubry, 1994), which correspond to the "breathing" of DNA observed by biologists. It is important to notice that the existence of these nonlinear solutions is not linked to a particular mathematical expression of the potentials. Instead, it is a generic feature of nonlinear lattices having interactions qualitatively similar to those that connect the bases in DNA. Moreover, it has also been shown that thermal fluctuations can self-localize in such lattices so it is likely that related nonlinear excitations could exist in DNA. But discreteness has another consequence. Large-amplitude modes are strongly localized due to their high nonlinearity. Their width becomes of the order of the spacing between the bases and they lose the translational invariance of solitons in continuum media. The image of freely moving solitons has to be corrected by the pinning effect of discreteness, and the translation of the nonlinear excitations in DNA, if it occurs, has to be activated, for instance, by thermal fluctuations.

Proteins are much more complex than DNA because they do not have a quasi-periodic structure, but some of their substructures are nevertheless fairly regular. They are biological polymers composed of amino acids of the general formula

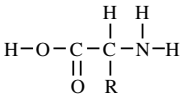

where R is an organic radical that determines the amino acid. These building blocks are linked by a peptide bond that can be viewed as a result of the elimination of a water molecule between consecutive amino acids, leading to the generic formula

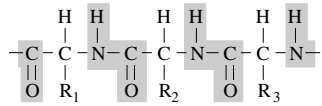

A given protein is defined by its sequence of amino acids chosen by 20 possible types and the length of the chain (typically 150–180 residues), but this so-called primary structure does not determine the function that depends on the spatial organization of the residues. Segments of the chain tend to fold into secondary structures having the shape of helices (called α-helices) or sheets (called β-sheets) stabilized by hydrogen bonds formed mainly between the negatively charged C = O groups and the positively charged protons linked to the nitrogen atom of a peptide bond. The different components of the secondary structure assemble in the tertiary structure, which is the functional form of the protein.

Proteins perform numerous functions and one of them is the storage and transport of the energy released by the hydrolysis of adenosine-triphosphate (ATP), which plays the role of the fuel necessary for many biological processes, such as muscle contraction. The hydrolysis of a single ATP molecule releases approximately 0.4 eV, which is transmitted to a protein for later use. This raises a puzzling question because, if this energy were distributed among all the degrees of freedom of a protein, each atom would carry such a small amount that the energy would be useless. There must be a mechanism that maintains this energy sufficiently localized, and moreover, as it will not be used at the site where it has been released, it must be transported efficiently within the molecule. Recent experiments at the molecular scale have shown that the hydrolysis of a single ATP molecule can be used for *several* steps of a molecular motor involved in muscle contraction (Kitamura et al., 1999), providing evidence of the temporary storage of the energy.

Attempting to understand these phenomena in 1973, Alexander Davydov noticed that the energy released by ATP hydrolysis almost coincides with 2 quanta of the vibrational energy of the C = O bond, which led him to the conclusion that this energy was stored as vibrational energy in the peptide bond (Scott, 1992). He conjectured that it could stay localized through an extrinsic nonlinearity associated with a distortion of the chain of hydrogen bonds that spans the α-helix. The underlying mechanism is similar to the one leading

to the formation of a polaron in solid-state physics (Ashcroft & Mermin, 1976). The vibration of the C = O bond strains the lattice in its vicinity, resulting in slight displacements of the neighboring amino acids. But, as the frequency of the C = O vibration is affected by its interactions with the neighboring atoms, the frequency of the excited C = O bond becomes slightly shifted and no longer coincides with the resonating frequencies of the neighboring C = O bonds, preventing an efficient transfer of energy to the neighboring sites. As a consequence, the energy released by the ATP hydrolysis does not spread along the protein.

Therefore, the basic idea behind the mechanism proposed by Davydov is nonlinear energy localization due to the shift of the frequency of an oscillator when it is excited. For the protein, it is not due to an intrinsic nonlinearity of the C = O bond (as was the case for the Morse potential linking the bases in a pair for DNA), but due to a coupling with another degree of freedom, which is an acoustic mode of the lattice of amino acids connected by hydrogen bonds.

As only a few quanta of the C = O vibrational motion are excited, the theory cannot ignore quantum effects, and in order to go beyond the qualitative picture discussed above, one has to solve the time-dependent Schrödinger equation. Davydov proposed a simple *ansatz* to describe the quantum state of the system. In this simple approximation, the motion of the self-trapped energy packet is described by a discrete form of the nonlinear Schrödinger equation. When one introduces proper parameters for the α-helix, the calculation of the soliton width shows that it is much broader than the lattice spacing, which should allow its motion without pinning by discreteness. As a result, energy transfer by solitons in the α-helix is plausible, but a definitive conclusion about the existence of such solitons is still pending. This is because the role of thermal fluctuations, which could destroy the coherence of the lattice distortion around the excited C = O site and hence the self-trapping, and the extent of quantum effects are hard to evaluate quantitatively (Peyrard, 1995). A direct experimental observation on a protein has not been possible up to now.

These uncertainties prompted physicists and physical chemists to experimentally investigate model systems that are simpler than proteins but, nevertheless, show chemical bonds comparable to the peptide bonds in proteins. Crystalline acetanilide consists of quasi-one-dimensional chains of hydrogen-bonded peptide groups. In the early 1980s, it was recognized by spectroscopic studies that the C = O stretching and N−H stretching bands of crystalline acetanilide exhibit anomalies, and tentative explanations involve self-trapped states similar to the Davydov solitons. These ideas have been confirmed by recent pump–probe experiments (Edler et al., 2002). A direct observation of self-trapping could be achieved, and it appears that the crystal structure is essential to stabilize the excitation that decays 20 times faster for isolated molecules than for molecules linked by hydrogen bonds in the crystal. Although the lifetime of the self-trapped state (20 ps) is shorter than expected by Davydov, this study supports the original idea of the importance of the coupling with the lattice degrees of freedom. A possible translational motion of the self-trapped state and its possible role for biological functions are still open questions.

The *News and Views* section of the journal *Nature* attests that nonlinear excitations in biomolecules have been the object of strong controversy, ranging from enthusiastic approval (Maddox, 1986, 1989) to harsh criticisms (Frank-Kamenetskii, 1987), which were justified by some of the overstatements by theoreticians. Today, passionate opinions have subsided and experiments at the scale of a single molecule have become feasible, showing us how biomolecules work or take their shape. Thus, it appears likely that while freely moving solitons along DNA or protein α-helices may not exist, nonlinear excitations leading to energy localization or storage, and perhaps transport, could well provide useful clues to understand some of the phenomena occurring in biomolecules.

MICHEL PEYRARD

See also **Davydov soliton; DNA premelting; DNA solitons; Pump-probe measurements**

Further Reading

Ashcroft, N.W. & Mermin, D.A. 1976. *Solid State Physics*, Philadelphia: Saunders Company

Calladine, C.R. & Drew, H.R. 1997. *Understanding DNA: The Molecule and How It Works*, 2nd edition, San Diego and London: Academic Press

Dauxois, T., Peyrard, M. & Bishop, A.R. 1993. Dynamics and thermodynamics of a nonlinear model for DNA denaturation. *Physical Review E*, 47: 684–695 and R44–R47

Edler, J., Hamm, P. & Scott, A.C. 2002. Femtosecond study of self-trapped vibrational excitons in crystalline acetanilide. *Physical Review Letters*, 88 (1–4): 067403

Englander, S.W., Kallenbach, N.R., Heeger, A.J., Krumhansl, J.A. & Litwin, S. 1980. Nature of the open state in long polynucleotide double helices: Possibility of soliton excitations. *Proceedings of the National Academy of Sciences USA*, 777: 7222–7227

Frank-Kamenetskii, M. 1987. Physicists retreat again. *Nature*, 328: 108

Kitamura, K., Tokunaga, M., Iwane A.H. & Yanagida, T. 1999. A single myosin head moves along an actin filament with regular steps of 5.3 nanometres. *Nature*, 397: 129–134

MacKay, R.S. & Aubry, S. 1994. Proof of existence of breathers for time-reversible or Hamiltonian networks of weakly coupled oscillators. *Nonlinearity*, 7: 1623–1643

Maddox, J. 1986. Physicists about to hi-jack DNA? *Nature*, 324: 11

Maddox, J. 1989. Towards the calculation of DNA. *Nature*, 339: 577

Peyrard, M. (editor). 1995. *Nonlinear Excitations in Biomolecules*, Berlin and New York: Springer

Schrödinger, E. 1944. *What is Life? The Physical Aspect of the Living Cell*, Cambridge: Cambridge University Press
Scott, A.C. 1992. Davydov's soliton. *Physics Reports*, 217: 1–67
Sievers, A.J. & Takeno, S. 1988. Intrinsic localized modes in anharmonic crystals. *Physical Review Letters*, 61: 970–973
Takeno, S. & Homma, S. 1983. Topological solitons and modulated structures of bases in DNA double helices. *Progress of Theoretical Physics*, 70: 308–311
Yakushevich, L.V. 1998. *Nonlinear Physics of DNA*, Chichester and New York: Wiley
Yomosa, S. 1984. Solitary excitations in deoxyribonucleic acid (DNA) double helices. *Physical Review* A, 30: 474–480

BIONS

See **Breathers**

BIRGE–SPONER RELATION

See **Local modes in molecules**

BIRKOFF–SMALE THEOREM

See **Phase space**

BISTABILITY

See **Equilibrium**

BISTABLE EQUATION

See **Zeldovich–Frank-Kamenetsky equation**

BJERRUM DEFECTS

Ice is the most common and important member in a class of solids in which the conduction of electricity is carried almost exclusively by protons. Its dc electrical conductivity reaches the level of $10^{-7}\ \Omega^{-1}\ \mathrm{m}^{-1}$, placing ice among the semiconductors. Known protonic semiconductors include disordered forms of solid water and several salt hydrates and gas hydrates. In the case of lithium hydrazinium sulfate ($LiN_2H_5SO_4$), one finds quasi-one-dimensional hydrogen-bonded chains (HBCs) along the c-crystallographic axis. Electrical conductivity is three orders of magnitude larger in the c-direction (compared with the perpendicular directions), demonstrating that proton conductivity is directly related to the presence of hydrogen bonds. In addition to inorganic crystals, protonic conductivity plays a significant role in biological systems, where it participates in energy transduction and formation of proton pumps. Of particular significance is proton transport across cellular membranes through the use of hydrogen-bonded side-chains of proteins embedded in membrane pores.

As is shown in Figures 1 and 2, protonic conductivity in HBCs takes place through ionic defects and bonding or "Bjerrum" defects (named after Danish physical chemist Niels Bjerrum). Ionic defects are formed by an excess proton (H_3O^+) or a proton vacancy (HO^-), while bonding defects are misfits in the orientations of neighboring atoms resulting in either vacant bonds (L defect) or placing two protons in the same bond (D defect). Bonding defects do not obey the Bernal–Fowler rule of one proton per hydrogen bond for the ideal ice crystal.

When a proton is transported along an HBC through an ionic defect, after the passage of the proton, the chain remains blocked to further proton movement since all chain protons have been moved, say, from the left-hand to the right-hand side of each hydrogen bond. The chain gets unblocked through cooperative rotations, that is, through the passage of a bonding defect. Thus, protons move in an HBC through coordinated ionic and Bjerrum defects, using a mechanism that is also found in hydrogen-bonded protein side chains. Coordinated proton transport in biological macromolecules leads to the formation of proton pumps that channel protons across membranes and, through reversals, produce cyclic motor actions of mechanical nature. Defects in HBCs are topological in nature, with the rotational activation energy being smaller than that of ionic defect energy. The total charge of the topological ionic and bonding defects is not the same; in ice, the ionic defect charge is $e_I = 0.64e$ (e is the proton charge), while the bonding defect charge is $e_B = 0.36e$. Only after a coordinated passage of an ionic and bonding defect is one entire proton charge transferred across the HBC.

A simple one-dimensional cooperative model of an HBC is similar to the Frenkel–Kontorova model but with two alternating barriers modeling bonding and ionic activation energies. The minima separating the barriers correspond to equilibrium positions of protons that interact mutually through dipole-dipole interactions. In equilibrium under this model, there is initially one proton per hydrogen bond; transitions of protons over the large barriers correspond to ionic defects, while bonding defects result from transitions over the smaller barrier. Both classes of defects are modeled through topological solitons. There are two kink solutions corresponding to HO^- and L-bonding defects, while the corresponding antikinks are the H_3O^+ and D-bonding defects, respectively.

This simple model can be made quantitative through the introduction of the one-dimensional Hamiltonian

$$H = \sum_n \left[\frac{p_n^2}{2} + \frac{1}{2}(u_{n+1} - u_n)^2 + \omega V(u_n) \right], \quad (1)$$

where u_n and p_n are the dimensionless displacement from an equilibrium position and momentum, respectively, of the nth hydrogen that is coupled to its nearest

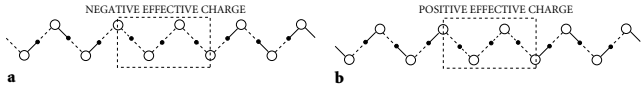

Figure 1. Ionic defects present in a hydrogen bonded chain: (a) negative ionic defect HO^- and (b) positive ionic defect H_3O^+. Large open circles denote ions, for example, oxygen ions in ice, while small black dots are protons. A hydrogen bond that links two ions contains a covalent part (solid line) that places in equilibrium the proton closer to one of the two oxygens. In the ionic defect region, there is a gradual transition in the equilibrium locations of protons within the hydrogen bonds; this transitional region is modeled through a topological soliton.

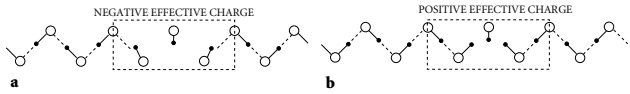

Figure 2. Bonding defects in a hydrogen bonded chain: (a) negative bonding defect (L) and (b) positive bonding defect (D). Molecular rotations introduce additional protons or remove protons from the quasi-one-dimensional HBC and produce bonding defects.

neighboring protons through harmonic spring interaction, while ω sets the energy scale. A typical choice for $V(u_n)$, the nonlinear substrate potential that models the ionic and bonding barriers, is

$$V(u_n) = \frac{2}{1-\alpha^2}\left[\cos(\frac{u_n}{2}) - \alpha\right]^2. \qquad (2)$$

The substrate potential (2) is periodic and (for appropriate values of the parameter α) is doubly periodic with two distinct alternating maxima that separate degenerate minima. In this model, one assumes one proton per unit cell, the latter consisting of the larger ionic barrier with its adjacent minima, one on each side. In the strongly cooperative limit, where neighboring hydrogen displacements do not differ substantially, one obtains for the proton displacement $u(x,t)$ that becomes a function of the continuous space variable x as well as time t the double sine-Gordon partial differential equation:

$$u_{tt} - c^2 u_{xx} + \frac{\omega^2}{1-\alpha^2}\left[-\sin u + 2\alpha \sin\frac{u}{2}\right] = 0, \qquad (3)$$

where c is the speed of sound of the linearized lattice oscillations. This sine-Gordon model has as solutions two sets of soliton kinks as well as their corresponding antikinks representing L-Bjerrum (kink I), D-Bjerrum (antikink I), HO^- ionic (kink II) and H_3O^+ (antikink II). More complex nonlinear models can be constructed that also include an acoustic interaction between neighboring ions as well as coupling of protons with ions. In these cases, one obtains two component solitons where the defects in the proton sublattice are topological solitons that induce a polaronic-like deformation in the ionic lattice. This more complex defect can travel along an HBC when an external electric field is applied in the system. Numerical simulations demonstrate that these nonlinear defects do indeed encompass some of the basic dynamical properties of the ionic and bonding defects found in hydrogen-bonded networks.

G.P. Tsironis

See also **Frenkel–Kontorova model; Hydrogen bond; Sine-Gordon equation; Topological defects**

Further Reading

Hobbs, P.V. 1974. *Ice Physics*, Oxford: Clarendon Press

Pnevmatikos, St. 1988. Soliton dynamics of hydrogen-bonded networks: a mechanism for proton conductivity. *Physical Review Letters,* 60: 1534–1537

Pnevmatikos, St., Tsironis, G.P. & Zolotaryuk, A.V. 1989. Nonlinear quasiparticles in hydrogen-bonded systems. *Journal of Molecular Liquids*, 41: 85–103

Savin, A.V, Tsironis, G.P. & Zolotaryuk, A.V. 1997. Reversal effects in stochastic kink dynamics. *Physical Review* E, 56: 2457–2466

Zolotaryuk, A.V., Pnevmatikos, St. & Savin, A.V. 1991. Charge transport by solitons in hydrogen-bonded materials. *Physical Review Letters*, 67: 707–710

BLACK HOLES

A massive body like the Earth is characterized by an "escape velocity," which is the speed that a moving particle must have on leaving the surface of the body to leave the attraction of gravity. Consider a bullet at the surface of the Earth that is moving upward with a speed of 11.2 km/s and neglect atmospheric friction. Such a bullet will just escape Earth's gravitational field by exchanging its kinetic energy for the potential energy of the gravitational field. If the mass of the Earth were compressed into a smaller radius, this escape velocity would be larger, because the gravitational energy to be overcome by the kinetic energy of the bullet would be larger.

In 1916, Karl Schwarzschild used Einstein's gravitational field equations to show that if a body of mass m is compressed to a radius

$$r_s = \frac{2Gm}{c^2}, \quad (1)$$

where G is the gravitational constant, then an object traveling at the speed of light c will be unable to escape the influence of gravity (Schwarzschild, 1916). For a body having the mass of the Earth, this "Schwarzschild radius" is about 1 cm, and for the Sun, it is about 3 km. Interestingly, Schwarzschild's idea was first suggested in the 18th century (Mitchell, 1783; Laplace, 1796).

The term "black hole" was coined by John Archibald Wheeler in 1967 to denote a cosmic object with its mass concentrated within the Schwarzschild radius. Neither particles nor light can overcome gravitational attraction and travel outside the sphere of radius r_s. Interestingly, Stephen Hawking (1974) has shown that—due to quantum fluctuations—a black hole should radiate as a black body with the temperature

$$T = \frac{hc}{4\pi k r_s}, \quad (2)$$

where k and h are, respectively, the Boltzmann and Planck constants. Indirect evidence for black holes is provided by the fact that there do not exist stable cold stars with masses larger than about three Sun masses. Under its own gravitational field, according to theory, such a star should collapse into a black hole. In 1931, Subrahmanyan Chandrasekhar was the first to conclude that above some critical mass of white dwarfs, the equation of state (of a quantum relativistic gas of degenerate Fermi particles) is too weak to counter the gravitational forces, leading to the formation of black holes. Both Lev Landau (1932) and Arthur Eddington (1924) rejected this implication of relativistic quantum mechanics rather than accept the possibility of black holes. Albert Einstein also concluded that Schwarzschild singularities do not exist in the real world (Einstein, 1939).

In 1939, however, J. Robert Oppenheimer and his colleagues used general relativity (rather than Newtonian gravity) to show that when all thermonuclear sources of energy are exhausted (with no further outward pressure due to radiation), a sufficiently heavy star will continue to contract indefinitely, never reaching equilibrium (Oppenheimer & Volkoff, 1939; Oppenheimer & Snyder, 1939). Oppenheimer et al. further noted that if one considers stellar collapse from the inside, a stationary observer sees the stellar surface moving inward to the Schwarzschild sphere and finally sees the surface freeze as it nears the Schwarzschild sphere. Moreover, they showed that observers who move inward with the collapsing matter do not observe such freezing; these observers could cross the critical surface ("event horizon") after a finite time on their own clocks, after which they have no possibility of sending a signal that could be detected by an observer located outside the collapsing matter.

Recently, the scientific history of black holes has been characterized by a rapid growth of observational, theoretical, and mathematical studies, in which the discovery of such compact objects becomes the main purpose (Thorne et al., 1986). Currently, the most important classes are black holes of stellar masses (about 3–10 solar masses) and super-massive black holes. The most convincing candidates for stellar black holes are binary X-ray sources, one component of which is an ordinary star and the other component is a black hole or neutron star (Novikov & Zeldovich, 1966). Estimates of the masses of compact objects in these systems are essentially greater than three solar masses, and one example of such a system is Cygnus X-1 (V 1357 Cyg). The present number of systems mentioned as possible candidates for black holes with stellar masses is about 20, all of which are X-ray sources in binary systems (Novikov & Frolov, 2001). In the case of super-massive black holes and nuclei of Seyfert galaxies, interpretations of the observable effects using the black hole theory seem the most simple and natural; for example, Galaxy M 31 is a black hole candidate having a mass of about 3×10^7 the Sun's mass (Novikov & Frolov, 2001).

Presently, the concept of black holes continues to be confirmed by direct observations and is used to explain observable astronomical effects related to exceptionally strong emission of energy. Thus, it is expected that in the future new astronomical objects will be detected near black holes, and new physical phenomena will be discovered that can be interpreted using the black hole concept. Along these lines, it is interesting to note recent work in which concepts from thermodynamics and information theory (such as temperature and entropy) are connected with black holes based on Hawking's ideas (Markov, 1965; Hawking, 1977). Also of interest are "artificial black holes," which do not compress a large amount of mass into a small volume, but reduce the speed of light in a moving medium to less than the speed of the medium, thereby creating an event horizon (Leonhardt, 2001).

VIATCHESLAV KUVSHINOV

See also **Binding energy; Einstein equations; General relativity**

Further Reading

Chandrasekhar, S. 1931. The maximum mass of ideal white dwarfs. *Astrophysical Journal*, 74: 81

Eddington, A. 1924. A comparison of Whitehead's and Einstein's formulae. *Nature*, 113: 192

Einstein, A. 1939. On a stationary system with spherical symmetry consisting of many gravitating masses. *Annals of Mathematics*, 40: 922

Hawking, S.W. 1974. Black hole explosions. *Nature*, 248: 30–31

Hawking, S.W. 1977. Gravitational instantons. *Physics Letters* A, 60: 81
Landau, L.D. 1932. On the theory of stars. *Physikalische Zeitschrift der Sowjetunion*, 1: 285
Laplace, P.-S. 1796. *Exposition du système du monde*, [Description of the World System], Paris
Leonhardt, U. 2001. A laboratory analogue of the event horizon using slow light in an atomic medium. *Nature*, 415: 406–409
Markov, M.A. 1965. Can the gravitational field prove essential for the theory of elementaryparticles? *Progress of Theoretical Physics*, (Suppl): 85–95
Mitchell, J. 1783. *Transactions of the Royal Society of London*, 74: 35
Novikov, I.D. & Frolov, V.P. 2001. Black holes in the Universe. *Physics-Uspekhi*, 44(3): 291
Novikov, I.D. & Zeldovich, Ya.B. 1966. *Nuovo Cimento*, 4 (Suppl.): 810
Oppenheimer, J.R. & Snyder, M. 1939. On continued gravitational contraction. *Physical Review*, 56: 455
Oppenheimer J.R. & Volkoff, G.M. 1939. On massive neutron cores. *Physical Review*, 55: 374–381
Schwarzschild, K. 1916. Über das Gravitational eines Massenpunktes nach der Einsteineschen Theory. *Sitzungsberichte der Preusischen Akademie der Wissenschaften zu Berlin, Physik-Mathematik, Kl.*: 189–196
Thorne, K.S., Price, R.H. & MacDonald, D.A. (editors). 1986. *Black Holes: The Membrane Paradigm*, New Haven: Yale University Press

BLOCH DOMAIN WALL

See **Domain walls**

BLOCH FUNCTIONS

See **Periodic spectral theroy**

BLOWOUT BIFURCATION

See **Intermittency**

BLOW-UP (COLLAPSE)

See **Development of singularities**

BOHR–SOMMERFELD QUANTIZATION

See **Quantum theory**

BOOMERONS

See **Solitons, types of**

BORN–INFELD EQUATIONS

Classical linear vacuum electrodynamics with point massive charged particles has two limiting properties: the electromagnetic energy of a point particle field is infinity, and a Lorentz force must be postulated to describe interactions between point particles and an electromagnetic field. Nonlinear vacuum electrodynamics can be free of these imperfections.

Gustav Mie (1912–1913) considered a nonlinear electrodynamics model in the framework of his "Fundamental unified theory of matter." In this theory the electron is represented by a nonsingular solution with a finite electromagnetic energy, but Mie's field equations are noninvariant under the gauge transformation for an electromagnetic four-potential (addition of the four-gradient of an arbitrary scalar function).

Max Born (1934) considered a nonlinear electrodynamics model that is invariant under the gauge transformation. A stationary electron in this model is represented by an electrostatic field configuration that is everywhere finite, in contrast to the case of linear electrodynamics when the electron's field is infinite at the singular point (see Figure 1). The central point in Born's electron is also singular because there is a discontinuity of electrical field at this point (hedgehog singularity). The full electromagnetic energy of this electron's field configuration is finite.

Born and Leopold Infeld (1934) then considered a more general nonlinear electrodynamics model, which has the same solution associated with the electron. Called Born–Infeld electrodynamics, this model is based on the Born–Infeld equations, which have the form of Maxwell's equations, including electrical and magnetic field strengths $\boldsymbol{E}$, $\boldsymbol{H}$, and inductions $\boldsymbol{D}$, $\boldsymbol{B}$ with nonlinear constitutive relations $\boldsymbol{D} = \boldsymbol{D}(\boldsymbol{E}, \boldsymbol{B})$, $\boldsymbol{H} = \boldsymbol{H}(\boldsymbol{E}, \boldsymbol{B})$ of a special kind. For inertial reference frames and in the region outside of field singularities, these equations are

$$\begin{cases} \operatorname{div} \boldsymbol{B} = 0, \\ \dfrac{1}{c}\dfrac{\partial \boldsymbol{B}}{\partial t} + \operatorname{curl} \boldsymbol{E} = 0, \\ \operatorname{div} \boldsymbol{D} = 0, \\ \dfrac{1}{c}\dfrac{\partial \boldsymbol{D}}{\partial t} - \operatorname{curl} \boldsymbol{H} = 0, \end{cases} \tag{1}$$

where

$$\boldsymbol{D} = \frac{1}{\mathcal{L}}\left(\boldsymbol{E} + \chi^2 \mathcal{J}\boldsymbol{B}\right),$$
$$\boldsymbol{H} = \frac{1}{\mathcal{L}}\left(\boldsymbol{B} - \chi^2 \mathcal{J}\boldsymbol{E}\right), \tag{2}$$

$$\mathcal{L} \equiv \sqrt{|\,1 - \chi^2 \mathcal{I} - \chi^4 \mathcal{J}^2\,|},$$
$$\mathcal{I} = \boldsymbol{E}\cdot\boldsymbol{E} - \boldsymbol{B}\cdot\boldsymbol{B}, \quad \mathcal{J} = \boldsymbol{E}\cdot\boldsymbol{B}. \tag{3}$$

Relations (2) can be resolved for $\boldsymbol{E}$ and $\boldsymbol{H}$:

$$\boldsymbol{E} = \frac{1}{\mathcal{H}}\left(\boldsymbol{D} - \chi^2 \boldsymbol{\mathcal{P}} \times \boldsymbol{B}\right),$$
$$\boldsymbol{H} = \frac{1}{\mathcal{H}}\left(\boldsymbol{B} + \chi^2 \boldsymbol{\mathcal{P}} \times \boldsymbol{D}\right), \tag{4}$$

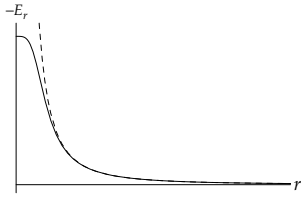

Figure 1. Radial components of electrical field for Born's electron and purely Coulomb field (dashed).

where $\mathcal{H}=\sqrt{1+\chi^2\left(\boldsymbol{D}^2+\boldsymbol{B}^2\right)+\chi^4\,\boldsymbol{\mathcal{P}}^2}$, $\boldsymbol{\mathcal{P}}\equiv\boldsymbol{D}\times\boldsymbol{B}$. Using relations (4) for Eq. (1), the fields $\boldsymbol{D}$ and $\boldsymbol{B}$ are unknown.

The symmetrical energy-momentum tensor for Born–Infeld equations has the following components:

$$T^{00}=\frac{1}{4\pi\,\chi^2}\,(\mathcal{H}-1)\,,\quad T^{0i}=\frac{1}{4\pi}\,\mathcal{P}^i,$$
$$T^{ij}=\frac{1}{4\pi}\left\{\delta^{ij}\left[\boldsymbol{D}\cdot\boldsymbol{E}+\boldsymbol{B}\cdot\boldsymbol{H}-\chi^{-2}\,(\mathcal{H}-1)\right]-\left(D^i\,E^j+B^i\,H^j\right)\right\}. \tag{5}$$

In spherical coordinates, the field of Born's static electron solution may have only radial components

$$D_r=\frac{e}{r^2},\quad E_r=\frac{e}{\sqrt{\bar r^4+r^4}}, \tag{6}$$

where e is the electron's charge and $\bar r\equiv\sqrt{|\chi\,e|}$. At the point $r=0$, the electrical field has the maximum absolute value

$$|E_r(0)|=\frac{|e|}{\bar r^2}=\frac{1}{\chi}\,, \tag{7}$$

which Born and Infeld called the absolute field constant.

The energy of field configuration (6) is

$$m=\int T^{00}\,\mathrm{d}V=\frac{2}{3}\,\beta\,\frac{\bar r^3}{\chi^2}, \tag{8}$$

where the volume integral is calculated over the whole space, and

$$\beta\equiv\int_0^\infty\frac{\mathrm{d}r}{\sqrt{1+r^4}}=\frac{\left[\Gamma\left(\frac{1}{4}\right)\right]^2}{4\sqrt{\pi}}\approx 1.8541. \tag{9}$$

In view of the definition for $\bar r$ below (6), Equation (8) yields

$$\bar r=\frac{2}{3}\,\beta\,\frac{e^2}{m}. \tag{10}$$

Considering m as the mass of electron and using (7), Born & Infeld (1934) estimated the absolute field constant $\chi^{-1}\approx 3\times 10^{20}\,\mathrm{V/m}$. Later, Born & Schrödinger (1935) gave a new estimate (two orders of magnitude less) based on some considerations taking into account the spin of the electron. (Of course, such estimates may be corrected with more detailed models.)

An electrically charged solution of the Born–Infeld equations can be generalized to a solution with the singularity having both electrical and magnetic charges (Chernitskii, 1999). A corresponding hypothetical particle is called a dyon (Schwinger, 1969). Nonzero (radial) components of fields for this solution have the form

$$D_r=\frac{\mathscr{E}}{r^2},\quad E_r=\frac{\mathscr{E}}{\sqrt{\bar r^4+r^4}},$$
$$B_r=\frac{\mathscr{B}}{r^2},\quad H_r=\frac{\mathscr{B}}{\sqrt{\bar r^4+r^4}}, \tag{11}$$

where $\mathscr{E}$ is the electric charge and $\mathscr{B}$ is the magnetic one; $\bar r\equiv\left[\chi^2\left(\mathscr{E}^2+\mathscr{B}^2\right)\right]^{1/4}$. The energy of this solution is given by Equation (8) with this definition for $\bar r$. It should be noted that space components of electromagnetic potential for the static dyon solution have a line singularity.

A generalized Lorentz force appears when a small, almost constant field $\tilde{\boldsymbol{D}}$, $\tilde{\boldsymbol{B}}$ is considered in addition to the moving dyon solution. The sum of the field $\tilde{\boldsymbol{D}}$, $\tilde{\boldsymbol{B}}$ and the field of the dyon with varying velocity is taken as an initial approximation to some exact solution. Conservation of total momentum gives the following trajectory equation (Chernitskii, 1999):

$$m\,\frac{\mathrm{d}}{\mathrm{d}t}\,\frac{\boldsymbol{v}}{\sqrt{1-\boldsymbol{v}^2}}=\mathscr{E}\left(\tilde{\boldsymbol{D}}+\boldsymbol{v}\times\tilde{\boldsymbol{B}}\right)+\mathscr{B}\left(\tilde{\boldsymbol{B}}-\boldsymbol{v}\times\tilde{\boldsymbol{D}}\right), \tag{12}$$

where $\boldsymbol{v}$ is the velocity of the dyon, and m is the energy for static dyon defined by (8).

A solution with two dyon singularities (called a bidyon) having equal electric ($\mathscr{E}=e/2$) and opposite magnetic charges can be considered as a model for a charged particle with spin (Chernitskii, 1999). Such a solution has both angular momentum and magnetic moment.

A plane electromagnetic wave with arbitrary polarization and form in the direction of propagation (without coordinate dependence in a perpendicular plane) is an exact solution to the Born–Infeld equations. The simplest case assumes one nonzero component of the vector potential ($A_y\equiv\phi(t,x)$), whereupon Equations (1) reduce to the linearly polarized plane wave equation

$$\left(1+\chi^2\,\phi_x^2\right)\phi_{tt}-\chi^2\,2\,\phi_x\,\phi_t\,\phi_{xt}-\left(c^2-\chi^2\,\phi_t^2\right)\phi_{xx}=0 \tag{13}$$

with indices indicating partial derivatives. Sometimes called the Born–Infeld equation, Equation (13) has solutions $\phi=\zeta(x^1-x^0)$ and $\phi=\zeta(x^1+x^0)$, where $\zeta(x)$ is an arbitrary function (Whitham, 1974). Solutions

comprising two interacting waves propagating in opposite directions are obtained via a hodograph transform (Whitham, 1974). Brunelli & Ashok (1998) have found a Lax representation for solutions of this equation.

A solution to the Born–Infeld equations, which is the sum of two circularly polarized waves propagating in different directions, was obtained by Erwin Schrödinger (1943).

Equations (1) with relations (2) have an interesting characteristic equation (Chernitskii, 1998)

$$g^{\mu\nu}\frac{\partial\Phi}{\partial x^{\mu}}\frac{\partial\Phi}{\partial x^{\nu}}=0, \quad g^{\mu\nu}\equiv g^{\mu\nu}-4\pi\,\chi^{2}\,T^{\mu\nu}, \quad (14)$$

where $\Phi(x^{\mu})=0$ is an equation of the characteristic surface and $T^{\mu\nu}$ are defined by (5). This form for $g^{\mu\nu}$, including in addition the energy-momentum tensor, is special for Born–Infeld equations.

The Born–Infeld model also appears in the quantized string theory (Fradkin & Tseytlin, 1985) and in Einstein's unified field theory with a nonsymmetrical metric (Chernikov & Shavokhina, 1986). In general, this nonlinear electrodynamics model is connected with ideas of space-time geometrization and general relativity (see Eddington, 1924; Chernitskii, 2002).

ALEXANDER A. CHERNITSKII

See also **Einstein equations; Hodograph transform; Matter, nonlinear theory of; String theory**

Further Reading

Born, M. 1934. On the quantum theory of the electromagnetic field. *Proceedings of the Royal Society of London* A, 143: 410–437

Born, M. & Infeld, L. 1934. Foundation of the new field theory. *Proceedings of the Royal Society of London* A, 144: 425–451

Born, M. & Schrödinger, E. 1935. The absolute field constant in the new field theory. *Nature*, 135: 342

Brunelli, J.C. & Ashok, D. 1998. A Lax representation for Born–Infeld equation. *Physics Letters* B, 426: 57–63

Chernikov, N.A. & Shavokhina, N.S. 1986. The Born–Infeld theory as part of Einstein's unified field theory. *Soviet Mathematics*, (Izvestiya Vgsikish Uchebnykh Zaverdenii), 30(4): 81–83

Chernitskii, A.A. 1998. Light beams distortion in nonlinear electrodynamics. *Journal of High Energy Physics*, 11, 15: 1–5

Chernitskii, A.A. 1999. Dyons and interactions in nonlinear (Born–Infeld) electrodynamics. *Journal of High Energy Physics*, 12, 10: 1–34

Chernitskii, A.A. 2002. Induced gravitation as nonlinear electrodynamics effect. *Gravitation & Cosmology*, 8 (Suppl.), 123–130

Eddington, A.S. 1924. *The Mathematical Theory of Relativity*, Cambridge: Cambridge University Press

Fradkin, R.S. & Tseytlin, A.A. 1985. Nonlinear electrodynamics from quantized strings. *Physics Letters* B, 163: 123–130

Mie, G. 1912–13. Grundlagen einer theorie der materie. *Annalen der Physik*, 37: 511–534; 39: 1–40: 40: 1–66

Schrödinger, E. 1942. Dynamics and scattering-power of Born's electron. *Proceedings of the Royal Irish Academy* A, 48: 91–122

Schrödinger, E. 1943. A new exact solution in non-linear optics (two-wave system). *Proceedings of the Royal Irish Academy* A, 49: 59–66

Schwinger, J. 1969. A magnetic model of matter. *Science*, 165: 757–761

Whitham, G.B. 1974. *Linear and Nonlinear Waves*, New York: Wiley

BOSE–EINSTEIN CONDENSATION

Bose–Einstein condensation (BEC) is the occupation of a single quantum state by a large number of identical particles, which implies that the particles are bosons, satisfying Bose–Einstein statistics and allowing for many particles to pile up in the same quantum state. This is in contrast to fermions, satisfying Fermi–Dirac statistics, for which the Pauli exclusion principle forbids the occupation of any single quantum state by more than one particle.

The role of quantum correlations caused by Bose–Einstein statistics is crucial for the occurrence of BEC. These statistics were advanced by Satyendranath Bose (1924) for photons, having zero mass, and generalized by Albert Einstein (1924) to particles with nonzero masses. Einstein (1925) also described the phenomenon of condensation in ideal gases. The possibility of BEC in weakly nonideal gases was theoretically demonstrated by Nikolai Bogolubov (1947). The wave function of Bose-condensed particles in dilute gases satisfies the Gross–Pitaevskii equation, suggested by Gross (1961) and Pitaevskii (1961). Its mathematical structure is that of the nonlinear Schrödinger equation. Experimental evidence of BEC in weakly interacting confined gases was achieved 70 years after Einstein's prediction, almost simultaneously, by three experimental groups (Anderson et al., 1995; Bradley et al., 1995; Davis et al., 1995).

To say that many particles are in the same quantum state implies that these particles display state coherence, a particular example of coherence phenomena requiring the particles to be strongly correlated with each other. The necessary conditions may be qualitatively understood by applying the de Broglie duality arguments to an ensemble of atoms in thermodynamic equilibrium at temperature T. Then the thermal energy of an atom is given by $k_{\mathrm{B}}T$, where k_{B} is the Boltzmann constant. This energy defines the thermal wavelength

$$\lambda_{\mathrm{T}}\equiv\sqrt{2\pi\hbar^{2}/m_{0}k_{\mathrm{B}}T} \quad (1)$$

for an atom of mass m_0, with $\hbar$ being the Planck constant. Thus, an atom can be associated with a matter wave characterized by the wavelength (λ_{T}). Atoms become correlated with each other when their related waves overlap, which requires that the wavelength be larger than the mean interatomic distance, $\lambda_{\mathrm{T}}>a$. The average atomic density $\rho\equiv N/V$ for N atoms in

volume V is related to the mean distance a through the equality $\rho a^3 = 1$. Hence, condition $\lambda_T > a$ may be rewritten as $\rho\lambda_T^3 > 1$. With the thermal wavelength (1), this yields the inequality

$$T < \frac{2\pi\hbar^2}{m_0 k_B}\,\rho^{2/3}, \tag{2}$$

which implies that state coherence may develop if the temperature is sufficiently low or the density of particles is sufficiently high.

An accurate description of BEC for an ideal gas is based on the Bose–Einstein distribution

$$n(\boldsymbol{p}) = \left[\exp\left(\frac{\varepsilon_p - \mu}{k_B T}\right) - 1\right]^{-1}, \tag{3}$$

describing the density of particles with a single-particle energy $\varepsilon_p = p^2/2m_0$ for a momentum $\boldsymbol{p}$ and with a chemical potential μ. The latter is defined from the condition $N = \sum_p n(\boldsymbol{p})$ for the total number of particles. Assuming the thermodynamic limit

$$N \to \infty, \qquad V \to \infty, \qquad \frac{N}{V} \to \text{const}$$

allows the replacement of summation over $\boldsymbol{p}$ by integration. Then, the fraction of particles, condensing to the state with $\boldsymbol{p} = 0$ is

$$n_0 \equiv \frac{N_0}{N} = 1 - \left(\frac{T}{T_c}\right)^{3/2} \tag{4}$$

below the condensation temperature

$$T_c = \frac{2\pi\hbar^2\rho^{2/3}}{m_0 k_B \zeta^{2/3}}, \tag{5}$$

where $\zeta \approx 2.612$. Above the critical temperature (5), $n_0 = 0$. The latter is about half of the right-hand side of inequality (2).

The condensate fraction (4) is derived for an ideal (noninteracting) Bose gas. A weakly nonideal (weakly interacting) Bose gas also displays Bose–Einstein condensation, although particle interactions deplete the condensate so that at zero temperature the condensate fraction is smaller than unity ($n_0 < 1$). A system is called weakly interacting if the characteristic interaction radius r_{int} is much shorter than the mean interparticle distance ($r_{int} \ll a$). This inequality can be rewritten as $\rho r_{int}^3 \ll 1$, and such a system is termed dilute.

Superfluid liquids, such as liquid ^{4}He, are far from being dilute, but it is commonly believed that the phenomenon of superfluidity is somehow connected with BEC. Although an explicit relation between the superfluid and condensate fractions is not known, theoretical calculations and experimental observations for superfluid helium estimate the condensate fraction at $T = 0$ as $n_0 \approx 0.1$.

A strongly correlated pair of fermions can be treated approximately as a boson, allowing superfluidity in liquid ^{3}He to be interpreted as the condensation of coupled fermions. Similarly, superconductivity is often compared with the condensation of the Cooper pairs that are formed by correlated electrons or holes. One should understand, however, that the superconductivity of fermions is analogous to but not identical to BEC of bosons.

An ideal object for the experimental observation of BEC is a dilute atomic Bose gas confined in a trap and cooled down to temperatures satisfying condition (2). Such experiments with different atomic gases have been recently realized, BEC has been explicitly observed, and a variety of its features have been carefully investigated. It has been demonstrated that the system of Bose-condensed atoms displays a high level of state coherence.

There exist different types of traps (single- and double-well), magnetic, optical, and their combinations, which make it possible to confine atoms for sufficiently long times of up to 100s. Using a standing wave of laser light, multi-well periodic effective potentials called optical lattices have been obtained, which have allowed the demonstration of a number of interesting effects, including Bloch oscillations, Landau–Zener tunneling, Josephson current, Wannier–Stark ladders, Bragg diffraction, and so on.

Displaying a high level of state coherence, an ensemble of Bose-condensed atoms forms a matter wave that is analogous to a coherent electromagnetic wave from a laser. Therefore, a device emitting a coherent beam of Bose atoms is called an atom laser.

The realization of BEC of dilute trapped gases is important for several reasons. First, this demonstrated the phenomenon predicted by Einstein in the 1920s. Note that a direct observation of BEC in superfluid helium—despite enormous experimental efforts—has never been achieved. Second, dilute atomic gases are simple statistical systems that can serve as a touchstone for testing different theoretical approaches. Finally, Bose-condensed trapped gases display a variety of interesting properties that promise diverse practical applications.

V.I. Yukalov

See also **Coherence phenomena; Critical phenomena; Lasers; Nonequilibrium statistical mechanics; Nonlinear optics; Nonlinear Schrödinger equations; Order parameters; Phase transitions; Quantum nonlinearity; Quantum theory; Superconductivity; Superfluidity**

Further Reading

Anderson, M.H., Ensher, J.R., Matthews, M.R., Wieman, C.E. & Cornell, E.A. 1995. Observation of Bose–Einstein condensation in a dilute atomic vapor. *Science*, 269: 198–201

Bogolubov, N.N. 1947. On the theory of superfluidity. *Journal of Physics*, 11: 23–32

Bose, S.N. 1924. Plancks gesetz und lichtquantenhypothese. *Zeitschrift für Physik*, 26: 178–181

Bradley, C.C., Sackett, C.A., Tollett, J.J. & Hulet, R.G. 1995. Evidence of Bose–Einstein condensation in an atomic gas with attractive interactions. *Physical Review Letters*, 75: 1687–1690

Coleman, A.J. & Yukalov, V.I. 2000. *Reduced Density Matrices*, Berlin: Springer

Courteille, P.W., Bagnato, V.S. & Yukalov, V.I. 2001. Bose–Einstein condensation of trapped atomic gases. *Laser Physics*, 11: 659–800

Dalfovo, F., Giorgini, S., Pitaevskii, L.P. & Stringari, S. 1999. Theory of Bose–Einstein condensation in trapped gases. *Reviews of Modern Physics*, 71: 463–512

Davis, K.B., Mewes, M.O., Andrews, M.R., van Drutten, N.J., Durfee, D.S., Kurn, D.M. & Ketterle, W. 1995. Bose–Einstein condensation in a gas of sodium atoms. *Physical Review Letters*, 75: 3969–3973

Einstein, A. 1924. Quantentheorie des einatomigen idealen gases. *Sitzungsberichte der Preussischen Akademie der Wissenschaften, Physik-Mathematik*, 261–267

Einstein, A. 1925. Quantentheorie des einatomigen idealen gases. Zweite abhandlung. *Sitzungsberichte der Preussischen Akademie der Wissenschaften, Physik-Mathematik*, 3–14

Gross, E.P. 1961. Structure of a quantized vortex in boson systems. *Nuovo Cimento*, 20: 454–477

Huang, K. 1963. *Statistical Mechanics*, New York: Wiley

Klauder, J.R. & Skagerstam, B.S. 1985. *Coherent States*, Singapore: World Scientific

Lifshitz, E.M. & Pitaevskii, L.P. 1980. *Statistical Physics: Theory of Condensed State*, Oxford: Pergamon

Nozières, P. Pines, D. 1990. *Theory of Quantum Liquids: Superfluid Bose Liquids*, Redwood, CA: Addison-Wesley

Parkins, A.S. & Walls, D.F. 1998. The physics of trapped dilute-gas Bose–Einstein condensates. *Physics Reports*, 303: 1–80

Pitaevskii, L.P. 1961. Vortex lines in an imperfect Bose gas. *Journal of Experimental and Theoretical Physics*, 13: 451–455

Ter Haar, D. 1977. *Lectures on Selected Topics in Statistical Mechanics*, Oxford: Pergamon

Yukalov, V.I. & Shumovsky, A.S. 1990. *Lectures on Phase Transitions*, Singapore: World Scientific

Ziff, R.M., Uhlenbeck, G.E. & Kac, M. 1977. The ideal Bose-Einstein gas revisited. *Physics Reports*, 32: 169–248

BOSONS

See **Quantum nonlinearity**

BOUNDARY LAYERS

The Navier–Stokes system is the basic mathematical model for viscous incompressible flows. It reads

$$(\mathrm{NS}_\nu) \qquad \begin{cases} \partial_t \boldsymbol{u} + \boldsymbol{u}\cdot\nabla\boldsymbol{u} - \nu\Delta\boldsymbol{u} + \nabla p = 0, \\ \operatorname{div}(\boldsymbol{u}) = 0, \\ \boldsymbol{u} = 0 \quad \text{on} \quad \partial\Omega, \end{cases} \tag{1}$$

where $\boldsymbol{u}$ is the velocity, p is the pressure, and ν is the viscosity. We can define a typical length scale L and a typical velocity U. The dimensionless parameter or Reynolds number, $Re = UL/\nu$, is very important to compare the properties of different flows. Indeed, two flows having the same Re have the same properties. When Re is very large (ν very small), the Navier–Stokes system (NS_ν) behaves like the Euler system

$$(\text{Euler}) \qquad \begin{cases} \partial_t \boldsymbol{U} + \boldsymbol{U}\cdot\nabla\boldsymbol{U} + \nabla p = 0, \\ \operatorname{div}(\boldsymbol{U}) = 0, \\ \boldsymbol{U}.n = 0 \quad \text{on} \quad \partial\Omega. \end{cases} \tag{2}$$

In the region close to the boundary, the length scale becomes very small and we cannot neglect viscous effects. In 1905, Ludwig Prandtl suggested that there exists a thin layer called the boundary layer, where the solution $\boldsymbol{u}$ undergoes a sharp transition from a solution to the Euler system to the no-slip boundary condition $\boldsymbol{u} = 0$ on $\partial\Omega$ of the Navier–Stokes system. In other words, $\boldsymbol{u} = \boldsymbol{U} + \boldsymbol{u}_{\mathrm{BL}}$ where $\boldsymbol{u}_{\mathrm{BL}}$ is small except near the boundary.

To illustrate this, we consider a two-dimensional (planar) flow $\boldsymbol{u} = (u, v)$ in the half-space $\{(x, y) \mid y > 0\}$ subject to the following initial condition $\boldsymbol{u}(t = 0, x, y) = \boldsymbol{u}_0(x, y)$, boundary condition $\boldsymbol{u}(t, x, y = 0) = 0$, and $\boldsymbol{u} \to (U_0, 0)$ when $y \to \infty$.

Taking the typical length and velocity of order one, the Reynolds number reduces to $Re = \nu^{-1}$. Let $\varepsilon = Re^{-1/2} = \sqrt{\nu}$.

Near the boundary, the Euler system is not a good approximation. We introduce new independent variables and new unknowns

$$\tilde{t} = t, \quad \tilde{x} = x, \quad \tilde{y} = \frac{y}{\varepsilon},$$

$$(\tilde{u}, \tilde{v})(\tilde{t}, \tilde{x}, \tilde{y}) = \left(u, \frac{v}{\varepsilon}\right)(\tilde{t}, \tilde{x}, \varepsilon\tilde{y}).$$

Notice that when $\tilde{y}$ is of order one, $y = \varepsilon\tilde{y}$ is of order ε. Rewriting the Navier–Stokes system in terms of the new variables and unknowns yields

$$\begin{cases} \tilde{u}_{\tilde{t}} + \tilde{u}\tilde{u}_{\tilde{x}} + \tilde{v}\tilde{u}_{\tilde{y}} - \tilde{u}_{\tilde{y}\tilde{y}} - \varepsilon^2\tilde{u}_{\tilde{x}\tilde{x}} + p_{\tilde{x}} = 0, \\ \varepsilon^2(\tilde{v}_{\tilde{t}} + \tilde{u}\tilde{v}_{\tilde{x}} + \tilde{v}\tilde{v}_{\tilde{y}} - \tilde{v}_{\tilde{y}\tilde{y}}) - \varepsilon^4\tilde{v}_{\tilde{x}\tilde{x}} + p_{\tilde{y}} = 0, \\ \tilde{u}_{\tilde{x}} + \tilde{v}_{\tilde{y}} = 0. \end{cases} \tag{3}$$

Neglecting the terms of order ε^2 and ε^4 yields

$$\begin{cases} \tilde{u}_{\tilde{t}} + \tilde{u}\tilde{u}_{\tilde{x}} + \tilde{v}\tilde{u}_{\tilde{y}} - \tilde{u}_{\tilde{y}\tilde{y}} + p_{\tilde{x}} = 0, \\ p_{\tilde{y}} = 0, \qquad \tilde{u}_{\tilde{x}} + \tilde{v}_{\tilde{y}} = 0. \end{cases} \tag{4}$$

Since p does not depend on $\tilde{y}$, we deduce that the pressure does not vary within the boundary layer and can be recovered from the Euler system (2) when $y = 0$, namely $p_x(t, x) = -(U_t + UU_x)(t, x, y = 0)$, since $V(t, x, y = 0) = 0$.

Going back to the old variables, we obtain

$$\begin{cases} u_t + uu_x + vu_y - \nu u_{yy} + p_x = 0, \\ u_x + v_y = 0 \end{cases} \tag{5}$$

which is the so-called Prandtl system. It should be supplemented with the following boundary conditions:

$$\begin{cases} u(t, x, y = 0) = v(t, x, y = 0) = 0, \\ (u, v)(t, x, y) \to (U(t, x, 0), 0) \quad \text{as} \quad y \to \infty. \end{cases} \tag{6}$$

Formally, a good approximation of $\boldsymbol{u}$ should be $\boldsymbol{U}+\boldsymbol{u}_{\mathrm{BL}}$, where U is the solution of the Euler system (2) and $\boldsymbol{u}_{\mathrm{BL}}+\boldsymbol{U}(t,x,0)$ is the solution of the Prandtl system (5), (6).

Replacing the Navier–Stokes system by the Euler system in the interior and the Prandtl system near the boundary requires a justification. Mathematically, this can be formulated as a convergence theorem when ν goes to 0; namely, $\boldsymbol{u}-(\boldsymbol{U}+\boldsymbol{u}_{\mathrm{BL}})$ goes to 0 when ν goes to 0 in L^∞ or in some energy space (see Masmoudi, 1998 for a special case). In its whole generality, this is still a major open problem in fluid mechanics. This is due to problems related to the well-posedness of the Prandtl system as well as problems related to the instability of some solutions to the Prandtl system, which may prevent the convergence.

Let us explain the first problem for the steady Prandtl system

$$\begin{cases} uu_x+vu_y-\nu u_{yy}+p_x=0, \\ u_x+v_y=0 \end{cases} \tag{7}$$

in $\Omega=\{(x,y)\,|\,0<x<X\,,\,y>0\}$ subject to the following extra boundary condition $u(x=0,y)=u_0(y)$. Here, x should be thought of as a time-like variable. If we assume that $U,u_0\geq 0$ and $u>0$ if $y>0$, we can introduce the von Mises transformation

$$(x,y)\;\rightarrow\;(x,\psi)\quad\text{and}\quad w=u^2,$$

where $\psi_y=u$, $\psi_x=-v$ and $\psi(x,0)=0$. In (x,ψ), the steady Prandtl system reads

$$w_x=\nu\sqrt{w}w_{\psi\psi}-2p_x,$$

which is a degenerate parabolic equation, with the boundary conditions

$$\begin{gathered} w(x,0)=0,\quad w(0,\psi)=w_1(\psi), \\ w(x,\psi)\rightarrow U^2(x)\quad\text{as }\psi\rightarrow\infty, \end{gathered}$$

where $w_1(\int_0^y u_1(s)\mathrm{d}s)=u_1^2(y)$. Using this new equation, one can prove existence for the steady Prandtl system (see Oleinik and Samokhin, 1999). In the case of favorable pressure gradient, namely $p_x\leq 0$, the solution is global ($X=+\infty$). If $p_x>0$, then a separation of the boundary layer may occur. x_0 is said to be a point of separation if $u_y(x_0,0)=0$ and $u_y(x,0)>0$ for $0<x<x_0$. Qualitatively, the separation of the boundary layer is caused by a downward flow that drives the boundary layer away from the boundary. In that case, the assumption that the tangential velocity is large compared with the normal one is not valid, and the derivation of the Prandtl system is not justified.

A second obstacle to the convergence can come from the instability of the solution to the Prandtl system itself, if we consider a two-dimensional shear flow $\boldsymbol{u}^{\mathrm{s}}=(u^{\mathrm{s}}(y),0)$, which is a steady solution of the Euler system. It is well known that the linear stability of such a flow is linked to the presence of inflection points in the profile u^{s}. A necessary condition of instability is that the profile has an inflection point. The solution to the Prandtl system with initial data $\boldsymbol{u}^{\mathrm{s}}$ and $U=0$ is just the solution of a heat equation $u_t=\nu u_{yy}$. If the profile $\boldsymbol{u}^{\mathrm{s}}$ is linearly unstable for the Euler system, then u is not a good approximation of the Navier–Stokes system when ν goes to 0 (see Grenier, 2000).

The boundary layer theory is a very powerful tool in asymptotic analysis and is present in many different fields of partial differential equations, including the magnetohydrodynamic flow boundary layer. In fluid mechanics and atmospheric dynamics, we can also mention the Ekman layer, which is due to the balance between the viscosity and the rapid rotation of a fluid (Coriolis forces). In kinetic theory, systems of conservation laws, passage to the limit from a parabolic to a hyperbolic system, different types of boundary layers arise.

NADER MASMOUDI

See also **Fluid dynamics; Navier–Stokes equation**

Further Reading

Grenier, E. 2000. On the nonlinear instability of Euler and Prandtl equations. *Communications on Pure and Applied Mathematics*, (53): 1067–1091

Grenier, E. & Masmoudi, N. 1997. Ekman layers of rotating fluids, the case of well prepared initial data. *Communications in Partial Differential Equations*, 22: 953–975

Masmoudi, N. 1998. The Euler limit of the Navier-Stokes equations, and rotating fluids with boundary. *Archive Rational Mechanics and Analysis*, 142(4): 375–394

Oleinik, O.A. & V.N. Samokhin. 1999. *Mathematical Models in Boundary Layer Theory*, Boca Raton, FL: Chapman & Hall

Prandtl, L. 1905. Mathematiker-Kongresses. *Boundary Layer*, Heidelberg: *Verhandlung Internationalen*, pp. 484–494

Weinan, W.E. 2000. Boundary layer theory and the zero-viscosity limit of the Navier–Stokes system. *Acta Mathematica Sinica*, 16(2): 207–218

BOUNDARY VALUE PROBLEMS

For a given ordinary or partial differential equation, a boundary value problem (BVP) requires finding a solution of the equation valid in a bounded domain and satisfying a set of given conditions on the boundary of a domain. To define a boundary value problem, therefore, one needs to give an equation, a domain, and an appropriate number of functions supported on the boundary of the given domain, defining the boundary conditions. For example,

$q_t+q_x+q_{xxx}=0$, the PDE,
$x\in[0,\infty)$, $t\in[0,T]$, the domain,
$q(x,0)=f_0(x)$, $q(0,t)=g_0(t)$, the boundary conditions.

Finding a solution of a given BVP is more difficult than finding a function that satisfies the PDE, because of

the constraint imposed on the solution at the boundary of the domain. Indeed, for nonlinear equations, there exists no general method to find the solution of a given BVP. The question of the solvability of such a problem must also be addressed, and in general, it does not have an easy answer (in the above example, if we prescribe two rather than just one condition at the boundary $x = 0$, there exists, in general, no solution). The existence and uniqueness of the solution of a given BVP can be guaranteed only when a specific, well-defined number of boundary conditions are prescribed, and this number depends on the highest-order derivatives appearing in the equation with respect to each variable (Coddington & Levinson, 1955).

For linear ordinary differential equations (ODEs), there is a general methodology for solving a BVP, based on defining the particular solution of a related problem. This particular solution is called the Green function associated with the BVP, and it depends on the boundary conditions. The Green function is used to define an integral operator, and if this operator is sufficiently regular, one can use it to express the solution of the original problem (Stackgold, 1979). This approach is powerful and fairly general, but it is not always successful, and it cannot be used for nonlinear equations.

No general methods are available to construct solutions for nonlinear ODEs or even to assert their existence. Most techniques rely on perturbing in some way the solution of an associated linearized problem or an integrable nonlinear problem. If one hopes to extract information about the nonlinear problem by studying a corresponding linearized one, the correct way to linearize must also be evaluated. Examples of such techniques are branching theory, eigenvalue perturbation, and boundary conditions or domain perturbation.

For linear PDEs in two variables, the classical approach for solving a BVP (going back to Jean D'Alembert's work in the 1740s) is separation of variables. The aim of this technique is to reduce the problem to two distinct linear problems for two ODEs. However, the separability of the problem depends on the specific domain and boundary conditions. For example, depending on the specific boundary conditions prescribed, the ODE one obtains may lead, via the associated Green function, to a non-self-adjoint transform problem, for which few general results are available.

An important theoretical result for the solvability of BVP for linear PDEs is the fundamental principle of Ehrenpreis (1970), which states that there always exists an appropriate generalization of the Fourier transform capable of representing the general solution of a BVP for a linear PDE in the variables (x_1, x_2), posed in a smooth convex domain. This result assumes the well-posedness of the problem. It then ensures that there exists a measure $\rho(k)$ and a contour Γ in the complex plane such that the solution of the problem can be expressed as an integral in the form

$$\int_\Gamma \mathrm{e}^{f_1(k)x_1 + f_2(k)x_2} \mathrm{d}\rho(k),$$

where k is a complex parameter. The functions $f_1(k)$ and $f_2(k)$ are given explicitly. For example, in the case of an evolution equation $u_t = Lu$, where $u = u(x, t)$ and L is a linear differential operator, the representation takes the form

$$u(x, t) = \int_\Gamma \mathrm{e}^{\mathrm{i}kx - \mathrm{i}\omega(k)t} \mathrm{d}\rho(k), \tag{1}$$

where $\omega(k)$ is the dispersion relation of the equation. In representation (1), the dependence on the solution variables (x, t) is explicit; the integration variable k is called the spectral parameter, and such a representation is said to be spectrally decomposed. However, this result is, in general, not constructive, as $\rho(k)$ and Γ are not known. In some cases, it is possible, to obtain this representation via separation of variables, but this is not always the case. Consider, for example, the second-order BVP

$$\begin{aligned} \mathrm{i}q_t + q_{xx} &= 0, 0 < x < \infty, \ 0 < t < \infty, \\ q(x, 0) &= q_0(x), q(0, t) = f(t), \end{aligned} \tag{2}$$

where $q = q(x, t)$ and it is assumed that all functions are infinitely differentiable and vanish as $x \to \infty$. By separating variables, one obtains an ODE in x, which can be solved using the sine transform. Assuming that a unique solution exists, this procedure yields the representation

$$\begin{aligned} q(x, t) = \frac{2}{\pi} \int_0^\infty & \sin(kx) \mathrm{e}^{-\mathrm{i}k^2 t} \\ & \times \left(\hat{q}_0(k) + \mathrm{i}k \int_0^t \mathrm{e}^{\mathrm{i}k^2 s} f(s) \mathrm{d}s \right) \mathrm{d}k, \end{aligned}$$

where

$$\hat{q}_0(k) = \int_0^\infty \sin(kx) q_0(x) dx.$$

This representation is not in form (1) as the variable t also appears as a limit of integration. This fact not only makes this representation less convenient for extracting information about the t dependence of the solution but also makes the rigorous proof of existence and uniqueness of a solution more cumbersome, as the relevant integral is not uniformly convergent as $x \to 0$.

For nonlinear PDEs, no general method is available (Logan, 1994). Perturbation techniques can be of some use in the study of evolutionary PDEs of the form $u_t + P(u) = 0$, where $u = u(t, x)$ and Pu is a nonlinear ODE containing the x-derivatives. Solutions of this problem such that $u_t = 0$ are called steady-state

solutions: these are the solutions that are independent of time. In this context, one studies the linearized stability of the steady state by using the same perturbative techniques discussed for ODEs, as this yields information about the qualitative behavior in time of the solution of the nonlinear problem. The results available in this area are, in general, of limited applicability and practical use for finding explicit solutions.

The special class of nonlinear PDEs known as integrable deserves separate consideration. For these equations, there exists a particular linearizing technique, the inverse scattering transform, which yields the solution of the Cauchy problem. Some of these equations, such as the Korteweg–de Vries and sine-Gordon equations, have been considered on simple domains, and specific BVPs have been solved by ad hoc PDE techniques. The first such result was obtained already 40 years ago (Cattabriga, 1959), but recently this field has witnessed a new surge of interest. To obtain such results, the nonlinear problem is often considered as a linear problem, with the nonlinear term considered as a nonhomogeneous (or forcing) term; thus, the analysis is based on the analysis of the linearized equations by classical PDE techniques (Bona et al., 2001). A different approach involves the attempt to extend the inverse scattering linearizing technique to BVPs, as done, for example, in Leon (2002) for the sine-Gordon equation.

Recently, a general approach to solving BVPs for two-dimensional linear PDEs has been proposed and successfully used to solve many different types of such problems (Fokas, 2000). Its relevance is enhanced by the fact that this approach can be generalized to treat integrable nonlinear PDEs. This methodology yields a spectral transform associated directly to the PDE rather than to transforms associated to the two ODEs obtained by separating variables. For Example (2), this yields, for the solution, the representation

$$q(x,t) = \frac{1}{2\pi}\int_0^\infty e^{ikx-ik^2t}\hat{q}_0(k)dk + \frac{1}{2\pi}\int_\Gamma e^{ikx-ik^2t}\hat{q}(k)dk,$$

where Γ is the boundary of the first quadrant of the complex k-plane, and

$$\hat{q}(k) = \frac{\hat{q}_0(k)+\hat{q}_0(-k)}{2} - k\int_0^\infty e^{ik^2t}f(t)dt.$$

This representation is in Ehrenpreis form, and in addition, measure and contour are explicitly constructed.

The above-mentioned approach provides a unification of the integral representation of the solution of a linear PDE in terms of the Ehrenpreis fundamental principle with the inverse scattering transform for integrable nonlinear PDEs. Indeed, when the problem reduces to an initial value problem for decaying solutions (i.e., the domain for the spatial variable is the whole real line, and the solution is assumed to vanish at $\pm\infty$), the transform obtained is precisely the inverse scattering transform.

The essential ingredients of this approach are the reformulation of the PDE as the closure condition of a certain differential form, and the definition in the complex plane of a Riemann–Hilbert problem depending on both the PDE and the domain. The differential form can be found algorithmically for linear PDEs and is equivalent to the Lax pair formulation for integrable nonlinear PDEs (Lax, 1968). The solution of this Riemann–Hilbert problem (which can be found in closed form in many cases) takes the role of the classical Green formula, and yields an integral representation for the solution, which is independent of the particular boundary conditions and indeed contains all the boundary values of the solution. What this approach crucially provides (when the definition domain is connected) is a global relation among these boundary values, which is the tool necessary to express the solution only in terms of the given boundary conditions and to prove rigorously problems with well-posedness, as well as existence and uniqueness results.

BEATRICE PELLONI

See also **Integrability; Inverse scattering method or transform; Riemann–Hilbert problem; Separation of variables**

Further Reading

Bona, J., et al. 2001. A non-homogeneous boundary value problem for the Korteweg–de Vries equation. *Transactions of the American Mathematical Society*, 354: 427–490

Cattabriga, L. 1959. Un problema al contorno per una equazione parabolica di ordine dispari. *Annali della Scuola Normale Superiore di Pisa*, 13: 163–203.

Coddington, E.A. & Levinson, N. 1955. *Theory of Ordinary Differential Equations*, New York: McGraw-Hill

Ehrenpreis, L. 1970. *Fourier Analysis in Several Complex Variables*, New York: Wiley-Interscience

Fokas, A.S. 2000. On the integrability of linear and nonlinear PDEs. *Journal of Mathematical Physics*, 41: 4188

Ghidaglia, J.L. & Colin, T. 2001. An initial-boundary value problems for the Korteweg–de Vries equation posed on a finite interval. *Advances in Differential Equations*, 6(12): 1463–1492

Lax, P.D. 1968. Integrals of nonlinear equations of evolution and solitary waves. *Communications in Pure and Applied Mathematics*, 21: 467–490

Leon, J. 2002. Solution of the Dirichlet boundary value problem for the sine-Gordon equation. *Physics Letters* A, 298, 343–252

Logan, J.D. 1994. *An Introduction to Nonlinear Partial Differential Equations*, New York: Wiley-Interscience

Stackgold, I. 1979. *Green's Functions and Boundary Value Problems*, New York: Wiley-Interscience

BOUSSINESQ EQUATIONS

See **Water waves**

BOX COUNTING

See **Dimensions**

BRAIN WAVES

See **Electroencephalogram at large scales**

BRANCHING LAWS

In this entry, we briefly trace the history of a familiar phenomenon, branching, in physical and biological systems and the laws governing them. The simplest type of branching tree is one in which a single conduit enters a vertex and two conduits emerge. This dichotomous process is clearly seen in the patterns of biological systems, such as botanical trees, neuronal dendrites, lungs, and arteries, as well as in the patterns of physical systems, such as lightning, river networks, and fluvial landscapes. The quantification of branching through the construction of the mathematical laws that govern them can be traced back to Leonardo da Vinci (1452–1519). In his *Notebooks*, he writes (Richter, 1970):

> All the branches of a tree at every stage of its height when put together are equal in thickness to the trunk [below them]. All the branches of a water [course] at every stage of its course, if they are of equal rapidity, are equal to the body of the main stream.

He also admonished his readers with: "Let no man who is not a Mathematician read the elements of my work." This statement increases in significance when we consider that da Vinci wrote nearly two centuries before Galileo (Galilei, 1638), who is generally given the credit for establishing the importance of mathematics in modern science.

The first sentence in the da Vinci quote is further clarified in subsequent paragraphs of the *Notebooks*. With the aid of da Vinci's sketch reproduced in Figure 1, this sentence has been interpreted as follows: if a tree has a trunk of diameter d_0 that bifurcates into two limbs of diameters d_1 and d_2, the three diameters are related by

$$d_0^a = d_1^a + d_2^a \tag{1}$$

Simple geometrical scaling yields the diameter exponent $\alpha = 2$, which corresponds to rigid pipes carrying fluid from one level of the tree to the next, while retaining a fixed cross-sectional area through successive generations of bifurcation. Although the pipe model has a number of proponents from hydrology, the diameter exponent for botanical trees was determined empirically by Cecil D. Murray in 1927 to be insensitive to the kind of botanical tree and to have a value 2.59 rather than 2 (Murray, 1927). Equation (1) is referred to as Murray's law in the physiology literature.

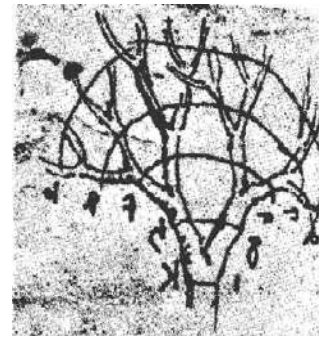

Figure 1. Sketch of tree from Leonardo da Vinci's Notebooks, PL XXVII (Richter, 1970).

The significance of Murray's law was not lost on D'Arcy Thompson (1942). In the second edition of his classic *On Growth and Form*, first published in 1917, Thompson argues that the geometrical properties of biological systems can often be the limiting factor in the development and final function of an organism. This is stated in his principle of similitude, which is a generalization of certain observations made by Galileo regarding the trade-off between the weight and strength of bone (Galilei, 1638). Thompson goes on to argue that the design principle for biological systems is that of energy minimization.

The second sentence in the da Vinci quotation is as suggestive as the first. In modern language, we would interpret it to mean that the flow of a river remains constant as tributaries emerge along the river's course. This equality must be true in order for the water to continue flowing in one direction and not stop and reverse course at the mouth of a tributary. Using the pipe model introduced above, and minimizing the energy with respect to the pipe radius, yields $\alpha = 3$, in Equation (1). Thus, the value of the diameter exponent obtained empirically by Murray falls between the theoretical limits of geometric self-similarity and hydrodynamic conservation, $2 \leq \alpha \leq 3$.

In da Vinci's tree, it is easy to assign a generation number to each of the limbs, but the counting procedure can become complicated in more complex systems like the generations of the bronchial tubes in the mammalian lung. One form taken by the branching laws is that the ratio of the radii of the tubes (from one generation to the next) is constant, that is, by the scaling relation

$$\frac{r_j}{r_{j+1}} = R. \tag{2}$$

Equation (2) is analogous to Horton's law for river trees and fluvial landscapes, which involves the ratio

of the number of branches in successive generations of branches, rather than radii (Mandelbrot, 1977). In either case, the parameter R determines the branching law and Equation (2) implies a geometrical self-similarity in the tree, as anticipated by Thompson. In the branching of bronchial airways, $d_1 = d_2$ at each stage of the tree, so that from Equation (1) we deduce the relationship between the radii of the pipes between successive generations as

$$r_j = 2^{1/\alpha} r_{j+1}. \tag{3}$$

In the case of the lung, the diameter of an airway is reduced by a factor $2^{-1/3}$ at each generation, since $\alpha = 3$ for the bronchial tree. Therefore, after j generations, $r_j = r_0 \exp(-j/\lambda)$, where the exponential rate of reduction, $\lambda = \ln(2)/3$, is the same for each generation beyond the trachea r_0, as argued by Weibel (2000).

A less space-filling value of the scaling index is obtained for the arterial system, where it is empirically determined that $\alpha = 2.7$. For a general non-integer branching index, the scaling relation Equation (3) defines a fractal tree. Such trees have no characteristic scale length and were first organized and discussed as a class by Benoit Mandelbrot (1977)—the father of fractals. The classical approach relied on the assumption that biological processes, like their physical counterparts, are continuous, homogeneous, and regular. However, most biological systems and many physical ones are discontinuous, inhomogeneous, and irregular and are necessarily that way in order to perform a particular function, such as gas exchange in lungs and arteries.

An entirely different kind of fractal tree is that of neuronal dendrites. The branching trees of neurons interleave the brain and form the communication system within the body. In the neurophysiology literature, Equation (1) is known as Rall's law with $\alpha = 1.5$ (Rall, 1959). More recent measurements of the scaling index, at each generation of dendritic branching, show a change with generation number; that is, the single parameter R is replaced with R_j. This non-constant scaling coefficient implies that Thompson's principle of similitude is violated.

A fractal model of the bronchial tree assumes that the ratio of successive generations of radii is dependent on the generation number, giving rise to a renormalization group relation, with the solution given by

$$r_j = \frac{a(j)}{j^u}, \quad j > 0. \tag{4}$$

Here, the average radius is an inverse power law in the generation number j, modulated by a slowly oscillating function $a(j)$ as observed in the human, dog, rat, and hamster data shown in Figure 2 (West & Deering, 1994). In this way, the fractal concept is used as a design principle in biology (Weibel, 2000; West, 1999; Mandelbrot, 1977) and in the development of branching laws.

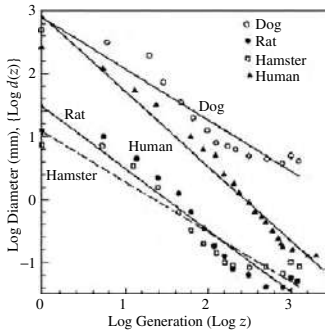

Figure 2. The variation in diameter d of the bronchial airways is depicted as a function of generation number j for rats, hamsters, humans, and dogs. The modulated inverse power law from the fractal model of the bronchial airway is observed in each case (West & Deering, 1994).

BRUCE J. WEST

See also **Fibonacci series; Geomorphology and tectonics; Martingales; Multiplex neuron**

Further Reading

Galilei, G. 1638. *Dialogue Concerning Two New Sciences*, translated by H. Crew & A. deSalvio in 1914, New York: Dover, 1954

Mandelbrot, B.B. 1977. *The Fractal Geometry of Nature*, San Francisco: W.H. Freeman

Murray, C.D. 1927. A relationship between circumference and weight and its bearing on branching angles. *Journal of General Physiology*, 10: 725–729

Rall, W. 1959. Theory of physiological properties of dendrites. *Annals of New York Academy of Science*, 96: 1071–1091

Richter, J.P. 1970. *The Notebooks of Leonardo da Vinci*, vol. 1, New York: Dover, unabridged edition of the work first published in London in 1883

Thompson, D.W. 1942. *On Growth and Form*, 2nd edition, Cambridge: Cambridge University Press, republished New York: Dover, 1992

Weibel, E.R. 2000. *Symmorphosis: On Form and Function in Shaping Life*, Cambridge, MA: Harvard University Press

West, B.J. 1999. *Physiology, Promiscuity and Prophecy at the Millennium: A Tale of Tails*, Singapore: World Scientific

West, B.J. & Deering, W. 1994. Fractal physiology for physicists: Levy statistics. *Physics Reports*, 246: 1–100

BREATHERS

The term *breather* (also called a "bion") arose from studies of the sine-Gordon (SG) equation

$$u_{tt} - u_{xx} + \sin u = 0, \tag{1}$$

which has localized solutions that oscillate periodically with time and decay exponentially in space. Such a

solution of Equation (1) is given by

$$u(x,t) = 4\tan^{-1}\left[\frac{\lambda \sin \omega t}{\omega \cosh \lambda x}\right], \quad \lambda = \sqrt{1-\omega^2}, \tag{2}$$

which is shown in Figure 1.

Although the breather of Equation (2) is a non-topological soliton of Equation (1), it can be considered as a bound state of two topological solitons of the SG equation (kink and antikink), one of which is shown in Figure 2(a). The kink and antikink oscillate with respect to each other with the period $T = 2\pi/\omega$. Thus, such a soliton is also called a "doublet." A sketch of the bion at small frequencies ($\omega \ll 1$) and large enough t is presented in Figure 2(b). At some initial time, the kink and antikink move outward in opposite directions and separate in space with increasing time up to some finite distance (at $t = T/4$). The kink and antikink components of the breather never become fully free of distortions in their shapes due to interactions between each other, and finally oscillate in a kind of bound state.

At $1-\omega^2 \ll 1$, Equation (2) reduces to a small-amplitude breather $u(x,t) = 4\,Re\,\psi(x,t)$, where

$$\psi(x,t) = -\mathrm{i}\,\frac{\lambda \exp(-\mathrm{i}\omega t)}{\cosh \lambda x} \tag{3}$$

and $\lambda = \sqrt{2(1-\omega)}$. Equation (3) is a soliton solution of the nonlinear Schrödinger (NLS) equation

$$\mathrm{i}\psi_t + \tfrac{1}{2}\,\psi_{xx} - \psi + |\psi|^2\psi = 0, \tag{4}$$

which is regarded as a breather and can be written as $\psi(x,t) = \phi(x)\exp(\mathrm{i}\omega t)$. In this form, the spatial dependence of the soliton amplitude and the time dependence of the phase (of the complex function ψ) are separated. As a result, the nonlinearity appears only in the amplitude, but not in the phase of the NLS soliton. Although such a separation of the spatial and time dependencies in a soliton expression does not take place in the general form of the SG breather, the limiting case of the SG breather coincides with the amplitude of the NLS soliton.

At present, it is not known whether other nonlinear Klein–Gordon equations similar to Equation (1), but differing from it only by the nonlinear term, possess exact breather solutions (Segur & Kruskal, 1987). However, if certain nonlinear terms in a Klein–Gordon-type equation differ only slightly from $\sin u$ (slightly perturbed SG equation), a breather-like solution may persist in the first order with respect to the perturbation (Birnir et al., 1994).

The breather of the SG equation can move along the space coordinate axis with a stationary velocity V. As Equation (1) is a relativistic invariant equation (invariant under a Lorentz transformation

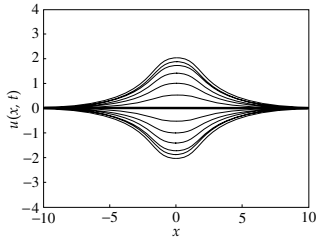

Figure 1. $u(x,t)$ from Equation (2) versus x for 26 different times equally spaced and covering one period, with $\lambda = 0.5$.

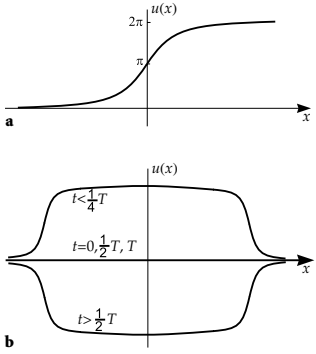

Figure 2. (a) A sketch of the sine-Gordon kink. (b) Three profiles of the kink-antikink oscillations.

of the independent variables), one can obtain a moving breather from Equation (2) substituting $x \to (x - Vt)/(1-V^2)^{1/2}$ and $t \to (t - Vx)/(1-V^2)^{1/2}$. Consequently, the moving breathers form a two-parametric (ω and V) family of solutions of the SG equation.

Possible values of the breather parameters ω and V can be compared with the dispersion relation ($\omega^2 = 1 + k^2$) for small vibrations (phonons) described by the linearized version of Equation (1). These phonons have frequencies $\omega > 1$ and phase velocities $\omega/k > 1$. A breather frequency, on the other hand, is smaller than the minimum frequency of the phonons ($\omega < 1$), and the breather velocity is smaller than the minimum phonon phase velocity ($V < 1$). Therefore, the dynamical breather parameters lie outside of the spectrum of the linear vibrations. Although the time dependence of the breather includes the higher temporal harmonics of the oscillations, the phonons cannot be resonantly excited by the breather. Thus, breathers and phonons are asymptotically independent vibrational

modes of the system described by the SG equation. This asymptotic independence of nonlinear excitations (breathers and kinks) and phonons follows from the integrability of Equation (1).

An important way to study nonlinear integrable equations is the inverse scattering method. According to this method, breathers are characterized by poles in the complex phase plane of scattering parameters for the equation under consideration.

It is known that several nonlinear differential equations possess breather solutions. The Landau–Lifshitz (LL) equation provides an example of a nonlinear equation generalizing the results that are described by the SG and NLS equations. The breather-like solution of the LL equation has a more complicated form than the one presented above; however, it is also a two-parameter soliton called a dynamic magnetic soliton (Kosevich et al., 1977). Its oscillatory behavior is characterized by a frequency ω, and its center can move with a velocity V. In the general case, the magnetic soliton can be described by some complex function of x and t, but the time and spatial dependencies are not separated in the analytical expression for such a soliton.

An important class of breathers the so-called discrete breathers (also known as intrinsic localized modes, self-localized anharmonic modes, or nonlinear localized excitations). These are solutions of a nonlinear equation on a lattice, and they are periodic in time and localized in space. Although most such investigations are performed by numerical calculations, there exist nonlinear dynamic equations on a lattice possessing exact analytical breather solutions. One of them is the following discrete version of the NLS equation proposed by Ablowitz and Ladik (AL) in 1976 (Ablowitz & Ladik, 1976):

$$\mathrm{i}\partial_t \psi_n - (\psi_{n+1} + \psi_{n-1})(1 + |\psi_n|^2) = 0. \quad (5)$$

The AL lattice is integrable and it allows for breather-like solutions, the simplest of which has a form close to that of Equation (2):

$$\psi = \frac{\sinh\beta \exp(-\mathrm{i}\omega t)}{\cosh\beta(n - x_0)}, \quad (6)$$

where n is the integer number of a lattice site, $x_0 = \text{constant}$, and $\omega = -2\cosh\beta$.

ARNOLD KOSEVICH

See also **Discrete breathers; Discrete nonlinear Schrödinger equations; Integrability; Inverse scattering method or transform; Sine-Gordon equation; Solitons**

Further Reading

Ablowitz, M.J. & Ladik, J.F. 1976. Nonlinear differential-difference equations and Fourier analysis. *Journal of Mathematical Physics*, 17: 1011

Birnir, B., McKean, H.P. & Weinstein, A. 1994. The rigidity of sine-Gordon breathers. *Communications on Pure and Applied Mathematics*, 47: 1043

Flach, S. & Willis, C.R. 1998. Discrete breathers. *Physics Reports*, 295: 181

Kosevich, A.M., Ivanov, B.A. & Kovalev, A.S. 1977. Nonlinear localized magnetization wave of a ferromagnet as a bound-state of a large number of magnons. *Pis'ma Zhurnal Eksperimental'noy i Teoreticheskoy Fiziki*, 25: 516 (in Russian); *JETP Letters*, 25: 486

Kosevich, A.M., Ivanov, B.A. & Kovalev, A.S. 1990. Magnetic solitons. *Physics Reports*, 194: 117

Segur, H. & Kruskal, M.D. 1987. Nonexistence of small-amplitude breather solutions in ϕ^4 theory. *Physical Review Letters*, 58: 747

BROUWER'S FIXED POINT THEOREM

See **Winding numbers**

BROWNIAN MOTION

In 1828, Robert Brown, a leading botanist, observed that a wide variety of particles suspended in liquid exhibit an intrinsic, irregular motion when viewed under a microscope. While not the first to witness such motion, his experimental focus on this phenomenon, which would bear his name, established its universality and intrinsic nature, thereby raising it as an issue for fundamental scientific inquiry (Nelson, 1967). Deutsch has recently raised the question of whether Brown actually witnessed Brownian motion or fluctuations due to some external contaminating influence (Peterson, 1991). Indeed, while Brownian motion is a ubiquitous phenomenon, not all irregular motions can be ascribed to Brownian motion. The dancing of dust particles in sunlight is dominated by imperceptible turbulent currents, not Brownian motion. True Brownian motion is generally only visible on scales of microns and below, but has important macroscopic ramifications because all microscopic particles manifest it. For example, Brownian motion makes possible both the fine-scale mixing of initially segregated substances in nature and industry, as well as the passive transport of ions, nutrients, and fuel, which allow biological cells to support life.

The origin of Brownian motion remained under debate throughout the 19th century, with Cantoni, Delsaux, Gouy, and C. Weiner proposing that thermal motions in the suspending liquid were responsible, as discussed in Einstein (1956, pp. 86–88), Gallavotti (1999, Chapter 8), and Russel et al. (1989, pp. 65–66). Attempts to examine this hypothesis quantitatively were hampered by the inability to measure accurately the velocity of particles undergoing Brownian motion, since such motion loses coherence over time scales (microseconds) that are shorter than those which experimental observations were able to resolve. In

one of three ground-breaking papers that Einstein published in 1905, he offered a statistical mechanical means for theoretical calculations involving Brownian motion (Einstein, 1956). Einstein realized that the quantity involving Brownian motion that can be best observed under a microscope in an experiment is the "diffusivity":

$$D = \lim_{t\to\infty} \frac{|X(t) - X(0)|^2}{2t}, \tag{1}$$

where $X(t)$ denotes the observed displacement of the Brownian particle along a fixed direction at time t. In practice, t is simply taken as some satisfactorily long time of observation, and there is no need for fine temporal resolution as there would be if the velocity were to be measured. Einstein employed a random walk model for his analysis and showed that the diffusivity defined in (1) is identical to the diffusion constant that describes the macroscopic evolution of the concentration density $n(\boldsymbol{x}, t)$ of a large number of Brownian particles:

$$\frac{\partial n(\boldsymbol{x}, t)}{\partial t} = D \sum_{j=1}^{3} \frac{\partial^2 n(\boldsymbol{x}, t)}{\partial x_j^2}. \tag{2}$$

Through an elegant argument based on *equilibrium* statistical mechanical arguments, Einstein showed that the diffusivity D of a Brownian particle must be related to its friction coefficient ξ in the following way:

$$D = \frac{k_B T}{m\xi}, \tag{3}$$

where k_B is Boltzmann's constant and T is the absolute temperature (measured in Kelvin scale), and m is the particle's mass. The friction coefficient ξ appears in the relation between the drag force F_{drag} and velocity v of the particle in steady-state motion (assuming a low Reynolds number):

$$F_{\text{drag}} = m\xi v. \tag{4}$$

For a sphere of radius a moving through a fluid with dynamic viscosity μ, the friction coefficient is given by $\xi = 6\pi\mu a/m$. The remarkable property of the "Einstein relation" in (3) is that it links a quantity D pertaining to statistically unpredictable dynamical fluctuations to a quantity ξ, which involves deterministic, steady-state properties. Later work generalized the Einstein relation (3) to "fluctuation-dissipation theorems," which express the structure of the spontaneous statistical fluctuations in a wide class of physical systems to the structure of the dissipative (frictional) dynamics (Kubo et al., 1991, Chapter 1).

The basic theory of Brownian motion was developed by Einstein in 1905, a time when the premises of the atomic theory of matter were still not yet fully agreed upon (Gallavotti, 1999; Nelson, 1967). Einstein realized that a careful observation of Brownian motion and his relation between the diffusivity of a Brownian particle and its mobility could be used to calculate the number of particles making up a given mass of fluid if the atomic theory were valid. Under a microscope sufficient to resolve the Brownian motion of a particle, all quantities in (3) are directly observable except for Boltzmann's constant k_B. Therefore, the Einstein relation (3) can be used to compute a value for k_B based on Brownian motion data. Now, k_B is in turn related to Avogadro's number N_A, which is the number of molecules in a "mole" (a certain well-defined macroscopic amount) of a substance. The Brownian motion data and the Einstein relation, therefore, furnish an independent prediction for Avogadro's number N_A and, thereby, the number of molecules per unit mass of the fluid. In other words, the number (and therefore mass) of the individual fluid particles could be calculated without having to observe them at an individual level, an experimental feat that has become possible only in recent years. Instead, their individual mass and number could be assessed through their collective influence on a much larger and, therefore, observable immersed particle. In 1908, Jean Perrin experimentally confirmed that the value of N_A computed in this way agreed with those obtained from other techniques (Gallavotti, 1999), providing strong support for the atomic theory of matter. Since the 1970s, Brownian motion has been investigated in the laboratory through dynamic light scattering techniques (Russel et al., 1989, Chapter 3).

The most idealized mathematical representation of Brownian motion with diffusivity D is defined as $(2D)^{1/2}W(t)$, where $W(t)$ is a canonical continuous random process with Gaussian statistics such that $W(0) = 0$, $\langle W(t)\rangle = 0$, and

$$\langle (W(t) - W(t'))^2 \rangle = |t - t'|. \tag{5}$$

This mathematical Brownian motion is often referred to as the Wiener process (Borodin & Salminen, 2002; Gallavotti, 1999; Nelson, 1967). This idealized Brownian motion has independent increments (no inertia). Physical Brownian motion, of course, has some small inertia as well as several other complicating influences from the fluid environment and from the presence of other nearby Brownian particles (Russel et al., 1989). These extra features can be built into a dynamical description using the mathematical Brownian motion as the basic noise input with influence mediated by the other physical parameters. The mathematical Brownian motion has a similar role in modeling noise input in a wide variety of stochastic models in physics, biology, finance, and other fields. More precisely, the Levy–Khinchine theorem indicates that in any system affected by noise in a continuous way such that the noise on disjoint time intervals is independent can be modeled in terms of mathematical Brownian motion (Reichl, 1998, Chapters 4, 5).

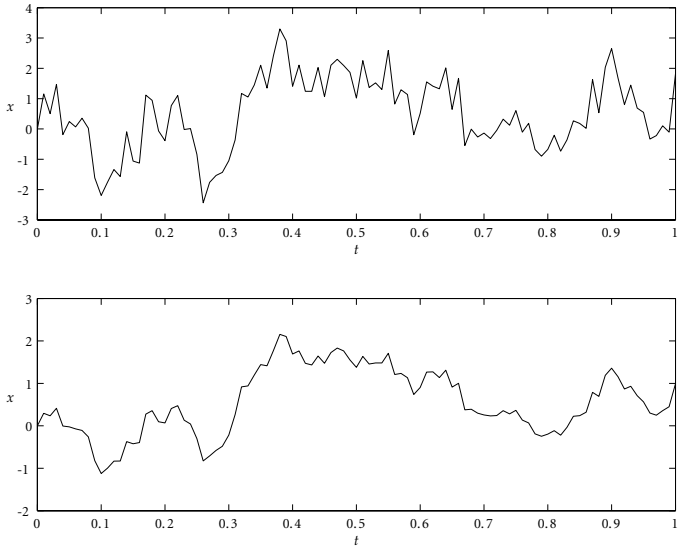

Figure 1. Sample trajectories of fractional Brownian motion using Fourier-wavelet method (Elliott et al., 1997). Top panel: $H = \frac{1}{3}$, lower panel: $H = \frac{2}{3}$. Both simulations used the same random numbers.

Discontinuous noise-induced jumps, in contrast, are modeled in terms of Poisson processes or more generally Lévy processes (Reichl, 1998, Chapters 4, 5). Continuous noise with long-range correlations (so that the independent increment property is not satisfied), on the other hand, can often be usefully modeled in terms of "fractional Brownian motion" (FBM) (Mandelbrot, 2002). This is an idealized Gaussian random process $Z(t)$ with $Z(0) = 0$, $\langle Z(t)\rangle = 0$, and

$$\langle (Z(t) - Z(t'))^2 \rangle = |t - t'|^{2H} \tag{6}$$

where the Hurst exponent H is chosen from the interval $0 < H < 1$. The FBM with $H = \frac{1}{2}$ corresponds to ordinary Brownian motion with independent increments. FBMs with $\frac{1}{2} < H < 1$ have positive, long-ranged correlations with less rough trajectories and large excursions, while FBMs with $0 < H < \frac{1}{2}$ have negative, long-ranged correlations with rougher trajectories and a more oscillatory character (Figure 1). All FBMs have a statistical self-similarity property; the statistics of the rescaled FBM $\lambda^{-H} Z(\lambda t)$ are identical to those of the original $Z(t)$. That is, these processes have no finite length or time scale associated to them and can be thought of as random fractals. Fractional Brownian motions are therefore particularly appropriate for modeling systems with fluctuations occurring over a wide range of scales; cutoff lengths can be introduced by filtering an input FBM. Models built from FBMs have been developed in turbulence theory, natural landscape and cloud structures, surface adsorption processes, neural signals in biology, and self-organized critical systems such as earthquakes, forest fires, and sandpiles.

PETER R. KRAMER

See also **Fluctuation-dissipation theorem; Fluid dynamics; Fokker–Planck equation; Lévy flights; Random walks**

Further Reading

Borodin, A.N. & Salminen, P. 2002. *Handbook of Brownian Motion: Facts and Formulae*, 2nd edition, Basel: Birkhäuser

Einstein, A. 1956. *Investigations on the Theory of the Brownian Movement*, edited with notes by R. Fürth, translated by A.D. Cowper, New York: Dover

Elliott, Jr, F.W., Horntrop, D.J. & Majda, A.J. 1997. A Fourier-wavelet Monte Carlo method for fractal random fields. *Journal of Computational Physics*, 132(2): 384–408

Gallavotti, G. 1999. *Statistical Mechanics*, Berlin: Springer

Kubo, R., Toda, M. & Hashitsume, N. 1991. *Statistical Physics*, vol. 2, 2nd edition, Berlin: Springer

Mandelbrot, B.B. 2002. *Gaussian Self-affinity and Fractals*, Chapter IV. New York: Springer

Mazo, R.M. *Brownian Motion. Fluctuations, Dynamics and Applications*, Oxford and New York: Oxford University Press

Nelson, E. 1967. *Dynamical Theories of Brownian Motion*, Princeton, NJ: Princeton University Press
Peterson, I. 1991. Did Brown see Brownian motion? *Science News*, 139: 287
Reichl, L.E. 1998. *A Modern Course in Statistical Physics*. 2nd edition, New York: Wiley
Russel, W.B., Saville, D.A. & Schowalter, W.R. 1989. *Colloidal Dispersions*. Cambridge and New York: Cambridge University Press

BRUSSELATOR

The Brusselator is an autocatalytic model involving two intermediates. It illustrates how the fundamental laws of thermodynamics and chemical kinetics as applied to open systems far from equilibrium can give rise to self-organizing behavior and to dissipative structures in the form of temporal oscillations and spatial pattern formation.

Chemical kinetics imposes stringent conditions on the concentrations of the species involved in a reaction scheme and on the associated parameters. In a scheme consisting entirely of elementary steps, the overall rates are given (in an ideal system) by mass action kinetics, featuring particular combinations of products of concentrations preceded by stoichiometric coefficients (integer numbers specifying how the relevant constituents are produced or consumed). This guarantees the positivity of the solutions of the mass balance equations. A second condition is detailed balance, which requires that in chemical equilibrium, each individual reaction step is balanced by its inverse (*See* **Detailed balance**). This gives rise to relations linking the concentrations of initial reactants and final products to the rate constants, independent of the concentrations of the intermediates.

An additional set of requirements stems from the fact that self-organization in chemical kinetics must arise through an instability. One reason for this is that equilibrium and the states in its vicinity, obtained as the constraints are gradually increased (called the "thermodynamic branch"), are stable. To overcome this property and evolve to states that are qualitatively different from equilibrium, new branches of solutions must be generated, which can only take place through the mechanisms of instability and bifurcation. This, in turn, requires that the non-equilibrium constraints exceed a critical value (Glansdorff & Prigogine, 1971). Because the evolution laws generated by chemical kinetics at the macroscopic level of description are dissipative, the bifurcating states are attractors, attained by families of initial conditions belonging to an appropriate part of phase space. This guarantees structural stability, that is to say, the robustness of the solution toward small perturbations—a condition to be fulfilled by a model aiming to describe a physical phenomenon. Note that non-equilibrium instabilities and self-organization collapse when the system becomes closed to the external environment or when the kinetics involves only first-order steps, in which case one obtains a monotonic decay to a unique steady state (Denbigh et al., 1948).

Following the pioneering work of Alfred Lotka, several authors in the late 1940s, proposed models of open nonlinear systems deriving from mass action kinetics and giving rise to sustained oscillations (Lotka, 1956; Moore, 1949). These models do not have structural stability (as they give rise to a continuum of initial condition-dependent solutions), and they do not exhibit the role of the constraints in a transparent manner (as they are usually formulated in the limit of irreversible reactions). When the non-equilibrium constraints are explicitly accounted for, it is found (Lefever et al., 1967) that there is no instability threshold in these models. As the first known chemical model that is both fully compatible with the laws of thermodynamics and chemical kinetics and generates dissipative structures through non-equilibrium instabilities, the Brusselator is free from such deficiencies.

Model Presentation

In the interest of transparency, one desires a minimal model, and if oscillatory behavior is one of the required properties, this necessitates two coupled variables representing the concentrations of intermediate products. As in the models of the Lotka family, one seeks steps that are not only nonlinear but also include feedback processes, the simplest chemical version of which is autocatalysis. But contrary to these models, one now needs to scan the whole range of near to far from equilibrium situations and to undergo an instability somewhere in this range. As the Lotka-type models contain only second-order steps, a natural solution is to amend them by replacing these steps by a third-order one. This leads to the scheme (Prigogine & Lefever, 1968)

$$A \underset{k_{-1}}{\overset{k_1}{\rightleftharpoons}} X, \quad B + X \underset{k_{-2}}{\overset{k_2}{\rightleftharpoons}} Y + D,$$
$$2X + Y \underset{k_{-3}}{\overset{k_3}{\rightleftharpoons}} 3X, \quad X \underset{k_{-4}}{\overset{k_4}{\rightleftharpoons}} E \qquad (1)$$

Hanusse, Tyson, and Light have shown that a two-variable system compatible with the above requirements necessarily comprises a third-order step. Here A, B are the initial reactants, D, E the final products, and X, Y the intermediates: X can be thought of as an activator generating Y at its own expense, which acts as an inhibitor if the B concentration is large.

From the standpoint of irreversible thermodynamics, the Brusselator can be driven out of equilibrium through two independent constraints (affinities) related to the

overall reactions

$$A \underset{k_{-1}k_{-4}}{\overset{k_1k_4}{\rightleftharpoons}} E, \; B \underset{k_{-3}k_{-2}}{\overset{k_3k_2}{\rightleftharpoons}} D.$$

This offers sufficient flexibility to allow one to take the limit of purely irreversible steps and of fixed reactant and product concentrations (also referred to as pool chemical approximation, ensuring that the (X, Y) subsystem becomes open to the external environment), while satisfying the positivity of concentrations, detailed balance, and mass conservation (Lefever et al., 1988). When diffusion is also included, and upon performing a suitable scaling transformation, this leads to the Brusselator equations

$$\begin{aligned} \frac{\partial X}{\partial t} &= A - (B+1)X + X^2Y + D_x\nabla^2 X, \\ \frac{\partial Y}{\partial t} &= BX - X^2Y + D_y\nabla^2 Y \end{aligned} \qquad (2)$$

in which B, D_x/D_y, and the system size usually play the role of the parameters controlling the instabilities.

A number of variants of this canonical form have also been developed, including Brusselator in an open well-stirred reactor, Brusselator in a non-ideal system, including coupling between non-equilibrium instabilities and phase transitions, and coupling with external fields or advection.

Behavior of the Solutions

Since the first bifurcation analysis of the Brusselator equations (Nicolis & Auchmuty, 1974), several studies have been devoted to the various modes of spatiotemporal organization generated by Equations (2): limit cycles, Turing patterns, and traveling waves in one-dimensional systems (Nicolis & Prigogine, 1977); spatiotemporal chaos arising from the diffusive coupling of local limit cycle oscillators (Kuramoto, 1984); patterns in two- and three-dimensional systems including patterns arising from the interference of different instability mechanisms such as Turing, Hopf (De Wit, 1999); and the effect of confinement (Herschkowitz-Kaufman & Nicolis, 1972). Many phenomena now known to be generic have first been discovered on these Brusselator-based analyses, which have also helped to test the limits of traditional theoretical approaches and to explore new methodologies such as normal forms and phase dynamics.

The Brusselator has also been used to explore possible thermodynamic signatures of dissipative structures. No clearcut tendencies seem to exist, suggesting that global thermodynamic quantities like entropy and entropy production do not provide adequate measures of dynamic complexity. Finally, attention has been focused on the new insights afforded when the mean-field equations (2) are augmented to account for fluctuations, a study for which the Brusselator is well suited thanks to its mechanistic basis. The interest here is to provide a fundamental understanding of how large-scale order can be sustained despite the locally prevailing thermal disorder. Early accounts of the results, with emphasis on critical behavior in the vicinity of bifurcations, can be found in Nicolis & Prigogine (1977) and in Walgraef et al. (1982).

G. NICOLIS

See also **Chemical kinetics; Detailed balance; Emergence; Turing patterns**

Further reading

Denbigh, K.G., Hicks, M. & Page, F.M. 1948. Kinetics of open systems. *Transactions of the Faraday Society*, 44: 479–494

De Wit, A. 1999. Spatial patterns and spatio-temporal dynamics in chemical systems. *Advances in Chemical Physics*, 109: 453–513

Glansdorff, P. & Prigogine, I. 1971. *Thermodynamic Theory of Structure, Stability and Fluctuations*, London and New York: Wiley

Herschkowitz-Kaufman, M. & Nicolis, G. 1972. Localized spatial structures and nonlinear chemical waves in dissipative systems. *Journal of Chemical Physics*, 56: 1890–1895

Kuramoto, Y. 1984. *Chemical Oscillations, Waves and Turbulence*, Berlin and New York: Springer

Lefever, R., Nicolis, G. & Prigogine, I. 1967. On the occurrence of oscillations around the steady state in systems of chemical reactions far from equilibrium. *Journal of Chemical Physics*, 47: 1045–1047

Lefever, R., Nicolis, G. & Borckmans, P. 1988. The Brusselator: it does oscillate all the same. *Journal of the Chemical Society, Faraday Transactions*, 1. 84: 1013–1023

Lotka, A. 1956. *Elements of Mathematical Biology*, New York: Dover

Moore, M.J. 1949. Kinetics of open reaction systems: chains of simple autocatalytic reactions. *Transactions of the Faraday Society*, 45: 1098–1109

Nicolis, G. & Auchmuty, J.F.G. 1974. Dissipative structures, catastrophes, and pattern formation: a bifurcation analysis. *Proceedings National Academy of Sciences USA*, 71: 2748–2751

Nicolis, G. & Prigogine, I. 1977. *Self-organization in Nonequilibrium Systems*, New York: Wiley

Prigogine, I. & Lefever, R. 1968. Symmetry-breaking instabilities in dissipative systems. II. *Journal of Chemical Physics*, 48: 1695–1700

Walgraef, D., Dewel, G. & Borckmans, P. 1982. Nonequilibrium phase transitions and chemical instabilities. *Advances in Chemical Physics*, 491: 311–355

BULLETS

See **Solitons, types of**

BURGERS EQUATION

In 1915, Harry Bateman considered a nonlinear equation whose steady solutions were thought to describe certain viscous flows (Bateman, 1915). This equation, modeling a diffusive nonlinear wave, is now

widely known as the Burgers equation, and is given by

$$u_t + uu_x = \frac{\mu}{2}u_{xx}, \tag{1}$$

where μ is a constant measuring the viscosity of the fluid. It is a nonlinear parabolic equation, simply describing a temporal evolution where nonlinear convection and linear diffusion are combined, and it can be derived as a weakly nonlinear approximation to the equations of gas dynamics.

Although nonlinear, Equation (1) is very simple, and interest in it was revived in the 1940s, when Dutch physicist Jan Burgers proposed it to describe a mathematical model of turbulence in gas (Burgers, 1940). As a model for gas dynamics, it was then studied extensively by Burgers (1948), Eberhard Hopf (1950), Julian Cole (1951), and others, in particular; after the discovery of a coordinate transformation that maps it to the heat equation. While as a model for gas turbulence the equation was soon rivaled by more complicated models, the linearizing transformation just mentioned added importance to the equation as a mathematical model, which has since been extensively studied. The limit $\mu \to 0$ is a hyperbolic equation, called the inviscid Burgers equation:

$$u_t + uu_x = 0. \tag{2}$$

This limiting equation is important because it provides a simple example of a conservation law, capturing the crucial phenomenon of shock formation. Indeed, it was originally introduced as a model to describe the formation of shock waves in gas dynamics.

A first-order partial differential equation for $u(x, t)$ is called a conservation law if it can be written in the form

$$u_t + (f(u))_x = 0\,.$$

For Equation (2), $f(u) = u^2/2$. Such conservation laws may exhibit the formation of shocks, which are discontinuities appearing in the solution after a finite time and then propagating in a regular manner. When this phenomenon arises, an initially smooth wave becomes steeper and steeper as time progresses, until it forms a jump discontinuity—the shock.

Once a discontinuity forms, the solution is no longer a globally differentiable function; thus, the sense in which it can be considered as a solution of the PDE must be clarified. A discontinuous function $(u(x, t))$ can still be considered as a solution in the weak sense if it satisfies

$$\int\int_D \left(u\varphi_t + \frac{1}{2}u^2\varphi_x\right) \mathrm{d}x\mathrm{d}t = 0, \tag{3}$$

where D is any rectangle in the (x, t) plane, and $\varphi(x, t)$ is any smooth function vanishing on the boundary ∂D. Any regular solution is a weak solution, as is seen by multiplying the equation by $\varphi(x, t)$, integrating by parts along ∂D, and using Green's theorem.

In physical applications, one often considers the discontinuous solution as the limit, as $\mu \to 0$, of smooth solutions of the viscous Equation (1). This idea is correct from a physical point of view, as it takes into account the significance of these solutions as a physical description of gas dynamics. From the form of the equation (or its weak formulation (3)), one can derive the velocity v_s of a shock separating two regimes, u_r to the right and u_l to the left of a discontinuity. The result is the Rankine–Hugoniot formula, valid in general for conservation laws, which for the case of the Burgers equation yields

$$s = \tfrac{1}{2}(u_r + u_l). \tag{4}$$

Even this, however, is not enough to guarantee uniqueness of the solution, because there are several ways of writing the equation in the form of a conservation law. Often, the way to select the physically relevant solution is to consider the vanishing viscosity limit. To obtain this solution mathematically, an additional entropy condition, that $u_l > s > u_r$, must be imposed.

Besides its significance as a model for shocks, the Burgers equation is prominent among PDEs because it is completely integrable. Indeed, the nonlinear change of variable

$$u = -\mu(\log \psi)_x \tag{5}$$

transforms Equation (1) into the heat equation $\psi_t = \psi_{xx}$, with initial conditions transforming simply into initial conditions for this latter equation: if $u(x, 0) = f(x)$ is the given condition, then the corresponding initial condition for the heat equation is given by

$$\psi(x, 0) = \exp\left[-\frac{1}{\mu}\int_0^x f(\xi)\mathrm{d}\xi\right].$$

The relation between the Burgers and the heat equation was already mentioned in an earlier book (Forsyth, 1906), but the former had not been recognized as physically relevant; hence, the importance of this connection was seemingly not noticed at the time. Using the transformation of Equation (5), known as the Cole–Hopf transformation, it is easy to solve the initial value problem for this equation. Recently, a generalization of the Cole–Hopf transformation has been successfully used to linearize the boundary value problem for the Burgers equation posed on the semiline $x > 0$ (Calogero & De Lillo, 1989).

The existence of this linearizing transformation, which is a transformation of Bäcklund type (Rogers & Shadwick, 1982) relating the solutions of two different PDEs, stimulated work to extend this approach to a generalized version of the Burgers equation, such as the Korteweg–de Vries–Burgers equation, given by

$$u_t + uu_x = \frac{\mu}{2}u_{xx} - \varepsilon u_{xxx}, \quad \varepsilon > 0. \tag{6}$$

Although it was found out that such a directly linearizing transformation did not exist, efforts in this direction were rewarded by several discoveries. Indeed, the importance of a linearizing transformation became evident when the inverse scattering transform (IST) was discovered, leading to the full analytical understanding of the solution of the Cauchy problem for the Korteweg–de Vries (KdV) equation, and later all integrable evolution equations in one spatial dimension, such as KdV, the nonlinear Schrödinger, and the sine-Gordon equations.

A crucial step in the discovery of the IST was an observation made by Robert Miura. In analogy to gas dynamics, he noted that one needs conservation laws to compute jump conditions across the region where the solution is small and essentially dispersive, isolating the solitonic part, which is thought of as a kind of reversible shock. This led to the connection between the KdV and modified KdV equation via the Miura transformation and eventually to the IST through which these nonlinear equations are solved through a series of linear problems (Gardner et al., 1967).

Nowadays, the Burgers equation is used as a simplified model of a kind of hydrodynamic turbulence (Case & Chiu, 1969), called Burgers turbulence. Burgers himself wrote a treatise on the equation now known by his name (Burgers, 1974), where several variants are proposed to describe this particular kind of turbulence. Generalizations such as the KdV–Burgers equation (6) arose from the need to model more complicated physical situations and introduce more factors than those that the Burgers equation takes into account. Lower-order friction terms may be considered that reduce the amplitude of the wave, although in a different scale and manner than the reduction due to the higher-order diffusion term u_{xx}. For example, the KdV–Burgers equation is an appropriate model when a different higher-order amplitude-reducing effect, namely dispersion, is introduced. Depending on the relative sizes of μ and ε, this equation may exhibit either an essentially shock-like structure, with the presence of dispersive tail, or mainly dispersive phenomena; thus, Equation (6) has been proposed as a natural model for hydrodynamic turbulence. In the context of the study of gas dynamics (particularly turbulent and vorticity phenomena), the Burgers equation has also been used to model phase diffusion along vortex filaments.

BEATRICE PELLONI

See also **Constants of motion and conservation laws; Inverse scattering method or transform; Shock waves; Turbulence**

Further Reading

Bateman, H. 1915. Some recent research on the motion of fluids. *Monthly Weather Review*, 43: 163–170

Burgers, J. 1940. Application of a model system to illustrate some points of the statistical theory of free turbulence. *Proceedings of the Nederlandse Akademie van Wetenschappen*, 43: 2–12

Burgers, J. 1948. A mathematical model illustrating the theory of turbulence, *Advances in Applied Mechanics*, 1: 171–199

Burgers, J. 1974. *The Nonlinear Diffusion Equation: Asymptotic Solutions and Statistical Problems*, Dordrecht and Boston: Reidel

Calogero, F. & De Lillo, S. 1989. The Burgers equation on the semiline. *Inverse Problems*, 5: L37

Case, K.M. & Chiu, S.C. 1969. Burgers turbulence models. *Physics of Fluids*, 12: 1799–1808

Cole, J. 1951. On a quasilinear parabolic equation occuring in aerodynamics. *Quarterly Journal of Applied Mathematics*, 9:225–236

Forsyth, A.R. 1906. *Theory of Differential Equations*, Cambridge: Cambridge University Press

Gardner, C.S., Greene, J.M., Kruskal, M.D. & Miura, R.M. 1967. Method for solving the Korteweg-de Vries equation. *Physical Review Letters*, 19: 1095–1097

Hopf, E. 1950. The partial differential equation $u_l + uu_x = \mu u_{xx}$. *Communications in Pure and Applied Mathematics*, 3: 201–230

Lax, P.D. 1973. *Hyperbolic Systems of Conservation Laws and the Mathematical Theory of Shock Waves*, Philadelphia: Society for Industrial and Applied Mathematics

Newell, A.C. (editor). 1974. *Nonlinear Wave Motion*, Providence, RI: American Mathematical Society

Rogers, C. & Shadwick, W.F. 1982. *Bäcklund Transformations and Their Applications*, New York: Academic Press

Sachdev, P.L. 1987. *Nonlinear Diffusive Waves*, Cambridge and New York: Cambridge University Press

Smoller, J. 1983. *Shock Waves and Reaction-Diffusion Equations*, Berlin and New York: Springer

Whitham, G.B. 1974. *Linear and Nonlinear Waves*, New York: Wiley-Interscience

BUTTERFLY EFFECT

The Butterfly Effect serves as a metaphor for what in technical language is called "sensitive dependence on initial conditions" or "deterministic chaos," the fact that small causes can have large effects.

As recounted by Gleick (1987, Chapter 1), in the early 1960s, Edward Lorenz was carrying out computer simulations on a 12-dimensional weather model. One day, he decided to run a particular time series for longer. In order to save time, he restarted his code from data from a previous printout. After returning from a coffee break, he found that the weather simulation had diverged sharply from that of his earlier run. After some checks, he could only conclude that the difference was caused by the difference in initial conditions: he had typed in only the first three of the six decimal digits that the computer worked with internally. Apparently, his assumption that the fourth digit would be unimportant was false.

Lorenz realized the importance of his observation: "If, then, there is any error whatever in observing the present state—and in any real system such errors seem inevitable—an acceptable prediction of an instantaneous state in the distant future may well be

impossible" (Lorenz, 1963, p. 133). Indeed, the error made by discarding the fourth and higher digits is so small that it can be imagined to represent the effect of the flap of the wings of a butterfly. Lorenz originally used the image of a seagull. The more lasting name seems to have come from his address at the annual meeting of the American Association for the Advancement of Science in Washington, December 29, 1972, which was entitled "Predictability: does the flap of a butterfly's wings in Brazil set off a tornado in Texas?" The text of this talk was never published but is presented in its original form as an appendix in Lorenz (1993).

Sensitive dependence on initial conditions forces us to distinguish between determinism and predictability, two concepts often confused by scientists and popular writers alike. Determinism has to do with how Nature (or, less ambitiously, any system under consideration) behaves, while predictability has to do with what we, human beings, are able to observe, analyze, and compute. We have determinism if we have a law or a formula describing exactly, and fully, how the system behaves given its present state. To have predictability we need, in addition, to be able to measure the present state of the system with sufficient precision and to compute with the given formula (to solve the equations) in a sufficiently accurate computational scheme.

Determinism is most famously expressed by Pierre-Simon Laplace (1814, p.2):

> An intelligence that, at a given instant, could comprehend all the forces by which nature is animated and the respective situation of the beings that make it up, if moreover it were vast enough to submit these data to analysis, would encompass in the same formula the movements of the greatest bodies of the universe and those of the lightest atoms. For such an intelligence nothing would be uncertain, and the future, like the past, would be open to its eyes.

Laplace's dramatic statement is often erroneously interpreted as a belief in perfect predictability now rendered untenable by the chaos theory. But he was describing determinism: given the state of the system (the universe) at some time, we have a formula (a set of differential equations) that gives, in principle, the state of the system at any later time. Nowhere will one find a claim about the computability, by us humans, of all the consequences of the laws of mechanics. Indeed, the quote appears in the introduction of a book on probability. Laplace is, in fact, assuming incomplete knowledge from the start and uses probabilities to make rational inferences. If it were not for quantum mechanics, Laplace's statement would still stand, unaffected by deterministic chaos.

To illustrate the problems with computability, consider the simple but important example of the (deterministic) Bernoulli shift map defined by

$$f : [0, 1] \to [0, 1] : \; x_{n+1} = 2x_n \,(\mathrm{mod}\, 1).$$

On numbers in binary representation, this map has a particularly simple effect: shift the binary point one place to the right and discard the first digit. For example, if $x_0 = 0.10110$ (which corresponds to the decimal 0.6875), then $x_1 = 0.01100$ (decimal 0.375). Now, any rational starting number x_0 is represented by a repeating sequence of 0s and 1s and hence leads to a periodic orbit of f, while any irrational x_0 is represented by a nonrepeating sequence of 0s and 1s and hence leads to a nonperiodic orbit. This latter sequence would appear as unpredictable as the sequence of heads and tails generated by flipping a coin, the quintessentially random process. Since there is an irrational number arbitrarily close to every rational number and vice versa, the map exhibits a sensitive dependence on initial conditions. In practice, on a computer, numbers are always represented with finite precision; hence, the computations become completely meaningless once—after a finite number of iterations—all significant digits have been removed. In the standard 32-bit (4-byte) floating point arithmetic with 23-bit mantissa, this will be after roughly 23 iterations.

The significance of the Bernoulli shift map is that dynamical systems theory tells us that its dynamics lies at the heart of the so-called "horseshoe dynamics," which in turn is commonly found in (the wide class of) systems with homoclinic (i.e., expanding and reinjecting) orbits (Wiggins, 1988). It means that in many situations, all we can say about a system's dynamics is of a statistical nature. A quantitative measure of the sensitivity on initial conditions, and therefore a measure of the predictability horizon, is provided by the leading Lyapunov exponent.

The possibility of small causes having large effects (in a perfectly deterministic universe) was anticipated by many scientists before Lorenz, and even before the birth of dynamical systems theory, which is generally accepted to have its origins in Poincaré's work on differential equations toward the end of the 19th century. Maxwell (1876, p. 20) wrote: "There is a maxim which is often quoted, that 'The same causes will always produce the same effects.'" After discussing the meaning of this principle, he adds: "There is another maxim which must not be confounded with [this], which asserts that 'Like causes produce like effects.' This is only true when small variations in the initial circumstances produce only small variations in the final state of the system." He then gives the example of how a small displacement of railway points sends a train on different courses.

Others have often used the image of the weather:

Wiener (1954/55):

> It is quite conceivable that the general outlines of the weather give us a good, large picture of its course for hours or possibly even for days. However, I am profoundly skeptical of the unimportance of the unobserved part of the weather for longer periods.

> To assume that these factors which determine the infinitely complicated pattern of the winds and the temperature will not in the long run play their share in determining major features of weather, is to ignore the very real possibility of the self-amplification of small details in the weather map. A tornado is a highly local phenomenon, and apparent trifles of no great extent may determine its exact track. Even a hurricane is probably fairly local where it starts, and phenomena of no great importance there may change its ultimate track by hundreds of miles.

Poincaré (1908, p. 67):

> Why have meteorologists such difficulty in predicting the weather with any certainty? Why is it that showers and even storms seem to come by chance, so that many people think it quite natural to pray for rain or fine weather, though they would consider it ridiculous to ask for an eclipse by prayer? We see that great disturbances are generally produced in regions where the atmosphere is in unstable equilibrium. The meteorologists see very well that the equilibrium is unstable, that a cyclone will be formed somewhere, but exactly where they are not in a position to say; a tenth of a degree more or less at any given point, and the cyclone will burst here and not there, and extend its ravages over districts it would otherwise have spared. If they had been aware of this tenth of a degree, they could have known it beforehand, but the observations were neither sufficiently comprehensive nor sufficiently precise, and that is the reason why it all seems due to the intervention of chance.

Even earlier, Franklin (1898, p. 173) had used an analogy surprisingly similar to Lorenz's:

> . . . an infinitesimal cause may produce a finite effect. Long range detailed weather prediction is therefore impossible, and the only detailed prediction which is possible is the inference of the ultimate trend and character of a storm from observations of its early stages; and the accuracy of this prediction is subject to the condition that the flight of a grasshopper in Montana may turn a storm aside from Philadelphia to New York!

Duhem (1954, p. 141) used Hadamard's theorem of 1898 on the complicated geodesic motion on surfaces of negative curvature to "expose fully the absolutely irremediable physical uselessness of certain mathematical deductions." If such incomputable behavior is possible in mechanics, "the least complex of physical theories," Duhem goes on to ask rhetorically, "Should we not meet that ensnaring conclusion in a host of other, more complicated problems, if it were possible to analyse the solutions closely enough?"

Many had contemplated the possibility of sensitive dependence on initial conditions, but Lorenz was the first to see it actually happening quantitatively in the numbers spit out by his Royal McBee computing machine, and to be sufficiently intrigued by it to study it more closely in the delightfully simple system of equations now bearing his name (Lorenz, 1963). Indeed, while most scientists, with Duhem, had looked to complicated systems for unpredictable behavior, Lorenz found it in simple ones and thereby made it amenable to analysis.

GERT VAN DER HEIJDEN

See also **Chaotic dynamics; Determinism; General circulation models of the atmosphere; Horseshoes and hyperbolicity in dynamical systems; Lorenz equations**

Further Reading

Bricmont, J. 1995. Science of chaos or chaos in science? *Physicalia Magazine*, 17: 159–208

Duhem, P. 1954. *The Aim and Structure of Physical Theory*, translated by Ph.P. Wiener, Princeton: Princeton University Press (original French edition, *La Théorie Physique: Son Objet, Sa Structure, 2ème éd.*, Paris: Marcel Rivière & Cie, 1914; 1st edition, 1906)

Franklin, W.S. 1898. A book review of P. Duhem, *Traité Elémentaire de Méchanique Chimique fondée sur la Thermodynamique*, vols. I and II, Paris, 1897, *The Physical Review*, 6: 170–175

Gleick, J. 1987. *Chaos: Making a New Science*, London: Heinemann, and New York: Viking

Laplace, P.-S. 1814. *Philosophical Essay on Probabilities*, translated from the fifth French edition of 1825 by A.I. Dale, Berlin and New York: Springer, 1995 (first edition published in French, 1814)

Lorenz, E.N. 1963. Deterministic nonperiodic flow. *Journal of the Atmospheric Sciences*, 20: 130–141

Lorenz, E.N. 1993. *The Essence of Chaos*, Seattle: University of Washington Press and London: University College London Press

Maxwell, J.C. 1876. *Matter and Motion*, New York: Van Nostrand

Poincaré, H. 1908. *Chance*. In *Science and Method*, pp. 64–90, translated by F. Maitland, London: Thomas Nelson and Sons, 1914 (original French edition, *Science et Méthode*, Paris: E. Flammarion, 1908)

Wiener, N. 1954/55. Nonlinear prediction and dynamics. *Proceedings of the Third Berkeley Symposium on Mathematical Statistics and Probability*, Berkeley: University of California Press, vol. 3, pp. 247–252; *Mathematical Reviews*, 18: 949 (1957); reprinted in 1981. *Norbert Wiener: Collected Works with Commentaries*, vol. III, edited by P. Masani, Cambridge, Massachusetts: MIT Press, pp. 371–376

Wiggins, S. 1988. *Global Bifurcations and Chaos*, Berlin and New York: Springer

C

CALOGERO–MOSER MODEL

See **Particles and antiparticles**

CANDLE

At about the time that John Scott Russell was systematically studying hydrodynamic solitons on a Scottish canal, Michael Faraday, the brilliant English experimental physicist and physical chemist, organized his annual Christmas Lectures on facets of natural philosophy for young people. These included a series on the candle that began with the claim (Faraday, 1861):

> There is no better, there is no more open door by which you can enter into the study of natural philosophy than by considering the physical phenomena of a candle.

Although this assertion may have startled some of his listeners, Faraday went on to support it with a sequence of simple yet elegant experiments that clearly expose the structure and composition of a candle flame, demonstrating a stream of energy-laden vapor feeding into the flame and suggesting an analogy with the process of respiration in living organisms (Day & Catlow, 1994). (An engraving showing Faraday presenting one of these lectures can be found on a recent British 20-pound note.)

While the details are intricate (Fife, 1988), the flame of a candle can be regarded globally as a dynamic process balancing two flows of energy: the rate at which energy is dissipated by the flame (through emission of heat and light) and the rate at which energy is released from the wax as the flame eats its way down the candle. Let us define variables as follows.

- P is the power dissipation by the flame, in units of (say) joules per hour.
- E is the chemical energy stored in the wax of the candle, in units of (say) joules per centimeter.
- v is the speed at which the flame moves down the candle.

If the rates of dissipation and energy input are equal, then the velocity of the flame is determined by the power balance condition

$$P = vE, \tag{1}$$

implying $v = P/E$ (cm/h). Metaphorically, the flame must digest energy at the same rate at which it is eaten.

Consider a family of cylindrical candles with various diameters (d), and assume the dissipation rates of their flames to be independent of the sizes of the candles. Since stored chemical energy is proportional to the area of cross section ($E \propto d^2$), power balance implies

$$v \propto 1/d^2. \tag{2}$$

Some measured flame speeds for typical candles are plotted on a log–log scale in Figure 1, where the dashed line of slope -2 indicates a $1/d^2$ dependence. From this figure, it is evident that the inverse square dependence of Equation (2) is obeyed for larger candles. For smaller candles, v is somewhat less than expected, because the flames are not so large.

Although Equation (2) was derived for candles, Equation (1) is quite general, expressing a global constraint that governs the dynamics of many kinds of nonlinear diffusion, including the propagation of nerve impulses (Scott, 2002). For a smooth axon described by the Hodgkin–Huxley equations, power balance is established between electrostatic energy released from the fiber membrane and ohmic dissipation by circulating ionic currents, implying $v \propto \sqrt{d}$. (Plotted in Figure 1, this dependence would have a slope of $+\frac{1}{2}$.) For myelinated nerves, on the other hand, evolutionary pressures require that $v \propto d$, corresponding to a slope of unity in Figure 1.

In the language of nonlinear dynamics, a candle flame provides a physical example of an attractor, which is evidently stable because moderate disturbances (small gusts of air) do not extinguish the flame by forcing it out of its basin of attraction. As the air becomes still, the flame returns to its original shape and size. The task of lighting a candle, on the other hand, requires getting the wick hot enough—above an

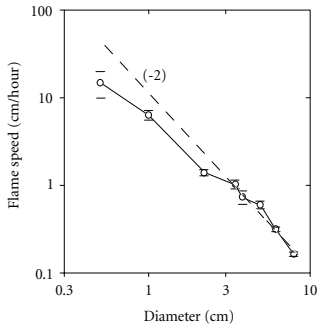

Figure 1. Measurements of flame speeds (v) for candles of different diameters (d). The error bars indicate rms deviations of about six individual measurements. (Data courtesy of Lela Scott MacNeil Scott (2003).)

ignition threshold and into the basin of attraction—so that a viable flame is established. Qualitatively similar conditions govern the firing of a nerve axon, leading to an all-or-nothing response.

From a more intuitive perspective, an ignition threshold implies the power balance indicated in Equation (1), where the corresponding flame is unstable. Above the threshold, instability arises from the establishment of a positive feedback loop, in which the flame releases more than enough chemical energy than is needed to maintain its temperature. Such a positive feedback loop is represented by the diagram

$$\begin{array}{c}\textbf{Release of energy } (vE)\\ \downarrow \quad \uparrow \\ \textbf{Dissipation of energy } (P),\end{array}$$

with the gain about the loop being greater than unity, implying an increase in the flame size with time (Scott, 2003). Eventually, this temporal increase is limited by nonlinear effects in the release and dissipation of energy, reducing the loop gain to unity as the fully developed flame is established.

The candle flame is an example of a reaction-diffusion (or autocatalytic) process, going back to an early suggestion by Robert Luther, a German physical chemist (Luther, 1906). Following a lecture demonstration of a chemical wave, Luther claimed that such systems should support traveling waves at a speed proportional to $\sqrt{D/\tau}$ where D is the diffusion constant for the reacting components (in units of distance squared per unit of time) and τ is a delay time for the onset of the reaction. During the 1930s, autocatalytic systems were studied in the context of genetic diffusion through spatially dispersed biological species, and in 1938 the equation

$$D\frac{\partial^2 u}{\partial x^2} - \frac{\partial u}{\partial t} = \frac{1}{\tau}u(u-a)(u-1), \qquad (3)$$

where a is a threshold parameter lying in the range $(0, \frac{1}{2}]$, was used by Soviet scientists Yakov Zeldovich and David Frank-Kamenetsky to represent a flame front. These authors showed that uniform traveling waves solutions of Equation (3) propagate at a fixed speed given by the expression

$$v = (1-2a)\sqrt{D/2\tau}, \qquad (4)$$

which includes both Luther's factor $\left(\sqrt{D/\tau}\right)$ and the power balance condition. Long overlooked by the neuroscience community, this early work on flame propagation offers a convenient model for the leading edge of a nerve impulse, confirming Faraday's intuition (Scott, 2002).

ALWYN SCOTT

See also **Attractors; Flame front; Hodgkin–Huxley equations; Power balance; Zeldovich–Frank-Kamenetsky equation**

Further Reading

Day, P. & Catlow, C.R.A. 1994. *The Candle Revisited: Essays on Science and Technology*, Oxford and New York: Oxford University Press

Faraday, M. 1861. *A Course of Six Lectures on the Chemical History of a Candle*. Reprinted as *Faraday's Chemical History of a Candle*, Chicago: Chicago Review Press, 1988

Fife, P.C. 1988. *Dynamics of Internal Layers and Diffusive Interfaces*, Philadelphia: Society for Industrial and Applied Mathematics

Luther, R. 1906. Räumliche Fortpflanzung chemischer Reaktionen. *Zeitschrift für Elektrochemie* 12(32): 596–600 (English translation in *Journal of Chemical Education* 64 (1987): 740–742)

Scott, A.C. 2002. *Neuroscience: A Mathematical Primer*, Berlin and New York: Springer

Scott, A.C. 2003. *Nonlinear Science: Emergence and Dynamics of Coherent Structures*. 2nd edition, Oxford and New York: Oxford University Press

CANONICAL VARIABLES

See **Hamiltonian systems**

CANTOR SETS

See **Fractals**

CAPACITY DIMENSION

See **Dimensions**

CAPILLARY WAVES

See **Water waves**

CARDIAC ARRHYTHMIAS AND THE ELECTROCARDIOGRAM

In the early 1900s, Willem Einthoven developed the string galvanometer to measure the potential differences in the body surface associated with the heartbeat and introduced a nomenclature for the deflections of the electrocardiogram that are still used today. For this work, Einthoven was awarded a Nobel prize in 1924 (Katz & Hellerstein, 1964).

The electrocardiogram (ECG) is a measurement of the potential difference between two points on the surface of the body. Because the heart generates waves of electrical activation that propagate through the heart during the cardiac cycle, ECG measurements reflect cardiac activity. Over the past century, physicians have learned how to interpret the electrocardiogram to diagnose a variety of different cardiac abnormalities. Although interpreting an ECG is difficult, this entry introduces the basic principles.

In order to appreciate the ECG, it is first necessary to have a rudimentary knowledge about the spread of the cardiac impulse in the heart. The heart is composed of four chambers, the right and left atria, and the right and left ventricles (see Figure 1). The atria are electrically connected to each other, but are insulated from the ventricles everywhere except in a small region called the atrioventricular (AV) node. The ventricles are also electrically connected to each other. The rhythm of the heart is set by the sinoatrial node located in the right atrium, which acts as the pacemaker of the heart. From a mathematical perspective, this pacemaker is an example of a nonlinear oscillator. Thus, if the rhythm is perturbed, for example, by delivering a shock to the atria, then in general the timing of subsequent firings of the sinus node may be reset (i.e., they occur at different times than they would have if the shock had not been delivered), but the frequency and amplitude of the oscillation will remain the same. A wave of excitation initiated in the sinus node travels through the atria, then through the atrioventricular node, and then through specialized Purkinje fibers to the ventricles. The wave of electrical excitation is associated with a wave of mechanical contraction so that the cardiac cycle is associated with contraction and pumping of the blood through the body. The right and left atria are comparatively small chambers and act as collection points for blood. The right atrium collects blood from the body and the left atrium collects blood from the lungs. The right ventricle pumps blood to the lungs to be oxygenated, whereas the left ventricle pumps blood that has returned to the heart from the lungs to the rest of the body. The right atrium and right ventricle are separated by the tricuspid valve that prevents backflow of blood during the ventricular contraction. Similarly, the left atrium and left ventricle are separated by the mitral valve. In order to pump the blood, the ventricles are comparatively large and muscular.

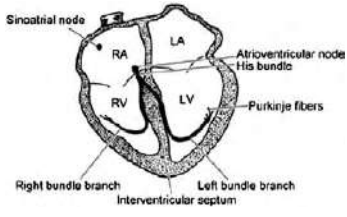

Figure 1. A schematic diagram of the heart. Adapted from Goldberger & Goldberger (1994) with permission.

In the normal ECG, there are several main deflections labeled the P wave, the QRS complex, and the T wave, Figure 2a (Goldberger & Goldberger, 1994). The P wave is associated with the electrical activation of the atria, the QRS complex is associated with the electrical activation of the ventricles, and the T wave is associated with the repolarization of the ventricles. The duration of the PR interval reflects the conduction time from the atria to ventricles, which is typically 120–200 ms. The duration of the QRS complex reflects the time that it takes for the wave of excitation to activate the ventricles. Because of the specialized Purkinje fibers, the wave of activation spreads rapidly through the ventricles so that the normal duration of the QRS complex is less than 100 ms. The time interval from the beginning of the QRS complex to the end of the T wave, called the QT interval, reflects the time that the ventricles are in the contraction phase. The

Figure 2. Sample electrocardiograms. In all traces, one large box represents 0.2 s. (a) The normal electrocardiogram. The P wave, QRS complex, and T wave are labeled. (b) 3:2 Wenckebach rhythm, an example of a second-degree heart block. There are 3 P waves for each R wave in a repeating pattern. (c) Parasystole. The normal beats, labeled N, occur with a period of about 790 ms, and the abnormal ectopic beats, labeled E, occur with a regular period of 1300 ms s. However, when ectopic beats fall too soon after the normal beats, they are blocked. Normal beats that occur after an ectopic beat are also blocked. If a normal and ectopic beat occur at the same time, the complex has a different geometry, labelled F for fusion. In this record, the number of normal beats occurring between ectopic beats is either 4, 2, or 1, satisfying the rules given in the text. Panels (a) and (b) are adopted from Goldberger & Goldberger (1994), with permission. Panel (c) is adapted from Courtemanche et al. (1989) with permission.

duration of QT interval depends somewhat on the basic heart rate. It is shorter when the heart is beating faster. For heart beats in the normal range, the QT interval is typically of the order of 300–450 ms.

On examining an ECG, one first looks for P waves. The presence of the P wave indicates that the heart beat is being generated by the normal pacemaker. In the normal heart, each P wave is followed by a QRS complex and then a T wave. The heart rate is often measured by time intervals between two consecutive R waves. Abnormally fast heart rates, faster than about 90 beats per minute, are called tachycardia, and abnormally slow heart rates, slower than about 50 beats per minute, are called bradycardia.

Reduced to the basics, all cardiac arrhythmias (i.e., abnormal cardiac rhythms) are associated with abnormal initiation of a wave of cardiac excitation, abnormal propagation of a wave of cardiac excitation, or some combination of the two. Given such a simple underlying concept, it is not surprising that mathematicians have been attracted to the study of cardiac arrhythmias, or that many cardiologists are mathematically inclined. However, despite the apparent simplicity, cardiac arrhythmias can manifest themselves in many different ways, and it is still not always possible to figure out the mechanism of an arrhythmia in any given individual. The following is focused on some arrhythmias that are well understood and that have interesting mathematical analyses.

One class of cardiac arrhythmias is associated with conduction defects through the AV node. In first-degree heart block, the PR interval is elevated above its normal value, but each P wave is followed by a QRS complex and T wave. However, in second-degree heart block, there are more P waves than QRS complexes, as some of the atrial activations do not propagate to the ventricles. This type of cardiac arrhythmia, sometimes called Wenckebach rhythms (after Karel Frederik Wenckebach, a Dutch-born Austrian physician, who studied these rhythms at the beginning of the 20th century), has repeatedly attracted theoretical interest (Katz & Hellerstein, 1964). It is common to classify Wenckebach rhythms by a ratio giving the number of P waves to the number of QRS complexes. For example, Figure 2b shows a 3:2 heart block.

In the 1920s, Balthasar van der Pol and J. van der Mark developed a mathematical model of the heart as coupled nonlinear oscillators that displayed striking similarities to the Wenckebach rhythms. We now understand that in a number of different models, as the frequency of atrial activation is increased, different types of $N:M$ heart block can be observed (van der Pol & van der Mark, 1928). In fact, theoretical models have demonstrated that if there is $N:M$ heart block at one stimulation frequency and an $N':M'$ heart block at a higher frequency, then the $N+N':M+M'$ heart block is expected at some intermediate stimulation frequency. This result provides a mathematical classification complementary to the cardiological classification, and can be confirmed in clinical settings (Guevara, 1991). Finally, in third-degree heart block, there is a regular atrial rhythm and a regular ventricular rhythm (at a slower frequency), but there is no coupling between the two rhythms. Such rhythms in mathematics are called quasi-periodic.

A different type of rhythm that appeals to mathematicians is called parasystole. In the "pure" case, the normal sinus rhythm beats at a constant frequency, and an abnormal (ectopic) pacemaker in the ventricles beats at a second slower frequency (Glass et al., 1986; Courtemanche et al., 1989). Figure 2c shows the normal (N) beats and the ectopic (E) beats. If the ectopic pacemaker fires at a time outside the refractory period of the ventricles, then there is an abnormal ectopic beat, identifiable on the ECG by a morphology distinct from the normal beat, and the following normal sinus beat is blocked. If the normal and abnormal beats occur at the same time, this leads to a fusion (F) beat.

Surprisingly, this simple mechanism has amazing consequences that can be appreciated by forming a sequence of integers that counts the number of sinus beats between two ectopic beats. In general, for fixed sinus and ectopic frequencies and a fixed refractory period, in this sequence, there are at most three integers, where the sum of the two smaller integers is one less than the largest integer. Moreover, given the values of the parameters, it is possible to predict the three integers. The mathematics for this problem is related to the "gaps and steps" problem in number theory. Both AV heart block and parasystole lead to mathematical predictions of cardiac arrhythmias in humans, which have been tested in experimental models and in humans. Such arrhythmias are diagnosed and treated when necessary, by physicians who have no knowledge of the underlying mathematics. Thus, to date, the mathematical analysis of these arrhythmias is of little medical interest.

From a medical perspective, the most important class of arrhythmias is called re-entrant arrhythmias. In these arrhythmias, the period of the oscillation is set by the time an excitation takes to travel in a circuitous path, rather than the period of oscillation of a pacemaker. The re-entrant circuit can be found in a single chamber of the heart or can involve several anatomical features of the heart (Josephson, 2002). In typical atrial flutter, there is a wave circulating around the tricuspid valve in the right atrium; in Wolf–Parkinson–White syndrome, there can be excitation traveling in the normal circuit from atria to the AV node to the ventricles, but then traveling retrogradely back to the atria via an abnormal accessory pathway between the ventricles and the atria. Also in some patients who have had a heart attack, there is a re-entrant circuit contained entirely in the ventricles. In all these three re-entrant arrhythmias, a

part of the circuit is believed to be a comparatively thin strand of tissue.

Considering these re-entrant arrhythmias from a mathematical perspective, the wave often appears to be circulating on a one-dimensional ring. This conceptualization developed by cardiologists has an important implication for therapy: "if you cut the ring, you can cure the rhythm." By inserting catheters directly into a patient's heart and delivering radio frequency radiation to precisely identified loci, the cardiologist destroys heart tissue and can often cure these serious arrhythmias. In these cases, the cardiologist is thinking like a topologist since changing the topology of the heart cures the arrhythmia. Moreover, there is a body of mathematics that has studied the properties of excitation traveling on one-dimensional rings (Glass et al., 2002).

Other reentrant arrhythmias are not as well understood and are not as easily treated. Many theoretical and experimental studies (*See* **Cardiac muscle models**) have documented spiral waves circulating stably in two dimensions and scroll waves circulating in three dimensions (Winfree, 2001). Since real hearts are three-dimensional, and there is still no good technology to image excitation in the depth (as opposed to the surface) of the cardiac tissue, the actual geometry of excitation waves in cardiac tissue associated with some arrhythmias is not as well understood and is now the subject of intense study.

From an operational point of view, it is suggested that any arrhythmia that cannot be cured by a small localized lesion in the heart is a candidate for a circulating wave in two or three dimensions. Such rhythms include atrial and ventricular fibrillation. In these rhythms, there is evidence of strong fractionation (breakup) of excitation waves giving rise to multiple small spiral waves and patterns of shifting blocks. Tachycardias can also arise in the ventricles in patients other than those who have experienced a heart attack, or perhaps occasionally in hearts with completely normal anatomy, and in these individuals it is likely that spiral and scroll waves are the underlying geometries of the excitation. A particularly dangerous arrhythmia, polymorphic ventricular tachycardia (in which there is a continually changing morphology of the ECG complexes), is probably associated with spiral and scroll waves that undergo a meander. New technologies are presenting unique opportunities to image cardiac arrhythmias in model systems and the clinic, and nonlinear dynamics is suggesting new strategies for controlling cardiac arrhythmias. For a summary of advances up until 2002 see the collection of papers in Christini & Glass (2002).

Despite the great advances in research and medicine over the past 100 years, there is still a huge gap between what is understood and what actually happens in the human heart. The only way to appreciate this gap is to toss out the models and start looking at real data from patients who are experiencing complex arrhythmia as measured on the ECG. All who plan to model cardiac arrhythmias are encouraged to take this step.

LEON GLASS

See also **Cardiac muscle models; Scroll waves; Spiral waves; Van der Pol equation**

Further Reading

Christini, D. & Glass, L. (editors). 2002. Focus issue: mapping and control of complex cardiac arrhythmias. *Chaos*, 12(3)

Courtemanche, M., Glass, L., Bélair, J., Scagliotti, D. & Gordon, D. 1989. A circle map in a human heart. *Physica* D, 40: 299–310

Glass, L., Goldberger, A., & Bélair, J. 1986. Dynamics of pure parasystole. *American Journal of Physiology*, 251: H841–H847

Glass, L., Nagai, Y., Hall, K., et al. 2002. Predicting the entrainment of reentrant cardiac waves using phase resetting curves. *Physical Review* E, 65: 021908

Goldberger, A.L. & Goldberger, E. 1994. *Clinical Electrocardiography: A Simplified Approach*, 5th edition, St Louis: Mosby

Guevara, M.R. 1991. Iteration of the human atrioventricular (AV) nodal recovery curve predicts many rhythms of AV block. In *Biomechanics, Biophysics, and Nonlinear Dynamics of Cardiac Function*, edited by L. Glass, P. Hunter, P. & A., McCulloch Theory of Heart: New York: Springer, pp. 313–358

Josephson, M.E. 2002. *Clinical Cardiac Electrophysiology: Techniques and Interpretations*, Philadelphia and London: Lippincott Williams & Wilkins

Katz, L.N. & Hellerstein, H.K. 1964. Electrocardiography. In *Circulation of the Blood: Men and Ideas*, edited by A.P. Fishman & D.W. Richards, Oxford and New York: Oxford University Press, pp. 265–354

van der Pol, B. & van der Mark, J. 1928. The heartbeat considered as a relaxation oscillation, and an electrical model of the heart. *Philosophical Magazine*, 6: 763–765

Winfree, A.T. 2001. *The Geometry of Biological Time*, 2nd edition, Berlin and New York: Springer

CARDIAC MUSCLE MODELS

Cardiac muscle was created by evolution to pump the blood, and contractions of cardiac muscle, as of any muscle, are governed by calcium (Ca) ions. Increased concentration of calcium ions inside a cardiac cell ($[\mathrm{Ca}]_i$) induces a contraction, and diminished concentration induces relaxation (diastole). Calcium ion concentration in a cardiac cell is governed by many mechanisms. Importantly, a signal to increase $[\mathrm{Ca}]_i$ is given by an abrupt increase in membrane potential E, which is called an action potential (AP). The membrane potential E in cardiac cells is described by reaction diffusion equations.

Cardiac models have the mathematical structure of the well-known Hodgkin–Huxley (HH) equations:

$$\partial E/\partial t = -I(E, g_1, ..., g_N))/C + \nabla\cdot(D\nabla E), \quad (1)$$

$$\partial g_i/\partial t = (\tilde{g}_i(E) - g_i)/\tau_i(E), i = 1, ..., N, \quad (2)$$

where g_i are the gating variables (describing opening and closing of the gates of ionic channels), $\tilde{g}_i(E)$ are the steady values of those variables, $\tau_i(E)$ are associated time constants, $I(\cdots)$ is the transmembrane ionic current, and the diffusive term $\nabla \cdot (D\nabla E)$ describes the current flowing from the neighboring cells. In this description of the coupling, the anisotropy of the heart is properly described with an anisotropic diffusivity tensor. Equations (1) and (2) are similar to standard HH equations (with $N = 3$), and this formulation was used for the first cardiac model introduced by Denis Noble in 1962. As more and more ionic channels were discovered, they were incorporated into more detailed models: $N = 6$ for a modified Beeler–Reuter (BR) model, and $N > 10$ for the Luo–Rudy model and for recent Noble models. Although the original HH formulation was based on analytic functions for the $\tilde{g}_i(E)$ and $\tau_i(E)$, experimentally measured functions can be used in the equations, as shown in Figure 1. This results in both physical transparency and faster numerical calculations.

The functions $g_i(E)$ and $\tau_i(E)$ have a simple physical interpretation—the dynamics of each gating variable g_i are governed by the membrane potential E only. For fixed E, Equations (2) are linear and independent; each of them describes relaxation to the steady value $\tilde{g}_i(E)$ with the time constant $\tau_i(E)$. The characteristic times $\tau_i(E)$ scan four orders of magnitude (see Figure 1(a)), leading to qualitative understanding using time-scale separation.

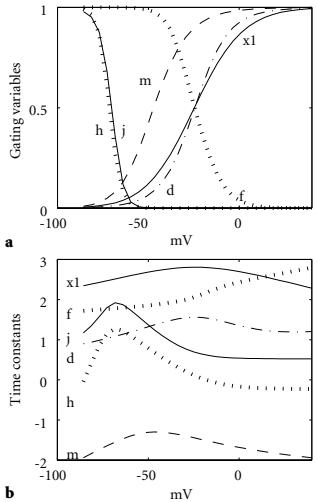

Figure 1. BR model with eight variables. (a) Gating variables $\tilde{g}_i(E)$. (b) Time constants $\tau_i(E)$ (log scale).

Noble's 1962 Model

This original cardiac model (N4 model), which is the key for understanding all subsequent models, consists of the following four equations (Noble, 1962).

$$\partial E/\partial t = -(I_{\mathrm{Na}}(E,m,h) + I_{\mathrm{K}}(E,n))/C + D\nabla^2 E, \quad (3)$$

$$\partial n/\partial t = (\tilde{n}(E) - n)/\tau_n, \quad (4)$$

$$\partial m/\partial t = (\tilde{m}(E) - m)/\tau_m, \quad (5)$$

$$\partial h/\partial t = (\tilde{h}(E) - h)/\tau_h, \quad (6)$$

where

$$I_{\mathrm{Na}}(E,m,h) = (g_{\mathrm{Na}} m^3 h + \varepsilon_1)(E - E_{\mathrm{Na}}), \quad (7)$$

$$I_{\mathrm{K}}(E,n) = (\alpha g_{\mathrm{K}} n^4 + \varepsilon_2)(E - E_{\mathrm{K}}), \quad (8)$$

A cardiac action potential has a duration of about 200 ms, which is about two orders of magnitude longer than that of a typical nerve impulse. To describe cardiac action potential, just one time constant in the HH equations was increased by a factor of 100, two small terms (ε_1 and ε_2) were added, and other time constants were adjusted to incorporate cardiac experimental results.

To observe how the N4 model works, note that it has three gating variables: m, n, and h. The characteristic time τ_n is about 100 ms, while τ_m and τ_h are almost two orders of magnitude faster (shorter). This permits adiabatic elimination of the fast equations (5) and (6), thereby replacing Equations (3)–(6) with a system of equations only (system N2) (Krinsky & Kokoz, 1973):

$$\partial E/\partial t = -(I_{\mathrm{Na}}(E,\tilde{m},\tilde{h}) + I_{\mathrm{K}}(E,n))/C + D\nabla^2 E, \quad (9)$$

$$\partial n/\partial t = (\tilde{n}(E) - n)/\tau_n. \quad (10)$$

Note that the current I_{Na} becomes

$$I_{\mathrm{Na}} = (g_{\mathrm{Na}} \tilde{m}^3(E)\tilde{h}(E) + \varepsilon_1)(E - E_{\mathrm{Na}}), \quad (11)$$

which contains only the known functions $\tilde{m} \equiv \tilde{m}(E)$ and $\tilde{h} \equiv \tilde{h}(E)$. The behavior of this model is illustrated in Figure 2.

Nullclines $\mathrm{d}E/\mathrm{d}t = 0$, and $\mathrm{d}n/\mathrm{d}t = 0$ for a Purkiknje fiber are shown in Figure 2(a). A Purkinje fiber has a pacemaker activity, which the nullclines (in the phase plane) show directly. Note that there is only one fixed point S, which is unstable, thus giving rise to limit cycle oscillations.

The nullclines for a myocyte are shown in Figure 2(b). There is no pacemaker activity in myocytes; thus, the nullclines show the absence of a limit cycle. Although there are two unstable fixed points (S′ and S″), they do not induce a limit cycle because there is a third fixed point (S) that is stable and determines the resting potential.

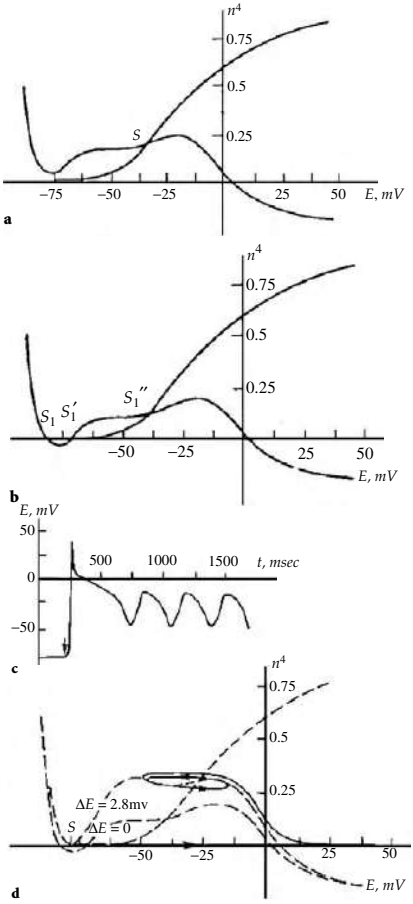

Figure 2. Analysis of the N4 model based on adiabatic elimination of two fast variables. (a) A Purkiknje fiber with a pacemaker activity. The nullclines of the reduced system N2 contain only one fixed point S that is unstable, thus giving rise to the limit cycle oscillations. (b) An excitable myocyte. There are three fixed points: S′ and S″ are unstable, and point S determines the resting potential. (c) Analysis of the effect of an arrhythmogenic drug aconitine, showing oscillations of the plateau of action potential (AP). (d) As in (c), where the nullclines show a small-amplitude limit cycle on the plateau of AP. (Parameters: (a) $\alpha = 1.2$; (b) $\alpha = 1.3$; (c) and (d) $\alpha = 1.3$; h $= \tilde{h}(E - \delta E)$; $\delta E = 2.8$ mV.)

Analysis of the effect of the arrhythmogenic drug aconitine (inducing oscillations on the plateau of the action potential) is shown in Figures 2(c) and (d). Aconitine induces dangerous oscillations because of a shift of the voltage dependence of Na

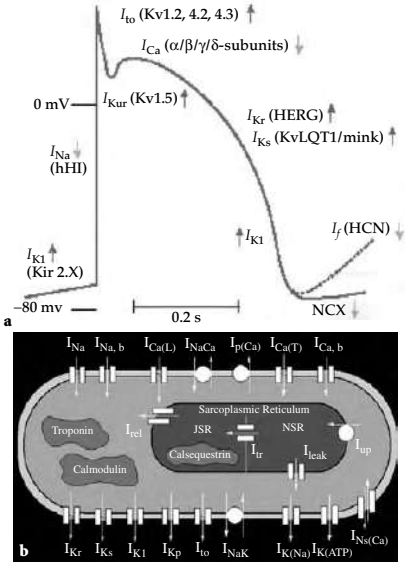

Figure 3. (a) Action potential showing the principal currents that flow in each phase, with the corresponding subunit clones shown in parentheses. (Courtesy of S. Nattel) (b) Main ionic currents (Courtesy of Y. Rudy).

inactivation variable h. Oscillations on the plateau of action potential are shown in Figure 2(c), and the corresponding nullclines are shown in Figure 2(d). The shift of $h(E)$ dependence results in the disappearance of the stable resting point and appearance of a small-amplitude limit cycle on the plateau of the AP. The electrophysiological characteristics in the full (N4) and reduced (N2) models are the same with an accuracy of 0.1–0.2 mV (Krinsky & Kokoz, 1973).

Contemporary Models

Recent models include more ionic currents (see Figures 1 and 3), and also incorporate a change of intracellular ionic concentrations. For example, the BR model contains an additional equation for the concentration $[Ca]_i$ of intracellular Ca:

$$\partial Ca_i/\partial t = I_{Ca}. \tag{12}$$

The Luo–Rudy (LR) model, and the Noble model are widely known. The LR model (Rudy, 2001) can be downloaded from http://www.cwru.edu/med/CBRTC/LRdOnline. Noble models are described at http://www.cellml.org/ and http://cor.physiol.ox.ac.uk/. The model of human ventricular myocyte (Ten Tusscher et al.

2003) is also available at http://www-binf.bio.uu.nl/khwjtuss/HVM.

In contemporary models the gap between the 100 and 1 ms time scales has been filled by many ionic currents, and (contrary to what was seen in the first cardiac model) the graphs even intersect each other (see Figure 1(b)). This makes the separation for fast and slow variables dependent upon the phase of AP, so results as in Figure 2 cannot be obtained directly. Instead, events on every time scale must be analyzed separately, eliminating adiabatically equations with a faster time scale and considering variables with a larger time scale fixed, or even postulating a model with only two to four equations (Keener & Sneyd, 1998; Fenton & Karma, 1998).

Models that do not follow the HH formalism are needed because HH-type models predict that a point stimulation will create a circular or an elliptical distribution of membrane potential, while in the experiments a quadrupolar distribution was found. Thus, *bidomain models* were created that describe separately potentials inside (E_i) and outside (E_o) of a cell instead of considering $E_o = 0$ as in the HH formulation. These models correctly reproduce many important electrophysiological effects, and turn out to be useful for understanding the mechanisms of cardiac defibrillation (Trayanova et al., 2002). The integration of these models, however, is computationally more expensive than the integration of HH models. *Markov chain models* are used to describe transitions between states of single ionic channels linking genetical defects with cardiac arrhythmias. They also depart from the HH formalism. *Anatomical models* incorporate cardiac geometry and tissue structure, but they require months of laborious measurements on anatomical slices cut from the heart. A new approach is being developed at INRIA in France, which aims to create models for every cardiac patient and is intended to be used in clinics. Cardiac contractions are measured and incorporated into the model. NMR tomography methods were used that permit obtaining anatomical data in a few minutes, not months, see http://www-sop.inria.fr/epidaure/. More cardiac models and authors can be found at http://www.cardiacsimulation.org/.

Dynamics of Myocardial Tissue

In the past, breakthroughs were due to very simple models beginning with the pioneering work of Norbert Wiener and Arturo Rosenbluth (Wiener & Rosenbluth, 1946). They led the way to understanding rotating waves using a cellular automata model, where a cardiac cell can be in three states only: rest, excitation, and refractory. This model explained anatomical reentry (a wave rotating around an obstacle (Wiener & Rosenbluth, 1946)), and predicted a free rotating wave. Partial differential equations yield more refined refined results (Keener & Sneyd, 1998).

As two- and three-dimensional studies of rotating waves are time consuming, it is often convenient to use a two-variable model, permitting increased speed of calculations by two orders of magnitude. Numerical simulation of ionic models can be accelerated either by adiabatic elimination of fast variable m (Na) activation or by slowing down its dynamics and increasing the diffusion coefficient to keep the propagation velocity unchanged.

Propagation Failure

As cardiac cells are connected via gap junctions, an excitation can be blocked when propagating from one cardiac cell to another, similar to the propagation failure in myelinated nerves. When an excitation propagates from auricles (A) to ventricles (V) via the AV node, a periodic pattern can be observed: for example, from every three pulses, only two pulses propagate, and the third pulse is blocked (3:2 Wenckebach periodicity). Other periodicities $N : (N - 1)$ can also be observed. Propagation block can be observed on any cardiac heterogeneity when the period T of stimulation is shorter than the restoration time R (refractory period). Usually, Wenckebach rhythms with only small periods N are observed because

$$T_N \sim N^{-2}, \tag{13}$$

where T_N is an interval of T that can yield. Wenckebach rhythms with period N. When an excitation block (Wenckebach rhythm) occurs in a two- or three-dimensional excitable medium, it generically gives rise to a wave break that evolves into a rotating wave. For cardiac muscle, initiation of a rotating wave is a dangerous event, often leading to life-threatening cardiac arrhythmias.

A new approach is being developed at INRIA in France, to create patient-specific models to be used in clinics. A 3-d electro-mechanical model of the heart is automatically adpted to a time series of volumetric cardiac images gated on the ECG (Ayache et al., 2001) providing useful quantitative parameters on the heart function in a few minutes, not months, see http://www-sop.inria.fr/epidaure/.

V. Krinsky, A. Pumir, and I. Efimov

See also **Hodgkin–Huxley equations; Myelinated nerves; Neurons; Scroll waves; Synchronization; Van der Pol equation**

Further Reading

Ayache, N., Chapelle, D., Clément, F., Coudiére, Y., Delingette, H., Désidéri, J.A., Sermesant, M. Sorine, M. & Urquiza, J. 2001. Towards model-based estimation of the cardiac electro-mechanical activity from ECG signals and ultrasound images. In *Functional Imaging and Modeling of the Heart* (*FIMH'01*), *Helsinki, Finland*, Lecture Notes in Computer Sciences, vol. 2230, Berlin, Springer, pp. 120–127

Chaos, topical issue: Ventricular fibrillation, 8(1), 1998
Fenton, F. & Karma, A. 1998. Vortex dynamics in three-dimensional continuous myocardium with fiber rotation: Filament instability and fibrillation. *Chaos*, 8: 20–47
Journal of Theoretical Biology, topical issue devoted to the work of Winfree, 2004
Keener, J. & Sneyd, J. 1998. *Mathematical Physiology*, New York: Springer
Krinsky, V. & Kokoz, Ju. 1973. Membrane of the Purkinje fiber. reduction of the noble equations to a second order system. *Biophysics*, 18: 1133–1139
Noble, D. 1962. A modification of the Hodgkin–Huxley equations applicable to Purkinje fiber action and pacemaker potential. *Journal of Physiology*, 160: 317–352
Noble, D. & Rudy, Y. 2001. Models of cardiac ventricular action potentials: iterative interaction between experiment and simulation. *Philosophical Transactions of the Royal Society A*, 359: 1127–1142
Rudy, Y. 2001. The cardiac ventricular action potential. In *Handbook of Physiology: A Critical, Comprehensive Presentation of Physiological Knowledge and Concepts. Section 2, The cardiovascular system. vol. 1, the heart*, edited by E. Page, H.A. Fozzard & R.J. Solaro, Oxford: Oxford University Press, pp. 531–547
Pumir, A., Romey, G. & Krinsky, V. 1998. De-excitation of cardiac cells. *Biophysical Journal*, 74: 2850–2861
Sambelashvili, A. & Efimov, I.R. 2002. Pinwheel experiment re-revisited. *Journal of Theoretical Biology*, 214: 147–153
TenTusscher, K.H.W.J., Noble, D., Noble, P.J. & Panfilov, A.V. 2003. A model of the human ventricular myocyte. *American Journal of Physiology*, 10: 1152
Trayanova, N., Eason, J. & Aguel, F. 2002. Computer simulations of cardiac defibrillation: a look inside the heart. *Computing and Visualization in Science*, 4: 259–270
Wiener, N. & Rosenbluth, N. 1946. The mathematical formulation of the problem of conduction of impulses in a network of connected excitable elements, specifically in cardiac muscle. *Archivos del Instituto de cardiologia de Mexico*, 16: 205–265

CASIMIRS

See **Poisson brackets**

CAT MAP

The cat map is perhaps the simplest area-preserving transformation that exhibits a high degree of chaos. In the development of the theory of dynamical systems, it served as a guiding example to illustrate new concepts such as entropy (Sinai, 1959) and Markov partitions (Adler & Weiss, 1967). The cat map owes its name to an illustration by V.I. Arnol'd showing the image of a cat before and after the application of the map. In the mathematical literature it is also referred to as "hyperbolic toral automorphism."

The torus M, which topologically has the shape of a doughnut, may be described by the points in the unit square (see Figure 1) where opposite sides are identified. Alternatively, one may think of a point on M as a point in the plane $\mathbb{R}^2$ modulo integer translations in $\mathbb{Z}^2$. This yields a representation of M as the coset space $\mathbb{R}^2/\mathbb{Z}:=\{x+\mathbb{Z}^2 : x \in \mathbb{R}^2\}$. The cat map is now a mapping $\phi : M \to M$ defined by $x \mapsto Ax \pmod{\mathbb{Z}^2}$, where

$$x = \begin{pmatrix} x_1 \\ x_2 \end{pmatrix}, \qquad A = \begin{pmatrix} a & b \\ c & d \end{pmatrix}, \tag{1}$$

provided $a, b, c, d \in \mathbb{Z}$ are chosen such that $|\det A| = 1$ and A has eigenvalues $\lambda_\pm$ with modulus not equal to one. (This implies that both eigenvalues are real and distinct.) The matrix A used in our illustration is

$$A = \begin{pmatrix} 2 & 1 \\ 1 & 1 \end{pmatrix}. \tag{2}$$

Let us now explore some of the dynamical properties that show that the cat map is indeed completely "chaotic" (*See* **Chaotic dynamics**). Sensitivity on initial conditions is measured by the rate of divergence of two nearby points, x and $x+\delta x$, under iterations of ϕ. For any smooth map ϕ, the Taylor expansion for small δx yields $\phi(x+\delta x) = \phi(x) + D\phi_x \delta x + O(\delta x^2)$ where $D\phi_x$ is the differential of ϕ at x; it may be viewed as a linear map from TM_x to $TM_{\phi(x)}$, the tangent spaces at x and $\phi(x)$, respectively.

Because ϕ is linear in the case of the cat map, the above Taylor expansion is in fact exact, that is, $\phi(x+\delta x) = \phi(x) + D\phi_x\, \delta x$ with $D\phi_x = A$. If $v_\pm$ are the eigenvectors of A corresponding to the eigenvalues $\lambda_\pm$, let us denote by E_x^+ and E_x^- the subspaces of TM_x spanned by v_+ and v_-, respectively. As $\lambda_+ \neq \lambda_-$, we have

$$TM_x = E_x^+ \oplus E_x^-. \tag{3}$$

Furthermore, since $|\lambda_+| = 1/|\lambda_-| > 1$, we find

$$\|D\phi_x(\xi)\| \geq \mathrm{e}^{\lambda}\|\xi\| \quad \text{if } \xi \in E_x^+, \tag{4}$$

$$\|D\phi_x(\xi)\| \leq \mathrm{e}^{-\lambda}\|\xi\| \quad \text{if } \xi \in E_x^-, \tag{5}$$

where $\lambda = \ln|\lambda_+| > 0$ and $\|\cdot\|$ is the Euclidean norm. Hence, ϕ is expanding in the direction of v_+, and contracting in the direction of v_-, which will therefore be referred to as the unstable and stable directions, respectively. [Here, inequalities (4) and (5) are in fact equalities; inequalities become necessary in the case of more general Anosov maps, if one seeks uniform bounds with λ independent of x.] For the nth forward or backward iterates of the map (n a positive integer), we have, by the above arguments with ϕ replaced by $\phi^{\pm n}$,

$$\|D\phi_x^n(\xi)\| \geq \mathrm{e}^{n\lambda}\|\xi\|, \quad \|D\phi_x^{-n}(\xi)\| \leq \mathrm{e}^{-n\lambda}\|\xi\|, \quad \text{if } \xi \in E_x^+, \tag{6}$$

$$\|D\phi_x^n(\xi)\| \leq \mathrm{e}^{-n\lambda}\|\xi\|, \quad \|D\phi_x^{-n}(\xi)\| \geq \mathrm{e}^{n\lambda}\|\xi\|, \quad \text{if } \xi \in E_x^-. \tag{7}$$

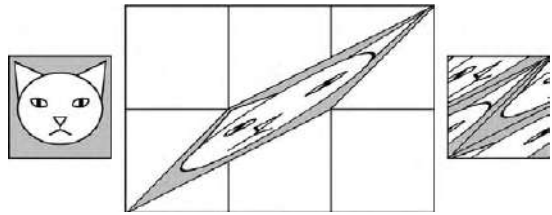

Figure 1. The cat map: the image of a cat in the unit square (left) is stretched by the matrix A (middle) and then re-assembled by cutting and translating (without rotation) the different parts of the cat's face back into the unit square (right). (Illustration by Federica Vasetti.)

The expansion/contraction is thus exponentially fast in time. Relations (3), (6), and (7) are equivalent to the statement that the cat map is an Anosov system. Special features of Anosov systems are ergodicity, mixing, structural stability, exponential proliferation of periodic orbits, and positive entropy h.

There is a particularly simple formula for the entropy h due to Sinai (1959), which states that $h = \lambda = \ln|\lambda_+|$. The number of fixed points of the nth iterate ϕ^n is equal to $|\det(1 - A^n)| = |(1 - \lambda_+^n)(1 - \lambda_-^n)|$ and is therefore asymptotically given by $\exp(nh)$, for large n. The notion of ergodicity implies that for any $f \in \mathrm{L}^1(M, \mathrm{d}x)$, for almost every $x \in M$ (that is, for all x up to a set of Lebesgue measure zero), we have

$$\lim_{N\to\infty} \frac{1}{N} \sum_{n=0}^{N-1} f(\phi^n x) = \langle f \rangle, \quad \langle f \rangle := \int_M f(x)\,\mathrm{d}x. \tag{8}$$

"Mixing" means that, if $f, g \in \mathrm{L}^2(M, \mathrm{d}x)$, then

$$\lim_{n\to\pm\infty} \int_M f(\phi^n x)\, g(x)\,\mathrm{d}x = \langle f \rangle \langle g \rangle. \tag{9}$$

Although the mixing property follows from general arguments for Anosov systems, it can be proved for ϕ directly by means of Fourier analysis. What is more, the rate of convergence in (9) is in fact exponentially fast in n for suitably smooth test functions f, g ("exponential decay of correlations") and super-exponentially fast for analytic ones.

Markov partitions are a powerful tool in the analysis of dynamical systems. In the case of the cat map the torus is divided into a finite collection of non-overlapping parallelograms $P_1, \ldots, P_N$ whose sides point in the directions of the eigenvectors v_+ and v_-, such that if $\phi(P_i)$ (or $\phi^{-1}(P_i)$) intersects with P_j, then it extends all the way across P_j. Let us construct an N by N matrix B whose coefficients are $B_{ij} = 1$ if the intersection of $\phi(P_i)$ with P_j is non-empty, and $B_{ij} = 0$ otherwise. A symbolic description of the dynamics of the cat map can now be obtained as follows. Consider doubly infinite sequences of the form $\cdots b_{-2}b_{-1}\underline{b_0}b_1b_2\ldots$, where b_n is an integer $1, \ldots, N$ with the condition that the number b_n can be followed by b_{n+1} only if $B_{b_n\, b_{n+1}} = 1$. To each such sequence we can associate a point x on M by requiring that for every $n \in \mathbb{Z}$, the parallelogram R_{b_n} contain the iterate $\phi^n(x)$. The symbolic dynamics of ϕ is now given by shifting the mark by one step to the right: the new word $\cdots b_{-1}b_0\underline{b_1}b_2b_3\cdots$ indeed represents the point $\phi(x)$. The dynamical properties of ϕ are thus encoded in the matrix B. In particular, the higher the rate of mixing of ϕ, the smaller the number of coefficients B_{ij} that are zero. This in turn means that we have fewer restrictions on $b_n \mapsto b_{n+1}$ and a typical orbit will be represented by a more "random" sequence of symbols.

Cat maps, as well as higher-dimensional toral automorphisms, are featured in most textbooks on dynamical systems and ergodic theory. An introduction to the basic concepts may be found in Arnol'd & Avez (1968), and more advanced topics, such as entropy, Markov partitions, and structural stability, are discussed, for example, in Adler & Weiss (1970), Katok & Hasselblatt (1995), Pollicott & Yuri (1998), and Shub (1987).

JENS MARKLOF

See also **Anosov and Axiom-A systems; Chaotic dynamics; Horseshoes and hyperbolicity in dynamical systems; Maps; Markov partitions; Measures**

Further Reading

Adler, R.L. & Weiss, B. 1967. Entropy, a complete metric invariant for automorphisms of the torus. *Proceedings of the National Academy of Sciences of the United States of America*, 57: 1573–1576

Adler, R.L. & Weiss, B. 1970. *Similarity of Automorphisms of the Torus*, Providence, RI: American Mathematical Society

Arnol'd, V.I. & Avez, A. 1968. *Ergodic Problems of Classical Mechanics*, New York and Amsterdam: Benjamin

Katok, A. & Hasselblatt, B. 1995. *Introduction to the Modern Theory of Dynamical Systems*, Cambridge and New York: Cambridge University Press

Pollicott, M. & Yuri, M. 1998. *Dynamical Systems and Ergodic Theory*, Cambridge and New York: Cambridge University Press

Sinai, Ya.G. 1959. On the concept of entropy for a dynamic system. *Doklady Akademii Nauk SSSR*, 124: 768–771

Shub, M. 1987. *Global Stability of Dynamical Systems*, Berlin and New York: Springer

CATALYTIC HYPERCYCLE

The concept of the "hypercycle" was invented in the 1970s in order to characterize a functional entity that integrates several autocatalytic elements into an organized unit (Eigen, 1971; Eigen & Schuster, 1977, 1978a,b). This concept is a key to understanding the dynamics of living organisms.

A catalytic hypercycle is defined as a cyclic network of autocatalytic reactions (Figure 1). Autocatalysts, in general, compete when they are supported by the same source of energy or material. Hypercyclic coupling introduces mutual dependence of elements and suppresses competition. Consequently, the fate of all members of a hypercycle is identical to that of the entire system and, in other words, no element of a hypercycle dies out provided the hypercycle as such survives.

The current view of biological evolution distinguishes periods of dominating Darwinian evolution based on variation, competition, and selection interrupted by rather short epochs of radical innovations often called *major transitions* (Maynard Smith & Szathmáry, 1995; Schuster, 1996). In the course of biological evolution major transitions introduce higher hierarchical levels. Examples are (i) the origin of translation from nucleic acid sequences into proteins including the invention of the genetic code, (ii) the transition from independent replicating molecules to chromosomes and genomes, (iii) the transition from the prokaryotic to the eukaryotic cell, (iv) the transition from independent unicellular individuals to differentiated multicellular organisms, (v) the transition from solitary animals to animal societies, and (vi) presumably a series of successive transitions from animal societies to humans. All major transitions introduce a previously unknown kind of cooperation into biology. The hypercycle is one of very few mechanisms that can deal with cooperation of otherwise competing individuals. It is used as a model system in prebiotic chemistry, evolutionary biology, theoretical economics, as well as in cultural sciences.

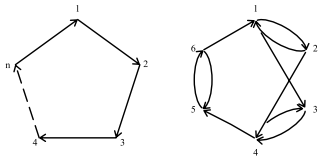

Figure 1. Definition of hypercycles. Replicator equations as described by the differential equation (2) can be symbolized by directed graphs: the individual species are denoted by nodes and two nodes are connected by an edge, $j \cdot \longrightarrow \cdot\, i$, if and only if $a_{ij} > 0$. The graphs of hypercycles consist of single Hamiltonian arcs as sketched on the left-hand side of the figure. These dynamical systems are permanent independent of the choice of rate parameters f_i. For $n \leq 5$ they represent the only permanent systems, but for $n \geq 6$ the existence of a single Hamiltonian arc is only a sufficient but not a necessary condition for permanence. The graph on the right-hand side, for example, does not contain a Hamiltonian arc but the corresponding replicator equation is permanent for certain choices of rate parameters (Hofbauer & Sigmund, 1998).

The simplest example of a catalytic hypercycle is the *elementary hypercycle*. It is described by the dynamical system

$$\frac{\mathrm{d}x_i}{\mathrm{d}t} = x_i \left(f_i x_{i-1} - \sum_{j=1}^{n} f_j x_{j-1} x_j \right);$$
$$i, j = 1, 2, \ldots, n;\ i, j = \bmod n. \qquad (1)$$

The catalytic interactions within a hypercycle form a directed closed loop comprising all elements, often called Hamiltonian arc: $1 \to 2 \to 3 \to \cdots \to n \to 1$ (Figure 1). Hypercycles are special cases of replicator equations of the class

$$\frac{\mathrm{d}x_i}{\mathrm{d}t} = x_i \left(\sum_{j=1}^{n} a_{ij} x_j - \sum_{j=1}^{n} \sum_{k=1}^{n} a_{jk} x_j x_k \right);$$
$$i, j, k = 1, 2, \ldots, n \qquad (2)$$

with $a_{ij} = f_i \cdot \delta_{i-1,j}$; $i, j = \bmod n$. (The 'mod n' function implies a cyclic progression of integers, $1, \ldots, n-1, n, 1, \ldots$. The symbol $\delta_{i,j}$ represents Kronecker's symbol: $\delta = 1$ for $i = j$ and $\delta = 0$ for $i \neq j$.)

For positive rate parameters and initial conditions inside the positive orthant (the notion of an *orthant* refers to the entire section of a Cartesian coordinate system in which the signs of variables do not change. In n-dimensions, the positive orthant is defined by $\{x_i > 0 \ \forall\, i = 1, 2, \ldots, n\}$.). The trajectory of a hypercycle remains within the orthant:

$$f_i > 0,\ x_i(0) > 0\ \forall i = 1, 2, \ldots, n \Longrightarrow x_i(t) > 0\ \forall t \geq 0.$$

In other words, none of the variables is going to vanish and hence, the system is *permanent* in the sense that no member of a hypercycle dies out in the limit of long times, $\lim_{t \to \infty} x_i(t) \neq 0\ \forall\, i = 1, \ldots, n$. The existence of a Hamiltonian arc, that is, a closed loop of directed edges visiting all nodes once, is a sufficient condition for permanence (Hofbauer & Sigmund, 1998). It is also a necessary condition for low-dimensional systems with $n \leq 5$, but there exist permanent

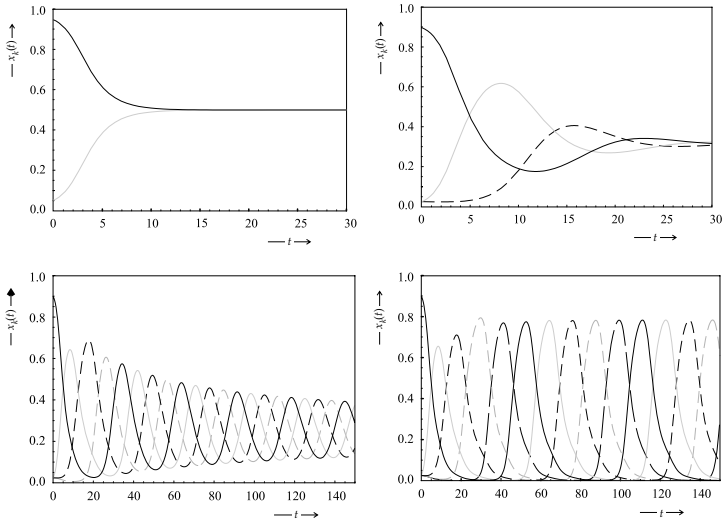

Figure 2. Solution curves of small elementary hypercycles. The figure shows the solution curves of Equation (1) with $f_1 = f_2 = \ldots = f_n = 1$ for $n = 2$ (upper left picture), $n = 3$ (upper right picture), $n = 4$ (lower left picture), and $n = 5$ (lower right picture). The initial conditions were $x_1(0) = 1 - (n-1) \cdot 0.025$ and $x_k(0) = 0.025 \,\forall\, k = 2, 3, \ldots, n$. The sequence of the curves $x_k(t)$ is $k = 1$ full black line, $k = 2$ full gray line, $k = 3$ hatched black line, $k = 4$ hatched grey line, and $k = 5$ black line with long hatches. The cases $n = 2$, 3, and 4 have stable equilibrium points in the middle of the concentration space $c = (1/n, 1/n, \ldots, 1/n)$; Equation (1) with equal rate parameters, $n = 4$, and linearized around the midpoint c exhibits a marginally stable "center" and very slow convergence is caused by the nonlinear term, which becomes smaller as the system approaches c. For $n = 5$, the midpoint c is unstable and the trajectory converges toward a limit cycle (Hofbauer et al., 1991).

dynamical systems for $n \geq 6$ without a Hamiltonian arc; one example is shown in Figure 1.

The dynamics of Equation (1) remains qualitatively unchanged when all rate parameters are set equal: $f_1 = f_2 = \ldots = f_n = f$, which is tantamount to a *barycentric* transformation of the differential equation (Hofbauer, 1981). The hypercycle is invariant with respect to a rotational change of variables, $x_i \Longrightarrow x_{i+1}$ with $i = 1, 2, \ldots, n$; $i \bmod n$, it has one equilibrium point in the center, and its dynamics depends exclusively on n. Some examples with small n are shown in Figure 2. The systems with $n \leq 4$ converge toward stable equilibrium points, whereas the trajectories of Equation (1) with $n \geq 5$ approach limit cycles. Independent of n, elementary hypercycles do not sustain chaotic dynamics.

Hypercycles have two inherent instabilities, which are easily illustrated for molecular species: (i) The members of the cycle may also catalyze the formation of nonmembers that do not contribute to the growth of the hypercycle, and thus hypercycles are vulnerable to parasitic exploitation (Eigen & Schuster, 1978a,b), and (ii) concentrations of individual species in oscillating hypercycles ($n \geq 5$) go through very small values, and these species might become extinct through random fluctuations. More elaborate kinetic mechanisms can stabilize the system in Case (ii). Exploitation by parasites, Case (i), can be avoided by compartmentalization. Competition between different hypercycles is characterized by a strong nonlinearity in selection (Hofbauer, 2002): once a hypercycle has been formed and established, it is very hard to replace it by another hypercycle. Epochs with hypercyclic dynamics provide explanations for "once for ever" decisions or "frozen accidents."

PETER SCHUSTER

See also **Artificial life; Biological evolution**

Further Reading

Eigen, M. 1971. Self-organization of matter and the evolution of biological macromolecules. *Naturwissenschaften*, 58: 465–523

Eigen, M. & Schuster, P. 1977. The hypercycle. A principle of natural self-organization. Part A: emergence of the hypercycle. *Naturwissenschaften*, 64: 541–565

Eigen, M. & Schuster, P. 1978a. The hypercycle. A principle of natural self-organization. Part B: The abstract hypercycle. *Naturwissenschaften*, 65: 7–41

Eigen, M. & Schuster, P. 1978b. The hypercycle. A principle of natural self-organization. Part C: The realistic hypercycle. *Naturwissenschaften*, 65: 341–369

Hofbauer, J. 1981. On the occurrence of limit cycles in the Volterra–Lotka equation. *Nonlinear Analysis, 5: 1003–1007*

Hofbauer, J. 2002. Competitive exclusion of disjoint hypercycles. Zeitschrift für Physikalische Chemie, 216: 35–39

Hofbauer, J. & Sigmund, K. 1998. *Evolutionary Games and Replicator Dynamics, Cambridge and New York: Cambridge University Press*

Hofbauer, J., Mallet-Paret, J. & Smith, H.L. 1991. Stable periodic solutions for the hypercycle system. Journal of Dynamics and Differential Equations, 3: 423–436

Maynard Smith, J. & Szathmáry, E. 1995. *The Major Transitions in Evolution, Oxford and New York: Freeman*

Schuster, P. 1996. How does complexity arise in evolution? Complexity, 2(1): 22–30

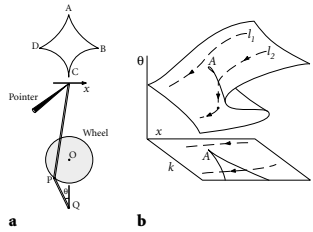

Figure 1. (a) Sketch of Zeeman's catastrophe machine, (b) A sketch of the three-dimensional solution surface and its projection onto two dimensions near the cusp A.

CATASTROPHE THEORY

Many natural phenomena (cell division, the bursting of bubbles, the collapse of buildings, and so on) involve discontinuous changes, whereas the majority of applied mathematics is directed toward modeling continuous processes. On the other hand, catastrophe theory is primarily concerned directly with singular behavior and as such deals with properties of discontinuities directly. This approach has found use in many and diverse fields and at one time was heralded as a new direction in mathematics, uniting singularity and bifurcation theories and their applications (Zeeman, 1976).

A simple mechanical system that illustrates the important ideas of discontinuous changes and hysteresis is provided by Zeeman's catastrophe machine (Zeeman, 1972, Poston & Stewart, 1996). A sketch showing its construction is given in Figure 1(a). It is recommended that readers make such devices for themselves and experiment with them.

The lines between Q, P, and the pointer represent rubber bands attached to a disk that rotates around O. Movement of the pointer such that it remains outside of the region ABCD results in a smooth motion of the wheel from one equilibrium state to another. This is illustrated by the path ℓ_1 in Figure 1(b), where x and θ are as defined in Figure 1(a) and k is a measure of the stiffness of the bands. However, starting with the pointer below AB and moving the pointer horizontally to cross AD will cause an anticlockwise jump in the wheel. This is equivalent to following the path ℓ_2 in Figure 1(b). This equilibrium will remain until AB is crossed when the pointer is moved backwards. The loci DAB form a cusp in the parameter space of the system where AD and AB are lines of folds that meet at the cusp point A. The cusp is a projection down onto the plane of a three-dimensional folded surface. The region labeled ABCD comprises four such cusps, each of which can be described by a simple cubic equation. Indeed, the set can be obtained from an approximate model for the machine (Poston & Stewart, 1996).

The term *catastrophe* was introduced by René Thom in 1972 to describe such discontinuous changes in a system where a parameter is changed smoothly. Zeeman (1976) then coined the phrase *catastrophe theory*, and an explosion of applications arose ranging from the physical to the social sciences. An important idea put forward is that there are seven elementary catastrophes that classify most types of observed discontinuous behavior. They are the fold, cusp, swallowtail, and butterfly catastrophes and the elliptic, hyperbolic, and parabolic umbilic catastrophes. These describe all possible discontinuities for potential systems that are controlled by up to four variables. They are ordered according to their typicality of occurrence with the fold being the most common. A path of folds will be represented by a line of singular behavior in parameter space and a cusp will be formed when two such lines meet. Indeed, these two singularities are sufficient to cover most of the observed macroscopic critical behavior in practical applications.

One area of application where catastrophe theory has been used with considerable success is in optical caustics (Nye, 1999). Common experience of this phenomenon is observation of a distant light source through a drop of water on a window pane where a web of bright lines separated by dark regions can often be seen. The bright lines on the bottom of swimming pools are also examples of caustics where the bright sunlight is focused by the surface of the water. In this case, the line caustics are examples of paths of folds in the ray surfaces. An example of an optical cusp is provided by strong sunlight focused on the surface of a cup of coffee where two principal fold lines are made to meet by the curvature of the cup. In an outstanding series of experiments (Berry, 1976), a laser beam was shone through a water drop and a whole sequence of catastrophes was uncovered including swallowtails. All of the observed patterns can be reproduced in detail using the equations of ray optics (Nye, 1999).

Catastrophe theory has also been used to explore in some detail the state selection process in Taylor–Couette flow between concentric cylinders. In this case, even numbers of vortices are generated in the flow field, and the number that is realized depends

on the length of the cylinders. For a given length of the cylinder, one state develops smoothly, with control parameter and neighboring states delimited by fold lines in parameter space. The fold lines meet in a cusp that has been observed experimentally (Benjamin, 1978) and calculated numerically (Cliffe, 1988) from the Navier–Stokes equations.

There has been considerable criticism of catastrophe theory on both technical and practical grounds (Arnol'd, 1986; Arnol'd et al., 1994). For example, it is known that critical behavior or bifurcations in some multidimensional gradient systems do not reduce to critical points of potentials (Guckenheimer, 1973). Also, the ideas have been applied to a wide range of social, financial, and biological applications where the governing rules are not known or are very primitive. Very often, it is a case of re-interpretation of common experience in terms of technical mathematical language, which is most often qualitative rather than quantitative (Arnol'd, 1986). Hence, it is often the case that disparate systems superficially appear the same, but closer examination reveals that they are quite different in terms of important details.

TOM MULLIN

See also **Bifurcations; Critical phenomena; Development of singularities; Equilibrium; Taylor–Couette flow**

Further Reading

Arnol'd, V.I. 1986. *Catastrophe Theory*, Berlin and New York: Springer

Arnol'd, V.I., Afrajmovich, V.S. Il'yashenko, Yu.S. & Shil'nikov, L.P. 1994. *Bifurcation Theory and Catastrophe Theory*, Berlin and New York: Springer

Benjamin, T.B. 1978. Bifurcation phenomena in steady flows of a viscous fluid. *Proceedings of the Royal Society of London*, Series A, 359: 1–43

Berry, M.V. 1976. Waves and Thomas theorem. J *Advances in Physics*, 25(1): 1–26

Cliffe, K.A. 1988. Numerical calculations of the primary-flow exchange process in the Taylor problem. *Journal of Fluid Mechanics*, 197: 57–79

Guckenheimer, J. 1973. *Bifurcation and catastrophe*. In *Dynamical Systems*: Proceedings of the Symposium of University of Babia Salvador, 1971, pp. 95–109

Nye, J.F. 1999. *Natural Focusing and Fine Structure of Light: Caustics and Wave Dislocation,* Bristol: Institute of Physics Publishing

Poston, T. & Stewart, I. 1996. *Catastrophe Theory and Its Applications*, New York: Dover

Saunders, P.T. 1980. *An Introduction to Catastrophe Theory*, Cambridge and New York: Cambridge University Press

Thom, R. 1972. *Structural Stability and Morphogenesis.* Reading, MA: Benjamin

Zeeman, E.C. 1976. Catastrophe theory: a reply to Thom. In *Dynamical Systems Warwick 1974*, edited by A. Manning, Berlin and New York: Springer, pp. 405–419

Zeeman, E.C. 1972. A catastrophe machine. In *Towards a Theoretical Biology*, vol. 4, edited by C.H. Waddington, Edinburgh: Edinburgh University Press, pp. 276–282

CAUSALITY

Basic to science as well to common sense is the root notion of causality, that things and processes in the world we experience are not totally random, but ordered in specific ways that allow for rational understanding through explanations of various types. In the transition from a mythological worldview to a rational one, the notion of guilt (in Greek *aitia*), as in a criminal being guilty of a crime, was metaphorically used to describe nonpersonal natural processes whenever one phenomenon would necessarily follow another. As one aim of modern science is to uncover the deep structure of the world beyond our immediate experience, its explanations deal with the different determinants (or causes) of processual order. Three classical conceptions of inquiry, associated with the traditions of Plato, Aristotle, and Archimedes, have provided influential ideas about the role of causal explanations in science.

In the Platonic tradition, certain properties of nature could be derived from a priori given mathematical structures. As discovered by the Pythagorean philosophers of nature, a specific mathematical structure (relations between small whole numbers) could be the key to a part of nature (such as acoustics), so why not see whether that same structure could also describe other areas (such as astronomy)? Although the latter attempt failed, the general idea of using the power of demonstrative or formal necessity in mathematics as a descriptive tool of natural causality is still vital in many areas of science, including cosmology and high-energy physics. Also, the use of analog mathematical structures to describe phenomena has become standard.

The Aristotelian tradition did not refuse mathematical description but saw it only as a tool in a search for the real causes of things. For Aristotle, there were four kinds of causes: the material cause (*hyle* or *causa materialis*) that describes the stuff of which something is made, the formal cause (*eidos* or *causa formalis*) that describes the organization of something, the efficient cause (*to kineti'kon* or *causa efficiens*) that describes the active forces by which the phenomenon comes into being, and the final cause (*to 'telos* or *causa finalis*) that describes the purpose that it serves. Thus, for a house, bricks and mortar are its material cause, the plan of the house is its formal cause, the mason building it is its efficient cause, and the purpose of sheltering a family is its final cause.

In that ancient world of Aristotle, each phenomenon generally served a purpose. Aristotle did not consider the four causes as necessarily separate aspects of nature, but more like principles of explanation that may sometimes merge, as in the sprouting acorn becoming an oak tree where the formal, efficient, and final causes work together to actualize the characteristics of an adult oak. The popular renaissance critique of the final cause as implying the paradox of a future state (a goal)

influencing a present state led to a dismissal of any pluralist conception of causes. In the subsequent mechanical world picture, only efficient causes were left as explanatory. The life sciences could not live up to this reduction but continued as a descriptive natural history with an essentially Aristotelian outlook, at least until Darwin would explain the final cause of adaptations by the efficient causes of natural selection and heredity. Yet, even the Darwinian paradigm could not account for the nonlinear mechanisms of self-organization in the organism's embryonic development. Such goal-like (teleological) properties of development and self-reproduction remained necessary yet unexplained preconditions for the mechanics of natural selection.

The Archimedean tradition was founded by disciplines more physical than mathematical, although combining the two, such as optics, astronomy, mechanics, and music theory. The mathematical relations discovered by Archimedes (ca. 287–212 BC) in his books on mechanics were not a priori, as in the Platonic tradition, but derived from experience. However, the Aristotelian pursuit after the causes of the phenomena, especially the final ones, was regarded as metaphysical and so ignored. The Archimedean tradition includes such names as Ptolemaios, Johannes Kepler, Galileo Galilei, and Isaac Newton. Kepler started out as a Platonic, aiming to explain the Copernican system (which placed the Sun at the center of the solar system, in opposition to the Ptolemaic system) by regular polyhedrons, but failed and found the right laws for planetary movements through a mathematical analysis of Tycho Brahe's empirical observations. Galileo found his laws of falling bodies by eschewing the search for a hypothetical cause of gravitational force and instead using measures proportional to the velocity of a moving body for the effect of this force.

Although the mechanical worldview emphasizes only the role of efficient causes as principles of explanation in physics, the very idea of cause gave way for a long period to skepticism about proving any real existence of causes (the positivism of David Hume), eventually seeing the concept of cause as a feature of the observing subject (the transcendental idealism of Immanuel Kant). Yet, in physics, the laws of nature as expressed in terms of mathematics came to play the explanatory role of the causes of a system's movement. It was assumed that any natural system could be encoded into some formalism (e.g., a set of differential equations representing the basic laws governing the system) and that the entailment structure of that formalism perfectly mirrored the (efficient) causal structure of that part of nature. This view was compatible with a micro-determinism where a system's macroscopic properties and processes are seen as completely determined by the behavior of the system's constituent particles, governed by deterministic laws. This view was deeply questioned by quantum physics, and by Rosen's work on fundamental limits on dynamic models of causal systems.

The complexity of causality, especially in goal-directed systems, was presaged by cybernetic research in the 1940s, dealing with negative feedback control (in animals and artifacts such as self-guiding missiles) and the role of information processing for the regulation of dynamic systems. A paradigmatic example is the closed causal loops connecting various physiological levels of hormones in the body, essential for maintaining a constant internal environment (homeostasis)—a modern version of the ancient symbol of uroboros, the snake biting its own tail.

The emergence of nonlinear science in the late 20th century increased interest in the old idea that causal explanations may not all reduce to simple one-to-one correspondences between cause and effect. The realization that complex systems may occupy different areas in phase space characterized by qualitatively distinct attractors, eventually separated by fractal borders, has questioned micro-determinism even more than the fact that many such nonlinear systems have a high sensitivity to the initial conditions (the butterfly effect).

Another insight is that complex things often self-organize as high-level patterns via processes of local interactions between simple entities. This emergence of wholes (or collective behavior of units) may be mimicked in causal explanations. Instead of top-down reductive explanations, nonlinear science provides additional bottom-up explanations of emergent phenomena. Although these explanations are still reductive (in the methodological sense that one can show exactly what is going on from step to step in a simulation of the system), the complexity makes prediction impossible; thus, computational shortcuts to predict a future state can rarely be found.

As an emergent whole is formed bottom-up, its organization constrains its components in a top-down manner, that has been called downward causation (DC). There are three interpretations of DC: in strong DC, the emergent whole (a human mind) effectuates a change in the very laws that govern the lower-level (like free will might suspend what normally determines the action of the brain's neurons). This interpretation is often related to vitalist and dualist conceptions of life and mind and is hard to reconcile with science. In medium DC, lower-level laws remain unaffected; yet, their boundary conditions are constrained by the emergent pattern (a mental representation), which is considered just as real as the components of the system (neuronal signaling). Here, the state of the higher level works as a factor selecting which of the many possible next states of the high level may emerge from the low level. In weak DC, the emergent higher levels are seen as regulated by stable (cyclic or chaotic) attractors for the dynamics of the lower level. The fact that a biological species consists of

stable organisms is not solely a product of natural selection, but is a result of such internal, formal properties in the system's organization—the job of natural selection being to sort out the possible stable organisms and find those most fit for the given milieu (Kauffman, 1993; Goodwin, 1994). It should be emphasized that DC is not a form of efficient causation (involving a temporal sequence from cause to effect), rather it is a modern version of the Aristotelian formal and final cause.

Nonlinear science may be said to integrate a Platonic appreciation of universality (as found in the equations governing the passage to chaos in systems of quite distinct material nature), an Aristotelian acceptance of several types of causes, and an Archimedean pragmatism regarding the deeper status of determinism and causality. The latter is reflected in the fact that although deterministic chaos characterizes a large class of systems, this does not imply that these systems (or nature) are fully deterministic. The determinism refers to the mathematical tools used rather than an ontological notion of causality.

CLAUS EMMECHE

See also **Biological evolution; Butterfly effect; Determinism; Feedback**

Further Reading

Depew, D.J. & Weber, B.H. 1995. *Darwinism Evolving: System Dynamics and the Genealogy of Natural Selection*, Cambridge, MA: MIT Press

Emmeche, C., Stjernfelt, F. & Køppe, S. 2000. Levels, Emergence, and three versions of downward causation. In *Downward Causation. Minds, Bodies and Matter*, edited by P.B. Andersen, C. Emmeche, N.O. Finnemann & P.V. Christiansen, aarhus: Aarhus University Press, pp. 13–34

Fox, R.F. 1982. *Biological Energy Transduction: The Uroboros*, New York: Wiley

Goodwin, B. 1994. *How the Leopard Changed Its Spots: The Evolution of Complexity*, New York: Scribner's

Kauffman, S.A. 1993. *The Origins of Order. Self-organization and Selection in Evolution*, Oxford and New York: Oxford University Press

Pedersen, O. 1993. *Early Physics and Astronomy: A Historical Introduction*, Cambridge and New York: Cambridge University Press

Rosen, R. 2000. *Essays on Life Itself*, New York: Columbia University Press

Weinert, F. (editor). 1995. *Laws of Nature: Essays on the Philosophical, Scientific and Historical Dimensions*, Berlin and New York: Walter de Gruyter

CAUSTICS

See **Catastrophe theory**

CAVITY SOLITONS

See **Solitons, types of**

CELESTIAL MECHANICS

Although its origins can be traced back in antiquity to the first attempts of explaining the apparently irregular wandering of the planets, celestial mechanics was born in 1687 with the release of Isaac Newton's *Principia*. In 1799, Pierre-Simon Laplace introduced the term *mécanique céleste* (Laplace, 1799), which was adopted to describe the branch of astronomy that studies the motion of celestial bodies under the influence of gravity. Celestial mechanics is researched and developed by astronomers and mathematicians; the methods used to investigate it including numerical analysis, the theory of dynamical systems, perturbation theory, the quantitative and qualitative theory of differential equations, topology, the theory of probabilities, differential and algebraic geometry, and combinatorics.

Ptolemy's idea of the epicycles—according to which planets are orbiting on small circles, whose centers move on larger circles, whose centers move on even larger circles around the Earth—dominated astronomy in antiquity and the Middle Ages. In 1543, after working for more than 30 years on a new theory, Copernicus finished writing *De Revolutionibus*, a book in which he expressed the motion of the planets with respect to a heliocentric reference system, that is, one with the Sun at its origin. This allowed Kepler to use existing observations and formulate three laws of planetary motion, published in 1609 in *Astronomia Nova*:

(i) *The law of motion*: every planet moves on an ellipse having the sun at one of its foci.
(ii) *The law of areas*: every planet moves such that the segment planet-sun sweeps equal areas in equal intervals of time.
(iii) *The harmonic law*: the squares of the periods of any two planets are to each other as the cubes of their mean distances from the sun.

But all these achievements were empirical, based on observations, not on deductions obtained from a more general physical law.

In 1666, Newton came up with the idea that the attractive force responsible for the free fall of objects might be the same as the one keeping the Moon in its orbit. He conjectured that the expression of this force is directly proportional to the product of the masses and inversely proportional to the square of the distance between bodies. The tools of calculus, which he had invented independent of—and at about the same time as—Gottfried Wilhelm von Leibniz, allowed him to proceed with the computations. Two decades later, in *Principia*, Newton proved the correctness of his theory. Kepler's laws follow as consequences. They are obtained from the differential equations of the Newtonian two-body problem (also called the Kepler problem) given by a potential energy of the form $U(r) = -Gm_1m_2/r$, where G is the gravitational

constant and r is the distance between the bodies of masses m_1 and m_2.

After Newton, mathematicians, such as Johann Bernoulli, Alexis Clairaut, Leonhard Euler, such as Jean d'Alembert, Laplace, Joseph-Louis Lagrange, Siméon Poisson, Carl Jacobi, Karl Weierstrass, and Spiru Haretu, attacked various theoretical questions of celestial mechanics (e.g., the 2- and 3-body problem, the lunar problem, the motion of Jupiter's satellites, and the stability of the solar system) mostly with the quantitative tools of analysis, algebra, and the theory of differential equations. On the practical side, the first resounding success in the field was the prediction of the return of Halley's comet, which occurred in 1758—as the calculations had shown. An even more spectacular achievement came in 1846 with the discovery of the planet Neptune on the basis of the perturbation theory through computations independently performed by John Couch Adams and Urbain Jean-Joseph Le Verrier. Having its origin in one of Euler's papers, which applied the calculus of trigonometric functions to the 3-body problem, perturbation theory is now an independent branch of mathematics (see, e.g., Verhulst, 1990; Guckenheimer & Holmes, 1983) that is often used in celestial mechanics.

An important theoretical advance was achieved by Henri Poincaré toward the end of the 19th century, when the questions of celestial mechanics—especially those concerning the Newtonian 3-body problem—received substantial attention. While working on this problem, Poincaré understood that the quantitative methods of obtaining explicit solutions for differential equations are not strong enough to help him make significant progress; thus, he tried to describe the qualitative behavior of orbits (e.g., stability, the motion in the neighborhood of collisions and at infinity, existence of periodic solutions) even when their expressions were too complicated or impossible to derive, which is the case in general. His ideas led to the birth of several branches of mathematics, including the theory of dynamical systems, nonlinear analysis, chaos, stability, and algebraic topology (Barrow-Green, 1997; Diacu & Holmes, 1996).

Today's astronomers working in celestial mechanics are primarily interested in questions directly related to the solar system, such as the accurate prediction of eclipses, orbits of comets and asteroids, the motion of Jovian moons, Saturn's rings, and artificial satellites. The invention of the electronic computer had a significant impact on the practical aspects of the field. The development of numerical methods allowed researchers to obtain good approximations of the planet's motion for long intervals of time. These types of results are also used in astronautics. No space mission, from the Sputnik, Apollo, and Pioneer programs to the space shuttle, the Hubble telescope launch, and the recent international space collaboration projects, could have been possible without the contributions of celestial mechanics.

Contemporary mathematicians active in the field are mostly dealing with theoretical issues, as, for example, the study of the general N-body problem and its particular cases (Wintner, 1947) ($N = 2, 3, 4$, the collinear, isosceles, rhomboidal, Sitnikov, and planetary problems, central configurations, etc.), attempting to answer questions regarding motion near singularities and at infinity, periodic orbits, stability and chaos, oscillatory behavior, Arnol'd diffusion, etc. Some researchers also study alternative gravitational forces like that suggested by Manev (Diacu et al., 2000; Hagihara, 1975; Moulton, 1970), which offers a good relativistic approximation at the level of the solar system.

Celestial mechanics and mathematics have always influenced each other's development, a trend that is far from slowing down today. The contemporary needs of space science bring a new wave of interest in the theoretical and practical aspects of celestial mechanics, making its connections with mathematics stronger than ever before.

FLORIN DIACU

See also ***N*-body problem; Perturbation theory; Solar system**

Further Reading

Barrow-Green, J. 1997. *Poincaré and the Three-Body Problem*, Providence, RI: American Mathematical Society

Diacu, F. & Holmes, P. 1996. *Celestial Encounters—The Origins of Chaos and Stability*, Princeton, NJ: Princeton University Press

Diacu, F., Mioc, V. & Stoica, C. 2000. Phase-space structure and regularization of Manev-type problems, *Nonlinear Analysis*, 41: 1029–1055

Guckenheimer, J. & Holmes, P. 1983. *Nonlinear Oscillations, Dynamical Systems, and Bifurcations of Vector Fields*, Berlin and New York: Springer

Hagihara, Y. 1975. *Celestial Mechanics*, vol. 2, part 1, Cambridge, MA: MIT Press

Laplace, P.-S. 1799. *Traité de mécanique céleste*. 5 vols. Paris, 1799–1825

Moulton, J.R. 1970. *An Introduction to Celestial Mechanics*, Dover

Verhulst, F. 1990. *Nonlinear Differential Equations and Dynamical Systems*, Berlin and New York: Springer

Wintner, A. 1947. *The Analytical Foundations of Celestial Mechanics*, Princeton, NJ: Princeton University Press

CELL ASSEMBLIES

The term *cell assembly* became well established as a neuropsychological concept with the publication in 1949 of Donald Hebb's book *The Organization of Behavior*. A cell assembly forms when a group of cortical neurons gets wired together through experience-dependent synaptic potentiation induced by nearly synchronous activity in pairs of connected neurons. Once formed, it serves as a cooperative and

holistic mental representation. The mutual excitation within the active cell assembly influences network dynamics such that (i) the entire group of cells can be activated by stimulating only a part of it and (ii) once active, the ensemble displays afteractivity outlasting the stimulus triggering it. An important extension of the concept was suggested by Peter Milner, who proposed that negative feedback from lateral inhibition is essential to prevent mass activation of the entire network and the emergence of epileptic-like activity (Milner, 1957). This also introduces an element of competitive interaction between the cell assemblies allowing one assembly at a time to dominate the network. Hebb further proposed that cell assemblies activated in succession would wire together to form "phase sequences" that might be the physiological substrate of chains of association and the flow of thought. The concept of cell assemblies has been extensively elaborated in the context of cortical associative memory (see, e.g., Fuster, 1995).

Notably, abstract attractor network models (Hopfield, 1982; Rolls and Treves, 1997) may be regarded as mathematical instantiations of Hebb's cell assembly theory. They have been useful, for example, to estimate how many assemblies can be stored in a network of a given size, the existence of spurious attractors, and the effect of sparse activity and diluted network connectivity.

The extensive recurrent neuronal circuitry required for the formation of cell assemblies is abundant in the cerebral cortex in the form of horizontal intracortical and cortico-cortical connections. The latter are myelinated and support fast communication over large distances. The existence of experience-dependent synaptic changes in the form of "Hebbian" long-term synaptic potentiation is very well experimentally established today. In light of what we now know about brain circuitry and neuronal response properties, it is reasonable to assume that a cell assembly may extend across large areas of sensory, motor, and association cortices, perhaps even involving subcortical structures like the thalamus and basal ganglia. Rather than individual neurons, the actual nodes of the cell assembly are likely to be cortical modules, that is, minicolumns, comprising a couple of hundred neurons and with a diameter of about 30 μm (Mountcastle, 1998). Feature detectors in primary sensory areas like the visual orientation columns described by David Hubel and Torsten Wiesel are typical examples. Although the modular organization of higher-order cortical areas is less obvious, it has been proposed that the cortical sheet actually comprises a mosaic of such minicolumns. A single-cell assembly would then engage a small fraction of them distributed over a large part of the brain.

The reverberatory afteractivity in an active cell assembly was proposed by Hebb (1949) to correspond to "a single content in perception" and last some hundred milliseconds to half a second. Notably, this is of the same order as the duration of visual fixations and the period of cognitively relevant neurodynamical phenomena evident in EEG (e.g., the theta rhythm) and evoked potentials (Pulvermueller et al., 1994). Persistent activity over seconds but otherwise of the same origin has recently been proposed as a mechanism underlying working memory (Compte et al., 2000).

The cell assembly theory connects the cellular and synaptic levels of the brain with psychological phenomenology. It suggests explanations for the close interaction between memory and perception, including the holistic and reconstructive nature of Gestalt perception, perceptual fusion of polymodal stimuli, and perceptual illusions. Typical examples are perceptual completion and filling in as when looking at the Kaniza triangle and perceptual rivalry as demonstrated by the slowly alternating perception of an ambiguous three-dimensional stimulus like the Necker cube (Figure 1). An analogy to Gestalt perception in the motor domain would be motor synergies, and their existence can also be understood based on the cell assembly theory. In the motor control domain, however, the

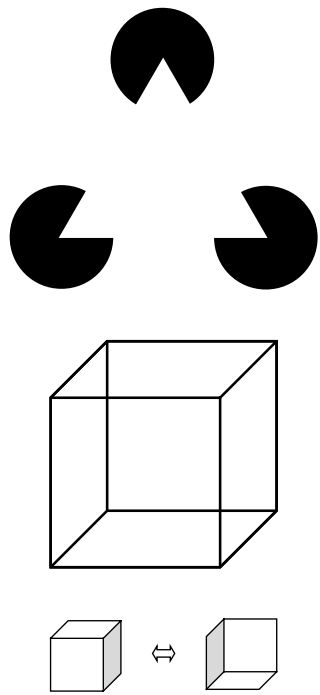

Figure 1. Two perceptual illusions that may be understood in terms of cell assembly dynamics.

temporal component of the underlying neurodynamics is critical, and for instance, finely tuned temporal sensory-motor coordination cannot be explained within this paradigm alone.

The neurodynamics of cell assemblies has been studied in a network with biophysically detailed model neurons (see, e.g., Lansner and Fransén, 1992; Fransén and Lansner, 1998), showing that the cellular properties of cortical pyramidal cells promote sustained activity. Moreover, the experimentally observed level of mutual excitation is sufficient to support such activity, and the measured magnitude of cortical lateral inhibition is effective in preventing coactivation of assemblies. The time to activate an entire assembly from a part of it was found to be within 50–100 ms in accordance with psychological experimental results. Modeling has further shown that neuronal adaptation due to accumulation of slow afterhyperpolarization (presumably together with synaptic depression) is a likely cause of termination of activity in an active assembly. Afteractivity may typically last some 300 ms, but the network dynamics is quite sensitive to endogenous monoamines such as serotonin, which acts by modulating the neuronal conductances underlying such adaptation. Further, simulations demonstrate that a cell assembly can survive even if the average conduction delay between the participating neurons increases to 10 ms, corresponding to a spatial extent of about 50 mm at axonal conduction velocities of 5 m/s. Despite quite powerful mutual excitation, reasonably low firing rates of cortical cells can be obtained in models with saturating synapses with slow kinetics (e.g., NMDA receptor gated channels) together with cortical feedback inhibition.

Although biologically highly plausible and supported by computational models, solid experimental evidence for the existence of cell assemblies is still lacking. Detection of their transient and highly distributed and diluted activity requires simultaneous noninvasive measurement in awake animals of the activity in a large number of neurons with high spatial and temporal resolution. This is still beyond the reach of current experimental techniques. Nevertheless, Hebb's original proposal has remained a vital hypothesis for more than half a century and it continues to inspire much experimental and computational research aimed at understanding how the brain works.

ANDERS LANSNER

See also **Attractor neural network; Electroencephalogram at large scales; Gestalt phenomena; Neural network models; Neurons**

Further Reading

Compte, A., Brunel, N., Goldman-Rakic, P.S. & Wang, X.-J. 2000. Synaptic mechanisms and network dynamics underlying visuospatial working memory in a cortical network model. *Cerebral Cortex*, 10: 910–923

Fransén, E. & Lansner, A. 1998. A model of cortical associative memory based on a horizontal network of connected columns. *Network: Computation in Neural Systems*, 9: 235–264

Fuster, J.M. 1995. *Memory in the Cerebreal Cortex*. Cambridge, MA: MIT Press

Hebb, D.O. 1949. *The Organization of Behavior*, New York: Wiley

Hopfield, J.J. 1982. Neural networks and physical systems with emergent collective computational properties, *Proceedings of the National Academy of Sciences, USA*, 81: 3088–3092

Lansner, A. & Fransén, E. 1992. Modeling Hebbian cell assemblies comprised of cortical neurons. *Network: Computation in Neural Systems*, 3: 105–119

Milner, P.M. 1957. The cell assembly: Mark II. *Psychological Review*, 64: 242–252

Mountcastle, V.B. 1998. *Perceptual Neuroscience: The Cerebral Cortex*. Cambridge, MA: Harvard University Press

Pulvermueller, F., Preissl, H., Eulitz, C., Pantev, C., Lutzenberger, W., Elbert, T. & Birbaumer, N. 1994. Brain rhythms, cell assemblies and cognition: evidence from the processing of words and pseudowords. *Psycoloquy*, 5(48)

Rolls, E. & Treves, A. 1997. *Neural Networks and Brain Function*. Oxford and New York: Oxford University Press

Scott, A.C. 2002. *Neuroscience: A Mathematical Primer*. Berlin and New York: Springer

CELLULAR AUTOMATA

Following a suggestion by Stanislaw Ulam, John von Neumann developed the concept of cellular automata (CA) in 1948. Von Neuman wanted to formalize a set of primitive logical operations that were sufficient to evolve the complex forms of organization necessary for life. In doing this, he constructed a two-dimensional self-replicating automaton and initiated not only the study of CA but also the idea, now popular among students of complexity theory, that highly complex global behavior can be generated from local interaction rules. Much of the interest in CA has been motivated by their ability to generate complex spatial and temporal patterns from simple rules. Because of this, they provide a rich modeling environment, having the twin virtues of mathematical tractability and representational robustness (see Burk, 1970, for discussion of much of the early work on CA).

The non-obvious connection between simple local rules of interaction and emergent complex global patterns offers a possible approach to an explanation of complexity through determination of its generating local interactions. Some researchers have gone so far as to suggest that the universe itself is a CA, or CA-like object, and that sets of local generative interaction rules can replace differential equations as the standard mathematical expression for physical models.

CA are spatially and temporally discrete symbolic dynamical systems defined in terms of a lattice of sites (or cells), an alphabet of symbols that can be assigned to lattice sites, and a local update rule that

determines what symbol is assigned to each site at time $t+1$ on the basis of the site values in a local neighborhood of that site at time t. Given the local neighborhood structure, a neighborhood state is defined by an assignment of symbols from the alphabet to each site in the neighborhood. The local update rule can be specified in terms of a look-up table that lists the set of neighborhood states together with the symbol that each one assigns to the designated site at the next time step.

For example, if the lattice is isomorphic to the integers, the alphabet is 0, 1, and the neighborhood of any site s is the set of sites $s-1$, s, $s+1$, then there are 256 possible update rules, defined by the look-up table:

000	001	010	011	100	101	110	111
x_0	x_1	x_2	x_3	x_4	x_5	x_6	x_7

(The updated symbol is entered in the central cell. This defines what are called nearest-neighbor rules.) Here, each of the x_i is either 0 or 1 depending on the specific rule. Thus, they can be thought of as components of the rule.

A cellular automaton can be defined in any number of dimensions. Von Neuman's original automaton was two dimensional, as is what is perhaps the best-known CA—Conway's Game of Life (Gardner, 1970). This is one of the simplest two-dimensional CA known to be equivalent to a universal Turing machine.

If Σ is the full state space for a CA, then the local update rule defines a global mapping $\psi : \Sigma \rightarrow \Sigma$. Much of the analytical work on CA has been directed at determining the mathematical properties of the map ψ. A fundamental paper published by Hedlund in 1969 showed that CA are just the shift-commuting endomorphisms of the shift dynamical system. It is also known that surjectivity (a function is surjective, or onto, if every state has at least one predecessor) of the map ψ is decidable only in dimension one and that for one-dimensional additive rules (i.e., those satisfying the condition $\psi(\mu+\mu') = \psi(\mu) + (\mu')$), injectivity is equivalent to a certain rule-dependent complex polynomial having no roots that are nth roots of unity for any n. (A function is injective, or one to one, if every state has at most one predecessor. A function that is both surjective and injective is called reversible.)

From the early 1960s until the early 1980s, much of the work on CA was either simple applications or mathematical analysis. The terminology was not settled, and work can be found under the names *cellular structures, cellular spaces, homogeneous structures, iterative arrays, tessellation structures*, and *tessellation arrays*.

As computers became powerful enough to support the intense calculations required, however, an experimental mathematics approach became possible. In addition, solution of systems of differential equations by computer makes use of numerical combination rules on a discrete lattice, and CA are the simplest examples of such rules, adding impetus to interest in their study.

Concurrent with the appearance of powerful computers, work was initiated on the physics of computation, and the construction of reversible automata that, it was supposed, would be a discrete equivalent to the time-invariant differential equations of physics. More or less simultaneously, Stephen Wolfram began to publish a series of papers that popularized the study of elementary automata (see Wolfram, 1994), and by the mid-1980s, CA had emerged as a major field of interest among research in the field of complex systems theory.

Because of their generality as a modeling platform, CA have found wide application in many areas of science. In chemistry and physics, they have provided models of pattern formation in reaction-diffusion systems, the evolution of spiral galaxies, spin exchange systems and Ising models, fluid and chemical turbulence (especially as lattice gas automata), dendritic crystal growth, and solitons, among other applications.

Spatially recurring patterns that propagate in the space-time evolution of certain CA have been likened to particles moving in physical space-time. The interactions of these "particles" are important in attempts to use CA for computational tasks (e.g., Crutchfield & Mitchell, 1995). It has also been pointed out that these particles are analogous to the defects, or coherent structures found in pattern formation processes in condensed matter physics, and to solitons in hydrodynamics. The best-known examples of such particles are the so-called "gliders" that occur in Conway's game of life.

Numerous connections have also been shown between fractals and cellular automata. Rescaling the space-time output of a CA often generates a fractal, as, for example, the two-site rule defined by $00, 11 \rightarrow 0$, $01, 10 \rightarrow 1$ generates the well-known Sierpinski gasket (Peitgen, Jürgen & Saupe, 1992).

In biology and medicine, CAs have been applied in models of heart fibrillation, developmental processes, evolution, propagation of diseases infectious, plant growth, and ecological simulations.

In computation, CAs have been used as parallel computers, sorters, prime number sieves, and tools for encryption and for image processing and pattern recognition. Some automata have the capacity for universal computation, although how to implement this capacity remains problematic.

Cellular automata have also been used to model social dynamics (Axtell & Epstein, 1996), the spread of forest fires, neural networks, and military combat situations. Extensive references to these applications and others can be found in Voorhees (1995) and Ilachinski (2001).

Work on CA has also stimulated work on other systems that generate complex patterns based on local rules. There are close connections to the fields of artificial life, random Boolean networks, genetic programming and evolutionary computation (Mitchell, 1996), and the general theory of computational mechanics.

A web search under the key word "cellular automata" will turn up literally hundreds of sites devoted to various aspects of their study. A particularly useful program for the study of CA, Boolean networks, and other discrete iterated systems is *Discrete Dynamics Lab* (Wuensche & Lesser, 1992), available for downloading from http://www.ddlab.com.

BURTON H. VOORHEES

See also **Artificial life; Chaotic dynamics; Emergence; Fractals; Game of life; Integrable cellular automata; Lattice gas methods; Neural network models; Solitons**

Further Reading

Axtell, R. & Epstein, J.M. 1996. *Growing Artificial Societies: Social Science from the Bottom Up*, Cambridge, MA: MIT Press

Burk, A.W. (editor). 1970. *Essays on Cellular Automata*, Champaign, IL: University of Illinois Press

Crutchfield, J.P. & Mitchell, M. 1995. The evolution of emergent computation. *Proceedings of the National Academy of Sciences*, 92(10): 10,742–10,746

Doolen, G.D. (editor). 1991. *Lattice Gas Methods: Theory, Applications, and Hardware*, New York: Elsevier

Gardner, M. 1970. The fantastic combinations of John Conway's new solitaire game of life. *Scientific American*, 223: 120–123

Ilachinski, A. 2001. *Cellular Automata*, Singapore: World Scientific

Mitchell, M. 1996. *An Introduction to Genetic Algorithms*, Cambridge, MA: MIT Press

Peitgen, H.-O, Jürgens, H. & Saupe, D. 1992. *Chaos and Fractals: New Frontiers in Science*, New York: Springer

Toffoli, T. & Margolis, N. 1987. *Cellular Automata Machines: A New Environment for Modeling*, Cambridge, MA: MIT Press

Voorhees, B.H. 1995. *Computational Analysis of One-Dimensional Cellular Automata*. Singapore: World Scientific

Wolfram, S. 1994. *Cellular Automata and Complexity*, Reading, MA: Addison-Wesley

Wuensche, A. & Lesser, M. 1992. *The Global Dynamics of Cellular Automata*, Reading, MA: Addison-Wesley

CELLULAR NONLINEAR NETWORKS

The development of cellular nonlinear networks (CNN) is embedded in the history of the electronic and computer industry, which is characterized by three revolutions: cheap computing power via microprocessors (since the 1970s), cheap bandwidth (since the end of the 1980s), and cheap sensors and MEMS (micro-electro-mechanical system) arrays (since the end of the 1990s). These research and technology breakthroughs led the way for several important economic enterprises such as the PC industry of the 1980s, the Internet industry of the 1990s, and the future analog computing industry, which is growing, together with optical and nanoscale implementations on the atomic and molecular level. Analog cellular computers have been the technical response to the sensors revolution, mimicking the autonomy and physiology of sensory and processing organs.

The CNN was invented by Leon O. Chua and Lin Yang in Berkeley in 1988. The main idea behind the CNN paradigm is Chua's so-called "local activity principle," which asserts that no complex phenomena can arise in any homogeneous media without local activity. Obviously, local activity is a fundamental property in microelectronics, where, for example, vacuum tubes and, later on, transistors are locally active devices in the electronic circuits of radios, televisions, and computers. The demand for local activity in neural networks was motivated by practical technological reasons. In 1985, John Hopfield theoretically suggested a neural network, which, in principle, could overcome the failures of pattern recognition in Frank Rosenblatt's perceptron (*See* **Perceptron**). However, its globally connected architecture was highly impractical for technical realizations in VLSI (very-large-scale-integrated) circuits of microelectronics: the number of wires in a fully connected Hopfield network grows exponentially with the size of the array. A CNN only needs electrical interconnections in a prescribed sphere of influence.

In general, a CNN is a nonlinear analog circuit that processes signals in real time. It is a multicomponent system of regularly spaced identical ("cloned") units, called cells, which communicate with each other directly only through their nearest neighbors. However, the locality of direct connections also permits global information processing. Communications between nondirectly (remote) connected units are obtained on passing through other units. The idea that complex and global phenomena can emerge from local activities in a network dates back to John von Neumann's first paradigm of cellular automata (CA). In this sense, the CNN paradigm is a higher development of the CA paradigm under the new conditions of information processing and chip technology. Unlike conventional cellular automata, CNN host processors accept and generate analog signals in continuous time with real numbers as interaction values. Furthermore, the CNN paradigm allows deep insights into the dynamic complexity of computational processes. While the classification of complexity by CA was more or less inspired by empirical observations of pattern formation in computer experiments, the CNN approach delivers a mathematically precise measure of dynamic complexity. The basic idea is to understand cellular automata as a special case of CNNs that can be characterized by a precise code for attractors of nonlinear dynamical systems and by a unique complexity index.

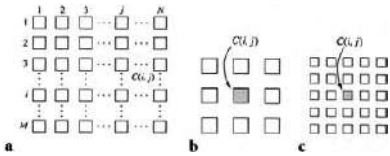

Figure 1. Standard CNN with array (a), 3×3 and 5×5 neighborhood (b,c).

Mathematical Definition

A CNN is defined by (1) a spatially discrete set of continuous nonlinear dynamical systems (cells or neurons) where information is processed into each cell via three independent variables (input, threshold, initial state) and (2) a coupling law relating relevant variables of each cell to all neighboring cells within a predescribed sphere of influence. A standard CNN architecture consists of an $M \times N$ rectangular array of cells $C(i, j)$ with cartesian coordinates (i, j) with $i = 1, 2, ..., M$ and $j = 1, 2, ..., N$ (Figure 1a). Figures 1b–c show examples of cellular spheres of influence as 3×3 and 5×5 neighborhoods. The dynamics of a cell's state is defined by a nonlinear differential equation (CNN state equation) with scalars for state x_{ij}, output y_{ij}, input u_{ij}, and threshold z_{ij}, and coefficients, called "synaptic weights", modeling the intensity of synaptic connections of the cell $C(i, j)$ with the inputs (feedforward signals) and outputs (feedback signals) of the neighboring cells $C(k, l)$. The CNN output equation connects the states of a cell with the outputs.

The majority of CNN applications use space-invariant standard CNNs with a cellular neighborhood of 3×3 cells and no variation of synaptic weights and cellular thresholds in the cellular space. A 3×3 sphere of influence at each node of the grid contains nine cells with eight neighboring cells and the cell in its center. In this case, the contributions of the output (feedback) and input (feedforward) weights can be reduced to two fixed 3×3 matrices, which are called feedback (output) cloning template $\mathbf{A}$ and feedforward (input) cloning template $\mathbf{B}$. Thus, each CNN is uniquely defined by the two cloning templates $\mathbf{A}$, $\mathbf{B}$, and a threshold z, which consist of $3 \times 3 + 3 \times 3 + 1 = 19$ real numbers. They can be ordered as a string of 19 scalars with a uniform threshold, nine feedforward, and nine feedback synaptic weights. This string is called a "CNN gene" because it completely determines the dynamics of the CNN. Consequently, the universe of all CNN genes is called the "CNN genome." In analogy to the human genome project, steady progress can be made by isolating and analyzing various classes of CNN genes and their influences on CNN genomes.

Applications

In visual computing, the triple $\mathbf{A}$, $\mathbf{B}$, z, and its 19 real numbers can be considered as a CNN macroinstruction on how to transform an input image into an output image. Simple examples are a subclasses of CNNs with practical relevance such as the class $C(\mathbf{A}, \mathbf{B}, z)$ of space-invariant CNNs with excitatory and inhibitory synaptic weights, the zero-feedback (feedforward) class $C(0, \mathbf{B}, z)$ of CNNs without cellular feedback, the zero-input (autonomous) class $C(\mathbf{A}, 0, z)$ of CNNs without cellular input, and the uncoupled class $C(\mathbf{A}^0, \mathbf{B}, z)$ of CNNs without cellular coupling. In $\mathbf{A}^0$, all weights are zero except for the weight of the cell in the center of the matrix. Their signal flow and system structure can be illustrated in diagrams that can easily be applied to electronic circuits as well as to typical living neurons.

CNN templates are extremely useful for standards in visual computing. Simple examples are CNNs detecting edges either in binary (black-and-white) input images or in gray-scale input images. An image consists of pixels corresponding to the cells of a CNN with binary or gray scale. Logic operators can also be realized by simple CNN templates in order to combine CNN templates for visual computing. The logic NOT CNN operation inverts intensities of all binary image pixels, the foreground pixels becoming the background, and vice versa. The logic AND (logic OR, respectively) CNN operation performs a pixel-wise logic AND (logic OR operation, respectively) on corresponding elements of two binary images. These operations can be used as elements of some Boolean logic algorithms that operate in parallel on data arranged in the form of images.

The simplest form of a CNN can be characterized via Boolean functions. We consider a space-invariant binary CNN belonging to the uncoupled class $C(\mathbf{A}^0, \mathbf{B}, z)$ with a 3×3 neighborhood that maps any static 3×3 input pattern into a static binary 3×3 output pattern. It can be uniquely defined by a Boolean function of nine binary input variables, where each variable denotes one of the nine pixels within the sphere of influence of a cell. Although there are infinitely many distinct templates of the class $C(\mathbf{A}^0, \mathbf{B}, z)$, there are only a finite number of distinct combinations of 3×3 pattern of black and white cells, namely, $2^9 = 512$. As each binary nine input pattern can map to either 0 (white) or 1 (black), there are 2^{512} distinct Boolean maps of nine binary variables. Thus, every binary standard CNN can be uniquely characterized by a CNN truth table, consisting of 512 rows with one for each distinct 3×3 black-and-white pattern, nine input columns with one for each binary input variable, and one output column with binary values of the output variable.

$2^{512} \approx 1.3408 \times 10^{154} > 10^{154}$ is an "immense" number (in the sense proposed by Walter Elsasser), although the uncoupled $C(\mathbf{A}^0, \mathbf{B}, z)$ CNNs are only

a small subclass of all CNNs. So, the question arises as to which subclass of Boolean functions exactly characterizes the uncoupled CNNs. In their critique of the perceptron (1969), M. Minsky and S. Papert introduced the concept of linearly separable and nonseparable Boolean functions. It can be proven that the class $C(\mathbf{A}^0, \mathbf{B}, z)$ of all uncoupled CNNs with binary inputs and binary outputs is identical to the linearly separable class of Boolean functions. Thus, linearly nonseparable Boolean functions such as, for example, the XOR function cannot be realized by an uncoupled CNN. But the uncoupled CNNs can be used as elementary building blocks that are connected by CNNs of logical operations. It can be proved that every Boolean function of nine variables can be realized by using uncoupled CNNs with nine inputs and either one logic OR CNN, or one logic AND CNN, in addition to one logic NOT CNN.

Every uncoupled CNN $C(\mathbf{A}^0, \mathbf{B}, z)$ with static binary inputs is completely stable in the sense that any solution converges to an equilibrium point. The waveform of the CNN state increases or decreases monotonically to the equilibrium point if the state at this point is positive or negative. Moreover, except for some degenerate cases, the steady-state output solution can be explicitly calculated by an algebraic formula without solving the associated nonlinear differential equations. Obviously, this is an important result to characterize a CNN class of nonlinear dynamics with robust CNN templates. Completely stable CNNs are the workhouses of the most current CNN applications. But there are also even simpler CNNs with oscillatory or chaotic behavior. Future applications will exploit the immense potentials of the unexplored terrains of oscillatory and chaotic operating regions. Then, Cellular Neural Networks will actually be transformed to Cellular Nonlinear Networks with all kinds of phase transitions and attractors of nonlinear dynamics.

Complexity Paradigm

From the perspective of nonlinear dynamics, it is convenient to think of standard CNN state equations as a set of ordinary differential equations with the components of the CNN gene as bifurcation parameters. Then, the dynamical behavior of standard CNNs can be studied in detail. Numerical examples deliver CNNs with limit cycles and chaotic attractors. The emergence of complex structures in nature can be explained by the nonlinear dynamics and attractors of complex systems. They result from the collective behavior of interacting elements in a complex system. The different paradigms of complexity research promise to explain pattern formation and pattern recognition in nature by specific mechanisms (e.g., Prigogine's chemical dissipation, Haken's work on lasers). From the CNN point of view, it is convenient to study the subclass of autonomous CNNs where the cells have no inputs. In these systems, it can be explained how patterns can arise, evolve, and sometimes converge to an equilibrium by diffusion-reaction processes. Pattern formation starts with an initial uniform pattern in an unstable equilibrium that is perturbed by small, random displacements. Thus, in the initial state, the symmetry of the unstable equilibrium is disturbed, leading to rather complex patterns. Obviously, in these applications, cellular networks do not refer only to neural activities in nerve systems, but to pattern formation in general.

A CNN is defined by the state equations of isolated cells and the cell coupling laws. For simulating reaction-diffusion processes, the coupling law describes a discrete version of diffusion (with a discrete Laplacian operator). CNN state equations and CNN coupling laws can be combined in a CNN reaction-diffusion equation, determining the dynamics of autonomous CNNs. If we replace their discrete functions and operators by their limiting continuum version, then we obtain the well-known continuous partial differential equations of reaction-diffusion processes that have been studied in different complexity approaches. Chua's version of the CNN reaction-diffusion equation delivers computer simulations of these pattern formations in chemistry and biology (e.g., concentric, auto, and spiral waves). On the other hand, for any nonlinear partial differential equation, many appropriate CNN equations can be associated with it. In many cases, it is sufficient to study the computer simulations of associated CNN equations, in order to understand the nonlinear dynamics of these complex systems.

CNN Universal Machine and Programming

There are practical and theoretical reasons for introducing a CNN Universal Machine (CNN-UM). From an engineering point of view, it is totally impractical to implement different CNN components or templates with different hardwired CNNs. Historically, John von Neumann's general-purpose computer was inspired by Alan Turing's universal machine in order to overcome all the different hardware machines of the 1930s and 1940s for different applications. From a theoretical point of view, CNN-UM opens new avenues of analog neural computers. In the CNN-UM, analog (continuous) and logic operations are mixed and embedded in an array computer. It is a complex nonlinear system, which combines two different types of operations, namely continuous nonlinear array dynamics and continuous time with local and global logic. Obviously, the mixture of analog and digital components considerably resembles to neural information processing in living organisms. The stored program, as a sequence of templates, could

be considered as a genetic code for the CNN-UM. The elementary genes are the templates.

After the introduction of the architecture with standard CNN universal cells and the global analog programming unit (GAPU), the complete sequence of an analog CNN program can be executed on a CNN-UM. The description of such a program contains the global task, the flow diagram of the algorithm, the description of the algorithm in a high level α (analog) programming language, and the sequence of macro-instructions by a compiler in the form of an analog machine code (AMC). At the lowest level, the chips are embedded in their physical environment of circuits. The AMC code will be translated into hardware circuits and electrical signals. At the highest level, the α compiler generates a macro-level code called analog macro-code (AMC). The input of the α compiler is the description of the flow diagram of the algorithm using the language. In Figure 2, the levels of the software and the core engines are described. The analog macro code is used for software simulations running on a Pentium chip in a PC and for applications in a CNN-UM Chip with a CNN Chip Prototyping System (CCPS).

The CNN-UM is technically realized by analog and digital VLSI implementation. It is well known that any complex system of digital technology can be built from a few implemented building blocks by wiring and programming. In the same way, the CNN-UM, also containing analog building blocks, can be constructed. A core cell needs only three building blocks of a capacitor, resistor, and a VCCS (voltage-controlled current source). If a switch, a logic register, and a logic gate are added to the three building blocks, the extended CNN cell of the CNN-UM can be implemented. In principle, six building blocks plus wiring are sufficient to build the CNN-UM: resistor, capacitor, switch, VCCS, logic register, logic gate. As in a digital computer, stored programmability can also be introduced for analog neural computers, enabling the fabrication of visual microprocessors. Similar to classical microprocessors, stored programmability needs a complex computational infrastructure with high-level language, compiler, macro-code, interpreter, operating system, and physical code, in order to make it understandable for the human user. Using this computational infrastructure, a visual microprocessor can be programmed by downloading the programs onto the chips, as in the case of classical digital microprocessors. Writing a program for an analog CNN algorithm is as easy as writing a BASIC program.

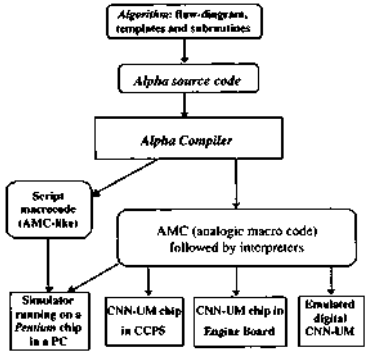

Figure 2. Levels of the software and the core engines in the CNN-UM.

With respect to computing power, CNN computers offer an orders-of-magnitude speed advantage over conventional technology when the task is complex. There are also advantages in size, complexity, and power consumption. A complete CNN-UM on a chip consists of an array of 64×64 0.5 μm micron CMOS cell processors. Each cell is endowed not only with a sensor for direct optical input of images and video but also with communication and control circuitries, as well as local analog and logic memories. CNN cells are interfaced with their nearest neighbors, as well as with the outside world. A CNN chip with 4096 cell processors on a chip means more than 3.0 Tera-OPS (operations per second) equivalent of computing power, which is about a 1000 times faster than the computing power of an advanced Pentium processor. By exploiting the state-of-the-art vertical packaging technologies, close to 10^{15} OPS CNN-UM architectures can be constructed on chips with 200×200 arrays. Thus, CNN universal chips will realize Tera-OPS or even Penta-(10^{15}) OPS, which are required for high-speed target recognition and tracking, real-time visual inspection of manufacturing processes, and intelligent machine vision capable of recognizing context-sensitive and moving scenes.

KLAUS MAINZER

See also **Attractor neural network; Cellular automata; Integrable cellular automata**

Further Reading

Chua, L.O. 1998. *A Paradigm for Complexity*, Singapore: World Scientific

Chua, L.O., Gulak, G., Pierzchala, E. & Rodriguez-Vázquez (editors). 1998. Cellular neural networks and analog VLSI. *Analog Integrated Circuits and Signal Processing. An International Journal*, 15(3)

Chua, L.O. & Roska, T. 2002. *Cellular Neural Networks and Visual Computing: Foundations and Applications*, Cambridge and New York: Cambridge University Press

Chua, L.O., Sbitnev, V.I. & Yoon, S. 2003. A nonlinear dynamics perspective of Wolfram's new kind of science. Part II: universal neuron. *International Journal of Bifurcation and Chaos in Applied Sciences and Engineering*, 13: 2377–2491

Chua, L.O. & Yang, L. 1988. Cellular neural networks: theory. *IEEE Transactions on Circuits and Systems*, 35: 1257–1272; Cellular neural networks: applications. *IEEE Transactions on Circuits and Systems*, 35: 1273–1290

Chua, L.O., Yoon, S. & Dogaru, R. 2002. A nonlinear dynamics perspective of Wolfram's new kind of science. Part I: threshold of complexity. *International Journal of Bifurcation and Chaos in Applied Sciences and Engineering*, 12: 2655–2766

Elsassee, W.M. 1987. *Reflections on a Theory of Organisms: Holism in Biology*, Frelighsburg, Quebec: Editions Orbis

Huertas, J.L., Che, W.K. & Madan, R.N. (editors). 1999. *Visions of Nonlinear Science in the 21st Century. Festshrift Dedicated to Leon O. Chua on the Occasion of his 60th Birthday*, Singapore: World Scientific

Mainzer, K. 2003. *Thinking in Complexity: The Computational Dynamics of Matter, Mind, and Mankind*, 4th edition, Berlin and New York: Springer

Tetzlaff, R. (editor). 2002. Cellular Neural Networks and Their Applications. *Proceedings of the 7th IEEE International CNN Workshop*, Singapore: World Scientific

CENTER MANIFOLD REDUCTION

A dynamical system might be difficult to solve, even numerically. To better understand its behavior in the neighborhood of an equilibrium, a reduction can be performed. For this, one starts with the eigenvalue spectrum λ of the linearized system. In the linear evolution $\sim \exp(\lambda t)$, eigenvalues with $\Re\lambda < 0$ ($\Re\lambda > 0$) are called stable (unstable), whereas those with $\Re\lambda = 0$ are called central.

In the neighborhood of an equilibrium point, P, of a dynamical system, in general, three different types of invariant manifolds exist: the trajectories belonging to the stable manifold M^{s} are being attracted by P, whereas those of the unstable manifold M^{u} are being repelled. The dynamics on the center manifold M^{c} depend on the nonlinearities. For the linearized problem, $E^{\mathrm{s}} \equiv M^{\mathrm{s}}$, $E^{\mathrm{u}} \equiv M^{\mathrm{u}}$, and $E^{\mathrm{c}} \equiv M^{\mathrm{c}}$ are uniquely determined linear subspaces that span the whole space. The transition to the nonlinear system causes (only) deformations of the linearly determined manifolds M_{s}, M_{u}, and M_{c}. However, the form of the latter critically depends on the nonlinear terms.

Let us elucidate that the behavior for the very simple system (Grosche et al., 1995)

$$\dot{x} = -xy, \quad \dot{y} = -y + x^2. \tag{1}$$

Here, the dot means differentiation with respect to time t. The equilibrium point P is $(0, 0)$, and the linearized system is

$$\dot{x} = 0, \quad \dot{y} = -y. \tag{2}$$

Here, we have the stable manifold E^{s} being identical to the y-axis and the center manifold E^{c} being identical to the x-axis. The linearized problem can be visualized by the graph shown in Figure 1.

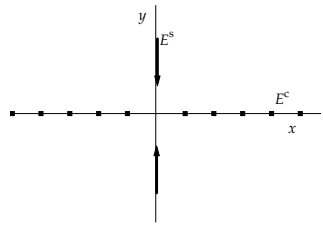

Figure 1. The linear stable (E^{s}) and center manifold (E^{c}) for example (1).

Both manifolds will be deformed in the transition to the nonlinear system. The (nonlinear, perturbed) center manifold can be described in the present example by

$$M^{\mathrm{c}} : y = h(x) \tag{3}$$

with $h(0) = h'(0) = 0$. Using that ansatz for the center manifold in (1), we obtain

$$\dot{x} = -x\, h(x). \tag{4}$$

Differentiating (3) with respect to t, leads to

$$\dot{y} = h'(x)\, \dot{x} \tag{5}$$

or

$$-h(x) + x^2 = h'(x)[-xh(x)], \tag{6}$$

that is, a differential equation for $h = h(x)$. Performing a power series ansatz $h(x) = cx^2 + dx^3 + \cdots$, we find that $c = 1$. The (nonlinear) center manifold is thus given by

$$y = x^2 + \cdots, \tag{7}$$

and the dynamics on it follows from

$$\dot{x} = -x^3; \tag{8}$$

that is, the trajectories are being attracted by P. For an illustration, see Figure 2.

More General Theoretical Background

Let us now generalize the idea and consider a system of ordinary differential equations (ODEs)

$$\dot{a} = Aa + N(a, b), \tag{9}$$

$$\dot{b} = Bb + M(a, b), \tag{10}$$

describing the dynamics of amplitudes $a_1, \ldots, a_n$ and $b_1, \ldots, b_m$ of n linear marginal stable modes and m linear stable modes, respectively $[(a_1, \ldots, a_n) := a$,

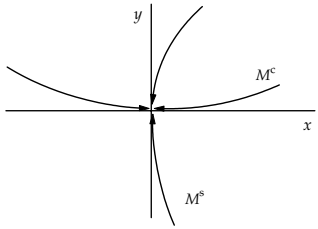

Figure 2. The stable (M^s) and center manifold (M^c) for example (1).

$(b_1, \ldots, b_m) := b]$. This implies that the real parts of eigenvalues of the matrix A vanish, and the real parts of the eigenvalues of the matrix B are negative. The functions $N(a, b)$, $M(a, b) \in C^r$ on the right-hand sides of Equations (9) and (10) represent the nonlinear terms. Let E^c be the n-dimensional (generalized) eigenspace of A and E^s be the m-dimensional (generalized) eigenspace of B. Under these assumptions, the center manifold theorem provides the following statement (Guckenheimer & Holmes, 1983):

> There exists an invariant C^r manifold M^s and an invariant C^{r-1} manifold M^c that are tangent at $(a, b) = (0, 0)$ to the eigenspaces E^s and E^c, respectively. The stable manifold M^s is unique but the center manifold M^c is not necessarily unique.

Locally, the center manifold M^c can be represented as a graph,

$$M^c = \{(a, b) | b = h(a)\}, \; h(0) = 0, \; Dh(0) = 0, \tag{11}$$

where the C^{r-1} function h is defined in a neighborhood of the origin, and Dh denotes the Jacobi matrix. Introducing (11) in Equations (9) and (10), we obtain

$$\dot{a} = Aa + N(a, h(a)), \tag{12}$$

$$Dh(a)\,[Aa + N(a, h(a))] = Bh(a) + M(a, h(a)). \tag{13}$$

The solution h of Equation (13) can be approximated by a power series. The ambiguity of the center manifold is manifested by the fact that h is determined only modulo C^∞, a non-analytic function; thus, the power series approximation of the function h is unique. The importance of the center manifold theory is reflected by the following theorem (Marsden & McCracken, 1976; Carr, 1981):

> If there exists a neighborhood U^c of $(a, b) = (0, 0)$ on M^c, so that every trajectory starting in U^c never leaves it, then there exists a neighborhood U of $(a, b) = (0, 0)$ in $\Re^n \times \Re^m$, so that every trajectory starting in U converges to a trajectory on the center manifold.

Therefore, it is sufficient to discuss the dynamics on the center manifold, described by Equation (12). If all solutions are bounded to some neighborhood of the origin, then we have described all features of the asymptotic behavior of Equations (9) and (10). In order to fulfill the condition, the function $N(a, h(a))$ has to be expanded up to a sufficiently high order. We end up with normal forms, for example, the third order may be adequate.

Very often, the problems contain parameters and, in addition, the systems may be infinite dimensional. In both cases, one can generalize the theory presented so far. Parameters can be taken into account by expanding Equations (9) and (10) to

$$\dot{a} = A(\Lambda)a + N(a, b, \Lambda), \tag{14}$$

$$\dot{b} = B(\Lambda)b + M(a, b, \Lambda), \tag{15}$$

$$\dot{\Lambda} = 0, \tag{16}$$

where $\Lambda = (a_{n+1}, \ldots, a_{n+l})$ contains l parameters. The center manifold now has dimension $n + l$.

PDE Reduction and Symmetry Considerations

The theory is also valid in the infinite-dimensional case, if the spectrum of the linear operator can be split into two parts. The first part contains a finite number of eigenvalues whose real parts are zero, and the second part contains (an infinite number of) eigenvalues with negative real parts that are bounded away from zero.

To elucidate the power of center manifold reduction, let us consider the partial differential equation (PDE)

$$\frac{\partial \phi}{\partial t} + \phi \frac{\partial \phi}{\partial y} + \alpha \frac{\partial^2 \phi}{\partial y^2} + \beta \frac{\partial^3 \phi}{\partial y^3} + \frac{\partial^4 \phi}{\partial y^4} + \nu \phi = 0. \tag{17}$$

All coefficients α, β, and ν are nonnegative. In the following, we treat β as a fixed parameter, and consider the dynamics in dependence in α and ν. The linearization with $\phi \equiv 0$ as the equilibrium solution leads to

$$\omega = -\beta k^3 + \mathrm{i}\left(-k^4 + \alpha k^2 - \nu\right) \tag{18}$$

when we assume a unit cell of length 2π with periodic boundary conditions. A typical dependence of the linear growth (or damping) rate $\gamma := \Im\omega$ is shown in Figure 3 for $\alpha = 5.25$ and $\nu = 3.8$.

The case of two unstable modes ($k = 1, 2$) is already highly nontrivial. Let us choose $\alpha = \alpha_c = 5$ and $\nu = \nu_c = 4$. Then, the modes $\phi^{(1)} = \sin y$, $\phi^{(2)} = \cos y$, $\phi^{(3)} = \sin 2y$, and $\phi^{(4)} = \cos 2y$ belonging to $k = 1$ and 2, respectively, are marginally stable. We introduce

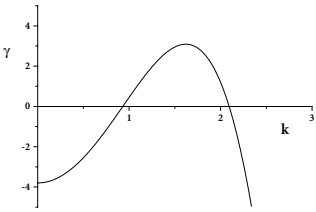

Figure 3. Growth rate curve, with two unstable modes at $k = 1$ and $k = 2$ for the PDE (17).

the four (real) amplitudes a_1, a_2, a_3, and a_4, as well as $\alpha_5 = \alpha - \alpha_c$ and $\alpha_6 = \nu - \nu_c$. The center manifold theory will allow us to derive a closed set of nonlinear amplitude equations

$$\dot{a}_n = f_n(a_1, \ldots, a_6), \ n = 1, \ldots, 6, \tag{19}$$

which are valid in the neighborhood of the critical point α_c, ν_c. One has $f_5 \equiv f_6 \equiv 0$. The other functions f_n are written as a power series in a_n,

$$f_n = \sum_{1 \le m \le 6} A_n^m \, a_m + \sum_{1 \le m \le p \le 6} A_n^{mp} \, a_m \, a_p + \cdots . \tag{20}$$

The dynamics on the center manifold is characterized by $a_1, \ldots, a_6$. Thus, we can make the ansatz (Carr, 1981)

$$\phi(y,t) = \sum_{1 \le n \le 4} a_n(t) \, \phi^{(n)}(y) + \sum_{1 \le n \le m \le 6} a_n(t) \, a_m(t) \phi^{(nm)}(y), \tag{21}$$

where the $\binom{7}{2} = 21$ new functions $\phi^{(nm)}$ and, of course, the next $\binom{8}{3} = 56$ functions $\phi^{(nmp)}$, and so on, can be chosen orthogonal to $\phi^{(n)}$, $n = 1, \ldots, 4$.

The technical procedure is now as follows. One inserts ansatz (21) into the basic equation (17) and compares equal orders in the amplitudes. For example, in the second-order, one collects equal powers $a_r a_s$; the "coefficients" (being equated to zero) will determine the unknown functions $\phi^{(nm)}$ via ODEs. Taking into account the (periodic) boundary conditions, we have to satisfy the solvability conditions. Collecting equal powers of the amplitudes a_n, we find the solutions for the coefficients A_r^{np}. With these values, we can solve for $\phi^{(mn)}$. This procedure should be continued to higher orders.

Actually, when written explicitly, one faces considerable work (in second order, we have to solve for 84, and in third order for 224 coefficients $A_r^{\cdots}$, and so on). One can simplify the calculations by making use of symmetries.

Translational invariance implies the following. If $\phi(y)$ is a solution,

$$T_{y_0}\phi(y) := \phi(y + y_0) \tag{22}$$

will also satisfy the dynamical equation (17), where y_0 is a real shift parameter. (In the case $\beta \equiv 0$, we also have the mirror symmetry $\phi(y) = \phi(-y)$.)

Remember the structure of the center manifold reduction: the modes $\phi^{(nm)}$, $\phi^{(nmp)}, \ldots$ have to be determined from inhomogeneous differential equations. The inhomogeneities contain (in nonlinear forms) the marginal modes $\phi^{(r)}$, $r = 1, \ldots, 4$. Thus, the so-called slaved modes can be written in symbolic form as

$$\phi^{(m\ldots)} = h^{(m\ldots)}\left[\{\phi^{(r)}\}\right]. \tag{23}$$

Thus, the following symmetry should hold:

$$T_{y_0} h^{(m\ldots)}\left[\{\phi^{(r)}\}\right] = h^{(m\ldots)}\left[T_{y_0}\{\phi^{(r)}\}\right]. \tag{24}$$

The consequences of the translational symmetry are most easily seen when combing the marginal modes to

$$\varphi := \sum_{r=1}^{4} a_r \phi^{(r)} \equiv \Im\left(c_1 e^{iy} + c_2 e^{2iy}\right) \tag{25}$$

with the complex amplitudes $c_1 := a_1 + ia_2$, $c_2 := a_3 + ia_4$. The (complex) amplitude equations are

$$\dot{c} = g_n(c_1, c_2, a_5, a_6), \ n = 1, 2, \tag{26}$$

$$\dot{a}_m = 0, \ m = 5, 6. \tag{27}$$

The translational symmetry (22) requires

$$e^{iny_0} g_n(c_1, c_2, a_5, a_6) = g_n\left(e^{iy_0}c_1, e^{i2y_0}c_2, a_5, a_6\right) \tag{28}$$

for $n = 1, 2$. The vector field (g_1, g_2) is called equivariant with respect to the operation

$$(c_1, c_2) \to \left(e^{iy_0}c_1, e^{i2y_0}c_2\right). \tag{29}$$

The most general form of vector fields being equivariant under operation (28) is

$$(g_1, g_2) = \left(c_1 P_1 + \bar{c}_1 c_2 Q_1, \ c_2 P_2 + c_1^2 Q_2\right), \tag{30}$$

where P_1, P_2, Q_1, and Q_2 are polynomials in $|c_1|^2, |c_2|^2$, and $\Re(c_1^2 \bar{c}_2)$; of course, they can also depend on a_5 and a_6.

Keeping in mind the symmetry properties, the general form of the amplitude equations reduces to

$$\dot{c}_1 = \lambda c_1 + \mathcal{A}\bar{c}_1 c_2 + \mathcal{C} c_1 |c_1|^2 + \mathcal{E} c_1 |c_2|^2 + \mathcal{O}(|c|^4), \tag{31}$$

$$\dot{c}_2 = \mu c_2 + \mathcal{B} c_1^2 + \mathcal{D} c_2 |c_1|^2 + \mathcal{F} c_2 |c_2|^2 + \mathcal{O}(|c|^4), \tag{32}$$

$$\dot{a}_5 = \dot{a}_6 = 0. \tag{33}$$

A straightforward analysis leads to

$$\begin{aligned} &\lambda = a_5 - a_6 - \mathrm{i}\beta, \quad \mu = 4a_5 - a_6 + \mathrm{i}8\beta, \\ &\mathcal{A} = \tfrac{1}{2}, \quad \mathcal{B} = -\tfrac{1}{2}, \\ &\mathcal{C} = 0, \quad \mathcal{D} = -\tfrac{3}{4(20-\mathrm{i}9\beta)}, \\ &\mathcal{E} = \tfrac{1}{2}D, \quad \mathcal{F} = -\tfrac{1}{12(15-\mathrm{i}4\beta)}. \end{aligned} \tag{34}$$

This completes the center manifold reduction.

Very interesting conclusions result, for example, with respect to the number of modes and their interplay in time, from the systematic treatment with the center manifold theory. For example, one interesting aspect is that the present codimension-two analysis can describe successive bifurcations of one unstable mode, which, in some cases can lead to chaos in time.

KARL SPATSCHEK

See also **Inertial manifolds; Invariant manifolds and sets; Synergetics**

Further Reading

Carr, J. 1981. *Applications of Center Manifold Theory*, New York: Springer

Grosche, G., Ziegler, V., Ziegler, D. & Zeidler, E. (editors). 1995. *Teubner-Taschenbuch der Mathematik, Teil II*, Stuttgart: Teubner

Guckenheimer, J. & Holmes, P. 1983. *Nonlinear Oscillations, Dynamical Systems, and Bifurcations of Vector Fields*, Berlin and New York: Springer

Marsden, J.E. & McCracken, M. 1976. *The Hopf Bifurcation and Its Applications*, New York: Springer

CENTRAL LIMIT THEOREM

See **Martingales**

CHAOS VS. TURBULENCE

The notion of chaos has its genesis in the work of Henri Poincaré (*See* **Poincaré theorems**) on the three-body problem of celestial mechanics. Poincaré realized that this problem cannot be reduced to quadratures and solved in the manner of the two-body problem. A precise definition of chaos or non-integrability can be given in terms of the absence of conserved quantities necessary to yield a solution. It took several decades for the full significance of non-integrable dynamical systems to be appreciated and for the term "chaos" to be introduced (*See* **Chaotic dynamics**). An important step was the 1963 paper by Edward N. Lorenz, entitled "Deterministic Nonperiodic Flow" (Lorenz, 1963), on a model describing thermal convection in a layer of fluid heated from below. The Lorenz model truncates the basic fluid dynamical equations, written in terms of Fourier amplitudes, to just three modes (*See* **Lorenz equations**):

$$\begin{aligned} \dot{x} &= -\sigma x + \sigma y, \\ \dot{y} &= -xz + rx - y \\ \dot{z} &= xy - bz. \end{aligned} \tag{1}$$

In this system, x is the time-dependent amplitude of a stream-function mode, while y and z are mode amplitudes of the temperature field. The parameters σ, r, and b depend on the geometry, the boundary conditions, and the physical parameters of the fluid. Equations (1) are a subset of the full, infinite system of mode amplitude equations, chosen such that it exactly captures the initial instability of the thermally conducting state to convecting rolls when the parameter r, known as the Rayleigh number, is increased.

What Lorenz observed in numerical solutions of (1), and verified by analysis, was that very complicated, erratic solutions would arise when r was increased well beyond the conduction-to-convection transition. In fact, Lorenz had found the first example of what is today called a strange attractor (*See* Figure 1 and **Attractors**). System (1) is clearly deterministic, yet it can produce non-periodic solutions. There were other intriguing aspects of the solutions to (1) in the chaotic regime. Solutions arising from close initial conditions would separate exponentially in time, leading to an apparently random dependence on initial conditions of the solution after a finite time (*See* **Butterfly effect**). Today, this would be associated with the existence of a positive characteristic Lyapunov exponent. A list of "symptoms" can be established that are shared by systems having the property of chaos, including: complex temporal evolution, exponential separation from close initial conditions, a strange attractor in phase space (if the system is dissipative), and positive Lyapunov exponents. An important difference from Poincaré's work was that Lorenz's system described a dissipative system in which energy is not conserved.

From the start, the potential connection between chaos and other concepts in statistical physics, such as ergodicity and turbulence, was of central interest. For example, chaos was thought to imply ergodic

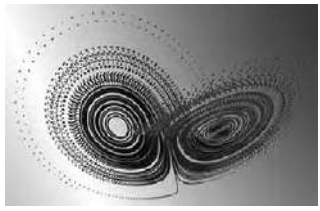

Figure 1. Strange attractor associated with the Lorenz equations. Reproduced with permission from Images by Paul Bourke, http://astronomy.swin.edu.au/ pbourke/fractals/lorenz/.

behavior in the sense of the "ergodic hypothesis" underlying equilibrium statistical mechanics (*See* **Ergodic theory**). Similarly, the connection between chaos and turbulence was sought, particularly appropriate given that Lorenz's model was of a fluid flow. Experiments on other fluid systems by Gollub, Swinney, Libchaber, and later many others established that the transition from laminar to turbulent flow typically takes place through a regime of chaotic fluid motion. The well-known route to chaos via period-doubling bifurcations of Mitchell J. Feigenbaum belongs here as well (Feigenbaum, 1980; Eckmann, 1981). In view of this, it is natural to think that turbulent flow itself is simply some kind of chaotic flow state.

Turbulence is a common state of fluid flow that shares several "symptoms" with chaotic dynamical systems, but also has distinct features not easily duplicated by chaos. The word "turbulence" was apparently first used by Leonardo da Vinci to describe a complex flow. In mathematical terms, turbulent flows should be solutions of the Navier–Stokes equation, usually written in the dimensionless form (*See* **Navier–Stokes equation**)

$$\frac{\partial \boldsymbol{u}}{\partial t} + \boldsymbol{u} \cdot \nabla \boldsymbol{u} = -\nabla p + R^{-1} \Delta \boldsymbol{u}, \tag{2}$$

$$\nabla \cdot \boldsymbol{u} = 0. \tag{3}$$

We have restricted attention to incompressible flows by insisting in (3) that the velocity field $\boldsymbol{u}(\boldsymbol{x}, t)$ be divergence free. In (2) the field p represents the pressure—the constant density has been absorbed in the nondimensionalization. The sole dimensionless parameter R is Reynolds number. In terms of physical variables $R = UL/\nu$, where U is a typical scale of velocity, L a typical length scale of the flow, and n is the kinematic viscosity of the fluid. For small values of R, say $0 < R \leq 1$, the flow is laminar. For moderate R, say $1 < R \leq 100$, various periodic flow phenomena may arise, such as the shedding of vortices from blunt bodies. For large R, the flow eventually breaks down into many interacting eddies—this is turbulent flow. Since most flowing fluid is, in fact, flowing at large R, turbulence is the prevailing flow state of fluids in our surroundings (oceans and atmosphere), in the universe in general, in many industrial processes, and to some extent, within our bodies.

The characterization of what makes a flow turbulent is not nearly so clear as what makes a dynamical system chaotic. First, the issue of whether the particular set of nonlinear partial differential equations (2) and (3) even has a smooth solution for all time, given smooth initial conditions, is still unsettled and is one of the prize challenges set by the Clay Mathematics Institute (http://www.claymath.org). In spite of several attempts, a convincing example of a flow with smooth initial conditions, evolving under (2) and (3), that develops a singularity in a finite time has not been found. Conversely, there is no proof that solutions with the requisite number of derivatives will exist for all time.

Turbulent flows are also recognized by a variety of "symptoms." The flow velocity as a function of time at any given point in a turbulent flow is a random function (roughly a Gaussian). However, the overall nature of the velocity field viewed as a random vector field is not Gaussian. The random nature of turbulent velocity fields is today thoroughly familiar to the flying public. The randomness is not just temporal at a fixed point in space; the spatial variation of the flow field at a given time constitutes a multitude of interacting eddies of different sizes. Because of their random character, turbulent flows stir vigorously, leading to rapid dispersal of a passively advected substance or a field, such as temperature, and to a rapid exchange of momentum with contiguous fluid. In the classic pipe flow experiment of Osborne Reynolds, for example, in which the transition from laminar to turbulent flow was first demonstrated to depend only on the dimensionless number R, a streak of dye introduced at the inlet would remain a thin streak (except for a bit of molecular diffusion) when the flow in the pipe was laminar. When the flow rate was increased and the flow became turbulent, the dye rapidly dispersed across the pipe.

In a turbulent flow, the large scales of motion, which are typically in contact with some kind of forcing from the outside, will generate smaller scales through interactions and instabilities. This process continues through a broad range of length scales, ultimately reaching small scales where molecular dissipation is effective and quells the motion altogether. The repeated process of "handing down" energy from larger scales to smaller scales is a key process in turbulence. It is usually referred to as the Kolmogorov cascade (*See* **Kolmogorov cascade**). The qualitative nature of this process was already envisaged by Lewis Fry Richardson and was described by him in an adaptation of a verse by Jonathan Swift:

> *Big whorls have little whorls,*
> *Which feed on their velocity;*
> *And little whorls have lesser whorls,*
> *And so on to viscosity (in the molecular sense).*

Because of its broad range of length scales, the energy in a turbulent flow may be considered partitioned among modes of different wavenumbers k. The energy spectrum $E(k)$ is defined such that $E(k)\,\mathrm{d}k$ is the amount of kinetic energy of the turbulent flow associated with motions with wavenumbers between k and $k + \mathrm{d}k$. The cascade implies a transfer of energy from scale to scale with a characteristic energy flux per unit mass, ε, which must also be equal to the rate at which energy is fed to the flow from the largest scales, and to the rate at which energy is dissipated by viscosity at the smallest scales. A simple dimensional argument then (*See* **Dimensional**

analysis) gives the dependence of $E(k)$ on ε and k to be

$$E(k) = C\varepsilon^{2/3}k^{-5/3}. \quad (4)$$

This is the well-known Kolmogorov spectrum, predicted by Andrei N. Kolmogorov in 1941 (Hunt et al., 1991; Frisch, 1995) and only subsequently verified by experiments in a tidal channel (see Figure 2).

Turbulence has many further intriguing statistical properties, which remain subjects of active research. A major shift in our thinking on turbulence occurred in the late 1960s and in the 1970s when experiments by Kline and Brown & Roshko demonstrated that even in turbulent shear flows at very large Reynolds number, one can identify coherent structures that organize the flow to some extent (Figure 3). Later investigations have shown that even in homogeneous, isotropic turbulence, the flow is often organized into strong filamentary vortices. The persistence of these organized structures, which can dominate the flow for long times and interact dynamically, forces a strong coupling among the spectral modes, reducing the effective number of degrees of freedom of the problem.

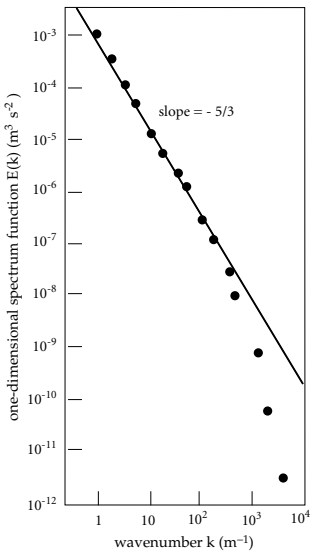

Figure 2. One-dimensional spectrum in a tidal channel from data in Grant et al. (1962).

Figure 3. Coherent structures in a turbulent mixing layer. From Brown & Roshko (1974), reprinted from *An Album of Fluid Motion*, M. Van Dyke, Parabolic Press, 1982.

Chaos and turbulence both describe states of a deterministic dynamical system in which the solutions appear random. Our current understanding of chaos is largely restricted to few-degree-of-freedom systems. Turbulence, on the other hand, is a many-degree-of-freedom phenomenon. It seems somewhat unique to fluid flows—related phenomena such as plasma turbulence or wave turbulence appear to be intrinsically different. The emergence of collective modes in the form of coherent structures in turbulence amidst the randomness is an intriguing feature, somewhat reminiscent of the mix between regular "islands" and the "chaotic sea" observed in chaotic, low-dimensional dynamical systems. The coherent structures themselves approximately form a deterministic, low-dimensional dynamical system. However, it seems impossible to fully eliminate all but a finite number of degrees of freedom in a turbulent flow—the modes not included explicitly form an essential, dissipative background, often referred to as an eddy viscosity, that must be included in the description.

Turbulence is intrinsically spatiotemporal, whereas chaotic behavior in a fluid system can be merely temporal with a simple spatial structure. It is possible for the flow field to be perfectly regular in space and time, yet the trajectories of fluid particles moving within the flow will be chaotic. This is the phenomenon of chaotic advection (*See* **Choatic advection**), which points out the hugely increased complexity of a turbulent flow relative to chaos in a dynamical system.

PAUL K.A.NEWTON AND HASSAN AREF

See also **Attractors; Butterfly effect; Celestial mechanics; Chaotic advection; Chaotic dynamics; Diffusion; Ergodic theory; Kolmogorov cascade; Lorenz equations; Lyapunov exponents; Navier–Stokes equation; *N*-body problem; Partial differential equations, nonlinear; Period doubling; Phase space; Poincaré theorems; Routes to chaos; Shear flow; Thermal convection; Turbulence**

Further Reading

Aref, H. & Gollub, J.P. 1996. Application of dynamical systems theory to fluid mechanics. *Research Trends in Fluid Dynamics, Report of the US National Committee on Theoretical and Applied Mechanics*, edited by J.L. Lumley et al., New York: AIP Press, pp. 15–30

Eckmann, J.P. 1981. Roads to turbulence in dissipative dynamical systems. *Reviews of Modern Physics*, 53: 643–654

Feigenbaum, M.J. 1980. Transition to aperiodic behavior in turbulent systems. *Communications in Mathematical Physics*, 77: 65–86

Frisch, U. 1995. *Turbulence—The Legacy of A. N. Kolmogorov*, Cambridge and New York: Cambridge University Press
Grant, H.L., Stewart, R.W. & Moilliet, A. 1962. Turbulent spectra from a tidal channel. *J. Fluid. Mech.*, 12: 241–268
Hunt, J.C.R., Phillips, O.M., & Williams, D. (editors). 1991. Turbulence and stochastic processes: Kolmogorov's ideas 50 years on. *Proceedings of the Royal Society, London* A, 434: 1–240
Lorenz, E.N. 1963. Deterministic nonperiodic flow. *Journal of Atmospheric Sciences*, 20: 130–141
Ruelle, D. 1991. *Chance and Chaos*, Princeton, NJ: Princeton University Press

CHAOTIC ADVECTION

In fluid mechanics, *advection* means the transport of material particles by a fluid flow, as when smoke from a chimney is blown by the wind. The term *passive advection* is sometimes used to emphasize that the substance being carried by the flow is sufficiently inert that it follows the flow entirely, the velocity of the advected substance at every point and every instant adjusting to that of the prevailing flow.

To describe the kinematics of a fluid, two points of view may be adopted: the Eulerian representation focuses on the velocity field $\mathbf{u}$ as a function of position and time, $\mathbf{u}(\mathbf{x}, t)$; the Lagrangian representation emphasizes the trajectories $\mathbf{x}_P(t)$ of a fluid particle as it is advected by the flow. The two points of view are linked by stating that the value of the velocity field at a given point in space and instant in time equals the velocity of the fluid element passing through that same point at that instant, that is,

$$\dot{\mathbf{x}}_P(t) = \mathbf{u}(\mathbf{x}_P(t), t). \tag{1}$$

The Eulerian representation is used extensively for measurements and numerical simulations of fluid flow since it allows one to fix the points in space and time where the field is to be determined. The Lagrangian representation, on the other hand, is often more natural for theoretical analysis, as it explicitly addresses the nonlinearity of the Navier–Stokes equation.

For a given flow, the equations of motion (1), sometimes called the *advection equations*, are a system of ordinary differential equations that define a dynamical system. These equations can be integrable or non-integrable. Chaotic advection appears when the equations are non-integrable and the trajectories of fluid elements become chaotic. The dynamical system defined by (1) has two or more degrees of freedom. For a two-dimensional time-independent or steady flow, there are just two degrees of freedom and no chaotic motion is possible. However, already for a 2-d time-dependent or a 3-d steady flow, there are enough degrees of freedom to allow for chaotic trajectories. In other words, chaotic advection can appear even for flows that would otherwise be considered laminar.

The phenomenon of chaotic advection is also known as Lagrangian chaos, or sometimes Lagrangian turbulence. Usually, the word turbulence refers to the Eulerian representation and to flows in which the velocity field fluctuates across a wide range of spatial and temporal scales with limited correlations. In such flows, the trajectories of fluid elements are always chaotic. By contrast, chaotic advection or Lagrangian chaos can arise in situations where the velocity field is spatially coherent and the time dependence is no more complicated than a simple periodic modulation.

Many examples have now been given to illustrate the point that the complexity of the spatial structure of material advected by a flow can be much greater than one might surmise from a picture of the instantaneous streamlines of the flow. Thus, in the paper that introduced the notion of chaotic advection (Aref (1984) and Figure 1), the case of two stirrers that act alternately on fluid confined to a disk was considered. Each stirrer was modeled as a point vortex that could be switched on and off. There are several parameters in the system, such as the strengths and positions of the vortex stirrer and the time interval over which each acts. For a wide range of parameter values, the dynamics is as shown in Figure 1; after just a few periods, the 10,000 particles being advected are spread out over a large fraction of the disk.

Chaotic advection gives rise to very efficient stirring of a fluid. Material lines are stretched at a rate given by the Lyapunov exponent. In bounded flows, these exponentially growing material lines have to be folded back over and over again, giving rise to ever finer and denser striations. They are familiar from the mixing of paint or from marbelized paper. On the smallest scales diffusion, takes over and smoothes the steep gradients, giving rise to mixing on the molecular scale. The interplay between stirring and diffusion is the

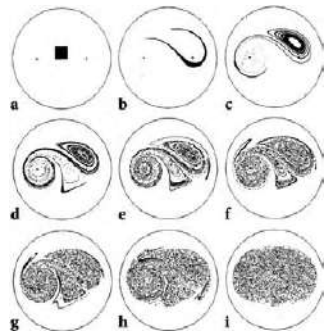

Figure 1. Spreading of 10,000 particles in a cylindrical container (disk) under the alternating action of two stirrers. The positions of the stirrers are marked by crosses. (a) initial distribution; (b)–(g) positions of the particles after 1, 2, …, 6 periods; (h) after 9 periods; (i) after 12 periods. From (Aref, 1984).

source of the efficient mixing in the presence of chaotic advection. This phenomenon is being exploited in various procedures for mixing highly viscous fluids, including applications to materials processing, in micro-fluidics, and even in large-scale atmospheric, oceanographic, and geological flows. It may play a role in the feeding of microorganisms.

In the case of 2-d incompressible flows the equations of motion allow for an interesting connection to Hamiltonian dynamics. The velocity field can be represented through a stream function $\psi(x, y, t)$, so that $\mathbf{u} = \nabla \times \psi \mathbf{e}_z$ and Equations (1) for the trajectories of fluid elements become

$$\dot{x} = \frac{\partial \psi}{\partial y}, \qquad \dot{y} = -\frac{\partial \psi}{\partial x}. \tag{2}$$

The relation to Hamilton's canonical equations is established through the identification x=position, y=momentum, and ψ=Hamilton function. Thus, what is the phase space in Hamiltonian systems can be visualized as the position space in the hydrodynamic situation. The structures that appear in 2-d periodically driven flows are, therefore, similar to the phase space structures in a Poincaré surface of section for a chaotic Hamiltonian system, and the same techniques can be used to analyze the transport of particles and the stretching and folding of material lines.

The phenomena that arise in chaotic advection by simple flows may be relevant to turbulent flows when a separation of length and time scales is possible. Consider, for example, the small-scale structures that appear in the density of a tracer substance when the molecular diffusivity κ of the tracer is much smaller than the kinematic viscosity ν of the liquid, that is, in a situation where the Schmidt number $\mathrm{Sc} = \nu/\kappa$ is much larger than one. Then, the velocity field is smooth below the Kolmogorov scale, $\lambda_K = (\nu^3/\varepsilon)^{1/4}$, where ε is the kinetic energy dissipation, but the scalar field has structures on even smaller scales, down to $\lambda_s = (\mathrm{Sc})^{-1/2}\lambda_K$. These arise from Lagrangian chaos with a randomly fluctuating velocity field. The patterns produced in this so-called Batchelor regime are strikingly similar to the ones observed in laminar flows.

On larger scales, ideas from chaotic advection are relevant when there are large-scale coherent structures with slow spatial and temporal evolution. Typical examples are 2-d or quasi-2-d flows, for example, in the atmosphere or in the oceans. Fluid volumes can be trapped in regions bounded by separatrices or by stable and unstable manifolds of stagnation points and may have very little exchange with their surroundings. Such a reduction in stirring appears to occur in the Wadden sea (Ridderinkhof & Zimmerman, 1992).

Equations (1) apply in this form to fluid elements and ideal particles only. For realistic particles with finite volume and inertia, further terms must be added. A significant change in the qualitative side is that the effective velocity field for inertial particles can have a nonvanishing divergence even for incompressible flows (Maxey & Riley, 1983).

The book by Ottino, (1989) and the two conference proceedings (Aref, 1994; IUTAM, 1991) provide good starting points for entering the many aspects of chaotic advection and Lagrangian chaos in engineering applications, geophysical flows, turbulent flows, and theoretical modeling. Historical remarks may be found in the Introduction to Aref, (1994) and in Aref, (2002). Today, the term chaotic advection designates an established subtopic of fluid mechanics that is used as a classification keyword by leading journals and conferences in the field.

HASSAN AREF AND BRUNO ECKHARDT

See also **Chaotic dynamics; Chaos vs. turbulence; Dynamical systems; Hamiltonian systems; Lyapunov exponents; Turbulence**

Further Reading

Aref, H. 1984. Stirring by chaotic advection. *Journal of Fluid Mechanics*, 143: 1–21

Aref, H. (editor). 1994. Chaos applied to fluid mixing. *Chaos, Solitons and Fractals*, 4: 1–372

Aref, H. 2002. The development of chaotic advection. *Physics of Fluids*, 14: 1315–1325

IUTAM Symposium on fluid mechanics of stirring and mixing. 1991. *Physics of Fluids*, 3: 1009–1496

Maxey, M. & Riley, J. 1983, Equation of motion for a small rigid sphere in a nonuniform flow. *Physics of Fluids*, 26: 883–889

Ottino, J.M. 1989. *The Kinematics of Mixing: Stretching, Chaos and Transport*, Cambridge: Cambridge University Press

Ridderinkhof, H. & Zimmermann, J.T.F. 1992. Chaotic stirring in a tidal system. *Science*, 258: 1107–1111

CHAOTIC BILLIARDS

See **Billiards**

CHAOTIC DYNAMICS

When we say "chaos", we usually imagine a very complex scene with many different elements that move in different directions, collide with each other, and appear and disappear randomly. Thus, according to everyday intuition, the system's complexity (e.g., many degrees of freedom) is an important attribute of chaos. It seems reasonable to think that in the opposite case, for example, a system with only a few degrees of freedom, the dynamical behavior must be simple and predictable. In fact, this point of view is Laplacian determinism.

The discovery of dynamical chaos has destroyed this traditional view. Dynamical chaos is a phenomenon that can be described by mathematical models for many natural systems, for example, physical, chemical, biological, and social, which evolve in time according to a deterministic rule and demonstrate capricious and

seemingly unpredictable behavior. To illustrate such behavior, consider a few examples.

Examples

Hyperion: Using Newton's laws, one can compute relatively easily all future solar eclipses not only for the next few hundred years but also for thousands and millions of years into the future. This is indicative of a real predictability of the system's dynamical behavior. But even in the solar system, there exists an object with unpredictable behavior: a small irregularly shaped moon of Saturn, Hyperion. Its orbit is regular and elliptic, but its altitude in the orbit is not. Hyperion is tumbling in a complex and irregular pattern while obeying the laws of gravitational dynamics. Hyperion may not be the only example of chaotic motion in the solar system. Recent studies indicate that chaotic behavior possibly exists in Jovian planets (Murray & Holman, 1999), resulting from the overlap of components of the mean motion resonance among Jupiter, Saturn, and Uranus. Chaos in Hamiltonian systems, which represent the dynamics of the planets, arises when one resonance is perturbed by another one (*See* **Standard map**).

Chaotic mixing is an example of the complex irregular motion of particles in a regular periodic velocity field, like drops of cream in a cup of coffee; see Figure 1. Such mixing, caused by sequential stretching and folding of a region of the flow, illustrates the general mechanism of the origin of chaos in the phase space of simple dynamical systems (*See* **Chaotic advection; Mixing**).

Billiards: For its conceptual simplicity, nothing could be more deterministic and completely predictable than the motion of a single ball on a billiard table. However, in the case of a table bounded by four quarters of a circle curved inward (Sinai billiard), the future fate of a rolling billiard ball is unpredictable beyond a surprisingly small number of bounces. As indicated by Figure 2, a typical trajectory of the Sinai billiard is irregular and a statistical approach is required for a quantitative description of this simple mechanical system. Such an irregularity is the result of having a finite space and an exponential instability of individual trajectories resulting in a sensitive dependence on initial conditions. Due to the curved shape of the boundary, two trajectories emanating from the same point but in slightly different directions with angle δ between them, hit the boundary $\partial\Omega$ (see Figure 2) at different points that are $c\delta$ apart where $c > 0$. After a bounce, the direction of the trajectories will differ by angle $(1 + 2c)\delta$, and because an actual difference between the directions is multiplied by a factor $\mu = (1 + 2c) > 1$, the small perturbation δ will grow more or less exponentially (Sinai, 2000). Such sensitive dependence on initial conditions is the main feature of every chaotic system.

A Markov map: To understand in more detail how randomness appears in a nonrandom system, consider a simple dynamical system in the form of a one-dimensional map

$$x_{n+1} = 2x_n \bmod 1. \tag{1}$$

Since the distance between any two nearby trajectories ($|x_n - x'_n| \ll 1$) after each iteration increases at least two times ($|\mathrm{d}x_{n+1}/\mathrm{d}x_n| = 2$), any trajectory of the map is unstable. The map has a countable infinity of unstable periodic trajectories, which can be seen as fixed points when one considers the shape of the map $x_{n+k} = F^{(k)}(x_n)$; see Figure 3(b). Since all fixed points and periodic trajectories are repelling, the only possibility left for the most arbitrarily selected initial condition is that the map will produce a chaotic motion that never exactly repeats itself. The irregularity of such dynamics can be illustrated using a binary symbolic description ($s_n = 0$ if $x_n < \frac{1}{2}$ and $s_n = 1$ if $x_n \geq \frac{1}{2}$). In this case, any value of x_n can be represented as a binary

Figure 1. Mixing of a passive tracer in a Newtonian flow between two rotating cylinders with different rotation axes. The rotation speed of the inner cylinder is modulated with constant frequency. The flow is stretched and folded in a region of the flow. The repetition of these operations leads to a layered structure—folds within folds, producing a fractal structure (Ottino, 1989).

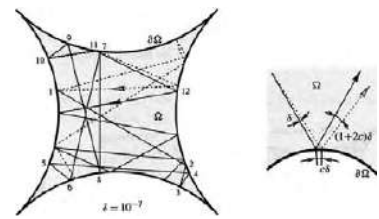

Figure 2. Illustration of the trajectory sensitivity to the initial conditions in a billiard model with convex borders.

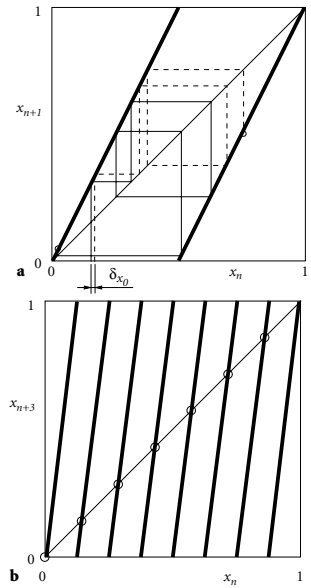

Figure 3. Simple map diagram: (a) two initially close trajectories diverge exponentially; (b) illustration of the increasing of the number of unstable periodic trajectories with the number of iterations.

decimal

$$x_n = 0.s_{n+1}s_{n+2}s_{n+3}\ldots \equiv \sum_{j=n+1}^{\infty} 2^{-j}s_j.$$

If the initial state happens to be a rational number, it can be written as a periodic sequence of 0's and 1's. For instance, 0.10111011101110111... is the rational number $\frac{11}{15}$. Each iteration $x_n \to x_{n+1}$ of map (1) corresponds to setting the symbol s_{n+1} to zero and then moving the decimal point one space to the right (this is known as a *Bernoulli shift*). For example, the iterations of the number $\frac{11}{15}$ yield

$$\begin{aligned}
&0.10111011101110111\ldots,\\
&0.01110111011101110\ldots,\\
&0.11101110111011101\ldots,\\
&0.11011101110111011\ldots,\\
&0.10111011101110111\ldots,
\end{aligned}$$

which illustrates a periodic motion of period 4. Selecting an irrational number as the initial condition, one chooses a binary sequence that cannot be split into groups of 0's and 1's periodically repeated an infinite number of times. As a result, each iteration of the irrational number generates a new irrational number. Since the irrational numbers appear in the interval $x_n \in [0, 1]$ with probability one, one can observe only the aperiodic (chaotic) motions. Random-like behavior of the chaotic motions is illustrated in a separate figure in the color plate section (See the color plate section for a comparison of chaos generated by Equation (1) and a truly random process).

The degree of such chaoticity is characterized by *Lyapunov exponents* that can be defined for one-dimensional maps ($x_{n+1} = f(x_n)$). The stability or instability of a trajectory with the initial state x_0 is determined by the evolution of neighboring trajectories starting at $\tilde{x}_0 = x_0 + \delta x_0$ with $|\delta x_0| \ll 1$. After one iteration

$$\tilde{x}_1 = x_1 + \delta x_1 = f(x_0 + \delta x_0) \approx f(x_0) + \left.\frac{\mathrm{d}f}{\mathrm{d}x}\right|_{x=x_0} \delta x_0.$$

Now, the deviation is $\delta x_1 \approx f'(x_0)\delta x_0$. After the nth iteration it becomes $\delta x_n = (\prod_{m=0}^{n-1} f'(x_m))\delta x_0$. The evolution of the distance between the two trajectories is calculated by taking the absolute value of this product. For infinitesimally small perturbations and large enough n, it is expected that $|\delta x_n| = \alpha^n |\delta x_0|$, where

$$\alpha \approx \lim_{n\to\infty} \left(\left|\frac{\delta x_n}{\delta x_0}\right|\right)^{1/n} = \left(\prod_{m=0}^{n-1} |f'(x_m)|\right)^{1/n}$$

or

$$\ln \alpha \approx \lambda = \lim_{n\to\infty} \frac{1}{n} \sum_{m=0}^{n-1} \ln\left(|f'(x_m)|\right). \qquad (2)$$

Limit (2) exists for a typical trajectory x_m and defines the Lyapunov exponent, λ, which is the time average of the rate of exponential divergence of nearby trajectories. For map (1) $f' = 2$ for all values of x and, therefore, $\lambda = \ln 2$ (*See* **Lyapunov exponents**).

Assuming that the initial state cannot be defined with absolute accuracy, the prediction of the state of the map after a sufficiently large number of iterations becomes impossible. The only description that one can use for defining that state is a statistical one. The statistical ensemble in this case is the ensemble of initial conditions. The equation of evolution for the initial state probability density $\rho_{n+1}(F(x))$ can be written as (Ott, 1993, p. 33)

$$\rho_{n+1}(F(x)) = \sum_{j=1,2} \rho_n(x) \Big/ \left|\frac{\mathrm{d}F(x)}{\mathrm{d}x}\right|_j, \qquad (3)$$

where the summation is taken over both branches of $F(x)$. Considering the evolution of a sharp initial distribution $\rho_0(x)$, one can see that at each step this distribution becomes smoother. As n approaches infinity, the distribution asymptotically approaches the steady state $\rho(x) = 1$.

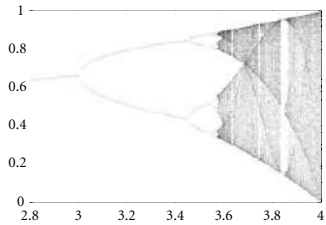

Figure 4. Bifurcation diagram for the logistic map.

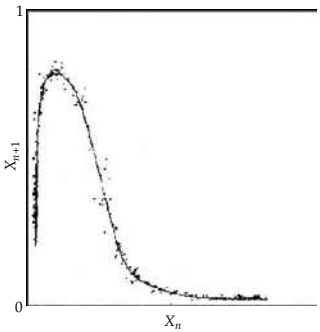

Figure 5. Return map measured in the Belousov–Zhabotinsky autocatalytic reaction.

Population dynamics: A popular model of population growth is the logistic map $x_{n+1} = \alpha x_n(1 - x_n)$, $0 \leq \alpha \leq 4$ (*See* **Population dynamics**). The formation of chaos in this map is illustrated in the bifurcation diagram shown in Figure 4. This diagram presents the evolution of the attracting set as the value of α grows. Below the Feigenbaum point $\alpha_\infty = 3.569\ldots$, the attractor of the map is periodic. Its period increases through a sequence of period-doubling bifurcations as the value of α approaches α_∞ (*See* **Period doubling**). For $\alpha > \alpha_\infty$, the behavior is chaotic but some windows of periodic attractors exist (*See* **Order from chaos**).

Belousov–Zhabotinsky (BZ) autocatalytic reaction: In the BZ reaction (*See* **Belousov–Zhabotinsky reaction**), an acid bromate solution oxidizes malonic acid in the presence of a metalion catalyst and other important chemical components in a well-stirred reactor (Roux et al., 1983). The concentration of the bromide ions is measured and parameterized by the return map (plotting a variable against its next value in time) $x_{n+1} = \alpha x_n \exp[-bx_n]$ (see Figure 5). This map exhibits chaotic behavior for a very broad range of parameter values.

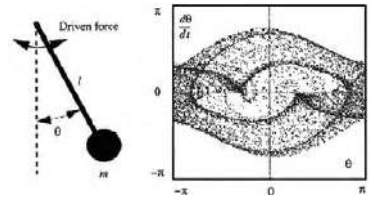

Figure 6. Chaotic oscillation of a periodically driven pendulum, in phase-space plot of angular velocity versus angular position (Deco & Schürmann, 2000).

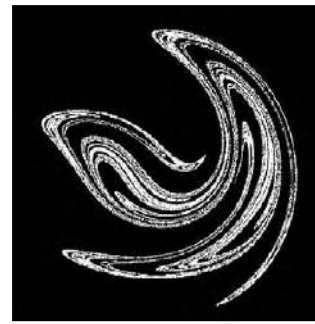

Figure 7. Ueda attractor. The fractal structure of the attractor is typical for all chaotic sets (compare this picture with Figure 1) (Ueda, 1992).

Simple chaotic oscillators: The dynamics of the periodically driven pendulum shown in Figure 6 is described by

$$\frac{d^2\Theta}{dt^2} + \nu\frac{d\Theta}{dt} + \frac{g}{l}\sin\Theta = B\cos 2\pi f t, \qquad (4)$$

where the term on the right-hand side is the forcing (sinusoidal torque) applied to the pivot and f is the forcing frequency. Chaotic motions of the pendulum computed for $\nu = 0.5$, $g/l = 1$, $B = 1.15$, $f = 0.098$, and visualized with stroboscopic points at moments of time $t = i/f$ are shown in Figure 6.

A similar example of chaotic behavior was intensively studied in an oscillator where the restoring force is proportional to the cube of the displacement (Ueda, 1992, p. 158)

$$\frac{d^2\Theta}{dt^2} + \nu\frac{d\Theta}{dt} + \Theta^3 = B\cos t. \qquad (5)$$

The stroboscopic image (with $t = i$) of the strange attractor in this forced Duffing-type oscillator computed with $\nu = 0.05$ and $B = 7.5$ is shown in Figure 7.

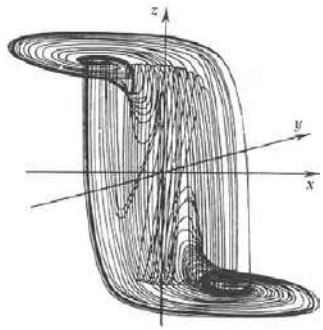

Figure 8. Chaotic attractor generated by electric circuit, which is a modification of van der Pol oscillator: $\dot{x} = hx + y - gz$; $\dot{y} = -x$; $\mu\dot{z} = x - f(x)$; where $f(x) = x^3 - x$ (Pikovsky & Rabinovich, 1978).

Figure 8 presents a chaotic attractor generated by an electronic circuit. Such circuits are a popular topic in engineering studies today.

Characteristics of Chaos

Lyapunov exponents: Consider the Lyapunov exponents for a trajectory $\tilde{\boldsymbol{x}}(t)$ generated by a d-dimensional autonomous system

$$\frac{\mathrm{d}\boldsymbol{x}}{\mathrm{d}t} = \boldsymbol{F}(\boldsymbol{x}), \tag{6}$$

with initial condition $\boldsymbol{x}_0$, $\boldsymbol{x} \in \Re^d$. Linearizing Equation (6) about this solution, one obtains a linear system which describes the evolution of infinitesimally small perturbations $\boldsymbol{w} = \boldsymbol{x}(t) - \tilde{\boldsymbol{x}}(t)$ of the trajectory, in the form

$$\frac{\mathrm{d}\boldsymbol{w}}{\mathrm{d}t} = M(\tilde{\boldsymbol{x}})\boldsymbol{w}, \tag{7}$$

where $M(\boldsymbol{x}) = \partial \boldsymbol{F}(\boldsymbol{x})/\partial \boldsymbol{x}$ is the Jacobian of $\boldsymbol{F}(\boldsymbol{x})$ that changes in time in accordance with $\tilde{\boldsymbol{x}}(t)$. In d-dimensional phase space of (7), consider a sphere of initial conditions for perturbations $\boldsymbol{w}(t)$ of diameter l, that is, $|\boldsymbol{w}(0)| \le l$. The evolution of this ball in time is governed by linear system (7) and depends on trajectory $\tilde{\boldsymbol{x}}(t)$. As the system evolves in time, the ball transforms into an ellipsoid. Let the ellipsoid have d principal axes of different length l_j, $j = 1, d$. Then, the values of Lyapunov exponents of the trajectory $\tilde{\boldsymbol{x}}(t)$ are defined as

$$\lambda_j(\tilde{\boldsymbol{x}}) = \lim_{t\to\infty}\left[\left(\frac{1}{t}\right)\ln\left(\frac{l_j(\tilde{\boldsymbol{x}}, t)}{l(\boldsymbol{x}_0, 0)}\right)\right]. \tag{8}$$

Although limit (8) depends on $\tilde{\boldsymbol{x}}(t)$, the *spectrum of the Lyapunov exponents* λ_j for the selected regime of chaotic oscillations generated by (6) is independent of the initial conditions for the typical trajectories and characterizes the chaotic behavior.

The Lyapunov exponents, λ_j, can be ordered in size: $\lambda_1 \ge \lambda_2 \ge \cdots \ge \lambda_d$. Self-sustained oscillations in autonomous time-continuous systems always have at least one Lyapunov exponent that is equal to zero. This is the exponent characterizing the stretching of phase volume along the trajectory. The spectrum of λ_j for chaotic trajectories contains one or more Lyapunov exponents with positive values.

Kolmogorov–Sinai entropy is a measure of the degree of predictability of further states visited by a chaotic trajectory started within a small region. Due to the divergence, a long-term observation of such a trajectory gives more and more information about the actual initial condition of the trajectory. In this sense, one may say that a chaotic trajectory creates information. Consider a partitioning of the d-dimensional phase space into small cubes of volume ε^d. Observing a continuous trajectory during T instances of time, one obtains a sequence $\{i_0, i_1, \ldots, i_T\}$, where $i_0, i_1, \ldots$ are the indexes of the cubes consequently visited by the trajectory. As a result, the type of the trajectory observed during the time interval from 0 to T is specified by the sequence $\{i_0, i_1, \ldots, i_T\}$. As Kolmogorov and Sinai showed, in dynamical systems whose behavior is characterized by exponential instability, the number of different types of trajectories, K_T, grows exponentially with T:

$$0 < H = \lim_{T\to\infty}\frac{1}{T}\log K_T.$$

The quantity H is the Kolmogorov–Sinai (KS) entropy.

The number of unique random sequences $\{i_0, i_1, \ldots, i_T\}$ that can be obtained without any rules applied increases exponentially with T. In the case of nonrandom sequences where there is a strict law for the generation of future symbols, like the periodic motion, the number of possible sequences grows in time slower than the exponent. Since the exponential growth takes place for the segments of trajectories in the unstable dynamical system producing chaos, such a dynamical system is capable of generating "random" sequences. The Kolmogorov–Sinai entropy is a measure of such "randomness" in a "nonrandom" system, for example, a dynamical system.

Since both KS entropy and Lyapunov exponents reflect the properties of the divergence of the nearby trajectories, these characteristics are related to each other. The formula describing this relation is given by Ruelle's Inequality

$$H \le K = \sum_{j=1}^{m}\lambda_j \ge 0 \tag{9}$$

where m is the number of positive λ_i ($K = 0$, when $m = 0$). The equality $H = K$ holds when the system

has a physical measure (Sinai–Ruelle–Bowen measure) (Young, 1998). The invariant set of trajectories characterized by a positive Kolmogorov–Sinai entropy is a chaotic set.

Forecasting

If a sufficiently long experimental time series capturing the chaotic process of an unknown dynamical system is available in the form of scalar data $\{x_n\}_{n=0}^{N}$, it is possible, in principle, to predict x_{N+m} with finite accuracy for some $m \geq 1$. Such predictions are based on the assumption that the unknown generating mechanism is time independent. As a result, "what happened in the past may happen again—even stronger: that what is happening now has happened in the past" (Takens, 1991). In classical mechanics (no dissipation), this idea of "what happens now has happened in the past" is related to the Poincaré Recurrence Theorem.

Usually, the prediction procedure consists of two steps: first, it is necessary to consider all values of n in the "past," that is, with $n < N$, such that $\sum_{k=0}^{K} |x_{n-k} - x_{N-k}| < \varepsilon$, where ε is a small constant. If there are only a few of such n, then one can try again with a smaller value of K or a larger value of ε. In the second step, it is necessary to consider the corresponding elements x_{n+l} for all the values of n found in the first step. Finally, taking a union of the ε-neighborhoods of all these elements, one can predict that x_{N+l} will be in this union.

To understand when and why forecasting is possible and when it is not, it is reasonable to use characteristics such as *dimension* and *entropy* that can be computed directly from time series (Takens, 1991). If we want to make a catalog of essentially different segments of length $k+1$ in $\{x_n\}_{n=0}^{N}$, this can be done with $C(k, \varepsilon, N)$ elements. $C(k, \varepsilon, N)$ is a function of N that has a limit $C(k, \varepsilon) = \lim_{N \to \infty} C(k, \varepsilon, N)$, and for prediction, we need $C(k, \varepsilon) \ll N$.

The quantitative measure for the way in which $C(k, \varepsilon)$ increases as ε goes to zero is

$$D = \lim_{k \to \infty} \left(\overline{\lim_{\varepsilon \to 0}} \frac{C(k, \varepsilon, N)}{\ln(1/\varepsilon)} \right). \tag{10}$$

If D is large, the prediction is problematic. The quantity D defined by (10) is the dimension of the time series.

The quantitative measure for the way in which $C(k, \varepsilon)$ increases with k is

$$H = \overline{\lim_{\varepsilon \to 0}} \left(\lim_{k \to \infty} \frac{C(k, \varepsilon, N)}{k} \right), \tag{11}$$

This is the entropy of the time series. For the time series generated by a differentiable dynamical system, both the dimension and entropy are finite, but for a random time series they are infinite. Suppose each x_n is taken at random in the interval [0,1] (with respect to the uniform distribution) and for each $n_1, \ldots, n_k$ (different), the choices of $x_{n_1}, \ldots, x_{n_k}$ are independent. For such time series, one can find: $C(k, \varepsilon) = (1 + \lfloor 1/2\varepsilon \rfloor)^{k+1}$, where $\lfloor 1/2\varepsilon \rfloor$ is the integer part of $1/2\varepsilon$. From this formula, it immediately follows that both dimension and entropy in such random time series are infinite.

Models of the Earth's atmosphere are generally considered as chaotic dynamical systems. Due to the unstability, even infinitesimally small uncertainties in the initial conditions grow exponentially fast and make a forecast useless after a finite time interval. This is known as the butterfly effect. However, in the tropics, there are certain regions where wind patterns and rainfall are so strongly determined by the temperature of the underlying sea surface, that they do not show such sensitive dependence on the atmosphere. Therefore, it should be possible to predict large-scale tropical circulation and rainfall for as long as the ocean temperature can be predicted (Shukla, 1998).

History

The complex behavior of nonlinear oscillatory systems was observed long before dynamical chaos was understood. In fact, the possibility of complex behavior in dynamical systems was discovered by Henri Poincaré in the 1890s in his unsuccessful efforts to prove the regularity and stability of planetary orbits. Later on, experiments with an electrical circuit by van der Pol and van der Mark (1927) and the double-disk model experiments of the magnetic dynamo (Rikitake, 1958) also indicated the paradoxically complex behavior of a simple system. At that time, several mathematical tools were available to aid the description of the nontrivial behavior of dynamical systems in phase space, such as homoclinic Poincaré structures (homoclinic tangles). However, at the time, neither physicists nor mathematicians realized that deterministic systems may behave chaotically. It was only in the 1960s that the understanding of randomness was revolutionized as a result of discoveries in mathematics and in computer modeling (Lorenz, 1963) of real systems. An elementary model of chaotic dynamics was suggested by Boris Chirikov in 1959. During the last few decades, chaotic dynamics has moved from mystery to familiarity.

Standard map and homoclinic tangle: The standard map (Chirikov, 1979) is an area-preserving map

$$\begin{aligned} I_{n+1} &= I_n + K \sin \Theta_n, \\ \Theta_{n+1} &= I_n + \Theta_n + K \sin \Theta_n, \end{aligned} \tag{12}$$

where Θ is an angle variable (computed modulo 2π) and k is a positive constant. This map was proposed as a model for the motion of a charged particle in a magnetic field. For K larger than K_{cr}, map

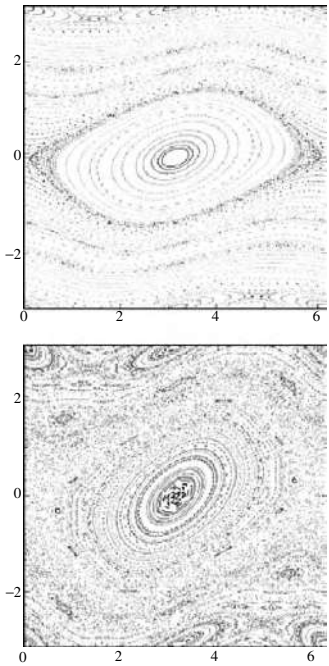

Figure 9. Examples of chaos in the standard map for two different values of K. The coexistence of the "chaotic sea" and "regular islands" that one can see in the panel on the right is typical for Hamiltonian systems with chaotic regimes (Lichtenberg & Lieberman, 1992).

(12) demonstrates an irregular (chaotic) motion; see Figure 9. The complexity of the phase portrait of this map is related to the existence of *homoclinic tangles* formed by stable and unstable manifolds of a saddle point or saddle periodic orbits when the manifolds intersect transversally. The complexity of the manifold's geometry stems from the fact that, if stable and unstable manifolds intersect once, then they must intersect an infinite number of times. Such a complex structure results in the generation of a horseshoe mapping, which persistently stretches and then folds the area around the manifolds generating a chaotic motion. The layers of the chaotic motion are clearly seen in Figure 9.

Lorenz system: The first clear numerical manifestation of chaotic dynamics was obtained in the Lorenz model. This model is a three-dimensional dynamical system derived from a reasonable simplification of the fluid dynamics equations for thermal convection in a liquid layer heated from below. The differential equations $\dot{x} = \sigma(y - x)$, $\dot{y} = rx - y - xz$, $\dot{z} = -bz + xy$ are written for the amplitude of the first horizontal harmonic of the vertical velocity (x), the amplitude of the corresponding temperature fluctuation (y), and a uniform correction of the temperature field (z) (Lorenz, 1963). σ is the Prandtl number, r is the reduced Rayleigh number, and b is a geometric factor. The phase portrait of the Lorenz attractor, time series, and the return mapping generated on the Poincaré cross section computed for $r = 28$, $\sigma = 10$, and $b = \frac{8}{3}$ are presented in Figure 10. A simple mechanical model illustrating the dynamical origin of oscillations in the Lorenz system is shown in Figure 11 (*See* **Lorenz equations**).

Definition of Chaos

As was shown above, dynamical chaos is related to unpredictability. For quantitative measurment of the unpredictability, it is reasonable to use the familiar characteristics *dimension* and *entropy*. These characteristics are independent: it is possible to generate a time series that has a high dimension and at the same time entropy equal to zero. This is a quasi-periodic motion. It is also simple to imagine a low-dimensional dynamical system with high entropy (see, e.g., the map in Figure 3).

Various definitions of chaos exist, but the common feature of these definitions is the sensitive dependence on initial conditions that was formalized above as positive entropy. Thus, dynamical chaos is the behavior of a dynamical system that is characterized by finite positive entropy.

Chaotic Attractors and Strange Attractors

A region in the phase space of a dissipative system that attracts all neighboring trajectories is called an attractor. An attractor is the phase space image of the behavior established in the dissipative system, for example, a stable limit cycle is the image of periodic oscillations. Therefore, the image of chaotic oscillations is a chaotic attractor.

A *chaotic attractor* (CA) possesses the following two properties that define any attractor of the dynamical system:

- There exists a bounded open region U containing a chaotic attractor ($\mathrm{CA} \in U$) in the phase space such that all points from this neighborhood converge to a chaotic attractor when time goes to infinity.
- A chaotic attractor is invariant under the evolution of the system,

In addition, the motion on a chaotic attractor has to be chaotic, for example:

- each trajectory of a chaotic attractor has at least one positive Lyapunov exponent.

Such types of attractors represent some regimes of chaotic oscillations generated by a Lorenz system and

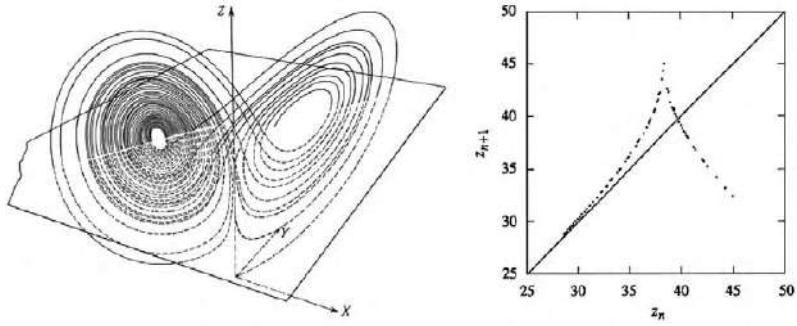

Figure 10. Lorenz attractor (left) and the return map $z_{n+1} = F(z_n)$ plotted for maximum values of variable z for the attractor trajectory (right).

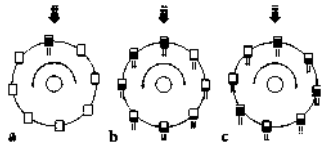

Figure 11. A toy model invented by Willem Malkus and Lou Howard illustrates dynamical mechanisms analogous to oscillations and chaos in the Lorenz system. Water steadily flowing into the top (leaky) bucket makes it heavy enough to start the wheel turning. When the flow is large enough, the wheel can start generating chaotic rotations characterized by unpredictable switching of the rotation direction; see Strogatz (1994, p. 302) for details.

the piece-wise linear maps. However, most of the chaotic oscillations observed in dynamical systems correspond to attractors that do not precisely satisfy the latter property. Although almost all trajectories in such attractors are unstable, some stable periodic orbits may exist within the complex structure of unstable trajectories. Chaos in such systems is persistent both in physical experiments and in numerical simulations because all of these stable orbits have extremely narrow basins of attraction. Due to natural small perturbations of the system, the trajectory of the system never settles down on one of the stable orbits and wanders within the complex set of unstable orbits.

The definition of a *strange attractor* is related to the complicated geometrical structure of an attractor. A strange attractor is defined as an attractor that cannot be presented by a union of the finite number of smooth manifolds. For example, an attractor whose topology can be locally represented by the direct product of a Cantor set to a manifold is a strange attractor. In many cases, the geometry of a chaotic attractor satisfies the definition of a strange attractor. At the same time, the definition of a strange attractor can be satisfied in the case of a nonchaotic strange attractor. This is an attractor that has fractal structure, but does not have positive Lyapunov exponents.

The origin of chaotic dynamics in dissipative systems and Hamiltonian systems in many cases is the same and is related to coexistence in the phase space of infinitely many unstable periodic trajectories as a part of homoclinic or heteroclinic tangles.

The Lorenz attractor, as for many other attractors in systems with a small number of degrees of freedom, can appear through a finite number of easily observable bifurcations. The bifurcation of a sudden birth and death of a strange attractor is called a crisis. Usually, it is related to the collision of the attractor with an unstable periodic orbit or its stable manifold (Arnol'd et al., 1993; Ott, 1993).

Order in Chaos

How does the dynamical origin imprint in chaos? Or in other words, how can the rules or order of the dynamical system be found inside a chaotic behavior? Consider the images (portraits) of the dynamical chaos shown in Figures 7, 8, and 10. The elegance of these images reflects the existence of order in dynamical chaos.

The dynamical origin of such elegance is very similar: different trajectories with close initial conditions have to be close in time $t_l \approx 1/\lambda$, where λ is the maximally positive Lyapunov exponent. The domain occupied by the strange attractor in phase space is finite; thus, the divergence of the phase space flow changes to convergence, and as a result of sequential action of divergence and convergence of the phase flow in the finite domain, the mixing of trajectories occurs. Such mixing can be illustrated with the motions of liquids in the physical space experimentally observed by Ottino (1989; see Figure 1).

Another way to recognize the existence of order in chaos is to analyze its dependence on a control parameter. The macroscopic features of real stochastic

Figure 12. Appearance of spatiotemporal chaos in the extended Faraday experiment: chaotic patterns on the surface of the liquid layer in the oscillating gravitational field. The irregular chain of the localized structures—dark solitons—can be seen beneath a background of the square capillary lattice (Gaponov-Grekhov & Rabinovich, 1988).

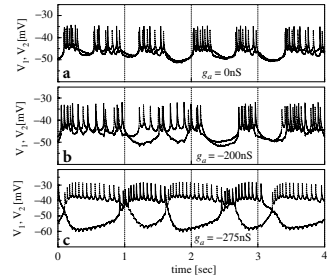

Figure 13. Dynamics of chaotic bursts of spikes generated by two living neurons coupled with an electrical synapse—a gap junction (Elson et al., 1998). Chaotic busts in naturally coupled neurons synchronize (a). When natural coupling is compensated by additional artificial coupling g_a, the chaotic oscillations are independent oscillations (b). The neurons coupled with negative conductivity fire in the regimes of antiphase synchronization (c).

processes, for example, Brownian motion or developed turbulence, depend on this parameter and change without any revolutionary events such as bifurcations. But for dynamical chaos, the picture is different. A continuous increase of control parameters of the logistic map does not necessarily gradually increase the degree of chaos: within chaos, there are windows—intervals of control parameter values in which the chaotic behavior of the system changes to stable periodic behavior, see Figure 4.

In a spatially extended system, for example, in convection or Faraday flow, order within chaos is related to the existence of coherent structures inside the chaotic sea (Rabinovich et al., 2001); see Figure 12.

Spatiotemporal Chaos

Similar to regular (e.g., periodic) motions, low-dimensional chaotic behavior is observed not only in simple (e.g., low-dimensional) systems but also in systems with many, and even with infinite number of degrees of freedom. The dynamical mechanisms behind the formation of low-dimensional chaotic spatiotemporal patterns in dissipative and nondissipative systems are different. In conservative systems, such patterns are related to the chaotic motion of particle-like localized structures. For example, a soliton that is described by a nonlinear Schrödinger equation with the harmonic potential

$$\mathrm{i}\frac{\partial a}{\partial t} + \beta\frac{\partial^2 a}{\partial^2 x} + \left(|a|^2 + \alpha \sin qx\right) a = 0 \qquad (13)$$

moves chaotically in physical space x and reminds us of the chaotic motion occurring in the phase space of a parametrically excited conservative oscillator (the equations of such an oscillator can be derived from (13) for slow variables characterizing the motion of the soliton center mass).

The interaction of the localized structures (particles) in a finite area, large in comparison with the size of the structure, can also lead to the appearance of spatiotemporal chaos. It was observed that collisions of solitons moving in two-dimensional space result in chaotic scattering similar to the chaotic motion observed in billiards (Gorshkov et al., 1992).

In dissipative nonlinear media and high-dimensional discrete systems, the role of coherent structures is also very important (such as defects in convection, clusters of excitations in neural networks, and vortices in the wake behind a cylinder; see Rabinovich et al., 2001). However, the origin of low-dimensional chaotic motions in such systems is determined by dissipation. There are two important mechanisms of finite dynamics (including chaos) that are due to dissipation: (1) the truncation of the number of excited modes (in hydrodynamic flows) due to high viscosity of the small-scale perturbations and (2) the synchronization of the modes or individual oscillators. Dissipation makes synchronization possible not only among periodic modes or oscillators but even in the case when the interacting subsystems are chaotic (Afraimovich et al., 1986). Figure 13 illustrates the synchronization of chaotic bursts of spikes observed experimentally in two coupled living neurons. In the case of a dissipative lattice of chaotic elements (e.g., neural lattices or models of an extended autocatalytic chemical reaction), complete synchronization leads to the onset

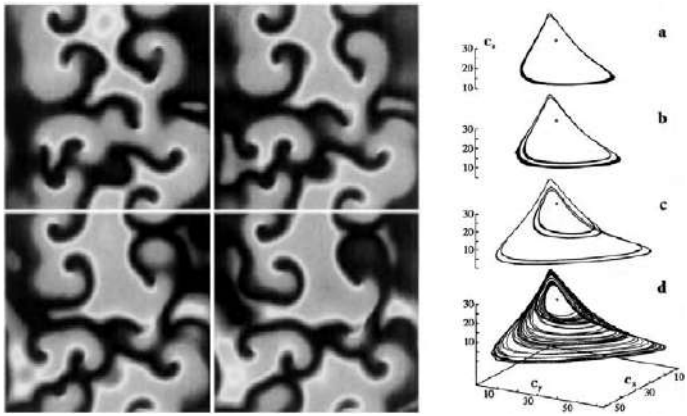

Figure 14. Coherent patterns generated in the chaotic medium with Rössler-type dynamics of medium elements. Left: an example of coherent patterns with defects. Right: evolution of the attractor with increasing distance r from a defect. The attractor changed from the limit cycle of period T at $r = r_1$ to the period $2T$ limit cycle at $r = r_2 > r_1$, then to the period $4T$ limit cycle at $r = r_3 > r_2$, and finally to the chaotic attractor for $r = r_4 > r_3$ (Goryachev & Kapral, 1996).

of a spatially homogeneous chaotic state. When this state becomes unstable against spatial perturbations, the system moves to the spatiotemporal chaotic state. A snapshot of such spatiotemporal chaos, which is observed in the model of chaotic media consisting of diffusively coupled Rössler-type chaotic oscillators, is presented in Figure 14. Figure 14 also illustrates the sequence of period-doubling bifurcations that are observed in the neighborhood of the defect in such a medium.

Edge of Chaos

In dynamical systems with many elements and interconnections (e.g., complex systems), the transition between ordered dynamics and chaos is similar to phase transitions between states of matter (crystal, liquid, gas, etc.). Based on this analogy, an attractive hypothesis named "edge of chaos"(EOC) appeared at the end of the 1980s. EOC suggests a fundamental equivalence between the dynamics of phase transitions and the dynamics of information processing (computation). One of the simplest frameworks in which to formulate relations between complex system dynamics and computation at the EOC is a cellular automaton. There is currently some controversy over the validity of this idea (Langton 1990; Mitchel et al., 1993).

Chaos and Turbulence

The discovery of dynamical chaos has fundamentally changed the accepted concept of the origin of hydrodynamic turbulence. When dealing with turbulence at finite Reynolds number, the main point of interest is the established irregular motion. The image of such irregularity in the phase space could be a chaotic attractor. Experiments in closed systems, for example, one in which fluid particles continuously recirculate through points previously visited, have shown the most common scenarios for the transition to chaos. These are (i) transition through the destruction of quasiperiodic motion that was observed in Taylor–Couette flow (Gollub & Swinney, 1975); (ii) period-doubling sequence observed in Rayleigh–Bénard convection (Libchaber & Maurer, 1980); and (iii) transition through intermittency (Gollub & Benson, 1980). Observation of these canonical scenarios for particular flows proved the validity of the concept of dynamical origin of the transition to turbulence in closed systems. It is possible to reconstruct a chaotic set in the phase space of the flow directly from observed data; see Brandstäter et al. (1982). At present it is difficult to say how dynamical chaos theory can be useful for the understanding and description of the developed turbulence.

The discovery and understanding of chaotic dynamics have important applications in all branches of science and engineering and, in general, to our evolving culture. An understanding of the origins of chaos in the last decades has produced many clear and useful models for the description of systems with complex behavior, such as the global economy (Barkly Russel, 2000), the human immune system (Gupta et al., 1998), animal behavior (Varona et al., 2002), and more. Thus, chaos theory provides a new tool for the unification of the sciences.

M.I. Rabinovich and N.F. Rulkov

See also **Attractors; Billiards; Butterfly effect; Chaos vs. turbulence; Controlling chaos; Dripping faucet; Duffing equation; Entropy; Fractals; Hénon map; Horseshoes and hyperbolicity in dynamical systems; Intermittency; Kicked rotor; Lorenz equations; Lyapunov exponents; Maps; Maps in the complex plane; Markov partitions; Multifractal analysis; One-dimensional maps; Order from chaos; Period doubling; Phase space; Quasiperiodicity; Rössler systems; Routes to chaos; Sinai–Ruelle–Bowen measures; Spatiotemporal chaos; Synchronization; Time series analysis**

Further Reading

Abarbanel, H.D.I. 1996. *Analysis of Chaotic Time Series*, New York: Springer

Afraimovich, V.S., Verichev, N.N. & Rabinovich, M.I. 1986. Stochastic synchronization of oscillations in dissipative systems. *Izvestiya Vysshikh Vchebnykh Zavedenii Radiofizika. RPQAEC*, 29: 795–803

Arnol'd, V.I., Afraimovich, V.S., Ilyashenko, Yu.S. & Shilnikov, L.P. 1993. Bifurcation theory and catastrophe theory. In *Dynamical Systems*, vol. 5, Berlin and New York: Springer

Barkly Russel, J., Jr. 2000. *From Catastrophe to Chaos: A General Theory of Economic Discontinuities*, 2nd edition, Boston: Kluwer

Brandstäter, A., Swift, J., Swinney, H.L., Wolf, A., Doyne Farmer, J., Jen, E. & Crutchfield, P.J. 1982. Low-dimensional chaos in a hydrodynamic system. *Physical Review Letters*, 51: 1442–1445

Chirikov, V.A. 1979. A universal instability of many-dimensional oscillator systems. *Physics Reports*, 52: 264–379

Deco, G. & Schürmann, B. 2000. *Information Dynamics: Foundations and Applications*, Berlin and New York: Springer

Elson, R.C., Selverston, A.I., Huerta, R., Rulkov, N.F., Rabinovich, M.I. & Abarbanel H.D.I. 1998. Synchronous behavior of two coupled biological neurons. *Physical Review Letters*, 81: 5692–5695

Gaponov-Grekhov, A.V. & Rabinovich, M.I. 1988. *Nonlinearity in Action: Oscillations, Chaos, Order, Fractals*, Berlin and New York: Springer

Gollub, J.P. & Benson, S.V. 1980. Many routes to turbulent convection. *Journal of Fluid Mechanics*, 100: 449–470

Gollub, J.P. & Swinney, H.L. 1975. Onset of turbulence in rotating fluid. *Physical Review Letters*, 35: 927–930

Gorshkov, K.A., Lomov, A.S. & Rabinovich, M.I. 1992. Chaotic scattering of two-dimensional solitons. *Nonlinearity*, 5: 1343–1353

Goryachev, A. & Kapral, R. 1996. Spiral waves in chaotic systems. *Physical Review Letters*, 76: 1619–1622

Gupta, S., Ferguson, N. & Anderson, R. 1998. Chaos, persistence, and evolution of strain structure in antigenically diverse infectious agent. *Science*, 280: 912–915

Langton, C.C. 1990. Computation at the edge of chaos—phase transitions and emergent computation. *Physica* D, 42: 12–37

Libchaber, A. & Maurer, J. 1980. Une expérience de Rayleigh-Bénard en géométrie réduite; multiplication, accrochage et démultiplication de fréquences. *Journal de Physique Colloques*, 41: 51–56

Lichtenberg, A.J. & Lieberman, M.A. 1992. *Regular and Chaotic Dynamics*, Berlin and New York: Springer

Lorenz, E.N. 1963. Deterministic nonperiodic flow. *Journal of Atmospheric Science*, 20: 130–136

Mitchel, M., Hraber, P. & Crutchfield, J. 1993. Revisiting the edge of chaos: evolving cellular automata to perform computations. *Complex Systems*, 7: 89–130

Murray, N. & Holman, M. 1999. The origin of chaos in the outer solar system. *Science*, 283: 1877–1881

Ott, E. 1993. *Chaos in Dynamical Systems*, Cambridge and New York: Cambridge University Press

Ottino, J.M. 1989. *The Kinetics of Mixing: Stretching, Chaos, and Transport*, Cambridge and New York: Cambridge University Press

Pikovsky, A.S. & Rabinovich, M.I. 1978. A simple generator with chaotic behavior. *Soviet Physics Doklady*, 23: 183–185 (see also Rabinovich, M.I. 1978. Stochastic self-oscillations and turbulence. *Soviet Physics Uspekhi*, 21: 443–469)

Rabinovich, M.I., Ezersky, A.B. & Weidman, P.D. 2001. *The Dynamics of Patterns*, Singapore: World Scientific

Rikitake, T. 1958. Oscillations of a system of disk dynamos. *Proceedings of the Cambridge Philosophical Society*, 54: 89–105

Roux, J.C., Simoyi, R.H. & Swinney, H.L. 1983. Observation of a strange attractor. *Physica* D, 8: 257–266

Shukla, J. 1998. Predictability in the midst of chaos: a scientific basis for climate forecasting. *Science*, 282: 728–731

Sinai, Ya.G. 2000. *Dynamical Systems, Ergodic Theory and Applications*, Berlin and New York: Springer

Strogatz, S.H. 1994. *Nonlinear Dynamics and Chaos: With Applications to Physics, Biology, Chemistry, and Engineering* Reading, MA: Addison-Wesley

Takens, F. 1991. Chaos, In *Structures in Dynamics: Finite Dimensional Deterministic Studies*, edited by H.W. Broer, F. Dumortier, S.J. van Strien & F. Takens, Amsterdam: North-Holland Elsevier Science

Ueda, Y. 1992. *The Road to Chaos*, Santa Cruz, CA: Aeirial Press

van der Pol, B. & van der Mark, B. 1927. Frequency demultiplication. *Nature*, 120: 363–364

Varona, P., Rabinovich, M.I., Selverston, A.I. & Arshavsky, Yu.I. 2002. Winnerless competition between sensory neurons generates chaos: A possible mechanism for molluscan hunting behavior. *CHAOS* 12: 672–677

Young, L.S. 1998. Developments in chaotic dynamics. *Notices of the AMS*, 17: 483–504

CHARACTERISTICS

Systems of first-order partial differential equations describe many different physical phenomena from the behavior of fluids, gases, and plasmas. To introduce the Method of Characteristics, consider the simple scalar conservation law of the form

$$\frac{\partial U}{\partial t} + A(U)\frac{\partial U}{\partial x} = 0. \tag{1}$$

Here, $U = U(x, t)$, where x is a spatial coordinate and t is the time coordinate. The function $A(U)$ defines the speed of propagation of a disturbance and either may be independent of U, in which case equation (1) is a linear partial differential equation, or it may depend explicitly on the dependent variable U, in which case the equation is a nonlinear partial differential equation.

It is important to specify the initial or boundary conditions that the solution $U(x, t)$ must satisfy.

Consider the simple case where the function is known at the initial time $t = 0$. Thus,

$$U(x, 0) = F(x). \tag{2}$$

The idea is to simplify Equation (1) by choosing a suitable curve in the x-t plane. This curve can be written in parametric form as

$$x = x(s), \quad t = t(s), \tag{3}$$

where s is the parameter that can be thought of as measuring the distance along the curve. To understand how to select the particular form of the curve, note that, using (3),

$$U(x, t) = U(x(s), t(s)), \tag{4}$$

implies that U is a function of s. Hence, the chain rule gives the derivatives of U along the curve as

$$\frac{\mathrm{d}U}{\mathrm{d}s} = \frac{\partial U}{\partial t}\frac{\mathrm{d}t}{\mathrm{d}s} + \frac{\partial U}{\partial x}\frac{\mathrm{d}x}{\mathrm{d}s}. \tag{5}$$

Comparing the right-hand side of (5) with the left-hand side of (1), it is clear that they are identical, provided the parametric form of the curve is chosen as

$$\frac{\mathrm{d}t}{\mathrm{d}s} = 1, \tag{6}$$

$$\frac{\mathrm{d}x}{\mathrm{d}s} = A(U), \tag{7}$$

and (1) reduces to

$$\frac{\mathrm{d}U}{\mathrm{d}s} = 0, \Rightarrow U = \text{constant along the curve.} \tag{8}$$

The curve satisfied by (6) and (7) is called the *characteristic curve*. Along this curve, U is constant. However, the value of the constant may be different on each characteristic curve. The solution of the characteristic equations requires some initial conditions for x and t. These are taken as

$$x = x_0, \quad t = 0, \quad \text{at } s = 0. \tag{9}$$

Note that x_0 covers the same domain as x. Solving (6)–(8) yields

$$t = s, \quad x = A(U)s + x_0, \tag{10}$$

on using the initial conditions (9). x_0 can be thought of as a constant of integration and so it has a fixed value along the characteristic curve. This implies, using (2), that

$$U(x, 0) = F(x_0). \tag{11}$$

Note that the particular characteristic curve is determined by the value of the parameter x_0. Hence, eliminating the parameter s and solving for x_0 in terms of x, U, and t, the solution given by (11) is

$$U(x, t) = F(x_0) = F(x - A(U)t). \tag{12}$$

If $A(U)$ is a constant, say c, then the solution is simply

$$U(x, t) = F(x - ct), \tag{13}$$

but if $A(U)$ depends explicitly on U, then the solution is an *implicit solution*.

The characteristic curves in this example are straight lines in the x-t plane with a gradient given by $A(U)$. When $A(U) = c$ is a constant, the characteristic curves are parallel straight lines. This means that the shape of the initial disturbance propagates unchanged, to the right if c is a positive constant. If $A(U)$ depends on U, then the characteristic curves are straight lines but with different gradients. There exists the possibility that the characteristic curves may cross, and this corresponds to the formation of a shock. When the characteristic curves diverge, the solution exhibits an expansion fan that can be expressed in terms of a similarity variable.

Note that the method of characteristics can be used when $A = A(U, x, t)$ depends explicitly on the space and time coordinates. In this case, the coupled equations, (6)–(8), may be solved numerically. A detailed description of the method of characteristics for general first-order partial differential equations is given in Rubenstein & Rubenstein (1993).

Example: Burgers Equation

Consider the case when $A(U) = U$. Then, (1) becomes the inviscid Burgers equation

$$\frac{\partial U}{\partial t} + U\frac{\partial U}{\partial x} = 0, \tag{14}$$

and the solution satisfying the initial condition

$$U(x, 0) = \begin{cases} 0, & x < -1, \\ 1 + x, & -1 \le x < 0, \\ 1 - x, & 0 \le x \le 1, \\ 0, & x > 1 \end{cases} \tag{15}$$

is

$$U = \begin{cases} 0, & x < -1 + Ut, \\ 1 + x - Ut, & -1 + Ut \le x < Ut, \\ 1 - x + Ut, & Ut \le x \le 1 + Ut, \\ 0, & x > 1 + Ut. \end{cases} \tag{16}$$

Thus, solving for U in each region gives the solution as

$$U = \begin{cases} 0, & x < -1, \\ (1 + x)/(1 + t), & -1 \le x < t, \\ (1 - x)/(1 - t), & t \le x \le 1, \\ 0, & x > 1. \end{cases} \tag{17}$$

Note that the solution becomes multi-valued for $t > 1$. This can be understood by considering the characteristic curves defined by (9). In the x-t plane, they are straight lines of the form

$$x = Ut + x_0, \tag{18}$$

so that the gradient depends on the value of U at $t = 0$ and $x = x_0$. Thus, using the initial conditions, the characteristic curves, valid in the region $t \leq x \leq 1$, can be expressed as

$$x = (1 - x_0)t + x_0, \tag{19}$$

for $0 \leq x_0 \leq 1$. Considering two different values of x_0, say x_a and x_b, the straight lines cross when

$$x = (1 - x_a)t + x_a = (1 - x_b)t + x_b,$$
$$\Rightarrow \qquad t = 1 \quad \text{and} \quad x = 1. \tag{20}$$

Hyperbolic Systems of Several Dependent Variables

Systems of first-order hyperbolic equations can be expressed in vector and matrix form as

$$\frac{\partial \boldsymbol{U}}{\partial t} + \boldsymbol{A}(\boldsymbol{U}, x, t)\frac{\partial \boldsymbol{U}}{\partial x} = 0, \tag{21}$$

where $\boldsymbol{U}$ is a column vector of n elements containing the dependent variables and $\boldsymbol{A}$ is an $n \times n$ matrix whose coefficients may depend on the dependent variables. The problem is linear if the matrix $\boldsymbol{A}$ has elements independent of $\boldsymbol{U}$ and nonlinear otherwise. The characteristic curves in this case are given by the equations

$$\frac{\mathrm{d}t}{\mathrm{d}s} = 1, \tag{22}$$

$$\frac{\mathrm{d}x}{\mathrm{d}s} = \lambda_i(\boldsymbol{U}, x, t) \tag{23}$$

for $i = 1, 2, ..., n$ and where λ_i is an eigenvalue of the matrix $\boldsymbol{A}$. Here, it is assumed that the matrix $\boldsymbol{A}$ has n distinct eigenvalues. For the linear problem, and in particular, for the case where the matrix $\boldsymbol{A}$ has constant coefficients, the full solution can be obtained by using a suitable linear combination of dependent variables so that the equations reduce to a set of simple advection equations. Hence, the first step is to determine the eigenvalues, λ_i, of the matrix $\boldsymbol{A}$ and the corresponding eigenvectors $\boldsymbol{z}_i$, where

$$\boldsymbol{A}\boldsymbol{z}_i = \lambda_i \boldsymbol{z}_i, \tag{24}$$

Next, use the change of variable

$$\boldsymbol{U} = \boldsymbol{Q}\boldsymbol{V}, \tag{25}$$

where $\boldsymbol{Q}$ is an $n \times n$ matrix whose jth column is the jth eigenvector $\boldsymbol{z}_j$. Substituting into (21) yields

$$\boldsymbol{Q}\frac{\partial \boldsymbol{V}}{\partial t} + \boldsymbol{A}\boldsymbol{Q}\frac{\partial \boldsymbol{V}}{\partial x} = 0. \tag{26}$$

Finally, pre-multiplying by $\boldsymbol{Q}^{-1}$, the inverse of $\boldsymbol{Q}$, results in a decoupled system of equation, since $\boldsymbol{Q}^{-1}\boldsymbol{A}\boldsymbol{Q}$ is a diagonal matrix whose elements are the eigenvalues λ_i. Thus, the final set of n equations are

$$\frac{\partial V_i}{\partial t} + \lambda_i \frac{\partial V_i}{\partial x} = 0, \tag{27}$$

for $i = 1, 2, ..., n$. The solutions to (27) are simply

$$V_i = F_i(x - \lambda_i t), \tag{28}$$

where F_i is an arbitrary function determined by the initial conditions. Once all the solutions for V_i are determined from the initial conditions, the solution in terms of the original variables is obtained using (25). Note that while the original variables may depend on all the characteristic variables, the V_i solution is *constant* along the ith characteristic curve.

Example: The Second-Order Wave Equation

The second-order wave equation

$$\frac{\partial^2 U}{\partial t^2} = c^2 \frac{\partial^2 U}{\partial x^2} \tag{29}$$

can be expressed as a pair of first-order equations as

$$\frac{\partial U}{\partial t} = -c\frac{\partial p}{\partial x},$$
$$\frac{\partial p}{\partial t} = -c\frac{\partial U}{\partial x}.$$

Thus,

$$\boldsymbol{A} = \begin{pmatrix} 0 & c \\ c & 0 \end{pmatrix}. \tag{30}$$

The eigenvalues are simply $\lambda_1 = c$ and $\lambda_2 = -c$ and the corresponding eigenvectors are

$$\boldsymbol{z}_1 = \begin{pmatrix} 1 \\ -1 \end{pmatrix}, \qquad \boldsymbol{z}_2 = \begin{pmatrix} 1 \\ 1 \end{pmatrix}. \tag{31}$$

Thus,

$$\boldsymbol{Q} = \begin{pmatrix} 1 & 1 \\ -1 & 1 \end{pmatrix}, \qquad \boldsymbol{Q}^{-1} = \frac{1}{2}\begin{pmatrix} 1 & -1 \\ 1 & 1 \end{pmatrix}. \tag{32}$$

Equation (27) reduces to the pair of equations

$$\frac{\partial V_1}{\partial t} - c\frac{\partial V_1}{\partial x} = 0, \qquad \frac{\partial V_2}{\partial t} + c\frac{\partial V_2}{\partial x} = 0. \tag{33}$$

The solutions are $V_1 = F_1(x+ct)$ and $V_2 = F_2(x-ct)$ and, in terms of the original variables, the solution is

$$\begin{aligned} U &= F_1(x+ct) + F_2(x-ct), \\ p &= -F_1(x+ct) + F_2(x-ct). \end{aligned} \tag{34}$$

Riemann Invariants

A Riemann invariant may be thought of as a function of the dependent variables that is constant along a characteristic curve. In the previous example, it is clear that $U+p = 2F_2(x-ct)$, so $U+p$ is a Riemann invariant along the characteristic curve defined by $x-ct =$ constant. Similarly, $U-p$ is constant along $x+ct =$ constant.

Example: Isentropic Flow

The dimensionless equations for *isentropic* fluid flow with $p/\rho^\gamma = 1$ can be expressed in terms of the fluid velocity, u, and the sound speed $c = (\gamma p/\rho)^{1/2}$ as

$$\frac{\partial u}{\partial t} + u\frac{\partial u}{\partial x} + \frac{2}{\gamma-1}c\frac{\partial c}{\partial x} = 0, \tag{35}$$

$$\frac{\partial c}{\partial t} + \frac{\gamma-1}{2}c\frac{\partial u}{\partial x} + u\frac{\partial c}{\partial x} = 0. \tag{36}$$

A detailed derivation of these equations is given in Kevorkian (1989). The matrix $\boldsymbol{A}$ is

$$\boldsymbol{A} = \begin{pmatrix} u & \frac{2}{\gamma-1}c \\ \frac{\gamma-1}{2}c & u \end{pmatrix} \tag{37}$$

having eigenvalues $\lambda_1 = u+c$ and $\lambda_2 = u-c$. There are two characteristic curves given by the solution of the coupled differential equations

$$\frac{\mathrm{d}t}{\mathrm{d}s} = 1,$$

$$\frac{\mathrm{d}x}{\mathrm{d}s} = \lambda_i,$$

where $i=1$ or $i=2$. For $i=1$, the initial conditions are $t=0$ and $x=\xi$ at $s=0$, which implies that the characteristic curve is defined by $\xi = x - \int_0^t (u+c)\,\mathrm{d}s =$ constant. For $i=2$, $t=0$, and $x=\eta$ at $s=0$, the second curve is defined by $\eta = x - \int_0^t (u-c)\,\mathrm{d}s =$ constant. Multiplying (35) by $(\gamma-1)/2$ and then adding and subtracting (36) gives two equations

$$\frac{\partial R}{\partial t} + (u+c)\frac{\partial R}{\partial x} = 0,$$

$$\frac{\partial S}{\partial t} + (u-c)\frac{\partial S}{\partial x} = 0,$$

where $R = c + (\gamma-1)u/2$ and $S = c - (\gamma-1)u/2$. R and S are Riemann invariants since R is constant along the characteristic curve defined by $\xi =$ constant) and S is constant along $\eta =$ constant). A more detailed derivation of Riemann invariants is described in Kevorkian (1989).

ALAN HOOD

See also **Burgers equation; Coupled systems of partial differential equations; Hodograph transform; Shock waves**

Further Reading

Kevorkian, J. 1989. *Partial Differential Equations: Analytical Solution Techniques*, New York: Chapman & Hall

Rubenstein, I. & Rubenstein, L. 1993 *Partial Differential Equations in Classical Mathematical Physics*, Cambridge and New York: Cambridge University Press

CHARGE DENSITY WAVES

A charge density wave (CDW) is a collective transport phenomenon, whose origin lies in the interaction between electrons and phonons in a solid (Grüner & Zettl 1985; Grüner, 1988). As envisioned by Rudolph Peierls in 1930 in some quasi-one-dimensional metals (where the influence of one electron to each other electron is much stronger than in higher dimensions), the elastic energy needed to displace the position of the atoms may be balanced by a lowering of conduction electron energy.

In such cases, the more stable configuration may have a periodic distortion of the lattice; thus, there is a modulation of the electronic charge density, which gives rise to a CDW. The wave vector turns out to be $Q = 2k_\mathrm{F}$, where k_F is the Fermi wave vector, and the electronic density becomes

$$\delta\rho = \rho_0 \cos(2k_\mathrm{F}x + \phi).$$

Due to this periodic lattice distortion, a gap at the Fermi level appears, and the conduction electrons lower their kinetic energy. At high temperatures, thermal excitation of electrons across the band gap makes the normal metallic state stable. When the temperature is sufficiently low, a second-order phase transition (known as the Peierls transition) takes place, and a CDW is formed.

In 1954, Herbert Fröhlich suggested that if Q was not commensurate with the lattice constant, the CDW energy would be independent of the phase ϕ, and thus, an electrical current would appear under any electric field, independent of its intensity. For a while, this phenomenon was speculated to be a possible origin of superconductivity. Interestingly, the interplay and relationship among CDWs, superconductivity, and spin density waves is still a field of study (Gabovich et al., 2002).

If the translational invariance of ϕ is disrupted, there is a phase for which the CDW energy is the

lowest, and there is also a minimum threshold field to overcome this energy reduction and to initiate the conduction. A possible cause of the invariance break could be that the CDW is commensurate with the lattice. Although this case is unusual and mostly of theoretical interest, such a CDW (with a period quasimultiple of the lattice constant) may contain solitons in the form of constant phase zones, separated by abrupt change areas. This soliton behavior is modeled by sine-Gordon-like equations. However, empirical evidence suggests that the origin of the pinning of the CDW to the lattice and the appearance of a threshold field stem from impurities.

Experimental evidence of CDW behavior became available in the 1970s, and nowadays several materials show CDW behavior, both inorganic, like $NbSe_3$, NbS_3, or $K_{0.3}MoO_3$ ("blue bronze"), and organic, like $(\text{fluoranthene})_2PF_6$. Evidence of this kind of transition is detected through magnitudes affected by the gap at the Fermi level, including magnetic susceptibility, resistivity, thermoelectric power, scattering experiments where the CDW wave vector manifests itself, and more recently, by means of scanning tunneling microscope images.

Conductivity is among the more interesting properties of CDWs. The dielectric constants for these materials are high, and conductivity suffers an abrupt change from insulating to metallic values of orders of magnitude. The Hall and thermoelectric effects suggest that their conductivity consists of an ohmic linear term and a CDW nonlinear term.

The response of the CDW to a field higher than the threshold value is twofold. First, there appears a high-frequency coherent current, or narrow band noise, which seems to be due to the displacement of the CDW over the pinning potential. Second, a low-frequency broad band noise, incoherent response, is also detected. It is also found that the conductivity saturates for high values of the external field, and it seems that this is due to electrons leaving the CDW region or due to the elimination of $2k_F$ phonons.

When an a.c. field is present, the CDW exhibits a strong dependence on the field frequency, and its conductivity, σ_{ac}, also saturates for high frequencies. There also appear an induced conductivity, σ_{dc}, which increases when V_{ac} increases, and some interference phenomena between the narrow band noise and the a.c. The external field $E_{ac}\cos\omega_e t$ causes oscillations of the current at frequency ω_e, and if there is also a d.c. field, E_{dc}, there are oscillations at frequency ω_i corresponding to the narrow band noise. These two frequencies may interact to produce mode-locking phenomena when they are commensurate ($n\omega_i = m\omega_e$).

In CDW systems, this locking shows up in the step structure of the differential resistance as a function of the d.c. field. As the external d.c. changes, the nonlinearity of the system keeps the relation between both frequencies constant, ω_i/ω_e, over a finite interval of the external parameter, corresponding to the intervals where dV/dI is constant. When the external parameter moves far from the locking region, the system undergoes a transition to an unlocked state, which is quasi-periodic, with two incommensurate frequencies. The interference between the internal frequency ω_i and the external one ω_e is the origin of the coherent and incoherent responses of the system. Usually, the low-frequency region of the power spectra consists of a broad band noise, while the narrow components show up at high frequencies as narrow band noise. A systematic elimination of the broad band noise when the CDW entered mode locking (Sherwin & Zettl, 1985) and a reinforcement of this noise in the unlocked regime have been observed. The interplay between the internal frequency and the external one may give rise to chaotic behavior, with a period-doubling route to chaos.

Studied in the context of self-organized criticality, CDWs are an example of systems that reorganize themselves near the edge of stability, and any small change in the external electrical field gives rise to a drastic change in the response of the CDW (high increase of conductivity).

Although several models have been proposed to explain CDW behavior, none is completely satisfactory. The classical model considers the CDW as a rigid carrier, without any internal degree of freedom, using the forced oscillator equations with some analogy to the Josephson junctions. The tunneling model focuses on the gap in the excitation spectrum of the CDW, explaining the nonlinear conductivity and the scale relationship between $\sigma_{ac}(\omega)$ and $\sigma_{dc}(E)$. However, these models do not explain the interference phenomena between the narrow band noise and the external field frequency ω.

There are other models that consider the internal degrees of freedom of the CDW (segmenting the CDW either through a hydrodynamical description or the Kelmm–Schrieffer model), but none of them completely explains the phenomenology observed in a CDW. Another interesting model is the Fukuyama–Lee–Rice model, which treats the CDW as a classical extended elastic medium, interacting with impurities and an electric field. Discrete versions of these models have also been used. For the commensurate case, Frenkel–Kontorova and soliton models (such as the sine-Gordon equation) have been used.

Several applications have been suggested for these materials, including tunable condensers, optical detectors, memory devices, and switches, among others.

LUIS VÁZQUEZ, P. PASCUAL, AND S. JIMÉNEZ

See also **Coupled oscillators; Frenkel–Kontorova model; Polarons; Sine-Gordon equation; Superconductivity**

Further Reading

Brown, S. & Grüner, G. 1994. Charge and spin density waves. *Scientific American*, April 1994: 50–56

Gabovich A.M., Voitenko, A.I. & Ausloos, M. 2002. Charge-and spin-density waves in existing superconductors: competition between Cooper pairing and Peierls or excitonic instabilities. *Physics Reports*, 367: 583–709

Grüner, G. & Zettl, A. 1985. Charge density wave conduction: a novel collective transport phenomenon in solids. *Physics Reports*, 119: 117–232

Grüner, G. 1988. The dynamics of charge-density waves. *Reviews of Modern Physics*, 60: 1129–1181

Sherwin, M. & Zettl A. 1985. Complete charge density-wave mode locking and freeze-out of fluctuations in $NbSe_3$. *Physical Review B*, 32: 5536–5539

Thorne, R.E. 1996. Charge-density-wave conductors. *Physics Today*, May 1996: 42–47

CHEMICAL KINETICS

Chemical kinetics is a well-defined field of physical chemistry that arose in the 1850s as a complement to the investigation of chemical equilibria. The question of how fast a reactive mixture in a closed vessel reaches equilibrium gave rise to the concept of reaction velocity. The mass action law, enunciated by Cato Guldberg and Peter Waage in 1863, provided a quantitative expression of the velocity of an elementary reaction step in a homogeneous medium in terms of the concentrations or the mole fractions of the reactants involved, and a parameter known as the rate constant. Chemical kinetics is intrinsically nonlinear, since the law of mass action features products of concentrations of the species involved.

Early Developments

Evidence that chemical reactions can generate complex behavior was reported in the early days of chemical kinetics (Pacault & Perraud, 1997). In 1899, Wilhelm Ostwald discovered that in a reaction involving chromium in concentrated acid solution, the release of hydrogen gas was periodic. In 1906, Robert Luther observed propagating chemical reaction fronts in connection with the catalytic hydrolysis of alkyl sulfates. These studies remained isolated for a long time. Possible origins, including the systematic study of reaction mechanisms, were hardly touched upon and there was little or no modeling effort. Not surprisingly, therefore, they came to be regarded by the scientific community as curiosities or even as artifices. On the theoretical side in the 1920s, Alfred Lotka devised a model formally deriving from chemical kinetics and giving rise to sustained oscillations. As the model did not apply to any known chemical system, it was discarded by chemists but was far better received in population dynamics where it played a seminal role. This connection was further enforced in 1926 when Vito Volterra advanced an explanation of ecological cycles in connection with predator-prey systems, using ideas similar to those of Lotka.

The Phenomenology of Nonlinear Chemical Kinetics

Nonlinear chemical kinetics in its modern form owes much to the Belousov–Zhabotinsky reaction (Zhabotinsky, 1964; Field et al., 1972) dealing with the oxidation of a weak acid by bromate in the presence of a metal ion redox catalyst. In addition to the possibility of displaying long records of oscillatory behavior in batch (closed reactor), this reaction gave rise for the first time to a thorough mechanistic study which highlighted the important role of feedback in the onset of complex behavior, in addition to nonlinearity.

Nonlinear phenomena in chemical kinetics have been observed on whole classes of systems giving rise to a large variety of complex behaviors, as reviewed in a Faraday discussion held in 2001. Quantitative phase diagrams have been constructed separating different behavioral modes as some key parameters are varied (Gray & Scott, 1990; Epstein & Pojman, 1998).

Open Well-Stirred Reactors

Simple periodic, multi-periodic, and chaotic oscillations are observed as the residence time of reactants (inversely proportional to their pumping rate into the reactor) is varied. A second type of phenomenon is multistability, the possibility of exhibiting more than one simultaneously stable steady-state concentration level. A third type of phenomenon is excitability whereby, once perturbed, a system performs an extended excursion resembling a single pulse of an aborted oscillation, before settling back to its stable steady state. Finally, an interesting phenomenology pertains to combustion reactions, where the dependence of the rate constant on temperature is the source of a universal (reaction mechanism-independent) positive feedback.

Open Unstirred Reactors

In the absence of stirring, chemical dynamics coexists with transport phenomena. This can give rise to the generic phenomenon of propagating wave fronts. In a bistable system, a typical front may join the two stable states, with one of them progressing at the expense of the other. In two- and three-dimensional reactors undergoing excitable or oscillatory dynamics, the fronts can take the more spectacular form of circles (target patterns), rotating spirals, and scrolls. An exciting form of spatial self-organization is spontaneous symmetry-breaking leading to sustained steady-state patterns, anticipated by Alan Turing in 1952 and realized experimentally by Patrick De Kepper and coworkers; see Figure 1 (Turing, 1952; De Kepper et al., 2000).

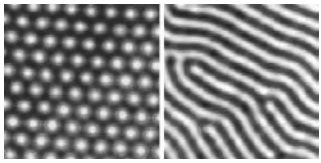

Figure 1. Stationary concentration patterns arising in the chlorite–iodide–malonic acid reaction beyond a symmetry-breaking instability (courtesy of P. De Kepper).

Heterogeneous Systems

Since the late 1980s, a series of novel developments has been initiated following the encounter of nonlinear chemical kinetics with surface science as it is manifested, for instance, in heterogeneous catalysis. Complex behavior in all the above-mentioned forms is observed. Furthermore, the development of sophisticated monitoring techniques, such as field ion microscopy, opens the perspective of monitoring chemical dynamics at the nanoscale level (Hildebrand et al., 1999).

Theoretical Developments: Dynamical Systems and Nonlinear Chemical Kinetics

The essence of nonlinear chemical kinetics is captured by the reaction-diffusion equations (Nicolis & Prigogine, 1977)

$$\frac{\partial c_i}{\partial t} = v_i(\{c_j\}, k_\alpha, \Delta H_\alpha, \cdots) + D_i \nabla^2 c_i, \qquad (1)$$

where $c_i (i = 1, \ldots, n)$ denotes the concentrations or the temperature, k_α and ΔH_α the rate constants and heats of reaction of the steps involved, and D_i the mass or heat diffusivity coefficients. The rate function v_i accounts for the nonlinearities and feedbacks, whereas the contribution of transport processes is linear.

The reaction-diffusion equations (1) exhibit nonlinearity in its simplest expression, as a property arising from intrinsic and local cooperative events. Because of this, complex behavior may arise in the absence of spatial degrees of freedom and persist even when few variables are present. In thermodynamic language, reactions are purely dissipative processes, whereas in nonlinear mechanics, inertia plays a very important role in the onset of complex behavior. Understanding how purely dissipative systems can come to terms with the restrictions imposed by the laws of thermodynamics and statistical mechanics has stimulated several fundamental developments (Glansdorff & Prigogine, 1971; Nicolis & Prigogine, 1977). It has also led to the design of canonical models, such as the Brusselator, that are being used with success to test ideas and to assess the limits of validity of approximations.

The intrinsic parameters k and D in Equations (1) has dimensions of $[\text{time}]^{-1}$ and $[(\text{length})^2/\text{time}]$, respectively. It follows that a reaction-diffusion system possesses intrinsic time (k^{-1}) and space $((D/k)^{1/2})$ scales. This places nonlinear kinetics at the forefront for understanding the origin of endogenous rhythmic and patterning phenomena as observed, in particular, in biology and in materials science. In thermodynamic equilibrium, these intrinsic time and length scales remain dormant, owing to detailed balance. Nonequilibrium allows for the excitation and eventual stabilization of finite amplitude disturbances bearing these characteristic scales.

Equations (1) form the basis of interpretation of the experiments surveyed above. They also constitute some of the earliest and most widely used models of bifurcation and chaos theories. The classical tools used in their analysis are stability theory and the reduction to normal form (amplitude) equations using perturbation techniques and/or symmetry arguments, complemented by interactive numerical simulations (Nicolis, 1995). A most interesting development is the prediction of an impressive variety of intrinsically generated spatial and spatiotemporal patterns, including spatiotemporal chaos, when two or more mechanisms of instability are interfering.

Nonlinear Chemical Kinetics in the Life Sciences

Research in nonlinear chemical kinetics has led to a semi-quantitative interpretation of a wide spectrum of dynamical behaviors in biochemistry (Goldbeter, 1996). This has been possible thanks to the development of models in which the involvement of cooperative enzymes in some key steps provides the principal source of nonlinearity and feedback. Glycolytic oscillations, calcium oscillations and waves, the cell division cycle, cAMP-induced aggregation in amoebae, and synchronization in cell populations are among the main achievements of this effort that helped to identify the principal mechanisms behind the observed behavior.

Nonlinear kinetics has also been a source of inspiration for approaching dynamical phenomena of crucial importance in biology, in which modeling involving a few variables and/or well-established molecular mechanisms is still not available. Immune response, the electrical activity of the brain, embryonic development, cooperative processes such as food recruitment or building activity in social insects, and, last but not least, chemical and biochemical evolution itself (Eigen & Schuster, 1979; *See* **Biological evolution**) have been explored in one way or the other in the light of the concepts and techniques of nonlinear kinetics.

As a closing remark, Equations (1) anticipate a decoupling between the evolution laws of the

macroscopic observables and dynamics at the microscopic level, which may actually break down when reactive systems are embedded on low-dimensional supports owing to the generation of anomalous inhomogeneous fluctuations. This leads to interesting synergies among nonlinear chemical kinetics, statistical mechanics, and computational science (Nicolis, 2001).

G. NICOLIS

See also **Belousov–Zhabotinsky reaction; Brusselator; Population dynamics; Reaction-diffusion systems; Turing patterns**

Further Reading

De Kepper, P., Dulos, E., Boissonade, J., De Wit, A., Dewel, G. & Borckmans, P. 2000. Reaction–diffusion patterns in confined chemical systems, *Journal of Statistical Physics*, 101: 495–508

Eigen, M. & Schuster, P. 1979. *The Hypercycle: A Principle of Natural Self-organization*, Berlin and New York: Springer

Epstein, I.R. & Pojman, J.A. 1998. *An Introduction to Nonlinear Chemical Dynamics*, Oxford and New York: Oxford University Press

Field, R.J., Körös, E. & Noyes, R. 1972. Oscillations in chemical systems. II. Thorough analysis of temporal oscillation in the bromate–cerium–malonic acid system. *Journal of the American Chemical Society*, 94: 8649–8664

Glansdorff, P. & Prigogine, I. 1971. *Thermodynamic Theory of Structure, Stability and Fluctuations*, London and New York: Wiley

Goldbeter, A. 1996. *Biochemical Oscillations and Cellular Rhythms*, Cambridge and New York: Cambridge University Press

Gray, P. & Scott, S.K. 1990. *Chemical Oscillations and Instabilities*, Oxford: Clarendon Press and New York: Oxford University Press

Hildebrand, M. Kuperman, M., Wio, H., Mikhailov, A.S. & Ertl, G. 1999. Self-organized chemical nanoscale microreactors. *Physical Review Letters*, 83: 1475–1478

Nicolis, G. 1995. *Introduction to Nonlinear Science*, Cambridge and New York: Cambridge University Press

Nicolis, G. 2001. Nonlinear kinetics: at the crossroads of chemistry, physics and life sciences. *Faraday Discussions*, 120: 1–10

Nicolis, G. & Prigogine, I. 1977. *Self-organization in Nonequilibrium Systems*, New York: Wiley

Pacault, A. & Perraud J.-J. 1997. *Rythmes et Formes en Chimie*, Paris: Presses Universitaires de France

Royal Society of Chemistry. 2002. *Nonlinear Chemical Kinetics: Complex Dynamics and Spatio-temporal Patterns*. Faraday Discussion no. 120, London: Royal Society of Chemistry; pp. 1–431

Turing, A.M. 1952. The chemical basis of morphogenesis. *Philosophical Transactions of the Royal Society of London, Series B*, 237: 37–72

Zhabotinsky, A.M. 1964. Periodic liquid phase oxidation reactions, *Doklady Akademie Nauk* SSSR, 157: 392–395

CHERENKOV RADIATION

Cherenkov radiation is the electromagnetic radiation of a charged particle moving uniformly in a medium with a velocity exceeding the velocity of light (c) in that medium. It was discovered experimentally by Pavel Cherenkov in 1934 and was theoretically explained by Igor Tamm and Il'ja Frank in 1937. (In 1958, Cherenkov, Tamm, and Frank were awarded a Nobel Prize in physics for this work.) Earlier, Cherenkov radiation was theoretically predicted by Arnol'd Sommerfeld, who, in 1904, solved a formal problem on the radiation of a charged particle moving in vacuum with a velocity $v > c$, and by Oliver Heaviside (Heaviside, 1950) at the end of the 19th century.

At present, all radiation phenomena of waves of any origin, created by a source that moves with a velocity exceeding the phase velocity of the waves, are regarded as Cherenkov radiation. Common examples that can be observed in ordinary life include waves created on a water surface by moving objects, the so-called bow waves according to a theory developed by Lord Kelvin (William Thomson) in the middle of the 19th century, and acoustic shock waves brought about in the atmosphere by a supersonic jet or a rocket, first described by Ernst Mach in 1877.

Essentially, Cherenkov radiation can be understood from the following simple considerations. A source moving steadily with a velocity $\boldsymbol{v}$ and depending on coordinates and time as $f(\boldsymbol{r} - \boldsymbol{v}t)$ can be presented in the form of a Fourier integral $f(\boldsymbol{r}, t) = \int f(\boldsymbol{k}) \mathrm{e}^{\mathrm{i}\boldsymbol{k}\boldsymbol{r} - \mathrm{i}\boldsymbol{k}\boldsymbol{v}t} \mathrm{d}^3k$, which suggests that each Fourier harmonic has frequency $\boldsymbol{k}v$. In electrodynamics, the role of the source is played by the distribution of charge density $\rho(\boldsymbol{r} - \boldsymbol{v}t)$ and current $\boldsymbol{j} = \rho\boldsymbol{v}(\boldsymbol{r} - \boldsymbol{v}t)$, and in hydrodynamics by external forces and moving particles.

If a source is to excite the waves in a medium whose wave vector $\boldsymbol{k}$ and frequency ω are related by the dispersion equation $\omega = \omega(\boldsymbol{k})$, a resonance condition must be satisfied, under which the wave frequency $\omega(\boldsymbol{k})$ coincides with the external force frequency $\boldsymbol{k}v$. This equality yields the Cherenkov condition

$$\omega(\boldsymbol{k}) = \boldsymbol{k} \cdot \boldsymbol{v}, \tag{1}$$

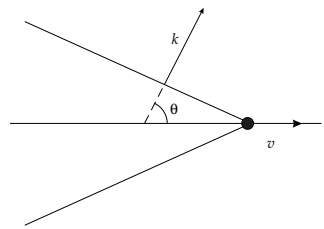

Figure 1. Wave front configuration by Cherenkov radiation, $\boldsymbol{v}$ is the particle velocity, and $\boldsymbol{k}$ is the wave vector of the emitted wave.

which can be fulfilled only if the moving source velocity exceeds the phase velocity of the waves $v > v_{\rm ph} = \omega(\boldsymbol{k})/k$.

The radiated wave vectors form a characteristic Cherenkov cone, which is similar to the Mach cone in hydrodynamics. Thus, the angle θ between the wave vector of the radiated wave and the direction of particle velocity is determined by the Cherenkov condition of Equation (1), which requires $\cos\theta = v_{\rm ph}/v$, showing that the frequency distributions of radiation are related to each other. Figure 1 shows the wave front configuration of a wave of frequency ω, emitted by a moving source.

Nowadays, Cherenkov radiation is used in high-energy physics as an important experimental tool (the Cherenkov counter), enabling identification and velocity measurements of fast charged particles, and in electronics for Cherenkov electron oscillators and amplifiers of electromagnetic waves, such as traveling-wave tubes and backward-wave oscillators. Many diverse phenomena can be related to manifestations of Cherenkov radiation, including Landau damping and instabilities in plasma physics, and the Kelvin–Helmholtz instability in hydrodynamics (excitation of waves on a water surface by wind).

VLADISLAV V. KURIN

See also **Dispersion relations; Shock waves**

Further Reading

Heaviside, O. 1950. *Electromagnetic Theory*, 3 vols, London: The Electrician; reprinted New York: Dover

Jackson, J.D. 1998. *Classical Electrodynamics*, New York: Wiley

Landau, L.D. & Lifshitz, E.M. 1963. *Theoretical Physics*, vol. 6: *Fluid Mechanics*, Oxford: Pergamon Press

Landau, L.D. & Lifshitz, E.M. 1963. *Theoretical Physics*, vol. 8: *Electrodynamics of Continious Media*, Oxford: Pergamon Press

Landau, L.D. & Lifshitz, E.M. 1963. Theoretical Physics, vol. 10: *Physical Kinetics*, Oxford: Pergamon Press

CHI(2) MATERIALS AND SOLITONS

See **Nonlinear optics**

CHIRIKOV MAP

See **Maps**

CHUA'S CIRCUIT

Having witnessed futile attempts at producing chaos in an electrical analog of the Lorenz equations while on a visit to Japan in 1983, Leon Chua was prompted to develop a chaotic electronic circuit. He realized that chaos could be produced in a piecewise-linear circuit if it possessed at least two unstable equilibrium points—one to provide stretching and the other to fold the trajectories. With this insight and using nonlinear circuit theory (Chua et al., 1987), he systematically identified those third-order piecewise-linear circuits containing a single voltage-controlled nonlinear resistor that could produce chaos. Specifying that the V–I characteristic of the nonlinear resistor N_R should be chosen to yield at least two unstable equilibrium points, he invented the circuit shown in Figure 1.

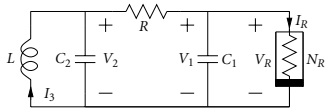

Figure 1. Chua's circuit consists of a linear inductor L, two linear capacitors (C_1 and C_2), a linear resistor R, and a voltage-controlled nonlinear resistor N_R (called a Chua diode).

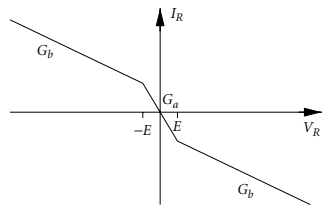

Figure 2. The V–I characteristic of the Chua diode N_R has breakpoints at $\pm E$ and slopes G_a and G_b in the inner and outer regions, respectively.

This circuit is described by three ordinary differential equations

$$\begin{aligned} C_1\frac{{\rm d}V_1}{{\rm d}t} &= -GV_1 - f(V_1) + GV_2, \\ C_2\frac{{\rm d}V_2}{{\rm d}t} &= GV_1 - GV_2 + I_3, \\ L\frac{{\rm d}I_3}{{\rm d}t} &= -V_2, \end{aligned} \tag{1}$$

where $G = 1/R$. Also, $f(\cdot)$ is the V–I characteristic of the nonlinear resistor N_R (known as a Chua diode), which has a piecewise-linear V–I characteristic defined by

$$f(V_R) = G_bV_R + \tfrac{1}{2}(G_a - G_b)(|V_R + E| - |V_R - E|), \tag{2}$$

where $\pm E$ are the breakpoints in the characteristic, and G_a and G_b are the slopes in the inner and outer regions, respectively, as shown in Figure 2.

If the values of the circuit parameters are chosen such that the circuit contains three equilibrium points (two in the outer regions and one at the origin), all of which are unstable with saddle-focus stability, then a homoclinic trajectory can be formed, potentially producing chaos.

Soon after its conception, the rich dynamical behavior of Chua's circuit was confirmed by computer simulation and experiment and in 1986 was proven to exhibit chaos in the sense of Shilnikov (Chua et al., 1986). An intensive effort since then to understand every aspect of the dynamics of this circuit has resulted in its widespread acceptance as a powerful paradigm for learning, understanding, and teaching about nonlinear dynamics and chaos (Madan, 1993; Chua, 1992).

By adding a linear resistor R_0 in series with the inductor, Chua's circuit has been generalized to the Chua oscillator (Chua, 1993), with the last of Equations (1) changing to

$$L\frac{\mathrm{d}I_3}{\mathrm{d}t} = -V_2 - R_0 I_3. \tag{3}$$

Chua's oscillator is canonical in the sense that it is equivalent (topologically conjugate) to a 13-parameter family of three-dimensional ordinary differential equations with odd-symmetric piecewise-linear vector fields. The circuit can exhibit every dynamical behavior known to be possible in a system described by a continuous odd-symmetric three-region piecewise-linear vector field. Unlike the Lorenz or Rössler equations, which have more complex multiplicative nonlinearities, the only nonlinearity in Chua's circuit is a scalar function of one variable. With an appropriate choice of parameters, the circuit can be made to follow the classic period-doubling, intermittency, and torus breakdown routes to chaos; in addition, over 60 different types of strange attractors have been reported in Chua's oscillator.

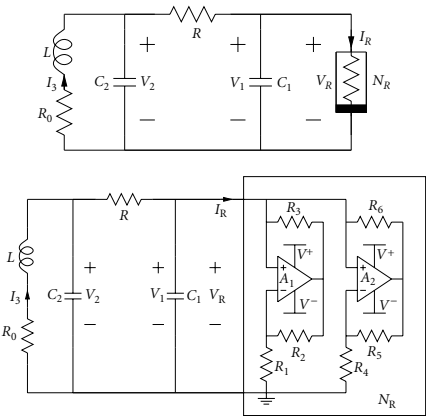

Figure 3. Robust practical implementation of Chua's circuit/oscillator using two op amps and six resistors to realize the Chua diode. In the case of Chua's circuit, R_0 is zero; in Chua's oscillator, R_0 may assume negative or positive values. Component values for Chua's circuit are listed in Table 1.

Chua's circuit oscillator can be realized in a variety of ways by using standard or custom-made electronic components. Since all of the linear elements (capacitors, resistors, and inductor) are readily available as two-terminal devices, only the nonlinear diode must be synthesized using a combination of standard electronic components. The most robust practical realization of Chua's circuit/oscillator, shown in Figure 3, uses two operational amplifiers (op-amps) and six resistors to implement the nonlinear diode (Kennedy, 1992).

The op-amp subcircuit consisting of A_1, A_2, and R_1 through R_6 functions as a Chua diode with V–I

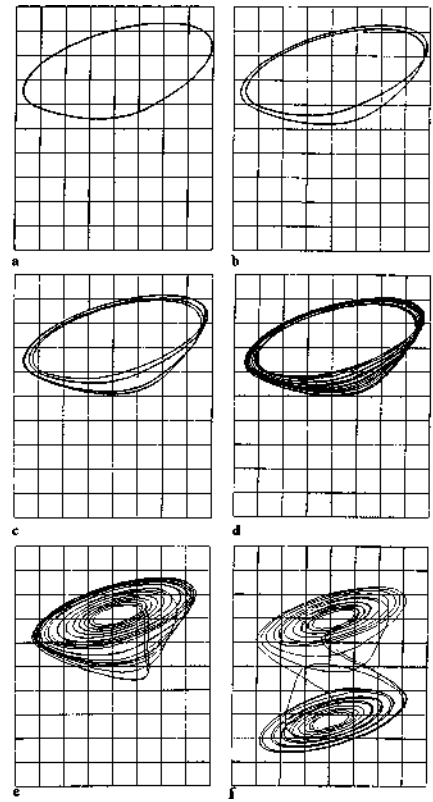

Figure 4. Typical experimental bifurcation sequence in Chua's circuit (component values as in Table 1) recorded using a Hitachi VC-6025 Digital Storage Oscilloscope. Horizontal axis V_2 200 mV/div; vertical axis V_1 1 V/div. (a) $R = 1.83$ kΩ, period 1; (b) $R = 1.82$ kΩ, period 2; (c) $R = 1.81$ kΩ, period 4; (d) $R = 1.80$ kΩ, Spiral attractor; (e) $R = 1.76$ kΩ, Spiral attractor; (f) $R = 1.73$ kΩ, double-scroll attractor [reproduced from Kennedy (1993)].

Element	Description	Value	Tolerance (%)
A_1	Op-amp ($\frac{1}{2}$ AD712 or TL082)		
A_2	Op-amp ($\frac{1}{2}$ AD712 or TL082)		
C_1	Capacitor	10 nF	± 1
C_2	Capacitor	100 nF	± 1
R	Potentiometer	2 kΩ	
R_1	$\frac{1}{4}$W Resistor	3.3 kΩ	± 1
R_2	$\frac{1}{4}$W Resistor	22 kΩ	± 1
R_3	$\frac{1}{4}$W Resistor	22 kΩ	± 1
R_4	$\frac{1}{4}$W Resistor	2.2 kΩ	± 1
R_5	$\frac{1}{4}$W Resistor	220 Ω	± 1
R_6	$\frac{1}{4}$W Resistor	220 Ω	± 1
L	Inductor (TOKO type 10RB)	18 mH	± 5

Table 1. Component list for Chua's circuit.

characteristic as shown in Figure 2. Using two 9 V power supplies for the analog devices AD712, op-amps set their saturation voltages at approximately ± 8.3 V, yielding breakpoints $E \approx$ 1V. With $R_2 = R_3$ and $R_5 = R_6$, the V–I characteristic of the Chua diode is defined by $G_a = -1/R_1 - 1/R_4 = -25/33$ mS and $G_b = 1/R_3 - 1/R_4 = -9/22$ mS. Note that the value of the resistance R_0 is ideally zero in Chua's circuit. In practice, the real inductor L has a small parasitic resistance that can be modeled by R_0; the TOKO-type 10RB inductor is preferred because it has a sufficiently low parasitic resistance R_0 for this application.

By reducing the value of the variable resistor R from 2000 Ω to zero, with all other components as in Table 1, the circuit exhibits a Hopf bifurcation from dc equilibrium, a sequence of period-doubling bifurcations to a spiral attractor, periodic windows, a double-scroll strange attractor, and a boundary crisis (Kennedy, 1995).

Although the diode characteristic in Equation (2) is piecewise-linear, qualitatively similar behavior is observed when a smooth nonlinearity such as a cubic is used instead. The piecewise-linear nonlinearity is more convenient for circuit realization, while the smooth nonlinearity is more appropriate for bifurcation analysis.

MICHAEL PETER KENNEDY

See also **Attractors; Bifurcations; Chaotic dynamics; Hopf bifurcation; Horseshoes and hyperbolicity in dynamical systems; Period doubling; Routes to chaos**

Further Reading

Chua, L.O. 1992. The genesis of Chua's circuit. *Archiv für Elektronik und Übertragungstechnik*, 46(4): 250–257

Chua, L.O. 1993. Global unfolding of Chua's circuit. *IEICE Transactions Fundamentals*, E76A(5): 704–734

Chua, L.O., Desoer, C.A. & Kuh, E.S. 1987. *Linear and Nonlinear Circuits*, New York: McGraw-Hill

Chua, L.O., Komuro, M. & Matsumoto, T. 1986. The double scroll family—Parts I and II. *IEEE Transactions on Circuits and Systems*, 33(11): 1073–1118

Kennedy, M.P. 1992. Robust op amp realization of Chua's circuit. *Frequenz*, 46(3–4): 66–80

Kennedy, M.P. 1993. Three steps to chaos—Parts I and II. *IEEE Transactions on Circuits and Systems—Part I*, 40(10): 640–674

Kennedy, M.P. 1995. Experimental chaos from autonomous electronic circuits. *Philosophical Transactions of the Royal Society London* A, 353(1701): 13–32

Madan, R.N. 1993. *Chua's Circuit: A Paradigm for Chaos*, Singapore: World Scientific

CIRCLE MAP

See **Denjoy theory**

CLEAR AIR TURBULENCE

Description

In 1966, the National Committee for Clear Air Turbulence officially defined *clear air turbulence* (CAT) as "all turbulence in the free atmosphere of interest in aerospace operations that is not in or adjacent to visible convective activity (this includes turbulence found in cirrus clouds not in or adjacent to visible convective activity)." FAA Advisory Circular AC 00-30B (1997) has simplified this somewhat to "turbulence encountered outside of convective clouds." Thus, CAT is considered to mean turbulence in the clear air, not in or near convective clouds, usually at upper levels of the atmosphere (above 6 km).

CAT was first observed by high-flying fighter aircraft in the mid-to-late 1940s. It was expected that turbulence encounters would be rare at high levels due to the lack of clouds at upper levels. However, it was soon discovered that turbulence encounters in clear air were not only frequent but sometimes quite severe. Since then, CAT encounters have become a significant problem for commercial aircraft flying at cruising altitudes (18,000–45,000 ft above the mean sea level). In fact, various reviews of National Transportation Safety Board (NTSB) reports indicate that in the U.S., turbulence encounters account for approximately 65% of all weather-related accidents or incidents for commercial aircraft; probably more than half of these are due to CAT. Although most turbulence encounters are generally just an annoyance to passengers and crew, on average there are about eight commercial aircraft turbulence-related incidents per year that are significant enough to be reported to the NTSB, accounting for 10 serious and 32 minor injuries. Fortunately, fatalities and substantial damage to the aircraft structure are rare but can occur, as shown in Figure 1.

It should be noted that only a certain range of frequencies or wavelengths of turbulent eddies is felt by aircraft as bumpiness. For most commercial aircraft, this wavelength is anywhere from about 10 m to 1 km.

Figure 1. Damage sustained to a DC-8 cargo aircraft in an encounter with CAT on 9 December 1992 at 31,000 ft over the Rocky Mountains near Evergreen, Colorado. Note the loss of left outboard engine and approximately 6 m of the wing. (Photo by Kent Meiries.)

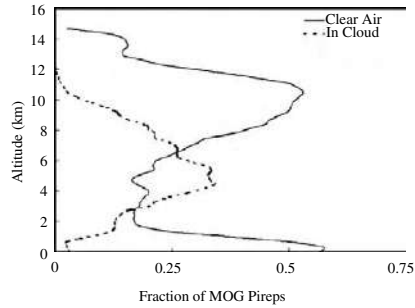

Figure 2. Vertical distribution of the fraction of moderate or greater-intensity (MOG) turbulence pilot reports taken over a two-year period. Solid lines indicate reports in clear air, and dashed lines indicate reports in cloud.

Shorter wavelengths are integrated out over the aircraft structure and longer wavelengths are felt as "waves" and do not generally have vertical accelerations large enough to be felt as "bumps."

CAT can be measured quantitatively with instrumented research aircraft or remotely by instruments such as clear air radar and lidar, but by far the majority of measurements are through pilot reports (PIREPs) of turbulent encounters. PIREPs usually report turbulence on intensity scales of smooth, light, moderate, severe, or extreme. Although definitions of these categories are provided in terms of normal accelerations or airspeed fluctuations, there is still an amount of subjectivity associated with these reports. The pilot reporting system is fairly successful in warning other aircraft of turbulence regions encountered, but to use PIREPs to deduce CAT climatology is difficult, since they are biased by air traffic patterns, non-uniform reporting practices, and the tendency to avoid known turbulence areas. One way to reduce these biases is to examine the ratio of moderate or severe PIREPs to total reports in the three-dimensional airspace averaged over many years of reports. This has been done over the continental U.S. (Sharman et al., 2002). The distribution of this ratio of moderate or greater (MOG) severity PIREPs to total PIREPs by altitude for both CAT and in-cloud encounters is shown in Figure 2. Note that above about 8 km, the majority of reports are in clear air. Similar analyses show the occurrence of CAT to be about twice as frequent in winter as in summer. CAT encounters also tend to be more frequent and more severe over mountainous regions, for example, the Colorado Rockies.

One characteristic of CAT is its patchiness in both time and space. These patches tend to be relatively thin compared with their length (the median thickness is about 500 m, whereas the median horizontal dimension is about 50 km); the median duration is about 6 hours (Vinnichenko et al., 1980). Within a patch, the turbulence may be continuous or may occur in discrete bursts that may be very severe but very narrow (1–2 km).

Relation to Kelvin–Helmholtz Instability

From Figure 2, it can be seen that the altitude of maximum occurrence of CAT is at upper levels near the tropopause and jet stream levels. This relation has been known since the 1950s. For example, Bannon (1952) noted that severe CAT tended to occur above and below the jet stream core on the low-pressure side. These areas tend to have large values of the vertical shear of the horizontal wind, and this led to the hypothesis (e.g., Dutton & Panofsky, 1970) that, at least in some cases, CAT may be related to Kelvin–Helmholtz (KH) instability (KHI, *See* **Kelvin–Helmholtz instability**). The KHI process occurs in stably stratified shear flows when dynamic instabilities due to wind shear exceed the restoring forces due to stability. KH waves (also known as "billows") are, in fact, commonly observed in the atmosphere near the top of clouds, where the KH distortions become visible (Figure 3).

Further, the KHI connection to CAT has been verified on occasion by simultaneous measurements of KH billows by high-powered radar and aircraft measurements of turbulence (Browning et al., 1970). Although the figure shows a KH wave train at an instant in time, the KHI process is an evolutionary one, where waves develop, amplify, roll up, and break down into turbulent patches. The resultant turbulent mixing will eventually destroy the wave structure and mix out the shear, and density distributions that created it, but if larger scale processes continue to reinforce the shears, the entire process may reinitiate.

The names associated with KHI derive from the early works of Hermann von Helmholtz (1868), who realized the destabilizing effects of shear, and later of Lord Kelvin (William Thomson) (1871), who posed and solved the instability problem mathematically. Richardson (1920), using simple energy considerations, deduced that a sufficient condition for

Figure 3. An example of Kelvin–Helmholtz billows observed in the presence of clouds. © 2003 University Corporation for Atmospheric Research.

stability of disturbances in shear flow occurs when the restoring force of stability (as measured by the buoyancy frequency N) is greater than the destabilizing force of the mean horizontal velocity shear ($\mathrm{d}U/\mathrm{d}z$) in the vertical (z) direction. Thus, when the ratio $N^2/(\mathrm{d}U/\mathrm{d}z)^2$ is greater than unity, the flow should be stable. In honor of Richardson's insight, it has become common to refer to this ratio as the Richardson number (Ri). The linear problem for various stratified shear flow configurations is well reviewed in the texts by Chandrasekhar (1961, Chapter 11) and by Drazin and Reid (1981). The sufficient condition for stability to linear two-dimensional disturbances is that $Ri > 0.25$; $Ri < 0.25$ is necessary but not sufficient for instability. More recently, Abarbanel et al. (1984), using the method of Arnol'd, were able to show that the necessary and sufficient condition for Liapunov stability to three-dimensional nonlinear disturbances is $Ri >$ unity, in agreement with Richardson's deduction.

Through these theoretical studies, laboratory experiments (e.g., Thorpe, 1987), and more recently, very high-resolution numerical simulations (e.g., Werne & Fritts, 1999), considerable progress has been made in understanding the intricacies of KHI. One (probably common) method in which KHI is initiated in the atmosphere is through longer wavelength gravity-wave-induced perturbations that lead to local reductions (e.g., in the crest of the wave) in Ri to a value small enough to initiate instability. Gravity waves are ubiquitous in the atmosphere and can be generated in a variety of ways, for example, by flow over mountains or by strong updrafts and downdrafts in convective storms. However, the processes by which KHI may lead to turbulent breakdowns within three-dimensional transient gravity waves is not yet completely understood. It should be mentioned that gravity wave breakdown into turbulent patches may also occur through other mechanisms besides KHI. Examples include convective overturning in large-amplitude waves or nonlinear wave–wave interactions (see the reviews by Wurtele et al. (1996) and Staquet & Sommeria (2002) for discussions of some of these effects). Further, other instability mechanisms besides KHI may lead to CAT, for example, inertial instability or critical-level instability. Thus, the processes by which CAT may be generated at any given time and place are complex, involving many different sources, making its forecasting quite difficult.

One new promising avenue of research is the use of high-resolution numerical simulations of the atmosphere to reconstruct the atmospheric processes that led to particularly severe encounters of CAT (e.g., Clark et al., 2000; Lane et al., 2003). These types of studies have only recently become possible with advances in computing capabilities that allow model runs to contain both the large-scale processes that create conditions conducive to turbulence and the smaller scales that may affect aircraft. Further studies such as these, along with continued theoretical and numerical studies and field measurement campaigns, should lead to a better understanding of CAT genesis and evolution processes.

Until this understanding is available, forecasting of CAT must be accomplished by empirical means. This is done by forecasting various large-scale atmospheric conditions that are known through experience to be related to CAT. Until recently, these diagnostics for likely regions of turbulence had to be performed by laborious weather map analyses of jet streams and upper-level fronts. Nowadays, these diagnostics can be computed from the output of routine numerical weather prediction forecast models. However, the reliability of these turbulence diagnostics is highly variable, and at the moment it seems that better success may be achieved by combining the various diagnostics within an artificial intelligence framework (Tebaldi et al., 2002).

ROBERT SHARMAN

See also **Kelvin–Helmholtz instability; Turbulence**

Further Reading

Abarbanel, H.D.I., Holm, D.D., Marsden, J.E. & Ratiu, T. 1984. Richardson number criterion for the nonlinear stability of three-dimensional stratified flow. *Physical Review Letters*, 52: 2352–2355

Bannon, J.K. 1952. Weather systems associated with some occasions of severe turbulence at high altitude. *Meteorological Magazine*, 81: 97–101

Browning, K.A., Watkins, C.D., Starr, J.R. & McPherson, A. 1970. Simultaneous measurements of clear air turbulence at the tropopause by high-power radar and instrumented aircraft. *Nature*, 228: 1065–1067

Chandrasekhar, S. 1961. *Hydrodynamic and Hydromagnetic Stability*, Oxford: Clarendon Press

Clark, T.L., Hall, W.D., Kerr, R.M., Middleton, D., Radke, L., Ralph, F.M., Nieman, P.J. & Levinson, D. 2000. Origins of aircraft-damaging clear-air turbulence during the 9 December 1992 Colorado downslope windstorm: numerical simulations and comparison with observations. *Journal of the Atmospheric Sciences*, 57: 1105–1131

Drazin, P.G. & Reid, W.H. 1981. *Hydrodynamic Stability*, Cambridge: Cambridge University Press

Dutton, J.A. & Panofsky, H.A. 1970. Clear air turbulence: a mystery may be unfolding. *Science*, 167: 937–944
von Helmholtz, H. 1868. On discontinuous movements of fluids. *Philosophical Magazine*, 36: 337–346 (originally published in German, 1862)
Lane, T.P., Sharman R.D., Clark T.L. & Hsu, H.-M. 2003. An investigation of turbulence generation mechanisms above deep convection. *Journal of the Atmospheric Sciences*, 60: 1297–1321
Kelvin, Lord. 1871. Hydrokinetic solutions and observations. *Philosophical Magazine*, 42: 362–377
Richardson, L.F. 1920. The supply of energy from and to atmospheric eddies. *Proceedings of the Royal Society, London*, A97: 354–373
Sharman, R., Fowler, T.L., Brown, B.G. & Wolff, J. 2002. Climatologies of upper-level turbulence over the continental U. S. and oceans. Preprints, 10th Conference on Aviation, Range, and Aerospace Meteorology, Portland OR: American Meteorological Society, J29–J32
Staquet, C. & Sommeria, J. 2002. Internal gravity waves: from instabilities to turbulence. *Annual Reviews of Fluid Mechanics*, 34: 559–593
Tebaldi, C., Nychka D., Brown B.G., and Sharman, R. 2002. Flexible discriminant techniques for forecasting clear-air turbulence. *Environmetrics*, 13(8): 859–878
Thorpe, S.A. 1987. Transitional phenomena and the development of turbulence in stratified fluids: a review. *Journal of Geophysical Research*, 92: 5321–5248
Vinnechenko, N.K., Pinus, N.Z., Shmeter, S.M. & Shur, G.N. 1980. *Turbulence in the Free Atmosphere*, 2nd edition, New York: Consultants Bureau
Werne, J. & Fritts, D.C. 1999. Stratified shear turbulence: evolution and statistics. *Geophysical Research Letters*, 26: 439–442
Wurtele, M.G., Sharman, R.D. & Datta, A. 1996. Atmospheric lee waves. *Annual Reviews of Fluid Mechanics*, 28: 429–476

CLUSTER COAGULATION

In 1916, nine years before he was awarded the Nobel prize for his studies of colloidal solutions, the Austro-Hungarian chemist Richard Zsigmondy (1865–1929) brought forth the first model for cluster coagulation. Interpreting the behavior of aqueous solutions of gold colloidal particles, he posited that each cluster of particles is surrounded by a sphere of influence. According to this model, clusters execute independent Brownian motions when their spheres of influence do not overlap. Whenever the spheres of influence of a pair of clusters touch, the clusters instantaneously stick together to form a new cluster. This kind of non-equilibrium kinetics (*See* **Nonequilibrium statistical mechanics**) has proven to be truly ubiquitous: bond formation between polymerization sites; the coalescence of rain drops, smog, smoke, and dust; the aggregation of bacteria into colonies; the formation of planetesimals from submicron dust grains; the coalescence arising in genetic trees; and even the merging of banks to form ever-larger financial institutions are all examples of cluster coagulation.

Cluster coagulation results in a broad distribution of cluster sizes described by $\{n_i(t)\}_{i=1,\ldots,\infty}$, where $n_i(t)$ is the number of clusters of size i present in the system at time t. The size of a cluster is defined as the number of unit clusters that it comprises. The primary goal of coagulation theory is to determine the evolution of $n_i(t)$ for all i.

The most important theory of coagulation was given by the Polish physicist Marian Smoluchowski (1872–1917) (Smoluchowski, 1916, 1917). In 1916, prompted by a request from Zsigmondy to provide a mathematical description of coagulation, Smoluchowski postulated that (1) clusters are randomly distributed in space and this feature persists throughout the coagulation process, (2) only collisions between pairs of clusters are significant, and (3) the number of new clusters of size $i+j$, formed per unit time and unit volume due to collisions of clusters of sizes i and j, is proportional to the product of the concentrations $c_i = n_i/V$ and $c_j = n_j/V$:

$$\frac{\text{number of new clusters}}{V\,\Delta t} = K_{i,j}c_i c_j. \qquad (1)$$

Here, V is the volume of the coagulating system and $K_{i,j}$ is the collision frequency factor, also called the *coagulation kernel*.

The rate equation describing the evolution of $c_i(t)$ follows from the balance between the total number of clusters of size i created and annihilated as a result of coagulation:

$$\dot{c}_i(t) = \frac{1}{2}\sum_{j=1}^{i-1} K_{i-j,j}c_{i-j}(t)c_j(t) - \sum_{j=1}^{\infty} K_{i,j}c_i(t)c_j(t), \quad i = 1, \ldots, \infty. \qquad (2)$$

Here, $\dot{c}_i(t)$ is the time derivative of the concentration $c_i(t)$.

This equation—in fact, the chain of nonlinear ordinary differential equations—is called the Smoluchowski coagulation equation (SCE). It describes the evolution of homogeneous aggregating systems with the distribution $c_i(t)$, provided knowledge of $K_{i,j}$ and an initial distribution $c_i(0)$. The SCE does not depend on the spatial dimension in which the coagulation process is taking place. According to modern terminology, Smoluchowski theory is a mean field (*See* **Phase transitions**) theory of nonequilibrium growth. It neglects fluctuations of the concentrations c_k; that is, it presumes the existence of the thermodynamic limit: $V \to \infty, n_k \to \infty, n_k/V \to c_k$. For a broad variety of aggregating systems, this proves to be a reasonable assumption. However, the first assumption of Smoluchowski, that correlations in the distribution of the cluster may be disregarded, is not always satisfied. Aggregating systems fulfilling this assumption are called well-mixed. In low-dimensional systems with no "external" mixing mechanism, the cluster

collisions are often not able to provide sufficient mixing. This may result in correlation build-up and, therefore, a breakdown of Equation (2).

The last, essential, albeit obvious, condition for the applicability of the SCE is that interactions between aggregating clusters be treated as instantaneous collisions, that is, $\tau_{\mathrm{col}} \ll \tau_{\mathrm{coag}}$, where τ_{col} is the characteristic time scale of collisions and τ_{coag} is the characteristic time scale of coagulation. Thus, similar to the Boltzmann kinetic equation (*See* **Nonequilibrium statistical mechanics**), the SCE describes a slow evolution of the distribution due to fast collisions.

For a continuous distribution $c(t, v)$, SCE takes the form of an integro-differential equation (Müller, 1928):

$$\partial_t c(t, v) = \frac{1}{2}\int_0^v K(u, v-u)c(t, u)c(t, v-u) - c(t, v)\mathrm{d}u \int_0^\infty K(u, v)c(t, u)\,\mathrm{d}u. \quad (3)$$

Here u, v are the physical sizes of clusters.

Although the SCE establishes a firm foundation for our understanding of a great variety of cluster coagulation processes, other models have also been devised. They include the Oort–van de Hulst–Safronov equation, which describes cluster coagulation as a continuous growth process, and various stochastic models, such as Kingman's coalescent and the Marcus–Lushnikov process. In this article, we limit ourselves to the Smoluchowski coagulation theory.

The mathematical structure of SCE can be traced to the master equation for stochastic processes:

$$\dot{P}_i(t) = \sum_j \left(w_{i,j}P_j(t) - w_{j,i}P_i(t)\right). \quad (4)$$

Here, $P_i(t)$ is the probability of finding the system in a state i at time t, and $w_{i,j}$ is the probability of transition from state j to state i per unit time. Under the aforementioned assumptions of Smoluchowski theory, $P_i = c_i$, $w_{i,j} = K_{i,j}P_i$. Thus, we arrive at the probabilistic interpretation of $K_{i,j}$ as the probability of coagulation of a pair of clusters i and j in unit volume per unit time.

Calculating the coagulation kernel for a particular coagulation mechanism is a separate problem that is beyond the scope of this article. However, a few remarks are appropriate. First, due to the aforementioned time-scale separation, calculation of K can be treated as a stationary problem. Second, the probability of cluster collisions will depend on the cluster geometry. Very often, the aggregates prove to be fractals (*See* **Fractals; Pattern formation**) having no characteristic size. The coagulation kernel K will then depend on their fractal dimension D_f. Third, the probability of coagulation of a pair of clusters is a product of the probability of their collision and the sticking efficiency E. The latter is defined as the probability of clusters merging once they have collided. Two practically important limiting cases are distinguished for coagulation of diffusing clusters: diffusion-limited cluster-cluster aggregation (DLCA), when $E \approx 1$, and reaction-limited cluster-cluster aggregation (RLCA), when $E \ll 1$. DLCA and RLCA produce aggregates of different fractal dimensions and have kinetics of different speeds. Fourth, when the coagulation mechanism is scale-free and the aggregates are fractals, the coagulation kernel K should also be scale-free. In mathematical terms this amounts to the following requirement on the function $K(u, v)$:

$$K(\lambda u, \lambda v) = \lambda^\alpha K(u, v) \quad (5)$$

for any real $\lambda > 0$. Such kernels are called homogeneous, and α is called the homogeneity index. Several examples of widely used kernels are listed in Table 1.

Our present knowledge of when solutions of (2) exist and are unique is limited, as the nonlinearity of SCE presents challenging problems for rigorous mathematical analysis. Existence and uniqueness of solutions for all times have been proven for the kernels $K(u, v) \le C(u + v)$, where C is a constant. This result has recently been extended to the kernels $K(u, v) \le r(u)r(v)$, where $r(v) = o(v)$, as $v \to \infty$ (Norris, 1999; Leyvraz, 2003).

The distribution function is significant because any macroscopic property characterizing a given coagulating system can be calculated in the continuous (discrete) case as an integral (sum) over the distribution. From a mathematical point of view, the distribution function is simply a time-dependent measure on the set of all cluster sizes. Therefore, it is natural to look for *weak solutions* to SCE. Weak solutions can be conveniently defined in the continuous case by means of a Laplace transformed SCE, which describes the time evolution of the Laplace transformation of the concentration.

Weak solutions are inverse Laplace transforms of the solutions to this equation. The discrete case can be treated analogously with the help of generating functions. In fact, most of the presently known exact solutions of SCE were obtained by this approach.

Since the total mass of clusters is, apparently, conserved during collisions, the SCE is expected to conserve the first moment of the distribution

$$M_1(t) = \int_0^\infty vc(t, v)\,\mathrm{d}v. \quad (6)$$

It appears as a deceptively simple exercise to prove this by substituting (6) into SCE. The proof, however, hinges on the condition that the infinite sums involved are convergent. Violation of this condition gives rise to the important phenomenon of *gelation*, also known as

Coagulation mechanism	Kernel	Originator (year)
"Mating"	2	Smoluchowski (1916)
Brownian motion	$\frac{(r(u)+r(v))^2}{r(u)r(v)}$; $r(v) \propto v^{1/D_f}$	Smoluchowski (1916)
Isotropic turbulent shear	$(r(u)+r(v))^3$; $r(v) \propto v^{1/D_f}$	Saffman and Turner (1956)
Gravitational coalescence	$(r(u)+r(v))^2 \lvert r(u)^2 - r(v)^2 \rvert$; $r(v) \propto v^{1/D_f}$	Findheisen (1939)
Polymerization (RA_∞ model)	uv	Flory (1953)
Polymerization (ARB_∞ model)	$u+v$	

Table 1. Examples of kernels. All kernels are given up to a non-dimensional prefactor. D_f is the fractal dimension of the coagulates.

the gel-sol transition or runaway growth. It was first predicted for the kernel $K(u, v) = uv$, which serves as a model of polymerization (*See* **Polymerization**) in which new links are formed randomly between polymerization sites. In the mean field approximation, this model also describes random graph growth and bond percolation (*See* **Percolation theory**). An exact solution of this problem shows that starting with monodisperse initial conditions, the first moment $M_1(t)$ begins to decay after a finite time, t_c, whereas the second moment $M_2(t)$, measuring the average cluster size, diverges. This behavior corresponds to the formation of an infinite cluster, or gel, in a finite time due to the coagulation kinetics "accelerating" with growing cluster sizes. The sol mass M_1 decreases, as part of it is being lost to the gel. This kind of kinetics has also proved to be a key to the explanation of the rapid growth of Jupiter and planetesimal growth in the terrestrial planets.

It has been shown that $M_1(t) = M_1(0)$ for all times; that is, the system is nongelling, when $K(u, v) \leq C(u + v)$. A wealth of data suggests that this is, in fact, the exact bound separating gelation at finite times from nongelling behavior, although a rigorous proof has not yet been given.

The nonlinear character of SCE complicates mathematical analysis for arbitrary kernels, and the set of exactly solvable kernels is limited. Considerable progress in understanding coagulation kinetics has been achieved for the wide class of homogeneous (or asymptotically homogeneous) kernels by looking for similarity solutions. This can be done in two different ways, which we shall refer to as the self-preservation theory and the self-similarity theory.

The first approach embodies the notion of a single characteristic size in the system, which can be chosen to be equal to an average cluster size, $s(t)$. The asymptotic solution of SCE is then expected to have a self-preserving (scaling) form:

$$c(t, v) = s(t)^{-2} \Phi\left(v/s(t)\right). \tag{7}$$

The self-preserving form has been further studied with the objective of identifying when it will lead to a power-law distribution asymptotically (Leyvraz, 2003). This approach allows one to obtain sensible results for a large variety of problems, including some extensions of SCE, in an almost automatic manner. However, since the scaling hypothesis is postulated, one cannot estimate a priori the accuracy of these solutions. Experimental data on coagulation often display a power-law distribution over some range of cluster sizes.

The second approach deals with a coagulating system maintained at steady state by an external source of monomers. By analogy with the scaling theories for turbulent flows and the theory of critical phenomena, it may be expected that the steady-state distribution at large sizes will "forget" the forcing scale v_0 and, therefore, will evolve to a scale-free form,

$$c(v) = \text{const} \times v^{-\tau}. \tag{8}$$

A careful mathematical analysis has shown that this is indeed the case for a wide range of homogeneous kernels, and that the asymptotic distribution equals

$$c(v) = \left(\frac{E}{\kappa}\right)^{1/2} v^{-(3+\alpha)/2}. \tag{9}$$

Here, E is the total influx of mass into the system due to the forcing and κ is a kernel-dependent constant.

DMITRI O. PUSHKIN AND HASSAN AREF

See also **Brownian motion; Dimensional analysis; Fractals; Nonequilibrium statistical mechanics; Pattern formation; Percolation theory; Phase transitions; Polymerization**

Further Reading

Aldous, D.J. 1999. Deterministic and stochastic methods for coalescence (aggregation, coagulation): review of the mean-field theory for probabilists. *Bernoulli*, 5: 3

Drake, R.L. 1972. A general mathematical survey of the coagulation equation. In *Topics in Current Aerosol Research*, edited by G.M. Hidy and J.R.Brock, part 2, Oxford: Pergamon Press

Family, F. & Landau, D.P. (editors). 1984. *Kinetics of Aggregation and Gelation*, Amsterdam and New York: Elsevier Science

Findheisen, W. 1939. Zur Frage der Regentropfenbildung in reinen Wasserwolken. *Meteorologische Zeitschrift*, 56: 365–368

Flory, P. 1953. Principles of Polymer Chemistry. Ithica: Cornell University Press

Friedlander, S.K. 1960. Similarity consideration for the particle-size spectrum of a coagulating, sedimenting aerosol. 17(5): 479

Friedlander, S.K. 2000. *Smoke, Dust, and Haze: Fundamentals of Aerosol Dynamics*, 2nd edition, Oxford and New York: Oxford University Press

Friedlander, S.K. & Wang, C.S. 1966. The self-preserving particle size distribution for coagulation by Brownian motion. *Journal of Colloid and Interface Science*, 22: 126

Galina, H. & Lechowicz, J.B. 1998. Mean-field kinetic modeling of polymerization: the Smoluchowski coagulation equation. *Advances in Polymer Science*, 137: 135–172

Hunt, J.R. 1982. Self-similar particle-size distributions during coagulation: theory and experimental verification. *Journal of Fluid Mechanics*, 122: 169

Leyvraz, F. 2003. Scaling theory and exactly solved models in the kinetics of irreversible aggregation. *Physics Reports*, 383: 95–212

Müller, H. 1928. Zur algemeinen Theorie der raschen Koagulation. *Kolloid-chemische Beihefte*, 27: 223

Norris, J.R. 1999. Uniqueness, non-uniqueness, and a hydrodynamic limit for the stochastic coalescent. *Annals of Applied Probability*, 9: 78

Pushkin, D.O. & Aref, H. 2002. Self-similarity theory of stationary coagulation. *Physics of Fluids*, 14(2): 694

Saffman, P.G. & Turner, J.S. 1956. On the collision of drops in turbulent clouds. *Journal of Fluid Mechanics*, 1: 16–30

Smoluchowski, M.V. 1916. Drei vorträge über diffusion, *Physikalische Zeitschrift*, 17: 557

Smoluchowski, M.V. 1917. Versuch einer mathematischen theorie der Koagulationskinetik kolloider lösungen. *Zeitschrift für Physikalische Chemie*, 92: 129

van Dongen, P.G.J. & Ernst, M.H. 1985. Dynamic scaling in the kinetics of clustering. *Physical Review Letters*, 54: 1396

van Dongen, P.G.J. & Ernst, M.H. 1988. Scaling solution of Smoluchowski coagulation equation. *Journal of Statistical Physics*, 50: 295

CNOIDAL WAVE

See **Elliptic functions**

COHERENCE PHENOMENA

The word *coherence* comes from the Latin *cohaerens*, meaning "being in relation." Thus, coherence phenomena are those displaying a high level of correlation between several objects.

From the physical point of view, it is necessary to distinguish between two types of coherence: state coherence, which characterizes correlations between static properties of the considered objects, and transition coherence, which describes correlated dynamical processes. These types of coherence are two sides of the same coin, and one obtains a better insight from considering them together.

To gain an intuitive idea of these two types of coherence, imagine a group of soldiers all standing at attention, without moving. This corresponds to state coherence. If the soldiers were all in different positions (some standing, some sitting, some lying down), there would be no state coherence between them. Now, imagine well-aligned rows of soldiers in a parade, moving synchronously with respect to each other. This corresponds to transition coherence. Also, if they were to march with different speeds and in different directions, transition coherence would be absent.

Coherence is related to the existence of a kind of order—be it a static order defining the same positions or an ordered motion of a group. Then, the antonym of *coherence* is *chaos*. Thus, state chaos means the absence of any static order among several objects, and transition chaos implies an absolutely disorganized motion of an ensemble of constituents.

The notion of coherence is implicit in the existence of correlation among several objects (enumerated with the index $i = 1, 2, \ldots, N$). Each object, placed in the spatial point $\boldsymbol{r}_i$, at time t, can be associated with a set $\{Q_\alpha(\boldsymbol{r}_i, t\}$ of observable quantities labeled by α. To formalize the definition of state and transition coherence, one may write $Q_i^\alpha = Q_\alpha(\boldsymbol{r}_i, t)$, where Q_i^z corresponds to a state property of an object, while Q_i^x and Q_i^y describe its motion. As an illustration, assume that Q_i^α are spin components. Another example assumes that Q_i^z is the population difference of a resonant atom, while Q_i^x and Q_i^y are its transition dipoles. Instead of considering the latter separately, it is convenient to introduce the complex combinations $Q_i^\pm \equiv Q_i^x \pm \mathrm{i} Q_i^y$. (In general, Q_i^α are not restricted to classical quantities but may be operators.)

If the system is associated with a statistical operator $\hat{\rho}$, then the observable quantities are the statistical averages

$$\langle Q_i^\alpha \rangle \equiv \mathrm{Tr}\hat{\rho}\, Q_i^\alpha, \tag{1}$$

expressed by means of the trace operation. A convenient way of describing the system features is by introducing dimensionless quantities, normalized to the number of objects N and to the maximal value $Q \equiv \max\langle Q_i^z \rangle$. Then, one may define the state variable

$$s \equiv \frac{1}{QN} \sum_{i=1}^{N} \langle Q_i^z \rangle \tag{2}$$

and the transition variable

$$u \equiv \frac{1}{QN} \sum_{i=1}^{N} \langle Q_i^- \rangle. \tag{3}$$

One may distinguish two opposite cases, when the individual states of all objects are the same and when they are randomly distributed. These two limiting cases give

$$|s| = \begin{cases} 1, & \text{state coherence,} \\ 0, & \text{state chaos.} \end{cases} \tag{4}$$

Next consider the transition characteristic (3) and collective motion of an ensemble of oscillators. Again, there can be two opposite situations, when the oscillation frequencies of all oscillators, as well as their initial phases, are identical and when these take randomly different values. For the corresponding limiting cases of completely synchronized oscillations and of an absolutely random motion, respectively, one has

$$|u| = \begin{cases} 1, & \text{transition coherence,} \\ 0, & \text{transition chaos.} \end{cases} \tag{5}$$

In the intermediate situation, one may say that there is partial state coherence if $0 < |s| < 1$ and partial transition coherence when $0 < |u| < 1$.

Accepting that coherence is not necessarily total, it is convenient to define qualitative characteristics for partial coherence by introducing correlation functions. Let $Q_\alpha^+(\boldsymbol{r}, t)$ denote the Hermitian conjugation for an operator $Q_\alpha(\boldsymbol{r}, t)$. When $Q_\alpha(\boldsymbol{r}, t)$ is a classical function, Hermitian conjugation means complex conjugation. For any two operators from the set $\{Q_\alpha(\boldsymbol{r}, t)\}$, one may define the correlation function

$$C_{\alpha\beta}(\boldsymbol{r}_1, t_1, \boldsymbol{r}_2, t_2) \equiv \langle Q_\alpha^+(\boldsymbol{r}_1, t_1) Q_\beta(\boldsymbol{r}_2, t_2) \rangle. \tag{6}$$

The function $C_{\alpha\alpha}(\ldots)$ for coinciding operators is called the autocorrelation function. There is also a shifted correlation function

$$B_{\alpha\beta} \equiv \langle Q_\alpha^+ Q_\beta \rangle - \langle Q_\alpha^+ \rangle \langle Q_\beta \rangle,$$

where, for brevity, the spatiotemporal variables are not written explicitly. For describing coherent processes, it is convenient to use the normalized correlation function

$$K_{\alpha\beta} \equiv \frac{\langle Q_\alpha^+ Q_\beta \rangle}{(\langle Q_\alpha^+ Q_\alpha \rangle \langle Q_\beta^+ Q_\beta \rangle)^{1/2}}, \tag{7}$$

which is sometimes termed a "coherence function." Functions (6) and (7) can be specified as second-order correlation functions since, in general, it is possible to define higher-order correlation functions, such as the $2p$-order function

$$C_{\alpha_1 \ldots \alpha_{2p}} = \langle Q_{\alpha_1}^+ \ldots Q_{\alpha_p}^+ Q_{\alpha_{p+1}} \ldots Q_{\alpha_{2p}} \rangle,$$

which are closely related to reduced density matrices.

Correlations are usually strongest among nearby spatiotemporal points. Thus, function (7) varies in the interval $0 \leq |K_{\alpha\beta}| \leq 1$, being maximal for the autocorrelation function $|K_{\alpha\alpha}| = 1$ at the coinciding points $\boldsymbol{r}_1 = \boldsymbol{r}_2$, $t_1 = t_2$. When either the spatial or temporal distance between two points increases, correlations diminish; this is named *correlation decay*. At an asymptotically large distance, the correlation function (6) for two local observables displays the property of correlation weakening (correlation decoupling)

$$\langle Q_\alpha^+(\boldsymbol{r}_1, t_1) Q_\beta(\boldsymbol{r}_2, t_2) \rangle \simeq \langle Q_\alpha^+(\boldsymbol{r}_1, t_1) \rangle \langle Q_\beta(\boldsymbol{r}_2, t_2) \rangle, \tag{8}$$

where either $|\boldsymbol{r}_1 - \boldsymbol{r}_2| \to \infty$ or $|t_1 - t_2| \to \infty$. It is important to stress that property (8) holds only for local observables; thus, for operators representing no observable quantities, correlation decoupling generally has no meaning.

Coherence characteristically implies correlations between similar objects, which require the use of autocorrelation functions. To describe coherence decay, it is also necessary to fix a point from which this decay is measured (usually at $\boldsymbol{r} = 0$ and $t = 0$), whereupon coherence decay is studied by considering an autocorrelation function

$$C_\alpha(\boldsymbol{r}, t) \equiv \langle Q_\alpha^+(\boldsymbol{r}, t)\ Q_\alpha(0, 0) \rangle. \tag{9}$$

In many cases, there exists a spatial direction of particular importance, for example, the direction of field propagation. It is natural to associate this special direction with the longitudinal z-axis and the transverse direction with the radial variable $r_\perp$. The characteristic scale of coherence decay in the longitudinal direction is called coherence length $l_{\rm coh}$, where

$$l_{\rm coh}^2 \equiv \frac{\int z^2 |C_\alpha(\boldsymbol{r}, t)|^2 \, d\boldsymbol{r}}{\int |C_\alpha(\boldsymbol{r}, t)|^2 \, d\boldsymbol{r}}, \tag{10}$$

and the integration is over the entire space volume. Coherence decay in the transverse direction is classified as transverse coherence radius $r_{\rm coh}$, where

$$r_{\rm coh}^2 \equiv \frac{\int r_\perp^2 |C_\alpha(\boldsymbol{r}, t)|^2 \, d\boldsymbol{r}}{\int |C_\alpha(\boldsymbol{r}, t)|^2 \, d\boldsymbol{r}}. \tag{11}$$

For isotropic systems, one replaces $r_\perp$ by the spherical radius r and obtains a coherence radius from equation (11). It is natural to call $A_{\rm coh} \equiv \pi r_{\rm coh}^2$ the coherence area and $V_{\rm coh} \equiv A_{\rm coh} l_{\rm coh}$ the coherence volume. The typical scale of temporal correlation decay is termed the coherence time $t_{\rm coh}$, where

$$t_{\rm coh}^2 \equiv \frac{\int_0^\infty t^2 |C_\alpha(\boldsymbol{r}, t)|^2 \, dt}{\int_0^\infty |C_\alpha(\boldsymbol{r}, t)|^2 \, dt}. \tag{12}$$

As seen, the coherence length (10) and coherence radius (11) are related to a fixed moment of time, while the

coherence time (12) defines the temporal coherence decay at a given spatial point. Equations (10)–(12) all have to do with a particular coherence phenomenon characterized by the correlation function (9).

Phase transitions in equilibrium statistical systems are collective phenomena demonstrating different types of state coherence arising under adiabatically slow variation of thermodynamic or system parameters (temperature, pressure, external fields, and so on). Phase transitions are conventionally specified by means of order parameters, which are defined as statistical averages of operators corresponding to some local observables. The order parameter is assumed to be zero in a disordered phase and nonzero in an ordered phase. For example, the order parameter at Bose–Einstein condensation is the fraction or density of particles in the single-particle ground state. The order parameter for superconducting phase transition is the density of Cooper pairs or the related gap in the excitation spectrum. Superfluidity is characterized by the fraction or density of the superfluid component. For magnetic phase transitions, the order parameter is the average magnetization. Thermodynamic phases can also be classified by order indices.

Let the autocorrelation function (9) be defined for the operator related to an order parameter. Then, for a disordered phase, the coherence length is close to the interparticle distance and the coherence time is roughly the interaction time. But for an ordered phase, the coherence length is comparable with the system size and the coherence time becomes infinite.

Taking account of heterophase fluctuations in the quasiequilibrium picture of phase transitions, there appear mesoscopic coherent structures, with the coherence length being much larger than interparticle distance, but much smaller than the system size. The coherence time of these mesoscopic coherent structures (their lifetime) is much longer than the local equilibrium time, although it may be shorter than the observation time. Such coherent structures are similar to those arising in turbulence.

Electromagnetic coherent radiation by lasers and masers presents a good example of transition coherence. Such radiation processes are accompanied by interference patterns, a phenomenon that is typical of coherent radiation and can be produced by atoms, molecules, nuclei, or other radiating objects. Interference effects caused by light beams are studied in nonlinear optics. But coherent radiation and related interference effects also exist in other ranges of electromagnetic radiation frequencies, including infrared, radio, or gamma regions. Moreover, there exist other types of field radiation, such as acoustic radiation or emission of matter waves formed by Bose-condensed atoms. Registration of interference between a reference beam and that reflected by an object is the basis for holography, which is the method of recording and reproducing wave fields.

The description of interference involves correlation functions. Let $Q_i(t)$ represent a field at time t, produced by a radiator at a spatial point $\boldsymbol{r}_i$. The radiation intensity of a single emitter may be defined as

$$I_i(t) \equiv \langle Q_i^+(t)\ Q_i(t)\rangle, \tag{13}$$

whereupon the radiation intensity for an ensemble of N emitters is

$$I(t) = \sum_{i,j=1}^{N} \langle Q_i^+(t)\ Q_j(t)\rangle. \tag{14}$$

Separating the sums with $i = j$ and with $i \neq j$ yields

$$I(t) = \sum_{i=1}^{N} I_i(t) + \sum_{i\neq j}^{N} \langle Q_i^+(t)\ Q_j(t)\rangle, \tag{15}$$

which shows that intensity (14) is not simply a sum of the intensities (13) of individual emitters but also includes the interference part, expressed through the autocorrelation functions of type (9). The first term in equation (15) is the intensity of incoherent radiation, while the second term corresponds to the intensity of coherent radiation.

V.I. YUKALOV

See also **Bose–Einstein condensation; Chaotic dynamics; Critical phenomena; Ferromagnetism and ferroelectricity; Lasers; Nonequilibrium statistical mechanics; Nonlinear optics; Order parameters; Phase transitions; Spatiotemporal chaos; Spin systems; Structural complexity; Superconductivity; Superfluidity; Turbulence**

Further Reading

Andreev, A.V., Emelyanov, V.I. & Ilinski, Y.A. 1993. *Cooperative Effects in Optics*, Bristol: Institute of Physics Publishing

Benedict, M.G., Ermolaev, A.M., Malyshev, V.A., Sokolov, I.V. & Trifonov, E.D. 1996. *Superradiance: Multiatomic Coherent Emission*, Bristol: Institute of Physics Publishing

Bogolubov, N.N. 1967. *Lectures on Quantum Statistics*, Vol. 1, New York: Gordon and Breach

Bogolubov, N.N. 1970. *Lectures on Quantum Statistics*, Vol. 2, New York: Gordon and Breach

Coleman, A.J. & Yukalov, V.I. 2000. *Reduced Density Matrices*, Berlin: Springer

Klauder, J.R. & Skagerstam, B.S. 1985. *Coherent States*, Singapore: World Scientific

Klauder, J.R. & Sudarshan, E.C.G. 1968. *Fundamentals of Quantum Optics*, New York: Benjamin

Lifshitz, E.M. & Pitaevskii, L.P. 1980. *Statistical Physics: Theory of Condensed State*, Oxford: Pergamon Press

Mandel, L. & Wolf, E. 1995. *Optical Coherence and Quantum Optics*, Cambridge and New York: Cambridge University Press

Nozières, P. & Pines, D. 1990. *Theory of Quantum Liquids: Superfluid Bose Liquids*, Redwood, CA: Addison-Wesley
Perina, J. 1985. *Coherence of Light*, Dordrecht: Reidel
Scott, A.C. 1999. *Nonlinear Science: Emergence and Dynamics of Coherent Structures*, Oxford and New York: Oxford University Press
Ter Haar, D. 1977. *Lectures on Selected Topics in Statistical Mechanics*, Oxford: Pergamon Press
Yukalov, V.I. 1991. Phase transitions anad heterophase fluctuations. *Physics Reports*, 208: 395–492
Yukalov, V.I. & Yukalova, E.P. 2000. Cooperative electromagnetic effects. *Physics of Particles and Nuclei*, 31: 561–602

COHERENT EXCITON

See **Excitons**

COHERENT STRUCTURES

See **Emergence**

COLE–HOPF TRANSFORM

See **Burgers equation**

COLLAPSE

See **Development of singularities**

COLLECTIVE COORDINATES

The soliton equations describe a number of important nonlinear physical phenomena. However, in real life, these phenomena are not precisely modeled by say the sine-Gordon (SG) equation, the nonlinear Schrödinger (NLS) equation, or some of the other pure soliton equations. Corrective and often small terms are added to include, for example, inhomogeneities, dissipation, or energy input. The resulting wave phenomena possess modified solitonic features that can be treated approximately starting with a pure soliton solution and then allow the parameters of the soliton solution to vary slowly with time under the influence of the perturbations instead of being constant. Solution parameters that are chosen to vary with time are called *collective coordinates*. They encompass the influence of the perturbations in the pure soliton equations. The advantage of introducing collective coordinates is to reduce a problem with infinitely many degrees of freedom to a problem with a few degrees of freedom (Kivshar & Malomed, 1989; Sánchez & Bishop, 1998).

To illustrate the use of a collective coordinate approach, we shall investigate the NLS equation with the perturbative term εR

$$\mathrm{i}u_t + u_{xx} + 2|u|^2 u = \varepsilon R. \tag{1}$$

Here, $u = u(x, t)$, where x is the spatial coordinate and t is time. Subscripts x and t denote partial derivatives with respect to these variables. The simple single soliton solution of the pure NLS equation ($\varepsilon = 0$) reads

$$u(x, t) = a\,\mathrm{sech}(a\theta)\exp(\mathrm{i}\xi\theta + \mathrm{i}\sigma), \tag{2}$$

where $\theta = x - x_0$. This solution possesses four parameters $(a, \xi, x_0, \sigma) = (y_1, y_2, y_3, y_4)$, which we shall choose as collective coordinates. For weak perturbations, $\varepsilon \ll 1$, we shall assume that the collective coordinates depend slowly on time t due to the influence of εR. In addition, the perturbation leads to a radiation field of small amplitude, which is neglected. A variational approach is employed to determine the time evolution of the collective coordinates, but this is not the only method available. In the framework of a variational approach, the collective coordinates are the generalized coordinates. Although perturbations may destroy the Hamiltonian property of the pure soliton equations, dissipative effects and external nonconservative forces can be accounted for in the variation of a Lagrangian function by introducing generalized forces associated with the generalized coordinates. Below, this is done by introducing a generalized force for each collective coordinate as in classical mechanics.

The unperturbed NLS equation (and its complex conjugate) can be derived from the Lagrangian density (Caputo et al., 1995; Scott, 2003);

$$\mathcal{L}(u, u^*, u_t, u_t^*, u_x, u_x^*) = \frac{\mathrm{i}}{2}(u^* u_t - u_t^* u) - |u_x|^2 + |u|^4. \tag{3}$$

The total Lagrangian function is

$$L(y_i, \dot{y}_i) = \int_{-\infty}^{\infty} \mathcal{L}\,\mathrm{d}x, \tag{4}$$

where we denote the collective coordinates $y_i(t)$, $i = 1, 2, 3, 4$, and $\dot{y}_i$ is the time derivative of y_i. Together with Equation (1), the variation of total Lagrangian leads to the Euler–Lagrange equations (Caputo et al., 1995; Scott, 2003)

$$\frac{\partial L}{\partial y_i} - \frac{\mathrm{d}}{\mathrm{d}t}\left(\frac{\partial L}{\partial \dot{y}_i}\right) = \varepsilon \int_{-\infty}^{\infty} R\frac{\partial u^*}{\partial y_i}\mathrm{d}x + \text{c.c.}, \tag{5}$$

where c.c. stands for complex conjugate of the preceding term on the right-hand side. The inhomogeneous term on the right-hand side is interpreted as the generalized force associated with the collective coordinate $y_i(t)$, which is a key result as we do not rely on a perturbation with a strict Hamiltonian nature. Another important feature is that the above approach provides as many dynamical equations as we choose collective coordinates; thus it is straightforward to determine the generalized forces associated with each collective coordinate.

To illustrate the method, we calculate the total Lagrangian for the NLS equation using the simple single soliton solution in (2)

$$L = \frac{2}{3}a^3 - 2a\xi^2 + 2a\xi\frac{\mathrm{d}x_0}{\mathrm{d}t} - 2a\frac{\mathrm{d}\sigma}{\mathrm{d}t}. \tag{6}$$

Consider the perturbation

$$\varepsilon R = -\mathrm{i}\Gamma u + \frac{\mathrm{i}g_0 u}{1 + p/p_\mathrm{s}}, \tag{7}$$

describing light propagation through an optical fiber amplifier with a loss factor Γ, gain g_0, and power $p = \int_{-\infty}^{\infty} |u|^2 \mathrm{d}x$. The constant p_s is a saturation power level that is characteristic for a given fiber amplifier. From Equation (5), the resulting dynamical equations for the collective coordinates are

$$\frac{\mathrm{d}a}{\mathrm{d}t} = -2\Gamma a + \frac{2g_0 a}{1 + 2a^2/p_\mathrm{s}}, \tag{8}$$

$$\frac{\mathrm{d}\xi}{\mathrm{d}t} = 0, \tag{9}$$

$$\frac{\mathrm{d}x_0}{\mathrm{d}t} = 2\xi, \tag{10}$$

$$\frac{\mathrm{d}\sigma}{\mathrm{d}t} = a^2 + \xi^2, \tag{11}$$

which is a drastic simplification compared to the original perturbed NLS problem. As for the sine-Gordon system, one can define a power balance condition by requiring $\dot{a}(t) = 0$, implying an equilibrium amplitude a_∞ given as $a_\infty = \sqrt{(g_0 - \Gamma)p_\mathrm{s}/2\Gamma}$.

A number of other strategies have been designed to determine slow time variation of collective coordinates in perturbed soliton solutions. These include slow variation of scattering data of the inverse scattering theory for pure solitons (Kivshar & Malomed, 1989; Lamb, 1980), more direct perturbation approaches (McLaughlin & Scott, 1978), and utilizing Hamiltonian structures in cases where the perturbation leads to Hamiltonian systems (Caputo & Flytzanis, 1991). An important result of perturbations is the formation of trailing radiation fields, which are low-amplitude linear waves created as perturbed solitons propagates (McLaughlin & Scott, 1978; Kivshar & Malomed, 1989; Willis, 1997). The solitons lose energy to the radiation field, and the variational approach used here can be extended to include such radiation.

MADS PETER SØRENSEN

See also **Constants of motion and conservation laws; Energy analysis; Euler–Lagrange equations; Hamiltonian systems; Inverse scattering method or transform; Nonlinear optics; Nonlinear Schrödinger equations; Perturbation theory; Solitons**

Further Reading

Caputo, J.G. & Flytzanis, N. 1991. Kink-antikink collisions in sine-Gordon and ϕ^4 models: problems in the variational approach. *Physical Review* A, 44(10): 6219–6225

Caputo, J.G., Flytzanis, N. & Sørensen, M.P. 1995. The ring laser configuration studied by collective coordinates. *Journal of the Optical Society of America* B, 12(1): 139–145

Kivshar, Y.S. & Malomed, B.A. 1989. Dynamics of solitons in nearly integrable systems. *Reviews of Moderen Physics*, 61: 763–915

Lamb, G.L. 1980. *Elements of Soliton Theory*, New York: Wiley

McLaughlin, D.W. & Scott, A.C. 1978. Perturbation analysis of fluxon dynamics. *Physical Review A*, 18: 1652–1680

Sánchez, A. & Bishop, A.R. 1998. Collective coordinates and length-scale competition in spatially inhomogeneous soliton-bearing equations. *SIAM Review*, 40(3): 579–615

Scott, A.C. 2003. *Nonlinear Science: Emergence and Dynamics of Coherent Structures*, 2nd edition, Oxford and New York: Oxford University Press

Willis, C.R. 1997. Spontaneous emission of a continuum sine-Gordon kink in the presence of a spatially periodic potential. *Physical Review E*, 55(5): 6097–6100

COLLISIONS

An interesting consequence of Hamiltonian structures is that there typically exist symmetries and invariances that allow one to generate mobile localized states from standing ones. For instance, the sine-Gordon (SG) equation (Dodd et al., 1982)

$$u_{tt} = u_{xx} - \sin(u), \tag{1}$$

where the subscripts denote partial derivatives, is invariant under the Lorentz transformation $x \rightarrow x' = \gamma(x - vt)$ and $t \rightarrow t' = \gamma(t - vx)$. $\gamma = \sqrt{1 - v^2}$. As a result, static kinks and antikinks, corresponding to the two signs of the solution

$$u(x, t) = \pm 4 \tan^{-1}(x - x_0), \tag{2}$$

can be boosted to any subluminal speed $v < 1$, as

$$u(x, t) = \pm 4 \tan^{-1}\left[\gamma(x - x_0 - vt)\right]. \tag{3}$$

Similarly, standing waves of the nonlinear Schrödinger (NLS) equation

$$\mathrm{i}u_t = -u_{xx} - |u|^2 u \tag{4}$$

can be boosted by Galilean invariance into traveling ones with any speed v of the form (Sulem & Sulem, 1999)

$$u(x, t) = (2\alpha)^{1/2} \mathrm{e}^{\mathrm{i}(v/2)x + \mathrm{i}(\alpha - (v^2/4))t} \times \mathrm{sech}\,(x - x_0 - vt)\,. \tag{5}$$

Note that localized solutions of dissipative partial differential equations do not typically share such features, because their traveling wave speeds are determined by the dynamics rather than initial conditions. Hereafter, we will focus on Hamiltonian models.

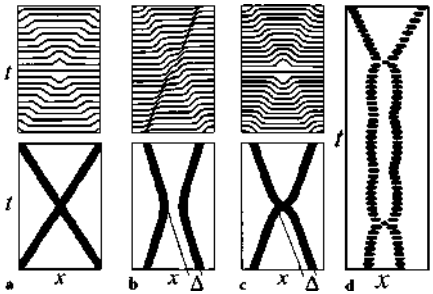

Figure 1. Elastic collisions: (a) linear-shaped antikink and kink in the linear wave equation; (b) kink-kink repulsive collision in SG; (c) antikink-kink attractive collision in SG. Top panels show $u(x, t)$, while bottom panels show the trajectories of soliton cores in the (x, t)-plane. (d) Inelastic collisions between two NLS solitons in the presence of weak perturbation.

Given the mobility of the localized coherent structures, it is natural to consider the outcome of their collisions. In fact, it was the "solitary" nature of such interactions (Zabusky & Kruskal, 1965) that inspired the term *soliton* in the case of integrable systems.

Linear versus Nonlinear Collisions

Consider the collision of two wavepackets that are governed by a linear wave equation. In this case, the superposition principle inherent in linearity guarantees that the two packets do not "feel" each other and survive the collision without change of shape, speed, or trajectory (see Figure 1(a)).

On the other hand, nonlinear dynamics offers more interesting collisions. Here, the result of the interaction of two excitations does not resemble their sum and (at least) a phase shift Δ is present (compare Figures 1(b) and 1(c) with 1(a)). In 1(b) and 1(c), the kink-kink and the antikink-kink collisions in the nonlinear SG equation are shown. The soliton cores do not merge in mutually repulsive collisions 1(b) while they do so in attractive collisions 1(c).

Elastic versus Inelastic Collisions

In fully integrable systems, solitons have the remarkable property (often used to define them) of colliding elastically (Ablowitz & Segur, 1981). In these special systems, the dynamics are severely restricted by the existence of an infinite set of conservation laws. Although realistic systems are typically non-integrable, the non-integrability in many applications is weak and can be treated by including small perturbative terms in integrable equations. Such perturbations are called Hamiltonian if the total energy of the perturbed system remains a dynamical invariant. While collisions in linear systems are much simpler than those in integrable nonlinear systems (such as the SG and NLS equations), the latter can, in turn, also be very different from the much more complex picture of inelastic collisions in near-integrable or more generally non-integrable systems.

In general non-integrable systems, the inelasticity of collisions may be manifested through emission of radiation, excitation of soliton internal modes, and energy exchange between solitons. Internal modes are the long-lived, spatially localized, oscillatory excitations (corresponding to the point spectrum of the linearization around the wave). These can typically be excited only for a particular sign of the perturbation (Campbell et al., 1983).

Small-amplitude radiation waves correspond to an irreversible chunk of energy lost in the collision (radiated toward the boundaries). Such modes are extended, plane waves of the continuous spectrum. Notice that the energy of internal modes can be partly restored to solitons if they collide again, while this is not possible for radiation waves (in the first-order approximation).

Strong energy exchange between nonlinear waves in near-integrable systems can also occur in the absence of the above two mechanisms (and for different types and signs of the original perturbation). There are two necessary conditions for this recently manifested mechanism (Dmitriev et al., 2001, 2002). It can be observed only if the energy exchange is not forbidden by the conservation laws existing in the perturbed system and if the collision is of attractive type, as in Figure 1(c). For example, in the SG equation perturbed by the term εu_{xxxx}, where energy and momentum are conserved for the one (free)-parameter kink-solitons, energy exchange is possible only when more than two solitons participate in the collision. The energy exchange between only kinks or only antikinks is also not possible because SG solitons with the same parity repel each other. Similarly, the effect is not possible in the Korteweg–de Vries (KdV) equation, where soliton interactions are always mutually repulsive.

In the NLS equation, in-phase solitons attract each other, while out-of-phase solitons repel. Each soliton has two parameters (amplitude and phase), and for many practically important perturbations, there are two conserved quantities: the Hamiltonian and L^2 norm of the solution. Thus, energy exchange between two nearly in-phase NLS solitons is possible in the presence of a weak perturbation. The effect of radiationless energy exchange between solitons survives even for a very weak perturbation, as it decreases linearly with a decrease in perturbation amplitude, while other effects of the perturbation decay faster. If the perturbation is not small, the energy exchange effect mingles with

radiation emission and possibly with the excitation of internal modes.

Probabilistic Nature of Soliton Collisions

In many examples of perturbed, non-integrable models related to applications in optics, fluid mechanics, or condensed-matter physics (Kivshar & Malomed, 1989), the result of soliton collisions can be predicted only in a probabilistic sense. The following sources of stochastic behavior can be identified. First, chaotic soliton scattering can arise from resonant interaction with the soliton internal modes (Campbell et al., 1986; Gorshkov et al., 1992). Second, in discrete systems, the result of inelastic collisions can be sensitive to the coordinate of collision point, x_c, with respect to the lattice site (Dmitriev et al., 2003; Papacharalampous et al., 2003). Because the coordinate of the collision point usually cannot be controlled, it is natural to describe the result of the collision as a function of the random variable x_c. Finally, the result of the collision can be extremely sensitive to some other uncontrolled characteristics, such as the relative phase of the colliding solitons, as has been demonstrated to dramatically affect the collisions between NLS solitons or between kinks and breathers in SG (Dmitriev et al., 2001, 2002, 2003; Papacharalampous et al., 2003).

This last source of randomness is important when energy exchange between solitons is possible. In Figure 1(d), an example of inelastic interaction between two NLS solitons in the presence of quintic perturbation, $\varepsilon|u|^4u$ in Equation (4), with a small $\varepsilon > 0$ is presented (Dmitriev & Shigenari, 2002). (The regions of the (x, t)-plane are shown, where the real part of the solution exceeds a certain value.) After each collision, the properties of the solitons such as the frequency and amplitude are different depending on the collision phase. With a certain probability, the solitons can attain (after a number of collisions) a velocity sufficient to overcome their weak mutual attraction. In the example presented, the solitons split after the fourth collision. Emission of extended wave radiation is monitored and found to be very weak in this case; as a result, the solitons may continue to collide for a very long time, forming a two-soliton bound state. However, the probability P to obtain a bound state with the lifetime T decays algebraically as $P \sim T^{-\alpha}$ (Dmitriev & Shigenari, 2002), which is a manifestation of the chaotic character of their interaction.

In conclusion, linear waves do not "feel" each other, and nonlinear waves of integrable equations emerge unscathed from collisions, retaining their solitary character. However, solitary wave collisions in more realistic, non-integrable models remain a fascinating topic, where a number of basic mechanisms (such as internal mode resonances, extended wave radiation, and radiationless energy exchange) have been elucidated, but the full picture is far from complete. The probabilistic interpretation of collisions mentioned above may prove a fruitful viewpoint in future studies.

P.G. Kevrekidis and S.V. Dmitriev

See also **Nonlinear Schrödinger equations; Partial differential equations, nonlinear; Sine-Gordon equation; Solitons; Solitons, types of**

Further Reading

Ablowitz, M.J. & Segur, H. 1981. *Solitons and the Inverse Scattering Transform*, Philadelphia: SIAM

Campbell, D.K., Schonfeld, J.F. & Wingate, C.A. 1983. Resonance structure in kink–antikink interactions in $\phi/4$ field theory. *Physica* D, 9: 1–32

Campbell, D.K., Peyrard, M. & Sodano, P. 1986. Kink-antikink interactions in the double sine-Gordon equation. *Physica* D, 19: 165–205

Dmitriev, S.V., Kivshar, Yu.S. & Shigenari, T. 2001. Fractal structures and multiparticle effects in soliton scattering. *Physical Review* E, 64: 056613

Dmitriev, S.V., Semagin, D.A., Sukhorukov, A.A. & Shigenari, T. 2002. Chaotic character of two-soliton collisions in the weakly perturbed nonlinear Schrödinger equation. *Physical Review* E, 66: 046609

Dmitriev, S.V. & Shigenari, T. 2002. Short-lived two-soliton bound states in weakly perturbed nonlinear Schrödinger equation. *Chaos*, 12: 324

Dmitriev, S.V., Kevrekidis, P.G., Malomed, B.A. & Frantzeskakis, D.J. 2003. Two-soliton collisions in a near-integrable lattice system. *Physical Review* E, 68: 056603

Dodd, R.K., Eilbeck, J.C., Gibbon, J.D. & Morris, H.C. 1982. *Solitons and Nonlinear Wave Equations*, London: Academic Press

Gorshkov, K.A., Lomov, A.S. & Gorshkov, M.I. 1992. Chaotic scattering of two-dimensional solitons. *Nonlinearity*, 5: 1343–1353

Kivshar, Yu.S. & Malomed, B.A. 1989. Dynamics of solitons in nearly integrable systems. *Reviews of Modern Physics*, 61: 763–915

Papacharalampous, I.E., Kevrekidis, P.G., Malomed, B.A. & Frantzeskakis, D.J. 2003. Soliton collisions in the discrete nonlinear Schrödinger equation. *Physical Review* E, 68: 046604

Sulem, C. & Sulem, P.L. 1999. *The Nonlinear Schrödinger Equation*, New York: Springer

Zabusky, N.J. & Kruskal, M.D. 1965. Interactions of solitons in a collisionless plasma and the recurrence of initial states. *Physical Review Letters*, 15: 240–243

COLOR CENTERS

Gemstones are brightly colored because of the presence of *color centers*, atomic-scale imperfections that absorb light in otherwise transparent crystals. Historically, the term *color centers* has been associated with such imperfections in a special class of crystals called alkali halides, because it was in these relatively simple transparent hosts that the scientific study of color centers flourished. A German research program that

began in the 1930s soon led to the recognition that alkali halides are excellent hosts for scientific studies of defects in nonmetallic solids, and the understanding of fundamental properties in these materials has been of great significance in the studies of similar phenomena in more complicated (and sometimes more practical) situations and materials.

Sodium chloride—common table salt—is the most familiar alkali halide. It consists of positively charged sodium and negatively charged chlorine ions, alternating positions in a simple cubic array. In the perfect crystal, each ion has six nearest neighbors of opposite charge. Simple defects may involve chemical impurities, such as a positively charged silver or thallium ion on an alkali site, or the removal of one or more ions from normal positions. The most fundamental of the latter class is the F center (from the German *Farbzentren*), a halogen ion vacancy that has trapped an electron. Defects involving more than one F center, or chemical impurities next to one or more F centers, may also occur.

Understanding the properties of color centers in detail requires some knowledge of quantum concepts. For example, the trapped electron of an F center can exist only in certain quantum states. In order for light to be absorbed, the energy of an incident photon must match the energy difference between the lowest quantum state and a higher one. This energy difference depends on the host crystal, and so F centers induce different colors in different alkali halides.

The situation becomes more complicated when one considers that the electron is not trapped in a static host, but rather that the neighboring ions are vibrating. The electron's interaction with these vibrations, whose time scale is long with respect to that of the (light) electron's motion, means that the energy difference between ground and excited electronic states does not have a single value, but rather a distribution of values about some mean. Thus, for example, whereas the mean photon absorption energy for F centers at low temperatures in NaCl is 2.77 eV, the mean width of the distribution of absorption energies is 0.26 eV.

This *electron-lattice interaction* has other consequences. In most cases, an F center at low temperature that has been excited by light will re-emit light. However, the mean energy of the emitted photon is found to be considerably smaller than that of the absorbed photon. This *Stokes shift* is exemplified in NaCl, where the mean photon emission energy at low temperatures is 0.98 eV.

Why is there a Stokes shift? In simple terms, the energy-level structure of the F center is determined by the mean position of the neighboring ions. However, the mean position of the neighboring ions is in turn determined by the quantum state of the F center electron. After the electron is excited from the ground state to another quantum state, the neighboring ions relax in response to the change in the average force exerted on them by the electron. This relaxation then leads to a change in the energy-level separations, as well as other fundamental aspects of their properties. The emitted photon has an energy smaller than the absorbed photon had, and energy is conserved in the total cycle as the relaxation processes create quanta of lattice vibrations, or phonons, which remove the excess energy.

This cyclic process may be visualized by means of a configuration coordinate diagram. In the simplest case, this diagram consists of two equal parabolas, displaced vertically (in energy, E) and horizontally (in the displacement of neighboring ions, R), as shown in Figure 1. Each parabola represents the vibration of neighboring ions and leads to quantized vibrational states. According to the Franck–Condon principle, electronic transitions take place vertically on the diagram—the massive ions do not respond instantly to the excitation by the photon—so absorption corresponds to a transition from A to B, emission C to D. This picture is highly oversimplified, but it does represent a physical and visual way to understand phenomena associated with the optical properties of F centers (and by extension, many other types of defects in both insulators and semiconductors).

We now consider a perfect alkali halide crystal in which one electron has been removed by light (ionizing radiation) from the array of negative ions. At low temperatures, this is found to lead to the phenomenon of self-trapping, whereas in semiconductors, the removal of an electron from a valence band of occupied states leads to motion of the empty state, or hole, and resulting electrical conduction; in most alkali halides the missing charge becomes localized in space, or self-trapped. What happens in detail is that the halogen ion that has lost one electron (and become a neutral atom) can form a chemical bond with a nearby halogen ion. In the process, both of these move toward each other, the lattice around them relaxes, and the missing charge is equally shared by this halogen molecule-ion.

Self-trapping is not a universal process; it "costs" energy to localize a quantum particle, and the energy

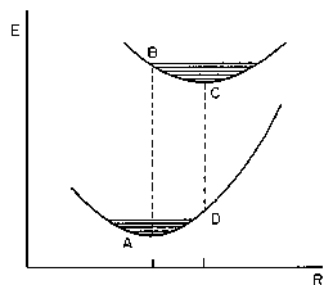

Figure 1. Schematic configuration coordinate diagram.

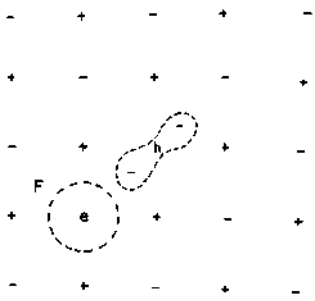

Figure 2. Adjacent F center and self-trapped hole center in an alkali halide. "+" and "−" denote alkali and halogen ions, respectively.

gained by chemical bonding and relaxation must overcome this. Self-trapping of holes occurs in most alkali halides, but not in semiconductors and not in many other insulators. Also of interest is the creation of defects by the self-trapping of excitation energy in alkali halides, leading to a *self-trapped exciton*. To approach this, we consider the trapping of an electron by a self-trapped hole. Since the hole is effectively positive (it resulted from the removal of an electron), we might imagine that the trapped electron would find itself in loosely bound quantum states about the self-trapped hole. However, there is another possibility. If it does not cost too much energy for the halogen molecule-ion to move into one halogen site, rather than be shared by two sites, then the electron may be trapped in the other, empty halogen site. One then has an F center next to a halogen molecule-ion; hence, two defects have been formed. This situation is shown in Figure 2. Since the two defects are adjacent, this may be an unstable arrangement, and indeed there is a finite probability that the system will revert back to the perfect crystal, either before or after the emission of a photon. But, in many cases, it is found that this nearest-neighbor arrangement is the precursor for the creation of a stable defect pair: the halogen molecule-ion may migrate through the halogen sublattice, not by long-range atomic motion, but rather by short-range halogen motion accompanied by motion of the hole. This results in sequential sharing of the hole by the halogens as the hole migrates away from the F center.

W. BEALL FOWLER

See also **Excitons; Franck–Condon factor; Quantum theory**

Further Reading

Crawford, J.H. & Slifkin, L.M. (editors). 1972 (vol. 1), 1975 (vol. 2). *Point Defects in Solids*, New York, Plenum

Fowler, W.B. (editor). 1968. *Physics of Color Centers*, New York: Academic

Hayes, W. & Stoneham, A.M. 1985. *Defects and Defect Processes in Nonmetallic Solids*, New York: Wiley

Schulman, J.H. & Compton, W.D. 1962. *Color Centers in Solids*, New York: Macmillan

Song, K.S. & Williams, R.T. 1993, 1996. *Self-Trapped Excitons*, Berlin and New York: Springer

COMMENSURATE-INCOMMENSURATE TRANSITION

When some local property in a crystalline solid (atomic positions or orientation of local magnetic moments) develops a spatial modulation with a wavelength b that differs from the underlying lattice spacing a, one speaks of a "modulated phase." A modulated phase is said to be "commensurate" when the ratio b/a is rational and "incommensurate" when b/a is irrational.

Modulated phases are experimentally observed by the appearance of "satellite spots" in X-ray, neutron, or electron diffraction patterns (Janssen & Janner, 1987; Cummins, 1990). Observations of spatially modulated structures are abundant in condensed matter physical systems, such as the ferrimagnetic phases of the rare earths and their compounds, long-period structures of binary alloys, graphite intercalation compounds, or the polytypic phases of spinelloids, perovskites, and micas, among other minerals.

The wavelength b characterizing the modulation varies with external parameters, such as temperature, pressure, or magnetic field. Sometimes, this variation is smooth, but often it remains constant at a rational locking value through some range of values of the external parameter before changing to another rational locking value, and so on.

The ubiquity of modulated phases shows that the physical origin of these behaviors cannot be tied to particularities of specific types of systems, but must be of a general character. It is widely recognized that modulated phases appear whenever different terms in the free energy of the system compete, each one trying to impose its own characteristic length scale. The external parameters control the relative strength of the competing interactions and new compromises are reached as they vary.

An insight into the physics of modulated phases was obtained through detailed analyses of simple model systems of competing interactions. Although these simple models are unlikely to fit experiments on specific materials, they help to understand the complexity of behaviors that emanate from length-scale competition and to discern essential features.

One of the best-studied model systems with competing interactions is the axial next-nearest-neighbors Ising (ANNNI) model (motivated by the

magnetic structures of erbium), which was introduced by R.J. Elliot in 1961 (Yeomans, 1988). This is an Ising model with a two-state spin, $S = \pm 1$, on each site of a cubic lattice. Interactions between spins on nearest-neighbor sites are ferromagnetic, but there are second (next-nearest) neighbor antiferromagnetic interactions along the axial direction, z. The Hamiltonian is

$$H = -\frac{1}{2}J_0 \sum_{i,j,j'} S_{i,j} S_{i,j'} - J_1 \sum_{i,j} S_{i,j} S_{i+1,j} - J_2 \sum_{i,j} S_{i,j} S_{i+2,j}, \quad (1)$$

where i indicates the two-dimensional layers perpendicular to the axial direction, and j, j' are nearest-neighbor sites within a layer. Both J_0 and J_1 are positive (ferromagnetic interactions), thus favoring the same value of neighboring spins, but $J_2 < 0$ (antiferromagnetic) so that it favors opposite values of second neighbor spins along the z-direction.

In the absence of thermal effects ($T = 0$), the favored spin configurations along the z-direction are the ferromagnetic alignment ($\cdots + + + + + + \cdots$) if $\kappa = -J_2/J_1 < \frac{1}{2}$, and the antiphase ($\cdots + + - - + + \cdots$) configuration if $\kappa > 1/2$. Exactly at $\kappa = \frac{1}{2}$, any configuration containing a stripe of two or more spins "+" followed by a stripe of two or more spins "−", etc., has the same energy; thus there is a multiphase point.

A convenient notation is to use $\langle n_1, \ldots, n_m \rangle$ to represent a state in which a set of stripes of width n_i of alternating spins repeat. For example, ($\cdots + + - - + + + - - + + - - \cdots$) is denoted by $\langle 223 \rangle$. Ferromagnetic and antiphase configurations are consistently denoted by $\langle \infty \rangle$ and $\langle 2 \rangle$, respectively. When temperature increases from zero, entropic effects regulate the competition among the ferro and antiferro interactions, and a flower (called a "devil's flower" by Per Bak) of petal-like phases of modulated structures opens up from the multiphase point.

Figure 1 shows how new commensurate phases appear as temperature increases, demonstrating qualitatively what is commonly observed in experiments—locking to a few short-wavelength commensurate phases separated either by first-order phase transitions (as in the low-temperature regime of Figure 1) or by regions where the wave vector appears to vary smoothly (as at higher temperatures).

The following question naturally arises: what determines the behavior of the modulation wave vector as parameters vary? The answer to this question is closely tied to a central paradigm of nonlinear science, the soliton concept in the context of its discrete counterpart called discommensuration.

To clarify this issue, consider the simplest model of competing interactions (Griffiths, 1990), the Frenkel–Kontorova model, which can be visualized as an array of atoms at positions (u_n), $-\infty < n < +\infty$, experiencing

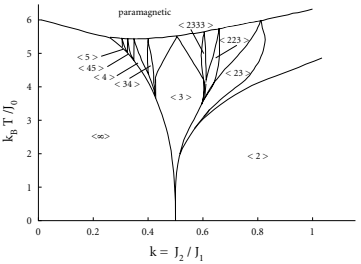

Figure 1. Mean-field phase diagram of the ANNNI model showing the main commensurate phases.

a periodic substrate potential $V(u) = V(u+1)$ and nearest-neighbor interaction $W(\Delta u)$. The Hamiltonian is

$$H = \sum_n [K V(u_n) + W(\Delta u_n)], \quad (2)$$

where the parameter K controls the relative strength of the interactions. The standard Frenkel–Kontorova model corresponds to

$$V(u) = \frac{1}{(2\pi)^2}[1 - 2\cos(2\pi u)],$$
$$W(\Delta u) = \frac{1}{2}(\Delta u)^2 - \sigma \Delta u. \quad (3)$$

Note that V favors an integer value of the interspacing Δu, while W favors a uniform value σ, so both interactions compete to determine the configuration (u_n), characterized here by the average interspacing $\omega = \langle \Delta u \rangle$.

If (as in the standard model) the interaction $W(\Delta u)$ is a convex function, a complete rigorous characterization of the model phase diagram was given by Aubry (1985). Thus, we restrict the analysis to convex $W(\Delta u)$.

In the thermodynamic limit of the system, care must be taken when defining what is meant by configurations of minimum energy or even by the energy of a configuration. Thus, the mean energy ε per particle of a configuration (u_n) is defined as

$$\varepsilon = \lim_{(N-M)\to\infty} \frac{1}{N-M} \times \sum_{j=M}^{N-1} [K V(u_j) + W(u_{j+1} - u_j)]. \quad (4)$$

A minimum energy configuration (MEC) (u_j) is that for which the arbitrary displacement of any finite segment $(u_j + \delta_j)$, $M < j < N$, of the configuration always produces a nonnegative energy change. For an MEC, both limits (ω and ε) exist. Moreover, for every real number ω, there is at least an MEC with average spacing ω, and its mean energy per particle $\varepsilon(\omega)$ is

a well-defined function. A ground state is an MEC that is "recurrent," meaning that any arbitrary finite segment of the configuration approximately reappears somewhere else, within arbitrary precision. One often speaks of the ground state that corresponds to fixed values of the parameters (K and σ for the standard model), meaning the ground-state configuration for which $\varepsilon = \min_\omega \varepsilon(\omega)$ occurs at the fixed values of the parameters. The minimum ε, which depends on the parameter values, is the ground state energy, and the value of ω where that minimum occurs is the ground-state average spacing.

The ground-state phase diagram of the standard Frenkel–Kontorova model is shown in Figure 2. Some low-order commensurate phases (rational ω) are shown there, but in between any two of them, there are an infinite number of others. The ground-state average spacing ω as a function of the tension σ, for a fixed value of $K = 1$, is shown in Figure 3. This is a continuous function with plateaus of (rational) constant value, which correspond to commensurate phases. This function is called "devil's staircase" or Cantor function. No first-order phase transitions between commensurate phases of different commensurabilities are allowed in convex models.

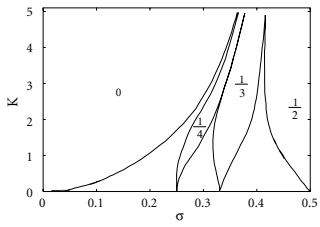

Figure 2. Ground-state phase diagram of the standard Frenkel–Kontorova model. Each point in the diagram is characterized by the value of ω, average spacing of the groundstate configurations for the parameters (K, σ) of the model. The numbers in the figure are values of ω. Only a few commensurate phases are plotted, as there are infinitely many commensurate and incommensurate phases in between any two of them.

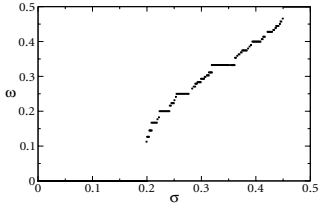

Figure 3. ω as a function of σ at K = 1, a devil's staircase, there being a "plateau" for each rational value of ω.

For rational values of $\omega_c = p/q$, commensurate ground states are periodic configurations: $\sigma_{qp}(u_n) := (u_{n+q} - p) = (u_n)$. But there are also two MECs with average spacing (ω_c) that are nonrecurrent and called elementary "discommensurations" (DC). These can be described as a localized compression (retarded DC) or a localized expansion (advanced DC) over a commensurate ground state. The distortion being localized, they have the same mean energy per particle $\varepsilon(\omega_c)$ of the ground state. However, the difference of the non-averaged energy of a DC and the ground state (the extra energy of the localized compression or expansion) is generally nonzero; this is called the "creation energy" of the DC.

If a configuration contains two elementary DCs superimposed on a commensurate ground state, the energy difference with respect to the ground state can be understood as the sum of the creation energies of the DCs plus the interaction energy. If both DCs are of the same type, the energy decreases with the interdistance (repulsive interaction). The interaction is attractive for DCs of opposite type. Elementary DCs have an *excess length* Δ with respect to the ground state, which is exactly $\Delta = 1/q$ for an advanced DC and $\Delta = -1/q$ for a retarded one.

The creation energy of a DC varies linearly with the tension σ, the slope being the excess length Δ of the DC. Inside the corresponding commensurate plateau, the creation energy of an advanced DC increases with σ and disappears at the left edge σ^-_{C-IC} of the plateau, while the creation energy of the retarded DC decreases with σ, disappears at the right edge σ^+_{C-IC} (see Figure 4). Inside the commensurate plateau, the creation of an elementary DC is energetically costly, but right after either edge (σ^-_{C-IC} or σ^+_{C-IC}) is crossed, it becomes energetically advantageous to create as many DCs (of the correct type) as possible, were it not for the repulsive interaction between them that prevents condensation of an infinite number of DCs.

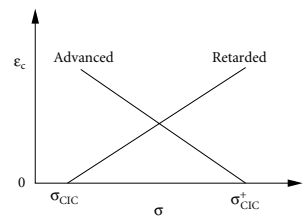

Figure 4. Creation energy ε_c of both types of elementary discommensurations for values of σ inside the tongue associated with a rational ω. At a certain critical value of σ this energy becomes negative and a commensurate–incommensurate transition occurs, changing the average spacing of the ground-state configuration.

The compromise between these two effects determines the density c of DCs, and, as each DC carries an excess length Δ, the average spacing of the new structure is $\omega = \omega_c + c\Delta$. For very small values of $|\sigma - \sigma_{C-IC}|$, where the interdistance (c^{-1}) is so large as to approximate a continuous variable, the scaling behavior of the ground-state average spacing ω in the commensurate-incommensurate transition is then

$$|\omega - \omega_c| \sim -(\ln|\sigma - \sigma_{C-IC}|)^{-1}. \quad (5)$$

For nonconvex interactions, the basis for an interpretation of the transitions between modulated phases in terms of interacting DCs is less rigorously supported. However, the central idea that the creation of localized defects or discommensurations drives these transitions and that the character (repulsive, attracting, or oscillatory) of their interaction determines the type of transition has been successfully applied, and undoubtedly it provides the most physical way of understanding why and how transitions between modulated phases occur. This fact adds to the many merits of the soliton paradigm in nonlinear science.

LUIS MARIO FLORÍA

See also **Aubry–Mather theory; Frenkel–Kontorova model; Ising model; Phase transitions**

Further Reading

Aubry, S. 1985. Structures incommensurables et brisure de la symmetrie de translation I [Incommensurate structures and the breaking of traslation simmetry I]. In *Structures et Instabilités*, edited by C. Godréche, Les Ulis: Editions de Physique, pp. 73–194

Cummins, H.Z. 1990. Experimental studies of structurally incommensurate crystal phases. *Physics Reports*, 185: 211–409

Griffiths, R.B. 1990. Frenkel–Kontorova models of commensurate–incommensurate phase transitions. In *Fundamental Problems in Statistical Mechanics VII*, edited by H. van Beijeren, Amsterdam: North-Holland, pp. 69–110

Janssen, T. & Janner, A. 1987. Incommensurability in crystals. *Advances in Physics*, 36: 519–624

Yeomans, J. 1988. The theory and application of axial Ising models. *Solid State Physics*, 41: 151–200

COMPACT SET

See **Topology**

COMPACTON

See **Solitons, types of**

COMPARTMENTAL MODELS

Compartmental models, which model the flow of material between components of a system, have been applied to the study of nutrient or energy flow in an ecosystem, to analyses of tracer kinetics in an organism, and to the theory of epidemics, among other applications.

The construction of a compartmental model is straightforward and intuitive, but the estimation of the associated parameters is not. The system is divided into homogeneous compartments, and the flow of "material" (meaning nutrients, energy, money, goods, electrons, radioactive tracers, information, etc.) between them is traced, keeping account of the level of material in each compartment. The compartments are represented by boxes and the flows are represented by arrows (see Figure 1).

This representation is a directed graph in which the compartments are vertices and the flows are arcs. To analyze a system, however, the model must be quantized by studying the rate of change of the level x_i of the ith compartment in time as

$$x_i = x_i(t). \quad (1)$$

The flow between the ith and jth compartment, designated f_{ij}, is a rate, measured in terms of quantity of material per unit time.

A differential equation describing the behavior of x_i may be obtained by equating the time rate of change of x_i to the difference between the flows coming in and those going out of the ith compartment. Thus,

$$\frac{dx_i}{dt} = \sum_k f_{ki} - \sum_j f_{ij}.$$
$$\text{rate of change} = \text{flows in} - \text{flows out} \quad (2)$$

The f_{ij} may be constant or variable in time and are usually functionally dependent on the x_i's.

A widely used assumption (particularly in physiology and medicine) is that

$$f_{ij} = a_{ij}x_i, \quad (3)$$

which corresponds to a certain fraction a_{ij} of the level of material x_i in compartment i passing to compartment j per unit time. In the ecological literature, this is often

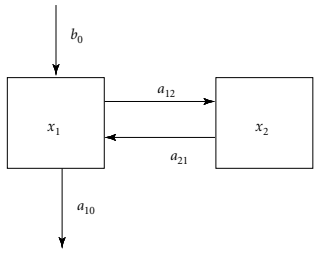

Figure 1. A compartmental model of tracer kinetics.

called donor-controlled flow. (The a_{ij} may be functions of time but are usually assumed to be independent of the x_is.)

Tracer Kinetics

Tracer kinetics refers to a technique for studying the flow of a drug or other material through a biological system (often a human body) near steady state. A small quantity of radioactive isotope or other recognizable form of the material (the tracer) is introduced, so that the tracer flows may be modeled by linear equations.

As a simple example, consider lipoprotein metabolism. One compartment corresponds to the blood plasma and the other corresponds to the extravascular space. A unit dose of tracer is injected into the blood and the flow follows the diagram in Figure 1. The quantity of interest is the flow out of compartment 1 (excretion), which cannot be measured directly, although the level of compartment 1 over time is known.

The differential equations are those obtained from (2) by taking the flow rates to be donor controlled; thus,

$$\begin{aligned} \mathrm{d}x_1/\mathrm{d}t &= -a_{10}x_1 - a_{12}x_1 + a_{21}x_2, \\ \mathrm{d}x_2/\mathrm{d}t &= a_{12}x_1 - a_{21}x_2, \end{aligned} \tag{4}$$

with initial conditions

$$x_1(0) = 1, \quad x_2(0) = 0. \tag{5}$$

These equations can be solved for $x_1(t)$ in terms of the three parameters a_{10}, a_{12}, a_{21}; since x_1 is known for all t, this result can be used to estimate these parameters by fitting a number of nonlinear equations.

General Differential Equations and Solutions

The differential equations for a system of n compartments can be written in vector form as

$$\mathrm{d}\boldsymbol{x}/\mathrm{d}t = A\boldsymbol{x} + \boldsymbol{f}, \tag{6}$$

where A is the matrix given by

$$A = \begin{bmatrix} a_{11} & a_{21} & \cdots & a_{n1} \\ a_{12} & a_{22} & \cdots & a_{n2} \\ \cdots & \cdots & \cdots & \cdots \\ a_{1n} & a_{2n} & \cdots & a_{nn} \end{bmatrix} \tag{7}$$

and $\mathbf{x} = [x_1, x_2, ..., x_n]^{\mathrm{T}}$ is the vector of levels of material in the n compartments and $\boldsymbol{f}$ is the input vector. The a_{ij} for $i \neq j$ are the flow rates, while the diagonal elements of A are

$$a_{ii} = -\sum_{j \pm i} a_{ij} - a_{i0}. \tag{8}$$

Although the input to a compartmental system is often to a single compartment, it may be distributed to input compartments. In general, we assume that the input to the system is $\boldsymbol{f} = B\boldsymbol{u}$, where $\boldsymbol{u}$ is a vector function distributed to the various compartments by B. Typically, B has one column but as many rows as there are compartments.

The outputs (measurements) of the system may be similarly combined. If the system is assumed donor to be controlled, the output will have the form

$$\boldsymbol{y} = C\boldsymbol{x}, \tag{9}$$

where the output of the compartments is directed to one or more measuring devices with measurements $\boldsymbol{y}(t)$. (Here, C is a general sampling matrix that is usually composed of 0s and 1s.)

The problem is then translated to the differential equation form

$$\begin{aligned} \frac{\mathrm{d}\mathbf{x}}{\mathrm{d}t} &= A\mathbf{x} + B\mathbf{u}, \\ \mathbf{y} &= C\mathbf{x}, \\ \mathbf{x}(0) &= \mathbf{0}. \end{aligned} \tag{10}$$

where we have assumed that the initial levels are $\mathbf{0}$. (This is no restriction as an initial value can be incorporated into $B\boldsymbol{u}$.) Solutions of the system are determined by matrices A, B, and C as

$$\mathbf{y}(t) = C\mathbf{x}(t) = C\int_0^t \mathrm{e}^{A(t-s)}B\mathbf{u}(s)\mathrm{d}s \tag{11}$$

where $\boldsymbol{x}(0) = 0$. Typically, however, the flow rates in the matrix A are unknown and must be determined from knowledge of $\mathbf{u}(t)$ and $\boldsymbol{y}(t)$, which is called the identification problem. A system is said to be identifiable if there is a unique solution to this problem, which is not always the case, and even if a solution does exist, it may be difficult to find.

Parameter Estimation

The problem of actually estimating the parameters of an identifiable problem is often an ill-posed problem, meaning that the estimated output may be close to the true output, while the parameters are still quite different from the true parameters. Moreover, such parameters are usually sensitive to slight perturbations of the data.

Suppose we are given a discrete set of observations/measurements made at times $t_i, i = 1, \ldots, m$ such that

$$y_i = y(t_i) + \varepsilon_i, \tag{12}$$

where ε_i are assumed to be independent normal random variables with mean 0 and constant variance. The standard approach to estimation is to solve for A in the least-squares sense

$$\min_{a_{ij}} \sum_i |y_i - y(t_i)|^2 \tag{13}$$

subject to the condition that A is a compartmental matrix of the appropriate model. (This is a nonlinear least-squares problem, since $y(t)$ is a linear combination of exponential functions.)

Another approach to estimation involves two stages; the data are first fitted to a sum of exponentials (Anderson, 1983)

$$g(t) = \sum_{k=1}^{n} c_k e^{\lambda_k t}. \tag{14}$$

In most nonpathological cases, the number of exponentials to be considered is the same as the size of the model. The estimates $\hat{c}_k$ and $\hat{\lambda}_k$ are obtained by least squares subject to $\lambda_k \leq 0$. Then, the Laplace transform of the fitted function $g(t)$ is compared with the Laplace transform of $y(t)$. As both are rational functions, the numerator and denominator are polynomials whose coefficients must be approximately equal.

There is also the method of peeling, which avoids least squares. This involves fitting an exponential function to the later data values. This corresponds to the eigenvalue of smallest magnitude. The difference between the data and this function is then used to approximate the second eigenvalue, and so on.

GILBERT G. WALTER

See also **Continuum approximations; Neural network models**

Further Reading

Anderson, D.H. 1983. *Compartmental Models and Tracer Kinetics,* Berlin and New York: Springer

Bellman, R.E. & Aström, K.J. 1970. On structural identifiability. *Mathematical Biosciences*, 7: 329–339

Dennis, J.E. & Schnabel, R. 1983. *Numerical Methods for Unconstrained Optimization and Nonlinear Equations*, Englewood Cliffs, NJ: Prentice-Hall

Godfrey, K. 1983. *Compartmental Models and Their Applications*, New York: Academic Press

Jacquez, S.A. 1996. *Compartmental Analysis in Biology and Medicine*, Ann Arbor: University of Michigan Press

Walter, E. 1987. *Identifiability of Parametric Models*, Oxford and New York: Pergamon

Walter, G.G. & Contreras, M. 1999. *Compartmental Modelling with Networks*, Boston: Birkhäuser

COMPLEX GINZBURG–LANDAU EQUATION

Ginzburg–Landau (GL) is a generic name for a class of basic models of nonlinear science, with a wide range of applications. They combine most fundamental features that underlie pattern formation in nonlinear media: dissipation (linear and nonlinear) and gain (provided by an intrinsic instability), conservative nonlinearity (accounting for wave mixing), and diffusion and/or dispersion (dependence of the dissipation rate and wave frequency on the wave number). Usually, the diffusion and dispersion are linear, but in more sophisticated models they may be both linear and nonlinear. In most cases, GL equations are local, but nonlocal (integral) generalizations are sometimes used. Both single GL equations and systems thereof play important roles as fundamental models.

The name of this class of equations first appeared in a seminal paper by Vitaly Ginzburg and Lev Landau (1950), which presented a phenomenological theory of superconductivity (V.L. Ginzburg was awarded the Nobel Prize in Physics in 2003 for this work.) In a standard form (Tinkham, 1996), these equations are

$$\begin{aligned} \eta\,(\partial_t + \mathrm{i}\kappa\phi)\,\psi &= -\left(\mathrm{i}\kappa^{-1}\nabla + \boldsymbol{A}\right)^2 \psi \\ &\quad + \left(1 - |\psi|^2\right)\psi, \qquad (1) \\ \boldsymbol{A}_t + \nabla\phi &= -\nabla\times(\nabla\times\boldsymbol{A}) + (2\mathrm{i}\kappa)^{-1} \\ &\quad \times\left(\psi^*\nabla\psi - \psi\nabla\psi^*\right) - |\psi|^2\boldsymbol{A} \\ &\quad + \nabla\times\boldsymbol{H}, \qquad (2) \end{aligned}$$

where ψ is the wave function of superconducting electrons, also known as the order parameter of the superconductivity, $\boldsymbol{A}$ and $\boldsymbol{H}$ are the vector potential of the intrinsic magnetic field and an externally applied field, ϕ is the electrostatic potential (related to $\boldsymbol{A}$ by an arbitrary gauge condition, e.g., $\phi_t + \nabla\cdot\boldsymbol{A} = 0$), η and κ are the dissipative and so-called GL parameters, ∇ is the gradient, and subscripts stand for the partial derivatives. A solution with $\psi = 0$ represents a normal state with no superconductivity. In their original work, Ginzburg and Landau (1950) introduced a time-independent version of the equations, while the full time-dependent system was proposed later.

In the modern theory of nonlinear pattern formation (Cross & Hohenberg, 1993), the name GL is applied to equations resembling Equation (1) [while there is usually no counterpart of Equation (2)], which govern the evolution of a physically or phenomenologically defined order parameter in a dynamical medium. For instance, in the case of chemical-reaction waves, the order parameter determines local concentrations of reactants (Ipsen et al., 2000); in applications to fluid mechanics, the velocity field is expressed in terms of the order parameter, and in numerous applications to optics the order parameter is a local amplitude of the electromagnetic field (Arecchi et al., 1999).

The first generic example of the GL equation of this type is the complex cubic GL (CCGL) equation ("cubic" refers to the nonlinearity), which is closest in its form to Equation (1), but the name "complex" stresses that its coefficients are complex:

$$\psi_t = g\psi + (a + \mathrm{i}b)\,\nabla^2\psi - (d + \mathrm{i}c)\,|\psi|^2\psi. \tag{3}$$

The first term on the right-hand side of Equation (3) accounts for the gain, provided that $g > 0$ (its imaginary part can be trivially removed), a and b are real coefficients accounting for the diffusion and

dispersion, while d and c are parameters controlling the nonlinear dissipation and frequency shift. Note that a and d must be positive, otherwise (3) is an ill-posed equation. In the case $|a| \ll |b|$, $|d| \ll |c|$, Equation (3) may be treated as a perturbed version of the nonlinear Schrödinger (NLS) equation.

In the case $b = c = 0$, Equation (3) is called a real GL equation, to stress that all its coefficients are real, although ψ remains complex. The real GL equation may be represented in the gradient form, $\psi_t = -\delta L\{\psi, \psi^*\}/\delta\psi^*$, where $\delta/\delta\psi^*$ stands for the functional derivative, and $\int \left(-|\psi|^2 + |\nabla\psi|^2 + (1/2)|\psi|^4\right) \mathrm{d}V$ is a real Lyapunov functional. A consequence of the gradient representation is that L may only decrease, $\mathrm{d}L/\mathrm{d}t \leq 0$. This fact simplifies the dynamics of the real GL equation.

A fundamental feature of Equation (3) is that its zero solution, $\psi = 0$, becomes unstable as the gain g changes its sign from negative to positive. In this case, a transition from the stable trivial solution to a nontrivial state is called *supercritical*. In particular, the supercritical transition in the one-dimensional (1-d) case yields a solitary-pulse (SP) solution that can be found in an exact analytical form,

$$u = A\,[\cosh(\kappa x)]^{-(1+\mathrm{i}\mu)} \exp(-\mathrm{i}\omega t), \tag{4}$$

where A, κ, μ, and ω are uniquely determined by parameters of Equation (3). If the CCGL equation reduces to a perturbed NLS equation, the SP (4) can be obtained from the NLS soliton by means of the perturbation theory, provided that $bc < 0$ (otherwise, the NLS equation does not have bright-soliton solutions). However, the SP solution (4) is always unstable because the zero background around it is unstable.

In many cases (for instance, in the case of thermal convection in a binary fluid), a nontrivial state may be excited by a finite-amplitude perturbation, while the trivial solution is stable against small perturbations. The simplest model that describes the corresponding *subcritical* transition to a nontrivial state is the cubic-quintic complex GL (CQCGL) equation, first proposed by Petviashvili and Sergeev (1984) as

$$\psi_t = -g\psi + (a + \mathrm{i}b)\nabla^2\psi + (d - \mathrm{i}c)|\psi|^2\psi - (f + \mathrm{i}h)|\psi|^4\psi. \tag{5}$$

Here, $g > 0$ implies stability of the zero solution, the last term with $f > 0$ guarantees overall stabilization of the system, the coefficient h accounts for a quintic nonlinear correction to the wave frequency, while $d > 0$ provides for a possibility of *nonlinear* gain. The CQCGL equation may give rise to nontrivial states, coexisting with the stable zero solution, if the nonlinear gain coefficient exceeds a value $d_{\min} = 2\sqrt{gf}$. An important result, obtained by means of analytical and numerical methods, is that the 1-d and 2-d versions of the CQCGL equation support SP solutions that may be *stable* (in the 2-d case, the localized pulse may carry vorticity, having a spiral structure). If all the parameters g, a, d, f, and h are small, the 1-d pulse can be constructed on the basis of the NLS soliton by means of the perturbation theory. However, the CQCGL equation does not make it possible to find stable SP solutions in an exact analytical form (one exact solution for a 1-d SP is known, but it is always unstable).

Patterns in nonlinear dissipative media may be supported not only by intrinsic gain; another possibility is to apply an external field, which is, for instance, the case for the pattern formation in laser cavities (Arecchi et al., 1999). In this case, the appropriate CCGL equation is

$$\psi_t = -g\psi + (a + \mathrm{i}b)\nabla^2\psi - (d + \mathrm{i}c)|\psi|^2\psi + P, \tag{6}$$

where the driving term, induced by the external field, may be of two different types: direct drive, $P = \varepsilon$, or parametric drive, $P = -\mathrm{i}\omega_0\psi + \varepsilon\psi^*$, where the asterisk stands for complex conjugation, ω_0 fixes the frequency, and ε is the drive's amplitude. Equation (6) with either type of drive can support stable SPs in 1-d and 2-d cases (in the case of the direct drive, SP settles on a nonzero background).

An important generalization is to consider systems of coupled GL equations. These may describe counter-propagating waves (for instance, in thermal convection in a binary-fluid layer), or second-harmonic generation in a lossy medium. In the latter case, the nonlinearity is not cubic, but *quadratic*, viz., $\psi_1^*\psi_2$ in the equation for the fundamental-frequency field ψ_1, and ψ_1^2 in the equation for the second-harmonic field ψ_2.

An alternative to the CQCGL equation is a system originating in nonlinear optics, in which the stability of the zero solution is provided by an extra linear equation,

$$\begin{aligned} \psi_t &= g\psi + (a + \mathrm{i}b)\nabla^2\psi - (d + \mathrm{i}c)|\psi|^2\psi - \mathrm{i}\kappa\chi, \\ \chi_t &= -G\chi - \mathrm{i}\kappa\psi, \end{aligned} \tag{7}$$

where κ is a real coupling constant, and $G > 0$ is the loss coefficient in the additional equation. The zero solution in this system is stable if the loss in the second equation and coupling are strong enough, $G > g$ and $\kappa^2 > Gg$. System (7) has exact SP solutions, in which both fields ψ and χ take the form (4) (with different amplitudes), but, in contrast to the CCGL equation proper, in this case the pulse may be *stable* (Atai & Malomed, 1998).

Yet another type of a system occurs if, due to a specific nature of the underlying physical problem, the complex order parameter ψ is coupled to an extra real-order parameter ϕ, which accounts for the existence of a conserved quantity in the medium (Matthews & Cox, 2000): $\psi_t = \psi + \nabla^2\psi - |\psi|^2\psi - \phi\psi$, $\phi_t = \nabla^2\left[\sigma\phi + \mu\left(|\psi|^2\right)\right]$. In this simplest version of the system, $\sigma > 0$ and μ are real constants.

A common feature of the various GL equations displayed above is their universality. Each is a generic representative of a class of models with given qualitative properties (for instance, super- or subcritical character of the excitation of nontrivial states, and the absence or presence of a conserved quantity). In more specific situations, there arise generic equations of other types. In particular, the complex Swift–Hohenberg (SH) equation describes a situation (for instance, in Rayleigh–Bénard convection) when the instability of the zero solutions appears at a finite wave number k_0 of small perturbations; thus,

$$\psi_t = g\psi - (a+\mathrm{i}b)\left(\nabla^2+k_0^2\right)^2\psi - (d+\mathrm{i}c)\,|\psi|^2\psi \quad (8)$$

with $g, a, d > 0$. Quasi-1-d solutions of Equation (8) can be looked for as $\psi(x, y, t) = \Psi(x, y, t)\exp(\mathrm{i}k_0 x)$, where Ψ is a slowly varying function, whose x- and y-dependences are characterized by large scales $X, Y \gg k_0^{-1}$. An asymptotic consideration is then consistent in the case $X \sim Y^2$, reducing the SH equation (8) to an anisotropic complex Newell–Whitehead–Segel equation, $\Psi_t = g\Psi + (a+\mathrm{i}b)\left(2i\partial_x + \partial_y^2\right)^2\Psi - (d+\mathrm{i}c)\,|\Psi|^2\Psi$.

GL equations generate rich dynamics. The simplest exact solutions are plane waves (PWs). In the case of the CCGL equation (3) (here, it is set by rescaling $g = a = d \equiv 1$), a family of PWs is

$$\psi = A\exp(\mathrm{i}Qx - \mathrm{i}\omega t),\ A = \sqrt{1-Q^2},\quad \omega = c + (b-c)Q^2, \quad (9)$$

where Q is a wave number (a parameter of the solution family) taking values $-1 < Q < +1$. Note that the group velocity of this PW is $\mathrm{d}\omega/\mathrm{d}Q = 2(b-c)Q$.

The CQCGL equation gives rise to two different PWs for given Q, with amplitudes $A_\pm = (2f)^{-1} \times \left[1 \pm \sqrt{1-4f\left(1+Q^2\right)}\right]$ (under the same normalization $g = a = d \equiv 1$). This solution exists in the interval $Q^2 < (4f)^{-1}(1-4f)$, and only A_+ may correspond to a stable PW.

The stability of PWs is an important issue. In the CCGL equation, a condition for stability against long-wave perturbations with a large wavelength takes a simple form, $Q^2 < (1+bc)/\left(3+2c^2+bc\right)$, which is called a generalized Eckhaus stability criterion (the original Eckhaus criterion, which applies to the real GL equation with $b = c = 0$, is $Q^2 < 1/3$). Obviously, this criterion cannot hold unless $1 + bc > 0$ (the Benjamin–Feir–Newell (BFN) condition). The consideration of finite-wavelength perturbations gives rise to more complex stability conditions. Therefore, following Aranson and Kramer (2002), the structure of a full stability region for the PWs can be shown by means of its cross sections in the space (b, c, Q); see Figure 1. The figure makes a distinction between convective and absolute instabilities, when, respectively, the growing perturbation is traveling away or staying put. The transition from the 1-d CCGL equation to its multidimensional counterpart does not import extra instabilities to the PWs.

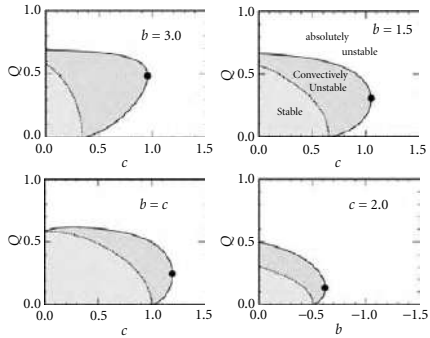

Figure 1. A set of cross sections of the stability region for the plane-wave solutions (9) of the cubic complex GL equation (3) in the space $(b, c, |Q|)$. The two top panels, the left bottom panel, and the right bottom panel show, respectively, the cross sections $b = \text{const}$, $b = -c$, and $c = \text{const}$. The filled circles mark turning points on the border between absolute and convective instabilities.

If the BFN combination $1 + bc$ becomes negative, the PW develops phase turbulence, which means that $|\psi|$ remains roughly constant, while the phase of the complex phase ψ demonstrates spatiotemporal chaos. In the 1-d case, close to the BFN instability threshold, the chaotic evolution of the phase gradient $p \equiv \phi_x$ obeys the Kuramoto–Sivashinsky equation, which, in a rescaled form, is $p_t + p_{xx} + p_{xxxx} + pp_x = 0$. Deeper into the instability region, phase-slip points (PSPs) arise, at which the amplitude $|\psi|$ disappears. Multiple creation of PSPs leads to a transition from the phase turbulence to defect turbulence, which is distinguished by random dynamics of the PSP ensemble. Mixed turbulence at the border between these two types also occurs (Aranson & Kramer, 2002).

In the case when PWs are stable, shock waves can be generated by collision between two PWs (9) with different wave numbers Q_1 and Q_2. Although exact solutions for shocks are not available, they can be obtained in an approximate form, provided that $Q_1 - Q_2$ is small, or the coefficients b and c are small. In particular, a transient layer between the two PWs moves at the velocity $v = (b-c)(Q_1+Q_2)$, which is exactly the mean of the group velocities of the colliding PWs. In the 2-d case, PWs can collide obliquely; in this case, shocks take the form of a domain wall. Generally, the shocks are stable.

Besides the shocks (which are sources that emit PWs), the 1-d CCGL equation also gives rise to sinks,

that is, localized hole-type structures that absorb PWs. If the CCGL equation (3) is a perturbed version of the NLS equation, sinks can be constructed as perturbed counterparts of NLS dark solitons, provided that $bc > 0$ (particular solutions for the sinks are available in an exact analytical form). A standing sink is actually a PSP, as $|\psi|$ vanishes at its center, and it may be dynamically stable. A moving sink is a finite dip in the profile of $|\psi|$; it is structurally unstable, as it is either decelerated (turning into a standing sink) or accelerated (eventually vanishing) by a quintic term added to the CCGL equation (Lega, 2001; Aranson & Kramer, 2002).

The 2-d CCGL equation displays spiral waves (SWs) in the form $\psi = A(r)\,\exp(\mathrm{i}N\theta - \mathrm{i}\omega t)$, where r and θ are the polar coordinates, N is an integer vorticity, and $A(r)$ is a complex function. An asymptotic form of the SW is $A(r) \approx \sqrt{1-Q^2}\exp(\mathrm{i}Qr)$ at $r \to \infty$, where Q is related to ω as in Equation (9), and $A(r) \sim r^N$ at $r \to 0$. (In the case of the real GL equation, the SW has $Q = 0$, which corresponds to a *vortex* solution. Similar solutions are generated by Equations (1) and (2), which represent *Abrikosov vortices* in superconductivity. For the prediction of these vortices, A.A. Abrikosov shared the Nobel Prize for Physics in 2003.) The asymptotic wave number Q is an eigenvalue of the 2-d CCGL equation, as it is uniquely selected by parameters of the equation. All the SWs with $N > 1$ are unstable. The SW with $N = 1$ may be subject to specific instabilities localized near its core (Aranson & Kramer, 2002).

An extension of the SW is a vortex line in three dimensions, which, in particular, may be closed into a ring. A vortex line with an additional wave number directed along its axis (twisted vortex) is also possible. The dynamics of 3-d vortex lines are quite complicated (Aranson & Kramer, 2002).

BORIS MALOMED

See also **Nonlinear Schrödinger equations; Partial differential equations, nonlinear; Pattern formation; Spatiotemporal chaos; Superconductivity**

Further Reading

Aranson, I.S. & Kramer, L. 2002. The world of the complex Ginzburg–Landau equation. *Reviews of Modern Physics*, 74: 99–143

Arecchi, F.T., Boccaletti, S. & Ramazza, P. 1999. Pattern formation and competition in nonlinear optics. *Physics Reports*, 318: 1–83

Atai, J. & Malomed, B.A. 1998. Exact stable pulses in asymmetric linearly coupled Ginzburg–Landau equations. *Physics Letters* A, 246: 412–422

Cross, M.C. & Hohenberg, P.C. 1993. Pattern-formation outside of equilibrium. *Reviews of Modern Physics*, 65: 851–1112

Ginzburg V.L. & Landau, L.D. 1950. On the theory of superconductivity. *Zhurnal Eksperimentalnoy i Teoreticheskoy Fiziki (USSR)*, 20: 1064–1082 (in Russian) [English translation: in *Men of Physics*, vol. 1. 1965. Oxford: Pergamon Press, pp. 138–167]

Ipsen, M., Kramer, L. & Sorensen, P.G. 2000. Amplitude equations for description of chemical reaction-diffusion systems. *Physics Reports*, 337: 193–235

Lega, J. 2001. Traveling hole solutions of the complex Ginzburg–Landau equation: a review. *Physica* D, 152: 269–287

Matthews, P.C. & Cox, S.M. 2000. Pattern formation with a conservation law. *Nonlinearity*, 13: 1293–1320

Petviashvili, V.I. & Sergeev, A.M. 1984. Spiral solitons in active media with an excitation threshold. *Doklady Akademii Nauk SSSR*, 276: 1380–1384 (in Russian)

Tinkham, M. 1996. *Introduction to Superconductivity*. New York: McGraw-Hill

COMPLEXITY, MEASURES OF

See **Algorithmic complexity**

CONDENSATES

See **Bose–Einstein condensation**

CONLEY INDEX

In a five-page paper published in the Proceedings of the 1970 International Congress of Mathematicians (Conley, 1971), Charles Conley gave the first definition of his index. For context, he chose the phase space to be a compact connected metric space X and F to be the space of flows on X with the compact open topology. (A flow is a continuous function such that $f(x,0) = x$, $f(x, t+s) = f(f(x,t), s)$ for all choices of x, t, s.)

For a compact subset Y of X define the set $\mathrm{Inv}(Y, f) = \{y \in Y : f(y,t) \in Y \text{ for all } t\}$. This set is the maximal invariant set contained in Y. An isolating neighborhood for a flow f is a compact subset N of X such that $\mathrm{Inv}(N, f)$ is contained in the interior of N. The set, $\mathrm{Inv}(N, f)$, is the isolated invariant set associated with N.

It is easy to show that isolating neighborhoods persist. If N is an isolating neighborhood for f, then there exists a neighborhood U of f in F such that N is an isolating neighborhood for every flow g in U. Suppose that M is an isolating neighborhood for g. If $\mathrm{Inv}(M, g) = \mathrm{Inv}(N, g)$ then the isolated invariant set $\mathrm{Inv}(M, g)$ is said to be a local continuation of the set $\mathrm{Inv}(N, f)$. Two invariant sets $\mathrm{Inv}(N, f)$ and $\mathrm{Inv}(M, g)$ are related by continuation if there is a finite sequence of local continuations linking one to the other.

For a flow f and an arbitrary compact subset W of X, one defines forward and backward exit time functions from W into the extended real line $[-\infty, \infty]$ as follows:

$$t^+(x) = \sup\{t \geq 0 : f(x, [0,t]) \subset W\},$$
$$t^-(x) = \inf\{t \leq 0 : f(x, [t,0]) \subset W\}.$$

Certain subsets of W are associated with these functions. The forward asymptotic set is the set $A^+ = \{x : t^+(x) = \infty\}$, and the backward asymptotic

set is the set $A^- = \{x : t^-(x) = -\infty\}$. Note that the maximal invariant set $\mathrm{Inv}(W, f)$ is the set $A^+ \cap A^-$. Forward and backward exit sets are the sets $W^\pm = \{x : t^\pm(x) = 0\}$.

An isolating block B for a flow f is a special type of isolating neighborhood with the following property. The boundary of B is the union of the exit sets B^+ and B^-. The intersection of these sets is the "tangency" set τ of boundary points that immediately exit in both time directions. Thus, a block has no internal tangencies where an orbit comes to the boundary from inside the block and does not exit.

If B is an isolating block for a flow f, one can show that the exit time functions are continuous. Using these functions and the flow, one may define deformation retractions of $B - A^+$ onto B^- and $B - A^-$ onto B^+. For example, a retraction r of $B - A^-$ onto B^+ is defined by the formula $r(x) = f(x, t^+(x))$ (This property was first used by Wazewski (1954).)

Suppose that f is a flow on R^3 and also that T is a solid torus that is an isolating block for the flow. Suppose that the exit set is a disk D on the boundary of T. Then, the invariant set $\mathrm{Inv}(T, f)$ must not be empty. If it were empty, one could define a deformation retraction of T onto D, which is impossible.

Under these definitions, the following theorem is fundamental (Conley & Easton, 1971). Given an isolating neighborhood N for a flow f, there exists an isolating block B contained in N such that $\mathrm{Inv}(N, f) = \mathrm{Inv}(B, f)$.

We use this theorem to define the Conley index of the set $\mathrm{Inv}(N, f)$ to be the homotopy types of the pair of quotient spaces $[B/B^+]$ and $[B/B^-]$. These spaces are obtained by collapsing the exit sets to points and using the quotient topology on the resulting spaces.

Consider, for example, the flow f defined on R^2 by $f((x, y), t) = (\mathrm{e}^{-t}x, \mathrm{e}^t y)$. This flow has the origin as a saddle point. Let B be a square centered at the origin. Then B is an isolating block for the flow. The exit set consists of the top and bottom sides of B. The quotient space $[B/B^-]$ has the homotopy type of the pair of spaces consisting of a circle and a point on this circle.

The Conley Index has the following properties (Conley, 1978; Herman et al., 1988; Smoller, 1983; Easton, 1998; Hofer & Zehnder, 1995; Mischaikow, 2002):

(i) The Conley index is well defined. Thus it is independent of the choice of block B.
(ii) If $\mathrm{Inv}(N, f)$ and $\mathrm{Inv}(M, g)$ are two isolated invariant sets that are related by continuation, then they have the same Conley index.
(iii) The index $[B/B^-]$ of a saddle point for a smooth flow on a manifold is a sphere together with a point on the sphere. The sphere has the same dimension as that of the unstable manifold of the saddle point. Thus, the Conley index is a generalization of the Morse index of a saddle point.
(iv) The index of two disjoint isolated invariant sets is the "sum" or "join" of their indices.

Traveling Waves

One of the early applications of the Conley index was to find traveling waves for reaction-diffusion equations (Smoller, 1983). We will use as an example the FitzHugh–Nagumo (FN) equations $u_t = \varepsilon v$, $v_t = v_{xx} + f(v) - u$, which are a simplification of the Hodgkin–Huxley equations used to model nerve impulses. The parameter ε is assumed to be small, and one seeks a solution of the form $U(x, t) = u(s)$, $V(x, t) = v(s)$, where $s = x + \theta t$ and θ is the wave velocity.

Substituting the trial solutions into the FN equations, one obtains the following system of ordinary differential equations: $\mathrm{d}u/\mathrm{d}s = (\varepsilon/\theta)v$, $\theta\,\mathrm{d}v/\mathrm{d}s = \mathrm{d}^2v/\mathrm{d}s^2 + f(v) - u$, where $f(v)$ is assumed have the general shape of a cubic equation that is decreasing, increasing, and then decreasing. To be specific, we take $f(v) = -v(v-1)(v-2)$. The corresponding first-order system of ordinary differential equations is $u' = \sigma v$, $v' = w$, $w' = \theta w + u - f(v)$, where $\sigma = \varepsilon/\theta$. Our goal is to find a periodic solution of this system for small values of the parameters sigma and theta, and thereby to find a periodic solution of the FN equations.

One can completely understand the phase portrait of system when the parameters σ and θ are set to zero. In this case, $u(t)$ is constant and the equations for v, w form a Hamiltonian system with Hamiltonian $H(v, w) = w^2/2 + F(v) - uv$ with $F(v) = \int_0^u f(r)\mathrm{d}r = -v^2(v-2)^2/4$. The phase portrait in the $u = 0$ plane has saddle points at $(v, w) = (0, 0)$, $(v, w) = (2, 0)$ and a center at $(v, w) = (1, 0)$. The saddle points are connected by heteroclinic orbits implicitly defined by the equation $H(v, w) = 0$, $0 < v < 2$. Note that the set of equilibrium points for the system is the set $\{(u, v, w) : u = f(v), w = 0\}$.

Next consider the system with $\sigma = 0$, $\theta > 0$. For this system, we have $(d/dt)H(u(t), v(t), w(t)) = \theta w^2(t)$. Let $a(u) < b(u) < c(u)$ denote the three solutions of the cubic equation $u - f(u) = 0$. One can show that there are values $0 < u_1 < u_2$ such that for $j = 1, 2$, there is a heteroclinic solution joining the equilibrium points $(u_j, a(u_j), 0)$ and $(u_j, c(u_j), 0)$ in the plane $u = u_j$. We now have a cycle consisting of the two heteroclinic orbits together with arcs of equilibrium points $\{(u, a(u), 0) : u_1 < u < u_2\}$ and $\{(u, c(u), 0) : u_1 < u < u_2\}$. This cycle is an invariant set for the system. However, the cycle is not isolated since it intersects the set of equilibrium points in two arcs. The two arcs of equilibrium points may be viewed as normally hyperbolic invariant manifolds, whose stable

and unstable manifolds intersect transversally along the two heteroclinic orbits.

Finally, consider the system for small positive values of sigma. In this case, u is increasing when u is positive and decreasing when negative. The hard part is to construct an isolating block, which topologically is a solid torus containing the cycle. The transversal intersection noted above is essential to this construction. The cycle is no longer invariant when sigma is positive. However, one shows that the isolating block must contain a periodic solution of the full system of equations. The periodic solution thus constructed may be viewed as a periodic traveling wave solution of the FN equations.

Applications to Discrete Dynamical Systems

Consider the discrete dynamics generated by iterating a homeomorphism f of a compact metric space X. It is natural to study orbits with "errors" such as truncation or round-off errors in numerical algorithms. Thus, an ε-chain for f is a finite sequence $(y_0, y_1, y_2, \ldots)$ such that $d(f(y_n), y_{n+1}) \leq \varepsilon$ where $d(x, y)$ is the distance function on X. Conley (1978) and Bowen (1975) both understood the importance of studying orbits with errors. Bowen asked when such an orbit could be shadowed by a true orbit of the system.

Conley defined the ε-chain recurrent set $\mathrm{CR}(f, \varepsilon)$ to be the set of points that are contained in periodic ε-chains of length at least 2. The chain recurrent set is the set $\mathrm{CR}(f) = \cap \{\mathrm{CR}(f, \varepsilon) : \varepsilon > 0\}$. Points in $\mathrm{CR}(f)$ are chain equivalent if for any positive epsilon there is a periodic ε-chain containing both points. He showed that every orbit uniformly approaches a unique chain equivalence class in $\mathrm{CR}(f)$. This result is known as the Conley decomposition theorem, and it generalizes Smale's decomposition of an Axiom A system into basic sets (Bowen, 1975).

An isolating block for f is a compact subset N of X such that whenever x, $f(x)$, $f^2(x) \in N$, then $f(x)$ is contained in the interior of N. This is something like having no internal tangencies. The exit set of N is the set $E = \{x \in N : f(x) \ni \mathrm{int}(N)\}$. Because N is a block, the exit set is compact. Define an equivalence relation on N making all points of E equivalent and all points not in E equivalent only to themselves. Let $N^{\#}$ denote the space of equivalence classes with the quotient topology obtained by projecting N onto $N^{\#}$ by sending a point to the equivalence class to which it belongs. Let $E^{\#}$ denote the image of E. The index space of N is the pair $(N^{\#}, E^{\#})$. Define an index map $f^{\#} : N^{\#} \to N^{\#}$ by $f^{\#}(x) = E^{\#}$ if $x = E^{\#}$ or $f(x) \in E^{\#}$. Otherwise, define $f^{\#}(x) = f(x)$. Note that the index map is continuous. The pair $(N^{\#}, f^{\#})$ plays the role of the Conley index in this context. If the index map is not homotopic to a constant, then one can prove that the set $\mathrm{Inv}(N, f)$ is non-empty.

Smale's horseshoe map in the plane may be used as an example. Suppose that a rectangle B is mapped across itself so that the image crosses the rectangle in a horizontal strip, then curves back and crosses the rectangle again in another horizontal strip above the first. In this case, the exit set consists of three vertical strips, one in the center of the rectangle and the other two on the left and right sides containing the vertical edges of B. The index space $[B/B^{-}]$ has the homotopy type of a figure of eight and the index map is non-trivial.

Sequences of compact sets (called "windows") may sometimes be constructed to contain an orbit with errors. If each window in the sequence is "correctly" mapped across the next one, then a true orbit runs through the sequence of windows and shadows the orbit with errors (Easton, 1998).

ROBERT W. EASTON

See also **Anosov and Axiom-A systems; FitzHugh–Nagumo equation; Horseshoes and hyperbolicity in dynamical systems**

Further Reading

Bowen, R. 1975. *Equilibrium States and the Ergodic Theory of Anosov Diffeomorphisms*, New York: Springer

Conley, C.C. 1971. On the continuation of invariant sets of a flow. In *Proceedings of the International Congress of Mathematicians 1970*, Paris: Gauthiers-Villars, pp. 909–913

Conley, C.C. & Easton, R.W. 1971. Isolated invariant sets and isolating blocks. *Transactions of the American Mathematical Society* 158: 35–61

Conley, C.C. 1978. *Isolated Invariant Sets and the Morse Index*, Providence, RI: American Mathematical Society.

Easton, R. 1998. *Geometric Methods for Discrete Dynamical Systems*, Oxford and New York: Oxford University Press.

Herman, M., McGehee, R., Moser, J. & Zehnder, E. (editors). 1988. Charles Conley Memorial Volume, Special Issue of *Ergodic Theory and Dynamical Systems*, 8

Hofer, H. & Zehnder, E. 1995. Symplectic invariants and Hamiltonian dynamics. *The Floer Memorial Volume Progress in Mathematics*, vol. 133, Basel: Birkhäuser.

Mischaikow, K. 2002. Topological techniques for efficient rigorous computations in dynamics, *Acta Numerica*,vol. 11, 435–477

Smoller, J. 1983. *Shock Waves and Reaction-diffusion Equations*, New York: Springer.

Wazewski, T. 1954. Sur un principe topologique de l'examen de l'allure asymptotique des integrales des equations differentielles, *Proceedings of the International Congress of Mathematicians*, vol. 3, 132–139

CONSTANTS OF MOTION AND CONSERVATION LAWS

Although nonlinear spatiotemporal processes may be very complicated, they frequently obey simple constraints in the form of conservation laws. It is sometimes possible to construct one or several constants of motion (also called dynamical invariants, DIs), in the form of spatial integrals of local densities expressed in terms

of the physical fields and their derivatives, which are conserved in time, as a consequence of the underlying dynamics. Such commonly known conserved quantities as energy, momentum, and angular momentum belong to this class.

Typically, the existence of conservation laws can be established if the underlying dynamics is dissipation-free; however, a specific DI may sometimes also exist in dissipative systems. Examples of the latter are provided by the diffusion equation, $u_t = u_{xx}$, and its important nonlinear counterparts in the form of the Burgers equation,

$$u_t = u_{xx} + uu_x, \tag{1}$$

and Cahn–Hilliard equation,

$$u_t + \left(u - u^3 + u_{xx}\right)_{xx} = 0 \tag{2}$$

(the subscripts stand for the partial derivatives). They all conserve $\int_{-\infty}^{+\infty} u(x,t)\mathrm{d}x$, which is simply the total mass of the substance in the case of diffusion.

A more sophisticated example of the "dissipative conservation" occurs in physically important models based on the nonlinear Schrödinger (NLS) equation with special additional terms:

$$\mathrm{i}u_t + u_{xx} + F'(|u|^2)u = \varepsilon Q, \tag{3}$$

where the function F' describes conservative nonlinearity of the medium (the prime stands for the derivative with respect to the argument of F; in particular, $F = \left(|u|^2\right)^2$ corresponds to the most generic case of the cubic NLS equation), ε is a real parameter, and the "special perturbation" is, for instance, the nonlinear Landau-damping term in the NLS equation for Langmuir waves in plasmas,

$$Q = -u\int_{-\infty}^{+\infty} \mathrm{d}x' \left(x - x'\right)^{-1} |u(x')|^2, \tag{4}$$

or the stimulated Raman scattering term in the equation for electromagnetic waves in nonlinear optical fibers, $Q = \left(|u|^2\right)_x u$. While these terms are dissipative ones, the corresponding perturbed NLS equation conserves the single DI, namely, the total *wave action* (alias "number of quanta"),

$$N = \int_{-\infty}^{+\infty} |u(x,t)|^2 \mathrm{d}x. \tag{5}$$

In the general case, equations that govern the dissipation-free spatiotemporal dynamics can be derived from the underlying action functional $S\left\{u^{(n)}\right\}$: $\delta S/\delta u^{(n)} = 0$, where $u^{(n)}(\boldsymbol{r},t)$ is the nth field variable, $\boldsymbol{r}$ is the set of the spatial coordinates, $\delta/\delta u^{(n)}$ stands for the variational (functional) derivative, and the action is expressed in terms of the Lagrangian density $\mathcal{L}$, so that

$$S = \int\int \mathcal{L}\left(u^{(n)}, \nabla u^{(n)}, u_t^{(n)}\right) \mathrm{d}\boldsymbol{r}\mathrm{d}t. \tag{6}$$

For instance, the density

$$\mathcal{L} = (1/2)\left[u_t^2 - (\nabla u)^2\right] - F(u) \tag{7}$$

yields a nonlinear Klein–Gordon (NKG) equation for a single real field u,

$$u_{tt} - \nabla^2 u + F'(u) = 0. \tag{8}$$

The fundamental nature of DIs in Lagrangian systems is established by a theorem that was published by Emmy Noether in 1918: any *continuous symmetry* of the system, that is a family of transformations of the field variables, spatial coordinates, and time, which depend on an arbitrary continuous parameter ξ and leave the action invariant, generates a constant of motion. If the infinitesimal symmetry transformation is written in the form

$$u^{(n)} \to u^{(n)} + U_n\,\mathrm{d}\xi,\ \boldsymbol{r} \to \boldsymbol{r} + \boldsymbol{R}\,\mathrm{d}\xi,$$
$$t \to t + T\,\mathrm{d}\xi, \tag{9}$$

then the main result following from the Noether theorem is the continuity equation $\mathcal{I}_t + \nabla\cdot\boldsymbol{J} = 0$, with the following density and current:

$$\mathcal{I} = \sum_n \frac{\partial\mathcal{L}}{\partial\left(u_t^{(n)}\right)}\left(\boldsymbol{R}\cdot\nabla u^{(n)} + Tu_t^{(n)} - U_n\right) + T\mathcal{L}, \tag{10}$$

$$\boldsymbol{J} = \sum_n \frac{\partial\mathcal{L}}{\partial\left(\nabla u^{(n)}\right)}\left(\boldsymbol{R}\cdot\nabla u^{(n)} + Tu_t^{(n)} - U_n\right) + \boldsymbol{R}\mathcal{L}, \tag{11}$$

$\left(\partial/\partial\left(\nabla u^{(n)}\right)\right.$ is realized as a vector with the components $\partial/\partial\left(u_x^{(n)}\right)$, $\partial/\partial\left(u_y^{(n)}\right)$, $\left.\partial/\partial\left(u_z^{(n)}\right)\right)$. Then, assuming, as usual, that the fields disappear at $|\boldsymbol{r}|\to\infty$, the continuity equation immediately yields the conservation law in the form of $\mathrm{d}I/\mathrm{d}t = 0$, with $I \equiv \int \mathcal{I}\,\mathrm{d}\boldsymbol{r}$. A detailed derivation of this fundamental result can be found in the book by Bogoliubov & Shirkov (1973); for discussion of the Noether theorem in various contexts, see also Sulem & Sulem (1999), and Whitham (1974) If the underlying equations are complex, the Lagrangian density and all the DIs are nevertheless real.

The obvious invariance of the action against arbitrary temporal and spatial shifts, which are described by Equation (9) with $U_n = 0$ and, respectively, $\boldsymbol{R} = 0$, $T = 1$, or $\boldsymbol{R}_j = \boldsymbol{e}_j$, $T = 0$ ($\boldsymbol{e}_j$ is the unit vector corresponding to the jth spatial coordinate) gives rise

to the conservation of the energy (Hamiltonian) H and momentum $\boldsymbol{P}$. For the important classes of the NKG and multidimensional NLS, Equations (8) and (3), Equation (10) yields

$$H_{\mathrm{NKG}} = \int \left[\frac{1}{2}\left(u_t^2 + (\nabla u)^2\right) + F(u)\right] \mathrm{d}\boldsymbol{r},$$

$$\boldsymbol{P}_{\mathrm{NKG}} = -\int u_t \nabla u \ \mathrm{d}\boldsymbol{r}, \tag{12}$$

$$H_{\mathrm{NLS}} = \int \left[|\nabla u|^2 - F(|u|^2)\right] \mathrm{d}\boldsymbol{r},$$

$$\boldsymbol{P}_{\mathrm{NLS}} = \mathrm{i}\int \left(u\nabla u^* - u^*\nabla u\right) \mathrm{d}\boldsymbol{r}, \tag{13}$$

where * stands for the complex conjugation (the transition from the Lagrangian to Hamiltonian density as per Equation (10) in the case of the temporal-shift invariance is called the Legendre transformation). The invariance against rotations in the three-dimensional space leads to the conservation of the angular momentum,

$$\boldsymbol{M} = \int (\boldsymbol{r} \times \mathcal{P}) \ \mathrm{d}\boldsymbol{r}, \tag{14}$$

where $\mathcal{P}$ is the density in the expressions for the momentum in Equations (12)–(14); in the two-dimensional case, there is only one component of the conserved angular momentum. Additionally, in the NLS-type equations, the invariance against the phase shift (alias *gauge invariance*), $u \to u \exp(\mathrm{i}\xi)$ with an arbitrary constant ξ, generates the conservation of the above-mentioned wave action (5), which is $\int |u|^2 \, \mathrm{d}\boldsymbol{r}$ in the multidimensional case.

Another important class of models in one dimension is based on equations of the Korteweg–de Vries (KdV) type for a real function $u(x, t)$,

$$u_t + u_{xxx} + F''(u)u_x = 0 \tag{15}$$

(the most important cases of the KdV equation proper and modified KdV equation correspond to $F = u^3$ and $F = u^4$, respectively). The Lagrangian representation of Equation (15) is possible in terms of the potential field v, defined so that $v_x \equiv u$, but the Hamiltonian and momentum are expressed solely in terms of the original field u,

$$H_{\mathrm{KdV}} = \int_{-\infty}^{+\infty} \left[\frac{1}{2}u_x^2 - F(u)\right] \mathrm{d}x,$$

$$P_{\mathrm{KdV}} = \int_{-\infty}^{+\infty} u^2 \, \mathrm{d}x. \tag{16}$$

The invariance of the action, written in terms of the potential v, against the arbitrary shift $v \to v + \xi$ additionally generates the conservation of the "mass," $\int_{-\infty}^{+\infty} u \, \mathrm{d}x$.

Besides being a dynamical invariant, the Hamiltonian gives rise to a canonical representation of the equation(s) in the Hamiltonian form, which is dual to the Lagrangian representation. In particular, for the complex and real equations of the NLS and KdV types, respectively, this representation is

$$u_t = -\mathrm{i}\frac{\delta H}{\delta u^*}, \quad u_t = \frac{\partial}{\partial x}\frac{\delta H}{\delta u}. \tag{17}$$

The conservation of H itself and the conservation of the mass in the KdV-type equations are immediate consequences of the general form of Equations (17). The conservation of the wave action in the NLS-type equation is also a consequence of its representation in the form of Equations (17).

If a multicomponent Lagrangian system possesses an additional ("isotopic") symmetry against linear transformations of the components, this also gives rise to a specific DI. An important example is a system of coupled NLS equations of Manakov's type (Manakov, 1973)

$$\mathrm{i}\begin{pmatrix} u_t \\ v_t \end{pmatrix} + \nabla^2 \begin{pmatrix} u \\ v \end{pmatrix} + F'\left(|u|^2 + |v|^2\right)\begin{pmatrix} u \\ v \end{pmatrix} = 0, \tag{18}$$

which are invariant against rotation in the plane of (u, v). In this case, Equation (10) gives rise to the DI ("isotopic spin") in the form

$$S = \mathrm{i}\int \left(uv^* - u^*v\right) \mathrm{d}\boldsymbol{r}. \tag{19}$$

A very special situation arises for the DIs in the case of integrable equations, that is, those that are amenable to the application of the inverse scattering transform (IST) (Ablowitz & Segur, 1981; Newell, 1984; Zakharov et al., 1984). Integrable equations have an infinite set of hidden dynamical symmetries, which, unlike the above-mentioned elementary invariances against temporal and spatial shifts, spatial rotations, phase shift, etc., do not have a straightforward meaning. In compliance with the Noether theorem, each hidden symmetry generates the corresponding DI, which is an integral expression with a density that, unlike those corresponding to the elementary DIs (see Equations (12), (4), and (16), involves higher-order derivatives. For instance, in the integrable KdV equation (15) with $F = u^3$, the first higher-order DI is

$$I = \int_{-\infty}^{+\infty} \left(u_{xx}^2 + 5u^2u_{xx} + 5u^4\right) \mathrm{d}x. \tag{20}$$

In fact, it was an empirical discovery of several higher-order DIs in the KdV equation that was a major incentive for the study that had resulted in the discovery of the IST technique.

The IST provides a systematic method to derive the infinite set of the DIs in terms of the corresponding scattering data, into which the original wave field is mapped to make the hidden integrability explicit (Ablowitz & Segur, 1981; Newell, 1984; Zakharov et al., 1984). The use of the scattering data makes it possible to explicitly introduce a full system of the action-angle variables for the integrable equations, and demonstrate that the infinite set of the action variables is in one-to-one correspondence with the set of the DIs. It is also possible to prove; that all the DIs are *in involution* among themselves; that is, the Poisson bracket between any two DIs, defined as per the corresponding symplectic (Hamiltonian) structure, is zero. Thus, integrable equations are direct counterparts, for the case of the infinite number of degrees of freedom, of finite-dimensional Hamiltonian systems that are Liouville-integrable; that is, with a set of DIs that are in involution, their number being equal to the number of the degrees of freedom.

The presence of the infinite set of the DIs in the integrable equations helps to understand such a well-known property as the completely elastic character of collisions between solitons (Ablowitz & Segur, 1981; Newell, 1984; Zakharov et al., 1984): roughly speaking, the necessity to satisfy the infinite set of the conservation laws leaves no room for changes of the solitons, except for phase shifts. On the other hand, some equations amenable to the application of the IST technique, such as, for instance, the standard three-wave system,

$$\left(u_{1,2}\right)_t + c_{1,2}\left(u_{1,2}\right)_x = \mathrm{i}u_{2,1}^* u_3, \quad (u_3)_t = \mathrm{i}u_1 u_2, \tag{21}$$

where $u_{1,2}$ and u_3 are, respectively, the "daughter" and pump waves, and $c_{1,2}$ are group velocities, feature nontrivial "soliton reactions"—for instance, a spontaneous split of a pump-wave soliton into separating daughter ones. This possibility is explained by the fact that the above-mentioned one-to-one correspondence between the infinite sets of the degrees of freedom and DIs does not really hold for these equations: the set of the DIs is not "infinite enough" (Fokas & Zakharov, 1992). Such equations are sometimes called "solvable," to stress their difference from the genuinely integrable ones (integrable in the sense of Liouville, as generalized to systems with infinitely many degrees of freedom).

Integrable lattice (discrete) models feature another important property: due to the lack of the continuous translational invariance, lattice systems lack the momentum conservation. Nevertheless, integrable lattice models do possess a conserved momentum, due to their hidden symmetry. For example, the Ablowitz–Ladik equation,

$$2\mathrm{i}\frac{\mathrm{d}u_n}{\mathrm{d}t} + (u_{n+1} + u_{n-1} - 2u_n) + |u_n|^2(u_{n+1} + u_{n-1}) = 0, \tag{22}$$

which is an integrable discretization of the cubic NLS equation, conserves the real momentum in the form of

$$P = \sum_{n=-\infty}^{+\infty} \left(\psi_n \psi_{n+1}^* - \psi_n^* \psi_{n+1}\right). \tag{23}$$

In fact, conservation of the momentum is a specific integrability feature of discrete models, in contrast to continuum ones.

Elementary DIs find specific applications in systems perturbed by small nonconservative terms to order ε. In that case, the conservation laws no longer hold; however, using evolution (balance) equations for the former DI(s) is a convenient way to derive effective equations of motion for solitons (or other collective nonlinear excitations) in the weakly perturbed model. For instance, in the cubic NLS equation (3) with the above-mentioned terms (Kerr and stimulated Raman scattering ones), $F = \left(|u|^2\right)^2$ and $Q = \left(|u|^2\right)_x u$, an exact soliton solution with arbitrary amplitude η and velocity c, in the case of $\varepsilon = 0$, is

$$u_{\mathrm{sol}} = \eta \,\mathrm{sech}\left(\eta\,(x - ct)\right) \times \exp\left[\mathrm{i}(c/2)x + \mathrm{i}\left(\eta^2 - c^2\right)t\right]. \tag{24}$$

In the presence of small $\varepsilon > 0$, the wave action (4) remains a DI (see above), and the balance equation for the formerly conserved momentum P_{NLS}, see Equation (13), is

$$\frac{\mathrm{d}P}{\mathrm{d}t} = 2\varepsilon \int_{-\infty}^{+\infty} \left[\left(|u|^2\right)_x\right]^2 \mathrm{d}x. \tag{25}$$

Substitution of the unperturbed soliton (24) into Equation (25), and into the conservation of the wave action, yields evolution equations for the amplitude and velocity:

$$\frac{\mathrm{d}\eta}{\mathrm{d}t} = 0, \quad \frac{\mathrm{d}c}{\mathrm{d}t} = \frac{16}{15}\varepsilon\eta^4. \tag{26}$$

For further details and references, see the review by Kivshar & Malomed (1989).

BORIS MALOMED

See also **Hamiltonian systems; Integrability; Integrable lattices; Inverse scattering method or transform; Korteweg–de Vries equation; N-wave interactions; Symmetry groups**

Further Reading

Ablowitz, M. & Segur, H. 1981. *Solitons and the Inverse Scattering Transform*, Philadelphia: SIAM

Bogoliubov, N.N. & Shirkov, D.V. 1973. *Introduction to the Theory of Quantized Fields*, Moscow: Nauka (in Russian); English translation, 2nd edition: New York: Wiley, 1980

Fokas, A.S. & Zakharov, V.E. 1992. The dressing method and nonlocal Riemann-Hilbert problems. *Journal of Nonlinear Science*, 2: 109–134
Kivshar, Y.S. & Malomed, B.A. 1989. Dynamics of solitons in nearly integrable systems. *Reviews of Modern Physics*, 61: 763–915
Manakov, S.V. 1973. Theory of two-dimensional stationary self-focusing of electromagnetic waves. *Zhurnal Eksperimentalnoy i Teoreticheskoy Fiziki*, 65: 505–516 (in Russian); translated in *Soviet Physics—Journal of Experimental and Theoretical Physics*, 38: 248 (1974)
Newell, A.C. 1984. *Solitons in Mathematics and Physics*, Philadelphia: SIAM
Sulem, C. & Sulem, P.-L. 1999. *The Nonlinear Schrödinger Equation*, New York: Springer
Whitham, G.B. 1974. *Linear and Nonlinear Waves*, New York: Wiley
Zakharov, V.E., Manakov, S.P., Novikov, S.P. & Pitaevskii, L.P. 1984. *Theory of Solitons*, New York: Consultants Bureau

CONTINUITY EQUATION

See **Constants of motion and conservation laws**

CONTINUOUS SPECTRUM

See **Inverse scattering method or transform**

CONTINUUM APPROXIMATIONS

In general, a physical system belongs to one of three broad classes: (i) media with distributed parameters (electromagnetic fields, fluids, or liquid), (ii) discrete media (crystal lattices, polymers, or macromolecules), and (iii) artificial periodic systems (layered structures, lattices of nano-dots, or Josephson arrays). In the first class, the dynamics of a system is described by partial differential equations (PDE) for the field variable $u(x, t)$ and in the other two cases by discrete differential equations (DDE) for the field variable at the lattice sites $u(n, t) = u_n(t)$. For simplicity, only one-dimensional (1-d) models are discussed here.

Well-known examples of discrete nonlinear dynamical systems include the following:

- The discrete 1-dimensional elastic chain with a nonlinear interaction between the nearest neighbors (generalized Fermi–Pasta–Ulam (FPU) model), whose equation of motion reads

$$m\frac{\mathrm{d}^2u_n}{\mathrm{d}t^2} = \varphi'(u_{n+1} - u_n) - \varphi'(u_n - u_{n-1}), \quad (1)$$

  where u_n is the displacement of the nth atom in a chain; a prime indicates the derivative with respect to the argument, and $\varphi(u_n - u_{n-1})$ is the energy of the interatomic interaction (Fermi et al., 1955). The particular choice $\varphi(\xi) = A\xi^2/2 + \alpha\xi^3/3 + \beta\xi^4/4$ and $\varphi(\xi) = c\exp(-p\xi) + q\xi$ represents α-FPU (for $\beta = 0$), β-FPU (for $\alpha = 0$), and Toda models.

- The discrete 1-d chain with linear interatomic interaction exposed to a nonlinear external field (discrete Frenkel–Kontorova (FK) model) with the following equation of motion:

$$m\frac{\mathrm{d}^2u_n}{\mathrm{d}t^2} = A(u_{n+1} + u_{n-1} - 2u_n) - w'(u_n), \quad (2)$$

  where $w(u_n)$ is the nonlinear on-site external potential. The particular choice $w = U(1 - \cos(2\pi u_n/a))$, where a is the interatomic distance, corresponds to the traditional FK-model (Frenkel & Kontorova, 1939).

- 1-d photonic crystals (periodic arrays of optical waveguides) or the discrete spin lattice, which may be described in the context of the discrete nonlinear Schrödinger equation (DNLS)

$$\mathrm{i}\frac{\mathrm{d}\psi_n}{\mathrm{d}t} + B(\psi_{n+1} + \psi_{n-1} - 2\psi_n) + F(|\psi_n|^2)\psi_n = 0, \quad (3)$$

  where in the simplest case F is a linear function of the argument. ψ_n denotes the value of the effective field at the nth element of the discrete system, which can be assigned different physical meanings for various applications.

Even in the 1-d case, the solution of the nonlinear DDE poses a fairly complicated mathematical problem and only a few of them can be solved exactly (the Toda and Ablowitz–Ladik equations). Thus, it is often easier to study discrete problems in the "continuum approximation" (CA) within the framework of PDEs. Clearly, some information about nonlinear dynamics of discrete systems is lost, and some phenomena cannot be described in this continuum limit; but in the long wave limit, this approach provides a good qualitative and even quantitative agreement with the results for a discrete system investigation.

In the CA, the discrete number of the atom site n is replaced with the continuous coordinate $x : na \to x$, with a being the interatomic equilibrium distance or the period of mesoscopic periodical structure, and $u_n(t) = u(na, t)$ is replaced with $u(x, t)$. The finite differences $u_{n\pm1} - u_n$ have to be expanded in Taylor series

$$u_{n\pm1} - u_n = \pm a\frac{\partial u}{\partial x} + \frac{a^2}{2}\frac{\partial^2 u}{\partial x^2} \pm \frac{a^3}{6}\frac{\partial^3 u}{\partial x^3} + \frac{a^4}{24}\frac{\partial^4 u}{\partial x^4}\cdots. \quad (4)$$

This expansion is valid under the condition

$$|(u_{n+1} - u_n)/u_n| \ll 1. \quad (5)$$

For linear waves of the form $u_n = u_0\sin(kna - \omega t)$ this expansion agrees with the long wavelength approximation $ak \ll 1$, where k is a wave number.

Substitution of expansion (4) in DDE (1) in the leading approximation yields for the α-FPU and Toda models the Boussinesq equation

$$m\frac{\partial^2 u}{\partial t^2} - Aa^2\frac{\partial^2 u}{\partial x^2} - \frac{Aa^4}{12}\frac{\partial^4 u}{\partial x^4} - 2\alpha a^3\frac{\partial u}{\partial x}\frac{\partial^2 u}{\partial x^2} = 0. \quad (6)$$

(In the case of the β-FPU model, the modification of this equation with the nonlinear term $3\beta a^4(\partial u/\partial x)^2(\partial^2 u/\partial x^2)$ is obtained.)

Equations (2) for discrete FK model within continuum limit are transformed in the leading approximation into the nonlinear Klein–Gordon (NKG) equation

$$m\frac{\partial^2 u}{\partial t^2} - A\,a^2\frac{\partial^2 u}{\partial x^2} + w'(u) = 0. \quad (7)$$

In the particular case of the periodic external potential $w = U(1 - \cos u_n)$, one obtains the sine-Gordon (SG) equation. Finally, the CA for DNLS equation (3) reduces to the usual partial differential nonlinear Schrödinger equation

$$\mathrm{i}\frac{\partial \psi}{\partial t} + Ba^2\frac{\partial^2 \psi}{\partial t^2} + F(|\psi|^2)\psi = 0. \quad (8)$$

Examples (6)–(8) demonstrate that a different number of terms in expansion (4) are to be taken into account in different situations. In the case of Equation (1), the dispersion relation is

$$\omega = 2\sqrt{(A/m)}\,\sin ak/2, \quad (9)$$

which is of acoustic type with a weak dispersion in the limit $k \to 0$. Within the CA, this weak dispersion is governed by the fourth spatial derivative alone in expansion (4), and it is necessary to retain the dispersion term in (6). The dispersion relation for Equation (6) is consistent with the exact formula (9) only in the long wave limit $ak \ll 1$.

Unfortunately, the dispersion term $-(Aa^4/12)\,\partial^4 u/\partial x^4$ in (6) necessitates an additional boundary conditions for this equation and results in the appearance of additional nonphysical solutions with small frequencies and $ak \sim 1$. To avoid these side effects, a regularization of the expansion over the discreteness parameter a can be performed (Rosenau, 1987). This corresponds to substitution of the relation $\partial^2/\partial x^2 \simeq (m/Aa^2)\partial^2/\partial t^2$ into the dispersion term in (6) and leads to yet another version of the CA for Equation (1) containing the term with mixed derivatives:

$$m\frac{\partial^2 u}{\partial t^2} - Aa^2\frac{\partial^2 u}{\partial x^2} - \frac{ma^2}{12}\frac{\partial^4 u}{\partial x^2 \partial t^2} - 2\alpha a^3\frac{\partial u}{\partial x}\frac{\partial^2 u}{\partial x^2} = 0. \quad (10)$$

The above estimation of CA application area ($ak \ll 1$) holds for long wave small amplitude envelope solitons in the nonlinear case as well. But in general, this condition can differ for solitons of different types. For example, CA descriptions of Boussinesq solitons of the type $u(x, t) = u(x - vt)$ describe the solutions of FPU model (1) only under the condition $v/v_c - 1 \ll 1$, where $v_c = \sqrt{Aa^2/m}$.

Only the lowest-order terms of expansion (4) have so far been taken into account for discrete systems within the CA. In general, retaining the next terms with higher powers of spatial derivatives exceeds the accuracy of CA. But in some way, such extended versions of the CA also take into account the discreteness of the systems and can lead to interesting and important physical results. Retaining the fourth order derivative in (4) transforms the nonlinear KGE (7) into

$$m\frac{\partial^2 u}{\partial t^2} - Aa^2\frac{\partial^2 u}{\partial x^2} - \frac{Aa^4}{12}\frac{\partial^4 u}{\partial x^4} + w'(u) = 0. \quad (11)$$

In the case of a sinusoidal external force, the corresponding generalized equation (dispersive SG equation) has steady-state bounded kinks solutions (4π-kink solitons) for some particular values of their velocities (Bogdan et al., 2001). This result obtained within the CA is in agreement with the numerical result for the corresponding discrete system (2) (Alfimov et al., 1993). The inclusion of yet higher terms of expansion (4) in the nonlinear parts of discrete equations in the CA gives rise to the nonlinear dispersion and leads to an existence of exotic solitons such as "compactons" and "peakons."

The CA is not restricted to the long-wave limit. For high-frequency short waves with wave numbers $k \simeq \pi/a$ and $\omega - \omega_{\max} \ll \omega_{\max}$ (where $\omega_{\max} = 2\sqrt{A/m}$ for (1) and (2)), the CA for the slowly varying envelope of antiphase oscillations ($u_n = (-1)^n v_n$) in the β-FPU-model results in a PDE with the Euclidean differential part

$$m\frac{\partial^2 v}{\partial t^2} + Aa^2\frac{\partial^2 v}{\partial x^2} + 4Av + 16\beta v^3 = 0. \quad (12)$$

The breather solution of this equation (Kosevich & Kovalev, 1975) within the CA describes the "intrinsic modes," which are currently being widely discussed since the pioneering paper of Sievers and Takeno (1988). In more complicated diatomic chains with the gap in the linear waves spectrum at $k = \pi/2a$, the so-called "gap solitons" (breathers with frequencies lying in the gap) can be described in CA for the envelopes of the antiphase oscillations of atoms from two sublattices.

To this point, applications of the CA for DDE models of discrete systems were discussed. Often, the opposite approach is used where the corresponding PDEs are investigated numerically in some discrete

schemes as a system of DDE (Dodd et al., 1982). The finite-differences method is one of the most popular in this case: the initial function $u(x,t)$ is defined on the rectangular net of the (x,t) plane at points $x = hn, t = h't$. The partial derivatives are replaced by the finite differences

$$\frac{\partial u(x,t)}{\partial x} = \frac{u_{n+1} - u_n}{h}, \quad \frac{\partial^2 u(x,t)}{\partial x^2} = \frac{u_{n+1} + u_{n-1} - 2u_n}{h^2}, \ldots \qquad (13)$$

Generally, sampling over all variables is performed, but in some hybrid methods space sampling alone is carried out and the resulting system of ODEs is solved by using standard computer codes.

Space sampling is commonly used for complicated biological systems. In order to simulate the behavior of a single neuron, for example, its continuous structure may be sliced into a large number of small segments (compartments). This procedure is called the "compartmental" approach, and within it the continuous PDEs are replaced by sets of ODEs. The advantage of this modeling approach is that it imposes no restrictions on the properties of each compartment and permits great flexibility at the level of resolution. Compartmental methods make it possible to develop the realistic models that have a close relationship with the relevant experimental data.

ALEXANDER S. KOVALEV

See also **Compartmental models; Delay-differential equations; Discrete nonlinear Schrödinger equations; Dispersion relations; Fermi–Pasta–Ulam oscillator chain; Frenkel–Kontorova model; Partial differential equations, nonlinear; Peierls barrier; Sine-Gordon equation**

Further Reading

Alfimov, G., Eleonskii, V., Kulagin, N. & Mitskevich, N. 1993. Dynamics of topological solitons in models with nonlocal interaction. *Chaos*, 3: 405–414

Bogdan, M., Kosevich, A. & Maugin, G. 2001. Soliton complex dynamics in strongly dispersive medium. *Wave Motion*, 34: 1–26

Dodd, R., Eilbeck, J., Gibbon, J. & Morris, H. 1982. *Solitons and Nonlinear Wave Equations*, London: Academic Press

Eisenberg, H., Silberberg, Y., Marandotti, R., Boyd, A. & Aitchison, J. 1998. Discrete spatial optical solitons in waveguide arrays. *Physical Review Letters*, 81: 3383–3386

Fermi, E., Pasta, J. & Ulam, S. 1955. Studies of nonlinear problems. 1965. *Collected Works of E. Fermi*, vol. II, Chicago: University Chicago Press

Frenkel, J. & Kontorova, T. 1939. On the theory of plastic deformation and twinning. *Physical Journal USSR*, I: 137–149 (originally published in Russia, 1938)

Kosevich, A. & Kovalev, A. 1975. Self-localization of vibrations in 1D anharmonic chain. *Soviet Physics, Journal of Experimental and Theoretical Physics*, 40: 891–896

Rosenau, P. 1987. Dynamics of dense lattices. *Physical Review*, B36: 5868–5876

Sievers, A. & Takeno, S. 1988. Intrinsic localized modes in anharmonic crystals. *Physical Review Letters*, 61: 970–973

CONTOUR DYNAMICS

A wide variety of fluid dynamical problems involve the material advection of a tracer field $q(\boldsymbol{x}, t)$, expressed by

$$\frac{\mathrm{D}q}{\mathrm{D}t} \equiv \frac{\partial q}{\partial t} + \boldsymbol{u} \cdot \nabla q = 0, \qquad (1)$$

where $\boldsymbol{u}(\boldsymbol{x}, t)$ is the fluid velocity. The value of q thus does not change following an infinitesimal element or particle. That is, for a particle at $\boldsymbol{x} = \boldsymbol{X}(\boldsymbol{a}, t)$, where $\boldsymbol{a}$ is a vector label (e.g., the initial position of the particle), Equation (1) implies that $q = q(\boldsymbol{a})$, a constant, and $\partial \boldsymbol{X}/\partial t = \boldsymbol{u}(\boldsymbol{X}, t)$, which is just the statement that the particle moves with the local fluid velocity. The collective effect of this transport is a rearrangement of the tracer field q by the velocity field $\boldsymbol{u}$.

Depending on the nature of $\boldsymbol{u}$, this may lead to highly intricate distributions of q, even starting from simple initial conditions. Moreover, there are important applications in which $\boldsymbol{u}$ depends on q itself, often in a nonlocal manner, that is, in which the entire field of q contributes to $\boldsymbol{u}$ at any given point $\boldsymbol{x}$. A specific example relevant to the present topic is provided by the two-dimensional Euler equations governing the behavior of an inviscid, incompressible fluid:

$$\frac{\mathrm{D}\boldsymbol{u}}{\mathrm{D}t} = -\frac{\nabla p}{\rho}, \qquad (2)$$

$$\nabla \cdot \boldsymbol{u} = 0, \qquad (3)$$

where p is the pressure and ρ is the density (here constant), and where now the velocity field is two dimensional: $\boldsymbol{u} = (u, v)$. Taking the curl of Equation (2) gives an equation for the scalar vorticity $\zeta \equiv \partial v/\partial x - \partial u/\partial y$:

$$\frac{\mathrm{D}\zeta}{\mathrm{D}t} = 0, \qquad (4)$$

which is identical to Equation (1) if we take $q = \zeta$. Thus, the vorticity is materially conserved in this system. But it also induces the velocity field $\boldsymbol{u}$, that transports it. Equation (3) is satisfied generally by considering

$$u = -\partial\psi/\partial y \quad \text{and} \quad v = \partial\psi/\partial x, \qquad (5)$$

where $\psi(\boldsymbol{x}, t)$ is called the streamfunction. Substituting these components into the definition of ζ leads to a Poisson equation for ψ:

$$\nabla^2 \psi = \zeta. \qquad (6)$$

Given the distribution of ζ, this equation (with suitable boundary conditions) may be inverted to find ψ, whose spatial derivatives provide u and v. The inversion of

this equation can be formally accomplished by using the Green function $G(\boldsymbol{x};\boldsymbol{x}')$ of Laplace's operator ∇^2; in two dimensions,

$$G(\boldsymbol{x};\boldsymbol{x}') = (2\pi)^{-1}\log|\boldsymbol{x}'-\boldsymbol{x}|. \tag{7}$$

(G is the solution to Equation (6) for $\zeta=\delta(\boldsymbol{x}'-\boldsymbol{x})$, a singular delta distribution of vorticity having a unit spatial integral.)

Consider henceforth an unbounded two-dimensional fluid. Then, the formal solution to the inversion problem is

$$\psi(\boldsymbol{x},t) = \iint G(\boldsymbol{x};\boldsymbol{x}')\zeta(\boldsymbol{x}',t)\,\mathrm{d}x'\mathrm{d}y', \tag{8}$$

which shows explicitly that the flow field at any point depends on the vorticity field at all points. Moreover, the integration over space implies that the field of ψ is generally smoother than that of ζ.

The evolution of the flow in this case consists of two basic steps:

- *inversion*—the recovery of the velocity field $\boldsymbol{u}$ from the distribution of ζ and
- *advection*—the transport of fluid particles to the next instant of time.

Now, a two-dimensional plane is carpeted by an infinite number of such particles, and therefore, this view of the evolution may appear to be quite complex. However, the material conservation of q (or ζ) affords an enormous simplification. First, note that, if one exchanges two particles labeled $\boldsymbol{a}$ and $\boldsymbol{a}'$ having the same value of q, this does not alter the distribution of q, and as a result the velocity field $\boldsymbol{u}$ remains unchanged. This is a "particle relabeling" symmetry, and in general, it gives rise to an infinite number of globally conserved quantities (the spatial integrals of any functional of q). This symmetry implies that contours of fixed q consist of the same set of fluid particles for all time. They are called material contours.

Contour dynamics arises from representing the distribution of q by a finite set of contours C_k, $k=1, 2, ..., n$, between which q is spatially uniform, and across which q jumps by Δq_k (defined to be the value of q to the left of C_k minus that to the right of C_k). The contours here are still material ones—the particles just on either side of a contour retain their distinct values of q. Between two contours, any two fluid particles may be exchanged without altering q or $\boldsymbol{u}$. This implies that only the contours matter for determining the velocity field. Also, since the contours are material, their advection suffices to evolve the entire distribution of q. This is the basis of contour dynamics.

To see how this works for the two-dimensional Euler equations, it remains to be shown as to how one can calculate the velocity field directly from the contours C_k. The starting point is Equation (8), in which we consider $\zeta=q$ to be a piecewise-uniform field. For the moment, we need only use the property $G(\boldsymbol{x};\boldsymbol{x}')=g(\boldsymbol{x}'-\boldsymbol{x})$ satisfied by the Green function of the Laplace operator. Also, we need only consider one contour at a time and afterwards linearly superpose the results, since the relation between q and $\boldsymbol{u}$ is linear. We may take $q=0$ outside of the (closed) contour, so that $q=\Delta q$ inside it (denoted by the region R below). Nonzero exterior q simply gives rise to solid-body rotation, and may be superposed afterwards. Then, from Equation (5), we have

$$\begin{aligned}(u(\boldsymbol{x},t),\,v(\boldsymbol{x},t)) &= \left(-\frac{\partial}{\partial y},\frac{\partial}{\partial x}\right)\Delta q\iint_R g(\boldsymbol{x}'-\boldsymbol{x})\,\mathrm{d}x'\mathrm{d}y' &(9)\\ &= -\Delta q\iint_R\left(-\frac{\partial}{\partial y'},\frac{\partial}{\partial x'}\right)g(\boldsymbol{x}'-\boldsymbol{x})\,\mathrm{d}x'\mathrm{d}y' &(10)\\ &= -\Delta q\oint_C g(\boldsymbol{X}'-\boldsymbol{x})\,(\mathrm{d}X',\mathrm{d}Y'), &(11)\end{aligned}$$

where we have used the symmetry of g with respect to $\boldsymbol{x}$ and $\boldsymbol{x}'$ in the second line and Stokes' theorem in the third, and where $\boldsymbol{X}'$ denotes a point on the contour C. The velocity field anywhere thus depends only on the shape of C.

For a set of contours, the velocity field is required only on the contours themselves to evolve q. The contours thus form a closed dynamical system, contour dynamics, governed by

$$\frac{\mathrm{d}\boldsymbol{X}_j}{\mathrm{d}t} = \boldsymbol{u}(\boldsymbol{X}_j) = -\sum_{k=1}^{n}\Delta q_k\oint_{C_k} g(\boldsymbol{X}_k'-\boldsymbol{X}_j)\mathrm{d}\boldsymbol{X}_k' \tag{12}$$

for all points $\boldsymbol{X}_j$ on contours C_j, $j=1, 2, ..., n$.

These equations were first derived for the two-dimensional Euler equations by Zabusky et al. (1979), following earlier work by Berk & Roberts (1967), who derived a similar contour-based model for the two-dimensional Vlaslov equations in plasma physics. These authors also developed numerical methods for contour dynamics in which the contours were discretized into a finite set of points or nodes, originally connected by straight line segments. A wide variety of numerical methods have since been developed, many of which are summarized in the review articles of Dritschel (1989) and Pullin (1992). They principally differ in terms of the choice of the interpolation between nodes (linear, quadratic, cubic; local and global splines); the method of numerical quadrature used to evaluate the contour integral over the segment connecting adjacent nodes (trapezoidal, Gaussian, explicit); the method of redistributing, inserting, and removing nodes to maintain an accurate representation of the contour shape; and the procedure used, if any, to remove fine-scale structure (e.g., filaments and

thin bridges connecting two separating regions)—a procedure coined "contour surgery" (Dritschel, 1988).

Contour dynamics has been used to study a wide variety of problems, from the interaction of two vortex patches (having just one contour each), to the filamentation and stripping of nested vortices (having many contours to represent a continuum) (Dritschel, 1989; Pullin, 1992). The numerical method illustrated next is described in Dritschel (1988, 1989). This method uses local cubic splines between contour nodes, explicit quadrature to first order in the departure of the contour from a straight line between nodes, node redistribution based on maintaining a local node density proportional to the square root of contour curvature, and automatic surgery whenever contours or contour parts get closer than a prescribed cutoff scale δ. This scale and the precise formula for the node density are chosen to balance the errors arising from surgery and node redistribution. A fourth-order Runge–Kutta scheme is used for the time integration.

An example is presented next of the collapse of three vortex patches (see also (Rogberg & Dritschel, 2000)). The centers of the vortices are initially chosen at points where equivalent delta-distributed point vortices of the same circulation (spatial integral of q) are known to collide in finite time. Two of the vortices have $q = +2\pi$ and radii 1 and $2/\sqrt{5}$, while the third has $q = -2\pi$ and radius $\frac{2}{3}$. The two positive vortices are initially separated by a distance $d = 5$, and the negative vortex is placed at a distance $d\sqrt{17/27}$ and at an angle 225° relative to the joint center of the two positive vortices. The vortices are then all shifted so that the joint center of all three vortices lies at the origin. Starting from this configuration, the collapse time for the point vortices is 7.70059886...

Figure 1 illustrates the evolution of the vortices—in the upper left-hand frame, the initial conditions are shown, while the remaining frames (to the right and then downwards) are spaced at unit increments in time starting from $t = 5$ and ending at $t = 15$. By $t = 6$, the two positive vortices begin to merge (they are separated by only a thin channel of irrotational fluid). Thereafter, the flow grows rapidly in complexity, as many filaments are generated and small vortices roll up at the tips of some of the filaments. Notably, the negative vortex does not distort significantly, but merely acts to bring the two positive vortices together.

The complexity just illustrated is typical of many vortex interactions. An accurate, robust numerical method must be able to capture this generic behavior, at least over time scales when the flow is reasonably predictable. To see how well the current method performs, we next examine how the results vary with spatial resolution. Two additional simulations were performed at half and double the average point spacing used in Figure 1. The results are compared in Figure 2 at the final time, $t = 15$, when the numbers of nodes in the three simulations are, from low to high resolution, 2740, 10,738 and 27,297 (at $t = 0$, the numbers of nodes are 183, 349, and 682). Note the cutoff scale $\delta = 0.000225$, 0.0009, and 0.0036 in the three simulations—there is a factor of 4 difference in δ between resolutions. The agreement is striking even in the detailed structure. The most visible differences show up in the lengths of the filaments, which are removed more readily at low resolution. These filaments, however, contribute negligibly to the velocity field, and retaining them makes little difference to the evolution of the flow.

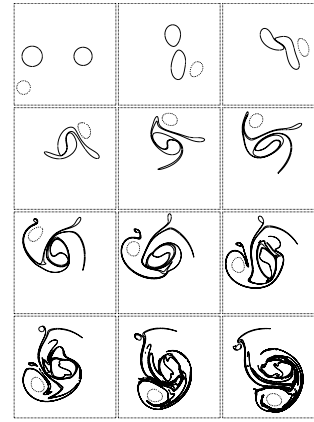

Figure 1. The collapse of three vortex patches. The initial condition is shown in the upper left frame. Time proceeds to the right and downwards in increments of one unit, from $t = 5$ to $t = 15$. The window of view is $-5.0 < x < 5.0$ and $-5.8 < y < 4.2$. The negative vortex is rendered with a short-dashed line (with a dash between each node), while the positive vortices are rendered with a continuous solid line.

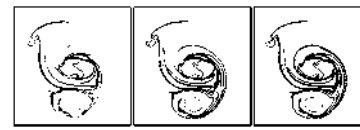

Figure 2. Comparison, at $t = 15$, of three contour dynamics simulations of vortex collapse. Resolution increases from left to right, doubling between each frame (the node spacing parameter is $\mu = 0.12, 0.06$, and 0.03, and the large-scale length $L = 1$ in all cases; consult Dritschel (1989) or Dritschel & Ambaum (1997) for further details). The domain of view is the same as used in the previous figure.

Contour dynamics has since been applied in a variety of diverse fields. Its largest growth has occurred in the field of atmospheric and oceanic dynamics, where the potential vorticity plays the role of the materially

conserved tracer q often to a very good approximation (Hoskins et al., 1985). Indeed, its application to this field is on a much sounder footing than it is to the fields it was originally developed for: plasma physics and aeronautics. The two-dimensional approximation is a particularly severe one in aeronautics, since real flows do not preserve two-dimensional symmetry, unless constrained in some manner. In the atmosphere and oceans, rotation and stratification serve to constrain the flow to be two dimensional, or more appropriately, layerwise two dimensional, and furthermore one may extend contour dynamics to study such flows (indeed, the equations are formally no different than given those by (12); see (Dritschel, 2002)).

Finally, the use of contours to carry out tracer advection—the fast and accurate part of contour dynamics—has been combined with more traditional approaches of computing the velocity field (the inversion step) to produce a particularly fast, accurate, and versatile numerical method called the contour-advective semi-Lagrangian (CASL) algorithm (Dritschel & Ambaum, 1997; Dritschel et al., 1999; Dritschel & Viúdez, 2003). This latest development allows the extension of the contour approach to much more realistic sets of equations, and has significantly widened the applicability of the original contour dynamics method.

DAVID DRITSCHEL

See also **Chaotic advection; Euler–Lagrange equations; Vortex dynamics of fluids**

Further Reading

Berk, H.L. & Roberts. K.V. 1967. The water-bag model. *Methods in Computational Physics*, 9: 87–134

Dritschel, D.G. 1988. Contour surgery: a topological reconnection scheme for extended integrations using contour dynamics. *Journal of Computational Physics*, 77: 240–266

Dritschel, D.G. 1989. Contour dynamics and contour surgery: numerical algorithms for extended, high-resolution modelling of vortex dynamics in two-dimensional, inviscid, incompressible flows. *Computer Physics Reports*, 10: 77–146

Dritschel, D.G. 2002. Vortex merger in rotating stratified flows. *Journal of Fluid Mechanics*, 455: 83–101

Dritschel, D.G. & Ambaum, M.H.P. 1997. A contour-advective semi-Lagrangian numerical algorithm for simulating fine-scale conservative dynamical fields. *Quarterly Journal of the Royal Meteorological Society*, 123: 1097–1130

Dritschel, D.G., Polvani, L.M. & Mohebalhojeh, A.R. 1999. The contour-advective semi-Lagrangian algorithm for the shallow water equations. *Monthly Weather Review*, 127(7): 1551–1565

Dritschel, D.G. & Viúdez, A. 2003. A balanced approach to modelling rotating stably-stratified geophysical flows. *Journal of Fluid Mechanics*, 488: 123–150. See also: www-vortex.mcs.st-and.ac.uk.

Hoskins, B.J., McIntyre, M.E. & Robertson, A.W. 1985. On the use and significance of isentropic potential-vorticity maps. *Quarterly Journal of the Royal Meteorological Society*, 111: 877–946

Pullin, D.I. 1992. Contour dynamics methods. *Annual Review of Fluid Mechanics*, 24: 89–115

Rogberg, P. & Dritschel, D.G. 2000. Mixing and transport in two-dimensional vortex interactions. *Physics of Fluids*, 12(12): 3285–3288

Zabusky, N.J., Hughes, M.H. & Roberts, K.V. 1979. Contour dynamics for the Euler equations in two dimensions. *Journal of Computational Physics*, 30: 96–106

CONTROL PARAMETERS

See **Bifurcations**

CONTROLLING CHAOS

It may seem paradoxical that chaotic systems—which are extremely sensitive to the tiniest fluctuations—can be controlled; yet, the earliest reference to this idea appears around 1950, when John von Neumann presaged just that. Nowadays, laboratory demonstrations of the control of chaos have been realized in chemical, fluid, and biological systems, and the intrinsic instability of chaotic celestial orbits is routinely used to advantage by international space agencies who divert spacecraft to travel vast distances using only modest fuel expenditures.

A variety of techniques for chaos control has been implemented since around 1990 when the first concrete analyses appeared, including traditional feedback and open-loop methods, neural network applications, shooting methods, Lyapunov function approaches, and synchronization to both simple and complex external signals. These techniques resolve the paradox implied by chaos control in different ways, but they all make use of the fact that chaotic systems can be productively controlled if disturbances are countered by small and intelligently applied impulses. Just as an acrobat balances about an unstable position on a tightrope by the application of small correcting movements, a chaotic system can be stabilized about any of an infinite number of unstable states by continuous application of small corrections.

Two characteristics of chaos make the application of control techniques even more fruitful. First, chaotic systems alternately visit small neighborhoods of an infinite number of periodic orbits. The presence of an infinite number of periodic orbits embedded within a chaotic trajectory implies the existence of an enormous variety of different behaviors within a single system. Thus, the control of chaos opens up the potential for tremendous flexibility in operating performance within a single system.

As an example, Figure 1 depicts the Lorenz attractor, used to model fluid convection. Embedded within the gray attractor are innumerable periodic orbits, such as the solid figure-8 orbit and the more complicated dashed one. For practical systems such as chemical reactors or fluidized beds, the presence of multiple

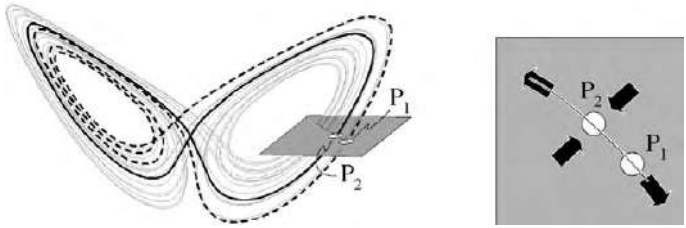

Figure 1. Left: Lorenz attractor with two of its embedded unstable periodic orbits highlighted. Right: unstable points P_1 and P_2 in the surface of section indicated. The unstable direction is denoted by outgoing arrows, and stable direction is denoted by ingoing arrows.

co-existing states implies that one chaotic system could be operated in multiple different states, thus potentially performing the function of several separate units.

A second characteristic of chaos that is important for control applications is the exponential sensitivity of the phenomenon. That is, the fact that the state of a chaotic system can be drastically altered by the application of small perturbations means two things: such a system if uncontrolled can be expected to fluctuate wildly, and if controlled can be directed from one state to a very different one using only very small controls.

Traditional feedback control remains among the most widely used methods of control for chaotic systems. To implement feedback control, one waits until a chaotic trajectory by chance lands near a desired periodic point and then applies small variations to an accessible system parameter in order to repeatedly nudge the trajectory closer to that point. As an example, consider the plot to the right in Figure 1, where we depict two periodic points as they appear on a "surface of section" formed in this case by recording every intersection between the Lorenz chaotic attractor and the half plane, $Z = 0$, $X > 0$. To control the state to remain near point P_2 (so the trajectory stays near the figure-8 trajectory shown to the left), one needs to apply variations in a parameter, p, that directs the state toward P_2 along the unstable direction (or directions in more complicated problems) indicated by outgoing arrows in Figure 1. One can establish the direction in which a parametric control moves the chaotic state either experimentally, by varying the parameter and recording the future variation of the system state, or analytically, by determining the Jacobian of the flow or mapping where available. Nudging the state closer to P_2 amounts to what is termed "pole placement" in traditional control literature, and numerous reports of alternative strategies for selecting parameter variations appear in the literature. Strategies include simple pole placement, optimal control, neural network approaches, simple proportional control, periodic forcing, and control dependent on the distance from P_2. Most of these strategies have proven successful under appropriate conditions, and the choice of strategy depends principally on details of the control goal required and the computational resources available to meet that goal.

All of these strategies require that the system state must lie close to the desired state in order to achieve control. In such a case, the system dynamics can be linearized, making control calculations rapid and effective. Fortunately, in chaotic systems, one can rely on ergodicity to ensure that the system state will eventually wander arbitrarily close to the desired state. By the same token, if it is desired to switch the system between one accessible state (say P_1) and a second (say P_2), one can merely release control from P_1 and reapply a new control algorithm once the system strays close to P_2, which it is certain to do by ergodicity.

In higher-dimensional or slowly varying systems, the time taken for the state to move on its own from one state to another can be prohibitive, and for this reason fully nonlinear control strategies have been devised that use chaotic sensitivity to steer the system state from any given initial point to a desired state. Since chaotic systems amplify control impulses exponentially, the time needed to steer such a system can be quite short. These strategies have been demonstrated both in systems in which a large effect is desired using very modest parameter expenditures (energy or fuel) and in systems in which rapid switching between states is needed (computational or communications applications).

On the other hand, in both linear and nonlinear control approaches, one needs to repeatedly re-apply control over a time that is short compared with the inverse of the fastest growing growth rate of the system in order to counter the potential amplification of ubiquitous noises. Computational and experimental analyses have demonstrated that this is readily done in typical chaotic systems and that control can be robustly achieved. Because large but rare noise events can occur, however, controlled states occasionally break free when the system encounters an anomalous large noise. In this case, bounds have been established for the frequency and duration of these noise-induced excursions.

Numerous biological control applications have been proposed since the first introduction of the notion of chaotic control. Among the first applications were studies of intrinsic nonlinear control mechanisms involved in autonomic and involuntary functions such as the regulation of internal rhythms and the control of gait and balance. These studies confirm that nontrivial control algorithms are involved in the maintenance of normal physiological function and that provocative insights into pathological conditions can be gained (such as cardiac and breathing arrythmias and motor tremor). Further work has shown that networks of chaotic devices, under prescribed conditions, can be brought into synchronization, and strong indications have been presented that neuronal signaling may rely on nonlinear synchronization. Additional experimental studies are promising for the control of unwanted fluctuations (e.g., during fibrillation of the heart) or for the so-called "anticontrol" of synchronized periodic signals in focal epilepsy. In both studies, the goal is to use feedback control methods to steer a diseased organ using small electrical stimulation: in the former state, toward a stabilized state, and in the latter, away from a synchronized state.

TROY SHINBROT

See also **Chaotic dynamics; Feedback; Lorenz equations**

Further reading

Alekseev, V.V. & Loskutov, A.Y. 1987. Control of a system with a strange attractor through periodic parametric action. *Soviet Physics Doklady*, 32: 1346–1348

Ditto, W.L. & Pecora, L.M. 1993. Mastering chaos. *Scientific American*, 78–84

Garfinkel, A., Spano, M.L., Ditto, W.L. & Weiss, J.N. 1992. Controlling cardiac chaos. *Science*, 257:1230–1235

Glass, L. & Zeng, W. 1994. Bifurcations in flat-topped maps and the control of cardiac chaos. *International Journal of Bifurcation & Chaos*, 4: 1061–1067

Hayes, S., Grebogi, C. & Ott, E. Communicating with Chaos. *Physical Review Letters*, 70: 3031–3014

Hübler, A., Georgii, R., Kuckler, M., Stelzl, W. & Lscher, E. 1988. Resonant Stimulation of nonlinear damped oscillators by Poincaré maps. *Helvetica Physica Acta*, 61: 897–900

Lima, R. & Pettini, M. 1990. Suppression of chaos by resonant parametric perturbations. *Physics Review A*, 41: 726–733

Ott, E., Grebogi, C. & Yorke, J.A. 1990. Controlling chaos. *Physical Review Letters*, 64: 1196–1199

Pecora, L.M. & Carroll, T.J. 1990. Synchronization in chaotic systems. *Physical Review Letters*, 64: 821–824

Schiff, S.J., Jerger, K., Duong, D.H., Chang, T., Spano, M.L. & Ditto, W.L. 1994. Controlling chaos in the brain. *Nature*, 370: 615–620

Shinbrot, T., Ott, E., Grebogi, C. & Yorke, J.A. 1993. Using small perturbations to control chaos. *Nature*, 363: 411–417

COSMOLOGICAL MODELS

Relativistic cosmology—the science of the structure and evolution of the universe—is based on the building and investigation of cosmological models (CMs), which describe geometrical properties of physical space-time, the matter, composition and structure of the universe, and physical processes at different stages of the universe's evolution. Prominent in cosmology is the hot big bang CM, which is based on solutions of Alexander Friedmann's cosmological equations for homogeneous isotropic models deduced in the framework of Einstein's general relativity theory (GR). Because of its large-scale structure (galaxies, clusters of galaxies, etc.), the universe is homogeneous and isotropic only on the largest scales from 100 Mpc. (The pc or parsec is an astronomical unit of distance equal to 3.2616 light years; thus, an Mpc is 3.2616 million light years.)

The most important feature of Friedmann's CM is its nonstationary character, which was confirmed by Edwin Hubble's discovery of cosmological expansion in 1929. In this formulation, the geometrical properties of physical space depend on the value of energy density ρ relative to a critical density

$$\rho_{\text{crit}} = \frac{3H_0^2}{8\pi G}, \tag{0}$$

where H_0 is the expansion rate (Hubble parameter) at the present epoch and G is Newton's gravitational constant. If $\Omega = \rho/\rho_{\text{crit}} = 1$, the 3-space is flat; if $\Omega > 1$, 3-space possesses positive curvature and if $\Omega < 1$, 3-space possesses negative curvature. Corresponding CMs are flat, closed, and open CM, respectively.

All Friedmann CMs have a beginning in time (or cosmological singularity), where energy density and curvature invariants diverge. Their evolutions depend on properties of matter. In the case of ordinary matter with a positive energy density and a nonnegative pressure, the evolution of flat and open models has the character of expansion, and closed models recollapse after an expansion stage. The assumption that the temperature was very high at the initial stage of cosmological explanation (hot CM) was confirmed by the discovery of the cosmic microwave background (CMB) radiation in 1965, with a present epoch temperature of about $T = 2.7$ K. The theory of nucleosynthesis of light elements (hydrogen, helium, deuterium, lithium, etc.) into the first few minutes of cosmological expansion based on the framework of the hot big bang CM is in accord with empirical data.

Advances in both theory and technology during the last 20 years have launched cosmology into a most exciting period of discovery. By using precise instruments (telescopes, satellites, spectroscopes), several cosmological research programs are being carried out, including investigations of the anisotropy

of CMB and supernovae observations. Cosmological observations have not only strengthened and expanded the hot big bang CM but they have also revealed surprises.

Recent measurements of the anisotropy of the CMB have provided convincing evidence that the spatial geometry is very close to being uncurved (flat) with $\Omega = 1.0 \pm 0.03$. The currently known components of the universe include ordinary baryonic matter, cold dark matter (CDM), massive neutrinos, the CMB and other forms of radiation, and dark energy. The sum of the values for these densities derived empirically is equal to the critical density (to within their margins of error). The largest contributions to energy density are from two components—CDM and dark energy. About 30% of the total mass-energy is dark matter, composed of particles probably formed early in the universe. Two thirds is in smooth dark energy whose gravitational effects began causing the expansion of the universe to speed up just a few billion years ago. The remarkable fact that the expansion is accelerating can be accounted for within GR, as the source of gravity is proportional to $(\rho + 3p)$, where the pressure p and energy density ρ describe the bulk properties of "the substance." A substance with pressure more negative than one-third its energy has repulsive gravity in GR. Such a situation occurs, for example, for gravitating vacuum (positive cosmological constant), for which $p = -\rho$.

In addition to breakthrough empirical observations, creative theoretical ideas are also driving progress in cosmology. The development of cosmology during the last 20 years shows that profound connections exist between the elementary particles on the smallest scales and the universe on the largest. Using unified gauge theories of elementary particles, an inflationary scenario was formulated, which resolves a number of problems of standard Friedmann cosmology: flatness and the problem of horizon, among others. According to inflation, small bits of the universe underwent a burst of expansion when the universe was extremely young, explaining the homogeneity and isotropy of the universe at initial stages of cosmological expansion. Based on the framework of an inflationary CM, the appearance of quantum fluctuations with a nearly scale-invariant distribution by transition to radiation-dominated era was predicted, explaining the large scale structure of the universe.

The inflationary CM as well as others discussed above are singular, which is an outstanding problem of GR. Assuming that the Planck era (when the universe was sufficiently dense to require a quantum mechanical treatment) existed, some quantum gravitation theory is necessary to construct a regular CM. At present, the superstring theory is a candidate for such a theory.

Some regular CMs have been constructed in a "brane world," under which our universe is thought to exist as a slice (or membrane) through a higher-dimensional space. By using scalar fields with a negative potential, a solution for an oscillating CM was obtained; thus, the Big Crunch takes place in such models before Big Bang. Resolving the problem of cosmological singularity requires that the gravitation theory not only admits regular solutions for CM but also excludes singular solutions. This suggests gauge theories of gravitation (Poincaré gauge theory or metric-affine gauge theory), leading to regular bouncing solutions for CMs.

The building of more realistic CMs requires the resolution of fundamental cosmological problems. According to present knowledge, our universe is flat and 13 Gyr old, and it is expanding at the current rate of $H_0 = 72 \pm 8\,\mathrm{km\ sec^{-1}\ Mpc^{-1}}$. Measurements of the past rate reveal that the universe is presently in a period of cosmic acceleration. The contribution of ordinary matter to the overall mass energy is small, with more than 95% of the Universe existing in new and unidentified forms of matter and energy. What is the composition of dark matter (axions, neutralinos, or other exotic particles)? What is the nature of dark energy (quantum vacuum energy or scalar fields)? What is the field that drives inflation? Answers to these and other questions will change the picture presented above.

VIACHASLAV KUVSHINOV AND ALBERT MINKEVICH

See also **Black holes; Einstein equations; Galaxies; General relativity**

Further Reading

Gasperini, M. & Veneziano, G. 2003. The pre-big bang scenario in string cosmology. *Physics Reports*, 373: 1–212

Khoury, J., Ovrut, B.A, Seiberg, N., Steinhardt, P.J. & Turok, N. 2002. From big crunch to big bang. *Physical Review* D, 65: 086007

Kolb, E.W. & Turner, M.S. 1990. *The Early Universe*, Reading, MA: Addison-Wesley

Linde, A.D. 1990. *Particle Physics and Inflationary Cosmology*, Chur: Harwood Academic

Steinhardt, P.J. & Turok, N. 2002. A Cyclic Model of the Universe. hep-th/0111030

CONVECTION

See **Fluid dynamics**

CONVECTIVE INSTABLITY

See **Wave stability and instability**

CORRELATION DIMENSION

See **Dimensions**

CORRESPONDENCE PRINCIPLE

See **Quantum nonlinearity**

COUPLED MAP LATTICE

Originally introduced in the study of spatiotemporal chaos, the coupled map lattice (CML) can be presented as a dynamical model for the evolution of a spatially extended system in time (Kaneko, 1983). CMLs have been widely used, not only as a tool for the study of spatiotemporal chaos but also for pattern dynamics in physics, chemistry, ecology, biology, brain theory, and information processing.

A CML is a dynamical system with discrete time (map), discrete space (lattice), and a continuous state. It consists of dynamical elements on a lattice, which interact (are coupled) with suitably chosen sets of other elements.

The construction of a CML is carried out as follows. First, choose a (set of) field variable(s) on a lattice. This (set of) variable(s) is on a macroscopic, not a microscopic level. Second, decompose the phenomenon of interest into independent units (e.g., convection, reaction, diffusion, and so on). Third, replace each unit by simple parallel dynamics (procedure) on a lattice, where the dynamics consists of a nonlinear transformation of the field variable at each lattice point and/or a coupling term among suitably chosen neighbors. Finally, carry out each unit dynamics (procedure) successively.

As a simple and widely used example, consider a phenomenon that is created by a locally chaotic process and by diffusion, and choose a suitable lattice model on a coarsegrained level for each process. As the simplest choice, we can adopt some one-dimensional map for chaos, and a discrete Laplacian operator for the diffusion. The former process is given by $x'_n(i) = f(x_n(i))$, where $x_n(i)$ is a variable at time n and lattice site i, $(i = 1, 2, \ldots, N)$, whereas $x'_n(i)$ is introduced as the intermediate value. The discrete Laplacian operator for diffusion is given by

$$x_{n+1}(i) = (1-\varepsilon)x'_n(i) + \frac{\varepsilon}{2}\{x'_n(i+1) + x'_n(i-1)\}. \quad (0)$$

Combining the above two processes, the CML is given by

$$x_{n+1}(i) = (1-\varepsilon)f(x_n(i)) + \frac{\varepsilon}{2}\{f(x_n(i+1)) + f(x_n(i-1))\}. \quad (1)$$

The mapping function $f(x)$ is chosen to depend on the type of local chaos. For example, one can choose the logistic map, $f(x) = rx(1-x)$, as a typical model for chaos. As the map dynamics are well studied, dynamical systems theory can be applied to understand behaviors of the CML.

By adopting different procedures, one can construct models for different types of spatially extended dynamical systems. For problems of phase transition dynamics, it is useful to adopt a map with bistable fixed points (e.g., $f(x) = \tanh x$) as a local dynamics. The choice of a different type of coupling, as well as the extension to a higher-dimensional space is straightforward. By changing the procedures in the CML, one can easily construct a model for dynamical phenomena in space-time. Examples include spinodal decomposition, crystal growth, boiling, convection, and cloud dynamics, among others.

Universality Classes of the Phenomena

Phenomena found in one CML are often observed in a wide variety of systems, and they form a universality class common to such systems. CMLs thus work as a tool to predict novel phenomenology forming such qualitative universality classes.

In the model of Equation (1), the following phenomena have been discovered: (i) spatial bifurcation and frozen chaos, (ii) spatiotemporal intermittency (STI), (iii) Brownian motion of chaotic defects, and (iv) global traveling wave by local phase slips. These phenomena are observed in a wide variety of systems, including experiments. In particular, STI is now regarded as a universal route to fully developed spatiotemporal chaos. In fully developed spatiotemporal chaos, statistical mechanics theory is developed by taking advantage of the discreteness in spacetime.

If one adopts a two-dimensional lattice system, spiral pattern dynamics are often observed. For example, by taking a local map with an excitable state, the formation of spiral waves is studied, including turbulence due to the break-up of a spiral wave pair. Such a model is studied in relation to the pattern dynamics in reaction-diffusion systems as well as wave propagation in cardiac tissue.

Another straightforward extension is a spatially asymmetric coupling. In an open fluid flow, for example, there is coupling from up-flow to down-flow, instead of the diffusion. The CML $x_{n+1}(i) = (1-\varepsilon) f(x_n(i)) + \varepsilon f(x_n(i))$ gives a prototype model for such a case. In this open flow system, it is important to distinguish absolute instability from convective instability. If a small perturbation against a reference state grows in a stationary frame, it is called "absolute instability," while if the perturbation grows only in a frame moving with a specific velocity, it is called "convective instability." This convective instability leads to spatial bifurcation from a homogeneous state to down-flow convective chaos.

Globally Coupled Maps with Applications to Biology

An extension of CML to global coupling is interesting, and often important for biological problems. Thus a globally coupled map (GCM) was introduced as a

mean-field-type extension of a CML, written as

$$x_{n+1}(i) = (1-\varepsilon) f(x_n(i)) + (\varepsilon/N) \sum_{j=1}^{N} f(x_n(j)). \quad (2)$$

One important notion here is clustering. The elements split into several clusters, within which all the elements oscillate in synchronization. Depending on the numbers of clusters in the GCM, there are phase transitions among a coherent phase, an ordered phase, a partially ordered phase, and a desynchronized phase, as the parameter describing the nonlinearity in $f(x)$ is increased. In the partially ordered phase, there are many attractors with different numbers of clusterings and with a variety of partitions. Dynamically, the system spontaneously switches between ordered states through disordered states, known as chaotic itinerancy. In the desynchronized phase, nontrivial collective motion is observed with some hidden coherence among elements. This demonstrates the existence of macroscopic chaos different from microscopic chaos represented by each map $x_{n+1} = f(x_n)$. This observation may shed new light on the origin of collective behavior by an ensemble of cells, such as an electroencephalogram (EEG) in the brain.

Often, a biological system has both internal dynamics and interactions. Chemical dynamics in a cell includes both intra-cellular reactions associated with gene expressions and cell-cell interactions. Since a CML or GCM is a model for such intra-inter dynamics, the concepts developed in this area will be relevant to biological problems. For example, clustering leads to differentiation of the states of elements. The theory for cell differentiation and robust developmental process may be based on this dynamic differentiation.

KUNIHIKO KANEKO

See also **Cellular automata; Cluster coagulation; Maps**

Further Reading

Chaté, H. & Courbage, M. (editiors). 1997. Special issue on lattice dynamics. *Physica* D, 103: 1–612

Kaneko, K. 1986. *Collapse of Tori and Genesis of Chaos in Dissipative Systems* Singapore: World Scientific 1986 (PhD thesis originally published 1983)

Kaneko, K. (editior). 1992. Chaos focus issue on coupled map lattices. *Chaos*, 2(3): 279–408

Kaneko, K. (editor). 1993 *Theory and Applications of Coupled Map Lattices*, Chichester and New York: Wiley

Kaneko, K. & Tsuda, I. 2000. *Complex Systems: Chaos and Beyond—A Constructive Approach with Applications in Life Sciences*, Berlin and New York: Springer

Kaneko, K. & Tsuda, I. 2003. Chaos focus issue on chaotic itinerancy. *Chaos*, 13(3): 926–1164

COUPLED OSCILLATORS

The simplest coupled oscillator is a pair of linearly coupled harmonic oscillators, which is used as a model for a wide variety of physical systems—including the interactions of musical instruments and tuning forks, lattice vibrations, electrical resonances, and so on—in which energy tunnels back and forth between two sites at a difference (beat) frequency. If there are many elementary oscillators that are nonlinear, coupled systems exhibit more varied nonlinear phenomena. There are two types of coupled nonlinear oscillators: those described by Hamiltonian (energy-conserving) dynamics, and systems in which energy is not conserved. In addition to coupled pendula, examples of the first kind include the Fermi–Pasta–Ulam model and the Toda lattice.

Coupled nonlinear oscillators that do not conserve energy can be viewed as coupled limit cycle oscillators. A limit cycle oscillator (also called a self-sustained oscillator) is described as an attractor in a dissipative dynamical system. A typical dissipative dynamical system that exhibits a limit cycle oscillation is van der Pol's equation

$$\frac{d^2x}{dt^2} - \varepsilon\left(1-x^2\right)\frac{dx}{dt} + \omega^2 x = 0 \quad (1)$$

in which the character of the oscillation varies from sinusoidal and energy-conserving to a strongly dissipative (blocking or relaxation) oscillation through the variation of a parameter (ε) from zero to large values (van der Pol, 1934).

Among the varieties of limit cycle oscillators, the behavior of a quasilinear oscillator (small ε) can be expressed by a sinusoidal wave, $x(t) = A\sin(\omega t + \phi_0)$. The wave shape of a relaxation oscillator (large ε), on the other hand, is composed of alternating fast and slow motions, similar to the spikes and slow recovery motions in a firing neuron, and stick-slip oscillations in frictional motions.

Although the limit cycle oscillation has a certain natural amplitude and frequency, the phase variable, for example, $\phi = \omega t + \phi_0$ for a quasilinear oscillator, is a neutral mode, sensitively perturbed by an external force. If the external force is periodic with a frequency close to the natural frequency of the limit cycle oscillator, the phase of the limit cycle oscillator tends to approach the phase of the external periodic force. If the external force is sufficiently strong, the phase difference $\Delta\phi(t) = \phi(t) - \phi_e(t)$ between the limit cycle oscillator and the external force is fixed. This phenomenon—termed *phase* or *frequency locking*—occurs more easily when ε is large, the frequency of the limit cycle oscillator is close to that of the external force, and the coupling (K) is large.

Regions in the (ω, ε, K) parameter space where frequency locking is observed are termed "Arnol'd

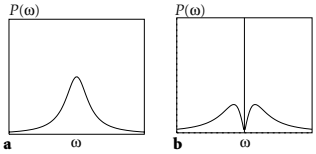

Figure 1. Frequency distribution $P(\omega)$ (a) in an asynchronous state for $K < K_c$ and (b) in a mutually entrained state for $K > K_c$.

tongues" owing to their peculiar shape. The frequency ratio between the limit cycle and the external force is 1:1 in the above frequency locking. In general, n:m frequency lockings are possible, where n and m are small integers.

For a collection of coupled limit cycle oscillators with slightly different natural frequencies, frequency locking (called mutual entrainment) also occurs, as was first observed by Christiaan Huygens in the 17th century. He found that the motions of pendulum clocks suspended from the same wooden beam come to coincide with each other perfectly. Nobert Wiener analyzed such systems in the 1950s, showing that the power spectrum of the waves should have a peak close to 10 Hz, and he inferred that a similar shape of the power spectra of electroencephalogram (EEG) is due to mutual entrainment in coupled neural oscillators (Wiener, 1958). Buck and Buck reported that rhythmical flashes of South Asian fireflies were mutually synchronized (Buck & Buck, 1976).

Mutual entrainment of coupled limit cycle oscillators has been studied by Winfree (2000) and also by Kuramoto, who considered a coupled phase oscillator model, noting the neutrality of phase variables (Kuramoto, 1984). The simplest model with global coupling has the form

$$\dot{\phi}_i = \omega_i + \frac{K}{N}\sum_{j=1}^{N}\sin(\phi_j - \phi_i), \qquad (2)$$

where ϕ_i and ω_i represent the phase and the natural frequency of the ith oscillator, N is the total number of oscillators, and K is a coupling constant.

For $K < K_c$, the motion of each oscillator is independent and the frequency of the ith oscillator is the same as ω_i. However, for $K > K_c$, collective oscillation appears and a number of oscillators are entrained to the collective oscillation. Figure 1 displays a typical frequency distribution for $K < K_c$ and $K > K_c$. The δ-function peak in the frequency distribution implies mutual entrainment and a depression is seen around the deserved frequency for $K > K_c$.

The Josephson junction is a quantum device composed of two weakly coupled superconductors. With the current bias current below a critical value, the superconducting current flows without a voltage drop. If the bias is above the critical current, the phase difference (ϕ) between the Josephson junction is not constant in time, and the voltage drop (V) between the Josephson junction equals $\hbar\dot{\phi} = 2\,\mathrm{eV}$. This is called the AC Josephson effect. Thus the Josephson junction behaves as a kind of limit cycle oscillator above the critical current. If microwaves with frequency ω_0 are applied to the Josephson junction, $n:1$ frequency locking occurs, and the voltage becomes $V = n\hbar\omega_0/2e$. With N Josephson junctions coupled in series, the total voltage across the array is given by $V = Nn\hbar\omega_0/2e$. Such series arrays are currently used to establish the international standard of voltage (*See* **Josephson junction arrays**).

HIDETSUGU SAKAGUCHI

See also **Chaotic dynamics; Phase dynamics; Synchronization; Van der Pol equation**

Further Reading

Buck, J. & Buck, E. 1976. Synchronous fireflies. *Scientific American*, 234: 74–85

Kuramoto, Y. 1984. *Chemical Oscillations, Waves, and Turbulence*, Berlin: Springer

van der Pol, B. 1934. The nonlinear theory of electric oscillations. *Proceedings of the IRE*, 22: 1051–1086

Wiener, N. 1958. *Nonlinear Problems in Random Theory*, Cambridge, MA: MIT Press

Winfree, A.T. 2000. *When Time Breaks Down*, Berlin and New York: Springer

COUPLED SYSTEMS OF PARTIAL DIFFERENTIAL EQUATIONS

Coupled systems of nonlinear partial differential equations (PDEs) are often derived to simplify complicated systems of governing equations in theoretical and applied sciences (Engelbrecht et al., 1988). Nonlinear electromagnetic theory, fluid dynamics, and systems in general relativity are difficult computational problems even with the help of numerical algorithms and the latest computer technologies. Using additional assumptions on properties of nonlinear wave processes in physical systems, however, one can derive coupled systems of nonlinear PDEs from the original governing equations, which simplify the analysis.

The main effects of nonlinear waves (such as nonlinearity, dispersion, diffraction, diffusion, damping and driven forces, and resonances) can be described with coupled nonlinear PDEs. Such systems may exhibit simple solutions such as traveling solitary waves and periodic waves, and some can be solved with the inverse scattering transform methods. Coupled systems comprise various combinations of nonlinear evolution equations that describe long solitary waves (Korteweg–de Vries and Boussinesq equations), envelope waves (nonlinear Schrödinger equations), kinks

and breathers (sine-Gordon equations), and traveling fronts and pulses (reaction-diffusion systems). Here, we present a few examples.

Long surface water waves occur in oceans, seas, and lakes. The tsunami wave (Bryant, 2001) is an example of a nonlinear surface wave that arises following underwater earthquakes or underwater volcano eruptions and may reach heights of 20–30 m as it comes ashore. Because tsunamis are as long as tens and hundreds of kilometers, the ocean can be considered as shallow for such waves. This shallow-water approximation reduces the Euler equations for water waves to the Boussinesq system of coupled PDEs (Whitham, 1974):

$$\begin{aligned} u_t + uu_x + g\eta_x - (h^3/3)u_{txx} &= 0, \\ \eta_t + hu_x + \eta u_x + u\eta_x &= 0, \end{aligned}$$

where $\eta = \eta(x,t)$ is the wave surface elevation, $u = u(x,t)$ is the horizontal velocity, h is the water depth, and g is the gravitational acceleration.

The linear Boussinesq equation takes the form of the wave equation: $\eta_{tt} - c^2\eta_{xx} = 0$, which exhibits a two-wave solution $\eta = f(x-ct) + g(x+ct)$, where $f(x)$, $g(x)$ are arbitrary functions and $c = \sqrt{gh}$ is the wave speed. When the two waves are separated in space, small nonlinearity and dispersion are captured in the unidirectional Korteweg–de Vries (KdV) equation (Johnson, 1997):

$$\eta_t + c\left(1 + \frac{3\eta}{2h}\right)\eta_x + \frac{ch^2}{6}\eta_{xxx} = 0.$$

Different modes of long weakly nonlinear waves may travel with the same speed, exchanging energy by means of wave resonances. Because ocean water is stratified in density and shear flow, gravity waves can propagate along internal interfaces of the ocean stratification. Resonant interaction of internal wave modes in stratified shear flows is described by the system of coupled KdV equations (Grimshaw, 2001):

$$\boldsymbol{u}_t + A\boldsymbol{u}_x + B(\boldsymbol{u})\boldsymbol{u}_x + C\boldsymbol{u}_{xxx} = 0,$$

where A, $B(\boldsymbol{u})$, C are matrices and $\boldsymbol{u} = \boldsymbol{u}(x,t)$ is the vector for amplitudes of different internal wave modes.

Optical pulses may consist of electromagnetic waves in optical fibers, waveguides, and transmission lines. The propagation of optical pulses due to a balance between nonlinearity and dispersion is based on the paraxial approximation of the Maxwell equations with nonlinear refractive indices. This perturbation technique results in the nonlinear Schrödinger (NLS) equation (Newell & Moloney, 1992):

$$\mathrm{i}\psi_t + \tfrac{1}{2}\omega''(k_0)\psi_{xx} + \gamma(k_0)|\psi|^2\psi = 0,$$

where $\psi = \psi(x,t)$ is the envelope amplitude of a wave packet with the carrier wave number k_0. Depending on the relative signs of the dispersion coefficient $\omega''(k_0)$ and the nonlinearity coefficient $\gamma(k_0)$, wave perturbations are focused or defocused in the time evolution of the NLS equation. Interactions between waves with two orientations of polarization (ψ_y and ψ_z with propagation in the x-direction) can be represented in a normalized form as

$$\begin{aligned} \mathrm{i}\psi_{y,t} + \psi_{y,xx} + 2(|\psi_y|^2 + |\psi_z|^2)\psi_y &= 0 \\ \mathrm{i}\psi_{z,t} + \psi_{z,xx} + 2(|\psi_y|^2 + |\psi_z|^2)\psi_z &= 0. \end{aligned}$$

These are a pair of coupled NLS equations that are integrable by the inverse scattering transform method and display vector solitons (Manakov, 1974). Under collisions, the polarization vectors of two vector solitons change.

In wavelength-division-multiplexing optical systems, optical signals are transmitted through parallel channels at different carrier wave numbers (up to 40 channels in latest communication lines). Incoherent interaction of optical pulses at nonresonant frequencies is described by the system of coupled NLS equations (Akhmediev & Ankiewicz, 1997):

$$\mathrm{i}\boldsymbol{\psi}_t + D\boldsymbol{\psi}_{xx} + E(|\boldsymbol{\psi}|^2)\boldsymbol{\psi} = 0,$$

where D and $E(|\boldsymbol{\psi}|^2)$ are matrices and $\boldsymbol{\psi} = \boldsymbol{\psi}(x,t)$ is the vector for optical pulses in different channels. If the coupling between optical pulses is coherent (as in birefringent fibers, waveguide couplers, phase mixers, and resonant optical materials), the system of coupled NLS equations takes a general form:

$$\mathrm{i}\boldsymbol{\psi}_t + A\boldsymbol{\psi} + \mathrm{i}B\boldsymbol{\psi}_x + \mathrm{i}C(\boldsymbol{\psi})\boldsymbol{\psi}_x + D\boldsymbol{\psi}_{xx} + E(\boldsymbol{\psi})\boldsymbol{\psi} = \boldsymbol{0}.$$

The coupled NLS equations describe phase-matching resonance in quadratic χ^2 materials, gap solitons in periodic photonic gratings under Bragg resonance, Alfvén waves in plasmas, and other applications (Newell & Moloney, 1992).

In conservative nonlinear systems, wave dynamics of small amplitudes occur typically in the neighborhood of local minima of potential energy. Wave oscillations in the system of nonlinear massive pendulums are described by the Frenkel–Kontorova dislocation model. In a continuous approximation, the Frenkel–Kontorova lattice model reduces to the sine-Gordon (SG) equation (Braun & Kivshar, 1998):

$$\varphi_{tt} - c^2\varphi_{xx} + \sin\varphi = 0,$$

where φ is the angle between a pendulum and the vertical axis in a mechanical model. The nonlinear pendulums swing on a rigid rod under the gravity force and couple to each other with elastic springs. More complicated models of molecular crystals and ferromagnetics in solid state mechanics, stacked Josephson contacts in superconductivity, and strings in

the general relativity theory are formulated as coupled systems of sine-Gordon equations (Maugin, 1999). The coupled Klein–Gordon equations take the form

$$\boldsymbol{\varphi}_{tt} - C\boldsymbol{\varphi}_{xx} + \boldsymbol{f}(\boldsymbol{\varphi}) = 0,$$

where C is a positive-definite matrix and $\boldsymbol{f}(\boldsymbol{\varphi})$ is the nonlinear vector function of components of the vector $\boldsymbol{\varphi} = \boldsymbol{\varphi}(x, t)$.

In more general systems, the energy of a nonlinear wave changes in time due to active and dissipative forces. The simplest system of this type is the nonlinear heat equation, which models the flame propagation (Zeldovich et al., 1985):

$$u_t = Du_{xx} + f(u),$$

where $u = u(x, t)$ is the temperature and D is the diffusivity constant. A complex form of the nonlinear heat equation (known as the Ginzburg–Landau equation) is derived for the amplitude of the most unstable wave mode (Newell & Moloney, 1992).

Active and dissipative systems include typically pairs of coupled activators and inhibitors. Coupled activator-inhibitor equations, known as the reaction-diffusion systems, are derived from the governing equations of thermodynamics in the form (Remoissenet, 1999):

$$\boldsymbol{u}_t = C\boldsymbol{u}_x + D\boldsymbol{u}_{xx} + \boldsymbol{f}(\boldsymbol{u}),$$

where C and D are matrices, and $\boldsymbol{f}(\boldsymbol{u})$ is a nonlinear vector function of components of the vector $\boldsymbol{u} = \boldsymbol{u}(x, t)$. Reaction-diffusion systems exhibit static, traveling, and pulsating nonlinear wave structures such as fronts and impulses. Coupled reaction-diffusion systems include the FitzHugh–Nagumo and Hodgkin–Huxley equations for nerve impulses, ephaptic coupling among nerve impulses, and models of the global dynamics of heart.

DMITRY PELINOVSKY

See also **Ephaptic coupling; Nonlinear optics; Reaction-diffusion systems; Sine-Gordon equation; Water waves**

Further Reading

Akhmediev, N. & Ankiewicz, A. 1997. *Solitons, Nonlinear Pulses, and Beams*, London: Chapman & Hall

Braun, O.M. & Kivshar, Yu.S. 1998. Nonlinear dynamics of the Frenkel–Kontorova model. *Physics Reports*, 306: 1–109

Bryant, T., 2001. *Tsunami: The Underrated Hazard*, Cambridge and New York: Cambridge University Press

Engelbrecht, J.K., Fridman V.E. & Pelinovski E.N., 1988. *Nonlinear Evolution Equations*, London: Longman and New York: Wiley

Grimshaw, R. (editor). 2001. *Environmental Stratified Flows*, Boston: Kluwer

Johnson, R.S. 1997. *A Modern Introduction to the Mathematical Theory of Water Waves*, Cambridge and New York: Cambridge University Press

Manakov, S.V. 1974. On the theory of two-dimensional stationary self-focusing of electromagnetic waves. *Soviet Physics, JETP*, 38: 248–253

Maugin, G.A. 1999. *Nonlinear Waves in Elastic Crystals*, Oxford and New York: Oxford University Press

Newell, A.C. & Moloney, J.V. 1992. *Nonlinear Optics*, Redwood City, CA: Addison-Wesley

Remoissenet, M. 1999. *Waves Called Solitons*. Berlin and New York: Springer

Whitham, G. 1974. *Linear and Nonlinear Waves*. New York: Wiley

Zeldovich, Ya.B., Barenblatt, G.I., Librovich, V.B. & Makhviladze, G.M. 1985. *The Mathematical Theory of Combustion and Explosions*. New York: Consultants Bureau

CRITICAL PHENOMENA

The term *critical phenomenon* is used synonymously with "phase transition," which involves a change of one system phase to another and occurs at a characteristic temperature (called a transition temperature or a critical temperature: T_c). There are several different kinds of phase transitions such as melting, vaporization, and sublimation, as well as solid-solid, conducting-superconducting, and fluid-superfluid transitions. In systems undergoing phase transitions, an emergence of long-range order is seen in which the value of a physical quantity at one arbitrary point in the system is correlated with its value at another point a long distance away.

A classification scheme of phase transitions which remains the most popular was originally proposed by Paul Ehrenfest. According to this scheme, a transition for which the first derivative of the free energy with respect to temperature is discontinuous is called a first-order phase transition; thus, the heat capacity, C_p, at a first-order transition is infinite. A second-order phase transition is one in which the first derivative of the thermodynamic potential with respect to temperature is continuous, but its second derivative is discontinuous, so the heat capacity is discontinuous but not infinite at the transition. Near a second-order phase transition (due to the reduction of rigidity of the system), critical fluctuations dominate as their amplitudes diverge.

A useful concept in analyzing phase transitions is that of a critical exponent. In general, if a physical quantity $Q(T)$ either diverges or tends to a constant value (see Figure 1) as T tends to T_c, it can be characterized by defining the reduced temperature ε as

$$\varepsilon \equiv \frac{T - T_c}{T_c}. \tag{1}$$

The associated critical exponent is

$$\mu = \lim_{\varepsilon \to 0} \frac{\ln Q(\varepsilon)}{\ln \varepsilon}. \tag{2}$$

The most important critical exponents are denoted as α, β, γ, δ, υ, and η and describe the specific heat, order parameter, isothermal susceptibility, response to an external field, the correlation length, and the pair correlation function, respectively. (See Table 1 where

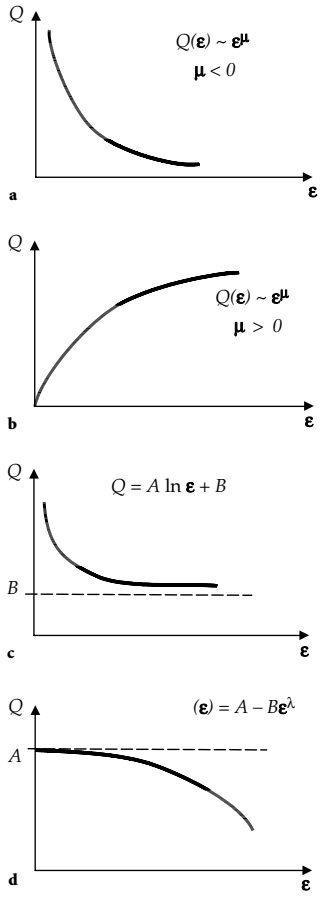

Figure 1. The four generic behaviors near criticality.

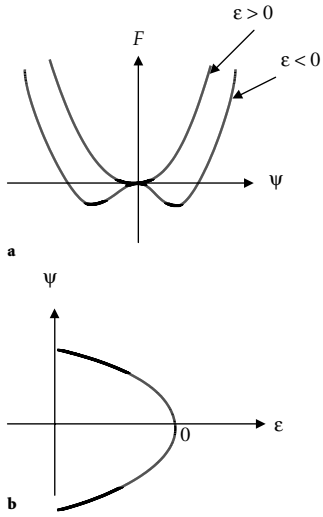

Figure 2. A prototype of second-order phase transitions according to Landau.

the primed exponents are introduced for temperatures below the critical temperature while the unprimed exponents are valid above the critical temperature.)

The mean field approximation (Landau theory) describes the physics of phase transitions well except in the immediate vicinity of the critical point where order parameter fluctuations are large. It is assumed that close to T_c, the free energy F can be expanded in a Taylor series of the order parameter ψ. Introducing the reduced temperature ε as a control parameter, the simplest such expansion is (see Figure 2)

$$F(T, V, \psi) = F_0 + a\varepsilon\psi^2 + A_4\psi^4, \tag{3}$$

where $a > 0$ and $A_4 > 0$. Solving the equilibrium conditions for ψ yields $\psi = 0$ for $\varepsilon > 0$ and

$$\psi = \pm\left(-\frac{a\varepsilon}{2A_4}\right)^{1/2} \quad \text{for } \varepsilon < 0, \tag{4}$$

thus $\beta = 0.5$ is obtained. Calculating the entropy

$$S = \frac{\partial F}{\partial T} = S_0 + \frac{a^2}{2A_4}\frac{\varepsilon}{T_c} \quad \varepsilon \le 0, \tag{5}$$

where for $\varepsilon > 0$, $S = S_0$ is the entropy of the disordered phase, which gives the specific heat as

$$C_v = T\frac{\partial S}{\partial T} = C_0 + \frac{a^2}{2A_4T_c}T \quad \varepsilon \le 0, \tag{6}$$

where for $\varepsilon > 0$, $C_v = C_0$ is the specific heat of the disordered phase. Hence, a discontinuity occurs at T_c (see Figure 3).

$$\Delta C = \frac{a^2}{2A_4T_c}. \tag{7}$$

Thus, $\alpha = 0$.

Including in F an external field h coupled to ψ

$$F = F_0 + a\varepsilon\psi^2 + A_4\psi^4 - h\psi \tag{8}$$

Exponent	Definition (liquid-vapor) Specific heat at constant volume	Definition (magnetic) Specific heat at constant H
α'	$C_v \sim (-\varepsilon)^{-\alpha'}$	$C_H \sim (-\varepsilon)^{-\alpha'}$
α	$C_v \sim \varepsilon^{-\alpha}$	$C_H \sim \varepsilon^{-\alpha}$
	Density difference	Magnetization
β	$\rho_L - \rho_G \sim (-\varepsilon)^{\beta}$	$M \sim (-\varepsilon)^{\beta}$
	Isothermal compressibility	Isothermal susceptibility
γ'	$\kappa_T \sim (-\varepsilon)^{-\gamma'}$	$\chi_T \sim -\varepsilon^{-\gamma'}$
γ	$\kappa_T \sim \varepsilon^{-\gamma}$	$\chi_T \sim \varepsilon^{-\gamma}$
	Pressure-density critical isotherm	Magnetic field-magnetization
δ	$P - Pc \sim \lvert\rho_L - \rho_G\rvert^{\delta}$	$H \sim \lvert M\rvert^{\delta}$
	$(T = T_c)$	$(T = T_c)$
	Correlation length	Correlation length
ν'	$\xi \sim (-\varepsilon)^{-\nu'}$	$\xi \sim -\varepsilon^{-\nu'}$
ν	$\xi \sim \varepsilon^{-\nu}$	$\xi \sim \varepsilon^{-\nu}$
	Density–density pair correlation	Spin-spin pair correlation
η	$\Gamma(r) \sim \lvert r\rvert^{-(d-2+\eta)}$	$\Gamma(r) \sim \lvert r\rvert^{-(d-2+\eta)}$

Table 1. The definitions of critical exponents for liquid-vapor and magnetic systems. [The primed (unprimed) exponents are for temperatures below (above) T_c.]

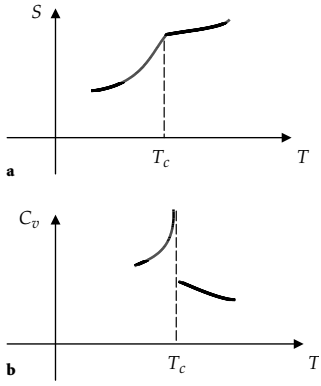

Figure 3. Plots of $S(T)$ and $C_v(T)$ in the Landau model of a second-order phase transition.

and minimizing F with respect to ψ yields an equation of state of the form

$$h = 2\psi\lfloor a\varepsilon + 2A_4\psi^2\rfloor. \tag{9}$$

Because the susceptibility $\chi \equiv \partial\psi/\partial h$, we find

$$\chi = [2a\varepsilon + 12A_4\psi^2]^{-1}. \tag{10}$$

As $\psi \to 0$ as $T \to T_c$, the third exponent is $\gamma = 1$. At $T = T_c$, the equation of state (9) simplifies to:

$$h \cong 4A_4\psi^3, \tag{11}$$

and hence $\psi \sim h^{1/3}$ giving $\delta = 3$. The quartic expansion in the Landau model invariably leads to the classical critical exponents: $\alpha = 0$, $\beta = 0.5$, $\gamma = 1$, and $\delta = 3$.

While the Landau theory cannot describe spatial fluctuations, following Ginzburg and Landau's proposal, it can be extended to consider the free energy to be a functional:

$$F(\psi(\vec{r}), T) = \int \mathrm{d}^3\mathbf{r}[A_2\psi^2 + A_4\psi^4 - h\psi + D(\nabla\psi)^2] \tag{12}$$

where D describes the energy due to spatial inhomogeneities. Applying a variational principle to F results in a nonlinear Klein–Gordon equation for the order parameter

$$h = 2A_2\psi + 4A_4\psi^3 - 2D\nabla^2\psi. \tag{13}$$

A linearized solution of Equation (13) in spherical coordinates is

$$\psi = \frac{h_0}{4\pi D}\frac{\mathrm{e}^{-r/\xi}}{r}, \tag{14}$$

where $\xi \sim A_2^{-1/2}$ is the correlation length that diverges as $T \to T_c$ so that the critical exponent $\upsilon = 0.5$. Fourier transforming the order parameter according to

$$\psi(\vec{r}) \equiv L^{-d/2}\sum_{k<k_0}\psi_k \mathrm{e}^{\mathrm{i}\vec{k}\cdot\vec{r}}, \tag{15}$$

where d is the spatial dimensionality and the cutoff wavelength $k_0 = \Lambda^{-1}$ corresponds to the smallest periodicity, F becomes (for $h = 0$)

$$F = \sum_{k<k_0}|\psi_k|^2(A_2 + Dk^2) + L^{-d}\sum_{k,k',k''<k_0} A_4\psi_k^*\psi_{k'}^*\psi_{k''}\psi_{k+k'-k''} \tag{16}$$

Ignoring mode-mode coupling provides the basis for a Gaussian approximation, where

$$F \cong \sum_{k<k_0} |\psi_k|^2 (A_2 + Dk^2). \tag{17}$$

The Fourier transform of the correlation function is found as

$$\begin{aligned} \Gamma(k) &= L^{-d} \int \mathrm{e}^{-\mathrm{i}\vec{k}(\vec{r}-\vec{r'})} < \psi(\vec{r})\psi(\vec{r'}) > \mathrm{d}\vec{r}\,\mathrm{d}\vec{r'} \\ &= \langle |\psi_k|^2 \rangle \cong \frac{n}{2}(A_2 + Dk^2)^{-1} \end{aligned} \tag{18}$$

Therefore, as $T \to T_c$, we find that $\Gamma(k) \sim k^{\eta-2}$ with $\eta = 0$ in the Gaussian approximation and also $\Gamma(r) \sim r^{-(d-2)}$. Furthermore, the Gaussian approximation introduces a new value of the specific heat critical exponent $\alpha = 2 - d/2$.

JACK A. TUSZYŃSKI

See also **Bifurcations; Ferromagnetism and ferroelectricity; Order parameters; Phase transitions**

Further Reading

Anderson, P.W. 1984. *Basic Notions of Condensed Matter Physics*, Menlo Park, CA: Benjamin Cummings

Landau, L.D. & Lifshitz, E.M. 1959. *Statistical Physics*, London: Pergamon

Ma, S.-K. 1976. *Modern Theory of Critical Phenomena*, New York: Benjamin

Reichl, L.E. 1979. *A Modern Course in Statistical Physics*, Austin: University of Texas Press

Stanley, H.E. 1971. *Introduction to Phase Transitions and Critical Phenomena*, Oxford: Clarendon Press and New York: Oxford University Press

White, R.H. & Geballe, T. 1979. *Long Range Order in Solids*, New York: Academic Press

Yeomans, J.M. 1992. *Statistical Mechanics of Phase Transitions*, Oxford: Clarendon Press and New York: Oxford University Press

CRITICAL POINTS

See **Critical phenomena**

CRYSTAL DISLOCATIONS

See **Dislocations in crystals**

CRYSTALS, MOLECULAR

See **Local modes in molecular crystals**

CUBIC MAP

See **Maps**

D

DAMPED-DRIVEN ANHARMONIC OSCILLATOR

Many problems in engineering and the applied sciences are modeled by low-dimensional forced oscillators. Examples include vibrating mechanical and structural engineering systems (beams, bridges), marine systems (ships, oil platforms), electronic circuits and devices (Josephson junctions), as well as biological oscillators. While the linear behavior of such systems has long been well understood, the potential dynamics of nonlinear oscillators is far more complex and many open problems remain.

Damped Nonlinear Pendulum

Let us consider a mathematical pendulum and denote with θ the angular displacement of the pendulum from the equilibrium (hanging down) position. The equation of motion for the oscillations of a damped nonlinear pendulum of unitary mass is

$$\frac{\mathrm{d}^2\theta}{\mathrm{d}t^2} + \eta\frac{\mathrm{d}\theta}{\mathrm{d}t} + \frac{g}{l}\sin(\theta) = 0, \qquad (1)$$

where l is the length of the pendulum and g is the gravitational acceleration. This equation expresses Newton's second law with the terms on the left-hand side, respectively, representing acceleration, damping, and gravitation. Equation (1) may be rewritten as two first-order equations:

$$\begin{cases} \dot{\theta} &= \omega, \\ \dot{\omega} &= -\eta\omega - \frac{g}{l}\sin(\theta), \end{cases} \qquad (2)$$

where ω denotes the angular velocity. Then, one can use (θ, ω) as phase space coordinates.

Fixed points: The dynamics of the nonlinear pendulum can be analyzed as trajectories in the phase space. The rest position $\theta = \omega = 0$ is called a *fixed point*. It is easy to see that almost all phase space trajectories spiral into the fixed point at $(0, 0)$. This is a linearly stable fixed point, since if a small perturbation is made from the fixed point, the perturbation decays in time (exponentially for small enough perturbations). There is a second fixed point at $(\pi, 0)$ corresponding to the pendulum pointing vertically up. The fixed point at $(\pi, 0)$ is linearly unstable because a small perturbation from this fixed point grows exponentially. Only very carefully tuned initial conditions will lead to a trajectory ending on the unstable fixed point, and almost all perturbations to the initial condition will lead to a trajectory that may approach close to the unstable fixed point, but eventually spirals into the stable fixed point. The $(0, 0)$ fixed point is attracting, and in this case the basin of attraction, that is, the set of initial conditions leading to trajectories that approach the fixed point, is the whole phase space except for a set of zero measure.

An example of a trajectory of system (2) converging towards the stable fixed point at $(0, 0)$ is shown in Figure 1.

The Periodically Driven Damped Pendulum

Let us now consider the nonlinear damped pendulum of Equation (1) when a harmonic driving force is applied. The equation of motion for the oscillations of a damped, sinusoidally driven nonlinear pendulum is

$$\frac{\mathrm{d}^2\theta}{\mathrm{d}t^2} + \gamma\frac{\mathrm{d}\theta}{\mathrm{d}t} + \sin(\theta) = A_{\mathrm{D}}\cos(\omega_{\mathrm{D}}t), \qquad (3)$$

where A_{D} is the forcing amplitude and the angular velocity of the forcing, ω_{D}, may be different from the natural frequency of the pendulum. Note, with respect to Equation (1), that the time variable has been rescaled so that the period of small oscillations of the undamped and undriven pendulum is unity, and the (scaled) dissipation coefficient is now denoted by γ. Physically, the situation corresponds to driving the pendulum, feeding in energy to resupply the energy dissipated.

Small-Amplitude Oscillations

For small driving amplitudes, A_{D}, and assuming a small initial condition, one can approximate $\sin\theta \approx \theta$ and

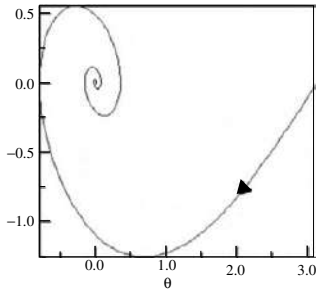

Figure 1. Typical trajectory for the nonlinear pendulum of Equation (2). All initial conditions lead to an orbit spiraling into the fixed point at (0, 0).

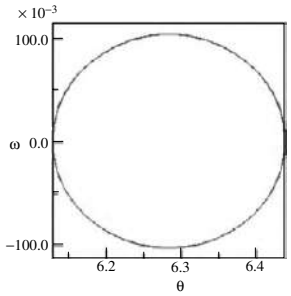

Figure 2. If small driving is turned on ($A_D = 0.1$), the steady-state solution is a stable limit cycle. Note that, for simplicity, the transient dynamics are not shown.

solve Equation (3) analytically:

$$\theta = \frac{A_D}{\sqrt{(1-\omega_D^2)^2+\gamma^2\omega_D^2}}\cos(\omega_D t+\Phi) + A_0 e^{-\gamma t/2}\cos(\omega t+\varphi_0), \quad (4)$$

where

$$\tan\Phi = -\frac{\gamma\omega_D}{(1-\omega_D^2)}, \quad \omega = \sqrt{1-\frac{\gamma^2}{4}}, \quad \gamma < 2 \quad (5)$$

while the constants A_0 and φ_0 depend upon the initial conditions (θ_0, ω_0), that is, for $t = 0$.

Equation (4) describes the resonant response (the first term) oscillating at the applied frequency, together with decaying free oscillations (the second term), depending on the initial conditions. This kind of solution is called an attracting *limit cycle*.

A typical limit cycle at this small amplitude, for $A_D = 0.1$, is shown in Figure 2 and is seen to be close to circular. From now on, although the transient may be quite complicated, only the asymptotic behavior, that is, the behavior of the attractors will be considered.

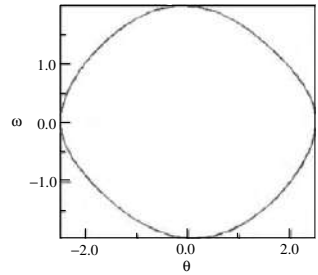

Figure 3. Large-amplitude limit cycle, for $A_D = 0.9$.

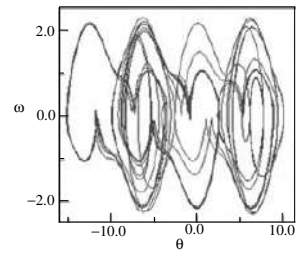

Figure 4. Chaotic attractor, for driving amplitude $A_D = 1.15$.

Large-Amplitude Solutions

What happens for large driving amplitudes? Here, there are no analytic solutions, and one must proceed numerically. To gain some intuition it is more convenient to view the dynamics in the phase space. To this end, Equation (3) may be converted to autonomous form by using three variables, as follows:

$$\begin{cases} \dot\theta = \omega, \\ \dot\omega = -\gamma\omega - \sin(\theta) + A_D\cos(\theta_D), \\ \dot\theta_D = \omega_D, \end{cases} \quad (6)$$

where the phase of the driving, θ_D, has been introduced.

If one increases the driving strength to $A_D = 0.9$, a large-amplitude limit cycle is observed, as shown in Figure 3. This limit cycle bifurcates for increasing values of the driving strength according to the well-known period-doubling route to chaos, leading to a chaotic attractor for $A_D = 1.09$.

Then, increasing the driving to $A_D = 1.15$ results in an even more irregular chaotic behavior, as illustrated in Figure 4. But, perhaps at first sight surprisingly, increasing the driving further, for example, to $A_D = 1.35$ gives periodic motion again. In this case, though, there is a drift along with the oscillation—the

pendulum is oscillating but also consistently rotating all the way around.

In summary, numerical simulations show that both periodic and chaotic solutions of the driven damped pendulum are possible, depending on the particular choice of the system parameters. Chaos may indeed occur since the driven pendulum equation is equivalent to a three-dimensional nonlinear autonomous system. Note the contrast with linear theory, where a damped system driven periodically *must* eventually respond periodically.

GIAN MARIO MAGGIO AND LJUPCO KOCAREV

See also **Chaotic dynamics; Coupled oscillators; Distributed oscillators; Pendulum; Relaxation oscillators; Semiconductor oscillators**

Further Reading

Andronov, A.A., Vitt, A.A. & Khaikin, S.E. 1966. *Theory of Oscillators*, New York: Dover

Baker, G.L. & Gollub, J.P. 1996. *Chaotic Dynamics*, Cambridge and New York: Cambridge University Press

Guckenheimer, J. & Holmes, P. 1983. *Nonlinear Oscillations, Dynamical Systems, and Bifurcations of Vector Fields*, New York: Springer

Hagedorn, P. 1988. *Non-Linear Oscillations*, Oxford: Clarendon Press

Mitropolskii, Y.A. & Van Dao, N. 1997. *Applied Asymptotic Methods in Nonlinear Oscillations*, Dordrecht: Kluwer

Ott, E. 1993. *Chaos in Dynamical Systems*, Cambridge: Cambridge University Press

Parker, T.S. & Chua, L.O. 1989. *Practical Numerical Algorithms for Chaotic Systems*, New York: Springer

Thompson, J.M.T. & Stewart, H.B. 2002. *Nonlinear Dynamics and Chaos*, 2nd edition, New York: Wiley

DARBOUX TRANSFORMATION

From a historical point of view, the Darboux transformation is the specialization of a more general result due to Théodore Moutard. The prior result is of application in the classical theory of surfaces (Darboux, 1887–96) and takes the following form.

Let $\phi_0(x, y)$ be any particular integral of the hyperbolic partial differential equation

$$\phi_{xy} + q(x, y)\phi = 0, \tag{1}$$

$q(x, y)$ being a given function. We may rewrite this equation in the form

$$(D_x^+ D_y^- + D_y^+ D_x^-)\phi = 0, \tag{2}$$

where the Ds are differential operators, $D_u^\pm = \partial_u \pm \phi_0^{-1}\phi_{0u}$. Now let $\psi(x, y)$ and $\phi(x, y)$ be functions satisfying the pair of first-order partial differential equations

$$\begin{aligned} D_x^-\phi &= -D_x^+\psi, \\ D_y^-\phi &= D_y^+\psi, \end{aligned} \tag{3}$$

then (1) is equivalent to the identity $[D_x^+, D_y^+]\psi = 0$. Alternatively, the identity $[D_x^-, D_y^-]\phi = 0$ yields an equation for ψ, namely,

$$\psi_{xy} + p(x, y)\psi = 0, \tag{4}$$

where $p(x, y) = q(x, y) + 2(\ln \phi_0)_{xy}$. The class of equations of form (1) is thus covariant under maps $\mu_{\phi_0} : (\phi, q) \mapsto (\psi, p)$.

The map μ_{ϕ_0} is the *Moutard* transformation and its value lies in its relating, and generating, hyperbolic equations integrable in finite terms (Darboux, 1887–96).

Darboux (1882) specialized this result to the case where (1) carries a symmetry, that is, where $q(x, y) = Q(x + y)$ is a function of $x + y$ only. Putting $z = x + y$, $\bar{z} = x - y$ and applying the standard technique of separation of variables leads to $\phi(x, y) = \exp(\lambda\bar{z})\Phi(z, \lambda)$ and the equation for Φ,

$$\Phi_{zz} + Q(z)\Phi = \lambda^2\Phi. \tag{5}$$

Given a solution Φ_0 to this equation with $\lambda = \lambda_0$, there is a corresponding $\phi_0(x, y) = \exp(\lambda_0\bar{z})\Phi_0(z, \lambda_0)$ and after a simple, constant rescaling of Φ, Equations (3) become

$$\begin{aligned} \Psi &= (\partial_z - \Phi_0^{-1}\Phi_{0z})\Phi, \\ (\lambda^2 - \lambda_0^2)\Phi &= (\partial_z + \Phi_0^{-1}\Phi_{0z})\Psi \end{aligned} \tag{6}$$

and Equation (5) becomes

$$\Psi_{zz} + P(z)\Psi = \lambda^2\Psi. \tag{7}$$

Here $P(z) = Q(z) + 2(\ln \Phi_0)_{zz}$.

The map $\delta_{\lambda_0} : (\Phi, Q) \mapsto (\Psi, P)$ is the *Darboux* transformation (DT). Note that it creates from the Φ equation one member of a family of equations depending on the free parameter λ_0.

Starting with $Q = 0$ and a specific choice λ_0 for λ, we may take $\Phi_0 = c_1 \cosh \lambda_0(z + c_2)$. Then $P(z) = 2\lambda_0^2 \operatorname{sech}^2 \lambda_0(z + c_2)$ and so, from the trivial ("vacuum") potential, the DT has generated a family of potential barriers involving the chosen λ_0 and a parameter of translation, c_2, in the z-direction.

The linear PDE (5) plays a crucial role in the Inverse Scattering Transform (IST). We suppose the potential Q to depend upon an additional parameter t ("time"): $Q = Q(z, t)$. The pair of linear PDE (Lax pair),

$$L_Q\Phi = \lambda^2\Phi, \tag{8}$$

$$M_Q\Phi = \partial_t\Phi, \tag{9}$$

where $L_Q = \partial_z^2 + Q$ and $M_Q = 4\partial_z^3 + 6Q\partial_z + 3Q_z$, is integrable in the Cauchy sense provided Q satisfies the nonlinear PDE

$$Q_t = Q_{zzz} + 6QQ_z, \tag{10}$$

namely, the Korteweg–de Vries (KdV) equation. This follows from the operator relation (Frobenius condition)

$$L_Q t = [M_Q, L_Q] \equiv M_Q L_Q - L_Q M_Q. \qquad (11)$$

The DT, $\Psi = \mathcal{D}\Phi$ for $\mathcal{D} = \partial_z + \alpha$, $\alpha = -\Phi_0^{-1}\Phi_{0z}$, is seen to play the role of an intertwining operator:

$$\mathcal{D}L_Q = L_P\mathcal{D}, \qquad (12)$$

and

$$\partial_t \Psi = M_P\Psi + \{\alpha_t + \mathcal{D}M_Q - M_P\mathcal{D}\}\Phi. \qquad (13)$$

Some calculation shows that the bracketed term is vanishing and we have the Lax pair

$$L_P\Psi = \lambda^2\Psi, \qquad (14)$$

$$M_P\Psi = \partial_t\Psi, \qquad (15)$$

in the DT transformed variables Ψ and P. Consequently, the transformed potential P will also satisfy the KdV equation (10).

Returning now to the simple example above, Φ_0 will satisfy Equation (9) with $Q = 0$, namely $\Phi_{0t} = 4\Phi_{0zzz}$, so that $\Phi_0 = c_1\cosh(\lambda_0 z + 4\lambda_0^3 t + c_3)$ and the DT generates the traveling wave (1-soliton) solution to the KdV,

$$P = 2\lambda_0^2\,\mathrm{sech}^2(\lambda_0 z + 4\lambda_0^3 t + c_3). \qquad (16)$$

Imagine now that we wish to form a sequence of DTs. Starting with (5), we make a choice Φ_0, λ_0 to form (7) via (6). Now for (7) we choose Ψ_1, λ_1 and use

$$\Theta = (\partial_z - \Psi_1^{-1}\Psi_{1z})\Psi$$

to generate Θ, satisfying

$$\Theta_{zz} + R(z)\Theta = \lambda^2\Theta,$$

where $R = P + 2(\ln\Psi_1)_{zz}$. But since Ψ_1 satisfies (6) with $\lambda = \lambda_1$, it can itself be constructed as

$$\Psi_1 = \Phi_{1z} - \Phi_0^{-1}\Phi_{0z}\Phi_1,$$

where Φ_1 satisfies (5) with $\lambda = \lambda_1$. Then simple algebra yields formulae for Θ and R:

$$\Theta = \begin{vmatrix} \Phi_0 & \Phi_1 \\ \Phi_{0z} & \Phi_{1z} \end{vmatrix}^{-1} \begin{vmatrix} \Phi_0 & \Phi_1 & \Phi \\ \Phi_{0z} & \Phi_{1z} & \Phi_z \\ \Phi_{0zz} & \Phi_{1zz} & \Phi_{zz} \end{vmatrix}, \qquad (17)$$

$$R = Q + 2\ln\left(\begin{vmatrix} \Phi_0 & \Phi_1 \\ \Phi_{0z} & \Phi_{1z} \end{vmatrix}\right)_{zz}. \qquad (18)$$

From the symmetry of these formulae under interchange of λ_0 and λ_1, it follows that the order of composition of DTs is immaterial. The fundamental result of Crum (1955) is that, starting with $n+1$ pairs (Φ_i, λ_i), $i = 0, \ldots, n$, associated with (5) one obtains the n-fold DT:

$$\begin{aligned}\delta_0 \ldots \delta_n(\Phi, Q) = {} & (W^{-1}(\Phi_0, \ldots, \Phi_n) \\ & \times W(\Phi_0, \ldots, \Phi_n, \Phi), Q \\ & + 2\ln W(\Phi_0, \ldots, \Phi_n)_{zz}),\end{aligned}$$

where W denotes the Wronskian function of its arguments.

This result, when applied to a set of n single soliton solutions of the KdV, yields an explicit n-soliton solution.

Generally speaking, a transformation of dependent variables that carries solutions of one DE to solutions of another is termed a *Bäcklund* transformation (BT). The term *Darboux* transformation refers to the special case of linear equations. We have described above a DT for a Lax pair that gives rise to a BT for the KdV equation.

For DTs of higher order, ordinary linear differential equations have been developed. For such results the intertwining property can be related to the factorization of differential operators, an approach to solvable Schrödinger potentials pioneered in quantum mechanics. This naturally leads to their algebraic formulation in terms of $\mathcal{D}$-modules. Moutard (sometimes called the Binary DT) and Darboux transformations have also been generalized to higher dimensions and utilized for solving associated analogues of the KdV with three independent variables, the Kadomtsev–Petviashvili, Novikov–Veselov, and Davey–Stewartson equations, to name but three.

The double logarithmic derivative occurring in the expression of the DT transformed potentials is of fundamental importance in the bilinear theory of soliton equations originally due to Hirota.

In the Hamiltonian theory of soliton equations the DT is seen to play the role of a canonical transformation.

A comparatively recent application of DTs has been in the theory of integrable systems with discrete variables, that is, systems defined on lattices (Antoniou & Lambert, 2000).

Finally, it should be remarked that the geometrical insights of Gaston Darboux, Luigi Bianchi, and their contemporaries are being rediscovered and developed within the modern theory of integrable systems and that Darboux and Moutard transformations are playing a key role in this resurgence (Rogers & Schief, 2002).

There are a number of monographs where further details about DTs and BTs may be found, for example, Calogero & Degasperis (1982); Konopelchenko (1987); Matveev & Salle (1991); Rogers & Shadwick (1982). For more recent reviews of work in this area see Coley (2001).

CHRIS ATHORNE

See also **Bäcklund transformations; Inverse scattering method or transform**

Further Reading

Antoniou, I. & Lambert, F. (editors). 2000. Integrability and chaos in discrete systems. Proceedings Brussels Meeting 1997. *Chaos, Solitons and Fractals*, 11(1–3)
Calogero, F. & Degasperis, A. 1982. *The Spectral Transform and Solitons*, Amsterdam: North-Holland
Coley, A. (editor). 2001. Bäcklund and Darboux transformations. The geometry of solitons, *Proceedings AARMS-CRM Workshop, Halifax, Nova Scotia, 1999*, Providence, RI: American Mathematical Society
Crum, M. 1955. Associated Sturm–Liouville systems. *Quarterly Journal of Mathematics*, 6: 121–128
Darboux, G. 1882. Sur une proposition relative aux équations linéaires. *Comptes Rendus de l'Academie des Sciences, Paris*, 94: 1343; 1456–1459
Darboux, G. 1887–96. *Leçons sur la Théorie des Surfaces*, Parts I–IV, Paris: Gauthier-Villars
Konopelchenko, B.G. 1987. *Nonlinear Integrable Equations*, Berlin and New York: Springer
Matveev, V.B. & Salle, M.A. 1991. *Darboux Transformations and Solitons*, Berlin and New York: Springer
Rogers, C. & Shadwick, W. 1982. *Bäcklund Transformations and their Applications*, New York: Academic Press
Rogers, C. & Schief, W.K. 2002. *Bäcklund and Darboux Transformations*, Cambridge and New York: Cambridge University Press

DAVEY–STEWARTSON EQUATION

See **Multidimensional solitons**

DAVYDOV SOLITON

In 1972, a meeting was convened in order to search for the general principles that underlie biological processes such as muscle contraction, active transport, enzyme catalysis, and oxidative phosphorylation (Green, 1974). One of the main questions asked was whether there was a crisis in bioenergetics. While some participants disagreed that a crisis existed, others proposed solutions to the crisis. One solution was the "conformon" of Green and Ji, defined as the free energy associated with a localized conformational strain, which was to store and transport energy (Green, 1974, pp. 419–437). McClare's paper, on the other hand, suggested that vibrational excited states and resonant energy transfer constitute a fundamental step in energy transduction in biological systems (Green, 1974, pp. 74–97). The main objection to McClare's proposal was that the lifetime of vibrational excited states, thought to be in the subpicosecond time range, was considered too short for these states to be useful. Alexander Davydov's model, proposed in connection with a mechanism for muscle contraction (Davydov, 1982), aimed to answer this objection.

The Davydov Model

The Davydov model describes energy transfer in the hydrogen-bonded spines that stabilize protein α-helices:

$$\begin{array}{ccccc} \cdots\ \text{H-N-C=O} & \cdots & \text{H-N-C=O} & \cdots & \text{H-N-C=O}\ \cdots \\ n-1 & & n & & n+1 \end{array}$$

The idea is that the energy liberated in the hydrolysis of adenosine triphosphate (ATP) creates up to two quanta of amide-I, an excited vibrational state in the peptide group that is essentially a stretching vibration in the C=O bond (Davydov, 1982). This vibration excitation propagates from one group to the next because of the dipole-dipole interaction between the groups. But it also interacts with the neighboring hydrogen bonds, leading to a deformation of the lattice and a lower energy state. This new state, which is constituted by an amide-I excitation and its associated hydrogen bond distortion, is the Davydov soliton. Structurally, the Davydov soliton is, in fact, a subtle local conformational change of the α-helix, similar to the conformon.

Davydov's Hamiltonian has three parts:

$$\hat{H} = \hat{H}_{\text{ex}} + \hat{H}_{\text{int}} + \hat{H}_{\text{ph}}, \tag{1}$$

where $\hat{H}_{\text{ex}}$, the exciton Hamiltonian, describes the transfer of an amide-I excitation between adjacent sites

$$\hat{H}_{\text{ex}} = -V \sum_{n=1}^{N} \left[\left(\hat{a}_n^{\dagger} \hat{a}_{n-1} + \hat{a}_n^{\dagger} \hat{a}_{n+1} \right) \right], \tag{2}$$

$-V$ being the dipole-dipole interaction energy between neighboring sites, $\hat{a}_n^{\dagger}(\hat{a}_n)$ the creation (annihilation) operator for a quantum quasiparticle (the amide-I excitation) at site n, and N being the number of sites (the peptide groups) in the lattice; $\hat{H}_{\text{ph}}$, the phonon Hamiltonian, describes the vibrations of the peptide groups n in the one-dimensional chain:

$$\hat{H}_{\text{ph}} = \frac{1}{2} \sum_{n=1}^{N} \left[\kappa \left(\hat{u}_n - \hat{u}_{n-1} \right)^2 + \frac{\hat{P}_n^2}{M} \right], \tag{3}$$

$\hat{u}_n$ being the displacement operator from the equilibrium position of site n, $\hat{P}_n$ the momentum operator of site n, M the mass of each site, and κ the elasticity constant of the lattice; $\hat{H}_{\text{int}}$, the interaction Hamiltonian, describes the interaction of amide-I excitation with the motions of the lattice sites:

$$\hat{H}_{\text{int}} = \chi \sum_{n=1}^{N} \left[\left(\hat{u}_{n+1} - \hat{u}_{n-1} \right) \hat{a}_n^{\dagger} \hat{a}_n \right], \tag{4}$$

χ being an anharmonic parameter arising from the coupling between the vibrational excitation and the lattice displacements.

Davydov's Hamiltonian (Equations (1–4)) is formally similar to the Holstein Hamiltonian for the interaction of electrons with a polarizable lattice. The

difference is that while Davydov's Hamiltonian couples quantum particles to acoustic phonons, the Holstein Hamiltonian couples quantum particles to optical phonons.

In Equations (1–4) both the excitation and the lattice are treated quantum mechanically. Exact wavefunctions for the system are yet to be determined in this approximation, and different solutions have been proposed in the literature (see references in Scott, 1992; Cruzeiro-Hansson & Takeno, 1997). On the other hand, when the lattice is treated classically, an approximation that has been called mixed quantum-classical (Cruzeiro-Hansson & Takeno, 1997), it is possible to determine exact wave functions. They are

$$|\psi(t)\rangle = \sum_{i=1}^{N} \varphi_i(\{u_m\}, \{p_m\}, t)\, \hat{a}_i^{\dagger}\, |0\rangle, \qquad (5)$$

where the dependence of the probability amplitude for an excitation at site i on the displacements and momenta of all the sites is not specified *a priori*. The equations of motion for the quantum variables are derived from Schrödinger's equation, while the equations of motion for the classical variables are derived from Hamilton's equations. For a one-quantum state they are

$$\begin{aligned} i\hbar \frac{d\varphi_n}{dt} &= -V\,(\varphi_{n-1} + \varphi_{n+1}) \\ &\quad + \chi\,(u_{n+1} - u_{n-1})\,\varphi_n, \end{aligned} \qquad (6)$$

$$\begin{aligned} M \frac{d^2 u_n}{dt} &= \chi\,(|\,\varphi_{n+1}\,|^2 - |\,\varphi_{n-1}\,|^2) \\ &\quad + \kappa\,(u_{n+1} + u_{n-1} - 2u_n) \end{aligned} \qquad (7)$$

The numerical simulation of these equations (and of extensions of these equations to the three interacting chains that are present in an α-helix (Scott, 1992)) confirmed Davydov's analytical studies in the continuum limit by showing that solitons can form and travel along the chains. It was also found that in the discrete chains there is a threshold in the nonlinearity parameter χ above which localized excitations can form. This threshold tends to zero as the length of the system increases.

Thermal Stability of Localized States

While the zero temperature results summarized above allow for the existence of soliton states in proteins, an important question is whether these states are stable at biological temperatures and, if not, how long they last. Coupling to a thermal bath was modeled by extending the equations of motion into Langevin equations, that is, adding stochastic forces $F(n)$ and damping terms $-\Gamma du_n/dt$ to the right-hand side of Equation (7), so that these terms obey the fluctuation-dissipation relations (Lomdahl & Kerr, 1985): $\langle F_n(t)\, F_m(t')\rangle \geq 2M\Gamma k_B T \delta_{nm}\delta(t-t')$, k_B being the Boltzmann constant and T the temperature. The result is that soliton solutions disperse in a few picoseconds at biological temperatures. On the other hand, exact quantum Monte Carlo (QMC) simulations (Wang et al., 1989) showed that the distortion induced by the excitation increased with temperature. This conflict was resolved by showing that the coupling of a classical bath to a mixed quantum-classical system leads to a classical behavior of the quantum part (Cruzeiro-Hansson & Takeno, 1997). While the states of a classical excitation at finite temperature are predominantly delocalized, the states of a quantum excitation are predominantly localized. A set of dynamic equations, that leads to the same equilibrium averages as the QMC, leads to the following dynamics (Cruzeiro-Hansson & Takeno, 1997): instead of coherent propagation along the chain, as is expected from solitons, localized amide-I excitations jump stochastically from site to site, changing their shape and their velocity as they travel. It has been suggested that this stochastic propagation is a very robust way of transferring energy in proteins because it can survive mutations more than coherent propagation. Thus these simulations indicate that the Davydov model is indeed a possible mechanism for energy transfer in proteins (Cruzeiro-Hansson & Takeno, 1997).

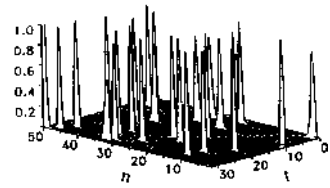

Figure 1. Dynamics of an amide-I excitation at biological temperatures.

Experimental Evidence

The first evidence for a Davydov-like state was obtained in a crystal of acetanilide (ACN), which includes hydrogen-bonded chains identical to those found in proteins. Careri and co-workers found an anomalous line, red-shifted by 15 cm^{-1} with respect to the amide-I vibration in that crystal (Scott, 1992). A series of studies established that this spectral line could not be attributed to a Fermi resonance, a Davydov splitting, or a phase transition. Its interpretation in terms of an interaction of an amide excitation with optical phonons provided good fits of the variation of its intensity with temperature as well as of its overtone frequencies. Careri and Wyman (see Scott, 1992) integrated the Davydov model in the so-called "turning wheel" model of enzyme action in which it is assumed that the binding

of ligands leads to the formation of solitons that are used to promote the enzymatic cycle.

An early objection to the role of vibrational excited states in proteins was their short lifetime, which was supposed to be in the subpicosecond range. Recently, Austin and co-workers have measured the lifetime of amide-I vibrations in myoglobin and found it to be 15 ps (Xie et al., 2000). Hamm and co-workers have also recently applied nonlinear spectroscopy to the study of ACN, not only to the amide-I band (Edler & Hamm, 2002) but also to the NH vibrations (Edler et al., 2002) that have approximately twice the energy of amide-I and a binding energy 20 times larger. In a pump-probe femtosecond spectroscopy experiment, they found that the ground state recovery for NH at room temperature is 20 ps and for amide-I at 90 K, it is 35 ps, and that the lifetime of NH stretch in the crystal is 20 times greater than in isolated ACN. Computer simulations show that vibrational excitations can travel tens of nanometers within the lifetime of these excitations (Cruzeiro-Hansson & Takeno, 1997). Edler & Hamm (2002) also find that while the low-temperature amide-I excitations are self-trapped, the higher temperature ones are Anderson-localized, in agreement with the predictions of the computer simulations (Cruzeiro-Hansson & Takeno, 1997).

Future Work

The theoretical work on the Davydov model shows that localized vibrational excited states can form in proteins and that they can be used to transfer energy from the active site to other regions of the proteins where this energy is used for work. The experimental evidence available corroborates this possibility. Further experiments should test the role of excited vibrational states in protein function in a more direct way. A theoretical challenge is to integrate the Davydov model in the full protein cycle and find out how vibrational energy transfer may eventually lead to a conformational change (Cruzeiro–Hansson & Silva, 2001), the well-known way in which proteins fold or transform into their permanent three-dimensional shapes.

LEONOR CRUZEIRO

See also **Biomolecular solitons; Excitons**

Further Reading

Cruzeiro-Hansson, L. & Takeno, S. 1997. Davydov model: the quantum, mixed quantum-classical and full classical systems. *Physical Review*, E 56(1): 894–906

Cruzeiro-Hansson, L. & Silva, P.A.S. 2001. Protein folding: thermodynamic versus kinetic control. *Journal of Biological Physics*, 27: S6–S9

Davydov, A.S. 1982. *Biology and Quantum Mechanics*, Oxford–Frankfurt: Pergamon

Edler, J. & Hamm, P. 2002. Self-trapping of the amide I band in a peptide model crystal. *Journal of Chemical Physics*, 117: 2415–2424

Edler, J., Hamm, P. & Scott, A.C. 2002. Femtosecond study of self-trapped vibrational excitons in crystalline acetanilide. *Physical Review Letters*, 88(6): 067403

Green, D.E. (editor). 1974. The mechanism of energy transduction in biological systems. *Annals of the New York Academy of Sciences*, 227: 1–668

Lomdahl, P.S. & Kerr, W.C. 1985. Do Davydov solitons exist at 300K? *Physical Review Letters*, 55(11): 1235–1238

Scott, A. 1992. Davydov's soliton. *Physics Reports*, 217(1): 1–67

Wang, X., Brown, D.W. & Lindenberg, K. 1989. Quantum Monte Carlo simulation of the Davydov model. *Physical Review Letters*, 62(15): 1796–1799

Xie, A.H., van der Meer, L., Hoff, W. & Austin, R.H. 2000. Long-lived amide I vibrational modes in myoglobin. *Physical Review Letters*, 84: 5435–5438

DELAY COORDINATES

See **Embedding methods**

DELAY-DIFFERENTIAL EQUATIONS

A delay-differential equation (DDE) comprises an unknown function and certain of its derivatives, evaluated at arguments that differ by fixed numerical values. For example, $\dot{x}(t) = F(t, x(t), x(t-r))$ is a retarded DDE for $r > 0$.

DDEs can be characterized by the number of variables, the differential order, the order of the highest derivative appearing, and the difference order (one less than the number of different arguments appearing). DDEs (also called functional differential equations or difference-differential equations) generalize the concept of differential equations by allowing the state of the system to depend on states different from the present one, via, for example, a feedback mechanism.

DDEs appear in many fields, from economics to biology and from chemistry to mathematics, as the following examples suggest.

Bacterial Infection

In a book on the study of malaria published in 1911 (Ross, 1911), Ross considered a differential equation model of malarial epidemics based on the interaction of two populations, that of infected humans, described by $h(t)$, and that of infected mosquitoes, by $m(t)$. The relevant nonlinear DDEs are

$$\dot{h}(t) = m(t-u)\frac{p - h(t-u)}{p} - (M+r)h(t),$$

$$\dot{m}(t) = h(t-v)\frac{q - m(t-v)}{p} - (N+s)m(t), \quad (1)$$

with p and q being the total populations, M and N the death rates, and r and s the recovery rates for human and mosquito populations, respectively. The delay from the time of a bite to the time at which the human or the mosquito is infective is $u = 0.5$ months for humans and $v = 0.6$ months for mosquitoes.

Enzyme Catalysis

Roussel (1996) presents a model of enzyme catalysis, proposed by Adrian Brown in 1902, in which the enzyme-substrate complex has a fixed lifetime τ before giving rise to its reaction products

$$E(t) + S(t) \rightarrow P(t+\tau) + E(t+\tau). \qquad (2)$$

The DDEs generated by this model are

$$\begin{aligned} \frac{\mathrm{d}S(t)}{\mathrm{d}t} &= -kE(t)S(t), \\ \frac{\mathrm{d}E(t)}{\mathrm{d}t} &= -kE(t)S(t) + kE(t-\tau)S(t-\tau), \\ \frac{\mathrm{d}P(t)}{\mathrm{d}t} &= kE(t-\tau)S(t-\tau), \end{aligned} \qquad (3)$$

where k is the rate constant and by $E(t)$, $P(t)$, and $S(t)$, we mean the enzyme, product, and substratum concentrations.

Economic Dynamics

Delays can emerge in the dynamics of economic processes in two ways. First, there is a lag between the time economic decisions are taken and the time the decisions bear fruit. Also, the expected future values of a variable are functions of its current and past values. Let us consider a world in which infinitely many houses are inhabited, and let us consider the problem of finding the best time for constructing a new house (Asea & Zak, 1999).

The individuals' preferences are represented by a continuous, strictly increasing, and concave utility function $U(c(t))$. Subjective discount rates are characterized by $\rho > 0$. In this model, it takes $r > 0$ periods to obtain new capital. The solution of this planning problem is given by

$$\max_{\{c(t)\}} \int_0^\infty U(c(t))\mathrm{e}^{-\rho t}\mathrm{d}t, \qquad (4)$$

subject to the DDE

$$\frac{\mathrm{d}k(t)}{\mathrm{d}t} = f(k(t-r)) - \delta k(t-r) - c(t), \qquad (5)$$

with initial condition $k(t) = \phi(t)$, for all $t\varepsilon[-r, 0]$. $f(\cdot)$ is the production function; $c(t)$, the rate at which capital depreciates, such that $0 < c(t) \leq f(k(t-r))$, $\delta \in [0, 1]$; and $k(t)$, the productive capital stock at time t.

Mathematics

If one considers the symmetry reduction of a nonlinear differential-difference equation with respect to a combination of continuous and discrete symmetries, then the initial equation reduces to a DDE. As an example, consider the Toda lattice (Levi & Winternitz, 1993)

$$\ddot{u}_n(t) = \mathrm{e}^{u_{n-1}(t)-u_n(t)} - \mathrm{e}^{u_n(t)-u_{n+1}(t)}, \qquad (6)$$

and assume a reduction with respect to $\partial_n + a\partial_t$ where a is an arbitrary real parameter. Equation (6) then reduces to

$$\frac{\mathrm{d}^2u(\eta)}{\mathrm{d}\eta^2} = \mathrm{e}^{u(\eta+a)-u(\eta)} - \mathrm{e}^{u(\eta)-u(\eta-a)}, \qquad (7)$$

where $\eta = t - an$.

The equations considered in these examples are all instances of a general DDE, which, in the simple case of a linear first-order equation for just one field, can be written as

$$\begin{aligned} a_0\frac{\mathrm{d}u(t)}{\mathrm{d}t} + a_1\frac{\mathrm{d}u(t-\sigma)}{\mathrm{d}t} + b_0u(t) + b_1u(t-\sigma) \\ = f(t). \end{aligned} \qquad (8)$$

An equation of the form (8) is said to be a DDE of *retarded* type if $a_0 \neq 0$ and $a_1 = 0$; it is said to be of *neutral* type if $a_0 \neq 0$ and $a_1 \neq 0$; and of *advanced* type if $a_0 = 0$ and $a_1 \neq 0$.

In applications, an equation of *retarded* type may represent the behavior of a system in which the rate of change of $u(t)$ depends on its past and present values. A *neutral* equation represents a system in which the present rate of change depends on past rates of changes as well as its present and past values. An *advanced* type equation may represent a system in which its rate of change depends on its present and future values.

If $a_0 = a_1 = 0$, Equation (8) is a pure difference equation, while if $a_0 = b_0 = 0$ or $a_1 = b_1 = 0$, it is a pure differential equation. In either case, $f(t)$ is a forcing function.

Let us compare the solution techniques for DDEs with those of ordinary differential equations (ODEs) and note some of their peculiar features. For simplicity we limit ourselves to retarded DDEs. For more details, see Bellman & Cooke (1963), Hale (1977), Hale & Verduyn Lunel (1993), Driver (1977), Bainov & Mishev (1991), Kuang (1993), and Gyori & Lada (1991).

Because retarded DDEs depend on previous history, the initial condition at one point is not sufficient to obtain the present time behavior. What one needs depends on the discrete order of the equation. If the equation is a DDE of first order, then the initial solution on a whole delay interval is needed.

For constant coefficient DDEs, an algebraic method of solution is provided by the "method of steps," which also provides a constructive proof of the existence of the solution. To illustrate this method, consider a DDE generalization of the logistic equation

$$\frac{\mathrm{d}x(t)}{\mathrm{d}t} = -cx(t-1)[1 + x(t)], \qquad t > 0, \qquad (9)$$

with the initial condition $x(t) = \phi(t)$ for $t \in [-1, 0]$. To solve Equation (9), we divide the interval $[0, \infty)$ into steps of the size of the delay and solve recursively in each interval. We use the solution obtained in one interval to solve Equation (9) in the next one. For example, the solution in the interval $[0, 1]$ is given by

$$x(t) = [\phi(0) + 1]e^{-c\int_0^t \phi(s-1)ds} - 1,$$

which is obtained as a solution of the ODE

$$\frac{dx(t)}{dt} = -c\phi(t-1)[1 + x(t)]. \qquad (10)$$

For linear DDEs we can construct, as in the case of linear ODEs, the characteristic equation, by looking at exponential solutions. In this case, however, the characteristic equation is given by a nonlinear algebraic equation. For example in the case of Equation (8), with $a_1 = 0$, we have

$$h(\lambda) = a_0\lambda + b_0 + b_1 e^{-\lambda\sigma} = 0. \qquad (11)$$

Once the characteristic equation is solved, a particular solution of the DDE is obtained by applying the Laplace transform (Bellman & Cooke, 1963).

As we have seen, the nature of the method of solution of a DDE is similar to that of an ODE. Nevertheless, DDEs exhibit more complicated behaviors, even in the linear case. For example, scalar linear first-order homogeneous DDEs with real coefficients can have nontrivial oscillating solutions unlike ODEs (Kalecki, 1935). Moreover, solutions to DDEs may be discontinuous and, depending on the initial conditions, a solution may also not exist (Winston & Yorke, 1969). As in the case of ODEs, series solutions can be used to approximate solutions to nonlinear DDEs (Bellman & Cooke, 1963); however, the solutions obtained are often complicated and obscure.

We can gain a better insight into the solution using qualitative theory and stability analysis to obtain properties of the dynamics of a nonlinear DDE by looking at its linearization.

The stability of a fixed point of a DDE is defined by examining the roots of the characteristic equation $h(\lambda)$. Thus, a fixed point of a DDE is stable if all roots of $h(\lambda)$ have negative real parts. As the characteristic equation (11) is transcendental, it has an infinity of roots, and it is not guaranteed that all roots will have real parts, strictly negative or positive. So fixed points of DDEs will often be saddle points. Moreover, stability may depend crucially on the initial data (Driver, 1977).

The stability of homogeneous scalar DDEs of the first order has been studied by Hayes (Bellman & Cooke, 1963). These results can be extended to nonlinear systems by linearizing the DDE around a stable solution and then using a generalization of the Poincaré–Lyapunov theorem. In such a way, one can show that DDEs often admit periodic solutions after a sequence of Hopf bifurcations. Chaotic orbits may also exist, with the structure of the orbits depending critically on the smoothness of the feedback mechanism.

DECIO LEVI

See also **Bifurcations; Equations, nonlinear; Feedback; Hopf bifurcation; Integral transforms; Ordinary differential equations, nonlinear; Poincaré theorems; Quasilinear analysis; Stability; Symmetry: equations vs. solutions**

Further Reading

Asea, P.K. & Zak, P.J. 1999. Time-to-build and cycles. *Journal of Economic Dynamics & Control*, 23: 1155–1175

Bainov, D.D. & Mishev, D.P. 1991. *Oscillation Theory for Neutral Differential Equations with Delay*, Bristol: Adam Hilger

Bellman, R. & Cooke, K.L. 1963. *Differential-Difference Equations*, New York: Academic Press

Driver, R.D. 1977. *Ordinary and Delay Differential Equations*, New York: Springer

Gyori, I. & Ladas, P. 1991. *Oscillation Theory of Delay Differential Equations: with Applications*, Oxford: Clarendon Press

Hale, J.K. 1977. *Theory of Functional Differential Equations*, New York: Springer

Hale, J.K. & Verduyn Lunel, S.M. 1993. *Introduction to Functional Differential Equations*, New York: Springer

Kalecki, M. 1935. A macroeconomic theory of business cycles. *Econometrica*, 3: 327–344

Kuang, Y. 1993. *Delay Differential Equations with Applications in Population Dynamics*, Boston: Academic Press

Levi, D. & Winternitz, P. 1993. Symmetries and conditional symmetries of differential-difference equations. *Journal of Mathematical Physics*, 34: 3713–3730

Ross, R. 1911. *The Prevention of Malaria*, 2nd edition, London: John Murray

Roussel, M.R. 1996. The use of delay differential equations in chemical kinetics. *Journal of Physical Chemistry*, 100: 8323–8330

Winston, E. & Yorke, J.A. 1969. Linear delay differential equations whose solutions become identically zero. *Académie de la République Popolaire Roumaine*, 14: 885–887

DENJOY THEORY

The theory developed by Arnaud Denjoy (1884–1974) showed that any sufficiently smooth orientation-preserving diffeomorphism T of the unit circle S^1 with an irrational rotation number ρ is topologically equivalent to a linear rotation by the angle $2\pi\rho$ (Denjoy, 1932). Informally, diffeomorphism is a smooth invertible map such that its inverse is also smooth.

Circle diffeomorphisms arise naturally in many physical problems. For instance, in the case of Hamiltonian systems with two degrees of freedom, such diffeomorphisms appear as Poincaré first return maps for the two-dimensional invariant tori. When the rotation number is irrational, circle diffeomorphisms represent an important model for quasi-periodic dynamics (*See* **Quasiperiodicity**). The Denjoy theory

implies the following important fact: if two smooth circle maps have the same irrational rotation number then the topological structure of their trajectories is exactly the same.

The topological equivalence means that circle diffeomorphisms are conjugated to a linear rotation with the help of a homeomorphic change of variables. Namely, there exists a homeomorphism, ϕ, which is an invertible map that is continuous together with its inverse, such that $T \circ \phi = \phi \circ T_\rho$, where T_ρ is the linear rotation by the angle $2\pi\rho$ and $\circ$ stands for a composition of two maps. Denjoy's theorem holds if T is absolutely continuous and $\log T'(x)$ has bounded total variation: $V = \mathrm{Var}_{S^1} \log T'(x) < \infty$. The last condition is satisfied if T is C^2-smooth and $T'(x) > 0$. The conjugacy ϕ is defined uniquely up to an arbitrary rotation T_α. In fact, a mapping ϕ of the unit circle S^1 that satisfies condition $T \circ \phi = \phi \circ T_\rho$ can be constructed for any quasi-periodic homeomorphisms T. This means that any homeomorphism T with irrational rotation number ρ is semiconjugate to T_ρ. However, if T is not regular enough, ϕ may not be a homeomorphism. To construct ϕ it is enough to take two arbitrary points x_0 and y_0 and define their forward trajectories by T and T_ρ, respectively: $x_i = T^i x_0$, $y_i = T_\rho^i y_0$, $i \geq 1$. Now one can define ϕ on $\{y_i\}$ by letting $\phi(y_i) = x_i$, $i \geq 0$ and extending ϕ by continuity to the whole unit circle. This can be done since any trajectory of a linear rotation by an irrational angle is everywhere dense. It is easy to see that a conjugacy ϕ is a homeomorphism if and only if T is transitive; that is, all its trajectories are dense on S^1.

When the total variation V is bounded, the transitivity of T follows from the Denjoy inequality:

$$\exp(-V) \leq \prod_{i=0}^{q_n-1} T'(x_i) \leq \exp(V),$$

where q_n are the denominators of the convergents $p_n/q_n = [k_1, k_2, \ldots, k_n]$, and $\rho = [k_1, k_2, \ldots, k_n, \ldots]$ is the continued fraction expansion for ρ. The condition $T \in C^2(S^1)$ that implies topological equivalence is almost sharp. Indeed, Denjoy constructed counterexamples where $T \in C^1(S^1)$ and the derivative $T'(x)$ is a Hölder continuous function with an arbitrary Höder exponent $0 < \alpha < 1$. In these examples T is not transient and, hence, is not conjugate to T_ρ.

An important extension of the Denjoy theory is connected with the problem of smoothness of the conjugacy ϕ. It is natural to ask when the homeomorphism ϕ is at least C^1-smooth, which implies not only topological but also asymptotic metrical equivalence between T and T_ρ. In this case, the unique probability invariant measure for T is absolutely continuous with respect to the Lebesgue measure. The first progress in this direction was made by Arnol'd (1961), who proved that for analytic diffeomorphisms, T that are close enough to the linear rotation T_ρ, a conjugacy ϕ is analytic provided the rotation number ρ is Diophantine, that is, $\|\rho - p/q\| \geq 1/q^{2+\delta}$ for some $\delta > 0$ and all integers p, q. Diophantine numbers form a set of positive Lebesgue measure and, hence, are typical in the Lebesgue sense. Arnol'd has also constructed counterexamples in the case of nontypical rotation numbers, which show that the smooth theory cannot be constructed for all irrational rotation numbers. In these counterexamples, ϕ is not differentiable, and the invariant measure for T is essentially singular with respect to Lebesgue measure. Arnol'd's results are of the KAM-type (Kolmogorov–Arnol'd–Moser) and, hence, have a local character. However, as it was conjectured by Arnol'd, in the one-dimensional case the local condition of T being close to T_ρ should not be necessary, and the global result should hold for all T smooth enough. Such a global result has been proven by Herman (1979) in the case when ρ satisfies certain Diophantine condition and $T \in C^3(S^1)$. Later Herman's results were extended to a wider class of rotation numbers (Yoccoz, 1984) and to diffeomorphisms $T \in C^{2+\varepsilon}(S^1)$ (Khanin & Sinai, 1987; Sinai & Khanin, 1989; Katznelson & Ornstein, 1989).

Finally, we mention another extension of the Denjoy theory to the case of diffeomorphisms with singularities. Such mappings appear, for example, in the case of critical invariant tori in Hamiltonian systems with two degrees of freedom. The extension of the Denjoy theory to this case is a subject of the so-called rigidity theory. The main aim is to find conditions which imply that two topologically equivalent homeomorphisms that have the same local structure of their singular points are, in fact, C^1-smoothly conjugate to each other. Significant progress in this direction has been made in the last 5 years in the case of mappings with one singular point (de Faria & de Melo, 1999, 2000; Yampolsky, 2001; Khanin & Khmelev, 2003). Note that the presence of singularities makes rigidity stronger than in the case of smooth diffeomorphisms. The arithmetical properties of the rotation numbers are less important, and one should expect C^1-rigidity for all irrational rotation numbers.

KONSTANTIN KHANIN

See also **Kolmogorov–Arnol'd–Moser theorem; Maps; Quasiperiodicity**

Further Reading

Arnol'd, V.I. 1961. Small denominators. I. Mapping the circle onto itself. *Izvestiya Akademii Nauk SSSR Seriya Mathematicheskaya*, 25: 21–86

Cornfeld, I. P., Fomin, S. V. & Sinai, Ya. G. 1982. *Ergodic Theory*, New York: Springer

Denjoy, A. 1932. Sur les courbes définies par les équations différentielles à la surface du tore. *Journal des Mathematiques Pures et Appliques*, ser. 9, 11: 333–375

de Faria, E. & de Melo, W. 1999. Rigidity of critical circle mappings. I. *Journal of the European Mathematical Society (JEMS)*, 1: 339–392
de Faria, E. & de Melo, W. 2000. Rigidity of critical circle mappings. II. *Journal of the European Mathematical Society (JEMS)*, 13: 343–370
Herman, M. 1979. Sur la conjugaison différentiable des difféomorphismes du cercle à des rotations. *Publications Mathématiques de l'Institut des Hautes Études Scientifiques*, 49: 5–233
Katznelson, Y. & Ornstein, D. 1989. The differentiability of the conjugation of certain diffeomorphisms of the circle. *Ergodic Theory & Dynamical Systems*, 9: 643–680
Khanin, K.M. & Sinai, Ya.G. 1987. A new proof of M. Herman's theorem. *Communications in Mathematical Physics*, 112: 89–101
Khanin, K. & Khmelev D. 2003. Renormalizations and rigidity theory for circle homeomorphisms with singularities of the break type. *Communications in Mathematical Physics*, 235: 69–124
Sinai, Ya.G. & Khanin, K.M. 1989. Smoothness of conjugacies of diffeomorphisms of the circle with rotations. *Russian Mathematical Surveys*, 44: 69–99
Yampolsky, M. 2001. The attractor of renormalization and rigidity of towers of critical circle maps. *Communications in Mathematical Physics*, 218: 537–568
Yoccoz, J.-C. 1984. Conjugaison différentiable des difféomorphismes du cercle dont le nombre de rotation vérifie une condition diophantienne. *Annales Scientifique de l'École Normale Superierieure*, 4(17): 333–359

DERIVATIVE NLS EQUATION

See **Nonlinear Schrödinger equations**

DERRICK–HOBART THEOREM

The Derrick–Hobart scaling argument concerns certain solutions of nonlinear partial differential equations that arise as models for elementary particles; thus they are mostly of the relativistic variety. To appreciate the context in which the argument arose and the way it is used, some introductory remarks on relativistic quantum field theory are in order.

There are only a few interacting relativistic quantum field theories that have been solved explicitly, in the sense that physically relevant quantities (particle spectrum, scattering, form factors, and so on) are known in closed form. For all of these models the dimension of space-time equals two. To gain more insight into higher-dimensional models, it has become standard practice to study the field theory first as a classical field theory. The underlying idea is that (via the Feynman path integral) one can use classical findings to obtain nonperturbative information on the quantum version. In particular, the presence of nonconstant, smooth, stable, time-independent, finite-energy, classical solutions is believed to signal the presence of an associated stable quantum particle.

The notion of "stability" refers to small fluctuations around such a classical finite-energy solution. To first order, such variations do not change the energy, as expressed by the Euler–Lagrange equation. To second order, however, the energy may become smaller, in which case the corresponding quantum particle is considered to be unstable. (Think of a ball resting on top of a hill. A little push makes it roll down.)

In order to study the existence of nonconstant finite-energy solutions (either stable or unstable), an argument due independently to Derrick (1964) and (in a somewhat different form) to Hobart (1963) is often useful. These authors were concerned with three-dimensional space (four-dimensional space-time), but the argument can be extended without difficulty to an arbitrary space dimension N. Briefly, the argument is as follows.

Assume $\phi(x,t)$, $x \in R^N$, $t \in R$, is a scalar field on $(N+1)$-dimensional space-time, whose dynamics is given by the Lagrangian

$$\mathcal{L} = \tfrac{1}{2}(\partial_t \phi^2 - \nabla\phi \cdot \nabla\phi) - V(\phi), \tag{1}$$

with $V(y)$ being a potential function. Now let $\phi(x)$ be a (smooth) time-independent nonconstant solution to the Euler–Lagrange equation, with finite energy

$$E = E_{\text{kin}} + E_{\text{pot}}, \quad E_{\text{kin}} = \frac{1}{2}\int_{R^N} \nabla\phi \cdot \nabla\phi \mathrm{d}x,$$

$$E_{\text{pot}} = \int_{R^N} V(\phi)\mathrm{d}x. \tag{2}$$

Starting from the above data, Derrick's key idea is to consider the family of scaled functions

$$\phi_\lambda(x) = \phi(\lambda x). \tag{3}$$

Clearly, the energy associated with ϕ_λ is given by

$$E_\lambda = \lambda^{(2-N)} E_{\text{kin}} + \lambda^{-N} E_{\text{pot}}, \tag{4}$$

so that

$$(\mathrm{d}E_\lambda/\mathrm{d}\lambda)_{\lambda=1} = (2-N)E_{\text{kin}} - NE_{\text{pot}}, \tag{5}$$

$$(\mathrm{d}^2 E_\lambda/\mathrm{d}\lambda^2)_{\lambda=1} = (2-N)(1-N)E_{\text{kin}} + N(N+1)E_{\text{pot}}. \tag{6}$$

Since ϕ_λ makes the energy stationary for $\lambda = 1$, we have

$$(\mathrm{d}E_\lambda/\mathrm{d}\lambda)_{\lambda=1} = 0. \tag{7}$$

Hence (5) yields

$$E_{\text{pot}} = \frac{2-N}{N} E_{\text{kin}}, \tag{8}$$

which entails

$$(\mathrm{d}^2 E_\lambda/\mathrm{d}\lambda^2)_{\lambda=1} = 2(2-N)E_{\text{kin}}. \tag{9}$$

Let us now draw the relevant conclusions from this simple calculation. Since $\phi(x)$ is nonconstant, its

kinetic energy E_{kin} is positive. For $N > 2$, then, (9) says that the finite-energy solution cannot be stable. This is the first consequence, an instability result for $N > 2$. It does not involve restrictions on the potential $V(y)$.

Assuming from now on that $V(y) \geq 0$, far stronger conclusions can be drawn. Indeed, since ϕ_λ is a solution for $\lambda = 1, \phi_1 = \phi$ makes the energy stationary. But since ϕ is nonconstant, we have $E_{\text{kin}} > 0$, and since $V \geq 0$, we also have $E_{\text{pot}} \geq 0$. Therefore, the right-hand side of (5) is negative for $N > 2$, a contradiction. A second consequence, therefore, is the absence of finite-energy nonconstant solutions for $V \geq 0$ and $N > 2$.

Retaining the assumption $V \geq 0$, one can draw a conclusion for $N = 2$, too. Indeed, it then follows that $E_{\text{pot}} = 0$, so that ϕ must satisfy $V(\phi) = 0$; moreover, the second variation (6) vanishes.

For $N = 1$ the variation formulas (5), (6) have no useful consequences. Indeed, in two-dimensional space-time there do exist stable time-independent finite-energy solutions, as exemplified by the one-soliton and one-antisoliton solutions of the sine-Gordon theory.

In applications of Derrick's argument, one usually encounters positive potentials and invokes the latter consequences sketched above. Thus, it is used to the effect that for $N \geq 2$, time-independent finite-energy solutions must be constant (the so-called vacuum solutions). Some caveats should be heeded, however.

First, it is important to keep track of the above steps in models that are not of the above form, since the reasoning may need to be suitably modified. Second, even when this can be done at face value, it should be observed that the above argument, although convincing at first sight, is not a rigorous proof. Indeed, the scaling variation that is involved has a global character, whereas the Euler–Lagrange equation is derived by considering local variations. More in detail, one needs to control boundary terms that can *a priori* spoil the above derivation. (This was already realized in Hobart (1963).)

We exemplify these related issues with two models described by Lagrangians that are different from the above, namely a (special) Yang–Mills/Higgs model in physical space ($N = 3$) and a class of nonlinear σ-models for $N \geq 2$. In the first setting, explicit static finite-energy solutions were obtained in Prasad & Sommerfield (1975) and Bogomolnyi (1976). (These are nowadays called BPS monopoles.) The energy of these solutions is manifestly not scale-invariant, contradicting (7) for the case at hand. Inspection of the solution shows that this is due to poor decay at spatial infinity; it entails that the pertinent boundary term cannot be ignored.

Turning to $O(3)$ σ-models, one can once more study the issue of finite-energy solutions by adapting Derrick's scaling argument. For $N = 2$ (now viewed as Euclidean space-time) this yields no conclusion, since the energy is scale-invariant. In this case, the so-called instanton and anti-instanton solutions do exist, and they are stable for topological reasons.

For $N > 2$, the scaling argument leads to the absence of finite-energy solutions. In this particular setting, the heuristic reasoning can be corroborated. More specifically, the boundary term can be rigorously controlled. The pertinent result (Garber et al. (1979), Theorem 5.1) has later been used by differential geometers to prove the nonexistence of harmonic maps, which are closely related to the above type of solution.

SIMON RUIJSENAARS

See also **Matter, nonlinear theory of; Skyrmions; Virial theorem; Yang–Mills theory**

Further Reading

Bogomolnyi, E.B. 1976. The stability of classical solutions. *Soviet Journal of Nuclear Physics*, 24: 449–454

Derrick, G.H. 1964. Comments on nonlinear wave equations as models for elementary particles. *Journal of Mathematical Physics*, 5: 1252–1254

Garber, W.-D., Ruijsenaars, S.N.M., Seiler, E. & Burns, D. 1979. On finite-action solutions of the nonlinear σ-model. *Annals of Physics*, 119: 305–325

Hobart, R.H. 1963. On the instability of a class of unitary field models. *Proceedings of the Physical Society, London*, 82: 201–203

Prasad, M.K. & Sommerfield, C.M. 1975. Exact classical solution for the 't Hooft monopole and the Julia-Zee dyon. *Physical Review Letters*, 35: 760–762

DETAILED BALANCE

This entry provides a qualitative discussion of equilibrium, a more quantitative discourse of principles such as detailed balance (which are needed in the description of equilibrium phenomenon), and a brief presentation of the Einstein relation between mobility and diffusion, which can be related to the above topics.

The Problem of Time

One often says that a system has reached an equilibrium state if its physical variables are constant in time. Because of fluctuations that cannot be removed, however, it is better to regard the system as in equilibrium when there are no systematic trends in the time averages of its physical parameters. Here, averages are considered over all the microscopic constituents of the system, whether they are elementary particles, atoms, molecules, or larger objects. Equilibrium can be established among these constituents.

Thus, a system that is in equilibrium cannot reveal the time variable among its broad characteristics. In other words, there is no way of telling which way time is running if one's observations are confined to an equilibrium system. Formulated as a philosophical puzzle about the nature of time, this subject has spawned a library of books and papers, with little

agreement among the authors (see Landsberg, 1982; Smith, 1993; Price, 1996; Davies, 1995).

Some Relevant Principles of Statistical Mechanics

Here and below, we shall deal with a number of important principles that may or may not hold in any given case and are related to each other. To make these matters quantitative, denote by P_i the probability of finding a system of interest in any one of the ith group of states, G_i in number. The probability per unit time that a transition occurs from a state of group i to a state of group j is denoted by A_{ij}. The transition rate $i \to j$ can be written as

$$R_{ij} = P_i A_{ij} G_j. \tag{1}$$

If there are W available groups of states, the time rate of change of P_i is

$$\dot{P}_i = \sum_{l=1}^{W} (R_{li} - R_{il}) \quad (i = 1, 2 \ldots W). \tag{2}$$

To be tractable the A_{ij} have to be independent of time. The first sum gives the transitions into states i and the second sum gives the transitions out of the states i. To simplify the picture one can replace a typical group of states i by a single state, i.e., one can put $G_i = 1$.

Now some additional general principles can be defined. The existence of the A_{ij} can be deduced from quantum mechanical perturbation theory, but it is then valid only for a restricted time interval. One often finds the symmetry relation

$$A_{ij} = A_{ji} \quad (\text{all } i, j) \tag{3}$$

as a result of the Hermitian character of the perturbation operator. In statistical mechanics, one also uses the principle of Equation (3). It can then be independent of perturbation theory and is regarded instead as resulting from adequate statistical assumptions. It is then called the *principle of microscopic reversibility*.

Next we have the principle of detailed balance which asserts that at a certain time t the forward and reverse transition rates between two groups of states are equal at a certain time; thus,

$$R_{ij} = R_{ji} \quad (\text{all } i, j). \tag{4}$$

If Equation (4) holds, one sees that $\dot{P}_i$ vanishes for all i. In fact, we can define a steady state by

$$\dot{P}_i = 0 \quad (\text{all } i). \tag{5}$$

Such a state need not be an equilibrium state since the system may, for example, be continuously raised to a high energy state by some external influence and then drop back continuously, for example, by the emission of radiation. Thus, one sees that Equation (4) implies Equation (5), but not conversely. For more details, see Lifschitz & Pitaewski (1981) and Landsberg (1991).

A Simple Example from the Solid State

One can use detailed balance arguments to infer the form of an unknown emission rate from a known absorption rate, as will now be shown by an example (Landsberg, 1991, p. 391). The idea is to obtain an expression for the equilibrium absorption rate per unit volume of photons of frequency ν_0 in a semiconductor of refractive index μ and, hence, to infer spontaneous emission rates per unit volume.

The probability of a single photon of vacuum wavelength λ_0 being absorbed per unit time per unit volume is

$$P(\lambda_0) = c\alpha(\lambda_0)/V\mu(\lambda_0). \tag{6}$$

The dimensions $(LT^{-1} \cdot L^{-1} \cdot L^{-3})$ are easily verified to be correct. To find the volume rate of excitation in the solid by photons in the vacuum wavelength range $\mathrm{d}\lambda_0$, $P(\lambda_0)$ has to be multiplied by the number of relevant photon modes $(8\pi\mu^3\lambda_0^{-4}V\mathrm{d}\lambda_0)$, and also by their equilibrium occupation probability at temperature T:

$$1/[\exp(ch/\lambda_0 kT) - 1]. \tag{7}$$

But not all photons of wavelength λ_0 will, when absorbed, produce one electron-hole pair. We denote by $\alpha'(\lambda_0)/\alpha(\lambda_0)(\leq 1)$ the probability of this happening per absorbed photon. Hence, the equilibrium absorption rate (per unit volume) of photons in the wavelength range $\mathrm{d}\lambda_0$ with production of an electron-hole pair is

$$\alpha'/\alpha \frac{8\pi\mu^2\alpha c\lambda^{-4}}{\exp(ch/\lambda_0 kT) - 1} d\lambda_0$$

or

$$\frac{8\pi\alpha'}{h^3}\frac{\mu}{c^2}(kT)^3 \frac{x^2 \mathrm{d}x}{\exp x - 1}. \tag{8}$$

Here $x = h\nu_0/kT$, and the second of these expressions is like the first, except that it is in terms of frequencies. According to detailed balance, the new inference is that these expressions give the rate per unit volume of spontaneous radiated recombination of electron-hole pairs with the emission of photons in the range $\mathrm{d}\lambda_0$ or $\mathrm{d}\nu_0$. Note that we have passed from absorption to emission data. This widely used result was first given by W. van Roosbroeck and W. Shockley in 1954. For other examples of the use of the principle of detailed balance in solid state physics, see Landsberg (1991).

The Einstein Relation

The Einstein Relation is basic to solid states physics and rests on the assumption that in a steady state the flux of charged particles due to an electric field must be balanced by diffusion of these particles induced by their density gradients. These two effects are due to well-known and simple forces. The first is a particle flux due

to diffusion (with diffusion coefficient D, say). It can be written $-D\mathrm{d}n/\mathrm{d}x$ for one-dimensional motion, where n is the density of particles and $\mathrm{d}n/\mathrm{d}x$ the gradient ("grad n" in three dimensions). The minus sign shows that the force acts to the left if the concentration n increases to the right. The second force on the charged particles is due to a built-in or externally applied electric field E, which is a vector in three dimensions. Here we deal merely with the one-dimensional problem, and note that E can be replaced by $-\mathrm{d}V/\mathrm{d}x$, where V is the electrostatic potential at the point considered. The flux of particles can be written as $nvE = -n\mu\mathrm{d}V/\mathrm{d}x$, where v is the so-called mobility of the particles.

In order to obtain the Einstein relation in its simplest form, one has to equate the two forces

$$-n\mu\frac{\mathrm{d}V}{\mathrm{d}x} = D\frac{\mathrm{d}n}{\mathrm{d}x}, \tag{9}$$

which implies that

$$\frac{\mathrm{d}(\ln n)}{\mathrm{d}x} = -\frac{\mu}{D}\frac{\mathrm{d}V}{\mathrm{d}x} \tag{10}$$

giving the simple result

$$n = n_0 \exp(-\mu V/D). \tag{11}$$

As we also know that the stationary state in an electric field at a temperature T is governed by the Boltzmann distribution

$$n = n_0 \exp(-eV/kT), \tag{12}$$

where n_0 is a constant and k is Boltzmann's constant. Comparison yields the Einstein relation

$$\mu = eD/kT. \tag{13}$$

This result connects the mobility of charged particles in a field with their diffusion coefficient. At first sight this seems unexpected because one side of the equation deals with the mechanical characteristic of diffusion.

The extension to three dimensions is not the only generalization that can be made. For example, a similar Einstein relation holds for thermal current density, and generalizations have also been made for large departures from equilibrium (Landsberg, 1991). A further variety of special cases arises for different assumptions about the shape of the semiconductor bands that can occur; for example, they can be degenerate or nondegenerate, parabolic or nonparabolic, etc., and the results can be given in a table of formulae. (Einstein's paper was published in *Annalen der Physik und Chemie* in 1905, the first of three important papers published by him in that year.)

The principle of detailed balance emerged somewhat hesitantly in the 1920s, based on Einstein's 1917 paper on transition possibilities. It was named by Fowler and Milne following other authors and other names. A brief historical survey is given by ter Haar (1955).

PETER LANDSBERG

See also **Diffusion; Stochastic processes**

Further Reading

Coveney, P. & Highfield, R. 1991. *The Arrow of Time*, London: Allen, 1990 and New York: Fawcett Columbine

Davies, P. 1995. *About Time: Einstein's Unfinished Revolution*, New York: Simon and Schuster

Einstein, A. 1905. Die von der molekularkinetischen Theorie der Wärme geforderte Bewegung. *Annalen der Physik und Chemie*, 17: 549–560

Landsberg, P.T. (editor). 1982. *The Enigma of Time*, Bristol: Adam Hilger

Landsberg, P.T. 1991. *Thermodynamics and Statistical Mechanics*, Oxford and New York: Oxford University Press

Landsberg, P.T. 1991. *Recombination in Semiconductors*, Cambridge and New York: Cambridge University Press

Lifschitz, E.M. & Pitaewski, L.P. 1981. *Physical Kinetics*, Oxford and New York: Pergamon Press

Price, H. 1996. *Time's Arrow and Archimedes' Point*, Oxford and New York: Oxford University Press

Smith, Q. 1993. *Language and Time*, Oxford and New York: Oxford University Press

ter Haar, D. 1955. Foundations of statistical mechanics. *Reviews of Modern Physics*, 27: 289

DETERMINISM

Determinism is a philosophical and scientific notion, and discussions about it are as old as philosophy and science themselves. Richard Taylor writes "Determinism is the general philosophical thesis which states that for everything that ever happens there are conditions such that, given them, nothing else could happen" (Taylor, 1996). This seems to be the most general formulation of determinism. In philosophy, he continues, "There are five theories of determinism to be considered, which can for convenience be called ethical determinism, logical determinism, theological determinism, physical determinism, and psychological determinism." Here we shall confine ourselves only to physical determinism in the natural sciences, except in the concluding section.

In physics, the deterministic view developed along with the experimental approach to research, in the sense that phenomena are reproducible under the same unchanged external conditions, implying that the same cause leads to the same consequences under the same conditions. The quantitative description of physical reality began with Galileo Galilei; although some early developments are due to Pythagoras. However, Isaac Newton was the first to lay down the complete basis of classical mechanics, which at the time was considered to be the origin of all physical phenomena. His laws of mechanics plus

the law of gravitation enabled him to reproduce and mathematically derive the motion of the planets, observations of which were empirically well known by the beginning of the 16th century and formulated in Johannes Kepler's laws of celestial mechanics. With the rise and development of classical mechanics the view of determinism developed, with the opinion that all natural laws can be described by dynamical equations, either ordinary differential equations (as, for example, in celestial mechanics) or partial differential equations (as, for example, in the dynamics of fluids). In each case precise knowledge of the initial conditions (all positions and all velocities) completely determines the entire future and entire past of the system. When pushed to its extremum, this view implies complete deterministic evolution of the entire universe, including all its smallest and largest details. The French mathematician Pierre Simon de Laplace, about one century after Newton, wrote (in an often quoted passage):

> We ought then to regard the present state of the universe as the effect of its antecedent state and the cause of the state that is to follow. An intelligence knowing, in any instant of time, all forces acting in nature, as well as the momentary positions of all things of which the universe consists, would be able to comprehend the motions of the largest bodies in the world and those of the smallest atoms in one single formula, provided it were sufficiently powerful to subject all data to analysis: to it, nothing would be uncertain, both future and past would be present before its eyes. (Laplace, 1814)

We can comment on Laplace's statement from our modern perspective. First, to store and process data of *infinite precision* about the state of the entire universe is problematic, as it would require a computer that would be of comparable size and complexity to the entire universe. Thus, its presence has to be taken into account, since—obeying the same mechanical laws as the rest of the universe—it would itself disturb the universe. Therefore, we can conclude that Laplace's "intelligence" (sometimes known as Laplace's daemon) cannot exist, and consequently his idea is fiction. Second, infinite precision of all the initial conditions (positions and momenta) can never be achieved in practice. And when the precision is finite, the existence of chaos (positive Lyapunov exponents) implies sensitive dependence on initial conditions and exponential divergence of nearby trajectories. In other words, there is a finite time horizon exists in general chaotic mechanic systems, beyond which nothing at all can be predicted (Lyapunov time). Therefore, the modern notion of omnipresent chaotic behavior makes Laplace's idea impossible to implement, even in principle. Third, the universe is not described by classical mechanics, but by quantum mechanics, classical mechanics being just a useful or even excellent approximation in observing and describing the motions of sufficiently large bodies. Quantum mechanics tells us, through Heisenberg's principle of uncertainty, that momenta and positions cannot be measured simultaneously with infinite precision, but we have instead the inequality $\Delta x \Delta p_x \geq \hbar/2$, where Δx and Δp_x are the uncertainties of position x and the conjugated momentum p_x. So, Laplace's initial conditions can never be known to arbitrary precision, even in principle.

Quantum mechanics is the correct description of physical reality, with the Schrödinger equation as the starting tool, for nonrelativistic systems. The quantum theory has been further developed by Paul Dirac for relativistic quantum systems and by the quantum field theory up to the unifying field theories, which capture three fundamental interactions (electromagnetic, weak, and strong interactions), but not yet gravity. The Schrödinger equation is a deterministic equation of motion of the wave function ψ, which contains the complete description of the quantum state of a given system. Importantly, ψ itself is a statistical quantity and thus not deterministic: it gives merely probabilities for the given system to be found (by measurement) in a given state.

This is the so-called Copenhagen interpretation of quantum mechanics, initiated by Max Born in 1926 and further developed by Niels Bohr and his colleagues, according to whom there is no determinism in physical reality. This view was strongly opposed by Albert Einstein and colleagues, who accepted the quantum theory as correct but thought that it was an incomplete theory, to be supplemented (through future research) by a more general deterministic theory, uncovering further "hidden variables," which seem to be ignored in present-day quantum mechanics. Many attempts have been made to find such a classical theory of fields to deduce the quantum theory but without success. There are also certain predictions such as Bell's inequalities that are the testing ground of whether quantum theory can in principle be an extended classical deterministic field theory. So far the answer is no, at least for a large class of "local hidden variables theories," and today we do have experimental confirmations where Bell's inequalities are experimentally violated, meaning that the quantum theory and its prediction for the outcome of such experiments is correct. Therefore, the statistical interpretation of quantum mechanics of Bohr's Copenhagen school, together with the strongly counter-intuitive notion of nonlocality, is proven to be correct, and these nondeterministic properties of quantum mechanics are being used in technological applications (such as quantum information theory, quantum teleportation, and quantum computing).

It is, of course, a philosophical shock to learn that the world is not deterministic, but there seems to be no way out. One of the main causes is the process of quantum measurement, which as a process is *not* described by the Schrödinger equation and seems to

be the primary source of quantum indeterminism. Quantum measurement is the main source for the generally accepted statistical interpretation of quantum mechanics. Still, the potential of a classical nonlinear field theory (including its turbulent solutions) seems largely unexplored as a description of physical reality. Even classical nonlinear dynamics is not deterministic (even in principle) due to the existence of chaos. A nonlinear classical field theory is even richer, for example the complex turbulent solutions of the Navier–Stokes equations.

In a deterministic world, there would be no place for free will in the lives of human beings or other living creatures. Everything would be predetermined by the initial state before our life, even if we do not have information about that, which implies that we cannot be aware of our predestination. Since the world is not deterministic, there is room for free will and free choice. However, it might be that the world is deterministic, if we do not observe it, and is not deterministic as soon as we "touch" it. Therefore, determinism can never be proved (in analogy with Kurt Gödel's famous incompleteness theorem). Thus, our free will may materialize as soon as we interact with the world, otherwise we would be completely predestined, but isolated from the rest of the world, which is of course not possible. The issue of classical and quantum measurement lies at the bottom of such discussions. It leads to the general conclusion that the world ultimately is not deterministic, but determinism might be a good approximation under certain conditions imposed on the measurement process.

MARKO ROBNIK

See also **Butterfly effect; Causality; Chaotic dynamics; Lyapunov exponents; Quantum theory; Turbulence**

Further Reading

Belavkin, V.P. 2002. Quantum causality, stochastics, trajectories and information. *Reports on Progress in Physics*, 65: 353–420

Bell, J.S. 1987. *Speakable and Unspeakable in Quantum Mechanics*, Cambridge and New York: Cambridge University Press

Edward U. Condon, author. Mechanics, Quantum. 1980. *The New Encyclopaedia Britannica: Macropaedia*, 15th edition, vol. 11, Chicago: Encyclopaedia Britannica: 793

Laplace, P.S. 1814. *Essai philosophique sur le probabilités*, Paris: Courier, 1814; as *Philosophical Essay on Probabilities*, Berlin and New York: Springer, 1995

Peres, A. 1995. *Quantum Theory: Concepts and Methods*, Dordrecht: Kluwer

Philip W. Goetz. (editor). 1980. Determinism. *The New Encyclopaedia Britannica: Micropaedia*, 15th edition, vol. III, Chicago: Encyclopaedia Britannica: 494

Taylor, R. 1996. Determinism. In *The Encyclopedia of Philosophy*, vol. 2, edited by Paul Edwards, New York: Macmillan and London: Simon & Schuster, 359

Wheeler, J.A. & Zurek, W.H. (editors). 1983. *Quantum Theory and Measurement*, Princeton, NJ: Princeton University Press

DETERMINISTIC WALKS IN RANDOM ENVIRONMENTS

A "deterministic walk in a random environment" (DWRE) is the name given to a system generated by the motion of some object (such as, a particle, signal, wave, ant, read/write head of the Turing machine) on a graph. At each time step, the object hops from a vertex to one of its neighboring vertices. The choice of neighbor is completely determined by the type of deterministic scattering rule or scatterer, located at the vertex. A random environment is formed by the scatterers that are assumed to be initially randomly (usually independently) distributed among the vertices. DWREs (in their simplest form and under different names) were introduced in various branches of science (Gunn & Ortuño, 1985; Langton, 1986; Ruijgrok & Cohen, 1988) as paradigms, for example, for propagation of a signal in a random media, evolutionary dynamics, growth processes, and the computational environment.

In the early numerical studies, graphs were regular lattices and usually two types of scatterers were considered in each model. The most studied case was that of the regular quadratic lattice with left and right rotators, which rotate the particle to the left or to the right by an angle $\pi/2$, or left and right mirrors aligned along the two diagonals of the lattice. Two classes of such models have been extensively studied numerically (Cohen, 1992). The first class corresponds to the case when there is no feedback of the moving particle to the environment; that is, a particular type of scatterer is fixed at each site of the lattice forever. Another class is formed by models with flipping scatterers, when a scatterer at a site changes (deterministically) after every visit of a particle to this site.

In statistical physics, these models naturally appear as deterministic Lorentz lattice gases (but with a random distribution of scatterers). The scatterers are not spheres (disks) as in the classical Lorentz gas. Instead, say in the d-dimensional cubic lattice, there are $(2d)^{2d}$ different types of scatterers because each vertex in this case has $2d$ incoming and $2d$ outcoming edges. In theoretical computer science, these models are referred to as many-dimensional Turing machines because the changes of scatterer type at each vertex occur deterministically—according to some program written on an infinite tape divided into commands, for example, to change a given scatterer to some other type (Bunimovich & Khlabystova, 2002a).

Although a DWRE reminds one of random walks, these systems are essentially different. The major difference with random walks is that instead of carrying out a random experiment (like flipping a

coin), the particle chooses each step deterministically. Formally, DWREs are deterministic cellular automata, but their behavior reflects a mixture of deterministic dynamics and a random environment. Their dynamics is often counterintuitive (Cohen, 1992) because one's intuition is essentially based on exactly understood (completely solved) systems and models. There are many such models among purely deterministic and purely stochastic systems; however, there were basically no completely understood systems with a mixture of deterministic and stochastic features. Some subclasses of DWREs provide such exactly solvable models (Bunimovich, 2000).

Although closest to stochastic systems, DWREs have fixed environments. This seems counterintuitive, but the evolution of scattering types makes the entire dynamics more deterministic than in the case where an (initially random) distribution of scatterers is frozen.

In many cases, DWRE systems are equivalent to various models from percolation theory (Bunimovich & Troubetzkoy, 1992). Not only the structure of the graph (lattice) but also the types of scatterer in the model determine the corresponding percolation problem. For instance, the mirror's model in the square lattice is reduced to the percolation problem on the square lattice, while the rotator's model is reduced to the percolation problem on some nonplanar graph (Bunimovich & Troubetzkoy, 1992).

Perhaps the most widely known DWRE models are Langton's Ant (Langton, 1986) or the flipping rotators model on the square lattice (Ruijgrok & Cohen, 1988), which are solvable again with rather counterintuitive results (Bunimovich & Troubetzkoy, 1993). If all vertices are occupied with rotators, then all orbits (particle's paths) are unbounded. If, on the other hand, one allows vertices to be empty with positive probability (i.e., the third, straight-ahead scatterer is allowed), then the particle's path becomes bounded with probability one.

The results, both numerical and mathematical, continued to surprise until "Walks in Rigid Environments" (WRE) were introduced and analyzed (Bunimovich, 2000). WREs employ a new integer parameter r, $1 \le r \le \infty$, which is called the rigidity of the environment. The rigidity determines how many times the particle must collide with the given scatterer in order to change its type. In other words, the scatterer at a given vertex changes its type immediately after the rth visit of the particle to this site. Therefore, WREs interpolate between DWREs with fixed environments (where $r = \infty$) and DWREs with flipping environments (where $r = 1$).

WREs on a one-dimensional lattice $\mathbb{Z}$ are completely solved (Bunimovich, 2000; Bunimovich & Khlabystova, 2002b). In this case, there are only four types of scatterers. Two of them (forward scatterer and backscatterer) are symmetric with respect to the reflection of $\mathbb{Z}$, which is the only nontrivial symmetry of the one-dimensional lattice. The other two scatterers, which always send the particle to the right (or to the left), do not respect this symmetry. Therefore, the WRE with the last two types of scatterers has the same behavior for all values of the rigidity r. This model demonstrates a diffusive type of behavior, in which the particle eventually visits all vertices and the mean square displacement of the particle is proportional to t. On the contrary, WREs with forward and back scatterers demonstrate totally different behavior depending on the parity of the rigidity r. For even rigidities, the particle eventually visits all vertices again but its motion is subdiffusive. The most interesting behavior occurs for odd values of the rigidity. In this case the particle—after a short initial period of seemingly irregular motion near the origin—starts to propagate in one direction with random velocity. This phenomenon of (eventual) propagation reminds one of "gliders" in Conway's Game of Life. However, in a WRE this propagation occurs for all initial configurations of environment, while in the Game of Life, gliders appear as only very special solutions. The phenomenon of eventual propagation in one direction is not restricted to one-dimensional WREs. For instance, the same behavior is demonstrated by the model with right and left rotators on the triangular lattice (Grosfils et al., 1999).

If the rigidity $r < \infty$, then one can also investigate the dynamics of the environment. Observe that if $r < \infty$, then it makes sense to consider not one but many moving particles as well. Indeed, even though the particles do not interact directly, they do effectively interact by changing environments with each other. The evolution of the environment in such models can be chaotic having a positive and even infinite metric entropy (Bunimovich & Troubetzkoy, 1993). This means, in particular, that the moving particle sees itself surrounded by almost any possible environment of scatterers at different moments of time.

An important difference between DWREs and random walks is that in the continuous limit DWREs become completely deterministic (Bunimovich & Khlabystova, 2002b), whereas biased random walks under proper scaling of probabilities become in the continuous limit stochastic diffusion processes.

LEONID BUNIMOVICH

See also **Game of life; Lorentz gas; Random walks**

Further Reading

Bunimovich, L.A. 2000. Walks in rigid environments. *Physica* A, 279:169–179

Bunimovich, L.A. & Khlabystova, M.A. 2002a. Lorentz lattice gases and many-dimensional Turing machines. In *Collision-Based Computing*, edited by A. Adamatzky, London: Springer

Bunimovich, L. A. & Khlabystova, M.A. 2002b. Walks in rigid environments: continuous limits. *Journal of Statistical Physics*, 108: 905–925

Bunimovich, L. A. & Troubetzkoy, S.E. 1992. Recurrence properties of the Lorentz lattice gases. *Journal of Statistical Physics*, 67: 289–302

Bunimovich, L. A. & Troubetzkoy, S.E. 1993. Topological properties of flipping Lorentz lattice gas models. *Journal of Statistical Physics*, 72: 297–307

Cohen, E.G.D. 1992. New types of diffusion in lattice gas cellular automata. In *Microscopic Simulations of Complex Hydrodynamic Phenomena*, edited by M. Mareschal & B.L. Holian, New York: Plenum

Grosfils, P., Boon, J.P., Cohen, E.G.D. & Bunimovich, L.A. 1999. Propagation and self-organization in lattice random media. *Journal of Statistical Physics*, 97: 575–608

Gunn, J.M.F. & Ortuño, M. 1985. Percolation and motion in a simple random environment. *Journal of Physics* A, 18: 1095–1099

Langton, C.G. 1986. Studying artificial life with cellular automata. *Physica* D, 22: 120–149

Ruijgrok, T.W. & Cohen, E.G.D. 1988. Deterministic lattice gas models. *Physics Letters* A, 133: 415–419

DEVELOPMENT OF SINGULARITIES

For some nonlinear PDEs, solutions of the Cauchy (initial-value) problem may exist only until a finite moment $t = t_c$, and they cannot be continued afterwards. At $t = t_c$, the solution loses its initial smoothness, and a singularity appears, which causes the blow-up of the solution. For conservative systems where the wavefield develops sharply diverging gradients, this blow-up phenomenon is often called collapse.

Historically, the first example of collapse follows from the so-called Hopf equation: $u_t + uu_x = 0$, which describes the one-dimensional velocity of dust with zero pressure. This equation admits the generic implicit solution $u = F(x - ut)$, where F is determined from the initial velocity profile. For any compact distribution F, there exists a couple of coordinates (x_c, t_c), at which the spatial derivative of u reaches infinity.

Collapse also occurs in the high-dimensional solutions to the nonlinear Schrödinger (NLS) equation, consisting of a point-singularity that achieves the fate of nonlinear waves undergoing self-focusing (Kelley, 1965). To describe this process, let us consider the NLS equation

$$i\partial_t \psi + \nabla^2 \psi + |\psi|^2 \psi = 0, \qquad (1)$$

where t is a time variable and the Laplacian $\nabla^2 = \partial_x^2 + \partial_y^2 + \partial_z^2 + \cdots$ accounts for the dispersion of a wave-packet along D orthogonal spatial axes $[\boldsymbol{r} = (x, y, z, ...)]$. The wave function ψ evolves from the spatially localized initial datum $\psi(\boldsymbol{r}, 0) \equiv \psi_0(\boldsymbol{r})$, assumed to belong to the Hilbert space H^1 with finite norm $\|\psi\|_{H^1} = (\|\psi\|_2^2 + \|\nabla\psi\|_2^2)^{1/2}$, where $\|f\|_p \equiv (\int |f|^p d\boldsymbol{r})^{1/p}$. Two invariants are associated with ψ, namely, the L^2 norm N (sometimes called mass, power, or number of particles) and the Hamiltonian H:

$$N = \|\psi\|_2^2, \quad H = \|\nabla\psi\|_2^2 - \tfrac{1}{2}\|\psi\|_4^4. \qquad (2)$$

From Equation (1), the following virial equality can be established (Glassey, 1977):

$$N d_t^2 \langle r^2 \rangle = 4\{2H + (1 - D/2)\|\psi\|_4^4\}, \qquad (3)$$

where $\langle r^2 \rangle = \int r^2 |\psi|^2 d\boldsymbol{r}/N$ denotes the mean-squared radius of the solution ψ. By a double integration in time, Equation (3) shows that, whenever $D \geq 2$, there exist initial conditions for which $\langle r^2 \rangle$ vanishes at finite time, which is the signature of a wave collapse. For finite norms N, the inequality $N \leq (2/D)^2 \langle r^2 \rangle \times \|\nabla\psi\|_2^2$ implies that the gradient norm diverges in collapse regimes. As H is finite, the collapse dynamics makes the L^4 norm $\|\psi\|_4^4$ blow up in turn and $\max|\psi|$ diverges, by virtue of the mean-value theorem $\int |\psi|^4 d\boldsymbol{r} \leq \max_r |\psi|^2 \times N$. This leads to a finite-time blow-up, at which the solution ψ ceases to exist in H^1. Blow-up generally occurs before $\langle r^2 \rangle$ reaches zero (Rasmussen & Rypdal, 1986).

While $H < 0$ arises from Equation (3) as a sufficient condition for collapse, sharper requirements can be derived by means of the so-called Sobolev inequality

$$\|\psi\|_4^4 \leq C \|\nabla\psi\|_2^D \times \|\psi\|_2^{4-D}. \qquad (4)$$

- In the critical case $D = 2$, this inequality can be used to bound H from below, so that the gradient norm blows up only if N fulfills the constraint $N > N_c$. The best constant in Equation (4) is exactly $C_{best} = 2/N_c$, and it involves the quantity $N_c = \int \phi_0^2 \, d\boldsymbol{r} = 11.68$, where ϕ_0 is the radially symmetric soliton solution of $-\phi_0 + \nabla^2\phi_0 + \phi_0^3 = 0$ (Weinstein, 1983). N_c provides the minimum power that ψ must necessarily contain at $t = 0$ for producing a collapse, justifying the existence of a critical power for the 2-dimensional self-focusing of optical beams in nonlinear Kerr media.
- In the supercritical case $D = 3$, a criterion for collapse, sharper than $H < 0$, can be established from a combination of Equations (3) and (4) as $H < N_c^2/N$ for gradient norms initially above $3N_c^2/N$ (Kuznetsov et al., 1995). N_c again corresponds to the mass of the three-dimensional soliton solution ϕ_0 satisfying $-\phi_0 + \nabla^2\phi_0 + \phi_0^3 = 0$.

Once the collapse is triggered, the solution self-focuses and shrinks isotropically in a self-similar way near the singularity point t_c. It is, thus, convenient to introduce the self-similar substitution:

$$\psi(\boldsymbol{r}, t) = a^{-\alpha}(t)\phi(\boldsymbol{\xi}, \tau) e^{i\lambda\tau - i\beta\xi^2/4}, \qquad (5)$$

where $\boldsymbol{\xi} = \boldsymbol{r}/a(t)$, $\tau(t) \equiv \int_0^t du/a^2(u)$, and $\beta = -a\dot{a}$ (dot indicates differentiation with respect to time). Here, the parameter λ is positive for localization of ϕ. The function $a(t)$ represents the scale length that vanishes as collapse develops, and ϕ converges to an exactly self-similar form $\phi(\boldsymbol{\xi})$, which no longer

depends explicitly on time [$\partial_\tau \phi \to 0$]. Inserting (3) into H shows that the right balance between the gradient and L^4 norms requires $\alpha = 1$, in order to preserve the finiteness of the Hamiltonian. With $\alpha = 1$, $N = a^{D-2}(t) \int |\phi|^2 \mathrm{d}\boldsymbol{\xi}$ and for radial solutions, Equation (1) transforms to

$$\mathrm{i}\partial_\tau \phi + \xi^{1-D} \partial_\xi \xi^{D-1} \partial_\xi \phi + |\phi|^2 \phi + \varepsilon[\xi^2 - \xi_\mathrm{T}^2]\phi = 0, \tag{6}$$

where $\xi_\mathrm{T}^2 \equiv \varepsilon^{-1}[\lambda + \mathrm{i}\beta(D/2 - 1)]$ is viewed as a turning point, with $\varepsilon \equiv \frac{1}{4}(\beta^2 + \partial_\tau \beta)$. As $a(t) \to 0$, ϕ can be treated by means of quasi-self-similar techniques (Bergé, 1998). In the limit $\partial_\tau \phi \to 0$, ε converges to $\beta^2/4$ and the solution ϕ is split into a nonlinear core (ϕ_c) extending in the range $\xi < \xi_\mathrm{T}$ and a linear tail (ϕ_T) defined in the complementary spatial domain $\xi > \xi_\mathrm{T}$, where the nonlinearity vanishes. As a result, the wave function ψ reads near the collapse point:

$$\psi(\boldsymbol{r}, t) = \frac{\mathrm{e}^{\mathrm{i}\lambda \int_0^t \mathrm{d}u/a^2(u)}}{a(t)} \times \left\{ \phi_\mathrm{c}\left(\frac{r}{a}, \varepsilon\right) \mathrm{e}^{-\mathrm{i}\beta r^2/4a^2} \Big|_{0 \le r < r_\mathrm{T}} + \frac{C(\beta)}{(r/a)^{1+\mathrm{i}\lambda/\beta}} \Big|_{r_T < r < r_\mathrm{max}} \right\}, \tag{7}$$

where $|C(\beta)|^2$ evolves like $(2/\beta|\xi_\mathrm{T}|^{D-2})\mathrm{e}^{-\lambda\pi/\beta}$, $r_\mathrm{T} = a(t)|\xi_\mathrm{T}|$ and r_max bounds the self-similarity domain. The length $a(t)$ is identified from the continuity equation describing the mass exchanges between the core and tail parts of ψ. The dynamics of self-similar collapses then vary with the space dimension number as follows.

- *Strong collapse*: For $D = 2$, the size $a(t)$ behaves with a double-logarithmic correction: $a(t) \simeq a_0 \sqrt{t_\mathrm{c} - t}/\sqrt{\ln \ln [1/(t_\mathrm{c} - t)]}$, coming from $\beta \simeq \lambda\pi/\ln[\tau(t)]$ and $\tau(t) \simeq \ln[1/(t_\mathrm{c} - t)]$. As $t \to t_\mathrm{c}$, the exponential contribution in tail (5) thus decreases to zero, while the core boundary ξ_T increases slowly to infinity. Collapse thus takes place with a core solution providing the principal contribution in the wavefunction ψ. N is mainly given by $\int |\phi_\mathrm{c}|^2 \mathrm{d}\boldsymbol{\xi}$, which relaxes to the critical value $N_\mathrm{c} = 11.68$. The mass stays mostly located around the center, which meets the definition of *strong collapse* (Zakharov & Kuznetsov, 1986).
- *Weak collapse*: For $D = 3$, β attains a fixed point $\beta_0 \neq 0$, leading to the scaling law $a(t) \simeq a_0 (t_\mathrm{c} - t)^{1/2}$. The power is no longer preserved self-similarly in space, since $N = a(t) \int |\phi|^2 \mathrm{d}\boldsymbol{\xi}$. This integral behaves as $N \simeq N_\mathrm{core}(t) + N_\mathrm{tail}(t)$, where $N_\mathrm{core}(t) \sim a(t)$ vanishes, while $N_\mathrm{tail}(t) \simeq 4\pi |C(\beta)|^2 r_\mathrm{max}$ contains almost all the initial mass as $a(t) \to 0$. A 3-d collapse is thus accompanied by an expulsion of particles towards the large-distance domain $r \gg r_\mathrm{T}(t)$, which characterizes a *weak collapse*. The solution ψ blows up at the center, where N_core becomes zero. Accordingly, ψ extends in the outer domain with the stationary density $r^2 |\psi|^2 \to |C(\beta_0)|^2 = \text{const}$.

These different collapses can be tested numerically by adding a small nonlinear dissipation term in Equation (1), i.e., by changing ψ_t into $\psi_t + \beta|\psi|^m \psi$ with $\beta \ll 1$ and $m > 1$. For $D = 2$, dissipation removes a substantial amount of energy per collapse event, because N remains mostly confined at the center. This leads to a step-wise decrease of N (Kosmatov et al., 1991). In contrast, for $D = 3$, nonlinear dissipation cannot remove much energy, the major part of $N \simeq N_\mathrm{tail}$ being transferred to large distances. This causes a monotonical decrease of N.

- *Superstrong collapse*: For weak and strong collapses, only the energy captured by the singularity dissipates. A different situation is realized if collapsing solutions can sustain dissipation through power loss into a persistent region of high intensity. Such solutions approach a quasi stationary state, described by $\psi_{rr} + (D - 1)\psi_r/r + |\psi|^2 \psi = 0$, in the limit of small $\beta \to 0$. For instance, when $D = 4$, Equation (1) admits the stationary radial state $\psi(r) = B\mathrm{e}^{\mathrm{i} \ln r \sqrt{B^2 - 1}}/r$ $(B > 1)$, for which the power density $|\psi|^2$ flows into the singularity with a constant energy flux equal to $B^2\sqrt{B^2 - 1}$. This collapse, which received the adjective of *superstrong*, has been numerically detected at high dimension numbers $D > 3$ (Kosmatov et al., 1991).

So far, the discussion has remained within the realm of the one-wave component NLS equation with a cubic nonlinearity. It is thus worth underlining the following.

- The previous results can be generalized to a power-law nonlinearity, when the cubic term $|\psi|^2\psi$ of Equation (1) is replaced by $|\psi|^{2n}\psi$ with $n > 1$ (Rasmussen & Rypdal, 1986; Bergé, 1998). Solutions with $D = 2/n$ follow the route of a strong collapse, while solutions defined for $D > 2/n$ collapse weakly. Superstrong collapses apply to the dimensional configurations $D > 2 + 1/n$.
- Several NLS equations coupled through their cubic nonlinearities often serve to model the self- and cross-interactions of multiple wave components (or different polarizations) in vector systems. Such systems promote blow-up phenomena, which can be examined by means of the above analytical tools (Bergé, 2001).
- Blow-up may take place in solutions of PDEs other than the NLS equation. For example, investigations of the solutions to the generalized D-dimensional Korteweg–de Vries (KdV) equation

$$q_t + q^n q_x + (\nabla^2 q)_x = 0 \tag{8}$$

suggest that, whereas no collapse occurs for values of the product $nD < 4$, collapsing states can arise and adopt a self-similar shape provided that $nD \geq 4$ (Blaha et al., 1989). The mathematical proof for this statement is presently incomplete.

LUC BERGÉ

See also **Filamentation; Kerr effect; Nonlinear Schrödinger equations; Virial theorem**

Further Reading

Bergé, L. 1998. Wave collapse in physics: Principles and applications to light and plasma waves. *Physics Reports*, 303: 259–370

Bergé, L. 2001. Nonlinear wave collapse. In *Spatial Solitons*, edited by S. Trillo & W. Torruellas, Berlin: Springer, pp. 247–267

Blaha, R., Laedke, E.W. & Spatschek, K.H. 1989. Collapsing states of generalized Korteweg–de Vries equations. *Physica* D, 40: 249–264

Glassey, R.T. 1977. On the blowing-up of solutions to the Cauchy problem for nonlinear Schrödinger equations. *Journal of Mathematical Physics*, 18: 1794–1797

Kelley, P.L. 1965. Self-focusing of optical beams. *Physical Review Letters*, 15: 1005–1008

Kosmatov, N.E., Shvets, V.F. & Zakharov, V.E. 1991. Computer simulation of wave collapses in the nonlinear Schrödinger equation. *Physica* D, 52: 16–35

Kuznetsov, E.A., Rasmussen, J., Rypdal, K. & Turitsyn, S.K. 1995. Sharper criteria for the wave collapse. *Physica* D, 87: 273–284

Rasmussen, J. & Rypdal, K. 1986. Blow-up in nonlinear Schrödinger equations-I: a general review. *Physica Scripta*, 33: 481–497

Weinstein, M.I. 1983. Nonlinear Schrödinger equations and sharp interpolation estimates. *Communications in Mathematical Physics*, 87: 567–576

Zakharov, V.E. & Kuznetsov, E.A. 1986. Quasiclassical theory of three-dimensional wave collapse. *Zhurnal Eksperimental'noi i Teoreticheskoi Fiziki* (USSR JETP), 91: 1310–1324 [Trans. in *Soviet Physics JETP*, 64: 773–780]

DEVIL'S STAIRCASE

See **Fractals**

DIFFEOMORPHISM

See **Maps**

DIFFERENTIAL GEOMETRY

A *topological manifold of dimension n* is a topological space M that can locally be identified with an open set in $\mathbb{R}^n$; a superscript on the symbol for M is often used to indicate the dimension. For example, a circle is a one-dimensional manifold, denoted S^1, while a figure-eight is not a manifold. In more detail, M must have a set of *coordinate charts* ϕ_α, each of which is a homeomorphism from an open set $U_\alpha \subset M$ to an open set in $\mathbb{R}^n$, such that every point of M is in the domain of a chart. If the intersection $U_{\alpha\beta}$ of two domains U_α and U_β is nonempty, then the change of coordinates $\phi_\alpha \circ \phi_\beta^{-1}$ is a continuous map from $\phi_\beta(U_{\alpha\beta})$ to $\phi_\alpha(U_{\alpha\beta})$ with a continuous inverse.

A *differentiable manifold* is a topological manifold M^n equipped with charts such that, on the overlaps, $\phi_\alpha \circ \phi_\beta^{-1}$ is differentiable with a differentiable inverse. (Here, "differentiable" or "smooth" functions are those whose partial derivatives exist and are continuous to all orders; however, for C^k *manifolds*, the changes of coordinates are only required to be differentiable up to order k.) If $x^1, \ldots, x^n$ and $\bar{x}^1, \ldots, \bar{x}^n$ are the coordinate functions for two overlapping charts, then the Jacobian determinant $||\partial x^i / \partial \bar{x}^j||$ must be nonzero at each point.

For example, the subset M of $\mathbb{R}^{n+1}$ defined by an equation form $f(x^0, x^1, \ldots, x^n) = 0$ is a differentiable manifold if f is a smooth function and at each point $p \in M$, at least one partial derivative (say, $\partial f / \partial x^0$) is nonzero. Then, by the Implicit Function Theorem, the projection from a neighborhood of p (i.e., an open subset of M containing p) onto the $x^1 \cdots x^n$ coordinate hyperplane is differentiable with a differentiable inverse. So, the n-dimensional spheres S^n are compact differentiable manifolds. Similarly, the group SL_n of $n \times n$ matrices with determinant one is a noncompact manifold of dimension $n^2 - 1$.

A function $f : M \to \mathbb{R}$ is smooth if $f \circ \phi$ is smooth for any chart ϕ. More generally, if M^m and N^n are two differentiable manifolds, we say a mapping $F : M \to N$ is smooth if it is smooth with respect to coordinate charts on both ends, that is, $\psi \circ F \circ \phi^{-1}$ is smooth from $\mathbb{R}^m$ to $\mathbb{R}^n$ for any charts ϕ on M and ψ on N. When $F : M \to N$ also has a smooth inverse, it is a *diffeomorphism*, and M and N are *diffeomorphic*. For example, the hyperboloid $x^2 + y^2 - z^2 = 1$ is diffeomorphic to the cylinder $x^2 + y^2 = 1$, and any open interval on the real line $\mathbb{R}$ is diffeomorphic to all of $\mathbb{R}$.

Vector Fields and 1-Forms

A *tangent vector* at a point $p \in M^n$ is a linear operator v on smooth functions f defined near p, such that (i) $\mathsf{v}(f_1 f_2) = f_1 \mathsf{v}(f_2) + f_2 \mathsf{v}(f_1)$, and (ii) $\mathsf{v}(f_1) = \mathsf{v}(f_2)$ if $f_1 = f_2$ on a neighborhood of p (i.e., f_1, f_2 have the same *germ* at p). For example, if $c : \mathbb{R} \to M$ defines a curve in M such that $c(t) = p$, then we define the tangent vector $c'(t)$ to the curve by $c'(t)(f) := (\mathrm{d}/\mathrm{d}t) f(c(t))$, where the symbol ":=" indicates a definition. If $\mathsf{v} = c'(t)$, then we say that the curve is *tangent to* v at p.

The set of tangent vectors at p form a vector space of dimension n, denoted $T_p M$. If $x^1, \ldots, x^n$ are local coordinates near p, then the partial derivative operators $\partial / \partial x^i$ are a basis for $T_p M$. The set of all tangent vectors at all points of M is itself a differentiable manifold of dimension $2n$, since we can adjoin coordinates

$y^1, \ldots, y^n$ and locally write all tangent vectors as

$$\mathsf{v} = \sum_{i=1}^{n} y^i \frac{\partial}{\partial x^i}.$$

This manifold is the *tangent bundle* of M, and is denoted TM.

A *vector field* on M smoothly assigns a tangent vector at each point; in local coordinates, we specify a vector field by giving the y^i as smooth functions of x^i. If f is a smooth function on M and $\boldsymbol{V}$ is a vector field, then $\boldsymbol{V}(f)$ is another smooth function.

Given a vector field $\boldsymbol{V}$ and a point $p \in M$ at which $\boldsymbol{V} \neq 0$, existence theorems for systems of ODE (e.g., Picard's Theorem) imply that there exist a neighborhood U of p and a one-parameter family of smooth, one-to-one mappings $F_t : U \to M$, such that for any fixed $q \in U$, the curve $F_t(q)$ is tangent to $\boldsymbol{V}$ for every t. The F_t's are called the *flow by vector field* $\boldsymbol{V}$.

The *Lie bracket* $[\boldsymbol{V}_1, \boldsymbol{V}_2]$ of two vector fields $\boldsymbol{V}_1, \boldsymbol{V}_2$ is a third vector field defined by

$$[\boldsymbol{V}_1, \boldsymbol{V}_2](f) := \boldsymbol{V}_1(\boldsymbol{V}_2(f)) - \boldsymbol{V}_2(\boldsymbol{V}_1(f)).$$

If y_1^i and y_2^i are the components of $\boldsymbol{V}_1, \boldsymbol{V}_2$ in local coordinates, then

$$[\boldsymbol{V}_1, \boldsymbol{V}_2] = \sum_{i,j=1}^{n} \left(y_1^i \frac{\partial y_2^j}{\partial x^i} - y_2^i \frac{\partial y_1^j}{\partial x^i} \right) \frac{\partial}{\partial x^j}. \quad (1)$$

The vector fields are said to *commute* if $[\boldsymbol{V}_1, \boldsymbol{V}_2]$ is identically zero; then, flow by $\boldsymbol{V}_1$ commutes with flow by $\boldsymbol{V}_2$.

A *differential 1-form at* p is a linear mapping function from T_pM to $\mathbb{R}$. For example, given a differentiable function f defined near p, we define the 1-form $\mathrm{d}f$ by $\mathrm{d}f(\mathsf{v}) := \mathsf{v}(f)$ for all $\mathsf{v} \in T_pM$. The vector space of 1-forms at p is denoted T_p^*M. Given local coordinates, the differentials $\mathrm{d}x^1, \ldots, \mathrm{d}x^n$, which satisfy $\mathrm{d}x^i(\partial/\partial x^j) = \delta_j^i$, are a basis for T_p^*M. While tangent vectors generalize directional derivatives in $\mathbb{R}^n$, 1-forms generalize gradients; however, 1-forms cannot be identified with tangent vectors without using some nondegenerate bilinear form on tangent vectors, for example, a Riemannian metric or symplectic form on M.

A *differential 1-form* on M assigns a 1-form at each point; in local coordinates, these appear as

$$\omega = \sum_{i=1}^{n} z_i \mathrm{d}x^i,$$

where the z_i are some smooth functions of the x^i. If $\boldsymbol{V}$ is a vector field on M, then $\omega(\boldsymbol{V})$ is a function on M.

Given a smooth mapping $F : M \to N$, we can transform a tangent vector $\mathsf{v} \in T_pM$ to a tangent vector $F_*\mathsf{v}$ at $F(p)$ by defining

$$F_*\mathsf{v}(f) := \mathsf{v}(f \circ F)$$

for any function $f : N \to \mathbb{R}$. This is called the *pushforward* of v. We similarly define the pushforward $F_*\boldsymbol{V}$ of a vector field $\boldsymbol{V}$ on M. We can also transform a 1-form ω on N to a 1-form $F^*\omega$ on M by defining

$$F^*\omega(\mathsf{v}) := \omega(F_*\mathsf{v})$$

for any tangent vector v to M. This is called the *pullback* of ω.

If $\boldsymbol{V}$ is a vector field and F_t is the flow by $\boldsymbol{V}$, we define the *Lie derivative* of a 1-form ω with respect to $\boldsymbol{V}$ by

$$\mathcal{L}_{\boldsymbol{V}}\omega := \left. \frac{\mathrm{d}}{\mathrm{d}t} \right|_{t=0} F_t^*(\omega).$$

If the components of $\boldsymbol{V}$ and ω in local coordinates are y^i and z_i, respectively, then

$$\mathcal{L}_{\boldsymbol{V}}\omega = \sum_{i,j=1}^{n} \left(y^i \frac{\partial z_j}{\partial x^i} - z_i \frac{\partial y^j}{\partial x^i} \right) \mathrm{d}x_j. \quad (2)$$

Some useful properties of the Lie derivative are that it obeys the product rule and commutes with d, that is,

$$\begin{aligned} \mathcal{L}_{\boldsymbol{V}}(f\boldsymbol{W}) &= (\mathcal{L}_{\boldsymbol{V}} f)\boldsymbol{W} + f\,\mathcal{L}_{\boldsymbol{V}}\boldsymbol{W}, \\ \mathcal{L}_{\boldsymbol{V}}(f\omega) &= f\,\mathcal{L}_{\boldsymbol{V}}\omega + (\mathcal{L}_{\boldsymbol{V}} f)\omega, \\ \mathcal{L}_{\boldsymbol{V}}(\mathrm{d}f) &= \mathrm{d}(\mathcal{L}_{\boldsymbol{V}} f), \end{aligned}$$

where we define $\mathcal{L}_{\boldsymbol{V}} f := \boldsymbol{V}(f)$ and $\mathcal{L}_{\boldsymbol{V}}\boldsymbol{W} := [\boldsymbol{V}, \boldsymbol{W}]$. (Note than one can derive (2) using these properties.)

Higher Degree Differential Forms and Topology

A *differential* k*-form at* p is a multilinear function on k-tuples of vectors in T_pM that is skew-symmetric; that is, its value is multiplied by -1 whenever two adjacent vectors in the k-tuple are exchanged. For example, a 2-form may be constructed from two 1-forms ω^1, ω^2 using the *wedge product*:

$$\omega^1 \wedge \omega^2(\mathsf{v}_1, \mathsf{v}_2) := \omega^1(\mathsf{v}_1)\omega^2(\mathsf{v}_2) - \omega^1(\mathsf{v}_2)\omega^2(\mathsf{v}_1).$$

(Note that this is zero if ω^1 and ω^2 are linearly dependent.) More generally, the wedge product of 1-forms $\omega^1, \ldots, \omega^k$ is defined by

$$\begin{aligned} &\omega^1 \wedge \ldots \wedge \omega^k(\mathsf{v}_1, \ldots \mathsf{v}_k) \\ &\quad := \sum_{\sigma} (-1)^\sigma \omega^1(\mathsf{v}_{\sigma(1)})\omega^2(\mathsf{v}_{\sigma(2)}) \cdots \omega^k(\mathsf{v}_{\sigma(k)}), \end{aligned}$$

where the sum is over all permutations σ of $1, 2, \ldots, k$ and $(-1)^\sigma$ is the sign of the permutation. On an n-dimensional manifold, the vector space of k-forms

at a point has dimension $\binom{n}{k}$ and is spanned by wedge products of 1-forms; in particular, there are no forms of degree higher than n.

A 2-form may also be constructed from a single 1-form ω by taking the *exterior derivative* $\mathrm{d}\omega$, which satisfies

$$\mathrm{d}\omega(\boldsymbol{V}_1, \boldsymbol{V}_2) = \boldsymbol{V}_1(\omega(\boldsymbol{V}_2)) - \boldsymbol{V}_2(\omega(\boldsymbol{V}_1)) - \omega([\boldsymbol{V}_1, \boldsymbol{V}_2]). \tag{3}$$

(Although the right-hand side is defined using vector fields, its value at a point p depends only on the values of $\boldsymbol{V}_1, \boldsymbol{V}_2$ at p.) The exterior derivative of a k-form is a $(k+1)$-form; it can be calculated inductively using linearity and the product rule

$$d(\alpha \wedge \beta) = \mathrm{d}\alpha \wedge \beta + (-1)^{\mathrm{degree}(\alpha)} \alpha \wedge \mathrm{d}\beta.$$

If the exterior derivative of a k-form is identically zero on M, the form is *closed*. If a k-form is an exterior derivative of a $(k-1)$-form, it is *exact*. An important property of the exterior derivative is that $\mathrm{d}(\mathrm{d}\alpha) = 0$, i.e., exact forms are closed. The *Poincaré Lemma* asserts that a closed k-form α is *locally* exact; that is, in the vicinity of any given point a $(k-1)$-form β is defined such that $\alpha = \mathrm{d}\beta$. However, not every closed form is *globally* exact (e.g., the 1-form $\mathrm{d}\theta$ on S^1). Moreover, the *de Rham Theorem* asserts that the dimension of the vector space of closed k-forms modulo exact k-forms is a topological invariant of M; that is, two manifolds cannot be homeomorphic (or diffeomorphic) unless these dimensions, known as the *Betti numbers*, match up. (For example, the Euler characteristic is determined by the Betti numbers.)

THOMAS A. IVEY

See also **Invariant manifolds and sets; Lie algebras and Lie groups; Topology**

Further Reading

Isham, C.J. 1999. *Modern Differential Geometry for Physicists*, Singapore: World Scientific

Ivey, T. & Landsberg, J.M. 2003. *Cartan for Beginners: Differential Geometry via Moving Frames and Exterior Differential Systems*, Providence, RI: American Mathematical Society

Warner, F.W. 1983. *Foundations of Differentiable Manifolds and Lie Groups*, Berlin and New York: Springer

DIFFUSION

When a small drop of ink is poured onto a soft gel, the ink molecules disperse through by diffusion. Similarly, the spread of heat through a medium can also be a diffusive process (called heat conduction). Many other applications of diffusion arise in biology, combustion, economics, chemical engineering, and geophysics, among other fields.

Mathematically, the diffusion equation takes the form (Crank, 1975)

$$u_t = \triangle u, \tag{1}$$

where $u = u(\boldsymbol{x}, t)$ is the state variable, representing, for example, the density of concentration of some substance, at time $t \geq 0$ and position $\boldsymbol{x}$ in R^n, where $\triangle u$ denotes the Laplacian of u with respect to the space variable $\boldsymbol{x}$. Equation (1) is an example of a parabolic equation of evolution. If it holds for all $\boldsymbol{x}$ in R^n, then the problem is fully specified once appropriate initial conditions

$$u(\boldsymbol{x}, 0) = u_0(\boldsymbol{x}) \tag{2}$$

are known. If Equation (1) holds in a limited domain $\Omega \subset R^n$, then some boundary conditions must be imposed on u at $\partial\Omega$ that are compatible with the physical situation.

The diffusion equation can be viewed as a balance law (Grindrod, 1996). Let $Q(\boldsymbol{x}, t)$ be the net creation rate of particles at $\boldsymbol{x} \in \Gamma \subset \Omega$ and time t, and let $\boldsymbol{J}(\boldsymbol{x}, t)$ be the flux density. For any unit vector $\boldsymbol{n} \in R^n$, the scalar product $\boldsymbol{J} \cdot \boldsymbol{n}$ is the net rate at which particles cross a unit area in a plane perpendicular to $\boldsymbol{n}$ (take the plus sign in the direction of $\boldsymbol{n}$). Assuming that the rate of change of mass in Ω is due to particle creation or degradation inside Γ and the inflow and the outflow of particles through the boundary $\partial\Gamma$, we have

$$\frac{\mathrm{d}}{\mathrm{d}t} \int_\Gamma u \, \mathrm{d}\boldsymbol{x} = -\int_{\partial\Gamma} \boldsymbol{J} \cdot \boldsymbol{n} \, \mathrm{d}S + \int_\Gamma Q \, \mathrm{d}\boldsymbol{x}, \tag{3}$$

where $\int_\Gamma u \, \mathrm{d}\boldsymbol{x}$ denotes the population mass in Γ. If the solution is smooth enough, then applying the divergence theorem to the right-hand side in (3) gives

$$\frac{\mathrm{d}}{\mathrm{d}t} \int_\Gamma u \, \mathrm{d}\boldsymbol{x} = \int_\Gamma \nabla \cdot \boldsymbol{J} \, \mathrm{d}S + \int_\Gamma Q \, \mathrm{d}\boldsymbol{x}. \tag{4}$$

As Γ was arbitrary in Ω, Equation (4) implies that

$$u_t = -\nabla \cdot \boldsymbol{J} + Q \tag{5}$$

at every point in Ω, which is the required balance law.

In practice, depending on the process studied, one must specify the flux $\boldsymbol{J}$ and the source term Q. For example, in combustion or in chemistry, one uses Fick's law:

$$\boldsymbol{J} = -D\nabla u. \tag{6}$$

Here $D > 0$ is a constant called diffusivity with physical units of $\mathrm{m}^2\mathrm{s}^{-1}$. The minus sign in (6) accounts for the fact that the particles are transported from high to low densities. Using (6) in (5) gives the usual reaction-diffusion equation

$$u_t = D\triangle u + Q(\boldsymbol{x}, t, u, \ldots). \tag{7}$$

A heuristic derivation of the diffusion equation (1) involves the notion of a random walk. Consider a one-dimensional (1-d) random walker that at each time step t_i hops from its position x_n one unit to the left or right, $x_{n\pm1}$. The change in probability $p(x_n, t_i)$ to find the walker at x_n at t_i is equal to the sum of probabilities

for it to hop into the point minus the sum of probabilities to hop off the point:

$$p(x_n, t_i) - p(x_n, t_{i-1}) = \frac{1}{2}\left(p(x_{n+1}, t_{i-1}) + p(x_{n-1}, t_{i-1})\right) - p(x_n, t_{i-1}). \tag{8}$$

Introducing the space and time scales of the motion, this equation can be rearranged as

$$\frac{p(x_n, t_i) - p(x_n, t_{i-1})}{\delta_t} = \frac{\delta_x^2}{2\delta_t}\left[\frac{p(x_{n-1}, t_{i-1}) - 2p(x_n, t_{i-1}) + p(x_{n+1}, t_{i-1})}{\delta_x^2}\right]. \tag{9}$$

Denoting $D = \delta_x^2/2\delta_t$, Equation (9) becomes a discrete approximation of Equation (1), and by taking the limit as $\delta_t, \delta_x \to 0$, keeping D finite, we recover Equation (1).

A rigorous derivation of the diffusion equation is obtained via stochastic calculus. The motion of individual particles is described by stochastic differential equations with the positions of the particles being modeled as random variables in R^n. The global behavior depends on the type of stochastic process governing the motion of the particles. Typically, one describes this in terms of the probability distribution of the random variable. In many cases, one finds that all its moments of order higher than 2 vanish. Consequently, the distribution of the population density, u, satisfies the second-order Fokker–Planck (or Kolmogorov's forward equation) (Øksendal, 2000)

$$u_t = \nabla(D(\boldsymbol{x}, t)u) - \nabla(C(\boldsymbol{x}, t)u). \tag{10}$$

Equation (10) is a diffusion equation with a nonconstant, inhomogeneous diffusivity and convective term. It often arises for particles whose individual speeds are random deviations from some externally applied convection velocity. Examples arise in fluid flow and in biology (dispersals of population dispersals, e.g. chemotaxis), among other fields.

Particularly important cases are when the diffusivity depends on the population density such as in biology or ecology (Aronson & Weinberger, 1975). For example, insect dispersal models use the fact that the rate of spread of the population is increased at higher insect density. This is usually modeled with an equation of the form

$$u_t = \triangle(D(u)\nabla u) + f(u), \tag{11}$$

where typically $D(u) = D_0 u^m$, $m > 0$ (Okubo & Levin, 2001; Murray, 2002). Density-dependent diffusion equations appear in many other fields. In physics, impurities are diffused into semiconductor materials (in the processing of silicon-based electronic devices) so the diffusivity is a function of the density of the semiconductor. Other examples include models of crystal growth, porous media, magnetic flux vortices in superconductors, surface reactions, and so on.

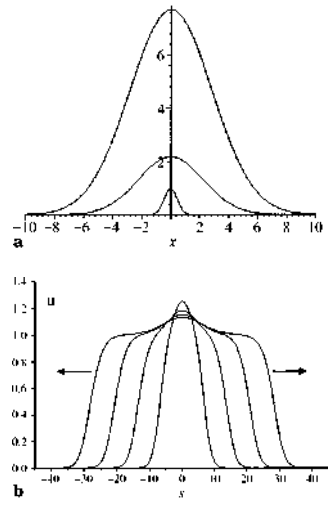

Figure 1. (a) Linear diffusion solutions of Equation (13). (b) Nonlinear diffusion solutions of Equation (14).

The behavior of the solution to Equation (1) is well understood. If Q is linear in u, then the solution is found by Fourier transform or eigenfunction-expansion techniques. For example, the linear diffusion equation

$$u_t = \triangle u + u \tag{12}$$

with the initial condition $u(x, 0) = \delta(x)$ (Dirac's delta function) has, in (1-d), the fundamental solution

$$u(x, t) = \frac{1}{2\sqrt{\pi t}} \exp\left(t - \frac{x^2}{4t}\right), t > 0. \tag{13}$$

Figure 1a illustrates the behavior of Equation (13) as a function of x for various times. Due to the linear source term, the solution grows exponentially (is unbounded). Another feature of solution (13) is the "paradox of infinite speed propagation." For all $x \neq 0$, $u(x, 0) = 0$, but $u(x, t) > 0$ for all $t > 0$. However, the diffusion equation describes well the global behavior of mass, as it can be easily verified that the center of mass does propagate with a finite speed.

The behavior of solutions of Equation (7) changes dramatically if Q is no longer linear in u. Consider the typical nonlinear autonomous form now called the Fisher–KPP equation and first investigated by Kolmogorov, Petrovsky, and Piscounoff (1937) and,

separately, by Fisher (1937) to model the process of genetic diffusion:

$$u_t = \triangle u + u(1 - u). \qquad (14)$$

The only solution evolving from a positive compactly supported initial data is always bounded and propagates in the form of a traveling wave with constant speed $v = 2$, see Figure 1b for an illustration. This is due to the combined action of diffusion and local nonlinearity and has been used in many models applied in biology (genetics, ecology, population dynamics, etc.), chemistry, combustion, economics, physics, etc. The equation similar to (14) but with a cubic nonlinearity (bistable model) instead of the quadratic was proposed in 1938 as a model for a flame front by Zeldovich and Frank-Kamenetsky (1938).

RAZVAN A. SATNOIANU

See also **Fokker–Planck equation; Heat conduction; Reaction-diffusion systems; Zeldovich–Frank-Kamenetsky equation**

Further Reading

Aronson, D.G. & Weinberger H.F. 1975. Nonlinear diffusion in population genetics, combustion and nerve pulse propagation. In *Partial Differential Equations and Related Topics*, edited by J.A. Goldstein, New York: Springer

Crank, J. 1975. *The Mathematics of Diffusion*, Oxford: Clarendon Press

Fisher, R.A. 1937. The wave of advance of advantageous genes. *Annuals of Eugenics*, 7, 353–369

Grindrod, P. 1996. *The Theory and Applications of Reaction–Diffusion Equations*, 2nd edition, Oxford: Clarendon Press and New York: Oxford University Press

Kolmogorov, A., Petrovsky, I. & Piscounoff, N. 1937. Etude de l'equation de la diffusion avec croissance de la quantité de matière et son application á un problème biologique. *Moscow Univ. Bull. Math.*, 1: 1–25

Murray, J.D. 2002. *Mathematical Biology*, vol. I, 3rd edition: *An Introduction*, Berlin and New York: Springer

Øksendal, B. 2000. *Stochastic Differential Equations*, Berlin and New York: Springer

Okubo, A. & Levin, S.A. 2001. *Diffusion and Ecological Problems: Modern Perspectives*, Berlin and New York: Springer

Zeldovich, Ya.B. & Frank-Kamenetsky, D.A. 1938. K teorii ravnomernogo rasprostranenia plameni [Toward a theory of uniformly propagating flames]. *Doklady Akademii Nauk SSSR*, 19: 693–697

DIMENSIONAL ANALYSIS

The dimensions of quantities in any equation (in physics these are mass, length, time, charge, temperature, angle, and so on) must be the same on both sides; otherwise an equality would be violated by changing units. From such reasoning, it is often possible to derive valuable insights without delving into mechanisms. This "dimensional analysis" is an old idea; Lord Rayleigh (John William Strutt), an early vigorous exponent of the method, called it the "principle of similitude,"

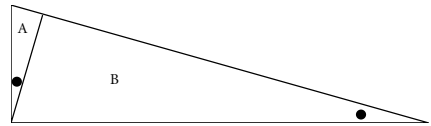

Figure 1. A right triangle is broken into two smaller right triangles of the same proportions.

which he extolled in the following terms (Rayleigh, 1915): "It happens not infrequently that results in the form of 'laws' are put forward as novelties on the basis of elaborate experiments, which might have been predicted a priori after a few minutes' consideration."

The principle was familiar to Galileo, Newton, Fourier, Reynolds, and Maxwell, and was widely used in engineering around 1900. Edgar Buckingham formalized it in what is now called the Pi (for "product") Theorem, that any functional relation among N quantities represented by real numbers and collectively involving $U < N$ basic units can be rewritten as a dimensionless, constant function of $N - U$ dimensionless, multiplicative combinations of those variables (Buckingham, 1914). Unless N and U are trivially small, some systematic procedure is helpful for finding all possible ways of combining variables into dimensionless constants (Birkhoff, 1950; Coyle & Ballico-Lay, 1984).

Interestingly, there have been attempts to discover the laws of economics and finance by similar procedures, starting of course from a different list of fundamental units (DeJong, 1967).

As most articles on dimensional analysis expound abstract principles, two examples are presented here, one drawn from the ancient roots of mathematics and one from the nonlinear physics of shock waves.

Pythagorean Theorem

The area of a right triangle is uniquely determined by the length of the "long" side and one of the other ("wrong") angles. Area is some universal function of Long and Angle, let us say the smaller Angle, dotted in Figure 1. Do we have to figure out exactly what function? Maybe not. We know Area has to be proportional to Long^2 to make the dimensions come out right, and the other factor must be some dimensionless function of the dimensionless Angle (or equivalently of the ratio between the two shorter sides). Break this triangle into two smaller ones of exactly the same shape by constructing a perpendicular from the right angle to the Long side. Call the two areas Area A and Area B. So Area = Area A + Area B.

Each of these similar triangles has for its own long side one of the big triangle's shorter sides,

and all the angles are the same as in the big one. Thus $\text{Long}^2 f(\text{Angle}) = \text{ShortA}^2 f(\text{Angle}) + \text{ShortB}^2 f(\text{Angle})$, where Angle means the dotted smaller angle, which is the same in all three cases. So unless $f(\text{Angle}) = 0$ (i.e., unless the areas are all 0 anyhow), then

$$\text{Long}^2 = \text{ShortA}^2 + \text{ShortB}^2. \qquad (1)$$

This is the theorem attributed to Pythagoras. We obtained it by merely insisting on dimensional consistency (Goldenfeld, 1992).

Atomic Explosions

From any big explosion in air, shock waves propagate outwards, slowing as the hemisphere of destruction expands. How fast does the hemisphere expand? You might think that an answer to this question necessarily involves a complex variety of considerations about sound, chemistry, thermal physics, and so on. Indeed it does, but let us consider an atomic explosion from the perspective of dimensional analysis.

Suppose the results are pretty much the same for any blast of the same total energy. If that were so, how could the expansion of the shock—its distance from ground zero (R) as a function of time (t)—depend on the energy (E) of the blast?

Let us denote the unit of length by the symbol L and the unit of time by the symbol T. (Thus L might be meters and T seconds.) Then energy (which is mass times velocity squared) has units (ML^2T^{-2}), where M denotes the unit of mass.

Since no combination of the three factors R, T, and E is unitless, we need to include another factor that involves mass. Such a factor is the air density, ρ. This factor is clearly important because without air there would be no shock wave but only bomb parts flying at fixed speeds through the vacuum of space. So throw ρ into the stew with units ML^{-3}. How to relate these four quantities (R, t, E, and ρ) to obtain a unitless result?

From the Pi Theorem, there is only one unitless combination of our four quantities (R, t, E, and ρ) that are expressed in terms of three basic units (L, t, and M). Thus,

$$\frac{R^5\rho}{t^2E} = a, \qquad (2)$$

where a is a dimensionless number that Geoffrey Taylor estimated (in 1941) to be 0.926 (Taylor, 1950a).

In 1949, Taylor verified his analysis by plotting the log of R (in meters) against the log of t (in seconds) for the first atomic explosion—the Trinity blast of 16 July 1945 in Alamogordo, New Mexico. According to Equation (2), $\log R$ versus $\log t$ should be a straight line with a dimensionless slope $\frac{2}{5}$. Except for the first point at 0.1 ms, the log-log plot in Figure 2 is indeed close to a straight line with slope $\frac{2}{5}$. In dimensional terms,

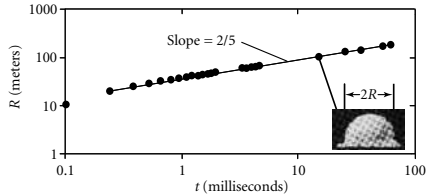

Figure 2. A log-log plot of the expansion of the Trinity fireball. From the origin of the blast, a hemispherical shock of radius R expands as a function of t during the first 62 ms. (The inset shows is a photograph of the blast at 15 ms, and the data are from Taylor, 1950b.)

$$\frac{R^5}{t^2} = 6 \times 10^{13}\text{m}^5\text{s}^{-2} \qquad (3)$$

to an experimental uncertainty of about 10%. Because a and ρ are known, the data in Figure 2 reveal the blast energy, which Taylor computed to be the equivalent of about 20 ktons of TNT (Taylor, 1950b).

In 1947, several of the photographs upon which Figure 2 is based were published by *Life*, a popular magazine of the time. Using these data, assuming $a = 1$, and taking $\rho = 1.25\ \text{kg m}^{-3}$, Equations (2) and (3) imply a blast energy of $8.4 \times 10^{10}\ \text{kg m}^2\ \text{s}^{-2}$ (or joules), which is equivalent to about 20 ktons of TNT. It may be presumed that interested parties made this simple estimate without delay.

Although these two examples may seem like magic, dimensional analysis has some limitations (Rayleigh, 1915). For example, this approach is useless in the absence of clear functional relations among mathematical quantities. Furthermore, one may doubt that the list of dimensioned variables presumed to be relevant is complete and does not include superfluous items. Finally, the desired relations may be unknown functions of dimensionless combinations of the pertinent variables.

A.T. WINFREE

See also **Explosions; Nerve impulses; Shock waves**

Further Reading

Birkhoff, G. 1950. *Hydrodynamics: A Study in Logic, Fact, and Similitude*, Princeton, NJ: Princeton University Press (Chapter 3 especially is a primary source and particularly lucid)

Bridgman, P.W. 1922. *Dimensional Analysis*, New Haven, CT: Yale University Press; often reprinted

Buckingham, E. 1914. On physically similar systems: illustrations of the use of dimensional equations. *Physical Review*, 4: 345–376

Buckingham, E. 1915. Model experiments and the form of empirical equations. *Transactions of the Americal Society of Mechanical Engineers*, 37: 263

Coyle, R.G. & Ballico-Lay, B. 1984. Concepts and software for dimensional analysis in modeling. *IEEE Transactions on*

Systems, Man, and Cybernetics SMC-14(3): 478–482 (Other than MatLab, the only source I know for software in this area)
DeJong, F.J. 1967. *Dimensional Analysis for Economists*, Amsterdam: North-Holland (The only effort I know to adapt dimensional analysis to economics and finance)
Goldenfeld, N. 1992. *Lectures on Phase Transitions and the Renormalization Group*, Reading, MA: Addison-Wesley (Contains full analysis of shock wave from explosions, esp. nuclear, following Taylor, 1952)
Rayleigh, Lord, 1915. The principle of similitude. *Nature*, 95: 66–68
Taylor, G.I. 1950a. The formation of a blast wave by a very intense explosion. I. Theoretical discussion. *Proceedings of the Royal Society of London*, 201A: 159–174
Taylor, G.I. 1950b. The formation of a blast wave by a very intense explosion. II. The atomic explosion of 1945. *Proceedings of the Royal Society of London*, 201A: 175–186

DIMENSIONS

The classical, integer-valued definition of dimension (see Hurewicz & Wallman, 1941) is defined inductively: the empty set has dimension -1, and a set has dimension n if n is the smallest integer such that every point has arbitrarily small neighborhoods whose boundaries have dimension less than n. This gives the "right" answer for smooth curves and surfaces, whose dimension we know intuitively.

In order to describe more accurately the complicated fractal sets that arise in nonlinear dynamics, we need to introduce more subtle definitions. Surprisingly, there are several generalizations of dimensions that still assign the intuitively correct dimensions to the above-noted well-behaved sets, and we recall two of them here.

The first of these is the "box-counting" dimension, also known as the Minkowski dimension, the fractal dimension, the entropy dimension, the capacity dimension, and the limit capacity: a litany of names that testifies to its popularity. For a subset X of $\mathbb{R}^n$, take a fixed array of boxes of side δ, and count the number $N_\delta(X)$ of these boxes that intersect with X. If $N_\delta(X) \sim \delta^{-d}$ as $\delta \to 0$, then X has box-counting dimension d. This can be made mathematically precise by defining

$$d_{\text{box}}(X) = \limsup_{\delta \to 0} \frac{\log N_\delta(X)}{-\log \delta}. \tag{1}$$

(For alternative definitions that give the same quantity see Falconer (1990).) While the box-counting dimension is simple to define, it is not without problems. For example, the set $S = \{0\} \cup \{1/n : n = 1, 2, \ldots\}$, an unlikely candidate for a fractal, has box-counting dimension $\frac{1}{2}$. We now introduce another widely used definition of dimension that does not suffer from this anomaly.

We could try to define a notion of the "d-dimensional volume" of X as the limit of $N_\delta(X)\delta^d$ as $\delta \to 0$, but such a definition does not even agree with the standard definition of volume (Lebesgue measure) when d is an integer. Instead, the proper generalization of Lebesgue measure to non-integer dimensions is d-dimensional Hausdorff measure. Essentially, we cover a set $X \subset \mathbb{R}^n$ by a collection of balls of radii $r_i \le \delta$, and then let $\mathcal{H}^d(X)$ be the limit of $\sum r_i^d$ as δ tends to zero. More precisely, we define

$$\mathcal{H}^d(X) = \liminf_{\delta \to 0} \left\{ \sum_i r_i^d : r_i \le \delta \text{ and } X \subseteq \cup_i B_{r_i}(x_i) \right\}$$

(the notation $B_r(x)$ denotes an open ball centered at x of radius r). The resulting measure is proportional to Lebesgue measure when d is an integer. The "Hausdorff dimension" of X is the smallest value of d for which $\mathcal{H}^d(X)$ is finite,

$$d_{\text{H}}(X) = \inf\{d > 0 : \mathcal{H}^d(X) < \infty\}.$$

Since $\mu_d(X, \delta) \le N_\delta(X)\delta^d$, we always have $d_{\text{H}}(X) \le d_{\text{box}}(X)$ (and this inequality can be strict: the set S defined above has zero Hausdorff dimension). While harder to estimate in practice, the Hausdorff dimension is easier to deal with theoretically.

If we want to estimate the dimension of the attractor $\mathcal{A}$ of a dynamical system, it is useful to have a method based on dynamical quantities. In 1980, Douady & Oesterlé showed how to obtain a bound on $d_{\text{H}}(\mathcal{A})$, the dimension of the attractor of an iterated C^1 map f on $\mathbb{R}^n$. Denote by $\text{D}f(x)$ the matrix of partial derivatives of f, i.e., $[\text{D}f]_{ij} = \partial f_i / \partial x_j$, and let $\lambda_1(x) \ge \lambda_2(x) \ge \lambda_n(x)$ be the logarithms of the eigenvalues of $[\text{D}f(x)^T \text{D}f(x)]^{1/2}$. Now set

$$d(x) = j + \frac{\lambda_1(x) + \cdots + \lambda_j(x)}{|\lambda_{j+1}(x)|}, \tag{2}$$

where j is the largest integer for which $\lambda_1(x) + \cdots + \lambda_j(x) \ge 0$ (note that $j \le d(x) < j + 1$). If $d > d(x)$, then any infinitesimal d-volume near x is contracted under the application of f, so

$$d_{\text{H}}(\mathcal{A}) \le \sup_{x \in \mathcal{A}} d(x). \tag{3}$$

Hunt (1996) showed that the right-hand side of (3) also bounds $d_{\text{box}}(\mathcal{A})$. (A similar approach also works for the attractors of flows by taking f to be the time T map, for some suitable T. Constantin & Foias (1985) have proved a version of (3) for the attractors of infinite-dimensional dynamical systems.)

However, the box-counting and Hausdorff dimensions give equal weighting to all points in the attractor, while it is possible to have regions of the attractor that are visited very rarely. In such a situation, it can be more natural to consider invariant measures rather than attractors. As a (canonical) example of such a measure, suppose that $f : \mathbb{R}^n \to \mathbb{R}^n$ generates a dynamical system on $\mathbb{R}^n$. Then for any set X, we can define

$$\mu(X) = \lim_{m \to \infty} \frac{1}{m} \text{card}\{k : f^k(x) \in X,\ 1 \le k \le m\},$$

where x is a point in the basin of attraction of $\mathcal{A}$. The quantity $\mu(X)$ is the proportion of time spent in X by a "typical trajectory" on the attractor.

There are various ways of defining the dimension of a measure μ. We could define the Hausdorff/box-counting dimension of μ to be the dimension of its support,

$$d_{\mathrm{box/H}}(\mu) = \inf\{d_{\mathrm{box/H}}(E) : \mu(E) = 1\},$$

but this still discounts the dynamical information contained in μ. Kaplan & Yorke (1979) defined the *Lyapunov dimension* of μ, $d_{\mathrm{L}}(\mu)$, precisely as in (2), but replacing $\lambda_j(x)$ by the Lyapunov exponents associated with μ (the asymptotic growth rates of infinitesimal displacements about trajectories through μ-almost every choice of initial condition). In 1981, Ledrappier showed that for a very general class of dynamical systems, $d_{\mathrm{H}}(\mu) \le d_{\mathrm{L}}(\mu)$ (the inequality can be strict), while

$$d_{\mathrm{box}}(\mathcal{A}) \le \sup_{\text{all invariant ergodic } \mu} d_{\mathrm{L}}(\mu).$$

(Kaplan & Yorke had originally conjectured that $d_{\mathrm{box}}(\mathcal{A}) = d_{\mathrm{L}}(\mu)$.)

We now give two definitions of dimension that take into account the spatial structure of μ. The correlation at scale δ is defined by

$$C(\delta) = \int_{X\times X:\ |x-y|\le\delta} \mathrm{d}\mu(x)\,\mathrm{d}\mu(y),$$

which gives the probability that two points chosen according to the probability measure μ lie within δ of each other. If $C(\delta) \sim \delta^d$ as $\delta \to 0$, then d is the *correlation dimension* $d_{\mathrm{corr}}(\mu)$. This was introduced by Grassberger & Procaccia (1983), who demonstrated that this quantity is particularly suited to numerical calculation.

Alternatively, define the "δ-entropy" $K_\delta(\mu) = -\sum_i \mu(B_i)\ln\mu(B_i)$, where $\{B_i\}$ is an array of boxes of side δ; the *information dimension* is given by

$$d_{\mathrm{inf}}(\mu) = \lim_{\delta\to 0} \frac{K_\delta(\mu)}{-\log\delta}.$$

(Ruelle (1989) refers to $d_{\mathrm{H}}(\mu)$ as the "information dimension" of μ: this should serve to emphasize how important it is when discussing dimensions to be explicit about the definition.)

Three of these dimensions occur as part of a scale of dimension-like quantities (see Grassberger, 1983). If B_i is an array of boxes of side δ, set

$$K_\delta(q) = \frac{1}{1-q}\log\sum_i \mu(B_i)^q$$

("the Renyi q entropy"). Note that $K_\delta(0) = \log N_\delta$ (supp μ),

$$\lim_{q\to 1} K_\delta(q) = -\sum_i \mu(B_i)\ln\mu(B_i) = K_\delta(\mu)$$

and that since $C(\delta) \le \sum_i \mu(B_i)^2 \le C(\delta\sqrt{n})$, we have $\log C(\delta) \le K_\delta(2) \le \log C(\delta\sqrt{n})$. Now define the *Renyi dimensions* $D_q(\mu)$ by

$$D_q(\mu) = \lim_{\delta\to 0} \frac{K_\delta(q)}{-\log\delta}.$$

Then $D_0(\mu) = d_{\mathrm{box}}(\mu)$, $D_1(\mu) = d_{\mathrm{inf}}(\mu)$, and $D_2(\mu) = d_{\mathrm{corr}}(\mu)$. Since D_q is non-increasing in q, we have in particular $d_{\mathrm{corr}}(\mu) \le d_{\mathrm{inf}}(\mu) \le d_{\mathrm{box}}(\mu)$.

The Renyi dimensions are similar to quantities used to define the "multi-fractal spectrum." The theory relates the numbers $\tau(q) = (1-q)D_q$ to the frequency of various scaling behaviors about points on a fractal set: roughly, if for some small ε the number of δ-mesh cubes B_i with

$$\delta^{\alpha+\varepsilon} \le \mu(B_i) < \delta^\alpha$$

scales like $\delta^{-f(\alpha)}$, then

$$f(\alpha(q)) = \tau(q) + q\alpha(q),$$

where $q = f'(\alpha(q))$. The curve $f(\alpha)$ is the multi-fractal spectrum of the measure μ. (As remarked by Falconer (1990), the tempting interpretation of the "fractal spectrum" as the dimension of sets of points x where $\mu(B_\delta(x)) \sim \delta^\alpha$ is incorrect: typically the dimension of such sets will be zero or the same as that of the whole space, see Genyuk (1997/98).) Although these ideas have proved useful in the theory of turbulence (e.g. Frisch, 1995), their mathematical foundations have still to be fully resolved.

JAMES C. ROBINSON

See also **Attractors; Fractals; Lyapunov exponents; Measures**

Further Reading

Constantin, P. & Foias, C. 1985. Global Lyapunov exponents, Kaplan–Yorke formulas and the dimension of the attractor for 2D Navier–Stokes equation. *Communications in Pure and Applied Mathematics*, 38: 1–27

Douady, A. & Oesterlé, J.D. 1980. Dimension de Hausdorff des attracteurs. *Compes Rendus de l'Academies des Sciences, Paris Sèries A–B*, 290: A1135–A1138

Falconer, K. 1990. *Fractal Geometry*, Chichester and New York: Wiley

Frisch, U. 1995. *Turbulence*, Cambridge and New York: Cambridge University Press

Genyuk, J. 1997/98. A typical measure typically has no local dimension. *Real Analysis Exchange*, 23: 525–537

Grassberger, P. 1983. Generalized dimensions of strange attractors. *Physics Letters A*, 97: 227–230

Grassberger, P. & Procaccia, I. 1983. Measuring the strangeness of strange attractors. *Physica* D, 9: 189–208

Hunt, B. 1996. Maximal local Lyapunov dimension bounds the box dimension of chaotic attractors. *Nonlinearity*, 9: 845–852

Hurewicz, W. & Wallman, H. 1941. *Dimension Theory*, Princeton, NJ: Princeton University Press

Kaplan, J.L. & Yorke, J.A. 1979. Chaotic behavior of multidimensional difference equations. In *Functional Differential Equations and Approximation of Fixed Points*, Berlin: Springer, 204–227

Ledrappier, F. 1981. Some relations between dimension and Lyapounov exponents. *Communications in Mathematical Physics*, 81: 229–238

Ruelle, D. 1989. *Chaotic Evolution and Strange Attractors*, Cambridge and New York: Cambridge University Press

DIODES

Many of the desirable features of a wide variety of solid-state electronic devices are based on nonlinear current-voltage characteristics. These involve situations where a sufficiently high bias is applied to the device so that it either switches from one conductive state to another or oscillates between different conductive states.

A two-terminal electronic device is called a diode. In general, the current I through a diode depends upon the polarity of the applied voltage U and exhibits a nonlinear voltage dependence. This includes the important special case of a rectifier diode that conducts the current for one polarity of voltage and blocks it for the other. A rectifier can be realized by a p–n junction (a semiconductor that is p-doped on one side and n-doped on the other side), and it can be described approximately by the current-voltage characteristic

$$I = I_s \left(e^{eU/k_B T} - 1 \right), \qquad (1)$$

where I_s is the saturation current for reverse bias $U < 0$, k_B is Boltzmann's constant, and T is the temperature (Figure 1a). For forward bias (positive voltage applied to the p side), the majority carriers (holes from the p side and electrons from the n side) flow towards the junction where they recombine, while for reverse bias they are pulled away from the junction.

The Schottky diode is a rectifier diode, which consists of a metal-semiconductor contact. Interface states and to a small degree the difference in work functions between the metal and the semiconductor give rise to a potential barrier (Schottky barrier) and depletion of majority carriers in the barrier region for reverse bias. The current-voltage characteristic is similar to Equation (1).

Depending upon bias conditions, doping profiles, and device geometry, various other terminal functions of diodes are possible, which involve nonlinear behavior of the conductivity, the capacitance, and the inductance of the device.

The Zener diode is a p–n junction that exhibits a sharp increase in the magnitude of the current at a certain well-controlled reverse bias (Figure 1b). Depending upon the specific device structure, it is either due to avalanche breakdown (multiplication of carriers by impact ionization occurring at high voltage) or due to tunneling across the bandgap (occurring at lower voltage). It is used to stabilize and limit the dc voltage in

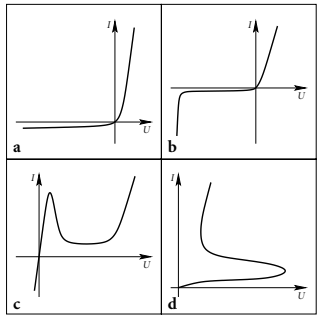

Figure 1. Typical nonlinear current-voltage characeristics of diodes. (a) p–n diode, (b) Zener diode, (c) Tunnel diode, (d) p–i–n diode (schematic).

circuits, utilizing the property that the current can vary over a large range at the breakdown threshold without noticeable change in voltage.

A class of diodes exhibits a nonmonotonic dependence of the current I upon voltage U. Negative differential conductance $dI/dU < 0$ can arise due to various mechanisms and may result in self-generated oscillations and complex self-organized spatiotemporal patterns. A famous example is the Esaki tunnel diode (Figure 1c) that, in its original version, consists of a heavily doped p–n junction. In thermal equilibrium, the Fermi level lies within the conduction band on the n side and within the valence band on the p side. When a small forward bias is applied, electrons can tunnel from the n- to the p-side where they find empty states in the valence band. With increasing bias, the filled conduction band states on the n side move up, and the overlap with empty states in the valence band decreases; consequently, the tunneling current decreases, and $dI/dU < 0$. With a further increase of the bias, diffusion of the electrons over the barrier sets in as in a normal p–n junction, and the current increases again.

Modern variants of the tunnel diode are double-barrier resonant tunneling structures and superlattices that consist of alternating layers of different semiconductor materials (heterostructures) forming potential barriers and quantum wells on length scales of a few nanometers. The current density across the barrier between two wells is maximum if there is maximum overlap between the occupied states in one well and the available unoccupied states in the other, that is, if the energies are in resonance. For low bias, equivalent levels in adjacent wells are approximately in resonance, while for higher bias the ground energy level in one quantum well becomes aligned with the second level in the neighboring well. Thus, resonant tunneling produces an $I(U)$ characteristic similar to Figure 1c. High-frequency

oscillations up to 150 GHz can be generated in resonant tunneling structures and superlattices.

Gunn diodes are used to generate and amplify microwaves at frequencies typically beyond 1 GHz (these devices are called "diodes" because they are two-terminal devices, but no p–n junction is involved). The mechanism is based upon field-induced intervalley transfer of electrons from a high- to a low-mobility valley in the conduction band, and the manifestation of the current instability (oscillations or switching) is determined primarily by the cathode contact boundary condition. Traveling high-field domains (Gunn domains), which show up as transit time oscillations, represent an important mode of operation.

Multilayered structures with alternating p- and n-doping represent another class of diodes that exhibit negative differential conductance, high-power microwave oscillations well above 30 GHz, and complex spatiotemporal current density patterns. Starting from the basic n^+–p–i–p^+ structure, where "+" denotes high doping and i is an intrinsic (undoped) layer, various modifications like IMPATT (impact ionization avalanche transit time) diodes, TRAPATT (trapped plasma avalanche-triggered transit) diodes, p–i–n diodes (with double injection of electrons and holes), or $n^+p^+np^-p^+$ devices, where "−" denotes low doping, have been studied. These structures typically display bistability and switching from a low- to a high-conductivity state where carrier multiplication and avalanche breakdown set in (Figure 1d). Negative differential conductance is also exhibited by multilayer systems composed of layers of different semiconductor materials (heterojunctions) like the heterostructure hot electron diode or real-space transfer devices.

A p–n diode may also be operated as a nonlinear capacitor. As the depletion-layer width increases with increasing reverse bias, its capacitance decreases in a controlled way depending upon the doping profile. This effect is used in varactor (*vari*able re*actor*) diodes to tune the capacitance and for parametric amplification. State-of-the-art developments include studies on p–n diodes with embedded quantum dot nanostructures, which strongly exhibit nonlinear capacitance-voltage characteristics as signatures of the charging of these quantum dots.

Nonlinear inductors represent another class of two-terminal devices. A Josephson junction consists of two superconductors separated by a thin nonsuperconducting region. The tunneling of superconducting electron pairs produces a current at zero voltage called the Josephson current. Switching can be obtained from this state to a voltage state by either current overdrive or a magnetic field. The dynamic response of the Josephson junction can be represented by an equivalent circuit with an intrinsic field-dependent inductance.

ECKEHARD SCHÖLL

See also **Avalanche breakdown; Josephson junctions; Nonlinear electronics; Semiconductor oscillators**

Further Reading

Böer, K.W. 2002. *Survey of Semiconductor Physics*, 2nd edition, New York: Plenum

Ibach, H. & Lüth, H. 2003, *Solid-State Physics*, Berlin: Springer

Schöll, E. 2001. *Nonlinear Spatio-Temporal Dynamics and Chaos in Semiconductors*, Cambridge and New York: Cambridge University Press

Shaw, M.P., Mitin, V.V., Schöll, E. & Grubin, H.L. 1992. *The Physics of Instabilities in Solid State Electron Devices*, New York: Plenum Press

Sze, S.M. 1981. *Physics of Semiconductor Devices*, New York: Wiley

Sze, S.M. 1998. *Modern Semiconductor Device Physics*, New York: Wiley

DIRAC'S DELTA FUNCTION

See **Generalized functions**

DISCRETE BREATHERS

The study of dynamical nontopological localization in translationary invariant nonlinear Hamiltonian lattices has experienced considerable development during the late 1990s (Sievers & Page, 1995; Aubry, 1997; Flach & Willis, 1998). The discreteness of space—that is, the use of a spatial lattice—is crucial in order to provide structural stability for spatially localized excitations. Spatial discreteness is a very common situation for various applications from, for example, solid-state physics.

To make things precise, consider a d-dimensional hypercubic spatial lattice with discrete translational invariance. Each lattice site is labeled by a d-dimensional vector l with integer components. To each lattice site we associate one pair of canonically conjugated coordinates and momenta X_l, P_l that are real functions of time t. Let us then define some Hamiltonian H being a function of all coordinates and momenta and further require that H has the same symmetries as the lattice. The dynamical evolution of the system is given by the usual Hamiltonian equations of motion. Without loss of generality, let us consider that H is a nonnegative function and that $H = 0$ for $X_l = P_l = 0$ (for all l's). We call this state the classical ground state. Generalizations to other lattices and larger numbers of degrees of freedom per lattice site are straightforward.

When linearizing the equations of motion around $H = 0$, we obtain an eigenvalue problem. Due to translational invariance the eigenvectors will be spatially extended plane waves, and the eigenvalues Ω_q (frequencies) form a phonon spectrum, that is, Ω_q is a function of the wave vector q. Due to the translation symmetry of the Hamiltonian, Ω_q will be periodic in

q. Moreover, the phonon spectrum will be bounded, that is, $|\Omega_q| \leq \Omega_{\max}$. Depending on the presence or absence of Goldstone modes Ω_q might be gapless (zero belongs to the spectrum, spectrum is acoustic) or exhibit a gap ($|\Omega_q| \geq \Omega_{\min}$, spectrum is optical). Increasing the number of degrees of freedom per lattice site induces several branches in Ω_q with possible gaps between them.

Let us search for spatially localized time periodic solutions of the full nonlinear equations of motion, that is, $X_{|l|\to\infty} \to 0$, and

$$X_l(t) = X_l(t + T_b) + \lambda k_l,\ P_l(t) = P_l(t + T_b), \quad (1)$$

with k_l being integers and λ a spatial period (the equations of motion should be invariant under shifts of X_l by multiples of λ if applicable.) These solutions are called discrete breathers. If $k_l \neq 0$ for a finite subset of lattice sites, the solutions are sometimes called "rotobreathers."

If a solution exists, we can expand it into a Fourier series in time, that is, $X_l(t) = \sum_k A_{k_l} e^{ik\omega_b t}$ ($\omega_b = 2\pi/T_b$). Spatial localization implies $A_{k_l\to\infty} \to 0$. Inserting these series into the equations of motion results in a set of coupled algebraic equations for the Fourier amplitudes (Flach & Willis, 1998). Consider the spatial tail of the solution where all Fourier amplitudes are small and should further decay to zero with growing distance from the excitation center. Since all amplitudes are small, the equations of motion can be linearized. This procedure decouples the interaction in k-space, and we obtain for each k a linear equation for A_{k_l} with coupling over l. This equation will contain $k\omega_b$ as a parameter. It will, in fact, be identical to the above-discussed equation linearized around $H = 0$, and it will contain $k\omega_b$ instead of Ω_q (Flach & Willis, 1998). If $k\omega_b = \Omega_q$, the corresponding amplitude A_{k_l} will not decay in space, instead it will oscillate. To obtain localization, we arrive at the nonresonance condition (Flach & Willis, 1998)

$$k\omega_b \neq \Omega_q. \quad (2)$$

This condition has to be fulfilled for all integer k. For an optical spectrum Ω_q, frequency ranges for ω_b exist, which satisfy this condition. For acoustic spectra, $k = 0$ has to be considered separately (Flach et al., 1997).

The nonresonance condition is only a necessary condition for generic occurrence of discrete breathers. More detailed analysis shows that breathers being periodic orbits bifurcate from band edge plane waves (Flach, 1996). The condition for this bifurcation is an inequality involving parameters of expansion of H around $H = 0$ (Flach, 1996). Rigorous existence proofs for weakly coupled anharmonic oscillators use, for example, the implicit function theorem (MacKay & Aubry, 1994).

Discrete breathers (periodic orbits) appear generically as one-parameter families of periodic orbits. The parameter of the family can be, for example, the frequency (or energy, action, etc.). Note that we do not need any topological requirement on H (no energy barriers). Indeed, breather families possess limits where the breather delocalizes and its amplitude becomes zero.

With the help of the nonresonance conditions, we can exclude the generic existence of spatially localized solutions that are quasi-periodic in time. Indeed, in the simplest case, we would have to satisfy a nonresonance condition $k_1\omega_1 + k_2\omega_2 \neq \Omega_q$ for ω_1/ω_2 being irrational and all possible pairs of integers k_1, k_2. This is impossible (Flach, 1994).

The nonresonance condition also explains why breather solutions are nongeneric for nonlinear Hamiltonian field equations, since Ω_q becomes unbounded for a spatially continuous system. Consequently, generically an infinite number of unavoidable resonances destroys the breather existence there.

Note that in many cases breathers can be easily excited by choosing some localized perturbation of the lattice system. Integrating numerically the equations of motion, we find that the energy distribution is not delocalizing but stays essentially localized over several orders of magnitude of the characteristic phonon periods. These numerical results clearly show that breathers are not only interesting solutions but can be rather typical and robust depending on the system's parameters.

Note that breathers can also exist for autonomous forced damped systems (MacKay & Sepulchre, 1998). In these systems, contrary to the Hamiltonian ones, breather periodic orbits do not come in one-parameter families of the frequency ω_b, but correspond to limit cycle attractors that are isolated in the system's phase space.

SERGEJ FLACH

See also **Breathers; Discrete nonlinear Schrödinger equations; Discrete self-trapping system; Fermi–Pasta–Ulam oscillator chain; Josephson junction arrays; Local modes in molecular crystals; Multidimensional solitons; Nonlinear Schrödinger equations; Solitons**

Further Reading

Aubry, S. 1997. Breathers in nonlinear lattices: existence, linear stability and quantization. *Physica* D, 103: 201

Flach, S. 1994. Conditions on the existence of localized excitations in nonlinear discrete systems. *Physical Review* E, 50: 3134

Flach, S. 1996. Tangent bifurcation of band edge plane waves, dynamical symmetry breaking and vibrational localization. *Physica* D, 91: 223

Flach, S., Kladko, K. & Takeno. S. 1997. Acoustic breathers in two-dimensional lattices. *Physical Review Letters*, 79: 4838

Flach, S. & Willis, C.R. 1998. Discrete breathers. *Physics Reports*, 295: 182

MacKay, R.S. &. Aubry, S. 1994. Proof of existence of breathers for time-reversible or Hamiltonian networks of weakly coupled oscillators. *Nonlinearity*, 7: 1623

MacKay, R.S. & Sepulchre, J.A. 1998. Stability of discrete breathers. *Physica* D, 119: 148

Sievers, A.J. & Page, J.B. 1995. Unusual Anharmonic Local Mode Systems. In *Dynamical Properties of Solids VII Phonon Physics The Cutting Edge*, edited by G.K. Horton and A.A. Maradudin, Amsterdam: Elsevier

DISCRETE NONLINEAR SCHRÖDINGER EQUATIONS

With a fairly generous definition, a discrete nonlinear Schrödinger (DNLS) equation is any equation that can be obtained from a nonlinear Schrödinger (NLS) equation of general form

$$\mathrm{i}\frac{\partial \phi}{\partial t} + \Delta\phi + f(|\phi|^2)\phi = 0, \qquad (1)$$

by employing some finite-difference approximation to the operators acting on the space-time-dependent continuous field $\phi(\boldsymbol{r}; t)$. In (1), $\Delta = \nabla^2$ is the Laplace operator acting in one, two, or three spatial dimensions, and f is a quite general function that, for most purposes, is taken to be differentiable and with $f(0) = 0$. In the most well-known case of cubic nonlinearity, $f(|\phi|^2) = \gamma|\phi|^2$, Equation (1) is often referred to as *the* NLS equation, and is integrable with the inverse scattering method if the number of spatial dimensions is one. Here we use the term DNLS equation to denote the set of coupled ordinary differential equations resulting from discretizing *all* spatial variables in (1), while keeping the time-variable t continuous. However, one may also consider equations with discrete time ("fully discrete NLS equations"), as well as equations with only some of the spatial dimensions discretized ("discrete-continuum NLS equations"). The former are of interest as algorithms for numerical solution of (1), while the latter may describe pulse propagation in *arrays* of coupled nonlinear optical fibers (Aceves et al., 1995).

The simplest example of a DNLS equation can be formally obtained by just replacing the Laplacian operator in (1) with the corresponding discrete Laplacian. Thus, for the one-dimensional (1-d) case, we let $\phi_n(t) \equiv \phi(x = na; t)$ where a is the lattice parameter, so that for the particular case of cubic nonlinearity, the following equation is obtained:

$$\mathrm{i}\frac{\mathrm{d}\phi_n}{\mathrm{d}t} + C(\phi_{n+1} - 2\phi_n + \phi_{n-1}) + \gamma|\phi_n|^2\phi_n = 0, \qquad (2)$$

where $C = 1/a^2$. This set of differential–difference equations with purely diagonal ("on-site") nonlinearity is sometimes called the diagonal DNLS (DDNLS) equation, but since it is by far the most studied example of a DNLS equation, it is most commonly referred to as simply *the* DNLS equation. Extensions to higher dimensions are straightforward, so that, for example, for a 2-d lattice with $x = ma$, $y = na$, the DNLS equation reads

$$\mathrm{i}\frac{\mathrm{d}\phi_{m,n}}{\mathrm{d}t} + C(\phi_{m+1,n} + \phi_{m-1,n} + \phi_{m,n+1} + \phi_{m,n-1} - 4\phi_{m,n}) + \gamma|\phi_{m,n}|^2\phi_{m,n} = 0. \qquad (3)$$

The study of DDNLS equations has a long and fascinating history, beginning in the 1950s within solid-state physics with Holstein's model for polaron motion in molecular crystals (Holstein, 1959); reappearing in the 1970s within biophysics with Davydov's model for energy transport in biomolecules (see, e.g., Scott, 1999, Chapter 5.6), in the 1980s within physical chemistry in the theory of local modes of small molecules (see, e.g., Scott, 1999, Chapter 5.4), and within nonlinear optics modeling coupled nonlinear waveguides (see, e.g., Hennig & Tsironis, 1999, Chapter 1.4); and most recently around the turn of the century within matter wave physics in the description of a dilute Bose–Einstein condensate trapped in a periodic potential (Trombettoni & Smerzi, 2001). A brief account of experimental verifications of the validity of the DNLS description in the two latter contexts available at the time of writing was given in Eilbeck & Johansson (2003, Chapter 10). In addition, the DDNLS equation has played a central role in the development of the general theory for intrinsic localized modes ("discrete breathers") in systems of coupled anharmonic oscillators during the 1990s (Flach & Willis, 1998). The reader should also note that the DDNLS equation is a particular example of the more general "discrete self-trapping" (DST) systems (described under a separate entry), where the general DST dispersion matrix describing interactions between lattice sites is restricted to nearest-neighbor couplings. Thus, the general theory described for DST systems is also applicable for the DDNLS equation.

The reason for the ubiquity of the DDNLS equation in nonlinear lattice systems is analogous to that of the NLS equation for continuum systems: it takes into account dispersion (through the nearest-neighbor interaction terms) as well as nonlinearity (the term $\gamma|\phi_n|^2\phi_n$) at the lowest order of approximation. It can be derived, for example, from a general system of coupled anharmonic oscillators using a "rotating wave approximation" (RWA), where it is assumed that each oscillator approximately can be described by a complex rotating-wave amplitude as $u_n(t) = \mathrm{Re}(\phi_n \mathrm{e}^{-\mathrm{i}\omega t})$ (see, e.g., Flach & Willis, 1998, Chapter 2.3; Scott, 1999, Chapter 5.3.1). Thus, the RWA assumes time-periodic solutions to have a purely harmonic time dependence, neglecting the generation of all higher harmonics. This approximation can be justified for small-amplitude oscillations in weakly coupled oscillator chains, using

perturbational techniques with expansions on multiple time scales (see, e.g., Flach & Willis, 1998, Chapter 2.2, for a general outline, and Morgante et al., 2002, Chapter 2.2, for details).

As for general DST systems, the DDNLS equation has, in addition to the energy (Hamiltonian) $H = \sum_n \left(C|\phi_{n+1} - \phi_n|^2 - \frac{\gamma}{2}|\phi_n|^4\right)$ (where $\mathrm{i}\phi_n$ and ϕ_n^* are canonical conjugated variables), a second conserved quantity, which is the excitation number $N = \sum_n |\phi_n|^2$. The conservation of excitation number results (through Noether's theorem) from the invariance of the equation under infinitesimal transformations of the overall phase ($\phi_n \to \phi_n \mathrm{e}^{\mathrm{i}\varepsilon}$). As a consequence, the DDNLS equation is integrable for two degrees of freedom but nonintegrable for larger systems. Still, the existence of a second conserved quantity has some notable consequences, which makes the DDNLS equation nongeneric among general Hamiltonian lattice systems, such as:

- It has purely harmonic time-periodic solutions $\phi_n(t) = A_n \mathrm{e}^{-\mathrm{i}\omega t}$ with time-independent A_n ("stationary solutions").
- It has continuous families of time-quasi-periodic solutions, with two incommensurate frequencies, which may be spatially exponentially localized also in infinite systems ("quasi-periodic breathers") (see, e.g., Eilbeck & Johansson, 2003, Chapter 7; Kevrekidis et al., 2001, Chapter 2.4).

From a mathematical point of view, it is highly interesting that there also exist discretizations of the integrable 1-d cubic NLS equation that conserve its integrability. The most famous integrable DNLS equation is the so-called Ablowitz–Ladik (AL) DNLS equation, the integrability of which was first proven by Ablowitz & Ladik (1976). It is obtained by replacing the nonlinear term $\gamma|\phi|^2\phi$ with an "off-diagonal" discretization $\frac{\gamma}{2}|\phi_n|^2(\phi_{n+1} + \phi_{n-1})$, yielding

$$\mathrm{i}\frac{\mathrm{d}\phi_n}{\mathrm{d}t} + C(\phi_{n+1} - 2\phi_n + \phi_{n-1}) + \frac{\gamma}{2}|\phi_n|^2(\phi_{n+1} + \phi_{n-1}) = 0. \qquad (4)$$

Due to its integrability, it is possible to obtain exact analytical solutions to (4) describing, for example, traveling waves (in terms of elliptic functions, see, e.g., Scott, 1999, Chapter 5.3.2), solitons, and multisolitons. In particular, for $\gamma/C > 0$, there is a (bright) one-soliton solution given by (with rescalings such that $C = 1$, $\gamma = 2$):

$$\phi_n(t) = \sinh\beta\,\mathrm{sech}[\beta(n - vt)]\mathrm{e}^{\mathrm{i}(kn+\omega t+\alpha)}, \qquad (5)$$

where β, k, and α are free parameters,

$$v = (2/\beta)\sinh\beta\sin k,$$

and $\omega = 2(\cosh\beta\cos k - 1)$. On the other hand, when $\gamma/C < 0$, there are dark-soliton solutions with nonvanishing amplitude as $|n| \to \infty$ (Vekslerchik & Konotop, 1992).

The ALDNLS equation (4) also has a Hamiltonian structure with

$$H = \sum_n \left[-C\phi_n^*(\phi_{n+1} + \phi_{n-1}) + \frac{4C^2}{\gamma}\log\left(1 + \frac{\gamma}{2C}|\phi_n|^2\right)\right],$$

although the conjugated variables $\mathrm{i}\phi_n$ and ϕ_n^* are noncanonical and the corresponding Poisson bracket deformed (see, e.g., Faddeev & Takhtajan, 1987, p. 303; Scott, 1999, Chapter 5.3.2). There is, at this writing, no known direct physical application of the ALDNLS equation; however, it is commonly used as a starting point for perturbational studies of physically more relevant equations such as (2). A particularly interesting model allowing interpolations between Equations (2) and (4) is the so-called "Salerno equation," which is described under a separate entry.

As a final example, we mention a rather complicated DNLS equation, which was introduced and proven to be integrable by Izergin and Korepin in 1981. This Izergin–Korepin equation reads

$$\mathrm{i}\frac{\mathrm{d}\phi_n}{\mathrm{d}t} = 4\phi_n + \frac{P_{n,n+1}}{Q_{n,n+1}} + \frac{P_{n,n-1}}{Q_{n,n-1}}, \qquad (6)$$

where

$$P_{n,n\pm1} = -\phi_n - \phi_{n\pm1}\sqrt{\left(1 - \frac{\gamma}{8}|\phi_n|^2\right)\left(1 - \frac{\gamma}{8}|\phi_{n\pm1}|^2\right)} + \frac{\gamma}{4}\phi_n|\phi_{n\pm1}|^2 + \frac{\gamma}{16}\left(|\phi_n|^2\phi_{n\pm1} + \phi_n^2\phi_{n\pm1}^*\right) \times\sqrt{\frac{1 - \frac{\gamma}{8}|\phi_{n\pm1}|^2}{1 - \frac{\gamma}{8}|\phi_n|^2}}$$

and

$$Q_{n,n\pm1} = 1 - \frac{\gamma}{8}\left(|\phi_n|^2 + |\phi_{n\pm1}|^2\right) - \frac{\gamma}{8}\left(\phi_n\phi_{n\pm1}^* + \phi_n^*\phi_{n\pm1}\right) \times\sqrt{\left(1 - \frac{\gamma}{8}|\phi_n|^2\right)\left(1 - \frac{\gamma}{8}|\phi_{n\pm1}|^2\right)} + \frac{\gamma^2}{32}|\phi_n|^2|\phi_{n\pm1}|^2.$$

It is associated with a lattice Heisenberg magnet model, and turns into the cubic NLS equation in the continuum limit (see Faddeev & Takhtajan, 1987, pp. 299, for details).

MAGNUS JOHANSSON

See also **Discrete self-trapping system; Nonlinear Schrödinger equations; Rotating wave approximation; Salerno equation**

Further Reading

Ablowitz, M.J. & Ladik, J.F. 1976. Nonlinear differential-difference equations and Fourier analysis. *Journal of Mathematical Physics*, 17(6): 1011–1018

Aceves, A.B., De Angelis, C., Luther, G.G., Rubenchik, A.M. & Turitsyn, S.K. 1995. All-optical-switching and pulse amplification and steering in nonlinear fiber arrays. *Physica* D, 87(1–4): 262–272

Eilbeck, J.C. & Johansson, M. 2003. The discrete nonlinear Schrödinger equation—20 years on. In *Localization and Energy Transfer in Nonlinear Systems: Proceedings of the Third Conference, San Lorenzo de El Escorial, Spain, 17–21 June 2002*, edited by L. Vázquez, M.P. Zorzano and R. MacKay. Singapore: World Scientific

Faddeev, L.D. & Takhtajan, L.A. 1987. *Hamiltonian Methods in the Theory of Solitons*. Berlin and Heidelberg: Springer

Flach, S. & Willis, C.R. 1998. Discrete breathers. *Physics Reports*, 295(5): 181–264

Hennig, D. & Tsironis, G.P. 1999. Wave transmission in nonlinear lattices. *Physics Reports*, 307(5–6), 333–432

Holstein, T. 1959. Studies of polaron motion. *Annals of Physics*, 8: 325–389

Kevrekidis, P.G., Rasmussen, K.Ø. & Bishop, A.R. 2001. The discrete nonlinear Schrödinger equation: a survey of recent results. *International Journal of Modern Physics* B, 15(21): 2833–2900

Morgante, A.M., Johansson, M., Kopidakis, G. & Aubry, S. 2002. Standing wave instabilities in a chain of nonlinear coupled oscillators. *Physica* D, 162(1–2): 53–94

Scott, A. 1999. *Nonlinear Science: Emergence & Dynamics of Coherent Structures*. Oxford and New York: Oxford University Press

Trombettoni, A. & Smerzi, A. 2001. Discrete solitons and breathers with dilute Bose-Einstein condensates. *Physical Review Letters*, 86(11): 2353–2356

Vekslerchik, V.E. & Konotop, V.V. 1992. Discrete nonlinear Schrödinger equation under non-vanishing boundary conditions. *Inverse Problems*, 8(6): 889–909

DISCRETE SELF-TRAPPING SYSTEM

In the early 1980s, experimental evidence suggested that vibrational energy in natural proteins (specifically the CO stretch oscillation of the peptide unit) might become self-localized, with implications for the storage and transport of energy in biological organisms (Careri et al., 1984). Because the structures of natural proteins take a wide variety of shapes, the following equation—called the discrete self-trapping (DST) equation (Eilbeck et al., 1985)—was proposed to capture the essential features of self-localization:

$$\left(\mathrm{i}\frac{\mathrm{d}}{\mathrm{d}t} - \omega_0\right)\boldsymbol{U} + \gamma D(|\boldsymbol{U}|^2)\boldsymbol{U} + \varepsilon \boldsymbol{M}\boldsymbol{U} = 0. \quad (1)$$

Here, $\boldsymbol{U}(t) \equiv \mathrm{col}(u_1, u_2, \ldots, u_f)$ is a column vector representing the amplitudes of f oscillatory modes, each of which is described in the rotating wave approximation by the complex amplitudes: $u_1(t), u_2(t)$, …, $u_f(t)$. With $\gamma = 0$ and $\varepsilon = 0$, these modes (sites) oscillate independently and sinusoidally at the site frequency ω_0.

In the last term of Equation (1), $M = [m_{jk}]$ is an $f \times f$ dispersion matrix, expressing energetic interactions among the f modes stemming from electromagnetic couplings. This matrix is real and symmetric ($m_{ij} = m_{ji}$), and its diagonal elements can be chosen to represent small variations in the site frequencies from ω_0. Thus, with $\gamma = 0$ but with the dispersion parameter ε not zero, there will be f modes of oscillation given by eigenvectors of the matrix $(M - \omega_0 I)$.

In the second term of Equation (1), the parameter γ introduces nonlinearity into the formulation, where $D(|\boldsymbol{U}|^2) \equiv \mathrm{diag}|(|u_1|^2, |u_2|^2, \ldots, |u_f|^2)$ is a diagonal matrix. Thus, with $\varepsilon = 0$ but with the nonlinear parameter γ not equal to zero, each site is an independent (uncoupled) anharmonic oscillator.

From a physical perspective, there are two types of nonlinearity: intrinsic (stemming from weakening of electronic bonding with mode amplitude) and extrinsic (arising from interactions between localized vibrations and the lattice) (Scott, 2003). Intrinsic nonlinearity governs energy localization in small molecules (such as "local modes" of the CH stretch oscillations in benzene), which has been known to physical chemists since the 1920s (Ellis, 1929).

With both γ and ε not equal to zero, the DST equation displays an interesting variety of regular and chaotic motions for various values of the energy

$$H = \sum_j \left(\omega_0 |u_j|^2 - \frac{\gamma}{2}|u_j|^4\right) - \varepsilon \sum_{j,k} m_{jk} u_j^* u_k \quad (2)$$

and the "mass" $N = |u_1|^2 + |u_2|^2 + \cdots + |u_f|^2$. Numerical studies of these motions provide insights into the dynamics of vibrational energy in proteins and in small molecules. (For descriptions at small levels of oscillatory energy, Equation (1) is conveniently quantized, Scott et al., 1994.)

The scaling $\boldsymbol{U} \to \boldsymbol{U}\exp(-\mathrm{i}\omega_0 t)$ reduces (1) to the standard form of the DST equation

$$\mathrm{i}\frac{\mathrm{d}}{\mathrm{d}t}\boldsymbol{U} + \gamma D(|\boldsymbol{U}|^2)\boldsymbol{U} + \varepsilon \boldsymbol{M}\boldsymbol{U} = 0. \quad (3)$$

An important class of solutions of the DST equation are the so-called stationary solutions ("stationary" because amplitudes are time-independent), which satisfy the ansatz

$$\boldsymbol{U}(t) = \boldsymbol{y}\exp(\mathrm{i}\omega t).$$

Inserting this into (3), we see that the constant vector $\boldsymbol{y} = \mathrm{col}(y_1, y_2, \ldots, y_f)$ satisfies the nonlinear eigenvalue problem

$$-\omega \boldsymbol{y} + \gamma D(|\boldsymbol{y}|^2)\boldsymbol{y} + \varepsilon \boldsymbol{M}\boldsymbol{y} = 0, \quad (4)$$

where ω plays the role of the eigenvalue. In many cases, the vector $\boldsymbol{y}$ can be chosen to be real. In the limit $\varepsilon \to 0$ (alternatively $\gamma \to \infty$), called the "anti-integrable" limit, we have $y_i = 0$ or $|y_i|^2 = \omega/\gamma$, and in the real case, we have $y_i = \pm\sqrt{N/K}$, where K is the

number of nonzero y_i on the chain. Starting from these solutions, branches of solutions for nonzero ε can then be generated numerically by path-following methods (Eilbeck et al., 1984). In the limit $\gamma \to 0$, (4) becomes a linear eigenvalue problem.

The values of y_i in the anti-integrable limit serve as a useful classification scheme for the branch, where we denote the three different (real) limits by the symbols $\cdot$, $\uparrow$, and $\downarrow$, respectively. The simplest stationary localized solution has only one nonzero mode or site amplitude in the anti-integrable limit, with $y_k = \sqrt{N}$, $y_i = 0, i \neq k$. For small but nonzero ε the amplitudes on the sites $\neq k$ are small and tend to zero exponentially as $|k - i| \to \infty$.

Such a localized solution was called a soliton in the early work on the DST equation but is now more often referred to as a breather due to its internal degree of freedom ω. A single breather in the center of a 1-dimensional lattice would be written as $(\ldots\cdots\uparrow\cdots\ldots)$, and would appear as in Figure 1. More complicated breather structures are possible, such as $(\ldots\cdots\uparrow\uparrow\cdots\ldots)$ and $(\ldots\cdots\uparrow\downarrow\cdots\ldots)$.

Breathers satisfying (4) are referred to as stationary breathers; more general mobile solutions are of interest. Feddersen (1991b) carried out a numerical study of solutions of the form

$$U_n(t) = \psi(n - ct)\mathrm{e}^{\mathrm{i}(kn-\omega t)}$$

in the case where M is a tridiagonal matrix with constant coefficients (nearest-neighbor interactions). This case is now known as the discrete nonlinear Schrödinger (DNLS) equation. Note that the "carrier wave" speed ω/k is different from the "envelope" speed c. He found branches of localized solutions to high accuracy, but the existence of such solutions is still an open question.

The stability criteria for stationary solutions of the DST equation were studied by Carr & Eilbeck (1985). An important step is to consider perturbations in a frame rotating with the stationary solutions

$$U_n(t) = [y_n + \varepsilon_n(t)]\,\mathrm{e}^{\mathrm{i}\omega t}.$$

Once this trick is carried out, the study of linear stability reduces to an algebraic eigenvalue problem, at least when f is finite, which greatly simplifies the problem. One noteworthy point is that the resulting stability matrix is not self-adjoint, so branches can change stability at points away from bifurcation points.

On a finite lattice, modeling vibrational modes on small molecules, the stationary solutions of the DST equation can often be found exactly. For $f = 3$ and $M_{ij} = 1$ if $i \neq j$ (modeling NH_3 stretching oscillations in ammonia), we obtain the bifurcation diagram shown in Figure 2. Details are discussed in Eilbeck et al. (1985). Note the change of stability of the $\uparrow\downarrow$ 0 branch at two places, and the local-mode branch, where the vibrational energy is localized on a single degree of freedom.

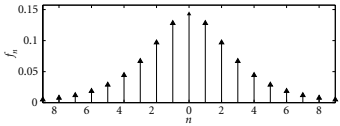

Figure 1. Stationary Breather on a DST (DNLS) lattice.

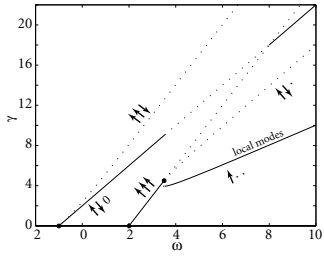

Figure 2. Stationary solutions on a DST lattice with $f = 3$. Solid (dotted) lines indicate stable (unstable) solutions.

In the large f case, in an application of the DST formulation to the dynamics of a globular protein, Feddersen considered interactions among CO stretch oscillations in adenylate kinase, which comprises 194 amino acids ($f = 194$) (Feddersen, 1991a). Since the structure of this enzyme has been determined by X-ray analysis, the $f(f-1)/2 = 18721$ off-diagonal elements of the dispersion matrix (M) were calculated from Maxwell's equations. Also, diagonal elements were selected from a random distribution, and the degree of localization of a particular solution was defined by evaluating the quotient $\sum |u_j|^4 / \sum |u_j|^2$.

In this study at experimentally reasonable levels of nonlinearity (γ), stable localized solutions were observed near some but not all of the amino acids. Interestingly, this anharmonic localization was observed to be distinctly different from Anderson localization, a property of randomly interacting linear systems. Thus, none of the stationary states, that were observed to be highly localized at large γ, remained so as γ was made small. Also, none of the states, that were localized at $\gamma = 0$ (i.e., Anderson localized), remained so as γ was increased to a physically reasonable level.

Other studies and applications of the DST equation include models for Bose–Einstein condensates and coupled optical fiber arrays. On the theoretical side, work has been carried out in the study of nonstationary and chaotic solutions on both small and large lattices. A list of citations to Eilbeck et al. (1985) is presently maintained at http://www.ma.hw.ac.uk/∼chris/dst/.

ALWYN SCOTT AND CHRIS EILBECK

See also **Anderson localization; Discrete breathers; Discrete nonlinear Schrödinger equations; Local modes in molecular crystals; Local modes in molecules; Rotating wave approximation**

Further Reading

Careri, G., Buontempo, U., Galluzzi, F., Scott, A.C., Gratton, E. & Shyamsunder, E. 1984. Spectroscopic evidence for Davydov-like solitons in acetanilide. *Physical Review* B 30: 4689–4702

Carr, J. & Eilbeck, J.C. 1985. Stability of stationary solutions of the discrete self-trapping equation. *Physics Letters* A 109: 201–204

Eilbeck, J.C., Lomdahl, P.S. & Scott, A.C. 1984. Soliton structure in crystalline acetanilide. *Physical Review* B, 30: 4703–4712

Eilbeck, J.C., Lomdahl, P.S. & Scott, A.C. 1985. The discrete self-trapping equation. *Physica* D 16: 318–338

Ellis, J.W. 1929. Molecular absorption spectra of liquids below 3 μ. *Transactions of the Faraday Society*, 25: 888–897

Feddersen, H. 1991a. Localization of vibrational energy in globular protein. *Physics Letters* A, 154: 391–395

Feddersen, H. 1991b. Solitary wave solutions to the discrete nonlinear Schrödinger equation. In *Nonlinear Coherent Structures in Physics and Biology*, edited by M. Remoissenet & M. Peyrard, Berlin and New York: Springer, 159–167

Scott, A.C., Eilbeck, J.C. & Gilhøj, H. 1994. Quantum lattice solitons. *Physica* D, 78: 194–213

Scott, A.C. 2003. *Nonlinear Science: Emergence and Dynamics of Coherent Structures*. 2nd edition, Oxford and New York: Oxford University Press

DISLOCATIONS IN CRYSTALS

Dislocations in crystals are linear topological defects near which the regular crystalline atomic arrangement is broken. The dislocation as a structural defect is characterized by the following peculiarity: the regular crystal lattice structure is greatly distorted only in the near vicinity of an isolated line (the dislocation axis), and the region of irregular atomic arrangement has transverse dimensions of the order of the interatomic distance. Nevertheless, deformation occurs even far from the dislocation core, and this is a consequence of a topological property of the dislocation. The deformation at a distance from the dislocation axis may be seen by passing along a closed contour around the dislocation core and considering the displacement vector of each crystalline site from its position in an ideal lattice. Upon calculating the total increment of this displacement vector at the end of the pass, one sees that the total atomic displacement is nonzero and equals one atomic translation period.

Among the many microscopic models of dislocations, the simplest takes the dislocation to be the edge of an extra half-plane present in the crystal lattice. In the conventional atomic scheme of this model (Figure 1), the trace of the half-plane coincides with the upper semiaxis y, and its edge coincides with the z-axis; thus, one has an "edge" dislocation. If one surrounds

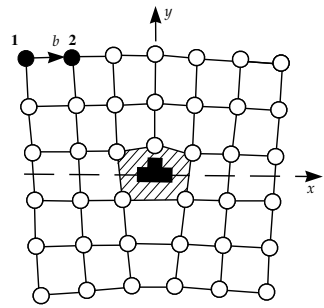

Figure 1. Schematic atomic arrangement in the vicinity of an edge dislocation.

the dislocation axis with a tube with radius of the order of several interatomic distances, the crystal outside this tube may be regarded as ideal and subject only to elastic deformation (crystal planes are connected to one another almost regularly), and inside the tube the atoms are considerably displaced relative to their equilibrium positions and form the "dislocation core." The atoms of the dislocation core are distributed over the contour of the shaded pentagon in Figure 1. The closed pass is the external contour starting from point 1 and finishing at point 2. The vector connecting atoms 1 and 2 is denoted by $\boldsymbol{b}$ and called the "Burgers vector." Possible values of the Burgers vectors in a crystal are determined by its crystallographic structure and correspond, as a rule, to a small number of certain directions in a crystal. The dislocation lines are arranged arbitrarily, although their arrangement is limited by a set of definite crystallographic planes. The dislocation line cannot end inside a crystal. It must either leave the crystal with each end on the crystal surface or form a dislocation loop.

The main topological property of the dislocation implies that a dislocation in a crystal is a specific line D having the following general property. After a circuit around the closed contour L enclosing the line D (see Figure 2), the elastic displacement vector $\boldsymbol{u}$ changes by a certain finite increment $\boldsymbol{b}$ equal to one of the lattice periods. This property can be written as

$$\oint_L \mathrm{d}u_i = \oint_L \frac{\partial u_i}{\partial x_k}\mathrm{d}x_k = -b_i, \qquad (1)$$

assuming that the direction of the circuit is related to a chosen direction of the tangent vector $\boldsymbol{\tau}$ to the dislocation line. The dislocation line is in this case a line of singular points of the elastic fields.

Macroscopic considerations (based on elasticity theory) allow one to find a concentration of strains and stresses near the dislocation. The elastic field created by a dislocation leads to its interaction with

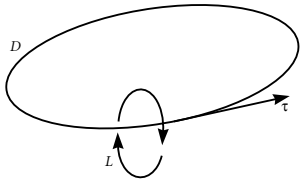

Figure 2. Mutual coordination of the vector $\boldsymbol{\tau}$ and circuit around the contour L.

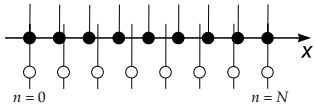

Figure 3. Edge dislocation in the Frenkel–Kontorova model.

other dislocations and other types of crystal defects. In particular, the dislocation can accumulate point defects near its core. If such defects are color centers, the dislocation line can be decorated (*See* **Color centers**).

Displacements of the dislocation line in the plane determined by the vectors $\boldsymbol{b}$ and $\boldsymbol{\tau}$ (called a "slip plane") have no effect on the crystal continuity. Therefore, a comparatively easy mechanical motion of the dislocation is possible in principle in this plane. But any displacement of the dislocation produces some plastic deformation, so moving dislocations are carriers of crystal plasticity.

Macroscopic dislocation theory can describe a contribution of the dislocations to mechanical properties of real crystals and proposes a physical explanation of the crystal plasticity. However, the macroscopic theory cannot propose a structure of the dislocation core and explain possible mechanisms of the dislocation motion. The Soviet scientists Yakob Frenkel and Tatiana Kontorova were the first to present a simple 1-dimensional microscopic dislocation model (Frenkel & Kontorova, 1938). To formulate their model, it is convenient to analyze the following picture. The atomic chain (a set of black circles in Figure 3) is an edge series of one half of a plane crystal ($y > 0$, Figure 1) displaced in a certain way with respect to another half of a crystal (a substrate at $y < 0$). The influence of the nondisplaced half of the crystal on the atoms distributed along the x-axis can be qualitatively described assuming that those atoms are in a given external periodic field whose period coincides with the interatomic distance on the substrate a. The chain energy is then determined not only by a relative displacement of neighboring atoms but also by an absolute displacement of separate atoms u_n (n is the atomic number) in the external field. If the external periodical field has a simple sine-shaped dependence, the equation of chain motion has the form

$$m\frac{\mathrm{d}^2u_n}{\mathrm{d}t^2} = \alpha(u_{n+1} + u_{n-1} - 2u_n) - U_0\sin(2\pi u_n/a)\,, \qquad (2)$$

where m is the atom mass and α and U_0 are constant parameters. The displacements of the atoms in the chain are performed in such a way that $N+1$ atoms are situated over N crystal sites on the substrate. This atom distribution corresponds to the following boundary conditions for the displacements:

$$u_n = a \quad \text{at} \quad n = -\infty\,, \quad u_n = 0 \quad \text{at} \quad n = \infty. \qquad (3)$$

Equation (2) and the boundary conditions (3) are basic in the Frenkel–Kontorova model.

In a long-wavelength approximation, the function of the discrete number u_n is replaced by a continuous function of the coordinate $u(x)$ where $x = na$, and Equation (2) transforms into the sine-Gordon equation (SG) equation

$$\frac{\partial^2 w}{\partial t^2} = s^2\frac{\partial^2 w}{\partial x^2} - \omega_0^2\sin w, \quad w = 2\pi u/a, \qquad (4)$$

where $s^2 = a^2\alpha/m$ and $\omega_0^2 = U_0/m$.

The SG equation (4) possesses the following (kink-soliton) solution satisfying the boundary conditions (3): $u(x) = \tan^{-1}\exp[-(x - x_0/l)]$, where $l = s/\omega_0$ and $x_0 =$ constant. This kink describes the distribution of atoms in the core of the Frenkel–Kontorova dislocation, the parameter l determines the dislocation semiwidth, and x_0 is the coordinate of the dislocation center. Later Peierls (1940) proposed a semimicroscopic model of a straight dislocation line (directed along the z-axis in Figure 1) in a 3-d isotropic elastic medium. In this model, it was assumed that strains around the dislocation are described by the theory of elasticity; however, the interaction energy of both semi-spaces above (+) and under (−) the slide plane depends periodically on the relative displacements $v(x) = w(x)^+ - w(x)^-$ (the x-axis is a trace of the slide plane) and is described by a sine-shaped periodic function of $v(x)$. The main equation of Peierls's theory has the following form:

$$a\int_{-\infty}^{\infty}\left(\frac{\mathrm{d}v}{\mathrm{d}x}\right)\frac{\mathrm{d}\xi}{x-\xi} + M\ \sin v = 0\,, \qquad (5)$$

where the integral means its principal value and M is some dimensionless combination of elastic modules. Equation (5) has a soliton solution very close to the Frenkel–Kontorova dislocation $w(x) = \pi + 2\tan^{-1}[(x - x_0)/l]$ where $l = \pi a/M$.

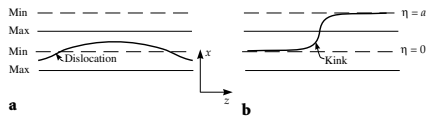

Figure 4. Two types of dislocation motion in the Peierls potential field. (a) Dislocation oscillates in its own trough. (b) The dislocation forms a kink moving along the z-axis.

Both the chain energy in the 1-d case and crystal energy in the 3-d case (calculated for the Frenkel–Kontorova and Peierls models, respectively) do not depend on the coordinate of the dislocation center x_0. Thus, the dislocation can glide, changing its location on the slide plane without action of any external field. This fact is a result of using the continuous approximation. Taking into account discreteness of the crystal and following the Peierls theory, Nabarro (1947) showed that a moving dislocation is influenced by some crystal field periodically depending on the dislocation center x_0 (later called the "Peierls relief"). Therefore, the dislocation can start moving only if an external stress acting on it exceeds a certain value called the "Peierls barrier."

Many dynamic problems in dislocation theory can be analyzed using the so-called "string model." This model treats the dislocation line as a heavy string under tension lying on a corrugated surface. An effective mass per unit length of the dislocation m and its line tension T_D are of a field origin and are associated with the inertia and energy of dislocation dynamic elastic field (Kosevich, 1964). The corrugated surface describes the Peierls relief. Troughs of this surface correspond to the potential minima of the slide plane occupied by a straight-line dislocation in equilibrium (see Figure 4). If the z-axis is directed along the equilibrium position of the dislocation and its transverse displacements η go along the x-axis, then the equation of motion of the dislocation has the form (Seeger, 1956):

$$m\frac{\partial^2\eta}{\partial t^2} - T_D\frac{\partial^2\eta}{\partial x^2} + b\sigma_p \sin(2\pi\eta/a) = b\sigma\ , \qquad (6)$$

where σ_p is the Peierls stress and σ is the applied stress. In the case $\sigma = 0$, this equation is equivalent to Equation (4), proposed by Frenkel and Kontorova. Equation (6) describes both small amplitude vibrations of the dislocation effected by an external oscillation force and the so-called kink-mechanism of the transverse displacements of the dislocation along the x-axis effected by a strong stationary driving force.

ARNOLD KOSEVICH

See also **Color centers; Frenkel–Kontorova model; Peierls barrier; Sine-Gordon equation; Topological defects**

Further Reading

Frenkel, J. & Kontorova, T. 1938. On the theory of plastic deformation and twinning. *Physikalische Zeitschrift der Sowjetunion*, 13: 1

Kosevich, A.M. 1964. Dynamical theory of dislocations. *Uspekhi Fizicheskikh Nauk*, 84: 579 (in Russian); translated in 1965. *Soviet Physics, Uspekhi*, 7: 837

Kosevich, A.M. 1979. Crystal dislocations and the theory of elasticity, in *Dislocations in Solids*, edited by F.R.N. Nabarro Amsterdam: North Holland, p. 33

Nabarro, F.R.N. 1947. Dislocations in a simple cubic lattice *Proceedings of Physical Society, London*, A59: 256

Nabarro, F.R.N. 1967. *Theory of Crystal Dislocations*, Oxford: Clarendon Press

Peierls, R.E. 1940. The size of a dislocation. *Proceedings of Physical Society, London*, A52: 34

Seeger, A. 1956. On the theory of the low-temperature internal friction peak observed in metals. *Philosophical Magazine*, 1: 651

DISPERSION MANAGEMENT

The propagation of optical pulses in fiber lines is usually limited by dispersion and nonlinearity. Dispersion causes a broadening of the pulses whereas nonlinearity is the reason for four-wave mixing (FWM). A balance of dispersion and nonlinearity may produce the so-called optical soliton. Dispersion management (manipulations of the chromatic dispersion along the line) is an attractive technique that allows enhancement of the performance of fiber communication links both for soliton and nonsoliton transmission. Dispersion-managed solitons can be viewed as novel kinds of information carriers with many attractive features that will lead to further improvement of the transmission capacity of fiber links. The starting point of all considerations in this area is the cubic nonlinear Schrödinger (NLS) equation for an optical mode in a cylindrical fiber with (constant) dispersion and Kerr nonlinearity (Newell & Maloney, 1992):

$$\mathrm{i}\,\frac{\partial u}{\partial z} + \frac{1}{2}\,\frac{\partial^2 u}{\partial t^2} + |u|^2 u = 0. \qquad (1)$$

This equation is written in dimensionless form (u is the normalized intensity, z the normalized propagation distance, and t is the normalized time); for more details, see, for example, Hasegawa & Kodama (1995).

From FWM calculations (Agrawal, 1995), one knows that the FWM efficiency depends on the phase mismatch and thereby on the dispersion coefficient, D. The larger the phase mismatch (proportional to dispersion), the smaller the efficiency of FWM. On the other hand, small D values are necessary for high bit-rates B. One reason is the so-called Gordon–Haus effect (Gordon & Haus, 1986). Solitons adjust themselves to external perturbations, and thereby they can be considered as quite robust. However, this adjustment also has disadvantages. Any re-shaping, for example, in the presence of amplifier noise, also has consequences

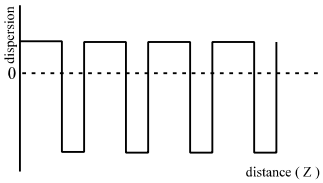

Figure 1. Schematic plot of the dispersion coefficient that varies in space when dispersion management is applied.

for the velocities. Changing velocities cause a timing jitter, and the latter limits the maximal possible bit-rate. Note that the general soliton solution of Equation (1)

$$u_s = A\ \mathrm{sech}\,[A(t+\Omega z) - q_0]\,\mathrm{e}^{-\mathrm{i}\Omega t - (\mathrm{i}/2)(A^2-\Omega^2)z + \mathrm{i}\phi_0} \tag{2}$$

is moving with velocity $v = -1/\Omega$. The detailed calculation (Gordon & Haus, 1986) gives an upper limit for the bit-rate B and the length L of the system in the form

$$(BL)^3 \leq \text{upper limit} \sim \frac{1}{D}. \tag{3}$$

One clearly recognizes that low dispersion favors high bit-rates over large distances. On the other hand, as was mentioned already, low dispersion is dangerous with respect to FWM. Dispersion management is an elegant way out of this dilemma.

Principle of Dispersion Management

The idea of using a dispersion-compensating fiber (DCF) to overcome the dispersion of the standard mono-mode fiber (SMF) was proposed in 1980 (Lin et al., 1980). The simplest optical-pulse equalizing system consists of a transmission fiber (SMF or dispersion-shifted fiber (DSF)) and an equalizer fiber with the opposite dispersion (DCF to compensate SMF or, for instance, SMF to compensate DSF with normal dispersion). The incorporation of a fiber with normal dispersion reduces (or, in the ideal case, eliminates) the total dispersion of the fiber span between two amplifiers. Low average dispersion is good for reducing the Gordon–Haus effect while high local dispersion reduces the FWM efficiency. In Figure 1, we indicate the principle of dispersion management by a schematic drawing.

Dispersion management means that the coefficient in front of the second time derivative becomes Z-dependent (we change notation in order to allow for different normalization parameters), that is, the simplest form of the dispersion-managed nonlinear Schrödinger equation becomes (Kodama, 1998)

$$\mathrm{i}\,\frac{\partial q}{\partial Z} + \frac{1}{2}\,\mathrm{d}(Z)\,\frac{\partial^2 q}{\partial T^2} + |q|^2 q = 0. \tag{4}$$

A short remark: if $\mathrm{d}(Z)$ would be $\neq 0$ everywhere in the fiber, the variation of $\mathrm{d}(Z)$ can be eliminated by using a new coordinate Z' via

$$\frac{\mathrm{d}Z'}{\mathrm{d}Z} = d(Z). \tag{5}$$

Then a Z-dependent coefficient would appear in front of the nonlinear term. Again, we would end up with an equation with a rapidly varying coefficient. However, characteristic for nearly all practical dispersion management arrangements is the vanishing of $d(z)$ at certain positions z.

Weak Dispersion Management

For weak dispersion management of small-amplitude pulses, one can start with the equation

$$\mathrm{i}\frac{\partial u}{\partial z} + d(z)\frac{\partial^2 u}{\partial t^2} + \varepsilon|u|^2 u = 0. \tag{6}$$

Here,

$$\begin{aligned} d(z) &= \langle d\rangle + \tilde{d} \quad \text{for } 0 \leq z \leq l, \\ d(z) &= \langle d\rangle - \tilde{d} \quad \text{for } l \leq z \leq 2l, \end{aligned} \tag{7}$$

and so on, is the z-dependent dispersion. The z-coordinate is made dimensionless with the dispersion length of the local dispersion, that is, $\tilde{d} \sim O(1)$. The averaged dispersion $\langle d\rangle$ is assumed to be small, and we introduce the smallness parameter $\varepsilon \ll 1$ via $\langle d\rangle \approx \varepsilon$. Nonlinearity will also be scaled by ε. The strength of the dispersion management is characterized by

$$R(z) = \int_0^z (d - \langle d\rangle)\,\mathrm{d}s. \tag{8}$$

Weak dispersion management means $R \sim O(\varepsilon^{1/2})$; that is, R is assumed to be small. From the definition $R \sim O(\tilde{d}\cdot l)$ holds. Therefore, the length l (of the parts with constant dispersion) is also small compared with the dispersion length, $l \sim O(\varepsilon^{1/2})$.

One can use (at least three different) averaging methods to calculate the average behavior of pulses over large distances. The first one is a direct method, starting with an expansion. The second one uses the Lie-transform technique; it is, therefore, much more systematic than the direct method. The third method makes use of a Bogolyubov transformation, which is very elegant in practice, but the ansatz is not as straightforward as the Lie transformation. The ansatz has to be specifically chosen for each problem. In the direct method (Kivshar & Spatschek, 1995; Yang et al., 1997), one expands u in orders of $\varepsilon^{1/2}$ and applies a multiple scale technique,

$$\begin{aligned} u &= U + u_1 + u_2 + \cdots, \\ \frac{\partial}{\partial z} &= \frac{\partial}{\partial \xi} + \frac{\partial}{\partial z_0} + \frac{\partial}{\partial z_1} + \cdots \end{aligned} \tag{9}$$

with $U = U(z_0, z_1, z_2, \ldots)$ and $u_k = u_k(\xi, U)$. One may use the scaling $\xi \sim O(\varepsilon^{-1/2})$, $z_k \sim O(\varepsilon^{k/2})$, $u_k \sim O(\varepsilon^{k/2})$, where $\langle u \rangle = U$, $\langle u_k \rangle = 0$.

The Lie transformation technique was originally developed for ordinary differential equations but can also be used for a partial differential equation (Neyfeh, 1973). To apply the Lie transformation one rearranges Equation (6) into the form

$$\frac{\partial u}{\partial z} = \mathrm{i}\langle d \rangle u_{tt} + \mathrm{i}\varepsilon|u|^2 u + \mathrm{i}\tilde{d}u_{tt} = X_0 + \tilde{d}X_{0D} = X[u, u^*]. \tag{10}$$

X depends on the infinite set of variables $(u, u_t, u_{tt}, \ldots, u^*, u_t^*, u_{tt}^*, \ldots)$, indicated by $X[u, u^*]$. Obviously $X_0 \sim O(\varepsilon)$, $X_{0D} \sim O(1)$. The transformation

$$u = \mathrm{e}^{\vec{\phi}\nabla} v = v + \phi + \frac{1}{2!}\left(\vec{\phi}\cdot\nabla\right)\phi + \frac{1}{3!}\left((\vec{\phi}\cdot\nabla)\phi\cdot\nabla\right)\phi + \cdots \tag{11}$$

transforms Equation (10) into

$$\frac{\partial v}{\partial z} = Y[v, v^*]. \tag{12}$$

The right-hand side can, in principle, be derived appropriately in order to identify v with the averaged intensity. Here, $\vec{\phi} = (\phi, \phi_t, \ldots)$ and $\nabla = (\frac{\partial}{\partial v}, \frac{\partial}{\partial v_t}, \ldots)$ are infinite-dimensional vectors.

In the third method (Arnol'd, 1988), one uses a Floquet–Lyapunov transformation

$$u(z, t) = \mathrm{e}^{\mathrm{i}R(z)\partial_t^2} B(z, t) \tag{13}$$

as well as the Bogolyubov–Krylov transformation

$$B = v + \mathrm{i}f|v|^2 v + (g + p)N_1(v) + \mathrm{i}hN_2(v) + q|v|^4 v + O(\varepsilon^{5/2}), \tag{14}$$

with coefficients to be determined appropriately during the calculation. All three methods lead to the same result. Over fairly large distances, the averaged solution is still a fundamental soliton, that is, robust. This follows from the fact that *to lowest order*, the basic equation for the averaged pulse intensity is the *integrable* cubic nonlinear Schrödinger equation

$$\mathrm{i}v_z + \langle d \rangle v_{tt} + \varepsilon|v|^2 v = \frac{1}{2}\varepsilon\left\langle R^2 \right\rangle N_2(v). \tag{15}$$

The correction term on the right-hand side contains a polynomial N_2 in v, v_t, $v_{tt}, \cdots$. One should bear in mind, on the other hand, that on the short scale (length $2l$ of one of the periodic elements), the exact (non-averaged) solution is oscillating (breathing) with the frequency following from the periodicity in the dispersion map. Besides the scaling $\tilde{d} \sim O(1)$ and $R \sim O(\varepsilon^{1/2})$, other scalings are possible and tractable by the methods mentioned above, as long as R is small (weak dispersion management).

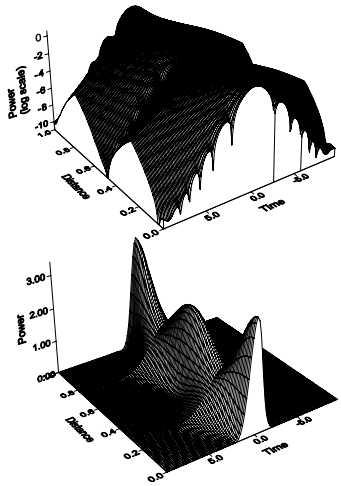

Figure 2. Plot of a DM soliton. The lower part shows the breathing over one element of the dispersion map. The upper graph shows the fine structure on a logarithmic axis, indicating the characteristic deviations from the fundamental soliton.

Strongly Dispersion-Managed Solitons

Recently (Nijhof et al., 1998), the strong dispersion management (R is no longer small) became of increasing interest. The chirp (pulse phase has a quadratic time-dependence) is a new and one of the most important features of the (strongly dispersion managed) DM soliton (recall that the conventional soliton is unchirped). In addition, the DM soliton is not anymore of the sech-type. The DM soliton consists of a self-similar energy-containing core surrounded by oscillating tails. Such tails manifest themselves as non-self-similar modulations of the soliton profile during the compensation period, although their amplitudes are rather small compared with the main peak (see Figure 2).

The most surprising feature of the DM soliton is that it can propagate stably along the line with zero or even with normal average dispersion (in contrast to the fundamental soliton that propagates stably only in the anomalous dispersion region). These observations indicate that an average model describing the evolution of the breathing pulse differs from the nonlinear Schrödinger equation. In other words, strong dispersion management imposes such a strong perturbation that a carrier pulse in this case is no longer the NLS soliton. For more details, see Nijhof et al. (1998).

Experimental Results

One can estimate the potential of dispersion management from successful experiments, for example, Carter et al. (1999).

KARL SPATSCHEK

See also **Nonlinear optics; Optical fiber communications**

Further Reading

Agrawal, G.P. 1995. *Nonlinear Fiber Optics*, San Diego: Academic Press

Arnol'd, V.I. 1988. *Geometrical Methods in the Theory of Ordinary Differential Equations*, New York: Springer

Carter, G.M., Grigoryan, V.S., Mu, R.-M., Menyuk, C.R., Sinha, P., Carruthers, T.F., Dennis, M.L. & Duling, I.N. 1999. Transmission of dispersion-managed solitons at 20 Gbit/s over 20 000 km. *Electronics Letters*, 35(3): 233

Gordon, J.P. & Haus, H.A. 1986. Random walk of coherently amplified solitons in optical fiber transmission. *Optics Letters*, 11: 665

Hasegawa, A. & Kodama, Y. 1995. *Solitons in Optical Communications*, Oxford: Clarendon Press

Kivshar, Yu.S. & Spatschek, K.H. 1995. Nonlinear dynamics and solitons in the presence of rapidly varying periodic perturbations. *Chaos, Solitons, and Fractals*, 5: 2551–2569

Kodama, Y. 1998. Nonlinear pulse propagation in dispersion managed system. *Physica* D, 123: 255–266

Lin, C., Kogelnik, H. & Cohen, L.G. 1980. Optical pulse equalization and low dispersion transmission in single-mode fibers in the 1.3–1.7 mm spectral region. *Optics Letters*, 5: 476–478

Newell, A.C. & Moloney, J.V. 1992. *Nonlinear Optics*, Redwood City, CA: Addison-Wesley

Neyfeh, A.H. 1973. *Perturbation Methods*, New York: Wiley

Nijhof, J., Doran, N., Forysiak, W. & Bernston, A. 1998. Energy enhancement of dispersion-managed solitons and WDM. *Electronics Letters*, 34: 481–482

Yang, T.-S., Golovchenko, A., Pilipetskii, A.N. & Menyuk, C.R. 1997. Dispersion-managed soliton interactions in optical fibers. *Optics Letters*, 22: 793–795

DISPERSION RELATIONS

Dispersion relations (DRs) are associated with wave equations to characterize the nature of their temporal and spatial evolution. For a linear wave equation in one dimension, the DR expresses the wavenumber ($k = 2\pi/\lambda$) as a function of the frequency ($\omega = 2\pi/T$), or vice-versa, where λ and T are, respectively, the wavelength and temporal period of an elementary periodic solution. Through the superposition principle, the behaviors of all solutions of linear equations are determined by the DR. In nonlinear cases, DRs also depend on wave amplitude and can be used in perturbative analyses of quasiharmonic systems. For more than one spatial dimension, the wave number is a vector.

Dispersion Relations for Linear Equations

Fourier analysis establishes a one-to-one correspondence between DRs and equations in such a way that we can obtain one from the other. Consider as an example, the Klein–Gordon equation,

$$u_{tt} - u_{xx} + m^2 u = 0, \tag{1}$$

where m is a constant and the subscripts indicate partial derivatives. Substituting a plane-wave solution of the form $u(t, x) = \mathrm{a}e^{\mathrm{i}(\omega t - kx)}$ into (1), we obtain the DR

$$\omega^2 = m^2 + k^2. \tag{2}$$

For linear equations, the phase velocity $v_\varphi(k)$ and the group velocity $v_\mathrm{g}(k)$ are defined as

$$v_\varphi(k) = \frac{\omega(k)}{k}, \quad v_\mathrm{g}(k) = \frac{\mathrm{d}\omega(k)}{\mathrm{d}k}. \tag{3}$$

The phase velocity of a wave number k is the speed of propagation of the corresponding harmonic wave component or mode. The group velocity corresponds to the propagation speed of a wave packet, and thus is the speed of energy transmission for the system (Whitham, 1974). This distinction is especially important in the propagation of wave trains, where signals travel with the group velocity.

An equation (or the wave that is represented by its solution) is said to be *dispersive* if $v_\varphi(k)$ is not a constant (or equivalently if $v_\varphi \neq v_\mathrm{g}$ for all k). In such cases, the initial profile of the wave is not conserved. For the Klein–Gordon equation we have

$$v_\varphi(k) = \pm\frac{\sqrt{m^2 + k^2}}{k}, \quad v_\mathrm{g}(k) = \pm\frac{k}{\sqrt{m^2 + k^2}}, \tag{4}$$

and the equation is dispersive except in the special case $m = 0$ (which corresponds to the wave equation).

The DR also plays an important role in simulations of Equation (1) by finite differences. The usual (von Neumann) stability conditions are equivalent to requiring that the phase velocity in the mesh be greater or equal to the phase velocity of the equation (Ritchmyer & Morton, 1967). Other aspects that mark deviations of numerical solutions from continuous solutions are governed by discrete DRs (Trefethen, 1982).

Amplitude-Dependent Dispersion Relations

For nonlinear equations, solutions cannot, in general, be expressed as a superposition of plane waves and thus, in principle, there is not dispersion relation. There are nevertheless two possible applications of the concept. The first is in the small-amplitude regime where an approximate DR can be established by neglecting the higher order terms, and the second is when plane waves are particular solutions of the nonlinear equation. In both cases, the DRs are amplitude dependent. We illustrate both cases with a nonlinear Klein–Gordon equation and the cubic Schrödinger equation.

The nonlinear Klein–Gordon equation with cubic term

$$u_{tt} - u_{xx} + m^2 u + g u^3 = 0 \qquad (5)$$

does not have exact plane wave solutions. (The case $m = 1$, $g = -1/3!$ corresponds for instance to the first two terms expansion of the sine-Gordon equation.) Nevertheless, we may assume a term of the form $a\cos(\omega t - kx)$ in the solution. Substituting and retaining only the lower-order terms, we obtain the approximate DR

$$-\omega^2 + k^2 + m^2 + \frac{3}{4} g a^2 + \cdots = 0 \qquad (6)$$

provided $m^2 \gg g a^2$. The presence of coupled higher-order terms together with the approximate DR gives a picture of how such modes get excited and evolve.

The previous analysis can also be applied, for instance, to the cubic nonlinear Schrödinger equation

$$\mathrm{i}\phi_t - \phi_{xx} + |\phi|^2 \phi = 0, \qquad (7)$$

but this equation is special in the sense that it has particular solutions in the form of plane waves $\phi = a e^{\mathrm{i}(\omega t - kx)}$. Although the general solution cannot be expressed as a superposition of such plane waves, we have an amplitude-dependent DR of the form

$$\omega = k^2 + a^2. \qquad (8)$$

In this case, wave dispersion can be compensated by nonlinearity and solitons may appear.

L. VÁZQUEZ AND S. JIMÉNEZ

See also **Modulated waves; Wave packets, linear and nonlinear**

Further Reading

Ritchmyer, R.D. & Morton, K.W. 1967. *Difference Methods for Initial-Value Problems*, New York: Wiley-Interscience

Trefethen, L.N. 1982. Group velocity in finite difference schemes. *SIAM Review*, 24: 113–136

Whitham, G.B. 1974. *Linear and Nonlinear Waves*, New York: Wiley-Interscience

DISTRIBUTED OSCILLATORS

Two modes of oscillation sharing a common source of energy may have a stationary solution of equal mode amplitudes, but this solution may be unstable for the following reason. One of the modes will inevitably gain a bit of amplitude (due to noise), and if it then consumes more than its share of the available power, it will grow further, causing the other mode to decrease. Interestingly, this effect depends upon the spatial dimension of the oscillating system. Related dynamics arise in diverse areas of engineering and science, including flip-flop circuits, multimode lasers, interacting biological species, and the neocortex of a human brain.

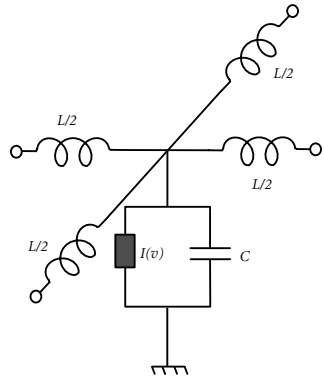

Figure 1. A unit cell of a two-dimensional oscillator array.

As a model for mode interactions, consider a two-dimensional array of identical oscillators, each interacting only with its nearest neighbors. Power flow among the modes of such an array can be studied using the method of harmonic balance, introduced by Balthasar van der Pol in 1934 (van der Pol, 1934) and developed by applied mathematicians and engineers in the Soviet Union during the 1930s and 1940s (Andronov et al., 1966; Kryloff & Bogoliuboff, 1947).

As shown in Figure 1, a unit cell of the array consists of a nonlinear conductance $I(v)$ in parallel with a capacitance C, connecting a lattice point to a ground plane. Each lattice point is attached to its four nearest neighbors through an inductance L. The nonlinear conductance is represented as

$$I(v) = -Gv\left(1 - 4v^2/3V_0^2\right), \qquad (1)$$

so for $-V_0/2 < v < +V_0/2$ the differential conductance $(\mathrm{d}I/\mathrm{d}v)$ is negative.

Assume a large, square $(N \times N)$ lattice of these unit cells with zero-voltage (short circuit) boundary conditions on the edges, as in Figure 2. In a zero-order approximation, the nonlinear conductance can be neglected, and in a continuum approximation, this linear, lossless system supports an arbitrary number (say n) modes. Thus, the total voltage is

$$v(x, y, t) = \mathcal{V}_1(x, y)\cos\theta_1 + \mathcal{V}_2(x, y) \times \cos\theta_2 + \cdots + \mathcal{V}_n(x, y)\cos\theta_n, \qquad (2)$$

which depends on space (x and y) and time (t) where

$$\mathcal{V}_i(x, y) \equiv V_i \cos k_{xi} x \cos k_{yi} y \quad \text{and} \quad \theta_i \equiv \omega_i t + \phi_i.$$

Noting that the energy in the ith mode is related to its amplitude by $U_i = (N^2 C/8) V_i^2$ and averaging the

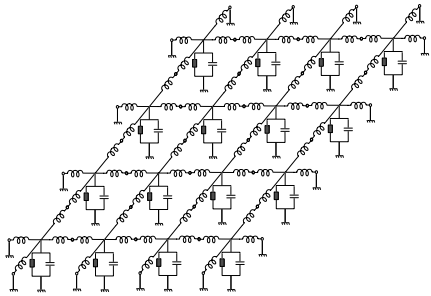

Figure 2. A 4×4 array ($N^2 = 16$) of the unit cells in Figure 1.

product of current (given by Equation (1)) and voltage (given by Equation (2)) over space and time gives the rate of change in mode energies as functions of mode energies (Scott, 2003).

The rate of change of energy (or power) into the first mode is

$$\frac{\mathrm{d}U_1}{\mathrm{d}\tau} = U_1\left[1 - \alpha\left(\frac{9}{8}U_1 + U_2 + \cdots + U_n\right)\right], \quad (3)$$

with $\tau \equiv Gt/C$ and $\alpha \equiv 4/(N^2 C V_0^2)$. For n excited modes, there is a set of n equations—each similar to Equation (3) but with the indices appropriately altered—for the rates of change of the mode energies as functions of those energies. These nonlinear, autonomous equations have the same form as those introduced by Vito Volterra to describe the interaction of biological species competing for the same food supply (Volterra, 1937), and they are similar to a formulation suggested by Peter Greene (Greene, 1962) to describe interactions between assemblies of neurons in the brain.

Generalizing to a system of d-space dimensions, equations of interacting mode energies become

$$\begin{aligned} \frac{\mathrm{d}U_1}{\mathrm{d}\tau} &= U_1\left[1 - \alpha\left(KU_1 + U_2 + \cdots + U_n\right)\right], \\ &\vdots \\ \frac{\mathrm{d}U_n}{\mathrm{d}\tau} &= U_n\left[1 - \alpha\left(U_1 + U_2 + \cdots + KU_n\right)\right], \end{aligned} \quad (4)$$

where

$$K = 3^d/2^{d+1}.$$

For $K > 1$ (implying $d \geq 2$), analysis of Equations (4) indicates multimode stability. In other words, several modes can stably exist for two or more spatial dimensions. For one spatial dimension, on the other hand, two modes of equal amplitude are unstable, and only a single mode can be stably established. This observation is important in the design of semiconductor lasers, where large transverse dimensions are introduced to increase the power output.

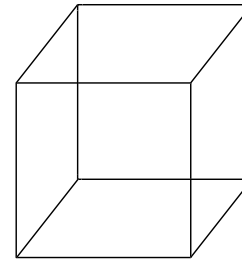

Figure 3. A Necker cube.

Unfortunately, such a design allows several modes to oscillate together, thereby decreasing the coherence and spectral purity of the output beam.

Multimode oscillator arrays have been realized using semiconductor tunnel diodes (Scott, 1971), superconductor tunnel diodes (Hoel, et al., 1972), and integrated circuits (Aumann, 1974). In these experiments, a variety of stable multimode oscillations have been observed, some quasiperiodic and others periodic, indicating mode locking. In a manner qualitatively similar to that proposed by Greene in his model of the brain's neocortex (Greene, 1962), the oscillator array can be induced to switch from one stable multi-mode configuration to another.

At the level of subjective perception, similar switchings in the brain are observed as one stares at Figure 3. Constructed by Louis Albert Necker (a Swiss geologist) in the mid-1800s, this image seems to jump from one metastable orientation to another, like the flip-flop circuit of a computer engineer. Defining order parameters (ξ_1 and ξ_2) to represent neural activities corresponding to the two perceptions of the Necker cube, Hermann Haken has recently suggested the equations

$$\begin{aligned} \frac{\mathrm{d}\xi_1}{\mathrm{d}t} &= \xi_1[1 - C\xi_1^2 - (B + C)\xi_2^2], \\ \frac{\mathrm{d}\xi_2}{\mathrm{d}t} &= \xi_2[1 - C\xi_2^2 - (B + C)\xi_1^2] \end{aligned} \quad (5)$$

as an appropriate dynamic description (Haken, 1996). With $U_j = \xi_j^2$ ($j = 1, 2$), Equations (5) are identical to Equations (4), showing only single-mode stability for $B > 0$. Study of this system in the (ξ_1, ξ_2) phase plane reveals two stable states: $(1/\sqrt{C}, 0)$ and $(0, 1/\sqrt{C})$, and jumping back and forth between these two states models one's subjective experience of Figure 3.

ALWYN SCOTT

See also **Cell assemblies; Lasers; Population dynamics; Quasilinear analysis; Synergetics; Tacoma Narrows Bridge collapse**

Further Reading

Andronov, A.A., Vitt, A.A. & Khaikin, S.E. 1966. *Theory of Oscillators*, Oxford and New York: Pergamon

Aumann, H.M. 1974. Standing waves on a multimode ladder oscillator. *IEEE Transactions on Circuits and Systems*, CAS-21: 461–462

Greene, P.H. 1962. On looking for neural networks and "cell assemblies" that underlie behavior. *Bulletin Mathematical Biophysics* 24: 247–275 and 395–411

Haken, H. 1996. *Principles of Brain Functioning: A Synergetic Approach to Brain Activity, Behavior and Cognition*, Berlin: Springer

Hoel, L.S., Keller, W.H., Nordman, J.E. & Scott, A.C. 1972. Niobium superconductive tunnel diode integrated circuit arrays. *Solid State Electronics*, 15: 1167–1173

Kryloff, N. & Bogoliuboff, N. 1947. *Introduction to Nonlinear Mechanics*, Princeton, NJ: Princeton University Press

Scott, A.C. 1971. Tunnel diode arrays for information processing and storage. *IEEE Transactions on Systems, Man, and Cybernetics*, SMC-1: 267–275

Scott, A.C. 2003. *Nonlinear Science: Emergence and Dynmaics of Coherent Structures*, 2nd edition. Oxford and New York: Oxford University Press

van der Pol, B. 1934. The nonlinear theory of electric oscillations. *Proceedings of the Institute of Radio Engineers*, 22: 1051–1086

Volterra, V. 1937. Principes de biologie mathématique. *Acta Biotheoretica*, 3: 1–36

DNA PREMELTING

DNA premelting phenomena are spontaneous dynamical processes that occur well below the melting temperature of DNA. They reflect DNA "breathing," a process that combines the transient unstacking of base-pairs (allowing planar drugs and dyes to intercalate into DNA), with the transient breaking and rejoining of hydrogen-bonds connecting base-pairs in limited DNA regions (allowing tritium nuclei in hydrogen bonds connecting base-pairs to exchange with protons in water). The formation and propagation of chain-slippage structures either within or between homologous DNA molecules, along with a variety of structural phase transitions in DNA are also included in discussions of premelting. This entry describes how concepts of kink-antikink-bound states (breather solitons) have been used to assist in understanding a wide range of DNA premelting phenomena.

Conceptually, the lowest energy kink-antikink-bound state in DNA (termed a "premelton") contains a central hyperflexible beta-DNA core region modulated into B-DNA on either side through kink and antikink boundaries. As the kink and antikink move together, for example, the energy density in the central beta-DNA core region rises. This energy is used first to enhance (alternate) base-pair unstacking, and next, to stretch and to eventually break hydrogen-bonds connecting base-pairs. As kink and antikink move apart, the reverse occurs. Energy within this central core region falls, allowing hydrogen-bonds to reform, and (alternate) base-pairs to partially restack. Isoenergetic breather-motions such as these can facilitate the intercalation of drugs and dyes into DNA and allow tritium exchange to occur at temperatures well below the melting temperature.

Beta-DNA is a structural form that differs from either B- or A-DNA. Evidence for its existence comes from studies of intercalation by drugs and dyes into DNA and the binding of certain proteins to DNA. Although double-stranded, beta-DNA is unique in being both hyperflexible and metastable. Its hyperflexibility suggests it be a liquid-like phase, lying intermediate between the more rigid B- and A-forms and the melted single-stranded form. Both properties necessitate beta-DNA to be pinned by an intercalator or held by a protein in order to be studied in detail. The structure is composed of repeating units called beta-structural elements. These are a family of base-paired, dinucleotide structures, each possessing the same mixed sugar-puckering pattern (i.e., C3′ endo (3′–5′) C2′ endo) and having similar backbone conformational angles, but varying in the degree of base-unstacking. Lower energy forms contain base-pairs that are partially unstacked, while higher energy forms contain base-pairs completely unstacked.

Beta-DNA is an intermediate in DNA melting, lying on the minimal energy pathway connecting B-DNA with single-stranded melted DNA. Three distinctly different sources of nonlinearity appear as DNA chains unwind, and these determine the sequence of conformational changes that occur along this pathway.

The first two sources of nonlinearity stem from changes in the sugar-pucker conformations and base-pair stacking. These changes require small energies (ca. kT) and appear as part of the initial structural distortions accompanying DNA unwinding. Starting with B-DNA, the effect of unwinding DNA is to counterbalance this with an equal but opposite right-handed superhelical writhing to keep the linking invariant. This is achieved through a modulated beta-alternation in sugar-puckering along the chains, accompanied by the gradual partial unstacking of alternate base-pairs. The lowest energy beta-DNA structure emerges as an end result. Its metastability reflects the presence of additional energies in its structure that cause the partial unstacking of alternate base-pairs.

The third source of nonlinearity arises from the stretching and ultimate rupture of hydrogen bonds connecting base-pairs. At first, beta-DNA accommodates further unwinding through the gradual loss of superhelical writhing. This reflects the appearance of beta-structural elements having increasingly higher energy (these have base-pairs further unstacked and unwound). Eventually, however, a limit is reached and further unwinding begins to stretch hydrogen-bonds that connect the base-pairs. Continued unwinding results in the disruption of these hydrogen-bonds, and the appearance

Figure 1. Molecular structure of a B–B premelton.

Figure 2. Molecular structure of a B–A premelton.

of single-stranded DNA. This final sequence of conformational change defines the boundary that connects beta-DNA to single-stranded melted DNA.

Using nonlinear least-squares methods, it has been possible to form premelton structures within B-DNA and within A-DNA (i.e., B–B premeltons, and A–A premeltons), as well as hybrid structures that connect the two (i.e., B–A premeltons and A–B premeltons) (see Figures 1 and 2). Such hybrid premeltons are constructed by connecting the central beta-DNA core with either type of kink-antikink boundary. Importantly, B–B and A–A premeltons are nontopological, whereas B–A and A–B premeltons are topological.

The B to A structural phase transition can be understood in the following way. In the presence of suitable thermodynamic conditions, kink and antikink within premeltons in B-DNA structure begin to move apart to form larger and larger core regions, whose centers modulate into A–DNA structure. Eventually, B–A premeltons and A–B premeltons form, and these continue to move apart, leaving a growing A-DNA region within. Such a mechanism is reversible and illustrates how a bifurcation within the central core region of this low-energy kink-antikink bound state structure can give rise to the B- to A-DNA structural phase transition.

Bifurcations arising within premeltons having higher energy (containing longer beta-DNA core regions that undergo more vigorous breather-motions) can lead to the formation of two additional types of higher energy kink-antikink bound states in DNA. These are called "branch-migratons" and "dislocatons." Each gives rise to different types of chain-slippage events, called double- and single-strand branch-migration.

Branch-migratons arise from breathing events that cause DNA chains to come apart transiently, and to then snap back, at nucleotide base sequences having 2-fold symmetry. Weakly hydrogen-bonded hairpin-like structures initially form. These are lengthened by a series of kinetic steps in which hydrogen-bonds connecting base-pairs within dinucleotide elements in vertical stems are broken and simultaneously reformed in horizontal stems (or vice versa) in a concerted 2-fold symmetric process. This phenomenon is called "cruciform-extrusion." A branch-migraton contains four stems; each stem contains kink (or antikink) boundaries connecting beta-DNA core regions with surrounding B–DNA.

Dislocatons arise at repetitive base sequences, for example, in poly-d(G-A): poly-d(C-T). Again, these structures form as a result of particularly energetic breathing events that cause DNA chains to come apart, and to then "snap back," forming small single-stranded bubble-like protrusions on opposite chains. These protrusions can then move apart, leaving growing regions of beta-DNA in between. The centers of these regions modulate into kink and antikink boundaries, and these, in turn, continue to move apart leaving B-DNA. The net result is the appearance of pairs of dislocatons, each moving in opposite directions along DNA. Movement involves single-chain slippage and is remarkably similar to the mechanism underlying moving crystal lattice dislocations, hence, the term dislocaton.

The formation of these two different kinds of higher energy kink-antikink bound state structures is another example of bifurcations emanating within the centers of premeltons. The underlying source of nonlinearity that determines the path of the bifurcation is the breaking and reforming (after chain-slippage) of hydrogen bonds connecting dinucleotide base-pairs. The decision as to whether branch-migratons or dislocaton pairs form is determined by information coded in the nucleotide base-sequence. This information constitutes the bias.

The combined presence of torsional and writhing strain energies found in negatively superhelical circular

DNA increases the probability that branch-migratons and dislocatons form at the appropriate sequences. These energies are first used to form premeltons. They are next used to form dislocatons or branch-migratons, and to propagate chain-slippage events.

Although B- and A-DNA are right-handed double-helical structures, DNA molecules containing the alternating poly-d(G–C): poly-d(G–C) sequence can, under certain conditions, assume a left-handed double-helical conformation (i.e., in the presence of high salt and/or negative superhelicity). This structure, called Z-DNA, contains the dinucleotide (G–C) as the asymmetric unit, held together by base-pairs. Being a left-handed double-helical structure, Z-DNA contains sugar-phosphate backbone conformations radically different from either B- or A-DNA.

The B to Z transition is proposed to occur as a result of a bifurcation that takes place during the formation of the dislocaton. As before, DNA breathing within the premelton takes place, followed by chains snapping back to form pairs of single-stranded, bubble-like protrusions on opposite chains. As pairs of protrusions move apart, Z-DNA forms within. The molecular boundaries that allow the helix to "swing left," capitalize on the additional flexibility and length provided by the single-stranded DNA regions on opposite DNA chains. B to Z boundaries form simultaneously on both ends in a concerted two-fold symmetric process. This is a direct consequence of the nonlinearity that ties the process together. A prediction of the model is the appearance of single-stranded DNA regions juxtaposed to beta-DNA regions within each B–Z junction, which is supported by experimental evidence.

HENRY M. SOBELL

See also **Biomolecular solitons; DNA solitons; Domain walls; Sine-Gordon equation**

Further Reading

Banerjee, A. & Sobell, H.M. 1983. Presence of nonlinear excitations in DNA structure and their relationship to DNA premelting and to drug intercalation. *Journal of Biomolecular Structure and Dynamics*, 1: 253–262

Bond, P.J., Langridge, R., Jennette, K.W. & Lippard, S.J. 1975. X-ray fiber diffraction evidence for neighbor exclusion binding of a platinum metallointercalation reagent to DNA. *Proceedings of the National Academy of Sciences*, 72: 4825–4829

Crothers, D.M. 1968. Calculation of binding isotherms for heterogeneous polymers. *Biopolymers*, 6: 575–583

Jessee, B., Gargiulo, G., Razvi, F. & Worcel, A. 1982. Analogous cleavage of DNA by micrococcal nuclease and a 1,10-phenanthroline-cuprous complex. *Nucleic Acids Research*, 10: 5823–5834

Lerman, L.S. 1961. Structural considerations in the interaction of DNA and acridines. *Journal of Molecular Biology*, 3, 18–30

Pohl, F.M., Jovin, T.M., Baehr, W., & Holbrook, J.J. 1972. Ethidium bromide as a cooperative effector of a DNA structure. *Proceedings of the National Academy of Sciences*, 69: 3805–3809

Printz, M.P. & von Hippel, P. 1965. Hydrogen exchange studies of DNA structure. *Proceedings of the National Academy of Sciences*, 53: 363–367

Sobell, H.M. 1985. Kink–antikink bound states in DNA Structure. In *Biological Macromolecules and Assemblies*, vol. 2: *Nucleic Acids and Interactive Proteins*, edited by F.A. Jurnack & A. McPherson, New York: Wiley, pp. 172–232

Sobell, H.M. 1985. Actinomycin and DNA transcription. *Proceedings of the National Academy of Sciences*, 82: 5328–5331

Stasiak, A., DiCapua, E. & Koller, T. 1983. Unwinding of duplex DNA in complexes with recA protein. *Cold Spring Harbor Symposia on Quantitative Biology*, 47: 811–820

DNA SOLITONS

In the early 1970s, Alexander Davydov and his colleagues began studies of nonlinear conformational waves in α-helix proteins. Englander et al. (1980) extended these ideas to DNA, interpreting open states (also called bubbles or local unwound regions, evidenced in hydrogen exchange experiments) as solitary waves, which can be viewed as kink solutions of the sine-Gordon (SG) equation. To understand the relation between the SG equation and DNA, we begin with models of the structure and dynamics of DNA.

Tightly packed in the nuclei of living cells, DNA consists of two polynucleotide chains (Figure 1). The chemical structure of each chain consists of periodically repeating phosphate groups and sugar rings (shown by dark ribbons), and irregular nitrous bases (shown in gray). Sequences of four types of bases (adenine, thymine, guanine, and cytosine) occur in DNA, forming the genetic code. These two polynucleotide chains interact weakly through hydrogen bonds and wind around each other to produce the double helix.

The internal structure of DNA is rather flexible. Thermal collisions with molecules of the surrounding solution, action of radiation, and local interactions with proteins, drugs, or other ligands induce several types of internal motions. Among these are

- small-amplitude oscillations of individual atoms;
- rotational, transverse, and longitudinal displacements of the atomic groups (phosphate groups, sugars, and bases);
- motions of the double chain fragments, having several base pairs lengths;

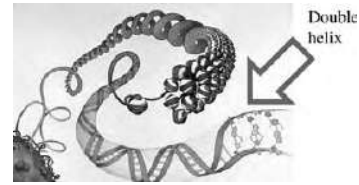

Figure 1. DNA molecule packing into the cell nucleus (courtesy of Nicolas Bouvier).

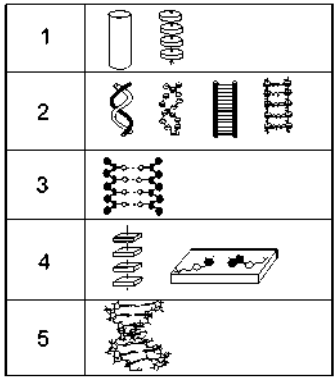

Figure 2. Hierarchy of models of DNA structure and dynamics.

- local unwinding of the double helix; and
- transitions of DNA fragments from one conformational form to another (e.g., from A- to B-form).

Thus, the DNA molecule is a complex dynamical system with many types of internal motions having different energies, velocities, amplitudes, frequencies, and lifetimes (McCammon & Harvey, 1987).

To describe the motions of DNA, different approximate models may be used, as indicated in Figure 2. The simplest model resembles a fragment of elastic thread (or rod), which ignores the internal structure. This model emerges naturally from microphotos where the DNA molecule does indeed resemble a thin elastic thread. Under this formulation only three coupled differential equations are needed: one for longitudinal displacements, another for angular displacements, and a third for transverse displacements. In Figure 2 a discrete analog of the model is placed nearby in the same row.

In the second row of Figure 2, a more complex model recognizes that DNA consists of two polynucleotide chains while ignoring the internal structure. Thus, the model has two weakly interacting elastic threads that wind around each other in a double helix. A mathematical formulation of this model requires six coupled differential equations—three for each of the two helices. The discrete version of the model and two simplified versions where the helical structure is neglected are shown nearby.

In the third row a more complex model is presented, taking into account that each of the polynucleotide chains comprises three types of atomic groups (phosphate groups, sugar rings, and nitrous bases) and representing solid-like motions of each of the atomic groups. Under this model, the required number of equations dramatically increases.

The model shown in the fourth row takes into account the internal motions of the atomic groups while neglecting variations of the base pairs (genetic code). Finally, the most accurate model is shown in the fifth line, which represents positions and motions of all atoms of the DNA molecule. The number of differential equations required to describe the motions in both of these models is inconveniently large at present levels of computer development.

To see the relation between DNA and the SG equation, apply the first model of the second row to study the opening of base pairs. The mathematical formulation of this model comprises six coupled differential equations that are nonlinear because base pair opening is a motion of large amplitude. Following Englander et al. (1980) we assume that rotational motions of bases around the sugar-phosphate chains make the greatest contribution to the process of opening, reducing the number of equations to two. Considering the rotational motions of bases in only one of the chains (accounting for the other chain as some averaged external field) reduces the number of equations from two to one.

To obtain the form of this single equation, an analogy between rotational motions of DNA bases and rotational motions of pendula in a mechanical model of the SG equation is convenient (*See* **Laboratory models of nonlinear waves**). Thus, the pendula of the mechanical model can be considered as analogs of DNA bases, the horizontal spring as an analog of one of the two sugar-phosphate chains, and the gravitational field as an averaged field formed by the second chain interacting with the first chain through hydrogen bonds. The analogy between these two dynamical systems suggests that the equation describing rotational motions bases in DNA should be an SG equation, with parameters defined as follows:

- I is the moment of inertia of bases.
- K is the coefficient of rigidity of the sugar-phosphate chain.
- V_0 is a potential function that represents interactions of bases through hydrogen bonds.
- R_0 is the radius of DNA.
- a is the distance between bases along the chains.

The variable of the equation is Ψ (the angle of rotations of bases around one of the two sugar-phosphate chains), and the equation itself is

$$I\frac{\partial^2}{\partial t^2}\Psi - KR_0^2a^2\frac{\partial^2}{\partial z^2}\Psi + V_0\sin\Psi = 0, \qquad (1)$$

where z indicates distance along the molecule. Kink solutions of this equation describe the opening of base pairs.

Another type of DNA soliton has been obtained by Peyrard & Bishop (1989), who studied melting and denaturation of DNA. Supposing that transverse (rather than rotational) motions of bases make the most contribution to the process, they reduced the number of equations from six to two, and after a simple linear

transformation, they obtained two independent equations describing transverse displacements in phase and out of phase. The first of the equations was nonlinear and its solitary wave solutions were interpreted as bubbles appearing in the DNA structure as temperature was increased.

Solitary wave solutions obtained by Englander et al. (1980) and by Peyrard and Bishop (1989) were improved later by investigators who considered other types of internal motions and their interactions, effects of dissipation and inhomogeneity, and interactions with surroundings. These refinements led to additional solitary wave solutions that have been used to interpret experimental data on hydrogen-tritium exchange, resonant microwave absorption, and neutron scattering by DNA. Such studies help us to understand transitions between different DNA forms, long-range effects, regulation of transcription, DNA denaturation, protein synthesis (e.g., insulin production), and carcinogenesis (Scott, 1985; Gaeta et al., 1994; Yakushevich, 1998).

LUDMILA YAKUSHEVICH

See also **Biomolecular solitons; Davydov soliton; DNA premelting; Laboratory models of nonlinear waves; Sine-Gordon equation**

Further Reading

Davydov, A.S. & Kislukha, N.I. 1973. Solitary excitations in one-dimensional chains. *Physica Status Solidi* B, 59: 465–470

Davydov, A.S. & Suprun, A.D. 1974. Configurational changes and optical properties of alpha-helical proteins. *Ukrainian Physical Journal*, 19: 44–50

Englander, S.W., Kallenbach, N.R., Heeger, A.J., Krumhansl, J.A. & Litwin, A. 1980. Nature of the open state in long polynucleotide double helices: possibility of soliton excitations. *Proceedings of the National Academy of Sciences (USA)*, 77: 7222–7226

Gaeta, G., Reiss, C., Peyrard, M. & Dauxois, T. 1994. Simple models of nonlinear DNA dynamics. *Rivista del Nuovo Cimento*, 17: 1–48

McCammon, J.A. & Harvey, S.C. 1987. *Dynamics of Proteins and Nucleic Acids*. Cambridge: Cambridge University Press

Peyrard, M. (editor). 1995. *Nonlinear Excitations in Biomolecules*, Berlin and New York: Springer

Peyrard, M. & Bishop, A.R. 1989. Statistical mechanics of a nonlinear model for DNA denaturation. *Physical Review Letters*, 62: 2755–2758

Scott, A.C. 1969. A nonlinear Klein–Gordon equation. *American Journal of Physics*, 37: 52–61

Scott, A.C. 1985. Solitons in biological molecules. *Comments on Molecular and Cellular. Biophysics*, 3: 5–57

Yakushevich, L.V. 1998. *Nonlinear Physics of DNA*, Chichester and New York: Wiley

DOMAIN WALLS

In ferromagnetic materials, small regions of correlated magnetic moments formed below the critical temperature are called domains. Domain walls are two-dimensional structures that separate distinct domains of order and form spontaneously when a discrete symmetry (such as time-reversal symmetry in magnets) is broken at a phase transition. With each subdivision of a substance into distinct domains, there is a decrease in the bulk energy because the order parameter value inside each domain minimizes its free energy. However, there is a simultaneous increase in the energy of interaction between differently aligned domains giving rise to an extra surface energy at the boundaries between neighboring domains. Consequently, this competition leads to an average domain size that gives the lowest overall free energy in a material sample, which is quantified below.

The energy of a ferromagnetic domain wall is calculated as arising from the exchange interactions between spins augmented by the anisotropy energy, while the exchange energy for N spins of magnitude S comprising a domain wall varies as

$$E_{\text{exch}} = \frac{\pi^2 J S^2}{N}, \tag{1}$$

where J is the exchange constant and the anisotropy energy is

$$E_{\text{anis}} = K N a^3, \tag{2}$$

where a is the lattice constant and K the anisotropy constant. Minimizing the sum with respect to N yields

$$N = \sqrt{\frac{\pi^2 J S^2}{K a^3}} \tag{3}$$

giving the domain width as $\Delta = Na$.

A Bloch domain wall is a region separating two (magnetic) domains within which magnetization changes gradually by rotating in the plane perpendicular to the line along the direction from one domain to the next. This way the magnetization direction experiences a reversal by 180° without changing its magnitude. The energy associated with a domain wall decreases with the width of the wall, and domain wall thickness is found as a minimization problem involving the anisotropy energy. A Neel domain wall, on the other hand, involves magnetization reversal in the plane perpendicular to the boundary between two domains.

Domains undergo reorganization under the effects of applied fields and can move in space. This occurs especially in the initial phase of remagnetization favoring those domains that are aligned with it and thus setting their boundary in motion to occupy more space, and it is followed by reorientation of the magnetization within each domain that is not aligned with the field.

Domain walls also exist in other systems, including crystals, ferroelectrics, metals, alloys, liquid crystals, and so on. In annealing metals, for example, domain walls appear as the grain boundaries between two sharply different compositions. Generically, the underlying physical quantity is called the order

parameter and is specific for a given substance. (For the annealing metal it is a real field, while in superfluid helium it is a complex-valued field.) Over most of the sample, the order parameter has a constant magnitude, but the sign (when it is real) or the phase (when complex) is not fixed and can change from place to place. A real order parameter field may be positive in one region of space and negative in its neighborhood, the continuity of the field implies that it must cross the zero value on a surface between them. This transition region is a domain wall.

In all types of critical systems, domain walls arise due to the competition between the bulk part of the free energy, which in the Landau theory of phase transitions is a quartic polynomial in the order parameter ϕ, and the surface energy term, which is due to inhomogeneities and varies as the square of the order parameter gradient following Ginzburg. Minimizing this type of free energy functional

$$F = \int \left[A_2\phi^2 + A_4\phi^4 + D\left(\frac{\mathrm{d}\phi}{\mathrm{d}x}\right)^2 \right] \mathrm{d}x \quad (4)$$

leads to a stationary nonlinear Klein–Gordon (NLKG) equation for the order parameter as a function of the spatial variable

$$D\phi'' = A\phi + B\phi^3, \quad (5)$$

where $A = A_2$ and $B = 2A_4$. One of its stable solutions is proportional to $\phi_0 \tanh(x/\xi)$ where $\xi = \sqrt{-8D/A}$, which describes a smooth function that interpolates between the two homogeneous phases $\phi = \pm\sqrt{-A/B}$. For magnetization as an order parameter, this solution represents a magnetic domain wall (in one space dimension), and for ferroelectrics, where the order parameter is a polarization vector, this represents a ferroelectric domain wall. For crystals undergoing structural phase transitions, there can also be a kinetic energy term in the free energy functional leading to a standard form of the NLKG equation

$$-m\ddot{\phi} + D\phi'' = A\phi + B\phi^3. \quad (6)$$

This solution is a moving domain wall (or kink)

$$\phi = \phi_0 \tanh[(x - vt)/\xi] \quad (7)$$

as shown in Figure 1 (Krumhansl & Schrieffer, 1975).

Nonlinear traveling solitary waves have also been investigated in ferroelectrics where kinks representing domain walls were shown to carry an electric dipole flip (Benedek et al., 1987). Domain walls in ferroelectrics are typically several unit cells wide, while in ferromagnets their thickness is several hundred or even thousands of unit cells. This difference is due to the exchange interactions between spins that are much stronger than the dipole-dipole interactions in ferroelectric crystals.

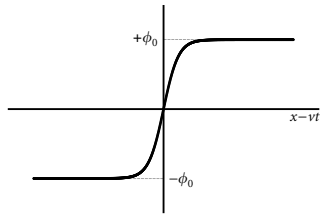

Figure 1. A typical form of a domain wall (or kink).

Geometry	Defect
Sheet-like	domain walls, membranes
Line-like	vortices, strings
Point-like	monopoles, hedgehogs

Table 1. Geometry of space and the corresponding topological defects.

There also exist cylindrical domains in magnets. As can be seen from Table 1, domain walls are examples of topological defects, and as such, they are very common in all broken-symmetry phenomena that take place slowly enough to allow for the generation of defects. Modern particle physics predicts that phase transitions occurred in the early universe following the Big Bang. Of particular interest to cosmology is the production of topological defects, which may be sheet-like, line-like, or point-like concentrations of energy.

JACK A. TUSZYŃSKI

See also **Critical phenomena; Ferromagnetism and ferroelectricity; Order parameters; Topological defects**

Further Reading

Anderson, P.W. 1984. *Basic Notions of Condensed Matter Physics*, Menlo Park, CA: Benjamin Cummings

Benedek, G., Bussmann-Holder, A. & Bilz, H. 1987. Nonlinear travelling waves in ferroelectrics. *Physical Review*, B36: 630–638

Kittel, C. 1996. *Introduction to Solid State Physics*, 7th edition, New York: Wiley

Krumhansl, J.A. & Schrieffer, J.R. 1975. Dynamics and statistical mechanics of a one-dimensional model Hamiltonian for structural phase transitions. *Physical Review*, B11: 3535–3545

White, R.H. & Geballe, T. 1979. *Long Range Order in Solids*, New York: Academic Press

DOPPLER SHIFT

The Doppler shift (or Doppler effect) is named after the Austrian scientist Christian Doppler, who in 1842 noticed that the observed frequency of waves from a source depends on how it is moving relative to the observer. In its simplest form, applicable to motions that are slow compared with the wave speed, it is quite easy

to visualize and understand. If a source of waves at some frequency f is approaching an observer, the frequency f' that the observer detects is higher than would be the case were the two at rest with respect to each other. From the point of the observer, he is "running into" the waves, while from the point of view of the source, the waves are being "bunched up." The opposite effect occurs when a source is moving away from an observer, and the general situation can be expressed as

$$\frac{f'}{f} = 1 + (v/c)\cos\theta, \tag{1}$$

where v is the relative speed, c the speed of the waves, and θ the angle between the wave propagation and the relative velocity. The $\cos\theta$ factor is simply a statement that the only important component of the relative velocity which can contribute to the shift is that along the direction of wave propagation. As long as v is small compared with the speed of light, this expression works well for most applications, and is quite appropriate to discuss the frequency shift of reflected radar signals used to detect speeding motorists (where c would be the speed of light) or the rise and fall in the pitch of a train whistle or an ambulance siren as it approaches and passes (in which case c would be the speed of sound).

One of the most famous experiments ever done to demonstrate the Doppler shift was done by the Dutch meteorologist Buys-Ballot who put a group of musicians on a train and then had them hold a constant note while racing past him as he stood on the platform.

The Doppler shift often appears more than once in a single application. For example, in police radar, electrons in the metal of an approaching car see a higher frequency radar signal than the police officer emits. They then re-emit radio waves at a higher frequency that is in turn seen at a still higher frequency by the officer being approached.

When speeds involved are very large, the effects of special relativity come into play. While it is possible to outrun a sound wave, the speed of light is the same no matter how the source moves. If we take c to be the speed of light and consider the Doppler shift for light (or any other electromagnetic wave), we have

$$\frac{f'}{f} = \frac{1 + (v/c)\cos\theta}{\sqrt{1 - v^2/c^2}}. \tag{2}$$

A good discussion of special relativity including the Doppler shift is that of Rindler (1991), and a particularly elegant geometric derivation of the formula under very general conditions can be found in Burke (1980). The additional term in the denominator of Equation (2) is due to time dilation whereby a moving clock appears to go more slowly than one at rest. In this case there is a Doppler shift even when $\cos\theta = 0$, which is referred to as the "transverse Doppler effect." One might imagine that it would be very difficult to detect, but in the special case where the sources are in random thermal motion, the leading $(v/c)\cos\theta$ term averages to zero and merely broadens spectral lines of atoms without actually shifting them. This "thermal Doppler effect" due to the transverse Doppler effect was measured by Pound and Rebka in 1960 using the Mössbauer effect. Interestingly, the nontransverse Doppler shift itself played an important role in that measurement.

The Doppler effect has numerous practical applications. In addition to its use already mentioned in measuring automobile velocities, these include Doppler radar for studying weather based on measuring the speeds of raindrops blown by wind (see, e.g., Doviak & Zrnic, 1993) and imaging moving tissues such as the heart in echocardiography, or measuring the speed of blood flow through an artery (see, e.g., Evans & McDicken, 2000).

The Doppler effect is also a valuable tool for pure science and has played a key role in many experiments upon which our present view of the world is based. Edwin Hubble used it to determine the velocities of distant objects in space from shifts in their spectral lines (shifted toward the red end of the spectrum, hence redshift), finding that distant objects seem to be moving away from us with speeds that increase with their distance (Christianson, 1995). This discovery is the basis of modern cosmology and is one of the strongest pieces of evidence that the universe had its origins in a Big Bang. The Doppler shift has also been used in delicate and beautiful experiments that demonstrate the time dilation effects of gravity. Both these gravitational effects on time and the relativistic effect in the transverse Doppler shift must be taken into account in order for the Global Positioning System (GPS) to function properly.

JOHN DAVID SWAIN

See also **Einstein equations; Gravitational waves**

Further Reading

Burke, W.L. 1980. *Spacetime, Geometry, Cosmology*, Mill Valley, CA: University Science Books

Christianson, G.E. 1995. *Edwin Hubble: Mariner of the Nebulae*, New York: Farrar Straus & Giroux

Doviak, R.J. & Zrnic, D.S. 1993. *Doppler Radar and Weather Observations*, New York: Academic Press

Evans, D.H. & McDicken, W.N. 2000. *Doppler Ultrasound: Physics, Instrumental, and Clinical Applications*, 2nd edition, New York: Wiley

Rindler, W. 1991. *Introduction to Special Relativity*, 2nd edition, Oxford and New York: Oxford University Press

DOUBLE-WELL POTENTIAL

See **Equilibrium**

DRESSING METHOD

The dressing method is a technique of constructing and solving nonlinear partial differential equations of

integrable models. It is based on dressing transformations that are symmetries of nonlinear partial differential equations and act on the Lax operators as gauge transformations on the connection (Zakharov & Shabat, 1974). Accordingly, the form of the linear spectral problem and the zero-curvature conditions are preserved.

The basic concept of the dressing method (Zakharov & Shabat, 1974) is that starting from known solutions of the underlying linear problem, one obtains new solutions of the transformed ("dressed") linear problem. Suppose Ψ_0 is a solution of the following linear problems:

$$\left(\frac{\partial}{\partial t_i} - E_i^{(0)}\right)\Psi_0\,(t_1, \ldots, t_n, \lambda) = 0, \quad i = 1, \ldots, n, \tag{1}$$

where $t_1, t_2, \ldots, t_n$ are independent flow variables and $E_i^{(0)}$ are complex $m \times m$ mutually commuting matrices that depend on the spectral parameter λ. The matrix Ψ_0 is referred to as a "bare" wave function and commuting operators $L_i^{(0)} = \partial/\partial t_i - E_i^{(0)}$ as "bare" Lax operators.

For the soliton equations in $1+1$ (one spatial and one time) dimensions, the dressing transformations are generated by the dressing matrices $\Theta_\pm$ which can be defined by the Riemann–Hilbert factorization problem (Zakharov & Shabat, 1974; Faddeev & Takhtajan, 1987). Given a Lie group of functions $g(\lambda)$ on the contour $\mathcal{C}$ in the complex plane, one finds a new (dressed) wave function through the factorization problem:

$$\Psi_0(t_1, \ldots, t_n, \lambda)g(\lambda)\Psi_0^{-1}(t_1, \ldots, t_n, \lambda) = \Theta_-^{-1}(t_1, \ldots, t_n, \lambda)\Theta_+(t_1, \ldots, t_n, \lambda), \tag{2}$$

where $\Theta_-^{-1} = (\Psi_0 g \Psi_0^{-1})_-$ and $\Theta_+ = (\Psi_0 g \Psi_0^{-1})_+$ have analytic continuation inside or outside the contour $\mathcal{C}$, respectively. The dressing transformation defines a new wave function $\Psi^{(g)} = \Theta_- \Psi_0 g = \Theta_+ \Psi_0$, which is a solution of new linear problems:

$$\left(\frac{\partial}{\partial t_i} - E_i\right)\Psi^{(g)}(t_1, \ldots, t_n, \lambda) = 0, \tag{3}$$

where

$$E_i = \frac{\partial \Theta_-}{\partial t_i}\Theta_-^{-1} + \Theta_- E_i^{(0)}\Theta_-^{-1} = \frac{\partial \Psi^{(g)}}{\partial t_i}(\Psi^{(g)})^{-1} \tag{4}$$

satisfy the compatibility conditions also known as zero-curvature conditions:

$$\frac{\partial E_j}{\partial t_i} - \frac{\partial E_i}{\partial t_j} - \left[E_i\,,\ E_j\right] = 0. \tag{5}$$

Comparing the expression for E_i from Equation (4) with $E_i^{(0)} = (\partial \Psi_0/\partial t_i)\Psi_0^{-1}$, following from Equation (1), one sees that the dressing transformations preserve the form of the Lax connections $L_i = \partial/\partial t_i - E_i$. A related approach also exists, which yields the dressing matrix in terms of the Fredholm type of integral operator entering the Gel'fand–Levitan–Marchenko equation (Zakharov & Shabat, 1974). Both dressing approaches are equivalent.

By considering two successive dressing transformations associated with two group elements g_1 and g_2, one naturally arrives at the concept of the group of the dressing transformations with $\Psi^{(g_1 g_2)} = (\Psi^{(g_1)})^{(g_2)}$. The general theory of dressing transformations and its group was developed by Semenov–Tian–Shansky (1985), who also introduced a Poisson bracket covariant under the dressing group action on the phase space of functions E_i. With such a bracket, the group of the dressing transformations induces on a phase space a Lie–Poisson action and turns out to be a symmetry of the phase space. Furthermore, it was observed that the group of the dressing transformations appears as a semi-classical limit of the quantum group symmetry of the two-dimensional integrable quantum field theories. Hence the group of the dressing transformations appears to be a classical precursor of the quantum group structure of an integrable field system in two dimensions (Babelon & Bernard, 1992). In many integrable models, the N-soliton solutions can be thought of as elements of the dressing group orbit of the vacuum state. Accordingly, successive dressing transformations can be used to build N-soliton solutions from the vacuum solution. In Babelon & Bernard (1993), the authors presented the construction of N-soliton solutions by dressing transformations in the sine-Gordon model. The dressing group also admits an elegant interpretation within the Kyoto school (Date et al., 1983) approach to the integrable models appearing in this context as a transformation group of the τ-function.

For equations in $2+1$ (two spatial and one time), dimensions, one applies the dressing technique based on a nonlocal Riemann–Hilbert problem for Kadomtsev–Petviashvili I and Davy–Stewartson I equations as well as the N-wave equations. The nonlocal (D-bar) $\bar\partial$ problem is required for the Kadomtsev-Petviashvili II and Davey–Stewartson II equations (Zakharov & Manakov, 1985).

The nonlocal (D-bar) $\bar\partial$-problem gives rise to the $\bar\partial$-dressing method in which an $N \times N$ quasi-analytical matrix function of $\lambda, \bar\lambda\ \chi(\lambda, \bar\lambda, x)\,, x \in \mathbb{C}^n$ satisfies the following nonlocal $\bar\partial$-problem:

$$\frac{\partial \chi(\lambda, \bar\lambda)}{\bar\lambda} = \hat{R}\chi = \int\int_C \mathrm{d}\lambda' \mathrm{d}\bar\lambda' \chi(\lambda', \bar\lambda') R(\lambda', \bar\lambda', \lambda, \bar\lambda), \tag{6}$$

with R being a kernel of a linear integral operator $\hat{R}$. The set of commuting differential operators defined in terms of commuting rational matrix functions I_i:

$$D_i\chi = \frac{\partial \chi}{\partial x_i} + \chi I_i(\lambda), \qquad i = 1, \ldots, n, \tag{7}$$

defines an integrable system. Let the integral linear operator $\hat{R}$ commute with all differential operators D_i, $[D_i, \hat{R}] = 0$. Then, the choice $I_1 = \lambda$, $I_2 = \lambda^2$, $I_3 = \lambda^3$ leads for $N = 1$ to the KP II equation: $(u_t + u_{xxx} + + 6uu_x)_x + 3u_{yy} = 0$ with $u = 2\partial\chi_1/\partial x_1$ where χ_1 is the term in an asymptotic expansion ($\lambda \to \infty$) of $\chi = 1 + \chi_1/\lambda + \chi_2/\lambda^2 + \ldots$.

HENRIK ARATYN

See also **Bäcklund transformations; Darboux transformation; Hirota's method; Inverse scattering method or transform; Multidimensional solitons; *N*-soliton formulas; Riemann–Hilbert problem**

Further Reading

Babelon, O. & Bernard, D. 1992. Dressing symmetries. *Communications in Mathematical Physics*, 149: 279–306

Babelon, O. & Bernard, D. 1993. Affine solitons: a relation between tau functions, dressing and Bäcklund transformations. *International Journal of Modern Physics A*, 8: 507–543

Date, E., Jimbo, M., Kashiwara, M. & Miwa, T. 1983. Transformation groups for soliton equations. In *Nonlinear Integrable Systems-Classical and Quantum Theory*, edited by M. Jimbo & T. Miwa. Singapore: World Scientific

Faddeev, L.D. & Takhtajan, L.A. 1987. *Hamiltonian Methods in the Theory of Solitons*, Berlin and Heidelberg: Springer

Semenov–Tian–Shansky, M.A. 1985. Dressing transformations and Poisson group actions, *Publications of Research Institute of Mathematical Sciences, Kyoto University*, 21: 1237–1260

Zakharov, V.E. & Manakov, S.V. 1985. Construction of multidimensional integrable non-linear systems and their solutions, *Functional Analysis and Applications*, 19 (N2): 11–25

Zakharov, V.E. & Shabat, A.B. 1974. A scheme for integrating the nonlinear equations of mathematical physics by the method of the inverse scattering problem. I. *Functional Analysis and Applications*, 8: 226–235

Zakharov, V.E. & Shabat, A.B. 1979. Integration of the nonlinear equations of mathematical physics by the method of the inverse scattering problem. II. *Functional Analysis and Applications*, 13: 166–174

DRIPPING FAUCET

A dripping faucet may easily be seen in everyday life. Its rhythm is sometimes regular but sometimes not, which sensitively depends on the flow of water. If the rhythm is irregular, one might blame it on noise due to unseen influences such as small air vibrations. However, it is nowadays well known that the irregularity arises from deterministic chaos instead of stochastic noise. In fact, this system is a good example showing that chaos is not only a mathematical product but also a phenomenon ubiquitous in the real world.

Chaotic dripping was originally suggested by Otto Rössler (Rössler, 1977) and the first experimental study was performed by Robert Shaw and his colleagues (Shaw, 1984; Martien et al., 1985). They measured the time interval (T_n) between the nth drip and its successor, and obtained a time series $\{T_1, T_2, \cdots\}$. To detect

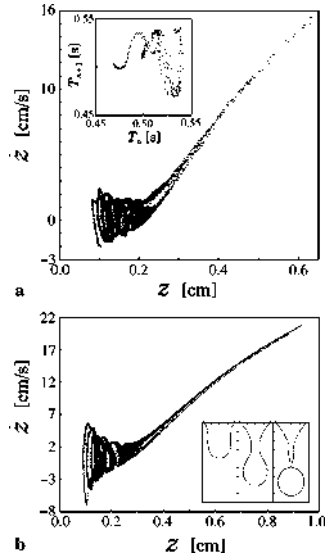

Figure 1. (a) An experimental strange attractor reconstructed from the observation of the oscillation, deformation, and breakup of drops hanging from a nozzle (7 mm inner diameter and 10 mm outer diameter). The projection of the orbit onto the plane $(z, \dot{z})$ is presented, where z is the center of mass and $\dot{z}$ is its velocity. The flow rate $Q = 0.24$ g/s (~ 2 drips/s on average). Inset of (a): return map of the dripping time interval (T_n). (b) Fluid dynamic simulation for 7 mm nozzle diameter. $Q = 0.32$ g/s. Inset of (b): drop deformation.

possible determinism from a nonperiodic time series, they made a return map (plot of (T_n, T_{n+1}) for each n). A return map for nonperiodic dripping is shown in the inset of Figure 1(a). If irregular numbers $T_1, T_2, \cdots$ were generated stochastically by throwing the dice, the plots would look like a set of random points with no particular structure. The observed map actually exhibited a clear structure, which implies a deterministic rule existing in the seemingly random outcomes.

As suggested by Rössler, the deterministic randomness, chaos is expected if two oscillating variables couple: (i) damped oscillation of the drop position (z, the center of mass) due to the surface tension of the water and (ii) relaxation oscillation of the mass of the drop (m) due to the filling-and-discharging process. A minimal model including these variables is the so-called mass-spring model described as

$$\frac{\mathrm{d}}{\mathrm{d}t}\left(m\frac{\mathrm{d}z}{\mathrm{d}t}\right) = -kz - \gamma\frac{\mathrm{d}z}{\mathrm{d}t} + mg, \qquad (1)$$

where g is the acceleration of gravity, k is the spring constant, and γ is the damping parameter. The mass

increases at a constant flow rate Q as

$$\frac{dm}{dt} = Q. \tag{2}$$

The model assumes that when the position z reaches a critical point, a part of the total mass (Δm) breaks away. Shaw used this model to explain the dripping dynamics as low-dimensional chaos.

Since then, dripping faucets have attracted many physicists, and a wide range of nonlinear behavior has been reported, such as strange attractor, period-doubling bifurcation, Hopf bifurcation, intermittency, hysteresis, crisis, and satellite drop formation. On the other hand, theoretical studies mainly rested on the mass-spring model, and any direct link between this simple model and the physics of drop formation was not known. The basic dynamics inherent in the complex behavior of the dripping faucet system was revealed quite recently, owing to detailed analyses of (i) experiments for a wide range of flow rates (Katsuyama & Nagata, 1999), (ii) fluid dynamic simulations using a new algorithm (Fuchikami et al., 1999), and (iii) the improved mass-spring model based on the fluid dynamic simulations (Kiyono & Fuchikami, 1999).

The fluid dynamic simulations clearly visualized how drops are formed and pinched off repeatedly (see figures in color plate section):

- The water under the faucet, increasing at a constant flow rate, forms a drop, which bulges until m reaches $\sim m_{\mathrm{crit}}$ (the maximum mass for the static stable state) and the surface tension is overwhelmed by the gravitational force.
- Then its sides begin to shrink, forming a rapidly narrowing neck (necking process) and the drop is soon pinched off (breakup). In the necking process, the drop undergoes almost free-fall.
- Because the water is stretched downward at the breakup moment, the surface tension works as a restoring force just after the breakup, which causes oscillation of the water. Thus the position z, the center of mass of the water, moves downward with up-and-down oscillation.
- After m reaches m_{crit} again, the necking followed by the breakup is repeated.
- The phase of oscillation at the onset of the necking process affects the breakup moment, the mass at that moment, and so the remnant mass ($m_{\mathrm{r}} = m - \Delta m$).
- If the phase changes periodically, the motion is periodic (for example, in the period-two motion T_1, T_2, T_1, T_2, $\cdots$, the phase changes as θ_1, θ_2, θ_1, θ_2, $\cdots$), while the phase is random in chaotic motion.

The essential information obtained from the fluid dynamic simulations is as follows:

(i) The state point of the water is well described in the limited phase space $(z, dz/dt, m)$, even if the water, an infinite-dimensional system, deforms its shape in a complex way. (Remember z denotes the center of mass.)

(ii) The instability of the shape of water induces the instability of the chaotic orbit. In other words, stretching of the chaotic attractor mainly occurs in the beginning of the necking process.

(iii) After the breakup, the renewed (i.e., remnant) mass realizes various values, while the renewed position and velocity are confined in a small region, well approximated as constants. Thus the attractor is compressed and becomes low dimensional.

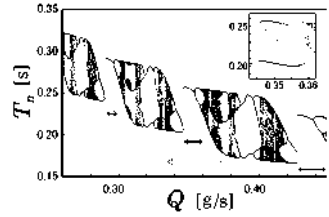

Figure 2. A section of the bifurcation diagram of the improved mass-spring model obtained by decreasing the control parameter Q, the flow rate. Hysteresis is observed in certain ranges of Q (indicated with $\leftrightarrow$). Inset: a hysteresis curve.

These features have also been confirmed experimentally. Figure 1 presents a recent experiment (a) and the corresponding fluid dynamic simulation result (b). The low-dimensional (almost one-dimensional) pattern of the return map (inset of (a)) suggests that the system can be described by a low-dimensional dynamical system. The experimental trajectory in the phase space $(z, dz/dt, m)$ was reconstructed from the continuous change of the drop shape observed. The spiral orbit indicates that the drop oscillates several times and then makes free-fall in the necking process before breakup. The drop shape obtained from the simulation (inset of (b)) is very close to the experimental result.

The observation of the drop formation process made it possible to improve the traditional mass-spring model by taking account of several points ignored so far, which include

- the mass dependence of the spring constant: $k = k(m)$;
- the necking process by setting $k = 0$ for $m > m_{\mathrm{crit}}$; and
- the mass dependence of the remnant mass: $m_{\mathrm{r}} = m_{\mathrm{r}}(m)$, where m is the mass just before the breakup.

Bifurcation diagrams (plot of T_n versus Q) obtained from the improved mass-spring model reproduce the global structure of experimental bifurcation diagrams for a wide range of flow rates, Q. As seen in Figure 2,

one distinct feature is a repetition of similar "units." The neighboring units are very similar but gradually become complex as Q is increased. Each unit is characterized by an integer that is the number of oscillations of each drop before breakup. This number decreases with increasing Q because the drop mass reaches the critical value sooner. In Figure 2, for example, there are three units and the corresponding numbers are 6, 5, 4 from left to right. Units in a range of relatively large Q include various types of bifurcations, such as period-doubling cascade to chaos, intermittency, and hysteresis (inset of Figure 2), while units in a range of sufficiently small Q include just period one motion. The bifurcation diagrams for small faucet diameters also exhibit a relatively simple structure.

The improved mass-spring model systematically explains the characteristic complexities of low-dimensional chaos (Ott, 1993) inherent in dripping dynamics. However, the model can be applied only when Q is small enough so that drops are clearly separated from each other. For larger flow rates, experimental results are so complex that approximations used in the fluid dynamic simulations do not work. New theoretical approaches are required, especially to interpret Hopf bifurcation and statistical features of satellite drops.

NOBUKO FUCHIKAMI AND KEN KIYONO

See also **Bifurcations; Chaotic dynamics**

Further Reading

Fuchikami, N., Ishioka, S. & Kiyono, K. 1999. Simulation of a dripping faucet. *Journal of the Physical Society of Japan*, 68: 1185–1196

Katsuyama, T. & Nagata, K. 1999. Behavior of the dripping faucet over a wide range of the flow rate. *Journal of the Physical Society of Japan*, 68: 396–400

Kiyono, K. & Fuchikami, N. 1999. Dripping faucet dynamics by an improved mass-spring model. *Journal of the Physical Society of Japan*, 68: 3259–3270

Kiyono, K., Katsuyama, T., Masunaga, T. & Fuchikami, N. 2003. Picture of the low-dimensional structure in chaotic dripping faucets. *Physics Letters* A, 320: 47–52

Martien, P., Pope, S.C., Scott, P.L. & Shaw, R.S. 1985. The chaotic behavior of the leaky faucet. *Physics Letters* A, 110: 399–404

Ott, E. 1993. *Chaos in Dynamical Systems*, Cambridge and New York: Cambridge University Press

Rössler, O.E. 1977. Chemical turbulence. In *Synergetics: Proceedings of the International Workshop on Synergetics at Schloss Elmau, Bavaria*, edited by Hermann Haken, Berlin: Springer, 174–183

Shaw, R. 1984. *Dripping Faucet as a Model Chaotic System*, Santa Cruz: Aerial Press

DRUDE MODEL

In 1900, Paul Drude developed his theory of metallic conduction of electricity, following the discovery of the electron by Joseph John Thomson in 1897. Applying the kinetic theory of gases to a metal, considered as a gas of electrons, he made the following assumptions:

(i) Each electron moves according to Newton's law of motion in the presence of external fields until it collides with other electrons or ions. Between collisions, interactions with both the other electrons and with the ions are neglected.
(ii) Collisions are instantaneous events that abruptly alter the velocity of an electron. The probability per unit time that an electron experiences a collision is given by $1/\tau$, where τ is called the collision time, mean free time, or relaxation time.
(iii) Electrons are assumed to achieve thermal equilibrium with their surroundings only through collisions. After each collision, the electron emerges with a randomly directed velocity whose magnitude is given by the temperature.

Note that in contrast to a classical gas of neutral molecules, the electrons move against a background of positively charged immobile ions.

The Drude model considers an average electron representative for the whole ensemble. Newton's equation of motion is

$$m\frac{\mathrm{d}^2}{\mathrm{d}t^2}\boldsymbol{r} + \frac{m}{\tau}\frac{\mathrm{d}}{\mathrm{d}t}\boldsymbol{r} = -e\boldsymbol{E}, \tag{1}$$

where $\boldsymbol{r}$ is the spatial drift coordinate (excluding the random thermal motion), m is the effective mass of the electron, $e > 0$ is the electron charge, and $\boldsymbol{E}$ is the applied electric field. The second term is a friction term arising from collisions. This equation can be rewritten in terms of the electron momentum $\boldsymbol{p} = m\boldsymbol{v} = m\mathrm{d}\boldsymbol{r}/\mathrm{d}t$, where $\boldsymbol{v}$ is the drift velocity,

$$\frac{\mathrm{d}}{\mathrm{d}t}\boldsymbol{p} + \frac{\boldsymbol{p}}{\tau} = -e\boldsymbol{E}\,. \tag{2}$$

In the overdamped case the momentum induced by the electric field is given by

$$\boldsymbol{p} = -e\tau\boldsymbol{E}\,. \tag{3}$$

The current density is obtained by multiplying the drift velocity of the mean electron by the electron charge and by the density per unit volume n of all electrons

$$\boldsymbol{j} = -en\boldsymbol{v} = en\frac{e}{m}\tau\boldsymbol{E} = en\mu\boldsymbol{E}\,, \tag{4}$$

where the drift mobility $\mu = (e/m)\tau$ has been introduced. This is Ohm's law, with constant conductivity $\sigma = en\mu$.

The classical Drude model neglects electron-electron interactions, heating of the electrons, non-equilibrium dynamics, and quantum transport effects, and is thus restricted to low fields, moderate carrier densities and temperature ranges. If any of these

conditions are violated, nonlinear and non-Ohmic conduction arises. Such effects are abundant in metals and semiconductors and may lead to instabilities and bifurcations of self-sustained oscillations or self-organized spatiotemporal patterns (Shaw et al., 1992, Schöll, 2001).

In the simplest case, a local, instantaneous conductivity $\sigma = en\mu$ still exists, but n or μ depends upon the field E (generation-recombination or drift instability, respectively), leading to a nonlinear or even nonmonotonic current density-field relation $j = en(E)\mu(E)E$, possibly with a range of negative differential conductivity (NDC), where $\mathrm{d}j/\mathrm{d}E = en\mu + e(\mathrm{d}n/\mathrm{d}E)\mu(E)E + en(\mathrm{d}\mu/\mathrm{d}E)E < 0$.

In an extension of the simple Drude picture, those nonlinearities may be due to a dependence of the momentum relaxation time upon the field (drift instability) or upon the electron temperature that, in turn, depends upon E (electron overheating instability, as a result of changes in the dissipation of energy and momentum). They may also be due to dependence of the carrier density upon field (generation-recombination instability, as in avalanche breakdown). More complex situations arise if the (semi)conductor consists of several layers of different materials, and intrinsic inhomogeneities render the notion of a local conductivity inappropriate. In particular, this applies to low-dimensional nanoscale structures (Ferry & Goodnick, 1997) or mesoscopic conductors (Datta, 1995), where the characteristic length scales may be such that the device dimension becomes smaller than the mean free path, the quantum mechanical phase relaxation length, and the de Broglie wavelength of the electron. Then various nonlinear transport regimes occur, where ballistic or non-equilibrium or coherent quantum effects dominate.

ECKEHARD SCHÖLL

See also **Avalanche breakdown; Diodes; Semiconductor oscillators**

Further Reading

Ashcroft, N.W. & Mermin, N.D. 1976. *Solid State Physics*, Philadelphia: Saunders College

Datta, S. 1995. *Electronic Transport in Mesoscopic Systems*, Cambridge and New York: Cambridge University Press

Drude, P. 1900. Zur Elektronentheorie der Metalle. *Annalen der Physik*, 1: 566–613

Ferry, D.K. & Goodnick, S.M. 1997. *Transport in Nanostructures*, Cambridge and New York: Cambridge University Press

Schöll, E. 2001. *Nonlinear Spatio-temporal Dynamics and Chaos in Semiconductors*, Cambridge: Cambridge University Press

Schöll, E. (editor). 1998. *Theory of Transport Properties of Semiconductor Nanostructures*, London: Chapman & Hall

Shaw, M.P., Mitin, V.V., Schöll, E. & Grubin, H.L. 1992. *The Physics of Instabilities in Solid State Electron Devices*, New York: Plenum Press

DUFFING EQUATION

Serious studies of forced nonlinear oscillators appeared early in the 20th century when Georg Duffing (1918) examined mechanical systems with nonlinear restoring forces and Balthasar van der Pol studied electrical systems with nonlinear damping. Subsequently, any equation of the form

$$a\ddot{x} + b\dot{x} + f(x) = F\sin\omega t \tag{1}$$

was called Duffing's equation, the nonlinearity often being polynomial, usually cubic (Hayashi, 1964). Here, $\dot{x}$ represents the time derivative $\mathrm{d}x/\mathrm{d}t$.

Linear resonance has $f(x) = cx$ $(c > 0)$, and Duffing's extension models many mechanical and electrical phenomena. With symmetry, f is odd, giving the first nonlinear approximation

$$f(x) = cx + dx^3. \tag{2}$$

If $d > 0$, the system is *hardening* and the resonant peak tilts to the right. A *softening* system $(d < 0)$ has a peak tilted to the left (as in Figure 2). Duffing's method of successive approximation and a variety of averaging and perturbation techniques can estimate these tilts for conditions of weak nonlinearity.

Twin-Well Duffing Oscillator

Taking Equations (1) and (2) with $c < 0$, $d > 0$ gives the "twin-well" Duffing oscillator governed by the potential energy $V(x) = \frac{1}{2}cx^2 + \frac{1}{4}dx^4$. Trajectories lie in and across the two symmetric potential wells separated by the hill-top at $x = 0$. This is a useful archetypal model for studies of chaos (Guckenheimer & Holmes, 1983). The undamped, unforced system $(b = F = 0)$ has two symmetrically placed orbits that (in infinite time) leave and return to the phase-space saddle at $x = 0$, $\dot{x} = 0$: we say they are "homoclinic to the saddle." For small b and F the corresponding invariant manifolds exhibit a homoclinic tangency on an arc in the (b, F) control space. Beyond this global bifurcation a homoclinic tangle generates "horseshoe dynamics" giving chaos and fractal basin boundaries (see Figure 3). The (b, F) arc can be estimated by Mel'nikov perturbation analysis.

Ueda's Chaos

For hardening with $c = 0$, Ueda (1980, 1992) mapped intricate regimes of subharmonics and chaos. Ueda's equation is

$$\ddot{x} + k\dot{x} + x^3 = B\cos t. \tag{3}$$

With $k = 0.05$, $B = 7.5$, all solutions settle onto a unique chaotic attractor, irrespective of $x(0), \dot{x}(0)$: its basin of attraction is the whole starting plane.

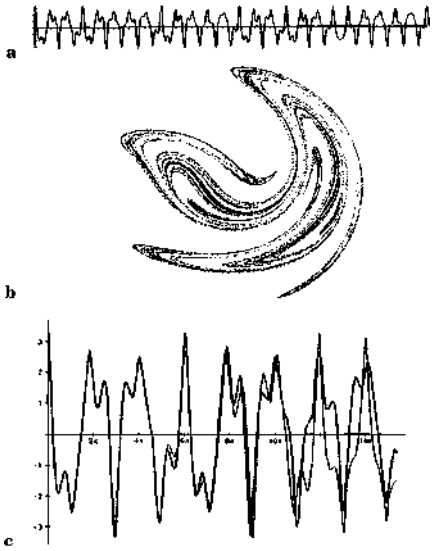

Figure 1. Waveform (a) shows a plot of $x(t)$ at the end of a long computer time integration during which any start-up transient is effectively dissipated, while the large fractal dot diagram (b) shows this chaotic attractor in a Poincaré section sampling $x(t)$ and $\dot{x}(t)$ stroboscopically at the period of the forcing. Two waveforms in (c) show the exponential divergence from two adjacent starts on the attractor where $(x(0), \dot{x}(0))$ are $(3, 4)$ and $(3.01, 4.01)$, respectively. Reproduced from Thompson & Stewart (2002) with the permission of John Wiley.

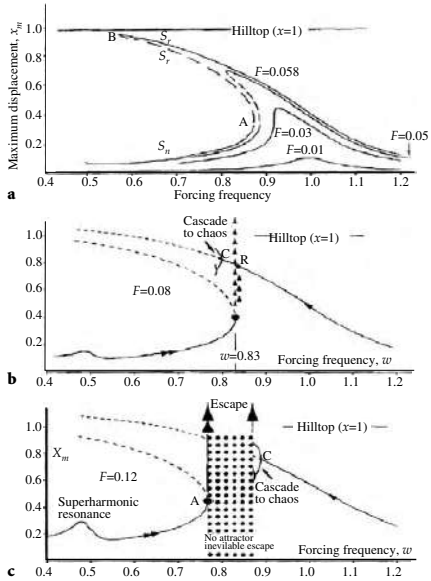

Figure 2. Three resonance response diagrams for Equation (4), where the maximum of the steady-state response, x_m, is plotted against the forcing frequency, ω, for fixed values of F (all with $\beta = 0.1$). At higher F, in (c), there is a regime with no attractor, implying inevitable escape from either fold A or the chaotic crisis ending the cascade from C. Reproduced from Thompson & Stewart (2002) with the permission of John Wiley.

The steady chaotic response is shown in Figure 1. In each cycle, sheets of trajectories are folded and compressed, as in making flaky pastry. This mixing produces divergence (Figure 1(c)) that quickly makes adjacent motions totally uncorrelated, although both remain on the fractal attractor. This divergence serves to identify chaos: it is quantified by Lyapunov exponent techniques (Guckenheimer & Holmes, 1983).

Escape from a Potential Well

Asymmetric models were used by Hermann Helmholtz to model vibrations in the human ear. An archetypal example introduced by Thompson (1989) is

$$\ddot{x} + \beta\dot{x} + x - x^2 = F\sin\omega t. \tag{4}$$

This Helmholtz–Thompson equation governs escape from the well,

$$V(x) = \tfrac{1}{2}x^2 - \tfrac{1}{3}x^3. \tag{5}$$

Such escape is a universal problem in science, from activation energies of molecular dynamics to the gravitational collapse of massive stars. Failures in electrical systems are triggered when the underlying system escapes from a well: if power generators slip out of synchronization, an entire city can be blacked out. Naval research (Thompson, 1997) is directed toward the capsizing of vessels under sinusoidal forcing by ocean waves.

Equation (4) is used by Thompson & Stewart (2002) to illustrate a variety of complex phenomena including chaos, fractal boundaries, and indeterminacies. These arise in a wide class of systems involving nonlinear damping, different well shapes, different direct and parametric forcing, and hardening characteristics. They are not detected by perturbation and averaging methods.

Chaos in Nonlinear Resonance

Three response diagrams for Equation (4) are shown in Figure 2. The quadratic form of the restoring force is technically *softening* for $x > 0$ and *hardening* for $x < 0$, but its overall effect is *softening*. Thus in 2(a), the peaks tilt to the left, as for a cubic Duffing oscillator with

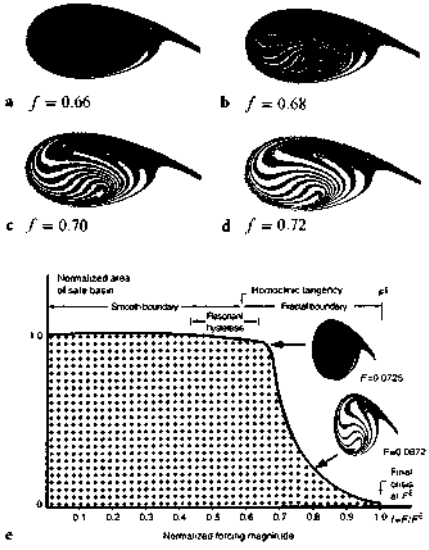

Figure 3. In the space of the coordinates $x(0), \dot{x}(0)$, the four safe basins of attraction, (a)–(d), comprise all those starts that do not give escape: we see how they vary with f, the basin being dramatically eroded by fractal fingers at $f \approx 0.68$. This basin erosion is quantified in (e) by plotting the area of the safe basin against f to give an integrity diagram. Reproduced from Thompson & Stewart (2002) with the permission of John Wiley.

$d < 0$. At the low value of $F = 0.01$, where the small response is almost linear, the untilted peak lies over $\omega = 1$ (the natural frequency). At $F = 0.056$ we see the hysteresis response of a softening oscillator, with a jump to resonance at fold A as ω increases, and a jump from resonance at B as ω decreases. Between these *cyclic folds*, there are three steady periodic solutions with frequency ω: nonresonant attractor, $S_{\rm n}$; resonant attractor, $S_{\rm r}$; unstable saddle, $D_{\rm r}$.

In 2(b), the resonant branch loses stability in a period-doubling cascade to chaos, and the jump at A is indeterminate.

Fractal Boundaries, Indeterminate Bifurcations

Transient motions arise from different starting values of $x(0), \dot{x}(0)$, and Figure 3 shows how the safe basin of attraction varies with $f = F/F^{\rm E}$. Here $F^{\rm E}$ is the steady-state escape magnitude, at which a slowly evolving system would jump out of the well. The observed fractal structure is generated at a homoclinic tangency. The sudden drop in the integrity diagram at the "Dover cliff" can be used as a design criterion. An engineering system should not be operated at values of $f > 0.68$, even though there are still stable motions within the well up to $f = 1$ (Thompson & Stewart, 2002).

Fractal basin boundaries and their chaotic transients generate great complexities in all forms of Duffing's equation once the response is significantly nonlinear: they are a topic of active research (Stewart et al., 1995). An example is the indeterminate jump from fold A in Figure 2(b). Locally, this is a normal saddle-node fold, but it is located precisely on a fractal boundary. The outcome from such a "tangled saddle-node" is unpredictable (Thompson & Soliman, 1991). Depending sensitively on how A is approached, the jump may settle onto attractor R or escape out of the well; it may also settle onto a co-existing subharmonic motion.

MICHAEL THOMPSON

See also **Attractors; Chaotic dynamics; Damped-driven anharmonic oscillator; Mel'nikov method; Van der Pol equation**

Further Reading

Duffing, G. 1918. *Erzwungene Schwingungen bei Veränderlicher Eigenfrequenz*, Braunschweig: Vieweg

Guckenheimer, J. & Holmes, P. 1983. *Nonlinear Oscillations, Dynamical Systems and Bifurcations of Vector Fields*, New York: Springer

Hayashi, C. 1964. *Nonlinear Oscillations in Physical Systems*, Princeton, NJ: Princeton University Press

Stewart, H.B., Thompson, J.M.T., Ueda, Y. & Lansbury, A.N. 1995. Optimal escape from potential wells: patterns of regular and chaotic bifurcation. *Physica* D, 85: 259–295

Thompson, J.M.T. 1989. Chaotic phenomena triggering the escape from a potential well. *Proceedings of the Royal Society of London*, A, 421: 195–225

Thompson, J.M.T. 1997. Designing against capsize in beam seas: recent advances and new insights. *Applied Mechanics Reviews*, 50: 307–325

Thompson, J.M.T. & Soliman, M.S. 1991. Indeterminate jumps to resonance from a tangled saddle-node bifurcation. *Proceedings of the Royal Society of London*, A, 432: 101–111

Thompson, J.M.T. & Stewart, H.B. 2002. *Nonlinear Dynamics and Chaos*, 2nd edition, Chichester and New York: Wiley

Ueda, Y. 1980. Steady motions exhibited by Duffing's equation: a picture book of regular and chaotic motions. In *New Approaches to Nonlinear Problems in Dynamics*, edited by P.J. Holmes, Philadelphia: SIAM, pp. 311–322

Ueda, Y. 1992. *The Road to Chaos*, Santa Cruz: Aerial Press

DUNE FORMATION

Dunes are sand formations, found on land, that have heights ranging from 1 to 500 m and have been shaped by the wind. These topographical structures are found typically where large masses of sand have accumulated, which can be in the desert or along the beach; thus, one distinguishes desert dunes and coastal dunes. Dunes can be mobile or fixed. Fixed dunes are older and are either "fossilized," that is, transformed into a cohesive material, a precursor to sandstone, or fixed because of

Figure 1. Barchan dunes near Laâyoune, Morocco.

the vegetation or because the average wind over some period at their location is zero. Otherwise the sand moves if the winds are strong enough, which means typically stronger than $4\,\mathrm{ms}^{-1}$.

The beautiful landscapes (Figure 1; see also color plate section) formed by dunes are characterized by very gentle hills interrupted by sharp edges called brink lines, delimiting regions of steeper slope, called slip-faces, lying in the wind shadow. Depending on the amount of available sand and the variation of the wind direction, one distinguishes different typical dune morphologies that have been classified by geographers into over a hundred categories. The most well known are longitudinal, transverse, and barchan dunes. Barchans (from an Arabic word) are crescent-shaped mobile dunes that appear when the wind always comes from the same direction and there is not much sand present. Their movement ranges from 5 to 50 m per year and is inversely proportional to their height. If sufficient sand is available to cover all the surface, then transverse dunes appear (from the merger of many barchans). Longitudinal dunes, that is, along the direction of the wind, are observed when the wind periodically changes its direction over about 30°. Other famous dune types are star dunes, ergs, parabolic dunes, and draas.

The driving force for sand motion is the drag imposed by the wind on the grains at the surface. A given dune morphology can therefore be understood as an aerodynamic instability close to a mobile surface. A complete mathematical description of the problem therefore needs the equation of motion of the wind velocity field coupled with an equation of motion of the granular surface. The right formulation of these equations requires a good understanding of the transport mechanism of sand.

Three types of transport can be distinguished according to the size of a sand grain: creep, saltation (bouncing), and suspension. The only mechanism relevant for dune formation is saltation, which drags grains typically of 100–300 μm diameter. The mechanism of saltation, first described by Ralph Bagnold in his pioneering work (Bagnold, 1941), consists of grains, which once lifted out from their granular bed are accelerated by the wind and then impact against the surface, ejecting new grains. These grains are again accelerated and eject a further splash of grains, so that the number of grains flying above the surface increases exponentially until the total momentum transferred from the air to the grains saturates to its maximum capacity, and the wind can no longer pick up more sand from the dune. On dunes in the field, these saltating grains form a sheet of grains floating typically 5 cm above the surface. The wind typically is turbulent and has a logarithmic profile as a function of height, which (due to the presence of the grains) is strongly modified close to the surface. The height of the boundary layer is less than 1 cm. Using the techniques of Jackson & Hunt (1975), one can calculate the shear force of the wind at the surface in an approximate form and obtain reasonable agreement with measurements on dunes. The saturated flux of sand at the surface is a function of this shear stress and has been described by various phenomenological expressions, the first one given by Bagnold (1941) and subsequent ones by Lettau & Lettau (1969), and by Sørensen (1981). A full description also requires taking into account the transient length before (or after) reaching saturation. Together with mass conservation one can then close the system of equations, giving at the end a full set of equations of motions (Sauermann et al., 2001).

When the local slope exceeds a value of typically 35°, the angle of repose, the sand begins to slide in the form of avalanches giving a second mechanism of sand transport driven by gravity. The slip-faces all have this slope. The edges separating them from the purely wind-driven regions are just given by the brink lines. Over these regions the wind field develops recirculation eddies of velocities typically below the minimum threshold for grain motion. When the saturation length is less than the size of these low-velocity regions, the sand grains get trapped. This is the principal instability underlying dune morphology: the dunes become traps of sand for more sand. The typical saturation length of about 10 m also means that no dune below 1.5 m in height is stable under Earth's meteorological conditions; the dune is too short for the air to reach its saturation point, and the dune suffers erosion.

Dunes have been studied on all continents and their shape, sand flux, velocity, and granulometry have been presented in many publications. Several

books review the subject (Pye & Tsoar, 1990). For different morphologies one finds specific shapes and scaling laws, but systematic studies exist only for barchans. Sand fluxes are typically measured with traps, but a more sophisticated metrology (e.g., acoustic, optic) is evolving. The limitation factors are the fluctuations of the wind fields and the climate. In the arid regions of the world, in particular the poor countries in the Sahara, dune motion poses an important threat to housing, roads, and fields, and sand removal constitutes a significant economic factor in these countries. Many empirical techniques of dune fixing and dune destruction have been developed, mostly applied to coastal dunes, which are in fact disappearing in many places, sometimes damaging the fragile dune ecosystem.

H.J. HERRMANN

See also **Avalanches; Geomorphology and tectonics; Sandpile model**

Further Reading

Bagnold, R.A. 1941. *The Physics of Blown Sand and Desert Dunes*, London: Methuen

Hersen, P., Douady, S. & Andreotti, B. 2002. Relevant length scale of barchan dunes. *Physical Review Letters*. 89: 264301

Jackson, P. S. & Hunt, J.C.R. 1975. Turbulent wind flow over a low hill. *Quarterly Journal of the Royal Meteorological Society*, 101–929

Lettau, K. & Lettau, H. 1969. Bulk transport of sand by the barchans of the Pampa de La Joya in Southern Peru. Zeitschrift für Geomorphologie, N.F. 13(2): 182–195

Pye, K. & Tsoar, H. 1990. *Aeolian Sand and Sand Dunes*, London: Unwin Hyman

Sauermann, G., Kroy, K. & Herrmann, H.J. 2001. A continuum saltation model for sand dunes. *Physical Review* E, 64: 31305

Sørensen, M. 1991. An analytic model of wind-blown sand transport. *Acta Mechanica*, (Suppl.) 1: 67–81

DYM EQUATION

See **Solitons, types of**

DYNAMIC PATTERN FORMATION

See **Synergetics**

DYNAMIC SCALING FUNCTION

See **Routes to chaos**

DYNAMICAL SYSTEMS

A dynamical system is a time-dependent, multicomponent system of elements with local states determining a global state of the whole system. In a planetary system, for example, the state of the system at a certain time is the set of values that completely describe the system (the position and momentum of each planet). The states can also refer to moving molecules in a gas, excitation of neurons in a neural network, nutrition of organisms in an ecological system, supply and demand of economic markets, or behavior of social groups in human societies.

The dynamics of a system (the change of system states with time) is given by linear or nonlinear differential equations. In the case of nonlinearity, several feedback activities take place between the elements of the system: in the solar system, the movement of the Earth is determined by the gravitation not only of the Sun, but of all the other celestial bodies of the system, which attract each other gravitationally.

For deterministic processes (for example, movements in a planetary system), each future state is uniquely determined by the present state. A conservative (Hamiltonian) system such as an ideal pendulum is characterized by the reversibility of time direction and conservation of energy. Dissipative systems, for example, a real pendulum with friction, are irreversible. The time-dependent development of a system's state is geometrically represented by orbits (trajectories) in a state space or phase space, which is defined by the multidimensional vectors of the nonlinear system (*See* **Phase space**).

In addition to continuous processes, we can also consider discrete processes of changing states at certain points of time. Difference equations are important for modeling measured data at discrete points of time, which are chosen equidistant or defined by other measurement devices.

Random events (Brownian motion in a fluid, mutation in evolution) are represented by additional fluctuation terms. Classical stochastic processes, such as the billions of unknown molecular states in a fluid, are defined by time-dependent differential equations with distribution functions of probabilistic states. Stochastic nonlinear differential equations (such as Fokker–Planck equation, Master equation) are also used to model phase transitions of complex systems, including migration dynamics of populations, traffic dynamics, data dynamics in the Internet, among others.

In quantum systems, the dynamics of quantum states are determined by Schrödinger's equation. Although it is a deterministic differential equation of a wave function, its observables (position and momentum of a particle) depend on Heisenberg's uncertainty principle, which only allows probabilistic forecasts.

During the 17th–19th centuries, classical physics viewed the universe as a deterministic and conservative system. The astronomer and mathematician Pierre-Simon Laplace assumed that all future states of the universe could be computed or determined if all forces acting in nature and the initial states of all celestial bodies are known at one instant of time (Laplacian determinism). Laplace's assumption was correct for

linear and conservative dynamical systems such as a harmonic oscillator. However, at the end of the 19th century, Henri Poincaré discovered that celestial mechanics is not a completely computable system even if it is considered as a deterministic and conservative system. The mutual gravitational interactions of more than two celestial bodies (the many-body problem) correspond to nonlinear and non-integrable equations with instabilities and sometimes chaos (*See* ***N*-body problem**).

According to Laplacian determinism, similar causes effectively determine similar effects. Thus, in the phase space, trajectories starting close to each other also remain close to each other during time evolution. Dynamical systems with deterministic chaos exhibit an exponential dependence on initial conditions for bounded orbits: the separation of trajectories with close initial states increases exponentially. (The rate at which nearby orbits diverge from each other after small perturbations is measured by Lyapunov exponents.) Consequently, tiny deviations of initial states lead to exponentially increasing computational efforts for future data, limiting long-term prediction, although the dynamics is, in principle, uniquely determined.

The sensitivity of chaotic dynamics to small changes in initial conditions is known as the "butterfly effect": small and local causes (local perturbations of the weather, for example) can lead to unpredictable large and global effects in unstable states (*See* **Butterfly effect**). According to the famous KAM theorem of Andrei Kolmogorov, Vladimir Arnol'd, and Jürgen Moser, trajectories in the phase space of classical mechanics are neither completely regular nor completely irregular, but depend sensitively on the chosen initial conditions. Changes of states in a dynamical system that change the stability of solutions to its nonlinear equations are associated with bifurcations of orbits in the corresponding phase space (*See* **Bifurcations**).

Dynamical systems can be classified by the effects of their dynamics on a region of the phase space. A conservative system is defined by the fact that, during time evolution, the volume of a region remains constant, although its shape may be transformed. An attractor is a region of a phase space into which all trajectories departing from an adjacent region, the so-called basin of attraction, converge. There are different kinds of more or less complex attractors. Chaotic attractors are highly complex structures of nonperiodic orbits in a bounded region of the phase space between regular behavior and stochastic behavior or noise. Although high-dimensional dynamical systems (such as the stock market, the economy, and society) cannot be formulated in all detail, approximate models may provide qualitative insights into their complex behavior.

KLAUS MAINZER

See also **Chaotic dynamics; Determinism; Equations, nonlinear**

Further Reading

Abarbanel, H.D.I. 1996. *Analysis of Observed Chaotic Data*, New York: Springer

Abraham, R.H. & Shaw, C.D. 1992. *Dynamics: The Geometry of Behavior*, 2nd edition, Redwood City, CA: Addison-Wesley

Arnol'd, V.I. 1978. *Mathematical Methods of Classical Mechanics*, Berlin and New York: Springer

Guckenheimer, J. & Holmes, P. 1983. *Nonlinear Oscillations, Dynamical Systems, and Bifurcations of Vector Fields*, New York: Springer

Hirsch, M.W. & Smale, S. 1974. *Differential Equations, Dynamical Systems, and Linear Algebra*. New York: Academic Press

Kaplan, D. & Glass, L. 1995. *Understanding Nonlinear Dynamics*, New York: Springer

Mainzer, K. 2003. *Thinking in Complexity. The Computational Dynamics of Matter, Mind, and Mankind*, 4th edition, New York: Springer

Rand, D.A. & Young, L.S. (editors). 1981. *Dynamical Systems and Turbulence*, Berlin and New York: Springer

Shilnikov, L.P., Shilnikov, A.L., Turaev, D.V. & Chua, L.O. 2001. *Methods of Qualitative Theory of Nonlinear Dynamics*, Singapore: World Scientific

DYNAMICAL ZETA FUNCTIONS

See **Periodic orbit theory**

DYNAMOS, HOMOGENEOUS

Dynamos convert mechanical energy into electromagnetic energy, the most familiar example being the bicycle dynamo. Nearly all electricity consumed by mankind is generated by dynamos in power plants—electrochemical processes also generate electric power, for example, in batteries, but these play only a minor role. The simplest dynamo is the disk dynamo originally invented by Faraday and shown in Figure 1. A metal disk rotates about its axis with an angular velocity $\boldsymbol{\Omega} = \boldsymbol{k}\Omega$. When the disk is permeated by an initial magnetic field $\boldsymbol{B}_0$ parallel to the axis, an electromotive force is generated between the axis and rim of the disk,

$$U = \boldsymbol{\Omega} \cdot \int_{r_1}^{r_0} \boldsymbol{B}_0 \mathrm{d}r, \tag{1}$$

where r_1 and r_0 denote the radii of axis and disk. The electromotive force U can be used to drive an electric current J through the circuit indicated in Figure 1. Denoting by L and R the inductivity and the ohmic resistance of the circuit, we obtain for the current J

$$L\frac{\mathrm{d}J}{\mathrm{d}t} + RJ = U. \tag{2}$$

The current J flowing through the circuit is associated with a magnetic field $\boldsymbol{B}_1$, which may replace the initial field $\boldsymbol{B}_0$. The integral $2\pi \int_{r_1}^{r_0} \boldsymbol{k} \cdot \boldsymbol{B}_1 \mathrm{d}r/J$ describes

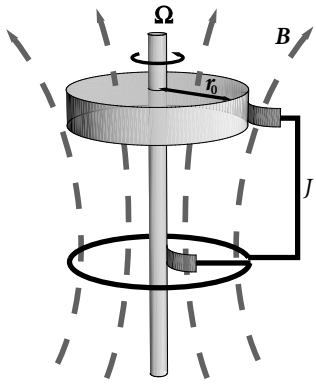

Figure 1. The disk dynamo.

the mutual inductivity M between circuit and disk. Equation (2) for the self-exited disk dynamo can thus be written in the form

$$L\frac{\mathrm{d}J}{\mathrm{d}t} = (\Omega M/2\pi - R)J, \tag{3}$$

which allows for exponentially growing solutions once the dynamo condition

$$\Omega > 2\pi R/M \tag{4}$$

is satisfied.

The disk dynamo is an inhomogeneous dynamo since it depends on an inhomogeneous distribution of electrical conductivity as given by the wiring of the circuit. The dynamo would not work if the sense of wiring around the axis would be opposite to that shown in the figure or if it would be short-circuited by immersion in a highly conducting fluid. While it is generally believed that planetary and stellar magnetic fields are generated by dynamos in the electrically conducting interiors of these celestial bodies, these dynamos must be homogeneous ones because they operate in singly connected finite domains of essentially homogeneous electrical conductivity. In 1919, Larmor first proposed this idea as an explanation for the magnetic field of sunspots. It was doubtful for a long time whether homogeneous dynamos were possible. Cowling proved in 1934 that axisymmetric fields could not be generated by a homogeneous dynamo. But, in 1958, Backus and Herzenberg independently demonstrated in a mathematically convincing way that homogeneous dynamos are indeed possible.

The velocity fields that are required to drive a homogeneous dynamo are necessarily more complex than the simple rotation velocity of the disk dynamo. A new mathematical discipline called dynamo theory has evolved and continues to be an active field of research. One distinguishes between the kinematic dynamo problem based on a linear equation such as (3) with a prescribed velocity field and the magnetohydrodynamic dynamo problem in which the influence of the growing magnetic field on the velocity field is taken into account. Obviously, a magnetic field cannot grow exponentially forever. Just as the Lorentz force produced by the magnetic field together with the current density in the disk opposes the rotation of the disk in Figure 1, it also changes the velocity field of the magnetohydrodynamic dynamo. The external torque T_e applied to the disk in the figure must be increased in the presence of dynamo action in order to sustain the rotation rate Ω. The equilibrium strength of the magnetic field will thus be determined by the available torque T_e.

In the case of the geodynamo driven by convection flows in the liquid iron core of the Earth, as well as in the case of other planetary or stellar dynamos, the equations of motions together with the equation of magnetic induction (*See* **Magnetohydrodynamics**) must be solved to determine the strength of the generated magnetic field as a function of the relevant parameters. Extensive computer simulations have been performed in recent years. Some examples can be found in Jones et al. (2003). The complex numerical simulations of magnetohydrodynamic dynamos share the following properties with the simple disk dynamo:

(i) For given external parameters, there always exists a solution without magnetic field besides the dynamo solution, just as the disk of Figure 1 can rotate with $\Omega > \Omega_c$ in the absence of any initial field $\boldsymbol{B}_0$.

(ii) The existence of a dynamo solution requires that the magnetic Reynolds number Rm exceeds a critical value Rm_c. Rm is defined by

$$Rm = V\mathrm{d}\sigma\mu, \tag{5}$$

where V is a typical velocity, d is a characteristic length such as the radius of the iron core in the case of the Earth, and σ and μ are the electrical conductivity and the magnetic permeability of the fluid. The inverse product $\lambda = 1/\sigma\mu$ is called the magnetic diffusivity. The dimensionless parameter Rm corresponds to the quantity $\Omega M/R$ in the case of the disk dynamo. The nonmagnetic solution exists, but it is unstable for $Rm > Rm_c$.

(iii) Magnetohydrodynamic dynamos exist in two forms that are identical except for the sign of the magnetic field $\boldsymbol{B}$. This property reflects the fact that the Lorentz force is given by an expression quadratic in $\boldsymbol{B}$.

Property (iii) is the basic reason that the geomagnetic field has often switched its polarity in the geologic past. These "reversals" have occurred nearly randomly about

every 200,000 years on average. In contrast, the solar magnetic field reverses every 11 years in a surprisingly periodic fashion.

For the description of magnetic fields associated with a spherical system, one often uses the general representation for a solenoidal vector field,

$$\boldsymbol{B} = \nabla \times (\nabla h \times \boldsymbol{r}) + \nabla g \times \boldsymbol{r}, \qquad (6)$$

in terms of a poloidal and a toroidal component each of which is described by a scalar function, the poloidal function h, and the toroidal function g. Without loss of generality, the averages of h and g over surfaces $|\boldsymbol{r}| =$ constant can be assumed to vanish. A homogeneous dynamo usually requires the interaction of both components of the magnetic field. It can be shown (Kaiser et al., 1994) that a magnetic field with vanishing toroidal part cannot be generated. It is also generally believed that a purely poloidal field cannot be generated either. But a proof of this hypothesis has not yet been given. The functions h and g can be separated into their axisymmetric parts $\bar{h}$ and $\bar{g}$ and non-axisymmetric parts, $\breve{h} = h - \bar{h}$ and $\breve{g} = g - \bar{g}$. The component $\bar{g}$ can easily be generated in a spherical dynamo through a stretching of the axisymmetric poloidal field by a differential rotation. This process is known as the ω-effect. The amplification of $\bar{h}$ requires the interaction of the non-axisymmetric components of magnetic fields and velocity fields. This is often called the α-effect. This latter effect can, of course, also be used for the generation of $\bar{g}$ in the absence of a differential rotation. Accordingly, one distinguishes between $\alpha\omega$- and α^2-dynamos. These concepts were originally introduced within the framework of mean-field magnetohydrodynamics for which the reader is referred to the book by Krause & Raedler (1980).

F.H. BUSSE

See also **Alfvén waves; Fluid dynamics; Magnetohydrodynamics; Nonlinear plasma waves**

Further Reading

Childress, S. & Gilbert, A.P. 1995. *Stretch, Twist, Fold: The Fast Dynamo*, Berlin and New York: Springer

Davidson, P.A. 2001. *An Introduction to Magnetohydrodynamics*, Cambridge and New York: Cambridge University Press

Jones, C.A., Soward, A.M. & Zhang, K. 2003. *Earth's Core and Lower Mantle*, London and New York: Taylor & Francis

Kaiser, R., Schmitt, B.J. & Busse, F.H. 1994. On the invisible dynamo. *Geophysical and Astrophysical Fluid Dynamics*, 77: 91–109

Krause, F. & Raedler, K.-H. 1980. *Mean-field Magnetohydrodynamics and Dynamo Theory*, Oxford and New York: Pergamon Press

Moffatt, H.K. 1978. *Magnetic Field Generation in Electrically Conducting Fluids*, Cambridge and New York: Cambridge University Press

E

EARTHQUAKES

See **Geomorphology and tectonics**

ECKHAUS INSTABILITY

See **Wave stability and instability**

ECONOMIC SYSTEM DYNAMICS

Economic dynamics is concerned with fluctuations in the economy. Most economic variables, such as gross domestic product (GDP), production, unemployment, interest rates, exchange rates, and stock prices, exhibit perpetual fluctuations over time. These fluctuations are characterized by sustained growth of production and employment as well as large oscillations in relative changes or growth rates. The fluctuations vary from fairly regular business cycles in macroeconomic variables to very irregular fluctuations, for example, in stock prices and exchange rates, in financial markets. In this note, we discuss some approaches to the theory of economic fluctuations, emphasizing the role of nonlinear dynamic models.

In contrast to many dynamic phenomena in natural sciences, uncertainty always plays a role in an economy, at least to some extent. Therefore, a purely deterministic model seems inappropriate to describe fluctuations in the economy, and a stochastic dynamic model is needed. Nevertheless, a key question in economic dynamics is whether a simple, nonlinear dynamic model can explain a *significant part* of observed economic fluctuations.

Brief History

There are two contrasting viewpoints concerning the explanation of observed economic fluctuations. According to the first (New Classical) viewpoint, the main source of fluctuations is to be found in exogenous, random shocks (news about economic fundamentals) to an inherently stable, often linear economic system. Without any external shocks to economic fundamentals (preferences, endowments, technology, etc.), the economy would be stable and converge to the unique steady-state (growth) path. According to the second, opposing (Keynesian) viewpoint, economic fluctuations are not caused by chance or random impulses, but should be explained by nonlinear economic laws of motion. Even without any external shocks to the fundamentals of the economy, fluctuations in prices or other economic variables may arise. It is an old Keynesian theme that fluctuations are not determined by economic fundamentals only, but are also driven by volatile, self-fulfilling expectations ("animal spirits," market psychology).

The view that business cycles are driven by external random shocks was propagated in the 1930s, for example, by Ragnar Frisch and Jan Tinbergen (sharing the first Nobel Prize in Economic Sciences in 1969 "for having developed and applied dynamic models for the analysis of economic processes"). They observed that simple, linear systems buffeted with noise can mimic time series similar to those observed in real business cycle data. To several economists this approach was unsatisfactory, however, because it does not provide an *economic* explanation of business cycles, but rather attributes them to external, random events. In the 1940s and 1950s Nicholas Kaldor, John Hicks, and Richard Goodwin developed nonlinear dynamic models with locally unstable steady states and stable limit cycles as an explanation for business cycles. These early nonlinear business cycle models, however, suffered from a number of serious shortcomings. First of all, the laws of motion were too "ad hoc," and in particular they were *not* derived from rational behavior, that is, from utility and profit maximizing principles. Secondly, the simulated time series from the models were too regular compared with observed business cycles, even when small dynamic noise was added to the models. Finally, expectation rules were "ad hoc," and along the regular cycles, agents made "systematic" forecasting errors.

The Role of Expectations

The most important difference between economics and natural sciences is perhaps the fact that an economic system is an *expectations feedback* system. Decisions

of economic agents are based upon their expectations and beliefs about the future state of the economy. Through these decisions, expectations feed back into the economy and affect actual realization of economic variables. These realizations lead to new expectations, in turn affecting new realizations, implying an infinite sequence of expectational feedback. For example, in the stock market, optimistic expectations that stock prices will rise will lead to a larger demand for stocks, which will cause stock prices to rise. This process may lead to a self-fulfilling speculative bubble in the stock market. A theory of expectation formation is, therefore, a crucial part of economics, in particular for modeling dynamic asset markets.

In the early business cycle models, simple, ad hoc expectations rules were employed, such as naive expectations (where the forecast of the economic variable is simply the latest observation of that variable) or adaptive expectations (where the forecast is a weighted average of the previous forecast and the latest observation). An important problem with simple forecasting rules is that typically agents make systematic forecasting errors, especially when there are regular cycles. A smart agent would learn from her mistakes and adapt her expectations rule accordingly. Another problem is that if an agent is to use a simple forecasting rule, it is far from clear which simple rule to choose in a particular model. With the development of empirical, econometric analysis of business cycles, it became clear that unrestricted models of expectations preclude a systematic inquiry into business fluctuations. These considerations led to the development of *rational expectations*, a solution to the expectations feedback system proposed by John Muth (1961) and applied to macroeconomics, for example, by Robert Lucas and Thomas Sargent. Rational expectations means that agents use all available information, including economic theory, to form optimal forecasts and that, on average, expectations coincide with realizations. In a deterministic model, without noise and randomness, rational expectations implies perfect foresight (no mistakes at all); in a stochastic model, rational expectations coincides with the conditional mathematical expectations given all available information (no mistakes on average, no systematic bias).

In the 1970s and 1980s, the rational expectations critique culminated in the development of New Classical economics and real business cycle models, based upon rational expectations, intertemporal utility and profit maximization, and perfectly competitive markets. This approach outdated the early Keynesian nonlinear business cycle models of the 1950s. Due to the discovery of deterministic chaos and other developments in nonlinear dynamics, however, the last two decades have witnessed a strong revival of interest in nonlinear endogenous business cycle models.

Nonlinear Dynamics

In mathematics and physics, things changed dramatically in the 1970s due to the discovery of deterministic chaos, the phenomenon that simple, deterministic laws of motion can generate unpredictable time series. This discovery shattered the Laplacian deterministic view of perfect predictability and made scientists realize that long-run prediction may be fundamentally impossible, even when laws of motion are known exactly. Inspired by "chaos theory," economists (e.g., Richard Day and Jean-Michel Grandmont) started looking for nonlinear, deterministic models generating erratic time series similar to the patterns observed in real business cycles. This search led to new, simple nonlinear business cycle models within the paradigm of rational expectations, optimizing behavior and perfectly competitive markets, generating chaotic business fluctuations.

In the 1980s, several economists (e.g., William Brock, Davis Dechert, Jose Scheinkman, and Blake LeBaron) also employed nonlinear methods, such as correlation dimension tests, from the natural sciences to look for evidence of nonlinearity and low deterministic chaos in economic and financial data. This turned out to be a difficult task because the methods employed require very long time series and the methods are very sensitive to noise. One can say that evidence for low-dimensional deterministic chaos in economic and financial data is weak (but it seems fair to add that because of the sensitivity to noise, the hypothesis of chaos buffeted with dynamic noise has not been rejected) but evidence for nonlinearity is strong. In particular, Brock, Dechert, and Scheinkman have developed a general test (the BDS-test), based upon ideas from U-statistics theory and correlation integrals, to test for nonlinearity in a given time series; see Brock et al. (1996) and Brock, Hsieh, & LeBaron (1991) for the basic theory, references, applications, and extensions. The BDS test has become widely used in economics and also in physics.

Bounded Rationality

Already in the 1950s, Herbert Simon pointed out that rationality requires unrealistically strong assumptions about the computing abilities of agents and proposed that *bounded rationality*, with limited computing capabilities and with agents using habitual rules of thumb instead of perfectly optimal decision rules, would be a more accurate description of human behavior. Nevertheless, as noted above, rational expectations became the dominating paradigm in dynamic economics in the 1970s and 1980s. Nonlinear dynamics, the possibility of chaos, and its implications for limited predictability shed important new light on the expectations hypothesis, however. In a simple (linear) stable economy with a unique steady-state path, it seems natural that

agents can learn to have rational expectations, at least in the long run. A representative, perfectly rational agent model nicely fits into a linear view of a globally stable and predictable economy. But how could agents have rational expectations or perfect foresight in a complex, nonlinear world, with prices and quantities moving irregularly on a strange attractor and sensitivity to initial conditions? A boundedly rational world view with agents using simple forecasting strategies, perhaps not perfect but at least approximately right, seems more appropriate for a complex nonlinear world. These developments contributed to a rapidly growing interest in bounded rationality in the 1990s (see, e.g., the survey in Sargent (1993)). A boundedly rational agent forms expectations based upon observable quantities and adapts her forecasting rule as additional observations become available. Adaptive learning may converge to a rational expectations equilibrium, or it may converge to an "approximate rational expectations equilibrium," where there is at least some degree of consistency between expectations and realizations (see, e.g., Evans & Honkapohja (2001) for an extensive and modern treatment of adaptive learning in macroeconomics).

Interacting Agents and Evolutionary Models

The representative agent model has played a key role in economics for a long time. An important motivation for the dominance of the rational agent model dates back to the 1950s, to Milton Friedman who argued that nonrational agents will be driven out of the market by rational agents, who will trade against them and simply earn higher profits. In recent years, however, this view has been challenged, and heterogeneous agent models are becoming increasingly popular, especially in financial market modeling (see, e.g., Kirman (1992) for a critique on representative agent modeling).

Many heterogeneous agent models are artificial, computer simulated markets. This work views the economy as a complex evolving system composed of many different, boundedly rational, interacting traders, with strategies, expectations and realizations co-evolving over time (see, e.g., work at the Santa Fe Institute collected in Anderson et al. (1988)). Two typical trader types arising in many heterogeneous agent financial market models are fundamentalists and chartist or technical traders. Fundamentalists base their investment decisions upon market fundamentals such as dividends, earnings, interest rates, or growth indicators. In contrast, technical traders pay no attention to economic fundamentals but look for regular patterns in past prices and base their investment decision upon simple trend following trading rules. An evolutionary competition between these different trader types, where traders tend to follow strategies that have performed well in the recent past, may lead to irregular switching between the different strategies and result in complicated, irregular asset price fluctuations. It has been shown, for example, by Brock and Hommes (1997, 1998), that in these evolutionary systems, rational agents and/or fundamental traders do not necessarily drive out all other trader types, but that the market may be characterized by perpetual evolutionary switching between competing trading strategies. Nonrational traders may survive evolutionary competition in the market (see, e.g., Hommes (2001) for a survey and many relevant references). Lux & Marchesi (1999) show that these types of interacting agent models are able to generate many of the stylized facts, such as unpredictable returns, clustered volatility, fat tails, and long memory, observed in real financial markets.

Future Perspective

A good feature of the rationality hypothesis is that it puts natural discipline on agents' forecasting rules and minimizes the number of free parameters in dynamic economic models. In contrast, the "wilderness of bounded rationality" leaves too many degrees of freedom in modeling, and it is far from clear which out of a large class of habitual rules of thumb is most reasonable. Stated differently in a popular phrase: "there is only one way (or perhaps a few ways) one can be right, but there are many ways one can be wrong." The philosophy underlying the evolutionary approach is to use simple forecasting rules based upon their performance in the recent past. In this type of modeling, "evolution decides who is right." Bounded rationality, heterogeneity, adaptive learning, and evolutionary competition all create natural nonlinearities. Nonlinearity is, therefore, likely to play an increasingly important role in the future of economic dynamics.

CARS HOMMES

See also **Dynamical systems; Forecasting; Game theory; Time series analysis**

Further Reading

Anderson, P.W., Arrow, K.J. & Pines, D. (editors). 1988. *The Economy as a Complex Evolving System*, Redwood City, CA: Addison-Wesley

Brock, W.A. Dechert, W.D., Scheinkman, J.A. & LeBaron, B. 1996. A test for independence based upon the correlation dimension. *Econometric Review*, 15: 197–235

Brock, W.A. & Hommes, C.H. 1997. A rational route to randomness. *Econometrica*, 65: 1059–1095

Brock, W.A. & Hommes, C.H. 1998. Heterogeneous beliefs and routes to chaos in a simple asset pricing model. *Journal of Economic Dynamics and Control*, 22: 1235–1274

Brock, W.A., Hsieh, D.A. & LeBaron, B. 1991. *Nonlinear Dynamics, Chaos and Instability: Statistical Theory and Economic Evidence*, Cambridge, MA: MIT Press

Day, R.H. 1996. *Complex Economic Systems*, Cambridge, MA: MIT Press

DeGrauwe, P., DeWachter, H. & Embrechts, M. 1993. *Exchange Rate Theory. Chaotic Models of Foreign Exchange Markets*, Oxford: Blackwell

Evans, G.W. & Honkapohja, S. 2001. *Learning in Macroeconomics*, Princeton, NJ: Princeton University Press
Friedman, M. 1953. The case of flexible exchange rates. In *Essays in Positive Economics*, Chicago: University of Chicago Press
Frisch, R. 1933. Propagation problems and impulse problems in dynamic economics. In *Economic essays in honor of Gustav Cassel*, London: George Allen and Unwin, Ltd; reprinted in *Readings in Business Cycles*, edited by R.A. Gordon and L.R. Klein, Homewook, IL: Richard D. Irwin, Inc, 1965
Gabisch, G. & Lorenz, H.W. 1987. *Business Cycle Theory. A Survey of Methods and Concepts*. Berlin: Springer
Goodwin, R.M. 1951. The nonlinear accelerator and the persistence of business cycles. *Econometrica*, 19: 1–17
Grandmont, J.M. 1985. On endogenous competitive business cycles. *Econometrica*, 53: 995–1045
Hicks, J.R. 1950. *A contribution to the theory of the trade cycle*. Oxford: Clarendon Press
Hommes, C.H. 2001. Financial markets as nonlinear adaptive evolutionary systems. *Quantitative Finance*, 1: 149–167
Kaldor, N. 1940. A model of the trade cycle. *Economic Journal*, 50: 78–92
Kirman, A. 1992. Whom or what does the representative individual represent? *Journal of Economic Perspectives*, 6: 117–136
Lorenz, H.W. 1993. *Nonlinear Dynamical Economics and Chaotic Motion*, 2nd edition, Berlin: Springer
Lucas, R.E. 1971. Econometric testing of the natural rate hypothesis. In *The Econometrics of Price Determination*, edited by O. Eckstein, Washington, DC: Board of Governors of the Federal Reserve System and Social Science Research Council
Lux, T. & Marchesi, M. 1999. Scaling and criticality in a stochastic multi-agent model of a financial market. *Nature*, 397: 498–500
Muth, J.F. 1961. Rational expectations and the theory of price movements. *Econometrica*, 29: 315–335
Sargent, T.J. 1993. *Bounded Rationality in Macroeconomics*, Oxford: Clarendon Press
Simon, H.A. 1957. *Models of Man*, New York: Wiley

EFFECTIVE MASS

Effective mass is a physical quantity characterizing the dynamics of a particle or quasiparticle with an energy ($\mathcal{E}$) that is quadratic in the components of the momentum ($\boldsymbol{p}$). With a dispersion relations of the form

$$\mathcal{E} = \mathcal{E}_0 + \tfrac{1}{2}\,\mu_{ik}\,p_i\,p_k\,, \quad \mathcal{E}_0 = \text{const.}, \tag{1}$$

the tensor $\mu_{ik} = m_{ik}^{-1}$ is a tensor of reciprocal effective masses, and m_{ik} is an effective mass tensor. Considering Equation (1) as the Hamiltonian function of a free particle, one can determine a particle velocity using a canonical equation of motion

$$v_i = \partial\mathcal{E}/\partial p_i, \quad i = 1, 2, 3. \tag{2}$$

From the Hamiltonian function (1) and relations (2) a Lagrangian function of the particle is

$$L = L_0 + \tfrac{1}{2}\,m_{ik}\,v_i\,v_k, \quad L_0 = \text{const.} \tag{3}$$

As the Lagrangian function of a free particle coincides with its kinetic energy, the effective mass tensor can be associated with kinetic energy (3), which is quadratic in components of the velocity.

Having its origin in the mechanics of particles, the definition of the effective mass can be connected with the dynamics of wave packets. According to the de Broglie principle of wave-corpuscular dualism, the energy $\mathcal{E}$ and momentum $\boldsymbol{p}$ of a particle correspond to the frequency ω and wave vector $\boldsymbol{k}$ of some wave packet, as $\mathcal{E} = \hbar\omega$ and $\boldsymbol{p} = \hbar\boldsymbol{k}$ where $\hbar$ is Planck's constant. From this point of view, any quasiparticle excitation in condensed matter behaves as a particle-like wave packet, and Equation (2) coincides with the definition of a group velocity of the wave packet.

The effective mass tensor for a free Newtonian particle or quasiparticle in an isotropic media (for example, excitations in the superfluid liquid He) has the simple form: $m_{ik} = m\,\delta_{ik}$, $i, k = 1, 2, 3$.

The dispersion relation of type (1) for the quasiparticles described by band theory in a periodic structure (electrons in metals and phonons in crystals) takes place at vicinities of singular points in the **p**-space. These are at the points where energy $\mathcal{E}(\boldsymbol{p})$ has a minimum (then μ_{ik} is positively definite), at the points near the maximum of $\mathcal{E}(\boldsymbol{p})$ (then μ_{ik} is negatively definite), and at the so-called conical points, when the main values of the tensor μ_{ik} have different signs.

In the general band theory of electrons and semiconductors, energy is a more complicated (arbitrary) function of the momentum $\mathcal{E} = \mathcal{E}(\boldsymbol{p})$, and the tensor of the reciprocal effective mass is defined as

$$\mu_{ik} = \frac{\partial^2\mathcal{E}}{\partial p_i \partial p_k}, \quad i, k = 1, 2, 3, \tag{4}$$

which can be a function of the momentum. The effective mass tensor allows one to calculate the acceleration of a particle under the action of the external force $\boldsymbol{f}$. As an equation of the particle motion is

$$\frac{\mathrm{d}\boldsymbol{p}}{\mathrm{d}t} = \boldsymbol{f}, \tag{5}$$

Equations (2) and (5) lead to the following equation for the acceleration:

$$m_{ik}\,\frac{\mathrm{d}v_k}{\mathrm{d}t} = f_i, \quad i = 1, 2, 3. \tag{6}$$

The force $\boldsymbol{f}$ is determined, for example, by the electric field effect on a charged particle.

The effective mass has another definition for an electron (or a charged particle) moving in a static magnetic field $\boldsymbol{B}$. In such a case the force $\boldsymbol{f}$ is

a Lorentz force, and Equation (5) implies that the electron moves under the following conditions: $\mathcal{E}(\boldsymbol{p}) =$ constant and $p_B =$ constant, where p_B is a projection of the momentum on the magnetic field direction. Thus, an electron trajectory in $\boldsymbol{p}$-space is a section of the isoenergy surface $\mathcal{E}(\boldsymbol{p}) = \mathcal{E}$ with the plane $p_B = p$. If this section is a closed curve and has a sectional area $S(\mathcal{E}, p)$, the electron motion is periodic in time and characterized by the "cyclotron frequency" $\omega_c = eB/(m^*c)$, where e is the electron charge, and c is the velocity of light. Thus, the effective mass m^* is equal to

$$m^* = \frac{1}{2\pi} \frac{\partial S}{\partial \mathcal{E}}. \tag{7}$$

Cyclotron resonance is the most convenient experimental method for measuring the effective mass defined in Equation (6).

ARNOLD KOSEVICH

See also **Dispersion relations; Group velocity; Wave packets, linear and nonlinear**

Further Reading

Haken, H. 1976. *Quantum Field Theory of Solids*, Amsterdam: North-Holland

Kittel, C. 1987. *Quantum Theory of Solids*, New York: Wiley

Slater, J.C. 1951. *Quantum Theory of Matter*, New York: McGraw-Hill

EIFFEL JUNCTION

See **Long Josephson junction**

EIGENVALUES AND EIGENVECTORS (BOUND STATE)

See **Inverse scattering method or transform**

EIKONAL CURVATURE EQUATION

See **Geometrical optics, nonlinear**

EINSTEIN EQUATIONS

After Albert Einstein (1905) published his special theory of relativity, Hermann Minkowski (1908) delivered a seminar in which he said

> Henceforth space by itself, and time by itself, are doomed to fade away into mere shadows, and only a kind of union of the two will preserve an independent reality.

This "kind of union" is called space-time. In special relativity, two observers in inertial frames moving at constant velocity with respect to each other will not, in general, agree on the distance between two objects or the duration of some interval of time they both observe. However, suppose an observer sees a particle at time t and at (cartesian) coordinates (x, y, z) and later observes the particle at time $t + \mathrm{d}t$ to be at the point $(x + \mathrm{d}x, y + \mathrm{d}y, z + \mathrm{d}z)$. If both observers record these measurements, they will both agree on the value of the quantity

$$\mathrm{d}s^2 = c^2\mathrm{d}t^2 - \mathrm{d}x^2 - \mathrm{d}y^2 - \mathrm{d}z^2 \tag{1}$$

(where c is the speed of light in vacuum), which is called the metric on Minkowski space-time. In tensor notation, $\mathrm{d}s^2 = \sum \eta_{\mu\nu}\,\mathrm{d}x^\mu \mathrm{d}x^\nu$, where the four values of the subscripts μ, ν correspond to the coordinates on the four-dimensional space-time, and $\eta_{\mu\nu} = \mathrm{diag}(1, -1, -1, -1)$ is the metric tensor. Minkowski space-time is flat; that is, it can be identified with its tangent space.

In general relativity, described by the Einstein equations, the constants $\eta_{\mu\nu}$ are replaced by more general, coordinate-dependent metric coefficients $g_{\mu\nu}$, and space-time is allowed to have nonzero curvature. This curvature manifests itself as gravitation and is caused by the presence of matter. In any space-time, test particles follow geodesics (paths that minimize distance locally, i.e., generalizations of straight lines) of the space-time. In the now-famous words of the astrophysicist John Archibald Wheeler (Misner, Thorne & Wheeler, 1973),

> Matter tells space-time how to curve and curved space tells matter how to move.

The latter part of the sentence corresponds to the geodesics; the first part is the content of the Einstein equations, which in tensor notation are

$$G_{\mu\nu} = 8\pi\, T_{\mu\nu}, \qquad \mu, \nu = 0, 1, 2, 3, \tag{2}$$

where we are using units in which the speed of light and Newton's gravitational constant both have the value 1. The tensor $T_{\mu\nu}$ is called the stress-energy or energy-momentum tensor, and its components measure several physical properties of continuous matter. In vacuum, $T_{\mu\nu} = 0$. The tensor $G_{\mu\nu}$ is called the Einstein tensor. It is constructed from $g_{\mu\nu}$ and its first two derivatives, and it is a measure of the curvature of space-time. In short, the left-hand side of the Einstein equations (2) measures curvature, which encodes the geometry of the space-time, while the right-hand side of the equations measures energy, momentum, and stress, and so encodes the physical properties of the matter. The Einstein equations can be derived from an action principle and are constructed in such a way as to satisfy a generalization of the law of conservation of energy.

Apart from the flat space-time of Minkowski, the most important solutions of the Einstein equations

are those with spherical symmetry. In Schwarzschild coordinates, the metric of any vacuum, asymptotically flat, spherically symmetric space-time has the form

$$ds^2 = \left(1 - \frac{2M}{r}\right) dt^2 - \left(1 - \frac{2M}{r}\right)^{-1} dr^2 - r^2(d\theta^2 + \sin^2\theta\, d\phi^2), \quad (3)$$

where M is a constant (Schwarzschild, 1916). The Schwarzschild metric (3) is used to describe the external field of a nonrotating spherically symmetric matter distribution (such as a star) of mass M. Expression (3) becomes singular at the so-called Schwarzschild radius $r = 2M$. In ordinary stellar models, the Schwarzschild radius lies deep in the interior of the star where the vacuum metric (3) does not apply. However, if a star undergoes gravitational collapse, then its radius shrinks to zero and the Schwarzschild radius is in the vacuum region.

By computing certain curvature invariants, it can be shown that there is no physical singularity at $r = 2M$. In other words, there is nothing wrong with the space-time manifold at $r = 2M$; it is simply that the coordinates r and t are bad here. This phenomenon is called a coordinate singularity. Use of the so-called Kruskal–Szekeres coordinates allow us to explicitly extend the space-time past this singularity. The surface $r = 2M$ is the event horizon of a black hole. Nothing can escape from the interior of the event horizon, including light, and will eventually fall into the (physical) singularity at $r = 0$ in finite proper time, where the theory breaks down.

Although a great number of exact solutions of the Einstein equations are known (Stephani et al., 2003), they describe very special and often unphysical situations. In order to study more general situations, extensive numerical studies have been undertaken. There are many ways in which the numerical evolution of the Einstein equations is especially difficult. The dependent variables of the Einstein equations are metric coefficients which describe the space-time manifold on which the independent variables (the space-time coordinates) live. Many issues stem from the fact that there is no preferred frame in general relativity meaning that one has to deal with the choice of an appropriate gauge and to recognize and avoid coordinate singularities. The Einstein equations are a system of ten strongly coupled nonlinear PDEs.

The Einstein equations as written in (2) are not in evolution form. For numerical purposes the Einstein equations are usually written in terms of an evolution variable λ. A Cauchy or characteristic approach corresponds to the normal of the $\lambda = \text{const}$ hypersurfaces being time-like or null, respectively. Einstein's equations then project to a set of constraint equations on the hypersurfaces and a set of evolution equations. If the constraint equations are satisfied on an "initial" hypersurface, then they are preserved under evolution to other hypersurfaces.

Numerical studies using the Cauchy approach have been used to model the collision of axisymmetric black holes (Anninos et al., 1995), and they have led to the discovery of critical phenomena in spherical collapse (Choptuik, 1993). One drawback of this method is that boundary conditions are usually artificially imposed on the hypersurfaces to avoid integrating out to infinity (although sometimes conformal methods can be used to include space-like infinity). The characteristic approach has led to the first unlimited evolution of a single black hole space-time (Gomez et al., 1998). While this approach allows for long-time simulations, it is only valid in the absence of crossing characteristics or caustics.

General relativity makes a number of predictions that have been tested. These include the excess advance in the perihelion of Mercury, the bending of light rays near the sun, time delays in radar signals passing near the sun, and gravitational lensing of distant galaxies by nearer ones. The most important prediction still awaiting confirmation is the existence of gravitational waves. A number of detectors have now been built around the world and observations are expected soon.

ROD HALBURD AND GINO BIONDINI

See also **Black holes; Cosmological models; General relativity; Gravitational waves**

Further Reading

Anninos, P., Hobill, D., Seidel, E., Smarr, L. & Suen, W.-M. 1995. Head-on collision of two equal mass black holes, *Physical Review* D, 52: 2044–2058

Choptuik, M.W. 1993. Universality and scaling in gravitational collapse of a massless scalar field. *Physical Review Letters*, 70: 9–12

Einstein, A. 1905. Zur elecktrodynamik bewegter Körper. *Annalen der Physik*, 17: 891–921

Gomez, R., Lehner, L., Marsa, R.L. & Winicour, J. 1998. Moving black holes in 3D, *Physical Review*, D57: 4778–4788

Minkowski, H. 1908. Space and time. Translated in *The Principle of Relativity*, New York: Dover, 1923

Misner, C.W., Thorne, K.S. & Wheeler, J.A. 1973. *Gravitation*, San Francisco: Freeman

Schwarzschild, K. 1916. Über das Gravitationsfeld einer Kugel aus inkompressibler Flussigkeit nach der Einsteinschen Theorie, *Sitzungsberichte der Preussischen Akademie der Wissenschaften, Sitzung der Physikalisch-mathematischen Klasse*, 424–434

Stephani, H., Kramer, D., MacCallum, M., Hoenselaers, C. & Herlt, E. 2003. *Exact Solutions of Einstein's Field Equations*, Cambridge and New York: Cambridge University Press

Wald, R.M. 1984. *General Relativity*, Chicago: University of Chicago Press

ELASTIC AND INELASTIC COLLISIONS

See **Collisions**

ELECTROENCEPHALOGRAM AT LARGE SCALES

Since the first human scalp recordings of the tiny electric currents generated by the brain (electroencephalogram or EEG) were obtained in the mid-1920s, EEG has been recognized as a genuine (if often opaque) window on the mind, allowing observations of brain processes to be correlated with behavior and cognition. EEG has important applications in medicine, including epilepsy, head trauma, drug overdose, brain infection, sleep disorder, coma, stroke, tumor, monitoring anesthesia depth, and fundamental cognitive studies. Most EEG power occurs at frequencies below about 15 Hz in scalp (not cortical) recordings. EEG and magnetoencephalography (MEG) are the only technologies with sufficient temporal resolution to follow the fast dynamic changes associated with cognition; however, EEG spatial resolution is poor relative to modern brain structural imaging methods such as positron emission tomography (PET), computed tomography (CT), and magnetic resonance imaging (MRI). Each scalp electrode records electrical activity at very large scales, involving cortical tissue containing perhaps 10^7–10^9 neurons.

Mesoscopic and Microscopic Sources

Scalp potentials are generated by micro-current sources at cell membranes. Sorting out the complex relations between micro-sources and macroscopic scalp potentials is facilitated by assuming an intermediate (mesoscopic) descriptive scale that recognizes the columnar structure of the neocortex. From this perspective, the mesoscopic source strength of a volume of tissue is its electric current dipole moment per unit volume (microamps/mm^2), designated as $\boldsymbol{P}(\boldsymbol{r}', t)$. This function represents the weighted average of micro-source activity in a volume of the neocortex (near $\boldsymbol{r}'$) that is large compared with the scale of individual neurons yet small compared with the size of a typical EEG electrode. For the idealized case of micro-sources of one sign confined to a superficial cortical layer and micro-sources of opposite sign confined to a deep layer, $\boldsymbol{P}(\boldsymbol{r}', t)$ is roughly the mesoscopic current density across a cortical column (≈ 1 mm^2). The contributing electrical activities are primarily dendritic post-synaptic currents, although currents associated with axonal action potentials (spikes) may also contribute (see Figure 1).

Mesoscopic Sources and Scalp Recordings

Human neocortical sources form dipole layers over which the function $\boldsymbol{P}(\boldsymbol{r}', t)$ varies with cortical location ($\boldsymbol{r}'$), measured in and out of cortical folds. In a few special cases, $\boldsymbol{P}(\boldsymbol{r}', t)$ may be approximated by a few cm-scale active regions, consisting of focal sources as in focal epilepsy or mid-latency components of evoked potentials (before tangential spread to other cortical locations). In general, however, $\boldsymbol{P}(\boldsymbol{r}', t)$ is widely distributed, perhaps over the entire cortical surface. Most EEGs are believed to be generated as a linear sum of contributions from cortical sources, in which case cortical or scalp potential may be approximated by the following integral of dipole moment over the cortical surface:

$$\Phi(\boldsymbol{r}, t) = \int_S \boldsymbol{G}(\boldsymbol{r}, \boldsymbol{r}') \cdot \boldsymbol{P}(\boldsymbol{r}', t)\, \mathrm{d}S(\boldsymbol{r}'). \qquad (1)$$

The Green function $\boldsymbol{G}(\boldsymbol{r}, \boldsymbol{r}')$ contains all geometric and conductive information about the head volume conductor. Cortical dipole moment may in turn be expanded in a series of basis functions $\boldsymbol{p}_n(\boldsymbol{r})$:

$$\boldsymbol{P}(\boldsymbol{r}, t) = \sum_{n=0}^{\infty} \xi_n(t)\, \boldsymbol{p}_n(\boldsymbol{r}). \qquad (2)$$

An idealized model neocortex consists of a thin spherical shell with $\boldsymbol{P}(\boldsymbol{r}', t)$ everywhere normal to the surface, reflecting the columnar structure of the closed neocortical surface. An appropriate choice of basis functions for this idealized cortex is the set of spherical harmonics $Y_{lm}(\theta, \phi)\boldsymbol{a}_r$, where $\boldsymbol{a}_r$ is a unit vector in the radial direction and (θ, ϕ) are the usual spherical coordinates. The single sum over n in Equation (2) may then be expressed as a double sum $l = 0, \infty$; $m = -l, +l$, associated with the spherical geometry. Combining Equations (2) and (1) yields the following series expansion for the cortical $\boldsymbol{r}_\mathrm{C}$ or scalp $\boldsymbol{r}_\mathrm{S}$ surface potential $\Phi(\boldsymbol{r}, t)$ in terms of a new set of basis functions $\phi_n(\boldsymbol{r})$ that are surface integrals of the dot product of the Green's function $\boldsymbol{G}(\boldsymbol{r}, \boldsymbol{r}')$ with the

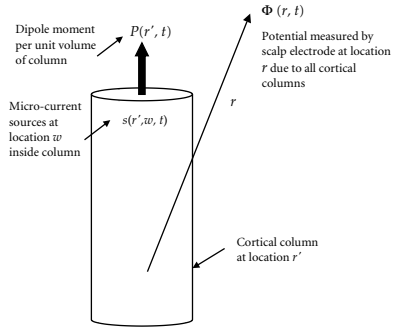

Figure 1. A mesoscopic tissue mass (for example, a mm-scale cortical column containing millions of volume micro-current sources $s(\boldsymbol{r}', \boldsymbol{w}, t)$) produces a current dipole moment per unit volume $\boldsymbol{P}(\boldsymbol{r}', t)$, or meso-source strength. Cortical or scalp potential due to brain sources is the weighted integral of $\boldsymbol{P}(\boldsymbol{r}', t)$ over the brain volume or, in the case of exclusively cortical sources, the integral over the cortical surface.

basis functions $\boldsymbol{p}_n(\boldsymbol{r})$. Thus,

$$\Phi(\boldsymbol{r}, t) = \sum_{n=0}^{\infty} \xi_n(t)\phi_n(\boldsymbol{r}). \tag{3}$$

General Dynamic Properties of Cortical and Scalp Potentials

As summarized below, EEG exhibits many dynamic behaviors, depending on recording location, physiologic state, and subject.

(i) Often complex physical or biological systems can be adequately characterized by only a few terms in Equation (3). The time-dependent coefficients $\xi_n(t)$ are called order parameters in the field of synergetics and may be governed by nonlinear differential or integral equations. The basis functions $\phi_n(\boldsymbol{r})$ may be chosen (bottom up) by physiological theory or (top down) by experimental data, for example, by constructing Karhunen–Loeve expansions (also called principal components analysis) in which the $\phi_n(\boldsymbol{r})$ are chosen as the most efficient set of orthogonal functions representing a data record.

(ii) The basis functions $\phi_n(\boldsymbol{r})$ are typically ordered in terms of progressively higher spatial frequencies as in Fourier series. The index n is then a measure of the two-dimensional spatial frequency of the corresponding basis function. Many systems exhibit a correspondence between spatial and temporal frequencies such that Fourier transforms of the order parameters $\xi_n(\omega)$ peak at higher frequencies ω for higher spatial frequencies n. For linear wave phenomena, such a correspondence is called the dispersion relation.

(iii) The large-scale spatiotemporal dynamics of cortical potential $\Phi(\boldsymbol{r}_c, t)$ are believed to be very similar to the dynamics of the mesoscopic cortical sources $\boldsymbol{P}(\boldsymbol{r}, t)$. The head volume conductor acts as a low-pass spatial filter, resulting mainly from the low electrical conductivity of skull and the physical separation (1–2 cm) between sources and electrodes. Scalp potential $\Phi(\boldsymbol{r}_s, t)$ is then a spatial low-pass representation of cortical potential $\Phi(\boldsymbol{r}_c, t)$ or mesoscopic source function $\boldsymbol{P}(\boldsymbol{r}, t)$. Comparisons of cortical potential (ECoG) with scalp potential (EEG) show that this spatial filtering results in temporal filtering. That is, the Fourier transform of cortical potential $\Phi(\boldsymbol{r}_c, \omega)$ typically contains much more relative power at higher frequencies (say 15–40 Hz) than the scalp potential transform $\Phi(\boldsymbol{r}_s, \omega)$, recorded in the same brain state, an observation qualitatively consistent with normal wave dispersion relations.

(iv) EEG phenomena typically exhibit larger amplitudes at lower frequencies. In deep sleep and moderate to deep anesthesia, $\Phi(\boldsymbol{r}_S, t)$ is typically a few 100 μV with nearly all power in the delta range (0–4 Hz) at all scalp locations. The eyes closed, waking alpha rhythm (ca. 40 μV) is normally dominated by one or two spectral peaks in the 8–13 Hz range at widespread scalp locations. Low-amplitude beta activity (ca. 13–20 Hz) superimposed on alpha rhythms is more evident in frontal cortex. Alcohol and hyperventilation typically lower alpha frequencies and increase amplitudes; barbiturates increase beta activity. Scalp EEG activity is more consistent with limit cycle modes $\xi_n(t)$ than low-dimensional chaos.

(v) Scalp EEG is a weighted space average of many cortical rhythms that can look different in different cortical regions. Alpha rhythms have been recorded from nearly the entire upper cortical surface, including frontal and prefrontal areas. Differences in ECoG waveforms between cortical areas are largely eliminated with anesthesia, suggesting shifts from more functional localization to more globally dominated brain states.

(vi) Both globally coherent and locally dominated behavior can occur within the alpha band, depending on narrow band frequency, measurement scale and brain state. Upper alpha (ca. 10 Hz) and theta (ca. 4–6 Hz) phase locking between cortical regions during mental calculations often occurs, consistent with neural network formation. At the same time, quasi-stable alpha phase structures consistent with global standing waves have been observed.

Neocortical Dynamic Theory

The apparent balance among locally and globally dominated dynamic processes has been estimated by phase synchronization among other measures. Cortical or thalamic interactions with time delays due to rise and decay times of post-synaptic potentials (local theory) have been modeled. Network frequencies are then determined only by local tissue properties. In global theories, characteristic frequencies depend on the entire neocortex/cortico-cortical fiber system. Excitatory synaptic action density $F(\boldsymbol{r}, t)$ may be expressed in terms of action potential density $\Gamma(\boldsymbol{r}, t)$ by

$$F(\boldsymbol{r}, t) = \int_0^{\infty} \mathrm{d}v \int_S R(\boldsymbol{r}, \boldsymbol{r}_l, v) \times \Gamma\left(\boldsymbol{r}_l, t - \frac{|\boldsymbol{r} - \boldsymbol{r}_l|}{v}\right) \mathrm{d}S(\boldsymbol{r}_l) \tag{4}$$

The outer integral is over distributed cortico-cortical propagation speeds v, and the inner integral is over the neocortical surface S. The dependence of cortico-cortical fiber density with distance $|\boldsymbol{r} - \boldsymbol{r}_l|$ is expressed by the function $R(\boldsymbol{r}, \boldsymbol{r}_l, v)$. This linear relation between the dependent variables $F(\boldsymbol{r}, t)$ and $\Gamma(\boldsymbol{r}, t)$ may

be combined with a variety of nonlinear local equations in the same dependent variables. Such local/global theories include both network-to-global and global-to-network interactions.

PAUL NUÑEZ

See also **Cell assemblies; Electroencephalogram at mesoscopic scales; Gestalt phenomena; Synergetics**

Further Reading

Edelman, G.M. & Tononi, G. 2000. *A Universe of Consciousness*, New York: Basic Books

Freeman, W.J. 1975. *Mass Action in the Nervous System*, New York: Academic Press

Haken, H. 1983. *Synergetics. An Introduction*, 3rd edition, Berlin: Springer

Malmuvino, J. & Plonsey R. 1995. *Bioelectromagetism*, New York: Oxford University Press

Niedermeyer, E. & Lopes da Silva, F.H. (editors). *electroencephalography. Basic Principals, Clinical Applications, and Related Fields*, 4th edition. London: Williams and Wilkins

Nuñez, P.L. 1981. *Electric Fields of the Brain: The Neurophysics of EEG*, New York: Oxford University Press

Nuñez, P.L. 1995. *Neocortical Dynamics and Human EEG Rhythms*, New York: Oxford University Press

Nuñez, P.L., Wingeier, B.M. & Silberstein, S.B. 2001. Spatial-temporal structure of human alpha rhythms: theory, microcurrent sources, multiscale measurements, and global binding of local networks. *Human Brain Mapping*, 13: 125–164

Nuñez, P.L. 2000. Toward a quantitative description of large scale neocortical dynamic function and EEG. *Behavioral and Brain Sciences*, 23: 371–437

Penfield, W. & Jasper, H.D. 1954. *Epilepsy and the Functional Anatomy of the Human Brain*, London: Little, Brown and Co

Scott, A.C. *Stairway to the Mind*, Berlin and New York: Springer, 1995

Uhl, C. (editor). 1999. *Analysis of Neurophysiological Brain Functioning*, Berlin: Springer 1999

Wilson, H.R. & Cowan, J.D. 1973. A mathematical theory of the functional dynamics of cortical and thalamic nervous tissue. *Kybernetik*, 13: 55–80

ELECTROENCEPHALOGRAM AT MESOSCOPIC SCALES

The two most dominant theoretical positions that have influenced the development of explanations of behavior are functional modularity, where specific behaviors are believed to reside in distinct cortical locations, and mass action, in which behavior is posited to arise out of the cooperative activity of distributed neural structures comprising the brain. The first of these positions predominates in the medical and cognitive sciences, based upon observations collected over many years in which selective behavioral deficits were observed to occur in response to the specific destruction or stimulation of various areas of the brain. This has led to considering the brain as a collection of interconnected functionally specialized modules. This view is generally known as modularism and in the context of higher functions is also referred to as cortical localizationism. Modules are thought to embody algorithms, acting mechanistically on input to produce output, in a computer-like manner. Mass action, however, considers behavior as best understood as arising out of cooperative neural activity occurring over a number of interacting spatial and temporal scales. The consequence of this view is that behavior can now be characterized by the observation of dynamical patterns of brain activity.

The dynamics of the brain can be observed at a number of different spatial and temporal scales. These range from the level of the ion channel, synapse, and neuron (microscopic), to the level of neuronal population (mesoscopic), up to the level of large aggregates of brain tissue (macroscopic). The associated methods can generally be divided into those that measure some form of electromagnetic activity and those that reflect the metabolic correlates of neural activity. At the mesoscopic scale electromagnetic measures typically have millisecond temporal resolution whereas metabolic measures (e.g., fMRI, PET, near-infrared spectroscopy, diffuse optical tomography) have comparatively poor temporal resolution (s), while both mesoscopic and metabolic measures have comparable spatial resolution (mm). Electromagnetic measurements of brain activity better reflect the time scales of neuronal activity associated with the dynamics of behavior. For these reasons theories of mesoscopic brain dynamics are built around state variables that characterize the electromagnetic activity associated with neural populations. The most important mesoscopic electromagnetic measures are those of the local field potential (LFP) and the electrocorticogram (ECoG) which predominately reflect the quasi-static electromagnetic fields produced in response to the ionic currents generated by synchronized synaptic activity. It is generally thought that in the cortex this synchronized activity is linearly related to the spatially averaged soma membrane potential of populations of excitatory (pyramidal) neurons.

For both excitatory and inhibitory neuronal populations the mean soma membrane potential determines the mean rate of neuronal action potential generation (or firing rate). In the simplest case, the mean population firing rate is a sigmoidal function of the mean soma membrane potential for functionally equivalent members of the same neuronal population. More generally, such a relationship will be time-variant. Because the mean soma membrane potential is a function of neuronal population synaptic input which itself is a function of the mean neuronal population firing rates, the mean soma membrane potential can be used as a canonical state variable to both characterize and develop theories of the dynamics of neuronal populations.

At the level of the neuronal population, the spatially averaged soma membrane potential is typically defined over the characteristic scales of the short-range

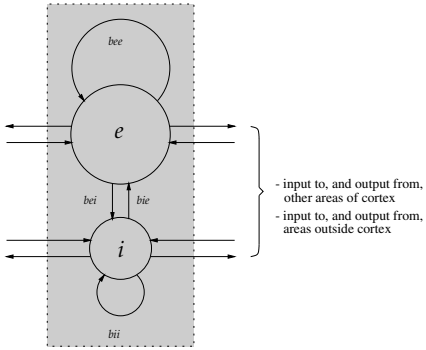

Figure 1. The neurons of mammalian cortex interact with each other locally (by short range connections) and globally (by long-range connections). Short-range connections serve to diffusely interconnect the intermixed excitatory (e) and inhibitory (i) neuronal populations of cortex. The characteristic scales of these connections loosely organize cortex into a sheet of overlapping "modules" or cylinders that span the entire thickness of cortex. The resulting pattern is often referred to as columnar organization with a single one of these cylinders known as a cortical macrocolumn. One way of quantifying the strength of interaction between these local neuronal populations is to specify the mean number of connections (or synapses) neurons of one population receive from neurons of the same or another population (b_{ij}).

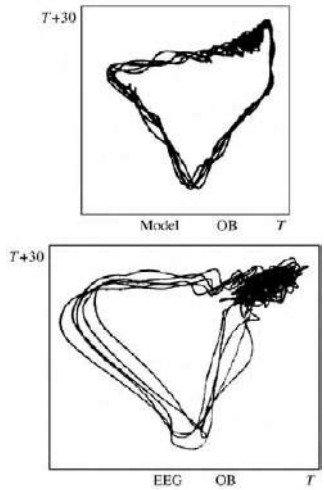

Figure 2. Delay embedded phase plane plots comparing EEG seizure activity recorded from rat olfactory bulb (a phylogenetically primitive form of cortex present in all mammals), top panel, and with a mesoscopic theory of olfactory bulb dynamics (bottom panel). The delay embedding is 30 ms for experimental and simulated time series of 1s duration, with time increasing counterclockwise. Figure reproduced with permission from Freeman (1987), Copyright Springer-Verlag.

intracortical fibers. These intracortical fibers comprise the recurrent axonal branchings of the pyramidal neurons as well as all the axonal fibres of the inhibitory interneurons. Detailed morphometric studies of cortex have established that the typical characteristic spatial scale of these fibers ranges anywhere between 30 μm to 1 mm (Braitenberg & Schüz, 1998). The advantage of using this spatially averaged state variable is that it has a commensurate spatial scale to LFP and ECoG recordings.

Most mesoscopic theories of neuronal dynamics have considered cerebral cortex to consist of two functionally distinct neural populations—excitatory (e) and inhibitory (i)—reflecting the respective pyramidal and interneuron populations. The earliest models of cortical mass action attempted to describe neuronal dynamics exclusively in terms of short- and long-range excitatory interactions between excitatory populations. While a number of interesting analytical solutions were obtained using this approach, they are no longer of any significant physiological relevance because they did not incorporate the activity of inhibitory neurons. Subsequent models, based on anatomical considerations, have addressed this deficiency by the incorporation of all forms of feedforward and feedback connectivity between excitatory and inhibitory neuronal populations. Starting with Wilson & Cowan (1972), most modern theories functionally incorporate local $e \to e$, $e \to i$, $i \to e$, and $i \to i$ connections, as illustrated in Figure 1. However, a notable exception is the influential body of work by Lopes da Silva et al. in which all the significant population neurodynamics arise out of the reciprocal interactions between excitatory and inhibitory neurons.

In the majority of theories the dynamical response of the mean soma membrane potential to synaptic activity induced by population neuronal firings is generally described using a differential formalism.

$$\dot{h}_n = -a_n h_n + \sum_{r=1}^{N} g_{nr}(h_n) I_{nr}, \qquad (1)$$

$$\mathcal{D}_{nr} I_{nr} = S_{nr}(h_r) \quad n, r = 1 \ldots N, \qquad (2)$$

where N is the number of locally interacting neuronal populations and the a_n are real constants which correspond approximately to the reciprocal of the mean neuronal membrane time constant. In most theories $N = 2$. h_n is the mean soma membrane potential of the nth neuronal population, and S_{nr} defines functions that take into account the topology of neuronal population connectivity as well as the sigmoidal relationships between mean soma membrane potential and mean firing rate. $g_{nr}(h_n)I_{nr}$ represents the postsynaptic current induced in local neuronal population n by neuronal population r, whose temporal evolution is

determined by the temporal differential operator $\mathcal{D}_{nr}$. This operator takes into account bulk neurotransmitter kinetics and neuronal cable properties.

Theories of mesoscopic dynamics can generally be distinguished by the form and order of $\mathcal{D}_{nr}$, g_{nr} and S_{nr}, and N. For instance, in the original work of Wilson and Cowan, $\mathcal{D}_{nr}$ was of zero order in time, whereas in the theories of Lopes da Silva, $\mathcal{D}_{nr}$ is of first order and $g_{nr}(h_n) =$ constant. More recent theories have considered $g_{nr}(h_n)$ linear in h_n and $\mathcal{D}_{nr}$ second order in time due to more detailed physiological considerations, (Liley et al., 2002). Differing forms and parametrizations of $\mathcal{D}_{nr}$, g_{nr}, and S_{nr} have been shown to give rise to a wide range of dynamics (e.g., limit cycle, chaos, and filtered noise) some of which bear strong similarities to experimental recordings (see Figure 2; see also figures in color plate section).

DAVID LILEY AND MATHEW DAFILIS

See also **Cell assemblies; Electroencephalogram at large scales; Nerve impulses; Neurons; Synergetics**

Further Reading

Braitenberg, V. & Schüz, A. 1998. *Cortex: Statistics and Geometry of Neuronal Connectivity*. Berlin and New York: Springer

Freeman, W.J. 1975. *Mass Action in the Nervous System*. New York: Academic Press

Freeman, W.J. 1987. Simulation of chaotic EEG patterns with a dynamic model of the olfactory system. *Biological Cybernetics*, 56(2–3): 139–150

Freeman, W.J. 2000. *Neurodynamics: An Exploration in Mesoscopic Brain Dynamics*. London and New York: Springer

Liley, D.T.J., Cadusch, P.J. & Dafilis, M.P. 2002. A spatially continuous mean field theory of electrocortical activity. *Network: Computation in Neural Systems*, 13(1): 67–113

van Gelder, T. 1999. Dynamic approaches to cognition. In *The MIT Encyclopedia of the Cognitive Sciences*, edited by R.A. Wilson & F.C. Keil, Cambridge, MA: MIT Press

van Rotterdam, A., Lopes da Silva, F.H., van den Ende, J., Viergever, M.A. & Hermans, A.J. 1982. A model of the spatial-temporal characteristics of the alpha rhythm. *Bulletin of Mathematical Biology*, 44(2): 283–305

Wilson, H.R. & Cowan, J.D. 1972. Excitatory and inhibitory interactions in localized populations of model neurons. *Biophysical Journal*, 12: 1–24

ELECTRON BEAM MICROWAVE DEVICES

Electron beam devices have been used in a wide variety of applications since the beginning of vacuum technology early in the 20th century. These include simple diodes and triodes, used in early radio; cathode-ray tubes, used for display in oscilloscopes, televisions, and computers; lithography; high-voltage devices used to produce X-rays; sources for electron accelerators; and the energy source for microwave devices, with applications in communications, microwave ovens, industrial processes, and electronic warfare. For the purposes of this entry, we will limit our discussion to just one application, the production of electromagnetic energy at microwave frequencies, where nonlinear space charge effects tend to play a major role. For a wider range of applications, including the basic theory, texts are available such as Harmon (1953) and Gilmour (1994). It should be noted that solid state devices, not involving electron beams, are now often used at low power, particularly as oscillators to drive microwave electron-beam amplifiers.

Generation of microwaves with electron beams involves the interaction of a beam with electromagnetic fields across gaps of discrete cavities or synchronously with electromagnetic fields propagating on a slow wave structure. The basic physical principle is that a bunched beam interacts with the decelerating phase of an electric field to transfer energy from the beam to the field. This mechanism is the converse of the interaction in linear accelerators and synchrotrons that operate by interaction of a field in an accelerating phase with a bunched beam to transfer energy from the fields to the beam. In a device such as a traveling-wave tube (TWT) or magnetron, in which the beam interacts with a traveling wave, there is a natural bunching action as the wave develops, such that most of the beam particles are decelerated, producing the wave amplification. In a klystron, with a bunching cavity and an energy extraction cavity, the proper phase relation must be established, which is, in fact, equivalent to the synchronous condition in the TWT.

The earliest beam-type device to be extensively used for microwave generation is the magnetron, a coaxial cylindrical device with a potential between inside cathode and outside anode cylinders, and a magnetic field along the cylindrical axis. The electrons accelerated from the cathode toward the anode perform cycloidal motion due to the magnetic field with an average azimuthal drift velocity in the combined electric and magnetic fields given by $\boldsymbol{v}_{\mathrm{d}} = \boldsymbol{E} \times \boldsymbol{B}/B^2$. The anode consists of a series of microwave cavities with the operating frequency, chosen such that the cavities operate in the π-mode, that is, 180° phase shift between cavities. The fields and dimensions are chosen such that the electrons are in synchronism with the fundamental Fourier component of the fields that appear across the cavity openings. Through a complicated nonlinear process, the electrons bunch at a phase with respect to the traveling microwave field to give energy to the field, finally being collected on the anode structure with an energy considerably less than the energy eV, where V is the cathode-anode accelerating voltage. Simplified models describe some of the processes (Hutter, 1965), but most development has been experimental, assisted more recently by detailed numerical calculations (Lemke et al., 2000). The magnetron configuration described above operates naturally as an oscillator. It has high efficiency and

usually operates at high power. It was an essential element in the development of radar during World War II, which was important in winning the air war over Great Britain. The magnetron has become ubiquitous in the consumer market, as the power source in the household microwave oven. Magnetrons, despite being inexpensive and robust, have a number of unfavorable characteristics, including excess noise, narrow bandwidth, and difficulty in tuning, which limit their applications.

The klystron, which was developed roughly during the same period of time as the magnetron, is more flexible because it can operate, with small modifications, as either an amplifier or an oscillator, and versions operate over very large ranges of power and frequency. The basic configuration is two cylindrical microwave cavities with an electron beam passing through their center. The cavities have a reentrant shape such that the central hole consists of a narrow gap. The beam is velocity modulated by an alternating electric field across the first cavity gap which becomes density modulated in the second gap. At very low beam density, the electron trajectories can be taken to be kinematic, with the bunching distance related to the beam velocity and the perturbed velocity created by the gap fields. However, the usual operation is in a regime where space charge effects are fundamental to the operation. The excitation produces two waves, fast and slow space charge waves, which give a beat modulation distance $\lambda_b/4 = \pi v_o/2\omega_{pb}$, where v_o is the beam velocity and ω_{pb} is the plasma frequency of the beam. The trajectories are shown schematically in Figure 1. The beam plasma frequency is reduced from the natural electron oscillation $\omega_p = ne^2/m\epsilon_0$ due to the transverse beam dimensions. A second cavity at a position $z = \lambda_b/4$ from the first cavity is excited by a maximum of the radio-frequency current in the beam. The amplifier is converted into an oscillator by either feeding back some of the signal externally from the second cavity to the first cavity or by reflecting the modulated beam, after traversing only a single cavity, to self-excite it as a reflex klystron. See a basic text such as Harmon (1953), or more detail in Hutter (1965), for mathematical analysis.

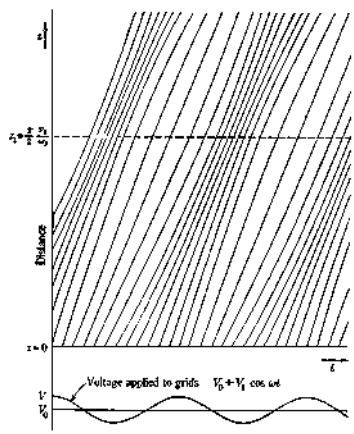

Figure 1. Distance-time diagram of a klystron indicating how velocity variations at the input grids result in density variations farther down the electron stream (after Harmon, 1953).

The traveling-wave tube (TWT), developed somewhat later, competes for applications with the klystron at all but the highest powers. The device transfers energy from a beam to a slow wave structure, usually a helix, by a resonant interaction in which the beam becomes naturally modulated in the presence of the wave. A linear, or small signal, analysis is sufficient to obtain the amplifying properties of the device for many low-power applications. However, as the microwave power becomes comparable to the beam power, nonlinear considerations become very important. As in the klystron, space charge is a fundamental source of nonlinearity. If significant power is extracted from the beam, the wave velocity on the circuit must be reduced along its length to maintain the coherent synchronous interaction. Due to the periodicity of slow wave structures, the propagation characteristics have operating regions for which the group velocity $v_g = d\omega/dk$ is opposite in direction to the phase velocity $v_{ph} = \omega/k$ (Brillouin, 1953). If the TWT is operated with such parameters, then wave energy is propagated backward from the direction in which the beam is moving and in which the wave amplitude, by interaction with the beam, is growing. This feedback allows the beam to self-excite the wave and therefore become an oscillator, which is called a backward wave oscillator (BWO). The operating conditions of a BWO are inherently nonlinear. In addition to the general books already mentioned, a detailed account of TWTs by one of the scientists associated with their development, is Pierce (1950). Sketches of the three basic types of devices are shown in Figures 2, 3, 4. There are many variants of these basic configurations.

Because electron beams are the power source and the active interacting medium for both klystron and TWT amplifiers and their associated oscillators, beam design is of great importance in obtaining good operating

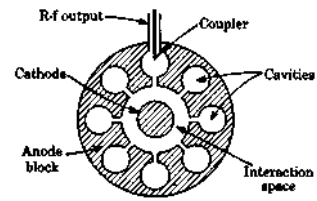

Figure 2. Multicavity magnetron (after Hutter, 1965).

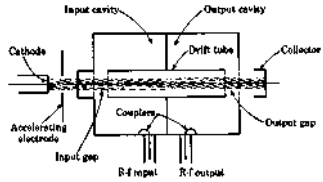

Figure 3. Two-cavity klystron (after Hutter, 1965).

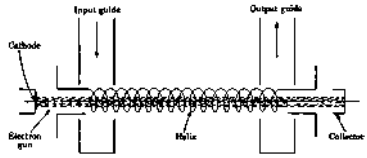

Figure 4. Helix-type traveling-wave tube (after Hutter, 1965).

characteristics. Some of the issues involved are collimation (minimizing transverse emittance), energy spread (minimizing longitudinal emittance), and high current and/or current density. The collimation is often accomplished with a uniform magnetic field along the beam axis, but radial space charge forces also lead to beam rotation. Alternatively, electric or magnetic lenses can be employed. An important consideration is to launch the beam from an accelerating region in a smooth manner; this led to the electrode shape known as the Pierce diode. An important method of confining a beam with significant space charge is to inject the beam into a uniform magnetic field from a magnetic field-free region. The proper choice of magnetic field leads to azimuthal rotation that just takes up the space charge potential, lending to smooth, uniform axial flow, called Brillouin flow. Many of the basic topics of beam dynamics and beam design are covered in Pierce (1954).

Some of the important considerations that have motivated the development of various microwave beam devices have been noise characteristics, particularly achieving low noise to amplify very low signals; frequency ranges, particularly pushing devices to increasingly high frequencies for broadband applications; tunability; and power and efficiency, particularly to obtain high power at high efficiency. For certain applications, there are also other types of constraints such as ruggedness, reliability, and weight limits, which we will not consider here. Low noise requirements have tended to favor TWTs over klystrons on the front end of receivers. Higher frequencies, used to obtain more bandwidth in communication applications, have led to miniaturization of klystrons, but other types of devices such as free electron lasers can obtain even higher frequencies for some applications (Freund & Antonsen, 1996). Some of the key issues motivating nonlinear analysis have arisen from the requirement of obtaining high efficiency at high power. Currently, the state of the art in high power is to produce 1GW in a pulse of 0.1kJ. For studies of more recent analysis and developments the reader is referred to Benford & Swegle (1992) and Barker & Schamiloglu (2001).

To obtain high efficiency the majority of the electrons should be trapped in the wave field, such that they can be decelerated. This requires matching the phase space of the beam emittance to the acceptance of the wave field, usually by some additional bunching mechanisms. Some of the basic ideas are treated in Lichtenberg (1969), but each device needs detailed numerical trajectory calculations to optimize trapping. In addition to trapping, the exiting spent beam must be decelerated to retrieve the excess energy (a depressed collector). Reducing the collector voltage is limited by the requirement that the average beam energy of the exiting beam must be greater than its energy spread so as not to turn electrons around. This condition requires knowledge of the nonlinear characteristics of the longitudinal phase space emittance.

ALLAN J. LICHTENBERG AND JOHN P. VERBONCOEUR

See also **Particle accelerators**

Further Reading

Barker, R.J. & Schamiloglu, E. (editors). 2001. *High Power Microwave Sources and Technologies*. New York: IEEE Press
Benford, J. & Swegle, J. 1992. *High Power Microwaves*, Norwood, MA: Artech House
Brillouin, L. 1953. *Wave Propagation in Periodic Structures*. New York: Dover
Freund, H.P. & Antonsen, Jr., T.M. 1996. *Principles of Free Electron Lasers*, London: Chapman & Hall
Gilmour, A.S. 1994. *Principles of Traveling Wave Tubes*, Boston: Artech House
Harmon, W.W. 1953. *Fundamentals of Electronic Motion*, New York: McGraw-Hill
Hutter, R.G.E. 1965. *Beam and Wave Electronics in Microwave Tubes*, Cambridge, MA: Boston Technical Publishers
Lemke, R.W., Genoni, T.C. & Spencer, T.A. 2000. Effects that limit efficiency in relativistic magnetrons. *IEEE Transactions on Plasma Science*, 28: 887–897
Lichtenberg, A.J. 1969. *Phase-Space Dynamics of Particles*, New York: Wiley
Pierce, J.R. 1950. *Traveling-Wave Tubes*, New York: Van Nostrand
Pierce, J.R. 1954. *Theory and Design of Electron Beams*, 2nd edition, New York: Van Nostrand

ELLIPTIC FUNCTIONS

Elliptic functions were first introduced as inverses of elliptic integrals, so called because the integral for the arclength of the ellipse studied by John Wallis in the 17th century (Stillwell, 1989) was the first such example. By the end of the 18th century, in particular after the work of Leonhard Euler, Joseph-Louis Lagrange, and Adrien-Marie Legendre, mathematicians had realized

that integrals of the form $\int \mathrm{d}x/\sqrt{P(x)}$, where $P(x)$ is a cubic or quartic polynomial, could not be expressed in terms of elementary functions (or their inverses). Many elliptic integrals arise naturally in the solutions of problems in mechanics (Lawden, 1989). For example, the solution of the simple pendulum equation

$$\dot{\theta} + \omega^2 \sin\theta = 0$$

can be obtained using conservation of energy $\frac{1}{2}(\dot{\theta})^2 - \omega^2 \cos\theta = E$, $E > -\omega^2$, to arrive at the inversion problem for the integral

$$t - t_0 = \int_0^{\theta} \frac{\mathrm{d}\theta}{\sqrt{2E + \omega^2 - \omega^2 \sin^2(\theta/2)}}\,\mathrm{d}\theta.$$

Substituting $z = \sin(\theta/2)$ and defining $k^2 = \omega^2/(E+\omega^2) \in (0, 1)$, one arrives at the expression

$$K(z;k) = \int_0^z \frac{\mathrm{d}z}{\sqrt{1-z^2}\sqrt{1-k^2z^2}} = \frac{\omega}{k}(t - t_0). \quad (1)$$

In the late 19th century, Niels Henrik Abel, Carl Jacobi, and Carl Friedrich Gauss observed the similarity between $K(z;k)$ and the integral defining the transcendental function arcsin z as

$$\operatorname{arcsine} z = \int_0^z \frac{\mathrm{d}z}{\sqrt{1-z^2}}$$

(which is indeed the limiting case of (1) as $k \to 0$, giving the solution for the small amplitude oscillations of the pendulum), and introduced the *Jacobi elliptic sine function* $\operatorname{sn}(z;k)$ as the inverse of $K(z;k)$

$$z = K(\operatorname{sn}(z;k);k).$$

While the circular (trigonometric) functions $\sin z$, $\cos z$, $\tan z$, etc., are singly periodic functions of the complex variable z, satisfying $f(z + 2\pi) = f(z)$, elliptic functions can be characterized as the doubly periodic functions, which only possess pole singularities. Elliptic functions satisfy

$$f(z + 2\omega_1) = f(z), \quad f(z + 2\omega_2) = f(z),$$

where ω_1 and ω_2 (the *periods* of f) are complex numbers such that ω_1/ω_2 is not purely real. The region of the complex plane with vertices $\{0, 2\omega_1, 2\omega_2, 2\omega_1 + 2\omega_2\}$ is called the *fundamental period parallelogram* (see Figure 1).

The simplest elliptic functions are those with two poles: the *Jacobi elliptic functions*, with two simple poles of opposite residues, and the *Weierstrass elliptic functions*, with a single double pole with zero residue, all others can be constructed from these.

Jacobi Elliptic Functions

The three most common Jacobi elliptic functions are $\operatorname{sn}(z;k)$, introduced earlier, and the associated

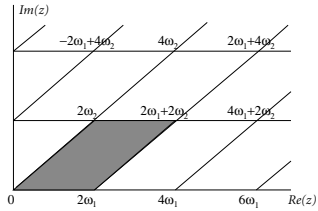

Figure 1. The period lattice of an elliptic function.

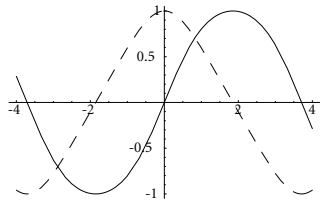

Figure 2. Graphs of $\operatorname{sn}(x;k)$ (solid line) and $\operatorname{cn}(x;k)$ (dashed line), for real x, $k = 0.5$.

$\operatorname{cn}(z;k) = \sqrt{1 - \operatorname{sn}^2(z;k)}$ (a generalization of the cosine function) and $\operatorname{dn}(z;k) = \sqrt{1 - k^2\operatorname{sn}^2(z;k)}$. Some of their main properties, analogues of the properties of trigonometric functions, are listed below; their proofs are elementary (Whittaker & Watson, 1943) (see Figure 2):

Symmetry:

$$\operatorname{sn}(-u) = -\operatorname{sn} u, \quad \operatorname{cn}(-u) = \operatorname{cn} u, \quad \operatorname{dn}(-u) = \operatorname{dn} u.$$

Derivatives:

$$\frac{\mathrm{d}}{\mathrm{d}u}\operatorname{sn} u = \operatorname{cn} u \operatorname{dn} u, \quad \frac{\mathrm{d}}{\mathrm{d}u}\operatorname{cn} u = -\operatorname{sn} u \operatorname{dn} u,$$

$$\frac{\mathrm{d}}{\mathrm{d}u}\operatorname{dn} u = -k^2 \operatorname{sn} u \operatorname{cn} u.$$

Addition formulas: For example,

$$\operatorname{sn}(u+v) = \frac{\operatorname{sn} u \operatorname{cn} v \operatorname{dn} v + \operatorname{sn} v \operatorname{cn} u \operatorname{dn} u}{1 - k^2 \operatorname{sn}^2 u \operatorname{sn}^2 v.}$$

Periods: Define the *complete elliptic integral*

$$K = \int_0^1 \frac{\mathrm{d}z}{\sqrt{(1-z^2)(1-k^2z^2)}},$$

the *complementary modulus* k' such that $k^2 + k'^2 = 1$, and the constant $K' = K(1;k')$. Then, for example,

$$\operatorname{sn}(u + 4K) = \operatorname{sn} u, \quad \operatorname{sn}(u + 2\mathrm{i}K') = \operatorname{sn} u.$$

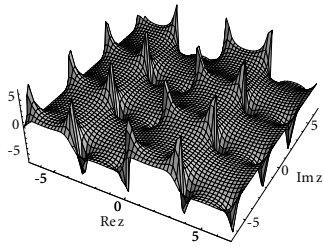

Figure 3. The doubly periodic function $\mathrm{sn}(z;k)$: graph of $Re[\mathrm{sn}(z;0.3)]$.

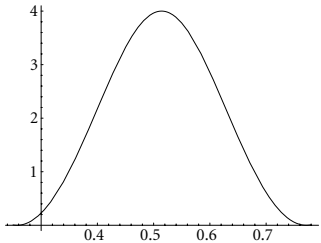

Figure 4. The profile of the cnoidal wave solution of the KdV equation, $A=4$, $k=0.3$.

Poles: For example, $\mathrm{sn}(z;k)$ is analytic except at points congruent to iK' and $2K+iK'$ (mod $2K, 2iK'$), which are simple poles.

Weierstrass Elliptic Functions

This class of elliptic functions was introduced by Weierstrass by means of infinite partial-fraction and product expansions, rather than as inversions of elliptic integrals. Indeed, such construction exists for all elliptic functions. Given $\omega_1, \omega_3 \in \mathbb{C}$, $\omega_2 = \omega_1 + \omega_2$, we define the most famous of Weierstrass' elliptic functions, the $\wp$-function, on the period lattice $\{m2\omega_1 + n2\omega_3 \mid m, n \in \mathbb{Z}\}$:

$$\wp(z) = \frac{1}{z^2} + \sum_{(m,n)\neq(0,0)} \left\{ \frac{1}{(z-(m2\omega_1+n2\omega_3))^2} - \frac{1}{(m2\omega_1+n2\omega_3)^2} \right\}. \tag{2}$$

$\wp(z)$ is a meromorphic function with double poles at each point of the period lattice and satisfies the following differential equation:

$$[\wp'(z)]^2 = 4[\wp(z)]^3 - g_2[\wp(z)] - g_3 = 4(\wp(z)-e_1)(\wp(z)-e_2)(\wp(z)-e_3), \tag{3}$$

where $e_i = \wp(\omega_i)$.

Among applications of the Weierstrass $\wp$-function is the profile of a wave traveling in water (see, e.g., Walker, 1996), as described by the Korteweg–de Vries (KdV) equation

$$u_t + u_x + 12uu_x + u_{xxx} = 0. \tag{4}$$

Seek a traveling-wave solution by setting $u(x,t) = f(x-ct)$, for some constant speed c. Then f satisfies the ordinary differential equation $(1-c)f' + 12ff' - + f''' = 0$ which, after twice integrating, leads to

$$(f')^2 = 4f^3 - (1-c)f^2 + Af + B,$$

A, B constants of integration. By comparison with (3), the form of f must be $f(s) = \alpha\wp(\beta s) + \gamma$, for suitable constants α, β, γ. Since the Weierstrass $\wp$-function can be shown to be related to the square of Jacobi elliptic functions (Whittaker & Watson, 1943), this leads to the notable *cnoidal wave* solution of KdV (see Figure 4):

$$u(x,t) = A\,\mathrm{cn}^2\left(\frac{\sqrt{A}}{k}(x-ct);k\right),$$

$$c = 1 + 4A\,\frac{2k^2-1}{k^2}.$$

Finally, we briefly mention hyperelliptic functions (or abelian functions), as inverses of integrals of rational functions $R(z, \sqrt{P(z)})$, with $P(z)$ a quintic or higher-degree polynomial (Baker, 1995). For example, the equations for the Kovalevsky top were shown by Sophia Kovalevsky to be integrable in terms of hyperelliptic functions (Whittaker, 1960).

ANNALISA M. CALINI

Further Reading

Baker, H.F. 1995. *Abelian Functions: Abel's Theorem and the Allied Theory of Theta Functions*. Reissue of the 1897 edition, Cambridge and New York: Cambridge University Press

Byrd, P.F. & Friedman, M.D. 1954. *Handbook of Elliptic Integrals for Engineers and Physicists*, New York: Wiley

Lawden, D.F. 1989. *Elliptic Functions and Applications*, Berlin and New York: Springer

Rauch, H.E. & Lebowitz, A. 1973. *Elliptic Functions, Theta Functions and Riemann Surfaces*, Baltimore: Williams and Wilkins

Stillwell, J. 1989. *Mathematics and Its History*, 2nd edition, Berlin and New York: Springer, Chapter 12

Walker, P.L. 1996. *Elliptic Functions: A Constructive Approach*, Berlin and New York: Springer

Whittaker, E.T. 1960. *A Treatise on the Analytical Dynamics of Particles and Rigid Bodies: With an Introduction to the Problem of Three Bodies*, Cambridge: Cambridge University Press (originally published 1904)

Whittaker, E.T. & Watson, G.N. 1943. *A Course of Modern Analysis*, 4th edition, Cambridge: Cambridge University Press

EMBEDDING METHODS

The modeling of a deterministic dynamical system relies on the concept of a phase space, which is a theoretical representation of the totality of possible system states. In general, a system state consists of information of positions and velocities needed to specify all future system states. For a system that has a mathematical model, the phase space is known from the equations of motion.

For experimental and natural chaotic dynamical systems, the full state space is unknown. Embedding methods have been developed as a means to reconstruct the phase space and develop new predictive models. One or more signals from the system must be observed as a function of time. The time series are then used to build a proxy of the observed states.

Mathematical theorems show how the observed time series can be used. A famous theorem of Hassler Whitney from the 1930s holds that a generic map from an n-manifold to $2n+1$-dimensional Euclidean space is an embedding. In particular, the image of the n-manifold is completely unfolded in the larger space because $2n+1$ signal traces measured from a system can be considered as a map from the set of states to $2n+1$-dimensional space, Whitney's theorem implies that each state can be identified uniquely by a vector of $2n+1$ measurements, thereby reconstructing the phase space.

The contribution of Floris Takens (1981) was to show that the same goal could be reached with a single measured quantity. He proved that instead of $2n+1$ generic signals, the time-delayed versions $[y(t), y(t-\tau), y(t-2\tau), \ldots, y(t-2n\tau)]$ of one generic signal would suffice to embed the n-dimensional manifold. There are some technical assumptions that must be satisfied, restricting the number of low-period orbits with respect to the time-delay τ and repeated eigenvalues of the periodic orbits. This result was roughly contemporaneous with similar theoretical results by D. Aeyels and a more empirical account by Packard et al. (1980).

The idea of using time delayed coordinates to represent a system state is reminiscent of the theory of ordinary differential equations, where existence theorems say that a unique solution exists for each $[y(t), \dot{y}(t), \ddot{y}(t), \ldots]$. For example, in Newtonian many-body dynamics, current knowledge of the position and momentum of each body suffices to uniquely determine the future dynamics. The time derivatives can be approximated by delay-coordinate terms as

$$\left[y(t), \frac{y(t)-y(t-\tau)}{\tau}, \frac{y(t)-2y(t-\tau)+y(t-2\tau)}{\tau^2}, \ldots\right].$$

The emergence of chaos and fractal geometry in physical systems motivated a reassessment of the original theory, which applies to smooth manifold attractors. It was shown (Sauer et al., 1991) that an attractor of (possibly fractional) box-counting dimension d can always be reconstructed with m generic observations, or with m time-delayed versions of one generic observation, where m is any integer greater than $2d$.

Embedding ideas were later extended beyond autonomous systems with continuously measured time series. A version was designed for excitable media, where information may be transmitted by spiking events, extending usage to possible neuroscience applications. An embedding theorem for skew systems by J. Stark explores extensions of the methodology when one part of a system is driving another.

Although the theory implies that an arbitrary time delay is sufficient to reconstruct the attractor, efficiency with a limited amount of data is enhanced by particular choices of the time delay τ. Methods for choosing an appropriate time delay have centered on measures of linear autocorrelation and mutual information (Fraser & Swinney, 1986). Further, in the absence of knowledge of the phase space dimension n, a choice of the number of embedding dimensions m must also be made. A number of ad hoc methods have been proposed that try to estimate whether the image has been fully unfolded by a given m-dimensional map.

The success of embedding in practice depends heavily on the specifics of the application. In particular, the hypothesis of a generic observation function creating the time series is often problematic. A mathematically generic observation monitors by definition all degrees of freedom of the system. The extent to which this is true affects the faithfulness of the reconstruction. If there is only a weak connection from some degrees of freedom to the observation function, the data requirements for a satisfactory reconstruction may be prohibitive in practice. Other factors that limit success are difference in time scales between different parts of the system, as well as system and observational noise.

Applications of embedding time-series data (Ott et al., 1994; Kantz & Schreiber, 1997) have been extensive since Takens's theorem was published. Many techniques of system characterization and identification were made possible, including determination of periodic orbits and symbolic dynamics, as well as approximation of attractor dimensions and Lyapunov exponents of chaotic dynamics. In addition, researchers have focused on methods of time series prediction and nonlinear filtering for noise reduction, the use of chaotic signals for communication, and the control of chaotic systems.

TIM SAUER

See also **Chaos vs. turbulence; Controlling chaos; Fractals; Phase space; Time series analysis**

Further Reading

Eckmann, J.-P. & Ruelle, D. 1985. Ergodic theory of chaos and strange attractors. *Reviews of Modern Physics*, 57: 617–652

Fraser, A.M. & Swinney, H.L. 1986. Independent coordinates for strange attractors from mutual information. *Physical Review* A, 33: 1134–1140

Kantz, H. & Schreiber, T. 1997. *Nonlinear Time Series Analysis*, Cambridge and New York: Cambridge University Press

Ott, E., Sauer, T. & Yorke, J.A. 1994. *Coping with Chaos: Analysis of Chaotic Data and the Exploitation of Chaotic Systems*, New York: Wiley Interscience

Packard, N., Crutchfield, J., Farmer, D. & Shaw, R. 1980. Geometry from a time series. *Physical Review Letters*, 45: 712–715

Sauer, T., Yorke, J.A. & Casdagli, M. 1991. Embedology. *Journal of Statistical Physics*, 65: 579–616

Takens, F. 1981. *Detecting Strange Attractors in Turbulence*, Berlin: Springer

EMERGENCE

Like many commonly used words, the term *emergence* has several meanings. In its weakest sense, a metaphor is provided by Michelangelo Buonarroti's famous sculptures entitled *The Prisoners*, which show human figures struggling to free themselves from their lithic confines, suggesting the artist's view of the creative process.

In simplest terms, there is little mystery here; the sculptor merely removes the unnecessary marble to expose the finished work, as Michelangelo himself is said to have pointed out. Thus, his prisoners are emerging only in an elementary sense which philosopher Robert Van Gulick calls "specific value emergence" and defines as follows (Van Gulick, 2001):

> SPECIFIC VALUE EMERGENCE: The whole and its parts have features of the *same kind,* but have different *specific subtypes* or *values* of that kind. For example, a bronze statue has a given mass as does each of the molecular parts of which it is composed, but the mass of the whole is different in value from that of any of its material parts.

Moving beyond this limited sense, Van Gulick defines various degrees of "modest emergence" in these terms.

> MODEST EMERGENCE: The whole has features that are *different in kind* from those of its parts (or alternatively that *could* be had by its parts). For example, a piece of cloth might be purple in hue even though none of the molecules that make up its surface could be said to be purple. Or a mouse might be alive even if none of its parts (or at least none of its subcellular parts) were alive.

Modest emergence thus arises in a spectrum of different ways depending upon the degree of difference between a phenomenon and the base out of which it emerges, with the coherent structures of nonlinear science providing many examples (Scott, 2003).

Among the more modest types of emergence, one would include solitons of the Korteweg–deVries (KdV) equation, which emerge out of a nonlinear partial differential equation (PDE) in response to certain initial conditions. Although KdV solitons are independent dynamic entities, their speeds and shapes are determined via the inverse scattering transform (IST) method from the initial conditions applied to the system. Somewhat less modest would be the various solitary wave solutions of Hamiltonian (energy conserving) systems for which IST formulations are not currently known and may not exist, precluding the prediction of solitary wave speeds from initial conditions.

Further decreasing modesty (increasing robustness) of emergence leads to the nerve impulse, which has several model PDEs (Hodgkin–Huxley, FitzHugh–Nagumo, etc.) in addition to those many physiological manifestations (the action potentials of the brain) which compose our mental activity (Scott, 2002). While propagating on a uniform system with constant speed and shape, a nerve impulse differs fundamentally from solitary waves of Hamiltonian systems for the following reason: a nerve impulse (like the flame of a candle) does not conserve energy. The nonlinear dynamics of a nerve impulse involves a balance between the release and dissipation of energy, so the process is open and thus does not have a Hamiltonian formulation. This, in turn, implies that the dynamic behavior of a nerve impulse changes greatly upon reversal of the direction of time, whereas the qualitative behavior of a Hamiltonian system is insensitive to time reversal.

Under this distinction, we can gauge the relative modesty of several other types of emergence that arise in the realms of nonlinear science. Vortex solutions of viscosity-free fluids (superfluids, for example) would be more modestly emergent than those of (more or less) viscous fluids, in which dissipative processes cause the dynamics to (more or less) rapidly forget the information received from the initial conditions. As residents of Tornado Alley in the U.S. midlands know well, tornados are famously ill-behaved, detached from their initial conditions and moving quite wildly in response to local variations of pressure, humidity, temperature, and so on.

A deeper meaning of Michelangelo's metaphor suggests the emergence of living organisms from the oily brine of the Hadean oceans some three thousand million years ago. Life is even less modestly (more robustly) emergent, with the "arrow of time" clearly constraining us all and playing a key role in the unpredictable drama of biological evolution (Gould, 1989). In other words, the emergence of life is far more intricate than the emergence of John Scott Russell's soliton from the prow of his test vessel on the Union Canal.

Yet more robust (less immodest) than the emergence of life is the phenomenon of human consciousness, which philosophers have struggled for centuries to

understand and many find qualitatively different from its material substrate. To include the qualitative aspects of emergence at this far end of the scale, Van Gulick introduces the following definition.

> RADICAL EMERGENCE: The whole has features that are both different in kind from those had by its parts, and of a kind whose nature and existence is not necessitated by the features of its parts, their mode of combination and the law-like regularities governing the features of its parts.

Whether human consciousness offers an example of radical emergence is currently controversial among cognitive scientists, neuroscientists, psychologists, cultural anthropologists, philosophers, and others interested in the nature of mind. On the one hand, reductive materialists assert that all of reality must "in principle" reduce to a physical basis (Kim, 1999), whereas substance dualists claim that the human mind differs ontologically (in its nature) from physical reality (Chalmers, 1996). Situated between these two positions, property dualists suggest that the human mind may radically emerge from intricate interactions among the various nonlinear dynamic levels of body, brain, and culture (Scott, 1995; Van Gulick, 2001).

ALWYN SCOTT

See also **Biological evolution; Game of life; Morphogenesis, biological**

Further Reading

Chalmers, D. 1996. *The Conscious Mind: In Search of a Fundamental Theory*, Oxford and New York: Oxford University Press

Gould, S.J. 1989. *Wonderful Life: The Burgess Shale and the Nature of History*, New York and London: Norton

Kim, J. 1999. *Mind in a Physical World*, Cambridge, MA: MIT Press

Scott, A.C. 1995. *Stairway to the Mind: The Controversial New Science of Consciousness*, Berlin and New York: Springer

Scott, A.C. 2002. *Neuroscience: A Mathematical Primer*, Berlin and New York: Springer

Scott, A.C. 2003. *Nonlinear Science: Emergence and Dynamics of Coherent Structures*, 2nd edition, Oxford and New York: Oxford University Press

Van Gulick, R. 2001. Reduction, emergence and other recent options on the mind/body problem. *Journal of Consciousness Studies*, 8(9–10): 1–34

ENDOMORPHISM

See **Maps**

ENERGY ANALYSIS

In time-reversible Hamiltonian systems, the total energy of the system is constant in time. A local change of the energy density W at a point x in time t is balanced by the energy flux S from/to the point x according to the energy balance equation:

$$\frac{\partial W}{\partial t} + \frac{\partial S}{\partial x} = 0.$$

In irreversible (active and/or dissipative) systems, the total energy changes in time due to the energy sinks/sources of density ρ are given by the extended the extended energy balance equation:

$$\frac{\partial W}{\partial t} + \frac{\partial S}{\partial x} = -\rho.$$

In mathematical physics, energy balance is used for analysis of well-posedness of partial differential equations. Solutions of well-posed differential equations remain bounded in a suitable function space, starting with a bounded initial data (Strauss, 1992). For illustration, we consider the energy balance for the heat equation $u_t = u_{xx}$ that takes the form

$$\frac{\partial}{\partial t}\left(u^2\right) - 2\frac{\partial}{\partial x}\left(uu_x\right) = -2\left(u_x\right)^2.$$

Suppose the initial data $u(x,0)$ belong to space of real-valued $L^2(\mathcal{R})$ functions such that the initial energy is bounded: $E(0) = \int_{-\infty}^{\infty} u^2(x,0)\,\mathrm{d}x < \infty$. The energy $E(t)$ decreases at later times such that $0 \le E(t) = \int_{-\infty}^{\infty} u^2(x,t)\,\mathrm{d}x \le E(0)$. These simple estimates of energy analysis immediately imply the following properties of the heat equation:

(i) The zero solution $u(x,t) = 0$ is unique.
(ii) A general solution $u(x,t)$ is asymptotically stable in space of $L^2(\mathcal{R})$ functions.
(iii) A general solution $u(x,t)$ decays uniformly to zero in the L^2-norm sense: $\lim_{t\to\infty} ||u(\cdot,t)||_{L^2(\mathcal{R})} = 0$.

A real-valued energy can be introduced for complex functions, for example, in the Schrödinger equation $\mathrm{i}u_t = u_{xx}$, where the energy balance takes the form

$$\frac{\partial}{\partial t}|u|^2 + \mathrm{i}\frac{\partial}{\partial x}\left(\bar{u}u_x - \bar{u}_x u\right) = 0.$$

The Schrödinger equation is reversible, and the total energy is constant in time such that $0 \le E(t) = \int_{-\infty}^{\infty} |u|^2(x,t)\,\mathrm{d}x = E(0)$. As a result, the solution is well-posed in the space of complex-valued $L^2(\mathcal{R})$ functions with the following properties:

(i) The zero solution $u(x,t) = 0$ is unique.
(ii) A general solution $u(x,t)$ is neutrally stable in the L^2-norm sense.

Partial differential equations can be well-posed in energy space, which is different from the space of square integrable functions. For the wave equation $u_{tt} = c^2 u_{xx}$, two balance equations take the form

$$\frac{\partial}{\partial t}\left(u_t^2 + c^2 u_x^2\right) - 2c^2\frac{\partial}{\partial x}\left(u_t u_x\right) = 0$$

and

$$\frac{\partial}{\partial t}\,(u_t u_x) - \frac{1}{2}\,\frac{\partial}{\partial x}\left(u_t^2 + c^2 u_x^2\right) = 0.$$

The first equation prescribes the positive-definite quantity, $E(t) = \int_{-\infty}^{\infty}\left(u_t^2 + c^2 u_x^2\right)\mathrm{d}x$, which defines the energy space $H^1(\mathcal{R})$ for solutions of the wave equation, such that $0 \le E(t) = E(0)$. The second equation prescribes the sign-indefinite quantity, $P(t) = \int_{-\infty}^{\infty} u_t u_x\,\mathrm{d}x$, referred to as the momentum, such that $P(t) = P(0)$.

In modeling of various physical phenomena, momentum balance equations are useful for analysis of integral properties of solutions of underlying equations at infinite or finite intervals. For instance, adiabatic dynamics of localized pulses, envelope wave packets, and radiative wave trains can be studied with the momentum balance equations, when a solitary wave changes under the action of external perturbations, variations of physical parameters, internal instabilities, various resonances, and interactions with other wave structures (Kivshar & Malomed, 1989). In the simplest version of the soliton perturbation theory, effects of external perturbations to a physical system are captured by slow variations of soliton parameters. The dynamical rate of change of soliton parameters is found by substituting the soliton solutions in the momentum balance equations. For illustration, we consider the perturbed sine-Gordon equation with dissipative and external harmonic forces:

$$\begin{aligned} u_{tt} - u_{xx} + \sin u &= \varepsilon\, R(u) \\ &= \varepsilon\,\left[-\alpha u_t + \Gamma \sin(\omega t)(1-\cos u)\right], \end{aligned}$$

where $\varepsilon \ll 1$, α is a damping parameter and Γ is the amplitude of the external force such that $\omega < 1$ (no resonance occurs). With the account of the perturbation, the balance equation for momentum is

$$\frac{\partial}{\partial t}\,(u_t u_x) - \frac{1}{2}\,\frac{\partial}{\partial x}\left(u_t^2 + u_x^2 + 2\cos u\right) = \varepsilon\, R(u) u_x.$$

As a result, the rate of change of momentum $P(t) = \int_{-\infty}^{\infty} u_t u_x\,dx$ is given by

$$\frac{\mathrm{d}P}{\mathrm{d}t} = \varepsilon \int_{-\infty}^{\infty} u_x R[u]\mathrm{d}x.$$

provided that $\lim_{|x|\to\infty}\left(u_t^2 + u_x^2\right) = 0$ and $\lim_{x\to\infty} \cos u = \lim_{x\to-\infty}\cos u = 1$. The unperturbed sine-Gordon equation at $\varepsilon = 0$ has the kink solution:

$$u_k(x,t) = 4\arctan\left(\exp\left(\frac{x - vt - x_0}{\sqrt{1-v^2}}\right)\right),$$

where $|v| < 1$ is the kink's velocity and x_0 is its position. The momentum of the unperturbed kink is a function of its velocity: $P_k(v) = -8v/\sqrt{1-v^2}$. The kink solution satisfies the aforementioned vanishing conditions at infinity. Assuming that the velocity of the kink $v = v(t)$ changes due to the external perturbation, we use the momentum balance equation and find a particle-like equation of motion for the kink's adiabatic dynamics:

$$\frac{\mathrm{d}P_k}{\mathrm{d}t} + \varepsilon\,\alpha P_k = 2\pi\,\varepsilon\,\Gamma \sin(\omega t).$$

The equation has a simple solution:

$$\begin{aligned} P_k(t) \;=\; & C\mathrm{e}^{-\varepsilon\alpha t} \\ & - \frac{2\pi\varepsilon\omega\Gamma}{\omega^2 + \varepsilon^2\alpha^2}\cos\omega t \\ & + \frac{2\pi\varepsilon^2\alpha\Gamma}{\omega^2 + \varepsilon^2\alpha^2}\sin\omega t, \end{aligned}$$

where C is found from initial condition: $P_k(0) = P_0$.

Adiabatic dynamics of kinks and solitary waves often generate a strong radiation field that takes away part of momentum of the localized solution. The radiation field can be taken into account from other balance equations, such as the mass balance. Radiative effects usually occur in the second order of the perturbation theory, leading to radiative decay of solitary waves or their perturbations (Pelinovsky & Grimshaw, 1996). For illustration, we consider dynamics of solitary waves in the critical KdV equation:

$$u_t + 15u^4 u_x + u_{xxx} = 0.$$

The balance equations for mass and momentum of a nonlinear field are:

$$\frac{\partial}{\partial t}(u) + \frac{\partial}{\partial x}\left(3u^5 + u_{xx}\right) = 0$$

and

$$\frac{\partial}{\partial t}(u^2) + \frac{\partial}{\partial x}\left(5u^6 + 2uu_{xx} - u_x^2\right) = 0.$$

Solitary waves are given by special solutions of the critical KdV equation:

$$u_{\mathrm{s}}(x,t) = \left[\sqrt{v}\,\mathrm{sech}(2\sqrt{v}(x - vt - x_0))\right]^{1/2}.$$

Solitary waves may change adiabatically due to internal perturbation of the initial data, such that v becomes a function of t. The radiation field is generated behind the solitary wave due to the uni-directional property of the dispersion relation for the linear KdV equation: $u_t + u_{xxx} = 0$. The radiation field can be found from the mass balance equation

$$\lim_{x\to-\infty} u(x,t) = -\frac{1}{v}\,\frac{\mathrm{d}M_{\mathrm{s}}}{\mathrm{d}t},$$

where $M_{\mathrm{s}}(v) = \int_{-\infty}^{\infty} u_{\mathrm{s}}(x,t)\,\mathrm{d}x = M_0/v^{1/4}$ and M_0 is constant. The momentum balance equation leads to a closed particle-like equation of motion for the solitary

wave's adiabatic dynamics:

$$\frac{\mathrm{d}}{\mathrm{d}t}\left[\left(\frac{\mathrm{d}M_s}{\mathrm{d}v}\right)^2\frac{\mathrm{d}v}{\mathrm{d}t}\right] = -v\left[\lim_{x\to-\infty}u(x,t)\right]^2$$
$$= -\frac{1}{v}\left(\frac{\mathrm{d}M_s}{\mathrm{d}v}\right)^2\left(\frac{\mathrm{d}v}{\mathrm{d}t}\right)^2.$$

The dynamical equation has a unique solution:

$$v(t) = v_0\left(\frac{t_0}{t_0 - t}\right)^2,$$

where v_0 and t_0 are constants. The exact solution defines the scaling law for self-similar blowup in the critical KdV equation. The blowup rate is modified due to generation of the radiation field, which makes the balance between the left- and right-hand sides of the momentum balance equation. To summarize, the balance equations for energy, momentum, and mass can be used for both qualitative and quantitative estimates of the interaction between localized and radiative components of the nonlinear wave in solutions of nonlinear wave equations.

DMITRY PELINOVSKY

See also **Constants of motion and conservation laws; Multisoliton perturbation theory; Power balance**

Further Reading

Kivshar, Yu.S. & Malomed, B.A. 1989. Dynamics of solitons in nearly integrable systems. *Reviews of Modern Physics*, 61: 763–915

Pelinovsky, D.E. & Grimshaw, R.H.J. 1996. An asymptotic approach to solitary wave instability and critical collapse in long-wave KdV-type evolution equations. *Physica* D, 98: 139–155

Strauss, W.A. 1992. *Partial Differential Equations: An Introduction*, New York: Wiley

ENERGY CASCADE

See **Turbulence**

ENERGY OPERATORS

See **Quantum nonlinearity**

ENTRAINMENT

See **Coupled oscillators**

ENTROPY

Entropy is a quantity characterizing disorder, or randomness. This conclusion is the result of successive advances since the pioneering works by Sadi Carnot on the fundamentals of steam engines in 1824 and by Rudolf Clausius, who, between 1851 and 1865, developed the concept of entropy (from $\tau\rho o\pi\eta$ meaning "transformation" in Greek) as a thermodynamic state variable. Called S, this quantity varies as $\mathrm{d}S = \mathrm{d}Q/T$ in an equilibrium system at temperature T exchanging a quantity $\mathrm{d}Q$ of heat and no matter reversibly with its environment.

Thereafter, Ludwig Boltzmann (1896/1898), Max Planck (1901), Josiah Willard Gibbs (1902), and others discovered the statistical meaning of entropy. Boltzmann and Gibbs introduced the concepts of probability and statistical ensemble in the context of mechanics. If P_α is the probability (satisfying $0 \le P_\alpha \le 1$ and $\sum_\alpha P_\alpha = 1$) that the system is found in the microstate α specified by a set of observables such as energy and linear or angular momenta, the thermodynamic entropy is given by

$$S = -k_\mathrm{B}\sum_\alpha P_\alpha \ln P_\alpha, \tag{1}$$

where $k_\mathrm{B} = 1.38065\ 10^{-23}\,\mathrm{J\,K^{-1}}$ is the so-called Boltzmann constant, although it was originally introduced by Planck (Sommerfeld, 1956).

The entropy S measures the disorder in a statistical ensemble composed of a very large number, $\mathcal{N}$, of copies of the system. Each copy is observed in a microstate α occurring with the probability P_α. The microstates of all the $\mathcal{N}$ copies form a random list $\{\alpha_1, \alpha_2, \ldots, \alpha_\mathcal{N}\}$. Typically, $\mathcal{N}_\alpha = \mathcal{N}P_\alpha$ copies are found in the microstate α, and $\sum_\alpha \mathcal{N}_\alpha = \mathcal{N}$. The copies being statistically independent, the total number of possible lists of the microstates of the ensemble is thus equal to

$$W = \frac{\mathcal{N}!}{\prod_\alpha \mathcal{N}_\alpha!}, \tag{2}$$

where $\mathcal{N}! = \mathcal{N}\times(\mathcal{N}-1)\times\cdots\times 3\times 2$ denotes the factorial of the integer $\mathcal{N}$. In the limit $\mathcal{N}\to\infty$, according to Stirling's formula $\mathcal{N}! \simeq (\mathcal{N}/\mathrm{e})^\mathcal{N}$, where $\mathrm{e} = 2.718\ldots$ denotes the Naperian base, entropy (1) is given in terms of the logarithm of the number W of possible lists (originally called complexions by Boltzmann):

$$S \simeq \frac{k_\mathrm{B}}{\mathcal{N}}\ln W. \tag{3}$$

If the system is perfectly ordered, all the copies in the ensemble would be in the same microstate, and there would be a single possible complexion $W = 1$ so that the entropy would vanish ($S = 0$). In contrast, if the system were completely disordered with A equiprobable microstates α, the entropy would take the maximum value $S = k_\mathrm{B}\ln A$. For partial disorder, the entropy takes an intermediate value.

In spatially extended homogeneous systems, the thermodynamic entropy is an extensive quantity. If the

system is covered by $\mathcal{N}$ disjoint windows of observations of volume V, the microstates $\{\alpha_1, \alpha_2, \ldots, \alpha_\mathcal{N}\}$ in the $\mathcal{N}$ windows form one among W possible lists (2). If the volume V of the observation window is large enough, the thermodynamic entropy is again given by Equation (3). In this case, the entropy per unit volume obtained by dividing the entropy S by the volume V is a measure of spatial disorder.

Entropy can also be interpreted as a quantity of information required to specify the microstate of the system. Indeed, the recording of the random microstates $\{\alpha_1, \alpha_2, \ldots, \alpha_\mathcal{N}\}$ of the statistical ensemble requires one to allocate at least $I = \log_2 W$ bits of information in the memory of a computer. This number of bits is related to the entropy (1) by $I \simeq \mathcal{N} S/(k_B \ln 2)$. Such connections between entropy and information have been developed since the works by Leo Szilard in 1929 and Léon Brillouin around 1951.

Equation (1) for the entropy is very general. It applies not only to equilibrium but also to out-of-equilibrium systems provided the states α are understood as coarse-grained states. In a classical system of N particles, the coarse-grained states α should correspond to cells of volume h^{3N} in the phase space of the positions and momenta of the particles, where $h = 6.626\ 10^{-34}$ Js is Planck's constant of quantum mechanics.

In 1902, Gibbs suggested that the second law of thermodynamics is a consequence of a dynamics having the mixing property according to which the statistical averages of observables or the coarse-grained probabilities P_α converge to their equilibrium values. Not all systems are mixing, but for those that are, entropy (1) converges toward its equilibrium value. In mixing systems, the statistical correlations in the initial probability distribution tend to disappear on finer and finer scales in phase space and are shared among more and more particles during a causal time evolution. The approach to the thermodynamic equilibrium may thus be described in terms of asymptotic expansions of the probability distributions in the long-time limits $t \to \pm\infty$. Both limits are not equivalent because, in the limit $t \to +\infty$, the probability distributions remain smooth in the unstable phase-space directions but become singular in the stable ones and vice versa in the other limit $t \to -\infty$, which may appear as an irreversibility or time arrow in the long-time description. The irreversibility in the increase of the entropy is thus closely related to the problems of identifying all the degrees of freedom guaranteeing the causality of the time evolution and of reconstructing the initial conditions, which is of great importance for the understanding of historical processes such as biological and cosmological evolution.

During recent decades, it has been shown that the increase of entropy does not preclude the formation of structures in equilibrium or non-equilibrium systems, nor in self-gravitating systems. At equilibrium, the homogeneity of pressure, temperature, and chemical potentials does not prevent inhomogeneities in the densities as is the case in crystals, in vortex states of quantum superfluids, and in mesomorphic phases of colloidal systems where equilibrium self-assembly occurs. Besides, open non-equilibrium systems can remove entropy to their environment, leading to far-from-equilibrium self-organization into spatial structures such as Turing patterns, self-sustained oscillations in such systems as chemical clocks, or complex processes such as biological morphogenesis.

While the entropy per unit volume characterizes spatial disorder at a given time, a concept of entropy per unit time was introduced in 1949 by Claude Shannon in development of his information theory, as a measure of temporal disorder in random or stochastic processes. It is defined in the same way as standard entropy but replacing space by time. In 1959, Andrei N. Kolmogorov and Yakov G. Sinai applied Shannon's idea to deterministic dynamical systems with an invariant probability measure, and they defined a metric entropy per unit time in analogy with Equation (1), considering the states α as the sequences $\omega_1\omega_2 \ldots \omega_n$ of the phase space cells ω_j successively visited at time intervals Δt by the trajectories during the time evolution of the system. In order to get rid of the arbitrariness of the coarse-grained cells ω_j, Kolmogorov and Sinai considered the supremum (least upper bound) of the entropy per unit time with respect to all possible partitions $\mathcal{P}$ of the phase space into cells ω_j, defining

$$h_{KS} = \mathrm{Sup}_\mathcal{P} \lim_{n\to\infty} -\frac{1}{n\Delta t} \times \sum_{\omega_1\omega_2\ldots\omega_n} P_{\omega_1\omega_2\ldots\omega_n} \ln P_{\omega_1\omega_2\ldots\omega_n}, \quad (4)$$

where the probability P is evaluated with the given invariant measure (Cornfeld et al., 1982).

In isolated chaotic dynamical systems, the temporal disorder of the trajectories finds its origin in the sensitivity to initial conditions because the Kolmogorov–Sinai entropy per unit time is equal to the sum of positive Lyapunov exponents λ_i, $h_{KS} = \sum_{\lambda_i>0} \lambda_i$, as proved by Yakov B. Pesin in 1977 (Eckmann & Ruelle, 1985). We notice that the entropy per unit time h_{KS} differs from the irreversible entropy production defined by the time derivative of the standard thermodynamic entropy S in an isolated system. Indeed, the entropy per unit time may take a positive value for a system of particles already at thermodynamic equilibrium where entropy production vanishes. In spatially extended chaotic systems, the spatiotemporal disorder can be characterized by a further concept of entropy per unit time and unit volume.

A so-called topological entropy has also been introduced as the rate of proliferation of cells in

successive partitions iteratively refined by the dynamics (Eckmann & Ruelle, 1985). In finite chaotic systems, the topological entropy is the rate of proliferation of periodic orbits as a function of their period. The topological entropy is not smaller than the Kolmogorov–Sinai entropy: $h_{\rm top} \geq h_{\rm KS}$.

PIERRE GASPARD

See also **Algorithmic complexity; Biological evolution; Cosmological models; Information theory; Lyapunov exponents; Measures; Mixing; Morphogenesis, biological; Nonequilibrium statistical mechanics; Pattern formation; Phase space; Stochastic processes; Turing patterns**

Further Reading

Boltzmann, L. 1896/1898. *Vorlesungen über Gastheorie*, 2 vols, Leipzig: Barth; as *Lectures on Gas Theory*, translated by S.G. Brush, Berkeley, University of California Press, 1964

Cornfeld, I.P., Fomin, S.V. & Sinai, Ya.G. 1982. *Ergodic Theory*, Berlin: Springer

Eckmann, J.-P. & Ruelle, D. 1985. Ergodic theory of chaos and strange attractors. *Reviews of Modern Physics*, 57: 617–656

Gibbs, J.W. 1902. *Elementary Principles in Statistical Mechanics*, New Haven, CT: Yale University Press

Planck, M. 1901. Uber das Gesetz der Energieverteilung im Normalspektrum. *Annalen der Physik*, 4: 553–563 (First historical publication of $S = k_{\rm B} \ln W$)

Sommerfeld, A. 1956. *Thermodynamics and Statistical Mechanics*, New York: Academic Press

ENVELOPE EQUATIONS

See **Nonlinear Schrödinger equations**

ENVELOPE SOLITONS

See **Solitons, types of**

EPHAPTIC COUPLING

Neurons communicate with each other by different means. The most investigated of these is synaptic transmission, which can be either chemical or electrical. Chemical synapses transmit neural signals from presynaptic to postsynaptic membranes via neurotransmitters and are widely found in vertebrate neurons, while electrical synapses correspond to an electronic coupling through specialized gap junctions and are more common in invertebrates (Jefferys, 1995). Therefore, both transmission processes need a specialized anatomical structure to create points of contact between neurons but there are other possibilities.

Since the work of Elwald Hering in 1882, it has been known that electrical communication can also occur between neurons when neuronal membranes are closely apposed but not contiguous (Scott, 2002). Called ephaptic coupling by Angelique Arvanitaki (who defined the term *ephapse* as "... the locus of contact or close vicinity of the active functional surfaces, whether this contact be experimental or brought by natural means"), this process relies on current spread through the extracellular space, which may influence the membrane dynamics of a second fiber (Arvanitaki, 1942). Early experimental evidence of ephaptic interactions was also provided by Bernhard Katz and Otto Schmitt on a pair of naturally adjacent unmyelinated fibers from the limb nerve of a crab (Katz & Schmitt, 1940). They showed that an impulse traveling on one fiber changes the excitability of the other fiber. Furthermore, impulses on adjacent fibers with similar speed and launched at about the same time become synchronized.

In the 1970s, Markin proposed a theoretical description of ephaptic coupling between two parallel unmyelinated fibers based on the assumption that they share an external series resistance per unit length proportional to the ionic resistivity of the extracellular medium (Markin, 1970). Using a piecewise constant function for the transmembrane ionic current, yielding to a leading-edge analysis, Markin concluded that under normal physiological conditions, ephaptic coupling does not allow transmission of an impulse from a fiber to an adjacent one, as verified in numerous experiments. Nevertheless, he also suggested that a synchronization of two impulses is to be expected with a longitudinal distance δ equal to zero.

A recent leading-edge analysis (Scott, 2002) considered a more appropriate representation of the ionic current (sodium ions), the resulting system corresponding to the Zeldovich–Frank-Kamenetsky (ZF) equation. In the case of a small ephaptic coupling, a perturbation theory showed that $\delta = 0$ corresponds to a stable locking of pairs of impulses if the threshold parameter a of the membrane is above a critical value, otherwise stability occurs with δ increasing when a decreases.

Other possibilities of synchronization have been found when studying the influence of complete impulses including a leading edge and a recovery part. Based on the FitzHugh–Nagumo model, studies have shown that two other locking distances δ are also stable and separated by two unstable ones (Scott, 2002; Eilbeck et al., 1981). Recently, it has also been shown that ephaptic coupling influences the speed of conduction of synchronized impulses, the speed decreasing when the coupling increases (Binczak et al., 2001).

In mammals, motor or sensory nerves are often organized in fiber bundles. These fibers are myelinated, and the active nodes of the membrane are separated

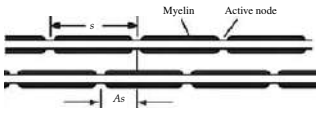

Figure 1. Sketch of two adjacent and parallel myelinated nerve fibers.

by a myelin sheath, which acts as an insulator. Thus, ephaptic coupling may be influenced by the alignment of the active nodes between two adjacent fibers (Binczak et al., 2001), as illustrated in Figure 1 where A is an alignment parameter.

Using a ZF description for the ionic current, a leading-edge analysis suggests that synchronization of impulses occurs whatever the alignment A. Nevertheless, an alignment of the nodes ($A = 1$) leads to a stronger synchronization while staggered nodes ($A = \frac{1}{2}$) allow a broader impulse coupling. Furthermore, when impulses are synchronized, an alignment of adjacent nodes reduces the critical longitudinal internodal distance at which propagation fails. Staggered nodes, on the other hand, lead to a more robust medium in order to prevent propagation failure.

From a functional perspective, synchronization of impulses on parallel and adjacent fibers might provide a means to adjust and organize the timing of impulses necessary for coordination and computation of neuronal information. Furthermore, ephaptic interactions may be important in neurological pathophysiology. Indeed, it has been observed that the transmission of impulses occurs from a fiber to an adjacent one when nerves are damaged, as when the nerves end in a neurisma after a nerve crush injury or a nerve compression (Seltzer & Devor, 1979) or when the ionic composition of the extracellular medium is changed (Ramon & Moore, 1978). Demyelination diseases, such as multiple sclerosis, are also a cause of ephaptic connections leading to pathological synchronization (Jefferys, 1995). Finally, ephaptic phenomena have been reported between muscles and motor nerves causing possible cramps and spasms and between cardiac cells, implying a possible involvement of ephaptic coupling in cardiac arrhythmias (Suenson, 1984).

STEPHANE BINCZAK

See also **FitzHugh–Nagumo equation; Myelinated nerves; Neurons; Zeldovich–Frank-Kamenetsky equation**

Further Reading

Arvanitaki, A. 1942. Effects evoked in an axon by the activity of a contiguous one. *Journal of Neurophysiology*, 5: 89–108

Binczak, S., Eilbeck, J.C. & Scott, A.C. 2001. Ephaptic coupling of myelinated nerve fiber. *Physica D*, 148: 159–174

Eilbeck, J.C., Luzader, S.D. & Scott, A.C. 1981. Pulse evolution on coupled nerve fibers. *Bulletin of Mathematical Biology*, 43(3): 389–400

Jefferys, J.G.R. 1995. Nonsynaptic modulation of neuronal activity in the brain: electric currents and extracellular ions. *Physiological Reviews*, 75 (4): 689–723

Katz, B. & Schmitt, O.H. 1940. Electric interaction between two adjacent nerve fibers. *Journal of Physiology*, 97: 471–488

Markin, V.S. 1970. Electrical interactions of parallel nonmyelinated fibers. I and II. *Biophysics*, 15: 122–133 and 713–721

Ramon, F. & Moore, J.W. 1978. Ephaptic transmission in squid giant axons. *American Journal of Physiology: Cell Physiology*, 234: C162–C169

Seltzer, Z. & Devor, M. 1979. Ephaptic transmission in chronically damaged peripherical nerves. *Neurology*, 29: 1061–1064

Scott, A.C. 2002. *Neuroscience: A Mathematical Primer*, Berlin and New York: Springer

Suenson, M. 1984. Ephaptic impulse transmission between ventricular myocardial cells in vitro. *Acta Physiologica Scandinavica*, 120: 445–455

EPIDEMIOLOGY

Throughout human history diseases have played an important role. The black death in Europe in the middle ages is one example, and more recent examples include the flu pandemic of 1918 and 1919 and diseases such as AIDS and various childhood diseases. Additionally, the study of population dynamics in ecology has been greatly advanced by the study of diseases for several reasons. First, the data on the incidence of childhood diseases are both extensive and accurate. Second, the processes involved in the dynamics of childhood diseases (essentially, infection and either recovery or death) are relatively simple and straightforward and well understood.

In particular, many questions of scientific or practical interest can be answered using relatively simple models. A fundamental question is why does a disease die out before everyone has the disease? And, what fraction of the population needs to be vaccinated so a disease can be controlled or eliminated? Answering this question can explain why smallpox was more easily eradicated than other so-called childhood diseases.

Perhaps the simplest epidemic model, which also introduces many of the ideas, is the case of a single epidemic of a disease, first studied in detail by Kermack and McKendrick (1927). We focus here on diseases that are caused by microparasites, so individuals either have the disease or do not, as opposed to diseases caused by macroparasites (such as tapeworms) where the number of infectious agents in individuals needs to be considered explicitly in order to understand the disease dynamics. Different models are needed to understand epidemics and diseases which are endemic (Kermack & McKendrick, 1932).

We assume a constant population size and divide the population into three classes: susceptible, infective, and removed. Since the time scale of an epidemic is much shorter than the time scale of changes in human population sizes, we can simplify the system by ignoring any demographic influences in the simplest model for an epidemic, which corresponds to the assumption of a constant population size. In other words, the population size is assumed constant, and births and deaths are ignored (although there are models that do take this into account) because the time scale of an epidemic is short relative to the time scale of human population dynamics.

We assume that the rate at which susceptibles become infected is simply proportional to the product of the number of susceptible and infective individuals, corresponding to an assumption of random encounters. The rate at which infective individuals recover is assumed to be a constant. Then, with S the number of susceptibles, I the number of infectives, and R the number of removed individuals, the dynamics are given by

$$\frac{dS}{dt} = -\beta SI, \tag{1}$$

$$\frac{dI}{dt} = \beta SI - \gamma I, \tag{2}$$

$$\frac{dR}{dt} = \gamma I. \tag{3}$$

Under the assumption that the total population size N remains constant, we can use the relationship $N = S + I + R$, and reduce the system (1)–(3) to one based on just the first two equations. The phase plane analysis of the resulting system is facilitated by the fact that the formula

$$\frac{dI}{dS} = \frac{\gamma}{\beta S} - 1 \tag{4}$$

is so simple. As first discussed by Kermack and McKendrick (1927), one can solve this system explicitly by integration and using approximations. From this one can see that the solution curves which start with I arbitrarily small return to $I = 0$ before all individuals in the population become infected, or in other words the number of susceptibles at $t = \infty$ is positive.

The qualitative behavior of the system (1)–(3) essentially depends on a single nondimensional parameter, the reproductive number for the disease. The reproductive number is defined as the mean number of infective individuals produced by a single infective individual, which can clearly be calculated by multiplying the rate at which a single infective individual produces new infections by the mean period of infectivity for a single individual. Under our assumptions, the mean rate of infection is simply βS and the mean infective period is $1/\gamma$. Thus the reproductive number is simply

$$R_0 = \frac{\beta S}{\gamma}. \tag{5}$$

The dynamics are governed by the observation that the number of infectives will increase if $R_0 > 1$ and will decrease if $R_0 < 1$. For the case of a single infective introduced into a population of susceptibles, we can use the total population N instead of S in the formula for R_0.

The import of the observation about the importance of R_0 (and results from integrating (4)) is typically summarized in the *threshold theorem* which states that there will be an epidemic if the population initially satisfies $R_0 > 1$, which may be a reflection of the population size. From integrating (4) one finds that the total number of individuals who get the disease is dramatically larger if the population is initially above the threshold.

Kermack & McKendrick (1932) further studied the cases of endemic diseases, where it is necessary to take into account the demography of the population, since the time scale is long enough that births and deaths need to be explicitly included. Other more complex systems were also studied (Kermack & McKendrick, 1933).

Modifications of the basic equations have been used to study the dynamics of sexually transmitted diseases, including AIDS. Here, an important modification has been to break up the population into classes based on different encounter rates.

More recent work on disease dynamics has played a central role in population biology, as the data sets for the incidence of childhood diseases in the United Kingdom and many large U.S. cities are among the longest, most accurate, and most detailed records of populations available (Bjornstad & Grenfell, 2001). In particular, the prevaccination dynamics of measles has been carefully analyzed using a variety of approaches, based essentially on extensions of the basic model (Equations (1)–(3)), modified to include a seasonally varying contact rate and, in some cases, stochasticity. Studies of this data has led to important substantial advances in the analysis of the kinds of time series available: relatively short with substantial stochastic influences. Analysis of these time series using nonlinear methods have demonstrated that at least some of the dynamics may be chaotic. Further and more recent efforts have focussed on spatiotemporal dynamics (Rohani et al., 1999) and on applied questions (Keeling et al., 2002) like the recent hoof and mouth epidemic in the UK.

ALAN HASTINGS

See also **Chaotic dynamics; Phase plane; Population dynamics**

Further Reading

Bjornstad, O.N. & Grenfell, B.T. 2001. Noisy clockwork: time series analysis of population fluctuations in animals. *Science*, 293: 638–643

Diekmann, O. & Heesterbeek, J.A.P. 2000. *Mathematical Epidemiology of Infectious Diseases*, Chichester and New York: Wiley

Keeling, M.J., Woolhouse, M.E.J., Shaw, D.J., Matthews, L., Chase-Topping, M., Haydon, D.T., Cornell, S.J., Kappey, J., Wilesmith, J. & Grenfell, B.T. 2002. Dynamics of the 2001 UK foot and mouth epidemic: stochastic dispersal in a heterogeneous landscape. *Science*, 294: 813–817

Kermack, W.O. & McKendrick, A.G. 1927. Contributions to the mathematical theory of epidemics. *Proceedings of the Royal Society of London A*, 115: 700–721

Kermack, W.O. & McKendrick, A.G. 1932. Contributions to the mathematical theory of epidemics. *Proceedings of the Royal Society of London A*, 138: 55–83

Kermack, W.O. & McKendrick, A.G. 1933. Contributions to the mathematical theory of epidemics. *Proceedings of the Royal Society of London A*, 141: 94–122

Rohani, P., Earn, D.J.D. & Grenfell, B.T. 1999. Opposite patterns of synchrony in sympatric disease metapopulations. *Science*, 286: 968–971

EQUATIONS, NONLINEAR

Nonlinear equations arise in a wide variety of forms in all branches of science, engineering, and technology as well as in other fields such as economics and social dynamics. These include algebraic, differential (ordinary/partial/delay), difference, differential-difference, integro-differential, and integral equations.

Nonlinear algebraic equations such as polynomial (quadratic, cubic, quartic, etc.) and transcendental equations in one or more variables and simultaneous equations have a chequered history. A large number of root-searching algorithms and methods of solutions are available in the literature.

With the advent of differential calculus in the 17th century, differential equations started to play a pivotal role in scientific investigations. This is particularly so for evolutionary problems, as differential equations are obvious candidates for the dynamical description of natural phenomena. Since most natural processes are nonlinear, it is no wonder that nonlinear differential equations arise frequently in theoretical descriptions (Ablowitz & Clarkson, 1991; Murray, 2002; Lakshmanan & Rajasekar, 2003; Scott, 2003).

Nonlinear ordinary differential equations (ODEs) occur in a wide variety of situations depending upon the nature of the problem. Their solution properties, such as integrability, non-integrability, and chaos, depend upon the order of the highest derivative, number of dependent variables, degree of nonlinearity, whether homogeneous or inhomogeneous, and on the values of the parameters. Some ubiquitous nonlinear ODEs and their significance are indicated in Table 1.

Nonlinear partial differential equations (PDEs) also have a long history dating back to the early days of differential calculus. For example, the basic equations of fluid dynamics, such as the Euler equation and the Navier–Stokes equation, are highly nonlinear. Many of the equations describing nontrivial surfaces in geometry are essentially nonlinear. The properties of solutions of nonlinear PDEs depend heavily on the number of dependent and independent variables, the order, the nature of nonlinearity, and the boundary conditions. However, it is also useful to classify the nonlinear PDEs into nonlinear dispersive and nonlinear diffusive/dissipative types. Further, they can

	Name	Equation	Significance
1.	Logistic equation	$\dot{x} = ax - bx^2$	Population growth model
2.	Bernoulli equation	$\dot{x} + P(t)x = Q(t)x^n$	Linearizable
3.	Riccati equation	$\dot{x} + P(t) + Q(t)x + R(t)x^2 = 0$	Admits nonlinear superposition principle
4.	Lotka–Volterra equation	$\dot{x} = ax - xy$, $\dot{y} = xy - by$	Population dynamics; exhibits limit cycle
5.	Anharmonic oscillator	$\ddot{x} + \omega_0^2 x + \beta x^3 = 0$	Integrable by Jacobian elliptic function(s)
6.	Pendulum equation	$\ddot{\theta} + \frac{g}{L}\sin\theta = 0$	Integrable by Jacobian elliptic function(s)
7.	Painlevé II equation	$\ddot{x} = 2x^3 + tx + \alpha$	Satisfies Painlevé property
8.	Duffing oscillator	$\ddot{x} + p\dot{x} + \omega_0^2 x + \beta x^3 = f\cos\omega t$	Exhibits chaotic dynamics
9.	Damped driven pendulum	$\ddot{\theta} + \alpha\dot{\theta} + \omega_0^2 \sin\theta = \gamma\cos\omega t$	Exhibits chaotic dynamics
10.	Lorenz equation	$\dot{x} = \sigma(y - x)$, $\dot{y} = -xz + rx - y$, $\dot{z} = xy - bz$	Prototypical example of chaotic motion
11.	Hénon–Heiles system	$\ddot{x} + x + 2xy = 0$, $\ddot{y} + y + x^2 - y^2 = 0$	Hamiltonian chaos
12.	Mackey–Glass equation	$\dot{x} + \frac{ax_\tau}{(1+x_\tau^{10})} + bx = 0$, $x_\tau = x(t-\tau)$, τ : constant	Delay-differential system

Table 1. Some important nonlinear ordinary differential equations ($\cdot = \mathrm{d}/\mathrm{d}t$)

	Name	Equation	Significance
I	*Dispersive Equations*		
1.	Korteweg–de Vries equation	$u_t + 6uu_x + u_{xxx} = 0$	Integrable soliton eqn. in (1+1) dimensions
2.	Sine-Gordon equation	$u_{xt} = \sin u$	Integrable soliton eqn. in (1+1) dimensions
3.	Nonlinear Schrödinger equation	$\mathrm{i}q_t + q_{xx} + 2\lvert q\rvert^2 q = 0$	Integrable soliton eqn. in (1+1) dimensions
4.	Heisenberg ferromagnetic spin equation	$\mathbf{S}_t = \mathbf{S} \times \mathbf{S}_{xx}$, $\mathbf{S} = (S_1, S_2, S_3)$	Integrable soliton eqn. in (1+1) dimensions
5.	Kadomtsev–Petviashvili equation	$(u_t + 6uu_x + u_{xxx})_x + 3\sigma^2 u_{yy} = 0$, $\sigma^2 = \pm 1$	Integrable soliton eqn. in (2+1) dimensions
6.	Davey–Stewartson equation	$\mathrm{i}q_t + \frac{1}{2}(q_{xx} + q_{yy}) + \alpha\lvert q\rvert^2 q + q\phi = 0$, $\phi_{xx} - \phi_{yy} + 2\alpha(\lvert q\rvert^2)_{xx} = 0$, $\alpha = \pm 1$	Integrable soliton eqn. in (2+1) dimensions
7.	ϕ^4 equation	$u_{tt} - u_{xx} + u - u^3 = 0$	Nonintegrable equation
II	*Diffusive equations*		
8.	Burgers equation	$u_t + uu_x - u_{xx} = 0$	Linearizable through Cole–Hopf transformation
9.	FitzHugh–Nagumo equation	$u_t = u_{xx} + u - u^3 - v$, $v_t = a(u - b)$	Nerve impulse propagation model
10.	Kuramoto–Sivashinsky equation	$u_t = -u - u_{xx} - u_{xxxx} - uu_x$	Spatiotemporal patterns and chaos
11.	Ginzburg–Landau equation	$u_t = (a + \mathrm{i}b)\nabla^2 u + (c + \mathrm{i}d)(\lvert u\rvert^2)u$	Spatiotemporal patterns and chaos

Table 2. Some important nonlinear partial differential equations (suffix denotes partial derivative with respect to that variable)

be classified into integrable and non-integrable PDEs. A select set of such equations along with their significance is given in Table 2.

Another class of interesting nonlinear equations is the so-called difference equations/recurrence equations/iterated maps of the form $\boldsymbol{x}_{n+1} = \boldsymbol{F}(\boldsymbol{x}_n, n)$, where the independent/time variable n takes discrete values $n = 0, 1, 2, \ldots$, and $\boldsymbol{x}_n$ stands for the m dependent variables, while $\boldsymbol{F}$ is an m-dimensional nonlinear function. These equations often correspond to various finite-difference schemes of nonlinear ODEs/PDEs, such as the explicit Euler or implicit midpoint. For example, the logistic differential equation $\mathrm{d}x/\mathrm{d}t = ax - bx^2$ can be approximated by Euler's forward difference scheme as $x_{n+1} - x_n = h(ax_n - bx_n^2)$, where $h > 0$. But nonlinear difference equations can arise as dynamical systems on their own merit as in population dynamics or radioactive decay. The most famous example is the logistic map,

$$x_{n+1} = \lambda x_n(1 - x_n), \quad 0 \le x \le 1, \quad 0 \le \lambda \le 4,$$

as a prototypical model exhibiting a period-doubling bifurcation route to chaos. A two-dimensional example is the Hénon map, $x_{n+1} = 1 - ax_n^2 + y_n$, $y_{n+1} = bx_n$, $a, b > 0$ showing self-similar and fractal nature. Spatiotemporal patterns have been identified in coupled logistic map lattices. There also exist several integrable families of maps (Kosmann-Schwarzbach et al., 1997): for example, the McMillan map,

$$x_{n+1} + x_{n-1} = \frac{2\mu x_n}{1 - x_n^2}. \tag{1}$$

Other examples include integrable discrete Painlevé equations; Quispel, Robert, and Thompson (QRT) map; and so on. Several integrable nonlinear differential-difference and difference-difference equations also exist (Ablowitz & Clarkson, 1991). The Toda lattice equation

$$\ddot{x}_n = \exp(-(x_n - x_{n-1})) - \exp(-(x_{n+1} - x_n)),$$
$$n = 0, 1, 2, \ldots, N \tag{2}$$

is an integrable soliton system. Examples of integrable nonlinear difference-difference equations can be constructed from integrable PDEs.

Nonlinear integro-differential equations arose (Davis, 1962) with the work of Vito Volterra when he introduced a hereditary component composed of the sum of individual factors encountered in the past as a modification to the logistic equation as

$$\frac{\mathrm{d}y}{\mathrm{d}t} = ay - by^2 + y\int_c^t K(t - s)y(s)\,\mathrm{d}s, \tag{3}$$

where a, b, c are parameters and $K(t)$ is a given function. A special case of such an equation is the nonlinear integral equation

$$y(x) = f(x) + \lambda \int_a^b K(x, s, y(s))\, \mathrm{d}s, \qquad (4)$$

where λ is a parameter. Some interesting special cases correspond to $f = 0$, $K = \bar{k}(x, t)y^n$ and $f = 0$, $K = G(x, t)\exp y$ (Bratu equation), where $\bar{k}$ and G are specified functions. One of the most important nonlinear integro-differential equations in physics is the Boltzmann transport equation for the distribution function $f(\boldsymbol{r}, \boldsymbol{v}, t)$ of a dilute gas

$$\left(\frac{\partial}{\partial t} + \boldsymbol{v}_1 \cdot \nabla_r + \frac{\boldsymbol{F}}{m} \cdot \nabla_{\boldsymbol{v}_1}\right) f(\boldsymbol{r}, \boldsymbol{v}_1, t) = \int d^3 v_2 \int d\Omega\, \sigma(\Omega) |\boldsymbol{v}_2 - \boldsymbol{v}_1| (f_1' f_2' - f_1 f_2), \quad (5)$$

where $f_i' = f(\boldsymbol{r}, \boldsymbol{v}_i', t)$, $f_i = f(\boldsymbol{r}, \boldsymbol{v}_i, t)$, $i = 1, 2$. In the integrable soliton case, there exist several interesting integro-differential equations, for example, the Benjamin–Ono equation,

$$u_t + 2uu_x + Hu_{xx} = 0, \qquad (6)$$

where Hu is the Hilbert transform.

MUTHUSAMY LAKSHMANAN

See also **Maps; Ordinary differential equations, nonlinear; Partial differential equations, nonlinear**

Further Reading

Ablowitz, M.J & Clarkson, P.A. 1991. *Solitons, Nonlinear Evolution Equations and Inverse Scattering*, Cambridge and New York: Cambridge University Press

Davis, H.T. 1962. *Introduction to Nonlinear Differential and Integral Equations*, New York: Dover

Ince, E.L. 1956. *Ordinary Differential Equations*, New York: Dover

Kosmann-Schwarzbach, Y., Grammaticos, B. & Tamizhmani, K.M., (editors). 1997. *Integrability of Nonlinear Systems*, Berlin and New York: Springer

Lakshmanan, M. & Rajasekar, S. 2003. *Nonlinear Dynamics: Integrability, Chaos and Patterns*, Berlin: Springer

Murray, J.D. 2002. *Mathematical Biology*, Berlin and New York: Springer

Scott, A.C. 2003. *Nonlinear Science: Emergence and Dynamics of Coherent Structures*, 2nd edition, Oxford: Oxford University Press

EQUILIBRIUM

The word *equilibrium* suggests a balance, typically between antagonistic forces, which in turn often implies absence of motion. Consider a rigid rod, which can freely (i.e., with almost no friction) rotate in a vertical plane about a horizontal axis located near one of its ends. Because of gravity, the rod naturally assumes a position where it is suspended from the horizontal axis, and points downward (see Figure 1a). In this situation, the gravity force acting on the rod is balanced by the reaction force at the suspension point, and no motion occurs. The rod is in equilibrium. If displaced a little bit from this position, the rod oscillates about the horizontal axis and, because of friction, eventually returns to its initial position, which is therefore stable. The other equilibrium position of the rod, which is unstable, is that shown in Figure 1b, where the rod points upward. A slight perturbation will take the rod away from this position, toward the stable equilibrium. Consider now a marble rolling on an uneven floor. Typically, it will keep rolling until it stops in a depression of the floor or reaches a wall or a corner of the room. It is clear from this example that depending on the configuration of the floor, there may be more than one stable equilibrium position. As in the case of the rod, there also exist unstable equilibria, which correspond to local maxima of the floor surface. In both of these examples, motion takes place as to decrease the potential energy of the system, which increases with elevation.

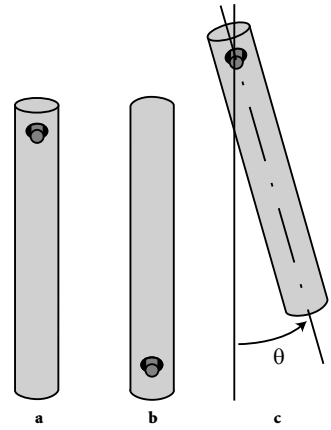

Figure 1. Stable (a) and unstable (b) equilibrium positions of a simple pendulum. (c) The angle θ is measured from the vertical.

From a mathematical point of view, an equilibrium corresponds to a stationary solution of a differential system or a map (see, for instance, Arnol'd, 1992). Quite often, these equations are mathematical models of physical, chemical, or biological systems. Consider the differential equation

$$\frac{\mathrm{d}^2\theta}{\mathrm{d}t^2} = -\sin(\theta) \qquad (1)$$

describing the motion (in dimensionless form) of a simple pendulum, similar to the rigid rod discussed above but without friction. Here, the variable θ measures the angle between the pendulum and the vertical (see Figure 1c). Time-independent solutions of (1) are obtained by setting the right-hand side of this equation to zero. This gives an infinite number of critical points $\theta = 2p\pi$ and $(2p+1)\pi$, where p is an integer. The first family of solutions can be identified with the stable equilibrium of the pendulum discussed above; the second family corresponds to its unstable equilibria.

Nondissipative mechanical systems conserve their total energy. Typically, the latter can be written in dimensionless form as

$$E(u) \equiv \tfrac{1}{2}(\dot{u})^2 + V(u) = \text{constant}, \tag{2}$$

where u is a time-dependent variable which describes the position of the system and $\dot{u}$ is its derivative. Taking the derivative of (2) with respect to time and dividing by $\dot{u}$ gives

$$\frac{\mathrm{d}^2u}{\mathrm{d}t^2} = -\frac{\mathrm{d}V}{\mathrm{d}u}. \tag{3}$$

In the case of the pendulum, $u = \theta$ and E is obtained by multiplying (1) by $\dot{\theta} = \mathrm{d}\theta/\mathrm{d}t$ and integrating over time. It reads

$$E = \frac{1}{2}\left(\frac{\mathrm{d}\theta}{\mathrm{d}t}\right)^2 - \cos(\theta). \tag{4}$$

The first term on the right-hand side of E corresponds to the (dimensionless) kinetic energy of the pendulum and the second term to its potential energy V. The graph of V as a function of θ is plotted in Figure 2a. We see that solutions $\theta = 2p\pi$ are minima of V, and solutions of the form $\theta = (2p+1)\pi$ are maxima of V. This can be understood in general as follows. Since the right-hand side of (3) vanishes at an equilibrium point, the latter corresponds to an extremum of the potential energy $V(u)$. Because $-\mathrm{d}V/\mathrm{d}u$ can be interpreted as a force, a minimum of V corresponds to a stable equilibrium, for which the force is restoring. Similarly, maxima of V identify unstable equilibria, as illustrated in Figure 2b. In dynamical systems terminology (see, for instance, Guckenheimer & Holmes, 1990), solutions $\theta = 2p\pi$ of (1) are centers and are *neutrally* stable; solutions $\theta = (2p+1)\pi$ are saddles and are unstable. If we now add a friction term to Equation (1), we get

$$\frac{\mathrm{d}^2\theta}{\mathrm{d}t^2} = -\sin(\theta) - c\frac{\mathrm{d}\theta}{\mathrm{d}t}. \tag{5}$$

This equation has the same equilibria as (1) but now the total energy E decreases as a function of time, $\mathrm{d}E/\mathrm{d}t = -c\ (\mathrm{d}\theta/\mathrm{d}t)^2$, and as a consequence,

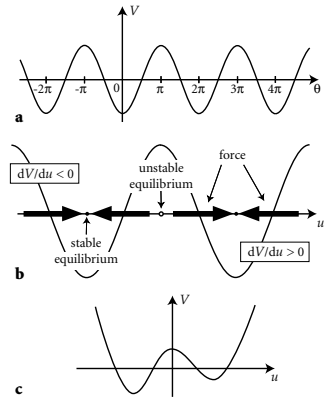

Figure 2. (a) Potential energy $V(\theta) = -\cos(\theta)$ of the simple pendulum. (b) Minima of the potential energy correspond to stable equilibria, whereas maxima describe unstable equilibria. (c) Double-well potential.

the equilibrium corresponding to solutions of the form $\theta = 2p\pi$, where p is an integer, is *globally asymptotically* stable.

In the situation depicted in Figure 2c, V is a double-well potential and the system is *bistable*. Generically, the two minima correspond to different values of the potential energy; the absolute minimum is then the most stable equilibrium of the system; the other minimum corresponds to a metastable equilibrium position.

In the case of maps, equilibria (i.e., stationary solutions) are often called fixed points. For instance, the map

$$u_{n+1} = 2u_n - |u_n|^2 u_n \tag{6}$$

with $u_n \in \mathbb{R}$ has three fixed points, given by $u_n = u_\mathrm{e}$ for all values of n, where $u_\mathrm{e} = 0$ or $u_\mathrm{e} = \pm 1$. They are obtained by substituting the unknown equilibrium value u_e for u_n in Equation (6) and solving for u_e. If we now consider the same map but let u_n be complex, we see that we have, together with the solution $u_\mathrm{e} = 0$, a whole family of equilibria, given by $u_\mathrm{e} = \exp(\mathrm{i}\varphi)$, where φ is an arbitrary real number. This happens because Equation (6) with u_n complex has the following gauge symmetry: if u_n is a sequence of iterates of the map, then so is $u_n \exp(\mathrm{i}\varphi)$, but with, of course, a different initial condition, $u_0 \exp(\mathrm{i}\varphi)$. More generally, by applying a symmetry of the equation to one of its solutions, one typically obtains another solution. If one starts this iterative process with an equilibrium, a collection of other equilibria is generated. Moreover, if the symmetry is continuous, as it is the case for

the gauge invariance of Equation (6) with u_n complex, a continuous family of relative equilibria is created. Similarly, if the symmetry is discrete, a discrete family of equilibria is obtained. For instance, Equation (6) with u_n real has the symmetry $u_n \to -u_n$; as a consequence if $u_e = 1$ is an equilibrium, so is $u_e = -1$.

Similar ideas apply to differential equations. Equations (1) and (5) have the discrete symmetry $\theta \to \theta + 2\pi$. The Landau equation

$$\frac{du}{dt} = u - |u|^2 u, \quad u \in \mathbb{C}, \tag{7}$$

which is the continuous version of Equation (6) with $u_n \in \mathbb{C}$, has the continuous symmetry $u \to u\exp(i\varphi)$, and its equilibria are given by $u = 0$ and $u = \exp(i\varphi)$, where φ is an arbitrary real number.

JOCELINE LEGA

See also **Pendulum; Stability; Symmetry: equations vs. solutions**

Further Reading

Arnol'd, V.I. 1992. *Ordinary Differential Equations*, 3rd edition, Berlin and New York: Springer

Guckenheimer, J. & Holmes, P. 1990. *Nonlinear Oscillations, Dynamical Systems, and Bifurcations of Vector Fields*, New York and London: Springer

EQUIPARTITION OF ENERGY

In 1845, the Scottish scientist John James Waterston submitted a large manuscript outlining a kinetic theory of gases to the Royal Society of London for publication in *Philosophical Transactions*. The central idea of this theory was that heat should be viewed as nothing but the energy associated with the motions of the enormous numbers of molecules, which themselves constitute the gas. Among his results, Waterston noted that "in mixed media the mean square molecular velocity is inversely proportional to the specific weight of the molecules," where the constant of proportionality is to be identified as a measure of thermodynamic temperature. This result is the essence of the Principle of Equipartition of Energy. The manuscript was rejected for publication at the time (as "nonsense, unfit even for reading before the Society") and then published (Waterston, 1893) almost 50 years later when it was (re)discovered by Lord Rayleigh who prefaced the paper with the suggestion that Waterston should be ranked "among the very foremost theorists of all ages."

In the years while Waterston's manuscript lay dormant, the kinetic theory of gases became established, mainly through the collected works of Rudolf Clausius, James Clerk Maxwell, and Ludwig Boltzmann (Brush, 1965, 1966) utilizing statistical methods to describe equilibrium properties. In 1868 Boltzmann obtained one of the most important results of this period, the (Maxwell–Boltzmann) distribution of energy among the molecules for a gas in thermal equilibrium. Let ε denote the energy of a molecule with r degrees of freedom, and position and momentum coordinates in the range $d\omega = \delta q_1 \ldots \delta q_r \delta p_1 \ldots \delta p_r$; the number of such molecules is proportional to the product of the extension $d\omega$ and the Boltzmann factor

$$\exp(-\varepsilon/kT).$$

In the Boltzmann factor, $k = 1.38 \times 10^{-16}$ erg/deg is a constant and T is the absolute temperature. The statistical justification for the Maxwell–Boltzmann distribution is that it is the most probable distribution for the distribution of energy among the possible states for a large number of molecules making up a system at constant energy.

Boltzmann derived the Principle of Equipartition of Energy from the Maxwell–Boltzmann distribution in 1871. In Boltzmann's formulation the mean energy associated with each variable that contributes a quadratic term to the total energy of the molecule has the same value $kT/2$. Thus, the mean energy of a molecule in a system is independent of mass—lighter molecules travel faster. From the mean energy per molecule, it is a simple matter to multiply by the total number of molecules to find the total energy and then to differentiate the total energy with respect to the temperature to find the specific heat at constant volume.

For example, for a perfect monatomic gas of N point atoms where $E = \sum_{i=1}^{N} m v_i^2/2$, there are $3N$ quadratic terms. Thus the internal energy of the gas is $U = 3NkT/2$, and the specific heat at constant volume is $C_V = 3Nk/2$. A simple thermodynamic calculation for the ratio of the specific heat at constant pressure to the specific heat at constant volume yields $\gamma = \frac{5}{3}$ in good agreement with experimental values for the inert gases. In the case of a crystal of N point atoms vibrating about their equilibrium positions according to Hooke's law (harmonic oscillators), there are three quadratic terms for the kinetic energy and three for the potential energy for each particle. Thus, the total internal energy is $U = 3NkT$ and the specific heat is $C_V = 3Nk$, in agreement with the empirical result obtained by Pierre-Louis Dulong and Alexis-Thérèse Petit in 1819.

In 1918 Richard Tolman derived the general Equipartition Principle (Tolman, 1918),

$$\left\langle q_i \frac{\partial \varepsilon}{\partial q_i} \right\rangle = \left\langle p_j \frac{\partial \varepsilon}{\partial p_j} \right\rangle = kT$$

which agrees with Boltzmann's result in the case where ε is a quadratic function of the q_i and p_j but can be applied more generally when ε is not a quadratic function.

Toward the end of the 19th century, some of the predictions from the classical Equipartition Principle were found to be at odds with experimental results.

Examples include the energy distribution from black body radiation, the specific heats of low temperature solids, and the specific heats of diatomic gases. The eventual resolution of these problems played a pivotal role in the upheaval of classical mechanics and the subsequent revolution of quantum mechanics but paradoxically strengthened the atomistic and probabilistic basis on which this principle was founded. The essential new idea of the quantum mechanics is that atoms have sets of discrete energy levels and radiation is absorbed and emitted in discrete quanta. Boltzmann's method of obtaining the Maxwell–Boltzmann distribution as the most probable distribution according to the way that small units of energy could be partitioned was employed by Max Planck in his famous derivation of the radiation law (Planck, 1972) in 1900. The Boltzmann factor is immediately adaptable to the quantum situation. In thermal equilibrium the ratio of the number of particles n_i in one given energy level E_i to the number of particles n_j in another energy level E_j is given by

$$\frac{n_i}{n_j} = \exp\left(-\frac{E_i - E_j}{kT}\right).$$

The word *particle* in this context embraces molecules, electrons, sound waves, light waves, and other dynamical quantities with well-defined energies. As an example, the Boltzmann ratio leads to the average energy of a harmonic oscillator whose quantum energy is an integer multiple of $h\nu$ as

$$\bar{\varepsilon} = \frac{1}{2}h\nu + \frac{h\nu}{e^{h\nu/kT} - 1}.$$

In the low-temperature regime this provides reasonable agreement with the experimental result, but it only agrees with the classical Equipartition Principle $\bar{\varepsilon} = kT$ at high temperatures, $T \gg h\nu/k$.

The Maxwell–Boltzmann distribution is a stationary or steady-state distribution. It can be derived (Tolman, 1948) from the steady-state micro-canonical ensemble distribution for which the density of ensemble copies in phase space is uniform in a narrow energy range $E, E + \delta E$ but zero elsewhere. The dynamical justification for the Maxwell–Boltzmann distribution then rests upon the (quasi-)ergodic hypothesis that the time spent by the phase space trajectory for the dynamical system in a given region of the energy surface will be proportional to the micro-canonical density of ensemble copies in that region. Thus, from a dynamical perspective, ergodicity is a necessary condition for Equipartition of Energy. It follows that in isolated integrable systems Equipartition of Energy has no dynamical justification.

The Equipartition principle emerged again as a catalyst for change in the mid-20th century when its failure observed in computer experiments (Fermi et al., 1955) triggered studies into solitons on the one hand and deterministic Hamiltonian chaos on the other (Ford, 1992). The systems investigated by Fermi, Pasta, and Ulam (FPU) could be considered as collections of harmonic oscillators (harmonic modes of vibration) weakly coupled by nonlinear interactions. The expectation of FPU was that energy initially supplied to one of the harmonic oscillators would become uniformly distributed among all harmonic oscillators. Following the FPU experiments, there has been an enormous literature, attempting to recover the equipartition result, particularly for larger nonlinearities and larger numbers of oscillators. Note however that Boltzmann's principle of equipartition of energy predicts uniform energy sharing among the harmonic modes of an isolated linear chain (a result that cannot be justified dynamically), and it does not make predictions for an isolated nonlinear chain. For energy sharing in an isolated nonlinear chain Tolman's general principle of equipartition can be employed, but the result of uniform energy sharing among the harmonic modes should not generally be expected (Henry & Szeredi, 1995). Moreover, nonlinear chains can sustain intrinsic local nonlinear modes that may persist for very long times, and integrable nonlinear chains support nonlinear normal modes that are more fundamental than the harmonic modes.

The principle of equipartition of energy is one of the most fundamental results in the history of the atomistic description of matter. Inconsistencies between this principle and experimental results in different settings have provided a catalyst for some of the most profound theoretical developments in science in the 20th century. A contemporary problem is the failure of the Equipartition Principle in granular materials (Feitosa & Menon, 2002), the resolution of which may play a fundamental role in the development of a comprehensive kinetic theory of granular systems.

BRUCE HENRY

See also **Ergodic theory; Fermi–Pasta–Ulam oscillator chain; Local modes in molecules; Quantum theory**

Further Reading

Boltzmann, L. 1896. *Lectures on Gas Theory*, New York: Dover (English Translation by S.G. Brush. Originally published in German in two parts by J.A. Barth, Leipzig, 1896 (Part I) and 1898 (Part II), under the title *Vorlesungen über Gastheorie*)

Brush, S.G. 1965, 1966. *Kinetic Theory*, vols. 1(2), Oxford: Pergamon Press

Ehrenfest, P. & Ehrenfest, T. 1959. *The Conceptual Foundations of the Statistical Approach in Mechanics*, Ithaca: Cornell University Press (English Translation of No. 6, vol. IV 2II, *Encyklopädie der mathematischen Wissenschaften*, 1912)

Feitosa, K. & Menon, N. 2002. Breakdown of energy equipartition in a 2D binary vibrated granular gas. *Physical Review Letters*, 88(19): 198301

Fermi, E., Pasta, J.R. & Ulam, S.M. 1955. *Studies of Nonlinear Problems*, Los Alamos Scientific Laboratory Report N. LA-1940 (Electronic Access: http://www.osti.gov/accomplishments/pdf/A80037041/A80037041.pdf)

Ford, J. 1992. The Fermi–Pasta–Ulam problem: paradox turns discovery. *Physics Reports*, 213(5): 271–310

Henry, B.I. & Szeredi, T. 1995. New equipartition results for normal mode energies of anharmonic chains. *Journal of Statistical Physics*, 78: 1039–1053

Planck, M. 1972. On the theory of the energy distribution law of the normal spectrum. In *Planck's Original Papers in Quantum Physics*, edited by H. Kangro with D. ter Haar, & S. Brush (transl.). London: Taylor & Francis (English translation of Planck, M. 1900. Zur Theorie des Gesetzes der Energieverteilung im Normalspectrum. *Verh deutsch phys ges*, 2: 202–237)

Tolman, R.C. 1918. A general theory of energy partition with applications to quantum theory. *Physical Review*, 11: 261–275

Tolman, R.C. 1948. *The Principles of Statistical Mechanics*, Oxford: Oxford University Press, Chapter IV.

Waterston, J.J. 1893. On the physics of media that are composed of free and perfectly elastic molecules in a state of motion. *Philosophical Transactions of the Royal Society London*, 183A: 5–79

ERGODIC THEORY

Ergodic theory is the statistical study of groups of motions of a space, either physical or mathematical, with a measurable structure on it. The origins of ergodic theory can be traced back to the mid-19th century when containers of gas particles were first viewed as sets of randomly moving objects rather than as a collection of individual particles moving under known forces. The word *ergodic* was introduced by Ludwig Boltzmann in the context of the statistical mechanics of gas particles, and it comes from two Greek words *ergon* (work) and *odos* (path).

The mathematical setting in which ergodic theory is studied is as follows. Starting with a space X that represents all possible states of some system which changes over time under known forces, a point $x \in X$ corresponds to one state in the space. The measurable structure consists of a collection of measurable sets $\mathcal{B}$ on X along with a probability measure μ. The measure μ is a function that associates to each set B in $\mathcal{B}$ a number between 0 and 1; this number is the measure of B and we write its measure as $\mu(B)$. A probability measure has the property that $\mu(X) = 1$. Instead of tracking the path of each object in the system, one studies the statistical properties of the motion. The subject evolved from statistical mechanics applied to the study of systems of gas particles moving according to classical laws of physics. In principle, the path of each gas particle can be tracked and its entire history and future can be known; in practice, the complete determination of the paths of the gas molecules is not feasible.

After t units of time, $F_t(x)$ is the point in X corresponding to where x ends up. If $t \in \mathbb{R}$, then the *orbit* of x is the set $\{F_t(x) | t \in \mathbb{R}\}$; F_t is called a flow and defines an action of the group $\mathbb{R}$ on X. Frequently, one uses discrete time intervals and writes $T^n(x) \equiv F_n(x)$ for each integer n, so the orbit of x is a discrete set $\{T^n(x) | n \in \mathbb{Z}\}$ and the group acting on X is $\mathbb{Z}$. In the discrete setting the transformation T is the generating map T^1, and T^n is T composed with itself n times. In classical ergodic theory, the measure μ is preserved under the action; i.e., for any set $A \in \mathcal{B}$, $\mu(A) = \mu(F_t A)$ for all $t \in \mathbb{R}$ or $\mu(A) = \mu(T^n A)$ for all $n \in \mathbb{Z}$. One of the main advantages of the ergodic theoretic point of view is that one can ignore some orbits if they only form a set of measure 0 in the space X; therefore, one uses the terminology *μ-almost everywhere* (or *for μ-a.e. x*) to refer to a property that holds on a set of points of measure 1 in X but perhaps fails to hold on some set of measure 0.

Boltzmann's original ergodic hypothesis has come to be known as the statement that *time average equals space average*; he conjectured (in a certain classical setting) that for any integrable function f, for μ-a.e. x,

$$\lim_{n\to\infty} \frac{1}{n} \sum_{k=0}^{n-1} f(T^k x) = \int_X f \mathrm{d}\mu. \tag{8}$$

In this expression, the time average of f for n time steps along the orbit of x is represented by averaging $f(x)$ with $f(Tx)$, $f(T^2x)$, ..., and $f(T^{n-1}x)$, since each application of T represents the passage of one unit of time (the left-hand side of the expression). The space average of f is obtained by integrating f over the entire space X, giving the right-hand side of the expression. For a flow the ergodic hypothesis is

$$\lim_{t\to\infty} \frac{1}{t} \int_0^t f[F_s(x)]\mathrm{d}s = \int_X f \mathrm{d}\mu. \tag{9}$$

The conjecture is false as stated; it only holds when the action is μ-ergodic, and this realization led to the definition of an ergodic action.

The setting of ergodic theory has been greatly enlarged to include the actions of many other groups (Zimmer, 1984). A nonsingular action Φ of a group G on a space $(X, \mathcal{B}, \mu)$ consists of an action of G on X such that the map $\Phi : G \times X \to X$ is measurable and for each $g \in G$ the map $\phi_g(x) = \Phi(g, x)$ is a nonsingular automorphism of X; that is, ϕ_g is an invertible measurable transformation and for any $B \in \mathcal{B}$, $\mu(B) = 0$ if and only if $\mu(\phi_g^{-1} B) = \mu(\phi_{g^{-1}} B) = 0$. The group operation on G is reflected in the action since $\phi_{g_1 g_2}(x) = \phi_{g_2}(\phi_{g_1} x)$ for all $g_1, g_2 \in G$ and almost every (μ-a.e.) x.

An action is *ergodic* if whenever $\phi_g(A) = A$ for all $g \in G$, then $\mu(A) = 0$ or 1. The study has been extended beyond group actions to the study of ergodic equivalence relations, and the assumption that the measure μ be a probability measure is frequently dropped. One also considers the actions of semigroups when the action being studied is not invertible.

The Birkhoff ergodic theorem for a measure-preserving transformation T states that the limit of the left-hand side in Equation (8) exists for μ-a.e. x, is an integrable function f^*, and $f^*(Tx) = f^*(x)$ for μ-a.e. x. Furthermore, f^* is the constant $\int_X f \, d\mu$, the space average of f, precisely when the action is ergodic (Birkhoff, 1931). Any point x satisfying the theorem is called a generic point and generates a *typical orbit*. There are many ergodic theorems; perhaps the simplest is the von Neumann ergodic theorem (von Neumann, 1932). By definition, a function $f \in L^2$ if $\int |f|^2 d\mu < \infty$; moreover defining $f \circ T^k(x) = f(T^k x)$, for measure-preserving T, $f \circ T^k \in L^2$ as well. Von Neumann's theorem is also called the Mean or L^2 ergodic theorem because while no individual orbit is tracked (no x appears in the statement), the average difference (L^2 integral) between the time average and the limit function f^* must be small.

Theorem 1. (von Neumann or L^2 Ergodic Theorem) *If T is a measure-preserving transformation and $f \in L^2$, then there is a function $f^* \in L^2$ such that*

$$\int_X \left| \frac{1}{n} \sum_{k=0}^{n-1} f \circ T^k - f^* \right|^2 d\mu \to 0 \quad as \quad n \to \infty.$$

If $(X, \mathcal{B}, \mu)$ is a probability space and the transformation T (or group action) on X is non-ergodic, there is a disintegration or decomposition of μ into measures μ_y, indexed by points y in another probability space Y, with its own measure ρ, such that $\mu(A) = \int_Y \mu_y(A) \, d\rho$ for every $A \in \mathcal{B}$. Furthermore, the limit function f^* in the ergodic theorems is constant with respect to each measure μ_y; that is, T is μ_y ergodic for ρ–a.e. y. The decomposition is independent of the function f; this is referred to as the *ergodic decomposition* of the measure μ with respect to T (Rohlin, 1949). One of the central problems in ergodic theory is to determine when two measure-preserving group actions are conjugate via a measure-preserving isomorphism. To this end, invariants such as entropy and spectral properties have been the subject of much study.

There is a hierarchy of statistical properties associated to ergodic actions, including weak mixing, mixing, K-automorphisms, and Bernoulli automorphisms. As a transformation moves up the hierarchy (in the order listed), the more chaotic the behavior of the system is expected to be.

Applications to Dynamical Systems and Chaos

The simplest example of an ergodic transformation is irrational rotation on the circle with respect to Lebesgue measure. The most random transformation is a Bernoulli shift with an independent identically distributed measure on it; this includes coin tosses.

Overlaps of the topological setting of dynamical systems with ergodic theory exist, and much of ergodic theory highlights the interface between the topological and measurable structure of a group G acting on $(X, \mathcal{B}, \mu)$. In 1935, Hedlund proved the ergodicity of the geodesic flow on the unit tangent bundle of a surface of constant negative curvature; in 1940, Hopf extended the result to establish ergodicity of the geodesic flow on arbitrary manifolds with negative sectional curvature. In this setting the invariant measure is the Liouville measure.

Modern ergodic theory was started by Andrei Kolmogorov with the formal development of Boltzmann's notion of entropy, and developed in the 1960's and 1970's to include many differentiable actions. Applications include fluid dynamics, coding theory, number theory, complex dynamics, and cellular automata.

JANE HAWKINS

See also **Chaotic dynamics; Dynamical systems; Entropy; Symbolic dynamics**

Further Reading

Birkhoff, G. 1931. Proof of the ergodic theorem. *Proceedings of the National Academy of Sciences USA*, 17: 656–660

Cornfeld, I., Fomin, S. & Sinai, Y. 1982. *Ergodic Theory*, New York: Springer

Furstenberg, H. 1981. *Recurrence in Ergodic Theory and Combinatorial Number Theory*, Princeton: Princeton University Press

Halmos, P. 1956. *Ergodic Theory*, New York: Chelsea Publishing

Katok, A. & Hasselblatt, B. 1995. *Introduction to the Modern Theory of Dynamical Systems*, Cambridge and New York: Cambridge University Press

Petersen, K. 1983. *Ergodic Theory*, Cambridge and New York: Cambridge University Press

Rohlin, V. A. 1949. On the fundamental ideas of measure theory. *American Mathematical Society Translations*, 10 (1): 1–54 (original Russian article 1949)

von Neumann, J. 1932. Proof of the quasiergodic hypothesis. *Proceedings of the National Academy of Sciences USA*, 18: 70–82

Walters, P. 1982. *An Introduction to Ergodic Theory*, New York: Springer

Zimmer, R. 1984. *Ergodic Theory and Semisimple Groups*, Boston: Birkhäuser

ESAKI TUNNEL DIODE

See **Diodes**

EULER'S METHOD

See **Numerical methods**

EULERIAN DESCRIPTION

See **Fluid dynamics**

EULER–LAGRANGE EQUATIONS

In the dynamics of energy conserving systems there are two equivalent formulations: one based on differential equations and the other based on the principle of least action (Goldstein, 1951). At first glance, these two approaches seem to have little in common as one stems from iterating infinitesimal changes along a solution trajectory, whereas the other depends on evaluating all possible paths between two end points and selecting the path with the minimum action.

To see how this goes, consider a simple classical system: the nonrelativistic point particle of unit mass. In three dimensions this particle has three degrees of freedom each labeled by coordinates $q_i(t)$ for $i = 1, 2, 3$. The motion of the particle is determined by a Lagrangian functional $L(q_i, \dot{q}_i)$ which depends on both the position components, $q_i(t)$, and the velocity components, $\dot{q}_i(t)$, of the particle. This functional is

$$L = \sum_i \left[\dot{q}_i^2/2 - V(q_i)\right], \tag{1}$$

where $V(q_i)$ is some potential in which the particle moves; thus, the Lagrangian is defined as the difference between the kinetic and the potential energy of the system. The motion of the particle is determining by minimizing the action, which is the time integral of the Lagrangian

$$S = \int_{t_1}^{t_2} L(q_i, \dot{q}_i)\, \mathrm{d}t, \tag{2}$$

and the path taken by the particle is the one for which the action is a minimum. In other words, $\delta S = 0$, where δ implies a differential change in S under a small change in the path.

In calculating the equations of motion, a small variation in the path of the particle $\delta q_i(t)$ is assumed with the endpoints fixed, that is, $\delta q_i(t_1) = \delta q_i(t_2) = 0$. To calculate δS, the Lagrangian is varied with respect to both changes in the position and the velocity

$$\delta S = \int_{t_1}^{t_2} \sum_i \left(\frac{\partial L}{\delta q_i} \delta q_i + \frac{\partial L}{\partial \dot{q}_i} \delta \dot{q}_i \right) \mathrm{d}t. \tag{3}$$

Integration by parts of the last term gives

$$\delta S = \int_{t_1}^{t_2} \sum_i \left[\frac{\partial L}{\partial q_i} \delta q_i - \frac{\mathrm{d}}{\mathrm{d}t} \left(\frac{\partial L}{\partial \dot{q}_i} \right) \delta q_i \right] \mathrm{d}t, \tag{4}$$

so the condition $\delta S = 0$ implies that

$$\frac{\partial L}{\partial q_i} - \frac{\mathrm{d}}{\mathrm{d}t} \left(\frac{\partial L}{\partial \dot{q}_i} \right) = 0 \tag{5}$$

for all i. These are the Euler–Lagrange (EL) equations of motion. For the system of Equation (1), they are $\mathrm{d}^2 q_i/\mathrm{d}t^2 + \partial V/\partial q_i = 0$, which is Newton's second law.

In some cases the motion is constrained, for example to curves or surfaces. Such a constraint can be expressed as a function $f(q_i) = 0$. Augmenting the Lagrangian to $\tilde{L} = L + \lambda f$ (where λ is called a Lagrange multiplier) and minimizing S with respect to $\tilde{L}$ then yields equations for motion under the constraint (Gel'fand & Fomin, 2000). As a simple example, consider the system of Equation (1) with $V = (q_1^2 + q_2^2 + q_3^2)/2$ moving under the constraint $q_1 = q_2$ or $q_1 - q_2 = 0$. Then the EL equations for the augmented Lagrangian $\tilde{L} = L + \lambda(q_1 - q_2)$ are $\mathrm{d}^2(q_1 + q_2)/\mathrm{d}t^2 + (q_1 + q_2) = 0$ and $\mathrm{d}^2 q_3/\mathrm{d}t^2 + q_3 = 0$.

An alternative to the Lagrangian formulation (where positions and velocities are the fundamental variables) is the Hamiltonian formulation. Here the positions and momenta (p_i) are independent variables, where

$$p_i \equiv \partial L/\partial \dot{q}_i \tag{6}$$

and a Hamiltonian is defined through the Legendre transformation

$$H(q_i, p_i) \equiv \sum_i p_i \dot{q}_i - L(q_i, \dot{q}_i). \tag{7}$$

Because this Hamiltonian is conserved under the dynamics, it is often interpreted as the energy of a dynamical system. For the example of Equation (1),

$$H = \sum_i \left[\dot{q}_i^2/2 + V(q_i)\right], \tag{8}$$

the sum of kinetic and potential energies.

The generalization from a point particle to a three-dimensional field may be viewed as the replacement of $q_i(t)$ by a field amplitude: $\phi(x, y, z, , t)$ (Goldstein, 1951). In this case, EL equations can be derived from a variational principle applied to an action integral of the form

$$S = \int \mathcal{L}\left(\phi, \phi_t, \phi_x, \phi_y, \phi_z\right) \mathrm{d}x\, \mathrm{d}y\, \mathrm{d}z\, \mathrm{d}t, \tag{9}$$

where $\mathcal{L}$ is a Lagrangian density and the subscripts indicate partial derivatives. The condition for minimum

action then gives

$$\frac{\partial \mathcal{L}}{\partial \phi} - \frac{\partial}{\partial t}\frac{\partial \mathcal{L}}{\partial \phi_t} - \frac{\partial}{\partial x}\frac{\partial \mathcal{L}}{\partial \phi_x} - \frac{\partial}{\partial y}\frac{\partial \mathcal{L}}{\partial \phi_y} - \frac{\partial}{\partial z}\frac{\partial \mathcal{L}}{\partial \phi_z} = 0, \tag{10}$$

which is the EL equation in field theory.

A simple example of this field formulation is provided by the sine-Gordon equation in three-dimensional space. The Lagrangian density is given by

$$\mathcal{L} = \tfrac{1}{2}\left(\phi_t^2 - \phi_x^2 - \phi_y^2 - \phi_z^2\right) + (\cos\phi - 1), \tag{11}$$

for which Equation (10) implies

$$\phi_{xx} + \phi_{yy} + \phi_{zz} - \phi_{tt} = \sin\phi. \tag{12}$$

Because not all dynamics conserve energy, the Lagrangian formulation is not applicable to all physically motivated systems. Reaction-diffusion equations, for example, are excluded from this class (Scott, 2003).

ALWYN SCOTT

See also **Extremum principles; Hamiltonian systems; Newton's laws of motion; Poisson brackets**

Further Reading

Gel'fand, I.M. & Fomin S.V. 2000. *Calculus of Variations*, New York: Dover

Goldstein, H. 1951. *Classical Mechanics*, Reading, MA: Addison–Wesley

Scott, A.C. 2003. *Nonlinear Science: Emergence and Dynamics of Coherent Structures*, 2nd edition, Oxford and New York: Oxford University Press

EVANS FUNCTION

Traveling waves are one-dimensional patterns that arise in numerous applications, for instance, as defects, flame fronts, nerve impulses, shock waves, and solitons. Typically, traveling waves are only observed in experiments or in numerical simulations if they are stable.

In the early 1970s, Evans developed a number of tools designed to determine the stability of pulses, that is of traveling waves that are localized in space as solutions to a system of partial differential equations (PDEs) (Evans, 1975). The class of PDEs considered by Evans serve as models for the propagation of impulses in nerve axons that include the FitzHugh–Nagumo equation and the Hodgkin–Huxley equations. The strategy to determine the stability of waves consists of two steps: (i) linearize the nonlinear PDE about the wave and calculate the spectrum of the resulting linear operator, and (ii) show that the wave is stable for the nonlinear PDE if the spectrum contains no unstable elements. This entry focuses on the first step, see Sandstede (2002) for references concerning (ii).

The spectrum of the linearization $\mathcal{L}$ about a pulse or a front is the union of two sets, namely the point spectrum (which consists of all isolated eigenvalues) and the essential spectrum (which is also often referred to as the continuous or radiation spectrum). The essential spectrum can be computed easily as it involves only the homogeneous background states of the pulse or front.

The key problem is therefore to find all isolated eigenvalues in the complement Ω of the essential spectrum in the complex plane. To address this issue for his class of nerve-axon models, Evans constructed an analytic function $D(\lambda)$ (now referred to as the Evans function) that maps the region Ω into the complex plane with the property that $D(\lambda)$ vanishes precisely at isolated eigenvalues of the linear operator $\mathcal{L}$. In fact, the order of a root λ_* of the Evans function $D(\lambda)$ coincides with the algebraic multiplicity of λ_* as an eigenvalue of $\mathcal{L}$. Here, ℓ is the order of a root λ_* of $D(\lambda)$ if the first $\ell - 1$ derivatives of $D(\lambda)$ vanish at λ_* but the ℓth derivative does not.

Note that, if the underlying PDE is invariant under space translations, then $\lambda = 0$ is an eigenvalue. The corresponding eigenfunction is given by the spatial derivative of the wave. Hence, if $\lambda = 0$ is not in the essential spectrum, the Evans function $D(\lambda)$ vanishes at $\lambda = 0$. Proving linear stability of a pulse, therefore, amounts to calculating the Evans function $D(\lambda)$ and showing that it does not have any zero in the closed right half-plane except possibly a simple zero at $\lambda = 0$.

The derivative $D'(0)$ is actually given by the Mel'nikov integral, computed with respect to the wave speed, c, of the pulse. This integral measures how the stable and unstable manifolds of the background state intersect as the wave speed c of the pulse is varied. In other words, if the existence problem of the wave is understood well enough, then $D'(0)$ is computable.

This can be exploited as follows. The Evans function $D(\lambda)$ is, in fact, real whenever λ is real, and $D(\lambda)$ can be normalized so that $D(\lambda) > 0$ for all sufficiently large $\lambda \gg 1$. Here, λ is the temporal growth rate so that unstable eigenvalues have positive real part. Thus, if $D'(0) < 0$, then the pulse is necessarily unstable with an odd (and therefore nonzero) number of unstable real eigenvalues. Consequently, the derivative $D'(0)$ of the Evans function provides a parity instability index.

The function $D(\lambda)$ introduced by Evans was then later used by Jones and by Yanagida to prove that the fast pulse arising in the FitzHugh–Nagumo equation is stable. Both proofs used the parity index introduced above: after establishing that there is precisely one eigenvalue besides $\lambda = 0$ that lies close to the imaginary axis or in the right half-plane, a computation of the parity index at $\lambda = 0$ showed that it is positive, so that the other eigenvalue must lie in the left half-plane.

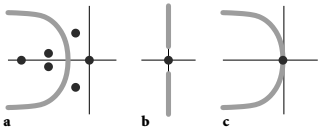

Figure 1. The three illustrations show typical spectra of the linearization about (a) a stable pulse in a dissipative PDE, (b) a soliton in an integrable system, and (c) a viscous shock wave. The horizontal and vertical axes are ($\mathrm{Re}\,\lambda$, $\mathrm{Im}\,\lambda$). The point and essential spectrum are shown as discs and lines, respectively.

Alexander et al. (1990) developed the Evans function further and also related it to certain topological invariants. Since then, Evans-function calculations have been utilized in various applications, for instance, in nonlinear optics, plasma physics, and thin films (Sandstede, 2002; Zumbrun, 2001).

An important class of PDEs to which the Evans function has been applied is singularly perturbed equations that exhibit two different spatial scales. In this situation, the Evans function can often be calculated from the Evans functions for the slow and the fast subsystem (Doelman et al., 2002).

The Evans function is also a useful tool for investigating the stability of multi-hump pulses, or n-pulses, which are composed of n widely separated copies of a primary pulse. If the primary pulse is stable, so that $\lambda = 0$ is a simple eigenvalue, then such an n-pulse has exactly n critical eigenvalues near the origin which encode the interaction properties of the n individual pulses. These eigenvalues can be calculated using the Evans function (Sandstede, 2002).

The original construction of the Evans function works only outside of the essential spectrum. For Hamiltonian PDEs, the essential spectrum of stable pulses lies on the imaginary axis, see Figure 1(b). Thus, it is possible that eigenvalues move out of the essential spectrum and into the right half-plane once a small perturbation is added to the underlying PDE. The points in the essential spectrum from which such eigenvalues can potentially emerge and the exact location of the bifurcating eigenvalues for concrete perturbations can be found by extending the Evans function across the essential spectrum. For integrable PDEs such as the Korteweg–de Vries or the nonlinear Schrödinger equation, it is possible to compute the extended Evans function explicitly using inverse scattering theory (see Kapitula & Sandstede (2002) for references).

Similar issues occur for the linearization about viscous shock waves where the essential spectrum always touches the origin, see Figure 1(c). An extension of the Evans function across the essential spectrum to a full neighborhood of $\lambda = 0$ allows one to generalize the parity instability index, given by an appropriate sign condition on the derivative $D'(0)$, to viscous shocks. In addition, the extended Evans function plays an important role in the nonlinear stability analysis of viscous shocks (Zumbrun, 2001).

BJÖRN SANDSTEDE

See also **Shock waves; Stability; Wave stability and instability**

Further Reading

Alexander, J.C., Gardner, R.A. & Jones, C.K.R.T. 1990. A topological invariant arising in the stability analysis of travelling waves. *Journal für die Reine und Angewandte Mathematik*, 410: 167–212

Doelman, A., Gardner, R.A. & Kaper, T.J. 2002. A stability index analysis of 1-D patterns of the Gray–Scott model. *Memoirs of the American Mathematical Society*, 155(737): xii+64 pp.

Evans, J. 1975. Nerve axon equations (iv): The stable and unstable impulse. *Indiana University Mathematics Journal*, 24: 1169–1190

Kapitula, T. & Sandstede, B. 2002. Edge bifurcations for near integrable systems via Evans-function techniques. *SIAM Journal on Mathematical Analysis*, 33: 1117–1143

Sandstede, B. 2002. Stability of travelling waves. In *Handbook of Dynamical Systems,* vol. 2, edited by B. Fiedler, Amsterdam: North-Holland

Zumbrun, K. 2001. Multidimensional stability of planar viscous shock waves. In *Advances in the Theory of Shock Waves*, edited by H. Freistühler, A. Szepessy, T.-P. Liu & G. Métiver, Boston: Birkhäuser

EVAPORATION WAVE

Under special conditions a liquid can be superheated to a few hundred degrees Celsius above its nominal boiling point. The thermal energy associated with this excess temperature can be released by rapid evaporation, also called a *vapor explosion*. The largest explosions on Earth are vapor explosions in the form of volcanic eruptions. For example, the Mount St. Helens blast was estimated at 400 Mtons TNT equivalent (Decker & Decker, 1981), which is nearly the sum of all worldwide nuclear explosions to date (about 500 Mtons).

Vapor explosions also pose a hazard in industry. In one incident, 100 lb of molten steel fell into an open trough containing 78 gallons of water. The resulting explosion killed one person and injured many, cracked the 20-in. thick concrete floor, and shattered 6000 panes of glass (Reid, 1976). If a vapor explosion involves a flammable liquid, then the physical explosion can transition to a more powerful chemical explosion.

An *evaporation wave* is a vapor explosion that proceeds across the system with an identifiable propagation velocity. Evaporation waves are an interesting example of self-organized dynamical complexity and comprise a controlled form of vapor explosion that facilitates the detailed study of liquid fragmentation and dispersal mechanisms.

Liquid superheating is caused by cohesion between molecules. Hence, bubbles—even very small

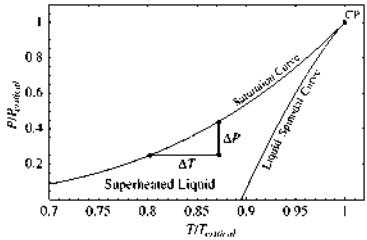

Figure 1. Existence region for superheated liquid from the Redlich–Kwong (R–K) equation of state. R–K predicts universal behavior in a reduced coordinate system.

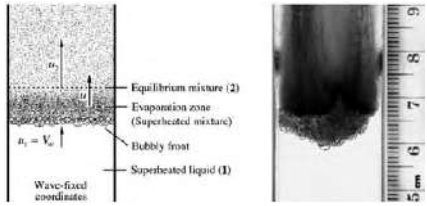

Figure 2. Schematic diagram of an evaporation wave (a), and a photograph of an evaporation wave in freon-12 at 20°C (b). The front is moving down at 0.6 m s^{-1}.

ones that reside in most liquids under normal conditions—comprise weak spots that inhibit superheating. Even a completely pure liquid can only be superheated to a point, called the superheat limit, where it becomes mechanically unstable. The theoretical superheat limit occurs at a locus of states called the *spinodal curve* (Debenedetti, 1996). Superheated liquid can exist between the saturation and spinodal curves as shown in Figure 1. The amount of superheat is quantified by the excursion of the liquid state from the saturation curve, for example, the degree ΔT by which the liquid temperature exceeds the equilibrium temperature at its pressure.

The specific enthalpy required to evaporate a liquid is the latent heat of evaporation L. A superheated liquid stores an excess specific enthalpy $C_p \Delta T$, where C_p is the liquid specific heat at constant pressure. The Jakob number, $\mathrm{Ja} \equiv (C_p \Delta T)/L$, is equal to the liquid mass fraction χ that can evaporate adiabatically at constant pressure. If $\mathrm{Ja} > 1$ then complete evaporation can occur. This condition is possible in *retrograde* liquids, which are those possessing a sufficiently large specific heat (Thompson et al., 1986). Nowhere near complete evaporation is required to produce quasisteady evaporation waves. However, sufficient evaporation must occur so that the liquid phase is swept along by the vapor; otherwise, the upstream liquid will cool and the process will quench.

The first mention of an evaporation wave appears to have been by Terner (1962), who performed vertical shock tube experiments on heated water. Terner believed that an evaporation wave followed depressurization, though he did not definitively show it.

The first direct observation appears to have been by Friz (1965), who studied the expulsion of superheated water from a vertical glass tube into the atmosphere. The tube was sealed on top by a diaphragm, and the water was heated to temperatures from 105°C to 125°C. The gas space above the water was pressurized to 3.5 bar, whereupon a cutter was activated to puncture the seal. Friz describes that upon depressurization "a great number of bubbles" formed throughout the water column. An "acceleration front" several centimeters thick then propagated into the bubbly mixture at 1–2 m s^{-1}, transforming it into a spray that was ejected upward. The many bubbles were probably caused by pre-pressurization, which increased the amplitude of the initial expansion wave so that it reflected from the test cell base in tension, causing cavitation.

Grolmes and Fauske (1970) performed similar experiments in heated water, freon-11, and methanol. Their configuration was like Friz's, except that (i) the initial pressure was the vapor pressure, and (ii) the fluid was expelled into a nearly evacuated reservoir. By paying careful attention to the liquid purity and test cell cleanliness, they were able to suppress *all* nucleation within the liquid column. Upon depressurization boiling erupted on the liquid surface and proceeded with sufficient vigor to expel the generated spray from the container as depicted in Figure 2a. The boiling surface receded at a constant average rate of 0.3–0.5 m s^{-1}, depending on the liquid and conditions.

Thompson et al. (1987) performed similar experiments on the retrograde fluorocarbon perfluoro-*n*-hexane (C_6F_{14}). At the highest (nearly critical) temperatures, the lead expansion wave attempted to lower the pressure past the superheat limit, whereupon homogeneous nucleation erupted and blocked the drop. An approximate plateau was maintained near the spinodal, into which a slower evaporation wave propagated in a manner similar to Friz's. Such *wave splitting* occurs when material properties abruptly change within the wave, in a way that lowers the sound speed. At lower temperatures, homogeneous nucleation likely erupted upon reflection of the initial expansion wave from the test cell base, and an evaporation wave initiated after the reflected wave reached the free surface. The waves became progressively less distinct as the initial temperature was lowered, presumably because heterogeneous nucleation from the metal side-walls and the transducer ports became increasingly important.

Shepherd and Sturtevant (1982) performed experiments on butane drops that were heated slowly in an ethylene glycol host fluid to the superheat limit

($\Delta T = 105°C$), whereupon they exploded with a sharp "crack." High-speed photographs showed that evaporation initiated at a single nucleation site at or near the drop surface and spread into pure liquid as a miniature evaporation wave resembling Grolmes and Fauske's. Thus, heating to the superheat limit has produced waves in pure liquid, whereas depressurizing to the superheat limit has produced waves in bubbly liquid.

Shepherd and Sturtevant suggested that the *Landau instability* of premixed flames was the essential fragmentation mechanism. Frost and Sturtevant (Frost, 1988) repeated the exploding droplet experiments in pentane, iso-pentane, and ethyl ether. They obtained several photographs in which the evaporating interface had a mottled texture resembling an orange peel. This suggested that they had caught the interface at the early stages of instability, which they believed grew to the point of pinching off droplets to produce the observed rough-looking interfaces and spray flow. About the same time Mesler (1988) proposed that the *secondary nucleation* mechanism of surface boiling—whereby receding film-caps from ruptured bubbles strike the liquid surface and entrain vapor to create new nucleation sites—was responsible.

Hill and Sturtevant (Hill, 1991) performed Grolmes and Fauske-type experiments in freons 12 and 114, with the goal of observing detailed propagation mechanisms. Figure 2b is a photograph from that study. Several observations suggested that a three-step cycle occurs: (i) bubbles grow at the leading edge in accordance with classical theory; (ii) these are consumed en masse by fragmentation waves that sweep around the bubbly layer transversely to the main propagation at speeds of order the axial flow, and which shatter the superheated interstitial liquid into droplets; (iii) a small fraction of the droplets are propelled forward to strike the leading edge and nucleate new bubbles à la Mesler. Whether such behavior extends toward the superheat limit, or whether a nucleation-free evaporative instability dominates at some point, is unknown.

Simões-Moreira and Shepherd (1999) performed similar experiments in heated dodecane ($C_{12}H_{26}$)—a highly retrograde liquid—with the intention of observing complete evaporation waves. For $\mathrm{Ja} > 1$ a simple plane evaporation wave, or a convoluted but simply connected surface like Frost's "orange peel," would be energetically admissible. Instead they observed a scenario qualitatively like previous experiments, except that the droplets evaporated in the downstream flow.

From a gas-dynamic viewpoint an evaporation wave is analogous to a flame in a combustible mixture. Both are classified as *deflagrations*, or *exothermic discontinuities*. The ideal theory (e.g., Hayes, 1958) considers a plane, steady wave. The conservation equations for mass, momentum, and energy are applied between the upstream state **1**, and an arbitrary state in the reaction or evaporation zone. The flow is assumed to be one-dimensional (no turbulence), and viscosity and heat conduction are neglected. Eliminating the fluid velocities between the three conditions yields the Hugoniot curve $\mathcal{H}$, which specifies the locus of possible downstream states given **1**:

$$h_1 - h(v, P) = \tfrac{1}{2}(P_1 - P)(v_1 + v), \tag{1}$$

where h is the specific enthalpy, P is the pressure, and v is the specific volume. Combining the mass and momentum equations gives the Rayleigh line $\mathcal{R}$:

$$\frac{P - P_1}{v - v_1} = -(\rho_1 V_w)^2 = -\dot{m}^2, \tag{2}$$

a line in P–v space with negative slope equal to the square of the mass flux $\dot{m}$. Since the same value of $\dot{m}$ applies throughout the structure of the steady wave, $\mathcal{R}$ traces the locus of states in the reaction or evaporation zone. Steady wave solutions are given by the intersection of $\mathcal{R}$, with $\mathcal{H}$ evaluated at the end state **2**.

We now specialize the analysis to an evaporation wave with pure (or nearly pure) upstream liquid, with a two-phase downstream mixture described by

$$h = h_l(1 - \chi) + h_v\chi \quad \text{and} \quad v = v_l(1 - \chi) + v_v\chi, \tag{3}$$

where χ is the mass fraction of vapor, and l and v denote the liquid and vapor phases. We neglect slip between the two phases keep to and invoke four additional assumptions that are each usually accurate to a percent or better: (i) the liquid enthalpy is conserved upon depressurization from the initial state **0** to the established upstream state **1** ($h_0 = h_1$); (ii) the liquid density is constant throughout ($\rho_0 = \rho_1 = \rho_l = \rho_{l2}$); (iii) the vapor density is small compared with the liquid density ($\rho_v \ll \rho_l$)—true except near the critical point; (iv) the kinetic energies are small compared with the thermal energy ($\chi_2 = \mathrm{Ja}_2$).

In the evaporation zone the liquid droplets are still somewhat superheated, with bulk enthalpy (averaged over a cross-section) h_l. Motivated by the reaction progress variable used in combustion, we define an *evaporation progress variable*, $0 \le \lambda \le 1$:

$$\lambda \equiv \frac{h_0 - h_l}{h_0 - h_{l\phi}(P)}, \tag{4}$$

where $h_{l\phi}(P)$ is the equilibrium liquid enthalpy. The Jakob number is then written as

$$\mathrm{Ja}(P) \equiv \frac{h_0 - h_{l\phi}(P)}{h_v(P) - h_{l\phi}(P)}. \tag{5}$$

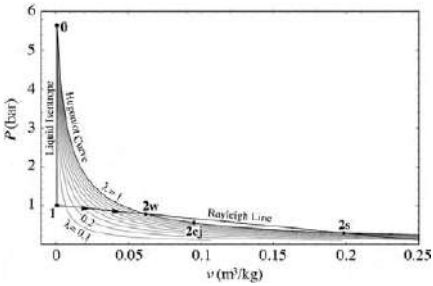

Figure 3. Thermodynamic construction for an evaporation wave—the liquid expansion isentrope, Hugoniot curve, Rayleigh line, and Chapman–Jouguet point.

Combining Equations (3b)–(5) with the energy equation gives an implicit formula for $\mathcal{H}$:

$$v = v_0 + \frac{v_v(P)\lambda\,\mathrm{Ja}(P)}{1-\mathrm{Ja}(P)(1-\lambda)}. \tag{6}$$

Equation (6) is plotted in Figure 3 for several values of λ. A particular $\mathcal{R}$ is overlaid, which intersects $\mathcal{H}$ in two places. The high-pressure intersection at **2w** is the *weak solution*; the low-pressure intersection at **2s** is the *strong solution*. One can show that the end state **2** is subsonic for the weak branch and supersonic for the strong branch. In progressing along $\mathcal{R}$ from **1** to **2w**, the local state crosses increasing values of λ. This is a physically realizable process. But there is no physical way for evaporation to proceed beyond **2w** to **2s**—which is why strong deflagrations are not observed.

In the special case where $\mathcal{R}$ intersects $\mathcal{H}$ at the tangency point the emerging flow is exactly sonic; this is the Chapman–Jouguet (**cj**) point. It is clear from Equation (2) and Figure 3 that for a given **1**, **2cj** defines the maximum allowable wave speed. In some experiments, the test cell is *choked*, which corresponds to sonic outflow in the laboratory frame. In an evaporation wave, the two-phase flow speed is much faster than the wave speed, such that the difference between the laboratory and wave frames is negligible. Therefore, if an unobstructed test cell of constant cross-sectional area is choked, the wave can be considered **cj**.

Combining $\mathcal{R}$ with $\mathcal{H}$ evaluated at **2** gives an explicit equation for the wave speed:

$$V_w = \sqrt{\frac{v_0\ \delta P_2}{\mathrm{Jk}(P_2)}},\ \text{where}\ \mathrm{Jk}(P) \equiv \mathrm{Ja}(P)\left(\frac{v_v(P)}{v_0}\right)$$

and

$$\delta P \equiv P_1 - P. \tag{7}$$

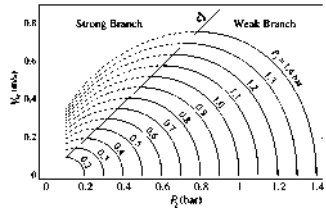

Figure 4. Plot of the evaporation wave speed relation, Equation (7), for freon-12.

δP_2 is the overall wave pressure-amplitude, one measure of its strength. Jk is a useful alternative definition of the Jakob number that arises about as frequently as Ja, and which unfortunately goes by the same name (and usually the same symbol).

The liquid initial conditions v_0 and h_0, and the external reservoir pressure P_r, are set a priori and remain essentially unchanged after depressurization. Assuming that the test cell is long enough for equilibrium to be achieved at or before the exit: if the flow is unchoked (weak solution), then $P_2 = P_\mathrm{r}$; if the flow is choked (**cj** solution), then $P_2 > P_\mathrm{r}$ and a sonic condition applies that specifies P_2. But P_1, and therefore δP_2, is unknown.

Figure 4 plots Equation (7) for various values of P_1. Each curve has a velocity maximum, representing its own **cj** solution, the locus of which is given by

$$V_{w\mathbf{cj}}(P_2) = \sqrt{\frac{v_0}{-\mathrm{d}Jk/\mathrm{d}P_2}}. \tag{8}$$

Predicted and measured wave speeds can deviate by up to 50%. Two issues likely dominate. First, the theory assumes the flow to be strictly one dimensional, but Hill's experiments show that the transient lateral flow velocity in the evaporation zone is of order the mean axial velocity. This results in a higher-than-calculated pressure drop. Second, evaporation is very rapid where fragmentation occurs, but slows downstream where droplets are convecting. Thus, the end state **2** may not exist within the tube.

To close the theory—to calculate the wave speed without measuring P_1—we must add a statement about the physical mechanisms peculiar to evaporation waves. This task is actually simpler for waves in bubbly liquids than for waves in pure ones. For Thompson et al.'s highest-temperature experiments, the upstream state was essentially at the superheat limit, which can be computed from initial conditions. In Friz's experiments, there was time for multiple acoustic reflections in the upstream liquid. He assumed P_1 to be the equilibrium value at the initial temperature, which gave reasonable results.

For waves in pure liquids there is no upstream nucleation to modulate the pressure, and one must address the boiling dynamics in the evaporation zone. The problem is analogous to the calculation of flame speed, which is controlled by the rate of heat conduction (and often convection) from the reaction zone to the reactants. This is where transport properties such as thermal and mass diffusivity enter. No such physically based model exists for evaporation waves, although Reinke and Yadigaroglu (2001) have proposed an empirical correlation based on existing data.

LARRY HILL

See also **Dimensional analysis; Explosions; Flame front; Fluid dynamics**

Further Reading

Debeneditti, P.G. 1996. *Metastable Liquids: Concepts & Principles*. Princeton, NJ: Princeton University Press

Decker, R. & Decker, B. 1981. The eruptions of Mount St Helens. *Scientific American*, 244(3): 68–80

Friz, G. 1965. Coolant ejection studies with analogy experiments. *Proceedings of the Conference on Safety Fuels & Core Design in Large Fast Power Reactors*, US Atomic Energy Commission Report ANL-7120: 890–894

Frost, D.L. 1988. Dynamics of explosive boiling of a droplet. *Physics of Fluids*, 31(9): 2554–2561

Grolmes, M.A. & Fauske, H.K. 1970. Modeling of sodium expulsion with freon-11. *ASME Paper* 70-HT-24

Hayes, W.D. 1958. The basic theory of gasdynamic discontinuities. In *Fundamentals of Gas Dynamics*, edited by H.W. Emmons, Princeton, NJ: Princeton University Press

Hill, L. 1991. An experimental study of evaporation waves in a superheated liquid. Ph.D. Thesis, California Institute of Technology, Pasadena, CA, USA

Mesler, R. 1988. Explosive boiling: a chain reaction involving secondary nucleation. *Proceedings of the ASME National Heat Transfer Conference*, 96: 487–491

Reid, R.C. 1976. Superheated liquids. *American Scientist*, 64: 146–156

Reinke, P. & Yadigaroglu, G. 2001. Explosive vaporization of superheated liquids by boiling fronts. *International Journal of Multiphase Flow*, 27: 1487–1516

Shepherd, J.E. & Sturtevant, B. 1982. Rapid evaporation at the superheat limit. *Journal of Fluid Mechanics*, 121: 379–402

Simões-Moreira, J.R. & Shepherd, J.E. 1999. Evaporation waves in superheated dodecane. *Journal of Fluid Mechanics*, 382: 63–86

Terner, E. 1962. Shock tube experiments involving phase changes. *Industrial and Engineering Chemistry Process Design and Development*, 1(2): 84–86

Thompson, P.A., Carofano, G.C. & Kim, Y.-G. 1986. Shock waves and phase changes in a large-heat-capacity fluid emerging from a tube. *Journal of Fluid Mechanics*, 166: 57–92

Thompson, P.A., Chaves, H., Meier, G.E.A., Kim, Y.-G. & Speckmann, H.-D. 1987. Wave splitting in a fluid of large heat capacity. *Journal of Fluid Mechanics*, 185: 385–414

EXCITABILITY

Nineteen century natural history identified irritability—the active response to stimulation—as a characteristic of living systems; this vague concept has developed into excitability, a characteristic of some nonlinear systems.

An excitable system has a stable resting state, and the response to a small brief perturbation is small, with an amplitude that varies smoothly with the perturbation amplitude. The response to a sufficiently large perturbation, above a threshold, is qualitatively different, undergoing a stereotyped, large amplitude excursion in at least one of the state variables before return to the resting state. For a spatially extended excitable system, the subthreshold response is localized while the suprathreshold response is a traveling wave, or traveling wave train. This dynamics—a stable steady state (a mathematical, but not thermodynamic equilibrium), a threshold, and a return to the steady state—requires at least two processes, a fast nonlinear excitation and a slower recovery process.

The excitation process can be exemplified by the bistability of a candle. The unlit candle is stable, and the threshold for igniting the candle arises from a positive feedback, with heat melting and vaporizing the wax, and the vapor providing the fuel sustaining the flame. This positive feedback loop gives the all-or-none nature of the flame—either it is self-sustaining or not, and the threshold separates these two states. The burnt candle is stable; there is no recovery process.

An example of excitation and recovery is provided by the nerve impulse, where the resting state potential is stable and the energy required for the action potential is obtained from the electrochemical gradients across the membrane. The voltage dependence of the Na^+ conductance provides the positive feedback. Recovery is by the slower, voltage-dependent K^+ conductance, and propagation by spread of depolarization along the fiber (Cole, 1968; Aidley, 1998). In both these examples, the spatial spread of activity can be considered as traveling-wave solution of a reaction-diffusion equation in which there is a balance between the active nonlinear term and the diffusive term. In typical chemical excitable systems, all the variables diffuse, with similar diffusion coefficients; in nerve and muscle excitation only the fast excitation variable (transmembrane voltage) spreads and there is only one nonzero diffusion coefficient. The velocity of the traveling-wave solution varies as the root of the diffusion coefficient.

The simplest excitable dynamical system has two kinetic variables, a fast excitation u and a slower recovery v

$$\varepsilon \, \mathrm{d}u/\mathrm{d}t = f(v,u), \quad \mathrm{d}v/\mathrm{d}t = g(v,u), \qquad (1)$$

and the nullcline for the fast excitation system has the characteristics of a cubic that is, for a range of u values the solution of $f(v,u) = 0$ has three branches. If, as in Figure 1, the nullclines have a single intersection

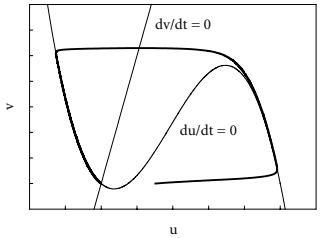

Figure 1. State space of two-variable excitable system, with u the fast excitation variable and v the slower recovery variable. There is a stable equilibrium and a single suprathreshold response.

on the left branch, there is a single globally stable, but excitable, steady state. A large enough perturbation gives a trajectory that jumps to the right branch, moves slowly close to the right branch, and then jumps back to the left branch, returning slowly to rest. If the nullclines intersect on the central branch the resultant equilibrium can be unstable, and the system is no longer excitable but oscillatory.

The key concepts of excitability—threshold and all-or-none response—came from the physiology of nerve and muscle tissue. Nerve and muscle are electrically excitable tissues; their excitability is electrochemical, due to nonlinear membrane current-voltage relations produced by voltage-dependent conductances. The suprathreshold response is the action potential that acts as a trigger, where the intensity of the response is determined by the rate of action potentials. Repetitive activity—that can be idealized as a periodic response—is a biologically significant behavior and may be forced, by inputs to an excitable system, or endogenous, as in a pacemaking system, due to stable limit cycle surrounding an unstable equilibrium when the equilibrium state loses its stability at a Hopf bifurcation as a parameter (say, an applied current or maximal membrane conductance) is changed. Also rate coding phase synchronization effects can be significant—synchronization of bursting discharges in the mammalian central nervous systems provides a candidate mechanism for cognitive effects (Eckhorn, 1999). In spatially extended cells, there can be repetitive traveling-wave trains—effectively one-dimensional in a nerve fiber, and three-dimensional in heart muscle. In the heart three-dimensional scroll waves provide the mechanism for re-entrant arrhythmias that can lead to sudden cardiac death. Some intracellular systems show chemical excitability: a localized increase in intracellular $[Ca^{2+}]$ can trigger calcium-induced calcium release from intracellular organelles, producing intracellular calcium oscillations, or traveling waves. An example is a $[Ca^{2+}]$ wave triggered by fertilization of an oocyte (Dupont & Goldbeter, 1997). Chemical excitability, via cyclic AMP triggering cellular release of cyclic AMP, underlies the wave phenomena seen in the aggregation of the slime mold *Dictyostelium*, a simple example of morphogenesis (Tyson & Murray, 1989). In all these biological examples, high-order, mechanistically detailed stiff systems of equations have been developed, validated, and investigated numerically, but much of the essential phenomenology can be captured by low-order caricatures. Simple models of biological populations can also show excitable behavior, for example, the initiation of an epidemic.

The Belousov–Zhabotinsky reaction, initially developed as an oscillatory organic reaction as an analogue of biochemical oscillations, was the first of several autocatalytic chemical reactions that, in a flow reactor with concentrations that allow bistability, addition of a feedback species can lead to oscillations (Sagues & Epstein, 2003). These chemical oscillatory systems, in thin films and bulk media, also show traveling waves—target patterns, spirals, and scrolls—and with some parameter values are excitable. Models of autocatalytic processes with cubic excitable kinetics are widely used to represent oscillatory and wave phenomena in chemistry, especially combustion problems (Gray & Scott, 1990).

ARUN V. HOLDEN

See also **FitzHugh–Nagumo equation; Hodgkin–Huxley equations; Hopf bifurcation; Nerve impulses; Neurons; Periodic bursting; Threshold phenomena**

Further Reading

Aidley, D.J. 1998. *The Physiology of Excitable Cells*, Cambridge and New York: Cambridge University Press

Cole, K.S. 1969. *Membranes, Ions and Impulses*, Berkley: University of California Press

Dupont, G. & Goldbeter, A. 1997. Modelling oscillations and waves of cytosolic calcium. *Nonlinear Analysis—Theory, Methods and Applications*, 30: 1781–1792

Eckhorn, R. 1999. Neural mechanisms of visual feature binding investigated with microelectrodes and models. *Visual Cognition* 6: 231–265

Gray, P. & Scott, S.K. 1990. *Chemical Oscillations and Instabilities: Non-linear Chemical Kinetics*, Oxford: Clarendon Press and New York: Oxford University Press

Holden, A.V., Markus. M. & Othmer, H.G. 1991. *Nonlinear Wave Processes in Excitable Media*, New York: Plenum

Keener, J.P & Sneyd, J. 1998. *Mathematical Physiology*, New York: Springer

Sagues F. & Epstein, I.R. 2003. Nonlinear chemical dynamics. *Dalton Transactions*, (7): 1201–1217

Tyson, J.J. & Murray, J.D. 1989. Cyclic-AMP waves and aggregation of *Dictyostelium amebas*. *Development*, 106: 421–426

EXCITABLE MEDIUM

See **Reaction-diffusion systems**

EXCITONS

Traditionally, an exciton is defined as a quantum of electronic excitation energy traveling in a periodic structure, whose motion is characterized by a wave vector. It is generated when an electron from a filled electronic orbital of a molecule is transferred through an optical or electrical excitation to a high-energy unoccupied electronic orbital, leaving behind it a hole. Coulomb interaction binds the excited negative electron and the positively charged hole producing an electrically neutral bound state, and this bound electron-hole pair is the exciton. Once created the exciton can be destroyed through emission of light (radiative recombination) or heat (nonradiative recombination), electron-hole separation (exciton dissociation), and subsequent absorption of the electron by an acceptor site (electron transfer). It can change its spin state through intersystem crossing, while at high excitation densities, excitons can mutually collide and dissociate (exciton-exciton annihilation). Furthermore, the whole excitation can move to other sites leading to energy transfer, one of its most important properties.

Excitons occur in molecular crystals, inorganic semiconductors, and conjugated polymers. Three different types of excitons are known. The Frenkel exciton is an electronic excitation of a single molecular unit with both electron and hole located on the same molecule. As any molecule is equally likely to be excited and if there is nonzero coupling between adjacent molecules, this exciton is transferred from one molecular unit to another. Frenkel excitons appear in ionic, molecular, and noble gas crystals having a typical binding energy of 1 eV. In the Wannier exciton the electron-hole distance is much larger than the lattice spacing, and the Coulomb interaction gets screened by the crystal dielectric constant forming a hydrogen-like bound system. They appear mostly in inorganic semiconductors and have a small binding energy of about 0.1 eV and a large radius of typically 50 Å. Finally, the charge-transfer exciton is intermediate between Frenkel and Wannier excitons with an electron-hole distance of a few lattice spacings.

Although excitons are neutral they can be found in definite spin states depending on the relative orientation of electron and hole spins. For antiparallel electron-hole spins a singlet exciton with total spin zero is formed with short lifetime of the order of picoseconds due to fast decay through an optically allowed transition leading to fluorescent emission from this state. There are also three degenerate spin one states leading to a triplet exciton that produces emission termed "phosphorescence." Optical transitions between triplet excited and single ground state are not allowed due to the forbidden spin flip, resulting in conjugated polymers in triplet exciton lifetime of the order of milliseconds at low temperatures. Thermal energy assists triplet motion and at higher temperatures exciton motion process in an incoherent diffusive mode, although some quantum mechanical coherence may be retained. Coherent exciton dynamics at finite temperatures is investigated theoretically through generalized Langevin equations.

Self-trapped excitons (STEs) form a special class of excitations that involve excitons coupled strongly to vibrational degrees of freedom of molecules. Low-dimensional and, in particular, quasi-one-dimensional materials are ideal systems for studying STEs because reduced dimensionality results in strong electron-phonon interaction. Systems under experimental study include halogen-bridged MX materials, where X is a halogen (chlorine, bromine, etc.) and the metal is, for instance, platinum or crystalline hydrogen-bonded acetanilide (ACN).

The STE can be of electronic or vibrational nature if, in the latter case, specific vibrational modes couple strongly to other phonon system modes leading to vibron excitons. In ACN, C=O as well as NH stretching modes have been linked with STEs through the temperature dependence of specific peaks in their absorption spectra, while in the metal-halogen material PtCl, resonant Raman spectroscopy experiments have indicated the existence of self-localized modes.

From a more formal point of view, STEs can be classified as polarons, solitons, or (discrete) breathers, and depending on their specific nature, they may have some differences in their precise physical properties. A generic mathematical model for exciton self-trapping is provided by the discrete nonlinear Schrödinger equation (DNLS) or discrete self-trapping equation

$$i\frac{d\psi_n}{dt} = \varepsilon_n\psi_n + V(\psi_{n+1} + \psi_{n-1}) - \gamma|\psi_n|^2\psi_n, \quad (1)$$

where ψ_n is the probability amplitude for an exciton to be located in a molecular unit at a crystal site n with local energy ε_n, V is the nearest neighbor overlap, and γ is proportional to exciton-phonon coupling. In this approximate, semiclassical description, the nonlinear term in the equation arises from strong electron-phonon coupling in the original exact problem that can be introduced, for instance, by a model such as the Holstein model for molecular crystals. The conserved number $\sum_n |\psi_n|^2 = N$ of the DNLS equation corresponds to the number of excitation quanta present in the system. In the weak coupling limit where $V \to 0$, the STEs of DNLS are completely localized in a given site with energy equal to

$$E_N = N\varepsilon - \frac{\gamma}{2}N^2, \quad (2)$$

where all local site energies are taken to be identical, that is, $\varepsilon_n = \varepsilon$ for all n. The energy of the STE is thus lower than $N\varepsilon$, the energy of the delocalized exciton and also red-shifted by an amount that grows quadratically in the number of quanta N. These spectral features have been observed experimentally in spectra of both PtCl and ACN as well as in other systems. Precise theoretical analysis of resonant Raman spectra of PtCl as well as femtosecond infrared pump-probe spectroscopy experiments in ACN that go beyond the weak coupling DNLS energy in Equation (2) have demonstrated the existence of STEs in these systems. In the case of ACN, an amide-I exciton lifetime of the order of 2 ps was found. If, as originally conjectured by Davydov, similar modes with larger lifetimes exist in biological macromolecules such as proteins, STEs may participate in energy transfer processes of biological significance.

G.P. TSIRONIS

See also **Davydov soliton; Discrete breathers; Discrete nonlinear Schrödinger equations; Discrete self-trapping system; Polaritons; Polarons**

Further Reading

Dexter, D.L. & Knox, R.S. 1965. *Excitons*, New York: Wiley

Edler, J, Hamm, P. & Scott, A. C. 2002. Femtosecond study of self-trapped vibrational excitons in crystaline acetanilide. *Physical Review Letters*, 88, 067403: 1–4

Eilbeck, J.C, Lomdahl, P.S. & Scott, A.C. 1985. The discrete self-trapping equation. *Physica D*, 16: 318–338

Hennig, D. & Tsironis, G.P. 1999. Wave transmission in nonlinear lattices. *Physics Reports*, 307: 333–432

Kenkre, V.M. & Reineker P. 1982. *Exciton Dynamics in Molecular Crystals and Aggregates*, Berlin: Springer

Pope, M. & Swenberg, C.E. 1982. *Electronic Processes in Organic Crystals*, Oxford: Clarendon Press and New York: Oxford University Press; 2nd edition, 1999

Scott, A.C. 1992. Davydov's soliton. *Physics Reports*, 217: 1–67

Voulgarakis, N.K., Kalosakas, G., Bishop, A.R. & Tsironis, G.P. 2001. Multiquanta breather model for PtCl. *Physical Review* B, 64 (020301): 1–4

EXPLOSIONS

The English word *explode* comes from the Latin word *explodere*, which means to drive an actor from the stage by rhythmic clapping. In applied science, a sudden deposition of energy leads to an explosion. Since on a streamline of a flow we have $\mathrm{d}E/\mathrm{d}t = -p\mathrm{d}v/\mathrm{d}t$ (where E is internal energy, t is time, p is pressure, and v is volume), rapid deposition of energy will give high pressure, or rapid motion as volume expands, or both. How large and how rapid the energy deposition must be to have an explosion depends on external circumstances, so the concept of explosion is investigated here by looking at some examples.

Low Explosives and Propellants

The words *energetic materials* are used to describe substances that have fuel and oxidizer in the same molecule or in separate molecules intimately mixed. Production and purification of potassium nitrate (KNO_3) were the keys to making materials that burned rapidly and could be used for fireworks, frightening enemies, setting enemy ships on fire, and entertainment at fairs. After 1300 AD, these materials were used in guns, and the mixtures were improved for better performance. High-strength black powder is about six parts of potassium nitrate and one part each of charcoal and sulfur. Black powder has been replaced by smokeless powders made from nitrocellulose or nitrocellulose with nitroglycerin, with various additives. Modern rocket motors usually use a coarse mixture of ammonium perchlorate (NH_4ClO_4) as oxidizer, and rubber, aluminum powder, and high explosive molecules as fuels. Black powder was used in mining from 1650 to 1900; it has since been replaced by high explosives.

All of these materials deliver their energy by burning, which is also called deflagration. That is, energy is transferred from the reacting region forward to ignite the unreacted material mainly by heat conduction. The wave speed of the flame is slow compared with the speed of sound, so that the pressure is nearly constant in the flame. The distance from the reacting region to the wave front varies with the pressure, so the speed of the flame and its rate of release of energy depend on the external confinement. In a mine, the apparent power of black powder varies with the strength of the rock and the existing cracks in the rock. The powder in a gun is usually in the form of separate pellets or grains, and the rate of burning depends on the exposed surface area that supports the flame. As the projectile moves along the barrel, the volume to be occupied by the gases increases at an accelerating rate. It is advantageous to have the rate of burning also accelerate, and this is accomplished by shaping the grains. For example, the grains may be in the form of cylindrical pellets with a number of holes parallel to the axis. As the pellet burns, the holes are enlarged, exposing more area and accelerating the rate of gas production.

High Explosives

High explosives are also energetic materials with the fuel and oxidizer in intimate mixture or in the same molecule. They explode by a process called detonation, and the speed of the reaction is 100,000–10,000,000 times faster than burning in the same material. The rapid reaction produces extremely high pressures and speeds. It also makes the detonation process almost independent of confinement or boundary effects. High explosives detonate the same way every time, without being influenced by exterior changes.

Detonation proceeds as a wave traveling at high speed, from 4000 to 9000 ms^{-1} in various explosives, with a shock wave at the front of the wave structure. The compression in the shock heats the explosive enough to make it react rapidly. The energy released in the reaction supports the shock. The shock is supersonic, going as fast as the available energy can drive it, so nothing occurs ahead of the shock. In the reaction zone the flow is subsonic so energy can be transferred, but at the end of the reaction zone the flow becomes supersonic, and anything that happens in that supersonic flow cannot come forward to affect the reaction zone. It is for these reasons that the detonation is almost independent of the external conditions. Only at the edges can it be perturbed.

High explosives were discovered about the middle of the 19th century by chemists developing new dyes. Ascanio Sobrero, an Italian chemist, first prepared nitroglycerin and several other high explosives in 1846 and 1847. Alfred Nobel in 1864 developed a method of initiating nitroglycerin reliably by a fast compression wave, or shock wave, but it was dangerous to handle and ill-suited to mining operations. In 1867 Nobel was granted a patent for an explosive prepared by mixing nitroglycerin with a porous absorbent such as charcoal, diatomaceous earth, or fine sawdust. This explosive, called dynamite, proved to be just what was needed for the developing industrial revolution. In a few years it replaced black powder throughout the world. Many compositions competed with dynamite: a dictionary of explosives published in 1891 listed more than a thousand explosives.

After the middle of the 20th century, dynamite was replaced by explosives prepared from ammonium nitrate and fuel oil as granular mixtures, as slurries, or as emulsions. In the United States alone the annual use of high explosives is more than five billion pounds per year, or nearly 20 pounds for each person. A pound of explosive will break about 3000 pounds of rock, so about 60,000 pounds of rock is broken for each person in the United States each year. A large fraction of the explosive is employed to break the rock overburden of coal seams, other uses are in other mining, road construction, lumbering, and farming. Almost any product we purchase has had explosive used for it at some stage.

The first high-precision application of high explosives was to nuclear weapons, developed during World War II, where explosive was used for the precise dynamic assembly of the fissionable material. The nuclear weapons laboratories around the world have contributed to the detailed theory of detonation, to numerical modeling of detonations, to the development of powerful and safe explosives, and to the experimental techniques for studying explosives.

Nonlinear relations are especially important to detonation. The shock wave forms because the stress-strain behavior of the explosive is nonlinear. Materials become stiffer as they are compressed, so the sound speed increases with pressure, and a compression wave steepens to become a shock. The extremely strong nonlinear dependence of the reaction rate on temperature is also very important. It is the on-off switch for the release of energy. For example, a typical rate law for an explosive might be $d\lambda/dt = k(1-\lambda)e^{(-T^*/T)}$, where k is the limiting rate; λ is a progress variable for the reaction, going from zero to one as the explosive goes to products; t is the time; T is the temperature; and T^* is the activation temperature. If $k = 10^{20}\ s^{-1}$ and $T^* = 25{,}000$ K, the time required for half of the explosive to react when kept at constant temperature is 341 million years at 300 K (room temperature), 8.64 ms at 600 K, and 8.03 ns at 900 K.

Nuclear Weapons

In nuclear fission weapons, U^{235} or Pu^{239} is bombarded by neutrons that cause it to split into two lighter nuclei, releasing a large amount of energy and also emitting more neutrons. If more neutrons are generated than escape through the surface, the exponential increase in the number of neutrons leads to an explosion. A fusion weapon is initiated by a fission weapon and releases energy as hydrogen, deuterium, tritium, and lithium fuse to make heavier nuclei. These weapons release a million or more times as much energy as the same weight of conventional chemical explosive. The energy is often quoted in kilotons or megatons. These units are based on an assumed yield for TNT of 1000 $calg^{-1}$ or 4187 Jg^{-1}. The metric tonne is 10^6 g and the kiloton is a thousand times that, so a kiloton is 10^{12} cal or 4.187×10^{12} J, and a megaton is 4.187×10^{15} J.

Asteroid Collision with Earth

About 65 million years ago an asteroid hit the earth leaving the crater Chicxulub in Yucatan, Mexico, and perturbing the conditions on earth to the extent that dinosaurs and many other animals and plants became extinct. The energy deposited was the kinetic energy of the asteroid. The exact details cannot be known, but if the asteroid was 12 km in diameter with density 2500 kg m^{-3} and relative speed 20 km s^{-1}, its kinetic energy was 4.5×10^{23} J. An obvious time constant for the energy release is the diameter divided by the speed, 0.6 s. The kinetic energy divided by the time gives the power as 7.5×10^{23} W; the actual value is a few times smaller.

An asteroid of the Chicxulub size is not slowed much by the Earth's atmosphere and reaches the Earth's surface. A smaller asteroid is slowed more, and the compression wave from the air travels through the asteroid. If the asteroid is small enough, the compression wave reaches the rear surface before the asteroid reaches the ground. The high pressure inside

the asteroid causes it to expand and break up into small pieces that are then slowed more by the air. The kinetic energy is transferred suddenly to the air, and there is an explosion above the surface of the earth. The Tunguska Event in Central Siberia in 1908 flattened trees over an area of about 2000 km^2. It was caused by an asteroid about 60 m diameter that exploded about 8 km above the surface. Its kinetic energy was about 4×10^{16} J.

Volcanoes

The 1883 eruption of the Indonesian volcano Krakatau, which blew ash to a height of 80 km and ejected 22 km^3 of rock, was heard in Australia 4600 km away. Tsunamis caused by the eruption reached heights of 40 m and killed 34,000 people.

Mount St. Helens, in the state of Washington, erupted in 1980 and has been studied extensively. It ejected 2.7 km^3 of rock, devastated an area of 550 km^2, and blew down an estimated 10^7 trees.

A huge volcanic explosion occurred in Yellowstone, United States, about 2,000,000 years ago. About 3000 km^3 of rock were ejected. No explosion of such a magnitude has been experienced during the period of human civilization.

Novae and Supernovae

A nova occurs in a close binary star system made up of a red giant and a white dwarf. Hydrogen-rich matter from the red giant is pulled onto the surface of the white dwarf. When enough matter is accumulated, a nuclear fusion detonation occurs, causing the ejection of hot surface gases and resulting in an extraordinary increase in luminosity. A supernova occurs when a massive star exhausts its nuclear fuel and its core collapses to become a neutron star. The outer layers of the star are attracted by the gravitational pull of the core, and then rebound from it. A shock wave generated in the collision propagates outward and blows off the surface gases.

W.C. Davis

See also **Dimensional analysis; Flame front; Shock waves**

Further Reading

Baker, W.E., 1973. *Explosions in Air*, Austin: University of Texas Press

Baker, W.E., Cox, P.A., Westine, P.S., Kulesz, J.J. & Strehlow, R.A. 1983. *Explosion Hazards and Evaluation*, Amsterdam and New York: Elsevier

Federoff. B.T. et al. 1960. *Encyclopedia of Explosives and Related Items*, 10 vols, Dover, NJ: US Army Armament Research and Development Command (Picatinny Arsenal), (PATR-2700)

Glasstone, S. & Dolan, P.J. (editiors). 1977. *The Effects of Nuclear Weapons*, 3rd edition, Washington: United States Department of Defences

International Astronomical Union, 1991. *Physics of Classical Novae*, Berlin and New York: Springer

Kinney, G.F. & Graham, K.J. 1985. *Explosive Shocks in Air*, 2nd edition, Berlin and New York: Springer

Sigurdsson, H. et al. (editors). 2000. *Encyclopedia of Volcanoes*, San Diego and London: Academic Press

Wheeler, J. Craig 2000. *Cosmic Catastrophes: Supernovae, Gamma Ray Bursts, and Adventures in Hyperspace*, Cambridge and New York: Cambridge University Press

EXTREMUM PRINCIPLES

Extremum principles are ubiquitous in mathematics, with wide applications in areas ranging from genetic theory (Narain, 1993) to thermodynamics (Velasco & Fernandez-Pineda, 2002). The simplest sort of extremum principle occurs in differential geometry, whenever one considers a differentiable function $f(x_1, \ldots, x_N)$ of N variables and wishes to determine the critical points of f, namely those $\boldsymbol{x}$ that satisfy

$$\nabla f(\boldsymbol{x}) = 0.$$

The Hessian matrix H has entries given by the second derivatives

$$H_{jk} = \frac{\partial^2 f}{\partial x_j \partial x_k}(\boldsymbol{x})$$

(assuming these exist). If all the eigenvalues of the Hessian are positive (negative), then this ensures that $\boldsymbol{x}$ is a local minimum (maximum); eigenvalues of mixed sign correspond to a saddle point. The general characterization of functions in terms of their behavior near critical points is the subject of Morse theory (Morse & Cairns, 1969).

Probably the most widespread type of extremum principles are those arising from the application of the calculus of variations (Gel'fand & Fomin, 1963). One of the first historical examples of this sort is the brachistochrone problem posed by Johann Bernoulli the elder in 1696: given a particle sliding from rest along a path between two fixed points under the influence of gravity, find the plane curve such that the time taken is minimized. The solution curve (a cycloid) was obtained by both Johann and Jakob Bernoulli, and also by Newton, Leibniz, and l'Hôpital. Nowadays, the problem is usually solved directly through the use of the total time functional

$$T = \int_{x_0}^{x_1} \sqrt{\frac{1 + (y')^2}{2g(y_0 - y)}}\, \mathrm{d}x \equiv \int_{x_0}^{x_1} F(y, y')\, \mathrm{d}x,$$
$$y' = \frac{\mathrm{d}y}{\mathrm{d}x}, \qquad (1)$$

where $y(x)$ is the plane curve joining the points (x_0, y_0) and (x_1, y_1) and g is the acceleration due to gravity. To

minimize the time, it is necessary that the first variation of the functional T should vanish,

$$\delta T = 0,$$

which leads to the Euler–Lagrange equations

$$\frac{\partial F}{\partial y} - \frac{\mathrm{d}}{\mathrm{d}x}\left(\frac{\partial F}{\partial y'}\right) = 0 \tag{2}$$

The solution of (2) is given parametrically in terms of (x_0, y_0) and another constant h by

$$x(\theta) = x_0 + (\theta - \sin\theta)/(2h^2),$$
$$y(\theta) = y_0 - (1 - \cos\theta)/(2h^2).$$

In complete analogy to the Hessian condition in finite dimensions, the positivity of the second variation $\delta^2 T$ ensures that the cycloid yields a minimum of the functional $T[y]$.

In physics perhaps the most important extremum principle of all is the Principle of Least Action. An early proponent of this notion was Pierre Louis de Maupertuis, who employed an extremality argument to solve a problem in statics (Beeson, 1992). Maupertuis, who was tutored by Johann Bernoulli, was in regular correspondence with Leonhard Euler, and the work of the latter laid the foundation for the subsequent development of the subject. The enormous generality of the least-action principle became apparent from the Lagrangian formulation of classical mechanics (Goldstein, 1950), as derived from the action functional

$$S[\boldsymbol{q}] = \int_{t_0}^{t_1} L(\boldsymbol{q}, \dot{\boldsymbol{q}}, t)\,\mathrm{d}t. \tag{3}$$

The variable t is the time, and the vector $\boldsymbol{q}$ and its time derivative $\dot{\boldsymbol{q}}$ denote the generalized coordinates and velocities, respectively. Requiring that the action should be stationary with respect to variations that vanish at the initial and final times, so

$$\delta S = 0, \quad \text{with } \delta\boldsymbol{q}(t_0) = 0 = \delta\boldsymbol{q}(t_1), \tag{4}$$

it follows (after an integration by parts) that L must satisfy the Euler–Lagrange equations

$$\frac{\partial L}{\partial \boldsymbol{q}} - \frac{\mathrm{d}}{\mathrm{d}t}\left(\frac{\partial L}{\partial \dot{\boldsymbol{q}}}\right) = 0.$$

The extremality condition (4) is truly fundamental, since once the Lagrangian L has been specified appropriately, then all the classical equations of motion for a mechanical system (in particular, Newton's Second Law) are a direct consequence. Even the geodesic equations for a Riemannian manifold arise in this way (Choquet-Bruhat, 1968), by taking the purely kinetic (free particle) Lagrangian

$$L(\boldsymbol{q}, \dot{\boldsymbol{q}}) = g_{jk}(\boldsymbol{q})\dot{q}^j\dot{q}^k,$$

where g_{jk} is the metric tensor (the Einstein summation convention is assumed).

In parallel to the development of mechanics, a corresponding extremum principle was employed in optics, namely Fermat's Principle of Least Time. This is more correctly formulated within the theory of geometrical optics (Kline & Kay, 1965), as the requirement that the path taken by light traveling between two points P_1 and P_2 is such that the optical distance is *extremized*, that is,

$$\delta \int_{P_1}^{P_2} n(x, y, z)\,\mathrm{d}s = 0, \tag{5}$$

where $n(x, y, z)$ is the refractive index at the point (x, y, z) in the medium and s denotes arc length along the path. Contrary to Fermat's original formulation, if the optical distance is extremal, then in general, the time taken for the light to travel between P_1 and P_2 need not be minimized—this only holds in certain special cases.

The precise analogy between geometrical optics and mechanics was fully appreciated and exploited by Hamilton. Choosing a parameter τ along the light path such that $\boldsymbol{q} = (x, y, z)^T$ satisfies

$$|\dot{\boldsymbol{q}}|^2 = n^2, \quad \mathrm{d}s = |\dot{\boldsymbol{q}}|\,\mathrm{d}\tau, \tag{6}$$

the equations arising from the variational principle (5) are just

$$\ddot{\boldsymbol{q}} = \nabla\left(\tfrac{1}{2}n^2\right), \quad n = n(\boldsymbol{q}),$$

which are equivalent to Newton's equations for a particle of unit mass moving in a potential $-\frac{1}{2}n^2$. In this mechanical analogy, τ should be reinterpreted as the time, while the first equation (6) implies that the total energy of the particle is zero.

The Principle of Least Action is also essential in field theory. A scalar field theory in N dimensions has the action

$$S[\phi] = \int_V \mathcal{L}(\phi, \phi_\mu, \ldots)\,\mathrm{d}^N x$$

with the Lagrangian density $\mathcal{L}$ being a function of the field ϕ, its first derivatives ϕ_μ $(\mu = 1, \ldots, N)$, and possibly higher derivatives. The appropriate variational principle for the classical field equations is

$$\delta S = 0 \quad \text{with } \delta\phi(\boldsymbol{x}) = 0 \quad \text{for } \boldsymbol{x} \in \partial V,$$

so that the variations vanish on the boundary of the space-time volume V. In the path integral formalism of quantum field theory, as pioneered by Richard Feynman (Feynman & Hibbs, 1965), the central object is the

partition function, defined in terms of the action by

$$Z = \int \mathrm{e}^{\mathrm{i}S[\phi]}\,\mathcal{D}\phi,$$

where $\mathcal{D}\phi$ = path integral measure. When the action is coupled to an external source, $S \to S + \int J(\boldsymbol{x})\phi(\boldsymbol{x})\,\mathrm{d}^N x$, then the vacuum expectation values of the field operators are obtained by taking successive functional derivatives $\delta/\delta J$ of Z. This is the key technique for calculating Feynman rules and perturbative scattering amplitudes in gauge field theory (Bailin & Love, 1986).

Another sort of extremum principle appears in game theory (Owen, 1982). In the simplest case of two-person zero-sum games, with two players denoted "row" and "column" and strategies labelled by an index j ($j = 1, \ldots, M$) for the row player and an index k ($k = 1, \ldots, N$) for the column player, the payoffs to the row player form an $M \times N$ matrix $\mathcal{A}$. The matrix element $\mathcal{A}_{jk}$ is just the payoff to the row player arising from the pure strategy combination (j, k); since the game is zero-sum, the corresponding payoff to the column player is $-\mathcal{A}_{jk}$. If the maximum of the row minima in the payoff matrix is equal to the minimum of the column maxima, then this is a saddle point (or minimax point), corresponding to an optimum solution of the game. However, a saddle point does not exist in general, and so it is necessary to resort to mixed strategies, taking the set of probability distributions $\mathcal{S}_X \times \mathcal{S}_Y$ on the strategy space, where

$$\mathcal{S}_X = \left\{ \boldsymbol{x} \in \mathbb{R}^M \mid x_j \in [0,1],\ \sum_{j=1}^{M} x_j = 1 \right\},$$

$$\mathcal{S}_Y = \left\{ \boldsymbol{y} \in \mathbb{R}^N \mid y_k \in [0,1],\ \sum_{k=1}^{N} y_k = 1 \right\}.$$

Then the Minimax Theorem, due to John von Neumann (von Neumann & Morgenstern, 1947), states that

$$\max_{\boldsymbol{x}\in\mathcal{S}_X} \min_{\boldsymbol{y}\in\mathcal{S}_Y} \boldsymbol{x}^{\mathrm{T}}\mathcal{A}\boldsymbol{y} = v = \min_{\boldsymbol{y}\in\mathcal{S}_Y} \max_{\boldsymbol{x}\in\mathcal{S}_X} \boldsymbol{x}^{\mathrm{T}}\mathcal{A}\boldsymbol{y}. \quad (7)$$

The quantity v is the expected payoff to the row player corresponding to some optimal mixed strategy combination $(\boldsymbol{x}, \boldsymbol{y})$ and is called the *value* of the game. The existence of a more general sort of equilibrium in n-person, noncooperative games has been proved by John Nash (1951). Nash's proof relies on properties of convex functions (as does the standard proof of the Minimax Theorem). Convex analysis has also been used recently in thermodynamics, for a general proof of the minimum energy principle, starting from the maximum entropy principle and using the concavity of the entropy (Prestipino & Giaquinta, 2003).

ANDREW HONE

See also **Euler–Lagrange equations; Game theory; Geometrical optics, nonlinear; Quantum field theory**

Further Reading

Bailin, D. & Love, A. 1986. *Introduction to Gauge Field Theory*, Bristol: Adam Hilger

Beeson, D. 1992. *Maupertuis: An Intellectual Biography*, Oxford: Voltaire Foundation

Choquet-Bruhat, Y. 1968. *Géométrie Différentielle et Systèmes Extérieurs*, Paris: Dunod

Feynman, R.P. & Hibbs, A.R. 1965. *Quantum Mechanics and Path Integrals*, New York: McGraw-Hill

Gel'fand, I.M. & Fomin, S.V. 1963. *Calculus of Variations*, Englewood Cliffs, NJ: Prentice-Hall

Goldstein, H. 1950. *Classical Mechanics*, Reading, MA: Addison-Wesley

Kline, M. & Kay, I.W. 1965. *Electromagnetic Theory and Geometrical Optics*, New York: Interscience Publishers, Wiley

Morse, M. & Cairns, S.S. 1969. *Critical Point Theory in Global Analysis and Differential Topology*, New York: Academic Press

Narain, P. 1993. On an extremum principle in the genetical theory of natural selection. *Journal of Genetics*, 72(2–3): 59–71

Nash, J. 1951. Non-cooperative games. *Annals of Mathematics*, 54: 286–295

Owen, G. 1982. *Game Theory*, 2nd edition, London: Academic Press

Prestipino, S. & Giaquinta, P.V. 2003. The concavity of entropy and extremum principles in thermodynamics. *Journal of Statistical Physics*, 111(1-2): 479–493

Velasco, S. & Fernandez-Pineda, C. 2002. A simple example illustrating the application of thermodynamic extremum principles. *European Journal of Physics*, 23: 501–511

von Neumann, J. & Morgenstern, O. 1947. *Theory of Games and Economic Behaviour*, Princeton, NJ: Princeton University Press

F

FABRY–PEROT RESONANCES

See **Laser**

FAIRY RINGS OF MUSHROOMS

Much of the mythology and mysticism formerly associated with fairy rings is summed up by the words of Prospero in Shakespeare's *The Tempest*, V.i: "Ye elves of hills. . .that/ By moonshine do the green sour ringlets make,/ Whereof the ewe not bites, and you whose pastime/ Is to make midnight mushrooms. . .." However, in what could be interpreted as a minor triumph of reason over superstition, Prospero's invocation is not to the sorcery that was supposedly imbued in fairy rings, but a declaration that he is giving up magic forever.

Fairy rings are not caused by supernatural beings, witches, moles, snails mating, or lightning—these being some of the early explanations, all the more hilarious *now* for being propounded so seriously back *then*, for the annular rings of dead grass, fringed on both edges by concentric rings of over-lush grass, that are often evident in grassy fields. They are caused by fungi. One of the first scientific investigations to establish this fact was reported by Wollaston (1807), whose explanation of fairy rings is still broadly accepted today. Despite this demystification, their appeal to the human imagination remained strong. Kipling (1906) wrote *Puck of Pooks Hill*, a story in which magical manifestations occur when children perform *A Midsummer Night's Dream* in a fairy ring, and Conan Doyle in *The Coming of the Fairies* (1923) only reluctantly admitted that fairy rings were due to fungal growth.

The mode of life involving progressive radial increase from a central point is not unusual among fungi. As pointed out by Ramsbottom (1953), hundreds of fungi grow in circular patterns, including microscopic ones such as *Penicillium* molds as well as those with macroscopic fruiting bodies such as mushrooms and puff-balls. Although the conditions governing initiation of a ring are still obscure, many scientific studies have documented the kinetics of expansion, the species involved, and the biology and ecology of fairy rings. Two excellent and complementary studies are reported in Shantz & Piemeisel (1917) and Dowson et al. (1989).

The underground body of a fairy ring fungus, consisting of a network of filaments called the mycelium, grows radially outwards as it consumes organic matter in the soil. Behind the fungus front, the mycelial mass dies, so that the advancing live fungus front is actually a strange sort of disconnected organism. The dead filaments form a dense and water-repellant mat. Grass in this advancing annular region dies, due simply to physiological drought. Inside this bare region, the grass can grow luxuriantly because the dead filaments eventually decay, providing nitrogen-rich fertilizer. In advance of the fungal front, the grass also grows dark and luxuriant because of the peculiar (to us) eating habits of fungi: they exude digestive enzymes into the medium, then absorb this pre-digested food. Left-over digested food stimulates the grass forward of the fungus.

The radial growth rate of grassland fairy rings has been measured between 99 and 350 mm/year (Dickinson, 1979) and diameters of tens and hundreds of meters have been recorded. The obvious but rather awesome conclusion is that fairy rings may be among the world's oldest living organisms, since many rings are estimated to be several centuries old and some are believed to be 600 or 700 years old. It would be a fascinating exercise to obtain supporting evidence, such as historical records or results from scientific dating methods, for the ages of large fairy rings.

At favorable times of the year, fruiting bodies—mushrooms or toadstools—may be put forth around the circumference of a fairy ring. In woodlands these are often the only obvious manifestation of a fairy ring, since leaf-litter usually covers the ground (Figure 1). Because they depend on the roots of a tree for nutrient supply, woodland fairy rings are referred to as "tethered" rings, whereas those in grassland, for which the nutrient source is spread though the ground, are called "free" rings. The growth of tethered rings is coupled to the radial growth of the host tree roots, and they tend to reach an equilibrium diameter, determined

Figure 1. A typical fairy ring in grass.

by the mature size of the tree, rather than increase indefinitely (Gregory, 1982).

What happens when two or more fairy rings meet? Usually, the putative intersecting portions of same-species rings are extinguished, because of direct competition for resources or as each reaches the other's annular dead zone where nutrients and moisture are depleted in any case. Rings of different species either continue growing through each other or only the dominant species may survive. Rings of different species may also form inside one another.

A simple mathematical model for the ecology of fairy ring systems was developed by Parker-Rhodes (1955), from which was derived estimates for the proportion of ground covered by rings at a given time, the age distribution of rings, and geometric factors affecting inter- and intra-specific competition, such as rate of birth of new rings per unit area and distance between their centers. This model was extended by Stevenson & Thompson (1976) to include boundary effects and a more realistic treatment of the rings as annuli rather than discs. Their conclusions had some interesting implications for the management and control of fairy rings.

Why would anyone want to control them? Some people, sadly, consider fairy rings to be a pathogenic nuisance, a disease to be eradicated; and it is true that they can spoil the appearance and functionality of lawns, golf courses, playing fields, and pastures. The modeling results of Stevenson & Thompson (1976) indicated that if one's aim is to control a population of harmful rings by using an antagonistic but innocuous species of rings, it is more effective in the long term to choose the *smallest* growth rate available. In their work, the rings' growth rate was assumed constant.

If we admit, however, that the growth rate is variable, then fairy rings must be modeled as a dynamical system, and since they spread in two spatial dimensions, the appropriate dynamical description is a system of partial differential equations. Davidson et al. (1997) modeled the spatiotemporal dynamics of fungal mycelia by nonlinear reaction-diffusion equations describing the coupled evolution of the mycelial biomass and nutrient substrate concentration. They found that qualitative features of the development of fairy rings, such as the annular advancing front, degeneration of colony centers, and extinction of the interface between two colliding fronts, were reflected in the structure of solutions to the equations.

This type of predictive computational modeling and simulation of radial growth patterns is likely to become more important in future—and not only because it gives fairy rings the ultimate modern imprimatur and authority of the computer. Other organisms are known to exhibit the fairy ring habit of growth. In the semi-arid rangelands of Australia, for example, certain species of saltbush grow radially outwards from a central origin forming a slowly increasing ring of foliage, the interior of which is bare ground. The patterns on the landscape formed by these blue-gray saltbush rings on the red soil are very striking from the air. The saltbush is a nutritious food source for sheep; thus one might be interested in management strategies that *increase* the covering fraction of saltbush and in factors that affect its growth. In this and other similar problems, the results from mathematical modeling of fungus fairy rings will provide valuable insights.

ROWENA BALL

See also **Growth patterns; Pattern formation; Reaction-diffusion systems**

Further Reading

Davidson, F.A., Sleeman, B.D., Rayner, A.D.M., Crawford, J.W. & Ritz, K. 1997. Travelling waves and pattern formation in a model for fungal development. *Journal of Mathematical Biology,* 35: 589–608

Dickinson, C.H. 1979. Fairy rings in Norfolk. *Bulletin of the British Mycological Society,* 13: 91–94

Dowson, C.G., Rayner, A.D.M. & Boddy, L. 1989. Spatial dynamics and interactions of the woodland fairy ring fungus, *Clitocybe nebularis*. *New Phytologist,* 111: 699–705

Gregory, P.H. 1982. Fairy rings: free and tethered. *Bulletin of the British Mycological Society,* 16: 161–163

Parker-Rhodes, A.F. 1955. Fairy ring kinetics. *Transactions of the British Mycologcal Society,* 38 (1): 59–72

Ramsbottom, J. 1953. *The New Naturalist Mushrooms & Toadstools,* London: Collins

Shantz, H.L. & Piemeisel, R.L. 1917. Fungus fairy rings in eastern Colorado and their effect on vegetation. *Journal of Agricultural Research,* 11: 191–247

Stevenson, D.R. & Thompson, C.J. 1976. Fairy ring kinetics. *Journal of Theoretical Biology,* 58: 143–163

Wollaston, W.H. 1807. On fairy-rings. *Philosophical Transactions of the Royal Society of London,* 2: 133–138

FARADAY WAVES

See **Surface waves**

FEEDBACK

Long before the invention of electrical amplifiers and generators, feedback was used widely in mechanical

control devices, including the governor that was devised by James Watt in 1784 to stabilize the speed of a steam engine. The theory of such a governor was developed in the latter half of the 19th century by James Clerk Maxwell and by Ivan Alekseevich Vyshnegradskiy. Although the results obtained by Maxwell and Vyshnegradskiy seem contradictory, they present complementary aspects of the analysis. We consider briefly the detailed discussion of these results as given by Neimark et al. (1985).

The Lagrange equations for a steam engine with a governor are

$$I(\vartheta)\ddot{\varphi} + I'_\vartheta(\vartheta)\dot{\vartheta}\dot{\varphi} = M_r(\dot{\varphi}, \vartheta) - M_l,$$
$$I_g\ddot{\vartheta} - \tfrac{1}{2} I'_\vartheta(\vartheta)\dot{\varphi}^2 + U'_\vartheta(\vartheta) + h\dot{\vartheta}, \qquad (1)$$

where $I(\vartheta)$ is the moment of inertia of the engine and governor about the engine shaft, φ is the rotation angle of the engine shaft, ϑ and I_g are, respectively, the angular deviation and the moment of inertia of the governor balls, $M_r(\dot{\varphi}, \vartheta)$ is the driving torque, M_l is the moment of load, and $-U'_\vartheta(\vartheta)$ and $\dot{\vartheta}$ are, respectively, the moments of gravity and viscous friction.

For ideal functioning, Maxwell assumed that the friction factor h must be as small as possible and the governor sensitivity $d\vartheta_0/d\Omega$ (where $\Omega = \dot{\varphi}_0$, φ_0 and ϑ_0 are the equilibrium values of φ and ϑ) must be as large as possible, and he gave recommendations how these conditions could be fulfilled. Vyshnegradskiy, on the other hand, understood that the friction plays an important role by promoting the stability of control. Therefore, he proposed adding a new element to the governor, called the cataract. In addition, Vysnegradskiy showed that for stability of control $d\Omega/dM_l$ must be negative and constructed his famous diagram in the plane $d\Omega/dM_l$, Ih/I_g, now known as the Vysnegradskiy diagram. Maxwell's ideas have also been realized in practice by a device called an "isodromic" in which feedback is effected by a rod that changes its length due to stretching or compressive force.

In the context of electronic amplifier theory, a detailed mathematical treatment of linear feedback was given by Henrik Bode (1950). Here the basic formula is

$$G = \frac{A}{1 - \mu A}, \qquad (2)$$

which was famously discovered by Harold Black in 1927 (Brittain & Black, 1997). In this equation, A is the (large) forward gain of an amplifier, μ is the loss of a passive feedback circuit, μA is the open-loop gain, and G is the closed-loop gain. Assuming the amplifier does not oscillate and making $\mu A \gg 1$ implies $G \approx 1/\mu$. Thus, the closed-loop gain is essentially determined by the properties of a passive circuit (μ), which is far less sensitive to variations in temperature and aging than the forward gain (A). Long-distance telephone service—which requires a large number of highly stable repeater amplifiers—was made possible by Black's invention.

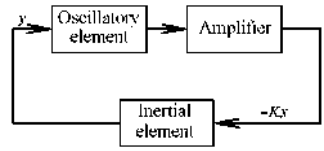

Figure 1. The block diagram of the simplest self-oscillatory system with inertial excitation.

To avoid low-frequency oscillations, the amplifier system of Equation (2) is designed with the open-loop gain having a phase shift of 180° at low frequencies, which corresponds to negative feedback. To avoid oscillations resulting from positive feedback at higher frequencies (where the phase shift approaches 360°), it is necessary and sufficient that the complex mapping of the frequency axis by the open-loop gain function does not surround the point +1 in the μA-plane—the Nyquist criterion (Bode, 1950).

Positive feedback reveals itself in the appearance of negative friction or negative resistance, whereas negative feedback causes the stabilization of device parameters. In Watt's governor, for example, negative feedback stabilizes the speed of rotation, and in other devices it can stabilize frequency variations, the gain factor, and so on. In certain systems, however, negative feedback can result in self-excitation of oscillations. Such systems were called "systems with inertial excitation" by Babitzky & Landa (1982, 1984), and they often arise in physical and engineering studies. The excitation of oscillations in such systems is conditioned by the so-called inertial interaction between dynamical variables occurring as a result of inertia in the feedback loop.

A block diagram of the simplest self-oscillatory system with inertial excitation is shown in Figure 1. The inertial interaction between dynamical variables, like negative friction, can be both linear and nonlinear. A linear interaction can, under certain conditions, lead to spontaneous oscillations, whereas a nonlinear interaction can result in the hard excitation of oscillations (requiring that a threshold be overcome).

A simple system with linear inertial interaction is

$$\ddot{x} + 2\delta\dot{x} + \omega_0^2 x = -ky + f(x, \dot{x}, y),$$
$$\dot{y} + \gamma y = ax + \varphi(x, \dot{x}, y), \qquad (3)$$

where $f(x, \dot{x}, y)$ and $\varphi(x, \dot{x}, y)$ are nonlinear functions free from linear terms, and the parameter a is proportional to the gain of the amplifier. The inertia of the feedback loop is characterized by the parameter γ. The condition of self-excitation of oscillations can

be shown to be $\gamma \leq \gamma_{\rm cr}$, where

$$\gamma_{\rm cr} = -\delta + \sqrt{\delta^2 + ak/2\delta - \omega_0^2}.$$

Because $\gamma_{\rm cr}$ should be positive, self-excitation can occur only for $ak \geq 2\delta\omega_0^2$. The condition $\gamma \leq \gamma_{\rm cr}$ signifies that the feedback loop must be sufficiently inertial (an inertia-less feedback loop corresponds to $\gamma \to \infty$).

Systems with inertial feedback need not be self-excited. A child on a swing, for example, is an inertial system that is not self-excited. Interestingly, the oscillation of a swing is often inaccurately presented in textbooks as an example of parametric excitation. If oscillations are excited by a child who stands on the swing and lifts her center of gravity up and down at the proper moments, the system is not parametrically excited, because the oscillation frequency of the center of gravity is not constant but tuned according to variations of the frequency of the oscillations of the swing. Thus, a child on a swing is a control system with feedback that is self-oscillatory but not self-excited. For excitation of self-oscillations some finite initial perturbation is necessary (i.e., the excitation of oscillations is hard).

The simplest equations describing oscillations of a swing are

$$\ddot{x} + 2\delta\dot{x} + \omega_0^2 x = -bxy, \quad \dot{y} + \gamma y = ax^2, \qquad (4)$$

where the variable y describes the position of the child's center of gravity and γ is the inertial factor of the control circuit. If the feedback is slightly inertial (i.e., γ is too large to put $y \approx (a/\gamma)x^2$), then the variable x obeys the Duffing equation, which has no self-oscillatory solution. Self-oscillations exist only for modest values of γ, when the feedback loop is sufficiently inertial.

Examples of self-oscillatory systems with inertial excitation include the Lorenz system, the Helmholtz resonator with non-uniformly heated walls, a heated wire with a weight at its center, the Vallis model for nonlinear interaction between ocean and atmosphere, a modified Brusselator, an air-cushioned body, and a lumped model of the "singing" flame (Landa, 1996, 2001). Note that the mechanism of self-excitation of oscillations in some continuous system is similar to the examples considered above. Among these are the Rijke tube and a distributed model of the "singing" flame (Landa, 1996).

It must be emphasized that feedback can be nonlinear as well as linear. Although nonlinear feedback cannot cause self-excitation of oscillations, it is of primary importance in their development, and many examples are known. In addition to the swing, noted above, nonlinear feedback plays a role in population dynamics, and it is related to the development of turbulence in a subsonic submerged jet, where the feedback is realized via an acoustic wave. In general, positive feedback plays a key role in the emergence of coherent structures (Landa, 1996).

POLINA LANDA

See also **Candle; Flame front; Nerve impulses; Population dynamics; Tacoma Narrows Bridge collapse**

Further Reading

Babitzky, V.I. & Landa, P.S. 1982. Self-excited vibrations in systems with inertial excitation. *Soviet Physics, Doklady*, 27: 826–827

Babitzky, V.I. & Landa, P.S. 1984. Auto-oscillation systems with inertial self-excitation. *Zeitschrift fuer Angewandte Mathematik und Mechanik*, 64: 329–339

Bode, H.W. 1950. *Network Analysis and Feedback Amplifier Design*, New York: Nostrand

Brittain, J.E. & Black, 1997. Black and the negative feedback amplifier. *Proceedings of the IEEE*, 85: 1335–1336

Landa, P.S. 1996. *Nonlinear Oscillations and Waves in Dynamical Systems*, Dordrecht and Boston: Kluwer

Landa, P.S. 2001. *Regular and Chaotic Oscillations*, Berlin and New York: Springer

Neimark, Yu.I., Kogan, N.Ya. & Savel'ev, V.P. 1985. *Dinamicheskie Modeli Teorii Upravleniya* [*Dynamical Models of the Control Theory*], Moscow: Science

FEIGENBAUM THEORY

See **Routes to chaos**

FERMI ACCELERATION AND FERMI MAP

In a seminal paper, Enrico Fermi (1949) proposed two related methods of producing cosmic rays by accelerating charged particles by repeated collisions with moving magnetic fields. The particles could either be trapped by magnetic mirroring (*See* **Averaging methods**) or be deflected without trapping. In either case, the charged particles gain energy if the magnetic field is moving opposite to the particle's motion and lose energy if the motions are in the same direction. For random motions of the magnetic fields the net effect is stochastic acceleration; that is, the probability is higher for an accelerating collision, due to the relative velocities. The mechanism could explain the power law of proton energies and was consistent with the magnitude of the cosmic ray energies. However, because of the competition between energy loss due to ionization and energy gain from the stochastic heating, the process could not reasonably explain the existence of high mass cosmic rays. More recently, after the discovery of supernovas, and observing magnetic fields and motions of supernova remnants (SNRs), the trapping version of Fermi's acceleration mechanism has been closely examined. A general understanding, developed over the last few years, is that shock waves in SNRs can repeatedly accelerate trapped charged

particles to produce both proton and higher mass cosmic rays (see a recent account by Malkov et al. (2002), and references therein).

Well before the recent interest in cosmic ray production by SNRs, the original basic idea of Fermi acceleration was being investigated with simple models. In particular, the question was asked whether the nonlinear dynamics of the particle motion would lead to stochastic acceleration even if the particles were acted on by periodic forces. A simple mapping model to detect this effect is that of a ball bouncing between a fixed and an oscillating wall. The model, developed by Ulam in 1961, was very straightforward to implement on a computer. The results were explained analytically and confirmed numerically in work during the 1960s and early 1970s by, among others, Zaslavsky and Chirikov, Brahic, and Lieberman and Lichtenberg (see Lichtenberg & Lieberman, 1991). They showed that for smooth forcing functions, the phase plane divides up into three distinct regions with increasing ball velocity: (1) a low-velocity region in which all period 1 fixed points are unstable, leading to stochastic motion over almost the entire region; (2) an intermediate velocity region in which islands of stability, surrounding elliptic fixed points, are imbedded in a stochastic sea; and (3) a higher-velocity region in which bands of stochastic motion, near the separatrices of the island trajectories joining the hyperbolic fixed points, are isolated from each other by regular orbits. The existence of region (3), in which invariant curves span the entire range of phase, bounds the energy gain of the particle. If the forcing function is not sufficiently smooth, then region (3) does not exist, in agreement with the Kolmogorov–Arnol'd–Moser (KAM) theory.

Because the Fermi particle acceleration mechanism was one of the first considered for determining the regions of parameter space where KAM surfaces exist and is easily approximated by simple mappings for which numerical solutions are attainable for "long times," it has become a bellweather problem in understanding the dynamics of nonlinear Hamiltonian systems with the equivalent of two degrees of freedom. Various versions both with analytic and non-analytic wall oscillation functions, and with physically moving walls or walls that just impart momentum, have been analyzed. The basic Ulam model, together with an interesting variant of it, is shown in Figure 1. The model in (a) is homologous to many physical problems (see below) and has therefore been of considerable importance. A simplified version of the model in (b) leads to the *standard map*.

A simplified form of the Ulam map can be constructed if the oscillating wall imparts momentum to the ball, according to the wall velocity, without the wall changing its position in space. The problem defined in this manner has many of the features of the more physical problem and can be analytically treated with

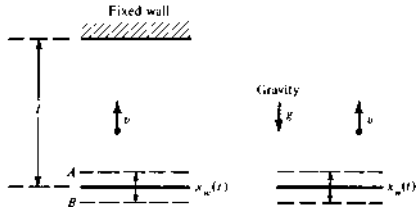

Figure 1. Fermi acceleration models. (a) Version in which a particle bounces between an oscillating wall and a fixed wall. (b) Version in which the particle returns to an oscillating wall under the action of a constant gravitational acceleration.

various wall-forcing functions. In this simplified form, the mapping is

$$u_{n+1} = |u_n + f(\psi_n)|,$$
$$\psi_{n+1} = \psi_n + \frac{2\pi M}{u_{n+1}}, \tag{1}$$

where u is the velocity, normalized to the maximum wall velocity, and ψ is the phase of the oscillating wall at impact, with $2\pi M/u$ a conventionally used form for phase advance. Equation (1) is the product of two involutions and is, therefore area, preserving; that is, it satisfies the Jacobian condition

$$\frac{\partial(u_{n+1}, \psi_{n+1})}{\partial(u_n, \psi_n)} = 1. \tag{2}$$

The mapping in (1) serves as an approximation (with suitably defined variables) to many physical systems in which the transit time between kicks is inversely proportional to a velocity. The absolute-value signs correspond to the velocity reversal, at low velocities, $u < 1$ but have no effect on the region $u > 1$, which is the primary region of interest. The forcing function $f(\psi)$ is often a sinusoid in physical problems, but it may have other forms.

The basic method to analyze mapping models is to expand about a fixed point $u_{n+1} = u_n$, $\psi_{n+1} = \psi_n + 2\pi n$, and examine the linear stability. Alternatively, a local linearization of the phase advance equation about the phase-stable value of u linearizes the phase-advance equation but retains the nonlinearity in the forcing term. This expansion leads to the standard map, whose nonlinear stability properties have been extensively analyzed. These procedures have determined the basic phase-plane motion, as described above. A difference between the exact and simplified mappings, which should be noted, is that the canonical variables are different, leading to different variables in which an invariant distribution is uniform. For the simplified problem, a proper canonical set of variables is the ball velocity and phase just before the nth impact

with the moving wall. The normalized velocity u then has a uniform invariant distribution. A detailed theoretical and numerical study of various forms of the Fermi map can be found in Lichtenberg & Lieberman (1991, Chapters 3 and 4), where many of the original references can be found. The Fermi map together with the standard map has also led to extensive analysis of phase space diffusion and correlations, which can also be found in the above reference, Chapter 5.

Various elaborated forms of the Fermi map have been applied to a variety of problems. Two such mapping models are electron cyclotron resonance heating (ECRH) in magnetic mirrors (Lieberman & Lichtenberg, 1973) and radio-frequency heating in capacitively driven discharges (Goedde et al., 1988). Although these physical models are generally more complicated than that given in (1), much of the basic analysis is similar. In particular, the expansion around fixed points can be made to investigate linear stability, and nonlinear expansions can obtain the standard mapping from which the KAM barriers to heating can be obtained. Weak dissipation can also be included in models, but this results in a contracting phase space not discussed here (*See* **Chaotic Dynamics**).

Another variant of the basic mapping is one for which the sign in the phase advance equation changes at some value of the action. Such mappings naturally occur in the dynamics of particles in circular accelerators where the sign transition occurs with increasingly relativistic motion in two frequency cyclotron heating and is an underlying cause of the period 3 "catastrophe" of the standard map. When the phase advance equation changes sign, the stable and unstable fixed points exchange their ψ-values, and the phase space structure between these fixed points undergoes a change in topology called reconnection. For further discussion of this phenomenon and references to the original literature, see Lichtenberg & Lieberman (1991, Sections 3.3 and 5.5).

ALLAN J. LICHTENBERG

See also **Averaging methods; Chaotic dynamics; Kolmogorov–Arnol'd–Moser theorem; Maps; Phase space diffusion and correlations; Standard map**

Further Reading

Fermi, E. 1949. On the origin of cosmic radiation. *Physical Review*, 75: 1169–1174

Goedde, C.G., Lichtenberg, A.J. & Lieberman, M.A. 1988. Self-consistent stochastic electron heating in radio frequency discharges. *Journal of Applied Physics*, 64: 4375–4383

Lichtenberg, A.J. & Lieberman, M.A. 1991. *Regular and Chaotic Dynamics*, 2nd edition, New York: Springer

Lieberman, M.A. & Lichtenberg, A.J. 1973. Theory of electron cyclotron resonance heating—II. Long-time and stochastic effects. *Plasma Physics*, 15: 125–150

Malkov, M.A., Diamond, P. & Jones, T.W. 2002. On the possible reason for non-detection of TEV protons in SNRs. In *Bifurcation Phenomena in Plasmas*, edited by S.I. Itoh & Y. Kawai, Fukuoka: Kyushu University

FERMI RESONANCE

See **Harmonic generation**

FERMI–PASTA–ULAM OSCILLATOR CHAIN

A closely examined model of a high-dimensional system comprises a number of masses constrained to move along a line, with a specified force law governing their interaction. In the early 1950s, Enrico Fermi, John Pasta, and Stan Ulam (FPU) (Fermi et al., 1955) numerically examined such a chain of coupled oscillators, with a Hamiltonian of the general form

$$H(p,q) = \sum_{k=1}^{N} \left[\frac{1}{2} p_k^2 + \frac{1}{2}(q_{k+1} - q_k)^2 + \frac{1}{3}\alpha(q_{k+1} - q_k)^3 + \frac{1}{4}\beta(q_{k+1} - qk)^4 \right], \tag{1}$$

where each of N particles has unit mass and unit harmonic coupling constant and the end points are either fixed (vertical position $q_1 = q_{N+1} = 0$) or periodic ($q_{N+1} = q_1$). The parameters α, β represent the nonlinearity in the forces between the particles in the chain. In the original FPU numerical computations either α or β was set equal to zero, and fixed end points were used to correspond to a discretized nonlinear spring. Most subsequent work was done with $\alpha = 0$ and is known as the FPU-β model. The FPU-β model can be normalized so that the significant parameter is βE, where E is the total energy, $H(p,q) = E$.

The original idea of Fermi was that the nonlinearity of the springs would lead to mode mixing such that thermodynamic properties in the lattice could be studied. The original numerical work placed the initial energy in the lowest mode of the linearized system, which at low energy becomes a quasimode of the nonlinear system. The N independent normal modes Q_k of the harmonic system with fixed end point boundary conditions give

$$q_i = \sqrt{\frac{2}{N+1}} \sum_{k=1}^{N} Q_k \sin\left(\frac{ik\pi}{N+1}\right), \tag{2}$$

for which the amplitudes q_i of the mass points form a half-sine for the lowest mode and pick up an additional zero for each higher mode. The harmonic mode frequencies are

$$\omega_k = 2\sin\left(\frac{\pi k}{2N+2}\right). \tag{3}$$

The original numerical study surprisingly showed recurrences, rather than a thermodynamic spreading of energy among the modes. Subsequent studies explained these recurrences as resulting from near resonances among various combinations of modes (Bivins et al., 1973). However, the question of whether the nonlinearity led to long-term mixing of the energy remained an open question.

Although the original question of whether the nonlinearity led to equipartition among the degrees of freedom went unanswered during the 1960s, the FPU-β system became rightly famous for having inspired the early development of soliton theory. Zabusky & Kruskal (1965) showed that a Taylor expansion to transform the FPU chain into a continuous differential equation resulted in the Korteweg–de Vries (KdV) or the modified Korteweg–de Vries (mKdV) equation, depending on whether the α or β term in (1) was retained. For the FPU-β chain (mKdV equation), we have

$$u_\tau + 12u^2u_\xi + u_{\xi\xi\xi} = 0, \tag{4}$$

where time and length variables have been rescaled by $\tau = h^3t/24$ and $\xi = x - ht$; subscripts τ, ξ denote differentiation with respect to that variable.

The periodic solutions of (4), stationary in the frame $\xi - c\tau$, may be obtained by integrating to give

$$\tfrac{1}{2}u_\xi^2 + u^4 - \tfrac{1}{2}cu^2 + A \equiv \tfrac{1}{2}u_\xi^2 + P(u) = 0, \tag{5}$$

where A is a constant of integration. Equation (5) is in the form of a one-degree-of-freedom Hamiltonian, which is therefore integrable. Solutions have been obtained in terms of the Jacobi elliptic functions (or cnoidal waves) $\mathrm{cn}(\xi, q)$, with q (the modulus) taken as a parameter with $0 \le q^2 < 1$. This formalism led to the observations of the stability properties of solitons, and more generally motivated the development of the inverse scattering technique (Gardner et al., 1967). However, the explanation that long-time recurrences were due to initial conditions that were superpositions of stable solitons was not a complete picture and was ultimately misleading.

An explanation for the mechanism leading to stochastic diffusion of energy over the $2N$-dimensional phase space, which also predicted a transition from regular to stochastic motion with increasing energy, was put forward by Izrailev & Chirikov (1966). Using the transformation to modes as in (2), they postulated that if the interaction of pairs of neighboring modes was sufficient to create overlapping beat modes, then the overlap would create global stochasticity. The concept that had been developed by Chirikov for low degree-of-freedom Hamiltonian systems, known as the Chirikov overlap criterion, was applied to the high-dimensional system by isolating a few modes containing the energy. The criterion had been confirmed numerically and later studied in great detail using the *standard map*. The criterion can be shown to be roughly equivalent to requiring that the nonlinear frequency shift with the energy in a single mode be equal to the mode separation (Lichtenberg & Lieberman, 1991, Section 6.5b). Substituting (2) into (1), the nonlinear shift in mode frequency of mode k can be calculated approximately as $\Delta\omega_k \simeq 3\beta E_k\omega_k/4N$. From (3), the frequency separation between low-frequency modes with $\omega_k \simeq \pi k/N$, $k \ll N$, is $\delta\omega_k \simeq \pi/N$, such that for overlap ($\Delta\omega_k/\delta\omega_k \ge 1$)

$$\beta E_k/N \ge 4/3k. \tag{6}$$

Stochastic energy transfer among modes, leading to approximate equipartition among modes, has been numerically found at much lower values of energy density than given by (6). Numerical studies of equipartition (e.g., Livi et al. (1985); Pettini & Landolphi, 1990) found that (6) roughly corresponds to a transition between an inverse time to obtain some measure of equipartition that scales as $\tau^{-1} \propto (E/N)^2$ at low energy, to a time scaling as $\tau^{-1} \propto (E/N)^{2/3}$ at high energy. The latter scaling models a random process that is very strongly stochastic. Furthermore, the prediction that mode overlap determines the transition between regular motion and stochastic diffusion leading to equipartition does not hold if the energy is initially placed in one or a few high-frequency modes. There is local mode mixing, but the high-frequency modes interact only weakly with the low frequencies, as theoretically predicted by Benettin et al. (1987), such that equipartition is not observed above the mode overlap transition on a fast time scale.

The mKdV soliton was found to become unstable from a low-frequency mode, leading to exponential growth of higher frequencies, which correspond quite closely to similar growth of higher frequencies in an oscillator chain (Driscoll & O'Neil, 1976). However, this low-frequency instability is neither a necessary nor sufficient condition for a transition to equipartition, as the soliton theory does not describe the high-frequency modes, but it does present a physical picture of the process that can hold a low-frequency mode together in the absence of coupling to high-frequency modes and how it can break down.

A more coherent picture of the underlying processes leading to equipartition has been developed recently. Basic phase space arguments indicate that, for relatively high-dimensional systems with not too small a perturbation strength, the probability will be high that a generic initial condition will lie in a stochastic portion of the phase space. Arnol'd diffusion will then transport energy over most of the degrees of freedom, essentially leading to equipartition, on some time scale. However, the time to equipartition can be exponentially slow.

Focusing on the region of weaker stochasticity, a transition was numerically found between power law and exponentially long time scales as the energy

density $\varepsilon = E/N$ of the system is decreased. This latter transition is of prime importance for the observation of equipartition, as it essentially separates observable times from those that are not observable. For the FPU chain, the main mechanisms leading to equipartition in this lower energy regime are that resonant interaction of some set of low-frequency modes, in which a significant portion of the energy resides, can lead to local superperiod (very low frequency) beat oscillations that are stochastic. The beat oscillations, which increase with energy, can become comparable to frequency differences between high-frequency modes. This results in Arnol'd diffusion transferring energy to high-frequency modes, on a power law time scale (DeLuca et al., 1995). Furthermore, the appearance of stochasticity corresponds to the onset of the mKdV instability. The driving frequency for diffusion is associated with the libration frequency of the resonance, Ω_B. Using resonant normal form perturbation theory to isolate the most important coupling to the high-frequency modes, the energy transfer to high-frequency modes by Arnol'd diffusion, depends exponentially on the frequency ratio as

$$\frac{dE}{dt} \propto \exp(-\pi\delta\omega_h/2\Omega_B), \tag{7}$$

where $\delta\omega_h$ is the difference frequency between two high-frequency modes. When $\Omega_B \sim \delta\omega_h$, the exponential factor is of order unity, allowing strong diffusion of energy to high-frequency modes, and equipartition on computationally observable time scales. In a separate work, an estimate of the scaling, with energy density, of the equipartition time for $E \gg E_c$ was found theoretically to be $T_{eq} \propto (N/E)^3$, which agrees with numerical computations (De Luca et al., 1999). The somewhat weaker quadratic scaling found in earlier work, as quoted above, was probably due to the use of a less accurate measure of equipartition.

If the energy is initially placed in high-frequency modes, the equipartition process is significantly different from that starting from low-frequency initial conditions. In this case, the dynamics is transiently mediated by the formation of unstable nonlinear structures. First, there is an initial fast stage in which the mode breaks up into a number of breather-like structures. Second, on a slower time scale, these structures coalesce into one large unstable structure. These structures have been called chaotic breathers (CB). Because a single large CB closely approximates a stable breather, the final decay stage, toward equipartition, can be very slow. This behavior has been observed in oscillator chains approximating the Klein–Gordon equation with various force laws and the FPU-β model (Cretegny et al., 1998; Mirnov et al., 2001). In Cretegny et al. (1998), the energy was placed in the highest frequency mode with strict alternation of the amplitudes from one oscillator to the next (periodic boundary conditions). This configuration is stable up to a particular energy, for which there exist exact discrete solutions. Beyond this energy a parametric instability occurs, leading to the events described above. However, the nonlinear evolution does not depend on special initial conditions but will generically evolve from any high-frequency mode initial condition that has predominantly the alternating amplitude symmetry. One does not know, in this generic situation, whether there exists any true energy threshold. As discussed with respect to low-frequency mode initial conditions, the practical thresholds refer to observable time scales. From a phase space perspective, it is intuitively reasonable that for a large number of oscillators and not too low an initial energy, the generic set of initial conditions will lie in a chaotic layer, but the chaotic motion can remain close to a regular orbit for very long times (Lichtenberg & Lieberman, 1991).

Considerable insight into the behavior of a nonlinear oscillator chain, starting from high-frequency mode initial conditions, can be obtained by introducing an envelope function for the displacements of the oscillators. Low-order expansions produce PDEs that have integrable solutions in the form of envelope solitons, analogous to the solitons produced from low-frequency initial conditions (Kosevich, 1993). Higher-order terms usually destroy the integrability.

Substituting the envelope function $\psi_i(t) = (-1)^i q_i(t)$ in (1) (with $\alpha = 0$), using the continuous variable $x = ai$, a Taylor's expansion in a, the lattice period, yields

$$\begin{aligned}\psi_{tt} + 4\psi + 16\beta\psi^3 \\ +a^2\{\psi_{xx} + \beta(12\psi\psi_x^2 + 12\psi^2\psi_{xx})\} \\ +a^4\{(1/12)\psi_{xxxx} + \beta(3\psi_x^2\psi_{xx} + 3\psi\psi_{xx}^2 \\ +4\psi\psi_x\psi_{xxx} + \psi^2\psi_{xxxx})\} + \cdots = 0.\end{aligned} \tag{8}$$

Comparing (8) with (4) qualitatively explains why relaxation is accompanied by the formation of sharply localized states if energy is initially deposited in the high-frequency part of the spectrum where the effect of dispersion is small, while only broad nonlinear structures are formed if the energy is initially in the low-frequency modes where the dispersion is large. Using a dimensionless variable, introducing the rotating wave approximation (RWA) $\cos^3 \omega t \simeq (\frac{3}{4})\cos\omega t$ and neglecting terms proportional to a^4 and higher, (8) can be integrated to yield

$$(-\omega^2 + 4)\psi^2 + \psi_x^2 + \beta(6\psi^4 + 9\psi^2\psi_x^2) = C_1, \tag{9}$$

which has integrable trajectories in phase space similar to (5) but includes a high-frequency drive ω. Depending on the boundary conditions, these phase trajectories represent multiple or single breathers.

As with low-frequency initial conditions, the soliton solution of the envelope, obtained from (9), becomes unstable with increasing energy. For most numerical studies of oscillator chains, the initial state imposed on the system is mainly that of a single linear mode. This state is generally not close to an equilibrium. The initial state rapidly relaxes, governed by the nonlinear equations. Numerical studies indicate that the chaotic breathers that are formed in the nonlinear processes are probably marginally stable, which accounts for their long-lived existence.

After a set of chaotic breathers has been formed, on a short time scale by a modulational instability or breakup relaxation, the breathers coalesce, on a longer time scale into a single chaotic breather. This process has been well documented numerically (Cretegny et al., 1998; Mirnov et al., 2001) and an analytic estimate of the process made (Kosevich & Lepri, 2000; Mirnov et al., 2001) with the breather coalescence time found to scale as $\tau_B^{-1} \propto E_B/N$, the breather energy density. The background mode spectrum beats with the breather to transfer energy to low-frequency modes, resulting in equipartition on a slower time-scale as $T_{eq} \propto (E/N)^{-2}$ (Mirnov et al., 2001).

Although we have concentrated on the seminal problem of the FPU-β lattice, the results are qualitatively connected to other types of oscillator chains. For example, if the cubic, rather than the quartic, potential is retained in (1), then the Hamiltonian is equivalent to the lowest-order nonlinear expansion of the integrable Toda lattice. Consequently, the chain is considerably more stable. Other interesting types of lattices are composed of discretizations of Klein–Gordon equations. In particular, with a quartic potential, the dynamics of the Klein–Gordon Hamiltonian

$$H = \sum_{i=1}^{N} \left[\tfrac{1}{2} p_i^2 + \tfrac{1}{2}(q_{i+1} - q_i)^2 + \tfrac{1}{2} m^2 q_i^2 + \tfrac{1}{4} \beta q_i^4 \right], \tag{10}$$

has been compared with the FPU-β chain, showing both similarities and differences (Pettini & Cerruti-Sola, 1991). The stability of "discrete breathers" has also been examined for various chains (Cretegny et al., 1998).

ALLAN J. LICHTENBERG

See also **Arnol'd diffusion; Breathers; Discrete breathers; Frenkel–Kontorova model; Korteweg–de Vries equation; Phase space diffusion and correlations; Solitons; Solitons, a brief history; Standard map; Toda lattice**

Further Reading

Benettin, G., Galgani, L. & Giorgilli, A. 1987. Realization of holonomic constraints and freezing of high frequency degrees of freedom in the light of classical perturbation theory. *Communications in Mathematical Physics*, 113: 87–103

Bivins, R.L., Metropolis, N. & Pasta, J.R. 1973. Nonlinear coupled oscillators: model equation approach. *Journal of Computational Physics*, 12: 65–87

Cretegny, T., Dauxois, T., Ruffo, S. & Torcini, A. 1998. Localization and equipartition of energy in the β-FPU chain: chaotic breathers. *Physica* D, 121: 109–126

De Luca, J., Lichtenberg, A.J. & Lieberman, M.A. 1995. Time scale to ergodicity in the Fermi–Pasta–Ulam system. *Chaos*, 5: 283–297

De Luca, J., Lichtenberg, A.J. & Ruffo, S. 1999. Finite times to equipartition in the thermodynamic limit. *Physical Review* E, 60: 3781–3786

Driscoll, C.F. & O'Neil, T.M. 1976. Explanation of instabilities observed on the Fermi–Pasta–Ulam lattice. *Physical Review Letters*, 37: 69–72

Fermi, E., Pasta, J.R. & Ulam, S.M. 1955. Studies of nonlinear problems. *Los Alamos Scientific Report*, LA-1940; also in *Collected Works of Enrico Fermi* 1965. Chicago: University of Chicago Press, 2: 978–988

Gardner, C.S., Greene, J.M., Kruskal, M.D. & Mura, R.M. 1967. Method for solving the Korteweg–de Vries equation. *Physical Review Letters*, 19: 1095–1097

Izrailev, F.M. & Chirikov, B.V. 1966. Statistical properties of the nonlinear string. *Soviet Physics-Doklady*, 11: 30–32

Kosevich, Y.A. 1993. Nonlinear envelope-function equation and strongly localized vibrational modes in anharmonic lattices. *Physical Review* B, 47: 3138–3151

Kosevich, Y.A. & Lepri, S. 2000. On modulation instability and energy localization in harmonic lattices at finite energy density. *Physical Review* B, 61: 299–314

Lichtenberg, A.J. & Lieberman, M.A. 1991. *Regular and Chaotic Dynamics*, 2nd edition, New York: Springer

Livi, R., Pettini, M., Ruffo, S., Sparglioni, M. & Vulpiani, A. 1985. Equipartition threshold in nonlinear large Hamiltonian systems: the Fermi–Pasta–Ulam model. *Physical Review* A, 31: 1039–1045

Mirnov, V.V., Lichtenberg, A.J. & Guclu, H. 2001. Chaotic breather formation, coalescence, and evolution to energy equipartition in an oscillator chain. *Physica* D, 157: 251–282

Pettini, M. & Cerruti-Sola, M. 1991. Strong stochasticity threshold in nonlinear large Hamiltonian systems: effect on mixing times. *Physical Review* A, 44: 975–987

Pettini, M. & Landolphi, M. 1990. Relaxation and ergodicity breaking in nonlinear Hamiltonian dynamics. *Physical Review* A, 41: 768–783

Zabusky, N.J. & Kruskal, M.D. 1965. Interactions of solitons in a collisionless plasma, and the recurrence of initial states. *Physical Review Letters*, 15: 240–243

FERROMAGNETISM AND FERROELECTRICITY

Iron, nickel, cobalt, and some rare earths (e.g., gadolinium) are characterized by long-range ferromagnetic order. This originates at the atomic level and causes the unpaired electron spins to line up parallel to each other within a region of space called a magnetic domain. Domains range from 0.1 mm to a few mm in size. Within each domain, the net magnetization is large and homogenous, but over the entire sample it averages out to zero due to random orientations of spins. An externally applied magnetic field can cause the material to become macroscopically magnetized, as the magnetic

domains already aligned in the direction of this field grow at the expense of their neighbors and those neighbors reorient their magnetizations towards the field direction.

Ferromagnets have very high magnetic susceptibilities (χ), ranging from 1000 up to 100,000 (meaning the ferromagnet is that much easier to magnetize than free space), and they tend to stay magnetized following the application of an external magnetic field. This tendency to remember magnetic history is called "hysteresis." All ferromagnets have a maximum temperature, called the Curie temperature (T_c), which for iron is about 1043 K. Above T_c the ferromagnetic phase changes into a paramagnetic phase, in which induced magnetism is proportional to the applied field. Ferromagnets also respond mechanically to an applied magnetic field, changing length slightly in the direction of the applied field, a property that is called magnetostriction.

In addition to ferromagnets, there exist other magnetically ordered compounds with parallel-oriented sublattices. The simplest such example is antiferromagnetism with two antiparallel sublattice magnetizations. To measure the degree of order in a complex magnetic phase, as many order-parameter components as there are distinct sublattices may be needed. For ferromagnets, the order parameter is the net magnetization. In antiferromagnets, the order parameter is the staggered magnetization: $\boldsymbol{M}_1 - \boldsymbol{M}_2$, where $\boldsymbol{M}_1$ and $\boldsymbol{M}_2$ are the magnetization vectors for the two sublattices.

In 1907, Pierre Weiss proposed a phenomenological theory of ferromagnetism, building on the model of paramagnetism that Paul Langevin introduced in 1905. The Langevin function: $L = \coth(x) - 1/x$ (where $x = \mu H/kT$) describes the paramagnetic susceptibility of N non-interacting classical spins in a magnetic field of intensity H. Weiss assumed that spins interact with each other through a molecular field proportional to the average magnetization in the sample. So that

$$H_{\text{eff}} = H + \lambda M. \tag{1}$$

By replacing spin-spin interactions with the interaction of a single spin (S) and all its neighbors taken as an average field, the nonlinear problem was approximately solved giving rise to ferromagnetism for T below $T_c = \lambda C$, where

$$C = \frac{N\mu^2 S(S+1)}{3k} \tag{2}$$

with k denoting the Boltzmann constant.

As a consequence, the Langevin expression for susceptibility in paramagnetism

$$\chi = \frac{M}{H} = \frac{C}{T} \tag{3}$$

becomes the Curie–Weiss relation

$$\chi = \frac{C}{T - T_c} \tag{4}$$

above T_c, with spontaneous magnetization below T_c for ferromagnets. This is characteristic of a second-order phase transition. Spin alignment stems from the exchange interactions between spins whose energy can be expressed via the Ising Hamiltonian $\mathcal{H}$ in the case of strong uniaxial anisotropy favoring alignment parallel or antiparallel to the z-axis of quantization depending on the sign of the exchange constant J:

$$\mathcal{H} = -\sum_{i,j} J S_i^z S_j^z, \tag{5}$$

where S_i^z and S_j^z are the z-components of the spin vectors at the lattice sites i and j, respectively. In the absence of anisotropy, one uses the Heisenberg Hamiltonian that couples the spin vectors in a scalar product. Free-energy expansion of the Landau type can be obtained within the Curie–Weiss approximation for a Hamiltonian that includes the Zeeman interaction with an external magnetic field and an Ising-type spin-spin interaction.

Ferroelectricity was discovered in the beginning of the 20th century as a property of ionic, covalent, molecular crystals, and even polymers that possess electrical polarization either spontaneously (e.g., Rochelle salt) or under mechanical stress (piezoelectricity) or temperature changes (pyroelectricty). The net polarization of a ferroelectric crystal can be reoriented by applying an electric field. In ferroelectric phase transitions, a change in the crystal structure is accompanied by the appearance of spontaneous polarization. Ferroelectric phase transitions can be either displacive or order-disorder type. In displacive transitions (e.g., $BaTiO_3$), atoms or molecules exhibit small (compared with the unit cell) positional shifts with long-range correlations. These transitions are caused by phonons and the order parameter is the amplitude of the related lattice distortion giving rise to a change of the lattice structure. Displacive transitions are described using a continuous Landau–Ginzburg model with ensuing solitary waves. In order-disorder transitions (e.g., $NaNO_2$), atoms or molecules order themselves on distances comparable to the unit cell. A transformation between randomly distributed atomic positions of their local double-well potential bottoms ($T > T_c$) and an ordered arrangement ($T < T_c$) takes place. Models of order-disorder transitions use the Ising Hamiltonian with an effective (not real) spin variable.

Ferroelectric phase transitions involve symmetry changes in the crystal structure that are manifested by the emergence of an order parameter: spontaneous polarization vector $\boldsymbol{P}$. For second-order transitions, the symmetry group of the ferroelectric phase is a

subgroup of that in the paraelectric phase (in which $\boldsymbol{P}$ is proportional to the applied electric field $\boldsymbol{E}$). In some cases, such as the onset of ferroelectricity with a transverse optical branch, a so-called soft mode is responsible for the transition. The soft-mode's frequency ω_k for the wave vector k tends to 0 as $T \to T_c$. A special type of ferroelectric phase transition involves incommensurate phases where spontaneous polarization develops a spatial modulation with a wavelength that is incommensurate with lattice periodicity. The occurrence of incommensurate phases is usually explained by competition between long- and short-range forces, for example, in the Frenkel–Kontorova model. As in ferromagnets, ferroelectrics develop domains in which a particular orientation of polarization is selected. These domains can range in sizes from submicroscopic to macroscopic, and the region between two neighboring domains is called a domain wall.

JACK A. TUSZYŃSKI

See also **Critical phenomena; Domain walls; Frenkel–Kontorova model; Hysteresis; Ising model; Order parameters**

Further Reading

Bruce, A.D. & Cowley, R.A. 1981. *Structural Phase Transitions*, London: Taylor & Francis

Kittel, C. 1996. *Introduction to Solid State Physics*, 7th edition, New York: Wiley

Landau, L.D. & Lifshitz, E.M. 1959. *Statistical Physics*, London: Pergamon Press

Lines, M.E. & Glass, A.M. 1977. *Principles and Applications of Ferroelectric and Related Materials*, Oxford: Clarendon Press

Stanley, H.E. 1971. *Introduction to Phase Transitions and Critical Phenomena*, Oxford: Clarendon Press and New York: Oxford University Press

White, R.H. & Geballe, T. 1979. *Long Range Order in Solids*, New York: Academic Press

FIBERS, OPTICAL

See **Optical fiber communications**

FIBONACCI SERIES

Leonardo of Pisa (approx. 1175 to around 1250), also known as Leonardo Pisano, referred to himself as Fibonacci (or son of Bonacci), the name by which he is usually called today. As the son of a customs officer, he had opportunities to travel around the Mediterranean coast and observe many commercial practices. He saw that the Hindu-Arabic system of ten digits and its algorithms for arithmetic had many advantages over Roman numerals. His book of 1202 (revised 1228), *Liber Abaci*, meaning *The Book of the Abacus* or *The Book of Reckoning*, described the system in the Italian vernacular, and so the decimal system became common in Europe.

In his book are some problems and puzzles that were meant as arithmetic practice using the new system. One referred to a problem about rabbits in a field: "A certain man put a pair of rabbits in a place surrounded on all sides by a wall. How many pairs of rabbits can be produced from that pair in a year if it is supposed that every month each pair begets a new pair, which from the second month on becomes productive?" It is based on the assumption that the pairs mate according to the same conditions. Each month, the number of rabbit pairs in the field is 1, 1, 2, 3, 5, 8, 13, 21, 34, 55, 89, 144. So the answer is 144 pairs after 12 months. The number of rabbits in any month is found by adding the number of rabbits alive in the last month (since we assume none die or are eaten) and adding to it the number of new rabbits born that month, which is one for each pair that was alive in the month before that. The rule is therefore "add the last two numbers to get the next." The next number in the series is 89 plus 144, or 255. The series was probably known before this and Fibonacci merely copied it from another source. The sequence is now called the Fibonacci sequence in his honor, but this name was not given until the late 1800s when Edouard Lucas rediscovered the series and wrote about some of its many properties.

Earlier than this, it had been noticed that the Fibonacci numbers (though not called that) appear in the number of petals of flowers of many plant species, in the arrangements of leaves round a branch, or seed whorls on a seed head. The study of such features of plants is termed phyllotaxis. There are flowers with 3 petals (clover) and many with 5, but none with 7 or 9 leaves or petals. The numbers 4, 6, and 10 also occur but the arrangement is of two sets of 2, 3, or 5. No scientific justification for this was given until Douady and Couder wrote about it in 1993 where they showed that if the growing tip of a plant (the meristem) produces a new primordial cell that becomes a leaf or petal or branch, then the optimal arrangement is for the new cell to be produced at the rate of 1.618 per turn of the growing point. This produces the least overlapping for leaves and the maximum exposure to collect sunlight, or for seeds, it provides the most compact packing (given the simple method of growth of the meristem) with even placing of seeds no matter how large the seed head becomes.

This number, precisely computed as $g \equiv (\sqrt{5}+1)/2 = 1.6180339887\ldots$, is a famous number in geometry called the golden section (also golden ratio, golden mean, divine proportion). It appears as the ratio of diagonals to sides in a pentagon. The golden section as a decimal number never recurs, and so cannot be expressed exactly as a fraction (i.e., it is irrational). It has the property that its reciprocal (1 divided by the golden section) is 0.6180339887.... This is

exactly 1 less than the golden section itself, giving rise to the definition of the golden section as "the positive number that is 1 less than its reciprocal." In other words, $1/g = g - 1$ or $1 = g^2 - g$, a quadratic equation that is solved by the value above together with $-1/g = -0.6180339887\ldots$.

The fractions that best approximate g are the ratios of two successive Fibonacci numbers: 3/2, 5/3, 8/5, 13/8, 21/13 in the sense that no fraction with numbers smaller than the numerator of one of these terms will give a better approximation. It is this that explains why the Fibonacci numbers appear in phyllotaxis since the optimal arrangements are best approximated using Fibonacci numbers (or, indeed any series where the last two numbers are added to produce the next).

Since the Fibonacci rule is so simple, it is also found in other mathematical situations. For instance, suppose that houses can be made in two sizes, single (separate) and double (two attached), the latter taking twice the frontage along a road as the single ones. Given a road that is long enough for n houses on one side, how many arrangements are there that the architect can choose from? For instance, a road that can have 3 houses on it could have 3 singles, or else a double followed by a single or a single first and then a double—3 ways. For 4 houses there are 5 arrangements; for 5 houses, 8 possibilities. The number of arrangements is always a Fibonacci number.

The rule also applies to the family tree of a male honeybee. Male bees are produced from unfertilized eggs and female bees from fertilized eggs. So males have one parent and females have two. A male bee thus has one parent (F) and two grandparents (M and F), three great-grandparents and so on with 5, 8, 13, 21 as we go back each generation.

In two dimensions, a rectangle with sides in the golden ratio is called a golden rectangle. It has been observed in the shape of many parts of the Parthenon on the Acropolis in Athens, although none of the original plans of the building are extant. The Greeks knew of the ratio, and Euclid's *Elements* shows how to find and construct the golden section point on any line.

RON KNOTT

See also **Branching laws**

Further Reading

For further information, references, applications, and related mathematics, see www.mcs.surrey.ac.uk/Personal/R.Knott/Fibonacci/

Boncompagni, B. 1852. *Della vita e delle opere di Leonardo Pisano*, Rome: Tipografia delle Belle Arti (The only complete printed version of Fibonacci's 1228 edition of *Liber Abbaci*.)

Gies, J. & Gies, F. 1969. *Leonard of Pisa and the New Mathematics of the Middle Ages*, New York: Crowell (Another book with much on the background to Fibonacci's life and work.)

Grimm, R.E. 1973. The autobiography of Leonardo Pisano. *Fibonacci Quarterly*, 11: 99–104

Horadam, A.F. 1985. Eight hundred years young. *The Australian Mathematics Teacher*, 31: 123–134 (An interesting and readable article on Fibonacci, his names and origins as well as his mathematical works. It refers to and expands upon the article by Grimm.)

Parshall, Karen Hunger. *The Art of Algebra from al-Khwarizmi to Viète: A Study in the Natural Selection of Ideas*, http://www.lib.virginia.edu/science/parshall/algebra.html (Contains a brief biography of Fibonacci if you want to read more about the history of mathematics.)

Smith, D.E. 1923. *History of Mathematics*, vol. 1, Boston and London: Ginn; reprinted, New York: Dover, 1958 (Gives a complete list of other books that he wrote and is a fuller reference on Fibonacci's life and works.)

FIBRILLATION

See **Cardiac arrhythmias and electrocardiogram**

FILAMENTATION

When we look at a window on rainy days, we may observe a curious phenomenon: the rain forms a sheet of water on the glass. A single drop—from time to time—introduces a perturbation on this surface that is sufficient to trigger small-scale channels breaking the layer of liquid and escaping from it. Filamentary structures of water emerge from the unstable flow, destroying the initial expanse. The water sheet has thus decayed into filaments through an instability that is called filamentation.

Filamentation also occurs in plasma physics and nonlinear optics. In this context, an intense optical beam propagating in a focusing (Kerr) medium may break up into several spots due to the small inhomogeneities affecting its initial distribution, as evidenced by self-focusing experiments in solids, liquids, and gases (see, e.g., Bespalov & Talanov, 1966; Campillo et al., 1973). This phenomenon can be understood from the equation for the paraxial self-focusing of optical beams that describes the propagation of the slowly varying complex envelope ψ of a scalar electric field with central frequency ω_0 through a nonlinear medium. The envelope ψ, expressed in the frame moving with the group velocity, obeys the nonlinear Schrödinger (NLS) equation

$$\mathrm{i}\partial_z\psi + \nabla_\perp^2\psi + f(|\psi|^2)\psi = 0, \qquad (1)$$

where $\nabla_\perp^2 \equiv \partial_x^2 + \partial_y^2$ represents wave diffraction and $f(|\psi|^2)$ models the nonlinear response of the medium. Here, the radial (x, y) and longitudinal (z) variables are normalized with respect to the beam waist w_0 and to the Rayleigh length $z_0 = \pi n_0 w_0^2/\lambda_0$, depending on the linear refractive index n_0 and central wavelength λ_0.

For an unsaturated Kerr medium, $f(s) = s$ and solutions of Equation (1) collapse at finite distance whenever their power $P = \int |\psi|^2 \mathrm{d}\boldsymbol{r}$ exceeds the threshold $P_c \simeq 11.7$. Nonlinear responses of optical materials are, however, generally saturating, for example,

like $f(s) = s/(1+\beta s)$ with $\beta = |\psi|^{-2}_{\max} \ll 1$. Such saturations occur in two-level systems, such as sodium and rubidium atomic vapors (Soto-Crespo et al., 1992).

Modeling filament formation requires a perturbation theory, following which small fluctuations break up steady-state solutions, expressed as $\psi_s(\boldsymbol{r}, z) = \phi(\boldsymbol{r})e^{i\lambda z}$, where ϕ satisfies the differential equation

$$-\lambda\phi + \nabla_\perp^2\phi + f(\phi^2)\phi = 0 \tag{2}$$

and $\lambda =$ const. Stability of ϕ can thus be investigated from the perturbed solution

$$\psi(x, y, z) = [\phi(x, y, \lambda) + \varepsilon\{v(x, y, z) + iw(x, y, z)\}]e^{i\lambda z}, \tag{3}$$

where v and w are real-valued functions with amplitude parameter $\varepsilon \ll 1$.

Linearizing Equation (1) with respect to these functions yields the eigenvalue problem

$$\partial_z v = L_0 w, \quad -\partial_z w = L_1 v, \tag{4}$$

where L_0 and L_1 represent the self-adjoint operators

$$L_0 = \lambda - \nabla_\perp^2 - f(\phi^2),$$
$$L_1 = \lambda - \nabla_\perp^2 - [f(\phi^2) + 2f'(\phi^2)\phi^2], \tag{5}$$

with $f'(\phi^2) = \partial f(u)/\partial u|_{u=\phi^2}$. Combining Equations (4), we then obtain $\partial_z^2 v = -L_0 L_1 v$, and different filamentation-like instabilities may be investigated from this general formalism.

- *Modulational instability (MI):* Originally, Bespalov & Talanov (1966) proposed a modulational instability theory, following which oscillatory perturbations with an exponential growth rate split the beam envelope taken as a background uniform solution into small-scale cells. Perturbative modes are chosen as $v, w \sim \cos(k_x x)\cos(k_y y)e^{\gamma z}$, and they apply to a plane wave ϕ which, by definition, satisfies $\nabla_\perp^2\phi = 0$, so that $\lambda = f(\phi^2)$. The growth rate γ is then given by Equation (4):

$$\gamma^2 = k^2[2A - k^2], \quad A \equiv uf'(u)|_{u=\phi^2},$$
$$k^2 = k_x^2 + k_y^2. \tag{6}$$

  Plane waves are unstable with $\gamma^2 > 0$ in the range $0 < k < \sqrt{2A}$ and the maximum growth rate $\gamma_{\max} = A$ is attained for $k = k_{\max} = \sqrt{A}$. This instability promotes the beam breakup into a wave-train of small-scale filaments regularly distributed in the diffraction plane with the transversal spacing $\lambda_{\text{mod}} \simeq 2\pi/k_{\max}$ and longitudinal length $\sim\gamma^{-1}$. In practical uses, the number of filaments is close to the ratio $P_{\text{in}}/P_{\text{fil}}$, where P_{in} is the power of the input beam and P_{fil} the power enclosed in one filament. Considering each filament with radial symmetry, the evaluation $P_{\text{fil}} \simeq 2\pi\int_0^{\lambda_{\text{mod}}/2} r|\phi|^2\,dr \simeq 2.65P_c$ holds for unsaturated Kerr media [$f(s) = s$].

- *Filamentation on a ring*: For broad beams, self-focusing often takes place as a regular distribution of dots superimposed upon ring-like diffraction patterns, so that filamentation may not develop over the entire surface of the input beam. To model this instability, the Laplacian in Equation (1) can be rewritten as $\nabla_\perp^2 = r^{-1}\partial_r r\partial_r + r^{-2}\partial_\theta^2$, where θ denotes the azimuthal angle. Unstable modes $v, w \sim \cos(m\theta)e^{\gamma_m z}$ with azimuthal index number m break up a spatial ring, which is modeled by a uniform background solution ϕ lying on a circular path with length $s = \bar{r}\theta$, where $\bar{r}$ is the mean radius of the ring. Equation (4) then yields (Soto-Crespo et al., 1992)

$$\gamma_m^2 = \left(\frac{m}{\bar{r}}\right)^2\left(2A - \frac{m^2}{\bar{r}^2}\right) \tag{7}$$

  and the maximum number of modulations on the ring is provided by the integer part number $m_{\max} = \text{int}\{\bar{r}^2 A\}^{1/2}$. An example of filamentation on a ring-diffraction pattern emerging from a tenth-order super-Gaussian beam is shown in Figure 1 for $f(s) = s$ in the presence of a random-phase noise. About seven to eight filaments emerge and rapidly collapse.

- *Transverse instability*: Although elementary, MI theory has been considered as the starting point for understanding laser filamentation, until plane waves are replaced by bounded solutions. These can be the soliton modes of the NLS equation, and the resulting instability is termed transverse instability. It appears when a soliton ϕ is perturbed by oscillatory modulations developing along one axis. For instance, when the Laplacian reduces to the 1-dimensional operator $\nabla_\perp^2 = \partial_x^2$ in Equation (2), a soliton solution $\phi(x, \lambda) = \sqrt{2\lambda}\,\text{sech}(\sqrt{\lambda}x)$ can undergo perturbative modes v, w decomposed as $V(x), W(x)\cos(k_y y)e^{\gamma z}$. These perturbations are local in x and they promote the formation of bunches, periodically distributed over the y-axis. The operators L_0 and L_1 in Equation (5) are transformed as $L_0 = \lambda - \partial_x^2 - f(\phi^2) + k_y^2$ and $L_1 = L_0 - 2f'(\phi^2)\phi^2$. For the cubic nonlinearity ($f(s) = s$), the instability growth rate is close to the theoretical curve $\gamma^2 = 1.08k_y^2(3\lambda - k_y^2)$ (Rypdal & Rasmussen, 1989). The same reasoning holds when the Laplacian of Equation (1) includes a third dimension, for example, a time variable, along which 2-dimensional spatial solitons are subject to periodic fluctuations. Because bounded solutions ϕ are not always accessible analytically, numerical computations are often required for determining γ^2 (Akhmediev et al., 1992).

Besides filament formation, Equations (4) and (5) provide information on the inner stability of solitons, known as orbital stability, which refers to the ability

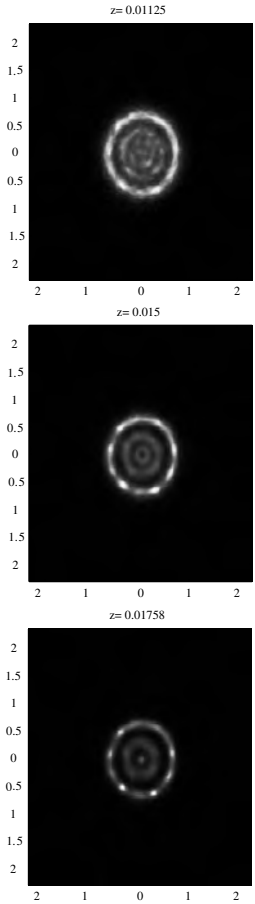

Figure 1. Filamentation pattern numerically computed for a tenth-order super-Gaussian beam with $P_{in} = 30P_c$ in a cubic medium.

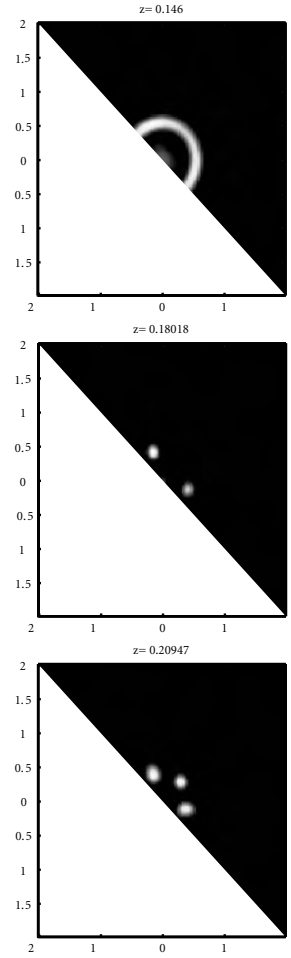

Figure 2. Filamentation pattern numerically computed for a Gaussian beam with $P_{in} = 20P_c$ in a saturable medium.

of initial solutions near equilibrium states to converge to robust soliton shapes. Standard procedures allow the stability criterion $dP(\phi)/d\lambda > 0$ to be established, where $P(\phi) \equiv \int \phi^2 d\boldsymbol{r}$ is the soliton power (Kuznetsov et al., 1986). Orbital stability applies to filaments formed in saturable media with $f(s) = \alpha s - \beta s^2$, $f(s) = \alpha s/(1 + \beta s)$, or $f(s) = \alpha(1 - e^{-s})$, where α and β are positive constants. Relaxation of filaments to stable solitons promoted by the nonlinearity $f(s) = s/(1 + 2 \times 10^{-3} s)$ is shown in Figure 2.

On the whole, filamentation follows from linear stability analyses, which are valid as long as $\varepsilon(v + iw)$ remains smaller than ϕ, thus applying to early stages in the beam propagation. At later stages, filaments develop into a fully nonlinear regime, and they may interact. From the interplay between diffraction and nonlinearity, two filaments with radius ρ and separated by the distance $\Delta > 2\rho$ can fuse whenever Δ is below a critical value, Δ_c. This critical distance can be evaluated by the balance between the free and interaction contributions in the Hamiltonian of Equation (1) (Bergé et al., 1997). With no saturation, each filament whose

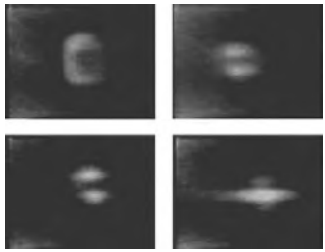

Figure 3. Filamentation and coalescence event in a two-spot pattern produced by a 50 fs pulse with 5 mJ energy propagating in air at the increasing distances (from left to right and from top to bottom): $z = 2.5$, 4.5, 6.5, and 8.5 m (Tzortzakis et al., 2001).

power is above critical creates its own attractor, at which it mostly freely collapses. This constraint is softened by including saturation, so that filaments with powers above critical are able to coalesce into an intense central lobe. As an example, the coalescence of two spots resulting from the propagation of modulationally unstable femtosecond pulses in air is shown in Figure 3 (Tzortzakis et al., 2001).

Modulational instability and multisoliton-like generation take place in various nonlinear media, such as biased photorefractive crystals or quadratically nonlinear optical materials favoring the coupling of fundamental and second harmonic fields (Fuerst et al., 1997). Filamentation moreover occurs in inertial fusion confinement (IFC) experiments as a harmful instability destroying the homogeneity in the beam energy distributed in the focal spot. For IFC, it has detrimental consequences to the hydrodynamics of the plasma created by a laser beam and contributes to the growth of parametric instabilities, which dissipate part of the laser energy. To limit its influence, optical smoothing techniques can be employed. For instance, random phase plates are used to generate a diffraction pattern composed of speckles, whose size λ_{sp} is smaller than the optimal wavelength λ_{mod} that maximizes the filamentation growth rate. This contributes to suppress laser filamentation (Labaune et al., 1992).

LUC BERGÉ

See also **Development of singularities; Kerr effect; Nonlinear optics**

Further Reading

Akhmediev, N.N., Korneev, V.I. & Nabiev, R.F. 1992. Modulational instability of the ground state of the nonlinear wave equation: optical machine gun. *Optics Letters*, 17: 393–395

Bergé, L., Schmidt, M.R., Rasmussen, J. Juul, Christiansen, P.L. & Rasmussen K.Ø. 1997. Amalgamation of interacting light beamlets in Kerr-type media. *Journal of the Optical Society of America* B, 14: 2550–2562

Bespalov, V.I. & Talanov, V.I. 1966. Filamentary structure of light beams in nonlinear media. *Zhurnal Eksperimental'noi i Teoreticheskoi Fiziki, Pis'ma v Redaktsiyu* (USSR JETP), 3: 471–476 [Translated in *JETP Letters*, 3: 307–310]

Campillo, S.L., Shapiro, S.L. & Suydam, B.R. 1973. Periodic breakup of optical beams due to self-focusing. *Applied Physics Letters*, 23: 628–630

Fuerst, R.A., Baboiu, D.-M., Lawrence B., Torruellas, W.E., Stegeman, G.I., Trillo, S. & Wabnitz, S. 1997. Spatial modulational instability and multisolitonlike generation in a quadratically nonlinear optical medium. *Physical Review Letters*, 78: 2756–2759

Kuznetsov, E.A., Rubenchik, A.M. & Zakharov, V.E. 1986. Soliton stability in plasmas and hydrodynamics. *Physics Reports*, 142: 103–165

Labaune, C., Baton, S., Jalinaud, T., Baldis, H.A. & Pesme, D. 1992. Filamentation in long scale length plasmas: experimental evidence and effects of laser spatial incoherence. *Physics of Fluids* B, 4: 2224–2231

Rypdal, K. & Rasmussen, J. Juul. 1989. Stability of solitary structures in the nonlinear Schrödinger equation. *Physica Scripta*, 40: 192–201

Soto-Crespo, J.M., Wright, E.M. & Akhmediev, N.N. 1992. Recurrence and azimuthal-symmetry breaking of a cylindrical Gaussian beam in a saturable self-focusing medium. *Physical Review* A, 45: 3168–3175

Tzortzakis, S., Bergé, L., Couairon, A., Franco, M., Prade, B. & Mysyrowicz, A. 2001. Break-up and fusion of self-guided femtosecond light pulses in air. *Physical Review Letters*, 86: 5470–5473

FINGERING

See **Hele-Shaw cell**

FINITE ELEMENT METHODS

See **Numerical methods**

FINITE-DIFFERENCE METHODS

See **Numerical methods**

FISHER'S EQUATION

See **Zeldovich–Frank-Kamenetsky equation**

FISKE STEPS

See **Josephson junctions**

FITNESS LANDSCAPE

The notion of landscape is chosen in analogy to terrestrial landscapes, which are functions over a two-dimensional space, $f(x, y)$. Commonly, landscape is altitude h as a function of latitude θ and longitude φ: $h(\theta, \varphi)$. In the history of physics, the landscape concept was first applied to motion in the gravitational field resulting in the concept of a potential energy surface. The gravitational potential V depends on altitude, latitude, the mass of the particle m, and the gravitational

acceleration on the surface of the Earth as a function of latitude, $g(\theta)$: $V(\theta, \varphi) = m\, g(\theta)\, h(\theta, \varphi)$. The metaphor of a landscape embedded in the gravitational field suggests an exploration of optimal downhill paths following the negative gradient of the potential, $-\mathbf{grad}\ V(\boldsymbol{x}) = -(\partial V/\partial x_1, \partial V/\partial x_2, \ldots, \partial V/\partial x_n)$, with infinitesimal step width and vanishing kinetic energy corresponding to infinitesimally slow motion.

The landscape metaphor is used today in many different disciplines where the optimization of a nonsimple cost function is the primary goal. Such a cost function may depend on any number of variables, for example, spatial coordinates and strengths of external fields, and then the space upon which a landscape is built will be high-dimensional. Landscapes describing complex systems exhibit a large number of local minima and maxima. Models of disordered systems, spin glasses in particular, were the first examples studied in detail. Spin glasses are traditionally studied by statistical mechanics and still represent the best-studied cases of statistics on complex landscapes (Binder, 1986; Dotsenko et al., 1990).

The notion of fitness landscape was introduced into evolutionary biology by Sewall Wright in 1932 as a metaphor for the visualization of Darwinian evolution as an optimization process (see Wright, 1967). The Darwinian mechanism operates on populations over the course of many generations. It is based on genetic variation of individuals through mutation and recombination and selection of the variants with largest reproductive success. Reproductive success of a genotype I is measured in terms of its fitness value f, which counts the number of (fertile) descendants in the next generation. The concept of a fitness landscape or mapping ϕ assigns a fitness value f_k to every genotype I_k: $\phi(I_k) = f_k$. Population genetics describes the evolution of a population by means of the time dependence in the distribution of genotypes: At time t the genotype I_k is assumed to be present with frequency $x_k(t)$ in a population of N individuals distributed over n types or variants. The frequencies fulfill $\sum_{k=1}^{n} x_k = 1$, and for asexual reproduction, we have $\mathrm{d}x_k/\mathrm{d}t = x_k(f_k - \bar{f})$ with $\bar{f} = \sum_{k=1}^{n} x_k f_k$ being the mean fitness of the population. The time derivative of the mean fitness,

$$\frac{\mathrm{d}\bar{f}}{\mathrm{d}t} = \overline{f^2} - \left(\overline{f}\right)^2 = \mathrm{var}\{f\} \geq 0, \qquad (1)$$

is equal to the variance of the fitness. The mean fitness of a population is a nondecreasing function of time and, hence, subjected to optimization. The frequencies of all variants with fitness values larger than average, $f_k > \bar{f}$, increase whereas those of genotypes that are less productive than average, $f_k < \bar{f}$ decrease until the genotype becomes extinct. This process continues until the mean fitness $\bar{f}$ has reached its maximum because all variants except the fittest have disappeared. The optimization principle also holds for sexual reproduction with recombination, as long as variants at a single gene locus are considered, and is called Fisher's fundamental theorem in this context. More general models of population dynamics describe variation explicitly. When mutation is included and several genetic loci are considered, the optimization principle is no longer valid. However, it works in the mild form as an optimization heuristic in the sense that optimization is observed in almost all cases.

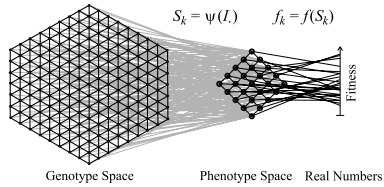

Figure 1. Fitness landscapes illustrated by two consecutive mappings, one from genotype space into phenotype space and the other from phenotype space into the positive real numbers, $\mathbb{R}_+$, representing the fitness values. In agreement with the available data on biopolymer landscapes, we are dealing with the phenomenon of neutrality: There are many more genotypes than phenotypes, and different phenotypes may have fitness values that cannot be distinguished by selection.

The dichotomy of biological evolution—genetic variation in the form of mutation and recombination changes genotypes, whereas selection operates on phenotypes—suggests a splitting of the conventional fitness landscapes into two successive mappings: Genotypes are mapped onto a space of phenotypes, and the phenotypes are evaluated by a second map to yield fitness values (Figure 1):

Biological evolution:
genotype $\Longrightarrow$ phenotype $\Longrightarrow$ fitness,
RNA evolution:
sequences $\Longrightarrow$ structure $\Longrightarrow$ replication rate.

Evolution experiments with RNA molecules in the test tube (Biebricher & Gardiner, 1997) are sufficiently simple to allow for a description of the fitness landscape in molecular terms. The RNA sequence forms a molecular structure that determines the replication rate parameters that are the molecular counterparts of fitness values.

In biological landscape metaphors, the genotypes are materialized as polynucleotide sequences, DNA or RNA. These are strings built from four classes of symbols, $\{\mathbf{A}, \mathbf{T}(\mathbf{U}), \mathbf{G}, \mathbf{C}\}$. In RNA $\mathbf{T}$ is replaced by $\mathbf{U}$. All sequences of given chain length are subsumed in a discrete sequence space, $\mathcal{I}$, with the Hamming distance between two sequences I_i and I_j, $d_{ij}^{(h)}$ serving as metric. The fitness landscape can be expressed by

$$\phi : \{\mathcal{I}; d_{ij}^{(h)}\} \Longrightarrow \mathbb{R}_{(+)}, \qquad (2)$$

where the plus sign implies a restriction to strictly positive fitness values. The structures are points in another discrete metric space $\mathcal{S}$ with some distance measure between structures $d_{ij}^{(s)}$. The fitness landscape is properly split into two mappings

$$\psi : \{\mathcal{I}; d_{ij}^{(h)}\} \Longrightarrow \{\mathcal{S}; d_{ij}^{(s)}\}$$

and

$$f : \{\mathcal{S}; d_{ij}^{(s)}\} \Longrightarrow \mathbb{R}_{(+)}. \tag{3}$$

Sequence-structure maps of RNA have been studied by means of computer models (Schuster, 2001, 2003) on the simplified level of RNA secondary structure. As sketched in Figure 1, the number of sequences is much larger than the number of secondary structures. Hence, many sequences may give rise to the same structure. In population biology this phenomenon is known as neutrality in sequence space, and it was discussed already in the 1980s by Kimura (1983) when the first biopolymer sequences became accessible. Neutrality was also found to be highly relevant for the efficiency of evolutionary processes because it allows for escape from local optima that would otherwise trap populations for long times (Fontana & Schuster, 1998).

The nature of landscapes can be analyzed by means of an expansion of the landscape in eigenfunctions of the Laplacian on the underlying discrete space (Reidys & Stadler, 2002). The expansion coefficients of this expansion allow for estimates of the hardness of optimization. Whenever we have only a single dominating expansion coefficient, the optimization problem is much simpler than in the case of equally important blending of two or more eigenfunctions. Biopolymer landscapes of free energies of conformations or other relevant properties turned out to be rather complex as several eigenfunctions of the Laplacian were found to be important.

PETER SCHUSTER

See also **Biological evolution; Spin systems**

Further Reading

Biebricher, C.K. & Gardiner, W.C. 1997. Molecular evolution of RNA in vitro. *Biophysical Chemistry*, 66: 179–192

Binder, K. 1986. Spin glasses: experimental facts, theoretical concepts and open questions. *Reviews of Modern Physics*, 58: 801–976

Dotesenko, V.S., Feigel'man, M.V. & Ioffe, L.B. 1990. Spin glasses and related problems. *Soviet Science Reviews A. Physics*, 15: 1–250

Fontana, W. & Schuster, P. 1998. Continuity in evolution. On the nature of transitions. *Science*, 280: 1451–1455

Kimura, M. 1983. *The Neutral Theory of Molecular Evolution*, Cambridge and New York: Cambridge University Press

Reidys, C.M. & Stadler, P.F. 2002. Combinatorial landscapes. *SIAM Review*, 44: 3–54

Schuster, P. 2001. Evolution *in silico* and in vitro: the RNA model. *Biological Chemistry*, 382: 1301–1314

Schuster, P. 2003. Molecular insights into the evolution of phenotypes. In *Evolutionary Dynamics—Exploring the Interface of Accident, Selection, Neutrality, and Function*, edited by J.P. Crutchfield & P. Schuster, Oxford and New York: Oxford University Press, pp.163–215

Wright, S. 1967. "Surfaces" of selective value. *Proceedings of the National Academy of Sciences USA*, 58: 165–172

FITZHUGH–NAGUMO EQUATION

Around 1960, Jin-ichi Nagumo (from the University of Tokyo) visited with Richard FitzHugh (at the U.S. National Institutes of Health), who was adapting the relaxation-oscillator models of Karl Bonhoeffer and Balthasar van der Pol to provide a more simple formulation of nerve membrane switching than the four-variable Hodgkin–Huxley system. From this visit emerged the FitzHugh–Nagumo (FN) system as a two-variable oscillator model (FitzHugh, 1961), which led to a simplified formulation of neural action potentials (Nagumo et al., 1962).

Neurons display relaxation oscillations par excellence. When the voltage across the cell membrane (in the trigger zone of the soma) exceeds a threshold, they fire an action potential and then gradually decay to the resting state. If the exciting input is constantly above the threshold, the neuron fires repeatedly. The frequency of such firing depends on the intensity of the input (total input coming from neighboring neurons). FitzHugh sought to reduce the Hodgkin–Huxley model of this dynamics to a two-variable model for which phase-plane analysis applies. His general observations were that the gating variables of the Hodgkin–Huxley model, n (potassium activation) and h (sodium inactivation), have slow kinetics relative to m (or sodium activation), and that for typical nerves $n+h \approx 0.8$. Furthermore, FitzHugh noticed that the voltage nullcline had the shape of a cubic function and the n-nullcline could be approximated by a straight line, both within the physiological range of the variables. This led to the following two-variable model that provides a phase space qualitative explanation of the formation and decay of the action potential.

$$\begin{aligned} \dot{v} &= +v(v-\theta)(1-v) - y + I, \\ \dot{y} &= \varepsilon(v - \gamma y), \end{aligned} \tag{1}$$

where the dots indicate time derivatives.

Like all relaxation oscillators, this oscillator has a slow accrual phase and a fast release phase. Here v is the scaled voltage or membrane potential (namely, the output of the neuron), and y the single recovery variable accounting for the slow dynamics (sodium inactivation and potassium activation variables). The difference in time scales between sodium activation (m) and sodium inactivation and potassium activation (n and h) is represented by $\varepsilon \ll 1$. As ε increases, so does the frequency of oscillation. The constant γ

is a shunting parameter, $0 < \theta < 1$ is a thresholding parameter, and I is an externally applied current.

Such oscillators exhibit the characteristic dynamics of a real neuron. When fed by a constant amount of low current, the oscillator gradually increases its voltage (or membrane charge) until it reaches the threshold. Upon reaching threshold, the neuron fires and quickly releases the accumulated charge. If the current source is sufficient and is constantly applied, this results in stable limit-cycle oscillations.

The FN oscillator is applied in neuroscience to study the synchronization properties of neurons, which is particularly easy for relaxation oscillators such as the FN model. Following the Hebbian rule, neurons that fire closely in time strengthen their synaptic connections, and therefore synchronization in neural activity is important to the way the states of a brain evolve in time. Furthermore, information in neural tissues seems to be coded in the spatiotemporal firing of sets of neurons that fire synchronously, and tissues that are anatomically separated may operate together when they are synchronized.

An ensemble of coupled excitable oscillators of the FN type makes up an excitable medium, through which electrical signals can propagate. This is the case for a nerve and for other excitable media such as muscles. To model the spatiotemporal evolution of membrane potential and its generated current flows in such structure, one treats the axon or dendrite branch of the nerve as a membrane cylinder, with x denoting the distance along the cylinder. If ρ is the intracellular resistivity (in ohm-cm) and d the diameter, then the axial current is

$$I_i = -(\pi d^2/4\rho)\frac{\partial V}{\partial x}\,, \tag{2}$$

which follows directly from Ohm's law. Conservation of current then requires

$$C_m \frac{\partial V}{\partial t} = \frac{d}{4\rho}\frac{\partial^2 V}{\partial x^2} - I_{\text{ion}} + I(x,t), \tag{3}$$

where I_{ion} is the ionic current flowing through a unit area of the membrane surface and $I(x,t)$ and C are an external current and membrane capacitance per unit area.

Applying Equation (3) to the FN case, suggests that the electrical propagation in nerves can be represented as a reaction-diffusion system of the form

$$\begin{aligned} \frac{\partial^2 V}{\partial x^2} - \frac{\partial V}{\partial t} &= +F(V) - Y + I(x,t), \\ \frac{\partial Y}{\partial t} &= \varepsilon(V - \gamma Y)\,. \end{aligned} \tag{4}$$

Here $F(V)$ is a function with cubic shape such as $F(V) = V(V-\alpha)(1-V)$ or some similar function. [Such diffusion models can also be extended to more dimensions with $\partial^2 V/\partial x^2 + \partial^2 V/\partial y^2$ and $V(x, y; t)$.]

Under a traveling-wave analysis, let $I(x,t) = 0$ and $z = x + ct$ and define $\mathrm{d}V/\mathrm{d}z \equiv W$. Then Equations (4) become a system of ordinary differential equations

$$\begin{aligned} \frac{\mathrm{d}V}{\mathrm{d}z} &= W, \\ \frac{\mathrm{d}W}{\mathrm{d}z} &= F(V) - Y + cW, \\ \frac{\mathrm{d}Y}{\mathrm{d}z} &= \frac{\varepsilon}{c}(V - \gamma Y)\,, \end{aligned} \tag{5}$$

where one seeks traveling-waves solutions as trajectories $(V(z), W(z), Y(z))$ that approach the origin $(0, 0, 0)$ as $z \to \pm\infty$ (Scott, 2003).

With $\varepsilon = 0$, Y is constant. In this case, the only stable traveling wave solution is a level change from one of the outer zeros of $F(V) - Y$ to the other; in other words, a moving impulse-like solution does not exist. For $0 < \varepsilon \ll 1$, however, there is an impulse-like traveling-wave solution (or solitary wave). At arbitrarily small values of ε, this solitary wave continues to exist but with the front and back edges of the wave becoming far apart. These front and back edges interpolate between the slowly varying regions and are called boundary layers (as in hydrodynamics). As $\varepsilon \to 0$ on a scale where the impulse length is unity, the boundary layers reduce to step functions.

One of the main research areas related to these reaction-diffusion models in electrophysiology focuses on pattern formation and cardiac rhythm disturbances. FN equations have been used to investigate a variety of unusual front-bifurcation and pattern-formation processes. The precise conditions for wave front formation and subsequent wave propagation in an excitable medium are critical for understanding the genesis and possible control of re-entrant (spiral-wave) cardiac arrhythmias.

L. Vazquez and M.-P. Zorzano

See also **Boundary layers; Hodgkin–Huxley equations; Neurons; Reaction-diffusion systems; Relaxation oscillators**

Further Reading

FitzHugh, R. 1961. Impulses and physiological states in theoretical models of nerve membranes. *Biophysiscal Journal*, 1: 445–466

Nagumo, J., Arimoto, S. & Yoshizawa, S. 1962. An active pulse transmission line simulating nerve axons. *Proceedings of the Institute of Radio Engineering and Electronics*, 50: 2061–2070

Scott, A. 2002. *Neuroscience: A Mathematical Primer*, Berlin and New York: Springer

Scott, A. 2003. *Nonlinear Science: Emergence and Dynamics of Coherent Structures*, 2nd edition, Oxford and New York: Oxford University Press

FIXED POINTS

See **Equilibrium**

FLAME FRONT

Combustion waves can propagate over a wide range of burning velocities that differ by more than three orders of magnitude for the same mixture. At one end of the velocity spectrum, we have a laminar flame (deflagration) that propagates at a typical velocity of about half a meter per second for common fuel-air mixtures at normal conditions. At the other end, the combustion wave propagates as a detonation whose speed is of the order of a couple of thousand meters per second in the same mixture. In between these limits, we have an almost continuous range of turbulent burning velocities. Both laminar flames and detonation wave are intrinsically unstable and have the morphology of a transient cellular structure (Figure 1).

A laminar flame is essentially an isobaric diffusion-reaction wave. Its propagation speed is determined by the rate of diffusion transport of heat from the reaction zone to the cold unburned mixture and the characteristic time of heat release of the chemical reactions. A laminar flame speed (S_L) is proportional to the square root of the product of thermal diffusivity (D_{th}) and the reaction rate (w_r) (i.e., $S_L \sim \sqrt{D_{th} w_r}$). The reaction rate is given by $w_r \sim \exp(-E/RT_f)$ in which E is the activation energy and T_f is the flame temperature. Because the activation energy is very large in general, the reaction rate is extremely temperature sensitive. Thus, any fluctuation in the flame temperature will result in a large variation in the reaction rate leading to the development of instability of the flame front. Due to the large density and temperature changes across the flame, a strong thermal expansion of the burned gas results from the conservation of mass. The flame as a strong density interface as well as an expansion wave is subject to a number of dynamic instability mechanisms in the presence of an acceleration field. Furthermore, competition between heat and mass diffusion across the flame results in thermal diffusion instability. Rapid density changes across the flame also give rise to acoustic wave generation that can couple with increase in burning rate to induce acoustic driven instability. Thus, in practice, there is a wealth of instability mechanisms that render laminar flames unstable. Various instability mechanisms can be at work simultaneously and can influence each other. However, historically, each instability mechanism was isolated and studied individually and was, thus, named after the original researchers.

The flame as a density interface is unstable when subjected to an acceleration field (for example, gravity). If the flame propagates upward, the light burned gas (ρ_b) is at the bottom and the heavy unburned gas (ρ_u) is on the top. The lighter fluid will be driven upward (i.e., buoyancy) whereas the heavier fluid is driven downward by gravity (g). This motion will destabilize the interface, and hence, small perturbations on the flame surface will grow with time (t). If the perturbed flame surface (F) is defined as $A \exp(\sigma t + ikx)$, where k is the wave number and x the space coordinate, the disturbance growth rate σ can be determined from normal mode stability analysis as

$$\sigma = \sqrt{gk\gamma/(2-\gamma)}, \quad \gamma = 1 - \rho_b/\rho_u. \qquad (1)$$

Therefore, instability occurs at all wavelengths but growth is faster at shorter wavelengths. This phenomenon was first discovered by Lord Rayleigh (1883) and later by Geoffrey Ingram Taylor (1950), and thus, it is referred to as the Rayleigh–Taylor instability. This instability is common to all density gradient fields in the presence of an acceleration field normal to it.

Due to the density change across the flame, the flow velocity increases as the density ratio because the flame is approximately isobaric. The expansion across

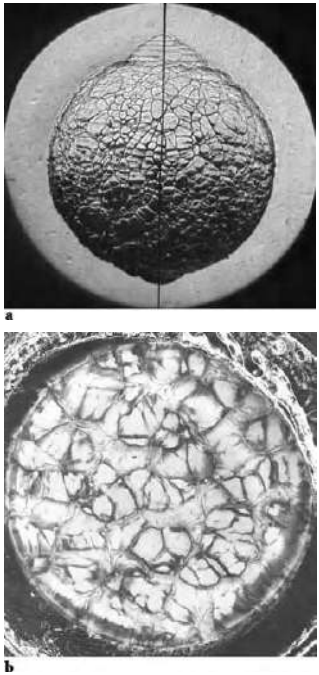

Figure 1. Cellular structures of laminar flame and detonation front. (a) Laminar outward propagating spherical flame (rich dimethyl ether–air at equivalence ratio of 1.2 and 10 atm). (b) Detonation: unstable cellular detonation front as recorder upon reflection from a soot-coated glass plate (C_2H_2–O_2 mixture at 10 mmHg).

the front will induce a divergent flow field ahead of a curved flame (Williams, 1985). This divergence slows down the local flow speed ahead of the curved flame front, and assuming the flame speed to be constant, this will result in a growth of the curvature of the flame. This instability was first discovered by G. Darrieus (1938) and Lev Landau (1944). The Darrieus–Landau instability was obtained by treating the flame as a surface of discontinuity moving at a constant speed. In the limit of small density change, stability analysis gives the growth rate as

$$\sigma = \gamma k S_{\mathrm{L}}/2. \tag{2}$$

Therefore, it was concluded that a flame front is unstable to perturbations at all wavelengths, with growth rate proportional to wave number (i.e., perturbations grow faster for small wavelengths). Unfortunately, this conclusion was contrary to later laboratory observations of small-scale stable flames.

The deficiency of this model was the result of neglecting the finite thicknesses of the flame front, which influences the flame speed when the flame is curved. To include the effect of flame thickness, George Markstein (1951) proposed a phenomenological model by adding a modification of flame speed due to curvature and showed that curvature decreases the flame speed and tends to stabilize the flame at short wavelengths inhibiting its growth. A more rigorous derivation of the dispersion equation including diffusion effect on the flame speed (in the limit of small density jump) was given later by Gregory Sivashinsky (1983) as

$$\sigma = \frac{\gamma k S_{\mathrm{L}}}{2} - \left[\frac{\beta}{2}(\mathrm{Le}-1)+1\right] \times D_{\mathrm{th}}k^2 - 4\frac{D_{\mathrm{th}}^3}{S_{\mathrm{L}}^2}k^4 + \sqrt{gk\gamma/(2-\gamma)}, \tag{3}$$

where $D_{\mathrm{th}}k^2$ in the second term of Equation (3) represents the thermal relaxation via transverse thermal diffusion that stabilizes the flame. Le is the Lewis number (i.e., the ratio of thermal diffusivity to mass diffusivity) and $(\mathrm{Le}-1)$ in the second term denotes the competition between heat loss via thermal diffusion and the enthalpy gain via mass diffusion. As a result, flame temperature will increase or decrease if Le is less or larger than unity. Equation (3) shows that if $\mathrm{Le}-1$ is less than $-2/\beta$ (β is the reduced activation energy), diffusion transport will destabilize the flame. This is the mechanism of the cellular instability. The third term in Equation (3) is the thermal relaxation to the modification of flame temperature caused by the heat and mass diffusion (Clavin, 1985). Therefore, for long wavelength disturbance, the hydrodynamic instability dominates (Figure 1a). At short wavelengths, diffusion relaxation stabilizes the flame. At moderate wavelengths, the competition between heat and mass transfer induces cellular instability at small Le. At large Le, flame temperature is very sensitive to the mass diffusion of the deficient reactant. Coupling between the diffusion and temperature sensitive reaction yields pulsating and spinning waves. This traveling wave is often seen in lean propane-air flames.

By further considering the effect of flame curvature on flow field, Equation (3) can be normalized as an evolution equation of flame front

$$F_t + \tfrac{1}{2}(\nabla F)^2 + \nabla^2 F + 4\nabla^4 F = 0 \tag{4}$$

This is the so-called Kuramoto–Sivashinsky equation which was independently developed by Yoshiki Kuramoto (Kuramoto & Tsuzuki, 1976) for the study of phase turbulence in the Belousov–Zhabotinsky reaction and by Gregory Sivashinsky (1983) for thermal diffusive instabilities of flame fronts. This equation has also been used to model directional solidification and weak fluid turbulence. However, the assumption of small density jump used in Equations (3) and (4) is not rigorous in practical flames. A unified model considering large density jump and Le was obtained by Class Andreas et al. (2003).

Heat release by combustion results in an increase in the specific volume of the product gases and thus generates acoustic waves (Chu, 1956). The acoustic waves play two roles in affecting combustion: (1) inducing pressure-heat release coupling via pressure-dependent reactions, and (2) increasing flame surface area via the baroclinic torque (Meshkov instability). If the changes of pressure and chemical heat release are in phase, the acoustic instability occurs (Rayleigh, 1877; Markstein, 1953; Clavin, 2002). Lord Rayleigh first used this criterion (Rayleigh criterion) to explain the singing flame and Rijke's tone (where heating the bottom of a tube causes it to produce sound). The acoustic instability causes the major problems of noise and vibration in combustors (Putnam & Dennis, 1953). On the other hand, volumetric heat loss reduces the flame speed and changes the resident time of the emitting gases. This coupling triggers the radiation induced instability for weak flames (Ju et al., 2000).

At the upper limit of propagation of combustion waves, the propagation mechanism is not due to diffusion. The flame instability mechanisms discussed above are too slow to be relevant in detonation wave instability. A detonation wave is a supersonic compression wave where mixture is ignited by the adiabatic compression of the leading shock. The classical structure of a detonation wave was formulated by Yakov Zeldovich, John von Neumann, and W. Döring (ZND) independently in the early 1940s and consists of a leading shock followed by the reaction zone after a short induction length (Zeldovich, 1940; von Neumann, 1942; Döring, 1943). Gas dynamic theory gives the detonation wave speed as proportional

to the square root of the chemical heat release and does not involve any non-equilibrium rate processes. Again due to the high-temperature sensitivity of the reaction rates, small temperature fluctuations due to variation of the leading shock speed will result in large variations in the induction length and reaction rates, hence the coupling between the energy release zone and the leading shock. The instability yields a transient three-dimensional cellular detonation front (Lee, 1984). The unstable cellular detonation front consists of an ensemble of interacting transverse shock waves with the leading shock front. The cell boundaries (Figure 1b) are formed by the intersections of the transverse shocks. Shock interactions (Mach reflections) also give rise to the formation of shear layers which lead to turbulence generation due to Kelvin–Helmholtz instability. Chemical reactions in cellular detonations occur in disjointed piecemeal zones embedded within the complex of interacting shocks and shear layers.

The instability of the laminar ZND detonation structure was demonstrated theoretically by standard normal mode stability analysis using the one-dimensional Euler equation (e.g., Erpenbeck, 1964; Lee & Stewart, 1990). In one dimension, unstable detonations are referred to as pulsating detonations that go from harmonic oscillations near the stability limit to highly nonlinear and eventually to chaotic oscillations with the increase of the activation energy. By examining the bifurcation diagram, it is interesting to find that the path to higher instability mode follows closely the Feigenbaum route (Feigenbaum, 1983) of a period-doubling cascade observed in many nonlinear systems. One-dimensional pulsating detonation as well as two- and three-dimensional cellular detonations have been reproduced qualitatively via numerical simulation using the reactive Euler equations (Bourlioux et al., 1991; Short & Stewart, 1999). However, the detailed description of the turbulent structure and chemical reactions requires resolutions far beyond current computing capabilities.

In between the two limits of laminar flames and detonations, there is a continuous range of flame speeds that depend on turbulence. The morphology of a turbulent flame is a time-dependent cellular or wrinkled surface. Turbulent flame is, in fact, an unstable flame, and the effect of turbulence is to increase the burning rate via faster transport and increase in burning surface area. In the limit of very intense turbulence where mixing and reaction rates are comparable, auto-ignition may result, and thus, the mechanism becomes similar to that of a detonation. It differs only in the manner in which auto-ignition is achieved by turbulent mixing of fresh mixture with hot products or by adiabatic heating of the leading shock. Thus, nature tends to maximize the burning rate of a mixture, and instability is a route to optimize the burning rate for given initial and boundary conditions.

YIGUANG JU AND JOHN LEE

See also **Candle; Explosions; Forest fires; Kuramoto–Sivashinsky equation; Reaction-diffusion systems; Zeldovich–Frank-Kamenetsky equation**

Further Reading

Bourlioux, A., Majda, A.J. & Roytburd, V. 1991. Theoretical and numerical structure for unstable one-dimensional detonations. *SIAM Journal of Applied Maths*, 51: 303–343

Class Andreas G., Matkowsky, B.J. & Klimenko, A.Y. 2003. Stability of planar flames as gas dynamic discontinuities. *Journal of Fluid Mechanics*, 491: 51–63

Clavin, P. 1985. Dynamic behaviour of premixed flame fronts in laminar and turbulent flows. *Progress in Energy and Combustion Science*, 11: 1–39

Clavin, P. 2002. Dynamics of combustion fronts in premixed gases: from flames to detonation. *Proceedings of the Combustion Institute*, 29: 569

Chu, B.T. 1956. Stability of systems containing a heat source—the Rayleigh criterion, National Advisory Committee for Aeronautics research memorandum, RM56D27

Darrieus, G. 1938. Propagation d'un front de flame, unpublished work presented at La Technique Moderne and le Congrès de Méchanique Appliquée, Paris

Döring, W. 1943. On detonation processes in gases. *Annals of Physics, Leipzig*, 43: 421–436

Erpenbeck, J. 1964. Stability of idealized one-reaction detonations. *Physics of Fluids*, 7: 684–696

Feigenbaum, M. 1983. Universal behaviour in nonlinear systems. *Physica* D, 7: 16–39

Ju, Y., Law, Chung K., Maruta, K. & Niioka, T. 2000. Radiation induced instability of stretched premixed flames. *Proceedings of the Combustion Institute*, 28: 1891–1900

Kuramoto, Y. & Tsuzuki, T. 1976. Persistent propagation of concentration waves in dissipative media far from thermal equilibrium. *Progress of Theoretical Physics*, 55: 356–369

Landau, L.D. 1944. On the theory of slow combustion. *Acta Physiocochimica URSS*, 19: 77–85

Lee, J.H.S. 1984. Dynamic parameters of gaseous detonation. *Annual Reviews of Fluid Mechanics*, 16: 311–316

Lee, H. & Stewart, D. 1990. Calculation of linear detonation instability: one-dimensional instability of plane detonation. *Journal of Fluid Mechanics*, 216: 103–132

Markstein, G.H. 1951. Experimental and theoretical studies of flame front instability. *Journal of the Aeronautical Sciences*, 18: 199–209

Markstein, G.H. 1953. Instability phenomena in combustion waves. *Proceedings of the Combustion Institute*, 14: 44–59

Putnam, A.A. & Dennis, W.R. 1953. A study of burner oscillations of the organ-pipe type. *Transaction of the ASME*, 75: 15–28

Rayleigh, L. (John William Strutt). 1877. *The Theory of Sound*, vol.2, London: Macmillan; reprinted New York: Dover, 1945, p. 226

Rayleigh, L. (John William Strutt). 1883. Investigation of the character of the equilibrium of an incompressible heavy fluid of variable density. *Proceedings of the London Mathematical Society*, 14: 170–177

Short, M. & Stewart, D. 1999. Multi-dimensional stability of weak-heat-release detonation. *Journal of Fluid Mechanics*, 382: 103–135

Sivashinsky, G.I. 1983. Instabilities, pattern formation, and turbulence in flames. *Annual Reviews of Fluid Mechanics*, 15: 179–199

Taylor, G.I. 1950. The instability of liquid surfaces when accelerated in a direction perpendicular to their planes.

Proceedings of the Royal Society of London A, 201: 192–196

von Neumann, J. 1942. Theory of detonation waves, Proj. Report No. 238, OSRD report No.549. In *Von Neumann*, *Collected Works*, vol. 6, edited by A.J. Taub, Oxford: Pergamon Press, 1963

Williams, F.A. 1985. *Combustion Theory*, 2nd edition, New York: Benjamin Cumming

Zeldovich, Y.B. 1940. On the theory of the propagation of detonations in gaseous systems. *Experimental and Theoretical Physics SSSR*, 10: 542

FLIP-FLOP CIRCUIT

A bistable circuit is one that can exist indefinitely in either one of two stable states and that can be induced to make an abrupt transition from one stable state to the other by means of an external excitation. Bistable circuits are known by a variety of names, such as bistable multivibrator, Eccles–Jordan circuit (after the inventors), trigger circuit, binary, and flip-flop, the latter being the term that we adopt. Flip-flops are used for the performance of many digital operations such as counting and storing of binary information.

In general, digital (switching) circuits may be either combinational or sequential. In combinational circuits the Boolean relation that describes the output function is at any moment uniquely determined by the inputs. The output function is independent of all prior input or output conditions and the circuit is without memory. In contrast, the sequential circuit contains feedback and its outputs depend not only on the present inputs but, in general, also on the entire past history of inputs. The flip-flop is a basic sequential circuit that functions as a basic logic memory element. It has two distinct states of equilibrium and may, therefore, be used as a single binary-digit (bit) storage device. The two stable states are referred to by various names such as TRUE and FALSE, HIGH and LOW, or 1 and 0.

Sequential circuits can be presented using a graphical tool known as a state diagram. In a state diagram, nodes are used to represent the different states of a circuit, and connections between nodes are used to show transitions between states with different inputs that act as conditioning signals. Figure 1 represents a general bistable circuit. Let us denote the present state of the circuit as $Q(t)$ and the state that follows after a time interval Δt as $Q(t + \Delta t)$. Then the circuit stays in state 1 as long as condition 1 is applied, but moves to state 0 when condition 2 is applied. Similarly, it stays in state 0 as long as condition 3 is applied, and moves to state 1 when condition 4 occurs.

Four types of flip-flops are presently in use, RS (conditional **S**et and **R**eset), JK (unconditional set and reset), D (**D**elay), and T (**T**rigger), and they have different sets of conditions for transition between the two states. For example, the characteristic equation for

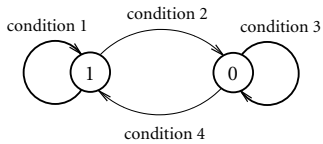

Figure 1. State diagram of a general bistable circuit.

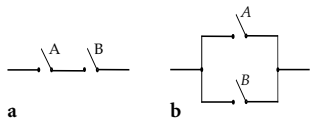

Figure 2. Basic switching elements, (a) AND and (b) OR. An ideal switch consists of a pair of contacts that have zero internal (or switch closed) resistance and infinite leakage (or switch open) resistance. Transitions from one state to the other should be instantaneous. It should attain the open and closed states with equal probability. Although these characteristics have been approached most closely with every new technological generation, we deal in reality with approximations to them.

the RS flip-flop is given as

$$Q(t + \Delta t) = S + Q(t) \cdot \overline{R} \tag{1}$$

under the constraint

$$S \cdot R = 0. \tag{2}$$

Here $+$ (OR), $\cdot$ (AND), and $-$ (NOT, also known as inversion and complement) are operations from switching algebra. Switching circuits which represent the AND, $A \cdot B$, and the OR, $A + B$, functions are presented in Figures 2a and b, respectively.

The mathematical theory of switching circuits, first postulated by Shannon (1938, 1949), is based on Boolean algebra. It is defined on a set U that consists of two values, 0 and 1, two basic binary operations, $\cdot$ (which is also called AND, product or conjunction), and $+$ (which is also called OR, sum or disjunction), and a set of basic postulates that were derived and proven by Edward Huntington in 1904, based on the work of George Boole in 1847.

Switching circuits have been designed from various technologies; for example, vacuum tubes were used in their early development. They have become dramatically faster and dramatically smaller in size with every new technology. The advent of integrated circuits (ICs), in which many discrete components (diodes, transistors, and resistors) are fabricated at the same time on one chip of silicon, has led to many different types of switching circuits in IC form. Recent research in nanoelectronics has introduced the concepts of resonant tunneling diodes, electronic quantum cellular automata, single electron transistors, and molecular electronic devices.

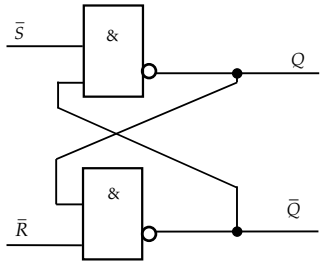

$Q(t)$	$Q(t+\Delta t)$	S	R
0	0	0	×
0	1	1	0
1	0	0	1
1	1	×	0

Figure 3. The RS flip-flop with NAND gates (top) and its truth-table (bottom). Its characteristic equation is $Q(t+\Delta t) = \overline{\bar{S}\cdot\overline{Q(t)}} = \bar{S}\cdot\overline{Q(t)\cdot\bar{R}} = S + Q(t)\cdot\bar{R}$. Here we used de Morgan's laws: for any two subsets A and B of the U, we have $\overline{A\cdot B} = \bar{A}+\bar{B}$ and $\overline{A+B} = \bar{A}\cdot\bar{B}$.

The basic switching circuits are called gates. Often NAND and NOR gates are used, as they are easier to implement. The RS flip-flop can be designed simply by interconnecting a pair of two-input NAND gates, with appropriate feedback, as shown in Figure 3. The truth-table in Figure 3 gives input values, R and S, that condition changes from a present state $Q(t)$ to a next state $Q(t+\Delta t)$. It is constructed by considering the physical action of the circuit shown in the same figure. For example, to stay in state 1, the equivalent to input condition 1 in Figure 1 is $R = 0$, and S need not be defined; its value is $\times$. The entries marked with $\times$ correspond to "not allowed" or "don't care" inputs because, under these conditions, when both R and S are present simultaneously, the operation of the circuit becomes uncertain.

The Δt is a delay that occurs between the present state and the next state. This delay is essential in the operation of sequential circuits. With respect to the delay, two types of sequential circuits can be distinguished: synchronous and asynchronous. The synchronous sequential circuits trigger on receiving a certain clock pulse. The maximum frequency of the clock is defined by the operational time of the slowest element in the circuit. State transitions in a synchronous sequential circuit thus occur with a constant frequency. The delay in asynchronous sequential circuits changes from transition to transition, i.e. $\Delta t \neq \text{const}$.

The RS flip-flop, introduced above, is a bistable multivibrator. It stays in one of two states that can be changed only when an external input is applied. If there are no external inputs, but one state causes a transition to the other state and this repeats continuously, the multivibrator is said to be astable. It is not stable in either state and alternates between them at a specific frequency. The astable multivibrator is, in fact, a free-running oscillator. The frequency is usually determined by a capacitor placed between the two gates and a resistor in parallel with each gate. Thus the delay, Δt, and consequently the frequency, are determined by the values of the capacitor and resistors.

In general, every oscillator contains a positive and negative feedback loop at the same time. For example, a unit with one excitatory and one inhibitory neuron that are mutually connected is a neuronal oscillator. The model proposed by Wilson and Cowan (*See* **Inhibition**), who introduced an inhibitory neuron and by this a positive along with the negative feedback loop, is today known as the Wilson–Cowan oscillator. As the exchange of energy and matter is continuous in every biological process that is based on existence of both positive and negative feedback loops, an oscillator can be seen as a basic biological unit.

Flip-flop circuits are today used as a general paradigm for bistability in a very wide range of nonlinear systems, one of many examples being the phenomenon of stochastic resonance (Fauve & Heslot, 1983).

ANETA STEFANOVSKA

See also **Coupled oscillators; Feedback; Inhibition; State diagrams**

Further Reading

Fauve, S. & Heslot, F. 1983. Stochastic resonance in a bistable system. *Physics Letters* A, 97: 5–7

Shannon, C.E. 1938. A symbolic analysis of relay and switching circuits. *Transactions of the AIEE*, 57: 713–723

Shannon, C.E. 1949. The synthesys of two-terminal switching circuits. *Bell Systems Technical Journal*, 28: 59–98

FLOQUET THEORY

See **Periodic spectral theory**

FLUCTUATION-DISSIPATION THEOREM

In the 19th century, there were two schools of thought on the existence of atoms, those that believed in them and those that did not. Remarkably, it was not until the early 20th century that the experiments of Jean Perrin—summarized in his 1913 book *Atoms* (Perrin, 1913)—established once and for all the existence of atoms. One of the laws Perrin experimentally verified was the fluctuation-dissipation relation, which interrelates the physical notions of randomness (through fluctuations) and determinism (through dissipation) (Montroll & West, 1979).

No matter how carefully experiments are done, they never yield the same value of a physical

observable from one measurement to the next. The collection of values from such measurements is called an ensemble, and the number of times a measurement falls in an assigned interval divided by the total number of measurements in the ensemble yields a probability, which when all the intervals are taken together yields a probability distribution function. The best representation of this ensemble of measurements is the mode of the distribution (or ensemble average) as first noted by Carl Friedrich Gauss (1809). The deviations of a physical observable from its average value are called fluctuations, which are typically small and random. In physical systems, the source of these fluctuations is thermal agitation of the atoms. Thus, the thermodynamic properties of an equilibrium physical system are determined by the probability density, through the averages, and not by the instantaneous values of the positions and velocities of the atoms.

The changes in macroscopic physical systems over time comprise a combination of deterministic dynamics and microscopically induced macroscopic fluctuations. Albert Einstein, in 1905, was the first to fully appreciate the influence of these fluctuations on macroscopic transport phenomena in his investigations of the phenomenon of equilibrium diffusion (Furth, 1956). Einstein showed that the strength of the fluctuations, as measured by their mean-square level through the diffusion coefficient, D, is directly proportional to the temperature of the ambient fluid, $kT/2$, which is the average kinetic energy per degree of freedom of the ambient fluid particles. The constant of proportionality between the temperature and the diffusion coefficient is the dissipation time per unit mass, λ/m, thereby inter-relating the fluctuations and dissipation of the medium through the particle's motion

$$D = \frac{2\lambda kT}{m}. \tag{1}$$

Equation (1) was the first fluctuation-dissipation relation and demonstrates that macroscopic fluctuations and dissipation have the same microscopic origin.

Two decades before Einstein's analysis of diffusion, Walther Nernst (1884) investigated the combined process of mobility and diffusion to determine the size of the charge on an individual particle. He established that the mobility is proportional to the ratio of the diffusion coefficient to the temperature, and the charge of the particle is the proportionality constant. This ratio is usually called the Einstein equation even though Nernst discovered it. One can more generally define the mobility of a particle as the terminal velocity per unit force, through a generalized Nernst relation

$$D = kT \times \text{mobility} \tag{2}$$

for any sort of particle that is free to move but is subject to frictional drag. The linear transport coefficient (here the mobility) was only partially understood until Harry Nyquist (in considering the fluctuations in the current flowing through an electrical resistance) showed that the circuit impedance can be used to compute the fluctuations arising from the thermal agitation of the electrons (Nyquist, 1928). Nyquist's form of the fluctuation-dissipation theorem gives the mean-square voltage fluctuations as proportional to the product of the temperature and resistance, with the proportionality constant being the bandwidth. Alternatively, the temperature can be written as the ratio of the spectral density of the random fluctuations of the electromotive force $S_e(\omega)$ to the real part of the impedance $Z(\omega)$:

$$S_e(\omega) = 2kT \operatorname{Re} Z(\omega) \tag{3}$$

at the frequency ω. When the Nyquist relation (3) was first derived, the applicability of the underlying reasoning to other linear transport processes involving thermal noise was not appreciated.

Let us consider the dynamical equation constructed by Paul Langevin concerning the forces acting on a particle in a fluid (Langevin, 1908). The equation of motion for a particle of mass m is

$$m\frac{du}{dt} + \frac{u}{\mu} = F + f, \tag{4}$$

where u is the particle velocity, μ is the mobility (the inverse of the dissipation), F is an external driving force, and f is a fluctuating force with zero mean produced by the thermal agitation of the ambient fluid particles. The Fourier transform of Equation (4) yields the impedance for the particle $Z(\omega) \equiv \bar{F}(\omega)/\bar{u}(\omega) = im\omega + \mu^{-1}$. The average of the transformed equation yields the Nernst relation for a constant external force: $\langle \bar{u}(0) \rangle = \mu F$. The diffusion coefficient is given by the integral over the velocity autocorrelation function, which using Parseval's theorem can be written in terms of the velocity spectral density, $S_u(\omega)$, as

$$D = 2S_u(0). \tag{5}$$

This expression for the diffusion coefficient is valid for any form of the velocity autocorrelation function and velocity spectral density, under the condition that the underlying process is stationary in time.

In general, one can conclude that the autocorrelation function of the random force in a physical system is proportional to the dissipation in that system, with the proportionality constant given by the temperature kT. This relation can be summarized as

$$\langle f(t) f(t') \rangle = 2D\delta(t - t'), \tag{6}$$

so that the diffusion coefficient determines the strength of the fluctuations. Further, there are time-dependent

generalizations of this form of the fluctuation–dissipation relation, where the δ function is replaced with a memory kernel, as well as extensions from the classical to the quantum domain, see, for example, Lindenberg & West (1990) for a review. However, each elaboration contains essentially the same information, namely, that microscopic dynamics are amplified to macroscopic fluctuations and dissipation. A complete understanding of the macroscopic phenomena of fluctuations and dissipation therefore requires an understanding of microscopic dynamics.

BRUCE J. WEST

See also **Brownian motion; Diffusion; Fokker–Planck equation**

Further Reading

Furth, R. (editor). 1956. *Albert Einstein, Investigations on the Theory of Brownian Motion*, New York: Dover; originally published in German, 1926

Gauss, F. 1809. *Theoria Motus Corporum Coelestrium*, Hamburg:

Langevin, P. 1908. Comptes Rendus Acad. Sci. Paris, 530

Lindenberg, K. & West, B.J. 1990. *The Nonequilibrium Statistical Mechanics of Open and Closed Systems*, New York: VCH

Montroll, E.W. & West, B.J. 1979. An enriched collection of stochastic processes. In *Fluctuation Phenomena*, edited by E.W. Montroll & Lebowitz, J. Amsterdam: North-Holland

Nernst, W. 1884. *Zeitschrift für Physikalische Chemie*, 9: 613

Nyquist, H. 1928. Thermal agitation of electric charge in conductors. *Physical Review*, 32: 110

Perrin, J. 1990. *Atoms*, Woodbridge: Ox Bow Press; originally published as *Les Atomes* in French, 1913

FLUID DYNAMICS

The field of fluid dynamics is devoted to the study of flows of matter in the liquid or gaseous state or in the form of multiple phases including suspensions of solid particles in liquids or gases. While it is in principle possible (and sometimes appropriate) to apply Newton's laws to individual molecules of a fluid and to describe the flow as an average over trajectories of the particles (*See* **Molecular dynamics**), it is usually far more efficient to consider liquids and gases as a continuum and to apply the equations for the dynamics of continuous media.

Conservation Laws of Continuous Media

The laws of the conservation of mass, momentum, and energy can be written in the form

$$\frac{\mathrm{d}}{\mathrm{d}t}\int_V \rho\,\mathrm{d}^3V = \int_V \frac{\partial\rho}{\partial t}\,\mathrm{d}^3V = -\oint_{\partial V} \rho n_j v_j\,\mathrm{d}^2A, \tag{1a}$$

$$\frac{\mathrm{d}}{\mathrm{d}t}\int_V \rho v_i\,\mathrm{d}^3V = -\oint_{\partial V} \rho v_i n_j v_j\,\mathrm{d}^2A + \int_V \rho F_i\,\mathrm{d}^3V + \oint_{\partial V} S_{ij}n_j\,\mathrm{d}^2A, \tag{1b}$$

$$\begin{aligned}\frac{\mathrm{d}}{\mathrm{d}t}&\int_V \rho(e + v_j v_j/2)\,\mathrm{d}^3V \\ &= -\oint_{\partial V} v_j n_j \rho(e + v_i v_i/2)\mathrm{d}^2A \\ &+ \int_V \rho F_i v_i \mathrm{d}^3V + \int_V \rho q\,\mathrm{d}^3V \\ &+ \oint_{\partial V} v_i S_{ij} n_j\,\mathrm{d}^2A - \oint_{\partial V} h_j n_j\,\mathrm{d}^2A,\end{aligned} \tag{1c}$$

where V denotes an arbitrary volume fixed in space and ∂V denotes its surface. ρ is the density of the continuous medium, v_i is the velocity vector, and ρF_i is the body force density acting on the medium. A typical example for F_i is the acceleration of gravity. e is the internal energy per unit mass, ρq is the heat source density, and h_i denotes the heat flux. Contributions like absorption and emission of radiation have not been included explicitly in the energy balance (1c). But in optically thick media they can be subsumed under q and h_i. The index notation has been used where the index i refers to the coordinates 1, 2, 3 of a Cartesian system of coordinates and where the summation over indices occurring twice in any term is implied. Relativistic effects have been neglected in writing Equations (1) that are thus valid only for velocities small compared with the velocity of light.

The fundamental quantity of the dynamics of a continuous medium is the stress tensor S_{ij} which describes the surface force $S_{ij}n_j$ exerted on a surface element with the normal unit vector n_i. More exactly, $S_{ij}n_j$ is the force per unit area exerted by the material pierced by n_i on the material pierced by $-n_i$. The concept of the surface force was advanced long before the atomistic nature of materials became generally accepted. Surface forces in the ideal sense do not exist in nature. But since the forces between molecules in materials act only over atomic distances, the concept of surface forces has turned out to be very useful. The limitation should be kept in mind, however, in the fluid dynamical treatment of the dynamics of galaxies, for instance.

For applications of the conservation laws (1) it is convenient to formulate them in differential form by taking the limit $V \to 0$ and using Gauss' theorem,

$$\left(\frac{\partial}{\partial t} + v_j\partial_j\right)\rho + \rho\partial_j v_j = 0, \tag{2a}$$

$$\rho\frac{\partial}{\partial t}v_i + \rho v_j\partial_j v_i = \rho F_i + \partial_j S_{ij}, \tag{2b}$$

$$\frac{\partial}{\partial t}\rho e + \partial_j(\rho v_j e) = S_{ij}\partial_j v_i + \rho q - \partial_j h_j. \tag{2c}$$

In deriving (2b) from (1b) and (2c) from (1c), we have used relationships (2a) and (2b), respectively. While Equations (2) apply to all continua, including solid materials, for applications to fluids the stress tensor is separated into two parts,

$$S_{ij} = -p\delta_{ij} + S'_{ij}, \tag{3}$$

where p is the thermodynamic pressure and S'_{ij} is the part of the stress tensor which depends on viscous friction and other dissipative effects. Then $S'_{ij}\partial_j v_i \equiv \rho\Phi$ is the irreversible conversion of work into heat. After using (2b), we may write (2c) in the form

$$\frac{\mathrm{D}e}{\mathrm{D}t} + p\frac{\mathrm{D}\rho^{-1}}{\mathrm{D}t} = \Phi + q - \rho^{-1}\partial_j h_j, \tag{4}$$

where the material derivative

$$\frac{\mathrm{D}}{\mathrm{D}t} \equiv \frac{\partial}{\partial t} + v_j\partial_j \tag{5}$$

has been introduced that describes the change in time with respect to the frame of reference moving with the fluid. This is also referred to as the Lagrangian description in contrast to the Eulerian description where the time derivative at a fixed point in space is taken.

In applications, the pressure p and the temperature T are usually the most readily known thermodynamic variables. We thus use the relationship $e = h - p/\rho$ for simple materials where h is the specific enthalpy and obtain

$$\mathrm{d}h = c_p\,\mathrm{d}T + \left.\frac{\partial h}{\partial p}\right|_T \mathrm{d}p = c_p\,\mathrm{d}T + \frac{1}{\rho}(1-\alpha T)\,\mathrm{d}p, \tag{6}$$

where some simple thermodynamic relationships have been used and $\alpha \equiv \rho(\partial\rho^{-1}/\partial T)_p$ is the coefficient of thermal expansion. As a final result, we thus obtain the energy equation in its most useful form

$$T\frac{\mathrm{D}s}{\mathrm{D}t} \equiv c_p\frac{\mathrm{D}T}{\mathrm{D}t} - \frac{\alpha T}{\rho}\frac{\mathrm{D}p}{\mathrm{D}t} = \Phi + q - \frac{1}{\rho}\partial_j h_j. \tag{7}$$

Fourier's law, $h_i = -\lambda\partial_i T$, is commonly used for the heat flux, and for laboratory applications, it is a good approximation to neglect $\alpha T\rho^{-1}\mathrm{D}\rho/\mathrm{D}t + \Phi$ in comparison with $c_p\,\mathrm{D}T/\mathrm{D}t$. In this case, the familiar heat equation

$$\left(\frac{\partial}{\partial t} + v_j\partial_j\right)T = q + \kappa\partial_j\partial_j T \tag{8}$$

is obtained where $\lambda =$ const. has been assumed and where $\kappa = \lambda/\rho c_p$ is the thermal diffusivity.

Dynamics of Inviscid Fluids

The simplest equation of fluid dynamics is obtained when viscous, elastic, and other effects are neglected and $S_{ij} = -p\delta_{ij}$ is assumed. The resulting Euler equation,

$$\left(\frac{\partial}{\partial t} + v_j\partial_j\right)v_i = -\rho^{-1}\partial_i p + F_i, \tag{9}$$

is most easily solved when the fluid is incompressible and $\rho =$ const. can be assumed. In that case

$$\partial_j v_j = 0 \tag{10}$$

holds and an equation of state connecting ρ and p is not needed.

A more general form of the equations is obtained in the barotropic case when the density is prescribed as a function of the pressure alone as, for instance, in the form of a polytropic relationship

$$p = p_0\left(\frac{\rho}{\rho_0}\right)^{\gamma}. \tag{11}$$

This expression is valid, for example, for adiabatic changes of an ideal gas in which case γ equals the ratio of specific heats, $\gamma = c_p/c_v$. The equation for sound waves can be obtained when Equations (2a) and (9) are linearized around the static equilibrium state with $\rho = \rho_0$, $p = p_0$,

$$\frac{\partial^2}{\partial t^2}\rho = \gamma\frac{p_0}{\rho_0}\partial_j\partial_j\rho, \tag{12}$$

where $\gamma p_0/\rho_0 = c_s^2$ is the square of the speed of sound. For general fluids, the relationship $c_s^2 = \partial p/\partial\rho$ holds. The ratio of a characteristic velocity divided by the sound speed is called the Mach number Ma. The domains of fluid flow with $\mathrm{Ma} > 1$ are usually separated from regions with $\mathrm{Ma} < 1$ by shock fronts in which energy is dissipated and frictional processes must be taken into account.

A fundamental consequence of Equation (9) is Kelvin's theorem,

$$\frac{\mathrm{D}}{\mathrm{D}t}\oint_C \boldsymbol{v}\cdot\mathrm{d}\boldsymbol{l} = 0, \tag{13}$$

where the integral is called the circulation and must be taken over a closed curve C moving with the fluid. Theorem (13) holds for barotropic fluids when the force field F_i is conservative; that is, it can be written as the gradient of a single-valued scalar function. The property that the circulation is an invariant of fluid motion represents an elegant formulation of Helmholtz's vortex theorem, which states that the strength of a vortex tube moving with the fluid remains unchanged,

$$\frac{\mathrm{D}}{\mathrm{D}t}\int_S \nabla\times\boldsymbol{v}\cdot\mathrm{d}^2\boldsymbol{A} = 0, \tag{14}$$

where the surface S is bounded by a closed material curve, C. $\nabla\times\boldsymbol{v}$ is called the vorticity field of the velocity field $\boldsymbol{v}$. The manifold of vorticity vectors

intersecting the curve C generates as tangential vectors the surface of the vortex tube. Kelvin's theorem and Helmhotz's theorem are connected, of course, by Stokes' theorem.

An important consequence of theorem (13) or (14) is that motions starting in a fluid from rest have vanishing vorticity if the force field is conservative and viscous effects can be neglected. An incompressible fluid with vanishing vorticity obeys the equation

$$\boldsymbol{v} = \nabla\phi \quad \text{with} \quad \nabla^2\phi = 0. \tag{15}$$

Such flows are called potential flows.

Dynamics of Viscous Fluids

In the general case, the stress tensor S'_{ij} may be a rather complex function of the properties of the fluid and its motions. The various problems arising in this connection are the subject of the field of rheology. Fortunately, the most important fluids such as air and water and many others can be described as Newtonian fluids for which a linear homogeneous relationship holds between S'_{ij} and the velocity gradient tensor $\partial_i v_j$,

$$S'_{ij} = \mu(\partial_i v_j + \partial_j v_i - \tfrac{2}{3}\delta_{ij}\partial_k v_k) + \tilde{\mu}\delta_{ij}\partial_k v_k, \tag{16}$$

where μ is the dynamic viscosity and $\tilde{\mu}$ is the bulk viscosity. It is difficult to measure the latter property. Because $\tilde{\mu} = 0$ can be shown to hold for mono-atomic gases, this relationship is often generally applied in which case the Navier–Stokes equations are obtained,

$$\rho\left(\frac{\partial}{\partial t} + v_j\partial_j\right)v_i = -\partial_i p + \rho F_i + \partial_j\left(\mu(\partial_i v_j + \partial_j v_i - \tfrac{2}{3}\delta_{ij}\partial_k v_k)\right). \tag{17}$$

For a given force field F_i, this equation together with the equation of continuity (2a) and a barotropic equation of state, $\rho = \rho(p)$, provides a complete set for the determination of the variables v_i, ρ, p (*See* **Navier–Stokes equations**).

An even simpler set of equations can be obtained for incompressible fluids with $\rho = \text{const.}$, $\mu = \text{const.}$,

$$\left(\frac{\partial}{\partial t} + v_j\partial_j\right)v_i = -\partial_i\frac{p}{\rho} + F_i + \nu\partial_j\partial_j v_i, \tag{18a}$$

$$\partial_j v_j = 0, \tag{18b}$$

where the kinematic viscosity $\nu = \mu/\rho$ has been introduced. Using U as typical velocity and d as a typical length scale, we find for the ratio of the last terms on the left- and right-hand sides of Equation (18a)

$$\frac{Ud}{\nu} = \text{Re} \tag{19}$$

which is called the Reynolds number. In the low Reynolds number limit, the Stokes equation is obtained in which the term $v_j\partial_j v_i$ in Equation (18a) is dropped. In the high Reynolds number limit, the Euler equation does not become applicable, in general, because of the existence of a turbulent cascade where energy is transferred to smaller and smaller scales such that the term $\nu\partial_j\partial_j v_i$ cannot be neglected in the limit $\nu \to 0$ (*See* **Turbulence**).

Buoyancy-driven Flows

Among the force fields that are not conservative and therefore tend to generate motions with vorticity, buoyancy forces are the most common ones. Especially in atmospheric, oceanic, and astrophysical applications, buoyancy-driven flows are of fundamental importance. In order to keep as much as possible of the convenient properties of the Navier–Stokes equations for incompressible fluids, the Boussinesq approximation is usually introduced in which the temperature dependence of the density, say $\rho = \rho_0(1 - \gamma(T - T_0))$, is taken into account in the gravity force term only, while ρ is replaced by ρ_0 elsewhere in the equations. Together with the heat equation, the following set of equations is obtained:

$$\left(\frac{\partial}{\partial t} + \boldsymbol{v}\cdot\nabla\right)\boldsymbol{v} = -\nabla\pi - \gamma(T - T_0)\boldsymbol{g} + \nu\nabla^2\boldsymbol{v}, \tag{20a}$$

$$\nabla\cdot\boldsymbol{v} = 0, \tag{20b}$$

$$\left(\frac{\partial}{\partial t} + \boldsymbol{v}\cdot\nabla\right)T = \kappa\nabla^2 T, \tag{20c}$$

where $\boldsymbol{g}$ is the gravity vector and where $\nabla\pi$ includes all terms that can be written as a gradient. Because the pressure dependence of the density is neglected in the Boussinesq approximation, the contribution Φ must also be neglected (Busse, 1989).

A simple solution described by these equations is the flow between two parallel plates with separation d that are kept at different temperatures and that are inclined at an angle χ with respect to the horizontal plane (see Figure 1).

$$\boldsymbol{v} = z(z^2 - d^2/4)\gamma g\sin\chi(T_2 - T_1)\boldsymbol{i}, \tag{21a}$$

$$T = T_0 + (T_2 - T_1)z/d. \tag{21b}$$

A Cartesian system of coordinates has been assumed with the z-coordinate normal to the plates and the origin in the middle between the plates. $\boldsymbol{i}$ is the unit vector in the direction of inclination parallel to the x-axis as shown in Figure 1. T_1 and T_2 are the fixed temperatures at the boundaries $z = -0.5$ and $+0.5$, respectively, and $T_0 = (T_2 + T_1)/2$. Since in laboratory realizations of this configuration the space between the plates will be enclosed by side walls, the condition that the total mass transport between the plates vanishes has been imposed. Of special interest is the case $\gamma(T_2 - T_1) < 0$

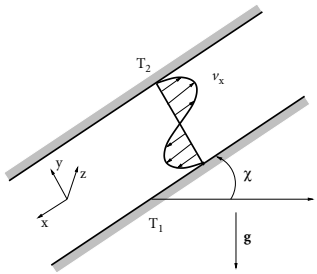

Figure 1. Inclined fluid layer heated from above.

when the density increases opposite to the direction of gravity such that an unstable stratification results. In a horizontal layer where solution (21a) vanishes, the instability occurs in the form of Rayleigh–Bénard convection. The dimensionless control parameter for this case, $\mathrm{Ra} \equiv \gamma g(T_2 - T_1)d^3/\kappa\nu$, is called the Rayleigh number. Convection rolls set in when Ra exceeds a critical value $\mathrm{Ra_c}$ depending on the boundary conditions. Besides buoyancy driven rolls aligned with the x-axis for $\chi \neq 0$ hydrodynamic, instabilities may set in in the form of transverse vortices. Since these forms of secondary states of motion are themselves subject to secondary instabilities, sequences of bifurcations are observed leading to increasingly complex patterns of fluid flow as indicated in Figure 2 for a few examples. The variety of patterns that can be realized continue to be a subject of intense experimental and theoretical research (*See* **Taylor–Couette flow**).

A role similar to that of buoyancy is played by the temperature dependence of surface tension that may give rise to instabilities much like Rayleigh–Bénard convection. Instead of the parameter Ra, the Marangoni number $M = \xi(T_2 - T_1)d/\kappa\eta$ is used as a control parameter, in this case where $\xi = \partial\sigma/\partial T$ denotes the derivative with respect to temperature of the surface tension σ.

Dynamics of Rotating Fluids

The Navier–Stokes equations (17) are invariant with respect to a Galileo transformation; that is, they retain their form in the transition from one inertial frame of reference to another one. When the transformation is made from an inertial to a frame of reference rotating with the constant angular velocity $\boldsymbol{\Omega}$, it must be taken into account that the transformation of a vector field $\boldsymbol{a}$ is different from that of a scalar field ϕ,

$$\frac{\partial}{\partial t'}\boldsymbol{a} = \left(\frac{\partial}{\partial t} + \boldsymbol{\Omega}\times\boldsymbol{r}\cdot\nabla - \boldsymbol{\Omega}\times\right)\boldsymbol{a}, \qquad (22a)$$

$$\frac{\partial}{\partial t'}\phi = \left(\frac{\partial}{\partial t} + \boldsymbol{\Omega}\times\boldsymbol{r}\cdot\nabla\right)\phi; \qquad (22b)$$

that is, a constant vector field in an inertial frame becomes time dependent as seen from the rotating frame. Using $\boldsymbol{v}' = \boldsymbol{v} - \boldsymbol{\Omega}\times\boldsymbol{r}$ where $\boldsymbol{r}$ is the position vector, we find as Navier–Stokes equation in the rotating frame

$$\left(\frac{\partial}{\partial t'} + \boldsymbol{v}'\cdot\nabla\right)\boldsymbol{v}' + 2\boldsymbol{\Omega}\times\boldsymbol{v}' = -\nabla\frac{p}{\rho} - \nabla\Psi + (\boldsymbol{\Omega}\times\boldsymbol{r})\times\boldsymbol{\Omega} + \nu\nabla^2\boldsymbol{v}' \qquad (23a)$$

$$\nabla\cdot\boldsymbol{v}' = 0. \qquad (23b)$$

We have restricted our attention to the incompressible case with $\rho = \text{const.}$ and have assumed that the force field $\boldsymbol{F}$ is conservative, that is, $\boldsymbol{F} = -\nabla\Psi$. Because the centrifugal force is also conservative it can be combined with $\boldsymbol{F}$; that is, $\Psi' = \Psi - |\boldsymbol{\Omega}\times\boldsymbol{r}|^2/2$ can be used as the potential. The other new term in Equations (23) is the Coriolis force, $-2\boldsymbol{\Omega}\times\boldsymbol{v}'$, which is responsible for the fact that the dynamics of rotating systems is quite different from that of nonrotating systems. Since the Coriolis force is typically the largest term on the left-hand side of Equation (23a) and since viscous friction is usually negligible in the interior of the fluid, the approximate relationship

$$2\boldsymbol{\Omega}\times\boldsymbol{v} = -\nabla\pi \qquad (24)$$

is obtained which is called the geostrophic balance because of its importance in meteorology and oceanography. Here, $\rho\pi$ is the dynamic pressure, $\pi = p/\rho + \Psi'$, and for simplicity, the prime of $\boldsymbol{v}$ has been dropped. When the curl of balance (24) is taken and Equation (23b) is used, the famous Proudman–Taylor theorem is obtained,

$$2\boldsymbol{\Omega}\cdot\nabla\boldsymbol{v} = 0. \qquad (25)$$

This theorem states that in a rapidly rotating system, a steady velocity field of a nearly inviscid fluid must be independent of the coordinate in the direction of the axis of rotation. As a consequence, $\boldsymbol{v}$ will depend only on the x-, y-coordinates of a cartesian system with the z-coordinate pointing in the direction of $\boldsymbol{\Omega}$. Since $\boldsymbol{v}$ must also satisfy $\nabla\cdot\boldsymbol{v} = 0$, a single scalar function, the stream function ψ, is sufficient to describe $\boldsymbol{v}$. Assuming boundaries perpendicular to $\boldsymbol{\Omega}$, we find

$$\boldsymbol{v} = \nabla\psi\times\boldsymbol{\Omega}/\Omega \quad \text{with} \quad \psi = -\pi(x, y)/2\Omega$$

and

$$\Omega = |\boldsymbol{\Omega}|. \qquad (26)$$

The form of the velocity field indicates that the flow parallels the isobars in contrast to the situation in a nonrotating system where the flow is usually directed perpendicular to the pressure gradient. The

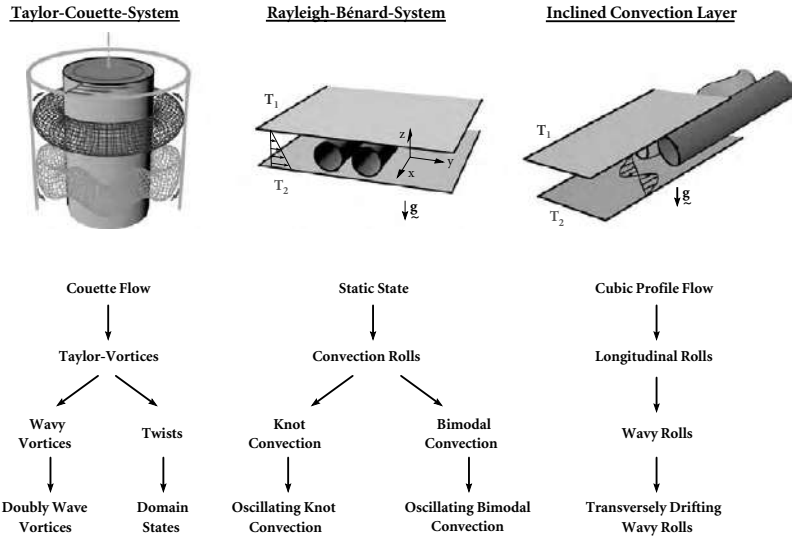

Figure 2. Examples of bifurcation sequences.

geostrophic wind (26) flows cyclonically (i.e., in the sense of rotation) around low-pressure regions and anticyclonically around high-pressure regions, as can be seen on weather maps.

The fact that the function $\pi(x, y)$ has remained undetermined so far is known as the geostrophic degeneracy. Terms of higher order in the equations of motion are needed to remove this degeneracy and to introduce time dependences on scales much longer than the rotation period $2\pi/\Omega$ of the system. A three-dimensional nature of the velocity field enforced, for instance, by boundary conditions can thus be introduced as a perturbation of the geostrophic solution. Rossby waves are a typical example for the quasigeostrophic dynamical response of rotating fluid systems.

The friction term in Equation (23a) is characterized by the highest spatial derivatives and thus can become large wherever strong variations of the velocity field occur, as, for example, near solid boundaries where the tangential velocity component must vanish. Thin Ekman boundary layers are formed here with the typical thickness $\sqrt{\nu/\Omega}$. But internal shear layers in the interior of the fluid can also be realized. The Ekman number defined by

$$E = \nu/\Omega d^2, \tag{27}$$

where d is a typical length scale of the system in the direction of the axis of rotation, is often used as a dimensionless parameter in the dynamics of rotating fluids.

F.H. Busse

See also **Boundary layers; Molecular dynamics; Navier–Stokes equation; Taylor–Couette flow; Thermal convection; Turbulence; Vortex dynamics of fluids**

Further Reading

Acheson, D.J. 1990. *Elementary Fluid Dynamics*, Oxford: Clarendon Press and New York: Oxford University Press

Batchelor, G.K. 1967. *An Introduction to Fluid Dynamics*, Cambridge: Cambridge University Press

Busse, F.H. 1989. Fundamentals of Thermal Convection. In *Mantle Convection*, edited by W. Peltier, London: Gordon and Breach

Greenspan, H.P. 1968. *The Theory of Rotating Fluids*, Cambridge and New York: Cambridge University Press

Swinney, H.L. & Gollub, J.P. (editors). 1985. *Hydrodynamic Instabilities and Transition to Turbulence*, 2nd edition, Berlin and New York: Springer

Tritton, D.J. 1988. *Physical Fluid Dynamics*, 2nd edition, Oxford: Clarendon Press and New York: Oxford University Press

FLUX FLOW OSCILLATOR

See **Long Josephson junction**

FLUX QUANTIZATION

See **Josephson junction**

FLUXON

See **Long Josephson junction**

FOCUSING SYSTEM

See **Nonlinear optics**

FOKKER–PLANCK EQUATION

The Fokker–Planck equation (FPE) plays a role in stochastic systems analogous to that of the Liouville equation in deterministic mechanical systems. Namely, the FPE describes in a statistical sense how a *collection* of initial data evolves in time. To be precise, let the phase space describing the system be parameterized by the state vector $\boldsymbol{y}$, and let $\boldsymbol{Y}(t)$ denote the value of the state vector assumed by the system at time t. Suppose the dynamics of the system is governed by a stochastic differential equation (SDE) of the form

$$\mathrm{d}\boldsymbol{Y}(t) = \boldsymbol{U}(\boldsymbol{Y}(t), t)\,\mathrm{d}t + \sigma(\boldsymbol{Y}(t), t) \cdot \mathrm{d}\boldsymbol{W}(t). \quad (1)$$

The deterministic component of the dynamics is described by the drift vector $\boldsymbol{U}(\boldsymbol{y}, t)$, while the random part is driven by a vector of independent Brownian motions $\boldsymbol{W}(t)$ that are coupled to the system through the matrix $\sigma(\boldsymbol{y}, t)$.

Alternatively, we can define the system dynamics as a "diffusion process" in the relevant phase space such that

$$\begin{cases} \lim\limits_{\tau \downarrow 0} \tau^{-1} \langle \boldsymbol{Y}(t+\tau) - \boldsymbol{Y}(t) \rangle = \boldsymbol{U}(\boldsymbol{Y}(t), t), \\ \lim\limits_{\tau \downarrow 0} \tau^{-1} \langle (\boldsymbol{Y}(t+\tau) - \boldsymbol{Y}(t)) \\ \quad \otimes (\boldsymbol{Y}(t+\tau) - \boldsymbol{Y}(t)) \rangle = 2\mathsf{D}(\boldsymbol{Y}(t), t), \\ \lim\limits_{\tau \downarrow 0} \tau^{-1} \langle |\boldsymbol{Y}(t+\tau) - \boldsymbol{Y}(t)|^{\gamma} \rangle = 0 \text{ for } \gamma > 2, \end{cases} \quad (2)$$

where $\langle \cdot \rangle$ denotes an average over the random component of the dynamics. The SDE and diffusion process descriptions are equivalent, with $2\mathsf{D} = \sigma\sigma^{\dagger}$.

One useful way to describe the evolution of stochastic systems over a finite (rather than infinitesmal) time interval is through the probability transition density $p(t, \boldsymbol{y}|t', \boldsymbol{y}')$, which describes the likelihood that if the state variable assumes the value $\boldsymbol{y}'$ at time t', then it will assume a value near $\boldsymbol{y}$ at the later time t. More precisely, p is defined in terms of conditional probability as

$$\mathrm{Prob}(\boldsymbol{Y}(t) \in B | \boldsymbol{Y}(t') = \boldsymbol{y}') = \int_B p(t, \boldsymbol{y}|t', \boldsymbol{y}')\,\mathrm{d}\boldsymbol{y} \quad (3)$$

for all nice (Borel) sets B in the phase space. The FPE, also known as the Kolmogorov forward equation, is a partial differential equation that describes how the probability transition density evolves when the system can be described as an SDE (1) or diffusion process (2):

$$\begin{cases} \dfrac{\partial p(t, \boldsymbol{y}|t', \boldsymbol{y}')}{\partial t} \\ \quad = \dfrac{\partial}{\partial \boldsymbol{y}} \left(-\boldsymbol{U}(\boldsymbol{y}, t) p + \dfrac{\partial}{\partial \boldsymbol{y}} \left(\mathsf{D}(\boldsymbol{y}, t) p \right) \right), \\ p(t = t', \boldsymbol{y}|t', \boldsymbol{y}') = \delta(\boldsymbol{y} - \boldsymbol{y}'). \end{cases} \quad (4)$$

This equation is to be solved for $t > t'$ with fixed data for the source variables $(t', \boldsymbol{y}')$ and appropriate boundary conditions in $\boldsymbol{y}$ (Risken, 1989, Chapter 4).

The probability transition density can be used to describe the probability density for the state vector at any moment of time:

$$\mathrm{Prob}(\boldsymbol{Y}(t) \in B) = \int_B \phi(t, \boldsymbol{y})\,\mathrm{d}\boldsymbol{y} \quad (5)$$

by simply integrating against the prescribed probability distribution of the states at the initial time t':

$$\phi(t, \boldsymbol{y}) = \int p(t, \boldsymbol{y}|t', \boldsymbol{y}') \phi(t', \boldsymbol{y}')\,\mathrm{d}\boldsymbol{y}'. \quad (6)$$

Alternatively, $\phi(t, \boldsymbol{y})$ can be shown to satisfy the FPE (4) but with initial data $\phi(t', \boldsymbol{y}')$ prescribed more generally as a nonnegative function with integral one rather than as a delta function.

The FPE was first applied to describe Brownian motion. In the most idealized case, where inertia is completely neglected, Einstein showed that the statistics of the position $\boldsymbol{x} = \boldsymbol{X}(t)$ of a Brownian particle obeys an FPE that coincides with the ordinary diffusion equation:

$$\frac{\partial \phi(t, \boldsymbol{x}|t', \boldsymbol{x}')}{\partial t} = \kappa \Delta_{\boldsymbol{x}} \phi, \quad (7)$$

where $\Delta_{\boldsymbol{x}}$ is the Laplace operator and the diffusion coefficient $\mathsf{D} = \kappa \mathsf{I}$ is a constant scalar multiple of the identity matrix. The stochastic differential description of this model is simply

$$\mathrm{d}\boldsymbol{X}(t) = (2\kappa)^{1/2}\,\mathrm{d}\boldsymbol{W}(t). \quad (8)$$

The effects of inertia and external forces can be incorporated by passing to a phase space description including both the position $\boldsymbol{x} = \boldsymbol{X}(t)$ and the velocity $\boldsymbol{v} = \boldsymbol{V}(t)$ of the Brownian particle. The equations of

motion can then be written in terms of Newton's law with a random forcing component proportional to $\mathrm{d}\boldsymbol{W}$:

$$\begin{cases} \mathrm{d}\boldsymbol{X}(t) = \boldsymbol{V}(t)\,\mathrm{d}t, \\ m\,\mathrm{d}\boldsymbol{V}(t) = -m\xi\boldsymbol{V}(t)\,\mathrm{d}t + \boldsymbol{f}(\boldsymbol{X}(t), t)\,\mathrm{d}t \\ \qquad\qquad + (2k_{\mathrm{B}}Tm\xi)^{1/2}\,\mathrm{d}\boldsymbol{W}(t), \end{cases} \tag{9}$$

where ξ is a friction coefficient, k_{B} is Boltzmann's constant, T is the absolute temperature, and $\boldsymbol{f}(\boldsymbol{x}, t)$ represents the deterministic part of the external applied force. The equivalent Fokker–Planck description for the phase space probability transition density in this system reads

$$\begin{aligned} &\frac{\partial p(t, \boldsymbol{x}, \boldsymbol{v}|t', \boldsymbol{x}', \boldsymbol{v}')}{\partial t} \\ &\quad = \mathbf{grad}_{\boldsymbol{v}} \cdot \left[\left(\xi \boldsymbol{v} - \frac{\boldsymbol{f}(\boldsymbol{x}, t)}{m} + \frac{k_{\mathrm{B}}T\xi}{m} \mathbf{grad}_{\boldsymbol{v}} \right) p \right] \\ &\qquad - \mathbf{grad}_{\boldsymbol{x}} \cdot (\boldsymbol{v} p) \end{aligned} \tag{10}$$

Observe how this equation generalizes the Liouville equation for deterministic mechanics to include Brownian motion. The simplified diffusion equation (7) can be obtained through an asymptotic limit of the full FPE (10) with $\kappa = k_{\mathrm{B}}T/(m\xi)$, when $\boldsymbol{f}(\boldsymbol{x}, t) = 0$ and $(k_{\mathrm{B}}T/(m\xi^2\ell^2))^{1/2} \ll 1$ with ℓ a characteristic length of the system (Bocquet, 1997; Risken, 1989). A similar reduction to a partial differential equation in coordinate space, called the Smoluchowski equation, is also possible for collections of interacting particles where the friction tensor depends on the particle configuration (Titulaer, 1980). From the FPE for Brownian motion, one can compute various statistical properties such as its mean-square displacement, the spectrum of its fluctuations, the rate of relaxation of initial velocity to thermal equilibrium values, and the probability distribution for the time at which the particle first achieves a certain location or surmounts a potential barrier (Wax, 1954).

The FPE has found useful application in computing similar statistical properties in numerous other systems, such as lasers, polymers, particle suspensions, quantum electronic systems, molecular motors, and finance. In some instances, the system is not at first formulated in one of the senses (1) or (2) which immediately imply an FPE. Rather, the systems are more naturally represented in terms of a master equation with a complete description of the rates at which the system (randomly) jumps from one state to another. The FPE is an appropriate approximation to this system when certain asymptotic conditions, such as small jumps, a large system size, or a separation of time scales between resolved and unresolved variables, are met (Grabert, 1982; Risken, 1989; van Kampen, 1981).

A variety of techniques for practical analysis of FPEs can be found in Risken (1989). The main alternative to analyzing stochastic systems through the FPE is through the stochastic differential (or Langevin) formulation (1). The FPE has the merit of being a deterministic partial differential equation that can be solved once through either analytical or numerical methods. The stochastic differential description (1) by contrast consists of ordinary differential equations for which individual realizations (samples) are faster to simulate through Monte Carlo methods (Kloeden & Platen, 1992). But obtaining a statistical description of the general behavior of the system requires the generation of a large number of realizations.

Certain statistical quantities described above can be easily calculated using either the solution of the FPE or by operating directly on the FPE itself. On the other hand, the stochastic differential system (1) must be used if one wishes to characterize particular realizations of the stochastic system. Moreover, the stochastic differential description can be readily generalized to cases in which the random driving has temporal correlations (Kubo et al., 1991; Moss & McClintock, 1989). The FPE formulation can be modified to a "fractional" formalism for certain self-similar temporal correlation structures (Metzler & Klafter, 2000), but further generalizations are much more complicated and usually require some sort of approximation (Moss & McClintock, 1989).

PETER R. KRAMER

See also **Brownian motion; Fluctuation-dissipation theorem; Nonequilibrium statistical mechanics; Phase-space diffusion and correlations; Stochastic processes**

Further Reading

Bocquet, L. 1997. High friction limit of the Kramers equation: The multiple time-scale approach. *American Journal of Physics*, 65(2): 140–144

Grabert, H. 1982. *Projection Operator Techniques in Nonequilibrium Statistical Mechanics*, Berlin and New York: Springer [FPE as approximation to more detailed models when separation of time scales exists]

Kloeden, P.E. & Platen, E. 1992. *Numerical Solution of Stochastic Differential Equations*, Berlin and New York: Springer [Sections 1.7, 2.4, 4.1, 4.7]

Kubo, R., Toda, M. & Hashitsume, N. 1991. *Statistical Physics*, 2 vols, 2nd edition, Berlin and New York: Springer [Chapter 2 has a derivation of hierarchy of statistical descriptions for physical systems]

Metzler, R. & Klafter, J. 2000. The random walk's guide to anomalous diffusion: a fractional dynamics approach. *Physics Reports*, 339(1): 1–77

Moss, F. & McClintock, P.V.E. (editors). 1989. *Noise in Nonlinear Dynamical Systems*, vol. 1. Cambridge and New York: Cambridge University Press [A collection of expository articles on FPE methods with extensions to temporal correlations in noise]

Risken, H. 1989. *The Fokker–Planck Equation*, 2nd edition, Berlin: Springer

Titulaer, U.M. 1980. Corrections to the Smoluchowski equation in the presence of hydrodynamic interactions. *Physica* A, 100(2): 251–265

van Kampen, N.G. 1981. *Stochastic Processes in Physics and Chemistry*, Amsterdam: North-Holland [Chapter 8 has a careful discussion of physical applicability of FPE]
Wax, N. (editor). 1954. *Selected Papers on Noise and Stochastic Processes*, New York: Dover

FORCED SYSTEMS

See **Damped-driven anharmonic oscillator**

FORECASTING

The success of Newtonian classical mechanics led in the 18th and 19th centuries to a strong belief in determinism; that is, the notion that the past determines the present and the future. As a consequence, a superior intellect ("Laplace's Daemon") would be able to forecast the future given enough information about the present and the past. However, the discovery of chaos in a large class of deterministic nonlinear dynamical systems sets a limit as to what Laplace's Daemon can forecast.

One of the characteristics of deterministic chaos is that the future state of a dynamical system depends sensitively on the initial conditions—infinitesimal perturbations will grow exponentially. This effect is also known more poetically as the "butterfly effect" (from a lecture by Edward Lorenz in 1972: "Does the flap of a butterfly's wings in Brazil set off a tornado in Texas?"). Since there will always be some uncertainty—however small—about the observed state of any physical system, a consequence of extreme sensitivity on the initial conditions is that the future state of such a system can only be forecast to lie within a given error tolerance a limited time ahead. As even Laplace's Daemon would not be able to determine the exact present state of the system, she would not be able to forecast the state of the future, but as she would know the uncertainty about the present, she would be able to work out all possible future states.

Uncertainty in the initial conditions is appropriately expressed in terms of a multivariate probability density function (pdf). A forecast is then given by the time evolution of the initial pdf, subject to the underlying dynamical system. Typically, the initial pdf is sharp, centered around the best estimate of the observed state of the physical system, but with time the pdf is smeared out in a complicated fashion until, eventually, all information about the initial condition is lost. For the short-range evolution, when the pdf remains "sufficiently" sharp, a forecast can be given in deterministic terms. For the intermediate-range evolution, when the pdf still has sufficient structure, a forecast can (and should) be given in probabilistic terms. Beyond that, a forecast will be no better than a guess based on the observed long-term behavior of the system.

When the governing dynamical equations are known, the time evolution of the pdf can be expressed in terms of the Liouville equation, which is a special case of the stochastic-differential Fokker–Planck equation. In theory, the Liouville equation could be applied to weather forecasting where dynamical models have been developed of the atmospheric circulation, but in practice, numerical problems and computational limits need to be overcome. An alternative approach is to make a Monte Carlo-type estimation of the time evolution of the pdf, that is, numerical integration of an ensemble of a large number of initial conditions that are generated by random sampling of the initial pdf. Application to weather forecasting of this Monte–Carlo approach is, however, also problematic, primarily due to the very high dimension ($\sim 10^7$) of the phase space of atmospheric circulation models that requires a very large number of Monte Carlo integrations to be performed (beyond the capacity of present-day supercomputers) in order to sufficiently reduce sampling uncertainty.

The practical approach that is applied to today's weather forecasting is to generate a relatively small ensemble (comprising typically 50–100 members) of initial perturbations to the observed initial state of the atmosphere. The perturbations are calculated in a way that ensures that the corresponding trajectories of the dynamical model equations initially diverge rapidly from the observed initial state. Thus, the time evolution of the individual ensemble members is not representative of the time evolution of the "true" pdf, but the ensemble is useful for the weather forecaster who is often most interested in the most likely development of the weather and possible major deviations from this development.

Forecasting becomes increasingly problematic when we also take into account that the forecast model is not perfect; that is, there are errors in the model (perhaps due to incorrect assumptions or poor spatial resolution), the effect of which is that the model does not behave like the real world. In the area of weather forecasting, model errors cause severe problems for long-range forecasts. A long-range weather forecast, or seasonal forecast, valid out to typically six months ahead, aims at predicting slowly varying surface conditions, such as sea surface temperature, sea ice cover, and soil moisture, and the effect they have on the preferred state of the atmospheric circulation in certain regions. A prominent example is prediction of El Niño conditions (increased sea surface temperature in the central and eastern tropical Pacific), which have an influence on worldwide weather.

The effect of model errors is in practice taken into account by basing seasonal weather forecasts on ensembles made up of integrations of more than one model. In this way, a pseudo-stochastic element is introduced into the forecast through the different

formulations of the models, particularly for processes that take place on spatial scales that are smaller than the resolution of the model grid.

Forecasting is also of interest in areas in which models are not readily expressed in terms of known physical laws, most notably, in economics. When a physical model is not available, forecasting has to be based on more empirical methods. For example, a statistical forecast model would be based on the forecaster's notion of cause and effect, while an empirically constructed dynamical model could be derived from analysis of the combined behavior of many observed variables.

Due to the nondeterministic nature of economic evolution, economic forecasts will often be associated with substantial uncertainty. However, it is worth noting that a forecast need not be very accurate to be useful. If, in the long run, an economic forecast is just slightly better than a guess, then money can be made from the forecast.

In practical forecasting, no matter in what field, there is almost always an element of human expert judgment involved, and overall the expert judgment probably remains the most widespread forecasting method.

HENRIK FEDDERSEN

See also **Butterfly effect; Chaotic dynamics; Determinism; Economic system dynamics; Fokker–Planck equation; General circulation models of the atmosphere**

Further Reading

Ehrendorfer, M. 1994. The Liouville equation and its potential usefulness for the prediction of forecast skill. Part I: theory. *Monthly Weather Review*, 122: 703–713

Houghton, J. 1991. The Bakerian lecture, 1991. The predictability of weather and climate. *Philosophical Transactions of the Royal Society of London* A, 337: 521–572

Lorenz, E. 1963. Deterministic non-periodic flow. *Journal of Atmospheric Sciences*, 20: 130–141

Sivillo, J.K., Ahlquist, J.E. & Toth, Z. 1997. An ensemble forecasting primer. *Weather and Forecasting*, 12: 809–818

Smith, L.A. 2000. Disentangling uncertainty and error: On the predictability of nonlinear systems. In *Nonlinear Dynamics and Statistics* (Chapter 2), edited by A.I. Mees, Boston: Birkhauser

FOREST FIRES

The modeling of forest fires (FF) is based upon the concept of interacting particle systems (Liggett, 1985) for the description of complex systems. Within this framework, attention is on the interactions among particles (i.e., the trees), disregarding any attempt to understand the behavior of each particular tree. Using local interaction rules among neighboring trees, interesting collective behavior can be observed on a global scale.

FF models are defined so that trees may grow on the nodes of a surface network with periodic boundary conditions (Bak et al., 1990; Drossel & Schwabl, 1992, 1993; Christensen et al., 1993; Grassberger, 1993; Albano, 1995). Each node can assume three different states: (s1) occupied by a growing tree, (s2) occupied by a burning tree, and (s3) empty. The last corresponds to the absence of a tree that occurs after the completion of the tree burning process. Local interaction rules govern the dynamics of the system, which is updated as a cellular automation. For a given configuration, the time evolution is obtained by applying the following rules: (r1) a tree grows on an empty node with probability P; (r2) a burning tree evolves into an empty node; and (r3) a tree catches fire from a neighbor burning tree with probability $1 - G$. Thus, P is the growing probability of trees and G is the immunity of each tree to catch fire (Drossel & Schwabl, 1993).

Qualitatively, one expects that if the immunity is nonzero, the fire fronts present for $G = 0$ will become more and more fuzzy when G is increased. Of course, the fire cannot propagate for $G = 1$. For large values of P ($P \to 1$) and if the immunity is low ($G \to 0$), one observes coexistence of fire, trees, and empty nodes. Within this active state, fire fronts exhibit a rich variety of spatiotemporal patterns, including the development of spirals, and the collision between fronts. However, by keeping P constant and increasing G, the fire will eventually cease and the system will become trapped in an inactive state where the network is completely occupied by trees (see Figure 1). Since the spontaneous ignition of trees is not considered, the system will remain in the inactive state forever. So, for some critical values of the parameters $P \equiv P_c$ and $G \equiv G_c$, this simple kind of FF model exhibits irreversible phase transitions (Marro & Dickman, 1999) between active states with fire propagation and an inactive state where the fire becomes irreversibly extinguished. Figure 1 shows the critical curve at the border between these two states. In the case of standard reversible phase transitions and in marked contrast to forest fire models, the state of the system can be reversibly selected by tuning the control parameter (Binder & Heermann, 2002), that is, the temperature or pressure.

In spite of the irreversible nature of the transitions, a statistical treatment of this kind of FF model reveals that they share the relevant features of many phase transitions and critical phenomena occurring under equilibrium conditions. Therefore, FF models can be described by using a well-established framework in the field of statistical physics. In fact, close to the transition point, it is well known that the correlation length among particles is quite large—diverging to infinite at the critical point (Binder & Heermann, 2002). Therefore, at the critical state $P \to P_c$, $G \to G_c$, the burning of a single tree would affect the whole forest. The onset of this collective behavior, characteristic of critical phenomena, washes out the microscopic details (i.e., the mechanisms keeping every tree alive)

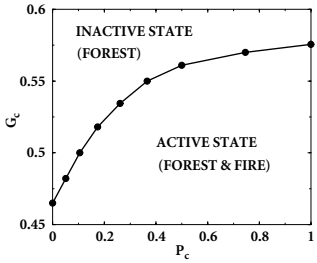

Figure 1. Plot of the critical threshold G_c versus P_c. Filled circles are critical values determined quite accurately by means of epidemic simulations. The critical line (solid curve) is drawn to guide the eye. The upper part of the figure corresponds to the inactive state of the system where the fire becomes irreversibly extinguished, while the lower part corresponds to the stationary state with fire fronts.

allowing the relevant behavior of the whole system to be caught by means of a small set of simple local rules, in agreement with the concept of interacting particle systems (Liggett, 1985).

A powerful method used to characterize and study an irreversible transition consists of performing the so-called epidemic (or spreading) simulations (ES) (Grassberger, 1989). The idea behind ES is to start the simulations from a configuration very close to the inactive state and follow the temporal evolution of the system under consideration. For this purpose, a network fully occupied by trees, except for a small patch of burning trees, is employed. Depending on the values of the parameters P and G, such a small fire would either propagate or become extinguished. During the propagation the following quantities are measured:

(i) The average number of burning trees $N(t)$;
(ii) The survival probability of the fire $P(t)$, that is, the probability that the fire is still ignited at time t;
(iii) The average mean-square distance $R^2(t)$ over which the fire has spread.

Due to the existence of a diverging correlation length, it is usually assumed that the measured quantities obey simple power laws given by

$$N(t) \propto t^{\eta}, \quad P(t) \propto t^{-\delta} \quad \text{and} \quad R^2 \propto t^{z}, \qquad (1)$$

where η, δ, and z are critical exponents. These exponents have been evaluated by means of extensive numerical simulations, yielding $\eta = 0.212 \pm 0.005$, $\delta = 0.459 \pm 0.005$, and $z = 1.115 \pm 0.010$ (Albano, 1995). This result allows us to place the FF model with immune trees within the universality class of directed percolation (DP) (Grassberger, 1989). It should be stressed that DP was previously proposed in the field of physics as a model for the systematic dripping of a fluid through a lattice with randomly occupied bonds (Kinzel, 1983), and similar irreversible behavior is observed in many disciplines, such as catalysis (the interruption of chemical reactions due to the poisoning of the catalysts (Loscar & Albano, 2003)), biology (the epidemic propagation of a disease (Marro & Dickman, 1999)), ecology (the extinction of species when resources become exhausted or the environment is changed (Rozenfeld & Albano, 2001)), and sociology (models for a society of interacting individuals (Monetti & Albano, 1997)).

By introducing an additional parameter given by the lightning probability F, which can be thought of as the probability of spontaneous ignition of a tree, to the above-formulated FF model, an interesting behavior with two characteristic time scales is observed. In the limit $F \to 0$, the onset of fire is quite sporadic and occurs on large time scales. After ignition, however, fire propagates during relatively short periods of time (Drossel & Schwabl, 1992; Christensen et al., 1993; Grassberger, 1993). By analogy to sandpile models, these rapid events are called avalanches. A statistical analysis of the area of the forest reached by fire shows that it lacks a characteristic size. So, in contrast to the standard Gaussian distribution, which describes many natural phenomena exhibiting a typical (average) size, avalanches of all magnitude are expected to be observed. Under these circumstances, it is believed that the time-scale separation effectively tunes the system into a scale-free state. This behavior is the typical sign of criticality observed in studies of the phase transitions of many substances and is due to the existence of a diverging correlation length.

Finally, several attempts to reproduce forest fires in the laboratory should be mentioned. Nahmias et al. (1989, 1996) have built a square network sample containing combustible and noncombustible blocks randomly distributed with a variable concentration. The effect of randomness on the propagation of the fire is studied by considering both the presence and absence of wind. It is found that the results are consistent with critical models of percolation. Also, Zhang et al. (1992) have studied forest-fire propagation by means of paper-burning experiments. It is found that fire fronts exhibit self-affine scaling behavior that can be described by a nonlinear stochastic differential equation of the Kardar–Parisi–Zhang type with Gaussian noise.

EZEQUIEL ALBANO

See also **Cellular automata; Critical phenomena; Flame front; Reaction-diffusion systems; Sandpile model**

Further Reading

Albano, E.V. 1995. Spreading and finite-size scaling study of the critical behaviour of a forest-fire model with immune trees. *Physica* A, 216: 213–226

Bak, P., Chen, K. & Tang, C. 1990. A forest-fire model and some thoughts on turbulence. *Physics Letters*, 147A: 297–300
Binder, K. & Heermann, D. 2002. *Monte Carlo Simulations in Statistical Physics: An Introduction*, 4th edition, Berlin and New York: Springer
Christensen, K., Flyvbjerg, H. & Olami, Z. 1993. Self-organized critical forest-fire model: mean-field theory and simulation results in 1 to 6 dimensions. *Physical Review Letters*, 71: 2737–2740
Drossel, B. & Schwabl, F. 1992. Self-organized critical forest-fire model. *Physical Review Letters*, 69: 1629–1632
Drossel, B. & Schwabl, F. 1993. Forest-fire model with immune trees. *Physica* A, 199: 183–97
Grassberger, P. 1989. Directed percolation in $2 + 1$ dimensions. *Journal of Physics A* (*Mathematical & General*), 22: 3673–3680
Grassberger, P. 1993. On a self-organized critical forest-fire model. *Journal of Physics A* (*Mathematical & General*), 26: 2081–2089
Kinzel, W. 1983. Directed percolation. In *Percolation Structures and Processes.* Annals of the Israel Physical Society. vol. 5, edited by G. Deutscher, R. Zallen & J. Adler Jerusalem: Israel Physical Society, pp.425–445
Liggett, T.M. 1985. *Interacting Particle Systems*, New York: Springer
Loscar, E.S. & Albano, E.V. 2003. Critical behaviour of irreversible reaction systems. *Reports on Progress in Physics*, 66: 1343–1382
Marro, J. & Dickman, R. 1999. *Nonequilibrium Phase Transitions and Critical Phenomena*, Cambridge and New York: Cambridge University Press
Monetti, R.A. & Albano, E.V. 1997. On the emergence of large-scale complex behaviour in the dynamics of a society of living individuals: the stochastic game of life. *Journal of Theoretical Biology*, 187: 183–194
Nahmias, J., Téphany, H. & Duarte, J. 1996. Percolation de sites en combustion. *Comptes Rendues de l´Academie des Sciences Paris*, 332: 113–119
Nahmias, J., Téphany, H. & Guyon, E. 1989. Propagation de la combustion sur un réseau hétérogène bidimensionnel. *Revue Physique Applique*, 24: 773–777
Rozenfeld, A.F. & Albano, E.V. 2001. Critical and oscillatory behaviour of a system of smart preys and predators. *Physical Review* E, 63: 061907-1–061907-6
Zhang, J., Zhang, Y.-C., Alstrom, P. & Levinsen, M.T. 1992. Modeling forest fire by paper-burning experiment, a realization of the interface growth mechanism. *Physica* A, 189: 383–389

FOURIER TRANSFORM

See **Integral transforms**

FOUR-WAVE MIXING

See N**-wave interactions**

FRACTAL BASIC BOUNDARIES

See **Attractors**

FRACTAL DIMENSION

See **Dimensions**

FRACTALS

Many spatial patterns and objects in nature are either irregular or fragmented to such an extreme degree that it is very hard to describe their form. For example, the coastline of a typical oceanic island or of a continent is neither straight, nor circular, nor elliptic, and no other classical curve can serve to describe it. Similarly, there is no Euclidean surface to capture adequately the boundaries of clouds or of rough turbulent wakes. To fill this gap, Benoit Mandelbrot proposed to use a family of shapes called *fractals* for geometric representation of the shapes mentioned above and many other irregular patterns. The word *fractal* derives from the Latin *fractus* (an adjective from the verb *frangere*, meaning "to break"), capturing the irregular characteristics of geometrical objects it describes. One can think of a fractal as an irregular set consisting of parts similar to the whole. It means that a fractal is a rough or fragmented geometrical shape that can be subdivided into parts, each of which is (at least approximately) similar at reduced size to the whole. Roughness present at any resolution of a fractal object distinguishes it from Euclidean shapes. The transition from a Euclidean geometry to a fractal one reflects the conceptual jump from translational invariance of traditional Euclidean shapes to continuous scale invariance of fractal objects. The concept of fractals is useful for describing various natural objects, such as clouds, coasts, and river or road networks. However, the fractal structure of natural objects is only observed over a limited range of scales, beyond which the fractal description breaks down.

During the study of geometry of irregular patterns, it became clear that a proper understanding of irregularity or fragmentation must, among other things, involve an analysis of the intuitive notion of dimension. Topological dimension cannot properly describe strongly irregular fractal structures. Let us consider the simplest example of a fractal, namely the Cantor set, see Figure 1. For the construction of the Cantor set an iteration procedure is used. At the zeroth level, the construction of the triadic Cantor set begins with the unit interval, that is, all points on the line between 0 and 1. The first level is obtained from the zeroth one by deleting all points between $\frac{1}{3}$ and $\frac{2}{3}$, that is the middle third of the initial interval. The second level is obtained from the first level by deleting the middle third of each remaining interval at the first level. In general, the next level is obtained from the previous one by deleting the middle third of all intervals obtained from the previous level. This process continues ad infinitum. The result is a collection of points with topological dimension $d_t = 0$ since its total measure (length) is zero.

It is seen that the notion of dimension from Euclidean geometry is not very useful for the Cantor set and similar objects since it does not distinguish between the rather complex set of elements and a single point that also has a vanishing topological dimension. To cope

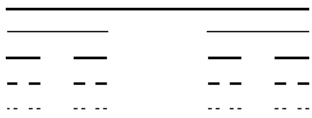

Figure 1. The construction of the Cantor set.

with this degeneracy, concepts of fractal dimensions were introduced for quantifying such fractal sets. Many paradoxical aspects of the Cantor set can be traced to the fact that it is dimensionally discordant. Furthermore, the discordant character of basic fractals is not at all a minor nuisance. Rather, it is such a basic feature that we shall use it to give a tentative definition of the concept of fractal. The simplest nontrivial dimension that generalizes the topological dimension is the so-called fractal dimension, which in this context can be defined as follows:

$$D_{\mathrm{c}} = \lim_{n \to +\infty} \frac{\ln N_n}{\ln 1/l_n}. \tag{1}$$

Here, N_n is the number of observable elements at the nth level, l_n is the measure (length) of the smallest element at the nth level, and $1/l_n$ is the resolution. For the triangle Cantor set at the nth level, the set consists of $N_n = 2^n$ segments, each of which has length $l_n = \frac{1}{3}^n$. Therefore, the capacity dimension of the triangle Cantor set equals

$$D_{\mathrm{c}}^{\mathrm{cantor}} = \frac{\ln 2}{\ln 3} \simeq 0.63. \tag{2}$$

We see that fractal dimension is noninteger. Mathematically, we can say that a fractal is a set of points whose fractal dimension exceeds its topological dimension.

Felix Hausdorff developed another way to quantify a fractal set. He suggested examining the number $N(\varepsilon)$ of small intervals needed to cover the set at a scale ε. The Hausdorff dimension is defined by considering the quantity

$$M \equiv \lim_{\varepsilon \to 0} \inf_{\varepsilon_m < \varepsilon} \sum_m \varepsilon_m^d, \tag{3}$$

which is constructed by summing d-dimensional volumes ε_m^d of balls of radii ε_m not exceeding ε that cover the fractal set. The "inf" means that all partitions of balls of radius less than ε that cover the set are considered and the one that gives the smallest possible value for the sum is kept. Hausdorff demonstrated that there is a special value D_{H} for the exponent d, called the *Hausdorff dimension*, such that for $d < D_{\mathrm{H}}$ measure $M = \infty$ as $\varepsilon \to 0$ and for $d > D_{\mathrm{H}}$ measure $M = 0$ in the limit $\varepsilon \to 0$.

Now the reader may ask, why do we need more than one fractal dimension? Actually, as is seen below, there is an infinite set of fractal dimensions. The reason for this number of quantities describing a single fractal object is the *fractal form*. The form of Euclidean shapes is well described by topology. However, as was noted by Mandelbrot the concept of form possesses mathematical aspects other than topological ones. Topology is the branch of mathematics that teaches us, for example, that all pots with two handles are of the same form because, if they were made of an infinitely flexible clay, each could be molded into any new opening, closing up any old one. Obviously, this particular aspect of the notion of form is not useful in the study of individual coastlines, since it simply indicates that they are all topologically identical to each other (and to a circle). This identity is underlined by the fact that the topological dimension in each case equals 1. By way of contrast, it will be seen that coastlines of different "degrees of irregularity" tend to have different fractal dimensions. Differences in fractal dimensions express differences in nontopological aspects of form, which can be called the *fractal form*.

Now let us consider the cumulative distribution function of mass along the Cantor set. Let the initial line's length and mass both be equal to 1, and define the cumulative distribution function for the abscissa x as being the mass contained between 0 and x. It is assumed that the total mass of the pattern is not changed while building the Cantor set. It means that we do not take away one-third of each line, but divide it in to two parts and compress them until the length of each part equals one-third of the initial line length at the previous step. Iterating this procedure up to infinity, we obtain the massive Cantor set. Because there is no mass in the intermissions, the distribution function remains constant along almost the whole length of the unit interval. However, since hammering does not affect the total mass, the distribution must manage to increase somewhere from the point of coordinates $(0, 0)$ to the point of coordinates $(1, 1)$. It increases over infinitely many, infinitely small, highly clustered jumps corresponding to the points of the Cantor set. The plot of the cumulative distribution function shown in Figure 2 is called the *Devil's staircase*. It is the plot of a continuous function on the unit interval, whose derivative is 0 almost everywhere, but it rises from 0 to 1 (see Figure 2). The cumulative sums of the widths and of the heights of the steps are both equal to 1, and one finds in addition that this curve has a well-defined length equal to 2. A curve of finite length is called *rectifiable* and is of dimension $D = 1$. This example has the virtue of demonstrating that sharp irregularities do not necessarily prevent a curve from being of dimension $D = 1$, as long as they remain sufficiently few and scattered.

You can see from Figure 2 that the Devil's staircase is a function which is not differentiable at the Cantor set points, but has zero derivative everywhere else. Because a Cantor set has measure zero, this function has

Figure 2. The Devil's staircase.

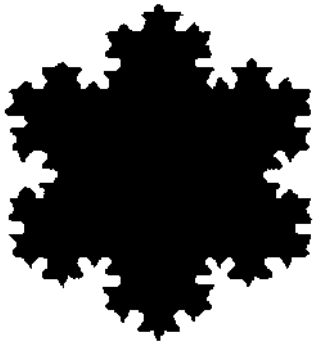

Figure 3. The Koch snowflake.

zero derivative practically everywhere and rises only on Cantor set points.

Now we consider the fractal whose dimension, in contrast to the Cantor set, exceeds unity. As an example we consider the *Koch snowflake*; see Figure 3. This is a fractal, also known as the Koch island, which was first described by Helge von Koch in 1904. It is built by starting with an equilateral triangle, removing the inner third of each side, building another equilateral triangle at the location where the side was removed, and then repeating the process indefinitely (see Figure 4). The border of the snowflake is a curve. Indeed, its area vanishes, but on the other hand each stage of its construction increases its total length by the ratio $4/3$. Thus, the limit border is of infinite length. It is also continuous, but it has no definite tangent in almost all of its points because it has, so to speak, a corner almost everywhere. Its nature borders on that of a continuous function without a derivative. This object has a fractal nature. The capacity dimension of the Koch snowflake equals $D_c^{\text{Koch}} = \ln 4/\ln 3 \simeq 1.26$. Though the total length of the border is infinite, the area

Figure 4. The construction of the Koch snowflake.

of the Koch island originated from the initial triangle with unit side is finite and equals $S^{\text{Koch}} = 2\sqrt{5}/5$.

Fractals arising in nature usually have a more complex scaling relation than simple fractals (like the Cantor set) described above. The single fractal dimension is not enough to describe their structure, because these fractal sets usually involve a range of scales that depend on their location within the set (the simplest example is the Cantor set with some measure distributed on it). Such fractals are called *multifractals*.

The multifractal formalism is a statistical description that provides global information on the self-similarity properties of fractal objects. For practical realization of the method, one primarily covers the fractal set under study by a regular array of cubic boxes of some given mesh size l. The measure of weight p_n of a given box n is then defined as the sum of the measure of interest within the box. A simple fractal dimension α is defined by the relation:

$$p_n \sim l^{\alpha}. \tag{4}$$

Multifractal analysis is a generalization in which α may change from point to point and is a local quantity. The standard method to test for multifractal properties consists in calculating the moments of order q of the measure p_n defined by

$$M_q(l) = \sum_{n=1}^{n(l)} p_n^q. \tag{5}$$

Here $n(l)$ is the total number of non-empty boxes. Varying q, one can characterize the inhomogeneity of the pattern, for instance, the values of moments with large q are controlled by the densest boxes. If scaling holds, then the generalized dimension D_q is defined by the relation:

$$M_q(l) \sim l^{(q-1)D_q}. \tag{6}$$

For instance, D_0, D_1, and D_2 are called *capacity* (defined above), *information*, and *correlation* dimensions, respectively.

In multifractal analysis, one also determines the number $N_\alpha(l)$ of boxes having similar local scaling characterized by the same exponent α. Using it, one can introduce the multifractal singularity spectrum $f(\alpha)$ as the fractal dimension of the set of singularities of strength α according to the following relation:

$$N_\alpha(l) \sim (1/l)^{f(\alpha)}. \tag{7}$$

There is a general relationship between a moment of order q and a singularity strength α, expressed

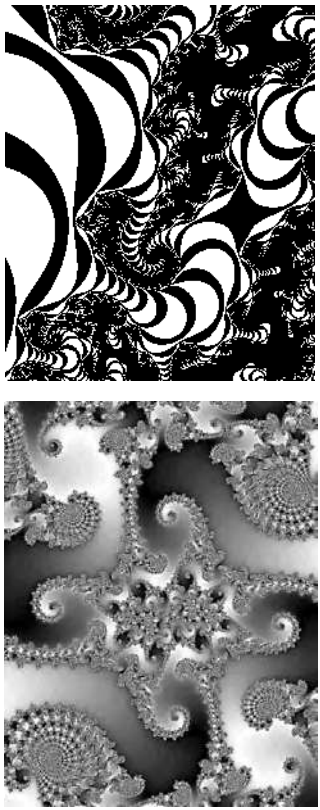

Figure 5. Examples of Julia sets.

mathematically as a Legendre transformation:

$$f(\alpha) = q\alpha - (q-1)D_q. \tag{8}$$

Fractal sets can be impressive. For example, see Figure 5 where a number of so-called *Julia sets* is shown. (See also color plate section.)

Mathematically, the Julia set can be introduced as follows. Take some function $f(z)$ and consider the sequence obtained when $f(z)$ is iterated starting from the point $z = a$:

$$a,\ f(a),\ f(f(a)),\ f(f(f(a))),\ \text{etc.} \tag{9}$$

Depending on the initial condition a and form of the function f, it may happen that these values stay small or they do not, that is, repeatedly applying f to yield arbitrary large values. So the set of all numbers (initial conditions) is partitioned; into two parts, and the Julia set associated with the function f is the boundary between these sets. The "filled" Julia set includes those numbers $z = a$ for which the iterates of f applied to remain bounded. If one considers complex numbers rather than real ones, it is the complex plane that is partitioned into two sets, and the resulting picture can be quite striking; see Figure 5. That is an example of iterating a quadratic function defined in the complex plane. Linear functions do not yield interesting partitions of the complex plane, but quadratic and higher-order polynomials do.

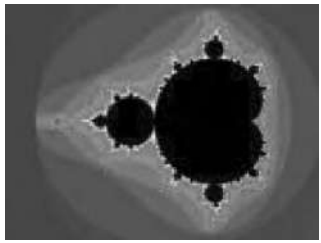

Figure 6. The Mandelbrot set.

Consider the most studied family of quadratic polynomials $f(z) = z^2 + \mu$ parametrized by a complex variable μ. As μ varies, the Julia set will vary on the complex plane. Some of these Julia sets will be connected, and some will be disconnected. Those values of μ for which the Julia set is connected are called the *Mandelbrot set* in the parameter plane. The boundary between the Mandelbrot set and its complement is often called *Mandelbrot separator curve*. The Mandelbrot set is the black shape in Figure 6 (see also color plate section). The Mandelbrot set is the set of points in the complex μ-plane that do not go to infinity when iterating the map $z_{n+1} = z_n^2 + \mu$ starting with $z = 0$. One can avoid the use of the complex numbers by substitution $z = x + \mathrm{i}y$ and $\mu = a + \mathrm{i}b$, and computing the orbits in the ab-plane for two-dimensional mapping:

$$\begin{aligned} x_{n+1} &= x_n^2 - y_n^2 + a, \\ y_{n+1} &= 2x_n y_n + b, \end{aligned} \tag{10}$$

with initial conditions $x = y = 0$ or equivalently $x = a$, $y = b$.

Now let us consider a natural phenomenon exhibiting fractal properties, namely, Brownian motion. Consider a fluid mass in equilibrium, for example, water in a glass; all the parts appear completely motionless. However, if one puts a small enough particle into the water, it is observed that instead of rising or descending regularly (depending on the density of the particle),

Figure 7. The example of Brownian motion of a colloidal particle.

it moves with a perfectly irregular movement. The segment of motion of a colloidal particle is presented in Figure 7 as it is seen under the microscope. The successive positions of a particle in equal time intervals are marked by points, then joined by straight lines having no physical reality whatsoever. If this particle's position were marked down 100 times more frequently, each segment would be replaced by a polygon relatively just as complicated as the whole drawing, and so on. Here, we have the natural example of the *scaling property* of the colloidal particle's motion. It is easy to see that in practice the notion of tangent is meaningless for such curves. This property of the trajectory reminds one of the Koch's snowflake described above, because when a Brownian trajectory is examined increasingly closely, its length increases without bound. Thus, we see that the trajectory of a colloidal particle has features peculiar to fractal objects, and we can qualify Brownian motion as being *fractal* and giving us a natural example of a fractal pattern.

VITCHESLAV KUVSHINOV AND ANDREI KUZMIN

See also **Brownian motion; Dimensions; Multifractal analysis**

Further Reading

Barnsley, M. 1988. *Fractals Everywhere*, Boston: Academic Press

Devaney, R. & Keen, L. (editors). 1989. *Chaos and Fractals: The Mathematics Behind the Computer Graphics*, Providence, RI: American Mathematical Society

Falcone, K.J. 1985. *The Geometry of Fractal Sets*, Cambridge and New York: Cambridge University Press

Feder, J. 1988. *Fractals*, New York and London: Plenum Press

Mandelbrot, B.B. 1988. *Fractal Geometry of Nature*, New York: Freeman

Sornette, D. 2000. *Critical Phenomena in Natural Sciences. Chaos, Fractals, Self-organization, and Disorder: Concepts and Tools*, Berlin and New York: Springer

FRAMED SPACE CURVES

The Frenet–Serret Frame

Let $\gamma : I \to \mathbb{R}^3$ be a C^3 regular parametrized space curve, with I an open interval on the real line; by regular we mean that $\gamma'(t)$ is never zero. We define the unit tangent vector $\boldsymbol{t}$ by $\boldsymbol{t} = \gamma'/|\gamma'|$ and an arclength coordinate s by $s = \int |\gamma'| \, dt$. An inflection point of the curve is one where $\boldsymbol{t}'$ is zero; away from such points, we may define the unit normal by $\boldsymbol{n} = \boldsymbol{t}'/|\boldsymbol{t}'|$. Then the binormal vector is $\boldsymbol{b} = \boldsymbol{t} \times \boldsymbol{n}$, where $\times$ denotes the cross product of vectors in $\mathbb{R}^3$.

Expressing the derivatives of these mutually orthogonal unit vectors in terms of themselves produces the Frenet equations

$$\dot{\boldsymbol{t}} = \kappa \boldsymbol{n},$$
$$\dot{\boldsymbol{n}} = -\kappa \boldsymbol{t} + \tau \boldsymbol{b},$$
$$\dot{\boldsymbol{b}} = -\tau \boldsymbol{n},$$

where the dot denotes derivative with respect to arclength s, and κ and τ are the *curvature* and *torsion* functions of the curve, respectively. Curvature may be defined in terms of $\boldsymbol{t}$ by $\kappa = |\dot{\boldsymbol{t}}|$, so that if κ is identically zero then $\gamma(t)$ is a straight line; more generally, inflection points, where κ vanishes, may be defined as points where the curve has at least second-order contact with a line.

We will say that a regular curve is *nondegenerate* if it has no inflection points. For such curves, we may define τ in terms of the scalar triple product as $\tau = (\boldsymbol{t}, \dot{\boldsymbol{t}}, \ddot{\boldsymbol{t}})/\kappa^2$. Thus, τ depends on the third derivative of γ while κ is a second-order quantity. Moreover, τ is identically zero if and only if $\gamma(t)$ lies in a fixed plane parallel to $\boldsymbol{t}$ and $\dot{\boldsymbol{t}}$.

Curvature and torsion are unchanged if we reverse the orientation of the curve (i.e., the direction of $\boldsymbol{t}$), or if the curve is rotated or translated within $\mathbb{R}^3$. (However, τ is changed by a minus sign if the curve is reflected, and both functions are multiplied by ρ^{-1} when the curve is scaled by a factor $\rho > 0$.) Conversely, uniqueness theorems for linear systems of differential equations, as applied to the Frenet equations, imply that two nondegenerate space curves with the same curvature and torsion, as functions of arclength, are congruent under an orientation-preserving isometry of $\mathbb{R}^3$ (congruence theorem).

Natural Frames

Although the vector $\kappa \boldsymbol{n}$ is well defined for any regular curve, by itself $\boldsymbol{n}$ is undefined at inflection points, and even at simple inflection points (where $\boldsymbol{t} \times \dot{\boldsymbol{t}}$ vanishes only to first order), κ is nondifferentiable and $\boldsymbol{n}$ is discontinuous. One can get around this problem and obtain a C^1 orthonormal framing along the curve, by using *natural frames*, also known as relatively parallel adapted frames (Bishop, 1975). Such frames satisfy

equations of the form

$$\begin{aligned} \dot{\boldsymbol{t}} &= k_1 \boldsymbol{m}_1 + k_2 \boldsymbol{m}_2, \\ \dot{\boldsymbol{m}}_1 &= -k_1 \boldsymbol{t}, \\ \dot{\boldsymbol{m}}_2 &= -k_2 \boldsymbol{t}, \end{aligned} \tag{1}$$

where $\boldsymbol{t}$ is the usual unit tangent vector, $\boldsymbol{m}_1$ is a unit normal to $\boldsymbol{t}$, $\boldsymbol{m}_2 = \boldsymbol{t} \times \boldsymbol{m}_1$, and k_1, k_2 are the *natural curvatures*. The natural frame is not unique, but any two such frames for the same oriented curve differ only by rotating $\boldsymbol{m}_1$ and $\boldsymbol{m}_2$ around $\boldsymbol{t}$ through an angle which is constant along the curve.

Any regular curve that is C^k for $k \geq 2$ has a C^{k-1} natural frame. When the curve also has a Frenet frame, and we suppose $\boldsymbol{n} = \cos\theta\, \boldsymbol{m}_1 + \sin\theta\, \boldsymbol{m}_2$, then $k_1 = \kappa \cos\theta, k_2 = \kappa \sin\theta$, and $\theta = \int \tau \, \mathrm{d}s$. Thus, a space curve is planar when its natural curvatures (k_1, k_2), when graphed in $\mathbb{R}^2$, lie along a fixed line through the origin. More generally, a space curve lies on a fixed sphere of radius ρ when (k_1, k_2) lie along a line distance $1/\rho$ from the origin.

The above congruence theorem is true for regular curves with degeneracies when suitably rephrased in terms of natural frames and natural curvatures.

The Hasimoto Correspondence

The vortex filament flow

$$\frac{\partial \gamma}{\partial t} = \frac{\partial \gamma}{\partial x} \times \frac{\partial^2 \gamma}{\partial x^2} \tag{VFF}$$

is an evolution equation for space curves that models the self-induced motion of a vortex filament in an ideal fluid taking only local effects into account. This model, originally formulated by L. Da Rios in 1906 (Ricca, 1996), is also known as the *localized induction approximation*. Note that if x is an arclength parameter at a given time, then it remains so for all t. We will take x as such, and then the right-hand side of (VFF) is κB when expressed in terms of the Frenet frame.

Hasimoto (1972) showed that solutions to this equation induce solutions to the focusing cubic nonlinear Schrödinger equation

$$\mathrm{i}q_t + q_{xx} + \tfrac{1}{2}|q|^2 q = 0, \tag{NLS}$$

by virtue of letting

$$q = \kappa \mathrm{e}^{\mathrm{i}\theta} \quad \text{with} \quad \theta = \int \tau \, \mathrm{d}s. \tag{H}$$

However, the "constant of integration" cannot be taken to be an arbitrary function of t; in fact, substituting (H) into (NLS) shows that we must have $\theta_t = \kappa^{-1}\ddot{\kappa} - \tau^2 + \frac{1}{2}\kappa^2$. Thus, $q(x, t)$ is unique up to multiplication by a unit modulus constant. Unfortunately, definition (H) for the Hasimoto map does not work at points of inflection (unless $\ddot{\kappa}$ vanishes to the same order as κ). However, it may be defined for arbitrary regular curves by using the natural curvatures of an evolving natural frame (see Calini, 2000, Section 1.4), whereupon $q = k_1 + \mathrm{i}k_2$.

DNA and White's Formula

At its lowest level of structure, DNA consists of two right-handed helices connected by base pairs, resembling the rungs of a twisted ladder. At lesser magnification the double helix, seen as a single strand, usually coils around itself in a left-handed fashion called *negative supercoiling*. Moreover, as the base pairs are separated during DNA replication and the ladder is untwisted, the supercoiling relaxes (becomes less negative) or may even reverse itself to become positive supercoiling. The dynamic interplay of these two levels of structure in DNA is governed by White's formula (White, 1970; Pohl, 1980). Although the formula, as stated below, applies only to closed loops of DNA (which occur in bacteria and in the mitochondria of some cells), it also governs the behavior of long strands of DNA, since in living cells the DNA is clamped to a protein scaffold at intervals of roughly 100,000 base pairs (Cozzarelli, 1992).

Let $\mathcal{C} \subset \mathbb{R}^3$ be a closed oriented regular curve and let $\boldsymbol{v}$ be a C^1 unit normal vector field along $\mathcal{C}$. (In DNA, we should regard $\mathcal{C}$ as one of the helices and $\boldsymbol{v}$ as pointing along the base pairs.) Let $\tilde{\mathcal{C}} = \mathcal{C} + \varepsilon \boldsymbol{v}$ have the same orientation. For $\varepsilon > 0$ sufficiently small, the linking number $\mathrm{Lk}(\mathcal{C}, \tilde{\mathcal{C}})$ is independent of ε and will be denoted by Lk. Define the total twist of $\boldsymbol{v}$ by the integral

$$\mathrm{Tw} = \frac{1}{2\pi} \int (\boldsymbol{t}, \boldsymbol{v}, \dot{\boldsymbol{v}}) \, \mathrm{d}s.$$

The twisting of $\boldsymbol{v}$ about γ obviously contributes to $\mathrm{Lk}(\mathcal{C}, \tilde{\mathcal{C}})$, but there is also a contribution independent of $\boldsymbol{v}$, due to the "writhing" of $\mathcal{C}$ about itself.

White's formula says that

$$\mathrm{Lk} = \mathrm{Tw} + \mathrm{Wr},$$

where Wr is the *writhe* of $\mathcal{C}$, defined as follows. On $D = \{(x, y) \in \mathcal{C} \times \mathcal{C} | x \neq y\}$, define the vector-valued function $\boldsymbol{e} = (x - y)/|x - y|$. Extend $\boldsymbol{e}$ continuously to the two components of ∂D, as the forward- and backward-pointing unit tangent vector. Then

$$\mathrm{Wr} = \frac{1}{4\pi} \int_{\overline{D}} \boldsymbol{e}^* \, \mathrm{d}S,$$

where $\mathrm{d}S$ is the standard element of area on the unit sphere S^2 and $\overline{D}$ is the closure of D. If s_1 and s_2 are arclength parameters on D, then we may also write

$$\mathrm{Wr} = \frac{1}{4\pi} \int \int \left(\boldsymbol{e}, \frac{\partial \boldsymbol{e}}{\partial s_1}, \frac{\partial \boldsymbol{e}}{\partial s_2} \right) \mathrm{d}s_1 \, \mathrm{d}s_2.$$

When $\mathcal{C}$ is nondegenerate and $\boldsymbol{v} = \boldsymbol{n}$, the Frenet normal, Lk is called the *self-linking* or *helicity* of $\mathcal{C}$, and White's formula specializes to

$$\mathrm{SL}(\mathcal{C}) = \mathrm{Wr} + \int \tau \, \mathrm{d}s,$$

a formula which was discovered much earlier by Calagareanu and later extended to regular closed curves (Pohl, 1980).

In DNA, with each base pair twisting the ladder by about 34°, Tw is positive and on the order of 10^5. The fact that DNA supercoiling is left-handed is reflected by a negative value of Wr, leading to a relatively small overall linking number. However, this number is rarely zero; the surgery that unlinks each of the two strands, a necessary step in cell division, is accomplished by enzymes known as *topoisomerases* (Sumners, 1995).

THOMAS A. IVEY

See also **DNA premelting; DNA solitons**

Further Reading

Bishop, R. 1975. There is more than one way to frame a curve. *American Mathematical Monthly*, 82: 246–251

Calini, A. 2000. Recent developments in integrable curve dynamics. In *Geometric Approaches to Differential Equations*, edited by P. Vassiliou & I. Lisle, Cambridge and New York: Cambridge University Press

Cozzarelli, N. 1992. Evolution of DNA topology: implications for its biological roles. In *New Scientific Applications of Geometry and Topology*, edited by D. Sumners, Providence, RI: American Mathematical Society

Hasimoto, H. 1972. A soliton on a vortex filament. *Journal of Fluid Mechanics*, 51: 477–485

Pohl, W. 1980. DNA and differential geometry. *Mathematical Intelligencer*, 3: 20–27

Ricca, R. 1996. The contributions of Da Rios and Levi–Civita to asymptotic potential theory and vortex filament dynamics. *Fluid Dynamical Research*, 18: 245–268

Sumners, D. 1995. Lifting the curtain: using topology to probe the hidden action of enzymes. *Notices of the American Mathematical Society*, 42: 528–537

White, J. 1970. Some differential invariants of submanifolds of Euclidean space. *Journal of Differential Geometry*, 4: 207–223

FRANCK–CONDON FACTOR

The concept of Franck–Condon transitions between electronic energy levels originates from the Born–Oppenheimer approximation, which adiabatically separates the fast electronic degrees of freedom of a molecule from the much slower nuclear degrees of freedom (since the nuclei are much heavier than the electrons, electronic motions occur as if the nuclei were fixed in place). Within the Born–Oppenheimer approximation, the total wave function $\Psi(q, Q)$ can be written as a product of an electronic and a nuclear (vibrational) wave function:

$$\Psi(q, Q) = \Psi^{(\mathrm{el})}(q; Q)\varphi^{(\mathrm{vib})}(Q), \tag{1}$$

where the electronic wave function $\Psi^{(\mathrm{el})}(q; Q)$ depends only parametrically on the nuclear coordinates Q. One first calculates the electronic eigenstates for a particular nuclear configuration Q, which is assumed to be fixed in space, and assembles electronic potential energy surfaces by varying the nuclear coordinates Q step-by-step. The nuclear wave function is subsequently calculated by solving the Schrödinger equation on these potential energy surfaces, assuming that the electrons can adapt adiabatically to a changing nuclear configuration.

As usual, the intensity of a transition between two electronic states k and l with vibrational quanta n and m is given by the transition dipole matrix element

$$\mu^2_{kn,lm} = \langle \Psi_{k,n} | \hat{\mu} | \Psi_{l,m} \rangle^2 = \left(\frac{\partial \mu}{\partial q} \right)^2 \langle \Psi_{k,n} | \hat{q} | \Psi_{l,m} \rangle^2. \tag{2}$$

When incorporating the product wave function of Equation (1), we obtain

$$\mu^2_{kn,lm} = \left(\frac{\partial \mu}{\partial q} \right)^2 \langle \Psi^{(\mathrm{el})}_k | \hat{q} | \Psi^{(\mathrm{el})}_l \rangle^2 \langle \varphi^{(\mathrm{vib})}_{k,n} | \varphi^{(\mathrm{vib})}_{l,m} \rangle^2 . \tag{3}$$

The transition dipole matrix element separates into a product because (a) the transition dipole operator $\partial \mu / \partial q \cdot \hat{q}$ acts on the electronic coordinates q only and (b) we have assumed that the transition dipole operator does not depend on the nuclear coordinate Q (*Franck–Condon approximation*). The second term $\langle \varphi^{(\mathrm{vib})}_{k,n} | \varphi^{(\mathrm{vib})}_{l,m} \rangle^2$ is the *Franck–Condon factor*.

Figure 1a shows possible transitions between two electronic potential energy surfaces (S_0 and S_1). At not too high temperatures, only the vibrational ground state $\nu = 0$ in the electronic ground state S_0 will be populated. When both potential energy surfaces have the same shape and their lowest points are not displaced, the Franck–Condon factors $\langle \varphi^{(\mathrm{vib})}_n | \varphi^{(\mathrm{vib})}_m \rangle^2$ reduce to the condition of orthonormality of the vibrational eigenstates (i.e., the vibrational wave functions are the same on both potential energy surfaces). Hence, in that case, only the $\nu = 0 \rightarrow \nu' = 0$ transition (the *zero-phonon transition*) carries oscillator strength, while all others are dark. However, when both potential energy surfaces are displaced (i.e., the excited state has a different nuclear coordinate to the ground state), the absorption spectrum will consist of a series of absorption lines (a Franck–Condon progression) as depicted in Figure 1b. The intensity of these lines scales with the Frank–Condon factors $\langle \varphi^{(\mathrm{vib})}_{k,n} | \varphi^{(\mathrm{vib})}_{l,m} \rangle^2$. In the spectra of Figure 1b, the energy origin relates to the frequency of the zero-phonon transition, and

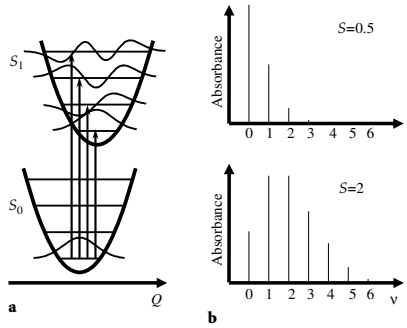

Figure 1. (a) Displaced potential energy surfaces of the electronic ground state S_0 and the first electronic excited state S_1 with the possible transitions depicted at a temperature of 0 K. The overlap integrals $\langle\varphi_i^{(\mathrm{vib})}|\varphi_j'^{(\mathrm{vib})}\rangle^2$ of the vibrational wave functions in both electronic states determine the strength of the individual absorption lines. (b) Absorption spectra for Huang–Rhys parameters $S = 0.5$ and 2, respectively.

the energy spacing between the various lines is given by the frequency ω of the oscillator. We call normal modes with such a displacement of the potential energy surfaces Franck–Condon active modes.

An analytic expression for the Franck–Condon factors can be given when the potential energy surfaces are assumed to be harmonic (as in Figure 1a):

$$V_{S_0} = \frac{1}{2}\hbar\omega Q^2,$$
$$V_{S_1} = E_{01} + \frac{1}{2}\hbar\omega Q^2 - \bar{x}\hbar\omega Q, \qquad (4)$$

where Q is the dimensionless oscillator coordinate, E_{01} the energy separation between the electronic ground and first excited states at $Q = 0$, and ω the vibrational frequency. The dimensionless displacement $\bar{x}$ between potential energy surfaces is a measure of the strength of the coupling between electronic and vibrational transition. It is common to introduce an alternative coupling parameter, the Huang–Rhys parameter:

$$S \equiv \frac{x^2}{2} \qquad (5)$$

with which the Franck–Condon factors can be expressed as (Fitchen, 1968)

$$\langle\varphi_{S_1,n}^{(\mathrm{vib})}|\varphi_{S_0,m}^{(\mathrm{vib})}\rangle^2 = \mathrm{e}^{-S}\frac{m!}{n!}S^{n-m}\left[L_m^{n-m}(S)\right]^2, \qquad (6)$$

where $L_j^{i-j}(S)$ are the Laguerre polynominals. For the important case where $T = 0$ K, the only occupied initial level is $m = 0$ and $L_0^n(S) = 1$, and we obtain

$$\langle\varphi_{S_1,n}^{(\mathrm{vib})}|\varphi_{S_0,0}^{(\mathrm{vib})}\rangle^2 = \frac{S^n}{n!}\mathrm{e}^{-S}. \qquad (7)$$

For $S < 1$, the zero phonon line is the most intense transition, while for larger displacements, $S > 1$, the intensity is shifted toward transitions with higher vibrational quanta on the electronically excited state S_1 (Figure 1b). This finding can be explained in simple words with the Franck–Condon principle, which states that in a classical picture, an electronic transition occurs very quickly and is most likely to occur without changes in the positions of the nuclei. Hence, the transition is vertical from the bottom of the S_0 potential energy surface to the S_1 surface. The quantum mechanical formulation of this principle is that the intensity of a vibronic transition is proportional to the square of the overlap integral between the vibrational wave functions of the two states that are involved in the transition.

The concept of a Franck–Condon transition was originally formulated for electronic states. However, it can be used in a more general sense and appears whenever an adiabatic separation of timescales can be made between two molecular degrees of freedom. For example, this is the case when a high-frequency vibrational mode is coupled to a low-frequency vibrational mode. In that case, $\Psi^{(\mathrm{el})}$ in the expressions above is replaced by the wave function of the high-frequency mode, but the rest of the formalism remains unchanged. Most prominent examples are hydrogen bonds XH$\cdots$Y, where the high-frequency X$-$H stretching vibration is coupled to the low-frequency XH$\cdots$Y hydrogen bond vibration. One of the striking features of hydrogen bonds is an extraordinarily large anharmonic coupling between both modes that leads to a Franck–Condon-like progression in the absorption spectrum of the X$-$H stretching band.

PETER HAMM

See also **Color centers; Hydrogen bond**

Further Reading

Fitchen, D.B. 1968. Zero-phonon transitions. In *Physics of Color Centers*, edited by W.B. Fowler, New York: Academic Press, pp. 293–350

FREDHOLM THEOREM

The Fredholm theorem gives a necessary and sufficient condition for the existence of a solution to a linear equation of the form $A\boldsymbol{x} = \boldsymbol{y}$, where A is a linear operator and $\boldsymbol{x}$ and $\boldsymbol{y}$ are vectors. Consider the matrix

$$A = \begin{pmatrix} 1 & 4 & 5 \\ 2 & 5 & 7 \\ 3 & 6 & 9 \end{pmatrix}, \qquad (1)$$

and the linear map $\mathcal{F}$, which associates the vector $A\boldsymbol{x}$ to each vector $\boldsymbol{x}$ in $\mathbb{R}^3$. If x_i, $i = 1 \ldots 3$, are the

components of $\boldsymbol{x}$, we have

$$\mathcal{F}\boldsymbol{x} = A\boldsymbol{x} = x_1 \begin{pmatrix} 1 \\ 2 \\ 3 \end{pmatrix} + x_2 \begin{pmatrix} 4 \\ 5 \\ 6 \end{pmatrix} + x_3 \begin{pmatrix} 5 \\ 7 \\ 9 \end{pmatrix} = (x_1 + x_3) \begin{pmatrix} 1 \\ 2 \\ 3 \end{pmatrix} + (x_2 + x_3) \begin{pmatrix} 4 \\ 5 \\ 6 \end{pmatrix}. \tag{2}$$

The third equality comes from the fact that the last column of A can be written as the sum of its first two columns. It is then clear that the equation $\mathcal{F}\boldsymbol{x} = \boldsymbol{y}$ has a solution if and only if $\boldsymbol{y}$ is a linear combination of the first two columns of A. In this case, there is more than one solution because the kernel or null space of A is not trivial.

If we equip $\mathbb{R}^3$ with the inner product $\langle \boldsymbol{x}, \boldsymbol{y} \rangle = \sum_{i=1}^{3} x_i\, y_i$, the transpose A^{T} of A, defined by $\{A^{\mathrm{T}}\}_{ij} = \{A\}_{ji}$, is such that

$$\langle A\boldsymbol{x}, \boldsymbol{v} \rangle = \langle \boldsymbol{x}, A^{\mathrm{T}}\boldsymbol{v} \rangle, \tag{3}$$

for any two vectors $\boldsymbol{x}$ and $\boldsymbol{v}$ in $\mathbb{R}^3$. This equality shows that $\boldsymbol{v}$ is orthogonal to the range of A (i.e., $\langle A\boldsymbol{x}, \boldsymbol{v} \rangle = \boldsymbol{0}$ for every $\boldsymbol{x}$ in $\mathbb{R}^3$) if and only if $\boldsymbol{v}$ is in the kernel of A^{T}; that is, $A^{\mathrm{T}}\boldsymbol{v} = \boldsymbol{0}$. As a consequence, the existence of a solution to the equation $\mathcal{F}\boldsymbol{x} = \boldsymbol{y}$ (i.e., $A\boldsymbol{x} = \boldsymbol{y}$), which is equivalent to $\boldsymbol{y}$ being in the range of A, can be restated as $\boldsymbol{y}$ being orthogonal to the kernel of A^{T}. This is the contents of the Fredholm theorem, which is often presented as the following alternative theorem.

Fredholm alternative: For a matrix A, either the equation $A\boldsymbol{x} = \boldsymbol{y}$ always has a solution or the kernel of A^* is nontrivial. Here A^* is the adjoint of A, which is its transpose (resp. Hermitian transpose) if A has real (resp. complex) entries. The Fredholm alternative can be stated in a similar fashion for a special class of infinite-dimensional linear operators. In this case, $A = \lambda I - \mathcal{L}$, where $\mathcal{L}$ is a compact operator, λ is a nonzero complex number, and I is the identity operator (see for instance Reed & Simon, 1980; Kreyszig, 1989; Dunford & Schwartz, 1988).

Applications of this theorem involve multiple scales analysis and perturbation theory. Assume for instance that we want to solve the eigenvalue problem $\mathcal{L}\boldsymbol{x} = \lambda\boldsymbol{x}$, where the linear operator $\mathcal{L}$ can be written as $\mathcal{L} = \mathcal{L}_0 + \varepsilon\mathcal{L}_1$ and ε is a small parameter. If we look for expansions of the eigenvector $\boldsymbol{x} = \boldsymbol{x}_0 + \varepsilon\boldsymbol{x}_1 + \cdots$ and eigenvalue $\lambda = \lambda_0 + \varepsilon\lambda_1 + \cdots$ in powers of ε, substitute in the equation, and equate the left-and right-hand sides at each power of ε, we obtain a hierarchy of linear equations of the form

$$(\mathcal{L}_0 - \lambda_0 I)\, \boldsymbol{x}_i = \mathcal{J}_i, \quad i = 0,\, 1,\, \ldots, \tag{4}$$

where I is the identity operator and the right-hand side, $\mathcal{J}_i$, of (4) only depends on $\boldsymbol{x}_k$ for $k < i$. In particular, $\mathcal{J}_0 = \boldsymbol{0}$ and $\mathcal{J}_1 = \lambda_1\boldsymbol{x}_0 - \mathcal{L}_1\boldsymbol{x}_0$. At each step of this iterative process, the linear equation $(\mathcal{L}_0 - \lambda_0 I)\, \boldsymbol{x}_i = \mathcal{J}_i$ has a solution if and only if $\mathcal{J}_i$ is orthogonal to the kernel of the adjoint of $\mathcal{L}_0 - \lambda_0 I$. This typically gives the value of the coefficient λ_i of the expansion of the eigenvalue λ in powers of ε. Once λ_i is known, one can then solve the equation $(\mathcal{L}_0 - \lambda_0 I)\, \boldsymbol{x}_i = \mathcal{J}_i$ for $\boldsymbol{x}_i$. A similar method can be applied to solve equations of the form

$$\mathcal{L}\boldsymbol{x} = \mathcal{G}(\boldsymbol{x}), \tag{5}$$

where $\mathcal{L} = \mathcal{L}_0 + \varepsilon\mathcal{L}_1$ and $\mathcal{G}$ is a nonlinear function of $\boldsymbol{x}$. Such equations are often encountered in bifurcation theory. Assume for instance that $\mathcal{G}$ is polynomial, say $\mathcal{G} = \langle \boldsymbol{x}, \boldsymbol{x} \rangle \boldsymbol{x}$, and that one knows a solution $\boldsymbol{x}_0$ to the linear equation $\mathcal{L}_0\boldsymbol{x}_0 = \boldsymbol{0}$. Small-amplitude solutions to the nonlinear problem can be approximated by introducing a small parameter that measures the size of $\boldsymbol{x}$ and rescaling. For instance, the scaling $\boldsymbol{x} = \sqrt{\varepsilon}\, \boldsymbol{y}$ turns (5) into $(\mathcal{L}_0 + \varepsilon\mathcal{L}_1)\, \boldsymbol{y} = \varepsilon \langle \boldsymbol{y}, \boldsymbol{y} \rangle \boldsymbol{y}$. A solution of the form $\boldsymbol{y} = \boldsymbol{y}_0 + \varepsilon\boldsymbol{y}_1 + \cdots$ can then be sought, using an iterative process similar to the one discussed above.

JOCELINE LEGA

See also **Perturbation theory**

Further Reading

Dunford, D. & Schwartz, J.T. 1988. *Linear Operators. Part I: General Theory*, New York and Chichester: Wiley

Kreyszig, E. 1989. *Introductory Functional Analysis with Applications*, New York and Chichester: Wiley

Reed, M. & Simon, B. 1980. *Methods of Modern Mathematical Physics. I. Functional Analysis*, Boston and London: Academic Press

FREE ENERGY

The concept of "free energy" is a key concept to characterize physically relevant states in statistical mechanics (see, e.g., Mandl, 1988; Reichl, 1998). Given an equilibrium system of statistical mechanics with energy levels E_i of the microstates i, the (Helmholtz) free energy F is defined as

$$F(\beta) = -\frac{1}{\beta} \log Z(\beta), \tag{1}$$

where

$$Z(\beta) = \sum_i \mathrm{e}^{-\beta E_i} \tag{2}$$

is the partition function and β is the inverse temperature. Apparently, the free energy is different from the internal energy U given by

$$U = -\frac{\partial}{\partial\beta} \log Z(\beta) = \langle E_i \rangle. \tag{3}$$

The difference is given by the entropy S times the absolute temperature T:

$$F = U - TS. \tag{4}$$

This equation can also be regarded as describing a Legendre transformation from U to F. Equilibrium states minimize the free energy (rather than the internal energy)—in this sense F is more relevant than U. The minimum of F can be achieved in two contrasting ways, either by making the internal energy U small, or by making the entropy S large (or both). Changes of the free energy are related to the maximum amount of work a system can do at constant pressure and temperature.

The basic principle underlying statistical mechanics, the maximum entropy principle, can also be formulated as a "principle of minimum free energy" (Beck & Schlögl, 1993). In this formulation, one starts from fixed intensive quantities (e.g., the inverse temperature β) and considers a free energy function $F[p]$ as a function of an a priori arbitrary set of probabilities $[p] = \{p_1, p_2, \ldots\}$. The probabilities p_i can describe any state, for example, also non-equilibrium and nonthermal states. One then requires

$$F[p] = \sum_i p_i E_i + \beta^{-1} p_i \log p_i = U - \beta^{-1} S \quad (5)$$

to have a minimum in the space of all possible probability distributions. This minimum is achieved for the canonical distribution

$$p_i = \frac{1}{Z} \mathrm{e}^{-\beta E_i}. \quad (6)$$

There are straightforward generalizations of this principle for systems with several intensive quantities, for example, grand canonical ensembles.

For nonlinear dynamical systems, the concept of free energy is often seen in a much broader sense. Various generalized types of free energies can be defined. A key ingredient for this more general approach is the so-called thermodynamic formalism of dynamical systems (Beck & Schlögl, 1993). One defines partition functions that contain information on certain fluctuating quantities associated with the dynamical system, for example, local singularities of the invariant density or local Lyapunov exponents. To proceed to a (formal) statistical mechanics description, one then defines a free energy function for these partition functions quite analogous to Equation (1).

Examples are "static," "dynamic," and "expansion" free energies of dynamical systems, as well as the so-called "topological pressure." Let us here consider the static free energy in somewhat more detail. This free energy function contains information on the spectrum of singularities of the invariant density of the dynamical system and is closely related to very important quantities that characterize multifractals, the so-called Rényi dimensions. One covers the attractor (or repeller) under consideration with small d-dimensional cubes ("boxes") of volume ε^d, where d is an integer dimension large enough to embed the attractor. The static partition function is then defined as

$$Z(\beta) = \sum_i p_i^\beta = \sum_i \mathrm{e}^{-\beta \alpha_i V}, \quad (7)$$

where p_i is the invariant probability measure associated with box i and β is a formal "inverse temperature" parameter. To illustrate the similarities with statistical mechanics, we have written in the above equation $p_i =: \varepsilon^{\alpha_i} = e^{-\alpha_i \cdot V}$, where α_i is like a fluctuating energy associated with each box i and $V = -\log \varepsilon$ plays the role of a formal volume variable. One can then study the free energy density associated with this partition function,

$$f(\beta) := \lim_{V \to \infty} -\frac{1}{\beta V} \log Z(\beta). \quad (8)$$

This static free energy, up to a trivial factor, is indeed identical with the Rényi dimensions D_β:

$$f(\beta) = \frac{\beta - 1}{\beta} D_\beta. \quad (9)$$

In this way, methods borrowed from statistical mechanics play an important role for the statistical description of dynamical systems.

While the above generalized free energies, of relevance for nonlinear dynamical systems, have only formal analogies with conventional free energies, a more fundamental generalization of statistical mechanics suitable for complex systems has been suggested by Tsallis (1988). In this so-called non-extensive statistical mechanics approach (Abe & Okamoto, 2001; Kaniadakis et al., 2002), the entire formalism of statistical mechanics is generalized by starting from more general entropy measures, the Tsallis entropies. These are defined by

$$S_q = \frac{1}{q-1} \left(1 - \sum_i p_i^q \right). \quad (10)$$

Here the p_i are probabilities associated with the microstates i of a physical system. Note that the Tsallis entropies look somewhat similar to the Rényi information measures but are indeed different (there is no logarithm). The parameter q, called "entropic index," can take on any real value but is in practice often close to 1. For $q \to 1$, one can easily check that the Tsallis entropies reduce to the ordinary Shannon entropy $S_1 = -\sum_i p_i \log p_i$. The principal idea of non-extensive statistical mechanics is to do everything we know from ordinary statistical mechanics, but start from the more general entropy measures. Naturally, ordinary statistical mechanics is contained as a special case ($q = 1$) in this more general formalism.

The maximum entropy principle yields power-law generalizations of the canonical ensemble,

$$p_i = \frac{1}{Z_q(\beta)}(1 + (q-1)\beta E_i)^{-1/(q-1)}, \qquad (11)$$

which reduce to Equation (6) for $q \to 1$. As a consequence, there is then also a more general free energy $F_q(\beta)$, which is parametrized by the entropic index q. One can basically show that the entire formalism of thermodynamics has simple q-generalizations, for example, for the generalized free energy there is a relation of the form

$$F_q = U_q - TS_q, \qquad (12)$$

where the index q indicates that the q-generalized canonical ensemble is chosen. This type of formalism has interesting physical applications, for example, for fully developed turbulence and for scattering processes in high-energy physics (Beck, 2002).

CHRISTIAN BECK

See also **Chaotic dynamics; Dimensions; Entropy; Fractals; Multifractal analysis**

Further Reading

Abe, S. & Okamoto, Y. (editors). 2001. *Nonextensive Statistical Mechanics and Its Applications*, Berlin and New York: Springer

Beck, C. & Schlögl, F. 1993. *Thermodynamics of Chaotic Systems*, Cambridge and New York: Cambridge University Press

Beck, C. 2002. Nonextensive methods in turbulence and particle physics. *Physica A*, 305: 209-217

Kaniadakis, G., Lissia, M. & Rapisarda, A. (editors). 2002. *Nonextensive Thermodynamics and Physical Applications*, Physica A, 305 (special volume)

Mandl, F. 1988. *Statistical Physics*, 2nd edition, Chichester and New York: Wiley

Reichl, L.E. 1998. *A Modern Course in Statistical Physics*, 2nd edition, New York: Wiley

Tsallis, C. 1988. Possible generalization of Boltzmann–Gibbs statistics. *Journal of Statistical Physics*, 52: 479-487

FREE PROBABILITY THEORY

A new probabilistic context emerged in the 1980s (Voiculescu, 1985) from studies in operator algebras, a mathematical subject with ties to quantum physics. Free probability theory (FPT) is developing along a parallel to the basics of usual probability theory, drawn from assumptions designed for quantities with the highest degree of noncommutativity. FPT has turned out to have important connections to random matrix theory (Voiculescu, 1991) as well as to some combinatorics (Speicher, 1998) and to certain models in physics (Voiculescu, 1997).

To introduce FPT, one takes the view that "a probability theory" deals with expectation values $\varphi(a)$ for the elements a, called random variables, of a set A endowed with operations of addition, multiplication, and multiplication by scalars. We may describe FPT as noncommutative probability theory (i.e., the products ab and ba can be different for $a, b \in A$) with independence defined by a new relation called free independence. In usual probability theory, A consists of numerical functions on some space of events and clearly $ab = ba$ in this case. By contrast, noncommutative probability occurs typically when A consists of quantum mechanical observables Q. These are linear operators on a vector space $\mathcal{H}$ with an inner product $\langle \cdot, \cdot \rangle$ and $\varphi(Q) = \langle Q\xi, \xi \rangle$ where $\xi \in \mathcal{H}$ is a fixed vector with $\langle \xi, \xi \rangle = 1$. Under quantum mechanics, the usual definition of independence of Q_1 and Q_2 requires commutation $Q_1Q_2 = Q_2Q_1$ and $\varphi(f(Q_1)g(Q_2)) = \varphi(f(Q_1))\varphi(g(Q_2))$ for polynomials f and g. Free independence of Q_1, Q_2, by contrast requires that

$$\varphi(\dots f(Q_1)g(Q_2)h(Q_1)\dots) = 0 \qquad (1)$$

whenever

$$\dots, \varphi(f(Q_1)) = 0, \varphi(g(Q_2)) = 0, \quad \varphi(h(Q_1)) = 0, \dots, \qquad (2)$$

where $\dots, f, g, h, \dots$ are polynomials and Q_1, Q_2 alternate as arguments. The definition of free independence extends to sets of variables by replacing the one-variable polynomials $f, g, h, \dots$ by corresponding polynomials in noncommuting variables from those sets. Note that if Q_1, Q_2 satisfy free independence, then in most cases $Q_1Q_2 \neq Q_2Q_1$.

The FPT analogue of the central limit theorem (Voiculescu, 1985; Voiculescu et al., 1992) states $\varphi(Q_j) = 0$, $\varphi(Q_j^2) = 1$ and $|\varphi(Q_j^k)| \leq C_k$, then

$$S_n = n^{-1/2}(Q_1 + \dots + Q_n) \qquad (3)$$

will have in the limit, the moments of a semicircle distribution, that is,

$$\lim_{n\to\infty} \varphi(S_n^k) = (2\pi)^{-1} \int_{-2}^{2} t^k (4 - t^2)^{1/2}\, \mathrm{d}t. \qquad (4)$$

Many other topics in classical probability theory have FPT analogs. The list includes the following (Voiculescu et al., 1992; Biane & Speicher, 1998; Voiculescu, 2002):

- Addition and multiplication of freely independent random variables corresponds to highly nonlinear free convolution operations on the distributions.
- The FPT infinitely divisible laws and stable laws have been classified, and there are corresponding processes with free increments.
- Semicircular processes are the FPT analog of Gaussian processes, and in particular there is a concept of free Brownian motion.
- There are stochastic integrals with respect to free Brownian motion.

- There is a free entropy theory that deals with FPT analogues of Shannon's differential entropy and of the Fisher information.

The semicircle distribution, which plays the role of the Gauss law in FPT, was well known from Wigner's work as the limit-distribution of eigenvalues of large symmetric random matrices with independent identically distributed Gaussian entries (the Gaussian orthogonal ensemble). The explanation of this surprising coincidence was found to be that free independence often occurs asymptotically among large random matrices (Voiculescu, 1991). For instance, if for each n we are given two sets $\{A_1^{(n)}, \ldots, A_m^{(n)}\}$ and $\{B_1^{(n)}, \ldots, B_p^{(n)}\}$ of $n \times n$ Hermitian random matrices, then the requirement that their joint distribution (as matrix-valued random variables) be the same as that of $\{UA_1^{(n)}U^{-1}, \ldots, UA_m^{(n)}U^{-1}, B_1^{(n)}, \ldots, B_p^{(n)}\}$ for all unitary matrices U is the key to asymptotic free independence of the two sets (Voiculescu, 1998). For $n \times n$ random matrices T, the expectation functional is $\varphi_n(T) = n^{-1}E(TrT)$, where E denotes the expectation of the numerical random variable TrT. Asymptotic free independence means the equalities of free independence hold after taking the limit $n \to \infty$.

A random matrix T is thus a classical matrix-valued random variable and at the same time a noncommutative random variable. Passing to the noncommutative context discards information about the entries, since the expectation values $\varphi_n(T^k)$ remember only the eigenvalue distribution of T.

Asymptotic free independence results for random matrices imply that their limit behavior is governed by FPT. For instance, for the sum or product of random matrices satisfying free independence asymptotically, the limit distribution of eigenvalues is computed by the free convolution operations.

Among the simplest cases of asymptotic free independence are a pair of independent matrices from the Gaussian ensembles or a constant matrix and one from a Gaussian ensemble. Also, if X_n is a rectangular $[\alpha n] \times n$ Gaussian random matrix with independent and identically distributed (i.i.d.) entries, then $X_n^* X_n$ and a constant $n \times n$ random matrix will exhibit asymptotic free independence. Besides these simplest instances of asymptotic free independence, there are many others involving unitary matrices, random permutation matrices or matrices with non-Gaussian i.i.d. entries (Voiculescu, 2000). Also, Gaussian random band-matrices can be handled with more involved FPT techniques (Shlyakhtenko, 1996). Most asymptotic free independence results for complex Hermitian or unitary matrices also hold for real symmetric or orthogonal matrices. The differences between distributions of eigenvalue spacings between the real and complex cases occur at another scale, which is wiped out by taking the limit of the φ_n as $n \to \infty$.

FPT methods have also been used for physics models related to asymptotics of random matrices, like the large N Yang–Mills two-dimensional quantum chromodynamics in papers of I.M. Singer, R. Gopakumar and D. Gross, and M. Douglas (Voiculescu, 1997). Also occurring in physics are multimatrix-models, corresponding to ensembles of k-tuples of $N \times N$-matrices with the densities $c_N \exp(-NTrP(T_1, \ldots, T_k))$ that have connections to the analog of entropy in FPT (Voiculescu, 2002). An indication about where FPT and quantum field theory connect is given by the combinatorial approach to FPT (Speicher, 1998) that deals with noncrossing partitions of $\{1, \ldots, n\}$, that is, with planar Feynman diagrams.

DAN VIRGIL VOICULESCU

See also **Quantum field theory; Random matrix theory I, II, III, IV**

Further Reading

Biane, P. & Speicher, R. 1998. Stochastic calculus with respect to free Brownian motion and analysis on Wigner space. *Probability Theory and Related Fields*, 112: 373–409

Shlyakhtenko, D. 1996. Random Gaussian band matrices and freeness with amalgamation. *International Mathematics Research Notices*, 20: 1013–1025

Speicher, R. 1998. Combinatorial theory of the free product with amalgamation and operator-valued free probability theory. *Memoirs of the American Mathematical Society*, 627

Voiculescu, D. 1985. Symmetries of some reduced free product C^*-algebras. In *Operator Algebras and Their Connections with Topology and Ergodic Theory*, edited by H. Araki et al., Berlin and New York: Springer

Voiculescu, D. 1991. Limit laws for random matrices and free products. *Inventiones Mathematicae*, 104: 201–220

Voiculescu, D.V. (editor). 1997. *Free Probability Theory*, Providence, RI: American Mathematical Society

Voiculescu, D. 1998. A strengthened asymptotic freeness result for random matrices with applications to free entropy. *International Mathematics Research Notices*: 41–63

Voiculescu, D. 2000. Lectures on free probability theory. In *Lectures on Probability Theory and Statistics, École d'Été de Probabilities de Saint–Flour XXVIII –1998*, edited by M. Emery, A. Nemirovski & D. Voiculescu, New York: Springer

Voiculescu, D. 2002. Free entropy. *Bulletin of the London Mathematical Society*, 34: 257–278

Voiculescu, D.V., Dykema, K.J. & Nica, A.M. 1992. *Free Random Variables*, Providence, RI: American Mathematical Society

FRENKEL–KONTOROVA MODEL

In 1938, Yakob Frenkel and Tatiana Kontorova developed in some detail a model originally proposed by Ulrich Dehlinger (see Nabarro, 1967) for studying stationary dislocations in a crystal, and its motion. A perfect crystalline (regular lattice) solid subjected to small deformations returns to a perfect lattice arrangement of atoms after the forces causing the deformations are released. This regime of small

deformations is called "elastic." Larger deformations can lead to rearrangements of the crystal lattice. In this other regime, called "plastic," the perfect lattice is not restored after tension is released. The attempt to describe the energetics involved in those irreversible rearrangements (or lattice dislocations, see Figure 1(b)) led to the posing of a theoretical physics problem of a discrete elastic one-dimensional field of displacements (atomic positions) experiencing a spatially periodic potential (Dehlinger, 1929; Frenkel & Kontorova, 1939; Frank & Van der Merwe, 1949). Figure 1(c) shows a schematic representation of Dehlinger's *Verhakung* (interlocking), as he named his idea.

The Frenkel–Kontorova (FK) model has been used for modeling nanostructural properties of adsorbed monolayers of atoms on crystalline surfaces, nonlinear magnetic excitations in magnets, ionic conductors, and many other solid-state physics problems. Today it has become a textbook mathematical model with direct applications in condensed matter, statistical physics, nonlinear fields, and material science, often under different names, notably the "discrete sine-Gordon" or "periodic Klein–Gordon" equation.

The Generalized Frenkel–Kontorova Model

In the generalized FK model, a discrete one-dimensional field (u_n) $(-\infty < n < +\infty)$, has a potential energy density

$$H(u_{n+1}, u_n) = K\,V(u_n) + W(\Delta u_n), \qquad (1)$$

where $W(\Delta u)$ is the interaction between neighbor components of the field, $V(u)$ is a periodic function $V(u+1) = V(u)$, and K is a parameter controlling the relative strength of both (V and W) contributions to the energy density.

The standard version of the model corresponds to the simplest choices of sinusoidal on-site potential V and harmonic spring interaction W:

$$V = \frac{1}{(2\pi)^2}\,[1 - \cos(2\pi u)]\,,$$

$$W(\Delta u) = \frac{1}{2}\,(\Delta u)^2 - \sigma\,\Delta u, \qquad (2)$$

where σ is the unstretched length of the spring, the value at which W is a minimum.

Keeping V as above, the following choice for W

$$W = \frac{1}{(2\pi)^2}\left[1 - \cos(2\pi(\Delta u - \gamma))\right] \qquad (3)$$

(known as a "chiral XY model" in a magnetic field) models a system of magnetic moments with strong planar (XY) anisotropy (here described by the angles $2\pi u_n$), with chiral (preferred relative angle γ) interactions W, and K in Equation (1) measuring the intensity of the external magnetic field. Other choices are motivated by different physical situations of interest.

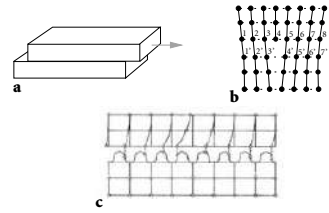

Figure 1. (a) Schematic net outcome of a plastic deformation. Relative shift between layers does not occur uniformly: The slip process can take place sequentially by the mechanism of dislocation motion shown in (b). (c) Dehlinger's picture of the imperfection, that he named *Verhakung*, where the atoms of the upper row, in this displacement, experience a periodic potential on account of their interaction with atoms in the lower row.

To complete the formal definition of the generalized FK model, one must define its time evolution and this choice depends on the specific application one has in mind. The standard model with Hamiltonian dynamics

$$\frac{\mathrm{d}^2 u_n}{\mathrm{d}t^2} = u_{n+1} - 2u_n + u_{n-1} - \frac{K}{2\pi}\sin(2\pi u_n) \qquad (4)$$

corresponds to the simplest discretized version of the integrable partial differential equation known as sine-Gordon (SG):

$$\frac{\mathrm{d}^2 u}{\mathrm{d}t^2} = \frac{\mathrm{d}^2 u}{\mathrm{d}x^2} - \sin(2\pi u). \qquad (5)$$

This justifies the name of "discrete SG model" often used for the FK model.

Some physical applications, for example, in Josephson junction devices, suggest introducing dissipative terms in Equation (4) (involving first-time derivatives $\dot{u}_n$) and more complicated functional forms of the right-hand-side dependence on u_n and u_{n+1}. The richness of dynamical behaviors shown by the different dynamical FK models is a continuing source of interest in both theory development and applications (Braun & Kivshar, 1998, 2004; Floría & Mazo, 1996).

The Equilibrium Problem for Convex FK Models

A simpler problem, but quite complex, is the characterization of equilibrium properties of the generalized FK model. The physical motivation for studying this problem comes mainly from the observed abundance of modulated phases in minerals and man-made materials

and compounds, and the need to understand the peculiar multiphase diagrams shown by experimental studies.

For the case in which W is not a convex function, like the chiral XY example above, the difficulties of a complete rigorous characterization of equilibria are much greater than in the case of convex W interaction. For the latter, Aubry's work allowed a satisfactory theory in the infinite system size (thermodynamic) limit, by showing a one-to-one correspondence between equilibrium configurations (u_n), which satisfy the (force-equilibrium) equations

$$\frac{\partial(H(u_n, u_{n-1}) + H(u_{n+1}, u_n))}{\partial u_n} = 0 \qquad (6)$$

and orbits of a symplectic twist map of the cylinder.

When an equilibrium configuration is such that any segment of length $L = M - N + 1$, $(u_N, \ldots, u_M)$, can only increase its energy as result of arbitrary fluctuations of $u_{N+1}, \ldots, u_{M-1}$, the field configuration is called a minimum energy configuration (MEC).

There are two types of MEC, which are both recurrent—meaning that given any integer p and any number $\varepsilon > 0$, there are integers m and $q > 0$ such that both inequalities: $|u_{p+q} - u_p - m| < \varepsilon$ and $|u_{p+q+1} - u_{p+1} - m| < \varepsilon$ are satisfied. These two types of recurrent MEC are called commensurate (or periodic) phases and incommensurate (or quasi-periodic) phases, respectively. Remarkably, there are nonrecurrent MECs, which are rigorous discrete versions of the soliton solutions of continuous partial differential equations (like the integrable sine-Gordon model). These are called "discommensurations" or "homoclinic field configurations," and they correspond to the original motivation (Dehlinger's *Verhakung*) of the FK model: localized dislocations over the recurrent (periodic or quasi-periodic) substrate phase.

Commensurate Phases

These are periodic configurations with rational p/q average spacing ω (defined as $\lim_{L\to\infty}(u_M - u_N)/L$), where $u_{n+p} - q = u_n$. Such field configurations are generically pinned, meaning that one has to put some finite energy E_{PN} on the system to displace the configuration over the path-dependent barriers of energy (called "Peierls–Nabarro barriers") separating configurations that are equivalent by translations σ_{mn}.

A pinned configuration has a finite coherence length (or decay range) ξ of fluctuations, meaning that if a field component (the center u_{n_0}) is kept displaced by an external force, the rest of components u_n are displaced with exponentially decaying amplitude $\exp(-|n - n_0|/\xi)$. Also, the linear spectrum of small oscillations (phonon spectrum) of a pinned configuration has a finite gap $\Delta > 0$.

Incommensurate or Quasi-periodic Phases

Recurrent configurations with irrational average spacing ω can be viewed as limits of sequences of periodic phases of mean spacing $\omega_n \to \omega$ as $n \to \infty$. The physical properties of these structures depend on the parameter K of the model: For each irrational ω there is a critical value $K_c(\omega)$ such that:

- For $K < K_c$, the quasi-periodic MEC is sliding (unpinned), so that $E_{\mathrm{PN}} = 0$. Consequently, localized induced fluctuations extend through the system so that the decay range diverge, $\xi \to \infty$. The spectrum of phonons of a sliding configuration is gapless, $\Delta = 0$. The distribution function of the fractional parts $\mathrm{Frac}(u_n)$ in this phase is a continuous function.
- For $K > K_c$, the incommensurate phase is pinned, $E_{\mathrm{PN}} > 0$, the decay range is finite, and a gap Δ appears in the phonon spectrum. The distribution function of the values $\mathrm{Frac}(u_n)$ is now a Cantor function; there are infinitely many forbidden intervals (gaps) of values of the field (modulo 1).

MacKay (1993) has characterized this drastic change in the physical properties of quasi-periodic fields as a critical phenomenon (already called by Aubry as a "transition by breaking of analiticity") using renormalization group methods for the case of noble irrational ω and the standard model (2).

Discrete Solitons (DSs) or Discommensurations (DCs)

Field configurations can connect asymptotically $(n \to \pm\infty)$ two commensurate configurations (usually one is a translation of the other, though they can be different in general) by an energy minimizing path of exponentially localized length (the width of the DS) around a lattice site (the center of the DS). The width is of the order of the decay range ξ of the recurrent (periodic) substrate.

These structural defects are the elementary excitations of the modulated phase, or localized compressions (advanced DCs) or expansions (retarded DCs) superimposed on the regular substrate modulation. If ω is close to a rational ω_0, the modulated phase corresponding to a mean spacing ω can be correctly described as an array of localized DCs (advanced if $\omega > \omega_0$, retarded if $\omega < \omega_0$) over a periodic substrate of mean spacing ω_0. The interaction energy between neighboring DCs decays exponentially with the quotient interdistance/width, $\exp(-1/(\xi|\omega - \omega_0|))$, so that for ω very close to ω_0 and/or high values of the pinning parameter K (ξ small), the elementary excitations are almost non-interacting (and pinned). However, at lower values of K the tail overlapping of the DCs makes the interactions strong enough, and the array of strongly interacting DCs becomes sliding.

Though with less rigorous formal basis, the DC theory of modulated phases is a well-established formal description of equilibrium for nonconvex FK models. In these cases, interactions between DCs can be of either (attractive or repulsive) sign and even alternating with interdistance. Also, the inner structure of DC can be more complex than in the convex case.

LUIS MARIO FLORÍA AND PEDRO JESÚS MARTÍNEZ

See also **Aubry–Mather theory; Commensurate-incommensurate transition; Dislocations in crystals; Josephson junction arrays; Peierls barrier; Sine-Gordon equation**

Further Reading

Braun, O.M. & Kivshar, Yu. S. 1998. Nonlinear dynamics of the Frenkel–Kontorova model. *Physics Reports*, 306: 1–108

Braun, O.M. & Kivshar, Yu. S. 2004. *The Frenkel–Kontorova Model*, Berlin and New York: Springer

Dehlinger, U. 1929. Zur theorie der rekristallisation reiner metalle [On the theory of recrystallization in pure metals]. *Annalen der Physik*, (5)2: 749–793

Floría, L.M. & Mazo, J.J. 1996. Dissipative dynamics of the Frenkel–Kontorova model. *Advances in Physics*, 45: 505–598

Frank, F.C. & van der Merwe, J.H. 1949. One dimensional dislocations I & II. *Proccedings of the Royal Society* (*London*) A, 198: 205–225

Frenkel, Y. & Kontorova, T. 1939. On the theory of plastic deformation and twinning. *Journal of Physics* (*Moscow*), 1: 137–149 (original Russian publication 1938)

MacKay, R.S. 1993. *Renormalisation in Area-preserving Maps*, Singapore: World Scientific

Nabarro, F.R.N. 1967. *Theory of Crystal Dislocations*, Oxford: Clarendon Press

FREQUENCY DOUBLING

Frequency doubling, or second-harmonic generation, is the process in which an intense laser beam propagating through a nonlinear optical medium produces light at double the frequency of the input beam (Bloembergen, 1969; Boyd, 2002; Shen, 1984; Zernike & Midwinter, 1973). It was the first laser-induced nonlinear optical effect to be reported, and its observation by Franken et al. (1961) marked the beginning of the field of nonlinear optics. This work involved the use of ruby laser radiation at 694.3 nm propagating though a quartz crystal to produce second-harmonic radiation at 347.2 nm (Franken et al., 1961).

Our laboratory demonstration of second-harmonic generation is shown in Figure 1 (also in color plate section). The 800 nm radiation of a titanium-doped sapphire laser is converted into the second harmonic at 400 nm in passing through a lithium niobate crystal. A prism is used to separate the second harmonic from the fundamental radiation exiting of the crystal. A side view showing the ray trajectories is represented in Figure 1c. We can see the red light of the laser beam illuminating the crystal and the blue light of the second harmonic exiting the crystal, together with some portion of unconverted red light. Typically, not all of the incident radiation is converted into the second harmonic. The quantity describing the effectiveness of converting the incident radiation into a harmonic is called the conversion efficiency.

The physical origin of the process of second-harmonic generation can be understood as follows. The electric field of a monochromatic optical wave incident upon a nonlinear medium forces the electrons bound in atoms and molecules to oscillate about their equilibrium positions. Thus, it induces a polarization (dipole moment per unit volume) in the medium that depends on the strength of the electric field. This polarization plays the role of a secondary source of electromagnetic radiation.

The Lorentz model, which treats the atom as a harmonic oscillator, provides a good description of the linear atomic response. The electric force F_{E} exerted on the electron by the electromagnetic field displaces the electron with respect to the nucleus. The restoring force F_{rest} has the opposite action, tending to return the electron to its equilibrium position. If the applied field is weak, the restoring force is linear with respect to the electron displacement x from equilibrium, that is,

$$F_{\mathrm{rest}} = -m\omega_0^2 x.$$

Here m is the mass of the electron and ω_0 is the resonance frequency of the oscillator. Therefore, the potential energy function of the medium is quadratic with respect to x (see Figure 2a, the solid line):

$$U = -\int F_{\mathrm{rest}}\,\mathrm{d}x = \tfrac{1}{2}\,m\omega_0^2 x^2.$$

The parabolic shape of the potential energy function describes harmonic oscillations of the electron at the applied optical field frequency. In such a way, the induced polarization gives rise to the radiation at the applied field frequency. Figure 2b shows the waveform of the incident monochromatic electromagnetic wave of frequency ω (the top graph). For the case of a medium with linear response, there is no distortion of the waveform associated with the polarization of the medium (the middle graph).

In order to describe the nonlinear response, the model has to be extended by allowing the possibility of a nonlinearity in the restoring force (Boyd, 2002). The lowest-order nonlinear response is modelled by adding a contribution quadratic in the displacement so that

$$F_{\mathrm{rest}} = -m\omega_0^2 x - max^2.$$

Here a characterizes the strength of the nonlinearity. The potential energy function of such a system has an additional term that is cubic with respect to x (Figure 2a, the dashed line):

$$U = -\tfrac{1}{2}\,m\omega_0^2 x^2 + \tfrac{1}{3}\,max^3.$$

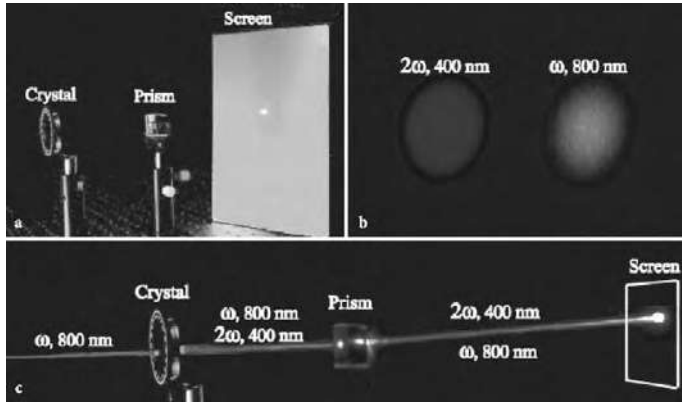

Figure 1. Second-harmonic generation in lithium niobate: (a) Experimental setup; (b) close-up view of the observation screen; (c) side view showing ray trajectories.

Because of the nonlinearity of the restoring force, the atomic response can show a harmonic distortion of the waveform associated with polarization oscillation (Figure 2b the bottom graph). In this case, the induced polarization will give rise to radiation not only at the same frequency as the applied field, but also at higher frequencies (harmonics) as well. A nonlinear effect can occur only if the applied field is sufficiently strong to produce a large displacement x.

More formally, the nonlinear response of a medium to a strong incident field can be described by a nonlinear susceptibility (Bloembergen, 1969; Boyd, 2002; Shen, 1984). In the case of a linear response to the applied field, the induced polarization P depends linearly upon the electric field strength E according to the relationship

$$P = \chi^{(1)} E, \tag{1}$$

where the constant of proportionality $\chi^{(1)}$ is the linear susceptibility. In the case of a nonlinear response, optical response can be described by expanding polarization P as a power series in the field strength E:

$$P = \chi^{(1)} E + \chi^{(2)} E^2 + \chi^{(3)} E^3 + \cdots . \tag{2}$$

The quantities $\chi^{(2)}$ and $\chi^{(3)}$ represent the second- and third-order nonlinear optical susceptibilities, respectively. Here, we will consider only the second-order nonlinear response.

Second-order nonlinear interactions can occur only in noncentrosymmetric media. A typical value of the second-order nonlinear susceptibility in crystals is $\chi^{(2)} \simeq 5 \times 10^{-8}$ esu (6.3×10^{-7} SI). We refer to

$$P^{(2)} = \chi^{(2)} E^2 \tag{3}$$

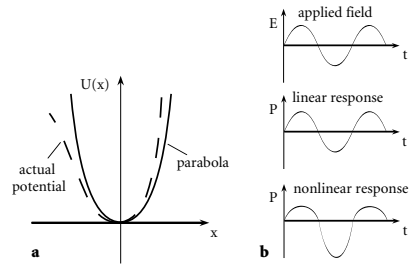

Figure 2. (a) Potential energy function in case of linear response (solid line) and nonlinear noncentrosymmetric response (dashed line); (b) polarization waveforms associated with the atomic response.

as the second-order nonlinear polarization. The strength of the applied optical field can be represented by

$$E = E_0 \exp^{-i\omega t} + \text{c.c.} \tag{4}$$

Substituting (4) into the equation for the second-order nonlinear polarization (3), we can obtain

$$P^{(2)} = 2\chi^{(2)} E E^* + (\chi^{(2)} E^2 \exp^{-i2\omega t} + \text{c.c.}). \tag{5}$$

We can see from (5) that the second-order polarization consists of a constant contribution (the first term) and a contribution at frequency 2ω (the second term). This doubled frequency contribution leads to the generation of radiation at the second-harmonic frequency 2ω.

Frequency doubling can also be understood by means of a virtual energy level description (Figure 3) (Boyd, 2002). The diagram shows that for a lossless

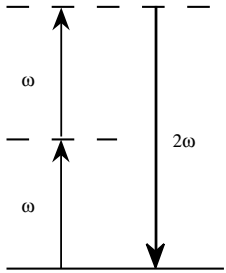

Figure 3. Energy-level diagram describing second-harmonic generation.

medium, the creation of a photon at a doubled frequency 2ω must be accompanied by the destruction of two photons at frequency ω, or according to Manley–Rowe relations: the rate at which a photon at frequency 2ω is created is equal to the rate at which two photons at frequency ω are destroyed.

Second-harmonic generation is a process in which the initial and final quantum mechanical states (energy levels) are identical. Therefore, the energy conservation and momentum conservation laws need to be satisfied. According to the momentum conservation law, the momentum of the two incident photons of frequency ω, $2\hbar\boldsymbol{k}_\omega$, must be equal to the momentum of the radiated photon of frequency 2ω, $\hbar\boldsymbol{k}_{2\omega}$:

$$2\hbar\boldsymbol{k}_\omega = \hbar\boldsymbol{k}_{2\omega}. \tag{6}$$

Here $\boldsymbol{k}_\omega$ and $\boldsymbol{k}_{2\omega}$ are the wave vectors of the incident wave and the second harmonic, respectively. According to (6), in order for the second-harmonic generation to effectively occur, it is necessary for the following phase matching condition to be satisfied:

$$2\boldsymbol{k}_\omega = \boldsymbol{k}_{2\omega}. \tag{7}$$

The dispersion relation for light propagating in a medium is

$$k_\omega = n(\omega)\frac{\omega}{c}, \tag{8}$$

where $n(\omega)$ is the index of refraction for the wave of frequency ω. Thus, condition for perfect phase matching with collinear beams (7) requires that

$$n(\omega) = n(2\omega). \tag{9}$$

In practice, the condition of perfect phase matching is often difficult to achieve because the refractive index of materials displays an effect of normal dispersion: $n(\omega)$ increases monotonically with ω. Thus, condition (9) cannot be satisfied.

There are several ways to achieve phase matching. One of the most common ways is to use the birefringence displayed by many crystals. Birefringence is the dependence of the refractive index on the direction of polarization of the optical radiation. In order to achieve phase matching through the use of birefringent crystals, the highest-frequency wave (2ω) should be polarized in the direction that gives it the lower of two possible refractive indices. There is another technique, known as quasi-phase matching, that can be used when normal phase matching cannot be implemented (Armstrong et al., 1962; Boyd, 2002). This technique involves the use of periodically poled materials, that are fabricated so that the orientation of one of the crystalline axis is inverted periodically as a function of position within the material. It results in periodic alternation of the sign of $\chi^{(2)}$, that can compensate for a nonzero wave vector mismatch $\Delta\boldsymbol{k}$.

Second-harmonic generation can usefully convert the coherent output of a fixed-frequency laser to a different spectral region (Zernike & Midwinter, 1973). For example, the infrared radiation of an Nd:YAG laser operating at 1064 nm can be converted into 532 nm visible radiation with a conversion efficiency of more than 50%.

KSENIA DOLGALEVA, NICK LEPESHKIN, AND ROBERT W. BOYD

See also **Harmonic generation; Manley–Rowe relations; Nonlinear optics**

Further Reading

Armstrong, J.A., Bloembergen, N., Ducuing, J. & Pershan, P.S. 1962. Interaction between light waves in a nonlinear dielectric. *Physical Review*, 127: 1918–1939

Bloembergen, N. 1969. *Nonlinear Optics*, New York: Plenum Press

Boyd, R.W. 2002. *Nonlinear Optics*, San Diego: Academic Press

Franken, P.A., Hill, A.E., Peters, C.W. & Weinreich, G. 1961. Generation of optical harmonics. *Physical Review Letters*, 7: 118–119

Shen, Y.R. 1984. *The Principles of Nonlinear Optics*, New York: Wiley

Zernike, F. & Midwinter, J.E. 1973. *Applied Nonlinear Optics*, New York: Wiley

FREQUENCY LOCKING

See **Coupled oscillators**

FRÖHLICH THEORY

Starting in the late 1960s and continuing until his death in 1991, Herbert Fröhlich developed a theory of biological coherence that was based on quantum interactions between dipolar constituents of biomolecules. Fröhlich advocated momentum-space correlations within a living system such as a membrane, a cell, or an organism. This dynamic order would be a characteristic feature that distinguishes living systems from inanimate matter. The key assumptions

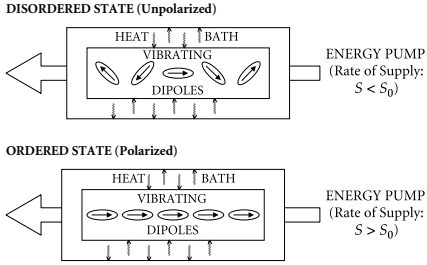

Figure 1. Illustration of the Fröhlich model.

of Fröhlich's theory can be listed as follows:

(i) a continuous supply of metabolic energy (also referred to as energy pumping) above a threshold level,
(ii) the presence of thermal noise due to physiological temperature,
(iii) internal organization of the biosystem that promotes functional features,
(iv) the existence of a large transmembrane potential difference, and
(v) a nonlinear interaction between two or more types of degrees of freedom.

As a result of these nonlinear interactions, in addition to the global minimum that characterizes a biological system in its nonliving state, a metastable energy minimum is achieved in the living state.

The Fröhlich model of biological coherence is based on a condensate of quanta of collective polar vibrations. It is a non-equilibrium property due to the interactions of the system with both the surrounding heat bath and an energy supply (see Figure 1). The energy is channeled into a single collective mode that becomes strongly excited. Most importantly, the Fröhlich model relies on the nonlinearity of internal vibrational mode interactions and in this respect is somewhat reminiscent of the laser action principle. Associated with this dynamically ordered macroscopic quantum state is the emergence of polarization due to the ordering of dipoles in biomolecules such as membrane head groups. Furthermore, Fröhlich predicted the generation of coherent modes of excitation such as dipole oscillations in the microwave frequency range. Nonlinear interactions between dynamic degrees of freedom were predicted to result in the local stability of the polarized state and in the long-range frequency-selective interactions between two systems with these properties.

In the search for empirical support of this model, Fröhlich placed an emphasis on the presence of dipole moments in many biomolecular systems that would then oscillate in synchrony in the frequency range of $10^{11}-10^{12}$ Hz due to their nonlinear interactions. Consequently, due to the resonant dipole-dipole coupling in a narrow frequency range, the entire biological system can be seen as a giant oscillating dipole. An alternative picture developed within the Fröhlich theory was that of a Bose–Einstein condensation in the space of dipole oscillations. The Hamiltonian postulated by Wu and Austin (1977) takes the form

$$\begin{aligned} H = {} & \sum_i \omega_i {a_i}^\dagger a_i + \sum_i \Omega {b_i}^\dagger b_i + \sum\nolimits_i \Theta_i {P_i}^\dagger P_i \\ & + \frac{1}{2}\sum_{i,j,k} (\chi {a_i}^\dagger a_j {b_k}^\dagger + \chi^* a_j {a_i}^\dagger b_k) \\ & + \sum_{i,j} (\lambda b_i {a_j}^\dagger + \lambda^* {b_i}^\dagger a_j) \\ & + \sum_{i,j} (\xi P_i {a_j}^\dagger + \xi^* {P_i}^\dagger a_j), \end{aligned} \tag{1}$$

where $({a_i}^\dagger, a_i)$, $({b_i}^\dagger, b_i)$, and $({P_i}^\dagger, P_i)$ are the cell, heat-bath, and energy-pump creation and annihilation (boson-type) operators, respectively. A kinetic rate equation was derived for this model that indicates Bose-type condensate in the frequency domain with a stationary occupation number dependence of the dipole modes given by

$$N_i = \left[\mathrm{e}^{\beta(\omega_i - \mu)} - 1 \right]^{-1}. \tag{2}$$

The nonlinear coupling comes from the dipole-phonon interaction proportional to χ. Provided that the oscillating dipoles are within a narrow band of resonance frequencies ($\omega_{\min} \le \omega_i \le \omega_{\max}$) and the coupling constants (χ, λ and ξ) are large enough, long-range ($\sim 1\,\mu$m) attractive forces are expected to act between the dipoles.

The effective potential between two interacting dipoles which initially vibrate with frequencies ω_1 and ω_2 is given by

$$U(r) = \frac{E}{r^3} + \frac{F}{r^6}. \tag{3}$$

The van der Waals coefficient F is negative (attractive) unless the average distance between the interacting particles is very short. However, the van der Waals attraction between particles rapidly decreases with distance making it an unlikely candidate mechanism for biological coherence. The coefficient E can be both positive (repulsion) and negative (attraction) depending on the occupation of the new eigenstates of the system. Population inversion leads to attraction while thermal equilibrium for occupation numbers leads to repulsion between particles. In particular, E is given by

$$E = \frac{\hbar e^2 Z \mid \bar{A} \mid \gamma}{4\bar{\omega} M} \left(\frac{1}{\varepsilon'(\omega_+)} - \frac{1}{\varepsilon'(\omega_-)} \right), \tag{4}$$

where M is the mass of a dipole, e is the electron charge, Z is the number of elementary charges on each dipole, A is an angle constant, and $\varepsilon'(\omega)$ is the real part of the frequency-dependent dielectric constant. The quantities $\omega_\pm$ are the new dipole vibration frequencies

$$\omega_\pm = \left[\frac{1}{2}(\omega_1{}^2+\omega_2{}^2)\pm\left(\frac{1}{4}(\omega_1{}^2-\omega_2{}^2)+\frac{\beta_0{}^4}{(\varepsilon'_\pm)^2}\right)^{1/2}\right]^{1/2}, \quad (5)$$

where $\beta_0 = \gamma^2 e^2 \sqrt{Z_1 Z_2}/Mr^3$. In the resonant frequency case, the effective interaction energy between two oscillating dipoles was found to be long-range, depending on distance as r^{-3}.

Most of the expected condensation of dipolar vibrations was envisaged by Fröhlich to take place in the cell membrane due to its strong potential on the order of 10–100 mV across the thickness of 5–10 nm giving an electric field intensity of $1–20 \times 10^6$ V/m. The resultant dipole-dipole interactions were calculated to show a resonant long-range order at a high-frequency range of $10^{11}–10^{12}$ Hz with a propagation velocity of about 10^3m/s. In addition to membrane dipoles, several other candidates for Fröhlich coherence were considered, including double ionic layers, dipoles of DNA and RNA molecules, and plasmon oscillations of free ions in the cytoplasm.

Applications of the Fröhlich theory were made to explain cancer proliferation, where a shift in the resonant frequency was seen to affect the cell-cell signaling, the brain waves, and enzymatic chemical reactions.

Various experiments have been reported that appeared to demonstrate the sensitivity of metabolic processes to certain frequencies of electromagnetic radiation above the expected Boltzmann probability level. Raman scattering experiments by Webb (1980) found non-thermal effects in *E. coli* but these could not be reproduced by other labs. Irradiation of yeast cells by millimeter waves showed increased growth at specific frequencies (Grundler, et al., 1983). Rouleaux formation of human erythrocytes was explained in terms of Fröhlich's resonant dipole-dipole attraction (Paul et al., 1983) but did not rule out standard coagulation processes. While some of these experiments illustrate nonthermal effects in living matter that would require nonlinear and non-equilibrium interactions for explanation, no unambiguous experimental proof has been furnished to date to support Fröhlich's hypothesis.

It is interesting to note that while Fröhlich sought evidence for frequency selection in biological systems, another famous physicist, Alexander S. Davydov tried to find spatial localization of vibrational energy in biological systems such as DNA and peptides. There is a conceptual link between these two approaches as shown by Tuszyński et al. (1983) that involves self-focusing in reciprocal (Fröhlich) or real space (Davydov).

Jack A. Tuszyński

See also **Bose–Einstein condensation; Cluster–coagulation; Davydov soliton; Synergetics**

Further Reading

Davydov, A.S. 1982. *Biology and Quantum Mechanics*, Oxford: Pergamon Press

Fröhlich, H. 1968. Long range coherence and energy storage in biological systems. *International Journal of Quantum Chemistry*, 2: 641–649

Fröhlich, H. 1972. Selective long range dispersion forces between large systems. *Physics Letters*, 39A: 153–155

Fröhlich, H. 1980. The biological effects of microwaves and related questions. In *Advances in Electronics and Electron Physics*, vol. 53, edited by L. Marton and C. Marton, New York: Academic Press, pp. 85–152

Grundler, W., Eisenberg, C.P. & Sewchand, L.S. 1983. *Journal of Biological Physics*, 11: 1

Paul, R., Chatterjee, R., Tuszyński, J.A. & Fritz, O.G. 1983. Theory of long-range coherence in biological systems. I: the anomalous behaviour of human erythrocytes. *Journal of Theoretical Biology*, 104: 169

Tuszyński, J.A., Paul, R., Chatterjee, R. & Sreenivasan, S.R. 1983. Relationship between Fröhlich and Davydov models of biological order. *Physical Review* A, 30: 2666

Webb, S.J. 1980. Laser-Raman spectroscopy of living cells. *Physics Reports*, 60: 201–224

Wu, T.M. & Austin, S. 1977. Bose condensation in biosystems. *Physics Letters* A, 64: 151

FRONT PROPAGATION

See **Reaction-diffusion systems**

FRUSTRATION

Frustration is the inevitable consequence of trying to simultaneously satisfy a number of conflicting constraints. In general, when faced with such conflicting requirements one's only way out is to compromise. Inevitably, there are usually many widely different ways to compromise, some better than others. In physical systems, frustration arises from competition between different contributions to the total energy of a system. Generally, each contribution can be separately minimized by a unique choice of state but the different contributions have different minimum-energy states. The presence of frustration then typically leads to a situation in which there are many, very different, states with similar low energies separated from one another by "barriers" of much higher energy states. This leads to a proliferation of low-energy dynamical modes in the system and, especially in the presence of disorder, slow (glassy) dynamics.

A simple physical example that shows the way in which frustration leads to complexity is afforded by the Ising model (*See* **Spin systems**). Each site of a regular lattice bears a simple binary variable—a spin than can

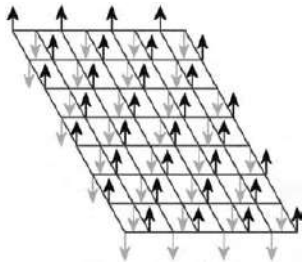

Figure 1. The ground state configuration of the 2-d Ising model on a square lattice.

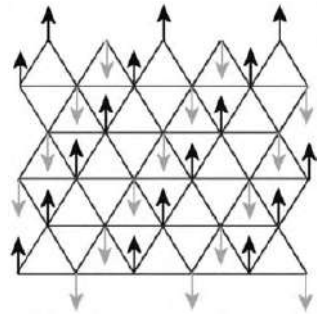

Figure 2. One of the degenerate ground state configurations of the 2-d Isig model on a triangular lattice.

point either up or down. The energy of the whole system has a contribution from each bond on the lattice. A given bond contributes an energy $+J$ if the spins at either end of the bond point in the same direction and an energy $-J$ if they point in opposite directions (this corresponds to the anti-ferromagnetic Ising model). First, consider the model on a two-dimensional square lattice with N sites (this model was solved exactly by Lars Onsager in 1940) as shown in Figure 1.

We can divide the lattice into two sub-lattices such that each site on one sub-lattice is surrounded entirely by sites on the other sub-lattice. The lowest energy state of the system is trivially found—we make all the spins on one sub-lattice point in one direction and all the spins on the other sub-lattice point in the opposite direction (clearly there are two such states with the same energy related by global inversion of all the spins). Each bond of the lattice connects two oppositely oriented spins so that the total energy is $-2NJ$. Any other configuration of spins must result in at least four bonds connecting like spins and so has energy $\geq -2JN + 4J$. This situation is simple and unfrustrated—all bonds can be simultaneously "happy."

Now consider the same simple model, with the same rules for assigning energy, but on a triangular lattice as shown in Figure 2. It is fairly simple to see that there is no way of simultaneously making all the bonds happy. Each elementary plaquette of the lattice has three spins, each of which wants to be in a different state to its neighbors—at least one bond must be unsatisfied (i.e., have energy $+J$). The minimum energy states of this system have alternate "stripes" of aligned spins so that each plaquette has only one unsatisfied bond giving a minimum energy of $-NJ$. A little thought will tell one that there are six equivalent configurations with this minimum energy: three choices for the direction of the stripes as well as the possibility of reversing all spins.

A very simple situation in which there is geometrical frustration arises when one considers the adsorption of one material onto a surface of a different material. Suppose that we have a substrate of material A, which is flat, and we deposit atoms of material B onto it. Further suppose that a bulk sample of pure A atoms has a lattice parameter a, while a bulk sample of pure B atoms has a lattice parameter b. When only a few atoms of material B have been deposited, they will simply bond with A atoms at the surface. Once a large number of B atoms have been deposited, they will begin to come into contact and be able to bond with each other. In the case that $b \approx a$, there is no frustration—the B atoms simply attach themselves to surface A atoms and quite happily bond to other B atoms when they are adjacent. This happy situation is referred to as epitaxial growth and happens for the technologically important situation in which material A is the semiconductor gallium arsenide and material B is the alloy aluminium gallium arsenide. However if $b \ncong a$, then the growth of B is frustrated—there is a competition between the desire of the B atoms to attach themselves to A atoms and their desire to be a distance b from the nearest B atom. If the energetics are such that one set of bond energies is much greater than the other, the system will either form an adsorbed, strained layer, with B–B neighbor distance set by the substrate (a) or it will detach itself entirely. If the energetics are more closely balanced, then the system will find a compromise, often involving the formation of dislocations in the surface layer. There are, of course, many ways of introducing such dislocations to relieve the strain. A simple model for this effect was proposed by Frenkel and Kontorova (*See* **Frenkel–Kontorova model**).

An interesting system in which the frustration can be continuously tuned experimentally is the Josephson junction array (*See* **Josephson junction arrays**). This is a system composed of a lattice of superconducting islands separated by weak links. Each island is characterized by a phase variable and the total energy of the array can be written

$$E = -\varepsilon_J \sum_{\langle i,j \rangle} \cos\left(\theta_i - \theta_j - A_{ij}\right),$$

where the sum is over nearest-neighbor sites, θ_i is the phase on the ith island, ε_J is the Josephson energy, and A_{ij} is a twist variable along a nearest-neighbor bond. The twist variables must satisfy

$$\sum A_{ij} = 2\pi \frac{\Phi}{\phi_0},$$

where the sum is around all the bonds on an elementary plaquette of the lattice, Φ is the magnetic flux through that plaquette, and ϕ_0 is the flux quantum $h/2e$. When the flux per plaquette is an integer number of flux quanta, the system is unfrustrated and its ground state simply has all phases equal. When Φ/ϕ_0 is a rational fraction, the system is uniformly frustrated and its ground states exhibit periodic spatial ordering. If Φ/ϕ_0 is irrational (or, in finite-sized systems if the commensuration length exceeds the system size), then the system exhibits complex, aperiodic ordering. The introduction of frustration introduces a greater range of elementary excitations and a greater degeneracy in the lowest energy states.

Spin glasses are magnetic alloys in which there are competing interactions between magnetic ions that can be of either sign. The canonical model of a spin glass was devised by S.F. Edwards and P.W. Anderson (Edwards & Anderson, 1975) in which each site of a regular lattice bears a classical vector spin. Nearest-neighbor pairs of spins interact via an exchange coupling drawn from a quenched (i.e., nondynamical) random distribution that includes both ferromagnetic and antiferromagnetic possibilities. The energy of a given configuration of spins is then given by

$$E = -\sum_{\langle i,j \rangle} J_{ij} \mathbf{S}_i \cdot \mathbf{S}_j.$$

The combination of frustration and quenched randomness leads to very rich behavior. A mean field version of this model in which all pairs of spins interact weakly was proposed by Sherrington and Kirkpatrick (1975) and solved by Parisi (1979) by introducing the notion of replica symmetry breaking. An alternative approach based on an equation (the so-called TAP equation) for the number of metastable states was presented by Thouless, Anderson, and Palmer (Mezard et al., 1987; Fischer & Hertz, 1991). The relevance of the notions developed for this mean field model to real finite range spin glasses (the EA model) has been questioned and the so-called droplet picture for these was developed (Fischer & Hertz, 1991). The debate over the relative merits of the droplet picture and the broken replica symmetry picture has resurfaced recently and is still highly contentious. Irrespective of which detailed picture is correct, it is clear that the combination of frustration and quenched randomness leads to spin glass systems having many, closely competing low-energy configurations. This leads to a hierarchy of free energy valleys and barriers causing the dynamics of these systems to show very complex and slow dynamical behavior such as aging in which the dynamical response of the system depends on its thermal history. Much current attention is focussed on quantum mechanical frustrated systems both regular (spin liquid states in quantum antiferromagnets) and disordered (quantum spin glasses, etc.).

KEITH BENEDICT

See also **Ferromagnetism and ferroelectricity; Frenkel–Kontorova model; Ising model; Josephson junction arrays; Spin systems**

Further Reading

Binder, K. & Young, A.P. 1996. Spin glasses: experimental facts, theoretical concepts and open questions. *Reviews of Modern Physics*, 58: 801–976

Edwards, S.F. & Anderson, P.W. 1975. Theory of spin glasses. *Journal of Physics* F, 5: 965–974

Fischer, K.H. & Hertz, J.A. 1991. *Spin Glasses*, Cambridge and New York: Cambridge University Press

Mezard, M., Parisi, G. & Virasoro, M.A. 1987. *Spin Glass Theory and Beyond*, Singapore: World Scientific

Parisi, G. 1979. Infinite number of order parameters for spin-glasses. *Physical Review Letters*, 43: 1754–1756

Sherrington, D. & Kirkpatrick, S. 1975. Solvable model of a spin glass. *Physical Review Letters*, 35: 1792–1796

Young, A.P. 1997. *Spin Glasses and Random Fields*, Singapore: World Scientific

FUNCTION SPACES

There are classes of spaces that, while maintaining some essential features of the n-dimensional Euclidean space ($\mathbb{R}^n$), are still general enough to include spaces of functions as particular examples. This entry covers both these abstract classes and some particular function spaces.

A *metric space* retains only the notion of distance. To be a metric on a space X, $d(x, y)$ should be nonnegative and satisfy

(i) $d(x, x) = 0$ for every $x \in X$;
(ii) $d(x, y) = d(y, x)$ for every $x, y \in X$; and
(iii) the triangle inequality: $d(x, y) \leq d(x, z) + d(z, y)$ for every x, y, and $z \in X$.

More precisely, it is the pair (X, d), rather than X alone, that is the metric space. For $x, y \in \mathbb{R}^n$, the standard metric is just given by $d(x, y) = |x - y|$.

A metric leads to a notion of convergence: $x_j \to x$ in X as $j \to \infty$ if for any $\varepsilon > 0$, there is an N such that $d(x_j, x) < \varepsilon$ whenever $j \geq N$. In Euclidean spaces, a sequence converges if and only if it is a Cauchy sequence. In the context of a metric space, $\{x_j\}_{j=1}^{\infty}$ is Cauchy if for any $\varepsilon > 0$, there exists an N such that $d(x_i, x_j) < \varepsilon$ whenever $i, j \geq N$. A metric space

in which every Cauchy sequence converges is called *complete*.

The general version of a length is a norm. Consider a real (or complex) vector space X [which satisfies the property: if x and y are elements of X, then so is $x + \lambda y$ for any $\lambda \in \mathbb{R}$ (or $\mathbb{C}$)]. Then a norm on X is a nonnegative function $\| \cdot \|$ such that

(iv) $\|x\| \geq 0$ with equality if and only if $x = 0$;
(v) $\|\lambda x\| = |\lambda| \|x\|$ for every $x \in X$ and $\lambda \in \mathbb{R}$ (or $\mathbb{C}$); and
(vi) $\|x + y\| \leq \|x\| + \|y\|$ for every $x, y \in X$ (the triangle inequality again).

Note that X needs to be a vector space so that if x and y are in X, so are λx (as in (v)) and $x + y$ (as in (vi)). The pair $(X, \| \cdot \|)$ is called a *normed space*. A complete normed space is called a *Banach space*.

Given a norm, the distance between x and y, $d(x, y) = \|x - y\|$, defines a metric; thus, normed spaces are less general than metric spaces.

The standard notion of the length of a vector in $\mathbb{R}^n$ is not just an ad hoc definition satisfying (iv)–(vi). Vectors are specified relative to n orthogonal coordinate axes, and the expression for the length follows from Pythagoras's theorem. Since the mathematical formalization of orthogonality involves the dot product ($\mathbf{x} \cdot \mathbf{y} = \sum_{j=1}^{n} x_j y_j$), it is natural to consider generalizing this concept.

An *inner product space* is a real (or complex) vector space X equipped with an inner product: that is, a function (x, y) that associates a real (or complex) number with any two elements $x, y \in X$ and satisfies

(vii) $(x, x) \geq 0$, with equality if and only if $x = 0$;
(viii) $(x, y) = \overline{(y, x)}$ for all $x, y \in X$; and
(ix) $(\lambda x + \mu y, z) = \lambda (x, z) + \mu (y, z)$ for every $x, y, z \in X$ and every $\lambda, \mu \in \mathbb{R}$ (or $\mathbb{C}$).

A complete inner product space is called a *Hilbert space*.

Due to (vii), it is possible to set $\|x\| = (x, x)^{1/2}$; the Cauchy–Schwarz inequality

$$|(x, y)| \leq \|x\| \, \|y\| , \tag{1}$$

a consequence of (vii)–(ix), can then be used to show that $\| \cdot \|$ is a norm on X. Thus, every inner product space can also be viewed as a normed space, implying that inner product spaces are more restrictive than normed spaces.

There is one abstract setting that includes all the above: the only concept retained is the notion of an open set. Such *topological spaces* (Sutherland, 1975) consist of a space X and a topology $\mathcal{T}$—the collection of all the open sets in X. This collection must satisfy:

(x) $\emptyset$ and X are elements of $\mathcal{T}$;
(xi) if $O_1, O_2 \in \mathcal{T}$, then $O_1 \cap O_2 \in \mathcal{T}$; and
(xii) the union of any collection of sets in $\mathcal{T}$ is also in $\mathcal{T}$.

Any metric space gives rise to a topological space by taking $\mathcal{T}$ to be the collection of all of its open sets, but there are some notions of convergence (e.g.,weak convergence, *See* **Functional analysis**) that do not correspond to any choice of metric. Because of this, topological vector spaces (vector spaces equipped with a topology) form the basis of advanced functional analysis (Rudin, 1991).

We now give some simple examples of function spaces, in which I denotes any interval (finite or infinite) in $\mathbb{R}$.

The space $C^0(I)$ consists of all real-valued continuous functions on I. The standard norm on this space is the supremum or uniform norm $\| \cdot \|_\infty$, defined as

$$\|f\|_\infty = \sup_{x \in I} |f(x)| \tag{2}$$

(essentially the maximum value of f on the interval I, provided that this is attained). Since the uniform limit of continuous functions is itself continuous, equipped with the uniform norm $C^0(I)$ is complete, and so a Banach space. For functions defined on the whole real line, such uniform convergence is often too strong. More realistic is uniform convergence on compact intervals, that is, equivalent to convergence in the metric

$$d_K(f, g) = \sum_{j=1}^{\infty} 2^{-j} \times \min \left(\sup_{x \in [-j, j]} |f(x) - g(x)|, 1 \right) \tag{3}$$

which cannot be derived from a norm.

The space $C^k(I)$ consists of all continuous functions whose first k derivatives are also continuous,

$$C^k(I) = \{ f \in C^0(I) : \mathrm{d}^j f / \mathrm{d}x^j \in C^0(I), \; j = 1, \ldots, k \} . \tag{4}$$

Its standard norm (which makes C^k a Banach space) is formed by adding the maximum value of f and its first k derivatives,

$$\|f\|_{C^k} = \sum_{j=0}^{k} \|\mathrm{d}^j f / \mathrm{d}x^j\|_\infty . \tag{5}$$

The theory of generalized functions uses the space $\mathcal{D}(\mathbb{R})$ of infinitely differentiable functions with compact support in $\mathbb{R}$ ("test functions"). A sequence $\{\phi_n\}_{n=1}^{\infty} \in \mathcal{D}(\mathbb{R})$ converges to ϕ in $\mathcal{D}$ if there is a fixed compact set K containing the support of each ϕ_n, and $\mathrm{d}^j \phi_n / \mathrm{d}x^j$ converges uniformly to $\mathrm{d}^j \phi / \mathrm{d}x^j$ for every

$j = 0, 1, 2, \cdots$. This form of convergence gives rise to a topology, but there is no corresponding metric.

Another family of Banach spaces are the "Lebesgue spaces" $L^p(I)$, consisting of all Lebesgue integrable functions on I for which the L^p norm defined by

$$\|f\|_{L^p} = \begin{cases} \left(\int_I |f(x)|^p \, \mathrm{d}x\right)^{1/p}, 1 \le p < \infty, \\ \inf\{M : |f(x)| \le M \text{ almost everywhere in } I\}, \\ p = \infty \end{cases} \tag{6}$$

is finite. (See Priestley (1997) for a readable introduction to Lebesgue integration.) The space $L^2(I)$ of square integrable functions is a Hilbert space: for two functions $f, g \in L^2(I)$ one can define an inner product by setting

$$(f, g) = \int_I f(x)\overline{g(x)} \, \mathrm{d}x. \tag{7}$$

Note that this is a very natural space of functions to consider physically: if $u(x)$ denotes a velocity then the L^2 norm of $u(x)$ is proportional to the kinetic energy.

The modern theory of partial differential equations relies heavily on *Sobolev spaces* (Adams, 1975; Evans, 1998; Gilbarg & Trudinger, 1983). These allow discussion of the degree of differentiability of functions that are only weakly differentiable: a function f defined on an open interval I has weak derivative $Df = g$ if there is a function $g \in L^1(I)$ such that for every infinitely differentiable function ϕ with compact support in I

$$\int_I g(x)\phi(x) \, \mathrm{d}x = -\int_I f(x)\phi'(x) \, \mathrm{d}x. \tag{8}$$

(The right-hand side would be the result of integrating $\int f'(x)\phi(x) \, \mathrm{d}x$ by parts if f were a C^1 function. Although this is similar to the definition of the derivative of a generalized function, the weak derivative must be an element of L^1.) By requiring successive weak derivatives $D^j f$ to be in $L^p(I)$, we obtain the Sobolev space $W^{k,p}(I)$:

$$W^{k,p}(I) = \{f \in L^p(I) : D^j f \in L^p(I), \; j = 1, \ldots, k\}. \tag{9}$$

Given the norm

$$\|f\|_{W^{k,p}} = \left(\sum_{j=0}^{k} \|D_j f\|_{L^p}^p\right)^{1/p}, \tag{10}$$

these are Banach spaces. The spaces $H^k(I) \equiv W^{k,2}(I)$ are Hilbert spaces when equipped with the inner product

$$(f, g)_{H^k} = \sum_{j=0}^{k} (D^j f, D^j g)_{L^2}. \tag{11}$$

JAMES C. ROBINSON

See also **Functional analysis; Generalized functions; Topology**

Further Reading

Adams, R.A. 1975. *Sobolev Spaces*, New York: Academic Press
Evans, L.C. 1998. *Partial Differential Equations*, Providence, RI: American Mathematical Society
Gilbarg, D. & Trudinger, N.S. 1983. *Elliptic Partial Differential Equations of Second Order*, Berlin: Springer
Priestley, H.A. 1997. *Introduction to Integration*, Oxford: Clarendon Press and New York: Oxford University Press
Rudin, W. 1991. *Functional Analysis*, New York: McGraw-Hill
Sutherland, W.A. 1975. *Introduction to Metric and Topological Spaces*, Oxford: Clarendon Press

FUNCTIONAL ANALYSIS

Introduction

Systems that are extended in space are usually modeled by partial differential equations (PDEs). The solution of such an equation will be a function of both space and time, for example, $u(x, t)$, and so the state of the system is specified by the *function* $f(\cdot) = u(\cdot, t)$. Since the resolution of such a function as a Fourier series

$$f(x) = \sum_{k \in \mathbb{Z}} c_k \mathrm{e}^{\mathrm{i}kx}, \qquad c_{-k} = \overline{c_k},$$

requires an infinite number of coefficients, the appropriate phase space for a PDE is generally infinite-dimensional. For example, the stability of a solution (be it stationary, periodic, or more general still) will depend on the eigenvalues of some linear operator that acts on this infinite-dimensional phase space.

Broadly speaking, functional analysis can be viewed as the study of infinite-dimensional spaces and the properties of maps (often linear) defined on them. Functional analysis is required for any rigorous treatment of PDEs (e.g., Evans, 1998, or Robinson, 2001) and many problems in the theory of ordinary differential equations.

In this entry we discuss two topics, both central to the subject. First, we give a very brief outline of spectral theory, which generalizes ideas familiar from linear algebra; and then we discuss the notion of "weak convergence" that goes some way to circumventing the problems arising from a fundamental difference between finite- and infinite-dimensional spaces.

For the sake of simplicity, we will discuss these two topics only in the context of a Hilbert space rather than for a general Banach space (*See* **Function spaces**). We denote this Hilbert space by H, its norm by $\|\cdot\|$, and its inner product by $(\cdot, \cdot)$. Note that $\mathbb{R}^n$ is a finite-dimensional Hilbert space. For more details and a more general treatment, see the suggestions for further reading.

Spectral Theory

Initially motivated by Sturm–Liouville boundary value problems and the related theory of integral equations, spectral theory has become an important part of functional analysis. The theory generalizes ideas from finite-dimensional linear algebra to linear operators on infinite-dimensional spaces.

A map $A : H \to H$ is *linear* if

$$A(x + \lambda y) = Ax + \lambda Ay \quad \text{for every } x, y \in H, \lambda \in \mathbb{R},$$

and is *bounded* if, for some $M > 0$,

$$\|Ax\| \leq M\|x\| \qquad \text{for every } x \in H. \tag{1}$$

[If $H = \mathbb{R}^n$, then any linear map is bounded, but this is not true when H is infinite-dimensional.]

When $H = \mathbb{R}^n$, the eigenvalues of a matrix A are all those complex numbers λ for which $A - \lambda I$ is not invertible (so that $Ax = \lambda x$ for some nonzero x). When A is a linear operator on an infinite-dimensional space, the *spectrum* of A consists of all the values of λ for which $R_\lambda(A) = (A - \lambda I)^{-1}$ lacks one or more of the following "nice" properties:

(i) $R_\lambda(A)$ exists,
(ii) $R_\lambda(A)$ is bounded, and
(iii) $R_\lambda(A)$ can be defined on a dense subset of H (another "nice" property whose exact meaning is unimportant here).

In general, this spectrum can be divided into three distinct pieces:

- the point spectrum $\sigma_p(A)$ (eigenvalues): (i) does not hold, so that there is a nonzero $x \in H$ (the "eigenfunction") with $Ax = \lambda x$;
- the continuous spectrum $\sigma_c(A)$: (i) and (iii) hold, but not (ii), and
- the residual spectrum $\sigma_r(A)$: (i) holds but (iii) does not.

If $H = \mathbb{R}^n$, then whenever (i) holds so do (ii) and (iii), and the spectrum consists only of the eigenvalues of A.

When $H = \mathbb{R}^n$ and A is a real symmetric matrix, results from linear algebra guarantee that (a) all its eigenvalues are real, (b) the eigenvectors corresponding to distinct eigenvalues are orthogonal, and (c) the eigenvectors form a basis for $\mathbb{R}^n$. To obtain a similar result when H is infinite-dimensional we have to impose certain restrictions on A. The original applications to boundary value problems and integral equations motivated the following two definitions that are useful here: an operator $A : H \to H$ is *compact* if the image $\{Ax_n\}_{n=1}^{\infty}$ of any bounded sequence $\{x_n\}_{n=1}^{\infty}$ has a convergent subsequence [if $H = \mathbb{R}^n$, then any linear map is compact, cf. below]; and a bounded map from a Hilbert space H into itself is *self-adjoint* if

$$(Ax, y) = (x, Ay) \quad \text{for every} \quad x, y \in H$$

[when $H = \mathbb{R}^n$, this means that A is a real symmetric matrix].

If A is a compact, self-adjoint operator that is also invertible, then it behaves much like a real symmetric matrix: (a) all of its eigenvalues are real; (a′) the residual spectrum is empty and there are at most a countable number of eigenvalues, which are bounded and can only have zero as an accumulation point; (b) eigenfunctions corresponding to distinct eigenvalues are orthogonal; and (c) the eigenfunctions form a basis for H. This is the celebrated Hilbert–Schmidt theorem, the rigorous result that justifies the approach of Sturm–Liouville theory, that is, using eigenfunctions as a basis in which to expand solutions as a "generalized Fourier series" (see Kreyszig, 1978; Renardy & Rogers, 1992, for example).

Weak Convergence

A space is finite-dimensional if and only if its unit ball is compact. Put another way, any bounded sequence in a finite-dimensional space has a convergent subsequence (in $\mathbb{R}$ this is the Bolzano–Weierstrass theorem): this result is extremely useful, but it is not true in an infinite-dimensional space.

However, it is possible to define a weaker notion of convergence ("weak convergence") and so recover a form of this compactness property in certain infinite-dimensional spaces. To motivate the definition we make two observations. First, if x and y are two distinct elements of a Hilbert space H, then, it is possible to find a $z \in H$ such that

$$(z, x) \neq (z, y),$$

"inner products can distinguish elements of H." Second, it is also possible to show that if $(z, x) = (z, y)$ for every $z \in H$, then we must have $x = y$: "inner products can determine elements of H."

Because of these two results, it is reasonable to define a notion of convergence based on inner products. In a Hilbert space, a sequence x_n converges weakly to x, written $x_n \rightharpoonup x$, if

$$(z, x_n) \to (z, x) \quad \text{for every element} \quad z \in H.$$

Although a bounded sequence in an infinite-dimensional Hilbert space need not have a convergent subsequence, it will have a subsequence that converges weakly. Such convergence is often sufficient for applications; in particular, it is fundamental to many results in the theory of existence and uniqueness for solutions of PDEs.

[The Riesz Representation theorem guarantees that for any bounded linear map $\rho : H \to \mathbb{R}$, there is a $z \in H$ such that $\rho(x) = (z, x)$ for all $x \in H$. In a general Banach space B, the "inner product with" z used above is replaced by "any bounded linear map from B into $\mathbb{R}$". These maps are known as "linear functionals," and

gave rise to the name of the subject to which they are central.]

JAMES C. ROBINSON

See also **Function spaces; Generalized functions; Topology**

Further Reading

Evans, L.C. 1998. *Partial Differential Equations*, Providence, RI: American Mathematical Society

Kreyszig, E. 1978. *Introductory Functional Analysis with Applications*, New York: Wiley

Meise, R. & Vogt, D. 1997. *Introduction to Functional Analysis*, Oxford: Clarendon Press and New York: Oxford University Press

Renardy, M. & Rogers, R.C. 1992. *An Introduction to Partial Differential Equations*, New York: Springer

Robinson, J.C. 2001. *Infinite-dimensional Dynamical Systems*, Cambridge and New York: Cambridge University Press

Rudin, W. 1991. *Functional Analysis*, New York: McGraw-Hill

Yosida, K. 1980. *Functional Analysis*, Berlin: Springer

G

GALAXIES

Galaxies are dense agglomerations of matter in the Universe. They consist of gas, dust, and stars as a major fraction. In addition, for kinematical reasons a hypothetical "dark matter" component is required. Their formation dates back to the early Universe, almost 14 billion years ago. Although some galaxies were already listed as nebulous objects in Charles Messier's catalogue of nebulae and star clusters from 1784, their discovery as detached "island universes" only dates from 1924, when Edwin Hubble resolved the outer parts of Messier Object 31 (M31, the Andromeda Nebula) into stars and measured their distances.

Within 2.2 million light years ($1\,\mathrm{ly} = 9.46 \times 10^{12}$ km), M31 is the closest massive galaxy and is similar to our Milky Way galaxy, both belonging to a galaxy type that is characterized by a rotating disk of stars and gas showing spiral patterns. In addition, such spiral galaxies possess a central spheroid of old stars called a bulge and an extended spheroidal halo of old single stars and bound star clusters, called globular clusters.

All spiral galaxy labels today begin with the prefix "*S*". For decreasing bulge-to-disk ratios, Hubble classified the sequence of spirals from Sa to Sc, some of which also show an innermost bar structure where the spiral arms emerge at the ends. Hubble distinguished these as SBs as distinct from normal Ss.

Another morphological galaxy type exists with an elliptical shape, almost no particular substructure, relatively old stars, and depleted in gas: ellipticals. According to their minor-to-major axes ratio b/a, Hubble denoted them by E10$(1 - b/a)$ reaching from E0 (circular) to E7 ($b/a = 0.3$) at most.

Lenticular galaxies (SOs) form the link between spirals and ellipticals in Hubble's famous "tuning-fork diagram" (see Figure 1). Hubble galaxies have masses between several 10^{10} to 10^{12} solar masses ($m_s = 1.9891 \times 10^{30}$ kg) and diameters of 100,000 light years and more. More refined classification schemes are possible such as those by de Vaucouleurs (1959) and Sandage (1961). Today an extension exists to Sds, and even further to irregularly shaped galaxies (Is) with lower mass and brightness and no central bulge.

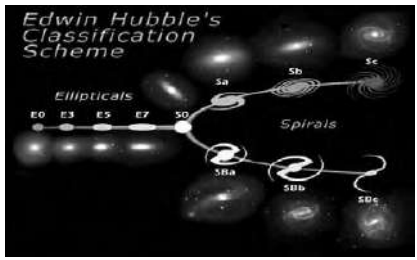

Figure 1. Hubble's "tuning-fork diagram" of galaxies. With courtesy from STScI.

Internal and Dynamical Structure of Galaxies

Ellipticals

According to the stellar mass distribution, any galaxy becomes dimmer with distance R from the geometrical center. The radial dependence however, differs between morphological types and their components. Ellipticals follow in all directions the empirical de Vaucouleurs law with brightness falling off with $\exp(-R^{1/4})$. Although it seems plausible that rotation causes ellipticity, since the 1970s, it has been known that in most ellipticals their regular rotation velocity is smaller than the irregular proper motion of stars with speeds of 200–250 km/s. They are therefore denoted as "hot stellar systems." The elliptical shape is thus formed by the anisotropic velocity dispersion of stars. Moreover, triaxiallity of the figure axes, as for a flattened cigar, can be derived for some elliptical galaxies if the elliptical contours of equal brightness are somehow twisted. Most elliptical galaxies can be divided additionally into boxy- or disky-shaped contours considering the fourth-order cosine in a trigonometric expansion.

Spirals

Spiral galaxies are the most complex systems. While their bulges' brightness profiles resemble ellipticals,

they are rotationally supported. Although the halos are not dense enough to show a continuous stellar distribution, one can take, for example, globular clusters as representative and find a power law for the density of $R^{-2} \ldots R^{-3.5}$. While in the halo, the large irregular velocities of stars (determined in our Milky Way) and globular clusters, their age, and the lack of significant amounts of gas are similar to those of ellipticals (without knowing the halo's ellipticity), disks consist of 10–20% gas and of stars, both rotating with velocities of 200–250 km/s. Because the velocity dispersion of stars is much less, in the range of only 10–60 km/s, disks are therefore "cold systems" and rotationally flattened. Their radial face-on brightness drops with $\exp(-R/\alpha)$ where α is the so-called scale length of around 10,000 light years.

Although spiral arms are exceptionally trailing, they are not the result of structures wound by differential rotation because their pitch angles, that is, the angle between an arm and a circle, should be much smaller than observed. Because the arm structure is pronounced in the visual by the brightness of young stars that form out of cold gas condensed within the arms, among different possible processes of arm formation, density waves are the most favored.

Since the characteristic velocities v, for example, the rotation of spiral disks and velocity dispersion in elliptical galaxies, are almost constant with R, although the visible mass decreases, this invokes the existence of dark matter. Because in equilibrium the centrifugal force $F_c = mv^2/R$ acting on the mass element m is balanced by the gravitational force of a mass M_R included within R, $F_g \propto mM_R/R^2$, for observed v=const. M_R has to increase with R. This means that the dark matter contribution dominates in the outermost regime. In contrast, less bright ellipticals have been found recently where a decline of velocities at large radii is measured, so the dark matter content remains controversial.

Formation and Evolution of Galaxies

Galaxies assemble into larger units by means of gravitation, thus forming galaxy groups like our Local Group and galaxy clusters with numerous members, as for example, the Virgo Cluster at a distance of 50 million light years. In the center of the clusters, ellipticals dominate while spirals permeate the whole cluster. This leads to the suggestion that ellipticals are formed by merging events in the densest cluster regions and in the early universe.

While the Hubble-type galaxies are massive, dwarf galaxies with less mass exist. In our vicinity the large and small magellanic clouds (LMC, SMC) as satellites of the Milky Way represent a dwarf irregular type, consisting of gas and stars as spirals but with less regular structures. With masses of $5 \times 10^9 m_s$, the LMC lies at the upper-mass range of dwarf galaxies, while other Milky Way galaxy satellites, dwarf spheroidals, form the low-mass end of the dwarf ellipticals. With 10^6–$10^7 m_s$ their brightness is so low that observations are still incomplete. Dwarf ellipticals are the most frequent galaxy type in the present Universe resembling Hubble's Es.

The class of dwarf galaxies is of substantial importance for our understanding of galaxy formation and the evolution of the Universe, because they serve as the building blocks of massive galaxies in the cosmological picture of hierarchical clustering. Although their accretion by mature galaxies by means of tidal friction is observable, their destruction rate during the course of the universe is yet unclear because it is also possible that the dwarf galaxy types are replenished by other processes such as tidal tails of merging galaxies.

GERHARD HENSLER

See also **Cosmological models; Gravitational waves; Hénon–Heiles system; Spiral waves**

Further Reading

Binney, J. & Merrifield, M. 1998. *Galactic Astronomy*, Princeton Series in Astrophysics, Princeton, NJ: Princeton University Press

Binney, J. & Tremaine, S. 1987. *Galactic Dynamics*, Princeton Series in Astrophysics, Princeton, NJ: Princeton University Press

Combes, F., Mazure, A. & Boisse, F. 2001. *Galaxies and Cosmology*, Berlin and Heidelberg: Springer

Sandage, A. 1961. *Hubble Atlas of Galaxies*, Washington, DC: Carnegie Institution of Washington

Sparke, L.S. & Gallagher, J.S. 2000. *Galaxies in the Universe*, Cambridge and New York: Cambridge University Press

de Vaucouleurs, G. 1959. Classification and morphology of external galaxies, vol. 53, *Handbuch der Physik*, Berlin: Springer, p. 275

GAME OF LIFE

The rules underlying Life are simple, according to computer scientists. Biologists are inclined to be skeptical, but they do agree that the cellular automaton known as the Game of Life provides fascinating insights into the phenomena of self-organization and emergence in systems of interacting agents.

Biological life has been around for at least 3.8 billion years, but the Game of Life was invented by mathematician John Conway in 1970 and publicized by Martin Gardner in his "Mathematical Games" column in *Scientific American*. It is probably the best-known example of the class of algorithms known as cellular automata (CA). A CA is a one- or two-dimensional array of cells, each of which can exist in a number of states. Time in a CA is discrete; at each time step, every cell updates itself on the basis of its current state and those of its neighbors. Cellular automata can exhibit surprisingly complex global temporal

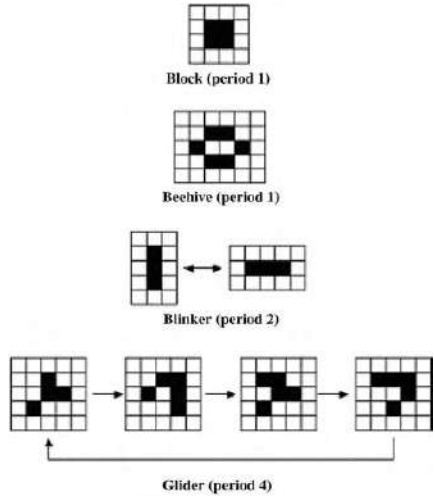

Figure 1. Some commonly seen patterns in the Game of Life.

dynamics, arising from extremely simple rules applied on a local scale.

The standard Game of Life uses a two-dimensional grid. Cells can be either on (alive) or off (dead). The neighborhood of a cell is the eight cells surrounding it. The rules of Life are, indeed, simple; if a live cell has two or three live neighbors, it stays alive. A dead cell with exactly three live neighbors comes alive (is born). In all other cases the cell dies, either of overcrowding (with more than three live neighbors) or loneliness (with fewer than two). At each time step, all cells update their states simultaneously. That's all there is to Life! No wonder the biologists are dubious. But from this simple foundation, complex, consistent patterns of activity emerge. If the grid is seeded at random with live cells, the first few time steps are a turmoil of apparently random activity. However, identifiable patterns of live cells quickly emerge. Interesting patterns exhibit periodic behavior, cycling between a number of different states in a deterministic manner. Many patterns settle into a limit cycle of length one—a stable point attractor, or "still life" in the Life terminology. Others, known to Life practitioners as "oscillators," have longer limit cycles.

So consistent are these patterns that hundreds have been identified, named, and studied by Life enthusiasts all over the world (see e.g., Figure 1). There are several catalogues of Life patterns available on the Web; a particularly nice site is http://hensel.lifepatterns.net/.

Although most initial configurations eventually settle to a stable state or cyclic set of states, this is not always the case. Life aficionados have identified initial states that generate new states indefinitely.

So is Life more than just a generator of interesting patterns? The answer, of course, is "yes." Cellular automata in general, and Life in particular, have interesting theoretical properties. Stephen Wolfram identified four broad classes of dynamic behavior common to one-dimensional (Wolfram, 1984) and two-dimensional (Wolfram, 1985) CAs.

Class 1: Evolution leads to a homogeneous state (analogous to a point attractor in a nonlinear dynamic system),

Class 2: Evolution leads to a set of separated simple stable or periodic structures (analogous to limit cycles),

Class 3: Evolution leads to a chaotic pattern (analogous to the chaotic attractors found in continual dynamic systems),

Class 4: Evolution leads to complex localized structures, sometimes long-lived.

Although the universal applicability and hence usefulness of Wolfram's classification system has been questioned (e.g., Eppstein, 2000), it is still widely accepted. The Game of Life falls, serendipitously, into class 4, the class for which Wolfram hypothesizes that "class-4 cellular automata are generically capable of universal computation, so that they can implement arbitrary information-processing procedures" (Wolfram, 1985). It has, in fact, been proven that Life is a universal cellular automaton—one which can emulate a Turing machine, capable of performing universal

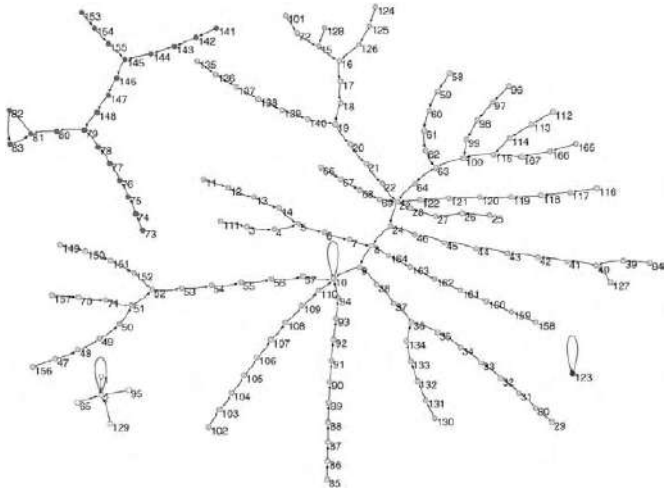

Figure 2. State transition graph for a cellular automaton. States are arbitrarily numbered. The state space contains four basins of attraction, three of which contain a point attractor, while the fourth leads to a limit cycle of length three (states 81, 82 and 83).

computation. The universality of Life was proved in the early 1980s (Berlekamp et al., 1982), and a Turing machine that can be extended to a universal Turing machine was implemented by Paul Rendell in 2000 (Adamatzky, 2002).

An overview of the temporal dynamics of a two-dimensional CA such as the Game of Life can be provided by a state transition graph, in which each possible pattern of on and off cells in the CA makes up a unique state. If the number of cells in the lattice is s and the number of cell states is k, then there are k^s possible states for that CA. Each state forms a node in the graph. Since the rules are deterministic, each state will map to a single new state in the next timestep, and the transition between the two states is represented by a directed link (an arc) between the two nodes. A state transition graph depicts the course of evolution of the CA from any given starting point (Figure 2).

Inspection of a state transition diagram leads to the conclusion that evolution in a CA is not deterministically reversible; some states have two or more antecedent states. Some states, in contrast, have no preceding states. The latter are known as Garden of Eden states. The existence of Garden of Eden states in the Game of Life was predicted by CA theory, but actually identifying such a state is a nontrivial task. Several Garden of Eden states have been identified by trial and error, but the search for a reliable algorithm for their identification continues.

The rules of Life are simple, but from them arise complex, emergent behaviors—coherent forms arising at different levels of organization and interacting to produce new forms and patterns. This complexity arising from underlying simplicity makes the Game of Life an ideal toy world for the study of many of the fascinating phenomena of complex systems.

JENNIFER HALLINAN

See also **Artificial life; Attractors; Biological evolution; Cellular automata; Order from chaos; State diagrams**

Further Reading

Adamatzky, A. (editor). 2002. *Collision-based Computing*, Heidelberg: Springer

Berlekamp, E.R., Conway, J.H. & Guy, R.K. 1982. *Winning Ways for Your Mathematical Plays*, vol. II. *Games in Particular*, London: Academic Press

Eppstein, D. 2000. Searching for spaceships. In *More Games of No Chance*, edited by R.J. Nowakowski, Cambridge and New York: Cambridge University Press, pp. 433–453

Gardner, M. 1970. Mathematical games: the fantastic combinations of John Conway's new solitaire game "life." *Scientific American*, 223: 120–123

Wolfram, S. 1984. Universality and complexity in cellular automata. *Physica* D, 10: 1–35

Wolfram, S. 1985. Two-dimensional cellular automata. *Journal of Statistical Physics*, 38: 901–946

The Game of Life can be played online at:
http://www.math.com/students/wonders/life/life.html
http://www.bitstorm.org/gameoflife/
http://hensel.lifepatterns.net/

GAME THEORY

Humans play games. From the formalized warfare of chess to the Machiavellian machinations of politics to the subtleties of sexual pursuit, interactions between individuals with desires and priorities that are often conflicting and contradictory lies at the heart of human society. The formal study of games, however, is a relatively recent phenomenon and has moved rapidly from its beginnings as a mathematical tool to aid gamblers to its current status as an essential paradigm in fields as diverse as economics and evolutionary biology.

Today, *game theory* can be defined as "the analysis of rational behavior under circumstances of strategic interdependence, when an individual's best strategy depends upon what his opponents are likely to do" (Varoufakis, 2001). Individuals may be people, corporations, nations, animals, species, or any other entity that can be said to exhibit strategic behavior.

Formal game theory began in 1713, when Pierre-Rémond de Montmort first proposed the concept of a minimax solution to a card game called Le Her. A minimax solution to a two-player game is one in which an individual chooses his strategy so as to minimize the maximum loss or risk that he/she will incur. It was James Waldegrave, the originator of Le Her, who actually produced a minimax solution to the game.

Other concepts of fundamental importance to modern game theory also emerged in the 18th century, a result of work by Daniel Bernoulli in his 1738 analysis of the St. Petersburg paradox (Dimand & Dimand, 1992). These concepts included utility (a measure of the desirability to the player of each possible outcome of the game), the maximization of expected utility, diminishing marginal utility (the decrease in the amount of benefit derived from consuming each additional unit of a product or service), and risk aversion as a parameter of a utility function.

The work on minimax game solutions remained an isolated curiosity until the 1920s, when Émile Borel published a series of short papers on strategic games in the Proceedings of the French Academy of Sciences between 1921 and 1927. In these papers, he defined the normal form of a game: a matrix representation of the game in which each player tries to work out the best strategy independent of the sequence of moves. Borel later claimed to have proven the minimax theorem, but this does not appear to be the case. In fact, he may not even have stated the theorem.

The first formal proof of the minimax theorem for two-person games with any finite number of pure strategies was given by John von Neumann in a paper presented to the Gottingen Mathematical Society on December 7, 1926 (Dimand & Dimand, 1992). He proved that in a zero-sum game (one in which one player's gain is the other's loss), there exists a unique set of mixed strategies, one per player, which equalizes the payoffs that each player can gain regardless of the strategy adopted by the other player.

At about the same time, the Princeton economist Oskar Morgenstern was pondering mixed strategy game theoretic issues, as exemplified by that master of bluff, Sherlock Holmes, and the strategies he should adopt to avoid his arch enemy, Professor Moriarty. In 1944, von Neumann and Morgenstern collaborated to produce *The Theory of Games and Economic Behavior*, the seminal publication in this area. In 1947, they revised the book to include expected utility theory, under which games are expressed in terms of the players' perceptions of the inherent desirability and likelihood of their outcomes, and players never expect other players to hold mistaken beliefs—the assumption of complete rationality, which has been fundamental to much ensuing work. Economists were initially reluctant to accept game theory, but since the publication of von Neumann and Morgenstern's book, the theory has undergone extensive development, and has been applied to an enormous variety of problems in economics, to the point where Leonard (1992) could assert that "game theory plays a central role in economic theory."

Minimax theory assumes that each player has perfect knowledge about the game and that the game is zero-sum. In such a case, the best strategy for each player is independent of the strategy adopted by the other player. In most real-world situations, this is not the case; more often, the best strategy for one player depends on what the other players choose to do. The extension of minimax theory to n-player, noncooperative games was achieved by the Princeton mathematician John Nash in a paper published in 1950. In this paper, he defined the Nash equilibrium. A Nash equilibrium is a set of strategies such that no player could improve his/her payoff, given the strategies of all other players in the game, by changing his/her strategy. Nash proved that all noncooperative games have a Nash equilibrium and, thereby, established an analytical structure within which all situations of conflict and cooperation could be studied. For this work, he received the 1994 Nobel Prize for Economics, together with John Harsanyi and Reinhard Selten.

Game theory was also applied with considerable success to other fields of research, perhaps most notably to evolutionary biology. The concepts of game theory transfer readily to evolutionary biology—the values of different outcomes, which in economic theory are measured as utility, are readily interpreted in terms of Darwinian fitness. Moreover, the somewhat sweeping assumption of complete rationality in the behavior of the agents is replaced by the concept of evolutionary stability.

Game-theoretic concepts were first explicitly applied to the study of evolution by Lewontin (1961), who saw the agents in the game as a species on the one hand,

against nature on the other. The utility of this approach was quickly recognized, and the focus shifted to modeling interactions between individuals. In this context, the concept of the Nash equilibrium was rediscovered independently by John Maynard Smith and G.R. Price in 1973 as the Evolutionarily Stable Strategy (ESS—"a strategy such that, if all the members of a population adopt it, no other strategy can invade" (Maynard Smith, 1982, p. 204). An ESS represents the solution to a game.

In the last three decades, game theory has been used to provide a framework for the analysis of a wide range of biological phenomena, including the evolution of sex ratios, parental investment in offspring, patterns of animal dispersal, competition for resources (see, e.g., Maynard Smith, 1982) and the evolution of cooperation (Axelrod, 1984). In biology, as in economics, game theory has become an essential tool for the theorist, providing a structured framework for the analysis of a wide range of phenomena.

JENNIFER HALLINAN

See also **Artificial life; Biological evolution; Economic system dynamics**

Further Reading

Axelrod, R. 1984. *The Evolution of Cooperation*, New York: Basic Books

Dimand, R.W. & Dimand, M. 1992. The early history of the theory of strategic games from Waldegrave to Borel. In *Toward a History of Game Theory*, edited by E.R. Weintraub, Durham: Duke University Press

Leonard, R.J. 1992. Creating a context for game theory. In *Toward a History of Game Theory*, edited by E.R. Weintraub, Durham: Duke University Press

Lewontin, R.C. 1961. Evolution and the theory of games. *Journal of Theoretical Biology*, 1: 382–403

Maynard Smith, J. 1982. *Evolution and the Theory of Games*, Cambridge: Cambridge University Press

Nash, J. 1950. Equilibrium points in N-person games. *Proceedings of the National Academy of Sciences*, 36: 48–49

Varoufakis, Y. 2001. General introduction: game theory's quest for a single, unifying framework for the social sciences. In *Game Theory: Critical Concepts in the Social Sciences*, edited by Y. Varoufakis, vol. 1. London and New York: Routledge

von Neumann, J. & Morganstern, O. 1953. *Theory of Games and Economic Behavior*, 3rd edition, New York: Wiley (1st edition, 1944)

GAP SOLITONS

See **Solitons, types of**

GARDNER (GGKM) EQUATION

See **Inverse scattering method**

GAUSSIAN BEAM

See **Nonlinear optics**

GAUSSIAN ENSEMBLES

See **Free probability theory**

GEL'FAND–LEVITAN THEORY

In inverse problems, sometimes also called backward problems, one is given the solution and required to find the underlying equation. Inverse spectral problems deal with the recovery of unknown coefficients of a differential operator from the knowledge of its spectral data. Their importance stems from the fact that coefficients in a differential equation usually model the physical structure or composition of a certain material. Nondestructive testing, geophysical prospecting, radar, and medical imaging are just some of the important applications of inverse problems. By analyzing reflected waves, radar can locate, track, and sometimes identify a target. In geophysical prospecting, the travel time of reflected underground acoustic waves can reveal deposits of petroleum and natural gas. The field of medical imaging has witnessed the development of many non-invasive and safe procedures using the above ideas. For example, ultrasonography using the three-dimensional Doppler effect can help visualize the fetal vascular system for prenatal diagnosis. High-resolution ultrasound cardiovascular imaging not only reconstructs a real-time picture of the heart but also measures the rate of blood flow, thus giving early warnings for clogged arteries, heart attacks, and strokes.

A simple rule of the thumb is that data used should be equivalent to the information to be reconstructed. For example, if we are looking for a square integrable function, the data should be equivalent to its sequence of Fourier coefficients, while an analytic function is equivalent to its Taylor coefficients. Can we recover a matrix of size $n \times n$ from its n eigenvalues? Although in general to define a matrix we would need n^2 entries, possible exceptions would be matrices that are fully determined by their first rows—symmetric Toeplitz or Hankel matrices, for example. In all kinds of inverse problems, one faces two major issues: uniqueness of the solution and the algorithm for its reconstruction. One of the best understood inverse problems, which deals with the Schrödinger operator, was solved by Gel'fand and Levitan in 1951 (see Gel'fand & Levitan, 1955).

The One-dimensional Schrödinger Equation

Consider the one-dimensional Schrödinger operator

$$\begin{cases} L(y) = -y''(x,\lambda) + q(x)y(x,\lambda) = \lambda y(x,\lambda), \\ \quad x \in [0,\ \infty), \\ y'(0,\lambda) - hy(0,\lambda) = 0, \end{cases} \tag{1}$$

where q is a real continuous function and h is a real constant. The continuity of q ensures the existence of a

unique solution of the initial value problem at $x = 0$ for every $\lambda \in \mathbb{C}$. The boundary value problem (1) is regular at $x = 0$ and singular at $x = \infty$. The operator L, which acts in the Hilbert space of square integrable functions on the positive half line, is self-adjoint so its eigenvalues are real. We usually normalize solutions of (1) by the condition $y(0, \lambda) = 1$, which leads to $y'(0, \lambda) = h$. To determine the spectrum of L (the set of values λ such that the inverse operator of $L - \lambda I_d$ either does not exist or is unbounded), we need to examine the behavior of the solutions $y(x, \lambda)$ as $x \to \infty$. If the solution decays fast enough and is square integrable, that is, has a finite energy $\alpha_n = \int_0^\infty |y(x, \lambda_n)|^2 \, dx < \infty$, then λ_n is an eigenvalue and belongs to the discrete part of the spectrum. For other solutions that could be approximated by continuous functions or do not grow faster than a polynomial in x, λ belongs to the continuous spectrum; otherwise λ is not in the spectrum. A more precise result using the theory of distributions (Gel'fand & Shilov, 1967) shows that λ is in the spectrum if and only if the solution $y(x, \lambda)$ is the derivative of a function that cannot grow faster than $x^{3/2+\varepsilon}$ as $x \to \infty$. This characterization threw a new light on the mysterious behavior of the continuous spectrum.

For example, when $q = h = 0$, the spectrum of L is continuous on $[0, \infty]$. Indeed its "eigenfunctions" are $\cos\left(x\sqrt{\lambda}\right)$ which are not square integrable and so there are no eigenvalues, while for $\lambda > 0$ the solutions $\cos\left(x\sqrt{\lambda}\right)$ are bounded and so grow less than $x^{3/2+\varepsilon}$ as $x \to \infty$, which means that $\lambda > 0$ is in the continuous spectrum. On the other hand, when $\lambda < 0$, the solutions $\cos\left(x\sqrt{\lambda}\right) = \cosh\left(x\sqrt{-\lambda}\right)$ have an exponential growth, and so $\lambda < 0$ cannot be not in the spectrum.

Once the operator L is known to be self-adjoint, the solution $y(x, \lambda)$ forms the kernel of a transform, which is similar to the Fourier cosine transform,

$$F(\lambda) = \int_0^\infty f(x) y(x, \lambda) \, dx,$$

and its inverse transform is defined explicitly by

$$f(x) = \int_\sigma F(\lambda) \overline{y(x, \lambda)} \, d\rho(\lambda).$$

The function ρ, which is called the spectral function, is nondecreasing, is right-continuous, has jumps at the eigenvalues $\rho(\lambda_n) - \rho(\lambda_n - 0) = 1/\alpha_n$, and is continuous and increasing only on the continuous part of the spectrum. For example, when $q = h = 0$, the spectral function is simply

$$\rho_0(\lambda) = \begin{cases} (2/\pi)\sqrt{\lambda} & \text{if } \lambda \geq 0, \\ 0 & \text{if } \lambda < 0. \end{cases}$$

Obviously when $q \neq 0$, the new spectral function ρ would record all new spectral changes, which leads to the inverse spectral problem: by comparing ρ to ρ_0 can we recover the perturbation q?

Gel'fand–Levitan Theory

If we are given a spectral function ρ, can we find its associated Sturm–Liouville differential operator given in (1)? This is in essence the Gel'fand–Levitan theory, which produced an elegant algorithm for the recovery of the potential q and the boundary condition at $x = 0$.

As explained earlier, the spectrum depends on the growth of solutions and a key point is their representations by the Fourier transform,

$$y(x, \lambda) = \cos\left(x\sqrt{\lambda}\right) + \int_0^x K(x, t) \cos\left(t\sqrt{\lambda}\right) dt. \quad (2)$$

The kernel $K(x, t)$ is continuous and contains all information about q, namely, that

$$\frac{d}{dx} K(x, x) = \frac{1}{2} q(x) \text{ and } K(0, 0) = h. \quad (3)$$

Thus, it is a matter of finding $K(x, t)$ in order to recover q. To do so, we first form the function

$$F(x, t) = \int_{-\infty}^{\infty} \frac{\sin\left(x\sqrt{\lambda}\right)}{\sqrt{\lambda}} \frac{\sin\left(t\sqrt{\lambda}\right)}{\sqrt{\lambda}} \, d\sigma\left(\lambda\right), \quad (4)$$

where the given spectral function ρ is used in

$$\sigma(\lambda) = \begin{cases} \rho(\lambda) - \frac{2}{\pi}\sqrt{\lambda} & \text{if } \lambda \geq 0, \\ \rho(\lambda) & \text{if } \lambda < 0 \end{cases} \quad (5)$$

and set

$$f(x, t) = \frac{\partial^2 F(x, t)}{\partial x \partial t}.$$

The crux of the theory is that $f(x, t)$ and $K(x, t)$ satisfy a linear integral equation, for each fixed x

$$K(x, t) + \int_0^x K(x, s) f(s, t) \, ds = -f(x, t) \quad \text{for } 0 \leq t \leq x. \quad (6)$$

Thus given the spectral function ρ, we can form $F(x, t)$ by (4), yielding the kernel $f(x, t)$ and then for each fixed x solve the Fredholm integral equation (6) for $K(x, t)$. As for matrices, a Fredholm integral equation has a solution if the null space contains only the trivial solution. Once the existence of a solution K is guaranteed, its smoothness is examined. It is shown that $f(x, t)$ and $K(x, t)$ have the same degree of smoothness which implies the smoothness of q by (3). The original

Gel'fand–Levitan result in (1951) is based on the linear equation (6) and can be summarized as follows:

Theorem 1 (Gel'fand and Levitan Theory). *If a non-decreasing function $\rho(\lambda)$ satisfies*

(A) *for arbitrary real x the integral*

$$\int_{-\infty}^{0} \exp\left(x\sqrt{|\lambda|}\right) \mathrm{d}\rho(\lambda) \text{ exists},$$

(B) *the integral*

$$a(x) = \int_{1}^{\infty} \frac{\cos\left(x\sqrt{\lambda}\right)}{\lambda} \mathrm{d}\sigma(\lambda)$$

exists for all $0 \leq x < \infty$, while $a(x)$ has continuous derivatives up to the fourth order for all $0 \leq x < \infty$ and if the set of points of increase of ρ has at least one finite accumulation point, then there exists just one differential operator of the second order defined by (1) *which has $\rho(\lambda)$ as its spectral function. The function $q(x)$ and the number h are defined by* (3)*, where $K(x,t)$ is a solution of* (6).

However, the original theory had a gap between the necessary and sufficient conditions. Ten years later, Levitan and Gasymov proved a stricter version, which we state as the Gel'fand–Levitan–Gasymov theory found in Gasymov & Levitan (1964) that contains necessary and sufficient conditions.

Theorem 2 (Gel'fand–Levitan–Gasymov). *The monotonically increasing function ρ is the spectral function of a Sturm–Liouville of type* (1) *with a function q having m integrable derivatives and a number h if and only if the following conditions are satisfied:*

(A) *If $E(\lambda) = \int_0^\infty f(x)\cos\left(x\sqrt{\lambda}\right) \mathrm{d}x$, where $f \in L^2(0,\infty)$ and of compact support, then*

$$\int |E(\lambda)|^2 \mathrm{d}\rho(\lambda) = 0 \Longrightarrow f = 0 \text{ almost everywhere}.$$

(B) *The limit $\boldsymbol{\Phi}(x) = \lim_{N\to\infty} \int_{-\infty}^{N} \cos\left(x\sqrt{\lambda}\right)\mathrm{d}\sigma(\lambda)$, where $\sigma(\lambda)$ is defined by* (5)*, exists boundedly in every finite range of values of x and $\boldsymbol{\Phi}$ has $m+1$ locally integrable derivatives with $\boldsymbol{\Phi}(0) = -h$.*

There are also interesting results for the regular case that is defined by

$$\begin{cases} L(y) = -y''(x,\lambda) + q(x)y(x,\lambda) = \lambda y(x,\lambda), \\ \quad 0 \leq x \leq \pi, \\ y'(0,\lambda) - hy(0,\lambda) = 0, \\ y'(\pi,\lambda) - Hy(\pi,\lambda) = 0, \end{cases} \tag{7}$$

where q is continuous and $q, h, H \in \mathbb{R}$. Let the norming constants be defined by $\alpha_n = \int_0^\pi |y(x,\lambda_n)|^2 \mathrm{d}x$. Note that since q is continuous, its knowledge is equivalent to its sequence of Fourier coefficients. Thus, the data ought to be at least an infinite sequence of numbers in order to recover the potential q.

Theorem 3. *If all the $\alpha_n > 0$,*

$$\sqrt{\lambda_n} = n + \frac{a_0}{n} + \frac{a_1}{n^3} + O\left(\frac{1}{n^4}\right)$$

and

$$\alpha_n = \frac{\pi}{2} + \frac{b_0}{n^2} + O\left(\frac{1}{n^3}\right),$$

where a_0, a_1, and b_0 are constants, then there exists an absolutely continuous function $q(x)$ corresponding to the given λ_n and α_n.

Theorem 4. *The numbers $\{\lambda_n\}_{n=0}^\infty$ and $\{\alpha_n\}_{n=0}^\infty$ are the spectral data of some boundary value problem (7) with q'' being square integrable if and only if the following asymptotic estimates hold:*

$$\sqrt{\lambda_n} = n + \frac{a_0}{n} + \frac{a_1}{n^3} + \frac{\gamma_n}{n^3}$$

and

$$\alpha_n = \frac{\pi}{2} + \frac{b_0}{n^2} + \frac{\tau_n}{n^3},$$

where $\lambda_n \neq \lambda_m$ and $\alpha_n > 0$ and the series $\sum_{n=1}^\infty \gamma_n^2$ and $\sum_{n=1}^\infty \alpha_n^2$ are convergent.

The problem of generalizing the theory to higher dimensional operators remains open and depends heavily on the idea of transformation operators that map generalized functions. In Boumenir (1991), it is also proved that the Gel'fand–Levitan theory is based on the factorization of operators whose symbol is given by the spectral functions.

Discrete Case

Consider now a discrete version of the Sturm–Liouville problem

$$Bv = \lambda Av, \tag{8}$$

where B is a Jacobi matrix and A is a diagonal matrix with positive entries (positive definite). Expressing (8) in a vectorial form, we end up with recurrence relation defined by

$$\begin{cases} c_n y_{n+1} = (a_n\lambda + b_n)\, y_n - c_{n-1}y_{n-1}, \\ \quad n = 0, \ldots, m-1, \\ y_{-1} = 0, \quad \text{and} \quad y_m + hy_{m-1} = 0, \end{cases} \tag{9}$$

where $b_n \in \mathbb{R}$, $a_n > 0$, and $c_n > 0$. We look for a nontrivial finite sequence $y_{-1}, \ldots, y_m$ which satisfies (9). To this end, we normalize the solution vectors by $y_0 = 1/c_{-1}$, then knowing the first terms y_{-1} and

y_0 allows us to compute recursively the remaining entries that are now functions of λ. It is easy to see that eigenvalues λ_r are nothing other than the zeros of the last condition $y_m(\lambda) + hy_{m-1}(\lambda) = 0$. For a given eigenvector, define its squared norm by $\alpha_r = \sum_{k=0}^{m-1} a_k |y_k(\lambda_r)|^2$. The following theorem is found in Atkinson (1964) or in Teschl (2000).

Theorem 5. *Assume that we are given* $h \in \mathbb{R}$, $\{a_k > 0\}$, *eigenvalues* $\{\lambda_r\}_{0 \le r \le m-1}$, *norming constants* $\{\rho_r\}_{0 \le r \le m-1}$, *then there exists* $\{c_k\}_{-1 \le k \le m-1}$ *which are positive and constants* $\{b_k\}_{0 \le k \le m-1}$ *such that the boundary value problem has the set* $\{\lambda_r\}_{0 \le r \le m-1}$ *as its eigenvalues.*

AMIN BOUMENIR

See also **Inverse problems; Inverse scattering method or transform; Quantum inverse scattering method**

Further Reading

Atkinson, F.V. 1964. *Discrete and Continuous Boundary Problems*, New York and London: Academic Press

Boumenir, A. 1991. A comparison theorem for self-adjoint operators. *Proceedings of the American Mathematical Society*, 111(1): 161–175

Gasymov, M.G. & Levitan, B.M. 1964. Determination of a differential equation by two of its spectra. *Russian Mathematical Surveys*, 19(2): 1–63

Gel'fand, I.M. & Levitan, B.M. 1955. On the determination of a differential equation from its spectral function. *American Mathematical Society Translations*, (2)1: 253–304

Gel'fand, I.M. & Shilov, G.E. 1967. *Generalized Functions*, vol. 3: *Theory of Differential Equations*, New York and London: Academic Press

Levitan, B.M. 1987. *Inverse Sturm–Liouville Problems*, Utrecht: VNU Science Press

Marchenko, V.A. 1986. *Sturm–Liouville Operators and Applications*, Basel: Birkhäuser

Teschl, G. 2000. *Jacobi Operators and Completely Integrable Nonlinear Lattices*, Providence, RI: American Mathematical Society

GENERAL CIRCULATION MODELS OF THE ATMOSPHERE

Atmospheric general circulation models (AGCMs) simulate the dynamical, physical, and chemical processes of planetary atmospheres. For the Earth's atmosphere (*See* **Atmospheric and ocean sciences**), they are based on the thermo-hydrodynamic equations, which consist of the conservation of momentum, mass, and energy with the ideal gas law in coordinates suitable for the rotating planet.

In the presently used form, they were first derived by Vilhelm Bjerknes in 1904; subsequently, Lewis Fry Richardson (1922) proposed numerical weather prediction (NWP) as a practical application which, in 1950, was successfully performed by Jule Charney, R. Fjørtoft, and John von Neumann on an electronic computer based on a simplified set of these equations. While numerical weather prediction models utilize the atmospheric short-term memory for forecasting, AGCMs developed since the 1960s extend applications to longer time scales simulating seasonal and climate variability (for a personal recollection, see Smagorinsky, 1983).

Since then, numerical weather prediction and atmospheric general circulation modeling have enjoyed continuous advances, which are attributed to the following gains and improvements: (1) observational data accuracy, analysis, and assimilation; (2) insight into dynamical and physical processes, numerical algorithms, and computer power; and (3) the use of model hierarchies to study individual atmospheric phenomena. With simulations of the Earth system and that of other planets envisaged, a broad field of science has been established, which is of vital importance socio-economically, agriculturally, politically, and strategically.

Observations

Since the foundation of the World Meteorological Organization (WMO) and international treaties to monitor and record meteorological and oceanographical data, the collection of global data through local weather and oceanic stations has been systematically organized and has become a truly globalized system through the deployment of satellites and introduction of remote sensing facilities. The availability of extensive global data has enabled the extension of NWP models to complex global GCMs, thus facilitating simulations on larger time scales (months and years instead of hours and days) and validation of NWPs in return. Furthermore, it has become possible to study climate history and make estimates of future climates, which is particularly important due to likely anthropogenic impacts.

General Circulation Models

Atmospheric general circulation models have two basic components. First, the dynamical core consists of the primitive equations (the conservation equations with vertical momentum equation approximated by hydrostatic equilibrium, that is, balancing the vertical pressure gradient and the apparent gravitational forces) under adiabatic conditions. Second, physical processes contribute to the diabatic sources and sinks interacting with the dynamical core. They are incorporated as parameterizations, mostly in a modular format: solar and terrestrial radiation, the hydrological cycle (with phase transitions manifested in evaporation and transpiration, cloud, and precipitation processes), the planetary boundary layer communicating between the free atmosphere and the ground (soil with vegetation, snow and ice cover; ocean with sea ice), and atmospheric chemistry. Most of these parameterizations enter the thermodynamic energy equation as heat sources or sinks.

Dynamical core

State-of-the-art atmospheric general circulation models commonly utilize the so-called primitive equation approximation of the Navier–Stokes equations. In addition to the dry dynamics, equations describing the transport of other constituents such as water vapor, cloud liquid water and ice, trace gases, and particles (aerosols) can be an integral part of the dynamical core. To integrate the equations, they are discretized in space and time where finite differences and spectral methods are the most dominant. For more details on the governing equations; *See* the entries for **Atmospheric and ocean sciences; Fluid dynamics; Navier–Stokes equation**.

(i) Horizontal discretization: In the horizontal, grid point, or spectral representations of the dependent model variables are used. Different grid structures and finite difference schemes have been designed to reduce the error (Messinger & Arakawa, 1976). An alternative approach is the spectral method. The dependent variables are represented in terms of orthogonal functions where appropriate basis functions are the spherical harmonics. The maximum wave number of the expansion defines the resolution of the model. Since the computation of products is expensive, only linear terms are evaluated in the spectral domain. To compute the nonlinear contributions, the variables are transformed into grid point space every time step, where the respective products are computed and transformed back to spectral space. Necessary derivatives are computed during the transformation. This spectral-transform procedure (Eliassen et al.,1970; Orszag, 1970) makes the spectral approach computationally competitive with finite difference schemes. For low resolutions, the spectral method is, in general, more accurate than the grid point method. However, spectral methods are less suitable for the treatment of scalar fields, which exhibit sharp gradients and, for physical reasons, must maintain a positive-definite value (e.g., water vapor, cloud water, chemical tracers). Therefore, selected fields are often treated separately in the grid point domain using, for example, semi-Lagrangian techniques. Recently, with increasing model resolutions and the need for transporting more species (e.g., for chemical submodels), grid point models are attracting more attention again, while novel grid structures are introduced, for instance, the spherical icosahedral grid of the German Weather Service model GME (Majewski et al., 2000).

(ii) Vertical discretization: In general, finite differences and numerical integration techniques are used for the derivatives and integrals in the vertical. The vertical coordinate can be defined in different ways. The isobaric coordinate eliminates the density from the equations and simplifies the continuity equation compared with a z-coordinate system. However, the intersection of low-level pressure surfaces with the orography enforces time-dependent lower boundary conditions which are difficult to treat numerically. This problem can be avoided if terrain following sigma (σ) coordinates are used, where sigma is defined by the pressure divided by the surface pressure $\sigma = p/p_0$. Unfortunately, the sigma coordinate leads to a formulation of the pressure gradient force which, in the presence of steep orography, is difficult to treat. The advantages of both sigma and pressure coordinates are combined by introducing a hybrid coordinate system with a smoothed transition from σ to p with height.

Physical Processes and Parameterizations

Many processes that are important for large-scale atmospheric flow cannot be explicitly resolved by the model due to its given spatial and temporal resolution. These processes need to be parameterized; that is, their effect on the large-scale circulation needs to be formulated in terms of the resolved grid-scale variables. The most prominent processes in building a parameterization package of an atmospheric general circulation model are long- and short-wave radiation, cumulus convection, large-scale condensation, cloud formation and the vertical transport due to turbulent fluxes in the planetary boundary layer, and the effect of different surface characteristics such as vegetation on the surface fluxes. Additional processes such as the excitation of gravity waves and their impact on the atmospheric momentum budget or the effect of vertical eddy fluxes above the boundary layer are often considered. Because the land surface provides a time-dependent boundary condition that acts on time scales comparable to the atmosphere, great effort has been made to include land surface and soil processes in the atmospheric parameterization package. More recently, the effect of the interaction of various chemical species and their reactions with atmospheric circulation are also being considered. In addition to the direct relation between the resolved atmospheric flow and the effect of the parameterized processes, there are various other interactions among the individual processes that have to be taken into account. For typical comprehensive atmospheric general circulation models, Figure 1 displays the interrelations between the adiabatic dynamics, providing the spatial and temporal distribution of the dependent model variables and the various processes being parameterized.

Model Hierarchy

General circulation models of reduced complexity are continuously developed to supplement comprehensive

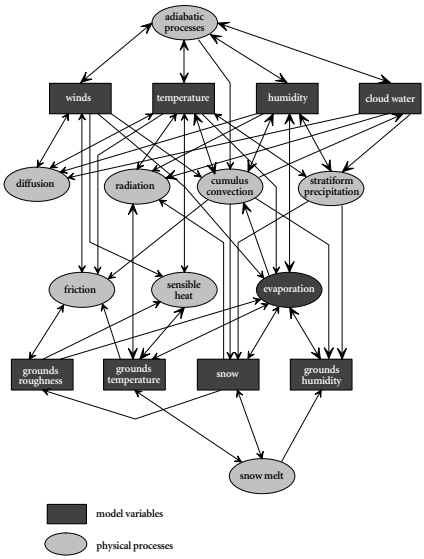

Figure 1. Interactions in comprehensive GCMs (schematic).

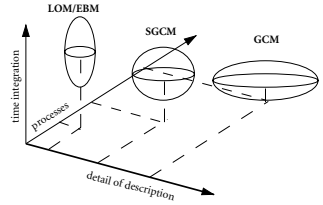

Figure 2. A model hierarchy of general circulation models.

GCMs, to gain insight into atmospheric phenomena (see Figure 2) and for educational purposes: when utilizing the full set of equations, the model spectrum ranges from simple GCMs (SGCMs) with analytic forms of heating and friction to low-order models (LOMs). A prominent LOM is the Lorenz model (*See* **Lorenz equations**), which approximately describes the nonlinear convection dynamics in the vicinity of a critical point for the stream function and temperature in a set of ordinary differential equations. It can be regarded as including first-order nonlinear effects (temperature advection) to a linear model, which leads to chaotic behavior. The Lorenz model is used to study predictability and serves as a paradigm for phase-space behavior of atmospheric GCMs. Utilizing thermal energy conservation only, another spectrum of models (energy balance models, or EBMs) is obtained by averaging in certain spatial directions. This leads to the horizontally averaged one-dimensional radiative-convective models; the one-dimensional energy balance model when averaged vertically and longitudinally for studying climate feedback and stability; and two-dimensional statistical–dynamical models when averaged longitudinally where dynamical processes are being parameterized. A prominent EBM example is the globally averaged or zero-dimensional energy balance model. With ice-albedo and water vapor-emissivity feedbacks included, climate catastrophes leading to a snowball earth and runaway greenhouse can be demonstrated. With random forcing and periodic solar radiation input (e.g., Milankovich cycles), stochastic resonance emerges.

KLAUS FRAEDRICH, ANDREAS A AIGNER, EDILBERT KIRK, AND FRANK LUNKEIT

See also **Atmospheric and ocean sciences; Fluid dynamics; Forecasting; Lorenz equations; Navier–Stokes equation**

Further Reading

Eliassen, E., Machenhauer, B. & Rasmussen, E. 1970. *On a Numerical Method for Integration of the Hydrodynamical Equations with a Spectral Representation of the Horizontal Fields.* Report No. 2, Institut for Teoretisk Meteorologi, University of Copenhagen

Majewski, D., Liermann, D., Prohl, P., Ritter, B., Buchhold, M., Hanisch, T., Paul, G., Wergen, W. & Baumgardner, J. 2000. *The global icosahedral–hexagonal grid point model GME-operational version and high resolution tests*, ECMWF, Workshop Proceedings, Numerical methods for high resolution global models, pp. 47–91

McGuffie, K. & Henderson-Sellers, A. 1997. *A Climate Modelling Primer*, New York: Wiley

Messinger, R. & Arakawa, A. (1976). *Numerical Methods Used in Atmospheric Models*, Geneva: WMO

Orszag, S.A. 1970. Transform method for calculation of vector coupled sums: application to the spectral form of the vorticity equation. *Journal of Atmospheric Sciences*, 27: 890–895

Richardson, L.F. 1922. *Weather Prediction by Numerical Process*, Cambridge: Cambridge University Press

Smagorinsky, J. 1983. The beginnings of numerical weather prediction and general circulation modeling: early recollections. In *Theory of Climate*, edited by B. Saltzman, New York: Academic Press, pp. 3–38

Trenberth, K. 1992. *Climate System Modelling*, Cambridge and New York: Cambridge University Press

GENERAL RELATIVITY

Called *general relativity*, Albert Einstein's theory of gravitation was created as a generalization of his special relativity theory. As special relativity is a theory of physical space-time (neglecting gravitational effects), general relativity is a theory of physical space-time in the presence of gravitation.

While Maxwell's theory of electromagnetism is a relativistic theory that is covariant with respect to Lorentz transformations, Newton's theory of gravitation is incompatible with special relativity. In 1907,

two years after proposing special relativity, Einstein was preparing a review of special relativity when he suddenly wondered how Newtonian gravitation would have to be modified to fit in with special relativity. Einstein described this as "the happiest thought of my life." He proposed the *equivalence principle* as "the complete physical equivalence of a gravitational field and the corresponding acceleration of the reference frame" that "extends the principle of relativity to the case of uniformly accelerated motion of the reference frame."

In fact, Einstein's equivalence principle is a generalization of the so-called *weak* equivalence principle, which dates from Galileo and Newton and states that the inertial mass and gravitational mass of any object are equal. Thus (neglecting friction), the acceleration of different bodies in a gravitational field is independent of their masses and other physical characteristics, and hence, with given initial conditions, their motions will be the same.

The next important step was made by Einstein in his 1912 papers, where he concluded that "if all accelerated systems are equivalent, then Euclidean geometry cannot hold in all of them." Further investigations by Einstein to find the correct form of equations for a gravitational field were connected with applications of Riemannian geometry and tensor analysis. The final form of equations of general relativity was given by Einstein in his paper "The Field Equations of gravitation," submitted on 25 November 1915. At about the same time, David Hilbert submitted a paper entitled "Foundations of Physics," which also contains the correct field equations for gravitation, introduced by applying a variation principle.

Physical Space-time and Gravitating Matter in General Relativity

According to general relativity, physical space-time in a gravitational field is non-Euclidean; so to describe the properties of space-time, Einstein applied Riemannian geometry. Without gravitation, physical space-time is a flat pseudo-Euclidean Minkowski 4-continuum, where free particles move uniformly and linearly along geodesic worldlines of Minkowski space-time. Einstein's key idea is that in a gravitational field, particles move along geodesic lines of curved space-time, and in accordance with the Equivalence principle, their movement does not depend on the particles' characteristics. Thus, motion for an observer is motion along curves in 3-space with variable velocity. Curvature of space-time in general relativity is created by sources of gravitational field. In general relativity, the role of sources of gravitational field is played by the energy-momentum tensor describing the distribution and motion of gravitating matter. Energy (or mass) density (the source of gravitation in Newton's theory) is only a component of the energy-momentum tensor. Besides energy (mass), a gravitational field in general relativity is also created by momentum and other components of an energy-momentum tensor. The dependence between geometrical properties of physical space-time and gravitating matter is described by Einstein's gravitational equations.

Einstein Gravitational Equations

The principal geometrical characteristics of a gravitational field in general relativity are given by the metric tensor g_{ik}, which determines the square of distance between two infinitesimally close points of pseudo-Riemannian 4-space-time

$$ds^2 = g_{ik}\,dx^i\,dx^k \quad (i, k = 0, 1, 2, 3). \tag{1}$$

By means of the metric tensor, time intervals and spatial distances can be defined; thus the formula for proper time fixed by a clock at rest in some reference frame is $d\tau = (1/c)\sqrt{g_{00}\,dx^0\,dx^0}$. Because the value of g_{00} in a gravitational field depends on location, time flow depends on gravitational field.

Einstein's gravitational equations are nonlinear second-order differential equations with respect to the metric tensor and have the form

$$R_{ik} - 1/2 g_{ik} R = 8\pi G/c^4 T_{ik}, \tag{2}$$

where R_{ik} is the so-called Ricci tensor (a contraction of the curvature tensor), R is the scalar curvature, T_{ik} is the energy-momentum tensor, G is Newton's gravitational constant, and c is the velocity of light in a vacuum. Einstein's equations are covariant with respect to arbitrary coordinate transformations.

Equation (2) can be changed by adding to the right-hand side, the so-called cosmological term Λg_{ik}, where Λ is a cosmological constant introduced by Einstein. This term describes energy density and pressure of the vacuum, and it plays an essential role in cosmology, leading to the effect of gravitational repulsion if $\Lambda > 0$. In the case of weak gravitational fields, when the variation of metric with respect to the Minkowski metric is small, the Einstein equations lead to Newton's law of gravitational attraction and allow one to find first relativistic corrections. In the case of strong gravitational fields, Einstein equations can give new physical results, including black holes and gravitational waves.

Experimental Verification and Bounds of Applicability

Several classical effects of general relativity have been verified observationally, including the bending of light in a gravitational field, gravitational redshift, the advance of the perihelion of the planet Mercury (43 s

of arc per century), and retarding of the propagation of light in a gravitational field. The first three effects were discussed by Einstein even before the creation of general relativity.

The *weak* equivalence principle has been verified to high precision (10^{-12}), and general relativity provides a basis for relativistic astrophysics and cosmology. The Hot Big Bang model was built within the framework of general relativity. Over the past two decades, the role of general relativity has grown in connection with discoveries in cosmology—in particular, acceleration of cosmological expansion, dark matter and dark energy, and other problems that need to be resolved.

General relativity is a classical theory, and a consistent quantum theory of gravitation has not yet been developed. In fact, the formulation of a quantum-gravitation theory requires a unified theory of all fundamental physical interactions. At present, the most popular candidate for such a unified theory is the superstring theory. This theory is in higher-dimensional space, and it leads to a generalization of Einstein's gravitation theory. A second problem with general relativity is the presence of gravitational singularities (cosmological singularities, collapsing systems, etc.). According to theorems by Stephen Hawking and Roger Penrose, this problem is connected under certain conditions with internal properties of the gravitational equations of general relativity. As with classical theory, general relativity is inapplicable near singular states.

The creation and development of Einstein's gravitation theory was a triumph of 20th-century science, providing the basis of gravitation theory, relativistic astrophysics, and cosmology. Within the frame of its applicability, general relativity will remain a great achievement of human culture.

VIACHASLAV KUVSHINOV AND ALBERT MINKEVICH

See also **Black holes; Cosmological models; Einstein equations; Gravitational waves; String theory; Tensors; Twistor theory**

Further Reading

Einstein, A. 1989–1996. *The Collected Papers of Albert Einstein*, vol. 2: The Swiss Years: Writings, 1900–1909, vol. 3: The Swiss Years: Writings, 1909–1911; vol. 4: The Swiss years: Writings, 1912–1914, Princeton, NJ: Princeton University Press

Fok, V.A. 1961. *The Theory of Space, Time and Gravitation*, New York: Pergamon Press

Landau, L.D. & Lifshitz, E.M. 1973. *Therie of field*, Moscow: Nauka

Landau, L.D. & Lifshitz, E.M. 1984. *The Classical Theory of Fields*, 4th edition, Oxford and New York: Pergamon Press

Misner, C., Thorne, K. & Wheeler, J. 1973. *Gravitation*, San Francisco: Freeman

Weinberg, S. 1972. *Gravitation and Cosmology: Principles and Applications of the General Theory of Relativity*, New York: Wiley

Zel'dovich, Ya.B. & Novikov, I.D. 1971. *Relativistic Astrophysics*, 2 vols. Chicago: University of Chicago Press

GENERALIZED FUNCTIONS

Generalized functions were introduced into quantum mechanics by Paul Dirac, who defined the delta function $\delta(x)$ as follows (Dirac, 1958):

$$\delta(x) = 0 \text{ for } x \neq 0$$

and

$$\int_{-\varepsilon}^{+\varepsilon} \delta(x) = 1 \text{ for } \varepsilon > 0. \tag{1}$$

Although $\delta(x)$ is not a true function (from a mathematical perspective) because it is undefined at $x = 0$, the delta function is widely used in physics to approximate functions that are localized in space or time. Examples of such idealizations include the concepts of point mass or point charge and the spatially localized action of a pick on a guitar string.

In an engineering context, the delta function is called the unit impulse function and is used to approximate functions of large amplitude and short duration such as the striking of a golf ball or the instantaneous charging of an electrical capacitor (Guillemin, 1953). Since such point sources are only idealizations, they can be represented by the limiting procedure, $\delta(x) = \lim_{a\to\infty} \delta_a(x)$ for a family of piecewise continuous functions $\delta_a(x)$, where a is a continuous parameter. Among others, the following four functions, $\delta_a(x)$, are popular approximations of the delta function $\delta(x)$ (Pauli, 1973):

- *Unit impulse* (*box*): $\delta_a(x) = a/2$ for $|x| < 1/a$, and $\delta_a(x) = 0$ for $|x| > 1/a$.
- *Finite impulse response filter*: $\delta_a(x) = \sin ax/\pi x$.
- *Gaussian pulse*: $\delta_a(x) = a\mathrm{e}^{-\pi a^2 x^2}$.
- *Lorentzian pulse*: $\delta_a(x) = a/(1 + \pi^2 a^2 x^2)$.

In the limit $a \to \infty$, all representations $\delta_a(x)$ have zero width, infinite peak amplitude, and unit area, that is, all the approximations converge to the delta function $\delta(x)$ (see Figure 1).

Closely related to Dirac's delta function is Oliver Heaviside's step function, which was introduced in the late 19th century and has been widely used in electronics and communications research since the 1920s (Heaviside, 1950; Guillemin, 1953). The Heaviside step $H(x)$ is defined as follows:

$$H(x) = 1 \text{ for } x > 0 \text{ and } H(x) = 0 \text{ for } x < 0. \tag{2}$$

The derivative of the Heaviside step function is recognized as Dirac's delta function because $H'(x) = 0$ for $x \neq 0$ and for $\varepsilon > 0$

$$\int_{-\varepsilon}^{+\varepsilon} H'(x)\,\mathrm{d}x = H(+\varepsilon) - H(-\varepsilon) = 1. \tag{3}$$

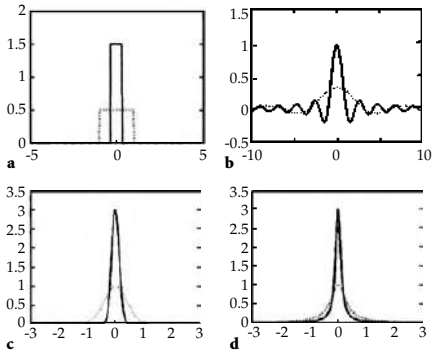

Figure 1. Approximations of the Dirac delta function $\delta(x)$ for $a=1$ (dotted curves) and $a=3$ (solid curves): (a) the box, (b) the impulse response filter, (c) the Gaussian pulse, and (d) the Lorentzian pulse.

In engineering terms, the step function represents an instantaneous jump from zero to unit value of some physical quantity such as the signal voltage at the input terminals of an amplifier.

Because the delta and step are not defined at $x=0$, they are not true functions; thus mathematicians call them distributions, implying rules that assign numbers to integral expressions (Strauss, 1992). To understand this perspective, consider a real function, $f(x)$ which has derivatives for all values of x that approach zero faster than any power of x. In other words, $\lim_{|x|\to\infty}|x|^p f^{(m)}(x)=0$ for any $m\geq 0$ and $p\geq 0$. Such functions $f(x)$ are called test functions for integral distributions. As is seen from the box approximation of $\delta_a(x)$ in the limit $a\to\infty$, the delta function $\delta(x)$ assigns the number $f(0)$ to the integral distribution associated with a test function $f(x)$:

$$\int_{-\infty}^{\infty} f(x)\delta(x)\,\mathrm{d}x = f(0). \tag{4}$$

More generally, the delta function $\delta(x)$ and its derivatives $\delta^{(m)}(x)$ satisfy the following fundamental property:

$$\begin{aligned}\int_{-\infty}^{\infty} & f(x)\delta^{(m)}(x-\xi)\,\mathrm{d}x \\ &= (-1)^m\int_{-\infty}^{\infty} f^{(m)}(x)\delta(x-\xi)\,\mathrm{d}x \\ &= (-1)^m f^{(m)}(\xi),\end{aligned} \tag{5}$$

where $f(x)$ is a test function. A brief list of useful delta function properties follows from the fundamental property in Equation (5) (Gel'fand & Shilov, 1964):

- *Even function*: $\delta(-x)=\delta(x)$.
- *Scaling transformation*: $|\xi|\delta(\xi x)=\delta(x)$.
- *Factorization*: $2|\xi|\delta(x^2-\xi^2)=\delta(x-\xi)+\delta(x+\xi)$.
- *Projection formula*: $\frac{1}{(x-\xi\mp\mathrm{i}0)}=\mathrm{PV}\left[\frac{1}{(x-\xi)}\right]\pm\pi\mathrm{i}\delta(x-\xi)$ (where PV stands for principal value).
- *Fourier transform*: $\hat{\delta}(k)=\int_{-\infty}^{\infty}\delta(x)\mathrm{e}^{-\mathrm{i}kx}\,\mathrm{d}x=1$.
- *Spectral representation*: $2\pi\delta(x)=\int_{-\infty}^{\infty}\mathrm{e}^{\mathrm{i}kx}\,\mathrm{d}x$.

Dirac studied orthogonality relations for the wave function $\psi_\lambda(x)$ of the stationary Schrödinger equation with a potential

$$-\frac{h}{2m}\psi_\lambda''(x)+U(x)\psi_\lambda(x)=\lambda\psi_\lambda(x). \tag{6}$$

In this context, square integrable wave functions for different levels of energy λ are orthogonal with respect to the inner product

$$\langle\psi_{\lambda'}|\psi_\lambda\rangle=\int_{-\infty}^{\infty}\bar{\psi}_{\lambda'}(x)\psi_\lambda(x)\,\mathrm{d}x=\delta_{\lambda',\lambda}, \tag{7}$$

where $\delta_{\lambda',\lambda}=0$ for $\lambda'\neq\lambda$ and $\delta_{\lambda,\lambda}=1$. Similar orthogonality relations for wave functions of continuous spectra diverge. For example, linear waves in free space (when $U(x)=0$) take the form $\psi_\lambda(x)=\Psi(x;k)=\mathrm{e}^{\mathrm{i}kx}$ for $\lambda=hk^2/2m$. They are periodic in x with period $L=2\pi/k$. If $k=k_n=2\pi n/L$, the periodic function satisfies the following orthogonality relations on the finite interval $x\in[-L/2, L/2]$:

$$\langle\Psi(k_{n'})|\Psi(k_n)\rangle=\int_{-L/2}^{L/2}\mathrm{e}^{\mathrm{i}(k_n-k_{n'})x}\,\mathrm{d}x=L\delta_{n',n}. \tag{8}$$

When linear waves in free space are taken over the whole real axis (i.e., $L\to\infty$), the inner product of the wave function $\Psi(x;k)$ with itself diverges. The delta function $\delta(k)$ replaces this divergence in the closed form

$$\begin{aligned}\langle\Psi(k')|\Psi(k)\rangle &= \int_{-\infty}^{\infty}\bar{\Psi}(x;k')\Psi(x;k)\,\mathrm{d}x \\ &= 2\pi\delta(k'-k),\end{aligned} \tag{9}$$

where $\delta(k)=0$ for $k\neq 0$ and $\delta(0)=\infty$. The singularity of the delta function $\delta(k)$ is uniquely specified in the distribution (integral) sense by requiring that

$$\int_{-\infty}^{\infty}\delta(k)\,\mathrm{d}k=1. \tag{10}$$

The delta function $\delta(x)$ represents not only the orthogonality of the wave functions $\psi_\lambda(x)$ of

the stationary Schrödinger equation, but also their completeness with the completeness relation:

$$\frac{1}{2\pi}\int_{-\infty}^{\infty}\bar{\Psi}(x';k)\Psi(x;k)\,\mathrm{d}k+\sum_n\bar{\Psi}_n(x')\Psi_n(x)=\delta(x'-x), \tag{11}$$

where $\Psi(x;k)$ are wave functions of the continuous spectrum and $\Psi_n(x)$ are wave functions of the discrete spectrum. With the use of the delta function $\delta(x)$, a test function $f(x)$ can be expanded into a complete and orthogonal set of wave functions:

$$f(x)=\frac{1}{2\pi}\int_{-\infty}^{\infty}\hat{f}(k)\Psi(x;k)\,\mathrm{d}k+\sum_n\hat{f}_n\Psi_n(x), \tag{12}$$

where coefficients of the expansion are

$$\hat{f}(k)=\langle\Psi(k)|f\rangle,\quad \hat{f}_n=\langle\Psi_n|f\rangle. \tag{13}$$

Generalized functions are widely used in electric circuit theory, communications, spectral analysis, integral transforms, and Green function solutions of equations of mathematical physics (Guillemin, 1953; Pauli, 1973; Strauss, 1992). For example, the Fourier transform is based on the spectral decomposition above for $\Psi(x;k)=\mathrm{e}^{\mathrm{i}kx}$ and $\Psi_n(x)=0$.

DMITRY PELINOVSKY

See also **Function spaces; Functional analysis; Integral transforms; Quantum theory; Spectral analysis**

Further Reading

Dirac, P.A.M. 1958. *The Principles of Quantum Mechanics*, 4th edition, Oxford: Clarendon Press

Gel'fand, I.M. & Shilov, G.E. 1964. *Generalized Functions,* vol. 1, *Properties and Operations*, New York and London: Academic Press

Guillemin, E.A. 1953. *Introductory Circuit Theory*, New York: Wiley

Heaviside, O. 1950. *Electromagnetic Theory*, New York: Dover

Pauli, W. 1973. *Pauli Lectures on Physics:* Vol. 5, *Wave Mechanics*, Cambridge, MIT Press

Strauss, W.A. 1992. *Partial Differential Equations, An Introduction*, New York: Wiley

GEOMETRICAL OPTICS, NONLINEAR

Nonlinear geometric optics arose in the second half of the 20th century in several areas of research, including nonlinear optics and reaction-diffusion systems. To understand the origin of such problems and the underlying physical phenomena, it is helpful to consider briefly the historical path that has led to them.

Classical Results

Traditionally, geometric optics comprised all of optics. It developed from empirical laws of propagation for light beams, which are bent in a non-uniform medium and refract and reflect at the interfaces of media possessing different optical properties. Remarkable successes were achieved, including inventions of the microscope and the telescope around the beginning of the 17th century. At the same time, some important scientific problems were studied; thus in 1620, Willebrord Snell established the law of refraction at the interface of two transparent media. Assuming angles are measured with respect to a line normal to the boundary, Snell's law states that at any angle of incidence (ψ_1), the ratio

$$\frac{\sin\psi_1}{\sin\psi_2}=\text{constant}\equiv n_{12}, \tag{1}$$

where ψ_2 is the angle of refraction and the constant n_{12} is the reciprocal refractive index. Interestingly, this important law was independently discovered by René Descartes about a decade later. Pierre Fermat's subsequent formulation of the principle of least time—which governs the propagation of light rays—completed the phenomenological theory of geometric optics.

In the 17th century, two competitive hypotheses were advanced for the physical nature of light: the corpuscular hypothesis of Isaac Newton and the wave theory of Christian Huygens. Two centuries later, after the theoretical studies and experimental works of Thomas Young, Augustin-Jean Fresnel, and François Arago, the wave theory of light triumphed. The true nature of light was revealed in the 19th century to be based on James Clerk Maxwell's theory of electromagnetism, which predicted the existence of electromagnetic waves that propagate in vacuum with constant velocity $c=1/\sqrt{\varepsilon_0\mu_0}\approx 3\times 10^8$ m/s, where ε_0 and μ_0 are the dielectric permittivity and magnetic permeability of vacuum, respectively.

This value—obtained entirely from independent measurements of electric and magnetic fields—is precisely equal to the light velocity in vacuum, which was first measured by Ole Roemer two centuries before (using astronomical data on time intervals between eclipses of Jupiter's satellites). Together with the subsequent experimental discovery and investigation of properties of electromagnetic waves inspired by Hermann Helmholtz and performed by Heinrich Hertz, this result has convinced physicists of the electromagnetic nature of light.

This electromagnetic theory of light explains most optical phenomena. For example, it yields Snell's law of refraction, giving the constant in Equation (1) as

$$n_{12}=v_1/v_2=\sqrt{\varepsilon_2/\varepsilon_1}=n_2/n_1. \tag{2}$$

Here v_i is the velocity of light in the ith medium ($i = 1, 2$), and ε_i and $n_i = c/v_i = \sqrt{\varepsilon_i/\varepsilon_0}$ are the dielectric permittivity and the absolute refractive index of this medium, respectively.

Physical mechanisms underlying the refractive index were studied by Helmholtz, Paul Drude, and Hendrik Lorentz at the close of the 19th century. They merged the electromagnetic theory with the idea of electrons as charged particles bound in atoms and molecules which are dislocated under the influence of an electromagnetic field of a light wave. (From the modern point of view, such electrons occupy exterior atomic shells; thus, they are referred to as optical electrons.) Further developments of such ideas connect optical phenomena with the dynamic response of an optical medium to the electromagnetic waves propagating through it.

When a light wave propagates through a dielectric medium, its electric field ($\boldsymbol{E}$) displaces the optical electrons, inducing a wave of electric polarization ($\boldsymbol{P}$). The latter generates a secondary electromagnetic wave which is added to the primary wave, modifying the polarization wave, and so on, ad infinitum. In other words, the electromagnetic wave and the response of an optical medium determine each other. As the relations

$$\begin{aligned} \varepsilon \boldsymbol{E} &= \varepsilon_0 \boldsymbol{E} + \boldsymbol{P}, \quad \boldsymbol{P} = \varepsilon_0 \chi \boldsymbol{E}, \\ n &= c/v = \sqrt{\varepsilon/\varepsilon_0} \end{aligned} \tag{3}$$

are always fulfilled (where χ is the dielectric susceptibility of the medium), the absolute refraction index of the medium can be expressed via χ by the formula

$$n = \sqrt{\varepsilon/\varepsilon_0} = \sqrt{1 + \chi}. \tag{4}$$

If the light wave is sinusoidal and sufficiently weak, the response of the medium is readily calculated; thus the susceptibility χ is expressed via the oscillatory parameters of optical electrons which, in turn, depend on the frequency (ω), but not on the wave amplitude. Weakness of a light wave means that intensity $\boldsymbol{E}$ of an electric field in the wave must be much smaller than characteristic intensities of intra-atomic electric fields. The greatest intra-atomic intensities (reached in the hydrogen atom) are about 5×10^9 V/cm, whereas the intensities of light fields generated by ordinary (nonlaser) sources of light are about 1 V/cm. Thus, the constitutive equation relating the electric polarization $\boldsymbol{P}$ with the electric field intensity $\boldsymbol{E}$ is linear for ordinary light.

Nonlinear Optics

In the latter half of the 20th century, lasers were invented, which could generate fields with intensities of about 10^7 V/cm, and in 1989, beams of light were produced with electric fields of more than ten times the intra-atomic values. In such strong fields, dielectric susceptibility χ becomes dependent on the electric field intensity, making the constitutive equation nonlinear. Both the dielectric permittivity ε and the absolute refraction index n of the medium also depend on the electric field intensity $\boldsymbol{E}$, and these dependencies are modified by additional influences, such as heating of the medium.

Studies of optical effects in strong light fields use the basic ideas of geometric optics, for example, the concept of refractive index. Consider a uniform isotropic dielectric medium. Adverting to Equation (3), let us write the expansion

$$\boldsymbol{P} = \varepsilon_0 \chi^{(1)} \boldsymbol{E} + \varepsilon_0 \chi^{(2)} |\boldsymbol{E}|^2 + \varepsilon_0 \chi^{(3)} |\boldsymbol{E}|^2 \boldsymbol{E} + \cdots. \tag{5}$$

Here, even powers of $\boldsymbol{E}$ are excluded by symmetry consideration, so $\chi = \boldsymbol{P}/\varepsilon_0 \boldsymbol{E} = \chi^{(1)} + \chi^{(3)} |\boldsymbol{E}|^2 + \cdots$, which implies (see Equation (4))

$$\begin{aligned} n &= \sqrt{1 + \chi^{(1)} + \chi^{(3)} \boldsymbol{E}|^2} \approx n_0 + 2 n_3 |\boldsymbol{E}|^2, \\ n_0 &= \sqrt{1 + \chi^{(1)}}, \quad n_3 = \frac{\chi^{(3)}}{4\sqrt{1 + \chi^{(1)}}}, \end{aligned} \tag{6}$$

because the nonlinear term is small. Averaging n on the time period $T = 2\pi/\omega$ of oscillations of electric field $\boldsymbol{E} = \boldsymbol{E}_0(x, y, z) \sin \omega t$ yields

$$n = n_0 + n_3 |\boldsymbol{E}_0|^2, \tag{7}$$

where n_0 is the linear refractive index and $n_3 |\boldsymbol{E}_0|^2$ describes the nonlinear correction to this index.

Equations (3) and (7) indicate that a bounded cylindrical beam of light can create an optical heterogeneity in the medium through which it propagates. Suppose the beam is Gaussian so the amplitude of electric oscillations varies transversely as $|\boldsymbol{E}_0|(r) = A_0 \exp[r^2/(2r_0^2)]$, where A_0 is the value of amplitude on the axis of beam, r is distance from the beam axis, and r_0 is a phenomenological constant determining the typical width of the beam. Then,

$v = c/(n_0 + n_3 A_0^2)$ on the axis of the beam;
$v = c/n_0$ far from the axis of the beam.

If the inequality $n_3 > 0$ ($n_3 < 0$) is fulfilled, the axial velocity of light is smaller (greater) than the peripheral velocity. In first case, the plane wave front will become concave in the direction of light propagation, and self-focusing of the beam will occur; while in the second case, self-defocusing of the beam will occur. Both these phenomena have been observed; in particular, self-focusing was predicted by Gurgen Askarian in 1962 and then experimentally observed by N.P. Pilipetsky and A.R. Rustamov in 1965.

Nonlinear Reaction-Diffusion Systems

One can image an excitable medium (EM) as a spatial region G occupied by a medium, in which the processes of autocatalytic production, destruction, and diffusion of some substances occur. In the simplest case, when only one substance of concentration $u = u(\mathbf{r}, t)$ is involved (here $\mathbf{r}$ is a point in three-dimensional space and t is time), the dynamics of u are described by two relationships: the continuity equation

$$u_t + \operatorname{div} \boldsymbol{J} = f(u) \tag{8}$$

(where $u_t = \partial u/\partial t$), and the Fick diffusion law

$$\boldsymbol{J} = -D \operatorname{grad} u. \tag{9}$$

For constant diffusivity D, these two equations reduce to the single parabolic reaction-diffusion equation

$$u_t = D\Delta u + f(u). \tag{10}$$

Here, the symbols div, grad, and Δ designate the spatial divergence, gradient operator, and Laplace operator, respectively; $\mathbf{J} = \mathbf{J}(\mathbf{r}, t)$ is the vector of diffusion flux density of the substance; and the function $f(u)$ (called the kinetic function of the active medium) determines the dependence of the production/destruction rate of substance per unit volume of the concentration u.

In general, an EM is able to support the propagation of traveling-wave fronts and impulses. In the steady regime, plane excitation waves propagate with constant speed preserving their spatial profile. Both the speed and the wave profile are determined by physical parameters of the medium in which the waves propagate and are independent of initial conditions; thus such waves are called *autowaves* (AW). This term was coined by Rem Khokhlov (an early Russian specialist on nonlinear physics and president of Moscow State University) in a 1974 presentation as an official opponent during Anatol Zhabotinsky's defense of his doctoral thesis on periodic chemical reactions. (An enthusiastic mountain climber, Khokhlov sadly perished in the Caucasian mountains in 1977.) The significance of AWs stems from the fact that they frequently occur in physical, chemical and biological applications, including muscles, the nervous system, and the heart.

To reveal the qualitative properties of AW propagation, one needs to solve these equations; but even in the spatially homogeneous case—when the medium is described by Equation (10) with constant D—this problem is challenging. Thus, it is of interest to consider an approach in which the general properties of EM are specialized by means of some simple axioms. Interestingly, this approach leads to an analog of traditional geometric optics, as was first shown by Israel Gel'fand and Sergei Fomin in 1961 (Gel'fand & Fomin, 1961).

When either a traveling-wave front or the leading edge of an impulse moves through an EM, the latter switches from the resting state to the excited state (in the case of impulse, the life time of excitable state is finite and equal to the pulse duration). Neglecting the front width, one may imagine the leading edge as a surface that separates the resting and excited zones, and a motion of this surface (which models the motion of an AW) is interpreted as propagation of excitation. Thus, Gel'fand and Fomin introduced two axioms: (i) each spatial point of the EM can be in one of two states: either in the resting state or in the excited one; (ii) if at some time moment t the excitation has reached some spatial point P, then P immediately becomes a source of propagating excitation. In the case of a nonhomogeneous anisotropic EM, the time period $\mathrm{d}t$ of motion of excitation along the infinitesimal path connecting the points $x(s)$ and $x(s + \mathrm{d}s) = x(s) + (\mathrm{d}x/\mathrm{d}s)\,\mathrm{d}s$ (here s is the parameter) depends both on the point $x(s)$ and on the vector $[\mathrm{d}x/\mathrm{d}s : \mathrm{d}t = f(x, \mathrm{d}x/\mathrm{d}s)\,\mathrm{d}s]$. The function $f(x, \mathrm{d}x/\mathrm{d}s)$ (which is assumed to be a strict convex function of the second argument) is a key element of the theory; thus, if the point $x_1 = x(s_1)$ is excited, then the time period after which the point $x_2 = x(s_2)$ will be excited is given by the expression

$$\min \int_{x_1}^{x_2} f(x, \mathrm{d}x/\mathrm{d}s)\,\mathrm{d}s,$$

where the minimum is taken over all curves connecting the points x_1 and x_2. (Indeed, if the excitation propagating from the point x_1 along all possible paths has already reached the point x_2 along some path, then all paths that connect x_1 and x_2, but take more time, are insignificant.) This is equivalent to Fermat's principle of least time, adapted to dynamic processes in EM. Thus, Gel'fand and Fomin developed a variational theory of propagation of excitation, endowing it with proper Lagrange–Hamiltonian–Jacobian equations that are formally equivalent to the variational formalism of geometric optics based on Fermat's principle.

The Gel'fand–Fomin formulation follows earlier studies of cardiology by Norbert Wiener and Arturo Rosenblueth, whose system of axioms involves an additional (refractory) state (Wiener & Rosenblueth, 1946). Any point goes to the refractory state immediately upon being excited, after which it cannot be excited during the finite time period R. Supposing the velocity v of propagation of excitation to be constant, Wiener and Rosenblueth developed the theory of circulation of an excitation around nonexcitable obstacles and determined the least critical length λ of the obstacle, around which the excitation can stationary circulate: $\lambda = Rv$. Further development of these geometric approaches was undertaken by

those involved in a seminar on mathematical biology (organized by Gel'fand at Moscow State University in the early 1960s) and led to a prediction of the existence of spiral waves (Balakhovsky, 1965).

Current geometric theories of spiral waves are concerned with properties that were long ignored, including the dependence of an AW leading-edge velocity on the curvature of the edge. Around 1980, Werner Ebeling, Yakov Zeldovich, Yoshiki Kuramoto, and Vladimir Zykov independently showed that the velocity of a curved leading edge must differ from the velocity of a plane edge—if the edge is concave (convex) in the direction of its propagation then it must accelerate (decelerate). This fact is readily understood in the case of a combustion wave where ignition occurs more rapidly (slowly) ahead of concave (convex) parts of the flame front than ahead of the plane parts due to focusing (diverging) the lines of heat flux. The formula for the velocity v of a weakly bent wave front that propagates in two-dimensional EM and obeys Equation (10) is

$$v = v_0 - DK, \tag{11}$$

where v_0 is the velocity of plane front and K is the curvature of the wave front. The domain of applicability of this equation is given by the inequality $Kl_f \ll 1$, where l_f is a characteristic width of the front.

Equation (11) implies that excitation of sufficiently small circular patches of EM will die out. The radii of such patches are bounded above by the critical value $\rho_c = |K_c|^{-1} = Dv_0^{-1}$ which corresponds to the zero value of v in Equation (11). In a more precise theory of curved AW dynamics (Kuramoto, 1980), Equation (11) emerges as an eikonal equation in the "nonlinear geometric optics" of an AW; thus, it is deeply involved in the modern geometric theory of spiral waves (Mikhailov et al., 1994; Elkin et al., 1998).

Interestingly, a version of Snell's law for AWs emerges from such studies which differs from that of classical optics in several important ways:

- Assuming the underlying reaction-diffusion equation to be Equation (10), Equation (1) is replaced by

$$\frac{\tan\psi_1}{\tan\psi_2} = \text{constant} = \frac{D_1}{D_2}, \tag{12}$$

  where D_1 and D_2 are the diffusion constants in the incident and refractive regions.
- This is a *local* law which determines the structure of refracted concentration fronts only near the interface between homogeneous regions rather than far from it.
- Equation (12) is obeyed for nonstationary as well as stationary refractions.
- In the regime of stationary refraction, when the incident wave and the refracted one shape a planar form and move with constant velocities, the angles of incidence and refraction are determined by the conditions (Mornev, 1984)

$$\sin\psi_1 = \sqrt{D_1/(D_1 + D_2)}$$

  and

$$\sin\psi_2 = \sqrt{D_2/(D_1 + D_2)}.$$

If a plane AW is normally incident on the boundary ($\psi_1 = 0$) and D_2 is sufficiently larger than D_1, the wave will be forced to stop. Assuming $f(u)$ to be a cubic-shaped function possessing three zeroes $u_0 < u_b < u_1$ and satisfying the conditions $f(u) > 0$ at $(u < u_0)$ and $(u_b < u < u_1)$, $f(u) < 0$ at $(u_0 < u < u_b)$ and $(u > u_1)$, the condition for the AW to die at the boundary is

$$\frac{D_2}{D_1} > \frac{\sigma_+}{\sigma_-},$$

where $\sigma_-(\sigma_+)$ denotes the least (greatest) of two values $\left|\int_{u_0}^{u_b} f(u)\,du\right|, \int_{u_b}^{u_1} f(u)\,du$ (Mornev, 1984).

O. A. MORNEV

See also **Diffusion; Fairy rings of mushrooms; Nonlinear optics; Reaction-diffusion systems; Spiral waves; Zeldovich–Frank-Kamenetsky equation**

Further Reading

Balakhovsky, I.S. 1965. Nekotorye rezhimy dvizheniya vozbuzhdeniya v ideal'noi vozbudimoi tkani. [Some regimes of motion of excitations in ideal excitable tissue.] *Biofizika*, 10(6): 1063–1067

Born, M. & Wolf, E. 2002. *Principles of Optics*, 7th edition, Cambridge and New York: Cambridge University Press

Elkin, Yu.E., Biktashev, V.N. & Holden, A.V. 1998. On the movement of excitation wave breaks. *Chaos, Solitons, and Fractals*, 9: 1597–1610

Gel'fand, I.M. & Fomin, S.V. 1961. *Variatsionnoe ischislenie* [*Variational Calculus*], Moscow: Gosudarstvennoe Izdatel'stvo Fiziko-Matematicheskoii Literatury

Kuramoto, Y. 1980. Instability and turbulence of wavefronts in reaction–diffusion systems. *Progress of Theoretical Physics*, 63(6): 1885–1903

Mikhailov, A.S., Davydov, V.A. & Zykpv, V.S. 1994. Complex dynamics of spiral waves and motion of curves. *Physics* D, 70: 1–39

Mornev, O.A. 1984. Elements of the "optics" of autowaves. In *Self-Organization of Autowaves and Structurees Far from Equilibrium*, edited by V.I. Krinsky, Berlin: Springer

Vinogradova, M.B., Rudenko, O.V. & Sukhorukov, A.P. 1990. *Teoriya Voln* (*Wave Theory*), 2nd edition, Moscow: Nauka

Wiener, N. & Rosenblueth, A. 1946. The mathematical formulation of the problem of conduction of impulses in a network of connected excitable elements, specially in cardiac muscle. *Archivos del Instituto de Cardiologia de Mexico* XVI (3–4): 205–265

GEOMORPHOLOGY AND TECTONICS

Geomorphology deals with the evolution of Earth's surface by gravity (e.g., landslides) and the sculpting

action of wind, river flow, and ice. Tectonics deals with the deformation and uplift of rocks, including the behavior of earthquakes. Nonlinearity arises in many geomorphic systems in the feedbacks between the shape of the surface and the fluid flow above the surface. The shapes of sand ripples and dunes, for example, control the flow of wind above the surface, which, in turn, controls the spatial distribution of erosion and deposition. Over time, erosion and deposition modify the shape of the surface and the flow of wind in a positive feedback loop. The flow of wind over a dune and the sediment transport caused by the wind are both nonlinear processes. The relationship between the sediment flux moved by the wind over a dune, for example, and the shear stress exerted by the wind is strongly nonlinear, including both a threshold shear stress for particle entrainment and a nonlinear power-law relationship between flux and shear stress above that threshold.

Some of the nonlinear feedback relationships in geomorphic systems affect practical issues. The feedback between vegetation density and soil erosion, for example, can lead to dust bowl conditions if low vegetation density promotes wind erosion, stripping the soil to further inhibit vegetation growth in a positive feedback loop. In tectonic systems, nonlinear feedbacks also govern much of the interesting behavior. Deformations in rock or along a fault plane, for example, can become localized by the feedback between shear strength and strain rate. Rocks often become weaker as they are strained, in turn focusing more deformation to the areas of highest strain. The rheology of rocks, including their nonlinear dependence on strain rate and time, thus plays a very important role in our understanding of mountain belts.

Self-organized, periodic landforms have received considerable attention in geomorphology. Sand ripples, dunes, and yardangs (all examples of eolian landforms), flutes (elongated ridges of subglacial sediment), drumlins (sculpted large mounds of subglacial debris), finger lakes, cirques, sorted stone stripes and circles (all glacial and periglacial landforms), discontinuous ephemeral streams and step-pool sequences (fluvial landforms), beach cusps and spits (coastal landforms) all have a characteristic width or spacing (Figure 1) that is controlled in part by the fluid movement on or above the surface and its relationship to erosion and deposition. The dynamic processes governing these systems are disparate and complex, but feedback between the surface and the fluid flow on or above the surface plays a key role in all of these examples. Finger lakes, for example, are elongated glacial troughs that developed on the margins of former ice sheets as glacier flow was focused into incipient bedrock depressions, concentrating glacial erosion in troughs in a positive feedback that forms deeper basins when the ice retreats. The Finger Lakes of central New York are the typical examples, but similar lakes occur along other former ice margins. Step-pool sequences form in mountain river channels by feedback between the roughness of the channel bed, the flow velocity in the channel, and the selective entrainment of particles on the bed. A channel reach with an initially rougher bed than nearby reaches will have slower flow velocity, promoting the deposition of coarse particles along the channel reach and a further decrease in flow velocity. This feedback produces channel reaches characterized by shallow gradients and fine particles alternating with steep gradients and coarse particles. In some cases, numerical models have been developed that enable the wavelengths of these periodic landforms to be predicted.

Figure 1. Sand ripples with a characteristic width or spacing. White Sands, New Mexico, courtesy of National Park Service.

In many if not most cases, landform evolution does not lead to periodic topography at all. River networks, coastal erosion of a rugged shoreline, and the dissolution of limestone to form cave networks (or karst topography above ground) are all examples of processes that create chaotic landforms with no apparent characteristic scale. Many of these landforms have an underlying order, however, by virtue of their self similarity. Self-similar landforms are those that have a similar appearance and statistical structure at a wide range of spatial scales. Rugged coastlines are the classic example of fractals popularized by Benoit Mandelbrot (1982). Long before the fractal structure of coastlines had been described, however, geomorphologists were interested in the self-similarity of river networks. To examine this self-similarity, streams are first ordered according to their position in a drainage network. The Strahler order defines all channels with no upstream tributaries as first-order channels. Whenever any two streams of like order join at a tributary, they form a stream of the next highest order. Horton's law states the principle of self-similarity of drainage networks mathematically: the ratio of the number of streams of order n to the number of streams of order $n+1$ is equal to approximately 4 and is independent of n (Rodriguez-Iturbe and Rinaldo (2001) provide an excellent review). Similar relationships exist between channel lengths, areas, and the Strahler order.

Horton's laws are satisfied in many different kinds of networks; however, so the modern view is that Horton's laws are not unique properties of drainage networks (Kirchner, 1993). Other relationships, such as the angles of tributary junctions and the relationships between channel slope and the Stahler order, contain important information about the self-organization of channel networks.

The Earth's crust exhibits nonlinear, critical behavior in several ways. First, earthquakes occur over a wide range of sizes with a frequency-size distribution characterized by a power law. This observation, known as the Gutenberg–Richter law, is the most fundamental rule of seismology. Seismicity also exhibits temporal correlations that have self-similar properties. Omori's law, for example, states that the frequency of foreshocks or aftershocks is inversely proportional to the time before or since the mainshock. Theoretical models for fault behavior have been devised based upon a simple model of blocks (representing one fault plane) frictionally coupled to a table (the other fault plane) and elastically coupled to one another and to a driver plate (representing the regional tectonic stress) (e.g., Turcotte, 1997). The model builds up stress until all the elements are near the threshold for slipping. At that point, the slippage of one block can transfer stress to other blocks in a cascade that produces earthquakes that follow the Gutenberg–Richter law. This phenomenon is called stick-slip friction. The discrete nature of the slider-block model appears to have an analog in real faults; the behavior of faults can be characterized according to the size and strength of asperities (sticky spots) on the fault plane, which are like the individual blocks in the slider-block system. The aftershock behavior of earthquakes does not appear to arise naturally in the simplest slider-block models; instead, some viscous coupling between blocks is necessary to reproduce Omori's law (Pelletier, 2000), suggesting that the punctuated process of seismic events is linked to a steady, creeping motion of the fault motion over longer time scales.

The crust also exhibits nonlinear critical behavior in the way that magma makes its way through the crust and is released as volcanic eruptions. The frequency–size distribution of volcanic eruptions appears to follow a power-law distribution analogous to the Gutenberg–Richter distribution in terms of the volume of material released. Magmatic and volcanic activity is also clustered in time in a way that is generally analogous to Omori's law. The processes of fluid movement through the crust are very different compared with the stresses on an earthquake fault, but a model for the spatial interaction of many fluid conduits all near the threshold for eruption produces a model very similar to the slider-block model (Pelletier, 1999). This kind of model appears to be most consistent with the Rayleigh distillation model of geochemical mixing (Turcotte, 1997), which describes the abundances of certain geochemical elements in the crust.

JON D. PELLETIER

See also **Avalanches; Branching laws; Dune formation; Evaporation wave; Feedback; Fractals; Glacial flow; Rheology; Sandpile model**

Further Reading

Kirchner, J.W. 1993. Statistical inevitability of Horton's laws and the apparent randomness of stream channel networks. *Geology*, 21: 591–594

Mandelbrot, B.B. 1982. *Fractal Geometry of Nature*, New York: W.H. Freeman

Pelletier, J.D. 1999. Statistical self-similarity of magmatism and volcanism. *Journal of Geophysical Research*, 104: 15,425–15,438

Pelletier, J.D. 2000. Spring-block models of seismicity: review and analysis of a structurally heterogeneous model coupled to a viscous asthenosphere. In *GeoComplexity and the Physics of Earthquakes*, edited by J.B. Rundle, D.L. Turcotte, & W. Klein, Washington, DC.: American Geophysical Union

Rodriguez-Iturbe, I. & Rinaldo, A. 2001. *Fractal River Basins: Chance and Self-Organization*, Cambridge and New York: Cambridge University Press

Turcotte, D.L. 1997. *Fractals and Chaos in Geology and Geophysics*, 2nd edition, Cambridge and New York: Cambridge University Press

GESTALT PHENOMENA

The Gestalt idea was introduced to science by Ernst Mach (1868) and Christian von Ehrenfels (1890). Mach stated that the spontaneous creation of order, that is, order arising without any external control, can be shown in inanimate nature. Von Ehrenfels characterized Gestalt qualities, that is, higher order qualities emerging from basic elements, by two criteria: (1) supersummativity, which means that the elements of a pattern presented individually to a person give, in the totality of the experience, a poorer impression than the total experience of a person to whom all the elements are presented; and (2) transposition, which means the characteristics of a Gestalt quality are retained even if all the elements which exhibit the Gestalt quality are changed in a certain way (for example, the transposition of a melody).

Wolfgang Köhler (1920) delivered the earliest formulation of a concept of self-organization of perception. The idea that perception must necessarily be understood as a process of autonomous creation of order runs through all his works. Starting from the observation of spontaneous Gestalt tendencies in experience, Köhler made it his primary task to design and test a model of brain function in which the phenomenal organization of the perceptual world is explained as not only stimulus-dependent, but as strongly dependent upon the perceptual system's own inner dynamics. In the development of Gestalt theory, Köhler was mainly oriented to the observations

and theoretical concepts of physics. In accordance with the assumption of linear thermodynamics, the general systemic tendency towards final equilibrium was considered in Köhler's time to be the only basic principle of self-organization. This principle can easily be demonstrated in cognition by recursive experiments of serial reproduction of complex patterns. These patterns follow the "principle of prägnanz" towards very simple and stable configurations (Stadler & Kruse, 1990; Kanizsa & Luccio, 1990). In perception, this principle states that people will perceive the most orderly or regular thing they can out of the stimuli that are presented to them. Köhler applied the model of physical fields striving independently to balance forces directly to the way in which the visual system functions. At the time, this almost provocatively contradicted the findings of neuroanatomy and neurophysiology. On the basis of his theoretical model of perception, the brain is not seen as a complex network of many different interacting neurons but as a homogeneous conductor of bioelectric forces.

Köhler's argument was not primarily the postulation of electromagnetic field forces acting in the brain independently of neuroanatomical structures (which has been refuted by most contemporary brain scientists) but the idea of self-organization in the brain. He was fully aware of the fact that the general principle of development of linear thermodynamics has been rather unsuitable for application to biological systems as long as it was oriented exclusively towards the final equilibrium. This was criticized by Köhler himself in 1955: "Although this is a perfectly good principle, it cannot, in its present formulation, be applied to the organism. For the organism is obviously not a closed system; moreover, while the direction indicated by the principle may be called 'downward', the direction of events in healthy organisms is on the whole clearly not 'downward' but, in a good sense, 'upward'."

Modern Developments

The brain is conceived as a self-organizing system that can be treated by means of synergetics (Haken, 1983, 1990). Pattern recognition is understood as pattern formation (of activities of the neural net). Incomplete (visual) data are complemented by a dynamic associative memory. In both cases (pattern formation and recognition), incomplete data generate order parameters that compete with each other. In general, one order parameter wins and generates, according to the slaving principle of synergetics, the complete pattern. In this processes, idealized (Gestalt) patterns may be incorporated. Of particular interest are ambiguous figures, such as Figure 1 (young woman vs. old woman). Here, two or more interpretations (percepts) are possible, and two (or more) order

Figure 1. Young woman vs. old woman.

parameters may win the competition. The final outcome is determined by an order parameter dynamics in which the dynamics of attention parameters is included.

The mathematical approach (algorithm of the "synergetic computer") is as follows: The images of different objects are decomposed into their pixels that are lumped together as pixel vectors

$$\boldsymbol{v}_\mu = (v_{\mu 1}, v_{\mu 2}, ..., v_{\mu N}), \quad \mu = 1, ..., M. \tag{1}$$

The label μ is associated with an interpretation (the name of a person, say), and the adjoint vectors $\boldsymbol{v}_\mu^+$ are defined by

$$(\boldsymbol{v}_\mu^+ \boldsymbol{v}_\nu) = \delta_{\mu\nu}. \tag{2}$$

The activity pattern of the neural net is written as

$$\boldsymbol{q}(t) = \sum_{\mu=1}^{M} \xi_\mu(t) \boldsymbol{v}_\mu + \boldsymbol{r}(t), \tag{3}$$

where $\boldsymbol{r}$ is a residual term that vanishes in the course of time. The order parameters are defined by

$$\xi_\mu(t), \tag{4}$$

where the initial value at the observation time t_0 is given by

$$\xi_\mu(0) = (\boldsymbol{v}_\mu^+ \boldsymbol{q}(0)). \tag{5}$$

The order parameters obey competition equations that can be derived from a potential function V

$$\mathrm{d}\xi_\mu(t)/\mathrm{d}t = -\partial V/\partial\xi_\mu, \tag{6}$$

where

$$V = V(\xi_1, ..., \xi_M; \lambda_1, ..., \lambda_M) \tag{7}$$

does not only depend on the order parameters but also on the attention parameters λ_j. The competition equations read explicitly

$$\mathrm{d}\xi_\mu(t)/\mathrm{d}t = \left(\lambda_\mu - B\sum_{\mu'\neq\mu}^{M}\xi_{\mu'}^2 - D\sum_{\mu'=1}^{M}\xi_{\mu'}^2\right)\xi_\mu \tag{8}$$

with positive constants λ_μ, B, C. The winning order parameter fixes the activity pattern (3). In the case of ambiguous patterns (such as that of Figure 1), equations for the order parameters ξ_1 and ξ_2 and the attention parameters read

$$\mathrm{d}\xi_1/\mathrm{d}t = (\lambda_1 - C\xi_1^2 - (B+C)\xi_2^2)\xi_1 - \partial V_\mathrm{b}/\partial\xi_1, \tag{9}$$

$$\mathrm{d}\xi_2/\mathrm{d}t = (\lambda_2 - C\xi_2^2 - (B+C)\xi_1^2)\xi_2 - \partial V_\mathrm{b}/\partial\xi_2, \tag{10}$$

$$\mathrm{d}\lambda_j/\mathrm{d}t = \gamma(1 - \lambda_j - \xi_j^2), \quad j = 1, 2. \tag{11}$$

The bias potential V_b is defined by

$$V_\mathrm{b} = 2B\xi_1^2\xi_2^2\left(1 - 4\alpha\frac{\xi_1^2 - \xi_2^2}{\xi_1^2 + \xi_2^2}\right). \tag{12}$$

The parameter α is determined by the percentage of that perception that is seen first. It also determines the relative length of the perception times that occur in the oscillatory motion of the order parameters ξ_1, ξ_2 that represent the switch from one percept to the other one and back again.

HERMANN HAKEN AND MICHAEL A. STADLER

See also **Cell assemblies; Emergence; Synergetics**

Further Reading

von Ehrenfels, C. 1890. Über Gestaltqualitäten [On Gestalt qualities]. In *Foundations of Gestalt Theory*, edited by B. Smith, München: Philosophia-Verlag, pp. 82–117

Haken, H. 1983. Synopsis and introduction. In *Synergetics of the Brain*, edited by E. Başar, H. Flohr, H. Haken & A.J. Mandell, Berlin and New York: Springer, pp. 3–25

Haken, H. 1990. *Synergetic Computers and Cognition: A Top-down Approach to Neural Nets*, Berlin and New York: Springer

Kanizsa, G. & Luccio, R. 1990. The phenomenology of autonomous order formation in perception. In *Synergetics of Cognition*, edited by H. Haken & M. Stadler, Berlin and New York: Springer, pp. 186–200

Köhler, W. 1920. *Die physischen Gestalten in Ruhe und im stationären Zustand*, Braunschweig: Vieweg

Köhler, W. 1955. Direction of processes in living systems. *Scientific Monthly*, 8: 29–32

Mach, E. 1868. Die Gestalten der Flüssigkeit [The Gestalts of fluids]. In *Populärwissenschaftliche Vorlesungen*, 4th edition, 1910, Leipzig: Barth

Stadler, M. & Kruse, P. 1990. The self-organization perspective in cognition research: historical remarks and new experimental approaches. In *Synergetics of Cognition*, edited by H. Haken & M. Stadler, Berlin and New York: Springer, pp. 32–52

GINZBURG–LANDAU EQUATION

See **Complex Ginzburg–Landau equation**

GLACIAL FLOW

Glaciers are defined as multi-year features, consisting of snow and ice, which flow down-slope under the force of gravity. The broadness of this definition means that there exists a continuum of glaciers that ranges from small, multi-year snow patches with surface areas of the order of 100 square meters, to the Columbia Glacier in Alaska, with a surface area of over 1100 square kilometers (the District of Columbia would fit within its terminus). Yet, in spite of the broad range of features encapsulated in this definition, the same basic physical processes are common to all of the world's roughly 160,000 different glaciers, and most of these processes are nonlinear.

Glaciers deform under their own weight, behaving like highly viscous fluids. Mass input is greatest at the glacier's upper elevations where colder temperatures result in a greater percentage of precipitation falling as snow. Mass loss is greatest at the glacier terminus, the lowest point on the glacier, where temperatures and melting are highest and where ablation (mass loss from melting, evaporation, sublimation, and in special cases, iceberg formation) equals flow. This imbalance results in a continuous mass transfer from the upper reaches to the lower reaches. The basis of the equations governing glacial flow is therefore mass conservation. However, unlike liquid water, where an applied stress, τ, (i.e., a squeeze) causes a linear, proportional deformation or strain, glaciers have a nonlinear stress-strain response. Although measurements in remote mountain locations are difficult and limited, field studies and laboratory experiments have shown that

$$\dot{\varepsilon} = A\tau^n, \tag{1}$$

where n is constant and generally assigned a value of 3 (though values ranging from 1.5 to 4.2 can be found

in the literature), $\dot{\varepsilon}$ is the rate of deformation, and $1/A$ is a nonlinear measure of the viscosity. This glacier "flow law" is a version of pseudoplastic flow and is similar to dry sand dune flows (which use a value of 2 for n). Viscoplastic flows, such as clay-water mixtures, and Bagnold macro-viscous flows, such as mud-flows, are also similar, differing primarily in the value of the exponent n.

The nonlinear flow law is the source of many fractal, self-similar, and nonlinear scaling properties. The basic scaling relationships are simple: discharge of ice through a given cross section of the glacier is proportional to glacier depth raised to the power $(n+2)$, and glacier flow velocity is proportional to glacier depth raised to the power $(n+1)$ (Patterson, 1994). However, Bahr (1997) has shown that in conjunction with mass and momentum conservation, the nonlinear flow law implies nonlinear scaling relationships between surface area (a parameter easily measured with satellites) and many difficult to measure but fundamental properties. Glacier thickness, volume, mass balance, velocity, flux, and other parameters relate to the surface area by exponents of 3/8, 11/8, etc. Using these unusual scaling exponents, the volume of ice in the world's glaciers can be predicted based solely on observed surface areas.

Equation (1) applies to basic glacier flow under constant stress. In reality, glaciers are rarely under consistent stress throughout. In areas where glaciers are under tensional stress, if the stress becomes too high, the ice becomes brittle and fractures, resulting in crevassing. Crevassing can be mathematically described using fracture mechanics (Smith, 1976; Sassolas et al., 1995). Crevassing can occur as the glacier flows over large drops in the bed as a result of varying flow speeds (Harper et al., 1998). Particularly dramatic crevassing occurs in the lower reaches of retreating tidewater glaciers as a result of faster flow at the glacier terminus than in the ablation zone (the area of the glacier that is annually losing more mass than it is gaining). Because the lower sections of tidewater glaciers are near or at floatation, unlike land-based glaciers, tidewater glacier crevassing can result in calving (the formation of icebergs from pieces that are broken off the terminus). Calving from tidewater glaciers can be modeled using both fracture mechanics and percolation theory (Bahr, 1995).

Tidewater glacier calving contributes to an unexpected nonlinearity in the tidewater glacier terminus position. Most glaciers move back and forth with changes in climate as the balance between melt and accumulation shifts. For tidewater glaciers, however, there is an additional loss of mass through calving. The tidewater glacier calving rate increases with water depth, but water depth is typically minimized by a pile of debris deposited at the end of the glacier. If the glacier terminus retreats backwards off the debris pile, then the water depth increases and the calving rate increases, further increasing glacier retreat (Meier, 1993; van der Veen, 2002). This is a classic positive feedback loop scenario, and is the cause of the dramatic and rapid retreats recently seen in many glaciers that terminate in water, such as the Columbia Glacier in Alaska and many of the New Zealand glaciers that terminate in lakes. While many of the world's glaciers are slowly retreating due to changes in climate, these tidewater glaciers retreat nonlinearly in response to even the smallest climatic perturbations.

In addition to surface and internal processes, such as flow and crevassing, glaciers exhibit nonlinear behavior in their basal processes. For temperate glaciers (those not frozen to their beds), glacial flow is a combination of ice deformation and sliding at the glacier bed. Motion tends to be stick-slip, very similar to the nonlinear slider-block models of earthquakes (Bahr & Rundle, 1996; Fischer & Clarke, 1997). This gives rise to the grinding of the underlying rock, plucking of rocks out of the bed, and deformation of the bed in places where it is a fine-grained matrix. Lubrication appears to increase flow rates, as it does in sub-surface faults (Patterson, 1994). At the extreme end of lubricated basal flow, we find surging glaciers. These glaciers appear to build up water and water pressure at the glacier bed. Some mechanism or pressure trigger allows this water to be periodically catastrophically released (the Variegated Glacier in Alaska, for example, surged in 1906, 1947, 1964–65, and 1982–83), resulting in rapid flow and over-extension of the glacier (Patterson, 1994).

Finally, the overall structure of large glaciers is fractal. Large glaciers, such as the Talkeetna and Columbia Glaciers in Alaska have multiple upper branches that coalesce into one outlet tongue, similar to a river system or branching tree. Measurements have shown that the structure is statistically self-similar with fractal dimensions ranging from roughly 1.6 for small- to mid-sized mountain glaciers, to 2.0 for large glaciers and space-filling ice sheets such as Greenland (Bahr & Peckham, 1996).

KAREN LEWIS MACCLUNE AND DAVID BAHR

See also **Avalanches; Dune formation; Geomorphology and tectonics; Sandpile model**

Further Reading

Bahr, D.B. 1995. Simulating iceberg calving with a percolation model. *Journal of Geophysical Research*, 100(B4): 6225–6232

Bahr, D.B. 1997. Global distributions of glacier properties: a stochastic scaling paradigm. *Water Resources Research*, 33(7): 1669–1679

Bahr, D.B. & Peckham, S. 1996. Observations of self-similar branching topology in glacier networks. *Journal of Geophysical Research*, 101(B11): 25511–25521

Bahr, D.B. & Rundle, J.B. 1996. Stick-slip statistical mechanics of motion at the bed of a glacier. *Geophysical Research Letters*, 23(16): 2073–2076

Fischer, U.H. & Clarke, G.K.C. 1997. Stick-slip sliding behavior at the base of a glacier. *Annals of Glaciology*, 24: 390–396
Harper, J.T., Humphrey N.F. & Pfeffer, W.T. 1998. Crevasse patterns and the strain rate tensor: a high-resolution comparison. *Journal of Glaciology*, 44(146): 68–76
Hooke, R. 1998. *Principles of Glacier Mechanics*, Saddle River, NJ: Prentice-Hall
Meier, M.F. 1993. Columbia Glacier during rapid retreat: interactions between glacier flow and iceberg calving dynamics. *Workshop on the Calving Rate of West Greenland Glaciers in Response to Climate Change*, Copenhagen
Patterson, W.S.B. 1994. *The Physics of Glaciers*, 3rd edition, New York: Elsevier
Sassolas, C., Pfeffer, T. & Amadei, B. 1995. Stress interaction between multiple crevasses in glacier ice. *Cold Regions Science and Technology*, 24: 107–116
Sharp, R.P. 1988. *Living Ice*, Cambridge and New York: Cambridge University Press
Smith, R.A. 1976. The application of fracture mechanics to the problem of crevasse penetration. *Journal of Glaciology*, 17(76): 223–228
van der Veen, C.J. 2002. Calving glaciers. *Progress in Physical Geography*, 26(1): 96–122

GLOBAL WARMING

Few modern scientific concerns have achieved such notoriety as the possibility of relatively rapid anthropogenic global warming through increased CO_2 emissions. This complex problem became a matter of considerable public attention during the 1980s, and during the 1990s, the first attempt was made at international management of the challenge (the Kyoto Protocol under the United Nations Framework Convention on Climatic Change). However, scientific awareness of CO_2-induced climatic change is not new, and the underlying physical processes were understood from the beginning of studies concerning the absorption of radiation by the atmosphere. Later research resulted in a deeper understanding of the dynamics of the biospheric carbon cycle, and global atmospheric circulation models have been adopted, and adapted, for assessing the future course of tropospheric CO_2 levels. In spite of all of these advances, much remains unclear and uncertain.

Early Studies

Several years before his death in 1830, the French mathematician Joseph Fourier concluded that the atmosphere acts like the glass of a greenhouse, letting light through and retaining the invisible rays emanating from the ground (Fourier, 1822). In modern scientific terms, the atmosphere is highly (though not perfectly) transparent to incoming (shortwave) solar radiation, but it is a strong absorber of certain wavelengths in the outgoing (longwave) infrared spectrum produced by the reradiation of absorbed sunlight.

John Tyndall was the first scientist to study this process in detail by measuring the absorptive properties of air and its key constituent molecules (water vapor and about a dozen different compounds). He used a sensitive galvanometer to measure the electric current passing through gases irradiated by heat. In 1861, Tyndall concluded that water vapor accounts for most of the atmospheric absorption and hence "every variation of this constituent must produce a change in climate. Similar remarks would apply to the carbonic acid diffused through the air. . ." (Tyndall, 1861). The next major contribution to the field came just before the end of the 19th century when Svanté Arrhenius offered the first calculations of the global surface temperature rise resulting from naturally changing atmospheric CO_2.

Arrhenius's conclusions contained all of the key qualitative modern results. He found that geometric increases of CO_2 will produce a nearly arithmetic rise in surface temperatures, that the warming will be smallest near the equator and highest in polar regions, that the Southern hemisphere will be less affected, and that the warming will reduce temperature differences between night and day (Arrhenius, 1896). His quantitative results also resembled those of today's best global climatic models: he predicted that the increase in average annual temperature will be about 50°C in the tropics and just over 6°C in the Arctic. All of these findings applied to natural fluctuations of atmospheric CO_2: Arrhenius concluded (correctly) that future anthropogenic carbon emissions would be largely absorbed by the ocean and (incorrectly, as he grossly underestimated future fossil fuel combustion) that the accumulation would amount to only about 3 ppm in half a century.

The link between CO_2 and climate change was resurrected in 1938 by George Callendar who calculated a more realistic temperature rise with doubling of CO_2 concentrations (1.5°C rise) and documented a slight global warming trend of 0.25°C for the preceding half a century (Callendar, 1938). In his later writings, he also recognized the importance of carbon emissions from land-use changes. In 1956, Gilbert Plass performed the first computerized calculation of the radiation flux in the main infrared region of CO_2 absorption (Plass, 1956). His results (average surface temperature rise of 3.6°C with the doubled atmospheric CO_2) were published a year before Roger Revelle and Hans Suess summarized the problem with continuing large-scale fossil fuel combustion in such a way that the key sentence has become a citation classic:

> Thus human beings are now carrying out a large scale geophysical experiment of a kind that could not have happened in the past nor be reproduced in the future. Within a few centuries we are returning to the atmosphere and oceans the concentrated organic carbon stored in sedimentary rocks over hundreds of millions of years. (Revelle & Suess, 1957)

An almost instant response to this concern was the setting up of the first two permanent stations for

the measurement of background CO_2 concentrations, at Mauna Loa in Hawai'i and at the South Pole. Accumulating measurements began showing a steady rise of atmospheric CO_2 at these two remote locations, but, once again, attention to the problem of potential global warming eased during the 1960s and began to grow only in the aftermath of OPEC's two sudden oil price hikes during the 1970s.

Numerical Models of Anthropogenic Global Warming

By the late 1960s, improvements in computer capabilities made it possible to run the first three-dimensional models of global atmospheric circulation and use them to simulate the effects of higher CO_2 levels. Most of these simulations looked at possible effects arising from the doubling of preindustrial CO_2, that is, after reaching levels around 600 ppm. Initial simulations indicated a 2.93°C rise with the doubling of the CO_2 level to 600 ppm (Manabe & Wetherald, 1967). Increases in computing power (subject to Moore's famous law) and better understanding of interactions between the atmosphere, oceans, and the terrestrial biosphere has led to increasingly more realistic models of global climate. Another important refinement was the inexplicably delayed consideration of other greenhouse gases (above all, of CH_4, N_2O, and chlorofluorocarbons) whose combined radiative forcing is now slightly higher than that of carbon dioxide (about 1.5 and 1.4 $W\,m^{-2}$).

By the late 1990s, the best models coupled the atmosphere's physical behavior with changes on land and in the ocean, and with simulations of some key features of carbon and sulfur cycles and of atmospheric chemistry (Houghton et al., 2001). At the same time, even our best numerical models still represent the atmosphere with a relatively coarse grid and are incapable of reproducing the intricacies and multiple feedbacks that determine the course and the rate of climate change.

One of the most important sources of potential error in the climate models is the treatment of clouds. The best general circulation models represent fairly well some essential gross features of global atmospheric physics but their iterative calculations are done at such widely spaced points of three-dimensional grids that it is impossible to treat cloudiness in a realistic manner. And yet clouds are key determinants of the planetary radiation balance because they have, on balance, a pronounced net cooling effect. Because clouds account for about half of the Earth's albedo (the fraction of incident radiation that is reflected), even relatively small changes in their properties could have an appreciable effect on the course of global warming.

Other unresolved matters include the response of terrestrial biota (Will carbon sequestration take place mostly in short- or long-lived tissues or in soil?), marine algae (especially their role in forming clouds), sudden releases of methane (rising temperatures may lead to catastrophic emissions from methane hydrates), and effects of orbital and solar influences (particularly a very high correlation between the solar cycles shorter than the 11-year mean and higher average land temperature of the Northern Hemisphere, and a link between mid-atmospheric temperature and changing intensity of radiation over the sunspot cycle). If the global forecasts are uncertain, regional predictions are particularly questionable. The most complex coupled models now provide reasonably reliable simulations of climate down to the sub-continental level but their results still have unacceptably large variations on regional scales.

Geological Evidence for Global Warming and Cooling

Indirect or proxy markers (such as isotopic and trace chemical analysis on tree rings, ice, or sediment cores) make it clear that a substantial decline of atmospheric CO_2 preceded the most extensive and longest lasting (some 70 million years, or Ma) glaciation of the entire Phanerozoic era that began about 330 Ma ago. Approximate reconstruction of CO_2 levels for the past 300 Ma—since the formation of the Pangea whose eventual break-up led to the current distribution of oceans and land masses—indicates, first, a pronounced rise (about five times the current level during the Triassic period), followed by a steep decline (Berner, 1998; Figure 1, top). Boron-isotope ratios of planktonic foraminifer shells point to CO_2 levels above 2000 ppm 60–50 Ma ago (with peaks above 4000 ppm), followed by an erratic decline to less than 1000 ppm by 40 Ma ago, and relatively stable and low (below 500 ppm) concentrations ever since the early Miocene 24 Ma ago (Pearson & Palmer, 2000; Figure 1, bottom).

Reliable record of atmospheric CO_2 is available only for the past 420,000 years thanks to the analyses of air bubbles from ice cores retrieved from Antarctica and Greenland. Preindustrial CO_2 levels never dipped below 180 ppm and never rose above 300 ppm (Raynaud et al., 1993; Petit et al., 1999; Figure 2) and their oscillations are highly positively correlated with changing temperatures. But these correlations are not a proof of a clear cause-and-effect relationship as there are no obvious lead-lag sequences. Other recent paleoclimatic studies actually found signs of decoupling of atmospheric CO_2 and global climate during the Phanerozoic eon and particularly during the early to middle Miocene, when a warm period coexisted with low CO_2 levels (Veizer et al., 2000; Pagani et al., 1999). These findings confirm the complexity of climate change where cause and effect are difficult to assign: atmospheric CO_2 may have

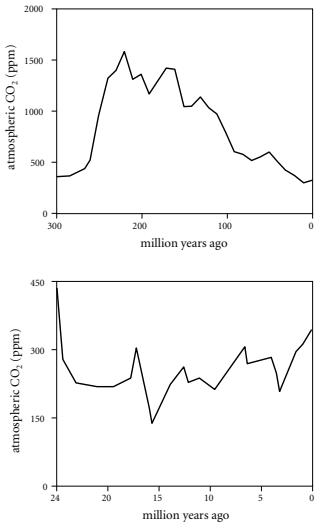

Figure 1. Atmospheric CO_2 concentrations during the past 300 and 24 million years. Based on Berner (1998) and Pearson and Palmer (2000).

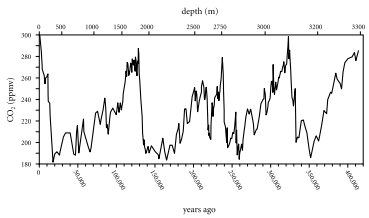

Figure 2. Atmospheric CO_2 concentrations during the past 420,000 years derived from air bubbles in Antarctica's Vostok ice core. Based on Petit et al. (1999).

been a primary climate driver but the evidence is not conclusive (Kump, 2002). The most likely pacemaker during the Pleistocene period was small changes in the Earth's orbit around the Sun; massive methane releases from gas hydrates and volcanic activity must be also considered.

Recent Evidence for Global Warming

During the time between the rise of the first high civilizations (5000–6000 years ago) and the beginning of the fossil fuel era, atmospheric CO_2 levels had fluctuated within an even narrower range of 250–290 ppm. Subsequent anthropogenic emissions pushed atmospheric concentrations of CO_2 to a high of 370 ppm by the year 2000. Paleoclimatic studies of the Northern Hemisphere during the last millennium show

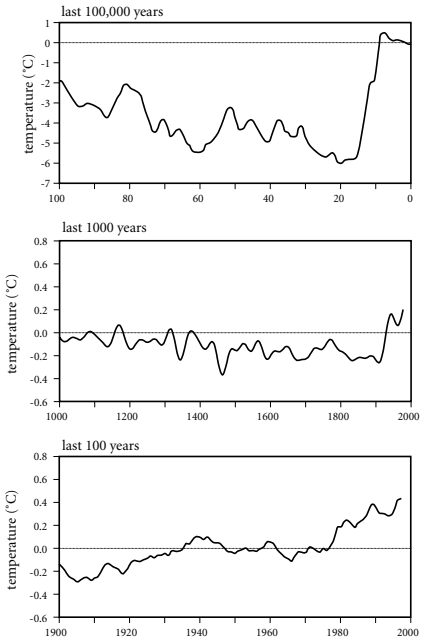

Figure 3. Reconstructed temperature trends during the past 100,000 years (from the Vostok ice core), 1000 years (for the Northern Hemisphere), and a 5-year running mean from instrumental temperature measurements for the past 100 years. Reproduced from Smil (2002).

warming periods during the 12th and 18th centuries and pronounced cooling during the 15th century (the Little Ice Age). A demonstrable cooling trend between the late 18th and the early 20th centuries was followed by an unprecedented rate of warming that has brought the average planetary temperature to levels higher than at any time during the past 1000 years (Figure 3).

The most extensive studies of the existing global record of surface temperatures have detected long-term planetary warming of, respectively, 0.5°C and 0.78°C since the middle of the 19th century (Jones et al., 1986; Hansen & Lebedeff, 1988). Changes in measurement techniques (different thermometers), station locations (from downtowns to suburbs) and station environment (increasing urban heat island effect), and until very recently, highly inadequate coverage of large areas of the Southern Hemisphere complicate the interpretation of this shift, which has distinct spatial patterns with areas of more pronounced warming and regions of slight cooling. However, the most recent (post-1976) spell of warming has been almost global and the 1990s were the warmest decade since the beginning of the

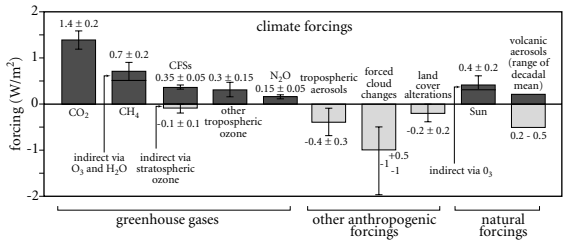

Figure 4. Estimates of cumulative radiation forcings by greenhouse gases and aerosols between 1850 and 2000 according to Hansen et al. (2000).

instrumental record in the 1850s and the warmest ten years of the millennium in the Northern Hemisphere.

According to the general circulation models, the warming should have been more pronounced. The best explanation of the discrepancy between the models and the actual temperature record is that the warming was partially counteracted by sulfate aerosols. The combined direct and indirect effect of all greenhouse gases resulted in a total anthropogenic forcing of about $2.8\,W\,m^2$ by the late 1990s (Hansen et al., 2000; Figure 4). This is equal to a little more than 1% of solar radiation reaching the ground.

Future Climate

If the atmospheric warming was primarily the function of radiative forcing, then the level of greenhouse gas emissions would be the key variable. Recent emission scenarios for CO_2 alone offer a very large range of concentrations, 540–970 ppm, by the year 2100. CH_4 levels may range even wider, from just above 1500 ppb to more than 3600 ppb. The aggregate radiative forcing may thus be anywhere between 4 and $9\,W\,m^{-2}$ and the climate sensitivity would then range between 1.5°C and 4°C with 2.2–3°C considered to be the most likely by the latest IPCC assessment. Broad consensus from the latest generation of models foresees that this climatic change would cool the stratosphere while raising the tropospheric temperatures in a distinct spatial pattern, with the warming more pronounced on the land (and during nights) and with increases of about two to three times the global mean in higher latitudes in winter than in the tropics, and greater in the Arctic than in the Antarctic.

There are many effective ways to slow down the greenhouse gas emissions and reduce their environmental impact. Most significantly, the affluent countries could largely retain their quality of life while reducing their energy and material consumption by at least a third. While the means are available, the will to act, nationally and internationally, is mostly absent. Global warming is a complex natural process but its anthropogenic enhancement calls for a fundamentally moral solution that runs against some basic human propensities: consume less and do so more efficiently.

VACLAV SMIL

See also **Atmospheric and ocean sciences; Forecasting; General circulation models of the atmosphere**

Further Reading

Alverson, K.D., Bradley, R.S. & Pedersen, T.F. (editors). 2003. *Paleoclimate, Global Change, and the Future*, Berlin and New York: Springer

Arrhenius, S. 1896. On the influence of carbonic acid in the air upon the temperature of the ground. *Philosophical Magazine, Series 5*, 41: 237–276

Berner, R.A. 1998. The carbon cycle and CO_2 over Phanerozoic time: the role of land plants. *Philosophical Transactions of the Royal Society of London* B, 353: 75–82

Callendar, G.S. 1938. The artificial production of carbon dioxide and its influence on temperature. *Quarterly Journal of the Royal Meteorological Society*, 64: 223–237

Fourier, J.B.J. 1822. *Théorie Analytique de la Chaleur*, Paris: Firmin Didot

Hansen, J. & Lebedeff, S. 1988. Global surface air temperatures: update through 1987. *Geophysical Research Letters*, 15: 323–326

Hansen J., Sato, M., Ruedy, R., Lacis, A. & Oinas, V. 2000. Global warming in the twenty-first century: an alternative scenario. *Proceedings of the National Academy of Sciences USA*, 97: 9875–9880

Houghton, J.T., Ding, Y., Griggs, D.J., Noguer, M., van der Linden, P.J. & Xiaosu, D. (editors). 2001. *Climate Change 2001: The Scientific Basis*, Cambridge and New York: Cambridge University Press

Jones P.D., Wigley, T.M.L. & Wright, P.B. 1986. Global temperature variations between 1861 and 1984. *Nature*, 322: 430–434

Kump, L.R. 2002. Reducing uncertainty about carbon dioxide as a climate driver. *Nature*, 419: 188–190

Lozán, J.L., Grassl, H. & Hupfer, P. (editors). 2001. *Climate of the 21st Century: Changes and Risks, Scientific Facts*, Hamburg: Wissenschaftliche Auswertungen

Manabe, S. & Wetherald, R.T. 1967. The effects of doubling CO2 concentration on the climate of a general circulation model. *Journal of the Atmospheric Sciences*, 32: 3–15

Pagani, M., Arthur, M.A. & Freeman, K.H. 1999. Miocene evolution of atmospheric carbon dioxide. *Paleoceanograohy*, 14: 273–292

Pearson, P.N. & Palmer, M.R.. 2000. Atmospheric carbon dioxide concentrations over the past 60 million years. *Nature*, 406: 695–699

Petit, J.R., Jouzel, J., Raynaud, D., Barkov, N.I., Barnola, J.-M., Basile, I., Bender, M., Chappellaz, J., Davis, M., Delaygue, G., Delmotte, M., Kotlyakov, V.M., Legrand, M., Lipenkov, V.Y., Lorius, C., Pepin, L., Ritz, C., Saltzman, E. & Stievenard, M. 1999. Climate and atmospheric history of the past 420,000 years from the Vostok ice core, Antarctica. *Nature*, 399: 429–426

Plass, G.N. 1956. The carbon dioxide theory of climatic change. *Tellus*, 8: 140–154

Raynaud, D., Jouzel, J., Barnola, J.M., Chappellaz, J., Delmas, R.J. & Lorius C. 1993. The ice record of greenhouse gases. *Science*, 259: 926–934

Revelle, R. & Suess, H.E. 1957. Carbon dioxide exchange between atmosphere and ocean and the question of an increase of atmospheric CO_2 during the past decades. *Tellus*, 9: 18–27

Smil, V. 2002. *The Earth's Biosphere: Evolution, Dynamics, and Change*, Cambridge, MA: MIT Press

Tyndall, J. 1861. On the absorption and radiation of heat by gases and vapours, and on the physical connection of radiation, absorption, and conduction. *Philosophical Magazine and Journal of Science*, 22: 169–194, 273–285

Veizer, J., Godderis, Y. & François, L.M. 2000. Evidence for decoupling of atmospheric CO_2 and global climate during the Phanerozoic eon. *Nature*, 408: 698–701

Woodwell, G.M. & Mackenzie, F.T., eds. 1995. *Biotic Feedbacks in the Global Climatic System*, Oxford and New York: Oxford University Press

GOLDEN MEAN

See **Fibonacci series**

GRADIENT SYSTEM

In the study of dynamic systems, it is often observed that the rate of evolution of some system in its phase space is proportional to the gradient of a state function. A system of this type is called a *gradient system*, and the state function—which governs the course of its evolution—is its *potential*.

If the state s of a system is given by n state variables $s_1, \ldots, s_n$ and $G(s) = G(s_a, \ldots s_{,n})$ is the potential of the system, then one can write (in matrix form)

$$\dot{s} = -\hat{k} \cdot \left(\frac{\partial G}{\partial s}\right)^{\mathrm{T}}. \tag{1}$$

Here the rate of change of state s is given by the column vector $\dot{s} = |\dot{s_1}, \ldots, \dot{s_n}|^{\mathrm{T}}$, where the superscript T indicates transposition; $\partial G(s)/\partial s = |\partial G/\partial s_1, \ldots, \partial G/\partial s_n|$ is the row vector of gradient of potential $G(s)$; and $\hat{k}$ is a coefficient of proportionality, represented by the nonsingular matrix $\hat{k} = |k_{ij}|$, $\det |k_{ij}| \neq 0$. The minus sign in Equation (1) is chosen for convenience. The coordinate representation of this equation is

$$\dot{s_i} = -\sum_{j=1}^{n} k_{ij} \frac{\partial G}{\partial s_j} \quad (i = 1, \ldots, n). \tag{2}$$

Equations (1) and (2) are quite general. For example, if the order n is an even number ($n = 2m$, $m \geq 1$), and $\hat{k}$ is a $2m \times 2m$ block-diagonal matrix composed of the skew-symmetric blocks,

$$\hat{k} = \mathrm{diag}|\hat{k}_1, \ldots, \hat{k}_m|, \hat{k}_1 = \hat{k}_2 = \ldots = \hat{k}_m = \begin{pmatrix} 0 & -1 \\ 1 & 0 \end{pmatrix}, \tag{3}$$

then Equations (1) and (2) are the usual Hamiltonian system (Fomenko, 1995).

However, gradient systems differ radically from Hamiltonian systems. Essential restrictions that specialize the definition of gradient systems and predetermine their qualitative properties are on the structure of matrix $\hat{k}$. For a gradient system: (i) The nonsingular matrix $\hat{k}$ is assumed to be symmetric: ($\hat{k} = \hat{k}^{\mathrm{T}}$ or $k_{ij} = k_{ji}$); hence, it possesses exactly n nonzero eigenvalues that the real numbers. (ii) All eigenvalues of $\hat{k}$ are assumed to have the same signs, either positive or negative.

Note that requiring that the rates $\dot{s}$ be proportional to the gradient of potential $G(s)$ does not oblige the coefficient of proportionality $\hat{k}$ to be a constant matrix. In general, the elements of $\hat{k}$ can (smoothly) depend on the current state $s : k_{ij} = k_{ji}(s)$, suggesting a third requirement of a gradient system: (iii) The properties (i) and (ii) must be fulfilled everywhere in the state space of system. Thus, a gradient system is defined as a system, whose evolution follows Equations (1) and (2), with a matrix satisfying conditions (i)–(iii).

The key dynamic difference between Hamiltonian and gradient systems is that Hamiltonian systems preserve the values of system potential, the Hamiltonian function ($\dot{G}(s) = 0$). The behavior of a gradient system is quite different because the matrix $\hat{k}$ in (3) is symmetric rather then skew-symmetric; thus $\dot{G}(s) \neq 0$.

From conditions (i)–(iii), one can demonstrate that the evolution of a gradient system preserves the sign of $\dot{G}(s)$; hence, the potential $G(s)$ either decreases or increases monotonically. To see this, consider the dissipative function of a gradient system, which is introduced by the quadratic form

$$\Gamma = \frac{1}{2}\dot{s}^{\mathrm{T}}\hat{\gamma}\dot{s} = \frac{1}{2}\sum_{i,j=1}^{n} \gamma_{ij}\dot{s}_i\dot{s}_j \quad \text{where} \quad \hat{\gamma} = \hat{k}^{-1}. \tag{4}$$

The matrix $\hat{\gamma}$ inherits the properties (i)–(iii) of matrix $\hat{k}$, and the constancy of sign $\dot{G}(s)$ under the evolution of a gradient system follows directly from the relation

$$\dot{G}(s) = -2\Gamma. \tag{5}$$

Relation (5) indicates that the sign of $\dot{G}(s)$ is opposite to the sign of dissipative function; thus, as the latter is

positively (negatively) definite, the potential of gradient system strictly decreases (increases).

As an elementary example, the ordinary equation $\dot{u} = f(u)$ is a gradient system because it admits the representation $\dot{u} = -k[\mathrm{d}G(u)/\mathrm{d}u]\,, k = 1\,, G(u) = -\int f(u)\mathrm{d}u$. The corresponding dissipative function is $\Gamma = \dot{u}^2/2$, and under time-dependent solutions of this equation, the potential decreases monotonically.

As a second example, consider a Newtonian particle of mass m that is changing its position $\boldsymbol{r}$ with the speed $\dot{\boldsymbol{r}}$ and acceleration $\ddot{\boldsymbol{r}}$ by the action of forces of two kinds: a potential force $\boldsymbol{Q}^{(\mathrm{P})} = -\,\mathrm{grad}G(\boldsymbol{r})$ (where $G(\boldsymbol{r})$ is the potential energy), and a friction force $\boldsymbol{Q}^{(\mathrm{D})} = -\gamma\dot{\boldsymbol{r}}, \gamma = \mathrm{const} > 0$. The Newtonian vector equation of motion of this particle is $m\ddot{\boldsymbol{r}} = \boldsymbol{Q}^{(\mathrm{D})} + \boldsymbol{Q}^{(\mathrm{P})} \equiv -\gamma\dot{\boldsymbol{r}} - \mathrm{grad}G(\boldsymbol{r})$, or, equivalently,

$$\dot{\boldsymbol{r}} = \boldsymbol{v}, \quad m\dot{\boldsymbol{v}} + \gamma\boldsymbol{v} = -\mathrm{grad}G(\boldsymbol{r}). \tag{6}$$

This system has two different limits—"Galilean" and "Aristotelian." The Galilean limit corresponds to the situation when dissipative force $\boldsymbol{Q}^{(\mathrm{D})}$ is negligible in comparison with the d'Alembert inertia force $\boldsymbol{Q}^{(\mathrm{I})} = -\,m\dot{\boldsymbol{v}}$. At this limit—which is realized under motion through a vacuum—the term $\gamma\boldsymbol{v}$ in Equations (6) vanishes, and it reduces to the form

$$\dot{\boldsymbol{r}} = \boldsymbol{v}, \quad m\dot{\boldsymbol{v}} = -\mathrm{grad}G(\boldsymbol{r}). \tag{7}$$

We refer to this limit as Galilean because Galileo proposed and experimentally demonstrated that gravitational force determines the acceleration of a falling body rather then its speed.

The Aristotelian limit, on the other hand, describes so-called creeping motions, in which the d'Alembert inertia force $\boldsymbol{Q}^{(I)}$ is much weaker than the dissipative force $\boldsymbol{Q}^{(D)}: |\boldsymbol{Q}^{(D)}| = m|\dot{\boldsymbol{v}}| \ll |\boldsymbol{Q}^{(I)}| = \gamma|\boldsymbol{v}|$. This limit is realized in the viscosity limited motion of particle, which occurs in a strongly viscous medium in the presence of a potential force field. In this limit, Equations (6) asymptotically reduce to

$$\dot{\boldsymbol{r}} = -k\mathrm{grad}G(\boldsymbol{r})\,, \quad k = \gamma^{-1}\,. \tag{8}$$

The order of Equation (8) with respect to time is less by half then corresponding order of (6). In this case, the current state s of particle is fully determined by current value of radius-vector $\boldsymbol{r}$. Now, the rate of change of state is proportional to the gradient of potential energy; therefore, the Newtonian particle undergoes creeping motion in a gradient system. The dissipative function of this system is

$$\Gamma = \gamma\boldsymbol{v}^2/2 \quad (\gamma > 0)\,, \tag{9}$$

and the potential $G(\boldsymbol{r})$ always decreases monotonically as $\dot{G} = -\gamma|\mathrm{grad}G(\boldsymbol{r})|^2$. This limit is called Aristotelian because it manifests the Aristotelian principle that "velocity of a body is proportional to a force acting upon the body." (This principle is not wrong; it merely corresponds to one of two possible limits of classical macroscopic dynamics which is realized in the presence of strong friction.)

The Newtonian example can be extended to the more general case of constrained system of n degrees of freedom, which move under stationary holonomic constraints and generalized forces of three types: the potential forces $Q_i^{(\mathrm{P})}$, the dissipative forces $Q_i^{(\mathrm{D})}$ of viscous friction, and the d'Alembert inertia forces $(Q_i^{(1)} = 1, \ldots, n)$. A related example is provided by electrical networks that are constructed with linear lumped elements: resistances (R), inductances (L), and capacitances (C). From an electromechanical analogy (Gantmacher, 1975), the considerations discussed above are extended to this case almost automatically. The analogs of Galilean and Aristotelian limits also exist here. The first limit corresponds to the situation when all resistances are negligible; it displays the LC subclass of general RLC networks. The networks belonging to this subclass are described by systems of ordinary differential equations that involve second-order time derivatives; as a rule, they are not gradient systems. The electrical analog of the Aristotelian limit corresponds to the networks with negligible inductances (RC subclass of general RLC networks). The networks making up this subclass are gradient systems.

The gradient systems considered in these examples are characterized by the monotonic diminution of potential G in their motions. Formally, this property follows from positiveness of dissipative functions related to these systems. In the mechanical examples, where the potential G is given by the potential energy of a mechanical system, its diminution can be explained physically by the action of viscous friction, which dissipates the energy of system and fully converts it to heat Q at a rate $\mathrm{d}Q/\mathrm{d}t = 2\Gamma$.

The opposite case, which corresponds to a monotonic *increase* of G, can be viewed as the action of "negative friction" transferring energy from exterior sources to the moving system; for example, processes during evolution of the genetic structure of biological populations which are described by classical Fisher–Haldane–Wright equations. The gradient representations of these equations were developed by Svirezhev in 1972 and by Shahshahani in 1979. (Svirezhev's results now can be found in the comprehensive monograph of Svirezhev & Pasekov, 1990.) In the context of their results, the famous Fisher's Fundamental Theorem of Natural Selection—which asserts that the mean fitness of population always increases with the rate proportional to the genotypical diversity of the population—is

a simple consequence of the gradient properties of the equations. In this case, the role of potential of the corresponding gradient system is played by the mean fitness of population, whereas the dissipative function is connected with a certain measure of genotypical diversity.

Owing to the presence of the monotonically varying quantity G, any gradient system is forbidden to return to states it once already left. In particular, such a system cannot perform nontrivial periodic motions (different from the states of rest). These properties are widely used in applied mathematics, including numerical gradient methods of searching for minima and maxima of multivariable functions.

In the above examples, gradient systems with finite degrees of freedom were considered. However, in various problems one deals with nonlocal spatially distributed systems in continuous media, occupying some d-dimensional region X of physical space, whose dynamics inherits the main features of finite-dimensional gradient systems. These objects form a class of gradient systems of an infinite number of degrees of freedom, which are referred to as *continuum gradient systems*. A nontrivial example is the system

$$\dot{u} = -k(u, \boldsymbol{x})\frac{\delta G[u]}{\delta u},$$

$$G[u] = \int_X g(u, \nabla u, \boldsymbol{x})\mathrm{d}X, \tag{10}$$

where $u = u(\boldsymbol{x}, t)$ is a function describing the state of the system at the spatial point $\boldsymbol{x} \equiv (x_i, \ldots, x_d) \in X$ and time t, and the integral functional $G[u]$ is a potential of the continual gradient system. Also ∇u denotes the spatial gradient, $\nabla u = |\partial u/\partial x_1, \ldots, \partial u/\partial x_d|$; $\mathrm{d}X = \mathrm{d}x^1 \ldots \mathrm{d}x^d$ is the space volume element of the region X occupied by the continuous medium; and $\delta/\delta u$ is a functional derivative, which acts upon the functional $G[u]$ according to the rule

$$\frac{\delta G}{\delta u} = \frac{\partial g}{\partial u} - \mathrm{div}\left[\frac{\partial g}{\partial(\nabla u)}\right] = \frac{\partial g}{\partial u} - \sum_{\mu=1}^{d}\frac{\partial}{\partial x^\mu}\frac{\partial g}{\partial(\partial u/\partial x^\mu)}. \tag{11}$$

Substituting (11) into the second part of (10), one can show that equations (10) are equivalent to the equation

$$\dot{u} + \mathrm{div}\,\boldsymbol{J} = Q \tag{12}$$

where $\boldsymbol{J}$ and Q are given by the expressions

$$\boldsymbol{J} = -k\frac{\partial g}{\partial(\nabla u)}, \tag{13}$$

$$Q = -k\frac{\partial g}{\partial u} - \nabla k \cdot \frac{\partial g}{\partial(\nabla u)}. \tag{14}$$

Equation (12) has the form of standard continuity equations for some substance filling the spatial region X; therefore, the quantities u and $\boldsymbol{J}$ can be interpreted as the density of this substance and as a vector of density of the corresponding spatial transport flux, respectively. From this standpoint, the function in the second part of continuity equation (12), defined by relationship (14), describes the rate of production of these substances per unit space volume, whereas expression (13) relating the flux $\boldsymbol{J}$ to the density u and its spatial gradient ∇u can be interpreted as a peculiar nonlinear generalization of well-known linear phenomenological laws such as Fick's law of diffusion or Ohm's law of electrical conduction. Hence, the continuum physical systems obeying the functional gradient equation (10) constitute a specific subclass in the class of reaction diffusion systems. This subclass comprises many physically important systems, including the parabolic equation

$$\gamma(\boldsymbol{x})\dot{u} = \mathrm{div}[D(\boldsymbol{x})\nabla u] + f(u, \boldsymbol{x}) = D(\boldsymbol{x})\Delta u + \nabla D(\boldsymbol{x}) \cdot \nabla u + f(u, \boldsymbol{x}) \tag{15}$$

defined in the space region X. Here $\gamma(\boldsymbol{x}) > 0$, $D(\boldsymbol{x}) > 0$, and $f(u, \boldsymbol{x})$ are the given functions of their arguments. Special cases of (15) include the linear diffusion equation $\dot{u} = \Delta u$, as well as the nonlinear reaction diffusion equation

$$\dot{u} = \Delta u + f(u), \tag{16}$$

which arises in several branches of natural science.

In mathematical genetics, Equation (16) describes the gene exchange waves traveling in the populations of biological organisms (Fisher's equation). In addition, this equation describes flame propagation as well as the switching processes in some physical, chemical, and biological nonlinear media (Zeldovich–Frank-Kamenetsky equation). Also, the time-dependent Ginzburg–Landau equation, which arises in physical kinetics and in synergetics for the phase transitions in spatially distributed self-organizing systems, has the form of Equation (16).

Remarkably, all these examples can be interpreted as processes of time evolution of certain gradient continuum systems. The functional gradient representation (10) is important because it suggests their general qualitative properties by the analogy with finite-dimensional case. For example, the potential $G[u]$ in (10) decreases monotonously in all time-dependent solutions if the latter is endowed with impermeability boundary conditions [see (18)]

$$J_n|_{\partial X} = 0 \leftrightarrow \boldsymbol{n}\left.\frac{\partial g}{\partial(\nabla u)}\right|_{\partial X} = 0, \tag{17}$$

where the subscript ∂X indicates that corresponding expressions are considered at the boundary ∂X of space region X enclosing the continual system, $J_n|_{\partial X}$ is the normal component of $\boldsymbol{J}$ at the boundary, and $\boldsymbol{n}$ is unit normal vector at ∂X. Indeed, the full derivative of the energy functional $G[u]$ with respect to time t is given by the elegant relation

$$\frac{\mathrm{d}G}{\mathrm{d}t} = -\int_X k\left(\frac{\delta G}{\delta u}\right)^2 \mathrm{d}X \le 0\,. \tag{18}$$

Defining the *dissipative functional* by the formula

$$\Gamma[u,\dot{u}] = \int_X \frac{1}{2k}\dot{u}^2 \mathrm{d}X = \frac{1}{2}\int_X \gamma\dot{u}^2 \mathrm{d}X,$$
$$\gamma = k^{-1},$$

puts (18) into the simple form of Equation (5), which appeared in the finite-dimensional case.

As in the finite-dimensional case, the monotone decrease of potential means that time evolution is *unidirectional*—these systems cannot return to the states once left. In particular, they can have neither solutions that are periodic in space and time nor traveling-impulse solutions with complete recovery of the initial state. If they possess moving wave-front solutions, contra directional wave fronts cannot be reflected after collisions with each other. On the contrary, if some spatially distributed system isolated from the outer world by the impermeable boundaries can modify its state supporting the propagation of solitary/periodic traveling pulses, then it cannot be described by continuum gradient equations.

O.A. Mornev

See also **Diffusion; Flame front; Nerve impulses; Reaction-diffusion systems; Synergetics; Zeldovich–Frank-Kamenetsky equation**

Further Reading

Fomenko, A.T. 1995. *Symplectic Geometry: Methods and Applications*, 2nd edition, New York: Gordon and Breach (original Russian edition 1988)

Gantmacher, F. 1975. *Lectures in Analytical Mechanics*, Moscow: Mir Publications (original Russian edition 1966)

Loskutov, A.Yu. & Mikhailov, A.S. 1996. *Foundations of Synergetics*, 2nd edition, Berlin and New York: Springer (original Russian edition 1990)

Mornev, O.A. 1997. Dynamical principle of minimum energy dissipation for systems with ideal constraints and viscous friction. *Russian Journal of Physical Chemistry*, 71(12): 2077–2081 [Translated from *Zhurnal Fizicheskoi Khimii*, 1997, 71(12): 2293–2298]

Mornev, O.A. 1998. Modification of the biot method on the basis of the principle of minimum dissipation (with an application to the problem of propagation of nonlinear concentration waves in an autocatalytic medium). *Russian Journal of Physical Chemistry*, 72(1): 112–118 [Translated from *Zhurnal Fizicheskoi Khimii*, 1998, 72(1): 124–131]

Mornev, O.A. & Aliev, R.R. 1995. Local variational principle of minimum dissipation in the dynamics of reaction-diffusion systems. *Russian Journal of Physical Chemistry*, 69(8): 1325–1328 [Translated from *Zhurnal Fizicheskoi Khimii*, 1995, 69(8): 1466–1469]

Scott, A.C. 2002. *Neuroscience: A Mathematical Primer*, Berlin and New York: Springer

Scott, A.C. 2003. *Nonlinear Science: Emergence and Dynamics of Coherent Structures*, 2nd edition, Oxford and New York: Oxford University Press

Svirezchev, Yu.M. & Pasekov, V.P. 1990. *Fundamentals of Mathematical Evolutionary Genetics*, Dordrecht: Kluwer (original Russian edition 1982)

GRANULAR MATERIALS

What do coffee powder, wheat, mustard seeds, granulated sugar, cement, sand, and rocks have in common? They are granular materials, assemblies of solid objects, from tens of micrometers to meter sized, that are generally not bound together by significant attractive forces. Such assemblies of objects possess unique physical and dynamic characteristics. Even though individual grains are solid particles, the assembly of grains behaves distinctly from ordinary solids, fluids, or gases (Jeager et al., 1996; Duran, 1997). For example, a sand dune is reliably solid-like and can sustain the weight of a person. However, if the sand from the dune is placed in an hourglass, it will flow rapidly and at a predictable rate.

The curious behavior of granular matter has long attracted the attention of scientists. In 1885, Osborne Reynolds observed that in order for grains to flow past each other, they have to move out of each other's way, leading to a dilation of granular matter under shear (Reynolds, 1885).

Some of the first modern work on granular matter was inspired by Per Bak, C. Tang, and K. Wiesenfeld (1987), who developed the concept that many systems may self-organize into a critical state. Granular avalanching was thought to be one of the prominent experimental realizations of their theory of self-organized criticality (SOC). The idea was that on a sandpile, grains might self-organize through avalanching to form a heap with a critical angle, which is called the angle of repose of the sandpile.

While experiments showed that SOC does not describe the behavior of real sandpiles (Nagel, 1992), the initial experiments showed some of the puzzling properties of granular matter and inspired a significant resurgence of research into granular matter. Here we describe three of the main questions of recent work:

When and How Does Granular Matter Flow?

In most situations when granular matter flows, such as during emptying of silos or during natural rock avalanches, only part of the material behaves like a fluid. This is illustrated in Figure 1 in a long exposure image of the side of an avalanche flowing down the

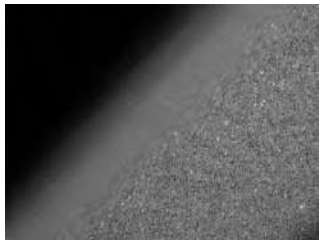

Figure 1. Long exposure image of the side of an avalanche flowing down the side of a granular pile. A clear separation into fluid-like and solid-like regions is visible. (Courtesy of N. Taberlet and P. Richard, University of Rennes).

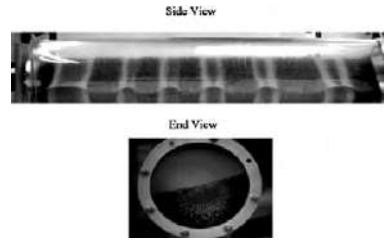

Figure 2. Unmixing of grains of three different sizes in a rotating horizontal cylinder. After 5 min of rotation at 15 rpm, material is separated into axial and radial bands. Both a side view and end view of the cylinder are shown.

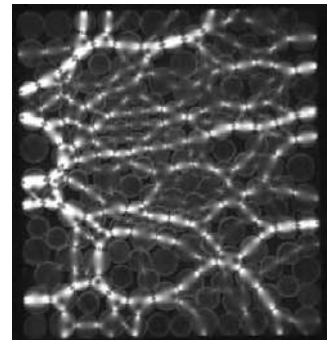

Figure 3. Forces in a 2-dimensional assembly of disks sheared between concentric cylinders. The disks are birefringent and placed between crossed polarizers, so that only points subject to large forces are visible as bright regions. (Courtesy of B. Utter and R.P. Behringer, Duke University).

side of a granular pile. The flow leaves behind a pile with a known surface angle, the angle of repose (Nagel, 1992). Predicting the timing and extent of such partial fluidization is part of the current challenge of modeling dense granular flows.

Once flowing, hydrodynamic equations may describe the flow behavior (Losert et al., 2000), though velocity gradients on length scales of a few particle diameters can call the validity of continuum models with local equilibria into question.

More dilute flows can be modeled as a system of hard spheres in which some energy is lost during each collision. Based on such a picture, kinetic theories of driven granular media have been developed, for example by Goldhirsch & Zanetti (1993). Since energy is continuously lost in collisions and must be added through gravity or shaking, granular flows are non-equilibrium driven, dissipative systems that exhibit interesting instabilities. One example is the clustering instability, in which a dilute system of particles can spontaneously develop localized, dense clusters (Goldhirsch & Zanetti, 1993). The basic mechanism for and clustering is that a local increase in particle density increases the number of collisions in that region, and, thus, slowing particles down and trapping them in the dense region.

How Can Different Kinds of Particles be Mixed or Separated?

During flow, mixtures of grains tend to spontaneously unmix (Shinbrot & Muzzio, 2000), as illustrated in Figure 2. The figure shows unmixing in a mixture of glass particles of three different sizes after several rotations in a half-filled horizontal cylinder. The phenomenology of granular unmixing is complex. In a horizontally rotating drum, for example, materials can segregate both radially and axially by size or by density. There is, to date, no simple model for unmixing, but a wealth of empirical experimental data and several simple physical mechanisms, such as percolation through voids, shear flows, and convection, all play some role in the unmixing process.

How Are Forces Transmitted Through Granular Matter?

In civil engineering, the mechanical behavior of granular matter is modeled by solid-like equations (Nedderman, 1992). Zooming in to the scale of grains, forces can only be transmitted at particle contacts, and only repulsive forces are permitted at each contact. This can lead to very inhomogeneous force distributions and locally very large forces as is indeed seen, for example, in grain silos. Experiments with birefringent disks that highlight the location and magnitude of contact forces (Howell et al., 1999) have helped in our microscopic understanding of the way forces are transmitted through granular matter (Figure 3). Strong inhomogeneities in the force magnitude, anisotropies in the direction of stress

transmission, and large rearrangements in the force distribution, even for small changes in structure are observed.

Two emerging concepts to explain the properties of such dense granular matter are jamming, the property of a system to get trapped in some intermediate state which may be generic to granular matter as well as thermal systems such as glasses, and the idea of stress chains, lines of particles that carry disproportionately large stress, as can be seen in Figure 3.

To conclude, basic questions about granular matter remain. Granular matter encompasses different kinds of particles with many variables, such as the frictional properties of grain-grain or grain-boundary contacts, the deformability, surface roughness, polydispersity, and grain shape. It remains difficult to predict whether a particular granular parameter, such as the shape of individual grains will qualitatively alter flow, forces, or mixing behavior, and thus, has to be taken into account in modeling. While models for flow, forces, and segregation have been developed that agree with experimental data under various conditions, a broadly valid model of granular flow based on simple physical insights similar to the Navier–Stokes equation for fluids has so far proven elusive. Similarly, no consensus about the most suitable equation for granular solids has yet emerged, nor has a clear separation between the solid-like and liquid-like regime emerged.

WOLFGANG LOSERT

See also **Avalanches; Cluster coagulation; Dune formation; Sandpile model**

Further Reading

Bak, P., Tang, C. & Wiesenfeld, K. 1987. Self-organized criticality: an explanation of the 1/f noise. *Physical Review* A, 59: 381–384

Duran, J. 1997. *Sands, Powders, and Grains: An Introduction to the Physics of Granular Materials*, Berlin and New York: Springer

Goldhirsch, I. & Zanetti, I. 1993. Clustering instability in dissipative gases. *Physical Review Letters*, 70: 1619–1622

Howell, D.W., Veje, C.T. & Behringer, R.P. 1999. Stress fluctuations in a 2D granular couette experiment: a critical transition. *Physical Review Letters*, 82: 5241–5244

Jaeger, H.M., Nagel, S.R. & Behringer, R.P. 1996. *Reviews of Modern Physics*, 68: 1259–1273

Knight, J.B., Jaeger, H.M. & Nagel, S.R. 1993. *Physical Review Letters*, 70: 3728–3731

Losert, W., Bocquet, L., Lubensky, T.C. & Gollub, J.P. 2000. Particle dynamics in sheared granular matter. *Physical Review Letters*, 85: 1428–1431

Nagel, S.R. 1992. Instabilities in a sandpile. *Reviews of Modern Physics*, 64: 321—325

Nedderman, R.M. 1992. *Statics and Kinematics of Granular Materials*, Cambridge and New York: Cambridge University Press

Reynolds, O. 1885. On the dilatancy of media composed of rigid particles in contact. *Philosophical Magazine*, 20: 469

Shinbrot, T. & Muzzio, F.J. 2000. *Physics Today*, March 25

GRAVITATIONAL WAVES

In 1687, Newton published *The Philosophiae Naturalis Principia Mathematica* in which he first proposed his law of gravitation. According to this law, the gravitational force of attraction between two bodies is always proportional to their masses and inversely proportional to the square of their distance apart, and it acts instantaneously through infinite distance. Less than two and half centuries later, Newton's theory was radically revised.

According to Einstein's general theory of relativity (published in 1913), gravitation is not a force of attraction but rather the force required to prevent the natural motion of matter, which is to follow a geodesic in space time. The geodesic or shortest path in four-dimensional space time describes a free-fall trajectory such as the motion of a planet around the sun. The space time is curved by the presence of matter or energy. The predictions of general relativity are very close to those of Newtonian theory as long as gravity is weak and velocities are slow, but they diverge in strong gravity due to two aspects of the theory. The first is the change in geometry due to the non-Euclidean properties of space time. The second stems from the nonlinear aspects of general relativity, which arise because gravitational energy is itself a source of curvature.

Eight years prior to publishing his general relativity theory, Einstein published the special theory of relativity, which predicted that neither matter nor information could ever travel faster than the speed of light. This means that the curvature at a point generated by a mass at another point only achieves its value at a retarded time, a time set by the travel time for light between the two points.

The general theory of relativity changed our vision of a Euclidean flat space that had been assumed since the days of Newton. In non-Euclidean space, the sum of the angles of a triangle does not equal 180° and the area of a circle is not always πr^2. Space time can be considered as an elastic membrane. The deformations are described by the Einstein curvature tensor G, while the sources of curvature (i.e., the mass-energy distribution) are described by the stress-energy tensor T. Einstein's field equations are then expressed by the equation (Misner et al., 1973)

$$\mathsf{T} = \frac{c^4}{8\pi G}\mathsf{G}. \qquad (1)$$

The constant $c^4/8\pi G$ (where c is the speed of light and G is Newton's gravitational constant) is a very large number which can be considered as the "spring constant" of space time. Because it is so large, only very small curvatures are generated even by very large values of mass-energy distribution. A natural consequence of the membrane analogy is the existence

of waves; ripples in the curvature of the membrane which propagate through the membrane. This concept can also be deduced from Einstein's field equations.

Equation (1) is a set of ten nonlinear equations. Except in simplified situations, these equations are difficult to solve directly. Matter creates curvature and curvature influences the motion of matter. This mutual influence gives rise to nonlinear phenomena in gravitational wave propagation. Unlike the theory of electromagnetism, the theory of general relativity is intrinsically nonlinear. Since gravity is itself a source of curvature, there can be a gravitational interaction between gravitational waves. While gravitational wave signals are normally expected to be very small (and hence amenable to a linearized theory), at their sources, the nonlinear aspect of the theory makes prediction extremely difficult. The following list offers some examples of expected nonlinear phenomena in gravitational wave propagation:

- For gravitational waves emerging from the birth of a black hole, the gravitational redshift of the waves reduces the total emitted energy. The mass-energy of the gravitational waves themselves constitute the redshift.
- Like electromagnetic radiation, gravitational waves can undergo gravitational lensing. A mass in the path of the waves creates a background curvature. This curvature focuses the waves by modifying the wave front. This effect can enhance the intensity of dim sources. The gravitational lensing effect has successfully been observed for electromagnetic radiation.
- A time-varying curvature can amplify waves. If a wave modulates the space curvature, a second incident wave will be amplified or its frequency shifted. An optical parametric oscillator represents the equivalent phenomena for optical radiation. Similar to the optical Kerr effect, a gravitational wave can interact with its own self-generated background curvature. In the early universe, it is predicted that gravitational waves from the Big Bang may have been parametrically amplified by the action of inflation.
- A strong background curvature (e.g., from a black hole) can scatter a gravitational wave passing in its vicinity.

Under gravitational wave astronomy, it may be possible to find evidence of these predicted phenomena. The first indirect experimental proof of gravitational waves was provided in 1984 by Weisberg and Taylor. By studying the pulsar PSR 1913+16, they showed that the period of the pulsar around its companion star decreased exactly as predicted by the Einstein equations (Weisberg et al., 1981). A part of the pulsar orbital energy is converted to gravitational radiation.

The orbital parameters of binary stars are usually deduced from measurements of the Doppler shift of the radiated electromagnetic waves. According to Newtonian gravitational theory, the mass m_1 of the pulsar and the mass m_2 of its companion cannot be determined with confidence. All results obtained are proportional to an unknown parameter: the sine (normally denoted $\sin i$) of the angle between the orbital plane and the line of sight. This parameter can be evaluated in the framework of general relativity. From this theory, five independent parameters (among them, the advance of the periastron (the point of closet approach of the two stars), the evolution of the period, or the Einstein parameter) which are functions of m_1, m_2, and $\sin i$ can be measured. The overdetermined system of five equations determines with an unprecedented accuracy (error less than 0.5%) the mass of the pulsar. Moreover, the compatible results from the five independent equations confirm the general theory of relativity in the strong field and radiative regime. This high-precision validation of general relativity indirectly implies that the velocity of gravitational waves is equal to the speed of light.

Direct detection of gravitational waves on Earth is one of the most exciting challenges of today's science. In the 1960s, Joseph Weber invented and developed the first gravitational wave detectors, consisting of large (about a ton) vibration-isolated cylinders of aluminium or niobium (Weber, 1960). The gravitational waves excite the longitudinal resonance in the cylinder, which behaves as an extremely low-loss mechanical oscillator. The motion of the cylinder is monitored to very high precision. Most of its motion is thermal vibration but the small effect of the gravitational waves appear as very small perturbations in the amplitude or phase of the vibration. The mechanical oscillations, converted into an electrical signal, are recorded and analyzed by sophisticated predictive filter algorithms. A worldwide network of five resonant bars still uses Weber's technique (see Figure 1).

A new generation of gravity-wave detectors is based on laser interferometry (Blair, 1991). Gravitational waves passing through a Michelson interferometer change the relative length difference between the two perpendicular arms of the interferometer. Thus the variation of the gravitational field can be converted to an optical phase variation. Due to the weakness of gravitational wave interaction with matter, the detectors must be able to measure a length variation of less than 10^{-18} m, which is close to the quantum limit. Compared with the resonant bar, the interferometric devices exhibit a larger bandwidth and higher sensitivity. The sensitivity is limited by seismic and thermal noise at low frequency and photon-counting noise at higher frequency.

Five international projects, similar to the example shown in Figure 2, are using long base interferometry

Figure 1. Photograph of the interior of Niobe, the resonant bar at the University of Western Australia. The bar is a one and half ton cylinder of niobium cooled to 5 K to limit the thermal noise.

Figure 2. Aerial view of the French–Italian gravitational waves detector VIRGO near Pisa in Italy. On this photo, the two perpendicular 3 km vacuum pipes containing the arms of the interferometer are clearly distinct (Bradaschia et al., 1990) (Reproduced with permission from EGO).

to detect gravitational waves. The network of, interferometers (situated in the United States, Europe, Japan, and Australia) will enable the localization of sources of gravitational radiation in space as well as determination of their polarization. By measuring the arrival time of the waves at different detectors, the speed of the gravity waves can be calculated. This speed could be influenced by two independent factors: a coupling of the wave with a strong curvature background (difficult to detect on Earth) and the possibility that the graviton, the particle associated with the gravitational waves, is not massless (Will, 1998).

The direct detection of gravitational waves is expected to occur before 2012. This gravitational spectrum will open a new window to studying the universe, comparable to the revolution fathered by the invention of radio astronomy in the 1950s. The direct mapping of the gravity spectrum will broaden our knowledge about the universe, from the earliest moment of the Big Bang to the end of stars.

JEROME DEGALLAIX AND DAVID BLAIR

See also **Einstein equations; General relativity**

Further Reading

Blair, D.G. 1991. *The Detection of Gravitational Waves*, Cambridge and New York: Cambridge University Press

Bradaschia, C. et al. 1990. The VIRGO project: a wide band antenna for gravitational wave detections. *Nuclear Instruments and Methods in Physics Research* A, 289: 518–528

Misner, C.W., Thorne, K.S. & Wheeler, J.A. 1973. *Gravitation*, San Francisco: W.H. Freemann

Weber, J. 1960. Detection and generation of gravitational waves. *Physical Review*, 117: 306–313

Weisberg, J.M., Taylor, J.H. & Fowler, L.A. 1981. *Gravitational Waves from an Orbiting Pulsar*, Scientific American, p. 74

Will, C.M. 1998. Bounding the mass of the graviton using gravitational waves observations of inspiralling compact binaries. *Physical Review* D, 57: 2061–2068

GRAVITY WAVES

See **Water waves**

GREEN'S FUNCTION

See **Boundary layer problems**

GREY SOLITON

See **Solitons, types of**

GROSS-PITAEVSKII EQUATION

See **Nonlinear Schrödinger equations**

GROUP VELOCITY

Waves often propagate as a packet, or group, within which there are several wave crests. A common illustration is given by the wave pattern formed when a stone is thrown into a pond. An axially symmetric ring of waves on the water surface propagates outwards as a wave group; within the group, however, one can see that the wave crests propagate through the group, apparently from the rear to the front. The speed of the wave crests, called the *phase velocity*, is different from that of the group as a whole, this speed being called the *group velocity*. For water waves, the phase velocity is greater than the group velocity, except for the very short waves dominated by surface tension.

This important distinction between phase and group velocity arises in all physical systems which support waves. The concept of group velocity appears to have been first formulated by William Hamilton in 1839 (quoted by Havelock, 1914). The first recorded observation of the group velocity of a (water) wave is due to John Scott Russell in 1844 (Russell, 1844) (note also his remark that "the sound of a cannon travels faster than the command to fire it" (Russell, 1885)). However, our present understanding of group velocity is usually

attributed to George Stokes, who used it as the topic of a Smith's Prize examination paper in 1876.

For simplicity, consider a linearized system, with a single spatial variable x and time represented by t. Then a sinusoidal wave has the representation,

$$u(x,t) = a\cos(kx - \omega t + \phi). \tag{1}$$

Here k is the wave number, ω is the wave frequency, a is the constant amplitude, and ϕ is a constant phase. Thus, this sinusoidal wave has a wavelength $\lambda = 2\pi/k$ and a wave period $T = 2\pi/\omega$. Equation (1) is a kinematic expression, valid for all physical systems which support waves. The dynamics of the system are governed by the dispersion relation

$$\omega = \omega(k), \tag{2}$$

defining the frequency as a function of wave number. The phase velocity $c = \omega/k$ is likewise a function of wavenumber.

To obtain the group velocity, consider an argument first advanced by Stokes (1876) and later in more general form by Lord Rayleigh (1881). Form the linear superposition of two sinusoidal waves, each of the form (1) with frequencies $\omega \pm \Omega$, wave numbers $k \pm K$, and with equal amplitudes a and phases ϕ which can be written as

$$u(x,t) = 2a\cos(kx - \omega t\phi)\cos(Kx - \Omega t). \tag{3}$$

This expression can be viewed as a wave packet, or group, with a dominant wave number k and frequency ω, and with a group velocity of Ω/K. Taking the limit $K \to 0$, one sees that the group velocity is given by

$$c_g = \frac{d\omega}{dk}, \tag{4}$$

which can be obtained by differentiation of the dispersion relation (2).

A more general argument that links the origin of a wave packet to initial conditions uses Fourier superposition to represent the solution of an initial-value problem in the form

$$u(x,t) = \int_{-\infty}^{\infty} F(k)\exp(\mathrm{i}(kx - \omega t))\,dk + \text{c.c.}, \tag{5}$$

where $F(k)$ is the Fourier transform of $u(x,0)$ and c.c. stands for complex conjugate. Thus, the initial conditions determine the Fourier transform, each component of which evolves independently with frequency ω related to the wave number k through the dispersion relation (2). To obtain a wave packet, we suppose that the initial conditions are such that $F(k)$ has a dominant component centered at $k = k_0$. The dispersion relation is then approximated by

$$\omega = \omega_0 + b_1(k - k_0) + b_2(k - k_0)^2, \tag{6}$$

where

$$b_1 = \frac{d\omega}{dk} = c_g, \quad \text{and} \qquad b_2 = \frac{1}{2}\frac{d^2\omega}{dk^2}. \tag{7}$$

Here, both b_1, b_2 are evaluated at $k = k_0$. Expression (5) then becomes

$$u(x,t) \approx A(x,t)\exp(\mathrm{i}(k_0 x - \omega_0 t)) + \text{c.c.}, \tag{8}$$

where

$$A(x,t) = \int_{-\infty}^{\infty} F(k_0+\kappa)\exp[\mathrm{i}(\kappa(x - c_g t)) - \mathrm{i}b_2\kappa^2 t]\,d\kappa, \tag{9}$$

where the variable of integration has been changed from k to $\kappa = k - k_0$. Here, the sinusoidal factor $\exp(\mathrm{i}(k_0 x - \omega_0 t))$ is a carrier wave with a phase velocity ω_0/k_0, while the (complex) amplitude $A(x,t)$ describes the wave packet. Since the term proportional to κ^2 in the exponent in (9) is a small correction term, it can be seen that to the leading order, the amplitude A propagates with the group velocity c_g, while the aforementioned small correction term gives a dispersive correction term proportional to $t^{-1/2}$. Indeed, it can be shown that as $t \to \infty$

$$A(x,t)|_{x=c_g t} \sim F(k_0)\left(\frac{2\pi}{|b_2|t}\right)^{1/2}\exp\left(\frac{\mathrm{i}\pi}{4}\operatorname{sign} b_2\right). \tag{10}$$

This same result can be obtained directly from (5) by using the method of stationary phase, valid here in the limit when $t \to \infty$ (see, for instance, Lighthill, 1978); In this case, it is not necessary to also assume that $F(k)$ is centered at k_0, and so wave packets are the generic long-time outcome of initial-value problems.

It is useful to note that the group velocity appears naturally in the kinematic theory of waves (Lighthill, 1978; Whitham, 1974). Thus, let the wave field be defined asymptotically by

$$u(x,t) \sim A(x,t)\exp(\mathrm{i}\theta(x,t)) + \text{c.c.}, \tag{11}$$

where $A(x,t)$ is the (complex) wave amplitude, and $\theta(x,t)$ is the phase, which is assumed to be rapidly

varying compared with the amplitude. Then it is natural to define the local wave frequency and wave number by

$$\omega = -\frac{\partial\theta}{\partial t}, \qquad k = \frac{\partial\theta}{\partial x}. \tag{12}$$

Note that expression (10) has the required form (11). Then cross-differentiation leads to the kinematic equation for the conservation of waves,

$$\frac{\partial k}{\partial t} + \frac{\partial\omega}{\partial x} = 0. \tag{13}$$

But now, if we suppose the dispersion relation (2) holds for the frequency and wave number defined by (12), then we readily obtain

$$\frac{\partial k}{\partial t} + c_{\mathrm{g}}\frac{\partial k}{\partial x} = 0 \tag{14}$$

with a similar equation for the frequency. Thus, both the wave number and frequency propagate with the group velocity, a fact that can also be seen in (10). Equation (14) is itself a simple wave equation, which can be readily integrated by the method of characteristics, or rays. It is important to note that the group velocity c_{g} is a function of k, so that (14) is a nonlinear equation.

Next, suppose that the physical system contains several spatial variables, represented by the vector $\boldsymbol{x}$. Then the phase variable $(kx - \omega t)$ in (1, 5) is replaced by $(\boldsymbol{k}\cdot\boldsymbol{x} - \omega t)$, where $\boldsymbol{k}$ is the vector wave number. The dispersion relation (2) is replaced by

$$\omega = \omega(\boldsymbol{k}). \tag{15}$$

The phase velocity is now a vector $(\boldsymbol{c})$, has a magnitude $\omega/|\boldsymbol{k}|$, and is in the direction of $\boldsymbol{k}$, and the definition of group velocity, replacing (4), is

$$\boldsymbol{c}_{\mathrm{g}} = \nabla_{\boldsymbol{k}}\omega. \tag{16}$$

Thus, the group velocity can differ from the phase velocity in both magnitude and direction. A striking example of the latter arises for internal waves, whose group velocity is perpendicular to the phase velocity (see Lighthill, 1978).

Since the group velocity is the velocity of the wave packet as a whole, it is no surprise to find that it can also be identified with energy propagation. Indeed, it can be shown that in most linearized physical systems, an equation of the following form can be derived:

$$\frac{\partial\boldsymbol{E}}{\partial t} + \nabla\cdot(\boldsymbol{c}_{\mathrm{g}}\boldsymbol{E}) = 0\,, \tag{17}$$

where $\boldsymbol{E}$ is the wave action density, and is proportional to the square of the wave amplitude $|A|^2$, with the factor being a function of the wavenumber $\boldsymbol{k}$. Typically, the wave action is just the wave energy density divided by the frequency, at least in inertial frames of reference.

So far the discussion has remained within the realm of linearized theory, and it remains to mention the consequences of nonlinearity. Analogous definitions and concepts can be developed, and at least for weakly nonlinear waves, the main outcome is that a dependence on wave amplitude (more strictly, on $|A|^2$) appears in the dispersion relation. This has the consequence that the phase and group velocities both inherit a weak dependence on the wave amplitude. It can be shown that at least within the confines of weakly nonlinear theory, in the case of just a single active spatial dimension, the complex wave amplitude A is governed by the nonlinear Schrödinger (NLS) equation,

$$\mathrm{i}\left(\frac{\partial A}{\partial t} + c_{\mathrm{g}}\frac{\partial A}{\partial x}\right) + b_2\frac{\partial^2 A}{\partial x^2} + \mu|A|^2 A = 0. \tag{18}$$

Here recall that b_2 is defined in (7), and μ is a nonlinear coefficient which is system-dependent.

If A is assumed to depend only on t then Equation (18) has the plane wave solution

$$A = A_0\exp(\mathrm{i}\mu|A_0|^2 t), \tag{19}$$

which shows that the nonlinear coefficient μ has the physical interpretation that $-\mu|A_0|^2$ is the nonlinear correction to the wave frequency. It can be shown that this plane wave is stable (unstable) according as $\mu b_2 < (>)0$ (see Whitham, 1974). In the unstable case, $\mu b_2 > 0$, a perturbed plane wave will evolve into one or more solitons, where the soliton family is given by (see Zakharov and Shabat, 1972),

$$A(x,t) = \alpha\exp(-\mathrm{i}\mu\alpha^2 t)\mathrm{sech}(\gamma\alpha(x - c_{\mathrm{g}}t - x_0)),$$
$$\text{where}\quad \gamma^2 = \frac{\mu}{b_2}. \tag{20}$$

Here, x_0 is a phase constant determining the location of the soliton at $t = 0$, and the amplitude α is a free parameter. In linear theory, the wave packet profile is determined by the initial conditions, whereas the influence of even weak nonlinearity, when it is balanced by weak dispersion, results in the generic sech profile.

ROGER GRIMSHAW

See also **Modulated waves; Nonlinear Schrödinger equations; Wave packets, linear and nonlinear**

Further Reading

Havelock, T.H. 1914. *The Propagation of Disturbances in Dispersive Media*, Cambridge: Cambridge University Press

Lighthill, M.J. 1978. *Waves in Fluids*, Cambridge: Cambridge University Press
Rayleigh, Lord, 1881. On the velocity of light. *Nature*, XXIV: 382
Russell, J.S. 1844. *Report on Waves*, 14th meeting of the British Association for the Advancement of Science, London: BAAS, pp. 311–339
Russell, J.S. 1885. *The Wave of Translation in the Oceans of Water, Air and Ether*, London: Trübner
Stokes, G.G. 1876. Problem 11 of the Smith's Prize examination papers (February 2, 1876). In *Mathematical and Physical Papers of George Gabriel Stokes*, vol. 5, New York: Johnson Reprint Co., 1966, p. 362
Whitham, G.B. 1974. *Linear and Nonlinear Waves*, New York: Wiley
Zakharov, V.E. & Shabat, A.B. 1972. Exact theory of two-dimensional self-focusing and one-dimensional self-modulation of waves in nonlinear media. *Soviet Physics, JETP*, 34: 62–69

GROWTH PATTERNS

Patterns are ubiquitous in nature. They can range from the broad stripes on a zebra, to the intricate design of a snowflake, to the rib patterns on a saguaro cactus. The idea that naturally occurring patterns might have some underlying and universal governing mathematical structure has long been a source of fascination to researchers. The study of biological patterns was pioneered by D'Arcy Thompson in his landmark treatise *On Growth and Form* (Thompson, 1942). This was followed by a notable contribution by the mathematician (and Enigma code breaker) Alan Turing in a now famous paper "The Chemical Basis of Morphogenesis" (Turing, 1952). A more contemporary account of many biological patterns and their mathematical modeling is given in James D. Murray's textbook *Mathematical Biology* (Murray, 2003). But to what extent are patterns universal? Are there any connections among the three examples cited above? Inevitably, the underlying physical and biological processes governing a particular pattern-forming process can be very different, even if the topology of the resultant patterns and certain "defects" in those patterns look very similar. In some cases, different governing physical processes end up having essentially the same mathematical formulation, and in these cases, commonality of pattern structure is less surprising.

Here, we will concentrate on two physical pattern-forming systems that are popular topics of contemporary research in condensed-matter physics, namely, the fingering patterns at the interface of fluid mixtures and formation of dendritic crystals in solidification. Some of the patterns seen in these two systems are also seen in growing bacterial colonies.

The Hele-Shaw Cell: Fluid Fingering

This classic problem was first studied at the end of the 19th century, but even to this day there are still unresolved issues relating to the stability of the patterns exhibited. The experimental setup is relatively simple, consisting merely of a thin film of fluid sandwiched between two glass plates into which air (or another fluid) is pumped. As the air is pumped into the fluid film, one might imagine that it simply forms an expanding circular planar bubble. Initially this appears to be the case, but the circular perimeter rapidly becomes wavy and these "waves" then grow into long finger-like structures which, in turn can split or side branch forming highly complicated patterns. A typical pattern is shown in Figure 1a. The physical principles governing the growing air-fluid interface are well understood. The key idea is that the normal velocity of the air-fluid boundary (i.e., the velocity in the direction normal to each point of the interface) is governed by the gradient of the pressure across the interface. Because the fluid layer is so thin, the equations of fluid mechanics are greatly simplified, and one ends up with governing equations of the form

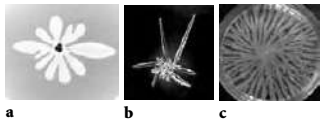

Figure 1. Three different types of growth patterns: (a) Hele-Shaw fingers; (b) dendritic crystals; (c) *Bacillus substilis* bacterial colonies.

$$\nabla^2 p = 0, \tag{1}$$

$$u_{\mathrm{n}} = -\frac{b^2}{12\mu}(\nabla p)\cdot \boldsymbol{n}, \tag{2}$$

$$\Delta p|_{\partial\Omega} = \sigma\kappa. \tag{3}$$

The first equation, in which $p = p(x, y)$ denotes the pressure, is a statement of the incompressibility of the fluid. In the second equation, u_{n} denotes the normal velocity (in the normal direction $\boldsymbol{n}$) of the interface. This is determined by the pressure gradient, the thickness of the fluid film b, and the fluid viscosity μ. The third equation describes the pressure jump Δp across the air-fluid interface $\partial\Omega$, and this depends on the surface tension σ and the interface curvature κ (the Young–Laplace law). Unlike more standard systems of partial differential equations in which the equation and boundary conditions are specified, the solution to this problem involves finding the boundary, $\partial\Omega$, itself. This is an example of a Stefan problem. At first sight the equations might look linear, but the coupling to the boundary dynamics makes them effectively highly nonlinear. Finding an exact solution of these equations is very difficult. A standard "linear stability" analysis is relatively straightforward and can explain why the initial circular air-fluid interface becomes

wavy. But beyond this, finding solutions for the finger-like structures, let alone fingers whose tips split, is (still) a difficult problem. A pioneering early study of the Hele-Shaw cell is due to Philip Saffman and Geoffrey Taylor (1958), and many hundreds of papers have been published on the problem in subsequent years.

Solidification and Dendritic Crystal Growth

At first sight this seems like a very different process. Cooling a drop of a molten substance (or a supersaturated salt solution) can produce very striking needle crystals that grow with approximately constant velocity and develop side branches. A typical pattern is shown in Figure 1b. Many questions come to mind: why do finger-like structures form; what determines their propagation speed; why do they form side branches; and is there any connection with the finger-like structures seen in the Hele-Shaw cell? Before addressing these questions it is worth noting that historically the study of dendritic growth had its origins in metallurgical studies associated with the casting of canons. It was discovered that during the casting process the solidifying metal developed a crystalline structure that could weaken the canon—to the point of its shattering when it was fired!

The physical process determining the growth of the solid phase is that of cooling, with the rate of cooling being determined by the rate at which heat can diffuse away from the solid-melt interface. The speed at which the the solid front advances is determined by the temperature gradient across the interface. Using these basic principles, the governing equations are found to be

$$\frac{\partial T}{\partial t} = \nabla^2 T, \tag{4}$$

$$u_{\mathrm{n}} = -\alpha(\boldsymbol{\nabla} T).\boldsymbol{n}, \tag{5}$$

$$T|_{\partial\Omega} = T_{\mathrm{m}} - \beta\kappa. \tag{6}$$

Here, the first equation is just the diffusion equation for the temperature field T. The second equation for the normal velocity, u_{n}, of the solidification front is exactly analogous to the one for the Hele-Shaw cell. The third equation expresses the temperature drop at the solid-melt interface $\partial\Omega$ in which the normal melting temperature T_{m} is corrected by subtle effects related to the curvature of the interface (the Gibbs–Thompson effect). In more sophisticated theories, there is an additional correction proportional to the velocity of the moving front itself. Here, α and β are certain parameters reflecting the physical properties of the crystalizing substance. Thus, despite the very different physics, the mathematical description of the Hele-Shaw cell and a solidifying melt are almost identical Stefan problems. Again, solving the equations is difficult. Apart from a linear stability analysis (leading to the so-called Mullins–Sekerka instability criterion (Langer 1980)), solutions for the dendritic structures and a description of the side-branching structure in particular are very difficult. A classic review of dendritic growth is Langer (1980) and a more recent textbook is Davis (2001).

Other Pattern-Forming Systems

The formulation of the above problems indicates that two quantities appear to play a key role: the gradient of a field variable (pressure or temperature in the above examples) that drives the evolution of the pattern, and curvature of the interface (Pelcé, 1988; Ben-Jacob & Garik, 1990). In fact, these two quantities also play important roles in other pattern-forming systems. In almost every problem whose pattern is in the form of a propagating front or interface (another classic example is flame propagation), the curvature, and the parameter that multiplies it (e.g., surface tension in the case of the Hele-Shaw cell), plays an important role in determining the basic pattern wavelength.

In the introduction, we cited bacterial colony formation as another example of a pattern-forming system. A typical pattern, of a colony of *Bacillus subtilis* on an agar plate, is shown in Figure 1c. What drives the formation of these patterns? A fundamental concept is that of chemotaxis, namely, the response of the organisms to a concentration gradient. Thus, flux of cells in a medium is typically determined by the nutrient gradient. This principle enables one to write down systems of coupled diffusion and hydrodynamic equations for the concentration of cells responding to the nutrient gradient, and for the nutrient concentration itself, which is clearly going to be depleted in regions of high cell concentration. The ensuing nonlinear feedback between these quantities can lead to a rich, and much-studied, pattern structure (Lega & Passot, 2003).

MICHAEL TABOR

See also **Branching laws; Cluster coagulation; Flame front; Hele-Shaw cell; Navier–Stokes equation; Pattern formation; Turing patterns**

Further Reading

Ben-Jacob, E. & Garik, P. 1990. The formation of patterns in non-equilibrium growth. *Nature*, 343: 523–530

Bensimon, D., Kadanoff, L.P., Liang, S., Shraiman, B.I. & Tang, C. 1986. Viscous flows in two dimensions. *Reviews of Modern Physics*, 58: 977–999

Davis, S.H. 2001. *Theory of Solidification*, Cambridge and New York: Cambridge University Press

Langer, J.S. 1980. Instabilities and pattern formation in crystal growth. *Reviews of Modern Physics*, 52: 1–28

Lega, J. & Passot, T. 2003. Hydrodynamics of bacterial colonies: a model. *Physical Review* E, 67: 031960

Murray, J.D. 2003. *Mathematical Biology*, 3rd edition, Berlin and New York: Springer

Pelcé, P. 1988. *Dynamics of Curved Fronts*, Boston: Academic Press

Saffman, P.G. & Taylor, G.I. 1958. The penetration of a fluid into a porous medium or Hele-Shaw cell containing a more viscous fluid. *Proceedings of the Royal Society of London* B, 245: 312–329

Thompson, D.W. 1942. *On Growth and Form*, 2nd edition, Cambridge: Cambridge University Press

Turing, A.M. 1952. The chemical basis of morphogenesis. *Philosophical Transactions of the Royal Society of London* B, 237: 37–72

GUTZWILLER TRACE FORMULA

See **Quantum theory**

H

HAMILTONIAN SYSTEMS

A system of $2n$, first order, ordinary differential equations

$$\dot{z} = J\nabla H(z,t), \quad J = \begin{pmatrix} 0 & I \\ -I & 0 \end{pmatrix} \tag{1}$$

is a Hamiltonian system with n degrees of freedom. (When this system is non-autonomous, it has $n + 1/2$ degrees of freedom.) Here H is the Hamiltonian, a smooth scalar function of the extended phase space variables z and time t; the $2n \times 2n$ matrix J is called the "Poisson matrix"; and I is the $n \times n$ identity matrix. The equations naturally split into two sets of n equations for *canonically conjugate* variables, $z = (q, p)$, as follows.

$$\dot{q} = \partial H/\partial p, \quad \dot{p} = -\partial H/\partial q.$$

Here the n coordinates q represent the configuration variables of the system (positions of the component parts), and their canonically conjugate momenta p represent the impetus associated with movement. These equations generalize Newton's second law: $F = ma = \mathrm{d}p/\mathrm{d}t$, to systems (like particles in magnetic fields, or motion in non-inertial reference frames) where the momentum is not simply mass times velocity. The Hamiltonian usually represents the total energy of the system; thus, if $H(q, p)$ does not depend explicitly upon t, then its value is invariant, and Equations (1) are a conservative system. More generally, however, Hamiltonian systems need not be conservative.

William Rowan Hamilton first gave this reformulation of Lagrangian dynamics in 1834 (Hamilton, 1835). However, Hamiltonian dynamics is much more than just a reformulation. It leads, for example, to Henri Poincaré's geometrical insight that gave rise to symplectic geometry, and it provides a compact notation in which the concept of integrability is most naturally expressed and in which perturbation theory can be efficiently carried out. Moreover, nearly integrable Hamiltonian systems exhibit a remarkable stability expressed by the famous results of Kolmogorov–Arnol'd–Moser (KAM) theory and also Nekhoroshev theory. The Hamiltonian formulation also provides the foundation of both statistical and quantum mechanics.

Importantly, virtually all of the dynamical laws of physics—from the motion of a point particle to the interaction of complex quantum fields—have a formulation based on Equations (1). For example, frictionless mechanical systems are described by a Hamiltonian $H(q, p) = K(p) + V(q)$, where K is the kinetic energy (which is often quadratic in p) and V is the potential energy. For example, an ideal planar pendulum consists of a point particle of mass m attached to a massless rigid rod of length L whose other end is attached to a frictionless pivot. The most convenient configuration variable for the pendulum is $q = \theta$, the angle of the rod from the vertical. The gravitational potential energy of the system is then $V = -mgL\cos\theta$, and its kinetic energy is $K = p^2/(2mL^2)$, where p is the angular momentum about the pivot. For this case Equations (1) become

$$\dot{\theta} = \frac{\partial H}{\partial p} = \frac{p}{mL^2}, \quad \dot{p} = -\frac{\partial H}{\partial q} = -mgL\sin\theta. \tag{2}$$

The point $(0, 0)$ is a stable (elliptic) equilibrium corresponding to the pendulum hanging down, at rest. The point $(\pm\pi, 0)$ is also an equilibrium but is an unstable (saddle) point. The unstable eigenvector of the saddle is the beginning of the unstable manifold, W^{u}, a trajectory that is backwards asymptotic to the saddle. By energy conservation, the unstable manifold corresponds to a branch of the energy contour $E = mgL$, which again joins the saddle point (after the pendulum has undergone one full rotation). Thus, this trajectory is forward asymptotic to the saddle as well; that is, it lies on the stable manifold, W^{s}, of the saddle. Orbits of this kind are called *homoclinic*. In this case the homoclinic orbit separates the trajectories oscillating about the elliptic equilibrium from those in which the pendulum undergoes complete rotations, thus it is called a *separatrix*. Orbits near the elliptic equilibrium oscillate with the frequency of the linearized, harmonic oscillator, $\omega = \sqrt{g/L}$. The frequency of oscillation decreases monotonically as the amplitude increases, approaching zero logarithmically

at the separatrix. The frequency of rotation of the solution grows again from zero as the energy is further increased.

Canonical Structure

The geometrical structure of Hamiltonian systems arises from the preservation of the loop action, defined by

$$A[\gamma] = \oint_{\gamma} p\,\mathrm{d}q - H\,\mathrm{d}t, \tag{3}$$

where γ is any closed loop in (q, p, t)-space. A consequence of Equations (1) is that if each point on a loop γ_0 is evolved with the flow to obtain a new loop γ_t, then $A[\gamma_0] = A[\gamma_t]$: the loop action is known as the *Poincaré invariant*.

The Hamiltonian form of Equations (1) is not preserved under an arbitrary coordinate transformation (unlike the Euler–Lagrange equations for a Lagrangian system). A canonical transformation $(q, p) \to (q', p')$ preserves the form of the Equations (1). Canonical transformations can be obtained by requiring that the Poincaré invariant of Equation (3) be the same in the new coordinate system, or locally that

$$\left(p'\,\mathrm{d}q' - H'\,\mathrm{d}t\right) - (p\,\mathrm{d}q - H\,\mathrm{d}t) = \mathrm{d}F$$

is the total differential of a function F. If F is represented as a function of a selection of half of the variables (q, p) and the complementary half of (q', p'), it is a "generating" function for the canonical transformation. For example, a function $F(q, q', t)$ implicitly generates a canonical transformation through

$$p = -\frac{\partial F}{\partial q}, \quad p' = \frac{\partial F}{\partial q'},$$
$$H'(q', p', t) = H(q, p, t) - \frac{\partial F}{\partial t}. \tag{4}$$

In order that this transformation be well defined, the first equation must be inverted to find $q'(q, p)$; this requires that the matrix $\partial^2 F/\partial q \partial q'$ be nonsingular. An autonomous canonical transformation is also called a *symplectic map*. Canonical transformations are often employed to simplify the equations of motion. For example, Hamilton's equations are especially simple if the new Hamiltonian is a function of only the momentum variables, $H'(p')$. If we can find a transformation to such a coordinate system then the system is said to be integrable. In general, such transformations do not exist; one of the consequences is chaotic motion.

Integrability

Loosely speaking, a set of differential equations is integrable if it can be explicitly solved for arbitrary initial conditions (Zakharov, 1991). The explicit solution, when inverted, yields the initial conditions as invariant functions along the orbits of a system—the initial conditions are constants of motion. A Hamiltonian $H(q, p)$ is said to be Liouville integrable if it can be transformed to a canonical coordinate system in which it depends only on new momenta. When the energy surfaces are compact and the new momenta are everywhere independent, Arnol'd showed that it is always possible to choose the momentum variables so that their conjugate configuration variables are periodic angles ranging from 0 to 2π (Arnol'd, 1989). These coordinates are called *action-angle variables*, denoted $(\theta, \mathcal{J})$.

As the Hamiltonian is a function only of the actions, $H(\mathcal{J})$, Equation (1) becomes $\dot{\mathcal{J}} = 0$, and $\dot{\theta} = \Omega(\mathcal{J}) = \partial H/\partial \mathcal{J}$. A system is anharmonic when the frequency vector Ω has a nontrivial dependence on $\mathcal{J}$. Thus, for an integrable system, motion occurs on the n-dimensional tori $\mathcal{J}$ = constant. Orbits helically wind around the torus with frequencies Ω that depend upon the torus chosen. When the frequency is nonresonant (there is no integer vector m for which $m \cdot \Omega = 0$), then the motion is dense on the torus.

Any one degree-of-freedom, autonomous Hamiltonian system is locally integrable. A Hamiltonian with more than one degree of freedom, such as pendulum with an oscillating support, is typically not integrable. Systems that are separable into non-interacting parts are integrable, and there are also a number of classical integrable systems with arbitrarily many degrees of freedom. These include the elliptical billiard, the rigid body in free space, the Neumann problem of the motion of a particle on a sphere in a quadratic potential, the Toda lattice, and the Calogero–Moser lattice (Arnol'd, 1988).

Hamiltonian Chaos

The problem of understanding the motion of a slightly perturbed integrable system originated with the desire to understand the motion of the planets. The Kepler problem corresponding to the gravitational interaction of two spherical bodies is integrable; however, once other effects (such as the mutual forces among planets) are included, there appear to be no general, explicit solutions. Poincaré in particular addressed the question of the stability of the solar system, finally realizing that the convergence of perturbation series for the solutions could not be guaranteed and discovering the phenomenon of transverse homoclinic intersections that is a harbinger of chaos (Poincaré, 1892).

Consider the problem

$$H(\theta, \mathcal{J}) = H_0(\mathcal{J}) + \varepsilon H_1(\theta, \mathcal{J}) + \cdots,$$

where the perturbation H_1 depends periodically on the angles and can be expanded in a Fourier series. When

$\Omega(\mathcal{J})$ is nonresonant, a formal sequence of canonical transformations can be constructed to find a set of coordinates in which H is independent of the angle. The problem is the occurrence of denominators in the coefficients proportional to resonance conditions $m \cdot \Omega(\mathcal{J})$ for integer vectors m. Even for actions where the frequencies are incommensurate, it is always possible to make $m \cdot \Omega(\mathcal{J})$ arbitrarily small by choosing large enough integers m. Thus, a priori bounds on the convergence fail. This is called the *problem of small denominators*.

Chirikov realized that small denominators signal the creation of topologically distinct regions of motion (Chirikov, 1979; MacKay & Meiss, 1987). Near a typical resonance, one can use averaging methods to approximate the motion by an integrable pendulum-like Hamiltonian, effectively discarding all of the terms in H_1 except for those that are commensurate with the resonance, that is, the Fourier modes $H_m(\mathcal{J})$ with $m \cdot \Omega = 0$. Thus, orbits near to a resonance are trapped in an effective potential well. The domain of the trapped motion has the width in action of the corresponding pendulum separatrix; it is typically proportional to the square root of the mth Fourier amplitude of H_1. If we can treat the resonances independently, then each gives rise to a corresponding separatrix. However, as the perturbation amplitude grows, this approximation must break down as it predicts the overlap of neighboring separatrices. In 1959, Chirikov proposed this resonance overlap condition as an estimate of the onset of global chaos. Renormalization theory gives a more precise criterion (*See* **Standard map**).

This picture, together with the fact that rational numbers are dense, leads to the expectation that none of the invariant tori of an integrable system persist when it is perturbed with an arbitrarily small perturbation. Surprisingly, the Fermi–Pasta–Ulam computational experiment in 1955 (Fermi et al., 1965; Weissert, 1997) failed to find this behavior. Indeed, KAM theory, initiated by Andrei Kolmogorov in the 1950s and developed in the 1960s by Vladimir Arnol'd and Jürgen Moser, proves persistence of most of the invariant tori (de la Llave, 2001; Pöschel, 2001). This holds when the perturbation is small enough, provided that the system satisfies an anharmonicity or nondegeneracy condition, it is sufficiently differentiable, and the frequency of the torus is sufficiently irrational. The irrationality condition is that $|m \cdot \Omega| > c/|m|^\tau$ for all nonzero integer vectors m and some $c > 0$ and $\tau \geq 1$; this is a *Diophantine condition*. Each of these conditions is essential, though some systems (such as the solar system for which the frequencies are degenerate) can be reformulated so that KAM theory applies.

Resonant tori and tori whose frequencies are nearly commensurate lie between the Diophantine tori. Generally, these tori are destroyed by a small perturbation and either form new, secondary tori trapped in a resonance or are replaced by a zone of chaotic motion that is found in the neighborhood of the stable and unstable manifolds of the resonance. These generically intersect and give rise to a homoclinic tangle or trellis that contains a Smale horseshoe. In the case that the Hamiltonian is analytic, the size of the chaotic region is exponentially small in ε and, thus, can be difficult to detect (Gelfreich & Lazutkin, 2001).

For small perturbations of an integrable Hamiltonian, it remains an open problem to show that a nonzero volume of initial conditions behaves chaotically, in the sense that they have positive Lyapunov exponents. Numerical investigations indicate that orbits in the chaotic zones do have positive Lyapunov exponents, and that these domains form a "fat fractal" (a fractal with positive measure). There are also many examples of uniformly hyperbolic dynamics (especially for the case of billiards (Bunimovich, 1989)) which can also have properties such as mixing and ergodicity.

The problem of the nonlinear stability of a typical system is also open (*See* **Symplectic maps**). However, N.N. Nekhoroshev showed in 1977 that for an analytic system, the actions drift very little for very long times (at most by an amount that is proportional to a power of ε for times that are exponentially long in ε (Lochak, 1993; Pöschel, 1993)). Thus, while it is possible that a KAM torus is unstable, for most practical purposes, they appear to be stable.

Generalizations

Many partial differential equations (PDEs) also have a Hamiltonian structure. For a PDE with independent variables (x, t), the canonical variables are replaced by fields $(q(x, t), p(x, t))$ and the partial derivatives in (1) by functional or Frechêt derivatives, so that

$$\frac{\partial q}{\partial t} = \frac{\delta H}{\delta p}, \quad \frac{\partial p}{\partial t} = -\frac{\delta H}{\delta q}.$$

The Hamiltonian functional H is the integral of an energy density. For example, the wave equation has the Hamiltonian $H[q, p] = \int \mathrm{d}x \, \frac{1}{2}\left(p^2 + c^2(\partial_x q)^2\right)$. Other nonlinear wave equations such as the integrable nonlinear Schrödinger, Korteweg–de Vries, and sine-Gordon equations also have Hamiltonian formulations.

JAMES D. MEISS

See also **Adiabatic invariants; Chaotic dynamics; Constants of motion and conservation laws; Ergodic theory; Euler–Lagrange equations; Fermi–Pasta–Ulam oscillator chain; Hénon–Heiles system; Horseshoes and hyperbolicity in dynamical systems; Lyapunov exponents; Mel'nikov method; Pendulum; Phase space; Poisson brackets; Standard map; Symplectic maps; Toda lattice**

Further Reading

Arnol'd, V.I. (editor). 1988. *Dynamical Systems III*, New York: Springer

Arnol'd, V.I. 1989. *Mathematical Methods of Classical Mechanics*, New York: Springer

Bunimovich, L.A. 1989. Dynamical systems of hyperbolic type with singularities. In *Dynamical Systems*, edited by Ya. Sinai, Berlin: Springer, p. 278

Chirikov, B.V. 1979. A universal instability of many-dimensional oscillator systems. *Physics Reports*, 52: 265–379

de la Llave, R. 2001. A tutorial on KAM theory. In *Smooth Ergodic Theory and Its Applications (Seattle, WA, 1999)*, Providence, RI: American Mathematical Society, pp. 175–292

Fermi, E., Pasta, J. & Ulam, S. 1965. Studies of nonlinear problems. In *Collected Papers of Enrico Fermi*, vol. 2, edited by E.Segré, Chicago: University of Chicago Press, pp. 977–988

Gelfreich, V.G. & Lazutkin, V.F. 2001. Separatrix splitting: perturbation theory and exponential smallness. *Russian Mathematical Surveys*, 56(3): 499–558

Hamilton, W.R. 1835. On the application to dynamics of a general mathematical method previously applied to optics. *British Association Report, 1834*, pp. 513–518

Lochak, P. 1993. Hamiltonian perturbation theory: periodic orbits, resonances and intermittancy. *Nonlinearity*, 6: 885–904

MacKay, R.S. & Meiss, J.D. (editors). 1987. *Hamiltonian Dynamical Systems: A Reprint Selection*, London: Adam Hilger

Poincaré, H. 1892. *Les Methodes Nouvelles de la Mechanique Celeste*, Paris: Gauthier–Villars

Pöschel, J. 1993. Nekhoroshev estimates for quasi–convex Hamiltonian systems. *Mathematische Zeitschrift*, 213:187–216

Pöschel, J. 2001. A lecture on the classical KAM theorem. In *Smooth Ergodic Theory and Its Applications (Seattle, WA, 1999)*, Providence, RI: American Mathematical Society, pp. 707–732

Weissert, T.P. 1997. *The Genesis of Simulation in Dynamics: Pursuing the Fermi–Pasta–Ulam Problem*, New York: Springer

Zakharov, V.E. (editor). 1991. *What Is Integrability?* Berlin: Springer

HARMONIC GENERATION

Harmonic generation is the phenomenon whereby new frequency components of a wave are created upon interaction with a nonlinear medium. The concept of a harmonic frequency is familiar to anyone with a basic knowledge of music: two notes whose frequencies form a ratio of small whole numbers (e.g., 2:1, 3:2, 5:4) produce a sound that is pleasing or "harmonious" compared with two notes with incommensurate frequencies. More generally, any periodic function $f(t+T)=f(t)$ can be written as an infinite Fourier series containing the first harmonic (fundamental frequency) $\omega=2\pi/T$, the second harmonic, and higher harmonic frequencies $\omega_m=m\omega$:

$$f(t)=\sum_{m=-\infty}^{\infty} c_m\,\mathrm{e}^{-\mathrm{i}\omega_m t}. \qquad (1)$$

The function $f(t)$ could represent the displacement of a guitar string, the amplitude of a wave in the ocean, or the electric field strength of a radio wave or a beam of light. If f satisfies a linear dynamic equation, then the principle of superposition holds, and no energy can be exchanged among the different Fourier coefficients c_m. Under nonlinear dynamics, however, the coefficients c_m are coupled to each other, and energy can be transferred back and forth among them.

Harmonic generation refers to the case in which energy originally at frequency ω generates a new wave component at a harmonic frequency ω_m. A closely related phenomenon is that of parametric amplification, in which a frequency ω_m provides the energy source to amplify a signal at a related frequency $\omega_{m'}$.

In optics, harmonic generation is based upon the nonlinear response of some medium to electromagnetic radiation at optical frequencies. The origin of harmonic generation is related to Theodore Maiman's invention of the ruby laser in 1960. Exploiting the high intensities and the coherency properties of the newly available laser output, in 1961 Peter Franken and his colleagues used the nonlinear polarization response of crystal quartz to produce second-harmonic light at a free-space wavelength of 347 nm from the ruby laser output at 694 nm, marking the birth of nonlinear optics.

By the late 1960s, lithium niobate ($LiNbO_3$) had emerged as the nonlinear crystal of choice for parametric amplification and harmonic generation. Much of the work taking place in the following decades was dedicated to improving the efficiency of the generation of harmonics, either by finding materials with better properties (higher transparency, stronger nonlinearity, etc.) or by aiding the energy transfer through phase matching the various waves involved in the process. More recently, improvements in material processing have made possible the technique of quasi-phase-matching (QPM), in which better phase matching is achieved through the engineering of a spatial variation of the nonlinear coefficient of the medium. In contrast to previous phase-matching techniques, QPM allows a wide, continuous range of frequencies to be coupled to their harmonics without imposing constraints on the orientation of the crystal; the orientation can then be chosen to maximize the nonlinear coefficient seen by the fundamental frequency and its harmonic as they pass through the crystal.

In optics, harmonic generation is often used to convert energy from one frequency band to another. The generated frequency may be more suitable for telecommunications or spectroscopy, for example, and may be in a region of the electromagnetic spectrum

that is not directly available from high-powered lasers. The generation of a harmonic might also be a way of obtaining a coherent copy of an optical pulse, where the copy can be compressed, broadened, chirped, squeezed, or simply measured to determine the properties of the original pulse. Depending on the type of physical process involved and the particular application considered, one refers to the relevant phenomena as second-harmonic generation, sum- or difference-frequency generation, optical parametric generation, or optical parametric oscillation.

The canonical example for studying harmonic generation is an anharmonic oscillator, which can be taken as a simplified model of coherent light propagating through a nonlinear medium. In optics, the nonlinearity can arise due to the material polarization (electronic response) of the medium, or due to a coupling between the light and lattice vibrations in the medium (optical phonons). Referring to the former phenomenon, the polarization response can be expanded in a power series of the applied field, where the coefficients, the nonlinear susceptibility tensors of the material, can be obtained through quantum-mechanical calculations. In general, the quadratic polarization of a medium will be its leading order nonlinear response unless symmetries of the medium rule it out. In this case, one can then reduce Maxwell's equations to the nonlinear wave equation

$$\frac{\partial^2 E}{\partial z^2} - \frac{n^2}{c^2}\frac{\partial^2 E}{\partial t^2} = \frac{\chi^{(2)}}{c^2}\frac{\partial^2 (E^2)}{\partial t^2}, \tag{2}$$

where n is the refractive index of light in the medium, c is the speed of light, and $E(z,t)$ is the electromagnetic field strength which depends on a longitudinal dimension z and on time t.

The nonlinear susceptibility $\chi^{(2)}$ characterizes the quadratic response of the medium to an incident field, where the linear susceptibility has been included in the definition of the refractive index n. To observe the exchange of energy between two frequencies ω_1 and ω_2 mediated by this nonlinearity, the Fourier expansion of Equation (1) can be augmented as

$$E(z,t) = c_1(z)\,\mathrm{e}^{\mathrm{i}\theta_1(z,t)} + c_2(z)\,\mathrm{e}^{\mathrm{i}\theta_2(z,t)} + \text{c.c.}, \tag{3}$$

where "c.c." denotes the complex conjugate, $\theta_j(z,t) = k_j z - \omega_j t$ is a rapidly varying optical phase, and $k_j = n\omega_j/c$ is the linear wave number. Under the assumption that the coefficients $c_j(z)$ vary much more slowly in z than the optical phase (slowly varying envelope approximation), substituting Equation (3) into Equation (2) gives

$$2\mathrm{i}k_1 c_1'(z)\mathrm{e}^{\mathrm{i}\theta_1} + 2\mathrm{i}k_2 c_2'(z)e^{\mathrm{i}\theta_2} + \text{c.c.}$$

$$= \frac{\chi^{(2)}}{c^2}\frac{\partial^2}{\partial t^2}(E^2), \tag{4}$$

where

$$E^2 = c_1^2\mathrm{e}^{\mathrm{i}(2\theta_1)} + c_2^2\mathrm{e}^{\mathrm{i}(2\theta_2)} + 2c_1^* c_2\mathrm{e}^{\mathrm{i}(-\theta_1+\theta_2)} + 2c_1 c_2\mathrm{e}^{\mathrm{i}(\theta_1+\theta_2)} + |c_1|^2 + |c_2|^2 + \text{c.c.} \tag{5}$$

In order for the terms on the right of Equation (4) to contribute significantly to the growth of $c_1(z)$ or $c_2(z)$ on the left, the rapid phase rotations given by the exponentials must resonate, which occurs if $\theta_2 = 2\theta_1$, or $\omega_2 = 2\omega_1$. The resulting equations will then be

$$c_1'(z) = \frac{\mathrm{i}\omega_1\chi^{(2)}}{n_1 c} c_1^* c_2 \mathrm{e}^{\mathrm{i}\Delta k z}, \tag{6a}$$

$$c_2'(z) = \frac{\mathrm{i}\omega_2\chi^{(2)}}{n_2 c} c_1^2 \mathrm{e}^{-\mathrm{i}\Delta k z}. \tag{6b}$$

The phase mismatch term $\Delta k = k_1 - 2k_2$ arises from a more careful calculation that takes into account that the medium's linear susceptibility (and therefore the refractive index n) is a function of frequency ω; thus, it is not generally true that $\omega_2 = 2\omega_1$ implies $k_2 = 2k_1$.

Equations (6) can be solved exactly, but it is more instructive to consider the quantities that are invariant in this system of equations. These invariants reflect physical quantities that are conserved during the mixing process (called Manley–Rowe invariants):

$$I_0 = \frac{1}{2}\varepsilon_0 c\left(n_1|c_1|^2 + n_2|c_2|^2\right), \tag{7a}$$

$$I_1 = \frac{1}{2}\varepsilon_0 c\left(\frac{n_1|c_1|^2}{\hbar\omega_1} + 2\frac{n_2|c_2|^2}{\hbar\omega_2}\right). \tag{7b}$$

The first of these, I_0, is the total irradiance, or incident optical power per unit of surface area. That I_0 is invariant follows from conservation of energy, which is to be expected given that no absorption has been accounted for here in the linear susceptibility. The quantity I_1 sums the irradiance from the two frequencies, dividing each by the energy of a single photon at the respective frequency ($E_j = \hbar\omega_j$) before summing. The invariance of I_2, therefore, reflects a law of conservation of photon flux, as the destruction of two photons at the fundamental frequency ω_1 must bring about the creation of a single photon at the second harmonic, $\omega_2 = 2\omega_1$.

In the spectroscopy of molecular crystals, the fundamental frequency of a vibrating mode sometimes lies close to an overtone or combination of other mode frequencies, whereupon both frequencies are pushed away from each another. In such a case, the overtone or combination band borrows intensity

from the fundamental in a phenomenon called Fermi resonance.

RICHARD O. MOORE AND GINO BIONDINI

See also **Frequency doubling; Manley–Rowe relations; Nonlinear optics; Parametric amplification**

Further reading

Armstrong, J.A., Bloembergen, N., Ducuing, J. & Pershan, P.S. 1962. Interactions between light waves in a nonlinear dielectric. *Physical Review*, 127: 1918

Bloembergen, N. 1965. *Nonlinear Optics*, Singapore: World Scientific

Boyd, R.W. 2003. *Nonlinear Optics*, 2nd edition, San Diego: Academic Press

Dunn, M.H. & Ebrahimzadeh, M. 1999. Parametric generation of tunable light from continuous-wave to femtosecond pulses. *Science*, 286: 1513

Franken, P.A., Hill, A.E., Peters, C.W. & Weinreich, G. 1961. Generation of optical harmonics. *Physical Review Letters*, 7: 118

Maiman, T.H. 1960. Stimulated optical radiation in ruby. *Nature*, 187: 493

Schubert, M. & Wilhelmi, B. 1986. *Nonlinear Optics and Quantum Electronics*, New York: Wiley

HARMONIC OSCILLATORS

See **Damped-driven anharmonic oscillator**

HARTREE APPROXIMATION

In the quantum-mechanical treatment of a system with many degrees of freedom, the Hartree approximation writes the multidimensional correlated wave function as a simple product of one-dimensional or low-dimensional (orbital) functions. This ansatz reduces the full Schrödinger equation to a set of simpler equations for the orbital functions. The Hartree product approximation, first proposed by Douglas R. Hartree (1928) for many-electron atoms, can in principle be applied to any many-particle system, for example, electrons in an atom, molecule, or crystal. However, the Hartree ansatz is often physically inadequate as it disregards the fundamental permutation symmetry requirements for wave functions of nondistinguishable particles (fermions or bosons). In the case of electron systems, the Hartree approximation soon gave way to the more appropriate Hartree–Fock (HF) approximation that is based on a fully antisymmetrized product representation (Slater determinant) of the many-electron wave function proposed by Vladimir A. Fock (Fock, 1930a). For systems with distinct degrees of freedom, on the other hand, such as the multimode nuclear dynamics in molecules, the Hartree product representation still represents a basic approximation. (see, e.g., Beck et al., 2000).

For the many-electron system of an atom or molecule, the (nonrelativistic) stationary Schrödinger equation can be written in the form (see, e.g., Landau & Lifshitz, 1977)

$$\hat{H}\Phi_n = E_n\Phi_n, \tag{1}$$

where the Hamiltonian $\hat{H} = \hat{H}_o + \hat{V}$ consists of a one-particle part,

$$\hat{H}_o = \sum_i \hat{h}_i, \quad \hat{h}_i = -\frac{\hbar^2}{2m}\nabla^2 - \sum_\alpha \frac{Z_\alpha e^2}{|\boldsymbol{R}_\alpha - \boldsymbol{r}_i|} \tag{2}$$

i.e., $\hat{H}_o$ is the sum of the Hamiltonians $\hat{h}_i$ associated with the motion of the ith electron in the field of the nuclei with charges eZ_α at positions $\boldsymbol{R}_\alpha$, and a two-particle part,

$$\hat{V} = \frac{1}{2}\sum_{i\neq j} \frac{e^2}{|\boldsymbol{r}_i - \boldsymbol{r}_j|} \tag{3}$$

corresponding to the Coulomb repulsion of the electrons. The complexity of the many-electron problem is due to the latter part of the Hamiltonian, as it prevents a separation of the N-electron Schrödinger equation into N independent single-particle equations. The idea underlying the Hartree and the Hartree–Fock approximation is to replace the full electron-electron interaction by a new approximately separable effective Coulomb repulsion (or "mean field"). In the Hartree case, the optimal mean-field formulation is obtained by making use of a variational principle (Fock, 1930b),

$$\delta\langle\Phi|\hat{H}|\Phi\rangle = 0 \tag{4}$$

with the trial wave function given by a Hartree product

$$\Phi(\boldsymbol{x}_1, \boldsymbol{x}_2, \ldots, \boldsymbol{x}_N) = \phi_1(\boldsymbol{x}_1)\phi_2(\boldsymbol{x}_2)\ldots\phi_N(\boldsymbol{x}_N) \tag{5}$$

of normalized single-electron functions (orbitals) $\phi_i(\boldsymbol{x}_i)$. Here $\boldsymbol{x}_i = (\boldsymbol{r}_i, s_i)$ comprises in a short-hand notation the set of spatial and spin variables of the ith electron. The resulting equations for the orbitals read

$$(\hat{h} + \hat{v}_k^H)\phi_k(\boldsymbol{x}) = \varepsilon_k\phi_k(\boldsymbol{x}), \quad k = 1, 2, \ldots, N, \tag{6}$$

where for each orbital $\phi_k(\boldsymbol{x})$ a distinct mean field

$$\hat{v}_k^H = \sum_{l\neq k} \hat{J}_l, \qquad \hat{J}_l = e^2\int \frac{|\psi_l(\boldsymbol{r}')|^2}{|\boldsymbol{r}' - \boldsymbol{r}|}\,\mathrm{d}\boldsymbol{r}' \tag{7}$$

augments the one-particle Hamiltonian $\hat{h}$. The physical meaning of $\hat{v}_k^H$ is the Coulomb energy arising from the interaction of the electron in orbital $\phi_k(\boldsymbol{x})$ and the charge distribution associated with the other orbitals (the operators $\hat{J}_l$ are referred to as Coulomb operators).

Equations (6) are a set of nonlinear integro-differential equations in the orbitals $\phi_1(\boldsymbol{x}_1)$, $\phi_2(\boldsymbol{x}_2), \ldots, \phi_N(\boldsymbol{x}_N)$. Starting with an initial guess for the orbitals $\phi_k(\boldsymbol{x})$, these equations have to be solved in

an iterative way until self-consistency is reached. Here it is essential to select appropriate orbital solutions of the individual one-particle eigenvalue problems (6) so that in the N-electron product wave function the Pauli exclusion principle is at least approximately fulfilled. The resulting potential energy operators (7) constitute the Hartree self-consistent field (SCF).

In the many-electron problem, the Hartree approximation is only of historical or pedagogical interest. It was soon succeeded by the more rigorous and practical Hartree–Fock (HF) approximation (Fock, 1930a) based on the proper antisymmetrized product (Slater determinant) representation

$$\Phi(\boldsymbol{x}_1, \boldsymbol{x}_2, \ldots, \boldsymbol{x}_N) = \begin{vmatrix} \phi_1(\boldsymbol{x}_1) & \phi_1(\boldsymbol{x}_2)\ldots & \phi_1(\boldsymbol{x}_N) \\ \phi_2(\boldsymbol{x}_1) & \phi_2(\boldsymbol{x}_2)\ldots & \phi_2(\boldsymbol{x}_N) \\ \vdots & \vdots & \vdots \\ \phi_N(\boldsymbol{x}_1) & \phi_N(\boldsymbol{x}_2)\ldots & \phi_N(\boldsymbol{x}_N) \end{vmatrix} \tag{8}$$

of the N-electron wave function. This leads to one common eigenvalue problem for the HF orbitals,

$$(\hat{h} + \hat{v}^{\mathrm{HF}})\phi_k(\boldsymbol{x}) = \varepsilon_k \phi_k(\boldsymbol{x}), \quad k = 1, 2, \ldots, N, \tag{9}$$

where the HF mean field operator

$$\hat{v}^{\mathrm{HF}} = \sum_{l=1}^{N} (\hat{J}_l - \hat{K}_l) \tag{10}$$

now contains in addition to the Coulomb contributions a so-called exchange part $-\sum_{l=1}^{N} \hat{K}_l$, and the nonlocal exchange operators $\hat{K}_l$ are defined by

$$\hat{K}_l \phi(\boldsymbol{x}) = e^2 \int \frac{\phi_l^*(\boldsymbol{x}')\phi(\boldsymbol{x}')\,\mathrm{d}\boldsymbol{x}'}{|\boldsymbol{r}' - \boldsymbol{r}|} \phi_l(\boldsymbol{x})\,. \tag{11}$$

Here the integration sums over the spin variable. The HF eigenvalue equation (9) represents a nonlinear problem that again has to be solved in a self-consistent way. It should be noted that because of $(\hat{J}_l - \hat{K}_l)\phi_l = 0$, there arise no self-interaction contributions in the self-consistent HF mean field. Usually, the HF or "molecular" orbitals (MO) are written as linear combinations (LC) of basis functions or "atomic" orbitals (AO). This LCAO representation transforms the integro-differential HF equation (9) into an algebraic eigenvalue problem, and the self-consistency solution is achieved by successive matrix diagonalization. Both with respect to practical applicability and theoretical significance, the HF (or SCF) method is fundamental for electronic structure computations in atoms, molecules, and the solid state. In the LCAO form it is a main ingredient in all existing quantum chemistry program packages. Most of the methods aiming at the description of electron correlation, that is, the effects beyond the HF one-particle picture, are based on the SCF orbital energies and integrals as input data.

Although in electronic structure calculations the Hartree approximation is no longer used, it is still a viable means in the description of nuclear dynamics, that is, the nuclear motion accompanying electronic states and processes. Because one deals here with distinguishable "particles" and not with fermions, the Hartree and not the Hartree–Fock approximation is the appropriate choice. Here one assumes a specific kind of separation of the nuclear and electronic degrees of freedom that has its physical foundation on the large mass differences of electrons and nuclei and correspondingly large differences in the respective velocities (Born & Oppenheimer, 1927). Setting molecular rotations aside, one may write the total wave function as a product of an electronic wave function $\Phi(\boldsymbol{x}; \boldsymbol{R})$ and a wave function $\chi(\boldsymbol{R})$ associated with the vibrational motion of the nuclei:

$$\Psi(\boldsymbol{x}, \boldsymbol{R}) = \Phi(\boldsymbol{x}; \boldsymbol{R})\chi(\boldsymbol{R}) \tag{12}$$

Here $\boldsymbol{x}$ and $\boldsymbol{R}$ denote collectively the electronic and nuclear variables. The electronic function is an eigenfunction of the electronic Hamiltonian at spatially fixed nuclei and, thus, depends parametrically on the nuclear coordinates $\boldsymbol{R}_\alpha$. The product approximation (12) is referred to as Born–Oppenheimer approximation. Having determined the electronic wave function and energy $E(\boldsymbol{R})$, the Schrödinger equation for the vibrational wave function can be formulated as follows:

$$\left(\sum_\alpha -\frac{\hbar^2}{2M_\alpha} \nabla_\alpha^2 + \hat{U}(\boldsymbol{R}) \right) \chi(\boldsymbol{R}) = E_{\mathrm{tot}}\, \chi(\boldsymbol{R}) \tag{13}$$

Here the potential energy term $\hat{U}(\boldsymbol{R})$ is the sum of the nuclear repulsion energy and the electronic energy $E(\boldsymbol{R})$. Since we are here not interested in translational or rotational motion of the molecule as a whole, it is advantageous to replace the Cartesian coordinates used so far by a set of $M = 3N - 6$ nuclear coordinates $Q_1, Q_2, \ldots, Q_M$ describing, for example, the displacements from a reference nuclear configuration. Assuming a separable form of the kinetic energy in the new variables Q_i, that is,

$$\hat{T} = \sum_{i=1}^{M} \hat{t}_i \tag{14}$$

the Hartree ansatz

$$\chi(Q_1, Q_2, \ldots, Q_M) = \chi_1(Q_1)\chi_2(Q_2)\ldots\chi_M(Q_M) \tag{15}$$

leads to the following M nonlinear coupled one-dimensional eigenvalue equations,

$$(\hat{t}_i + \hat{u}_i)\chi_i(Q_i) = e_i \chi_i(Q_i), \quad i = 1, \ldots, M, \tag{16}$$

where the Hartree mean fields $\hat{u}_i$ are given by

$$\hat{u}_i = \int U(Q_1, Q_1, \ldots, Q_M) \prod_{j \neq i} (|\chi(Q_j)|^2\, \mathrm{d}Q_j). \tag{17}$$

The Hartree product representation is particularly useful in the context of time-dependent methods which solve the time-dependent Schrödinger equation by propagating an initial wave fuction numerically over a sufficiently long period of time. A very efficient and accurate example of such methods is the multi-configuration time-dependent Hartree (MCTDH) method (Beck et al., 2000). Here the representation of the wave function is given by a linear combination of several Hartree products.

PETER SCHMELCHER AND JOCHEN SCHIRMER

See also **Quantum theory**

Further Reading

Beck, M.H., Jäckle, A., Worth, G.A. & Meyer, H.-D. 2000. The multiconfiguration time-dependent Hartree method: a highly efficient algorithm for propagating wavepackets. *Physics Reports*, 324: 1–105

Born, M. & Oppenheimer, R. 1927. On the quantum theory of molecules. *Annalen der Physik*, 84: 457

Fock, V. 1930a. Self-consistent field mit Austausch für Natrium. [Self-consistent field with exchange for Sodium]. *Zeitschrift für Physik*, 62: 795–805

Fock, V. 1930b. Näherungsmethode zur Lösung des quantenmechanischen Mehrkorperproblems. [Approximate method for solution of quantum many body problem]. *Zeitschrift für Physik*, 61: 126–148

Hartree, D.R. 1928. *Proceedings of the Cambridge Philosophical Society*, 24: 111

Landau, L.D. & Lifshitz, E.M. 1977. *Course of Theoretical Physics*, vol. 3: *Quantum Mechanics*, Oxford: Pergamon Press

HAUSDORFF DIMENSION

See **Dimensions**

HEAT CONDUCTION

There are two main aspects of the theory of heat conduction that are intensively treated in nonlinear science. The first is related to the possibility of nonlinear terms in the phenomenological equations of heat conduction. The second aspect is related to the microscopic nature of heat conduction and especially to deriving Fourier's law (proportionality of heat flux to the temperature gradient) from the fundamental laws of motion at an atomic level.

Equations of Heat Conduction

In the phenomenological theory of heat conduction, the nonlinearity is normally manifested in temperature dependence of the thermal conductivity coefficient (or concentration dependence of the diffusion coefficient in the related diffusion problem). Such dependence leads to a nonlinear modification of Fourier's law. In the one-dimensional case, this equation may be written as

$$\frac{\partial T}{\partial t} = \frac{\partial}{\partial x}\left[\kappa(T)\frac{\partial T}{\partial x}\right], \tag{1}$$

where $T(x,t)$ is the temperature field, $\kappa(T) = \vartheta/\rho C$, ϑ is the heat conductivity coefficient, ρ is the density, and C is the heat capacity of the specimen. All parameters introduced above may be significantly temperature-dependent.

As an example of nonlinear heat conduction, consider heat transfer in a hot plasma driven primarily by radiation. The internal energy of the photon gas is $(4\sigma/c)T^4$, where c is the velocity of light and σ is the Stefan–Boltzmann constant. The heat capacity $C = 16\sigma T^3/3c$. Using results of kinetic theory and plasma physics,

$$\lambda \sim T^{7/2}\rho^{-2}, \tag{2}$$

where λ is the mean free path one can derive the final temperature dependence of the thermal conductivity coefficient: $\kappa(T) \sim T^{13/2}$. In the more common case of molecular heat conduction, the transfer is realized by gas molecules, and therefore, the average velocity of the molecules $v \sim T^{1/2}$ and λ is independent of the temperature ($\lambda \sim 1/\rho$); accordingly, the heat conductivity $\kappa \sim T^{1/2}$. More general models deal with the general form of the temperature dependence, like $\kappa = \kappa_0 T^\nu$, $\nu > 0$.

Probably, the most impressive consequence of the temperature dependence of the thermal conductivity coefficient is the phenomenon of so-called "heat inertia" when the heat energy remains localized in the system and does not dissipate away. If $T(x,t)$ is the solution of the Cauchy problem for Equation (1) with initial temperature

$$T(x,t_0) = \begin{cases} T_m(1-|x|/x_0)^{2/\nu}, & |x| \le x_0, \\ 0, & |x| \ge 0, \end{cases}$$

then $T(x,t) = 0$ for $|x| \ge x_0$, $t_0 < t < t_0 + t^*$, $t^* = x_0^2\nu/2\kappa_0(\nu+2)T_m^\nu$; that is, the heat energy is localized in the initial region for a certain time interval.

Microscopic Nature of Heat Conduction

The problem of heat conduction in dielectric crystals goes back to Rudolph Peierls (1926). A linear model of the crystalline lattice, being useful in many other physical problems, turns out to be insufficient when explaining the finiteness of the coefficient of thermal conductivity. The normal process of the heat conduction implies formation of a linear temperature gradient as the temperatures of the boundaries of the specimen are different. In an ideal linear crystal, however, any excitation is presented as a sum of independent vibrational modes that transfer energy from one boundary to the other without any loss. Therefore, a

temperature gradient cannot be formed. This is why an account of the nonlinearity of interactions is necessary to describe the finite heat conductivity. Peierls has suggested that this condition is also a sufficient one because the phonon collision in a weakly nonlinear crystal is governed by the following relationships:

$$\omega_1 + \omega_2 = \omega_1' + \omega_2', \qquad \boldsymbol{k}_1 + \boldsymbol{k}_2 = \boldsymbol{k}_1' + \boldsymbol{k}_2' + m\boldsymbol{p}. \tag{3}$$

The values with a prime correspond to the state after collision. The relationship for frequencies ω_i expresses the energy conservation. However the conservation of the quasimomenta $\boldsymbol{k}_i$ can be violated by a multiple of Bragg vector $\boldsymbol{p}$. The processes with $m = 0$ are referred to as normal phonon scattering. The case with $m \neq 0$ is referred to as Umklapp process. The latter case means that a certain quantity of the quasimomentum is transferred to the lattice. According to Peierls, the fact that the heat flux is scattered due to the Umklapp processes leads to normal heat conductivity. This picture was accepted until Fermi, Pasta, and Ulam examined it in one of the first computer simulations ever accomplished, finding that a one-dimensional chain with weak anharmonicity of the interaction potential did not demonstrate normal heat conduction (*See* **Fermi–Pasta–Ulam oscillator chain**). Instead, the energy was preserved in a few low-frequency vibrational modes. This famous numerical experiment led to great progress in nonlinear dynamics, including the discovery of lattice solitons, but the problem of the finite heat conductivity of a dielectric crystal again turned out to be unsolved.

It is easy to understand the essence of the problem of finding a sufficient condition for normal heat conductivity. Let us consider a set of equivalent particles arranged along a straight line and interacting only via purely elastic collisions. In every collision the interacting particles mutually exchange their velocities. Any pulse propagates through the system without loss, and therefore, a temperature profile is not formed. Similar properties were proved for the chain with exponential potential of interaction between the nearest neighbors (the so-called Toda lattice).

This problem remains unsolved to date despite numerous efforts. The lack of reliable analytical methods has resulted in many numerical simulations dealing with various lattice models. For one-dimensional systems the results available may be summarized as follows.

- A narrow class of completely integrable systems demonstrates no formation of linear temperature profile at all. Consequently, the coefficient of thermal conductivity cannot be defined. Examples are the linear chain and the Toda lattice.
- For many non-integrable chains, a linear temperature profile is formed and the coefficient of thermal conductivity may be defined for any given size N of the specimen. However, in the thermodynamic limit $N \to \infty$, the coefficient diverges: $\kappa \to \infty$. Therefore, such systems cannot be treated as having normal heat conductivity. Examples are the chain with parabolic and quartic potential among many others.
- A few one-dimensional chains were recently demonstrated to have normal heat conductivity. These examples are the chain of rotators, the Frenkel–Kontorova chain, and some other models.

It should be mentioned that some chains seem to "switch" between different types of behavior with respect to normal heat conductivity with changes of temperature and/or parameters of the potential of interaction.

It seems that different regimes of heat conduction in one-dimensional systems are related to the properties of nonlinear excitations in every concrete model. For instance, the normal heat conduction in the chain of rotators was found to be related to the breakdown of nonlinear acoustic waves and formation of localized breathers, which scatter the heat flux. Similar mechanisms were discovered in other models exhibiting normal heat conduction.

For two-dimensional systems very little information is available, but some investigations suggest that the heat conductivity for different types of potentials is finite or logarithmically divergent. No classification similar to the one-dimensional case can yet be provided.

For the three-dimensional case the situation is as unknown, but the field of molecular dynamics is developing very rapidly and new results are expected to arrive soon.

OLEG GENDELMAN AND LEONID MANEVITCH

See also **Fermi–Pasta–Ulam oscillator chain; Frenkel–Kontorova model; Integrable lattices; Solitons; Toda lattice**

Further Reading

Bonetto, F., Lebowitz, J. & Rey-Bellet, L. 2000. In *Mathematical Physics 2000*, edited by A. Fokas, A. Grigoryan, T. Kibble, & B. Zegarlinski, River Edge, NJ : Imperial College Press

Fermi, E., Pasta, J.R. & Ulam, S.M. 1955. *Studies of Nonlinear Problems*, Los Alamos Scientific Laboratory Report No. LA–1940

Gendelman, O.V. & Savin, A.V. 2000. Normal heat conductivity in one-dimensional chain of rotators. *Physical Review Letters*, 84: 2381–2384

Lepri, S., Livi, R. & Politi, A. 2001. Thermal conduction in classical low-dimensional lattices, preprint: www.lanl.gov, arXiv:cond-mat/0112193

Peierls, R.E. 1955. *Quantum Theory of Solids*, London: Oxford University Press

Samarskii, A.A., Galaktionov, V.A., Kurdiumov, S.P. & Mikailov, A.P. 1987. *Regimes with Sharpening in the Problems for Quasilinear Parabolic Equations*, Moscow, Nauka (in Russian)

Toda, M. 1967. Vibration of a chain with nonlinear interactions. *Journal of the Physical Society of Japan*, 22: 431–36; Wave propagation in anharmonic lattices. *Journal of the Physical Society of Japan*, 23: 501–06

HEAVISIDE STEP FUNCTION

See **Generalized functions**

HELE-SHAW CELL

A very simple device invented by Henry Selby Hele-Shaw in the late 1890s, the Hele-Shaw cell consists of two closely spaced parallel plates, held in place by a frame, between which is a layer of a viscous liquid. Hele-Shaw invented this simple instrument in order to be able to exhibit the streamlines of a flow to students at University College of Liverpool by projecting the flow in the thin liquid layer onto a large screen. He found that minute air bubbles provided excellent flow tracers, and developed the technique to be able to display in a spectacular manner the flow patterns past a variety of objects.

Hele-Shaw discovered that when the distance between the two plates was very small (he used water as the fluid, and glass plates mounted within 0.02 in. of each other), the flow pattern around a circular cylinder perpendicular to the plates closely matched the potential flow solution that was known from the theory of two-dimensional flow of an ideal fluid. Apparently, the viscous liquid between the plates was flowing in this narrow space as though it were an inviscid fluid. George Stokes explained these observations by writing the equation of motion for a viscous fluid—today known as the Navier–Stokes equation—and averaging the flow (today known as plane Poiseuille flow) across the narrow gap between the two bounding plates in the Hele-Shaw cell. One then finds that the averaged, essentially two-dimensional flow velocity, $\boldsymbol{v}$, is proportional to the gradient of the pressure, p, in the fluid:

$$\boldsymbol{v} = -(d^2/12\mu)\nabla p, \tag{1}$$

where d is the separation between the plates and μ is the viscosity of the fluid. Thus, flow in a Hele-Shaw cell is potential flow, with a velocity potential proportional to the pressure, and this explains the coincidence between Hele-Shaw's observations and the theory of two-dimensional, ideal flow. As Stokes wrote, "[Hele-Shaw's experiments] afford a complete graphical solution, experimentally obtained, of a problem which from its complexity baffles mathematicians except in a few simple cases."

Hele-Shaw flows illustrate two-dimensional potential flow around objects with sharp edges and thus show no separation. This is quite remarkable, because even the slightest viscosity would immediately alter the flow pattern were the fluid not constrained by the two plates of the Hele-Shaw cell.

Figure 1. Viscous fingering patterns in a Hele-Shaw cell at a gravitationally unstable interface between two immiscible fluids—viscous silicone oil and air. (Reprinted with permission from Gallery of Fluid Motion, *Physics of Fluids*, 28(9). Copyright 1985, American Institute of Physics. Courtesy of T. Maxwell.)

A controversy with Osborne Reynolds ensued about the validity of the experiments since they appeared to invalidate Reynolds' criterion of a transition to turbulence based solely on the value of "Reynolds number." This led to several acrimonious exchanges of notes and letters in *Nature* in 1898 and 1899 between Reynolds and Hele-Shaw.

The Hele-Shaw cell has found wide application in later years, after it was realized that Equation (1) has the form of the velocity-pressure relationship one would expect for fluid flow in a porous material obeying Darcy's law. Thus, the Hele-Shaw cell became a paradigmatic instrument for studying flows in porous media, a subject of great interest to petroleum engineering.

When two immiscible fluids of different viscosities are present in a Hele-Shaw cell, a number of interesting phenomena occur. In the late 1950s, Geoffrey Taylor and Philip Saffman explored the evolution of "fingers" when a less viscous fluid (air) was pushed into a more viscous fluid (water, glycerin, or oil) in a Hele-Shaw cell. Similar "fingering" occurs when water is forced into oil-carrying porous rock in secondary oil recovery.

The subject of viscous fingering is similar to other pattern-forming instabilities, dendritic crystal growth in

particular, and has become a much studied experimental system. The experimental data tend to be very visually appealing (Figure 1). Many variations on the basic setup have been explored and a voluminous literature exists. The degree of structure of the two-fluid interface depends sensitively on the ratio of viscosities of the two fluids in the Hele-Shaw cell, and the pattern is sensitive to small perturbations, such as imperfections on either plate or tiny air bubbles resident in the cell.

The scale of the smallest fingers observed in a two-fluid Hele-Shaw experiment is set by the surface tension at the interface between the two immiscible fluids. When the surface tension is very small, apparently fractal patterns emerge.

HASSAN AREF

See also **Fractals; Navier–Stokes equation; Pattern formation; Rayleigh–Taylor instability**

Further reading

Hele-Shaw, J.H.S. 1898. The flow of water. *Nature*, 58: 34–36

Lamb, H. 1932. *Hydrodynamics*, 6th edition, Cambridge: Cambridge University Press

Saffman, P.G. & Taylor, G.I. 1958. The penetration of a fluid into a porous medium or Hele-Shaw cell containing a more viscous liquid. *Proceedings of the Royal Society of London* A, 245: 312–329

Wooding, R.A. & Morel-Seytoux, H.J. 1976. Multiphase fluid flow through porous media. *Annual Reviews of Fluid Mechanics*, 8: 233–274

HELICAL WAVES

See **Nonlinear plasma waves**

HELICITY

Intuitively, it is clear that a vortex having a component of velocity along its axis is a helical structure. Many structures fall under this category, including such diverse structures as Taylor–Gortler vortices, leading edge and trailing vortices shed from wings and slender bodies, streamwise vortices in boundary layers and free shear flows, Langmuir circulations in the ocean and analogous structures in the atmosphere, tornados, and rotating storms. Similar structures are observed in space and in laboratory plasmas. Such structures lack reflection symmetry. One of the key quantities characterizing reflection symmetry (or its lack) of a fluid flow is the so-called helicity, which roughly measures how parallel velocity and vorticity are in a fluid flow.

Definition

Helicity $\mathcal{H}_B$ of a solenoidal vector field $\boldsymbol{B}$ ($\mathrm{div}\boldsymbol{B}=0$) in a domain D within any surface S on which $\boldsymbol{n}\cdot\boldsymbol{B}=0$ is defined as the integral

$$\mathcal{H}_B = \int_D \boldsymbol{A}\cdot\boldsymbol{B}\,\mathrm{d}V \tag{1}$$

with $\boldsymbol{A}$ being the vector potential of $\boldsymbol{B}$. Here $\boldsymbol{B}=\mathrm{curl}\boldsymbol{A}$ and the quantity $\mathfrak{h}_B=\boldsymbol{A}\cdot\boldsymbol{B}$ is the helicity density of the field $\boldsymbol{B}$. Both $\mathcal{H}_B$ and $\mathfrak{h}_B$ are pseudoscalars: they change sign under the parity transformation, that is, under change from a right-handed to a left-handed frame of reference. Helicity as defined in Equation (1) is gauge invariant, that is, invariant under replacement of $\boldsymbol{A}$ by $\boldsymbol{A}+\mathrm{grad}\phi$, where ϕ is any single-valued scalar field. This type of invariance should not be confused with time invariance of $\mathcal{H}_B$ in a nondissipative medium (see below). It is important that $\mathcal{H}_B$ is gauge invariant only as defined in Equation (1) for volumes bounded by the field surfaces, that is, $\boldsymbol{n}\cdot\boldsymbol{B}|_s=0$. Generalizations of Equation (1) for open field structures (i.e., such that $\boldsymbol{n}\cdot\boldsymbol{B}|_s\neq 0$) are not gauge invariant. As a rule these generalizations are also not well-defined topologically. Another generalization is the cross-helicity for two solenoidal fields $\boldsymbol{B}_1$ and $\boldsymbol{B}_2$ defined as $\mathcal{H}_{B_1,B_2}=\int_D \boldsymbol{A}_1\cdot\boldsymbol{B}_2\,\mathrm{d}V$. For closed structures, that is, $\boldsymbol{n}\cdot\boldsymbol{B}_{1,2}|_s=0$, cross-helicity is gauge invariant and is symmetric, $\mathcal{H}_{B_1,B_2}=\mathcal{H}_{B_2,B_1}$. Of special interest in physics is a magnetic field, $\boldsymbol{B}$, in electrically conducting fluids or plasmas (with $\mathcal{H}_B$ termed magnetic helicity) and vorticity $\boldsymbol{\omega}$ in fluid flows with $\mathcal{H}_\omega=\int_D \boldsymbol{u}\cdot\boldsymbol{\omega}\,\mathrm{d}V$ (kinetic helicity), where $\boldsymbol{u}$ is the velocity and $\boldsymbol{\omega}=\mathrm{curl}\,\boldsymbol{u}$.

Geometrical and Topological Meaning

Helicity is important at a fundamental level in relation with the linkage(s) of field lines, such as magnetic lines or vortex lines of fluid flow (see Figure 1). The simplest example of two linked vortex tubes is shown in Figure 1 with fluxes $\Phi_{1,2}$ associated with each tube, that are equal to their circulations $\kappa_{1,2}$. Hence, $\mathcal{H}_B$ is directly related to the most basic topological invariant of two

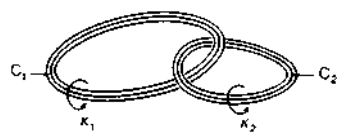

Figure 1. Prototype configuration of linked field tubes with nonzero helicity (Moffatt & Tsinober, 1992). Here the field is assumed to be identical to zero except in two closed tubes with axes $C_{1,2}$ and vanishingly small cross section. The field lines are untwisted within each tube, i.e. each line is a closed curve passing once round the tube, and unlinked with its neighbors in the same tube. In such a case $H_B=\pm 2L_{1,2}F_1F_2$, where $L_{1,2}$ is the linking (or winding) number of the two tubes (in the figure $L_{1,2}=1$), $F_{1,2}$ are the fluxes (equal to their circulations $\kappa_{1,2}$) associated with each tube, and the + or − sign is chosen depending on whether the linkage is right- or left-handed.

linked curves—their linking (winding) number $L_{1,2}$, which was defined by Gauss in 1833 as

$$L_{12} = L_{21} = \frac{1}{4\pi} \oint_{C_1} \oint_{C_2} \frac{\boldsymbol{R} \cdot (\mathrm{d}\boldsymbol{x}_1 \times \mathrm{d}\boldsymbol{x}_2)}{R^3}, \quad (2)$$

where $\boldsymbol{R} = \boldsymbol{x}_1 - \boldsymbol{x}_2$, $\boldsymbol{x}_1 \varepsilon C_1$, and $\boldsymbol{x}_2 \varepsilon C_2$. In the general case of an infinite number of field lines, one can approximate the field via a finite number of N of small flux tubes each with flux Φ_i $(i = 1, \ldots, N)$. Then $\mathcal{H}_B = L_{ij} \Phi_i \Phi_j$, where L_{ij} is the linking number of tubes i and j, and summation is assumed over the repeated indices. In other words, the helicity $\mathcal{H}_B$ can be interpreted as the sum of linking numbers of all pairs of the field lines weighted by the flux. This interpretation remains valid also in the case when the field lines are not closed upon themselves and even may wander chaotically, and the integral of Equation (1) is interpreted as the asymptotic Hopf invariant, that is, asymptotic linking number. The cross-helicity $\mathcal{H}_{B,\omega}$ is interpreted as a measure of mutual linkage of the two fields $\boldsymbol{B}$ and $\boldsymbol{\omega}$.

Invariance in Nondissipative Media

The magnetic field, $\boldsymbol{B}$, in a perfectly conducting fluid and vorticity, $\boldsymbol{\omega}$, in an inviscid fluid is governed by the equations

$$\frac{\partial \boldsymbol{B}}{\partial t} = \mathrm{curl}(\boldsymbol{u} \times \boldsymbol{B}), \quad (3)$$

$$\frac{\partial \boldsymbol{\omega}}{\partial t} = \mathrm{curl}(\boldsymbol{u} \times \omega), \quad (4)$$

describing frozen-field transport of the vector fields $\boldsymbol{B}$ and $\boldsymbol{\omega}$. Under this nondissipative evolution both the magnetic helicity $\mathcal{H}_B$ and the helicity of vorticity $\mathcal{H}_\omega$ are conserved. Invariance of helicity is directly associated with invariance of the topology of $\boldsymbol{B}$ and $\boldsymbol{\omega}$.

In cases when the fluid flow is influenced by the presence of the magnetic field, that is, by the Lorenz force (the term $\mathrm{curl}(\boldsymbol{j} \times \boldsymbol{B})$ added to the left-hand side of Equation (4)), the helicity of vorticity $\mathcal{H}_\omega$ is not conserved whereas the magnetic helicity remains conserved. Another conserved quantity in this latter case is the cross-helicity $\mathcal{H}_{B,\omega} = \int \boldsymbol{u} \cdot \boldsymbol{B}\, \mathrm{d}V$. In principle, one can choose the gauge ϕ in such a way that the helicity density $\mathfrak{h}_B = \boldsymbol{A} \cdot \boldsymbol{B}$ is a Lagrangian invariant, that is, it is pointwise conserved along the paths of fluid particles and therefore for any fluid volume. Such a choice is possible both for magnetic field and for nonconducting fluid flows.

Dissipative effects (finite electrical resistivity and viscosity) are responsible for the reconnection of field lines and thus for the evolution of helicity. In such a case, helicity is either created or destroyed just as if $\boldsymbol{n} \cdot \boldsymbol{B} \neq 0$ on the boundary of the domain.

Kinetic Helicity and Turbulent Dynamo

Helicity plays an important role in the process of growth of magnetic fields in electrically conducting fluids due to fluid motion, called the dynamo process. In turbulent flows with nonzero kinetic helicity, there exists the so-called α-effect, the main ingredient of which is that the large-scale (mean) magnetic field results from currents induced by an electromotive force that is (roughly) proportional to the kinetic helicity $\mathcal{H}_\omega$. An important aspect is that this electromotive force is (generally) nonvanishing for nonvanishing electrical resistivity. There is a buildup of magnetic helicity of the generated large-scale magnetic field, and the importance of finite electrical resistivity is in the dissipation of the small scale (on the energy containing scales of fluid turbulence) magnetic helicity of the opposite sign that allows the build up of the large magnetic helicity (Brandenburg, 2001). Recent laboratory experiments with liquid sodium confirm the possibility of generating a magnetic field by helical fluid flows. The growing magnetic field reacts back on the fluid flow via the Lorenz force that results in a decrease of the electromotive force driving the electrical currents (α-quenching), that is, in a nonlinear saturation in the growth of the mean magnetic field.

Kinetic Helicity and Fluid Turbulence

Present knowledge of the effects of helicity on fluid turbulence is controversial. A difficulty in the assessment of the role of helicity in the dynamics of turbulence stems from the fact that—unlike kinetic energy—helicity is not a positively defined quantity. At a speculative level it is expected that nonvanishing helicity comprises a constraint reducing in some sense the nonlinear processes, and thereby turbulence. The simplest argument is that since $(\boldsymbol{u} \cdot \boldsymbol{\omega})^2 + (\boldsymbol{u} \times \boldsymbol{\omega})^2 = \boldsymbol{u}^2 \boldsymbol{\omega}^2$, larger $\langle |\boldsymbol{u} \cdot \boldsymbol{\omega}| \rangle$ implies reducing of nonlinear processes associated with $\langle |\boldsymbol{u} \times \boldsymbol{\omega}| \rangle$. Indeed, the so-called Beltrami flows with $\boldsymbol{\omega} = \boldsymbol{\lambda} u$, possessing in some sense maximal helicity, are linear. However, existing evidence weakly supports the above argument (Moffatt & Tsinober, 1992; Tsinober, 2001). On the other hand, if $\langle \boldsymbol{u} \cdot \boldsymbol{\omega} \rangle \neq 0$, this is a clear indication of direct and bidirectional coupling of large and small scales. Therefore, in flows with nonzero mean helicity, the coupling between small and large scales is stronger than otherwise. This stronger coupling may aid creation of large scale structures out of small scale turbulence—a process that is frequently called inverse energy cascade. There is little understanding of these processes, although there are suggestions that in the presence of kinetic helicity in compressible fluids there exists an effect (Hα-effect) analogous to the above-mentioned α-effect for a magnetic field.

More subtle issues include spontaneous breaking of relexional symmetry and emergence of helicity in initially helicity-free flows. The evidence is based on indications from stability analysis, laboratory observations and quantitative measurements of helicity, and direct numerical simulations of Navier–Stokes equations (Kholmyansky et al., 2001). Finally, kinetic helicity has a considerable effect on the effective diffusivity of a passive scalar that may be enhanced by the presence of helicity by more than a factor of two. In addition, helicity leads to a new "skew-diffusion" effect, that is, appearance of a component of turbulent flux of passive scalar perpendicular to the local mean gradient of a passive scalar.

Applications

In atmospheric physics, the so-called storm-relative environmental (kinetic) helicity (SREH) is routinely used in the U.S. with moderate success as a parameter for characterizing, interpreting, and forecasting tornado and supercell rotating storms (Weisman & Rotunno, 2000). The origin of these strucures is not understood, though there are suggestions that the Hα-effect (due to the Coriolis force) and intensive heat transport in turbulent convection are among the important physical mechanisms contributing to their formation (Levina et al., 1999). One has to add to this list at least one more factor, the vertical wind shear.

In plasma physics, magnetic helicity plays a central role in magnetic confinement and in the relaxation of plasmas to a minimum-energy state, for example, in toroidal laboratory plasmas and spheromaks. Interestingly, during this process involving reconnection due to small but finite resistivity and turbulence, the total magnetic helicity is approximately conserved and constrains the energy of the magnetized plasma in equilibrium. This minimum energy state is generally a force-free (Beltrami) field, curl $\boldsymbol{B} = \lambda \boldsymbol{B}$ with λ constant.

In astrophysics, magnetic helicity is important in a number of aspects in solar physics (coronal loops, solar wind), the astrophysical dynamo problem (Brown et al., 1999), and cosmology (primordial magnetic field).

ARKADY TSINOBER

See also **Alfvén waves; Magnetohydrodynamics; Nonlinear plasma waves; Topology; Vortex dynamics of fluids; Winding numbers**

Further Reading

Brandenburg, A. 2001. The inverse cascade and nonlinear alpha-effect in simulations of isotropic helical hydromagnetic turbulence. *Astrophysical Journal*, 550: 824–840

Brown, M.R., Canfield, R.C. & Pevtsov, A.A. 1999. *Magnetic Helicity in Space and Laboratory Plasmas*, Washington, DC: American Geophysical Union

Kholmyansky, M., Shapiro-Orot, M. & Tsinober, A. 2001. Experimental observations of spontaneous breaking of reflexional symmetry in turbulent flows, *Proceedings of the Royal Society of London*, 457: 2699–2717

Levina, G.V., Moiseev, S.S. & Rutkevich, P.B. 1999. Hydrodynamic alpha-effect in a convective system. In *Nonlinear Instability, Chaos and Turbulence*, edited by L. Debnath & D.N. Riahi, Southampton and Boston: WIT Press

Moffatt, H.K. & Tsinober, A. 1992. Helicity in laminar and turbulent flows. *Annual Reviews of Fluid Mechanics*, 24: 281–312

Ricca, R.L. (editor). 2001. *An Introduction to the Geometry and Topology of Fluid Flows*, Dordrecht and Boston: Kluwer

Tsinober, A. 1995. Variability of anomalous transport exponents versus different physical situations in geophysical and laboratory turbulence. In *Levy Flights and Related Topics in Physics*, edited by M. Schlesinger, G. Zaslavsky & U. Frisch, Berlin and New York: Springer

Tsinober, A. 2001. *An Informal Introduction to Turbulence*, Dordrecht and Boston: Kluwer

Weisman, M. & Rotunno, R. 2000. The use of vertical wind shear versus helicity in interpreting supercell dynamics. *Journal of Atmospheric Sciences*, 57: 1452–1472

HÉNON MAP

By the mid-1970s, examples such as the Lorenz equations had convinced researchers that strange attractors could arise in differential equations modeling physical systems. Unfortunately, the length of time needed to compute solutions coupled with strong contraction rates made it very difficult to observe fractal structures numerically in these examples with the computers then available. The Hénon map provided the first simple equation in which this fractal structure is easily observed.

Michel Hénon's approach was based on the idea of return maps. The dynamics of differential equations can be modelled by invertible maps, and so evidence of fractal structure in the attractor of an invertible map shows that these objects can exist in differential equations. The Hénon map is a very simple nonlinear difference equation

$$\begin{aligned} x_{n+1} &= y_n + 1 - a x_n^2, \\ y_{n+1} &= b x_n, \end{aligned} \tag{1}$$

where the parameters a and b were chosen as $a = 1.4$ and $b = 0.3$ by Hénon (1976), although other values are also interesting. The attractor, together with some blowups of parts of the attractor, are shown in Figure 1. These pictures are very easy to generate: successive points on an orbit are obtained by evaluating the algebraic expressions on the right-hand side of (1) as the following rough MATLAB program shows:

```
x(1)=0.3; y(1)=0.2;
  %% Initial conditions
N=5000;
  %% N is the number of iterates
a=1.4;b=0.3;
  %% Sets the parameters
for i=1:N
```

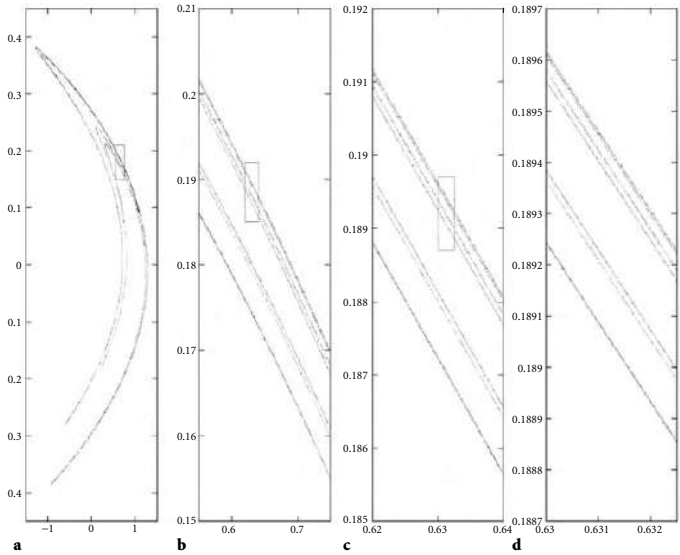

Figure 1. (a) Numerically computed attractor of the Hénon map, (1) with $a = 1.4$ and $b = 0.3$; (b), (c), and (d) are blowups of the boxed regions of (a), (b), and (c), respectively, showing the fractal structure of the attractor. Each figure contains the first 5000 points to land in the displayed region.

```
  %% Begin the iteration loop here
x(i+1)=y(i)+1-a*x(i)^2;
y(i+1)=b*x(i);
  %% That calculated the next
  point
end
plot(x,y,'k.')
  %% Plot the iterates in the
  %% (x,y) plane
```

Despite the simplicity of this program, Hénon used a mainframe (IBM 7040) to perform the 5 million iterates he needed to get a reasonable number of points in the equivalent of Figure 1(d). Figure 1 uses a slightly more sophisticated program to generate the attractor and zoom in on the rectangular regions indicated so that 5000 points can be plotted in each of the blowup regions. This involved 35,724,657 iterations of the map order to get 5000 points in the smallest blowup region of Figure 1(d). This level of computation would have been almost unthinkable when Hénon wrote his paper.

The Hénon attractor pictured in Figure 1 is computationally cheap, requiring no more than the most simple algebraic operations. Also, the numerical evidence for fractal structure in the attractor is sufficiently convincing that most researchers have come to accept that it is a strange attractor or, at least, to suspend their disbelief. For this reason it has become a canonical example of chaotic motion. Almost every new technique or relevant theoretical result is applied to the Hénon map as part of the evaluation of the method. Early papers on phase space reconstruction, dimension calculations, chaotic prediction, chaotic control and synchronization, periodic orbit expansions, invariant measure algorithms, etc., have all used the Hénon map as an important test example. Given this general level of acceptance, it may come as a surprise to learn that it is still not known whether there really is a strange attractor for the Hénon map at the standard parameter values ($a = 1.4$, $b = 0.3$).

Hénon (1976) gave a number of reasons for looking at orbits of (1):

> ... we try to find a model problem which is as simple as possible, yet exhibits the same essential properties as the Lorenz system. Our aim is (i) to make the numerical exploration faster and more accurate...; (ii) to provide a model which might lend itself more easily to mathematical analysis.

As we have seen, Hénon's aim of making the numerical exploration of apparently chaotic attractors more straightforward succeeded spectacularly. However, he could not have imagined how hard it would be to answer the theoretical questions posed by this deceptively simple map.

Hénon's intuitive explanation for his map in terms of folding, stretching, and contraction is much closer to the formation of horseshoes rather than to the Lorenz model, which has discontinuities in the natural return map. As such, the Hénon map has become a paradigm for the formation of horseshoes as parameters vary (see Devaney & Nitecki, 1979), and it is the more general question of how the attractors of the Hénon map change as the parameters vary that has occupied most theoretical approaches.

By defining a new y variable $y_{\text{new}} = b^{-1} y_{\text{old}}$, Equation (1) can be written in the form of a more general, Hénon-like map:

$$\begin{aligned} x_{n+1} &= -\varepsilon y_n + f_a(x_n), \\ y_{n+1} &= x_n, \end{aligned} \tag{2}$$

where $\varepsilon = -b$ and $f_a(x) = 1 - ax^2$ gives the Hénon map in the new coordinates. This formulation emphasizes the relationship between Hénon-like maps and one-dimensional maps: if $\varepsilon = 0$ then the x equation decouples and x evolves according to the one-dimensional difference equation $x_{n+1} = f_a(x_n)$, which in the original case, (1), is just the standard quadratic family. The Jacobian of the map is ε, so positive ε corresponds to orientation-preserving maps, which is more natural in the context of return maps, although this means that $b < 0$ in Hénon's original formulation, (1). Early efforts toward proving that strange attractors exist in the Hénon map concentrated on extending results for one-dimensional maps to the two-dimensional case with $\varepsilon > 0$ small. On the negative side, Holmes & Whitley (1984) showed that however small ε is, some periodic orbits of the Hénon map appear in a order different from the order in which they appear in the quadratic family. On the positive side, Gambaudo, van Strien, & Tresser (1989) showed that for sufficiently small $\varepsilon > 0$, the first complete period-doubling cascade is associated with the original period two orbit.

The major breakthrough on the existence of strange attractors was made by Benedicks & Carleson (1991). Using delicate mathematical analysis, they were able to show that if $\varepsilon > 0$ is small enough and a is close to $a = -2$ (the equivalent of $\mu = 4$ for the standard formulation of the quadratic map, $\mu x(1-x)$), then there is a positive measure of parameter values for which the Hénon map has a strange attractor. This result was generalized by Mora & Viana (1993) who showed that Hénon-like maps arise naturally near homoclinic bifurcations of maps. It had long been recognized that these bifurcations occur in the Hénon map (see, for example, Holmes & Whitley (1984)), so this made it possible to deduce the existence of strange attractors at values of ε that are not small. Indeed, this important paper provides a method of proving the existence of strange attractors for a set of parameter values with positive measure in a wide variety of model systems. Despite all these advances, these results only prove that there exist such parameter values and they do not give methods for proving that a strange attractor exists at a *given* parameter value.

Two other avenues of research suggested by the one-dimensional, $\varepsilon = 0$, limit in (2) have led to interesting developments. We have already noted that the one-dimensional order of periodic orbits is not preserved if $\varepsilon > 0$. However, a beautiful theory of partial orders based on period and knot type has emerged, which shows that the existence of some periodic orbits implies the existence of some others in two-dimensional maps (see Boyland (1994) for more details). The second adaptation of one-dimensional approaches is based on the idea of the symbolic dynamics (or *kneading theory*) of unimodal maps. The main idea, introduced by Cvitanovic et al. (1988) and developed by de Carvalho (1999), is to produce symbolic models of the dynamics of the Hénon map by relating the dynamics to modifications of the full horseshoe. This is done by *pruning* the horseshoe, that is, identifying regions of the horseshoe with dynamics that are not present in the Hénon map under consideration and judiciously removing these regions together with their images and preimages, leaving a pruned horseshoe that can still be accurately described.

Much of the current interest in the Hénon map involves the existence and construction of invariant measures for the attractors. This work should lead to a good statistical description of properties of orbits and averages along orbits. So, even now, this simple two-dimensional map with a single nonlinear term is motivating important questions in dynamical systems.

PAUL GLENDINNING

See also **Attractors; Bifurcations; Chaotic dynamics; Horseshoes and hyperbolicity in dynamical systems; Markov partitions; One-dimensional maps; Routes to chaos; Sinai–Ruelle–Bowen measures; Symbolic dynamics**

Further Reading

Benedicks, M. & Carleson, L. 1991. The dynamics of the Hénon map. *Annals of Mathematics*, 133: 73–169

Boyland, P. 1994. Topological methods in surface dynamics. *Topology and Its Applications*, 58: 223–298

de Carvalho, A. 1999. Pruning fronts and the formation of horseshoes. *Ergodic Theory and Dynamical Systems*, 19: 851–894

Cvitanovic, P., Gunaratne, G. & Procaccia, I. 1988. Topological and metric properties of Hénon-type strange attractors. *Physical Review* A, 38: 1503–1520

Devaney, R. & Nitecki, Z. 1979. Shift automorphisms in the Hénon mapping. *Communications in Mathematical Physics*, 67: 137–146

Gambaudo, J.-M., van Strien, S. & Tresser, C. 1989. Hénon-like maps with strange attractors: there exist C^∞

Kupka–Smale diffeomorphisms on $\mathbf{S}^2$ with neither sinks nor sources. *Nonlinearity*, 2: 287–304

Hénon, M. 1976. A two-dimensional mapping with a strange attractor. *Communications in Mathematical Physics*, 50: 69–77

Holmes, P. & Whitley, D. 1984. Bifurcations of one- and two-dimensional maps. *Philosophical Transactions of the Royal Society (London)* A, 311: 43–102

Mora, L. & Viana, M. 1993. Abundance of strange attractors. *Acta Mathematica*, 171: 1–71

HÉNON–HEILES SYSTEM

Although the molecules of a gas move freely and collide frequently, the stars in a galaxy move under the constraint of long-range interactions and do not collide. The motion of any one star in a galaxy can be modeled as if it moves alone under the constraint of a fixed gravitational galactic potential with cylindrical symmetry. The energy of the star is conserved as is the angular momentum with respect to an axis through the center of the galactic plane and at right angles to it. These two conserved quantities are isolating integrals of the motion. In the absence of a third isolating integral, the distribution of stellar velocities in a galaxy with an axisymmetric potential should be circularly symmetric in the meridian plane, a result contrary to observation (Ollongren, 1965).

The astronomer Michel Hénon and a graduate student Carl Heiles introduced a mathematical model to numerically investigate the third integral problem when Hénon visited Princeton University in 1962. In "order to have more freedom of experimentation" in their numerical studies, they considered the simplified model system, with two degrees of freedom, described by the Hamiltonian (Hénon & Heiles, 1964)

$$H = \tfrac{1}{2}\left(\dot{x}^2 + \dot{y}^2\right) + \tfrac{1}{2}\left(x^2 + y^2\right) + x^2 y - \tfrac{1}{3}y^3,$$

where the last three terms are called V. The choice of coefficients in the cubic potential confers a ternary symmetry on the equipotential lines. The equipotential line for $V = \frac{1}{6}$ is an equilateral triangle, and this is the limiting energy at which the motion is bounded. In the Hénon–Heiles model, the original problem of the third isolating integral is transformed into whether there exists an isolating integral other than the constant energy itself. The Hénon–Heiles Hamiltonian also describes the center of mass reduction of a three-particle periodic chain with linear and quadratic nearest neighbor elastic forces and is, thus, a member of the class of systems investigated in the numerical studies of Fermi, Pasta, and Ulam (Ford, 1992). More generally, the Hénon–Heiles Hamiltonian is one of the simplest non-integrable Hamiltonian systems known. It has become a paradigm for studies of chaos and non-integrability in Hamiltonian systems with two degrees of freedom.

The solutions of the equations of motion corresponding to the Hénon–Heiles Hamiltonian can be represented by trajectories in the four-dimensional phase space spanned by $(x, \dot{x}, y, \dot{y})$. If the energy is fixed in the range $0 \le E \le \frac{1}{6}$ then these trajectories are bounded and recurrent on a three-dimensional energy surface. No techniques are known to construct exact algebraic formulae for the trajectories for arbitrary initial conditions. Approximate solutions can be obtained using perturbation methods or numerical methods. In their numerical studies, Hénon and Heiles plotted the points of intersection between phase-space trajectories and a two-dimensional surface of section in the phase-space. For recurrent trajectories, successive intersection points on the surface of section define an area-preserving two-dimensional discrete time dynamical system or map that shares the important dynamical features of the original system (Poincaré, 1993).

A convenient Poincaré map for the Hénon–Heiles Hamiltonian at fixed energy, in the range $0 \le E \le \frac{1}{6}$, is obtained with the surface of section $x = 0$ and $\dot{x} \ge 0$. The coordinate pair $(y, \dot{y})$ in this case uniquely determines an initial point for a trajectory since $\dot{x} = \sqrt{2E - \dot{y}^2 - y^2 + 2y^3/3}$. Thus, the dynamical description is reduced to a study of the Poincaré map from one intersection point $(y_n, \dot{y}_n)$ to the next intersection point $(y_{n+1}, \dot{y}_{n+1})$. The existence of an additional isolating integral in the Hénon–Heiles Hamiltonian would restrict a trajectory to intersect an invariant curve in the surface of section. In the absence of an additional isolating integral, the pattern of intersection points should fill an area on the surface of section. In numerical studies, where the number of intersection points is finite, discrimination between these two signatures is subjective since any finite set of points can be aligned to a smooth curve. Despite this, the interpretation of the intersection points as invariant curves or filled area in the Hénon–Heiles study has been regarded as unambiguous.

Figure 1 shows the intersection points between numerical phase space trajectories and a Poincaré surface of section in the Hénon–Heiles system at four different values of the energy, $E = \frac{1}{24}, \frac{1}{12}, \frac{1}{8}$, and $\frac{1}{6}$.

At $E = \frac{1}{24}$ and $E = \frac{1}{12}$, the intersection points appear to lie on invariant curves. At $E = \frac{1}{8}$, intersection points for some trajectories appear to lie on invariant curves whereas intersection points for other trajectories explore areas on the surface of section. At $E = \frac{1}{6}$, intersection points for most trajectories do not appear to lie on invariant curves (and typically the separation distance between trajectories started from nearby initial conditions diverges exponentially in time, a signature of chaos). A feature that is not revealed in the surface of section portraits at $E = \frac{1}{6}$, but is clear in three-dimensional phase space portraits (Henry & Grindlay, 1994), is intermittency whereby a single trajectory switches in time between regular behavior (close to invariant curves) and irregular behavior (filling areas).

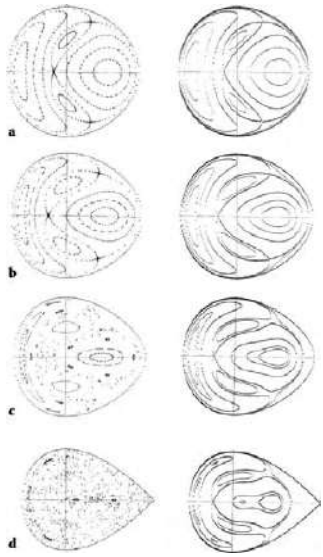

Figure 1. Surface of section portraits for the Hénon–Heiles Hamiltonian at four different values of the energy; (a) $E = 1/24$, (b) $E = 1/12$, (c) $E = 1/8$, (d) $E = 1/6$. The figures on the left are from numerical integrations and the figures on the right are from Birkhoff–Gustavson normal form theory. The figures have been reproduced from Gustavson (1966).

The transition from regular behavior to irregular behavior as the system energy is increased in the Hénon–Heiles model is characteristic of a more general transition from regular behavior to irregular behavior in Hamiltonian systems with two degrees of freedom and in two-dimensional area-preserving maps. A detailed theoretical understanding of this phenomena encompasses collective results from the Birkhoff–Gustavson normal form theory, the Kolmogorov–Arnol'd–Moser (KAM) theory, the Poincaré–Birkhoff theory, the Aubry–Mather theory, the theory of heteroclinic tangles (Poincaré, 1993), and the theory of overlapping resonances (Ford, 1992).

The Birkhoff–Gustavson normal form (Gustavson, 1966) represents the Hamiltonian as an infinite series of harmonic oscillator Hamiltonians through an infinite series of successive canonical transformations. The Hénon–Heiles Hamiltonian is strictly non-integrable at all values of the system energy (Ito, 1985); thus the normal form series for this Hamiltonian does not converge. On the other hand, any finite truncation of the normal form series constitutes an integrable Hamiltonian that can be considered to be "close" in some sense to the Hénon–Heiles Hamiltonian. The additional conserved quantity for an integrable normal form Hamiltonian can be readily calculated and used to plot the associated invariant curves on the Poincaré surface of section. The KAM theory proves that for a non-integrable Hamiltonian sufficiently close to an integrable Hamiltonian, most of the phase space trajectories are confined to invariant tori, similar to the invariant tori of the integrable system. Thus the surface of section portraits for the Hénon–Heiles Hamiltonian should map out the invariant curves from the truncated normal form Hamiltonian whenever this Hamiltonian is sufficiently close to the Hénon–Heiles Hamiltonian. The difference between the truncated normal form series and the Hénon–Heiles Hamiltonian increases with system energy. This can be seen in Figure 1 where the invariant curves from an eighth order truncation (Gustavson, 1966) are compared side by side with the numerical results for the Hénon–Heiles Hamiltonian.

In Hamiltonian systems with two degrees of freedom, the tori are characterized by a winding number ω_1/ω_2. The KAM theory proves the existence of invariant tori whose winding numbers are sufficiently irrational that

$$\left|\frac{\omega_1}{\omega_2} - \frac{r}{s}\right| > \frac{k(\varepsilon)}{s^{5/2}}$$

where r and s are co-prime integers and $k(\varepsilon)$ approaches zero as ε approaches zero. Here ε measures the strength of the non-integrable perturbation on the integrable Hamiltonian. The volume of phase-space not filled by invariant tori approaches zero as ε approaches zero. Tori whose winding numbers do not satisfy the stability condition under perturbation breakup according to the Poincaré–Birkhoff theory (rational winding numbers) or the Aubry–Mather theory (irrational winding numbers). The numerical results for the Hénon–Heiles Hamiltonian are consistent with an increasing breakup of tori with increasing energy as less and less tori satisfy the stability criteria.

The motion of an asteroid around the Sun can also be described approximately by a simplified model Hamiltonian with two degrees of freedom. The simplest non-trivial model is a plane circular restricted three-body problem involving the asteroid, the Sun, and Jupiter (Berry, 1978). The two-body motion of the asteroid around the Sun is a Kepler ellipse with frequency ω_A, and the two-body motion of Jupiter about its center of mass with the Sun is taken to be a circle with frequency ω_J. In the restricted three-body problem the effect of the asteroid on the motion of the Sun and Jupiter is neglected, the motion of the asteroid is dominated by the Sun, and the motion of Jupiter is considered to be a perturbation on the motion of the asteroid. The Hamiltonian for this restricted three-body problem is non-integrable, and an application of KAM theory to the problem identifies the frequency ratio ω_A/ω_J with the winding number for invariant tori. Thus, asteroids

should be expected to be found in stable orbits at distances from the Sun where ω_A/ω_J is sufficiently irrational. Indeed, as had been noted by Daniel Kirkwood in 1866, there is an abundance of asteroids at these locations but gaps in the asteroid belt at locations where the frequency ratio is 3:1, 5:2, 7:3, or 2:1; however a detailed understanding of the Kirkwood gaps is still an area of active research (Ferraz-Mello, 1999).

BRUCE HENRY

See also **Kolmogorov–Arnol'd–Moser theorem; *N*–body problem; Normal forms theory; Poincaré theorems; Solar system**

Further Reading

Berry, M.V. 1978. Regular and irregular motion. In *Topics in Nonlinear Dynamics*, edited by S. Jorna, New York: American Institute of Physics, pp.16–120

Contopoulos, G. 1963. On the existence of a third integral of motion. *The Astronomical Journal*, 68(1): 1–14

Ferraz-Mello, S. 1999. Slow and fast diffusion in asteroid-belt resonances: a review. *Celestial Mechanics & Dynamical Astronomy*, 73(1–4): 25–37

Ford, J. 1992. The Fermi–Pasta–Ulam problem: paradox turns discovery. *Physics Reports*, 213(5): 271–310

Gustavson, F.G. 1966. On constructing formal integrals of a Hamiltonian system near an equilibrium point. *The Astronomical Journal*, 71(8): 670–686

Gutzwiller, M.C. 1990. *Chaos in Classical and Quantum Mechanics*, New York: Springer

Hénon, M. & Heiles, C. 1964. The applicability of the third integral of motion: some numerical experiments, *The Astronomical Journal*, 69(1): 73–99

Henry, B.I. & Grindlay, J. 1994. From dynamics to statistical mechanics in the Hénon–Heiles model: dynamics. *Physical Review* E, 49(4): 2549–2558

Ito, H. 1985. Non-integrability of Hénon-Heiles system and a theorem of Ziglin. *Kodai Mathematical Journal*, 8: 120–138

Ollongren, A. 1965. Theory of stellar orbits in the galaxy. *Annual Review of Astronomy and Astrophysics*, 3: 113–134

Poincaré, H. 1993. *New Methods of Celestial Mechanics, vol. 3. Integral Invariants and Asymptotic Properties of Certain Solutions*. Woodbury, New York: American Institute of Physics. (English translation of *Les Méthodes nouvelles de la Mécanique Céleste, vol. 3: Invariants integraux. Solutions periodiques du deuxieme genre Solutions doublement asymptotiques*, 1899)

HETEROCLINIC INTERSECTION

See **Phase space**

HETEROCLINIC TRAJECTORY

See **Phase space**

HIERARCHIES OF NONLINEAR SYSTEMS

Although we must deal with many hierarchical structures in the course of life—social, military, and monetary, among others—two are of particular interest to practitioners of nonlinear science: the biological and cognitive hierarchies.

Biological Hierarchy

It is an empirical fact that living creatures are hierarchical in structure, organized according to a scheme that is roughly as follows.

Biosphere
Species
Organisms
Organs
Cells
Processes of replication
Genetic transcription
Biochemical cycles
Biomolecules
Molecules
Atoms

Several comments are in order. First, it is only the general nature of this hierarchy that is of interest here, not the details. Second, the nonlinear dynamics at each level of description generate emergent structures, and nonlinear interactions among these structures provide a basis for the dynamics at the next higher level (Scott, 2003). Thus, molecules emerge from the nonlinear forces among their constituent atoms, biomolecules emerge from molecules, biochemical cycles (such as the Krebs cycle, which processes energy in a living cell) emerge from interactions among biomolecules, and so on. Third, the emergence of a new dynamic entity usually involves presence of a closed causal loop, which leads to positive feedback and exponential growth that is ultimately limited by nonlinear effects.

Finally, it should be noted that philosophers disagree about the ontological status of an emergent entity. Are the levels mere designations, convenient for academic organization, or do they mark qualitatively different realms of reality?

In attempting to answer this question, it is important to know whether the upper levels of the biological hierarchy can be derived from lower levels, which leads to the concept of reductionism. In other words, can the upper levels of the hierarchy (organisms, species, biosphere) be logically derived from the properties of the lower levels? Or are they in some sense independent? In response to such questions, condensed matter physicist Philip Anderson has commented (Anderson, 1972): "The ability to reduce everything to simple fundamental laws does not imply the ability to start from those laws and reconstruct the universe."

Why not? Like the flame of a candle, the Belousov–Zhabotinsky reaction, or a nerve impulse, the dynamics of biological systems arise from nonlinear reaction-diffusion processes, in which the particular atoms participating in the reactions change with time. Thus, exact knowledge of the positions and velocities of the

constituent atoms of an organism at one time tells little about the behavior at a later time (Bickhard & Campbell, 2000; Scott, 2002). Of course, a dedicated reductionist would respond that the explanatory net has not been cast far enough—all the atoms and radiation that wander into and out of the organism must be followed—but few seriously propose to do this as it would require computing in detail the dynamics of the entire universe.

Cognitive Hierarchy

Just as the phenomenon of life arises from the hierarchical nature of the biological realm, it has been suggested that the mysteries of mind may stem from an analogous hierarchy, describing levels of activity of the brain. Again ignoring details, this cognitive hierarchy may be sketched as follows.

Human cultures
Phase sequences
Complex assemblies
. . .
Assemblies of assemblies of assemblies
Assemblies of assemblies
Assemblies of neurons
Neurons
Nerve impulses
Nerve membranes
Membrane proteins
Molecules
Atoms

To the previous comments on the biological hierarchy, the following can be added. Although the biological levels are observed—through x-ray diffraction, via electron and light microscopy, or more directly—several levels of the cognitive hierarchy are theoretical constructs. This is particularly so for the cell assemblies and their constituent subassemblies, which Donald Hebb proposed to underlie the dynamic nature of human thought (Hebb, 1949). Thus a particular complex cell assembly that embodies a particular idea (your memory of your grandmother, for example) might involve interactions among several (visual, auditory, conceptual) subassemblies as suggested by Figure 1.

In this figure, the shaded areas do not suggest that all neurons in that region are firing, but only those (perhaps ten thousand or so) that have become specific to this particular memory through many related experiences and interactions. The neurons of this assembly are interconnected in such a manner that they are "capable of interacting briefly as a closed system, delivering facilitation to other such systems and usually having a specific motor facilitation" (Hebb, 1949). As a complex assembly comprises subassemblies that in turn are composed of yet more basic constituent assemblies, the concept is inherently hierarchical.

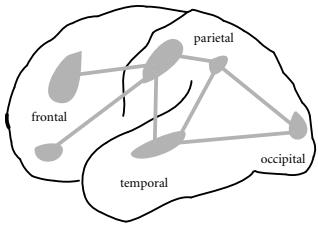

Figure 1. A sketch of the left side of the human brain, suggesting how the active subassemblies (shaded areas) of a complex cell assembly might be distributed over various lobes of the neocortex.

Although Hebb's theory is in accord with a substantial amount of psychological data (Hebb, 1980; Scott, 2002), it is difficult to imagine placing electrodes in the neocortex so that the simultaneous firings of a substantial number of these assembly neurons could be recorded. Nontheless, a substantial amount of experimental and numerical data is accumulating in support of this theory.

At higher levels of the cognitive hierarchy, we recognize the phase sequence, in which the focus of thought moves from one complex assembly to the next in a train of thought or a dream. At yet higher levels, important aspects of cultural dynamics—ingrained social prejudices, for example, or an aversion to eating certain foods—may remain unrecognized as they play important roles in human behavior.

ALWYN SCOTT

See also **Cell assemblies; Electroencephalogram at large scales; Emergence; Neural network models**

Further Reading

Anderson, P.W. 1972. More is different: broken symmetry and the nature of the hierarchical structure of science. *Science*, 177: 393–396

Bickhard, M.H. & Campbell, D.T. 2000. Emergence. In *Downward Causation: Minds, Bodies and Matter*, edited by P.B., Andersen, C. Emmeche, N.O. Finnemann & P.V. Christiansen, Aarhus, Denmark: Aarhus University Press

Hebb, D.O. 1949. *Organization of Behavior: A Neuropsychological Theory*, New York: Wiley

Hebb, D.O. 1980. The structure of thought. In *The Nature of Thought*, edited by P.W. Jusczyk & R.M. Klein, Hillside, NJ: Lawrence Erlbaum Associates, pp. 19–35

Scott, A.C. 1995. *Stairway to the Mind*, New York: Springer

Scott, A.C. 2002. *Neuroscience: A Mathematical Primer*, Berlin and New York: Springer

Scott, A.C. 2003. *Nonlinear Science: Emergence and Dynamics of Coherent Structures*, 2nd edition, Oxford and New York: Oxford University Press

HIGGS BOSON

Particle physics is devoted to discovering and investigating the fundamental constituents of all the matter in the universe (at all times), and the forces of nature by which these constituents interact with each other. The theoretical framework that currently aids our understanding is called the Standard Model. Although there is no experimental result that significantly disagrees with the Standard Model, it is not a complete theory; indeed, there are several reasons why the Standard Model is not a theory at all in the normal sense of the word. Perhaps the most important of these is that it contains a large number of parameters (such as the fundamental particle masses) that are not predicted but determined experimentally and then incorporated into the theoretical framework.

A principle mission of particle physics is the development of a complete, fundamental theory that unifies all of the known forces into one. Historically, this process seems to be taking place one pair of forces at a time (for example, James Clerk Maxwell famously unified electricity and magnetism in the 19th century), and an important feature of the Standard Model is that it contains the unification of the short-range weak nuclear force and the long-range electromagnetic force. The strong nuclear force is not yet unified and gravity is completely excluded from the standard model.

Although the successful implementation of electroweak unification encourages particle physicists to consider the Standard Model as a low energy approximation of a more fundamental theory, electroweak unification comes at a price. The quantum of the electromagnetic field is the photon, which has zero rest mass. The weak field has a chargeless quantum, known as the Z particle, and a charged quantum, known as the W particle. The rest masses of the Z and the W are both almost 100 times the proton rest mass. This huge difference in the masses of the particles associated with the electromagnetic and weak force fields is known as electroweak symmetry breaking, and in order to interpret it, physicists have introduced into the Standard Model an arbitrary mathematical trick.

In a series of papers some 40 years ago, Englert and Brout (and independently, Higgs) pointed out that a symmetry-breaking idea used in the theory of superconductivity could also be used to break the electroweak symmetry. This mathematical trick is known in particle physics as the Higgs mechanism. In the theory of superconductivity, the idea explains how photons appear to acquire mass inside a superconductor. Introducing it into the Standard Model provides an explanation of where the Z and W masses come from.

The Higgs mechanism is most readily viewed in terms of a constant, ubiquitous energy field that has no preferred direction in space. This field is known as the Higgs field. It is this Higgs field that breaks the electroweak symmetry, giving mass to both Z and W while retaining a massless photon. Just as there are well-defined quanta, known as bosons, associated with each of the known force fields, so it is with the hypothetical Higgs field. In the simplest version of the Higgs mechanism, there is just one quantum and it is known as the Higgs particle or Higgs boson.

So, to recap, the Higgs particle is intimately associated with the Higgs field, and the Higgs field is assumed to be responsible for the mass difference between the quanta of the electromagnetic and weak fields. It is not too much of a stretch to expect that the masses of all matter particles (quarks and leptons) somehow get their masses from the Higgs mechanism. Indeed, the coupling of every particle to the Higgs field has strength proportional to its mass, and so this interpretation seems natural. Unfortunately, the Higgs mechanism does not reduce the number of unknown parameters of the Standard Model—there is still one per particle, plus a few more.

Curiously, the assumed Higgs particle has quite well-determined properties. Its mass, like all other particle masses, is not predicted but must be measured. As a function of an assumed mass, however, one can use the Standard Model to calculate the rate at which it will be produced in a high-energy collision of two elementary particles. The Higgs particle is expected to be highly unstable, and it is also straightforward to calculate, using the Standard Model, how it will decay. In other words, what it will decay into and with what relative rates. These Standard Model predictions provide a basis for experimental searches for the Higgs particle.

The particle experimentalists perform experiments in which they collide, at the highest available energy, protons with protons, or protons with antiprotons, or electrons with positrons. They then examine the debris of the collision for evidence of a Higgs particle whose properties match those suggested by the Standard Model.

In this manner, the experimental techniques of particle physics have been able, over the past decade or so, to eliminate the possibility of a Higgs particle with mass below about 120 proton masses or above about 200 proton masses. When the Higgs mechanism was first introduced to particle physics, the mass of the Higgs particle could have been anywhere between zero and about 1000 times the proton mass. One of the remarkable achievements of particle physics over the past few decades has been the elimination of most of this mass region. Of course, this elimination is of a statistical nature and the best thing that physicists can do is to assign a measure of the statistical confidence to these limits. In late 2002, most particle physicists were confident that if the Standard Model Higgs particle exists, its mass is probably in the mass range of approximately 120–200 proton masses (somewhere between the atomic masses of tin

and gold). The Tevatron (proton-antiproton collider accelerator at Fermilab with energy close to 2 TeV) has a chance to investigate the lower 10% of this mass range; the Large Hadron Collider (LHC; proton-proton collider accelerator under construction at CERN with energy 14 TeV, scheduled to start operation in or after 2007) will finish the job. Thus, by 2020 at the latest, we will know whether there is a Higgs particle, and therefore whether Nature uses the Higgs mechanism to generate the masses of fundamental particles.

STEPHEN REUCROFT

See also **Born–Infeld equations; Matter, nonlinear theory of; Particles and antiparticles; Skyrmions; String theory**

Further Reading

Englert, F. & Brout, R. 1964. Broken symmetry and the mass of the gauge vector mesons. *Physical Review Letters*, 13(9): 321

Gunion, J., Haber, H., Kane, G. & Dawson, S. 2000. *The Higgs Hunter's Guide*, Reading, MA: Perseus

Halzen, F. & Martin, A. 1984. *Quarks and Leptons*, New York: Wiley

Higgs, P. 1964. Broken symmetries and the masses of gauge bosons. *Physical Review Letters*, 13(16): 508

Higgs, P. 1964. Broken symmetries, massless particles and gauge fields. *Physics Letters*, 12(2): 132

Kane, G. 1993. *Perspectives on Higgs Physics*, River Edge, NJ: World Scientific

HILL'S EQUATION

See **Periodic spectral theory**

HIROTA'S METHOD

Ryogo Hirota originally proposed his bilinear method as a "direct method" for constructing multisoliton solutions to integrable equations. The method is "direct" in the sense that one can apply it without resorting to deeper mathematical properties, for example, to those that are needed in order to apply the inverse scattering transform (IST). In practice, this means that Hirota's method is applicable to a wider class of equations. Nevertheless, the bilinear method is related to deep mathematical foundations of soliton theory (Sato theory), as has been shown by the members of the Kyoto school (Sato, Date, Jimbo, Miwa, Kashiwara).

Prototypical Result: The KdV Equation

Let us see how Hirota's bilinear method works for the Korteweg–de Vries (KdV) equation

$$u_{xxx} + 6uu_x + u_t = 0. \tag{1}$$

It is known from IST that multisoliton solutions can be written as $u = 2\partial_x^2 \log(\det M)$, where the entries in M are of the form $c_0 + c_1 \mathrm{e}^{c_2 x + c_3 t}$ for some constants c_i. Thus, $\det M$ is a sum of exponentials and, therefore, an entire function. This inspired Hirota to write the KdV equation in terms of a new dependent variable F defined by (Hirota, 1971)

$$u = 2\partial_x^2 \log F. \tag{2}$$

Then the KdV equation (1) becomes

$$\partial_x [F_{xxxx}F - 4F_{xxx}F_x + 3F_{xx}^2 + F_{xt}F - F_x F_t] = 0. \tag{3}$$

Note the derivative outside the brackets, which means that the bilinearization actually works most naturally for the potential KdV equation.

In order to shorten the notation, let us introduce the bilinear derivative operator D as follows:

$$\begin{aligned} D_x^n f \cdot g &= (\partial_{x_1} - \partial_{x_2})^n f(x_1) g(x_2)\big|_{x_2 = x_1 = x} \\ &\equiv \partial_\varepsilon^n f(x+\varepsilon) g(x-\varepsilon)\big|_{\varepsilon = 0}. \end{aligned} \tag{4}$$

Then the KdV equation may be written in the simple form

$$(D_x^4 + D_x D_t)\, F \cdot F = 0. \tag{5}$$

Since F was assumed to be a sum of exponentials, let us try to construct a one-soliton solution (1SS) to (5) using the ansatz

$$F = 1 + \mathrm{e}^{\eta}, \quad \eta = px + \omega t + \eta^0. \tag{6}$$

A direct computation shows that this is indeed a solution, provided that $\omega = -p^3$; this condition on the parameters is called the *dispersion relation*. From (2) we get the usual soliton solution

$$u = \frac{2p^2 \mathrm{e}^{\eta}}{(1+\mathrm{e}^{\eta})^2} = \frac{p^2}{2\cosh^2(\eta/2)}, \tag{7}$$

where $\eta = px - p^3 t + \eta^0$.

A particularly nice feature of the bilinear method is that two-soliton solutions (2SSs) are also very easy to obtain. We assume that a 2SS is constructed from two 1SSs perturbatively as follows:

$$F = 1 + e^{\eta_1} + \mathrm{e}^{\eta_2} + a_{12} \mathrm{e}^{\eta_1 + \eta_2}, \tag{8}$$

where $\eta_i = p_i x - p_i^3 t + \eta_i^0$.

A direct computation then shows that this is indeed a solution of (5), provided that the *phase factor* is given by

$$a_{12} = \left(\frac{p_1 - p_2}{p_1 + p_2} \right)^2. \tag{9}$$

Using (2) one gets the nonlinear form of the 2SS, which is already rather complicated. The above 1SS and 2SS ansätze actually work (with suitable a_{12}) for *any* equation having a bilinear form of type $P(D)F\cdot F=0$, with $P(0)=0$.

The above can be extended to a 3SS. By considering various asymptotic limits (where one of the three solitons is far away), one finds that the proper ansatz cannot have new free coefficients, but must have the form

$$F = 1+\mathrm{e}^{\eta_1}+\mathrm{e}^{\eta_2}+\mathrm{e}^{\eta_3}+a_{12}\mathrm{e}^{\eta_1+\eta_2}+a_{13}\mathrm{e}^{\eta_1+\eta_3} +a_{23}\mathrm{e}^{\eta_2+\eta_3}+a_{12}a_{13}a_{23}\mathrm{e}^{\eta_1+\eta_2+\eta_3}. \quad (10)$$

In contrast to the 2SS case, this ansatz only works for *integrable* equations of type $P(D)F\cdot F=0$, for example, the KdV, Sawada–Kotera, and Kadomtsev–Petviashvili equations. In fact, the existence of multisoliton solutions can be used as a criterion of integrability (Hietarinta, 1990).

Examples of Bilinear Equations

Let us next consider the nonlinear Schrödinger equation (NLS)

$$\mathrm{i}\phi_t+\phi_{xx}+2|\phi|^2\phi=0. \quad (11)$$

It is bilinearized with the substitution

$$\phi=G/F, \quad G \text{ complex, } F \text{ real}, \quad (12)$$

which yields

$$F\,[(\mathrm{i}D_t+D_x^2)G\cdot F]-G\,[D_x^2F\cdot F-2|G|^2]=0. \quad (13)$$

For normal (bright) solitons we split this into two equations for two functions:

$$\begin{cases} (\mathrm{i}D_t+D_x^2)G\cdot F=0, \\ D_x^2F\cdot F=2|G|^2. \end{cases} \quad (14)$$

The 1SS ansatz is given by

$$G=\mathrm{e}^{\eta}, \quad F=1+a\,\mathrm{e}^{\eta+\eta^*}, \quad \eta=px+\omega t, \quad p \text{ and } \omega \text{ complex} \quad (15)$$

and from the equations one finds a dispersion relation for the complex parameters, $\mathrm{i}\omega+p^2=0$, and the value of the phase factor, $a=1/(p+p^*)^2$.

Hirota's method works also for discrete systems. Consider the (semi-)discrete Toda-lattice equation

$$\ddot{y}_n=\mathrm{e}^{-(y_n-y_{n-1})}-\mathrm{e}^{-(y_{n+1}-y_n)}. \quad (16)$$

First one goes over to the dependent variable $r_n=y_n-y_{n-1}$, and then the substitution $\mathrm{e}^{r_n}=1+\partial_t^2\log f_n$ yields

$$(D_t^2+2)f_n\cdot f_n=2f_{n-1}f_{n+1}. \quad (17)$$

Since $e^{\alpha D_x}f(x)\cdot g(x)=f(x+\alpha)g(x-\alpha)$, we can write (17) also in the form

$$\left[D_t^2-4\sinh^2\left(\tfrac{1}{2}D_n\right)\right]f_n\cdot f_n=0. \quad (18)$$

The 1SS is given by

$$f_n(t)=1+\mathrm{e}^{2(pn+\omega t)}, \quad (19)$$

where $\omega=\pm\sinh(p)$.

The above types of bilinearizations work, *mutatis mutandis*, for several classes of equations, but unfortunately there is no algorithmic method of finding the bilinearizing substitution for a given nonlinear equation. In fact, it is not even clear a priori how many dependent or even independent variables one should use. There are some general guidelines; for example, in order to bilinearize higher members in a hierarchy, one usually needs extra independent variables. If the 1SS and 2SS are known, one may use them in order to make an educated guess about the bilinearizing substitution.

The ultimate bilinear equation, from which many other bilinear equations can be derived as particular limits, is the Hirota–Miwa equation

$$(z_1\mathrm{e}^{D_1}+z_2\mathrm{e}^{D_2}+z_3\mathrm{e}^{D_3})F\cdot F=0, \quad (20)$$

where z_i are constants and D_i are arbitrary linear combinations of $D_x, D_y, \ldots$.

The General Perturbative Approach for Constructing Soliton Solutions

Once a reasonable bilinear form has been found, one can try to find soliton solutions using a perturbative expansion in a fictitious parameter ε (Hirota, 1976):

$$F=f_0+\varepsilon f_1+\varepsilon^2f_2+\cdots, \quad (21)$$

and similarly for the other dependent variables appearing in the bilinear equations. One first chooses a suitable "vacuum" solution (no solitons), that is, constant values for the ε^0 terms, with all other terms vanishing. Next for a 1SS, one uses a minimal nontrivial entry (typically $\mathrm{e}^{px+qy+\omega t}$) at order ε, that is, for f_1, and normally one should then be able to truncate the expansion at this or the next level (cf. (6) or (15)). For a 2SS, the previous 1SS solution is generalized at the ε level by taking the sum of two terms (cf. (8)), and as a result the expansion will truncate later (for KdV at ε^2, but for NLS we need even powers up to 4 for F and odd powers up to 3 for G). If the expansion does not truncate, it is probable that the equation is non-integrable. What helps here is that since $P(\boldsymbol{D})\mathrm{e}^{\boldsymbol{a}\cdot\boldsymbol{x}}\cdot\mathrm{e}^{\boldsymbol{b}\cdot\boldsymbol{x}}=P(\boldsymbol{a}-\boldsymbol{b})\mathrm{e}^{(\boldsymbol{a}+\boldsymbol{b})\cdot\boldsymbol{x}}$, the highest order terms in $P(\boldsymbol{D})F\cdot F$ vanish automatically.

In a systematic construction of multisoliton solutions, one uses determinants of Wronskian or Grammian type, or Pfaffians (Nimmo, 1990). Their applicability follows from the fact that determinants often

satisfy quadratic identities, of which the Laplace expansion (a Plücker relation) is a typical example. The type of the matrix used is intimately related to the above-mentioned phase factor of the 2SS.

Bäcklund Transformations

In addition to providing a simple method for constructing multisoliton solutions, Hirota's method is also natural for studying Bäcklund transformations (BTs). In general terms, the starting set of equations and variables is doubled (while adding a new free parameter), and their combination is manipulated in order to get a pair of bilinear equations that are *linear* in each set of variables. Furthermore, if variables of one set are eliminated, one should get back the original equations. For example, the BT of the KdV equation is (Hirota, 1980)

$$\begin{cases} (D_x^3 + 3\lambda D_x + D_t)F' \cdot F = 0, \\ (D_x^2 - \mu D_x - \lambda)F' \cdot F = 0, \end{cases} \tag{22}$$

and if one eliminates F' from this pair, one obtains (a derivative of) (5).

Sato Theory

The reason Hirota's bilinear method works so well is that it is a reflection of an elegant fundamental theory called Sato theory, where bilinear identities (expressed using Young or Maya diagrams) play a major role. The theory naturally yields several infinite hierarchies of equations in an infinite number of variables, and their finite-dimensional reductions are the usual soliton equations. For an introduction, see Ohta et al. (1988) and Miwa et al. (2000).

Because there is so much mathematical structure underlying the bilinear approach, it is not surprising that bilinear forms of various equations have appeared before in the literature (although only in passing). For example, in 1902, Painlevé found bilinear forms for the first three of the six Painlevé equations using a substitution like (2); his idea was to express the equations in terms of entire functions. Indeed, the functions that arise in Sato theory are also entire functions, called τ-functions, and so one often refers to the bilinearizing functions (F and G above, for example) as τ-functions.

Summary

Hirota's bilinear method is a very effective technique in constructing multisoliton solutions. For a given equation, one should first find a one-soliton solution, and using it, one can often guess a method for bilinearizing the nonlinear equation. If that is successful, one can search for multisoliton solutions using the perturbative approach.

It is believed that all integrable evolution equations are obtained as reductions from a limited number of hierarchies, as described in Miwa et al. (2000), although the reductions can be highly nontrivial. Conversely, for a given new integrable equation, one should try to understand its origin as a reduction of one of the known hierarchies, and the bilinear form and the phase factor are helpful in this process.

In practical applications, one must nevertheless be careful, first to avoid bilinearizations that trivialize the system. The usual bilinearizing substitution (2) usually yields a multilinear system. One can forcibly bilinearize it by separating it into smaller bilinear parts and requiring each one of them to vanish independently. But if at the end there are more equations than unknown functions, the set of bilinear equations so obtained may include conditions that did not exist in the original equations.

Also, the existence of a bilinear form does not imply integrability. Bilinear forms have also been written for many non-integrable models, and the existence of a bilinear form does not even imply the existence of N-soliton solutions, nor can one always assume that the bilinearizing functions are τ-functions. Indeed, for a large class of bilinear equations (containing non-integrable equations), it is possible to find two-soliton solutions exhibiting elastic scattering, but that does not imply the existence of a *general* N-soliton solution for any $N > 2$.

JARMO HIETARINTA

See also **Bäcklund transformations; Inverse scattering method or transform; N-soliton formulas; Solitons**

Further Reading

Hietarinta, J. 1990. Hirota's bilinear method and integrability. In *Partially Integrable Evolution Equations in Physics*, edited by R. Conte & N. Boccara, Dordrecht: Kluwer, pp. 459–478

Hirota, R. 1971. Exact solution of the Korteweg–de Vries equation for multiple collision of solitons. *Physical Review Letters*, 27: 1192–1194

Hirota, R. 1976. Direct method of finding exact solutions of nonlinear evolution equations. In *Backlund Transformations, the Inverse Scattering Method, and Their Applications*, edited by R. Miura, New York: Springer, pp. 40–68

Hirota, R. 1980. Direct methods in soliton theory. In *Solitons*, edited by R. Bullough & P.J. Caudrey, New York: Springer, pp. 157–176

Miwa, J., Jimbo, M. & Date, E. 2000. *Solitons: Differential Equations, Symmetries and Infinite Dimensional Algebras*, Cambridge and New York: Cambridge University Press

Nimmo, J.J.C. 1990. Hirota's method. In *Soliton Theory: A Survey of Results*, edited by A.P. Fordy, Manchester: Manchester University Press, pp. 75–96

Ohta, Y., Satsuma, J., Takahashi, D. & Tokihiro, T. 1988. An elementary introduction to Sato theory. *Progress in Theoretical physics, Supplementum*, 94: 210–241

HODGKIN–HUXLEY EQUATIONS

Classical experiments on the compound action potential produced by vertebrate nerve trunks provided all the components for a reaction-diffusion model for the propagation of an action potential, with the nerve impulse as a nonlinear traveling wave produced by the nonlinear "reaction" of excitation and the diffusive spread of voltage. Even as late as the 1930s, however, it was not clear if nerve excitation was a membrane phenomenon, or if the the extracellular potential changes were a consequence of some chemical excitation propagating through the axoplasm.

The identification of the 100–500 μm diameter giant axons of the squid as single nerve fibers provided a preparation large enough for excitation and propagation in a single nerve fiber to be analyzed in detail. Wires can be inserted down the axoplasm, one to pass current, one to record potential, and one to short circuit the resistance of the intracellular axoplasm, providing a space clamp under which the membrane potential is spatially uniform. Current can be passed between the internal electrode and external electrodes, exciting a membrane action potential that is recorded as the difference in potential V across the membrane.

The membrane current I_m is the sum of a capacitative and an ionic current:

$$I_m = C_m \, dV/dt + I_{ion} \tag{1}$$

with the membrane capacitance $C_m = 1\,\mu F\,cm^{-2}$. Direct recordings of the membrane action potential show that the potential changes sign, from a resting value of -60 mV to a peak value of $+40$ mV. The peak of the action potential varies logarithmically with the extracellular Na^+ concentration, showing the role of sodium ion (Na^+) current in the generation of the action potential.

The voltage clamp technique uses a feedback circuit to control the potential across the membrane. Using rectangular command pulses, the membrane potential can be changed from its resting value to an arbitrary value within a fraction of a millisecond. During a voltage clamp, the only current flowing across the membrane is ionic and is equal and opposite to the current that is injected to maintain the clamp. Net ionic currents can be measured, and dissected into their components by ion substitution experiments. From the estimated ionic currents and their electrochemical gradients, the ionic conductances changes can be calculated. Under a depolarizing voltage clamp, the sodium(Na^+)-conductance change is fast and transient, while the potassium (K^+)-conductance change is slower, delayed, and maintained.

Hodgkin & Huxley (1952) fitted their extensive series of experimental measurements of ionic currents obtained under voltage clamp and synthesized their empirical equations into a quantitative model for the propagating action potential.

For axoplasmic resistance R and membrane capacitance C, both per unit length of axon, the spread of membrane potential V with distance x (cm) and time t (ms) is described by a reaction–diffusion equation:

$$C\frac{\partial V}{\partial t} = \frac{1}{R}\frac{\partial^2 V}{\partial x^2} - I_{ion}, \tag{2}$$

where I_{ion} is a nonlinear function of V and t .

The membrane ionic current I_{ion} is assumed to be composed of three independent components, a Na^+-current I_{Na}, a K^+-current I_K, and a leakage current density I_L ($\mu A\,cm^{-2}$) that flow through separate conductance pathways that have different ion-selectivities, maximal conductances, and voltage-dependent kinetics. Thus,

$$I_{ion} = I_{Na} + I_K + I_L. \tag{3}$$

The instantaneous current-voltage relation for each pathway is linear, so the current is the product of a conductance and a driving force—the difference between the potential V and the equilibrium (Nernst) potential for the pathway. The Nernst potential is determined by the intracellular (axoplasm) and extracellular (artificial sea water) ionic concentrations, and $V_{Na} = -115$, $V_K = +12$, and $V_L = -10.613$ mV (the unreasonable precision for V_L is to fix $V = 0$ as a stable equilibrium solution). The conductance is the product of the maximal conductance $\bar{g}$ and gating variables—activation m and inactivation h for Na^+-channels activation n for K^+-channels. The activation variables are raised to a certain power (3 for m, 4 for n) that empirically reproduces the delayed, sigmoid increase in current and may be interpreted as the number of gating structures per channel. Thus

$$\begin{aligned} I_{Na} &= \bar{g}_{Na} m^3 h (V - V_{Na}), \\ I_K &= \bar{g}_K n^4 (V - V_K), \\ I_L &= g_L (V - V_L). \end{aligned} \tag{4}$$

Each gating variable obeys first-order kinetics

$$\begin{aligned} dm/dt &= \alpha_m (1 - m) - \beta_m m, \\ dh/dt &= \alpha_h (1 - h) - \beta_h h, \\ dn/dt &= \alpha_n (1 - n) - \beta_n n \end{aligned} \tag{5}$$

with rate coefficients α and β for opening or closing that are empirical functions of voltage:

$$\begin{aligned} \alpha_n &= \frac{0.01(10 - V)}{\exp(10 - V)/10 - 1}, \\ \beta_n &= 0.125 \exp(-V/80), \\ \alpha_m &= \frac{0.1(25 - V)}{\exp(25 - V)/10 - 1}, \\ \beta_m &= 4 \exp(-V/18), \\ \alpha_h &= 0.07 \exp(-V/20), \\ \beta_h &= \frac{1}{\exp(30 - V)/10 + 1}. \end{aligned} \tag{6}$$

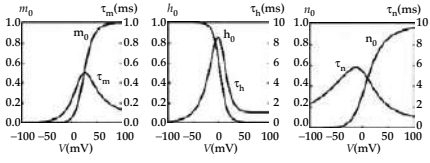

Figure 1. Voltage dependence of time coefficients and steady state values for gating variables m, h, and n of HH equations.

The rate coefficients α and β are derived from the experimentally estimated time constants τ and steady-state values illustrated in Figure 1, for example,

$$\tau_m = 1/(\alpha_m + \beta_m), \quad m_0 = \alpha_m/(\alpha_m + \beta_m). \quad (7)$$

Numerical solution (on a mechanical hand calculator) of the membrane equations reproduced both the subthreshold and action potential responses to initial depolarizations and a decrease in latency seen with increasing amplitude above threshold.

Computations of the total conductance change during the membrane action potential; total ion fluxes, time course of refractory period, and damped oscillatory responses matched experimental observations. The equations were based on experiments performed at 6.3°C; a Q_{10} of 3 (increasing temperature by 10° caused the rates to increase by a factor of 3) allowed simulation of the temperature dependence of the action potential. A solitary propagating solution of Equations (1)–(6) was obtained by assuming a wave solution traveling with a constant velocity of θ and making a coordinate transformation $\xi = x - \theta t$ to reduce Equation (1) to an autonomous system of ordinary differential equations. A value of $\theta = 18.8\,\mathrm{ms}^{-1}$ was found by trial and error to give an appropriately bounded solution in this traveling-coordinate system, which is close to the experimental estimate of $20\,\mathrm{ms}^{-1}$. For this work Alan Hodgkin and Andrew Huxley shared the Nobel Prize in Physiology or Medicine in 1963.

Early digital computations showed the continuous HH membrane equations to have a quasi-threshold, with the size of the action potential increasing smoothly with stimulus intensity. This contradiction of the "all-or-none" nature of the nerve impulse required control of variables to a higher resolution than thermal noise would allow in practice. However, similar behavior was found both numerically and experimentally at high temperatures (Cole et al., 1970). The membrane equations respond to steady injected currents by a repetitive discharge with a rate from 50 to $125\,\mathrm{s}^{-1}$, with a logarithmic relation between rate and injected current density, as found in sensory coding. The numerical and experimental responses to periodic stimulation include phase-locked, entrained, and even chaotic responses. The close agreement between numerical and experimental results has allowed chaos in the periodically forced squid axon to be a test signal for the validation of methods of quantifying chaos.

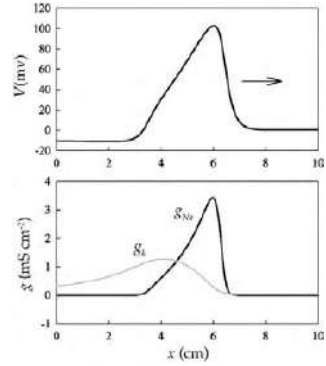

Figure 2. Constant velocity travelling wave solution of HH equations. Transmembrane voltage (upper) and membrane permeability (lower).

The equations successfully reproduced experimental data on membrane potential, ionic currents, and ion fluxes and provided a quantitative theory for the excitation and propagation of the nerve impulse. The equations were an empirical description of the currents seen under voltage clamp that also gave a quantitatively accurate reconstruction of the action potential. The form of the equations suggested a simple model of gated pores, with each pore gated by a system of four independent gates, and each gate opening or closing independently, with voltage-dependent, first-order kinetics. This physical model, of gated ionic conductance channels, has been substantiated by the electrophysiological and molecular biological characterization of single ionic channels, their kinetics and gating (Hille, 2001). The Hodgkin–Huxley formalism has also been successfully applied to the analysis of excitable membranes of nerve, smooth, skeletal, and cardiac muscle.

The introduction of digital computing into bioscience laboratories allowed numerical solution of the full partial differential equation system (Cooley & Dodge, 1966). Both stable and unstable traveling- wave solutions are found (Rinzel & Keller, 1973), and the effects of changes in diameter and axonal branching have been described.

As the first quantitatively accurate description of excitation, the HH equations have been used as a prototype for studying the behavior of excitation cells in general, as well as in circumstances with parameter values that may have no biological relevance for the squid axon. The development of autorhythmicity, by changes in parameters (injected steady current, maximal conductances, extracellular ionic concentrations,

temperature), has been shown to be by simple Hopf bifurcation; the bifurcation curves in parameter space have been mapped (Holden & Winlow, 1984) and explained using singularity theory (Golubitsky & Schaeffer, 1985). The HH equations were in fact a case study for the first numerical package for using continuation algorithms to track Hopf bifurcation curves. Phase-resetting behavior and annihilation of repetitive activity by appropriately timed perturbations has been computed and found in experiments (Guttman et al., 1984).

The importance of the HH equations in physiology has led to interest from mathematicians, either by generalizing the equations to characterize the mathematical aspects of excitation (Carpenter, 1977) or to allow exotic behavior such as bursting or by simplifying the equations to allow analysis or to facilitate numerical computations.

ARUN V. HOLDEN

See also **Excitability; FitzHugh–Nagumo equation; Hopf bifurcation; Markin–Chizmadzhev model; Nerve impulses; Neurons; Periodic bursting**

Further Reading

Carpenter, G. 1977. A geometric approach to singular perturbation problems with applications to nerve impulse equations. *Journal of Differential Equations*, 23: 335–367

Cole, K.S. 1969. *Membranes, Ions and Impulses*, Berkley: University of California Press

Cole, K.S., Guttman, R. & Bezanilla, F. 1970. Nerve membrane excitation without threshold. *Proceedings of the National Academy of Science of the USA*, 65: 884–891

Cooley, J.W. & Dodge, F.A., Jr. 1966. Digital computer solutions for excitation and propagation of the nerve impulse. *Biophysical Journal*, 6: 583–599

Golubitsky, M. & Schaeffer, D.G. 1985. *Singularities and Groups in Bifurcation Theory: vol. 1*, Berlin and New York: Springer, pp. 382–396

Guttman, R., Lewis, S. & Rinzel, J. 1984. Control of repetitive firing in squid axonal membrane as a model of a neurone oscillator. *Journal of Physiology*, 305: 377–395

Hille, B. 2001. *Ion Channels of Excitable Membranes*, 3rd edition, Sunderland, MA: Sinauer

Hodgkin, A.L. & Huxley, A.F. 1952. A quantitative description of membrane current and its application to conduction and excitation in nerve. *Journal of Physiology*, 117: 500–544

Holden, A.V. & Winslow, W. 1984. Neuronal activity as the behaviour of a differential system. *IEEE Transactions SMC*, 13: 711–719

Rinzel, J. & Keller, J.B. 1973. Traveling wave solutions of a nerve conduction equation. *Biophysical Journal*, 13: 1313–1337

HODOGRAPH TRANSFORM

Consider an N-component system with dependent variables

$$u(x,t) = [u_1(x,t), u_2(x,t), \dots u_N(x,t)]$$

that satisfy the partial differential equations

$$\frac{\partial u_i}{\partial t} = \sum_{j=1}^{N} v_{ij}(u)\,\frac{\partial u_j}{\partial x}, \quad v_{ij}(u) \in \mathbb{R}, \quad i = 1, \dots, N. \tag{1}$$

Under invertible smooth changes of variables of the form

$$u_i = u_i(w_1, w_2, \dots, w_N), \quad i = 1, 2, \dots, N, \tag{2}$$

the coefficients v_{ij} transform as a tensor,

$$v_{ij}(u_1, u_2, \dots, u_N) \to \tilde{v}_{rs}(w_1, w_2, \dots, w_N) = \sum_{i,j=1}^{N} \frac{\partial w_r}{\partial u_i} v_{ij}(u(w)) \frac{\partial u_j}{\partial w_s}.$$

Now let us assume that the eigenvalues $\lambda_1, \lambda_2, \dots, \lambda_N$ of the matrix v_{ij} are real and distinct, so system (1) is hyperbolic. Then it is possible to reduce (1), using transformation (2) to a diagonal form

$$\frac{\partial w_i}{\partial t} = \lambda_i(w)\frac{\partial w_i}{\partial x}, \quad i = 1, 2, \dots, N, \tag{3}$$

where $w(x,t) = (w_1(x,t),\ w_2(x,t), \dots, w_N(x,t))$. The variables $w_1, w_2, \dots w_N$ are called "Riemann invariants," and the coefficients $\lambda_1(w), \lambda_2(w), \dots, \lambda_N(w)$ are the corresponding characteristic velocities.

For $N = 2$ it is always possible locally to reduce (1) to Riemann invariant form, while for $N \geq 3$ this is not true in general. When system (1) is reducible to the diagonal form (3), it is sometimes possible to integrate it through the so-called hodograph transform. For $N \leq 2$, this fact is well known (see Courant & Hilbert, 1962); while for $N \geq 3$, the result was proved by Tsarev (1985). Let us consider the two-component system

$$\frac{\partial w_1}{\partial t} = \lambda_1(w_1, w_2)\frac{\partial w_1}{\partial x}, \quad \frac{\partial w_2}{\partial t} = \lambda_2(w_1, w_2)\frac{\partial w_2}{\partial x}. \tag{4}$$

To integrate (4), we map it into a linear set of equations, by interchanging the role of the dependent and independent variables, the so-called hodograph transform $(x,t) \to (w_1, w_2)$. In this transformation

$$\partial_2 x = -\frac{\partial_t w_1}{J}, \quad \partial_1 x = \frac{\partial_t w_2}{J}, \quad \partial_2 t = \frac{\partial_x w_1}{J}, \quad \partial_1 t = -\frac{\partial_x w_2}{J},$$

where $x = x(w_1, w_2)$, $t = t(w_1, w_2)$, $\partial_i = \partial/\partial w_i$, $i = 1, 2$ and $J = \partial_x w_1 \partial_t w_2 - \partial_t w_1 \partial_x w_2$ is the Jacobian. Then system (4) is mapped into the linear equations

$$\partial_2 x + \lambda_1\, \partial_2 t = 0, \quad \partial_1 x + \lambda_2\, \partial_1 t = 0. \tag{5}$$

The hodograph transform guarantees a linear equation, but it may not be useful in practice. Let us write (5) in the equivalent form

$$\partial_2 \underbrace{(x+\lambda_1 t)}_{\chi_1} = t\,\partial_2\lambda_1,$$
$$\partial_1 \underbrace{(x+\lambda_2 t)}_{\chi_2} = t\,\partial_1\lambda_2. \tag{6}$$

Then the functions $w_1(x,t)$ and $w_2(x,t)$, defined implicitly by

$$\chi_1(w_1,w_2) = \lambda_1(w_1,w_2)t + x,$$
$$\chi_2(w_1,w_2) = \lambda_2(w_1,w_2)t + x, \tag{7}$$

solve (4) if

$$\frac{\partial_2\chi_1}{\chi_1-\chi_2} = \frac{\partial_2\lambda_1}{\lambda_1-\lambda_2}, \quad \frac{\partial_1\chi_2}{\chi_2-\chi_1} = \frac{\partial_1\lambda_2}{\lambda_2-\lambda_1}. \tag{8}$$

Indeed from (7)

$$t = \frac{\chi_1-\chi_2}{\lambda_1-\lambda_2},$$

and substituting the above into (6), we obtain the linear overdetermined system (8).

As an example, consider the Born–Infeld equation

$$(1-\psi_t^2)\psi_{xx} + 2\psi_x\psi_t\psi_{xt} - (1+\psi_x^2)\psi_{tt} = 0, \tag{9}$$

which was formulated by Max Born in the early 1930s as a nonlinear field model for elementary particles. It is a simple matter to check that either

$$\psi = \Psi(x-t) \qquad \text{or} \quad \psi = \Psi(x+t)$$

are solutions of (9) for any function Ψ. In particular, the solution can be chosen in the form of a single hump to give the solitary wave appearance. The equation is hyperbolic for solution with $1+\psi_x^2-\psi_t^2>0$. We notice that the solitary waves have constant characteristic velocity ±1 and avoid the usual breaking expected for nonlinear hyperbolic waves. Interacting waves for system (9) were obtained through the hodograph method by Barbishov & Chernikov (1966). First, if new variables

$$\xi = x-t, \quad \eta = x+t, \quad u_1 = \psi_\xi, \quad u_2 = \psi_\eta$$

are introduced, we obtain the equivalent system

$$\partial_\eta u_1 - \partial_\xi u_2 = 0,$$
$$u_2^2\partial_\xi u_1 - (1+2u_1u_2)\partial_\eta u_1 + u_1^2\partial_\eta u_2 = 0. \tag{10}$$

The Riemann invariants are

$$w_1 = \frac{\sqrt{1+4u_1u_2}-1}{2u_2}, \quad w_2 = \frac{\sqrt{1+4u_1u_2}-1}{2u_1},$$

so system (10) reduces to the form

$$\partial_\xi w_1 = w_2^2\partial_\eta w_1, \quad \partial_\xi w_2 = \frac{1}{w_1^2}\partial_\eta w_2. \tag{11}$$

Performing the hodograph transform $(\eta,\xi)\to(w_1,w_2)$, system (11) is mapped to

$$w_1^2\partial_1\xi + \partial_1\eta = 0, \qquad \partial_2\xi + w_2^2\partial_2\eta = 0,$$

where $\partial_1\equiv\partial_{w_1}$ and $\partial_2\equiv\partial_{w_2}$. Eliminating η leads to the simple form

$$\partial_1\partial_2\xi = 0.$$

The above equation is readily integrated as

$$x-t = \xi = F(w_1) - \int w_2^2 G'(w_2)\,\mathrm{d}w_2,$$
$$x+t = \eta = G(w_2) - \int w_1^2 F'(w_1)\,\mathrm{d}w_1,$$

where F and G are arbitrary functions, and it follows that

$$\partial_1\psi = w_1F'(w_1), \quad \partial_2\psi = w_2G'(w_2).$$

It is convenient to introduce

$$F(w_1)=\rho, \quad G(w_2)=\sigma,$$
$$w_1 = \Phi_1'(\rho), \quad w_2 = \Phi_2'(\sigma),$$

so that the corresponding expression for ψ reads

$$\psi = \Phi_1(\rho) + \Phi_2(\sigma),$$
$$x-t = \rho - \int_{-\infty}^{\sigma} \Phi_2'^2(\sigma)\,\mathrm{d}\sigma,$$
$$x+t = \sigma + \int_{\rho}^{+\infty} \Phi_1'^2(\rho)\,\mathrm{d}\rho.$$

If $\Phi_1(\rho)$ and $\Phi_2(\sigma)$ are localized, say, they are nonzero in $-1<\rho<0$ and $0<\sigma<1$, then

$$\psi = \Phi_1(x-t) + \Phi_2(x+t), \quad t<0,$$

while for $t\to+\infty$, the solution approaches

$$\psi = \Phi_1\left(x-t+\int_{-\infty}^{\infty}\Phi_2'^2(\sigma)\,\mathrm{d}\sigma\right) + \Phi_2\left(x+t-\int_{-\infty}^{+\infty}\Phi_1'^2(\rho)\,\mathrm{d}\rho\right).$$

Each wave receives a displacement in the direction opposite to its direction of propagation equal to

$$\int_{-\infty}^{+\infty}\Phi_i'^2(\tau)\,\mathrm{d}\tau, \quad i=1,2.$$

The interaction is remarkably similar to the interaction of solitary waves even though the Born–Infeld equation belongs to a different class of systems. We remark that the above analysis is valid provided that the mapping from the (x,t) plane to the (ρ,σ) plane is nonsingular.

Application to Multiphase Averaging

The generalized hodograph method is used to integrate (Dubrovin & Novikov, 1989) the multiphase averaged equations or Whitham equations (Whitham, 1974; Flaschka et al., 1980). These equations are obtained by averaging conservation laws over the family of multiphase solutions of one-dimensional integrable nonlinear evolution equations like, for example, the Korteweg–de Vries equation. The Whitham equations describe the modulation of the wave parameters and wave numbers of the multiphase solutions over time and space scales of order εt and εx, where t and x are the independent variables of the original nonlinear evolution equations and $0 < \varepsilon \ll 1$. When the Whitham equations are hyperbolic, the technique of integration follows from a result of Tsarev (1985) that generalizes the hodograph transform to many dependent variables. The following condition is sufficient for integrability

$$\partial_i \left(\frac{\partial_k \lambda_j}{\lambda_k - \lambda_j} \right) = \partial_k \left(\frac{\partial_i \lambda_j}{\lambda_i - \lambda_j} \right), \quad i \neq j \neq k,\ i, j, k = 1, \ldots, N.$$

The integration of (3) is obtained as follows. If $\chi_1(w), \ldots, \chi_N(w)$ solves the linear over-determined system

$$\partial_i \chi_j = \frac{\chi_i - \chi_j}{\lambda_i - \lambda_j} \partial_i \lambda_j, \quad i \neq j,\ i, j = 1, \ldots, N, \quad (12)$$

then the solution $w_1(x, t), \ldots, w_N(x, t)$ of the generalized hodograph transform

$$x + \lambda_i(w)t = \chi_i(w), \quad i = 1, \ldots, N,$$

satisfies (3). Conversely, every solution of (3) can be obtained in this way in the neighborhood of a point (x_0, t_0) where $\partial_x w_i$, $i = 1, 2, \ldots, N$, is not vanishing. The solution of the linear overdetermined system (12) corresponding to the Whitham equations can be obtained by algebro-geometric integration.

GREGORIO FALQUI AND TAMARA GRAVA

See also **Born–Infeld equations; Characteristics; Horseshoes and hyperbolicity in dynamical systems; Modulated waves; Periodic spectral theory; Shock waves; Solitons**

Further Reading

Barbishov, B.M. & Chenikov, N.A. 1966. Solution of the two plane wave scattering problem in a nonlinear scalar field theory of the Born–Infeld type, *JETP*, 23: 1025–1033

Courant, R. & Hilbert, D. 1962. *Methods of Mathematical Physics*, New York: Interscience

Dubrovin, B. & Novikov, S.P. 1989. Hydrodynamic of weakly deformed soliton lattices. Differential geometry and Hamiltonian theory, *Russian Mathematical Surveys*, 44(6): 35–124

Flaschka, H., Forest, M. & McLaughlin, D.W. 1980. Multiphase averaging and the inverse spectral solution of the Korteweg–de Vries equation, *Communications on Pure and Applied Mathematics*, 33: 739–784

Tsarev, S.P. 1985. Poisson brackets and one-dimensional Hamiltonian systems of hydrodynamic type. *Soviet Mathematics Doklady*, 31: 488–491

Whitham, G.B. 1974. *Linear and Nonlinear Waves*, New York: Wiley

HOLE BURNING

Hole burning is a nonlinear technique for high-resolution spectroscopy, which was first demonstrated in magnetic resonance spectroscopy (Bloembergen et al., 1948). Hole burning employs the spectral purity of a laser to remove from an inhomogeneously broadened spectral line a narrow homogeneous line, causing a dip (or hole) in the spectrum. Thus, the technique is aimed at revealing the homogeneous line shape in the presence of strong inhomogeneous broadening.

The homogenous line shape is usually a Lorentzian whose full width $\Delta\omega_h$ is determined by the phase relaxation time T_2 of the system being considered

$$\Delta\omega_h = 1/T_2 . \quad (1)$$

T_2 is itself composed of two different times T_1 and T_2^*. T_1 is the energy relaxation time, that is, the time by which a non-equilibrium population reaches equilibrium. T_2^* is the pure dephasing time, the time in which an ensemble of molecules randomizes its initial coherent motion. From the Bloch equation, it can be readily shown that

$$1/T_2 = 1/T_1 + 2/T_2^* . \quad (2)$$

Hence, the homogeneous line shape function contains all the information on energy relaxation and dephasing processes (Abragam, 1961).

The inhomogeneous width $\Delta\omega_i$ is often much larger than $\Delta\omega_h$, so that the homogeneous line shape is completely masked. Inhomogeneous line broadening occurs since the microenvironments of the molecules, atoms, etc. under consideration are different, so the respective resonance frequencies experience a dispersion. Accordingly, the associated line shape is, as a rule, a Gaussian. In magnetic resonance this dispersion has its origin in the field inhomogeneities, in optical spectroscopy it comes from structural imperfections of the matrix in which the probe molecule is embedded.

Hole burning is one possible method for revealing the homogenous line shape. It is a special variant of saturation spectroscopy for the case that $\Delta\omega_h \ll \Delta\omega_i$. There are two main branches of this technique, namely saturation via the power and saturation via the radiation dose of the applied field. A two-state system, for example, an electronic two-level system of a probe molecule in an imperfect lattice, can only be saturated

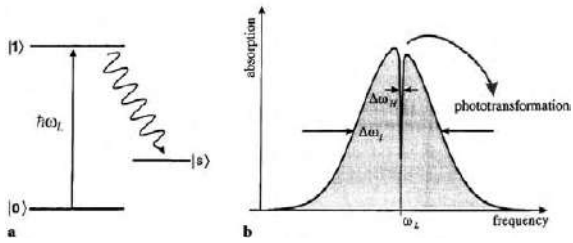

Figure 1. (a) Saturation of a three-level system. The storage level $|s\rangle$ is accessible from the excited state $|1\rangle$ by nonradiative processes. ω_L: laser frequency. (b) Schematic representation of the spectrum associated with saturation of the three-level system. $\Delta\omega_H$: holewidth. In the limit of vanishing saturation $\Delta\omega_H \rightarrow 2\Delta\omega_h$.

via the power of the radiation field: power is absorbed as long as there is a population difference between the lower and the upper state. As the power is increased, the population of the two states may equalize. Absorption and stimulated emission are balanced and the sample becomes transparent at the frequency of the radiation field. This phenomenon is called saturation. Note that power saturation of a two-level system is nonpersistent; that is, it decays with the energy relaxation time T_1. If the radiation field is tuned through the saturated transition, a dip or "hole" appears in the spectrum. The width of the hole in a power-saturated transition, $\Delta\omega_p$, however, deviates from the width of the homogenous line-shape function because it depends via the so-called Rabi frequency ω_1 on the power of the saturating radiation:

$$\Delta\omega_p = \Delta\omega_h[1 + \omega_1^2 T_1 T_2]^{1/2}. \tag{3}$$

ω_1 is proportional to the amplitude of the radiation field. Note that although the width becomes power dependent, the shape of the power-saturated transition retains its Lorentzian shape.

A very different saturation process is associated with hole burning involving three levels (Gorokhovskii et al., 1974; Kharlamov et al., 1974). Although power-saturation of an electronic two-level system is possible, it is of much less importance compared with saturation processes involving three levels, say the groundstate of a molecule $|0\rangle$, its first excited singlet state $|1\rangle$, and a long-lived intermediate $|s\rangle$ that acts as a storage state (Figure 1a). This intermediate, for instance, could be a photochemical state, a structural (e.g., a conformational) state or a long-lived spin state. It is not directly accessible to the radiation field, but can only be populated from state $|1\rangle$ via some radiative or radiationless process. Upon irradiating the $|0\rangle \rightarrow |1\rangle$ transition with a laser, population from a small range around the laser frequency ω_L is transferred to $|s\rangle$. Accordingly, a hole appears around ω_L in the absorption spectrum (Figure 1b). This hole may be persistent if the storage state $|s\rangle$ lives sufficiently long, as is the case for many photochemical states. In this case, the technique is called "photochemical hole burning." At sufficiently low temperatures, say, a few K, T_2^* becomes very large so that $\Delta\omega_h$ becomes lifetime-limited (Equations (1) and (2)). For a dye molecule with a typical lifetime of 10 ns dissolved in an organic glass, which gives rise to a typical inhomogeneous width of 300 wave numbers, this means that the burnt-in hole can be 4 to 5 orders of magnitude narrower than the inhomogeneous width. Because of this improvement in resolution, spectral hole burning is essentially a low-temperature technique (Friedrich & Haarer, 1984).

Persistent spectral hole burning may be characterized as a zero-power technique because holes can be burnt with vanishingly small power just by increasing the irradiation time. Yet, despite the fact that power saturation can be avoided, there is saturation broadening that, in contrast to the two-level case, depends on the irradiation dose: as population is transferred to the level $|s\rangle$, the number of absorbers in the center of the hole decreases steadily. Hence, the population transfer slows down in the center but still continues in the margins of the hole. This gives rise to an additional broadening in a similar way as has been discussed above for power broadening. Accordingly, $\Delta\omega_h$ is obtained from an extrapolation of the hole width to zero radiation dose.

Since the power of the radiation field can be made vanishingly small, the optics itself is perfectly linear. The nonlinear behavior of optical hole burning comes in via the persistent changes of the complex index of refraction through the irradiated energy. The advantage of the technique lies in the persistency of these changes. This makes it easy to exploit the high resolution, for instance, in measuring the influence of small external perturbations in the presence of strong inhomogeneous broadening, such as the influence of small electric, magnetic, or pressure fields. Persistent hole burning has been one of the major techniques to investigate the dynamics of low-temperature glasses via so-called spectral diffusion experiments

(Friedrich & Haarer, 1986), and it has gained much attraction in high-resolution spectroscopy of biological molecules (Friedrich, 1995). There are also quite a few technical applications, mostly in optical data storage (Moerner, 1988).

JOSEF FRIEDRICH

See also **Nonlinear optics**

Further Reading

Abragam, A. 1961. *Principles of Nuclear Magnetism*, Oxford and New York: Oxford University Press

Bloembergen, N., Purcell, E.M. & Pound, R.V. 1948. Relaxation effects in nuclear magnetic resonance absorption. *Physical Review*, 73: 679–712

Friedrich, J. 1995. Hole burning spectroscopy and physics of proteins. In *Biochemical Spectroscopy*, edited by K. Sauer, San Diego: Academic Press

Friedrich, J. & Haarer, D. 1984. Photochemical hole burning: a spectroscopic study of relaxation processes in polymers and glasses. *Angewandte Chemie*, International Edition, 23: 113–140

Friedrich, J. & Haarer, D. 1986. Structural relaxation processes in polymers and glasses as studied by high resolution optical spectrocopy. In *Optical Spectrocopy of Glasses*, edited by I. Zschokke, Dordrecht: Reidel

Gorokhovskii, A.A., Kaarli, R.K. & Rebane, L.A. 1974. Hole burning in the contour of a purely electronic line in a Shpol'skii system. *JETP Letters*, 20: 216–218

Kharlamov, B.M., Personov, R.I. & Bykovskaya, L.A. 1974. Stable gap in absorption spectra of solid solutions of organic molecules by laser irradiation. *Optics Communications*, 12: 191–193

Moerner, W.E. (editor). 1988. *Persistent Spectral Hole Burning: Science and Application*, Berlin and New York: Springer

HOLONS

In the literature on nonlinear science, the term *holon* has arisen in two quite different senses: as a type of elementary quantum excitation and in the context of emergent biological and social phenomena.

Holons in Physics

In the physics community, holons are particles with zero spin and charge ± 1 (in units of electron charge e) obtained in the fractionalization of an electron or a hole. They are related to the phenomena of spin-charge separation and fractionalization and are the supersymmetric partner of spinons—particles with zero charge and spin $\frac{1}{2}$. Holons and spinons are neither bosons (statistics 0) nor fermions (statistics -1) (statistics α represents the phase that the two-particle wavefunction accumulates when one particle is taken and moved around another), but obey fractional statistics $\frac{1}{2}$ and are, therefore, called semions.

Recently, it has become possible to experimentally realize one-dimensional samples by growing crystals, such as $KCuF_3$, $SrCuO_2$, or Sr_2CuO_3, with strong anisotropy due to antiferromagnetic spin-spin interaction. Photoemission spectroscopy experiments on these crystals show two distinct bands in the energy dispersion, one belonging to the spinon, and the other to the holon. In theory and in experiments, holons have been observed only in one spatial dimension (Kim et al., 1996, 1997; Fujisawa et al., 1998, 1999), with credible efforts to discover them in higher dimensions having remained so far unsuccessful.

The simplest model where holons show up is the supersymmetric t-J model with $1/r^2$ interaction (Kuramoto–Yokohama (KY)-model) (Kuramoto & Yokohama, 1991). This is a system of electrons on a lattice with periodic boundary conditions, where it is forbidden that two electrons be on the same lattice site. Electrons can hop from site to site, there is a Coulomb interaction term, and there are also antiferromagnetic spin-spin interactions. The Hamiltonian is supersymmetric, in the sense that it costs zero energy for a charge to be introduced in the system. The elementary excitations of the system are spinons and holons. The holons have a dispersion relation:

$$E = -\frac{J}{2}\left[\left(\frac{\pi}{2}\right)^2 - q^2\right], \tag{1}$$

where E is the holon energy, q is the holon momentum, and J is an energy scale in the system. The configuration space of positive energy holons is halved with respect to that of an integral particle. Although the equations governing the dynamics of spinons and holons are different, they yield the same form for the interaction between a holon and a spinon and between two spinons. The interaction between the holon and the spinon in one spatial dimension is inversely proportional to the distance between these particles. When the holon and the spinon are at the same point in space, the interaction between them is divergent and together they form the electron. However, the interaction does not diverge fast enough to prevent an instability of the electron toward decay into the two particles, and indeed there is a small but finite matrix element for electron to holon and spinon decay.

An experimentally accessible quantity is the spectral function for a holon-spinon pair:

$$\begin{aligned} A_{\text{holon-spinon}}(\omega, q) = {} & \frac{1}{\pi^2 J q}\sqrt{\frac{J[q+\frac{\pi}{2}]^2 - \omega}{\omega - J[q-\frac{\pi}{2}]^2}} \\ & \times \Theta\left[\omega - J[q-\frac{\pi}{2}]^2\right] \\ & \Theta\left[J[\frac{\pi^2}{4} + q(\pi - q)] - \omega\right], \end{aligned} \tag{2}$$

where ω and q are the energy and momentum at which the measurements are being conducted and J is the relevant energy scale in the system. The

physical consequence of these measurements is the proof of instability of the electron, which is no longer a legitimate excitation of the system but breaks up into a holon and a spinon (Bernevig et al., 2001, 2002).

Holons in Biological and Social Systems

Biological and social systems are typically organized as hierarchies, in which nonlinear dynamics at each level of the hierarchy leads to the emergence of new dynamic entities that provide a basis for the nonlinear dynamics of the next higher level (Scott, 1995).

A well-known example of such a hierarchy is the structure of a military unit. Thus, an infantry division comprises four regiments, each of which comprises four battalions, which consist of four companies, and so on, up to 15,000 individual riflemen. Similar hierarchical structure is displayed by living organisms—for example, a human being is composed of a collection of organs, and the organs are composed of cells, which are made up of biochemicals (proteins, DNA, etc.), down to our constituent atoms.

In the 1960s, Arthur Koestler proposed the term *holon* to imply a general feature of a biological or social system that has a unique identity, yet is made up of lower-level features that comprise parts of the whole (Koestler, 1968). In this sense, holons are components of complex dynamic systems that are efficient and adaptable to disturbances, both internal and external. For example, you are a holon, as is your liver and each of your skin cells.

Interestingly, the human neocortex seems also to be hierarchically organized into closely interconnected assemblies of neurons that embody the holonic components of complex thought (Scott, 1995, 2002).

BOGDAN A. BERNEVIG

See also **Cell assemblies; Emergence; Hierarchies of nonlinear systems; Quantum field theory**

Further Reading

Bernevig, B.A., Giuliano, D. & Laughlin, R.B. 2001. Spinon attraction in spin-$\frac{1}{2}$ antiferromagnetic spin chains. *Physical Review Letters*, 86: 3392–3395

Bernevig, B.A., Giuliano, D. & Laughlin, R.B. 2002. Coordinate representation of the one-spinon one-holon wave function and spinon-holon interaction. *Physical Review* B, 65: 195112

Fujisawa, H. et al. 1998. Spin-charge separation in single chain compound Sr_2CuO_3 studied by angle resolved photo emission. *Solid State Communications*, 106: 543

Fujisawa, H. et al. 1999. Angle-resolved photoemission study of Sr_2CuO_3. *Physical Review* B, 59: 7358–7361

Kim, C. et al. 1996. Observation of spin-charge separation in one-dimensional $SrCuO_2$. *Physical Review Letters*, 77: 4054

Kim, C. et al. 1997. Separation of spin and charge excitations in one-dimensional $SrCuO_2$. *Physical Review* B, 56: 15,589–15,595

Koestler, A. 1968. *Ghost in the Machine*, New York: Macmillan

Kuramoto, Y. & Yokohama, M. 1991. Exactly soluble supersymmetric t–J-type model with long-range exchange and transfer. *Physical Review Letters*, 67: 1338–1341

Scott, A. 1995. *Stairway to the Mind*, Berlin and New York: Springer

Scott, A. 2002. *Neuroscience: A Mathematical Primer*, Berlin and New York: Springer

HOLSTEIN MODEL

See **Davydov soliton**

HOLSTEIN–PRIMAKOV TRANSFORMATION

See **Spin systems**

HOMEOMORPHISM

See **Maps**

HOMOCLINIC INTERSECTION

See **Phase space**

HOMOCLINIC TRAJECTORY

See **Phase space**

HOPF BIFURCATION

The term *Hopf bifurcation* (also called Poincaré–Andronov–Hopf bifurcation) refers to the local birth or death of a periodic solution (self-excited oscillation) from an equilibrium as a parameter crosses a critical value. It is the simplest bifurcation not just involving equilibria and, therefore, belongs to what is sometimes called dynamic (as opposed to static) bifurcation theory. In a differential equation, a Hopf bifurcation typically occurs when a complex conjugate pair of eigenvalues of the linearized flow at a fixed point becomes purely imaginary. This implies that a Hopf bifurcation can only occur in systems of dimension two or higher.

That a periodic solution should be generated in this event is intuitively clear from Figure 1. When the real parts of the eigenvalues are negative the fixed point is a stable focus (Figure 1(a)); when they cross zero and become positive the fixed point becomes an unstable focus, with orbits spiralling out. But this change of stability is a local change, and the phase portrait sufficiently far from the fixed point will be qualitatively unaffected. If the nonlinearity makes the far flow contracting, then orbits will still be coming in and we expect a periodic orbit to appear

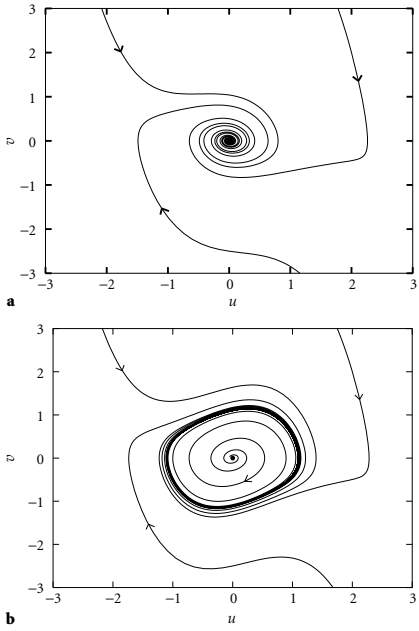

Figure 1. Phase portraits of (2) for (a) $\mu = -0.2$, (b) $\mu = 0.3$. There is a supercritical Hopf bifurcation at $\mu = 0$.

where the near and far flow find a balance (as in Figure 1(b)).

The Hopf bifurcation theorem makes the above precise. Consider the planar system

$$\begin{aligned} \dot{x} &= f_\mu(x, y), \\ \dot{y} &= g_\mu(x, y), \end{aligned} \tag{1}$$

where μ is a parameter. Suppose it has a fixed point that without loss of generality, we may assume to be located at the origin of the (x, y) plane. Let the eigenvalues of the linearized system about this fixed point be given by $\lambda(\mu), \bar{\lambda}(\mu) = \alpha(\mu) \pm \mathrm{i}\beta(\mu)$. Suppose further that for a certain value of μ (which we may assume to be zero), the following conditions are satisfied:

(i) $\alpha(0) = 0, \quad \beta(0) = \omega \neq 0$
(nonhyperbolicity condition: conjugate pair of imaginary eigenvalues);

(ii) $\left.\dfrac{\mathrm{d}\alpha(\mu)}{\mathrm{d}\mu}\right|_{\mu=0} = d \neq 0$
(transversality condition: eigenvalues cross imaginary axis with nonzero speed);

(iii) $a \neq 0$, where

$$\begin{aligned} a = {} & \frac{1}{16}\left(f_{xxx} + f_{xyy} + g_{xxy} + g_{yyy}\right) \\ & + \frac{1}{16\omega}\left(f_{xy}(f_{xx} + f_{yy}) - g_{xy}(g_{xx} + g_{yy})\right. \\ & \left. - f_{xx}g_{xx} + f_{yy}g_{yy}\right), \end{aligned}$$

with $f_{xy} = \left.(\partial^2 f_\mu/\partial x\,\partial y)\right|_{\mu=0}(0, 0)$, etc. (genericity condition).

Then a unique curve of periodic solutions bifurcates from the origin into the region $\mu > 0$ if $ad < 0$ or $\mu < 0$ if $ad > 0$. The origin is a stable fixed point for $\mu > 0$ (resp. $\mu < 0$) and an unstable fixed point for $\mu < 0$ (resp. $\mu > 0$) if $d < 0$ (resp. $d > 0$), while the periodic solutions are stable (resp. unstable) if the origin is unstable (resp. stable) on the side of $\mu = 0$, where the periodic solutions exist. The amplitude of the periodic orbits grows like $\sqrt{|\mu|}$ while their periods tend to $2\pi/|\omega|$ as $|\mu|$ tends to zero. The bifurcation is called "supercritical" if the bifurcating periodic solutions are stable, and "subcritical" if they are unstable.

This two-dimensional version of the Hopf bifurcation theorem was known to Alexandr A. Andronov and his co-workers from around 1930 (Andronov et al., 1966) and had been suggested by Henri Poincaré (1892). Eberhard Hopf (1942) proved the result for arbitrary (finite) dimensions. Through center-manifold reduction, the higher-dimensional version essentially reduces to the planar one provided that apart from the two purely imaginary eigenvalues no other eigenvalues have zero real part. In his proof (which predates the center-manifold theorem), Hopf assumes the functions f_μ and g_μ to be analytic, but C^5 differentiability is sufficient (a proof can be found in Marsden & McCracken (1976)). Extensions exist to infinite-dimensional problems such as differential delay equations and certain classes of partial differential equations (including the Navier–Stokes equations) (e.g., Marsden & McCracken, 1976, Sections 8 and 9).

Example. Consider the oscillator $\ddot{x} - (\mu - x^2)\dot{x} + x = 0$ (an example of a so-called Liénard system), which, with $u = x$, $v = \dot{x}$, we can write as the first-order system

$$\begin{aligned} \dot{u} &= v, \\ \dot{v} &= -u + (\mu - u^2)v. \end{aligned} \tag{2}$$

The origin is a fixed point for each μ, with eigenvalues $\lambda(\mu), \bar{\lambda}(\mu) = \frac{1}{2}\left(\mu \pm \mathrm{i}\sqrt{4 - \mu^2}\right)$. The system has a Hopf bifurcation at $\mu = 0$. We have $d = \frac{1}{2}$ and $a = -\frac{1}{8}$, so the bifurcation is supercritical and there is a stable isolated periodic orbit (limit cycle) if $\mu > 0$ for each sufficiently small μ (see Figure 1).

Hopf Bifurcation for Maps

There is a discrete-time counterpart of the Hopf bifurcation that occurs when a pair of complex conjugate eigenvalues of a map crosses the unit circle. It is slightly more complicated than the version for flows. The corresponding theorem was first proved independently by Naimark (1959) and Sacker (1965), and the bifurcation is, therefore, sometimes called the Naimark–Sacker bifurcation. A proof can again be found in Marsden & McCracken (1976).

Consider the planar map $f_\mu : \mathbb{R}^2 \to \mathbb{R}^2$, with parameter μ, and suppose it has a fixed point that without loss of generality, we may assume to be located at $(x, y) = (0, 0)$. Suppose further that at this fixed point, Df_μ has a complex conjugate pair of eigenvalues $\lambda(\mu), \bar{\lambda}(\mu) = |\lambda(\mu)|e^{\pm i\omega(\mu)}$ and that for a certain value of μ (which we may assume to be 0), the following conditions are satisfied:

(i) $|\lambda(0)| = 1$ (nonhyperbolicity condition: eigenvalues on the unit circle);

(ii) $\lambda^k(0) \neq 1$ for $k = 1, 2, 3, 4$ (nonstrong-resonance condition);

(iii) $$\left.\frac{d|\lambda(\mu)|}{d\mu}\right|_{\mu=0} = d \neq 0$$ (transversality condition);

(iv) $a \neq 0$, where

$$a = -\mathrm{Re}\left[\frac{(1-2e^{ic})e^{-2ic}}{1-e^{ic}}c_{11}c_{20}\right] - \tfrac{1}{2}|c_{11}|^2 - |c_{02}|^2 + \mathrm{Re}(e^{-ic}c_{21}), \qquad c = \omega(0),$$

with

$$c_{20} = \tfrac{1}{8}[(f_{xx} - f_{yy} + 2g_{xy}) + i(g_{xx} - g_{yy} - 2f_{xy})],$$

$$c_{11} = \tfrac{1}{4}[(f_{xx} + f_{yy}) + i(g_{xx} + g_{yy})],$$

$$c_{02} = \tfrac{1}{8}[(f_{xx} - f_{yy} - 2g_{xy}) + i(g_{xx} - g_{yy} + 2f_{xy})],$$

$$c_{21} = \tfrac{1}{16}[(f_{xxx} + f_{xyy} + g_{xxy} + g_{yyy}) + i(g_{xxx} + g_{xyy} - f_{xxy} - f_{yyy})]$$

(genericity condition).

Then an invariant simple closed curve bifurcates into either $\mu > 0$ or $\mu < 0$, depending on the signs of d and a. This invariant circle is attracting if it bifurcates into the region of μ where the origin is unstable (a supercritical bifurcation) and repelling if it bifurcates into the region where the origin is stable (a subcritical bifurcation).

Note that this result says nothing about the dynamics *on* the invariant circle. In fact, the dynamics on the circle has the full complexity of so-called "circle maps" (including the possibility of having attracting periodic orbits on the invariant circle) and depends sensitively on any perturbation (see the example below). Consequently, unlike the Hopf bifurcation for flows, the Hopf bifurcation for maps is not structurally stable.

Example. Consider the following family of maps:

$$f_\mu \begin{pmatrix} x \\ y \end{pmatrix} = (1 + d\mu + a(x^2 + y^2)) \times \begin{pmatrix} \cos(c + b(x^2 + y^2)) & -\sin(c + b(x^2 + y^2)) \\ \sin(c + b(x^2 + y^2)) & \cos(c + b(x^2 + y^2)) \end{pmatrix} \times \begin{pmatrix} x \\ y \end{pmatrix}. \tag{3}$$

The origin $(x, y) = (0, 0)$is a fixed point for each μ. The Jacobian matrix of f_μ at this fixed point is

$$Df_\mu(0, 0) = (1 + d\mu) \begin{pmatrix} \cos c & -\sin c \\ \sin c & \cos c \end{pmatrix} \tag{4}$$

and the eigenvalues are $\lambda(\mu), \bar{\lambda}(\mu) = (1 + d\mu)e^{\pm ic}$. The map takes a simpler, semi-decoupled form in polar coordinates $r = \sqrt{x^2 + y^2}$, $\theta = \arctan(y/x)$:

$$\begin{pmatrix} r \\ \theta \end{pmatrix} \mapsto \begin{pmatrix} r(1 + d\mu + ar^2) \\ \theta + c + br^2 \end{pmatrix}. \tag{5}$$

This five-parameter map is in fact the *normal form* for the Hopf bifurcation up to cubic terms (i.e., by a smooth change of coordinates, we can bring any f_μ into this form (plus higher-order terms)). The parameters a, c, and d in (3) and (5) are precisely those defined in the conditions above. We choose $a = -0.02$, $b = c = 0.1$, $d = 0.2$. The map then undergoes a supercritical Hopf bifurcation at $\mu = 0$, as can be confirmed by a simple graphical analysis of the decoupled r map (for $a > 0$, it would be subcritical). For sufficiently small $\mu > 0$, we have an attracting invariant circle given by $r = \sqrt{-d\mu/a}$ (see Figure 2). On the circle the map is given by $\theta \mapsto \theta + c - bd\mu/a$. This is simply a rotation through a fixed angle $\phi = c - bd\mu/a$, giving periodic orbits if $2\pi/\phi \in \mathbb{Q}$, or dense (irrational) orbits if $2\pi/\phi \in \mathbb{R} \setminus \mathbb{Q}$.

If the Hopf bifurcation occurs in a map associated with the return map (Poincaré map) near a periodic orbit of an autonomous flow, then the bifurcation is often called a secondary Hopf bifurcation. In this case, the invariant curve corresponds to an invariant torus because the flow and attracting periodic orbits on the circle correspond to mode-locked periodic motion on the torus, while dense orbits correspond to quasi-periodic motion.

Degenerate Hopf Bifurcations

If one or more of the listed conditions for a Hopf bifurcation are not satisfied (for instance, because of symmetry), one may still have the emergence of a

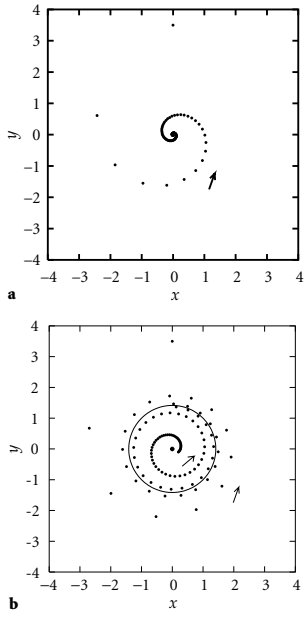

Figure 2. Phase portraits of (3) for (a) $\mu = -0.2$, (b) $\mu = 0.2$. There is a supercritical Hopf bifurcation at $\mu = 0$. ($a = -0.02$, $b = c = 0.1$, $d = 0.2$.)

periodic orbit, but some of the conclusions of the theorem may cease to hold true. The bifurcation is then called a "degenerate Hopf bifurcation." For instance, if the transversality condition is not fulfilled, the fixed point may not change stability, or multiple periodic solutions may bifurcate. An important case is provided by a Hamiltonian system for which complex eigenvalues come in symmetric quadruples, and therefore, the transversality condition cannot be satisfied. This is why the analogous bifurcation in Hamiltonian systems (the so-called "Hamiltonian–Hopf bifurcation" (van der Meer, 1985)) is much more complicated requiring, for one thing, a four-dimensional phase space.

Applications

The balance between local excitation and global damping mentioned above occurs commonly in physical systems. Thus, the Hopf bifurcation underlies many spontaneous oscillations, including airfoil flutter and other wind-induced oscillations (for example, the Tacoma–Narrows bridge collapse) in structural engineering systems, vortex shedding in fluid flow around a solid body at sufficiently high stream velocity, LCR oscillations in electrical circuits, relaxation oscillations (the van der Pol oscillator), the periodic firing of neurons in nervous systems (the FitzHugh–Nagumo equation), oscillations in autocatalytic chemical reactions (the Belousov–Zhabotinsky reaction) as described by the Brusselator and similar models, oscillations in fish populations (as described by Volterra's predator-prey model), and periodic fluctuations in the number of individuals suffering from an infectious disease (as described by epidemic models), among others.

GERT VAN DER HEIJDEN

See also **Bifurcations; Center manifold reduction; Normal forms theory; Phase space; Tacoma Narrows Bridge collapse**

Further Reading

Andronov, A.A., Vitt, A.A. & Khaikin, S.E. 1966. *Theory of Oscillators*, translated from the Russian by F. Immirzi, edited and abridged by W. Fishwick, Oxford: Pergamon Press

Hopf, E. 1942. Abzweigung einer periodischen Lösung von einer stationären Lösung eines Differentialsystems. *Berichten der Mathematisch-Physischen Klasse der Sächsischen Akademie der Wissenschaften zu Leipzig*, XCIV: 1–22. An English translation, with comments, is included as Section 5 in Marsden & McCracken (1976)

Marsden, J.E. & McCracken, M. 1976. *The Hopf Bifurcation and Its Applications*, Berlin and New York: Springer

Naimark, J. 1959. On some cases of periodic motions depending on parameters. *Doklady Akademii Nauk SSSR*, 129: 736–739

Poincaré, H. 1892. *Les Méthodes Nouvelles de la Mécanique Céleste, vol. 1*, Paris: Gauthier-Villars

Sacker, R.S. 1965. On invariant surfaces and bifurcations of periodic solutions of ordinary differential equations. *Communications on Pure and Applied Mathematics*, 18: 717–732

van der Meer, J.C. 1985. *The Hamiltonian Hopf Bifurcation*, Berlin and New York: Springer

HOPFIELD MODEL

See **Cellular nonlinear networks**

HORSESHOES AND HYPERBOLICITY IN DYNAMICAL SYSTEMS

In dynamical systems, *hyperbolicity* refers to the phenomenon in which nearby orbits diverge exponentially fast. It implies instability and sensitive dependence on initial conditions; when occurring on a wide enough scale, it implies *chaos*. This entry surveys and puts into perspective the core ideas in hyperbolic theory, one of the most developed branches in the mathematical theory of dynamical systems today.

For definiteness, we discuss only discrete-time systems, that is, systems generated by the iteration of a map f of a space (usually Euclidean space or a manifold) to itself, leaving analogous results in the continuous-time case to the reader.

Hyperbolic Fixed Points

A linear map $T : \mathbb{R}^n \to \mathbb{R}^n$ is called hyperbolic if none of its eigenvalues lies on the unit circle. A nonlinear map f is said to have a hyperbolic fixed point at p if $f(p) = p$ and $Df(p)$ is a hyperbolic linear map. Thus, there are three kinds of hyperbolic fixed points: attracting (when the moduli of all the eigenvalues of $Df(p)$ are < 1), repelling (when they are all > 1), and saddle type (when some are > 1 and some are < 1). In the saddle case, p has a stable manifold $W^{\mathrm{s}}(p)$ and an unstable manifold $W^{\mathrm{u}}(p)$ consisting of points the orbits of which tend to p in forward and backward time, respectively.

Smale's Horseshoe

Stephen Smale's horseshoe (Smale, 1967) can be seen as a globalization of the idea of a saddle-type fixed point to an invariant set with complicated dynamics. Geometrically, the presence of a horseshoe implies stretching and folding. In terms of orbit types, it implies the existence of random motion as unpredictable as the repeated flipping of a coin (see below).

A version of the horseshoe map is shown in Figure 1: f stretches the square B in the horizontal direction, compresses it in the vertical direction, bends the resulting rectangle into the shape of a horseshoe, and puts it back on top of B as shown. The two shaded vertical strips are mapped onto the two shaded horizontal strips, the union of which is equal to $B \cap f(B)$. Reasoning inductively, we see that after n iterates, $\cap_{i=0}^{n} f^i(B)$ is the union of 2^n disjoint horizontal strips. Iterating backwards as well as forwards, we see that Λ, the set of points that remain in B in all forward and backward times, is the product of two Cantor sets.

If we label the left vertical strip in B "L" and the right one "R" (or "head" and "tail"), then every point x in Λ can be coded into a bi-infinite sequence of L and R where the ith coordinate is L if and only if $f^i x$ is in the left strip. It is easy to see that this defines a one-to-one correspondence between the points in Λ and the set of all possible bi-infinite strings in L and R. An immediate consequence of this coding is that Λ contains many periodic points, one corresponding to each finite block of L and R.

By *horseshoes*, one generally refers to a much larger class of objects than that depicted in Figure 1. The map f is assumed to be invertible, but it does not have to be linear anywhere. There is a box B (or a region B that can be deformed into a box) that is stretched and compressed by f and mapped to a set, which crosses over B finitely many times. Moreover, for points that remain in B, f has well-defined expanding and contracting directions, that is, it is hyperbolic. For an n-dimensional analog of the linear

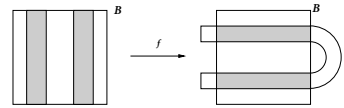

Figure 1. The horseshoe map: f sends the square B to the horseshoe on the right.

model in Figure 1, imagine $B = D_k \times D_{n-k}$, where the "horizontal" direction represents a k-dimensional disk and the "vertical" direction an $(n-k)$-dimensional disk (see also the Smale solenoid picture in the color plate section).

Smale's idea for the horseshoe was influenced by the work of Norman Levinson, who in the late 1940s studied a simplified version of the periodically forced van der Pol equation and proved that the resulting oscillator contains infinitely many periodic orbits with distinct periods. This map was shown to have a horseshoe by M. Levi many years later.

Dynamical complexity near homoclinic orbits was noted by Henri Poincaré. (A homoclinic point is a point in $W^s(p) \cap W^u(p)$ where p is a fixed point of saddle type; *See* **Phase space**.) An important result due to Smale says that transverse homoclinic orbits are always accompanied by horseshoes. Thus, locating transverse, homoclinic points is a means of detecting chaos.

Finally, while the presence of horseshoes implies the existence of chaotic behavior, it should be pointed out that from the probabilistic or observational point of view, this may be transient chaos. The reasons are as follows. Horseshoes have Lebesgue measure zero. It is possible to have a horseshoe Λ and at the same time for the orbit of almost every point to go to a stable equilibrium. In such a scenario, a typical orbit may come near Λ, spend some time near Λ mimicking its orbits, before it heads for its eventual destination. An experimenter tracking this orbit will observe chaotic behavior but only for a finite time period.

Uniform and Non-uniform Hyperbolicity

More general than the idea of a horseshoe is that of a uniformly hyperbolic invariant set. Let f be a smooth invertible map. A compact f-invariant set Λ is called uniformly hyperbolic if everywhere on Λ, the tangent space splits into Df-invariant subspaces $E^{\mathrm{u}} \oplus E^{\mathrm{s}}$, with $\|Df(v)\| > \|v\|$ for $v \in E^{\mathrm{u}}$, $\|Df(v)\| < \|v\|$ for $v \in E^{\mathrm{s}}$, $v \neq 0$. From the 1960s to 1970s, a detailed theory was developed for a class of dynamical systems that are uniformly hyperbolic either on their entire phase spaces or on certain important invariant sets. This theory is called Axiom A theory or uniform hyperbolic theory.

A weaker form of hyperbolicity was introduced in the 1970s. The setting here consists of a pair (f, μ) where f is a map and μ is an f-invariant Borel probability measure. Oseledec's multiplicative

ergodic theorem says that at μ-almost every x, the limit $\lim_{n\to\infty} \frac{1}{n} \log \|Df^n(x)v\| = \lambda(x, v)$ exists for every tangent vector v. These asymptotic growth rates are called *Lyapunov exponents*. The pair (f, μ) is said to be non-uniformly hyperbolic if there is a positive measure set of x such that $\lambda(x, v) > 0$ for some v and < 0 for other v; that is, there is some expansion and some contraction. Pesin's paper (Pesin, 1977) helped launch a systematic study of these systems. The hyperbolicity here is non-uniform in the sense that there may be points that take arbitrarily long for the expanding and contracting behaviors to manifest themselves. Indeed, on a set of μ-measure zero, the limit above may not exist.

We put into perspective the ideas introduced: Horseshoes are examples of uniformly hyperbolic sets. They occur widely, and their occurrence does not preclude other types of dynamical behaviors. Axiom A is a more stringent condition; it requires that all important parts of the phase space be uniformly hyperbolic. This idealized picture excludes many real-life examples; at the same time it has permitted the development of a rich and extensive theory, one that is useful beyond Axiom A. As for the relation between uniform and non-uniform settings, the latter is clearly more flexible and therefore larger in scope. But the contexts are not identical: the properties of (f, μ) depend on μ, and most maps have many invariant measures. Not all invariant measures are equally important, however (*See* **Sinai–Ruelle–Bowen measures**). To complete this circle of ideas, we mention the following result of Katok: if a non-uniformly hyperbolic system has positive entropy and no zero Lyapunov exponents, then nearly all of its entropy is carried by horseshoes.

For more on uniform hyperbolic theory, *See* **Anosov and Axiom-A systems**.

Highlights from General Non-uniform Theory

The results below are very general. They hold for *all* invertible maps f (for which both f and f^{-1} are twice continuously differentiable) acting on compact domains in finite dimensions. For more detailed expositions, see Eckmann and Ruelle (1985) and Young (1993).

(1) *Local nonlinear theory* (Pesin, 1977): It is shown that corresponding to negative and positive Lyapunov exponents are measurable families of local stable and unstable manifolds.

(2) *Structure of conservative systems*, that is, when μ has a density (Pesin, 1977): Assume there are no zero Lyapunov exponents. Then the phase space is made up of at most countably many ergodic components, each one of which is, up to a permutation of sets, mixing.

(3) *Relation among entropy, Lyapunov exponents, and dimension*: For conservative systems, there is the following entropy formula (Pesin, 1997):

$$h_\mu(f) = \int \sum_{\lambda_i > 0} \lambda_i m_i \, d\mu.$$

Here $h_\mu(f)$ is Kolmogorov–Sinai entropy, and the λ_i are distinct Lyapunov exponents with multiplicity m_i. In general, i.e. for arbitrary invariant measures, "=" in the formula above is replaced by "$\leq$" (Ruelle, 1978), and dimension enters to give the following equalities (Ledrappier-Young, 1985):

$$h_\mu(f) = \int \sum_{\lambda_i > 0} \lambda_i \delta_i \, d\mu = -\int \sum_{\lambda_i < 0} \lambda_i \delta_i \, d\mu.$$

Here δ_i is a notion of *partial dimension*; it gives the dimension of μ in the direction of the subspace of vectors whose growth rates are equal to λ_i; in particular $0 \leq \delta_i \leq m_i$. Together the results in (3) express the following two basic principles: randomness is created entirely from expansion; and dissipation can be measured in "wasted" expansion, that is, by the gap in Ruelle's inequality or, equivalently, by the dimensions of the invariant measure.

(4) *Sinai–Ruelle–Bowen (SRB) measures*: A special invariant measure (to play the role of volume) has been identified for dissipative systems with strange attractors (*See* **Sinai–Ruelle–Bowen measures**).

Examples

A large number of dynamical systems are believed to fit into the framework of non-uniform hyperbolic theory, but relatively few (that are not uniformly hyperbolic) have been rigorously studied. This is due in part to technical difficulties in proving the positivity of Lyapunov exponents in the absence of invariant cones (*See* **Lyapunov exponents**). Among the systems successfully analyzed, the most prominent are (1) Billiards flows, both scattering billiards (including the periodic Lorentz gas) and some focusing billiards (including the stadium), and geodesic flows on manifolds of nonpositive curvature. These systems are conservative and have natural invariant measures. (2) One-dimensional maps (such as the logistic family) and a class of attractors with one direction of instability (including the Hénon maps). For these maps, μ either has a density or is an SRB measure.

LAI-SANG YOUNG

See also **Anosov and Axiom-A systems; Chaotic dynamics; Lyapunov exponents; Sinai–Ruelle–Bowen measures**

Further Reading

Eckmann, J.-P. & Ruelle, D. 1985. Ergodic theory of chaos and strange attractors. *Reviews of Modern Physics*, 57: 617–656

Guckenheimer, J. & Holmes, P. 1983. *Nonlinear Oscillations, Dynamical Systems, and Bifurcations of Vector Fields*, New York: Springer

Pesin, Ya.B. 1977. Characteristic Lyapunov exponents and smooth ergodic theory. *Russian Mathematics Surveys*, 32: 55–114

Smale, S. 1967. Differentiable dynamical systems. *Bulletin of the American Mathematical Society*, 73: 747–817

Young, L.-S. 1993. Ergodic theory of differentiable dynamical systems. In *Proceedings of the NATO Advanced Study Institute, Hillerød, June 20–July 2, 1993*, edited by B. Branner & P. Hjorth, Dordrecht: Kluwer

Young, L.-S. 1999. Ergodic theory of chaotic dynamical systems. In *Proceedings of the 12th International Congress of Mathematics and physics, Brisbane, Australia, 1997*, International Press, pp. 131–143

Figure 1. Satellite view of Hurricane Andrew (1992), 25 August 1992 at 20:20 UT. Courtesy of National Oceanic and Atmospheric Administration.

HURRICANES AND TORNADOES

As examples of nonlinear emergent structures, hurricanes and tornadoes are both violent and destructive atmospheric storms, albeit of different scales: a hurricane is much larger than a tornado and lives longer. The word *hurricane* derives from the Spanish word *huracan* which, in turn, stems from the Caribbean name for the god of evil; *tornado* is a variant of the Spanish *tronada* for thunderstorm. Both are associated with very strong winds circling around a center, called the eye, which is the calmest region of the storm with the lowest pressure.

Due to the Coriolis force (which stems from the Earth's rotation), hurricane winds spiral around the eye in a counter-clockwise direction in the Northern Hemisphere, whereas in the Southern Hemisphere the opposite is true. The term *hurricane* is often restricted to storms occurring in the North Atlantic Ocean; the same phenomenon over the West Pacific Ocean is called a typhoon, and in the South Pacific, a cyclone. For simplicity, in what follows, the term *hurricane* is used for the entire phenomenon.

A hurricane forms as a tropical cyclone in areas over warm ocean waters (at temperatures over 26.5°C) under a number of other preconditions such as a moist atmosphere with a sufficiently strong vertical temperature gradient, and latitudes exceeding approximately 8° from the equator (the latter condition provides sufficient Coriolis force to create a wind rotation). Its energy source is associated with latent heat release. The low-pressure center takes in thermal energy and moisture from the ocean surface, the warm air ascends because of convection, and the higher pressure in the cold upper levels of the atmosphere pushes it outward. When the warm air ascends it cools and the temperature of the air may fall below its dew point, releasing water vapor that is able to condense into water droplets. The condensation releases heat that in turn warms the air, increasing its ascent; at this stage the storm works as a self-sustaining heat engine. When the wind speed exceeds 74 mph (119 km h^{-1}), the tropical cyclone is classified as a hurricane. In some hurricanes wind speeds reach over 280 km h^{-1}. A mature hurricane is nearly circularly symmetrical (see Figure 1) and is moved by the airstreams in which it is embedded.

Figure 2. Photo of a tornado in Seymour, Texas (1979). Courtesy of National Oceanic and Atmospheric Administration.

A tornado is a dark, funnel-shaped cloud containing violently rotating air that extends downward to the Earth (Figure 2). It is often accompanied by lightning and a roaring sound. Although it is not yet completely known how tornadoes form, the mechanism of tornado formation is presently attributed to mechanical and thermodynamical processes (the role of atmospheric electricity is disputable). Tornadoes are formed within massive and powerful storms called supercells. The supercells develop inside cumulonimbus clouds, which owe their name to the Latin *cumulus*, meaning mound or heap, and *nimbus*, which refers to rain. Cumulonimbus clouds may reach up to 18 km into the stratosphere, where the distinctive anvil-shaped top of a cloud

consisting of ice crystals is formed. Cumulonimbus clouds often form along a squall line (a wall of clouds and harsh weather often associated with a cold front) where, as a result of convective instability, a supercell is generated.

Once a supercell storm is formed, wind shear creates a mesocyclone, a region of rotating updrafts within a mature thunderstorm. Eventually, the mesocyclone reaches below the cumulonimbus cloud, whereupon it is considered a tornado cyclone. As air is pulled into the tornado cyclone, the water vapor condenses into a visible funnel cloud. When the latter touches the surface of the Earth, it is finally considered a full-fledged tornado. As time goes on, the tornado takes on a brownish color because of the dirt and debris it has drawn in. This whole process is termed the organizational stage, which leads to the mature stage when the tornado is at its largest and strongest. Eventually, when its source of warm, humid air is gone, the tornado begins to degenerate. This occurs when the atmosphere is finally stabilized due to convective processes. The tornado enters a shrinking stage and begins gradually weakening as it loses fuel. The funnel decreases to a thin column and becomes fragmented and disorganized in the decaying stage, although it may still remain destructive.

Hurricanes and tornadoes are destructive atmospheric phenomena, and not only because of strong winds. Since both hurricanes and tornadoes are storms, they are typically associated with excessive rainfall that can cause flooding. Another side effect of a hurricane is the so-called storm surge, which occurs when the ocean rises above its normal tide level. In fact, a hurricane can cause even more damage through storm surge than through strong winds. Still another potential side effect is the formation of tornadoes by thunderstorms embedded in the rainbands of a hurricane.

Both hurricanes and tornadoes are categorized by their wind speeds, from weak to devastating or violent, under the Saffir–Simpson scale for hurricanes and the Fujita–Pearson scale for tornadoes. While a hurricane can be hundreds of kilometers in diameter, the diameter of an average tornado is approximately 400 m. Tornadoes generally last from several minutes to several hours, and they travel up to several hundred kilometers before dying, whereas hurricanes last for several days and travel much greater distances. In the United States, about six hurricanes and 600 tornadoes are reported in an average year.

Some typical parameters of hurricanes and tornadoes are given in Table 1.

	Hurricanes	Tornadoes
Wind speed (kph)	119–300	60–over 500
Diameter	200–1300 km	few m–1.5 km
Lifetime	1–30 days	1–180 min

Table 1. Some parameters of hurricanes and tornadoes (by order of magnitude).

Since 1950, hurricanes have been given human names, such as Betty or George. Each year a new list of names is made, with male and female names alternating alphabetically, and the lists are reused every six years. Examples of exceptionally deadly hurricanes are the one that occurred in the Bay of Bengal in 1737, which claimed about 300,000 lives, many lost to the huge sea waves; and an 1881 typhoon in China with a similar death toll. More recent examples include the typhoon Vera (1959) that struck central Japan, causing over 5000 deaths and destroying about 40,000 homes; the hurricane Flora (1963), which presumably killed more than 6000 people in the Caribbean area, and Camille (1969), with 256 casualties and over 5 billion dollars of damage in the southern United States. The most destructive United States hurricane of record was hurricane Andrew. It blasted its way across south Florida on August 24, 1992; Louisiana and the Bahamas were also impacted. The hurricane caused 26.5 billion dollars in damage in the United States, mainly due to the winds.

Regarding tornadoes in the United States, extremely destructive was the Tri-State Tornado of 1925, which killed 689 people and injured nearly 2000. In the United States, tornadoes are most prevalent in "Tornado Alley," a group of central plains states. Since the terrain there is relatively flat, warm air coming up from the Gulf of Mexico and cold air coming down from Canada often clash, to form some of the most fertile tornado-producing storms in the world. One such tornado hit central Oklahoma in May 1999. Actually, it was a tornado outbreak—a collection of tornadoes all striking at the same time in the same general area. More than 70 tornadoes were observed in the region of Kansas, Oklahoma, and Texas. They caused 40 deaths and injured 675 people, with total damages estimated at 1.2 billion dollars.

From the physical viewpoint, hurricanes and tornadoes are examples of environmental vorticity, requiring interdisciplinary, nonlinear studies for their comprehension. Appropriate mathematical models comprise a set of nonlinear hydrodynamic and thermodynamic equations, and for hurricanes it is crucial to account for the Earth's rotation through the Coriolis force. Although a wide network of meteorological stations exists and available models provide some useful insights, the detailed modeling and prediction of hurricanes and tornadoes remains an

exciting challenge for future practitioners of nonlinear science.

LEV OSTROVSKY AND MASHA SVERDLOV

See also **Atmospheric and ocean sciences; General circulation models of the atmosphere; Vortex dynamics of fluids**

Further Reading

Elsner, J. & Birol Kara, A. 1999. *Hurricanes of the North Atlantic*, Oxford and New York: Oxford University Press

Grazulis, T. 2001. *The Tornado: Nature's Ultimate Windstorm*, Norman: University of Oklahoma Press

Longshore, D. 1998. *Encyclopedia of Hurricanes, Typhoons, and Cyclones*, New York: Facts on File

Pielke, R., Jr. & Pielke, R., Sr. 1997. *Hurricanes: Their Nature and Impacts on Society*, New York: Wiley

Tufty, B. 1987. *1001 Questions Answered about Hurricanes, Tornadoes, and Other Natural Air Disasters*, New York: Dover

HUYGENS PRINCIPLE

Huygens principle (HP) is a notion that goes back to the classical *Traité de la Lumière* (Treatise on Light) by Christiaan Huygens, which was published in 1690. In its original meaning, HP gives the following geometric description of the wave fronts. Consider a wave front at the moment t as the source of the new (secondary) waves emanating from points of this front. HP states that the new wave front at a later time is the envelope of the fronts of these secondary waves (see Figure 1). This principle was further elaborated by Augustin Fresnel who added the superposition principle for the amplitudes of the secondary waves to explain the phenomenon of diffraction.

In the second half of the 19th century, various mathematical aspects of the HP were discussed in the pioneering works of Gustav Kirchhoff, Eugenio Beltrami, and Vito Volterra. At the same time it, became evident that different authors were using the term *Huygens principle* with different meanings. It was Jacques Hadamard who brought clarity in this area. In his fundamental "Lectures on Cauchy's Problem" published in 1923, Hadamard introduced the notion of the "Huygens principle in the narrow sense" (minor premise) (Hadamard, 1923). In physical language one can formulate this principle in the following way: *an instantaneous signal remains instantaneous for every observer at each later time*. This property implies that a localized disturbance will have an effect localized in time at any point (for example, for sound waves after some time there will be complete silence).

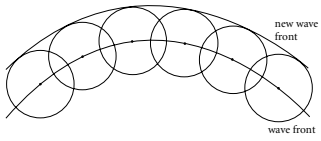

Figure 1. Diagram related to Huygens' principle.

Mathematically, HP in the narrow sense means that the fundamental solution of the corresponding hyperbolic equation vanishes not only outside but also inside the characteristic conoid and, thus, must be located on it. Equivalently, a hyperbolic equation satisfies the HP in the narrow sense if the solution of the Cauchy initial-value problem at a point P depends not on all the Cauchy data, but only on its part on the intersection of the characteristic conoid with vertex P with the Cauchy surface.

In contrast to the original principle ("major premise" in Hadamard's terminology), which holds for a general class of wave propagations, HP in the narrow sense is actually a remarkable property valid only for very special equations. In particular, this never happens in two dimensions, where one has wave diffusion. One can see this when a pebble falls in water, where the front wave is followed by the so-called "residual waves," and any object on the water surface is hit by the subsequent waves many times.

To explain this phenomenon, consider the fundamental solution of the wave equation

$$\left(\frac{\partial^2}{\partial t^2} - \frac{\partial^2}{\partial x_1^2} - \cdots - \frac{\partial^2}{\partial x_n^2}\right)\Phi = 0,$$

$$\Phi(x,0) = 0, \quad \frac{\partial \Phi}{\partial t}(x,0) = \delta(x).$$

This solution has the form

$$\Phi = \frac{1}{2\pi}\frac{\theta(t^2 - |x|^2)}{\sqrt{t^2 - |x|^2}}$$

when $n = 2$, and

$$\Phi = \frac{1}{2\pi}\delta(t^2 - |x|^2)$$

when $n = 3$. Here θ is the Heaviside step-like function and δ is the Dirac delta-function. Thus, we see that indeed for $n = 3$, Φ is located on the characteristic cone $t^2 - |x|^2 = 0$, which explains the sharpness of signal transmission in our three-dimensional world, while in two dimensions this is not the case.

Corresponding formulas for the solutions of the Cauchy problem for the wave equation in two and three spatial dimensions were found by Simeon Poisson and Kirchhoff, and for general n by Orazio Tedone. From these formulas it follows that for the Euclidean spaces, the HP in the narrow sense holds in all odd dimensions starting from 3 and never holds in even dimensions.

Hadamard raised the question of how to describe all second-order hyperbolic equations that satisfy the HP in the narrow sense (*Hadamard's problem*). Hadamard found a criterion for this, but it was not effective enough to answer this question. There was a common belief

that the HP in the narrow sense holds only for the wave equations in the Euclidean spaces of odd dimensions until 1953 when Karl Stellmacher found other examples (Stellmacher, 1953). He showed that the hyperbolic equation

$$\left(\frac{\partial^2}{\partial t^2} - \frac{\partial^2}{\partial x_1^2} - \cdots - \frac{\partial^2}{\partial x_n^2} + \frac{m(m+1)}{x_1^2}\right)\phi = 0$$

with integer nonnegative m satisfies the HP in the narrow sense if the dimension n is odd and large enough: $n \geq 2m+3$.

Later in 1967–68, Stellmacher and Lagnese solved the Hadamard problem in the class of the hyperbolic equations of the special form

$$\left(\frac{\partial^2}{\partial t^2} - \frac{\partial^2}{\partial x_1^2} - \cdots - \frac{\partial^2}{\partial x_n^2} + u(x_1)\right)\phi = 0,$$

when the potential depends only on one of the coordinates. They showed that the corresponding potentials are rational and (in modern terminology) can be described as the results of the Darboux transformations applied to $u = 0$ (Lagnese & Stellmacher, 1967).

The first examples of the Huygensian potentials $u(x)$ depending on more than one coordinate were found in 1993 by Berest and Veselov, who discovered a close relation of the Hadamard problem with the theory of quantum integrable systems of Calogero–Moser type (Berest & Veselov, 1994; Chalykh et al., 1999).

For the hyperbolic equations on the manifolds with nontrivial metrics, the Hadamard problem is still open even when the number of spatial variables is three. There are known only several particular cases when HP in the narrow sense is satisfied, including the modified wave equation on the symmetric spaces with even multiplicities, in particular on the spheres (Lax & Phillips, 1978) and simple compact Lie groups (Helgason, 1984), and wave equations on the spaces with the plane wave metrics (Günther, 1965). For a review of the results on the HP for other relativistic wave equations (e.g., Maxwell's equations), see Günther (1988).

Because the HP in the narrow sense is a very rare phenomenon, it is natural to ask about a weaker version. Such a version called the "generalized Huygens' principle" was introduced by Lax and Courant and is valid for a general hyperbolic equation. It states that the singularities of the solution at the point P depend only on the singularities of the initial data and only so far as these data are presented on the characteristic conoid of P. This implies that "in an approximate, and for that matter, usually satisfactory, sense any hyperbolic system does preserve the sharp signals, though in general slightly blurred" (Courant & Hilbert, 1962).

Finally, one should mention that the theory of HP is closely related to the deep theory of lacunae in the domains of dependence of hyperbolic equations (Petrovskii, 1945; Atiyah et al., 1970, 1973).

ALEXANDER P. VESELOV

See also **Characteristics; Darboux transformation; Generalized functions; Gravitational waves; Quantum nonlinearity**

Further Reading

Atiyah, M., Bott, R. & Gårding L. 1970 and 1973. Lacunae for hyperbolic differential equations with constant coefficients. *Acta Mathematica,* 124: 109–89 and 131: 145–206

Berest, Yu.Yu. & Veselov, A.P. 1994. Huygens' principle and integrability. *Russian Mathematical Surveys*, 49(6): 5–77

Chalykh, O.A., Feigin, M.V. & Veselov, A.P. 1999. Multidimensional Baker–Akhiezer functions and Huygens' principle. *Communications in Mathematical Physics*, 206: 533–566

Courant, R. & Hilbert, D. 1962. *Methods of Mathematical Physics*, New York: Interscience Publishers

Günther, P. 1965. Ein Beispiel einer nichttrivialen Huygensschen Differentialgleichung mit vier unabhängigen Variablen. *Archive for Rational Mechanics and Analysis*, 18: 103–106

Günther, P. 1988. *Huygens' Principle and Hyperbolic Equations*, Boston: Academic Press

Hadamard, J. 1923. *Lectures on Cauchy's Problem in Linear Partial Differential Equations*, New Haven: Yale University Press

Helgason, S. 1984. Wave equations on homogeneous spaces. *Lecture Notes in Mathematics*, 1077: 252–287

Huygens, Ch. 1690. *Traité de la Lumière*, Hague: Pierre vander Aa; as *Treatise on Light*, New York: Dover, 1962, and London: Dawson, 1966

Lagnese, J.E. & Stellmacher, K.L. 1967. A method of generating classes of Huygens' operators. *Journal of Mathematics and Mechanics*, 17: 461–472

Lax, P.D. & Phillips, R.S. 1978. An example of Huygens' principle. *Communications in Pure and Applied Mathematics*, 31: 415–421

Petrovskii, I.G. 1945. On the diffusion of waves and lacunas for hyperbolic equations. *Matematicheskii Sbornik,* 17: 289-370 (Russian) (Also in Petrowsky, I.G. *Selected works.* Part I. Gordon and Breach, London, 1996)

Stellmacher, K.L. 1953. Ein Beispiel einer Huygensschen Differentialgleichung. *Nachrichten der Akademie der Wissenschaften in Goettingen. Mathematisch-physikalisches Klasse,* IIa, 10: 133–138

HYDRAULIC JUMPS

See **Jump phenomena**

HYDRODYNAMIC LIMIT

See **Fluid dynamics**

HYDRODYNAMIC SOLITARY WAVES

See **Water waves**

HYDROGEN BOND

The hydrogen bond is a weak chemical bond, which nevertheless is fundamentally important in stabilizing secondary structure motifs in biological macromolecules such as proteins and DNA. Also, the peculiar properties of liquid water are attributed to a complex hydrogen bond network between neighboring water molecules. A hydrogen bond is mediated by a proton sitting in between two negatively charged atoms, the more negative of which is called the hydrogen bond donor and the other the hydrogen bond acceptor. Figure 1a shows a prototype hydrogen bond, using the N–H and the C=O group of two peptide units in an α-helix as an example (one of the most important secondary structure motif of proteins).

Hydrogen bonding leads to a dramatic distortion of the potential energy surfaces that determine the nuclei positions, giving rise to strongly anharmonic or even double-well potentials. Much of our knowledge about hydrogen bond potentials stems from vibrational spectroscopy, see, for example, Pimentel & McClellan (1976); Hadzi & Bratos (1976); Henri-Rousseau & Blaise (1998). The absorption band of the high-frequency vibration of the donor-proton bond (i.e., the NH bond in the example considered here) changes considerably upon formation of a hydrogen bond. The most evident effects are a strong red-shift with respect to the free group, an intensity increase and band broadening, often accompanied by a peculiar band shape with rich substructure. These effects could be reasonably explained using a model of the electronic (ground state) potential energy surface as a function of two coordinates, the high-frequency N–H stretching coordinate q, and the low-frequency hydrogen bond coordinate Q (see Figure 1a). A Taylor expansion of that potential energy surface yields (Hadzi & Bratos, 1976; Henri-Rousseau & Blaise, 1998)

$$V(Q,q) = \tfrac{1}{2}m\omega^2 q^2 + \tfrac{1}{2}M\Omega^2 Q^2 + \chi' Q q^2 + \cdots, \quad (1)$$

where the first two terms represent the harmonic normal modes of the N–H stretching and the hydrogen bond vibration with oscillation frequencies ω and Ω and effective masses m and M, respectively. Typical vibrational frequencies of N–H stretching modes lie in the range of $\omega = 3000$–$3600\,\mathrm{cm}^{-1}$, while hydrogen bond vibrations are found around $\Omega = 50$–$300\,\mathrm{cm}^{-1}$, depending on the masses of the molecular groups involved. This translates into typical spring constants of $k_{\mathrm{N-H}} \approx 650\,\mathrm{N/m}$ for the N–H bond and $K_{\mathrm{N-O}} \approx 10 - 20\,\mathrm{N/m}$ for the hydrogen bond. In the case of most molecular systems, the harmonic approximation is extremely good, and higher order terms in Equation (1) can be treated as weak perturbation (being responsible, for example, for energy dissipation). Harmonic normal modes have the property to decouple completely. Linear phenomena, such as propagation of linear phonon wave packets, can be fully understood in the harmonic approximation.

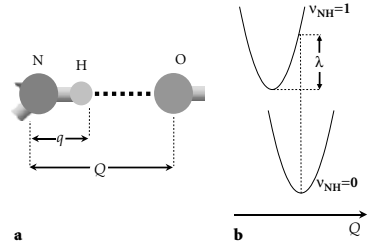

Figure 1. (a) A prototype hydrogen bond. The discussion presented here applies for other hydrogen bonds in essentially the same way. (b) Potential energy surfaces of the $\nu_{\mathrm{NH}} = 0$ and the $\nu_{\mathrm{NH}} = 1$ level.

However, one of the striking features of hydrogen bonds is an extraordinarily large anharmonicity, described by third, and higher, order terms in the expansion Equation (1). This anharmonicity leads to appreciable nonlinear behavior, a property that makes hydrogen-bonded crystals interesting objects to study in nonlinear science.

The problem can be simplified significantly when taking into account the more than one order of magnitude difference in the N–H and the hydrogen bond vibration frequency, allowing an adiabatic separation of timescales to be introduced. This is done in exactly the same way as the Born–Oppenheimer approximation separates off the fast motion of the electrons from the slow motion of the nuclei. In the case of a hydrogen bond, the motion of the fast N–H vibration adiabatically adapts to the position of the coordinate Q of the hydrogen bond. When the coordinate Q is held fixed, one can recast Equation (1) in the form

$$V(Q,q) = \tfrac{1}{2}m\omega_{\mathrm{eff}}^2 q^2 + \tfrac{1}{2}M\Omega^2 Q^2 \quad (2)$$

with

$$\omega_{\mathrm{eff}} \approx \omega + \frac{\chi'}{m\omega} Q \equiv \omega + \chi Q. \quad (3)$$

In this approximation, the vibration frequency of the N–H stretching mode, and hence its excitation energy, varies linearly with the hydrogen bond distance Q. The other third-order term not considered in Equation (1) ($\sim Q^2 q$) leads to a Q-dependent shift of the N–H-bond-length without change of its excitation energy. Such a linear dependence is observed experimentally for a large variety of hydrogen-bonded crystals (Pimentel & McClellan, 1976), which allows direct measurement of the nonlinear coupling constant: $\chi_{\mathrm{N-H}} \approx 500 - 1500\,\mathrm{cm}^{-1}/\mathrm{Å}$ or

$\chi_{N-H} \approx 1-3 \times 10^{-10}$ N. The nonlinear coupling constant varies significantly with hydrogen bond type.

Starting from Equations (2) and (3), one can construct potential energy surfaces (see Figure 1b), leading to the displaced oscillator picture that is well known from electronic Franck–Condon transitions. However, keep in mind that all this is happening on the *electronic ground state* potential surface! Each potential energy surface corresponds to a vibrational excitation level $v_{N-H} = 0, 1, \ldots$ of the N–H stretching mode, and describes the total energy of the system as a function of the hydrogen bond coordinate Q. It is the nonlinear coupling term χ that gives rise to the displacements of the potential energy surfaces. The reorganization energy λ, that is, the energy the system gains by relaxation towards the bottom of excited state potential energy surface after a vertical "Franck–Condon"-like excitation (see Figure 1b), is given by

$$\lambda = \frac{\chi^2}{2M\Omega^2} = \frac{\chi^2}{2K_{N\cdots O}}. \qquad (4)$$

Biological macromolecules, such as proteins and DNA, often form one-dimensional quasicrystals with approximate translational symmetry, whose structures are stabilized by hydrogen bonds. This observation motivated Alexander Davydov to speculate about nonlinear collective phenomena in bio-macromolecules (Davydov, 1979). Davydov discussed only the C=O vibration in a N–H$\cdots$OC-hydrogen bond, which shows the same phenomenon with a smaller, yet still appreciable, nonlinearity $\chi_{CO} \approx 300$ cm^{-1}/Å or $\chi_{CO} \approx 6 \times 10^{-11}$ N (Careri et al., 1984). Dipole–dipole interaction between adjacent C=O and N–H vibrations tends to delocalize the excitation along the crystal, forming a vibrational exciton (vibron). Coupling of the vibron to lattice-deformation modes, mediated through the nonlinearity χ of the hydrogen bonds, subsequently self-localizes the excitation. The hydrogen bond is getting stronger after excitation of the high frequency vibration (see Figure 1b), leading to a contraction of the macromolecular backbone. As a result, solitons and/or polarons may be formed.

PETER HAMM

See also **Color centers; Davydov soliton; Frank–Condon factor**

Further Reading

Careri, G., Buontempo, U., Galluzzi, F., Scott, A.C., Gratton, E. & Shyamsunder, E. 1984. Spectroscopic evidence for Davydov-like solitons in acetanilide *Physical Review* A, 30(8): 4689–4702

Davydov, A.S. 1979. Solitons in molecular systems. *Physica Scripta*, 20: 387–394

Hadzi, D. & Bratos, S. 1976. Vibrational spectroscopy of the hydrogen bond. In *The Hydrogen Bond: Recent Developments in Theory and Experiment*, edited by P. Schuster, G. Zundel & C. Sandorfy, Amsterdam: Elsevier, pp. 565–611

Henri-Rousseau O. & Blaise P. 1978. The infrared spectral density of weak hydrogen bonds within the linear response theory. *Advances in Chemical Physics*, 103: 1–186

Pimentel, G.C. & McClellan, A. 1960. *The Hydrogen Bond*, San Francisco: Freemann

HYDROTHERMAL WAVES

Hydrothermal waves are traveling waves produced by a supercritical instability of the thermocapillary flow of a thin liquid layer with a free surface subjected to a horizontal temperature gradient.

This article presents experiments in one spatial dimension, then gives some indications about the physical basis for wave effects. Extended systems are then considered and applications are described.

Experimental Observation in One Spatial Dimension

Hydrothermal waves were first experimentally observed in hot-wire convection experiments (Vince & Dubois, 1992), and a geometrically simpler system was then imagined by Daviaud & Vince (1993) that led to the first clear experimental observation of hydrothermal waves.

The classical experiment is as follows: a channel whose long sides are thermoregulated copper blocks contains a fluid with free surface. Its typical section is depicted in Figure 1. The horizontal gradient of temperature on the free surface leads to a gradient of surface tension. This results in a stationary flow of the surface from the hot side (low surface tension) toward the cold side (high surface tension): this is the Marangoni effect. Due to mass conservation, there is a return flow in the bottom of the layer. This is the basic thermocapillary flow (Kuhlnan, 1999; Schatz & Neitzel, 2001), the instability of which leads to hydrothermal waves (Smith & Davis, 1983; Davis, 1987). A similar flow is present in the melted wax of a candle (the cold side being the external boundary and the hot side being the wick). For visualization purposes, silicon oil is used because it is transparent and allows shadowgraphy.

For fluid depth h larger than the capillary length λ_c, one observes first when increasing the temperature gradient corotative rolls with their axis parallel to the cold and hot side of the container. Then hydrothermal waves of type 1 (HW1, plane waves) appear on top of the rolls (Figure 2a) (Riley & Neitzel, 1998). HW1 are emitted by "line"-sources that extend over the whole extension between the hot and the cold sides. For smaller depth $h < \lambda_c$, waves of type 2 (HW2) are observed (Figure 2b,c); they are circular and emitted by point sources located on the cold side of the container (Burguete et al., 2001; Garnier & Chiffaudel, 2001).

When the fluid depth is even larger (typically larger than the depth λ_{th} for which thermocapillary

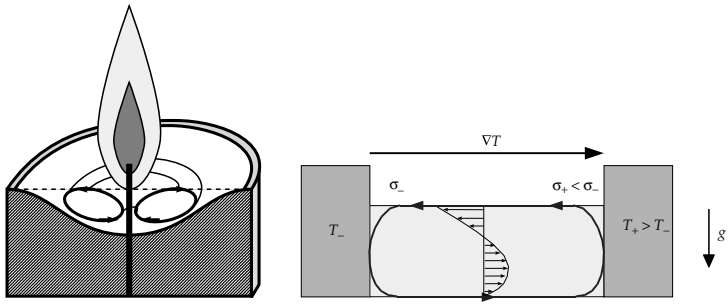

Figure 1. Thermocapillary basic flow created by Marangoni effect and susceptible to instability into hydrothermal waves. Left: the melted wax below the flame of a candle is an example of thermocapillary flow. Right: typical section of a laboratory setup. A horizontal temperature gradient is applied to a thin liquid layer with a free surface. Hydrothermal waves (not drawn) will propagate in the horizontal direction orthogonal to the temperature gradient ∇T, and with a small component along the gradient.

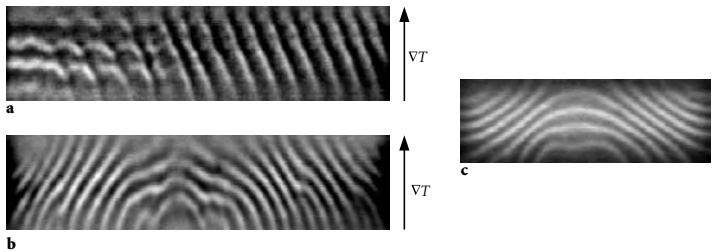

Figure 2. Shadowgraphic images of hydrothermal waves in rectangular cells. (a): $L_x = 30$ mm, $L_y = 180$ mm, $h = 2.75$ mm, $\Delta T = 7$ K. A single right-going wave of type 1 is present. The left side is a source, the amplitude of the wave is weak, and stationary corotative rolls orthogonal to the gradient are present. (b): $L_x = 30$ mm, $L_y = 180$ mm, $h = 1$ mm, $\Delta T = 7.3$ K. (c): $L_x = 30$ mm, $L_y = 90$ mm, $h = 1$ mm, $\Delta T = 5$ K. Hydrothermal waves of type 2, with a source located at the center of the cold side of the channel.

forces balances thermogravity forces), hydrothermal wave instability is replaced by a stationary instability: parallel rolls with axis aligned with the temperature gradient.

Physical Mechanisms

Vertical Temperature Gradient: Bénard–Marangoni Instability

Pearson (1958) gave a simple mechanism to explain hexagon formation in Bénard–Marangoni convection. In that case, the temperature gradient is purely vertical (cold at the surface, and hot at the bottom) and the velocity of the fluid is zero before the instability. Let us consider a positive temperature perturbation at the surface of the fluid: a point has a temperature larger than its surroundings. Because surface tension decreases with temperature for simple fluids, the surface tension is smaller at that point. This implies a differential stress on the free surface, and according to the equations of motion, the fluid has to flow away from that point (fluids flow from regions of small surface tension toward regions of large surface tension). But due to mass conservation, some fluid must rise up from the bulk of the fluid to the point on the surface (in the same way that wax climbs around the wick and flows away on the surface towards cooler regions). This ascending fluid is at a higher temperature because of the vertical temperature gradient. In conclusion, any positive temperature perturbation at the free surface is amplified; this means that there is an instability, namely, the Bénard–Marangoni instability into stationary hexagons, as can be shown by a linear stability analysis.

Horizontal Temperature Gradient: Hydrothermal Waves

Basically, the mechanism is the same, but one has to take into account, first, that the basic flow has

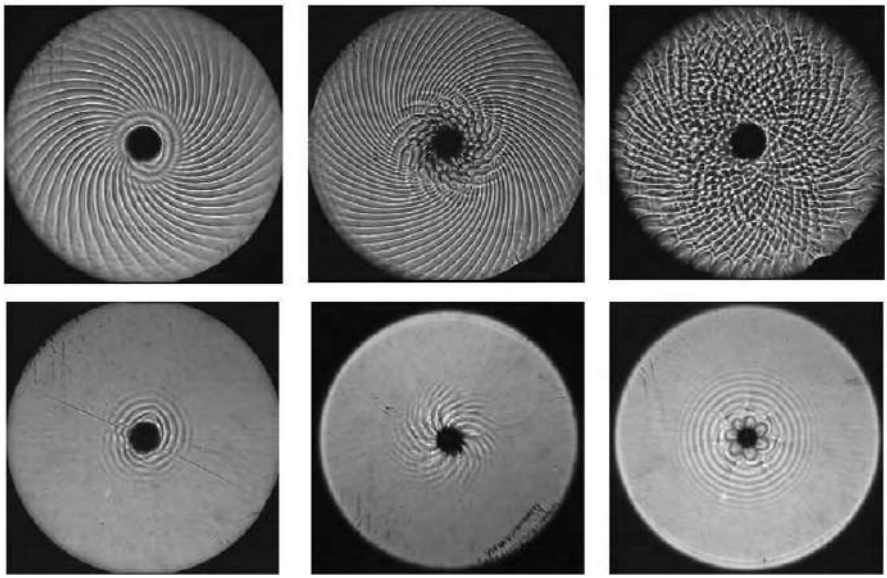

Figure 3. Top three pictures: extended patterns: single HW1 ($h = 1.9$ mm, $\Delta T = 14.25$ K), HW1 and HW2 together ($h = 1.2$ mm, $\Delta T = 20$ K), turbulent HW1 ($h = 1.9$ mm, $\Delta T = 25$ K). Bottom three pictures: localized patterns: HW2 ($h = 1.2$ mm, $\Delta T = 10$ K), inverted spirals ($h = 1.2$ mm, $\Delta T = -9$ K), and flowers ($h = 1.9$ mm, $\Delta T = -7$ K).

a finite velocity (see Figure 1), and second, that the vertical temperature profile is nonmonotonous. This intricacy results in a time-dependent pattern, in contrast to the stationary hexagons described above. Time-dependence is due to the existence of two different timescales: one for the relaxation of thermal perturbations (depending on the thermal diffusion coefficient) and the other for the relaxation of velocity perturbations (depending on kinematic viscosity). The ratio of those two timescales is called the Prandtl number, Pr.

Smith (1988) expressed two different tentative mechanisms depending on Pr in the limit cases of a flow dominated by inertial effects ($\mathrm{Pr} \to 0$) or by viscous effects ($\mathrm{Pr} \to \infty$). The relaxation of temperature and velocity perturbations then occur on very different timescales. Depending on the signs of the temperature and velocity gradients, an oscillatory behavior is shown to be unstable and to propagate along the horizontal temperature gradient (small Pr), or perpendicularly to it (large Pr).

Finally, note that hydrothermal waves are not necessarily associated with surface deflections (in contrast to gravity waves for example): they are an instability mode of the temperature field in the bulk (Pelacho & Burguete, 1999).

Experiments in 2-d

Recent experiments in extended geometries (the two horizontal dimensions are large compared to the fluid height) revealed a large variety of hydrothermal waves instability modes. Several of these obtained in cylindrical geometry (the candle geometry) are reproduced in Figure 3. The control parameter is defined as $\Delta T = T_{\mathrm{ext}} - T_{\mathrm{int}}$. This quantity can be positive or negative, and both cases are not equivalent. This is due to the presence of curvature (Garnier & Normand, 2001) that may also localize patterns near the center.

Applications

Many technological applications in which the Marangoni effect is present will involve hydrothermal waves—even when manufacturing is carried out in low gravity, where gravity-dependent, buoyancy-driven flow is reduced, for example, floating zone purification of silicon crystals, photographic films production, and melting of metals. In all of these processes, the aim is to avoid hydrothermal waves, which are detrimental to the final product, for example, by reducing the homogeneity of crystals.

In the physics laboratory, hydrothermal waves represent an ideal experimental nonlinear waves system. They are well modeled by a complex Ginzburg–Landau equation (Garnier et al., 2003) and can be used as a robust model for the study of the transition to spatiotemporal chaos. For example, as their group velocity is finite, they are subject to the convective/absolute distinction. Modulated amplitude waves have also been reported.

NICOLAS GARNIER AND ARNAUD CHIFFAUDEL

See also **Candle; Complex Ginzburg–Landau equation; Fluid dynamics; Thermo-diffusion effects**

Further Reading

Burguete, J., et al. 2001. Buoyant-thermocapillary instabilities in extended liquid layers subjected to a horizontal temperature gradient. *Physics of Fluids*, 13: 2773–2787

Daviaud, F. & Vince, J-M. 1993. Traveling waves in a fluid layer subjected to a horizontal temperature gradient. *Physical Review* E, 48: 4432–4436

Davis, S.H. 1987. Thermocapillary Instabilities. *Annual Reviews of Fluid Mechanics*, 19: 403–435

Garnier, N. & Chiffaudel, A. 2001. Two dimensional hydrothermal waves in an extended cylindrical vessel. *European Journal of Physics* B, 19: 87–95

Garnier, N. & Normand, C. 2001. Effects of curvature on hydrothermal waves instability of radial thermocapillary flows. *Comptes Rendus de l'Academie des Sciences, Series IV*, 2(8): 1227–1233

Garnier, N., et al. 2003. Nonlinear dynamics of waves and modulated waves in 1D thermocapillary flows. I. General presentation and periodic solutions. *Physica* D, 174: 1–29

Kuhlman, D. 1999. *Thermocapillary Flows*, New York: Springer

Pearson, J.R. 1958. On convection cells induced by surface tension. *Journal of Fluid Mechanics*, 4: 489–500

Pelacho, M.A. & Burguete, J. 1999. Temperature oscillations of hydrothermal waves in thermocapillary-buoyancy convection. *Physical Review* E, 59: 835–840

Riley, R.J. & Neitzel, G.P. 1998. Instability of thermocapillary–buoyancy convection in shallow layers. Part 1. Characterization of steady and oscillatory instabilities. *Journal of Fluid Mechanics*, 359: 143–164

Schatz, M.F. & Neitzel, G.P. 2001. Experiments on thermocapillary instabilities. *Annual Reviews of Fluid Mechanics*, 33: 93–127

Smith, M.K. 1986. Instabilty mechanisms in dynamic thermocapillary liquid layers. *Physics of Fluids*, 29: 3182–3186

Smith, M.K. & Davis, S.H. 1983. Saturation of Rayleigh-Taylor instability. *Journal of Fluid Mechanics*, 132: 119–144 and 132: 145–162

Vince, J-M. & Dubois, M. 1992. Hot wire below the free surface of a liquid: Structural and dynamical properties of a secondary instability. *Europhysics Letters*, 20: 505–510

HYPERBOLIC MAPPINGS

See **Maps**

HYPERCHAOS

See **Rössler systems**

HYPERCYCLE

See **Catalytic hypercycle**

HYPERELLEPTIC FUNCTIONS

See **Elliptic functions**

HYSTERESIS

The word *hysteresis* is derived from the Greek where it meant "shortcoming." In the present physical context it describes a retardation effect when the forces acting upon a body are changed. In particular, in magnetism hysteresis represents a lagging in the values of the net magnetization in a magnetic material due to a changing magnetizing field. In general, hysteresis signifies the history of dependence of physical quantities in systems responding to changes in external conditions. The term is most commonly, but not exclusively, applied to magnetic materials; for example, there is a class of metals called shape memory alloys that can be bent or stretched plastically over large distances back and forth many times without hardening.

Consider a ferromagnetic material that is originally unmagnetized. As the external magnetic field (H) is increased, the induced magnetization (M) also increases. The induced magnetization eventually saturates. Now, if the external field is reduced, the induced magnetization also is reduced, but it does not follow the original curve. Instead, the material retains a certain permanent magnetization called the remanent magnetization M_r when $H = 0$. The remanent magnetization is the permanent magnetization that remains after the external field is removed. If the external field is reduced more, the remanent magnetization will eventually be removed. The external field applied in the opposite direction for which the remanent magnetization goes to zero is termed the coercivity H_c. The product of M_r and H_c is termed the strength of the magnet. As the external field continues to reverse, permanent magnetization of the opposite polarity is created in the magnet. A similar curve is traced for the negative direction with saturation, remanent magnetization and coercivity. The hysteresis curve then retraces the previous points as the field cycles, and the shape of the loop after the first cycle is roughly the same as after many cycles. Note that the area under the hysteresis loop corresponds to the work done on the system by an external field that reorients the magnetization in a single cycle.

When an electric field (E) is applied to a ferroelectric crystal, the domains that are favorably oriented with respect to this field grow in size at the expense of those that are misaligned. In addition, favorably oriented domains may nucleate and grow until the whole crystal becomes one domain. The relation between

the resulting polarization P and E is described by a hysteresis loop in analogy to the relationship between M and H for ferromagnets.

Suppose now, in general, that the system under consideration can be described by a macroscopic order parameter η. Under the influence of an external field σ coupled linearly to η, the state of the system is determined by an equation of state that expresses a minimum condition of the associated thermodynamic potential V. Assuming the presence of at least one control parameter leads directly to the problem of catastrophes, an area investigated by René Thom. The cusp catastrophe is described by the potential

$$V(\eta) = \frac{\varepsilon}{4}\eta^4 + \frac{1}{2}a\eta^2 - \sigma\eta, \tag{1}$$

where a is a control parameter. This potential describes second-order phase transitions both in the absence ($\sigma = 0$) and in the presence ($\sigma \neq 0$) of external fields as proposed by Lev Landau. The butterfly catastrophe, on the other hand, is described by

$$V(\eta) = \frac{1}{6}\eta^6 + \frac{a}{4}\eta^4 - \frac{b}{3}\eta^3 + \frac{c}{2}\eta^2 - \sigma\eta \tag{2}$$

and has been used to model first-order phase transitions.

To illustrate the related phenomenon of hysteresis we first investigate the bifurcation effect by minimizing Equation (1), which yields the equation of state

$$\varepsilon\eta^3 + a\eta = \sigma. \tag{3}$$

A transition between a single stable solution for $a > 0$ and a bistable situation for $a < 0$ takes place when $a = 0$. However, a new feature is the phenomenon of external-field-induced hysteresis and metastability. Stability corresponds to a solution for which $\partial^2 V/\partial\eta^2 > 0$ and, if more than one solution of the equation of state exists that is stable, we call the higher energy solutions metastable. Figure 1 shows the difference in the response of the order parameter to the application of an external field. In unistable situations, η as a function of σ is a smooth single-valued function. Multistability results in multi-valuedness in some ranges of the external fields. Figure 1c demonstrates the regions of multistability in the parameter space. The dividing line in the cusp catastrophe case is given by the equation

$$-4a^3 + 27\sigma^2 = 0. \tag{4}$$

This indicates the parameter set for which a triple solution of the cubic equation in (4) is obtained. Figure 2 is an extension of these concepts to the butterfly catastrophe case that exhibits thermal hysteresis (if the control parameter a involves a temperature dependence) and a double hysteresis under the influence of an external field.

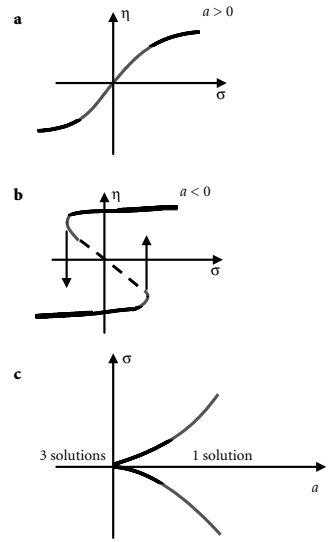

Figure 1. The order parameter's response to an externally applied field (a) in a unistable state, (b) in a bistable state (hysteresis), and (c) separation of the control parameter space into solution's multiplicity regions.

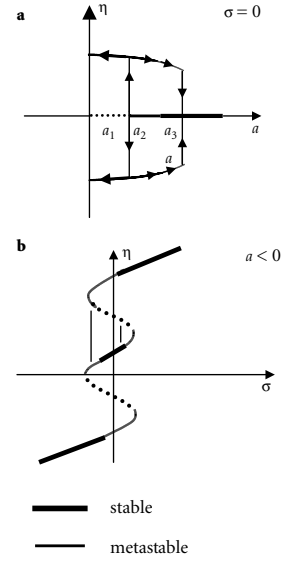

Figure 2. (a) Bifurcation plot (thermal hysteresis) and, (b) double field-induced hysteresis in the butterfly catastrophe case.

The sixth power free energy expansion for the order parameter η

$$F = F_0 + a\varepsilon\eta^2 + A_4\eta^4 + A_6\eta^6 - h\eta \qquad (5)$$

has been widely used to model first-order phase transitions provided $A_4 < 0$. The equation of state gives the order parameter in equilibrium

$$\eta_0 = \left\{\left[-A_4 - \left({A_4}^2 - 3a\varepsilon A_6\right)^{1/2}\right]/3A_6\right\}^{1/2} . \qquad (6)$$

The transition temperature is

$$T_c^* = T_c + \frac{{A_4}^2}{4aA_6}, \qquad (7)$$

where $\varepsilon = T - T_c$, and the disordered phase ($\eta = 0$) terminates its stability at $T = T_c$ while the ordered one (η_0) does so at $T = {T_0}^*$, where

$${T_0}^* = T_c + \frac{{A_4}^2}{3aA^6} . \qquad (8)$$

Importantly, the existence of a thermal hysteresis phenomenon is associated with first-order phase transition. Thermal hysteresis means that on cooling, the disordered phase is stable below the equilibrium transition temperature, while on heating, the ordered phase is stable above it. The associated effects are called supercooling and superheating, respectively.

JACK A. TUSZYŃSKI

See also **Catastrophe theory; Critical phenomena; Ferromagnetism and ferroelectricity; Order parameters**

Further Reading

Kittel, C. 1956. *Introduction to Solid State Physics*, New York: Wiley

Landau, L.D. & Lifshitz, E.M. 1959. *Statistical Physics*, London: Pergamon

Thompson, J.M.T. & Stewart, H.B. 1986. *Nonlinear Dynamics and Chaos*, New York: Wiley

I

IDEMPOTENT ANALYSIS

Definition and Introduction

The analyses that we all know and use (differentiation, integration, Fourier analysis, matrix analysis, etc.) are tacitly based on algebra defined by means of the conventional operations: addition, multiplication, and their inverses. In idempotent analysis, the starting point is not conventional algebra but instead the idempotent semiring.

Definition 1. *A semiring is a set $\mathcal{D}$ with two binary operations, $\oplus$ (called "sum" or "addition") and $\otimes$ (called "product" or "multiplication") and two specific elements ε and e such that*

- *$(\mathcal{D}, \oplus, \varepsilon)$ is a commutative monoid with identity element ε,*
- *$(\mathcal{D}, \otimes, e)$ is a monoid with identity element e,*
- *$a \otimes \varepsilon = \varepsilon \otimes a = \varepsilon$, for all $a \in \mathcal{D}$,*
- *$a \otimes (b \oplus c) = (a \otimes b) \oplus (a \otimes c)$, for all $a, b, c \in \mathcal{D}$.*

The semiring is called idempotent if in addition

- *$a \oplus a = a$, for all $a \in \mathcal{D}$.*

The semiring is called commutative if

- *the multiplication $\otimes$ is commutative.*

A monoid here is a set of elements with one operation. An idempotent semiring is sometimes referred to as a "dioid," which means "twice a monoid." It is the property $a \oplus a = a$ that distinguishes a dioid from conventional algebra. The most well-known example of a dioid is the so-called max-plus algebra, where $\mathcal{D} = R \cup \{-\infty\}$, the $\oplus$ operation is the maximum, with identity element $\varepsilon = -\infty$, and the $\otimes$ operation is (conventional) addition, with the identity element $e = 0$. As a numerical example, $5 \otimes (3 \oplus -2) = 8$. A noticeable difference between max-plus algebra and conventional algebra is that linear equations do not always have a solution (e.g., what is x in $5 \oplus x = 4$?). Addition is not cancellative in the sense that $a \oplus b = a \oplus c$ does not in general imply $b = c$.

The pioneering work in the max-plus algebra is Cuninghame-Green (1979), which has been extended into a system-theoretic direction in Baccelli et al. (1992). The phrase *idempotent analysis* was coined by Kolokoltsov & Maslov (1997). In Gunawardena (1998), it is shown that idempotency shows up in many different areas of mathematics; Gunawardena (1998, pp. 1–49) is an excellent survey. Applications are described in Le Boudec & Thiran (2001); and Heidergott et al. (2004).

We choose the max-plus algebra setting to introduce some analysis. Consider the recurrence relation

$$x(k+1) = A \otimes x(k), \tag{1}$$

which represents a model with state $x \in R^n$ and where A is an $n \times n$ matrix with elements a_{ij}. More explicitly, this relation is defined by its component-wise writing

$$\begin{aligned} x_i(k+1) &= \bigoplus_j (a_{ij} \otimes x_j) = (a_{i1} \otimes x_1) \\ &\quad \oplus (a_{i2} \otimes x_2) \oplus \cdots \oplus (a_{in} \otimes x_n), \\ i &= 1, 2, \ldots, n. \end{aligned}$$

The conventional way of writing this would be $x_i(k+1) = \max_j (a_{ij} + x_j)$. Such a model is sometimes referred to as a discrete event dynamic system.

If $x(0)$ is an eigenvector of A in the max-plus algebra defined as

$$A \otimes x(0) = \lambda \otimes x(0), \tag{2}$$

equivalently written as $\max_j (a_{ij} + x_j(0)) = \lambda + x_j$, with not all components $x_i(0)$ equal to ε, and where λ is called the eigenvalue, then $x_i(k+1) = \lambda + x_i(k) = x_i(0) + (k+1)\lambda$. The new state is obtained by adding λ to the previous state. In graph-theoretic terms, λ can be characterized as follows.

Theorem 1. *If the square matrix A is irreducible, equivalently, its corresponding graph is strongly connected and, there exists one and only one eigenvalue (with possibly several eigenvectors). This eigenvalue is equal to the maximum cycle mean of the graph:*

$\lambda = \max_\zeta |\zeta|_w/|\zeta|_l$, *where* ζ *ranges over the set of circuits in the graph, where* $|\zeta|_l$ *is the number of arcs of* ζ *and* $|\zeta|_w$ *its weight, that is, the addition of all* a_{ij} *which correspond to arcs of* ζ.

This theorem is referred to as the spectral theorem. A practical interpretation for this model and analysis is given below.

Examples

The first example of a dioid already encountered is $R \cup \{-\infty\}$ with $\oplus$ as max and $\otimes$ as addition. Other examples are:

- The set of $n \times n$ matrices with $A \oplus B$ and $A \otimes B$ defined as $(A = \{a_{ij}\},\ B = \{b_{ij}\})$

$$\{A \oplus B\}_{ij} = \max(a_{ij}, b_{ij}),\ \{A \otimes B\}_{ij} = \max_k (a_{ik} + b_{kj}).$$

- The set $R \cup \{-\infty\}$ with min as $\oplus$ and addition as $\otimes$ is isomorphic to the max-plus algebra.
- The set $R \cup \{-\infty\} \cup \{+\infty\}$ with $\oplus$ defined as max and $\otimes$ as min.
- The set $\{0, 1\}$ with $\oplus$ defined as max and $\otimes$ as min. This is the Boolean algebra.
- The set of all subsets of the R^2 plane, including $\emptyset$ and the whole R^2 itself, with $\oplus$ defined as $\cup$ and with $\oplus$ defined as the vector sum of subsets.
- Extension to polynomials or formal power series by defining (a polynomial or formal power series is given by $f(z) = \bigoplus_{k=0,1,\ldots} f_k z^k$):

$$f \oplus g:\ (f \oplus g)_k = f_k \oplus g_k;\ f \otimes g:\ (f \otimes g)_k = \max_{i+j=k} f_i \otimes g_j.$$

Relation to Nonlinear Theory and Practice

One must be careful using the word *nonlinear*. System (2) for instance is nonlinear with respect to conventional algebra, but it is considered linear in the max-plus algebra.

Relationship with Other Mathematical Disciplines

An interpretation in graph-theoretic terms is often possible. The occurrences of events in timed event graphs, the latter forming a subclass of Petri nets, can be modeled by means of an equation of the form (1). If $x \in R^n$, define $||x||$ to be its l^∞ norm, that is, $||x|| = \max_i |x_i|$. A mapping $f : R^n \to R^n$ is called non-expansive if $||f(x) - f(y)|| \leq ||x - y||$. As an example, $f(x) = A \otimes x$ is non-expansive. An important theme is the study of periodic solutions of non-expansive mappings; that is, does λ exist such that $f^k(x) = k\lambda + f(x)$? Another theme is that of the finiteness of the transient behavior (before one reaches a periodic behavior), if one starts with an arbitrary initial condition.

Some Applications

Consider the system (2). Interpret a_{ij} as the traveling time of a train on a track (if existing) between departure station j and arrival station i. Quantity $x_i(k+1)$ refers to the earliest departure time of trains at station i that depart for the $(k+1)$th time. The model states that in order to depart (for the $(k+1)$th time), the train must wait until all trains, which departed for the kth time, have arrived; $\max_j(a_{ij} + x_j)$ reflects the maximum of all arrival times. This allows passengers to change trains (one could add some minutes to all a_{ij} to account for the changeover times). If a track between two stations, say l and m, does not exist, set $a_{ml} = \varepsilon$. If one assumes that the departures take place as soon as possible subject to the restriction of passengers changing over, then the model $x(k+1) = A \otimes x(k)$, with an initial condition $x(0)$, determines all future departure times. If this $x(0)$ is an eigenvector, then one has a timetable with constant interdeparture times, this constant being λ. This constant is a lower bound for the interdeparture times of any periodic timetable obeying the changeover rule.

In the above, trains can be viewed as discrete flows on networks. If one replaces "trains" by "messages" and "all railway tracks" by "computer network" or "internet," one enters another field of application that has been described and analyzed in Le Boudec & Thiran (2001).

In discrete-time optimal control theory, or in decision processes on Markov chains, one encounters the equation

$$V(k, x) = \max_u (V(k+1, f(x, u)) + g(x, u)),$$

which is a consequence of Bellman's principle of optimality. The underlying model is $x(k+1) = f(x(k), u(k))$, and the costs during step k are $g(x(k), u(k))$. The function V is the value function. This equation, with the operations of addition and maximization can be interpreted and analyzed in the max-plus algebra sense (Akian et al., 1998). Applications in automata theory can also be found in Gunawardena (1998).

GEERT JAN OLSDER

See also **Markov partitions**

Further Reading

Akian, M., Quadrat, J.-P. & Viot, M. 1998. Duality between probability and optimization. In *Idempotency*, edited by J. Gunawardena, Cambridge and New York: Cambridge University Press

Baccelli, F., Cohen, G., Olsder, G.J. & Quadrat, J.-P. 1992. *Synchronization and Linearity*, New York: Wiley

Cuninghame-Green, R.A. 1979. *Minimax Algebra*, Berlin: Springer

Gunawardena, J. (editor). 1998. *Idempotency*, Cambridge and New York: Cambridge University Press

Heidergott, B., Olsder, G.J. & van der Woude, J.W. 2004. *Max Plus at Work*, Princeton, NJ: Princeton University Press

Kolokoltsov, V.N. & Maslov, V.P. 1997. *Idempotent Analysis and Its Applications*, Boston: Kluwer
Le Boudec, J.-Y. & Thiran, P. 2001. *Network Calculus, A Theory of Deterministic Queuing Systems for the Internet*, Berlin and New York: Springer

IKEDA MAP

See **Maps**

IMPULSE, NERVE

See **Nerve impulses**

INCOHERENT SOLITONS

Until 1996, solitons were considered to be exclusively coherent entities. However, experimental observations of self-trapping of partially spatially incoherent light (Mitchell et al., 1996) and of white light (Mitchell et al., 1997) in photorefractive media have shown that incoherent beams can also form solitons (Figure 1). These solitons are multimode or speckled beams for which the instantaneous intensity distribution varies randomly in space and/or time. They can exist only in non-instantaneous media whose response time is much longer than the random fluctuation time across the incoherent beam. Such a medium responds to the time-averaged envelope and not to the instantaneous speckles that constitute the incoherent beam. An incoherent soliton forms when the time-averaged intensity induces a multimode wave and traps itself in the waveguide by populating the guided modes in a self-consistent fashion. These random-phase and weakly correlated self-trapped entities exhibit a host of unique properties that have no analog in the coherent regime. Moreover, their existence is related to many other areas of physics, in which nonlinearities, stochastic behavior, and statistical averaging are involved. For example, incoherent modulation instability effects and incoherent pattern formation relate to many systems in nature: from clustering in a cooled atomic gas to self-supported "stripes" of electrons in semiconductors, from high-T_c superconductors to structures in fluids and gravitational effects.

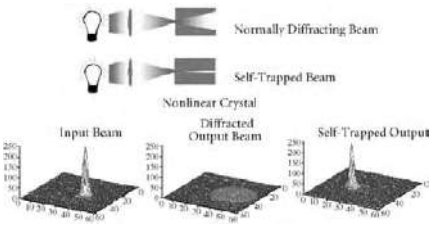

Figure 1. Self-trapping of spatially and temporally incoherent white light from an incandescent light bulb.

Numerous theoretical and experimental works followed the pioneering experiments (see Segev & Christodoulides (2001) and references within). This rapid progress in the area of incoherent solitons offers a number of interesting fundamental ideas as well as possible applications. For example, coherence engineering can be used to control modulation instabilities and to create interesting stable patterns in nonlinear materials for various applications. There is also an exciting possibility of using self-trapped light beams from incoherent sources, such as light-emitting diodes, for creating reconfigurable optical interconnects and beam steering.

Several theories have been developed to describe the propagation of partially incoherent beams and soliton formation in noninstantaneous nonlinear materials (Segev & Christodoulides, 2001). These include the coherent density theory (Christodoulides et al., 1997), the modal theory (Mitchell et al., 1997), and the mutual coherence theory (Shkunov & Anderson, 1998). Other, more approximate theories relying on ray optics (Snyder & Mitchell, 1998) and on the Wigner distribution (Hall et al., 2002) have also been suggested. The first three approaches are rather complete and equivalent to one another (Christodoulides et al., 2001). Here, we briefly overview the two most widely used theories.

Coherent Density Theory

The coherent density method is a dynamic approach suited for studying the evolution dynamics of incoherent solitons, their interactions, instabilities, and correlation statistics. In this formalism, the incoherent field is described by means of a so-called coherent density function, from which one can deduce the optical intensity distribution as well as the associated correlation statistics. Mathematically, the self-trapping process is described by an infinite set of nonlinear Schrödinger-like equations, provided that each coherent component at the input is appropriately weighted with respect to the incoherent angular power spectrum of the source (Christodoulides et al., 1997). These equations can be solved numerically by using modified beam propagation procedures.

Modal Theory

The modal theory is currently widely considered as the method of choice in terms of identifying static incoherent solitons, their range of existence, and correlation properties. The fundamental requirements of incoherent self-trapping were the starting point of this formulation. Incoherent solitons are identified by solving the underlying coupled (stationary) nonlinear Schrödinger-like equations in a self-consistent fashion (Mitchell et al., 1997). To solve these equations self-consistently, one needs to start with an arbitrary index profile, then solve for the guided modes and sum them incoherently to get the intensity profile, and finally

use this intensity profile to calculate the new induced-index profile. This process should be repeated until the solutions are stationary. The stationary solutions give the incoherent soliton intensity profile as well as its modal distribution and statistical properties.

1-d and 2-d Dark Incoherent Solitons

The existence of dark incoherent solitons and requirements for their observations were predicted (Coskun et al., 1998) two years after the observation of bright incoherent solitons. Such dark incoherent solitons were experimentally observed soon thereafter (Chen et al., 1998). In that experiment, (1 + 1)-dimensional dark incoherent solitons were observed, along with the self-trapping of a (2 + 1)-d dark incoherent beam. That is, a self-trapped 2-d void nested in spatially incoherent beam was demonstrated (Chen et al., 1998). As in the coherent case, fundamental dark incoherent solitons were found to exist only in defocusing nonlinear media and to require an initial transverse phase shift at the center of the dark stripe. 2-d dark incoherent solitons were initiated from a vortex beam that was generated by replacing a step mirror with a helicoidal phase mask, which created an optical vortex of unit topological charge. For bright solitons, only guided modes (bound modes) are self-trapped, whereas dark incoherent solitons involve a belt of radiation modes (unbound states). Unlike their coherent counterparts, fundamental dark and vortex solitons were always found to be gray because of the presence of both odd and even radiation modes at the center of the notch (Christodoulides et al., 1998). Furthermore, the grayness depends on the coherence length of the carrier beam. Dark soliton splitting and "phase memory" effects were also observed theoretically and experimentally (Coskun et al., 1999).

Modulation Instability, Pattern Formation, and Soliton Clustering

Both theory and experiment have revealed that modulation instabilities can take place with incoherent light beams provided that the nonlinearity exceeds a well-defined threshold, which depends on the correlation properties of the beam (Soljacic et al., 2000). This shows that modulation instabilities (MI) can be totally suppressed by properly adjusting the correlation distance of the wave front. A natural by-product of this suppression is the observation of anti-dark incoherent solitons (a bright beam on a constant background) in self-focusing environments. Periodic trains of 1-d filaments and self-ordered 2-d lattices of light spots due to incoherent modulation instabilities were observed by carefully increasing the nonlinearity (Kip et al., 2000). Spontaneous clustering of solitons in partially coherent wave fronts initiated by random noise was also demonstrated experimentally and numerically (Chen et al., 2002). It is, in fact, an outcome of the interplay between random noise, weak correlation, and high nonlinearity. Together, this process leads to incoherent MI, formation of 2-d solitary filaments, and eventually to clustering of 2-d solitons or in other words, aggregates of fine-scale structures. This clustering phenomenon has no counterpart with solitons in coherent systems. The rapid progress in this new area of incoherent solitons brings about many interesting fundamental ideas and possible applications. We have concentrated here on the basic features, but new ideas arise very quickly in this new, dynamic area of soliton science.

TAMER COSKUN, DEMETRIOS CHRISTODOULIDES, AND MORDECHAI SEGEV

See also **Nonlinear optics; Optical fiber communications; Solitons, types of**

Further Reading

Chen, Z., Mitchell, M., Segev, M., Coskun, T.H. & Christodoulides, D.N. 1998. Self-trapping of dark incoherent light beams. *Science*, 280: 889–892

Chen, Z., Sears, S.M., Martin, H., Christodoulides D.N. & Segev, M. 2002. Clustering of solitons in weakly correlated systems. *Proceedings of the US National Academy of Science*, 99(8): 5223–5227

Christodoulides, D.N., Coskun, T.H., Mitchell, M., Chen, Z.C. & Segev, M. 1998. Theory of incoherent dark solitons. *Physical Review Letters*, 80(23): 5113–5116

Christodoulides, D.N., Coskun, T.H., Mitchell, M. & Segev, M. 1997. Theory of incoherent self-focusing in biased photorefractive media. *Physical Review* E, 59(5): R4777–R4780

Christodoulides, D.N., Eugenia, D.E., Coskun, T.H., Segev, M.& Mitchell, M. 2001. Equivalence of three approaches describing partially incoherent wave propagation in inertial nonlinear media. *Physical Review* E, 63: 035601-1–035601-4

Coskun, T.H., Christodoulides, D.N., Chen, Z. & Segev, M. 1999. Dark incoherent soliton splitting and "phase memory" effects: theory and experiment. *Optics Letters*, 23(6): 418–420

Coskun, T.H., Christodoulides, D.N., Mitchell, M., Chen, Z. & Segev, M. 1998. Dynamics of incoherent bright and dark self-trapped beams and their coherence properties in photorefractive crystals. *Optics Letters*, 23(6): 418–420

Hall, B., Lisak, M., Anderson, D., Fedele, R. & Semenov, V.E. 2002. Statistical theory for incoherent light propagation in nonlinear media. *Physical Review* E, 65: 035602-1–035602-4

Kip D., Soljacic M., Segev, M., Eugenieva, E., Christodoulides, D.N. 2000. Modulation instability and pattern formation in spatially incoherent light beams. *Science*, 290: 495–498

Mitchell, M., Chen, Z., Shih, M. & Segev, M. 1996. Self-trapping of partially spatially incoherent light. *Physical Review Letters*, 77(3): 490–493

Mitchell, M. & Segev, M. 1997. Self-trapping of incoherent white light. *Nature*, 387: 880–883

Mitchell, M., Segev, M., Coskun, T.H. & Christodoulides, D.N. 1997. Theory of self-trapped spatially incoherent light beams. *Physical Review Letters*, 79(25): 4990–4993

Segev, M. & Christodoulides, D.N. 2001. Incoherent solitons: self-trapping of weakly-correlated wave-packets. In *Spatial Solitons*, edited by S. Trillo & W.E. Torruellas, New York: Springer

Shkunov, V.V. & Anderson, D.Z. 1998. Radiation transfer model of self-trapping spatially incoherent radiation by nonlinear media. *Physical Review Letters*, 81(13): 2683–2686

Snyder, A.W. & Mitchell, D.J. 1998. Big incoherent solitons. *Physical Review Letters*, 80(7): 1422–1924
Soljacic, M., Segev, M., Coskun, T.H., Christodoulides, D.N. & Vishwanath, A. 2000. Modulation instability of incoherent beams in noninstantaneous nonlinear media. *Physical Review Letters*, 84(3): 467–470

INERTIAL MANIFOLDS

In studying the dynamics of nonlinear systems, it is sometimes observed that all trajectories rapidly converge to a subspace of the phase space, leading to a simplification of the analysis through dimensional reduction. Such subspaces are called inertial manifolds (IMs) and the underlying dynamics are called inertial. In phase spaces of infinite dimension, the question is whether a finite-dimensional dynamical system can reproduce the dynamics of an infinite-dimensional one. In finite-dimensional systems, one tries to find a system of smaller dimension.

Related concepts have been introduced in sciences. In meteorology, for example, the slow manifold introduced and studied by Lorenz and others, is expected to reproduce the slow dynamics, taking into account interaction with the rapidly changing regions of the phase space. From a somewhat different perspective, the Reynolds equations in turbulence and some large eddies simulation models are finite-dimensional systems that attempt to reproduce the dynamics of the large eddies of the fluid, taking into account the action of the small eddies.

Definition

Denote by H the phase space, a Hilbert space of finite or infinite dimension, and consider on H a semigroup of operators $\{S(t)\}_{t\geq 0}$ generating the dynamical system: $u_0 \mapsto S(t)u_0 = u(t)$.

If it exists, an inertial manifold for this system is a smooth finite-dimensional manifold $\mathcal{M}$ in H that enjoys the following properties:

(i) $S(t)\mathcal{M} \subset \mathcal{M}, \forall t > 0$ (positive invariance);
(ii) all orbits converge to $\mathcal{M}$, as $t \to \infty$, at an exponential rate;
(iii) the rate of convergence is uniform for all orbits starting in a bounded set of initial data.

If a global attractor $\mathcal{A}$ exists, then necessarily $\mathcal{A}$ is included in $\mathcal{M}$ as well as any stationary solution, periodic orbit, etc. Comparing $\mathcal{A}$ to $\mathcal{M}$ when they both exist, we see that $S(t)\mathcal{A} = \mathcal{A}$, instead of (i), and we know that orbits may converge to $\mathcal{A}$ at arbitrarily slow rates, in contrast with (ii). Finally, attractors are believed to be sometimes fractal sets, whereas smoothness is required for $\mathcal{M}$.

When an inertial manifold exists, the restriction of the semigroup to $\mathcal{M}$ is a group—due to (i)—whose dynamics are the same as that of the initial systems. In particular, their attractor is the same if $\{S(t)\}_{t\geq 0}$ has an attractor, and this reduced dynamical system is called an inertial system. When the dynamical system is defined by a differential equation, as in Equation (1), its restriction to $\mathcal{M}$ is a finite-differential system, also called an inertial system.

Examples

Inertial manifolds have been studied for dynamical systems in infinite dimensions corresponding to dissipative parabolic evolution equations, written in functional form as

$$\frac{\mathrm{d}u(t)}{\mathrm{d}t} = F(u(t)), \quad u(0) = u_0. \tag{1}$$

Here $u(t) = S(t)u_0$, where u_0 and $u(t)$ belong to H.

The space H is decomposed as the sum of a finite-dimensional space $Y = P_y H$ and of its complement $Z = P_z H$, $u = y + z$. In all examples studied, the inertial manifold is then searched for as a graph:

$$z = \Phi(y), \quad y \in Y. \tag{2}$$

Usually, Y and Z are spectral spaces for the underlying linear dissipative operator A, Y representing hence the low-frequency component of the flow and z its high-frequency component.

The existence of inertial manifolds has been proven for the Kuramoto–Sivashinsky equation, the Ginzburg–Landau equation, reaction-diffusion equations in one and two spatial dimensions, and the Navier–Stokes equations with added (hyper-)viscosity.

The initial hope (Foias et al., 1988) was to find an IM for the Navier–Stokes equation at least in space two, justifying the name coined by Foias, since the role of the inertial terms over the viscous terms would be dominant on this manifold. However, the existence of an inertial manifold for the Navier–Stokes equations has not yet been proven nor disproven.

Several proofs of existence have been derived beyond those of Foias et al. (1988); the key hypothesis and limitation in all the proofs is the so-called spectral gap condition, involving a sufficiently large gap in the spectrum of the dissipative operator A. It is believed (but not proved) that this difficulty could be overcome with IMs that are less smooth and are not graphs. Alternatively, this difficulty has been overcome by removing the condition that $\mathcal{M}$ be a manifold. The corresponding concept was introduced in Eden et al. (1994) where it was called an inertial set or an exponential attractor.

The existence of inertial sets was proven in Eden et al. (1994) for numerous dynamical systems generated by evolutionary dissipative equations, in fact, for all systems for which the existence of a compact finite-dimensional attractor has been established (Hale, 1988; Sell & You, 2002; Temam, 1997).

Despite these limitations, inertial manifolds are a natural concept, giving a precise form to the idea that infinite-dimensional dynamical systems produce a finite-dimensional dynamics. Remember that a less explicit form of this idea is the property of the attractor to be finite-dimensional.

When IMs do not exist or are not easy to construct, approximate inertial manifolds (AIMs) are sometimes used, which are finite-dimensional smooth manifolds that attract the orbits in a small neighborhood. Extensive applications of AIMs in numerical analysis have been developed (Temam, 1997; Sell & You, 2002).

ROGER TEMAM

See also **Center manifold reduction; Invariant manifolds and sets; Synergetics**

Further Reading

Eden, A., Foias, C., Nicolaenko, B. & Temam, R. 1994. *Exponential Attractors for Dissipative Evolution Equations*, Collection Recherches en Mathématiques Appliquées, Paris: Masson, Paris, and New York: Wiley

Foias, C., Sell, G.R. & Temam, R. 1988. Inertial manifolds for nonlinear evolutionary equations, *Journal of Differential Equations*, 73: 309–353

Hale, J. 1988. *Asymptotic Behavior of Dissipative Systems*, Providence, RI: American Mathematical Society

Sell, G.R. & You, Y. 2002. *Dynamics of Evolutionary Equations,* New York: Springer

Temam, R. 1988. *Infinite Dimensional Dynamical Systems in Mechanics and Physics,* New York: Springer (2nd augmented edition, 1997)

INFELD EQUATION

See **Born–Infeld equation**

INFORMATION DIMENSION

See **Dimensions**

INFORMATION THEORY

Although the word *information* is commonly used and its engineering applications influence our lives, the quantitative meaning is often unclear. Among several measures of information, the most common is called Shannon information (denoted as I_S with units of the bit), which was introduced by Claude Shannon in 1948.

As an example, suppose your friend (whose wife has been pregnant for nearly nine months) telephones with the information: It's a girl. Since the prior probability (P) of a girl being born is $\frac{1}{2}$, the Shannon information is computed as

$$I_S = \log_b\left(\frac{1}{P}\right) = \log_2\left(\frac{1}{1/2}\right) = 1\,\text{bit}, \qquad (1)$$

with the logarithmic base $b = 2$. In other words, one bit of Shannon information is gained in a message that resolves one of two equally probable events.

Strings of such events (e.g., 100110100011100) are the language of computers, and their Shannon information can be computed by thinking of a string as a set of N switches, each of which can be on (1) or off (0). Since there are 2^N possible sequences of N switches, the probability of any particular sequence is 2^{-N}, leading to a Shannon information of N bits, which is conveniently equal to the number of switches.

Shannon's information takes the particular form, Equation (1), under the assumption that the received message (an observed switch sequence) is completely reliable. A more general Shannon measure allows for generally unreliable messages; thus

$$\begin{aligned}&(\text{source event } B_1 \text{ or } B_2 \text{ or } \ldots B_N)\\ &\quad\rightarrow \text{observed message } A. \end{aligned} \qquad (2)$$

Here a particular source event $B_n \equiv B$ occurs, and the observer receives a message A, providing evidence of what was actually intended. The arrow implies transmission through a real, imperfect communication channel, in which transmission errors may occur. For example, the actual source event B might be the switch sequence given above that is transmitted to an observer. Because of transmission errors, the received message might be $A = 010110100011100$.

As when a detective observes a fingerprint, the message A implies that an event B has occurred, where each B_n is a different possible switch sequence. Shannon information was designed to answer the question: How much evidence does the observed (garbled) message A constitute for the hypothesis that the event B actually occurred?

Intuitively, the evidence provided by A will be strong if the probability of B having occurred is now greater than before receiving A. That is, if the probability $P(B|A)$ (of B in the presence of A) much exceeds $P(B)$ (the probability of B in the absence of A). This suggests that the ratio $P(B|A)/P(B)$ measures the weight of the evidence. Strong evidence would give a large ratio, weak evidence a small ratio. Because any monotonic function of this ratio works as well, taking the logarithm defines the Shannon information

$$I_S(A, B) \equiv I_S \equiv \log_b \frac{P(B|A)}{P(B)}. \qquad (3)$$

Although the choice of a logarithmic base b is at the user's discretion, probabilities in computer codes are often powers of 2 for which $b = 2$ is the most convenient choice. Then I_S is assigned the unit of a *bit*. For a fixed channel probability ($P(B|A)$), Equation (3) discloses that the information increases as $P(B)$ becomes smaller. (In editing a newspaper, for example, an article entitled "Dog Bites Man" is not unusual enough to merit publication, but "Man Bites Dog" most definitely is.)

There is a problem with this definition of information—the observer, by hypothesis, does not know which event B_n has occurred. Therefore, he or she cannot know which information quantity, $I_S(A, B_1)$ or ... or $I_S(A, B_N)$ to compute. Furthermore, the message A may be one of a set of possibilities A_m, $m = 1, \ldots, M$. All such possibilities can be taken into account by forming the grand average

$$\left\langle \log_b \frac{P(B|A)}{P(B)} \right\rangle \equiv \sum_{m=1}^{M} \sum_{n=1}^{N} P(A_m, B_n) \log_b \frac{P(B_n|A_m)}{P(B_n)} \equiv I(A, B). \tag{4}$$

Called Shannon's "mutual information," this is the quantity commonly used to evaluate the quality of communication systems. Notice that it depends upon properties of the source (the $P(B_n)$) as well as the channel (the $P(B_n|A_m)$); thus, this is a total system perspective.

If just the quality of the channel (as specified by its fixed channel probabilities $P(B_n|A_m)$) is to be evaluated, the information $I(A, B)$ is maximized through choice of a source $P(B_n)$. The resulting information, then, only depends upon the channel probabilities and is called the channel capacity since it measures the intrinsic capacity of the channel for transmitting information.

Note that Equation (4) may be evaluated in its continuous limit; thus,

$$I(X, Y) = \int \int \mathrm{d}x\, \mathrm{d}y\, p(x, y) \log_b \frac{p(y|x)}{p(y)}. \tag{5}$$

Is there an information measure that is appropriate for describing growth processes? Consider a generalization of Equation (5) to

$$I_{\mathrm{KL}}(p, r) \equiv -\int \mathrm{d}\boldsymbol{x}'\, p(\boldsymbol{x}') \log_b \frac{p(\boldsymbol{x}')}{r(\boldsymbol{x}')}, \tag{6}$$

which is called the Kullback–Leibler (K–L) information. The ratio p/r is describes a "cross entropy" between the probability law $p(\mathbf{x}')$ and the reference law $r(\mathbf{x}')$, where the vector $\mathbf{x}'$ is general. In the special case $\mathbf{x}' = (\mathbf{x}, \mathbf{y})$, $r(\mathbf{x}') = p(\mathbf{x})p(\mathbf{y})$, Equation (6) becomes the mutual information in Equation (5). Another important case of the K–L information is when $r(\mathbf{x}') = 1$, whereupon Equation (6) takes the form

$$-\int \mathrm{d}\boldsymbol{x}' p(\boldsymbol{x}') \log_b p(\boldsymbol{x}') \equiv H, \tag{7}$$

which is called the entropy.

Yet another special case of K–L information is obtained when $\mathbf{x}' \equiv x$, a single coordinate, and the reference function $r(x)$ is made to be a slightly displaced version of the probability law, $r(x) \equiv p(x+\Delta x)$, $\Delta x \to 0$. In this limit, the K–L information is found to obey

$$-\lim_{\Delta x \to 0} \frac{1}{\Delta x^2} \int \mathrm{d}x\, p(x) \log_b \frac{p(x)}{p(x+\Delta x)} = -\frac{1}{2} \int \mathrm{d}x \frac{p'^2(x)}{p(x)} \equiv -\frac{1}{2} I_{\mathrm{F}}, \tag{8}$$

where I_{F} is the Fisher information and the usual derivative notation $p'(x) \equiv \mathrm{d}p(x)/\mathrm{d}x$ is used.

A useful variant of I_{F} is obtained by using a probability amplitude $q(x)$, where $p(x) \equiv q^2(x)$. The right-hand integral of Equation (8) then gives directly

$$I_{\mathrm{F}} = 4 \int \mathrm{d}x\, q'^2(x), \quad q'(x) \equiv \mathrm{d}q(x)/\mathrm{d}x. \tag{9}$$

Thus, Fisher information measures the gradient content of the probability amplitude curve.

Because the smallest possible mean-square error one can achieve in forming an estimate of the parameter is the reciprocal of Fisher's information, this also describes our ability to know a parameter from its measurements. Assuming all knowledge is based upon measurement, Fisher information describes quite generally our ability to know.

Physicists Leon Brillouin and David Bohm long sought a measure of information that would explain the mysteries of physics in general, including those of quantum mechanics. In particular, the question of quantum entanglement has long perplexed physicists. Consider a pair of particles that are created simultaneously as reactants from a mother particle. Measurement of one member of the pair supplies important information (such as spin) about the other member, even without measuring the latter. (This is called the Einstein–Podolsky–Rosen–Bohm, or EPRB, paradox.) In what way could information about the unmeasured particle be transmitted into a measurement of the detected one? This seems to require the realities of the two particles to be somehow "entangled." Hence, an "active information" was sought that could supply the needed information. Of course, they tried the Shannon variety, but this did not work.

Surprisingly, a form of information exists for generating the probability laws of physics that is aptly called the physical information and defined as follows. Let I be the Fisher information that is acquired in an actual measurement. Depending upon the measurement scenario, there may or may not be another, unmeasured particle accompanying the measured particle. The physical information K is the difference $K \equiv I - J$ of two Fisher informations (for simplicity we now drop the subscript F), where

$$I \equiv \sum_n I_n, \quad I_n = 4 \int \mathrm{d}x\, q_n'^2(x)$$

and

$$J \equiv I/\kappa, \quad 0 \leq \kappa \leq 1. \tag{10}$$

Notice that the information I in the measurement is actually a sum of individual Fisher terms I_n. It turns out that the additive sum also defines the maximum possible value of the Fisher information. Hence, I is called the Fisher information channel capacity (as in the Shannon case). The integral form of the second Equation (10) shows that I is also a functional of the amplitude functions $q_n(x)$. This is a scalar number whose value depends upon an integral over all values x of the functions $q_n(x)$.

By the third Equation (10), J is likewise a functional of the amplitude functions; however, its form is not fixed but dependent upon the particular measurement scenario. J must be computed in any application.

Recall that I is the information level of the particle in a measurement space. In all measurements of quantum phenomena $\kappa = 1$, so $J = I$ by the third Equation (10). Thus J represents information that arises out of entanglement with that of the measured particle. We, therefore, call J the entangled information. Mathematically, it is I as evaluated in an "entanglement space." If only the measured particle is present, entanglement space is the Fourier conjugate space to measurement space. If another, unmeasured particle is present, entanglement space is the (unused) measurement space of that particle.

In Equations (10), the form of I is a sum of squares of functions q_n' (an L^2 norm or measure). Like any squared length, such a norm is invariant to rotation, and rotations may be performed in either the space of coordinates x (which are more generally of dimension 4 or higher) or of the functions $q_n'(x)$. Because J is linear in I, it also obeys such invariance, and likewise for their difference K. Such invariance suggests a state of stationarity

$$K \equiv I - J = \text{extrem}. \tag{11}$$

Equation (10), supplemented by Equations (11), is called the principle of extreme physical information or EPI (Frieden, 1998). Its solutions $q_n(x)$ obey corresponding Euler–Lagrange equations

$$\frac{\mathrm{d}}{\mathrm{d}x}\left(\frac{\partial k}{\partial q_n'}\right) = \frac{\partial k}{\partial q_n}, \quad k \equiv k(x),$$

$$K \equiv \int \mathrm{d}x\, k(x). \tag{12}$$

These are wave equations whose solutions $q_n(x)$ are the amplitude functions of science. An example is the Schrodinger wave equation. Other examples are provided by growth phenomena, ranging from energy growth to crystal growth to cancer growth, with the preceding formulation leading to exponential, power law, or logarithmic growth depending on the boundary conditions and integration constants that are assumed (Gatenby & Frieden, 2002).

In summary, Shannon information and cross entropy are valuable forms of information in communication theory, and two important outgrowths of these definitions are Fisher information and physical information. Fisher information permits one to estimate the expected error in the estimate of a parameter. Physical information permits one to derive physical laws via the EPI principle.

B. Roy Frieden

See also **Algorithmic complexity; Entropy; Euler–Lagrange equations**

Further Reading

Bohm, D. & Hiley, B.J. 1993. *The Undivided Universe*, London: Routledge

Brillouin, L. 1956. *Science and Information Theory*, New York: Academic Press

Fisher, R.A. 1922. On the mathematical foundations of theoretical statistics. *Philosophical Transactions of the Royal Society of London*, 222: 309–368

Frieden, B.R. 1998. *Physics from Fisher Information*, Cambridge and New York: Cambridge University Press (see also 2nd edition, 2004)

Gatenby, R. & Frieden, B.R. 2002. Application of information theory and extreme physical information to carcinogenesis. *Cancer Research*, 62: 4675

Kullback, S. 1959. *Information Theory and Statistics*, New York: Wiley

Shannon, C.E. 1948. A mathematical theory of communication. *Bell System Technical Journal*, 27: 379–423; 623–656

INHIBITION

In what is certainly one of the best-known experiments on learning, Ivan Pavlov sounded a bell and shortly after presented food to a hungry dog. After several pairings of the bell and the food, the bell came to elicit salivation, a response that it had not elicited previously. We say that the bell become an excitatory conditioned stimulus. *Excitatory* means that it acquired the ability to excite, arouse, or elicit a new behavior. But Pavlov did not limit his work to excitatory conditioning; he performed and described (Pavlov, 1927) a variety of procedures that would endow the conditioned stimulus with exactly the opposite properties. Such conditioned stimuli acquire the ability to oppose conditioned excitation and are said to be inhibitory.

The term originates from the Latin word *inhibere* and means to restrain. *Inhibere* consists of *in* "in" and *habere* "to hold." The word *inhibition* is widely used in many disciplines, such as medicine, biochemistry, physiology, neuroscience, and psychology, and its general meaning is the arrest or restraint of a process, partial or complete. In psychoanalytic theory, it describes a conscious or unconscious restraining of an impulse or desire. In neurophysiology, to which we will return shortly in more detail, it is the process opposite to

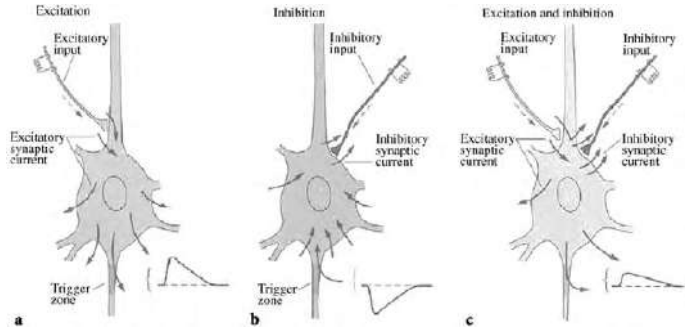

Figure 1. Excitatory and inhibitory currents have competitive effects on a single nerve cell. (a) An excitatory input in the base of a dendrite causes inward current which produces a large synaptic potential that brings the membrane potential close to its threshold. (b) An inhibitory input causes synaptic potential thus generated changes the membrane potential further below its threshold. (c) The shunting action of inhibition. When the cell receives both excitatory and inhibitory synaptic currents, the channels opened by the inhibitory pathway shunt the excitatory current, thereby reducing the excitatory synaptic potential. From Kandel et al. (2000).

excitation, or as Charles Sherrington (1933) wrote ". . . to refrain from an act is no less an act than to commit one, because inhibition is co-equally with excitation a nervous activity." By "nervous activity" he meant "the activity of the nervous system."

In fact, the function of all living systems and at all levels of complexity can be perceived as continuous adjustment between excitatory and inhibitory processes. The metabolic pathways are, for example, regulated by means of enzyme synthesis and inhibition. Almost all of the thousands of chemical reactions that occur in a living organism require catalysis by a specific enzyme. The character of any cell is based on its particular chemistry, which is determined by its specific enzyme composition. Genetic traits are expressed through synthesis of enzymes, which catalyze reactions that establish the phenotype. Many genetic diseases result from altered levels of enzyme production with changes in enzyme synthesis and/or inhibition. Much current drug therapy is based on the inhibition of a specific enzyme.

The nervous system continuously processes excitatory and inhibitory signals. Sherrington first pointed out that the quintessential action of the nervous system is its ability to weigh the consequences of different types of information and then decide on appropriate responses (Sherrington, 1947). He named it "the integrative action of the nervous system." The point at which one neuron communicates with another is called a synapse, and synaptic transmission is fundamental to processes such as perception, voluntary movement, or learning. Although many synaptic connections are highly specialized, all neurons make use of two basic forms of synaptic transmission: electrical and chemical.

Each neuron in the central nervous system, whether in the spinal cord or in the brain, is continuously bombarded by synaptic inputs from other neurons. Some are excitatory, others inhibitory. The effect of the synaptic potential—whether it is excitatory or inhibitory—is determined, not by the type of transmitter released from the presynaptic neuron, but by the type of ion channels gated by the transmitter in the postsynaptic cell. Most transmitters are recognized by types of receptors that mediate either excitatory or inhibitory potentials (for details see Kandel et al., 2000).

Synaptic contact can occur on the cell body, the dendrites, or the axon of a postsynaptic cell. The location of inhibitory inputs in relation to excitatory ones is critical for their functional effectiveness. Inhibitory short-circuit actions are more significant when they are initiated at the cell body near the initial axon segment. As a result, they can strongly curtail the influence of excitatory current on the membrane potential at the trigger zone, as illustrated in Figure 1c. In contrast, inhibitory action at a remote part of a dendrite is much less effective in shunting excitatory actions or in affecting the more distant trigger zones. Thus, in the brain, significant inhibitory input frequently occurs on the cell bodies of neurons.

Excitatory and inhibitory signals are integrated into a single response by the cell. In motor neurons and most interneurons, the decision to initiate an action potential is made by the initial segment of the axon (Figure 1, trigger zone). This region of cell membrane has a lower threshold for action potentials than the cell body or dendrites because it has a high density of voltage-dependent Na^+ channels. The neural integration involves the summation of synaptic potentials that spread passively to the trigger zone. It is critically affected by two passive membrane

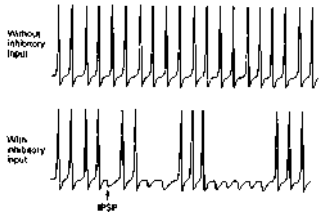

Figure 2. The *sculpturing* effect of inhibition. Without inhibitory input the neuron spontaneously fires at a fixed interval. With inhibitory input that produces an inhibitory postsynaptic potential (IPSP), some action potentials are inhibited, resulting in a distinctive pattern of impulses. From Kandel et al. (2000).

properties. First, the *time constant* affects *temporal summation*, the process by which consecutive synaptic potentials at the same site are added together in the postsynaptic cell. The larger the time constant, the greater the likelihood that two consecutive inputs from an excitatory presynaptic neuron will sum to bring the cell membrane to its threshold for an action potential. Second, the *length constant* affects *spatial summation*. Neurons with a large length constant are more likely to be brought to threshold by two different inputs arising from different sites than are neurons with a short space constant.

In addition to counteracting synaptic excitation, synaptic inhibition can exert control over spontaneously active nerve cells. Many cells in the brain are spontaneously active, as are the pacemaker cells of the heart. By suppressing the spontaneous generation of action potential in these cells, synaptic inhibition can shape the pattern of firing in a cell (Figure 2).

Many mathematical models have been introduced to describe the function of the nervous system. Their complexity ranges from that of individual nerve cells to assemblies of neurons. Hodgkin & Huxley (1952) constructed a model, known as the Hodgkin–Huxley model, to explain the electrical excitability of nerve axons in terms of discrete Na^+ and K^+ currents. The Hodgkin–Huxley model is probably the best-known and the most elegant model of a biological system, exemplifying a balance between experiment and theory that has rarely been matched. To explain how trains of impulses occur in the Hodgkin–Huxley model FitzHugh (1961) used the Hodgkin–Huxley model as one member of a large class of nonlinear systems showing excitable and oscillatory behavior. The model was further analyzed by an approximately distributed pulse transition line using analog simulations (Nagumo et al., 1962) and today is known as FitzHugh–Nagumo model.

Wilson and Cowan (1972) further increased the complexity of the system. The model they proposed was based on the properties of populations, and the single cell activity was represented not by a single spike, but rather by the spike frequency. They based their model on two main assumptions. First, the existence of spatially localized neuronal populations, based on physiological and anatomical evidence that many cells in a small volumes of cortical tissue have very nearly identical responses to identical stimuli. Second, all nervous processes of any complexity are dependent upon the interaction of excitatory and inhibitory cells. Wilson and Cowan were the first to treat inhibition as arising from exclusively inhibitory neurons. Wilson–Cowan oscillators are now widely used to describe higher functions, such as sensory information processing, learning, memory, or pattern recognition. Neural networks and chips are built for signal and image processing.

Much progress has been made in recent years toward a detailed understanding of the complex and nonlinear dynamics that underlie the Hodgkin–Huxley, FitzHugh–Nagumo, and Wilson–Cowan models. In addition, a large number of new models of synchronous oscillations have been introduced, attempting to describe features observed in the electrical activity of the brain as measured by EEG or MEG. They range from those involving details of receptors and inter-inhibitory interactions, to models depending on various nonlinear principles (see, for example, Haken, 2002).

ANETA STEFANOVSKA

See also **FitzHugh–Nagumo equation; Flip-flop circuit; Hodgkin–Huxley equations; Integrate and fire neuron; Multiplex neuron; Myelinated nerves; Nerve impulses; Neurons**

Further Reading

FitzHugh, R. 1961. Impulses and physiological states in models of nerve membrane. *Biophysical Journal*, 1: 445–466

Haken, H. 2002. *Brain Dynamics. Synchronization and Activity Patterns in Pulse-Coupled Neural Nets with Delays and Noise*, Berlin and New York: Springer

Hodgkin, A.L. & Huxley, A.F. 1952. A quantitative description of membrane current and its application to conduction and excitation in nerve. *Journal of Physiology*, 117: 500–544

Kandel, E.R., Schwartz, J.H. & Jessell, T.M. (editors). 2000. *Principles of Neural Science*, 4nd edition, New York: McGraw-Hill

Nagumo, J.S., Arimoto, S. & Yoshizawa, S. 1962. An active pulse transmission line simulating nerve axon. *Proceedings of IRE*, 50: 2061–2071

Pavlov, I.P. 1927. *Conditioned Reflexes*, London: Oxford University Press (original Russian edition 1926)

Sherrington, C. 1933. *The Brain and Its Mechanism*, REDE Lecture, Cambridge: Cambridge University Press

Sherrington, C. 1947. *The Integrative Action of the Nervous System*, 2nd edition, New Haven: Yale University Press

Wilson, H.R. & Cowan, J.D. 1972. Excitatory and inhibitory interactions in localised populations of model neurons. *Biophysical Journal*, 12: 1–24

INSTABILITY

See **Stability**

INSTANTONS

A remarkable feature of the Yang–Mills action is that there are finite-action topological soliton solutions to the classical field equations. These solitons are known as instantons or, in early papers, as pseudoparticles. The Yang–Mills action is important in particle physics; in particular, it describes the behavior of gluons, the particles that carry the strong nuclear force. Before instanton solutions were discovered in 1975 by Belavin et al. (1975), the Yang–Mills theory of the strong force appeared to have a symmetry not found in nature. This was known as the axial U(1) problem and was solved by 't Hooft who realized that one effect of the instanton solutions was to break this unwanted symmetry. This was the first example of an extended classical solution having a physical consequence in a field theory of particle physics.

In four Euclidean dimensions, the pure SU(2) Yang–Mills action is

$$S[A] = -\frac{1}{2}\int \mathrm{d}^4x \,\mathrm{trace}\, F_{\mu\nu}F_{\mu\nu}, \tag{1}$$

where μ and ν are space indices running from 1 to 4 and repeated indices are summed. $F_{\mu\nu}$ is a field strength tensor, a skew Hermitian 2×2 matrix field in four-dimensional space, related to a gauge potential A_μ by

$$F_{\mu\nu} = \frac{\partial}{\partial x_\mu}A_\nu - \frac{\partial}{\partial x_\nu}A_\mu + [A_\mu, A_\nu]. \tag{2}$$

The action is invariant under local gauge transformations

$$A_\mu \to A'_\mu = gA_\mu g^{-1} - \frac{\partial g}{\partial x_\mu}g^{-1}, \tag{3}$$

where g is a special unitary matrix function in four dimensions. Under this transformation $F_{\mu\nu} \to F'_{\mu\nu} = gF_{\mu\nu}g^{-1}$. One key consequence of this is that $F_{\mu\nu}$ not only vanishes when $A_\mu = 0$, but also, whenever A_μ is a gauge transformation of zero. This means that the asymptotic condition required for finiteness of the action is that A_μ approaches a gauge transformation of zero:

$$A_\mu \to -\frac{\partial g}{\partial x_\mu}g^{-1} \tag{4}$$

for $r = \sqrt{x_\mu x_\mu} \to \infty$. Now, the group of special unitary 2×2 matrices is topologically a three-sphere, and so the gauge potential on the large three-sphere at infinity gives a map from that three-sphere to the three-sphere of values of g. Maps between three-sphere are classified topologically by a single integer: the winding number. This integer, therefore, classifies finite-action field configurations; in fact, it is the only gauge-invariant information determined by the asymptotic field behavior. The topologically nontrivial stationary points of the action $S[A]$ are instantons.

Since they are stationary points of the action, instantons obey the Euler–Lagrange equation for the action:

$$\frac{\partial}{\partial x_\mu}F_{\mu\nu} = 0. \tag{5}$$

This is known as the Yang–Mills equation. It can be shown that minimal action solutions obey a first-order equation called the self-dual equation:

$$F_{\mu\nu} = \tfrac{1}{2}\varepsilon_{\mu\nu\lambda\sigma}F_{\lambda\sigma}, \tag{6}$$

where $\varepsilon_{\mu\nu\lambda\sigma}$ is totally skewsymmetric in its indices with $\varepsilon_{1234} = 1$. Solutions to this equation obey the second-order Yang–Mills equation. A solution with winding number one is given by

$$A_\mu = -\frac{r^2}{r^2 + R^2}\frac{\partial g}{\partial x_\mu}g^{-1}, \tag{7}$$

where R is an arbitrary scale and g has the hedgehog form

$$g = \frac{x_4}{r}\mathbf{I}_2 + \frac{i}{r}\left(x_1\sigma_1 + x_2\sigma_2 + x_3\sigma_3\right), \tag{8}$$

where $\mathbf{I}_2$ is the 2×2 identity matrix and the σ_i's are the Pauli matrices. Allowing for gauge equivalence, there is an eight-dimensional space of winding number one instantons, four of these dimensions correspond to the choice of position in space, one to the choice of scale, and three to an overall group orientation. Although these results are particular to SU(2), other groups can be studied; the main difference is in the number of overall group orientation parameters.

The self-dual equations are integrable. In fact, many of the integrable equations of mathematical physics can be derived from the self-dual equations by demanding that the solution has some translational or rotational symmetry. Because of this integrability, solutions to the self-dual equations with winding numbers greater than one may be constructed, in principle, by twistor theory and by algebraic methods (Christ et al., 1978). There is also a simple ansatz (Jackiw et al., 1977), but this does not give a general solution.

In the 1980s, the self-dual equations revolutionized the study of smooth four-dimensional manifolds: by studying the space of solutions to the self-dual equations over different manifolds, it is possible to derive invariants, known as the Donaldson invariants (Donaldson & Kronheimer, 1990). This approach has since been largely superceded by Seiberg–Witten theory.

In the path integral approach to quantum field theory, physical values are derived by certain weighted integrations over all possible field configurations. These path integrals are often intractable, and it is common to expand the integration about the stationary points of the action. This works because of the way the action appears in the integrand of the path integral. Calculations of this type are known as semi-classical calculations because they are effectively an expansion in Planck's constant, $\hbar$. This expansion must include a sum over all possible stationary points, and so, in Yang–Mills theory, it includes a sum over instanton configurations. By studying the symmetry properties of the measure in quantum chromodynamics (QCD), the Yang–Mills theory describing the strong nuclear force, it can be shown that terms in this expansion break the axial U(1) symmetry. This symmetry is unbroken if the instanton terms are omitted. The symmetry breaking allows processes that violate baryon and lepton conservation; however, the amplitudes for these effects are highly suppressed. One useful approach is to consider these processes as tunneling events between different vacua, in fact, instanton calculations in quantum field theory are very similar to Wentzel–Kramers–Brillouin (WKB) calculations in quantum mechanics.

While instantons provide a qualitative explanation for a host of phenomena in quantum chromodynamics, useful quantitative results are not available within the semi-classical approach, and even qualitatively, instanton calculations are not rigorous since they relate only to the semi-classical approximation, a truncation of the full quantum theory. The modern approach to quantum chromodynamics is lattice QCD. It is possible within lattice QCD to verify the original ideas about the role of instantons in the physics of the strong force; however, there are limits to the precision with which the lattice and semi-classical approaches can be compared (Negele, 1998).

Finite action soliton solutions in other equation systems are sometimes referred to as instantons. Examples include the finite action solutions to the forced Burgers equation, which arises in the study of turbulence, and the vortex-like solutions in the abelian Higgs model, which is related to condensed matter physics. Instantons have many similarities to the lump solitons found in certain sigma models.

CONOR HOUGHTON

See also **Burgers equation; Higgs boson; Particles and antiparticles; Quantum field theory; Solitons; Yang–Mills theory**

Further Reading

Belavin, A.A., Polyakov, A.M., Schwarz, A.S. & Tyupkin, Yu.S. 1975. Pseudoparticle solutions of the Yang–Mills equations. *Physics Letters* B, 59: 85–87

Christ, N.H., Weinberg, E.J. & Stanton, N.K. 1978. General self-dual Yang–Mills solutions. *Physical Review* D, 18: 2013–2025 (Includes a review of the complete solution to the self-dual equations originally due to Atiyah, Hitchin, Drinfeld, and Manin)

Coleman, S. 1985. *Aspects of Symmetries*, Cambridge and New York: Cambridge University Press (Chapter 7 gives a celebrated description of instantons in QCD)

Donaldson, S.K. & Kronheimer, P.B. 1990. *The Geometry of Four-manifolds*, Oxford: Clarendon Press and New York: Oxford University Press

Jackiw, R., Nohl, C. & Rebbi, C. 1977. Conformal properties of pseudoparticle configurations. *Physical Review* D, 15: 1642–1646 (A large, but incomplete, family of solutions to the self-dual equations.)

Negele, J.W. 1998. Instantons, the QCD vacuum, and hadronic physics. *Nuclear Physics* B *Proceedings Supplements*, 73: 92–104

't Hooft, G. 1976. Symmetry breaking through Bell-Jackiw anomalies. *Physical Review Letters*, 37: 8–11

Weinberg, S. 1996. *Quantum Field Theory*, vol. 2, Cambridge and New York: Cambridge University Press (Chapter 23 concerns extended field configurations in particle physics and has a very clear treatment of instantons.)

INTEGRABILITY

Central problems in the integrability theory for nonlinear ordinary differential equations (ODEs) or partial differential equations (PDEs) are knowing which systems can be solved analytically and developing appropriate solution techniques. Although in some contexts the term *integrability* is not well defined, let us begin by considering two physically motivated nonlinear ODE systems that can be analytically solved.

Nonlinear Pendulum

Here, the nonlinear system is

$$\ddot{x} = ax + bx^2 + cx^3, \quad a, b, c = \text{constants}. \qquad (1)$$

Multiplying both sides of this equation by $\dot{x}$ and integrating yields an intermediate integral $I = \dot{x}^2/2 - ax^2/2 - bx^3/3 - cx^4/4$, which is determined by the initial conditions: $x(t_0)$ and $\dot{x}(t_0)$. In terms of I, the solution $x(t)$ can be written implicitly as

$$t - t_0 = \int_{x_0}^{x} \frac{\mathrm{d}x}{\sqrt{2I + ax^2 + 2bx^3/3 + cx^4/2}}, \qquad (2)$$

where $x(t_0) = x_0$. The inversion of this formula is expressed in terms of Jacobi elliptic functions (Bryd & Friedman, 1954). Note that this system has one degree of freedom, and one intermediate integral was sufficient to obtain a solution. Because it is related to an area, the intermediate integral (I) is sometimes called a quadrature, and by extension, Equation (2) is said to be obtained by the method of quadratures.

Calogero–Moser N-Body Problem

In this example, the nonlinear system is

$$\ddot{q}_n = \sum_{m=1, m\neq n}^{N} 2g^2 (q_n - q_m)^{-3}, \quad g = \text{constant}, \quad (3)$$

generalizations of which were studied extensively in the last three decades of the 20th century. Using a Lax isospectral deformation technique, the solution matrix $\text{diag}\,[q_1(t), \ldots, q_N(t)]$ is found to be similar to the matrix $\tilde{Q} = [\tilde{Q}_{nm}(t)]$ defined by

$$\tilde{Q}_{nm}(t) = \delta_{nm}\big[q_n(0) + \dot{q}_n(0)t\big] + \mathrm{i}(1-\delta_{nm})g\big[q_n(0) - q_m(0)\big]^{-1}t. \quad (4)$$

Thus, the solution to the initial value (Cauchy) problem is reduced to the algebraic task of finding the N eigenvalues of the matrix $\tilde{Q}$, and the solution formula for initial data, $q_i(0)$ and $\dot{q}_i(0)$, can be constructed from linear functions, through a finite number of algebraic operations and compositions of functions (Calogero, 2001). Equations (1) and (3) are completely integrable.

In the 19th century, Evariste Galois, Niels Henrik Abel, Joseph Liouville, and Sophus Lie tried to rationalize the process of solving differential equations by quadratures, or failing that, massaging them in such a way that useful information might be extracted. Mainly based on geometry and algebra, these efforts initiated much of the mathematics—such as classifications of differential equations in term of symmetries and conservation laws—that has dominated the 20th century. Attempts by Karl Weierstrass and Henri Poincaré to create a systematic theory of integrability are based on complex function theory.

An achievement of 19th-century mathematics was the elaboration of the theory of elliptic and Abelian functions, particularly the introduction of theta functions. A solution comprising such rapidly convergent power series is quite efficient computationally; thus, a natural question for 19th-century mathematicians was this: Which differential equations admit solutions as quotients of power series that converge in large regions, independent of initial or boundary conditions? The Cauchy–Kovalevsky theorem gives local existence for such expressions. This theme traces through the work of Sophia Kovalevsky and Paul Painlevé for nonlinear ODEs and through Bernhard Riemann and Immanuel Fuchs and their successors for linear ODEs (Hermann, 1984).

There are several results about local and global solutions of differential equations that establish existence, uniqueness, smoothness, stability, approximations, and so on; yet attempts to find exact solution formulas in the 19th century were largely unsuccessful. This is because solutions to nonlinear systems may exhibit complex behaviors—such as blow-up, shocks, chaos, fractals, and bifurcation—which are obstacles to integrability. Poincaré put an end to the search for new integrable equations by showing that among all dynamical systems integrable ones are exceptional. Indeed, a small structural perturbation of an integrable system often destroys integrability.

Although Poincaré's results dampened interest in the search for new integrable equations during the first half of the 20th century, the situation changed dramatically with the discovery of the inverse scattering transform as a method of solving the initial value (Cauchy) problem for the Korteweg–de Vries (KdV) equation (Gardner et al., 1967). Rapidly extended to several other nonlinear systems of scientific interest (nonlinear Schrödinger equation, sine-Gordon equation, Toda lattice, and so on), this discovery also led to the emergence of "soliton factories" during the 1980s (Zakharov, 1991).

More generally, integrability theory aims to find global information on solutions and, if possible, to solve differential equations analytically. Integrability itself is an intrinsic characteristic of differential equations, imposing constraints on the way solutions evolve in phase space and suggesting the following working definition.

Definition A differential equation is completely integrable if all solutions to well-posed initial or boundary value problems can be presented beginning with elementary functions, using finitely many algebraic operations and compositions of functions, and evaluating limits.

Algebraic operations include inverting or diagonalizing matrices; compositions of functions include inverses; and the limits can be integrals, infinite series, or asymptotes. Thus, this definition holds for cases in which solutions can be constructed explicitly. It also generalizes the notion of integrability by quadratures (Liouville integrability) that only requires computation of intermediate integrals in addition to algebraic operations and compositions of functions.

For ODEs, the Liouville–Arnol'd theorem on finite-dimensional Hamiltonian systems gives sufficient conditions, called the Liouville conditions, for guaranteeing the integrability by quadratures (Arnol'd, 1989). For a Hamiltonian system of N degrees of freedom, these conditions are:

- the existence of N integrals of motion $\{F_1, F_2, \ldots, F_N\}$,
- that are functionally independent on the level surface $\{F_i = a_i\}$ containing the initial data, and
- that commute with each other under the associated Poisson bracket.

If the level surface $\{F_i = a_i\}$ is compact and connected, then the Liouville–Arnol'd theorem says that the underlying Hamiltonian system can be expressed as

$$\dot{I}_i = 0, \ \dot{\varphi}_i = \omega_i(I_1, \ldots, I_N), \quad (5)$$

in the action-angle coordinate system (I_i, φ_i) of a neighborhood of the level surface. Thus, the motion is conditionally periodic along an N-dimensional torus with the frequencies ω_i, and the solution to the Cauchy problem can be completely determined by the method of quadratures. The Euler top, the Lagrange top, Kowalewski's top, the Stäckel systems, and geodesic flows on a surface are Liouville-integrable systems (Perelomov, 1990).

For PDEs, there also exist some results on integrability properties from a Hamiltonian perspective, including the bi-Hamiltonian theory (Magri, 1978) from which infinitely many symmetries and conservation laws for PDEs can be deduced. Motivated by the Liouville–Arnol'd theorem, a notion of integrability for PDEs is the existence of infinitely many conservation laws. The KdV equation is integrable in this sense, and it can also be put into a Hamiltonian form in action-angle coordinates like integrable ODEs (Zakharov & Faddeev, 1971).

The existence of infinitely many conservation laws can lead to infinitely many finite-dimensional solution varieties that can be determined analytically (Fuchssteiner, 1992), but it is not clear whether these subvarieties generate the whole infinite-dimensional solution variety. Indeed, the infinitely many degrees of freedom of PDEs introduce large diversity, obscuring their solvability and integrability properties.

The notion of partial integrability arises when systems of differential equations (both ODEs and PDEs) possess more degrees of freedom than conservation laws (Conte & Boccara, 1990). Symmetry constraints developed in soliton theory (Ma & Zhou, 2001) suggest a way to show partial integrability for PDEs through relating PDEs to integrable ODEs. The method was motivated by Moser's work on Hill's equation (Moser, 1980) and nonlinearization of Lax pairs (Cao, 1990). The results generalize the theory of finite-dimensional integrable stationary equations, suggesting the possibility of establishing a Liouville–Arnol'd theorem for infinite-dimensional Hamiltonian systems.

Since the 1970s, several criteria have arisen for testing the integrability of nonlinear PDEs, and corresponding theories include infinitely many symmetries, infinitely many conservation laws, Lax structure, bi-Hamiltonian structure, the Bäcklund transform, Hirota's bilinear form, the inverse scattering transform, and the Painlevé property (Degasperis, 1998; Gu, 1995).

An ODE or a PDE is said to possess the Painlevé property, respectively, if the movable singularities of solutions of the ODE are only poles (Ablowitz & Clarkson, 1991) or if solutions of the PDE are "single-valued" in the neighborhood of noncharacteristic, movable singularity manifolds (Weiss et al., 1983), suggesting that the Painlevé property is an indication of complete integrability (Conte, 1999). One advantage of the Painlevé property is that it can be a tool for computing Lax pairs and conservation laws. Lax pairs, as we have seen in Equation (3), provide linear objects for solving Cauchy problems of nonlinear equations. A thorough understanding of the relationship between Painlevé singularities and integrability may suggest alternatives to the KAM notion of near-integrability (Zakharov, 1991).

The term S-integrability implies integrability of Cauchy problems by the inverse spectral transform technique (Calogero & Degasperis, 1982) or the inverse scattering transform (Ablowitz & Clarkson, 1991; Fokas, 1997). C-integrability, on the other hand, means that a differential equation can be transformed into a linear one by an appropriate change of variables. Examples of C-integrable equations are the Burgers equation and the Calogero–Dagasperis–Ibragimov–Shabat equation:

$$u_t = u_{xx} - 2uu_x, \tag{B}$$

$$u_t = u_{xxx} + 3u^2u_{xx} + 9uu_x^2 + 3u^4u_x. \tag{CDIS}$$

These two equations are, respectively, cast into the heat equation ($v_t = v_{xx}$) and the linear KdV equation ($v_t = v_{xxx}$) under appropriate dependent variable transformations. Calogero and colleagues have made a systematic study of the construction and classification of C-integrable equations, both in $1 + 1$ dimensions and $N + 1$ dimensions (Zakharov, 1991). Although the property of C-integrability often leads to an infinity of conservation laws, the Burgers equation has only one local conservation law of differential polynomial type.

WEN-XIU MA

See also **Burgers equation; Constants of motion and conservation laws; Hamiltonian systems; Hirota's method; Inverse scattering method or transform; Painlevé analysis; Solitons**

Further Reading

Ablowitz, M.J. & Clarkson, P.A. 1991. *Solitons, Nonlinear Evolution Equations and Inverse Scattering*, Cambridge and New York: Cambridge University Press

Arnol'd, V.I. 1989. *Mathematical Methods of Classical Mechanics*, 2nd edition, New York: Springer

Bryd, P.F. & Friedman, M.D. 1954. *Handbook of Elliptic Integrals*, New York: Springer

Calogero, F. 2001. *Classical Many-Body Problems Amendable to Exact Treatments*, Berlin and Heidelberg: Springer

Calogero, F. & Degasperis, A. 1982. *Spectral Transform and Solitons*, vol. I. *Tools to Solve and Investigate Nonlinear Evolution Equations*, Amsterdam and New York: North-Holland

Cao, C.W. 1990. Nonlinearization of the Lax system for AKNS hierarchy. *Science in China, Series A: Mathematics, Physics, Astronomy*, 33: 528–536

Conte, R. (editor). 1999. *The Painlevé Property, One Century Later*, New York: Springer

Conte, R. & Boccara, N. (editors). 1990. *Partially Integrable Evolution Equations in Physics*, Dordrecht: Kluwer

Degasperis, A. 1998. Resource letter Sol-1: solitons. *American Journal of Physics*, 66: 486–497
Fokas, A.S. 1997. A unified transform method for solving linear and certain nonlinear PDEs. *Proceedings of the Royal Society of London, Series A: Mathematical, Physical and Engineering Sciences*, 453: 1411–1443
Fuchssteiner, B. 1992. Hamiltonian structure and integrability. In *Nonlinear Equations in the Applied Sciences*, Boston, MA: Academic Press, pp. 211–256
Gardner, C.S., Greene, J.M., Kruskal, M.D. & Miura, R.M. 1967. Method for solving the Korteweg–de Vries equation. *Physical Review Letters*, 19: 1095–1097
Gu, C.H. (editor). 1995. *Soliton Theory and Its Applications*, Berlin and Heidelberg: Springer and Hangzhou: Zhejiang Science and Technology Publishing House
Hermann, R. 1984. *Topics in the Geometric Theory of Integrable Mechanical Systems*, Brookline, MA: Math Science Press
Ma, W.-X. & Zhou, Z. X. 2001. Binary symmetry constraints of N-wave interaction equations in $1+1$ and $2+1$ dimensions. *Journal of Mathematical Physics*, 42: 4345–4382
Magri, F. 1978. A simple model of the integrable Hamiltonian equation. *Journal of Mathematical Physics*, 19: 1156–1162
Moser, J. 1980. Various aspects of integrable Hamiltonian systems. In *Dynamical Systems*, Boston: Birkhäuser, pp. 233–289
Perelomov, A.M. 1990. *Integrable Systems of Classical Mechanics and Lie Algebras*, vol. I, Basel: Birkhäuser
Weiss, J., Tabor, M. & Carnevale, G. 1983. The Painlevé property for partial differential equations. *Journal of Mathematical Physics*, 24: 522–526
Zakharov, V. E. (editor). 1991. *What Is Integrability?* Berlin and Heidelberg: Springer
Zakharov, V.E. & Faddeev, L.D. 1971. The Korteweg–de Vries equation is a fully integrable Hamiltonian system. *Functional Analysis and Its Applications*, 5(4): 18–27

INTEGRABLE CELLULAR AUTOMATA

Integrable cellular automata (CAs) are discrete dynamical systems that possess attributes of integrability including conserved quantities, symmetries, and localized solutions. They show how to discretize a given integrable system of differential equations, maintaining the integrability property, suggesting that integrability of discrete systems and their coherent structures are inherently connected with the iterated string processing performed by automata.

The propagating solutions (or coherent objects) on certain cellular automata have been found to exhibit nondestructive collisions similar to those observed for soliton systems like the Korteweg–de Vries equation. In such cases, pulse-like disturbances propagating along a uniform nonlinear medium are represented by strings of symbols (zero-one patterns), passing through a one-way structure—the pipeline of identical automata M. The analysis of these moving objects reduces to investigating the repeated automaton action over strings, also called an iterated automaton map (IAM); $M(a^t) = a^{t+1}$, $t = 0, 1, \ldots$.

All known models capable of supporting such discrete localized structures are described by automata (Siwak, 2001, 2002), and a method (called ultra-discretization) leads to discrete systems in which solutions of some familiar soliton equations are preserved as soliton-like patterns (Tokihiro et al., 1999). Thus, an IAM is a fundamental discrete mechanism that supports localized soliton-like periodic structures. This is why a new term *iterons* (Siwak, 2001, 2002) has been proposed for these objects. Note also that fractals owe their existence to the iterating process of some maps.

There are two classes of iterons. The first consists of particles well known in cellular automata models (Delorme & Mazoyer, 1999) where the parallel processing of strings occurs. The second class is not widely known and consists of so-called filtrons. The filtrons are emergent coherent objects occurring in serial processing of strings (Siwak, 2001).

In parallel processing of a string a^t at a given time t all symbols a_i^{t+1} of the next string a^{t+1} are updated simultaneously, for example, by the function $a_i^{t+1} = f(a_{i-r}^t, \ldots, a_i^t, \ldots, a_{i+r}^t)$. When the same function f is used for all positions i, one has a 1-dimensional CA, with f being called its local function or rule. The arguments of f are determined by the so-called neighborhood window $N_i = (-r, \ldots, +r)$; here N_i designates r neighbors on both sides of position i.

The listing of consecutive strings a^t for $t = 0, 1, \ldots$ one under another forms what is called a space-time (ST) diagram. This diagram visualizes the evolution of a given string a^0—the dynamics of a CA system in phase space for initial global state a^0. Occasionally, some moving and periodic patterns of symbols or segments of a string are seen on ST diagrams of CA processing. These are just particles or signals of CAs (Delorme & Mazoyer, 1999).

The serial processing of strings is performed by a computational model called a finite (state) automaton. The Mealy type automaton is described by $M = (S, \Sigma, \Omega, \delta, \beta, s_0)$, where S, Σ, and Ω are nonempty finite sets of—respectively—states, inputs, and outputs; $\delta\colon S \times \Sigma \to S$ is called the next state function of M, $\beta\colon S \times \Sigma \to \Omega$ is called the output function of M, and s_0 is the initial (extinction) state of the automaton. The automaton converts sequences of symbols, preserving their length. Any input string is read sequentially from left to right, one symbol at each instant of time (pulse of clock). For all $\tau = 1, 2, \ldots$ the automaton:

(i) reads input symbol $\sigma(\tau)$,
(ii) changes its current state $s(\tau)$ onto the next one according to $\delta(s(\tau), \sigma(\tau)) = s(\tau + 1)$, and
(iii) generates the symbol $\beta(s(\tau), \sigma(\tau)) = \omega(\tau)$ of the resulting string.

Thus the complete one step conversion at $a^t \to a^{t+1}$ requires a series of clock pulses τ. To consider IAMs, one has to assume the unified input-output alphabet $A = \Sigma = \Omega = 0, 1, \ldots, m$. Then the automaton's operation can be described by a

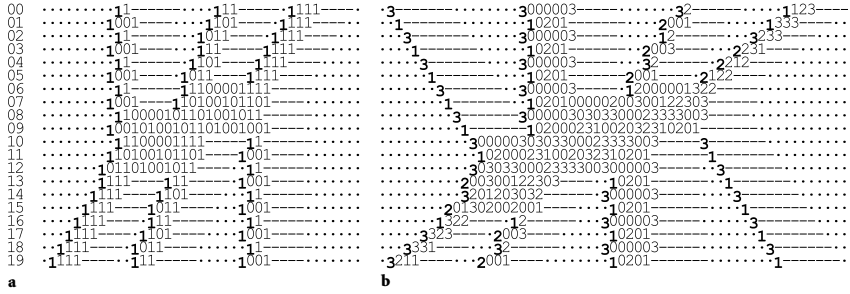

Figure 1. Nondestructive collisions of filtrons ($q = 2$). (a) PST model. (b) Automaton M_1.

sequence of operations $f_s: A \to A$, each f_s such that $f_s(a) = \beta(s, a)$.

Coherent objects of serial string processing were not known for a long time. The first model that established a bridge between discrete systems of string processing and soliton-like phenomena was the filter CA (Park et al., 1986). The PST (Park, Steiglitz, & Thurston) model was defined for $A = \{0, 1\}$ by a special space-time window (FCA window) and a nonlinear updating Boolean function $f_{\mathrm{PST}} : A^{2r+1} \to A$. It operates by moving the window to the right along a given string a^t. At each position the function f_{PST} computes consecutive elements

$$a_i^{t+1} = f_{\mathrm{PST}}\left(a_i^t, a_{i+1}^t, \ldots, a_{i+r}^t, , a_{i-r}^{t+1}, a_{i-r+1}^{t+1}, \ldots a_{i-1}^{t+1}\right)$$

of the resulting string a^{t+1} in such a way that $a_i^{t+1} = 1$ if and only if the sum of all window elements (which are arguments of f_{PST}) is even but not zero. It is assumed that the conversion $a^t \to a^{t+1}$ starts somewhere at left with the zero content of window (zero boundary conditions).

The PST model is an automaton and is classified as a digital parity infinite impulse response (IIR) filter. The dynamics of the PST model reveal discrete moving coherent objects capable of colliding in a nondestructive way. An example of such objects is shown in Figure 1(a).

Formal analysis of filter CAs has been given by Goldberg (1988). Goldberg has also given its first automaton-like description by means of a rapid updating rule.

Various generalizations of this model soon appeared. New updating functions were introduced, and the FCA window was modified (Jiang, 1992). A model with an infinite FCA window was given by Takahashi and Satsuma and called a soliton CA. Then, the working alphabet A was enlarged beyond binary (Fokas et al., 1990), and algebraic group operations were considered in computations of updating function.

Another approach was based on deriving the filter-CA-like description from the equations of motion of some systems and from so-called spectral problems (Bruschi et al., 1992).

It was observed that most of the models based on the FCA window perform very special cyclic processing. This led Siwak (2002) to a class of filter automata (FAs). FAs are described by three notions that are useful in physical interpretation of the IAM as a medium, namely:

— the activating function $\iota : A \to \{false, true\}$ such that $\iota(a) = true \leftrightarrow \delta(s_0, a) \neq s_0$;
— the cyclic sequence $(h_j, f_1, \ldots, f_k)$ of mappings f_s (the medium is excited); and
— the extinction conditions (the automaton returns to its extinction state s_0).

Note that the automaton equivalent of PST processing is activated by $a = 1$ (nonzero symbol). Its cyclic sequence of operations f_s is of the form $(N, A, \ldots, A) = NA^r$ where N denotes negate operation, and A is identity id (or accept). The extinction condition is based on a coincidence of some string's current segment $w \in \{a0^r\}$ with the cycle of activity.

The example of IAM dynamics of some cyclic automaton M_1 for $A = \{0, 1, 2, 3\}$ is shown in Figure 1(b). When the automaton M_1 is extinguished, it rewrites input zeroes; $h_0(0) = 0$, but activated by a symbol $j \neq 0$, it performs the cycles of operations $(h_0, f_1, f_2, f_3), (h_j, f_1, f_2, f_3), \ldots$ where

$$h_0 = \begin{pmatrix} 0 & 1 & 2 & 3 \\ 0 & 0 & 0 & 0 \end{pmatrix}, h_1 = \begin{pmatrix} 0 & 1 & 2 & 3 \\ 3 & 0 & 2 & 2 \end{pmatrix},$$

$$h_2 = \begin{pmatrix} 0 & 1 & 2 & 3 \\ 2 & 3 & 0 & 1 \end{pmatrix}, h_3 = \begin{pmatrix} 0 & 1 & 2 & 3 \\ 1 & 2 & 3 & 0 \end{pmatrix},$$

$$f_1 = f_3 = h_3 = \begin{pmatrix} 0 & 1 & 2 & 3 \\ 0 & 1 & 2 & 3 \end{pmatrix} = \mathrm{id},$$

$$f_2 = \begin{pmatrix} 0 & 1 & 2 & 3 \\ 0 & 1 & 3 & 2 \end{pmatrix}.$$

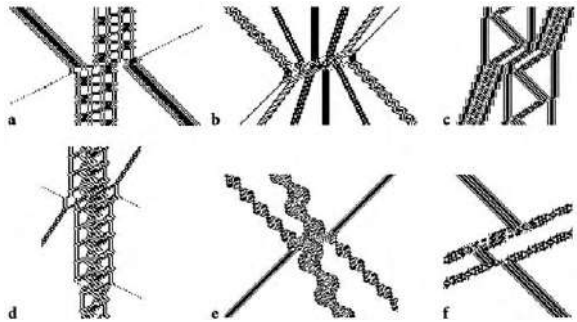

Figure 2. Exemplary images of IAM dynamics—various phenomena of colliding filtrons.

Extinction occurs when the segment $w = 0000$ is read within a cycle.

The symbols of A are shown on ST diagram in order to expose so-called M-segments within strings. Each M-segment begins with an activating symbol, which is printed in bold. The tail zeroes of an M-segment, that is all consecutive zeros immediately preceding the extinction of M are denoted by bar. All zeroes read by the automaton in its state s_0 are shown as dots, and all remaining zeroes as digits 0. With this convention one can recognize whether any two M-segments are distant, adjacent, or overlap and actually form a complex object. Also, a shift q per row to the left is sometimes applied to ST diagrams.

The filtron x of automaton M within the IAM dynamics is defined to be periodic M-segment of the string $a^0 = \ldots 0x0 \ldots$.

Among the discrete models supporting coherent objects there are also the following. For most of them the appropriate equivalent automata have been identified (Siwak, 2001, 2002):

— iterated arrays of finite state automata (Atrubin, 1965);
— filter CA, soliton CA, and other generalizations of PST model based on FCA window;
— digital recursive (IIR) filters and filter automata family (Siwak, 2001);
— classical CAs and higher order CAs (Delorme & Mazoyer, 1999);
— CAs with mixed serial and parallel scenarios of their updating schedule;
— rapid-updating rule-type procedures called also fast rules;
— integrable CAs derived from so-called spectral problems (Bruschi et al., 1992), and discrete versions of some classical soliton equations;
— box–ball systems introduced by D. Takahashi;
— crystal systems and combinatorial data processing;
— techniques of accelerating the convergence of numerical algorithms;
— affine Lie algebras.

Let us illustrate the dynamics of IAM with automata $M_{\mathrm{BBSC}}(m, n)$, which are equivalent to the model called the box-ball system with carrier (BBSC). In BBSC each position i represents a box, and each symbol $0 < a_i \leq m$ from A is interpreted as the number of balls. A single step of the evolution of a string is performed by a carrier of capacity n that runs to the right once and moves each ball exactly once. At each box, the carrier puts as many balls into the box as possible and simultaneously takes as many balls from the box as possible.

This means that if the carrier contains $0 \leq c_j \leq n$ balls at box j, then it will take $\min(a_j, n - c_j)$ balls from this box and, simultaneously, will leave $\min(c_j, m - a_j)$ balls. The finite state automaton $M_{\mathrm{BBSC}}(m, n)$ that performs exactly the same string processing as this BBSC is such that: the set of states $S = \{0, 1, \ldots, n\}$ and the alphabet of input/output symbols $A = \{0, 1, \ldots, m\}$ are sets of integers; $s_0 = 0$ is the initial state of $M_{\mathrm{BBSC}}(m, n)$; and the next states of $M_{\mathrm{BBSC}}(m, n)$ are given by $\delta(s, \sigma) = s + \min(\bar{s}, \sigma) - \min(s, \bar{\sigma})$, while the output symbols are determined by $\omega = \beta(s, \sigma) = \sigma + \min(s, \bar{\sigma}) - min(\bar{s}, \sigma)$. Here $\bar{s} = n - s$ and $\bar{\sigma} = m - \sigma$.

An example of colliding filtrons of the automaton $M_{\mathrm{BBSC}}(16, 22)$ is given in Figure 2.

Further examples of IAM dynamics for some other automata are given in Figure 3 where among the multi-filtron nondestructive (solitonic) collisions the following phenomena can be especially seen: complex filtrons (a), (c), jumps of the filtron over a bundle (a), (b), trapped or bouncing filtrons and collision of such complexes (c), decaying object (or quasifiltron) and its earlier solitonic collision (d), vibrating filtrons (e), steady filtrons (a), (b), and attraction and repelling of filtrons (f). Also the fusion, annihilation of filtrons and

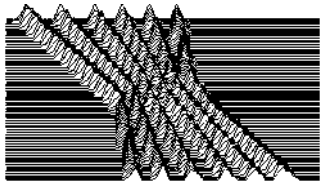

Figure 3. Six filtrons of the automaton $M_{\mathrm{BBSC}}(16, 22)$ collide solitonically (shift $q = 1$).

many other events are possible and can be seen in computer simulations—the realm of the behaviors of filtrons of automata is fascinating and amazingly rich.

The automaton approach and explanation of discrete coherent structures phenomena by IAMs leads to many applications, including computing by means of streams of filtrons (solitonic processing idea of Steiglitz), transmission and conversion of information via fiber optical lines, and signals and waves processing (e.g., by an interaction of electromagnetic waves with a shock wave background or another precisely shaped medium).

PAWEL SIWAK

See also **Cellular automata; Cellular nonlinear networks; Game of life; Integrable lattices; Solitons, types of**

Further Reading

Atrubin, A.J. 1965. An iterative one-dimensional real-time multiplier. *IEEE Transactions on Electronic Computers*, EC-14: 394–399

Adamatzky, A. (editor). 2002. *Collision-Based Computing*, London: Springer

Bruschi, M., Santini, P.M. & Ragnisco, O. 1992. Integrable cellular automata. *Physics Letters* A, 169: 151–160

Delorme, M. & Mazoyer, J. (editors). 1999. *Cellular Automata*, Dordrecht: Kluwer

Fokas, A.S., Papadopoulou, E.P. & Saridakis, Y.G. 1990. Coherent structures in cellular automata. *Physics Letters* A, 147(7): 369–379

Jiang, Z. 1992. An energy-conserved solitonic cellular automaton. *Journal of Physics* A: *Mathematical and General*, 25(11): 3369–3381

Park, J.K., Steiglitz, K. & Thurston, W.P. 1986. Soliton-like behavior in automata. *Physica* D, 19: 423–432

Siwak, P. 2001. Soliton-like dynamics of filtrons of cyclic automata. *Inverse Problems*, 17(4): 897–918

Siwak, P. 2002. Iterons of automata. In *Collision-Based Computing*, edited by A. Adamatzky, London: Springer, pp. 299–353

Tokihiro, T., Nagai, A. & Satsuma, J. 1999. Proof of solitonical nature of box and ball systems by means of inverse ultra-discretization. *Inverse Problems*, 15: 1639–1662

INTEGRABLE LATTICES

Lattices, or differential-difference equations (DDEs), are a special class of ordinary differential equations, with an infinite number of dependent variables $q_n = q_n(t)$ numbered by integer indices n, admitting a translational invariance with respect to the shift $n \to n + 1$. Due to this property, such equations are well suited for describing processes in translationally symmetric systems like crystals. By imposing suitable boundary conditions, such as periodic ones ($q_n(t) \equiv q_{n+N}(t)$ for all n), one can also model finite systems. In the notation above the dependent variable t plays the role of time; the range where the dependent variables q_n take values can be a multidimensional vector space or even a more general manifold. Sometimes it is convenient to think of n as the second, discrete independent variable, so that $q_n(t) = q(t, n\Delta x)$ is thought of as a sampling of a function $q(t, x)$ of two continuous variables (time t and space coordinate x) for the discrete sequence of values of $x = n\Delta x$. In such a context differential-difference systems appear as semi-discretizations of systems of partial differential equations (PDEs). For instance, the lattice model

$$\ddot{q}_n = \omega_0^2(q_{n+1} - 2q_n + q_{n-1}) - \sin(q_n), \qquad (1)$$

used by Yakov Frenkel and Tatiana Kontorova in their study (1939) of the relation between dislocation and deformation of crystals, can be considered as a semi-discretization of the sine-Gordon (SG) equation $q_{tt} - q_{xx} = -\sin(q)$ (in this interpretation $\omega_0 = 1/\Delta x$). Subsequent developments revealed that the discrete model (1) is non-integrable, unlike its continuous counterpart SG. Thus, in hindsight, already this early example illustrates the difficult problem of integrable discretization: how to discretize one or several independent variables in a given integrable system, maintaining the integrability property.

Another early example of a physically important system of DDEs is the model used by Enrico Fermi, John Pasta and Stan Ulam in their 1955 study of the dynamics of energy partition in crystals:

$$\ddot{q}_n = -\omega_0^2(q_{n+1} - 2q_n + q_{n-1}) - \alpha\big((q_{n+1} - q_n)^2 - (q_n - q_{n-1})^2\big). \qquad (2)$$

In this model, only nearest neighbors interact with the potential depending on their relative displacement, $U(\Delta q) = \frac{\omega_0^2}{2}(\Delta q)^2 + \frac{\alpha}{3}(\Delta q)^3$. Also this model is, strictly speaking, non-integrable. However, by an interesting historical twist, the studies by Fermi, Pasta, and Ulam played the precursor role for the theory of solitons. Presumably, due to the closeness of Equation (2) to integrable models, it demonstrated a lack of thermalization (the FPU recurrence phenomenon), and in attempts to understand this, Kruskal and Zabusky studied the KdV equation and eventually discovered its solitons (*See* **Fermi–Pasta–Ulam oscillator chain**).

The story of integrable lattices began with the discovery by Toda (1989) of the lattice with an exponential interaction of nearest neighbors, which

carries nowadays his name (*See* **Toda lattice**):

$$\ddot{q}_n = \mathrm{e}^{q_{n+1}-q_n} - \mathrm{e}^{q_n-q_{n-1}}. \tag{3}$$

He found a number of exact soliton-like solutions of this systems, both in the infinite and in the periodic setting. Multisoliton solutions were constructed in 1973 by Hirota with the help of his ingenious "direct" (or bilinear) method (*See* **Hirota's method**). The integrability of this model in the sense of classical mechanics (existence of an infinite number of independent integrals of motion, which are in involution with respect to the standard Poisson bracket with canonically conjugate momenta $p_n = \dot{q}_n$), as well as in the sense of the solitons theory (Lax representation and applicability of the inverse scattering, or inverse spectral, transformation (IST)) was demonstrated in 1974 independently by Flaschka and by Manakov. Other important early work on this system includes the treatment of scattering in the finite nonperiodic Toda lattice by Moser (1975), finding the Bäcklund transformation by Wadati and Toda (1975), and the solution of the periodic lattice in terms of multidimensional theta-functions given independently by Date and Tanaka and by Krichever (1976). One has a rare possibility to read the first-hand presentation of the whole body of relevant results, including the authentic story of the original discovery, in Toda (1989).

Once the mechanism of integrability via IST for lattice systems was uncovered, new integrable DDEs began to be discovered in quick succession. The next one was the lattice

$$\dot{a}_n = a_n(a_{n+1} - a_{n-1}), \tag{4}$$

having plenty of applications and known today under various names (Volterra, Kac–van Moerbeke, discrete KdV, etc.). Its integrability was established independently by Manakov (1974) and by Kac and van Moerbeke (1975), while the multisoliton solutions for it and for its modification,

$$\dot{a}_n = (1 + a_n^2)(a_{n+1} - a_{n-1}), \tag{5}$$

had been found by Hirota in 1973.

An important paper by Ablowitz & Ladik (1976) contained a lattice version of the zero-curvature (Zakharov–Shabat) representation of integrable systems and integration methods based on it. This deepened understanding of the algebraic structures behind integrable lattices, and opened an opportunity to construct in a unified manner arbitrarily many examples. One of the celebrated systems introduced and studied there is an integrable spatial discretization of the nonlinear Schrödinger equation (DNLS):

$$\mathrm{i}\dot{\psi}_n = -(\psi_{n+1} - 2\psi_n + \psi_{n-1})/(\Delta x)^2 + \nu \mid \psi_n \mid^2 \times(\psi_{n+1} + \psi_{n-1}). \tag{6}$$

A different but gauge equivalent discretization of NLS was found by Isergin and Korepin in 1981 (*See* Faddeev & Takhtajan, 1987 and **Discrete nonlinear Schrödinger equations**).

Dozens of integrable lattices have been found since then (which, of course, has led to a certain devaluation of this sort of activity). It seems, however, that only a few of them are of really fundamental importance for theory and applications. Such a "short list" depends naturally on personal tastes, but the following systems (apart from those already mentioned) should be included in any case.

A sort of a relativistic generalization of the Toda lattice is due to Ruijsenaars (1990):

$$\ddot{q}_n = (1 + \alpha\dot{q}_{n+1})(1 + \alpha\dot{q}_n)\,\frac{\mathrm{e}^{q_{n+1}-q_n}}{1 + \alpha^2\mathrm{e}^{q_{n+1}-q_n}} - (1 + \alpha\dot{q}_n)(1 + \alpha\dot{q}_{n-1})\,\frac{\mathrm{e}^{q_n-q_{n-1}}}{1 + \alpha^2\mathrm{e}^{q_n-q_{n-1}}}. \tag{7}$$

A Toda-type lattice with nearest neighbors interactions that encounter elliptic functions but depends not only on their relative displacements was discovered by Shabat & Yamilov (1990) and independently by Krichever (2000):

$$\ddot{q}_n = (\dot{q}_n^2 - 1)\big(V(q_n, q_{n+1}) + V(q_n, q_{n-1})\big), \tag{8}$$

where $V(q, q') = \zeta(q + q') + \zeta(q - q') - \zeta(2q)$ is an elliptic function in both arguments q, q' (here $\zeta(q)$ is the Weierstrass ζ-function).

A neat spatial discretization of the Landau–Lifshitz (LL) equation has been derived by Adler (2000):

$$\dot{s}_n = \langle s_n, Js_n\rangle\left(\frac{s_n \times s_{n+1}}{1 + \langle s_n, s_{n+1}\rangle} + \frac{s_n \times s_{n-1}}{1 + \langle s_n, s_{n-1}\rangle}\right) - 2s_n \times (Js_n). \tag{9}$$

Here $s_n \in S^2$, and J is a constant 3×3 matrix. In the isotropic case $J = I$ and this model reduces to a discrete Heisenberg magnetic discovered independently by Sklyanin and by Ishimori in 1982. Sklyanin found also a discretization of the LL equation different from (9); the relation between both models is discussed in Adler (2000).

In the rest of this article we briefly discuss some mathematical aspects of integrable lattices. We illustrate them mainly with the example of the Toda lattice (3), but almost all of this holds in one form or another for all integrable DDEs.

Lax Representations

The results by Flaschka and by Manakov of 1974 serve as a first application of IST in the differential-difference context. It is based upon the Lax representation of the Toda lattice, that is, the fact that (3) is equivalent to an operator equation

$$\dot{L} = [L, A_\pm], \tag{10}$$

in terms of linear difference operators L and $A_\pm$ with coefficients depending on $q_n, \dot{q}_n$ and on the so-called

spectral parameter λ:

$$L = \sum b_n E_{n,n} + \lambda^{-1} \sum a_n E_{n,n+1} + \lambda \sum E_{n+1,n}, \quad (11)$$

$$A_+ = \sum b_n E_{n,n} + \lambda \sum E_{n+1,n},$$

$$A_- = -\lambda^{-1} \sum a_n E_{n,n+1}, \quad (12)$$

where the Flaschka–Manakov variables a_n, b_n are expressed through q_n, $p_n = \dot{q}_n$ as

$$a_n = \mathrm{e}^{q_{n+1}-q_n}, \quad b_n = p_n. \quad (13)$$

Here we represent difference operators as infinite matrices, with $E_{m,n}$ being the matrix with the only nonvanishing element equal to 1 in the position (m, n). In the case of the finite open-end lattice, the operators are $N \times N$ matrices; summation in the above formulas is performed for n from 1 to N, and it is assumed that $E_{N+1,N} = E_{N,N+1} = 0$. The N-periodic case differs in that it is assumed that $E_{N+1,N} = E_{1,N}$ and $E_{N,N+1} = E_{N,1}$. In the infinite and the finite open-end case, the spectral parameter λ can be removed by a conjugation with a diagonal matrix $\mathrm{diag}(\lambda^n)$; it is not so in the periodic case, which makes the latter analytically much more difficult and demanding.

An alternative to the Lax representation is the discrete zero-curvature representation

$$\dot{L}_n = M_n L_n - L_n M_{n-1}, \quad (14)$$

first developed by Ablowitz and Ladik in 1975. It uses the same second-order operators (11), (12), but in terms of the spectral parameter-dependent 2×2 matrices

$$L_n = \begin{pmatrix} b_n + \lambda & a_{n-1} \\ -1 & 0 \end{pmatrix}, \quad M_n = \begin{pmatrix} -\lambda & -a_n \\ 1 & b_n \end{pmatrix}. \quad (15)$$

Such a representation is somewhat more flexible from the technical viewpoint.

Inverse scattering

The matrix L is similar to a symmetric tri-diagonal matrix, which means that the operator L is gauge equivalent to a second-order and self-adjoint matrix. The direct and inverse spectral theory of such operators is well-developed (see Teschl, 2000), and parallel, to a large extent, to the direct and inverse spectral theory of second-order differential operators. In the rapidly decaying case ($q_n \to c$, $\dot{q}_n \to 0$ as $n \to \pm\infty$) the standard IST scheme is illustrated by the following diagram.

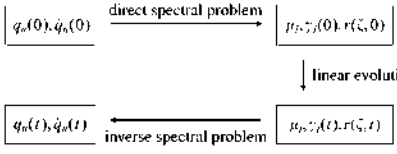

The set of spectral data allowing for a solution of the inverse problem consists of the discrete eigenvalues μ_j, the normalizing coefficients γ_j of the corresponding discrete eigenfunctions, and the reflection coefficient $r(\zeta)$ of the continuous spectrum. Equation (10) yields that the evolution of the operator L, induced by the fact that $q_n(t)$ satisfy the Toda lattice equations (3), is isospectral. More precisely, the discrete eigenvalues are constants of the motion, while the evolution of other spectral data is governed by simple linear equations:

$$\mu_j = \text{const}, \quad \gamma_j(t) = \gamma_j(0)\mathrm{e}^{(\mu_j - \mu_j^{-1})t},$$

$$r(\zeta, t) = r(\zeta, 0)\mathrm{e}^{(\zeta - \zeta^{-1})t}.$$

Solution of the inverse spectral problem is given in terms of the Riemann–Hilbert problem or its variants, such as the Gel'fand–Levitan equation. Multisoliton solutions correspond to reflectionless potentials, for which $r(\zeta, t) \equiv 0$.

In the periodic case, the set of the spectral data is more complicated: it includes a hyperelliptic Riemann surface $\mathcal{R}$ of genus $N - 1$ determined by the eigenvalues of the periodic boundary value problem for the operator L; further, it includes $N - 1$ points P_k on $\mathcal{R}$, which correspond to the eigenvalues of L with vanishing boundary conditions. Due to (10), the Riemann surface $\mathcal{R}$ itself is an integral of motion, and the evolution of points P_k is such that the image of the divisor $P_1 + \ldots + P_{N-1}$ under the Abel map moves along a straight line in the Jacobi variety of $\mathcal{R}$. Solution of the inverse spectral problem is given in terms of multidimensional theta-functions. An important technical device in this type of problems constitute Baker–Akhiezer functions, which have essential singularities at P_k and are meromorphic elsewhere on $\mathcal{R}$; their analytic properties define them uniquely.

Hierarchies

Integrable lattices (and, more generally, integrable systems) do not appear separately, but are organized in hierarchies. To describe the Toda lattice hierarchy, note that the matrices $A_\pm$ in (12) may be seen as $A_\pm = \pm\pi_\pm(L)$, where $\pi_\pm$ stands for the nonnegative (resp. negative) part of the Laurent series with respect to the spectral parameter λ. This is a particular instance of a very general construction, known as the Adler–Kostant–Symes (AKS) method, dealing with a splitting of a Lie algebra g into a direct sum of its two subspaces that are also Lie subalgebras $g_\pm$; in this general setting, $\pi_\pm : g \mapsto g_\pm$ are the corresponding projections. The higher members of the Toda lattice hierarchy (enumerated by $m \in \mathbb{N}$) are characterized by Lax equations of form (10) with the same Lax matrix L as in (11) and $A_\pm = \pm\pi_\pm(L^m)$, see also Kupershmidt (1985).

"Explicit" Solution in Terms of a Factorization Problem

A further important ingredient of the AKS method is a formula for the solution of the initial value problem for such Lax equations. It is given in terms of the factorization problem in the Lie group G corresponding to the Lie algebra g in terms of its Lie subgroups $G_\pm$ corresponding to $g_\pm$: if the elements $U_\pm(t) \in G_\pm$ solve the factorization problem $\exp(tL^m(0)) = U_+U_-$, then $L(t) = U_+^{-1}(t)L(0)U_+(t) = U_-(t)L(0)U_-^{-1}(t)$ is the solution of the mth member of the hierarchy. The factorization problem in G is, in general, a sort of Riemann–Hilbert problem, intimately related to the one participating in the inverse scattering transformation.

Darboux–Bäcklund Transformations and Discretization

The above-mentioned factorization problem in G also leads to an effective construction of Darboux–Bäcklund transformations, which are a further indispensable attribute of integrable systems. For the Toda lattice, a Bäcklund transformation $(q_n, p_n) \mapsto (\widetilde{q}_n, \widetilde{p}_n)$ with a parameter h, which serves also as an integrable discretization with the time step h, is a result of the following factorization: $I + hL = U_+U_-$, with a subsequent flipping of factors: $I + h\widetilde{L} = U_-U_+$, where the factors are given by

$$U_+ = \sum \mathrm{e}^{\widetilde{q}_n - q_n} E_{n,n} + h\lambda \sum E_{n+1,n} \in G_+, \quad (16)$$

$$U_- = I + h\lambda^{-1} \sum \mathrm{e}^{q_{n+1} - \widetilde{q}_n} E_{n,n+1} \in G_-. \quad (17)$$

The formulas for the Bäcklund transformation seen from these factorizations, are

$$\begin{aligned} 1 + hp_n &= \mathrm{e}^{\widetilde{q}_n - q_n} + h^2 \mathrm{e}^{q_n - \widetilde{q}_{n-1}}, \\ 1 + h\widetilde{p}_n &= \mathrm{e}^{\widetilde{q}_n - q_n} + h^2 \mathrm{e}^{q_{n+1} - \widetilde{q}_n}. \end{aligned} \quad (18)$$

This is a canonical transformation, possessing a classical generating function. This result was first obtained by Wadati and Toda in 1975, see also Suris (2003).

Hamiltonian Structure

The last immanent feature of integrable lattices (and, more generally, integrable systems) is their Hamiltonian structure. Often, they are even bi- or multi-Hamiltonian, as it is the case for the Toda lattice. In the Flaschka–Manakov variables (13) the equations of motion of the Toda lattice (3) are rewritten as

$$\dot{a}_n = a_n(b_{n+1} - b_n), \quad \dot{b}_n = a_n - a_{n-1}. \quad (19)$$

The canonical Poisson bracket for the variables q_n, p_n reads in the variables a_n, b_n as follows:

$$\{b_n, a_n\}_1 = -a_n, \quad \{a_n, b_{n+1}\}_1 = -a_n \quad (20)$$

(all other brackets of the coordinate functions vanish), and system (19) is Hamiltonian with respect to this bracket, with the Hamilton function $H_2 = \frac{1}{2}\sum b_n^2 + \sum a_n$. However, one can define also a different Poisson bracket for the variables a_n, b_n:

$$\begin{aligned} \{b_n, a_n\}_2 &= -b_n a_n, \\ \{a_n, b_{n+1}\}_2 &= -a_n b_{n+1}, \\ \{b_n, b_{n+1}\}_2 &= -a_n, \\ \{a_n, a_{n+1}\}_2 &= -a_n a_{n+1}, \end{aligned} \quad (21)$$

with the following properties: it is compatible with the first one (i.e., their linear combinations are again Poisson brackets), and system (19) is Hamiltonian with respect to this bracket, with the Hamilton function $H_1 = \sum b_n$. So, the Toda lattice in the form (19) is a bi-Hamiltonian system. This was found by M. Adler in 1979. The bi-Hamiltonian property, introduced by Magri in 1978 on the example of KdV, has been established since then as an alternative (and highly effective and informative) definition of integrability. Actually, the Toda lattice (19) is even tri-Hamiltonian, since there exists one more local Poisson bracket for the variables a_n, b_n with similar properties, discovered in Kupershmidt (1985).

Higher Dimensions

Up to now, we have considered integrable lattices with one continuous and one discrete independent variables. This clearly allows for a further generalization. Integrable systems with two continuous and one discrete independent variables are well known and widely used as the models in the field theory. For instance, the Toda field theory deals with the system

$$(q_n)_{xy} = \mathrm{e}^{q_{n+1} - q_n} - \mathrm{e}^{q_n - q_{n-1}}, \quad (22)$$

introduced into soliton theory by Mikhailov (1979). Later it was realized that the equivalent equation $(\log v_n)_{xy} = v_{n+1} - 2v_n + v_{n-1}$, which is obtained by setting $v_n = \exp(q_{n+1} - q_n)$, appeared already in studies by Darboux in 1888, as the equation satisfied by the so-called Laplace invariants of the chain of Laplace transformations of a given second-order hyperbolic partial differential equation.

YURI B. SURIS

See also **Bäcklund transformations; Darboux transformation; Discrete nonlinear Schrödinger equations; Hamiltonian systems; Inverse scattering method or transform; Quantum inverse scattering method; Toda lattice**

Further Reading

Ablowitz, M. & Ladik, J. 1976. Nonlinear differential-difference equations and Fourier analysis. *Journal of Mathematical Physics*, 17: 1011–1018

Adler, V.E. 2000. On discretization of the Landau–Lifshits equation. *Teoreticheskaya i Matematicheskaya Fizika*, 124: 48–61

Faddeev, L.D. & Takhtajan, L.A. 1987. *Hamiltonian Methods in the Theory of Solitons*, Berlin and New York: Springer

Flaschka, H. 1974. On the Toda lattice II. Inverse scattering solution. *Progress in Theoretical Physics*, 51: 703–716
Kac, M. & van Moerbeke, P. 1975. On an explicitly soluble system of nonlinear differential equations related to certain Toda lattices. *Advances in Mathematics*, 16: 160–169
Krichever, I. 2000. Elliptic analog of the Toda lattice. *International Mathematics Research Notices*, 8: 383–412
Kupershmidt, B.A. 1985. Discrete Lax equations and differential-difference calculus. *Asterisque*, 123
Manakov, S.V. 1974. On the complete integrability and stochastization in discrete dynamical systems. *Soviet Physics, JETP*, 40: 269–274
Moser, J. 1975. Finitely many mass points on the line under the influence of an exponential potential—an integrable system. In *Dynamic Systems Theory and Applications*, edited by J. Moser (see *Math. Reviews* MR0393426). Berlin and New York: Springer, pp. 467–497
Ruijsenaars, S.N.M. 1990. Relativistic Toda systems. *Communications in Mathematical Physics*, 133: 217–247
Suris, Yu.B. 2003. *The Problem of Integrable Discretization: Hamiltonian Approach*, Basel: Birkhäuser
Teschl, G. 2000. *Jacobi Operators and Completely Integrable Nonlinear Lattices*. Providence, RI: American Mathematical Society
Toda, M. 1989. *Theory of Nonlinear Lattices*, Berlin and New York: Springer
Wadati, M. & Toda, M. 1975. Bäcklund transformation for the exponential lattice. *Journal of the Physical Society of Japan*, 39: 1196–1203

INTEGRABLE TOPS

See **Rotating rigid bodies**

INTEGRAL EQUATIONS

See **Equations, nonlinear**

INTEGRAL TRANSFORMS

Integral transforms have their genesis in the 19th century work of Joseph Fourier and Oliver Heaviside, subsequently set into a general framework during the 20th century. The fundamental idea is to represent a function $f(x)$ in terms of a *transform* $F(p)$, using an integral transform pair,

$$F(p) = \int K(p,x) f(x)\,\mathrm{d}x,$$
$$f(x) = \int L(x,p) F(p)\,\mathrm{d}p. \qquad (1)$$

The functions $K(p,x)$ and $L(x,p)$ are *kernels*. If either of $f(x)$, $F(p)$ is discontinuous, further interpretation must be supplied at those points.

Oliver Heaviside invented his operational calculus to solve differential equations, such as those which arise in the theory of electrical transmission lines. A simple example is the diffusion problem (Whittaker, 1928),

$$\partial^2 u/\partial x^2 = k\,\partial u/\partial t, \quad x \geq 0, \quad t \geq 0,$$
$$u(0,t) = U_0. \qquad (2)$$

Heaviside treated differentiation as a symbolic operation, $p = \partial/\partial t$, to write the operational solution

$$u(x,t) = \mathrm{e}^{-x\sqrt{kp}} \cdot U_0. \qquad (3)$$

Using Euler's formula for differentiation,

$$\frac{\mathrm{d}^n(x^p)}{\mathrm{d}x^n} = \frac{p!}{(p-n)!}\,x^{p-n} \qquad (4)$$

with n not restricted to the integers, Heaviside was able to extract all the information he required from such an approach. However, his methods met with general disapproval, leading to lifelong difficulties for him.

Heaviside's work was formalized, using the Laplace integral, to give the Laplace transform pair:

$$F(p) = \int_0^\infty \mathrm{e}^{-px} f(x)\,\mathrm{d}x,$$
$$f(x) = \frac{1}{2\pi\mathrm{i}} \int_{c-\mathrm{i}\infty}^{c+\mathrm{i}\infty} \mathrm{e}^{+px} F(p)\,\mathrm{d}p. \qquad (5)$$

In the normal case, the transform integral converges for all p in a complex half-plane $\Re(p) > \alpha$, in which case the constant c in the inversion integral must be chosen to satisfy the restriction $c > \alpha$. Subjecting Equation (2) to the Laplace transform leads to the same formula (3) for the *transform* $U(x,p)$. Everything may be extracted from this using complex variable techniques; the complex variable p is just a placeholder for Heaviside's operational symbol $p = \partial/\partial t$.

The Laplace transform has simple properties with respect to differentiation and convolutions (Schiff, 1999). For the former, if $F(p)$ is the transform of $f(t)$, then the transform of $f'(t)$ is $pF(p) - f(0)$. Again, if $h(t)$ is the convolution of $f(t)$ with $g(t)$, defined as

$$h(t) = \int_0^t f(s) g(t-s)\,\mathrm{d}s, \qquad (6)$$

then the transform is given by simple multiplication:

$$H(p) = F(p)\,G(p). \qquad (7)$$

An important area of application is systems of ordinary differential equations with constant coefficients, such as (Barnett & Cameron, 1992)

$$\boldsymbol{x}' = A\boldsymbol{x} + B\boldsymbol{u}, \qquad \boldsymbol{y} = C\boldsymbol{x}. \qquad (8)$$

Here $\boldsymbol{x}$ is a set of n internal state variables, $\boldsymbol{u}$ a set of r inputs, $\boldsymbol{y}$ a set of s outputs; A, B, and C are matrices. Taking the Laplace transform and using elementary matrix algebra, the response of the system is given by

$$\mathbf{Y}(p) = G(p)\mathbf{U}(p),$$
$$G(p) = C(pI - A)^{-1}B. \qquad (9)$$

The transform being a product, the solution is a matrix of convolutions. However, the essential information

about the system may be extracted directly, without recourse to inversion.

The Fourier transform represents functions as linear combinations of periodic functions, an idea pioneered by Fourier. A one-dimensional form is

$$F(\omega) = \int_{-\infty}^{\infty} f(t)\, \mathrm{e}^{\mathrm{i}\omega t}\, \mathrm{d}t,$$

$$f(t) = \frac{1}{2\pi \mathrm{i}} \int_{-\infty}^{\infty} F(k)\, \mathrm{e}^{-\mathrm{i}\omega t}\, \mathrm{d}\omega. \qquad (10)$$

The most common uses are (i) with time as the original variable—transformation from the time domain to the frequency domain and (ii) with spatial position as the original variable—transformation from configuration space to momentum space. The Fourier transform also has simple properties with respect to differentiation and convolution (the integral in (6) now extends from $-\infty$ to $+\infty$), making it useful for investigation of partial differential equations, as well as many more complex systems.

Other important transforms are the Hankel transform, which uses Bessel functions for the kernels in pair (1), alternative forms of the Fourier transform using sine or cosine functions, and many other lesser known pairs (Davies, 2002). In fact, every Sturm–Liouville problem generates integral transforms (Antimirov et al., 1993). In addition, there are transforms that involve complex integration in an essential way, such as the Hilbert transform and Cauchy integrals, which use principal values.

The Mellin transform pair

$$F(p) = \int_0^{\infty} x^{p-1} f(x)\, \mathrm{d}x,$$

$$f(x) = \frac{1}{2\pi \mathrm{i}} \int_{c-\mathrm{i}\infty}^{c+\mathrm{i}\infty} x^{-p} F(p)\, \mathrm{d}p \qquad (11)$$

has great utility, particularly in asymptotics (Ninham et al., 1992; Davies, 2002). For example, the Mellin transform representation of the exponential integral

$$\mathrm{Ei}(x) = \int_x^{\infty} \frac{\mathrm{e}^{-u}}{u}\, \mathrm{d}u, \qquad (12)$$

is

$$\mathrm{Ei}(x) = \frac{1}{2\pi \mathrm{i}} \int_{c-\mathrm{i}\infty}^{c+\mathrm{i}\infty} \frac{(p-1)!x^{-p}}{p}\, \mathrm{d}p,\ c>0, \qquad (13)$$

$$= -\ln x - \gamma - \sum_{k=1}^{\infty} \frac{(-1)^k x^k}{k!\, k}, \qquad (14)$$

where the infinite sum is obtained by the standard theory of residues.

The Fourier transform is particularly well suited to linear evolution problems. Typically, there is an initial configuration, $u(x, 0)$, which is represented as a linear superposition of plane waves,

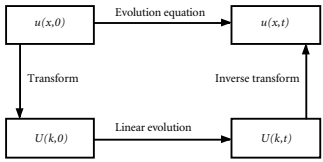

Figure 1. Solution of evolution equations using transforms.

$$u(x, 0) = \frac{1}{2\pi} \int_{-\infty}^{\infty} U(k, 0)\, \mathrm{e}^{-\mathrm{i}kt}\, \mathrm{d}k. \qquad (15)$$

The individual waves evolve according to a simple dispersion relation, $\omega = \omega(k)$, which means that the functions $\exp[-\mathrm{i}kx + \mathrm{i}\omega(k)t]$ satisfy the partial differential equation. As a consequence, the solution at later time is

$$u(x, t) = \frac{1}{2\pi} \int_{-\infty}^{\infty} U(k, 0)\, \mathrm{e}^{-\mathrm{i}kx + \mathrm{i}\omega(k)t}\, \mathrm{d}k. \qquad (16)$$

The process can be visualized as in Figure 1. The top arrow indicates the required evolution of the initial state $u(x, 0)$ to the later state $u(x, t)$. The circuitous route has three steps: (i) map the initial state $u(x, 0)$ to some wave data $U(k, 0)$, (ii) evolve the wave data under the evolution equation to the later wave data $U(k, 0)\mathrm{e}^{i\omega(k)t}$, and (iii) use an inverse transform to reconstruct the new state from the new wave data.

Beginning in the 1970s, it was realized that a large number of nonlinear evolution equations may be solved using an analogous process that has come to be known as the inverse scattering method (Dodd et al., 1982). It is more complicated than the linear methods, but reduces to them in the limit of small nonlinearity. Briefly, the nonlinear equation is associated with a linear one, and there is a mechanism for mapping the data of the former onto the data of the latter. The method again proceeds according to the scheme of Figure 1. However the inverse transform, which recovers the state from the "scattering data," is not so simple, and the method derives its name from it. The first explicit use of this scheme was for the solution of the Korteweg–de Vries (KdV) equation, which is associated with a linear Schrödinger equation in which the function $u(x, t)$ plays the role of the potential. The evolution of the spectrum of the Schrödinger operator, in response to the nonlinear evolution of KdV equation, is linear; furthermore, in the limit of weak nonlinearity, the transform and its inverse reduce to the Fourier transform.

BRIAN DAVIES

See also **Ablowitz–Kaup–Newell–Segur system; Burgers equation; Gel'fand–Levitan theory; Hirota's method; Inverse scattering method or transform; Korteweg–de Vries equation; Nonlinear Schrödinger equations; Sine-Gordon equation; Solitons**

Further Reading

Antimirov, M.Ya., Kolyshkin, A.A. & Vaillancourt, R. 1993. *Applied Integral Transforms*, New York: Springer

Barnett, S. & Cameron, R.G. 1992. *Introduction to Mathematical Control Theory*, 2nd edition, Oxford: Clarendon Press

Davies, B. 2002. *Integral Transforms and Their Applications*, 3rd edition, New York: Springer

Dodd, R.K., Eilberg, J.C., Gibbon, J.D. & Morris, H.C. 1982. *Solitons and Nonlinear Wave Equations*, London and New York: Academic Press

Duffy, D.G. 1994. *Transform Methods for Solving Partial Differential Equations*, Boca Raton, FL: CRC Press

Moore, D.H. 1971. *Heaviside Operational Calculus*, New York: Elsevier

Ninham, B.W., Hughes, B.D., Frankel, N.E. & Glasser, M.L. 1992. Möbius, Mellin, and mathematical physics. *Physica* A, 186: 441–481

Schiff, J.L. 1999. *The Laplace Transform: Theory and Applications*, New York: Springer

Whittaker, E.T. 1928. Oliver Heaviside. *Bulletin of the Calcutta Mathematical Society*, 20: 199–220 (The article is reprinted in Moore, 1971.)

INTEGRALS OF MOTION

See **Constants of motion and conservation laws**

INTEGRATE AND FIRE NEURON

Classical electrophysiology using extracellular recording methods established the all-or-none nature of the nerve impulse—a stimulus has to be above a threshold θ for an action potential to be generated, and for rectangular stimuli, θ depends on stimulus duration T. A plot of θ–T, a strength-duration curve is approximated by

$$\theta = \theta_{\mathrm{rh}}/[1 - \exp(-T/\tau], \tag{1}$$

where θ_{rh} is a constant called the rheobase and τ is a time constant. Lapicque (1907) produced the strength-duration curve of Equation (1) by a model in which subthreshold inputs $x(t)$ are integrated and decay with an exponential time course

$$V(t) = \int_0^t \exp(-(t-u)/\tau)\,\mathrm{d}u, \tag{2}$$

for $0 < V(t) < \theta$, and when $V(t)$ reaches threshold, an idealized action potential (a Dirac δ-function) is triggered and V is instantaneously reset to its resting value (say, $V = 0$). The subthreshold changes in $V(t)$ were represented as the response to an applied current of a resistance and capacitance in parallel. This separates the slow time scales of the subthreshold integrative processes from the fast time scales of the action potential mechanisms. The values of the resistance and capacitance reflect not membrane parameters, but cell parameters, and so depend via surface area on cell size. Guided by the strength-duration curve, nerve or muscle, or different diameter nerve fibers can be excited.

Lapicque's integrate-and-fire model is also known as the leaky integrator and, in the case $\tau \to \infty$, the perfect integrator. Unlike the FitzHugh–Nagumo, Hodgkin–Huxley, and Markin–Chizmadzhev models, it considers only subthreshold, integrative processes, not the processes generating the action potential, and so is more suitable for modeling neuronal information processing than action potential transmission. Originally formulated as a phenomenological model for the conditions for the initiation of an action potential, it is still widely used as a model today, but as a model for the generation of neuronal spike trains and mass activity in neuronal networks. It has been modified to include both absolute and relative refractory periods, obtained as a limiting case for the Hodgkin–Huxley equations, and extended into multiple time constant and spatially extended models (Tuckwell, 1988).

If the input $u(t)$ is a constant c, the interspike intervals t_i are a solution of

$$\theta = \int_0^{t_i} \exp(-(t-u)/\tau)\,\mathrm{d}u, \tag{3}$$

and so the rate of firing is $1/t_i = 1/[-\tau \ln(1 - 1/c\tau)]$, showing an increased sensitivity to small amplitude inputs. Such a logarithmic relation between discharge rate and the magnitude of a constant input is observed in some primary sensory neurons, and is used as an explanation for the Weber–Fechner law of sensory psychophysics.

Gerstein & Mandelbrot (1964) introduced a random walk model for neuronal spike trains, in which the input to a perfect integrator model was a random sequence of small positive and negative steps. This was motivated by the observation that the interspike interval and scaled interval (sums of adjacent intervals) of some auditory, neurons had the same unimodal, asymmetric shape; that is, assuming the spike train was a realization of a renewal point process, the interval density function was invariant under self-convolution or has a stable, or infinitely divisible, distribution. The subthreshold response of the integrate-and-fire model to small and brief positive or negative current pulses could represent the postsynaptic response of a neuron to synaptic inputs. Superposition of a (large) number of independent point processes generates a Poisson process: with appropriate constraints on how the amplitude of the steps decreases while the rate increases, the random walk becomes a white noise, leading to diffusion models for stochastic activity of neurons. The diffusion process models for $V(t)$ are approximations of the discontinuous, random walk models and are constructed to have the same first

and second infinitesimal moments. For the perfect integrator, the subthreshold $V(t)$ is a Wiener process; for the leaky integrator, an Ornstein–Uhlenbeck process. The interspike-interval probability density functions for these diffusion models are first passage time densities to an absorbing barrier, the threshold. These densities are obtained as solutions for forward or backward Chapman–Kolmogorov equations (see Holden, 1976; Tuckwell, 1988). These equations have been solved for different diffusion models, mostly numerically, but for some special cases solutions are available in closed form. The diffusion models have been extended to include time-varying threshold, temporal modulation of the rates of the excitatory and inhibitory inputs, and spatial separation filtering of the inputs. In the derivation of these diffusion models the synaptic inputs are assumed to be uncorrelated, producing a white noise input: correlation in the input, producing colored inputs, is more likely for central neurons and has profound effects on the output variability of the integrate-and-fire models (Feng, 2001).

The perfect and leaky integrators respond to a cosinusoidal input by modulated spike trains with a periodically modulated spike density. At large modulation depths both models show rectification, and the leaky integrator also shows phase-locked responses. Both these nonlinear distortions are reduced by adding noise to the input (Stein et al., 1972), and so additive noise can increase the ability of a neuron to transmit signals about narrow-band, high frequencies. This provides a functional explanation for the association between the variability in sensory mechanoreceptors and the frequency of their adequate stimulus: the discharge of auditory neurons is almost random, and velocity sensitive primary muscle spindle afferents have a higher variability than length sensitive secondary muscle spindle afferents, leading to ideas of stochastic resonance. The phase locked and aperiodic responses of the leaky integrator to a periodic input has been characterized in terms of the Arnol'd tongue structure for the dominant modes, where there are low order ratios between the spiking and forcing rhythms (Coombes & Bressloff, 1999).

The success of the integrate-and-fire models in accounting for general properties of spike trains has allowed it, with simple modifications, to be applied to model spike trains from specific neurons, see for example, Herrmann & Gerstner (2002). The simplicity of the model also allows it to be used as an element in constructing population dynamic equations for large systems of coupled neurons, as in Sirovich et al. (2000).

ARUN V. HOLDEN

See also **Excitability; FitzHugh–Nagumo equation; Hodgkin–Huxley equations; Markin–Chizmadzhev model; Nerve impulses; Neurons**

Further Reading

Coombes, S. & Bressloff, P.C. 1999. Mode locking and Arnol'd tongues in integrate-and-fire neural oscillators. *Physical Review* E, 60: 2086–2096

Feng. J. 2001. Is the integrate-and-fire model good enough? A review. *Neural Networks*, 14,955–14,975

Gerstein, G.L. & Mandelbrot. 1964. Random walk models for the spike activity of a single neuron. *Biophysical Journal*, 4: 41–68

Herrmann, A. & Gerstner, W. 2002. Noise and the PSTH response to current transients: II. Integrate-and-fire model with slow recovery and application to motoneuron data. *Journal of Computational Neuroscience*, 12: 83–95

Holden, A.V. 1976. *Models of the Stochastic Activity of Neurones*, Berlin: Springer

Lapicque, L. 1907. Recherches quantitatives sur l'excitation electrique des nerfs traite comme une polarization. *Journal de Physiologie et Pathologie Generale*, 9: 620–635

Sirovich, L., Omurtag, A. & Knight, B.W. 2000. Dynamics of neuronal populations: the equilibrium solution. *SIAM Journal on Applied Mathematics*, 6: 2009–2028

Stein, R.B., French, A.S. & Holden, A.V. 1972 The frequency response, coherence, and information capacity of two neuronal models. *Biophysical Journal*, 12: 295–322

Tuckwell, H.C. 1988. *Introduction to Theoretical Neurobiology.* vol. 1. Cambridge and New York: Cambridge University Press

INTEGRO-DIFFERENTIAL EQUATIONS

See **Equations, nonlinear**

INTERMITTENCY

Consider a dynamical system with x as the observed variable. As a function of time t, if $x(t)$ exhibits segments of relative constant values (laminar phase) interspersed by erratic bursts, we say the system dynamics is intermittent (see Figure 1). Pomeau and Manneville (1980) were the first to identify the three bifurcations in low-dimensional maps that are associated with commonly observed intermittencies. An additional mechanism for generating intermittency is related to the transverse instability of chaotic attractors confined to a manifold whose dimension is smaller than that of the full phase space, which is called on-off intermittency (Pikovsky, 1984; Fujisaka & Yamada, 1985; Platt et al., 1993).

Pomeau–Manneville type I intermittency stems from a saddle-node bifurcation. Near the bifurcating point ($x=0$) in one-dimensional maps, the dynamics are described by $x_{n+1}=x_n+\varepsilon+x_n^2$. For positive but small ε, a narrow channel near $x=0$ is formed between the nonlinear map function and the diagonal line $x_{n+1}=x_n$. When a trajectory enters the channel, it moves through it very slowly, giving rise to the appearance of a quiet laminar phase. After exiting the channel, the trajectory can display wild swings governed by nonlinear mechanisms, forming the bursting phase of the dynamics. As time progresses, ergodicity will bring the trajectory back to the channel

again, and the process starts anew. The re-injected trajectory can land at different points inside the channel. As a result, the laminar phase has variable length, the mean of which is a statistical quantity of interest. It has been shown that the mean length of the laminar phase scales with the parameter ε as $\sim \varepsilon^{-1/2}$. As ε decreases through zero, a saddle-node bifurcation occurs, creating a stable fixed-point attractor at $-\sqrt{-\varepsilon}$ and an unstable fixed point at $\sqrt{-\varepsilon}$. Intermittency terminates at the bifurcation point $\varepsilon = 0$.

Pomeau–Manneville type II intermittency is related to a subcritical Hopf bifurcation; thus a two-dimensional map is needed for this phenomenon. In polar coordinates, the dynamics near the bifurcation point (assumed to be the origin) is $r_{n+1} = (1+\varepsilon)r_n + r_n^3$, $\theta_{n+1} = \theta_n + \alpha$, where α is a constant rotation. For $\varepsilon > 0$, the origin is an unstable spiral. Viewing the r equation as a one-dimensional map, one again finds a channel for small r. When the trajectory is randomly injected into the channel, a quiet laminar period ensues, which is followed by a burst of chaotic behavior. The mean length of the laminar phase is shown to scale with ε as $\sim \varepsilon^{-1}$. At $\varepsilon = 0$ a subcritical Hopf bifurcation occurs. For $\varepsilon < 0$, intermittency is replaced by a stable fixed-point attractor at the origin that is accompanied by an unstable invariance circle centered at the origin.

Pomeau–Manneville type III intermittency is created near an inverse period-doubling bifurcation. Near the bifurcation point ($x = 0$), the equation of motion is $x_{n+1} = -(1+\varepsilon)x_n + \alpha x_n^2 + \gamma x_n^3$. For this map, the channel dynamics is best seen by examining the second iterate of the above map that is easily obtained (after discarding higher-order terms) to be $x_{n+1} = (1+2\varepsilon)x_n + \beta x_n^3$, where $\beta = -2(\alpha^2 + \gamma)$. As ε decreases from positive values to negative values, intermittency is replaced by a stable fixed-point attractor and an unstable period-two orbit. The channel near $x = 0$ here is analogous to the channel near $r = 0$ in the type II intermittency. It is, thus, not surprising that the mean length of the laminar phase scales with the parameter ε as $\sim \varepsilon^{-1}$.

Consider an m-dimensional dynamical system that has an n-dimensional invariant manifold where $n < m$. (By invariant we mean that a trajectory initialized in the manifold stays there for all time.) Suppose that the dynamics on the manifold has a chaotic attractor that is also an attractor for the full phase space. Suppose also that, as a parameter varies across a threshold, a blowout bifurcation takes place (Ott & Sommerer, 1994) and the attractor becomes transversely unstable. If one monitors the distance between the trajectory and the bifurcating invariant manifold, this distance typically exhibits on-off intermittency (see Figure 1) immediately after the blowout bifurcation. During the laminar phase, in other words, the trajectory spends a great deal of time close to the invariant manifold,

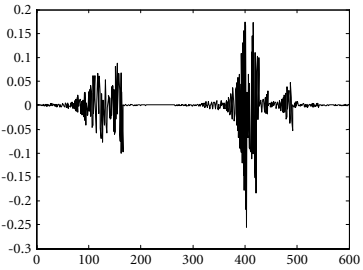

Figure 1. An intermittent function.

producing a nearly zero value for the distance variable. The trajectory then departs the manifold rapidly and displays erratic bursting behavior for the distance variable until the dynamics brings it back close to the invariant manifold again, and the process repeats. During the laminar phase, the distance variable can be studied via a random walk model, and the interval between successive bursts follows a distribution akin to that of the first return time (Ding & Yang, 1995).

All four types of intermittencies have been studied in experimental systems. For example, Jeffries and Perez found Pomeau–Manneville type I intermittency in a nonlinear circuit oscillator (Jeffries & Perez, 1982). Pomeau–Manneville type II intermittency is characterized in a chemical reaction system by Herzel et al. (1991). Dubois et al. (1983) observed Pomeau–Manneville type III intermittency in Rayleigh–Bénard convection. Experimental studies of on-off intermittency are relatively recent. Hammer et al. (1994) are the first to report evidence of on-off intermittency in a nonlinear electronic circuit. On-off intermittency in a laser system was observed by Pisarchik and Pinto-Robledo in 2002.

MINGZHOU DING

See also **Bifurcations; Hénon–Heiles system; Hopf bifurcations; Phase space; Routes to chaos**

Further Reading

Berge, P., Pomeau, Y. & Vidal, C. 1986. *Order Within Chaos, Toward a Deterministic Approach to Turbulence*, New York: Wiley

Ding, M. & Yang, W. 1995. Distribution of the first return time in fractional Brownian motion and its application to the study of on–off intermittency. *Physical Review* E, 52: 207–213

Dubois, M., Rubio, M.A. & Berge, P. 1983. Experimental evidence of intermittencies associated with a subharmonic bifurcation. *Physical Review Letters*, 51: 1446–1449

Fujisaka, H. & Yamada, T. 1985. A new intermittency in coupled dynamical systems. *Progress in Theoretical Physics*, 74: 918–921

Hammer, P.W., Platt, N., Hammel, S.M., Heagy, J.F. & Lee, B.D. 1994. Experimental observation of on-off intermittency. *Physical Review Letters*, 73: 1095–1098

Herzel, H., Plath, P. & Svensson, P. 1991. Experimental evidence of homoclinic chaos and type-II intermittency during the oxidation of methanol. *Physica* D, 48: 340–352

Jeffries, C. & Perez, J. 1982. Observation of a Pomeau-Manneville intermittent route to chaos in a nonlinear oscillator. *Physical Review* A, 26: 2117–2122

Ott, E. 2002. *Chaos in Dynamical Systems*, 2nd edition, Cambridge and New York: Cambridge University Press

Ott, E. & Sommerer, J. 1994. Blowout bifurcation: the occurrence of riddled basins and on–off intermittency. *Physics Letters* A, 188: 39–47

Pikovsky, A. 1984. A new type of intermittent transition to chaos. *Journal of Physics* A, 16: L109–L112

Pisarchik, A.N. & Pinto-Robledo, V.J. 2002. Experimental observation of two-state on–off intermittency. *Physical Review* E, 027203

Platt, N., Spiegel, E.A. & Tresser, C. 1993. On–off intermittency: a mechanism for bursting. *Physical Review Letters*, 70: 279–282

Pomeau, Y. & Manneville, P. 1980. Intermittent transition to turbulence in dissipative dynamical systems. *Communications in Mathematical Physics*, 74: 189–197

INVARIANT MANIFOLDS AND SETS

An invariant set S of a dynamical system has the property that every trajectory (or orbit) that starts in S remains in S. Invariant sets are the basic building blocks of dynamical systems and almost every set that is dynamically interesting has some invariance property. Every trajectory is an invariant set, and so equilibria and periodic orbits are simple examples of such objects. Attractors are also examples of invariant sets.

An invariant set that is also a manifold (i.e., it looks like R^n locally) is called an invariant manifold. Invariant manifolds provide a natural description of the dynamics close to an equilibrium or periodic orbit (using linearization) and can also make it possible to work in lower dimensions than the phase space of the problem, since a smooth dynamical system restricted to an invariant manifold is itself a dynamical system. This reduction in dimension is at the heart of center manifold techniques and inertial manifold methods.

Invariance is a topological property and does not depend upon stability. This is often useful, and the sudden appearance or disappearance of attractors, as parameters are varied, can sometimes be understood as a change in stability of an invariant set that exists throughout the parameter region of interest. Indeed, many invariant sets, and particularly invariant manifolds, have persistence properties under perturbations of the dynamical system that make them useful when working with families of systems.

The basic definitions will be given for differential equations $\dot{\boldsymbol{x}} = \boldsymbol{f}(\boldsymbol{x})$ with $\boldsymbol{x} \in R^n$ and solutions $\boldsymbol{x}(t)$, and maps $\boldsymbol{v}_{n+1} = \boldsymbol{g}(\boldsymbol{v}_n)$, $\boldsymbol{v} \in R^n$. In both cases, the complications that arise if solutions do not exist for all time will be ignored.

For differential equations, a set S is a *forward invariant* set (resp. *backward invariant* set) if $\boldsymbol{x}(0) \in S$ implies that $\boldsymbol{x}(t) \in S$ for all $t \geq 0$ (resp. all $t \leq 0$). S is *invariant* if it is both forward invariant and backward invariant.

For maps, a set S is a *forward invariant* set (resp. *backward invariant* set) if $\boldsymbol{v} \in S$ implies that $\boldsymbol{g}(\boldsymbol{v}) \in S$ (resp. $\boldsymbol{g}^{-1}(\boldsymbol{v})$). S is *invariant* if it is both forward invariant and backward invariant.

In the remainder of this entry, some different sorts of invariant sets that arise in dynamics will be considered, illustrated by the Lorenz equations

$$\dot{x} = \sigma(y - x), \quad \dot{y} = -y + rx - xz,$$
$$\dot{z} = -bz + xy, \tag{1}$$

where σ, r, and b are positive constants.

Trapping Regions

A set R is a trapping region if it is forward invariant and if all solutions are eventually contained in R. Trapping regions provide the first approximation to the location of any attractors in the system.

For the Lorenz equations, (1), with $\sigma = 10$ and $b = \frac{8}{3}$ Sparrow (1982) shows that the region

$$R = \{(x, y, x) \mid rx^2 + 10y^2 + 10(z - 2r)^2 \leq 5r^2\} \tag{2}$$

is a trapping region. This can be proved using the Lyapunov function $V(x, y, z) = rx^2 + 10y^2 + 10(z - 2r)^2$.

Stable and Unstable Manifolds of Stationary Points

A stationary point of the differential equation $\dot{\boldsymbol{x}} = \boldsymbol{f}(\boldsymbol{x})$ is a solution that is constant for all time, so it must satisfy $\boldsymbol{f}(\boldsymbol{x}) = \boldsymbol{0}$. The three equations obtained by setting $\dot{x} = \dot{y} = \dot{z} = 0$ in (1) can be solved to show that the origin is always a stationary point of the Lorenz equations, and provided $r > 1$, there are two other stationary points: $(\pm\sqrt{b(r-1)}, \pm\sqrt{b(r-1)}, r-1)$. Near a stationary point, the most important terms of the differential equation are the linear terms, so it is natural to ask whether the solutions of the linearized equation at the origin

$$\dot{x} = \sigma(y - x), \quad \dot{y} = -y + rx, \quad \dot{z} = -bz \tag{3}$$

obtained by ignoring the nonlinear terms in (1) reflect properties of the full equations close to the stationary point at the origin. These results are usually stated in terms of the eigenvalues of the matrix that defines the linear equation (3):

$$M = \begin{pmatrix} -\sigma & \sigma & 0 \\ r & -1 & 0 \\ 0 & 0 & -b \end{pmatrix}. \tag{4}$$

If M has no eigenvalues with zero real parts, then the manifold (vector space) spanned by the eigenvectors with eigenvalues having negative real parts contains all the stable directions and, hence, is called the stable manifold of the linear system, (3), while the manifold spanned by the eigenvectors with eigenvalues having positive real parts contains the unstable directions. The former manifold is called the stable manifold, E^{s}, of the origin, and the latter is the unstable manifold, E^{u}. If $0 < r < 1$, then all the eigenvalues of M are negative, so the stable manifold of the linear system is the whole space, and the unstable manifold is the empty set. If $r > 1$, then M has two negative eigenvalues and one positive eigenvalue, so the unstable manifold of the linear system is a line, and the stable manifold is a plane.

This provides definitions of stable and unstable manifolds for linear systems such as (3) with no eigenvalues with zero real parts. To extend the definition to nonlinear systems, we begin by noting that in the definition used for linear systems, the stable manifold of the origin contains the solutions that tend to the origin in forward time, and the unstable manifold contains those that tend to the origin in backwards time. These properties can be used to define the stable and unstable manifolds of a stationary point $\boldsymbol{x}^*$ for a nonlinear system: the stable manifold of $\boldsymbol{x}^*$, $W^{\mathrm{s}}(\boldsymbol{x}^*)$ is the set of initial conditions for which the solution $\boldsymbol{x}(t)$ tends to $\boldsymbol{x}^*$ as $t \to \infty$, while the unstable manifold, $W^{\mathrm{u}}(\boldsymbol{x}^*)$, is the set of initial conditions for which the solution $\boldsymbol{x}(t)$ tends to $\boldsymbol{x}^*$ as $t \to -\infty$. The stable manifold theorem states that provided the matrix that defines the linearized equation near a stationary point has no eigenvalues with zero real parts, then $W^{\mathrm{s}}(\boldsymbol{x}^*)$ and $W^{\mathrm{u}}(\boldsymbol{x}^*)$ exist, are invariant sets, and are of the same dimension as the corresponding linear stable and unstable manifolds. Moreover, they are each tangential to the corresponding linear manifold at the stationary point itself. See Guckenheimer & Holmes (1983) for more details.

Calculating Stable and Unstable Manifolds

The stable manifold theorem suggests how approximations to the stable and unstable manifolds of a stationary point can be calculated close to a stationary point. First, it is tangential to the corresponding linear manifold, and second, it is invariant. This is enough to obtain a power series solution, and this will be illustrated using the unstable manifold of the origin of the Lorenz equations with $\sigma = 1$ and $r = 4$.

Step 1 (Linear approximation): The eigenvalues of M in equation (4) are 1, -3, and $-b$ if $\sigma = 1$ and $r = 4$. The unstable manifold is one-dimensional, and the unstable manifold of the linear approximation is the eigenvector corresponding to the positive eigenvalue, that is, $(1, 2, 0)$ or $y = 2x$, $z = 0$.

Step 2 (Canonical form): It is good practice to bring the linear part into canonical form at this stage, see Guckenheimer & Holmes (1983). For brevity this step will be omitted.

Step 3 (Power series): Since the unstable manifold is tangential to the linear approximation of Step 1 at the stationary point, it can be represented *locally* as a function of one of the variables. From the form of the linear approximation, either x or y can be used here. If the defining equations are smooth, then the stable and unstable manifolds are smooth, so choosing x as the independent variable we write

$$y = 2x + \alpha x^2 + O(x^3), \quad z = \beta x^2 + O(x^3), \tag{5}$$

where the linear terms are obtained from the linear approximation, α and β are constants to be determined, and $O(x^3)$ denotes the terms of order x^3 and higher that are small (locally) compared with the linear and quadratic terms. To identify the constants α and β, two different ways of calculating $\dot{y}$ and $\dot{z}$ are used and then compared in the next three steps.

Step 4 (Power series evolution): Differentiating (5) gives $\dot{y} \sim 2\dot{x} + 2\alpha x\dot{x}$ and $\dot{z} \sim 2\beta x\dot{x}$ (ignoring the higher order terms). Now, on the unstable manifold given by (5) $\dot{x} = -x + y \sim x + \alpha x^2$, so

$$\begin{aligned} \dot{y} &\sim 2(x + \alpha a x^2) + 2\alpha x^2 \sim 2x + 4\alpha x^2, \\ \dot{z} &\sim 2\beta x^2, \end{aligned} \tag{6}$$

where higher-order terms have been ignored again.

Step 5 (Differential equation evolution): From (1) and (5) with $r = 4$ and $\sigma = 1$,

$$\begin{aligned} \dot{y} &= 4x - y - xz \sim 2x - \alpha x^2, \\ \dot{z} &= -bz + xy \sim -b\beta x^2 + 2x^2. \end{aligned} \tag{7}$$

Step 6 (Equate coefficients): To determine the two constants α and β, we now simply equate coefficients of powers of x in (6) and (7). From the $\dot{y}$ equations $4\alpha = -\alpha$, so $\alpha = 0$, and from the $\dot{z}$ equations $2\beta = -b\beta + 2$, so $\beta = 2/(2 + b)$. This gives the second-order approximation to the unstable manifold:

$$y = 2x + O(x^3), \quad z = \tfrac{2}{2+b}x^2 + O(x^3), \tag{8}$$

which is valid close to the stationary point at the origin. Higher-order terms can be calculated by including more terms in the power series expansions.

Center Manifolds

If the matrix that defines the linearized differential equation at a stationary point has eigenvalues with zero real parts, then three invariant manifolds can be defined: a strong stable manifold corresponding to

eigenvalues with negative real parts, a strong unstable manifold corresponding to eigenvalues with positive real parts, and a center manifold that is tangential at the stationary point to the space spanned by the eigenvectors corresponding to eigenvalues with zero real parts. The motion on the strong stable and unstable manifolds is defined by the dominant linear terms, that is, towards and away from the stationary point, respectively. The motion on the center manifold depends on the nonlinear terms of the differential equation and may be stable or unstable or neutral. Center manifolds can be approximated locally using the same ideas as the approximation of the unstable manifold above, and this leads to the technique of center manifold reduction, which is central to the development of bifurcation theory. The origin of the Lorenz equations has a one-dimensional center manifold if $r = 1$ (M in (4) has an eigenvalue of zero), which signals the bifurcation creating the nontrivial pair of stationary points if $r > 1$.

Unstable Chaotic Sets

The chaotic sets created by horseshoes are not stable, but they can be important from two points of view. First, if an unstable chaotic set exists in a system then it can manifest itself in chaotic transients before a stable attractor is reached. Second, if there are parameters in the system then the chaotic set may gain stability and so the sudden appearance of strange attractors can be explained by understanding the change of stability of a chaotic invariant set. Grebogi et al. (1982) describe some of these mechanisms as *crises*. In the Lorenz equations with $b = \frac{8}{3}$ and $\sigma = 10$, a strange invariant set (an unstable chaotic set with a fractal structure) is created by a homoclinic bifurcation as r is increased through $r \approx 13.93$, but it does not become stable until $r \approx 24.06$; see Sparrow (1982); for details.

There are many other types of invariant sets and properties of these sets that could have been described here—the selection above is only the tip of an invariant iceberg.

PAUL GLENDINNING

See also **Attractors; Bifurcations; Center manifold reduction; Chaotic dynamics; Horseshoes and hyperbolicity in dynamical systems; Inertial manifolds; Linearization; Lorenz equations; One-dimensional maps; Routes to chaos**

Further Reading

Grebogi, C., Ott, E. & Yorke, J.A. 1982. Chaotic attractors in crisis. *Physics Review Letters*, 48: 1507–1510

Guckenheimer, J. & Holmes, P. 1983. *Nonlinear Oscillations, Dynamcal Systems, and Bifurcations of Vector Fields*, New York: Springer

Sparrow, C. 1982. *The Lorenz Equations: Bifurcations, Chaos, and Strange Attractors*, New York: Springer

INVARIANT MEASURE

See **Measures**

INVERSE PROBLEMS

Scientists try to interpret the world in terms of mathematical models that depend on parameters by relating their models to the results of measurements. Thus, a model is given when a set $\mathcal{C}^0$ of parameters is mapped into a set $\mathcal{E}^0$ of experimental results. Explicit calculations of this mapping $\mathcal{M}$ are called "solving the direct problem." Providing an exact or approximate way for going back from experimental results to parameters by $\mathcal{M}$ is called "solving the inverse problem" (Sabatier, 2000).

Because the exact limits of $\mathcal{C}^0$ and $\mathcal{E}^0$ are difficult to define, they are embedded in convenient mathematical spaces, $\mathcal{C}$ and $\mathcal{E}$, usually linear normed spaces, where it is understood that $\mathcal{C}$ is the domain of $\mathcal{M}$ and $\mathcal{M}(\mathcal{C}) \subseteq \mathcal{E}$. Because of measurement errors, there may be measurement results belonging to $\mathcal{E}$ but not to $\mathcal{M}(\mathcal{C})$, and if it is so, the inverse problem is said to be overdetermined. To appraise uncertainties on measurements, the norm of $\mathcal{E}$ must be reasonably defined, corresponding to our physical knowledge of errors.

The inverse problem is said to be "well-posed" if the norm of $\mathcal{E}$ is reasonably defined, $\mathcal{C} = \mathcal{C}^0$, $\mathcal{M}(\mathcal{C}) = \mathcal{E}$, and $\mathcal{M}$ has a two-sided inverse $\mathcal{M}^{-1}$, which is continuous for the canonical distance in $\mathcal{E}$. Then given any measurement result $e \in \mathcal{E}$, $\mathcal{M}^{-1}e$ yields parameters $x \in \mathcal{C}$ such that

$$\mathcal{M}x = e. \tag{1}$$

If a small error in the experimental data e implies that the error in the parameters x is small, the solution x is stable. Unfortunately, almost all inverse problems of physics or engineering are "ill-posed" (i.e., not well-posed).

For an ill-posed problem, a regularized solution is a continuous mapping $\overline{\mathcal{M}}$ from $\mathcal{E}$ to $\mathcal{C}^0$ such that $\mathcal{M}(\overline{\mathcal{M}}e)$ is close to $e \in \mathcal{E}$. Because experimental observations define $\mathcal{C}^0$ only approximately, one often imposes additional requirements to ease the regularizing processes, for example, that $\mathcal{C}^0$ is compact (Engl et al., 2000).

Classical examples of regularized solutions for Equation (1) are obtained by minimizing over x in one of two ways: either successively as a Euclidean distance in $\mathcal{E}$ that models the misfit and a Euclidean distance in $\mathcal{C}$ that models the non-reliability or as a combination of their squares into a cost function. Typical is the Tikhonov cost

$$C(x, x_0, \lambda) = \|x - x_0\|_{\mathcal{C}}^2 + \lambda \|\mathcal{M}x - e\|_{\mathcal{E}}^2, \lambda > 0, \tag{2}$$

where two parameters (the "first guess" x_0 and the balance parameter λ) are to be chosen. (λ may be related to an evaluation of the noise/signal ratio or to the stability, whereas "physical" information on x_0 may be suggested by previous results.)

If $\mathcal{M}$ is differentiable, the cost function (2) is also differentiable, and elementary variational calculus applies. Information from statistical analyses is more conveniently represented by quadratic cost functions similar to Equation (2), but involving noncanonical distances in $\mathcal{C}$ and $\mathcal{E}$ that are constructed from covariance matrices (having many more arbitrary parameters). The minimum x_m is unique for a given quadratic cost function and Hilbert spaces $\mathcal{C}$ and $\mathcal{E}$ if $\mathcal{M}$ is linear and continuous and satisfies the requirements of a regularized solution. This minimum can be derived either by solving linear equations or by choosing among many ones an efficient iterative algorithm.

The value $C(x_m)$ is a trade-off between requirements on $\mathcal{C}$ and $\mathcal{E}$. Either it is larger than the largest number C_M allowed for this trade-off, so that there is no admissible regularized solution of this form, or it is smaller than C_M, and all values of x such that $C(x_m) \leq C(x) \leq C_M$ are also admissible solutions of Equation (2). Hence the range of this non-uniqueness can be appraised along the principal axes of the ellipsoid $C(x) = C_M$, whose center is x_m. In this linear case, the center is given by the formula $(M^*M + \lambda I)^{-1} M^*e$, where the regularising process is clearly due to adding λ^{-1} to the eigenvalues of M^*M (the "singular values of M). Extensions along the axes are trivially related to the inverse of $\mathcal{M}$ singular values, damped by means of λ.

Instabilities related to the small singular values (high spatial frequencies) make this kind of regularized solution more sensitive to accidental large deviations of data (less robust) than regularized solutions obtained from cost functions involving L^1 or L^∞ norms. However, choosing the later norms usually leads one to more complicated algorithms and to (bang–bang) solutions piecewise equal to the possible upper and lower bounds. Hence, simple and efficient analyses can be adapted to almost any linear (or linearized) inverse problem, including those important for medical tomography and most medical imaging (Bertero & Bocacci, 1998).

Among many examples of nonlinear inverse problems is the case when the a priori information on a first guess x_0 is so convincing that we seek a unique approximate solution of Equation (1) in a narrow neighborhood of x_0, allowing linearization $\mathcal{M}$. The only difference between such a linearized inverse problem and a linear one is that the conditions limiting $\mathcal{C}_0$ must involve those that ensure the relevance of our approximation.

A quite different case involves nonlinear inverse problems for which $\mathcal{M}$ is so general (with weak a priori conditions) that we cannot escape an exhaustive exploration of $\mathcal{C}^0$ for seeking the exact or approximate solutions of (1). Random walks through $\mathcal{C}^0$ can do the job, for example, Monte-Carlo methods, simulated annealing, or genetic algorithms.

Between these extreme cases are those that correspond to important physical or engineering problems, for which studies either give an exact method of solution or allow solution of the inverse problem by numerical techniques. Defining cost functionals and minimizing them by gradient iterative or other methods (Engl et al., 2000; Ghosh Roy & Couchman, 2002) is then possible, but the occurrence of several secondary minima can also make the job difficult, raising questions about their relevance as admissible solutions.

Solving an inverse problem means that we are able to derive all the admissible regularized solutions. If the non-uniqueness is due not only to small data or parameters deviations but to the structure of $\mathcal{M}$, these equivalent solutions should be classified into identified families. This is essential either to derive ways of restoring uniqueness (for instance, by making other kinds of measurements), to use the non-uniqueness (e.g., to design stealth targets), or to modify the nature of the model. In decisive as opposed to descriptive modeling, well-posed questions seek significant pieces of information instead of trying to get an image of the parameters.

A One-dimensional Example

Inverse scattering in one spatial dimension offers some completely solved examples, the simplest one being the Schrödinger problem on the line (Chadan & Sabatier, 1989; Aktosun & Klaus 2002), which may model observations of quantum, acoustic, or electromagnetic scattering. Experimental results are the scattering coefficients $R(k)$ and $T(k)$, $k \in \mathbb{R}$, related to the parameter $V(x)$ by the following formulas, where indices $\pm$ at the same level correspond :

$$\left[-\frac{\mathrm{d}^2}{\mathrm{d}x^2} + V(x)\right] f^{\pm}(k,x) = k^2 f^{\pm}(k,x)\,, \qquad (3)$$

$$\mathrm{e}^{\mp \mathrm{i}kx} f^{\pm}(k,x) \to 1 \quad \text{as} \quad x \to \pm\infty\,, \qquad (4)$$

$$T(k) f^{-}(k,x) = f^{+}(-k,x) + R(k) f^{+}(k,x)\,, \qquad (5)$$

where $\int_{-\infty}^{+\infty} |V(x)| \left(1 + x^2\right) \mathrm{d}x < \infty$. Equation (3) shows that $\mathbb{R}$ is the continuous part of the spectrum of $-\mathrm{d}^2/\mathrm{d}x^2 + V$, which has also a finite number of eigenvalues $k = \mathrm{i}\kappa_n$, $n = 1, 2, \ldots N$, corresponding to eigenfunctions in $L^2(\mathbb{R})$, with normalizing constants

ρ_n. The set $\{R(k),\ \kappa_n,\ \rho_n\}$, called the scattering (or spectral) data, defines the following function on $\mathbb{R}^+$:

$$S(z) = \frac{1}{2\pi}\int_{-\infty}^{+\infty} \mathrm{d}k\, R(k)\mathrm{e}^{\mathrm{i}kz} + \sum_{p=1}^{N} \rho_p \mathrm{e}^{-\kappa_p z}. \quad (6)$$

Although knowledge of $R(k)$ and $T(k)$ is not sufficient to determine V, the spectral data is sufficient to determine everything $\left(V,\ f^{\pm}, T,\ \text{etc}\right)$. In fact, $\int_x^{\infty} V(t)\,\mathrm{d}t$ is equal to $2K\left(x, x^+\right)$, where $K(x, y)$ has been derived from S by solving the linear integral equation:

$$K(x, y) + S(x + y) + \int_x^{\infty} \mathrm{d}z K(x, z)\, S(z + y) = 0. \quad (7)$$

Only the step $K \to V$ is (weakly) instable; hence, the inverse problem $(R \to V)$ is completely solved but with a structural non-uniqueness distributed into families labeled by κ_n and ρ_n.

If we let t be an evolution parameter (time) and assume that the evolution of $S(k, t)$ is described by a linear equation, the evolution of the corresponding $V(x, t)$ is generally not linear. Hence, the couple direct-inverse problem can be used to linearize special nonlinear equations. This observation provides the basis of the inverse scattering transform (IST), where the discrete eigenvalues (κ_n) correspond to solitons.

Three-dimensional Inverse Scattering

The simplest model for inverse scattering in three spatial dimensions obeys the equations:

$$(-\Delta + V)\,\Psi(\boldsymbol{k}, \boldsymbol{x}) = k^2 \Psi(\boldsymbol{k}, \boldsymbol{x}) \quad (8)$$

$$\Psi(\boldsymbol{k}, \boldsymbol{x}) = \exp\left[\mathrm{i}\boldsymbol{k}\cdot\boldsymbol{x}\right] + x^{-1}\exp\left[\mathrm{i}kx\right] F\left(\widehat{x}, \widehat{\boldsymbol{k}}, k\right) + 0\left(x^{-1}\right), \quad (9)$$

where the bold font indicates vectors (italics their length) and the hatted letters are elements of the unit sphere.

The scattering potential V is the parameter to be determined, and F the experimental observation, which in the general case depends on 5 variables, whereas V depends only on 3. Hence, the most general inverse problem is severely ill-posed. On the other hand, spherical symmetry may reduce it to a one-dimensional problem.

If V is a piecewise continuous parameter, the general case at fixed k can be treated by standard optimization techniques. However, in most target identifications (including sonar and radar), the scatterer is not modeled by a medium function $V(\boldsymbol{x})$ but by a reflecting (or absorbing) surface. In some cases, approximate methods are relevant—ray theory, physical optics, Rytov approximation, distorted wave Born approximation (DWBA)—and they often yield linear relations between well-chosen parameters and data, for example, the (inversable) Abel integral, which relates the velocity of an earthquake signal as a function of depth to the measured travel time as a function of the ray parameter. If in mineral prospecting by seismic reflection surveys, geological information and rough identification of the signals suggest that the underground structure may be represented as a homogeneous medium with few reflectors, so-called migration methods may be useful. (Migration methods reposition returned signals that are time-distorted to their true location in time, for example, for dipping structures.)

Unfortunately, the exact relations between scatterers and data are highly nonlinear. Inversion of the DWBA fails in diffraction tomography as the structural complexity increases and so do optimization methods in seismic problems (nonconvexity of cost functions, secondary minima, etc.). Studies of stealth targets also involve nonlinear inverse problems, but of course they are not well documented in the open literature.

Full studies of the inverse problems of target identification are available in well-known works (for approximations, see Langenberg, 1987; Hopcraft & Smith, 1992; for mathematics, see Colton & Kress, 1992; for comprehensive studies, see topics 1.3 to 1.5 in Pike & Sabatier, 2002. For direct and inverse problems of elastic waves, see topics 1.7 and 1.8 in Pike & Sabatier, 2002.) Acoustic soundings used in clinical medicine (i.e., ultrasound scans) show graphs of travel times between source and reflectors (i.e., impedance discontinuities), giving evidence of imaging reflectors without need of solving inverse problems and so do more precisely devices transmitting back a time-reversed version of the recorded wave field (Fink & Prada, 2001).

A few techniques of medical imaging yield inverse problems that are either linearizable or nonlinear, according to a priori information and constraints. Among these, electrocardiography (Johnston, 2001), electroencephalography, and magnetoencephalography try to determine the electrical activity in the heart and the brain as functions of space and time. In brain imaging, the number of data points ($\sim$100) and that of unknowns ($\sim$10, 000) make the linear problem severely underdetermined, leading to arbitrary choices in the space of parameters (Bayesian approaches are commonly used) and to low resolution. From improved a priori knowledge, on the other hand, one can assume relatively few localized active groups at a given time, which are the sources of activity, but the problem becomes nonlinear (Baillet et al., 2001).

PIERRE C. SABATIER

See also **Gel'fand–Levitan theory; Integrability; Inverse scattering method or transform**

Further Reading

Aktosun, T. & Klaus, M. 2002. Inverse theory: problem on the line. In *Scattering*, edited by E.R. Pike & P.C. Sabatier, San Diego and London: Academic Press, pp. 770–785

Baillet, S., Mosher, J.C. & Leahy, R.M. 2001. Electromagnetic brain mapping. *IFEE Signal Processing Magazine*, 18(6): 14–30

Bertero, M. & Bocacci, P. 1998. *Introduction to Inverse Problems in Imaging*, Bristol and Philadelphia: Institute of Physics Publishing

Chadan, K. & Sabatier, P.C. 1989. *Inverse Problems in Quantum Scattering Theory*, 2nd edition, Berlin and New York: Springer

Colton, D. & Kress, R. 1992. *Inverse Acoustic and Electromagnetic Scattering Theory*, Berlin and New York: Springer

Engl, H.W., Hanke, M. & Neubauer, A. 2000. *Regularisation of Inverse Problems*, Dordrecht and Boston: Kluwer

Fink, M. & Prada, C. 2001. Acoustic time-reversal mirrors. *Inverse Problems*, 17(1): R1–R38

Ghosh Roy, D.N. & Couchman, L.S. 2002. *Inverse Problems and Inverse Scattering of Plane Waves*, San Diego and London: Academic Press

Hopcraft, K.I. & Smith, P.R. 1992. *An Introduction to Electromagnetic Inverse Scattering*, Boston and Dordrecht: Kluwer

Johnston, P. (editor). 2001. *Computational Inverse Problems in Electrocardiography*, Southampton: WIT Press

Langenberg, K.J. 1987. Applied inverse problems for acoustic electromagnetic and elastic wave scattering. In *Basic Methods of Tomography and Inverse Problems*, edited by P.C. Sabatier, Bristol: Adams Hilger, pp. 125–467

Pike, E.R. & Sabatier, P.C. (editors). 2002. *Scattering*, San Diego and London: Academic Press

Sabatier, P.C. 2000. Past and future of inverse problems. *Journal of Mathematical Physics*, 41(6): 4082–4124

INVERSE SCATTERING METHOD OR TRANSFORM

The story begins one August day in 1834 on the Union Canal near Edinburgh. John Scott Russell observed a mass of water, displaced by the motion of a barge, race away along the channel and disintegrate into a series of waves, the likes of which he had not seen before. Following on horseback, he noted the lead wave was about 30 ft long and about a foot high. It was a wave purely of elevation above the mean level of the canal, and it traveled at about eight miles/hr without change of shape or loss of speed for a great distance. It took another 40 years before Joseph Boussinesq and Lord Rayleigh verified that such a solitary wave was indeed a solution of the shallow water equations. Twenty years later, in 1895, Diederik Korteweg and Hendrik de Vries (KdV) wrote down the now famous, universal, and ubiquitous KdV equation

$$q_t + 6qq_x + q_{xxx} = 0 \qquad (1)$$

for the scaled elevation $q(x, t)$ of a right-going wave in a frame of reference moving with the shallow water speed $\sqrt{gh_0}$ on a layer of water of depth h_0 and its solitary wave solution

$$q(x, t) = 2\eta^2 \operatorname{sech}^2\eta(x - x_0 - 4\eta^2 t). \qquad (2)$$

In the shallow water context, the elevation is

$$Ah_0 \operatorname{sech}^2 \left\{ \frac{\sqrt{3A}}{2h_0} \left(x - \sqrt{gh_0}\,(1 + A/2)\, t - x_o \right) \right\},$$

where g is the acceleration of gravity, A is the arbitrary dimensionless (small) height, and x_0 is the starting position of the wave.

The story continues almost 60 years later in Los Alamos. The question under address was totally different. Why do solids have finite rather than infinite heat conductivity? Peter Debye had suggested in 1916 that the anharmonicity (weak nonlinearity) of the interatomic forces hindered energy transport by coupling all the natural vibrations of the solid; thus, the relaxation time to thermal equilibrium would be a measure of conductivity. Enrico Fermi, John Pasta, and Stan Ulam (FPU) decided in the early 1950s to simulate numerically a model embracing this idea. The model consisted of 63 equal masses m attached by 64 springs with the force in each of them given by $k(\Delta + \alpha\Delta^2)$, a nonlinear modification of Hooke's law where Δ represents displacement from equilibrium. The initial energy was all in the lowest mode. As expected, very soon energy spread to the first few harmonics. But then a surprising thing occurred. The energy did not thermalize! Instead, after a while, it all recollected into the lowest mode. The pattern repeated. The negative outcome of the FPU experiment, one of the first scientific discoveries by computer experiment, was considered a great mystery (*See* **Fermi–Pasta–Ulam oscillator chain**).

Carpe Diem

The moment was seized by two young applied mathematicians, Martin Kruskal and Norman Zabusky (KZ). Because most of the energy of the FPU experiment resided in the low modes, Kruskal and Zabusky argued that they could replace the spring equations for the lateral displacements $y_n(t)$, $n = 1 \ldots 63$ by a continuum approximation $y(x = nh, t) = y_n(t)$, where h was the unstretched spring length. For disturbances traveling in one direction in a frame moving with the lattice velocity $c = \sqrt{k/m}\,h$, the suitably scaled strain $q(x, t) = y_x/6$ obeyed the KdV equation (1). They numerically simulated solutions of (1) on a periodic domain of length L beginning with $q(x, 0) = (\pi a/6)\cos(2\pi x/L)$. They found that the solution evolved toward a sequence of solitary wave pulses each very close to (2) in shape that ran around the interval with the taller, faster ones periodically catching up with the slower ones, thereby

producing partial, and occasionally nearly perfect, recurrences. Moreover, they made one startling observation. After a pairwise collision, the two solitary waves would emerge with their former identities (amplitude, width, and speed) intact. The only evidence that the interaction was nonlinear was a phase shift. The faster (slower) pulse seemed to advance (regress) by a fixed amount. Because the solitary waves exhibited such robust, particle-like properties, Kruskal and Zabusky called them solitons (*See* **Solitons, a brief history**).

Such behavior indicated that the KdV equation was somehow special and that its special properties were connected with hidden symmetries and conservation laws, beyond those connected with mass, momentum, and energy. A systematic search led to the Miura–Gardner transformation, $q(x,t) = w(x,t) + i\varepsilon w_x(x,t) + \varepsilon^2 w^2(x,t)$, a Riccati equation mapping solutions of a modified KdV equation $w_t + 6(w + \varepsilon^2 w^2)w_x + w_{xxx} = 0$ into solutions of (1). The single conservation law $w_t + (3w^2 + 2\varepsilon^2 w^3 + w_{xx})_x = 0$ and the corresponding conserved quantity $\int w\,dx$ (the integration interval is either infinite with $w(\pm\infty, t) = 0$ or finite with $w(x + L, t) = w(L, t)$) gave rise to an infinite number of conservation laws or conserved quantities for KdV, found by solving w iteratively in power of ε. Solving the Riccati equation by setting $w + 1/2\varepsilon^2 = iv_x/\varepsilon v$ gives

$$v_{xx} + (q(x,t) + \lambda)v = 0, \tag{3}$$

the Schrödinger equation with energy λ and potential $-q(x,t)$. This connection of solutions of KdV with the Schrödinger operator $L(t) = -d^2/dx^2 - q(x,t)$ gave rise to the inverse scattering method. By this stage Kruskal had been joined by colleagues Gardner, Greene, and Miura (GGKM).

A Natural Question

In the late 1960s, GGKM began by asking: As the potential $-q(x,t)$, defined on $-\infty < x < \infty$ and decaying to zero as $x \to \pm\infty$, evolves according to (1), how does the spectrum (the set of eigenvalues) of (3) change? The character of the spectrum was already well known. It consists of a discrete number N of negative energy levels $\lambda_n < 0$, $(1 \le n \le N)$, with corresponding eigenfunctions that are square integrable and a positive continuous spectrum $\lambda > 0$. Direct substitution of $q(x,t)$ from (3) into (1) gave $\lambda_t v^2 + (uQ_x - u_x Q)_x = 0$ with $Q \equiv v_t + v_{xxx} - 3(\lambda - q)v_2$. For bound state eigenvalues, the integral of the second term vanishes giving $\lambda_{nt} \int_{-\infty}^{\infty} v_n^2\,dx = 0$ so that λ_n is a motion constant. It turns out that $-2\lambda_n$ is the amplitude of the nth soliton which is contained in $q(x,t)$. The fact that it is constant is the reason for the special collision property of solitons. Because $\lambda_t = 0$, $uQ_x - u_x Q = \text{constant}$, which can easily be solved for Q to give an equation for the evolution of the eigenfunction $v(x,t)$

$$v_t = B \cdot v = -4v_{xxx} - 6qv_x + (C - 3q_x)v, \tag{4}$$

which is also equal to (remember $\lambda v = -v_{xx} - qv$)

$$v_t = B \cdot v = (q_x + C)v + (4\lambda - 2q_x)v_x. \tag{5}$$

The parameter C is a constant of integration that is used to normalize in a convenient way solutions of (3) called Jost functions. The compatibility $(v_{xx})_t = (v_t)_{xx}$ of (3) and (4) or (5) gives (1).

Peter Lax provided an elegant formalism for this compatibility. Differentiating $L(t)v = [-v_{xx} - q(x,t)v] = \lambda v$ with respect to t and using (4), one obtains $L_t = [B, L]$, which is (1) and is called the Lax equation. L and B are called the Lax pair. The Lax equation guarantees that the flow is an isospectral deformation; namely, that as the potential in (3) deforms according to (1), the spectrum remains unchanged.

The Inverse Scattering Method

The stage is now set to introduce the inverse scattering method (ISM)—or inverse scattering transform (IST)—which is done in three steps. First, one is given the potential $-q(x)$ and from this one defines solutions of (3) and calculates a set of data called the scattering data S. Second, one determines how S evolves as $q(x,t)$ evolves according to (1). Finally, one recovers the potential $-q(x)$ from the time-advanced scattering data S. This is analogous to the set of steps one uses in solving linear PDEs via the Fourier transform, and in a suitable "small" $-q(x)$ limit, S is the Fourier transform. The IST algorithm is

$$\begin{aligned} &\text{Step 1}: \ q(x,0) \to S(0). \\ &\text{Step 2}: \ S(0) \to S(t). \\ &\text{Step 3}: \ S(t) \to q(x,t). \end{aligned}$$

Interestingly, IST can be interpreted as a canonical map from the original coordinates $q(x,t)$ to suitable combinations of S that are action-angle variables.

In the first step, one defines two sets of linearly independent solutions $\{\varphi(x,k), \ \varphi(x,-k)\}$, $\{\psi(x,k), \ \psi(x,-k)\}$, $\lambda = k^2$ for real values of k (called Jost functions) by their asymptotic properties for all t as $x \to \pm\infty$,

$$\varphi(x,k) \to e^{-ikx}, \quad x \to -\infty; \ \psi(x,k) \to e^{ikx}, \quad x \to +\infty. \tag{6}$$

Because of unit (time-independent) coefficients, the choice of C in (5) for $\varphi(x,t,k)$ is $4ik^3$ and the choice of C in (5) for $\psi(x,t,k)$ is $-4ik^3$. Since (3) is linear, and second order, the pairs of Jost functions are related

$$\varphi(x,t,k) = a(k,t)\psi(x,t,-k) + b(k,t)\psi(x,t,k), \tag{7}$$

where $2ika(k,t)$ and $2ikb(k,t)$ are, respectively, the Wronskians $\varphi(k)\psi_x(+k)-\varphi_x(k)\psi(+k)$ and $\varphi(k)\psi_x(-k)-\varphi_x(k)\psi(-k)$. For a bound state $\lambda_n<0$ so that $k_n=\sqrt{\lambda_n}=i\eta_n$. Since $\psi(x,t,-k)$ diverges as $x\to+\infty$ for $\operatorname{Im}k>0$, the coefficient $a(k,t)$ must vanish for a bound state so that at $\lambda=i\eta_n$, $\varphi(x,t,i\eta_n)=b_n(t)\psi(x,t,i\eta_n)$. Dividing (7) by $a(k,t)$ and using (6), one sees that

$$\frac{\varphi}{a}\to\frac{1}{a}e^{ikx}\text{ as }x\to-\infty$$
$$\to e^{ikx}+\frac{b}{a}e^{ikx}\text{ as }x\to+\infty. \tag{8}$$

In wave scattering or quantum mechanical language, φ/a is a solution which represents an incoming wave of amplitude unity from $x=\infty$ and waves partially reflected and partially transmitted by the potential $-q(x)$. The coefficients $T(k)=1/a(k)$ and $R(k)=b(k)/a(k)$ are called the transmission and reflection coefficients, respectively.

It turns out that $\varphi(x,t;k)e^{ikx}(\varphi(x,t;-k)e^{-ikx})$, $\psi(x,t,k)e^{-ikx}(\psi(x,t,-k)e^{ikx})$ and $a(k,t)(a(-k,t))$, originally defined for real k, admit analytic continuation to $\operatorname{Im}k>0$ ($\operatorname{Im}k<0$). Each tends to unity as $|k|\to\infty$. The zeros of $a(k)$, $k_n=i\eta_n$, $n=1,\dots,N$ are the bound states. There is only a finite number of them. The set of data $S(t)=\{(k_n=i\eta_n,b_n)_1^N;\ R(k),\ k\text{ real}\}$ is called the scattering data. From S, $a(k)$ can be found.

In step 2, one uses (5) to calculate the time dependence of $S(t)$. Differentiate (7) with respect to t and use (5) with $C=4ik^3$ for $\varphi(x,k)$ and $\psi(x,-k)$ and $C=-4ik^3$ for $\psi(x,k)$ to find

$$a_t=0,\ b_t=8ik^3b. \tag{9}$$

For the bound state at $k_n=i\eta_n$, differentiating $\varphi(x,k_n)=b_n\psi(x,k_n)$ gives $b_{nt}=8\eta_n^3b_n$. Therefore, the discrete eigenvalues $k_n=i\eta_n$ are motion constants and $S(t)=\{(k_n=i\eta_n,\ b_n(0)\exp 8\eta_n^3t)_1^N,\ R(k,0)\exp 8ik^3t,\ k\text{ real}\}$.

In step 3, one uses $S(t)$ to reconstruct $q(x,t)$ via the Riemann–Hilbert algorithm, which seeks to reconstruct a meromorphic function for $\operatorname{Im}k>0$ (think $\frac{\varphi(x,k)}{a(k)}e^{ikx}$) tending to unity as $|k|\to\infty$, $0<\arg k<\pi$ and an analytic function for $\operatorname{Im}k<0$ (think $\psi(x,-k)e^{ikx}$) tending to unity as $|k|\to\infty$, $-\pi<\arg k<0$, whose difference on the real axis $\operatorname{Im}k=0$ is given (think $R(k)\psi(x,k)e^{ikx}$). To achieve this, consider for $\operatorname{Im}k>0$,

$$I=\frac{1}{2\pi i}\int_{-\infty}^{\infty}\frac{\varphi(x,k')e^{ik'x}}{a(k')(k'+k)}\,dk' \tag{10}$$

in two ways. First, close the contour at $|k|=\infty$ along $0<\arg k<\pi$. Second, after using (7), close the contour for that part analytic for $\operatorname{Im}k<0$ in the lower half-plane. Identifying the two results, one finds a linear integral equation

$$\psi(x,k)e^{-ikx}=1-\sum_{n=1}^{N}\frac{\gamma_k\psi(x,k_n)}{k+k_n}e^{ik_nx}$$
$$+\frac{1}{2\pi i}\int_{-\infty}^{\infty}R(k)\frac{\psi(x,k')e^{ik'x}}{k'+k}\,dk', \tag{11}$$

where $k_n=i\eta_n$, $\gamma_n=b_n(a'(k_n))^{-1}$. The potential $-q(x)$ is recovered from (11) by the formula

$$q(x)=\lim_{k\to\infty}-2ik\frac{d}{dx}(\psi(x,k)e^{-ikx}-1). \tag{12}$$

A simple transformation converts (11) into the famous Gel'fand–Levitan equation which, since the mid-1950s, was known as a means for reconstructing potentials from scattering data.

For a special set of initial conditions $q(x,0)$ called reflectionless potentials, the reflection coefficient $R(k)$ is identically zero. In that case, the Riemann–Hilbert algorithm yields a set of linear algebraic equations found by putting $k=i\eta_r$, $r=1,\dots,N$ in (11). The simplest is the single soliton solution for which $R(k)=0$, $a(k)=(k-i\eta)/(k+i\eta)$, $b_1(0)=\exp 2\eta x_0$, $b_1(t)=\exp 2\eta\bar{x}$, $\bar{x}=x_0+4\eta^2t$, $\psi(x,k_1)=e^{-\eta x}(1+e^{2\eta(\bar{x}-x)})^{-1}$ and $q(x,t)=2\eta^2\operatorname{sech}^2\eta(x-\bar{x})$. Multisoliton solutions can be similarly calculated. They can also be found by a nonlinear superposition principle—the Bäcklund transformation—which is introduced below.

For $q(x,0)=Q\delta(x)$, $a(k)=(Q+2ik)/2ik$ and $R(k)=-Q/(Q+2ik)$, and there is one bound state at $k=iQ/2$. The field consists of a single soliton with $\eta=Q/2s$ and a trailing radiation component. The two components are tied together with the self-similar solution

$$q(x,t)=\frac{1}{(3t)^{2/3}}f\left(\frac{x}{(3t)^{1/3}}\right),$$

which we will meet again when we discuss isomonodromic deformations.

The question: "Is the complete integrability of KdV an isolated miracle or are there lots of integrable PDEs?" was quickly resolved. The pioneering GGKM work of the late 1960s was followed within a few years by the discovery of the complete integrability via ISM of the equally ubiquitous nonlinear Schrödinger (NLS) equation by Zakharov and Shabat and the characterization and integrability via ISM of families of integrable PDEs by Ablowitz, Kaup, Newell, and Segur (AKNS), (*See* **Ablowitz–Kaup–Newell–Segur system**).

More Space Dimensions

Completely integrable systems in more than one space dimension were also found. Two of the most important were the two-dimensional analogues of the KdV and NLS equations, the Kadomtsev–Petviashvili (KP) and the Benney–Roskes–Davey–Stewartson (BRDS) equations. The KP equation describes the evolution of slightly oblique waves either on shallow water or in a two-dimensional FPU lattice where the linear spring force in one direction is much weaker than it is in the other. It is given by (1) with $\int_{-\infty}^{x} q_{yy}$ added. It is also the compatibility condition of two linear operators with coefficients depending on $q(x, y, t)$ and its derivatives.

Unexpected connections of integrable PDEs with other exactly integrable models (Ising, Yang–Baxter) were found in the late 1970s and the 1980s. Most notable among them was the discovery by Sato, Miwa, and Jimbo (SMJ) that in the scaling limit, the n-point correlation function of the nearest neighbor, two-dimensional Ising model satisfies a system of very special deformation equations. These express the fact that the monodromy group of an associated linear system, which contains the correlation functions as coefficients, is preserved as the correlation functions change with their arguments. (The monodromy group of matrices encodes information about how the fundamental solution matrix of the linear system changes on taking it through a loop surrounding regular and irregular singular points.) Much of their work has deep connections with classical work on isomonodromic deformations by Ludwig Schlesinger and Paul Painlevé on systems of Fuchsian differential equations (*See* **Monodromy preserving deformations**) and by Albert Bäcklund on superposition principles for nonlinear equations (*See* **Bäcklund transformations**). Indeed, soliton theory has had a major impact in many areas of mathematical physics. It has led, for example, to the solution of the Schottky problem of algebraic geometry, to the discovery of quantum groups, to models for quantum gravity, and to useful connections with arithmetic algebraic geometry and, in particular, Jones' polynomials.

Bäcklund Transforms and Hirota's Method

To see the connection with Bäcklund transformations, it is useful to consider further the KdV family of completely integrable PDEs given by

$$q_{t_{2n+1}} = \frac{\partial}{\partial x} L^n q, \quad L = -\frac{1}{4}\partial_x^2 - q - \frac{1}{2}\int_{\infty}^{x} \mathrm{d}x\, q_x, \quad n = 0, 1, \ldots, \tag{13}$$

where $t_{3/4}$ is the t of Equation (1) and $L^0 q = q$. To find them is easy. Write (5) as

$$v_t = A(\lambda; q, q_x, \ldots)v - D(\lambda; q, q_x, \ldots)v_x + Cv, \tag{14}$$

where A, D are polynomials in λ with coefficients depending on q and its x derivatives and C is the normalizing constant. The compatibility of (3) and (14), $(v_{xx})_t = (v_t)_{xx}$, tells one that $A = \frac{1}{2}D_x$ and $q_t = (-\frac{1}{2}\partial_x^3 - 2q\partial_x - q_x - 2\lambda\partial_x)D$. Solve for D as $D = -\lambda^n + D_1\lambda^{n-1} + \ldots + D_n$. Comparing powers of λ determines each D_r in terms of its predecessor as $2\partial_x D_{r+1} = (-\frac{1}{2}\partial_x^3 - 2q\partial_x - q_x)D_r$, $r = 0, \ldots, n$ with $D_0 = 1$ and D_{n+1} defined by $r = n$. The λ^0 balance gives $q_t = 2\partial_x D_{n+1} = \partial_x L^n q$.

Equations (13) are a completely integrable family of Hamiltonian commuting flows containing at level $n = 1$ the KdV equation. They all share the same constants of motion $\{H_{2r+1}\}_{-1}^{\infty}$ with $H_{-1} = \int_{-\infty}^{\infty} q\,\mathrm{d}x$, $H_1 = \int_{-\infty}^{\infty} \frac{1}{2}q^2\mathrm{d}x$, $H_3 = \frac{1}{8}\int_{-\infty}^{\infty}(q_x^2 - 2q^3)\,\mathrm{d}x$, each of which serves as the Hamiltonian for one of the flows $q_{t_{2n+1}} = \partial_x \frac{\delta H_{2n+1}}{\delta q}$ where $\frac{\delta H}{\delta q}[q]$ is the variational derivative of $H[q]$ and ∂_x is the skew symmetric symplectic operator. They are also bi-Hamiltonian in that $\partial_x \frac{\delta H_{2n+1}}{\delta q} = \left(-\frac{1}{4}\partial_x^3 - q\partial_x - \frac{1}{2}q_x\right)\frac{\delta H_{2n-1}}{\delta q}$. They commute under the Poisson bracket

$$\{H_{2m+1},\ H_{2n+1}\} = \int \frac{\delta H_{2m+1}}{\delta q}\,\frac{\delta}{\delta n}\frac{\delta H_{2n+1}}{\delta q}\,\mathrm{d}x = 0.$$

One consequence of commutativity is that if one begins with the shape $q(x, 0, 0, \ldots)$ and evolves q with respect to t_{2n+1} for a time t_{2n+1}, $n = 0, \ldots$, in any order, one always obtains the same shape $q(x, t_1, t_3, \ldots, t_{2n+1}, \ldots)$. This means that the phase shift experienced by any two solitons is the same for each member of the family. Why? Start with the larger, faster moving solution behind the smaller, slower one (the velocity of the soliton of flow n is proportional to η^{2n}). Evolve $q(x, t_{2m+1} = 0, t_{2n+1} = 0)$ via the t_{2m+1} flow for t_{2m+1} time units sufficient for the faster soliton to overtake the slower one and then for t_{2n+1} units via the t_{2n+1} flow. Now do it in the reverse order. Because $q(x, t_{2m+1}, t_{2n+1})$ is the same no matter which order is used, the phase shift must be the same.

A second consequence of commutativity is that one can express the vector made up of the string $L^n q$ as the x derivative of the gradient of a potential which we call $2\ln\tau(x, t_1, t_3, \ldots)$, namely, $L^n q = 2\frac{\partial}{\partial x}\cdot\frac{\partial}{\partial t_{2n+1}}\ln\tau$. The function $\tau(x, t_1, t_3, \ldots)$, called the Hirota τ function, has remarkable properties. It converts each member of the family (13) into bilinear form. For $n = 1$, the KdV equation under $q = 2\frac{\partial^2}{\partial x^2}\ln\tau$ becomes (recall $q_{t_1} = q_x$ and take $4t_3 = t$)

$$D_x^2\tau\cdot\tau = \tau\tau_{xt} - \tau_x\tau_t + \tau\tau_{xxxx} - 4\tau_x\tau_{xxx} + 3\tau_{xx}^2 = 0, \tag{15}$$

where the symbol D_x acting on the ordered pair σ, τ is defined as the limit as $\varepsilon \to 0$ of $\frac{\partial}{\partial \varepsilon}\sigma(x+\varepsilon)\tau(x-\varepsilon) = \sigma_x\tau - \sigma\tau_x$. For the KP equation, one adds $\tau\tau_{yy} - \tau_y^2$ to the left-hand side of (15). From (15), one can build multisoliton solutions. The solution $\tau = 1$ corresponds to the vacuum state $q = 0$. The solution $\tau = 1 + \exp\theta(x,t)$, $\theta(x,t) = 2k(x - x_0) - 8k^3t$ corresponds to the single solution solution $q(x,t) = 2k^2\mathrm{sech}^2 k(x - x_0 - 4k^2t)$. The next solution in the sequence is $\tau = 1 + \exp\theta_1(x,t) + \exp\theta_2(x,t) + \exp(\theta_1(x,t) + \theta_2(x,t) + A_{12})$, $\theta_j(x,t) = 2k_j(x - \bar{x})$, $x_j = 4k_j^2 t + x_{j0}$, $j = 1, 2$, $A_{12} = 2\ln\left|\frac{k_1 - k_2}{k_1 + k_2}\right| < 0$, and is a superposition of two solitons with amplitudes $2k_1^2$ and $2k_2^2$, which for large negative t and large positive t are separated with the faster one (assume $k_1^2 > k_2^2$) being on the left(right) when $t = -\infty(+\infty)$. For $t \to -\infty(+\infty)$, near $x \simeq \bar{x}_2$, the center of the slower pulse, it is the second and fourth (first and third) terms that dominate τ so that for large negative (positive) t, the second soliton looks like

$$2k_2^2\mathrm{sech}^2 k_2\left(x - \bar{x}_2 - \frac{1}{2k_2}|A_{12}|\right)$$
$$\times(2k_2^2\mathrm{sech}^2 k_2(x - \bar{x}_2)).$$

The collision shifts the slower soliton back by $\frac{1}{2k_2}|A_{12}|$ and, by a similar argument, the faster soliton ahead by $\frac{1}{2k_1}|A_{12}|$.

What does the interaction look like? For k_1 much greater than k_2, $|A_{12}| \simeq 0$, and the faster soliton rides adiabatically over the slowly changing slower one. For k_1 greater than but close to k_2, there is an exchange of identities with the slower soliton assuming the form of the faster one as soon as the trailing edge of the former feels the leading edge of the latter.

But a century before Ryogo Hirota's work in the 1970s (*See* **Hirota's method**), the works of Bäcklund, Darboux, and Schlesinger had shown how to build, for certain classes of nonlinear equations, complicated solutions from simple ones. Applied to any member of the KdV family, the idea is this. Define

$$q = -u_x = 2\partial_x^2 \ln\tau \quad \text{and} \quad \tilde{q} = -\tilde{u}_x = 2\partial_x^2 \ln\tilde{\tau}$$

Then there are two relations, called Bäcklund transformations, which express $\tilde{u}_x + u_x$ and $\tilde{u}_t + u_t$ as functions of $\tilde{u} - u$ and a new free parameter ζ^2. Then, if q satisfies KdV, the enriched solution $\tilde{q}$ also satisfies KdV. These expressions take on a beautifully simple form that reveals the algebraic structure underlying the hidden symmetries of the KdV family when they are expressed in terms of τ functions as $\tilde{\tau} = \tau v$ where $v(x, \zeta^2)$ solves (3) with the q corresponding to τ and $\lambda = \zeta^2$. But one can also express v as a combination of $\frac{X(\zeta)\tau}{\zeta}$ and $\frac{X(-\zeta)\tau}{\zeta}$, where the operator

$$X(\zeta) = \exp\left(\mathrm{i}\sum_o^\infty \zeta^{2k+1} t_{2k+1}\right)$$
$$\times \exp\left(\sum_0^\infty \frac{\mathrm{i}}{(2k+1)\zeta^{2k+1}} \frac{\partial}{\partial t_{2k+1}}\right),$$

so that $\tilde{\tau} = \tau_{\text{new}} = (AX(\zeta) + BX(-\zeta))\tau_{\text{old}}$.

For example, choose $\zeta = i\eta$. Then if $\tau_{\text{old}} = 1$, $\tau_{\text{new}} = Ae^{\theta} + Be^{-\theta} = 2\sqrt{AB}\cosh(\theta - \theta_0)$, where $\frac{A}{B} = e^{2\theta_0}$ and $\theta = \sum_0^\infty (-1)^k \eta^{2k+1} t_{2k+1}$ and τ_{new} is the one soliton solution. Because of the logarithm, we can also write τ_{new} as $(1 + \beta Y(\zeta))\tau_{\text{old}}$ where $Y(\zeta)$ is called the vertex operator

$$Y(\zeta) = \exp\left(-2\mathrm{i}\sum_0^\infty \zeta^{2k+1} t_{2k+1}\right)$$
$$\times \exp\left(\sum_{k=0}^\infty \frac{2}{\mathrm{i}(2k+1)\zeta^{2k+1}} \frac{\partial}{\partial t_{2k+1}}\right), \quad (16)$$

which has the property that $Y(\zeta) \cdot Y(\zeta')1 = 0$ if $\zeta = \zeta'$. Thus $Y^2 = 0$ and we can replace $1 + \beta Y(\zeta)$ by $\exp\beta Y(\zeta)$. The Bäcklund transformation is therefore

$$\tau_{\text{new}} = \exp\beta Y(\zeta) \cdot \tau_{\text{old}} \quad (17)$$

namely, the action of the "group" (infinite-dimensional groups are not rigorously defined) element corresponding to the algebraic element $Y(\zeta)$, which can be expressed as a Laurent series $\sum_{-\infty}^{\infty} Y_{2k+1}\zeta^{2k+1}$. The coefficients Y_{2k+1} obey a nontrivial set of commutator relations that form an infinite dimensional, graded Lie algebra (Kac–Moody algebra), the central extension of the loop algebra of Sl $(2, C)$. Under repeated application of (17), solutions of KdV trace out the orbit of the highest weight vector $\tau = 1$ in the basic representation of the Kac–Moody algebra. The algebra acts as an algebra of symmetries. There is also a complementary treatment where the algebra is used as the phase space on which there is defined both a natural Poisson bracket and Hamiltonian vector field.

Other Topics

Multisoliton solutions of the KdV family are a special case of finite gap solutions. The latter are defined by adding a nonlinear, constant coefficient ODE called the Lax–Novikov equation

$$\sum_0^N a_{2r+1}(L^r q)_x = \sum_0^N a_{2r+1}\, q_{t_{2r+1}} = 0 \quad (18)$$

as a constraint on (3) and (14). To illustrate the basic idea, assume traveling wave solutions

$q(x,t) = q(x - ct)$ satisfy $-cq_x + (q_{xx} + 3q^2)_x = 0$,

which is (18) with $a_1 = -c$, $a_3 = 4$, and $a_{2k+1} = 0$, $n > 1$. The Lax–Novikov equation, together with (3) and (14) gives rise to a Riemann surface, the analogue of the spectrum for potentials decaying at infinity, $y^2 = \Pi_{j=1}^{2N}(\lambda - \lambda_j)$ which remains invariant on the finite gap solution family. The τ function for the general N gap solution is the Riemann theta function.

Another class of solutions, the multiphase self-similar solutions, is found by attaching a nonlinear non-autonomous ODE

$$a_0 q + \sum_0^N a_{2r+1}\, t_{2r+1} (L^r q)_x = a_0 q + \sum a_{2r+1}\, t_{2r+1}\, q_{t_{2r+1}} = 0 \quad (19)$$

as a constraint to (3) and (14). It is closely related to the string equation of modern physics, and it leads to a system of linear ODEs for

$$\lambda \frac{\partial}{\partial \lambda} \begin{Bmatrix} v(x, t_{2r+1}, \lambda) \\ v_x(x, t_{2r+1}, \lambda) \end{Bmatrix}$$

with coefficients depending on self-similar scalings of q and its derivatives. Solutions of the multiphase self-similar family are isomonodromic deformations of this system of ODEs in that they leave the monodromic structure invariant. At $\lambda = \infty$, an irregular singular point, the monodromic structure is expressed in terms of Stokes multipliers; at $\lambda = 0$, a regular singular point, the monodromy is that of a simple pole. Members of this family include the Painlevé equations.

For example, (19) with $a_0 = -2$, $a_1 = -1$, $a_3 = 3$, $t_3 = t$ is $-2q - xq_x + 3t(q_{xx} + 3q^2)_x = 0$ which forces $q(x, t)$ to have the form

$$\frac{1}{(3t)^{2/3}} f\left(X = \frac{x}{(3t)^{1/3}}\right),$$

which satisfies an ODE that is a close cousin of the second Painlevé equation. This solution plays a key role in joining the soliton component of the solution with the trailing wave-like radiation. Isomonodromic deformations provide the link between soliton equations and the exactly solvable models of statistical physics. For example, the two-point correlation function for the nearest-neighbor Ising model in the scaling limit satisfies the third Painlevé equation.

The existence of so many completely integrable systems of physical interest (KdV, Boussinesq, nonlinear Schrödinger, derivative nonlinear Schrödinger, massive Thirring, sine-Gordon, Maxwell–Bloch with inhomogeneous broadening, KP, BRDS, three-wave scattering, Raman scattering) leads one to ask how important to applications these integrable models are. In the set of all PDEs, they are of measure zero. On the other hand, there are two reasons for their importance. The first is that many systems such as shallow waves traveling over a channel of slowly varying depth can be treated as perturbations of PDEs integrable by ISM, and there are simple algorithms for computing how the previously constant action variables slowly evolve. The second reason is more subtle and remains to be rigorously proven. Many of the equations of physical interest arise as asymptotic approximations, as reductions of more complicated systems assuming (as one does in deriving KdV) weak nonlinearity and weak dispersion, or (as one does in deriving NLS) weak nonlinearity and strong dispersion of an almost monochromatic wavepacket. If the process of reduction preserves integrability, then as long as there is one integrable equation among the class that reduces to the universal equation of interest, the reduced equation will also be integrable.

Finally, how does one test for integrability? How does one uncover the hidden symmetries, the algebraic structure of a PDE or ODE? There is yet no foolproof method that works in all circumstances. As in the original discovery of the integrability of KdV, serendipity often plays the main role. Two of the more promising semi-algorithmic approaches are the Painlevé test (the location of any algebraic, logarithmic or essential singularity is independent of initial conditions and only the location of poles can depend on arbitrary constants of integration). and the Wahlquist–Estabrook method, which seeks to uncover the hidden symmetries by embedding the equation of interest as an integrability condition of a pair of linear systems whose algebraic structure it is the goal of the method to find. Each has its advantages and each has proven to be successful in extracting the appropriate Lax pair in several contexts. But the challenge of determining a foolproof method to determine whether a particular equation is integrable is still open.

ALAN NEWELL

See also **Ablowitz–Kaup–Newell–Segur system; Bäcklund transformations; Hirota's method; Kadomtsev–Petviashvili equation; N-soliton formulas; Painlevé analysis**

Further Reading

Ablowitz, M.J., Kaup, D.J., Newell, A.C. & Segur, H. 1974. The inverse scattering transform-Fourier analysis for nonlinear problems. *Studies in Applied Mathematics*, 53: 249–315

Ablowitz, M.J. & Segur, H. 1981. *Solitons and the Inverse Scattering Transform*, Philadelphia: SIAM

Faddeev, L.D. & Takhtajan, L.A. 1987. *Hamiltonian Methods in the theory of solitons.* Berlin: Springer

Flaschka, H. & Newell, A.C. 1980. Monodromy and spectrum preserving deformations. *Communications in Mathematical Physics*, 76: 65–116

Fokas, A.S. & Zakharov, V.E. 1993. *Important Developments in Soliton Theory*, Berlin and New York: Springer

Gardner, C.S., Greene, J.M., Kruskal, M.D. & Miura, R.M. 1974. The Korteweg de Vries equation and generalization. VI. Methods of exact solution. *Communications in Mathematical Physics*, 27: 97–133

Newell, A.C. 1985. *Solitons in Mathematics and Physics*, Philadelphia: SIAM

ION ACOUSTIC WAVES

See **Nonlinear plasma waves**

ISING MODEL

The Ising or Lenz–Ising model was introduced by Wilhelm Lenz in 1920 as a simplified model of a ferromagnet. Lenz's student Ernst Ising studied the one-dimensional case (a linear chain of coupled magnetic moments) for his doctoral dissertation at the University of Hamburg, and his results published in 1925 showed the absence of a phase transition between a ferromagnetic and paramagnetic state. In 1942, Lars Onsager applied an ingenious mathematical method to the two-dimensional model and showed analytically the existence of a phase transition in the absence of an external magnetic field. Interest in the model has increased in recent years as it became the foundation for modeling changes of state in new areas such as spin glasses and neural networks. In 1975, David Sherrington and Scott Kirkpatrick introduced long-range competing interactions in the model and showed the emergence of a new type of glassy order, while John Hopfield in 1982 used the connection between spins and neurons in extending the Ising model into a model of neuronal networks.

The original motivation for the introduction of the model came from the knowledge that certain metals, such as iron, are ferromagnetic; that is, they form macroscopic domains with nonzero magnetization when the temperature is less than a characteristic Curie temperature (T_c), but this long-range order is lost at temperatures $T > T_c$. Because magnetic properties of atoms are a result of the orbital angular momentum as well as spin of their electrons, the existence of macroscopic size domains with nonzero magnetization stems from mutual alignment of permanent atomic dipole moments induced by dipole-dipole interactions. The Lenz–Ising simplification ignores quantum mechanics and assigns to an atom located in crystal site i a magnetic moment or "spin" S_i that takes only two values, namely, $S_i = \pm 1$. The energy or Hamiltonian for the system of N spins is

$$H = -\frac{1}{2}\sum_{i,j=1}^{N} J_{ij} S_i S_j - \sum_{i=1}^{N} B_i S_i, \qquad (1)$$

where J_{ij} is the interaction between spins at sites i and j; respectively; B_i is a local magnetic field at site i; and the sums extend independently over all N sites. Any of the 2^N spin configurations can be thought of as a chemical solution of two species with N_+ and $N_- = N - N_+$ spins in up and down states, respectively, with number densities $n_\pm = N_\pm/N$; the entropy of this state is determined by the number of ways N spins are partitioned in up and down configurations, giving

$$S = -Nk_B\,(n_+ \ln n_+ + n_- \ln n_-)\,. \qquad (2)$$

Furthermore, the density of $++$, $--$, and $+-$ pairs that determine short-range order is approximated in the Bragg–Williams approximation respectively, by n_+^2, n_-^2, and $2n_+n_-$. Thus, Equation (1) becomes

$$H = -\tfrac{1}{2}zNJ\left(n_+^2 + n_-^2 - 2n_+n_-\right) - NB\,(n_+ - n_-,)\,, \qquad (3)$$

where only interactions of strength J between z nearest-neighbor spins are included. Introducing the macroscopic magnetization $M = N_+ - N_- = N(n_+ - n_-)$, expressing the densities as $n_\pm = (1 \pm M/N)/2$, and substituting in the energy and entropy, respectively, one obtains

$$H = -\frac{zJM^2}{2N} - MB$$
$$S = NK\left[\ln 2 - \frac{1}{2}\left(1+\frac{M}{N}\right)\ln\left(1+\frac{M}{N}\right) - \frac{1}{2}\left(1-\frac{M}{N}\right)\ln\left(1-\frac{M}{N}\right)\right] \qquad (4)$$

The thermodynamics of the model is now completely determined from the minimization of the Helmholtz free energy $F = H - TS$ with respect to the magnetization M at constant external field B and temperature T. It yields

$$\frac{M}{N} = \tanh\beta\left(B + zJ\frac{M}{N}\right), \qquad (5)$$

where $\beta = 1/k_BT$. Equation (5) is identical to that obtained through the Weiss mean field theory predicting, after linearization and for zero external field, a Curie temperature determined by $k_BT_c = zJ$.

If the interaction J_{ij} is not fixed but taken to be random, distributed according to a Gaussian with mean J_0/N and variance J^2/N, then

$$P(J_{ij}) = \left(\frac{N}{2\pi J^2}\right)^{1/2}\exp\left[-\left(J_{ij} - \frac{J_0}{N}\right)^2\frac{N}{2J^2}\right]. \qquad (6)$$

The resulting Ising model is referred to as the Sherrington–Kirkpatrick model, and its low-temperature phase at zero-external-field is a spin glass. This phase is not characterized by the long-range order typical in ferromagnets but by partial system freezing in time showing persistent but spatially random configurations whose thermodynamic signature is a sharp cusp in the zero field cooled susceptibility. A spin glass is typically characterized by metastability, frustration, and slow relaxation resulting from the multiple high barriers (introduced by disorder in the

free energy) that force the system to remain trapped in local free energy minima for long times.

Introducing some changes in the Ising spin-glass model and with proper interpretation, one obtains a model for a network of neurons. Ising spins are now states of a neuron found in a firing ($S_i = +1$) or inhibitory state ($S_i = -1$), the interaction elements J_{ij} are synaptic strengths between neurons while the external field depends on a neuron firing threshold potential. In the learning mode, the network stores information on patterns in the synaptic strengths, while in the retrieval mode, these patterns are accessed when the network is exposed to partial information on the desired memories. If $S^\nu \equiv \{S_1^\nu, S_2^\nu, \ldots, S_N^\nu\}$ (for $\nu = 1, \ldots, p$) represent p patterns of N neurons, employment of the following version of Hebb's rule:

$$J_{ij} = \frac{1}{N} \sum_{\nu=1}^{p} S_i^\nu S_j^\nu \tag{7}$$

stores the p patterns in memory. In the Hopfield model for $p/N \leq 0.14$, these states, as well as several other spurious ones, become attractors to the evolution flow of neuron updating rules. Whenever a spin-glass phase is present, either alone or in coexistence with the memory states, information retrieval is corrupted.

While the phase diagrams of Ising spin glasses and neural networks are quite complex, the one determined analytically by Onsager for the two-dimensional Ising model with nearest-neighbor interaction J is much simpler, demonstrating the presence of a Curie temperature at $k_B T_c \approx 2.269J$ with a low-temperature ferromagnetic phase. This shows that even though quite simple, the Ising model contains the essential features of the problem that motivated its introduction, the ferromagnetic-paramagnetic transition. The absence of a transition in one dimension as found by Ising can be understood qualitatively by the following argument of Wannier. Energy equal to $2J$ can introduce a spin down defect in an ordered chain of $N + 1$ spins that are all in state up, and this can be done in N ways resulting in entropy $k_B \ln N$. The free energy for this change is $\Delta F = 2J - k_B T \ln N$ and favors always the entropic term except at $T = 0$; thus, there cannot be long-range order in one dimension at finite temperatures.

G.P. TSIRONIS

See also **Attractor neural network; Ferromagnetism and ferroelectricity; Frustration**

Further Reading

Baxter, R.J. 1982. *Exactly Solvable Models in Statistical Mechanics*, London: Academic Press

Binder, K. & Young, A.P. 1986. Spin glasses: experimental facts, theoretical concepts and open questions. *Reviews of Modern Physics*, 58: 801–976

Müller B., Reinhardt, J. & Strickland, M.T. 1995. *Neural Networks: An Introduction*, Berlin: Springer

Sompolinski H. 1988. Statistical mechanics of neural networks. *Physics Today*, 41 (12 Dec): 70–80

Wannier, G.H. 1966. *Statistical Physics*, New York: Wiley

ITO'S FORMULA

See **Stochastic processes**

IZERGIN–KOREPIN EQUATION

See **Discrete nonlinear Schrödinger equations**

J

JACOBI ELLIPTIC FUNCTIONS

See **Elliptic functions**

JOSEPHSON JUNCTION ARRAYS

Josephson junction arrays (JJAs) consist of islands of superconductor arranged in an ordered lattice, coupled by Josephson junctions. Large JJAs are useful model structures for studying the dynamics of coupled nonlinear oscillators, phase transitions, frustration effects, vortex dynamics, and macroscopic quantum phenomena (Newrock et al., 2000).

JJAs are generally divided into classical arrays ($E_J/E_C \gg 1$) and quantum arrays ($E_J/E_C \ll 1$), depending on the ratio of the Josephson energy, E_J, to the charging energy, E_C (Fazio & van der Zant, 2001). Classical JJAs can be divided into overdamped arrays ($\beta_C \ll 1$) and underdamped arrays ($\beta_C \gg 1$), referring to the fact that the equation of motion for a single Josephson junction is identical to a damped pendulum. The dividing line is determined by the McCumber parameter, β_C, which defines the amount of damping in terms of the junction capacitance and resistance.

Modeling of classical JJAs is essentially based on solving a system of coupled ordinary differential equations for the superconducting phase differences φ_n of Josephson junctions that constitute the array. Typically, JJAs are fabricated using photolithography and the standard fabrication processes for superconductive electronics. They are very well characterized, leading to an interesting synergy between experiments, theory, and simulations.

The properties of JJAs depend on their dimensionality and the way Josephson junctions are connected. In the series one-dimensional (1-d) JJAs shown in Figure 1a, there is no direct interaction between Josephson junctions. The junctions can be coupled, for example, via a load resistor connected between the extremities of the array. Under certain conditions (Jain et al., 1984), when biased by a bias current flowing along the array, Josephson junctions perform coherent oscillations.

Parallel 1-d arrays shown in Figure 1b have inherent mutual coupling between Josephson junctions due to screening currents and magnetic flux quantization in superconducting loops. Such an array is essentially similar to a long Josephson junction, and it is described by the discrete sine-Gordon (SG) model. Due to the similarity between the discrete SG and continuous SG models, properties of vortices in parallel 1-d JJAs are similar to those of Josephson vortices (solitons called fluxons) in long Josephson junctions (Ustinov & Parmentier, 1996; Watanabe et al., 1996).

The two-dimensional (2-d) JJA illustrated in Figure 1c has attracted a great deal of interest as it is isomorphic to a 2-d XY spin system, which is a 2-d lattice of spins free to rotate in the XY plane. In its simplest form, the Hamiltonian of an array can be written as

$$H = -\sum_{\langle n,m \rangle} E_J \cos(\varphi_m - \varphi_n - f), \qquad (1)$$

where $\langle n, m \rangle$ means summing over nearest neighbors and f is the frustration factor depending on the externally applied magnetic field. It should be noted that model (1) is valid only under the condition that both E_J and the array cell size are small enough, i.e., that inductance effects play no role. In practical JJAs, this is typically not the case and these effects significantly complicate JJA dynamics.

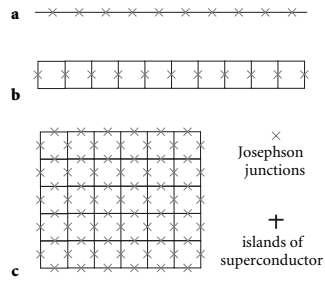

Figure 1. Schematic view of (a) 1-d series JJA; (b) 1-d parallel JJA; (c) 2-d JJA.

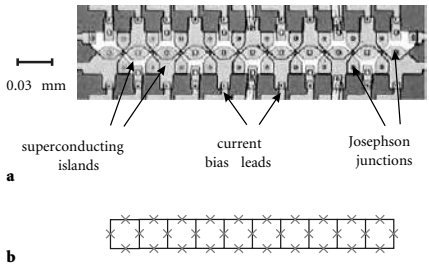

Figure 2. (a) Micro-photograph of a Josephson ladder (Binder et al., 2000). (b) The equivalent circuit of the ladder.

Starting from the mid-1990s, a special type of JJA called the Josephson ladder has received much interest. The ladder is essentially one row of cells cut from the standard 2-d JJA. Floría et al. (1996) studied a ladder driven by an ac bias current and found both oscillating and rotating localized modes. Such intrinsically localized modes, often called discrete breathers, are spatially localized time-periodic dynamical states that occur in various nonlinear lattices. The oscillating modes in Josephson arrays are difficult to detect experimentally as they are accompanied by zero average dc voltage. In contrast to oscillating discrete breathers, rotating discrete breathers induce a localized nonzero dc voltage and can be easily measured. Moreover, rotating discrete breathers can also be supported by a dc bias current. Experiments that followed the theoretical proposals successfully demonstrated dynamical localization in the form of discrete breathers in JJA (Ustinov, 2001).

There are several useful applications of JJA. At microwave frequencies, Josephson junctions can be used as sources and detectors of radiation. The Josephson relation $\Phi_0 \nu = V$ (where $\Phi_0 = h/(2e) = 2.07 \times 10^{-15}$ Vs is the magnetic flux quantum) states that at constant voltage V, the current through the junction will oscillate with a frequency ν, proportional to V. Utilizing this unique property, Josephson junction arrays have for the last two decades been studied as microwave sources (Darula et al., 1999). The advantages of using arrays as opposed to junctions are higher power outputs and better impedance matching to typical loads. Another important application of JJA, based on the same equation, is to define the voltage standard. Since frequency can be measured extremely accurately, locking Josephson junctions to a microwave source provides excellent accuracy for measuring the voltage. Using a series JJA instead of a single Josephson junction allows the upper voltage level to be brought from less than a millivolt up to the range of several volts.

ALEXEY V. USTINOV

See also **Breathers; Frenkel–Kontorova model; Frustration; Josephson junctions; Long Josephson junctions; Sine-Gordon equation; Superconducting quantum interference device; Superconductivity**

Further Reading

Binder, P., Abraimov, D. & Ustinov, A.V. 2000. Diversity of discrete breathers observed in a Josephson ladder. *Physical Review E*, 62: 2858–2862

Darula, M., Doderer, T. & Beuven S. 1999. Millimetre and sub-mm wavelength radiation sources based on discrete Josephson junction arrays. *Superconductor Science and Technology*, 12: R1–R25

Fazio, R. & van der Zant, H. 2001. Quantum phase transitions and vortex dynamics in superconducting networks. *Physics Reports*, 355: 235–334

Floría, L.M., Marin, P.J., Martinez, J.L., Falo, F. & Aubry, S. 1996. Intrinsic localization in the dynamics of a Josephson junction ladder. *Europhysics Letters*, 36: 539–544

Jain, A.K., Likharev, K.K., Lukens, J.E. & Sauvageau, J.E. 1984. Mutual phase-locking in Josephson junction arrays. *Physics Reports*, 109: 309–426

Newrock, R.S., Lobb, C.J., Geigenmüller, U. & Octavio, M. 2000. The two-dimensional physics of Josephson junction arrays. *Solid State Physics*, 54: 263–412

Ustinov, A.V. 2001. Experiments with discrete breathers in Josephson arrays. In *Nonlinearity and Disorder: Theory and Applications*, edited by F. Abdullaev, O. Bang & M.P. Soerensen, Dordrecht: Kluwer, pp. 183–185

Ustinov, A.V. & Parmentier, R.D. 1996. Coupled solitons in continuous and discrete Josephson transmission lines. In *Nonlinear Physics: Theory and Experiment*, edited by E. Alfinito, M. Boiti, L. Martina & F. Pempinelli, Singapore: World Scientific, pp. 582–589

Watanabe, S., van der Zant, H., Strogatz, S.H. & Orlando, T. 1996. *Physica* D, 97: 429

JOSEPHSON JUNCTIONS

Predicted theoretically by Brian Josephson in 1962, the Josephson junction (JJ) consists of two superconductors that are so weakly coupled that the Cooper pairs may quantum mechanically tunnel between the superconductors without destroying the integrity of their individual macroscopic wave functions, Ψ_1 and Ψ_2. A typical example is the trilayer tunnel junction (see Figure 1) consisting of two overlapping niobium (Nb) thin films separated by a thin (2–5 nm) insulating layer of aluminum oxide (Al_2O_3).

Extremely fast and highly nonlinear, the JJ is described by the two Josephson equations

$$I = I_c \sin \phi, \tag{1}$$

$$\frac{\partial \phi}{\partial t} = \frac{2\pi}{\Phi_0} V, \tag{2}$$

where I is the pair-current through the junction. The critical current I_c is a constant parameter given by the materials, the barrier, and the geometry of the structure. $\Phi_0 = h/2e$ is the flux quantum, $\phi = \theta_1 - \theta_2$ is the difference between the phases θ_1 and θ_2 of Ψ_1 and Ψ_2, respectively, and V is the voltage across the junction. These equations assume a constant current density over the junction area.

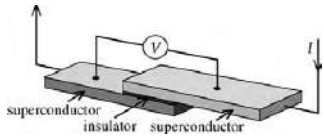

Figure 1. Typical Josephson tunnel junction consisting of two superconducting thin-films separated by a very thin insulating oxide layer.

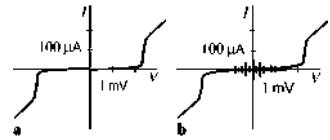

Figure 2. dc current–voltage characteristic of $Nb/Al_2O_3/Nb$ trilayer Josephson tunnel junction at 4.2 K. Note the supercurrent in the zero-voltage state and the steep gap structure near 2.7 mV. (a) No applied microwaves and (b) with applied microwaves. The small vertical zero-crossing steps are equidistantly spaced with a voltage difference of $\Delta V = hf/2e$. These nonlinear quantum phenomena allow for the practical construction of the Josephson voltage primary standard.

If one applies a dc bias current $I < I_c$ to the junction, the phase difference ϕ of the macroscopic wave functions automatically adjusts itself so that Equation (1) is satisfied; i.e., the junction remains in the zero-voltage state carrying a supercurrent up to the critical current. For $I \geq I_c$, the junction switches to the voltage state, and ϕ oscillates in time according to the second Josephson equation.

If the junction is supplied with a constant voltage, V_{DC}, the phase difference increases steadily with time, and the junction current oscillates with the frequency

$$f = \frac{1}{\Phi_0} V_{DC}; \tag{3}$$

that is, the junction functions as a voltage controlled oscillator (VCO) that may generate microwave power into the gigahertz range. (The pre-factor $1/\Phi_0 \approx 0.5\,\mathrm{GHz}/\mu\mathrm{V}$.)

The capacitance between the two electrodes in Figure 1 shunts the Josephson tunneling and leads to hysteresis in the current-voltage characteristic (I–V curve) as shown in Figure 2a. Starting at zero and increasing the bias current, there is a vertical supercurrent (zero-voltage state) up to I_c where the junction switches (horizontally) to the steep so-called quasi-particle curve (near 2.7 mV), which reflects the superconducting gap of the two niobium electrodes. The quasi-particle curve is followed both when the bias current is further increased and when the current is returned to $I = 0$. The hysteretic I–V curve is point-symmetric around $(V, I) = (0, 0)$.

The I–V curve near the gap is strongly nonlinear and temperature dependent. Tunnel junctions biased close to the knee are used as low-noise bolometers to detect broad band signals in the millimeter and sub-mm range. Due to its strong nonlinearity, heterodyne receivers based on this SIS-mixer (superconductor-insulator-superconductor) can be operated near the quantum limit ($hf \approx k_B T$). The SIS-mixer may be pumped by the microwave signal emitted from a long JJ (see below). Most modern radio-telescopes employ SIS-mixers for spectral measurements in the frequency range 10–1000 GHz.

Figure 2b shows the I–V curve when a microwave signal is applied to the junction. The supercurrent is suppressed and small equidistantly spaced replica appear as vertical (Shapiro) steps with a voltage difference of $\Delta V = hf/2e$. These zero-crossing steps and the fact that voltage and frequency are related only through fundamental constants allow for the practical realization of the Josephson voltage primary standard. When pumped by a 70 GHz signal, $\Delta V \approx 140\,\mu\mathrm{V}$; thus a small chip with more than 20.000 dc series connected JJs can generate a reference voltage of 10 V with an accuracy of 0.1 nV. Josephson junctions are strongly nonlinear elements which when pumped by external high-frequency signals may not only generate very high-numbered higher harmonics but also via parametric processes generate both even and odd subharmonics (e.g., period-doubling bifurcations) and chaos. The stability of the Josephson voltage standard is limited by chaotic behavior.

JJs are highly sensitive to magnetic fields. The gradient of the phase difference ϕ is proportional to the magnetic field applied in the plane of the junction, and for constant current density the net critical current is zero each time ϕ has a twist of 2π, which happens when the flux Φ threading the junction is exactly one flux quantum Φ_0. Included in a superconducting ring, JJs constitute the so-called Superconducting Quantum Interference Device (SQUID), which is used, for example, for magnetoencephalographic measurements of electrical activity in the human brain.

The magnetic twist of the phase difference along the junction also leads to the so-called Fiske steps. These are nearly constant-voltage steps in the I–V curve at voltages $V_{FSn} \approx \Phi_0 c_s/2L$, where $n = 1, 2, \ldots$ and L is the junction length perpendicular to the magnetic field. Also, c_s is the Swihart velocity of electromagnetic waves propagating in the junction (about 3% of the light velocity in vacuum). The physical mechanism is as follows. The Josephson oscillations at the voltages V_{FSn} excite standing electromagnetic waves inside the junction (cavity) with wavelengths $\lambda_n = 2L/n$ and resonance frequencies $f_n = c_s/\lambda_n$. Whenever the spatial twist in $\Phi(x)$ fits to the nth mode of the standing wave, there is a strong resonant nonlinear interaction

that phase-locks the Josephson oscillation at f_n, giving Fiske steps at voltages $V_{\mathrm{FS}n}$.

Until now we have considered only JJs with small dimensions compared with the so-called Josephson penetration length λ_{J}, which is of the order of 10 μm. Longer tunnel junctions are well modeled by the perturbed sine-Gordon (SG) equation. If we consider a linear one-dimensional (1-d, x-direction) junction with dc current bias, the SG equation in normalized units reads

$$\phi_{xx} - \phi_{tt} = \sin\phi + \alpha\phi_t - \eta, \tag{4}$$

where the normalized magnetic field $\kappa_{1,2}$ (perpendicular to the x-direction) enters as the boundary condition

$$\phi_x(0,t) = \kappa_1 \text{ and } \phi_x(l,t) = \kappa_2, \tag{5}$$

specifying the magnetic field at the two ends of the junction. The normalized bias current η here is assumed to be evenly distributed along the junction (overlap geometry). In the above equations, time t is normalized to the inverse maximum plasma frequency, ω_0, length x to λ_{J}, currents to the maximum critical current, I_{c}, and magnetic fields to the critical field, H_{c}, needed to force the first fluxon into the junction. Magnetic fields can only enter the junction in the form of fluxons, which are individual soliton-like localized 2π phase shifts each containing one flux quantum Φ_0.

Many solutions to the nonlinear SG equation have been found by numerical integration. For zero magnetic field and low values of the damping coefficient α, fluxons oscillate resonantly back and forth inside the junction driven by the Lorentz-like force from the bias current. This gives rise to a 4π phase shift per period and leads to the so-called zero-field steps, which are nearly constant-voltage steps located at voltages $V_{\mathrm{ZFS}n} \approx n\Phi_0 c_{\mathrm{s}} L$, $n = 1, 2, ..$ in the I–V curve. Note that zero-field step voltages are twice as large as the voltages of the Fiske steps discussed above for short junctions.

For every fluxon collision at $x = l$ (where l is the normalized junction length), a small electromagnetic field is emitted and the junction may be used as a microwave oscillator when biased on either a Fiske step or a zero-field step, but applications of this resonant soliton oscillator (RSO) are rather limited. First, the resonance frequencies are fixed (given by L and c_{s}) and the tunability is very small (steep steps). Second, the emitted power is relatively low and has high harmonic content (fluxon collision delta-function-like in time domain). However, due to its frequency stability and rather narrow linewidth, the RSO may be used as an on-chip clock oscillator.

When a stronger external magnetic field is applied (e.g., from a dc current, I_{CL}, in an overlaying control line), the junction will contain many fluxons, and since the fluxons repel each other, they will form an equidistant chain. Under a very strong field, the fluxons are forced so close to each other that the phase gradient becomes nearly uniform and proportional to the field strength. (One may compare the phase variation to a household corkscrew where the pitch is given by the applied magnetic field.) If a dc bias current I_{B} (uniformly distributed along the x-direction) is also applied to the junction, the fluxon chain is forced to move with constant velocity along the junction leading to a unidirectional flux flow through the junction. In our analogy, the bias current forces the corkscrew to rotate with constant angular velocity. The total phase shift per second and, thus, the frequency of the microwave signal emitted at $x = l$ can therefore be adjusted independently by the dc bias current (rotation) and the dc magnetic field (pitch). In the I–V curve, one observes a flux flow step (FFS) where the voltage, V_{FFS}, depends on both I_{B} and I_{CL}. Because the pitch for a dense chain of fluxons increases proportional to the magnetic field, V_{FFS}, the oscillator frequency in this limit depends linearly on I_{CL} for fixed I_{B}.

This explains the dynamics of the important flux flow oscillator (FFO). Its easy tunability not only permits wide band frequency coverage but also allows for accurate phase locking of the FFO. The power emitted from the FFO depends in a complicated way on the junction parameters as well as on I_{B} and I_{CL}, but with appropriate microwave design the power is sufficient to pump an SIS-mixer placed on the same chip. In 2002, a fully superconducting integrated receiver (SIR) with FFO, stripline circuit, SIS-mixer, and antenna (all placed on a $5 \times 5\,\mathrm{mm}^2$ chip) has been operated in phase-locked mode up to 712 GHz with a frequency resolution of less than 1 Hz relative to the reference oscillator used in the phase-locking loop. At 500 GHz the noise temperature was less than 100 K, just above the quantum limit. The low-noise in combination with the high-frequency resolution in the submillimeter frequency range is very promising for spectral investigations in astronomy, chemistry, and biophysics.

Numerical simulations of the SG equation have confirmed that the unidirectional flux flow mode can also be sustained for very large values of the damping parameter α. Often the damping per normalized length $\alpha l > \pi$ is used to define the flux flow range. For low values of αl the FFS consists of a distinct Fraunhöfer pattern of Fiske steps localized in the vicinity of the average FFS voltage given by I_{B} and I_{CL}. The correct boundary conditions, the geometry, and especially the paths along which the two bias currents are supplied to the junction are very important for the free-running linewidth of the FFO and thus for the practical implementation of the SIR.

For simplicity, we have restricted ourselves to a single Josephson junction with linear 1-d geometry. Considerable work has been devoted to 1- and 2-d arrays of both short and long junctions, and vertically stacked junctions (*See* **Josephson junction arrays**; **Long Josephson junctions**). Many structures and

circuits have been fabricated in both low-T_c and high-T_c superconductors. The 1-d long Josephson junction with annular geometry is of considerable interest, not least because the cyclic boundary conditions are combined with flux quantization and flux trapping. Whole families of *single flux quantum* (SFQ) and *rapid single flux quantum* (RSFQ) electronics based on propagation of single fluxons in superconducting circuits containing Josephson junctions and SQUIDs (*See* **Superconducting quantum interference device**) have been developed and partially tested for applications. Josephson junction science and technology now is mature, and many applications are waiting to be implemented in future electronics.

JESPER MYGIND

See also **Diodes; Hysteresis; Josephson junction arrays; Long Josephson junctions; Parametric amplification; Period doubling; Sine-Gordon equation; Solitons; Superconducting quantum interference device; Superconductivity**

Further Reading

Duzer, T. Van & Turner, C.W. 1998. *Principles of Superconductive Devices and Circuits*, 2nd edition, Upper Saddle River, NJ: Prentice-Hall, pp. 158–325

Kadin, A.M. 1999. *Introduction to Superconducting Circuits*, New York: Wiley, pp. 178–340

Orlando, T.P. & Delin, K.A. 1990. *Foundations of Applied Superconductivity*, Reading, MA: Addison-Wesley, pp. 393–486

JOST FUNCTIONS

See **Inverse scattering method or transform**

JULIA SETS

See **Fractals**

JUMP PHENOMENA

Jump phenomena or surfaces of discontinuity occur when a field or gradient of a field exhibits finite jumps (discontinuities) due to the system changing nature (such as a liquid-gas interface) or the geometry of the domain changing abruptly in a given hyperplane (such as an acoustical tube with an abrupt widening). A particularly dramatic example of a hydraulic jump (see Figure 1) appeared regularly on the river Seine early in the 20th century.

In nature, systems are often governed by conservation laws of the various quantities. For example, for a fluid, we can write equations for the conservation of mass, momentum, and energy, and in an electrical system, current is conserved. There may be a hierarchy of these laws so when the system is perturbed the lower order ones are approximately maintained while the higher order ones are clearly broken.

Following the discussion of Landau (Landau & Lifschitz, 1959), one can classify discontinuities in two main groups. Let us illustrate this with the example of a continuous medium for which mass flux, momentum flux, and energy flux are continuous across a discontinuity. In the first case, mass flux is zero across the discontinuity, implying that the tangential derivative of the velocity has a jump. This is called a tangential discontinuity, a familiar example being the ocean surface separating water circulation from wind circulation. In the other case, called a shock wave (*See* **Shock Waves**), mass flow is nonzero, implying a jump in the velocity normal to the discontinuity. The existence of such discontinuous fields is strongly connected to the hyperbolic nature of the system of equations for which wave fronts can propagate along definite directions (characteristics).

In reality, the velocity normal to the interface is not discontinuous but varies on a very small scale due to viscosity and damping which are not taken into account in the original model. In particular, energy is dissipated in such an event so that the energy flux is not conserved. A way to remove this difficulty is to assume a given dissipation and modify the energy jump condition. It is remarkable that such modified jump conditions can describe accurately the state of a system where dissipation occurs even without an accurate description of the (microscopic) dissipation mechanism.

Examples

Example (i)

As an example of a normal discontinuity (shock wave), consider a one-dimensional compressible fluid flow. The conservation of mass and momentum of the fluid can be written as

$$\rho_t + (\rho v)_x = 0, \tag{1}$$

$$v_t + v v_x + \frac{c^2}{\rho} h_x = 0, \tag{2}$$

where the subscripts indicate partial derivatives, ρ is the gas density, v the velocity along the x axis, and $c(\rho)$ is the velocity of sound.

In 1860, Bernard Riemann obtained a solution of this system by assuming a single dependence of the two fields $\rho(\alpha(x,t))$ and $v(\alpha(x,t))$ on an unknown function α. He obtained the compatibility condition linking ρ and v:

$$v = \pm \int \frac{c(\rho)}{\rho} \mathrm{d}\rho, \tag{3}$$

and showed that α should satisfy the one-dimensional partial differential equation

$$\alpha_t + (v \pm c)\alpha_x = 0, \tag{4}$$

Figure 1. A tidal bore (or *mascaret*) on the Seine at Quillebeuf, France. The site is 19 km from the mouth of the river, where tides up to 10 m occur. Due to dredging in the 1960s, this striking nonlinear phenomenon has disappeared. (Courtesy of J.J. Malandain.)

whose formal solution is $\alpha = f(x - (v \pm c)t)$. This indicates that given values of v and ρ move to the right along the characteristic lines $x = (v \pm c)t$ at speeds $v \pm c$, allowing shock waves across which the velocity and density fields are discontinuous. Consequently, an initial condition with $v > c$ will only propagate to the right, whereas if $v < c$, it will propagate over the whole domain.

Consider how to derive jump conditions; from (1). Assume $c^2 = \rho g$ where g is a constant; this is not physical in the context of gases but it simplifies the derivation. The conservation of the mass flux is obtained by integrating the first equation on a small domain $-\varepsilon < x < \varepsilon$ centered on $x = 0$; thus,

$$\int_{-\varepsilon}^{\varepsilon} \rho_t \, \mathrm{d}x + [\rho v]_{x=-\varepsilon}^{x=\varepsilon} = 0. \tag{5}$$

Assuming that ρ_t has a finite discontinuity at $x = 0$, we obtain in the limit $\varepsilon = 0$

$$[v\rho] = 0\,. \tag{6}$$

The momentum conservation law is obtained by examining the time evolution of the average momentum ρv:

$$(\rho v)_t + \left(\rho v^2 + \frac{g\rho^2}{2}\right)_x = 0. \tag{7}$$

The last conservation law involves the total energy e of the fluid, which is the sum of the kinetic and potential energy

$$(\rho v^2 + g\rho^2)_t + (\rho v^3 + 2\rho^2 v g)_x = 0. \tag{8}$$

Proceeding in a similar way as for the mass flux, we obtain jump conditions for the momentum and energy of the fluid so the entire set of jump conditions are

$$[v\rho] = 0, \left[\rho v^2 + \frac{g\rho^2}{2}\right] = 0,$$
$$[v^3\rho + 2g\rho^2 v] = 0. \tag{9}$$

Example (ii)

The second kind of discontinuity occurs when considering compression waves in an inhomogeneous beam made of two beams of different materials soldered at some point. The equation describing the displacement u is the one-dimensional generalized wave equation

$$\rho\sigma u_{tt} - (\sigma E u_x)_x = 0, \tag{10}$$

where σ is the beam section, ρ its density, and E the Young modulus such that $E = E_\mathrm{l}$ for $x < 0$ and $E = E_\mathrm{r}$ for $x > 0$. To obtain the jump condition at $x = 0$, one integrates equation (10) over a small domain $-\varepsilon < x < \varepsilon$ to obtain

$$\int_{-\varepsilon}^{\varepsilon} \mathrm{d}x \rho\sigma u_{tt} - [\sigma E u_x]_{x=-\varepsilon}^{x=\varepsilon} = 0\,. \tag{11}$$

Now consider the limit $\varepsilon = 0$, assuming the displacement u to be continuous across $x = 0$. The first term is the acceleration which should tend to zero. The second term is the stress, and relation (11) shows that it too should be continuous. At $x = 0$, we then have the following relations:

$$u_l = u_\mathrm{r}, \quad E_\mathrm{l} u_x|_\mathrm{l} = E_\mathrm{r} u_x|_\mathrm{r}, \tag{12}$$

so the gradient u_x exhibits a finite jump.

Hydraulic Jumps

Shallow water flows for which the depth h_0 is much smaller than the length l are governed by the following equations for the water elevation h and velocity v in the direction of propagation (Landau & Lifschitz, 1959)

$$h_t + (hv)_x = 0, \tag{13}$$
$$v_t + vv_x = -gh_x, \tag{14}$$

which are the same as (1) if we write $h = \rho$ and assume $c^2 = \rho g = gh$.

Consider a so-called hydraulic jump solution occurring, for example, when a dam breaks. The conservation of the mass flux, momentum flux, and energy flux are given by (9). The first two conditions imply the following relations between the fields indexed l (left) or r (right) on each side of the jump.

$$h_\mathrm{l} v_\mathrm{l} = h_\mathrm{r} v_\mathrm{r} \equiv j, \quad h_\mathrm{l} v_\mathrm{l}^2 + \frac{g h_\mathrm{l}^2}{2} = h_\mathrm{r} v_\mathrm{r}^2 + \frac{g h_\mathrm{r}^2}{2}, \tag{15}$$

where we introduced the (continuous) mass flux j. From these we deduce the velocities $v_{\mathrm{l,r}}$:

$$v_\mathrm{l}^2 = \frac{g}{2} h_\mathrm{r} \left(1 + \frac{h_\mathrm{r}}{h_\mathrm{l}}\right), \quad v_\mathrm{r}^2 = \frac{g}{2} h_\mathrm{l} \left(1 + \frac{h_\mathrm{l}}{h_\mathrm{r}}\right). \tag{16}$$

To gain further insight consider the energy flux across the hydraulic jump. From the original equations (13) this should be conserved; however (as we discussed above), discontinuities are in general not physical,

indicating that the model should be completed by some dissipation process. Without considering the details of this, we just write that energy per unit time (power) is being taken out of the system at the jump. Integrating as above, the energy conservation equation (8), from $-\varepsilon$ to ε and passing to the limit, gives the power dissipation at the jump,

$$w_{\mathrm{lr}} \equiv \lim_{\varepsilon \to 0} \int_{-\varepsilon}^{\varepsilon} e_t \, \mathrm{d}x = -[v^3 h + 2gh^2 v]_{\mathrm{l}}^{\mathrm{r}}. \qquad (17)$$

Using (16) we obtain the final result for the power dissipation at the jump,

$$w_{\mathrm{lr}} = jg \frac{(h_{\mathrm{l}} - h_{\mathrm{r}})^3}{2h_{\mathrm{l}} h_{\mathrm{r}}}. \qquad (18)$$

Assuming that energy is absorbed at the jump so $w_{\mathrm{lr}} < 0$, we get from (18) $h_{\mathrm{l}} < h_{\mathrm{r}}$, and from (16)

$$v_{\mathrm{l}}^2 = gh_{\mathrm{l}} \frac{h_{\mathrm{r}}}{h_{\mathrm{l}}} \frac{h_{\mathrm{r}} + h_{\mathrm{l}}}{2h_{\mathrm{l}}} > gh_{\mathrm{l}}$$

so that $v_{\mathrm{l}} > c_{\mathrm{l}}$, the local wave speed while $v_{\mathrm{r}} < c_{\mathrm{r}}$. These inequalities indicate the stability of the hydraulic jump.

Numerical Problems and Applications

As seen above, jump conditions come from conservation laws so an accurate numerical scheme should satisfy the conservation laws. Because the jump conditions are flux conditions, it is natural to use methods that involve integrating the operator over the spatial domain to satisfy them. One way to do this is the so-called finite volume approach, where the equation is integrated over reference volumes yielding naturally the flux conditions. Another approach is to use finite element methods, where the solution is decomposed on a basis of trial functions. The relation that gives the coefficients is obtained by integrating the equation over the whole domain.

For shock waves it is essential to have numerical schemes that do not artificially smooth the shock but respect the jump conditions. Here, special staggered finite difference schemes have been suggested by Lax, Wendroff, and Godunov.

As a final application, we present the case of a wave guide whose section changes abruptly at some point. This occurs in neurons for which varicosities are known to block the propagation of nerve impulses (Scott, 2003). To simplify the discussion, let us consider the following sine-Gordon nonlinear wave equation

$$\phi_{tt} - \phi_{xx} - \phi_{yy} + \sin(\phi) = 0, \qquad (19)$$

propagating in a two-dimensional T-shaped domain as shown in Figure 2 and assuming a zero normal gradient on the boundary. This describes the electrodynamics of a Josephson junction superconducting device obtained by inserting a small oxide layer between two metallic plates (Scott, 2003).

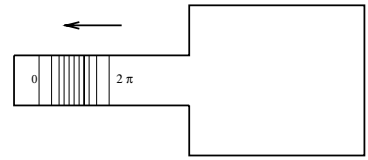

Figure 2. A T-shaped Josephson junction. The kink solution (21) is shown in the left region as contour lines. Kink propagation is easy from right to left but is inhibited in the other direction.

First note that the total energy of the system

$$E = \int \mathrm{d}x \, \mathrm{d}y \frac{1}{2}[\phi_t^2 + \phi_x^2 + \phi_y^2 + 2(1 - \cos(\phi))] \qquad (20)$$

is a constant in time. This can be seen by multiplying (19) by ϕ_t and integrating over the domain using the boundary conditions. Consider the propagation of a front (kink)

$$\phi(x, t) = 4 \arctan\left(\exp\left(\frac{x - vt}{\sqrt{1 - v^2}}\right)\right) \qquad (21)$$

which is an exact solution of the one-dimensional sine-Gordon equation for which ϕ is independent of y. Inserting (21) into (20) and calculating the integrals, it can be shown that the energy is

$$E_k = 8 \frac{w}{1 - v^2}, \qquad (22)$$

where w is the width in the y direction of the domain.

Let us now consider the propagation of such a front in the domain and assume it starts at $t = 0$ from the right-hand side with a negative velocity so that it will encounter the discontinuity. First, notice that because of the boundary conditions, it travels unaffected in the straight section. When it hits the discontinuity, it will cross into the small section with no apparent change in shape apart from reflected waves (see Figure 2). On the contrary, if the kink is started from the left side whose section is narrow, it will get reflected by the discontinuity unless its velocity is quite large.

The explanation of these observations lies in the conservation of the energy of the system, assuming that most of this energy is in the front. For a kink to exist in a domain of lateral extension w, its energy should be greater than $E_k(v = 0) = 8w$. When the kink is started in the right domain, its energy $E/8 = w_{\mathrm{r}}/(1 - v^2) > w_{\mathrm{r}} > w_{\mathrm{l}}$, so we expect it to cross without trouble into the smaller section. Indeed it should gain speed, and it does. On the contrary, if the kink is started in the left domain, its speed v_{l} must be very large (so that $w_{\mathrm{l}}/(1 - v_{\mathrm{l}}^2) > w_{\mathrm{r}}$ where $8w_{\mathrm{r}}$ is the energy of a static kink in the region on the right) in order to cross into the

region on the right. This provides a means to realize a rectifying gate, through which signals pass in only one direction.

JEAN GUY CAPUTO

See also **Constants of motion and conservation laws; Long Josephson junctions; Shock waves**

Further Reading

Ames, W. 1992. *Numerical Methods for Partial Differential Equations*, 3rd edition, New York: Academic Press

Caputo, J.G. & Stepanyants, Y. 2003. Bore formation, evolution and disintegration into solitons in shallow inhomogeneous channels. *Nonlinear Processes in Geophysics*, 10: 407–424

Landau, L. & Lifchitz, E. 1959. *Fluid Mechanics*, vol. 6 of *Course in Theoretical Physics*, London: Pergamon Press and Reading, MA: Addison-Wesley

LeVeque, R. 2002. *Finite Volume Methods for Hyperbolic Problems*, Cambridge and New York: Cambridge University Press

Lin, C.C., Segel, L.A. & Handelman, G.H. 1995. *Mathematics Applied to Deterministic Problems in the Natural Sciences*, 4th edition, Philadelphia: SIAM

Scott, A.C. 2003. *Nonlinear Science: Emergence and Dynamics of Coherent Structures*, 2nd edition, Oxford and New York: Oxford University Press

JUPITER'S GREAT RED SPOT

Jupiter's Great Red Spot is a large swirling cloud mass of reddish-brown appearance (see figure in color plate section). Situated in Jupiter's southern hemisphere, it straddles the south tropical zone and, to the north of this, the south equatorial belt. The Great Red Spot (GRS) is roughly elliptical in shape, with the semi-major axis zonally aligned (east-west) and with dimensions approximately 22, 000 km (twice the diameter of the Earth) by 11, 000 km. The atmospheric motions associated with the GRS are visible in the cloud layer near the tropopause. It is generally agreed to be a vortex (Mitchell et al., 1981); and Smith et al. (1979a) give an estimate of the vorticity. This vortex is anticyclonic (rotating in the opposite sense to that induced by the planetary rotation), that is, anticlockwise, but with a weakly counter-rotating, or possibly quiescent inner region. The GRS is at high pressure and low temperature relative to its surroundings. A striking feature associated with the GRS is the turbulent oscillating cloud system to the northwest.

In 1664, Robert Hooke observed a small dark spot in one of the southern belts of Jupiter, reported in Hooke (1665). This is considered by some contemporary authors to be an early manifestation of the GRS (see also Rogers, 1995). By observation of this feature, Hooke was able to make a good estimate of Jupiter's rate of rotation. Many further observations of this and other features of Jupiter were made by Hooke and by Giovanni Cassini over the next five years (e.g., Cassini, 1672), and intermittently by others over the next 50 years (see Denning, 1899). However, it was not until 1831 that Samuel H. Schwabe identified what can be clearly recognized as a feature called the Hollow, in his drawing reproduced in Rogers (1995). As the Hollow is clearly apparent above the GRS in contemporary observations, this is taken to imply the presence of the GRS. Continuous observations began in 1872 (Peek, 1958) and from these it appears that the GRS was considerably larger in the late 1800s than it is now (Beebe & Youngblood, 1979; Rogers, 1995). Very much more detailed observations became available once space probes reached Jupiter; first was Pioneer 10 in 1973, then Pioneer 11 in 1974, Voyagers 1 and 2 in 1979, Galileo in 1996, and then most recently Cassini from October 1, 2000 through until March 22, 2001. The Voyager and Galileo missions (Smith et al., 1979a, b; Vasavada et al., 1998) provided very high resolution still images, while Cassini (Porco et al., 2003) gave more dynamic information. From 1994, after corrections were made to faulty optics by the Endeavour crew, the Hubble telescope has been providing good images of Jupiter and the GRS. These, along with the Cassini sequences, clearly show vortex interactions between the GRS and smaller, intermittent vortices, thus allowing a much better understanding of the underlying dynamical processes (Morales-Juberías et al., 2002).

Attempts have been made since 1961 to model the GRS and to understand the processes giving rise to the motions observed, beginning with Hide (1961), who suggested that the GRS was the visible manifestation of a Taylor column. The quantity of relevance to these calculations is the potential vorticity q. As the atmosphere of Jupiter is stably stratified and there are significant rotational effects at the scale of the GRS, the most commonly used model is the quasi-geostrophic approximation (a simplification of the complete atmospheric dynamic equations, giving a balance of horizontal pressure gradient forces and horizontal Coriolis forces due to Jupiter's rotation). Here q is defined as

$$q = f + \nabla^2\psi + \frac{1}{\rho_0}\frac{\partial}{\partial z}\left(\rho_0 \frac{f_0^2}{N^2}\frac{\partial \psi}{\partial z}\right), \qquad (1)$$

where $\psi(x, y, z, t)$ is the stream function for the flow and (x, y, z) are local cartesian coordinates, with x and y being the zonal and meridional directions, respectively, and z being a measure of the depth. The basic state density profile is $\rho_0(z)$ and the effects of Jupiter's rotation are introduced by the beta-plane approximation, the assumption that we can treat part of Jupiter as a plane, over which the Coriolis parameter f varies linearly: $f = f_0 + \beta y$, where f_0 is the reference value at the latitude of the GRS and β is the ambient potential vorticity gradient. The buoyancy frequency $N(z)$, the frequency with which a parcel of fluid

displaced from equilibrium will oscillate, is determined by the vertical temperature variation. The potential vorticity is materially conserved, according to

$$\frac{\partial q}{\partial t} + \boldsymbol{v} \cdot \nabla q = 0, \tag{2}$$

where the horizontal velocity $\boldsymbol{v} = (-\partial\psi/\partial y, \partial\psi/\partial x)$.

Many researchers have modeled the vortical motions associated with the GRS by assuming a thin upper layer of constant density (of order 100 km; Dowling & Ingersoll, 1989) above a much deeper lower layer of slightly higher density in which there is a uniform steady zonal flow, for example, Ingersoll and Cuong (1981), Marcus (1988), and Marcus et al. (1990). The surface of the upper layer is above the visible cloud level. These models assume barotropic motions, that is, uniform in depth with no horizontal component of vorticity, in the upper layer where isolated vortices are assumed to be generated by mechanisms such as zonal shear flow instability. Merger of vortices can lead to the formation of larger vortices, and the relevant issues are then the stability and lifetime of isolated vortices such as the GRS in the observed zonal shear. A statistical mechanics approach to such equilibria is provided in Michel and Robert (1994).

There have also been discussions on the role of vertical density stratification, allowing baroclinic instability, but generally limited to the quasi-geostrophic case of (1) and (2). For example, Achterberg and Ingersoll (1994) studied the barotropic and the first two baroclinic modes, and Cho et al. (2001) used as many as 60 vertical modes. The high horizontal resolution used in Cho et al. (2001) allowed the authors to generate features such as the counter-rotating core (Vasavada et al., 1998, Figure 7, reporting Galileo data and similar Voyager data), but as in all other studies to date, the turbulent cloud system to the northwest of the spot does not appear.

A deficiency of the quasigeostrophic model is that vortices with radius significantly greater than the Rossby radius of deformation, L_R, tend to decay by radiation of Rossby waves in the absence of any external forcing. (L_R is a measure of the scale at which Coriolis forces become significant.) This would imply a lifetime for the GRS much shorter than the observed period, which is certainly greater than 150 years. In addition, the quasigeostrophic equations have the disadvantage that neither anticyclonic nor cyclonic vortices are preferentially created or destroyed, whereas observations show that the GRS is anticyclonic, as are 90% of the other (typically much smaller) vortices observed on Jupiter (Mac Low & Ingersoll, 1986).

For two-layer models, the zonal flows in the bottom layer can be incorporated in a reduced gravity single-layer shallow water model with meridionally varying topography and a free surface, which is taken to be above the visible cloud layer (Dowling & Ingersoll, 1989). There are various levels of approximation to the shallow-water equations beyond the quasi-geostrophic approximation. The intermediate geostrophic (IG) approximation (Williams & Yamagata, 1984; Nezlin & Sutyrin, 1994) arises when there is significant nonlinearity giving rise to finite free-surface distortion, as is to be expected for vortices with a scale much greater than the Rossby radius, such as the GRS. A more complete discussion of the asymptotic treatment of the nonlinear terms, along with higher-order approximations, is given in Stegner and Zeitlin (1996).

An alternative approach to understanding the GRS as a solitary wave was first introduced by Maxworthy and Redekopp (1976a,b) and Redekopp (1977). They considered the quasigeostrophic equations (1) and (2) and were able to find elementary soliton solutions in the limit of small amplitude disturbance, which obeyed either the Korteweg–de Vries equation (KdV) or the modified KdV equation. These balance zonal shear and dispersion to give isolated disturbances that could be regarded as vortices. However, as noted by several authors (e.g., Ingersoll & Cuong, 1981), these soliton solutions of the KdV equation pass through one another unchanged in form (elastic collisions). This is contrary to the behavior of vortices generally, and more particularly the GRS, where merger with smaller vortices is observed (Morales-Juberías et al., 2002). However, Petviashvili (1980), by going beyond quasigeostrophy, was able to derive solitary axisymmetric vortex solutions, without an imposed zonal shear, for a curved shallow layer, with anticyclones living longer. Nezlin et al. (1990) refer to this anticyclonic vortex as a Rossby soliton, with weak nonlinearity balanced by Rossby wave dispersion. These solitary solutions undergo inelastic collisions and were later thought to be found experimentally in parabolic water tank experiments (Nezlin et al., 1990), although Nycander (1993) and Stegner and Zeitlin (1996) demonstrated that this weakly nonlinear balance could not in fact exist in the parabolic geometry and that stronger nonlinearity was required to explain the laboratory observations. Stegner and Zeitlin (1996) go on to show that axisymmetric soliton-like solutions of a 2-d KdV equation are found for spherical geometry, corresponding to the surface of Jupiter, using a nonlinear model. Furthermore, only an anticyclonic vortex can be supported in this case, which is in accord with the observed rotation of the GRS. However, this cannot explain the preferential formation of anticyclonic vortices smaller than the Rossby radius, where the quasigeostrophic approximation remains appropriate. Finally, as explained by Stegner and Zeitlin (1996), their 2-d KdV solutions do not apply directly to the GRS as neither the elliptical shape nor the counter-rotating inner core can be accounted for.

C. MACASKILL AND T.M. SCHAERF

See also **Atmospheric and ocean sciences; Fluid dynamics; Korteweg–de Vries equation; Solitons**

Further Reading

Achterberg, R.K. & Ingersoll, A.P. 1994. Numerical simulation of baroclinic Jovian vortices. *Journal of the Atmospheric Sciences*, 51(4): 541–562

Beebe, R.F. & Youngblood, L.A. 1979. Pre-Voyager velocities, accelerations and shrinkage rates of Jovian cloud features. *Nature*, 280: 771–772

Cassini, G. 1672. A relation of the return of a great permanent spot in the planet Jupiter, observed by Signor Cassini, one of the Royal Parisian Academy of the Sciences. *Philosophical Transactions of the Royal Society of London*, 7: 4039–4042

Cho, J. Y-K., de la Torre Juárez, M., Ingersoll, A.P. & Dritschel, D.G. 2001. A high-resolution, three-dimensional model of Jupiter's Great Red Spot. *Journal of Geophysical Research—Planets*, 106(E3): 5099–5105

Denning, W.F. 1899. Early history of the Great Red Spot on Jupiter. *Monthly Notices of the Royal Astronomical Society*, 59: 574–584

Dowling, T.E. & Ingersoll, A.P. 1989. Jupiter's Great Red Spot as a shallow water system. *Journal of the Atmospheric Sciences*, 46(21): 3256–3278

Hide, R. 1961. Origin of Jupiter's Great Red Spot. *Nature*, 190: 895–896

Hooke, R. 1665. A spot in one of the belts of Jupiter. *Philosophical Transactions of the Royal Society of London*, 1: 3

Ingersoll, A.P & Cuong, P.G. 1981. Numerical model of long-lived Jovian vortices. *Journal of the Atmospheric Sciences*, 38(10): 2067–2076

Mac Low, M.-M. & Ingersoll, A.P. 1986. Merging of vortices in the atmosphere of Jupiter: an analysis of Voyager images. *Icarus*, 65: 353–369

Marcus, P.S. 1988. Numerical simulation of Jupiter's Great Red Spot. *Nature*, 331: 693–696

Marcus, P.S., Sommeria, J., Meyers, S.D. & Swinney, H.L. 1990. Models of the Great Red Spot. *Nature*, 343: 517–518

Maxworthy, T. & Redekopp, L.G. 1976a. A solitary wave theory of the Great Red Spot and other observed features in the Jovian atmosphere. *Icarus*, 29: 261–271

Maxworthy, T. & Redekopp, L.G. 1976b. New theory of the Great Red Spot from solitary waves in the Jovian atmosphere. *Nature*, 260: 509–511

Michel, J. & Robert, R. 1994. Statistical mechanical theory of the Great Red Spot of Jupiter. *Journal of Statistical Physics*, 77: 645–666

Mitchell, J.L., Beebe, R.F, Ingersoll, A.P. & Garneau, G.W. 1981. Flow fields within Jupiter's Great Spot and White Oval BC. *Journal of Geophysical Research—Space Physics*, 86(NA10): 8751–8757

Morales-Juberías, R., Sánchez-Lavega, A., Lecacheux, J. & Colas, F. 2002. A comparative study of Jovian anticyclone properties from a six-year (1994–2000) survey. *Icarus*, 157(1): 76–90

Nezlin, M.V., Rylov, A. Yu., Trubnikov, A.S. & Khutoreski, A.V. 1990. Cyclonic–anticyclonic asymmetry and a new soliton concept for Rossby vortices in the laboratory, oceans and the atmospheres of giant planets. *Geophysical and Astrophysical Fluid Dynamics*, 52: 211–247

Nezlin, M.V. & Sutyrin, G.G. 1994. Problems of simulation of large, long-lived vortices in the atmospheres of the giant planets (Jupiter, Saturn, Neptune). *Surveys in Geophysics*, 15: 63–99

Nycander, J. 1993. The difference between monopole vortices in planetary flows and laboratory experiments. *Journal of Fluid Mechanics*, 254: 561–577

Peek, B.M. 1958. *The Planet Jupiter*, London: Faber & Faber

Petviashvili, V.I. 1980. Red spot of Jupiter and the drift soliton in a plasma. *JETP Letters*, 32(11): 619–622

Porco, C.C., West, R.A., McEwen, A., et al. 2003. Cassini imaging of Jupiter's atmosphere, satellites and rings. *Science*, 299: 1541–1547

Rogers, J.H. 1995. *The Giant Planet Jupiter*, Cambridge and New York: University Press

Redekopp, L.G. 1977. On the theory of solitary Rossby waves. *Journal of Fluid Mechanics*, 82(4): 725–745

Smith, B.A., Soderblom, L.A., Johnson, T.V., et al. 1979a. The Jupiter system through the eyes of Voyager 1. *Science*, 204: 951–957 and 960–972

Smith, B.A., Soderblom, L.A., Beebe, R., et al. 1979b. The Galilean satellites and Jupiter: Voyager 2 imaging science results. *Science*, 206: 927–950

Stegner, A. & Zeitlin, V. 1996. Asymptotic expansions and monopolar solitary Rossby vortices in barotropic and two-layer models. *Geophysical and Astrophysical Fluid Dynamics*, 83: 159–194

Vasavada, A.R., Ingersoll, A.P., Banfield, D., et al. 1998. Galileo imaging of Jupiter's atmosphere: The Great Red Spot, equatorial region, and White Ovals. *Icarus*, 135(1): 265–275

Williams, G.P. & Yamagata, T. 1984. Geostrophic regimes, intermediate solitary vortices and Jovian eddies. *Journal of the Atmospheric Sciences*, 41(4): 453–478

K

KADOMTSEV–PETVIASHVILI EQUATION

The Kadomtsev–Petviashvili (KP) equation was derived by Kadomtsev & Petviashvili (1970) to examine the stability of the one-soliton solution of the Korteweg–de Vries (KdV) equation under transverse perturbations, and it is relevant for most applications in which the KdV equation arises. After rescaling of its coefficients, the equation takes the form

$$(-4u_t + 6uu_x + u_{xxx})_x + 3\sigma^2 u_{yy} = 0, \qquad (1)$$

where indices denote differentiation, and σ is a constant parameter. If $\sigma^2 = -1$ $(+1)$, the equation is referred to as the KP1 (KP2) equation. All other real values of σ^2 can be rescaled to one of these two cases. In what follows, a reference to KP (as opposed to KP1 or KP2) implies that the result in question is independent of the sign of σ^2.

Depending on the physical context, an asymptotic derivation can result in either the KP1 or the KP2 equation. In all such derivations, the equation describes the dynamics of weakly dispersive, nonlinear waves whose wavelength is long compared with its amplitude, and whose variations in the second space dimension (rescaled y) are slow compared with their variations in the main direction of propagation (rescaled x). Two examples are as follows:

- *Surface waves in shallow water*: In this case, u is a rescaled wave amplitude with a rescaled velocity. The wavelength is long compared with the depth of the water h, which is large compared with the wave amplitude. The sign of σ^2 is determined by the magnitude of the coefficient of surface tension τ. KP1 results for large surface tension $\tau/(gh^2) > 1/3$ (thin films); otherwise, KP2 results. Here g is the acceleration of gravity. For most applications in shallow water, surface tension plays a sufficiently unimportant role, and KP2 is the relevant equation (Ablowitz &, 1979, *See* **Water waves**).
- *Magneto-elastic waves in antiferromagnetic materials*: Here u is a rescaled strain tensor with a rescaled velocity. The sign of σ^2 is determined by the difference between the linear velocities of the magnons and phonons, and the strength and direction of the external magnetic field (Turitsyn & Fal'kovich, 1986).

The KP equation has different classes of soliton solutions. The first class is a generalization of the solitons of the KdV equation. These solutions decay exponentially as $x, y \to \pm\infty$, in all but a finite number of directions along which they approach a constant value. For this reason these solutions are referred to as line solitons. By appropriately choosing their parameters, the direction of propagation of each line soliton can be chosen to be anything but the y-direction. In the simplest case, the solitons all propagate in the x-direction, adding a second dimension to the KdV solitons. Many other scenarios are possible. Two line solitons can interact with different types of interaction regions to produce two line solitons, but two line solitons can also merge to produce a single line soliton. Alternatively, a single line soliton can disintegrate in to two line solitons. The production or annihilation of a line soliton is sometimes referred to as soliton resonance. Although both KP1 and KP2 have line soliton solutions, soliton resonance occurs only for the KP2 equation. Line soliton solutions of the KP2 equation are stable, whereas line soliton solutions of the KP1 equation are unstable. More possibilities exist when more than two line solitons are involved. Two distinct line soliton interactions are illustrated in Figure 1.

Another class of soliton solutions exists for only the KP1 equation and decays algebraically in all directions as $\sqrt{x^2 + y^2} \to \infty$. These soliton solutions are referred to as lumps and are unstable. Individual lumps in multi-lump solutions do interact with each other but leave no trace of this interaction. A lump soliton is shown in Figure 2 (Ablowitz & Segur, 1981).

Another important class of solutions of the KP equation generalizes the exact periodic and quasi-periodic solutions of the KdV equation. A (quasi-) periodic solution with g phases is expressed in terms of

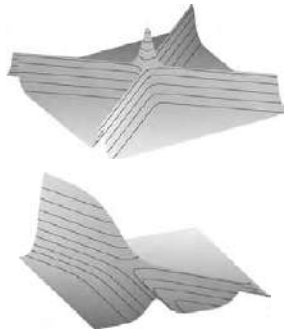

Figure 1. Two types of spatial ($t = 0$) line soliton interactions for the KP2 equation: (a) Two identical line solitons with an interaction that does not change their characteristics; (b) Two line solitons merge to produce one line soliton.

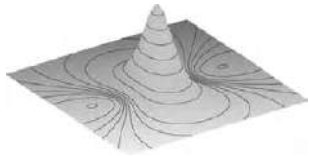

Figure 2. A lump soliton ($t = 0$) solution of the KP1 equation.

the Riemann theta function $\theta(\boldsymbol{z}|\boldsymbol{B})$ by

$$u(x, y, t) = c + 2\frac{\partial^2}{\partial x^2} \ln \theta(\boldsymbol{k}x + \boldsymbol{l}y + \boldsymbol{\omega}t + \boldsymbol{\phi}|\boldsymbol{B}). \quad (2)$$

Here, c is a constant, and $\boldsymbol{k}$, $\boldsymbol{l}$, $\boldsymbol{\omega}$, and $\boldsymbol{\phi}$ are g-dimensional vectors that are interpreted as wave vectors ($\boldsymbol{k}$, $\boldsymbol{l}$), frequencies ($\boldsymbol{\omega}$), and phases ($\boldsymbol{\phi}$). These parameters and the $g \times g$ Riemann matrix $\boldsymbol{B}$ are determined by a genus g compact connected Riemann surface and a set of g points on it.

For $g = 1$, solution (2) generalizes the cnoidal-wave solution of the KdV equation to two spatial dimensions. For $g = 2$, the solution is still periodic in space. Its basic period cell is a hexagon, which tiles the (x, y)-plane. These solutions translate along a direction in the (x, y)-plane. For $g \geq 3$, solution (2) is typically no longer periodic or translating in time. For some values of their parameters, these (quasi-)periodic solutions can be interpreted as infinite nonlinear superpositions of line solitons. Solutions with $g \leq 2$ have been compared with experiments in shallow water, with agreement being more than satisfactory (Hammack et al., 1995). A two-phase solution of the KP2 equation is shown in Figure 3. A good review of the finite-phase solutions of the KP equation is given by Dubrovin (1981).

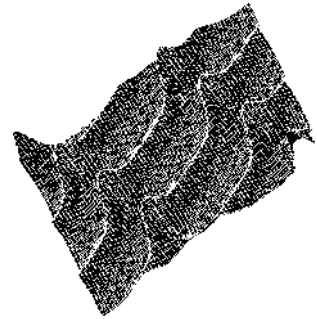

Figure 3. A two-phase periodic solution of the KP2 equation.

Unlike for the KdV equation, where only a restricted class of Riemann surfaces arises, any compact connected Riemann surface gives rise to a set of solutions of the KP equation. The reverse statement is also true: if (2) is a solution of the KP equation, then matrix $\boldsymbol{B}$ is the normalized period matrix of a genus g Riemann surface. This statement is due to Novikov. It provides a solution to the century-old Schottky problem, and its proof is by Shiota (1986).

The KP equation is the compatibility condition $\Psi_{yt} = \Psi_{ty}$ of the two linear equations

$$\sigma\Psi_y = \Psi_{xx} + u\Psi,$$
$$\Psi_t = \Psi_{xxx} + \tfrac{3}{2}u\Psi_x + \tfrac{3}{4}(u_x + w)\Psi, \quad (3)$$

with $w_x = \sigma u_y$. These equations constitute the Lax pair of the KP equation. Using the inverse scattering method, it is the starting point for the solution of the initial-value problem for the KP equation on the whole (x, y)-plane with initial conditions that decay at infinity. The inclusion of line solitons is also possible (Ablowitz & Clarkson, 1991). Although the initial-value problem with periodic boundary conditions for KP2 was solved by Krichever (1989), this approach was unable to solve the same problem for the KP1 equation. In this context, solutions (2) are referred to as finite-gap solutions, as they give rise to operators (3) with spectra that have a finite number of forbidden gaps in them.

More details and different aspects of the theory of the KP equation are found in Ablowitz & Clarkson (1991), Ablowitz & Segur (1981), Dubrovin (1981), Krichever (1989), Shiota (1986), and references therein.

BERNARD DECONINCK

See also **Inverse scattering method or transform; Korteweg–de Vries equation; Multidimensional solitons; Plasma soliton experiments; Theta functions; Water waves**

Further Reading

Ablowitz, M.J. & Clarkson, P.A. 1991. *Solitons, Nonlinear Evolution Equations and Inverse Scattering*, Cambridge and New York: Cambridge University Press

Ablowitz, M.J. & Segur, H. 1979. On the evolution of packets of water waves. *Journal of Fluid Mechanics*, 92: 691–715

Ablowitz, M.J. & Segur, H. 1981. *Solitons and the Inverse Scattering Transform*, Philadelphia: SIAM

Dubrovin, B.A. 1981. Theta functions and non-linear equations. *Russian Mathematical Surveys*, 36: 11–92

Hammack, J., McCallister, D., Scheffner, N. & Segur, H. 1995. Two-dimensional periodic waves in shallow water. Part 2. Asymmetric waves. *Journal of Fluid Mechanics*, 285: 95–122

Kadomtsev, B.B. & Petviashvili, V.I. 1970. On the stability of solitary waves in weakly dispersive media. *Soviet Physics Doklady*, 15: 539–541

Krichever, I.M. 1989. Spectral theory of two-dimensional periodic operators and its applications. *Russian Mathematical Surveys*, 44: 145–225

Shiota, T. 1986. Characterization of Jacobian varieties in terms of soliton equations. *Inventiones Mathematicae*, 83: 333–382

Turitsyn, S.K. & Fal'kovich, G.E. 1986. Stability of magnetoelastic solitons and self-focusing of sound in antiferromagnets. *Soviet Physics JETP*, 62: 146–152

KELVIN–HELMHOLTZ INSTABILITY

The Kelvin–Helmholtz (KH) instability was originally investigated by Lord Kelvin (William Thomson) and Hermann von Helmholtz (Kelvin, 1871; Helmholtz, 1868; Chandrasekhar, 1981; Drazin & Reid, 1981; Gerwin, 1968) in the context of wind flowing over water. Their main motivation was to understand how wind ruffles the ocean surface to produce the ripples, eddies, and whitecaps that we see on our trips to the beach.

The KH instability has subsequently been observed in a variety of space, astrophysical, and geophysical settings involving sheared fluid and plasma flows. In addition to the original situations relating to ocean waves, relevant configurations include the interface between the solar wind and the upper magnetosphere, coronal streamers moving through the solar wind, the boundaries between adjacent sectors of the solar wind, the structure of the tails of comets, and the boundaries of the jets propagating from the core of extragalactic double radio sources into their lobes. Another interesting application of KH instability in this age of unexplained air disasters is the phenomenon known as clear air turbulence, where an aircraft flying through a clear sky is suddenly buffeted (*See* **Clear air turbulence**).

With an initial or equilibrium configuration consisting of two superposed incompressible and inviscid fluids streaming in the horizontal or z-direction at differential speeds U_1 and U_2 (see Figure 1), consider how disturbances to this configuration evolve in time. Because the velocity differential occurs at different heights (or the transition in the speed from U_1 to U_2 occurs over some finite range of x), the equilibrium configuration

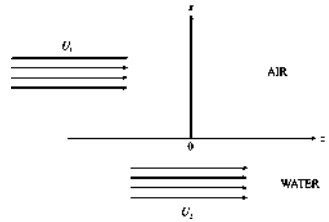

Figure 1. The basic configuration for shear flow across a vortex sheet.

has finite geometrical extent in the x-direction. Note that the inviscid assumption, which holds well for air and water as well as for very low-density interstellar media, allows an arbitrary profile for the velocity transition from U_1 to U_2 with the x transition length chosen to fit experiments. By contrast, the equilibrium is of semi-infinite extent in the horizontal or z-direction, and of infinite extent in y. Thus, one may represent field variables as Fourier series in the directions y and z which are of infinite extent, thereby assuming elementary disturbances of the form

$$\chi \sim f(x)\exp[\mathrm{i}(k_y y + k_z z - \omega t)] \qquad (1)$$

for all variables χ. Here, k_y and k_z are the y and z wave numbers, and ω is the angular frequency. (Note also that only a single mode among the infinite number needed to expand the variable χ as a Fourier series has been displayed in this equation.)

Substitution of Equation (1) into the equations governing the fluid flow yields a functional relationship between the angular frequency and the wave number called the dispersion relation, which provides key information regarding the propagation of the mode of Equation (1). Importantly, there are situations where the dispersion relation yields complex angular frequencies, that is,

$$\omega = \omega_r + \mathrm{i}\omega_i\,. \qquad (2)$$

The temporal exponential growth or decay of the mode is then controlled by ω_i (called the growth rate), while its oscillation frequency is governed by ω_r. Important for us are the unstable cases where $\omega_i > 0$ so the disturbance grows in time. In such cases, χ does not settle back to the original equilibrium, and one must consider the consequences of this growth.

A driving parameter for KH instability is the differential flow speed (velocity shear) of the two layers of fluid, and it suffices to consider one Fourier mode while investigating the stability of a system. The key concept here is that the wave number of the normal mode is left arbitrary, and the system is unstable if $\omega_i > 0$ for any wave number. In general, the system is stable for some range of the driving parameter and becomes unstable beyond a critical value

of the parameter. The wave number that first becomes unstable as this critical parameter value is reached selects the most unstable mode, which usually guides the further development of the instability.

Let us apply these concepts by substituting Equation (1) into the dynamical equations governing the flow. In the simplest form of the analysis (linear theory), one neglects all nonlinear terms (where any of the field variables are raised to higher than linear powers, or where there are products of different field variables) to obtain a dispersion relation. This relation satisfies boundary conditions at the discontinuity corresponding to the continuity of the normal (perpendicular) speed, the normal magnetic field (if any), and the normal total (fluid plus electromagnetic) stress. The resulting dispersion relation in the incompressible fluid case is given by (Chandrasekhar, 1981)

$$\omega = k_z(\alpha_1 U_1 + \alpha_2 U_2) \pm \left[gk \left\{ (\alpha_1 - \alpha_2) + \frac{k^2 T}{g(\rho_1 + \rho_2)} \right\} - k_z^2 \alpha_1 \alpha_2 (U_1 - U_2)^2 \right]^{1/2}.$$

Here, g is the acceleration of gravity, T is the coefficient of surface tension, and

$$\alpha_1 = \frac{\rho_1}{\rho_1 + \rho_2}, \quad \alpha_2 = \frac{\rho_2}{\rho_1 + \rho_2}, \tag{3}$$

where ρ_i is the density of the i-th fluid. Analysis of Equation (3) reveals instability ($\omega_i > 0$) for (Kelvin, 1871; Chandrasekhar, 1981)

$$(U_1 - U_2)^2 > \frac{2}{\alpha_1 \alpha_2} \sqrt{\frac{Tg(\alpha_1 - \alpha_2)}{\rho_1 + \rho_2}}. \tag{4}$$

For air over sea water, this implies instability at $U_1 - U_2 > 650$ cm/s (14.8 mph) manifested as surface waves of about 1.71 cm wavelength.

The sea, however, is ruffled by winds of smaller speeds than this, and a variety of effects have been advanced to explain this discrepancy. These include continuous velocity variation rather than an abrupt jump at the surface, continuously varying density profiles, rotational effects (due to the Earth's rotation), as well as Lord Kelvin's original suggestion—the effects of viscosity (Chandrasekhar, 1981; Drazin & Reid, 1981).

In addition, compressibility and various electromagnetic fields (Choudhury, 1986; Choudhury & Lovelace, 1984; Miura, 1990; Miura & Pritchett, 1982) become important in magnetospheric, geophysical, and astrophysical settings where there are high-speed shear flows and large fields. An important effect of compressibility is to introduce a second unstable traveling-wave mode with nonzero ω_r, in addition to the standing-wave unstable mode (with zero ω_r) which exists in the incompressible limit.

There have been numerous computer simulation studies of KH instability in a variety of settings (Miura, 1995; Normal et al., 1982). The effect of anisotropic pressure has also been comprehensively considered (Brown & Choudhury, 2000).

Finally, it is important to consider nonlinear effects on the instability since the temporal growth of the linear fields in Equation (1) will eventually reach amplitudes large enough so that product terms can no longer be ignored. From physical considerations, one may also argue that exponential linear growth as predicted by Equation (1) for $\omega_i > 0$ is not tenable indefinitely because the energy is proportional to the square of the field amplitude and this energy is limited. Clearly, nonlinear effects must come into play and limit the linear growth (Debnath & Choudhury, 1997; Drazin & Reid, 1981; Weissman, 1979). Such nonlinear evolution studies reveal a variety of interesting dynamical behaviors from quasi-periodicity and chaos at one extreme (Choudhury & Brown, 2001) to self-organization and coherent structures at the other (Miura, 1999). A formulation of the problem in terms of noncanonical Hamiltonians for the fluid dynamical equations (Benjamin & Bridges, 1997) enables one to follow instability evolution well into its late stages where the interface has become appreciably folded.

S. Roy Choudhury

See also **Clear air turbulence; Coherence phenomena; Dispersion relations; Shear flow; Wave stability and instability; Water waves**

Further Reading

Batchelor, G. K., Moffatt, H. F. & Worster, M. G. (editors) 2000. *Perspectives in Fluid Dynamics*, Cambridge and New York: Cambridge University Press

Benjamin, T. B. & Bridges, T.J. 1997. Reappraisal of the Kelvin–Helmholtz problem I & II. *Journal of Fluid Mechanics*, 333: 301, 327

Brown, K.G. & Choudhury, S.R. 2000. Kelvin–Helmholtz instabilities of high-velocity magnetized shear layers with generalized polytrope laws. *Quarterly Journal of Applied Mathematics*, LVIII, 401–423

Chandrasekhar, S. 1981. *Hydrodynamic and Hydromagnetic Stability*, Oxford: Clarendon Press

Choudhury, S.R. 1986. Kelvin–Helmholtz instabilities of supersonic, magnetized shear layers. *Journal of Plasma Physics*, 35: 375–392

Choudhury, S. R. & Brown, K.G. 2001. Novel dynamics in the nonlinear evolution of the KH instability of supersonic anisotropic tangential velocity discontinuities. *Mathematics and Computers in Simulations*, 55: 377

Choudhury, S.R. & Lovelace, R.V. 1984. On the Kelvin–Helmholtz instabilities of supersonic shear layers. *Astrophysical Journal*, 283: 331–334

Debnath, L. & Choudhury, S.R. 1997. *Nonlinear Instability Analysis*, Southampton: Computational Mechanics
Drazin, P.G. & Reid, W.H. 1981. *Hydrodynamic Stability*, Cambridge and New York: Cambridge University Press
Gerwin, R.A. 1968. Stability of the interface between two fluids in relative motion. *Reviews of Modern Physics*, 40: 652–658
Helmholtz, H. von 1868. Über discontinuirliche Flüssigkeits-bewegungen. *Wissenschaftliche Abhandlungen. Monats. Konigl. Preuss. Akad. Wiss. Berlin*, 23: 215–228; as On discontinuous movements of fluids. *Philosophical Magazine*, 36: 337–36 (1868)
Kelvin, Lord (William Thomson). 1871. Hydrokinetic solutions and observations. *Philosophical Magazine*, 42(4): 362–377; with On the motion of free solids through a liquid; Influence of wind and capillarity on waves in water supposed frictionless. In *Mathematical and Physical Papers*, vol. 4: *Hydrodynamics and General Dynamics*, Cambridge: Cambridge University Press, 1910
Miura, A. 1990. Kelvin–Helmholtz instability for supersonic shear flow at the magnetospheric boundary. *Geophysical Research Letters*, 17: 749–752
Miura, A. 1995. Kelvin–Helmholtz instability at the magnetopause: computer simulations. In *Physics of the Magnetopause, Geophysical Monogr*, edited by P. Song, B.U. Sonnerup & F. Thomsen, Washington, DC: American Geophysical Union
Miura, A. 1999. Self-organization in the two-dimensional Kelvin–Helmholtz instability. *Physical Review Letters*, 83: 1586–1589
Miura, A. & Pritchett, P.L. 1982. Nonlinear stability analysis of the MHD Kelvin–Helmholtz instability in a compressible plasma. *Journal of Geophysical Research*, 87: 7431–7444
Normal, M. L., Smarr, L., Winkler, K.H. & Smith, M.D. 1982. Supersonic jets. *Astronomy and Astrophysics*, 113: 285
Weissman, M. 1979. Nonlinear wave packets in the KH instability. *Philosophical Transactions of the Royal Society, London*, 290: 639

KEPLER PROBLEM

See **Celestial mechanics**

K-EPSILON METHOD

See **Turbulence**

KERMACK–MCKENDRICK SYSTEM

See **Epidemiology**

KERR EFFECT

Discovered by John Kerr in 1875, the electro-optical effect opened new trends in the world of optics. This effect refers to the modifications that a light beam undergoes in amplitude, phase, or direction when it propagates in an optical material that responds to an external electric field. An example is the modulation of optical radiation in crystals in which two possible linearly polarized modes exist with unique directions of polarization and corresponding indices of refraction. For crystals with no inversion symmetry, $(n^2)_{ij}$ denotes the squared ray index along the directions $(i, j) = 1, 2, 3$, such as $x = 1$, $y = 2$, $z = 3$. The linear change in the coefficients $(1/n^2)_{ij}$ due to an applied low-frequency electric field $\boldsymbol{E}(E_x, E_y, E_z)$ is then defined by

$$\Delta\left(\frac{1}{n^2}\right)_{ij} = \sum_k r_{ijk} E_k \quad (k = 1, 2, 3), \tag{1}$$

where the 6×3 matrix with elements r_{ijk} is called the electro-optical tensor. Current applications of this property are electro-optic retardation, amplitude or phase modulation, and beam deflection (Yariv, 1975).

Optical nonlinearities result from an analogous effect arising when the low-frequency electric field applied is replaced by a second optical frequency. Let us consider the electric field of an optical beam along the j-direction with frequency ω_1: $E_j^{\omega_1}(t) = \mathrm{Re}(A_j^{\omega_1} \mathrm{e}^{-\mathrm{i}\omega_1 t})$ while a second field at ω_2 is $E_k^{\omega_2}(t) = \mathrm{Re}(A_k^{\omega_2} \mathrm{e}^{-\mathrm{i}\omega_2 t})$. If the medium is nonlinear, these fields generate polarizations at frequencies $\omega_3 = n\omega_1 + m\omega_2$, where n and m are any integers. The susceptibility tensor $d_{ijk} = -\varepsilon_i \varepsilon_j r_{ijk}/2\varepsilon_0$ then enters the polarization vector as $P_i^{\omega_3} = \sum_j \sum_k d_{ijk} A_j^{\omega_1} A_k^{\omega_2}$, where ε_i and ε_j are the dielectric constants along i and j at ω_1, and ε_0 is the vacuum permittivity.

A single optical beam is able to induce nonlinear effects. The origin of the nonlinear response is then related to anharmonic motions of bound electrons under the influence of a primary optical field. As a result, the induced polarization $\boldsymbol{P}$ created from the electric dipoles is not linear in the electric field $\boldsymbol{E}$, but it satisfies the more general relation

$$\begin{aligned} \boldsymbol{P} &= \boldsymbol{P}_{\mathrm{L}} + \boldsymbol{P}_{\mathrm{NL}} \\ &= \varepsilon_0 \{\chi^{(1)} \cdot \boldsymbol{E} + \chi^{(2)} : \boldsymbol{EE} \\ &\quad + \chi^{(3)} \vdots \boldsymbol{EEE} + \cdots\}, \end{aligned} \tag{2}$$

where $\chi^{(n)}$ $(n = 1, 2, ...)$ is the nth-order susceptibility tensor of rank $n + 1$. The linear susceptibility $\chi^{(1)}$ represents the dominant, linear contribution to $\boldsymbol{P}$,

$$\boldsymbol{P}_{\mathrm{L}} = \varepsilon_0 \int_{-\infty}^{+\infty} \chi^{(1)}(t - t') \cdot \boldsymbol{E}(\boldsymbol{r}, t')\, \mathrm{d}t', \tag{3}$$

including the linear refractive index n_0 and related attenuation coefficient. $\chi^{(2)}$ is the second-order susceptibility responsible, for example, for second-harmonic generation in crystals with a lack of inversion symmetry. For centro-symmetric media such as optical fibers, silica samples, and gases, this contribution is zero and the first nonlinearities are provided by the third-order susceptibility $\chi^{(3)}$ through

$$\begin{aligned} \boldsymbol{P}_{\mathrm{NL}} = \varepsilon_0 \int\int\int_{-\infty}^{+\infty} &\chi^{(3)}(t - t_1, t - t_2, t - t_3) \\ &\vdots \boldsymbol{E}(\boldsymbol{r}, t_1) \boldsymbol{E}(\boldsymbol{r}, t_2) \boldsymbol{E}(\boldsymbol{r}, t_3)\, \mathrm{d}t_1\, \mathrm{d}t_2\, \mathrm{d}t_3. \end{aligned} \tag{4}$$

This causes an intensity dependence in the total refractive index of the form

$$n = n_0 + n_2|\boldsymbol{E}|^2 \tag{5}$$

with nonlinear coefficient $n_2 = 3\chi^{(3)}_{xxxx}/8n_0$ for a linearly polarized electric field involving a single $\chi^{(3)}$ component of four-rank tensor. This intensity dependence induced in the refractive index through $\chi^{(3)}$ contributions is called the Kerr effect.

The Kerr effect affects the evolution of the electric field $\boldsymbol{E}$, which is governed by Maxwell's equations. Straightforward combination of the latter, after eliminating the magnetic and electric flux density ($\boldsymbol{D} = \varepsilon_0\boldsymbol{E} + \boldsymbol{P}$), provides the wave equation

$$\boldsymbol{\nabla} \times \boldsymbol{\nabla} \times \boldsymbol{E} + \frac{1}{c^2}\partial_t^2 \boldsymbol{E} = -\mu_0 \partial_t^2 \boldsymbol{P}, \tag{6}$$

where $\mu_0\varepsilon_0 = 1/c^2$ and c is the speed of light in vacuum. For treating Equation (6) conveniently, certain assumptions can be made, among which are the following:

- $|\boldsymbol{P}_{\mathrm{NL}}|$ is a small perturbation to the total induced polarization.
- Optical losses are weak, so that the imaginary part of the frequency-dependent dielectric constant $\varepsilon(\omega)$ is negligible, that is, $\varepsilon(\omega) = 1 + \tilde{\chi}^{(1)}(\omega) \simeq n^2(\omega)$.
- $\boldsymbol{\nabla} \cdot \boldsymbol{D} \simeq \varepsilon \boldsymbol{\nabla} \cdot \boldsymbol{E} = \boldsymbol{0}$, and thus $\boldsymbol{\nabla} \times \boldsymbol{\nabla} \times \boldsymbol{E} = \boldsymbol{\nabla} \cdot (\boldsymbol{\nabla} \boldsymbol{E}) - \boldsymbol{\nabla}^2 \boldsymbol{E} \simeq -\boldsymbol{\nabla}^2 \boldsymbol{E}$.
- The polarization state is preserved, so that a scalar approach is valid.
- The optical field is quasi-monochromatic; that is, its spectrum centered at $\omega_0 = 2\pi c/\lambda_0$ for the wavelength λ_0 has a spectral width $\Delta\omega = \omega - \omega_0$ satisfying $\Delta\omega/\omega_0 \ll 1$.

It is then useful to separate out the rapidly varying part of the electric field, like $\boldsymbol{E}(\boldsymbol{r}, t, z) = \hat{\boldsymbol{x}} A(\boldsymbol{r}, t, z)\, \mathrm{e}^{-\mathrm{i}(\omega_0 t - k_0 z)}$ for a wavefield propagating along the z axis with wave number $k_0 = k(\omega_0) = n_0\omega_0/c$. As a result, the complex envelope A is described by the nonlinear Schrödinger (NLS) model (Brabec & Krausz, 1997)

$$\mathrm{i}\partial_\xi A + \frac{1}{2k_0} T^{-1} \nabla_\perp^2 A + \hat{D}A + \frac{\omega_0 n_2}{c} T(|A|^2 A) = 0, \tag{7}$$

after passing over to the frame moving with the group-velocity, by means of the new variables $\xi = z$, $\tau = t - \beta_1 z$ where $\beta_1 \equiv \partial k/\partial\omega|_{\omega_0}$. Here, the assumptions of paraxiality ($|\partial_\xi A| \ll k_0|A|$) and slow variations in time ($|\partial_\tau A| \ll \omega_0|A|$) have been made. The transverse Laplacian $\nabla_\perp^2 = \partial_x^2 + \partial_y^2$ accounts for wave diffraction in the x–y plane [$\boldsymbol{r} = (x, y)$]. $\hat{D} \equiv \sum_{m=2}^{+\infty} \frac{1}{m!}(\partial^m k/\partial\omega^m|_{\omega_0})(\mathrm{i}\partial_\tau)^m$ is the dispersion operator, where only the leading-order contribution ($m = 2$) is considered below, which corresponds to group-velocity dispersion (GVD) with coefficient $\beta_2 \equiv \partial^2 k/\partial\omega^2|_{\omega_0}$. The operator $T = 1 + (\mathrm{i}/\omega_0)\partial_\tau$ originates from the cross derivatives $\partial^2_{\xi,\tau}$ retained in the derivation of Equation (7), and it reduces to unity, whenever $\Delta\omega/\omega_0 \ll 1$ holds. For $n_2 > 0$, the principal physical processes caused by the Kerr effect can be listed as follows:

- The Kerr effect creates spectral broadening through self-phase modulation (SPM). Solving for $\mathrm{i}\partial_\xi A = -\omega_0 n_2 |A|^2 A/c$ indeed yields the exact solution $A = A_0 \mathrm{e}^{\mathrm{i}\omega_0 n_2 |A_0|^2 \xi/c}$ with $A_0 = A(\xi = 0)$, which describes a self-induced phase shift experienced by the optical field during its propagation. This intensity-dependent phase shift refers to SPM, which is responsible for the spectral broadening of short pulses by virtue of the relation $\Delta\omega/\omega_0 = -\partial_\tau \arg(A)/\omega_0$. The pulse shape does not change in time, but the frequency spectrum is expanded by the nonlinearity.
- In optical fibers for which diffractive effects are negligible, pulses mainly undergo GVD and Equation (7) reduces to the standard cubic NLS equation in the limit $T \to 1$. With $\beta_2 < 0$ (so-called anomalous GVD), this equation describes the balance between 1-d dispersion and nonlinearity, which gives rise to sech-shaped, "bright" temporal solitons. With $\beta_2 > 0$ (normal GVD), "dark" solitons appear as localized dips against a uniform background. Both types of solitons have been detected experimentally (Agrawal, 1989). Solitons in dispersion-managed optical fibers, prepared with alternating spans of normal and anomalous GVD, have important applications in high-rated data communication systems over distances of many kilometers.
- For ultrashort pulses developing sharp temporal gradients, the operator T in front of the Kerr term in (7) induces shock dynamics: the field intensity without GVD and diffraction is governed by the continuity relation $\rho_\xi + 3n_2\rho\rho_\tau/c = 0$ with $\rho = |A|^2$. For localized pulses with compact distribution F, ρ has the exact implicit solution $\rho = F(\tau - 3n_2\xi\rho/c)$, which gives rise to a singular shock profile with $|A_\tau| \to +\infty$ in the trail ($\tau > 0$) of the pulse. This effect is usually called self-steepening (Anderson & Lisak, 1983). A comparable formation of a trailing shock edge, called space-time focusing, follows from the operator T^{-1} acting on diffraction (Rothenberg, 1992).
- For beams with no temporal dispersion ($T = 1$, GVD = 0), Equation (7) describes the self-focusing of optical wave packets (Marburger, 1975). Self-focusing arises as a shrinking of the beam in the diffraction plane, which is achieved by a transverse collapse when no saturation of the Kerr nonlinearity takes place. This process develops when the input power $P_{\mathrm{in}} = \int |A|^2 \,\mathrm{d}\boldsymbol{r}$ exceeds the critical value $P_{\mathrm{cr}} \simeq \lambda_0^2/2\pi n_0 n_2$. The beam waist then decreases

more and more, as the field amplitude $|A|$ diverges. In media such as CS_2 liquids (Campillo et al., 1973), the optical field distribution is modulationally unstable, and self-focusing often produces filamentation, along which the background beam is broken up into small-scale cells that self-focus in turn. Their growth is, however, generally arrested by higher-order nonlinearities coming from Equation (2), which can form stable spatial solitons.

- By mixing GVD and spatial diffraction when $T \simeq 1$, the Kerr nonlinearity causes defocusing in time for $\beta_2 > 0$ and temporal compression for $\beta_2 < 0$, in addition to wave focusing in the transverse direction. The interplay of these processes results in the symmetric splitting of the pulse along the time axis with normal GVD and to a 3-d spatiotemporal collapse with anomalous GVD (Bergé, 1998).
- Finally, the Kerr response of optical media favors cross-phase modulation (XPM). XPM refers to the nonlinear phase shift of an optical field induced by a copropagating beam at a different wavelength. Noting the total electric field as $\boldsymbol{E} = \hat{\boldsymbol{x}}\,\mathrm{Re}[A_1 e^{-i\omega_1 t} + A_2 e^{-i\omega_2 t}]$ for two components with different frequencies ω_1 and ω_2, the phase shift for the field at ω_1 over a length L is given by $\phi_{\mathrm{NL}} = n_2 k_0 L(|A_1|^2 + 2|A_2|^2)$. The last term refers to XPM, from which spectral broadening is larger than that for one wave alone. Coupling of several wave components belongs to the category of parametric processes, among which are the third-harmonic generation, four-wave mixing and parametric amplification (Shen, 1984; Agrawal, 1989).

LUC BERGÉ

See also **Development of singularities; Filamentation; Harmonic generation; Nonlinear optics**

Further Reading

Agrawal, G.P. 1989. *Nonlinear Fiber Optics*, San Diego: Academic Press, pp 14–36

Anderson, D. & Lisak, M. 1983. Nonlinear asymmetric self-phase modulation and self-steepening of pulses in long optical waveguides. *Physical Review* A, 27: 1393–1398

Bergé, L. 1998. Wave collapse in physics: Principles and applications to light and plasma waves. *Physics Reports*, 303: 259–370

Brabec, T. & Krausz, F. 1997. Nonlinear optical pulse propagation in the single-cycle regime. *Physical Review Letters*, 78: 3282–3285

Campillo, S.L., Shapiro, S.L. & Suydam, B.R. 1973. Periodic breakup of optical beams due to self-focusing. *Applied Physics Letters*, 23: 628–630

Marburger, J.H. 1975. Self-focusing: theory. *Progress in Quantum Electronics*, 4: 35–110

Rothenberg, J.E. 1992. Space-time focusing: breakdown of the slowly varying envelope approximation in the self-focusing of femtosecond pulses. *Optics Letters*, 17: 1340–1342

Shen, Y.R. 1984. *The Principles of Nonlinear Optics*, New York: Wiley, pp 242–333

Yariv, A. 1975. *Quantum Electronics*, 2nd edition, New York: Wiley, pp 407–507

KICKED ROTOR

The properties of a classical and/or quantum kicked rotor can be understood by examining how nonlinearities influence the dynamics of conservative dynamical systems. The story begins with the French mathematician Henri Poincaré and his famous study of planetary motion (Poincaré, 1892). Unlike the integrable two-body problem, a third body added to the system experiences nonperiodic motion (*See* ***N*-body problem**). Indeed, the trajectory of a light mass moving under the influence of the gravity of two heavy masses is very complex, and we know that such an orbit is fractal. This is one end of the spectrum of dynamical possibilities; on the other end are the integrable Hamiltonian equations of the Kolmogorov–Arnol'd–Moser (KAM) theory.

Thus, in one limit we have the integrable Hamiltonians that are the subject of the KAM theory, and in another we have non-integrable Hamiltonians, an example of which is the three-body problem of Poincaré. So how do we get from one side to the other using a perturbed Hamiltonian? In the unperturbed system, the various degrees of freedom are uncoupled, given by the action-angle variables, and the motion unfolds on KAM tori. Small perturbations leave the motion essentially unchanged, but even then nonlinear resonances are introduced in restricted regions of phase space. These nonlinear resonances change the dynamics of the system and deform the tori on all scales as the strength of the perturbation increases, leading to breakup of the KAM tori and chaos.

The properties of such nonlinear resonances can be examined using maps, which in a Hamiltonian system is equivalent to using a strobe lamp to register the momentum and displacement at equally spaced time intervals. One map that approximates several physical systems is the Taylor–Chirikov or standard map (Chirikov, 1979). For the nth flash we have for this map the momentum p_n and displacement x_n,

$$p_{n+1} = p_n \frac{K}{2\pi} \sin(2\pi x_n), \quad x_{n+1} = x_n + p_{n+1}. \quad (1)$$

Figure 1 shows a sequence of standard map plots for increasing values of the coupling strength K. Each of the continuous curves is the result of a mapping of a single initial condition. The orbits in the vicinity of $p = 0.5$ in Figure 1a are those of a simple pendulum, which is the "harmonic oscillator" of nonlinear dynamics. As the size of K is increased, Figure 1b shows that the nonlinear resonances generate more and more structure in the phase space as well as deforming the already existing KAM tori. The tori break up into sprays of

points, beginning in the vicinity of the nonlinear resonances, whose exact locations are sensitively dependent on initial conditions. This is chaos, and as K is further increased, the chaos spreads throughout the phase space among the islands of stability, as in Figure 1c. There is no way to predict the motion of the trajectory in the chaotic sea. Further increases in the coupling parameter result in more tori disintegrating until the phase space appears to be completely dominated by chaos and all but the most stable of the KAM tori have disappeared, as in Figure 1d.

The standard map is also called a kicked rotor because it describes the strobe plot of the phase space trajectories for a rotor kicked every T units of time with a strength that depends on the angular position of the rotor. The Hamiltonian for the classical kicked rotor (CKR) can be written as (Chirikov, 1979; Reichl, 1992)

$$H = \frac{J^2}{2I} + K\cos\theta \sum_{k=-\infty}^{k=\infty} \delta(t - nT)\,, \qquad (2)$$

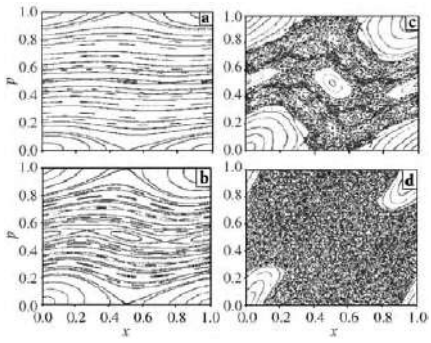

Figure 1. The phase space orbits for the kicked rotor are depicted for four values of the coupling strength: (a) $K = 0.1716354$; (b) $K = 0.4716354$; (c) $K = 1.1716354$, and (d) $K = 3.9716354$ (from Reichl, 1992).

where J is the angular momentum of the rotor, θ is its angular position, and I is the moment of inertia. Reichl (1992) reviews how to obtain the discrete map (2) by integrating the Hamiltonian equation of motion generated by (3) from one pulse to the next.

Hamiltonian (3) provides a classical description of an electron subjected to a periodically pulsed electric field. The nonlinear mechanisms are present in the motion of charged particles in accelerators and storage rings, as well as in the motion of planets and man-made celestial bodies. In the classical case, the particle dynamics in the chaotic sea are interpreted as diffusion, under which the mean-square separation of trajectories increases linearly in time with a diffusion coefficient given by $2D \approx K^2$. Thus, for the coupling strength (K) sufficiently large, the dynamical system behaves like simple Brownian motion. This has led a number of investigators to conjecture that chaos provides the dynamical foundation of thermodynamics, rather than the usual heat bath, with an infinite number of degrees of freedom (Ford & Waters, 1963; Chirikov, 1979). For example, the fluctuation-dissipation relation has been generated using nonlinear dynamical systems (Bianucci et al., 1995).

The quantum kicked rotor (QKR) employs a quantized version of the Hamiltonian, where the angular momentum J is replaced with the operator $i\hbar\,\partial/\partial\theta$. The mapping is carried out using the Floquet theory on the Schrödinger equation, because the Hamiltonian is periodic in time. There is a remarkable similarity between the QKR and the one-dimensional tight-binding model of Anderson localization in solid state physics. The dynamical evolution of the QKR can be determined analytically in terms of a Floquet map, where the Floquet momentum eigenstates are exponentially localized for irrational kicks and extended for rational kicks (Reichl, 1992). It has been established that the quantum density for the momentum states is a truncated Levy distribution in direct analogy with the classical probability density as shown in Figure 2 (Stefancich et al., 1998). The peaks on either side of the classical and quantum

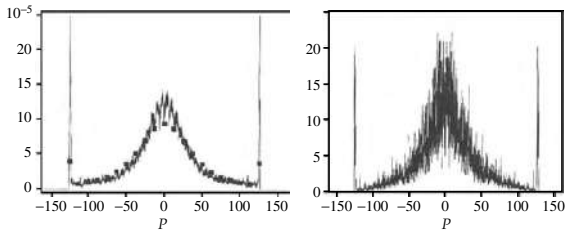

Figure 2. On the left is depicted the classical probability density for the dimensionless momentum of the CKR after 20 iterations of the map (2) and the solid curve is the theoretical prediction of the truncated Lévy distribution. On the right is the quantum probability density after 20 iterations for the QKR (Stefancich et al., 1998).

distributions correspond to the outward propagation of the initial states at maximum velocity. Finally, the CKR and QKR have been used to describe the experimental "quasifractal" structures resulting from a periodically kicked spin system in the semiclassically large-spin regions (Nakamura, 1993).

BRUCE J. WEST

See also **Chaotic dynamics; Fluctuation-dissipation theorem; Hamiltonian systems; Kolmogorov–Arnol'd–Moser theorem; Standard map**

Further Reading

Bianucci, M., Mannella, R., West, B.J. & Grigolini, P. 1995. From dynamics to thermodynamics: linear response and statistical mechanics. *Physical Review* E, 51: 3002–3022

Chirikov, B.V. 1979. A universal instability of many-dimensional oscillator systems. *Physics Reports*, 52: 263–379

Ford, J. & Waters, J. 1963. Computer studies of energy sharing and ergodicity for nonlinear oscillator systems. *J. Math. Phys*., 4: 1293–1305.

Nakamura, K. 1993. *Quantum Chaos: A New Paradigm of Nonlinear Dynamics*, Cambridge and New York: Cambridge University Press

Ott, E. 2003. *Chaos in Dynamical Systems*, 2nd edition, Cambridge and New York: Cambridge University Press

Poincaré, H. 1892–1899. *Les Methodes nouvelles de la méchanique céleste*, Paris: Gauthier-Villars; as *New Methods of Celestial Mechanics*, 3 vols, Woodbury, NY: American Institute of Physics, 1993

Reichl, L.E. 1992. *The Transition to Chaos*, New York: Springer

Stefancich, M., Allegrini, P., Bonci, L., Grigolini, P. & West, B.J. 1998. Anomalous diffusion and ballistic peaks: a quantum perspective. *Physical Review* E, 57: 6625–6633

KINKS AND ANTIKINKS

See **Sine-Gordon equation**

KIRCHHOFF'S LAWS

Introduction

Kirchhoff's laws are conservation rules for networks; given a particular network topology, they prescribe how its currents and voltages are related. This not only facilitates understanding of the behavior of a network, but also allows an analyst to write down the equations that govern its behavior. These laws were named after Gustav Robert Kirchhoff, who in 1845 published one of the first systematic treatises on the laws of circuit analysis. Kirchhoff's current law (KCL) states that the sum of all currents into any node (or single point) of the network is zero; thus the charge flowing in and out is balanced, which makes intuitive sense. In the network of Figure 1, this means that I_1 and I_4 are equal in magnitude (KCL at node A), and that the algebraic sum of I_1, I_2, and I_3 is zero (KCL at node B).

Kirchhoff's voltage law (KVL) states that the sum of voltages around a closed loop is zero, which is expected because traversing a loop brings one back to the starting point. In Figure 1, this means that V_2 and V_3 are equal (KVL around loop D), and that the algebraic sum of V_1, V_2, and V_4 is zero (KVL around loop C). Signs and directions can be confusing in both cases, and it is important to note these correctly. A positive current entering a node is the same as a negative current leaving a node. Also, moving from the negative to positive voltage (potential) terminal of an element entails a potential rise, while moving in the opposite direction entails a drop. Passive network elements create voltage drops; active ones such as voltage sources can create voltage rises.

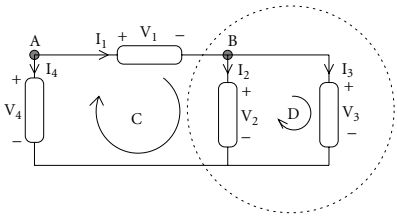

Figure 1. A simple electric network.

As with any such rules, there are some caveats. KCL actually specifies that current into a "cutset," not just a node, is zero; a cutset is any part of the network that is enclosed by a closed curve, such as the dotted circle in Figure 1. Moreover, KCL does not hold if nodes (or cutsets) can store, consume, or produce charge. KVL, on the other hand, is only valid if the voltage (or potential) between two points is independent of the path one takes between the points. If energy is lost or created as it moves around a loop, KVL does not hold.

Applications to Electronic Circuits

Kirchhoff's laws find their most common use in electronics. In Figure 2, for example, KVL around the left- and right-hand loops, respectively, yields $-V + V_1 + V_2 = 0$ and $-V_2 + V_3 = 0$, and KCL written at the point where the three resistors join yields $I_1 - I_2 - I_3 = 0$. These relationships are fairly obvious in such a simple network, assuming one gets the directions and the associated signs right. KVL and KCL become important when the network topology is complex or when one wants to automate the process in a computer algorithm.

If the constitutive relations (voltage-current characteristics) of the elements in a network are known, one can rewrite either set of equations in terms of the other state variables. Resistors, for example, obey Ohm's law ($V = IR$), so the first KVL equation can be rewritten in terms of the currents: $V = I_1 R_1 + I_2 R_2$.

The governing equations for a simple resistor circuit as in Figure 2 are linear and algebraic. When the

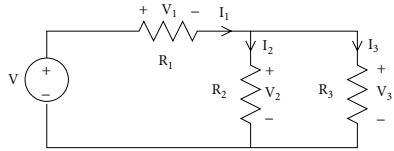

Figure 2. A resistor network.

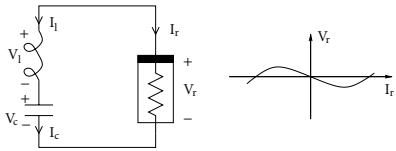

Figure 3. A simple oscillator circuit.

circuit includes inductors and capacitors, the equations become integro-differential, but Kirchhoff's laws work just as well, and they also handle nonlinear components easily. The circuit of Figure 3, for instance, is an example of the van der Pol oscillator. In this case, KCL simply states that the currents through all three elements are identical. KVL implies that $V_\mathrm{l} + V_\mathrm{c} - V_\mathrm{r} = 0$. The constitutive relations for the capacitor and inductor are $I_\mathrm{c} = C\,\mathrm{d}V_\mathrm{c}/\mathrm{d}t$ and $V_\mathrm{l} = L\,\mathrm{d}I_\mathrm{l}/\mathrm{d}t$, and the resistor in this circuit is nonlinear: $V_\mathrm{r} = -aI_\mathrm{r} + bI_\mathrm{r}^3$. Thus, KVL can be rewritten as

$$L\frac{\mathrm{d}I_\mathrm{l}}{\mathrm{d}t} + \frac{1}{C}\int I_\mathrm{c}\mathrm{d}t + aI_\mathrm{r} - bI_\mathrm{r}^3 = 0.$$

Other Applications

These ideas generalize beyond electronic circuit analysis. Many other systems, ranging from vehicle suspensions to social groups, can be described by networks. Moreover, KVL and KCL are actually instances of a more general set of laws. In the late 1950s and early 1960s, inspired by the realization that the principles underlying KCL and Newton's third law were identical (summation of {forces, currents} at a point is zero, respectively; both are manifestations of the conservation of energy), researchers began combining multi-port methods from a number of engineering fields into a generalized engineering domain with prototypical components (Paynter, 1961). The basis of this generalized physical networks (GPN) paradigm is that the behavior of an ideal two-terminal element—the "component"—can be described by a mathematical relationship between two dependent variables: generalized flow and generalized effort, where flow × effort = power. This pair of variables

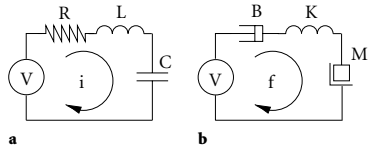

Figure 4. (a) An electrical circuit that is mathematically equivalent to (b) a mechanical circuit.

is different in each domain: (flow, effort) is (current, voltage) in an electrical domain and (force, velocity) in a mechanical domain.

The GPN representation brings out similarities between components and properties in different domains. Electrical resistors ($v = iR$) and mechanical dampers or "dashpots" ($v = fB$) are analogous, as both dissipate energy. Both of the networks in Figure 4, for example, can be modeled by a series inertia-resistor-capacitor GPN. Thus network (a) is an electronic RLC circuit (like the van der Pol example of Figure 3), and network (b) is a mechanical mass-spring-damper system that has identical behavior. Similar analogies exist for generalized inertia, capacitance, flow, and effort source components for mechanical rotational, hydraulic, and thermal domains (Karnopp et al., 1990, Sanford, 1965). These correspondences and generalizations allow applications of KVL and KCL to mechanical structures (buildings, vehicle suspensions, aircraft, etc.), which can be modeled as interconnected networks of masses, springs, and dashpots. This approximation gives analytic insight into the vibrational modes of buildings (important for earthquake protection) and of aircraft (to keep engine frequencies from damaging wings).

ELIZABETH BRADLEY

Further Reading

Karnopp, D., Margolis, D. & Rosenberg, R. 1990. *System Dynamics: A Unified Approach*, 2nd edition, New York: Wiley
Paynter, H. 1961. *Analysis and Design of Engineering Systems*, Cambridge MA: MIT Press
Sanford, R. 1965. *Physical Networks*, Englewood Cliffs, NJ: Prentice-Hall

KLEIN–GORDON EQUATION

See **Sine-Gordon equation**

KNOT THEORY

A simple closed curve in three-dimensional space is a knot; more precisely, if M denotes a closed orientable three-manifold, then a smooth embedding of S^1 in M is called a knot in M. A link in M is a finite collection of disjoint knots, where each knot is a component of the link. Knot theory deals with the study and application

of mathematical properties of knots and links in pure and applied sciences. As purely mathematical objects, knots are studied for the purpose of classifying three-dimensional surfaces according to the degree of topological complexity, regardless of their specific embedding and geometric properties (Figure 1). In this sense, knot theory is part of topology. In recent years, however, knot theory has embraced applications in dynamical systems, stimulated by the challenging difficulties associated with the study of physical knots (Kauffman, 1995). In this context knots and links are representatives of virtual and numerical objects (given by dynamical flows, phase space trajectories, and visiometric patterns), and are used to model tube-like physical systems, such as vortex filaments, magnetic loops, electric circuits, elastic cords, or even high-energy strings. For physical knots, topological issues and geometric and dynamical aspects are intimately related, influencing each other in a complex fashion. Virtual or numerical knots are studied in relation to the generating algorithms and the probability of forming knots, whereas the study of physical knots addresses questions relating topology and physics, as in the case of the topological quantum field theory (Atiyah, 1990) and topological fluid mechanics (Arnol'd & Khesin, 1998; Ricca, 2001).

Mathematical Aspects

Let us introduce some basic mathematical concepts (see, for example, Adams, 1994). A knot is said to be oriented in M, if it is a smooth embedding of an oriented curve. Two knots K and K' are said to be equivalent if there exists a smooth orientation-preserving automorphism $f : M \to M$ such that $f(K) = K'$; in particular, if the knot K is continuously deformed by f (preserving the curve orientation) to the knot K', then the two knots K and K' are said to be equivalent by ambient isotopy, and the isotopy class of K is represented by its knot type. Since knot theory deals essentially with the properties of knots and links up to isotopy, the knot parametrization, as well as any other geometric information, is irrelevant. A knot diagram of K is a plane projection with crossings marked as under or over; among the infinitely many diagrams representing the same knot K, the minimal diagram is the diagram with a minimum number of crossings. According to the type of crossing, it is customary to assign to each crossing in the knot diagram the value $\varepsilon = +1$ or $\varepsilon = -1$, as shown in Figure 2: by switching one crossing in the knot diagram from positive to negative (or the other way round), we obtain a different knot type, which is identical except for this crossing. By switching all the crossings we obtain the mirror image of the original knot. If the knot is isotopic to its mirror image, then its knot type is said to be achiral, otherwise it is chiral.

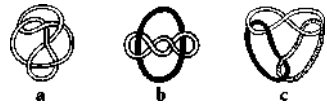

Figure 1. Three examples of knot and link types: (a) the six-crossing knot 6_3; (b) the two-component six-crossing link 6_3^2; (c) the three-component seven-crossing link 7_1^3.

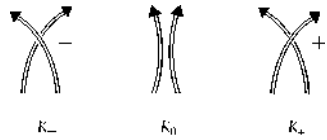

Figure 2. Standard crossing notation and algebraic sign convention for oriented strands: $\varepsilon(K_-) = -1$; $\varepsilon(K_0) = 0$; $\varepsilon(K_+) = +1$.

A knot invariant is a quantity whose value does not change when it is calculated for different isotopic knots. There are many types of invariants of knots and links, but the most common are of numerical or algebraic nature. One of the most important is the genus $g(K)$ of the knot K: recall that closed orientable surfaces are classified by genus, given by the number of handles in a handle-body decomposition. The genus $g(K)$ is defined as the minimum genus over all orientable surfaces S, which span an oriented knot K, where $\partial S = K$. One of the simplest combinatorial invariants of a knot is the minimum number of crossings of a knot K in any projection, called the crossing number $c(K)$. A fundamental invariant of links is the linking number $\mathrm{Lk}(K_1, K_2)$, that measures the topological linking between the knots K_1 and K_2; this invariant, discovered by Carl Friedrich Gauss in 1833, can be easily calculated by the crossing sign convention of Figure 2:

$$\mathrm{Lk}(K_1, K_2) = \frac{1}{2} \sum_{r \in K_1 \sqcap K_2} \varepsilon_r \,, \tag{1}$$

where $\varepsilon_r = \pm 1$ and $K_1 \sqcap K_2$ denotes the total number of crossings (not necessarily minimal) between K_1 and K_2. Following the pioneering work of James W. Alexander, who used a Laurent polynomial $\Delta_K(q)$ in q to compute a polynomial invariant for the knot K by using its projection on a plane, many other polynomial invariants have been introduced; most notably the Jones polynomial $V_K(t)$ in $t^{1/2}$, defined by the following set of axioms:

(i) Let K and K' be two oriented knots (or links), which are ambient isotopic. Then

$$V_K(t) = V_{K'}(t). \tag{2}$$

(ii) If U is the unknotted loop (that is the unknot), then

$$V_U(t) = 1. \quad (3)$$

(iii) If K_+, K_-, and K_0 are three knots (links) with diagrams that differ only as shown in the neighborhood of a single crossing site for K_+ and K_- (see Figure 2), then the polynomial satisfies the following skein relation

$$t^{-1}V_{K_+}(t) - tV_{K_-}(t) = (t^{1/2} - t^{-1/2})V_{K_0}(t)\,. \quad (4)$$

An important property of the Jones polynomial (which is not shared by previous polynomials) is that it can distinguish between a knot and its mirror image. Later work has led to other polynomial invariants, namely, the HOMFLY and Kauffman polynomials, and to a more abstract approach to algebraic invariants (Vassiliev invariants and Lie algebras). There are also invariants of different nature: among these, we mention the fundamental group $\pi_1(S^3/K)$ of the knot complement and its hyperbolic volume $v(K)$. The classification of knots and links has led to the important study of braids: these are given by a set of n interlaced strings, with ends defined on two parallel planes, placed at some distance h apart. According to specific topological characteristics, we may consider special types of knot sub-families, such as torus knots, alternating knots, two-bridge knots, tangles, and many others (see Hoste et al., 1998).

Virtual Knots

Virtual knots arise from dynamical flows, generated by the vector field of a specific ordinary differential equation (Ghrist, 1997), in connection with phase-space dynamics and statistical mechanical models (Millett & Sumners, 1994) or, as recently done, from application of ideas from the quantum field theory with an appropriate Lagrangian. This latter approach, originated in work by E. Witten in 1989, has led to the creation of a new area, called the topological quantum field theory, that has proven to be extremely fruitful in providing new results on invariants of low-dimensional manifolds. Soliton knots are given by solutions to soliton equations for one-dimensional systems: in this context there are intriguing questions relating topological invariants, integrability, and conservation laws. Virtual knots and links are generated in visiometrics by numerical simulations: in this case, smooth knots are replaced by polygonal knots, where the number of segments (or sticks) is the result of numerical discretization. Stimulating questions address the minimum number of sticks of given length for each knot type and the generation of knots and links by minimal random walks. Other questions regard charged knots: these are knots and links charged by potentials that generate self-attraction or repulsion on the knot strands (see Figure 3). Under volume-preserving diffeomorphisms, the knot is led to relax by minimizing the knot energy (defined by an appropriate functional), by shrinking or extending the length as far as possible, depending on the potential, to attain an ideal shape (Stasiak et al., 1998). Questions relating to topology and geometry of ideal shapes, and uniqueness of minimum energy states, pose challenging problems at the crossroads of topology, differential geometry, functional analysis, and numerical simulation.

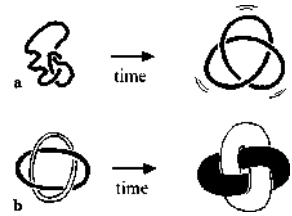

Figure 3. Examples where a topological barrier prevents further relaxation under a volume-preserving diffeomorphism: (a) an electrically charged trefoil knot is maximally extended by the Coulomb repulsion forces to its minimum energy state; (b) a magnetic link attains ground state energy by the action of the Lorentz force on the magnetic volume.

Physical Knots

By physical knots we mean tube models, centered around the knot K, with length $L(K)$, tubular neighborhood of radius $r(K)$, and volume $V(K)$. The tube is filled by vector field lines, whose distribution gives physical properties in terms, for example, of elasticity, vorticity, or magnetic field. A wide variety of filamentary systems present in nature at very different scales can be modeled by physical knots: from DNA molecules, polymer chains, vortex filaments, to elastic cords, strings, and magnetic flux tubes. In fluid systems, the action at a microscopic level of physical processes, such as viscosity and resistivity, may imply changes in knot topology by local recombination of the knot strands (known as knot surgery) and consequential rearrangement of energy distribution. In elastic systems, the material breaking point and internal critical twist are strongly influenced by knot strength and rope length, the latter given by the ratio L/r. All these systems are free to relax their internal energy to states of equilibrium: lower bounds on equilibrium energy for given measures of topological complexity (based, for example, on crossing number information) can be expressed by relationships of the kind

$$E_{\min} \geq h(c, \Phi, V, n), \quad (5)$$

where $E_{\min}$ is the equilibrium energy and $h(\cdot)$ gives the relationship between physical quantities—such as flux Φ, number of components n, knot volume V—and topology, given here by the crossing number c.

Understanding the interplay between topology and energy localization and redistribution can be very important in many fields of science and applications.

RENZO L. RICCA

See also **Differential geometry; Dynamical systems; Structural complexity; Topology**

Further Reading

Adams, C. 1994. *The Knot Book*, New York: W.H. Freeman
Arnol'd, V.I. & Khesin, B.A. 1998. *Topological Methods in Hydrodynamics*, Berlin and New York: Springer
Atiyah, M. 1990. *The Geometry and Physics of Knots*, Cambridge and New York: Cambridge University Press
Ghrist, R., Holmes, P. & Sullivan, M. 1997. *Knots and Links in Three-Dimensional Flows*, Berlin and New York: Springer
Hoste, J., Thistlethwaite, M. & Weeks, J. 1998. The first 1,701,936 knots. *Mathematical Intelligencer*, 20: 33–48
Kauffman, L. (editor). 1995. *Knots and Applications*, Singapore: World Scientific
Millett, K.C. & Sumners, D.W. (editors). 1994. *Random Knotting and Linking*, Singapore: World Scientific
Ricca, R.L. (editor). 2001. *An Introduction to the Geometry and Topology of Fluid Flows*, Dordrecht: Kluwer
Stasiak, A., Katritch, V. & Kauffman, L.H. (editors). 1998. *Ideal Knots*, Singapore: World Scientific

KOCH CURVE

See **Fractals**

KOLMOGOROV CASCADE

The velocity fluctuations of a high Reynolds number flow in a three-dimensional velocity field are typically dispersed over all possible wavelengths of the system, from the smallest scales, where viscosity dominates the advection and dissipates the energy of fluid motion, to the effective size of the system. This is not so bizarre: our everyday experience tells us it is so. On the corner of a city street, one might watch the fluttering and whirling of a discarded tram ticket as it is swept by an updraught, driven by localized thermal gradients from traffic or air-conditioning units; later, on the television news, one might see reports or predictions of storms on the city or district scale, and a weather map with isobars spanning whole continents. If you are a sailor you will know how to sail, or not, the multi-scaled surface of a turbulent ocean (Figure 1). The mechanism for this dispersal is vortex stretching and tilting: a conservative process whereby interactions between vorticity and velocity gradients create smaller and smaller eddies with amplified vorticity, until viscosity takes over (Tennekes & Lumley, 1972; Chorin, 1994).

An alternative, crude but picturesque, description of multi-scale turbulence was offered by the early 20th century meteorologist Lewis Fry Richardson (1922) in an evocative piece of doggerel: "big whirls have little whirls that feed on their velocity, and little whirls have lesser whirls and so on to viscosity." Richardson's

Figure 1. Turbulent action on many different scales in a high Reynolds number flow: woodcut print by Katsushika Hokusai (1760–1849).

often-quoted rhyme is apparently a parody of Irish satirist Jonathan Swift's verse: "So, naturalists observe, a flea—Has smaller fleas that on him prey—And these have smaller still to bite'—And so proceed *ad infinitum*."

The statistics of the velocity fluctuation distribution in turbulent flows were quantified rather more elegantly and rigorously by the mathematician Andrei N. Kolmogorov (1941b), who derived the subsequently famous "$-5/3$ law" for the energy spectrum of the intermediate scales, or inertial scale subrange, of high Reynolds number flows which are ideally homogeneous (or statistically invariant under translation) and isotropic (or statistically invariant under rotation and reflection) in three velocity dimensions. Two thorough, but different in style and emphasis, accounts of Kolmogorov's turbulence work are Monin & Yaglom (1971) and Frisch (1995).

Kolmogorov's idea was that the velocity fluctuations in the inertial subrange are independent of initial and boundary conditions (i.e., they have no memory of the effects of anisotropic excitation at smaller wave numbers). The turbulent motions in this subrange, therefore, show universal statistics, and the flow is self-similar. From this premise Kolmogorov proposed the first hypothesis of similarity as: "For the locally isotropic turbulence the [velocity fluctuation] distributions F_n are uniquely determined by the quantities ν, the kinematic viscosity, and ε, the rate of average dispersion of energy per unit mass [energy flux]." His second hypothesis of similarity is: "For pulsations [velocity fluctuations] of intermediate orders where the length scale is large compared with the scale of the finest pulsations, whose energy is directly dispersed into heat due to viscosity, the distribution laws F_n are uniquely determined by F and do not depend on ν."

Kolmogorov derived the form of the distribution or energy spectrum, which we denote as $\mathcal{E}(k)$, where k is the wave number given by $k^2 = k_x^2 + k_y^2 + k_z^2$, over the inertial subrange simply by dimensional analysis. By the first and second hypotheses, the spectrum must

be a function of the energy flux and wave number and independent of the viscosity or any other parameters:

$$\mathcal{E}(k) = f(\varepsilon, k).$$

By reference to the table below (after Vallis, 1999) we find

$$\begin{aligned}\mathcal{E}(k) &\sim \varepsilon^{2/3} g(k) \quad \text{(since } k \text{ is time-independent)} \\ &= C\varepsilon^{2/3} k^{-5/3}, \end{aligned} \tag{1}$$

where C is a dimensionless constant which Kolmogorov (and subsequently many others, see Sreenivasan, 1995) deduced from experimental data to be of order 1.

Quantity	Dimension
Wave number	1/length
Energy per unit mass	length^2/time^2
Energy spectrum $\mathcal{E}(k)$	length^3/time^2
Energy flux ε	energy/time $\sim$ length^2/time^3

The physical picture associated with Equation (1) is that the kinetic energy of large-scale motions (whirls or eddies) is successively subdivided and redistributed among stepwise increasing wave number components (or smaller and smaller whirls and eddies), until the action of viscosity becomes competitive. Although this process has come to be known as the "Kolmogorov cascade," the cascade metaphor was not used by Kolmogorov. Its first use in this context is apparently due to Onsager (1945), who also highlights another assumption underlying the $-5/3$ law: that the modulation of a given Fourier component of the velocity field is mostly due to those others that belong to wave numbers of comparable magnitude.

So Kolmogorov's energy distribution says that ε is the only relevant parameter for turbulence in the inertial scale range. Can this really be true? Does the notorious "problem of turbulence" really boil down to such a simple relation for intermediate wavenumbers? (The fabled Problem of Turbulence was well summed up by Horace Lamb in 1932: "When I die and go to Heaven there are two matters on which I hope enlightenment. One is quantum electro-dynamics and the other is turbulence of fluids. About the former, I am really rather optimistic.") Understandably, for a turbulence result that seems so simple and universal, so flimsily derived yet so powerful, much effort has gone into verifying the wave number spectrum, Equation (1). It is difficult to create extremely high Reynolds number flows in the laboratory, but they exist naturally in the ocean. The first and still the most exciting verification of Equation (1) was carried out by Grant et al. (1962), who made a remarkable series of measurements of turbulent velocities from a ship in the Seymour Narrows, part of the Discovery Passage on the west coast of Canada, where the Reynolds number is $\sim 10^8$ (see Figure 2). A spectral exponent close to $-5/3$ has since been measured many

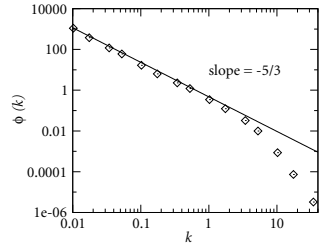

Figure 2. Data re-plotted from Grant et al. (1962), showing a Kolmogorov cascade over nearly three decades. $\phi(k)$ is the measured one-dimensional spectrum function, related to the three-dimensional spectrum function as $\mathcal{E}(k) = k^2\partial^2\phi(k)/\partial k^2 - k\partial\phi(k)/\partial k$.

times in materially different flows with high Reynolds number (e.g., Zocchi et al. (1994) in helium).

All this would seem to wrap up the problem of turbulence in the inertial scale range. Or does it? There must surely be a catch somewhere! As usual, the devil is in the details. Kolmogorov himself made a "refinement," as he delicately put it, of his hypotheses (Kolmogorov, 1962). It relates to the problem of small-scale intermittency, or the uneven distribution in space of the small scales. Clearly, intermittency is inherited from initial and boundary conditions, and the side-effects on ε, the assumed-constant rate of energy transfer, are not insignificant.

In fact, there is now quite a log of complaints about the $-5/3$ law, despite its all-pervasive influence on turbulence theoretical and experimental research:

- The hypothesis of local isotropy refers to infinite Reynolds number so is not applicable to a real fluid.
- No-one has ever extracted the $-5/3$ law from the Navier–Stokes equation or vice versa.
- Is it not a circular argument that to define an inertial subrange one has to assume a cascade process, and to postulate a cascade one has to assume that an inertial subrange exists?
- What about stochastic backscatter?
- Direct interaction between large and small scales can short-circuit the cascade.
- Katul et al. (2003) found that the effects of boundary conditions were evident in the inertial subrange of an atmospheric surface layer.
- The $-5/3$ law is demonstrably invalid in two dimensions. And so on.

What is the verdict on the Kolmogorov cascade? Chorin (1994, pp. 55–57) has a bet each way; in the light of experimental verifications of the $-5/3$ law, he considers that it may be correct *despite* flaws in the arguments supporting it. The scenario proposed as being entirely consistent with Kolmogorov's theory is

that energy can and does slosh back and forth across the spectrum, once the inertial range has been set up, with the energy dissipation ε being the (presumably average) difference between energy flows in both wave number directions.

The Kolmogorov cascade is starting to sound less and less like a waterfall, which *is* one-way, and more and more like an energy exchange network.

ROWENA BALL

See also **Chaos vs. turbulence; Dimensional analysis; Navier–Stokes equation; Turbulence**

Further Reading

Chorin, A.J. 1994. *Vorticity and Turbulence*, New York: Springer

Frisch, U. 1995. *Turbulence: The Legacy of A. N. Kolmogorov*, Cambridge and New York: Cambridge University Press

Grant, H.L., Stewart, R.W. & Moilliet, A. 1962. Turbulence spectra from a tidal channel. *Journal of Fluid Mechanics*, 12: 241–268

Katul, G.G., Angelini, C., De Canditiis, D., Amato, U., Vidakovic, B. & Albertson, J.D. 2003. Are the effects of large scale flow conditions really lost through the turbulent cascade? *Geophysical Research Letters*, 30(4), 1164,doi:10.1029/2002GL015284

Kolmogorov, A.N. 1941a. Local structure of turbulence in an incompressible fluid for very large Reynolds numbers. *Comptes rendus (Doklady) de l'Academie des Sciences de l'U.R.S.S.*, 31: 301–305 Reprinted in, S.K. Friedlander & L. Topper 1961. *Turbulence: Classic Papers on Statistical Theory*, New York: Interscience Publishers

Kolmogorov, A.N. 1941b. On degeneration of isotropic turbulence in an incompressible viscous liquid. *Comptes Rendus (Doklady) de l'Academie des Sciences de l'U.R.S.S.*, 31: 538–540, *ibidem.*

Kolmogorov, A.N. 1962. A refinement of previous hypotheses concerning the local structure of turbulence in a viscous incompressible fluid at high Reynolds number. *Journal of Fluid Mechanics*, 13: 82–85

Monin, A. S. & Yaglom, A.M. 1971. *Statistical Fluid Mechanics: Mechanics of Turbulence*, vol. 2, Cambridge: MIT Press

Onsager, L. 1945. The distribution of energy in turbulence. *Physical Review*, 68: 286

Richardson, L.F. 1922. *Weather Prediction by Numerical Process*, Cambridge: Cambridge University Press

Sreenivasan, K.R. 1995. On the universality of the Kolmogorov constant. *Physics of Fluids*, 7(11), 2778–2784

Tennekes, H. & Lumley, J.A. 1972. *A First Course in Turbulence*, Cambridge: MIT Press

Vallis, G. 1999. Geostrophic turbulence: the macroturbulence of the atmosphere and ocean. Lecture notes, www.gfdl.gov/~gkv/geoturb/

Zocchi, G., Tabeling, P., Maurer, J. & Willaime, H. 1994. Measurement of the scaling of the dissipation at high Reynolds numbers. *Physical Review* E, 50(5): 3693–3700

KOLMOGOROV, PETROVSKY AND PISCOUNOFF EQUATION

See **Diffusion**

KOLMOGOROV–ARNOL'D–MOSER THEOREM

In 1954, the Russian mathematician Andrei N. Kolmogorov, already famous for his contribution to measure theory and probability theory, delivered to the International Conference of Mathematics in Amsterdam, a lecture based on a paper entitled "On the General Theory of Dynamical Systems and Classical Mechanics." In this lecture he addressed the question of how much structure remains when a "regular" (or integrable) Hamiltonian system is replaced by one that differs from the original by only a small perturbation. Kolmogorov's original paper was not completely detailed, and clarifying work was done independently in the early 1960s by Jürgen Moser and Vladimir Arnol'd (the latter had been a student of Kolmogorov). Since then, a large body of work on this subject within the mathematical theory of Hamiltonian dynamics has been assembled.

Thus, the so-called Kolmogorov–Arnol'd–Moser (KAM) theorem is not a single theorem but rather a body of work with a common theme, which can be roughly described as the persistence of quasi-periodic motions in perturbed systems. These results were a breakthrough in the understanding of the ergodic properties of dynamical systems. The original theorems dealt with Hamiltonian systems and their discrete analogues, while more recent results have been extended to volume-preserving systems, reversible systems, and dissipative systems.

The central ideas in Kolmogorov's original paper can be formulated as follows. Under some general assumptions, the phase space M^{2n} of an integrable Hamiltonian system is foliated by invariant tori: $\mathbb{T}^n$. This system will be referred to as the unperturbed system. In the neighborhood of each torus are defined action-angle variables $(I, \phi(\mathrm{mod}\, 2\pi))$, such that the Hamiltonian H_0 is the function of only action variables I.

The motion on each torus is conditionally periodic with frequency vector $\omega(I) = \partial H_0/\partial I$. A torus is said to be nonresonant if all the n frequencies are rationally independent (incommensurable). The unperturbed system is called nonresonant if the frequencies are functionally independent:

$$\det\left(\frac{\partial \omega}{\partial I}\right) = \det\left(\frac{\partial^2 H_0}{\partial I^2}\right) \neq 0\,.$$

In a nondegenerate system, the nonresonant tori form a dense set of full measure. The resonant tori form a set of measure zero, which, however, is also dense.

The system with the Hamiltonian

$$H(I, \phi, \varepsilon) = H_0(I) + \varepsilon H_1(I, \phi, \varepsilon)$$

is called the perturbed system, where the function εH_1 is the perturbation. Note that usually the perturbed system is no longer integrable. Kolmogorov's theorem

describes the fate of the nonresonant tori under perturbation.

Theorem (A.N. Kolmogorov). *If the unperturbed system is nondegenerate, then for a sufficiently small ε most nonresonant invariant tori do not vanish but are only slightly deformed, so that in the phase space of the perturbed system there are invariant tori densely filled with conditionally periodic phase curves winding around them, with the number of independent frequencies equal to the number of degrees of freedom. These invariant tori form a majority in the sense that the measure of the complement to their union is small when the perturbation is small.*

The persistence of quasi-periodic motion is consistent with numerical experiments, well-known examples being the standard map (also called the Chirikov map) and the Hénon–Heiles system.

Discussion

KAM theory has several important implications, in particular for the stability theory. Suppose that phase space is four-dimensional. A perturbed system always has one first integral, the Hamiltonian function $H(I, \phi, \varepsilon)$ itself. The energy levels $H = h$ are three-dimensional, while the invariant tori are two-dimensional. Thus, a trajectory that starts in a region between two invariant tori of the perturbed system is forever trapped in the region between the tori. This means that the values of the action variables remain forever near their initial values, which in turn implies stability.

If, however, the number n of degrees of freedom is greater than two, the n-dimensional tori do not separate the $(2n-1)$-dimensional energy level manifold into disjoint regions, and the invariant tori do not prevent a phase curve from wandering far away. There are examples of such drift, when the action variables change from their original value by a quantity of order 1, an effect known as "Arnol'd diffusion" (*See* **Arnol'd diffusion**). Although in the latter case the system is unstable, KAM theory does guarantee "metric stability," that is, stability for most initial conditions.

Examples

1. Assume the masses of the planets are sufficiently small compared with the mass of the Sun in the gravitational n-body problem. Then a large portion of the region of phase space corresponding to unperturbed motion of all planets (on identically oriented Keplerian ellipses having small eccentricities and inclinations) is filled up by conditionally periodic motions. KAM theory provides important estimates for the long-time evolution of such a system. Note that Henri Poincaré's groundbreaking work *Les méthodes nouvelles de la mécanique céleste* (1892) was motivated by questions of the stability of the solar system.
2. Consider the motion of a heavy rigid body fixed at a point. If the kinetic energy of the body is sufficiently large in comparison with its potential energy at the initial moment of time, then the length of the angular momentum vector and its inclination to the horizon remain forever near their initial values, provided that the initial values of the energy and the angular momentum differ sufficiently from values for which the body can rotate around its medium principal axis.
3. For plasma confinement in toroidal chambers, the plasma particles tend to follow magnetic field lines. The equations for these magnetic field lines can be put into Hamiltonian form. When the system is azimutally symmetric, the Hamiltonian is integrable, deviation from azimutal symmetry creates a perturbation, and KAM theory is applicable.

M.V. Deryabin and P.G. Hjorth

See also **Hénon–Heiles system; Standard map**

Further Reading

Arnol'd, V.I. 1962. The classical theory of perturbations and the problem of stability of planetary systems. *Soviet Mathematics Doklady*, 3: 1008–1012

Arnol'd, V.I. 1963. Proof of A.N. Kolmogorov's theorem on the preservation of quasiperiodic motions under small perturbations of the Hamiltonian. *Russian Mathematical Surveys*, 18(5): 9–36

Arnol'd, V.I. (editor). 1988. *Dynamical Systems III*, Berlin and New York: Springer

Kolmogorov, A.N. 1954. Théorie générale des systémes dynamiques et mécanique classique. In *Proceedings of the International Congress of Mathematicians*, vol. 1, Amsterdam: North-Holland, pp. 315–333

Moser, J.K. 1962. On invariant curves of area-preserving mappings of an annulus. *Nachrichten der Akademic der Wissenschatten in Goettingen II, Mathematisch-physikalische klasie* 1–20

KORTEWEG–DE VRIES EQUATION

Historical Introduction

The Korteweg–de Vries (KdV) equation, given here in canonical form,

$$u_t + 6uu_x + u_{xxx} = 0, \tag{1}$$

is widely recognized as a paradigm for the description of weakly nonlinear long waves in many branches of physics and engineering. Here, $u(x, t)$ is an appropriate field variable, t is the time, and x is the space coordinate in the relevant direction. It describes how waves evolve under the competing but comparable effects of weak nonlinearity and weak dispersion. Indeed, if it is supposed that x-derivatives scale as ε where ε is the small parameter characterizing long waves (i.e., typically the ratio of a relevant background length scale to a wavelength scale), then the amplitude scales as ε^2

and the time evolution takes place on a scale of ε^{-3}. The KdV equation is characterized by its family of solitary wave solutions,

$$u = a\,\mathrm{sech}^2(\gamma(x - Vt)),$$
$$\text{where} \quad V = 2a = 4\gamma^2. \tag{2}$$

This solution describes a family of steady isolated wave pulses of positive polarity, characterized by the wave number γ; note that the speed V is proportional to the wave amplitude a and also to the square of the wave number γ^2.

The KdV equation (1) owes its name to the famous paper of Diederik Korteweg and Hendrik de Vries, published in 1895, in which they showed that small-amplitude long waves on the free surface of water could be described by the equation

$$\zeta_t + c\zeta_x + \frac{3c}{2h}\zeta\zeta_x + \frac{ch^2}{6}\delta\zeta_{xxx} = 0. \tag{3}$$

Here, $\zeta(x,t)$ is the elevation of the free surface relative to the undisturbed depth h, $c = (gh)^{1/2}$ is the linear long wave phase speed, and $\delta = 1 - 3B$, where $B = \sigma/gh^2$ is the Bond number measuring the effects of surface tension ($\rho\sigma$ is the coefficient of surface tension and ρ is the water density). Transformation to a reference frame moving with the speed c (i.e., (x,t) is replaced by $(x - ct, t)$, and subsequent rescaling readily establishes the equivalence of (1) and (3). Although Equation (1) now bears the name KdV, it was apparently first obtained by Joseph Boussinesq (1877) (see Miles (1980) and Pego and Weinstein (1997) for historical discussions on the KdV equation). Korteweg and de Vries found the solitary wave solutions (2), and importantly, they showed that they are the limiting members of a two-parameter family of periodic traveling-wave solutions, described by elliptic functions and commonly called cnoidal waves,

$$u = b + a\,\mathrm{cn}^2(\gamma(x - Vt)|m),$$
$$\text{where} \quad V = 6b + 4(2m - 1)\gamma^2\,,\ a = 2m\gamma^2. \tag{4}$$

Here, $\mathrm{cn}(x|m)$ is the Jacobi elliptic function of modulus m $(0 < m < 1)$. As $m \to 1$, $\mathrm{cn}(x|m) \to \mathrm{sech}(x)$, and then the cnoidal wave (4) becomes the solitary wave (2), now riding on a background level b. On the other hand, as $m \to 0$, $\mathrm{cn}(x|m) \to \cos 2x$, and so the cnoidal wave (4) collapses to a linear sinusoidal wave (note that in this limit, $a \to 0$).

This solitary wave solution found by Korteweg and de Vries had earlier been obtained directly from the governing equations (in the absence of surface tension) independently by Boussinesq (1871, 1877) and Lord Rayleigh (1876), who were motivated to explain the now very well-known observations and experiments of John Scott Russell (1844). Curiously, it was not until quite recently that it was recognized that the KdV equation is not strictly valid if surface tension is taken into account and $0 < B < \frac{1}{3}$, as then there is a resonance between the solitary wave and very short capillary waves.

After the ground-breaking work of Korteweg and de Vries, interest in solitary water waves and the KdV equation declined until the dramatic discovery of the soliton by Zabusky and Kruskal in 1965. Through numerical integrations of the KdV equation, they demonstrated that the solitary wave (2) could be generated from quite general initial conditions, and could survive intact collisions with other solitary waves, leading them to coin the term *soliton*. Their remarkable discovery, followed almost immediately by the theoretical work of Gardner et al. (1967) showing that the KdV equation was *integrable* through an inverse scattering transform, led to many other startling discoveries and marked the birth of soliton theory as we know it today (*See* **Solitons, a brief history**). The implication is that the solitary wave is the key component needed to describe the behavior of long, weakly nonlinear waves.

An alternative to the KdV equation is the Benjamin–Bona–Mahony (BBM) equation in which the linear dispersive term $c\zeta_{xxx}$ in (3) is replaced by $-\zeta_{xxt}$. It has the same asymptotic validity as the KdV equation, and since it has rather better high wave number properties, it is somewhat easier to solve numerically. However, it is not integrable and, consequently, has not attracted the same interest as the KdV equation.

Both the KdV and BBM equations are uni-directional. A two-dimensional version of the KdV equation is the KP equation (Kadomtsev & Petviashvili, 1970),

$$(u_t + 6uu_x + u_{xxx})_x \pm u_{yy} = 0. \tag{5}$$

This equation includes the effects of weak diffraction in the y-direction, in that y-derivatives scale as ε^2 whereas x-derivatives scale as ε. Like the KdV equation it is an integrable equation. When the "+"-sign holds in (5), this is the KP2 equation, and it can be shown that then the solitary wave (2) is stable to transverse disturbances. On the other hand, if the "−"-sign holds, this is the KP1 equation for which the solitary wave is unstable; instead this equation supports "lump" solitons. Both KP1 and KP2 are integrable equations. To take account of stronger transverse effects and/or to allow for bi-directional propagation in the x-direction, it is customary to replace the KdV equation with a Boussinesq system of equations; these combine the long wave approximation to the dispersion relation with the leading-order nonlinear terms and occur in several asymptotically equivalent forms.

Although the KdV equation (1) is historically associated with water waves, it in fact occurs in many other physical contexts, where it arises as an asymptotic multiscale reduction from the relevant

governing equations. Typically, the outcome is

$$A_t + cA_x + \mu AA_x + \lambda A_{xxx} = 0. \tag{6}$$

Here, c is the relevant linear long wave speed for the mode whose amplitude is $A(x,t)$, while μ and λ, the coefficients of the quadratic nonlinear and linear dispersive terms, respectively, are determined from the properties of this same linear long wave mode and, like c, depend on the particular physical system being considered. Note that the linearization of (6) has the linear dispersion relation $\omega = ck - \lambda k^3$ for linear sinusoidal waves of frequency ω and wave number k; this expression is just the truncation of the full dispersion relation for the wave mode being considered, and immediately identifies the origin of the coefficient λ. Similarly, the coefficient μ can be identified with the an amplitude-dependent correction to the linear wave speed. Transformation to a reference frame moving with a speed c and subsequent rescaling shows that (6) can be transformed to the canonical form (1). Equations of the form (6) arise in the study of internal solitary waves in the atmosphere and ocean, mid-latitude and equatorial planetary waves, plasma waves, ion-acoustic waves, lattice waves, waves in elastic rods, and in many other physical contexts (see, for instance, Ablowitz & Segur, 1981; Dodd et al., 1982; Drazin & Johnson, 1989; Grimshaw, 2001).

In some physical situations, it is necessary to complement the KdV equation (6) with a higher-order cubic nonlinear term of the form $\nu A^2 A_x$. After transformation and rescaling, the amended equation (6) can be transformed to the so-called Gardner equation

$$u_t + 6uu_x + 6\delta u^2 u_x + u_{xxx} = 0. \tag{7}$$

Like the KdV equation, the Gardner equation is integrable by the inverse scattering transform. Here the coefficient δ can be either positive or negative, and the structure of the solutions depends crucially on which sign is appropriate. Again, in some physical situations, solitary waves propagate through a variable environment which means that the coefficients c, μ, and λ in (6) are functions of x, while an additional term $c(\sigma_x/2\sigma)A$ needs to be included, where $\sigma(x)$ is a magnification factor. After transforming to new variables, $\theta = (\int^x dx/c) - t, x$ with $U = \sigma^{1/2}u$, the variable-coefficient KdV equation is obtained,

$$U_x + \alpha(x)UU_\theta + \beta(x)U_{\theta\theta\theta} = 0. \tag{8}$$

Here, $\alpha = \mu/c\sigma^{1/2}$, $\beta = \lambda/c^3$. In general, this is not an integrable equation and must be solved numerically, although we shall exhibit some asymptotic solutions below. Another modification of the KdV equation occurs when it is necessary to take account of background rotation, leading to the rotation-modified KP equation (see, for instance, Grimshaw, 2001), in which a term $-f^2 u$ is added to the left-hand side of Equation (5), where f is a measure of the background rotation.

Solitons

The remarkable discovery of Gardner et al. (1967) that the KdV equation was integrable through an inverse scattering transform marked the beginning of soliton theory. Their pioneering work was followed by the work of Zakharov and Shabat (1972) which showed that another well-known nonlinear wave equation, the nonlinear Schrödinger equation, was also integrable by an inverse scattering transform. Their demonstration that the integrability of the KdV equation was not an isolated result, was followed closely by analogous results for the modified KdV equation (Wadati, 1972) and the sine-Gordon equation (Ablowitz et al., 1973). In 1974, Ablowitz, Kaup, Newell, and Segur provided a generalization and unification of these results in the AKNS scheme. From this point there has been an explosive and rapid development of soliton theory in many directions (see, for instance, Ablowitz & Segur, 1981; Dodd et al., 1982; Newell, 1985; Drazin & Johnson, 1989).

For the KdV equation (1) the starting point is the Lax pair (Lax, 1968) for an auxiliary function $\phi(x,t)$,

$$L\phi \equiv -\phi_{xx} - u\phi = \lambda\phi, \tag{9}$$

$$\phi_t = B\phi \equiv (u_x + C)\phi + (4\lambda - 2u)\phi_x. \tag{10}$$

Here, $C(t)$ depends on the normalization of ϕ. The first of these equations (9), with suitable boundary conditions at infinity (see below) defines a spectral problem for ϕ in the spatial variable x with a spectral parameter λ, and with the time variable t as a parameter. The second equation (10) then describes how the spectral function ϕ evolves in time. If it is now assumed that λ is independent of time (i.e., $\lambda_t = 0$ then the KdV equation (1) is just the compatibility condition for these two equations (9, 10); that is, it emerges as a result of the condition that $(\phi_{xx})_t = (\phi_t)_{xx}$. In terms of the operators L, B defined in the Lax pair (9,10), the KdV equation can be written in the symbolic form $L_t = BL - LB$ (Lax, 1968). This form indicates the path to further generalizations, in that other nonlinear wave equations can be obtained by choosing different operators L, B. The general strategy for integration of the KdV equation now consists of three steps. Here, we will describe the process under the hypothesis that we seek solutions $u(x,t)$ of the KdV equation (1), which decay to zero sufficiently fast as $x \to \pm\infty$ and have the initial condition $u(x,0) = u_0(x)$. First, we insert the initial condition into the spectral problem (9) to obtain the scattering data (these will be defined precisely below). Then (10) is used to move the scattering data forward in time; it transpires that is a very simple process, and note in particular that the spectral parameter λ is independent of t and hence is determined by the initial condition. The third step is to invert the scattering data at time $t > 0$ and so recover $u(x,t)$; this is the most difficult step, but for the KdV equation can be reduced

to solution of a linear integral equation. Thus, the three steps constitute a linear algorithm for the solution of the KdV equation, and it is in this sense that it is said that the Lax pair (9,10) constitutes integrability of the KdV equation.

The spectral problem (9) for the KdV equation consists of two parts. The *discrete* spectrum is found by seeking solutions such that $\phi \to 0$ as $x \to \pm\infty$, which requires that $\lambda < 0$. It can be shown that there then exists a *finite* set of discrete eigenvalues $\lambda = -\kappa_n^2$, $n = 1, 2, \ldots, N$, and corresponding real eigenfunctions ϕ_n such that

$$\phi_n \sim c_n \exp(-\kappa_n x) \quad \text{as} \quad x \to \infty. \tag{11}$$

There is a similar condition as $x \to -\infty$, namely, that $\phi_n \sim d_n \exp(\kappa_n x)$. The real constants c_n, d_n are determined once the normalization condition is satisfied, that is,

$$\int_{-\infty}^{\infty} \phi_n^2 \, \mathrm{d}x = 1. \tag{12}$$

The continuous spectrum consists of all $\lambda > 0$, and so we set $\lambda = k^2$ where k is real. Then we define the scattering problem for solutions $\phi(x; k)$ of (9) by the boundary conditions,

$$\phi \sim \exp(-\mathrm{i}kx) + R(k)\exp(\mathrm{i}kx) \quad \text{as } x \to \infty, \tag{13}$$

$$\phi \sim T(k)\exp(-\mathrm{i}kx) \quad \text{as} \quad x \to -\infty. \tag{14}$$

The scattering data then consists of the set $(\kappa_n, c_n, n = 1, 2, \ldots, N)$ together with the reflection coefficient $R(k)$. It is useful to note that $R(k)$ may be continued into the upper half of the complex k-plane, has there a set of simple poles at $k = \mathrm{i}\kappa_n$, and $R \to 1$ as $|k| \to \infty$.

The next step is to determine from (10) how the scattering data evolves in time (note that the dependence on time t has been suppressed in the preceding paragraph). First, we recall that the discrete eigenvalues κ_n are independent of t. Next, we multiply (10) by ϕ_n and integrate the result over all x; also, on using (9), it is readily found that

$$\frac{\mathrm{d}}{\mathrm{d}t}\int_{-\infty}^{\infty} \phi_n^2 \, \mathrm{d}x = C_n \int_{-\infty}^{\infty} \phi_n^2 \, \mathrm{d}x,$$

where the constant C in (10) here must be indexed with n to become C_n. But then the normalization condition (12) implies that $C_n = 0$. Now substitute (11) into (10) to show that

$$\frac{\mathrm{d}c_n}{\mathrm{d}t} = 4\kappa_n^3 c_n$$
$$\text{so that} \quad c_n(t) = c_n(0)\exp(\kappa_n^3 t). \tag{15}$$

For the continuous spectrum, the asymptotic expressions (13), (14) are substituted into (10). Now it is found that the constant $C(k) = 4\mathrm{i}k^3$, and that

$$\frac{\mathrm{d}R}{\mathrm{d}t} = 8\mathrm{i}k^3 R$$
$$\text{so that} \quad R(k; t) = R(0; k)\exp(8\mathrm{i}k^3 t). \tag{16}$$

Similarly, it can be shown that $T(k; t) = T(k; 0)$.

The final step is the inversion of the scattering data at time t to recover the potential $u(x, t)$ in 9). This is accomplished through the Marchenko integral equation for the function $K(x, y)$

$$K(x, y) + F(x + y) + \int_x^{\infty} K(x, z)\, F(y + z)\, \mathrm{d}z = 0. \tag{17}$$

Here the function $F(x)$ is known in terms of the scattering data at time t,

$$F(x) = \sum_{n=1}^{N} c_n^2(t)\exp(-\kappa_n x) + \frac{1}{2\pi}\int_{-\infty}^{\infty} R(k; t)\, \exp(\mathrm{i}kx)\, \mathrm{d}k. \tag{18}$$

Here the t-dependence of K, F has been suppressed as the linear integral equation (17) is solved with t fixed. Then

$$u(x, t) = 2\frac{\partial}{\partial x}\{K(x, x; t)\}, \tag{19}$$

where the t-dependence in K has been restored.

The inverse scattering transform described by (17), (18) enables one to find the solution of the KdV equation (1) for an arbitrary localized initial condition. The most important outcome is that as $t \to \infty$, the solution evolves into N rank-ordered solitons propagating to the right ($x > 0$), and some decaying radiation propagating to the left ($x < 0$),

$$u \sim \sum_{n=1}^{N} 2\kappa_n^2 \operatorname{sech}^2(\kappa_n(x - 4\kappa_n^2 t - x_n)) + \text{radiation}. \tag{20}$$

Here the N solitons are derived directly from the discrete spectrum, where each eigenvalue $-\kappa_n$ generates a soliton of amplitude $2\kappa_n^2$, while the phase shifts x_n are determined from the constants $c_n(0)$. The continuous spectrum is responsible for the decaying radiation, which decays at each fixed $x < 0$ as $t^{-1/3}$.

The important special case when the reflection coefficient $R(k) \equiv 0$ leads to the N-soliton solution, for which there is no radiation. Indeed, the N-soliton solution can be obtained as an explicit solution of the Marchenko equation (17). We illustrate the procedure for $N = 1, 2$. First, for $N = 1$, $F(x) = c^2 \exp\kappa(x - 4\kappa^2 t)$, where we have omitted the subscript $n = 1$ for simplicity. Then seek a solution of

(17) in the form $K(x, y, t) = L(x, t)\exp(-\kappa y)$, where L can be found by simple algebra. The outcome is that

$$L(x,t) = \frac{-2\kappa c(0)^2 \exp(-\kappa x + 8\kappa^2 t)}{2\kappa + c(0)^2 \exp(-2\kappa x + 8\kappa^2 t)}.$$

Finally u is found from (19),

$$u = 2\kappa^2 \mathrm{sech}^2(\kappa(x - 4\kappa^2 t) - x_1).$$

This is just the solitary wave (2) of amplitude $2\kappa^2$; the phase shift x_1 is such that $c(0)^2 = 2\kappa \exp(2\kappa x_1)$. The procedure for $N = 2$ follows a similar course. Thus, with $R \equiv 0, N = 2$ in F (18), seek a solution of the Marchenko equation (17) in the form $K(x, y, t) = L_1(x, t)\exp(-\kappa_1 y) + L_2(x, t)\exp(-\kappa_2 y)$, and again $L_{1,2}$ can be found by simple algebra. The outcome is the two-soliton solution. For instance, with $\kappa_1 = 1, \kappa_2 = 2$, this is

$$u = 12\frac{3 + 4\cosh(2x - 8t) + \cosh(4x - 64t)}{[3\cosh(x - 28t) + \cosh(3x - 36t)]^2}. \quad (21)$$

It can be readily shown that

$$u \sim 8\mathrm{sech}^2(2(x - 16t \mp x_2) + 2\mathrm{sech}^2(x - 4t \mp x_1) \quad \text{as} \quad t \to \pm\infty, \quad (22)$$

where the phase shifts $x_{1,2} = (-\frac{1}{2}, \frac{1}{4})\ln 3$. Thus, the two-soliton solution describes the elastic collision of two solitons, in which each survives the interaction intact, and the only memory of the collision is the phase shifts; note that $x_1 < 0, x_2 > 0$, so that the larger soliton is displaced forward and the smaller soliton is displaced backward. The general case of an N-soliton is analogous and is essentially a sequence of pair-wise two-soliton interactions.

The integrability of the KdV equation (1) is also characterized by the existence of an infinite set of independent conservation laws. The most transparent conservation laws are

$$\int_{-\infty}^{\infty} u\,\mathrm{d}x = \text{constant}, \quad (23)$$

$$\int_{-\infty}^{\infty} u^2\,\mathrm{d}x = \text{constant}, \quad (24)$$

$$\int_{-\infty}^{\infty} \left(u^3 - \frac{1}{2}u_x^2\right)\mathrm{d}x = \text{constant}, \quad (25)$$

which may be associated with the conservation of mass, momentum, and energy, resepectively. Indeed (23) is obtained from the KdV equation (1) by integrating over x, while (24), (25) are obtained in an analogous manner after first multiplying (1) by u, u^2, respectively. However, it transpires that these are just the first three conservation laws in an infinite set, where each successive conservation law contains a higher power of u than the preceding one. This may be demonstrated using the inverse scattering transform (see Ablowitz & Segur, 1981; Dodd et al., 1982; Newell, 1985). However, here we use the original method based on the Miura transformation as adapted by Gardner. The Miura transformation is

$$u = -v_x - v^2, \quad (26)$$

$$v_t - 6v^2 v_x + v_{xxx} = 0. \quad (27)$$

Here (27) is the modified KdV equation. Direct substitution of (26) into the KdV equation shows that if v solves the modified KdV equation (27), then u solves the KdV equation (1). This discovery was the starting point for the discovery of the inverse scattering transform, since if one considers (26) as an equation for v and writes $v = \phi_x/\phi$, followed by a Galilean transformation for u (i.e., $u \to u - \lambda, x \to x - 6\lambda t$), one obtains the spectral problem (9). Here we follow a different route and write

$$v = \frac{1}{2\varepsilon} - \varepsilon w,$$

which (after a shift $x \to x + 3t/2\varepsilon^2$) converts the mKdV equation (27) into the Gardner equation (7) with $\delta = -\varepsilon^2$. Apart from a constant, which may be removed by a Galilean transformation, the corresponding expression for u is the Gardner transformation,

$$u = w + \varepsilon w_x - \varepsilon^2 w^2. \quad (28)$$

Thus, if w solves the Gardner equation

$$w_t + 6ww_x - 6\varepsilon^2 w^2 w_x + w_{xxx} = 0, \quad (29)$$

then u solves the KdV equation (1).

Next, we observe that the Gardner equation (29) has the conservation law

$$\int_{-\infty}^{\infty} w\,\mathrm{d}x = \text{constant}. \quad (30)$$

Since $w \to u$ as $\varepsilon \to 0$, we write the formal asymptotic expansion

$$w \sim \sum_{n=0}^{\infty} \varepsilon^n w_n.$$

It follows from (30) that then

$$\int_{-\infty}^{\infty} w_n\,\mathrm{d}x = \text{constant},$$

for each $n = 0, 1, 2, \ldots$. But substitution of this same asymptotic expansion for w into (28) generates a sequence of expressions for w_n in terms of u, of which the first few are

$$w_0 = u\,, \quad w_1 = -u_x\,, \quad w_2 = -u^2 + u_{xx}.$$

Thus, we see that $n = 0, 2$ give the conservation laws (23), (24), respectively, while $n = 1$ is an exact differential. It may now be shown that all even values of

n yield nontrivial and independent conservation laws, while all odd values of n are exact differentials.

The KdV equation belongs to a class of nonlinear wave equations, which have Lax pairs and are integrable through an inverse scattering transform. It shares with these equations several other remarkable features, such as the Hirota bilinear form, Bäcklund transformations, and the Painlevé property. Detailed descriptions of these and other properties of the KdV equation can be found in the other entries and referenced texts.

Solitary Waves in a Variable Environment

In a variable environment, the governing equation which replaces (1) is the variable-coefficient KdV equation (8). In general, this is not an integrable equation and is usually solved numerically. However, there are two distinct limiting situations in which some analytical progress can be made. First, let it be supposed that the coefficients $\alpha(x), \beta(x)$ in (8) vary rapidly with respect to the wavelength of a solitary wave, and then consider the case when these coefficients make a rapid transition from the values α_-, β_- in $x<0$ to the values α_+, β_+ in $x>0$. Then a steady solitary wave can propagate in the region $x<0$, given by

$$U = a\mathrm{sech}^2(\gamma(\theta - Wx)),$$
$$\text{where} \quad W = \frac{\alpha_- a}{3} = 4\beta_-\gamma^2. \tag{31}$$

It will pass through the transition zone $x \approx 0$ essentially without change. However, on arrival into the region $x>0$, it is no longer a permissible solution of (8), which now has constant coefficients α_+, β_+. Instead, with $x=0$, expression (31) now forms an effective initial condition for the new constant-coefficient KdV equation. Using the spectral problem (9) and the inverse scattering transform, the solution in $x>0$ can now be constructed; indeed, in this case, the spectral problem (9) has an explicit solution (e.g., Drazin & Johnson, 1989). The outcome is that the initial solitary wave *fissions* into N solitons and some radiation. The number N of solitons produced is determined by the ratio of coefficients $R = \alpha_+\beta_-/\alpha_-\beta_+$. If $R>0$ (i.e., there is no change in polarity for solitary waves), then $N = 1 + [((8R+1)^{1/2} - 1)/2]$ ($[\cdots]$ denotes the integral part); as R increases from 0, a new soliton (initially of zero amplitude) is produced as R successively passes through the values $m(m+1)/2$ for $m = 1, 2, \ldots$. But if $R<0$ (i.e., there is a change in polarity), no solitons are produced and the solitary wave decays into radiation. For instance, for water waves, $c = (gh)^{1/2}$, $\mu = 3c/2h$, $\lambda = ch^2/6$, $\sigma = c$, and so $\alpha = 3/(2hc^{1/2})$, $\beta = h^2/(6c^2)$, where h is the water depth. It can then be shown that a solitary water wave propagating from a depth h_- to a depth h_+ will fission into N solitons where N is given as above with $R = (h_-/h_+)^{9/4}$; if $h_- > h_+$, $N \geq 2$, but if $h_- < h_+$ then $N=1$ and no further solitons are produced (Johnson, 1973).

Next, consider the opposite situation when the coefficients $\alpha(x), \beta(x)$ in (8) vary slowly with respect to the wavelength of a solitary wave. In this case a multi-scale perturbation technique (see Grimshaw, 1979, or Grimshaw & Mitsudera, 1993) can be used in which the leading term is

$$U \sim A\mathrm{sech}^2\gamma\left(\theta - \int_{x_0}^{x} W\,\mathrm{d}x\right), \tag{32}$$

where

$$W = \frac{\alpha A}{3} = 4\beta\gamma^2. \tag{33}$$

Here the wave amplitude $a(x)$ and, hence, also $W(x), \gamma(x)$ are slowly varying functions of x. Their variation is most readily determined by noting that the variable-coefficient KdV equation (8) possesses a conservation law,

$$\int_{-\infty}^{\infty} U^2\,\mathrm{d}\theta = \text{constant}, \tag{34}$$

which expresses conservation of wave-action flux. Substitution of (32) into (34) gives

$$\frac{2A^2}{3\gamma} = \text{constant},$$
$$\text{so that} \quad A = \text{constant}\left(\frac{\beta}{\alpha}\right)^{1/3}. \tag{35}$$

This is an explicit equation for the variation of the amplitude $A(x)$ in terms of $\alpha(x), \beta(x)$. However, the variable-coefficient KdV equation (8) also has a conservation law for mass,

$$\int_{-\infty}^{\infty} U\,\mathrm{d}\theta = \text{constant}. \tag{36}$$

Thus, although the slowly varying solitary wave conserves wave-action flux, it cannot simultaneously conserve mass. Instead, it is accompanied by a trailing shelf of small amplitude but long length scale given by U_s, so that the conservation of mass gives

$$\int_{-\infty}^{\phi} U_s\,\mathrm{d}\theta + \frac{2A}{\gamma} = \text{constant},$$

where $\phi = \int_{x_0}^{x} W\,\mathrm{d}x$ ($\theta = \phi$ gives the location of the solitary wave) and the second term is the mass of the solitary wave (32). Differentiation then yields the amplitude $U_- = U_s(\theta = \phi)$ of the shelf at the rear of the solitary wave,

$$U_- = \frac{3\gamma_x}{\alpha\gamma^2}. \tag{37}$$

This shows that if the wavelength γ^{-1} increases (decreases) as the solitary wave deforms, then the trailing shelf amplitude U_- has the opposite (same)

polarity as the solitary wave. Once U_- is known, the full shelf $U_s(\theta, x)$ is found by solving (8) with the boundary condition that $U_s(\theta = \phi) = U_-$ (see El & Grimshaw, 2002, where it is shown that the trailing shelf may eventually generate secondary solitary waves).

For a solitary water wave propagating over a variable depth $h(x)$, these results show that the amplitude varies as h^{-1}, while the trailing shelf has positive (negative) polarity relative to the wave itself accordingly as $h_x < (>)\ 0$. A situation of particular interest occurs if the coefficient $\alpha(x)$ changes sign at some particular location (note that in most physical systems the coefficient β of the linear dispersive term in (8) does not vanish for any x). This commonly arises for internal solitary waves in the coastal ocean, where typically in the deeper water, $\alpha < 0$, $\beta > 0$ so that internal solitary waves propagating shorewards are waves of depression. But in shallower water, $\alpha > 0$ and so only internal solitary waves of elevation can be supported. The issue then arises as to whether an internal solitary wave of depression can be converted into one or more solitary waves of elevation as the critical point, where α changes sign, is traversed. This problem has been intensively studied (see, for instance, Grimshaw et al., 1998 and the references therein), and the solution depends on how rapidly the coefficient α changes sign. If α passes through zero rapidly compared with the local width of the solitary wave, then the solitary wave is destroyed and converted into a radiating wave train (see the discussion above in the first paragraph of this section). On the other hand, if α changes sufficiently slowly for the present theory to hold (i.e., (35) applies), we find that as $\alpha \to 0$, then $A \to 0$ in proportion to $|\alpha|^{1/3}$, while $U_- \to \infty$ as $|\alpha|^{-8/3}$. Thus, as the solitary wave amplitude decreases, the amplitude of the trailing shelf, which has the opposite polarity, grows indefinitely until a point is reached just prior to the critical point where the slowly varying solitary wave asymptotic theory fails. A combination of this trailing shelf and the distortion of the solitary wave itself then provide the appropriate "initial" condition for one or more solitary waves of the opposite polarity to emerge as the critical point is traversed. However, it is clear that in situations, as here, where $\alpha \approx 0$, it will be necessary to include a cubic nonlinear term in (8), thus converting it into a variable-coefficient Gardner equation (cf. (7)). This case has been studied by Grimshaw et al. (1999), who show that the outcome depends on the sign of the coefficient (ν) of the cubic nonlinear term at the critical point. If $\nu > 0$, so that solitary waves of either polarity can exist when $\alpha = 0$, then the solitary wave preserves its polarity (i.e., remains a wave of depression) as the critical point is traversed. On the other hand, if $\nu < 0$, so that no solitary wave can exist when $\nu = 0$, then the solitary wave of depression may be converted into one or more solitary waves of elevation.

ROGER GRIMSHAW

See also **Inverse scattering method or transform; Kadomtsev–Petviashvili equation; Solitons; Water waves**

Further Reading

Ablowitz, M.J., Kaup, D.J., Newell, A.C. & Segur, H. 1973. Method for solving the sine-Gordon equation. *Physcs Letters*, 30: 1262–1264

Ablowitz, M.J., Kaup, D.J., Newell, A.C. & Segur, H. 1974. The inverse scattering transform–Fourier analysis for nonlinear problems. *Studies in Applied Mathematics*, 53: 249–315

Ablowitz, M.J. & Segur, H. 1981. *Solitons and the Inverse Scattering Transform*, Philadelphia: SIAM

Boussinesq, M.J. 1871. Theórie de l'intumescence liquid appellée onde solitaire ou de translation, se propageant dans un canal rectangulaire. *Comptes Rendus Acad. Sci (Paris)*, 72: 755–759

Boussinesq, M.J. 1877. Essai sur la theorie des eaux courantes, *Memoires presentees par diverse savants a l'Academie des Sciences Inst. France (Series 2)* 23: 1–680

Dodd, R.K., Eilbeck, J.C., Gibbon, J.D. & Morris, H.C. 1982. *Solitons and Nonlinear Wave Equations*, London: Academic

Drazin, P.G. & Johnson, R.S. 1989. *Solitons: An Introduction*, Cambridge and New York: Cambridge University Press

El, G.A. & Grimshaw, R. 2002. Generation of undular bores in the shelves of slowly-varying solitary waves. *Chaos*, 12: 1015–1026

Gardner, C.S., Greene, J.M., Kruskal, M.D. & Miura, R.M. 1967. Method for solving the Korteweg–de Vries equation. *Physical Review Letters*, 19: 1095–1097

Grimshaw, R. 1979. Slowly varying solitary waves. I Korteweg–de Vries equation. *Proceedings of the Royal Society*, 368A: 359–375

Grimshaw, R. 2001. Internal solitary waves. In *Environmental Stratified Flows*, edited by Boston: Kluwer, Chapter 1: 1–28

Grimshaw, R. & Mitsudera, H. 1993. Slowly-varying solitary wave solutions of the perturbed Korteweg–de Vries equation revisited. *Studies in Applied Mathematics*, 90: 75–86

Grimshaw, R., Pelinovsky, E. & Talipova, T. 1998. Solitary wave transformation due to a change in polarity. *Studies in Applied Mathematics*, 101: 357–388

Grimshaw, R., Pelinovsky, E. & Talipova, T. 1999. Solitary wave transformation in a medium with sign-variable quadratic nonlinearity and cubic nonlinearity. *Physica* D, 132: 40–62

Johnson, R.S. 1973. On the development of a solitary wave moving over an uneven bottom. *Proceedings of the Cambridge Philosophical Society*, 73: 183–203

Kadomtsev, B.B. & Petviashvili, V.I. 1970. On the stability of solitary waves in weakly dispersive media. *Soviet Physics Doklady*, 15: 539–541

Korteweg, D.J. & de Vries, H. 1895. On the change of form of long waves advancing in a rectangular canal, and on a new type of long stationary waves. *Philosophical Magazine*, 39: 422–443

Lax, P.D. 1968. Integrals of nonlinear equations of evolution and solitary waves. *Communications in Pure and Applied Mathematics*, 21: 467–490

Miles, J.W. 1980. Solitary waves. *Annual Review of Fluid Mechanics* 12: 11–43

Newell, A.C. 1985. Solitons in mathematics and physics. In *CBMS-NSF Series in Applied Mathematics*, Vol. 48, edited by Philadelphia: SIAM

Pego, R.L. & Weinstein, M.J. 1997. Convective linear stability of solitary waves for Boussinesq equations. *Studies in Applied Mathematics*, 99: 311–375
Rayleigh, Lord. 1876. On waves. *Philosophical Magazine* 1: 257–279
Russell, J.S. 1844. Report on waves, *14th Meeting of the British Association for the Advancement of Science*, pp. 311–390
Wadati, M. 1972. The exact solution of the modified Kortewegde Vries equation. *Journal of the Physical Society of Japan*, 32: 62–69
Zabusky, N.J. & Kruskal, M.D. 1965. Interactions of solitons in a collisionless plasma and the recurrence of initial states. *Physical Review Letters*, 15: 240–243
Zakharov, V.E. & Shabat, A.B. (1972). Exact theory of two-dimensional self focussing and one dimensional self-modulation of waves in nonlinear media. *Soviet Physics JETP*, 34: 62–69

KRYLOV–BOGOLYUBOV METHOD

See **Quasilinear analyses**

KURAMOTO–SIVASHINSKY EQUATION

Derived by Yoshiki Kuramoto and Takeo Tsuzuki in the context of reaction-diffusion systems (Kuramoto & Tsuzuki, 1975, 1976), and by Gregory Sivashinsky in the study of flame front propagation (Sivashinsky, 1977), the Kuramoto–Sivashinsky equation (KS) is a prime example of a system that possesses a rich variety of spatial and temporal behaviors. The mathematical and statistical (thermodynamic) analyses and classification of both elementary solutions and observed complex behaviors have generated many advances in the understanding of the often complex patterns that arise in many experimental simulations.

The KS equation in one spatial dimension may be written

$$u_t + uu_x + u_{xx} + u_{xxxx} = 0, \qquad (1)$$

where the subscripts denote the partial derivatives w.r.t. the space variable x, and the time variable t. One important class of solutions is defined by a periodic boundary condition, say, with a $2\pi L$-periodicity. Here we may interpret such solutions as being restricted to a cell of size $2\pi L$ and the cellular state size serving as the control (or bifurcation) parameter. For small values of $L > 0$, the solutions of (1) behave periodically; then as L is increased, the system passes through a wide variety of behavior including exhibiting spatiotemporal chaos. Via a simple rescaling, the parameter dependence can be made explicit in (1), and the solutions then satisfy $u(x,t) = u(x + 2\pi, t)$. Equation (1) possesses both translation and Galilean symmetries.

Physically, the form of Equation (1) models the small perturbations from a reference Poiseuille flow of a film layer on an inclined plane (Pumir et al., 1983). The name KS often refers in the literature to the closely related equation formed by letting $u = w_x$ in (1) and integrating. Higher-dimensional equivalents of this form are found in the independent derivations of Kuramoto and Sivashinsky. The first is in the context of angular-phase turbulence for a system of reaction-diffusion equations modeling the Belouzov–Zabotinsky reaction in three spatial dimensions. Here, the solution is considered to be a small perturbation of a global periodic solution. The Sivashinsky laminar flame front derivation models small thermal diffusive instabilities, where the solution is the perturbation of an unstable planar front in the direction of propagation. Further derivations of the system can be found in the review by Nicolaenko (1986) and references therein.

The KS equation has been shown to posses an inertial manifold, that is, the infinite-dimensional solution space of the system is spanned by the solutions to a coupled system of ordinary differential equations with a low number of degrees of freedom (Foias et al., 1988). Hence, the system may be effectively studied by Fourier mode expansion, where the number of Fourier modes determining the dynamics is proportional to L.

The nontrivial behavior of the KS equation stems from the linear instability of the laminar state $u(x,t) = \text{constant}$—the evolution of the system is governed by the quadratic nonlinear coupling term uu_x and a second-order instability term u_{xx} that is balanced by the dissipation term u_{xxxx}. Long-wavelength k-numbered modes with $k < L$ are unstable. However, the linearly unstable low modes of the system are stabilized by the strong nonlinear coupling while the extremely stable high modes, with intermediate wavelengths with mode number $k \sim L$ play the important role of maintaining a "chaotic dynamical equilibrium."

For $L \geq 1$, standing and traveling waves may coexist with solutions having complicated oscillatory behavior. For example, antisymmetrically pulsating standing waves and waves that change both form and velocity periodically with time are considered in Demekhin et al. (1991). There exist windows of the parameter L in which many of these cellular states are stable. Windows of intermittency and strange (chaotic) attractors are also observed. For L not too large, these complex motions can be reached quite suddenly after extremely long transients. Figure 1 displays typical evolution once transients have died away. The KS equation also possesses persistent homoclinic and heteroclinic saddle connections which can be effectively explained via symmetry arguments (Kevrekidis et al., 1990).

The KS equation may be damped by the addition of the term νu on the left-hand side of (1), where ν parameterizes the level of damping. For zero damping the KS equation exhibits highly chaotic motions for large L. In the transition to these weakly turbulent motions, temporal intermittency is observed. Here, chaotic motions passing close to simple and weakly unstable states will feel regularizing effects for a

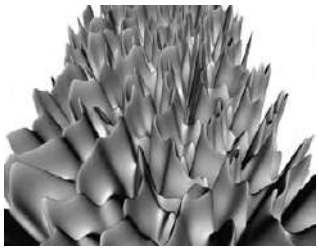

Figure 1. Spatiotemporally chaotic solution $u(x, t)$, computed from a 64-d Fourier truncation at $L = 10$. Coordinate x horizontal, amplitude u vertical, with plots of different times t overlapped at t progresses.

short while, for example. However, for large L and with damping, the intermittent behavior in the transition to weak turbulence also has a spatial element (Chaté & Manneville, 1986). In this scenario, a fluctuating mixture of both regular and chaotic patches with well-defined boundaries are observed in the solution surface $u(x, t)$. Choosing the parameters so that a weakly turbulent solution can be reached by spatiotemporal intermittency, one will observe chaotic domains slowly occupying the system; setting parameter values below such a threshold one will see the domains recede.

SAM GRATRIX AND JOHN N. ELGIN

See also **Belousov–Zhabotinsky reaction; Chaotic dynamics; Pattern formation; Turbulence**

Further Reading

Chang, H.-C. 1986. Travelling waves on fluid interfaces: normal form analysis of the Kuramoto–Sivashinsky equation. *The Physics of Fluids*, 29(10): 3142–3147

Chaté, H. & Manneville, P. 1986. Transition to turbulence via spatiotemporal intermittency. *Physical Review Letters*, 58(2): 112–115

Christiansen, F., Cvitanović, P. & Putkaradze, V. 1997. Spatiotemporal chaos in terms of unstable recurrent patterns. *Nonlinearity*, 10(1): 55–70

Demekhin, Y.A., Tokarev, G.Yu. & Shkadov, Ya.V. 1991. Hierarchy of bifurcations of space-periodic structures in a nonlinear model of active dissipative media. *Physica* D, 52 (2–3): 338–361

Elgin, J.N. & Wu, X. 1996. Stability of cellular states of the Kuramoto–Sivashinsky equation. *SIAM Journal on Applied Mathematics*, 56(6): 1621–1638

Foias, C., Nicolaenko, B., Sell, G.R. & Temam, R. 1988. Inertial manifolds for the Kuramoto–Sivashinsky equation and estimates of their dimension. *Journal de Mathématiques Pures et Appliquèes. Neuvième Série*, 67(3): 197–226

Hooper, P.A. & Grimshaw, R. 1988. Travelling wave solutions of the Kuramoto–Sivashinsky equation. *Wave Motion*, 10(5): 405–420

Kent, P. 1992. *Bifurcations of the travelling-wave solutions of the Kuramoto–Sivashinsky equation*, PhD Thesis, University of London

Kevrekidis, J.G., Nicolaenko, B. & Scovel, J.G. 1990. Back in the saddle again: A computer assisted study of the Kuramoto–Sivashinsky equation. *SIAM Journal on Applied Mathematics*, 50(3): 760–790

Kuramoto, Y. & Tsuzuki, T. 1975. On the formation of dissipative structures in reaction–diffusion systems. *Progress of Theoretical Physics*, 54(2): 687–699

Kuramoto, Y. & Tsuzuki, T. 1976. Persistent propagation of concentration waves in dissipative media far from thermal equilibrium. *Progress of Theoretical Physics*, 55(2): 356–369

Michelson, D. 1986. Steady solutions of the Kuramoto–Sivashinsky equation. *Physica* D, 19(1): 89–111

Nicolaenko, B. 1986. Some mathematical aspects of flame chaos and flame multiplicity. *Physica D*, 20(1): 109–121

Nicolaenko, B., Scheurer, B. & Temam, R. 1985. Some global dynamical properties of the Kuramoto–Sivashinsky equations: nonlinear stability and attractors. *Physica* D, 16(2): 155–183

Pumir, A., Manneville, P. & Pomeau, Y. 1983. On solitary waves running down an inclined plane. *Journal of Fluid Mechanics*, 135: 27–50

Sivashinsky, G.I. 1977. Nonlinear analysis of hydrodynamic instability in laminar flames: I. Derivation of basic equations. *Acta Astronautica*, 4(11–12): 1177–1206

L

LABORATORY MODELS OF NONLINEAR WAVES

In the decade following his 1834 discovery of the hydrodynamic solitary wave on Edinburgh's Union Canal, John Scott Russell constructed a water tank, allowing nonlinear wave phenomena to be studied in a laboratory environment (Russell, 1844). Among other results of these experiments, Russell observed, first, that the speed (v) of a solitary wave is related to its height (h) by the empirical relation $v = \sqrt{g(d+h)}$, where d is the resting depth of the water and g is the acceleration of gravity. Second, two solitary waves pass smoothly through each other without scattering. Third, two or more solitary waves can be generated from a sufficiently large "initial heap" of water. In the case sketched in Figure 1, for example, a volume (V) of water is released (by raising a sliding panel at the left-hand side of the tank) that is sufficiently large to generate two hydrodynamic solitons but not large enough to generate three of them. Also the soliton of larger amplitude is observed to have a higher velocity, leading to a separation between the two components that increases with time.

Since Russell's seminal work, hydrodynamic wave tanks have been widely used to investigate nonlinear wave propagation in a variety of settings, and several tanks suitable for undergraduate laboratories have been developed and described (Bettini et al., 1983; Olsen et al., 1984; Remoissenet, 1999). Tank experiments allow students to quantitatively investigate various properties of the Korteweg–de Vries (KdV) equation, which can be written in normalized form as

$$\frac{\partial u}{\partial t} + \frac{\partial u}{\partial x} + u\frac{\partial u}{\partial x} + \frac{\partial^3 u}{\partial x^3} = 0, \qquad (1)$$

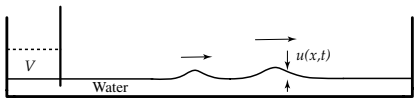

Figure 1. A sketch of John Scott Russell's wave tank, generating two solitons.

where $u(x, t)$ represents the vertical displacement of the wave from its resting level. Such experiments include quantitative comparisons of the number of solitons produced by an initial amount of water V as determined by eigenvalues of the corresponding time-independent linear Schrödinger equation through the inverse scattering transform method (Olsen et al., 1984). Similar tank experiments on deep water (where the depth is much larger than the lateral extent of the waves) allow quantitative studies of the nonlinear Schrödinger equation (Remoissenet, 1999).

In addition to wave tanks, mechanical wave models have been constructed for other nonlinear systems, including mechanical models of the normalized sine-Gordon (SG) equation

$$\frac{\partial^2 u}{\partial x^2} - \frac{\partial^2 u}{\partial t^2} = \sin u. \qquad (2)$$

As shown in the model of Figure 2, a number of pendula (dressmaker pins) are connected to a longitudinal spring (elastic band), whereupon $u(x, t)$ is the angle of rotation of the pendulum located at position x as a function of time t. The first term in Equation (2) represents the elastic restoring torque between adjacent pendula, the second term represents their angular acceleration, and the right-hand term is the angular-dependent torque of gravity. With a bit of practice, this simple model allows one to observe and demonstrate kink propagation, kink-kink collisions, breathers, and kink-antikink annihilation (Scott, 1969, 1970). The latter, in turn, is a model for electron-positron annihilation in elementary-particle physics.

More detailed mechanical models of the SG equation have been designed and constructed, which are suitable for undergraduate laboratory experiments (Scott, 1969, 1970; Remoissenet, 1999). As is evident from Figure 3, such models allow quantitative studies of the Lorentz contraction experienced by a kink as it approaches the limiting speed (Mach 1) of the system. For research purposes, Matteo Cirillo developed a mechanical model of fluxon propagation on a long Josephson junction, including an adjustable torque on the pendula (from air jets) that models the bias current acting in a

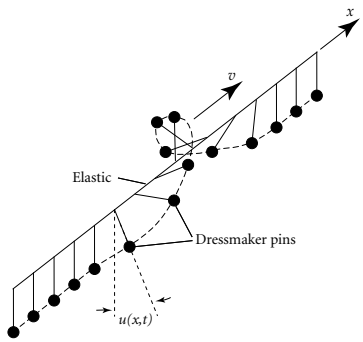

Figure 2. A kink on a simple mechanical model of the sine-Gordon equation that can be made from dressmaker pins and an elastic band.

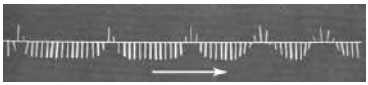

Figure 3. Strobe photos of an SG kink propagating on a mechanical model that was designed for student experiments (Scott, 1969). The kink is traveling to the right and slowing down due to friction. Spacing between the pendula is 1.59 cm and the time between successive images is 0.6 s.

typical experiment (Cirillo et al., 1981). Also, Michel Remoissenet and his colleagues have developed a model of the nonlinear Klein–Gordon equation with a double-well potential (the "phi-fourth model") to study the properties of compactons and the propagation of domain walls in ferroelectric and ferromagnetic materials (Duseul, 1998).

Complementing the family of mechanical models for nonlinear wave phenomena are nonlinear electrical transmission lines (Scott, 1970; Ostrovsky et al., 1972; Lonngren, 1978; Remoissenet, 1999). In energy-conserving versions of these models, nonlinearity is usually introduced through voltage-dependent capacitors (varactor diodes), and models of the KdV equation, Boussinesq equations, and the Toda lattice are readily constructed.

Allowing energy dissipation, it has long been known that the candle (or dynamite fuse or Japanese incense) models the leading edge of a nerve impulse as described by the Zeldovich–Frank-Kamenetsky (ZF) equation

$$\frac{\partial^2 u}{\partial x^2} - \frac{\partial u}{\partial t} = u(u-a)(u-1), \qquad (3)$$

where $u(x,t)$ represents temperature of a candle flame or transmembrane voltage of a nerve impulse. This equation can also be modeled by a nonlinear electrical transmission in which the transverse (shunt) conductive element is nonlinear with a region of negative slope (negative differential conductance) as provided by an Esaki tunnel diode or by a Giaever-type superconductive diode (Scott, 1970; Remoissenet, 1999).

In the 1920s, R.S. Lilly showed that nerve impulse propagation can be modeled by a piece of iron wire immersed in a strong nitric- or sulfuric-acid solution (Lilly, 1925). At rest, the wire is stabilized (passivated) by a thin oxide layer that prevents further oxidation. If this passivated layer is disturbed by mechanical or electrical means, however, a deoxidized region propagates along the wire, followed by re-establishment of the stabilizing oxide layer. In this manner, the iron-wire model simulates the recovery property of biological nerves that is missed by Equation (3).

A more complete electrical representation of impulse conduction along a nerve fibre was developed by Jin-ichi Nagumo and his colleagues in collaboration with Richard FitzHugh (Nagumo et al., 1962). Known as the FitzHugh–Nagumo equation, this model augments the ZF equation to allow for recovery to the initial resting state. Finally, the neuristor is an electronic device that functions like a nerve fiber and can be used as the basic element in a family of computing elements.

ALWYN SCOTT

See also **FitzHugh–Nagumo equation; Korteweg–de Vries equation; Neuristor; Sine-Gordon equation; Solitons, a brief history; Zeldovich–Frank-Kamenetsky equation**

Further Reading

Bettini, A., Minelli, T.A. & Pascoli, D. 1983. Solitons in an undergraduate laboratory. *American Journal of Physics*, 51: 977–984

Cirillo, M., Parmentier, R.D. & Savo, B. 1981. Mechanical analog studies of a perturbed sine–Gordon equation. *Physica* D, 3: 565–576

Duseul, S., Michaux, P. & Remoissenet, M. 1998. From kinks to compacton-like kinks. *Physical Review* E, 57: 2320–2326

Lilly, R.S. 1925. Factors affecting the transmission and recovery in the passive iron wire nerve model. *Journal of General Physiology*, 7: 473–507

Lonngren, K.E. 1978. Obsrvations of solitons on nonlinear dispersive transmission lines. In *Solitons in Action*, edited by K.E. Lonngren and A.C. Scott, New York: Academic Press

Nagumo, J., Arimoto, S. & Yoshizawa, S. 1962. An active pulse transmission line simulating nerve axon. *Proceedings of IRE*, 50: 2061–2071

Olsen, M., Smith, H. & Scott, A.C. 1984. Solitons in a wave tank. *American Journal of Physics*, 52: 826–830

Ostrovsky, L.A., Papko, V.V. & Pelinovsky, E.N. 1972. Solitary electromagnetic waves in nonlinear lines. *Radiophysics and Quantum Electronics*, 15: 438–446

Remoissenet, M. 1999. *Waves Called Solitons: Concepts and Experiments*, 3rd edition, Berlin and New York: Springer

Russell, J.S. 1844. Report on waves. *14th Meeting of the British Association for the Advancement of Science*, London: BAAS: pp. 311–339

Scott, A.C. 1969. A nonlinear Klein–Gordon equation. *American Journal of Physics*, 37: 52–61
Scott, A.C. 1970. *Active and Nonlinear Wave Propagation in Electronics*, New York: Wiley
Scott, A.C. 2003. *Nonlinear Science: Emergence and Dynamics of Coherent Structures*, 2nd edition, Oxford and New York: Oxford University Press

LAGRANGE–EULER EQUATIONS

See **Euler–Lagrange equations**

LAGRANGIAN DESCRIPTION

See **Fluid dynamics**

LAMB DIAGRAM

See **Bäcklund transformations**

LANDAU EQUATION

See **Equilibria**

LANDAU–LIFSHITZ EQUATION

The principal assumption of macroscopic ferromagnetism theory is that a magnetic crystal state is described unambiguously by the magnetization vector $\boldsymbol{M}$, so the dynamics and kinetics of a ferromagnet are determined by variations in its magnetization. The magnetization of a ferromagnet as a function of space coordinates and time $\boldsymbol{M}(\boldsymbol{x}, t)$ is a solution of the Landau–Lifshitz (LL) equation, which was first used by Soviet scientists Lev Landau and Evgeni Lifshitz for describing the dynamics of a small velocity domain wall, the magnetic susceptibility of ferromagnets with a domain structure, and ferromagnetic resonance (Landau & Lifshitz, 1935). Later, the macroscopic theory of spin waves as small vibrations of the magnetization vector was developed on the basis of the linearized LL equation (Akhieser et al., 1968). At present, the LL equation is the theoretical foundation of phenomenological magnetization dynamics in magnetically ordered solids, including ferromagnets, antiferromagnets, and ferrites.

The LL equation in a ferromagnet has the following form:

$$\frac{\partial \boldsymbol{M}}{\partial t} = -\frac{2\mu_0}{\hbar}[\boldsymbol{M} \times \boldsymbol{H}_{\text{eff}}] - \gamma[\boldsymbol{M} \times [\boldsymbol{M} \times \boldsymbol{H}_{\text{eff}}]], \quad (1)$$

where μ_0 is the Bohr magneton and γ is the relaxation constant determining the damping motion of the vector $\boldsymbol{M}$. The effective magnetic field $\boldsymbol{H}_{\text{eff}}$ is equal to the variational derivative of the magnetic crystal energy E with respect to the vector $\boldsymbol{M}$: $\boldsymbol{H}_{\text{eff}} = -\delta E/\delta \boldsymbol{M}$. The energy E is assumed to be a function of $\boldsymbol{M}$, its spatial derivatives, and depends on the external magnetic field $\boldsymbol{H}$.

In the case of a many-sublattice magnet, an LL equation for the magnetization of an α-sublattice $\boldsymbol{M}^\alpha$ coincides with Equation (1) after the replacement $\boldsymbol{M} \to \boldsymbol{M}^\alpha$.

Equation (1) for ferromagnets has an integral of motion $M^2 = M_0 =$ constant and is consistent with the assumption that the $\boldsymbol{M}$-vector length in a ferromagnet is its equilibrium parameter. In the ground state, the quantity M_0 is equal to a so-called spontaneous magnetization $M_0 = 2\mu_0 S/a^3$, where S is the atomic spin and a is the interatomic separation. Conservation of the $\boldsymbol{M}$-vector length allows one to rewrite the LL equation in angular variables that are convenient for describing the magnetization dynamics in ferromagnets with axial symmetry. Assuming the external magnetic field directed along the anisotropy axis (the z-axis), let us define (Figure 1)

$$\begin{aligned} M_x + \mathrm{i}M_y &= M_0 \sin\theta \exp \mathrm{i}\psi, \\ M_z &= M_0 \cos\theta. \end{aligned} \quad (2)$$

Then in a dissipativeless case ($\gamma = 0$)

$$\begin{aligned} \sin\theta \frac{\partial \theta}{\partial t} &= -\frac{2\mu_0}{\hbar M_0}\frac{\delta E}{\delta \varphi}, \\ \sin\theta \left(\frac{\partial \varphi}{\partial t} - \frac{2\mu_0 H}{\hbar}\right) &= \frac{2\mu_0}{\hbar M_0}\frac{\delta E}{\delta \theta}, \end{aligned} \quad (3)$$

where the magnetic energy E is written as a function of the angular variables.

The magnetic energy E of a ferromagnet includes two parts: the exchange energy E_{ex} and the magnetic anisotropy energy E_{a}:

$$\begin{aligned} E_{\text{ex}} &= \frac{1}{2}\alpha \int \frac{\partial \boldsymbol{M}}{\partial x_k}\frac{\partial \boldsymbol{M}}{\partial x_k}\,\mathrm{d}^3x, \\ E_a &= -\frac{1}{2}\beta_1 \int M_x^2\,\mathrm{d}^3x - \frac{1}{2}\beta_3 \int M_z^2\,\mathrm{d}^3x, \end{aligned} \quad (4)$$

where α is the nonuniform exchange energy constant and β_1 and β_3 are uniaxial anisotropy constants. (When all $\beta = 0$, we have an isotropic ferromagnet; when $\beta_1 = 0$, we have a uniaxial ferromagnet, the easy-axis anisotropy corresponds to $\beta = \beta_3 > 0$ and easy-plane anisotropy to $\beta < 0$; and when $\beta_1 \neq 0$ and $\beta_3 \neq 0$, we have biaxial anisotropy.)

Equations (3) for easy-axial ferromagnets can be written in the form

$$\begin{aligned} l_0^2 \triangle\theta - \left(1 + l_0^2(\nabla\varphi)^2\right)\sin\theta\cos\theta \\ + \frac{1}{\omega_0}\left(\frac{\partial \varphi}{\partial t} - \omega_H\right)\sin\theta = 0, \end{aligned} \quad (5)$$

$$l_0^2 \operatorname{div}(\sin^2\theta \nabla\varphi) - \frac{1}{\omega_0}\frac{\partial \theta}{\partial t}\sin\theta = 0, \quad (6)$$

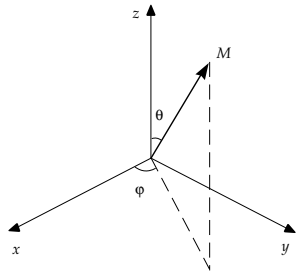

Figure 1. The angular variables for the magnetization $\boldsymbol{M}$.

where $\Delta = \nabla^2$ is the Laplacian, l_0 is the magnetic length ($l_0^2 = \alpha/\beta$), ω is the homogeneous ferromagnetic resonance frequency ($\hbar\omega_0 = 2\mu_0\beta M_0$), and $\omega_H = 2\mu_0 H/\hbar$ is the spin magnetic frequency.

Equations (5) and (6) have two additive integrals of motion, namely, the total momentum of the magnetization field $\boldsymbol{P}$ and z-component (projection) of the total magnetic moment written after normalization as a number of spin deviations N in the excited state of the magnet:

$$\boldsymbol{P} = -\frac{\hbar M_0}{2\mu_0}\int(1-\cos\theta)\nabla\varphi\,\mathrm{d}^3x,$$
$$N = \frac{M_0}{2\mu_0}\int(1-\cos\theta)\,\mathrm{d}^3x. \qquad (7)$$

In a slightly excited state of ferromagnets ($\theta = \theta_0 =$ constant, $\theta_0 \ll 1$, $\psi = \omega t - \boldsymbol{kr}$) the magnetization dynamics is equivalent to a set of precessional spin waves that are solutions of linearized Equations (5), (6) with the following dispersion relation:

$$\omega(\boldsymbol{k}) = \omega_0 + \omega_H + (l_0 k)^2. \qquad (8)$$

The simplest static solution of Equations (5), (6) is a domain wall (Figure 2c)

$$\sin\theta = \mathrm{sech}[(x - x_0)/l_0], \qquad (9)$$

separating two semispace ferromagnet domains at $x < x_0$ and $x > x_0$. Equation (9) presents a topological soliton of the LL equation.

Interesting nontopological soliton solutions of Equations (5) and (6) are two-parametric dynamic magnetic solitons. Magnetic solitons of a general type are given by the following solutions

$$\theta = \theta(\boldsymbol{r} - \boldsymbol{V}t)\,, \varphi = (\omega + \omega_H)t + \psi(\boldsymbol{r} - \boldsymbol{V}t), \quad (10)$$

where the function θ vanishes at infinity ($\theta = 0$ for $r = \infty$) and $\nabla\psi$ is limited for $r = \infty$, $\boldsymbol{V}$ is the translational velocity of the soliton, and $\omega + \omega_H$ is the precessional frequency of the magnetization vector in the frame of reference moving along with the soliton. Typical diagrams for the function θ in the 1-d case are

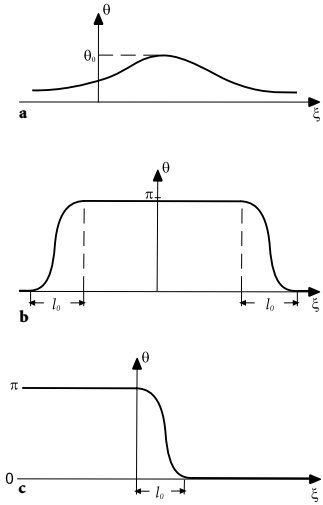

Figure 2. Magnetization distribution in (a) a low-amplitude soliton, (b) a magnetic soliton for small values V and ω, (c) a domain wall.

presented in Figure 2. There are the following Hamilton equations for a dynamic soliton (Kosevich et al., 1977):

$$\boldsymbol{V} = \left(\frac{\partial E}{\partial \boldsymbol{P}}\right)_N, \quad \hbar\omega = \left(\frac{\partial E}{\partial N}\right)_{\boldsymbol{P}}. \qquad (11)$$

The 1-dimensional version of Equations (5) and (6) is a totally integrable nonlinear equation in both isotropic (Lakshmanan, 1977; Takhtajan, 1977) and easy-axial (Borovik, 1978) cases and possesses a set of multiple-soliton solutions. The total integrability of 1-d LL equations in the case of biaxial anisotropy was proved by Sklyanin (1979).

If θ is small enough, the 1-d version of Equations (5) and (6) can be reduced to the nonlinear Schrödinger (NLS) equation for the complex function $\psi = M_x + \mathrm{i}M_y$ (Volzhan et al., 1976)

$$\frac{\mathrm{i}}{\omega_0}\frac{\partial\Psi}{\partial t} - l_0^2\frac{\partial^2\Psi}{\partial x^2} + (1+h)\Psi - \frac{1}{2M_0}|\Psi|^2\Psi = 0, \qquad (12)$$

which is used for description of small amplitude long-wave excitations in one-dimensional easy-axial ferromagnets.

Another limiting case arises for a ferromagnet with the biaxial anisotropy ($\beta_1 < 0$ and $\beta_3 > 0$) under the condition $\varepsilon = -\beta_1/\beta_3 \gg 1$. Then the plane YOZ plays easy-plane, the magnetization vector lies nearly in this plane, $\chi = \pi/2 - \theta \ll 1$, and the LL equation is transformed to the following equations:

$$l_0^2\frac{\partial^2\phi}{\partial x^2} - \frac{1}{\varepsilon\omega_0}\frac{\partial^2\phi}{\partial t^2} + \sin\phi\cos\phi = 0,$$

$$\omega_0 \chi = -\frac{1}{\varepsilon}\frac{\partial \phi}{\partial t}, \tag{13}$$

where the new angle variable ϕ is introduced with the equation $M_x + iM_y = M_0 \cos\chi \exp i\phi$.

At present, the LL equation is widely used for models of nonlinear macroscopic dynamic phenomena such as spin waves in inhomogeneous or spatially limited magnets, magnetostatic vibrations, magnetization dynamics, interaction of magnetically ordered media with electromagnetic and elastic waves, nonlinear magnetization waves, and magnetic solitons.

ARNOLD KOSEVICH

See also **Domain walls; Ferromagnetism and ferroelectricity; Nonlinear Schrödinger equations; Sine-Gordon equation; Solitons**

Further Reading

Akhieser, A.I., Bar'yahtar V.G. & Peletminskii S.V. 1968. *Spin Waves*, Amsterdam: North-Holland

Borovik, A.E. 1978. *N*-soliton solutions of Landau-Lifshitz equation, *Pis'ma Zhurnal Experimental'noy i Teoreticheskoy Fiziki*, 28: 629 (in Russian); *JETP Letters*, 28: 581

Kosevich, A.M. 1986. Dynamical and topological solitons in ferromagnets and antiferromagnets. In *Solitons*, edited by S.E. Trullinger, V.E. Zakharov & V.L. Pokrovsky, Amsterdam: North-Holland

Kosevich, A.M., Ivanov, B.A. & Kovalev, A.S. 1977. Nonlinear localized magnetization wave of a ferromagnet as a bound-state of a large number of magnons. *Pis'ma Zhurnal Eksperimental'noy i Teoreticheskoy Fiziki* 25: 516 (in Russian); *JETP Letters*, 25: 486

Kosevich, A.M., Ivanov, B.A. & Kovalev, A.S. 1990. Magnetic solitons. *Physics Reports*, 194: 117

Lakshmanan, M. 1977. Continium spin system as an exactly solvable dynamic system. *Physics Letters* A, 61: 53

Landau, L.D. & Lifshitz, E.M. 1935. On the theory of the dispersion of magnetic permability in ferromagnet bodies. *Physikalische Zeischrift der Sowjetunion*, 8: 153

Lifshitz, E.M. & Pitaevskii, L.P. 1980. *Statistical Physics, Part 2*, Oxford: Pergamon Press

Sklyanin, E.K. 1979. On complete integrability of Landau-Lifshitz equation, *Preprit/ Academy of Sciences of USSR*, Leningrad Department Steklov Mathematical Institute, E-3

Takhtajan, L.A. 1977. Integration of the continium Heisenberg spin chain through the inverse scattering method, *Physics Letters* A, 64: 235

Volzhan, E.B., Giorgadze, N.P. & Pataraya A.D. 1976. Weakly nonlinear magnetization density waves in magnetically ordered media. *Fizika Tverdogo Tela*, 25: 516 (in Russian); *Soviet Physics, Solid State*, 18: 1487

LANGEVIN EQUATION

See **Ferromagnetism and ferroelectricity**

LANGMUIR WAVES

See **Nonlinear plasma waves**

LANGMUIR–BLODGETT FILMS

The calming effect of oil on water has been known for centuries, and one early account of the phenomenon, on clay tablets, dates from the 18th century BCE in Babylonia. In 1879, a provisional British patent was filed by John Shields, the proprietor of a Scottish linen mill, for a simple device for spreading oil from valves in undersea pipes to calm the waves at the entrances to harbors. However, the first account of an experiment to investigate this effect was probably that of Benjamin Franklin in 1773, who wrote the following in a letter to a colleague.

> At length being at Clapham, where there is on the common a large pond, which I observed one day to be very rough with the wind, I fetched out a cruet of oil, and dropped a little of it on the water, and there the oil, though not more than a teaspoonful, produced an instant calm over a space several yards square, which spread amazingly, and extended itself gradually till it reached the lee side, making all that quarter of the pond, perhaps half an acre as smooth as a looking-glass.

A quick calculation reveals that Franklin's oil film was 1–2 nm thick—about the same as the size of an oil molecule, but this implication was not realized for many years. Although Lord Rayleigh was the first to propose that such films were only one molecule in thickness, he was not able to make a direct measurement to confirm this. The simple equipment for monolayer studies, now known as a Langmuir trough, was first introduced by Agnes Pockels. In a letter to Lord Rayleigh in 1891, she described the methods that formed the foundation of monolayer research.

Irving Langmuir provided most of the early scientific evidence for the existence of monolayer films. In 1917, he published a substantial paper outlining the properties of such films on a water surface. Some years later, Katharine Blodgett, working with Langmuir at the General Electric Company Research Laboratories in Schenectady, New York, devised a method for transferring the floating monolayers onto solid surfaces. The resulting films now bear the name of these two researchers.

Until the outbreak of World War II, research into the properties of monolayer films flourished, the work being undertaken mainly by surface chemists. However, few uses were found for monolayer and multilayer structures so activity in the area declined. Interest was rekindled in the 1970s following some stimulating experiments on energy transfer in multilayer systems by Hans Kuhn working in Germany. At about this time, organic chemists became aware of the limited range of monolayer forming materials that was available. Novel electroactive compounds were synthesized (dyes, semiconductors, polymers), and a new series of investigations began. This coincided with the birth of molecular electronics, a new interdisciplinary research

activity focused on the exploitation of organic materials in electronic and optoelectronic devices. Related thin film technologies, such as self-assembly and layer-by-layer electrostatic deposition, were also developed. By the end of the 20th century, a number of organic thin film deposition technologies and materials, suitable for fabricating organic molecular architectures, was available. The era of molecular nanotechnology had begun.

Materials that produce organized monomolecular layers on the surface of water invariably consist of molecules possessing both water-attracting (hydrophilic) and water-repelling (hydrophobic) chemical groups. Such organic compounds are called amphiphiles. One of the simplest materials suitable for forming such a monomolecular layer is stearic acid, $C_{17}H_{35}COOH$. The molecule consists essentially of 16 CH_2 groups forming a long hydrocarbon chain; one end of the chain terminates in a hydrophilic carboxylic acid COOH group.

Langmuir–Blodgett (LB) films are prepared by first depositing a small quantity of the amphiphilic material, dissolved in a volatile solvent such as chloroform, on the surface of carefully purified water (subphase). When the solvent has evaporated, the organic molecules may be compressed to form a floating two-dimensional solid. The hydrophilic and hydrophobic terminations of the molecules ensure that the individual molecules are aligned in the same way during this process. During compression the monolayer undergoes a number of phase transformations. The different phases are almost analogues of three-dimensional gases, liquids and solids. The phase changes may be readily identified by monitoring the surface pressure Π as a function of the area occupied by the film. This is the two-dimensional equivalent of the pressure versus volume isotherm for a gas/liquid/solid. Figure 1 shows such a plot for a hypothetical long-chain organic monolayer material (e.g., a long-chain fatty acid).

In the "gaseous" state (G in Figure 1), the molecules are far enough apart on the water surface that they exert little force on one another. As the surface area of the monolayer is reduced, the hydrocarbon chains will begin to interact. The "liquid" state that is formed is generally called the expanded monolayer phase (E). The hydrocarbon chains of the molecules in such a film are in a random, rather than a regular orientation, with their polar groups in contact with the subphase. As the molecular area is progressively reduced, condensed (C) phases may appear. There may be more than one of these, and the emergence of each condensed phase can be accompanied by constant pressure regions in the isotherm, as observed in the cases of a gas condensing to a liquid and a liquid solidifying. These regions will be associated with enthalpy changes in the monolayer. In the condensed monolayer states, the molecules are closely packed and are oriented with their hydrocarbon chains pointing away from the water surface. The area per molecule in such a state will be similar to the cross-sectional area of the hydrocarbon chain, that is, $\approx 0.19\,\mathrm{nm}^2\,\mathrm{molecule}^{-1}$.

The LB technique requires that the surface pressure and temperature of the floating monolayer are controlled so that the organic film is in a condensed and stable state. Figure 2 shows the commonest form of LB deposition. The substrate is hydrophilic and the first layer is transferred, like a carpet, as the substrate is raised vertically through the water. Subsequently, a monolayer is deposited on each traversal of the monolayer/air interface. As shown, these stack in a head-to-head and tail-to-tail pattern; this

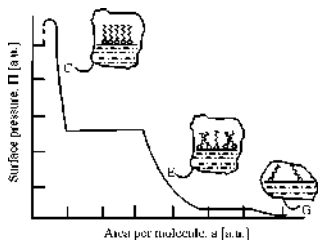

Figure 1. Surface pressure versus area per molecule for a long-chain organic compound. (The surface pressure and area are in arbitrary units (a.u.).)

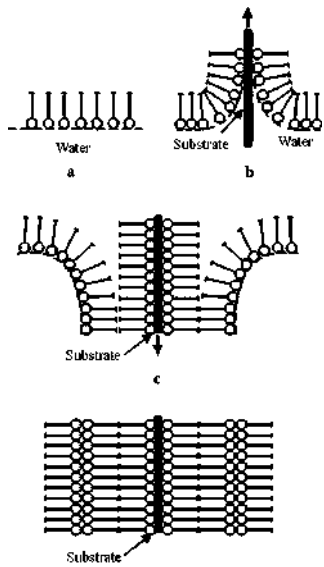

Figure 2. Y-type Langmuir–Blodgett film deposition.

deposition mode is called Y-type. Although this is the most frequently encountered situation, instances in which the monolayer is transferred to the substrate as it is being inserted into the subphase, or only as it is being removed, are often observed. These deposition modes are called X-type (monolayer transfer on the downstroke only) and Z-type (transfer on the upstroke only).

It is also possible to build up thin film architectures containing more than one type of monomolecular layer. In the simplest case, alternate-layer films may be produced by raising the substrate through a monolayer of one material (consisting of molecules of compound A, say) and then lowering the substrate through a monolayer of a second substance (compound B). An asymmetric multilayer structure consisting of ABABAB... layers is produced. This control over the molecular architecture permits the fabrication of organic superlattices with precisely defined symmetry properties. Such molecular assemblies can exhibit pyroelectric, piezoelectric, and second-order nonlinear optical phenomena.

Film transfer is characterized by measurement of the deposition ratio, τ (also called the transfer ratio). This is the decrease in the area occupied by the monolayer (held at constant pressure) on the water surface divided by the coated area of the solid substrate, that is,

$$\tau = A_L/A_S, \tag{1}$$

where A_L is the area occupied by the monolayer on the water surface and A_S is the coated area of the solid substrate. Transfer ratios significantly outside the range 0.95–1.05 suggest poor film homogeneity.

A schematic diagram of one experimental arrangement to deposit LB films is shown in Figure 3, together with a photograph of the equipment. The Langmuir trough is made from PTFE (polytetrafluoroethylene) and a working area is defined by a PTFE-coated glass fiber barrier, which can be moved using a low-geared electric motor. The barrier motor is coupled to a sensitive electronic balance, which continuously monitors, via a sensing plate (Wilhelmy plate), the surface pressure of the monolayer. Using a feedback arrangement, this pressure can be maintained at a predetermined value. The physical dimensions of the Langmuir trough arrangement are not critical (the system in the photograph is approximately 30 cm in length) and are governed by the size of the substrate used.

Many analytical techniques, such as X-ray and electron diffraction, and infrared spectroscopy may be used to study the orientation of molecules in an LB assembly. Figure 4 shows an 9 nm × 9 nm atomic force micrograph of the surface of a 12-layer fatty acid LB film. The lighter parts of the image relate to the higher part of the surface and the darker regions correspond to deeper down. Lines of individual molecules are evident at the magnification shown, confirming the highly ordered arrangement of organic molecules in the LB film.

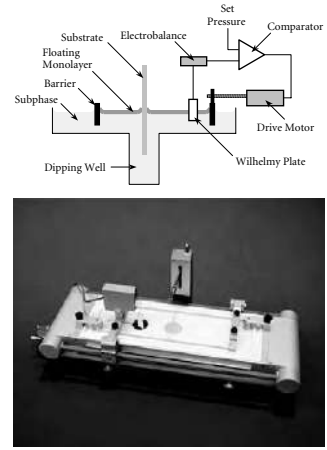

Figure 3. Langmuir–Blodgett trough (courtesy Molecular Photonics).

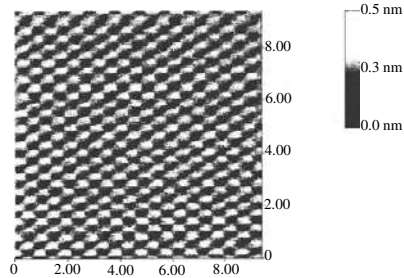

Figure 4. An atomic force micrograph of a fatty acid LB film.

The vertical dipping LB process is not the only way to transfer a floating molecular film to a solid substrate or to build-up multilayer films. Other methods are based on touching one edge of a hydrophilic substrate with the monolayer-covered subphase or lowering the substrate horizontally so that it contacts the hydrophobic ends of the floating molecules. Chemical means, for example, self-assembly of a thiol group onto a gold-coated substrate, can also be used to deposit monolayer organic films. In contrast, electrostatic layer-by-layer assembly relies on the forces between positively and negatively charged polyelectrolytes.

The earliest technical application of organic monolayer films is believed to be the Japanese printing art called *sumi-nagashi*. The dye comprising a suspension

of submicron particles and protein molecules is first spread on the surface of water; the application of gelatin to the uniform layer converts the film into a patchwork of colorless and dark domains. These distinctive patterns can then be transferred by lowering a sheet of paper onto the water surface.

There are, of course, many methods available to deposit thin films of organic materials, including: thermal evaporation, sputtering, spaying, painting, dip- and spin-coating, electrodeposition, and molecular beam epitaxy. However, the LB technique is one of the few thin film technologies that actually permits the manipulation of materials at the molecular level. It should, therefore, be appropriate for exploitation by workers in nanotechnology wishing to fabricate interesting material architectures (bottom-up approach to nanotechnology) or to build up novel electronic device structures.

A range of possible applications for LB and related films is evident from the literature. Many of the ideas exploit the physical and chemical properties of the ultra-thin films to provide surface coatings with particular catalytic, adhesive, or mechanical properties (e.g., low friction). The availability of new polymeric amphiphiles has led to an interest in semi-permeable membranes. The extreme thinness of monolayer and multilayer films could provide key benefits in a variety of chemical sensing structures. For gas sensing, adequate sensitivities to some important gases and vapors have already been achieved using a variety of transduction techniques (chemiresistor, surface plasmon resonance, acousto-electric coupling, and so on).

For commercial exploitation, it is imperative to establish those areas in which LB films offer significant advantages over layers produced by other (and perhaps cheaper) means. In the case of second-order nonlinear optics, the LB method offers a means of aligning the molecules in a film of micrometer dimensions. Materials with high second-order hyperpolarizabilities (for example, leading to significant second-harmonic generation) already exist. Further work is needed on the development of practical electro-optic structures with attention to important considerations such as encapsulation and device degradation.

It is also interesting to note that a large number of biological materials form monolayers on a water surface. Chlorophyll a, the green pigment in higher plants; vitamins A, E and K; and cholesterol are all examples. Monomolecular films resemble naturally occurring biological membranes, which are based on a bilayer arrangement of long-chain phospholipid molecules. The LB technique might, therefore, be used as a means to fabricate artificial structures that emulate certain biological functions, such as photosynthesis, molecular recognition, or parallel information processing.

MICHAEL PETTY

See also **Bilayer lipid membranes; Liquid crystals; Nonlinear optics**

Further Reading

Gaines, G.L., Jr. 1966. *Insoluble Monolayers at Liquid-Gas Interfaces*, New York: Wiley-Interscience
Petty, M.C. 1996. *Langmuir–Blodgett Films: An Introduction*, Cambridge: Cambridge University Press
Roberts, G. G. (editor). 1991. *Langmuir–Blodgett Films*, New York: Plenum Press
Tredgold, R.H. 1994. *Order in Organic Films*, Cambridge and New York: Cambridge University Press
Ulman, A. 1991. *Ultrathin Organic Films*, San Diego: Academic Press

LAPLACE TRANSFORM

See **Integral transforms**

LASERS

An acronym for Light Amplification by Stimulated Emission of Radiation, a laser involves interaction of light with matter at the molecular, atomic, or nuclear levels and requires a quantum mechanical description of both light and matter. According to quantum mechanics, when an electron decays from an excited level E_+ to a lower energy level $E_- < E_+$, a photon of energy $E_+ - E_-$ and frequency $\nu = (E_+ - E_-)/h$ is emitted, where $h \doteq 6.672 \times 10^{-34}$ J s is Planck's constant.

The decay of electrons from excited states and the consequent emission of light is stimulated by the interaction of photons (of the appropriate energy) with the electrons (Einstein's stimulated emission). The emitted photons can then interact with excited electrons to produce a cascade of coherent photons, making up the familiar laser beam.

For a laser to work, three basic elements are required: (i) an energy level structure for the electrons (e.g., atomic or molecular fluids (gases or liquids), solids (crystals or glasses), or semiconducting junctures); (ii) a pumping mechanism (such as electrical current or light) to populate the upper energy level; and (iii) an optical cavity to partially confine the photons, enhancing their probability of interacting with the excited electrons.

The most common laser structures are Fabry–Perot cavities (where light is confined between two opposite mirrors) and ring lasers (in which light travels in one direction along the border of a rectangle with mirrors appropriately oriented in the corners) (Siegman, 1986) (see Figure 1). Industrial lasers are normally of Fabry–Perot type while ring lasers are often preferred in research laboratories.

The simplest laser model, describing only the first two required elements, consists of the laser rate equations, which model a laser medium in terms of the number of photons (proportional to the light

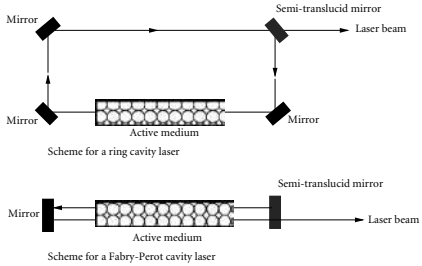

Figure 1. Ring and Fabry-Perot laser cavities.

intensity, I) and the number of excited electrons inside the laser cavity. Because the photon field can induce upward as well as downward transitions, the excited electrons are measured by the population inversion $N \equiv N_+ - N_-$, where N_+ (N_-) denotes the number of electrons in the upper (lower) level.

The photon population (I) is diminished due to the laser output as well as through other losses at a rate εI. Stimulated emission decreases the population inversion and increases the photon number at a rate αN_+, while absorption of photons produce the inverse effect at a rate αN_-. (The equivalence between emission and absorption rate per electron is a quantum mechanical result. Note that for each photon emitted, the population inversion decreases by two as N_+ decreases by one, while N_- increases by the same amount.) Excited electronic states (N_+) are also produced by the pumping mechanism at a rate $A/2$ (which may be a function of time) and diminished by nonradiative processes at a rate $\gamma(N - N_{\text{eq}})$ (where N_{eq}, a negative number, derives from the population inversion at thermal equilibrium). A simple formulation of the laser rate equations is, therefore,

$$\frac{\mathrm{d}I}{\mathrm{d}t} = [-\varepsilon + \alpha N]\, I, \tag{1}$$

$$\frac{\mathrm{d}N}{\mathrm{d}t} = (A + \gamma N_{\text{eq}}) - \gamma N - 2\alpha N I. \tag{2}$$

These laser rate equations have either one or two fixed points corresponding to steady operation of the laser. The laser-off state with $I = 0$ and $N = N_0 = A/\gamma + N_{\text{eq}}$ is always present. The stability of the laser-off solution depends on the sign of $\lambda = -\varepsilon + \alpha N_0$. If this quantity is positive, small disturbances such as those produced by spontaneous emission are amplified and laser action develops. If $\lambda < 0$, disturbances die out, hence $\lambda = 0$ implies a threshold value for the pumping of $A = \gamma(\varepsilon/\alpha - N_{\text{eq}})$. Steady operation of a laser above threshold is represented by the laser-on state $N = N_1 = \varepsilon/\alpha$ and $I = (\gamma/2\alpha)\,(N_0 - N_1)\,/N_1$.

These equations correspond to birth and death processes of photons and electrons that resemble those of predator and prey species in population dynamics. This analogy is somewhat tenuous, however, because quantum theory does not allow a photon or electron to be localized in time and energy simultaneously. Hence, the statistical description of a laser requires of entrained electron-photon states and the descriptions of quantum jump processes (Carmichael, 1999).

A more detailed set of equations is obtained by considering a laser operating in a single longitudinal cavity mode (i.e., having a fixed spatial pattern within the optical cavity). With a simple quantum mechanical model for electron energy levels and a classical description of the electromagnetic field (i.e., a large number of photons), the dynamics of the laser are described by Maxwell–Bloch equations, which involve complex amplitudes of the electric and polarization fields in addition to the population inversion (N) (Narducci & Abraham, 1988).

An aim of laser design has long been to achieve lasers of higher photon energies. While ultraviolet lasers were developed early, X-ray lasers have only recently been demonstrated (Rocca, 1999), and gamma-ray lasers are not yet realized.

Lasers can be classified in various ways according to their dynamics, the active media, the optical cavity, the pumping scheme, optical frequency, among others. Considering the active media, lasers can be grouped as follows.

Solid State Lasers

Solid state lasers, such as the ruby laser (the first laser, announced in 1960), which has a three-level pumping scheme for which Cr^{3+} impurities are essential, require a high-energy source for pumping and operate intermittently. In contrast, Nd-YAG (neodymium-doped yttrium aluminum garnet) and Nd-glass lasers are based in a four-level scheme, operate under moderate pump power, and display different dynamical regimes. Ruby and Nd-YAG lasers represent the two basic pumping schemes for solid state lasers.

In the three-level pumping scheme, the light emitting transition has the ground state as the final state, while in the four-level scheme the state reached by the electron after the transition is an excited state.

There are a large number of solid state lasers operating at different frequencies, each with particular features. Many of them employ a host crystal (or glass) doped with an impurity such as $Al_2O_3(Cr^{3+})$, $Y_2O_3(Eu^{3+})$, $Gd_2O_3(Nd^{3+})$, or $BaF_2(U^{3+})$.

Gas Lasers

Several active media fall in this category: helium-neon, argon, and the powerful CO_2 are among the best-known representatives. The standard method for the excitation

of the molecular states is an electric discharge in the gaseous medium where collisions between exited ions provide the pumping mechanism. However, optical pumping and other pumping mechanisms have been demonstrated for some gas lasers.

Gas lasers can be operated in continuous wave and pulsed modes and are particularly important at the low-frequency (infrared) region of the electromagnetic spectrum. Other members of this class include H_2O, HCN, CH_2I, and HF lasers.

Liquid Lasers

The best-known representatives are dye lasers, where a stream of organic liquid is excited using visible or ultraviolet radiation from a flash lamp or a laser beam. The pumping mechanism involves radiative fluorescence at a lower frequency than that of the pumping source, a mechanism known as Stokes-shift.

Other lasers in this class are based on solutions of rare earth elements. In contrast with gas and solid state lasers, dye lasers usually operate in cavities with relatively high losses.

Semiconductor Lasers

Because of their small size, semiconductor lasers play an important role in electronic applications. While earlier lasers were built as semiconductor diodes using p–n junctions as in GaAs diodes (or PbS, PbSe, PbTe, SnTe, InSb, etc.) new generations of lasers, such as the Vertical Cavity Surface Emitting Laser (VCSEL) are produced modifying semiconductor surfaces and reducing the size and power requirements of the laser significantly. Semiconductor lasers are pumped by direct electrical current using the band structure of the semiconductor and electron-hole recomposition to produce the photons.

Nuclear Magnetic Resonance

The unique NMR laser relies on the (permanent) magnetic momentum of nuclei, which are pumped using a radio-frequency field. Optical pumping has also been demonstrated recently.

For gas lasers, some liquid lasers, and solid state lasers, the lasing threshold is reached only with high reflectivity mirrors minimizing the cavity losses (small ε). Such lasers operate just above threshold in a mode that is almost resonant with the frequency of the atomic transition and can be viewed as weakly nonlinear systems. Wide cavities, higher pumping levels, feedback, and other effects can induce multimode dynamics, where several empty cavity modes are required for the spatial description of the dynamics.

When laser devices are based on lossy electromagnetic cavities, as in dye and semiconductor lasers, the relation between cavity modes and monochromatic states (or solutions) is obscured. Nevertheless, these are also called multimode lasers when a description of the spatial extension is required.

Despite the diversity of active media, pumping mechanisms, and lasing frequencies, the dynamics of lasers are often rather similar, the main differences accounted for by different parameter values in Maxwell–Bloch type equations. The dynamics of most lasers are described by simple dynamical attractors (fixed points) under constant pumping. There are, however, situations in which complex behavior emerges; thus, optical reinjection of the emitted light can destabilize a laser. Such a process might occur when the laser is coupled to optic fibers in a communication system. The Lang–Kobayasi equations (Lang & Kobayashi, 1980) (a modification of the rate equations including a delayed field) describe this situation for very small amounts of reinjected signal. In the case of semiconductor lasers, even small amounts of optical feedback require a spatial description of the laser cavity (multimode operation) (Huyet et al., 1998; Duarte & Solari, 1998). Attempts to control, or mode lock, a (usually powerful) slave laser with a (usually weak) master laser also generate a rich dynamical spectrum at the unlocking transition (Zimmermann et al., 2001).

HERNÁN G. SOLARI AND MARIO NATIELLO

See also **Maxwell–Bloch equations; Nonlinear optics; Semiconductor laser**

Further Reading

Carmichael, H.J. 1999. *Statistical Methods in Quantum Optics*, vol. 1, *Master equations and Fokker–Plank equations*, Berlin and New York: Springer

Duarte, A.A. & Solari, H.G. 1998. The metamorphosis of the monochromatic spectrum in a double-cavity laser as a function of the feedback rate. *Physical Review* A, 58: 614–619

Huyet, G., Balle, S., Giudici, M., Green, C., Giacomelli, G. & Tredicce, J.R. 1998. Low frequency fluctuations and multi-mode operation of a semiconductor laser with optical feedback. *Optical Communications*, 149: 341–347

Lang, R. & Kobayashi, K. 1980. External optical feedback effects on semiconductor injection laser properties. *IEEE Journal of Quantum Electronics*, QE-16: 347

Narducci, L.M. & Abraham, N.B. 1988. *Laser Physics and Laser Instabilities*, Singapore: World Scientific

Rocca, J.J. 1999. Table-top soft X-ray lasers. *Review of Scientific Instruments*, 70: 3799

Siegman, A.E. 1986. *Lasers*, Mill Valley, CA: University Science Books

Zimmermann, M., Natiello, M. & Solari, H. 2001. Global bifurcations in a laser with inhected signal: beyond Adler's approximation. *Chaos*, 11: 500–513

LATTICE GAS METHODS

When one is interested in studying the dynamical behavior of fluid systems starting at the microscopic

level, it is logical to begin with a molecular dynamics description of the interactions between the constituting particles. This is often a formidable task, as the fluid evolves into a nonlinear regime where chaos, turbulence, or reactive processes take place. But one may question whether a realistic description of the microscopic dynamics is necessary to gain insight on the underlying mechanisms of large-scale nonlinear phenomena. Around 1985, a considerable simplification was introduced (Frisch et al., 1986). These pioneering studies established (theoretically and computationally) the feasibility of simulating fluid dynamics via a microscopic approach based on a new paradigm. A virtual simplified micro-world is constructed as an automaton universe, based not on a realistic description of interacting particles but merely on the laws of symmetry and of invariance of macroscopic physics.

Suppose we implement point-like particles on a regular lattice where they move from node to node at each time step and undergo collisions when their trajectories meet at the same node. As the system evolves, we observe its collective dynamics by looking at the lattice from a distance. A remarkable fact is that—if the collisions occur according to some simple logical rules (satisfying fundamental conservations) and if the lattice has the proper symmetry—this "lattice gas automaton" (LGA) shows global behavior very similar to that of a real fluid. So we can infer that despite its simplicity at the microscopic scale, the LGA should contain the essential features that are responsible for the emergence of complex behavior and, thereby, can help us understand the basic mechanisms involved.

An LGA consists of a set of particles moving on a regular d-dimensional lattice $\mathcal{L}$ at discrete time steps, $t = n\Delta t$, with n an integer. The lattice is composed of V nodes, labeled by the d-dimensional position vectors $\boldsymbol{r} \in \mathcal{L}$. Associated to each node are b channels, labeled by indices $i, j, \ldots$, running from 1 to b. At a given time t, a channel can be either occupied by one particle or empty, so that the occupation variable $n_i(\boldsymbol{r}, t) = 1$ or 0. When channel i at node $\boldsymbol{r}$ is occupied, then the particle at the specified node $\boldsymbol{r}$ has velocity $\mathbf{c}_i$. The set of allowed velocities is such that the condition $\boldsymbol{r} + \boldsymbol{c}_i \Delta t \in \mathcal{L}$ is fulfilled. The "exclusion principle" requirement that the maximum occupation be of one particle per channel allows for a representation of the automaton configuration in terms of a set of bits $\{n_i(\boldsymbol{r}, t)\}$; $\boldsymbol{r} \in \mathcal{L}$, $i = \{1, b\}$. The evolution rules are thus simply logical operations over sets of bits.

The time evolution of the automaton takes place in two stages: propagation and collision. In the propagation phase, particles are moved according to their velocity vector, and in the (local) collision phase, the particles occupying a given node are redistributed among the channels associated to that node. So the microscopic evolution equation of the LGA reads

$$n_i(\boldsymbol{r} + \boldsymbol{c}_i\,\Delta t, t + \Delta t) = n_i(\boldsymbol{r}, t) + \Delta_i(\{n_j(\boldsymbol{r}, t)\}), \tag{1}$$

where $\Delta_i(\{n_j\})$ represents the collision term that depends on all channel occupations at node $\boldsymbol{r}$. By performing an ensemble average (denoted by angular brackets) over an arbitrary distribution of initial occupations, one obtains a hierarchy of coupled equations for the successive n-body distribution functions. This hierarchy can be truncated to yield the lattice Boltzmann equation for the single particle distribution function $f_i(\boldsymbol{r}, t) = \langle n_i(\boldsymbol{r}, t)\rangle$:

$$f_i(\boldsymbol{r} + \boldsymbol{c}_i\,\Delta t, t + \Delta t) - f_i(\boldsymbol{r}, t) = \Delta_i^{\mathrm{Boltz}}(\{f_j(\boldsymbol{r}, t)\}). \tag{2}$$

The left-hand side is recognized as the discrete version of the left-hand side of the classical Boltzmann equation for continuous systems, and the right-hand side denotes the collision term, where the precollisional uncorrelated state *ansatz* has been used to factorize the b-particle distribution function.

The lattice Boltzmann equation (2) is one of the most important results in LGA theory. It can be used as the starting point for the derivation (via multi-scale analysis) of the macroscopic equations describing the long wavelength behavior of the lattice gas. The LGA macroscopic equations are found to exhibit the same structure as the classical hydrodynamic equations, and under the incompressibility condition, one retrieves the Navier–Stokes equations for nonthermal fluids. Another important feature of the lattice Boltzmann equation is that it can be used as an efficient and powerful simulation algorithm. In practice, one usually prefers to use a simplified equation where the collision term is approximated by a single relaxation time process inspired by the Bhatnagar–Gross–Krook model, known in its lattice version as the LBGK equation:

$$f_i(\boldsymbol{r} + \boldsymbol{c}_i\,\Delta t, t + \Delta t) - f_i(\boldsymbol{r}, t) = -\frac{1}{\tau}\left[f_i(\boldsymbol{r}, t) - f_i^{\mathrm{leq}}(\boldsymbol{r}, t)\right], \tag{3}$$

where the right-hand side is proportional to the deviation from the local equilibrium distribution function.

There is a wealth of applications of the lattice gas methods that have established their validity and their usefulness. LGA simulations, based on Equation (1), are most valuable for fundamental problems in statistical mechanics, such as the study of fluctuation correlations in equilibrium and non-equilibrium systems (Rivet & Boon, 2001; Rothman & Zaleski, 1997). As an example, Figure 1 shows

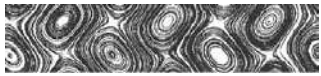

Figure 1. Lattice gas simulation of the Kolmogorov flow: the tracer trajectories reflect the topology of the ABC flow in the regime beyond the critical Reynolds number ($\mathrm{Re} = 2.5 \times \mathrm{Re}_c$).

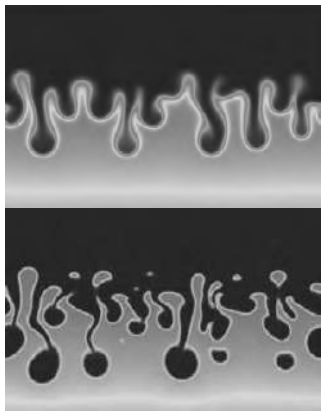

Figure 2. Lattice Boltzmann (LBGK) simulation of viscous fingering in miscible fluids (upper panel) showing the interface sharpening effect of a reactive process between the two fluids (lower panel).

the trajectories of tracer particles suspended in a Kolmogorov flow (above the critical Reynolds number) produced by a lattice gas automaton and from where turbulent diffusion was analyzed (Boon et al., 2000).

Simulations of more direct practical interest, such as, for instance, profile optimization in car design or turbulent drag problems, are most efficiently treated with the lattice Boltzmann method, in particular using the LBGK model. The example given in Figure 2 illustrates the method for the study of viscous fingering in Hele-Shaw geometry, showing the effect of reactivity between the two fluids as a determinant factor in the dynamics of the moving interface (Grosfils & Boon, 2002).

Applications of the LGA approach and of the lattice Boltzmann equation cover a wide variety of theoretical and practical problems ranging from the dynamics of thermal fluctuations and quantum lattice gas automata to multi-phase flow, complex fluids, reactive systems, and inhomogeneous turbulence.

JEAN PIERRE BOON

See also **Cellular automata; Hele-Shaw cell; Molecular dynamics; Navier–Stokes equation**

Further Reading

Boghosian, B.M., Coveney, P.V. & Emerton, A.N. 1996. A lattice gas model of microemulsions. *Proceedings of the Royal Society* A, 452: 1221–1250

Boon, J.P., Dab, D., Kapral, R. & Lawniczak, A. 1996. Lattice gas automata for reactive systems. *Physics Reports*, 273(2): 55–148

Boon, J.P., Hanon, D. & Vanden Eijnden, E. 2000. Lattice gas automaton approach to turbulent diffusion. *Chaos, Solitons and Fractals*, 11: 187–192

Coveney, P.V. & Succi, S. (editors). 2002. Discrete modeling and simulation of fluid dynamics. *Philosophical Transactions of the Royal Society*, 360: 291–573

Frisch, U., Hasslacher, B. & Pomeau, Y. 1986. Lattice gas automata for the Navier–Stokes equation. *Physical Review Letters*, 56: 1505–1508

Grosfils, P. & Boon, J.P. 2002. Viscous fingering in miscible, immiscible, and reactive fluids. *International Journal of Modern Physics* B, 17: 15–20

Meyer, D. 1996. From quantum cellular automata to quantum lattice gases. *Journal of Statistical Physics*, 85: 551–574

Rivet, J.P. & Boon, J.P. 2001. *Lattice Gas Hydrodynamics*, Cambridge and New York: Cambridge University Press

Rothman, D. & Zaleski, S. 1997. *Lattice Gas Cellular Automata*, Cambridge and New York: Cambridge University Press

Succi, S. 2001. *The Lattice Boltzmann Equation for Fluid Dynamics and Beyond*, Oxford: Clarendon Press and New York: Oxford University Press

LATTICE KINK

See **Solitons, types of**

LATTICE SOLITONS

See **Solitons, types of**

LAX OPERATORS

See **Inverse scattering method or transform**

LEADING EDGE DYNAMICS

See **Nerve impulses**

LEBESQUE MEASURE

See **Measures**

LEGENDRE TRANSFORMATION

See **Euler–Lagrange equations**

LENNARD–JONES POTENTIAL

See **Molecular dynamics**

LÉVY FLIGHTS

In 1937, the French mathematician Paul Lévy (1886–1971) introduced statistical descriptions of motion that

extend beyond the more traditional Brownian motion discovered over one hundred years earlier. A diverse range of both natural and artificial phenomena is now being described in terms of Lévy statistics, from the flight of an albatross across the Antarctic skies to the trajectories followed by the abstract painter Jackson Pollock as he constructed his famous drip paintings.

In 1828, Robert Brown published his studies of the random motion of soot particles in a dish of water as they were buffeted from random directions by the thermal motion of water molecules. In 1905, Albert Einstein provided a theoretical basis for this diffusion process. A particle's Brownian motion is pictured as a sequence of jumps. For a single jump, the probability dependence on jump size x has a Gaussian distribution. A consequence of Gaussian statistics is that the size distribution for N jumps is also described by a Gaussian.

Paul Lévy generalized beyond Brownian motion by considering other distributions for which one jump and N jumps share the same mathematical form. These Lévy distributions decrease according to the power law $1/x^{1+\gamma}$ for large x values, where γ lies between 0 and 2. Compared with Gaussian distributions, Lévy distributions do not fall off as rapidly at long distances. For Brownian motion, each jump is usually small and the variance of the distribution, $\langle x^2 \rangle$, is finite. For Lévy motion, however, the small jumps are interspersed with longer jumps, or "flights," causing the variance of the distribution to diverge. As a consequence, Lévy jumps do not have a characteristic length scale.

This scale invariance is a signature of fractal patterns. Indeed, Lévy's initial question of "When does the whole look like its parts?" addresses the fractal property of self-similarity. An important parameter for assessing the scaling relationship of fractal patterns is dimension. What, then, is the dimension of the pattern traced out by Lévy motion? The short jumps making up Brownian motion build a clustered pattern that is so dense that area is a more appropriate measure than length—the pattern is actually two-dimensional. In contrast, although the short jumps of Lévy motion produce a clustering, the longer, less frequent jumps initiate new clusters. These clusters form a self-similar pattern with a dimension of less than two. Fractional dimensions are an exotic property of fractals.

Today, Lévy motion is as widely explored in nonlinear, chaotic, turbulent, and fractal systems as Brownian motion is in simpler systems. Following Mandelbrot's research in the 1970s demonstrating the prevalence of fractal patterns in nature, an increasing number of natural phenomena have been described using Lévy statistics (Mandelbrot, 1982). Lévy distributions are also having an impact on artificial systems. A recent example concerns nano-scale electronic devices in which chaotic electron trajectories produce Lévy statistics in the electrical conduction properties (Micolich et al., 2001). Other examples include diffusion in Josephson junctions (Geisel et al., 1985) and at liquid-solid interfaces (Stapf et al., 1995).

It is even possible to picture relatively simple systems in which both Brownian and Lévy motion appear and a transition between the two can be induced. Consider, for example, dropping tracer particles into a container of liquid. This, of course, is Brown's original experiment. In 1993, Harry Swinney extended this experiment by considering a rotating container of liquid shaped like a washer. As turbulence set in, vortices appeared in the liquid and Swinney's group showed that the tracer particles followed Lévy flights between the vortices with $\gamma = 1.3$ (Solomon et al., 1993).

In addition to spatial distributions, Lévy statistics can also be applied to distributions measured as a function of time. A famous example is the dripping faucet (*See* **Dripping faucet**). In 1995, Thadeu Penna's group showed that the fluctuations in the time intervals between drips follow a Lévy distribution with $\gamma = 1.66-1.85$. A significant appeal of this result lies in a comparison with earlier medical work by Ary Goldberger's group showing that fluctuations in the human heart beat follow $\gamma = 1.7$ (Goldberger, 1996). This prompted Penna to ask, "Is the heart a dripping faucet?"

Goldberger suggested that the Lévy statistics describing the human heart arise from nonlinear processes that regulate the human nervous system. He has since extended his research of the fractal dynamics of physiology to other examples of involuntary behavior. This includes studies of the human gait that show that fluctuations in stride intervals display fractal variations (Hausdorff et al., 1996). Fractal variations might therefore be a general signature of healthy human behavior, exhibited whenever conscious control is not involved.

It is interesting to consider this speculation within the context of the results of the British Antarctic Survey in 1996, which showed that albatrosses follow Lévy flights. Other species of animals, such as ants and bees, also follow Lévy flights when foraging for food. Due to the diverging variance of the flight distribution, Lévy trajectories represent an efficient way of covering large regions of space, especially when compared with Brownian motion. Significantly, these animal behavioral patterns represent yet another example of Lévy behavior generated by actions that are devoid of intellectual deliberation.

This relationship between unconscious actions and Lévy statistics has even touched on human creativity. In particular, the Surrealist art movement developed a technique called automatic painting, in which artists painted with such speed that any conscious involvement was thought to be eliminated. Jackson Pollock adopted this approach during the 1940–1950s when he dripped paint onto large horizontal canvases (see *Autumn Rhythm*, Figure 1). Remarkably, his paintings are fractal

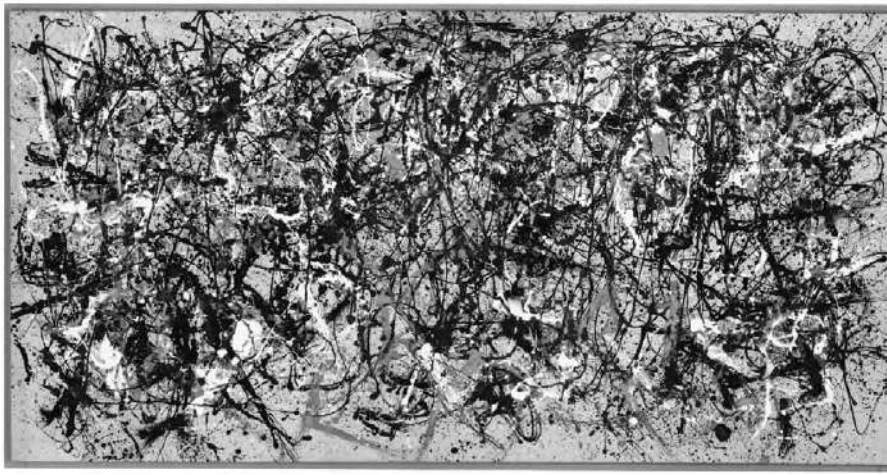

Figure 1. *Autumn Rhythm (Number 30)*, by Jackson Pollock, 1950. © 2003 The Pollock-Krasner Foundation / Artists Rights Society (ARS) New York. Courtesy The Metropolitan Museum of Art, George A. Hearn Fund, 1957. (57.92)

and his motions have been described in terms of Lévy flights (Taylor et al., 1999). This work triggered visual perception tests that identified an aesthetic preference for fractal patterns with dimensions between 1.3 and 1.5 (Taylor, 2001).

Lévy distributions represent a truly interdisciplinary phenomenon that will continue to be useful as novel artificial and natural systems are explored.

RICHARD TAYLOR

See also **Brownian motion; Dimensions; Dripping faucet; Fractals**

Further Reading

Geisel, T., Nierwetberg, J. & Zacherl, A. 1985. Accelerated diffusion in Josephson junctions and related chaotic systems. *Physical Review Letters*, 54: 616–620

Goldberger, A.L. 1996. Non-linear dynamics for clinicians: chaos theory, fractals, and complexity at the bedside. *The Lancet*, 347: 1312–1314

Haussdorff, J.M., Purdon, P.L., Peng, C.K., Ladin, Z., Wei, J.Y. & Goldberger, A.L. 1996. Fractal dynamics of human gait: stability of long-range correlations in stride interval fluctuations. *Journal of Applied Physiology*, 80: 1448–1457

Mandelbrot, B., 1982. *The Fractal Geometry of Nature*, San Francisco: Freeman

Micolich A.P., Taylor, R.P., Davies, A.G., Bird, J.P., Newbury, R., Fromhold, T.M., Ehlert, A., Linke, H., Macks, L.D., Tribe, W.R., Linfield, E.H., Ritchie, D.A., Cooper, J., Aoyagi, Y. & Wilkinson, P.B. 2001. The evolution of fractal patterns during a classical-quantum transition. *Physical Review Letters*, 87: 036802-1–036802-4

Solomon, T., Weeks, E. & Swinney, H. 1993. Observation of anomalous diffusion and Lévy flights in a two-dimensional rotating flow. *Physical Review Letters*, 71: 3975–3979

Stapf, S., Kimmich, R. & Seitter, R. 1993. Proton and deuteron field-cycling NMR relaxometry of liquids in porous glasses: evidence of Lévy-walk statistics. *Physical Review Letters*, 75: 2855–2859

Taylor, R.P., Micolich, A.P. & Jonas, D. 1999. Fractal analysis of Pollock's drip paintings. *Nature*, 399: 422 and *Physics World*, 12: 25–29

Taylor, R.P. 2001. Architect reaches for the clouds. *Nature*, 410: 18

LIE ALGEBRAS AND LIE GROUPS

Lie groups were introduced by the 19th century Norwegian mathematician Sophus Lie through his studies in geometry and integration methods for differential equations (Hawkins, 1999). Further developments by W. Killing, É. Cartan and H. Weyl established Lie's theory as a cornerstone of mathematics and its physical applications. General references include Duistermaat & Kolk (1999), Sattinger & Weaver (1986), and Varadarajan (1984).

An r parameter Lie group is defined as an r-dimensional manifold that is also a group with smooth multiplication and inversion maps. A key example is the $r = n^2$-dimensional general linear group $\mathrm{GL}(n)$ of (either real or complex) $n \times n$ nonsingular matrices, $\det A \neq 0$, under matrix multiplication. Most Lie groups can be realized as matrix groups, that is, subgroups of $\mathrm{GL}(n)$. Important examples include the

- special linear group $\mathrm{SL}(n) \subset \mathrm{GL}(n)$ with $\det A = 1$, and $r = n^2 - 1$;
- orthogonal group $\mathrm{O}(n) \subset \mathrm{GL}(n, \mathbb{R})$ with $A^{\mathrm{T}} A = I$, and $r = n(n-1)/2$;

- unitary group $\mathrm{U}(n) \subset \mathrm{GL}(n, \mathrm{C})$ with $A^\dagger A = I$, and $r = n^2$;
- symplectic group $\mathrm{Sp}(2n) \subset \mathrm{GL}(2n, \mathbb{R})$ with $A^{\mathrm{T}} J A = J = \begin{pmatrix} 0 & -I \\ I & 0 \end{pmatrix}$, and $r = n(2n+1)$.

A Lie algebra $\mathfrak{g}$ is a vector space equipped with a skew-symmetric, bilinear bracket $[\,\cdot,\cdot\,]\colon \mathfrak{g} \times \mathfrak{g} \to \mathfrak{g}$ that satisfies the Jacobi identity

$$[\,u, [\,v, w\,]\,] + [\,v, [\,w, u\,]\,] + [\,w, [\,u, v\,]\,] = 0.$$

The Lie algebra $\mathfrak{g}$ of left-invariant vector fields on an r-parameter Lie group G can be identified with the tangent space at the identity, and so $\dim \mathfrak{g} = r$. The Lie algebra $\mathfrak{gl}(n)$ of $\mathrm{GL}(n)$ consists of all $n \times n$ matrices under matrix commutator $[\,A, B\,] = AB - BA$. A finite-dimensional Lie algebra with basis $v_1, \ldots, v_r$ is specified by its structure constants c_{jk}^i, defined by the bracket relations $[\,v_j, v_k\,] = \sum_{i=1}^r c_{jk}^i v_i$. Each finite-dimensional Lie algebra corresponds to a unique connected and simply connected Lie group G^*; any other is obtained by quotienting by a discrete normal subgroup: $G = G^*/N$.

A subspace $\mathfrak{h} \subset \mathfrak{g}$ is a subalgebra if it is closed under the Lie bracket: $[\,\mathfrak{h}, \mathfrak{h}\,] \subset \mathfrak{h}$. Lie subalgebras are in one-to-one correspondence with connected Lie subgroups $H \subset G$. The subalgebra is an ideal if $[\,\mathfrak{g}, \mathfrak{h}\,] \subset \mathfrak{h}$. A Lie algebra is simple if it contains no nontrivial ideals, and semi-simple if it contains no nontrivial abelian (commutative) ideals. Semi-simple algebras are direct sums of simple algebras. A Lie algebra is solvable if the sequence of subalgebras $\mathfrak{g}^{(0)} = \mathfrak{g}$, $\mathfrak{g}^{(k+1)} = [\,\mathfrak{g}^{(k)}, \mathfrak{g}^{(k)}\,]$ eventually terminates with $\mathfrak{g}^{(n)} = \{0\}$. The Levi decomposition says that every Lie algebra is the semi-direct sum of a semi-simple subalgebra and its radical—the maximal solvable ideal.

The Killing–Cartan classification of complex simple Lie algebras contains four infinite families, denoted A_n, B_n, C_n, D_n, corresponding to the simple Lie groups $\mathrm{SL}(n+1)$, $\mathrm{O}(2n+1)$, $\mathrm{Sp}(2n+1)$, $\mathrm{O}(2n)$. In addition, there are five exceptional simple Lie groups, G_2, F_4, E_6, E_7, E_8, of respective dimensions 14, 52, 78, 133, 248. The last plays an important role in modern theoretical physics. Extending the classification to infinite-dimensional simple Lie algebras leads to the Kac–Moody Lie algebras, of importance in integrable systems, theoretical physics, differential geometry, and topology (Kac, 1990).

Lie groups typically arise as symmetry groups of geometric objects or differential equations. A (Lie) group G acts on a manifold M, for example, Euclidean space, provided $m \mapsto g \cdot m$ for $g \in G, m \in M$, defines a sufficiently smooth invertible map that respects the group multiplication. Lie classified all transformation groups acting on one- and two-dimensional real and complex manifolds (Olver, 1995). According to Klein's Erlanger Program, geometric structure is prescribed by an underlying transformation group; thus, Euclidean, affine, conformal, projective geometries are based on the eponymous Lie groups. If G acts transitively, then $M = G/H$ is a homogeneous space, obtained by quotienting by a closed Lie subgroup. The group orbits—minimal invariant subsets—form a system of submanifolds, and the invariant functions are constant on orbits. The infinitesimal generators of the group action form a Lie algebra $\mathfrak{g}$ of vector fields tangent to the orbits whose flows generate the group action.

A linear action $\rho\colon G \to \mathrm{GL}(V)$ on a vector space V is known as a representation. Representation theory plays a fundamental role in quantum mechanics since linear symmetries of the Schrödinger equation induce actions on the space of solutions, which decompose into irreducible representations. The structure of atoms, nuclei, and elementary particles is governed by the representations of particular symmetry groups (Hamermesh, 1962). Important special functions, for example, Bessel and hypergeometric, arise as matrix entries of representations of particular Lie groups (Vilenkin & Klimyk, 1991). The representation theory of the orthogonal group SO(2) leads to trigonometric functions and, hence, Fourier analysis, as the simplest case of harmonic analysis on semi-simple Lie groups (Warner, 1972).

A Lie group acts on its Lie algebra $\mathfrak{g}$ by the adjoint representation and on the dual space $\mathfrak{g}^*$ by the coadjoint representation. The coadjoint orbits are symplectic submanifolds with respect to the natural Lie–Poisson structure on $\mathfrak{g}^*$, and are of importance in classifying representations (Kirillov, 1999), geometric mechanics, and geometric quantization (Woodhouse, 1992). The Euler equations of rigid body motion and of fluid mechanics are realized as the Lie–Poisson equations on, respectively, the Lie algebra of the Euclidean group and the infinite-dimensional diffeomorphism group (Marsden, 1992).

A transformation group is called a symmetry group of a system of differential equations if it maps solutions to solutions. Symmetry groups are effectively computed by solving the infinitesimal symmetry conditions, which form an overdetermined linear system of partial differential equations, usually amenable to automatic solution by computer algebra packages (Olver, 1993, 1995). Applications include integration of ordinary differential equations, determination of explicit group-invariant (similarity) solutions of partial differential equations, Noether's theorems relating symmetries of variational problems and conservation laws (Noether, 1918), bifurcation theory (Golubitsky & Schaeffer, 1985), asymptotics and blow-up (Barenblatt, 1979), and the design of geometric numerical integration schemes (Hairer et al., 2002).

Classification of differential equations and variational problems admitting a given symmetry group relies on its differential invariants. The simplest examples

are the curvature and torsion of space curves, and the mean and Gaussian curvatures of surfaces under the Euclidean group acting on $\mathbb{R}^3$. Cartan's method of moving frames, and its more recent extensions to general Lie group and Lie pseudo-group actions (Olver, 2001), provides a general mechanism for construction and classification of differential invariants, with applications to differential geometry, the calculus of variations, soliton theory, computer vision, classical invariant theory, and numerical methods.

Modern developments in applications of Lie group methods have proceeded in a variety of directions. General theories of infinite-dimensional Lie groups and algebras (Kac, 1990) and Lie pseudo-groups, arising in relativity, field theory, fluid mechanics, solitons, and geometry, remain elusive. Higher order or generalized symmetries, in which the infinitesimal generators also depend upon derivative coordinates, first proposed by Noether (1918), have been used to classify integrable (soliton) systems. Recursion operators are used to generate such higher order symmetries and, via Noether's theorem, higher order conservation laws (Olver, 1993). Most recursion operators are derived from a pair of compatible Hamiltonian structures, and demonstrate the integrability of bi-Hamiltonian systems. The higher-order symmetries also appear in series expansions of Bäcklund transformations in the spectral parameter.

PETER J. OLVER

See also **Bäcklund transformations; Inverse scattering method or transform; Maps; Symmetry groups**

Further Reading

Barenblatt, G.I. 1979. *Similarity, Self-Similarity, and Intermediate Asymptotics*, New York: Consultants Bureau

Duistermaat, J.J. & Kolk, J.A.C. 1999. *Lie Groups*, Berlin and New York: Springer

Golubitsky, M. & Schaeffer, D.G. 1985. *Singularities and Groups in Bifurcation Theory*, 2 vols, New York: Springer

Hairer, E., Lubich, C. & Wanner, G. 2002. *Geometric Numerical Integration: Structure-preserving Algorithms for Ordinary Differential Equations*, Berlin and New York: Springer

Hamermesh, M. 1962. *Group Theory and Its Application to Physical Problems*, Reading, MA: Addison-Wesley, 1962

Hawkins, T. 1999. *The Emergence of the Theory of Lie Groups. An Essay on the History of Mathematics 1869–1926*, New York: Springer

Kac, V.G. 1990. *Infinite Dimensional Lie Algebras*, Cambridge and New York: Cambridge University Press

Kirillov, A.A. 1918. Merits and demerits of the orbit method, *Bulletin of the American Mathematical Society*, 36: 433–488

Marsden, J.E. 1992. *Lectures on Mechanics*, Cambridge and New York: Cambridge University Press

Noether, E. 1918. Invariante variationsprobleme. *Nachricheten von der Konig. Gesellschaft der Wissenschaften zu Gottingen, Mathematisch–Physikalische Klasse*, 235–257

Olver, P.J. 1993. *Applications of Lie Groups to Differential Equations*, 2nd edition, London and New York: Springer

Olver, P.J. 1995. *Equivalence, Invariants, and Symmetry*, Cambridge and New York: Cambridge University Press

Olver, P.J. 2001. Moving frames—in geometry, algebra, computer vision, and numerical analysis. In *Foundations of Computational Mathematics*, edited by R. DeVore, A. Iserles & E. Suli, Cambridge and New York: Cambridge University Press, pp. 267–297

Sattinger, D.H. & Weaver, O.L. 1986. *Lie Groups and Algebras with Applications to Physics, Geometry, and Mechanics*, New York: Springer

Varadarajan, V.S. 1984. *Lie Groups, Lie Algebras, and Their Representations*, New York: Springer

Vilenkin, N.J. & Klimyk, A.U. 1991. *Representation of Lie Groups and Special Functions*, Dordrecht: Kluwer

Warner, G. 1972. *Harmonic Analysis on Semi-simple Lie Groups*, Berlin and New York: Springer

Woodhouse, N.M.J. 1992. *Geometric Quantization*, 2nd edition, Oxford: Clarendon Press and New York: Oxford University Press

LIFETIME

As the word implies, *lifetime* is a measure of the time that something manages to persist and properly function. Often lifetime is a statistically defined quantity, as is evident from thinking about the failure of light bulbs. Clearly, one can exactly measure the lifetime of any particular bulb at the cost of burning it out, but it is more interesting to know the probability of failure in a given interval of time for a particular type of bulb. To obtain this information, it is necessary to measure the average burnout rate for a large number of bulbs that have been manufactured under identical conditions and use that information to characterize bulbs newly manufactured under the same conditions. A related approached is used by actuaries, who compute risks and premiums for human life insurance.

Failure of a Nuclear Power Plant

Statistical ideas are sometimes applied to more special situations, for example, a nuclear power plant, where neighbors ask: "What are the chances of it blowing up or melting down?" Engineers usually answer with soothing words. "It's very safe. This reactor can't blow up, and it has less than a fifty percent chance of melting down in the next thousand years." But the engineers have only built a few dozen plants, all of which seem to be working fine. How do they come up with such an estimate?

One procedure is to consider the various failure mechanisms (onset of corrosion, earthquakes, operators falling asleep, terrorist attacks, and so on), and assign a mean lifetime to each failure mechanism. Then the total failure probability up to time t_1 is defined as

$$P(t_1) = \int_0^{t_1} \frac{\mathrm{d}t}{\tau}\,, \qquad (1)$$

where τ is the mean lifetime, taking all failure mechanisms into account. If these mechanisms are independent (do not influence one another), then

$$\frac{1}{\tau} = \frac{1}{\tau_1} + \frac{1}{\tau_2} + \cdots + \frac{1}{\tau_N}, \qquad (2)$$

where $\tau_1, \tau_2, \ldots, \tau_N$ are mean lifetimes estimated for N failure mechanisms. (Note that the τ_i may be functions of time.) A key result of this simple formulation is that the total lifetime is less than the smallest constituent lifetime, making it imperative to consider all possible failure mechanisms.

Lifetime of a Quantum State

Given a quantum state $\psi(\mathbf{r})$, where $\mathbf{r}$ is a spatial coordinate, it is interesting to know the mean time (τ) before ψ makes a transition (decays) into one of N other states: $\phi_1(\mathbf{r})$, $\phi_2(\mathbf{r})$, …, $\phi_N(\mathbf{r})$. According to "Fermi's Golden Rule", the transition probability into ϕ_i is proportional to the square of an overlap integral (Slater, 1951; Dirac, 1935)

$$|\langle\psi|\phi_i\rangle|^2 \equiv \left[\int \psi\phi^* \, \mathrm{d}\mathbf{r}\right]^2; \qquad (3)$$

thus the total lifetime is

$$\tau \propto \frac{1}{|\langle\psi|\phi_1\rangle|^2 + |\langle\psi|\phi_2\rangle|^2 + \cdots + |\langle\psi|\phi_N\rangle|^2}. \qquad (4)$$

Although this equation is simple to write, it is difficult to compute because computation requires detailed knowledge of the wave functions of all states into which ψ can decay. Just as with a nuclear power plant, the total lifetime will be less than the smallest individual decay time, but τ is easier to measure, as it is often a small faction of a second.

Soliton Lifetimes

When John Scott Russell first observed a hydrodynamic soliton on the "happiest day of [his] life" in August of 1834, he was struck by its remarkable stability, giving him time to follow it on horseback until it became "lost in the windings of the canal" (Russell, 1844). Although this and subsequent observations suggest that solitons are long-lived objects, the conclusion is somewhat misleading. It is the spatial localization of soliton energy that persists in time rather than the energy itself. Detailed perturbation calculations for the Korteweg–de Vries equation and for the nonlinear Schrödinger equation show that the times for energy decay under dissipative perturbations are less for nontopological solitons than for delocalized wave packets (Scott, 2003). Solitons of the sine-Gordon (SG) equation, on the other hand, have infinite lifetimes, as their decay is prevented by a topological constraint. Thus, the kinetic energy of a SG kink decays (the soliton slows to a stop), but its rest mass does not disappear. The property of topological stability is shared by Skyrmions, which makes these objects interesting as models for elementary particles.

In studies of nontopological solitons in molecular crystals and of biological solitons, lifetime is a central issue, as the energy must remain localized long enough to be of technical or biological interest. When such solitons are also quantum objects (as is often the case), accurate lifetime calculations require estimates of the type sketched in Equation (4). This is a daunting theoretical task for three reasons: the wave function of a quantum soliton (ψ) is quite complicated (Davydov, 1991; Scott, 2003), biological molecules are often irregular structures for which all the possible final states $\{\phi_i\}$ are not known, and the temperatures at which biological organisms exist (ca. 300 K) introduce structural uncertainties that depend irregularly on time.

Using femtosecond pump-probe spectroscopy, however, it has recently become feasible to measure lifetimes in molecular crystals of the order of a picosecond or more (Elsaesser et al., 2000). Importantly, the response of such observations is null unless nonlinear effects are present, which occurs only for localized energy; thus the measurements focus specifically on soliton-like entities. From data produced by such experiments, the relevance of various theoretical proposals for solitons in molecular crystals and biomolecules should become better understood in coming years.

ALWYN SCOTT

See also **Biomolecular solitons; Davydov soliton; Pump-probe measurements; Skyrmions**

Further Reading

Davydov, A.S. 1991. *Solitons in Molecular Systems*, 2nd edition, Dordrecht and Boston: Reidel

Dirac, P.A.M. 1935. *The Principles of Quantum Mechanics*, Oxford: Clarendon Press

Elsaesser, T., Mukamel, S., Murnanae, M.M. & Scherer N.F. (editors). 2000. *Ultrafast Phenomena XII*, Berlin: Springer

Russell, J.R. 1844. Report on waves. *14th Meeting of the British Association for the Advancement of Science*, London: BAAS: 311–339

Scott, A.C. 2003. *Nonlinear Science: Emergence and Dynamics of Coherent Structures*, 2nd edition, Oxford and New York: Oxford University Press

Slater, J.C. 1951. *Quantum Theory of Matter*, New York: McGraw-Hill

LIGHTHILL CRITERION

See **Wave stability and instability**

LINDSTEDT–POINCARÉ METHOD

See **Perturbation analysis**

LINEARIZATION

Linear systems are much easier to analyze than nonlinear systems because they satisfy the superposition principle, which can be stated as follows: if R_1 is the output of a linear system to input S_1 and R_2 is the output to input S_2, then the output to the cumulative input $aS_1 + bS_2$ is $aR_1 + bR_2$. Applied iteratively, this property allows the inputs and outputs of a linear system to be decomposed in various ways to simplify analysis. From a more general perspective, linear systems do not confuse the lines of causality between the input and output (stimulation and response) of a linear system. Fully nonlinear systems, on the other hand, do not share this useful property; thus, the causal implications of each stimulation must be individually studied.

Linearization is an attempt to carry some of the attractive properties of linear systems into the nonlinear domain. Linearization methods can be classified in two approaches: reductions of nonlinear systems to linearized approximations for small perturbations and extensions of linearized approximations to weakly nonlinear systems. Linearization methods of the first approach are used for stability analyses of special solutions of a nonlinear system, such as critical points, periodic orbits, solitary waves and periodic waves. In the neighborhood of such special solutions of nonlinear systems, linear equations are derived for small perturbations that are then studied using standard methods (Fourier or Laplace transforms, Green functions, etc.). Linearization methods of the second approach are based on specific parameters of a linearized system, such as dominant eigenvalues or resonant wave numbers. Thus, linearized systems are extended to weakly nonlinear systems, such as normal forms and amplitude equations, by means of asymptotic multiple scale expansion methods and Fredholm's alternative theorem for linear nonhomogeneous equations.

For systems of partial differential equations (PDEs), linearization methods can be illustrated with the example of a nonlinear Schrödinger (NLS) equation (Whitham, 1974):

$$iu_t + u_{xx} - \left(\omega_0 + \omega_2|u|^2\right) u = 0, \tag{1}$$

where ω_0 and ω_2 are parameters such that $\omega_2 > 0$ and $\omega_2 < 0$ occur for defocusing and focusing cases, respectively. The NLS equation (1) has a constant wave solution of the form:

$$u_0(x,t) = a\, e^{-i(\omega_0+\omega_2 a^2)t}, \tag{2}$$

where the wave frequency $\omega = \omega_0 + \omega_2 a^2$ depends on the constant wave amplitude a. Linearizing the NLS equation (1) at the wave solution (2), one expands $u(x,t)$ as

$$u(x,t) = a\, e^{-i(\omega_0+\omega_2 a^2)t}\,[1 + V(x,t) + iW(x,t)], \tag{3}$$

where V and W are real. When the expansion is substituted into the NLS equation and the nonlinear terms in V and W are neglected, the linearized problem can be transformed to the linear Boussinesq equation (4) with constant coefficients:

$$W_{tt} - 2\omega_2 a^2 W_{xx} + W_{xxxx} = 0. \tag{4}$$

The Fourier spectrum of the linear Boussinesq equation consists of two counter-propagating waves:

$$W(x,t) = W_+ e^{ikx - i\Omega(k)t} + W_- e^{ikx + i\Omega(k)t}, \tag{5}$$

where $\Omega(k) = k\sqrt{2\omega_2 a^2 + k^2}$. When $\omega_2 > 0$ (the defocusing case), the wave spectrum is stable, that is, $\Omega(k)$ is real for any k. When $\omega_2 < 0$ (the focusing case), the wave spectrum is unstable, that is, $\Omega(k)$ is complex for an interval of k, namely for $0 < k < \sqrt{2|\omega_2|}a$. Thus, the linearization method of the first approach enables us to check stability of the constant wave solutions of the NLS equation.

The linear Boussinesq equation (4) with $\omega_2 > 0$ is a hyperbolic system. With dispersive effects neglected in a long-wave approximation, the Boussinesq equation reduces to the wave equation: $W_{tt} - c^2 W_{xx} = 0$, where $c^2 = 2\omega_2 a^2$. The wave equation has a solution in the form of two dispersionless counter-propagating waves: $W(x,t) = W_+(x - ct) + W_-(x + ct)$. Unidirectional long-wave, small-amplitude approximation can be captured by the asymptotic multi-scale expansion method in the perturbation series (Zakharov & Kuznetsov, 1986):

$$u(x,t) = a\, e^{-i(\omega_0+\omega_2 a^2)t} \times \left[1 + i\varepsilon R(\xi,\tau) + \varepsilon^2\left(\frac{1}{c}R_\xi - R^2\right) + O(\varepsilon^3)\right], \tag{6}$$

where $\xi = \varepsilon(x - ct)$, $\tau = \varepsilon^3 t$, and ε is a small parameter. Applying the Fredholm's alternative theorem to a linear nonhomogeneous equation at order $O(\varepsilon^3)$, one can derive the Korteweg–de Vries (KdV) equation for $W = R_\xi$:

$$-2cW_\tau - 6cWW_\xi + W_{\xi\xi\xi} = 0. \tag{7}$$

With quadratic nonlinear terms neglected, the KdV equation (7) reproduces the dispersion relation of the linear Boussinesq equation, which has been reduced in the unidirectional long-wave approximation. Thus, the linearized method of the second approach enables us to derive the nonlinear evolution equation for wave propagation over the background of the constant wave solution of the NLS equation (1).

Linearization methods for systems of ordinary differential equations (ODEs) are illustrated with the example of an autonomous nonlinear dynamical system (Glendinning, 1994):

$$\frac{d\boldsymbol{u}}{dt} = \boldsymbol{f}(\boldsymbol{u}), \tag{8}$$

where $\boldsymbol{u} = \boldsymbol{u}(t)$ is a vector observable and $\boldsymbol{f}(\boldsymbol{u})$ is a vector nonlinear function. Critical points of the dynamical system occur for $\boldsymbol{u} = \boldsymbol{u}_0$ such that $\boldsymbol{f}(\boldsymbol{u}_0) = 0$. Linearizing the nonlinear system (8) at the critical point $\boldsymbol{u}_0$, one expands $\boldsymbol{u}(t)$ as

$$\boldsymbol{u}(t) = \boldsymbol{u}_0 + \boldsymbol{v}(t). \tag{9}$$

Neglecting quadratic terms in $\boldsymbol{v}(t)$ reduces the linearized problem to the linear system with constant coefficients:

$$\frac{\mathrm{d}\boldsymbol{v}}{\mathrm{d}t} = \mathcal{J}\boldsymbol{v}, \quad \mathcal{J} = \nabla_{\boldsymbol{u}} f\Big|_{\boldsymbol{u}=\boldsymbol{u}_0}, \tag{10}$$

where $\mathcal{J}$ is the Jacobian matrix. Solutions of the linearized system (10) depend on eigenvalues and eigenvectors of the Jacobian matrix: $\mathcal{J}\boldsymbol{w} = \lambda\boldsymbol{w}$. If all eigenvalues are located in the left half-plane of λ, that is, $\mathrm{Re}(\lambda) < 0$, then the critical point $\boldsymbol{u}_0$ is asymptotically stable and the perturbation $\boldsymbol{v}(t)$ decays to zero exponentially in t. If there exists at least one eigenvalue in the right half-plane of λ, then the critical point $\boldsymbol{u}_0$ is linearly unstable and the perturbation $\boldsymbol{v}(t)$ grows exponentially in t.

Some or all eigenvalues may be located at the imaginary axis of λ, that is, $\mathrm{Re}(\lambda) = 0$. In such systems, when no other eigenvalues exist for $\mathrm{Re}(\lambda) > 0$, the critical point $\boldsymbol{u}_0$ is neutrally (weakly) stable. Perturbations may however grow algebraically in t, if eigenvalues of λ are multiple with algebraic multiplicity exceeding the geometric multiplicity. Local linearization is often insufficient for full description of such weak instability and the nonlinear stability analysis is desired.

When eigenvalues cross or coalesce on the axis $\mathrm{Re}(\lambda) = 0$, bifurcations may occur in the spectrum of a linearized system (Glendinning, 1994). Normal forms for bifurcations can be derived by extending the linearized system into the nonlinear domain. For example, a Hopf bifurcation occurs when two simple eigenvalues $\lambda = \Gamma(\varepsilon) + \mathrm{i}\Omega(\varepsilon)$ and $\bar{\lambda} = \Gamma(\varepsilon) - \mathrm{i}\Omega(\varepsilon)$ cross the imaginary axis at the bifurcation parameter $\varepsilon = 0$, such that $\Gamma(0) = 0$ and $\Omega(0) = \Omega_0$. The normal form for the Hopf bifurcation can be derived by the asymptotic multi-scale expansion method in the perturbation series:

$$\boldsymbol{u}(t) = \boldsymbol{u}_0 + \varepsilon\left[A(T)\boldsymbol{w}\mathrm{e}^{\mathrm{i}\Omega_0 t} + \bar{A}(T)\bar{\boldsymbol{w}}\mathrm{e}^{-\mathrm{i}\Omega_0 t}\right] + \mathrm{O}(\varepsilon^2), \tag{11}$$

where $T = \varepsilon^2 t$ and $\boldsymbol{w}$ is the eigenvector of $\mathcal{J}\boldsymbol{w} = \lambda\boldsymbol{w}$ for $\lambda = \mathrm{i}\Omega_0$ at $\varepsilon = 0$. The normal form for Hopf bifurcation follows from the Fredholm's alternative theorem at order $\mathrm{O}(\varepsilon^3)$ in the form

$$\frac{\mathrm{d}A}{\mathrm{d}T} = \left[\Gamma'(0) + \mathrm{i}\Omega'(0)\right]A - \beta(0)|A|^2 A, \tag{12}$$

where $\beta(0)$ is constant. $A(T)$ bifurcates into a periodic orbit at the Hopf bifurcation when $\Gamma'(0)\mathrm{Re}(\beta(0)) > 0$. Thus, linearization methods allow for linear and nonlinear stability analyses, resulting in simplifications of the nonlinear dynamical system (8).

DMITRY PELINOVSKY

See also **Causality; Multiple scale analysis; Quasi-linear analysis; Stability**

Further Reading

Glendinning, P. 1994. *Stability, Instability and Chaos: An Introduction to the Theory of Nonlinear Differential Equations*, Cambridge and New York: Cambridge University Press

Whitham, G.B. 1974. *Linear and Nonlinear Waves*, New York: Wiley

Zakharov, V.E. & Kuznetsov, E.A. 1986. Multi-scale expansions in the theory of systems integrable by the inverse scattering transform. *Physica* D, 18

LIOUVILLE EQUATION

See **Sine-Gordon equation**

LIOUVILLE THEOREM

See **Phase space**

LIPSCHITZ CONDITION

See **Phase space**

LIQUID CRYSTALS

Discovery and Basic Properties

Liquid crystals do not follow the conventional classification of matter into three states: gas, liquid, and solid. In solids the orientation and position of the molecular building blocks are well determined, whereas in liquids the molecules move around in a disordered mixture. In liquid crystals the molecules can change their position, but their orientation is largely determined by neighboring molecules. The liquid crystal phase was discovered by Friedrich Reinitzer in 1888, when he noticed that solid cholesterol benzoate melted at 145°C into a scattering liquid crystal phase which transformed into a clear liquid after further heating to 178°C (Priestly et al., 1976, Chapter 2).

The type of ordering is related to the shape of the molecules or mesogens building the liquid crystal (De Gennes & Prost, 1993, Chapter 1). Calamitic molecules are rod-shaped and form nematic (molecules are aligned) or smectic phases (molecules are aligned and ordered in layers) as shown in Figure 1. Discotic molecules are disc-shaped and form nematic or stacked phases (with the molecules stacked on top of each other). The ordering of the molecules is not perfect due to thermal motion. With increasing temperature, ordering decreases until the liquid crystal is transformed into an isotropic liquid. Because the phase transitions are

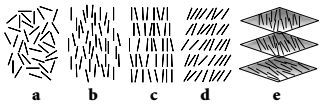

Figure 1. Different phases of liquid crystal materials. (a) isotropic, (b) nematic, (c) smectic-A, (d) smectic-C, (e) cholesteric.

related to temperature, these materials are called thermotropic liquid crystals. The organic molecules have low molecular weight (200–500) and can go through several phases from low to high temperature: solid–smectic-C–smectic-A–nematic–liquid (Figure 1). Chiral (handed) molecules do not have mirror symmetry and this may lead to a cholesteric phase in which the nematic orientation rotates slowly from one layer to the next (Figure 1e). Chiral phases have the property to reflect circularly polarized light that has the same handedness and periodicity as the molecule's structure. In lyotropic liquid crystals which have one hydrophobic and one hydrophilic part, the crystalline ordering depends on the concentration of certain molecules in the solvent. At very low concentrations individual molecules move freely in the liquid, at higher concentrations droplets, cylinders, or planes of attached molecules can be formed. Lyotropic liquid crystals are important in biological systems, in cell membranes, and dispersions (De Gennes & Prost, 1993, Chapter 1).

The nematic and smectic-A phases have uniaxial symmetry with the preferential axis parallel with the molecules. The preferential axis is characterized by a vector, the director $\bar{n}$. Other properties such as permittivity, refractive index, magnetic susceptibility, and conductivity are described by a tensor. The index of refraction of calamitic liquid crystals may, for example, vary between $n_\perp$=1.5 and $n_\parallel$=1.6. The smectic-C phase has biaxial properties. The deformation of a liquid crystal leads to elastic energy. The energy in nematic liquid crystals is due to three types of variations in the orientation: splay, twist, and bend (see De Gennes & Prost, 1993, Chapter 3; Blinov & Chigrinov, 1994, Chapter 4). The elastic energy is then expressed by the following equation:

$$F_{\text{elastic}} = \tfrac{1}{2}\left(K_{11}\,(\nabla\cdot\bar{n})^2 + K_{22}\,(\bar{n}\cdot\nabla\times\bar{n})^2 + K_{33}\,(\bar{n}\times\nabla\times\bar{n})^2\right). \quad (1)$$

Surfaces can prefer either homeotropic (perpendicular) or parallel alignment of the director. If the interface is treated by rubbing a polyimide surface layer, this dictates a preferential azimuth for the director. The minimization of the combined elastic energy and surface energy determines the orientation of the director between the surfaces. This can lead to a pure twist as shown in Figure 2.

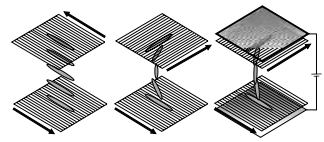

Figure 2. Nematic liquid crystal between two glass plates. The grid represents the alignment layer and the arrow the rubbing direction. Left: antiparallel rubbing with all molecules parallel; Middle: 90° twisted nematic; Right: when a voltage is applied between the electrodes, the molecules tilt.

Nonlinear Properties

In smectic liquid crystals, linear elasticity theory and linear hydrodynamics no longer hold because higher order terms come into play in the elastic energy (De Gennes & Prost, 1993, Chapter 8). The elasticity constants then depend on the deformation strength and this can lead to undulation instabilities, buckling, or focal conic structures. In a similar way, hydrodynamic nonlinearities yield frequency-dependent viscosities. If liquid crystal is illuminated with a high optical power, the physical properties may be modified. The processes leading to optical nonlinearities can be of electronic or non-electronic origin (Khoo, 1995). Electronic nonlinear effects involve processes in which the electronic wave functions of the liquid crystal molecules are perturbed by the optical field. These very fast processes are similar to electronic nonlinearities in solid crystals. These processes lead to second and third harmonic generation and optical phase conjugation (Khoo, 1995). Beside the electronic structure of the molecules, other physical properties can change because of an applied optical field, such as the molecular structure or orientation, the temperature, and the density (Elston & Sambles, 1998, Chapter 6). Slow temperature effects occur when a liquid crystal in a nematic phase is heated by an optical beam. The difference between the ordinary and extraordinary index of refraction decreases until the liquid crystal reaches the transition temperature and becomes isotropic. Another important effect is the molecular reorientation by the optical field. In the static case, the molecules will reorient due to the difference in dielectric constant ($\varepsilon_\parallel$ and $\varepsilon_\perp$); and in the optical case, due to the difference in refractive index ($n_\parallel$ and $n_\perp$).

Applications

Because of the anisotropy in the permittivity (or magnetic susceptibility), calamitic molecules with $\varepsilon_\parallel > \varepsilon_\perp$ prefer to orient their long axis parallel with an applied electric (or magnetic) field. By applying a voltage over a cell filled with liquid crystal, it is possible to make the molecules tilt out of the plane, as illustrated in Figure 2. In a uniaxial liquid crystal,

linearly polarized ordinary and extra-ordinary waves propagate with refractive indices $n_\perp$ and n_e (with n_e between $n_\parallel$ and $n_\perp$) (Iizuka, 2002, Ch.4). Because of the difference in propagation speed, the polarization state of the combined wave changes continuously. In a twisted nematic display (Figure 2), the linearly polarized light roughly follows the orientation of the director (Mauguin regime) and rotates over 90° (Priestly et al., 1976, Chapter 14). If the top polarizer is also rotated over 90° compared to the bottom polarizer, all light will be transmitted. If a voltage is applied to the cell and the molecules orient perpendicularly, the linear polarization is unchanged, and no light passes through the analyser. Cholesteric liquid crystals appear in nature, for example, in the cuticle of insects. The result is a colored and polarized reflection, depending on the angle of observation.

KRISTIAAN NEYTS AND JEROEN BEECKMAN

See also **Dislocations in crystals; Harmonic generation; Nonlinear optics**

Further Reading

Blinov, L.M. & Chigrinov, V.G. 1994. *Electrooptic Effects in Liquid Crystal Materials, Partially Ordered Systems*, New York: Springer

De Gennes, P.G. & Prost, J. 1993. *The Physics of Liquid Crystals*, 2nd edition, Oxford: Clarendon Press and New York: Oxford University Press

Elston, S. & Sambles, R. 1998. *The Optics of Thermotropic Liquid Crystals*, London: Taylor & Francis

Iizuka, K. 2002. *Elements of Photonics, in Free Space and Special Media*, New York: Wiley-Interscience

Khoo, I.C. 1995. *Liquid Crystals, Physical Properties and Nonlinear Optical Phenomena*, New York: Wiley

Priestly, E.B., Wojtowicz, P.J. & Shent, P. 1976. *Introduction to Liquid Crystals*, New York and London: Plenum Press

LOCAL MODES IN MOLECULAR CRYSTALS

Energy transfer in molecular crystals occurs through exciton hopping from molecule to molecule. It is possible, however, that nonlinear localization takes place due to coupling between excitonic and vibrational degrees of freedom, transforming the exciton into a local mode. Such a mode is generated by an effective local nonlinear potential induced by the exciton-phonon coupling, and it has features similar to a polaron, a soliton, and a breather.

The experimental search for nonlinear local modes was initiated by Careri in the early 1970s in crystalline acetanilide ($CH_3CONHC_6H_5$), or ACN, which has structure similar to a polypeptide; thus, positive findings in ACN could be of biological significance. In particular, if nonlinear local modes exist and are sufficiently long-lived, they could be agents of energy transfer in biomolecules.

In ACN and in proteins, one finds hydrogen-bonded quasi-one-dimensional polypeptide chains with the following structure:

$$\cdots H-N-C=O\cdots H-N-C=O\cdots H-N-C=O\cdots. \tag{1}$$

Careri focused on the amide-I (C=O stretching) vibration and found its infrared absorption spectrum to have two peaks: a "normal" one at 1665 cm^{-1} and an "anomalous" one at 1650 cm^{-1}. The basic feature of the latter is its strong temperature dependence and its disappearance at biological temperatures, as shown in Figure 1.

In 1982, Careri and Scott hypothesized that this anomalous peak is a spectral signature of a self-trapped state similar to the Davydov soliton, while the normal peak is the delocalized free exciton of the amide-I vibration. An approximate way to represent the ACN local mode is by assuming an adiabatic separation between the faster amide-I exciton vibration and a slower local (Einstein) oscillator with which the hydrogen bond interacts. The corresponding Hamiltonian has three terms:

$$H = H_{ex} + H_{ph} + H_{int}, \tag{2}$$

where

$$\begin{aligned} H_{ex} &= \sum_n \left[\varepsilon_0 a_n^\dagger a_n - J(a_n^\dagger a_{n+1} + a_n^\dagger a_{n-1})\right], \\ H_{ph} &= \frac{1}{2}\sum_n \left[\frac{{p_n}^2}{m} + m\omega_0{}^2 {q_n}^2\right], \\ H_{int} &= \chi \sum_n q_n a_n^\dagger a_n \,. \end{aligned} \tag{3}$$

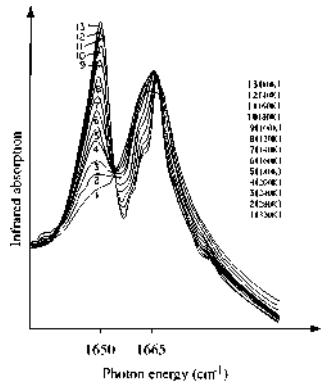

Figure 1. Infrared absorption spectra of crystalline acetanilide in the region of the amide-I mode. The free exciton peak is at 1665 cm^{-1} while the anomalous peak that is at 1650 cm^{-1} has strong temperature dependence and is associated with a self-trapped state (Careri et al., 1984).

Here $a_n^{\dagger}$ (a_n) creates (destroys) a quantum of amide-I excitation of energy ε_0 at the nth CO unit, J is the energy of exciton-exciton interaction between adjacent CO units, p_n and q_n are the momentum and position, respectively, of the local Einstein oscillator at the nth location representing a low frequency optical mode, and χ determines the strength of the interaction between the exciton and Einstein mode.

One way to analyze this complex problem is by treating the slow ($p_n \approx 0$) Einstein oscillators classically while evaluating the expectation value of the total Hamiltonian with respect to the exciton wave function $|\Psi\rangle = \sum_n c_n(t) a^{\dagger}_n |0\rangle_{\mathrm{ex}}$, where $|0\rangle_{\mathrm{ex}}$ is the exciton system vacuum. Variational minimization of $\mathcal{H} \equiv \langle \Psi | H | \Psi \rangle$ with respect to the oscillator variable q_n leads to $q_n = -\chi/(m\omega_0{}^2)|c_n(t)|^2$, which upon substitution to $\mathcal{H}$ transforms the latter to the classical Hamiltonian

$$\mathcal{H} = \sum_n \left[\varepsilon_0 |c_n|^2 \quad -J(c*_n c_{n+1} + c*_n c_{n-1}) - \frac{\chi^2}{2m\omega_0^2} |c_n|^4 \right]. \tag{4}$$

Hamilton's equations then lead to a discrete self-trapping system or a discrete nonlinear Schrödinger (DNLS) equation:

$$\mathrm{i}\hbar \dot{c}_n + J(c_{n+1} + c_{n-1}) + \frac{\chi^2}{m\omega_0{}^2} |c_n|^2 c_n = 0. \tag{5}$$

This equation admits two types of solutions: one is an extended plane wave corresponding to the free exciton, while the other is localized and corresponds to a self-trapped state. The difference of the energies of these two solutions is

$$E_{\mathrm{b}} = \frac{\chi^2}{2m\omega_0{}^2} - 2J, \tag{6}$$

corresponding to the binding energy of the self-trapped state. A combination of calculations and fitting to data suggests that $J \approx 4\,\mathrm{cm}^{-1}$, $\chi^2/m\omega_0^2 \approx 45\,\mathrm{cm}^{-1}$, and E_{b} is equal to $1665 - 1650 = 15\,\mathrm{cm}^{-1}$.

This picture is in accord with the presence of the two peaks in the amide-I region shown in Figure 1. Use of these parameter values in the context of a more sophisticated model gives also the correct temperature dependence of the anomalous peak. Because in the present case $J \ll \chi^2/m\omega_0^2$, the local mode can also be viewed as a DNLS discrete breather close to the anti-continuous limit (where $J \to 0$).

Although the above proposed was furnished in the 1980s, both the essence of Davydov's idea as well as its specific application to ACN were challenged during this period. The possibility that the anomalous peak is a result of Fermi resonance of the amide-I mode with an overtone of an alternative ACN vibrational mode was suggested as well as a possible structural source for the mode. These possibilities were to a large degree eliminated by the experimental work of Barthes and her collaborators. Definitive experimental information on the ACN local mode was furnished in 2002 by Edler and Hamm.

Using time-resolved pump-probe experiments with infrared beams of femtosecond duration, Edler and Hamm were able to excite the amide-I region and follow the time development of the various modes in that region. Their experiments showed a clear difference in the behavior of the normal and anomalous modes with the latter one being strongly anharmonic. Although the lifetime of the anomalous mode was only about 2 ps, return of this energy to the ground state took about 35 ps. Thus, the local mode initially relaxes into a state that is either spectroscopically dark or outside the spectral window of the probe. Interestingly, similar pump-probe experiments for the region of the NH stretching demonstrate the presence of nonlinear local mode structure in this range as well.

The initial experiments of Careri, the subsequent work of Barthes, and finally the experiments of Edler and Hamm along with Davydov's theory and its application to ACN by Scott present a convincing 30-year story that attributes the source of the anomalous ACN peak to a highly localized, relatively short-lived self-trapped state.

Another molecular crystal with different structure that is believed to form nonlinear local modes is the halide-bridged mixed-valence transition metal complex $\{[Pt(en)_2][Pt(en)_2Cl_2](ClO_4)_4\}$, where en = ethylenediamine. In PtCl, essentially one-dimensional chains of platinum alternating with chlorine atoms are formed, and an intra-molecular vibrational excitation of the $PtCl_2$ trimer caused by energy transfer between Pt^{4+} and Pt^{2+} seems to become effectively localized as a result of coupling with other crystal vibrational modes. Raman spectra show a clear red-shifted PtCl overtone spectrum induced by anharmonicity that reduces in PtBr crystals due to smaller effective anharmonicity and disappears in PtI due to absence of nonlinearity. A multiquanta generalization of the theoretical ACN approach of Equations (1)–(4) demonstrates that the overtone redshifts in the PtCl Raman spectrum can be accounted for quantitatively as well as qualitatively by a nonlinear local mode picture.

G.P. Tsironis

See also **Breathers; Davydov soliton; Discrete nonlinear Schrödinger equations; Discrete self-trapping system; Pump-probe measurements**

Further Reading

Barthes M., Nunzio, G.D. & Ribet, M. 1996. Polarons or protontransfer in chains of peptide groups? *Synthetic Metals*, 76: 337–340

Bushmann, W.E., McGrane, S.D. & Shreve, A.P., 2003. Chemical tuning of nonlinearity leading to intrinsically localized modes in halide-bridged mixed-valence platinum materials. *Journal of Physical Chemistry* A, 107(40): 8198–8207

Careri, G., Buontempo, U., Galluzzi, F., Scott, A.C., Gratton, E. & Shyamsunder, E. 1984. Spectroscopic evidence for Davydov-like solitons in acetanilide. *Physical Review* B, 30: 4689–4702

Edler, J. & Hamm, P. 2002. Self-trapping of the amide I band in a peptide model crystal. *Journal of Chemical Physics*, 117: 2415–2424

Scott, A.C. 1992. Davydov's soliton. *Physics Reports*, 217: 1–67

Swanson, B.I., Brozik, J.A., Love, S.P., Strouse, G.F., Shreve, A.P., Bishop, A.R., Zang, W.-Z. & Salkola, M.I. 1999. Observation of intrinsically localized modes in a discrete low-dimensional material. *Physical Review Letters*, 82: 3288–3291

Voulgarakis, N.K., Kalosakas, G., Bishop, A.R. & Tsironis, G.P. 2001. Multiquanta breather model for PtCl. *Physical Review* B, 64: 020301

LOCAL MODES IN MOLECULES

The local mode model was introduced in the 1970s to describe highly excited vibrational overtone states. It has been used to describe XH stretching overtone spectra where X is some heavier atom like C, N, or O. However, the genesis of the local mode model in molecules dates back to the work of J.W. Ellis (1929). Ellis measured the overtone spectrum of benzene in the liquid phase to $\Delta v_{CH} = 8$ (a transition from the ground vibrational state to a state with 8 quanta in CH-stretching). He found that the spectra were pseudo-diatomic in character, in that the CH overtone frequencies could be fitted by a simple Birge–Sponer relationship that had been used to describe a diatomic anharmonic oscillator. Thus, if the observed overtone peak frequencies, $\tilde{\nu}_{v_0}$, are divided by v, the number of CH-stretching quanta in the excited overtone state, and plotted versus v, a straight line is obtained. The slope yields the local mode anharmonicity, $\tilde{\omega}x$, and the intercept can be used to determine the local mode frequency, $\tilde{\omega}$.

$$\tilde{\nu}_{v_0}/v = \tilde{\omega} - (v+1)\tilde{\omega}x. \qquad (1)$$

In 1968, Henry and Siebrand used the localization ideas of Ellis to model the overtone spectrum of benzene on the basis of the assumption that the six local CH-stretching modes were anharmonic but only weakly coupled (Henry & Siebrand, 1968). They derived values for CH-stretching anharmonicity constants expressed in the normal mode basis and calculated the energies of all of the components of the overtone bands expressed in terms of normal modes. At $\Delta v_{CH} = 6$, there are 462 such components of which 150 (the 75 doubly degenerate E_{1_u} states) are allowed. The spectra were then modeled on the basis of a weighted combination of the allowed normal modes. Subsequently, Hayward and Henry postulated that the radiation field selectively excites only the most anharmonic of the normal mode components (Hayward & Henry, 1975). In such a state, all the vibrational energy is effectively localized in one XH bond (X = C, N, O, etc.) and absorption to this pure local mode state is said to account for the overtone spectra. Some of these ideas had been published in 1936 in Germany by Mecke and his collaborators (Mecke & Ziegler, 1936). However, Mecke's work seemed to have been largely unknown and ignored. The description that emerges is that XH-stretching overtone spectra can be described by a local mode model in which the local oscillators are anharmonic but only weakly coupled. The radiation field selectively excites a state whose components have all of the vibrational energy localized in one of a set of equivalent XH bonds. Such a description predicts only a single transition for a given type of XH oscillator in agreement with experiment. The local mode model is now generally accepted, and because of the localization of energy for spectrally active states in a single chemical bond, XH-stretching overtone spectra are very sensitive to bond properties. Such spectra have been used to investigate molecular structure, molecular conformation, intermolecular forces, nonbonded intramolecular interactions, and intramolecular vibrational energy redistribution.

The Harmonically Coupled Anharmonic Oscillator Model

In a molecule like water, the two OH bonds can be treated as Morse potentials. In accord with the local mode model, the OH oscillators are anharmonic but only weakly coupled. It turns out that this off-diagonal potential and kinetic energy coupling is well approximated by the rules that govern coupling of harmonic oscillators.

The harmonically coupled anharmonic oscillator (HCAO) model was formulated independently by Mortensen et al. (1981) and by Child & Lawton (1981). Coupling is allowed only between states within a given vibrational manifold, that is, between states with the same value of the XH-stretching vibrational quantum number v. Coupling is restricted to the harmonic limit where oscillator population differs by ±1. All of the parameters in this model are obtained either directly from the spectra or from ab initio calculations.

The model has been very successful in accounting for the observed energies of overtone peaks in XH-stretching overtone spectra and, thus, has proved useful in the assignment of these spectra. It has been generalized to more than two equivalent oscillators and to sets of non-equivalent oscillators. No identification of the wave functions is needed for the HCAO model to calculate peak energies. However, if one uses a basis set consisting of products of one-dimensional Morse oscillators, the HCAO model can be used to generate vibrational wave functions. If such wave functions are used along with ab initio calculations of dipole moment

functions (expanded in local coordinates), simple but highly successful calculations of overtone intensities are possible (Kjaergaard et al., 1990).

Overtone Intensities

Typically, these calculations: (i) identify transitions to pure local mode states, whose components have all of the vibrational energy localized in one of a set of equivalent XH oscillators, as the dominant peaks for $\Delta v_{XH} \geq 3$; (ii) indicate that the intensity of these pure local mode peaks is determined primarily by second-order diagonal terms involving $\partial^2\mu/\partial R^2$ in the dipole-moment operator μ; (iii) account for the fall-off in intensity with increasing v and the intensity distribution within a given manifold; (iv) account for the intensity distribution at $\Delta v_{XH} = 2$ where coupling between the local oscillators is important; and (v) account for relative intensities for different oscillators within a molecule. For example, calculations on cyclohexane (Kjaergaard & Henry, 1992) and naphthalene (Kjaergaard & Henry, 1995) successfully predict the relative intensities of the two non-equivalent ring hydrogens. These calculations have also been applied to the determination of accurate absolute overtone intensities for a number of species that are important in atmospheric photochemistry so that effects on the absorption of solar radiation can be estimated (Fono et al., 1999; Vaida et al., 2001).

One surprising result in these intensity calculations is that electron correlation in the dipole moment function affects the calculated fundamental intensity but has no significant effect on overtone intensities. One factor in this insensitivity to correlation is likely to be the primary importance of nonlinear terms in the dipole moment operator.

The HCAO intensity model has been generalized to include torsional motion in the Hamiltonian and to include the torsional coordinate in the ab initio calculation of the dipole moment function. As a result of coupling between torsion and stretching, both in the Hamiltonian and through the dipole-moment function, a very large number of transitions carry intensity and contribute to the overall methyl spectral profile. This model has successfully accounted for the methyl spectral profiles in the overtone spectra of methyl substituted aromatic molecules (Kjaergaard et al., 2000).

One early interest in the local mode field was the possibility that these highly localized states could be pumped with high power lasers and the result would be selective bond photochemistry. To date, no practical example of such behavior has arisen. The reason probably lies in the very rapid decay of these highly vibrationally excited states on a subpicosecond timescale. The dynamics of these local mode states continues to be a very active research area.

BRYAN R. HENRY

Further Reading

Child, M.S. & Lawton, T.R. 1981. Local and normal vibrational states: a harmonically coupled anharmonic oscillator model. *Faraday Discussions of the Chemical Society*, 71: 273

Ellis, J.W. 1929. Molecular absorption spectra of liquids below 3 μ. *Transactions of the Faraday Society*, 25: 888–897

Fono, L., Donaldson, D.J., Proos, R.J. & Henry, B.R. 1999. OH overtone spectra and intensities of pernitric acid. *Chemical Physics Letters*, 311: 131–138

Hayward, R.J. & Henry, B.R. 1975. A general local-mode theory for high energy polyatomic overtone spectra and application to dichloromethane. *Journal of Molecular Spectroscopy*, 57: 221–235

Henry, B.R. & Siebrand, W. 1968. Anharmonicity in polyatomic molecules. The CH stretching overtone spectrum of benzene. *Journal of Chemical Physics*, 49: 5369–5376

Kjaergaard, H.G. & Henry, B.R. 1992. The relative intensity contributions of axial and equatorial CH bonds in the local mode overtone spectrum of cyclohexane. *Journal of Chemical Physics*, 96: 4841–4851

Kjaergaard, H.G. & Henry, B.R. 1995. CH-stretching overtone spectra and intensities of vapor phase naphthalene. *Journal of Physical Chemistry*, 99: 899–904

Kjaergaard, H.G., Rong, Z., McAlees, A.J., Howard, D.L. & Henry, B.R. 2000. Internal methyl rotation in the CH stretching overtone spectra of toluene-α-d_2, -α-d_1, and -d_0. *Journal of Physical Chemistry* A, 104: 6398–6405

Kjaergaard, H.G., Yu, H., Schattka, B.J., Henry, B.R. & Tarr, A.W. 1990. Intensities in local mode overtone spectra: propane. *Journal of Chemical Physics*, 93: 6239–6248

Mecke, R. & Ziegler, R. 1936. Das Rotationsschwingungsspektrum des Acetylens (C_2H_2). *Zeitschrift für Physik*, 101: 405–417

Mortensen, O.S., Henry, B.R. & Mohammadi, M.A. 1981. The effects of symmetry within the local mode picture: a reanalysis of the overtone spectra of the dihalomethanes. *Journal of Chemical Physics*, 75: 4800–4808

Vaida, V., Daniel, J.S., Kjaergaard, H.G., Gross, L.M. & Tuck, A.F. 2001. Atmospheric absorption of near infrared and visible solar radiation by the hydrogen bonded water dimer. *Quarterly Journal of the Royal Meteorological Society*, 127: 1627–1644

LOCALIZATION

See **Solitons, types of**

LOCKING

See **Coupled oscillators**

LOGIC, DENDRITIC

See **Multiplex neuron**

LOGISTIC EQUATION

See **Population dynamics**

LOGISTIC MAP

See **One-dimensional maps**

LONG JOSEPHSON JUNCTIONS

The long Josephson junction is an excellent example of an experimental solid-state system that in a straightforward and measurable way, supports the existence and propagation of solitons (Parmentier, 1978; Pedersen, 1986; Ustinov, 1998). In this system, the soliton is called a fluxon, because it contains one quantum of magnetic flux, $\Phi_0 = h/2e \doteq 2.064 \times 10^{-15}$ webers (h is Planck's constant and e is the electron charge), in accord with the particle nature of solitons (Scott, 2003).

A Josephson junction consists of two weakly coupled superconductors separated by a thin (typically 1–10 nm) insulating layer. An important dynamical variable is the phase difference between the macroscopic quantum mechanical phases of the two superconductors, $\phi(x, t)$. Under an appropriate time normalization, the small Josephson junction obeys approximately the same equation as the damped and driven pendulum. If the Josephson junction is long with respect to an intrinsic length scale (called the Josephson penetration depth, of order 1–1000 μm), the equation becomes the damped and driven sine-Gordon equation (often called the perturbed sine-Gordon equation) (McLaughlin & Scott, 1978):

$$-\phi_{xx} + \phi_{tt} + \alpha\phi_t + \sin\phi = i\,. \qquad (1)$$

Here, the damping parameter α (with typical experimental values in the range $0.01 < \alpha < 0.1$) is related to the Josephson junction parameters per unit area: conductance G, capacitance C, and supercurrent J; thus $\alpha = G\sqrt{\hbar/2eCJ}$. Also $i = I_{\text{bias}}/I_0$ is a bias current normalized to the maximum Josephson current, x is the direction of the long side of the junction normalized to the Josephson penetration depth, and time t is normalized to the so-called plasma frequency, which corresponds to the pendulum oscillation frequency. The plasma frequency is of order 1–500 GHz, depending on fabrication parameters (composition and thickness of insulating layer, superconducting materials, etc.).

A particularly interesting solution to Equation (1) is the sine-Gordon soliton (kink), or rather a slightly modified kink because of the damping and bias terms. Such a kink carries one quantum of magnetic flux (an antikink carries a flux quantum pointed in the opposite direction), and it has a steady state velocity determined as a balance between energy input from the bias current (i) and losses stemming from α. This solution has particle-like properties, behaving approximately as a Lorentz invariant, relativistic particle with the velocity of light in the system being the limiting velocity. This so-called Swihart velocity is determined by the junction fabrication parameters and is typically 1–5% of the velocity of light in vacuum.

The simple form of the dynamical equation shown in Equation (1) refers to the so-called overlap geometry shown in Figure 1(a), in which the externally applied current is fed uniformly to the long dimension of the long Josephson junction. In addition to Equation (1), boundary constraints must be satisfied. For an overlap junction of length L, the longitudinal (x-directed) surface current (j) is zero at $x = 0$ and $x = L$ if no external magnetic field is applied.

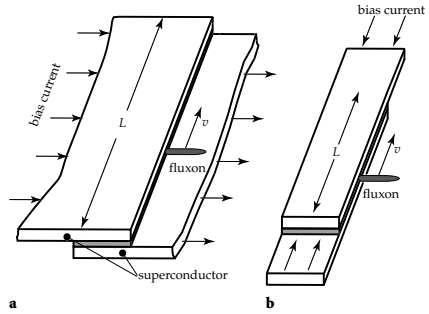

Figure 1. Rectangular-shaped long Josephson junctions (not to scale). (a) Overlap geometry. (b) Inline geometry.

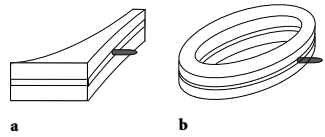

Figure 2. Other long junction geometries (bias not shown). (a) Eiffel junction. (b) Annular junction.

Because the long Josephson junction is typically fabricated using photolithographic and evaporation techniques borrowed from the semiconductor chip industry, it is easy to produce different geometries. Besides the overlap junction, inline junctions, Eiffel junctions, and annular junctions are of experimental and practical interest.

For the inline junction shown in Figure 1(b), the external current is fed from the narrow ends of the junction. The right-hand side of Equation (1) becomes zero, and the bias enter through the boundary conditions at $x = 0$ and L. In the Eiffel junction shown in Figure 2(a), the width of the junction is varied in an exponentially tapered shape approximating that of the Eiffel tower. For reasons of energy conservation, the propagation becomes unidirectional, with the fluxon tending to move in the direction of decreasing junction width (Benabdallah et al., 1996, 2000). The Eiffel junction has been proposed as a dc to ac converter and a microwave oscillator.

The annular junction, shown in Figure 2(b), is like a long overlap junction where the two ends are

joined. For topological reasons connected with the superconducting phase quantization, periodic boundary conditions apply; that is, $j(0,t) = j(L,t) + 2p\pi$ with $p = 0, 1, 2, \ldots$, where j is the longitudinal surface current. A relatively clean soliton (fluxon) can be studied here since there are no collisions with boundaries. The total number of fluxons minus antifluxons is a conserved number (p) and fluxons can only disappear in a fluxon-antifluxon annihilation processes, conserving the total flux in the ring. In a variant of the annular junction, periodic changes in the junction width give rise to deceleration and acceleration of the fluxons, thereby producing radiation (McLaughlin & Scott, 1978).

The long Josephson junction has a potential as a microwave oscillator in the hundreds of Gigahertz range (100–1000 GHz). This is a frequency range, interesting for applications such as fast superconducting electronics, radio astronomy, and satellite-to-satellite communication. In this frequency range, competing oscillators are often bulky, noisy, and expensive. Importantly, the line width of the fluxon oscillator with proper stabilization can become very narrow—of the order 50 kHz. Since the line width of a local oscillator sets the frequency resolution for a heterodyne receiver, this is an important property for spectroscopy and for determining the frequency of radio sources in the universe.

For radio astronomy ($\sim$100–500 GHz), the standard today is a superconducting superheterodyne receiver, for which all components (mixer, local oscillator, filters, etc.) are fabricated in superconducting electronics, and the local oscillator is typically a long Josephson junction. In practice, two different schemes for a fluxon oscillator have been used. In one scheme, the fluxon propagates back and forth within the junction. At each collision with boundary some radiation is coupled out to an external circuit. The frequency of the radiation is given by the time of flight of the fluxon in the junction.

In another mode—the so-called flux flow mode—a unidirectional stream of fluxons is created. This can be done either by the above mentioned Eiffel junction or by applying a magnetic field that breaks the symmetry, giving rise to energy absorption at one end of the junction and energy creation at the other. With proper parameter adjustment, fluxons will be continuously created at one end of the junction, propagated through the junction, and absorbed in an external load (mixer) at the other end.

The power obtainable in such schemes is at best a few microwatts at 300–500 GHz with a narrow line width (of order 100 kHz). Nonetheless, this power level is sufficient for local oscillators of superconducting receivers.

As a concluding remark, we mention that it has been known since the early days of the long Josephson junction research, that the fluxon has properties related to a relativistic particle. Recent experiments have demonstrated that it also has quantum mechanical properties (Wallraff et al., 2003).

NIELS FALSIG PEDERSEN

See also **Josephson junctions; Sine-Gordon equation; Superconductivity**

Further Reading

Benabdallah, A., Caputo, J.G. & Scott, A.C. 1996. Exponentially tapered Josephson flux flow oscillator. *Physics Review* B, 54: 16139–16146.

Benabdallah, A., Caputo, J.G. & Scott, A.C. 2000. Laminar phase flow for an exponentially tapered Josephson oscillator. *Journal Applied Physics*, 88: 16139–16146

McLaughlin, D.W. & Scott, A.C. 1978. Perturbation analysis of fluxon dynamics. *Physics Review A*, 18: 1652–1680.

Parmentier, R.D. 1978. Fluxons in long Josephson junction. In *Solitons in Action*, edited by K. Lonngren & A.C. Scott, New York: Academic Press, 173–199

Pedersen, N.F. 1986. Solitons in Josephson transmission lines. In *Solitons: Modern Problems in Condensed Matter Sciences*, edited by A.A. Maradudin & V.H. Agranovich, Amsterdam: Elsevier, 469–501

Scott, A.C. 2003. *Nonlinear Science: Emergence and Dynamics of Coherent Structures*, 2nd edition, Oxford and New York: Oxford University Press

Ustinov, A.V. 1998. Solitons in Josephson junctions. *Physica* D, 123 (1–4): 315–329

Wallraff, A., Lukashenko, A., Lisenfeld, A., Kemp, A., Fistul, M.V., Koval, Y., & Ustinov, A.V. (2003). Quantum dynamics of a single vortex. *Nature*, 425: 155–158

LONG WATER WAVE APPROXIMATIONS

See **Water waves**

LONG-WAVELENGTH APPROXIMATION

See **Continuum approximation**

LOOP SOLITONS

See **Solitons, types of**

LOOP, CLOSED CAUSAL

See **Causality**

LORENTZ GAS

The Lorentz gas is a model dynamical system generated by the motion of non-interacting point particles ("electrons") in a field of immovable (infinitely heavy) spherical particles, called scatterers. The particles move by inertia according to Newton's law and are reflected from the scatterers elastically. The scatterers may

overlap and are assumed to be randomly or periodically distributed.

Hendrik Lorentz introduced this model as a simplified version of the Drude model for metallic conductance of electricity (Lorentz, 1905). Lorentz's goal was to modify the Drude model in such a way that the Boltzmann equation becomes linear. This is so for the Lorentz gas because of the lack of interactions between particles, which do not influence the positions of the scatterers. As it is sufficient to consider just one moving particle, a one particle model is now usually called the Lorentz gas.

The Lorentz gas appeared to be an inadequate model to describe a gas of electrons in metals. However, it became one of the most popular models in non-equilibrium statistical mechanics, which is used to study the most fundamental problems such as irreversibility, the existence of transport coefficients, and the derivation of kinetic and hydrodynamic equations from mechanical laws. The Lorentz gas with random distribution of scatterers also serves as a relevant model of a dilute gas in equilibrium, consisting of a mixture of two types of (spherical) particles with one much larger and heavier than the other. Almost all collisions are between smaller and larger particles, rather than among smaller particles, even though there are many more smaller particles than heavy particles (Dettmann, 2000).

The kinetic stage of the Lorentz gas evolution is described by the Boltzmann equation, which refers to dilute gases. The appropriate limit procedure was suggested by Grad (1958) and is called the Boltzmann–Grad limit. In this limit, the density of a gas (density of scatterers) tends to zero while the mean free path of the moving particle remains constant. For the Lorentz gas, the kinetic Boltzmann equation goes in the Boltzmann–Grad limit into the linear Fokker–Planck–Kolmogorov equation for the corresponding Markov process. It has been proven for a dilute random Lorentz gas in the Boltzmann–Grad limit that the Boltzmann equation holds for almost any (Poisson distributed) configuration of scatterers (Boldrighini et al., 1983). This result allows a comparison of the theory with the results of computer experiments, because it refers to an individual configuration of scatterers rather than to characteristics averaged over the ensemble of all such configurations.

Rigorous results on the hydrodynamics of the Lorentz gas are available only for periodic configurations of scatterers. This problem for a random Lorentz gas currently looks hopeless because it can be reduced to a problem of random walks in random environments that is far beyond the present abilities of this theory. Clearly, the hydrodynamic equation for the Lorentz gas must be the diffusion equation because the momentum is not preserved in this model, and the conservation of energy is just equivalent to the conservation of mass. Therefore, the diffusion coefficient is also the only transport coefficient in the Lorentz gas.

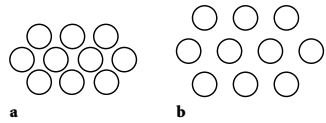

Figure 1. Periodic Lorentz gas: (a) With bounded free path. (b) With unbounded free path.

Consider a periodic Lorentz gas where a free path of the particle is uniformly bounded by some constant. The simplest such configuration of scatterers in the plane is obtained by taking the hexagonal lattice of sufficiently large scatterers (Figure 1(a)). Observe that a periodic Lorentz gas is just Sinai billiards (*See* **Billiards**) when restricted to an elementary cell of a periodic configuration of scatterers. Such a cell can always be chosen to be a rectangle $B = \{q = (q_1, q_2) : 0 \le q_1 \le b_1, 0 \le q_2 \le b_2\}$, where (q_1, q_2) are planar coordinates of the moving particle. Let the particle initially (at $t = 0$) have a random position in B and its velocity (which in a Lorentz gas can always be taken as equal to one) be also randomly distributed in the unit circle. Suppose that this distribution μ (in the direct product Π of B and the unit circle) has a well-behaved density with respect to the volume in Π. Then $x(t) = (q(t), v(t))$ is a random vector, where $q(t) = (q_1(t), q_2(t))$ is a position of the particle at time t and $v(t)$ is its velocity. Rescale trajectories of the particle by setting $q_t(s) = \frac{1}{\sqrt{t}}\, q(st)$, $0 \le s \le t$. The probability distribution μ on the initial conditions induces a probability distribution on μ_t on the set of all possible trajectories $q_t(s)$, $0 \le s \le t$. To study a hydrodynamic behavior one should consider large times. The measures μ_t converge (weakly) as $t \to \infty$ to a Wiener measure (Bunimovich & Sinai, 1981). This result provides a rigorous derivation of (time non-invertible macroscopic) hydrodynamic diffusion equations from first principles (time invertible microscopic Newtonian equations). It shows that at large scales in space and time, trajectories of the periodic Lorentz gas look the same as trajectories of the stochastic diffusion process. Indeed, the transition probabilities of Wiener processes are the fundamental solutions of the diffusion equation. The same result holds for the periodic Lorentz gas with bounded free path in dimensions ≥ 3 (Chernov, 1994).

According to the Einstein formula,

$$D = \frac{2}{d} \int_0^\infty \int_M [v(x(0)) \cdot v(x(t))\, \mathrm{d}\mu(x(0)]\, \mathrm{d}t, \quad (1)$$

where d is a dimension, M is the phase space, and $v(x(0))$ is the velocity of the particle at the moment $t = 0$. The Einstein formula is the first in the infinite

hierarchy of Green–Kubo formulas that relate transport coefficients with the integrals of time correlations of some phase functions. Therefore, the problem of existence of the transport coefficients is reduced to an estimate of the rate of time-correlations decay, which for the periodic Lorentz gas is fast enough (Chernov & Young, 2000).

The condition that a free pass must be bounded is important. Periodic Lorentz gases with an unbounded free path (Figure 1(b)) behave super-diffusively rather than diffusively (Bleher, 1992) and time correlations there decay only according to a power law because the particle gets trapped for a long time in the part of the phase space with arbitrarily long free paths.

Until the 1960s, it was generally believed that time correlations in many-body systems decay exponentially. This opinion was based on the analysis of completing solvable models, such as Markov processes. Therefore, the discovery of long tails of time correlations in numerical experiments came as a surprise (Alder & Wainwright, 1967). It is now believed that time correlations in a random Lorentz gas decay according to a power law. This is confirmed by numerical experiments and physical theories but not by rigorous mathematical results.

Interesting models arise by placing the Lorentz gas in an external field. A periodic Lorentz gas in a magnetic field can demonstrate ergodic as well as integrable behavior (Berglund & Kunz, 1996). The Lorentz gas in a (weak) electric field becomes a non-Hamiltonian system, with the energy of the moving particle increasing indefinitely. One can connect this system to a thermostat to keep the energy fixed and to make the dynamics time reversible, whereupon it is possible to establish rigorously Ohm's law (Chernov et al., 1993). Presently, studies of the thermostated Lorentz gas are popular both in non-equilibrium statistical mechanics and in molecular dynamics (Dettmann, 2000).

LEONID BUNIMOVICH

See also **Billiards; Deterministic walks in random environments; Drude model**

Further Reading

Alder, B.J. & Wainwright, T.E. 1967. Velocity autocorrelations for hard spheres. *Physical Review Letters*, 18: 988–990

Berglund, N. & Kunz, H. 1996. Integrability and ergodicity of classical billiards in a magnetic field. *Journal of Statistical Physics*, 83: 81–126

Bleher, P.M. 1992. Statistical properties of two-dimensional periodic Lorentz gas with infinite horizon. *Journal of Statistical Physics*, 66: 315–373

Boldrighini, C., Bunimovich, L.A. & Sinai, Ya G. 1983. On the Boltzmann equation for the Lorentz gas. *Journal of Statistical Physics*, 32: 477–501

Bunimovich, L.A. & Sinai, Ya.G. 1981. Statistical properties of Lorentz gas with periodic configuration of scatterers. *Communications in Mathematical Physics*, 78: 479–497

Chernov, N.I. 1994. Statistical properties of the periodic Lorentz gas. Multidimensional case. *Journal of Statistical Physics*, 74: 11–53

Chernov, N. & Young, L.S. 2000. Decay of correlations for Lorentz gas and hard balls. In *Hard Ball Systems and the Lorentz Gas*, edited by D. Szasz, Berlin and New York: Springer

Chernov, N.I., Eyink, G.I., Lebowitz, J.L. & Sinai, Ya.G. 1993. Steady state electrical conduction in the periodic Lorentz gas. *Communications in Mathematical Physics*, 154: 569–601

Dettmann, C.P. 2000. The Lorentz gas: a paradigm for nonequilibrium stationary states. In *Hard Ball Systems and the Lorentz Gas*, edited by D. Szasz, Berlin and New York: Springer

Grad, H. 1958. Principles of the kinetic theory of gases. In *Handbuch der Physik* 12, edited by S. Flügge, Berlin: Springer

Lorentz, H.A. 1905. The motion of electron in metallic bodies. *Proceedings of Amsterdam Akademie*, 7: 438–441

LORENTZ TRANSFORM

See **Symmetry groups**

LORENZ ATTRACTOR

See **Attractors**

LORENZ EQUATIONS

A revolutionary development in the realms of nonlinear science over the past four decades has been an understanding of how ubiquitously systems of deterministic equations exhibit complicated behavior. Although the possibility of complicated aperiodic solutions was known much earlier from the work of Henri Poincaré and George D. Birkhoff on the so-called three-body problem (the Earth, Sun, and Moon) in celestial mechanics in the late 19th and early 20th centuries, such behavior was believed to be exceptional (*See* **Poincaré theorems**).

Two crucial pieces of work in the 1960s, the first by Edward Lorenz in 1963 on a continuous model relating to weather prediction (*See* **Butterfly effect**) and the second by Stephen Smale in 1967 in the context of discrete mathematical maps, altered this perception completely, showing that complex aperiodic behavior is generic for most deterministic nonlinear systems.

The basic equations introduced by Lorenz are

$$\begin{aligned} \dot{x} &= \sigma(y - x), \\ \dot{y} &= rx - y - xz, \\ \dot{z} &= xy - bz, \end{aligned} \tag{1}$$

which were obtained by a drastic simplification of the fluid dynamical equations governing convection currents in the atmosphere. Equations (1) resulted from truncating a Fourier series description after the first few modes (Bergé et al., 1984), and the parameters σ

and r are physically important dimensionless numbers known, respectively, as the Prandtl and Rayleigh numbers in fluid mechanics.

Solutions of the Lorenz equations can be organized around a classification of their attractors (Glendinning, 1994; Strogatz, 1994; Nayfeh & Balachandran, 1995), which are regions of the space of physical variables or phase space (also called state space) to which solutions are attracted if the attractor is stable, or from whence they are repelled if the attractor is unstable.

Nonlinear systems may have several different kinds of attractors, including point attractors (also known as fixed, or critical, or equilibrium, points), isolated periodic attractors (or limit cycles), as well as more complex attractors called quasi-periodic and chaotic attractors. The nature and number of the attractors may change as the parameters (σ, r, and b) vary, leading to a qualitative change in behavior referred to as a bifurcation.

A straightforward calculation showed Lorenz that his system contracted volumes in phase space—a dissipative system. This meant that any ball or volume of initial conditions in the phase space must shrink down to zero volume at large times under evolutions governed by the Lorenz equations. In other words, any attractors of the system must have zero volume.

Also, the model has a critical point at the origin ($x = y = z = 0$) and a pair of critical points $C^{\pm}$ at $x = y = \pm\sqrt{b(r-1)}$ for $r > 1$. Lorenz's stability analysis showed that the first fixed point at the origin of the phase space is always stable for $r < 1$ and a global attractor to which all initial points (or initial conditions) in the phase space are attracted for this parameter range. For $r > 1$, he found that the first fixed point at the origin becomes linearly unstable and is longer a bona fide attractor. However, the new fixed points are stable for

$$1 < r < r_{\mathrm{H}} = \frac{\sigma(\sigma + b + 3)}{\sigma - b - 1}. \qquad (2)$$

In this parameter range, calculation shows that these fixed points coexist with an unstable limit cycle. At $r = r_{\mathrm{H}}$, this limit cycle is absorbed by the fixed point in a bifurcation that is known as a subcritical Hopf bifurcation. The fixed points $C^{\pm}$ go unstable in the process, being transformed into saddle points.

For $r > r_{\mathrm{H}}$, there are no simple stable point attractors, so Lorentz considered other stable limit cycles (periodic attractors) or solutions flying off to infinity. He showed that any possible limit cycles should be unstable for $r > r_{\mathrm{H}}$ and also that all trajectories must eventually enter, and be confined within, a certain large ellipsoid.

Clearly, any attractor had to be relatively complex, and the trajectories could not cross while evolving on the attractor. Together with the earlier-mentioned fact of volume contraction (which means that any attractor to which the solution trajectories or orbits are attracted must have zero volume asymptotically in time), Lorenz

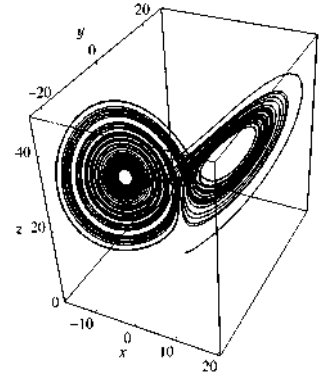

Figure 1. Lorenz attractor in (x, y, z) phase space for $\sigma = 10, r = 28, b = 8/3$.

was left with a perplexing question: What must such an attractor be like?

He numerically studied the case $\sigma = 10, r = 28$, $b = \frac{8}{3}$ with the $r > r_{\mathrm{H}} = 24.74$ in Equation (2). He also chose initial conditions $(x, y, z) = (0, 1, 0)$ close to the saddle point nearer the origin. The resulting solutions in (x, y, z) phase-space, and for $x(t)$ as a function of time are shown in Figures 1 and 2, respectively, where the solution trajectory settles onto a strange butterfly-shaped attractor set after an initial transient. The clearly aperiodic dynamics on this attractor is emphasized in Figure 2. In addition, the attractor appears to be infinitesimally thin and thus satisfies the requirement of zero volume. Hence, all three requirements of aperiodicity of the dynamics on the attractor, zero volume, and nonself-crossing of the orbit were reconciled on this "strange attractor"—a term subsequently coined by Ruelle and Takens. Among other observations, Lorenz noted that this strange attractor has a self-similar structure at all scales, which is now a well-known feature of chaotic attractors.

Subsequent work has revealed that trajectories on chaotic attractors exhibit sensitivity to initial conditions (SIC) where initially contiguous phase points diverge exponentially in time. Other work, some still in progress (Abraham & Shaw, 1983; Bergé et al., 1984), has elucidated the complex process leading to the structure of strange attractors and the properties of the orbits on them. In particular, there is convergence of orbits along the stable manifolds of saddle fixed points (this enables dissipation or volume contraction to be satisfied), divergence of trajectories along the corresponding unstable manifolds (this accounts for SIC), and foldings leading to bounded strange attractors.

Based on a combination of topological and numerical ideas to reconstruct chaotic attractors from

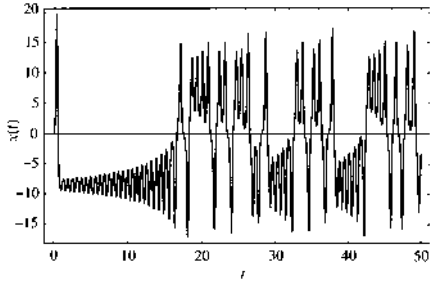

Figure 2. A solution $x(t)$ for $\sigma = 10, r = 28, b = 8/3$.

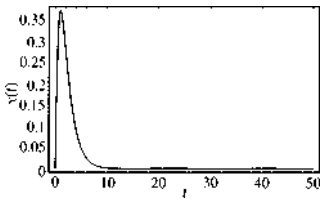

Figure 3. A solution $x(t)$ for $\sigma = 1, b = 2, r = 1/9$.

time series such as that in Figure 2, numerical procedures have been developed to compute various properties such as the fractal dimension (a measure of the global dimension of the attractor in phase space), Lyapunov exponents (measures of sensitivity to initial conditions on the attractor), power spectra and autocorrelation functions, and the so-called Kolmogorov entropy (Nayfeh & Balachandran, 1995). In particular, the chaotic attractor in Figure 1 has a dimension of about 2.05; that is, it occupies a region of the phase space that has infinite area or fills up any area (since the dimension is greater than 2), but has zero volume (since the dimension is less than 3).

The occurrence of sensitivity to initial conditions as indicated by at least one positive Lyapunov exponent or the envelope of the autocorrelation function going to zero in finite time signify the eventual loss of memory of past history (or equivalently the impossibility of prediction far into the future), which are integral features of chaotic dynamics.

Note that the Lorenz equations also exhibit completely deterministic or nonchaotic behavior for isolated parameter sets obtained via Painlevé analysis that are the so-called integrable cases (Tabor & Weiss, 1981). Figure 3 shows the completely regular dynamics for the parameter set $\sigma = 1, b = 2, r = 1/9$. Note how much more regular and orderly, the behavior of $x(t)$ is than that shown in Figure 2.

In conclusion, two features of the Lorenz model continue to make it topical. First, it remains a useful model in which to study essential basic features of chaotic systems. Second, the model has popped up in topical settings as diverse as atmospheric dynamos, lasers, and nonlinear optics, as well as the control of chaos (Ning & Haken, 1990; Pecora & Carroll, 1990; Nayfeh & Balachandran, 1995; Batchelor et al., 2000).

S. Roy Choudhury

See also **Attractors; Butterfly effect; Chaotic dynamics; Lyapunpov exponents; Phase space**

Further Reading

Abraham, R.H. & Shaw, C.D. 1983. *Dynamics: The Geometry of Behavior*, Santa Cruz: Aerial Press

Batchelor, G.K., Moffatt, H.F. & Worster, M.G. (editors). 2000. *Perspectives in Fluid Dynamics*, Cambridge and New York: Cambridge University Press

Bergé, P., Pomeau, Y. & Vidal, C. 1984. *Order Within Chaos*, New York: Wiley

Choudhury, S.R. 1992. On bifurcations and chaos in predator-prey models with delay. *Chaos, Solitons and Fractals*, 2: 393–409

Dodd, R.K., Eilbeck, J.C., Gibbon, J.D. & Morris, H.C. 1982. *Solitons and Nonlinear Wave Equations*, London: Academic Press

Glendinning, P. 1994. *Stability, Instability, and Chaos*, Cambridge and New York: Cambridge University Press

Lorenz, E.N. 1963. Deterministic nonperiodic flow. *Journal of Atmospheric Science*, 20: 130–141

Nayfeh, A.H. & Balachandran, B. 1995. *Applied Nonlinear Dynamics*, New York: Wiley

Ning, C.Z. & Haken, H, 1990. Detuned lasers and the complex Lorenz equations: Subcritical Hopf bifurcations. *Physical Review* A, 41: 3826–3837

Nusse, H. & Yorke, J.A. 1992. *Dynamics: Numerical Explorations*, New York: Springer

Pecora, L.M. & Carroll, T.L. 1990. Synchronization in chaotic systems. *Physical Review Letters*, 64: 821–824

Sparrow, C. 1982. *The Lorenz Equations*, New York: Springer

Strogatz, S.H. 1994. *Nonlinear Dynamics and Chaos*, Reading, MA: Addison-Wesley

Tabor, M. & Weiss, J. 1981. Analytic structure of the Lorenz system. *Physical Review* A, 24: 2157

LOTKA–VOLTERRA EQUATIONS

See **Population dynamics**

LYAPUNOV EXPONENTS

The sequence of powers $a^k, k = 1, 2, \ldots$, of a complex number $a \neq 0$ has one of three types of asymptotic behavior: exponential growth, exponential decay, or constant, according to the modulus $|a|$. A similar situation holds for powers $A^k, k = 1, 2, \ldots$, of an $n \times n$ matrix A. More precisely, for any vector $v \neq 0$, the following limit exists:

$$\lim_{k \to +\infty} \frac{1}{k} \log \|A^k v\| = \lambda(v). \qquad (1)$$

The possible values of $\lambda(v)$, $\lambda_1 < \cdots < \lambda_s$ are called Lyapunov exponents (LEs), and in this special case they are equal to $\log|a|$, where a is an eigenvalue of A (real or complex). Moreover, there is a strictly increasing sequence of subspaces in R^n

$$\{0\} = V_0 \subset V_1 \subset \cdots \subset V_s = \mathrm{R}^n, \tag{2}$$

such that $\lambda(v) = \lambda_i$ for all $v \in V_i \setminus V_{i-1}$, $i = 1, 2, \ldots, s$. The difference of dimensions $m_i = \dim V_i - \dim V_{i-1}$ is called the multiplicity of the Lyapunov exponent λ_i. The rates of growth of k-dimensional volumes of k-dimensional parallelepipeds under the action of A are sums of appropriate Lyapunov exponents. For example, the exponential rate of growth of the n-dimensional volume is equal to $\log|\det A| = m_1\lambda_1 + \cdots + m_s\lambda_s$.

A similar situation occurs for products $A^k = A_k A_{k-1} \ldots A_1$ when the sequence of matrices $A_1, A_2, \ldots$ is periodic (by direct reduction to the constant case we obtain so-called Floquet multipliers, and the LEs are logarithms of their moduli).

In the general nonperiodic case, the key Oseledec Multiplicative Ergodic Theorem (OMET) states that the same scenario holds, when the matrices we multiply $(A_1, A_2, \ldots)$ are supplied by a stationary stochastic process (with matrix values). In this case, the conclusions apply with probability one.

In the context of dynamical systems, the difference equation $x_{n+1} = \Phi(x_n)$, where $\Phi : M \to M$ is a diffeomorphism of a compact smooth manifold M (the phase space). For any ergodic invariant probability measure ν, the Lyapunov exponents are the limits

$$\lim_{k \to +\infty} ||D_x \Phi^k v|| = \lambda(v), \tag{3}$$

which exist for ν almost every $x \in M$ and all nonzero tangent vectors $v \in T_x M$. Thus, Lyapunov exponents characterize the growth in linear approximation of infinitesimal perturbations of initial conditions. Positive LEs lead to instability and negative LEs to stability for perturbations in the respective directions.

Applying OMET both to the future and the past (i.e., to Φ and to Φ^{-1}), we obtain a splitting of tangent spaces

$$T_x M = W_1 \oplus W_2 \oplus \ldots \oplus W_s, \tag{4}$$

such that

$$\lim_{k \to \pm\infty} ||D_x \Phi^k v|| = \pm\lambda_i \tag{5}$$

for ν almost every $x \in M$ and all nonzero tangent vectors $v \in W_i(x)$. It is of direct interest to know if this infinitesimal behavior translates to the behavior of actual orbits of the nonlinear system. We introduce the stable $E^{\mathrm{s}}(x)$ and unstable $E^{\mathrm{u}}(x)$ subspaces, which are the direct sums of subspaces $W_i(x)$ with negative, respectively positive, LEs. It is the content of Pesin Theory that the subspaces E^{s} and E^{u} can be integrated almost everywhere, that is, for ν almost every point $x \in M$ there are smooth submanifolds $W^{\mathrm{s}}(x)$ and $W^{\mathrm{u}}(x)$, which are at every point tangent to the stable and unstable subspaces, respectively.

The stable and unstable manifolds are crucial in understanding chaotic dynamics. Their importance stems from the fact that two orbits starting on one of these submanifolds have the same asymptotic behavior either in the future or in the past.

LEs are associated with the Kolmogorov–Sinai entropy. They enter into the Ruelle Inequality, which states that for any C^1 diffeomorphism Φ and any ergodic invariant probability measure ν

$$h_\nu(\Phi) \leq \sum_{\lambda_i > 0} m_i \lambda_i, \tag{6}$$

where $h_\nu(\Phi)$ is the K–S entropy. This inequality turns into equality (the Pesin formula) for absolutely continuous measures ν and C^2 diffeomorphisms. It was proven by Ledrappier and Young that equality holds if and only if ν is the Sinai–Ruelle–Bowen (SRB) measure.

For Hamiltonian systems (i.e., when Φ is a symplectomorphism), the LEs come in pairs of opposite numbers, which is related to the symmetry of spectra of symplectic matrices. Furthermore the subspace V_k is skew-orthogonal to V_{s-k}, $k = 1, 2, \ldots, s$: a property shared with eigenspaces of symplectic matrices.

Although analytic formulas for LEs are almost nonexistent, they can be readily obtained by numerical methods. Analytical estimates of LEs are available where all the matrices in question are J-separated for some quadratic form (field of forms) J. A matrix A is J-separated, if $J(Av) \geq 0$ for all v such that $J(v) \geq 0$.

MACIEJ P. WOJTKOWSKI

See also **Chaotic dynamics; Sinai–Ruelle–Bowen measures; Phase space**

Further Reading

Barreira, L. & Pesin, Y.B. 2002. *Lyapunov Exponents and Smooth Ergodic Theory*, Providence, RI: American Mathematical Society

Katok, A. & Hasselblatt, B. 1995. *Introduction to the Modern Theory of Dynamical Systems*, Cambridge and New York: Cambridge University Press

Wojtkowski, M.P. 2001. Monotonicity, J-algebra of Potapov and Lyapunov exponents. In *Smooth Ergodic Theory and Its Applications*, Providence, RI: American Mathematical Society, pp. 499–521

Wojtkowski, M.P. & Liverani, C. 1998. Conformally symplectic dynamics and symmetry of the Lyapunov spectrum. *Communications in Mathematical Physics*, 194: 47–60

LYAPUNOV STABILITY

See **Stability**

M

MACH STEM EFFECT

See **Shock waves**

MAGNETOHYDRODYNAMICS

Magnetohydrodynamics (MHD) is the special field of fluid dynamics that is concerned with the motions of electrically conducting fluids in the presence of magnetic fields. Flows of liquid metals or ionized gases (plasmas) are the main areas of applications of MHD.

For the theoretical description of MHD-problems, the basic equations of fluid dynamics must be supplemented by the Lorentz force $\boldsymbol{j} \times \boldsymbol{B}$ where $\boldsymbol{j}$ is the density of electric current and $\boldsymbol{B}$ is the magnetic flux density. To determine these fields Maxwell's equations are used in the magnetohydrodynamic approximation in which the displacement current is neglected. This represents a good approximation as long as the fluid velocity is small compared with the velocity of light. These equations together with Ohm's law for a moving conductor are given by

$$\nabla \cdot \boldsymbol{B} = 0, \quad \frac{\partial}{\partial t}\boldsymbol{B} = -\nabla \times \boldsymbol{E}, \quad \nabla \times \boldsymbol{B} = \mu \boldsymbol{j},$$
$$\boldsymbol{j} = \sigma(\boldsymbol{v} \times \boldsymbol{B} + \boldsymbol{E}), \tag{1}$$

where μ is the magnetic permeability of the fluid and σ is its electrical conductivity. These "pre-Maxwell" equations have the property that they are invariant with respect to a Galileo transformation, i.e., the equations remain unchanged in a new frame of reference moving with the constant velocity vector $\boldsymbol{V}$ relative to the original frame of reference. Indicating the variables of the new frame by a prime, we find

$$\boldsymbol{v}' = \boldsymbol{v} - \boldsymbol{V}, \quad \frac{\partial}{\partial t'} = \frac{\partial}{\partial t} + \boldsymbol{V} \cdot \nabla,$$
$$\boldsymbol{B}' = \boldsymbol{B}, \quad \boldsymbol{E}' = \boldsymbol{E} + \boldsymbol{V} \times \boldsymbol{B}, \quad \boldsymbol{j}' = \boldsymbol{j}. \tag{2}$$

This invariance is the basis for the combination in MHD of Equations (1) with the equations of hydrodynamics in their usual nonrelativistic form. The application of MHD to plasmas is limited to sufficiently low frequency and long wavelength phenomena. If these conditions are not satisfied, two-fluid equations may be used.

Elimination of $\boldsymbol{E}$ and $\boldsymbol{j}$ from Equation (1) yields the equation of magnetic induction

$$\nabla \times \left(\frac{1}{\sigma\mu}\nabla \times \boldsymbol{B}\right) = \frac{\partial}{\partial t}\boldsymbol{B} + \nabla \times (\boldsymbol{v} \times \boldsymbol{B}), \tag{3}$$

which for a solenoidal velocity field $\boldsymbol{v}$ and a constant magnetic diffusivity $\lambda \equiv (\sigma\mu)^{-1}$ can be further simplified,

$$\left(\frac{\partial}{\partial t} + \boldsymbol{v} \cdot \nabla\right)\boldsymbol{B} - \lambda\nabla^2\boldsymbol{B} = \boldsymbol{B} \cdot \nabla\boldsymbol{v}. \tag{4}$$

This equation has the form of a heat equation with the magnetic field line stretching term on the right-hand side acting as a heat source. This interpretation is useful in the dynamo problem of the generation of magnetic fields by fluid motions (*See* **Dynamos, homogeneous**). In order that a magnetic field $\boldsymbol{B}$ may grow, the term on the right-hand side of (3) must overcome the effect of the magnetic diffusion term on the left-hand side. Using a typical velocity U and a typical length scale d, the ratio of the two terms can be estimated by

$$Ud/\lambda \equiv \mathrm{Rm}, \tag{5}$$

which is called the magnetic Reynolds number in analogy to the ordinary Reynolds number used in fluid dynamics. A necessary condition for dynamo action is $\mathrm{Rm} > 1$, but this is by far not a sufficient condition (*See* **Dynamos, homogeneous**).

A typical problem of MHD is the flow in the channel in the presence of an applied homogeneous magnetic field $\boldsymbol{B}_0$. The equation for the plane parallel flow $\boldsymbol{v} = v_x(y)\boldsymbol{i}$ in the channel between two parallel plates with distance $2d$ is given by

$$\eta\frac{\mathrm{d}^2}{\mathrm{d}y^2}v_x(y) + \frac{1}{\mu}\boldsymbol{i} \cdot ((\nabla \times \boldsymbol{B}) \times \boldsymbol{B}) = -A, \tag{6}$$

where η is the dynamic viscosity, $\boldsymbol{i}$ is the unit vector in the x-direction along the channel, and A is the constant pressure gradient in the opposite direction. In accordance with the configuration of the problem, we have assumed that the steady solution depends only on the y-coordinate perpendicular to the plates. Using the

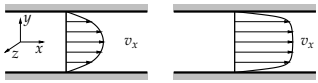

Figure 1. Profile of channel flow for small and large M.

notation $\boldsymbol{B} = \boldsymbol{B}_0 + \boldsymbol{b}$ we find after integrating Equation (4)

$$\lambda \frac{\mathrm{d}}{\mathrm{d}y} b_x(y) + B_{oy} v_x = -D, \tag{7}$$

where the constant of integration D represents the electric field directed in the z-direction; in other words, Equation (7) is the z-component of Ohm's law. Insertion of this expression into Equation (6) yields

$$\eta \frac{\mathrm{d}^2}{\mathrm{d}y^2} v_x(y) - \sigma B_{0y}^2 v_x(y) = -A + \sigma B_{oy} D \tag{8}$$

The solution of this equation is given by

$$v_x = v_0 \left(1 - \frac{\cosh(My/d)}{\cosh M}\right), \tag{9}$$

with

$$M \equiv B_{0y} d \sqrt{\sigma/\eta}$$

and

$$v_0 = (A - \sigma D B_{oy}) d^2/\eta M^2, \tag{10}$$

where M is the Hartmann number named after the scientist who first considered this type of problem. The constant D depends on the boundary condition applied in the transverse z-direction. D can be chosen, for example, such that the average electric current in the z-direction vanishes because of the insulating side walls. It is worth noting that only the y-component of $\boldsymbol{B}_0$ enters solution (9). The flow is not affected by the x- and z-components of $\boldsymbol{B}_0$ as long as it does not depend on those coordinates. Depending on the Hartmann number M, the velocity profile $v_x(y)$ varies between the two limiting cases sketched in Figure 1. For $M \to 0$, the parabolic Poiseuille profile is recovered from expression (9), while for $M \gg 1$, boundary layers of thickness d/M develop, which are called Hartmann layers. In geophysical and astrophysical applications of MHD, the Chandrasekhar number $Q = M^2$ is often used in place of the Hartmann number.

In many applications of MHD, it is justified to neglect magnetic diffusion in first approximation. Then the relationship

$$\frac{\partial}{\partial t} \boldsymbol{B} = \nabla \times (\boldsymbol{v} \times \boldsymbol{B}) \tag{11}$$

can be obtained from Equation (3) in the limit of large magnetic Reynolds numbers. This equation is the same as that obeyed by the vorticity of an inviscid fluid (*See* **Fluid dynamics**). By analogy to the vorticity laws of Kelvin and Helmholtz it can be concluded that the field line that is attached to a fluid element at some initial time continues to be attached to that fluid element at all times; that is, the field lines are "frozen" into the fluid. This statement is known as Alfvén's theorem.

In highly electrically conducting fluids, it is appropriate to consider Equation (11) together with the Euler equation of hydrodynamics,

$$\rho \left(\frac{\partial}{\partial t} \boldsymbol{v} + \boldsymbol{v} \cdot \nabla \boldsymbol{v}\right) = -\nabla p + \mu^{-1} (\nabla \times \boldsymbol{B}) \times \boldsymbol{B}, \tag{12}$$

where the Lorentz force has been included, but viscous friction has been neglected. In the case of an incompressible fluid with $\rho =$ constant, both, $\boldsymbol{v}$ and $\boldsymbol{B}$ are solenoidal vector fields and an exact steady solution of Equations (11) and (12) is given by

$$\boldsymbol{v} = (\rho\mu)^{-1/2} \boldsymbol{B}(x, y, z)$$
$$\text{with} \qquad p = p_0 + \rho \mid \boldsymbol{v} \mid^2 /2, \tag{13}$$

where the relationship $\boldsymbol{v} \cdot \nabla \boldsymbol{v} = (\nabla \times \boldsymbol{v}) \times \boldsymbol{v} + \nabla \mid \boldsymbol{v} \mid^2 /2$ has been used. The dependence of $\boldsymbol{B}$ on the cartesian coordinates x, y, z is arbitrary except for the condition $\nabla \cdot \boldsymbol{B} = 0$. Let us write $\boldsymbol{B}$ as the sum of its average and the remainder, $\boldsymbol{B} = B_0 \boldsymbol{i} + \boldsymbol{b}$, where it has been assumed without loss of generality that the average magnetic field is parallel to the x-direction given by the unit vector $\boldsymbol{i}$. Using a Galileo transformation with the constant velocity vector $V_A \boldsymbol{i}$, we obtain a time-dependent exact solution relative to the new frame of reference,

$$\boldsymbol{v}'(x - V_\mathrm{A} t, y, z) = (\rho\mu)^{-1/2} \boldsymbol{b}(x - V_\mathrm{A} t, y, z), \tag{14}$$

where the choice $V_\mathrm{A} = (\rho\mu)^{-1/2} B_0$ has been made. This solution describes dispersion-free waves called Alfvén waves. The physical interpretation of these waves of arbitrary amplitude is that the field lines of the basic magnetic field are embedded in the fluid-like rubber strings and provide a restoring force whenever a fluid parcel is displaced. The phase velocity V_A is called the Alfvén velocity. In compressible electrically conducting fluids a more complex spectrum of wave phenomena is found owing to combinations of Alfvén and acoustic modes.

F.H. Busse

See also **Alfvén waves; Dynamos, homogeneous; Fluid dynamics; Nonlinear plasma waves**

Further Reading

Davidson, P.A. 2001. *An Introduction to Magnetohydrodynamics*, Cambridge and New York: Cambridge University Press
Moreau, R. 1990. *Magnetohydrodynamics*, Dordrecht: Kluwer
Roberts, P.H. 1967. *An Introduction to Magnetohydrodynamics*, New York: Elsevier and London: Longmans

MANAKOV EQUATIONS

See **Nonlinear Schrödinger equations**

MANDELBROT SETS

See **Fractals**

MANLEY–ROWE RELATIONS

In lossless linear systems, a harmonic sinusoidal input at a frequency ω remains harmonic, the system's steady-state response to a linear combination of individual harmonic inputs is a linear combination of individual responses, and an average input power is zero at each frequency. In lossless nonlinear systems, on the other hand, harmonic inputs at some frequencies also generate inputs at multiple and combination frequencies. The average input powers at each frequency may not be zero but they are predicted from the general relations found by Jack Manley and Harrison Rowe in 1956 (Manley & Rowe, 1956).

Suppose the input applied to a nonlinear system consists of two harmonic signals of frequencies ω_1 and ω_2. The nonlinear system produces an output at all frequencies $m\omega_1 + n\omega_2$, where m and n are integers. For example, $m = 2$, $n = 0$ and $m = 0$, $n = 2$ are signals at the double frequencies $2\omega_1$ and $2\omega_2$, while $m = n = 1$ a signal with the combinational frequency $\omega_1 + \omega_2$. Denote $P_{m,n}$ the total input power at frequency $m\omega_1 + n\omega_2$. In lossless systems, the total power is zero; thus

$$\sum_{m,n} P_{m,n} = 0.$$

In other words, the power $P_{m,n}$ is negative if the signal at $m\omega_1 + n\omega_2$ is generated due to nonlinearity, and the power is positive if the signal is applied from input to the system.

The Manley–Rowe relations are relations between powers $P_{m,n}$ and frequencies $m\omega_1 + n\omega_2$ (Penfield, 1960):

$$\sum_{n=-\infty}^{\infty} \sum_{m=0}^{\infty} \frac{m P_{m,n}}{m\omega_1 + n\omega_2} = 0,$$

$$\sum_{m=-\infty}^{\infty} \sum_{n=0}^{\infty} \frac{n P_{m,n}}{m\omega_1 + n\omega_2} = 0. \qquad (1)$$

As an elementary example, we consider a heterodyne system, comprising an oscillator with frequency ω_1, which is mixed with the carrier incident frequency ω such that a combination frequency $\omega_2 = \omega - \omega_1$ occurs in the spectrum of the nonlinear system (Scott, 1970). We neglect signals at other frequencies and denote powers at frequencies ω_1, ω_2 and $\omega = \omega_1 + \omega_2$ as P_1, P_2, and $P = -P_1 - P_2$. The Manley–Rowe relations between the powers and frequencies of the three signals are

$$\frac{P_1}{\omega_1} = \frac{P_2}{\omega_2} = -\frac{P}{\omega}$$

Notice that these relations preserve conservation of powers $P_1 + P_2 + P = 0$ at the three resonant frequencies ω_1, ω_2, and ω. If $\omega > \omega_1, \omega_2$, the Manley–Rowe relations show that the power P_2 at the combinational frequency ω_2 is smaller than the input power P by a factor of ω_2/ω, while the power at the heterodyne frequency ω_1 is smaller than P by a factor of ω_1/ω. Therefore, when an input signal of larger frequency transforms into output signals of smaller frequencies, the powers of output signals become smaller.

As another application, we consider an electro-optical modulator that takes an input signal at frequency 1 GHz and multiplies with another signal at frequency 100 MHz to produce a modulated output signal at combinational frequency 1.1 GHz. If the power of the output signal has to be 1 mW, the Manley–Rowe relations require powers 0.0909 mW at 100 MHz and 0.9090 mW at 1 GHz. The 1 GHz signal is sometimes called the pump since it provides most of the power needed in the modulation process.

Manley–Rowe relations naturally describe constants of motion in the time evolution of the resonant nonlinear wave interactions. If three waves with frequencies ω_1, ω_2 and $\omega = \omega_1 + \omega_2$ and wavevectors $\mathbf{k}_1$, $\mathbf{k}_2$ and $\mathbf{k} = \mathbf{k}_1 + \mathbf{k}_2$ satisfy the phase matching conditions

$$\omega(\mathbf{k}_1 + \mathbf{k}_2) = \omega(\mathbf{k}_1) + \omega(\mathbf{k}_2),$$

then their interaction is resonant in time and is described by the system of three-wave interaction equations:

$$\begin{aligned}
\mathrm{i}\left(\frac{\partial}{\partial t} + \mathbf{v}\cdot\nabla\right) a &= \gamma a_1 a_2 \mathrm{e}^{-\mathrm{i}\Delta t},\\
\mathrm{i}\left(\frac{\partial}{\partial t} + \mathbf{v}_1\cdot\nabla\right) a_1 &= \gamma a \bar{a}_2 \mathrm{e}^{\mathrm{i}\Delta t},\\
\mathrm{i}\left(\frac{\partial}{\partial t} + \mathbf{v}_2\cdot\nabla\right) a_2 &= \gamma a \bar{a}_1 \mathrm{e}^{\mathrm{i}\Delta t}, \qquad (2)
\end{aligned}$$

where $\Delta = \omega(\mathbf{k}) - \omega(\mathbf{k}_1) - \omega(\mathbf{k}_2)$ is the frequency detuning from exact resonance. In other words, $\mathbf{v}$, $\mathbf{v}_1$, and $\mathbf{v}_2$ are group velocities of the three waves, for example, $\mathbf{v} = \nabla\omega(\mathbf{k})$; and γ is a real-valued coupling coefficient in nonlinear systems with quadratic nonlinearities. The system of amplitude equations (2) has integrals of motions:

$$\begin{aligned}
Q_1 &= \int \left(|a|^2 + |a_1|^2\right) \mathrm{d}\mathbf{x} = \text{const},\\
Q_2 &= \int \left(|a|^2 + |a_2|^2\right) \mathrm{d}\mathbf{x} = \text{const},\\
Q &= \int \left(|a_1|^2 - |a_2|^2\right) \mathrm{d}\mathbf{x} = \text{const}. \qquad (3)
\end{aligned}$$

The integrals of motions are the Manley–Rowe relations for the powers

$$P_1 = \omega_1 \int |a_1|^2 \, \mathrm{d}\mathbf{x},$$

$$P_2 = \omega_2 \int |a_2|^2 \, \mathrm{d}\mathbf{x},$$

$$P = \omega \int |a|^2 \, \mathrm{d}\mathbf{x}. \tag{4}$$

The resonant interaction of three waves results in decay of the wave with the larger frequency $\omega > \omega_1, \omega_2$ into waves of smaller frequencies ω_1; ω_2, which alternates with annihilation of the two waves of smaller frequencies ω_1, ω_2 into the wave of larger frequency ω (Gaponov-Grekhov & Rabinovich, 1992). This process has a simple quantum interpretation. Conservation of quantum momentums and energies of wave particles leads to the resonant relations:

$$\hbar\mathbf{k} = \hbar\mathbf{k}_1 + \hbar\mathbf{k}_2, \qquad \hbar\omega = \hbar\omega_1 + \hbar\omega_2,$$

where $\hbar$ is Planck's constant. If the wave of smaller frequency ω_1 is initially larger than the waves of frequencies ω and ω_2, it cannot decay into the other two waves, because there are not enough wave particles with frequencies ω_2 to merge into wave particles with frequency ω. On the other hand, if the wave of larger frequency ω is initially large, it can decay into two wave particles of smaller frequencies ω_1 and ω_2. Manley–Rowe relations follow from the conservation of number of particles in the quantum interpetation above. For instance, when a phonon with energy $\hbar\omega$ is absorbed, two phonons of energies $\hbar\omega_1$ and $\hbar\omega_2$ are emitted, such that the Manley–Rowe relations hold.

Manley–Rowe invariants play an important role in studies of properties of three-wave interactions in system (2). In particular, optical solitons are supported by dispersive and diffraction effects in nonlinear three-wave interactions. The stability of optical solitons is determined by the Vakhitov–Kolokolov criterion, which involves derivatives of the Manley–Rowe invariants (3) with respect to parameters of optical solitons (Buryak et al., 1997).

When the frequencies ω_1 and ω_2 of the two resonant waves coincide, the three-wave interactions degenerate into resonant second-harmonic generation; thus the wave $a_1 = a_2 = a_0$ with the fundamental frequency $\omega_1 = \omega_2 = \omega_0$ generates the wave a at the double frequency $\omega = 2\omega_0$. The system of equations (2) simplifies then to the form (Etrich et al., 2000)

$$\mathrm{i}\left(\frac{\partial}{\partial t} + \mathbf{v}_0 \cdot \nabla\right) a_0 = \gamma a \bar{a}_0 \mathrm{e}^{\mathrm{i}\Delta t},$$

$$\mathrm{i}\left(\frac{\partial}{\partial t} + \mathbf{v} \cdot \nabla\right) a = \gamma a_0^2 \mathrm{e}^{-\mathrm{i}\Delta t}. \tag{5}$$

System (5) for the second-harmonic generation has only one Manley–Rowe invariant:

$$Q_0 = \int \left(|a_0|^2 + |a|^2\right) \mathrm{d}\mathbf{x} = \text{const}.$$

DMITRY PELINOVSKY

See also **Frequency doubling; Harmonic generation; *N*-wave interactions**

Further Reading

Buryak, A.V., Kivshar, Yu.S. & Trillo, S. 1997. Parametric spatial solitary waves due to type II second-harmonic generation *Journal of the Optical Society of America* B, 14: 3110–3118

Etrich, C., Lederer, F., Malomed, B.A., Peschel, T. & Peschel, U. 2000. Optical solitons in media with a quadratic nonlinearity. *Progress in Optics*, 41: 483–568

Gaponov-Grekhov, A.V. & Rabinovich, M.I. 1992. *Nonlinearities in Action: Oscillations, Chaos, Order, Fractals*, Berlin and New York: Springer

Manley, J.M. & Rowe, H.E. 1956. Some general properties of nonlinear elements. *Proceedings of the Institute of Radio Engineers*, 44: 904–913

Penfield, P., Jr. 1960. *Frequency-power Formulas*, New York: Wiley

Scott, A.C. 1970. *Active and Nonlinear Wave Propagation in Electronics,* New York: Wiley

Weiss, M.T. 1957. Quantum derivation of energy relations analogous to those for nonlinear reactances. *Proceedings of the Institute of Radio Engineers*, 45: 1012–1013

MAPS

A *map* is a dynamical system with discrete time. Such dynamical systems are defined by iterating a transformation $\boldsymbol{\phi}$ of points $\mathbf{x}$

$$\mathbf{x}_{n+1} = \boldsymbol{\phi}(\mathbf{x}_n), \tag{1}$$

from a space $\mathcal{M}$ of dimension d (or a domain of this space) onto itself. $\mathbf{x}_n$ and $\mathbf{x}_{n+1}$ are thus points belonging to this so-called *phase space* $\mathcal{M}$, which can be a Euclidean space such as the space $\mathbb{R}^d$ of d-tuples of real numbers or a manifold such as a circle, a sphere, or a torus $\mathbb{T}^d$ (or a domain such as an interval or a square).

An *endomorphism* is a surjective (i.e., many-to-one) transformation $\boldsymbol{\phi}$ of the space $\mathcal{M}$ onto itself. Thus, the transformation $\boldsymbol{\phi}$ is not invertible. Examples of endomorphisms are one-dimensional maps of the interval such as the logistic map $\phi(x) = 1 - ax^2$ on $-1 \le x \le 1$, the Bernoulli map $\phi(x) = rx$ (modulo 1) with integer r (also called r-adic map), or the Gauss map $\phi(x) = 1/x$ (modulo 1) which generates continuous fractions. The last two maps are defined onto the unit interval $0 \le x \le 1$. There also exist multidimensional examples such as the exact map $\boldsymbol{\phi}(x, y) = (3x + y, x + 3y)$ (modulo 1) on the torus $\mathbb{T}^2$ (Lasota & Mackey, 1985).

An *automorphism* is a one-to-one (i.e., invertible) transformation $\boldsymbol{\phi}$ of the space $\mathcal{M}$ onto itself. Automorphisms for which the one-to-one

transformation $\boldsymbol{\phi}$ is continuous on $\mathcal{M}$ are called *homeomorphisms*. We speak about $\mathcal{C}^r$*-diffeomorphisms* if $\boldsymbol{\phi}$ is r-times differentiable and $\frac{\partial^r \boldsymbol{\phi}}{\partial \mathbf{x}^r}$ is continuous on $\mathcal{M}$. Examples of automorphisms are the circle maps defined with a monotonously increasing function $\phi(x) = \phi(x+1) - 1$ onto the circle; the baker map:

$$\boldsymbol{\phi}(x, y) = \begin{cases} (2x, \frac{y}{2}) & \text{if} \quad 0 \le x < 1/2, \\ \left(2x - 1, \frac{y+1}{2}\right) & \text{if} \quad 1/2 \le x < 1, \end{cases} \tag{2}$$

onto the unit square (Hopf, 1937); the cat map:

$$\boldsymbol{\phi}(x, y) = (x + y, x + 2y) \quad \text{(modulo 1)}, \tag{3}$$

onto the torus $\mathbb{T}^2$ (Arnol'd & Avez, 1968); the quadratic map:

$$\boldsymbol{\phi}(x, y) = (y + 1 - ax^2, bx) \ , \tag{4}$$

onto $\mathbb{R}^2$ also called the *Hénon map* (Hénon, 1976; Gumowski & Mira, 1980), among many others.

Iterating a noninvertible transformation $\boldsymbol{\phi}$ generates a semigroup of endomorphisms $\{\boldsymbol{\phi}^n(\mathbf{x})\}_{n \in \mathbb{N}}$, where $\mathbb{N}$ is the set of nonnegative integers. Iterating an invertible transformation $\boldsymbol{\phi}$ generates a group of automorphisms $\{\boldsymbol{\phi}^n(\mathbf{x})\}_{n \in \mathbb{Z}}$, where $\mathbb{Z}$ is the set of all the integers. Such groups or semigroups are deterministic dynamical systems with discrete time, called maps.

Link Between Maps and Flows

Maps naturally arise in continuous-time dynamical systems (i.e., flows) defined with $d+1$ ordinary differential equations

$$\frac{\mathrm{d}\mathbf{X}}{\mathrm{d}t} = \mathbf{F}(\mathbf{X}), \tag{5}$$

by considering the successive intersections of the trajectories $\mathbf{X}(t)$ with a codimension-one Poincaré section $\sigma(\mathbf{X}) = 0$. If $\mathbf{x}$ denotes d coordinates which are intrinsic to the Poincaré section, the successive intersections $\{\mathbf{X}_n = \mathbf{X}(t_n)\}_{n \in \mathbb{Z}}$ of the trajectory correspond to a sequence of points $\{\mathbf{x}_n\}_{n \in \mathbb{Z}}$ and return times $\{t_n\}_{n \in \mathbb{Z}}$ in the Poincaré section. According to Cauchy's theorem which guarantees the unicity of the trajectory $\mathbf{X}(t)$ issued from a given initial condition $\mathbf{X}(0)$ (i.e., by the determinism of the flow), the successive points and return times are related by

$$\begin{cases} \mathbf{x}_{n+1} = \boldsymbol{\phi}(\mathbf{x}_n), \\ t_{n+1} = t_n + T(\mathbf{x}_n), \end{cases} \tag{6}$$

where $\boldsymbol{\phi}(\mathbf{x})$ is the so-called *Poincaré map* and $T(\mathbf{x})$ the return-time (or ceiling) function. The knowledge of the Poincaré map and its associated return-time function allows us to recover the flow and its properties.

Consider a similar construction for ordinary differential equations which are periodic in time

$$\frac{\mathrm{d}\mathbf{x}}{\mathrm{d}t} = \mathbf{F}(\mathbf{x}, t) = \mathbf{F}(\mathbf{x}, t + T), \tag{7}$$

in which case the return-time function reduces to the period T in Equation (6) and the Poincaré map becomes a *stroboscopic map*.

Examples of Poincaré maps are the Birkhoff maps in the case of billiards. Billiards are systems of particles in free flights (or more generally following Hamiltonian trajectories) interrupted by elastic collisions. The knowledge of the collisions suffices to reconstruct the full trajectories. The Birkhoff map is thus the transformation ruling the dynamics of billiards from collision to collision.

Properties

Maps can be classified according to different properties. An important question is to know if a map is locally volume-preserving or not. If the map is differentiable, the volume preservation holds if the absolute value of its Jacobian determinant is equal to unity everywhere in $\mathcal{M}$:

$$\left| \det \frac{\partial \boldsymbol{\phi}}{\partial \mathbf{x}} \right| = 1. \tag{8}$$

This is the case for the baker map (2), the cat map (3), and the quadratic map (4) if $b = \pm 1$.

Maps that contract phase space volumes on average are said to be *dissipative*. In the limit $b \to 0$, the two-dimensional automorphism (4) contracts the phase space areas so much that it becomes an endomorphism given by the one-dimensional logistic map. This explains why highly dissipative dynamical systems are often very well described in terms of endomorphisms such as the logistic map.

A map is *symplectic* if its Jacobian matrix satisfies

$$\left(\frac{\partial \boldsymbol{\phi}}{\partial \mathbf{x}}\right)^{\mathrm{T}} \cdot \boldsymbol{\Sigma} \cdot \frac{\partial \boldsymbol{\phi}}{\partial \mathbf{x}} = \boldsymbol{\Sigma}, \tag{9}$$

where $^{\mathrm{T}}$ denotes the transpose and $\boldsymbol{\Sigma}$ is an antisymmetric constant matrix: $\boldsymbol{\Sigma}^{\mathrm{T}} = -\boldsymbol{\Sigma}$. Symplectic maps act onto phase spaces of even dimension. Poincaré maps of Hamiltonian systems as well as Birkhoff maps are symplectic in appropriate coordinates. Symplectic maps are volume-preserving. Area-preserving maps are symplectic, but there exist volume-preserving maps which are not symplectic in dimensions higher than two.

A map is symmetric under a group $\mathcal{G}$ of transformations $\mathbf{g} \in \mathcal{G}$ if

$$\mathbf{g} \circ \boldsymbol{\phi} = \boldsymbol{\phi} \circ \mathbf{g}. \tag{10}$$

A map is said to be *reversible* if there exists an involution, that is, a transformation $\boldsymbol{\theta}$ such that $\boldsymbol{\theta}^2 = 1$, which transforms the map into its inverse:

$$\boldsymbol{\theta} \circ \boldsymbol{\phi} \circ \boldsymbol{\theta} = \boldsymbol{\phi}^{-1}. \tag{11}$$

There exist reversible maps which are not volume-preserving (Roberts & Quispel, 1992).

Invariant Subsets

These are subsets of the phase space that are invariant under the action of the map. They include the fixed points $\boldsymbol{\phi}(\mathbf{x}_*) = \mathbf{x}_*$ (which correspond to periodic orbits of a corresponding flow) and the periodic orbits of prime period n defined as trajectories from the initial condition $\mathbf{x}_\mathrm{p}$ such that $\boldsymbol{\phi}^n(\mathbf{x}_\mathrm{p}) = \mathbf{x}_\mathrm{p}$ but $\boldsymbol{\phi}^j(\mathbf{x}_\mathrm{p}) \neq \mathbf{x}_\mathrm{p}$ for $0 < j < n$. Tori may also be invariant as in the case of KAM quasi-periodic motion.

An invariant subset $\mathcal{I}$ of the map is *attracting* if there exists an open neighborhood $\mathcal{U}$ such that $\boldsymbol{\phi}\,\mathcal{U} \subset \mathcal{U}$ and $\mathcal{I} = \cap_{n\in\mathbb{N}} \boldsymbol{\phi}^n \mathcal{U}$. The open set $\mathcal{B} = \cup_{n\in\mathbb{N}} \boldsymbol{\phi}^{-n}\mathcal{U}$ is called the *basin of attraction* of $\mathcal{I}$. An *attractor* is an attracting set which cannot be decomposed into smaller ones. A set which is not attracting is said to be *repelling*.

A closed invariant subset $\mathcal{I}$ is *hyperbolic* if (i) the tangent space $\mathcal{T}_\mathbf{x}\mathcal{M}$ of the phase space $\mathcal{M}$ splits into stable and unstable linear subspaces $\mathcal{E}^{(\mathrm{s})}_\mathbf{x}$ and $\mathcal{E}^{(\mathrm{u})}_\mathbf{x}$ depending continuously on $\mathbf{x} \in \mathcal{I}$,

$$\mathcal{T}_\mathbf{x}\mathcal{M} = \mathcal{E}^{(\mathrm{s})}_\mathbf{x} \oplus \mathcal{E}^{(\mathrm{u})}_\mathbf{x}; \tag{12}$$

(ii) the linearized dynamics preserves these subspaces; and (iii) the vectors of the stable (resp. unstable) subspace are contracted (resp. expanded) by the linearized dynamics (Ott, 1993). Hyperbolicity implies sensitivity to initial conditions of exponential type, characterized by positive Lyapunov exponents. By extension, a map is said to be *hyperbolic* if its invariant subsets are hyperbolic.

For the baker map (2), the unstable linear subspace is the x-direction while the stable one is the y-direction and the unit square is hyperbolic with a positive Lyapunov exponent. Moreover, the dynamics of the baker map can be shown to be equivalent to a so-called Bernoulli shift, that is, a symbolic dynamics acting as a simple shift on all the possible infinite sequences of symbols 0 and 1, so that most of its trajectories are random. The baker map is thus an example of a hyperbolic fully chaotic map.

A diffeomorphism is said to have the *Anosov* property if its whole compact phase space $\mathcal{M}$ is hyperbolic. Examples of Anosov diffeomorphisms are the cat map (3) and its nonlinear perturbations:

$$\begin{cases} x_{n+1} = x_n + y_n + f(x_n, y_n) \quad (\text{modulo } 1), \\ y_{n+1} = x_n + 2y_n + g(x_n, y_n) \quad (\text{modulo } 1), \end{cases} \tag{13}$$

with small enough periodic functions $f(x, y)$ and $g(x, y)$ defined on the torus. We notice that these nonlinear perturbations of the cat map are generally not area-preserving.

Dissipative maps may have chaotic attractors (i.e., attractors with positive Lyapunov exponents) which are not necessarily hyperbolic. This is the case for a set of $a > 0$ values of a positive Lebesgue measure in the logistic map (Jakobson, 1981), as well as in the quadratic map (4) if $b > 0$ is sufficiently small (Benedicks & Carleson, 1991).

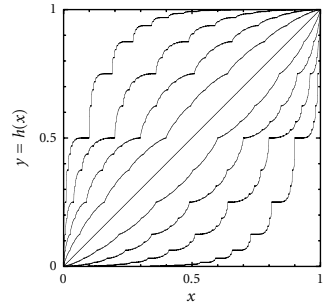

Figure 1. Homeomorphisms $y = h(x)$ transforming the dyadic map into maps (15) with $p = 0.1, 0.2, ..., 0.9$.

Maps may also have sensitivity to initial conditions of stretched-exponential type (with vanishing Lyapunov exponent) as it is the case for the intermittent maps $\phi(x) = x + ax^\zeta$ (modulo 1) with $\zeta > 2$.

Conjugacy Between Maps

In the study of maps, it is often important to modify the analytic form of the map by a change of variables $\mathbf{y} = \mathbf{h}(\mathbf{x})$. Such a conjugacy would transform map (1) into

$$\mathbf{y}_{n+1} = \boldsymbol{\psi}(\mathbf{y}_n)\,, \quad \text{with} \quad \boldsymbol{\psi} = \mathbf{h} \circ \boldsymbol{\phi} \circ \mathbf{h}^{-1}. \tag{14}$$

The Kolmogorov–Sinai entropy per iteration is known to remain invariant if the conjugacy $\mathbf{h}$ is a diffeomorphism, but it is only the topological entropy per iteration which is invariant if the conjugacy is a homeomorphism. For instance, the logistic map $\phi(x) = 1 - 2x^2$ is conjugated to the tent map $\psi(y) = 1 - 2|y|$ by the conjugacy $y = -1 + \frac{4}{\pi}\arcsin\sqrt{\frac{x+1}{2}}$, both maps having their Kolmogorov–Sinai entropy equal to $\ln 2$. On the other hand, the dyadic map $\phi(x) = 2x$ (modulo 1) is conjugated to the map

$$\psi(y) = \begin{cases} \frac{y}{p} & \text{if} \quad 0 \leq y \leq p, \\ \frac{y-p}{1-p} & \text{if} \quad p < y \leq 1, \end{cases} \tag{15}$$

with $p \neq \frac{1}{2}$ by a homeomorphism $h(x)$ which is not differentiable (see Figure 1). These two maps have their topological entropy equal to $\ln 2$ but different Kolmogorov–Sinai entropies.

Conjugacies are also important to transform a circle map such as $\phi(x) = x + \alpha + \varepsilon \sin(2\pi x)$ with $|\,\varepsilon\,| < \frac{1}{2\pi}$ into a pure rotation $\psi(y) = y + \omega$ of rotation number

$$\omega = \lim_{n\to\infty} \frac{1}{n}(x_n - x_0). \tag{16}$$

According to Denjoy theory, such a conjugacy is possible if the rotation number is irrational, in which

case the motion is quasi-periodic and nonchaotic. The circle map also illustrates the phenomenon of synchronization to the external frequency α, which occurs when the rotation number ω takes rational values corresponding to periodic motions. The motion may become chaotic if $|\varepsilon| > \frac{1}{2\pi}$.

Area-preserving Maps

Periodic, quasi-periodic, and chaotic motions are also the features of area-preserving maps which can be considered as Poincaré maps of Hamiltonian systems with two degrees of freedom. Area-preserving maps can be derived from a variational principle based on some Lagrangian generating function $\ell(x_{n+1}, x_n)$. The variational principle requires that the trajectories are extremals of the action

$$W = \sum_{n\in\mathbb{Z}} \ell(x_{n+1}, x_n). \tag{17}$$

The vanishing of the first variation, $\delta W = 0$, leads to the second-order recurrence equation

$$\frac{\partial \ell(x_{n+1}, x_n)}{\partial x_n} + \frac{\partial \ell(x_n, x_{n-1})}{\partial x_n} = 0. \tag{18}$$

This recurrence can be rewritten in the form of a two-dimensional map by expliciting the equations for the momenta

$$\begin{cases} p_{n+1} = \frac{\partial \ell(x_{n+1}, x_n)}{\partial x_{n+1}}, \\ p_n = -\frac{\partial \ell(x_{n+1}, x_n)}{\partial x_n}. \end{cases} \tag{19}$$

The Birkhoff map of a billiard is recovered if ℓ is the distance traveled by the particle in free flight between collisions and x_n is the arc of the perimeter at which the collision occurs. If a free particle or rotor is periodically kicked by an external driving, the Lagrangian function takes the form

$$\ell = \tfrac{1}{2}(x_{n+1} - x_n)^2 - V(x_n). \tag{20}$$

A famous map is the so-called *standard map*

$$\begin{cases} p_{n+1} = p_n + K \sin x_n, \\ x_{n+1} = x_n + p_{n+1} \quad (\text{modulo } 2\pi), \end{cases} \tag{21}$$

obtained for the kicked rotor with the potential $V(x) = K \cos x$ in Equation (20). The motivation for studying the standard map goes back to works on the origin of stochasticity in Hamiltonian systems (Chirikov, 1979; Lichtenberg & Lieberman, 1983, MacKay & Meiss, 1987).

Phase portraits of an area-preserving map typically present closed curves of KAM quasi-periodic motion, which form elliptic islands. Hierarchical structures of elliptic islands develop on smaller and smaller scales. The elliptic islands are surrounded by chaotic zones extending over finite area (see Figure 2).

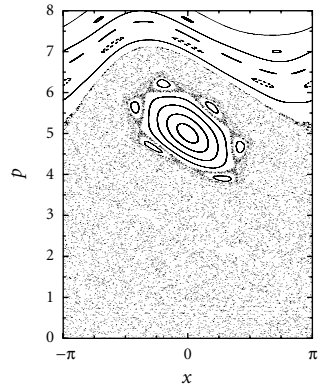

Figure 2. Phase portrait of the Fermi–Ulam area-preserving map, $p_{n+1} = |p_n + \sin x_n|, x_{n+1} = x_n + 2\pi M/p_{n+1}$ (modulo 2π), ruling the motion of a ball bouncing between a fixed wall and a moving wall oscillating sinusoidally in time, in the limit where the amplitude of the oscillations is much smaller than the distance between the walls. p is the velocity of the ball in units proportional to the maximum velocity of the moving wall. x is the phase of the moving wall at the time of collision. The parameter M is proportional to the ratio of the distance between the walls to the amplitude of the oscillations of the moving wall. (See Lichtenberg & Lieberman, 1983, for more details.)

Typical area-preserving maps such as the standard map (21) or the one of Figure 2 display a variety of motions that interpolate between two extremes, namely, the fully chaotic behavior of hyperbolic area-preserving maps such as the baker and cat maps and the fully regular motion of integrable maps such as the one given by the second-order recurrence:

$$x_{n+1} - 2x_n + x_{n-1} = -2\mathrm{i} \ln \frac{\kappa^2 + \mathrm{e}^{-\mathrm{i}x_n}}{\kappa^2 + \mathrm{e}^{+\mathrm{i}x_n}} \tag{22}$$

(Faddeev & Volkov, 1994).

Some area-preserving maps may have a repelling Smale horseshoe as the only invariant subset at finite distance. This is the case in the quadratic map (4) for $b = -1$ and large enough values of $a > 0$. Such horseshoes often arise in open two-degrees-of-freedom Hamiltonian systems describing the chaotic scattering of a particle in some time-periodic potential.

Complex Maps

Such maps are defined with some analytic function $\phi(z)$ of $z = x + \mathrm{i}y \in \mathbb{C}$ or some multidimensional generalizations of it. Complex maps are generally endomorphisms. An example is the complex logistic map $\phi(z) = z^2 + c$. Other examples are given by the Newton–Raphson method of finding the roots of a

function $f(z)=0$:

$$z_{n+1} = z_n - \frac{f(z_n)}{f'(z_n)}. \tag{23}$$

Complex maps have invariant subsets called Julia sets which are defined as the closure of the set of repelling periodic orbits (Devaney, 1986). The motion is typically chaotic on the Julia set which is repelling and often separates the basins of attraction of the attractors. For instance, the map

$$z_{n+1} = \frac{z_n}{2} + \frac{1}{2z_n}, \tag{24}$$

derived from Equation (23) with $f(z)=z^2-1$ has the attractors $z=\pm 1$. Their respective basins of attraction $x>0$ and $x<0$ are separated by the line $x=0$ where the dynamics is ruled by Equation (24) with $z=\mathrm{i}y$. This one-dimensional map is conjugated to the dyadic map

$$\chi_{n+1} = \begin{cases} 2\chi_n - \frac{\pi}{2} & \text{if} \quad 0 \le \chi_n \le \frac{\pi}{2}, \\ 2\chi_n + \frac{\pi}{2} & \text{if} \quad -\frac{\pi}{2} < \chi_n \le 0, \end{cases} \tag{25}$$

by the transformation $y=\tan\chi$, which shows that the dynamics is chaotic on this Julia set.

However, the boundaries between the basins of attraction are typically fractal (Ott, 1993) as is the case for the Newton–Raphson map (23) with $f(z)=\mathrm{e}^z-1$ (see Figure 3).

Maps and Probability

An important issue is to understand how maps evolve probability in their phase space. The time evolution of probability densities is ruled by the so-called Frobenius–Perron equation (Lasota & Mackey, 1985). The probability density at the current point $\mathbf{x}$ comes from all the points $\mathbf{y}$ that are mapped onto $\mathbf{x}$. Since the inverse of an endomorphism is not unique, the Frobenius–Perron equation is composed of the sum

$$\rho_{n+1}(\mathbf{x}) = \sum_{\mathbf{y}:\, \boldsymbol{\phi}(\mathbf{y})=\mathbf{x}} \frac{\rho_n(\mathbf{y})}{\left|\det \frac{\partial \boldsymbol{\phi}}{\partial \mathbf{x}}(\mathbf{y})\right|}. \tag{26}$$

For an automorphism, the sum reduces to the single term corresponding to the unique inverse. An invariant probability measure is obtained as a solution of the Frobenius–Perron equation such that $\rho_{n+1}(\mathbf{x})=\rho_n(\mathbf{x})$. The study of invariant measures is the subject of ergodic theory (Hopf, 1937; Arnol'd & Avez, 1968; Cornfeld et al., 1982). The knowledge of the ergodic invariant measure provides us with the statistics of the quantities of interest: observables, correlation functions, Lyapunov exponents, the Kolmogorov–Sinai entropy, etc. With these tools, transport properties such as normal and anomalous diffusion can also be studied in maps (Lichtenberg & Lieberman, 1983).

Some Applications

Dissipative maps are used to study chaos in hydrodynamics (Lorenz, 1963), chemical kinetics (Scott, 1991), biology (Olsen & Degn, 1985; Murray, 1993), nonlinear optics (Ikeda et al., 1980), and more. In particular, systems with time delay in some feedback can be approximated by maps, as in the nonlinear optics of a ring cavity (see Figure 4).

Dissipative maps are also used to study complex systems composed of many interacting units. The units may form a lattice or a graph and interact with each other by diffusive or global couplings. These high-dimensional maps are often called *coupled map lattices* in reference to their spatial extension.

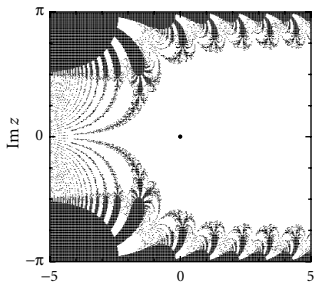

Figure 3. Complex map $z_{n+1}=z_n-1+\exp(-z_n)$: basin of attraction of the point at infinity in grey and of the attractors $z=0,\ \pm 2\pi\mathrm{i},\ \pm 4\pi\mathrm{i},\ \ldots$ in white. The dot is the attractor $z=0$.

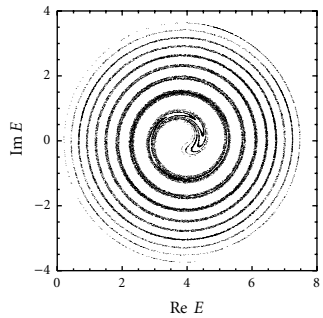

Figure 4. Chaotic attractor of the dissipative Ikeda map $E_{n+1}=a+bE_n\exp(\mathrm{i}\,|\,E_n\,|^2-\mathrm{i}c)$ ruling the complex amplitude $E_n\in\mathbb{C}$ of the electric field of light transmitted in a ring cavity containing a nonlinear dielectric medium, at each passage along the ring (Ikeda et al., 1980). The parameters take the values $a=3.9$, $b=0.5$, and $c=1$.

In addition, area-preserving and symplectic maps have become a fundamental tool to study the long-term evolution of the Solar system (Murray & Dermott, 1999).

PIERRE GASPARD

See also **Anosov and Axiom A systems; Attractors; Aubry–Mather theory; Billiards; Cat map; Chaotic dynamics; Coupled map lattice; Denjoy theory; Entropy; Ergodic theory; Hamiltonian systems; Horseshoes and hyperbolicity in dynamical systems; Kolmogorov–Arnol'd–Moser theorem; Lyapunov exponents; Maps in the complex plane; One-dimensional maps; Phase space; Symbolic dynamics**

Further Reading

Arnol'd, V.I. & Avez, A. 1968. *Ergodic Problems of Classical Mechanics*, New York: Benjamin

Benedicks, M. & Carleson, L. 1991. The dynamics of the Henon map. *Annals of Mathematics*, 133: 73–169

Chirikov, B.V. 1979. A universal instability of many-dimensional oscillator systems. *Physics Reports* 52: 263–379

Cornfeld, I.P., Fomin, S.V. & Sinai, Ya.G. 1982. *Ergodic Theory*, Berlin: Springer

Devaney, R.L. 1986. *An Introduction to Chaotic Dynamical Systems*, Menlo Park CA: Benjamin/Cummings

Faddeev, L. & Volkov, A.Yu. 1994. Hirota equation as an example of an integrable symplectic map. *Letters in Mathematical Physics*, 32: 125–135

Gumowski, I. & Mira, C. 1980. *Recurrences and Discrete Dynamical Systems*, Berlin: Springer

Hénon, M. 1976. A two-dimensional mapping with a strange attractor. *Communications in Mathematical Physics*, 50: 69–77

Hopf, E. 1937. *Ergodentheorie*, Berlin: Springer

Ikeda, K., Daido, H. & Akimoto, O. 1980. Optical turbulence: chaotic behavior of transmitted light from a ring cavity. *Physical Review Letters*, 45: 709–712

Jakobson, M.V. 1981. Absolutely continuous invariant measures for one-parameter families of one-dimensional maps. *Communications in Mathematical Physics*, 81: 39–88

Lasota, A. & Mackey, M.C. 1985. *Probabilistic Properties of Deterministic Systems*, Cambridge and New York: Cambridge University Press

Lichtenberg, A.J. & Lieberman, M.A. 1983. *Regular and Stochastic Motion*, New York: Springer

Lorenz, E.N. 1963. Deterministic nonperiodic flow. *Journal of Atmospheric Sciences*, 20: 130–141

MacKay, R.S. & Meiss, J.D. 1987. *Hamiltonian Dynamical Systems: A Reprint Selection*, Bristol: Adam Hilger

Murray, C.D. & Dermott, S.F. 1999. *Solar System Dynamics*, Cambridge and New York: Cambridge University Press

Murray, J.D. 1993. *Mathematical Biology*, Berlin and New York: Springer

Olsen, L.F. & Degn, H. 1985. Chaos in biological systems. *Quarterly Reviews of Biophysics*, 18: 165–225

Ott, E. 1993. *Chaos in Dynamical Systems*, Cambridge and New York: Cambridge University Press

Roberts, J.A.G. & Quispel, G.R.W. 1992. Chaos and time-reversal symmetry: Order and chaos in reversible dynamical systems. *Physics Reports*, 216: 63–177

Scott, S.K. 1991. *Chemical Chaos*, Oxford: Clarendon Press, and New York: Oxford University Press

MAPS IN THE COMPLEX PLANE

Iterates of rational functions in the complex plane form a class of dynamical systems that can be characterized in amazing detail and completeness. Gaston Julia (1918) and Pierre Fatou (1919/20) proved fundamental theorems on the invariant sets and the relation between critical points and attracting cycles. In some of the first numerical studies of the iterates of a quadratic polynominal, Benoit Mandelbrot discovered the set now named after him (Mandelbrot, 1980). Dennis Sullivan (1985) proved the complete classification of attractors and Adrien Douady & John Hubbard (1984) showed that the Mandelbrot set is connected. Because of their aesthetic beauty, their intricate details, and their omnipresence in iterations of complex functions, Mandelbrot and Julia sets belong to the most fascinating and most widely studied fractal objects. The book by Richter & Peitgen (1986) contains a good survey of the results and many color plates of Julia sets and Mandelbrot sets, as well as personal reflections by Mandelbrot and Douady.

In order to illustrate some of the ideas and concepts, consider the rational maps that result from Newton's method for roots of polynominals (Curry et al., 1983). Their roots can be found using Newton's method, where an initial point z_0 is iterated according to the rational map

$$z_{n+1} = g(z_n) = z_n - f(z_n)/f'(z_n)\,. \qquad (1)$$

For initial conditions sufficiently close to a root, the method converges faster than quadratically, hence its popularity in numerical mathematics. But a little numerical exploration shows that when the initial condition is further away from a root, the iterations can behave rather unpredictably.

Helpful for the investigation of the global dynamics of the iterates is a theorem due to Fatou (1919/20), according to which any attracting cycle will have a critical point in its basin of attraction. A point x_p on a cycle of period k returns after k iterations to its starting point, $z_p = g^{(k)}(z_p)$. At a critical point the derivative vanishes, $g'(z_c) = 0$. Newton's method for polynominals has $g'(z) = f(z)f''(z)/(f'(z))^2$; therefore, the critical points include the roots of the polynominal and the inflection points where $f''(z_c) = 0$. Since the roots of the polynominals are at the same time fixed points and critical points for Newton's method, each one of them is attracting. It thus suffices to investigate the dynamics of the inflection points.

Points that do not iterate to a root or to any other attracting object form the Julia set.

In 1879, Arthur Cayley solved the simplest case, Newton's method for the quadratic polynominal $z^2 - 1 = 0$, where the iteration reads

$$z_{n+1} = \frac{z_n^2 + 1}{2z_n}\,. \qquad (2)$$

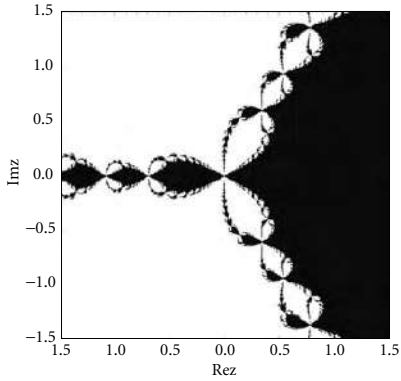

Figure 1. Initial conditions in Newton's method that converge to the root at 1 for the cubic equation z^3-1. The initial conditions for the other roots follow from symmetry by rotation through an angle of $\pm 2\pi/3$ around the origin.

There are no critical points besides the roots and hence no other attracting regions. The imaginary axis is the Julia set: it is mapped into itself and is the border between the two domains of attraction.

At the end of his paper Cayley comments that "the next succeeding case of the cubic equation appears to present considerable difficulty". Just how difficult is indicated in Figure 1 for the case $f(z)=z^3-1$. Evidently, not only the immediate neighborhood of 1 but also many points further away will map into the root $z_0=1$. The critical point $z_c=0$ is mapped to infinity, so that there are no other attractors. The boundary of the black region is the Julia set. It has the interesting feature that in an arbitrarily small neighborhood of every point, initial conditions can be found that iterate to any one of the possible roots. That is to say, at a boundary point, the attracting regions for all roots, and not just for two roots, meet. It has self-similar and fractal features (for instance, its Hausdorff dimension is about $1.429\ldots$ (Nauenberg & Schellnhuber, 1989)), but it is not of full measure.

For more general third-order polynominals, for example,

$$p_a(z)=z^3+(a-1)z-a\,, \tag{3}$$

it can happen that a set of initial conditions of finite measure will not converge to any one of the roots (Curry et al., 1983). Then the iterates of the critical point $z_c=0$ remain bounded but do not approach a root. For instance, for the parameter values underlying Figure 2, the critical point maps into a period-2 cycle. For initial conditions in the set shown, Newton's method will not find a root; instead, it will converge to a cycle of period 2.

Concerning the dependence on the parameter a, one can map out regions in the parameter space where the critical point $z_c=0$ does not iterate toward one of the roots or to infinity: for parameter a inside the black region in Figure 3, it approaches another attracting set and Newton's method fails. Besides the case of an attracting cycle of period 2 as in Figure 2, with parameters from the main cardioid of the set, one can find cycles of period 4 in the circular bud to the left, of period 8 even further to the left, and so on: the attracting periodic orbit undergoes period doubling. For parameters in other parts of the set, other sequences of bifurcations occur.

The object that appears in Figure 3 was first seen by Benoit Mandelbrot (1980) in investigations of iterates of the family of quadratic polynominals

$$z_{n+1}=z_n^2+c\,. \tag{4}$$

This map has only one critical point, $z_c=0$. For points outside the Mandelbrot set z_c iterates to infinity and there are no stable attracting cycles. The different compartments and regions inside the Mandelbrot set then contain parameter values where different cycles are stable, and transitions between regions correspond to various bifurcations. The cycles that are not attracting are dense in the Julia sets. For parameter values inside the Mandelbrot set, the Julia set is connected; for parameters outside, it dissolves into a Fatou dust. For $c=0$, the Julia set is a circle of dimension 1, and for small $c\neq 0$, it becomes a fractal with dimension

$$d\approx 1+\frac{|c|^2}{4\ln 2}\qquad \text{for small } c\,. \tag{5}$$

For real parameters and real z_n, the map belongs to the class of unimodal maps with quadratic maxima for which the period doubling cascade with its universal scaling laws in parameter and distance between periodic points applies. These relations then translate into scalings of the diameters of the buds in the Mandelbrot set and of structures in the Julia set. A fairly complete description of the structures in both the Mandelbrot set and the associated Julia sets can be achieved using methods from conformal mappings (Douady & Hubbard, 1984/85).

The previous examples already illustrate several kinds of behaviors of iterates. They can map to a fixed point of a periodic orbit, in which case the orbit is stable; if the derivative $M_{\rm p}=\mathrm{d}g^{(k)}(x_{\rm p})/\mathrm{d}x_{\rm p}$ along the orbit vanishes, as in the case of the roots for Newton's method, the orbit is superstable. Orbits that have derivatives $|M_{\rm p}|>1$ are repelling and belong to the Julia set. To complete the classification of all possible attractors as given by Sullivan (1985), we need to add the marginal cases when the derivative is of modulus one, $M_{\rm p}=\exp(2\pi\alpha)$: such orbits are called rationally or irrationally indifferent for rational and irrational α, respectively. Near irrationally indifferent

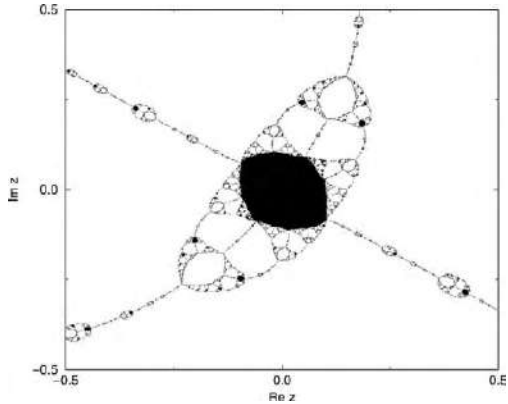

Figure 2. Initial conditions in Newton's method that do not converge to any one of the roots for the cubic polynominal (3) with parameter $a = 0.32 + 1.64$i. In the big blobs initial conditions converge to a period two cycle.

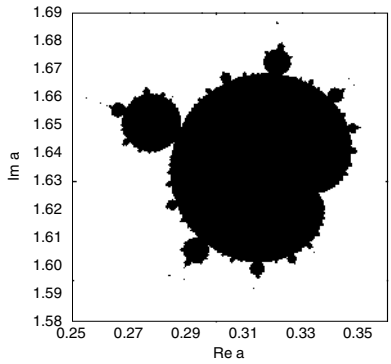

Figure 3. An example of the set of parameters a for which the iterates of the critical points for Newton's method for polynominal (3) do not approach one of the roots. In the main cardioid, the iterates approach a stable period 2 orbit, and in the buds attached to the main cardioid other orbits of higher period are stable. The small speckles outside the main object are also part of the Mandelbrot set that are connected to it by thin hairs and filaments which are not resolved in this plot.

orbits, Siegel disks, and Herman rings can appear. Sullivan's classification theorem now states that there are countably many attracting regions and that they can belong to superstable orbits, stable orbits, Siegel disks, or Herman rings. They can be identified by following iterates of critical points which will bring one to the attracting orbit or to the boundaries for the irrationally indifferent regions.

BRUNO ECKHARDT

See also **Fractals; Maps**

Further Reading

Curry, J., Garnett, L. & Sullivan, D. 1983. On the iteration of rational functions: computer experiments with Newton's method. *Communications of Mathematical Physics*, 91: 267–277

Douady, A. & Hubbard, J.H. 1984/85. Étude dynamique des polynômes complexes I et II. *Publications Mathematique D'Orsay* 84.02 (154 p.) and 85.04 (75 p.)

Fatou, P. 1919/20. Sur les Equations fonctionnelles. *Bulletin de la Société Mathematique de France*, 47: 161–271; 48: 33-94; 48: 208–314

Julia, G. 1918. Mémoire sur l'itération des fonctions rationelles. *Journal de Mathématiques Pures et Appliquées*, 4: 47–245

Mandelbrot, B.B. 1980. Fractal aspects of $z \to \lambda z(1 - z)$ for complex λ and z. *Annals of the New York Academy of Sciences*, 357: 249–259

Nauenberg, M. & Schellnhuber, H.J. 1989. Analytic evaluation of the multifractal properties of a Newtonian Julia set. *Physical Review Letters*, 62: 1807–1810

Richter, P.H. & Peitgen, H.O. 1986. *The Beauty of Fractals: Images of Complex Dynamical Systems*, Berlin and New York: Springer

Sullivan, D. 1985. Quasiconformal homoemorphisms and dynamics: I. Solution of the Fatou–Julia problem on wandering domains. *Annals of Mathematics*, 122: 401–418

MARANGONI CONVECTION

See **Fluid dynamics**

MARGINAL STABILITY

See **Stability**

MARKIN–CHIZMADZHEV MODEL

The Hodgkin & Huxley (1952) equations provide a quantitatively accurate and detailed model of the currents generating the propagating nerve impulse in the squid giant axon, and as the first such model they formed a prototype for nerve excitation. The equations are nonlinear, with four dynamical variables, and are in the form of a reaction-diffusion partial differential equation. Thus, the model is analytically intractable and numerical solution—now a trivial task on a PC—in the 1960s, required mainframe facilities. Simpler models were needed, both for understanding the mechanisms of propagation, and numerical exploration of propagation; such simple models are still used to simulate propagation in the anisotropic geometry of cardiac muscle (Panfilov, 1997). One approach is the FitzHugh–Nagumo equations, in which the nonlinear current-voltage relation of excitable membranes is caricatured by a cubic function (Rinzel & Keller, 1973). Another approach is to directly specify the currents flowing during the action potential.

Starting with the nonlinear cable equation for a nonmyelinated axon with axoplasmic resistance R and membrane capacitance C (both per unit length of axon), spread of membrane potential V with distance x (cm) and time t (ms) is described by

$$C\frac{\partial V}{\partial t} = \frac{1}{R}\frac{\partial^2 V}{\partial x^2} - I_{\text{ion}}, \tag{1}$$

where I_{ion} is a nonlinear function of V and t. Markin & Chizmadzhev (1967) assumed the following simple form for the membrane ionic current I_{ion}. This current was assumed to be switched to a constant inward current J_1 at the start of excitation and, after a time τ_1, switched to a smaller, longer constant outward current J_2 for a time period τ_2. The nonlinear diffusion equation (1) is thus replaced by a piecewise linear diffusion equation. Considering a solitary traveling-wave solution with a velocity θ ms^{-1}, moving to the coordinate system $\xi = x - \theta t$ reduces Equation (1) to an autonomous ordinary differential equation

$$\frac{\partial^2 V}{\partial \xi^2} + \theta RC\frac{\partial V}{\partial \xi} - RI(\xi) = 0. \tag{2}$$

For the Markin–Chizmadzhev model, I_{ion} in Equation (2) is linear in the four regions: (i) $\xi > 0$, (ii) $0 > \xi > -\theta\tau_1$, (iii) $-\theta\tau_1 > \xi > -\theta(\tau_1 + \tau_2)$, and (iv) $\xi < \theta(\tau_1 + \tau_2)$, so the traveling-wave solution can be constructed analytically from four components, as shown in Figure 1.

Analytic estimates for the velocities of the two traveling wave solutions, the larger being faster and stable, were obtained, these being analogous to earlier numerical studies on propagating activity of the Hodgkin–Huxley equations. This simple Markin–Chizmadzhev model for the membrane current generator retains the ratio of inward to outward current magnitudes and the relative time courses of the inward and outward membrane currents. A greater simplification is to consider the action potential as an event that is produced whenever a threshold is exceeded. Such an approach is widely used in modeling periodic and stochastic spike trains, for example, by the integrate and fire model.

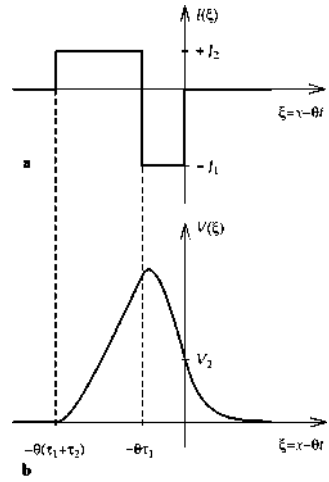

Figure 1. (a) Assumed membrane current and (b) computed potential during a solitary propagating action potential for the Markin–Chizmadzhev model for a nonmyelinated axon, with propagation velocity θ.

Markin et al. (1987) apply the membrane current generator model to provide estimates for the effects of branching and changes in axonal diameter on propagation, and the interaction between propagating activity in axons forming nerve trunks, where extracellular conduction pathways allow the possibility of ephaptic transmission (an action potential in one fiber inducing changes in potential in neighboring fibers), and an increased synchronization of propagating activity in a bundle of nerve fibers. They also applied the model to propagation of activity in syncytia—branching networks of coupled cells. The spread of excitation in such systems depends on the relative cell sizes and connections (it is easier for a large cell to excite a smaller adjacent cell). For systems of similar cells, the syncytium merges into an excitable medium as the cell-to-cell coupling is increased. Such excitable media models are widely used to model propagation in cardiac tissue.

A behavior of excitable media in which a drifting source emits periodic waves was believed to be associated with macroscopic inhomogeneities. Markin & Chizmadzhev (1972) showed that in two homogeneous coupled one-dimensional fibers, activity propagating

along one can excite activity in the other and vice-versa, setting up a reverberator that acts as a drifting source of periodic wave trains in a homogeneous system whose components all have stable equilibrium solutions. This provides a prototype, with two coupled one-dimensional fibers, for re-entry, which in two-dimensional excitable media appears as a spiral wave.

The basic phenomenology of propagation in excitable media was first studied with the Markin–Chizmadzhev model, as it allowed both piecewise linear analysis and rapid numerical solution. There is still a need for simple models for rapid simulation in three-dimensional media, but the Markin–Chizmadzhev model has been superceded by an efficient two-variable system for excitable media in general (Dowle et al., 1997), and the Fenton–Karma (1998) three current model for cardiac tissue.

ARUN V. HOLDEN

See also **FitzHugh–Nagumo equation; Hodgkin–Huxley equations; Integrate and fire neuron; Nerve impulses**

Further Reading

Dowle, M., Mantel, R.M. & Barkley, D. 1997. Fast simulations of waves in three-dimensional excitable media. *International Journal of Bifurcation and Chaos*, 7: 2529–2546

Fenton, F. & Karma, A. 1998. Vortex dynamics in three-dimesional continuous myocardium with fiber rotation: filamant instability and fibrillation. *Chaos*, 11: 20–47

Hodgkin, A.L. & Huxley, A.F. 1952. A quantitative description of membrane current and its application to conduction and excitation in nerve, *Journal of Physiology*, 117: 500–544

Markin, V.S. & Chizmadzhev, Yu. A. 1967. Spread of excitation in a model of the nerve fibre. *Biofizika*, 12: 900–907; *Biophyics GB*, 12: 1032–1040

Markin, V.S. & Chizmadzhev, Y.A. 1972. Properties of a multicomponent medium. *Journal of Theoreretical Biology*, 36: 61–80

Markin, V.V., Parushenko, V.F. & Chizmadzhev, Y.A. 1987. *Theory of Excitable Media*, New York: Wiley

Panfilov, A.V. 1997. Modelling of re-entrant patterns of excitation in an anatomical model of the heart. In *Computational Biology of the Heart*, edited by A.V. Panfilov & A.V. Holden, Chichester and New York: Wiley

Rinzel, J. & Keller, J.B. 1973. Traveling wave solutions of a nerve conduction equation. *Biophyical Journal*, 13: 1313–1337

Scott, A.C. 2002. *Neuroscience: A Mathematical Primer*, Berlin and New York: Springer

MARKOV CHAIN

See **Stochastic processes**

MARKOV PARTITIONS

To simplify analysis of a dynamical system, we often study a topologically equivalent system using symbolic dynamics, representing trajectories by infinite length sequences using a finite number of symbols. (A simple example of this idea is the writing of real numbers as sequences of digits, a finite collection of symbols.) To represent the state space of a dynamical system with a finite number of symbols, we must partition the space into a finite number of elements and assign a symbol to each one.

Definition. A topological partition of a metric space M is a finite collection $\mathcal{P} = \{P_1, P_2, ..., P_r\}$ of disjoint open sets whose closures cover M in the sense that $M = \overline{P_1} \cup \cdots \cup \overline{P_r}$ (Lind & Marcus, 1995).

In probability theory, the term Markov denotes memorylessness. In other words, the probability of each outcome conditioned on all previous history is equal to conditioning only on the current state; no previous history is necessary. The same idea has been adapted to the dynamical systems theory to denote a partitioning of the state space so that all of the past information in the symbol sequence is contained in the current symbol, giving rise to the idea of a Markov transformation.

One-dimensional Transformations

In the special, but important case that a transformation of the interval is Markov, the symbolic dynamic is simply presented as a finite directed graph. A Markov transformation in $\mathcal{R}^1$ is defined as follows (Góra & Boyarsky, 1997):

Definition. Let $I = [c, d]$ and let $\tau : I \to I$. Let $\mathcal{P}$ be a partition of I given by the points $c = c_0 < c_1 < \cdots < c_p = d$. For $i = 1, \ldots, p$, let $I_i = (c_{i-1}, c_i)$ and denote the restriction of τ to I_i by τ_i. If τ_i is a homeomorphism from I_i onto a union of intervals of $\mathcal{P}$, then τ is said to be Markov. The partition $\mathcal{P}$ is said to be a Markov partition with respect to the function τ.

There are two key elements of the Markov partition that allow the symbol dynamics to accurately represent the system. First, on each interval I_i of the partition, the map must be monotonic (a homeomorphism), which ensures that whenever the preimage of a point is inside an interval, the preimage is unique. Second, whenever the image of a partition element intersects another element, it covers that interval. Therefore, regardless of the trajectory before entering an interval I_j, the orbit may follow any allowed trajectory from I_j. (The future evolves only from the present state.)

As a one-dimensional example, consider map 1 (Figure 1a) which is a Markov map with the associated partition $\{I_1, I_2, I_3, I_4\}$. The symbol dynamics are captured by the transition graph (Figure 1b). Although map 2 (Figure 1c) is piecewise linear and is logically

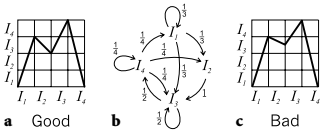

Figure 1. (a) A Markov map with partition shown. Note that on each interval, the map is a one-to-one and the image of the interval covers every interval that it intersects. (b) The transition graph for map 1. (c) The partition is not Markov ("Bad"): the image of I_2 stretches into interval I_3, but it does not completely cover that interval (and similarly for the image of I_3 with I_3).

partitioned by the same intervals as map 1, the partition is not Markov because interval I_2 does not map onto (in the mathematical sense) a union of any of the intervals of the partition. However, we are not able to say that map 2 is not Markov. There may be some other partition that satisfies the Markov condition. In general, finding a Markov partition or proving that such a partition does not exist is a difficult problem.

Higher Dimensions

Any topological partitioning of the state space will create symbol dynamics for the map. In the special case where the partition is Markov, the symbol dynamics capture the essential dynamics of the original system.

Definition. Given a metric space M and a map $f: M \to M$, a Markov partition of M is a topological partition of M into rectangles $\{R_1, \ldots, R_m\}$ such that whenever $x \in R_i$ and $f(x) \in R_j$, then (Bowen, 1975; Guckenheimer & Holmes, 1983)

$$f[W^{\mathrm{u}}(x) \cap R_i] \supset W_{\mathrm{u}}[f(x)] \cap R_j$$

and

$$f[W^{s}(x) \cap R_i] \subset W_{s}[f(x)] \cap R_j. \qquad (1)$$

To determine if the partition is Markov, in other words, we find the stable and unstable manifolds (W^{s} and W^{u}) of each point x and its image $f(x)$, and consider the restriction of these manifolds to the partition rectangles. Thus, whenever an image rectangle intersects a partition element, the image must stretch completely across that element in the expanding (unstable) directions, but the image must be inside that partition element in the contracting (stable) direction. (See Figure 2.)

It is important to use a "good" partition so that the resulting symbolic dynamics of orbits through the partition well represents the dynamical system. If the partition is Markov, then goodness is most easily ensured. However, a broader notion, called generating partition, may be necessary to capture the dynamics. A Markov partition is generating, but the converse is not generally true. See Bollt et al. (2001) and Rudolph

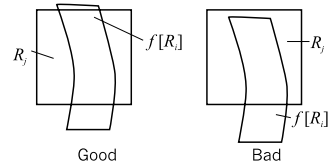

Figure 2. In the unstable (expanding) direction, the image rectangle must stretch completely across any of the partition rectangles that it intersects.

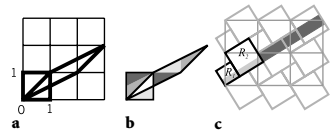

Figure 3. The cat map is a toral automorphism. (a) The operation of the linear map on the unit square. (b) Under the mod operation, the image is exactly the unit square. (c) Tessellation by rectangles R_1 and R_2 forms an infinite partition on $\mathbf{R}^2$. However, since the map is defined on the toral space $\mathbf{T}^2$, only two rectangles are required to cover the space. The filled gray boxes illustrate that R_1 and R_2 are mapped completely across a union of rectangles.

(1990) for a discussion of the role of partitions in representing dynamical systems.

The cat map, defined by

$$\mathbf{x} = (\mathbf{A}\mathbf{x}) \bmod 1, \qquad (2)$$

where

$$\mathbf{A} = \begin{bmatrix} 2 & 1 \\ 1 & 1 \end{bmatrix} \qquad (3)$$

yields a map from the unit square onto itself. This map is said to be on the toral space $\mathbf{T}^2$ because the mod 1 operation causes the coordinate $1 + z$ to be equivalent to z. A Markov partition for this map is shown in Figure 3 (see also color plate section). The cat map is part of a larger class of functions called toral Anosov diffeomorphisms and provides a detailed description of how to construct Markov partitions for this class of maps (Robinson, 1995).

Applications

In addition to establishing the link to symbol dynamics, the Markov partition has another direct application in the one-dimensional case. In a dynamical system, we are often interested in the overall behavior of the map—the evolution of an ensemble of initial conditions. The Frobenius–Perron operator is used to describe this evolution. When the map is Markov, this operator reduces to finite-dimensional stochastic transition matrix. Following the same development as in probability theory, the stationary (invariant) density associated with these maps is described by the eigenvector for the eigenvalue $\lambda = 1$. If the system

meets certain ergodic conditions, this density will describe the time average behavior of the system.

The analysis of the ensemble behavior of a dynamical system via its transition matrix is such a powerful tool that we would like to apply it to other one-dimensional systems, even when they may not be Markov. A general technique for approximating the invariant density of a map is called Ulam's method, conjectured by Ulam in 1960 and later proven by Li in 1976. The method relies upon the fact that Markov maps are dense in function space (Froyland, 2000).

ERIK M. BOLLT AND JOE D. SKUFCA

See also **Cat map; Symbolic dynamics**

Further Reading

Bollt, E., Stanford, T., Lai, Y. & Życzkowski, K. 2001. What symbol dynamics do we get with a misplaced partition? On the validity of threshold crossings analysis of chaotic time-series. *Physica* D, 154: 259–286

Bowen, R. 1975. *Equilibrium States and the Ergodic Theory of Anosov Diffeomorphisms*, Berlin and New York: Springer

Froyland, G. 2000. Extracting dynamical behavior via Markov models. In *Nonlinear Dynamics and Statistics: Proceedings, Newton Institute, Cambridge, 1998*, edited by A. Mees, Boston: Birkhäuser

Góra, P. & Boyarsky, A. 1997. *Laws of Chaos, Invariant Measures and Dynamical Systems in One Dimension*, Boston: Birkhäuser

Guckenheimer, J. & Holmes, P. 1983. *Nonlinear Oscillations, Dynamical Systems, and Bifurcations of Vector Fields*, New York: Springer

Lind, D. & Marcus, B. 1995. *An Introduction to Symbolic Dynamics and Coding*, Cambridge and New York: Cambridge University Press

Li, T.-Y. 1976. Finite approximation for the Frobenius–Perron operator. A solution to Ulam's conjecture. *Journal of Approximation Theory*, 17: 177–186

Robinson, C. 1995. *Dynamical Systems: Stability, Symbolic Dynamics, and Chaos*, Ann Arbor, MI: CRC Press

Rudolph, D.J. 1990. *Fundamentals of Measurable Dynamics, Ergodic Theory on Lebesgue Spaces*, Oxford: Clarendon Press, and New York: Oxford University Press

Ulam, S. 1960. *Problems in Modern Mathematics*, New York: Interscience Publishers

MARTINGALES

The classic setting for probability is that of independent random variables. An experiment is repeated many times, and whatever happens in one trial has no effect on what happens in future trials. However, many results of probability also hold true in a much more general setting, that of martingales. The word *martingale* is associated with the concept of a gambling scheme, but its importance in probability is quite general and goes far beyond gambling. The reason is that it is rather easy to find or construct martingales, and these give useful insights into probability problems.

In roulette, the "martingale system" is to double the bet (on black or red) after each bet, until one finally wins. (See Example 4.) The word *martingale* is also used for various arrangements of constraints: part of a horse's reins, lines controlling the jib of a yacht, and the belt at the back of a jacket. The word has been traced back to Middle French before 1600 and, in some accounts, comes from the town of Martigues, presumably a center for horses and gambling.

Definition

The mathematical definition of a martingale involves conditional expectation, and this is a nonlinear concept. If $X_1, \ldots, X_n$ are random variables, then they generate a larger set $\mathcal{F}_n$ of random variables. This set $\mathcal{F}_n$ is defined as the set of all random variables W such that there exists a function f (possibly very nonlinear) with $W = f(X_1, \ldots, X_n)$. If Z is a real random variable with well-defined expectation $E[Z]$, then the "conditional expectation" $E[Z \mid \mathcal{F}_n] = h(X_1, \ldots, X_n)$ is an element of $\mathcal{F}_n$. It is determined by the condition that for every bounded random variable W in $\mathcal{F}_n$ we have $E[E[Z \mid \mathcal{F}_n]\, W] = E[ZW]$. In other words, $E[Z \mid \mathcal{F}_n]$ is the orthogonal projection of Z onto the nonlinearly generated space $\mathcal{F}_n$.

A martingale is a fair game at each step. (There is also a concept of supermartingale, an unfavorable game, and a corresponding concept of submartingale, a favorable game. These are discussed in the references.) Thus, a martingale is a sequence of random variables S_n, one for each time step. These represent the fortune of the gambler at time n. Let $\mathcal{F}_n$ be generated by the random variables that are defined by what happens up to and including time n. Thus, in particular S_n belongs to $\mathcal{F}_n$. However, the fortune S_{n+1} at the next time step typically does not belong to S_n. Past history does not determine future performance.

The martingale condition is that the conditional expectation $E[S_{n+1} \mid \mathcal{F}_n] = S_n$. That is, given the past history up to time n, the expected change in fortune at the next step into the future is zero. It follows easily that the expected fortune $E[S_n]$ does not depend on n and is equal to $E[S_0]$.

A long-held dream of gamblers was to find a gambling scheme to play a fair game and win on the average. The situation is clarified by the following theorems. The dream can be realized, but only if one ignores constraints on time and capital.

Theorems and Examples

Some theorems involving martingales and examples are as follows.

Theorem. *A martingale that is bounded above or bounded below must converge almost surely. Thus there is a random variable S_∞ such that $S_n \to S_\infty$ as $n \to \infty$ with probability one.*

Theorem. *A martingale that is bounded above and below is fair in the limit. That is*, $E[S_\infty] = E[S_0]$.

Example 1. Symmetric random walk. A symmetric random walk is obtained by starting with zero and then making each future step equal to $+1$ or -1, each independently with probability $\frac{1}{2}$. The walk is the sum of the steps. This is a martingale. In fact, it is a sum of independent random variables. It is unbounded above and below, and it does not converge.

Example 2. Stop when ahead. Consider an integer b with $0 < b$. When the random walk first reaches b, make every future step equal to 0. Notice that these future steps are not independent of the past steps. This is a martingale. At each stage it is a fair game. There is no possibility of winning more than b, but one can be very far in debt. Since this martingale is bounded above, it must converge almost surely, and it can only converge to the constant value b. Thus, a gambler with unlimited credit and unlimited time can play a fair game and be almost sure to win a fixed specified amount.

Example 3. Stop when ahead or behind. Let $a < 0 < b$. When the random walk first reaches a or b, make every future step equal to 0. This is a martingale. It is bounded both above and below. This martingale converges almost surely to a random value that is either a or b. Furthermore, the expected value of the eventual winnings is zero.

Example 4. Double the bet and stop when ahead. The first step is ± 1 as before. For a while, each future step is either positive or negative with equal probability, but twice the size of the previous step. After the first positive step, future steps are zero. Thus, for example, the first steps might be $-1, -2, -4, -8, +16$. The result is that the gambler is ahead by one. This is again a martingale. Since it is bounded above, it converges almost surely to 1. This is favorable to the gambler.

Example 5. Double the bet, start again when ahead. The strategy is the same as in the previous example. However, once the gambler is ahead by one, the game is repeated until the gambler is ahead by two. Then it is repeated again, and so on. This too is a martingale. It has the remarkable property that it diverges almost surely to $+\infty$.

The same ideas may be formulated via the concept of martingale difference. Let $X_0, X_1, X_2, \ldots, X_n, \ldots$ be a sequence of random variables. This is a stochastic process with a discrete time index. (Most of the concepts discussed below extend to continuous time stochastic processes, but this generalization is left to the references.) Let $\mathcal{F}_n$ be the set of all random variables $f(X_0, X_1, X_2, \ldots, X_n)$ that are functions of $X_0, \ldots, X_n$. A sequence of real random variables Y_n belonging to $\mathcal{F}_n$ is called a "martingale difference" if for each $n \geq 0$ the conditional expectation

$$E[Y_{n+1} \mid \mathcal{F}_n] = 0. \tag{1}$$

It is easy to see that if S_0 is in $\mathcal{F}_0$ and the Y_n form a martingale difference, then the sum $S_n = S_0 + Y_1 + Y_2 + \cdots + Y_n$ is a martingale.

The advantage of martingales is that they are easy to create. One general method is to produce martingale differences by subtracting conditional expectations. Thus, if each Z_n is in $\mathcal{F}_n$, then

$$Y_{n+1} = Z_{n+1} - E[Z_{n+1} \mid \mathcal{F}_n] \tag{2}$$

is a martingale difference. However, it is also possible to create martingales by other natural constructions, as shown by the following examples.

Example 6. A branching process. Start with W_0 individuals at stage 0. At each stage n there are W_n individuals. The jth individual in the nth generation has $X_j^{(n+1)}$ children, independently of all other individuals. This number of children is random with expectation $\mu > 0$. Thus the $n+1$th generation has

$$W_{n+1} = X_1^{(n+1)} + \cdots + X_{W_n}^{(n+1)} \tag{3}$$

individuals. Since

$$E[W_{n+1} \mid \mathcal{F}_n] = \mu W_n, \tag{4}$$

the sequence $S_n = W_n/\mu^n$ is a martingale. In particular, the expected size of the nth generation is

$$E[W_n] = \mu^n E[W_0]. \tag{5}$$

However, this average behavior gives a rather misleading picture of the branching process. The martingale S_n is bounded below by zero, and so it converges to some random value S_∞ almost surely. When $\mu \leq 1$, then the population goes extinct, and so $S_n = W_n/\mu^n \to 0$ almost surely as $n \to \infty$. However, in the case $\mu > 1$, it may be shown that the martingale is fair in the limit. Thus $S_n = W_n/\mu^n \to S_\infty$, where $S_\infty \geq 0$ is random with expectation $E[S_\infty] = E[S_0] = E[W_0]$. If the population does not die out fairly soon, then it has exponential growth: asymptotically $W_n \sim S_\infty \mu^n$.

Example 7. Extinction of a branching process. Let $\mu > 1$ and let ρ be the probability of extinction starting with just one member of the population. Then ρ^{W_n} is a bounded martingale. It converges to 1 when the population goes extinct, and it converges to zero when the population goes to infinity. The fact that it remains fair in the limit says that the probability of extinction starting with w individuals is ρ^w. Each individual's line must die out independently.

Markov Chain Examples

Let $X_0, X_1, X_2, \ldots, X_n, \ldots$ be a Markov chain. (Continuous time Markov processes may also be treated, but that subject is also left to the references.) Let f be a real function of the state of the chain.

Then the present value $f(X_n)$ is a random variable. By the definition of a Markov chain, the expectation of a future value $f(X_{n+1})$, given the past $\mathcal{F}_n$, generated by $X_0, \ldots, X_n$, depends only on the present state X_n. That is,

$$E[f(X_{n+1}) \mid \mathcal{F}_n] = (Pf)(X_n), \tag{6}$$

where Pf is the application of the transition probability operator to the function f. (One can think of f as a column vector and P as multiplication by a square matrix, so Pf is another column vector.) Thus, in the special case when $Pf = f$, the sequence $f(X_n)$ is a martingale. It depends only on the current state. Such functions f are of particular interest when the chain has transient states that can lead to distinct recurrent classes.

Example 8. Asymmetric random walk (gambler's ruin). Let the Markov chain X_n be the random walk that starts at 0 and steps by $+1$ with probability p and steps by -1 with probability q, where $p + q = 1$. To be realistic in the gambling situation, take $0 < p < q < 1$. It is easy to check that the modified game $S_n = (q/p)^{X_n}$ is a martingale.

Example 9. Stop when ahead. Let $0 < b$. When the random walk X_n first reaches b, future steps are zero. Then $S_n = (q/p)^{X_n}$ is a bounded martingale. Therefore, it must converge almost surely and remain fair in the limit. The gambler either wins or goes further and further into debt. It follows from the fact that the modified game is fair in the limit that $1 = (q/p)^b P[X_n \to b]$. Thus, the probability of winning is $P[X_n \to b] = (p/q)^b$.

Example 10. Stop when ahead or behind. Let $a < 0 < b$. When the random walk X_n first reaches a or b, future steps are zero. It follows that $1 = (q/p)^a P[X_n \to a] + (q/p)^b P[X_n \to b]$. From this, it is easy to work out the probabilities of winning or losing. The probability of winning is less than in the last example, but the gambler is protected from catastrophe.

If f is a function of the state of a Markov chain, but $Pf \neq f$, then there is still an associated martingale, but it has a different character. Let

$$Y_{n+1} = f(X_{n+1}) - (Pf)(X_n). \tag{7}$$

Then Y_n forms a martingale difference sequence. Let $S_0 = f(X_0)$ and form the martingale S_n as before. Then the neighboring terms group together, and we get

$$\begin{aligned} S_n = {} & u(X_0) + u(X_1) + u(X_2) + \cdots + u(X_{n-1}) \\ & + f(X_n), \end{aligned} \tag{8}$$

where $u = f - Pf$. The martingale is a cumulative sum over the entire history.

For this result to be useful, it is necessary to find an interesting function u for which there is a solution f of $u = f - Pf$. This often happens in the context of an irreducible Markov chain with only positive recurrent states. Let π be the invariant probability vector for the Markov chain. (One can think of π as a row vector satisfying $\pi P = \pi$.) Then a necessary condition for a solution is that $\pi u = 0$. For instance, one can take a function h and define $u = h - (\pi h)1$. If f is bounded, then $f(X_n)/n \to 0$, and in suitable circumstances the strong law of large numbers for martingales (see below) gives

$$\frac{u(X_0) + u(X_1) + u(X_2) + \cdots + u(X_{n-1})}{n} \to 0 \tag{9}$$

almost surely. In terms of the function h this says that

$$\frac{h(X_0) + h(X_1) + u(X_2) + \cdots + h(X_{n-1})}{n} \to \pi h \tag{10}$$

almost surely, where πh is the expectation computed with the invariant probability (the product of the probability row vector π with the column vector h). This is a strong law of large numbers for Markov chains. It is the idea underlying the Monte Carlo calculation of unknown invariant probabilities π.

General Results

Many classical results for sums of independent random variables have generalizations to the martingale setting. These include the strong law of large numbers and the central limit theorem.

The Kolmogorov form of the strong law of large numbers says the following. Let $Y_1, \ldots, Y_n, \ldots$ be a sequence of martingale difference random variables with finite variances $\sigma_1^2, \ldots, \sigma_n^2, \ldots$. Assume that the variances are uniformly bounded, or more generally that

$$\sum_{n=1}^{\infty} \frac{\sigma_n^2}{n^2} < \infty. \tag{11}$$

Then as $n \to \infty$ the sample means

$$\bar{Y}_n = \frac{Y_1 + \cdots + Y_n}{n} \to 0 \tag{12}$$

almost surely (that is, with probability one). This is the law of averages in a very powerful and general form.

Fluctuations about the average are described by the central limit theorem. The setting for this theorem is a sequence $Y_1, \ldots, Y_n, \ldots$ of martingale difference random variables with finite variances $\sigma_1^2, \ldots, \sigma_n^2, \ldots$. Let

$$s_n^2 = \sigma_1^2 + \cdots + \sigma_n^2 \tag{13}$$

be the variance of the sum $Y_1 + \cdots + Y_n$.

The martingale differences satisfy the conditional variance normalization condition if

$$\frac{1}{s_n^2} \sum_{k=1}^{n} E[Y_k^2 \mid \mathcal{F}_{k-1}] \to 1 \tag{14}$$

in probability as $n \to \infty$.

Fix $\varepsilon > 0$. Consider one of the random variables Y_i. Say that it is large if $|Y_i| > \varepsilon s_n$. Define the large part of Y_i to be the random variable $Y_i^{\varepsilon s_n}$ that is equal to Y_i when Y_i is large and is equal to zero otherwise. The Lindeberg condition is that the contribution of the large values to the total variance is small, in the sense that for each $\varepsilon > 0$

$$\frac{1}{s_n^2}\sum_{i=1}^{n} E[(Y_i^{\varepsilon s_n})^2] \to 0 \tag{15}$$

as $n \to \infty$.

The central limit theorem states that if $Y_1, \ldots, Y_n, \ldots$ are martingale difference random variables with finite variances that satisfy the conditional variance normalization condition and the Lindeberg condition, then the distribution of

$$Z_n = \frac{Y_1 + \cdots + Y_n}{s_n} \tag{16}$$

approaches the distribution of a standard normal random variable Z as $n \to \infty$. That is, the Gaussian distribution gives a universal description of fluctuations of martingales.

WILLIAM G. FARIS

See also **Random walks; Stochastic processes**

Further Reading

Doob, J.L. 1953. *Stochastic Processes*, New York: Wiley

Durrett, R. 1991. *Probability: Theory and Examples*, Belmot, CA: Duxbury Press

Hall, P. & Heyde, C.C. 1980. *Martingale Limit Theory and Its Application*, New York: Academic Press

Nelson, E. 1987. *Radically Elementary Probability Theory*, Princeton, NJ: Princeton University Press (This book presents probability through the martingale central limit theorem in the context of finite but non-standard probability spaces. It is an unusual treatment, but inspiring.)

Neveu, J. 1975. *Discrete Parameter Martingales*, Amsterdam: North-Holland

MATHIEU EQUATION

See **Surface waves**

MATTER, NONLINEAR THEORY OF

A nonlinear theory of matter was first proposed in 1912 by Gustav Mie in a prescient series of papers that aimed to derive the elementary particles of matter as localized lumps of energy in a nonlinear field (Mie, 1912). To this end, Mie suggested a nonlinear augmentation of James Maxwell's electromagnetic equations out of which the electron would arise in a natural way.

Specifically, he defined a Lagrangian density ($\mathcal{L}$) depending upon electric field intensity ($\boldsymbol{E}$) and magnetic flux density ($\boldsymbol{B}$) and the four components of the electromagnetic potential ($\boldsymbol{A}, \phi$). Requiring dependence on the parameters $\eta \equiv (\boldsymbol{B}^2 - \boldsymbol{E}^2)$ and $\chi \equiv (\phi^2 - \boldsymbol{A}^2)$ ensured relativistic invariance, and the specific choice $\mathcal{L} = \eta/2 + a\chi^3/6$ led to a static, spherically symmetric electric potential (ϕ) of the form

$$\phi(r) \approx \frac{(3r_0^2/a)^{1/4}}{\sqrt{r^2 + r_0^2}}. \tag{1}$$

Setting $4\pi(3r_0^2/a)^{1/4} = e$ (the electronic charge) yielded a spherically symmetric model for the electron with a radius of r_0 and electric potential

$$\phi(r) \to e/4\pi r$$

as $r \to \infty$. The Lorentz invariance that is built into the theory permits this solution to travel with any speed up to the limiting velocity of light with an appropriate Lorentz contraction.

Mie's approach to a nonlinear theory of matter was supported by Albert Einstein, who offered the following opinion in the mid-1930s (Einstein, 1954).

> In the foundation of any consistent field theory, the particle concept must not appear in addition to the field concept. The whole theory must be based solely on partial differential equations and their singularity-free solutions.

Empirical support for this perspective was provided in the early 1930s by Carl Anderson's discovery of positron-electron creation from cosmic radiation. In other words, massive particles were observed to emerge from and collapse back into an electromagnetic field, which is not a property of the linear Maxwell equations.

Motivated by Anderson's observation, Max Born revisited Mie's nonlinear electromagnetics. Together with Leopold Infeld, he eliminated the χ-dependence in Mie's functional formulation and chose instead the Lagrangian density (Born & Infeld, 1934)

$$\mathcal{L} = E_0^2\sqrt{1 + (\boldsymbol{B}^2 - \boldsymbol{E}^2)/E_0^2} - E_0^2\,, \tag{2}$$

where E_0 sets the field intensities at which nonlinearities arise. At low-field amplitudes, Equation (2) reduces to the classical Lagrangian density for Maxwell's equations: $\mathcal{L} = (\boldsymbol{B}^2 - \boldsymbol{E}^2)/2$. (Even with the currently available, high-intensity lasers, these vacuum nonlinearities would be difficult to observe, as E_0 is estimated to be about 10^{20} V/m in laboratory units.)

Among the solutions of this system, Born and Infeld found a spherically symmetric model electron with $\boldsymbol{E}$ finite everywhere, although the electric displacement ($\mathbf{D}$) exhibits a singularity at the origin. Erwin Schrödinger became interested in Born's theory as early as 1935 and continued working on it through the 1940s when—as founding director of the Dublin Institute for Advanced Studies—he attempted to move research in physics toward key areas of nonlinear science (Schrödinger, 1935).

Plane waves derived from Equation (2) obey the equation $(1 - u_t^2)u_{xx} + 2u_x u_t u_{xt} - (1 + u_x^2)u_{tt} = 0$,

where u is a component of the vector potential. Called the Born–Infeld equation, this system has been studied as an interesting nonlinear wave equation (Barbashov & Chernikov, 1966).

Einstein's conviction that a consistent theory for particle physics must be based on localized solutions of nonlinear partial differential equations was shared by several of his colleagues. In addition to Mie, Born, Infeld, and Schrödinger, Werner Heisenberg (1966), Louis de Broglie (1960, 1963), and David Bohm (1957) have suggested nonlinear field theories that in their simplest representations, can be viewed as the augmentation of linear field equations by a nonlinear term of the form $|u|^2u$, as in the nonlinear Schrödinger equation. This nonlinearity conserves the integral

$$\int |u|^2 \, \mathrm{d}\mathbf{r}, \tag{3}$$

which can be interpreted as a mass.

The ideas of de Broglie and Bohm are related to those of the inverse scattering method (ISM). In their "theory of the double solution," the real particle is a localized solution of a nonlinear equation with the form

$$u = U\mathrm{e}^{\mathrm{i}\theta'}.$$

Associated with this localized nonlinear solution is the solution of a corresponding linear equation

$$\psi = \Psi \mathrm{e}^{\mathrm{i}\theta}$$

with

$$\theta = \theta' \tag{4}$$

except in a small region surrounding the real particle. The function ψ is taken to be a solution of Schrödinger's quantum mechanical wave equation, and the phase condition of Equation (4) allows the particle to be guided by ψ. Similarly, in the context of the ISM, the nonlinear solution of a soliton equation is guided through space-time by the linear asymptotic solution of the associated linear operator. Although proposed almost a half century ago, the de Broglie–Bohm theory continues to offer possibilities for further studies (Holland, 1993).

During the 1960s, several investigators proposed the sine-Gordon (SG) equation as a field theory for elementary particles in one space dimension and time (Scott, 2003). This work gained momentum in the 1970s when it became known that special properties of the SG equation allow the corresponding quantum problem to be solved, showing that certain qualitative properties of the classical solution survive quantization (Dashen et al., 1974; Faddeev, 1975; Goldstone & Jakiw, 1975). In particular, the classical field energy was found to be a useful first approximation for the soliton mass, with quantum effects coming in as second-order corrections. More recently, this approach has been developed into the concept of a skyrmion, which is a generalization of the SG kink, carrying its topological stability into three space dimensions.

These examples suggest that it may be possible to develop a nonlinear theory of matter by proceeding as follows. First, guess a classical version of the correct nonlinear field. Second, solve this classical system for salient aspects of localized behavior. Third, analyze the corresponding quantum theory to obtain exact values for the mass spectrum. Finally, compare calculated values of mass with measured mass spectra. As Einstein was aware, however, this is a daunting program because there are no theoretical bounds on the range of conceivable nonlinear theories; thus, it is not surprising to find a proliferation of partially evaluated theories. In addition to the Born–Infeld, de Broglie, and skyrmion formulations, present candidates include string theory and the Yang–Mills equation. What others are out there?

ALWYN SCOTT

See also **Born–Infeld equations; Hodograph transform; Inverse scattering method or transform; Particles and antiparticles; Skyrmions; String theory; Yang–Mills theory**

Further Reading

Barbashov, B.M. & Chernikov, N.A. 1966. Solution of the two plane wave scattering problem in a nonlinear scalar field theory of the Born–Infeld type. *Soviet Physics JETP*, 23: 1025–1033

Bohm, D. 1957. *Causality and Chance in Modern Physics*, London: Routledge & Kegan Paul

Born, M. & Infeld, L. 1934. Foundations of a new field theory. *Proceedings of the Royal Society* (*London*) A, 144: 425–451

de Broglie, L. 1960. *Nonlinear Wave Mechanics*, Amsterdam: Elsevier

de Broglie, L. 1963. *Introduction to the Vigier Theory of Elementary Particles*, Amsterdam: Elsevier

Dashen, R.F., Hasslacher, B. & Neveu, A. 1974. Particle spectrum in model field theories from semiclassical functional integral techniques. *Physical Review* D, 11: 3424–3450

Einstein, A. 1954. *Ideas and Opinions*, New York: Crown

Faddeev, L.D. 1975. Hadrons from leptons? *JETP Letters*, 21: 64–65

Goldstone, J. & Jakiw, R. 1975. Quantization of nonlinear waves. *Physical Review* D, 11: 1486–1498

Heisenberg, W. 1966. *Introduction to the Unified Field Theory of Elementary Particles*, New York: Wiley

Holland, P.R. 1993. *The Quantum Theory of Motion*, Cambridge and New York: Cambridge University Press

Mie, G. 1912. Grundlagen einer Theorie der Materie. *Annalen der Physil*, 37: 511–534; 39: 1–40; 40 (1913): 1–66

Schrödinger, E. 1935. Contributions to Born's new theory of the electromagnetic field. *Proceedings of the Royal Society* (*London*) A, 150: 465–477

Scott, A.C. 2003. *Nonlinear Science: Emergence and Dynamics of Coherent Structures*, 2nd edition, Oxford and New York: Oxford University Press

MAXWELL–BLOCH EQUATIONS

The Maxwell–Bloch (MB) equations arise in nonlinear optics, where they couple "two-level atoms" to Maxwell's electromagnetic field equations to model a nonlinear dielectric. Although the two-level atom is a pseudo-atom with only two nondegenerate energy levels, it can be realized in practice by real atoms excited by light close to a suitable atomic resonance, and it can be modeled as a two-state system: $|g\rangle$ (for ground) and $|e\rangle$ (for excited). Transitions between the two states are allowed, and there is a quantum mechanical matrix element $p = q\langle g|r|e\rangle \neq 0$ between them in dipole approximation, where q is the electronic charge and qr is the dipole transition operator.

The outer products of $|e\rangle$ and $|g\rangle$ form a Lie algebra with

$$S^z = \tfrac{1}{2}(|e\rangle\langle e| - |g\rangle\langle g|),$$
$$S^+ = |e\rangle\langle g|,$$
$$S^- = |g\rangle\langle e|.$$

By choosing $\langle e \mid e\rangle = \langle g \mid g\rangle = 1$, $\langle e \mid g\rangle = \langle g \mid e\rangle = 0$ (orthonormality), one finds that the Lie algebra is

$$[S^z, S^+] = S^+, \quad [S^z, S^-] = -S^-,$$
$$[S^+, S^-] = 2S^z,$$

where $[,]$ is the Lie bracket or "commutator" (Bullough et al., 1995b). Constructed from $|e\rangle$ and $|g\rangle$, this is a two-dimensional representation of su(2), corresponding to a spin-$\frac{1}{2}$ system in which $|e\rangle$ is spin-up and $|g\rangle$ is spin-down. In a magnetic field $\boldsymbol{B} = (B_x, B_y, B_z)$, a magnetic dipole μ has a Hamiltonian which can be taken in the form of a 2×2 Hamiltonian matrix with elements (Feynman et al., 1966, pp. 10–14)

$$H_{11} = -\mu B_z, \quad H_{12} = -\mu(B_x - \mathrm{i}B_y),$$
$$H_{21} = -\mu(B_x + \mathrm{i}B_y), \quad H_{22} = +\mu B_z.$$

There is an exact correspondence for the dipole p of the two-level atom in an electric field $\boldsymbol{E}$, and the two-level atom is a pseudo-spin-$\frac{1}{2}$ system (Bullough et al., 1995b). As any state $|\psi(t)\rangle$ at time t in the two-dimensional Hilbert space can be written $|\psi(t)\rangle = c_1(t)|e\rangle + c_2(t)|g\rangle$, the correspondence extends to the dynamics. From the Hamiltonian H_{ij}, Schrödinger's equation for the amplitudes $c_i(t)(i = 1, 2)$ becomes

$$\mathrm{i}\hbar\dot{c}_1 = -\mu[B_z c_1 + (B_x - \mathrm{i}B_y)c_2],$$
$$\mathrm{i}\hbar\dot{c}_2 = -\mu[(B_x + \mathrm{i}B_y)c_1 - B_z c_2].$$

When $B_x = B_y = 0$, $B_z =$ constant independent of t, $c_1(t), c_2(t)$ evolve as $c(0)\mathrm{e}^{\pm \mathrm{i}\omega_0 t}$, and $\omega_0 = 2\mu B_z \hbar^{-1}$ is a Larmor frequency for the spinning (precessing) magnet of moment μ. The free two-level atom with resonance frequency ω_0 thus *acts* as a true spin-$\frac{1}{2}$ in a fixed magnetic field B_z.

If we construct the Bloch vector $\boldsymbol{r}(t) = (r_1(t), r_2(t), r_3(t))$

$$r_1 = (c_1 c_2^* + c_1^* c_2), \; r_2 = -i(c_1 c_2^* - c_1^* c_2),$$
$$r_3 = (|c_1|^2 - |c_2|^2)$$

(c_1^* = complex conjugate of c_1), the equations of motion for $c_1(t)$, $c_2(t)$ become the Bloch equation

$$\dot{\boldsymbol{r}} \equiv \mathrm{d}\boldsymbol{r}/\mathrm{d}t = \boldsymbol{\omega} \times \boldsymbol{r} \tag{1}$$

for a spin-$\frac{1}{2}$ particle, where $\omega \equiv (-2\mu B_x \hbar^{-1}, -2\mu B_y \hbar^{-1}, -2\mu B_z \hbar^{-1})$. (For the two-level atom in a real electric field $E(t)$, $\boldsymbol{\omega} \equiv (-2pE\hbar^{-1}, 0, \omega_0)$.) The normalization $|c_1|^2 + |c_2|^2 = 1$ means $|\boldsymbol{r}|^2 = 1$, and the motion is confined to the surface of a sphere (the Bloch sphere) of unit radius: spin-up = (0,0,1), spin down = (0,0,-1) on this sphere. This description omits a Berry's phase.

Two-level atoms enter laser physics via the Jaynes–Cummings (JC) model, which couples one two-level atom to a single mode of the quantized electromagnetic field of frequency ω. The Hamiltonian is

$$H = \omega_0 S^z + \omega a^\dagger a + g(a^\dagger S^- + S^+ a),$$

where g is a (real and positive) coupling constant, S^z, $S^\pm$ satisfy the su(2) algebra given above, and $a, a^\dagger$ satisfy $[a, a^\dagger] = 1$ and the Heisenberg–Weyl algebra of standard bosons.

The number operator $N = S^z + a^\dagger a + 1/2$ commutes with H. The JC model is thus quantum integrable, there being two degrees of freedom (spin and the quantum oscillator), and there are exactly two commuting constants H and N. The model can be solved exactly in terms of 2×2 matrices (Bullough et al., 1995a) and also by the quantum inverse method in Bogoliubov et al. (1996). By coupling the JC model to a heat-bath, one obtains the master equation for a micromaser. (Such a nonlinear quantum device is in operation at the Max Planck Institute, Garching, Germany, using ^{85}Rb atoms which enter a cavity in their upper states $|e\rangle$ but may leave it in $|e\rangle$ or $|g\rangle$.)

The JC model evolves only in time and is a fundamental nonlinear quantum model. One obtains important nonlinear quantum field theories by coupling two-level atoms to Maxwell's electromagnetic field equations

$$\nabla^2 \hat{\boldsymbol{E}} - c^{-2}\partial^2 \hat{\boldsymbol{E}}/\partial t^2 = 4\pi n c^{-2}\, \partial^2 \hat{\boldsymbol{P}}/\partial t^2. \tag{2}$$

Here, c is the speed of light in a vacuum, n is the number of two-level atoms per unit volume, and $\hat{\boldsymbol{E}} = \hat{\boldsymbol{E}}(\boldsymbol{x}, t)$ and $n\hat{\boldsymbol{P}} = n\hat{\boldsymbol{P}}(\boldsymbol{x}, t)$ are, respectively, the electric field and dipole density operators. This operator Maxwell equation and the operator Bloch equation for the dipole density constitute the quantum operator form of the MB equations.

If the electric fields are strong enough (many photons), both $\hat{\boldsymbol{E}}$ and $\hat{\boldsymbol{P}}$ can be regarded as classical variables, while quantum mechanics still enters through the atoms. The classical electric field $\boldsymbol{E}(\boldsymbol{x}, t)$ acts on the atom at $\boldsymbol{x}$ at time t through vectors $\boldsymbol{\omega}(\boldsymbol{x}, t)$ given at points $\boldsymbol{x}$ and time t through

$$\boldsymbol{\omega}(\boldsymbol{x}, t) \equiv (-2\boldsymbol{p} \cdot \boldsymbol{E}(\boldsymbol{x}, t)\hbar^{-1}, 0, \omega_0)$$

and the Rabi frequency is $|2\boldsymbol{p} \cdot \boldsymbol{E}(\boldsymbol{x}, t)|\ \hbar^{-1}$. This form of $\boldsymbol{\omega}(\boldsymbol{x}, t)$ shows the coupling between the Maxwell equations and the Bloch equations to form the semiclassical MB equations, and the coupling is nonlinear since $\mathbf{E}(\mathbf{x}, t)$ is driven by $\boldsymbol{p}r_1(\boldsymbol{x}, t)$ for $\boldsymbol{P}(\boldsymbol{x}, t)$ in the (linear) Maxwell equation.

In one space dimension (x) one obtains the standard form of the semiclassical MB equations (Eilbeck et al., 1973). The (linear) Maxwell equations for such an $E(x, t)$ and $P(x, t) = pr_1(x, t)$ is

$$\partial^2 E/\partial x^2 - (1/c^2)\partial^2 E/\partial t^2 = (4\pi np/c^2)\partial^2 r_1/\partial t^2\,. \tag{3}$$

With $\omega(x, t) \equiv (-2pE(x, t)\hbar^{-1}, 0, \omega_0)$, the Bloch equation (1) can be written out explicitly as

$$\begin{aligned} \partial r_1/\partial t &= -\omega_0 r_2, \\ \partial r_2/\partial t &= \omega_0 r_1 + 2p\hbar^{-1} E r_3, \\ \partial r_3/\partial t &= -2p\hbar^{-1} E r_2. \end{aligned} \tag{4}$$

This system of four nonlinear partial differential equations (3) with (4) is not integrable, but it becomes an integrable field theory if the Maxwell equation is replaced by the unidirectional system (valid for small densities in the one space dimension)

$$\partial E/\partial x + (1/c)\partial E/\partial t = (-2\pi np/c)\partial r_1/\partial t. \tag{5}$$

Equations (4) and (5) comprise the reduced Maxwell–Bloch (RMB) equations, which can be explicitly integrated by the AKNS inverse scattering method as in Gibbon et al. (1973).

Under a slowly varying envelope and phase approximation (SVEPA), the envelope equations become the self-induced transparency (SIT) equations

$$\begin{aligned} &\partial \mathcal{E}/\partial x + (1/c)\partial \mathcal{E}/\partial t = \alpha P, \\ &\partial P/\partial t = \mathcal{E} N + \Delta\omega' Q, \\ &\partial N/\partial t = -\mathcal{E} P, \\ &\partial Q/\partial t = -\Delta\omega' P. \end{aligned} \tag{6}$$

In these SIT equations, $\Delta\omega' \equiv \omega_0' - \omega_0$ (called inhomogeneous broadening), and ω_0' is a shifted resonance frequency for any particular atom (induced by Doppler shifts, e.g.) while P, Q, N depend on $(x, t, \Delta\omega')$ and N replaces the inversion r_3 of the atom in the Bloch vector. It is an unfortunate confusion of the literature that what we call the SIT equations are also called the Maxwell–Bloch equations. Here, we reserve MB for the Maxwell equation coupled to the three Bloch equations which are *not* envelope equations.

The SIT equations (6) must be averaged over inhomogeneous broadening $\Delta\omega'$ but remain integrable. The soliton solution is the 2π-pulse of (McCall & Hahn, 1969) and there are multi-soliton solutions. Under a sharp line resonance condition, they further reduce to the standard form of the sine-Gordon (SG) equation

$$\partial^2\phi/\partial x^2 - \partial^2\phi/\partial t^2 = \sin\phi\,. \tag{7}$$

Under an SVEPA, the SG equation becomes the attractive case of the nonlinear Schrödinger (NLS) equation. The RMB, SIT, SG, and attractive NLS equations form a hierarchy of integrable nonlinear field theories in which integrability is handed down by the SVEPA in the fashion described by Calogero in 1995 (see Bullough, 2001).

The two-dimensional representations of su(2) for two-level atoms extend to three-dimensional representations of su(3) for three-level atoms, and the consequent appropriately generalized SIT equations are fundamental to electromagnetically induced transparency (EIT) and the storage of quantum information (Bullough, 2001; Hau, 2001; Haroche & Raimond, 1993; Bullough & Gibbs, 2004).

ROBIN BULLOUGH

See also **Berry's phase; Lie algebras and Lie groups; Nonlinear optics; Nonlinear Schrödinger equation; Sine-Gordon equation**

Further Reading

Bogoliubov, N.M., Rybin, A.V., Bullough, R.K. & Timonen, J. 1995. Maxwell–Bloch system on a lattice. *Physical Review* A, 52: 1487–1493

Bogoliubov, N.M., Bullough, R.K. & Timonen, J. 1996. Exact solution of generalized Tavis–Cummings models in quantum optics. *Journal of Physics A: Mathematics and General*, 29: 6305–6312

Bullough, R.K. 2001. Optical solitons: twenty-seven years of the last millennium and three more years of the new? In *Mathematics and the 21st Century*, edited by A.A. Ashour & A.-S.F. Obada, Singapore: World Scientific, pp. 69–121

Bullough, R.K. & Gibbs, H.M. 2004. Information storage and retrieval by stopping pulses of light. *Journal of Modern Optics*, 51(2): 255–284

Bullough, R.K., Nayak, N. & Thompson, B.V. 1995a. Cavity quantum electrodynamics: fundamental theory of the micromaser. In *Recent Developments in Quantum Optics*, edited by R. Inguva, New York: Plenum Press

Bullough, R.K., Thompson, B.V., Nayak, N. & Boguliubov, N.M. 1995b. Microwave cavity quantum electrodynamics: I, one and many Rydberg atoms in microwave cavities; and II, fundamental theory of the micromaser. In *Studies in Classical and Quantum Nonlinear Optics*, edited by Ole Keller, New York: Nova Science Publishers

Dirac, P.A.M. 1958. *The Principles of Quantum Mechanics*, 4th edition, Oxford: Oxford University Press

Dodd, R.K., Eilbeck, J.C., Gibbon, J.D. & Morris, H.C. 1982. *Solitons and Nonlinear Wave Equations*, London: Academic Press

Eilbeck, J.C., Gibbon, J.D., Caudrey, P.J. & Bullough, R.K. 1973. Solitons in nonlinear optics I. A more accurate description of the 2π pulse in self-induced transparency. *Journal of Physics A: Mathematics and General*, 6: 1337–1347

Feynman, R.P., Leighton, R.B. & Sands, M. 1965. *The Feynman Lectures on Physics*, vol. III. *Quantum Mechanics*, Reading, MA: Addison-Wesley (second printing, 1966)

Gibbon, J.D., Caudrey, P.J., Bullough, R.K. & Eilbeck, J.C. 1973. An N-soliton solution of a nonlinear optics equation derived by a general inverse method. *Lettre al Nuovo Cimento*, 8: 775–779

Haroche, S. & Raimond, J.-M. 1993. *Scientific American*, vol. 269, April: 26–33

Hau, L.V. 2001. Frozen light. *Scientific American*, vol. 284, July: 52–59

Maimstov, A.I., Basharov, A.M., Elyatin, S.O. & Sklyarov, Yu.M. 1990. The present state of self-induced transparency theory. *Physics Reports*, 191: 1–108

McCall, S.L. & Hahn, E.L. 1969. Self-induced transparency. *Phys. Rev*., 183(2): 457–485

MCCULLOCH–PITTS NETWORK

In 1943, Warren McCulloch and Walter Pitts published a seminal paper that described the first attempt to provide a mathematical model of a neuron (McCulloch and Pitts, 1943). This work explored the properties of networks of such mathematical neurons in relation to the working of the nervous system. The model arose from the following assumptions based on the knowledge of neurophysiology at the time

(i) The activity of the neuron is an "all-or-none" process.
(ii) A certain fixed number of synapses must be excited within the period of latent addition in order to excite a neuron at any time, and this number is independent of previous activity and position on the neuron.
(iii) The only significant delay within the nervous system is synaptic delay.
(iv) The activity of any inhibitory synapse absolutely prevents excitation of the neuron at that time.
(v) The structure of the net does not change with time.

The McCulloch–Pitts neuron is thus a binary threshold unit whose firing or activation is dependent on the values of its inputs. The neuron receives a number of excitatory (positive) or inhibitory (negative) inputs via "synaptic" connections. Excitatory synapses are equally weighted, and if the sum of these positive input signals exceeds some value, θ, the neuron fires. Otherwise, the neuron does not fire. If a signal is received on any of the negative inputs, the neuron cannot fire, regardless of the positive input values. The threshold value θ is a fixed threshold value unique to the neuron, and the model is assumed to be operating in discrete time steps.

A network of McCulloch–Pitts neurons can be assembled by connecting the outputs of neurons to the inputs of other neurons in some manner. In discussing networks of these artificial neurons,McCulloch and Pitts distinguish between nets with and without "circles." In a network without circles, it is not possible to follow a path of connections in the network from any given neuron and return to that same neuron. In other words, there are no closed causal loops. The activity in such a network will, therefore, have a feed-forward dynamic; any activity imposed on the network will propagate in a unidirectional fashion for a finite amount of time, terminating when neurons are encountered with no outgoing synaptic connections. The perceptron (Rosenblatt, 1962) and multi-layer perceptron (see e.g., Haykin, 1999) networks are examples of this kind of topology. A McCulloch–Pitts network without circles is capable of representing any statement within prepositional logic (i.e., any finite logical expression).

The dynamics of networks with circles are more complex. Activity in these networks may propagate indefinitely around the network in discrete time, so the firing activity of the network at any time may be dependent on the activity of the network at multiple stages in the past.

McCulloch and Pitts were able to show that such nets are equivalent to a Universal Turing Machine in principle. It should, however, be noted that the proofs for McCulloch–Pitts nets are existence proofs only in the sense that they do not imply an algorithm for constructing a network, with appropriate values of threshold and weight parameters, to compute a given function. Also, they do not consider computational time. Interestingly, the work of McCulloch and Pitts was also an influence in the development of the von Neumann stored program computer architecture.

Consider a McCulloch–Pitts net with circles. At any point in time, the state of the network can be defined by the current (binary) activity pattern of the neurons (i.e., which neurons are firing and which are not). The network can be thought of as a point in a configuration space of all possible activity patterns. Under some appropriately chosen scheme for updating the state of the network (synchronously or asynchronously), the activity may converge to an attractor in the configuration space, resulting in a stable state for subsequent time steps. This is the basis for attractor neural nets, as described by Hopfield in the context of simple associative memory networks (Hopfield, 1982).

MARCUS GALLAGHER

See also **Attractor neural network; Cell assemblies; Electroencephalogram at large scales; Electroencephalogram at mesoscopic scales; Neurons; Perceptron**

Further Reading

Haykin, S. 1999. *Neural Networks A Comprehensive Foundation*, 2nd edition, Upper Saddle River, NJ: Prentice-Hall

Hopfield, J.J. 1982. Neural networks and physical systems with emergent collective computational abilities. *Proceedings of National Academy of Sciences USA*, 81: 3088–3092

McCulloch, W.S. & Pitts, W. 1943. A logical calculus of ideas immanent in nervous activity. *Bulletin of Mathematical Biophysics*, 5: 115–133

Rosenblatt, F. 1962. *Principles of Neurodynamics*, New York: Spartan

MEAN FIELD THEORIES

See **Phase transitions**

MEASURES

Measures provide the means to introduce probabilistic methods into the study of a dynamical system by supplying a notion of the size or content of sets that is additive—the measure of a union of disjoint sets is the sum of the measures of these sets.

Sets correspond to events and the measure of a set to the probability of that event. The precursor to this general notion is that of the phase volume in a classical mechanical system, which is preserved under the phase flow (Liouville theorem). In other words, if a set of initial conditions is transported by the flow for a fixed time then the set of terminal conditions has the same volume as the set of initial conditions. Put differently, the phase flow consists of volume-preserving maps. In the general context of measures, this corresponds to measure-preserving transformations (see below), which are the subject of ergodic theory. For example, the Birkhoff ergodic theorem establishes a connection between the measure of a set and the proportion of time a typical orbit spends in it. The original result in ergodic theory is the Recurrence Theorem by Poincaré (1890) according to which almost every point in a volume-preserving system has to return arbitrarily close to its initial position.

The *Lebesgue measure* coincides with volume, but it is defined on a larger collection of sets. For example, the one-dimensional volume (length) of the set of rational numbers is not defined, but this set has zero Lebesgue measure. Closely related to the Lebesgue measure are *absolutely continuous* measures, that is, those defined by integrating a nonnegative density function over the set to be measured. The function can be interpreted as a probability density if the total integral is 1. (The bell curve $p(x) := \mathrm{e}^{-(x-b)^2/2a^2}/a\sqrt{2\pi}$ is a standard example.) Taking the Dirac δ-function as a (singular) "density," one obtains the *Dirac measure* defined by $\delta_p(U) = 1$ if $p \in U$, $\delta_p(U) = 0$ otherwise.

In general, a measure is a nonnegative additive set function. More precisely, it is a nonnegative function (with $+\infty$ an allowed value) defined on a collection of subsets (which are then said to be measurable) of the space in question, such that the union of any countable or finite union of disjoint measurable sets A_i is measurable (this is a requirement of the collection of measurable sets), and its measure is the sum of the measures of the A_i. (One cannot require an analogous property for unions of uncountably many sets because the real line is a disjoint union of points, each of which has zero Lebesgue measure.) One often is interested in finite measures, that is, those for which the measure of the whole space is finite. These can be rescaled to a *probability measure* (the whole space has measure 1). A set of measure zero is referred to as a *null set*, and a property is said to hold *almost everywhere* if it fails for only a null set of points.

If every open set is measurable and every compact set has finite measure, then the measure is said to be a *Borel measure*. This is a useful notion because a Borel measure μ is regular; that is

$$\begin{aligned}\mu(A) &= \inf\{\mu(O) : A \subset O \text{ and } O \text{ is open}\}\\ &= \sup\{\mu(B) : B \subset A \text{ and } B \text{ is compact}\}.\end{aligned}$$

Up to a scale factor, one defines the Lebesgue measure $\mu_n(A)$ of a set $A \subset \mathbb{R}^n$ by considering collections of balls whose union contains A and minimizing the sums of the volumes of these balls:

$$\mu_n(A) = \inf\left\{\sum r_i^n : A \subset \bigcup_i B(x_i, r_i)\right\}.$$

Replacing the exponent n of the radii by an arbitrary exponent α that is not necessarily related to the dimension of the ambient space, one obtains the α-dimensional *Hausdorff measure* μ_α. For example, for a smooth curve c of length $l(c)$ in the plane, we get $\mu_1(c) = l(c)$ and $\mu_2(c) = 0$. Indeed, one can characterize the *Hausdorff dimension* of a set S via Hausdorff measures. It is the number α_0 such that $\mu_\alpha(S) = +\infty$ for $\alpha < \alpha_0$ and $\mu_\alpha(S) = 0$ for $\alpha > \alpha_0$.

A measure is *invariant* under a map f and the map is said to be *measure-preserving*, if for any measurable set A the set $f^{-1}(A) := \{x: f(x) \in A\}$ is measurable and has the same measure as A. This preimage definition turns out to be the proper one for noninvertible maps. For example, circle rotations $z \mapsto z\mathrm{e}^{2\pi \mathrm{i}\theta}$ preserve the Lebesgue measure because they preserve length. The doubling map $z \mapsto z^2$ of the unit circle in the complex plane preserves the Lebesgue measure because the preimage of an arc consists of two arcs of half the length. The density $1/(1+x)$ on $[0, 1]$ defines a measure μ, which is invariant under the Gauss map $G: [0, 1] \to [0, 1]$ defined by $x \mapsto \{1/x\}$ (fractional part): $a = \{1/x\}$ if and only if $1/x = a + n$ for some $n \in \mathbb{N}$, so

$$\begin{aligned}\mu(G^{-1}([a, b])) &= \sum_{n\in\mathbb{N}} \int_{1/b+n}^{1/a+n} \frac{1}{1+x}\,\mathrm{d}x\\ &= \sum_{n\in\mathbb{N}} \log\left(1 + \frac{1}{a+n}\right)\end{aligned}$$

$$
\begin{aligned}
&\quad - \log\left(1 + \frac{1}{b+n}\right) \\
&= \sum_{n\in\mathbb{N}} \log(a+n+1) - \log(a+n) \\
&\quad - \log(b+n+1) + \log(b+n) \\
&= \log(b+1) - \log(a+1) \\
&= \int_a^b \frac{1}{1+x}\,\mathrm{d}x = \mu([a,b]).
\end{aligned}
$$

The Dirac measure δ_p concentrated on a fixed point p is always invariant.

The *Birkhoff ergodic theorem* guarantees the existence of time averages of orbits. If φ is an observable (a continuous or merely measurable scalar function on phase space) and μ is an f-invariant measure, then for almost every point the time (or Birkhoff or ergodic) average

$$\lim_{n\to\infty} \sum_{i=0}^{n-1} \varphi(f^i(x))/n$$

exists. A map f is said to be *ergodic* if the phase space is indecomposable in the following sense. If A is an invariant set (i.e., $f^{-1}(A) = A$), then either A or its complement is a null set. This is the case for the Lebesgue measure and the doubling map or rotations by an irrational angle, but not for rotations by a rational angle. For ergodic systems, the time average over almost every orbit equals the space average $\int \varphi\,\mathrm{d}\mu$.

A particularly interesting measure with respect to the study of hyperbolic attractors and strange attractors is the *Sinai–Ruelle–Bowen measure*. By definition it has a positive Lyapunov exponent almost everywhere and absolutely continuous conditionals (marginals) on unstable manifolds. If such a measure is ergodic and has no zero Lyapunov exponents, then it gives a natural or physical (physically observed) measure, which is defined by the following property. While for any invariant measure μ the Birkhoff ergodic theorem implies that almost every point is μ-equidistributed, the physical measure reflects the asymptotic distribution of Lebesgue-almost every point (or at least that of a set of points of positive Lebesgue measure). This means that if one picks a point at random (with respect to Lebesgue measure), its orbit will be equidistributed uniformly with respect to the physical measure. In other words, a physical (or natural) measure represents the density of points obtained from a computed orbit. For example, the Dirac measure concentrated on an attracting fixed point is a natural measure.

BORIS HASSELBLATT

See also **Ergodic theory; Poincaré theorems; Recurrence; Sinai–Ruelle–Bowen measures**

Further Reading

Hasselblatt, B. & Katok, A. (editors). 2002: *Handbook of Dynamical Systems*, vol. 1A. Amsterdam and New York: Elsevier (See also vol. 1B, 2005)

Hasselblatt, B. & Katok, A. 2003: *Dynamics: A First Course*, Cambridge and New York: Cambridge University Press

Katok, A. & Hasselblatt, B. 1995: *Introduction to the Modern Theory of Dynamical Systems*, Cambridge and New York: Cambridge University Press [Measure theory is summarized in an Appendix chapter.]

Petersen, K. 1983: *Ergodic Theory*, Cambridge and New York: Cambridge University Press

Poincaré, H.J. 1890. Sur le probléme des trois corps et les équations de la dynamique. *Acta Mathematica*, 13: 1–270

MECHANICS OF SOLIDS

Two aspects may be discerned in the historical development of the mechanics of solids. The first of these was motivated by technical requirements, and the second was motivated by studies in theoretical physics. Sometimes these two aspects interacted, but each of them has maintained its specificity.

From the fundamental continuum hypothesis, the mechanics of solids admits an introduction of vector and tensor fields describing the strained state of a solid as a result of its deformation: the displacement vector and tensors of stress and strain. Physical features are manifested by the constitutive relations (algebraic, differential, or integro-differential), which determine the coupling between stress and strain tensors, and Newton's equations of motion can be constructed taking into account all relations mentioned above.

There are two sources of nonlinearity in the mechanics of solids. If the constitutive relations are nonlinear, one deals with an intrinsically nonlinear problem. Nonlinearity also arises from purely geometric reasons (nonlinear dependence of the strains on displacements) and is called geometric nonlinearity. Four important approximations illustrating the basic nonlinear effects in the mechanics of solids are as follows.

Prerequisites of approximations:	*Result of approximation:*
(a) Rotational and translational invariance of infinite undeformed solid	Infinite isotropic media
(b) Discrete group of symmetry	Anisotropic crystal
(c) Details of microstructure	Media with weak or strong dispersion
(d) Smallness of one or two dimensions	Bar, plate, shell

Taking account of the shear, nonlinear dynamic equations for an infinite elastic body can be considered as an extension of the hydrodynamics of a compressible non-viscous fluid. Lagrange's equations of motion in

the main nonlinear approximation are written as follows (Blend, 1969):

$$\rho\frac{\partial^2 u_j}{\partial t^2}-\frac{\partial}{\partial u_j}\left(\frac{\partial U}{\partial u_{i,j}}\right)=X_{i,j},$$

$$U=\tfrac{1}{2}\lambda I_1^2+\mu I_2+T_0S-\kappa I_1 S+\text{higher-order terms},$$

$$i,\ j=1,2,3, \qquad (1)$$

where ρ_0 is the initial density of the elastic media, $X_{i,j}$ are components of external loading, u_j are components of the displacement vector, U is a potential, $I_1=\varepsilon_{ii}$ and $I_2=\varepsilon_{ij}\varepsilon_{ij}$ are the first and second invariants of the strain tensor, λ and μ are Lameé coefficients characterizing the elastic properties of isotropic media, S is entropy, κ is the coefficient of heat conductivity, and T_0 is the initial temperature. Lamé coefficients can be expressed via the Young's modulus E and Poisson coefficient ν, describing longitudinal elastic resistance and transversal deformation, respectively, for a specimen subjected to uniaxial longitudinal loading.

In this case, geometric nonlinearity is caused by nonlinear dependence of ε_{ij} on derivatives of displacements, and physical nonlinearity is accounted for by high-order terms involving strains ε_{ij}. A significant consequence of nonlinearity may be the possibility of shock waves manifested by discontinuity of the first or second derivatives of displacements (strong or weak discontinuities), respectively.

The simplest and most important problem admitting discontinuous solutions in nonlinear theory is the description of plane adiabatic shock waves propagation. In this case, nonlinear partial differential equations (1) are replaced by nonlinear algebraic relations. These relations are determined by conservation laws for mechanical and thermodynamical quantities as well as by the second law of thermodynamics. The main difference from shock waves in the fluid is manifested in the presence of shear shock waves.

Taking into account microstructure and intermolecular (physical) nonlinearity in the constitutive relations, one obtains in the lowest approximation for plane waves the Korteweg–de Vries (KDV) equation (Askar, 1985)

$$\frac{\partial w}{\partial\tau}+\frac{1}{2}\alpha_1 w\frac{\partial w}{\partial\zeta}+\frac{1}{24}\frac{\partial^3 w}{\partial\zeta^3}=0,$$

where τ and ζ are dimensionless time and space coordinates, respectively, and $w(\tau,\zeta)$ is a dimensionless deformation of the media. Due to the presence of nonlinear (second) and dispersion (third) terms, this equation has a stable soliton solution (compression wave) as well as multiple soliton solutions.

A second new aspect, important for media with microstructure, is the possibility of a short wavelength continuum approximation. Such an approximation is valid for the envelopes of short waves for which the wavelengths are comparable with the characteristic length of microstructure (Manevitch, 2001). In this case, equations of motion for the plane waves can be reduced to the dimensionless nonlinear Schrödinger (NLS) equation

$$\frac{\partial\varphi_0}{\partial\tau}-\mathrm{i}\alpha|\varphi_0|^2\varphi_0-\mathrm{i}\frac{\partial^2\varphi_0}{\partial\zeta^2}=0\,,$$

where $\varphi_0=[\exp\mathrm{i}\tau](w-\mathrm{i}u)$, u is the displacement, w is the velocity, α is a nonlinear parameter, and τ and ζ are dimensionless time and space coordinates. An important manifestation of nonlinearity in this case is the existence of envelope solitons

$$\varphi_0(\zeta,\tau)=\sqrt{2S/\alpha}\,\mathrm{e}^{\mathrm{i}(k\zeta-\omega\tau)}\mathrm{sech}[\sqrt{S}(\zeta-\nu\tau)],$$

where $k=\nu/2$ and $\omega=\nu^2/4-S$.

Dispersion effects can be also caused by the presence of boundaries as in the case of a rod embedded in another elastic external medium. Along with physical and/or geometric nonlinearity, this may lead to formation of solitons similar to solitons in media with microstructure (Samsonov et al., 1999).

Note that the formation of shock waves in three-dimensional elastic media requires much more energy than in the common case of sound waves. Contrary to this, geometric nonlinearity in thin elastic bodies described by simplified one- and two-dimensional models provides easy manifestation of nonlinear effects due to bifurcation of equilibrium states (elastic instability). Elastic instability may lead to localization of buckling and coupling of linear modes—a sign of strong nonlinearity (Thomson & Hupt, 1973). Thin-walled structures also demonstrate numerous other effects typical of common nonlinear systems, including period doubling and internal resonance, transition to spatial, and temporal chaos. Future developments in nonlinear mechanics of solids will focus on the study of these effects as well as the propagation of nonlinear waves in anisotropic and nonhomogeneous media and on mechanics of solids at the mesoscopic level (Alexander, 1998).

LEONID MANEVITCH

See also **Korteweg–de Vries equation; Nonlinear Shrödinger equations; Shock waves; Solitons**

Further Reading

Alexander, S. 1998. Amorphous solids theory, structure, lattice dynamics and elasticity. *Physics Reports*, 296: 68–256

Askar, A. 1985. *Lattice Dynamical Foundations of Continuum Theories*, Singapore: World Scientific

Blend, D.R. 1969. *Nonlinear Dynamic Elasticity*, Waltham, MA: Blaisdell Publishing

Manevitch, L.I. 2001. Solitons in polymer physics. *Polymer Science* C, 4(2): 117–181

Samsonov, A.M. et al. 1999. Strain solitons in solids: physics, numerics and fracture. In *Dynamics of Vibro-Impact Systems*, edited by V.I. Babitsky, Berlin: Springer, pp. 215–220

Thomson, J.M. & Hupt, G.M. 1973. *A General Theory of Elastic Stability*, New York: Wiley

MEL'NIKOV METHOD

In 1963, V.K. Mel'nikov developed an analytical method for the study of time-periodic perturbations of a planar autonomous system. This method permits determination of persistence and stability of subharmonic motions and measurement of infinitesimal separation of stable and unstable manifolds of hyperbolic fixed points. The Mel'nikov method is one of the few analytical tools for establishing conditions for homoclinic chaos, and it has been generalized to many settings, including Hamiltonian systems with higher degrees of freedom and partial differential equations.

The main ideas can be introduced in the context of a periodically forced planar Hamiltonian system:

$$\dot{x} = \frac{\partial H}{\partial y} + \varepsilon f_1(x, y, t),$$
$$\dot{y} = \frac{\partial H}{\partial x} + \varepsilon f_2(x, y, t).$$

$H(x, y)$ is the Hamiltonian function of the unperturbed system ($\varepsilon = 0$), and $\mathbf{f} = (f_1, f_2)^{\mathrm{T}}$ is a time-periodic perturbation vector field. Both H and $\mathbf{f}$ are assumed to be sufficiently smooth functions of their arguments.

Assume that the unperturbed system possesses a homoclinic orbit $q_{\mathrm{h}}(t)$ to a hyperbolic saddle point p_0, as shown in Figure 1. When $\varepsilon \neq 0$, a perturbation argument guarantees persistence of a hyperbolic fixed point p_ε, and local existence of its stable and unstable manifolds, parametrized, respectively, by solutions $q_\varepsilon^{\mathrm{s}}(t) = q_{\mathrm{h}}(t - t_0) + \varepsilon q_1^{\mathrm{s}}(t) + \mathcal{O}(\varepsilon^2)$ and $q_\varepsilon^{\mathrm{u}}(t) = q_{\mathrm{h}}(t - t_0) + \varepsilon q_1^{\mathrm{u}}(t) + \mathcal{O}(\varepsilon^2)$.

As the unperturbed separatrix is expected to split under perturbation, it is convenient to introduce the distance function

$$\begin{aligned} d(t_0) &= (\partial_x H, \partial_y H)^{\mathrm{T}}|_{q_{\mathrm{h}}(0)} \cdot [q_\varepsilon^{\mathrm{u}}(t_0) - q_\varepsilon^{\mathrm{s}}(t_0)] \\ &= \varepsilon[(\partial_x H, \partial_y H)^{\mathrm{T}}|_{q_{\mathrm{h}}(0)} \wedge (q_1^{\mathrm{u}}(t_0) - q_1^{\mathrm{s}}(t_0))] \\ &\quad + \mathcal{O}(\varepsilon^2), \end{aligned}$$

which measures the displacement of the stable and unstable manifolds of p_ε along a direction normal to the unperturbed separatrix (represented by vector $\mathbf{N}$ in Figure 1). After deriving an evolution equation for the perturbation expansion of the distance function $d(t)$, we arrive at the following expression:

$$d(t_0) = \varepsilon M(t_0) + \mathcal{O}(\varepsilon^2). \tag{1}$$

The Mel'nikov function $M(t_0)$ is defined by

$$M(t_0) = \int_{-\infty}^{+\infty} \mathbf{grad}\, H(q_{\mathrm{h}}(t - t_0)) \cdot \mathbf{f}(q_{\mathrm{h}}(t - t_0), t)\, \mathrm{d}t, \tag{2}$$

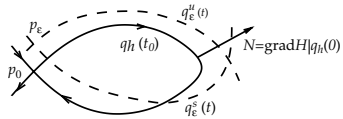

Figure 1. Unperturbed and perturbed separatrices.

where the integrand is the scalar product of vectorfields **grad** H and $\mathbf{f}$ and is evaluated along the unperturbed homoclinic orbit.

As an example, consider the following planar system of ordinary differential equations with periodic perturbation:

$$\dot{x} = y,$$
$$\dot{y} = -x + x^2 + \varepsilon \sin t.$$

The unperturbed system has Hamiltonian $H(x, y) = y^2/2 + x^2/2 - x^3/3$ and two fixed points: the origin (a center) and the point of coordinates $(1, 0)$ (a saddle point). The unperturbed homoclinic orbit (parametrizing the degenerate stable, unstable manifolds of the hyperbolic fixed point) is given by

$$q_{\mathrm{h}}(t - t_0) = \left(\frac{3}{2}\tanh^2\left(\frac{t - t_0}{2}\right) - \frac{1}{2}, \frac{3}{2}\tanh\left(\frac{t - t_0}{2}\right)\sinh^2\left(\frac{t - t_0}{2}\right)\right)^T, \tag{3}$$

and the corresponding Mel'nikov function is computed to be

$$\begin{aligned} M(t_0) &= \frac{3}{2}\int_{-\infty}^{+\infty} \tanh(t/2)\sinh^2(t/2)\sin(t + t_0)\, \mathrm{d}t \\ &= -\frac{3\pi\cos(t_0)}{2\sinh\pi/2\cosh\pi/2}. \end{aligned} \tag{4}$$

If, as in this example, $M(t_0)$ has an infinite sequence of nondegenerate zeros, an infinite number of transverse homoclinic orbits of the hyperbolic fixed point of the perturbed system is guaranteed to exist for all $\varepsilon \neq 0$ sufficiently small. Thus, the system exhibits homoclinic chaos.

For perturbations containing dissipative or constant forcing terms, the Mel'nikov integral may be nonvanishing. In such cases, the separatrix still splits under perturbation, but no transverse homoclinic points occur.

Generalizations of the Mel'nikov method to higher-dimensional systems have been discussed by various authors (see, for example, Yagasaki (1999), Gruendler (1992), and the monograph by Wiggins (1988, pp. 1–16)).

Autonomous Perturbations in Two Degrees of Freedom

Consider how this method applies to autonomous near-integrable Hamiltonian systems with two degrees of freedom. This case was first treated, and then generalized to integrable equations with $n+1$ degrees of freedom, by Holmes and Marsden (1982a,b). These authors assume that the unperturbed Hamiltonian has the form $H_0 = F(x, y) + G(I)$, where F is the Hamiltonian of a planar system with a homoclinic orbit to a hyperbolic fixed point, and G is the Hamiltonian of a planar system in action-angle coordinates. By restricting to the energy surface, the original equations are reduced to a single-degree-of-freedom non-autonomous system, to which the usual Mel'nikov technique is applied.

A more direct approach by Robinson (1996) assumes Hamiltonians of the general form

$$H_\varepsilon(\mathbf{x}) = H_0(\mathbf{x}) + \varepsilon H_1(\mathbf{x}), \quad \mathbf{x} \in \mathbb{R}^4. \tag{5}$$

The unperturbed system is assumed to be completely integrable, with a second constant of motion K, and to possess a hyperbolic periodic orbit $\gamma_\mathbf{0}$. The stable and unstable manifolds of γ_0, $\mathcal{W}^\mathrm{s}(\gamma_0) = \mathcal{W}^\mathrm{u}(\gamma_0)$, are parametrized by a two-dimensional family of homoclinic orbits $q_\mathrm{h}(t, \mathbf{x}_0)$, where $\mathbf{x}_0$ is a point on the corresponding level set $H_0(\gamma_0) = h_0$.

Because the perturbation is Hamiltonian, the perturbed hyperbolic periodic orbit γ_ε and its stable, unstable manifolds $\mathcal{W}^{\mathrm{s,u}}(\gamma_\varepsilon)$ continue to lie within the same energy surface $H_\varepsilon^{-1}(h_0)$. Thus **grad** H_0 no longer provides a good measurement of their transversal splitting.

Letting Π_0 be a two-dimensional plane transversal to the unperturbed separatrix at $\mathbf{x_0}$ and denoting by $\zeta^{\mathrm{s,u}}(\mathbf{x}_0, h_0; \varepsilon) = \Pi_0 \cap \mathcal{W}^{\mathrm{s,u}}(\gamma_\varepsilon)$ the corresponding points on the perturbed invariant manifolds, one computes the infinitesimal displacement in terms of the second integral K:

$$M(\mathbf{x_0}, h_0) = \frac{\partial}{\partial\varepsilon}[K \circ \zeta^u(\mathbf{x}_0, h_0; \varepsilon) - K \circ \zeta^s(\mathbf{x}_0, h_0; \varepsilon)]|_{\varepsilon=0}. \tag{6}$$

The Mel'nikov measurement can be reduced (Robinson, 1996) to the following conditionally convergent integral:

$$M(\mathbf{x}_0, h_0) = \lim_{j\to\infty} \int_{-T_j^*}^{T_j} \mathbf{grad}\, F \cdot \mathcal{J}\mathbf{grad}\, H_1|_{q_h(t,\mathbf{x}_0)}\, \mathrm{d}t, \tag{7}$$

where $\mathcal{J}\mathbf{grad}H_1$ is the Hamiltonian vector field of the perturbation, and $-T_j^*$, T_j are chosen so that $q_h(-T_j^*, \mathbf{x}_0)$ and $q_h(T_j, \mathbf{x}_0)$ converge to the same point of the periodic orbit γ_0.

An Elastic Pendulum

Consider the application of these ideas to the following four-dimensional dynamical system modelling an elastic pendulum (Holmes and Marsden, 1982a):

$$\begin{aligned}
\dot{x} &= y,\\
\dot{y} &= \sin x + \varepsilon\left(\sqrt{\frac{2I}{\omega}}\sin\theta - x\right),\\
\dot{I} &= \varepsilon\sqrt{\frac{2I}{\omega}}\left(\sqrt{\frac{2I}{\omega}}\sin\theta - x\right)\cos\theta,\\
\dot{\theta} &= \omega - \varepsilon\frac{1}{\sqrt{2I\omega}}\left(\sqrt{\frac{2I}{\omega}}\sin\theta - x\right)\sin\theta.
\end{aligned}$$

The unperturbed equations are completely integrable with constants of motion $H_0(x, y, I, \theta) = \frac{1}{2}y^2 - \cos x + \omega I$ and $K(x, y, I, \theta) = I$. The energy surface $H_0(\mathbf{x}) = 1 + \omega I = h_0$ contains a hyperbolic periodic orbit $\gamma_0 = (\pi, 0, I, \omega t)^\mathrm{T}$ and its two-dimensional stable and unstable manifolds, parametrized by the pair of homoclinic orbits

$$q_h^\pm(t, \theta_0) = (\pm 2\tan^{-1}(\sinh t), \pm 2\,\mathrm{sech}\, t, \frac{h_0 - 1}{\omega}, \omega t + \theta_0)^\mathrm{T}.$$

As $\mathbf{grad}\, K = (0, 0, 1, 0)^\mathrm{T}$, the quantities $M^\pm(\theta_0, h_0)$ are immediately computed as the following absolutely convergent integrals ($h_0 > 1$):

$$\frac{\sqrt{2(h_0-1)}}{\omega}\int_{-\infty}^{+\infty}\left[\frac{\sqrt{2(h_0-1)}}{\omega}\sin(\omega t + \theta_0) \mp 2\tan^{-1}(\sinh t)\right]\cos(\omega t + \theta_0)\,\mathrm{d}t. \tag{8}$$

The first term is odd and thus vanishes. Using integration by parts to simplify the second term yields the expression

$$M^\pm(\theta_0, h_0) = \pm\frac{\sqrt{2(h_0-1)}}{\omega^2} \times \int_{-\infty}^{+\infty}\mathrm{sech}(t)\sin(\omega t + \theta_0)\,\mathrm{d}t,$$

which can be evaluated using the method of residues as

$$M^\pm(\theta_0, h_0) = \pm 2\pi\frac{\sqrt{2(h_0-1)}}{\omega}\mathrm{sech}\left(\frac{\pi\omega}{2}\right)\sin(\theta_0).$$

An infinite sequence of simple zeros of $M^\pm(\theta_0, h_0)$ guarantees the existence of transversal homoclinic orbits on each energy surface $h_0 > 1$, for $\varepsilon \neq 0$ sufficiently small.

ANNALISA M. CALINI

See also **Chaotic dynamics; Hamiltonian systems; Horseshoes and hyperbolicity in dynamical systems; Phase space**

Further Reading

Gruendler, J. 1992. Homoclinic solutions for autonomous dynamical systems in arbitrary dimension. *SIAM Journal of Mathematical Analysis*, 23: 702–721

Guckenheimer, J. & Holmes, P. 1983. *Nonlinear Oscillations, Dynamical Systems, and Bifurcations of Vector Fields*, Berlin and New York: Springer

Holmes, P.J. & Marsden, J.E. 1982a. Mel'nikov's method and Arnol'd diffusion for perturbations of integrable Hamiltonian systems. *Journal of Mathematical Physics*, 23(4): 669–675

Holmes, P.J. & Marsden, J.E. 1982b. Horseshoes in perturbations of Hamiltonian systems with two degrees of freedom. *Communications in Mathematical Physics*, 82: 523–544

Mel'nikov, V.K. 1963. On the stability of the center for time periodic perturbations. *Transactions of Moscow Mathematical Society*, 12: 1–57

Robinson, C. 1996. Mel'nikov method for autonomous Hamiltonians. *Contemporary Mathematics*, 198: 45–53

Wiggins, S. 1988. *Global Bifurcations and Chaos: Analytical Methods*, Berlin and New York: Springer

Yagasaki, K. 1999. The method of Mel'nikov for perturbations of multi-degree-of-freedom Hamiltonian systems. *Nonlinearity*, 12(4): 799–822

METASTABILITY

See **Stability**

METEOROLOGY

See **Atmospheric and ocean sciences**

MISSING MASS (FOR KDV SOLITON)

See **Korteweg–de Vries equation**

MIURA TRANSFORMATION

See **Korteweg–de Vries equation**

MIXING

The word *mixing* is used both as a general term defining the operation of putting two or more substances together in order to achieve uniformity and as a mathematical term defining the property of random processes. Mixing as an operation is widespread as both a natural phenomenon and an industrial process. Putting milk into coffee, preparing cement, and pushing a car accelerator pedal involve mixing liquids, granular materials, and gases. On a molecular scale, it is diffusion that provides mixing. When diffusion is caused solely by the gradient of concentration $\theta(\boldsymbol{r}, t)$, it is described by the second-order partial differential equation

$$\frac{\partial \theta}{\partial t} = \operatorname{div}(\kappa \nabla \theta). \tag{1}$$

When the diffusivity κ is constant, (1) is a linear parabolic equation which can be solved by using the Green function: $\theta(\boldsymbol{r}, t) = (4\pi\kappa t)^{-d/2} \times \int \exp[-(\boldsymbol{r} - \boldsymbol{r}')^2/4\kappa t]\theta(\boldsymbol{r}', 0)\, \mathrm{d}\boldsymbol{r}'$.

The diffusivity of gases in gases is of order 10^{-1} cm^{2}s^{-1}, so it would take many hours for an odor to diffuse across the dinner table. Similarly, to diffuse salt to a depth of 1 km in the ocean molecular diffusion would take 10^7 years. It is the motion of fluids that provides large-scale mixing in most cases. In a moving fluid, θ satisfies the advection-diffusion equation:

$$\frac{\partial \theta}{\partial t} + (\boldsymbol{v} \cdot \nabla)\theta = \operatorname{div}(\kappa \nabla \theta). \tag{2}$$

If the velocity gradient is λ then one can define a diffusion scale $r_\mathrm{d} = \sqrt{\kappa/\lambda}$ comparing advective and diffusive terms in (2). Fluid motion and molecular diffusion provide for mixing at the scales respectively larger and smaller than r_d. Inhomogeneous flow brings into contact fluid parcels with different values of θ thus producing large gradients that are then eliminated by molecular diffusivity. How fast mixing proceeds and how concentration variance decays in time depends on how inhomogeneous the flow is.

When a velocity field fluctuates, the simplest quantity (and often most important) is the concentration averaged over velocity, $\langle\theta(\boldsymbol{r}, t)\rangle$. The behavior of this quantity is determined by the properties of Lagrangian velocity $\boldsymbol{V}(t) = \boldsymbol{v}[\boldsymbol{q}(t), t]$, which is taken on the trajectory that satisfies $\mathrm{d}\boldsymbol{q}/\mathrm{d}t = \boldsymbol{v}[\boldsymbol{q}(t), t]$. For times longer than the Lagrangian correlation time, $\langle\theta(\boldsymbol{r}, t)\rangle$ also satisfies the diffusion equation

$$\left[\partial_t - (\kappa\delta_{ij} + D_{ij})\nabla_i\nabla_j\right]\langle\theta(\boldsymbol{r}, t)\rangle = 0,$$

with so-called eddy diffusivity

$$D_{ij} = \frac{1}{2}\int_0^\infty \langle V_i(0)V_j(s) + V_j(0)V_i(s)\rangle\, \mathrm{d}s.$$

If we release a single spot of, say, a pollutant, then its average position is given by $\langle\theta(\boldsymbol{r}, t)\rangle$. On the other hand, the evolution of the spot itself depends on the spatial properties of the velocity field. In considering hydrodynamic mixing at a given scale, one usually distinguishes between two qualitatively different classes of velocity fields: spatially smooth and nonsmooth. Velocity can be considered spatially smooth on a given scale if the velocity gradient does not change much across the scale. Comparing the inertial term $(\boldsymbol{v}\cdot\nabla)\boldsymbol{v}$ with the viscous term $\nu\Delta\boldsymbol{v}$ in the Navier–Stokes equation for fluid motion, one defines the viscous scale η similarly to r_d. Turbulent flows are smooth at scales smaller than η (viscous interval) and nonsmooth at larger scales (intertial interval). Fluid particles separate exponentially with time in smooth flows and according to power laws in nonsmooth flows.

Despite the fact that the fluid viscosity ν (momentum diffusivity) is caused by the same molecular motion as κ (diffusivity of a substance), their ratio varies

widely depending on the type of material. That ratio is called the Schmidt number, or Prandtl number when θ is temperature. The Schmidt number is very high for viscous liquids and also for colloids and aerosols, since the diffusivity of, say, micron-size particles (e.g., cream globules in milk and smoke in the air) is six to seven orders of magnitude less than the viscosity of the ambient fluid. In those cases, $r_d \ll \eta$. At scales less than η, the flow is spatially smooth, and the velocity difference between two fluid particles can be presented as $\boldsymbol{v}(\boldsymbol{q}_1, t) - \boldsymbol{v}(\boldsymbol{q}_2, t) = \hat{\sigma}(t)\boldsymbol{R}(t)$ so that the separation $\boldsymbol{R} = \boldsymbol{q}_1 - \boldsymbol{q}_2$ obeys the ordinary differential equation

$$\dot{\boldsymbol{R}}(t) = \sigma(t)\,\boldsymbol{R}(t),$$

leading to the linear propagation $\boldsymbol{R}(t) = W(t)\,\boldsymbol{R}(0)$. The main statistical properties of $\boldsymbol{R}(t)$ can be established at the limit when t exceeds the correlation time of the strain matrix $\hat{\sigma}(t)$. The basic idea (going back to the works of Lyapunov, Furstenberg, Oseledec, and many others and developed in the theory of dynamical chaos) is to consider the positive symmetric matrix $W^{\mathrm{T}}W$ which determines R. The main result states that in almost every realization of $\hat{\sigma}(t)$, the matrix $t^{-1}\ln W^{\mathrm{T}}W$ stabilizes as $t \to \infty$. In particular, its eigenvectors tend to d fixed orthonormal eigenvectors $\boldsymbol{f}_i$. To understand that intuitively, consider some fluid volume, say, a sphere, which evolves into an elongated ellipsoid at later times. As time increases, the ellipsoid is more and more elongated, and it is less and less likely that the hierarchy of the ellipsoid axes will change. The limiting eigenvalues

$$\lambda_i = \lim_{t\to\infty} t^{-1} \ln |W\boldsymbol{f}_i| \tag{3}$$

define the so-called Lyapunov exponents. The major property of the Lyapunov exponents is that they do not depend on the starting point if the velocity field is ergodic.

Consider now a pollutant spot with size l released within a spatially smooth velocity and assume that the Peclet number l/r_d is large. The above consideration shows, in particular, that the spot will acquire an ellipsoid form. The direction that corresponds to the lowest Lyapunov exponent (necessarily negative in an incompressible flow) contracts until it reaches r_d, and further contraction is stopped by molecular diffusion. Because the exponentially growing directions continue to expand, the volume grows exponentially and the value of θ inside the spot decays exponentially in time. For an arbitrary large-scale initial distribution of θ, the concentration variance decays exponentially in a spatially smooth flow because this is how fast velocity inhomogeneity contracts θ "feeding" molecular diffusion which eventually decreases the variance. Even though it is diffusion that diminishes θ and the rate of decay is independent of κ, it is usually of order of the typical velocity gradient.

If the Schmidt number is small while the Reynolds number of the flow is large then the velocity field at scales larger than r_d cannot be considered spatially smooth. That means that the velocity difference $\delta v(r)$, measured between two points distance r apart, scales as r^a with $a < 1$ (of course, δv is random and the statement pertains to the moments). For example, for the energy cascade in incompressible fluids, a is close to $1/3$. The equation $\dot{\boldsymbol{R}} = \delta\boldsymbol{v}(\boldsymbol{R}) \propto R^a$ suggests that interparticle distance grows by a power law: $R(t) \propto t^{1/(1-a)}$. The volume of any spot also grows so that scalar variance decays by a power law: $\langle\theta^2\rangle \propto t^{d/(1-a)}$. Such estimates are supported by a rigorous theory only for a velocity field short-correlated in time. In this case, one can also show that the probability distribution $P(\theta, t)$ takes the self-similar form $t^{d/2(1-a)}Q(t^{d/2(1-a)}\theta)$ which is likely to be the case for a general scale-invariant velocity. On the contrary, $P(\theta, t)$ does not change in a self-similar way in a spatially smooth flow.

In finite vessels, the long-time properties of fluid mixing are usually determined by slowest parts, namely, the walls, where the velocity gradient may become zero, and corners with recirculating eddies.

In multiphase flows, not only mixing but also segregation can occur. The physical reason for that is a centrifugal force: when fluid streamlines are curved, heavier particles move out while lighter particles move in. It is a matter of everyday experience that air bubbles are trapped inside the sink vortex while heavy particles gather outside the vortices (which is used, in particular, for flow visualization).

Granular mixing is strikingly different from fluid mixing. In a granular flow, collisions of grains are inelastic and friction between grains makes it possible for static configurations (such as arches) to support a load and distribute stresses. As a result, granular motion has nonlocal properties, and no effective hydrodynamic description based on average over local kinetics (such as Equation (2)) is available. When a container partially filled with grains is vertically shaken with accelerations larger than the gravitational acceleration, convective rolls are observed with grains rising at the center and falling along the walls. Contrary to fluid convection, however, the grains move faster and mix better near the walls. Granular flows can also demonstrate segregation. The most celebrated example is the so-called Brazil nut effect whereby large particles (Brazil nuts) rise to the top of shaken container of mixed nuts.

The use of the term *mixing* in mathematics is based on the notion (introduced by Josiah Gibbs) that evolution is mixing when it leads asymptotically in time to some equilibrium invariant measure. Formally, one defines the evolution operator U_t acting on some phase space A and denotes the measure of any subset B as $P(B)$. The evolution is mixing if for any $B, C \in A$ one has $\lim_{t\to\infty} P(A \bigcap U_t B) = P(A)P(B)$. One can also define weak mixing property where

$\lim_{t\to\infty} t^{-1}\int P(A\bigcap U_s B)\,\mathrm{d}s = P(A)P(B)$. Mixing of a random process or dynamical system means ergodicity, that is equality between temporal and phase space average.

GREGORY FALKOVICH

See also **Chaotic advection; Diffusion; Entropy; Granular materials; Intermittency; Kolmogorov cascade; Lyapunov exponents; Turbulence**

Further Reading

Chate, H., Villermaux, E. & Chomaz, J.-M. (editors). 1999. *Mixing: Chaos and Turbulence*, New York: Kluwer

Falkovich, G., Gawędzki, K. & Vergassola, M. 2001. Particles and fields in fluid turbulence. *Reviews of Modern Physics*, 73: 913–975

MÖBIUS STRIP

See **Topology**

MODE LOCKING

See **Coupled oscillators**

MODE MIXING AND COUPLING

See **Coupled systems of partial differential equations**

MODIFIED KDV EQUATION

See **Korteweg–de Vries equation**

MODULATED WAVES

The term *modulated waves* implies waves in which some parameters vary slowly in time or in space–time compared with the main (carrier) variables. The term *modulation* comes from acoustics (music) and radio engineering, where signals of the type

$$A(t)\cos[\omega_0 t + \varphi(t)] \tag{1}$$

have long been used for transmitting and processing information. Here, the carrier frequency ω_0 is constant with respect to time t, whereas the amplitude A and phase φ are slowly varying functions of time as compared with variations of the carrier oscillations described by the function $\cos(\omega_0 t)$. If only one of the parameters A and φ is variable, the terms *amplitude modulation* or *phase modulation* are used. A more general form is $A(t)\cos[\Phi(t)]$, where Φ is the full phase, so that the frequency $\omega(t) = \mathrm{d}\Phi/\mathrm{d}t$ is slowly varying. Although this case is called frequency modulation, the terms *phase* and *frequency modulation* describe essentially the same process.

For spatially varying signals, a natural generalization of that is a modulated quasiharmonic wave

$$A(\mathbf{r},t)\cos[\omega_0 t + \varphi(\mathbf{r},t)] \text{ or } A(\mathbf{r},t)\cos[\Phi(\mathbf{r},t)], \tag{2}$$

where A, φ, and $\partial\Phi/\partial t$ are slowly varying functions of time. In the spectral representation, the first of these expressions yields a narrow frequency spectrum as compared with the carrier frequency ω_0, whereas the spectrum of the second expression can be arbitrarily wide. The cause of wave modulation can be different: modulation in initial or boundary (signaling) conditions, slow variation of the medium parameters in time and space, attenuation, and amplification.

A typical case is a one-dimensional traveling wave when functions (2) depend on time t and one spatial coordinate x, for example,

$$A(x,t)\cos[\omega_0 t - k_0 x + \varphi(x,t)], \tag{3}$$

where k_0 is the wave number. At constant A and φ, this wave is a sinusoid propagating with phase velocity $c_{\mathrm{ph}} = \omega_0/k_0$. If the envelope A and phase φ (sometimes called phase envelope, implying all slowly varying parameters of a modulated wave propagate as envelope waves) are slowly varying in space time, and the medium is linear, then up to some distance, they propagate as a wave, with the group velocity, $c_{\mathrm{gr}} = \mathrm{d}\omega_0/\mathrm{d}k_0$, where the dependence between ω_0 and k_0 (dispersion equation) is determined by the properties of the medium. Phase and group velocities are equal only in a nondispersive media, otherwise they are different. At even larger times in a dispersive medium, the wave envelopes are deformed. In particular, a finite-length impulse broadens and turns into a frequency-modulated wave in which each group propagates at its local group velocity depending on its frequency. Such dynamics can be represented by trajectories of groups on the (x,t) plane which are somewhat analogous to spatial rays in geometrical optics or geometrical acoustics and are called space-time rays.

In nonlinear dispersive media, the propagation of envelopes of a modulated dispersive wave is determined not only by its frequency but also by its amplitude (intensity). The interplay of these two factors—dispersion and nonlinearity—results in a variety of scenarios (Ostrovsky & Potapov, 1999; Scott, 1999; Whitham, 1974).

Under definite conditions, first, a non-modulated quasiharmonic wave can be unstable with respect to small modulating perturbations of its amplitude and phase (modulational or Benjamin–Feir instability). In other cases, modulation does not grow, but the envelope distorts with formation of steep (at a modulation scale) fronts (self-steepening). Finally, a steady propagation of envelopes is possible in the form of envelope solitons and envelope shocks.

The notion of modulation can be extended to significantly nonharmonic processes, such as cnoidal

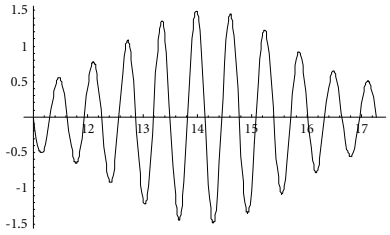

Figure 1. An example of a quasi-harmonic modulated wave.

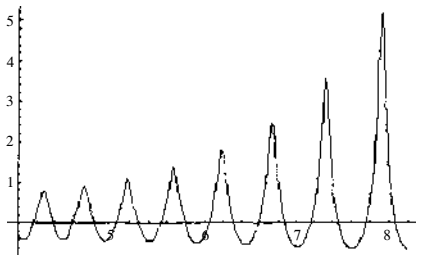

Figure 2. An example of a nonsinusoidal modulated wave.

waves which are typical elliptic function solutions of nonlinear wave equations. Also, in these solutions, slow modulation of their parameters (amplitude and period) in space and time can occur. Let the nonmodulated wave have the form $F(\omega t - kx, A_i)$, where F is a periodic function, the A_i are parameters defining the solution (such as the wave amplitude), and ω and k are effective frequency and wave number defined via the wave period T and its wavelength, Λ, as $\omega = 2\pi/T$ and $k = 2\pi/\Lambda$. Then at slow modulation of these parameters, the wave has the form

$$F[\theta(x,t), A_i(x,t)], \tag{4}$$

where F is a periodic function, A_i are slowly varying functions of x and t, and the phase θ is defined in such a way that $\omega = \partial\theta/\partial t$ and $k = -\partial\theta/\partial x$ are also slowly varying functions. Due to these slow variations, the wave profile can change continuously from an almost sinusoidal wave up to a train of pulses similar to solitary waves or solitons, as the modulus of the elliptic function increases.

Mathematical descriptions of modulated waves are based on asymptotic perturbation theory (Ostrovsky & Gorshkov, 2000) or on more heuristic descriptions. A rather general approach (Whitham's method) starts with a Lagrangian description of a wave field and employs the corresponding variational principle (Whitham, 1974; Ostrovsky & Potapov, 1999; Scott, 1999). For modulated quasi-periodic waves, substituting an expression of type (4) into the Lagrangian (L) and averaging over θ, one obtains an averaged Lagrangian $\mathcal{L}$ depending only on slowly varying parameters, A_i, ω, and k. Considering θ and A_i as new canonical variables, one then obtains from $\mathcal{L}$ variational equations describing the relation among A_i, ω, and k, and their variations in space and time.

This and other averaging methods can work for both nonharmonic nonlinear waves and for weakly nonlinear (or just linear) waves (2) or (3). For narrow-spectrum waves such as (3), a more detailed description can be developed that goes beyond the framework of space-time geometrical optics and takes into account time analogs of wave diffraction. In particular, the nonlinear Shrödinger equation has been obtained to describe such processes. This approach is useful, for example, for the study of envelope solitons having applications in nonlinear optics and for deep water waves.

Moreover, the evolution of a single soliton with slowly varying parameters (due to small losses or smooth inhomogeneities) can be represented in the form of Equation (4), where F is a localized function rather than a periodic one (Ostrovsky & Gorshkov, 2000; Ostrovsky & Potapov, 1999). This class of processes can also be referred to as modulation, and perturbation methods for slowly varying solitary waves have been constructed. Thus, such processes as damping, propagation in inhomogeneous media, and solitary-wave interactions have been analyzed. In the latter case, solitary waves can interact as particles (hence the term *soliton*) with different types of interactions, including repulsion when solitons retain their parameters after interaction and attraction when they may form an oscillating bound state or breather.

Finally, the term *modulation* can be extended to a wave that does not have a prescribed shape but a continuously but slowly distorting profile. A typical example is weakly nonlinear waves in nondispersive media—such as acoustic waves in fluids—where a cumulative steepening of a wave profile can occur up to the formation of weakly nonlinear shock waves. Provided the distortion is small at a wavelength scale, one can also refer to wave profile modulation.

LEV OSTROVSKY

See also **Averaging methods; Collective coordinates; Nonlinear acoustics; Nonlinear optics; Wave stability and instability**

Further Reading

Ostrovsky, L.A. & Gorshkov, K.A. 2000. Perturbation theories for nonlinear waves. In *Nonlinear Science at the Dawn of the 21st Century*, edited by P.L. Christiansen, M.P. Søerensen, & A.C. Scott, New York: Springer, pp. 47–65

Ostrovsky, L.A. & Potapov, A.I. 1999. *Modulated Waves: Theory and Applications*, Baltimore: John Hopkins University Press
Scott, A.C. 1999. *Nonlinear Science: Emergence and Dynamics of Coherent Structures*, Oxford and New York: Oxford University Press
Whitham, G.B. 1974. *Linear and Nonlinear Waves*, New York: Wiley

MODULATIONAL INSTABILITY

See **Wave stability and instability**

MOLECULAR CRYSTALS

See **Local modes in molecular crystals**

MOLECULAR DYNAMICS

Molecular dynamics (MD) refers to a family of computational methods aimed at simulating macroscopic behavior (thermodynamic or hydrodynamic) through the numerical integration of the classical equations of motion of a microscopic many-body system. Macroscopic properties are expressed as functions of particle coordinates and/or momenta, which are computed along a phase space trajectory generated by classical dynamics. At the core of the method is the assumption that over long times the system will reach an equilibrium state, or alternatively a steady state when simulating hydrodynamic conditions, in which temporal averages can be identified with statistical ensemble averages. This requires that mixing and Lyapunov instability be present in the phase space trajectories.

The field of MD simulations was born in the 1950s out of computational studies of the approach to equilibrium in a hard sphere system by B.J. Alder and T.E. Wainwright in 1957 (see Ciccotti et al. (1987) for a collection of seminal works illustrating the development and application of MD simulations). The first MD simulation employing continuous potentials was used to study radiation damage in a two-dimensional solid by Gibson et al. (1960). The first application of the methodology as it is used today, to an atomic fluid modeled by continuous potentials in three dimensions, was a study of structural and dynamical aspects of liquid argon by A. Rahman in 1964. Subsequently, MD simulations have been applied to the study of complex systems such as biomacromolecules and self-assembled systems, and to the elucidation of complex spatiotemporal phenomena in more simple systems. When performed under conditions corresponding to laboratory scenarios, molecular dynamics simulations can provide a detailed view of structure and dynamics at the atomic and mesoscopic levels that is not presently accessible by experimental measurements. The simulations can also be set to perform "computer experiments" that could not be carried out in the laboratory, either because they do not represent natural behavior or because the necessary controls cannot be achieved. Lastly, MD simulations can be implemented as simple test systems for condensed matter theory. In order to realize this wide spectrum of applications, several issues concerning system modeling, dynamical generation of statistical ensembles, and efficient numerical integrators must be considered.

To set the stage, consider the evolution of an isolated system of N point particles. In three dimensions, the canonical description of such system is given by a set of $6N$ first-order differential equations for the particles' positions $\boldsymbol{r}(t) = \{\boldsymbol{r}_1 \ldots \boldsymbol{r}_N\}$ and momenta $\boldsymbol{p}(t) = \{\boldsymbol{p}_1 \ldots \boldsymbol{p}_N\}$. The dynamics of the ith particle can be written in Hamiltonian form as

$$\begin{aligned} \dot{\boldsymbol{r}}_i &= \frac{\partial \mathcal{H}}{\partial \boldsymbol{p}_i} = \frac{\boldsymbol{p}_i}{m}, \\ \dot{\boldsymbol{p}}_i &= -\frac{\partial \mathcal{H}}{\partial \boldsymbol{r}_i} = -\frac{\partial V(\boldsymbol{r})}{\partial \boldsymbol{r}_i} \end{aligned} \tag{1}$$

with the Hamiltonian given by

$$\mathcal{H}(\boldsymbol{r}, \boldsymbol{p}) = \sum_{i=1}^{N} \frac{\boldsymbol{p}_i^2}{2m_i} + V(\boldsymbol{r}), \tag{2}$$

where $V(\boldsymbol{r})$ is the potential. The phase space trajectory generated is constrained to a hypershell parametrized by the conserved total energy of the system $\mathcal{H}(\boldsymbol{r}, \boldsymbol{p}) = E$. Microcanonical ensemble averages are constructed by means of the corresponding probability density function. For any observable A, either explicitly time-dependent or independent, the microcanonical ensemble average is given by

$$\langle A \rangle = \frac{\int \mathrm{d}\mu \; A(\boldsymbol{r}(t), \boldsymbol{p}(t)) \, \delta(\mathcal{H} - E)}{\int \mathrm{d}\mu \; \delta(\mathcal{H} - E)}, \tag{3}$$

where $\mathrm{d}\mu$ is the corresponding invariant measure, in this case $\mathrm{d}\mu = \mathrm{d}\boldsymbol{p} \, \mathrm{d}\boldsymbol{r}$. The chaotic nature of the phase space trajectory, in the sense indicated previously, allows the identification of (3) with the temporal average over an equilibrated simulation of time-length T:

$$\bar{A} = \frac{1}{T} \int \mathrm{d}t A(\boldsymbol{r}(t), \boldsymbol{p}(t)) = \langle A \rangle. \tag{4}$$

MD simulations use information (positions, velocities or momenta, and forces) at a given instant in time, t, to predict the positions and momenta at a later time, $t + \Delta t$, where Δt is the time step, usually taken to be constant throughout the simulation. Numerical solutions to the equations of motion are thus obtained by iteration of this elementary step. The most popular algorithms for propagating the equation of motion, or "integrators," are based on Taylor expansions of the positions (see Allen & Tildesley (1989) for a survey). For example, the Verlet algorithm uses the sum of third order expansions forward and backward in time of the

particle positions, $\boldsymbol{r}_i$,

$$\boldsymbol{r}_i(t+\Delta t) = \boldsymbol{r}_i(t) + \Delta t\,\boldsymbol{v}_i(t) + \frac{\Delta t^2}{2m_i}\boldsymbol{F}_i(t) + \frac{\Delta t^3}{6}\boldsymbol{b}_i(t) + \mathcal{O}(\Delta t^4), \quad (5)$$

$$\boldsymbol{r}_i(t-\Delta t) = \boldsymbol{r}_i(t) - \Delta t\,\boldsymbol{v}_i(t) + \frac{\Delta t^2}{2m_i}\boldsymbol{F}_i(t) - \frac{\Delta t^3}{6}\boldsymbol{b}_i(t) + \mathcal{O}(\Delta t^4), \quad (6)$$

where $\boldsymbol{v}_i$ is the velocity, $\boldsymbol{F}_i$ is the force, and $\boldsymbol{b}_i$ is the third derivative with respect to time, to obtain an equation for the predicted position that is accurate to third order in time (because of the cancellation of the terms containing odd powers of time):

$$\boldsymbol{r}_i(t+\Delta t) = 2\boldsymbol{r}_i(t) - \boldsymbol{r}_i(t-\Delta t) + \frac{\Delta t^2}{m_i}\boldsymbol{F}_i(t) + \mathcal{O}(\Delta t^4). \quad (7)$$

An equation for the velocities is obtained by subtracting the two expansions,

$$\boldsymbol{v}_i(t) = \frac{\boldsymbol{r}_i(t+\Delta t) - \boldsymbol{r}_i(t-\Delta t)}{2\Delta t} + \mathcal{O}(\Delta t^3). \quad (8)$$

Note that, according to Equation (7), the velocities are not necessary for prediction of the positions. Because the velocities are determined at time t while the positions are determined at time $t+\Delta t$, calculation of velocity-dependent quantities (e.g., the kinetic energy) coincident with the predicted positions is awkward. The Verlet algorithm can be modified to synchronize the prediction of the positions and velocities. One popular modification, the "velocity Verlet" algorithm, is described below.

A general approach to the development of MD integrators has been formulated based on the Liouville operator formalism of Hamiltonian mechanics, in which Hamilton's equations of motion (Equations (1)) are recast as

$$\dot{\Gamma} = \mathrm{i}L\Gamma. \quad (9)$$

Here, Γ is a $6N$-dimensional phase vector of the N particle coordinates and momenta (or velocities), and $\mathrm{i}L$ is the Liouville operator

$$\mathrm{i}L = \dot{\Gamma}\cdot\nabla_\Gamma = \sum_{i=1}^{N}\boldsymbol{v}_i\cdot\nabla_{\boldsymbol{r}_i} + \sum_{i=1}^{N}\left[\frac{\boldsymbol{F}_i(\boldsymbol{r})}{m_i}\right]\cdot\nabla_{\boldsymbol{v}_i}. \quad (10)$$

The formal solution to Equation (10) is

$$\Gamma(t) = \exp(\mathrm{i}Lt)\Gamma(0). \quad (11)$$

In practice, this is not useful because the action of the propagator, $\exp(\mathrm{i}Lt)$, on the phase vector cannot be determined analytically. However, it is possible to derive accurate short-time approximations to the propagator, whose action can be evaluated analytically, by factorizing the propagator. To this end, Equation (11) is rewritten so that the trajectory from 0 to t is generated in a sequence of P discrete time steps, $\Delta t = t/P$:

$$\Gamma(t) = \prod_{j=1}^{P}\left(\prod_{s}^{n}\exp(\mathrm{i}L_s\Delta t)\right)\Gamma(0). \quad (12)$$

Then the Trotter factorization may be used to decompose the propagator (Tuckerman & Martyna, 2000):

$$\exp(\mathrm{i}L\Delta t) = \exp\left(\mathrm{i}L_1\frac{\Delta t}{2}\right)\exp(\mathrm{i}L_2\Delta t)\exp\left(\mathrm{i}L_1\frac{\Delta t}{2}\right) + \mathcal{O}(\Delta t^3) \quad (13)$$

giving an approximate, short-time evolution operator that is time-reversible and has the same accuracy as typical MD integrators. The operators $\mathrm{i}L_1$ and $\mathrm{i}L_2$ are chosen so that their action on the phase vector can be determined analytically, with the restriction that $\mathrm{i}L_1 + \mathrm{i}L_2 = \mathrm{i}L$. For example, applying (13) to the phase vector, $\Gamma = (\boldsymbol{r}, \boldsymbol{v})$ (written here and in what follows in terms of velocities), with

$$\mathrm{i}L_1 = \sum_{i=1}^{N}\left[\frac{\boldsymbol{F}_i(\boldsymbol{r})}{m_i}\right]\cdot\nabla_{\boldsymbol{v}_i}, \quad (14)$$

$$\mathrm{i}L_2 = \sum_{i=1}^{N}\boldsymbol{v}_i\cdot\nabla_{\boldsymbol{r}_i} \quad (15)$$

gives the velocity Verlet integrator:

$$\boldsymbol{r}_i(t+\Delta t) = \boldsymbol{r}_i(t) + \Delta t\,\boldsymbol{v}_i(t) + \frac{\Delta t^2}{2m_i}\boldsymbol{F}_i(\boldsymbol{r}(t)), \quad (16)$$

$$\boldsymbol{v}_i(t+\Delta t) = \boldsymbol{v}_i(t) + \frac{\Delta t}{2m_i}[\boldsymbol{F}_i(\boldsymbol{r}(t)) + \boldsymbol{F}_i(\boldsymbol{r}(t+\Delta t))]. \quad (17)$$

In practice, computing meaningful time averages according to (4) requires sufficient sampling of an already equilibrated trajectory. This determines the total simulation time T. Once a model system and a dynamical system (i.e., an ensemble average) have been chosen, computational efficiency will rely on the choice of the numerical integrator. The total real computational time will depend on how many steps are required to reach the total time-length T. The choice of the time step size depends on the rate of accumulation of numerical errors as evaluated by the tolerance ΔE for the conserved quantity E. In molecular systems, the time step is determined by the highest frequency vibrational mode in the system. A rule of the thumb, is that, for numerical stability, one vibrational period should be covered by roughly 20 time steps. A popular approach to increasing the time step in MD simulations of molecular systems is to use holonomic constraints to freeze the motion of the

highest frequency bonds, or all of the bonds altogether. This is considered acceptable practice for most applications because the bond stretching motion is effectively decoupled from the other degrees of freedom that are typically of greater interest. To solve the equations of motion in the presence of constraints, the Lagrangian formalism of classical mechanics is used, and the constraint forces are expressed in terms of undetermined multipliers. There are a variety of algorithms for solving the resulting constraint equations and integrating the equations of motion (see Allen & Tildesley, 1989). The details depend on the choice of the integrator. The most popular are iterative methods known as SHAKE, designed to work with the Verlet integrator, and RATTLE, designed to work with the velocity Verlet integrator.

The utility of the constraint method rests on the fact that the fastest degrees of freedom place an upper bound on the time step, and the time step can therefore be increased if the fastest degrees of freedom are eliminated (constrained). A more general approach is based on the premise that the forces associated with different degrees of freedom evolve on different time scales, and the slower forces do not need to be computed as often as the faster forces. It turns out, for molecular systems, that the fastest forces, those associated with intramolecular interactions, require the least computational effort to evaluate ($\mathcal{O}(N)$), while the slowest forces, those associated with nonbonded interactions, require the most computational effort ($\mathcal{O}(N^2)$). Thus, in the interest of computational efficiency, it is clearly advantageous to calculate the rapidly evolving forces at each elementary time step, and only calculate the slowly evolving forces at a larger time interval that is several times the elementary time step. This is the essence of multiple time step MD (see Tuckerman & Martyna (2000) for a review), which is briefly summarized below.

Suppose that the total force on the particle i may be written

$$\boldsymbol{F}_i = \boldsymbol{F}_i^{\text{fast}} + \boldsymbol{F}_i^{\text{slow}}, \tag{18}$$

where $\boldsymbol{F}_i^{\text{fast}}$ and $\boldsymbol{F}_i^{\text{slow}}$ are the parts of the force that change rapidly and slowly, respectively. Now, according to Equation (13), we may write

$$\begin{aligned}&\boldsymbol{\Gamma}(t+\Delta t)\\ &= \{\exp(\mathrm{i}L_3\Delta t/2)[\exp(\mathrm{i}L_1\delta t/2)\exp(\mathrm{i}L_2\delta t)\\ &\quad\times\exp(\mathrm{i}L_1\delta t/2)]^n\exp(\mathrm{i}L_3\Delta t/2)\}\boldsymbol{x}(t)+\mathcal{O}(\Delta t^3),\end{aligned} \tag{19}$$

where $\mathrm{i}L_2$ is as before and

$$\mathrm{i}L_1 = \sum_{i=1}^{N}\left[\frac{\boldsymbol{F}_i^{\text{fast}}(\boldsymbol{r})}{m_i}\right]\cdot\nabla_{\boldsymbol{v}_i}, \tag{20}$$

$$\mathrm{i}L_3 = \sum_{i=1}^{N}\left[\frac{\boldsymbol{F}_i(\boldsymbol{r})-\boldsymbol{F}_i^{\text{fast}}(\boldsymbol{r})}{m_i}\right]\cdot\nabla_{\boldsymbol{v}_i} \tag{21}$$

with $\delta t = \Delta t/n$. Thus, to evolve the system from time t to $t+\Delta t$ in one step of an MD simulation, the total force needs to be evaluated only once, and the fast component of the force n times. The small time step, δt, is determined by the time scale of the fast forces. As the computational effort required to evaluate the fast component of the force is negligible compared with that required for the slow force, this scheme results in nearly a factor of n decrease in computational effort. The resulting algorithm is straightforward to implement because each action of the evolution operators translates directly into velocity Verlet-like integration steps (Tuckerman & Martyna, 2000).

The majority of microscopic systems modeled by MD simulations are collections of atoms or molecules in a condensed phase. The usual quantum mechanical treatment of molecular systems assumes that the problem is separable between electronic and nuclear (or ion-core) degrees of freedom. Within this context, the most common approach in MD simulations is to consider the classical limit for the nuclear degrees of freedom. Thus, the phase space trajectory describes the dynamics of the atomic nuclei as classical point particles, while the electronic degrees of freedom are accounted for by the interaction potential $V(\boldsymbol{r})$. There is not a single prescription for choosing the form of the potential energy function and determining its parameters. In general, analytical forms for model systems are taken from molecular mechanics, and the specific parameters are dependent on the kind of system that is being modeled. For simple systems, the available information from zero-temperature electronic structure calculations is directly fitted to a convenient analytical function. For complex systems, electronic structure calculations for small molecular moieties are complemented with relevant experimental data pertinent to the phase being modeled. For a detailed overview of commonly used empirical potentials, see Leach (2001).

Although the number and nature of the potential energy terms varies from one application to the next, the potential for an arbitrarily complicated molecule such as a polymer is generally written as the sum of "bonded" and "nonbonded" terms. The bonded terms include energy penalties, usually represented by harmonic potentials, for deforming chemical bonds and the angles between bonds from their equilibrium values, as well as periodic potentials to describe the energy change as a function of the torsion (dihedral) angle about rotatable bonds. The bonded terms are usually taken to be diagonal, that is, there are no terms describing coupling between deformations of bonds and angles, bonds and torsions, etc. These off-diagonal terms are important for accurate reproduction of vibrational properties, as are anharmonic terms (e.g., cubic, quartic). The nonbonded terms, as the name suggests, describe the interactions

between atoms in different molecules, or interactions within a molecule that are not completely accounted for by the bonded terms; that is, they are separated by more than two bonds. The nonbonded terms are typically assumed to be pairwise-additive functions of interatomic separation, r, and include van der Waals interactions and Coulomb interactions in polar or charged molecules in which the charge distribution is represented by partial charges (usually placed on the atoms). The van der Waals interactions include a term that is strongly repulsive (exponential or inverse 12th power of r), and a weakly attractive dispersion term (e.g., inverse 6th power of r, representing the induced dipole-induced dipole interaction). A popular form for the van der Waals interactions is the Lennard-Jones ("12-6") potential:

$$V(r) = 4\varepsilon\left(\left(\frac{\sigma}{r}\right)^{12} - \left(\frac{\sigma}{r}\right)^{6}\right) \tag{22}$$

Here, ε is the depth of the minimum, and σ is where the potential crosses zero and is a measure of the van der Waals diameter of the atom.

The number of bonded interactions grows in proportion to N, the number of atoms in the system, while the number of nonbonded interactions grows as N^2. Therefore, most of the computer time used for an MD simulation is spent on the evaluation of the nonbonded energies and forces. To reduce this burden, van der Waals interactions are typically ignored beyond some "cutoff" distance, usually around two or three atomic diameters. However, because the Coulomb potential is long-ranged, it is dangerous to truncate the electrostatic interactions. In condensed phase systems modeled using periodic boundary conditions (to eliminate surface effects in simulations of small systems that are meant to be in a bulk environment), the Ewald method can be used to sum all of the electrostatic interactions in an infinite, periodically replicated system. Details on the implementation of the Ewald sum may be found in Allen & Tildesley (1989).

Although MD simulations are most conveniently carried out in the microcanonical ensemble, there are disadvantages to doing so. An important aspect of performing simulation studies is to calculate experimentally measurable properties for comparison with measurements made at particular thermodynamic state points. Most experiments are carried out under the conditions of constant N and temperature, and either constant pressure or constant volume, that is, in the isobaric-isothermal or canonical statistical mechanical ensembles. In microcanonical simulations, the temperature and pressure are computed via averages of the kinetic energy and virial, respectively, and it is not known until after the simulation has been completed whether it was run at the desired state point. Moreover, in the canonical and isobaric-isothermal ensembles, the characteristic thermodynamic potentials are the Helmholtz free energy, $F(N, V, T)$, and Gibbs free energy, $G(N, P, T)$, respectively, and these free energies are easier to calculate from MD trajectories (see Frenkel & Smit (1996) for a discussion of methods for free energy calculations) than the entropy, $S(N, V, E)$, which is the characteristic thermodynamic potential of the microcanonical ensemble. In addition, constant pressure simulations are especially useful when the density of the system is not known a priori.

Several techniques for generating trajectories in ensembles other than the microcanonical ensemble have been developed (see Allen & Tildesley (1989) for an overview and Ciccotti et al. (1987) for a collection of key papers). The most powerful techniques are based on the concept of an "extended system" (ES), in which the atomic positions and momenta are supplemented by additional dynamical variables representing the coupling of the system to an external reservoir. For example, in the first application of the extended system concept to a simulation at constant pressure by H.C. Andersen in 1980, the system volume was taken to be a dynamical variable to simulate coupling to a pressure reservoir. In the Nosé implementation of constant temperature MD, a time-scaling "thermostat" variable was introduced. M. Parrinello and A. Rahman (1981) generalized Andersen's constant pressure method to allow the simulation cell to change shape as well as size by making the elements of the cell matrix dynamical variables. In these initial formulations of the ES concept, the additional dynamical variables were assigned fictitious kinetic and potential energies, and their equations of motion were derived using the Lagrangian formalism. Note that the choice of the form of the equations of motion for the additional degrees of freedom is not arbitrary, but rather should be made so that the resulting phase space distribution function is that of the desired ensemble. The Lagrangian formalism is not always the most convenient for handling extended systems. A more general approach is based on the formalism of non-Hamiltonian dynamics (Tuckerman & Martyna, 2000), which is sketched below. This approach was pioneered by W.G. Hoover, who rewrote the equations of motion for the Nosé thermostat in non-Hamiltonian form, leading to a much more straightforward implementation of constant temperature MD that was subsequently referred to as the Nosé–Hoover thermostat.

In the non-Hamiltonian dynamics approach, the equations of motion for the ES variables and a conserved Hamiltonian-like quantity, H', which includes terms for the kinetic and potential energies of the ES degrees of freedom, are chosen together such that the microcanonical distribution function generated by the extended system dynamics

is formally equivalent (within a normalization constant) to the desired phase space distribution function of the atoms (e.g., canonical, isobaric-isothermal). The "non-Hamiltonian" resides in the fact that the necessary equations of motion cannot be derived from H', as in the case of Hamilton's equations (see Equations (1)). A complication that arises for non-Hamiltonian systems is that the phase space compressibility,

$$\kappa = \nabla_\Gamma \cdot \dot{\mathbf{\Gamma}}, \tag{23}$$

where Γ is now the $6N + 2M$ dimensional vector of coordinates and momenta (or velocities) of the N particles and M extended system variables, does not vanish as it does for Hamiltonian systems. Consequently, a metric factor must be included in the phase space measure,

$$\mathrm{d}\mu = \sqrt{g(\mathbf{\Gamma}, t)}\mathrm{d}\mathbf{\Gamma}, \tag{24}$$

where

$$\sqrt{g(\mathbf{\Gamma}, t)} = \exp[-w(\mathbf{\Gamma}, t)], \tag{25}$$

$$\frac{\mathrm{d}w}{\mathrm{d}t} = \kappa, \tag{26}$$

so that the extended system phase space volume is conserved (i.e., Liouville's theorem is obeyed). Reversible, multiple time step integrators for extended system (Martyna et al., 1996) and non-equilibrium (Mundy et al., 2000) dynamics have been derived based on non-Hamiltonian mechanics using the Liouville operator formalism illustrated above for microcanonical dynamics.

In extended system MD simulations with temperature and pressure control, the instantaneous temperature (kinetic energy) and pressure (virial) fluctuate, and it is their average values that are equal to the values imposed by the thermal and pressure reservoirs. There are two other commonly employed approaches to temperature and pressure control (see Allen & Tildesley (1989) for a survey). In one class of methods, the instantaneous temperature and pressure are constrained to constant values. For large systems, the imposition of constraints is reasonable because fluctuations are small. By introducing Lagrange multipliers and applying Gauss's principle of least constraint, the constraints are applied in such a way so as to minimize the change in dynamics. The resulting phase space distribution functions are equal to the desired ones, multiplied by delta functions that account for the constraints on the temperature and pressure. Another technique is referred to as "coupling to an external bath," where the "bath" can be a temperature and/or pressure reservoir. This scheme drives the system to the desired temperature (pressure) at a rate determined by a preset temperature (pressure) relaxation time by scaling the velocities (volume and coordinates) at each time step. This method has the advantage that it is easily implemented, and the disadvantage that it does not generate states in any known statistical mechanical ensemble.

To date, most MD simulations have been driven by forces that were derived from assumed, empirical potentials. About two decades ago, the scope of MD simulations was greatly expanded by the introduction of a method by Car & Parrinello (1985) that, rather than relying on an empirical potential, utilizes interatomic potentials computed directly from the electronic structure which evolves simultaneously with the nuclear configuration. Thus, changes in electronic polarization and the possibility of chemical transformations are naturally included in the simulation. To this end, the wave function is expanded in a basis set, the expansion coefficients are treated as dynamical variables in an extended system Lagrangian, and the resulting equations of motion adiabatically propagate the electronic orbitals with respect to the nuclei, so that they remain on the ground state Born–Oppenheimer surface at each time step. Consequently, the need to solve the computationally burdensome electronic structure problem (self-consistent field) is avoided, and it is feasible to generate trajectories of sufficient length to study phenomena that were previously impossible to simulate. For technical details on the implementation of this so-called "ab initio MD" method, see Marx & Hütter (2000). Although the size of system (on the order of 100 atoms) and the length of trajectory (roughly tens of picoseconds) that can be simulated presently by ab initio MD are modest compared with simulations based on empirical potentials, it is clear that, as computational resources continue to evolve, applications of ab initio MD will become more and more prevalent and compelling.

Douglas J. Tobias and J. Alfredo Freites

See also **Hamiltonian systems; Local modes in molecular crystals; Lorentz gas; Newton's laws of motion; Protein dynamics**

Further Reading

Allen, M.P. & Tildesley, D.J. 1989. *Computer Simulation of Liquids*, Oxford: Oxford Science Publications

Car, R. & Parrinello, M. 1985. Unified approach for molecular dynamics and density-functional theory. *Physical Review Letters*, 55: 2471–2474

Ciccotti, G., Frenkel, D. & McDonald, I.R. (editors). 1987. *Simulation of Liquids and Solids: Molecular Dynamics and Monte Carlo Methods in Statistical Mechanics*, Amsterdam: North-Holland

Frenkel, D. & Smit, B. 1996. *Understanding Molecular Simulation: From Algorithms to Applications*, San Diego: Academic Press

Gibson, J.B., Golan, A.N., Milgram, M. & Vineyard, G.H. 1960. Dynamics of radiation damage. *Physical Review*, 120: 1229–1253

Leach, A.R. 2001. *Molecular Modelling: Principles and Applications*, 2nd edition, Harlow: Prentice-Hall

Martyna, G.J., Tuckerman, M.E., Tobias, D.J. & Klein, M.L. 1996. Explicit reversible integrators for

extended systems dynamics. *Molecular Physics*, 87: 1117–1137

Marx, D. & Hütter, J. 2000. *Ab initio* molecular dynamics: theory and implementation. In *Modern Methods and Algorithms of Quantum Chemistry*, edited by J. Grotendorst, Jülich: Forschungszentrum Jülich

Mundy, C.J., Balasubramanian, B., Bagchi, K., Tuckerman, M.E., Martyna, G.J. & Klein, M.L. 2000. Nonequilibrium molecular dynamics. *Reviews in Computational Chemistry*, 14: 291–397

Parrinello, M. & Rahman, A. 1981. Polymorphic phase transitions in single crystals: a new molecular dynamics method. *Journal of Applied Physics*, 52: 7182–7190

Tuckerman, M.E. & Martyna, G.J. 2000. Understanding modern molecular dynamics: techniques and applications. *Journal of Physical Chemistry* B, 104: 159–178

MONODROMY PRESERVING DEFORMATIONS

Suppose $z \to A(z)$ is a $p \times p$ matrix valued meromorphic function (analytic except for a finite number of poles) on the Riemann sphere (also called a "complex projective one space" and denoted as $\boldsymbol{P}^1$) with poles at the points $a_\nu, \nu = 1, \ldots, n$. Suppose Ψ is a fundamental solution for the linear system,

$$\frac{\mathrm{d}\Psi}{\mathrm{d}z} = A(z)\Psi, \tag{1}$$

defined in a neighborhood of a regular point, a_0. Analytic continuation of the fundamental solution along a closed curve γ which begins and ends at a_0 produces a change,

$$\Psi \to \Psi M_\gamma,$$

where M_γ is the *monodromy* associated with the path γ and the fundamental solution Ψ. The constant matrix M_γ depends only on the homotopy type of γ, and the map $\gamma \to M_\gamma^{-1}$ is a representation of the fundamental group $\pi_1\left(\boldsymbol{P}^1 \backslash \{a_\nu\}, a_0\right)$ called the monodromy representation of the differential equation.

In the 1850s, Bernhard Riemann solved the connection problem for solutions to the hypergeometric equation by exploiting the monodromy representation. The hypergeometric equation is the family of second-order equations on $\boldsymbol{P}^1$ with three regular singular points, and the connection problem is to understand how the local series solutions defined near the singularities are related to one another by analytic continuation. Riemann made some further speculations about monodromy representations, and (inspired by Riemann's work) David Hilbert asked if any representation of $\pi_1\left(\boldsymbol{P}^1 \backslash \{a_\nu\}, a_0\right)$ might be realized as the monodromy representation of a suitable differential equation. This is the 21st in the list of problems presented by Hilbert at the International Congress of Mathematicians in 1900. It always has a solution for differential equations with regular singular points (Plemelj, 1963), but it does not always have a solution if the differential equation is required to have simple poles. The book by Anasov and Bolibruch (1994) has a careful discussion of the history of this problem and its solution.

Suppose that the matrix $A(z)$ has simple poles,

$$A(z) = \sum_{\nu=1}^{n} \frac{A_\nu}{z - a_\nu}, \text{ with } \sum_{\nu=1}^{n} A_\nu = 0. \tag{2}$$

The second condition guarantees that ∞ is either a simple pole or a regular point. For simplicity, we also suppose that for each ν no pair of eigenvalues for A_ν differ by an integer. In this *nonresonant* case, the differential equation (1) is holomorphically equivalent to the differential equation,

$$\frac{\mathrm{d}\Phi}{\mathrm{d}z} = \frac{A_\nu}{z - a_\nu}\Phi, \tag{3}$$

in a neighborhood of $z = a_\nu$. In 1912, Ludwig Schlesinger asked how the residue matrices A_ν should depend on the pole locations $a = (a_1, a_2, \ldots, a_n)$ in order that the monodromy representation remain unchanged. In case ∞ is a regular point, he discovered that the matrices A_ν must satisfy a nonlinear differential equation,

$$\mathrm{d}A_\mu = -\sum_{\nu \neq \mu} \frac{A_\mu A_\nu - A_\nu A_\mu}{a_\mu - a_\nu} d(a_\mu - a_\nu).$$

This equation is known as the Schlesinger equation and is an example of a *monodromy preserving deformation*.

Schlesinger's treatment of the existence question for such deformations was clarified in the work of Malgrange (1983b). Let $D_{\mu\nu} = \{a \in \boldsymbol{C}^n : a_\mu = a_\nu\}$ denote the set of points in $\boldsymbol{C}^n$ where the μ and ν poles collide—evidently such points are singular points for the Schlesinger equations. Malgrange showed that if one starts with a monodromy representation that is realized for a differential equation with simple poles at a_ν^0 and residues A_ν^0, then the deformation equation has a solution $A_\nu(a)$ which is analytic on the simply connected covering of $\boldsymbol{C}^n \backslash \cup D_{\mu\nu}$ *except possibly for poles along a hypersurface in this space*. He also showed that the hypersurface on which the solutions $A_\nu(a)$ has poles consists of those points for which a variant of the Riemann–Hilbert problem fails to have a solution. It is simplest to describe this variant in the nonresonant case (although Malgrange does not make this assumption). The point a will be a pole of $A_\nu(a)$ provided that it is not possible to find a differential equation with simple poles at a_ν for $\nu = 1, 2, \ldots, n$ which reproduces the monodromy representation of the original equation,

$$\frac{\mathrm{d}\Psi}{\mathrm{d}z} = \sum_{\nu=1}^{n} \frac{A_\nu^0}{z - a_\nu^0}\Psi,$$

and is in the local holomorphic equivalence class of

$$\frac{\mathrm{d}}{\mathrm{d}z} - \frac{A_v^0}{z - a_v}$$

near $z = a_v$. It is possible that a given monodromy representation can be realized by a differential equation with simple poles without being able to specify the local holomorphic equivalence classes (see Bolibruch, 2002).

Nonlinear differential equations in the complex plane have the property that solutions can develop singularities away from the manifest singularities of the equations. The location of singularities of this sort depends on the initial conditions for the differential equation; thus, such points are called movable singularities. Differential equations with solutions whose only movable singularities are poles are said to have the Painlevé property. Paul Painlevé and Bertrand Gambier classified the simplest such nonlinear equations and determined six new families of transcendental functions that arise in the integration of these differential equations—now referred to as Painlevé I–VI (see Ince, 1956). Schlesinger understood, and as noted above, Malgrange proved that the Schlesinger equation has the Painlevé property. In a related development, Garnier (1912) showed that the Painlevé transcendents arise in the deformation of Fuchsian equations. Later, Jimbo, & Miwa (1981) showed how to obtain all six of the Painlevé equations by suitable specialization of the Schlesinger equations for 2×2 matrix systems. Painlevé VI arises for a linear system with simple poles of the type considered by Schlesinger. The other Painlevé equations arise by successive scaling that introduces irregular singularities and requires an extension of the Schlesinger analysis that was accomplished by Miwa, Jimbo, and Ueno in Jimbo, et al. (1981). Importantly, finding such representations for Painlevé equations is analogous to finding Lax pair representations for nonlinear equations such as the KdV equations (see Kapaev, 2002; Deift et al., 1999).

Flaschka & Newell (1980) first considered a generalization of the notion of monodromy preserving deformations to linear differential equations with higher rank singularities (equations with poles of order 2 or higher are said to have irregular singularities). More subtle local invariants, called Stokes multipliers, are fixed by the deformations, and in addition to the location of the singularities, the deformation parameters include formal expansion parameters that characterize the local asymptotics of solutions near the singularities. Based on Birkhoff's generalization of the Riemann–Hilbert problem (Birkhoff, 1913), Jimbo, Miwa, and Ueno (1981) generalized Flashka and Newell's work to the consideration of nonresonant differential equations with irregular singular points. They obtained the analogue of the Schlesinger equations for generalized monodromy preserving deformations of these equations. They also introduced the notion of a τ-function for such deformations. They conjectured that the τ-function is a holomorphic function of the deformation parameters whose 0 set is the set of pole locations for the solutions to the deformation equations. Miwa (1981) later showed that the τ-function is holomorphic and the Painlevé property is satisfied for the deformation equations in the domain of convergence for his explicit solution of the Birkhoff–Riemann–Hilbert problem. Malgrange (1983b) established the full conjecture for regular singularities without restrictions.

Geometric Perspectives

Röhrl (1957) formulated and solved a version of the Riemann–Hilbert problem on Riemann surfaces. The setting for the result involves vector bundles and holomorphic connections with singularities. Deligne (1970) developed a multidimensional generalization of the Riemann–Hilbert problem which took advantage of rather abstract categorical constructions. Malgrange (1983a) introduced Stokes' sheaves at irregular singular points to describe local holomorphic equivalence classes. More recently, progress in analyzing the local structure of differential equations at irregular singular points has come by introducing sophisticated ideas from algebraic geometry (see Varadarajan, 1996). Part of the impetus for these developments is the effort to achieve clarity in a subject that is subtle enough to have inspired the misinterpretation of fundamental results and even errors in proofs by such luminaries as George D. Birkhoff (see Anasov and Bolibruch (1994) for an account).

Among these developments, there is one geometric idea introduced by Röhrl and more fully realized by Malgrange (1983c), which provides helpful insight into the nature of the Birkhoff–Riemann–Hilbert deformation problem introduced in Jimbo et al. (1981). Suppose that $a^0 = \{a_1^0, a_2^0, \ldots, a_n^0\}$ is a collection of distinct points in $\boldsymbol{P}^1$ and $A^0(z)$ is a rational matrix valued function whose principal part at $z = a_v$ is

$$\frac{A_{r+1}^0}{(z - a_v)^{r+1}} + \frac{A_r^0}{(z - a_v)^r} + \cdots + \frac{A_1^0}{z - a_v}.$$

The integer $r = r_v$ is called the rank of the singularity. Let

$$\nabla^0 = \frac{\mathrm{d}}{\mathrm{d}z} - A^0(z)$$

denote the associated *connection*. We will say that the connection ∇^0 is *nonresonant* if the leading coefficient A_{r+1}^0 has distinct eigenvalues at each of the singularities with the additional requirement that these eigenvalues do not differ by integers in case $r = 0$. Incidentally, much of the machinery that has been introduced to study

irregular singular points is devoted to understanding the substantial complications that arise for *resonant* connections (Varadarajan, 1996).

It is a result of Deligne (1970) that the holomorphic equivalence class of ∇^0 on the *punctured* sphere $\boldsymbol{P}^1\backslash\{a_v^0\}$ is determined by its monodromy representation. On the other hand, in a neighborhood of each of the singularities, the connection ∇^0 belongs to a local holomorphic equivalence class of rank r connections. For nonresonant connections, this local equivalence class, is naturally a fiber bundle whose base consists of *diagonal* connections,

$$\frac{\mathrm{d}}{\mathrm{d}z} - \frac{H_r}{(z-a_v)^{r+1}} + \cdots + \frac{H_0}{z-a_v}, \tag{4}$$

whose leading coefficient, H_r, has distinct eigenvalues which do not differ by integers in case $r=0$. For $r=0$ the form (4) determines the local equivalence class, but for $r \geq 1$ the fibers in the bundle are essentially the Stokes multipliers, S. Each nonresonant connection ∇^0 has a *formal reduction* to a type (4) connection and the holomorphic equivalence class for ∇^0 is determined by this formal reduction together with the Stokes multipliers. The Stokes multipliers determine the relations between solutions to $\nabla^0\Psi=0$ that are sectorially asymptotic to flat sections of the connection (4) (see Sibuya, 1977; Malgrange, 1983c).

Let t denote the collection of diagonal entries for all the matrices H_j. The fiber bundle of local holomorphic equivalence classes has a natural flat connection (it is a so-called local system (Varadarajan, 1996)) and we let $t \to \sigma(t)$ denote the flat (locally constant) section of this bundle normalized to give the class of ∇^0 at the parameter value t^0 which corresponds to ∇^0. The generalized monodromy preserving deformation problem is to find a family of connections $\nabla(a,t)$ which reproduces the monodromy representation of ∇^0 in the punctured plane $\boldsymbol{P}^1\backslash\{a_v\}$ and whose local holomorphic equivalence class at each a_j is the equivalence class associated with the value of the flat section $\sigma(t)$ (i.e., locally constant Stokes multipliers).

The version of the Birkhoff–Riemann–Hilbert problem relevant to this deformation problem is: Given a representation of $\pi_1(\boldsymbol{P}^1\backslash a, a_0)$ and an assignment of a compatible local holomorphic equivalence class of a type r_v connection to each of the points a_v, find a connection on the trivial bundle over $\boldsymbol{P}^1$ which reproduces this data (compatible means that the local monodromy at a_v should reproduce the monodromy coming from the representation). Because noncanonical choices must be made to define the Stokes multipliers, this version of the Birkhoff–Riemann–Hilbert problem is even complicated to state if the connection with local holomorphic equivalence classes is not understood. Based on ideas of Malgrange, it has been shown that the τ-function introduced by Miwa, Jimbo, and Ueno (1981) has zeros for the deformation problem described above precisely when the associated Birkhoff–Riemann–Hilbert problem fails to have a solution (Palmer, 1999). It should also be mentioned that a crucial technique used both by Jimbo et al. (1981) and by Malgrange (1983b,c) has the prolongation of the connection originally defined on $\boldsymbol{P}^1$ to an integrable connection defined on $\boldsymbol{P}^1 \times \mathcal{D}$ where $\mathcal{D}$ is the space of deformation parameters. In this multidimensional setting, Malgrange adapts Röhrl's technique to prove the existence of a prolongation for the original connection on a vector bundle. The solution of the original deformation problem depends on the triviality of certain restrictions of this vector bundle.

Applications

The Riemann–Hilbert problem and the Painlevé transcendents have generated a steady stream of papers over the years, but interest in monodromy preserving deformations was largely dormant in the period from the early 1920s to the late 1970s. A rebirth of interest in the subject dates from the surprising discovery by Wu, McCoy, Tracy, and Baruch (WMTB) (1976) that the two-point scaling function for the two-dimensional Ising model can be expressed in terms of a Painlevé transcendent of type III. The two-dimensional Ising model is a statistical model of magnetism which exhibits a phase transition in the infinite volume limit. It is so far the only model with a phase transition in which the correlation functions can be studied exactly in the infinite volume limit. The scaling limit that was investigated in Wu et al. (1976) examines the asymptotics of the spin correlations at the length scale of the correlation length (which tends to ∞) as the temperature approaches the critical point. Not only is this analysis important for an understanding of critical phenomena in statistical physics, but it was understood at about the same time that the mathematics of critical phenomena in statistical physics was recognized as the same as the mathematics of renormalization for quantum field theory.

In a remarkable series of papers (Sato et al., 1978, 1979a,b,c, 1980) starting in 1978, Sato, Miwa, and Jimbo found a context for the WMTB result by showing that the n-point correlation for the Ising model could be expressed in terms of the solutions to "monodromy preserving deformations" of the Euclidean Dirac equation (with a mass term). Note that the equation which is the analogue of the Dirac equation in the earlier development is not the differential equation (1) but the Cauchy–Riemann equation $\bar{\partial}\psi = 0$. The correlation functions in the Ising model were the inspiration for their introduction of the τ-function in other contexts. See Palmer & Tracy (1983), Palmer (1993), Palmer et al. (1994), and Palmer (2002) for further developments of these ideas. In Jimbo et al. (1980), Sato, Miwa, Jimbo, and Mori explained the use of their techniques to analyze the impenetrable Bose gas and incidentally

remarked on a connection with an important function in random matrix theory.

The analysis of correlations in integrable models has since been developed by Its et al. (1990), who also codified some of the ideas in a theory of completely integrable integral operators (Korepin et al., 1993). The connection between the random matrix theory and Painlevé functions has been systematically worked out by Tracy & Widom (1994, 1996), who independently developed an integral equation approach to the nonlinear "deformation" equations.

Jimbo (1982) used the monodromy preserving deformation representation of Painlevé functions and the notion of the τ-function to analyze the connection problem for Painlevé functions. The problem is to understand how different families of solutions to the Painlevé equations defined by local asymptotic developments at different singular points are related to one another. Somewhat earlier the connection problem for Painlevé III was worked out by McCoy, Tracy, and Wu (1977) where the answer has consequences for the short distance behavior of the scaling function. Its and Novokshenov (1986) have developed these ideas further.

Although not quite a development in monodromy preserving deformation theory, a "steepest decent" technique based on Riemann–Hilbert ideas has emerged in work of Deift, Zhou and Its that is effective for the asymptotic analysis of solutions to nonlinear equations that arise from spectral or monodromy preserving deformations (Its, 1981; Deift et al., 1997; Bleher & Its, 1999; Deift et al., 1999).

Painlevé functions were discovered in two-dimensional quantum gravity and connections with monodromy preserving deformations are discussed in Moore (1990). Painelevé functions also arise in two-dimensional topological field theory (Dubrovin, 1999).

Further developments are discussed in Harnad & Its (2002).

JOHN PALMER

See also **Painlevé analysis; Riemann–Hilbert problem**

Further Reading

Anasov, D.V. & Bolibruch, A.A. 1994. *The Riemann–Hilbert problem*, Aspects of Mathematics E, vol. 22. Braunschweig; Wiesbaden: Vieweg

Birkhoff, G.D. 1913. The generalized Riemann problem for linear differential equations. *Proceedings of the American Academy of Arts and Sciences*, 32: 531–568

Bleher, P. & Its, A.R. 1999. Semiclassical asymptotics of orthogonal polynomials, Riemann–Hilbert problem, and universality in the matrix model. *Annals of Mathematics*, 150 (2): 185–266

Bolibruch, A. 2002. Inverse problems for linear differential equations with meromorphic coefficients. *CRM Workshop: Isomonodromic Deformations and Applications in Physics*, edited by J. Harnard & A. Its, Providence, RI: American Mathematical Society, pp. 3–25

Deift, P., Its, A., Kapaev, A. & Zhou, X. 1999. On the algebro-geometric integration of the Schlesinger equations. *Communications in Mathematical Physics*, 203: 613–633

Deift, P., Its, A. & Zhou, X. 1997. A Riemann–Hilbert approach to asymptotic problems arising in the theory of random matrix models, and also in the theory of integrable statistical mechanics. *Annals of Mathematics*, 146: 149–237

Deift, P., Kriecherbauer, T., McLaughlin, K., Venakides, S. & Zhou, X. 1999. Uniform asymptotics for polynomials orthogonal with respect to varying exponential weight and applications to universality questions in random matrix theory. *Communications in Pure and Applied Mathematics*, 52: 1335–1425

Deligne, P. 1970. *Équations différentielles à points singuliers réguliers*, Berlin and New York: Springer

Dubrovin, B. 1999. Painlevé transcendents in two-dimensional topological field theory. In *The Painlevé Property, One Hundred Years Later*, edited by R. Conte, New York: Springer, pp. 287–412

Flaschka, H. & Newell, A.C. 1980. Monodromy and spectrum preserving deformations I. *Communications in Mathematical Physics*, 76: 65–116

Garnier, R. 1912. Sur les équationes différentielles du troisième ordre dont l'intégrale générale est uniforme et sur une classe d'équations nouvelles d'ordre supérieur dont l'intégrale générale a ses points critique fixes. *Annales de l'Ecole Normale Supérieure*, (3) 29: 1–126

Harnad, J. & Its, A. 2002. *CRM Workshop: Isomonodromic Deformations and Applications in Physics*, edited by J. Harnard & A. Its, Providence, RI: American Mathematical Society

Ince, E.L. 1956. *Ordinary Differential Equations*, New York: Dover

Its, A.R. 1981. Asymptotics of solutions of the nonlinear Schrödinger equation and isomonodromic deformations of systems of linear differential equations. *Soviet Mathematics. Doklady*, 24: 454–456

Its, A.R., Izergin, A.G., Korepin, V.E. & Slavnov, N.A. 1990. Differential equations for quantum correlation functions. *International Journal of Modern Physics* B, 4: 1003–1037

Its, A.R. & Novokshenov, V.Yu. 1986. *The Isomonodromic Deformation Method in the Theory of Painlevé Equations*, Berlin: Springer

Jimbo, M. 1982. Monodromy problem and the boundary conditions for some Painlevé equations. *Publ. R.I.M.S. Kyoto University*, 18: 1137–1161

Jimbo, M. & Miwa, T. 1981. Monodromy preserving deformations of linear ordinary differential equations with rational coefficients II. *Physica* D, 2: 407–448

Jimbo, M. & Miwa, T. 1983. Monodromy preserving deformations of linear ordinary differential equations with rational coefficients III. *Physica* D, 2: 26–46

Jimbo, M., Miwa, T., Sato, M. & Mori, Y. 1980. Density matrix of an impenetrable bose gas and the fifth Painlevé transcendent. *Physica* D, 1: 80–158

Jimbo, M., Miwa, T. & Ueno, K. 1981. Monodromy preserving deformations of linear ordinary differential equations with rational coefficients I. *Physica* D, 2: 306–352

Kapaev, A.A. 2002. Lax pairs for Painlevé equations, *CRM workshop: Isomonodromic Deformations and Applications in Physics*, edited by J. Harnard & A. Its, Providence, RI: American Mathematical Society, pp. 37–47

Korepin, V.E., Bogoliubov, N.M. & Izergin, A.G. 1993. *Quantum Inverse Method and Correlation Functions*, Cambridge and New York: Cambridge University Press

Malgrange, B. 1983a. *La classification des connections irrégulieéres à une variable*, Boston: Birkhäuser, pp. 381–400
Malgrange, B. 1983b. *Sur les déformations isomonodromiques I, Singularités régulières*, Boston: Birkhäuser, pp. 401–426
Malgrange, B. 1983c. *Sur les déformations isomonodromiques II, Singularités irrégulières*, Boston: Birkhäuser, pp. 427–438
McCoy, B.M., Tracy, C.A. & Wu, T.T. 1977. Painlevé functions of the third kind. *Journal of Mathematical Physics*, 18: 1058–1092
Miwa, T. 1981. Painlevé property of monodromy preserving equations and the analyticity of τ-function. *Publ. R.I.M.S. Kyoto University*, 17: 703–721
Moore, G. 1990. Geometry of the string equations. *Communications in Mathematical Physics*, 133: 261–304
Palmer, J. 1993. Tau functions for the Dirac operator in the Euclidean plane. *Pacific Journal of Mathematics*, 160: 259–342
Palmer, J. 1999. Zeros of the Jimbo, Miwa, Ueno tau function. *Journal of Mathematical Physics*, 40: 6638–6681
Palmer, J. 2002. Short distance asymptotics of Ising correlations, *Journal of Mathematical Physics*, 43(2): 918–953
Palmer, J., Beatty, M. & Tracy, C. 1994. Tau functions for the Dirac operator on the Poincaré disk. *Communications in Mathematical Physics*, 165: 97–173
Palmer, J. & Tracy, C.A. 1983. Two dimensional Ising correlations: the SMJ analysis. *Advances in Applied Mathematics*, 4: 46–102
Plemelj, J. 1963. *Problems in the Sense of Riemann and Klein*, New York: Interscience
Röhrl, H. 1957. Das Riemann–Hilbertsche problem der theorie der linearen differentialgleichungen. *Mathematische Annalen*, 133: 1–25
Sato, M., Miwa, T. & Jimbo, M. 1978. Holonomic quantum fields I. *Publ. R.I.M.S. Kyoto University*, 14: 223–267
Sato, M., Miwa, T. & Jimbo, M. 1979a. Holonomic quantum fields II. *Publ. R.I.M.S. Kyoto University*, 15: 201–278
Sato, M., Miwa, T. & Jimbo, M. 1979b. Holonomic quantum fields III. *Publ. R.I.M.S. Kyoto University*, 15: 577–629
Sato, M., Miwa, T. & Jimbo, M. 1979c. Holonomic quantum fields IV. *Publ. R.I.M.S. Kyoto University*, 15: 871–972
Sato, M., Miwa, T. & Jimbo, M. 1980. Holonomic quantum fields V. *Publ. R.I.M.S. Kyoto University*, 16: 531–584
Schlesinger, L. 1912. Über eine klasse von differentialsystemen beliebiger ordnung mit festen kritischen punkten. *Journal für die reine und angewandte Mathematik*, 14: 95–145
Sibuya, Y. 1977. Stokes' phenomena. *Bulletin of the American Mathematical Society*, 83: 1075–1077
Tracy, C.A. & Widom, H. 1994. Fredholm determinants, differential equations and matrix models. *Communications in Mathematical Physics*, 163: 33–72
Tracy, C.A. & Widom, H. 1996. On orthogonal and symplectic matrix ensembles. *Communications in Mathematical Physics*, 177: 727–754
Varadarajan, V.S. 1996. Linear meromorphic differential equations: a modern point of view, *Bulletin of the American Mathematical Society*, 33(1): 1–41
Wu, T.T., McCoy, B., Tracy, C.A. & Barouch, E. 1976. Spin-spin correlation functions for the two dimensional Ising model: exact theory in the scaling region. *Physical Review* B, 13: 316–374

MONTE CARLO METHODS

Monte Carlo methods collectively refer to a set of computational tools based on random samples. These methods have a very long history that can be traced back to biblical times although a systematic foundation was established only in the early days of electronic computing. A group of mathematicians and physicists of the Los Alamos project during World War II, in particular, John von Neumann, Nick Metropolis, Jeffrey Kahn, Enrico Fermi, Stan Ulam, and their collaborators, developed Monte Carlo methods for estimating eigenvalues of the Schrödinger equation and for studying random neutron diffusion in fissile material used in atomic bombs. Since then, Monte Carlo methods have found applications in a vast number of scientific disciplines and are, becoming increasingly popular with the advent of cheap and powerful computers.

Starting with a space $\mathcal{X}$, let $\varphi : \mathcal{X} \to R$ be function and π be a probability density. In essence, Monte Carlo methods are concerned with

- *Integration*: Evaluate the expectation of φ under π; that is,

$$I_\pi(\varphi) = \int_{\mathcal{X}} \varphi(x)\, \pi(x)\, \mathrm{d}x. \tag{1}$$

- *Simulation*: Simulate some random samples $\{X_i\}_{i=1}^N$ distributed according to π.

Integration and simulation are essential elements of many scientific problems arising, for example, in statistical physics, statistics, engineering, and economics. The probability density π may correspond to a posterior density in the framework of Bayesian statistics or a Boltzmann–Gibbs distribution in equilibrium statistical thermodynamics.

In most applications, it is impossible to compute the expectations of interest in closed-form as the dimension of the space $\mathcal{X}$ is large; for example, $\mathcal{X} = R^{1000}$ or $\mathcal{X} = \{-1, 1\}^{5000}$. Moreover, π is often only known up to a normalizing constant, that is,

$$\pi(x) = cf(x), \tag{2}$$

where $f : \mathcal{X} \to R$ is known but c is unknown. Consequently, standard deterministic numerical integration schemes are very inefficient.

The basic idea of Monte Carlo methods is to compute the expectation(s) of interest in Equation (1) via random samples. Assume the random samples $\left\{X^{(i)}\right\}_{i=1}^N$ distributed according to π are available, then an estimate of $I_\pi(\varphi)$ can be given by the empirical average

$$\widehat{I}_\pi(\varphi) = \frac{1}{N} \sum_{i=1}^{N} \varphi\left(X^{(i)}\right).$$

In other words, π is approximated by

$$\widehat{\pi}(x) = \frac{1}{N} \sum_{i=1}^{N} \delta\left(x - X^{(i)}\right),$$

where $\delta(\cdot)$ is the Dirac delta function. This estimate has "good" theoretical properties. First, it is unbiased.

Second, if the samples $\left\{X^{(i)}\right\}_{i=1}^{N}$ are statistically independent, then the variance of this estimate is given by

$$\frac{\int [\varphi(x) - I_\pi(\varphi)]^2 \pi(x)\, \mathrm{d}x}{N}; \tag{3}$$

that is, the convergence rate of the estimation error to zero is independent of the dimension of $\mathcal{X}$. If the numerator of (3) is "small", then only a few hundreds/thousands of samples might be necessary to achieve a good precision even if $\mathcal{X} = R^{1000}$.

Thus far, it has been shown that estimates with good theoretical properties can be easily obtained from a large set of samples distributed according to the probability density of interest, but how to generate these samples? The Monte Carlo integration problem then becomes that of simulation. Generating samples from nonstandard probability distributions/densities only known up to a proportionality factor is a central problem in Monte Carlo methods.

In 1947, von Neumann, in a letter to Ulam, described an algorithm known as the Rejection Method, to simulate samples distributed according to a "target" probability density. Given a target probability density π that is only known up to a normalizing constant, that is, π is of the form in (2) and only f is known, one chooses a candidate density g that is easy to sample from and a number M satisfying $f(x) \leq Mg(x)$ for any $x \in \mathcal{X}$. The algorithm proceeds as follows:

(a) Sample $X^* \sim g$ ("$\sim$" is a standard notation for "distributed according to") and compute

$$\alpha\left(X^*\right) = \frac{f(X^*)}{Mg(X^*)}.$$

(b) Sample a uniform random variable U on [0, 1]. If $U \leq \alpha(X^*)$, return X^* otherwise go back to (a).

It can be easily verified that the accepted sample follows the target distribution π. The problem with this method is the difficulty in finding a candidate density g satisfying $f(x) \leq Mg(x)$ that is easy to sample from. Moreover, even if such a g can be found, the acceptance probability is $(Mc)^{-1}$, which can be extremely low when $\mathcal{X}$ is a high-dimensional space. Consequently, the algorithm may take a long time to generate a single sample.

A more powerful class of algorithms are the Markov chain Monte Carlo (MCMC) techniques. Given a "target" density π, the key idea of MCMC is to build a Markov chain $\{X_i\}_{i\geq 0}$ of transition kernel $K(\cdot|\cdot)$ such that

$$\int K\left(x'|x\right)\pi(x)\,\mathrm{d}x = \pi\left(x'\right), \tag{4}$$

i.e., if $X_{i-1} \sim \pi$ then any sample $X_i \sim K(\cdot|X_{i-1})$ is also distributed according to π. The target density π in (4) is known as the invariant (or stationary) distribution of the Markov chain. Under ergodicity conditions on the kernel $K(\cdot|\cdot)$, the samples $\{X_i\}_{i\geq 0}$ are distributed according to π asymptotically (as $i \to \infty$) regardless of the value of initial state X_0.

There are an infinity of kernels with invariant distribution π. However, the most frequently used are the Metropolis–Hastings kernels, first proposed by Metropolis et al. (1953), and then generalized by Hastings (1970). Green (1995) extended this to the case where $\mathcal{X}$ is a disjoint union of subspaces of different dimensions.

Given a candidate distribution $q(\cdot|\cdot)$ that is easy to sample from, the Metropolis–Hastings kernel can be constructed as follows: given X_{i-1}

(a) Sample a candidate $X^* \sim q(\cdot|X_{i-1})$ and compute

$$\alpha\left(X_{i-1}, X^*\right) = \frac{\pi(X^*)}{\pi(X_{i-1})}\frac{q(X_{i-1}|X^*)}{q(X^*|X_{i-1})}.$$

(b) Sample a uniform random variable U on [0, 1]. If $U \leq \alpha(X_{i-1}, X^*)$, then set $X_i = X^*$ otherwise set $X_i = X_{i-1}$.

It can be verified that the Markov chain $\{X_i\}_{i\geq 0}$ generated by the above kernel has invariant distribution π. Knowledge of the normalizing constant of π is not needed as it disappears in the acceptance ratio $\alpha(X_{i-1}, X^*)$. The major problem with such Markov chain techniques is that only samples from π are obtained as $i \to \infty$. Nevertheless, the Metropolis–Hastings algorithm and MCMC algorithms, in general, have been applied successfully in numerous applications. MCMC methods form the basis of global optimization algorithms such as simulated annealing (Van Laarhoven & Arts 1987). For a thorough treatment of the theory and applications of MCMC algorithms, the reader is referred to Robert & Casella, (1999).

Importance sampling (IS) is based on assigning weights (or importance) to samples generated from a candidate density q so as to approximate the target density π. Suppose that $\pi(x) = w(x)\, q(x)$, where q is a density that is easy to sample from. Then, given random samples $\left\{X^{(i)}\right\}_{i=1}^{N}$ distributed according to q, the expectation $I_\pi(\varphi)$ in Equation (1) can be estimated by the empirical average

$$\widehat{I_\pi}(\varphi) = \frac{1}{N}\sum_{i=1}^{N}\varphi\left(X^{(i)}\right)w\left(X^{(i)}\right).$$

In other words, π is approximated by

$$\widehat{\pi}_1(x) = \frac{1}{N}\sum_{i=1}^{N} w\left(X^{(i)}\right)\delta\left(x - X^{(i)}\right).$$

This strategy assumes full knowledge of π as $w\left(X^{(i)}\right) = \pi\left(X^{(i)}\right)/q\left(X^{(i)}\right)$ needs to be determined. When π is only specified upto normalizing constant,

write

$$\pi(x) = \frac{w(x)\, q(x)}{\int_{\mathcal{X}} w(x)\, q(x)\, \mathrm{d}x}$$

and apply importance sampling to both numerator and denominator to yield the following approximation:

$$\widehat{\pi}_2(x) = \sum_{i=1}^{N} \frac{w\left(X^{(i)}\right)}{\sum_{j=1}^{N} w\left(X^{(j)}\right)} \delta\left(x - X^{(i)}\right).$$

An approximate sample from π can be obtained by sampling from the discrete distributions $\widehat{\pi}_1$ or $\widehat{\pi}_2$.

Applications

The range of applications of Monte Carlo methods is vast. Listed below are some of the more well-known areas.

Integral equations: IS methods have been widely used to solve linear systems and integral equations appearing in particle transport problems. The basic idea is to give a probabilistic approximation of operators of the form $(I - H)^{-1} = \sum_{i=0}^{\infty} H^i$; see Sobol (1994) for details.

Computational physics and chemistry simulation: Monte Carlo methods are used in physics and chemistry to simulate from Ising models, simulate self-avoiding random walks, and compute the free energy, entropy, and chemical potential over systems; see, for example, Frenkel & Smith (1996).

Quantum physics: To compute the dominant eigenvalue and eigenvector of a positive operator, it is possible to use a stochastic version of the power method. This is often applied to the Schrödinger equation; see Melik-Alaverdian & Nightingale (1999) for a recent review.

Statistics: Performing inference in complex statistical models invariably requires sampling from high dimensional probability distributions. See Gilks et al. (1996) for applications of MCMC and Doucet et al. (2001) for applications of IS-type methods to such problems.

ARNAUD DOUCET AND BA-NGU VO

See also **Random walks; Stochastic processes**

Further Reading

Doucet, A., De Freitas, J.F.G. & Gordon, N.J. (editors). 2001. *Sequential Monte Carlo Methods in Practice*, New York: Springer

Frenkel, D. & Smith, B. 1996. *Understanding Molecular Simulation: From Algorithms to Applications*, Boston: Academic Press

Gilks, W.R., Richardson, S. & Spiegelhalter, D.J. (editors). 1996. *Markov Chain Monte Carlo in Practice*, London: Chapman & Hall

Green, P.J. 1995. Reversible jump MCMC computation and Bayesian model determination. *Biometrika*, 82: 711–732

Hastings, W.K. 1970. Monte Carlo sampling methods using Markov chains and their applications. *Biometrika*, 57: 97–109

Melik-Alaverdian, M. & Nightingale, M.P. 1999. Quantum Monte Carlo methods in statistical mechanics. *International Journal of Modern Physics* C, 10: 1409–1418

Metropolis, N., Rosenblutt, N., Rosenblutt, A.W., Teller, M.N. & Teller, A.H. 1953. Equations of state calculations by fast computing machines. *Journal of Chemical Physics,* 21: 1087–1092

Robert, C.P. & Casella, G. 1999. *Monte Carlo Statistical Methods*, New York: Springer

Sobol, I.M. 1994. *A Primer for the Monte Carlo Method*, Boca Raton, FL: CRC Press

Van Laarhoven, P.J. & Arts, E.H.L. 1987. *Simulated Annealing: Theory and Applications*, Amsterdam: Reidel

MORPHOGENESIS, BIOLOGICAL

One of the central problems in developmental biology is to understand how patterns and structures are laid down. From the initially almost homogeneous mass of dividing cells in an embryo emerges the vast range of pattern and structure observed in animals. For example, the skeleton is laid down during chondrogenesis when chondroblast cells condense into aggregates that lead eventually to bone formation. The skin forms many specialized structures such as hair, scales, feathers, and glands. Butterfly wings exhibit spectacular colors and patterns, and many animals develop dramatic coat patterns.

Although genes play a key role, genetics say nothing about the actual mechanisms that produce pattern and structure—the process known as morphogenesis—as an organism matures from embryo to adult. Tissue movement and rearrangement are the key features of almost all morphogenetic processes and arise as the result of complex mechanical, chemical, and electrical interactions. Despite the recent vast advances in molecular biology and genetics, little is understood of how these processes conspire to produce pattern and form. There is the danger of falling into the practices of the 19th century, when biology was steeped in the mode of classification and there was a tremendous amount of list-making activity. This was recognized by D'Arcy Thompson, in his classic work first published in 1917 (see Thompson (1992) for the abridged version). He was the first to develop theories for how certain forms arose, rather than simply cataloging different forms, as was the tradition at that time.

At the heart of a number of developmental phenomena is the process of convergence-extension, in which a tissue narrows along one axis while extending along another. This process represents the integration of local cellular behavior that produces forces to change the shape of the cell population. In fact, convergence-extension is essentially responsible for the transformation of the spherical egg into the elongated, bilaterally symmetric vertebrate body axis (Keller et al., 1992).

Cell fate and position within the developing embryo can be strongly influenced by environmental factors. Therefore, to investigate the process of morphogenesis, one must really address the issue of how the embryo organizes the complex spatiotemporal sequence of signalling cues necessary to develop structure in a controlled and coordinated manner. Structure can form through tissue movement and rearrangement. Theoretical studies in this area include the early purse-string model (Odell et al., 1981) for tissue folding in which, in response to a large deformation, cells were proposed to actively contract and, in doing so, cause a large deformation in neighboring cells which, in turn, also contract, setting up a propagating contraction wave which leads to tissue folding. This model was applied to a variety of developmental problems and provided the precursor to the mechanochemical theory of developmental patterning developed by Oster, Murray, and coworkers (for review, see Murray, 2003). This approach emphasized the link between tissue mechanics and chemical regulation and has been applied widely in both developmental biology and medicine.

Discrete-cell modeling approaches have subsequently been developed in which morphogenesis is hypothesized to occur via mechanical rearrangement of neighbors in an epithelial sheet, and computational finite elements have been developed to test various theoretical explanations for morphogenesis (Weliky et al., 1991; Davidson et al., 1995).

In all these models, individual cell movements within the tissue are determined by the balance of mechanical forces acting on the cell. Such models can exhibit tissue folding, thickening, invagination, exogastrulation, and intercalation, and have been shown to capture many of the key aspects of processes such as gastrulation, neural tube formation, and ventral furrow formation in *Drosophila*. Cells can also sort out depending on their type, and this has led to the theory of differential adhesion and energy minimization (Steinberg, 1970).

Models for tissue motion are not amenable to a mathematical analysis and tend to be highly computation based. However, models for how cells differentiate can be addressed mathematically. Broadly speaking, there are two classes of such models. In one class, the chemical pre-pattern models, it is hypothesized that a chemical signal is set up in some way and cells respond to this signal by differentiating. In the other class, the cell movement models, it is hypothesized that cells respond to mechanochemical cues and form aggregates. Cells in high density aggregates are then assumed to differentiate (see Murray, 2003, for details).

The fact that such models can lead to the generation of spontaneous order was first realized by Alan Turing (1952), who showed that a system of chemicals, stable in the absence of diffusion, could be driven unstable by diffusion. He proposed that such a spatial distribution of chemicals (which he termed *morphogens*) could set up a pre-pattern to which cells could respond and differentiate accordingly. He was one of the first to postulate the existence of such chemicals, and morphogens have now been discovered. It is still not clear that morphogen patterns in biology are set up by the mechanism proposed by Turing, but Turing patterns have been found in chemistry (see Maini et al., 1997, for a review).

A variety of models based on different biology give rise to mathematical formulations in terms of coupled systems of highly nonlinear partial differential equations. The analysis of these models has, to date, yielded a number of common behaviors. This has led to the idea of using such models to determine developmental constraints. That is, independent of the underlying biology, such models predict that only certain patterns are selected at the expense of others and thus there is a limited variation. This has consequences for evolution. For example, application of mitotic inhibitors to developing limbs produces smaller limbs with reduced elements. Some of the resultant variants look very similar to the pattern of evolution in other species, suggesting that these species may be more closely related than previously thought (Oster et al., 1988). Moreover, the construction rules generated by a study of developmental constraints is another, perhaps more mechanistic, way of describing how different species are related other than the topological deformation approach of D'Arcy Thompson.

Other approaches to morphogenesis and pattern formation include cellular automata models, in which individual entities (cells, for example) behave according to a set of rules. Such models allow one to include much more biological detail and to investigate finer grain patterns than those possible in the continuum approaches discussed above (see, for example, Alt et al., 1997). However, to date they lack a detailed mathematical underpinning.

The recent spectacular advances in molecular genetics raise the issue of how we can combine the enormous amount of data now being generated at this level with the data available from the classical experiments at the cell and tissue level to provide a coherent theory for pattern formation and morphogenesis. This leads to the problem of modeling across a vast range of spatial and temporal scales. The mathematics for this has not yet been developed and is one of the challenges presently being addressed.

PHILIP K. MAINI

See also **Brusselator; Cellular automata; Pattern formation; Reaction-diffusion systems; Turing patterns**

Further Reading

Alt, W., Deutsch, A. & Dunn G. (editors). 1997. *Dynamics of Cell and Tissue Motion*, Basel: Birkhäuser

Davidson, A., Koehl, M.A.R., Keller, R. & Oster, G.F. 1995. How do sea urchins invaginate? Using biomechanics to distinguish between mechanisms of primary invagination. *Development*, 121: 2005–2018

Keller, R., Shih, J. & Domingo, C. 1992. The patterning and functioning of protrusive activity during convergence and extension of the *Xenopus* organiser. *Development Supplement*, 81–91

Maini, P.K., Painter, K.J. & Chau, H.N.P. 1997. Spatial pattern formation in chemical and biological systems. *Faraday Transactions*, 93(20): 3601–3610

Murray, J.D. 2003. *Mathematical Biology II: Spatial Models and Biomedical Applications*, 3rd edition, Berlin and New York: Springer

Odell, G.M., Oster, G., Alberch, P. & Burnside, B. 1981. The mechanical basis of morphogenesis. I. Epithelial folding and invagination. *Developmental Biology*, 85: 446–462

Oster, G.F., Shubin, N., Murray, J.D. & Alberch, P. 1988. Evolution and morphogenetic rules. The shape of the vertebrate limb in ontogeny and phylogeny. *Evolution*, 45: 862–884

Steinberg, M.S. 1970. Does differential adhesion govern self-assembly processes in histogenesis? Equilibrium configurations and the emergence of a hierarchy among populations of embryonic cells. *Journal of Experimental Zoology*, 173: 395–434

Thompson, D.W. 1992. *On Growth and Form*, Cambridge and New York: Cambridge University Press

Turing, A.M. 1952. The chemical basis of morphogenesis. *Philosophical Transactions of the Royal Society of London* B, 327: 37–72

Weliky, M., Minsuk, S., Keller, R. & Oster, G.F. 1991. Notochord morphogenesis in *Xenopus laevis*: simulation of cell behaviour underlying tissue convergence and extension. *Development*, 113: 1231–1244

MULTIDIMENSIONAL SOLITONS

Although strict analogs of the Korteweg–de Vries soliton (exponentially localized solution with a specific relation between velocity and amplitude and particular scattering properties) have not been found in the multidimensional context, solvable equations with three or more independent variables exhibit a large variety of soliton-like solutions.

As with the Kadomtsev–Petviashvili equation, wide classes of exact explicit solutions have been constructed for other $(2+1)$-dimensional nonlinear equations solvable by the inverse scattering method. We consider here two basic examples, the first being the Davey–Stewartson (DS) equation

$$\begin{aligned} \mathrm{i}q_t + \tfrac{1}{2}\left(\sigma^2 q_{xx} + q_{yy}\right) + |q|^2 q - q\phi = 0\,, \\ \phi_{xx} - \sigma^2\phi_{yy} = 2\left(|q|^2\right)_{xx}\,, \end{aligned} \quad (1)$$

where $q(x, y, t)$ is a complex-valued function, ϕ is a real-valued function, and the parameter σ^2 takes two values $\sigma^2 = \pm 1$. The DS equation describes propagation of a two-dimensional long surface wave on water of finite depth. In the one-dimensional limit $q_y = \phi_y = 0$, it reduces to the nonlinear Schrödinger equation.

The DS equation (1) has a Lax representation with the two-dimensional Dirac operator as the Lax operator, but it has quite different properties for $\sigma^2 = 1$ (DS-I equation) and for $\sigma^2 = -1$ (DS-II equation). In both cases, there are multi-soliton solutions which do not decay in certain directions on the x, y plane. Similar to the Kadomtsev–Petviashvili equation these solutions describe elastic scattering of line solitons that decay exponentially in the direction of propagation and do not decay in the orthogonal direction. The phase shift can be explicitly calculated.

In addition, the DS equation possesses novel classes of solutions. Thus, the DS-II equation has an infinite set of nonsingular exponential-algebraic solutions, the simplest of which looks like

$$q(x, y, t) = \frac{2\nu \exp\left[\lambda(x + \mathrm{i}y) - \bar{\lambda}(x - \mathrm{i}y) - \mathrm{i}\left(\lambda^2 + \bar{\lambda}^2\right)t\right]}{|x + \mathrm{i}y + \mu - 2\mathrm{i}\lambda t|^2 + |\nu|^2}, \quad (2)$$

where λ, μ, and ν are arbitrary complex constants. It decays like $\left(x^2 + y^2\right)^{-1}$ as $x, y \to \infty$.

The DS-I equation also possesses solutions for which q decays exponentially in both space dimensions. The simplest of them is of the form

$$q(x, y, t) = \frac{4\rho\sqrt{\lambda\mu}\exp\left[\mu(x+y) + \lambda(x-y) + \mathrm{i}\left(\mu^2+\lambda^2\right)t\right]}{\left[1 + \mathrm{e}^{2\mu(x+y)}\right]\left[1 + \mathrm{e}^{2\lambda(x-y)}\right] + |\rho|^2}, \quad (3)$$

where λ, μ are arbitrary real parameters and ρ is an arbitrary complex parameter. The function ϕ has the nontrivial boundary values as $x, y \to \infty$. Called dromions, such solutions exhibit not only a two-dimensional phase shift during interaction but also a change of the form. Basically, these solutions are driven by the boundary conditions on the function ϕ.

Our second example—the Ishimori equation—is of the form

$$\begin{aligned} \boldsymbol{S}_t + \boldsymbol{S} \times \left(\boldsymbol{S}_{xx} + \sigma^2 \boldsymbol{S}_{yy}\right) + \phi_x \boldsymbol{S}_y + \phi_y \boldsymbol{S}_x = 0\,, \\ \phi_{xx} - \sigma^2\phi_{yy} + 2\sigma^2 \boldsymbol{S} \cdot \left(\boldsymbol{S}_x \times \boldsymbol{S}_y\right) = 0, \end{aligned} \quad (4)$$

where $\boldsymbol{S} = (S_1, S_2, S_3)$ is a unit vector $\boldsymbol{S}^2 = 1$, $\sigma^2 = \pm 1$, and ϕ is a scalar real-valued function. It represents an integrable $(2+1)$-dimensional generalization of the Heisenberg Ferromagnet model equation $\boldsymbol{S}_t = \boldsymbol{S} \times \boldsymbol{S}_{xx}$. An important feature of the Ishimori equation is that its solutions can be characterized by the topological invariant

$Q = (1/4\pi)\int\int \mathrm{d}x\,\mathrm{d}y\, \boldsymbol{S}\cdot(\boldsymbol{S}_x \times \boldsymbol{S}_y)$, which is conserved in time and takes integer values $N = 0, \pm 1, \pm 2, \ldots$.

The Ishimori equation for both signs of σ^2 possesses multisoliton solutions that describe elastic scattering of line solitons. The Ishimori-I equation ($\sigma^2 = 1$) has a rich variety of the dromion-like solutions. An interesting feature is that the Ishimori-II equation ($\sigma^2 = -1$) consists of the existence of the topologically nontrivial multi-vortex solutions. The one-vortex solution looks like

$$S_1 + \mathrm{i}S_2 = \frac{2\alpha\rho \mathrm{e}^{-\mathrm{i}\varphi}}{|\alpha|^2 + |\rho|^2}, \qquad S_3 = \frac{|\alpha|^2 - |\rho|^2}{|\alpha|^2 + |\rho|^2}, \quad (5)$$

where $\rho \mathrm{e}^{\mathrm{i}\varphi} = x + \mathrm{i}y - (x_0 + \mathrm{i}y_0)$, α is an arbitrary complex constant, and $Q = 1$. An anti-vortex solution with $Q = -1$ is also given by (5) under the substitution $x + \mathrm{i}y \to x - \mathrm{i}y$, that is, $\varphi \to -\varphi$. General N-vortex solution has $Q = N$ and describes the time dynamics of the spin-vortices and spin-anti-vortices of the form (5) which exhibits no phase shifts. These solutions are all regular and rational functions on x and y; in other words, they are lump solutions of the Ishimori-II equation.

Both the Davey–Stewartson and the Ishimori equations also possess infinite sets of exact solutions parameterized by finite number of arbitrary functions of one variable. As for the NLS equation and the Heisenberg ferromagnet equation, the DS equation and the Ishimori equation are related by the so-called gauge transformation.

Multidimensional nonlinear equations not solvable by the inverse scattering method do not possess multisoliton-like solutions. However, some of them, such as lumps, breathers, or spherical waves, have particular solutions which are similar to one soliton solution in some respects. Such solutions play roles in various nonlinear phenomena arising in classical and quantum field theories, in nonlinear theories of matter, and even in the theory of Jupiter's Great Red Spot.

BORIS B. KONOPELCHENKO

See also **Dressing method; Inverse scattering method or transform; Kadomtsev–Petviashvili equation**

Further Reading

Ablowitz, M.J. & Clarkson, P.A. 1991. *Solitons, Nonlinear Evolution Equations and Inverse Scattering*, Cambridge and New York: Cambridge University Press

Boiti, M. et al. 1995. Multidimensional localized solitons. *Chaos, Solitons and Fractals*, 12: 2377–2417

Coleman, S. 1977. Classical lumps and their quantum descendants. In *New Phenomena in Sub-Nuclear Physics*, edited by A. Zichichi, New York: Plenum Press

Konopelchenko, B. 1993. *Solitons in Multidimensions. Inverse Spectral Transform Method*, Singapore: World Scientific

Rajaraman, R. 1982. *Solitons and Instantons*, Amsterdam: North-Holland

MULTIFRACTAL ANALYSIS

A fractal is a geometrical shape that shows self-similarity, meaning that parts appear similar to the set as a whole (*See* **Fractals**). A multifractal is a fractal with a probability measure attributed to its geometrical support set. A typical multifractal can have different fractal dimensions in different parts of its support set, depending on the multifractal measure chosen. Typical examples of multifractals are attractors of nonlinear mappings, where the relevant probability measure is given by the invariant measure of the map. Often, quite a complicated structure is observed, and the invariant density may diverge at infinitely many points in the phase space with different exponents, that is, an entire spectrum of singularities is generated.

To statistically analyze this complex behavior, it is useful to evaluate the so-called Rényi dimensions D_q (Rényi, 1970). These are generalizations of the usual box dimensions (or capacity) that contain information not only on the topological structure of the fractal but on the probability measure as well. The simplest definition of the Rényi dimensions is as follows. Cover the fractal with small d-dimensional cubes ("boxes") of volume ε^d, where ε is the side length of the box and d is an integer dimension large enough to embed the fractal. For each such box i we consider the probability p_i that is associated with it:

$$p_i = \int_{i\text{th box}} \rho(\boldsymbol{x})\,\mathrm{d}\boldsymbol{x}. \quad (1)$$

Here $\rho(\boldsymbol{x})$ is the probability density considered. The Rényi dimensions are defined for any real parameter q as

$$D_q = \lim_{\varepsilon \to 0} \frac{1}{\log \varepsilon} \frac{1}{q-1} \log \sum_i p_i^q, \quad (2)$$

where the sum is over all i with $p_i \neq 0$. There are also more sophisticated definitions of the Rényi dimensions based on boxes of variable size (analogous to the definition of the Hausdorff dimension), see Beck & Schlögl (1993) for more details.

Generally, for a complicated multifractal (with lots of singularities of the probability density) the Rényi dimensions D_q depend on q, whereas for "simple" multifractals all D_q are the same and equal to the Hausdorff dimension. By changing the parameter q, one "scans" the structure of the multifractal. Large q values give more weight to large probabilities p_i, small q favor small probabilities p_i. Useful special cases of the Rényi dimensions are the box dimension (or capacity) D_0 (usually equal to the Hausdorff dimension, up to pathological cases), the information dimension D_1 (more precisely given by the limit $\lim_{q\to 1} D_q$), and the correlation dimension D_2. The correlation dimension can be easily extracted from experimental time series using the Grassberger–Procaccia algorithm (Grassberger & Procaccia, 1983). It is also of relevance

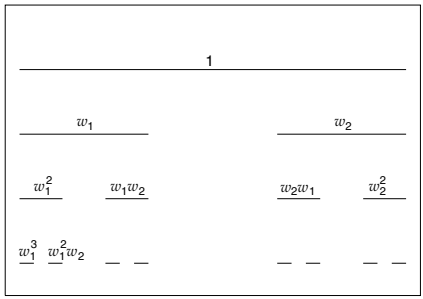

Figure 1. Construction of a classical Cantor set with a multiplicative non-uniform measure.

for the estimation of typical period lengths that are generated due to computer roundoff errors in chaotic dynamical systems (Beck, 1989). Also important are the limit dimensions $D_{\pm\infty}$ obtained for $q \to \pm\infty$. They describe the scaling behavior of the invariant density in the region of the phase space where the measure is most concentrated (D_∞) and least concentrated ($D_{-\infty}$).

From the Rényi dimensions, one can proceed to $f(\alpha)$, the spectrum of local scaling exponents α of the measure, by a Legendre transformation. The basic idea is very similar to thermodynamics. In fact, many of the ideas of the multifractal formalism are related to early work by Sinai, Ruelle, and Bowen on the so-called "thermodynamic formalism" of dynamical systems (Ruelle, 1978). For multifractals, one can regard the function $\tau(q) = (q-1)D_q$ as a kind of free energy, and q as a kind of inverse temperature (Tél, 1988; Beck & Schlögl, 1993). One then defines the variable α (the "internal energy") by $\partial\tau/\partial q =: \alpha$ and proceeds to the $f(\alpha)$ spectrum (the "entropy") by Legendre transformation:

$$f(\alpha) = q\alpha - \tau(q). \tag{3}$$

The advantage of the $f(\alpha)$ spectrum is that it has a kind of "physical meaning." Roughly speaking, it is the fractal dimension of the subset of points for which the probability density scales with a local exponent α, that is, $p_i \sim \varepsilon^{\alpha_i}$ with $\alpha_i \in [\alpha, \alpha + d\alpha]$. Hence, this is a kind of statistical mechanics of local Hölder indices.

Let us consider a simple example of a multifractal, given by the classical Cantor set with a multiplicative (non-uniform) measure (Figure 1). The classical Cantor set is constructed by cutting the middle third out of the unit interval, then cutting out the middle third out of the remaining two intervals, and so on (*See* **Fractals**). In this way, at the kth construction step there are 2^k intervals of length $(\frac{1}{3})^k$. We now attribute a product measure to each of the intervals, according to the rule sketched in Figure 1, with $w_1 + w_2 = 1$ but $w_1 \neq w_2$. In the limit $k \to \infty$ we obtain a multifractal.

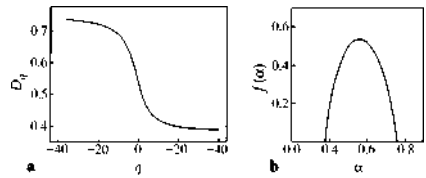

Figure 2. (a) Rényi dimensions and (b) $f(\alpha)$ spectrum of the Feigenbaum attractor.

Let us calculate the corresponding Rényi dimensions. We cover the multifractal with small intervals of size $\varepsilon_k = (\frac{1}{3})^k$. The number of boxes with probability $p_i = w_1^j w_2^{k-j}$ is

$$N_{k,j} = \begin{pmatrix} j \\ k \end{pmatrix} = \frac{j!}{k!(k-j)!}. \tag{4}$$

Hence,

$$\sum_i p_i^q = \sum_{j=0}^{k} N_{k,j} w_1^{jq} w_2^{(k-j)q} = (w_1^q + w_2^q)^k \tag{5}$$

and for the Rényi dimensions, one obtains from definition (2)

$$D_q = \frac{\log(w_1^q + w_2^q)}{(1-q)\log 3}. \tag{6}$$

In particular, the box dimension D_0 is given by the value $D_0 = \log 2/\log 3$, independent of w_1 and w_2. The other dimensions depend on the probabilities w_j, for example, for the information dimension one obtains $D_1 = -(1/\log 3)\sum_{j=1}^{2} w_j \log w_j$ by considering the limit $q \to 1$. The Legendre transform of (6) yields the $f(\alpha)$ spectrum.

Another interesting example is the attractor of the logistic map at the critical point of period doubling accumulation. Figure 2a shows the corresponding Rényi dimensions and Figure 2b the corresponding $f(\alpha)$ spectrum. Generally, the value of α where the function $f(\alpha)$ has its maximum is equal to the Hausdorff dimension of the attractor. The value of $f(\alpha)$ where the function has slope 1 is equal to the information dimension.

In practice, one often wants to evaluate the Rényi dimensions (or the $f(\alpha)$ spectrum) for a given time series (Kantz & Schreiber, 1997) of experimental data without explicitly knowing the underlying dynamics or the invariant measure. Here, various interesting methods are known (Grassberger–Procaccia algorithm (Grassberger & Procaccia, 1983), wavelet analysis (Arneodo et al., 1995), etc.). These algorithms can be implemented without explicitly knowing the underlying dynamics. The wavelet transform of an

experimental signal $s(x)$ is defined as

$$W_\Psi(x_0, a) = \frac{1}{a}\int_{-\infty}^{+\infty} \Psi^*\left(\frac{x - x_0}{a}\right) s(x)\,\mathrm{d}x, \quad (7)$$

($*$ indicates complex conjugate), where the analyzing wavelet Ψ is some localized function, often chosen to be the Nth derivative of a Gaussian function. For small a, the wavelet transform extracts local Hölder exponents from the signal s, and qth moments of W_Ψ can then be used to define suitable partition functions which yield the Rényi dimensions.

CHRISTIAN BECK

See also **Dimensions; Fractals; Free energy; Measures; Sinai–Ruelle–Bowen measures; Wavelets**

Further Reading

Arneodo, A., Bacry, E. & Muzy, J.F. 1995. The thermodynamics of fractals revisited with wavelets. *Physica* A, 213: 232–275

Beck, C. 1989. Scaling behavior of random maps. *Physics Letters* A, 136: 121–125

Beck, C. & Schlögl, F. 1993. *Thermodynamics of Chaotic Systems*, Cambridge and New York: Cambridge University Press

Grassberger, P. & Procaccia, I. 1983. Characterization of strange attractors. *Physical Review Letters*, 50: 346–349

Kantz, H. & Schreiber, T. 1997. *Nonlinear Time Series Analysis*, Cambridge and New York: Cambridge University Press

Rényi, A. 1970. *Probability Theory*, Amsterdam: North-Holland

Ruelle, D. 1978. *Thermodynamic Formalism*, Reading, MA: Addison-Wesley

Tél, T. 1988. Fractals, multifractals and thermodynamics – an introductory review. *Zeitschrift für Naturforschung* A, 43: 1154–1174

MULTIFRACTAL MEASURE

See **Dimensions**

MULTIPLE SCALE ANALYSIS

For a number of problems involving differential equations, we know methods that can provide exact solutions. However, the vast majority of modeling problems have a complexity that forbids finding an exact solution by paper and pencil. It may appear that the only way forward is to use numerical analysis. However, this is not necessarily the case since we can resort to finding good approximate solutions by various methods or strategies. In applications we usually encounter systems with dissipation and energy input, where neglecting these energy exchange terms leads to an exact solvable problem. We can then employ a strategy based on the assumption that the exact solution of the unperturbed problem is only modified slightly by adding the perturbation terms and hope that the difference between the two solutions can be estimated sufficiently accurately by assuming the perturbation is weak (Nayfeh, 1973, 1981, 2000).

Let us illustrate such a strategy by considering the damped harmonic oscillator. Denoting the displacement from equilibrium by $x(t)$ at time t, the dynamical equation reads

$$\ddot{x} + x = -\varepsilon\dot{x}. \quad (1)$$

A dot above the dependent variable $x(t)$ denotes differentiation with respect to time t. The damping parameter ε we shall vary, and accordingly it is natural to include ε in the argument list of $x = x(t; \varepsilon)$. The unperturbed oscillator corresponds to $\varepsilon = 0$, and using the initial conditions $x(0) = 1$ and $\dot{x}(0) = 0$, the solution of the unperturbed harmonic oscillator reads

$$x(t; 0) = x_0(t) = A\cos(t), \quad (2)$$

where the amplitude A equals unity. For the same initial conditions, the damped harmonic oscillator (1) with $\varepsilon \neq 0$ possesses the more complicated solution

$$x(t;\varepsilon) = \mathrm{e}^{-\varepsilon t/2}\left[\cos\left(t\sqrt{1-\varepsilon^2/4}\right) + \frac{\varepsilon/2}{\sqrt{1-\varepsilon^2/4}}\sin\left(t\sqrt{1-\varepsilon^2/4}\right)\right]. \quad (3)$$

The exact solution has features which can be used as a guide for developing a systematic way of finding an approximate solution assuming small damping, that is, $|\varepsilon| \ll 1$.

Without surprise, we recognize that the damping leads to a decreasing amplitude as time progresses but on a slow time scale of order $O(\varepsilon)$. Another result of the damping effect is an $O(\varepsilon^2)$ change of the frequency, which is $\omega = \sqrt{1-\varepsilon^2/4} \approx 1 - \varepsilon^2/8$. The damping slows down the oscillation, and accordingly the period increases, hence the frequency decreases. Suitable corrections are therefore to allow for a slow variation of the amplitude A and for an even smaller correction of the frequency. In general terms, this implies that we need to let $x(t; \varepsilon)$ depend on the slower time scales εt and $\varepsilon^2 t$. We can formalize this by introducing (Nayfeh, 1981)

$$T_0 = t\,, \quad T_1 = \varepsilon t\,, \quad T_2 = \varepsilon^2 t,$$
$$x(t) = x(T_0, T_1, T_2). \quad (4)$$

Thus, the time derivatives expand as

$$\frac{\mathrm{d}}{\mathrm{d}t} = \frac{\partial}{\partial T_0} + \varepsilon\frac{\partial}{\partial T_1} + \varepsilon^2\frac{\partial}{\partial T_2} + O(\varepsilon^3), \quad (5)$$

$$\frac{d^2}{dt^2} = \frac{\partial^2}{\partial T_0^2} + 2\varepsilon\frac{\partial^2}{\partial T_0 \partial T_1} + \varepsilon^2\left(\frac{\partial^2}{\partial T_1^2} + 2\frac{\partial^2}{\partial T_0 \partial T_2}\right) + O(\varepsilon^3), \quad (6)$$

by invoking the chain role for partial derivatives. The idea is to introduce slowly time-varying coefficients by regarding the new scaling variables in (4) as

independent variables. This is a somewhat mysterious trick, and it is not easy to understand why it works, since the scaling variables are all proportional to time, but it does. In perturbation theory, we often rely on such experience and tricks.

After having introduced the scaling into our original problem, we can add further corrections to the unperturbed solution by introducing a Taylor expansion around $\varepsilon = 0$ with respect to the perturbation parameter ε

$$x(\boldsymbol{T}; \varepsilon) = x_0(\boldsymbol{T}) + x_1(\boldsymbol{T})\varepsilon + x_2(\boldsymbol{T})\varepsilon^2 + O(\varepsilon^3), \quad (7)$$

where

$$\mathbf{T} = (T_0, T_1, T_2) \quad \text{and} \quad x_n(\mathbf{T}) = \frac{1}{n!}\frac{\partial^n x(\mathbf{T}; 0)}{\partial \varepsilon^n}.$$

Inserting the Taylor expansion into Equation (1) results in a polynomial in ε which equals zero. The coefficient of ε^n is a differential operator working on x_n, and as all these coefficients must vanish, we have a differential equation for each x_n, which normally is simple enough that it can be solved analytically, at least for the first few equations. Inserting the Taylor expansion into Equation (1) and ordering according to powers of ε we obtain

$$x_{0,T_0T_0} + x_0 = 0, \quad (8)$$

$$x_{1,T_0T_0} + x_1 = -x_{0,T_0} - 2x_{0,T_0T_1}, \quad (9)$$

$$x_{2,T_0T_0} + x_2 = -x_{1,T_0} - 2x_{1,T_0T_1} - x_{0,T_1} - x_{0,T_1T_1} - 2x_{0,T_0T_2}. \quad (10)$$

Subscript T_0 means a partial derivative with respect to T_0 and similarly for the analogous subscripts. The solution of the first equation reads

$$x_0 = A(T_1, T_2)\mathrm{e}^{\mathrm{i}T_0} + B(T_1, T_2)\mathrm{e}^{-\mathrm{i}T_0}. \quad (11)$$

The fact that A and B depend on T_1 and T_2 expresses the slow variation of these parameters with time. The solution of the equation for x_1 can now be found by inserting x_0 from (11) into the right-hand side of Equation (9),

$$x_{1,T_0T_0} + x_1 = -\mathrm{i}(A + 2A_{T_1})\mathrm{e}^{\mathrm{i}T_0} + \mathrm{i}(B + 2B_{T_1})\mathrm{e}^{-\mathrm{i}T_0}. \quad (12)$$

Terms proportional to the exponentials $\mathrm{e}^{\pm \mathrm{i}T_0}$ are resonant forcing terms, leading to a growth of x_1 proportional to time t. When t is of order $1/\varepsilon$, the term $\varepsilon x_1(t)$ has become of order unity, and our analysis breaks down. Such terms are called secular terms. In order to get a uniform and valid expansion, we need to avoid secular terms. However, due to the dependence on T_1 of A and B, we can demand that coefficients proportional to $\mathrm{e}^{\pm iT_0}$ vanish thereby providing simple differential equations for determining A

$$A + 2A_{T_1} = 0 \quad \Rightarrow \quad A(T_1, T_2) = A_1(T_2)\mathrm{e}^{-T_1/2}, \quad (13)$$

and similarly for B. Equation (12) now possesses the solution $x_1 = 0$. We can proceed by solving the $O(\varepsilon^2)$ equation (10) and invoke the initial conditions $x(0) = 1$ and $\dot{x}(0) = 0$. After rather straightforward calculations, we obtain the approximate solution (Scott, 2003)

$$x(t) = \mathrm{e}^{-\varepsilon t/2}\cos[(1 - \varepsilon^2/8)t] + \frac{\varepsilon}{2}\mathrm{e}^{-\varepsilon t/2} \times \sin[(1 - \varepsilon^2/8)t] + O(\varepsilon^3) \quad (14)$$

in agreement with the exact solution to the desired order in ε. Carrying out the analysis to order $O(\varepsilon^n)$ requires introduction of scaled variables up to the same order for the perturbation analysis to be consistent. The above approach is called the method of multiple scales, and it has been applied to many nonlinear ordinary differential equations as well as perturbed soliton equations (McLaughlin & Scott, 1978; Scott, 2003), including derivations of nonlinear partial differential equations (Dodd, 1984). An interesting extension of the method to nonlinear difference equations is presented in Broomhead & Rowlands (1983).

MADS PETER SØRENSEN

See also **Averaging methods; Damped-driven anharmonic oscillator; Fredholm theorem; Multi-soliton perturbation theory; Perturbation theory**

Further Reading

Broomhead, D.S. & Rowlands, G. 1983. On the analytic treatment of non-integrable difference equations. *Journal of Physics* A, 16: 9–24

Dodd, R.K., Eilbeck, J.C., Gibbon, J.D. & Morris, H.C. 1984. *Solitons and Nonlinear Wave Equations*, London: Academic Press

McLaughlin, D.W. & Scott, A.C. 1978. Perturbation analysis of fluxon dynamics. *Physical Review* A, 18: 1652–1680

Nayfeh, A.H. 1973. *Perturbation Methods*, New York: Wiley-Interscience

Nayfeh, A.H. 1981. *Introduction to Perturbation Techniques*, New York: Wiley-Interscience

Nayfeh, A.H. 2000. *Nonlinear Interactions: Analytical, Computational, and Experimental Methods*, New York: Wiley-Interscience

Scott, A.C. 2003. *Nonlinear Science: Emergence and Dynamics of Coherent Structures*, 2nd edition, Oxford and New York: Oxford University Press

MULTIPLEX NEURON

Under the view that dominated neuroscience around the middle of the 20th century, neural information processing involves three components (McCulloch & Pitts, 1943). First, incoming signals from chemical synapses on the dendritic trees are gathered as a linear, weighted sum of input signals. Second, this sum is compared with a threshold level at the base (initial segment) of the outgoing axonal tree. Finally, if the threshold level is exceeded, an active (all-or-nothing) nerve impulse is launched on the axonal tree, which propagates outward without failure to all of

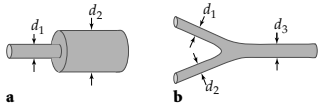

Figure 1. (a) Abrupt widening of a nerve fiber. (b) Branching region.

the distal (distant) twigs of the tree, providing inputs to other neurons or to muscle cells. A simplifying feature of this "McCulloch–Pitts model" is that the incoming dynamics are entirely linear, governed by inhomogeneous diffusion processes on the dendritic trees.

Before the end of the 1960s, there was no compelling evidence to abandon this simple view of dendritic dynamics, and two reasons for clinging to it. If all-or-nothing propagation is supposed to occur on dendrites, then the entire tree might be expected to ignite, preventing the dendrites from integrating incoming information. Additionally, the assumption of linear dendritic dynamics helps the theorist to sort out various causal influences, somewhat easing the difficulties of analyzing neural systems (Scott, 2002).

By the 1970s, three types of evidence began to indicate that dendritic and axonal dynamics are more complex. First, impulse blockage was experimentally observed in the optic nerves of cats, implying that impulses (spikes) can be extinguished at axonal branchings (Chung et al., 1970). Second, experimental studies showed that spikes do indeed propagate on the dendritic trees of some vertebrate neurons (Llinás & Nicholson, 1971). Third, numerical studies by Boris Khodorov and his colleagues in the Soviet Union on realistic models of nerve fibers confirmed that the propagation of active nerve impulses can indeed be blocked at changes in fiber geometry such as the abrupt widening and branching regions shown in Figure 1 (Khodorov, 1974).

These considerations suggested the concept of a "multiplex neuron," where the term (borrowed from communication engineering) implies the ability to handle two or more messages at the same time. As defined by Steven Waxman, a multiplex neuron has the following salient properties (Waxman, 1972).

- Impulse blockage at the branching regions of dendritic trees allows the possibility of Boolean logic, similar to the elementary operations of a digital computer. If the geometry of the branch is such that an impulse incoming on either daughter branch (one "or" the other) is able to ignite an outgoing impulse on the parent branch, this would be OR logic. If, on the other hand, coincident impulses on both incoming branches (one "and" the other) are required to ignite an outgoing impulse, it would be an example of AND logic. Thus the computational nature of a branching region may depend upon details of its geometry.
- Impulse blockage at branching regions of the axonal tree allows an impulse code transformation under which a time code on the trunk of the tree is transformed to space-time codes at the distal branches (twigs) of the tree.

Membrane model	Transmission	Blockage
H–H	5.5084	5.5126
M–L	2.2521	2.2563

Table 1. Widening ratios at which isolated impulses transmit and become blocked under Hodgkin–Huxley (H–H) and Morris–Lecar (M–L) membrane models (Altenberger et al., 2001).

Seminal Soviet studies of the propagation of impulses through the abrupt widening shown in Figure 1(a) showed that blockage of an isolated Hodgkin–Huxley impulse (Hodgkin & Huxley, 1952) (which corresponds to the dynamics of a squid giant axon) was to be expected at a widening ratio (d_2/d_1) greater than about 5.5. As indicated in Table 1, recent numerical studies by Altenberger et al. (2001) have confirmed the early Soviet results for the Hodgkin–Huxley model and extended them to the Morris–Lecar model (which represents dynamics on barnacle giant muscle fibers and more closely models the calcium dominated dynamics of typical dendritic fibers) (Morris & Lecar, 1981).

Although abrupt widenings of real nerve fibers are not observed, numerical blocking conditions in Figure 1(a) can be related to the corresponding blocking conditions in Figure 1(b) through the concept of a "geometric ratio" (GR) (Goldstein & Rall, 1974). Assuming a discontinuity with several outgoing fibers (of diameters d_{out}) and on which an impulse is incoming on a single fiber of diameter d_{in}, the GR is defined as $\sum d_{\text{out}}^{3/2}/d_{\text{in}}^{3/2}$, where the "3/2 powers" enter because branching currents divide in proportion to the characteristic admittance of the outgoing fibers (Scott, 2002).

Assuming the Morris–Lecar (M–L) model and an incoming impulse on daughter branch # 1 in the branch of Figure 1(b), the AND condition is

$$\frac{d_2^{3/2} + d_3^{3/2}}{d_1^{3/2}} > 2.2563^{3/2} = 3.389, \qquad (1)$$

requiring coincident inputs on both incoming branches (# 1 and # 2) for an impulse on the outgoing branch (# 3) to ignite. If this geometric inequality is not satisfied, the branch executes OR logic, in which incoming impulse either on daughter # 1 or on daughter # 2 is able to ignite an outgoing impulse on the parent branch (# 3).

Cell type	GR range
Purkinje	2.3–3.5
Stellate	2.4–3.5
Granule	2.3–4.8
Motoneuron	2.6–3.4
Pyramidal (apical)	2.5–3.4
Pyramidal (basal)	2.4–3.1

Table 2. The GR range for some typical dendrites (Scott, 2002).

Noting the GR values for typical dendritic trees given in Table 2 and considering the several ways in which critical GRs might be lowered in real neurons (changes in ionic concentrations, variations in channel membrane density, incomplete impulse recovery from previous interactions, and so on), it seems prudent to anticipate that dendritic trees can execute logical operations on the incoming (synaptic) codes, as is assumed in the multiplex neuron model (Stuart et al., 1999).

ALWYN SCOTT

See also **McCulloch–Pitts network; Nerve impulses; Neurons**

Further Reading

Altenberger, R., Lindsay, K.A., Ogden, J.M. & Rosenberg, J.R. 2001. The interaction between membrane kinetics and membrane geometry in the transmission of action potentials in non-uniform excitable fibres: a finite element approach. *Journal of Neuroscience Methods*, 112: 101–117

Chung, S.H., Raymond, S.A. & Lettvin, J.Y. 1970. Multiple meaning in single visual units. *Brain, Behavior and Evolution*, 3: 72–101

Goldstein, S.S. & Rall, W. 1974. Changes of action potential, shape and velocity for changing core conductor geometry. *Biophysical Journal*, 14: 731–757

Hodgkin, A.L. & Huxley, A.F. 1952. A quantitative description of membrane current and its application to conduction and excitation in nerve. *Journal of Physiology*, 117: 500–544

Khodorov, B.I. 1974. *The Problem of Excitability*, New York: Plenum

Llinás, R. & Nicholson, C. 1971. Electrophysiological properties of dendrites and somata in alligator Purkinje cells. *Journal of Neurophysiology*, 34: 532–551

McCulloch, W.S. & Pitts, W.H. 1943. A logical calculus of the ideas immanent in nervous activity. *Bulletin of Mathematical Biophysics*, 5: 115–133

Morris, C. & Lecar, H. 1981. Voltage oscillations in the barnacle giant muscle fibre. *Biophysical Journal*, 35: 198–213

Scott, A.C. 2002. *Neuroscience: A Mathematical Primer*, Berlin and New York: Springer

Stuart, G., Spruston, N. & Häusser, M. (editors). 1999. *Dendrites*, Oxford and New York: Oxford University Press

Waxman, S.G. 1972. Regional differentiation of the axon, a review with special reference to the concept of the multiplex neuron. *Brain Research*, 47: 269–288

MULTIPLICATIVE NOISE

See **Stochastic processes**

MULTIPLICATIVE PROCESSES

Random processes involving accumulation and/or reduction occur widely in nature and in mathematics. At the most basic level, the laws of accumulation (and reduction) may be represented either as the result of arithmetic summation (and differencing) or as the result of multiplications. The latter such processes are the subject of this article.

Any attempt to embody all multiplicative random processes in a single mathematical definition would be futile. However, it is possible to provide large classes of examples for which rich mathematical theories and applications are possible.

The "law of proportionate effect" provides the basis for the evolution of multiplicative stochastic processes $M_0, M_1, \ldots,$ found, for example, in materials science, biology, economics, and finance, in terms of the proportionate changes $r_{n+1} = \Delta M_n / M_n \equiv (M_{n+1} - M_n)/M_n, n = 0, 1, 2, \ldots.$ In finance, M_n may be the value of a unit of stock at the nth period of time when subjected to the hypothesis that the yields $r_1, r_2, \ldots$ are stationary and independent from time period to period. In materials science, on the other hand, M_n may represent the strength of a material after n repeated independent random impacts $R_1 = 1 + r_1, R_2 = 1 + r_2, \ldots.$ Similarly, M_n may represent the size of a biological population whose subsequent growth is in (random) proportions $r_1, r_2, \ldots$ to the amount of substance available. The law of proportionate effect is a widely observed statistical law according to which the sequence of proportionate changes $r_{n+1} = \Delta M_n / M_n, n = 0, 1, 2, \ldots,$ is a sequence of independent and identically distributed (iid) random variables. Equivalently, one may iterate this law to obtain the so-called geometric random walk model:

$$M_n = M_0 \prod_{k=1}^{n} R_k, \quad k = 1, 2, \ldots, \tag{1}$$

where

$$R_k = 1 + r_k, \quad k = 1, 2, \ldots. \tag{2}$$

The special case in which R_n has two possible values, corresponding to upward and downward price movements, yields the binomial tree model for stock prices popular in the modern mathematical finance literature (Föllmer & Schied, 2002).

A more general notion of "multiplicative processes", whose origins may be traced back to early 19th century genetics, occurs by consideration of a somewhat finer scale growth rule. In particular, changes to the process occur as M_{n+1} evolves from a previous random number

M_n of constituent members, each of which individually contributes its own growth and decay amounts (Y) to the whole in successive time steps. This more general stochastic law of evolution may be precisely expressed by the following iteration scheme: If $M_n = 0$ then define $M_{n+1} = 0$, else if $M_n > 0$ define

$$M_{n+1} = \sum_{k=1}^{M_n} Y_{n+1,k} \quad n = 0, 1, \ldots, \tag{3}$$

where M_0 is a nonnegative integer valued (counting) random variable representing an initial size, and for each $n \geq 0$, the random variables $Y_{n+1,1}, Y_{n+1,2}, \ldots Y_{n+1,M_n}$ are nonnegative integer valued, representing the respective numbers of offspring of each of the M_n elements composing the nth generation.

Two special cases may be noted. In the case that the $Y_{n+1,k} \equiv R_{n+1}$, $k \geq 1$, are the same for each k of the nth generation, but are independent and identically distributed (iid) from generation to generation n, Equation (3) is the law of proportionate effect. On the other hand, if for each n, the offspring sizes $Y_{n+1,1}, Y_{n+2,2}, \ldots$ are iid and independent of M_n, then Equation (3) defines the classical Bieneymé–Galton–Watson branching process (BGW) introduced in the early 19th century as a model for analyzing the survival of family names (Kendall, 1975).

A next generation of multiplicative processes arises out of these models by a still finer coding of the underlying phenomena. For simplicity, consider the BGW branching process and assume a single progenitor $M_0 = 1$. Then one may code the successive offspring as a random tree as follows: The single progenitor is coded by the empty sequence $\emptyset$. Its respective $Y_{1,1}$ offspring are coded (labeled) as $\langle 1 \rangle, \ldots, \langle Y_{1,1} \rangle$. The $Y_{2,k}$ next generation offspring of $\langle k \rangle$ can be coded as $\langle k1 \rangle, \langle k2 \rangle, \ldots, \langle kY_{2,k} \rangle$, and so on. In this way, the successive generations may be represented as a sequence of random family trees

$$\begin{aligned} \tau_0 = \{\emptyset\},\ \tau_1 &= \{\emptyset, \langle 1\rangle, \ldots, \langle Y_{1,1}\rangle\} \\ &\equiv \tau_0 \cup \{\langle 1\rangle, \ldots, \langle Y_{1,1}\rangle\}, \\ \tau_2 &= \tau_1 \cup \{\langle 11\rangle, \ldots, \langle 1Y_{2,1}\rangle, \ldots, \\ &\quad \langle Y_{1,1}1\rangle, \ldots, \langle Y_{1,1}Y_{2,Y_{1,1}}\rangle\}, \ldots. \end{aligned}$$

This, in fact, suggests an alternative description of the BGW process as a probability distribution P on a (metric) space of tree graphs. Specifically, let $\boldsymbol{T}$ be the space of (possibly infinite) labeled tree graphs rooted at $\emptyset$. As above, an element τ of $\boldsymbol{T}$ may be coded as a set of finite sequences of positive integers $\langle i_1, i_2, \ldots, i_n \rangle \in \tau$ such that:

(i) The root $\emptyset \in \tau$ is coded as the empty sequence.
(ii) If $\langle i_1, \ldots, i_k \rangle \in \tau$ then $\langle i_1, \ldots i_j \rangle \in \tau$ $\forall\ 1 \leq j \leq k$.
(iii) If $\langle i_1, i_2, \ldots, i_n \langle \in \tau$ then $\rangle i_1, \ldots i_{n-1}, j \rangle \in \tau$ $\forall\ 1 \leq j \leq i_n$.

Neighboring vertices are those of the form $\langle i_1, \ldots, i_n \rangle$ and $\langle i_1, \ldots, i_{n-1} \rangle$. The last condition (iii) specifies a left to right labeling of vertices, and (ii) connects all paths to the root via neighboring vertices without cycles. The space $\boldsymbol{T}$ of such trees may be viewed as a metric space with metric defined by $\rho(\tau, \gamma) = (\sup\{n+1 : \gamma|n = \tau|n\})^{-1}$, and $\tau|n = \{\langle i_1, \ldots, i_k \rangle \in \tau : k \leq n\}$ is the truncation of τ to the first n generations. This metric is complete and the countable dense subset $\boldsymbol{T}_0$ of finite labeled tree graphs rooted at $\emptyset$ makes $\boldsymbol{T}$ a separable metric space as well.

The BGW model may now be viewed as a probability distribution on the space $\boldsymbol{T}$, wherein the probability assigned to the ball B of radius $1/N$ centered at τ is given by

$$P(B) = \prod_{v \in \tau|N} p(\omega(\tau; v)), \tag{4}$$

where $p(j) = P(Y = j)$, $j = 0, 1, 2, \ldots$ is a prescribed offspring probability distribution, and $\omega(\tau; v) = \max\{j : \langle v1 \rangle, \ldots, \langle vj \rangle \in \tau\}$ counts the number of offspring of the vertex v in the tree τ.

A number of naturally occurring geophysical and biological structures admit natural tree codings, for example, river networks, lightning discharge patterns, and arterial and neural networks in human organs. Probabilistic models correspond to probability distributions on $\boldsymbol{T}$, leading to further generalizations of multiplicatively branching models; for example, see Barndorff-Nielsen et al. (1998) and references therein.

Random multiplicative cascade models provide another class of multiplicative processes of interest for their intermittency, extreme variability, and multiscaling structure in applications to phenomena ranging from fluid turbulence and spatial oceanic rainfall distributions to internet packet data on the world wide web (Barndorff-Nielsen et al., 1998; Gilbert et al., 1999; Jouault et al., 2000). The origins of this class of models trace back to classic work of Lewis Fry Richardson (1926), Andrei N. Kolmogorov (1962), and A.M. Yaglom (1966) in statistical turbulence theory. A rich geometrical and scaling perspective was subsequently advanced by Benoit Mandelbrot, and a more complete mathematical treatment was initiated by J.-P. Kahane and Jacques Peyrière (Kahane, 1985).

In the context of turbulence, one imagines introducing energy into the fluid by a large-scale stirring motion, whereby smaller-scale eddies split off and dissipate energy in random proportions R to those available. These eddies in turn split off smaller-scale eddies, and so on. In the simplest mathematical formulation, one considers random measures $M_n(\Delta)$ on the one-dimensional unit interval $[0, 1]$ having a piecewise constant density

$\rho_n(x)$ defined by a constant value over a dyadic subinterval

$$\Delta_n(j_1, \ldots, j_n) = \left[\sum_{k=1}^{n} j_k 2^{-k}, \sum_{k=1}^{n} j_k 2^{-k} + 2^{-n}\right], \quad j_k \in \{0, 1\},\ k \geq 1 \tag{5}$$

with constant value

$$\rho_n(x) = \prod_{k=1}^{n} R_{\langle j_1 j_2 \ldots j_k \rangle},\ \forall x \in \Delta_n(j_1, j_2, \ldots, j_k), \tag{6}$$

where the random factors R_v, $v = \langle\, j_1 j_2 \ldots j_k \,\rangle$, are iid nonnegative mean one random variables indexed by the vertices of the binary tree. The mean one condition provides conservation of the mass of M_n on average, where for any Borel subset G

$$M_n(G) = \int_G \rho_n(x)\, \mathrm{d}x. \tag{7}$$

The multiplicative cascade M_∞ is the random measure obtained by passing to the fine scale limit as $n \to \infty$.

The random cascade is defined by the branching number b $(=2$ in this exposition), and the random factors R_v, referred to as cascade generators. Kolmogorov's "log-normal hypothesis" refers to a choice of lognormal distribution for R. Tests of this hypothesis and physical arguments for alternative laws present significant challenges for modern statistical turbulence theory (e.g., She & Waymire, 1995; Jouault et al., 2000). On the mathematical side, the special choice of symmetrically distributed 0–2 valued generators yields the BGW process with binomial offspring distribution $p(j) = \binom{2}{j}\frac{1}{4}$, $j = 0, 1, 2$, for the total masses $M_n([0, 1])$, $n = 1, 2, \ldots$. Refinements for which the branching number b may be viewed as a random parameter are given in Burd & Waymire (2000), and as a continuous parameter in Barral & Mandelbrot (2002).

Branching random walk models of the type illustrated by this next application may also be viewed within the framework of random multiplicative cascades. An explicit representation of the Fourier transform of classes of solutions to 3-d incompressible Navier–Stokes equations

$$\frac{\partial u}{\partial t} + u \cdot \nabla u = \nu \Delta u - \nabla p + g, \quad \nabla \cdot u = 0, \tag{8}$$

in the form of an expected value of a certain product of initial and forcing data evaluated at the nodes of a branching random walk was recently uncovered (LeJan & Sznitman, 1997). While probability models have long enjoyed important connections to partial differential equations, most notable being the heat equation and reaction-diffusion equations, this ranks among the most striking recent connections between multiplicative cascades and nonlinear equations of fluid

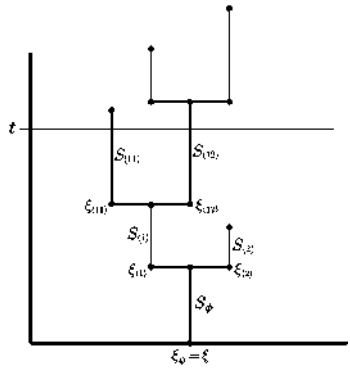

Figure 1. A sample tree graph for the Burgers equation.

motion. For a simple illustration of ideas made possible by refinements of the theory developed in Bhattacharya et al. (2003), consider the one-dimensional Burgers equation

$$u_t + uu_x = \nu u_{xx}, \quad u(0, x) = u_0(x). \tag{9}$$

Spatial Fourier transform will be denoted by $\hat{u}$. For simplicity of exposition, assume $\hat{u}_0(\xi) = 0$ for $\xi \leq 0$; that is, the initial data belongs to a Hardy function space. Taking spatial Fourier transforms one obtains, with the aid of an exponential integrating factor and $\xi > 0$ and writing

$$\lambda(\xi) = \nu\xi^2, \qquad m = -\frac{\mathrm{i}}{\nu}, \tag{10}$$

the result

$$\hat{u}(t, \xi) = \mathrm{e}^{-\lambda(\xi)t}\hat{u}_0(\xi) + \frac{m}{2}\int_0^t \lambda(\xi)\mathrm{e}^{-\lambda(\xi)s}\frac{1}{\xi} \times \int_0^\xi \hat{u}(t-s, \eta)\hat{u}(t-s, \xi-\eta)\, \mathrm{d}\eta. \tag{11}$$

Expressed in this form, Equation (11) takes on a probabilistic meaning. In particular, this is a recursive equation for the expected values of a multiplicative stochastic process initiated at $\xi_\emptyset = \xi$. The first term on the right-hand side $\mathrm{e}^{-\lambda(\xi)t}\hat{u}_0(\xi)$ is the product of the initial data $\hat{u}_0(\xi)$ times the probability $\mathrm{e}^{-\lambda(\xi)t}$ that an "exponentially distributed clock" with parameter $\lambda(\xi)$ rings after time t. The second integral term is an expected value in the complementary event of probability density $\lambda(\xi)\mathrm{e}^{-\lambda(\xi)s}$, that the clock rings at time s prior to t. Given that the clock rings at a time s prior to t, a product is formed with the factor $m(\xi)$ and a random selection of a pair of new "offspring" wave numbers (or Fourier frequencies) $\eta, \xi - \eta$ from the interval $[0, \xi]$ with (uniform) probability density $1/\xi$ to complete the recursion over the remaining time $t - s$. That is to say, the unique solution (in the appropriate

function space) is furnished by the expected value

$$\hat{u}(t,\xi) = EX(t,\xi), \quad \xi > 0, \tag{12}$$

for a multiplicative cascade $X(t,\xi)$ defined by the following stochastic recursion in Fourier wave number space (see Figure 1): A particle of type $\xi_\emptyset = \xi$ waits for an exponentially distributed time $S_\emptyset$ with mean $1/\lambda(\xi) = \frac{1}{\nu\xi^2}$. If $S_\emptyset > t$ then a value $\hat{u}_0(\xi)$ is assigned to the initial vertex $\emptyset$ and the process terminates. On the other hand, if $S_\emptyset \le t$ then an independent coin flip is made. If the outcome is a tail then the particle dies and a value 0 is assigned, but if a head occurs then the particle branches into two particles $\langle 1 \rangle$, $\langle 2 \rangle$ of respective types $\xi_{\langle 1 \rangle} = \eta$ and $\xi_{\langle 2 \rangle} = \xi - \eta$ selected according to the uniform distribution on $[0, \xi]$. Two independent exponential clocks $S_{\langle 1 \rangle}, S_{\langle 2 \rangle}$, with respective parameters $\lambda(\xi_{\langle 1 \rangle}), \lambda(\xi_{\langle 2 \rangle})$, are set, and the process is repeated independently from each of these two given types for the termination time t reduced to $t - S_\emptyset$. The multiplicative cascade $X(t,\xi)$ is, up to a (random) power of $m \equiv -\sqrt{-1/\nu}$, a product of the assigned values of $\hat{u}_0$ at the selected frequencies; for example, for the sample realization depicted in Figure 1, one has

$$X(t,\xi) = m^2 \cdot \hat{u}_0(\xi_{\langle 11 \rangle}) \cdot \hat{u}_0(\xi_{\langle 12 \rangle}) \cdot \hat{u}_0(\xi_{\langle 2 \rangle}) \cdot 0. \tag{13}$$

In particular, the premature death of $\langle 2 \rangle$ means that this particular sample realization will not contribute a positive value to the mathematical expectation in (12).

By presenting these models as a progression of modifications and extensions built on simpler structures, some sense of a mathematical theory begins to emerge, a large part of which directly rests on martingale theory. For example, for the BGW model one may observe, denoting the mean offspring number by μ, assumed positive and finite, that $M_n/\mu^n, n = 1, 2, \ldots,$ is a martingale. Similarly, for each fixed Borel set G, the cascade measure $M_n(G)$, as a function of (logarithmic) scale $n = 1, 2, \ldots,$ is a martingale. The latter property led Kahane to still further natural generalizations of widespread significance (Kahane, 1985). Such deep mathematical structure has made it possible to precisely analyze many of the singularities, intermittencies, and other critical phenomena associated with these models, as well as to provide precise statistical error bars required for scientifically sound empirical estimations and tests of hypothesis for multiplicative cascades. On the other hand, the overall theory is in its relative infancy and many questions of practical importance remain open (Ossiander & Waymire, 2000). Needless to say, the relationship with the incompressible Navier–Stokes equations provides a link to one of the most outstanding mathematical problems of our times.

EDWARD C. WAYMIRE

See also **Branching laws; Burgers equation; Martingales; Navier–Stokes equation**

Further Reading

Athreya, K. & Jagers, P. (editors). 1997. *Classical and Modern Branching Processes*, New York: Springer

Barndorff-Nielsen, O.E., Gupta, V.K., Perez-Abreu, V. & Waymire, E. (editors). 1998. *Stochastic Methods in Hydrology: Rain, Landforms and Floods*, Singapore: World Scientific

Barral, J. & Mandelbrot, B.B. 2002. Multifractal products of cylindrical pulses. *Probability Theory and Related Fields*, 124(3): 409–430

Bhattacharya, R., Chen, L., Dobson, S., Guenther, R., Orum, C., Ossiander, M., Thomann, E. & Waymire, E. 2003. Majorizing kernels & stochastic cascades with applications to incompressible Navier–Stokes equations. *Transactions of the American Mathematical Society*, 355: 5003–5040

Bramson, M. 1978. Maximal displacement of branching Brownian motion. *Communications in Pure and Applied Mathematics*, 31: 531–582

Burd, G. & Waymire, E. 2000. Self-similar invariance of critical binary Galton–Watson trees. *Proceedings of the American Mathematical Society*, 128: 2753–2761

Chen, L., Dobson, S., Guenther, R., Ossiander, M., Thomann, E. & Waymire, E. 2002. On Ito's complex measure condition, In *Probability, Statistics and Their Applications: Papers in Honor of Rabi Bhattacharya*, edited by K. Athreya, M. Majumdar, M. Puri & E. Waymire, Beachwood, OH: Institute of Mathematical Statistics

Föllmer, H. & Schied, A. 2002. *Stochastic Finance*, New York: Walter de Gruyter

Gilbert, A.C., Willinger, W. & Feldman, A. 1999. Scaling analysis of conservative cascades with applications to network traffic. *Institute of Electrical and Electronics Engineers Transactions on Information Theory*, 45: 971–991

Holley, R. & Waymire, E. 1992. Multifractal dimensions and scaling exponents for strongly bounded random cascades. *Annals of Applied Probability*, 2(4), 819–845

Jouault, B., Greiner, M. & Lipa, P. 2000. Fix-point multiplier distributions in discrete turbulent cascade models. *Physica* D, 136: 196–255

Kahane, J.P. 1985. Sur le chaos multiplicatif. *Annales des Sciences Mathématiques du Québec*, 9: 105–150

Kahane, J.P. & Peyrière, J. 1976. Sur certaines martingales de B. Mandelbrot. *Advances in Mathematics*, 22: 131–145

Kendall, D. 1975. Branching processes since 1873, the genealogy of genealogy: branching processes before (and after) 1873. *Bulletin of the London Mathematics Society*, 7: 385–406, 225–253

Kolmogorov, A.N. 1962. A refinement of previous hypothesis concerning the local structure of turbulence in a viscous incompressible fluid at high Reynold number. *Journal of Fluid Mechanics*, 13: 82–85

LeJan, Y. & Sznitman, A.S. 1997. Stochastic cascades and 3-dimensional Navier–Stokes equations. *Probability Theory and Related Fields*, 109: 343–366

Mandelbrot, B.B. 1974. Intermittent turbulence in self-similar cascades: divergence of high moments and dimension of the carrier. *Journal of Fluid Mechanics*, 62: 331–333

McKean, H.P. 1975. Applications of Brownian motion to the equation of Kolmogorov, Petrovskii, and Piskunov. *Communications in Pure and Applied Mathematics*, 28: 323–331

Ossiander, M. & Waymire, E. 2000. Statistical estimation theory for multiplicative cascades. *Annals of Statistics*, 28(6): 1–21

Ossiander, M. & Waymire, E. 2002. On estimation theory for multiplicative cascades. *Sankhyā: The Indian Journal of Statistics Series* A, 64(2): 323–343

Resnick, S., Samorodnitsky, G., Gilbert, A. & Willinger, G. 2003. Wavelet analysis of conservative cascades. *Bernoulli*, 9(1): 97–135

Richardson, L.F. 1926. Atmospheric diffusion shown on a distance-neighbour graph. *Proceedings of the Royal Society of London*, A110, 709–737

She, Z.S. & Waymire, E. 1995. Quantized energy cascade and logPoisson statistics in fully developed turbulence. *Physical Review Lettters*, 74(2): 262–265

Waymire, E. & Williams, S.C. 1996. A cascade decomposition theory with applications to Markov and exchangeable cascades. *Transactions of the American Mathematical Society* 348(2): 585–632

Yaglom, A.M. 1966. Effect of fluctuations in energy dissipation rate on the form of turbulence characteristics in the inertial subrange. *Dokladay Akademii Nauk SSSR*, 166: 49–52

MULTISOLITON PERTURBATION THEORY

Solitons appear as robust solutions of several important nonlinear partial differential equations and difference-differential equations, including the Korteweg–de Vries (KdV), nonlinear Schrödinger (NLS), and sine-Gordon (SG) equations and the Toda lattice (TL). It is a remarkable feature of these and other equations, integrable by means of the inverse scattering transform (IST), that one can find exact multisoliton solutions. Among other phenomena, multisoliton solutions describe collisions among several solitons and bound states of solitons (breathers).

Considering systems that conserve energy but lack integrability, multisoliton solutions, and breathers may be only approximate, their dynamics accompanied by emission of radiation. As a result, two colliding solitons may merge into a breather, and the energy of a breather gradually decreases until it completely decays.

The situation is yet more different from that in integrable models if the system is dissipative. The dissipative loss of energy may be offset by an external field (driving force). A well-known example is the damped-driven SG equation

$$\phi_{tt} - \phi_{xx} + \sin\phi = -\alpha\phi_t - \gamma, \tag{1}$$

which models magnetic flux propagation on a long Josephson junction (LJJ) (McLaughlin & Scott, 1978). In this equation, $\partial\phi/\partial x$ is the local magnetic field, α is a coefficient of dissipation, and γ is a bias-current density, which is the driving force. In the absence of perturbations ($\alpha = \gamma = 0$), (1) is the SG equation, whose fundamental soliton solution is the kink (it represents a magnetic-flux quantum, or fluxon, in LJJ),

$$\phi_{\rm k} = 4\tan^{-1}\left[\exp\left(\sigma\frac{x-\xi(t)}{\sqrt{1-c^2}}\right)\right]. \tag{2}$$

Here, $\sigma = \pm 1$, c, and $\xi(t)$ are, respectively, the polarity, velocity, and central coordinate of the kink (or fluxon). An exact breather solution to the unperturbed SG equation is

$$\phi_{\rm br} = 4\tan^{-1}\left[\frac{\sin(t\cos\mu)}{\cosh(x\sin\mu)}\tan\mu\right], \tag{3}$$

where the amplitude μ takes values $0 < \mu < \pi/2$. In the limiting case $\mu \to \pi/2$, (3) becomes a solution describing collision between two kinks with opposite polarities.

In the presence of perturbations, Equation (1) still has kink-like solutions, but the kink's steady-state velocity (c_0) is no longer arbitrary. It is determined by the condition that the power input from a constant driving force (γ) is in balance with the dissipation induced by the loss term, which yields

$$c_0 = \frac{\sigma\pi\gamma}{\sqrt{(\pi\gamma)^2 + 16\alpha^2}}. \tag{4}$$

According to Equation (4), kinks with opposite polarities move in opposite directions; hence, they may collide.

If an ac driving force is applied to the system [e.g., $\gamma = \gamma_0\cos(\omega t)$ in (1)], it may compensate the loss and support the breather whose frequency $\cos\mu$ is in resonance with the driving frequency ω. If γ in (1) is a random function of time, and α is small enough, the random force can split the breather into a free kink-antikink ($\rm k\bar{k}$) pair.

In the general case, basic effects produced by perturbations acting on two- or multi-soliton configurations may be classified as follows. Interaction between two solitons in the presence of conservative perturbations gives rise to emission of radiation, which appears at order ε^2, where ε is the strength of the perturbation. Adiabatic effects (those that neglect radiation) may be generated by conservative perturbations in a *three-soliton* system at order ε, in the form of energy exchange between colliding solitons (this may also occur in a two-soliton system if the conservative perturbation is not spatially uniform—for instance, if it is created by a local defect). In the case of dissipative perturbations, nontrivial effects are possible at order ε for two solitons, typical examples being fusion of a $\rm k\bar{k}$ pair into a breather or, inversely, breakup of a breather into a pair due to its collision with another kink.

If the model is a perturbed version of an integrable one, multi-soliton processes similar to those outlined above can be investigated by means of perturbation theory (PT), a powerful version of which is based on a perturbed variant of IST (Kaup & Newell, 1978). As in the integrable case, the initial configuration is mapped into scattering data of the corresponding scattering problem, but the time evolution of the scattering data is no longer trivial, discrete eigenvalues being no more

time-independent. Using a perturbative expansion, it is possible to derive ordinary differential equations (ODEs) for slow variations of the scattering data, which can be solved to obtain approximate solutions of the perturbed system. A comprehensive review of the IST-based PT for solitons in nearly integrable models was given by Kivshar & Malomed (1989).

An alternative multi-soliton PT is based on using a Green function (GF) for the underlying equation linearized around the unperturbed multi-soliton solution (Keener & McLaughlin, 1977). If the zero-order approximation is integrable, this method is equivalent to the IST-based PT, as the GF can be constructed—by means of IST—around any exact multi-solution solution. Although this approach has the advantage of being directly formulated in terms of physical parameters (soliton speeds, collision delays, breather frequencies, etc.), rather than more abstract IST characteristics (bound-state eigenvalues and reflection coefficients), finding the GF can be computationally demanding. Methods based on the Bäcklund transformation may ease some of these difficulties (McLaughlin & Scott, 1978).

The GF method often works for one-soliton problems in non-integrable models, as a full set of eigenmodes can often be found for an equation linearized about a soliton even if the equation is not integrable. An example is the nonlinear Klein–Gordon equation

$$\phi_{tt} - \phi_{xx} - \phi + \phi^3 = 0, \tag{5}$$

which describes ferroelectric phase transitions, among other applications. A comprehensive account of the GF method for kinks in non-integrable Klein–Gordon equations was given by Flesch & Trullinger (1987).

Another version of PT is based on the variational approximation (VA), which only demands that the full perturbed equation be derivable from a Lagrangian (e.g., the system is conservative), and that a one-soliton solution be available in the absence of perturbations. The method applies to the description of multisoliton effects in the adiabatic approximation, representing the wave field as a linear superposition of unperturbed solitons. Inserting this approximation into the model's Lagrangian and integrating over the spatial coordinate, one arrives at an effective Lagrangian, which is a function of the solitons' parameters (amplitude, velocity, and central coordinate and phase) and their first derivatives in time. Application of the Euler–Lagrange variational procedure to the effective Lagrangian then generates a system of ODEs that govern the evolution of the solitons' parameters. Because the linear-superposition assumption underlying VA is not valid in the general case (when solitons strongly overlap in the course of the interaction), a VA is restricted to cases when the solitons interact staying far apart or when they collide with a large relative velocity.

An early review of results obtained for multisoliton interactions by means of a VA was given by Gorshkov and Ostrovsky (1981), and an up-to-date review, including the interaction problems, was given by Malomed (2002). There is also an intermediate version of PT, which is based on IST for one soliton, but treats the interaction between solitons, even in an integrable equation, as a perturbation, assuming that the solitons are far separated. By means of this technique, Karpman and Solov'ev (1981) analyzed the interaction between solitons in the NLS and SG equations. Their results for NLS solitons were later checked in a direct experiment with solitons in a nonlinear optical fiber.

The approach based on the linear-superposition approximation for widely separated solitons makes it possible to calculate an effective potential of the interaction between solitons. To this end, one should isolate a part of the model's potential energy which depends on the separation between the solitons. For instance, the potential energy corresponding to the unperturbed SG equation (1) is

$$\Pi = \int_{-\infty}^{+\infty} \left[\tfrac{1}{2}\phi_x^2 + (1 - \cos\phi) \right] \mathrm{d}x \,. \tag{6}$$

In the vicinity of the first kink, the field is approximated as $\phi_1(x-\xi_1) + \delta\phi_2\,(x-\xi_2)$, where $\delta\phi_2$ is a small tail of the second kink (both are taken with $c=0$). Thus, in the lowest approximation, the contribution to the interaction potential from the vicinity of the first kink [which is, say, $-\infty < x < \Xi \equiv (1/2)\,(\xi_1+\xi_2)$] is

$$\begin{aligned} U_1 &= \int_{-\infty}^{\Xi} \left[(\phi_1)_x\,(\delta\phi_2)_x + (\sin\phi_1)\,\delta\phi_2 \right] \mathrm{d}x \\ &\equiv \int_{-\infty}^{\Xi} \left[-(\phi_1)_{xx} + \sin\phi_1 \right] \delta\phi_2 \,\mathrm{d}x + (\phi_1)_x\,\delta\phi_2 \big|_{-\infty}^{\Xi}, \end{aligned} \tag{7}$$

using integration by parts. A key observation, which holds in much more general situations, is that the integral term in (7) identically vanishes, as $\phi_1(x)$ is an exact stationary solution of the SG equation; hence, all the contribution comes solely from the last term in (7). This yields the interaction potential, $U = U_1 + U_2 = 32\sigma_1\sigma_2 \exp(-|\xi_1 - \xi_2|)$. Noting that each kink is a quasi-particle with mass $m=8$, this potential provides for full dynamical description of two- or multi-kink systems.

The derivation of the interaction potential based on the same principles applies to several other cases, including two- and three-dimensional solitons (Malomed, 1998). In the case of NLS solitons, the interacting pair is characterized by distance and relative phase between them, a peculiarity being that an effective mass corresponding to the phase difference is *negative*, which strongly affects stability of two-soliton

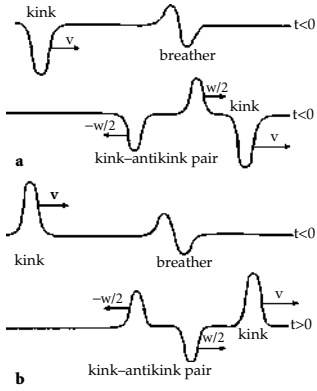

Figure 1. The breather's breakup into a kink-antikink pair as a result of the collision with another fast kink; shown is the field $\partial\phi/\partial x$. Panels (a) and (b) pertain to the polarities $\sigma = -1$ and $+1$ of the fast kink.

bound states induced by perturbations (Malomed, 2002).

The simplest nontrivial example of the two-soliton interaction is fusion of a $k\bar{k}$ pair as a result of collision. An analysis of this problem is outlined here for the case of small γ and α in (1). Because the collision-induced energy loss responsible for fusion is proportional to the dissipation (α) and can be found to be $\Delta E = 8\pi^2\alpha$, fusion occurs if the steady-state velocity given by (4) is small enough. This means that $|\gamma| \ll \alpha$ whereupon Equation (4) yields $c_0 \approx \sigma\pi\gamma\,/\,(4\alpha)$, the corresponding net kinetic energy of the pair being $E_{\rm kin} = 8c_0^2$. The collision results in pair annihilation if $E_{\rm kin} < \Delta E$, or $\gamma < \gamma_{\rm cr} \equiv 4\alpha^{3/2}$.

As shown in Figure 1, the collision of a breather with a moving kink may produce another interesting result in the same model: the breather may be split into a $k\bar{k}$ pair. The final result takes a simple form if the kink is ultrarelavitic, that is, c_0 is close to the limiting value 1: the breakup of the breather (3) into a $k\bar{k}$ pair is possible if $(\pi/2) - \mu < 2.91\sqrt{\alpha}$.

Some special types of conservative perturbations may greatly alter the dynamics. For instance, if the perturbation in the SG equation is $\varepsilon \sin(\phi/2)$ (double SG equation), free 2π-kinks do not exist; instead, their pairs form bound states (4π-kinks), $\phi_{4\pi} = 4\tan^{-1}\left(\sqrt{|\varepsilon|\,/\,2}\sinh x\right)$. It is possible to excite vibrations of this bound state, the eigenfrequency of which is $\sqrt{|\varepsilon|}$, as predicted by PT.

A typical example of two-soliton interactions generating radiation loss is the collision of two kinks (which may have both opposite and equal polarities) with a relative velocity c, the perturbing term in the SG equation being $\varepsilon \sin(2\phi)$. In the ultra-relativistic case, it can be shown directly that the radiation loss appears at order ε^2 and is the same for the $k\bar{k}$ and kk pairs. If the relative velocity of the collision is small, the $k\bar{k}$ pair may annihilate into a breather through the radiation loss, which takes place if $c < c_{\rm cr} \approx 2.22\,|\varepsilon|$.

Numerical simulations of $k\bar{k}$ collisions in non-integrable models, including Equation (5), reveal an interesting effect. There is a (probably infinite) set of critical relative velocities $c_{\rm cr}^{(n)}$, $n = 0, 1, 2, \ldots$, such that the annihilation takes place in intervals $0 < c < c_{\rm cr}^{(0)}$, $c_{\rm cr}^{(1)} < c < c_{\rm cr}^{(2)}$, $c_{\rm cr}^{(3)} < c < c_{\rm cr}^{(4)}$, …, while in transmission windows between them, $c_{\rm cr}^{(0)} < c < c_{\rm cr}^{(1)}$, $c_{\rm cr}^{(2)} < c < c_{\rm cr}^{(3)}$, ..., the collision is quasi-elastic.

An explanation for this effect is that the kink has an eigenmode of its internal oscillations, and the dominant collision-induced energy loss is caused not by the emission of radiation but by excitation of the internal mode. An ODE model of a variational type makes it possible to explain the alternating annihilation and transmission windows as a result of resonant transfer of kinetic energy of the colliding kinks into their internal modes and back (Campbell et al., 1986).

BORIS A. MALOMED

See also **Collisions; Long Josephson junctions; *N*-soliton formulas; Perturbation theory; Solitons**

Further Reading

Campbell, D.K., Peyrard, M. & Sodano, P. 1986. Kink-antikink interactions in the double sine-Gordon equation. *Physica* D, 19: 165–205

Flesch, R.J. & Trullinger, S.E. 1987. Green's function for nonlinear Klein–Gordon kink perturbation theory. *Journal of Mathematical Physics*, 28: 1619–1631

Gorshkov, K.A. & Ostrovsky, L.A. 1981. Interactions of solitons in non-integrable systems: direct perturbation method and applications. *Physica* D, 3: 428–438

Karpman, V.I. & Solov'ev, V.V. 1981. A perturbational approach to the two-soliton systems. *Physica* D, 3: 487–502

Kaup, D.J. & Newell, A.C. 1978. Solitons as particles and oscillators in slowly varying media. *Proceedings of the Royal Society of London* A, 361: 413–466

Keener, J.P. & McLaughlin, D.W. 1977. Solitons under perturbations. *Physical Review* A, 16: 777–790

Kivshar, Y.S. & Malomed, B.A. 1989. Dynamics of solitons in nearly integrable systems. *Reviews of Modern Physics*, 61: 762–915

Malomed, B.A. 1998. Potential of interaction between two- and three-dimensional solitons. *Physical Review* E, 58: 7928–7933

Malomed, B.A. 2002. Variational methods in nonlinear fiber optics and related fields. *Progress in Optics*, 43: 69–191

McLaughlin, D.W. & Scott, A.C. 1978. Perturbation analysis of fluxon dynamics. *Physical Review* A, 18: 1652–1680

MULTISTABILITY

See **Stability**

MUSHROOMS

See **Fairy rings of mushrooms**

MUTUAL ENTRAINMENT

See **Coupled oscillators**

MYELINATED NERVES

While smooth nerve fibers are common to invertebrates, for example, the giant axon of the squid (Hodgkin & Huxley, 1952), myelinated nerve fibers are widely found in vertebrates. A myelinated fiber is mainly composed of a membrane—interfacing the intracellular space and the extracellular one—surrounded by a myelin sheath which acts as an insulator (Waxman et al., 1995; Koch, 1998; Scott, 2002). This sheath, formed of Schwann cells, is periodically absent in gaps called nodes of Ranvier, making a nerve fiber a discrete and periodic structure, as illustrated in Figure 1. Therefore, ion currents through the membrane can only occur at the nodes of Ranvier, which implies a "saltatory" conduction, under which the wave of activity leaps from one node to the next.

One of the main constraints of neural processing is to develop robust and high-speed traveling waves. Compared with smooth fibers, myelinated structures allow an increased velocity of nerve impulses, while decreasing the diameter of the nerve fiber. Thus, the motor nerves of vertebrates may comprise several hundred individual saltatory fibers. For instance, the information transfer rate (bits/s) in a rabbit's sciatic nerve is about 1500 times greater than in a squid axon of the same diameter. In the context of biological evolution, it is interesting to know the link between internode spacing and impulse velocity, and whether this link is optimized in terms of speed and robustness. To this end, a mathematical model can provide some answers.

A single myelinated nerve can be modeled from Kirchhoff's law analysis by the system of difference-differential equations

$$V_n - V_{n+1} = RI_n,$$
$$I_{n-1} - I_n = C\frac{\mathrm{d}V_n}{\mathrm{d}t} + I_{\mathrm{ion},n}. \qquad (1)$$

In these equations, the index n indicates successive active nodes, each of which is characterized by a transverse (inside to outside) voltage across the membrane (V_n). A second dynamic variable is the current (I_n) flowing longitudinally through the fiber from node n to node $n+1$. Also, R is the sum of the inside and outside resistances between two nodes and is inversely proportional to the internode spacing s, and C is the membrane capacitance of a node.

To study the velocity of an impulse, it is sufficient to focus on its leading edge. Thus, we assume that the sodium ion (Na^+) current begins without delay, and the potassium (K^+) permeability remains equal to its resting value. In this case, the expression of the ion currents developed by Alan Hodgkin and Andrew Huxley (*See* **Hodgkin–Huxley equations**) can be reduced to the simple and yet physically reasonable expression:

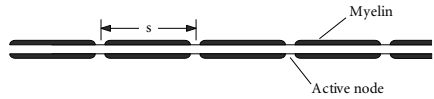

Figure 1. Sketch of a myelinated nerve fiber.

$$I_{\mathrm{ion},n} = I_{\mathrm{Na},n} = \left(\frac{G}{V_\mathrm{b}(V_\mathrm{b} - V_\mathrm{a})}\right) \times V_n(V_n - V_\mathrm{a})(V_n - V_\mathrm{b}), \qquad (2)$$

where V_a is a threshold potential, V_b is the Nernst potential, and G is the total ionic conductance near V_b.

The parameters of this model can be related to experimental measurements on a real myelinated nerve fiber (Binczak et al., 2001). From studies on frogs' motor nerves with a diameter of 14 μm, $R = 28\,\mathrm{M}\Omega$, $C = 3.7 \pm 1\mathrm{pF}$, $G = 0.57\,\mu\mathrm{S}$, $V_\mathrm{a} \sim 25\,\mathrm{mV}$, and $V_\mathrm{b} = 122\,\mathrm{mV}$, while the distance between nodes equals 2 mm.

In order to study the influence of the internode spacing s on the impulse velocity, s and therefore R become variable. A discreteness parameter D can be defined by setting $R_\mathrm{f} = 28\,\mathrm{M}\Omega$, as

$$D \equiv \frac{2\,\mathrm{mm}}{s} = \frac{R_\mathrm{f}}{R}, \qquad (3)$$

so that $D = 1$ implies the discreteness of a standard frog nerve. Using dimensionless voltage variables $v_n \equiv V_n/V_\mathrm{b}$ and $a \equiv V_\mathrm{a}/V_\mathrm{b}$, the dynamic equation becomes

$$D(v_{n+1} - 2v_n + v_{n-1}) = R_\mathrm{f}C\frac{\mathrm{d}v_n}{\mathrm{d}t} + \frac{R_\mathrm{f}G}{1-a}v_n(v_n - a)(v_n - 1), \qquad (4)$$

Equation (4) has been used to compute the wave front velocity, which is plotted against D in Figure 2.

If the internodal spacing is small enough, that is, $D \gg 1$, the relative change in voltage between nodes satisfies the inequality $|(v_{n+1} - v_n)/v_n| \ll 1$ and the voltages and currents are smooth functions of distance. Letting $ns \to x$ in this continuum limit, the system can be described by the partial differential equation

$$s^2 D\frac{\partial^2 v}{\partial x^2} - R_\mathrm{f}C\frac{\partial v}{\partial t} = \frac{R_\mathrm{f}G}{1-a}v(v-a)(v-1), \qquad (5)$$

which is the Zeldovich–Frank-Kamenetsky (ZF) equation. Initially formulated as a model for flame front

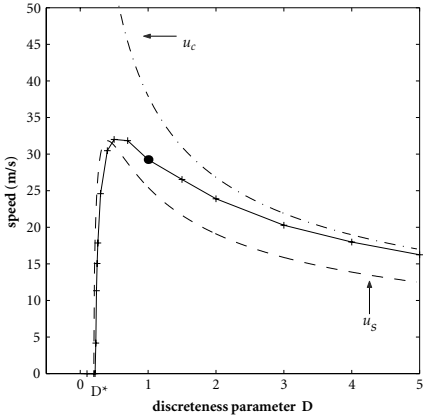

Figure 2. Leading edge impulse velocity on a myelinated axon as a function of the discreteness parameter D. The dot-dashed line indicates the continuum limit of Equation (6). The dashed line indicates the saltatory limit in Equation (8). Crosses indicates numerical results.

propagation, this equation is extensively used to study simple unmyelinated nerve models.

In the continuum limit, the wave speed u tends toward u_c (Zeldovich & Frank-Kamenetsky, 1938), where

$$u_c = s\left(\frac{1-2a}{\sqrt{2(1-a)}}\right)\sqrt{\frac{G}{RC^2}}, \tag{6}$$

corresponds to the dot-dashed line in Figure 2. As illustrated in this figure, the continuum approximation holds for $D > 5$.

Propagation failure (Keener, 1987) occurs when the distance between the active nodes becomes too large, that is, when D is above a critical value D^*. This critical value of the discreteness parameter is given to lowest order in a as (Erneux & Nicolis, 1993)

$$D^* \approx \frac{R_f G a^2}{4(1-a)}. \tag{7}$$

For D slightly larger than D^*, the impulse velocity $u \to u_s$, where

$$u_s = \frac{s}{\pi C}\sqrt{\frac{G(D-D^*)}{R_f(1-a)}}, \tag{8}$$

which corresponds to the dashed line in Figure 2.

When $D = 1$, the impulse velocity of a normal frog nerve has been calculated to be equal to 29 m/s, which matches the experimental results (Tasaki, 1982). The large dot in Figure 2 shows that the velocity is close to the maximum possible value, suggesting an optimal evolutionary design.

Failure of an impulse is expected to occur at an internode spacing of 1 cm, corresponding to $D = 0.2$, whereas the normal nerve is designed for $D = 1$, corresponding to a spacing of 2 mm. Thus, the process of evolution has provided a comfortable safety margin against accidental failure on the frog's motor nerve.

Because the impulse velocity reaches its maximum value near $D = 1$, we have an explanation for the fact that the conduction velocity of a frog's myelinated motor nerve is insensitive to the internode spacing. From an engineering perspective, operating in this region of parameter space makes the system robust. These observations are extendable to other myelinated fibers (Scott, 2002).

Finally, it should be noted that the transmission of an individual impulse expends much more energy on a smooth fiber, suggesting an additional reason that myelinated nerve fibers may have played an important role in the course of biological evolution.

STEPHANE BINCZAK

See also **Biological evolution; Nerve impulses; Zeldovich–Frank-Kamenetsky equation**

Further Reading

Binczak, S., Eilbeck, J.C. & Scott, A.C. 2001. Ephaptic coupling of myelinated nerve fiber. *Physica* D, 148: 159–174

Erneux, T. & Nicolis, G. 1993. Propagating waves in discrete bistable reaction–difusion systems. *Physica* D, 67: 237–244

Hodgkin, A.L. & Huxley, A.F. 1952. A quantitative description of membrane current and its application to conduction and excitation in nerve. *Journal of Physiology*, 117: 500–554

Keener, J.P. 1987. Propagation and its failure in coupled systems of discrete excitable cells. *SIAM Journal of Applied Mathematics*, 47: 556–572

Koch, C. 1998. *Biophysics of Computation: Information Processing in Single Neurons*, Oxford and New York: Oxford University Press

Scott, A.C. 2002. *Neuroscience: A Mathematical Primer*, Berlin and New York: Springer

Tasaki, I. 1982. *Physiology and Electrochemistry of Nerve Fibers*, New York: Academic Press

Waxman, S.G., Kocsis, J.D. & Stys, P.K. (editors). 1995. *The Axon: Structure, Function and Pathophysiology*, Oxford and New York: Oxford University Press

Zeldovich, Ya.B. & Frank-Kamenetsky, D.A. 1938. K teorii ravnomernogo rasprostranenia plameni (Toward a theory of uniformly propagating flames). *Doklady Akademii Nauk SSSR*, 19: 693–697

N

NATURAL MEASURE

See **Measures**

NAVIER–STOKES EQUATION

In 1822, the French engineer Claude Navier derived the Navier–Stokes equation, as an extension of Euler's equation to include viscosity. Navier was initially interested in blood flow, and he used a molecular approach to arrive at the viscous terms. Navier's equations were generalized to a compressible fluid by Poisson (1829), and one can find fully continuous derivations by De Saint-Venant (1843). A comprehensive treatment was given by George Stokes in 1845, who independently arrived at the results of Poisson and Saint-Venant using a continuous model. Stokes used the common assumption of linear relations between stress and strain rate and discovered "Stokes' law" for the terminal velocity of objects descending in fluids, which he deduced from experiments with slowing pendulums in viscous media.

The Navier–Stokes equation derives from a general equation for the conservation of momentum, balancing forces per unit volume on both sides. It is given by

$$\rho \frac{\mathrm{d}\boldsymbol{v}}{\mathrm{d}t} = \rho \boldsymbol{g} - \nabla p + \mu \left(\nabla^2 \boldsymbol{v} + \frac{1}{3} \nabla \nabla \cdot \boldsymbol{v} \right), \qquad (1)$$

where $\boldsymbol{v}(\boldsymbol{r}, t)$ is the velocity vector in a cartesian coordinate system, $\rho(\boldsymbol{r}, t)$ is the density, $\boldsymbol{g}$ is the acceleration due to external forces (for example, gravitational, magnetic, electro-static forces), $p(\boldsymbol{r}, t)$ the pressure, and μ the viscosity coefficient. The material derivative is given by

$$\frac{\mathrm{d}\boldsymbol{v}}{\mathrm{d}t} = \left(\frac{\partial}{\partial t} + \boldsymbol{v} \cdot \nabla \right) \boldsymbol{v}, \qquad (2)$$

where the first and second terms are the local time derivative of the quantity $\boldsymbol{v}(\boldsymbol{r}, t)$ with spatial coordinates fixed, and the convective (or advective) term accounting for the change of the quantity $\boldsymbol{v}(\boldsymbol{r}, t)$ at $\boldsymbol{r}$ due to the observer following the motion of the fluid with velocity $\boldsymbol{v}$. Both terms together are called the material derivative or convective derivative and are usually denoted by $\mathrm{d}/\mathrm{d}t$.

In an inertial coordinate system, the acceleration $\boldsymbol{g}$ originates solely from the gravitational potential of the Earth. Assuming a homogeneous mass at the center of the Earth, the acceleration $\boldsymbol{g}$ in Equation (1) is given by $\boldsymbol{g} = g\boldsymbol{k}$, where $\boldsymbol{k}$ is the local vertical direction, pointing to the center of gravity of the earth and g is the gravitational acceleration (982.1 cm s^{-2}), which is assumed constant in the first approximation. In a rotating coordinate system, the acceleration $\boldsymbol{g}$ consists of the centrifugal force and Coriolis force in addition to the gravitational acceleration, see Lamb (1906). Also, for large-scale processes, it is often necessary to account for tidal forces of the moon and sun. The term $-\nabla p$ is the force per unit volume due to a pressure gradient of the scalar pressure field $p(\boldsymbol{r}, t)$ acting on an infinitesimal volume of fluid with infinitesimal mass.

The last two terms of Equation (1)

$$\frac{\mu}{\rho} \left(\nabla^2 \boldsymbol{v} + \frac{1}{3} \nabla \nabla \cdot \boldsymbol{v} \right), \qquad (3)$$

are the frictional terms which derive from a shear stress tensor for a Newtonian viscous fluid with constant viscosity coefficients. A fluid is called Newtonian if there is a linear relation between stress and rate of strain assuming isotropy, which is true for the most common conditions. Non-Newtonian fluids have more complex molecular structure or are mixtures of fluids.

The frictional term $\nabla^2 \boldsymbol{v} = \nabla \nabla \cdot \boldsymbol{v} - \nabla \times (\nabla \times \boldsymbol{v})$ contains effects due to compression and rotation. If the fluid is incompressible then the divergence terms are missing from Equations (1) and (3), since $\nabla \cdot \boldsymbol{v} = 0$. Often the coefficient of kinematic viscosity $\nu = \mu/\rho$ is used instead of the viscosity μ. The viscosity of the fluid depends on temperature, and a table for typical values of viscosity μ, kinematic viscosity ν, and density ρ is shown in Table 1 for typical temperatures. If the temperature across the medium is not uniform then a variable viscosity may have to be accounted for (see Batchelor, 1970).

T (°C)	Air ρ (g cm^{-3})	μ (g cm^{-1} s^{-1})	ν (cm^2 s^{-1})	Water ρ (g cm^{-3})	μ (g cm^{-1} s^{-1})	ν (cm^2 s^{-1})
0	1.293×10^{-3}	1.71×10^{-4}	0.132	0.999	1.787×10^{-2}	1.787×10^{-2}
10	1.247×10^{-3}	1.76×10^{-4}	0.141	0.999	1.304×10^{-2}	1.304×10^{-2}
20	1.205×10^{-3}	1.81×10^{-4}	0.150	0.998	1.002×10^{-2}	1.004×10^{-2}

Table 1. Density ρ, viscosity μ and kinematic viscosity ν of air and water.

For an ideal (perfect) fluid without internal shear stress, the momentum equation reduces to Euler's equation of motion for $\mu = 0$. Note that if the flow is irrotational ($\nabla \times \boldsymbol{v} = 0$) and incompressible ($\nabla \cdot \boldsymbol{v} = 0$), it essentially behaves as if it is inviscid ($\mu = 0$), because of the incompressibility condition $\mathrm{d}\rho/\mathrm{d}t = -\rho \nabla \cdot \boldsymbol{v} = 0$. (Note that a fluid may be incompressible yet ρ may not be constant.)

The system of Equations (1) comprises three momentum equations, together with an additional equation for mass conservation; a thermodynamic equation of state; a relation of pressure, density, and either temperature or entropy; and an energy equation for the additional thermodynamic variable (temperature or entropy). These provide six scalar equations for the determination of the six independent variables, velocity $\boldsymbol{v}$, density ρ, pressure p, and temperature or entropy as functions of space $\boldsymbol{x}$ and time t. If the fluid is incompressible, the equation of state becomes obsolete and only four equations are needed, the three momentum equations and the equation for conservation of mass.

Numerical Problems

As with most complicated nonlinear partial differential equations, the Navier–Stokes equation is solved numerically to model a specific fluid flow that is of interest experimentally and theoretically. Because there are many different ways to write the Navier–Stokes equation, the first numerical difficulty is to pick the formulation most suitable to the numerical technique that one wishes to employ and the dimensions of the model. One distinguishes between two-dimensional and three-dimensional models. For two-dimensional incompressible Navier–Stokes equation, for example, there are four different kinds of formulations: the primitive-variable (velocity and pressure), stream function-vorticity, stream function, and velocity-vorticity formulation.

It is important to distinguish between the real dissipation ($\mu \neq 0$), given by the last term of Equation (1) and numerical dissipation, which is introduced by an accumulative error due to the limited order of accuracy of any numerical model. As the numerical dissipation of a good model is often negligible, it is sometimes appropriate to introduce an artificial viscosity that acts to damp growing high wave number modes, which can lead to numerical instability.

Euler's equation conserves linear and angular momentum and energy, so it is necessary to verify that the numerical model conserves these conserved quantities and preserves symmetry. In cases where it is not possible to satisfy all these requirements, properties that are most essential to the physical problem are given priority. In order to satisfy such conserved quantities, it is important that the numerical scheme treats the nonlinear convective term

$$\boldsymbol{v} \cdot \nabla \boldsymbol{\phi} \tag{4}$$

in a conservative manner, where ϕ represents the scalar quantity that is convected and could be one of the three velocity components u, v, w or density ρ in the conservation of mass. Expression (4) is known as the convection form and is nonconservative numerically, since fluxes across mesh boundaries do not cancel. The convection form thus represents a major flaw of every numerical scheme. The most commonly used corresponding conservative formulation is

$$\nabla \cdot (\boldsymbol{v}\phi), \tag{5}$$

which is also known as the divergence form. Recently it was shown that the skewsymmetric form

$$\tfrac{1}{2}\boldsymbol{v} \cdot \nabla \phi + \tfrac{1}{2}\nabla \cdot (\boldsymbol{v}\phi)$$

has advantages, because it reduces aliasing errors (see below) for yet unknown reasons and is preferable to the popular rotational form

$$(\nabla \times \boldsymbol{v}) \times \boldsymbol{v}.$$

It is important to note that although both equations (4) and (5) are formally equivalent, they are not in a corresponding numerical scheme and care must be taken to avoid this common pitfall when modeling equations that contain convective terms such as the Navier–Stokes equation or the equation for mass conservation (see Hirsch, 2000).

Nonlinear terms such as $\boldsymbol{v} \cdot \nabla \boldsymbol{v}$ also generate aliasing errors. These are high-frequency wave number modes appearing or being "aliased" as low-frequency modes that deteriorate the wave number spectrum and eventually lead to numerical blow-up.

Because a numerical model of the Navier–Stokes equation is coupled spatially and temporally, it is

helpful to approximate the spatiotemporal scales of the dynamics. One should determine whether the spatial and temporal scales are equal to, smaller, or larger than each other. If, for example, the temporal scale is larger than the spatial scale, it is sufficient to use low order integration in time such as finite-difference methods, and if smaller or equal, then higher-order temporal integration such as spectral methods becomes necessary. In a temporally extensive computation, it is sometimes possible to revert to finite differences, choosing a relatively small time-step.

Especially difficult numerical problems arise when it is necessary to invert nondiagonal, nonsparse, nontrivial matrices, for example, in implicit time integrations or inverting the Laplacian. In such cases iterative techniques using preconditioning and multi-grid methods have been successfully employed. Complications arising from specifying the correct boundary conditions to use along boundaries of the physical domain should also be mentioned.

Although the Navier–Stokes equation is a very good model for a real fluid, it is important to have an understanding of the process or phenomenon that one wishes to model as well as a sound knowledge of the applicability of the numerical methods that one wishes to employ to be able to faithfully represent the physical dynamics of the fluid.

Phenomena

A salient feature of the Navier–Stokes equation is the phenomenon of turbulence. Due to viscous effects the flow of a real fluid can be observed in two very different states: a laminar state and a turbulent state.

Turbulence induces a cascade to fine scales that are eventually dissipated. It is important in many engineering applications, as a loss of energy means increased costs and can possibly cause damage to the structural body that comes in contact with the fluid or which moves through the fluid (e.g., optimization of airfoils, loss of lift force due to turbulence and boundary layer separation).

Closely related to the phenomenon of turbulence is boundary layer theory and boundary layer separation. Fluid flowing past a surface at rest relative to the fluid will experience friction at the surface of the material, and for the velocity field to be continuous, it is required that the normal as well as tangential fluid velocity vanish at the material surface ($\boldsymbol{v} = 0$). For an idealized fluid ($\mu = 0$), only the normal velocity has to vanish.

It was the problem of matching the vanishing flow at the surface boundary to some nonzero fluid flow away from the boundary that led Prandtl (1905) to introduce the concept of boundary layer, which is a small "inner" fluid layer close to the surface where viscous effects dominate the flow. This inner layer is joined to an "outer" layer, where the fluid can be considered inviscid. The concept of boundary layer has led to great progress in fluid mechanics and perturbation methods, where matched asymptotic expansions feature prominently, but a complete understanding of boundary layer separation and its connection to turbulence is still missing.

A useful concept is vorticity, which can be regarded as a beautiful generalization of fluid motion. Formally vorticity is defined as

$$\omega = \nabla \times \boldsymbol{v},$$

which simplifies to twice the angular velocity for solid body rotation. A fluid is called irrotational if its vorticity is zero and rotational if it is not. Taking the curl of Euler's equation ($\mu = 0$) for an incompressible fluid in the absence of baroclinicity (and after some vector algebra) leads to the vorticity equation

$$\frac{\mathrm{d}\omega}{\mathrm{d}t} - \omega \cdot \nabla \boldsymbol{v} = 0.$$

Vortex lines and vortex strength are conserved, vortex lines move with the fluid, and an initially irrotational flow remains irrotational. Associated to vortices and turbulence is the, still not understood, phenomenon of vortex breakdown (Benjamin, 1978).

Among wave phenomena, the most striking is definitely the solitary wave, which appears as a nonlinear wave in a fluid internally as well as at fluid surfaces or interfaces. For free-surface wave phenomena, see Johnson (1997) and the references therein, and for a colorful overview, see Lighthill (1978). A beautiful picture gallery of fluid phenomena can be found in Van Dyke (1982). Other phenomena that can only be listed here include cavitation and thermal convection (Rayleigh–Bénard convection), sub- and supersonic flow, shock waves as well as most instability mechanisms and phenomena (Rayleigh–Taylor instability, Kelvin–Helmholtz instability, barotropic and baroclinic instability).

ANDREAS A. AIGNER

See also **Alfvén waves; Boundary layers; Burgers equation; Chaos vs. turbulence; Fluid dynamics; Hydrothermal waves; Kelvin–Helmholtz instability; Korteweg–de Vries equation; Lattice gas methods; Magnetohydrodynamics; Mixing; Rayleigh–Taylor instability; Solitons; Taylor–Couette flow; Turbulence; Water waves**

Further Reading

Batchelor, G.K. 1970. *An Introduction to Fluid Dynamics*, Cambridge and New York: Cambridge University Press

Benjamin, T.B. 1978. Theory of the vortex breakdown phenomenon. *Journal of Fluid Mechanics*, 14: 593–629

Chandrasekhar, S. 1961. *Hydrodynamic and Hydromagnetic Stability*, Oxford: Clarendon Press and New York: Dover

De Saint-Venant, J.-C. 1843. Note à joindre au mémoire sur le dynamique de fluides. *Comptes Rendu de l'Academie des Sciences Paris*, 17: 1240–1243
Drazin, P.G. 1981. *Hydrodynamic Stability*, Cambridge and New York: Cambridge University Press
Hirsch, C. 2000. *Numerical Computation of Internal and External Flows*, New York: Wiley
Johnson, R.S. 1997. *A Modern Introduction to the Mathematical Theory of Water Waves*, Cambridge and New York: Cambridge University Press
Lamb, H. 1906. *Hydrodynamics*, Cambridge: Cambridge University Press; 6th edition, Cambridge and New York: Cambridge University Press, 1993
Landau, L.D. & Lifshitz, E.M. 1987. *Fluid Mechanics*, vol.6 of *Course of Theoretical Physics*, London: Pergamon Press and Reading, MA: Addison-Wesley
Lighthill, J. 1978. *Waves in Fluids*, Cambridge and New York: Cambridge University Press
Milne-Thomson, L.M. 1968. *Theoretical Hydrodynamics*, 5th edition, New York: Macmillan Press
Navier, M. 1822. Mémoire sur les lois du mouvement des fluides. *Mémoires de l'Academie Royale des Sciences*, 6: 389–440
Poisson, S.D. 1829. Mémoire sur les équations générales de l'équilibre et du nouvement des corps silides élastiques et de fluides. *Journal de l'École Polytechnique*, 13: 1–174
Prandtl, L. 1905. *Verhandlungen des dritten internationalen Mathematiker-Kongresses, Heidelberg 1904*, Leipzig: 484–491
Stokes, G.G. 1845. On the theories of the internal friction of fluids in motion, and of the equilibrium and motion of elastic solids. *Transactions, Cambridge Philosophical Society*, 8: 287–319
Streeter, V.L. & Wylie, E.B. 1985. *Fluid Mechanics*, 8th edition, New York: McGraw-Hill
Van Dyke, M. 1982. *An Album of Fluid Motion*, Stanford: Parabolic Press
Vennard, J.K. 1954. *Elementary Fluid Mechanics*, New York: Wiley

N-BODY PROBLEM

The Newtonian N-body problem of celestial mechanics is a mathematical generalization of the solar system. In the Euclidean space $\mathbb{R}^3$, consider N points of masses $m_i > 0$, $i = 1, \ldots, N$, which attract each other by a force directly proportional to the product of the masses and inversely proportional to the square of the distance. The equations of motion are given by the $6N$-dimensional system of differential equations

$$\begin{cases} \dot{\boldsymbol{q}} = M^{-1}\boldsymbol{p}, \\ \dot{\boldsymbol{p}} = G\nabla U(q), \end{cases} \tag{1}$$

where the upper dot represents differentiation with respect to the time variable; $\boldsymbol{q} = (\boldsymbol{q}_1, \ldots, \boldsymbol{q}_N)$ is the configuration of the particle system, with $\boldsymbol{q}_i = (q_i^1, q_i^2, q_i^3)$; giving the coordinates of the point of mass m_i, $\boldsymbol{p} = M\dot{\boldsymbol{q}}$ is the momentum, where M is a $3N$-dimensional square matrix having on the diagonal the elements $m_1, m_1, m_1, \ldots, m_N, m_N, m_N$ and zeros in rest; G is the gravitational constant; and $U(\boldsymbol{q}) = \sum_{1 \le i < j \le N} \frac{m_i m_j}{|\boldsymbol{q}_i - \boldsymbol{q}_j|}$ is the potential function, $-U(\boldsymbol{q})$ representing the potential energy. Standard results of the theory of differential equations ensure the existence and uniqueness of an analytic solution for any initial value problem as long as the initial data do not belong to the collision set $\Delta = \bigcup_{1 \le i < j \le N} \Delta_{ij}$, where $\Delta_{ij} = \{\boldsymbol{q} \in \mathbb{R}^{3N} \,|\, \boldsymbol{q}_i = \boldsymbol{q}_j\}$.

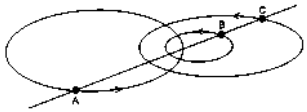

Figure 1. The Eulerian solutions of the three-body problem.

Isaac Newton formulated this problem in his master work *Principia*, but Leonhard Euler was the first to write the equations as we know them today. The case $N = 2$, also called the Kepler problem, is completely solved (see Albouy (2002) for a recent discussion of some early solutions). The relative motion of one body with respect to the other is planar and, depending on the initial conditions, can be a circle, an ellipse, a parabola, a branch of a hyperbola, or a line, in which case a collision takes place in the future or in the past. Kepler's laws (*See* **Celestial mechanics**) can be recovered from Equation (1).

For $N \ge 3$, very little is known about the N-body problem in spite of thousands of research papers written over more than three centuries. The case $N = 3$ was the most studied since many of the results obtained could be generalized to any larger N. The first attempts to understand the three-body problem were quantitative, aiming at finding explicit solutions. In 1767, Euler found the collinear periodic orbits, in which three bodies of any masses move such that they oscillate along a rotating line (Euler, 1767, Figure 1) and in 1772, Joseph-Louis Lagrange discovered some periodic solutions that lie at the vertices of a rotating equilateral triangle that shrinks and expands periodically (Lagrange, 1772, Figure 2). Those solutions led to the study of central configurations, for which $\boldsymbol{q}'' = k\boldsymbol{q}$ for some constant $k > 0$. Each central configuration provides a class of periodic orbits.

Another idea was to reduce the order of the system with the help of first integrals. Ten linearly independent integrals are known: three for the center of mass, three for the momentum, three for the angular momentum, and one for the energy (see Wintner, 1947). Together with a certain symmetry, these integrals allow the reduction of the three-body problem from dimension 18 to 7. But unfortunately the dimension of the problem cannot be further reduced. In 1887, Heinrich Bruns proved that there exist no more linearly independent integrals, algebraic with respect to $\boldsymbol{q}$, $\boldsymbol{p}$ and t (Bruns, 1887), thus showing the limitations of the quantitative methods. This led Henri Poincaré to

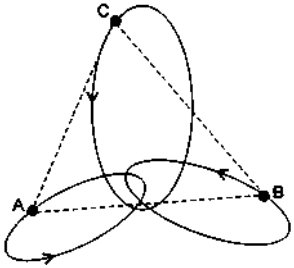

Figure 2. The Lagrangian solutions of the three-body problem.

attempt a qualitative approach. His first prolific ideas appeared in a memoir published in 1890 (Poincaré, 1890), for which he was awarded the King Oscar Prize (see Barrow-Green, 1997; Diacu & Holmes, 1996). There he laid the foundations of several branches of mathematics, including dynamical systems, chaos, KAM theory, and algebraic topology.

Poincaré aimed to understand the geometry of the phase space and the relative behavior of orbits and, thus, to answer questions regarding stability, asymptotic motion at infinity, existence of periodic orbits, etc. An important problem in this direction was that of singular solutions, that is, those that tend to the collision set Δ. It took mathematicians almost a century to prove that for $N \geq 5$, there exist singular solutions that do not end in collisions but in pseudocollisions, which are orbits that become unbounded in finite time (see Diacu & Holmes, 1996). For $N = 4$, the problem is still open.

Recently, a lot of interest has been in finding choreographies, that is, periodic orbits for which all the bodies move on the same closed curve. For more than two centuries the only known example was the class of Lagrangian solutions in the particular case that all the masses are equal and the ellipses are circles. With the help of variational methods, in 2000, a spectacular new class was proved to exist: three bodies of equal mass chase each other along a curve resembling the figure eight (Chenciner & Montgomery, 2000; Montgomery, 2001, Figure 3). There is numerical evidence that this periodic orbit is KAM stable, that is, the solutions through most initial conditions in some sufficiently small neighborhood of the orbit stay close to it for all time, while the other solutions leave the neighborhood very slowly. Unfortunately, the stability region seems to be very small. Numerical experiments suggest that the probability of finding an eight in the universe is somewhere between one per galaxy and one per universe. Hundreds of other choreographies have been numerically put into the evidence.

Still far from fully understood are the questions regarding various restricted three-body problems. In the

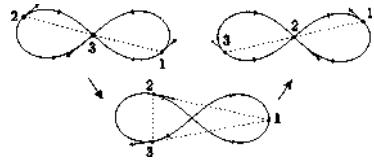

Figure 3. The figure eight solution of the 3-body problem.

elliptic one, for example, it is asked to determine the motion of one body, assumed to have zero mass, while the other two move on ellipses as in the Kepler problem with negative energy.

Numerical methods are also of help for getting insight into the problem. But due to the apparently chaotic character of the motion, they must be implemented with care. Recently, much progress has been made in successfully applying scientific computation to various aspects of the general and restricted three-body problem.

Many of the ideas of the classical N-body problem can be adapted to related problems for understanding the motion of particle systems given by other potentials, like those of Manev and Schwarzschild (also used in celestial mechanics), Coulomb (atomic and molecular theories), and Lennard-Jones (crystal formation). Based on the Coulomb potential, Niels Bohr's model of the hydrogen atom led to the development of quantum mechanics. Several other branches of science have profited from the study of the N-body problem.

FLORIN DIACU

See also **Celestial mechanics; Poincaré theorems; Solar system**

Further Reading

Albouy, A. 2002. Lectures on the two-body problem. In *Classical and Celestial Mechanics: The Recife Lectures*, edited by H. Cabral & F. Diacu, Princeton, NJ: Princeton University Press, pp. 71–135

Barrow-Green, J. 1997. *Poincaré and the Three-Body Problem*, Providence, RI: American Mathematical Society

Bruns, H. 1887. Über die Integrale des Vielkörper-Problems, *Acta Mathematica* 11: 25–96

Chenciner, A. & Montgomery, R. 2000. A remarkable periodic solution of the three-body problem in the case of equal masses. *Annals of Mathematics*, 152: 881–901

Diacu, F. & Holmes, P. 1996. *Celestial Encounters—The Origins of Chaos and Stability*, Princeton, NJ: Princeton University Press

Euler, L. 1767. De moto rectilineo trium corporum se mutuo attrahentium, *Novo Comm. Acad. Sci. Imp. Petrop.*, 11: 144–151

Lagrange, J.L. 1873. Essai sur le probl eme des trois corps. In *Ouvres de Lagrange*, vol. 6, pp. 229–324, Paris: Gauthier-Villars, 14 vols

Montgomery, R. 2001. A new solution to the three-body problem. *Notices of the American Mathematical Society* May, pp. 471–481

Poincaré, H. 1890. Sur le problème des trois corps et les équations de la dynamique. *Acta Mathematica*, 13: 1–270
Wintner, A. 1947. *The Analytical Foundations of Celestial Mechanics*, Princeton, NJ: Princeton University Press

NEEL DOMAIN WALL

See **Domain walls**

NEGATIVE RESISTANCE AND CONDUCTANCE

See **Diodes**

NEPHRON DYNAMICS

The kidneys play an important role in regulating the blood pressure and maintaining a proper environment for the cells of the body. The mammalian kidney contains a large number of functional units, the nephrons. For a human kidney the number of nephrons is of the order of 1 million, and for a rat kidney the number is approximately 30,000. The nephrons are organized in a parallel structure such that the individual nephron only processes a very small fraction of the total blood flow to the kidney. To distribute the blood that enters through the renal artery, the kidney makes use of a network of arteries and arterioles. Closest to the nephron, we have the afferent arteriole that leads the blood to the capillary network in the glomerulus where water, salts, and small molecules are filtered from the blood and into the tubular system of the nephron. On the other side of the glomerulus, the efferent arteriole leads the blood to another capillary system that receives the water and salts reabsorbed by the tubules.

Figure 1 provides a sketch of the main structural components of the nephron. Note how the terminal part of the loop of Henle passes within cellular distances of the afferent arteriole. As described below, this anatomical feature allows for a special feedback regulation.

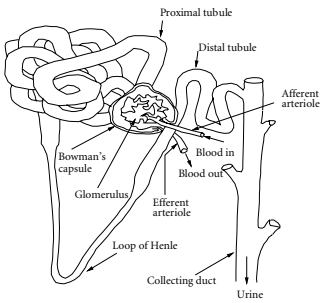

Figure 1. Sketch of the main structural components of the nephron.

In order to protect its function in the face of a varying blood pressure, the individual nephron disposes of a number of mechanisms to control the incoming blood flow. Most important is the tubuloglomerular feedback (TGF) mechanism that regulates the diameter of the afferent arteriole in response to variations in the NaCl concentration in the fluid that leaves the loop of Henle via the distal tubule. If the salt concentration in this fluid becomes too high, specialized cells (macula densa cells) near the terminal part of the loop of Henle elicit a signal that causes the smooth muscle cells at the downstream end of the afferent arteriole to contract. Hence, the incoming blood flow is reduced, and so is the glomerular filtration rate.

The TGF mechanism represents a negative feedback. However, by virtue of a delayed action associated with a finite transit time through the loop of Henle, the flow regulation tends to become unstable and produce self-sustained oscillations with a period of 30–40 s. While for rats with normal blood pressure, these oscillations have the appearance of a regular limit cycle with a sharply peaked power spectrum, highly irregular oscillations, displaying a broadband spectral distribution with strong subharmonic components are observed for spontaneously hypertensive rats. In a particular experiment, clear evidence of a period-doubling of the pressure oscillations has been found, indicating that the nephronic control system is operating close to a transition to chaos.

Figure 2 displays examples of the tubular pressure oscillations observed for normotensive rats (a) and for spontaneously hypertensive rats (b), respectively. The

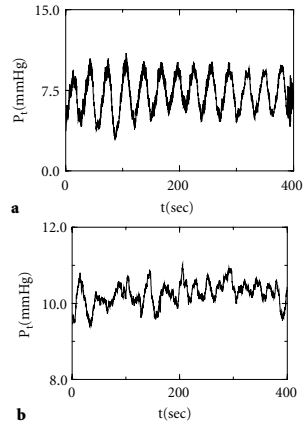

Figure 2. Regular (a) and irregular (b) tubular pressure oscillations from a normotensive and a spontaneously hypertensive rat, respectively.

pressure oscillations can be observed by means of a glass pipette inserted into the proximal tubule of a nephron at the surface of the kidney.

The processes involved in the nephron autoregulation are known in considerable detail. Besides the filtration of water and salts in the glomerulus, these processes include the passive (osmotic) and active (enzymatically controlled) processes by which water and salts are reabsorbed along the loop of Henle, the enzymatic processes through which the smooth muscle cells in the arteriolar wall are activated by the macula densa signal, and the dynamic response of the arteriolar wall to external stimulation.

The steady-state response of the TGF mechanism can be obtained from open-loop experiments in which a block of paraffin is inserted into the middle of the proximal tubule and the glomerular filtration rate is measured as a function of an externally forced flow of artificial tubular fluid into the loop of Henle. Reflecting physiological constraints on the diameter of the arteriole, this response follows an S-shaped characteristic with a maximum at low Henle flows and a lower saturation level at externally forced flows beyond 20−25 nl/min.

Together with the delay in the TGF regulation, the steepness of the response plays an essential role for the stability of the feedback system. The length of the delay can be estimated from the phase shift between the pressure oscillations in the proximal tubule and the oscillations of the NaCl concentration in the distal tubule. A typical value is 10–15 s. In addition, there is a transit time of 3–5 s for the signal from the macula densa cells to reach the smooth muscle cells in the arteriolar wall. The result is a total delay of 14–18 s. The steepness α of the steady state response curve is found to be significantly higher for spontaneously hypertensive rats than for normal rats.

By integrating the different physiological processes into a coherent, nonlinear dynamic model, it has been possible to show how these processes together produce the observed behavior, that is, the emergence of self-sustained oscillations as the slope of the response characteristic exceeds $\alpha \cong 11$ and the transition to chaos via sets of overlapping period-doubling cascades as the feedback slope exceeds $\alpha \cong 20$.

Figure 3 shows a two-dimensional bifurcation diagram for the single-nephron model. The dashed curve is a Hopf bifurcation curve. Period-doubling and saddle-node bifurcations are indicated as fully drawn and dotted curves, respectively. As before, T is the total delay in the TGF regulation, and α is the (maximal) slope of the open-loop feedback characteristic.

The single-nephron model can also be used to simulate the response to an external perturbation, for instance, the infusion of artificial tubular fluid into the loop of Henle or the administration of a drug to the rat. This last possibility is rapidly gaining in significance as the application of simulation models in the development of new drugs becomes more and more important.

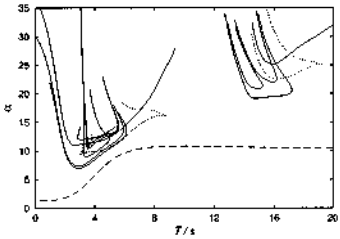

Figure 3. Two-dimensional bifurcation diagram for the single-nephron model. The diagram illustrates the complicated bifurcation structure in the region of 1:1, 1:2, and 1:3 resonances between the arteriolar dynamics and the TGF-mediated oscillations. In the physiologically interesting regime around $T = 16$ s, another set of complicated period-doubling and saddle-node bifurcations occur. Here, the nephron is operating close to a 1:4 (or 1:5) resonance.

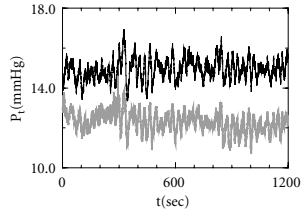

Figure 4. Example of chaotic phase synchronization for a pair of adjacent nephrons in a hypertensive rat.

A variety of cooperative phenomena that can arise from interactions among the nephrons may also be significant. The functional units are typically arranged in couples or triplets with their afferent arterioles branching off from a common interlobular artery. This structure allows neighboring nephrons to interact via signals that propagate along the arteriolar system. As experiments show, this interaction can lead to various forms of synchronization among the nephrons, including in-phase and antiphase synchronization for regularly oscillating nephrons, and chaotic phase synchronization for nephrons with irregular oscillations. By modeling these coupling phenomena in detail, one may be able to predict the typical size of the synchronization domains and to examine the role that synchronization among the nephrons plays in the overall regulation of the kidney.

Figure 4 shows an example of the tubular pressure oscillations observed for two adjacent nephrons in a hypertensive rat. The transition to synchronization can be observed as a locking of the average periods of the two signals in a 1:1 relation to one another. Alternatively, one can define and follow the temporal

variation of the instantaneous phases for the two signals.

E. Mosekilde, N.-H. Holstein-Rathlou, and O. Sosnovtseva

See also **Coupled oscillators**

Further Reading

Blekhman, I. 1988. *Synchronization in Science and Technology*, New York: ASME Press

Fung, Y.-C.B. 1981. *Biomechanics. Mechanical Properties of Living Tissues*, New York: Springer

Glass, L. & Makey, M.C. 1988. *From Clocks to Chaos: The Rhythms of Life*, Princeton, NJ: Princeton University Press

Keener, J. & Sneyd, J. 1998. *Mathematical Physiology, Interdisciplinary Applied Mathematics*, New York: Springer

Layton, H. & Weinstein, A. (editors). 2001. *Membrane Transport and Renal Physiology*, New York: Springer

Mosekilde, E. 1996. *Topics in Nonlinear Dynamics: Applications to Physics, Biology and Economic Systems*, Singapore: World Scientific

Mosekilde, E., Maistrenko, Yu. & Postnov, D. 2002. *Chaotic Synchronization — Applications to Living Systems*, Singapore: World Scientific

Pikovsky, A., Rosenblum, M. & Kurths, J. 2001. *Synchronization: A Universal Concept in Nonlinear Science*, Cambridge and New York: Cambridge University Press

Seldin, D.W. & Giebisch, G. (editors). 1992. *The Kidney: Physiology and Pathophysiology*, New York: Raven

NERVE IMPULSES

The scientific study of nerve impulses goes back to 1791, when Luigi Galvani reported that a frog's leg muscle twitches if the attached nerve is stimulated with a bimetallic contact (Brazier, 1961). This discovery was soon followed by Alessandro Volta's invention of the battery, which launched the science of electrophysiology and raised the question: Does animal electricity differ from chemical electricity?

Among attempts to answer this question was a key experimental study by young Hermann Helmholtz, who cleverly measured the speed of signal propagation on a frog's sciatic nerve (Helmoltz, 1850). In making this measurement, he ignored the advice of his father, a philosopher, who believed that muscular motion was identical to its motivation; thus, any time delay between thinking and doing was theoretically impossible. To the contrary, Helmholtz found a velocity of about 27 m/s, which is much less than the speed at which an electrical signals propagate along conducting wires. Although an outstanding theoretical physicist, Helmholtz was unable to understand why a nerve impulse should move so slowly. Was it the mechanical motion of some molecular substance that he had observed? Interestingly, nonlinear diffusion was suggested as an answer to this puzzle by Robert Luther at the beginning of the 20th century (Luther, 1906).

Among the wonders of electronics that appeared in the 20th century was the cathode-ray oscilloscope (CRO), which Kenneth Cole used to take the first photograph of a nerve impulse on the giant axon of the squid (see Figure 1) (Cole & Curtis, 1938). Time increases to the right as indicated in milliseconds by the marks on the lower margin, showing that horizontal CRO deflections were not yet uniform in the late 1930s. The solid line is the transmembrane voltage (V), which rises rapidly from a resting level, hesitates at a peak level of about 100 mV, and then falls back more slowly. The width of the band indicates the membrane permeability (or conductivity), which evidently increases greatly during passage of the nerve impulse.

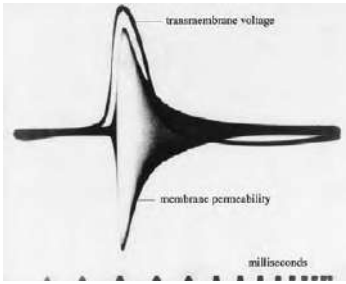

Figure 1. Time course of the transmembrane voltage and membrane permeability of an impulse on a squid nerve. (Courtesy of Kenneth Cole.)

Progress toward explaining these phenomena came soon after the Second World War, taking advantage of the significant advances in electronics during those years. In 1952, Alan Hodgkin and Andrew Huxley presented a series of papers on the squid giant axon, which culminated in a formulation of nerve impulse dynamics based on an empirically determined reaction-diffusion system, from which all details of Figure 1 were computed (Hodgkin & Huxley, 1952). In this Hodgkin–Huxley (HH) model, the initial rise of transmembrane voltage is caused by an inrush of positively charged sodium ions, and the maximum voltage is attained when the inward diffusion of sodium ions is balanced by outward conduction current through the membrane. On a longer time scale, positively charged potassium ions flow out of the nerve, bringing the transmembrane voltage back to its resting value, whereupon it is ready to conduct another impulse. Thus, the means by which squid nerves carry signals are explained by the nonlinear reaction-diffusion system

$$\frac{\partial^2 V}{\partial x^2} - rc\frac{\partial V}{\partial t} = rj_{\text{ion}}, \tag{1}$$

where r is the series resistance per unit length of the axon core, c is the capacitance per unit length, and j_{ion} is a rather complicated expression for the transmembrane ionic current per unit length.

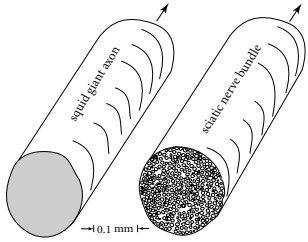

Figure 2. A squid giant axon and the sciatic nerve of a rabbit, to the same scale. (Data from Young, 1951).

In thinking about the HH formulation, it is important to be aware that a squid nerve differs from the sciatic nerve of the frog, which Galvani and Helmholtz studied. A sciatic nerve is actually a bundle of smaller fibers, whereas the squid nerve is a single "giant" axon. The squid nerve is uniform along the propagation direction; thus, the HH system is based on the partial differential equation system of Equation (1). The individual fibers of a sciatic nerve, on the other hand, are covered with an insulating layer (myelin) except at rather widely spaced active nodes (nodes of Ranvier). Thus, impulse propagation on a myelinated axon is described by a difference-differential equation, in which the wave of activity jumps from node to node (saltatory conduction). Among other differences, this means that impulse conduction velocity increases as the square root of diameter of a squid fiber, while it is roughly proportional to the first power of the diameter of a myelinated fiber. Importantly, the energy expended in transmitting a nerve impulse is much less in a myelinated fiber than in a smooth one.

These qualitative differences are emphasized in Figure 2, which compares a typical squid nerve with the sciatic nerve of a rabbit. The rabbit nerve contains about 375 small (myelinated) axons, each of which can conduct an impulse at up to 80 m/s, or about four times faster than a squid axon, leading to an increase in data transmission capacity of about three orders of magnitude. This dramatic increase in information carrying capacity is typical in vertebrate motor neurons, which are myelinated nerve bundles.

From an analytic perspective, the HH formulation is rather complicated, as it involves five dynamic variables, each of which depends on both longitudinal position and time. These are transmembrane voltage, axial current, sodium turn-on and turn-off variables, and a potassium turn-on variable. Thus, it has been of interest to consider other formulations that preserve qualitative properties of the HH system while simplifying their structure.

In the most simple approximation, the transmembrane ionic current is assumed to be a cubic nonlinear function of the transmembrane voltage; thus,

$$j_{\text{ion}} \approx \left(\frac{g}{V_{\text{th}} V_{\text{max}}}\right) V(V - V_{\text{th}})(V - V_{\text{max}}), \qquad (2)$$

where V_{th} is a threshold voltage and V_{max} is the amplitude of the impulse. Under this approximation, the HH dynamics reduce to the Zeldovich–Frank-Kamenetsky (ZF) equation, which describes the leading edge of an impulse but misses the return of the voltage to its resting value. From this perspective, a zero-order estimate of the impulse velocity is of order $\sqrt{g/rc^2}$. Several analytic formulas for the dependence of impulse velocity on axon parameters have been obtained under the ZF approximation (Scott, 2002).

A simple way to represent recovery was developed by Vladislav Markin and Yuri Chizmadzhev in the 1960s (Markin & Chizmadzhev, 1967). Under this MC approximation, a prescribed time course of transmembrane ionic current is assumed to be triggered if the membrane potential reaches a threshold variable. This prescribed current is a negative (inward) current (j_1) maintained for a time τ_1 followed by a positive (outward) current (j_2) maintained for a time τ_2. (The condition $j_1\tau_1 = j_2\tau_2$ then ensures that the net charge crossing the membrane during an impulse is zero.) With appropriate parameters, the MC model yields a recovering impulse having approximately the speed and threshold properties of the HH impulse.

To bring dynamics into the picture without invoking the complexities of the full HH model, Jin-Ichi Nagumo and his colleagues used a membrane model previously developed by Richard FitzHugh, in which the cubic ionic current of Equation (2) is augmented with a single dynamic recovery variable that drives the membrane voltage back to its resting level (Nagumo et al., 1962). This FitzHugh–Nagumo (FN) system was developed as an electronic equivalent of a nerve axon, which can be regarded as a *neuristor*. In the early 1970s, FN became of interest to applied mathematicians, who were beginning to study the theoretical properties of nonlinear reaction-diffusion systems, and in two or three spatial dimensions it has been used to study the emergence of spiral and scroll waves.

In addition to its inherent complexity, the HH system is driven by an initial inrush of sodium ions, whereas the exciting current in many nerve fibers, including dendrites of the human brain, are largely driven by calcium ion current. For many applications, therefore, it is currently of interest to use a version of the model developed by Catherine Morris and Harold Lecar for calcium ion induced membrane switching in the giant muscle fiber of the barnacle (Morris & Lecar, 1981). In this Morris–Lecar (ML) model, $j_{\text{ion}} \approx 2\pi a J_{\text{ml}}$, where a is the axon radius and

$$J_{\text{ml}} = G_{\text{K}} n\,(V - V_{\text{K}}) + G_{\text{Ca}} m\,(V - V_{\text{Ca}}) + G_{\text{L}}(V - V_{\text{L}})$$

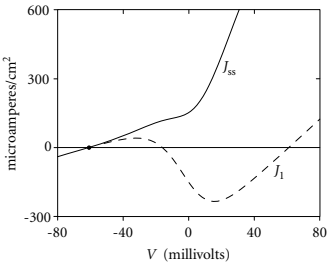

Figure 3. Plots of the initial ionic current (J_1) and the steady state current (J_{ss}) for a typical Morris–Lecar model (Fall et al., 2002; Scott, 2003).

with m and n being calcium and potassium turn-on variables, respectively. Also G_K, G_{Ca}, and G_L are membrane conductances, and V_K, V_{Ca}, and V_L are equilibrium potentials for potassium, calcium, and "leakage" ions, respectively. The turn-on variables are assumed to obey first-order dynamics as (Fall et al., 2002)

$$\frac{dm}{dt} = -[m - m_0(V)]/\tau_m(V),$$
$$\frac{dn}{dt} = -[n - n_0(V)]/\tau_n(V),$$

where

$$m_0(V) = [1 + \tanh((V - V_1)/V_2)]/2,$$
$$n_0(V) = [1 + \tanh((V - V_3)/V_4)]/2$$

and

$$\tau_m(V) = \tau_{m0}\,\mathrm{sech}[(V - V_1)/2V_2],$$
$$\tau_n(V) = \tau_{n0}\,\mathrm{sech}[(V - V_3)/2V_4].$$

At times short compared with τ_n, J_{ml} appears as the cubic function, which is plotted as a dashed line in Figure 3; thus the leading edge of an impulse will propagate as required by the ZF equation. At times long compared with τ_n, $m(t)$ remains equal to $m_0(V)$ and $n(t) \to n_0(V)$, so

$$J_{ml} \to J_{ss} = G_K n_0(V)(V - V_K) + G_{Ca} m_0(V)(V - V_{Ca}) + G_L(V - V_L).$$

This is a steady state membrane current (plotted as the solid line in Figure 3), which forces the system back to its resting state at

$$[V, m, n] = [V_R, m_0(V_R), n_0(V_R)].$$

For sufficiently large values of τ_{n0}, therefore, the ML equation supports a nerve impulse with recovery.

At the dawn of the 21st century, electrophysiology is becoming a highly sophisticated experimental science, generating data on ever more intricate neural structures; thus, it will be of interest to consider using these five approaches (HH, ZF, MC, FN, and ML) to understand the dynamics of nerve impulse propagation on axonal and dendritic branching regions of real neurons.

ALWYN SCOTT

See also **Candle; FitzHugh–Nagumo equation; Hodgkin–Huxley equations; Markin–Chizmadzhev model; Myelinated nerves; Neuristor; Reaction-diffusion systems; Zeldovich–Frank-Kamenetsky equation**

Further Reading

Brazier, M.A.B. 1961. *A History of Electrical Activity of the Brain*, London: Pitman

Cole, K.S. & Curtis, H.J. 1938. Electrical impedance of nerve during activity. *Nature*, 142: 209

Fall, C.P., Marland, E.S., Wagner, J.M. & Tyson, J.J. 2002. *Computational Cell Biology*, New York: Springer

Helmholtz, H. 1850. Messungen über den zeitlichen Verlauf der Zuckung animalischer Muskeln und die Fortpflanzungsgeschwindigkeit der Reizung in den Nerven. *Archiv für Anatomie und Physiologie*, 276–364

Hodgkin, A.L. & Huxley, A.F. 1952. A quantitative description of membrane current and its application to conduction and excitation in nerve. *Journal of Physiology (London)*, 117: 500–544

Luther, R. 1906. Räumliche Fortpflanzung chemischer Reaktionen. *Zeitschrift fuer Elektrochemie* 12(32): 596–600 [English translation in *Journal of Chemical Education*, 64 (1987):740–742]

Markin, V.S. & Chizmadzhev, Yu.A. 1967. On the propagation and excitation for one model of a nerve fiber. *Biophysics*, 12: 1032–1040

Morris, C. & Lecar, H. 1981. Voltage oscillations in the barnacle giant muscle. *Biophysical Journal*, 71: 193–213

Nagumo, J., Arimoto, S. & Yoshizawa, S. 1962. An active impulse transmission line simulating nerve axon. *Proceedings of the Institute of Radio Engineers*, 50: 2061–2070

Scott, A.C. 2002. *Neuroscience: A Mathematical Primer*, Berlin and New York: Springer

Scott, A.C. 2003. *Nonlinear Science: Emergence and Dynamics of Coherent Structures*, 2nd edition, Oxford and New York: Oxford University Press

Young, J.Z. 1951. *Doubt and Certainty in Science*, Oxford: Oxford University Press

NEUMANN BOUNDARY CONDITION

See **Partial differential equations, nonlinear**

NEURAL NETWORK MODELS

A neural network consists of units and connections corresponding to neurons and synapses in biological neural networks. We focus here on neural network models as a means to better understand the working principles of nervous systems, in particular the human brain. Quantitative modeling is today accepted as a very important tool in neuroscience that has potential to enable understanding of the very complex dynamical

and nonlinear processes underlying the functioning of biological nervous systems. So-called artificial neural networks have been developed mainly for technical applications with little concern for biological plausibility and modeling (Haykin, 1998), and we will not consider them further here.

A computational model may help to explain experimental findings and to make new experimentally testable predictions. By now, most parts of the brain have been modeled, and many different types of models exist of a system, for example, for the hippocampus, an evolutionary old part of cortex important for memory and memory consolidation. When designing a neural network model of a particular system, the constituent neurons and their synaptic connections have to be represented with the desired biophysical detail, for example, as a set of coupled ordinary differential equations that can be solved numerically on a computer (Koch & Segev, 1998; Scott, 2002). The level of biological detail in the models studied ranges from networks of very simple threshold logic units connected by binary weights to networks comprising elaborate compartmental cell models with thousands of compartments and parameters. In addition to the signal transduction and transmission processes of the neuron such a detailed cell model may also represent intracellular processes such as biochemical second messenger cascades and calcium dynamics including, for example, diffusion.

In an accurate network model of a particular system, its constituent neuron types and proportions as well as their synaptic interactions have to be adequately represented. Available data about the system must be collected from literature and experiments and be entered as parameter values. A problem with this approach is that often some part of the information required by the model is lacking, such as the distribution of different kinds of ionic channels over the cell membrane or the details of synaptic plasticity dynamics (for example, augmentation and depression). Thus, some parameters may have to be indirectly inferred, and the models need to be tuned to fit experimental recordings, for example, of the shape of excitatory and inhibitory postsynaptic potentials or neuronal firing patterns at different levels of injected current. This introduces some uncertainty with regard to the validity of the model.

The input to the network from sources outside the model must also be represented in some way. Moreover, conditions and values measured in an *in vitro* preparation like a brain slice, a cell culture, or a piece of isolated spinal cord may differ from those of the intact in vivo system, and the latter may be unaccessible.

Nervous systems, other than the most simple ones, typically comprise a very large number of neurons. With today's computers it is feasible to simulate hundreds of thousands of compartments and millions of synapses at a reasonable level of biophysical detail. For large models the turnaround time for simulations, however, may be in the order of days, so parallel simulators are therefore useful. It is still beyond the capacity of today's supercomputers to handle full scale models of biological networks. A common practice is, therefore, to work with dramatically subsampled network models in which the number of neurons is reduced to a small fraction of those actually present in the target system. As a consequence, the number of input synaptic connections on cells in the model is also dramatically reduced. With cell models tuned to single cell data, for example, with adequate input resistances and thresholds, it will become necessary to compensate by exaggerating the synaptic conductances in order for the model to reproduce the activity seen in the real system. Having few and large synaptic interaction events in the system may, however, distort network dynamics, thus, making the model a poor quantitative representation of the actual system. Such effects should be born in mind when interpreting result from simulations using subsampled models.

Furthermore, one sometimes excludes from the model altogether neuron types known to exist in the actual biological system. For one reason or another a cell type may be considered unimportant for the questions addressed. One example is the neuroglia cells that are on average about ten times more numerous than neurons in the brain. They are thought to mainly serve the purpose of structural support and maintenance of the internal environment and are rarely included in network models. But one cannot entirely exclude that these cells in some situations subserve functions important for signal processing.

At the other extreme from networks of complex multi-compartmental model neurons are neural network models in which the biophysical detail has been reduced to a minimum. Such abstraction serves the important purpose of helping to pinpoint and elucidate the fundamental mechanisms behind the functioning of a complex system, which may enable further theoretical analysis of the phenomena under study.

A network model may be simplified in several different ways. For instance, the neurons can be modeled as point neurons (a single isopotential compartment) lacking geometric extent. Network units may use a graded output (with, for example, a sigmoid transfer function) representing an instantaneous firing frequency, or they may be spiking as real neurons. The former may, in fact, represent the average population activity in a cortical module like a minicolumn rather than an individual neuron. An integrate-and-fire model neuron is a bit more elaborate with a simple membrane dynamics and a spiking threshold (Gerstner, 1999). Whether or not temporal timing at the millisecond range in the spike trains of neurons is fundamental for the information processing in the brain or if a rate code is

adequate for most purposes is presently a hotly debated issue. Yet another class of models is neural continuum field models that represent the neural structure as a continuous sheet of excitable neural tissue with a lattice connectivity (Bressloff et al., 2002).

In simplified network models, the details of synaptic transmission and plasticity may be replaced with weighted inputs and simple learning rules. Signal delays along axons are ignored, which may be reasonable at least for millimeter distances in small networks. Instead of an accurate representation of short- and long-term synaptic plasticity, one typically incorporates a correlation-based learning rule, for example, some form of Hebbian learning (Rolls & Treves, 1997). The adiabatic learning hypothesis (Caianiello, 1961) stating that synaptic weight changes occur on a much slower timescale than the neurodynamics itself, simplifies the model and network dynamics considerably. On the other hand, this assumption is now known to be invalid in, for instance, the neocortex where synaptic properties are modulated on a millisecond timescale.

A modeling strategy that has often proven fruitful is to develop a suite of models at different levels of abstraction for the same neuronal network. The most detailed model relates closely to the biological network under study, and the aim is to transform in a well-defined fashion to gradually more abstract descriptions, using the most abstract ones as the starting point for theoretical analysis.

ANDERS LANSNER

See also **Artificial intelligence; Attractor neural network; Cell assemblies; Compartmental models; Hodgkin–Huxley equations; Integrate and fire neuron; McCulloch–Pitts network; Multiplex neuron; Nerve impulses; Neurons; Perceptron**

Further Reading

Bressloff, P.C., Cowan, J.D, Golubitsky, M., Thomas, P.J. & Wiener, M. 2002. What geometric visual hallucinations tell us about the visual cortex. *Neural Computation*, 14: 473– 491

Caianiello, E. 1961. Outline of a theory of thought processes and thinking machines. *Journal of Theoretical Biology*, 1: 204–235

Gerstner, W. 1999. Spiking neurons. In *Pulsed Neural Networks*, edited by W. Maass & C. Bishop, Cambridge, MA:MIT Press, pp. 3–53

Haykin, S. 1998. *Neural Networks: A Comprehensive Foundation*, Upper Saddle River, NJ: Prentice–Hall

Koch, C. & Segev, I. (editors). 1998. *Methods in Neuronal Modeling: From Ions to Networks*, Cambrigde, MA: MIT Press

Rolls, E. & Treves, A. 1997. *Neural Networks and Brain Function*, Oxford and New York: Oxford University Press

Scott, A.C. 2002. *Neuroscience. A Mathematical Primer*, Berlin and New York: Springer

NEURISTOR

Coined by Hewitt Crane in 1962, the term *neuristor* implies "the whole class of lines that exhibit attenuationless propagation with recovery" (Crane, 1962). In principal, this definition was intended to include active nerve fibers and even forest fires, but Crane's motivation was to overcome certain problems associated with the miniaturization of electronic circuits. Based upon a half-dozen reports prepared by Crane and his colleagues at the Stanford Research Institute since the late 1950s, this carefully written paper provides a window into the thinking of electrical engineers at the threshold of the integrated circuit revolution.

As the dimensions of conventional (transistor) computing circuits are greatly reduced, Crane reasoned, at least two design problems must be faced. First, the density of interconnections increases, eventually requiring "a dense set of interconnections at a point." Second, the resistance per unit length of interconnecting wires may become inconveniently large. (Crane pointed out that the resistance of a 1 μm copper wire is about a $1000\,\Omega/\text{in.}$) Both of these problems may be mitigated by basing miniaturized computer design upon an "active wire" in which energy is stored uniformly over the system and continuously dissipated by nonlinear traveling-wave impulses, rather than at discrete and isolated amplifying elements. Some indication that neuristor design is a promising strategy is offered by the fact that it was selected by evolution for the development of our biological brains.

Being uniform in the direction of propagation, Crane's active wire supports a traveling-wave impulse in which the rate of energy release is equal to its rate of dissipation. Upon impulse passage, the line remains inactive for a certain time (the refractory period), after which it is able to transmit a new impulse. Because an impulse cannot propagate through a refractory region, two impulses will destroy one another in a head-on collision, and impulses are not reflected from the end of a neuristor line.

If two interconnection junctions are included—both of which seem feasible from an engineering perspective—a neuristor system is logically complete, meaning that it can realize all possible Boolean switching functions. These two neuristor interconnections are as follows. (a) A T junction is shown in Figure 1(a). An impulse entering on one of the branches proceeds outward on the other branches. Such a junction is not difficult to realize, requiring merely that the strength of the incoming impulse divided by the number of outgoing branches is above the threshold of the outgoing branches. (b) An R junction is shown in Figure 1(b). In an R junction, the refractory (or inhibitory) variable of one line is shared with an adjacent line (over the shaded area), while the excitatory variable is not. Thus, individual impulses traveling from A to B (on the upper line) can block individual impulses traveling from D to C (on the lower line) and vice versa. These two junctions can be interconnected in a variety of useful ways,

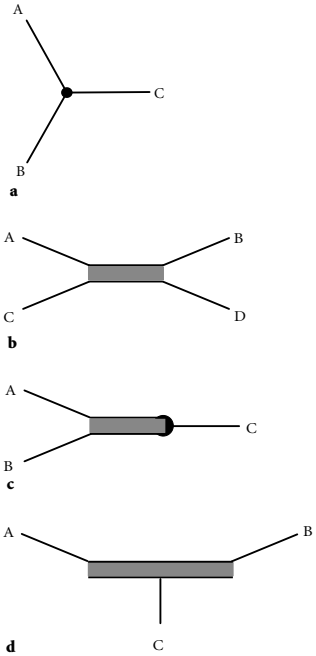

Figure 1. Some simple neuristor interconnections. (a) *T* junction. (b) *R* junction. (c) *T*–*R* junction. (d) Analog of a relay or transistor.

one being the *T*–*R* junction, shown in Figure 1(c). Here impulses incoming on line A will proceed through to C but will not be transmitted to B, effectively isolating the input lines (A and B) from each other.

In considering the switching possibilities of such neuristor systems, Boolean variables can be chosen in either of two ways, indicating the presence or absence of individual impulse or the presence or absence of impulse trains. From the latter perspective, the arrangement in Figure 1(d) can be viewed as equivalent to a relay or a transistor because an incoming impulse train on line C will block the transmission between A and B. As computing systems constructed from relays or transistors are known to be logically complete, it follows that neuristor systems are also logically complete.

The length of the refractory zone of an impulse is equal to the product of its velocity times the recovery interval. This is an important design parameter for a neuristor system, setting the scale for many functions. If a circular section of active line is used as a storage ring, for example, the circumference of this ring must be greater than the length of a refractory zone. Thus an insufficiently short refractory length is a major limitation on the degree to which a particular neuristor system can be miniaturized.

In his seminal paper, Crane offered several suggestions for neuristor realizations, taking advantage of the variety of interesting nonlinear diode structures that were being invented in the early 1960s—such as Esaki (tunnel) diodes and four-layer diodes. Also suggested was an ingenious combination of *T* and *R* junctions that allows two signal paths to cross without interference and without being lifted from a common substrate.

Although neuristors have been designed and fabricated in various laboratories (Beretovskii, 1963; Yoshizawa & Nagumo, 1964; Sato & Miyamoto, 1967; Parmentier, 1969; Scott, 1970; Reible & Scott, 1975; Nakajima et al., 1976), the neuristor strategy has not been important for the design of modern computing systems. Among other reasons for this failure must be counted the amazing progress in miniaturization of silicon metal-oxide-semiconductor transistors, which are now far smaller than the refractory length of any conceivable neuristor structure.

Beyond applications to electronic computing systems, however, the neuristor design concept may yet aid in understanding the behavior of neural systems, as was suggested by Crane in the early 1960s (Crane, 1964). Indeed, this possibility is more compelling today because dendritic fibers (in addition to axons) are now known to support action potentials and are, therefore, also neuristors in the original sense of the word (Stuart et al., 1999). Thus, possibilities arise for neuristor-like computations in the axonal and dendritic trees of real neurons (Scott, 2002). Neuroscientists studying the intricate networks of interwoven dendro-dendritic, currently being revealed by electron microscopy, may profit from a review of Crane's early work.

ALWYN SCOTT

See also **Multiplex neuron; Nerve impulses; Neurons**

Further Reading

Beretovskii, G.N. 1963. Study of single electric model of neuristor. *Radio Engineering and Electronic Physics*, 18: 1744–1751

Crane, H.D. 1962. Neuristor—a novel device and system concept. *Proceedings of the IRE*, 50: 2048–2060

Crane, H.D. 1964. Possibilities for signal processing in axon systems. In *Neural Theory and Modeling,* edited by R.F. Reiss. Stanford: Stanford University Press, pp. 138–153

Nakajima, K., Onodera, Y. & Ogawa, Y. 1976. Logic design of Josephson network. *Journal of Applied Physics*, 47: 1620–1627

Parmentier, R.D. 1969. Recoverable neuristor propagation on superconductive tunnel junction strip lines. *Solid-State Electronics*, 12: 287–297

Reible, S.A. & Scott, A.C. 1975. Pulse propagation on a superconductive neuristor. *Journal of Applied Physics*, 46: 4935–4945

Sato, R. & Miyamoto, H. 1967. Active transmission lines. *Electronics and Communications in Japan*, 50: 131–142
Scott, A.C. 1970. *Active and Nonlinear Wave Propagation in Electronics*, New York: Wiley
Scott, A.C. 2002. *Neuroscience: A Mathematical Primer*, Berlin and New York: Springer
Stuart, G., Spruston, N. & Häusser, M. (editors). 1999. *Dendrites*, Oxford and New York: Oxford University Press
Yoshizawa, S. & Nagumo, J. 1964. A bistable distributed line. *Proceedings of the IEEE*, 52: 308

NEURONS

Nerve cells, or neurons, are typically comprised of a cell body, dendrites, and an axon. The typical cortical neuron depicted in Figure 1 has both an apical dendrite and several basal dendrites. Dendrites and the soma are the sites at which axon terminals from other neurons make contacts and provide stimulation to a neuron. These sites of contact between neurons are termed synapses. The axon emanates from the cell body and contacts other neurons at distances varying from 1.0 mm up to almost 1 m, depending upon the the type and location of the neuron in question. The ends of axons terminate very close to the dendritic and cell body membranes of other neurons to form synpases. When the cell body of a neuron is sufficiently depolarized by its inputs, it reaches the threshold for action potential (or spike) generation, and one or more spikes are triggered. These spikes then propagate along the axon at speeds ranging from less than $1.0\,\mathrm{ms}^{-1}$ up to almost $100\,\mathrm{ms}^{-1}$.

Neurons receive both excitatory (depolarizing) and inhibitory (hyperpolarizing) stimulation from the axon terminals that synapse onto them, with a typical cortical neuron having about 10^3–10^4 synapses. When an action potential reaches a synapse, it causes the release of neurotransmitter molecules that rapidly diffuse across the very small extracellular space to the membrane of the postsynaptic cell's dendrite or soma. There they bind to receptor molecules and cause ion channels to open resulting in either depolarization (excitatory synapse) or hyperpolarization (inhibitory synapse). These potential changes propagate down the dendrites to the cell body, where they are combined approximately linearly. If this net potential change depolarizes the cell body past a threshold, the neuron will fire one or more spikes. These spikes in turn propagate along the axon of this cell, and the process repeats itself.

Nonlinear Dynamics of Action Potential Generation

In mathematical terms, a series of action potentials is a limit cycle oscillation in the neural state space. There are several distinct dynamical patterns of action potential generation that have been observed, and these will be characterized in terms of their dynamical foundations.

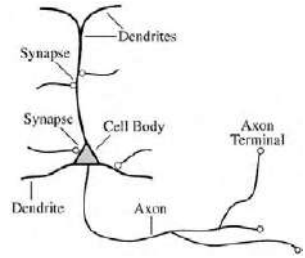

Figure 1. Schematic diagram of a typical neuron in the neocortex. The longest dendrites are between 1–3 mm in length, while the axon can be as short as a few mm or as long as 1.0 m.

As demonstrated by Hodgkin and Huxley (1952) in work that led to the Nobel Prize in 1963, the dynamics of spike generation is based upon two ionic currents: a sodium (Na^+) current that rapidly depolarizes the neuron followed by a slower potassium (K^+) current that repolarizes the neuron. Each current I_j is described by Ohm's law written as the product of a conductance (reciprocal of resistance) g_j and a voltage. For each ion, the voltage term is given by the difference between the membrane potential V and the equilibrium potential for the ion in question, E_j

$$I_j = g_j(V - E_j) \tag{1}$$

Due to the fact that the neural cell membrane functions as a capacitor, the membrane potential V is described by a differential equation of the form

$$\mathrm{C}\frac{\mathrm{d}V}{\mathrm{d}t} = g_{\mathrm{Na}}(V)\,(V - E_{\mathrm{Na}}) + g_{\mathrm{K}}(V)\,(V - E_{\mathrm{K}}) + I_{\mathrm{ext}}, \tag{2}$$

where I_{ext} is an external stimulating current (or a synaptic input). For typical cortical neurons, $E_{\mathrm{Na}} = 55\,\mathrm{mV}$ and $E_{\mathrm{K}} = -95\,\mathrm{mV}$. This equation would be linear except for one crucial observation: the two conductances $g_{\mathrm{Na}}(V)$ and $g_{\mathrm{K}}(V)$ are functions of V. This biophysical discovery by Hodgkin & Huxley (1952) means that ion conductances change with the voltage, thereby generating both positive and negative nonlinear feedback that produces the action potential.

A simple set of equations with normalized variables (Wilson, 1999a) can be used to elucidate the essential dynamics of Equation (2):

$$\frac{\mathrm{d}V}{\mathrm{d}t} = 4\left(V^2 - \frac{V}{10}\right)(V - 1) + R\left(V + \frac{1}{5}\right) + I_{\mathrm{ext}},$$

$$5\frac{\mathrm{d}R}{\mathrm{d}t} = R + 3V^2 \tag{3}$$

The term $(V^2 - V/10)$ on the right in the first equation represents the V dependence of the Na^+

conductance as a quadratic function, while the variable R (Recovery variable) represents the K^+ conductance governed by the second equation. Note that the time constant for the second equation is 5 times slower than that in the first equation. Normalization has shifted the resting potential from -70 mV to zero and has set $E_{Na} = 1$ here, which corresponds to 125 mV above the resting potential. Similarly, $E_K = -\frac{1}{5}$, or 25 mV below the resting potential. Finally, the unit of time here corresponds to 0.10 ms to produce spike durations of 1.0 ms. These simplifications make the mathematical analysis significantly easier. A version of these equations with parameter values optimized to describe human neocortical excitatory and inhibitory neurons may be found elsewhere (Wilson, 1999b).

For $I_{ext} = 0$, Equation (3) has three steady states at $V = 0, R = 0$ (resting state); $V = \frac{1}{7}, R = \frac{3}{49}$; and $V = \frac{2}{5}$, $R = \frac{12}{25}$. In order, these are an asymptotically stable node, a saddle point, and an unstable spiral point. The spike firing threshold occurs for $I_{ext} = 0.012$, where the saddle point and node coalesce in a saddle-node bifurcation to a limit cycle. This permits spike firing at arbitrarily low rates for I_{ext} just above threshold, which is characteristic of human and mammalian cortical neurons (Wilson, 1999a). A spike train for $I_{ext} = 0.013$ is depicted in Figure 2a. Above threshold, spike rate increases monotonically as a function of I_{ext}. Neurons that begin firing at arbitrarily low rates due to a saddle-node bifurcation are known as Class I neurons.

A different form of dynamics characterizes Class II neurons. The simplest example is obtained by replacing the dR/dt equation above with

$$5\frac{dR}{dt} = R + 2V. \tag{4}$$

For $I_{ext} = 0$, the equations now have a single steady state $V = 0$, $R = 0$. It can be shown that these neural equations undergo a subcritical Hopf bifurcation (Wilson, 1999a) to spiking at $I_{ext} = 0.062$. In this case firing begins at a relatively high spike rate, as arbitrarily low rates are precluded by the nature of the bifurcation to spiking. The original Hodgkin–Huxley (1952) equations, in fact, describe a Class II neuron (the giant axon of the squid).

Neurons in the cortex of humans and other mammals are Class I neurons. Thus, they begin firing at arbitrarily low spike rates (less than one spike per second), and this provides a greatly expanded dynamic range for encoding stimulus intensity into spike frequency. In addition, excitatory cortical neurons (but not most inhibitory neurons) typically have several additional currents that can produce even more complex spiking dynamics. For example, addition of a slow Ca^{2++} current and an even slower Ca^{2++}-driven K^+ current results in a neuron that fires bursts of spikes (Wilson, 1999a,b), as illustrated in Figure 2b.

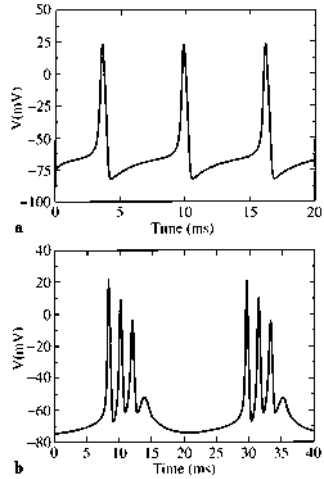

Figure 2. Spikes generated by neural equations. (a) Periodic spike train generated by Equation (3). (b) Pattern of spike bursts generated by a more complex cortical neuron with additional currents. Both graphs have been transformed back from the normalized form described in the text to reflect the mV range and ms time range actually encountered with cortical neurons.

Conclusions

Action potential dynamics are governed by two processes. Once threshold is reached, a rapid influx of Na^+ ions results in depolarization of the neuron causing the upswing of the spike. This process is described by the first term in the dV/dt equation in (3) above. Following this, the variable R increases, permitting K^+ to pass out of the neuron, thus hyperpolarizing it back toward its resting potential. The limit cycle is generated because the recovery variable R operates on a slower time scale than the very rapid Na^+ depolarization. There is also an inactivation of the Na^+ ion current that contributes to termination of the spike (Hodgkin & Huxley, 1952), but it is not essential to the dynamics of spike generation.

Virtually all brain function involves a dynamical interaction between excitatory and inhibitory neurons. For example, short-term memory circuits involve groups of neurons that are reciprocally interconnected by excitatory synapses, which enables them to continue firing following the cessation of stimulation. This ongoing neural activity makes up the short-term memory store. Inhibition is necessary both to shut off short-term memory activity and to prevent it from spreading to activate other neurons. Indeed, when there is too little inhibition in a brain area due to

an imbalance or injury, the spread of excitation may generate epileptic seizures. Many other examples of excitatory and inhibitory neural circuits may be found elsewhere (Wilson, 1999a; Dayan & Abbott, 2001).

HUGH R. WILSON

See also **Hodgkin–Huxley equations; Integrate and fire neuron; Nerve impulses**

Further Reading

Dayan, P. & Abbott, L.F. 2001. *Theoretical Neuroscience*, Cambridge, MA: MIT Press

Hille, B. 1992. *Ionic Channels of Excitable Membranes*, Sunderland, MA: Sinauer

Hodgkin, A.L. & Huxley, A.F. 1952. A quantitative description of membrane current and its application to conduction and excitation in nerve. *Journal of Physiology*, 117: 500–544

Koch, C. 1999. *Biophysics of Computation: Information Processing in Single Neurons*, Oxford and New York: Oxford University Press

Wilson, H.R. 1999a. *Spikes, Decisions, and Actions: Dynamical Foundations of Neuroscience*, Oxford and New York: Oxford University Press

Wilson, H.R. 1999b. Simplified dynamics of human and mammalian neocortical neurons. *Journal of Theoretical Biology*, 200: 375–388

NEWELL–WHITEHEAD–SEGEL EQUATION

See **Complex Ginzburg–Landau equation**

NEWTON'S LAWS OF MOTION

Isaac Newton's treatise *Philosophiae Naturalis Principia Mathematica* (Mathematical Principles of Natural Philosophy), often simply referred to as the *Principia*, was completed in May 1686. Publication and printing were overseen by the astronomer Edmund Halley, and the work became available to the public in 1687. In this work Newton sets out, in effect, a template for classical mathematical physics, the dynamics of particles and rigid bodies in particular. The text starts by defining certain basic quantities such as mass, momentum, inertia, force, and acceleration. Once these have been defined and some of their basic properties described, Newton states his "axioms" or "laws of motion" thus:

> *Law I*: Every body continues in its state of rest, or of uniform motion in a right line, unless it is compelled to change that state by forces impressed upon it;
> *Law II*: The change of motion is proportional to the motive force impressed; and is made in the direction of the right line in which that force is impressed;
> *Law III*: To every action there is always opposed an equal reaction: or, the mutual actions of two bodies upon each other are always equal, and directed to contrary parts.

(We have quoted the established 1729 translation from the original Latin to English by Andrew Motte.) In modern terms the first law, also known as the law of inertia, and already realized by Galileo, states that uniform translational motion is a "natural" state of motion for a particle or body requiring no cause or outside agent to maintain it. (This was an important departure from Aristotelian physics, which held that all motion required an explanation.) Not so with accelerated motion, according to the second law. If a change in the velocity of motion is to come about, it requires the action of a force acting on the particle or body. Finally, in the third law we have the requirement that if a body, A, is acted upon by a force due to another body, B, then B is subject to a force of the same magnitude but of opposite direction from its interaction with A.

Forces

Newtonian mechanics, then, operates with purely kinematic entities, such as position, velocity, and acceleration, and with a set of new, dynamical entities called forces. Newton's laws of motion instruct us to seek the cause of acceleration, a kinematic quantity, in the total force acting on a particle or body. Force is a dynamic quantity. The mass of the particle or body appears as the constant of proportionality in the relation between force (the cause) and acceleration (the effect). Like accelerations, forces are vectors. If two or more forces act simultaneously, they add vectorially and their resultant gives both the correct magnitude and the correct direction of the net force. Many well-known results about levers, systems with suspended masses, and various simple mechanical machines were immediately subsumed under Newtonian mechanics simply by recognizing that forces behave like vectors upon superposition.

Not only did Newton establish a framework for dynamics—and for much of physics—with his three laws, he provided also a new law of Nature for the attractive force of gravity acting between any two bodies. This development was, in some sense, extraneous to the three laws of motion but without it, the full force of Newton's dynamics might not have been appreciated and embraced. Newton's expression for the force acting on a particle, 1, of mass m_1 located at $\boldsymbol{x}_1$ due to a particle, 2, of mass m_2, located at $\boldsymbol{x}_2$, is

$$\boldsymbol{F}_{12} = Gm_1m_2\boldsymbol{e}_{12}/r^2. \qquad (1)$$

Here r is the distance between the two particles, $r = |\boldsymbol{x}_1 - \boldsymbol{x}_2|$ and $\boldsymbol{e}_{12}$ is the unit vector pointing from the location of particle "1" to the location of particle "2", that is, $\boldsymbol{e}_{12} = (\boldsymbol{x}_2 - \boldsymbol{x}_1)/r$. The coefficient G, now known as Newton's universal gravitational constant, has the approximate value $G \approx 6.672 \times 10^{-8}\,\mathrm{cm}^3\,\mathrm{g}^{-1}\,\mathrm{s}^{-2}$.

The first measurements of G were performed by Henry Cavendish in 1798 using a torsion balance. Expression (1) is fully consistent with Newton's third

law, which demands that $\boldsymbol{F}_{12} = -\boldsymbol{F}_{21}$. Force (1) represents action-at-a-distance in the sense that it does not result from direct contact between contiguous bodies or particles. Newton was severely criticized by his contemporaries for this notion, which they viewed as fanciful and unsubstantiated.

In modern terminology, in the *Principia* Newton accomplished (among many other things) integration of the two-body problem of celestial mechanics, that is, the following system of differential equations, which result by combining Newton's law of gravitation with his second law of motion:

$$m_1 \, \mathrm{d}^2\boldsymbol{x}_1/\mathrm{d}t^2 = Gm_1m_2(\boldsymbol{x}_2 - \boldsymbol{x}_1)/|\boldsymbol{x}_2 - \boldsymbol{x}_1|^3, \quad (2a)$$

$$m_2 \mathrm{d}^2\boldsymbol{x}_2/\mathrm{d}t^2 = Gm_1m_2(\boldsymbol{x}_1 - \boldsymbol{x}_2)/|\boldsymbol{x}_1 - \boldsymbol{x}_2|^3. \quad (2b)$$

Because of Newton's third law, addition of Equations (2) yields

$$m_1 \, \mathrm{d}^2\boldsymbol{x}_1/\mathrm{d}t^2 + m_2 \, \mathrm{d}^2\boldsymbol{x}_2/\mathrm{d}t^2 = 0, \quad (3)$$

which shows that the total momentum of the system, given by

$$\boldsymbol{P} = m_1 \mathrm{d}\boldsymbol{x}_1/\mathrm{d}t + m_2 \, \mathrm{d}\boldsymbol{x}_2/\mathrm{d}t, \quad (4)$$

is a constant of the motion. Thus, the center of mass of the two particles,

$$\boldsymbol{R} = (m_1\boldsymbol{x}_1 + m_2\boldsymbol{x}_2)/(m_1 + m_2), \quad (5)$$

moves with constant velocity $\boldsymbol{P}/M$ through space, where $M = m_1 + m_2$ is the total mass of the two-body system.

On the other hand, subtracting (2a) from (2b) gives

$$m\mathrm{d}^2\boldsymbol{r}/\mathrm{d}t^2 = -Gm_1m_2\boldsymbol{r}/r^3, \quad (6)$$

where $\boldsymbol{r} = \boldsymbol{x}_2 - \boldsymbol{x}_1$, $r = |\boldsymbol{r}|$, $M = m_1 + m_2$ as before, and $m = m_1m_2/(m_1 + m_2)$ is called the reduced mass. Equation (5) tells us that the problem of the relative motion of the two particles is equivalent to solving for the motion of a single (fictitious) particle of mass m in the same field of force centered at the origin of coordinates. Such a fixed force field pointing toward a given point in space (here chosen as the origin of coordinates) is called a central force.

Once (6) is solved, the original positions of the two gravitationally attracting particles may be reconstructed from the formulae

$$\boldsymbol{x}_1 = \boldsymbol{R} - m_2\boldsymbol{r}/M, \quad \boldsymbol{x}_2 = \boldsymbol{R} + m_1\boldsymbol{r}/M. \quad (7)$$

The differential equation for the vector function $\boldsymbol{r}$ is nonlinear because the magnitude of the force falls off with the square of the distance. Many force laws of interest in applications have the property that they are nonlinear functions of the positions of the constituent particles of the system. The force law for small extensions of a high-quality spring, known as Hooke's law, which states that the force is directly proportional to the deviation from equilibrium, is an important and notable exception.

Newton showed in the *Principia* that the general solution of (6) is that $\boldsymbol{r}$ traces out a conic section (ellipse or hyperbola, with a parabola as the "cross-over" possibility) corresponding to bounded or unbounded relative motions of the two original particles. The bounded motions apply to planets orbiting the Sun or the Moon orbiting the Earth. The effects of bodies farther away are to be treated subsequently by adding perturbations to the above analysis. Unbounded motions are realized by comets. Newton further considered the effects of the finite extension of the attracting body, for example, Earth's finite size relative to the Moon's orbit, and the effect of the deformation of the attracting body due to tidal forces.

HASSAN AREF

See also **Celestial mechanics; Determinism; *N*-body problem**

Further Reading

Chandrasekhar, S. 1995. *Newton's Principia for the Common Reader*, Oxford: Clarendon Press and New York: Oxford University Press

Newton, I. 1934. *Mathematical Principles of Natural Philosophy and System of the World*, translated by A. Motte (1729), edited by F. Cajori, 2 vols, Berkeley: University of California Press

NEWTON'S METHOD

See **Numerical methods**

NODES OF RANVIER

See **Myelinated nerves**

NOISE (WHITE, COLORED ETC.)

See **Stochastic processes**

NONATTRACTING CHAOTIC SETS

See **Chaotic dynamics; Invariant manifolds and sets**

NONAUTONOMOUS SYSTEMS

See **Phase space**

NONEQUILIBRIUM STATISTICAL MECHANICS

Nonequilibrium statistical mechanics aims to describe the behavior of large systems of particles removed from the state of thermodynamic equilibrium, in terms of the properties of the individual constituents and their interactions, as provided by the laws of classical and quantum mechanics. Such systems give rise to irreversible behavior in the form of an approach to thermodynamic equilibrium in the absence of permanent constraints (isolated systems), or to

a stationary nonequilibrium state in systems under constraint (referred to as thermostatted systems).

The fundamental problem of non-equilibrium statistical mechanics is to reconcile irreversible behavior at the macroscopic level with the reversible character of the underlying microscopic laws of mechanics. For a long time it was thought that irreversibility could not be understood entirely from mechanics, an idea that led to the systematic introduction of probabilistic ideas in the traditional deterministic description. As a result, the laws of statistical mechanics have frequently been regarded as analogs of the law of large numbers and similar universal laws of probability and statistics, independent of any explicit reference to the nature of the underlying dynamics. Since the 1980s, one has witnessed a change of perspective following the realization that the trajectories of individual particles in an N-body system are typically chaotic.

Boltzmann's Kinetic Theory. Ergodic and Mixing Hypotheses

In 1872, Ludwig Boltzmann derived by what appeared to be completely mechanical arguments his famous kinetic equation for dilute gases (Brush, 1965, 1966). This equation features the time-dependent probability distribution function f, of position $\boldsymbol{r}$ and velocity $\boldsymbol{v}$, for a particle in the gas and allows one to reproduce in a very satisfactory way the transport and flow properties of the system. The kinetic theory culminates in the derivation of the H-theorem, whereby in a homogeneous system the functional $H = k \int f \ln f \, d\boldsymbol{v}$ (k being the Boltzmann constant) decreases monotonously until f reaches its equilibrium form given by the Maxwell–Boltzmann distribution. The H-theorem should provide, then, a microscopic justification of the second law of thermodynamics. This claim prompted rather negative reactions, crystallized in the famous reversibility (Loschmidt's) and recurrence (Zermelo's) paradoxes. Boltzmann was unable to fully refute these objections since, as he himself recognized, his derivation makes use of a heuristic probabilistic assumption—the *Stosszahlansatz* or the assumption of molecular chaos—which allowed him to express approximately the rate at which binary collisions are taking place only in terms of the one-particle probability density f.

In trying to answer his critics Boltzmann enunciated the ergodic hypothesis, which eventually became a key concept in the entire field of statistical mechanics. Specifically, Boltzmann suggested that (a) in an isolated many-body system the overwhelming part of the phase space consists of regions where the macroscopic properties are very close to the equilibrium properties, (b) the system's trajectory will spend equal times in phase space regions of equal extent, and (c) the macroscopic properties of the system will essentially be constant throughout the allowable part of phase space and will coincide with the long-time averages of the corresponding microscopic quantities over the phase space trajectory. These statements were later completed by the equally ground-breaking discovery by Josiah W. Gibbs of the concept of mixing: the dynamical evolution of an isolated system initially occupying a limited phase space region compatible with some prescribed values of its macroscopic observables will lead it eventually to occupy uniformly (at least in a coarse-grained sense) the entire phase space available.

In their original forms, the ergodic hypothesis and the stronger mixing hypothesis had the serious drawback of relying to a considerable extent on the coarse-grained way one observes the system. Modern ergodic theory starts with the work of Henri Poincaré and George Birkhoff (Arnol'd & Avez, 1968), who were able to relate ergodicity to certain well-defined properties of the underlying deterministic evolution laws. Two examples are provided by Birkhoff's theorem on the existence of the limit $1/T \int_0^T A(t) \, dt$ as $T \to \infty$ of an integrable phase space function A provided that the motion remains bounded in phase space and by Poincaré's theorem that for systems satisfying suitable resonance conditions there exist no invariants other than total energy that are analytic in some parameter. Since the 1950s, a great deal of effort has been devoted to prove whether a system described by a given Hamiltonian will or will not fulfill these properties and to what extent these properties bear a clear-cut relationship with the type of dynamics going on in phase space. An early (negative) result of considerable historical importance was obtained by Enrico Fermi, John R. Pasta, and Stanislaw Ulam (1955), who showed that in a system of coupled nonlinear oscillators energy may remain localized rather than be equipartitioned among the individual degrees of freedom. At the other extreme, one finds Yakov Sinai's result (Sinai, 1970) on the ergodic and mixing behavior of a system of hard spheres. This work signaled the beginning of a series of developments aimed at relating the foundations of non-equilibrium statistical mechanics to the instability of motion of large classes of non-integrable dynamical systems giving rise to sensitivity to initial conditions and to deterministic chaos, known to be generic since the work of Andrei Kolmogorov.

Generalized Kinetic Theories

In parallel, and largely independently of progress in ergodic theory, the need to go beyond the assumptions underlying Boltzmann's equation became a central preoccupation from the mid-1940s. Three major attempts along this line were initiated by Nikolai Bogolubov, Leon Van Hove, and Ilya Prigogine and his colleagues (see, e.g., Balescu, 1975). Their

starting point was a systematic perturbation expansion of the Liouville equation and its quantum counterpart for the N-particle probability distribution or density matrix, or the hierarchy of equations for the reduced n-particle ($n = 1, \ldots, N$) distribution functions obtained by integrating the Liouville equation over the $N - n$ particles, known as the BBGKY hierarchy. This procedure led as a first step to exact, formal non-Markovian equations of the form

$$\frac{\partial \rho_s}{\partial t} + K\rho_s(t) = \int_0^t \mathrm{d}\tau\, G(t-\tau)\rho_s(\tau) + D(t), \quad (1)$$

where ρ_s is a reduced distribution, K stands for the contribution of the mean field, G is a memory kernel, and $D(t)$ depends on the initial correlations in the subspace of phase space complementary to the one of ρ_s. Closed kinetic equations for reduced probability densities could then be obtained under certain assumptions, linked to first principles in a more clear-cut way than Boltzmann's *Stosszahlansatz*: Bogolubov's ansatz of higher-order distributions becoming functionals of the one-particle one, Prigogine's ansatz on initial correlations, van Hove's random phase approximation. But even when these conditions are satisfied, it has so far proved impossible to establish a general H-theorem for the corresponding equations. Still, generalized kinetic equations have been at the foundation of spectacular progress in such fields as the study of dense fluids and plasmas and the microscopic theory of transport coefficients in the linear range of irreversible phenomena close to equilibrium.

Microscopic Chaos and Nonequilibrium Statistic Mechanics

Generalized kinetic theories rest on approximations whose validity is difficult to assess. Furthermore, there is no explicit link between the structure of the kinetic equations and the nature of the microscopic dynamics in phase space. In view of the fundamental importance and the ubiquity of irreversibility in the natural world, it would certainly be desirable to arrive at a description free of both these limitations. This has been achieved since the 1980s by the cross-fertilization between dynamical systems, nonequilibrium statistical mechanics, and microscopic simulation techniques.

Mapping to a Markov Process

A first series of attempts pertains to the class of strongly unstable systems known as Kolmogorov flows, in which each phase space point lies at the intersection of stable and unstable manifolds. It takes advantage of the existence in such systems of special phase space partitions—the Markov partitions—whose boundaries remain invariant under the dynamics, each partition cell being mapped at successive time steps into a union of partition cells. If the operator projecting the full phase space dynamics on such a partition commutes with the Liouville operator, then the Liouville equation can be mapped into an exact Markovian equation exhibiting an H-theorem. This provides a rigorous microscopic basis of coarse-graining (Penrose, 1970; Nicolis et al., 1991). The mapping is, however, not one-to-one as the projection operator is not invertible reflecting the loss of information associated with this process. Ilya Prigogine, Baidyanath Misra, and Maurice Courbage (Prigogine, 1980) succeeded in constructing a non-unitary, invertible, transformation operator Λ, which transforms the unitary evolution operator U_t (essentially the exponential of the Liouville operator) into a Markov semigroup W_t

$$W_t = \Lambda U_t \Lambda^{-1} \quad (2)$$

The idea of non-unitary transformations has also been extended to more general classes of systems, such as non-integrable systems generating Poincaré resonances.

Escape Rate Formalism and Deterministic Thermostats

A second line of approach aims to express transport coefficients and other macroscopic level properties including entropy production in terms of the quantifiers of the microscopic chaos prevailing at the level of individual particle trajectories (in a classical setting). Two different methodologies have been developed.

The escape rate formalism (Gaspard, 1998; Dorfman, 1999). In this formalism, transport in Lorentz gas type systems is linked to the escape from a fractal repellor formed by trajectories for which a certain microscopic quantity associated with the macroscopic flux of interest remains confined in phase space. The corresponding transport coefficients are then expressed in terms of the Lyapunov exponents of the repellor and its Kolmogorov–Sinai entropy or its fractal dimension. No boundary conditions need to be imposed. Furthermore, the hydrodynamic modes associated with the process are computed as generalized eigenmodes of the Liouvillian and turn out to be fractal distributions.

Deterministic thermostats. The question here is how to express in purely mechanical terms a constraint maintaining a system away from equilibrium. One of the most popular ways to achieve this is to augment (in a classical system) the Hamiltonian dynamics by dynamical friction terms preserving the time-reversal symmetry (Hoover, 1999). In this way, one obtains a dissipative dynamical system where the rate of phase space volume contraction and the entropy production are shown to be related to the sum of the Lyapunov exponents. The non-equilibrium steady states generated in this formalism are fractal attractors, contrary to the equilibrium states that extend over the entire phase space available. Furthermore, they are believed to satisfy an interesting fluctuation theorem (Gallavotti &

Cohen, 1995) expressing the probability of fluctuations associated with particles moving in a direction opposite to the applied constraint.

Statistical Mechanics of Dynamical Systems

Yakov Sinai, David Ruelle, and Rufus Bowen (see, for example, Ruelle, 1999) have shown that the long-time behavior of a large class of chaotic dynamical systems is determined by an invariant probability measure characterized by a variational principle, thereby establishing a link with ergodic theory and equilibrium statistical mechanics. A major difference is that contrary to equilibrium measures, Sinai–Ruelle–Bowen (SRB) measures are smooth only along the expanding directions while they possess a fractal structure along the contracting ones. This provides a rationale for characterizing the fractal character of the non-equilibrium steady states generated by deterministic thermostats. Furthermore, it has been the starting point of a series of developments aimed at characterizing low-order deterministic dynamical systems showing complex behavior through probability densities and the spectral properties of their evolution operators, such as the Liouville or the Frobenius–Perron operators (Lasota & Mackey, 1985). In a different vein, the transport induced by the overlap of resonances arising, in particular, around a separatrix has been investigated (Lichtenberg & Lieberman, 1983; Balescu, 1997). These approaches have provided insights to questions motivated by non-equilibrium statistical mechanics that had remained unsolved for a long time, owing to the formidable difficulties arising from the presence of a large number of interacting particles.

Non-equilibrium Statistical Mechanics as a Tool to Understand Cooperative Behavior in Complex Systems

Non-equilibrium statistical mechanics has been a source of inspiration providing interesting ways to analyze complex nonlinear systems arising in chemistry, fluid mechanics, biology, or even finance and sociology. One of the earliest applications was a mesoscopic approach describing the dynamics of fluctuations of the macroscopic observables of such systems around a reference state, using master equation or Langevin–Fokker–Planck equation descriptions (Nicolis & Prigogine, 1977; Haken, 1977). It led to a theory of nonequilibrium phase transitions showing how macroscopic level bifurcation phenomena are reflected at the microscopic level through the anomalous behavior of the non-equilibrium fluctuations. When applied to nanoscale systems, this approach provides interesting insights on energy transduction by non-equilibrium devices such as biological macromolecules, referred to as molecular motors (Astumian, 1997).

Finally, the formalism of non-equilibrium statistical mechanics is well suited to studying the cooperative behavior of interacting multi-agent systems involved in, for instance, food webs and other networks of connected elements, finance, or social phenomena. In this setting, the relevance of power laws describing the statistical behavior of certain systems has attracted considerable interest, the idea being that such laws reflect well the ability of complex systems to show adaptive behavior and to optimize information flows (Albert & Barabasi, 2002). The dynamical origin of these laws and the role of non-equilibrium constraints remain major open questions.

G. Nicolis

See also **Chaotic dynamics; Emergence; Ergodic theory; Fermi–Pasta–Ulam oscillator chain; Markov partitions; Recurrence; Sinai–Ruelle–Bowen measures; Synergetics**

Further Reading

Albert, R. & Barabasi, A.S. 2002. Statistical mechanics of complex networks. *Reviews of Modern Physics*, 74: 47–97

Arnol'd, V. & Avez, A. 1968. *Ergodic Problems of Classical Mechanics*, New York: Benjamin

Astumian, R.D. 1997. Thermodynamics and kinetics of a Brownian motor. *Science*, 276: 917–922

Balescu, R. 1975. *Equilibrium and Nonequilibrium Statistical Mechanics*, New York: Wiley

Balescu, R. 1997. *Statistical Dynamics*, London: Imperial College Press

Brush, S. 1965, 1966. *Kinetic Theory*, vols. I and II. London: Pergamon Press

Dorfman, J.R. 1999. *An Introduction to Chaos in Nonequilibrium Statistical Mechanics*, Cambridge and New York: Cambridge University Press

Fermi, E., Pasta, J.R. & Ulam S. 1955. *Studies of nonlinear problems*. Los Alamos Scientific Laboratory, Report NoLA-1940

Gallavotti, G. & Cohen, E.G.D. 1995. Dynamical ensembles in nonequilibrium statistical mechanics. *Physics Review Letters*, 74: 2694–2697

Gaspard, P. 1998. *Chaos, Scattering and Statistical Mechanics*, Cambridge and New York: Cambridge University Press

Haken, H. 1977. *Synergetics*, Berlin: Springer

Hoover, W.G. 1999. *Time Reversibility, Computer Simulation, and Chaos*, Singapore: World Scientific

Lasota, A. & Mackey, M. 1985. *Probabilistic Properties of Deterministic Systems*, Cambridge and New York: Cambridge University Press

Lichtenberg, A.J. & Lieberman, M.A. 1983. *Regular and Stochastic Motion*, Berlin: Springer

Nicolis, G., Martinez, S. & Tirapegui, E. 1991. Finite coarse-graining and Chapman–Kolmogorov equation in conservative dynamical systems. *Chaos, Solitons and Fractals*, 1: 25–37

Nicolis, G. & Prigogine, I. 1977. *Self-organization in Non-equilibrium Systems*, New York: Wiley

Penrose, O. 1970. *Foundations of Statistical Mechanics*, Oxford: Pergamon

Prigogine, I. 1980. *From Being to Becoming*, San Fransisco: Freeman

Ruelle, D. 1999. Smooth dynamics and new theoretical ideas in nonequilibrium statistical mechanics. *Journal of Statistical Physics*, 95: 393–468

Sinai, Ya. 1970. Dynamical systems with elastic reflections. *Russian Mathematical Surveys*, 25: 137–189

NONERGODICITY

See **Ergodic theory**

NONINTEGRABLE LATTICES

See **Integrable lattices**

NONLINEAR ACOUSTICS

As an area of physics and mechanics concerned with sound waves of finite amplitude, theoretical nonlinear acoustics stems from advances in classical fluid mechanics made in the 19th century. It was developed originally as a weakly nonlinear limit of gas dynamics and included the study of simple waves, weak shock waves, and their interactions. Nonlinear acoustics as a separate branch of science was formed mainly during and after World War II when, on the one hand, military applications of underwater acoustics became important, and on the other, more powerful sources of sound were developed.

The nature of finite-amplitude acoustic wave propagation in fluids depends on the value of the acoustic Reynolds number $\mathrm{Re} = \beta u_0 \lambda / \nu$, where u_0 is a characteristic amplitude of the particle velocity, λ is the wavelength, ν the kinematic viscosity (or a combination of viscosity and thermal conductivity), and β is the coefficient of nonlinearity (1.2 for air, 3.5 for water). For $\mathrm{Re} \leq 1$, the wave attenuates before significant nonlinear distortion accumulates. For $\mathrm{Re} \gg 1$, higher harmonics are generated, and the wave profile may undergo radical changes.

The physical process underlying waveform distortion for a plane (one-dimensional) traveling wave is the simple-wave characteristic relation $\mathrm{d}x/\mathrm{d}t = c_0 + \beta u$ for the propagation speed of individual points on the waveform, where c_0 is the small-signal (infinitesimal-amplitude) sound speed. Positive values of the particle velocity u (or sound pressure) in the waveform advance on the zero crossings propagating at speed c_0, and negative values recede. For $\mathrm{Re} \gg 1$, this process leads to waveform steepening up to the "breaking" point, beyond which this propagation law predicts a multivalued waveform (see Figure 1). Whereas water waves break, sound waves cannot, and instead an abrupt jump in the wave amplitude, referred to as a shock front, is formed. Shocks substantially increase attenuation of the wave, and their thickness is proportional to a combination of viscosity and thermal conductivity coefficients.

The process just discussed is well described for a plane traveling wave by the Burgers equation

$$\frac{\partial u}{\partial t} + (c_0 + \beta u)\frac{\partial u}{\partial x} = \delta \frac{\partial^2 u}{\partial x^2}, \qquad (1)$$

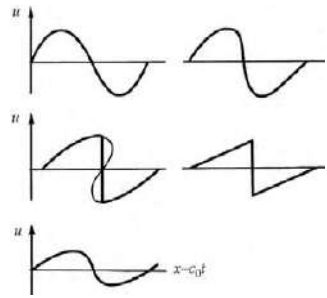

Figure 1. Schematic of the evolution of an initially sinusoidal nonlinear acoustic wave. Each plot corresponds to the one-period waveform as a function of coordinate at the successive time moments.

where δ is a dissipation coefficient that accounts for viscosity and thermal conductivity and equals $2\nu/3$ for shear viscosity alone. The left-hand side accounts for the finite-amplitude propagation speed given above. The Reynolds number, given above, characterizes the ratio of the nonlinear term to the dissipation term. Equation (1) is expressed in a form convenient for initial value problems, when an initial spatial waveform is prescribed. An alternative form of Equation (1), with the roles of x and t reversed, is used in signaling problems, in which a time waveform is prescribed on a boundary. Similar processes occur in spherical waves, such as those at sufficient distances from explosions, where the nonlinearity is weak.

An important role in the development of modern nonlinear acoustics has been played by the parametric array conceived by Westervelt in the USA and Zverev and Kalachev in Russia in the early 1960s. In the parametric array, two acoustic beams close in frequency interact nonlinearly and create a virtual antenna that radiates a secondary, low-frequency beam. Notwithstanding their low efficiency, these antennas prove useful in applications (such as sea bottom profiling) because of their high directivity and absence of side lobes.

Describing the parametric array and nonlinear sound beams, in general, is a complicated problem that requires taking into account the effect of diffraction. The combined effects of nonlinearity, attenuation, and diffraction on a sound beam may be modeled with an augmented form of Equation (1) called the Khokhlov–Zabolotskaya–Kuznetsov (KZK) equation. This equation contains an additional term that accounts for the diffraction of narrow beams. It is widely used for calculations of finite-amplitude sonars, such as the parametric array, and focused beams of high-intensity ultrasound used in imaging and medicine. Further augmentation of Equation (1) permits investigation of nonlinear propagation in inhomogeneous media

and leads to a theoretical formalism called "nonlinear geometrical acoustics," which is used to study the evolution of ray patterns.

Acoustic fields in fluids can also generate time-averaged effects such as acoustic streaming (steady flow) and radiation pressure. Acoustic streaming provides a basis for some microfluidic pumps, and in other applications, it influences heat transfer. Radiation pressures generated by standing waves are used to levitate and manipulate particles and bubbles, especially in microgravity environments. Accurate prediction of these time-averaged effects requires special care when defining the problem under consideration.

Nonlinear acoustics of solids includes a variety of interactions between different wave types, such as longitudinal, shear, and surface waves in isotropic solids. Additional types of wave interactions occur in anisotropic media (crystals). The different propagation speeds of the various waves lead to selection rules for particular wave interactions, usually connected with the direction of propagation. Surface (interface) waves exhibit nonlinear propagation effects that differ fundamentally from those of bulk longitudinal and shear waves. Their penetration depth away from an interface is proportional to wavelength, and this frequency-dependent property gives rise to nonlocal nonlinearity that does not occur in bulk waves. With nonlocal nonlinearity, the nonlinear perturbation of the wave velocity at any given point on a waveform is influenced by the entire wave field.

Along with "classical" homogeneous media in which the nonlinearity is due to anharmonicity of atomic forces, there exists an important class of "structurally" nonlinear media in which the nonlinearity is due to the presence of soft inclusions in a harder main body. Examples are small gas bubbles in liquids, pores in rubber-like materials, and grain contacts, microcracks, and dislocations in solids. Acoustic nonlinearities in such media can be several orders stronger than in homogeneous media. Moreover, the nonlinear equation of state (stress-strain relation) in such materials as metals and rock can predict irreversible behavior (hysteresis), which results in some unusual effects; for example, the third-harmonic amplitude in a strain wave can be proportional to the square of the primary-wave amplitude, rather than to its cube.

From a physical viewpoint, classical nonlinear acoustics deals mainly with non- or weakly-dispersive media, in which cumulative waveform steepening and harmonic generation occurs until shocks are formed. Dispersion in acoustics can be introduced by waveguide walls (geometrical dispersion) or by inhomogeneities such as grains and bubbles. As a result, many effects known in nonlinear optics and plasma physics have been realized in acoustics, such as self-focusing, phase conjugation (wave front reversal), and parametric amplification. Acoustic solitons, in which certain effects of nonlinearity and dispersion offset each another, are also possible. Even an acoustical analog of the maser, in which randomly phased oscillators (such as resonant bubbles) self-synchronize and radiate coherently, is possible.

Applications and manifestations of nonlinear acoustics are numerous. Besides the aforementioned processes, acoustic nonlinearities are important in explosion waves, sonic booms, thermoacoustic engines (in which sound waves serve as heat pumps), therapeutic and diagnostic medical ultrasound, materials characterization, and nondestructive testing. Shock waves also form inside collapsing cavitation bubbles, and they are thought to influence the resulting flashes of light referred to as sonoluminescence.

LEV OSTROVSKY AND MARK HAMILTON

See also **Burgers equation; Shock waves; Surface waves**

Further Reading

Beyer, R.T. 1997. *Nonlinear Acoustics*, 2nd edition, New York: Acoustical Society of America

Hamilton, M.F. & Blackstock, D.T. (editors). 1998. *Nonlinear Acoustics*, San Diego: Academic Press

Naugolnykh, K.A. & Ostrovsky, L.A. 1998. *Nonlinear Wave Processes in Acoustics*, Cambridge and New York: Cambridge University Press

Rudenko, O.V. & Soluyan, S.I. 1977. *Theoretical Foundations of Nonlinear Acoustics*, New York: Plenum Press

NONLINEAR ELECTRONICS

In the early part of the 20th century, vacuum tube devices dominated electronics circuitry. However with the advent of junction transistors in 1951 and integrated chips in 1957, semiconductor devices largely replaced vacuum tubes by the 1970s. Present-day electronic circuits make extensive use of active elements/devices that may behave either linearly or nonlinearly, depending upon their applications, operating currents, and voltages (as well as various physical effects including thermal effects, dielectric breakdown, and magnetic saturation). Typical modern nonlinear devices include semiconductor diodes, bipolar junction transistors (BJTs), and field effect transistors (FETs). For analysis and design, the nonlinear devices are often replaced by equivalent basic nonlinear circuit elements such as two-terminal, multiterminal, and multiport resistors, capacitors, and inductors. Thus, a nonlinear electronic circuit is an interconnection of the various circuit elements involving at least one nonlinear element.

The major nonlinear two-terminal circuit elements are typically characterized by nonlinear functional representations in contrast to their linear counterparts: (i) nonlinear resistor: nonlinear voltage $v(t)$ vs.

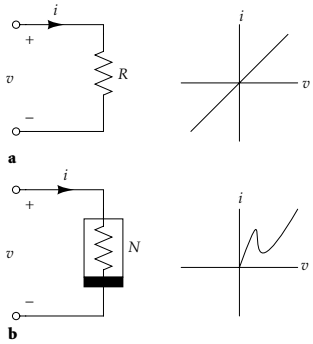

Figure 1. (a) Linear resistor and its v–i characteristic (b) Nonlinear resistor and its v–i characteristic.

current $i(t)$ characteristic curve, (ii) nonlinear capacitor: nonlinear charge $q(t)$ vs. voltage $v(t)$ curve, and (iii) nonlinear inductor: nonlinear $i(t)$ vs. magnetic flux Φ(t) curve (for an illustrative example, see Figure 1). More general circuit elements, such as three terminal transistors and multipliers, and multiterminal elements, such as operational amplifiers (opamps), are also frequently used (Chua et al., 1987; Schubert & Kim, 1996). An innovative nonlinear element is the piecewise-linear device, namely Chua's diode synthesized using opamps/diodes and linear elements (possessing a five-segment v–i characteristic curve, including three negative resistance pieces, see Figure 2), which plays a crucial role in understanding various nonlinear dynamical phenomena (Lakshmanan & Murali, 1996; Lakshmanan & Rajasekar, 2003). The state equations for the currents and voltages underlying a given nonlinear electronic circuit, which are deduced using Kirchhoff's laws for electrical circuits, turn out to be a system of coupled nonlinear differential equations. In particular, when a given circuit includes at least two energy storage elements such as capacitors and inductors and a nonlinear element (which can typically function as an amplifier), it behaves as an oscillator for appropriate feedback and circuit parameters. The underlying system of nonlinear differential equations can then be equivalently considered as a typical nonlinear oscillator dynamical system of dissipative type.

Historically, the relaxation oscillator investigated by the Dutch engineer Balthasar der Pol in his seminal paper, "Frequency Demultiplication" (van der Pol & van der Mark , 1927), may be considered as the earliest example of a nonlinear electronic circuit, exhibiting many of the characteristic features underlying bifurcations and chaos, though not fully understood at that time. The circuit typically consists of a high voltage dc source E attached via a large series

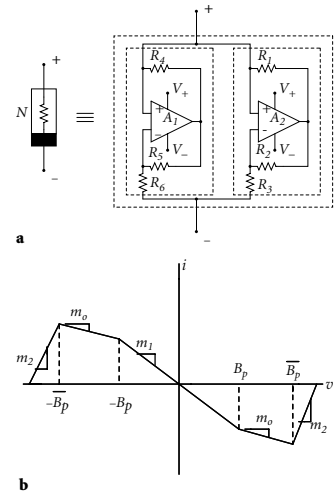

Figure 2. (a) Chua's diode and (b) its characteristic.

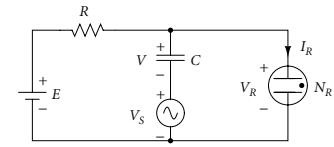

Figure 3. Van der Pol's original oscillator circuit.

resistance R to a neon bulb N_R (or a triode valve) and a capacitor C, which are connected in parallel (see Figure 3) along with an external periodic signal V_s. As the capacitance C is increased smoothly, the current exhibits "discrete jumps from one whole-submultiple of the driving frequency to the next." For a critical value of the amplitude of the driving signal, this pattern of modelockings has a self-similar fractal structure consisting of an infinite number of steps. In modern jargon, this is just the devil's staircase (Kennedy & Chua, 1986). Van der Pol also noted that "often an irregular noise is heard in the telephone receiver [monitoring the signal in some way] before the frequency jumps to the next level value." Now we know that this "noise" indeed corresponds to chaotic signals. Typically, the circuit is represented by the second-order non-autonomous nonlinear differential equation

$$\frac{\mathrm{d}^2x}{\mathrm{d}t^2} + \varepsilon\left(x^2 - 1\right)\frac{\mathrm{d}x}{\mathrm{d}t} + x = f\sin\omega t, \qquad (1)$$

where ε is the damping coefficient and f and ω represent the strength and frequency, respectively, of the periodic external forcing.

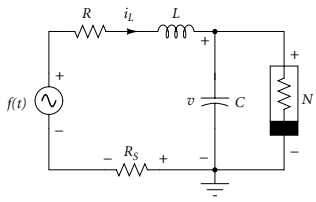

Figure 4. MLC Circuit: N is Chua's diode and $f(t)$ is the periodic signal.

Similar circuits are useful for modeling physical and biological systems; examples include flow of current across Josephson junctions or nerve impulse propagation in neuronal fiber in the form of Hodgkin–Huxley or FitzHugh–Nagumo equations (Scott, 2003). From the point of view of nonlinear dynamics, nonlinear electronic circuits arise either in analog simulation of typical nonlinear oscillators such as the Duffing oscillator or Lorenz system or as new dynamical systems per se constructed using typical nonlinear devices or ingeniously designed elements such as Chua's diode to act as black boxes to understand the various novel nonlinear phenomena. Examples of the latter include Chua's circuit/oscillator and Murali–Lakshmanan–Chua (MLC) circuit (Figure 4). In either case, these circuits are easy to build, analyse, and model, and help to scan the control parameter space quickly, thereby complimenting numerical and analytical studies of nonlinear phenomena.

Just like standard nonlinear dissipative dynamical systems, nonlinear electronic circuits typically exhibit various dynamical phenomena including bifurcations and chaos (Lakshmanan & Murali, 1996; Lakshmanan & Rajasekar, 2003; Thompson & Stewart, 1986).

- *Multistable states:* These correspond to point attractors (nodes and spiral points) as exhibited, for example, by any flip-flop or Schmitt trigger.
- *Periodic oscillations:* Autonomous nonlinear circuits can typically exhibit sinusoidal time response for weak nonlinearity (e.g., LC oscillators) and nearly square wave response (relaxation oscillators) for strong nonlinearity (e.g., square wave generators, Schmitt triggers). On the other hand, non-autonomous circuits often exhibit nonlinear resonant (harmonic, subharmonic, superharmonic, and dissipative) oscillations for weak nonlinearity (e.g., ferroresonant circuit with ac voltage source, hysteresis circuits, power amplifiers).
- *Bifurcations and chaos:* Almost the entire spectrum of bifurcations and chaos phenomena encountered in typical chaotic nonlinear dynamical systems is exhibited by numerous simple nonlinear electronic circuits/oscillators (e.g., Duffing oscillator, van der Pol oscillator, Chua's circuit, MLC circuit, RL diode circuit, Colpitts oscillator, Buck converters in power electronics).
- *Synchronization and controlling:* Nonlinear electronic circuits are versatile models to study and understand the phenomenon of synchronization in all its manifestations (such as identical, phase, lag, and generalized synchronizations) both with periodic and chaotic oscillations between two or a chain of oscillators. Similarly, to study various controlling techniques of periodic as well as chaotic oscillations, nonlinear circuits play a crucial role.
- *Secure communications and cryptography*: Because of the inherent advantage of miniaturization, nonlinear electronic circuits are natural choices for chaos application studies in secure communications, cryptography, and signal processing.

Nonlinear electronic circuits have become indispensable tools to understand a multitude of nonlinear dynamical phenomena, including chaos. In turn, nonlinear electronics has itself been enriched greatly by the advances in understanding various complex nonlinear phenomena, leading to the potential applications mentioned above.

MUTHUSAMY LAKSHMANAN

See also **Chaotic dynamics; Chua's circuit; Diodes; Duffing equation; Van der Pol equation**

Further Reading

Chua, L.O., Desoer, C.A. & Kuh, E.S. 1987. *Linear and Nonlinear Circuits*, New York: McGraw-Hill

Kennedy, M.P. & Chua, L.O. 1986. Van der Pol and chaos. *IEEE Transactions on Circuits and Systems*, 33: 974–980

Lakshmanan, M. & Murali, K. 1996. *Chaos in Nonlinear Oscillators: Controlling and Synchronization*, Singapore: World Scientific

Lakshmanan, M. & Rajasekar, S. 2003. *Nonlinear Dynamics: Integrability, Chaos and Patterns*, Berlin: Springer

Schubert, T.S. & Kim, E.M. 1996. *Active and Nonlinear Electronics*, New York: Wiley

Scott, A.C. 2003. *Nonlinear Science: Emergence and Dynamics of Coherent Structures*, 2nd edition, Oxford and New York: Oxford University Press

Thompson, J.M.T. & Stewart, H.B. 1986. *Nonlinear Dynamics and Chaos*, New York: Wiley

van der Pol, B. & van der Mark, J. 1927. Frequency demultiplication. *Nature*, 120: 363–364

NONLINEAR OPTICS

Maxwell's theory of electrical and magnetic fields and his idea that light is an electromagnetic wave were among the great milestones of scientific thought, unifying our understanding of a large and diversified range of physical phenomena. Indeed, by the late 19th century, the success of the classical electromagnetic theory of light led some to believe

that there were few fundamental discoveries to be made.

Nonlinear properties of Maxwell's constitutive relations $\boldsymbol{B}=\mu(\boldsymbol{H})\boldsymbol{H}$, $\boldsymbol{D}=\varepsilon(\boldsymbol{E})\boldsymbol{E}$ had been recognized from the beginning. For example, the nonlinear permeability of ferromagnetic media was of prime concern in the design of electrical machinery in the 19th century. Nonlinear properties in the optical region had to await the discovery of the ruby laser in 1960 by Theodore Maiman (Maiman, 1960). The defining experiment by Peter Franken and coworkers in 1961 (Franken et al., 1961) detected ultraviolet light ($\mathrm{l}=3470$Å) at twice the frequency of a ruby laser ($\mathrm{l}=6940$Å) when this beam traversed a quartz crystal. (There is a humorous story about this discovery: the detected radiation was so weak that it appeared as a very faint spot on the photograph submitted to *Physical Review Letters*. The typesetting staff assumed that it was a glitch and erased it in the published document!) This experiment spurred a flurry of activity and many nonlinear optical phenomena were rapidly discovered. A series of monographs by Nicolaas Bloembergen in the 1960s (see Bloembergen, 1996a,b) contain an excellent historical overview of the explosive growth of activity in this field in the early days (see also Marburger, 1977; Shen, 1977).

For the most part, the study of nonlinear optical phenomena assumes a quantum material system coupled to a classical electromagnetic field. Within this approximation, noise-driven phenomena can be adequately described by a Langevin-type driving force. A proper description of quantum effects such as spontaneous emission or scattering requires that the electromagnetic field itself be quantized. Most nonlinear optical materials are nonmagnetic, so one sets the magnetic permeability $\mu(\boldsymbol{H})=\mu_0$, a constant. The procedure then is to expand the dielectric permeability $\varepsilon(\boldsymbol{E})$ as a formal power series in the electric field. This is most commonly done by defining an induced polarization field in terms of the electric displacement vector $\boldsymbol{D}=\varepsilon_0\boldsymbol{E}+\boldsymbol{P}$, where $\boldsymbol{P}=\boldsymbol{P}_{\mathrm{L}}+\boldsymbol{P}_{\mathrm{NL}}$ (linear and nonlinear contributions). The first term on the right-hand side of the expression for the electric displacement vector $\boldsymbol{D}$ is the vacuum contribution. The polarization $\boldsymbol{P}$ describes the coupling of the light to induced dipoles in the material, and this physical quantity is expanded in series in powers of the electric field, $\boldsymbol{E}$, as follows.

$$\begin{aligned}\tfrac{1}{\varepsilon_0}\boldsymbol{P}=&\int\overline{\overline{\chi}}_1(\tau)\,\boldsymbol{E}(t-\tau)\,\mathrm{d}\tau\\&+\int\int\overline{\overline{\chi}}_2(\tau_1,\tau_2)\,\boldsymbol{E}(t-\tau_1)\\&\times\boldsymbol{E}(t-\tau_2)\,\mathrm{d}\tau_1\,\mathrm{d}\tau_2\\&+\int\int\int\overline{\overline{\chi}}_3(\tau_1,\tau_2,\tau_3)\,\boldsymbol{E}(t-\tau_1)\\&\times\boldsymbol{E}(t-\tau_2)\,\boldsymbol{E}(t-\tau_3)\,\mathrm{d}\tau_1\,\mathrm{d}\tau_2\,\mathrm{d}\tau_3+\cdots\\=&\tfrac{1}{2\pi}\int\widetilde{\overline{\chi}}_1(\omega)\,\widetilde{\boldsymbol{E}}(\omega)\,\mathrm{e}^{-\mathrm{i}\omega t}\,\mathrm{d}\omega\\&+\tfrac{1}{(2\pi)^2}\int\int\widetilde{\overline{\chi}}_2(\omega_1,\omega_2)\\&\times\widetilde{\boldsymbol{E}}(\omega_1)\,\widetilde{\boldsymbol{E}}(\omega_2)\,\mathrm{e}^{-\mathrm{i}(\omega_1+\omega_2)t}\mathrm{d}\omega_1\mathrm{d}\omega_2\\&+\tfrac{1}{(2\pi)^3}\int\int\int\widetilde{\overline{\chi}}_3(\omega_1,\omega_2,\omega_3)\,\widetilde{\boldsymbol{E}}(\omega_1)\,\widetilde{\boldsymbol{E}}(\omega_2)\\&\times\widetilde{\boldsymbol{E}}(\omega_3)\,\mathrm{e}^{-\mathrm{i}(\omega_1+\omega_2+\omega_3)t}\,\mathrm{d}\omega_1\,\mathrm{d}\omega_2\,\mathrm{d}\omega_3+\cdots\end{aligned}\tag{1}$$

Here, the dielectric susceptibility terms $\overline{\overline{\chi}}_j$, $j=1,2,3$ are second, third, and fourth rank tensors, respectively. The latter are causal functions and tensor product notation is assumed. The second equality is written in terms of Fourier transform variables. Although, in principle, the dielectric susceptibilities at each order could be obtained from fully ab initio quantum mechanical calculations on the relevant materials, in practice, such calculations are too complex and one usually has to rely on experimentally measured data. Higher order processes than those displayed explicitly in this equation are generally unimportant because the leading order accessible nonlinear effect dominates. (Exceptions occur when nonlinear saturation becomes important.) The above induced polarization term acts as a source for the electromagnetic field in Maxwell's vector wave equation,

$$\frac{\partial^2\boldsymbol{E}}{\partial t^2}-\frac{1}{c^2}\frac{\partial^2\boldsymbol{E}}{\partial z^2}-\nabla\cdot(\nabla\cdot\boldsymbol{E})=\frac{1}{\mu_0}\frac{\partial^2\boldsymbol{P}}{\partial t^2}.\tag{2}$$

The leading order term $\overline{\overline{\chi}}_1$ above is a second rank tensor that describes all linear optical interactions involving propagating optical fields of any arbitrary polarization. For virtually all nonlinear optical interactions, it is appropriate to expand the electric field vector as a linear combination of products of envelope functions and optical carrier waves

$$\boldsymbol{E}(\boldsymbol{r},t)=\sum_j\widehat{e}_jA_j(\boldsymbol{r},t)\exp\left(\mathrm{i}\left(\pm\boldsymbol{k}_j\cdot\boldsymbol{r}-\omega_jt\right)\right)+\mathrm{c.c.}\tag{3}$$

Here A_j are slowly varying envelope functions, and $\widehat{e}_j$ is a unit vector indicating the direction of polarization. Each wave vector or frequency pair $(\boldsymbol{k}_j,\omega_j)$ satisfies a linear dispersion relation $D(\boldsymbol{k}_j,\omega_j)=0$. A goal in nonlinear optics is to write down evolution equations for the complex slowly varying envelope functions A_j. The structure of these equations, which describe how almost monochromatic, weakly nonlinear, dispersive wave trains interact, is universal and so many of the properties of lightwaves

can be inferred from corresponding situations in other fields.

The leading nonlinear behavior in noncentrosymmetric crystals is due to the second order term $\overline{\overline{\chi}}_2$, a third rank tensor (with 9 components). This term is responsible for second harmonic generation as first observed by Franken et al. (1961). Significant quadratic nonlinear interactions between wave packets take place when triads of wave vectors and frequencies $\boldsymbol{k}_j, \omega_j$ obey

$$\boldsymbol{k}_1 + \boldsymbol{k}_2 + \boldsymbol{k}_3 = 0, \;\; \omega_1 \pm \omega_2 \pm \omega_3 = 0, \qquad (4)$$

where each $\boldsymbol{k}_j, \omega_j$ pair satisfies its own dispersion relation. Physical effects arising from this term include second harmonic generation ($2\omega_1 \rightarrow \omega_3$), dc rectification ($\omega_1 - \omega_1 \rightarrow 0$), and frequency up- and down-conversion ($\omega_1 \pm \omega_2 \rightarrow \omega_3$). The first two nonlinear interactions are termed degenerate because $\omega_1 = \omega_2$ and two photons ($2\hbar\omega_1$) in the incident laser beam are needed to create one second harmonic photon. For these three-wave interaction processes to be efficient both energy (i.e., $\hbar\omega_1 \pm \hbar\omega_2 = \hbar\omega_3$ for up-, down-conversion, $2\hbar\omega_1 = \hbar\omega_3$ for second harmonic generation) and momentum ($\hbar\boldsymbol{k}_1(\omega) \pm \hbar\boldsymbol{k}_2(\omega) = \hbar\boldsymbol{k}_3(\omega)$, for up-, down-conversion, $2\hbar\boldsymbol{k}_1(\omega) = \hbar\boldsymbol{k}_3(\omega)$ for harmonic generation) must be nearly conserved. (Here $\hbar\boldsymbol{k}$ is the photon momentum.) Three-wave interactions are generally difficult to observe in isotropic media as material dispersion precludes being able to satisfy the momentum conservation relation. A symmetry argument also shows that χ^2-processes are forbidden in materials possessing a center of symmetry. Noncentrosymmetric uniaxial and biaxial crystals (those in which the refractive index is different in different directions in the crystal) are employed to achieve efficient phase matching. This is because the magnitude of the optical wave vector is related to the material refractive index through the relation $k = n(\omega)\omega/c$, where the dispersion of the refractive index $n(\omega)$ is explicitly displayed. The complex envelopes A_1, A_2, and A_3 of the three wave packets obey the universal three-wave interaction equations of universal type

$$\frac{\partial A_j}{\partial t} + \boldsymbol{c}_j \cdot \nabla A_j = \theta_j A_l^* A_m^* \qquad (5)$$

with j, l, m cycled over 1,2,3, where $\boldsymbol{c}_j$ is the linear group velocity of the jth wave packet and θ_j is a coupling coefficient proportional to $\overline{\overline{\chi_2}}$.

Four-wave χ_3-processes are the leading order nonlinear optical processes in a medium possessing a center of symmetry. Here significant exchange of energy only takes place between resonant quartets $\left(\boldsymbol{k}_j, \omega_j\right)_{j=1}^4$, each obeying its dispersion relation. Contrary to the triad resonance condition, energy conservation and phase matching can always be satisfied with several trivial choices. The nonlinear dielectric susceptibility is now a fourth rank tensor although many of its components are either identical or zero, depending on crystal symmetry properties. Degenerate four-wave interactions include self-phase modulation (or Kerr effect, $\omega_1 + \omega_1 - \omega_1 \rightarrow \omega_1$) and third harmonic generation ($\omega_1 + \omega_1 + \omega_1 \rightarrow 3\omega_1$) (Terhune et al., 1962). Common nondegenerate third-order processes include four-wave-mixing (FWM) interactions.

Four-wave-mixing interactions can be used to create a "phase-conjugated wave." A nonlinear interference grating is created within the nonlinear material through the interaction of two strong pump waves satisfying $\boldsymbol{k}_1 + \boldsymbol{k}_2 = 0$ and $\omega_1 = \omega_2 = \omega$. A weak third wave scatters off this grating and generates a time-reversed phase-conjugated replica of itself. The incident and scattered waves satisfy $\boldsymbol{k}_3 + \boldsymbol{k}_4 = 0$ and $\omega_4 = \omega_3 = \omega$. FWM interactions can also lead to degradation in wavelength-division-multiplexed (WDM) long-haul fiber transmission systems as a result of energy transfer between equally spaced channels. Another important nondegenerate interaction involves the phenomenon of nonlinear birefringence where $\boldsymbol{k}_4, \omega_4 = -\boldsymbol{k}_2, -\omega_2, \boldsymbol{k}_3, \omega_3 = -\boldsymbol{k}_1, -\omega_1$ and the complex slowly varying functions A_1, A_2 represent envelope wave packets of different polarization direction. Coupled nonlinear Schrödinger (NLS) equations for the envelope fields $A_1(\boldsymbol{r}, t)$ and $A_2(\boldsymbol{r}, t)$ can be derived that describe nonlinear self- (i.e., $|A_1|^2 A_1$ in the A_1 equation and $|A_2|^2 A_2$ in the A_2 equation) and cross-phase modulation (i.e., $|A_2|^2 A_1$ in the A_1 equation and $|A_1|^2 A_2$ in the A_2 equation) for co- and counter-propagating laser pulses. The relative weighting of self- and cross-phase modulation nonlinearities depends on the material properties (Marburger, 1977) and plays an important role in polarization switching of soliton pulses in optical fibers. One can write down more general universal four-wave interaction equations along the lines described above for the three-wave interaction case.

A well-known degenerate χ_3-process is the optical Kerr effect. This self-interaction term induces a nonlinear phase change proportional to the intensity $|A|^2$ of the propagating light pulse. This phase change, called self-phase modulation, is an accumulative propagation effect that is central to applications that exploit the optical Kerr effect. A canonical form of the D-dimensional NLS equation, incorporating the Kerr effect, can be written as follows:

$$\mathrm{i}\left(\frac{\partial A}{\partial t} + \sum_{j=1}^{D}\left(\frac{\partial \omega}{\partial k_j}\right)\frac{\partial A}{\partial x_j}\right) - \sum_{j,l=1}^{D}\left(\frac{\partial^2 \omega}{\partial k_j k_l}\right)\frac{\partial^2 A}{\partial x_j x_l} + \left(\frac{\partial \omega}{\partial |A|^2}\right)|A|^2 A = 0. \qquad (6)$$

The first two terms combined describe the advection of a pulse (wave packet) with group velocity $v_g = \omega(k)$.

The second and third terms represent the balance between dispersion and weak nonlinearity. Higher order corrections terms can be derived as an asymptotic expansion in a small parameter as described in Newell & Moloney (1992). Dispersion in nonlinear optics is manifested in two physically distinct ways: diffraction describing spatial spreading of a tightly collimated beam or pulse in a direction transverse to the direction of propagation, and dispersive spreading in time (group velocity dispersion $\omega''(k)$) of an ultrashort laser pulse. The latter mechanism plays an increasingly influential role as the propagating laser pulse gets shorter and shorter.

In 1-d, the NLSE is integrable and the Kerr nonlinearity can balance group velocity dispersion to form temporal solitons in optical fibers. Both bright and dark temporal soliton pulses have been observed experimentally in fibers. Spatial soliton beams can be created in two-dimensional planar waveguides where there is strong confinement of the optical field in a single spatial dimension transverse to the propagation direction of the light beam. Spatial confinement in two (fibers) or one (planar waveguides) dimension is required to form stable soliton pulses or beams. In unconfined transparent bulk geometries, the optical Kerr effect is responsible for critical self-focusing, leading to extremely intense focused light that causes catastrophic damage in transparent glasses. Critical self-focusing was first observed experimentally by Chiao and coworkers in 1964 (Chiao et al., 1964).

There are other categories of nonlinear optical effects that can be described in terms of envelope functions and that depend sensitively on the finite response of some material oscillation. Stimulated scattering is a case in point. These processes are essentially three-wave interactions where one of the optical waves is replaced by a material oscillation. In transparent glasses for example, there are two characteristic modes of oscillation of the lattice as shown in Figure 1. The lower frequency acoustic phonon mode corresponds to an oscillation of all atoms in unison along a fixed direction in the lattice. The higher frequency optical phonon mode involves neighboring atoms in the lattice oscillating out of phase. The dispersion relation for lattice vibrations, therefore, contains an acoustic and optical branch, both of much lower frequency than the optical frequency.

Figure 1 shows a plot of the optical phonon (top curve) and acoustic phonon (bottom curve) dispersion for a diatomic crystal lattice within the first Brillouin zone. On the scale of this graph, the photon branch (light cone) is essentially vertical, making the acoustic and optical phonon dispersion essentially flat. An intense pump laser pulse at frequency ω_p entering a transparent glass can scatter off either a fluctuating low-frequency acoustic phonon (Stimulated Brillouin Scattering, SBS) or a fluctuating optical phonon (Stimulated Raman Scattering, SRS) at finite temperature. Energy conservation ensures that the scattered optical signal has a frequency $\omega_s = \omega_p - \omega_v$, where ω_v is the natural acoustic or optical phonon frequency. Technically, SBS and SRS processes look like a three-wave interaction where phase matching is easy as the dispersion of the material oscillation is locally flat on an optical frequency scale. In fact, it can be shown that these processes are essentially four-wave interactions, as the oscillator model, representing the material oscillation, is driven by the square of the optical field. Typically, SBS is generated in the backward direction and SRS can to be generated in the forward and/or backward direction relative to the propagating pump laser pulse. SRS processes in liquids and gases can generate a cascade of frequency down-shifted (Stokes) and frequency up-shifted (anti-Stokes) waves. Although both SBS and SRS processes are essentially phase matched for all directions, they can only exist by feeding off the intense pump pulse. There also exists a degenerate stimulated scattering process called Stimulated Rayleigh Scattering—this is essentially a Kerr-like process with finite memory. All of these stimulated scattering phenomena can be observed in bulk transparent materials (Marburger, 1977; Shen, 1977) and optical fibers (Agrawal, 1989). They can be stimulated from noise or seeded at the optical signal wavelength by injecting a weak laser field.

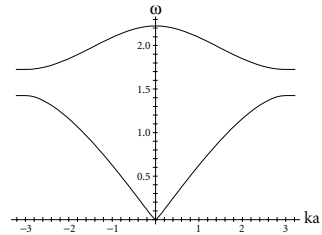

Figure 1. Acoustic (bottom)and optical (top) phonon branches of the dispersion curve for a diatomic lattice. The abscissa is scaled to the lattice constant "a."

Another important class of nonlinear optical phenomena involves direct resonant coupling to some form of material oscillation. The simplest physical manifestation of this category is the two-level atom. Absorbing/amplifying media that give rise to the phenomenon of self-induced transparency (SIT) and lasers belong to this category. The dielectric susceptibility is now complex with the real part corresponding to a refractive index change induced by the optical field and the imaginary part corresponding to absorption or amplification of light. The real and imaginary parts of the dielectric susceptibility are related through a Hilbert

transform—the Kramers–Kronig relation. Energy is directly transferred between optical fields and material oscillations. Self-induced transparency (SIT) solitons propagate when this coherent population or energy exchange can occur between the lower (L) and upper (U) level of a two-level atom on a timescale short relative to any irreversible energy decay processes such as spontaneous emission from the excited state (U). This population cycling between two levels occurs at a frequency $\omega_R = |\mu_{12}A|/\hbar$, where μ_{12} is the dipole matrix between the two levels and $\hbar$ is Planck's constant. The frequency ω_R is called the Rabi frequency, from the field of magnetic resonance spectroscopy. Figure 2a depicts this simple two-level atom scheme. For longer optical pulses, nonlinear saturation can occur in the presence of intense propagating optical fields. Population inversion, required for lasing action, cannot be achieved in a two-level atom (*See* **Lasers**). Optical amplification of light requires that a net inversion be achieved between the upper (U) and lower (L) atomic or molecular level involved in the light amplification process. Such inversion can be achieved by pumping atoms or molecules to energetically higher levels with a subsequent rapid nonradiative energy decay down to the upper excited level (U). Classical laser action can be described in terms of three-level and four-level quantum models. Figure 2b and c depict two classical lasing level schemes where the ground level population is pumped ($E = \hbar\omega_p$) into some upper excited state followed by a rapid (nonradiative) population decay (dashed arrows) to the upper excited lasing level (U). The original ruby laser, discovered by Maiman in 1961, is an example of a three-level (actually three band) system schematically shown in Figure 2b. Inversion is more difficult to achieve in a three-level laser as the upper lasing level must have a net population in excess of that in the ground level. This requires pumping of more than half of the atoms to the upper lasing level. In the four-level laser, the lower lasing state is not the ground state and its initial population can be zero or very small due to finite temperature populations. Efficient lasing is achieved by rapidly removing the populations from the lower lasing level (L).

Such energy level schemes are generally gross simplifications of a real laser although they provide useful models of solid state and gas lasers (Siegman, 1986). Fiber lasers with erbium and/or ytterbium-doped cores belong to the category of solid state lasers. Semiconductor lasers, on the other hand, are extremely complex many-body systems involving many bands rather than levels and the above descriptions prove inadequate.

Key current developments in the field of nonlinear optics have benefited from technical developments that have enabled experimentalists to produce ultrashort laser pulses and invent novel materials processing methodologies. We sketch some of the key areas of research where such effects have been exploited in recent years.

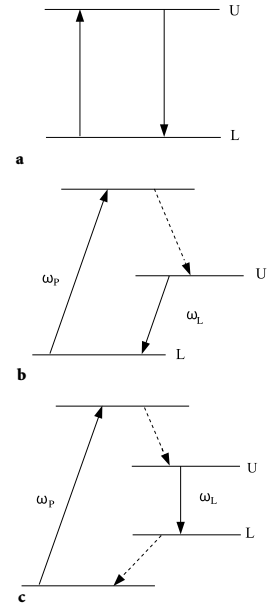

Figure 2. (a). Two-level energy level scheme. (b). Three-level lasing level scheme. (c). Four-level lasing level scheme.

Nonlinear Optical Data Processing

A cumulative intensity-induced phase shift due to the Kerr nonlinearity, of the order of p, provides one of the most useful all-optical data processing capabilities. High-speed optical sampling, switching, amplification and storage applications abound, based on this nonlinear mechanism. Optical switching and data sampling can be implemented in directional couplers and Mach–Zehnder interferometers in both waveguide and fiber arrangements. Optical amplification and storage of pulse trains representing digital information can be achieved by placing a nonlinear transparent Kerr medium in a ring or Fabry–Perot cavity arrangement. So-called optical bistable elements require an injected holding beam to maintain the cavity at some threshold level whereby an incremental input can lead to strong amplification or storage of the system in one of two stable accessible states. The latter situation is depicted in Figure 3. Here the system has a memory (hysteresis) whereby a lower (bit 0) and upper (bit 1) state can be switched by some external perturbation. Adjusting some cavity parameter can also lead to a single-valued but rapidly rising output transmission of the system. This is useful for amplifying injected pulse streams.

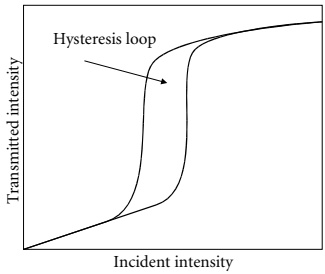

Figure 3. Hysteresis loop for a bistable optical cavity.

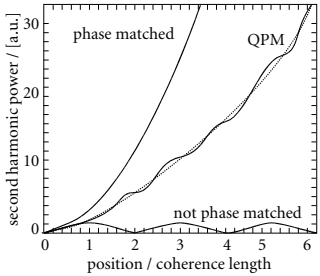

Figure 4. Comparison of energy transfer from the fundamental to the second harmonic for phase-matched, detuned and quasi-phase-matched conditions.

Such passive optical bistable cavities have also been shown to exhibit deterministic chaotic dynamics when the finite time delay of the optical signal circulating in the optical resonator has been taken into account. When transverse degrees of freedom of the external pump laser beam are included, so-called transverse spatial solitons have been observed. Although technology applications have been envisioned for both of these dynamical phenomena, there are no specific implementations to date.

Chaotic Synchronization and Communication with Lasers

Semiconductor lasers are highly susceptible to exhibiting chaotic dynamics even in the presence of extremely weak (10^{-4}) feedback from an external reflecting surface. This tendency to readily exhibit deterministic chaos means that semiconductor laser sources require greater than 40 dB optical isolation, making them the most expensive component in an optical fiber telecommunications network. Research in recent years has focused on taking advantage of this chaos by demonstrating that chaotic transmitter and receiver lasers can be synchronized and messages encoded and decoded at the transmitter and receiver end, respectively. Mathematically, these chaotic lasers are described at the simplest level by delay differential equations.

Quasi-phase Matching in Isotropic Media

Quasi-phase matching (QPM) is a means of beating the usual triad resonance condition needed to efficiently transfer energy between waves in second harmonic generation. Figure 4 shows the ideal phase-matched energy transfer to second harmonic as a function of propagation distance in a uniaxial crystal. When detuned from the phase-matching condition, energy transfer occurs less efficiently and there is a periodic transfer back and forth between the fundamental at frequency and the second harmonic signal at frequency 2ω. In this case, one observes the oscillatory nonphase-matched behavior depicted in the picture. This is typically the situation encountered in isotropic materials.

Quasi-phase matching entails taking a crystal with a nonlinear coefficient and periodically reverting the sign of the dipoles in such a way that the phase of the wave is reversed every coherence length along the crystal. The latter is proportional to the refractive index mismatch at the fundamental and second harmonic frequencies. A practical implementation of quasi-phase-matching is through the process of periodic polling whereby a ferroelectric material such as lithium niobate, for example, can effectively have its dipoles reversed periodically with patterned electrodes. QPM soliton propagation is an intense area of modern research and has the advantage that much larger nonlinear optical couplings can be achieved via the χ_2 nonlinearity.

Optical Breakdown in Intense Laser fields

Optical breakdown due to critical self-focusing of continuous wave laser beams or long pulses has been observed since the 1960s. The breakdown phenomenon itself is very complex and can involve nonlinear coupling to thermal, acoustic, vibrational, rotational, and electronic degrees of freedom. Thermally induced lensing, leading to critical self-focusing, is dominant for long microsecond-duration laser pulses. Nanosecond-duration laser pulses couple strongly to hypersonic acoustic waves and critical self-focusing is due to the physical mechanism of electrostriction. Picosecond-duration laser pulses typically generate electron/ion plasmas through the process of avalanche photoionization, whereas femtosecond-duration laser pulses breakdown materials predominantly via the mechanism of multiphoton ionization. The latter process is essentially instantaneous and the nonlinear ionization process is proportional to $|A|^{2N}$, where the minimum energy required to excite the bound electron to the ionization continuum is $E = N\hbar\omega$.

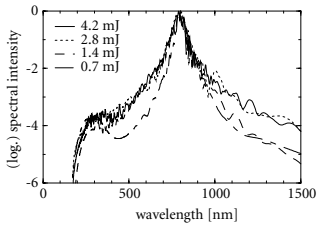

Figure 5. Calculated white-light supercontinuum for a high-power femtosecond laser pulse propagating in air.

Stimulated scattering processes usually accompany optical breakdown processes making it extremely difficult to unravel the relevant physics for longer duration laser pulses. Plasma, generated via avalanche ionization, acts as a shield, preventing the laser pulse from propagating further in the material. Shock waves generated in the nonlinear focal region can cause mechanical rupture for longer duration pulses.

Extreme Nonlinear Optics

The development of high-power femtosecond laser sources has led to some novel nonlinear interactions that exploit the optical Kerr effect. Single cycle pulses have been generated and very recent experimental evidence has been provided for the generation of attosecond pulses. These optical pulses are of such short duration that they interact with the atom or molecule on a timescale comparable to that taken by the electron to orbit the nucleus! The advantage of these laser sources is that many of the detrimental physical effects accompanying longer duration pulses are not operative in the femtosecond regime. Therefore, it is possible to achieve large local field intensities while maintaining low energies in the pulse. Recently, high-power femtosecond laser pulses, focused down to scales on the order of the wavelength of light, have been used to locally change the material properties of glass and write complicated integrated optics waveguiding structures. The actual mechanism for the transformation of the glass to a state with a higher refractive index is not yet fully understood.

High-power femtosecond laser pulses can propagate over anomalously long distances in air, achieving peak field intensities on the order of 10^{13}–$10^{14}\,\mathrm{W/cm^2}$. These huge intensities break down the air via multiphoton ionization in the vicinity of the nonlinear focus. Plasma, generated within the 100 μm diameter focal spot, can act as a defocusing lens, causing the trailing edge of the laser pulse to defocus and refocus multiple times as it propagates through the atmosphere. Accompanying the extreme self-focusing is white-light supercontinuum generation. The relatively narrow spectral peak of the initial pulse blows out asymmetrically and encompasses wavelengths ranging from the infrared to the ultraviolet. Figure 5 shows the change in the calculated white-light supercontinuum spectrum as a function of increasing pulse energy for a 100 fs-duration laser pulse propagating in air. The experimentally measured back-reflected white-light supercontinuum from a 2.6 TW 100 fs-duration laser pulse launched vertically into the atmosphere (Rairoux et al., 2000) exhibits the same qualitative features. The initial pulse spectrum is localized around the narrow peak at 800 nm. The mechanism, by which this high-power pulse sustains itself as a waveguide, is through a combination of recurring transverse modulational instabilities that create multiple intense chaotic self-focusing light strings and accompanying plasma filament generation that acts to limit the strong focusing effect (Mlejnek et al., 1999).

Another important application of high-power femtosecond laser pulses is in the generation of highly transient X-ray pulsed sources through higher harmonic cascades accompanying extreme pulse focusing. Hundreds of harmonics have been observed experimentally (Bartels et al., 2000), and novel algorithms are being developed to reshape the initial pulse so as to be able to efficiently extract a particular higher harmonic. When the pulse peak intensities exceed around $10^{17}\,\mathrm{W/cm^2}$, one enters the nonlinear regime where relativistic effects become important.

The extreme conditions encountered during critical focusing of high-power femtosecond-duration laser pulses have recently spurred theorists to question whether envelope equation models such as the NLS equation, even with higher order corrections included, can adequately describe pulse propagation under such extremes. As NLS describes quasi-monochromatic laser pulses, it is implicitly assumed in its derivation that the generated spectral bandwidth satisfies the inequality, which is the underlying optical carrier wave frequency. Experimental measurements of white-light generation in condensed media show that the spectral extent of the generated supercontinuum can exceed the initial pulse spectral bandwidth by a factor of 5 or more. The picture above for air shows that the supercontinuum extends well beyond the optical carrier frequency. Pulse propagation models that explicitly include the optical carrier wave and consequently allow for optical carrier shocks are currently under active development.

Nonlinear Optics in Photonic Bragg Structures

Periodic modulation of a material refractive index or gain offers a novel means of beating the intrinsic dispersion of available nonlinear optical materials. This idea goes back to the early days of nonlinear optics where 1-dimensional periodic index modulation allowed one

to manage or engineer the dispersion of a particular material. This is the photonic analog of the lattice periodicity leading to so-called Bloch states describing electron confinement in a semiconductor material. Just as the optical properties of semiconductor materials can be engineered by modifying the underlying lattice structure through the introduction of quantum wells or dots, so too can the optical confinement of photons be controlled by introducing a refractive index or gain periodicity in a transparent glass. Distributed feedback semiconductor lasers, based on this distributed feedback principal, are the workhorses of modern fiber-based telecommunications systems. 1-d Bragg or gap solitons have been experimentally generated in periodically modulated Kerr glass waveguides—these localized pulses have the property that they can be dramatically slowed down or even be nonpropagating within the nonlinear periodic structure.

2-d and 3-d photonic Bragg and crystal fiber structures have the special property that photonic bandgaps can be introduced in a structure consisting of a periodic lattice of holes or vertical columns. In principle, such structures can guide light around right angle bends in direct contrast to waveguide splitters, trap light in defects, and provide so-called omni-reflecting properties, that is, guide light at all angles and wavelengths. These properties are in marked contrast to conventional index-guided optical waveguides and, when combined with optical nonlinearity, offer many new potential technology applications (Mingaleev & Kivshar, 2002).

Electromagnetically Induced Transparency

Electromagnetically induced transparency (EIT) is a quantum interference effect that acts to reduce the usual absorption of light experienced when its frequency is tuned to the resonance frequency of the sample through which the light is propagating. The transparency is created by a second light (electromagnetic) source tuned to another resonance of the sample. Suppressing absorption through EIT leads to several other effects, including the focusing of one laser beam by another and the production of inversionless laser sources.

JEROME V. MOLONEY

See also **Filamentation; Kerr effect; Lasers; Nonlinear Schrödinger equations; Optical fiber communications; Photonic crystals; Pump-probe measurements; Rayleigh and Raman scattering and IR absorption**

Further Reading

Agrawal, G.P. 1989. *Nonlinear Fiber Optics*, San Diego: Academic Press

Bartels, R., Backus, S., Zeek, E., Misoguti, L., Vdovin, G., Christov, I.P., Murnane, M.M. & Kapteyn, H.C. 2000. Shaped-pulse optimization of coherent emission of high-harmonic soft X-rays. *Nature*, 406: 164

Bloembergen, N. 1996a. *Encounters in Nonlinear Optics: Selected Papers of Nicolaas Bloembergen*, Singapore: World Scientific

Bloembergen, N. 1996b. *Nonlinear Optics*, Singapore: World Scientific

Boyd, R.W. 1992. *Nonlinear Optics*, Boston and San Diego: Academic Press

Chiao, R.Y., Garmire, E. & Townes, C.H. 1964. Self-trapping of optical beams. *Physical Review Letters*, 13: 479–482

Franken, P.A., Hill, A.E., Peters, C.W. & Weinreich, G. 1961. Generation of optical harmonics. *Physical Review Letters*, 7: 118–120

Maiman, T.H. 1960. Stimulated optical radiation in ruby lasers. *Nature*, 187: 493

Marburger, J. 1977. Self focusing: theory. *Progress in Quantum Electronics*, 4: 35–110

Mingaleev, S. & Kivshar, Y. 2002. Nonlinear photonic crystals: toward all-optical technologies. *Optics and Photonics News*, 13: 48–51

Mlejnek, M., Kolesik, M., Moloney, J.V. & Wright, E.M. 1999. Optically turbulent femtosecond light guide in air. *Physical Review Letters*, 83: 2938–2941

Newell, A. & Moloney, J.V. 1992. *Nonlinear Optics*, Redwood City, CA: Addison-Wesley

Rairoux, P., Schillinger, H., Niedermeier, S., Rodriguez, M., Ronneberger, F., Sauerbrey, R., Stein, B., Waite, D., Wedekind, C., Wille, H. & Wöste, L. 2000. Teramobile: a nonlinear terawatt femtosecond lidar. *Applied Physics* B, 71: 573

Shen, Y.R. 1977. Self focusing: experimental. *Progress in Quantum Electronics*, 4: 1–34

Siegman, A.E. 1986. *Lasers*. Mill Valley, CA: University Science Books

Terhune, R.W., Maker, P.D. & Savage, C.M. 1962. Optical harmonic generation in calcite. *Physical Review Letters*, 8: 404–406

NONLINEAR PLASMA WAVES

In studying nonlinear plasma waves, one should recognize that there are several analytical methods, including single particle, fluid, and kinetic. Using the proper model is important, as different models can result in different nonlinear phenomena (Davidson, 1972; Horton & Ichikawa, 1996).

Because plasmas are composed of charged particles and are often immersed in external electric and magnetic fields, it is critical to determine when the self-consistent fields (fields produced by the charged particles directly) must be considered in the presence of externally applied fields. Typically, the self-consistent electric fields need to be considered, but we can often neglect self-consistent magnetic fields, because the forces produced by the self-consistent magnetic fields are usually much lower than those produced by external magnetic fields.

Transverse Plasma Waves

As an example of the single-particle approach, consider transverse electromagnetic (TEM) waves in a plasma. We begin with Maxwell's equations combining them to

produce the wave equation below:

$$\nabla \times \nabla \times \boldsymbol{E} = -\mu\sigma \frac{\partial \boldsymbol{E}}{\partial t} - \mu\varepsilon \frac{\partial^2 \boldsymbol{E}}{\partial t^2}, \tag{1}$$

Where σ, ε, and μ are the conductivity, electric permittivity, and magnetic permeability of the plasma, respectively. We shall assume that all of the plasma effects can be collected in the permittivity and that the conductivity is part of the permittivity, so we can set $\sigma = 0$ in Equation (1). If we now assume cartesian coordinates and that we have a transverse electromagnetic wave propagating in the z-direction with the propagation behaving like

$$\exp(\boldsymbol{k} \cdot \boldsymbol{r} - \omega t), \tag{2}$$

then we may substitute this notation into Equation (1) and represent Equation (1) as the matrix shown below:

$$\begin{pmatrix} -k_z^2 + \omega^2\mu\varepsilon & 0 & 0 \\ 0 & -k_z^2 + \omega^2\mu\varepsilon & 0 \\ 0 & 0 & -k_z^2 + \omega^2\mu\varepsilon \end{pmatrix} \times \begin{pmatrix} E_{0x} \\ E_{0y} \\ E_{0z} \end{pmatrix} = 0. \tag{3}$$

There are three possible eigenmodes (two of which are identical) for this equation. The first two are propagating disturbances, while the third mode is a time-invariant nonpropagating mode. In a plasma, this mode represents the electrostatic oscillations generated when the electrons are displaced with respect to the ions and allowed to move under the influence of the self-consistent (charge separation) electrostatic field. Vibrations of gelatin also exhibit this same property. If we assume that E_{0z} is zero, then the remaining two modes look just as they would in an ordinary dielectric. However, the permittivity of a plasma based on single-particle motions with stationary ions and no external d.c. magnetic field is expressed as

$$\varepsilon = \varepsilon_0 \left(1 - \frac{\omega_p^2}{\omega\,(\omega + \mathrm{i}\nu_m)}\right), \tag{4}$$

where ν_m is the electron momentum transfer collision frequency and ω_p is the electron plasma frequency defined as

$$\omega_p^2 = \frac{ne^2}{m\varepsilon_0}. \tag{5}$$

In Equation (5), n is the electron density, e is the charge of an electron, m is its mass, and ε_0 is the permittivity of free space. Since Equation (4) now has both real and imaginary parts, an effective conductivity of the plasma can now be obtained. Figure 1 shows a plot of the real part of ω vs. wave number k for two conditions: zero collision frequency and nonzero collision frequency. Because the relationship between k and ω is not a constant as frequency changes, we see that a TEM wave in a plasma exhibits dispersion. Examination of the real part of the propagation vector also shows that the wave amplitude will decrease as long as the collision frequency is not zero.

Nonlinear Ion-acoustic Waves

In this example, we consider the representation of a plasma as a fluid. Under these conditions, it is possible to excite longitudinal acoustic-type oscillations. We assume that the plasma mass is concentrated in its ions but that any electric fields that are generated by charge separation appear because of the higher mobility of the electrons. In this representation, we may write the equation of motion of a fluid element as follows (Chen, 1984):

$$Mn\left[\frac{\partial \boldsymbol{v}_i}{\partial t} + (\boldsymbol{v}_i \cdot \nabla)\boldsymbol{v}_i\right] = en\boldsymbol{E} - \nabla p, \tag{6}$$

where $\boldsymbol{v}_i$ refers to the ion species fluid velocity, p is the pressure, M is the ion mass, and n is the plasma density. Neglecting the electron mass (for simplicity), linearizing, and assuming propagating waves as previously, $\boldsymbol{E}$ is the negative gradient of a scalar potential ϕ. Using the equation of state gives

$$Mn(\mathrm{i}\omega + \nu_m)v = -en_0 \mathrm{i}k\phi - \gamma_i k T_i k n_1, \tag{7}$$

where n_0 is the steady-state density and n_1 is the perturbed density. Assuming that

$$e\phi/kT_e = n_1/n_0, \tag{8}$$

where T_e is the electron temperature, we obtain

$$(\omega + \mathrm{i}\nu_m)v = kV_s \frac{n_1}{n_0}. \tag{9}$$

In Equation (9) V_s is the sound speed $(kT_e/M)^{1/2}$. Applying a similar analysis to the continuity equation and substituting Equation (9) we obtain

$$\begin{aligned} -\mathrm{i}\omega n_1 + \mathrm{i}kn_0 v &= -\mathrm{i}\omega n_1 + \mathrm{i}k \frac{n_0}{(\omega + \mathrm{i}\nu_m)} [kV_s^2] \frac{n_1}{n_0} \\ &= 0 \end{aligned} \tag{10}$$

or

$$(\omega^2 + \mathrm{i}\nu_m\omega - k^2 V_s^2) = 0. \tag{11}$$

Longitudinal Plasma Oscillations (Langmuir Waves)

Now consider the kinetic representation of a plasma, in the case where the electric field is parallel to the direction of propagation. Assuming propagation in the z-direction, an electric field in the z-direction can be developed from an electrostatic potential of the form

$$\phi = \phi_0 \exp[\mathrm{i}(kz - \omega t)]. \tag{12}$$

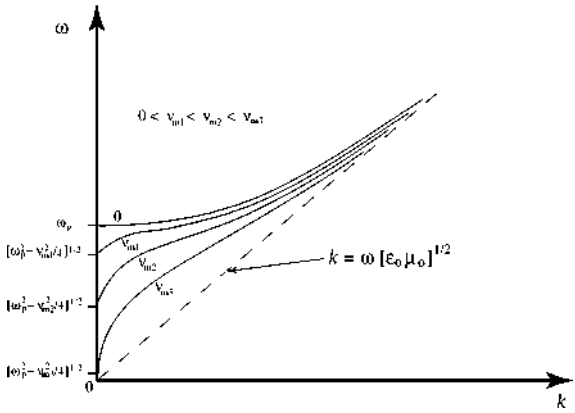

Figure 1. The real part of ω versus wave number k for increasing values of collision frequency ν_{m}.

If there are only electrostatic forces, the velocity distribution f of the electrons is governed by the Vlasov equation:

$$\frac{\partial f}{\partial t} + \boldsymbol{v} \cdot \nabla f + \frac{e}{m}\boldsymbol{E} \cdot \frac{\partial f}{\partial \boldsymbol{v}} = 0. \tag{13}$$

Writing a perturbation for f as $f = f_0 + f_1$ in which f_0 is only a function of velocity and f_1 can be a function of both position and velocity, we may write the perturbed part of the Vlasov equation as

$$\frac{\partial f_1}{\partial t} + \boldsymbol{v} \cdot \nabla f_1 + \frac{e}{m}\boldsymbol{E} \cdot \frac{\partial f_0}{\partial \boldsymbol{v}} = 0. \tag{14}$$

Writing Poisson's equation with this ordering results in

$$\nabla \cdot \boldsymbol{E} = \frac{n_0 e}{\varepsilon_0} \int f_1 \, \mathrm{d}\boldsymbol{v}. \tag{15}$$

Solving Equations (14) and (15) simultaneously yields the dispersion relation for these longitudinal plasma oscillations, often called Langmuir waves, as

$$1 = \frac{n_0 \varepsilon_0 e^2}{m} \frac{\boldsymbol{k}}{k^2} \cdot \int \frac{\partial f_0 / \partial \boldsymbol{v}}{(\boldsymbol{k} \cdot \boldsymbol{v} - \omega)} \, \mathrm{d}\boldsymbol{v}. \tag{16}$$

Note that the form of f_0 affects the dispersion relation. Also, the denominator in the integral of Equation (16) can have a singularity at which nonlinear effects can occur. It has been shown, for example, that the velocity distribution can draw energy from the wave or vice versa depending upon its slope. As a result, solitary waves can appear, expressing a balance between the driving and dissipative conditions.

In addition, Zakharov (1972) showed that Langmuir waves can evolve nonlinearly so that the electric field that results from the charge separation can become very large in a very small region. Under these "collapse" conditions, the field does not become infinitely large, but is limited by wave-particle interactions and often bursts of high-energy electrons are observed.

Plasmons

A plasmon is the resulting electrostatic oscillation described above when the velocity distribution can be neglected. For example, if it is assumed the ions in a plasma are stationary and the electrons are each uniformly displaced from their equilibrium position, then a Coulomb restoring force will be produced by the excess and deficiency of electrons at each end of the plasma, causing the electrons to oscillate about the ions. The frequency of oscillation is the electron plasma frequency:

$$\omega_{\mathrm{p}} = \left(\frac{ne^2}{m\varepsilon_0}\right)^{1/2}. \tag{17}$$

If the ion motion is considered, an ion plasma frequency also appears in the calculations. Plasmons, especially in solid state materials, can interact nonlinearly with electromagnetic fields and other radiation.

Plasma Turbulence

Turbulence appears when modeling for the three approaches (single particle, kinetic, and fluid) does not satisfactorily describe the experimental observations. For example, in hot plasmas, such as those appearing

in stars and fusion reactors, fluctuations in the plasma produce enhanced effects on mass, momentum and heat transport that must be studied in the context of turbulence.

If we could follow the motion of each and every particle in a plasma and its interactions with other particles and external electric and magnetic fields, we would be able to understand plasma turbulence. As that is not possible, alternative approaches must be undertaken.

Turbulence is said to appear in a plasma when the oscillations and fluctuations exhibit a continuous spectrum of frequencies. As a result of this state of turbulence, interactions between species in the plasma and the fluctuations can occur. For example, electrons, in addition to interacting with charged particles, can also interact with electric fields that are generated by the fluctuations. In addition, turbulent motion in a plasma has a very interesting effect: it can generate strong magnetic fields, producing a dynamo. This has been proposed as the mechanism for the generation of earth's magnetic field.

Numerical simulation has been shown to be a very powerful tool. In this case, the simulation involves a number of assumptions in order to make the problem solvable. The key method for these simulations involves following the trajectory of many simulation particles, as they interact with each other, that represent the plasma under various assumptions which can be applied to particular problems. By use of large supercomputers, it is possible to simulate astronomical and fusion plasma phenomena and examine the structure of the turbulence. A color figure in the color plate section shows a cross section of the results of such a simulation for a toroidal magnetic confinement system called a Tokamak. Calculations of this scale of detail could not be done without numerical simulations.

Whistlers and Helical Waves

Whistler waves have been detected in the ionosphere and have been attributed to the change of phase and group velocities of a right circularly polarized plasma wave that travels along the earth's magnetic field. The dispersion relation for this mode is

$$k^2 = \omega^2 \mu_0 \varepsilon_0 \left[1 - \frac{\omega_{\mathrm{pi}}^2 + \omega_{\mathrm{pe}}^2}{(\omega + \omega_{\mathrm{ci}})(\omega - \omega_{\mathrm{ce}})} \right]. \qquad (18)$$

In the ionosphere, the frequency of the waves is lower than the electron cyclotron frequency. Thus, the phase velocity (ω/k), which can be found from Equation (18) increases with frequency, and the group velocity also increases. When a lightning discharge takes place, an electromagnetic disturbance that has a large continuous spectrum of components is produced. The disturbance will travel to the ionosphere and then propagate along the Earth's magnetic field lines. However, the lower frequency components of the disturbance will take longer to arrive at a receiving station than the higher frequency components; thus, the received signal appears as a signal that decreases in frequency with time.

In examining the behavior of the electric field vector for a right circularly polarized wave, we note that as the wave propagates along an external magnetic field line, the direction of the electric field rotates around the direction of propagation which is, in this case, the direction of the magnetic field. As a result, this or any other mode can be represented as a helical wave in which the rotation of the end of the electric field vector traces out a helical path as it propagates.

MHD Kink Waves in Toroidally Confined Fusion Plasmas

The sine-Gordon equation has been shown to describe the trajectory of the "slinky" mode in a reversed-field-pinch magnetic fusion experiment (Ebraheem et al., 2002). A reversed-field-pinch experiment produces a magnetic field in a torus in which the portion of the field that is in the toroidal direction (the long way around) is reversed in its outer regions from that closer to the minor axis of the torus. Experimentally, it has been seen that during the operation of the system, magnetohydrodynamic (MHD) fluctuations in the center of the plasma can coalesce into a rotating "hot spot" that travels around the torus. Under some circumstances, the rotating mode may lock to other disturbances or to particular locations on the vacuum chamber torus.

As the mode may be envisaged as a helical solitary wave, it lends itself to being represented by the sine-Gordon equation. The mechanical transmission line analogy (Scott, 1971) can be applied here, if it is assumed that the MHD mode is a solenoid that wraps helically around the torus. The gravitational restoring torque can be represented as the gradient of the magnetic energy of the magnetic moment of the mode in the externally generated magnetic fields of the torus due to toroidal effects (the magnetic field on the inside of the torus is stronger than at the outside of the torus). The spring torque due to the adjacent pendula can be modeled by recognizing that the current flowing around the turns of the solenoid tends to make the solenoid align itself along its axis, so any disturbance from the alignment results in an equivalent spring torque.

Parametric Decay Instability

Consider two oscillators that have different resonant frequencies ω_1 and ω_2 that are nonlinearly coupled to each other through a third oscillator of resonant frequency ω_0. We assume that the oscillators are normal

modes of various types in the plasma such as described above. If each of these waves is considered from the point of view of quantum theory, interactions are governed by conservation of energy:

$$\hbar\omega = \hbar\omega_1 + \hbar\omega_2 \tag{19}$$

and conservation of momentum

$$k_0 = k_1 + k_2, \tag{20}$$

where k represents the wave number for each mode. The zero subscript refers to the "pump" mode and the other two modes are referred to as the "daughter" modes (Rost et al., 2002).

Assume that two of the oscillators obey the following equation of motion where each is driven by a time-dependent force that is proportional to the amplitude of a pump oscillator E_0:

$$\frac{\mathrm{d}^2 x_1}{\mathrm{d}t^2} + \omega_1^2 x_1 = c_1 x_2 E_0, \tag{21}$$

$$\frac{\mathrm{d}^2 x_2}{\mathrm{d}t^2} + \omega_2^2 x_2 = c_1 x_1 E_0, \tag{22}$$

where c_1 and c_2 are nonlinear coupling constants. If E_0 is made to vary in time at frequency ω_0, it can be seen that both modes can be driven by a frequency not equal to their natural frequency and, in addition, each oscillator's motion is coupled to the other oscillator's equation of motion.

J. Leon Shohet

See also **Alfvén waves; Magnetohydrodynamics; Plasma soliton experiments; Turbulence**

Further Reading

Chen, F.F. 1984. *Plasma Physics and Controlled Fusion*, 2nd edition, New York: Plenum Press.

Davidson, R.C. 1972. *Methods in Nonlinear Plasma Theory*, New York: Academic Press

Ebraheem, H.K., Shohet, J.L. & Scott, A.C. 2002. Mode-locking in reversed-field pinch experiments. *Physical Review Letters*, 88: 235003

Horton, C.W. & Ichikawa, Y.H. 1996. *Chaos and Structures in Nonlinear Plasmas*, River Edge, NJ: World Scientific

Rost, J.C., Porkolab, M. & Boivin, R.L. 2002. Edge ion heating and parametric decay during injection of ion cyclotron resonance frequency power on the Alcator C-Mod tokamak. *Physics of Plasmas*, 9: 1262–1270

Scott, A.C. 1971. *Active and Nonlinear Wave Propagation in Electronics*, New York: Wiley

Zakharov, V.E. 1972. Collapse of Langmuir waves. *Soviet Physics JETP*, 35: 908–912

NONLINEAR RESONANCE

See **Damped-driven anharmonic oscillator**

NONLINEAR SCHRÖDINGER EQUATIONS

The basic nonlinear Schrödinger (NLS) equations are

$$\mathrm{i}u_t \pm \tfrac{1}{2}u_{xx} + |u|^2 u = 0, \tag{1}$$

where $u(t, x)$ is a complex function, the real variables t and x are frequently (but not always, see below) time and space coordinates, and the subscripts indicate partial derivatives. The upper and lower signs in front of the second term in Equation (1) correspond, respectively, to self-focusing and self-defocusing NLS equations, to be denoted below as NLS(+) and NLS(−).

NLS equations attracted much attention after Zakharov & Shabat (1972) demonstrated that Equations (1) are integrable by means of the inverse scattering transform (IST) (Zakharov et al., 1984). Under this formulation, Equation (1) is viewed as a compatibility condition for a system of two auxiliary linear equations for a two-component function $\psi^{(1,2)}(x, t)$. The first of these equations is

$$\begin{pmatrix} -\mathrm{i}\partial_x & u^*(x) \\ -u(x) & \mathrm{i}\partial_x \end{pmatrix} \begin{pmatrix} \psi^{(1)} \\ \psi^{(2)} \end{pmatrix} = \lambda \begin{pmatrix} \psi^{(1)} \\ \psi^{(2)} \end{pmatrix}, \tag{2}$$

where λ is a spectral parameter and the asterisk stands for the complex conjugation. The first step in the application of IST is to solve the direct scattering problem for Equations (2) (also called Zakharov–Shabat (ZS) equations) with a given initial configuration $u_0(x)$ at $t = 0$, that is, to map $u_0(x)$ into a set of scattering data. In the general case, the set contains continuous and discrete components, which correspond, respectively, to real and complex λ. The temporal evolution of scattering data, generated by the temporal evolution of $u(x, t)$ under Equation (1), turns out to be trivial, so that, once the scattering data is known at $t = 0$, it is also known for any $t > 0$. Finally, at given t, one must recover the field $u(t, x)$ from the known scattering data, that is, to solve the inverse scattering problem, which is based on the Gel'fand–Levitan–Marchenko integral equation.

The simplest solution of NLS(+) represents a soliton (exponentially localized pulse)

$$\begin{aligned} u_{\mathrm{sol}} &= \eta \operatorname{sech}\left[\eta\,(x - ct - x_0)\right] \\ &\quad \times \exp\left(\mathrm{i}cx - \mathrm{i}\omega_{\mathrm{sol}} t + \mathrm{i}\phi_0\right), \end{aligned} \tag{3}$$

where $\omega_{\mathrm{sol}} = \left(c^2 - \eta^2\right)/2$, $\operatorname{sech} z \equiv 2\left(\mathrm{e}^z + \mathrm{e}^{-z}\right)^{-1}$, η and c are arbitrary amplitude and velocity of the soliton, and x_0 and ϕ_0 are the coordinate of the soliton's center and its phase at $t = 0$.

Note that frequencies of the zero-velocity ($c = 0$) solitons are negative ($\omega_{\mathrm{sol}} = -\eta^2/2 < 0$), while the frequencies of radiation modes, that is, solutions to the linearized version of NLS(+), $u_{\mathrm{rad}} = u_0 \exp\left(\mathrm{i}kx - \mathrm{i}\omega_{\mathrm{rad}} t\right)$, are positive ($\omega_{\mathrm{rad}} = k^2/2 > 0$, where k and u_0 are arbitrary wave number and amplitude). Thus, solitons exist

in a part of the frequency space where radiation modes are absent, exemplifying a general principle: solitons cannot share frequencies with radiation, as they would otherwise be losing energy through the emission of linear waves.

In terms of the IST, the soliton corresponds to a case when the continuous component of the scattering data is absent, while the discrete component consists of a single eigenvalue $\lambda = (-c + i\eta)/2$. All the solutions corresponding to an arbitrary set of complex eigenvalues can be found in an explicit form, describing collisions between solitons unless their velocities coincide. The solitons reappear after the collision with the same amplitudes and velocities, that they had prior to the collision, the only change being shifts of the constants x_0 and ϕ_0. If velocities coincide, the solution describes a bound state of solitons, which is dynamically unstable because its binding energy is zero. Thus, the simple soliton given by Equation (3) is the single stable solution to NLS(+) with a permanent wave shape.

Besides the solitons, Equations (1) have spatially uniform solutions in the form of continuous waves (CWs), $u_{\mathrm{CW}}(t) = \eta \exp\left(\pm i\eta^2 t\right)$, with an arbitrary real amplitude η. An important issue is stability of the CW solutions against small perturbations. To investigate the stability, one can represent a solution as $u(t,x) = a(x,t)\exp(i\phi(t,x))$, where $a(t,x)$ and $\phi(t,x)$ are real amplitude and phase. Rewriting Equation (1) as a system of real equations for a and ϕ leads to a perturbed CW with $a(t,x) = \eta + a_1(t,x)$, and $\phi(t,x) = \pm\eta^2 t + \phi_1(t,x)$, with infinitesimal perturbations a_1 and ϕ_1. Linearizing the equations with respect to a_1 and ϕ_1 yields a solution in the form

$$a_1(x,t) = a_1^{(0)} \exp(\sigma t)\cos(px)\,, \phi_1(x,t) = \phi_1^{(0)} \exp(\sigma t)\cos(px)\,, \tag{4}$$

where $a_1^{(0)}$ and $\phi_1^{(0)}$ are infinitesimal amplitudes of the perturbation, p is its arbitrary wave number $(-\infty < p < +\infty)$, and σ is an instability growth rate. The linearized equations imply the following relation between σ and p:

$$\sigma^2(p) = \pm p^2\left(\eta^2 \mp p^2/4\right). \tag{5}$$

The necessary and sufficient condition for the stability of CW against small perturbations is $\mathrm{Re}\,\sigma(p) \le 0$, which must hold for all p. As is seen from Equation (5), all the CW solutions to NLS(−) are stable, but in NLS(+) they all are unstable for p^2 in the range $0 < p^2 < 4\eta^2$. It follows from Equation (4) that growing perturbations break the uniformity of the CW, initiating spatial modulation. This is called modulational instability and also Benjamin–Feir instability, after the authors who discovered it in the context of water waves.

Although NLS(−) does not support solitary-wave solutions, it has a stable solution in the form of a dark soliton (DS), which is a region of low amplitude moving on top of a CW. The DS solution is

$$u_{\mathrm{DS}} = \eta \exp\left(i\eta^2 t\right) \times \{(\cos\theta)\tanh[\eta(\cos\theta)(x - ct)] + i\sin\theta\}\,, \tag{6}$$

where η is the amplitude of the CW background, and θ, which takes values between 0 and $\pi/2$, determines the minimum value of the field at the center of DS and its velocity (Kivshar & Luther-Davies, 1998). The solution of Equation (3) is sometimes called a bright soliton to stress its difference from the DS.

A fundamental property of NLS equations which is not related to the integrability and is therefore more generic, being shared by a broad class of equations, is a possibility to represent the equations in the Lagrangian and Hamiltonian forms. The general Lagrangian representation is $\delta S/\delta u^*(t,x) = 0$, where $S\{u(t,x), u^*(t,x)\}$ is an *action functional*, which must be real, and $\delta/\delta u^*$ stands for the variational (Fréchet) derivative of the functional (u and u^* are treated as independent functional arguments). The action functional that generates Equation (1) is

$$S = \int dt \int_{-\infty}^{+\infty} dx \left[i\left(u^* u_t - u u_t^*\right) \mp |u_x|^2 + |u|^4\right]. \tag{7}$$

The Hamiltonian representation of the NLS equations is

$$i\frac{\partial u}{\partial t} = \frac{\delta H\{u, u^*\}}{\delta u^*}, \tag{8}$$

where the Hamiltonian (H) is $\int dx \left(\pm|u_x|^2/2 - |u|^4/2\right)$. The representation in the form of Equation (8) is very general, applying to a large class of equations for complex fields.

For real H, it follows from Equation (8) that the Hamiltonian is conserved. From the perspective of the Noether theorem, conservation of H is a consequence of the fact that Equation (1) is invariant with respect to an arbitrary time shift, $t \to t + t_0$. The invariances with respect to an arbitrary phase shift, $u(t,x) \to u(t,x)\exp(i\phi_0)$, and to an arbitrary coordinate shift, $x \to x + x_0$, generate the conservation of the number N (alias "number of quanta") and momentum P, which are given by universal expressions, irrespective of the particular form of the equation:

$$N = \int_{-\infty}^{+\infty} dx\ |u(x)|^2\,, \quad P = \frac{1}{2}i\int_{-\infty}^{+\infty} dx\left(u u_x^* - u^* u_x\right). \tag{9}$$

If the equation is integrable by means of IST, it possesses, in addition to the dynamical invariants N,

P, and H, an infinite series of higher-order conserved quantities (Zakharov et al., 1984).

Despite the exact integrability of Equation (1) by means of IST, the solution provided by this technique may be too cumbersome; therefore, a more tractable approximate method for the construction of solutions is often desirable. To this end, a variational approximation (VA), whose applicability relies solely on the Lagrangian representation of the equation(s), has been developed for solitons of NLS(+) and for several other equations, including those described below. This method approximates the full PDE by a low-order system of ODEs, which are derived from the same action functional (Malomed, 2002).

NLS Models for Wave Envelopes in Weakly Nonlinear Dispersive Media

Equations (1) also appear as universal equations governing the evolution of slowly varying packets of quasi-monochromatic waves in weakly nonlinear media featuring dispersion (dependence of the wave's group velocity $c_{\rm gr}$ on its frequency ω).

To illustrate this point, one can take the sine-Gordon (SG) equation, $\psi_{tt} - \psi_{xx} + \sin\psi = 0$, for real $\psi(t, x)$. Assuming a small-amplitude wave with a slowly varying complex envelope function $u(t, x)$ carried by a high-frequency wave $\exp(-it)$, the solution is $\psi(t, x) = u(t, x)\exp(-it) + u^*(t, x)\exp(it)$, where the slow variation implies that $|u_t|^2 \ll |u|^2$. Substituting into SG, expanding $\sin\psi$ up to the cubic term, dropping the higher-order small terms u_{tt} and u^*_{tt}, and separately collecting terms in front of two independent rapidly varying functions $\exp(\pm it)$ yields two equations: NLS(+) for $u(t, x)$, and its complex conjugate for $u^*(t, x)$.

Thus, NLS equations can be derived as equations governing the evolution of weakly nonlinear wave packets in various media. An important example is light propagation in nonlinear optical fibers and planar waveguides. In the former case, NLS takes the normalized form $iu_z \pm (1/2)u_{\tau\tau} + |u|^2 u = 0$, where $u(\tau, z)$ is the local amplitude of the electromagnetic wave, which is a function of the propagation distance z and $\tau \equiv t - z/c_{\rm gr}$ ($c_{\rm gr}$ is the group velocity of light in the fiber). In the context of Equation (1), z plays the role of the evolutionary variable, and τ plays the role of the coordinate. The cubic term in the equation accounts for the Kerr effect (a nonlinear correction to the refractive index), while the upper and lower signs in front of $u_{\tau\tau}$ correspond to the anomalous and normal chromatic dispersion in the fiber, $dc_{\rm gr}/d\omega > 0$ and $dc_{\rm gr}/d\omega < 0$, respectively (ω is the frequency of the electromagnetic wave). Only anomalous dispersion gives rise to bright optical solitons (also called temporal solitons) as they are localized in τ (Agrawal, 1995). Temporal solitons are important in fiber-optic telecommunications.

In planar waveguides, spatial bright solitons are possible in the form of self-confined light beams. In this case, the propagation coordinate z again replaces t in Equation (1), while the transverse coordinate x appears the same way as in Equation (1), the term u_{xx} accounting for diffraction of light in the waveguide. The corresponding NLS equation is always self-focusing.

Other significant applications in which NLS equations arise are small-amplitude gravity waves on the surface of deep inviscid water and Langmuir waves in hot plasmas (collective oscillations of electrons relative to ions). However, these media are not really one-dimensional, which makes the corresponding NLS solitons unstable against transverse perturbations.

In plasma, NLS(+) approximates a more fundamental model—the Zakharov system

$$\begin{aligned} iu_t + \tfrac{1}{2}u_{xx} + nu &= 0, \\ n_{tt} - n_{xx} &= -\left(|u|^2\right)_{xx}, \end{aligned} \tag{10}$$

where $n(t, x)$ is a perturbation of the ion density, and $u(t, x)$ is the local amplitude of the Langmuir waves. Although Equations (10) are not integrable, they generate stable solitons and reduce to NLS(+) in the adiabatic limit, when the term n_{tt} may be neglected.

Zakharov's system is a universal model describing weakly nonlinear waves in dispersive media, where a dominating process is the interaction between high- and low-frequency waves (e.g., the Langmuir and ion-acoustic waves, respectively, in plasmas). Another example is the interaction of high-frequency (near infra-red) molecular vibrations and low-frequency (far infra-red) longitudinal deformations in a model of long biological molecules, which gives rise to the Davydov soliton.

Generalized Forms of the Nonlinear Schrödinger Equations

The NLS equation can be viewed as a paradigmatic representative of a large class of nonlinear PDEs, some of which are also integrable. Examples are the derivative NLS equation, $iu_t + u_{xx} + i\left(|u|^{2u}\right)_x = 0$, whose integrability was discovered by Kaup and Newell (this equation applies to Alfvén waves in magnetized plasmas), the Hirota equation, $iu_t + u_{xx} + i\left(u_{xxx} + 6|u|^2 u_x\right)$, and the Sasa–Satsuma equation, $iu_t + u_{xx} + i\left[u_{xxx} + 6|u|^2 u_x + 3\left(|u|^2\right)_x u\right] = 0$.

In applications to fiber optics, an important generalization considers two polarizations of light (or two different wavelengths in one fiber), leading to a

system of coupled NLS equations

$$\begin{aligned} \mathrm{i}u_z \pm \tfrac{1}{2}v_{\tau\tau} + \left(|u|^2 + \beta\,|v|^2\right)u = 0, \\ \mathrm{i}v_z \pm \tfrac{1}{2}v_{\tau\tau} + \left(|v|^2 + \beta\,|u|^2\right)u = 0. \end{aligned} \tag{11}$$

In the case of linear polarizations, $\beta = \frac{2}{3}$, and in the case of circular polarizations or different wavelengths, $\beta = 2$ (Agrawal, 1995). As demonstrated by Manakov, Equations (11) are integrable if $\beta = 1$ (Manakov, 1974).

Generalized NLS equations are not integrable in other cases of interest, including the multidimensional NLS equations

$$\mathrm{i}u_t \pm \tfrac{1}{2}\nabla^2 u + |u|^2\,u = 0, \tag{12}$$

where ∇^2 is the two- or three-dimensional (2-d or 3-d) Laplacian. Equation (12) describes light propagation in bulk media, and Langmuir waves in plasmas. Both the 2-d and 3-d solitons are unstable because NLS(+) gives rise to collapse, that is, formation of a singularity in finite time (Bergé, 1998) (nevertheless, the 2-d soliton, also called the Townes soliton, plays an important role, as it determines the critical power necessary for the collapse in the 2-d case).

The 2-d NLS(−) gives rise to vortex solutions, with important implications in nonlinear optics, which take the form

$$u = \eta \exp\left(\mathrm{i}\eta^2 t + \mathrm{i}S\chi\right) U\left(\sqrt{2}\eta r\right) \tag{13}$$

with arbitrary η and $U(\rho = \infty) = 1$. Here, χ is the angular coordinate in the 2-d space, and $S \geq 1$ is an integer vorticity. Only the vortex with $S = 1$ is stable, being a 2-d counterpart of the DS solution (6) with $\theta = 0$.

Multidimensional bright solitons (also called light bullets in 3-d optical models) may be stable if the cubic term $|u|^2\,u$ in NLS(+) is replaced by a saturable one, $|u|^2\left(1 + |u|^2/u_0^2\right)^{-1}$ ($u_0^2 = \text{const}$), or by a combination of self-focusing cubic and self-defocusing quintic terms, $\left(|u|^2 - |u|^4\right)u$. In the latter case, bright 2-d solitons with the embedded vorticity $S \geq 1$ and 3-d solitons with the vorticity $S = 1$ may also be stable.

Similar to Equation (12) is the Gross–Pitaevskii (GP) equation for the single-atom wave function $\psi(t, \boldsymbol{r})$, on which the mean-field description of Bose–Einstein condensates is based (Dalfovo et al., 1999):

$$\mathrm{i}\hbar\frac{\partial\psi}{\partial t} = -\frac{\hbar^2}{2m}\nabla^2\psi + U(\boldsymbol{r})\psi + g\,|\psi|^2\,\psi. \tag{14}$$

Here $\hbar$ is Planck's constant, m is the atom mass, $U(\boldsymbol{r})$ is a trapping potential, and g is proportional to the scattering length of collisions between atoms, which may be both positive and negative.

The simplest approach to GP is to seek a stationary solution, $\psi(t, \boldsymbol{r}) = \exp(-\mathrm{i}\mu t/\hbar)\,\Psi(\boldsymbol{r})$ (μ is called the chemical potential), and apply the Thomas–Fermi approximation to $\Psi(\boldsymbol{r})$, which amounts to dropping the Laplacian in Equation (14). This yields $|\Psi(\boldsymbol{r})|^2 = g^{-1}\left[\mu - U(\boldsymbol{r})\right]$ if it is positive, or $\Psi = 0$ otherwise.

Nonlinear optics motivate examples of coupled NLS equations that are different from Equations (11). Propagation of light in an optical fiber carrying a Bragg grating (a lattice of defects with the period equal to half the wavelength of light, which gives rise to mutual resonant conversion of right- and left-traveling waves) is described by equations for the amplitudes $u(t, x)$ and $v(t, x)$ of the counterpropagating waves,

$$\begin{aligned} \mathrm{i}u_t + \mathrm{i}u_x + \left(|u|^2 + 2\,|v|^2\right)u + v = 0, \\ \mathrm{i}v_t - \mathrm{i}v_x + \left(|v|^2 + 2\,|u|^2\right)v + u = 0 \end{aligned} \tag{15}$$

with the linear coupling accounting for the resonant Bragg scattering. The spectrum of the linearized version of Equations (15) is $\omega^2 = k^2 + 1$, hence it has a radiation-free gap, $-1 < \omega < +1$, where solitons may be expected. A family of gap solitons is generated by Equations (15) that can be found exactly although Equations (15) are not integrable and not all members of this family are stable (de Sterke & Sipe, 1994; Malomed, 2002).

Another NLS system describes a basic process in nonlinear optics—second harmonic generation (SHG). If the nonlinearity is quadratic, the system is

$$\begin{aligned} \mathrm{i}u_z + \tfrac{1}{2}u_{xx} + u^*v = 0, \\ 2\mathrm{i}v_z + \tfrac{1}{2}v_{xx} + \tfrac{1}{2}v^2 + qv = 0, \end{aligned} \tag{16}$$

where $u(z, x)$ and $v(z, x)$ are amplitudes of the fundamental-frequency and second harmonic waves, and real q is a wave number mismatch between the harmonics. Equations (16) are written for the realistic case of spatial fields in a planar waveguide. They give rise to a family of solitons in the form $u = \exp(\mathrm{i}kz)\,U(x)$, $v = \exp(2\mathrm{i}kz)\,V(x)$, with exponentially localized $U(x)$ and $V(x)$. Except for the case $k = q/3$, the solitons are not available in an analytical form, but most of them are stable (Etrich et al., 2000). Multidimensional generalizations of Equations (16) give rise to stable solitons too, as collapse does not take place in the SHG model.

Ginzburg–Landau (GL) equations, which are formally similar to NLS equations, provide general models of nonlinear dissipative media. The simplest GL equation is Equation (1) with all the coefficients made complex. In general, however, dynamics generated by GL equations is altogether different from that governed by NLS equations (Aranson & Kramer, 2002).

BORIS MALOMED

See also **Complex Ginzburg–Landau equation; Discrete nonlinear Schrödinger equations; Equations, nonlinear; Inverse scattering method or transform; Nonlinear optics**

Further Reading

Agrawal, G.P. 1995. *Nonlinear Fiber Optics*, San Diego: Academic Press

Aranson, I.S. & Kramer, L. 2002. The world of the complex Ginzburg–Landau equation. *Reviews of Modern Physics*, 74: 99–143

Bergé, L. 1998. Wave collapse in physics: principles and applications to light and plasma waves. *Physics Reports*, 303: 259–370

Dalfovo, F., Giorgini, S., Pitaevskii, L.P. & Stringari, S. 1999. Theory of Bose-Einstein condensation in trapped gases. *Reviews of Modern Physics*, 71: 463–512

Etrich, C., Lederer, F., Malomed, B.A, Peschel, T. & Peschel, U. 2000. Optical solitons in media with a quadratic nonlinearity. *Progress in Optics*, 41: 483–568

Kivshar, Y.S. & Luther-Davies, B. 1998. Dark optical solitons: physics and applications. *Physics Reports*, 298: 81–197

Malomed, B.A. 2002. Variational methods in nonlinear fiber optics and related fields. *Progress in Optics*, 43: 69–191

Manakov, S.V. 1974. On the theory of two-dimensional stationary self-focusing of electromagnetic waves. *Soviet Physics JETP*, 38: 248–253

de Sterke, C.M. & Sipe, J.E. 1994. Gap solitons. *Progress in Optics*, 33: 203–260

Zakharov, V.E., Manakov, S.V., Novikov, S.P. & Pitaevskii, L.P. 1984. *Solitons: The Method of Inverse Scattering Transform*, New York: Consultants Bureau

Zakharov, V.E. & Shabat, A.B. 1972. Exact theory of two-dimensional self-focusing and one-dimensional self-modulation of waves in nonlinear media. *Soviet Physics, JETP*, 34: 62–69

NONLINEAR SIGNAL PROCESSING

The field of nonlinear signal processing is an active area of research stimulated by a combination of new applications, advances in technology, and fundamental advances in mathematical theory. The breadth of applications has extended far beyond the original emphasis on communications to disciplines such as brain science, financial analysis, image and voice recognition, cryptography, virtual reality, digital photography and printing technology, and neural computing. Significant accelerations in computing speeds and the increasingly widespread availability of computer clusters have made more complex algorithms computationally feasible and motivated the investigation of a much larger range of algorithms. Included in these new algorithms are techniques extracted, for example, from chaos theory, partial differential equations, computational geometry, support vector machines, numerical analysis on manifolds, and optimization theory. Fundamental advances in nonlinear signal processing have centered around an increased mathematical understanding of the notion of information content and representation.

Nonlinear signal processing began with the realization that all components of a signal are not equal. For example, nonlinear filters have been used for compressing signals associated with telephone voice communications where the fidelity required depends on the frequency of the signal. In general, it is possible to retain fewer bits of high frequency data than lower frequency data and still maintain voice clarity. Additionally, median and min/max filters and histogram equalization represent traditional tools in nonlinear signal (and image) processing. In mathematical terms, the motivation for nonlinear signal processing techniques arises from the geometric structure, or organization, of the data. In some idealized sense, we can view data as either being flat, as possessing some degree of curvature, or having a fractal nature. The nature of this structure in the data dictates the best tool to be used for its analysis. For example, *signal dimension* is an important feature of a signal. Based on the geometry of the signal, one may employ, for example, basis dimension, topological dimension, or Hausdorff dimension. There are now a number of methods that have been proposed to detect nonlinear features in data including poly-spectral analysis, surrogate analysis, and more; see Barnett et al. (1997) for detailed comparisons.

As a consequence of the inherently complicated geometry, modeling nonlinear signals is significantly more challenging than their linear counterparts. For example, an n-dimensional linear signal may be written $f(x(t)) = Ax(t)$ where the model consists of the $m \times n$ matrix of parameters. If there are more points than unknowns to construct the model, then the approach of least squares may be used for solving over-determined systems. This theory, including the effect of perturbations on the data, is well understood. For nonlinear signals with n-dimensional domains, one encounters the well-known "curse of dimensionality" that suggests that the amount of data required to construct such nonlinear mappings is exponentially dependent on the dimension of the domain. However, the recognition that this problem is overcome by judiciously placing basis functions in the domain of the data has led to a large literature in the theory and applications of modeling nonlinear signals in high dimension. Radial basis functions (RBFs) are a popular choice and have the form

$$f(x) = w_0 + \sum_{k=1}^{N} w_k \phi(\|x - c_k\|),$$

where the vectors c_k are the special sites of the basis functions, x the domain value and the w_i the model parameters. The basis functions may be local, for example, $\phi(r) = \exp(-r^2)$ or global, for example, $\phi(r) = r^3$. Artificial neural networks (ANNs) have also been proposed for such nonlinear approximation tasks. These networks provide a flexible, or adaptive, tool to *learn* a function. Generally, a special type of ANN is employed, that is, a feed-forward sigmoidal network. Mathematically, this may be expressed as

$$y = \sum_i w_i^{(2)} \sigma \left(\sum_j w_{ij}^{(1)} x_j - \theta_i \right),$$

where σ is a monotonic nonlinear squashing function and $\{w_i^{(2)}, w_{ij}^{(1)}, \theta_i\}$ the model parameters. There exist universal approximation theorems that state under which conditions both the RBF and ANN approximations can produce models to essentially arbitrary accuracy. Of course, practical issues such as computation expense and parsimony of the model must be considered in the implementation of such methods. Further details on these issues may be found in Haykin (1994) and Kirby (2001).

Dynamical systems theory has provided a new paradigm for the analysis of nonlinear signals. Fuelled by observation that complex or chaotic signals can arise from simple nonlinear deterministic systems, a suite of new tools has been developed for their empirical detection, characterization, and design. Briefly, a discrete dynamical system may be viewed as the iteration of a mapping, that is

$$x^{(n+1)} = f(x^{(n)}). \tag{17}$$

Often the trajectory $\{x^{(0)}, x^{(1)}, x^{(2)}, \ldots\}$ traces out a complicated path. Here $x^{(n)}$ is viewed as a function of n. However, a *delay embedding* that plots a point as a function of the previous one or more points may produce a picture that reveals the structure of the simple underlying determinisitic system. For example, the well-known logistic map has the form

$$x^{(n+1)} = \alpha(1 - x^{(n)})x^{(n)}.$$

It possesses a complicated, apparently random trajectory with broad Fourier spectrum for $\alpha > 4$. However, clearly the locus of points $(x^{(n)}, x^{(n+1)})$ is a parabola. Thus, one is motivated to look for structure in a sequence of observations of a signal by constructing the delay embeddings $(x^{(n)}, x^{(n-1)})$ (one delay) or $(x^{(n)}, x^{(n-1)}, x^{(n-2)})$ (two delays) and so on. In practice, it is useful to explore delays of multiples of an integer, that is, $N, 2N, 3N, \ldots$.

This heuristic approach gains some credibility with the support of the Takens embedding theorem; see for example, Abarbanel (1996) and references therein. To get a flavor of the power of this theorem, consider a multidimensional discrete dynamical system, that is, the point $\mathbf{x}^{(n)}$ being iterated is a d-tuple. Takens's theorem basically says that if we are able to observe any one component of this system, for example $\{x_1^{(n)}\}$ then the delay embedding of this variable produces a geometrical structure that is in some sense equivalent to the original system. Furthermore, if only a function h of the first component is observed $h(x_1^{(n)})$, then we can still replicate the structure of the original system with the delay embedding approach. The number of delays required to achieve this embedding is prescribed by Takens, for example if the dynamical system resides on an m-dimensional manifold, then the number of delays need only be $2m + 1$ (Abarbanel, 1996).

The dynamical system described by Equation (17) or the delay mapping

$$x^{(n+1)} = f(x^{(n)}, x^{(n-1)}, \ldots),$$

where f is unknown but observed data are available may also be modeled using the RBF or ANN approaches. Note that the domain of this mapping of delay coordinates may be of high enough dimension to preclude the use of other standard methods. A first look at this procedure in the context of nonlinear signal modeling is described in Lapedes & Farber (1987).

Yet another promising direction of the dynamical systems approach is fractal image compression. Here a picture may be stored as an *iterated function system*, that is two or more systems of the form of Equation (17) where f is now an affine transformation. An image can be produced by iterating this system and only a small number of parameters need be stored. See Barnsley & Hurd (1993) for many interesting examples as well as mathematical details.

The richness of the nonlinear signal processing field is in part due to technology. Optical signal processing is based on the application of the characteristics of light to process and transmit information. For example, in optical image processing, holograms are used to store data while lenses are used to compute two-dimensional Fourier transforms and may also perform edge detection and filtering tasks (Poon & Banerjee, 2001). Most recently, the field of fiber optics has arisen from the observation that light emanating from a laser and passing through a tiny pure glass pipe can transmit more information than electrical signals transmitted along a wire. The ability to send and amplify multiple signals simultaneously along an optic fiber has give rise to data transmission rates of 10 Gbps with higher rates in view. This technique is referred to as dense wavelength division multiplexing (DWDM) (Ramaswami & Sivarajan, 2001). New efforts to model and exploit such technologies suggest that the field of nonlinear signal processing is at the dawn of a new era. For example, the emerging area of photonics addresses how light can be used to represent and process signals and the new discipline of biophotonics concerns how light may be used to discover the mechanisms by which the basic building blocks of living matter function. Signal processing problems such as these may prove to have significant impact on the human condition including the battle against diseases such as cancer.

MICHAEL J. KIRBY

See also **Attractor neural network; Embedding methods; McCulloch–Pitts network; One-dimensional maps; Standard map**

Further Reading

Abarbanel, H.D.I. 1996. *Analysis of Observed Chaotic Data*, Berlin and New York: Springer
Barnett, W., Gallant, A.R., Hinich, M.J., Jungeilges, J.A., Kaplan, D.T. & Jensen, M.J. 1997. A single-blind controlled competition among tests for nonlinearity and chaos. *Journal of Econometrics*, 82: 157–192
Barnsley, M.F. & Hurd, L.P. 1993. *Fractal Image Compression*, Wellesley, MA: AK Peters
Haykin, S. 1994. *Neural Networks*, New York: Macmillan
Kirby, M. 2001. *Geometric Data Analysis: An Empirical Approach to Dimensionality Reduction and the Study of Patterns*, New York: Wiley
Lapedes, A. & Farber, R. 1987. *Nonlinear signal processing using neural neworks: prediction and system modelling*, Techinical Report LA-UR-87-2662, Los Alamos National Laboratory
Poon, T.-C. & Banerjee, P.P. 2001. *Contemporary Optical Image Processing with Matlab*, New York: Elsevier
Ramaswami, R. & Sivarajan, K.N. 2001. *Optical Networks: A Practical Perspective*, 2nd edition, San Francisco: Morgan Kaufmanm

NONLINEAR SUPERPOSITION

See ***N*-solition formulas**

NONLINEAR TOYS

Toys are ubiquitous and some are unique to particular cultures. Many action toys are intriguing because they perform in unexpected ways as a result of underlying nonlinear principles, yielding both amusement and surprises for the unwary. Here we give several examples of toys and devices that operate on linear and nonlinear physical principles.

Frog on a Swing

Several toys are based on the mechanism of *parametric excitation*. Although primarily a linear mechanism, an increase in amplitude in parametric excitation leads to the nonlinear range of amplitude-dependent phenomena. One can demonstrate parametric excitation by taking a string with a weight attached to its end and make it into a pendulum by hanging it over the forefinger (see Figure 1(a)). Now, force the weight into a small amplitude oscillation, and then move the weight up and down with the same phase as the oscillation by pulling on the string periodically. The result is an increase in the amplitude of the oscillation of the pendulum. The phase of the oscillation will vary slowly as the amplitude increases and the inherently nonlinear nature of the pendulum becomes important. The basic linearized equation for parametric excitation of the nonlinear pendulum is the Mathieu equation

$$\frac{\mathrm{d}^2\theta}{\mathrm{d}t^2} + \left(\omega_0^2 - \alpha \sin 2\omega_0 t\right)\theta = 0$$

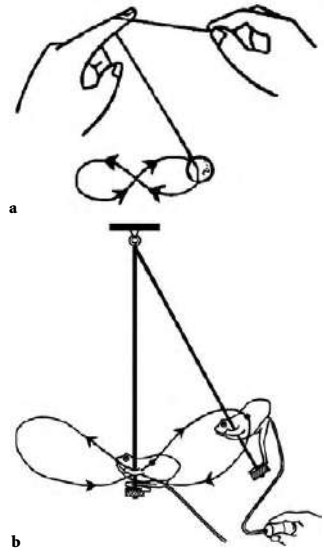

Figure 1. Parametric excitation demonstrated by (a) a pendulum over a finger and (b) a frog on a swing.

where θ is the angle of the pendulum from the vertical, ω_0 is the fundamental small amplitude frequency, and α is the amplitude of the periodically changing pendulum length.

This principle of parametric excitation is active in the toy called the "frog on a swing" (see Figure 1(b)). The frog in this toy is made of rubber and sits on a swing (pendulum). It can be inflated periodically with air using a tube and bulb. This causes the frog to stand up and sit down repeatedly and, hence, moves the center of mass of the frog up and down, as illustrated in Figure 1(b). With proper timing in inflating the bulb at the correct phase during each swing, the amplitude of the swing with the oscillating frog on it gradually increases. The same principle applies to the playground swing where children can increase the amplitude of their swing by "pumping" the swing in a standing position (Wirkus et al., 1998).

Handstand Pendulum

A related, but completely different, phenomenon occurs in the "handstand pendulum." The normal pendulum hangs stably downwards from its fulcrum as a result of gravity. However, applying a high-frequency forced oscillation to the fulcrum can cause the pendulum to be inverted, so that it now "hangs" stably pointing upwards

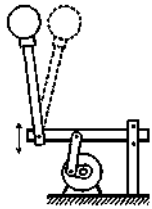

Figure 2. The handstand pendulum.

(Figure 2). Again the governing linearized equation is the Mathieu equation, but with the signs changed:

$$\frac{\mathrm{d}^2\theta}{\mathrm{d}t^2} + \left(-\frac{g}{\ell} + 2\alpha \sin 2\omega t\right)\theta = 0$$

where g is the acceleration due to gravity and ℓ is the length of the pendulum arm.

Shishi-odoshi

In some Japanese gardens, there is a device that was designed originally to scare deer and other animals away from rice fields. Now, its purpose is either to scare away the deer that may intrude into a garden to eat the plants or to serve as an aesthetic fixture in the garden for its novelty and silence breaking "clack." This device, while not strictly a toy, is based on nonlinear principles and is called a *shishi-odoshi* (deer-scarer) or *shika-oi*. The *shishi-odoshi* is made from a thick bamboo culm with a length of three internal cells, that is, four nodes (the raised rings at regular intervals along the bamboo). At one end, the last node has been cut off and the end shaped to receive water (see Figure 3). From this open end, the internal membrane of the first node also has been removed so there is a cylindrical cup that is two cells long. A pivot rod is inserted into the bamboo between the two inner nodes so that when the tube is empty, the closed end of the bamboo rests on a stone. However, the position of the pivot is chosen so that as a steady stream of water flows into the open end of the tube, the center of mass of the bamboo and water shifts across the pivot and the open end of the tube will dip down, thus pouring out the water. The empty tube now returns quickly to its stable position on the stone with a loud "clack," which is the noise that is supposed to scare the deer.

The oscillatory motion of the bamboo tube caused by the steady flow of water is called a *relaxation oscillation* and can be regarded as an example of a self-induced oscillation. There are many toys that use this principle to change their orientation periodically, namely, water filling up a reservoir, and then the water being discharged as a result of the change of orientation of the toy.

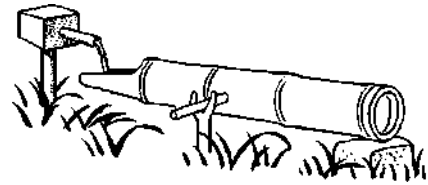

Figure 3. Bamboo deer alarm.

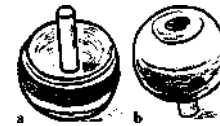

Figure 4. A tippe top in its stable resting position and stable rotating position.

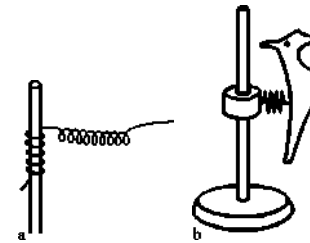

Figure 5. The pecking woodpecker with a detail of the spring in (a).

Tippe Top

A fascinating toy is the tippe top, which does not act like a conventional top. The tippe top consists of a little more than a hemisphere with a short cylindrical stem (see Figure 4(a)). It has a low center of gravity, so when placed on a surface, it will simply sit like an ordinary top on its hemispheric side. However, if the stem is held between a finger and the thumb and given a spin on the hemispheric end, then unlike a conventional top, the tippe top will readily turn over and continue to spin on the stem (see Figure 4(b)). As it turns over, the behavior of the tippe top is unusual in two respects: the center of gravity is raised and the spinning direction with respect to fixed body coordinates is reversed. When the top is spun, the low center of gravity is centrifugally moved away from the vertical spin axis. Before and after the top turns over, the angular momentum of the top about the vertical axis is the dominant momentum component. During the inversion process, the center of gravity is raised and the increase in potential energy reduces the rotational kinetic energy. The torque needed to execute

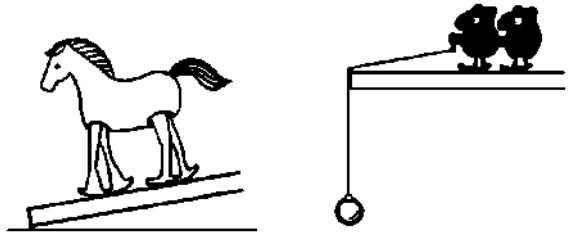

Figure 6. Two other toys that use self-induced oscillations.

this inversion comes from the sliding frictional forces between the top's hemispherical surface and the surface on which it is rotating. The mechanics of this top are described by nonlinear equations of motion that are solvable only in special cases (Cohen, 1977; Or, 1994; Gray & Nickel, 2001).

Pecking Woodpecker

A cute toy providing entertainment for young children is the pecking woodpecker going down a pole. To make this toy, coil a soft wire loosely around a smooth pole to make a soft spring. Now leave several turns of the coil on the pole and the remaining coils extended outwards from the pole (see Figure 5a). The weight of the protruding part of the spring will tilt the spring coiled around the pole so that the static friction is sufficient to keep it fixed on the pole. If one pushes the extended coil downwards and releases it, the extended coil vibrates up and down and the spring around the pole descends in a staccato fashion. The reason for the stuttering movement down the pole is that the coil around the pole oscillates periodically between being stopped by static friction and essentially free falling down the pole when the coil is aligned with the pole. Now attach a small wooden bird to the end of the extended wire, and the bird will peck the pole with its beak as it descends the pole (see Figure 5b).

There are many toys that move by the principle of self-induced excitation (see Figure 6). The basic equations for such oscillations are those of Duffing and van der Pol.

MORIKAZU TODA AND ROBERT M. MIURA

See also **Duffing equation; Equations, nonlinear; Laboratory models of nonlinear waves; Parametric amplification; Pendulum; Relaxation oscillators; Van der Pol equation**

Further Reading

Cohen, R.J. 1977. The tippe top revisited. *American Journal of Physics*, 45: 12–17

Gray, C.G. & Nickel, B.G. 2001. Constants of the motion for nonslipping tippe tops and other tops with round pegs. *American Journal of Physics*, 68: 821–828

Or, A.C. 1994. The dynamics of a tippe top. *SIAM Journal of Applied Maths*, 54: 597–609

Toda, M. 1979. *Toy Seminar.* Tokyo: Nihon-Hyoron-Sha (in Japanese)

Toda, M. 1982. *Toy Seminar (Continued).* Tokyo: Nihon-Hyoron-Sha (In Japanese)

Toda, M. 1983. *Mobile Toys.* Tokyo: Nihonkeizai-Shinbun-Sha (In Japanese)

Toda, M. 1993. *Science of Toys.* (6 vol.), Tokyo: Nihon-Hyoron-Sha, 1995 (In Japanese)

Wirkus, S., Rand, R. & Ruina, A. 1998. How to pump a swing. *The College Mathematics Journal*, 29: 266–275

NONLINEAR TRANSPARENCY

See **Nonlinear optics**

NONLINEARITY, DEFINITION OF

If a system's response to an applied force is directly proportional to the magnitude of that force, the system is said to be linear, otherwise the system is nonlinear. Nonlinear dynamics is concerned with systems whose time evolution equations are nonlinear.

As an example of a linear system, consider the one-dimensional motion of a point mass connected to a spring of force constant k, subject to a force

$$F_x(x) = -kx$$

in the x-direction. If k is changed, then the frequency and amplitude of resulting oscillations will change, but the qualitative nature of the behavior (simple harmonic oscillation in this example) remains the same. In fact, by appropriately rescaling the length and time axes, we can make the behavior for any value of k look just like that for some other value of k. For nonlinear systems, on the other hand, a small change in a parameter can lead to sudden and dramatic changes in both the qualitative and quantitative behavior of the system.

Although almost all natural systems are nonlinear, many of them respond in an approximately linear way provided that the amplitude of the force is

small enough. This is one of the reasons why traditional linear approximations are so popular in science. Another reason is that the analytical solution of nonlinear equations is often difficult. With the development and availability of computers, however, numerical solutions of nonlinear equations became relatively easy in the 1970s. This focused attention on important nonlinear phenomena such as deterministic chaos, although the idea of dynamic chaos was first glimpsed by Henri Poincaré (Poincare, 1908). Nonlinearity and the phenomena that result from it have a strong bearing on the concept of determinism.

Given a set of variables (position, velocity, acceleration, pressure, the number of species in a chemical reaction, etc.) or a function of two or more independent variables that describe the state of a system, the subsequent time evolution can be represented as causal relationship between its present state and its next state in the future. The existence of causality in such relationships is suggested by all our experience of experimenting with Nature, and it corresponds to the deterministic perception of the evolution of dynamical systems.

Consider, for example, the oscillatory motion of a damped pendulum in the phase space of two variables, the angle θ and the velocity v

$$\dot{\theta} = v,$$

$$\dot{v} = -\gamma v - \omega_0^2 \sin(\theta),$$

where γ and ω_0^2 are parameters that describe damping rate and frequency of small oscillations. These time evolution equations can be written in operator form as

$$L\theta = \frac{\mathrm{d}^2\theta}{\mathrm{d}t^2} + \gamma \frac{\mathrm{d}\theta}{\mathrm{d}t} + \omega_0^2 \sin(\theta) = 0. \qquad (1)$$

Formally, the dynamics is linear if the causal relation between the present state and the next state is linear, otherwise it is nonlinear. In the above example, the dynamics will be linear if we replace the term $\beta \sin(\theta)$ with its linear approximation $\beta\theta$ near the asymptotically stable equilibrium state $\theta = 0$, $v = 0$. The corresponding linear operator in this case satisfies the property that

$$L^{(\mathrm{lin})}(ax + by) = aL^{(\mathrm{lin})}x + bL^{(\mathrm{lin})}y,$$

where a and b are real numbers and x and y are differentiable functions. The property of linear superposition plays a fundamental role in the analysis of linear equations of motion, and represents one of the basic principles of quantum mechanics (Landau & Lifshitz, 1977). If the property of linear superposition does not hold the dynamics is nonlinear.

On physical grounds, dynamical systems are in general nonlinear. Indeed, if we consider small deviations of a pendulum from its state of unstable equilibrium $\theta = \pi$, $v = 0$ and replace the nonlinear term by its linear approximation $\omega_0^2 \sin(\pi + \delta\theta) \approx -\omega_0^2 \delta\theta$, we find unbounded growth of $\delta\theta$ in time. However, the experimentally observed motion of the pendulum is bounded; that is, the character of the motion changes when the deviation from the point of unstable equilibrium is large. Thus, nonlinearity corresponds to the situation that arises when the properties of the system depend directly on its state. The latter property, on one hand, makes a nonlinear system difficult to analyze but, on the other hand, gives rise to a rich diversity of nontrivial phenomena. We now consider briefly two consequences of nonlinearity.

First, the spectrum of oscillations of a nonlinear system is a complex function of its state (see, e.g., Sagdeev et al., 1988). For example, for weakly nonlinear oscillations of the pendulum near the state of stable equilibrium, we find (Hayashi, 1964), neglecting damping, that the frequency ω varies with the amplitude of the oscillations A as

$$\omega \approx \omega_0(1 - 3/64A^3).$$

The dependence of the frequency of oscillations on the state of the system is a key feature of many phenomena, including harmonic generation, synchronization, and the formation of solitons (*See* **Harmonic generation; Solitons; Synchronization**).

Second, a prominent effect of nonlinearity is the onset of deterministic chaos. Linear dynamical systems can have only three types of invariant sets: fixed points, cycles, and quasi-periodic orbits. The occurrence of a chaotic orbit is possible only in nonlinear systems and can be viewed in simple terms as arising from the interplay between the instability and nonlinearity. The instability is responsible for the exponential divergence of two nearby trajectories, whereas the nonlinearity bounds trajectories within a finite volume of the phase space of the system. The combination of these two mechanisms gives rise to a high sensitivity of the system to the initial conditions (*See* **Butterfly effect**). Consequently, the onset of deterministic chaos is restricted to nonlinear systems and involves repeated stretching and folding. The simplest example of a nonlinear system that demonstrates chaotic behavior through this process is a Bernoulli shift: $x_{n+1} = 2x_n \pmod 1$. An important consequence of chaos is that the predictability of even simple nonlinear systems is limited, so that ergodic theory has to be used to describe their statistical properties.

From these two brief examples it is already clear that in nonlinear science, the whole is more than the sum of its parts.

The complexity and diversity of the possible types of behavior in nonlinear systems have been widely explored in physics and chemistry, including analyses of solitons, nonlinear localization, pattern formation,

and formulation of the general principles of self-organization.

The formalism of nonlinear systems provides a framework for understanding and modeling of the hierarchy of complexity in the life sciences. However, there are many difficulties to be encountered on the way. In particular, Hermann Haken (in Tschacher & Dauwalder, 1999) notes:

> "While in physics or chemistry it is not too difficult to define the microscopic and macroscopic levels, with respect to the brain we must ask what adequate intermediate levels we have to choose between microscopic and macroscopic."

An example of a practical approach to the solution of this problem arose during the investigation of neurons (*See* **Neurons**). Although the ionic current through the axon membrane is successfully described by the Hodgkin–Huxley equations, heart fibrillation is more conveniently modeled by the continuous FitzHugh–Nagumo equation, which is a simplified version of Hodgkin–Huxley system. On passing to models of neural networks, the hierarchy of connections between neurons structured in time turn out to be of prime importance, but this raises new questions for nonlinear science related to the appearance of closed causal loops. Continuing this hierarchy, one may expect that the application to cognitive science of complexity theory derived from nonlinear analysis will have a major impact on our understanding of reasoning, thinking, behavior, and psychology generally (Tschacher & Dauwalder, 1999).

DMITRY G. LUCHINSKY AND ANETA STEFANOVSKA

See also **Causality; Chaotic dynamics; Determinism; Equations, nonlinear; Linearization; Pendulum; Van der Pol equation**

Further Reading

Hayashi, C. 1964. *Non-linear Oscillations in Physical Systems*, New York: McGraw-Hill

Landau, L.D. & Lifshitz, E. 1977. *Quantum Mechanics: Non-Relativistic Theory*, Oxford: Pergamon (original Russian edition 1947)

Poincaré, H. 1908. *Science et méthode*, Paris: Flammarion

Sagdeev, R.Z., Usikov, D.A. & Zaslavskii, G.M. 1988. *Nonlinear Physics: From the Pendulum to Turbulence and Chaos*, Chur: Harwood Academic

Tschacher, W. & Dauwalder, J.-P. (editors). 1999. *Dynamics, Synergetics, Autonomous Agents: Nonlinear Systems Approaches to Cognitive Psychology and Cognitive Science*, Singapore: World Scientific

NON-NEWTONIAN FLUIDS

See **Fluid dynamics**

NON-TOPOLOGICAL SOLITON

See **Solitons, types of**

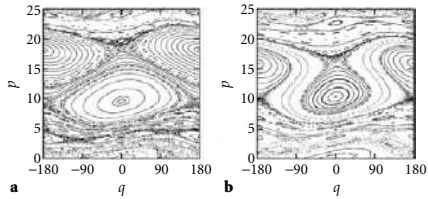

Figure 1. Standard nontwist map for $K = 1.5$ and (a) $\alpha = 0.036$, (b) $\alpha = 0.038$.

NONTWIST MAPS

Two-dimensional area-preserving mappings have become a standard tool for analyzing two-degrees-of-freedom autonomous and one-and-one-half dimensional time-periodic Hamiltonian systems (Lichtenberg & Lieberman, 1990). Prominent among such mappings are the radial twist maps

$$T : \begin{cases} p' = p - DU(q), \\ q' = q + f(p'), \end{cases} \tag{1}$$

where q and p are conjugate variables, $U(q)$ and $f(p)$ are smooth functions, and D is a derivative operator. For example, with $U = -K\cos q$ and $f(p) = p$, we recover the standard map, which has become a paradigm for chaotic Hamiltonian dynamics.

Usually $f(p)$ is monotonic, in which case the twist $\tau = \mathrm{d}f/\mathrm{d}p$ does not change sign. The twist condition, $\tau \neq 0$, is crucial for the validity of such linchpins of stability theory as the Moser twist theorem and the Kolmogorov–Arnol'd–Moser (KAM) theorem Arnol'd. Nevertheless, more and more instances have been found where the twist condition is violated, for example, plasma wave heating, zonal flows in planetary magnetospheres, beam dynamics in particle accelerators, and relativistic charged particle motion. The proliferation of such nontwist maps has challenged theorists to find alternatives to standard tools of nonlinear dynamics.

The Standard Nontwist Map

Many of the essential characteristics of nontwist maps are captured in the standard nontwist map (SNTM) (Howard and Hohs, 1984)

$$\begin{aligned} p' &= p - K\sin q, \\ q' &= q + p' - \alpha p'^2, \end{aligned} \tag{2}$$

where K and α are positive constants. Thus, the twist vanishes along the line $p = 1/2\alpha$. An equivalent version is discussed in del Castillo-Negrete et al. (1997). Generalizations employing higher order polynomial forms for $f(p)$ are discussed in Howard & Humphreys

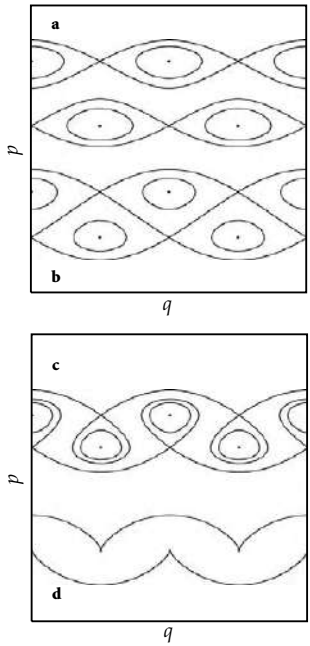

Figure 2. Reconnection scenario for standard nontwist map.

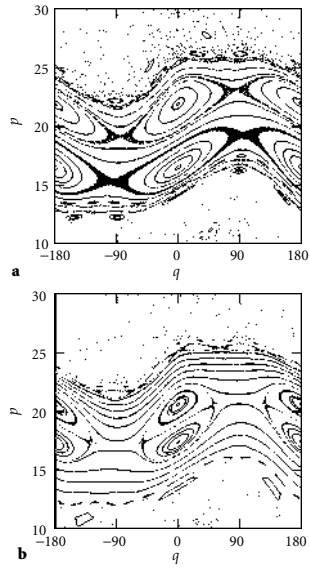

Figure 3. Vortex pair formation in the standard nontwist map for $K = 4.0$ and (a) $\alpha = 0.0260$, (b) $\alpha = 0.02634$.

(1995). Fixed points are located at $q \in (0, \pi)$ and

$$p_n^{\pm} = \frac{1 \pm \sqrt{1 - 8\pi n\alpha}}{2\alpha}. \tag{3}$$

For positive n both roots are positive real for $0 \le 8\pi n\alpha \le 1$, merging in a saddle-node bifurcation when $\alpha^* = (8\pi n)^{-1}$ at $p^* = 4\pi n$. Figure 1 shows the SNTM for $K = 1.5$ and two nearby values of α. Notice that, in contrast to the standard map, stable and unstable fixed points are staggered in phase rather than vertically aligned. This leads to a new kind of global bifurcation, called *reconnection* of KAM curves (by analogy with magnetic reconnection), which occurs when

$$K(\alpha) \approx \frac{1}{2}\int_{p^-(\alpha)}^{p^+(\alpha)} [f(\xi;\alpha) - 2\pi n]\,\mathrm{d}\xi = \frac{(1 - 8\pi n\alpha)^{3/2}}{12\alpha^2}. \tag{4}$$

The entire reconnection scenario is depicted schematically in Figure 2. We see that for a given configuration of X- and O-points, there are two topologically distinct arrangements of separatrices. Thus, in going from Figure 2(a) to (c), the upper separatrix is diverted downward, looping around the lower elliptic point. In between (b) the two separatrices merge, a process called *braiding*. Finally, Figure 2(d) shows the characteristic cusps resulting from the merging of X- and O-points via a saddle-node bifurcation. Naturally, the structure of the full mapping (Figure 1) is much more complicated than this approximate depiction. Of particular interest is the band of meandering curves seen in Figure 1(b), which constitute a new kind of barrier to chaotic transport. More complex sequences occur for more complex $f(p)$.

Higher-order fixed points also undergo reconnection. For example, the period-two islands near $p = 6\pi$ exhibit a second kind of reconnection, *vortex pair* formation, as shown in Figure 3. Here the elliptic and hyperbolic fixed points are vertically aligned, in contrast to the staggered pairs of period-one islands seen in Figure 1. An exhaustive classification of possible reconnection scenarios has not yet been accomplished.

As in the case of monotone twist maps, the location of higher order fixed points is facilitated by writing the map as a composition of involutions, $T = I_2 I_1$ ($I_1^2 = I_2^2 = I$). Fixed points of T then lie on the intersections of the invariant curves of I_1 and I_2. For the general twist map (1) we have

$$I_1 : \begin{cases} p' = p - DU, \\ q' = -q, \end{cases} \tag{5}$$

$$I_2 : \begin{cases} p' = p, \\ q' = -q + f(p). \end{cases} \quad (6)$$

Mappings with this decomposition are called *reversible*; that is, there exists a symmetry S such that $T^{-1} = STS$. Explicitly, $S = I_2$, so that $T^{-1} = I_1 I_2$.

Normal Forms

In investigating the structure of a 2-dimensional symplectic map near a stable fixed point (Howard & MacKay, 1987), it is useful to employ Birkhoff normal forms. Thus, the mapping T written in action-angle variables J and θ takes the simple form (Meyer & Hall, 1992)

$$\begin{aligned} J' &= J \\ \theta' &= \theta + 2\pi\Omega(J). \end{aligned} \quad (7)$$

Here the rotation number is given by

$$\Omega(J) = \omega + \tau_0 J + \tfrac{1}{2}\tau_1 J^2 + \cdots \quad (8)$$

and the twist by

$$\tau = \frac{\partial \Omega}{\partial J} = \tau_0 + \tau_1 J + \cdots, \quad (9)$$

where τ_0 and τ_1 are the zero and first-order twists. In this way it has been shown (Moeckel, 1990; Dullin et al., 1999) that a twistless torus is generated for any area-preserving map near a tripling bifurcation, where $\omega = \frac{1}{3}$.

Transition to Global Chaos

In many physical applications of nontwist maps, the transition to global chaos is of paramount importance, as space-spanning KAM curves (invariant rotational circles) act as barriers to particle or energy transport (Meiss, 1992; Lichtenberg & Lieberman, 1990). The breakdown of such barriers is usually studied via some kind of renormalization theory, such as that devised by Greene et al. (1981) for area-preserving maps satisfying the twist condition. Greene's method is based on the conjecture that the last KAM curve to break up with increasing perturbation strength has rotation number equal to the inverse of the golden mean, that is, $\omega_c = 1/\gamma = (\sqrt{5} - 1)/2$. Using the involution decomposition to locate a sequence of periodic orbits whose rotation number $\omega \to 1/\gamma$, he found the critical value $K_c = 0.9716\ldots$. Recently, del Castillo-Negrete et al. (1997) have succeeded in modifying Greene's semi-analytic method to obtain an accurate estimate for the breakup of the $\omega = 1/\gamma$ invariant circle for the SNTM. This calculation is complicated by the facts that (i) periodic orbits come in pairs for nontwist maps and may even fail to exist for certain parameters (K, α for the SNTM), and (ii) the sequence of periodic orbits actually has six convergent subsequences. Preliminary work has also been carried out on developing a suitable renormalization treatment for nontwist maps.

Extension to Higher Dimension

It is of interest to ask whether nontwist maps exist in higher dimension and what sort of reconnection processes might occur. This may be done in a natural way by letting p, $q \in \mathbb{R}^n$. The Birkhoff normal form then depends on the frequency map, $\Omega(J) = DS(J)$, where S is a scalar function of J. The twist, in turn, becomes the $n \times n$ Jacobian matrix $\tau(J) = D\Omega(J) = D^2 S(J)$, and the frequency map suffers a singularity whenever $\det \tau$ passes through zero. Dullin & Meiss (2003) have determined the behavior of four-dimensional symplectic maps near such a singularity. Again, a twistless torus appears near a $1:3$ resonance but with interesting topological complications. In four dimensions the frequency map can have a fold or a cusp singularity—in higher dimensions other catastrophies can occur.

JAMES E. HOWARD

See also **Hamiltonian systems; Maps; Standard map; Symplectic maps**

Further Reading

Arnol'd, V.I. 1990. *Mathematical Methods of Classical Mechanics*, 2nd edition, New York: Springer

del Castillo-Negrete, D., Greene, J.M. & Morrison, P.J. 1997. Renormalization and transition to chaos in area preserving nontwist maps. *Physica* D, 100: 311–329

Dullin, H.R. & Meiss, J.D. 2003. Twist singularities for symplectic maps. *Chaos*, 13(1): 1–16

Dullin, H.R., Meiss, J.D. & Sterling, D. 1999. Generic twistless bifurcations. *Nonlinearity*, 13: 203–224

Greene, J., MacKay, R.S., Vivaldi, F. & Feigenbaum, M.J. 1981. Universal behavior in families of area-preserving maps. *Physica* 3D, 13: 468–486

Howard, J.E. & Hohs, S.M. 1984. Stochasticity and reconnection in Hamiltonian systems. *Physical Review* A, 29: 203–224

Howard, J.E. & Humphreys, J. 1995. Nonmonotonic twist maps. *Physics Letters* A, 29: 256–276

Howard, J.E. & MacKay, R.S. 1987. Spectral stability of symplectic maps. *Journal of Mathematical Physics*, 28: 1036–1051

Lichtenberg, A.J. & Lieberman, M.A. 1990. *Regular and Chaotic Dynamics*, 2nd edition, New York: Springer

Meiss, J.D. 1992. Symplectic maps, variational principles, and transport. *Reviews of Modern Physics*, 64: 795–848

Meyer, K.R. & Hall, G.R. 1992. *Introduction to Hamiltonian Dynamical Systems and the N-Body Problem*, New York: Springer

Moeckel, R. 1990. Generic bifurcations of the twist coefficient. *Ergodic Theory of Dynamical Systems*, 10: 185–195

NORMAL FORMS THEORY

Many nonlinear systems can be modeled by ordinary, differential, or difference equations, and a central problem of dynamical systems theory is to obtain information on the long-time behavior of typical solutions. Because it is not possible, in general, to solve these equations explicitly, we identify particular solutions (such as equilibrium solutions or periodic

solutions) and try to infer global information from the behavior of nearby solutions.

As an example, consider an equilibrium state such as the downward position of a pendulum. Looking at small perturbations of this position to identify nearby periodic orbits (corresponding to small oscillations of the pendulum) shows that the downward pendulum is indeed stable. Analysis of the inverted pendulum reveals that it is unstable, in the sense that nearby solutions do not stay close to the equilibrium position.

Mathematically, an equilibrium is a fixed point of a dynamical system, and the stability analysis is carried out by linearizing the system, that is, by replacing (close to the fixed point) the nonlinear equations by linear equations for the perturbations. The resulting linear system can be solved exactly, and the analysis of these solutions may give information about the behavior of the solutions of the nonlinear system around the fixed point. This method is extremely powerful when it works, and is the basis of much dynamical system analysis. In some cases, however, the behavior of the linear system may be entirely different from that of the nonlinear system, and no information can be obtained from the linear analysis. This implies that there is crucial information contained in the nonlinear terms.

Normal forms theory is a general method designed to extract this information. The basic idea is to compute a local change of variables to transform a nonlinear system into a simpler nonlinear system that contains only the essential nonlinear terms—those that cannot be neglected without drastically changing the nature of the system. Hopefully, the new system is either linear or can be solved explicitly.

Consider the normal form analysis of the zero fixed point of systems of two differential equations of the form

$$\begin{aligned} \dot{x}_1 &= a_{11}x_1 + a_{12}x_2 + f_1(x_1, x_2), \\ \dot{x}_2 &= a_{21}x_1 + a_{22}x_2 + f_2(x_1, x_2), \end{aligned} \tag{1}$$

where the dots denote time derivatives and f_1 and f_2 are nonlinear analytic functions whose Taylor expansion about the origin contains no linear term. Linear analysis of the fixed point at the origin is carried out by neglecting the nonlinear terms and considering the linear system $\dot{x}_1 = a_{11}x_1 + a_{12}x_2$, $\dot{x}_2 = a_{21}x_1 + a_{22}x_2$. The dynamics of this system is governed by the eigenvalues λ_1, λ_2 of the matrix (a_{ij}), which is assumed to be diagonalizable. If the eigenvalues have nonvanishing real parts, then the dynamics of the original nonlinear system is qualitatively equivalent to the dynamics of the linear system and the fixed point is stable if both real parts are negative and unstable as soon as one of the real parts is negative. However, if the eigenvalues are imaginary, the behavior of the nonlinear system cannot be inferred from analysis of the linear system, and the information on the stability of the origin is contained in the nonlinear terms. For example, the origin of the system $\dot{x}_1 = x_2$, $\dot{x}_2 = -x_1 + \alpha x_1^2 x_2$ is either stable or unstable depending on the sign of α.

The first step in the normal form analysis of system (1) is to introduce a linear change of variables so it reads

$$\begin{aligned} \dot{y}_1 &= \lambda_1 y_1 + g_1(y_1, y_2), \\ \dot{y}_2 &= \lambda_2 y_2 + g_2(y_1, y_2). \end{aligned} \tag{2}$$

Second, look for a near-identity change of variables in the form of power series $y_1 = z_1 + P_1(z_1, z_2)$, $y_2 = z_2 + P_2(z_1, z_2)$ that simplifies system (2). To this end, expand g_1, g_2 in power series and choose the coefficients of the series P_1, P_2 so that in the z_1, z_2 variables, the system $\dot{z}_1 = \lambda_1 z_1 + h_1(z_1, z_2)$, $\dot{z}_2 = \lambda_2 z_2 + h_2$ (z_1, z_2) becomes simpler than the original system. Optimally, $h_1 = h_2 = 0$, which would provide an exact linearization of the original system. In general, however, some nonlinear terms remain after transformations.

It turns out that the ability to exactly linearize the original system is intimately connected to the eigenvalues λ_1, λ_2. If either $(n_1 - 1)\lambda_1 + n_2\lambda_2 = 0$ or $n_1\lambda_1 + (n_2 - 1)\lambda_2 = 0$ for some positive integers n_1, n_2, the eigenvalues are said to be resonant (or in resonance), and in general one of the functions (h_1 or h_2) contains resonant terms of the form $z_1^{n_1} z_2^{n_2}$. In the absence of resonance, therefore, no nonlinear terms remain and exact linearization is achieved.

If the eigenvalues are purely imaginary, z_2 is the complex conjugate of $z_1 = z$, and there are infinitely many resonance conditions. The stability of the fixed point is then decided by the first non-vanishing coefficient of h_1. As an example, consider again the system $\dot{x}_1 = x_2$, $\dot{x}_2 = -x_1 + \alpha x_1^2 x_2$. After the linear change of variable $x_1 = y_1 + y_2$, $x_2 = \mathrm{i}(y_1 - y_2)$, we have

$$\begin{aligned} \dot{y}_1 &= \mathrm{i}y_1 + (\alpha/2)\left(y_1{}^2 y_2 - y_1 y_2{}^2 - y_2{}^3 + y_1{}^3\right), \\ \dot{y}_2 &= -\mathrm{i}y_2 - (\alpha/2)\left(y_1{}^3 - y_1{}^2 y_2 + y_1 y_2{}^2 + y_2{}^3\right). \end{aligned} \tag{3}$$

The normal form transformation to third order reads:

$$\begin{aligned} y_1 &= z_1 + (\mathrm{i}\alpha/8)\left(2\, z_1{}^3 + 2\, z_1 z_2{}^2 - z_2{}^3\right) + \text{h.o.t.}, \\ y_2 &= z_2 + (\mathrm{i}\alpha/8)\left(z_1{}^3 - 2\, z_1{}^2 z_2 - 2\, z_2{}^3\right) + \text{h.o.t.}, \end{aligned} \tag{4}$$

where h.o.t. denotes higher-order terms of degree 5 and higher. Finally, the normal form becomes

$$\begin{aligned} \dot{z}_1 &= \mathrm{i}z_1 + (\alpha/2) z_1 z_2^2 + \text{h.o.t.}, \quad z_2 = z_1^*, \\ \dot{z}_2 &= -\mathrm{i}z_2 + (\alpha/2) z_2 z_1^2 + \text{h.o.t.}. \end{aligned} \tag{5}$$

From Equations (5), $\dot{\rho} = (\alpha/2)\rho^3 + \text{h.o.t.}$ where $\rho^2 = z_1 z_2$, which implies that the origin of the initial system is stable if $\alpha \leq 0$ and unstable otherwise.

If all coefficients of the normal forms vanish identically, then the fixed point is surrounded by an open set of periodic orbits (a nonlinear center). The downward position of the frictionless pendulum is an example of a center. Note, however, that the convergence of the power series P_1, P_2 is not guaranteed, in general, and further conditions on the eigenvalues and the transformation must be satisfied.

For a general N-dimensional system of differential equations, we can compute the linear eigenvalues $\lambda_1, \ldots, \lambda_N$. If the real part of one of these eigenvalues vanishes, there is no guarantee that the dynamics of the linear system is equivalent to the dynamics of the nonlinear system close to the fixed point. Again, one can find explicit near-identity power series change of variables that simplify the original system. If $n_1\lambda_1 + n_2\lambda_2 + \cdots + n_N\lambda_N = \lambda_i$ for any i between 1 and N and for positive integers $n_1, n_2, \ldots, n_N$, then the eigenvalues are in resonance, and the ith new equation will contain some resonant nonlinear terms. This resonance relation is one of the most fundamental relations in nonlinear dynamics. It determines whether linear modes (determined by the eigenvectors of eigenvalues λ) are coupled by the nonlinear terms. It is the same resonance relation that appears in different guises in the analysis of forced linear systems and in the resonance between frequencies in Hamiltonian and celestial mechanics. Essentially, in the absence of resonances, the system evolves following the linear modes and no interaction is possible. When resonances occur, the linear modes interact through the nonlinear terms and create complex dynamics.

Normal forms theory provide a systematic way to include the effect of the nonlinear terms. At the practical level, the method as presented tends to be rather tedious because the number of monomials that have to be taken into account grows rapidly with the dimension of the system and the degree of the normalizing transformation. There are several equivalent alternatives to the computation of normal forms, including the method of "amplitude equation" for ordinary and differential equations and the Birkhoff–Gustavson transformation for Hamiltonian systems. Nevertheless, at the conceptual level, normal forms theory is a central tool to understand the rich dynamics of nonlinear systems and this general framework can be used to study and give a rigorous foundation to many other problems beside stability.

A particularly important use of normal form theory is the theory of bifurcations. In order to identify generic bifurcations, one considers the parameters of the system $\mu_1, \ldots, \mu_M$ as additional variables satisfying trivial differential equations $\dot{\mu}_i = 0,\ i = 1, \ldots, M$ and studies the normal forms of this extended system of dimension $N + M$, revealing the nature of the bifurcation. Other applications of normal forms include the analysis of chaotic systems in systems of differential equations, the formation of patterns for partial differential equations, exponentially small effects in the splitting of separatrices, and the Painlevé theory of integrable systems.

ALAIN GORIELY

See also **Bifurcations; Damped-driven anharmonic oscillator; Painlevé analysis**

Further Reading

Arnol'd, V.I. 1973. *Ordinary Differential Equations*, Cambridge, MA: MIT Press (originally published in Russian, 1971); 3rd edition, Berlin and New York: Springer, 1992

Guckenheimer, J. & Holmes, P. 1983. *Nonlinear Oscillations, Dynamical Systems and Bifurcations of Vector Fields*, New York: Springer

N-SOLITON FORMULAS

A one-soliton solution of an evolutionary nonlinear partial differential equation in one spatial dimension $u_t = F(u, u_x, u_{xx}, \ldots)$ is a solitary wave (pulse) of finite energy and momentum. As an example, the Korteweg–de Vries (KdV) one-soliton is the exact solution

$$u(x,t) = \frac{-2\kappa_1^2}{\cosh^2\left(\kappa_1(x-\xi_1) - 4\kappa_1^3 t\right)}, \qquad (1)$$

to the KdV equation

$$u_t = -u_{xxx} + 6uu_x. \qquad (2)$$

Note that Equation (1) has the shape of a negative well, moving at a speed that is proportional to the depth.

N-soliton solutions are characterized by the fact that, for $t \to -\infty$ and $t \to +\infty$, the shape of the solution is composed by a quasi-exact superposition of N non-interacting pulses of the form (1). This means that the shape of the solution for $t \to -\infty$ is a sequence of N wells, ordered according to their depth, the deepest being the leftmost. For $t \to +\infty$, the shape is also a sequence of wells, with now the deepest being the rightmost, each of them retaining the original shape. The solution pictorially describes a family of N individual pulses traveling at their own characteristic speeds, the faster ones catching up with the slower, and, after an interaction, reemerging with their individual shapes. The overall effect of the nonlinear interaction is a phase shift between the pulses (that is, a difference in the relative distances of the dips of the wells). It can be proved that, in the collision process of N solitons, the total phase shifts are the sum of phase shifts of two-soliton processes.

The presence of N-soliton solutions, for arbitrary N, is often regarded as the hallmark for integrability of a nonlinear PDE. Three main methods have been devised for constructing and studying N-soliton solutions:

- The inverse scattering method (ISM), based on the Gel'fand–Levitan–Marchenko (GLM) equations
- Hirota's formalism
- Bäcklund transformations

Here we present formulas making explicit reference to the ISM. For direct ways of finding N-soliton solutions, we refer to the entries on Hirota's method and on the Darboux and Bäcklund transformations.

In the ISM, the existence of N-soliton solutions is associated with the following mathematical feature.

A nonlinear integrable evolution equation (say, for one dependent variable u defined on the real line), is presented as a Lax (isospectral) equation for a linear operator $L(u)$,

$$\frac{\mathrm{d}}{\mathrm{d}t}L(u) = [B(u), L(u)], \tag{3}$$

where the bracket indicates a commutator ($[B, L] \equiv BL - LB$). The spectrum of $L(u)$, as an operator in $L^2(R)$, is the union of the point spectrum $\lambda_1, \lambda_2, \ldots$ and the continuous spectrum, consisting of the intervals $I_1 \cup I_2 \ldots$. An N-soliton solution of (3) is a solution associated with an initial data $u(x, 0)$ whose spectrum contains only a finite number N of points. Such initial data are often called reflectionless potentials.

Given N-soliton initial data, the direct spectral problem for $L_0 = L(u(x, 0))$, gives (in addition to the spectrum) normalization coefficients β_i of the eigenfunctions corresponding to the eigenvalues λ_i, $i = 1, \ldots, N$. The evolution equations of the parameters $\beta_i = \beta_i(t)$ are linear equations with coefficients that depend on the constants λ_i. Accordingly, an N-soliton solution describes $2N$-dimensional families of solutions parametrized by the point spectrum of the linear operator and by the normalization coefficients β_i.

Two Soliton Solutions for Korteweg–de Vries and Sine-Gordon Equations

For the KdV equation (2) let $\lambda_1 = -\kappa_1^2$ and $\lambda_2 = -\kappa_2^2 |\kappa_1| > |\kappa_2|$ be the points in the spectrum of the Lax operator $L = -\mathrm{d}^2/\mathrm{d}x^2 + u$, and let ξ_i be quantities associated with the normalization coefficients $\beta_i(0)$ of the eigenvector of L. In other words, κ_i, ξ_i is the scattering data of the reflectionless potential $u(x, 0)$. A two-soliton solution for KdV is

$$u(x,t) = \frac{2\kappa_1^2 (\kappa_1-\kappa_2)(\kappa_1+\kappa_2)\left(\cosh^2(\phi_2) + (\kappa_2/\kappa_1)^2 \cosh^2(\phi_1) - 1\right)}{(\kappa_2 \cosh(\phi_1)\cosh(\phi_2) - \kappa_1 \sinh(\phi_1)\sinh(\phi_2))^2},$$

where $\phi_i = \kappa_i\,(x - \xi_i)\, - 4\,{\kappa_i}^3 t$.

This is an instance of the phenomenon described above. Indeed, for $t \to -\infty$ the solution describes two pulses traveling in the positive x-direction, with the faster one (that is, the one pertaining to the data κ_1, ξ_1) being the leftmost one.

The solution describes the process whereby the fast soliton catches up to the slow one, and finally (for $t \to +\infty$), the two emerge. The shape of the individual pulses remains unchanged, the effect of the nonlinear interaction being a phase shift. The fast soliton experiences a positive phase shift of

$$\Delta\phi_1 = \frac{1}{\kappa_1} \log\left|\frac{\kappa_1 + \kappa_2}{\kappa_1 - \kappa_2}\right|,$$

while the slow soliton loses the same phase (see Figure 1).

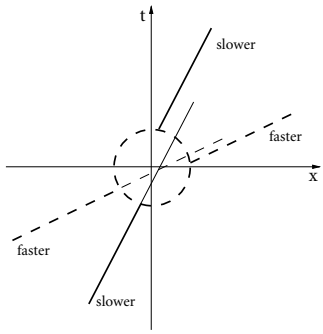

Figure 1. Phase shifts in two soliton collision.

The two-soliton solution of the sine-Gordon (SG) equation

$$\frac{\partial^2 u}{\partial^2 t} - \frac{\partial^2 u}{\partial^2 x} + \sin\, u = 0,$$

in terms of the points λ_1, λ_2 in the spectrum of the corresponding Lax operator and the constants c_1, c_2 is given by

$$u(x,t) = 4\mathrm{arctg}\frac{\frac{c_1}{2\lambda_1}\exp\left(-\frac{x-v_1 t}{\sqrt{1-v_1^2}}\right) + \frac{c_2}{2\lambda_2}\exp\left(-\frac{x-v_2 t}{\sqrt{1-v_2^2}}\right)}{1 - \frac{c_1 c_2}{4\lambda_1\lambda_2}\frac{(\lambda_1-\lambda_2)^2}{(\lambda_1+\lambda_2)^2}\exp\left(-\frac{x-v_1 t}{\sqrt{1-v_1^2}} - \frac{x-v_2 t}{\sqrt{1-v_2^2}}\right)},$$

where $v_i = (4\lambda_i^2 - 1)/(4\lambda_i^2 + 1)$, $i = 1, 2$. The fast soliton undergoes a positive phase shift given by

$$\Delta\phi_1 = \sqrt{1 - v_2^2}\,\log\frac{(\lambda_1 + \lambda_2)^2}{(\lambda_1 - \lambda_2)^2},$$

while the slow soliton undergoes a negative phase shift:

$$\Delta\phi_2 = -\sqrt{1 - v_1^2}\,\log\frac{(\lambda_1 + \lambda_2)^2}{(\lambda_1 - \lambda_2)^2}.$$

General Formulas

General formulas for N-soliton solutions of soliton equations are usually expressed in terms of determinants. For certain well-known soliton equations, one has the following results.

(1) Korteweg–de Vries (KdV) equation:

$$u_N(x,t) = -2\frac{\mathrm{d}}{\mathrm{d}x^2}\log\det(A),$$

where A is a $N \times N$ matrix with elements

$$A_{ij} = \delta_{ij} + \frac{\beta_i(t)}{\kappa_i + \kappa_j} \exp(-(\kappa_i + \kappa_j)x),$$

where $\beta_i(t) = \beta_i(0) \exp(8\kappa_i^3 t)$.

(2) Sine-Gordon (SG) equation:

$$u_N(x,t) = 2\mathrm{i} \log \frac{\det(A_+)}{\det A_-},$$

where

$$[A_\pm]_{ij} = \delta_{ij} \pm \frac{c_j}{\lambda_i + \lambda_j} \exp(\gamma_j(x,t)),$$

with $\gamma_j(x,t) = -i(\lambda_j + \frac{1}{4\lambda_j})t + i(\lambda_j - \frac{1}{4\lambda_j})x$.

(3) Nonlinear Schrödinger (NLS) equation:

$$\mathrm{i}\frac{\partial \psi}{\partial t} + \frac{\partial^2 \psi}{\partial^2 x} - 2g|\psi|^2\psi\,, \quad g = \pm 1.$$

The N-soliton solutions are given by

$$\psi(x,t) = \frac{\mathrm{i}}{\sqrt{g}} \frac{\det M_1(x,t)}{\det M(x,t)},$$

where

$$M_{ij}(x,t) = \frac{1 + \bar{\gamma}_i(x,t)\gamma_j(x,t)}{\bar{\lambda}_i - \lambda_j}$$

and the $N+1 \times N+1$ matrix $M_1(x,t)$ is described as follows:

$$M_1 = \begin{array}{|ccc|c|} \hline & M & & G \\ \hline 1 & \ldots & 1 & 0 \\ \hline \end{array}$$

where G is the vector $(\gamma_1(x,t), \ldots, \gamma_N(x,t))$, with $\gamma_i(x,t) = \gamma_i^{(0)} \exp(\mathrm{i}\lambda_i x - \mathrm{i}\lambda_i^2 t)$.

(4) Infinite Toda Lattice (ITL): The ITL equations are compactly written in the Lax form:

$$\frac{\mathrm{d}L}{\mathrm{d}t} = [B, L],$$

where L is the infinite matrix with b_i on the principal diagonal and a_i on the first lower and upper diagonal, and B is the antisymmetric matrix having a_i on the first lower diagonal; the coefficients $\{a_i, b_i\}$ are related to the canonical variables $\{Q_i, P_i\}$ by the transformation

$$a_i = \tfrac{1}{2} \exp(-(Q_{i+1} - Q_i)/2), \quad b_i = \tfrac{1}{2} P_i.$$

N-soliton solutions are given by the formula:

$$\exp(-(Q_i - Q_{i-1})) = \frac{\det B_i \det B_{i-2}}{(\det B_{i-1})^2},$$

$$P_i = \text{const.} + \frac{\mathrm{d}}{\mathrm{d}t} \log \frac{\det B_{i-1}}{\det B_i}.$$

In this formula the B_i's are $N \times N$ matrices with elements given by

$$[B_i]_{j,k} = \delta_{j,k} + \gamma_j(t)\gamma_k(t) \frac{(\lambda_j \lambda_k)^{i+1}}{1 - \lambda_j \lambda_k}, \quad j,k = 1, \ldots, N.$$

The λ_j are the N elements of the point spectrum of L, and the γ_j are normalization constants; the time dependence of the solution is given by

$$\gamma_j(t) = \gamma_j(0) \exp(\pm \sinh(\sigma_j)t), \quad \lambda_j = \pm \exp(-\sigma_j).$$

Further Comments

The formulas above can be interpreted as nonlinear superposition formulas for soliton solutions. Indeed, N-soliton solutions are constructed via the definition of suitable matrices determined by the spectral data associated with individual solitons. More precisely, the notion of nonlinear superposition principle can be better understood in the framework of the theory of Darboux–Bäcklund transformations.

In general, N-soliton solutions can be obtained as suitable limits of periodic solutions of the same system as the period tends to infinity. Periodic finite gap solutions are obtained by means of theta functions defined over Riemann surfaces. N-soliton solutions are obtained by letting suitable homology cycles of such Riemann surfaces shrink to a (degenerate) surface (with nodes and cusps) of genus equal to zero.

GREGORIO FALQUI AND TAMARA GRAVA

See also **Bäcklund transformations; Darboux transformation; Hirota's method; Inverse scattering method or transform; Theta functions**

Further Reading

Ablowitz, M.J. & Segur, H. 1981. *Solitons and the Inverse Scattering Transform*, Philadelphia: SIAM

Calogero, F. & Degasperis, A. 1982. *Spectral Transforms and Solitons: I*, Amsterdam: North-Holland

Drazin, P.G. & Johnson, R.S. 1989. *Solitons: An Introduction*, Cambridge and New York: Cambridge University Press

Faddeev, L.D. & Takhtajan, L.A. 1987. *Hamiltonian Methods in the Theory of Solitons*, Berlin: Springer

Miura, R.M. (editor). 1976. *Bäcklund Transformations*, Berlin: Springer

Newell, A.C. 1985. *Solitons in Mathematics and Physics*, Philadelphia: SIAM

Novikov, S.P., Manakov, S.V., Pitaevskii, L.P. & Zakharov, V.E. 1984. *Theory of Solitons*, New York: Consultants Bureau

Toda, M. 1988. *Theory of Nonlinear Lattices*, 2nd edition, Berlin: Springer

N-TORI

See **Quasiperiodicity**

NUMERICAL METHODS

Numerical methods are used for approximations of "exact" mathematical solutions, which either do not exist or are very complicated. With fast computer processors and advanced mathematical software, many problems become more attractive for numerical rather than for analytical solutions.

Computational Errors

Numerical computations are always uncertain because the results are only defined within the accuracy of a numerical error. Two main reasons account for errors in numerical approximations: finite precision in computer representation of numbers, and truncation of exact mathematical formulas in numerical algorithms.

Finite precision defines the tolerance interval, within which any further improvement in a numerical solution is impossible. For instance, the precision accuracy of MATLAB on the Windows platform is order of 10^{-16}. Therefore, it is meaningless to initialize irrational numbers (such as π or e) beyond the 16th digit after the period while carrying computations in MATLAB.

Round-off errors can be obstacles for accurate numerical approximations. Numerical differentiation algorithms are typically ill-posed since the round-off error increases with smaller step size of numerical discretization. Catastrophic cancellations can occur due to round-off errors, as in the example below when two large nearly identical numbers are subtracted:

$$f(x) = \sqrt{x+1} - \sqrt{x}.$$

If $x = 1.000000000000000 \times 10^{10}$, then $\sqrt{x+1} = 1.000000000050000 \times 10^5$, $\sqrt{x} = 1.000000000000000 \times 10^5$ and

$$f(x) = 4.999994416721165 \times 10^{-6}.$$

However, if the relative round-off error is order of 10^{-10}, the result is identical to zero. If the precision accuracy cannot be extended, a modification of the numerical procedure is required for a more accurate answer, as in the equivalent representation:

$$f(x) = \frac{1}{\sqrt{x+1} + \sqrt{x}}.$$

Within the same precision accuracy, the result is now $f(x) \approx 4.9999999999 \times 10^{-6}$.

Truncation errors occur due to chopping of an infinite series into a finite number of terms. For example, the Taylor series for analytical functions can be truncated with the Taylor polynomials, as in the example:

$$e^{x^2} = 1 + x^2 + \frac{1}{2!}x^4 + \frac{1}{3!}x^6 + E(x),$$

where $E(x)$ is the truncation error. The integral of e^{x^2} on $x \in [0, 1]$ is given in terms of a special function, called the error function. Equivalently, this integral can be approximated with the Taylor polynomial as

$$\int_0^1 e^{x^2}\,dx = \left(x + \frac{1}{3}x^3 + \frac{1}{10}x^5 + \frac{1}{42}x^7\right)\Big|_{x=0}^{x=1} + E_{\text{tr}}$$
$$= 1.457142857142857 + E_{\text{tr}},$$

where the truncation error is $E_{\text{tr}} \approx 5.508914448636659 \times 10^{-3}$.

Numerical algorithms are classified by the rate of convergence and by their numerical stability (i.e., will a small error decay or grow through the successive iterations). Convergence and stability of numerical algorithms are studied with analysis of the truncation error. If the truncation error depends on the step size h of the finite numerical discretization and reduces as h^n, then the numerical algorithm is said to converge to an exact solution as the nth-order algorithm. As an example, we consider a numerical computation of the integral, given by irrational number e:

$$e = \int_0^1 f(x)\,dx, \qquad f(x) = 1 + e^x.$$

Using the discretization of the unit interval with N equal subintervals of the step size $h = 1/N$, we can use the composite trapezoidal rule to approximate the integral as

$$e = \frac{h}{2}\left(f(0) + 2\sum_{n=1}^{N-1} f(hn) + f(1)\right) + E(h),$$

where the theoretical truncation error is $E(h) = \alpha_2 h^2$ and α_2 is constant, such that $\lim_{h\to 0} \alpha_2 \neq 0$. The composite trapezoidal rule converges to the integral as the second-order method. Indeed, computing the algorithm for $N = 100$ and 200, we have

$$N = 100: \quad e \approx 2.718296147450418,$$
$$E(0.01) = 1.431899137260828 \times 10^{-5}$$

and

$$N = 200: \quad e \approx 2.718285408211362,$$
$$E(0.005) = 3.579752316795748 \times 10^{-6},$$

and, therefore,

$$\frac{E(0.01)}{E(0.005)} = 3.999995001169598 \approx 2^2 = 4,$$

as predicted by the theoretical formula. An improved numerical algorithm for integration is the composite Simpson's rule, defined as

$$e = \frac{h}{3}\left(f(0) + 4\sum_{n=1}^{N/2} f(h(2n-1)) + 2\sum_{n=1}^{N/2-1} f(2hn) + f(1)\right) + E(h),$$

where the theoretical truncation error is $E(h) = \alpha_4 h^4$ and N is even. The composite Simpson's rule converges to the integral as the fourth-order method. Indeed, computing the algorithm for $N = 100$ and 200, we have

$$N = 100: \quad e \approx 2.718281828554504,$$
$$E(0.01) = 9.545830792490051 \times 10^{-11}$$

and

$$N = 200: \quad e \approx 2.718281828465013,$$
$$E(0.005) = 5.967226712755291 \times 10^{-12}$$

and, therefore,

$$\frac{E(0.01)}{E(0.005)} = 15.99709756642108 \approx 2^4 = 16,$$

as predicted by the theoretical formula.

Iteration Methods

Solutions of algebraic, differential, partial differential, and integral equations can be approximated with iteration methods. Numerical errors in iteration methods may grow during iterations. When this happens, numerical approximations cannot give the exact solution because instabilities lead to huge numerical errors. If the numerical iterations are unstable, it does not matter how accurately the truncation error converges to zero with smaller discretization step size. Propagation and growth of numerical errors can be illustrated with the linear iteration map:

$$x_{n+1} = q x_n, \quad |q| \geq 1.$$

The exact solution of the linear iteration map is $x_n = q^n x_0$, where x_0 is the starting value. If two iteration sequences are obtained from almost identical values $x_0^{(1)}$ and $x_0^{(2)}$, so the initial distance $e_0 = |x_0^{(1)} - x_0^{(2)}|$ is small, then the distance grows with larger n as $e_n = |q|^n e_0$. Two iteration sequences diverge from each other, even if the small error e_0 was generated by the round-off error!

Numerical instabilities and divergences often occur in solutions of algebraic equations, which represent the simplest numerical problems. A scalar algebraic equation $f(x) = 0$ can be reformulated as a root finding algorithm:

$$x_*: \quad f(x_*) = 0.$$

If we plot $f(x)$ as a function of x, the root x_* can be immediately found from the graph $y = f(x)$, if it exists. Algorithmically, we can try to approximate the root x_* from the iteration method:

$$x_{n+1} = x_n + f(x_n).$$

If the limit $x_\infty = \lim_{n\to\infty} x_n$ exists, then the root x_* is a fixed point of the iteration method such that $x_\infty = x_*$. If the limit x_∞ does not exist but x_* is known to exist, the numerical method fails and iterations $\{x_n\}_{n=1}^{\infty}$ diverge due to numerical instabilities. Analysis of convergence of the iteration method can be performed with the linearization of the iteration method. Let $e_n = x_n - x_*$ be the small distance of x_n from the fixed point x_* such that

$$\begin{aligned} e_{n+1} &= x_n + f(x_n) - x_* = e_n + f(x_* + e_n) - f(x_*) \\ &= q e_n + \alpha_n e_n^2, \quad q = 1 + f'(x_*), \end{aligned}$$

where α_n is constant, such that $\lim_{n\to\infty} \alpha_n$ exists. If $|q| \geq 1$, the error e_n grows with larger n and iterations $\{x_n\}_{n=1}^{\infty}$ and $\{e_n\}_{n=1}^{\infty}$ diverge. In this case, the fixed point x_* cannot be found from the iteration method. For example, when $f(x) = 3x - 6$, the fixed point $x_* = 2$ cannot be found iteratively, since $q = 4 > 1$.

An improved iteration algorithm is Newton's method which approximates a new point x_{n+1} from the root of the tangent line to the graph $y = f(x)$ at the previous point x_n. Thus

$$0 = f(x_n) + f'(x_n)(x_{n+1} - x_n) + \mathrm{O}(x_{n+1} - x_n)^2,$$

such that

$$x_{n+1} = x_n - \frac{f(x_n)}{f'(x_n)}.$$

Newton's method always converges to a fixed point x_*, if the fixed point x_* exists. The rate of convergence depends on whether the root $x = x_*$ is simple or multiple. For a single root when $f'(x_*) \neq 0$, the rate of convergence is quadratic in terms of the error e_n, since

$$q = \lim_{x\to x_*} \frac{f(x) f''(x)}{(f'(x))^2} = 0.$$

For a multiple root when $f(x) \sim (x - x_*)^m$ and $m > 1$, the rate of convergence is linear in terms of e_n, since $q = (m-1)/m$. When the function $f(x)$ is linear as in the example $f(x) = 3x - 6$, the convergence of the Newton–Raphson method occurs in a single iteration, no matter what x_0 is

$$x_1 = x_0 - \frac{3x_0 - 6}{3} = 2 = x_*.$$

Differential Equations

Numerical algorithms are particularly attractive for solutions of differential equations, which are widely used in all areas of physics and engineering. It is especially important because many applied differential equations cannot be solved in terms of analytical functions. The simplest differential equation is given by a scalar first-order quasilinear equation:

$$\frac{\mathrm{d}y}{\mathrm{d}t} = f(t, y),$$

starting with the initial condition: $y(0) = y_0$. Since $y(0) = y_0$ and $y'(0) = f(0, y_0)$ are known, it makes sense to step from $t = 0$ along the tangent line to the curve $y = y(t)$ at the point $(0, y_0)$. Using a number of steps from $t = 0$ to T with small step size h, we define a numerical approximation of $y(t_n)$ as y_n, such that $y(t_n) = y_n + e_n$, where e_n is the numerical error, accumulated after n steps. If all steps are taken alone the tangent line segments to the points (t_n, y_n), we have the Euler method (also known as the slope approximation):

$$y_{n+1} = y_n + hf(t_n, y_n).$$

When the time $t = T$ is reached in N steps, such that $T = Nh$, the global error is defined as $E_T = |y(T) - y_N|$. The global error for the Euler method is theoretically given by $E_T = \alpha_1 h$, such that the Euler method is the least accurate, first-order method. Figure 1 shows that oscillations of the undamped pendulum in the nonlinear second-order equation:

$$y'' + \sin y = 0$$

are destroyed in Euler's method. The inaccurate Euler's method introduces an effective damping due to numerical discretization.

Numerical methods for differential equations also produce numerical instabilities. For example, the linear first-order equation for exponential decay:

$$\frac{\mathrm{d}y}{\mathrm{d}t} = -\lambda y, \quad \lambda > 0,$$

has a simple solution: $y(t) = y_0 \mathrm{e}^{-\lambda t}$. Euler's method applied to this equation is equivalent to the linear iteration map:

$$y_{n+1} = (1 - \lambda h) y_n,$$

which diverges for $h > 2/\lambda$, when $|1 - \lambda h| > 1$. When $\lambda \to 0$, the differential equation for the exponential decay becomes stiff for numerical solution, since the step size h for numerical discretization must be very small to preserve stability of numerical approximation.

Advanced algorithms for numerical solutions of differential equations are developed with numerical integration methods. For example, integrating the first-order quasi-linear equation with the trapezoidal rule on the interval $t \in [t_n, t_{n+1}]$, we derive the implicit iteration method:

$$y_{n+1} = y_n + \frac{h}{2}\left[f(t_n, y_n) + f(t_{n+1}, y_{n+1})\right].$$

The global; truncation method of the method is $E_T = \alpha_2 h^2$, that is, it is the second-order method. The method is also implicit since the unknown values of y_{n+1} appear at the left and right sides of the equation. The implicit methods can be solved with iterations at each n, by means of root finding

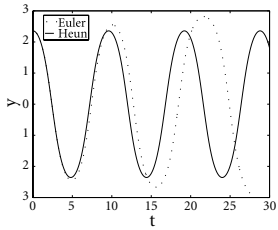

Figure 1. Oscillations of the undamped pendulum in Euler's and Heun's numerical methods.

algorithms. However, this modification makes the algorithm complicated and time-consuming. Predictor-corrector methods are used instead, either with single-step (Runge–Kutta) methods or with multi-step (Adams–Bashforth–Moulton) methods. For example, the second-order Runge–Kutta method (also known as the Heun's or improved Euler's method) is based on the trapezoidal rule in the form

$$p_{n+1} = y_n + hf(t_n, y_n),$$

$$y_{n+1} = y_n + \frac{h}{2}\left[f(t_n, y_n) + f(t_{n+1}, p_{n+1})\right],$$

where p_{n+1} is the predicted value at $t = t_{n+1}$ by using the slope approximation and y_{n+1} is the corrected value at $t = t_{n+1}$ by using the trapezoidal rule. The predictor–corrector method above has the same global truncation error $E_T = \tilde{\alpha}_2 h^2$ with a different numerical constant $\tilde{\alpha}_2$. Figure 1 shows that oscillations of the undamped pendulum are well preserved in the Heun's method based on predictions and corrections.

The most popular and accurate method is the fourth-order Runge–Kutta method, which takes four computations of the function $f(t, y)$ for a single step from $t = t_n$ to $t = t_{n+1}$ and has the global truncation error $E_T = \alpha_4 h^4$.

Higher-order predictor-corrector methods are still affected by numerical instabilities, especially in the case of stiff differential equations. More reliable methods for stiff problems are based on implicit integration formulas. Implicit methods can be rewritten as explicit methods if the function $f(t, y)$ is linear in y. For example, the equation for the exponential decay can be integrated with the implicit second-order method based on the trapezoidal rule, as follows:

$$y_{n+1} = \frac{2 - h\lambda}{2 + h\lambda} y_n.$$

Since $|(2 - h\lambda)/(2 + h\lambda)| \leq 1$ for any h and $\lambda > 0$, the implicit method is unconditionally stable, no matter how large the step size h is chosen. The accuracy of the method is still the same as in the second-order Heun's method, so the step size h must not be too large, to preserve accuracy of numerical approximation.

Partial Differential Equations

Partial differential equations are defined in two- and higher-dimensional domains. They represent most complicated and time-consuming problems for numerical methods. Initial values for partial differential equations at time $t = 0$ are supplemented by boundary values at the boundaries of a physical domain. A simple example of a linear partial differential equation is given by the heat equation, derived for a one-dimensional rod of finite length L:

$$\frac{\partial u}{\partial t} = \frac{\partial^2 u}{\partial x^2} + f(x,t), \quad 0 < x < L, \quad t > 0,$$

such that

$$u(0,t) = u_0(t), \quad u(L,t) = u_L(t), \quad u(x,0) = \phi(x).$$

The heat equation describes temperature $u(x,t)$ as function of time $t \geq 0$ and the point $0 \leq x \leq L$ in the rod. The heat sources $f(x,t)$, temperature values at the end points $u_0(t)$ and $u_L(t)$ and initial temperature $\phi(x)$ are all given as physical parameters of the problem. In the finite-difference methods, numerical approximations of $u(x,t)$ are defined at the equally spaced numerical grid with points at $x_n = nh$, $n = 0, 1, \ldots, N$, where h is the step size, such that $L = Nh$. Numerical approximations of $u(x,t)$ are also evaluated with equal time step τ at points $t_k = k\tau$, $k = 0, 1, \ldots$. Denoting $u_{n,k}$ as numerical approximation of $u(x_n, t_k)$, we approximate the second x-derivative of $u(x,t)$ by the central difference, derived from Taylor series expansions:

$$\begin{aligned} u_{n+1,k} &= u_{n,k} + hu_x(x_n,t_k) + \frac{1}{2}h^2 u_{xx}(x_n,t_k) \\ &\quad + \frac{1}{3!}h^3 u_{xxx}(x_n,t_k) + \mathrm{O}(h^4), \\ u_{n-1,k} &= u_{n,k} - hu_x(x_n,t_k) + \frac{1}{2}h^2 u_{xx}(x_n,t_k) \\ &\quad - \frac{1}{3!}h^3 u_{xxx}(x_n,t_k) + \mathrm{O}(h^4), \end{aligned}$$

such that

$$\frac{\partial^2 u}{\partial x^2}(x_n,t_k) = \frac{u_{n+1,k} - 2u_{n,k} + u_{n-1,k}}{h^2} + \mathrm{O}(h^2).$$

Using the slope approximation, we perform the time step from $u_{n,k}$ to $u_{n,k+1}$ according to the explicit finite-difference scheme:

$$u_{n,k+1} = (1-2r)u_{n,k} + r(u_{n+1,k} + u_{n-1,k}) + \tau f_{n,k},$$

where $r = \tau/h^2$, $n = 1, \ldots, N-1$, and $k = 0, 1, \ldots$. All boundary and initial values $u_{0,k}$, $u_{N,k}$ and $u_{n,0}$ are incorporated in computations of the explicit method for $n = 1, N-1$, and $k = 0$. Numerical approximations of $u_{n,k}$ are only computed at internal points of the grid. The total error of the explicit method is a composition of the truncation error of order $\mathrm{O}(h^2)$ for the central difference approximation and the truncation error of order $\mathrm{O}(\tau)$ for the Euler's method. The explicit method is least accurate with respect to time step size τ. It is also an unstable method for $r > 0.5$ when $\tau > h^2/2$. Figure 2 shows numerical solution of the heat equation with the explicit method for $f(x,t) = 0, u_0 = u_L = 0, \phi = \sin(\pi x), L = 2, h = 0.1$, and $r = 0.55$. Development of instabilities of the explicit method destroys validity of the numerical approximations.

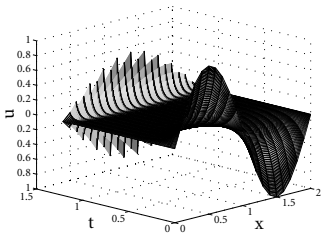

Figure 2. Solutions of the heat equation with the explicit method.

Implicit methods are more reliable in numerical computations. The implicit method, which is based on the trapezoidal rule of integration, is referred to as the Crank–Nicholson method. The method results in a linear system of equations:

$$\begin{aligned} A(r)\mathbf{u}_{k+1} &= A(-r)\mathbf{u}_k + \frac{\tau}{2}(\mathbf{f}_k + \mathbf{f}_{k+1}) \\ &\quad + \frac{r}{2}(\mathbf{b}_k + \mathbf{b}_{k+1}), \qquad k \geq 0, \end{aligned}$$

where

$$\mathbf{u}_k = \begin{bmatrix} u_{1,k} \\ u_{2,k} \\ \vdots \\ u_{N-2,k} \\ u_{N-1,k} \end{bmatrix}, \quad \mathbf{f}_k = \begin{bmatrix} f_{1,k} \\ f_{2,k} \\ \vdots \\ f_{N-2,k} \\ f_{N-1,k} \end{bmatrix},$$

$$\mathbf{b}_k = \begin{bmatrix} u_{0,k} \\ 0 \\ \vdots \\ 0 \\ u_{N,k} \end{bmatrix}$$

and

$$A(r) = \begin{bmatrix} 1+r & -r/2 & 0 & \cdots & 0 \\ -r/2 & 1+r & -r/2 & \cdots & 0 \\ 0 & -r/2 & 1+r & \cdots & 0 \\ \vdots & \vdots & \vdots & \vdots & \vdots \\ 0 & 0 & 0 & \cdots & 1+r \end{bmatrix}.$$

Although solving of the linear system at each time step is a time-consuming operation, the Crank–Nicholson

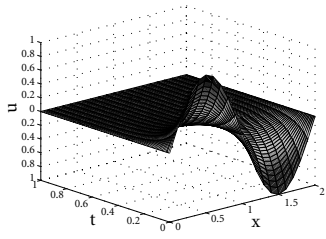

Figure 3. Solutions of the heat equation with the Crank–Nicholson method.

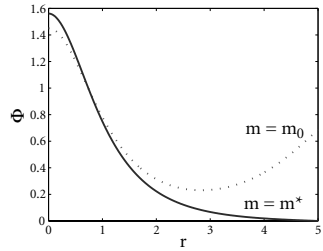

Figure 4. Bound state of the nonlinear Schrödinger equation with the numerical shooting method: starting (dotted) and final (solid) approximations.

method is more useful compared with the explicit method. In particular, the method has a symmetric numerical error $O(\tau^2 + h^2)$ and unconditional numerical stability for any $\tau > 0$. Figure 3 shows numerical solution of the heat equation with the Crank–Nicholson method for $h = 0.1$ and $r = 1$ when $\tau = h^2$. The numerical solution is stable in time evolution.

Finite-difference methods are used successfully in numerical solution of other boundary-value problems for partial differential equations. Explicit methods have a very straightforward form. Implicit methods are unconditionally stable and result in linear systems for linear differential equations. Implicit methods are usually replaced by the semi-implicit algorithms for nonlinear differential equations. As a drawback, finite-difference methods have low accuracy. More advanced (and also more involved) shooting, finite-element, and spectral methods are used for improved solutions of boundary-value problems.

Shooting methods are based on transformations of the boundary-value problems into the initial-value problems, which are iterated with the root finding algorithms. For simplicity, we illustrate with ordinary differential equations, although multi-dimensional shooting methods are also applied to partial differential equations. We consider a numerical approximation of radially symmetrical bound states of the two-dimensional nonlinear Schrödinger equations, which satisfy the boundary-value problem:

$$\frac{\mathrm{d}^2\Phi}{\mathrm{d}r^2} + \frac{1}{r}\frac{\mathrm{d}\Phi}{\mathrm{d}r} - \Phi + 2\Phi^3 = 0, \quad 0 < r < R,$$

such that

$$\Phi'(0) = 0, \quad \Phi(R) = 0,$$

where R is large length of the approximation interval. Using a shooting numerical method, we consider a solution of the initial-value problem for the same equation $\Phi = \Phi_m(r)$, such that

$$\Phi_m(0) = m, \quad \Phi'_m(0) = 0,$$

where the value of m is unknown. Solving the differential equation on $r \in [0, R]$ with an appropriate numerical method, such as the fourth-order Runge–Kutta method, we define the function of parameter m as

$$E(m) = \Phi_m(R).$$

The function $E(m)$ has a zero at $m = m_*$ if $\Phi_{m_*}(r)$ is the bound state of the nonlinear Schrödinger equation, such that $\Phi_{m_*}(R) = 0$. Starting with any value m_0, we can approach to the zero of $E(m)$ with a root finding algorithm, such as the Newton's method:

$$m_{k+1} = m_k - \frac{E(m_k)}{E'(m_k)},$$

where the value of

$$E'(m_k) = \left.\frac{\partial \Phi_m(R)}{\partial m}\right|_{m=m_k}$$

can be found from a linearization problem or from a secant method. The starting approximation $\Phi_{m_0}(r)$ and the final solution $\Phi_{m_*}(r)$ are shown on Figure 4 by dotted and solid lines, respectively. The value of $E(m_k)$ converges to zero, such that the sequence $\Phi_{m_k}(r)$ converges to the bound state $\Phi(r)$ of the nonlinear Schrödinger equation.

Finite-element methods approximate solutions of the boundary-value problems from a variational problem, which involves minimization of the energy functionals. The bound state $\Phi(r)$ of the nonlinear Schrödinger equation coincides with a minimizer of the energy functional:

$$H(u) = \frac{1}{2}\int_0^R \left[\left(\frac{\mathrm{d}u}{\mathrm{d}r}\right)^2 - u^4\right] r\,\mathrm{d}r,$$

such that the variation of $H(u)$ vanishes if and only if $u = \Phi(r)$:

$$\left.\frac{\delta H}{\delta u}\right|_{u=\Phi(r)} = -\frac{\mathrm{d}}{\mathrm{d}r}\left[r\frac{\mathrm{d}\Phi}{\mathrm{d}r}\right] - 2r\Phi^3 = 0.$$

Dividing the interval $r \in [0, R]$ into n subintervals $[0, r_1] \cup [r_1, r_2] \cup \cdots \cup [r_{N-1}, r_N]$, where $r_n = hn$ and $R = hN$, we approximate $\Phi(r)$ by a linear combination

of the finite elements $u_n(r)$:

$$u(r) = \sum_{n=0}^{N} \Phi_n u_n(r).$$

The finite elements $u_n(r)$ satisfy the constraints:

$$u_n(r_n) = 1, \quad \text{and} \quad u_n(r_m) = 0, \ m \neq n,$$

such that Φ_n are unknown values for the finite-element approximation of $u(r_n)$. The simplest finite elements (also known as the simplex elements) are given by the piecewise linear interpolation:

$$u_n(r) = \begin{cases} 0, & r \leq r_{n-1}, \\ \frac{r - r_{n-1}}{h}, & r_{n-1} \leq r \leq r_n, \\ \frac{r_{n+1} - r}{h}, & r_n \leq r \leq r_{n+1}, \\ 0, & r \geq r_{n+1}. \end{cases}$$

When $u(r)$ is substituted into the energy functional $H(u)$ and integrated numerically over $0 \leq r \leq R$, the function $H(u) = H(\Phi_0, \Phi_1, \ldots, \Phi_{N-1})$ with $\Phi_N = 0$ can be minimized with respect to parameters $\Phi_0, \Phi_1, \ldots, \Phi_{N-1}$. The minimization leads to a system of nonlinear algebraic equations:

$$\frac{\partial H(u)}{\partial \Phi_n} \equiv h_n(\Phi_0, \Phi_1, \ldots, \Phi_{N-1}) = 0, \quad n = 0, 1, \ldots, N-1.$$

This nonlinear system can be solved with a matrix root finding Newton's method, which completes the finite-element approximation of the bound states $\Phi(r)$. When the differential equations are linear and the exact integrations are replaced with the trapezoidal rule, the finite-element method with simplex elements recovers the finite-difference approximation. However, the finite-element method is more general and suitable for accurate numerical approximations. For example, the finite-element method can be used together with the Simpson's rule of numerical integration.

Spectral methods are based on Fourier series solutions of differential equations in finite intervals, subject to appropriate boundary conditions. Solutions of the homogeneous heat equation $u_t = u_{xx}$ on $x \in [0, L]$ with zero boundary conditions at the ends: $u(0, t) = u(L, t) = 0$ are given by the Fourier sine-series:

$$u(x, t) = \sum_{m=1}^{\infty} B_m(t) \sin \frac{\pi m x}{L},$$

where the set of Fourier amplitudes $B_m(t), m \geq 1$ solves the initial-value problems:

$$\frac{\mathrm{d}B_m}{\mathrm{d}t} = -\frac{\pi^2 m^2}{L^2} B_m, \quad m \geq 1.$$

The initial values of $B_m(0)$ are defined from $u(x, 0)$ by the Fourier integrals:

$$B_m(0) = \frac{2}{L} \int_0^L u(x, 0) \sin \frac{\pi m x}{L} \, \mathrm{d}x.$$

Truncating the Fourier series with the Galerkin method and defining the Fourier approximation at grid points $x_n = nh, n = 1, \ldots, N-1$, we replace the exact Fourier series solution with the discrete Fourier transform:

$$u(x_n, t) = \sum_{m=1}^{N-1} B_m(t) \sin \frac{\pi m n}{N},$$

where $B_m(t)$ solves the same initial-value problem for $m = 1, \ldots, N-1$ but $B_m(0)$ is defined by the inverse discrete Fourier transform:

$$B_m(0) = \frac{2}{N} \sum_{n=1}^{N-1} u(x_n, 0) \sin \frac{\pi m n}{N}.$$

We notice that the inverse discrete Fourier transform follows from Fourier integrals by means of the numerical trapezoidal rule. Solving systems of initial-value problems with Runge–Kutta methods, we define solutions of the heat equation at time steps $t_k = k\tau$, $k = 0, 1, \ldots$.

Spectral methods give more accurate solutions of the heat equation, compared with the finite-difference methods. First, all initial-value problems for Fourier coefficients $B_m(t)$ are uncoupled. Second, the spectral methods have superior accuracy, because the truncation error of the Galerkin approximation decays exponentially with larger number N of the Fourier amplitudes. Third, spectral methods can be applied to nonlinear differential equations. Performing time steps with the Runge–Kutta methods, discrete Fourier transform and its inverse can be employed for computations of the nonlinear terms. As a result, the spectral method is effectively uncoupled for Fourier amplitudes $B_n(t)$ as an explicit single-step method. Split-step spectral methods are especially important for nonlinear evolution equations, such as the nonlinear Schrödinger equations.

As computational power increases, the role of numerical methods will be increasingly important in coming years for efficient solutions of many problems in physical and engineering sciences. Presently, computations of three-dimensional equations for water waves, turbulence, and astrophysical problems can be run on workstations in reasonable time. Modern supercomputing resources based on multiprocessor clusters are designed to help scientists in their theoretical studies of nature. It is common nowadays that many research groups in physics and engineering replace analysis of a problem by numerical methods.

DMITRY PELINOVSKY

See also **Averaging methods; Compartmental models; Extremum principles; Lattice gas methods; Stability**

Further Reading

Akai, T.J. 1994. *Applied Numerical Methods for Engineers*, New York: Wiley

Chilling, R.J. & Harris, S.L. 2000. *Applied Numerical Methods for Engineers using MATLAB and C*, Pacific Grove, CA: Brooks/Cole
Fausett, L.V. 2003. *Numerical Methods: Algorithms and Applications*, Upper Saddle River, NJ: Prentice-Hall
Gerald, C.F. & Wheatley, P.O. 1999. *Applied Numerical Analysis*, 6th edition, Reading, MA: Addison-Wesley
Rao, S.S. 2002. *Applied Numerical Methods for Engineers and Scientists*, Upper Saddle River, NJ: Prentice-Hall

N-WAVE INTERACTIONS

Linear dispersive waves propagate according to a dispersion relation

$$\omega = \omega(\boldsymbol{k}),$$

which relates the frequency ω to the wave vector $\boldsymbol{k}$. In linear systems, waves of different wave vectors and frequencies do not interact due to the superposition principle. In nonlinear systems, the lowest-order nonlinear effect (expanding in the wave amplitudes) is the interaction between N waves of different wave vectors $\boldsymbol{k}_j$ and frequencies ω_j, which satisfy the spatial and temporal resonance conditions (Zaslavsky & Sagdeev, 1988)

$$\sum_{j=1}^{N} \boldsymbol{k}_j = \boldsymbol{0}, \quad \sum_{j=1}^{N} \omega(\boldsymbol{k}_j) = 0.$$

The simplest three-wave resonant interaction occurs if there are nontrivial solutions with

$$\boldsymbol{k} = \boldsymbol{k}_1 + \boldsymbol{k}_2, \quad \omega(\boldsymbol{k}) = \omega(\boldsymbol{k}_1) + \omega(\boldsymbol{k}_2). \qquad (1)$$

Resonant wave interactions are governed by the dispersion relation. Some dispersion relations do not exhibit nontrivial solutions of the resonance conditions (1) for any $\boldsymbol{k}_1$ and $\boldsymbol{k}_2$. Others may exhibit resonant three-wave interactions, for example the deep-water gravity-capillary waves satisfying the dispersion relation $\omega^2(\mathbf{k}) = g|\mathbf{k}| + T|\boldsymbol{k}|^3$, where g is the acceleration of gravity and T is the surface tension coefficient. When $T \neq 0$, the resonant configurations of the three waves occur already in one spatial dimension, as shown on a graphical solution on Figure 1. The solid curve on this figure shows the dispersion relation $\omega = \omega(k)$, while the dashed curve shows the same dispersion relation shifted relatively to the point (k_1, ω_1), such that $\omega - \omega_1 = \omega(k - k_1)$ and $\omega_1 = \omega(k_1)$. The intersection of the two curves defines a solution of the resonance equations (1) at the point $k = k_1 + k_2$, where $\omega(k) - \omega(k_1) = \omega(k_2)$.

When $T = 0$, the resonant three-wave configurations do not occur in space of any dimensions, but deep-water gravity waves satisfying the dispersion relation $\omega^2 = g|\boldsymbol{k}|$ exhibit the resonant four-wave interactions of the following type:

$$\boldsymbol{k}_1 + \boldsymbol{k}_2 = \boldsymbol{k}_3 + \boldsymbol{k}_4,$$
$$\omega(\boldsymbol{k}_1) + \omega(\boldsymbol{k}_2) = \omega(\boldsymbol{k}_3) + \omega(\boldsymbol{k}_4).$$

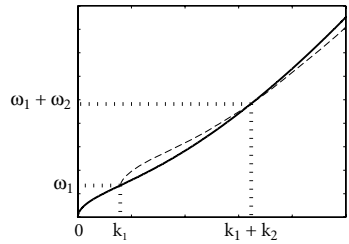

Figure 1. Graphical solution of Equations (1) for three resonant waves.

Given a dispersion relation $\omega(\boldsymbol{k})$ with one or more branches, one needs to compute all lowest-order resonances for $N = 3, 4$, and so on, in order to describe nonlinear dynamics of resonant wave interactions with the normal form analysis (Craig, 1996).

Time evolution of N resonant waves can be studied with an asymptotic multiscale expansion method. In this method, a solution of the system $u = u(\boldsymbol{x}, t)$ is assumed to be close to a linear superposition of N resonant waves with slowly varying amplitudes, where $\boldsymbol{x} = (x, y, z)$. For instance, resonant interaction of three waves is described by the following expansion (Gaponov-Grekhov & Rabinovich, 1992):

$$u(\boldsymbol{x}, t) = \varepsilon \Big[a(\varepsilon \boldsymbol{x}, \varepsilon t) \mathrm{e}^{\mathrm{i}(\boldsymbol{k}\boldsymbol{x} - \omega(\boldsymbol{k})t)} + a_1(\varepsilon \boldsymbol{x}, \varepsilon t) \mathrm{e}^{\mathrm{i}(\boldsymbol{k}_1 \boldsymbol{x} - \omega(\boldsymbol{k}_1)t)} + a_2(\varepsilon \boldsymbol{x}, \varepsilon t) \mathrm{e}^{\mathrm{i}(\boldsymbol{k}_2 \boldsymbol{x} - \omega(\boldsymbol{k}_2)t)} \Big],$$

where ε is a small parameter and ε^2 terms are dropped. The evolution equations for the wave amplitudes take the form

$$\begin{aligned} \mathrm{i}\left(\frac{\partial}{\partial t} + \boldsymbol{v} \cdot \nabla\right) a &= \gamma a_1 a_2 \mathrm{e}^{-\mathrm{i}\Delta t}, \\ \mathrm{i}\left(\frac{\partial}{\partial t} + \boldsymbol{v}_1 \cdot \nabla\right) a_1 &= \gamma_1 a \bar{a}_2 \mathrm{e}^{\mathrm{i}\Delta t}, \\ \mathrm{i}\left(\frac{\partial}{\partial t} + \boldsymbol{v}_2 \cdot \nabla\right) a_2 &= \gamma_2 a \bar{a}_1 \mathrm{e}^{\mathrm{i}\Delta t}. \end{aligned} \qquad (2)$$

Here $\Delta = \omega(\boldsymbol{k}) - \omega(\boldsymbol{k}_1) - \omega(\boldsymbol{k}_2)$ is the frequency detuning from the exact resonance; $\boldsymbol{v}$, $\boldsymbol{v}_1$, and $\boldsymbol{v}_2$ are group velocities of the three waves, for example $\boldsymbol{v} = \nabla\omega(\boldsymbol{k})$; and γ, γ_1, and γ_2 are coupling coefficients in systems with quadratic nonlinearities. In nonlinear dispersive systems with conserved energy, parameters γ, γ_1, and γ_2 are real.

Typical dynamics of the resonant three-wave interaction can be studied from system (2) for space-

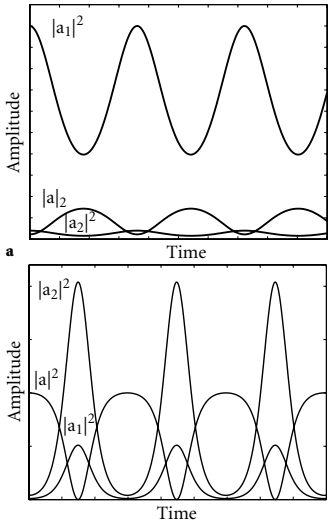

Figure 2. Two typical time evolutions of the three-wave resonant interaction: (a) the high-frequency wave a could not be generated from large low-frequency wave a_1 and small low-frequency wave a_2; (b) the large high-frequency wave a decays into pair of low-frequency waves a_1 and a_2.

independent waves $a(t)$, $a_1(t)$, and $a_2(t)$ in the case of exact resonance, when $\Delta = 0$. Without loss of generality, the real coupling coefficients can be normalized to be equal and positive: $\gamma = \gamma_1 = \gamma_2 > 0$. After these simplifications, system (2) has the following (Manley–Rowe) constants of motion:

$$|a|^2 + |a_1|^2 = C_1, \quad |a|^2 + |a_2|^2 = C_2,$$
$$|a_1|^2 - |a_2|^2 = C. \tag{3}$$

The time evolution of wave amplitudes $a(t)$, $a_1(t)$, and $a_2(t)$ displays two typical scenarios shown in Figure 2(a,b). If the wave with low frequency ($\omega_1, \omega_2 < \omega$) is initially pumped into the system (e.g., either $|a_1|^2 \gg |a|^2, |a_2|^2$ or $|a_2|^2 \gg |a|^2, |a_1|^2$ at $t = 0$), then the other two resonant waves remain small throughout the whole time evolution (see Figure 2(a)). Indeed, it is seen from Equations (3) that when $|a|^2$ grows, $|a_1|^2$ and $|a_2|^2$ decay. If either $|a_1|^2$ or $|a_2|^2$ were initially small, their decay (and the growth of $|a|^2$) is limited by a small value of C_1 and C_2.

If the wave of high frequency ω is initially pumped, however, the waves of low frequencies ω_1 and ω_2 may grow simultaneously. In this case, the resonant three-wave interactions display an exchange of energy between the high-frequency wave and the two low-frequency waves (see Figure 2(b)). This process is referred to as the "splitting" or "decaying" instability of the high-frequency wave. As seen from system (2) for small a_1 and a_2, the amplitude $a(t)$ does not change in time in the first-order approximation, while amplitudes $a_1(t)$ and $a_2(t)$ grow exponentially as $\sim e^{|\gamma a|t}$. The high-frequency wave $|a|^2$ decays into the two low-frequency waves $|a_1|^2$ and $|a_2|^2$, but the two waves merge back to the high-frequency wave later in the time evolution (see Figure 2(b)).

Resonant nonlinear three-wave interactions are known in many physical situations, such as in water waves, nonlinear optics, acoustics, and plasma physics. In nonlinear optics, resonant three-wave interactions are used in parametric amplifiers and oscillators, $\chi^{(2)}$ optical materials, self-induced transparency, and stimulated Raman scattering (Kaup et al., 1977). Four-wave mixing occur in optical communications and leads to growth of ghost pulses in an optical signal sequence. In water waves, resonant wave interactions explain effects of weak turbulence of gravity and gravity-capillary waves, as well as Rossby waves in the atmosphere (Zakharov, 1998). In plasma physics, nonlinear dynamics of high-temperature plasmas in a magnetic fields involve wave-particle and wave-wave interactions. Resonant three-wave interactions occur in ionospheric propagation, plasma heating with high-power electromagnetic sources, microwave sources, and laser sources (Kaup et al., 1977).

DMITRY PELINOVSKY

See also **Dispersion relations; Frequency doubling; Manley–Rowe relations**

Further Reading

Craig, W. 1996. Birkhoff normal forms for water waves. *Contemporary Mathematics*, 200: 57–74

Gaponov-Grekhov, A.V. & Rabinovich, M.I. 1992. *Nonlinearities in Action. Oscillations, Chaos, Order, Fractals*, Berlin: Springer

Kaup, D., Reiman, A. & Bers, A. 1977. Space–time evolution of nonlinear three-wave interactions. *Reviews of Modern Physics*, 51: 915

Zakharov, V.E. (editor). 1998. *Nonlinear Waves and Weak Turbulence*, Providence, RI: American Mathematical Society

Zaslavsky, G.M. & Sagdeev, R.Z. 1988. *Introduction to Nonlinear Physics: From the Pendulum to Turbulence and Chaos*, Moscow: Nauka (in Russian)

O

ONE-DIMENSIONAL MAPS

The term *one-dimensional map* usually indicates a dynamical system with discrete time, generated by some map f of a one-dimensional (1-d) space (the real line or an interval of it, a circle, or a graph) onto itself or, equivalently, the iterations of this map. To specify a 1-d space, the terms *interval map*, *circle map*, or *graph map* are used. The most famous examples of a 1-d maps are the so-called logistic map $x \mapsto \lambda x(1-x)$ of the interval $[0, 1]$ and the rotation $x \mapsto x + \alpha$ of the circle. The theory of 1-d maps can also be considered as the qualitative theory of the difference equations of the form $x_{n+1} = f(x_n)$, $n = 0, 1, 2 \ldots$.

Being part of the general theory of dynamical systems, the theory of 1-d maps includes studies relating to topological dynamics, symbolic dynamics, combinatorial dynamics, differential (or smooth) dynamics, and ergodic theory. The theory of 1-d maps is well developed and contains many deep and beautiful results. Even the simplest non-invertible (for example, quadratic) 1-d maps possess orbits with intricate dynamics, including those behaving like random processes. Thus, this theory offers comparatively simple tools for the understanding of general laws that govern the progression of real dynamic processes from regular to chaotic behaviors.

Many mathematical models, including those arising in population biology, can be reduced to investigations of 1-d maps. For organisms with non-overlapping generations, the population growth can be modeled with the difference equation $x_{n+1} = f(x_n)$, where x_n is the population density of the nth generation. When the density of the population is small and there are plenty of resources, the density x_n increases and follows approximately the linear law $x_{n+1} = \lambda x_n$, where λ is the reproduction coefficient. Because resources are bounded, density cannot increase forever; moreover, if the density x_n is very large, that is, close to 1, then x_{n+1}—the density of the next generation—must be close to 0. The logistic function $f(x) = \lambda x(1-x)$ with $0 < \lambda \leq 4$ is a canonical example.

Interval Maps

Let $f : J \to J$ be a map of the interval J onto itself and f^n be its iterations, defined by $f^n(x) = f(f^{n-1}(x))$, $n = 1, 2, \ldots$, $f^0(x) = x$. The orbit of a point $x_0 \in J$ under the map f is the sequence of points $x_n = f^n(x_0)$, $n = 0, 1, 2, \ldots$.

A point $\beta \in J$ is a periodic point if $f^m(\beta) = \beta$ for some natural m; the smallest m with this property is the *period* of β; if $m = 1$, β is called a fixed point. The points $f^n(\beta)$, $n = 0, 1, \ldots, m-1$ form a cycle of period m. To characterize the asymptotic behavior of an orbit, the set of its limiting points is used; it is called the ω-limit set of the orbit of x and denoted by $\omega(x)$. A cycle B is attracting if there exists a neighborhood U of B such that for any $x \in U$, $f^n(x) \in U$ for all $n > 0$ and $\omega(x) = B$. The basin of an attracting cycle B is the set $\{x \in J : \omega(x) = B\}$; it consists of a finite or countable number of (open) intervals. A cycle B is repelling if there exists a neighborhood U of B such that for any point $x \in U \setminus B$, there exists n such that $f^n(x) \notin U$. If f is differentiable and has a cycle $B = \{\beta_1, \ldots, \beta_m\}$, the quantity $\mu(B) = f'(\beta_1) \cdot \cdots \cdot f'(\beta_m)$ is the multiplier of B. B is attracting if $|\mu(B)| < 1$, and B is repelling if $|\mu(B)| > 1$. The smallest closed set that contains ω-limit sets of orbits for almost all points of J (with respect to Lebesgue measure), is called the (global) attractor of f and denoted by **A** below.

If f is a monotonic (and hence, invertible) continuous function, its dynamics are very simple. If f is monotonically increasing, the ω-limit set of each orbit consists of only a fixed point. If f is monotonically decreasing, the ω-limit set of each orbit is either a fixed point or a cycle of period 2.

The orbits of nonmonotonic (non-invertible) maps can be very complicated. Maps with a single extremum point are called unimodal. Many properties of continuous interval maps can be demonstrated with the simplest representative of unimodal maps—the family of logistic maps $f : x \mapsto \lambda x(1-x)$.

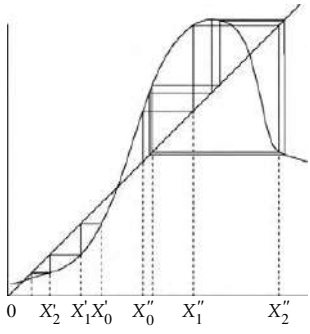

Figure 1. This Königs–Lamerey diagram gives a graphic representation of the orbit of x_0. If the graphs of two functions $y = f(x)$ and $y = x$ in the plane (x, y) are drawn, then the broken line consisting of vertical and horizontal segments that connect the points $(f^n(x_0), f^n(x_0))$ and $(f^n(x_0), f^{n+1}(x_0))$, $n = 0, 1, 2\ldots$, demonstrates the movement along the orbit. The orbit of x_0' tends to a fixed point, and the orbit of x_0'' tends to a cycle of period 3.

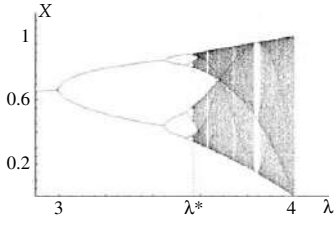

Figure 2. Bifurcation diagram of the attractors for the family of logistic maps.

Logistic Maps

The bifurcation diagram in Figure 2 shows what attractors the logistic map has when the parameter λ is changed.

With increasing λ up to $\lambda^* \approx 3.5699$, the consecutive doubling of period for attracting cycles holds and cycles of periods 2^n, $n = 0, 1, 2, \ldots$, appear: when $\lambda > 3$, the attracting fixed point $\beta_1 = 1 - 1/\lambda$ becomes repelling and a new attracting cycle of period 2 arises; for $\lambda > 1 + \sqrt{6} = 3.449\ldots$, this cycle becomes repelling and generates an attracting cycle of period 4, and so on. The period doubling for attracting cycles occurs with the speed

$$\frac{\lambda_{2^{n+1}} - \lambda_{2^n}}{\lambda_{2^{n+2}} - \lambda_{2^{n+1}}} \to 4.6692\ldots$$

(Feigenbaum–Coullet–Tresser constant), where λ_{2^n} is the parameter value when the cycle of period 2^n arises. The basin of each such attracting cycle is the interval $J = [0, 1]$ except for a countable set of repelling periodic points and their preimages.

If $\lambda = \lambda^*$, f has cycles of periods 2^n, $n = 0, 1, 2, \ldots$, only, and these cycles are repelling. The set K of limiting points for these cycles is an invariant Cantor set. The orbit of each point from K is everywhere dense on K. K is the attractor: the ω-limit set of each point from J, different from a periodic point or its preimages, coincides with K. The restriction of f^2 on the interval $[f^{-1}(\beta_1), \beta_1]$ is topologically conjugated to f on J, and hence, f is infinitely renormalizable.

For $\lambda = 3.83$, f has an attracting cycle of period 3, which is the attractor, and repelling cycles of all periods. The basin of the attracting cycle is J except for a Cantor set. This Cantor set is the closure of the set consisting of points of repelling cycles and their preimages.

If $\lambda = 4$, f is topologically expanding: for any interval $\widehat{J} \subset J$, there exists a number $m = m(\widehat{J})$ such that $f^m(\widehat{J}) = J$. Therefore, f has the property of sensitive dependence on initial conditions (sometimes called the "butterfly effect"). J is an attractor; periodic points lie everywhere dense on J. The map is topologically conjugate to the piecewise linear map

$$g:\ x \mapsto g(x) = \begin{cases} 2x, & 0 \le x \le 1/2, \\ 2(1-x), & 1/2 < x \le 1 \end{cases}$$

with the help of $h(x) = (2/\pi)\arcsin\sqrt{x}$. Because the Lebesgue measure is invariant under g, f has the invariant measure $\nu(\mathrm{d}x) = \mathrm{d}h(x) = \frac{1}{\pi}\mathrm{d}x\,/\sqrt{x(1-x)}$. This means, in particular, that for almost every orbit of f and for any $a_1, a_2 \in [0, 1]$, the frequency with which the orbit visits the interval (a_1, a_2) to $\int_{a_1}^{a_2} \nu(\mathrm{d}x)$.

The general characteristics of the logistic maps family are formulated as follows: for each $\lambda \in [0, 4]$, the attractor **A** of f is a cycle, or a Cantor set (as in the case $\lambda = \lambda^*$), or a cycle of intervals, that is, several closed non-intersecting intervals J_n, $n = 1, \ldots, m$, such that $f(J_n) = J_{(n+1) \bmod m}$ and $\cup_{n=1}^{m} J_n$ contain an everywhere dense orbit (in case $\lambda = 4$, $m = 1$).

The parameter values for which **A** is a cycle form an open and dense (on $[0, 4]$) set, and from the topological standpoint, a map with an attracting cycle is typical for the logistic family. The set of λ for which **A** is a Cantor set (and the map is infinitely renormalizable) has Lebesgue measure zero. The set of λ for which **A** is a cycle of intervals has positive Lebesgue measure. Moreover, for almost all value of these λ, **A** is the support of an ergodic absolutely continuous invariant measure.

The complication of dynamics in the logistic family stems, first of all, from the appearance of new attracting cycles resulting from the period-doubling bifurcation or the tangent bifurcation. With increasing λ, the multiplier of arising attracting cycle decreases from $+1$ to -1, and thereafter, this cycle becomes repelling and does not disappear in the sequel. If λ_m denotes the infinum (greatest lower bound) of the parameter

values for which f has an attracting cycle of period m, then $\lambda_{m'} < \lambda_m$ for $m' \prec m$, where "$\prec$" is the following ordering of the natural numbers:

$$1 \prec 2 \prec 2^2 \prec \cdots \prec 2^n \prec \cdots \prec 7 \cdot 2^n \prec 5 \cdot 2^n \prec 3 \cdot 2^n \prec \ldots \prec 9 \prec 7 \prec 5 \prec 3,$$

called "Sharkovsky's ordering." For $\lambda = \lambda_{2^n}$, $n > 0$, the cycle of period 2^n arises as a result of a period-doubling bifurcation; for $\lambda = \lambda_m$, $m \neq 2^n$, $n = 1, 2, \ldots$, the cycle of period m arises as a result of a tangent bifurcation.

If f has an attracting cycle of period m, then with increasing λ, the sequence of period-doubling bifurcations takes place until cycles of periods $2^n m$, $n = 1, 2, \ldots$, appear. For the limiting parameter value for this sequence of bifurcation values, the attractor is a Cantor set (as in the case $\lambda = \lambda^*$).

Smooth Maps

Analytic unimodal maps (briefly, AU-maps) and C^3-smooth unimodal maps with negative Schwarzian

$$Sf = f'''/f' - \tfrac{3}{2}\left(f''/f'\right)^2 \tag{1}$$

(briefly, SU-maps) are the most investigated classes of smooth maps. Any logistic map has negative Schwarzian.

As for logistic maps, the attractor **A** of each AU-map or SU-map includes (in general, not coincides with) one of the previous set: an (attracting) cycle, a Cantor set, or a cycle of intervals and always contains the ω-limit set of the extremum point. For an SU-map, **A** can have, in addition, only one attracting fixed point, and for an AU-map, **A** can have, in addition, any finite number of attracting cycles. If **A** is a cycle or a cycle of intervals, outside of **A**, f has only a finite number of isolated repelling cycles and isolated repelling invariant Cantor sets.

The period-doubling and tangent bifurcations are typical for smooth maps. The birth order of attractive cycles for the logistic family is kept, for example, for families of convex SU-maps of the form $\lambda f(x)$, $\lambda > 0$.

For almost all members of a typical family of SU-maps, the attractor is either a cycle or a cycle of intervals; the cycle of intervals is the support of an ergodic absolutely continuous invariant measure; and there is a closed invariant interval $\widehat{J} \subset J$ containing the extremum point and $m > 0$ such that the restriction of f^m on $\widehat{J}$ is topologically conjugated to some logistic map.

For a typical family of AU-maps, there exists an open and dense set of parameters for which the map attractor consists of a finite number of cycles, and the union of basins of these cycles has full Lebesgue measure.

A smooth (at least C^2) unimodal map f is structurally stable if an attractor consists of cycles; the multiplier of each cycle is not equal to ± 1; the extremum point c is nondegenerate (i.e., $f''(c) \neq 0$); and $f^n(c)$ is not a periodic point for any $n = 0, 1, 2 \ldots$. The class of structurally stable maps is open in the C^2 topology and dense in any smooth topology.

Some properties of unimodal maps (possibly somewhat modified) hold for maps with more than two branches of monotonicity. For example, the number of attracting cycles for any C^3-smooth map with negative Schwarzian is not greater than the number of extremum points plus two.

Continuous Maps

Due to the natural ordering of points on the real line and the continuity of f, the values of f on a finite set of points provides rich information about the behavior of orbits. So, if there exist points $\beta_1 < \beta_2 < \beta_3$ such that $f(\beta_1) = \beta_1$, $f(\beta_2) = \beta_3$, and $f(\beta_3) \leq \beta_1$, then f has cycles with any period.

Each finite set $B = \{\beta_1 < \beta_2 < \cdots < \beta_m\}$ such that $f(B) \subseteq B$ generates a permutation π on the set $\{1, 2, \ldots, m\}$: $\pi(i) = j$, if $f(\beta_i) = \beta_j$, $i = 1, \ldots, m$. If B is a cycle, such a permutation is cyclic. For $J_i = [\beta_i, \beta_{i+1}]$, $i = 1, 2, \ldots m-1$, $f(J_i) \supseteq J_{k(i)} \cup \cdots \cup J_{K(i)}$, where $k(i) = \min\{\pi(i), \pi(i+1)\}$, $K(i) = \max\{\pi(i), \pi(i+1)\} - 1$. This allows the construction of a Markov matrix of admissible transitions with elements $a_{ij} : a_{ij} = 0$, if $f(J_i) \not\supset J_j$, and $a_{ij} = 1$, if $f(J_i) \supset J_j$, and the corresponding Markov graph. An analysis of loops of Markov graph allows us to obtain the Sharkovsky theorem on the cycles coexistence: if a continuous interval map has a cycle of period m, then it has a cycle of any period m' such that $m' \prec m$.

Research on the coexistence of combinatorial objects, such as cycles, permutations, cyclic permutations, and graphs, is the subject of combinatorial dynamics. An important part of symbolic dynamics for 1-d maps is the kneading theory.

There are different criteria for the chaotic behavior of orbits. In particular, the following properties are equivalent: (i) the *topological entropy* of f is positive; (ii) there is a cycle with period $\neq 2^n$, $n \geq 0$; (iii) there is a *homoclinic orbit*; (iv) there is an ω-limit set containing a cycle, but different from it; and (v) there exist m and a closed invariant set $M \subset J$ such that the restriction of f^m on M is topologically conjugate to the *shift* on the *space of one-side sequences of two symbols*. Any of these involves the following: there is a continuum of many orbits such that for any two orbits $\{x'_n\}$ and $\{x''_n\}$, $\liminf_{n\to\infty} |x'_n - x''_n| = 0$, $\limsup_{n\to\infty} |x'_n - x''_n| > 0$.

If f has a cycle of intervals $\{J_1, J_2, \ldots, J_m\}$, then f on $\widehat{J} = \cup_{i=1}^m J_i$ is topologically expanding and has the property of the sensitive dependence on initial conditions, and the set of periodic points is everywhere dense on $\widehat{J}$.

The typical behavior of continuous maps differs from that of smooth maps. In particular, in the space of continuous maps with C^0-topology, the set of maps that have cycles of all periods contains an open and

dense subset. Moreover, almost every continuous (but nowhere differentiable!) interval map has infinitely many minimal Cantor sets that attract almost all orbits.

Discontinuous interval maps constitute another important class of 1-d maps, especially for applications including expanding interval maps and so-called interval exchange maps.

Circle Maps

Many of the properties of interval maps mentioned above are true for circle maps $f : S \to S$. Along with this, there are classes of circle maps with specific properties, for example, circle homeomorphisms semi-conjugated to rotation of S with rotation number α (corresponding to the discontinuous interval map: $\widehat{f} : x \mapsto x + \alpha \bmod 1$). If α is a rational number, the attractor **A** consists of cycles; if α is irrational, **A** is a minimal set and coincides with S or a Cantor set. Bifurcations in a family of circle homeomorphisms are described by Farey's sequences.

Circle maps, semi-conjugated to the discontinuous interval map $\widehat{f} : x \mapsto k\,x \bmod 1$ with an integer $|k| > 1$, are called circle maps of degree k and represent a further important class of circle maps, including expanding circle maps with $|f'(x)| > 1$ at $x \in S$. Any expanding map is topologically conjugate to the shift on the space of one-sided sequences of finite number of symbols; it is structurally stable and possesses an absolutely continuous invariant measure.

A.N. Sharkovsky and V.V. Fedorenko

See also **Anosov and Axiom-A systems; Bifurcations; Butterfly effect; Chaotic dynamics; Denjoy theory; Horseshoes and hyperbolicity in dynamical systems; Maps in the complex plane; Markov partitions; Measures; Mixing; Period doubling; Population dynamics; Routes to chaos; Sinai–Ruelle–Bowen measures; Symbolic dynamics**

Further Reading

Alseda, L., Llibre, J. & Misiurewicz, M. 2000. *Combinatorial Dynamics and Entropy in Dimension One*, 2nd edition, River Edge, NJ: World Scientific

Argonsky, S.J., Bruckner, A.M. & Laczkovich, M. 1989. Dynamics of typical continuous functions. *Journal of the London Mathematical Society*, 40: 227–243

Avila, A., Lyubich, M. & de Melo, W. 2003. Regular or stochastic dynamics in real analytic families of unimodal maps. *Inventiones Mathematicae*, 3(154): 451–550

Block, L. & Coppel, W.A. 1992. *Dynamics in One Dimension*, Berlin: Springer

Collet, P. & Eckmann, J.-P. 1980. *Iterated Maps on the Interval as Dynamical Systems*, Boston: Birkhäuser

de Melo, W. & van Strien, S.J. 1993. *One-Dimensional Dynamics*, Berlin: Springer

Devaney, R.L. 1992. *A First Course in Chaotic Dynamical Systems: Theory and Experiment*, Reading, MA: Addison-Wesley

Hao, Bai-Lin. 1989. *Elementary Symbolic Dynamics and Chaos in Dissipative Systems*, Singapore: World Scientific

Katok, A. & Hasselblatt, B. 1995. *Introduction to the Modern Theory of Dynamical Systems*, Cambridge and New York: Cambridge University Press

Kozlovski, O.S. 2003. Axiom A maps are dense in the space of unimodal maps in the C^k topology. *Annals of Mathematics*, 1 (157): 1–43

Milnor, J. & Thurston, W. 1988. On iterated maps of the interval. In *Dynamical Systems: Proceedings University of Maryland, 1986–87*, Berlin and New York: Springer, 425–563

Peitgen, H.-O., Jürgens, H. & Saupe, D. 1993. *Chaos and Fractals: New Frontiers of Science*, Berlin and New York: Springer

Sharkovsky, A.N., Kolyada, S.F., Sivak, A.G. & Fedorenko, V.V. 1997. *Dynamics of One-Dimensional Maps*, Boston and Dordrecht: Kluwer

OPEN SETS

See **Topology**

OPTICAL FIBER COMMUNICATIONS

The existence of temporal solitons in optical fibers and their use for optical communications were suggested in 1973 (Hasegawa & Tappert, 1973), and by 1980, such solitons had been observed experimentally (Mollenauer et al., 1980; Hasegawa & Kodama, 1995). Since then, rapid progress has converted temporal solitons into a practical candidate for designing modern communication systems based on optical-fiber technology (Agrawal, 2002; Kivshar & Agrawal, 2003).

Similar to other types of solitons, those in optical fibers emerge from a balance between the group-velocity dispersion (GVD) and self-phase modulation (SPM) induced by the Kerr nonlinearity. The GVD broadens optical pulses during their propagation inside an optical fiber, except when the pulse is initially chirped (compressed with linear frequency modulation) in the right way. More specifically, a chirped pulse can be compressed during the early stage of propagation whenever the GVD parameter β_2 and the chirp parameter C happen to have opposite signs such that $\beta_2 C$ is negative. The optical pulse then propagates undistorted in the form of an optical soliton.

The nonlinear Schrödinger (NLS) equation governing pulse propagation inside optical fibers can be written in the following form:

$$i\frac{\partial u}{\partial z} + \frac{1}{2}\frac{\partial^2 u}{\partial \tau^2} + |u|^2 u = 0\,, \tag{1}$$

where τ is a measure of time from the pulse center and is normalized to the input pulse width T_0, and L_D is the dispersion length. Noting that $z = Z/L_D$, the soliton period Z_0 is defined as

$$Z_0 = \frac{\pi}{2} L_D = \frac{\pi}{2}\frac{T_0^2}{|\beta_2|}. \tag{2}$$

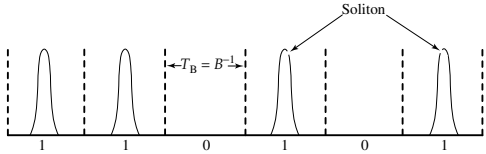

Figure 1. Soliton bit stream in the return-to-zero format where each soliton occupies a fraction of the bit slot representing 1 in a bit stream.

Temporal solitons are attractive for optical communications because they are able to maintain their width even in the presence of fiber dispersion, but their use requires substantial changes in the fiber system design, compared with conventional (nonsoliton) systems.

The basic idea is to use a soliton in each bit slot representing 1 in a bit stream. Figure 1 shows schematically a soliton bit stream in the return-to-zero (RZ) format. Typically, the spacing between two solitons exceeds a few times their full-width at half-maximum (FWHM), and individual solitons are well isolated. This requirement relates the soliton width T_0 to the bit rate B as $B = 1/T_B = 1/(2q_0T_0)$, where T_B is the duration of the bit slot and $2q_0 = T_B/T_0$ is the separation between neighboring solitons in normalized units.

The relatively large spacing necessary to avoid soliton interaction, limits the bit rate of soliton communication systems. The spacing can be reduced by up to a factor of two using unequal amplitudes for the neighboring solitons, so this scheme is feasible in practice and can be useful for increasing the system capacity.

Temporal solitons use the nonlinear phenomenon of SPM to maintain their width even in the presence of fiber dispersion. However, this property holds only if fiber losses are negligible. Optical amplifiers can be used for compensating fiber losses. Two approaches used for the management of losses through amplification of solitons are the lumped- and distributed-amplification techniques.

In the lumped-amplification scheme, optical amplifiers are placed periodically along the fiber link such that fiber losses between two amplifiers are exactly compensated by the amplifier gain. An important design parameter is the spacing L_A between amplifiers, which should be as large as possible to minimize the overall cost. For nonsoliton systems, L_A is typically 80–100 km. For soliton systems, L_A is restricted to smaller values because of the soliton nature of signal propagation.

The physical reason behind smaller values of L_A is that optical amplifiers boost soliton energy to the input level over a length of a few meters without allowing for gradual recovery of the fundamental soliton. The amplified soliton adjusts its width dynamically in the fiber section following the amplifier, but it also sheds a part of its energy as dispersive waves during this adjustment phase. The dispersive part can accumulate to significant levels over a large number of amplification stages and must be avoided. One way to reduce the dispersive part is to reduce the amplifier spacing L_A such that the soliton is not perturbed much over this short length. Numerical simulations show (Hasegawa & Kodama, 1995) that this is the case when L_A is a small fraction of the dispersion length ($L_A \ll L_D$). The dispersion length L_D depends on both the pulse width T_0 and the GVD parameter β_2 and can vary from 10 to 1000 km, depending on their values.

The condition $L_A \ll L_D$, imposed on loss-managed solitons when lumped amplifiers are used, becomes increasingly difficult to satisfy in practice as bit rates exceed 10 GB/s. This condition can be relaxed considerably when distributed amplification is used. The distributed-amplification scheme is inherently superior to lumped amplification because its use provides a nearly lossless fiber by compensating losses locally at every point along the fiber link. In fact, this scheme was used as early as 1985 using the distributed gain provided by Raman amplification (Agrawal, 2002) when the fiber carrying the signal was pumped at a wavelength of about 1.46 μm using a color-center laser (Hasegawa & Kodama, 1995). Alternatively, the transmission fiber can be doped lightly with erbium ions and pumped periodically to provide distributed gain. Several experiments have demonstrated that solitons can be propagated in such active fibers over relatively long distances.

Early soliton experiments on loss compensation used the Raman-amplification scheme. The situation changed with the application of erbium-doped fiber amplifiers from around 1989 for loss-managed soliton systems. In a typical experiment (Agrawal, 2002), 2.5 GB/s solitons were transmitted over 12,000 km by using a 75 km fiber loop containing three amplifiers, spaced 25 km apart (Agrawal, 2002). The bit rate–distance product of $BL = 30$ (TB/s)km is limited mainly by the timing jitter induced by amplifiers.

Dispersion management, which consists of a periodic change of the dispersion β_2 along the fiber

length, is employed commonly for modern wavelength-division multiplexed systems. The use of dispersion management forces each soliton to propagate in the normal-dispersion regime of a fiber during each map period. If the map period is a fraction of the nonlinear length, the nonlinear effects are relatively small, and the pulse evolves in a linear fashion over one map period. On a longer length scale, solitons can still form if the nonlinear effects are balanced by the average dispersion. As a result, solitons can survive in an average sense, even though not only the peak power but also the width and shape of such solitons oscillate periodically.

Since 1996, a large number of experiments have shown the benefits of using dispersion-managed solitons for optical communication systems (Agrawal, 2002). Presently, 10 GB/s dispersion-managed solitons can be transmitted over 16 Mm of standard fiber when soliton interactions are minimized by choosing the location of amplifiers appropriately. An important application of dispersion management consists of upgrading the existing terrestrial networks designed with standard fibers and operating in the linear regime.

YURI KIVSHAR

See also **Dispersion management; Kerr effect; Nonlinear optics; Nonlinear Schrödinger equations**

Further Reading

Agrawal, G.P. 2002. *Fiber-Optic Communication Systems*, New York: Wiley

Hasegawa, A. & Kodama, Y. 1995. *Solitons in Optical Communications*, Oxford: Clarendon Press

Hasegawa, A. & Tappert, F. 1973. Transmission of stationary nonlinear optical pulses in dispersive dielectric fibers. *Applied Physics Letters*, 23: 142–144

Kivshar, Yu.S. & Agrawal, G.P. 2003. *Optical Solitons: From Fibers to Photonic Crystals*, San Diego: Academic Press

Mollenauer, L.F., Stolen, R.H. & Gordon, J.P. 1980. Experimental observation of picosecond pulse narrowing and solitons in optical fibers. *Physical Review Letters*, 45: 1095–1098

OPTICAL NONLINEARITIES

See **Nonlinear optics**

ORBIT

See **Phase space**

ORDER FROM CHAOS

At first glance, the words *chaos* and *order* seem to be contradictory. Indeed they are contradictory in terms of common definitions of the words, but not in terms of their mathematical usages. The definition of *chaos* in the Oxford American Dictionary (1986) is "great disorder or confusion." In contrast, the mathematical notion of *chaos* explains that data that seems to be random may have been generated by a deterministic and ordered process. In this sense, the field might have profitably been called "order theory" instead of "chaos theory." There are two common usages of the phrase "order from chaos." The first refers to seeking deterministic "chaotic" models to explain complex phenomenon, thus "order *in* chaos." The second refers to the fact that some chaotic dynamical systems can also exhibit regular islands of simplicity within their phase space, or "order *from* chaos." We will discuss each in turn.

Order in Chaos

The fact that seemingly simple and deterministic evolution rules can give rise to extremely complicated motion dates to Henri Poincaré (1892), in the setting of celestial mechanics. Perhaps the most famous example of unpredictable behavior is due to Edward Lorenz (1963), who discovered that even the most simplified models of the weather could produce data for which it is impossible to make long-term forecasts. Lorenz identified the "butterfly effect," or "sensitive dependence to initial conditions," whereby even small measurement errors quickly grow to swamp the signal. In 1975, Tien Yien Li and James A. Yorke published a paper entitled, "Period Three Implies Chaos," (Li & Yorke, 1975). The most famous impact of this paper was that it coined the word *chaos*, the field of study describing the nonlinear effect in which even the simple systems of Poincaré, Lorenz, and others can display sensitive dependence in a bounded domain. The chaos theory has attracted a great deal of popular attention, partly, in fact, due to its sexy title. Part of the appeal is also due to the scientific tradition since the time of Newton of searching for mechanistic explanations of reality.

The concept of phase space is useful for mapping the behavior of a dynamical system. Phase space could be described as the set of all possible relevant variables, which creates a closed description of the time evolution of the system (*See* **Phase space**). For example, for a simple pendulum, we need to specify all possible angular position and angular momentum states to uniquely define all solutions; the phase space for the periodic oscillation is a closed curve, a circle. For an electronic tank oscillator (LRC) circuit, we need to specify capacitor charge and current through the inductor. The dimension of the system is the dimension of the phase space. A billiard table's worth of balls, for example, requires many variables for a complete description—two variables for position and two for momentum for each of the balls.

As a highly interdisciplinary field, chaos theory has been successful in finding deterministic chaos, or order, in what was once thought to be mere noise, or at

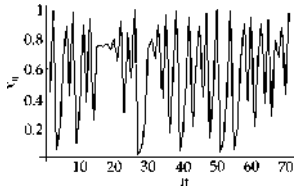

Figure 1. This seemingly stochastic data was actually generated by a "simple," low-dimensional, and deterministic process. This time-series plot of the state x_n versus time n was actually generated by the dynamical system $x_{n+1} = ax_n(1-x_n)$ called the logistic map. ($a = 4.0$, $x_0 = 0.44$).

least an extremely high-dimensional effect. There are numerous explicit examples of chaos in many areas, including biology, electrical engineering, chemistry, celestial mechanics, and brain and heart physiology. Thus, the old idea that extremely complicated data must always be due to extremely complicated effects is false (see Figure 1). One popular misuse of these ideas is a belief that all complicated data must have underlying order in chaos. This can be phrased as "Is what seems complicated always really simple?" The answer, of course, is no; it remains true that noise and other high-dimensional effects can also be responsible for complexity. What is true is that what seems complicated may *sometimes* be simple, in the sense of having a low-dimensional chaotic model. To cite one popular question, the stock market prices unarguably constitute extremely complicated data, but is there underlying order in chaos here, or is the explanation due to intractably high-dimensionality?

Order from Chaos

Some chaotic systems have an occasional tendency to exhibit simple behavior. This is often described as regular islands in an otherwise chaotic phase space. The classic mathematical example of regular islands arises in Hamiltonian systems, which can exhibit a phase space of solutions in which chaotic solutions are both intermingled and bounded by nested islands around islands around islands, and so on, of KAM-like tori (circle-like integrable solutions) (Arrowsmith & Place, 1990; Meiss, 1992).

Put differently, "order from chaos" and "regular islands" are terms commonly used to refer to the presence of an "attractor" (an imaginary point in the phase space about which the trajectories appear to orbit) in a system that one thinks should behave in a complicated manner. For example, consider a thought experiment of a game of pool in which we assume no friction so that the balls never stop moving (a two-dimensional Lorentz gas). Following the path of one specific ball, say the seven-ball, is an extremely complicated problem displaying sensitive dependence, since a small change in the velocity or position of the ball affects the next collision with the wall or with the next ball, an effect that multiplies upon subsequent collisions. However, there are several attractors near which the ball's motion becomes quite simple—the pocket holes. Once within the rim of a pocket (its basin of attraction), falling in becomes inevitable, as it would require a relatively large energy perturbation to prevent it from falling in. In this sense, we can say that the regions of phase space, corresponding to being stuck in the billiards pocket, are regular islands in a chaotic sea.

As analogies, such descriptions of islands in chaotic seas have been extended by some to explain the emergence of a coherent phenomenon from complicated processes. There is perhaps no more intriguing question than the origins of life. Proponents of emergence theories suggest that life in the original Hadean seas (the "primordial" seas on early Earth) gave rise to life through a capture process such as the billiards game (Waldrop, 1992; Kauffman, 1995). While randomly chosen initial conditions in the billiards game may each individually be unlikely to lead to capturing a ball in a pocket (and certainly any analogous attractors in chemical processes must be exceedingly unlikely), the way to win an unlikely bet is to play very quickly, over and over. This may have been the process that led to complex organic molecules, according to proponents of the emergence theory.

Emergence and order from chaos have also been used to describe processes whose attractors are surprisingly complicated themselves, as sets, but arise from surprisingly simple rules. Michael Barnsley has called the following "The Chaos Game" (Barnsley, 1993). First label the vertices of a triangle, 1, 2, 3. Using a random number generator (such as a six-sided die), assign probabilities to each triangle vertex, say die sides 1–2 to vertex 1, die sides 3–4 to vertex 2, and die sides 5–6 to vertex 3. Roll the die to randomly select one of the vertices, and record its planar coordinates (x, y). Then roll the die again to randomly select another vertex, and record the point halfway between the resulting new vertex and the current (x, y) as the new (x, y). Repeat indefinitely. For each newly defined (x, y), we record a dot for a pictorial record. Most people guess that the result will uniformly fill the triangle with a smattering of dots, but the mathematical fact is surprising. The result is an extremely intricate structure, a fractal called the Sierpinski gasket (see Figure 2). Because this simple rule gives rise to such a complicated structure, the argument goes, perhaps many of the other intricacies we see around us might have emerged from other simple rules.

Finally, we mention the meaning of "order from chaos," as developed from theories of the Nobel prize-winning physicist Ilya Prigogine, whose work on dissipative structures of systems held from thermal

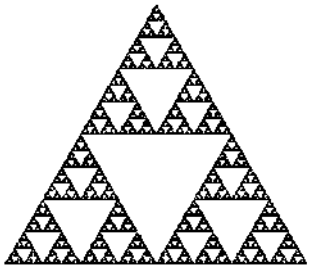

Figure 2. From such a simple algorithm as "The Chaos Game" (Barnsley, 1993) emerges the extremely intricate fractal shown, called the Sierpinski gasket.

equilibrium has been used to study self-organizing systems (Prigogine, 1984). Prigogine has defined complexity as the ability to switch between different modes of behavior as the environmental conditions vary. Thus, he has described a phenomenon in which far-from-equilibrium systems transition "from being to becoming," which some describe as order from chaos.

ERIK M. BOLLT

See also **Chaotic dynamics; Emergence; Kalmogorov–Arnol'd–Moser theorem; Phase space**

Further Reading

Arrowsmith, D.K. & Place, C.M. 1990. *An Introduction to Dynamical Systems*, Cambridge and New York: Cambridge University Press

Barnsley, M. 1993. *Fractals Everywhere*, 2nd edition, San Francisco: Morgan Kaufmann

Kauffman, S. 1995. *At Home in the Universe, the Search for the Laws of Self-Organization and Complexity*, Oxford and New York: Oxford University Press

Lorenz, E.N. 1963. Deterministic nonperiodic flow. *Journal of Atmospheric Science*, 20: 130–141

Li, T.Y. & Yorke, J.A. 1975. Period three implies chaos. *American Mathematics Monthly*, 82: 985–992

Meiss, J.D. 1992. Symplectic maps, variational principles, and transport. *Reviews of Modern Physics*, 64: 795

Poincaré, H. 1892–99. *Les méthodes nouvelles de la mécanique céleste*, Paris: Gauthier-Villars, 3 vols; as *New Methods of Celestial Mechanics*, New York: American Institute of Physics, 1993

Prigogine, S. 1984. *Order out of Chaos: Man's New Dialogue with Nature,* New York: Bantam Books

Waldrop, M. 1992. *Complexity: The Emerging Science at the Edge of Chaos and Order*, New York: Touchstone Press

ORDER PARAMETERS

Although the concept of an order parameter was introduced by Lev Landau in the 1930s, it does not yet have a precise definition. Broadly, an order parameter is a thermodynamic quantity that is invariant with respect

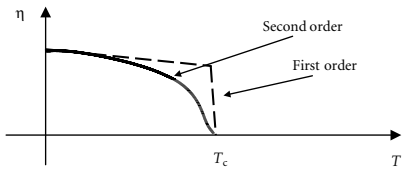

Figure 1. A typical plot of the scalar order parameter as a function of temperature.

to the symmetry group of the low-temperature phase and zero above a critical point or transition temperature, T_c. It is a measure of the amount of order that is built up in the system in the neighborhood of the critical point. In general, an order parameter has both an amplitude and a phase. To find the equation of state, a minimization procedure is followed for an appropriate thermodynamic potential.

From the original application to second-order phase transitions where it changes continuously from T_c to lower temperatures, the idea of an order parameter has been extended to first-order transitions involving an abrupt change at T_c (see Figure 1). The concept of an order parameter has been generalized from a globally defined scalar to a complex time- and space-dependent function. Note that first-order phase transitions are associated with discontinuities of the order parameter and thermal hysteresis effects. Second-order phase transitions have a continuous order parameter and show field-induced hysteresis. Diverse applications of the order parameter concept to both equilibrium and nonequilibrium critical phenomena are listed in Table 1.

Crystal formation is demonstrated by the existence of a regular diffraction pattern associated with the Fourier components of the mass density distribution $\rho(\mathbf{r})$

$$\rho(\boldsymbol{r}) = \sum_{\boldsymbol{g}} \rho(\boldsymbol{g}) e^{i\boldsymbol{g}\cdot\boldsymbol{r}}, \qquad (1)$$

where the $\boldsymbol{g}$ are vectors in the reciprocal space. The set of numbers $\rho(\boldsymbol{g})$ can be used as order parameters characterizing the low-temperature (crystal) phase. The nonzero coefficients $\rho(\boldsymbol{g})$ in Equation (1) define a multi-component order parameter.

The order parameter field for a magnet is defined at each position $\boldsymbol{x}$ by a direction of the local magnetization $\boldsymbol{M}(\boldsymbol{x})$ whose length is fixed. By becoming a magnet, this material has broken the rotational symmetry and its order parameter field defines the broken symmetry directions chosen in the material.

A number of metals, alloys, and ceramics below their critical temperature T_c exhibit an ordered state in the conduction electron degrees of freedom manifested by zero resistance. The order parameter for superconductors is the wavefunction of the Cooper pair

Phenomenon	Disordered phase	Ordered phase	Order parameter
Equilibrium			
Condensation	Gas	Liquid	Density difference $\rho_L - \rho_G$
Spontaneous magnetization	Paramagnet	Ferromagnet	Net magnetization M
Antiferromagnetism	Paramagnet	Antiferromagnet	Staggered magnetization $M_1 - M_2$
Superconductivity	Conductor	Superconductor	Cooper pair, wave function η
Alloy ordering	Disordered mixture	Sublattice ordered alloy	Sublattice concentration
Ferroelectricity	Paraelectric	Ferroelectric	Polarization
Superfluidity	Fluid	Superfluid	Condensate wavefunction
Nonequilibrium			
Laser action	Lamp (incoherent)	Laser (coherent)	Electric field intensity
Super-radiant source	Noncoherent polarization	Coherent polarization	Atomic polarization
Fluid convection	Turbulent flow	Bénard cells	Amplitude of mode

Table 1. Examples of order parameters (OPs).

condensate $\eta(\boldsymbol{r})$, and it exhibits a Hopf bifurcation at $T = T_c$.

The superfluid properties in ^{4}He and ^{3}He are manifested by the absence of viscosity. The ^{4}He atoms are bosons that below a transition temperature T_λ, undergo the so-called Bose condensation into a $k = 0$ mode. The associated order parameter is the condensate's quantum wavefunction. Because ^{3}He atoms are fermions, below T_λ they form Cooper pairs.

Liquid crystals are anisotropic fluids composed of strongly elongated molecules. The nematic phase is characterized by the existence of a direction to which most of the molecules are parallel, so the order parameter is a second rank tensor describing correlations along that direction. Numerous other examples of critical phenomena, such as binary fluids, the metal-insulator transition, polymer transitions and spin- and charge-density waves, have their own order parameters.

Landau deduced that second-order phase transitions are associated with symmetry breaking and can be qualitatively described by an order parameter η. Assuming that the free energy F depends on V, T, and η, the equilibrium conditions are:

$$\left.\frac{\partial F(T, V, \eta)}{\partial \eta}\right|_{\eta=\eta_0} = 0$$

and

$$\left.\frac{\partial^2 F(T, V, \eta)}{\partial \eta^2}\right|_{\eta=\eta_0} > 0, \qquad (2)$$

where η_0 is the equilibrium value of η.

The universality hypothesis states that any two physical systems with the same spatial dimensionality, d, and the same number of order parameter components, n, belong to the same universality class having identical critical exponents (see Table 2).

Universality class		System	Order parameter (OP)
$d = 2$,	$n = 1$	Absorbed films	Surface density
$d = 2$,	$n = 2$	Superfluid ^{4}He film	Superfluid wave function
$d = 3$,	$n = 1$	Uniaxial ferromagnets	Magnetization
$d = 3$,	$n = 1$	Fluids	Density difference
$d = 3$,	$n = 1$	Mixtures, alloys	Concentration difference
$d = 3$,	$n = 2$	Planar ferromagnets	Magnetization
$d = 3$,	$n = 2$	Superfluids	Superfluid wave function
$d = 3$,	$n = 3$	Isotropic ferromagnets	Magnetization

Table 2. Examples of universality classes.

Order parameters accompany broken symmetry phenomena where the new ground state of the system does not possess the full symmetry of the Hamiltonian. A classic example is the ferromagnetic-to-paramagnetic phase transition at T_c where the full rotational symmetry of the paramagnetic phase is broken by the axiality of the ground ferromagnetic state below T_c. When a symmetry that is broken is continuous, a vibrational mode appears whose frequency vanishes at long wavelengths. (Quanta of such modes are called "Goldstone bosons.") Examples include ferromagnetic domain walls and acoustic soft modes in structural phase transitions.

There exist several different types of broken symmetries: (a) translational (crystal formation, structural transitions); (b) gauge (superfluidity, superconductivity); (c) time reversal (ferromagnets); (d) local rotational (liquid crystals); (e) rotational (some structural phase transitions); and (f) space inversion (ferroelectricity). Gauge symmetry is a universal property of Hamiltonians whenever the total number of particles is conserved or a generalized charge-like conserved quantity exists. Then, the order parameter η is complex, and its local density $\rho = \eta^* \eta(r)$ is such that a phase shift $\eta \to \eta e^{i\omega}$ leaves the Hamiltonian invariant.

Defects in the order parameter space can be topological (i.e., kinks, also referred to as domain walls) and nontopological (i.e., solitons, also called nucleation centers). They are obtained as solutions to the equations of motion for the order parameter field. Also, point defects, line defects, vortices, dislocations, vacancies, and interstitials with attendant singularities are seen experimentally in critical systems (systems close to a phase transition).

Finally, note that Haken's separation of modes in synergetic systems into masters (order parameters) and slaves has been influenced by Landau's theory of phase transitions.

JACK A. TUSZYŃSKI

See also **Bose–Einstein condensation; Critical phenomena; Domain walls; Ferromagnetism and ferroelectricity; Hysteresis; Liquid crystals; Phase transitions; Solitons; Synergetics**

Further Reading

Anderson, P.W. 1984. *Basic Notions of Condensed Matter Physics*, Menlo Park, CA: Benjamin/Cummings

Haken, H. 1980. *Synergetics*, Berlin and New York: Springer

Landau, L.D. & Lifshitz, E.M. 1959. *Statistical Physics*, London: Pergamon

Ma, S.-K. 1976. *Modern Theory of Critical Phenomena*, Reading, MA: Benjamin

Reichl, L.E. 1979. *A Modern Course in Statistical Physics*, Austin, TX: University of Texas Press

White, R.H. & Geballe, T. 1979. *Long Range Order in Solids*, New York: Academic Press

Yeomans, J.M. 1992. *Statistical Mechanics of Phase Transitions*, Oxford: Clarendon Press and New York: Oxford University Press

ORDINARY DIFFERENTIAL EQUATIONS, NONLINEAR

An ordinary differential equation (ODE) is an equation

$$\Delta(t, f, f', f'', ..., f^{(N)}) = 0 \tag{1}$$

(with $f^{(j)} = \mathrm{d}^j f / \mathrm{d}t^j$), relating a function $f(t)$ to its derivatives. The order of an ODE is the size of the highest derivative that appears, so Equation (1) is Nth order. An ODE is *linear* if it can be written as a linear combination of f and its derivatives, that is,

$$\Delta \equiv a_N(t) f^{(N)} + a_{N-1}(t) f^{(N-1)} + \cdots + a_1(t) f' + a_0(t) f + b(t) = 0, \tag{2}$$

including the possible addition of an inhomogeneous term $b(t)$. All other ODEs, which are not of the form (2), are referred to as *nonlinear*.

More generally, one can consider systems of ODEs relating M functions $f_0, f_1, \ldots, f_{M-1}$ and their derivatives $f_k^{(j)}$ of different orders. In fact, if a system of ODEs can be solved for the highest derivatives appearing (which generally requires the implicit function theorem), then it can always be converted to a system of first-order equations,

$$\begin{aligned} f_0' &= F_0(t, f_0, f_1, \ldots, f_{M-1}), \\ f_1' &= F_1(t, f_0, f_1, \ldots, f_{M-1}), \\ &\vdots \\ f_{M-1}' &= F_{M-1}(t, f_0, f_1, \ldots, f_{M-1}). \end{aligned} \tag{3}$$

For example, suppose Equation (1) can be solved explicitly for the Nth derivative, as $f^{(N)} = F(t, f, f', f'', \ldots, f^{(N-1)})$. In that case, the single ODE (1) may be rewritten as the first-order system

$$\begin{aligned} f_0' &= f_1, \\ f_1' &= f_2, \\ &\vdots \\ f_{N-2}' &= f_{N-1}, \\ f_{N-1}' &= F(t, f_0, f_1, f_2, \ldots, f_{N-1}). \end{aligned}$$

In most applications of nonlinear ODEs, such as in the physical sciences or biology, they appear as coupled systems of either first or second order. For example, Newton's equations in mechanics (Arnol'd, 1989) are of the form

$$\boldsymbol{q}'' = \boldsymbol{F}(t, \boldsymbol{q}, \boldsymbol{q}'),$$

relating the acceleration $\boldsymbol{q}''$ of a particle (of unit mass) to the force $\boldsymbol{F}$ acting on it, which is a function of its position $\boldsymbol{q}$ and velocity $\boldsymbol{q}'$, and possibly the time t. Mechanical systems are often derived from an action functional $S = \int_{t_0}^{t_1} L(t, \boldsymbol{q}, \boldsymbol{q}', \ldots, \boldsymbol{q}^{(j)})\, \mathrm{d}t$. In particular, if $\boldsymbol{q}'$ is the highest derivative appearing in the Lagrangian, so that $L = L(t, \boldsymbol{q}, \boldsymbol{q}')$, then the corresponding Euler–Lagrange equations form a second-order system of ODEs, viz.

$$\frac{\partial L}{\partial \boldsymbol{q}} - \frac{\mathrm{d}}{\mathrm{d}t}\left(\frac{\partial L}{\partial \boldsymbol{q}'}\right) = 0.$$

In Hamiltonian mechanics, on the other hand, the equations of motion are given as a first-order system of ODEs,

$$\frac{\mathrm{d}\boldsymbol{x}}{\mathrm{d}t} = \boldsymbol{J}(\boldsymbol{x}) \nabla H(t, \boldsymbol{x}), \tag{4}$$

describing the evolution of a point $\boldsymbol{x}$ in the phase space with Poisson tensor $\boldsymbol{J}$ and Hamiltonian H. First-order equations are commonly used both in population dynamics, for example, the Verhulst model

$$\frac{\mathrm{d}P}{\mathrm{d}t} = rP(1 - P/K) \tag{5}$$

(with r, K constants), and in reaction kinetics applying the Law of Mass Action (Murray, 1989). The ODEs describing a system of N species or N chemical reagents typically take the form of N coupled first-order ODEs, but usually these are *not* Hamiltonian.

Given an ODE such as (1), the main task is to determine the nature of the solutions, namely, those functions $f(t)$ for which all the derivatives $f^{(j)}$ exist for $j = 1, \ldots, N$ and are related by Equation (1). More specifically, one may wish to solve an initial value problem, where the values $f(t_0), f'(t_0), \ldots, f^{(N-1)}(t_0)$ of the function f and its first $N-1$ derivatives are specified at some initial time $t = t_0$, and f is to be determined at subsequent times $t > t_0$. Alternatively, one might pose a boundary value problem where the values $f(t_0)$ and $f(t_1)$ (and maybe some of the derivatives) are given at the endpoints of the interval $[t_0, t_1]$, and $f(t)$ is to be found for $t_0 < t < t_1$.

For an Nth-order linear homogeneous ODE, of the form (2) with $b \equiv 0$, the general solution is just a linear combination of N-independent solutions s_j, that is, $f(t) = \sum_{j=1}^{N} A_j s_j(t)$ with N arbitrary constants $A_1, \ldots, A_N$. Ideally, one would like to express the general solution of an Nth-order nonlinear ODE as a function of N arbitrary integration constants, but in general this is not possible. However, for systems (3) where the F_j on the right-hand sides are suitably regular functions of all their arguments in the neighborhood of the initial data, the local existence of a solution to the initial value problem near $t = t_0$ can be proved by the Cauchy–Lipschitz method (Ince, 1926). In fact, whenever the F_j are analytic functions, then the existence of a local solution to the initial value problem is guaranteed in some circle around $t = t_0$ in the complex t plane (Hille, 1976). This means that, at least locally, the solution $f(t)$ can be considered as a function of the initial data $f(t_0), f'(t_0), \ldots, f^{(N-1)}(t_0)$. Only for ODEs of Painlevé type can this local solution be extended globally to a single-valued, meromorphic function of t (Hinkkanen & Laine, 1999). In contrast, the solutions of other ODEs can display chaotic behavior, with coalescing branch points in the complex plane (Sachdev, 1991).

For first-order equations ($N = 1$), there are various classes of ODEs that are amenable to exact integration methods. The simplest example is the class of *separable* equations, which are directly solvable by a quadrature:

$$\frac{\mathrm{d}f}{\mathrm{d}t} = T(t)/F(f),$$

whence

$$\int F(f)\,\mathrm{d}f = \int T(t)\,\mathrm{d}t + \text{constant}.$$

The Verhulst model (5) is a particularly simple example for we have

$$\int \frac{\mathrm{d}P}{P(1 - P/K)} = \log\left(\frac{P}{K - P}\right) = rt + c$$
$$\Rightarrow P(t) = \frac{K}{1 + \mathrm{e}^{-rt-c}} = \frac{KP_0}{P_0 + (K - P_0)\mathrm{e}^{-rt}},$$

where the constant $P_0 = K/(1 + e^{-c}) = P(0)$ is the initial population size. Other special classes of first-order equations include the Bernoulli equations $f' = P(t)f + Q(t)f^n$ and Riccati equations $f' = A(t)f^2 + B(t)f + C(t)$; both of these types can be converted to linear equations by a substitution (Ince, 1926).

Among higher-order ODEs, exactly solvable equations are rare, but nevertheless some exact solution methods exist. In particular, if there are first integrals (constants of motion) or symmetries for a system, then it is possible to reduce the order. For autonomous Hamiltonian systems of order $N = 2n$, Liouville's theorem on integrable systems states that if there are n independent first integrals, in involution with respect to the nondegenerate Poisson bracket defined by $\boldsymbol{J}$, then the ODEs (4) can be integrated by quadratures (Arnol'd, 1989). More generally, an ODE of order N with a first integral can be reduced to an equation of order $N-1$, while if it has a Hamiltonian or Lagrangian structure invariant under a symmetry of the system, then (using Noether's theorem) the order can be reduced to $N-2$. The approach to solving ODEs using their symmetries is originally due to Lie; for a modern treatment, see Olver (1993).

As an illustration of some of these ideas, consider the second-order ODE

$$f'' = \left(kt - \frac{(n-1)}{f}\right)(f')^2 + \frac{(n-1)}{t}f' \tag{6}$$

(k, n constants), which is a radial symmetry reduction of an n-dimensional partial differential equation appearing in differential geometry (Abreu, 1998). This can be derived from the action

$$S = \int_{t_0}^{t_1} L(t, f, f')\,\mathrm{d}t,$$
$$L = t^{n-1}\log(f^{n-1}f') - kt^n f. \tag{7}$$

By a Legendre transformation, setting $q = f$ and $p = \partial L/\partial f'$, (6) can also be converted to the first-order Hamiltonian form

$$\frac{\mathrm{d}}{\mathrm{d}t}\begin{pmatrix} q \\ p \end{pmatrix} = \begin{pmatrix} 0 & 1 \\ -1 & 0 \end{pmatrix}\begin{pmatrix} \partial_q H \\ \partial_p H \end{pmatrix}$$

with $H(t, q, p) = t^{n-1}\log(q^{n-1}/p) - kt^n q$. Because this is a non-autonomous system, with t appearing explicitly, the Hamiltonian H is *not* a constant of motion. However, (6) is invariant under the one-parameter group of scaling symmetries $r \to \mu r$, $f \to \mu^{-1} f$, so by introducing the new scale-invariant independent variable $y = ft$, and the dependent variables $v = v(y) = -\log t$, $w = \mathrm{d}v/\mathrm{d}y$, it reduces to a first-order equation for $w(y)$:

$$\frac{\mathrm{d}w}{\mathrm{d}y} = y(2n - ky)w^3 + (3n - 2ky)w^2 + ((n-1)/y - k)w.$$

Unfortunately, it is not possible to reduce this to a quadrature, since the action (7) is *not* invariant under scaling, unless $k = 0$ when the general solution to (6) is $f(t) = (At^n + B)^{1/n}$ (with A, B arbitrary constants).

Other important methods for ODEs include the Painlevé analysis of movable singularities (Kruskal & Clarkson, 1992), and asymptotic expansions around regular or irregular fixed singular points (Wasow, 1965; Tovbis, 1994).

ANDREW HONE

See also **Chaotic dynamics; Constants of motion and conservation laws; Euler–Lagrange equations; Extremum principles; Hamiltonian systems; Integrability; Painlevé analysis; Partial differential equations, nonlinear; Riccati equations**

Further Reading

Abreu, M. 1998. Kähler geometry of toric varieties and extremal metrics. *International Journal of Mathematics*, 9: 641–651

Arnol'd, V.I. 1989. *Mathematical Methods of Classical Mechanics*, 2nd edition, New York: Springer

Hille, E. 1976. *Ordinary Differential Equations in the Complex Domain*, New York: Wiley

Hinkkanen, A. & Laine, I. 1999. Solutions of the first and second Painlevé equations are meromorphic. *Journal d'Analyse Mathémathique*, 79: 345–377

Ince, E.L. 1926. *Ordinary Differential Equations*, London: Longmans Green; reprinted New York: Dover, 1956

Kruskal, M.D. & Clarkson, P.A. 1992. The Painlevé–Kowalevski and Poly–Painlevé tests for integrability. *Studies in Applied Mathematics*, 86: 87–165

Murray, J.D. 1989. *Mathematical Biology*, Berlin and New York: Springer

Olver, P.J. 1993. *Applications of Lie Groups to Differential Equations*, 2nd edition, Berlin and New York: Springer

Sachdev, P.L. 1991. *Nonlinear Ordinary Differential Equations and Their Applications*, New York: Marcel Dekker

Tovbis, A. 1994. Nonlinear ordinary differential equations resolvable with respect to an irregular singular point. *Journal of Differential Equations*, 109: 201–221

Wasow, W. 1965. *Asymptotic Expansions for Ordinary Differential Equations*, New York: Wiley

ORGANIZING CENTERS

See **Spiral waves**

OSCILLATOR, CLASSICAL NONLINEAR

See **Damped-driven anharmonic oscillator**

OVERTONES

When a tonal sound, such as a note played on a flute, a human vowel sound, or a bell, is analyzed in the frequency domain by applying a Fourier transform to the acoustic pressure waveform, the spectrum consists of a large number of sharp lines. The component of lowest frequency is termed the "fundamental", and the others are "upper partials" or "overtones." If the frequencies of the overtones are all exact integer multiples of the frequency of the fundamental, then they are termed "harmonics." The partial with frequency $f_n = nf_1$, where f_1 is the frequency of the fundamental, is the nth harmonic, so that the fundamental is the first harmonic.

A one-dimensional simple harmonic oscillator, or linear oscillator, in which the restoring force is proportional to displacement y from the equilibrium position, obeys the equation

$$m\frac{\mathrm{d}^2 y}{\mathrm{d}t^2} = -ky, \tag{1}$$

where m is the mass of the moving particle and k is the restoring force constant. A damping term can also be included, but this need not concern us here. Such an oscillator vibrates with a single frequency $f_1 = (1/2\pi)(k/m)^{1/2}$ that is independent of oscillation amplitude. It is useful to think of this oscillator in terms of its potential energy function, which is quadratic as shown in Figure 1(a). In real oscillators, the restoring force is not linear for large displacements, but nonlinear so that

$$m\frac{\mathrm{d}^2 y}{\mathrm{d}t^2} = -ky(1 + \alpha_1 y + \alpha_2 y^2 + \cdots), \tag{2}$$

where the α_n are constants. The energy curve then has a distorted parabolic form such as that shown as an example in Figure 1(b). In the absence of damping, the total energy must remain constant so that the magnitude of the velocity is a simple function of the displacement, and the motion repeats cyclically. This means that the spectrum of such a nonlinear oscillator consists of exact phase-locked harmonics of the fundamental frequency, though this fundamental frequency depends upon the amplitude of the motion. For a reason that is derived from molecular physics, as discussed below, such a nonlinear oscillator is often confusingly called an "anharmonic oscillator."

A thin taut string of length L ideally obeys an equation of the form

$$m\frac{\partial^2 y}{\partial t^2} = T\frac{\partial^2 y}{\partial x^2}, \tag{3}$$

where x measures length along the string, m is the mass per unit length, and T is the string tension.

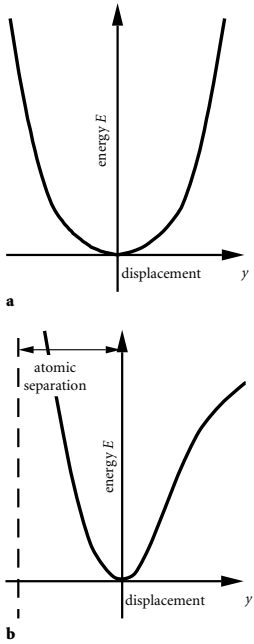

Figure 1. (a) Potential energy curve for a simple harmonic oscillator. (b) Potential energy curve for a typical nonlinear oscillator such as a diatomic molecule.

If its ends are rigidly fixed, then the mode frequencies are exact harmonics of the fundamental so that $f_n = (n/2L)(T/m)^{1/2}$. It is thus a multimode harmonic oscillator. The nonlinear frictional action of the bow on a violin reinforces the harmonicity of the modes and locks them into rigid phase relationship (Fletcher, 1999). Something very similar happens with wind instruments, which also have precisely harmonic spectra.

A thin stiff bar, on the other hand, obeys an equation of the form

$$m\frac{\partial^2 y}{\partial t^2} = K\frac{\partial^4 y}{\partial x^4}\,, \tag{4}$$

where K is the elastic stiffness. If the ends are free or rigidly clamped, then the mode frequencies are approximately $f_n \approx \frac{4}{9}(n+\frac{1}{2})^2 f_1$, and the overtones are very far from being harmonically related. Such an oscillator might be termed "inharmonic." The modes of a three-dimensional object such as a bell are even more complex (Fletcher & Rossing, 1998).

While sustained-tone musical instruments depend upon the nonlinearity of the active generator for their operation (bow, reed, or lip air-flow), the linear resonator (string or air column) determines the oscillation frequency, so that the pitch is nearly independent of loudness, and only the relative amplitudes of the harmonics change (Fletcher, 1999). Some Chinese opera gongs, however, make a virtue of nonlinearity so that, after an impulsive excitation, the pitch either rises or falls dramatically as the vibration dies away (Fletcher, 1985). The frequencies and relative intensities of upper partials determine the tone quality of a musical sound and have dictated the development of musical scales and harmonies (Sethares, 1998).

The human auditory system itself has some nonlinear aspects (Zwicker & Fastl, 1999), and, as in any forced nonlinear oscillator, these lead to the generation of harmonics ("harmonic distortion") and of multiple sum and difference tones ("intermodulation distortion"). In the ear these are chiefly apparent in the generation of the difference tone $|f_1 - f_2|$ when loud tones of frequencies f_1 and f_2 are heard simultaneously.

Optical absorption and emission spectra have many similarities to acoustic phenomena (Herzberg, 1950; Harmony, 1989). Diatomic molecules, for example, have interatomic potentials of the form shown in Figure 1(b) and thus constitute nonlinear oscillators. If the interatomic potentials were simply parabolic, as in Figure 1(a), then the quantum energy levels would have the form $E_n = (n+\frac{1}{2})h\nu$, where h is Planck's constant and ν is the classical vibration frequency labeled f_1 above. The wave functions describing the atomic vibration would then be either symmetric or antisymmetric, and the selection rule would dictate that n could change only by ± 1. There would thus be only a single absorption band consisting of the vibrational transition $0 \to 1$ surrounded by the allowed rotational transition lines.

For a more realistic model of the interatomic potential, as in Figure 1(b), the energy levels can be written as

$$E_n = (n+\tfrac{1}{2})h\nu[1 + \beta_1(n+\tfrac{1}{2}) + \beta_2(n+\tfrac{1}{2})^2 + \cdots]\,, \tag{5}$$

where β_n are usually called the "coefficients of anharmonicity" and β_1 is always negative in practice. The asymmetry of the potential also relaxes the selection rule so that in addition to the strong allowed absorption transition $0 \to 1$, there are much weaker transitions from $n = 0$ to higher levels. The absorption bands associated with these transitions have frequencies that are in approximate, but not exact, harmonic relationship to the fundamental, and are called "overtone bands."

Although the quantum treatment of a nonlinear oscillator may seem to conflict with the classical treatment, and the term *anharmonic* certainly suggests this, there is not really any disagreement. The infrared spectrum is derived from transitions between two levels of different energies, and therefore different classical amplitudes, and the classical frequency depends upon amplitude, as for the Chinese opera gong.

NEVILLE FLETCHER

See also **Damped-driven anharmonic oscillator; Harmonic generation; Molecular dynamics; Nonlinearity, definition of; Ordinary differential equations, nonlinear; Partial differential equations, nonlinear; Spectral analysis**

Further Reading

Fletcher, N.H. 1985. Nonlinear frequency shifts in quasi-spherical shells: pitch glide in Chinese gongs. *Journal of the Acoustical Society of America*, 78: 2069–2073

Fletcher, N.H. 1999. The nonlinear physics of musical instruments. *Reports on Progress in Physics*, 62: 721–764

Fletcher, N.H. & Rossing, T.D. 1998. *The Physics of Musical Instruments*, 2nd edition, New York: Springer

Harmony, M.D. 1989. Molecular spectroscopy and structure. *A Physicist's Desk Reference*, edited by H.L. Anderson, New York: American Institute of Physics, pp. 238–249

Herzberg, G. 1950. *Molecular Spectra and Molecular Structure*, 2nd edition, New York: Van Nostrand

Sethares, W.A. 1998. *Tuning, Timbre, Spectrum, Scale*, London and New York: Springer

Zwicker, E. & Fastl, H. 1999. *Psychoacoustics: Facts and Models*, 2nd edition, Berlin and New York: Springer

P

PAINLEVÉ ANALYSIS

Most problems of physics, chemistry, biology, engineering, and practically every applied science are nonlinear, in the sense that effects are not related to their causes by simple proportionality. Further, in most cases, these problems are described by differential equations, which provide the rules by which the main observables (such as displacements, velocities, fields, chemical concentrations, or populations) vary with respect to changes in the continuous independent variables (space and/or time). If the independent variables are discrete, the governing rules become difference equations.

Unfortunately, there is no general theory for integrating differential equations globally, that is, for finding their solutions analytically, over the full domain of the independent variables and for arbitrary initial and boundary data. That is why scientists often concentrate their analysis in regimes where the system behaves linearly, for example, small vibrations of lattices and solid structures, Fourier's law of heat conduction, Ohm's and Kirchhoff's laws in electrical circuits, and Laplace's and Maxwell's equations in electromagnetism.

However, even in such problems, the theory of linear differential equations often meets with serious difficulties, when the solutions possess singularities, that is, space and/or time values at which these solutions or their derivatives become infinite. In linear problems, these singularities appear explicitly in the equations, and if they are of special form, the general solution can still be found analytically near the singularity, for example, in terms of convergent series expansions. The theory of Lazarus Fuchs and Ferdinand Frobenius was especially developed for this purpose in the 1860s and led to the remarkable discovery of special functions, associated with such classic second-order ordinary differential equations (ODEs), as those of Bessel, Hermite, Legendre, or the hypergeometric equation.

By contrast, nonlinear ODEs possess singular points that are not evident by inspection of the equation itself. For example, the famous Riccati equation

$$\mathrm{d}x/\mathrm{d}t = a + bx + x^2 \tag{1}$$

(a, b constant parameters) known since the 1700s (*See* **Riccati equations**), has solutions which behave as

$$x(t) = \frac{1}{t-c} + a_0 + a_1(t-c) + a_2(t-c)^2 + \cdots, \tag{2}$$

where c is an arbitrary constant. Thus, this type of singularity, at $t = c$, is called movable, since its location depends on the choice of initial conditions. Furthermore, after the pioneering work of Augustin Cauchy in the 1830s showed the importance of complex variables, a new branch of mathematics developed in which ODEs are studied in the complex domain, with the independent variable taking values $t = t_{\mathrm{R}} + \mathrm{i}t_{\mathrm{I}}$, where $t_{\mathrm{R}}, t_{\mathrm{I}} \in \Re$ are, respectively, the real and imaginary parts of t and $\mathrm{i} = \sqrt{-1}$. As is well known, in this t-plane, the singularity at $t = c$ in (2) is called a pole and limits the convergence region of the Taylor expansion of the function $x(t)$ about any nearby point $t = t_0$ (where $x(t)$ is analytic), to $\mid t - t_0 \mid < \mid c - t_0 \mid$.

Still, when moving around a circle centered at the pole $t = c$ (and enclosing only this singularity), $x(t)$ always returns to the same values, implying that it is a single-valued function in that region. This is not what happens if $t = c$ is a branch point of $x(t)$ of the type

$$x(t) = (t-c)^{\alpha} + \cdots \quad \text{as } t \to c \tag{3}$$

with α not an integer. For example, if α is a rational number, $\alpha = p/q$, it takes q turns around $t = c$ for $x(t)$ to return to its starting value, demonstrating that it is a multi-valued function, describing a finitely sheeted Riemann surface, while $t = c$ is called an algebraic singularity. If, on the other hand, α in (3) is irrational or complex, $t = c$ is called a transcendental branch point and $x(t)$ describes an infinitely sheeted Riemann surface. Finally, if an expansion of $x(t)$ about $t = c$ contains logarithmic terms of the form $\log(t-c)$, it is again an infinitely multi-valued function and $t = c$ is called a logarithmic branch point.

Paul Painlevé, the great French mathematician and statesman (he was Prime Minister of France in 1917 and 1925), pursuing the idea that the problems with the

simplest singularities would be the easiest to solve, set out to determine which first-order ODEs of the form

$$dx/dt = f(t, x) \tag{4}$$

with f rational in x and analytic in t, are free from movable branch points; that is, their only movable singularities are poles. His remarkable discovery was that there is only one such equation: the Riccati equation (1), with the coefficients of 1, x, and x^2 being arbitrary analytic functions of t. Then, in a remarkable series of papers in the late 1890s and early 1900s, Painlevé and his coworkers (notably Bertrand Gambier) studied the same question on all second-order ODEs

$$d^2x/dt^2 = f(t, x, dx/dt) \tag{5}$$

with f rational in dx/dt, algebraic in x, and analytic in t. After painstaking analysis, they showed that there are 50 such equations, 44 of which can be explicitly integrated and solved in terms of known functions. For the remaining six equations (called Painlevé I–VI), such reduction was not possible, and new functions had to be introduced called the Painlevé transcendents. The first two of these equations are

$$\text{Painlevé I}: \quad d^2x/dt^2 = 6x^2 + t,$$

$$\text{Painlevé II}: \quad d^2x/dt^2 = 2x^3 + tx + a \tag{6}$$

with Painlevé III–VI being increasingly more complicated to write down. The interested reader will find them all discussed in the excellent books by Ince (1956) and Davis (1962), where Painlevé's approach to their discovery is also described.

It is important to recall, however, that independent of all this progress, the idea of using singularity analysis to solve systems of ODEs by requiring that their solutions have only poles was also used by the Russian mathematician Sophia Kovalevsky in 1888 to find one more solvable case of the rotating rigid body that bears her name (Kovalevsky's top). Still, the requirement that all solutions of a system of ODEs possess only poles as movable singularities in the complex t-plane has come to be referred to date as the Painlevé property.

Surprisingly enough, the Painlevé theory was not widely appreciated at first and remained largely unknown until it was revived, many decades later, in connection with exactly solvable partial differential equations (PDEs). More specifically, after the discovery that a number of PDEs are integrable by the inverse scattering transform (IST), Ablowitz and Segur observed in the mid-1970s that all ODE reductions of these PDEs had the Painlevé property and led, in fact, to some of the Painlevé I–VI equations, (6) (see Ablowitz & Segur, 1981, as well as Ablowitz & Clarkson, 1991).

Thus, the famous Ablowitz, Ramani, and Segur conjecture was formulated as follows: If a PDE is solvable by IST, all its ODE reductions obey the Painlevé property. Clearly, this conjecture provides a useful criterion to test the integrability of a given PDE by studying its ODE reductions—a much easier task than showing whether or not it is solvable by IST.

This discovery had enormous consequences, as it attracted the attention of many researchers working in the rapidly expanding field of nonlinear dynamics. The fact that most nonlinear dynamical systems of ODEs possess "irregular," "unpredictable," or chaotic solutions evidently suggests that they cannot be integrated and solved in terms of known functions, whose behavior is perfectly regular and predictable. It would thus be extremely interesting to find, in models of physical, chemical, or biological dynamics, integrable cases whose solutions would be clearly distinguished from those displaying chaotic behavior.

Such new, integrable systems could now be identified by means of the Painlevé property. Perhaps one of the most important applications occurred in Hamiltonian systems, like the famous Hénon–Heiles problem

$$H = \frac{1}{2}(\dot{x}^2 + \dot{y}^2 + Ax^2 + By^2) + x^2y + \frac{C}{3}y^3 \tag{7}$$

of two degrees of freedom (dots denote differentiation with respect to t). For $A = B = 1$ and $C = -1$, this problem had been extensively studied since the mid-1960s, as an example of a system whose chaotic regions grow dramatically as the total energy $H = E$ increases from 0 to $\frac{1}{6}$. Using the Painlevé analysis, it was first shown by Bountis et al. (1982) that (7) is completely integrable in exactly three cases:

(i) $C = 1$ and $A = B$ (known to be separable in the variables $s = x + y$, $d = x - y$).
(ii) $C = 6$ and any A and B.
(iii) $C = 16$ and $B = 16A$.

In each of the new cases (2) and (3), the second integral—besides Hamiltonian (7)—was also provided and their complete integrability in the sense of Liouville–Arnol'd was established.

Soon, many novel and highly nontrivial examples of Hamiltonian systems with N degrees of freedom were identified by requiring that their solutions possess the Painlevé property. Rigorous connections between integrability and the Painlevé property were also developed, mainly by Adler and van Moerbeke in the early 1980s, who used algebraic geometry to establish that if a Liouville–Arnol'd integrable Hamiltonian system has rational integrals which continue to describe tori in the complex domain, then its solutions have only movable poles (the converse, though not completely proved, is also believed to hold). A wealth of examples of integrable non-Hamiltonian systems were also discovered, related to models of physical, chemical, or biological interest. Finally, the Painlevé analysis was

extended and applied by Weiss, Tabor, and Carnevale to test integrability directly on a PDE, without reference to its ODE reductions (see Ramani et al., 1989).

But the importance of Painlevé analysis does not end here. After the early observation that any deviation from the Painlevé conditions generically introduces logarithmic terms, researchers began to look for connections between the violation of the Painlevé property and non-integrability, in the sense of non-existence of analytic, single-valued integrals such as (7). In that regard, the work of the Russian mathematicians V.V. Kozlov and S.L. Ziglin in the late 1970s turned out to be extremely important (see Kozlov, 1983). They showed, using Mel'nikov's theory, that one of the most fundamental causes of chaotic behavior, that is, the transverse intersection of stable and unstable manifolds of saddle fixed points on a Poincaré map, implies the presence of infinitely multi-valued solutions and non-existence of a second integral in a two-degree-of-freedom Hamiltonian systems.

Kozlov's and Ziglin's results inspired a series of interesting papers by H. Yoshida in the 1980s, where he used them to study the variational equations of simple periodic solutions in a large class of N-degree-of-freedom Hamiltonians. Yoshida was able to prove that when these variational equations do not satisfy certain conditions imposed by the existence of a full set of global single-valued integrals, such a set of constants cannot exist, thus demonstrating non-integrability for vast parameter ranges in many Hamiltonians of physical interest (see Ramani et al., 1989).

Finally, what about systems of ODEs (or PDEs) whose solutions possess only algebraic singularities, that is, points $t = c$, near which solutions have asymptotic expansions of the form

$$x(t) = (t-c)^{p/q} + \sum_{n=0}^{\infty} a_n (t-c)^{n/q} \tag{8}$$

without any other singularities present? In the 1980s, it was thought that this so-called weak Painlevé property, under some conditions on p/q, could also be related to complete integrability, in the Liouville–Arnol'd sense for N-degree-of-freedom Hamiltonian systems. In the 1990s, however, it was found that the situation is considerably more subtle.

First, it was shown by Goriely that many weak Painlevé examples could be transformed to systems having the usual Painlevé property after some rather general changes of coordinates (see Goriely, 2001). Then it was observed that there were weak Painlevé systems with chaotic solutions, which are evidently not integrable. Thus, the concept of globally finitely sheeted solutions (FSS) was introduced to distinguish integrable systems with algebraic singularities (8) from non-integrable ones, whose solutions are only locally finitely sheeted (see Bountis, 1992, 1995).

This is done as follows: every time a system of weak Painlevé ODEs, integrated numerically around arbitrarily large contours, showed evidence of "lattice" singularity patterns in the complex t-plane and FSS, it has been shown to be transformable to one that is completely integrable and possesses the usual Painlevé property. On the other hand, many such systems were also found which showed "dense" singularity patterns and evidence of globally infinitely sheeted solutions (ISS) for large enough contours. Although not solvable, such systems can still be integrable if they are hyperelliptically separable, that is, if they can be described by N holomorphic differentials on the Jacobian of a hyperelliptic curve of genus $g < N$ (see Abenda & Fedorov, 2000; Abenda et al., 2001).

Finally, in the 1990s, the connection between singularities and integrability was extended to discrete dynamical systems, described by difference equations. Here, since the methods of complex analysis for ODEs no longer apply, a novel criterion was introduced (see Grammaticos et al., 1991). It was based on the observation that if a difference equation such as

$$x_{n+1} = F(x_n, x_{n-1}), \quad n = 0, 1, 2 \ldots \tag{9}$$

with F rational, possesses an integral of the form

$$I(x_n, x_{n-1}) = \text{const.}, \quad n = 0, 1, 2 \ldots \tag{10}$$

yielding a family of curves in the x_n, x_{n+1} plane and precluding the presence of chaos, then x_n is infinite at some $n = m$ and becomes finite again at some later $n = m' > m$. This so-called singularity confinement criterion, whose success to date remains a mystery, has yielded a wealth of integrable discrete systems and has enabled many researchers to develop Painlevé difference equations, analogous to the famous Painlevé ODEs Painlevé I–VI (see Conte, 1999).

TASSOS BOUNTIS

See also **Hénon–Heiles system; Inverse scattering method or transform; Mel'nikov method; Riccati equations**

Further Reading

Abenda, S. & Fedorov, Y. 2000. On the weak Kowalevski–Painlevé property for hyperelliptically separable systems. *Acta Applicandae Mathematicae*, 60: 137

Abenda, S., Marinakis, V. & Bountis, T. 2001. On the connection between hyperelliptic separability and Painlevé integrability. *Journal of Physics* A, 34: 3521

Ablowitz, M.J. & Clarkson, P. 1991. *Solitons, Nonlinear Evolution Equations and Inverse Scattering*, Cambridge and New York: Cambridge University Press

Ablowitz, M.J. & Segur, H. 1981. *Solitons and the Inverse Scattering Transform*, Philadelphia: SIAM

Adler, M. & van Moerbeke, P. 1988. *Algebraically Completely Integrable Systems*, Boston: Academic Press,

Bountis, T. 1992. What can complex time tell us about real time dynamics? *International Journal of Bifurcation and Chaos*, 2(2): 217

Bountis, T. 1995. Investigating non-integrability and chaos in complex time. *Physica* D, 86 (1995): 256
Bountis, T., Segur H. & Vivaldi, F. 1982. Integrable Hamiltonian systems and the Painlevé property. *Physical Review* A, 25: 1257
Conte, R. (editor). 1999. *The Painlevé Property: One Century Later*, New York: Springer
Davis, H.T. 1962. *Introduction to Nonlinear Differential and Integral Equations*, London: Dover
Goriely, A. 2001. *Integrability and Non-integrability of Dynamical Systems*, Singapore: World Scientific
Grammaticos, B., Ramani, A. & Papageorgiou, V. 1991. Do integrable mappings have the Painlevé property? *Physical Review Letters*, 67(14): 1825–1828
Ince, E.L. 1956. *Ordinary Differential Equations*, London: Dover
Kozlov, V.V. 1983. Integrability and non-integrability in Hamiltonian mechanics. *Russian Mathematical Surveys* (Mathematical Review C) 38: 1
Ramani, A., Grammaticos, B. & Bountis, T. 1989. The Painlevé property and singularity analysis of integrable and non-integrable systems. *Physics Reports*, 180 (3): 160.
Tabor, M. 1989. *Chaos and Integrability in Nonlinear Dynamics*, New York: Wiley Interscience

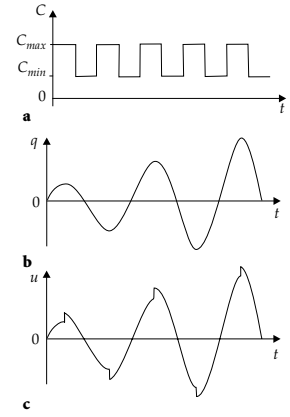

Figure 1. Periodic variations of capacitance C of capacitor (a), capacitor charge q (b), and voltage u (c) at parametric resonance.

PARAMETRIC AMPLIFICATION

Parametric generation and amplification of oscillations are based on the phenomenon of parametric resonance, using the work done by an external force under periodic variation of the parameters of an oscillatory system.

A simple mechanical system in which parametric resonance may occur is a pendulum, with the length of the cord (l) changing with time. If l is decreased when the pendulum is in the lower position and increased in its upper position, the average work done by an external force over one period is positive and oscillations of the pendulum build up. This phenomenon is the underlying principle of setting a swing into motion. When one stands on a swing, it is easier to rock it by squatting at the top position of the swing and standing up at the bottom position, thus shifting the center of mass of the person on the swing twice in one period.

An electric analog of a pendulum of variable length is an oscillatory circuit of variable capacitance. The capacitance C can be changed, for example, by mechanically moving the capacitor plates together or apart. For the amplitude of oscillations to build up, energy should be fed to the circuit by performing work against the electrostatic field forces of the capacitor. This means that the plates should be moved apart when the charge q on the capacitor is maximal and moved together when the charge on the capacitor returns to zero (Figure 1).

Such a periodic change in capacitance (pumping-up process) results in growing energy of the oscillations and appearance of instability in the system. The build-up of energy occurs at a pump frequency satisfying the relation

$$\omega_{\mathrm{p}} = 2\omega_0/n, \qquad (1)$$

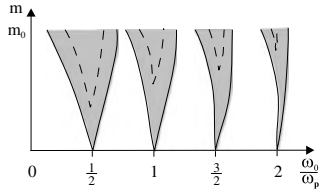

Figure 2. Mathieu instability zones within which parametric resonance may occur (solid line—without damping; dashed line—with damping; ω_0 natural frequency of the oscillatory circuit; ω_{p} pump frequency.

where n is an integer, ω_0 is the natural frequency of circuit oscillations, and ω_{p} is the pump frequency. Build-up is most effective for $n = 1$, that is, when the period of capacitance variation is half the period of natural oscillations of the circuit. Interestingly, energy build-up (parametric resonance) is possible not only for the values of ω_{p} satisfying Equation (1) but also at some deviations from these values within Mathieu instability zones (see Figure 2). The greater the width of Mathieu zones, the greater the extent of parameter variation $m = (C_{\max} - C_{\min}) / (C_{\max} + C_{\min})$.

In oscillatory systems with several degrees of freedom (e.g., in a system with two coupled circuits, coupled pendulums, and so on), normal modes with different natural frequencies ω_1 and ω_2 may exist. As parameters of such a system change, oscillations may build up (parametric resonance) not only at a frequency satisfying condition (1) for an arbitrary natural frequency, but also for their linear combination, for instance, when a parameter changes with sum

frequency

$$\omega_p = \omega_1 + \omega_2. \tag{2}$$

Resonance coupling is also possible at $\omega_p = \omega_1 - \omega_2$. In this case, however, no build-up of oscillations occurs. Instead, energy is periodically pumped between the modes ω_1 and ω_2. For such an oscillatory system, the pump power P_p input to the system at frequency ω_p and the powers P_1 and P_2 consumed at frequencies ω_1 and ω_2 are proportional to the corresponding frequencies (the Manley–Rowe relation):

$$\frac{P_p}{\omega_p} = \frac{P_1}{\omega_1} = \frac{P_2}{\omega_2}. \tag{3}$$

Parametric resonance may also provide conditions for excitation of normal modes in oscillatory media possessing an infinite number of degrees of freedom. In 1831, Michael Faraday had observed that standing waves are excited at frequency $\omega_{p/2}$ in the liquid in a vessel vibrating in the vertical direction at frequency ω_p. The classic experiment staged by Franz Melde in 1859 revealed excitation of transverse oscillations (standing waves) in a string, one end of which was fastened to the prong of a tuning fork. When the tuning fork vibrates and the string is tight, the string performs transverse oscillations with a frequency equal to half the frequency of the tuning fork.

A distinguishing feature of parametric resonance in systems with distributed parameters is that the build up of oscillations depends strongly on the relationship between the variation in space of the system parameters and the spatial structure of the forcing oscillations (waves). For example, if the pump that changes the parameters of the medium is a traveling wave with frequency ω_p and wave vector $\boldsymbol{k}_p$, then natural waves with frequencies ω_1 and ω_2 and wave vectors $\boldsymbol{k}_1$ and $\boldsymbol{k}_2$ are excited, provided the conditions of parametric resonance are fulfilled both in space and time; thus

$$\omega_p = \omega_1 + \omega_2, \quad \boldsymbol{k}_p = \boldsymbol{k}_1 + \boldsymbol{k}_2. \tag{4}$$

The potentialities of using parametric resonance for creating a parametric generator and amplifier were studied by Leonid I. Mandelshtam and Nikolai D. Papaleksi (1931–1933). They constructed capacitive and inductive parametric machines that transformed mechanical energy into electrical energy as a result of variation of the magnitudes of capacitance and inductance during shaft rotation. Parametric generators and amplifiers found practical application in the 1950s when semiconductor parametric diodes appeared, the capacitance of which depends on applied voltage, and when variable capacitors using the properties of ferroelectrics and variable inductors using the properties of ferrites and superconductors were developed. Low-noise variable capacitance parametric amplifiers based on high-frequency parametric diodes (varactors) are used in high-frequency receiving microwave devices employed in radar and radio astronomy, among other applications. Parametric generators are capable of generating oscillations whose phase can take one of two values differing by π. This feature of parametric generators was noted by Eiichi Goto who proposed in 1954 to use such generators, which he referred to as "parametrons," as logic switching elements in computers. Parametric generators are widely employed in optics as tunable coherent generators.

Note finally that parametric action on a nonlinear oscillatory system (for example, a nonlinear pendulum with variable-length cord or a nonlinear circuit with periodically varying capacitance and inductance) may also lead to dynamic oscillations.

VLADIMIR SHALFEEV

See also **Diodes; Dynamical systems; Harmonic generation; Manley–Rowe relations; Nonlinear toys**

Further Reading

Leven, R.W. & Koch, B.P. 1981. Chaotic behavior of a parametrically excited damped pendulum. *Physics Letters*, 86(2): 71–74

Rabinovich, M.I. & Trubetskov, D.I. 1989. *Oscillations and Waves in Linear and Nonlinear Systems*, Dordrecht and Boston: Kluver

Scott, A. 1970. *Active and Nonlinear Wave Propagation in Electronics*, New York: Wiley

PARAMETRIC DECAY INSTABILITY

See **Nonlinear plasma waves**

PARTIAL DIFFERENTIAL EQUATIONS, NONLINEAR

A partial differential equation (PDE) is a functional equation of the form

$$F\left(x_1, x_2, \ldots, x_n, z_1, \ldots, z_m, \frac{\partial z_\mu}{\partial x_\nu}, \ldots, \frac{\partial^2 z_\mu}{\partial x_1^2}, \frac{\partial^2 z_\mu}{\partial x_1 \partial x_2}, \ldots\right) = 0 \tag{1}$$

with m unknown functions $z_1, z_2, \ldots, z_m$ with n independent variables $x_1, x_2, \ldots, x_n$ ($n > 1$) and at least one of the partial derivatives of z_μ ($\mu = 1, 2, \ldots, m$) with respect to x_ν ($\nu = 1, 2, \ldots, n$). In general, there can be a system of coupled PDEs.

For a single equation, the order of the PDE is p if the highest derivative has order p, with an analogous definition for a system of equations. A PDE becomes an ordinary differential equation if the number of independent variables n is one. It is linear if the equation is linear with respect to z and its partial derivatives, meaning it is of the first degree in the unknown function as well as its derivatives. It is called quasilinear if

it is linear with respect to the highest-order partial derivatives which have coefficients that depend only on lower-order partial derivatives and the independent variables. In addition, a PDE is called semilinear if the coefficients of the highest-order derivatives depend on the independent variables only. A PDE is called nonlinear if it does not fit into any of the above categories.

Initial value problems (IVPs) for evolution equations arise where one of the independent variables x_i of Equation (1) represents time t and an initial condition at time $t = 0$ is given. Additionally, there are boundary value problems (BVPs), when spatial variables are involved and boundary conditions are specified along the n-dimensional boundary of the domain (where n is the number of independent spatial variables). There can also be mixed initial value-boundary value problems (IVBVPs), where both types of conditions are given.

For a single PDE, the number of initial conditions is generally one less than the highest temporal derivative, while the number of spatial boundary conditions is half the order of the highest spatial derivatives in the equation. For general nonlinear equations, there are no precise definitions.

Second-order semilinear PDEs have the general form

$$a\frac{\partial^2 z}{\partial x_1^2} + 2b\frac{\partial z}{\partial x_1 \partial x_2} + c\frac{\partial^2 z}{\partial x_2^2} + \text{l.o.t.} = 0,$$

where a, b, c are given functions of x_1 and x_2 or constants and l.o.t. stands for lower order terms. The coefficient matrix A of the corresponding second-order system has the determinant

$$\det A = \begin{vmatrix} a & b \\ b & c \end{vmatrix}. \tag{2}$$

A second-order semilinear PDE is said to be of elliptic type if $\det A \ (= ac - b^2) > 0$, of hyperbolic type if $\det A < 0$, and of parabolic type if $\det A = 0$ for all points x_1, x_2 of the domain D. The determinant of A is positive if both eigenvalues of the matrix A are positive or both negative. The determinant is negative if the eigenvalues are of opposite sign and zero if one of them is zero. The normal forms of the associated differential operators L are given by

$$\det A > 0: \qquad \frac{\partial^2}{\partial x_1^2} + \frac{\partial^2}{\partial x_2^2} \quad \text{(elliptic)},$$

$$\det A < 0: \qquad \frac{\partial^2}{\partial x_1^2} - \frac{\partial^2}{\partial x_2^2} \quad \text{(hyperbolic)},$$

and

$$\det A = 0: \qquad \frac{\partial^2}{\partial x_1^2} \quad \text{(parabolic)}.$$

Boundary value conditions may be "Dirichlet" (where the value of the solution is given along the boundary ∂D of the domain D), "Neumann" (where the normal derivative $\partial z / \partial n$ is specified along the boundary ∂D), and "Robin" (where both the value and the normal derivative of the solution $\partial z / \partial n + az$ satisfy an equation along the boundary of the domain ∂D).

The archetypical example for an elliptic PDE is the Laplace equation

$$\frac{\partial^2 z}{\partial x^2} + \frac{\partial^2 z}{\partial y^2} = 0;$$

for a hyperbolic PDE, it is the wave equation

$$\frac{\partial^2 z}{\partial t^2} - c^2\frac{\partial^2 z}{\partial x^2} = 0;$$

and for a parabolic PDE, it is the diffusion equation

$$\frac{\partial z}{\partial t} - \nu\frac{\partial^2 z}{\partial x^2} = 0.$$

The coefficient matrix A (2) can depend on first-order derivatives if the PDE is second-order quasilinear and the classes are analogous. Quasilinear and strictly linear second-order PDEs are classified according to these three classes. For a given nonlinear PDE of higher order or more than two variables, it is not useful to classify according to these three classes, instead, one classifies it according to the physical process it describes. In general, boundary value problems are often associated with elliptic equations and initial value problems with hyperbolic and parabolic equations.

Nonlinear PDEs describe many important processes in nature because often an approximate linear PDE is not sufficient to describe the process. Examples are the dynamics of fluids, gases, and elastic media; the equations from general relativity and quantum electrodynamics; and population dynamics in biology and chemistry.

The two main characteristics of such processes are the nonlinear interactions, due to the nonlinearities of the PDE and the possibility of self-organization into coherent structures.

There are three types of processes that one can distinguish. Reversible processes such as waves; irreversible; processes such as reaction, diffusion and heat flow; and stationary processes. A process is irreversible/reversible if it is impossible/possible to reverse the process in time and stationary processes are independent of time. In general, reversible processes are described by hyperbolic equations, irreversible processes by parabolic equations, and stationary processes by elliptic equations.

Most physical systems comprise a combination of all three types of processes, but often, some processes are dominant and by using a scaling argument, it is possible to neglect less dominant processes and

simplify the PDE to the degree that it describes the process adequately but is still easy to work with.

The nature of irreversible processes such as diffusion, is that they tend to smooth the solution in time, whereas for reversible processes singularities can develop, for example, shock waves in gas dynamics. For stationary processes, the solutions depend on the smoothness of the boundary conditions and external forces.

Solutions to nonlinear PDEs are often obtainable only by numerical integration. In integrable cases, on the other hand, analytic solutions can be found using advanced techniques such as the inverse scattering method, the associated Lax theory, and the Bäcklund transformation. There are other techniques that are helpful although not exact, such as Floquet and Mel'nikov theory.

In general, for nonlinear PDEs common tools such as the linear superposition principle are not valid anymore, although it is sometimes possible to find a nonlinear superposition principle. Methods such as the Fourier and Laplace transforms and Green's function, in general, are not applicable to nonlinear PDEs. Alternatively, one can attempt classical solution methods such as the separation of variables or transformation of variables to reduce the nonlinear PDE to a system of equations that is solvable analytically.

ANDREAS A. AIGNER

See also **Burgers equation; Korteweg–de Vries equation; Nonlinear Schrödinger equations; Separation of variables; Sine-Gordon equation**

Further Reading

Courant, R. & Hilbert, D. 1966. *Methods of Mathematical Physics II*, New York: Wiley

Debnath, L. 1997. *Nonlinear Partial Differential Equations*, Basel: Birkhäuser

Garabedian, P. 1964. *Partial Differential Equations*, New York: Wiley

Ockendon, J., Howison, S., Lacey, A. & Movchan, A. 1999. *Applied Partial Differential Equations*, Oxford and New York: Oxford University Press

PARTICLE ACCELERATORS

Particle accelerators have been used for much of the 20th century to investigate the properties of matter. The first accelerators of charged particles used steady (d.c.) electric fields, such as those obtained from a Van de Graaff generator. These devices could accelerate particles to above an energy of a million electron volts (MeV), which was sufficient to probe atomic nuclei. Applications needing higher energies continually emerged, leading to new types of devices, particularly ones having the charged particles move in a circular orbit. In that configuration, with the additional concept that electric fields and particles can be synchronized, such that on each crossing of a gap, particles encounter a field that is accelerating, the basic accelerator configuration was created. Such devices went through a series of developments from a fixed frequency cyclotron to a frequency modulated cyclotron and finally the synchrotron. In the first two devices, the equilibrium orbit spirals out as the energy increases, while in the last device, the orbit is held fixed, and the bending magnetic field is increased.

To keep the particles on a prescribed essentially circular orbit over many traversals of the device, the orbit must be stable to transverse perturbations. Furthermore, to achieve continuous acceleration, the particle motion must be stable about the equilibrium accelerating phase of the electric field. Because the particles are kept close to an equilibrium orbit, the transverse stability can be analyzed from linear stability analysis, using a first-order expansion of the fields about the equilibrium. When the gradients of the magnetic guide field are chosen to give stable oscillations around the equilibrium orbit, they are called betatron oscillations, after the betatron, an early circular induction accelerator for which the oscillations were first analyzed (Kerst & Serber, 1941). For particles traveling in a straight line, the forces resulting from magnetic gradients cannot focus in both transverse directions simultaneously. This is not true for circular orbits, as the gradient in the centrifugal force supplies an extra focusing force to allow focusing in both directions. The resulting homogenous linear equations of motion for the simplest, assumed azimuthally symmetric, device are

$$\frac{\mathrm{d}^2 z}{\mathrm{d}\theta^2} + nz = 0 \tag{1}$$

and

$$\frac{\mathrm{d}^2 x}{\mathrm{d}\theta^2} + (1-n)x = 0, \tag{2}$$

where z is the vertical position and x the horizontal deviation from the equilibrium orbit r_0, and θ is the azimuthal angle around the machine. Here, n is the field index

$$n = -\frac{r_0}{B_0}\frac{\partial B_z}{\partial r} \tag{3}$$

with B_0 the equilibrium magnetic field. From (1) and (2) the stability condition is $0 < n < 1$. The azimuthally symmetric focusing of this type is now called weak focusing because the limitations on stability make the relative frequencies or tunes $\nu_z \equiv \omega_z / \omega_0 = n^{1/2}$ and $\nu_x \equiv \omega_x / \omega_0 = (1-n)^{1/2}$ both less than 1. The weak restoring forces required large vacuum chambers, limiting the size and field strength of the devices and therefore the energy to which particles could be accelerated.

The breakthrough in developing a synchrotron in which particles could be closely contained around their

equilibrium orbit was the understanding that much stronger focusing could be achieved by alternating a section which strongly focused vertically while defocusing radially with a section that defocused vertically and focused radially. The net result, from simple lens theory, is that the pair can be strongly focusing. This led to the invention of the alternate gradient (AG) synchrotron (Courant et al., 1952). The simplest analysis of the linearized equations of motion is of the Hill equation

$$\frac{\mathrm{d}^2 y}{\mathrm{d}\theta^2} + K(\theta) y = 0 \tag{4}$$

with $K(\theta + \theta_L) = K(\theta)$, where θ_L is the repeating angular period. The transformation for a period can be analyzed for stability from Floquet theory by setting

$$y(\theta + \theta_L) = y(\theta) \mathrm{e}^{\pm \mathrm{i}\sigma} \tag{5}$$

and solving the transfer matrix, over the repeating period θ_L, for stability. This was done in the original paper, for a simple transfer matrix, leading to a stability diagram. However, even the early AG synchrotrons were more complicated, with bending magnets, focusing quadruple magnets, and straight sections in which resonators supplied the acceleration fields. For various reasons, described in part below, modern machines with very large radii, operating at many billions of electron volts (BeV or GeV), are much more complicated, leading to stability calculations with a very large number of elements.

However, even at the simplest level, calculating the linear stability of orbits is not sufficient. Nonlinear terms, although small, can have very important consequences. The motions given by (1) and (2), or more generally by (4), in each of the transverse directions are independent. The nonlinear terms couple the transverse dimensions and lead to a wide variety of resonances that can degrade the beam cross section. These difference resonances of various strengths must be avoided when finding a proper operating point in the $\nu_x - \nu_z$ parameter space. Additionally, magnet imperfections lead to entirely new classes of resonances. The effect of the increasing energy, coupled with the space charge of the beam of ions or electrons, leads to a movement of the operating point through the parameter space, such that all resonances cannot be avoided.

In addition to the primarily linear transverse oscillations, there are fundamentally nonlinear oscillations associated with the accelerating fields, called synchronous oscillations. For circular devices, these oscillations couple longitudinal and transverse motions. The frequencies of these electric-field-driven oscillations are generally much lower than the transverse betatron oscillations so that it is usually sufficient to consider their radial motion as adiabatic when studying the free oscillations, that is, using averaging methods. Depending on how relativistic the particles are, the phase motion may be either primarily longitudinal or radial. To simplify the treatment, we consider the synchronous motion in a linear accelerator such that transverse motions are unimportant to lowest order. The fields in both linear accelerators and synchrotrons are generated by high-power electromagnetic sources which operate in structures, for example, loaded waveguides in linear accelerators and resonant cavities in synchrotrons, that have a primary traveling-wave field synchronous with the particles. Nonsynchronous harmonic fields also exist, but are usually not important.

The equations of motion along the axis of a linear accelerator are the force equation

$$\frac{\mathrm{d}p}{\mathrm{d}t} = eE \sin\phi \tag{6}$$

and the equation for the change in phase

$$\frac{\mathrm{d}\phi}{\mathrm{d}t} = \omega \left(1 - \frac{v}{v_0}\right), \tag{7}$$

where v_0 is the wave velocity, ω the r.f. frequency, and E the applied field. The phase stable particle has $v = v_0$, and for stable acceleration, v_0 must be determined from (6), where p and v are relativistically related. The motion of particles around the stable phase is given by trajectories in the $p - \phi$ phase plane with the stable fixed point at $\phi = \phi_\mathrm{s}$, satisfying $\mathrm{d}\phi / \mathrm{d}t = 0$, and an unstable fixed point on a separatrix orbit satisfying, $\phi_\mathrm{u} = -\phi_\mathrm{s}$. The phase diagram indicates that particles injected between ϕ_u and some limiting ϕ on the separatrix trajectory with velocity v_0 oscillate nonlinearly about ϕ_s, while those outside the phase interval are not stably captured. For a general account of the basic ideas as described above, and also the many types of accelerators and variants on the concepts, the reader is referred to basic accelerator texts. Two such texts, which include many useful original references are Livingood (1961) and Kolomensky & Lebedev (1966). The early dates of publication indicate the maturity of this field.

As AG synchrotrons increased in size and energy, it became increasingly important to match the emittance phase space of the incoming particles to the acceptance phase space of the accelerator. This was to ensure the highest beam brightness, particularly as the long acceleration cycle led to low duty ratios. Phase space matching techniques were developed and exploited at the CERN high-energy physics center (Hereward et al., 1956). The transverse acceptance of a simplified AG synchrotron is illustrated in Figure 1.

The need for higher beam brightness led to the invention of the fixed field alternating gradient (FFAG) synchrotron which injected a number of pulses whose phase spaces were spatially separated by the energy increase. This phase space beam-stacking in the FFAG synchrotron further enhanced the usefulness of employing phase space matching concepts (Symon &

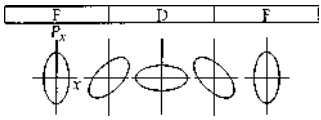

Figure 1. Phase-space transformations in an AG synchrotron.

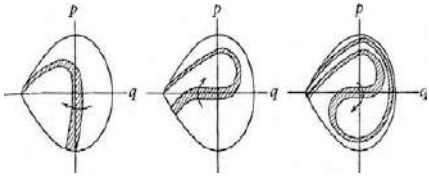

Figure 2. Filamentation of phase space due to nonlinear oscillations.

Sessler, 1956). Phase space matching was also used to increase the efficiency of linear accelerators, and of microwave devices (*See* **Electron beam microwave devices**). The effect of a mismatch of emittance and acceptance is illustrated in Figure 2 in which a beam with small momentum spread (cross-hatched region) is injected into the acceptance phase space of a synchronous oscillation in a linear accelerator or synchrotron, leading to an increase of the effective phase space area by filamentation (Lichtenberg, 1969).

The development of storage rings greatly increased the importance of keeping the phase space of the injected particles to a minimum. Conceived as a device to obtain high beam brightness, it rapidly became essential for operation of proton accelerators at energies many times the proton rest energy for which the energy in the center of mass of collisions with stationary matter was greatly reduced due to momentum conservation. This led to intersecting storage rings of particles traveling in opposite directions and a very severe requirement of high beam brightness (O'Neil, 1956). Storage rings, which store particles over many machine transits, have required the control of beam spreading. In electron storage rings, the synchrotron radiation which set a limit to electron energy is also effective in reducing the beam phase space (Robinson, 1958). For protons, which are little affected by radiation, stochastic cooling was invented to perform a similar function, a requirement that is essential for proton–antiproton colliders (Van der Meer, 1972).

The development of higher energy accelerators and higher intensity beams has led to new methods of analysis and various problems to be solved. The largest AG synchrotrons include many correcting magnets as well as the bending magnets, quadrupoles, and straight sections. Orbit calculations have required symplectic integrators to minimize numerical errors, which have involved the development of a Lie algebraic method (Dragt et al., 1988). Various resonances, coupled with machine errors, have led to exploration of resistive and Arnol'd diffusion explanations for beam spreading. Intense beams in electron linear accelerators have produced a pulse-shortening phenomenon that was analyzed as a nonlinear excitation of an electromagnetic mode in the accelerating structure, and methods of suppressing it were devised (Chao, 1993). Space-charge effects that become negligible at highly relativistic energies are again introduced by the beam-beam interaction in intersecting storage ring beams. Analysis of this subtle phenomenon within the environment of the very complicated beam dynamics has led to new exploration of simple mapping models (*See* **Fermi acceleration and Fermi map**), together with the use of averaging methods to smooth out various more rapid phenomena that do not play an essential role. In linear devices, to go beyond the 30 GeV two-mile long accelerator at SLAC (Stanford), which is field-strength limited, new ideas of structureless acceleration of ions in the wakefields produced by electron beams in plasmas and of electron acceleration, using the wakefield of an intense laser in a plasma, are being actively explored (see Esarey et al. (1996) and other articles in the same issue). The great challenges that face accelerator design above 300 GeV and intersecting beam interactions in storage rings keep a sense of excitement in a mature field. Much of the modern research and new ideas can be reviewed, with references, in Chao & Tigner (1999).

At the same time that the interaction energy has been increased to probe deeper into the fundamental properties of matter, new uses have been found for low-energy accelerators. On the atomic scale, materials are being probed with ultraviolet light and X-rays, using the natural radiation of electrons in circular devices or enhanced radiation employing undulators in combination with accelerators as advanced light sources. These latter devices typically have short period spatially oscillating magnetic fields with the accompanying electron oscillations relativistically doppler shifted to high frequencies (*See* **Electron beam microwave devices**). At still lower energies, accelerators are being used in various medical applications. Some of the technology-oriented work is treated by Scharf (1989).

ALLAN J. LICHTENBERG

See also **Arnol'd diffusion; Averaging methods; Electron beam microwave devices; Fermi acceleration and Fermi map; Hamiltonian systems**

Further Reading

Chao, A. 1993. *Physics of Collective Beam Instabilities in High Energy Accelerators*, New York: Wiley

Chao, A.W. & Tigner, M. (editors). 1999. *Handbook of Accelerator Physics and Engineering*, Singapore: World Scientific

Courant, E.D., Livingston, M.S. & Snyder, H.S. 1952. The strong-focusing synchrotron—a new high energy accelerator. *Physical Review*, 88: 1190–1196

Dragt, A.J., Neri, F. & Rangaranjan, G. 1988. Lie algebraic treatment of linear and nonlinear beam dynamics. *Annual Review of Nuclear and Particle Science*, 38: 455–496

Esarey, E., Sprangle, P., Krall, J. & Ting, A. 1996. Overview of plasma-based accelerator concepts. *IEEE Transactions on Plasma Science*, 24: 252–288

Hereward, H.G., Johnson, K. & Lapostolle, P. 1956. Problems of injection. *CERN Symposium*, 179–191

Kerst, D.W. & Serber, R. 1941. Electronic orbits in the induction accelerator. *Physical Review*, 60: 53–58

Kolomensky, A.A. & Lebedev, A.N. 1966. *Theory of Cyclic Accelerators*, Amsterdam: North-Holland

Lichtenberg, A.J. 1969. *Phase Space Dynamics of Particles*, New York: Wiley

Livingood, J.J. 1961. *Principles of Cyclic Particle Accelerators*, Princeton: Van Nostrand

O'Neil, G.K. 1956. Storage ring synchrotron: device for high energy physics research. *Physical Review*, 102: 1418–1419

Robinson, K.W. 1958. Radiation effects in circular electron accelerators. *Physical Review*, 111: 373–380

Scharf, W. 1989. *Particle Accelerator Applications in Technology and Research*, Taunton, England: Research Studies Press Ltd.

Symon, K.R. & Sessler, A.M. 1956. Methods of radiofrequency acceleration in fixed field accelerators with applications. *CERN Symposium*, 44–58

Van der Meer, S. 1972. Stochastic damping, of betatron oscillations in the ISR. *CERN Report ISR–PO*, pp. 72–81

PARTICLES AND ANTIPARTICLES

For a good understanding of the physical concept of *antiparticle* and the closely related concept of *charge*, it is important to appreciate how these notions emerged. Therefore, we begin with a brief sketch of the associated history.

In the early days of quantum mechanics, the material world was thought to be built from three elementary particles, namely, the electron, the proton, and the neutron. The idea that there might be associated particles with the same mass and opposite charge (now called antiparticles) first arose from the characteristics of the one-particle Dirac equation. Writing it in Hamiltonian form, the resulting Dirac Hamiltonian has spectrum $(-\infty, -m] \cup [m, \infty)$, where m is the particle mass. The negative part of the spectrum was already considered unphysical by Paul Dirac himself: no such negative energies had been observed, and their presence would give rise, for example, to instability of the electron.

This physical inadequacy of the "first-quantized" description quickly led to the introduction of "second quantization," as expressed in quantum field theory. In the quantum field theoretic version of the Dirac theory, the problem of unphysical negative energies is cured by a prescription that goes back to Dirac's hole theory.

Specifically, Dirac postulated that all of the negative energy states of his equation are filled by a sea of unobservable particles. In his picture, annihilating such a negative energy particle with a given charge yields a hole in the sea, which should manifest itself as a new type of positive energy particle with the same mass, but opposite charge. This intuitive idea led Dirac to the prediction that a charged particle should have an oppositely charged partner (its antiparticle).

Ever since, this prediction has been confirmed by experiment, not only for all electrically charged particles, such as the electron and proton, but also for most of the electrically neutral particles, such as the neutron. In the latter case, one still speaks of the particle having a charge, whereas the remaining electrically neutral particles are identical to their antiparticles.

As already mentioned, in the second-quantized Dirac theory no negative energies occur. In the Dirac quantum field, the creation/annihilation operators of negative energy states are replaced by annihilation/creation operators of positive energy holes. This hole theory substitution therefore leads to a physical arena with an arbitrary number of particles and antiparticles with the same positive mass, now called Fock space. (A mathematically precise account can be found in the monograph by Thaller, 1992.)

As it soon turned out, the number of particles and antiparticles in a high-energy collision is not conserved, a phenomenon that can be naturally accommodated in the Fock spaces associated with interacting relativistic quantum field theories. The quantum field theory model that is the most comprehensive description of real-world elementary particle phenomena arose in the early 1970s. During the last few decades, this so-called Standard Model has been abundantly confirmed by experiment.

In spite of these successes, the problem of obtaining nonperturbative insights into the Standard Model remains daunting. This is an important reason why its classical version and various related, but far simpler, classical nonlinear field theories have been, and still are, widely studied. It is a striking and relatively recent finding that within this classical framework, there exist localized, smooth, finite-energy solutions with characteristics that are very reminiscent of particles. The most conspicuous examples in this respect are the soliton field theories, where there exist such particle-like solutions for any given particle number and where the particle numbers and their velocities are preserved in a scattering process.

To be sure, the latter soliton equations arose independently of particle physics. They involve a lower space-time dimension (mostly two), and they have applications in a great many areas that are far removed from high-energy physics. (An early survey that is still one of the best and most comprehensive can be found in Scott et al., 1973.)

Returning briefly to the latter area, there are also various equations, typically within a gauge-theoretic context, where particle-like solutions (instantons, monopoles, vortices, and so on) have been found. A closely related field is classical gravity, where various previously known solutions (such as the Schwarzschild and Kerr black holes) came to be viewed as particle-like solutions, an interpretation strengthened by the occurrence of "many-particle" generalizations.

It should be pointed out that within this nonlinear classical context, there are no explicit many-particle solutions where "creation" and "annihilation" occur. Indeed, it is not even clear how this would manifest itself on the classical level (as compared with the quantum level, where this is a clear-cut matter).

Focusing once again on the notions of charge and particles vs. antiparticles, it is an even more striking fact that these concepts are naturally present within some of the above-mentioned nonlinear field theory models with particle-like solutions. A prime example for gauge theories is given by instanton solutions, which are accompanied by anti-instanton solutions. Roughly speaking, these are distinguished by opposite generalized winding numbers, viewed as charges of a topological nature. More precisely, these localized solutions minimize the energy in certain homotopy classes. This means they are stable under small perturbations.

Turning to soliton field theories, it should be mentioned at the outset that for most soliton equations (for instance, for their most well-known representative, the KdV equation), there exists only one type of soliton, hence no notion of charge. The sine-Gordon field theory is a paradigm for theories where more than one type of soliton occurs. We proceed by using it to exemplify the notions of particle, antiparticle, and charge at the classical level.

The sine-Gordon equation

$$\phi_{xx} - \phi_{tt} = \sin\phi \tag{1}$$

can be obtained as the Euler–Lagrange equation associated with the Lagrangian

$$\mathcal{L} = \tfrac{1}{2}(\phi_t^2 - \phi_x^2) - (1 - \cos\phi). \tag{2}$$

The corresponding energy functional reads

$$E = \int_R \left[\frac{1}{2}(\phi_t^2 + \phi_x^2) + (1 - \cos\phi)\right] \mathrm{d}x. \tag{3}$$

Obviously, the constant solutions

$$\phi_k = 2\pi k, \quad k \in Z, \tag{4}$$

yield $E = 0$. These are the so-called vacuum solutions.

There exist, however, two distinct classes of nonconstant, time-independent, finite-energy solutions, namely,

$$\phi_\pm = 4\arctan(\exp(\pm(x - x_0))), \quad x_0 \in R. \tag{5}$$

They connect the two vacuum solutions ϕ_0 and ϕ_1 for $x \to \pm\infty$. The functions $\exp(\mathrm{i}\phi_\pm(x)) : R \to S^1$ have winding numbers ± 1 and may be viewed as generators of the homotopy group $\pi_1(S^1) = Z$. They are interpreted as one-particle and one-antiparticle solutions (soliton and antisoliton) of the sine-Gordon equation, having charges ± 1. (By Lorentz invariance, they can be boosted to constant velocity v, with $|v|$ smaller than the speed of light, which is 1 for the units chosen in (1).)

The analogy with electrical charge is strengthened by the existence of soliton–antisoliton bound states, the so-called breathers. More generally, there exist solutions with N_+ solitons, N_- antisolitons, and N_0 breathers, where N_+, N_-, N_0 are arbitrary integers. These particle numbers and the velocities are conserved in the collision, the nonlinear interaction showing up only in factorized position shifts.

From the viewpoint of elementary particle physics, these findings are regarded as stepping stones for a better understanding of the associated quantum field theory. In particular, the existence of particle-like solutions stabilized by charges of a topological nature is believed to signal the existence of a corresponding stable quantum particle. A lucid survey in which this scenario is expounded is Coleman (1977).

Returning to the sine-Gordon example (also discussed in Coleman, 1977), the above scenario has not only been confirmed, but considerably enlarged: at the quantum level, the sine-Gordon theory yields a model of interacting solitons and antisolitons, whose scattering preserves particle numbers and other characteristics (such as the set of velocities), yielding an explicitly known factorized S-matrix. Thus, the classical picture is essentially preserved under quantization (cf. the review by Zamolodchikov & Zamolodchikov (1979)). It should be stressed that this absence of particle creation and annihilation is highly nongeneric for relativistic quantum field theories; it occurs for only completely integrable soliton type field theories in two space-time dimensions.

The phenomenon of oppositely charged particles and antiparticles with an attractive interaction between them has also come up in a setting quite different from the above field-theoretic one. Consider the classical Hamiltonian

$$H_N = \frac{1}{2}\sum_{j=1}^{N} p_j^2 + g^2 \sum_{1 \le j < k \le N} 1/\sinh^2(x_j - x_k) \tag{6}$$

on the phase space

$$\Omega = \{(x, p) \in R^{2N} \mid x_N < \cdots < x_1\}. \tag{7}$$

By contrast to the above partial differential equations, most of which are wave equations at face value, the Hamiltonian equations resulting from (6) have, from the outset, a point particle interpretation. To be specific,

they describe N nonrelativistic particles on the line with a repulsive pair interaction.

The special character of this Hamiltonian is already manifest from the scattering to which it leads: the particle velocities are conserved and the position shifts are factorized, just as for solitons. Indeed, Hamiltonian (6) is one version of the completely integrable nonrelativistic Calogero–Moser models. (These are surveyed at the classical and quantum levels in Olshanetsky & Perelomov (1981) and Olshanetsky & Perelomov (1983), respectively.) As pointed out first by Calogero, the substitution $x_k \to x_k + i\pi$, $k = 1, \ldots, N_-$, $N_- \in \{1, \ldots, N-1\}$ has the effect of turning the repulsive $1/\sinh^2$ interaction between particles $1, \ldots, N_-$ and particles $N_- + 1, \ldots, N$ into an attractive $-1/\cosh^2$ interaction. Thus, one obtains an integrable system that can be viewed as describing N_- antiparticles and $N_+ = N - N_-$ particles in interaction.

The nonrelativistic Calogero–Moser systems have been generalized to a relativistic setting, both on the classical and on the quantum levels. Again, there are versions describing particles and antiparticles, with repulsion between like charges and attraction between opposite charges. These versions have been studied at the classical level in Ruijsenaars (1994), where the intimate connection to the sine-Gordon solutions with arbitrary numbers of solitons, antisolitons, and breathers is also detailed. More generally, Ruijsenaars (2001) is a recent survey of this relation between the solitons and antisolitons of the sine-Gordon field theory and the point particles and antiparticles of certain relativistic Calogero–Moser systems, covering both classical and quantum aspects.

SIMON RUIJSENAARS

See also **Higgs boson; Instantons; Quantum field theory; Skyrmions; Solitons, types of; Yang–Mills theory**

Further Reading

Coleman, S. 1977. Classical lumps and their quantum descendants. In *New Phenomena in Subnuclear Physics, Proceedings Erice 1975*, edited by A. Zichichi, New York: Plenum, pp. 297–421

Olshanetsky, M.A. & Perelomov, A.M. 1981. Classical integrable systems related to Lie algebras. *Physics Reports*, 71: 313–400

Olshanetsky, M.A. & Perelomov, A.M. 1983. Quantum integrable systems related to Lie algebras. *Physics Reports*, 94: 313–404

Ruijsenaars, S.N.M. 1994. Action-angle maps and scattering theory for some finite-dimensional integrable systems. II. Solitons, antisolitons, and their bound states. *Publications RIMS Kyoto University*, 30: 865–1008

Ruijsenaars, S.N.M. 2001. Sine-Gordon solitons vs. relativistic Calogero-Moser particles. In *Integrable Structures of Exactly Solvable Two-dimensional Models of Quantum Field Theory*, edited by S. Pakuliak & G. von Gehlen Delft: Kluwer, pp. 273–292

Scott, A.C., Chu, F.Y.F. & McLaughlin, D.W. 1973. The soliton: a new concept in applied science. *Proceedings of the IEEE*, 61: 1443–1483

Thaller, B. 1992. *The Dirac Equation*, Berlin: Springer

Zamolodchikov, A.B. & Zamolodchikov, Al.B. 1979. Factorized S-matrices in two dimensions as the exact solutions of certain relativistic quantum field theory models. *Annals of Physics (NY)*, 120: 253–291

PATTERN FORMATION

Beautiful patterns and complex structures spontaneously emerge in a large variety of natural systems. Examples can be found on all length scales, ranging in size from Jupiter's red spot, to water waves, a zebra's stripes, mussel shell patterns, snowflake structures, and down to the nanoscale patterning of the scaffolding that gives stability to individual cells.

How do patterns form? The basic laws of physics should account for all forces driving pattern formation, but even with knowledge of all equations governing the pattern-forming process, it remains difficult to compute what patterns will emerge. A closer look at how the snowflake pattern develops illustrates the key challenges:

(i) *Patterns form under nonequilibrium conditions.* In order for an initial seed crystal to form, the air generally has to reach temperatures below the dew and freezing point. Once the seed crystal forms, surrounding air is filled with excess water not in thermodynamic equilibrium. Therefore, the crystal grows under non-equilibrium conditions, which means that the shape of the whole crystal may not obey equilibrium thermodynamics principles such as minimization of free energy. Instead of a spherical shape with minimal surface free energy, complex snowflake shapes emerge. This observation is quite general: patterns form while systems are driven out of equilibrium.

(ii) *Patterns can emerge from the competition of processes on various length and/or timescales.* What physical processes govern the pattern-formation process? In the snowflake example, the crystal grows so fast that heat and impurities, rejected from the growing crystal, build up ahead of the crystal-gas interface. They interfere with the growth of the initial spherical crystal and lead to the development of many fine fins. The length scale of the fins is determined by a competition between diffusion, which would lead to many fine fins (for which the diffusion distance becomes shortest) and surface tension, which inhibits very curved interfaces. In general, a variety of physical processes can drive pattern formation including diffusion, chemical reactions, and fluid flow. Patterns emerge from the competition

of processes on different length scales and timescales.

(iii) *Patterns are history-dependent.* As a non-equilibrium process, pattern formation is usually history dependent and sensitive to the initial conditions, thus it is difficult to predict patterns accurately. Small differences in temperature or water concentration in the atmosphere are amplified in snowflakes, so each snowflake looks distinct, reflecting the atmospheric conditions along the path it traveled. The theory of pattern formation provides insights into how pattern-forming systems can be analyzed and what one may learn about the underlying physical processes from observations of patterns.

General features of the pattern on the other hand, are often related to underlying symmetries in the system and can be predicted. For example, snowflakes often have six spikes, reflecting the symmetry of the anisotropy in the surface tension of ice.

However, each pattern-forming system may be driven by a unique combination of forces: similarities in the patterns may thus only reflect similar symmetries of the underlying equations, timescales, or length scales, not similarities in the underlying physics.

Driven by new mathematical tools, digital imaging, and powerful image analysis tools, numerous experimental and theoretical investigations of pattern-forming systems have been carried out over the past two decades. Cross & Hohenberg (1993) provide an excellent technical introduction into the mathematical concepts of pattern formation. Ball (1999) introduces the field of pattern formation in a non-mathematical way suitable for a broad audience. An update on the field can be found in Gollub & Langer (1999). Below, we briefly describe the basic principles and mathematical tools.

Model Systems of Pattern Formation

Pattern formation implies a change in symmetry. Spontaneous symmetry breaking is particularly evident in fluids, which are structureless in equilibrium but exhibit a surprising variety of patterns under non-equilibrium conditions. Fluid systems have yielded two model systems for detailed studies of pattern formation: surface waves and convection rolls.

Surface waves develop due to either wind or gravitational forces or, for example, when a stone is thrown into the fluid. Under vertical shaking, fluids can exhibit very ordered patterns, such as hexagonal structures as shown in Figure 1. Michael Faraday was the first to analyze ordered surface wave patterns more than a century ago (Faraday, 1831).

Spontaneous symmetry breaking into a patterned state can also be observed when a fluid is driven out of equilibrium through a thermal gradient. If a fluid is heated from below and cooled from above, the fluid near the bottom expands and rises to the top, while fluid near the top cools, contracts, and due to the increased density, drops back to the bottom. This leads to large-scale convection rolls, the so-called Rayleigh–Bénard convection, where streams of rising and falling fluid arrange into complex patterns, similar to the patterns found in surface waves shown in Figure 1.

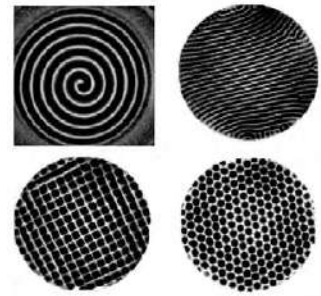

Figure 1. Surface wave patterns in a vertically vibrated fluid. Spirals, stripes, squares, and hexagonal patterns are characteristic of surface waves ("fluid" consists of 170 micron bronze spheres, a few layers deep. Courtesy of D. Goldman, P. Umbanhowar, B. Lewis, and H. Swinney, UT Austin).

While diffusion alone tends to create uniform states, Alan Turing suggested that diffusion coupled with chemical reactions may lead to spatial patterns in chemical composition. He speculated that such mechanisms would be sufficient to explain natural patterns such as zebra stripes or the regular shape and arrangement of leaves. An early experimental realization was the Belousov–Zhabotinsky reaction, which involves several intermediate chemical compounds. The original experiments were carried out in a well-stirred container and generated temporal patterns in which the concentration of intermediate components oscillated. Later experiments showed spatial patterns such as stripes and spirals.

Granular systems such as sand or coffee powder also spontaneously form patterns. Under vertical vibration, they form patterns resembling surface waves (see Figure 1). In addition, localized, stationary waves (so-called oscillons) are observed near the onset of surface waves (Umbanhowar et al., 1996). Unlike localized waves in fluids, oscillons do not spread out or dissipate over time. Mixtures of granular matter are also prone to pattern-forming instabilities. For example, when sand and sugar are mixed in a container and poured into a pile, the mixture spontaneously separates into bands under some conditions. Unlike the fleeting structure of surface waves or convection rolls in fluids, patterns in

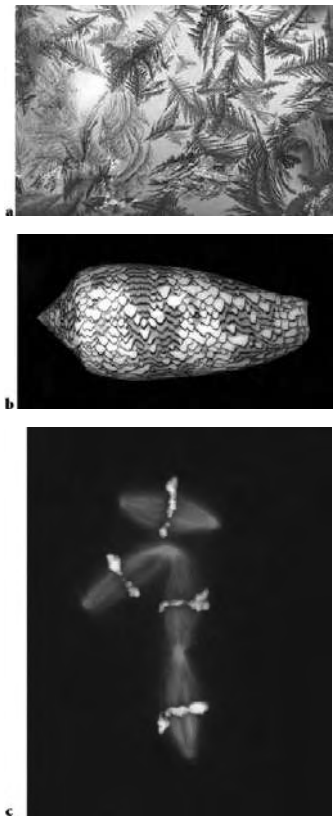

Figure 2. Pattern formation in nature on many scales: (a) Crystal growth pattern (rime on a windshield). (b) Mussel shell pattern (Conus textile, Courtesy of P. Egerton) (c) Scaffolding of a cell during cell division (Spindle assembly in *Xenopus* extracts. Microtubules (long) and DNA (rings), Courtesy of R. Ohi and T. Mitchison, Harvard Medical School, Boston).

granular flows can create lasting impressions such as bands of sugar and sand in a mixture, or sand ripples and sand dunes in wind-driven flows.

In solids, snowflakes are a well-known pattern (see Figure 2a) which we have discussed above. Similar patterns can be found in alloys and polymer blends, though they are hidden within the material micro- or nanostructure. Patterns in solids are technologically important, because they can determine material strength and flexibility.

Biological systems offer a rich variety of patterns. On large scales, patterns such as zebra stripes and mussel shell patterns (Gierer & Meinhard, 1972) (see Figure 2b) help animals blend in or send signals of intimidation or attraction. On a small scale, the microscopic mechanical structure within cells contains ordered arrangements of microtubules and other filaments, which assist, for example, in cell division (see Figure 2c).

Stability and Bifurcations

The first prerequisite for the emergence of patterns from a spatially uniform state is a symmetry-breaking instability. A linear stability analysis indicates whether a given set of equations is prone to a symmetry-breaking instability. For example, we start with a set of functions $\boldsymbol{u}(t)$:

$$\frac{\mathrm{d}\boldsymbol{u}}{\mathrm{d}t} = f(\boldsymbol{u}). \tag{1}$$

To assess the stability of a state $\boldsymbol{u}_0$, we linearize around that state $\boldsymbol{u} = \boldsymbol{u}_0 + \boldsymbol{\delta}$. This yields an equation for the perturbation $\boldsymbol{\delta}$:

$$\frac{\mathrm{d}\boldsymbol{\delta}}{\mathrm{d}t} = \left.\frac{\mathrm{d}f(\boldsymbol{u})}{\mathrm{d}u}\right|_{\boldsymbol{u}_0} \boldsymbol{\delta}. \tag{2}$$

The state $\boldsymbol{u}_0$ is linearly stable against perturbations if $\boldsymbol{\delta}$ shrinks for any shape of the initial perturbation and unstable if it grows. To test for all possible perturbations, $\boldsymbol{\delta}$ can be decomposed into Fourier modes $\delta = \delta_{\boldsymbol{q}} \exp(\mathrm{i}\boldsymbol{q}x)$. This indicates the range of wave numbers ($\boldsymbol{q}$) that are unstable.

Generally, pattern-forming systems become unstable when they are driven further from equilibrium. The transition point toward instability is called marginal stability. In the marginally stable state, perturbations of one, or a few, wave numbers neither grow nor decay; all other perturbations decay.

When parameters are changed further, the system will become unstable for a range of wave numbers (sometimes including $\boldsymbol{q} = 0$). In the example of crystal growth, a planar crystal growth front is stable for small $\boldsymbol{q}$ (due to diffusion) and for large $\boldsymbol{q}$ (due to surface tension), but unstable for a range of intermediate $\boldsymbol{q}$.

Once the perturbations grow, the linear approximation fails since δ will diverge, and other approaches are needed to predict patterns, but the range of unstable wave number is often a rough indicator of the characteristic length scales of the final patterns.

Model Equations

Beyond linear instability, modeling of pattern-forming systems becomes interesting: rather than going back to the full equations for the pattern-forming system, which are often too complex to be simply studied numerically or analytically, model partial differential equations have been developed to describe the main qualitative features

of patterns, and to highlight the universal features of many pattern-forming systems. They are discussed in great detail, for example, in the excellent review by Cross & Hohenberg (1993). Here we list the main equations.

The (complex) Ginzburg–Landau equation is an amplitude equation with an expansion in amplitudes and gradient terms. The equation applied, for example, to a two-dimensional plane can yield similar patterns as the vibrated fluid shown in Figure 1: squares, hexagons, and stripes. The equation provides insight into which gradient or higher-order terms must dominate in specific patterns. Long wavelength instabilities such as the Eckhaus instability are common and limit the range of stable patterns to a smaller range of wave numbers than the range of linearly stable wave numbers.

Other equations include the Swift–Hohenberg equation and the Kuramoto–Sivashinsky equation, which have been solved in various geometries and for different boundary conditions and parameter ranges. They provide a rich set of patterns and dynamical instabilities.

Experimentally and in simulations, the best model system has proven to be surface waves and Rayleigh–Bénard convection. The stability phase diagram of the convecting fluid—the range of stable wave numbers as a function of a measure of fluid convection such as the Rayleigh number—exhibits a region of stability, the so-called Busse balloon, bounded by various instabilities such as the Eckhaus instability, a zig-zag instability, or a cross roll instability. The range of stable patterns and the instability boundaries have been verified through extensive experiments.

Slightly different are equations that describe patterns in excitable media, which are often used to mimic biological processes. Reaction-diffusion equations yield wave fronts or spiral waves. Again, basic symmetries of the underlying processes dictate what patterns can occur, and the stability boundaries are crucial.

Finally, it should be noted that real patterns have boundaries and defects, which can strongly affect pattern selection and stability. Modeling defects and boundaries appropriately can be difficult, since it may only introduce small perturbations that change the system over long timescales (which are often beyond the reach of simulations). Recently, controlled experiments where defects are implanted deliberately into patterns have begun to allow quantitative tests of theories, but this work is only beginning.

Challenges for the future include application of these insights to real pattern forming systems, for example, to suppress or exploit crystal growth instabilities in the semiconductor industry. General theoretical descriptions of pattern formation in networks such as neural networks remains one of the open challenges.

WOLFGANG LOSERT

See also **Belousov–Zhabotinsky reaction; Dune formation; Emergence; Growth patterns; Kuramoto–Sivashinsky equation; Morphogenesis, biological; Rayleigh–Taylor instability; Reaction-diffusion systems; Turing patterns**

Further Reading

Ball, P. 1999. *The Self-made Tapestry: Pattern Formation in Nature*, Oxford and New York: Oxford University Press

Cross, M.C. & Hohenberg, P.C. 1993. Pattern formation out of equilibrium. *Reviews of Modern Physics*, 65: 851–1112

Faraday, M. 1831. On a peculiar class of acoustical figures; and on certain forms assumed by groups of particles upon vibrating elastic surfaces. *Philosophical Transactions of the Royal Society of London*, 52: 299–340

Gierer, A. & Meinhard, H. 1972. A theory of biological pattern formation. *Kybernetik*, 12: 30–39

Gollub, J.P. & Langer, J.S. 1999. Pattern formation in nonequilibrium physics. *Reviews of Modern Physics*, 71: S396–S403.

Turing, A. 1952. The chemical basis of morphogenesis. *Philosophical Transactions of the Royal Society of London B*, 237: 37–72

Umbanhowar, P.B., Melo, F. & Swinney, H.L. 1996. Localized excitations in a vertically vibrated granular layer. *Nature*, 382: 793–796

PATTERN SELECTION

See **Synergetics**

PEIERLS BARRIER

As a localized entity such as an electron, hole, polaron, soliton, or dislocation moves through a discrete lattice, it often experiences a potential barrier between one unit cell and the next. Called a Peierls barrier after the famed German/British physicist Rudolph Peierls, such potential barriers plays a key role in lattice dynamics.

More precisely, a Peierls barrier characterizes the dependence of the energy, $E(\bar{n})$, of a stationary localized entity (LE) on its position, $\bar{n}$, in a periodic lattice. The Peierls barrier, is the function $E(\bar{n}) - E_0$, where $E_0 = \min E(\bar{n})$ is the ground state energy of the LE. Because of lattice periodicity the barrier must be a periodic function with a period equal to the lattice constant a. Minima of the Peierls barrier correspond to stable positions and maxima to unstable positions. The barrier height $\Delta E = \max[E(\bar{n}) - E_0]$ is often called the pinning energy. To propagate along the chain, the LE must be activated with energy exceeding ΔE. For smaller energies, the LE vibrates near minima of the Peierls barrier, and for larger energies it can overcome the Peierls barrier and move through the lattice. The presence of a Peierls barrier also leads to the appearance of new eigenvalues corresponding to periodic oscillations of an LE near a minimum of the Peierls barrier.

The notion of the Peierls barrier goes back to the first quantitative explanation of the mechanism of plastic flow via the motion of dislocations in a lattice (Peierls, 1940; Naborro, 1967). From the perspective of the continuum theory of elasticity, a dislocation is an LE that involves a discontinuity in the displacement field, leading to singularities in strains and stresses. Peierls and Naborro showed how to overcome these artifacts of continuum idealizations by distributing the sharp discontinuity over a finite region, as in the one-dimensional nonlinear continuum Frenkel–Kontorova model of dislocation.

The dynamic influence of a Peierls barrier is greatest when the size of the LE is about equal to the lattice periodicity. Failure to include it in theoretical formulations can lead to erroneous calculations. When modeling the dynamics of protonic solitons in chains of hydrogen bonds, for example, inclusion of the Peierls barrier is necessary to find the temperature dependence of soliton mobility (Savin & Zolotaryuk, 1991).

Let us consider in more detail an autolocalized state of a quantum particle in a lattice (or molecular chain). In a simplified model, the dynamics of such a quasiparticle is described by the system of equations

$$\mathrm{i}\hbar\dot{\phi}_n = \chi u_n \phi_n - J(\phi_{n-1} + \phi_{n+1}), \tag{1}$$

$$m\ddot{u}_n = -K u_n - \chi |\phi_n|^2, \tag{2}$$

where $-\infty < n < +\infty$ is an integer, $\{\phi_n\}$ is a complex-valued wave function normalized by the condition

$$\sum_n |\phi_n|^2 = 1\,, \tag{3}$$

where u_n is the intramolecular displacement of the lattice, and χ, J, m, and K are parameters of the exciton–phonon interaction: energy of resonance or exchange interaction between neighboring lattice sites, reduced mass of the molecules, and stiffness of intermolecular interaction. Neglecting the inertia of intramolecular displacements implies that $u_n = -\chi|\phi_n|^2 / K$, whereupon Equations (1) and (2) reduce to a discrete nonlinear Schrödinger equation (DNLS), which can be written as

$$-\mathrm{i}\frac{\mathrm{d}\phi_n}{\mathrm{d}\tau} = \phi_{n-1} + \phi_{n+1} + g\phi_n|\phi_n|^2, \tag{4}$$

where $\tau = Jt / \hbar$ and $g = \chi^2 / KJ$ is a dimensionless parameter of nonlinearity.

In the continuum limit, Equation (4) reduces to the nonlinear Schrödinger (NLS) equation, which is integrable. In this limit, the Peierls barrier does not play any role because an envelope soliton can propagate freely along the chain. For the discrete model, which is not integrable, the situation is quite different.

A stationary autolocalized state of the quasiparticle can be found numerically by minimizing

$$H = -\sum_n \varphi_n\varphi_{n+1} + \tfrac{1}{4}g\varphi_n^4,$$

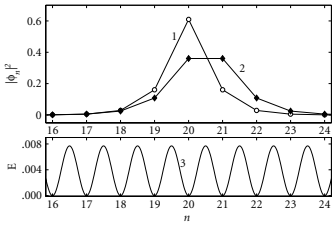

Figure 1. Stationary autolocalized state of the quantum quasiparticle with integer (curve 1) and half-integer (curve 2) centers of symmetry. Curve 3 (below) shows the Peierls barrier, i.e., the dependence of the energy of the stationary state E on the position of the center n. Nonlinear parameter $g = 3$.

subject to the constraint of Equation (3), where φ_n is the real-valued amplitude of quasiparticle wave function on nth site. If $\{\varphi_n\}_{n=-\infty}^{+\infty}$ is the solution of the minimization problem, the energy and position of the LE are $E = H$ and

$$\bar{n} = \sum_n n\varphi_n^2.$$

respectively.

Stationary states of quasiparticle have two types of symmetry. First is a solution with integer center of symmetry $\varphi_{n_0+n} \equiv \varphi_{n_0-n}$. In other words, the center of the LE is in one of the lattice sites. Second is a solution with half-integer center of symmetry, where the center of excitation is midway between two lattice sites ($\varphi_{n_0+n} \equiv \varphi_{n_0+1-n}$, $\bar{n} = n_0 + \frac{1}{2}$). The ground state is of the first type and corresponds to a minimum of the Peierls barrier. The second type is unstable and corresponds to a maximum of the Peierls barrier.

Numerical solution of the minimization problem allows one to find the energy profile of a Peierls barrier, as plotted in Figure 1. This profile has a sine-like character with minima at integer points and maxima in half-integer points. The height of the Peierls barrier depends on the value of nonlinear parameter g. If the nonlinearity parameter $g \to 0$, the size of the LE grows without bound, and the pinning energy ΔE goes monotonically to zero. One can calculate Peierls barriers analytically using the method of variational functions (Kuprievich, 1985).

Note that a specific discretization of the continuum NLS equation (Ablowitz & Ladik, 1976) leads to a discrete integrable system. In this case, the ground state energy does not depend on the position of the LE and the Peierls barrier is absent.

LEONID MANEVITCH AND ALEXANDER SAVIN

See also **Bjerrum defects; Discrete nonlinear Schrödinger equations; Dislocations in crystals; Frenkel–Kontorova model; Polarons**

Further Reading

Ablowitz, M.J. & Ladik, J.F. 1976. A nonlinear difference scheme and inverse scattering. *Studies in Applied Mathenatics*, 55(3): 213–229; Nonlinear differential-difference equations and Fourier analysis. *Journal of Mathematical Physics*, 17(6): 1011–1018

Kuprievich, V.A. 1985. Variational study of stationary autolocalized states of molecular chains in discrete model. *Theoretica Materialia Fizika (Soviet Theoretical and Mathematical Physics)*, 64(2): 269–276

Naborro, F.R.N. 1967. *Theory of Crystal Dislocations*, Oxford: Clarendon Press

Peierls, R.E. 1940. *Proceedings of the Physical Society of London*, 52: 34

Savin, A.V. & Zolotaryuk, A.V. 1991. Dynamics of ionic defects and lattice solitons in a thermalized hydrogen-bonded chain. *Physical Review* A, 44: 8167–8183

PENDULUM

With a history covering many centuries, the pendulum has been of primary importance in the development of physics. It is well known that in the 17th century, Dutch experimental physicist Christiaan Huygens discovered the synchronization phenomenon while studying pendulum clocks (Huygens, 1673). Using a pendulum as an example, Huygens formulated the conservation law for mechanical energy. In the 18th century, the French scientist Jean Charles Borda suggested using a pendulum for measuring the acceleration of gravity (Borda, 1792), and Wilhelm Bessel used a pendulum for an accurate verification of the equality of inertial and gravitational masses. There are many other applications of pendula for physical measurements; for example, a pendulum with a randomly vibrated suspension axis has turned out to be a good model for control of turbulence in subsonic submerged jets (Landa, 1996).

Two models of a pendulum are well known—mathematical and physical. The mathematical pendulum is defined as a ball suspended by a weightless thread in vacuum (Figure 1a). It is described by the equation

$$\ddot{\varphi} + \omega_0^2 \sin\varphi = 0, \tag{1}$$

where φ is the pendulum angle of deviation, $\omega_0 = \sqrt{g/l}$ is the angular frequency of small oscillations, g is the acceleration due to gravity, l is the thread length, and dots indicate derivative with respect to time. The physical pendulum can be defined as a body moving about a fixed horizontal axis O (Figure 1b).

Taking account of air friction, the motion equation for such a body is

$$I\ddot{\varphi} + h\dot{\varphi} + mga\sin\varphi = 0, \tag{2}$$

where I is the body's moment of inertia, h is the friction factor, m is the body's mass, and a is the distance between the axis and the body's center of gravity.

Equation (1) belongs to the class of nonlinear conservative (Hamiltonian) systems, whereas Equation (2) is a dissipative system. Solutions of these equations

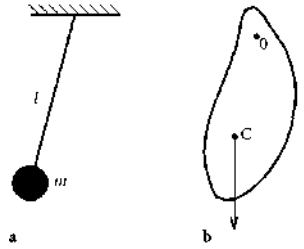

Figure 1. Schematic image of (a) mathematical pendulum and (b) physical pendulum.

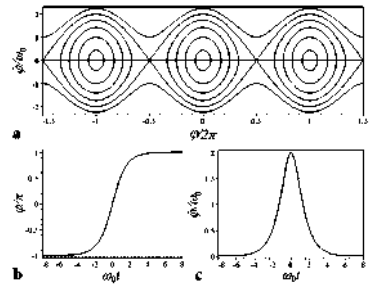

Figure 2. (a) Phase portrait of pendulum oscillations in the phase plane; (b,c) the time dependencies of the pendulum phase coordinates φ and $\dot{\varphi}$ at the motion of a representative point along a separatrix.

can be conveniently analyzed with the phase plane φ, $\dot{\varphi}$. We illustrate this for Equation (1).

Using the energy conservation law, we obtain an equation for a trajectory in the phase plane φ, $\dot{\varphi}$ in the form

$$\frac{ml^2\dot{\varphi}^2}{2} + mgl(1 - \cos\varphi) = E, \tag{3}$$

where E is the total pendulum energy. For $E < 2mgl$, Equation (3) describes closed trajectories corresponding to pendulum oscillations about the stable equilibrium position ($\varphi = 0$), and for $E > 2mgl$, nonclosed trajectories corresponding to the rotation of the pendulum (Figure 2a). These two kinds of trajectories are separated by peculiar trajectories passing through singular saddle points ($\dot{\varphi} = 0$, $\varphi = \pm\pi, \pm 3\pi, \ldots$). Such trajectories are said to be *separatrices*. Because values of φ differing from each other by 2π are physically indistinguishable, the phase plane shown in Figure 2a can be rolled into a cylinder.

In general, solutions of Equations (1) and (3) are Jacobi elliptic functions, but more simple solutions can be obtained in the case of small oscillations ($E \ll mgl$) and in the case when $E = 2mgl$ (this value of E

corresponds to the motion of a representative point along a separatrix). In the latter case, Equation (3) is split into two equations:

$$\dot{\varphi}_{\pm}(t) = \pm 2\omega_0 \cos\frac{\varphi}{2}. \tag{4}$$

By integrating (4) we find

$$\varphi_{\pm}(t) = \pm\left(4 \arctan\, \mathrm{e}^{\omega_0 t} - \pi\right). \tag{5}$$

The time dependencies of $\varphi = \varphi_+$ and $\dot{\varphi} / \omega_0 = \dot{\varphi}_+ / \omega_0$ are shown in Figure 2b and c. These solutions play an important part in soliton theory.

In the case of sufficiently small oscillations, when $\sin\varphi \approx \varphi - \varphi^3 / 6$, Equation (1) reduces to the Duffing equation

$$\ddot{\varphi} + \omega_0^2\left(1 - \frac{\varphi^2}{6}\right)\varphi = 0. \tag{6}$$

The general solution of Equation (6) is

$$\varphi = A\,\mathrm{sn}(\Omega t, k), \tag{7}$$

where sn is a Jacobi elliptic function of modulus $k = \sqrt{1 / 12}\, A / \Omega$, and $\Omega = \omega_0\sqrt{1 - A^2 / 12}$. Solution (7) is valid for $A \leq \sqrt{6}$, when $k \leq 1$. This constraint is certainly fulfilled because Equation (6) follows from (1) only for $A < 1$. Solution (7) describes periodic oscillations of period $4\mathrm{K}(k) / \Omega$, where $\mathrm{K}(k)$ is the full elliptic integral of the first kind. It follows from this that the period of oscillations increases with increasing amplitude. Such a property inherent in nonlinear systems is called anisochronism. It should be noted that Galileo was the first to discover the isochronism of small pendulum oscillations.

If a pendulum consisting of an iron ball suspended by a thread of length l is placed between the opposite poles of a magnet, its behavior essentially changes (Landa, 1996, 2001). Approximating the magnetic force acting on the ball by $F(\varphi) = ml(a_1\varphi - b_1\varphi^3)$ and restricting ourselves to small oscillations of the ball, then the pendulum angular deviation φ obeys the following approximate equation:

$$\ddot{\varphi} - (a - b\varphi^2)\varphi = 0, \tag{8}$$

where $a = a_1 - \omega_0^2$, $b = b_1 - \omega_0^2 / 6$, $\omega_0^2 = g / l$. In the case that $a_1 > \omega_0^2$ $(a > 0)$, the equilibrium position $x = 0$ becomes aperiodically unstable (the corresponding singular point $\varphi = 0$, $\dot{\varphi} = 0$ in the phase plane φ, $\dot{\varphi}$ becomes of saddle type). If, in addition to this, the inequality $b_1 > \omega_0^2 / 6$ holds, two stable equilibrium positions with coordinates $\varphi_{1,2} = \pm\sqrt{a / b}$ appear. These equilibrium positions correspond to singular points of center type. But if $b_1 < \omega_0^2 / 6$ and $a > 0$, then the ball adheres to one of the magnet poles. Equation (8) describes a so-called two-well oscillator, which is the subject of recent widespread interest in connection with stochastic and vibrational resonances (Landa, 2001).

If a pendulum is suspended from a uniformly rotating shaft, it can execute self-oscillations. Such a pendulum was discovered by William Froude and mentioned in the famous treatise by Lord Rayleigh (Rayleigh, 1877). Rayleigh showed that oscillations of such a pendulum are approximately described by an equation which came to be known as the Rayleigh equation. A controlled Froude pendulum was suggested by Neimark to be a model of stochastic oscillations (Neimark & Landa, 1992).

POLINA LANDA

See also **Damped-driven anharmonic oscillator; Duffing equation; Elliptic functions; Hamiltonian systems; Solitons**

Further Reading

Borda, J. 1792. *Mémoires sur la mesure du pendule* (*Mesure de la mńeridienne*), Paris

Huygens, C. 1673. *Christiani Hvgenii Zvlichemii Horologivm oscillatorivm, sive, De motv pendvlorvm ad horologia aptato demonstrationes geometricæ*. Paris: Muguet; as *Christiaan Huygens' The Pendulum Clock, or, Geometrical Demonstrations Concerning the Motion of Pendula as Applied to Clocks*, translated with notes by R.J. Blackwell, Ames: Iowa State University Press, 1986

Landa, P.S. 1996. *Nonlinear Oscillations and Waves in Dynamical Systems*, Dordrecht and Boston: Kluwer

Landa, P.S. 2001. *Regular and Chaotic Oscillations*, Berlin and New York: Springer

Neimark, Yu.I. & Landa, P.S. 1992 *Stochastic and Chaotic Oscillations*, Dordrecht and Boston: Kluwer (original Russian edition 1987)

Rayleigh, Lord (Strutt, J.W.) 1877–78. *The Theory of Sound*, London: Macmillan; reprinted New York: Dover, 1945

PERCEPTRON

The perceptron is one of the earliest computational models inspired by the human brain. Developed by Frank Rosenblatt from 1959–1962, the perceptron model is a parallel, distributed processing network intended to provide a means of modeling the capabilities and properties of the brain at a very simplified level (Rosenblatt, 1962).

Artificial neurons as mathematical processing elements of neurological (or artificial neural) networks were described earlier by Warren McCulloch & Walter Pitts (1943). Also earlier was the work of Donald Hebb, which presented a principal of learning or self-organization in neural networks (Hebb, 1949). The perceptron brought these concepts together by providing an algorithm for adjusting the parameters or weights of the network to learn to perform mappings or predicates. This model was implemented in analog electrical hardware by Rosenblatt and colleagues as the Mark I Perceptron and as such was the first neurocomputer to perform useful functions (Block, 1962). Accepting that biological brains possess "natural" intelligence, developing

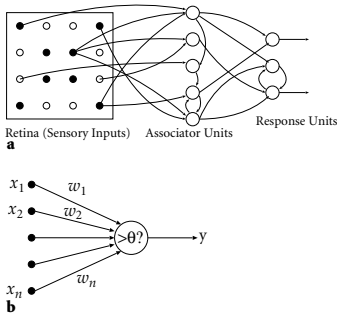

Figure 1. (a) General perceptron model. (b) Single perceptron unit.

computational models inspired by the brain represents one approach toward artificial intelligence.

The general perceptron model consists of a retina, associator units, and response units (see Figure 1a). The retina provides sensory inputs connected (many-to-many and at random) to a layer of associator units. The associator outputs are connected to response units. Connectivity can be sparse, and both associator and response units can be connected to other units in the same layer. An associator unit becomes active if its total input exceeds some threshold value and propagates a signal to the response units. This model appears to have the essential features to begin studying brain function (learning, pattern recognition, memory, generalization) in terms of brain structure.

A perceptron unit computes a threshold function of the values presented via its input connections

$$y = \begin{cases} 1 & \text{if } \sum_{i=1}^{n} w_i x_i > \theta, \\ 0 & \text{otherwise,} \end{cases} \tag{1}$$

where x_i is the value of the ith input signal. Each input connection is weighted by a real-valued weight w_i, and θ determines the threshold value. Geometrically, the perceptron unit implements a hyperplane in n-dimensional input space, where input vectors lying on one side of the line will result in an output of 1, and input vectors on the other side of the line will result in an output of 0. The position of the hyperplane is determined by the values of the weights and thresholds (zero threshold implies a hyperplane passing through the origin).

The simple perceptron unit provides a useful, simplified realization of the above model which can be implemented and trained to perform useful functions (Figure 1b). A set of inputs $X = \{x_1, \ldots, x_n\}$ are provided to a layer of associator units that compute a fixed value $\varphi(X)$. These values are then combined at the response unit to produce a binary output $\Psi(X)$. The response unit is adaptive in that there is an adjustable weight parameter α_i associated with each of its input connections. The output of the response unit Ψ is calculated as

$$\Psi = 1 \text{ if } \sum_{i=1}^{n} \alpha_i \varphi_i(X) > \theta, \tag{2}$$

$$\Psi = 0 \qquad \text{otherwise,} \tag{3}$$

where θ is a threshold value. The simple perceptron can compute any linear threshold function of the $\varphi_i(X)$ given appropriate values of the weights α_i and θ.

Given a set of data points in n-dimensional input space, labeled with desired (0 or 1) output values, Rosenblatt provided a rule for iteratively learning (modifying) the perceptron weights and thresholds, such that the outputs of the perceptron would match the desired output values. He also proved the convergence of the learning rule in a finite number of steps, provided that the perceptron has the capacity (ability) to learn an adequate linear threshold function. That is, if the n-dimensional (0,1)-labeled data is separable by an $(n-1)$-dimensional hyperplane in the input space, the perceptron can learn or be trained to find such a hyperplane.

An adaptive threshold value can be conveniently implemented by replacing θ with an additional input x_0, that always takes the value 1, and an adaptive weight w_0. Given input values and the desired (correct) value d for the output, the output of the model is computed from the inputs and the weights are adapted as follows:

$$\alpha_i = \begin{cases} \alpha_i & \text{if } d = y(X), \\ \alpha_i + x_i & \text{if } d = 1 \text{ and } y(X) = 0, \\ \alpha_i - x_i & \text{if } d = 0 \text{ and } y(X) = n1. \end{cases} \tag{4}$$

If the threshold function is changed to a continuous, differentiable function, it becomes possible to formulate a cost function for learning that is a differentiable function of the weight values. For example, a sigmoidal function is commonly used to approximate the threshold function. The delta rule can then be used to train the unit via an iterative gradient descent (Widrow & Hoff, 1960). Widrow and Hoff developed the delta (or Least Mean Squared) rule in the context of ADALINEs (ADAptive LInear NEurons), which are equivalent to McCulloch–Pitts neuron models with the bias weight (Widrow & Lehr, 1990). A quadratic error function resulting from the sum of squared error terms is used, making it possible to guarantee convergence of the delta rule under appropriate assumptions. In contrast, the perceptron learning rule does not converge if the data is nonlinearly separable.

In general, a perceptron may consist of a layer of k of the above perceptron units, each of which is fully connected to same set of inputs but has its own output. Both Rosenblatt's perceptron learning rule and the delta rule can be straightforwardly extended to train such a network.

The inability of single-layer perceptron to implement nonlinearly separable mappings and the lack of a procedure for training a multilayer perceptron model led to a lull in progress in the field for many years (Minsky & Papert, 1990). Recently, the back-propagation algorithm led to a resurgence of interest in the multilayer perceptrons and artificial neural network models. Such models have been very successfully applied to a wide range of data-driven learning tasks such as pattern recognition, classification, regression, and prediction (Haykin, 1999).

MARCUS GALLAGHER

See also **Artificial intelligence; Attractor neural network; Cell assemblies; Cellular automata; Cellular nonlinear networks; McCulloch–Pitts network; Neural network models**

Further Reading

Block, H.D. 1962. The perceptron: a model for brain functioning. I. *Reviews of Modern Physics*, 34(1): 123–135

Haykin, S. 1999. *Neural Networks A Comprehensive Foundation*, 2nd edition, Upper Saddle River, NJ: Prentice-Hall

Hebb, D.O. 1949. *The Organization of Behavior*, New York: Wiley

McCulloch, W.S. & Pitts, W. 1943. A logical calculus of ideas immanent in nervous activity. *Bulletin of Mathematical Biophysics*, 5: 115–133

Minsky, M. & Papert, S.A. 1990. *Perceptrons: An Introduction to Computational Geometry*, Cambridge, MA: MIT Press

Rosenblatt, F. 1962. *Principles of Neurodynamics*, New York: Spartan

Widrow, B. & Hoff, M.E., Jr. 1960. Adaptive switching circuits. In *1960 IRE WESCON Convention Record*, Part 4, New York: IRE, pp. 96–104

Widrow, B. & Lehr, M.A. 1990. 30 years of adaptive neural networks: perceptron, madaline, and backpropagation. *Proceedings of the IEEE*, 78: 1415–1442

PERCOLATION THEORY

For random site percolation, each site of a large lattice is randomly occupied with probability p and empty with probability $1-p$. A cluster is a set of neighboring occupied sites. A spanning cluster extends from one end of the sample to the opposite end. Percolation theory (PT) deals with the number and properties of spanning and nonspanning clusters as a function of p and of the cluster size s: the number of occupied sites in the cluster. Alternative variants are bond percolation where all sites are occupied but bonds between neighbor sites exist only with probability p. A cluster then is a set of sites connected directly or indirectly by existing bonds. One may also remove the lattice structure and place possibly overlapping circles on a piece of paper (or spheres in three dimensions). Instead of random variables, one can also study correlated percolation, such as Ising models where up spins are identified as occupied and down spins as empty sites. The following results are expected to be also valid for these variants as long as the correlations have a finite spatial extent (i.e., not at the Curie point of Ising models) (Stauffer & Aharony, 1994).

In 1941, Paul Flory published the first percolation theory (ignoring cyclic links and excluded volume effects). Physicists call this the Bethe lattice or mean field approximation, and it becomes exact for very high dimensions but is inaccurate in its critical behavior for the two or three dimensions we are mostly interested in. Percolation theory was continued by Stockmayer (1943), applied to immunology at the beginning of the 1950s, and a few years later, put onto square lattices by Broadbent & Hammersley (1957). The first computer simulations were published around 1960, and in 2001, these reached 4 million times 4 million sites (Tiggemann, 2001) and even larger lattices in Maloney & Pruessner (2003), using the Hoshen–Kopelman algorithm (Stauffer & Aharony, 1994). Exact polynomials for the number $n_s(p)$ of clusters of s sites were found for small and intermediate s, and exact results for many thresholds p_c and critical exponents are known in two dimensions.

For small p, we have only small clusters, and for p near unity, nearly the whole system forms a huge spanning cluster coexisting with rare small clusters. Thus, there is a sharp critical threshold p_c, where with increasing p for the first time, a spanning cluster appears in a very large lattice. For random site percolation on the triangular lattice with six neighbors or for random bond percolation on the square lattice, we have $p_c = \frac{1}{2}$, while for the square site problem, numerical estimates give $p_c \simeq 0.5927462\ldots$ and $p_c \simeq 0.31161\ldots$ for simple-cubic random site percolation. (Dimensions much higher than two and three were recently investigated by Grassberger (2003). Random percolation in one dimension has $p_c = 1$.) Only in infinite lattices are these thresholds defined as infinitely sharp.

Quantities of interest besides n_s are the probability $R(p)$ to have a spanning cluster, the fraction P_∞ of sites in the infinite (spanning) cluster, the mean cluster size

$$S = \frac{\sum_s n_s s^2}{\sum_s n_s} \quad \text{or} \quad \sum_s n_s s^2 , \tag{1}$$

the average cluster radius R_s, and the characteristic length ξ defined best through $\xi^2 = \sum_s R_s^2 n_s s^2 / \sum_s n_s s^2$ among other properties. (For $p > p_c$ in these sums, the spanning cluster is omitted.) Figure 1 shows S versus p, for random site percolation on nearest-neighbor simple-cubic lattices. From scaling laws or renormalization group arguments, the critical phenomena for large clusters and small $p - p_c$ are

$$\begin{aligned} n_s &\propto s^{-\tau} f[(p-p_c)s^\sigma] , \\ P_\infty &\propto (p-p_c)^\beta , \\ S &\propto |p-p_c|^{-\gamma} , \\ \xi &\propto |p-p_c|^{-\nu} , \\ R_s(p=p_c) &\propto s^{\sigma\nu} \end{aligned} \tag{2}$$

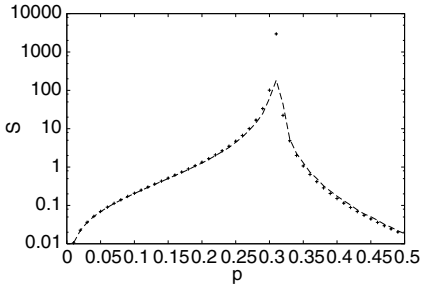

Figure 1. Mean cluster size from Equation (1) for seven nearest-neighbor simple-cubic lattices lattices $1000 \times 1000 \times 1000$ (+) compared with $100 \times 100 \times 100$ (line).

with the critical exponents given by Greek letters.

The first of these equations (Stauffer & Aharony, 1994) leads to Fisher's scaling laws $\beta = (\tau - 2)/\sigma$, $\gamma = (3 - \tau)/\sigma$, while additional hyperscaling assumptions valid for dimensionality d below six give $d\nu = \gamma + 2\beta = (\tau - 1)/\sigma$. The fractal dimensionality D of clusters at the percolation threshold, defined (Bunde & Havlin, 1996) through $s \propto R_s^D$, is then

$$D = 1/(\sigma\nu) = d - \beta/\nu = d/(\tau - 1)\,. \qquad (3)$$

Because an infinite cluster first appears for increasing p at $p = p_c$, it is plausible that for p slightly below p_c, we see finite but very large clusters; thus, the mean cluster size S diverges for $p \to p_c$ in an infinite system. In a finite system, S remains finite but the position of its maximum moves towards p_c and its height towards infinity, for system size $\to \infty$ (see Figure 1). The relation of its critical exponent γ with σ and τ can be easily derived from the above assumption for n_s by approximating the sum for S through an integral over s.

Flory's approximate solution is valid for the critical exponents only above six dimensions: $\beta = \gamma = 2\nu = 2\sigma = 1$, $\tau = \frac{5}{2}$, $D = 4$; the above scaling function f is then a Gaussian. For the more relevant case of $d = 2$, we have $\beta = 5/36$, $\gamma = 43/18$, while in three dimensions $\beta \simeq 0.42$, $\gamma \simeq 1.79$ with the other exponents following from the above scaling laws. The scaling function f is no longer a Gaussian but has a maximum below p_c; the cluster numbers n_s away from p_c decay as $\log(n_s) \propto -s$ above p_c and as $\propto -s^{1-1/d}$ below p_c. For $p < p_c$, the fractal dimension in three dimensions is $D = 2$, one of the rare cases where an exact solution was found in three but not in two dimensions.

Besides computer simulation, small-cell renormalization group methods also give reasonable approximations for thresholds and critical exponents. One divides the infinite lattice into cells of linear dimension b such that the cell centers themselves again form a lattice of the same type as the original lattice. A cell is occupied if the original occupied sites form a cluster spanning this cell. In this way, the original occupation probability p is renormalized into the cell occupation probability $p' = R(p)$. One may iterate this renormalization by computing $p'' = R(p')$ and then $R(p'')$ and so on. The fixed point p^* of this transformation obeys $p^* = R(p^*)$ and approaches, for large b, the true percolation threshold p_c. At this fixed point, the derivative $\mathrm{d}R(p)/\mathrm{d}p$ is related to the critical exponent ν. However, in contrast to many renormalization group publications, $R(p_c)$ is not equal to p_c (Ziff, 1992).

Some mathematical theorists in the 1980s claimed that the infinite cluster is unique, but this is not true at $p = p_c$ where several spanning clusters can coexist (Aizenman, 1997). Even above p_c in very elongated rectangles, one may find several clusters spanning in the short direction.

How do these theoretical and numerical results compare with applications and reality? Because the percolation thresholds p_c depend on the lattice structure, one should not expect them to agree with off-lattice experiments, but the exponents are more "universal" and should agree when comparing reality with PT. There are many applications (Sahimi, 1994) including flow in porous media, conductor-insulator mixtures, elasticity of composite materials, and breakdown of the internet. Sputtering metal drops onto a plane offers a particularly accurate realization of percolation.

Flory invented the percolation theory to describe the sol-to-gel transition of branched polymers, known from boiling your breakfast egg. But only half a century later was it experimentally confirmed that the gelation exponents are indeed those of three-dimensional lattice percolation theory.

Another application of percolation clusters is to speed up computer simulations of Ising models (ferromagnets) near their Curie point, using the clusters of correlated bond percolation formed by up spins connected by bonds with probability $p = 1 - \exp(-2J/k_B T)$. Flipping whole clusters instead of single spins equilibrates the system much faster. (In this Fortuin–Kasteleyn–Coniglio–Klein–Swendsen–Wang theory (Stauffer & Aharony, 1994), T is the absolute temperature, k_B the Boltzmann constant, and J the interaction energy such that $2J$ is the energy to change an isolated pair of parallel spins into antiparallel.) For example, right at the Curie point in a two-dimensional $L \times L$ lattice, the relaxation time no longer increases as $L^{2.17}$ but only as $\log(L)$ if these percolation clusters, instead of single spins, are flipped.

The above application stems from the relation between percolation clusters and the q-state Potts model ($q = 2$ is the Ising model again). The partition

function of this Potts model is $Z = \langle q^N \rangle$, where N is the total number of bond percolation clusters at the above $p = 1 - \exp(-2J/k_B T)$ and $\langle \cdots \rangle$ denotes the average over many realizations. Taking the limit $q \to 1$, we get $\ln(Z) / \ln(q) \to \langle N \rangle = \sum_s n_s$, recovering random percolation which is thus a $q \to 1$ Potts model.

Percolation is also a convenient teaching example. Filling a small triangular lattice at $p = p_c = \frac{1}{2}$ by throwing coins reveals in the classroom fractals, statistical errors, and (in the resulting number of isolated sites) strong systematic errors from the lattice boundaries.

DIETRICH STAUFFER

See also **Cluster coagulation; Polymerization; Sandpile model**

Further Reading

Aizenman, M. 1997. On the number of incipient spanning clusters. *Nuclear Physics* B, 485: 551–582

Broadbent, S.R. & Hammersley, J.M. 1957. Percolation processes. *Proceedings of the Cambridge Philosophical Society*, 53: 629–645

Bunde, A. & Havlin, S. 1996. *Fractals and Disordered Systems*, Berlin: Springer

Flory, P.J. 1941. Thermodynamics of high polymer solutions. *Journal of the American Chemical Society*, 63: 3083–3100

Grassberger, P. 2003. Critical percolation in high dimensions. *Physical Review* E, 67: 036101

Maloney, N.R. & Pruessner, G. 2003. Asynchronously parallelized percolation on distributed machines. *Physical Review* E, 67: 037701

Sahimi, M. 1994. *Applications of Percolation Theory*, London: Taylor & Francis

Stauffer, D. & Aharony, A. 1994. *Introduction to Percolation Theory*, London: Taylor & Francis

Stockmayer, W.H. 1943. Theory of molecular size distribution and gel formation in branched-chain polymers. *Journal of Chemical Physics*, 11: 45–55

Tiggemann, D. 2001. Simulation of percolation on massively-parallel computers. *International Journal of Modern Physics* C, 12: 871–878

Ziff, R.M. 1992. Spanning probability in 2D percolation. *Physical Review Letters*, 69: 2670–2673

PERIOD DOUBLING

Like many terms used in the nonlinear sciences, *period doubling* has more than one meaning. Well known is the response of a system at half the driving frequency, due to nonlinear coupling. Probably the earliest observation of period doubling was by Michael Faraday, in his investigations of shallow water waves (Faraday, 1831, arts. 98–101). The phenomenon was also investigated by Lord Rayleigh (Rayleigh, 1887). He wrote of an example:

> in which a fine string is maintained in transverse vibration by connecting one of its extremities with the vibrating prong of a massive tuning-fork, *the direction of motion of the point of attachment being parallel to the length of the string* the string may settle down into a state of permanent and vigorous vibration *whose period is double that of the point of attachment.*

A more everyday example is the fact that a child may set a swing into transverse motion by standing on the seat and moving up and down at twice the natural frequency. Such phenomena are in the province of *harmonic generation* and *parametric amplification* and are not treated in this entry.

Period doubling (as discussed in this entry) is the most common of several *routes to chaos* for a nonlinear dynamical system.

The dynamics of natural processes, and the nonlinear equations used to model them, depend on externally set conditions, such as environmental or physical factors. These take fixed values over the development of the system in any particular instance, but vary from instance to instance. Expressed as numerical quantities, such factors are called parameters, and their role is vital. Often, increasing a parameter increases the nonlinearity. The simplest example is the logistic model (May, 1976)

$$x_{n+1} = r x_n (1 - x_n), \tag{1}$$

a discrete system with state variable x_n and parameter r; n is the generation. (If x represents population, then r characterizes the underlying growth rate.)

For period doubling, it is sufficient to vary a single parameter. Over some range, the system may have a periodic attractor, that is, a periodic orbit that attracts neighboring orbits. Typically, the stability (attraction) decreases as the parameter increases, changing to instability (repulsion) at a critical value. This is a bifurcation, or change of structure, of the orbit. In period doubling, this change is accompanied by the "birth" of a new attracting period-doubled orbit, in which the system alternates between two states. In biological systems, these are known as alternans (Glass & Mackey, 1988). In the period-doubling route to chaos, each new periodic attractor loses its stability with increasing parameter value, whereupon the next period-doubled attractor is born. If the original attractor was a fixed point, this generates orbits of period 1, 2, 2^2, 2^3, ..., called the main period-doubling cascade.

A surprising *universality* was discovered by Mitchell Feigenbaum. In part, it relates to the sequence of parameter values at which successive period doubling occurs. Label the first by r_1, the second by r_2, and so on, and let the cascade end at the value r_∞. The differences $(r_\infty - r_n)$ decrease to zero; the surprising fact is that the ratios $(r_\infty - r_n)/(r_\infty - r_{n+1})$ converge to a universal constant δ, which takes the same value $\delta \approx 4.669202\ldots$ for all maps with a quadratic maximum (Feigenbaum, 1978). There is a second universal constant, $\alpha \approx 2.502908\ldots$, measuring the relative spatial scale of the orbits, which also becomes increasingly fine.

	Logistic		Hénon	
n	r_n	$\left(\frac{r_{n+1}-r_n}{r_{n+2}-r_{n+1}}\right)$	a_n	$\left(\frac{a_{n+1}-a_n}{a_{n+2}-a_{n+1}}\right)$
1	3.0000000000		0.3675000000	
2	3.4494897428		0.9125000000	
3	3.5440903596	4.751446	1.0258554050	4.807887
4	3.5644072661	4.656251	1.0511256620	4.485724
5	3.5687594195	4.668242	1.0565637582	4.646894
6	3.5696916098	4.668739	1.0577308396	4.659569

Table 1. Estimates of the Feigenbaum constant δ, for the logistic and Hénon maps.

Experiment		Observed number of period doublings	estimated value of δ	estimated value of α
Hydrodynamic:	helium	4	3.5 ± 1.5	
	mercury	4	4.4 ± 0.1	
Electronic:	diode	5	4.3 ± 0.1	2.4 ± 0.1
	Josephson	4	4.5 ± 0.3	2.7 ± 0.2
Laser:	feedback	3	4.3 ± 0.3	
Acoustic:	helium	3	4.8 ± 0.6	

Table 2. Selected experimental data on period doubling.

Numerical data for two main period-doubling sequences is given in Table 1. Columns 2–3 display data for the logistic map,

$$x_{n+1} = 1 - ax_n^2 + y_n, \qquad y_{n+1} = bx_n. \tag{2}$$

columns 4–5 for its two-dimensional cousin, the Hénon map. For Table 1, the parameter b has been kept constant. Experimental data has also been obtained in quite a few systems (Cvitanović, 1989); a selection is shown in Table 2. To appreciate the experimental difficulty involved, remember that for each successive period doubling, the significance of errors increases five-fold while the complexity of the dynamics doubles.

The mechanism for period doubling is already implicit in the fact that it is also known as a "flip bifurcation." Stability of a fixed point x^* of a smooth one-dimensional map f is the simplest case for theory. Consider a nearby point x that maps to x'. Linear approximation gives

$$(x' - x^*) \approx f'(x^*) \cdot (x - x^*). \tag{3}$$

This shows (and exact analysis confirms) that the fixed point is stable if $-1 < f'(x^*) < 1$ and unstable if $f'(x^*) < -1$ or $f'(x^*) > 1$. Successive iterates flip from side to side for negative $f'(x^*)$, so period doubling occurs at $f'(x^*) = -1$. For higher-dimensional systems, stability is determined by the eigenvalues of a matrix of partial derivatives; the occurrence of an eigenvalue $\lambda = -1$ leads to period doubling. Because $x^{**}_{n+2} = x^{**}_n$ for the new orbit, period doubling is connected with double iteration, controlled by the second composition map $f_2(x) = f(f(x))$. Elementary calculus shows that if f satisfies the two conditions

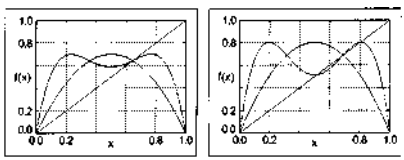

Figure 1. Mechanism: f and f_2 for $r = 2.8$ (left) and $r = 3.2$ (right).

$$f(x^*) = x^*, \qquad f'(x^*) = -1, \tag{4}$$

then f_2 satisfies three conditions:

$$f_2(x^*) = x^*, \quad f_2'(x^*) = +1, \quad f_2''(x^*) = 0. \tag{5}$$

As a result, $x - f_2(x)$ must be approximated by a cubic near the bifurcation. One of its zeros is the (now unstable) fixed point of f, the other two constitute the period-doubled orbit, because they are not fixed points of f.

In the case of the logistic map, the first period doubling occurs at $r = 3$. Graphs of f and f_2 show the mechanism (Figure 1). As the cascade proceeds,

the pictures and the analysis repeat but with increasing complication. The common thread is that, at each step, conditions (4) for a composition f_n imply conditions (5) for f_{2n}.

BRIAN DAVIES

See also **Attractors; Bifurcations; Dripping faucet; Harmonic generation; Hénon map; Maps; One-dimensional maps; Parametric amplification; Routes to chaos; Stability; Universality**

Further Reading

Cvitanović, P. 1989. *Universality in Chaos*, 2nd edition, Bristol: Adam Hilger

Davies, B. 1999. *Exploring Chaos: Theory and Experiment*, Reading, MA: Perseus Books

Faraday, M. 1831. On a peculiar class of acoustical figures; and on certain forms assumed by groups of particles upon vibrating elastic surfaces. *Philosophical Transactions of the Royal Society of London*, 121: 299–340

Feigenbaum, M.J. 1978. Quantitative universality for a class of nonlinear transformations. *Journal of Statistical Physics*, 19: 25–52

Glass, L. & Mackey, M.C. 1988. *From Chaos to Clocks: The Rhythms of Life*, Princeton, NJ: Princeton University Press

May, R.M. 1976. Simple mathematical models with very complicated dynamics. *Nature*, 261: 459–469

Rayleigh, Lord. 1887. Maintenance of vibrations by forces of double frequency, and propagation of waves through a medium with a periodic structure. *Philosophical Magazine*, 24: 145–159

Schuster, H.G. 1988. *Deterministic Chaos: An Introduction*, 2nd edition, Weinheim: VCH

PERIODIC BURSTING

Bursting systems show intervals of repetitive activity separated by intervals of relative quiescence, and have at least two different time scales; fast for the short period with spike-like oscillations that comprise the burst and slow for the longer period of the burst itself. Laboratory systems that exhibit bursting include the Belousov–Zhabotinsky reaction and neuronal systems. A simple conceptual model would be the bursting that is generated by switching between the active and inactive states, suggesting the coexistence of stable periodic and quiescent states. Bursting can be irregular, in which the periods between bursts are effectively random, or it can be strictly periodic. Some experimental bursting systems exhibit switching between different patterned periodic behaviors, suggesting two or more coexisting periodic states, and models have been shown to exhibit bi- or multi-rhythmicity. The exotic periodic dynamics of bursting systems—with patterning, multistability, and multi-rhythmicity provide a demonstrator for bifurcation and continuation algorithm packages.

A simple two-variable excitable or oscillatory system such as the FitzHugh–Nagumo equations can be driven to bursting by a slow periodic forcing term, so bursting can be viewed as the activity of a fast oscillatory system being modulated by a slower oscillatory system. For an autonomous bursting system, the fast and slow systems are coupled, and the burst is generated by the evolution of the slow system sweeping the dynamics of the fast subsystem between steady state and oscillatory dynamics (Chay & Rinzel, 1985). On the timescale of the fast system, the slow variable acts as a control parameter, so the fast variable approximates its attractors — its stable equilibrium during the period of quiescence and its oscillations during activity.

Bursting in neurons and other electrically excitable secretory cells may be part of their normal pattern generation behavior, as in the generation of the respiratory rhythm, or a sign of pathology, as in the abnormal bursting charges during epileptic fit. Synchronization of bursting activity between widely separate cells in the cortex excited by different features of the same visual input has been observed and proposed to underlay visual binding. Neural central pattern generators are networks of nerve cells, that generate periodic bursts as a result of their interconnections, but some single isolated cells can generate bursts. Both network and isolated cell bursting can be modeled by systems of differential equations. Specific models for isolated cells—the beta-pancreatic cell or the parabolic burster cell R15 of Aplysia—are ordinary differential systems, analogous to the Hodgkin–Huxley equations for the action potential, based on experimental measurements of currents and concentrations (Rinzel & Lee, 1986). They reproduce the observed bursting behaviors and can be reduced to simpler systems in which the dynamical mechanisms producing bursting are obtained by bifurcation analysis of these models.

In these models, the spiking is produced by oscillations of a fast subsystem that is modulated by the slower system. Bifurcation and topological analysis of the models has led to a classification of the types of bursting (Bertram et al., 1995). In type I, the fast subsystem is bistable, and the burst begins at a saddle node and ends at a homoclinic bifurcation. During the burst, the period between spikes increases illustrated by a simple three-variable polynomial model that retains the qualitative features of neuronal bursting, the Hindmarsh–Rose equations (1984) in Figure 1. The stable (thick solid line) and unstable (dotted line) Z-shaped steady state curves exchange stability at a Hopf bifurcation and a saddle-node bifurcation, and the periodic solutions that emerge at the Hopf bifurcation end at a homoclinic point. The $x\,y$ subsystem has a bistable range, with stable steady state and limit cycle. During the burst, z is approximately constrained to this bistable range, each spike increments z, and the period between spikes increases as the homoclinic point is approached. Between bursts, z decreases slowly close to the lower, stable limb of the steady-state curve, as x increases until the orbit is re-injected into the spiking region.

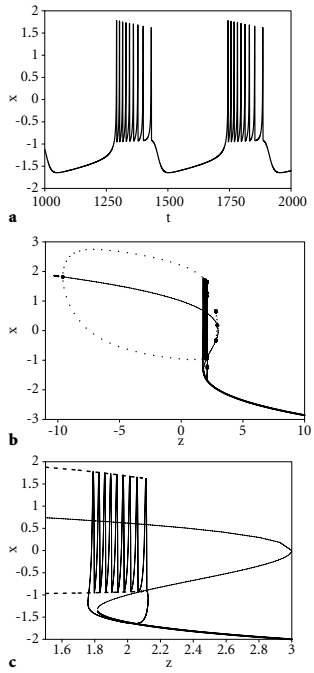

Figure 1. Example of type I burst generation in the three-variable (x, y, z) Hindmarsh & Rose (1984) model for neuronal oscillations, bursting and chaos. (a) Periodic bursting in the fast x variable representing membrane potential; (b) and (c) with z scale magnified: Bifurcation diagram for the fast $x-y$ subsystem with the slow variable z treated as a bifurcation parameter, and the periodic bursting of (a) is overlaid in the $x-z$ plane.

In type II bursting, two slow variables drive the fast system across a homoclinic bifurcation, so the spike period within the burst decreases and then increases parabolically, as the slow variables drive the system toward, and away from, the homoclinic point. This is illustrated by the parabolic burster R15 of Aplysia. The fast system has only a stable periodic limit cycle during the burst.

In type III bursting, as in type I, the fast system is bistable, but the burst ends at a saddle node rather than a homoclinic bifurcation, and the spike period need not increase during the burst.

Examples of all three types are seen in different bursting cells, and many bursting cells show more exotic, and chaotic, behaviors. An alternative approach is to reduce the models to interval maps, and to classify the bifurcations of these maps—see Fan & Holden (1993).

ARUN V. HOLDEN

See also **FitzHugh–Nagumo equation; Hodgkin–Huxley equations; Nerve impulses**

Further Reading

Bertram, R., Butte, M.J., Kiemel, T. & Sherman, A. 1995. Toplogical and phenomenological classification of bursting oscillations. *Bulletin of Mathematical Biology*, 57: 413–439

Chay, T.R. & Rinzel, J. 1985. Bursting, beating and chaos in an excitable embrane model. *Biophysical Journal*, 47: 357–366

Fan, Y-S. & Holden, A.V. 1993. Bifurcations, burstings, chaos and crises in the Rose–Hindmarsh model for neuronal activity. *Chaos Solitons and Fractals*, 3: 439–449

Hindmarsh, J.L. & Rose, R.M. 1984. A model for neuronal bursting using three coupled first order differential equations. *Proceedings of the Royal Society of London* B, 221: 87–112

Rinzel, J. & Lee, Y.S. 1986. On different mechanisms for membrane potential bursting. In *Nonlinear Oscillations in Biology and Chemistry*, edited by H.G. Othmer, New York: Springer, pp. 19–33

PERIODIC ORBIT THEORY

Many characteristic quantities for chaotic systems, such as Lyapunov exponents, correlation functions, or fractal dimensions, are defined as averages over the invariant measure (defined as a probability distribution on the phase space). For most chaotic systems, this measure is difficult to represent analytically, so it has to be approximated experimentally or numerically by averages over long trajectories. The periodic orbit theory rests on the idea that periodic orbits provide a skeleton that allows approximation of the invariant measure and that, therefore, ergodic averages can be determined from suitably weighted averages over periodic orbits. It combines mathematically established analytical expressions with well-controlled numerical input for highly accurate quantitative information about chaotic systems. It provides access to Lyapunov exponents, fractal dimensions, escape rates, diffusion constants, resonances, or even correlations between eigenvalues of quantum systems (Eckmann & Ruelle, 1985; Artuso et al., 1990; Chaos Focus Issue, 1992).

In order to motivate the basic expressions and to determine the weight of periodic orbits, consider the evolution of a density $\rho_n(\boldsymbol{x})$ at time n under the action of a discrete dynamical system, $\boldsymbol{x}_{n+1} = \boldsymbol{F}(\boldsymbol{x}_n)$ (Cvitanović & Eckhardt, 1991). After one time step, the density is given by

$$\rho_{n+1}(\boldsymbol{x}) = \int \mathrm{d}\boldsymbol{y}\, U(\boldsymbol{x}, \boldsymbol{y})\rho_n(\boldsymbol{y}) \qquad (1)$$

with the evolution kernel $U(\boldsymbol{x}, \boldsymbol{y})$. In the deterministic map, the points $\boldsymbol{y}$ at time n and $\boldsymbol{x}$ at $n+1$ are connected by a single trajectory, so that U is a δ-distribution, $U = \delta(\boldsymbol{x} - \boldsymbol{F}(\boldsymbol{y}))$. In the presence of noise, the evolution kernel will be more regular and some of the mathematical subtleties that appear when dealing with singular operators will disappear. Noise

regularization can also be used to define the "natural" invariant measure for a dynamical system, the Sinai–Ruelle–Bowen measure, as the measure obtained in the limit of vanishing noise (Eckmann & Ruelle, 1985). For an attractor, this invariant measure is the eigenvector to the eigenvalue 1 of the evolution operator.

Periodic orbits appear when traces of U are calculated: the trace requires that $\boldsymbol{x}$ and $\boldsymbol{y}$ coincide, and this singles out a periodic orbit. With p the label for the different periodic orbits, n_p their primitive period (the number of iterations need to first return to the starting point), and $J_p = \mathrm{d}\boldsymbol{x}(n_p) \,/\, \mathrm{d}\boldsymbol{x}(0)$ the Jacobian after one period, the trace for m iterations becomes

$$\begin{aligned} \operatorname{tr} U^m &= \int \mathrm{d}\boldsymbol{x}\, U^m(\boldsymbol{x}, \boldsymbol{x}) \\ &= \sum_p \sum_{r=1}^{\infty} \frac{n_p}{|\det(1 - J_p^r)|} \delta(m - r n_p); \end{aligned} \quad (2)$$

powers of U are defined as multiple mappings so that U^m is the evolution operator after m time steps. The first sum extends over the primitive, nonrepeated orbits p and the second over their multiple traversals r.

The Fredholm determinant for the evolution operator U can be related to traces of the evolution operator via

$$\det(1 - zU) = \exp(\operatorname{tr} \ln(1 - zU)) \quad (3)$$

$$= \exp\left(-\sum_{n=1}^{\infty} \frac{z^n}{n} \operatorname{tr} U^n \right) = \sum_{l=0}^{\infty} c_l z^l. \quad (4)$$

The right-hand side is then an expansion in terms of periodic orbits, first through the traces in the exponent and then through their contributions to the coefficients c_l in the final power series. The left-hand side can formally be expanded in terms of eigenvalues λ_ν of the operator, $\det(1 - zF) = \prod_\nu (1 - z\lambda_\nu)$. It vanishes whenever z equals the inverse of an eigenvalue.

The formal manipulations that lead to (4) can be made precise in the context of nice hyperbolic systems in which periodic orbits are dense ("Axiom A"). Simple maps and flows on surfaces of negative curvature belong to this class. Then the theory can be developed as discussed in Ruelle (1989) and Pollicott (2002). In particular, the eigenvalues with sufficiently small damping can be given an interpretation as experimentally accessible long-lived Ruelle–Pollicott resonances.

For the calculation of averages, the relation between the leading eigenvalue and the invariant density is important. If the average of a given phase space observable A is to be calculated, one can extend the transfer operator U to include the observable, $\tilde{U} = U \exp(-qA)$, and extract the phase space average from the variation of the leading, zero $z_0(q)$ of the Fredholm determinant with q,

$$\langle A \rangle = \frac{\mathrm{d}}{\mathrm{d}q} \ln z_0(q) \Big|_{q=0}. \quad (5)$$

The contribution to the trace is a term $\exp(q \sum_P A(\boldsymbol{x}_P))$ with the sum extending over all points P of the orbit p: it reflects the sampling of phase space along the orbit.

The dependence of the Fredholm determinant on periodic orbits and their properties can be spelled out completely, so that it can be written as a product over contributions from periodic orbits. For the case of a one-dimensional map, we find

$$\begin{aligned} \det(1 - zU) &= \prod_p \prod_{j=0}^{\infty} \left(1 - \frac{z^{n_p}}{|J_p| J_p^j} \right) \\ &= \prod_j \zeta_j^{-1}(z). \end{aligned} \quad (6)$$

The ζ_j are called dynamical zeta functions in analogy to the Riemann zeta function $\zeta_{\mathrm{R}}(s)$, which by the Euler product representation can be expressed as a product over prime numbers,

$$\zeta_{\mathrm{R}}^{-1}(s) = \left(\sum_{n=1}^{\infty} n^{-s} \right)^{-1} = \prod_p (1 - p^{-s}). \quad (7)$$

The analytic properties of the Fredholm determinant determine the decay of the coefficients c_l in the power series expansion in (4): if the Fredholm determinant is analytic then the coefficients fall off faster than exponentially (Rugh, 1992). This is particularly useful in numerical calculations where highly accurate and quickly converging results can be obtained using the shortest orbits.

For continuous flows, the discrete period z^{n_p} is replaced by the continuous equivalent $\exp s T_p$, and the contributions of observables becomes an integral along the orbit.

When the classical evolution operator is replaced by the quantum one, a relation between the quantum eigenvalues and classical periodic orbits emerges (Gutzwiller, 1990). For instance, the semiclassical periodic orbit expression for the density of states in a chaotic system is

$$\begin{aligned} \rho(E) &= \sum_i \delta(E - E_i) \\ &\sim \operatorname{Re} \frac{1}{\pi\hbar} \sum_p \sum_{r=1}^{\infty} \frac{T_p \exp(-\mathrm{i}\mu_p \pi r/2)}{\sqrt{|\det(1 - J_p^r)|}} \mathrm{e}^{\mathrm{i}r S_p(E)/\hbar}, \end{aligned} \quad (8)$$

where the symbol $\sim$ indicates the omission of a few regularizing terms, and where S_p and μ_p are the

classical action and the Maslov index, respectively. This Gutzwiller trace formula is at the heart of many developments in the field of quantum chaos.

Zeta functions for the counting of periodic orbits already appear in Smale (1967). The mathematical theory was developed prominently by David Ruelle, Rufus Bowen, and Yasha Sinai (see Eckmann & Ruelle, 1985; Ruelle, 1989; Pollicott, 2002). Practical aspects for calculating with periodic orbits are discussed by Artuso et al. (1990), by Gaspard (1998), and by many contributions to the Chaos Focus Issue (1992). Applications of this formalism to simple maps and the period-doubling attractor are given by Artuso et al. (1990), to diffusion in Lorentz gases in Chaos Focus Issue (1992), and to the dimension and resonances to the Lorenz model in Eckhardt & Ott (1994). The relation to quantum mechanics is discussed in Gaspard (1998), Gutzwiller (1990), Eckhardt (1993), and the Chaos Focus Issue (1992). As demonstrated by Flepp et al. (1991), a comparison between periodic orbits extracted from experimental data and from a numerical model can be used to fine tune and improve the model.

BRUNO ECKHARDT

See also **Phase space; Quantum chaos**

Further Reading

Artuso, R., Aurell, E. & Cvitanović, P. 1990. Recycling of strange sets: I. Cycle expansion; II. Applications. *Nonlinearity*, 3: 325–360 and 361–386

Chaos Focus Issue on Periodic Orbit Theory. 1992. *Chaos*, 2: 1–158

Cvitanović, P. & Eckhardt, B. 1991. Periodic orbit expansions for classical smooth flows. *Journal of Physics* A, 24: L237–L241

Eckhardt, B. 1993. Periodic orbit theory. *Proceedings of the International School of Physics "Enrico Fermi," Course CXIX, Quantum Chaos*, edited by G. Casati, I. Guarneri & U. Smilansky, Amsterdam: North-Holland, pp. 77–118

Eckhardt, B. & Ott, G. 1994. Periodic orbit analysis of the Lorenz attractor. *Zeitschrift für Physik* B, 94: 259–266

Eckmann, P. & Ruelle, D. 1985. Ergodic theory of chaotic systems. *Reviews of Modern Physics*, 57: 617–656 and 1115 (Addendum)

Flepp, L., Holzner, T., Brun, E., Finardi, M. & Badii, R. 1991. Model identification by periodic-orbit analysis for NMR-laser chaos. *Physical Review Letters*, 67: 2244–2247.

Gaspard, P. 1998. *Chaos, Scattering and Statistical Mechanics*, Cambridge and New York: Cambridge University Press

Gutzwiller, M.C. 1990. *Chaos in Classical and Quantum Mechanics*, New York: Springer

Pollicott, M. 2002. Periodic orbits and zeta functions. In *Handbook of Dynamical Systems*, vol 1A, edited by B. Hasselblatt & A. Katok, Amsterdam: Elsevier, pp. 409–452

Ruelle, D. 1989. *Elements of Differentiable Dynamical Systems and Bifurcation Theory*, New York: Academic Press

Rugh, H.H. 1992. The correlation spectrum for hyperbolic analytic maps. *Nonlinearity*, 5: 1237–1263

Smale, S. 1967. Differentiable dynamical systems. *Bulletin of the American Mathematical Society*, 73: 747–817

PERIODIC SPECTRAL THEORY

The direct problem of periodic spectral theory is that of constructing the spectral data of certain linear operators with periodic coefficients, that is, the determination of the spectrum of this operator and of the associated eigenfunctions. The inverse problem of periodic spectral theory is the problem of the reconstruction of such an operator (and thus its coefficients) from given spectral data. Although these questions can be asked for linear partial differential operators, this article focuses on linear ordinary differential operators.

The history of periodic spectral theory starts with the investigations of Sturm and Liouville on the eigenvalues of certain differential equations of second-order with given boundary conditions, now referred to as Sturm–Liouville theory. In 1836–1837, Charles François Sturm and Joseph Liouville examined independently different aspects of this problem, such as the asymptotics of eigenvalues, different comparison theorems on the solutions of similar equations with different coefficients, and theorems on the zeros of eigenfunctions. For the class of equations Sturm and Liouville considered, these results imply the existence of an infinite sequence of real, increasing eigenvalues, and orthogonality of eigenfunctions corresponding to different eigenvalues. Although their investigations did not as such deal with periodic spectral theory, many of their results carry over to this area.

Consider an ordinary differential operator of order n,

$$L = q_n(x)\frac{\mathrm{d}^n}{\mathrm{d}x^n} + q_{n-2}(x)\frac{\mathrm{d}^{n-2}}{\mathrm{d}x^{n-2}} + \cdots + q_1(x)\frac{\mathrm{d}}{\mathrm{d}x} + q_0(x), \tag{1}$$

where the coefficients $q_j(x)$, $j = 0, \ldots, n$ are periodic functions of x, sharing a common period: $q_j(x+T) = q_j(x)$, $j = 0, \ldots, n$, and $q_{n-1}(x) = 0$. They are referred to as potentials. Using this operator L, define the differential equation

$$L\psi = \lambda\psi. \tag{2}$$

The direct periodic spectral problem is the problem of (i) determining the set of all $\lambda \in \mathbb{C}$ for which this differential equation has at least one bounded solution, and (ii) for each such λ, determining all bounded solutions. There are many technical issues to be dealt with: which function space do the potentials belong to? Which function space does ψ belong to? These issues will be ignored here. Sometimes one restricts attention to periodic solutions ψ: $\psi(x+T) = \psi(x)$, or antiperiodic solutions $\psi(x+T) = -\psi(x)$. These and other choices lead to spectra that are subsets of the spectrum as obtained without making these choices.

One approach to solve the direct spectral problem is Floquet theory (Amann, 1990). Rewrite Equation (2) as

a first-order linear system:

$$\frac{\mathrm{d}\boldsymbol{\psi}}{\mathrm{d}x} = \boldsymbol{X}(x,\lambda)\boldsymbol{\psi}, \quad \boldsymbol{X}(x+T,\lambda) = \boldsymbol{X}(x,\lambda) \qquad (3)$$

with $\boldsymbol{\psi}_1 = \psi(x)$. Note that from $q_{n-1}(x) = 0$, it follows that $\mathrm{tr}\,\boldsymbol{X}(x,\lambda) = 0$. Thus, the flow determined by (3) is volume preserving. Define the monodromy matrix of this system as $\boldsymbol{M}(x_0,\lambda) = \boldsymbol{\Psi}(x_0+T, x_0, \lambda)$, where $\boldsymbol{\Psi}(x, x_0, \lambda)$ is a fundamental matrix of (3) such that $\boldsymbol{\Psi}(x_0, x_0, \lambda)$ is the identity matrix. Thus, $\boldsymbol{M}(x_0,\lambda)$ is the operator of translating x by T: $\boldsymbol{M}(x_0,\lambda)\boldsymbol{\psi}(x) = \boldsymbol{\psi}(x+T)$. Note that $\boldsymbol{\psi}(x)$ also depends on x_0 and λ, but this dependence is suppressed here. This operation commutes with $\mathrm{d}/\mathrm{d}x$, since $\boldsymbol{X}(x,\lambda)$ is periodic in x with period T. Thus, (3) has a set of solutions $\boldsymbol{\phi}(x)$ which are also eigenvectors of $\boldsymbol{M}(x_0,\lambda)$. These solutions are known as Bloch functions or Floquet functions. If the eigenvalue of $\boldsymbol{M}(x_0,\lambda)$ for any Bloch function has magnitude greater than one, then this Bloch function is unbounded as $x \to +\infty$ or $x \to -\infty$. Thus, the spectrum of (3) is the set of all λ such that at least one eigenvalue of $\boldsymbol{M}(x_0,\lambda)$ has magnitude one. This spectrum is independent of the choice of x_0 due to the requirement that the flow is volume preserving; that is, $\mathrm{tr}\,\boldsymbol{X}(x,\lambda) = 0$, or $q_{n-1}(x) = 0$.

An important class of periodic spectral problems is that of self-adjoint operators. These are operators whose spectrum is contained on the real line. For self-adjoint operators, the spectrum of the periodic spectral problem consists of the union of a (possibly infinite) sequence of intervals.

For the sake of explicitness, the remainder of this article will discuss the equation (Magnus & Winkler, 1979)

$$-\psi'' + q(x)\psi = \lambda\psi, \quad q(x+T) = q(x). \qquad (4)$$

Note that many of the results stated below are true for general classes of periodic spectral problems. Depending on the literature source, (4) goes by the name of Hill's equation or (after rescaling) the time-independent Schrödinger equation. This equation is self-adjoint. Its spectrum is bounded from below. It is a collection of intervals such that the length of the separating gaps between intervals $\to 0$ as $\lambda \to \infty$. Using Floquet theory, the condition for λ to be in the spectrum is found to be $|\mathrm{tr}\boldsymbol{M}(x_0,\lambda)| \leq 2$. The endpoints of the intervals are given by $|\mathrm{tr}\boldsymbol{M}(x_0,\lambda)| = 2$. Because (4) is a second-order equation, there are two linearly independent Bloch functions.

The time-independent Schrödinger equation (4) of course plays a fundamental role in quantum mechanics. In this case, $q(x)$ is the potential of the system, and λ plays the role of energy. The context of solid state physics is especially relevant here, because the potential $q(x)$ is periodic. The intervals constituting the spectrum are known as allowed (energy) bands and the gaps between them as forbidden (energy) bands.

The inverse periodic spectral problem for (4) is that of the reconstruction of $q(x)$, given a collection of spectral data. Various choices are possible for the collection of spectral data. In general, the inverse problem does not have a unique solution, using the knowledge of one spectrum. This can be resolved by also providing the eigenfunction. However, now the collection of spectral data is unnecessarily large. It is sufficient to provide two spectra (corresponding to different boundary conditions). Together with the known analyticity properties of the eigenfunction $\psi(x)$, this determines the potential $q(x)$. This is similar to the inverse scattering method where the knowledge of the scattering data and the analyticity properties of the eigenfunction determine the potential (decaying as $|x| \to \infty$) uniquely. A major difference is that in the inverse scattering method, the starting point is the asymptotic behavior as $x \to \pm\infty$. This behavior is simple, because it is governed by a differential equation with constant coefficients. This is one reason why the inverse scattering method is as efficient as it is. In the periodic problem, the role of $x \to \pm\infty$ is taken over by $x = x_0$, but there is no simple asymptotic behavior, resulting in a theory which is more technical and less explicit (Dubrovin et al., 1976; Novikov et al., 1984).

This lack of explicitness for solving the inverse periodic spectral problem is to some extent resolved by the consideration of so-called finite-gap potentials. These are potentials for which the number of intervals constituting the spectrum, and thus, the number of gaps separating these intervals, is finite. The simplest nontrivial example is that of the Lamé equation

$$-\psi'' + n(n+1)\wp(x - x_c)\psi = \lambda\psi. \qquad (5)$$

Here $\wp(x - x_c)$ is the Weierstrass elliptic function, x_c is a fixed complex number, and n is a positive integer. In this case, the number of gaps separating the intervals in the spectrum is n.

This classical example is a special case of a more recent theory of finite-gap potentials, whose development started with the works of Novikov (1974) and Lax (1975). They show that the stationary solutions of the nth member of the KdV hierarchy are n-gap potentials of (4). Here the KdV hierarchy is the collection of equations of the form $u_t = \partial_x(\delta H_n / \delta u)$, where H_n is any conserved quantity of the KdV equation, $\delta H_n / \delta u$ denotes the variational derivative of H_n with respect to u (*See* **Poisson brackets**), and indices denote differentiation. It was soon thereafter shown that all finite-gap potentials of (4) were of this nature. For example, the Lamé potential with $n = 1$ is a stationary solution of the KdV equation. This gives a nonspectral characterization of the finite-gap potentials.

To solve the direct spectral problem with an n-gap potential $q_n(x)$, one first considers the direct periodic spectral problem, as stated above. It is solved using

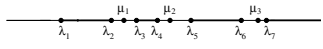

Figure 1. The main spectrum for a three-gap potential (thick solid line) and the auxiliary spectrum μ_1, μ_2 and μ_3.

Floquet theory. The outcome is the main spectrum, consisting of n finite intervals and one infinite interval. The endpoints of these intervals are labeled λ_1, λ_2, etc., in increasing order, as shown in Figure 1. At the endpoints, only one of the eigenfunctions is bounded. These eigenfunctions are periodic with period T or $2T$. There are an infinite number of isolated eigenvalues inside the interval of infinite length for which there are two bounded, periodic eigenfunctions. Next, one considers the Dirichlet problem

$$\begin{cases} -\psi'' + q_n(x)\psi = \lambda\psi, \\ \psi(x_0) = 0, \quad \psi(x_0 + T) = 0. \end{cases} \tag{6}$$

The spectrum of this problem is referred to as the auxiliary spectrum. It is discrete, and its points $\mu_k(x_0)$, $k = 1, 2, \ldots$ depend on x_0. All but n of its points lie inside the infinite interval of the main spectrum. Each remaining point lies in a different gap of the main spectrum. This is illustrated in Figure 1. The information contained in the main and auxiliary spectra determines the eigenfunction $\psi(x)$: it is a meromorphic function in the finite λ plane with zeros at $\lambda = \mu_k(x_0)$ and poles at $\lambda = \mu_k(x) = \mu_k(x_0)|_{x_0 = x}$ (Dubrovin et al., 1976; Novikov et al., 1984).

Using the main and auxiliary spectra, the inverse periodic spectral problem is solved by (Novikov et al., 1984)

$$q_n(x) = \sum_{j=1}^{2n+1} \lambda_j - 2\sum_{j=1}^{n} \mu_j(x). \tag{7}$$

This is the first of the so-called trace formulae. Other trace formulae give relationships between the potential $q_n(x)$ and its derivatives and the main and auxiliary spectra.

The proposed solution of the inverse periodic spectral problem for finite-gap potentials is not effective. It requires the solution of the direct spectral problem for all x_0 in a period of the potential in order to obtain the auxiliary spectrum as a function of x_0. It is possible to avoid this by determining $\mu_k(x_0), k = 1, \ldots, n$ as a solution of a set of differential equations (Novikov et al., 1984)

$$\frac{\mathrm{d}\mu_j}{\mathrm{d}x_0} = \frac{\pm 2\mathrm{i}\sqrt{\prod_{k=1}^{2n+1}(\mu_j - \lambda_k)}}{\prod_{k\neq j}^{n}(\mu_j - \mu_k)}, \quad j = 1, \ldots, n. \tag{8}$$

The choice of sign gives the direction in which $\mu_j(x_0)$ is going in between its two endpoints.

Another approach, which solves system (8), is the use of abelian functions and Riemann surfaces (Dubrovin, 1981; Belokolos, et al., 1994). An abelian function of n variables is a $2n$-periodic function. As such, abelian functions generalize elliptic functions to more than one variable. All abelian functions are expressible as ratios of homogeneous polynomials of Riemann's theta function. All finite-gap potentials of (4) are abelian functions. For example, the Lamé potentials in (5) are elliptic functions, which are special cases of abelian functions.

In the context of this method, the Bloch function $\phi(x) = \boldsymbol{\phi}_1(x)$ is often referred to as the Baker–Akhiezer function. One of the major results of the theory is the realization that the two Bloch or Baker–Akhiezer functions, regarded as a function of arbitrary complex λ, are distinct branches of one single-valued Baker–Akhiezer function, defined on a two-sheeted Riemann surface covering the complex λ plane (Krichever, 1989). This Riemann surface is already apparent in (8). It is

$$\eta^2 = \prod_{k=1}^{2n+1}(\lambda - \lambda_k), \tag{9}$$

which defines η as a double-valued function of λ. This surface has genus n. It is obtained from Figure 1 by choosing the intervals of the main spectrum as branch cuts and gluing the two resulting sheets together along these cuts. This Riemann surface defines a theta function $\theta(z_1, \ldots, z_n|\boldsymbol{B})$ through its normalized period (or Riemann) matrix $\boldsymbol{B}$. In terms of this theta function

$$q_n(x) = c - 2\frac{\mathrm{d}^2}{\mathrm{d}x^2}\ln\theta(k_1 x + \varphi_1, \ldots, k_n x + \varphi_n|\boldsymbol{B}). \tag{10}$$

The wave numbers $k_1, \ldots, k_n$ are determined as integrals of certain differentials on the Riemann surface (9) with a pole singularity at $\lambda = \infty$. The phase constants $\varphi_1, \ldots, \varphi_n$ are determined by the Riemann constants on (9) and the Abel transform. The constant c is determined by a differential on (9) with a double pole singularity at $\lambda = \infty$. Thus, (10) gives an explicit form for all finite-gap potentials of (4), providing a complete solution of the inverse periodic spectral problem.

Some remarks:

(i) The emphasis on finite-gap potentials is justified in the sense that any T-periodic function is approximated arbitrarily well by an infinite sequence of finite-gap potentials with period T and increasing number of gaps (Dubrovin, 1981).

(ii) The periodic spectral problem (4) is the first half of the Lax pair for the Korteweg–de Vries (KdV) equation. As such, it allows the solution of the KdV equation with periodic initial data. The full solution of this problem requires the solution of both the direct and the inverse periodic spectral problems. The schematics is identical to that of the inverse scattering method. First, the initial condition $u(x, t = 0) = U(x)$ is used

as a potential in (4) to solve the direct periodic spectral problem. This results in the main and auxiliary spectra. The time evolution of these spectra is implied from the second half of the Lax pair: the main spectrum is independent of time, whereas the auxiliary spectrum evolves according to differential equations similar to (8). The spectral data for any time is used to solve the inverse periodic spectral problem of (4). This gives the solution $u(x, t)$ of the KdV equation such that $u(x, t)|_{t=0} = U(x)$ (Novikov et al., 1984).

(iii) The spectral theory for the time-dependent Schrödinger equation is intimately connected to the initial-value problem for the Kadomtsev–Petviashvili equation. A solution of the inverse periodic spectral problem using Riemann's theta function and Riemann surfaces also exists here. However, here there are no restrictions on the form of Riemann surfaces that appear: all compact, connected Riemann surfaces arise. Hence, the periodic spectral theory of the time-dependent Schrödinger equation has important consequences for the theory of Riemann surfaces. It has provided, for instance, a solution to the Schottky problem, which was posed in 1903 (Novikov et al., 1984; Dubrovin, 1981).

(iv)The equation

$$\frac{\mathrm{d}^2 y}{\mathrm{d}x^2} + (a - 2k\cos(2x))y = 0 \qquad (11)$$

is Mathieu's equation. It arises from the three-dimensional Helmholtz equation by separation of variables using elliptical coordinates. It is a special case of (4), using a trigonometric potential. One is only interested in period solutions, resulting in a discrete subset of the main spectrum. The periodic solutions of this equation are referred to as Mathieu functions.

BERNARD DECONINCK

See also **Inverse scattering method or transform; Kadomtsev–Petviashvili equation; Korteweg–de Vries equation; Theta functions**

Further Reading

Amann, H. 1990. *Ordinary Differential Eequations: An Introduction to Nonlinear Analysis*, Berlin and New York: de Gruyter

Belokolos, E.D., Bobenko, A.I., Enol'skii, V.Z., Its, A.R. & Matveev, V.B. 1994. *Algebro-geometric Approach to Nonlinear Integrable Equations*, Berlin and New York: Springer

Dubrovin, B.A. 1981. Theta functions and non–linear equations. *Russian Mathematical Surveys*, 36: 11–92

Dubrovin, B.A., Matveev, V.B. & Novikov, S.P. 1976. Nonlinear equations of Korteweg–de Vries type, finite-zone linear operators, and Abelian varieties. *Russian Mathematical Surveys*, 31: 59–146

Krichever, I.M. 1989. Spectral theory of two-dimensional periodic operators and its applications. *Russian Mathematical Surveys*, 44: 145–225. (The introduction is a great overview of the development of periodic spectral theory.)

Lax, P.D. 1975. Periodic solutions of the KdV equation. *Communications on Pure and Applied Mathematics*, 28: 141–188

Magnus, W. & Winkler, S. 1979. *Hill's Equation*, New York: Dover and London: Constable

Novikov, S.P. 1974. The periodic problem for the Korteweg–de Vries equation. *Functional Analysis and Its Applications*, 8: 54–66

Novikov, S.P., Manakov, S.V., Pitaevskii, L.P. & Zakharov, V.E. 1984. *Theory of Solitons: The Inverse Scattering Method*, New York: Consultants Bureau (original Russian edition 1980)

PERMANENT WAVE

See **Wave of translation**

PERTURBATION THEORY

A limited number of nonlinear partial differential equations (PDEs) can be solved analytically for arbitrary initial conditions. Specific applications often lead to nonlinear PDEs that do not fall into the category that can be solved by means of the inverse scattering theory, Bäcklund transformations, or Hirota's bilinear method (Dodd et al., 1984). Examples of such PDEs with physical relevance include soliton equations with added perturbative terms describing energy gain and losses, where the original unperturbed problem is energy-conserving and hence Hamiltonian. Other problems involve nonconservative PDEs, such as nerve fibers and other reaction-diffusion type equations in general. In fluid mechanics, boundary layers possess a special challenge with singular perturbations requiring matching solutions close to a boundary and solutions far from a boundary layer. Perturbations can be additive or parametric (multiplicative), and they can be localized, periodic, quasi-periodic, or random, depending on the nature of the problem to be solved. In the case of a PDE that cannot be solved analytically, we resort to approximate analytical solutions or direct numerical analysis. The approximate solutions can be determined by various perturbation techniques. For soliton equations one procedure is to calculate the variation of the spectral data in the inverse scattering method due to external perturbations (Karpmann, 1979; Kivshar, & Malomed, 1989). Another method introduces slow variation of the parameters entering the soliton solution. Variants of the latter idea include multiple scales, energy methods, and the Lindsted–Poincaré technique. Here we shall illustrate the multiscale method applied to a perturbed nonlinear Schrödinger (NLS) equation. The method follows the ideas in Kaup (1990) with an extension presented in Nguyen et al. (1995). A general perturbed NLS equation is

$$\mathrm{i}\frac{\partial u}{\partial t} + \frac{\partial^2 u}{\partial x^2} + 2|u|^2 u = \varepsilon R(t, u). \qquad (1)$$

The complex function $u = u(x,t)$ depends on the spatial coordinate x and time t. The absolute value of the perturbation parameter ε is assumed to be much smaller than unity, and we expect that the perturbation εR on the right-hand side only slightly modifies soliton solutions of the pure NLS equation. We introduce multiple scales of the time variable according to

$$T_0 = t, \quad T_1 = \varepsilon t. \tag{2}$$

In the simplest case, we treat the single soliton solution and invoke the solution ansatz

$$u = q \exp(\mathrm{i}\xi(\Theta - \Theta_0) + \mathrm{i}(\sigma - \sigma_0)), \tag{3}$$

$$q = \eta \mathrm{sech}(\eta(\Theta - \Theta_0)),$$
$$\text{where} \quad \Theta = x - 2X(T_0, T_1). \tag{4}$$

The functions X and σ are defined by $\partial X/\partial T_0 = -2\xi(T_1)$ and $\sigma = (\eta^2(T_1) + \xi^2(T_1))T_0$. To proceed, we expand q according to $q = q_0 + \varepsilon(\phi + \mathrm{i}\psi)$ and insert into Equation (1), finding

$$Lq_0 = (\partial_{\Theta\Theta} + 2q_0^2 - \eta^2)q_0 = 0, \tag{5}$$

$$M\phi = (\partial_{\Theta\Theta} + 6q_0^2 - \eta^2)\phi = \mathrm{Re}[F], \tag{6}$$

$$L\psi = (\partial_{\Theta\Theta} + 2q_0^2 - \eta^2)\psi = \mathrm{Im}[F]. \tag{7}$$

Here, q_0 is assumed to be real, and F is a lengthy complex expression, omitted for brevity. $\mathrm{Re}[F]$ and $\mathrm{Im}[F]$ denote the real and imaginary parts of F, respectively. First a solution for q_0 is obtained and the next step is to solve the inhomogeneous Equations (6) and (7). In solving these, we shall invoke Fredholm's solvability condition, which states that the null spaces of the operators M and L are orthogonal to the right-hand sides $\mathrm{Re}[F]$ and $\mathrm{Im}[F]$, respectively. The null space of an operator L is the space spanned by the solutions of $L^\dagger z(\Theta) = 0$, where $L^\dagger$ is the adjoint operator of L. This condition guarantees a solution without secular terms and provides evolution equations for the slowly varying parameters of the form

$$\eta \frac{\partial \xi}{\partial T_1} = \int_{-\infty}^{\infty} \mathrm{Re}[R] \frac{\partial q_0}{\partial \Theta} \, \mathrm{d}\Theta, \tag{8}$$

$$\frac{\partial \eta}{\partial T_1} = \int_{-\infty}^{\infty} \mathrm{Im}[R] q_0 \, \mathrm{d}\Theta. \tag{9}$$

For a given perturbation R, we can solve these equations for the slowly varying soliton amplitude η and ξ.

In the previous discussion, we began with a soliton as the zero-order approximation and adjusted its parameters to achieve an approximate solution of the perturbed soliton equation. In nonlinear diffusion equations, solutions emerge from balancing sources of energy with diffusion and dissipative effects. The perturbation theory outlined above can also be applied to such systems. As an example let us consider the FitzHugh–Nagumo (FN) model for nerve pulse propagation (FitzHugh, 1961):

$$\frac{\partial^2 V}{\partial x^2} - \frac{\partial V}{\partial t} = F(V) + R, \tag{10}$$

$$\frac{\partial R}{\partial t} = \varepsilon V, \tag{11}$$

where $F(V)$ is the cubic-shaped function $V(V-a)(V-1)$. $V = V(x,t)$ is the voltage across the nerve cell membrane, and R is a recovery variable. The nerve pulse solution is localized in space and propagates by a velocity v to be determined from the model equations. Instead of using a multiscale approach, we invoke the Lindsted–Poincaré technique (Nayfeh, 1973) and expand the velocity parameter according to

$$v = v_0 + \varepsilon v_1 + O(\varepsilon^2). \tag{12}$$

The reason for introducing the above expansion is that nonlinearity will alter the propagation velocity. We also expand the dependent functions V and R

$$V = V_0 + \varepsilon V_1 + O(\varepsilon^2), \tag{13}$$

$$R = R_0 + \varepsilon R_1 + O(\varepsilon^2). \tag{14}$$

It is important to note that terms increasing to infinity for large times t, that is, secular terms in V_1 and R_1, are avoided by using the expansion of the velocity in Equation (12). Introducing a traveling wave assumption $\xi = x - vt$ in the solution and substituting expressions (12)–(14) into the FN equations (10) and (11) and ordering terms in power of ε leads to

$$\frac{\mathrm{d}^2 V_0}{\mathrm{d}\xi^2} + v_0 \frac{\mathrm{d}V_0}{\mathrm{d}\xi} - [F(V_0) - R_0] = 0, \tag{15}$$

$$\frac{\mathrm{d}R_0}{\mathrm{d}\xi} = 0. \tag{16}$$

To order $O(\varepsilon)$ we have

$$LV_1 = \frac{\mathrm{d}^2 V_1}{\mathrm{d}\xi^2} + v_0 \frac{\mathrm{d}V_1}{\mathrm{d}\xi} - F'(V_0)V_1 = R_1 - v_1 \frac{\mathrm{d}V_0}{\mathrm{d}\xi}, \tag{17}$$

$$\frac{\mathrm{d}R_1}{\mathrm{d}\xi} = -\frac{V_0}{v_0}. \tag{18}$$

Here it turns out that we can identify "boundary layers" for the determination of V and R together with appropriate matching. In the limit of $\varepsilon \to 0$, the nerve pulse voltage rises sharply from zero to a plateau value of order $O(1)$. The rapid change is equivalent to a boundary layer in fluid dynamics. Similarly a sharp decrease of the pulse appears at its rear end followed by a slow recovery interval due to a fading R. Matching of the solutions can be done in each region. The correction term v_1 in the expansion of the velocity is determined from Fredholm's solvability condition of

Equation (17). That is, the null space of the operator L should be orthogonal to the right-hand side of (17). This is equivalent to the requirement for the NLS equation in the previous section. For $a < \frac{1}{2}$ the traveling wave velocity v_0 of the leading edge is $v_0 = (1-2a)/\sqrt{2}$ and the first-order correction becomes

$$v_1 = \frac{\int_{-\infty}^{\infty} \left[\int_{\xi}^{\infty} V_0(\xi')\,\mathrm{d}\xi'\right](\mathrm{d}V_0/\mathrm{d}\xi)\mathrm{e}^{v_0\xi}\,\mathrm{d}\xi}{v_0\int_{-\infty}^{\infty}(\mathrm{d}V_0/\mathrm{d}\xi)^2\mathrm{e}^{v_0\xi}\,\mathrm{d}\xi}. \quad (19)$$

As we have used a traveling wave ansatz, the obtained solution for V_0 may not be stable. However, a closer analysis reveals that stable traveling wave solutions exist (Scott, 2003). Random perturbations make up a set of conceptually different problems that may be treated by methods of stochastic differential equations and statistics. For soliton equations, studies have been performed on random parameters modeling the stochastic variation of various physical properties, such as geometry or material. The influence of thermal noise and incoherence of amplitude and phase modulations of input pulses are other important examples (Abdullaev, 1994; Abdullaev et al., 2001).

MADS PETER SØRENSEN

See also **Averaging methods; FitzHugh–Nagumo equation; Fredholm theorem; Korteweg–de Vries equation; Multisoliton perturbation theory**

Further Reading

Abdullaev, F.Kh. 1994. *Theory of Solitons in Inhomogeneous Media*, Chichester: Wiley

Abdullaev, F.Kh., Bang, O. & Sørensen, M.P. 2001. *NATO Advanced Research Workshop on Nonlinearity and Disorder: Theory and Applications*, Boston and Dordrecht: Kluwer

Dodd, R.K., Eilbeck, J.C., Gibbon, J.D. & Morris, H.C. 1984. *Solitons and Nonlinear Wave Equations*, London: Academic Press

FitzHugh, R. 1961. Impulses and physiological states in theoretical models of nerve membrane. *Biophysical Journal*, 1: 445–466

Karpmann, V.I. 1979. Soliton evolution in the presence of perturbation. *Physica Scripta*, 20: 462–478

Kaup, D.J. 1990. Perturbation theory for solitons in optical fibers. *Physical Review* A, 24: 5689–5694

Kivshar, Y.S. & Malomed, B.A. 1989. Solitons in nearly integrable systems. *Reviews of Modern Physics*, 61: 763–915

Nayfeh, A.H. 1973. *Perturbation Methods*, New York: Wiley-Interscience

Nguyen, P., Skovgaard, P., Sørensen, M.P. & Christiansen, P.L. 1995. Solitons in fibre lasers and mode-locked systems. *Physical Review* A, 24: 5689–5694

Scott, A. 2003. *Nonlinear Science: Emergence and Dynamics of Coherent Structures*, 2nd edition, Oxford and New York: Oxford University Press

PHASE DYNAMICS

Phase as a physical term is most commonly used in reference to oscillatory processes. The concept of phase dynamics is particularly relevant to self-sustained or limit-cycle oscillations. The orbital shape of a limit cycle is more or less rigid against perturbations, while the remaining degree of freedom along the closed orbit (the phase) lacks such rigidity. Consequently, when a limit-cycle oscillator is slightly perturbed, the resulting nontrivial dynamics could well be described in terms of the phase alone. This is the intuition behind the phase description of a variety of oscillatory phenomena, among others biological oscillations (Winfree, 2000).

Mathematically, limit-cycle oscillations are described with a time-periodic solution of an autonomous nonlinear ordinary differential equation $\mathrm{d}X/\mathrm{d}t = F(X)$, $X \in R^n$. Let such a solution with angular frequency ω be given by a 2π-periodic function $X_0(\omega t + \phi_0)$ involving an arbitrary phase constant ϕ_0. One may also introduce a phase variable $\phi(t)$ to represent this one-parameter family of solutions as

$$X(t) = X_0(\phi(t)), \qquad \frac{\mathrm{d}\phi}{\mathrm{d}t} = \omega. \quad (1)$$

Suppose the oscillator is slightly perturbed, by which F is slightly modified. As the resulting deformation of the closed orbit would be negligibly small, the first equation in (1) still holds approximately, while the correction to the instantaneous frequency $\mathrm{d}\phi/\mathrm{d}t$, however small it may be, would give rise to a large difference in ϕ in the long run and hence is indispensable.

Further, suppose that the perturbation represents the influence from another oscillator with state vector X' coupled weakly to the first one. If these oscillators are identical in nature, one may also use the approximation $X'(t) = X_0(\phi'(t))$ for the second oscillator, so that the current state of our oscillator pair may well be specified only with their phases $\phi(t)$ and $\phi'(t)$. Therefore, the small term to be added to the phase equation in (1) should generally be given by some function $G(\phi, \phi')$ which is 2π-periodic both in ϕ and ϕ'. Due to the assumed smallness of G relative to ω, it turns out that the effect of G over one cycle of oscillation depends only on the phase difference $\phi - \phi'$. Thus, using a 2π-periodic function Γ, one may obtain

$$\frac{\mathrm{d}\phi}{\mathrm{d}t} = \omega + \Gamma(\phi - \phi') \quad (2)$$

and, if we need, a similar equation for the second oscillator also. The function Γ can be computed in principle with the knowledge of the original dynamical-system model. Note, however, that the formula for Γ requires an extension of the definition of phase slightly outside the limit-cycle orbit (Kuramoto, 1984a).

The above equation may readily be extended to larger assemblies of weakly coupled oscillators. Furthermore, the oscillators may be slightly dissimilar, with their effect appearing only through a small difference in natural frequency ω. Thus, for such an

assembly of N oscillators, we generally have

$$\frac{d\phi}{dt} = \omega_i + \sum_{j=1}^{N} \Gamma_{ij}(\phi_i - \phi_j), \quad i = 1, 2, ..., N. \quad (3)$$

This is called the phase oscillator model which is extremely useful for the study of complex collective behavior of large assemblies of coupled oscillators appearing in large varieties of fields ranging from physics to brain science (Pikovsky et al., 2001).

Phase dynamics are also useful when the oscillators constitute a continuous field. As a representative class of such continua, we will focus on oscillatory reaction-diffusion systems given by

$$\frac{\partial X}{\partial t} = F(X) + \hat{D}\nabla^2 X, \quad (4)$$

where $X(r, t)$ represents a space–time-dependent composition vector of dimension n and $\hat{D}$ is a diagonal matrix of n diffusion constants. If the spatial variation of X is of long wavelength, the diffusion term can be regarded as a small perturbation driving each local oscillator, so that the previous idea of phase dynamics should work. The approximation $X(r, t) = X_0(\phi(r, t))$ would again be valid at each spatial point. Its application to the diffusion term produces terms proportional to $\nabla^2\phi$ and $(\nabla\phi)^2$. According to a systematic perturbation theory, such terms actually appear in the phase equation. Specifically, we obtain a nonlinear phase diffusion equation

$$\frac{\partial \phi}{\partial t} = \omega + \nu\nabla^2\phi + \mu(\nabla\phi)^2 \quad (5)$$

to the nontrivial lowest order approximation with respect to the smallness in the spatial gradient of ϕ, where positive ν has been assumed. If ν is negative, the uniform oscillation is unstable. For small negative ν, the idea of phase dynamics still works. Then (5) is modified to give an equation equivalent to the Kuramoto–Sivashinsky equation, whose solution describes spatiotemporal chaos called phase turbulence.

In a more general context, phase is a degree of freedom appearing when a certain continuous symmetry of the system has been broken spontaneously (Mori & Kuramoto, 1998). For instance, the phase of a limit-cycle oscillator reflects the fact that the oscillation breaks the invariance of the governing evolution equation (assumed autonomous) with respect to temporal translations $t \to t + t_0$. Such symmetry-breaking solutions, not restricted to time-periodic solutions, generally involve an arbitrary phase constant, thus forming an infinite family recovering as a whole the original symmetry. This also means that phase has no prescribed value to which it is bound to relax or, equivalently, phase represents a neutrally stable dynamical variable. When the system is weakly perturbed, such neutrality is slightly violated causing the phase to evolve slowly, possibly apart from a constant drift. In contrast, all the other degrees of freedom will damp quickly, thus following adiabatically the slow motion of the phase. This explains why the phase so often dominates the pattern dynamics in nonlinear dissipative systems.

The general argument given above implies that the applicability of phase dynamics is by no means restricted to oscillatory systems. Two important non-oscillatory applications of phase dynamics, again in reference to reaction-diffusion systems with large spatial extension, will be touched upon next.

Reaction-diffusion systems may develop a spatially periodic static pattern out of a uniform state through the Turing instability, by which the spatial translational symmetry has been broken. When the local phase of the periodic pattern is subject to a large-scale spatial modulation, phase dynamics is applicable and describes the pattern dynamics through a slow evolution of the phase (Kuramoto, 1984b). For instance, the transient dynamics of recovery of a regular pattern can be described with a simple phase-diffusion equation.

Another important class of symmetry-breaking patterns arising in reaction-diffusion systems is localized structures such as moving domain boundaries and solitary pulses. In these cases, phase corresponds to the location of a moving front. For a planar front, the phase forms a uniform field advancing at a constant speed. When the planar front is deformed slightly in large spatial scale, the phase becomes slightly non-uniform and starts to evolve slowly. It is concluded from a systematic theory of phase dynamics that when the planar front is stable, the equation for the phase takes the same form as (5) with ∇ being replaced with a gradient of reduced dimension (Kuramoto, 1984a). A planar front that is weakly unstable due to small negative ν leads to phase turbulence described essentially by the Kuramoto–Sivashinsky equation.

YOSHI KURAMOTO

See also **Coupled oscillators; Kuramoto–Sivashinsky equation; Synchronization**

Further Reading

Kuramoto, Y. 1984a. *Chemical Oscillations, Waves, and Turbulence*, Berlin: Springer

Kuramoto, Y. 1984b. Phase dynamics of weakly unstable periodic structures. *Progress of Theoretical Physics*, 71(6): 1182–1196

Mori, H. & Kuramoto, Y. 1998. *Dissipative Structures and Chaos*, Berlin: Springer

Pikovsky, A., Rosenblum, M. & Kurths, J. 2001. *Synchronization: A Universal Concept in Nonlinear Sciences*, Cambridge and New York: Cambridge University Press

Winfree, A.T. 2000. *The Geometry of Biological Time*, 2nd edition, Berlin and New York: Springer

PHASE LOCKING

See **Coupled oscillators**

PHASE MATCHING

See **Nonlinear optics**

PHASE PLANE

The term *phase plane*, naturally enough, refers to the phase space of a two-dimensional dynamical system. The term is worthy of consideration in its own right because of the various special techniques that exist for the analysis of two-dimensional continuous-time dynamical systems (i.e., flows).

As an example, consider the two-dimensional flow induced by the following differential equations:

$$\begin{aligned} \dot{x}_1 &= x_1\,(1 - x_2)\,, \\ \dot{x}_2 &= x_2\,(x_1 - r)\,. \end{aligned} \tag{1}$$

Each of these equations specifies one component of a two-dimensional vectorfield on the plane, tangent at each point to the induced flow. Equations (1) were first employed by Alfred Lotka (1920) to describe a hypothetical bimolecular chemical reaction capable of sustained oscillations, assuming mass action kinetics. At about the same time and independently, Vito Volterra (1926) made use of the same equations to model the interaction of biological predator and prey populations. In Equations (1), x_1 denotes the density of the prey species and x_2 that of the predator. Figure 1a shows the relevant (positive) quadrant of the phase plane of Equations (1).

The most important aspects of the dynamics of smooth flows are determined by their α- and ω-limit sets. The former are those sets approached by an orbit as $t \to -\infty$; the latter, those approached as $t \to +\infty$. In smooth planar flows, these limit sets are of only three types: singular points (or equilibria), closed (or periodic) orbits, and homo- and heteroclinic chains. The last are made up of singular points together with bounded orbits, each of which has one singular point as α-limit and another (possibly identical) singular point as ω-limit. It should be noted that more complex behaviors such as quasi-periodicity and chaotic dynamics are not possible in two-dimensional flows.

Singular points are determined as the solutions of a system of two algebraic equations and classified, on the basis of linear stability analysis, into six types: stable and unstable nodes, stable and unstable foci, centers, and saddles. Useful information about the simultaneous existence of singular points and closed orbits can be obtained from consideration of the Poincaré index, an integer associated with each singular point (*See* **Winding numbers** and Andronov et al., 1966). For example, the Poincaré index can be used to show that every closed orbit encircles at least one singular point.

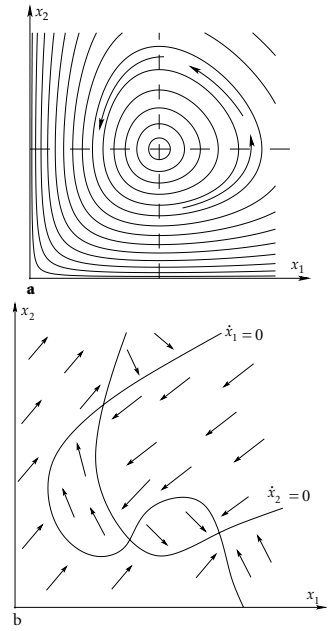

Figure 1. (a) Phase plane of the Lotka–Volterra equations (1). Representative orbits are shown as solid lines; the direction of flow is indicated by arrows. The isoclines are shown using dashed lines. The positive quadrant is filled with a family of closed orbits, corresponding to the fact that equations (1) are Hamiltonian. (b) Diagram showing a generic isocline analysis: many qualitative features of the dynamics are made plain. The isoclines show the loci where the vectorfield is horizontal or vertical. Intersections of the isoclines occur at singular points. From left to right, the three singular points are evidently of focus, saddle, and stable node types. It is not clear from the isocline analysis alone whether the focus is stable or unstable.

The method of isoclines is frequently invaluable in deriving qualitative information about the dynamics of a given smooth flow. An isocline is the locus where one of the vector field components vanishes. The two isoclines together split the phase plane into four divisions: within each such division each vector field component has a uniform sign. Figure 1b depicts a typical isocline analysis.

Closed orbits which attract or repel nearby orbits are called limit cycles. Systems possessing stable limit cycles are said to exhibit auto-oscillations. The method of Liénard can be used to demonstrate the existence of limit cycles in certain systems (Hartman, 2002). Sometimes, a limit cycle can also be found

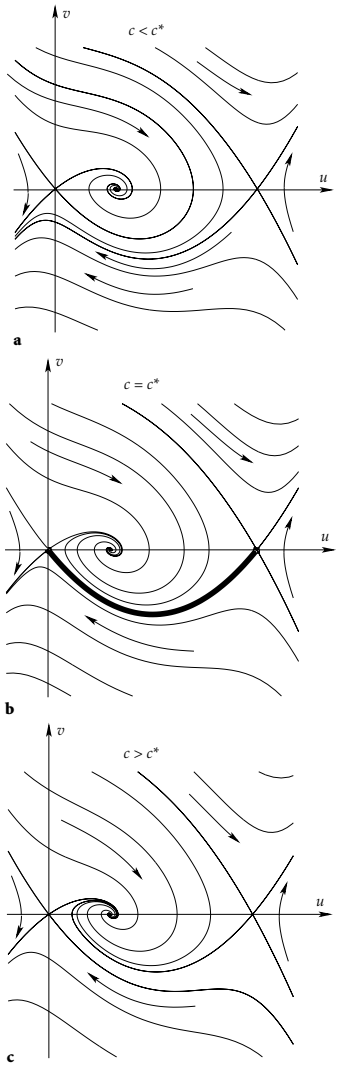

Figure 2. Determining a heteroclinic connection by shooting. Adjusting a parameter (in this case the wave speed c) causes the unstable manifold of the rightmost saddle point to move. For small positive values of c, one branch of the unstable manifold crosses the negative v-axis, never to return (a). At larger values of c, it is drawn into the stable focus point at $u = a$, $v = 0$ (c). There is precisely one intermediate value $c = c^*$ for which a branch of the unstable manifold of the rightmost saddle coincides with a branch of the stable manifold of the leftmost saddle, i.e., for which there is a heteroclinic connection (the emboldened orbit in b).

by association with a Hopf bifurcation (Arnol'd, 1973; Hale & Koçak, 1991). The Poincaré–Bendixson theorem can also be used to demonstrate the existence of limit cycles. It states that any non-empty compact α- or ω-limit set of a smooth planar flow which does not contain a singular point is a closed orbit.

Homo- and heteroclinic chains are, in general, more difficult to determine than equilibria. So-called shooting methods may sometimes be used to prove the existence of homoclinic or heteroclinic connections. For example, consider the following planar system, which arises as the traveling wave reduction of the Zeldovich–Frank-Kamenetsky equation

$$\begin{aligned} \dot{u} &= v, \\ \dot{v} &= u\,(u-a)\,(u-1) - c\,v. \end{aligned} \tag{2}$$

Here, the parameter c is a wave speed (*See* **Wave of translation**), and we assume (without loss of generality) that $0 < a < \frac{1}{2}$. It is readily seen that there are precisely three singular points (at $u = 0$, a, 1 and $v = 0$); the first and third are saddles; the intermediate is of focal type (see Figure 2). If we seek a rightward moving wave ($c > 0$), this focus is stable. For small values of c, the lower branch of the rightmost saddle's unstable manifold crosses the negative v-axis, where as for sufficiently large values of c, it crosses the positive u-axis before winding about the stable focus. It follows that there is an intermediate wave speed c^* for which a heteroclinic connection exists. It should be noted that this shooting argument depends on the fact that deleting a point from an interval in two-dimensional space topologically disconnects the interval. Shooting methods become more complicated in higher dimensions (see, e.g., Dunbar, 1984).

AARON A. KING

See also **Bifurcations; Chaotic dynamics; Chemical kinetics; Dynamical systems; Hamiltonian systems; Hopf bifurcation; Phase space; Poincaré theorems; Population dynamics; Wave of translation; Zeldovich–Frank-Kamenetsky equation**

Further Reading

Andronov, A.A., Vitt, A.A. & Khaikin, S.E. 1966. *Theory of Oscillators*, Oxford: Pergamon Press (translated from Russian)

Arnol'd, V.I. 1973. *Ordinary Differential Equations*, Cambridge, MA: MIT Press

Arnol'd, V.I. & Il'yashenko, Y.S. 1988. *Ordinary Differential Equations and Smooth Dynamical Systems*. *Dynamical Systems*, vol. 1, Berlin: Springer (original Russian edition 1985)

Dunbar, S.R. 1984. Traveling wave solutions of diffusive Lotka–Volterra equations: a heteroclinic connection in R^4. *Transactions of the American Mathematical Society*, 286: 557–594

Hale, J.K. & Koçak, H. 1991. *Dynamics and Bifurcations*, New York: Springer

Hartman, P. 2002. *Ordinary Differential Equations*, 2nd edition, Philadelphia: SIAM (corrected republication of edition published by Birkhäuser, Boston, 1982)
Hirsch, M.W. & Smale, S. 1974. *Differential Equations, Dynamical Systems, and Linear Algebra*, New York: Academic Press
Lotka, A.J. 1920. Undamped oscillations derived from the law of mass action. *Journal of the American Chemical Society*, 42: 1595–1598
Volterra, V. 1926. Fluctuations in abundance of a species considered mathematically. *Nature*, 118: 558–560

PHASE SPACE

The equations of motion of a mechanical system are usually of second order, and they determine the entire future from the initial *state*, which consists of both positions and velocities. The space of all states is called the *phase space*. For the mathematical pendulum (a point mass in the plane at one end of a massless rod whose other end is fixed), the configuration space is a circle, at each point of which one can choose any tangent vector as the velocity. Therefore, the phase space is a circle with a line attached to each point, that is, a cylinder. The pendulum equation for the position x and velocity v, $\ddot{x} + \sin x = 0$ converts to $(\dot{x}, \dot{v}) = (v, -\sin x)$, so the dynamics is described by integral curves of the vector field $R(x, v) = (v, -\sin x)$ on the cylinder.

That the notion of phase space is natural is also suggested by the Liouville theorem: the skew-symmetry of the Hamilton equation makes the Hamiltonian vector field divergence-free, and accordingly, a Hamiltonian flow preserves the volume on phase space.

Generally, a dynamical system consists of a phase space and a time-evolution of first order. The phase space is a set with some structure, such as differentiable (in the case of differential equations, this belongs to smooth dynamics), topological (one then speaks of topological dynamics), or measurable (this is the subject of ergodic theory, which arose from the Liouville theorem), and the time evolution is a one-parameter family of transformations that preserve this structure and that map initial states to states at another time. The time parameter may run through real numbers (continuous-time system) or integers (discrete-time system, iterations of a map and possibly its inverse). Specifically, a continuous-time system is given by a family $(f^t)_{t\in\mathbb{R}}$ of maps. If $f^t(f^s(x)) = f^{t+s}(x)$ for every s, t, x, then we say that this family is a flow. In the discrete-time case, one considers the iterates $(f^n)_{n\in\mathbb{Z}}$, where $f^0(x) = x$, $f^{n+1}(x) = f(f^n(x))$ for $n \geq 0$, and $f^n(x) = (f^{-1})^n(x)$ for $n < 0$, or if the map is not invertible, only positive iterates $(f^n)_{n\in\mathbb{N}}$. The maps $f_a(x) = ax(1-x)$ are a popular example of the latter (the so-called logistic map).

The long-term behavior of flows in the plane is well understood (*See* **Phase plane**): In the long run, any orbit either approaches fixed points or is asymptotically periodic (Poincaré–Bendixson theorem). This is ultimately due to the fact that a closed curve, such as a periodic orbit, divides the plane into separate regions. Already in three-space, one gets chaotic behavior, such as in the Lorenz attractor.

Qualitative Theory of Differential Equations and Dynamical Systems

On the phase space of a smooth continuous-time dynamical system, the time evolution is given by a first-order differential equation $\dot{x} = R(x, t)$. Suppose the right-hand side R satisfies a Lipschitz condition in x. This means that there is a constant M such that $d(R(x, t), R(x', t)) \leq M d(x, x')$ for all x, x'. The basic Picard theorem then guarantees existence and uniqueness of solutions for any initial condition. Otherwise solutions may not be unique ($\dot{x} = \sqrt[3]{x}$ has infinitely many solutions with initial value 0) or may not exist for any uniform amount of time (the solutions of $\dot{x} = x^2$ have singularities).

If solutions $x(t)$ exist for all time, as we henceforth assume, they define time-t-maps by $f^t(x(0)) = x(t)$. Each map f^t is as smooth as the right-hand side R of the differential equation (smooth dependence on initial conditions).

If R is independent of t, then the differential equation is said to be "autonomous," and R gives a vector field on the phase space that prescribes the velocity vectors of solutions. The family of time-t-maps is then a flow. The iterates of the time-1-map of a flow produce a discrete-time dynamical system whose study may yield useful information about the flow. If R depends on t, the system is said to be non-autonomous. Explicit time dependence can, for example, arise from forcing terms (forced pendulum $\ddot{x} + \sin x = \sin \omega t$) or from varying parameters (driving of a swing by parametric forcing, $\ddot{x} + \rho(t) \sin x = 0$).

An "orbit" or *trajectory* of a continuous-time system is a parametrized curve $(f^t(x))_{t\in\mathbb{R}}$. An orbit or trajectory of a map consists of the sequence of images of a point under iteration of the map: $(f^n(x))_{n\in\mathbb{Z}}$.

A singular point of a differential equation $\dot{x} = R(x, t)$ is a point x for which the right-hand side is zero for all t, that is, an equilibrium, or constant solution, or fixed point. Fixed points of a map f are those points x for which $f(x) = x$. A periodic point is a state that repeats at some positive time. For differential equations, this corresponds to solutions that are periodic functions of time; for maps, these are fixed points of an iterate. For the flow on the cylinder generated by $\ddot{x} + \sin x = 0$, all but four orbits are periodic; the point $(5 + \sqrt{5})/8$ is two-periodic for the map $4x(1-x)$.

Fixed and periodic points can be anchors for the study of the global orbit structure, and therefore, it is important to understand the behavior of nearby orbits. A fixed point is said to be attracting if orbits of nearby

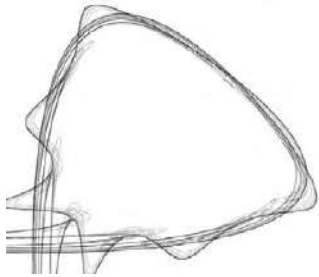

Figure 1. Stable and unstable manifold of a hyperbolic fixed point.

points stay nearby (Poisson stability) and converge to it for large positive time (asymptotic stability). (The example of a circle map like this ↻ with a fixed point at the top illustrates that the second condition does not imply the first.) This is the case if the differential of the map (or time-1-map in the case of a flow) at that point has only eigenvalues of absolute value less than 1. If all eigenvalues have absolute value greater than 1 then the point is repelling: There is a neighborhood which every other point leaves in positive time. The map $f_2(x) = 2x(1-x)$ has 0 and $\frac{1}{2}$ as fixed points. 0 is repelling and $\frac{1}{2}$ is attracting. In fact, $\frac{1}{2}$ is superattracting: $f_2'(\frac{1}{2}) = 0$ and orbits near $\frac{1}{2}$ approach $\frac{1}{2}$ faster than exponentially.

If eigenvalues of the differential are allowed to lie both inside the unit circle and outside it but not on it, then the fixed point is said to be "hyperbolic." In this case the Hartman–Grobman theorem states that there is a continuous coordinate change that maps orbits near the fixed point to orbits of the linearized map. Moreover, tangent to the contracting and expanding subspaces of the linearization, there are the stable and unstable manifold of points positively and negatively asymptotic to the fixed point, respectively. These are smooth subspaces without self-intersections, but they may be packed into the phase space in a complicated way.

For periodic points of maps, the analysis of stability can be carried out by studying the appropriate iterate; for a flow, one likewise studies Poincaré return maps as follows. Take a small hypersurface through the periodic point transverse (for example, orthogonal) to the flow. The orbit of every point sufficiently near the periodic point returns to this surface at a time close to the period, and this defines a map from a neighborhood of the periodic point in the hypersurface into the hypersurface, with the original periodic point as a fixed point.

If, for example, a periodic orbit is an attracting fixed point for the return map, then it is a limit cycle: All nearby orbits are asymptotic to it. For the mathematical pendulum from the introduction, the circle $\{v = 0\}$ is a

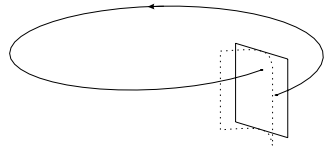

Figure 2. A section.

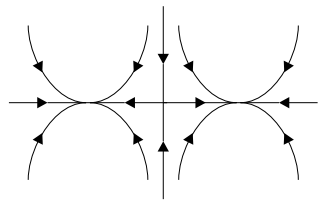

Figure 3. Two attracting points.

section of the cylinder, and the return map is defined for all of its points. It has two fixed points, and all other points are two-periodic.

A property complementary to stability of a fixed or periodic point as defined in terms of the behavior of nearby orbits (i.e., perturbations of the initial condition) is that of stability under perturbations of the dynamical system. An easy way to guarantee this is *transversality*, which is weaker than hyperbolicity: A fixed point $x = f(x)$ is said to be *transverse* if the derivative of f at x does not have 1 as an eigenvalue. (This implies that there are no other fixed points nearby.) In this case, any C^1-perturbation of f (i.e., one that changes derivatives only a little) also has a (transverse) fixed point near x. The origin is a nontransverse fixed point of $x(1-x)$, and indeed, it is absent for $x(1-x)+\varepsilon$ with $\varepsilon < 0$. The creation of two (hyperbolic) fixed points as ε changes from negative to positive is a basic local *bifurcation*. For differential equations, transversality corresponds to invertibility of the differential of the right-hand side.

An "invariant set" is a union of orbits; for example, $[0, 1]$ is invariant under $4x(1-x)$. It is a repeller if it has a neighborhood in which only orbits of points in the invariant set stay for all positive time. It is an "attractor" if there is a neighborhood that is mapped into itself and the intersection of whose positive-time iterates is the invariant set. (Usually, one also requires that there is no proper subset with the same property. Thus, Figure 3 shows two attracting fixed points, and the interval with these as endpoints is not considered an attractor.)

The "basin of attraction" is the set of points that are asymptotic to the attractor. For example, the interval $(0, 1)$ is the basin of attraction of $\frac{1}{2}$ for the map $2x(1-x)$.

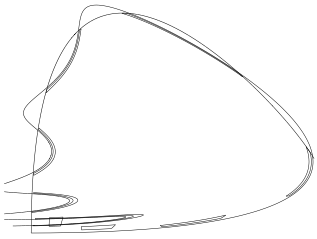

Figure 4. The Birkhoff–Smale theorem.

If two hyperbolic fixed points (saddles) in the plane are connected by a curve segment that lies in the unstable manifold of one of them and in the unstable manifold of the other, then this segment is called a "separatrix" (because it often separates two basins of attraction). More generally, the intersection of the stable manifold of one hyperbolic point with the unstable manifold of another is called a "heteroclinic intersection," and the orbit of every intersection point is called a "heteroclinic orbit." If the two fixed points coincide then one uses the terms "homoclinic intersection" and *homoclinic orbit* instead. The Birkhoff–Smale theorem asserts that if a homoclinic intersection is transverse (or if there is a pair of transverse heteroclinic intersections, that is, two hyperbolic points such that the unstable manifold of each of them intersects the stable manifold of the other point transversely), then there is a "horseshoe," that is, a rectangle that (under an iterate) gets mapped across itself in a horseshoe-like fashion as illustrated in Figure 4 and in Anosov and Axiom-A systems. This implies directly that there is an invariant Cantor set on which the dynamical system exhibits deterministic chaos.

There are several ingredients that make up chaotic behavior. One of these is recurrence. There are several recurrence properties. A point is said to be *recurrent* if it returns arbitrarily near to its initial condition. For a rigid rotation of a circle by an irrational number of degrees, all points have this property. By contrast, a point is said to be *transient* or *wandering* if it has a neighborhood all of whose images are pairwise disjoint. For the circle map $\circlearrowleft$ with a fixed point on top, all nonfixed points are wandering. The set of nonwandering points is called the nonwandering set. Nonwandering orbits can be closed by a localized C^1 perturbation of the map (Pugh closing lemma). A dynamical system is said to be "topologically transitive" if it has a dense orbit and "minimal" if every orbit is dense. Irrational circle rotations have both properties. Minimality does not reflect chaotic behavior. Existence of a dense orbit is equivalent to the condition that for any two open sets there are arbitrarily large times at which the image of one of these sets overlaps the other. A strengthening of this property is that such overlap occurs for all sufficiently large times; this is called topological mixing and implies sensitive dependence on initial conditions. Following Devaney, one can say that a dynamical system is *chaotic* if it is topologically transitive and the set of periodic points is dense. This also implies sensitive dependence. A condition stronger than sensitive dependence is "expansivity": There is a universal positive constant by which the images of any two points, no matter how close initially, are separated at some time. The cat map and horseshoes are good examples of dynamical systems with these properties.

The Poincaré return map is not the only construction that produces a new dynamical system with a different phase space. Another straightforward one is the product of two dynamical systems. For example, the flow of rotations of the unit circle given by $x_1 = \alpha \cos t$, $x_2 = \alpha \sin t$ can be combined with a similar flow $y_1 = \omega \cos t$, $y_2 = \omega \sin t$ to a flow on the two-torus in $\mathbb{R}^4$ defined by all four equations. (Note that the plane defined by $y_1 = y_2 = 0$ is a section on which the return map is a time-$2\pi/\omega$-map of the first flow.) If one projects this to the x_1y_1-plane, one gets Lissajous figures. In some applications, these readily show whether modes in weakly nonlinear oscillators are locked together.

BORIS HASSELBLATT

See also **Anosov and Axiom-A systems; Attractors; Cat map; Hamiltonian systems; Horseshoes and hyperbolicity in dynamical systems; Maps; Phase plane; Poincaré theorems; Population dynamics; Stability**

Further Reading

Arnol'd, V.I. 1989. *Mathematical Methods of Classical Mechanics*, 2nd edition, Berlin and New York: Springer (original Russian edition 1974)

Arnol'd, V.I. 1992. *Ordinary Differential Equations*, Berlin and New York: Springer (original Russian edition 1971, translated from 3rd edition 1984)

Fielder, B. (editor). 2002. *Handbook of Dynamical Systems*, vol. 2, Amsterdam and New York: Elsevier

Hasselblatt, B. & Katok, A. (editors). 2002. *Handbook of Dynamical Systems*, vol. IA, Amsterdam and New York: Elsevier

Hasselblatt, B. & Katok, A. 2003. *Dynamics: A First Course* (see also vol. 1B, 2005) Cambridge and New York: Cambridge University Press

Katok, A. & Hasselblatt, B. 1995. *Introduction to the Modern Theory of Dynamical Systems*, Cambridge and New York: Cambridge University Press

Katok, A., de la Llave, R., Pesin, Y. & Weiss, H. (editors). 2001. *Smooth Ergodic Theory and Its Applications (Summer Research Institute Seattle, WA, 1999), Proceedings of Symposia in Pure Mathematics*, vol. 69. Providence, RI: American Mathematical Society

Robinson, R.C. 1995. *Dynamical Systems, Stability, Symbolic Dynamics, and Chaos*, Boca Raton, FL: CRC Press
Strogatz, S. 1994. *Nonlinear Dynamics and Chaos*, Reading, MA: Addison-Wesley

PHASE-SPACE DIFFUSION AND CORRELATIONS

For problems concerned with particle acceleration and heating, which can be described in two degrees of freedom, surfaces of section in a two-dimensional phase space are usually appropriate for representing the motion (Lichtenberg & Lieberman, 1991, Chapter. 3). For periodically driven systems, a mapping representation is often convenient to describe the motion (*See* **Fermi acceleration and Fermi map; Standard map**). In the surface of section there is a characteristically divided phase space in which regular Kolmogorov–Arnol'd–Moser (KAM) curves and stochastic trajectories are intermingled. In the globally stochastic region of the phase space for a system with two degrees of freedom, in which KAM curves spanning the phase coordinate do not exist, a complete description of the motion is generally impractical. We can then seek to treat the motion in a statistical sense; that is, the evolution of certain average quantities can be determined, rather than the trajectory corresponding to a given set of initial conditions (Wang & Uhlenbeck, 1945). Such a formulation in terms of average quantities is also the basis for statistical mechanics (see Penrose, 1970, for example). The mathematical foundations for many of the results can be found in Arnol'd & Avez (1968).

In regions in which the trajectories are stochastic, nearby trajectories diverge exponentially in time. The divergence is usually measured by calculating the Lyapunov characteristic exponent σ of a trajectory $\boldsymbol{x}$ and a nearby trajectory $\boldsymbol{x} + \boldsymbol{w}$,

$$\sigma(\boldsymbol{x}, \boldsymbol{w}) = \lim_{t\to\infty,\ d(0)\to 0} \left(\frac{1}{t}\right) \ln \frac{\mathrm{d}(t)}{\mathrm{d}(0)}, \qquad (1)$$

where d is the distance separating the trajectories. Analytical and numerical calculations of the σ's (especially the maximum value of $\sigma = \sigma_1$ with respect to variations of $\boldsymbol{w}$) are widely used as measures of the degree of stochasticity in near-integrable systems. The commonly used numerical procedure for calculating the Lyapunov exponents was developed by Benettin et al. (1976).

In many problems, the density distribution in action space is the important quantity. Its dynamics is simplified by an average over phases to find the dynamical friction and diffusion coefficients for the action, which can then be used for determining its time evolution. If the phases are decorrelated after each mapping step, then a random phase approximation can be used which greatly simplifies the calculation. If the averaging over phase can be performed for a localized value of the action, then the resulting evolution is a Markov process, leading to the Fokker–Planck equation for the evolution of the distribution (Wang & Uhlenbeck, 1945)

$$\frac{\partial P}{\partial n} = -\frac{\partial}{\partial I}(BP) + \frac{1}{2}\frac{\partial^2}{\partial I^2}(DP), \qquad (2)$$

where P is the probability distribution in the action I, B and D are the friction and diffusion coefficients, appropriately averaged over the phases, and n is a characteristic time over which the averaging can be performed. For example, using the standard map

$$\begin{aligned} I_{n+1} &= I_n + K \sin\theta_n, \\ \theta_{n+1} &= \theta_n + I_{n+1}, \end{aligned} \qquad (3)$$

then one step of the mapping gives

$$\Delta I_1 = K \sin\theta_0, \qquad (4)$$

and the transport coefficients, with phases randomized on each step, are

$$F_{\mathrm{QL}} = F = \frac{1}{2\pi}\int_0^{2\pi} \Delta I_1 \,\mathrm{d}\theta_0 = 0, \qquad (5)$$

$$D_{\mathrm{QL}} = \frac{D}{2} = \frac{1}{4\pi}\int_0^{2\pi} (\Delta I_1)^2 \,\mathrm{d}\theta_0 = \frac{K^2}{4}, \qquad (6)$$

where the subscripts QL refer to quasilinear (phase randomized) values with no higher-order correlations. (The factor of 2 difference between D_{QL} and D is a convention.)

Phase correlations, which always exist in a phase space with both regular and stochastic regions, complicate the calculation procedures. Close to the borders between stochastic and regular regions, the correlations become pronounced, requiring entirely different procedures for determining the diffusion. The existence of accelerator modes in the standard map also leads to nondiffusive behavior. Other phenomena of interest for diffusion calculations are the effect of noise and the effect of slow changes of system parameters. For weak correlations, for example, large K in the standard map, corrections to the single-step transport coefficients can be obtained. The corrections were obtained using Fourier techniques by Rechester et al. (1981). In the opposite limit for which a phase-spanning KAM curve (torus) has just been broken, resulting in a cantorus (the KAM curve becomes a cantor set), an approximate rate of local diffusion can be calculated. These techniques were developed to analyze the standard map, but can be used in various approximations to describe other two-degree-of-freedom systems. For a review of the various techniques and limitations see Lichtenberg & Lieberman (1991, Chapter 5).

ALLAN J. LICHTENBERG

See also **Diffusion; Fermi acceleration and Fermi map; Kolmogorov–Arnol'd–Moser theorem; Standard map**

Further Reading

Arnol'd, V.I. & Avez, A. 1968. *Ergodic Problems of Classical Mechanics*, New York: Benjamin

Benettin, G., Galgani, L. & Strelcyn, J.M. 1976. Kolmogorov entropy and numerical experiments. *Physical Review* A, 14: 2338–2345

Lichtenberg, A.J. & Lieberman, M.A. 1991. *Regular and Chaotic Dynamics*, 2nd edition, New York: Springer

Penrose, O. 1970. *Foundations of Statistical Mechanics*, Oxford: Pergamon

Rechester, A.B., Rosenbluth, M.N. & White, R.B. 1981. Fourier-space paths applied to calculation of diffusion in the Chirikov–Taylor map. *Physical Review* A, 23: 2664–2672

Wang, M.C. & Uhlenbeck, G.E. 1945. On the theory of Brownian motion II. *Reviews of Modern Physics*, 17: 323–342

PHASE SPACE RECONSTRUCTION

See **Embedding methods**

PHASE SYNCHRONISM OF CHAOS

See **Synchronization**

PHASE TRANSITIONS

A phase transition is a change in the degree or nature of order in a system and/or a change in its symmetry caused by a change in a thermodynamic variable such as temperature or pressure. When water freezes as the temperature is lowered, it undergoes a phase transition from a liquid to a solid. In the liquid state, the positions of the water molecules are disordered and the system is isotropic. In the solid state, however, the molecules are fixed at the sites of a crystal lattice, so the system has positional order and the symmetry of the ice lattice. Other examples of phase transitions include the liquid-vapor transition, in which the ordering is related to a change in density of the material; the transition from paramagnet to ferromagnet, which involves the appearance of a net magnetization as the temperature is lowered through the Curie temperature; the isotropic-nematic transition in liquid crystals, in which the rod-like liquid crystal molecules all become oriented in the same direction; and the superfluid transition in liquid helium, in which a macroscopic fraction of the helium atoms condense into a single quantum mechanical energy level. There are many others.

For any phase transition, we can define an order parameter. This is a quantity related to the degree of ordering which changes as the system goes through the transition. One measure of the order in a system is its entropy: a more ordered system has a lower entropy. While the entropy could be used as an order parameter, it is normally difficult to measure. An order parameter is usually physically measurable and is typically chosen to be zero in the less-ordered phase and nonzero in the more-ordered phase. For the liquid-vapor transition, the order parameter is proportional to the difference in density between the liquid and vapor phases. The order parameter for the ferromagnetic transition is simply the magnetization. For the superfluid transition in liquid helium, the order parameter is a complex number describing the macroscopic wave function of the superfluid.

Phase transitions can be classified as first order or second order. The terminology refers to the fact that certain derivatives of the free energy are discontinuous at a phase transition. In a first-order transition, it is the first derivatives (entropy, density, magnetization) that are discontinuous, while in a second-order transition, the discontinuity occurs in the second derivatives. A more practical classification is in terms of the behavior of the order parameter. At a first-order transition, the order parameter changes discontinuously. These transitions exhibit hysteresis and a latent heat resulting from the discontinuous change in entropy. At a second-order transition, the order parameter changes continuously; there is no hysteresis and no latent heat. In equilibrium, a thermodynamic system has a well-defined free energy and stable states correspond to absolute minima of this free energy. At a phase transition, the position of the free energy minimum changes, corresponding to a change in phase.

A phase diagram for a typical liquid-vapor system is shown in Figure 1(a). In the pressure-temperature plane, there is a line of first-order phase transitions which ends at a point at which the transition is second order. The same system is shown in the temperature-density plane in Figure 1(b). The region under the coexistence curve in Figure 1(b) is forbidden; there are no stable states in this region. When the mean properties of the system would place it inside this curve, the system phase separates into coexisting liquid and vapor phases with different densities lying on the coexistence curve itself. In the center of this region, the high-temperature phase is globally unstable, while closer to the edge, it is metastable. A supersaturated vapor would lie in this metastable region.

Points in the phase diagram at which second-order transitions occur are called critical points. At these points, the equation of state of the system takes on a special form, and the order parameter and other thermodynamic quantities show a power law dependence on the distance from the critical point. For example, if we consider a magnetic system with magnetization M, temperature T, and Curie temperature T_c, then the magnetization behaves as $M \sim [(T_c - T)/T_c]^{\beta}$ for $T \leq T_c$. The magnetic susceptibility $\chi = \mathrm{d}M/\mathrm{d}H$, where H is an applied magnetic field, diverges at the critical point as

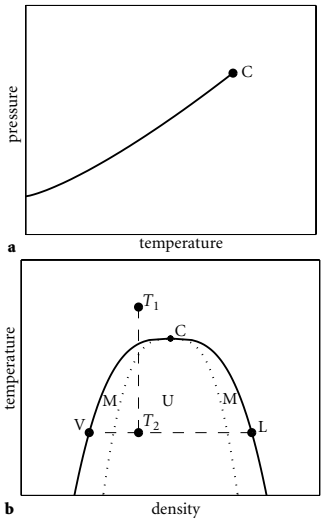

Figure 1. A typical liquid–vapor-phase diagram. (a) In the pressure–temperature plane a first-order phase transition occurs on crossing the solid line. The line of first-order transitions ends at the critical point C, at which the transition is second order. (b) The same phase diagram is shown in the temperature-density plane. The solid curve is the coexistence curve and corresponds to the solid line in (a). Outside the coexistence curve, the system exists as a single phase. In the region labeled **U** the one-phase state is unstable, and in the region labeled M it is metastable. If the system is cooled from the one-phase state at point T_1 into the unstable region at T_2, it will phase separate into a liquid component at the point L coexisting with a vapor component at V.

$\chi \sim |(T_c - T)/T_c|^{-\gamma}$. The quantities β and γ are called critical exponents. Interestingly, while T_c is different for different materials, the exponents β and γ have the same values for many different systems, including Ising ferromagnets and liquid-vapor systems, among others. This is known as "universality."

The simplest theoretical models used to describe phase transitions are called mean field theories. The van der Waals model for the liquid-gas transition and the Curie–Weiss model for the ferromagnetic transition are examples. Such theories assume that the order parameter at a particular point is determined by the average properties of the system—that is, by a mean field due to all other points of the system. Mean field theories are capable of describing first- and second-order-phase transitions qualitatively, but the values of the critical exponents are, in general, wrong. This is because mean field theories explicitly neglect the effects of spatial fluctuations in the order parameter, whereas it is these fluctuations which determine the behavior of the system near the critical point. Renormalization group theory provides a more complete description of critical point behavior.

When a system is quenched below a phase transition by suddenly changing a thermodynamic variable—for example, by suddenly dropping the temperature below the phase transition in a liquid-vapor system—it separates into two distinct phases. If the system is quenched into a region where the high-temperature phase is metastable (Figure 1), then macroscopic phase separation can only occur once large enough droplets of the unstable phase nucleate and grow. If it is quenched in the unstable region, then phase separation occurs by a process known as spinodal decomposition, whereby initially small perturbations to the local order parameter grow and coarsen with time. In a system with a conserved order parameter (e.g., a binary fluid mixture, in which the amount of each substance is fixed), the size of domains grows with time t as $L \sim t^{1/3}$, while if there is no conservation law (e.g., a ferromagnet) then $L \sim t^{1/2}$.

Phase transitions can also occur in systems out of equilibrium, for example, in the presence of a temperature gradient or a time-varying field. An important and interesting aspect of non-equilibrium systems is that the state of the system is no longer governed by the minima in the free energy, and indeed, a free energy functional may not even exist. Phase transitions can be significantly modified by non-equilibrium effects. In the case of a magnet in a time-varying field, for example, a competition between the time scale of the variations in the external field and the intrinsic relaxation time of the system itself leads to new behavior including spontaneous ordering that is not observed in the static case. Rather different phenomena, such as pattern-forming bifurcations in driven fluid systems, can also be thought of as nonequilibrium phase transitions.

JOHN R. DE BRUYN

See also **Critical phenomena; Ising model; Order parameters; Renormalization groups**

Further Reading

Chaiken, P.M. & Lubensky, T.C. 1995. *Principles of Condensed Matter Physics*, Cambridge and New York: Cambridge University Press

Chakrabarti, B.K. & Acharyya, M. 1999. Dynamic transitions and hysteresis. *Reviews of Modern Physics*, 71: 847–859

Gunton, J.D., San Miguel, M. & Sanhi, P.S. 1983. The dynamics of first order phase transitions. In *Phase Transitions and Critical Phenomena*, vol. 8, edited by C. Domb & J.L. Lebowitz, New York: Academic Press (Chapter 3). (The other volumes of this series contain review articles on many aspects of phase transitions.)

Stanley, H.E. 1971. *Introduction to Phase Transitions and Critical Phenomena*, Oxford: Oxford University Press

Tolédano, J.C. & Tolédano, P. 1987. *The Landau Theory of Phase Transitions*, Singapore: World Scientific

Uzunov, D.I. 1993. *Introduction to the Theory of Phase Transitions*, Singapore: World Scientific

PHASE TURBULENCE

See **Phase dynamics**

PHASE WINDING

See **Winding numbers**

PHI-FOUR EQUATION

See **Sine-Gordon equation**

PHOTONIC CRYSTALS

Photonic crystals are periodic dielectric (and/or metallic) structures, with periodicity comparable to a wavelength λ of interest, forming a *designable* optical medium where light propagation can exhibit unusual properties (Joannopoulos et al., 1995). The most important such property is a photonic band gap: a range of wavelengths in which there are no propagating modes in the crystal. Light in the band gap decays exponentially in the crystal, which acts like an optical "insulator." Nonlinear devices can exploit photonic crystals for enhanced phase sensitivity as well as to reduce power requirements, by means of tight spatial and long temporal confinement using the band gap and/or slow-light phenomena. Below are outlined two archetypical devices that greatly benefit from these properties of photonic crystals: Mach–Zender interferometers and bistable switches.

The simplest photonic crystals are one-dimensionally periodic multilayer films, or "Bragg mirrors," which were first studied in crystalline minerals by Lord Rayleigh (1887) (who observed that *any* periodic index variation will induce a band gap along that direction) and have since been the basis for a wide variety of applications: from reflective dielectric coatings, to distributed Bragg feedback (DFB) lasers, to fiber Bragg gratings for dispersion compensation and filters. It was not until 1987, however, that Yablonovitch (1987) and John (1987) applied the full principles of solid-state physics to electromagnetism and suggested that a three-dimensional (3-d) crystal could produce an omnidirectional gap. Since then, many photonic-crystal structures have been studied, both theoretically and experimentally, in two and three dimensions.

As a particular example, we consider a *two-dimensional* photonic crystal consisting of a square lattice of dielectric cylinders in air. This structure has a band gap for transverse-magnetic (TM) light (electric field perpendicular to the plane) and can, therefore, confine cavity and waveguide modes in point-like and linear defects of the crystal, as in Figures 1 and 2. For example, a single "defect" rod can be increased or decreased in size to trap a cavity mode within a diameter $\sim\lambda/2$, or a row of defect rods to form a waveguide. Bloch's theorem from solid-state physics (Ashcroft & Mermin, 1976) implies that modes in such a periodic waveguide propagate *without reflections*. Moreover, the waveguides form an effectively one-dimensional system, since the gap prohibits lateral scattering—this property allows photonic-crystal waveguides and cavities to be combined into complex device networks by adhering to simple design rules and symmetries. Alternatively, one can make a periodic sequence of cavities to form a coupled-cavity waveguide (CCW)—light slowly leaks from one cavity to the next, again trapping a guided mode (Yariv et al., 1999). The same principles apply in other photonic crystals, including those in three dimensions, and a direct analogue of this 2-d crystal can be made in 3-d (with an omnidirectional gap) by a stack of 2-d-like layers (Johnson & Joannopoulos, 2002).

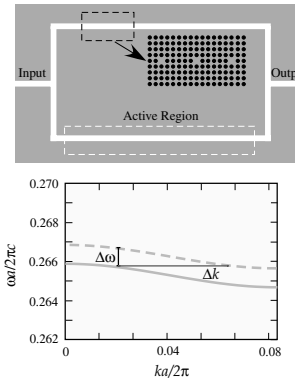

Figure 1. (Top) Schematic of a Mach–Zender interferometer: a waveguide that is split and recombined, with the relative phase modified by an active region to control the output transmission. Inset: a CCW slow-light waveguide to take advantage of photonic crystals. (Bottom) Band diagram of the CCW waveguide showing typical cosine dispersion curve. Because of the low group velocity, a slight shift of the curve (dashed) will cause a large change Δk in the wave number (horizontal axis). (The units are in terms of the distance a, the period of the square lattice.)

Mach–Zender Interferometers

The foundation of many optical device designs, from modulators to optical logic to switching, is the well-known Mach–Zender interferometer (Saleh & Teich, 1991) (Figure 1, Top).

Here, light in an incident waveguide is split into two branches and then recombined. If the two branches have the same optical path length, the recombination is in phase and light is transmitted; if their paths differ by half a period, then the recombination is out of phase and light is reflected. The relative optical path length is altered, for example, by changing the index by some Δn in the

branches with a linear electro-optic (external) or Kerr (self-induced) modulation, allowing the transmission to be switched continuously from "on" to "off." By using photonic-crystal line-defect waveguides in the interferometer, one can take advantage of their low group-velocity capability to significantly lower the power and size requirements of the device by a factor of the group velocity or better (Soljačić et al., 2002b).

To attain a low group-velocity waveguide in a photonic crystal, one simple strategy is to employ a coupled-cavity waveguide (CCW) like that in Figure 1 (top). The guided band of such a waveguide has a characteristic cosine-curve dispersion relation (Figure 1, bottom) with two important properties: (i) the mid-band group velocity is low and decreases exponentially with the cavity separation, and (ii) the group-velocity dispersion (frequency derivative of the group velocity) is zero at the center of the bandwidth, minimizing signal distortion.

Because the group velocity v_g is low, when the dispersion curve $\omega(k)$ (frequency vs. wave number) is slightly shifted by altering the index n of a waveguide branch, there will be a large change in k (Figure 1, bottom), causing a corresponding large phase shift $\Delta\phi = \Delta k L$ (where L is the propagation distance). Mathematically, if the curve is shifted by $\Delta\omega \sim \Delta n\omega$, then the phase shift is $\Delta\phi \cong L\Delta\omega/v_g$, inversely proportional to group velocity $v_g = \mathrm{d}\omega/\mathrm{d}k$. This means that the device size L to achieve a fixed phase shift $\Delta\phi = \pi$ (with a given Δn) varies proportionally to v_g. Moreover, the power required to modulate the index is proportional to L, so the switching power is also proportional to v_g. Alternatively, one could keep L fixed and reduce Δn by a factor of v_g; for a linear (Pockels) modulation, this reduces the modulation power by v_g^2.

If the Mach–Zender interferometer is modulated by the optical waveguide signal itself, say for all-optical logic, then there is an analogous benefit: the light is compressed in time by a factor of v_g/c, causing a greater field $|\boldsymbol{E}|^2$ for the same input power. Combined with the above mentioned power savings from length reduction, this means that Kerr self-modulated devices have their power reduced proportionally to v_g^2.

Of course, the low group velocity comes at a price: the bandwidth of the waveguide is reduced proportional to v_g. In optical telecommunications systems, however, the required bandwidth is relatively small; for example, a 40 Gbit/s channel has a bandwidth $\Delta\omega/\omega \sim 1/3000$, meaning that the group velocity could potentially be lowered by several hundred times without limiting the bandwidth, with corresponding decreases in the device size and power relative to conventional waveguides.

Optical Bistability

Optical bistability is a dramatic nonlinear phenomenon that can be exploited to implement all-optical transistors, switches, logic gates, amplifiers, and other functions (Saleh & Teich, 1991). Bistability stems from nonlinear feedback combined with resonant transmission through a cavity, produces an output power that is a sharp nonlinear function of input power, and may even display a hysteresis loop (Figure 2, right).

In this context, the ability of photonic crystals to minimize both cavity modal volume V and lifetime Q (number of temporal periods for energy to decay by $\mathrm{e}^{-2\pi}$) simultaneously allows them to greatly reduce the power threshold for optical bistability, in principle even down to the milliwatt level (Soljačić et al., 2002a).

An archetypical bistable device consists of an input waveguide coupled symmetrically into an output waveguide via a resonant cavity; this is shown in a photonic crystal setting of line and point defects in Figure 2 (left). In any such system, the transmission spectrum as a function of frequency will be a Lorentzian-like curve, peaked at 100% (in the absence of other loss mechanisms) at the resonant frequency (Figure 2, middle). In order to achieve bistability, one must include nonlinear feedback: the index (and thus the frequency) of the cavity depends on the field strength (e.g., via a Kerr nonlinearity $\Delta n \sim |\boldsymbol{E}|^2$). Furthermore, one must operate at a frequency ω_0 that lies *below* the linear resonant frequency ω_{res}. This combination, for continuous-wave (CW) sources, results in the bistable power-response curve shown in Figure 2 (right), which here includes a hysteresis. There are two stable system states for input powers in the bistable region (between the dashed vertical lines), and which one is realized depends upon whether one started from low or high power. (The middle, dashed, branch of the "S" curve is unstable.)

Intuitively, as the input power grows, the increasing index due to the nonlinearity will lower the resonant frequency through ω_0, as depicted by the dashed line in Figure 2 (middle), causing a rise and fall in transmission. This simple picture, however, is modified by feedback: as one moves into the resonance, coupling to the cavity is enhanced (positive feedback), creating a sharper "on" transition; and as one moves out of the resonance, the coupling is reduced (negative feedback), causing a delayed "off" transition.

The power threshold for the onset of bistability depends upon the power required to shift the cavity index sufficiently, which in turn depends upon the nonlinearity of the materials and the field strength $|\boldsymbol{E}|^2$ inside the cavity for a given input power. This field strength is inversely proportional to the modal volume V and is proportional to the lifetime Q (over which time the field builds up in the cavity). On the other hand, the required index shift of the cavity is proportional to the frequency width $1/Q$ of the Lorentzian transmission spectrum. Ultimately, therefore, the threshold power is proportional to V/Q^2; these simple arguments are confirmed by a more detailed analytical

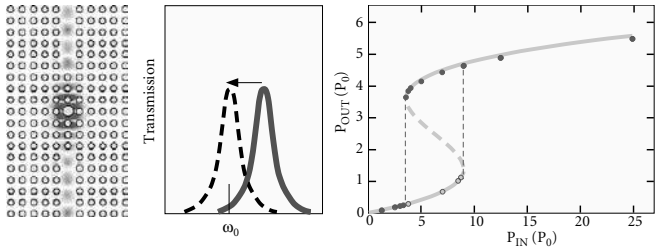

Figure 2. (Left) 100% (peak) resonant transmission from an input to an output waveguide through a cavity, formed by line and point defects, respectively, in a photonic crystal. Shaded regions indicate alternating positive/negative fields. (Middle) Lorentzian transmission spectrum (solid curve) of the linear resonant system. Increasing the power will nonlinearly shift the resonance curve (dashed) towards the operating frequency ω_0. (Right) Bistable transmission curve of output vs. input power resulting from the resonant transmission plus nonlinear feedback. The curve is an analytical theory and the dots are numerical calculations, with the vertical dashed lines indicating the region of hysteresis—for open dots the power was increased from a low value, while for closed dots the power was decreased from a high value.

theory that accurately predicts the bistability curve from the cavity characteristics (Soljačić et al., 2002a). Unlike traditional cavities such as ring resonators, photonic crystals impose no tradeoff between V and Q—the lifetime Q can be increased arbitrarily (up to the required signal bandwidth) while V is maintained near its minimum of $\sim(\lambda/2n)^3$, where n is the index of refraction. Indeed, in the example system of Figure 2, assuming reasonable material parameters and a $Q = 4000$ determined by the telecommunications bandwidth, one obtains a theoretical operating power of only a few milliwatts.

We conclude by presenting an analytical formula, derived from coupled-mode theory and perturbation theory, for the CW bistability relation in Figure 2 (right). The input/output power relation is given by

$$\frac{P_{\text{out}}}{P_{\text{in}}} = \frac{1}{1 + \left(P_{\text{out}}/P_0 - \delta\right)^2},$$

where δ is the frequency-detuning parameter $\delta \equiv 2Q(\omega_0 - \omega_{\text{res}})/\omega_{\text{res}}$ and P_0 is the characteristic power for bistability:

$$P_0 \equiv \frac{1}{\kappa Q^2 (\omega_{\text{res}}/c)^{d-1} \max(n_2)}.$$

Here, d is the dimensionality of the system, n_2 is the Kerr coefficient (index change per unit intensity of light), and κ ($\sim 1/V$) is a dimensionless, scale-invariant "nonlinear feedback parameter" quantifying the concentration of the cavity field $\boldsymbol{E}$ in the nonlinear material.

STEVEN G. JOHNSON, MARIN SOLJAČIĆ, AND J.D. JOANNOPOULOS

See also **Hysteresis; Nonlinear optics**

Further Reading

Ashcroft, N.W. & Mermin, N.D. 1976. *Solid State Physics*, Philadelphia: Holt Saunders

Joannopoulos, J.D. Meade, R.D. & Winn, J.N. 1995. *Photonic Crystals: Molding the Flow of Light*, Princeton, NJ: Princeton University Press

John, S. 1987. Strong localization of photons in certain disordered dielectric superlattices. *Physical Review Letters*, 58: 2486–2489

Johnson, S.G. & Joannopoulos, J.D. 2002. *Photonic Crystals: The Road from Theory to Practice*, Boston: Kluwer

Rayleigh, Lord (Strutt, W.J.). 1887. On the maintenance of vibrations by forces of double frequency, and on the propagation of waves through a medium endowed with a periodic structure. *Philosophical Magazine*, 24: 145–159

Saleh, B.E.A. & Teich, M.C. 1991. *Fundamentals of Photonics*, New York: Wiley

Soljačić, M., Ibanescu, M., Johnson, S.G., Fink, Y. & Joannopoulos, J.D. 2002a. Optimal bistable switching in non-linear photonic crystals. *Physics Review E Rapid Communincations*, 66: 055601(R)

Soljačić, M., Johnson, S.G., Shanhui Fan, Ibanescu, M., Ippen, E. & Joannopoulos, J.D. 2002b. Photonic-crystal slow-light enhancement of non-linear phase sensitivity. *Journal of the Optical Society of America B*, 19: 2052–2059

Yablonovitch, E. 1987. Inhibited spontaneous emission in solid-state physics and electronics. *Physical Review Letters*, 58: 2059–2062

Yariv, A., Xu, Y., Lee, R.K, & Scherer, A. 1999. Coupled-resonator optical waveguide: a proposal and analysis. *Optics Letters*, 24: 711–713

PIECEWISE LINEARITY

See **Ratchets**

PINNING TO LATTICE

See **Peierls barrier**

PITCHFORK BIFURCATION

See **Bifurcations**

PLASMA SOLITON EXPERIMENTS

Comprising a very large number of charged particles within a confined volume, a plasma is a convenient laboratory facility in which both linear and nonlinear phenomena can be experimentally investigated. The overall plasma is electrically neutral in that the density of positive particles is equal to the density of negative particles. If the negative particles are electrons, this is called a two-component or normal plasma. If a certain fraction ε of the electrons is replaced with negative ions, this is called a three-component or a negative ion plasma.

Washimi and Taniuti (1966) were the first to demonstrate that the evolution of perturbations of the charge density in a normal plasma can be described by the nonlinear fluid equations for the ions. This description includes a Boltzmann assumption for the electrons and Poisson's equation to reflect the local charge nonneutrality in a density perturbation that can be described with the Korteweg–de Vries (KdV) equation,

$$\frac{\partial \psi}{\partial t} + \psi^{\nu} \frac{\partial \psi}{\partial x} + \beta \frac{\partial^3 \psi}{\partial x^3} = 0. \qquad (1)$$

Here the dependent variable ψ represents the perturbations in the ion density, ion velocity, or the electric potential; β is a constant; and the parameter $\nu = 1$.

In 1984, Watanabe showed that perturbations in a negative ion plasma can also be described by the same equation if the fraction ε has certain values. In particular, if this parameter is very large, then the negative ions predominate and rarefactive solitons evolve from a negative ion density perturbation. Because the mass of the negative ions could be comparable with the mass of the positive ions, he found that the parameter ε had a critical value ε_c at which the derivation led to a modified Korteweg–de Vries (mKdV) equation with the parameter $\nu = 2$. Both of these equations describe solitons that propagate in one direction.

The first extension to include effects of higher dimensions was performed in 1970 by Kadomtsev and Petviashvili, who included weak effects in a direction that was perpendicular to the dominant direction of propagation of the ion acoustic soliton. This equation is now called the Kadomtsev–Petviashvili (KP) equation for $\nu = 1$ in a normal plasma and the modified Kadomtsev–Petviashvili (mKP) equation for $\nu = 2$ in a negative ion plasma; thus

$$\frac{\partial}{\partial x}\left(\frac{\partial \psi}{\partial t} + \psi^{\nu} \frac{\partial \psi}{\partial x} + \beta \frac{\partial^3 \psi}{\partial x^3}\right) + \frac{\partial^2 \psi}{\partial y^2} = 0. \qquad (2)$$

Both of these equations have certain predictions that have been experimentally verified in a plasma.

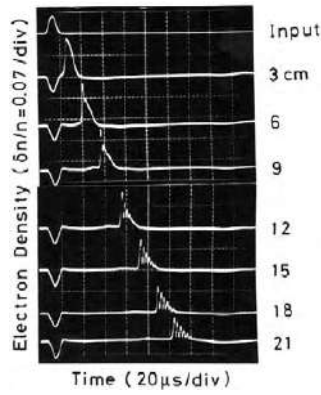

Figure 1. Evolution of a positive ion perturbation in a normal two component plasma. The pictures are taken at increasing distances from the source and illustrate the evolution of a burst of ions into a number of KdV solitons.

Laboratory experiments require the creation of a large volume of uniform collisionless plasma in which localized density perturbations are launched and movable probes monitor the evolution of the perturbation. Collisions between the particles are reduced with the evacuation of the chamber to a low pressure. Typically, a gas such as argon is inserted into the chamber and ionized to create a plasma with a volume of approximately $1\,m^3$. The density perturbations are created by applying a voltage signal to a fine-mesh grid or by introducing a charge density perturbation from one plasma into a second plasma. This is called a double-plasma (DP) machine and plasma solitons were first observed in a DP machine (Ikezi et al., 1970).

The spatial and temporal evolution of a compressive density perturbation in a normal plasma is illustrated in Figure 1. As this perturbation moves in the plasma, a number of solitary waves emerge for which the following KdV soliton properties have been observed: the product of the soliton amplitude (ψ) times the square of its width (W) is constant, and the soliton velocity $c_s = [1 + \psi/3]c$ where c is the linear ion acoustic velocity. In addition, the nondestructive collision of two solitons with different amplitudes was verified in the initial experiment performed in a normal plasma that existed in the DP machine.

By replacing a certain fraction of the free electrons in the normal plasma with negative ions to which these free electrons become attached, it is possible to realize a negative ion plasma. As a gas such as sulfur hexafluoride has a large attachment coefficient, a negative ion plasma can be created that consists of positive argon ions and negative fluorine ions whose

masses are comparable. The parameter ε can be altered to have values of $\varepsilon < \varepsilon_c$, $\varepsilon = \varepsilon_c$, or $\varepsilon > \varepsilon_c$. In the first case, the positive ions are compressed and the normal KdV soliton is excited. KdV solitons are also excited in the third case due to compression of the negative ions. In the second case, mKdV solitons have been excited and their properties have been verified. In particular, it was observed that the product of ψW^2 is constant. The first experimental detection of solitons in a negative ion plasma was in a DP machine (Ludwig et al., 1984; Nakamura & Tsukabayashi, 1984), and both solitons were later detected in a negative ion plasma using the grid excitation mechanism (Cooney et al., 1991).

Two solitons that propagate in a normal plasma or in a negative ion plasma but in directions that are not collinear can still interact and are described by the KP equation. In particular, Miles (1977) noted that at a particular angle, the amplitude of the soliton after such an interaction would be greater than the sum of the amplitudes of the two solitons that preceded the interaction. If the amplitudes of these two initial solitons were equal, the amplitude of the new soliton would be 4 times this amplitude. The critical amplitude and the amplitude enhancement predicted from this resonant interaction was first experimentally examined in a normal plasma (Ze et al., 1979). In the negative ion plasma, an amplitude enhancement of two was anticipated and has been experimentally verified (Nakamura et al., 1999).

A laboratory plasma has been found to be a convenient venue in which several of the fundamental properties of solitons that are described with the KdV, mKdV, KP, or mKP equations can be experimentally studied and verified. A summary of other experiments has recently appeared (Lonngren, 1998).

KARL E. LONNGREN AND YOSHIHARU NAKAMURA

See also **Kadomtsev–Petviashvili equation; Korteweg–de Vries equation; Multidimensional solitons; Nonlinear plasma waves; Nonlinear Schrödinger equations**

Further Reading

Cooney, J.L., Gavin, M.T. & Lonngren, K.E. 1991. Experiments on Korteweg–de Vries solitons in a positive ion-negative ion plasma. *Physics of Fluids* B, 3: 2758–2766

Ikezi, H., Taylor, R.J. & Baker, D.R. 1970. Formation and interaction of ion acoustic solitons. *Physical Review Letters*, 25: 11–14

Kadomtsev, B.B. & Petviashvili, V.I. 1970. On the stability of solitary waves in weakly dispersing media. *Soviet Physics Doklady*, 15: 539–541

Lonngren, K.E. 1998. Ion acoustic soliton experiments in a plasma. *Optical Quantum Electronics*, 30: 615–630

Ludwig, G.O., Ferreira, J.L. & Nakamura, Y. 1984. Observation of ion acoustic rarefaction solitons in a multicomponent plasma with negative ions. *Physical Review Letters*, 52: 275–278

Miles, J.W. 1977. Resonantly interacting solitary waves. *Journal of Fluid Mechanics*, 79: 171–179

Nakamura, Y., Bailung, H. & Lonngren, K.E. 1999. Oblique collision of mKdV ion-acoustic solitons. *Physics of Plasmas*, 6: 3466–3470

Nakamura, Y. & Tsukabayashi, I. 1984. Observation of modified Korteweg–de Vries solitons in a multicomponent plasma with negative ions. *Physical Review Letters*, 52: 2356–2359

Washimi, H. & Taniuti, T. 1966. Propagation of ion acoustic solitary waves of small amplitude. *Physical Review Letters*, 17: 996–998

Watanabe, S. 1984. Ion acoustic solitons in plasma with negative ions. *Journal of the Physical Society of Japan*, 53: 950–956

Ze, F., Hershkowitz, N., Chan, C. & Lonngren, K.E. 1979. Inelastic collision of spherical ion acoustic solitons. *Physical Review Letters*, 42: 1747–1750

PLASMA TURBULENCE

See **Nonlinear plasma waves**

PLASTIC DEFORMATION

See **Frenkel–Kontorova model**

PLUME DYNAMICS

Plumes and jets are naturally and frequently occurring transport phenomena arising in a variety of settings, ranging from dry convecting atmospheric motion on hot days through explosive volcanic eruptions, for example, the 1915 eruption of Lassen Peak shown in Figure 1. The fluid dynamical purpose of a plume is dynamic equilibration of a localized unstable distortion of the fluid density, which results in vertical, coherent motion of a parcel of fluid seeking an equilibrium density. Viscosity couples and draws fluid along with the parcel on its voyage (turbulent entrainment). If the parcel is miscible with the ambient fluid, turbulent mixing will result, accelerating the equilibration process.

A further complication is that ambient fluids typically develop stable stratifications in which the fluid density is higher at the bottom. Such is the case with the Earth's atmosphere, whose density drops to zero in outer space, and the steady-state density profile is merely the thermodynamic response of an air layer under gravitational compression. Equally interesting stratification processes occur with much sharper gradients in convective boundary layers and in the thermoclines found in lakes and oceans. In these situations, stable transitions from a high-density bottom fluid layer to a low-density upper fluid layer may occur across a very sharp, nearly interfacial, layer. Typical stratifying agents include localized high temperature and/or concentration gradients (e.g., salt in the ocean). The modifications introduced by such layers can be both naturally dramatic and socio-economically challenging. The discharge of pollutants into the atmosphere, lakes, and oceans

Figure 1. May 22, 1915, eruption of Lassen Peak, taken 50 miles away in Anderson, California, by photographer, R.I. Meyers. (Thanks to Cari Kreshak and Lassen Volcanic National Park for providing the high quality image.)

is frequently accompanied by trapping phenomena directly attributed to the formation of such stable density layers (thermal inversions), in which the discharged pollutants are confined away from mixing flows and may lead to hazardous air and water quality.

Plume Mixing and Entrainment: Modifying the Large Scale Observables

A light plume of fluid in a constant density environment is expected to rise continually until the Archimedian buoyancy force is reduced through mixing of the plume with the ambient to levels at which viscous balances occur. The complete evolution requires, at minimum, the solution of the Navier–Stokes equations, with an evolving density anomaly (the plume) allowed to mix with the ambient. The mixing is turbulent, and the computational simulations of these nonlinear partial differential equations are both difficult, and necessary in making first principle predictions. Modelers have turned to alternative, somewhat ad hoc, yet nonetheless fundamental attempts to describe the evolution with fewer degrees of freedom than the complete fluid equations. As discussed below, the pioneering work of Morton et al. (1956) utilized an entrainment hypothesis with a single entrainment coefficient in an attempt to describe jet (plume) profiles by reduced, nonlinear ordinary differential equations (involving only a few degrees of freedom).

The plume dynamics in stratified fluids are dramatically different (Morton et al., 1956; Morton, 1967; Turner, 1995). In such a situation, the buoyancy of a plume of light fluid is strongly height-dependent, and an initially (low altitude) light fluid parcel may well rise to a height at which a buoyancy reversal occurs and the parcel becomes neutrally buoyant. Such a situation was originally noted by Morton et al. to cause an arrestment of vertical jets of light fluid. Their experiments and modeling for a fluid with a linear stratification (linearly decreasing density with increasing height) indeed show vertical jets arresting. The implications for functioning smokestacks, modeling of volcanic plumes (Sparks et al., 1997), and the mixing of oceanic pollutants (Fischer et al., 1979) is clear.

When the density transitions sharply between two distinct values, one finds mixing between low-density jet (or plume) fluid and the ambient fluid, which may dramatically affect the large scale observables. Experiments, performed in the UNC Applied Mathematics Fluid Lab, further exhibit the need for improved modeling that is specifically designed to better understand turbulent mixing and entrainment.

Figure 2 shows two vertical jets, fired at approximately the same volumetric flow rate (roughly 0.2 gal/min) into two identically stratified fluid tanks with a prepared sharp transition from $1.06\,g/cm^3$ at the bottom to $1.015\,g/cm^3$ using varying salt concentrations, with a transition of approximately 1 in, thickness, centered around the 14 in. tick on the tape. The left jet fluid is a gauge oil, with density $0.8\,g/cm^3$ (lighter than all ambient tank fluid). Recall that oil and water do not mix. The right jet fluid is a dyed alcohol–water mixture, with density $0.8\,g/cm^3$, also (initially) lighter than everything in the tank. In this case, the alcohol-water mixture may mix with the ambient fluid.

Observe the striking difference in large-scale observables: The nonmixing case penetrates clear to the free surface, whereas the mixing case does not penetrate, but forms, at altitudes in the vicinity of the sharp density transition, a cloud. The alcohol jet, fired in nonstratified cases of either $1.06\,g/cm^3$ or $1.015\,g/cm^3$ constant density tanks will reach the free surface at these flow rates and does not form a cloud, which demonstrates the powerful effect that an ambient sharp stratification can have upon plume dynamics, and the effect of the turbulent mixing and entrainment. There has been considerable work on developing plume models for studying the types of behavior shown with the alcohol jet following the original work of (Morton et al., 1956; Sparks et al., 1997; Caulfield & Woods, 1998), and some attempts have been directed at the multi-phase aspects of the oil jet example (Asaeda & Imberger, 1993; Socolofsky et al., 2001). A successful and complete modeling approach handling a full range of cases in which the mixing properties between jet fluid and ambient fluid may be continuously varied is an open challenge.

Dynamic Plumes and Solid Wall Interactions: Transient Levitation of Falling Bodies

As an extreme example in which the injected quantity cannot mix with the ambient fluid, consider recently obtained experimental results concerning the motion of falling bodies through stratified fluids (similar to

Figure 2. Vertical buoyant jets through a strong stable density step: Left is oil (0.8 g/cm^3), right is alcohol-water mixture (0.8 g/cm^3). (Thanks to former UNC undergraduates Ryan McCabe and Daniel Healion for assistance with the experiment.)

the tank setup in Figure 2) (Abaid, Adalsteinsson, Agyapong, McLaughlin, 2004). This study has focused upon the effect of self-generated plumes upon the falling body and has documented situations in which a falling body may generate a dynamic plume that through hydrodynamic coupling, may temporarily arrest the body. Of course, any body moving through a fluid experiences a hydrodynamic drag (which sets terminal velocities of falling bodies) in which the viscous boundary condition of vanishing fluid flow at the solid boundary necessarily drags a blob of ambient fluid along the moving body. In a constant density fluid, there is no potential energy cost associated with moving such a parcel of ambient fluid vertically. However, in strongly stratified fluids, a parcel of fluid moved from one altitude to another may develop a potential energy (buoyancy), as when the body falls through a sharp density transition layer. The momentum of the attached blob of fluid thrusts it into the lower (heavier) fluid, at which point the blob becomes a density anomaly and rises sharply. This motion in turn drags the falling body along with it.

Figure 3 shows three montages of a descending sphere at uniformly spaced times. The (5 mm radius) sphere in this case has a density of 1.04 g/cm^3 and is falling in a stratified tank whose top is fresh water (0.997 g/cm^3) and whose bottom is salt water (1.039 g/cm^3), again with a transition thickness of approximately 1 in. The top montage demonstrates the arrest and transient rise of the initially falling bead, and subsequent return to slow descent, each image uniformly spaced 1.5 s apart. The bead ultimately comes to rest at the tank bottom. The middle montage is the same as the top, only uniformly spaced at 0.1 s intervals. The lower montage has the same time sequence as the middle row, only focusing upon the shadow on the back of the tank, which highlights the entrained, plume-forming fluid.

The nature of this phenomenon is both nonlinear and dynamic. The nonlinear effect of such plumes upon

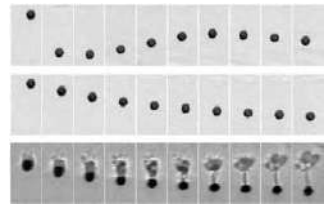

Figure 3. Top: Digital snapshots of bead position on uniform 1.5 s intervals, Middle: uniformly spaced on 0.1 s intervals, Bottom: shadowgraph depicting the dynamic plume on same time interval as middle row (Abaid, Adalsteinsson, Agyapong, McLaughlin, 2004). (Thanks to David Adalsteinsson for help with formatting the collage in his DataTank program and thanks to former UNC undergraduate Nicole Abaid for assistance with the experimental effort.)

the motion of solid bodies has been incorporated in a reduced system of ordinary differential equations in which the drag law for the falling body is modified to account for the dynamics of the plume which may modify the relative velocity of the falling sphere (Abaid, Adalsteinsson, Agyapong, McLaughlin, 2004). To describe the detailed dynamics of such transient plumes is quite difficult. Historically, there has been more success in the modeling of plume geometries under steady-state geometries. In pioneering work, Morton, Turner, and Taylor (Morton et al., 1956; Morton, 1967; Turner, 1995) were the first to model maintained plumes using an entrainment hypothesis which has become a standard in many fields (Fisher et al., 1979; Sparks et al., 1997).

Steady Plume Models in Stratified Environments

In 1956, Morton, Turner, and Taylor introduced what has become the standard maintained plume models for the shape of jet plumes (plumes emanating from

a maintained source of buoyancy and momentum) (Morton et al., 1956; Morton, 1967; Turner, 1995; Fischer et al., 1979; Sparks et al., 1997; Socolofsky et al., 2001). The entrainment hypothesis assumes that the rate of inflow of diluting, ambient fluid is proportional to the vertical velocity of the jet along its centerline. Much empirical data has been collected exploring the exact dependence of the constant of proportionality upon the various physical parameters describing the jet configuration (stratified profile, jet speed, jet fluid density). A considerable effort since the original work of Morton et al. has addressed the many algebraic fits for the entrainment coefficient as a function of Richardson numbers, etc. (Fischer et al., 1979; Turner, 1995; Socolofsky et al., 2001).

Armed with this entrainment assumption, Morton et al. (1956) developed the following system of nonlinear ordinary differential equations, the solution of which yields the jet (plume) profile in steady state:

$$\frac{\mathrm{d}(b^2 w)}{\mathrm{d}z} = 2\alpha b w, \tag{1}$$

$$\frac{\mathrm{d}(b^2 w^2)}{\mathrm{d}z} = 2g\lambda^2 b^2 Q, \tag{2}$$

$$\frac{\mathrm{d}(b^2 w Q)}{\mathrm{d}z} = \left(\frac{(1+\lambda^2)b^2 w}{\lambda^2 \bar{\rho}}\right)\frac{\mathrm{d}\rho_0}{\mathrm{d}z}. \tag{3}$$

Here, the plume parameters are the center-line vertical velocity, $w(z)$, the plume radius $b(z)$, and the nondimensional plume density $Q(z)$. All are functions of the height variable z. The entrainment coefficient is α, which in neutrally stratified cases is empirically seen to be approximately 0.08 (Fischer et al., 1979; Turner, 1995). The gravitational constant is g, $\bar{\rho}$ denotes some constant reference density, and the ambient stratification is contained within the given profile $\rho_0(z)$.

This system is based on the following assumptions. First, vertical derivatives of certain horizontally averaged, low-order moments (for plume mass, momentum, and buoyancy) are simplified in terms of single point, centerline field variables. Second, radial profiles for plume vertical velocity and buoyancy are postulated in terms of "collective variables": $w(z) = \hat{w}(z) f(r/(ab(z))$ and $Q(z) = \hat{Q}(z) f(r/(cb(z))$. Through these, the integrals defining the moments may be directly calculated, leading to the closed system of differential equations given above. For both velocity and plume density, the functional forms are taken to be Gaussians, following empirical observations (Morton, 1967; Fischer et al., 1979; Turner, 1995). The ratio of the velocity length scale a, to plume length scale c is $\lambda = c/a$ is taken to be approximately 1.2, but this must certainly vary considerably upon the mixing properties of the plume fluid with the ambient. Each of these steps involves numerous approximations, an excellent list of which may be found discussed in Chapter 9 of the text by Fischer et al., along with asymptotic solutions for limiting cases (Fischer et al., 1979).

The solution of these equations gives a rough picture for plume shapes in the environment and typically shows plumes arresting at heights below their heights of static neutral buoyancy (in the absence of any mixing) in stratified environments. A more systematic mathematical reduction of this system from the complete equations, along with a numerical simulation of the complete fluid equations for multiphase fluid flow would be valuable.

RICHARD M. MCLAUGHLIN

See also **Atmospheric and ocean sciences; Mixing; Navier–Stokes equation; Turbulence; Vortex dynamics of fluids**

Further Reading

Abaid, N., Adalsteinsson, D., Agyapong, A. & McLaughlin, R.M. 2004. An internal splash: Levitation of falling spheres in stratified fluids. *Physics of Fluids*, 16(5): 1567–1580

Asaeda, T. & Imberger, J. 1993. Structure of bubble plumes in linearly stratified environments. *Journal of Fluid Mechanics*, 249: 35–57

Caulfield, C.P & Woods, A.W. 1998. Turbulent gravitational convection from a point source in a non-uniformly stratified environment. *Journal of Fluid Mechanics*, 360: 229–248

Csanady, G.T. 1973. *Turbulent Diffusion in the Environment*, Dordrecht: Reidel

Fernando, H.J.S. 1991. Turbulent mixing in stratified fluids. *Annual Reviews of Fluid Mechanics*, 23: 455–493

Fischer, H.B., List, E.J., Koh, R.C.Y., Imberger, J. & Brooks, N.H. 1979. *Mixing in Inland and Coastal Waters*, New York: Academic Press

Larsen, L.H. 1969. Oscillations of a neutrally buoyant sphere in a stratified fluid. *Deep-Sea Research*, 16: 587–603

Morton, B.R., 1967. Entrainment models for laminar jets, plumes, and wakes. *Physics of Fluids*, 10(10): 2120–2127

Morton, B.R., Taylor, G.I. & Turner, J.S. 1956. Turbulent gravitational convection from maintained and instantaneous sources. *Proceedings of the Royal Society*, A, 234: 1–23

Socolofsky, S.A., Crounse, B.C. & Adams, E.E. 2001. Multi-phase plumes in uniform, stratified, and flowing environments. In *Environmental Fluid Mechanics–Theories and Applications*, edited by H. Shen, A. Cheng, K.-H. Wang & M.H. Teng, Reston, Va: American Society of Civil Engineers, Ch. 3

Sparks, R.S.J., Burksik, M.I., Carey, S.N., Gilbert, J.S., Glaze, L.Sl, Sigurdsson, H. & Woods, A.W. 1997. *Volcanic Plumes*, New York: Wiley

Srdic-Mitrovic, A.N., Mohamed, N.A. & Fernando, H.J.S. 1999. Gravitational settling of particles through density interfaces. *Journal of Fluid Mechanics*, 381: 175–198

Torres, C.R., Hanazaki, H., Ochoa, J., Castillo, J. & Van Woert, M. 2000. Flow past a sphere moving vertically in a stratified diffusive fluid. *Journal of Fluid Mechanics*, 417: 211–236

Turner, J.S. 1995. *Buoyancy Effects in Fluids*, Cambridge and New York: Cambridge University Press

POINCARÉ INDEX

See **Winding numbers**

POINCARÉ THEOREMS

One of the greatest of all French mathematicians, Jules Henri Poincaré (1854–1912) graduated from the École Polytechnique in Paris and later studied at the École des Mines. In 1879, he became a docteur es sciences at the University of Paris, where he was appointed as a professor in 1881. Poincaré became a member of Académie des Sciences in 1887.

A mathematical genius of rare power, Poincaré's approach to science was to solve concrete problems arising from mathematics, mechanics, and physics, rather than to present his results in a "pure axiomatic form." However, a complete understanding of Poincaré's scientific works has yet to be achieved. Outside mathematics, Poincaré is also known for his works in theoretical physics including his seminal contribution in the special theory of relativity (1904–1905) and for his works on the philosophy of science.

Many of Poincaré's papers gave birth to whole new branches of mathematics, a prime example being algebraic topology, but the matter that occupied his life throughout was the geometrical approach to nonlinear differential equations—in particular, the long-time behavior of orbits of the Newtonian N-body problem in celestial mechanics.

The qualitative approach to nonlinear dynamics, introduced by Poincaré in his seminal papers "Mémoire sur les courbes définies par une équation différentielle" (1881–1886), which focuses on orbits rather than formulas was of a geometric and global nature. This is how the qualitative theory of ordinary differential equations was born.

Studying smooth vector fields on the plane, he classified their simplest equilibria (i.e., points where the given vector field vanishes): foci, nodes, saddle points, and centers. The typical smooth planar vector field has only the first three types of equilibria, but those of a more complicated nature are not excluded.

Poincaré outlined the proof that if a half trajectory γ of the planar vector field v is confined in a compact domain K in which v is free of equilibrium points, but the whole trajectory γ is not confined in K, then K contains a closed orbit of v to which γ is asymptotically attracted (the Poincaré–Bendixson theorem in its simplest form). This type of closed orbit is called a limit cycle.

To generalize, let v be a smooth vector field on a two-dimensional compact manifold M. To each isolated equilibrium p of v, Poincaré associated an integer $\mathrm{Ind}(v, p)$, called the index of v at p, which is defined as follows. Let J be a small loop surrounding the isolated equilibrium p, and let $\Delta\theta$ be the total change of the angle θ that the vector of v makes with some fixed direction when one runs counterclockwise along the loop J. This number is independent of the choice of loop. The index of p is the number $\Delta\theta/2\pi$ which is always an integer. (The index of a focus, center, or node is $+1$, and the index of a saddle point is -1.)

If v has only a finite number of equilibria $p_1, \ldots, p_r$, then Poincaré showed that

$$\sum_{i=1}^{r} \mathrm{Ind}(v, p_i) = \chi(M), \tag{1}$$

where $\chi(M)$ is the Euler–Poincaré characteristic of M and no restrictions are imposed on the nature of equilibria $p_1, \ldots, p_r$. This result was generalized later by Heinz Hopf to the case of vector fields on compact manifolds of arbitrary dimension and is now called the Poincaré–Hopf theorem.

For a sphere, we have $\chi(M) = 2$, that is, an arbitrary smooth vector field on a two-dimensional sphere must vanish in at least one point—one cannot evenly comb the hair on a sphere! Another consequence of this theorem is that, for example, on the two-dimensional sphere, one cannot have a smooth vector field having as equilibria only two saddle points or having only three centers.

Poincaré's investigations of celestial mechanics led him to the study of Hamiltonian systems with n degrees of freedom

$$\frac{\mathrm{d}\, q_i}{\mathrm{d}\, t} = \frac{\partial\, H}{\partial\, p_i}, \quad \frac{\mathrm{d}\, p_i}{\mathrm{d}\, t} = -\frac{\partial\, H}{\partial\, q_i}, \quad i = 1, \ldots, n \tag{2}$$

with an analytic Hamiltonian function $H(q, p)$, $(q, p) \in \mathbb{R}^{2n}$. His researches in this area were summarized in his epoch-making three-volume treatise "Les méthodes nouvelles de la mécanique céleste" (1892, 1893, 1899).

The study of Hamiltonian systems close to integrable ones was called the "general problem of dynamics" by Poincaré. Specifically, he studied Hamiltonian equations (2) with a perturbed Hamiltonian of the form

$$H(q, p, \varepsilon) = H_0(p) + \varepsilon\, H_1(q, p) + \varepsilon^2\, H_2(q, p) + \cdots, \tag{3}$$

where $H_1, H_2, \ldots$ are periodic functions with respect to q of the same period. The system obtained by setting $\varepsilon = 0$ is integrable, and the phase space is foliated by n-dimensional invariant tori $p = \mathrm{const}$. For small nonzero ε, system (2) usually becomes non-integrable. In the case of two degrees of freedom, this means that the Hamiltonian function H is the only first integral of Equations (2) that is an analytic and uniform function of variables q, p and ε.

Poincaré's participation in a mathematical competition organized in 1885 by Oskar II, King of Sweden and Norway, led him to the discovery of homoclinic orbits and related phenomena explaining how a very complicated behavior now called dynamical chaos, occurs in nonlinear dynamical systems. In his prize-winning work (1889), Poincaré discusses mainly the restricted three-body problem, where one mass is negligible

compared with the other two, executing circular Keplerian motion.

Within the three-dimensional constant-energy manifold of this problem, he considered a two-dimensional surface Π transversal to most of the orbits. An orbit starting on this surface at a point x will pierce it again for the first time at some point y. The map $x \to y$ is the Poincaré return map induced on a surface of section Π.

It was in this framework that he discovered the existence of homoclinic orbits, that is, orbits which are asymptotically attracted by some periodic orbit γ when $t \to +\infty$ and $t \to -\infty$.

During his 1912 investigations on the restricted three-body problem, Poincaré conjectured that if one has a closed plane annulus Ω bordered by two concentric circles Γ_1 and Γ_2, then any area-preserving homeomorphism ϕ of Ω, such that $\phi(\Gamma_1) = \Gamma_1$, $\phi(\Gamma_2) = \Gamma_2$ and rotating these circles in opposite directions, has in Ω at least two different fixed points. This assertion, known as Poincaré's last geometric theorem, was proved in 1913 by George D. Birkhoff and is known also as the Poincaré–Birkhoff theorem.

Inspired by the analogy between a flow induced by a vector field and a flow of an incompressible fluid, Poincaré developed a theory of integral invariants, which was later refined by Elie Cartan.

Considering time t as an independent variable, we can study Hamiltonian system (2) in the extended phase space (q, p, t). A tube of trajectories is a two-dimensional cylindrical surface formed by the segments of trajectories of the vector field defined by (2) and bounded by two disjoint smooth closed curves. According to the Poincaré–Cartan theorem, in the extended phase space (q, p, t), the action integral $\oint_\gamma (p\,\mathrm{d}q - H\,\mathrm{d}t)$ has the same value for two different closed paths γ_1 and γ_2 encircling the same tube of trajectories and lying on it.

Poincaré also proved an important property of the long-time behavior of dynamical systems. In contemporary formulation, this proof shows that for any measure-preserving mapping of a measure space with a finite total measure, almost all trajectories starting from a given subset of positive measure eventually return to it. This is known as the Poincaré recurrence theorem, and it lies at the foundations of ergodic theory.

In his works on celestial mechanics, Poincaré provided the first formal definition of asymptotic series: divergent series giving nevertheless good numerical approximations for functions they represent.

Poincaré is the founder of the concept of normal forms in the theory of ordinary differential equations and of the contemporary bifurcation theory. His work was also at the beginning of modern variational methods in mathematics, in particular of the Morse theory which strongly links mathematical analysis to geometry and topology.

Other nonlinear problems studied by Poincaré include the problem of the existence of geodesics on convex surfaces, the problem of tides, and the stability of rotating fluid bodies.

Poincaré's impact on the theory of ordinary differential equations and dynamical systems is described in the books by Birkhoff (1927), Nemytskii & Stepanov (1960), Coddington & Levinson (1955), and Guckenheimer & Holmes (1990).

JEAN-MARIE STRELCYN AND ALEXEI TSYGVINTSEV

See also **Celestial mechanics; *N*-body problem; Phase plane; Phase space; Recurrence**

Further Reading

Barrow-Green, J. 1997. Poincaré and the three body problem, *History of Mathematics*, vol. 11, Providence, RI: American Mathematical Society and London: London Mathematical Society

Birkhoff, G.D. 1927. *Dynamical Systems*, Providence, RI: American Mathematical Society

Coddington, E.A. & Levinson, N. 1955. *Theory of Ordinary Differential Equations*, New York: McGraw-Hill

Guckenheimer, J. & Holmes, P. 1990. *Nonlinear Oscillations, Dynamical Systems and Bifurcations of Vector Fields*, 3rd edition, Berlin and New York: Springer

Milnor, J.W. 1965. *Topology from the Differentiable Viewpoint*, based on notes by David W. Weaver, Charlottesville, VA: University Press of Virginia; revised and reprinted, Princeton, NJ: Princeton University Press, 1997 Contains an elegant and simple proof of the Poincaré–Hopf theorem.

Nemytskii, V.V. & Stepanov, V.V. 1960. *Qualitative Theory of Differential Equations*, Princeton, NJ: Princeton University Press

Poincaré, H. 1904. L'état actuel et l'avenir de la physique mathématique. Conférence lue le 24 Septembre 1904 au Congrés d'arts et de sciences de Saint-Louis. *Bulletin des Sciences Mathématiques*, 28: 302–324; translation in *Bulletin of the American Mathematical Society*, 12 (1905–1906): 240–260, also published in Poincaré's book *La valeur de la science*, Paris: Flammarion, 1905, Chapters VII, VIII, and IX

Poincaré, H. 1905. Sur la dynamique de l'électron, *Comptes Rendus de l'Académie des Sciences*, 140: 1504–1508; also in *Œuvres*, vol. 9, pp. 489–493

Poincaré, H. 1906. Sur la dynamique de l'électron, Rendiconti del Circolo matematico di Palermo, 21: 129–176; also in *Œuvres*, vol. 9, pp. 494–550

Poincaré, H. 1916–1956. *Œuvres de Henri Poincaré*, 11 vols, Paris: Gauthier-Villars (This paper (Poincaré, 1904), which is not included in Poincaré (1916–1956), is in fact the first Poincaré's paper anticipating the special theory of relativity. The annoucement (Poincaré, 1905) and its full presentation in Poincaré (1906) is Poincaré's contribution to what is now called the special theory of relativity.)

Symposium on the Mathematical Heritage of Henri Poincaré. 1983. The Mathematical Heritage of Henri Poincaré, edited by Felix E. Browder, 2 vols., Providence, RI: American Mathematical Society

POINCARÉ–BENDIXSON THEOREM

See **Phase plane**

POISSON BRACKETS

Let M be an n-dimensional manifold (referred to as the phase space), and let f, g, and h denote analytic functions on M. A Poisson bracket of any two analytic functions on the phase space is defined as an operation which satisfies

(i) $\{\alpha f+\beta g, h\}=\alpha\{f, h\}+\beta\{g, h\}$, (linearity in the first component);
(ii) $\{f, g\}=-\{g, f\}$ (skew-symmetry);
(iii) $\{f,\{g, h\}\}+\{g,\{h, f\}\}+\{h,\{f, g\}\}=0$ (Jacobi identity);
(iv) $\{f, gh\}=g\{f, h\}+\{f, g\}h$ (Leibniz property),

where α, β are numbers. The first two properties ensure that a Poisson bracket is a bilinear operation on M. Properties (i)–(iii) imply that the analytic functions on M form a Lie algebra with respect to the Poisson bracket.

If local coordinates z_i, $i=1, \ldots, n$ are chosen on M, then the Poisson bracket has the coordinate representation

$$\{f, g\}=\sum_{j,k=1}^{n} J_{jk}(z)\frac{\partial f}{\partial z_j}\frac{\partial g}{\partial z_k}=(\nabla f)^T \boldsymbol{J}\nabla g, \quad (1)$$

where $\nabla f=(\partial f / \partial z_1, \ldots, \partial f / \partial z_n)$, and the Poisson matrix $\boldsymbol{J}(z)=(J_{jk}(z))_{j,k=1}^{n}$ is a skewsymmetric square matrix, satisfying a technical condition enforced by the Jacobi identity.

Any nonconstant function C on M that Poisson commutes with all other functions on M is called a Casimir of the Poisson bracket. From (1) it follows that the existence of a Casimir requires $\boldsymbol{J}$ to be singular, and ∇C is in the null space of $\boldsymbol{J}$. Furthermore, the number of independent Casimirs is the corank of $\boldsymbol{J}$. For a Poisson bracket with r Casimirs $C_1, \ldots, C_r$, Darboux's theorem states that it is always possible to find coordinates $(q_1, \ldots, q_N, p_1, \ldots, p_N, C_1, \ldots, C_r)$ on M such that in these coordinates

$$\boldsymbol{J}=\begin{pmatrix} \boldsymbol{0} & \boldsymbol{I}_N & \boldsymbol{0} \\ -\boldsymbol{I}_N & \boldsymbol{0} & \boldsymbol{0} \\ \boldsymbol{0} & \boldsymbol{0} & \boldsymbol{0} \end{pmatrix}, \quad (2)$$

where $\boldsymbol{I}_N$ is the N-dimensional identity matrix, and $\boldsymbol{0}$ is the zero matrix of the appropriate dimensions. In these coordinates,

$$\{f, g\}=\sum_{j=1}^{N}\left(\frac{\partial f}{\partial q_j}\frac{\partial g}{\partial p_j}-\frac{\partial f}{\partial p_j}\frac{\partial g}{\partial q_j}\right). \quad (3)$$

This representation of the Poisson bracket is called the canonical Poisson bracket, and the coordinates $(q_1, \ldots, q_n, p_1, \ldots, p_n)$ are called canonical coordinates.

The importance of Poisson brackets is derived from their relationship to Hamiltonian systems: let H be a function on M. Hamiltonian dynamics with Hamiltonian function H are defined on any function f on M by

$$\dot{f}=\{f, H\}. \quad (4)$$

Using the coordinate representation (1), the Hamiltonian dynamics for the coordinates is

$$\dot{z_j}=\{z_j, H\}=\sum_{k=1}^{n} J_{jk}\frac{\partial H}{\partial z_k}, \quad (5)$$

which reduces to the standard definition of a Hamiltonian system if canonical coordinates are used. From (4) it is clear that any function that Poisson commutes with the Hamiltonian is conserved for the Hamiltonian system defined by the Poisson bracket and the Hamiltonian H. In particular, H is conserved. Also, any Casimir is conserved. Because the conservation of the Casimirs is independent of the choice of H, they do not contain dynamical information. Rather, as is obvious from Darboux's theorem, they foliate the phase space and represent geometric restrictions on the possible motions in phase space. A Hamiltonian system can also be defined using the Hamiltonian function H and a symplectic two-form, of which $\boldsymbol{J}^{-1}$ (if it exists) is the coordinate representation (Weinstein, 1984).

As an example, consider Euler's equations of a free rigid body (Weinstein, 1984). Denote the angular momentum by (M_1, M_2, M_3) and the moments of inertia by I_1, I_2, I_3. The Poisson matrix is

$$\boldsymbol{J}=\begin{pmatrix} 0 & M_3 & -M_2 \\ -M_3 & 0 & M_1 \\ M_2 & -M_1 & 0 \end{pmatrix}. \quad (6)$$

The Hamiltonian is $H=(M_1^2 / I_1+M_2^2 / I_2+M_3^2 / I_3) / 2$. The Poisson matrix has rank 2 (except at the origin), and there is one Casimir: $C_1=M_1^2+M_2^2+M_3^2$.

The notion of Poisson brackets extends to infinite-dimensional phase spaces, so as to describe dynamics governed by evolution (partial differential) equations (Marsden & Morrison, 1984). In this case, the Poisson matrix $\boldsymbol{J}$ is replaced by a skew-adjoint differential operator B. If the evolution equation is first order in the dynamical variable t, this operator is scalar. Otherwise it is a matrix operator of the same dimension as the order of the evolution equation. Instead of functions on phase space, we consider functionals

$$F[\boldsymbol{u}]=\int f[\boldsymbol{u}]\,\mathrm{d}x. \quad (7)$$

Here $\boldsymbol{u}(x, t)$ is an infinite-dimensional coordinate on the phase space, indexed by the independent variable x. The square brackets denote that $f[\boldsymbol{u}]$ depends not only on $\boldsymbol{u}$, but possibly also on its derivatives with respect to x: $\boldsymbol{u}_x, \boldsymbol{u}_{xx}, \ldots$. The limits of integration depend on the boundary conditions imposed on the evolution equation. In the above, the variable x is assumed to be one dimensional. This is extended to higher dimensions in obvious fashion.

The Poisson bracket between any two functionals on phase space is the functional given by

$$\{F, G\}=\int \frac{\delta F}{\delta u}B\frac{\delta G}{\delta u}\,\mathrm{d}x, \quad (8)$$

where $\delta F / \delta \boldsymbol{u}$ is the variational (or Fréchet) derivative of F with respect to $\boldsymbol{u}$:

$$\frac{\delta F}{\delta \boldsymbol{u}} = \frac{\partial f}{\partial \boldsymbol{u}} - \frac{\partial}{\partial x}\frac{\partial f}{\partial \boldsymbol{u}_x} + \frac{\partial^2}{\partial x^2}\frac{\partial f}{\partial \boldsymbol{u}_{xx}} - \dots . \quad (9)$$

The Poisson bracket defined this way satisfies properties (i), (ii), and (iv). The operator B is chosen so that the Jacobi identity (iii) is also satisfied.

A functional H on the phase space defines Hamiltonian dynamics on any functional by

$$\frac{\partial F}{\partial t} = \{F, H\} \quad \Leftrightarrow \quad \frac{\partial \boldsymbol{u}}{\partial t} = \{\boldsymbol{u}, H\} = B\frac{\delta H}{\delta \boldsymbol{u}}. \quad (10)$$

As an example, consider the Korteweg–de Vries equation $u_t = uu_x + u_{xxx}$ (Gardner, 1971; Zakharov & Faddeev, 1971). This equation with $-\infty < x < \infty$ is Hamiltonian with $B = \partial/\partial x$ and $H = \int_{-\infty}^{\infty}(u^3/6 - u_x^2/2)\,\mathrm{d}x$. Thus, the Poisson bracket is

$$\{F, G\} = \int_{-\infty}^{\infty} \frac{\delta F}{\delta u}\frac{\partial}{\partial x}\frac{\delta G}{\delta u}\,\mathrm{d}x, \quad (11)$$

and $\int_{-\infty}^{\infty} u\,\mathrm{d}x$ is its only Casimir.

The Poisson bracket formulation of a Hamiltonian system is especially significant when a quantum description of the dynamics is required. Dirac's principle of canonical quantization postulates that such a quantum description is obtained by replacing all classical quantities by their quantum mechanical operator counterparts (generalized coordinates $q \to \hat{q}$, the operation of multiplying by q, momentum $p \to -\mathrm{i}\hbar\partial/\partial q$, etc., and all Poisson brackets by commutators/$(\mathrm{i}\hbar)$). Then, in the classical limit as $\hbar \to 0$, the quantum mechanical equations reduce to classical equations, as desired by the correspondence principle.

Poisson brackets were introduced by Siméon-Denis Poisson (1809) during his investigations on perturbation theory in classical mechanics. Poisson's *Traité de mécanique* (two volumes, 1811 & 1833) were standard texts for many years.

BERNARD DECONINCK

See also **Constants of motion and conservation laws; Hamiltonian systems; Korteweg–de Vries equation; Lie algebras and Lie groups**

Further Reading

Gardner, C.S. 1971. The Korteweg–de Vries equation and generalizations. IV. The Korteweg–de Vries equation as a Hamiltonian system. *Journal of Mathematical Physics*, 12: 1548–1551

Marsden, J.E. & Morrison, P. 1984. Noncanonical Hamiltonian field theory and reduced MHD. In *Fluids and Plasmas: Geometry and Dynamics*, edited by J.E. Marsden, Providence, RI: American Mathematical Society

Poisson, S.D. 1809. Mémoire sur la variation des constantes arbitraires dans les questions de mécanique [Memoir on the variation of arbitrary constants in mechanics]. *Journal de l'École Polytechnique*, cahier XV: 266–298

Weinstein, A. 1984. Stability of Poisson–Hamilton equilibria. In *Fluids and Plasmas: Geometry and Dynamics*, edited by J.E. Marsden, Providence, RI: American Mathematical Society

Zakharov, V.E. & Faddeev, L.D. 1971. Korteweg–de Vries equation: a completely integrable Hamiltonian system. *Functional Analysis and Its Applications*, 5: 280-287

POLARITONS

A simple view of a dielectric material is that it is just an insulator made from atoms that have bound positive and negative charges. The ratio of an electric field measured in vacuum to that measured inside a dielectric material is called the dielectric constant. The opposite signs of the charges make the atoms electrically neutral, but these charges can be pulled apart by an applied electric field and they are displaced in opposite directions. If this happens, the material is said to be polarized. A metal, on the other hand, appears to be more complicated; it is a conductor and a solid-state plasma. Often called the fourth state of matter, a plasma is an electrically neutral assembly of separated electrons and positively charged ions. A metal is precisely like this but, unlike a gaseous plasma, it has a highly mobile "sea" of electrons carrying charges that are exactly balanced by a virtually immobile set of positive charges residing on the ionic background making up the crystal lattice. The same can be said for a heavily doped semiconductor. In spite of the plasma nature of a metal, its interaction with electromagnetic waves is well modeled by a dielectric function that turns out to be frequency-dependent (Kittel, 1995).

To understand the physical interaction between an electromagnetic wave and a dielectric, it is instructive to look at a (deceptively) simple model of how electrons behave in a metal or a heavily doped semiconductor when exposed to an electromagnetic wave. The core, realistic assumption in this model is that the electrons are highly mobile and free to move against an immobile ionic background. Suppose that the electric field carried by the electromagnetic wave is $\boldsymbol{E} = (0, 0, E)$, with a time variation $\mathrm{e}^{\mathrm{i}\omega t}$, where ω is an angular frequency. For a free electron with mass m, charge $-e$, and velocity $\boldsymbol{v}$, moving in one dimension, the equation of motion becomes

$$\mathrm{i}\omega m\boldsymbol{v} = -e\boldsymbol{E}. \quad (1)$$

If N is the number density of the electrons, this particle motion creates a current density with a magnitude $\boldsymbol{j}$,

$$\boldsymbol{j} = -Ne\boldsymbol{v} = \mathrm{i}\left(\frac{Ne^2}{\omega m}\right)\boldsymbol{E} = \mathrm{i}\omega\boldsymbol{P}, \quad (2)$$

where $\boldsymbol{P}$ is called the polarization. The latter should be thought of as being excited as a dipole moment per unit volume by the electromagnetic wave. Defining the electric displacement vector of free space as $\boldsymbol{D}$, and the

magnetic field as $\boldsymbol{H}$, the appropriate Maxwell equation to incorporate (2) is

$$\begin{aligned}\operatorname{curl} \boldsymbol{E} &= \frac{\partial \boldsymbol{D}}{\partial t} + \boldsymbol{j} = \mathrm{i}\omega\varepsilon_0 \boldsymbol{E} - \mathrm{i}\frac{Ne^2}{\omega m}\boldsymbol{E} \\ &= \mathrm{i}\omega\varepsilon_0 \left[1 - \frac{\omega_\mathrm{p}^2}{\omega^2}\right]\boldsymbol{E} \end{aligned} \tag{3}$$

in which t is time and ε_0 is the permittivity of free space. Equation (3) shows that a metal is neatly modeled by the frequency-dependent relative permittivity

$$\varepsilon(\omega) = 1 - \frac{\omega_\mathrm{p}^2}{\omega^2}, \tag{4}$$

where $\omega_\mathrm{p}^2 = \left(\sqrt{Ne^2/\varepsilon_0 m}\right)$ is called the plasma frequency. For this to also be a useful description of a semiconductor, or to take into account that the ionic background of a metal may contribute a frequency-independent permittivity, all that is necessary is to replace unity in Equation (4) with a quantity ε_L, which can be much greater than unity for semiconductors. This model gives good agreement with experiment, and it also serves to introduce the polariton concept. Excitations other than those of a free-electron gas are easy to capture, once this basic example is accepted. In a one-dimensional system stretching along the x-axis, the electrons move a distance $\boldsymbol{x} = e\boldsymbol{E}/(\omega^2 m)$ and the polarization is $\boldsymbol{P} = -Ne\boldsymbol{x}$.

If a plane electromagnetic wave has a wave vector $\boldsymbol{k}$ and (4) is the dielectric function, then

$$\begin{aligned}\boldsymbol{k} \times \boldsymbol{E} &= \omega\mu_0 \boldsymbol{H}, \\ \boldsymbol{k} \times \boldsymbol{H} &= -\omega\varepsilon_0 \varepsilon(\omega)\boldsymbol{E}, \end{aligned} \tag{5}$$

where μ_0 is the magnetic permeability of free space. As a specific example, let the propagation be along the x-axis with wave vector $\boldsymbol{k} = (k, 0, 0)$ and let the electric field vector be $\boldsymbol{E} = (E_x, 0, E_z)$. The following modes are then implied (Boardman, 1982) by (5):

$$\text{Transverse}: \quad (\omega^2 - \omega_\mathrm{p}^2 - c^2k^2)E_z = 0, \tag{6}$$

$$\text{Longitudinal}: \quad (\omega^2 - \omega_\mathrm{p}^2)E_x = 0, \tag{7}$$

where $c^2 = 1/(\varepsilon_0\mu_0)$ is the velocity of light in vacuum and there are two independent solutions. The longitudinal mode is sustained when $E_x \neq 0$ and $\omega = \omega_p$. For this mode, the electrons move collectively in an oscillation that resembles the wobbling of a jelly.

At this stage, it should be pointed out that physicists are prone to call things by "ons" (Walker & Slack, 1970). All this started with the word *electron*. Unfortunately, the latter word does not, in itself, explain too much about the "on" part of the word, which is derived from the Greek word for "amber",—a fact that Benjamin Franklin would readily appreciate. Nevertheless, the electron is recognized to have a particle nature so physicists have become used to defining an "on" in association with an excited field, such as an electromagnetic wave or the jelly-like plasma oscillation. Thus, a *photon* is a particle, or quantum of energy, of light and the quantum of the wobbling electronic jelly, or plasma oscillation, is called the *plasmon*. The name *polariton* (Hopfield, 1958) is reserved for the quantum of an excitation in which electromagnetic waves cannot disentangle themselves from excitations such as plasmons.

The coupling of an electromagnetic field to the polarization excitations associated with electrons can be seen from the transverse solution (6). This shows that a finite value for E_z requires the dispersion equation to be

$$\omega^2 = \omega_\mathrm{p}^2 + c^2k^2 \tag{8}$$

Furthermore, this equation shows that the excitation is mixed because it involves not only the plasma frequency but also the velocity of light. It is for this reason that the quantum of this photon-plasmon field is called a polariton, as indicated earlier. The total energy is shared over the system because the mode has both plasmon and photon content, as can be seen by looking at the low and high wave number limits of (8). As $\boldsymbol{k} \to 0$, the frequency tends towards the plasma frequency, and the plasmon content grows at the expense of the photon contribution. The opposite is true as $\boldsymbol{k} \to \infty$, and the wave becomes a pure electromagnetic wave. The "on" labeling is not complete, however, unless the type of polariton is identified, so, in this case, they are referred to as plasmon-polaritons. This labeling is a reminder that only plasmons have been used here to introduce the concept of polaritons. The description is generic, however, and there are many types of polaritons. All that is necessary to generalize the discussion given here is to decide which polarization excitation the photons couple with and capture the material polarization properties through an effective permittivity. Well-known examples involve plasmons, excitons, and phonons.

After several decades of research, polaritons are still attracting attention (Baher & Cottam, 2003), in both guided and surface wave form, and the study of nonlinear polaritons in particular has opened new horizons (Boardman & Egan, 1985). The inclusion of nonlinearity means extending the permittivity to depend upon the amplitude of the electromagnetic wave through a functional dependence upon E, such as

$$\varepsilon(\omega, E) = \varepsilon(\omega) + \varepsilon^{\mathrm{NL}}(|E|) \tag{9}$$

Here $\varepsilon(\omega)$ is the relative permittivity for the excitation of choice, such as phonons, plasmons, or excitons. To reduce (9) to a tractable form, a Kerr-type of optical nonlinearity can be adopted, in which the total permittivity is expressed as

$$\varepsilon(\omega, E) = \varepsilon(\omega) + a\,|E|^2\,, \tag{10}$$

where a is a nonlinear coefficient.

This type of nonlinear process is not only popular in the literature but is genuinely applicable when the nonlinearity is well away from resonance and saturation. Immediately an interesting feature appears because the form of (10) permits an investigation of the kind of transverse electric (TE) waves that have no linear ($a \to 0$) limit. This dramatic conclusion culminates in the generation of an entirely new type of polariton. The TE waves can be guided or surface waves and for this discussion are assumed to be traveling along the x-axis. The field components are, therefore,

$$\begin{aligned} \boldsymbol{E} &= [0,\, E_y(k,\omega,z),\, 0]\mathrm{e}^{\mathrm{i}(kx-\omega t)}, \\ \boldsymbol{H} &= [H_x(k,\omega,z),\, 0,\, H_z(k,\omega,z)]\mathrm{e}^{\mathrm{i}(kx-\omega t)}. \end{aligned} \quad (11)$$

Substituting (11) into Maxwell's equations produces the following equations (Boardman et al., 1991):

$$\begin{aligned} \frac{\mathrm{d}}{\mathrm{d}z}E_y(k,\omega,z) &= -\mathrm{i}\omega\mu_0 H_x(k,\omega,z), \\ kE_y(k,\omega,z) &= \omega\mu_0 H_z(k,\omega,z), \\ \frac{\mathrm{d}}{\mathrm{d}z}H_z(k,\omega,z) &= \mathrm{i}kH_z(k,\omega,z) \\ &\quad +\mathrm{i}\omega\varepsilon_0\varepsilon(\omega,\mid E_y\mid^2)E_y(k,\omega,z). \end{aligned} \quad (12)$$

In general, E_y is complex so that $E_y = E(k,\omega,z)\,\mathrm{e}^{\mathrm{i}\phi(k,\omega,z)}$. Using $E \equiv E(k,\omega,z)$, $\phi \equiv \phi(k,\omega,z)$, and $\varepsilon \equiv \varepsilon(\omega)$ in (12) produces the following basic nonlinear equations:

$$\begin{aligned} &\frac{\mathrm{d}^2}{\mathrm{d}z^2}E - E\left(\frac{\mathrm{d}\phi}{\mathrm{d}z}\right)^2 + \left(\frac{\omega^2}{c^2}\varepsilon - k^2\right)E + \frac{\omega^2}{c^2}aE^2 = 0, \\ &\frac{\phi}{\mathrm{d}z} = \frac{K}{E^3}. \end{aligned} \quad (13)$$

The last equation expresses the conservation of energy flux along the z-axis, which is perpendicular to the propagation direction, and K is a constant of the integration process. The z-component of the time-averaged Poynting vector is

$$\langle S\rangle_z = -\frac{1}{2}\mathrm{Re}(E_y^* H_x) = \frac{c^2}{2\omega^2}\varepsilon_0 K. \quad (14)$$

Hence, $K = 0$ implies $\langle S\rangle_z = 0$. Finally,

$$\left(\frac{\mathrm{d}E}{\mathrm{d}z}\right)^2 + \left(\frac{\omega^2}{c^2}\varepsilon(\omega) - k^2\right)E + \frac{a}{2}\frac{\omega^2}{c^2}E^4 = C, \quad (15)$$

where C is another constant of integration. For a semi-infinite medium, $C = 0$, otherwise $C \neq 0$.

Consider now a $C = 0$ case describing a semi-infinite nonlinear medium interfaced to a semi-infinite linear medium. As it is well known that linear surface plasmon–polaritons are transverse magnetic (TM) polarized waves, the nonlinearity has added the extra functionality of making it possible to have TE-polarized surface plasmon-polariton waves. The field profile of these TE nonlinear waves is readily obtained from (15), since it factorizes when $C = 0$. The solution is

$$\begin{aligned} E = \frac{c}{\omega}\sqrt{\frac{2}{a}}\sqrt{\left(k^2 - \frac{\omega^2}{c^2}\varepsilon(\omega)\right)} \\ \times \operatorname{sech}\left[\sqrt{k^2 - \frac{\omega^2}{c^2}\varepsilon(\omega)}\right](z - z_0). \end{aligned} \quad (16)$$

This is a self-focused (self-guided) beam that has a peak in the nonlinear medium below the interface. This nonlinear surface wave looks exactly like a spatial soliton. Furthermore, there is no linear limit for the nonlinear TE-polarized surface plasmon-polaritons. The frequency dependence for guided modes is more complex and can have a linear limit.

Polaritons are being studied in a wide variety important of contexts. Some examples include nonlinear exciton-polariton dynamics in the experimental study of semiconductor microcavities (Savvides et al., 2000), two-dimensional electron systems in quantizing magnetic fields (Beletskii & Bludov, 2002), and plasmon-polaritons in dielectric films (Baher & Cottam, 2003). The idea that underpins the polariton concept can be put to dramatic use in an unusual way. This is possible because to create polaritons, photons must associate themselves with the quanta or the quasiparticles of collective excitations, be they plasmons, phonons, or related excitatons. The polariton is a genuine collaborative effect between the photons and particles that are acting in a prepared organized manner, which means that the particles are not absorbing or emitting the photons. If a stream of photons (a light beam) is sent through an atomic gas (Lukin et al., 2000), for example, then provided the gas atoms are not resonant with the laser wavelength, the atoms should swarm around the photons rather like bees around a honey pot. In other words, polaritons should be formed. Furthermore, these polaritons could be organized, through an appropriate choice of laser intensity, to travel at a speed that is much less than the velocity of light. The particle swarm that has associated itself with the photon will slow down the light dramatically. This is an elegant idea and is a striking illustration of the character of the polariton. It is not surprising that the phrase "to catch a moonbeam" has been used (Sincelli, 2000) to describe the polariton-based possibility of slowing down light to walking speed.

ALLAN BOARDMAN

See also **Alfvén waves; Drude model; Excitons; Nonlinear plasma waves; Plasma soliton experiments; Polarons**

Further Reading

Baher, S. & Cottam, M.G. 2003. Theory of nonlinear guided and surface plasmon-polaritons in dielectric films. *Surface Review and Letters*, 10: 13–22

Beletskii, N.N. & Bludov, Yu.V. 2002. Nonlinear surface polaritons in a two-dimensional electron system placed into a quantising magnetic field. *Telecommunications and Radioengineering*, 57: 67–78

Boardman, A.D. (editor). 1982. *Electromagnetic Surface Modes*, Chichester and New York: Wiley

Boardman, A.D. & Egan, P. 1985. s-polarised waves in a thin dielectric film asymmetrically bounded by optically nonliner media. *IEEE Quantum Electronics*, 21: 1701–1713

Boardman, A.D., Egan, P., Lederer, F., Langbein, U. & Mihalache, D. 1991. Third-order nonlinear electromagnetic TE and TM guided waves. In *Nonlinear Surface Electromagnetic Phenomena*, edited by H.-E. Ponath & G.I. Stegeman, Amsterdam and New York: North-Holland

Hopfield, J.J. 1958. Theory of the contribution of excitons to the complex dielectric constant of crystals. *Physical Review*, 112: 1555–1567

Kittel, C. 1995. *Introduction to Solid State Physics*, New York and London: Wiley

Lukin, M.D., Yelin, S. & Fleischhauer, M. 2000. Entanglement of atomic ensembles by trapping correlated photon states. *Physical Review Letters*, 84: 4232–4235

Savvides, P.G., Baumberg, J.J., Stevenson, R.M., Skolnick, M.S., Roberts, J.S. & Whittaker, D.M. 2000. Angular-asymmetric nonlinear polariton dynamics in semiconductor microcavities. *Physica Status Solidi* B, 221: 77–83

Sincelli, M. 2000. How to catch a moonbeam. *Physical Review Focus* 5, story 19

Walker, C.T. & Slack, G.A. 1970. Who named the -ON's? *American Journal of Physics*, 38: 1380–1389

POLARONS

The polaron concept goes back to 1933 when Lev Landau suggested the phenomenon of self-localization (self-trapping) of an electron (or a hole), slowly moving in a polar crystal (Landau, 1933). The electron locally polarizes and, therefore, distorts the ionic lattice in the region where it is located. This local lattice distortion, in turn, creates a potential well that traps the electron, lowering its energy. Therefore, the electron and the accompanying self-consistent polarization field can move in the crystal as a whole entity and may be considered as a quasi-particle. The term *polaron* was introduced in 1946 by Solomon Pekar, who studied the limiting (adiabatic) case of a sufficiently strong electron-lattice interaction and described the most-important properties of a stationary polaron, using a continuum model of electron motion (Pekar, 1946).

Pekar's theory of a polaron is based on the assumption that the polar coupling between electrons and optical phonons can be very large in ionic crystals. In ionic crystals, some of the ions are positively charged, while others are negatively charged, and an optical phonon has the different ions in the crystal vibrating out of phase. When the positive ions and negative ions oscillate in opposite directions (at a point $\boldsymbol{r}$ of the crystal), they create a polarization field $\boldsymbol{P}(\boldsymbol{r})$. This causes an electric field $\boldsymbol{E}(\boldsymbol{r})$, which is the source of the polar coupling. Polar coupling is only to longitudinal optical (LO) phonons, because only LO phonons set up a strong electric field when they vibrate. (This electric field is in the direction of the phonon wave vector $\boldsymbol{q}$.) Writing the expansion in normal modes:

$$\boldsymbol{E}(\boldsymbol{r}) = N^{-1/2} \sum_{\boldsymbol{q}} \boldsymbol{E}_{\boldsymbol{q}} \mathrm{e}^{\mathrm{i}\boldsymbol{q}\cdot\boldsymbol{r}}$$

$$\boldsymbol{P}(\boldsymbol{r}) = N^{-1/2} \sum_{\boldsymbol{q}} \boldsymbol{P}_{\boldsymbol{q}} \mathrm{e}^{\mathrm{i}\boldsymbol{q}\cdot\boldsymbol{r}} \qquad (1)$$

with N being the number of ions in the crystal and using the fact that there are no free charges, that is, $\nabla \cdot (\boldsymbol{E} + 4\pi\boldsymbol{P}) = 0$, one obtains the relation

$$\boldsymbol{E}_{\boldsymbol{q}} = -4\pi \boldsymbol{P}_{\boldsymbol{q}}. \qquad (2)$$

Each $\boldsymbol{P}_{\boldsymbol{q}}$ is proportional to the (quantized) displacement field

$$\boldsymbol{P}_{\boldsymbol{q}} = U_{\boldsymbol{q}} e \left(\frac{\hbar}{2M\omega_{\boldsymbol{q}}} \right)^{1/2} \mathrm{i} \frac{\boldsymbol{q}}{|\boldsymbol{q}|} \left(a_{\boldsymbol{q}}^{\dagger} + a_{-\boldsymbol{q}} \right), \qquad (3)$$

where the coefficient $U_{\boldsymbol{q}}$ is to be determined, e is the electron charge, M the ion mass, $\omega_{\boldsymbol{q}}$ is the frequency of the $\boldsymbol{q}$th mode, and $a_{\boldsymbol{q}}$ ($a_{\boldsymbol{q}}^{\dagger}$) is the annihilation (creation) operator of the $\boldsymbol{q}$th mode.

On the other hand, the electric field can be represented as a gradient of a potential field:

$$\boldsymbol{E}(\boldsymbol{r}) = -\nabla\phi(\boldsymbol{r}) = -\mathrm{i} \sum_{\boldsymbol{q}} \boldsymbol{q} \mathrm{e}^{\mathrm{i}\boldsymbol{q}\cdot\boldsymbol{r}} \phi_{\boldsymbol{q}} \,. \qquad (4)$$

Using Equations (1)–(4), the potential field for the electron is

$$\phi(\boldsymbol{r}) = 4\pi e \sum_{\boldsymbol{q}} U_{\boldsymbol{q}} \mathrm{e}^{\mathrm{i}\boldsymbol{q}\cdot\boldsymbol{r}} \left(\frac{\hbar}{2NM\omega_{\boldsymbol{q}}} \right)^{1/2} \times \frac{1}{|\boldsymbol{q}|} \left(a_{\boldsymbol{q}}^{\dagger} + a_{-\boldsymbol{q}} \right). \qquad (5)$$

Because each normal mode $\boldsymbol{q}$ assumes a new equilibrium configuration and oscillates in the vicinity of these new equilibria, the coupling constant $U_{\boldsymbol{q}}$ can be evaluated from the potential energy between two fixed electrons. For a dispersionless polar crystal, when the frequency $\omega_{\boldsymbol{q}}$ is nearly a constant ($\omega_{\boldsymbol{q}} \doteq \omega_0$), Pekar has derived the value

$$U_0^2 = \frac{\rho\omega_0^2}{4\pi} \left(\frac{1}{\varepsilon_\infty} - \frac{1}{\varepsilon_0} \right), \qquad (6)$$

where ρ is the mass density of the crystal (so $\rho V = NM$, with V being the crystal volume). The dielectric constants ε_0 and ε_∞ are both measurable: ε_0 is measured by putting the crystal between the parallel plates of a capacitor at low frequency and ε_∞ is the square of the refractive index.

Thus, it is possible to write the total Hamiltonian of a single electron that interacts with the phonons in the form

$$H = \frac{\boldsymbol{p}^2}{2m} + \omega_0 \sum_{\boldsymbol{q}} a_{\boldsymbol{q}}^{\dagger} a_{\boldsymbol{q}} + V^{-1/2} \sum_{\boldsymbol{q}} \frac{\chi_0}{|\boldsymbol{q}|} \mathrm{e}^{\mathrm{i}\boldsymbol{q}\cdot\boldsymbol{r}} \left(a_{\boldsymbol{q}}^{\dagger} + a_{-\boldsymbol{q}} \right). \qquad (7)$$

Here the unperturbed electron is taken to have free-particle motion with a momentum $\boldsymbol{p}$ and an effective mass m. Since there is only one electron in the problem, the results are independent of the statistics of the particle. The same results are obtained for any fermion or boson in the crystal, such as holes, excitons, or other particles, as long as they are free to move. Owing to Equations (5) and (6), the electron-phonon coupling constant χ_0 in Hamiltonian (7) is given by

$$\chi_0^2 = 4\pi\alpha\hbar(2m)^{-1/2}(\hbar\omega_0)^{3/2} \tag{8}$$

with the dimensionless polaron constant

$$\alpha = \frac{e^2}{\hbar}\left(\frac{m}{2\hbar\omega_0}\right)^{1/2}\left(\frac{1}{\varepsilon_\infty} - \frac{1}{\varepsilon_0}\right). \tag{9}$$

In Pekar's analysis of this model, the method of calculation is basically a variational procedure using a Gaussian wave function. The total wave function is assumed to be the product of electron and phonon coordinates (adiabatic approximation):

$$\Phi(\boldsymbol{r}; \boldsymbol{Q_q}) = \varphi(\boldsymbol{r})\psi_n(\boldsymbol{Q_q} + \delta\boldsymbol{Q_q}),$$
$$\varphi(\boldsymbol{r}) = \frac{\beta^{3/2}}{\pi^{3/4}}\exp\left(-\frac{\beta^2\boldsymbol{r}^2}{2}\right), \tag{10}$$

where β is a variational parameter to be determined. The phonon wave functions ψ_n are the wave functions for harmonic oscillators centered about new equilibrium displacements, which also need to be determined. Having carried out the variational procedure, one obtains the minimum value of β and the total energy $E = E(\beta)$ of the coupled electron–phonon system:

$$\beta_0 = \frac{2\alpha}{3}\sqrt{\frac{m\omega_0}{\pi}},$$
$$E(\beta_0) = -\frac{\alpha^2\omega_0}{3\pi} \simeq -0.106\alpha^2\omega_0. \tag{11}$$

This result shows the existence of a dynamically stable, self-localized state of an electron interacting with optical phonons in ionic crystals and having a finite binding energy, under the condition that the size of the self-trapped state is large compared with the lattice spacing constant (so the lattice discreteness becomes irrelevant in the theory).

Pekar's continuum polaron was the first model of a self-trapped state admitting a self-consistent theoretical treatment. The importance of this problem was soon understood by many theoretical and mathematical physicists working in solid state physics and quantum field theory, including N.N. Bogolyubov, S.V. Tyablikov, T.D. Lee, H. Fröhlich, R.P. Feynman, E.I. Rashba, T. Holstein, Y. Toyozawa, I.G. Lang, and Yu.A. Firsov. As a result, several pioneering works were published in the 1950s, favoring use of the methods of quantum field theory in solid state physics. Thus, the "polaron" concept has lost its original meaning as an electron interacting with long-wave-length polarized optical phonons and has been applied to a significantly wider class of self-trapped states, resulting in a large body of work that includes exciton-phonon interactions (Rashba, 1957) and even applications in biology (Scott, 1992), with very recent important contributions to the classical polaron theory (Romero et al., 1999). In this context, the following comments are relevant:

(i) The strong coupling limit in Pekar's theory is calculated in the adiabatic approximation, when the electron has a sufficient binding energy and its oscillatory motion in the potential well is much faster than the vibrational frequency of the phonons. Thus, the phonons do not have time to adjust to the individual oscillations of the electron. Instead, they adjust to the average motion of the electron. Quite a different picture applies to the weak coupling limit. In this case, the phonon energy is larger than that of the electron, so that the phonons (or ion polarization) follow the electron during its motion. The weak coupling limit was studied by Fröhlich within his polaron model, in which Hamiltonian (7) was generalized to (Fröhlich, 1954)

$$H = \sum_{\boldsymbol{k}} \frac{\boldsymbol{k}^2}{2m} c_{\boldsymbol{k}}^\dagger c_{\boldsymbol{k}} + \omega_0 \sum_{\boldsymbol{q}} a_{\boldsymbol{q}}^\dagger a_{\boldsymbol{q}}$$
$$+ V^{-1/2} \sum_{\boldsymbol{q},\boldsymbol{k}} \frac{\chi_0}{|\boldsymbol{q}|} c_{\boldsymbol{k}+\boldsymbol{q}}^\dagger c_{\boldsymbol{k}} \left(a_{\boldsymbol{q}}^\dagger + a_{\boldsymbol{q}}\right), \tag{12}$$

where $c_{\boldsymbol{k}}$ ($c_{\boldsymbol{k}}^\dagger$) is the annihilation (creation) operator of the electron with the wave number $\boldsymbol{k}$. However, the most sophisticated study of the "large" (or "continuum") polaron, using the Fröhlich Hamiltonian (12), is due to Feynman (1955) with the path-integral method, substantially extended in the past decade. For an extensive review of the large polaron studies in both the strong and weak coupling limits, see Mitra et al. (1987).

(ii) When the electron-phonon coupling constant is large, all the states in the Brillouin zone are involved in the formation of the polaron wave function. In this case, the polaron radius becomes comparatible with the lattice constant and the continuum approximation is no longer valid. For a "small" polaron, the theory should recognize the periodicity of the crystal and thereby assume that the motion of the electron, or another particle, is no longer translationally continuous. Therefore, one assumes that the electron may occupy an orbital state $\phi(\boldsymbol{r} - \boldsymbol{R}_j)$ centered on an atomic site $\boldsymbol{R}_j$. The orbital states are identical on each site, so that there is periodicity. The electron may move from site to site as in the tight-binding model. This motion may be caused by the overlap of the orbitals on adjacent

sites. Thus, the following Hamiltonian is suitable for the small polaron theory:

$$H = J\sum_{j,l} C^{\dagger}_{j+l}C_j + \sum_{\boldsymbol{q}} \omega_{\boldsymbol{q}} a^{\dagger}_{\boldsymbol{q}} a_{\boldsymbol{q}} + \sum_{j,\boldsymbol{q}} \chi_{\boldsymbol{q}} e^{i\boldsymbol{q}\cdot\boldsymbol{R}_j} C^{\dagger}_j C_j \left(a^{\dagger}_{\boldsymbol{q}} + a_{-\boldsymbol{q}}\right), \quad (13)$$

where the factor J describes the overlap of the orbitals and C_j ($C^{\dagger}_j$) is the annihilation (creation) operator of the electron on site $\boldsymbol{R}_j$. Basic features of the small polaron were well recognized a long time ago by Tyablikov, Holstein, Lang, and Firsov, among others, and are described in several review papers and textbooks (Appel, 1968; Böttger & Bryksin, 1985; Mahan, 1990; Alexandrov & Mott, 1995).

(iii) Another interesting case is a problem of the lattice polaron with a long-range Fröhlich interaction. This polaron has a small (atomic) size of wave function but a large radius of lattice deformation. As shown recently (Alexandrov & Kornilovitch, 1999), this "small Fröhlich polaron" can propagate in a narrow band with the effective mass much smaller than that of the Holstein small polaron of the same binding energy. Alexandrov and Kornilovitch argue that small as well as large Fröhlich (bi)polarons are relevant quasiparticles in the cuprates, describing holes in the CuO_2 plane coupled with the lattice distortion created by a long-range interaction.

(iv) The polaron concept appeared so ubiquitous that it was used even in biology to describe a possible mechanism of the localization and transport of vibrational energy in molecular chains, particularly in proteins. As was suggested by Davydov, the energy of the C=O stretching (amide-I) vibrations, being localized on a peptide group of the α-helix, distorts the structure of the helix in this place. In its turn, a (contractive) distortion of the helical chain creates a potential well that traps the amide-I oscillation energy preventing its dispersion. This mobile self-localized (or self-trapped) state that can travel along the chain, carrying the energy released under the adenosine triphosphate (ATP) hydrolysis, is called a "Davydov soliton" (Scott, 1992).

ALEXANDER V. ZOLOTARYUK

See also **Davydov soliton; Discrete self-trapping system; Local modes in molecular crystals**

Further Reading

Alexandrov, A.S. & Kornilovitch, P.E. 1999. Mobile small polaron. *Physical Review Letters*, 82: 807–810

Alexandrov, A.S. & Mott, N.F. 1995. *Polarons and Bipolarons*, Singapore: World Scientific

Appel, J. 1968. In *Solid State Physics*, edited by F. Seitz, D. Turnbull & H. Ehrenreich, New York: Academic Press

Böttger, H. & Bryksin, V.V. 1985. *Hopping Conduction in Solids*, Deerfield Beach, FL: VCH

Feynman, R.P. 1955. Slow electrons in a polar crystal. *Physical Review*, 97: 660–665

Fröhlich, H. 1954. Electrons in lattice fields. *Advances in Physics*, 3: 325

Landau, L.D. 1933. Über die Bewegung der Elektronen in Kristallgitter. *Physik Z. Sowjetunion*, 3: 664–665

Mahan, G.D. 1990. *Many-Particle Physics*, New York and London: Plenum Press

Mitra, T.K., Chatterjee, A. & Mukhopadhyay, S. 1987. Polarons. *Physics Reports*, 153: 91–207

Pekar, S.I. 1946. Autolocalization of an electron in a dielectric inertially polarized medium. *Soviet Physics, JETP*, 16: 335–340

Rashba, E.I. 1957. Theory of the strong interaction of electron excitations with lattice vibrations in molecular crystals. I & II. *Soviet Physics, Optika i Spektroskopiya (Optics and Spectroscopy)*, 2: 75–98

Romero, A.H., Brown, D.W. & Lindenberg, K. 1999. Polaron effective mass, band distortion, and self-trapping in the Holstein molecular-crystal model. *Physical Review* B, 59: 13728–13740; The self-trapping line of the Holstein molecular crystal model in one dimension. *Physical Review*, 60: 4618–4623

Scott, A.C. 1992. Davydov's soliton. *Physics Reports*, 217: 1–67

POLYMERIZATION

Polymers are long molecules made from one or more types of repeating units, called monomers. The simplest synthetic polymer consists of hundreds to even millions of monomers that are connected end to end in a linear chain. Polymers are essential to our modern world and our very life. Biochemical systems involve polymers because all enzymes are proteins, a type of polymer composed of about 20 different amino acids. DNA and RNA are also polymers but formed from four different bases (Nelson & Cox, 2000). Goldbeter (1995) discusses well the type of nonlinear phenomena that can occur. We focus only on synthetic polymers here.

A distribution of chain lengths always exists in a synthetic system. This molecular weight distribution can be quite broad, often spanning several orders of magnitude. However, biopolymers consist of a single molecular weight.

Linear polymers are often thermoplastic, meaning that they can flow at some temperature, which depends on the molecular weight. Common examples are poly(styrene) and poly(methyl methacrylate), whose trade name is Plexiglass.

Polymers need not be simple chains but can be branched or networked. Linear polymers are analogous to strings of spaghetti. Crosslinked polymers can be gels that swell in a solvent or thermosets, which form rigid three-dimensional networks. Home epoxy glue is an example of a crosslinked polymer. Figure 1 illustrates these variations.

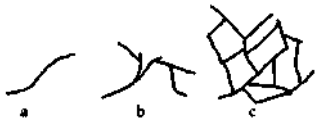

Figure 1. Illustration of three types of polymers: (a) linear, (b) branched, (c) crosslinked.

Polymer Kinetics and Mechanisms of Feedback

The mechanism of polymerization usually falls into one of two categories: chain growth or step growth. In chain-growth polymerization, a monomer is converted into a reactive species by an initiating species, either an ion or a free radical (a molecule containing an unpaired electron), that rapidly reacts with other monomers while always maintaining the reactive character. The reactive chain can be broken through some termination process. In most cases, even though relatively little of the monomer has reacted, high molecular weight molecules are produced in a few seconds. They usually do not participate further in the reaction. Plexiglass is produced via free-radical chain-growth polymerization.

For step-growth polymers, the monomers can usually react from both ends, and thus, all the monomers and polymers can react with each at any time from both ends. The molecular weight increases continuously throughout the reaction as monomers react to form dimers, and then dimers can react with each other or monomers, etc.

The physical properties of the polymer medium change dramatically during reaction. For example, the viscosity almost always increases orders of magnitude as the polymer concentration and/or molecular weight increases. This can be understood if you consider stirring a pot of penne versus a pot of spaghetti: the longer pasta pieces intertwine and resist flowing. Such physical changes will often affect the kinetic parameters of the reaction and the transport coefficients of the medium.

Synthetic polymer systems can exhibit feedback through several mechanisms. The simplest is thermal autocatalysis, which occurs in any exothermic reaction. The reaction raises the temperature of the system, which increases the rate of reaction through the Arrhenius dependence of the rate constants. Most chain-growth polymerizations, including free-radical polymerizations, are highly exothermic. Some step-growth polymerizations are highly exothermic (epoxies), but some are not (polyesters).

Free-radical polymerizations of certain monomers exhibit autoacceleration at high conversion via an additional mechanism, the isothermal "gel effect" or "Trommsdorff effect" (Odian, 1991). These reactions occur by the creation of a radical that attacks an unsaturated monomer, converting it to a radical, which can bond to another monomer, propagating the chain. The chain growth terminates when two radical chains ends encounter each other, forming a stable chemical bond. As the polymerization proceeds, the viscosity increases. The diffusion-limited termination reactions are thereby slowed down, leading to an increase in the overall polymerization rate. The increase in the polymerization rate induced by the increase in viscosity builds a positive feedback loop into the polymerizing system.

Some polymer hydrogels exhibit "phase transitions" as the pH and/or temperature are varied. Disposable diapers contain hydrogels that absorb great amounts of water because the polymers contain charged groups that bind the water. These charged groups can be affected by acid or base and are also temperature sensitive. The gel can swell significantly as the conditions are changed and can also exhibit hysteresis (Addad, 1996). Most polymers are immiscible, meaning that they will not dissolve with each other but will separate into different phases like oil and water. Introducing chemical reactions to an initially miscible polymer mixture often leads to phase separation. Autocatalytic behavior driven by chemical reactions and concentration fluctuations in miscible polymer mixtures can occur in photo-crosslinked polymer mixtures (Pojman & Tran-Cong-Miyata, 2003, Chapter 22). Concentration fluctuations increase as the reaction proceeds, leading to the reaction of photoreactive groups attached to one of the polymer components. This leads to an increase in the reaction yield that, in turn, accelerates the concentration fluctuations.

Finally, the polymer melts and the solutions are usually non-Newtonian fluids (Gupta, 2000), which means that there is no linear relationship between the stress applied to the fluid and strain that is measured. They often exhibit shear thinning, which means that the viscosity decreases as the shear is increased, but can also exhibit shear thickening. These properties make polymer additives important in the food and cosmetic industry.

Applications

There are two main scenarios by which nonlinear phenomena of possible utility arise with polymers. The first approach is to use a nonlinear system to drive the nonlinear behavior of a polymer or polymerization. Acrylonitrile will polymerize periodically when added to the Belousov–Zhabotinsky (BZ) reaction (Washington et al., 1999).

Yoshida et al. created a self-oscillating gel by coupling a pH oscillating reaction with a polymeric gel that expands and contracts with changes in pH (Yoshida et al., 1995). They have also used a gel in which the

ruthenium catalyst of the BZ reaction is chemically incorporated into polymer, causing local swelling and deswelling as chemical waves pass through the gel (Pojman & Tran-Cong-Miyata, 2003, Chapter 3).

The second approach is to use the inherent nonlinearities in a polymeric system. Polymerizations in a continuously stirred flow tank reactor (CSTR) can show nonlinear phenomena through the interaction of thermal feedback and the gel effect. Teymour and Ray showed in laboratory-scale CSTR experiments on vinyl acetate polymerization that oscillations with periods of 200 min could occur (Teymour & Ray, 1992). The gel effect causes the rate of polymerization to increase, but the increase in temperature lowers the viscosity, returning the polymerization to its lower rate.

Frontal Polymerization

One of the most promising applications of nonlinear dynamics to polymer science is the phenomenon of frontal polymerization. Frontal polymerization is a process of converting monomers into a polymer via a localized reaction zone that propagates through the monomer, much like a "liquid flame."

Thermal frontal polymerization involves the coupling of thermal diffusion and Arrhenius reaction kinetics of an exothermic polymerization (Pojman et al., 1996). Front temperatures are typically 200°C, and front velocities are from 1–20 cm/min. Because of the large composition and thermal gradients created in the front, convection can be a significant issue (Pojman et al., 1996). Simple convection can occur for thermosets in ascending fronts, but for thermoplastics, the Rayleigh–Taylor instability is a significant issue unless a filler is added to increase the viscosity.

Such systems exhibit many modes of nonplanar front propagation. Particularly fascinating are the spin modes in which the front propagates as a helix, and hot spots can be seen on the surface with an infrared camera (Figure 2). Even more complicated modes can be observed depending on the chemical composition.

Figure 2. Infrared image of a spin mode in the free-radical-frontal polymerization of an acrylate in a 1.5 cm diameter tube. (Image courtesy of J. Pojman.)

Isothermal frontal polymerization (IFP), also called interfacial gel polymerization, is a slow process in which polymerization occurs at a constant temperature and a localized reaction zone propagates because of the gel effect (Epstein & Pojman, 1998, Chapter 11). Using IFP, one can control the gradient of an added material to generate materials for optical applications.

JOHN A. POJMAN

See also **Belousov–Zhabotinsky reaction; DNA premelting; DNA solitons; Fluid dynamics; Morphogenesis, biological; Protein structure; Rayleigh–Taylor instability; Rheology**

Further Reading

Addad, J.P.C. 1996. *Physical Properties of Polymer Gels*, Chichester: Wiley

Epstein, I.R. & Pojman, J.A. 1998. *An Introduction to Nonlinear Chemical Dynamics: Oscillations, Waves, Patterns and Chaos*, Oxford and New York: Oxford University Press

Goldbeter, A. 1995. *Biochemical Oscillations and Cellular Rhythms*, Cambridge and New York: Cambridge University Press

Gupta, R.K. 2000. *Polymer and Composite Rheology*, New York: Marcel Dekker

Nelson, D.L. & Cox, M.M. 2000. *Lehninger Principles of Biochemistry*, 3rd edition, New York: Worth

Odian, G. 1991. *Principles of Polymerization*, New York: Wiley

Pojman, J.A., Ilyashenko, V.M. & Khan, A.M. 1996. Free-radical frontal polymerization: Self-propagating thermal reaction waves. *Journal of the Chemical Society Faraday Transactions*, 92: 2825–2837

Pojman, J.A. & Tran-Cong-Miyata, Q. (editors). 2003. *Nonlinear Dynamics in Polymeric Systems*, Washington, DC: American Chemical Society

Teymour, F. & Ray, W.H. 1992. The dynamic behavior of continuous polymerization reactors — V. Experimental investigation of limit-cycle behavior for vinyl acetate polymerization. *Chemical Engineering Science*, 47: 4121–4132

Washington, R.P., Misra, G.P., West, W.W. & Pojman, J.A. 1999. Polymerization coupled to oscillating reactions: I. A mechanistic investigation and numerical simulation of acrylonitrile polymerization in the Belousov–Zhabotinsky reaction in a batch reactor. *Journal of the American Chemical Society*, 121: 7373–7380

Yoshida, R., Ichijo, H., Hakuta, T. & Yamaguchi, T. 1995. Self-oscillating swelling and deswelling of polymer gels. *Macromolecular Rapid Communications*, 16: 305–310

POPULATION DYNAMICS

Biological populations have a propensity for exponential growth. This Malthusian principle is expressed by the linear, ordinary differential equation $dn/dt = rn$, $r > 0$, where $n = n(t)$ is a measure of population size or density (e.g., individual numbers, biomass, or dry weight) as a function of time t. Although populations can, under appropriate conditions, exhibit exponential growth over a finite period of time, no population can grow indefinitely according to this law. The field of nonlinear population dynamics involves the study of how

population numbers are regulated by biological and environmental effects. The equation

$$\frac{dn}{dt} = rn\,(1 - n/K) \tag{1}$$

is an example of a modification of the exponential growth equation. It is based on the assumption that per capita growth is a decreasing, linear function of population size. In the 1920s, many researchers, including Alfred J. Lotka, Lowell J. Reed, and, most notably, Raymond Pearl, considered Equation (1) as a fundamental law of population growth. It was later discovered that a Belgian mathematician, Pierre-François Verhulst, had used the equation in his studies of population growth in the 1840s. Equation (1) is called the Pearl–Reed equation, the Pearl–Verhulst equation, or more commonly, the "logistic equation" (a name adapted from Verhulst's name *logistique* for the equation).

Equation (1) implies all population densities monotonically approach the equilibrium K, called the carrying capacity. Before leveling off at this carrying capacity, low population numbers initially grow exponentially at the inherent growth rate r, and the resulting S-shaped trajectory is called a logistic growth curve. In their studies of human population dynamics, Pearl and his colleagues fit logistic curves to census numbers from many countries and states. Although today considered rather simplistic as a model of population growth, the logistic equation nonetheless encapsulates the notion of density self-regulation in population dynamics and has inspired many basic notions in ecology (e.g., habitat carrying capacity, the classification of species as "r or K selectors").

The logistic equation is a first-order differential equation of the Kolmogorov type

$$\frac{dn}{dt} = nf(n) \tag{2}$$

with per capita growth rate $f(n) = r\,(1 - n/K)$. Many theories of population growth use the Kolmogorov equations with other specialized forms for $f(n)$. One notable class of models arises from a modification of the negative feedback density regulation assumption of the logistic Equation (1) to include a positive feedback at low population numbers. This notion was put forth by W.C. Allee in order to account for increased growth rates associated with increased population size experienced by some (many biologists would say most) populations when at low numbers (although a negative feedback still comes into play at high numbers). An example is the equation

$$\frac{dn}{dt} = rn\left(1 - \frac{n}{K}\right)(n - \alpha K), \quad \alpha < 1.$$

The "Allee effect" entails a threshold αK such that populations go extinct unless their initial state $n(0)$ exceeds αK, in which case they equilibrate at the carrying capacity K.

Ordinary differential equation models based on equations of form (2) neglect important factors affecting the dynamics of real biological populations. Examples include temporal inhomogeneity (nonconstant vital rates and environment fluctuations), spatial inhomogeneity (diffusion and dispersal), and population inhomogeneity (differences among individuals). The inclusion of temporal inhomogeneities in Equation (2) produces a non-autonomous differential equation with $f = f(t, n)$. For example, a periodic carrying capacity K in the logistic Equation (1) reflects a seasonal habitat.

The movement of populations in a spatially extended habitat can be modeled by adding a diffusion or dispersal term to a growth model. For example, Fisher's equation

$$\frac{dn}{dt} = c\Delta n + rn\,(1 - n/K)$$

has been used to study the spread of populations by means of traveling waves. Other types of diffusion operators, including integral operators described by dispersal kernels, are often considered more appropriate for the movement of biological populations (Murray, 2003).

Differences in chronological age, body size, and other physiological characteristics of individual organisms can significantly affect birth and death rates and consequently, the entire population's dynamics. The McKendrick equation

$$\frac{\partial \rho}{\partial t} + \frac{\partial \rho}{\partial a} = -\delta\rho$$

describes the death processes of a population in terms of an age-specific density $\rho = \rho(t, a)$ and death rate δ. This equation is accompanied by a renewal or birth equation

$$\rho(t, 0) = \int \beta\rho \, da.$$

If the age-specific birth and death rates β and δ are independent of population density ρ, then these equations are linear and imply (under suitable conditions) the Fundamental Theorem of Demography. This theorem states that regardless of whether the population grows or decays exponentially, the normalized density approaches the positive, normalized eigensolution associated with the dominant eigenvalue. If β and/or δ are dependent on ρ, then the McKendrick model is nonlinear. This model can be used to study the effects that various life-cycle characteristics have on population level dynamics, effects such as maturation delays, gestation periods, and nonreproductive quiescent stages (Webb, 1985; Metz & Diekmann, 1986; Cushing, 1998).

Populations are often modeled using discrete time maps in which population numbers are predicted

from one census time to the next. The discrete time exponential growth is described by the linear map (or difference equation) $x_{t+1} = \lambda x_t$, $\lambda > 1$. An analog of logistic equation for density regulated growth is the Beverton–Holt equation

$$x_{t+1} = \lambda x_t \frac{1}{1 + (\lambda - 1)\, x_t/K},$$

whose solutions monotonically approach K as $t \to +\infty$. Other types of density-dependent, population growth models can lead to non-equilibrium asymptotic states. For example, in the Ricker model

$$x_{t+1} = \lambda x_t \exp(-c x_t),$$

larger population numbers, of sufficient magnitude, produce smaller population numbers at the next census. This type of density-dependent "depensation" produces a period-doubling, bifurcation route to chaos as the inherent growth rate λ increases. In the 1970s, Robert May stimulated the interest in complex and chaotic dynamics that flowered during the last decades of the 20th century by his studies of the Ricker model and similar one-dimensional maps as models of population growth (May, 1974).

There is a long tradition of using discrete time models to model structured populations (Caswell, 2001). The Leslie matrix model

$$\boldsymbol{x}_{t+1} = L\boldsymbol{x}_t \tag{3}$$

is an example. The components of the vector $\boldsymbol{x}_t$ are the number of individuals, at time t, in a finite collection of age classes. The nonnegative "projection" matrix L contains birth and survival rates per unit time. In other models, the structuring classes are based on other categories (such as body size and life cycle stage). If L is a constant in time, matrix model (3) implies (under suitable mathematical conditions) the Fundamental Theorem of Demography. If the entries of L depend on $\boldsymbol{x}_t$, then the model is nonlinear. Nonlinear matrix models can be used to study the effects of class specific density effects on birth and death rates. For example, a model of a population with three life cycle stages and Ricker-type negative feedback nonlinearities has been used in conjunction experimental studies to document the occurrence of a bifurcation route to chaos in a laboratory population of insects (Cushing et al., 2002).

Most populations interact with other populations in ways that affect each other's vital rates. A natural extension of the logistic equation to the interaction of two species' assumes per capita growth rates are linear expressions of species densities, an assumption that results in the Volterra–Lotka system

$$\begin{aligned} \frac{\mathrm{d}n_1}{\mathrm{d}t} &= n_1 (r_1 + c_{11} n_1 + c_{12} n_2), \\ \frac{\mathrm{d}n_2}{\mathrm{d}t} &= n_2 (r_2 + c_{21} n_1 + c_{22} n_2) \end{aligned}$$

of differential equations. A fundamental classification of two species' interactions can be based on the signs of the six coefficients in these equations. Two classical examples are

$$\begin{aligned} \frac{\mathrm{d}n_1}{\mathrm{d}t} &= r n_1 (1 - n_1/K) - c_1 n_1 n_2, \\ \frac{\mathrm{d}n_2}{\mathrm{d}t} &= -d n_2 + c_2 n_1 n_2 \end{aligned} \tag{4}$$

and

$$\begin{aligned} \frac{\mathrm{d}n_1}{\mathrm{d}t} &= r_1 n_1 (1 - n_1/K_1) - c_1 n_1 n_2, \\ \frac{\mathrm{d}n_2}{\mathrm{d}t} &= r_2 n_2 (1 - n_2/K_2) - c_2 n_1 n_2. \end{aligned} \tag{5}$$

The Lotka–Volterra predator-prey model (4) describes a logistically growing prey population n_1 that is preyed upon by a predator n_2 that dies out exponentially in the absence of n_1. In this model, the per predator uptake rate of prey is proportional to the amount of prey present, a mass-action type interaction that gives rise to the quadratic nonlinearity in (4). If $K < d/c_2$, this predator-prey model predicts predator extinction; if $K > d/c_2$, the model predicts coexistence (in terms of an asymptotically stable equilibrium state). The mass-action assumption is often replaced by one based on a predation rate that saturates (or even decreases) as the amount of prey increases. For example, the MacArthur–Rosenzweig predator-prey model,

$$\begin{aligned} \frac{\mathrm{d}n_1}{\mathrm{d}t} &= r n_1 (1 - n_1/K) - c_1 \frac{n_1}{a + n_1} n_2, \\ \frac{\mathrm{d}n_2}{\mathrm{d}t} &= -d n_2 + \frac{1}{\alpha} c_1 \frac{n_1}{a + n_1} n_2, \end{aligned}$$

assumes a per predator prey uptake rate $c_1 n_1/(a + n_1)$ of the so-called Holling II (or Monod, or Michaelis–Menten) type. This predator-prey model predicts a destabilization of the coexistence equilibrium, accompanied by a Hopf bifurcation to a stable limit cycle, for K large. Thus, an enrichment of the habitat results, paradoxically, in a destabilization of the predator-prey interaction and, for this reason, this phenomenon is called the "paradox of enrichment."

The Lotka–Volterra competition model (5) describes two logistically growing populations that adversely affect each other's growth rate through an interference competitive interaction measured by the quadratic mass–action terms. This model predicts a limited number of competitive outcomes. If the interspecific competition is weak compared with the intraspecific competition ($c_1 c_2 < r_1 r_2/(K_1 K_2)$), then the species coexist in an asymptotically stable equilibrium state. If interspecific competition is too strong ($c_1 c_2 > r_1 r_2/(K_1 K_2)$), then one species becomes extinct and the other survives (in an asymptotically stable equilibrium state). The Lotka–Volterra competition model gave rise to the

many fundamental ecological notions, including competitive exclusion, ecological niche (there can be no more species than there are limiting resources), and limiting similarity of competitors. Although not universal for theoretical competition models, these concepts are well supported by a large number of other competition models. For example, the exploitative competition model (the chemostat model)

$$\frac{dn_1}{dt} = -dn_1 + \frac{1}{\alpha_1}c_1\frac{R}{a_1+R}n_1,$$
$$\frac{dn_2}{dt} = -dn_2 + \frac{1}{\alpha_2}c_2\frac{R}{a_2+R}n_2,$$
$$\frac{dR}{dt} = d(R_0-R) - c_1\frac{R}{a_1+R}n_1 - c_2\frac{R}{a_2+R}n_2$$

describes the competition of two species for a (prey) resource R. This model also predicts the survival of only one species (Smith & Waltman, 1995).

Large-dimensional ecosystems can be modeled by coupling together any number of single species such as those described above (May, 2001). Such multispecies models can include temporal, spatial, and/or demographic inhomogeneities. For example, the dispersal and diffusion of many interacting species can be modeled by systems of reaction-diffusion equations, such as Fisher's equation, coupled together so as to describe predator-prey or competition interactions. Similarly, coupled systems of McKendrick equations or Leslie matrix models describe interactions among structured species.

J.M. Cushing

See also **Biological evolution; Brusselator; Epidemiology**

Further Reading

Caswell, H. 2001. *Matrix Population Models: Construction, Analysis and Interpretation*, 2nd edition, Sunderland, MA: Sinauer Associates

Cushing, J.M. 1998. *An Introduction to Structured Population Dynamics*, Philadelphia: Society for Industrial and Applied Mathematics

Cushing, J.M., Costantino, R.F., Dennis, B., Desharnais, R.A. & Henson, S.M. 2002. *Chaos in Ecology: Experimental Nonlinear Dynamics*, New York: Academic Press

Kingsland, S.E. 1995. *Modeling Nature: Episodes in the History of Population Ecology*, Chicago: University of Chicago Press

May, R.M. 1974. Biological populations with nonoverlapping generations: stable points, stable cycles and chaos. *Science*, 186: 645–647

May, R.M. 2001. *Stability and Complexity in Model Ecosystems*, Landmarks in Biology, Princeton: Princeton University Press

Metz, J.A.J. & Diekmann, O. 1986. *The Dynamics of Physiologically Structured Populations*, Berlin: Springer

Murray, J.D. 2003. *Mathematical Biology*, 3rd edition, Berlin and New York: Springer

Smith, H.L. & Waltman, P. 1995. *The Theory of the Chemostat: Dynamics of Microbial Competition*, Cambridge and New York: Cambridge University Press

Webb, G.F. 1985. *Theory of Nonlinear Age-Dependent Population Dynamics*, New York: Marcel Dekker

POWER BALANCE

As the dynamics of any real system includes dissipation, steady dynamic regimes are observed if energy loss is permanently compensated by energy input from some external or intrinsic source, which is a condition of power balance (PB). In the flame of a candle, for example, power input is supplied by the burning wax and dissipation by the emission of heat and light. Starting from the seminal theoretical work by Yakov Zeldovich & David Frank-Kamenetsky (1938), the modern combustion theory has developed a detailed mathematical analysis of the flame propagation in various combustible media, based on the PB concept (Williams, 1964).

The PB analysis in its general form underlies a variety of dynamical phenomena in physics, chemistry, biophysics, and engineering. A simple model is the van der Pol oscillator, which is described by the equation

$$\ddot{\xi} + \omega^2\xi = \alpha\dot{\xi} - \beta\xi^2\dot{\xi}. \tag{1}$$

Here, $\xi(t)$ is a dynamical variable, ω is the eigenfrequency of linear oscillations in the system, and the small positive coefficients α and β account for the linear intrinsic gain and nonlinear loss, respectively. As the energy (E) of this system is $(\dot{\xi}^2+\omega^2\xi^2)/2$, Equation (1) implies

$$dE/dt = (\alpha - \beta\xi^2)\dot{\xi}^2. \tag{2}$$

Assuming that $\xi = A\cos\omega t$, averaging Equation (2) over a cycle, and assuming that $\langle dE/dt\rangle = 0$, one finds that PB is established at the amplitude $A = 2\sqrt{\alpha/\beta}$.

Another generic case is the balance between intrinsic loss and energy supplied from an external source. An example is furnished by an equation for an ac-driven damped pendulum with sinusoidal nonlinearity,

$$\ddot{\xi} + \sin\xi = -\alpha\dot{\xi} + \gamma\cos(\omega_0 t), \tag{3}$$

where $\alpha > 0$ is a friction coefficient and γ and ω_0 are the amplitude and frequency of the drive. (An important realization of this equation is a Josephson junction. In this case, ξ is the phase difference of the superconducting wave function across the junction, α accounts for ohmic loss, and the ac drive is induced by bias current applied to the junction (Barone & Paternó, 1982).) The corresponding PB equation takes the form (cf. Equation (2))

$$dE/dt = -\alpha\dot{\xi}^2 + \gamma\dot{\xi}\sin(\omega_0 t). \tag{4}$$

In the lowest-order approximation, $\alpha = \gamma = 0$, two different types of exact solution are known: oscillating and rotating ones with zero and finite average velocity $\langle\dot{\xi}\rangle$, respectively. Substitution of the rotating solution into Equation (4) (where α and γ are treated as small parameters) and averaging over the period shows that PB is established for the solution whose frequency is

locked to the driving frequency ω_0, so that $\omega = \omega_0/n$, $n = 1, 2, \cdots$. In other words, the PB condition selects the solution's frequency. Further, it follows from Equation (4) that the PB condition cannot be met unless the drive's strength exceeds a finite threshold value, $\gamma_{\rm thr}$.

At $\gamma > \gamma_{\rm thr}$, the PB between the ac drive and loss selects a constant value of the phase shift ϕ_0 between the ac drive and the phase of the oscillating part of the solution. Indeed, averaging Equation (4) and demanding $\langle dE/dt \rangle = 0$ yield a general result, $\cos\phi_0 = \gamma_{\rm thr}/\gamma$; that is, there are two power-balanced solutions, $\phi_0 = \pm\cos^{-1}(\gamma_{\rm thr}/\gamma)$. Further analysis demonstrates that one solution is stable and the other one is unstable.

A similar mechanism underlies propagation of a magnetic-flux quantum (fluxon, or topological soliton) in a long weakly damped ac-driven Josephson junction with periodic spatial modulation, which is described by the following sine-Gordon (SG) equation:

$$\xi_{tt} - \xi_{xx} + [1 + \varepsilon \sin(2\pi x/\lambda)] \sin\xi = -\alpha\xi_t + \gamma\cos(\omega_0 t)\,. \tag{5}$$

Here x is the coordinate along the Josephson junction, the subscripts stand for partial derivatives, and ε and λ are the amplitude and period of the spatial modulation. In this case, the average velocity $\langle v \rangle$ of the ac-driven fluxon is determined by the condition of locking the frequency of the periodic passage of the spatially periodic relief by the fluxon to the ac-drive's frequency, which yields a spectrum of PB velocities: $\langle v \rangle = \lambda\omega_0/(2\pi n), n = \pm 1, \pm 2, \ldots$. Note that the sign of the velocity is determined by an initial push setting the fluxon in motion.

The latter phenomenon was observed in a direct experiment, in the form of an *inverse Josephson effect*, that is, dc voltage induced by ac bias current (Ustinov & Malomed, 2001). The periodic spatial modulation is necessary for the effect, as it opens a way to establish the PB between the ac drive and dissipation. Nevertheless, in an annular (ring-shaped) Josephson junction of a long but finite length, the same effect is possible without any spatial modulation, due to the interaction of the fluxon with its own tail (Goldobin et al., 2002). In that case, the average velocity is not "quantized," as above, but may take any value. A noteworthy feature, specific to the ring system, is the dependence of the threshold value $\gamma_{\rm thr}$ on the ring's length L (see Figure 1). (If the driving signal is slightly nonmonochromatic, progressive motion is still possible over a long time, but it is eventually destroyed by decoherence accumulating due to small fluctuations of the driving frequency (Filatrella et al., 2002.) PB for breathers in long lossy Josephson junctions is also possible (Lomdahl & Samuelsen, 1986).

Another class of PB problems can be formulated in terms of the complex Ginzburg–Landau equation, which may be regarded as a perturbed version of the nonlinear Schrödinger (NLS) equation:

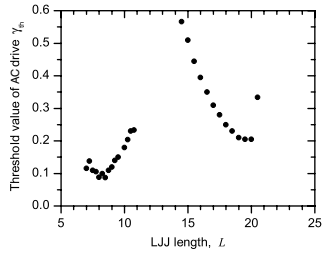

Figure 1. The minimum (threshold) value of the ac-drive's strength γ, in the case $\varepsilon = 0, \omega = 1.12$, and $\alpha = 0.1$ [see Equation (5)], which is necessary to support progressive motion (in either direction) of a fluxon in a long Josephson ring, vs. the length (L) of the ring. In regions without data, the ac-driven motion of the fluxon is impossible; in particular, the effect vanishes if L exceeds $L_{\rm max} \approx 21$.

$$iu_t + \tfrac{1}{2}u_{xx} + |u|^2 u = -i\alpha_0 u + i\alpha_1 u_{xx} + i\alpha_2|u|^2 u - i\alpha_3|u|^4 u, \tag{6}$$

where all the coefficients $\alpha_{0,1,2,3}$ are assumed to be positive and small. In this model, linear and quintic nonlinear losses are accounted for by α_0, α_1, and α_3, respectively, while α_2 is a cubic-gain coefficient. Equation (6) describes transmission of soliton signals in nonlinear fiber-optic telecommunication links with loss, gain, and filtering (the last being represented by the term α_2 term) (Iannone et al., 1998) and subcritical pulses observed in binary-fluid thermal convection in narrow channels (Kolodner, 1991).

The energy of the optical field in the fiber is $E = \int_{-\infty}^{+\infty} |u(x)|^2\,dx$, and the loss and gain terms on the right-hand side of Equation (6) give rise to the corresponding PB equation,

$$dE/dt = 2\left[-\alpha_0 E + \int_{-\infty}^{+\infty} \left(-\alpha_1|u_x|^2 - \alpha_3|u|^6 + \alpha_2|u|^4\right) dx\right]. \tag{7}$$

Approximating solutions by the NLS soliton, $u = \eta\,\mathrm{sech}(\eta x)\exp(i\phi)$, where η is an amplitude, substituting this in Equation (7) and equating dE/dt to zero lead to a PB condition in the form

$$\eta\left[8\alpha_3\eta^4 - 5(2\alpha_2 - \alpha_1)\eta^2 + 15\alpha_0\right] = 0. \tag{8}$$

The trivial solution, $\eta = 0$, is stable. The remaining factor in Equation (8) yields two nontrivial solutions if threshold conditions are satisfied: $\alpha_2 > \alpha_1/2$ and $5(2\alpha_2 - \alpha_1)^2 > 96\alpha_0\alpha_3$. The solution with a larger value of η gives a stable SP, and the one with smaller η is unstable.

Another manifestation of PB occurs in reaction-diffusion systems, such as the FitzHugh–Nagumo model (Cross & Hohenberg, 1993). Besides chemical systems—the Belousov–Zhabotinsky (BZ) reaction, heterogeneous catalysis, and so on—models belonging to this class find numerous other applications, including neural networks, cardiac tissue in biophysics, electron-hole plasmas in semiconductors, and gas-discharge plasmas. In this case, the PB takes place between energy release due to the chemical reaction, which is described by local terms of the model, and loss due to diffusion. As a result, various patterns may be supported as stable dynamical equilibria, including standing or traveling waves, fronts (shock waves) and periodic wave trains in one dimension, spiral vortices and localized spots in the two-dimensional case, and vortex rings in three dimensions, among others. An interesting experimental finding is the observation of two drastically different regimes of propagation of a BZ chemical wave in aqueous solution, which resemble deflagration and detonation waves in gas dynamics: a slow wave, which is driven by diffusion of chemical reactants, and a fast "big wave" (Inomoto et al., 1997), which is coupled to surface deformation and flow in the solution. The two modes of the chemical-wave propagation realize the PB in different forms, the choice between them being determined by the initial perturbation.

BORIS MALOMED

See also **Candle; Complex Ginzburg–Landau equation; Damped-driven anharmonic oscillator; FitzHugh–Nagumo equation; Flame front; Long Josephson junctions; Solitons; Zeldovich–Frank-Kamenetsky equation**

Further Reading

Barone, A. & Paternó, G. 1982. *Physics and Applications of the Josephson Effect*, New York: Wiley

Cross, M.C. & Hohenberg, P.C. 1993. Pattern-formation outside of equilibrium. *Reviews of Modern Physics*, 65: 851–1112

Filatrella, G., Malomed, B.A. & Pagano, S. 2002. Noise-induced dephasing of an ac-driven Josephson junction. *Physical Review* E, 65: 051116

Goldobin, E., Malomed, B.A. & Ustinov, A.V. 2002. Progressive motion of an ac-driven kink in an annular damped system. *Physical Review* E, 65: 056613

Iannone, E., Matera, F., Mecozzi, A. & Settembre, M. 1998. *Nonlinear Optical Communication Networks*, New York: Wiley

Inomoto, O., Kai, S., Ariyoshi, T. & Inanaga, S. 1997. Hydrodynamical effects of chemical waves in quasi-two-dimensional solution in Belousov–Zhabotinsky reaction. *International Journal of Bifurcation and Chaos*, 7: 989–996

Kolodner, P. 1991. Drifting pulses of traveling-wave convection. *Physical Review Letters*, 66: 1165–1168

Lomdahl, P.S. & Samuelsen, M.R. 1986. Persistent breather excitations in an ac-driven sine-Gordon system with loss. *Physical Review* A, 34: 664–667

Ustinov, A.V. & Malomed, B.A. 2001. Observation of progressive motion of ac-driven solitons. *Physical Review* B, 64: 020302(R)

Williams, F.A. 1964. *Combustion Theory*, Reading, MA: Addison-Wesley

Zeldozich, Ya.B. & Frank-Kamenetsky, D.A. 1938. K teorii ravnomernogo rasprostrane-niya plameni [On the theory of uniform propagation of frame]. Doklady Akademi Nauk SSSR, 19(10: 693–697.

POWER SPECTRA

See **Spectral analysis**

PRANDTL NUMBER

See **Fluid dynamics**

PREDATOR-PREY SYSTEMS

See **Population dynamics**

PREDICTABILITY OF FORECASTING

See **Forecasting**

PROTEIN DYNAMICS

Proteins carry out structural, catalytic, and molecular recognition roles that require a wide variety of motions over a broad range of timescales, from 10^{-15} to 10^{3} s, as sketched in Figure 1. Motions can be as mundane as coupled vibrations or as sophisticated as gene transcription by an RNA polymerase protein. The broad range of timescales is a principal difficulty in understanding protein dynamics. We will focus here on atomic motions and conformational changes of single proteins.

Although there are a wide variety of proteins displaying many remarkable dynamical phenomena, photoactive proteins play a special role in experimental studies of protein dynamics. This is because experiments can be initiated with a femtosecond laser pulse at any temperature from absolute zero to the unfolding temperature of the protein, allowing the wide variety of motions to be observed. Proteins which have been extensively studied this way are myoglobin (Austin et al., 1975), the photosynthetic reaction center, rhodopsin, photoactive yellow protein, and cytochrome coxidase.

An essential result of such studies is that there are three fundamentally different processes involved in modeling atomic motions of proteins. This distinction can be seen in the temperature-dependent rates of various processes observed in myoglobin, sketched in Figure 2 and described in Fenimore et al. (2002). These processes are labeled as fast fluctuations, bond formation, and conformational motions.

Fast fluctuations occur on the 100 picosecond timescale over the temperature range from 200 to 300 K, but their amplitude (or number) diminishes by a factor of ten over this range. Because these motions

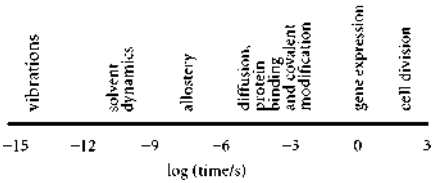

Figure 1. Types of protein motions which occur on timescales from femtoseconds to hours.

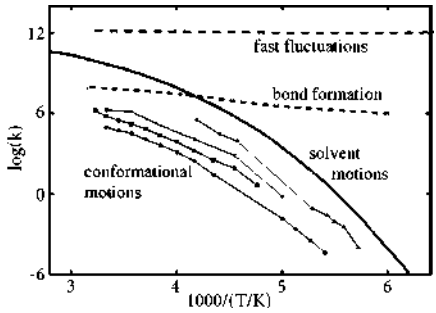

Figure 2. Arrhenius plot, showing the temperature-dependent rates of three types of experimentally measured protein motions, compared with the rate of solvent motions. (Taken from Fenimore et al., 2002, and references therein.)

occur in the absence of bulk solvent motions, they must involve relatively local rearrangements between the various possible meta-stable configurations possible in a protein. The network properties of water at the surface of the protein and the voids created by thermal expansion play an important role in these types of motion; the motions disappear when a protein sample contains less than about 30% water.

It is possible to capture the essence of these motions with a relatively simple potential energy function and Newton's law of motion, $F = ma$, V= bond stretch + bond angle + dihedral twist + atom-centered point charge electrostatics + Lennard–Jones.

The bond stretch and bond angle terms are simple harmonic potentials which allow the protein to vibrate. The dihedral twist term is a cosine function which allows transitions between rotamer states of single and double bonds. Dihedral twist parameters of the backbone will also influence the relative free energy of alpha helixes and beta sheets, two of the common secondary structure motifs described in the (*See* **Protein structure**). Much of the subtlety in this potential energy function lies in the electrostatics and Lennard–Jones terms. Both are pairwise additive interactions between atoms that are not bonded to each other or through another atom. The electrostatic interaction strength falls off as $1/d$, while the the Lennard–Jones term is of the form $A/d^{12} - B/d^6$, where d is the distance between atoms.

When the solvent is treated explicitly, parameters can be developed which reproduce important dynamic and thermodynamic properties that contribute to protein function. These include solvent properties, such as dielectric response time and amplitude, self-diffusion coefficients, and heat of vaporization. For amino acids and other small molecules, heats of solvation and heats of transfer from octanol to water are accurately reproduced. Heats of solvation and some aspects of the hydration shells of ions are also correctly modeled.

When this potential energy function is applied to protein folding and dynamics, it produces a prediction for the ensemble of protein conformations, as well as rates of water penetration, motions of loops, folding temperature, and the ensemble of unfolded states. In practice, it is difficult or impossible to obtain the necessary sampling to unambiguously quantify these properties. The reason is that a solvated protein simulation involves about 30,000 atoms; thus the integration time for the dynamics is limited to about 2 fs, while many of the motions of interest occur on the nanosecond to microsecond timescales (see Figure 2). Much effort in this field over the past two decades has centered on methods to improve the sampling through efficient implementation, parallelization, and statistical physics.

Covalent bond formation is the primary function of enzymes and involves many of the complexities of fast fluctuations combined with the need for a quantum-mechanical description of electronic polarizability, bond distortion, and bond formation. Such descriptions are available through all-electron quantum chemistry techniques, such as density functional theory, but calculations require approximately 1 cpu/day to evaluate energies and forces for 200 atoms. Calculations can be efficiently parallelized, and when more than 200 protein atoms are included, computation time scales linearly with system size. It is also possible to treat the bond-formation region quantum mechanically and the rest of the protein and solvent classically in a single calculation.

The difficulties involved in computing reaction rates include proper treatment of the vibrational dynamics of bond formation, sampling over hydration states, and sampling over the ensemble of protein conformations. One useful simplification is that many enzymes exclude water from their active site, considerably reducing the disorder.

Conformational motions of proteins can involve simple shifts of helixes, repacking of amino acid side chains, or more extensive changes between active

and inactive conformations. The molecular dynamics model described above makes a prediction for conformational changes of proteins, but it is only recently that computer power has reached the long times necessary to test these predictions (Karplus & McCammon, 2002; Mayor et al., 2003). It is likely that some tuning of parameters will be necessary to predict protein properties with the same reliability with which these models currently predict small molecule properties.

Because the solvent provides a cage which prevents the protein from moving freely, the fraction of possible configurations explored increases by several orders of magnitude when the solvent is considered implicitly (Takada, 1999). While it is doubtful that a single parameter set can be developed to treat all proteins with an implicit solvent, it is clear from models of protein folding that much can be learned from implicit solvent models which are explicitly, but weakly, biased toward a known folded conformation.

BENJAMIN H. MCMAHON AND PAUL W. FENIMORE

See also **Biomolecular solitons; Local modes in molecules; Molecular dynamics; Pump-probe measurements**

Further Reading

Austin, R.H., Beeson, K.W., Eisenstein, L., Frauenfelder, H. & Gunsalus, I.C. 1975. Dynamics of ligand-binding to myoglobin. *Biochemistry*, 14: 5355–5373

Fenimore, P.W., Frauenfelder, H., McMahon, B.H. & Parak, F.G. 2002. Slaving: solvent fluctuations dominate protein dynamics and functions. *Proceedings of the National Academy of Sciences, USA*, 99: 16047–16051

Karplus, M. & McCammon, J.A. 2002. Molecular dynamics simulations of biomolecules. *Nature Structural Biology*, 9: 646–652

Mayor, U., Guydosh, N.R., Johnson, C.M., Grossmann, J.G., Sato, S., Jas, G.S., Freund, S.M.V., Alonso, D.O.V., Daggett, V. & Fersht, A.R. 2003. Complete folding pathway of a protein from nanoseconds to microseconds. *Nature*, 421: 863–867

McMahon, B.H., Muller, J.D., Wraight, C.A. & Nienhaus, G.U. 1998. Electron transfer and protein dynamics in the photosynthetic reaction center. *Biophysical Journal*, 74: 2567–2587

Takada, S. 1999. Go-*ing* for the prediction of protein folding mechanisms. *Proceedings of the National Academy of Sciences, USA*, 96: 11698–11700

PROTEIN STRUCTURE

A protein's structure, flexibility, and activity depend on the primary sequence of amino acids encoded by DNA, the presence of small-molecule ligands, the presence of protein or nucleic acid binding partners, and its history of covalent modification by other enzymes. Figure 1 (in color plate section) shows the catalytic site of one protein, RNA polymerase. This protein is responsible for transcribing an organism's DNA into messenger RNA, initiating the process of protein production, an essential and highly regulated cellular process. The complex geometry of interactions which stabilize the DNA, RNA, and nucleotide being added to the RNA are highly conserved among polymerases from all organisms, from microbes to humans. It is typical of enzymes that they are precisely (within about 0.1 Å) constructed near the catalytic site in order to exclude water and polarize and orient the reactants, yet still maintain the flexibility to allow reactants to enter and exit the active site.

One reason proteins can adopt highly rigid active sites, yet still undergo the large motions necessary for substrate binding, is that the peptide backbone is stabilized by multiple interactions in particular structural motifs, such as helixes, sheets, and particular types of hairpin turns. Thus, not only are the residues directly responsible for catalysis highly conserved among organisms, but also the arrangement of helixes, sheets, and tightly packed hydrophobic residues which determine the large-scale dynamics of the protein. This is illustrated in page 7 of the color plate section, which shows the entire catalytic domain of RNA polymerase, color-coded according to the polarity and charge of the amino acids. It is useful, looking at this figure, to reflect on the numerous cooperative interactions among the 1034 amino acids of this protein which cause it to fold up in this shape, rather than the shape of any of the other 30,000 proteins, or a glob of tangled polymer. These interactions are predominantly hydrophobicity, shape, hydrogen bond formation, and charge complementarity.

Protein function entails not only catalysis, but also the ability to be regulated by other proteins. This is done either by covalent modification, such as phosphorylation (covalent attachment of PO_3^{2-}) or acetylation (covalent attachment of C_2O), or by complex formation with other proteins. In either case, all the residues at the surface and the geometry of rigid motifs communicating the surface interactions to the active site become important determinants of protein structure. This is illustrated in the color plate section, showing the complex of twelve proteins, DNA, and RNA that is required for RNA polymerase to transcribe DNA to messenger RNA, as an early step in protein synthesis.

We have used the polymerase protein to illustrate several aspects of protein structure. There are between 10,000 and 100,000 types of protein structures used in various organisms, and a significant fraction of them have had their structure experimentally determined by diffraction of X-rays from a protein crystal. These structures are collected in a publicly accessible protein data bank, and several free software programs exist to aid in visualizing various aspects of protein structures.

The single, most important determinant of a protein's structure is the primary sequence of amino acids, encoded by an organism's DNA. Advances in microbiology have allowed automated sequencing of

complete genomes of numerous organisms. While tens of thousands of protein structures are known, several million protein sequences are known, from all types of living creatures, from mammals to plants, microbes, and viruses. Proteins can be identified from their sequence of amino acids by searching for patterns of amino acids with BLAST (basic local alignment search tool), or tailoring a search algorithm based on numerous examples of a particular protein with a so-called hidden Markov model. Sequence analysis has been used to annotate both complete and partial genomes, and the results are available in several public databases.

The great excess of sequence data over structural data, combined with the insight into protein function and interactions provided by knowledge of the protein structure, provokes the question of whether it is possible to predict a protein structure from its primary sequence of amino acids. The essential reason this problem is difficult is that amino acids have an average of four dihedral angles which are equally stable in any of two or three positions (0°, $+120°$ and $-120°$), creating $3^{4\times150}$ possible structures for each protein. The second reason is that when proteins were optimized by evolution, they exploited subtleties of interactions which are not necessarily captured by simple potential energy functions. Thus, while it has long been clear what forces stabilize folded proteins (hydrophobic interactions, hydrogen bonding, and Coulomb interactions), it has only recently been possible to relate the folding of a sequence of 20 amino acids to interaction potentials derived from small-molecule thermodynamic properties.

When it is possible, the most reliable method to predict a protein's structure is to find a protein of known structure which has greater than about 30% sequence identity. The particular conformations of most amino acids can then be inferred from the known protein structure, and resulting problems can usually be corrected by a Monte Carlo search algorithm or by hand. This process is known as homology modeling. Systematic efforts have produced enough experimentally determined structures to cover most of the observed sequences.

If a suitable template protein is not available, the protein structure must be constructed from observed structural motifs. Three of the most useful rules are: (1) hydrophobic residues tend to occupy the interior of the protein; (2) beta sheets, alpha helices, and other types of turns have characteristic amino acid content; and (3) triplets of amino acids tend to make particular configurations. Progress in this so-called ab initio folding can be evaluated by observing the result of the CASP competition, where a dozen experimentally determined structures of novel proteins are held back, while competing research groups are given several months to enter predictions of their structures.

BENJAMIN H. MCMAHON AND MONTIAGO X. LABUTE

See also **Hydrogen bond; Molecular dynamics; Polymerization; Protein dynamics**

Further Reading

Alberts, B. et al. 2002. *Molecular Biology of the Cell*, 4th edition, New York: Garland Science
Branden, C. & Tooze, J. 1999. *Introduction to Protein Structure*, New York: Garland Science
Cramer, P., Bushnel, D.A. & Kornberg, R.D. 2001. Structural basis of transcription: RNA polymerase II at 2.8 Angstrom resolution. *Science*, 292: 1876
Petsko, G. A. & Ringe, D. 2003. *Protein Structure and Function*, Sunderland, MA: Sinauer Associates and Oxford: Blackwell Publishing
Valuable websites to persue:
THE PROTEIN DATA BANK: www.rcsb.org
CASP5 COMPETITION: predictioncenter.llnl.gov/casp5/Casp5.html.
BASIC LINEAR ALIGNMENT SEQUENCE TOOL (BLAST): www.ncbi.nlm.nih.gov/
MODELLER: www.salilab.org/modeller/modeller.html
VMD (A PROTEIN VISUALIZATION): www.ks.uiuc.edu/Research/vmd/
(SEARCHABLE GENE DATABASES): www.ensemble.org, www.ncbi.nlm.nih.gov/Entrez
PROTEIN FAMILY CATALOG: www.sanger.ac.uk/Software/Pfam/index.shtml.

PSEUDO-DIFFERENTIAL EQUATIONS

See **Equations, nonlinear**

PULSONS

See **Solitons, types of**

PUMP-PROBE MEASUREMENTS

Figure 1 shows a prototype pump-probe experiment in which short pump-laser pulse excites the vibrational oscillator (used here as a simple example) from the $\nu = 0$ vibrational state into the $\nu = 1$ vibrational state. A subsequent probe-laser pulse tests the $\nu = 1$ population by probing the $\nu = 1 \rightarrow \nu = 2$ excited state absorption, the $\nu = 1 \rightarrow \nu = 0$ stimulated emission, and/or the $\nu = 0 \rightarrow \nu = 1$ bleach. The time resolution of such an experiment is given by the pulse duration of the laser pulses, while the detector can be slow. With recent progress in laser technology, one can now perform pump-probe experiments in almost any spectral range, starting from far-IR (10 cm^{-1}) to soft X-ray radiation (1 keV) with a time resolution of much less than a picosecond (2000).

Pump-probe spectroscopy is a special form of third-order nonlinear spectroscopy. The theory of linear and nonlinear optical spectroscopy is generally performed in a perturbative expansion, where the electric fields of the light pulses act as weak perturbation onto the molecular Hamiltonian. The linear response, which

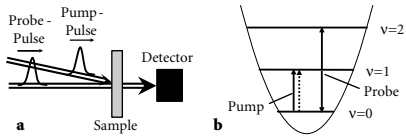

Figure 1. (a) A prototype pump-probe setup and (b) a prototype pump-probe experiment of a vibrator.

describes linear absorption spectroscopy, is given by

$$P^{(1)}(t) = \int_0^\infty \mathrm{d}t_1 R^{(1)}(t_1) \times E(t - t_1)\,. \qquad (1)$$

Expressed in simple words, the electric field E of the probe light interacts once with the sample through the first-order response function $R^{(1)}$, generating a first-order polarization $P^{(1)}$, which subsequently is measured in the detector. The first-order response function $R^{(1)}$ is a material property, which can be tested by this type of spectroscopy. For instance, if the electric field E is chosen to be a monochromatic wave, one can measure the absorption spectrum by tuning its frequency.

Third-order spectroscopy is given by

$$P^{(3)}(t) = \int_0^\infty \mathrm{d}t_3 \int_0^\infty \mathrm{d}t_2 \int_0^\infty \mathrm{d}t_1 R^{(3)}(t_1, t_2, t_3) \times E_1(t - t_3)E_2(t - t_3 - t_2)E_3(t - t_3 - t_2 - t_1). \qquad (2)$$

Again expressed in simple words, the electric fields E_1, E_2, and E_3 originating from a maximum of three laser pulses (in the example of Figure1a, both E_2 and E_3 originate from one pulse, i.e., the pump pulse) interact with the sample at three different time points $t - t_3$, $t - t_3 - t_2$, and $t - t_3 - t_2 - t_1$ through the third-order response function $R^{(3)}$, generating a third-order polarization $P^{(3)}$. The third-order response function $R^{(3)}$ contains significantly more information about the molecular system than the linear response function. Both can, in principle, be calculated once all eigenstates, transition dipole moments, and relaxation pathways of a system are known.

There are different types of third-order spectroscopies, the most important of which being pump-probe and photon echo spectroscopy. Both exist in many variations. They all measure the same third-order response function $R^{(3)}$ but differ by the choice of the three field interactions E_1, E_2, and E_3 (timing, frequency, beam direction, etc.). The different methods project different aspects of the complicated third-order response function $R^{(3)}$. A comprehensive discussion of the principles of nonlinear optical spectroscopy is given by (Mukamel, 1995). In the context of nonlinear science, the following advantages of third-order spectroscopies should be noted.

- In condensed phase systems, spectroscopic transitions are often significantly broadened. The most common broadening mechanisms are (i) lifetime broadening (T_1-relaxation), (ii) homogeneous broadening (T_2-relaxation), and (iii) inhomogeneous broadening. In solution phase systems, the situation becomes even more complicated since the distinction between homogeneous and inhomogeneous broadening becomes a question of the timescale of the fluctuating forces giving rise to dephasing. As a consequence, a continuous transfer between both regimes does, in general, occur. It is a common practice to fit absorption lines to certain line profiles such as a Lorentzian profile (homogeneous and/or lifetime broadening), a Gaussian profile (inhomogeneous broadening), a Voigt profile (a mixture of both), or a Kubo profile (intermediate regime). However, the assignment to different broadening mechanisms is model-dependent and often extremely questionable. Linear absorption spectroscopy principally cannot distinguish between different broadening mechanisms.

  The information boost of third-order nonlinear spectroscopy just makes that distinction possible. For example, pump-probe spectroscopy observes T_1-relaxation directly by populating a spectroscopic state with the pump-pulse and subsequently observing its relaxation back into the ground state with the probe-pulse (see Figure 1b). Photon echo experiments and transient hole burning experiments (a special form of pump-probe experiment with a spectrally narrow pump-pulses) can distinguish between the homogeneous, inhomogeneous, and the intermediate dephasing regime.
- When considering nonlinear vibrational states, such as the Davydov soliton and/or local modes in molecular crystals, a more subtle point is the following: The nonlinear third-order response of a system of linearly coupled harmonic oscillators (i.e., a crystal described in the harmonic approximation) vanishes exactly. This is because the three contributions to the nonlinear response function (bleach, stimulated emission, and excited state absorption, see Figure 1(b) all occur at the same frequency, and the transition dipoles are such that they cancel completely. Only anharmonicity (nonlinearity) of the molecular potential surfaces gives rise to a nonzero pump-probe signal. Hence, nonlinear pump-probe spectroscopy is specifically sensitive to that part of the molecular Hamiltonian which is also responsible for collective nonlinear phenomena. A linear absorption spectrum is, of course, nonzero also in the harmonic limit.

Using these properties, one can test predictions from soliton and self-trapping theories in a much more direct way than linear absorption spectroscopy can do. For example, Davydov has speculated about vibrational solitons in protein secondary structures, with the aim to

explain the capability of proteins to efficiently store small quanta of energy (Davydov, 1979). As a first experimental attempt to verify this prediction, Austin and coworkers (Xie et al., 2000) have investigated the lifetime of the amide-I band (mostly the C=O stretching mode of the protein backbone) of myoglobin, which typically relaxes on an ultrafast 1 ps timescale. Interestingly, they found a somewhat prolonged lifetime (15 ps) in the blue wing of the absorption spectrum. Pump-probe experiments on crystalline acetanilide (ACN), a simple model system used to study nonlinear collective phenomena in protein structures (Scott, 1992), have revealed useful information, including the following (Edler et al., 2002): (i) The NH free exciton self-traps on an ultrafast 400 fs timescale. (ii) The phonons that mediate self-trapping can be identified. (iii) The anharmonicity of the amide-I states is a measure of their degree of delocalization. The free exciton is delocalized at a temperature of 90 K but Anderson (disorder) localizes with increasing temperature. On the other hand, the band that has been assigned to a self-trapped state is localized at all temperatures. (iv) The lifetimes of the initially excited states are short (1–2 ps), yet the ground state recovery is somewhat longer (20–40 ps). Apparently, energy is stored in the meantime by mechanisms that still need to be explored. None of this information can be obtained from linear absorption spectroscopy.

PETER HAMM

See also **Biomolecular solitons; Davydov soliton, Local modes in molecular crystals; Nonlinear optics**

Further Reading

Davydov, A.S. 1979. Solitons in molecular systems *Physica Scripta*, 20: 387–394

Edler, J., Hamm, P. & Scott, A.C. 2002. Femtosecond study of self-trapped vibrational excitons in crystalline acetanilide. *Physical Review Letters*, 88: 067403. See also Edler, J. & Hamm, P. 2002. Self-trapping of the amide I band in a peptide model crystal. *Journal of Chemical Physics*, 117: 2415–2424

Elsaesser, T. Mukamel, S., Murnanae, M.M. & Scherer, N.F. (editors). 2000. *Ultrafast Phenomena XII*, Berlin: Springer and previous books of the same series

Mukamel, S. 1995. *Principles of Nonlinear Optical Spectroscopy*, New York: Oxford University Press

Scott, A.C. 1992. Davydov's soliton. *Physics Reports*, 217: 3–67

Xie, A., van der Meer, L., Hoff, W. & Austin, R.H. 2000. Long-lived amide I vibrational modes in myoglobin. *Physical Review Letters*, 84: 5435–5438

Q

Q-DEFORMATION

See **Salerno equation**

QUADRATIC FAMILY

See **One-dimensional maps**

QUANTUM BILLIARDS

See **Billiards**

QUANTUM CHAOS

Classical equations of motion can have arbitrary nonlinearities and thus can show a wide variety of chaotic behavior. The Schrödinger equation for quantum systems, in contrast, is a linear partial differential equation, and the initial value problem cannot show chaotic behavior in the usual sense. However, in the transition regions between classical and quantum descriptions, especially for highly excited systems or short de Broglie wavelengths, chaos in classical dynamics will have its effects on quantum dynamics, the eigenstates, and the eigenenergies. The field of quantum chaos deals with the characteristic properties that emerge in this transitional region. Some features are typical for the time evolution of wave functions and closely related to the classical dynamics of trajectories and phase space densities. Others deal with the properties of eigenenergies and eigenstates. Both aspects can nicely be illustrated for hydrogen atoms in external fields.

A first example for the close relation between classical and quantum dynamics is provided by excitations of hydrogen in microwave fields. Exposed to a microwave field of a frequency of 9.923 GHz, a hydrogen atom starting from a state with main quantum number $n = 66$ needs to absorb about 75 photons in order to ionize. Experiments show little ionization for small intensities of the field and a rapid increase to almost complete ionization for larger fields (Figure 1a). A full quantum calculation is prohibitively complicated because each photon adds one order of perturbation theory. However, an analysis of the classical dynamics of an electron in a Coulomb field and the external microwave field, with Hamiltonian

$$H = \frac{\mathbf{p}^2}{2m} - \frac{1}{4\pi\varepsilon_0}\frac{1}{r} + Ff(t)\cos\omega t, \qquad (1)$$

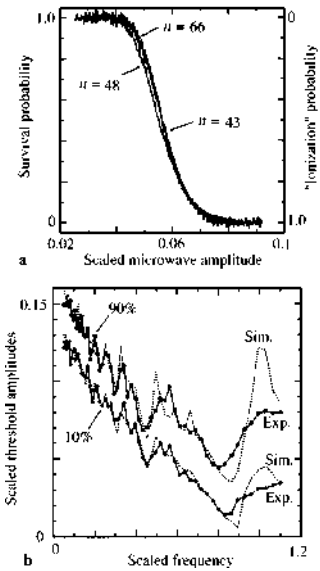

Figure 1. Microwave ionization of hydrogen atoms. The combinations $n_0\omega^3$ for the frequency and n_0^4F for the field strength are suggested by classical scaling. (Upper) Survival probability and ionization probability for different frequencies ω and different initial states n_0 that give the same scaled frequency as a function of field strengths. (Lower) Scaled threshold amplitude for the 10% and the 90% levels vs. scaled frequency. The comparison with classical simulations (dotted line) is very good and attests to the reliability of classical modelling of this process. For scaled frequencies $n_0^3\omega$ larger than 1, quantum effects become more important. (From Koch & van Leeuwen, 1995, with permission from Elsevier.)

where $f(t)$ describes the envelope of the field, reproduces the observed threshold amplitudes including many of the structures evident in Figure 1b very accurately.

The classical explanation for the fairly sharp onset is that for low field intensities, not all tori are destroyed, and the chaotic regions are separated by tori that block the transitions between them. For higher field intensities, the tori break up, the chaotic regions grow together, and electron trajectories can explore large regions of phase space, eventually escaping to infinity. This break up of tori is classically a rather dramatic event and can thus explain easily a fairly sharp onset of ionization. Many experiments since have verified the dependence on the initial state and the field intensities. Peculiar structures in the quantum ionization curves were also noted and could be explained as quantum effects due to almost degenerate quasienergy states. For the history of the problem and a careful analysis of the experiments and theories, see the review by Koch & van Leeuwen (1995).

Closely related to the microwave ionization of hydrogen is the dynamics of cold atoms in a standing light field. This problem is an experimental realization of the quantized kicked rotator, a standard model in classical and quantal chaos. Many properties of the quantized kicked rotator are described in Casati & Chirikov (1995); the first experimental realization is described in Moore et al. (1994).

For stationary problems, time can be separated and the eigenfunctions and eigenvalues of the Schrödinger equation can be analyzed. A good example is hydrogen in strong magnetic fields when the quadratic part of the vector potential cannot be neglected: the Hamiltonian then becomes

$$H = -\frac{\hbar^2}{2m}\Delta - \hbar\omega L_z - \frac{1}{4\pi\varepsilon_0}\frac{1}{r} + \frac{m\omega^2}{2}(x^2 + y^2) \quad (2)$$

with the magnetic field expressed through its cyclotron frequency $\omega_c = eB/(2m)$. In order for the energy content in the cyclotron motion to be compatible to the spacing between the ground state and the first excited state, the magnetic field has to be of the order of 10^5 T, values reached and exceeded on the surface of neutron stars only. However, if the initial state is an excited state with main quantum numbers of about $n = 40$, already a few Tesla suffice to bring the system way out of the linear Zeemann regime and to scramble the spectra completely (Figure 2). Many properties of the system are described in Friedrich & Wintgen (1989), and in the contribution by Delande to Giannoni et al. (1991).

In such strong fields, there are not enough quantum numbers anymore to allow one to label the eigenstates uniquely. In a similar situation, nuclear physicists introduced statistical measures for the distribution of eigenvalues (*See* **Random matrix theory**).

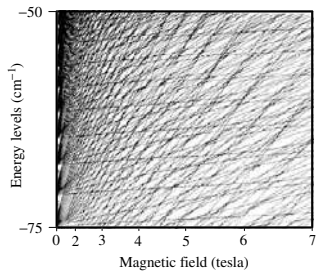

Figure 2. Energy levels for hydrogen in a magnetic field, for field strengths up to 7 T and initial quantum numbers between 38 and 45. The linear splitting within the Zeemann regime is limited to a region with very small fields. Most of the apparent crossings between eigenvalues are in fact avoided. (From Friedrich & Wintgen, 1989, with permission from Elsevier.)

Many investigations have shown that the statistics of eigenvalues for hydrogen in sufficiently strong magnetic fields, such as the level spacing distribution or two point correlation functions, are in very good agreement with random matrix theory (Friedrich & Wintgen, 1989). The same applies to many other classically chaotic systems, including vibrations of molecules, particles trapped in billiards, and model Hamiltonians with cubic and higher-order potentials, see the contribution by Bohigas to Giannoni et al. (1991) and the books by Brack & Bhaduri (1997), Haake (2001), and Stöckmann (1999).

While the distribution of eigenvalues shows statistical features, there are also deterministic ones: the Gutzwiller trace formula relates in the semiclassical limit eigenvalues E_i of the quantum system to classical periodic orbits and their properties (Gutzwiller, 1990; Chaos Focus Issue, 1992; Friedrich & Eckhardt, 1997),

$$\rho(E) = \sum_i \delta(E - E_i) \sim \mathrm{Re} \sum_p A_p \mathrm{e}^{\mathrm{i}S_p(E)/\hbar}, \quad (3)$$

$S_p = \oint \mathbf{p}\,\mathrm{d}\mathbf{q}$ is the classical action. The amplitude A_p carries information about caustics (through their phase shifts) and the instability of the classical orbits: the more unstable the smaller the weight. Because the density of states follows from a quantum amplitude (rather than a probability), the quantum amplitude is in magnitude the square root of the classical probability amplitude (*See* **Periodic orbit theory**). Expanding linearly around some reference energy E_r, the action becomes $S(E) \approx S(E_r) + T(E_r)(E - E_r)$, and a Fourier transform in E will results in peaks at the periods of periodic orbits in the system. This was noted in experiments by Karl Heinz Welge and his group and in numerical calculations by Friedrich & Wintgen (1989) (see also the comparison in Figure 3). Thus, on energy scales larger than a mean spacing

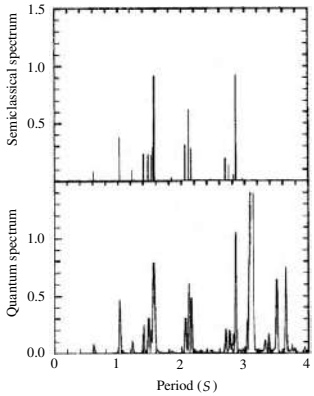

Figure 3. (Upper) The periodic orbits with periods S less than 3 and their semiclassical amplitudes and (Lower) a Fourier transform of a cross section of the quantum spectra in Figure 2.

and compatible with classical dynamics, the density of states is modulated by periodic orbits. Such periodic orbit spectroscopy can be used to extract the orbits and, thus, system specific properties.

In the presence of large-scale classical chaos and the accessibility of large parts of phase space by a single trajectory, one might expect that the wave functions are fairly uniformly spread out over the classically ergodic region. For billiards, this is the content of Shnirelman's theorem. However, as first discussed by Heller (1984) (see also Heller's contributions to Giannoni et al., 1991), periodic orbits leave their imprint on wave functions. One can find an enhanced intensity near a periodic orbit (a "scar") that can be detected in enhanced cross sections for certain processes.

The possibilities of quantum chaos are not limited to the realm of quantum phenomena proper: all that is needed is a wave theory, ideally with a classical dynamics for the propagation of wave fronts in the short wavelength limit. Examples outside the quantum world include resonances in microwave cavities, vibrations of solids, and acoustic waves in concert halls. In all cases level repulsion and other features can be found.

Many of the general properties of chaotic wave systems are discussed in the review Eckhardt (1988); in the textbooks by Brack & Bhaduri (1997), Gaspard (1998), Gutzwiller (1990), Haake (2001), and Stöckmann (1999); and in the contributions to Casati & Chirikov (1995), Giannoni et al. (1991), Chaos Focus Issue (1992), and Friedrich & Eckhardt (1997).

BRUNO ECKHARDT

See also **Periodic orbit theory; Random matrix theory I–IV; Regular and chaotic dynamics in atomic physics**

Further Reading

Brack, M. & Bhaduri, R.K. 1997. *Semiclassical Physics*, Reading, MA: Addison-Wesley

Casati, G. & Chirikov, B.V. 1995. *Quantum Chaos: Between Order and Disorder*, Cambridge and New York: Cambridge University Press

Cvitanoic, P. (editor). 1992. Chaos Focus Issue on Periodic Orbit Theory, *Chaos*, 2: 1–158

Eckhardt, B. 1988. Quantum mechanics of classically non-integrable systems. *Physics Reports*, 163: 205–297

Friedrich, H. and Eckhardt, B. (editors). 1997. *Classical, Semiclassical and Quantum Dynamics in Atoms*, Berlin and New York: Springer

Friedrich, H. & Wintgen, D. 1989. The hydrogen atom in a uniform magnetic field — an example of chaos. *Physics Reports*, 183: 37–79

Gaspard, P. 1998. *Chaos, Scattering and Statistical Mechanics*, Cambridge and New York: Cambridge University Press

Giannoni, M.J., Voros, A. & Zinn-Justin, J. (editors). 1991. *Chaos and Quantum Physics*. Proceedings Les Houches summer school 1989, Amsterdam and New York: North-Holland

Gutzwiller, M.C. 1990. *Chaos in Classical and Quantum Mechanics*, New York: Springer

Haake, F. 2001. *Quantum Signatures of Chaos*, Berlin: Springer

Heller, E.J. 1984. Bound-state eigenfunctions of classically chaotic Hamiltonian systems: scars of periodic orbits. *Physical Review Letters*, 53: 1515–1518

Koch, P.M. & van Leeuwen, K.A.H. 1995. The importance of resonances in microwave "ionization" of excited hydrogen atoms. *Physics Reports*, 255: 289–403

Moore, M.L., Robinson, J.C., Bharucha, C.F., Williams, P.E. & Raizen, M.G. 1994. Observation of dynamical localization in atomic momentum transfer: a new testing ground for quantum chaos. *Physical Review Letters*, 73: 2974–2977

Stöckmann, H.J. 1999. *Quantum Chaos: An Introduction*, Cambridge and New York: Cambridge University Press

QUANTUM FIELD THEORY

As our most fundamental description of physical phenomena, quantum field theory (QFT) is the natural culmination of classical mechanics, classical field theory, and quantum mechanics. To understand what QFT is and what makes it so special, it is worthwhile to briefly look at each of these structures in turn.

Classical mechanics describes the motion of objects in space and time in terms of well-defined positions and momenta that, taken together, form the phase space of the system. The location of an object in phase space can, in principle, be determined at any time, and once known suffices to predict its location at all future times given a complete enough knowledge of the forces at work. There are two main formulations of classical mechanics: the Hamiltonian formulation, which concentrates on how to find quantities at later times in terms of their known values at earlier times, and the Lagrangian one, which derives the same information from variational principles. These principles state that an object's trajectory in phase space extremizes a certain quantity called the action, which is the integral over the whole phase space history of a

functional called a Lagrangian. The dimension of the phase space is usually finite, but can be enlarged beyond the usual 3 + 3 dimensions for the location and velocity of a point particle to allow for rotations of a rigid body or changes of shape of a deformable body. Relativity can be accommodated, but the ideas of quantum mechanics do not appear.

The move to an infinite number of phase space dimensions takes one from classical mechanics to classical field theory. Fluid mechanics, for example, allows for an infinite variety of shapes that a fluid can take making the phase space infinite. Sums that arose in classical mechanics are now integrals, and the general problems of analysis become much more challenging. Nevertheless, many problems are tractable, and theories based on classical fields with an infinite number of degrees of freedom have had great success. Notable among these is Maxwell's electrodynamics, which describes the electromagnetic field in terms of electric and magnetic fields that can vary in space and time and are present at all points of space and time. The phase space of classical electromagnetism is then infinite dimensional, and this accounts for much of the richness of the physics that it can describe.

Another shift away from classical mechanics is to maintain a finite number of degrees of freedom but to allow that points in phase space cannot be arbitrarily well known. The Heisenberg uncertainty principle placed constraints on the accuracy with which position and momentum could be known simultaneously, and the points of the phase space acquired a certain fuzziness. For example, in place of a point with well-defined position x and momentum p_x in the x-direction, one had something like a fuzzy disk of area roughly equal to the square of the Planck length, and shape determined by whether one tried to accurately determine x or p_x—one could only know one with a consequent sacrifice of information about the other. A system cannot now be thought of as a well-defined classical point moving around in phase space. Rather, information about the system is encoded in a function on the phase space called the wave function Ψ, and the theory allows all that can be known about the system to be recovered by applying various linear operators to Ψ.

The step to QFT involves allowing an infinite number of degrees of freedom in quantum mechanics. Thus, one might say that QFT is to quantum mechanics what classical field theory is to classical mechanics. The shift is profound and carries a number of important implications.

The first is that QFT takes as its phase space classical fields upon which an uncertainty paralleling that in quantum mechanics has been imposed. For example, the role of x could be taken by a classical field ϕ, and the role of momentum p_x by the rate of change of something (the Lagrangian) with respect to the time derivative of ϕ. This quantity is called the momentum conjugate to ϕ, and it is impossible to know both it and ϕ with arbitrary precision.

Time and space are now just dummy labels (parameters) in the theory and are integrated over, their main use being to enforce the notion of locality in a Lagrangian. This point is often misunderstood as people look for the "locations" of field quanta in physical space. In QFT, one looks at ϕ as a dynamical quantity as opposed to x. An excellent discussion of this point can be found in Schwinger (1970).

It turns out, perhaps somewhat tautologically, that one can often expand fields in Fourier series and identify each of the modes as a "particle" with momentum given by the mode numbers. It is a remarkable fact that experiments to detect fields in nature, when performed with sufficient resolution, always find them occurring in (or at least interacting as) discrete chunks or quanta. In this sense, QFT is a theory of particles, and the degree to which these quanta can be identified as isolated, discrete objects determines how well they can be thought of as particles.

As a field changes in time so too do the various Fourier modes and this is interpreted as saying that particles appear and disappear; in other words, particles can be created and destroyed in QFT. This is something foreign to both quantum and classical mechanics and was needed with the advent of high-energy physics experiments in which particles are routinely created and destroyed.

Two of many excellent texts describing how QFT is used in the calculation of physical processes are those by Peskin & Schroeder (1995) and by Weinberg (1995). The text by Itzykson and Zuber (1980) is also very good. A more philosophically inclined and less calculationally oriented reader will find much to think about in the book by Teller (1995). It is easy to suppose that QFT is intrinsically, or somehow must be, relativistic. In fact, the concepts can be very successfully applied to problems in condensed matter physics in nonrelativistic situations, and the interested reader will find the delightful introductory book by Mattuck (1992) and the more advanced book by Abrikosov et al. (1975) excellent places to start.

Several caveats are in order. First of all, in the relativistic case (the real world), these quanta do not generally admit a localization in the sense of having well-defined classical-like positions. That is, they do not behave like billiard balls. Second, if interactions between them are very strong they may not act as intuition might suggest. For example, while electrons and photons are in many ways like what one might expect particles to be, protons and neutrons seem to be comprised of particles called quarks, which cannot be removed. One says that the interactions between quarks are so strong that they are "confined." Phonons are quantized vibrations in crystals that can be detected in neutron scattering experiments and act in many ways

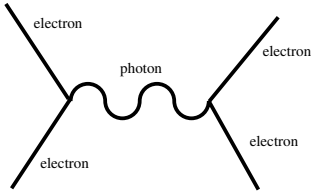

Figure 1. A Feynman diagram representing a first approximation to the scattering of one electron from another (the two straight lines) via the exchange of a photon (the wiggly line). Each diagram like this corresponds to a physically clear picture as well as to a well-defined mathematical expression contributing to the quantum mechanical amplitude for the process to take place. Only the topology of the diagram is important. Bending the lines around represents processes involving electrons and their antiparticles as different aspects of the same basic phenomenon, and connects scattering in space with scattering forward and backward in time, while not violating causality.

like particles, but they are only there insofar as there is a crystal lattice to vibrate. Any attempt to isolate a phonon by pulverizing a crystal and looking for one among the fragments is doomed to failure.

When it makes sense to think of weakly coupled particles, there is a well developed calculational framework called "perturbative quantum field theory" (pQFT), which allows one to make systematic estimates of physical quantities, often using sketches called Feynman diagrams. Figure 1 shows a Feynman diagram contributing to the scatting of one electron by another (the straight lines) via the exchange of a photon (the wiggly line).

The mathematical procedures involved are fraught with difficulties, and the series that arise are often divergent on physical grounds. In addition, the individual terms also tend to be infinite, and several procedures have been developed for handling such problems. The general approach is to first make ill-defined formal expressions finite by changing them ("regularizing" them) in a way controlled by some parameter, then comparing such regularized expressions only to one another and linking only such comparisons to observations ("renormalization"). Despite the feelings of many of the founders that there might be something deeply wrong with these procedures, it turns out that many quantities calculated in this way have given answers accurate to parts per million or better.

For strongly interacting theories the state of the art is much less well-developed. Powerful computers can be used to treat theories that are based on restricting fields to live on a grid or lattice that is meant to approximate space–time, but with a finite number of points. Analytic techniques also offer some hope, but the problems are formidable.

One of the most dramatic consequences of QFT is that the vacuum becomes a very complex object. Recalling the notion of the uncertainly principle applied to fields, one cannot set both a field and its conjugate momentum equal to zero. This, in fact is the case for each possible mode of a field and leads to an infinite energy in the vacuum due to these fluctuating, uncertain fields. As mentioned earlier, infinities like this are basically swept under the rug by insisting that only comparisons are meaningful, but in this case there are remarkable physical consequences.

For example, there are more modes that can exist for the electromagnetic field between two parallel metal plates that are far apart than for ones that are closer together. The infinite energies between the plates in these two cases can be compared and the result is finite—there is less energy between two plates that are close together than two that are far apart. This implies that two parallel metal plates, in order to reduce the energy between them (in empty space), will pull together. This is called the "Casimir effect" and has actually been observed in the laboratory, making it clear that QFT and its strange vacuum are more than theoretical fantasies.

Although it is often not made clear, one final aspect of QFT that differs from quantum mechanics is that QFT admits an infinite number of distinct vacua, all of zero energy. None of these vacua can be reached from another by a unitary transformation, making them physically distinct. This richness of "empty" space is a critical part of what makes QFT able to describe so much. To do justice to this point would require more space than is available, but the interested reader would do well to start with the book by Umezawa (1993). One consequence of this existence of unitarily inequivalent vacua is the amazing fact that the vacuum of one observer can be devoid of particles, while that of another may actually have particles present.

JOHN DAVID SWAIN

See also **Born–Infeld equations; Higgs boson; Quantum inverse scattering method; Skyrmions; String theory; Yang–Mills theory**

Further Reading

Abrikosov, A.A., Gorkov, L.P. & Dzyaloshinski, I.E. 1975. *Methods of Quantum Field Theory in Statistical Physics*, revised edition, translated and edited by Richard A. Silverman, New York: Dover

Itzykson, C. & Zuber, J.-B. 1980. *Quantum Field Theory*, New York: McGraw-Hill

Mattuck, R.D. 1992. *A Guide to Feynman Diagrams in the Many-Body Problem*, 2nd edition, New York: Dover

Peskin, M.E. & Schroeder, D.V. 1995. *An Introduction to Quantum Field Theory*, Reading, MA: Addison-Wesley

Schwinger, J. 1970. *Particles, Sources, and Fields*, Reading, MA: Addison-Wesley

Teller, P. 1995. *An Interpretative Introduction to Quantum Field Theory*, Princeton, NJ: Princeton University Press

Umezawa, H. 1993. *Advanced Field Theory*, New York: American Institute of Physics Press
Weinberg, S. 1995–2000. *The Quantum Theory of Fields*, 3 vols., Cambridge and New York: Cambridge University Press

QUANTUM INVERSE SCATTERING METHOD

The extension of the inverse scattering method to quantum theory, called the quantum inverse scattering method (QISM), was introduced at the end of the 1970s by the Leningrad (now St Petersburg) group and has been developed extensively since the 1980s. The QISM is significant in many respects. First, similar to the classical inverse scattering method, it provides a powerful method to solve the problem of quantum integrable systems. Second, it has a wide applicability to quantum particle systems, quantum field theoretic models, and quantum spin systems. Importantly, the QISM provides a unified view on exactly solvable models in physics. That is, it places completely integrable models in many-body theory and field theory and solvable models in statistical mechanics in a unified framework. Third, it has been the source of new mathematical objects and concepts such as Yangian algebra, quantum groups, q-deformation, and a revived knot theory. In these mathematical developments, the Yang–Baxter relation plays a central role.

As the simplest example, we begin with the quantum nonlinear Schrödinger (QNLS) model,

$$\mathrm{i}\phi_t + \phi_{xx} - 2\kappa\phi^\dagger\phi\phi = 0. \tag{1}$$

Here, $\phi(x,t)$ is the boson field operator, satisfying the equal-time commutation relation, $[\phi(x,t), \phi^\dagger(y,t)] = \delta(x-y)$. The Hamiltonian of the system is

$$H = \int \mathrm{d}x(\phi_x^\dagger\phi_x + \kappa\phi^\dagger\phi^\dagger\phi\phi). \tag{2}$$

The QNLS model (1) is considered to be the second-quantized theory of boson particles interacting via the pair-wise, delta-function potential. Motivated by the Zakharov–Shabat eigenvalue problem in the classical theory, we associate a linear auxiliary problem to (1),

$$\psi_{1x} + \frac{\mathrm{i}}{2}\lambda\psi_1 = \mathrm{i}\alpha\phi^\dagger\psi_2,$$
$$\psi_{2x} + \frac{\mathrm{i}}{2}\lambda\psi_2 = \mathrm{i}\varepsilon\alpha\psi_1\phi, \tag{3}$$

where $\alpha = |\kappa|^{1/2}$ and ε denotes the sign of κ. We further assume the boundary condition $\phi(x) \to 0$ as $|x| \to \infty$, which is interpreted as the weak relation (a relation for the matrix elements). The Jost function operator $\Psi(x,\lambda)$ is defined by

$$\Psi(x,\lambda) = \begin{bmatrix} 1 \\ 0 \end{bmatrix} \exp\left(-\tfrac{\mathrm{i}}{2}\lambda x\right), \qquad x \to \infty,$$
$$= \begin{bmatrix} A(\lambda)\exp\left(-\frac{\mathrm{i}}{2}\lambda x\right) \\ B(\lambda)\exp\left(\frac{\mathrm{i}}{2}\lambda x\right) \end{bmatrix}, \qquad x \to -\infty. \tag{4}$$

The coefficients $A(\lambda)$ and $B(\lambda)$, corresponding to the transmission coefficient $a(\lambda)$ and the reflection coefficient $b(\lambda)$ in the classical theory, are called scattering data operators. The auxiliary problem (3) with (4) is solved perturbatively to express $A(\lambda)$ and $B(\lambda)$ in terms of the operators ϕ and $\phi^\dagger$ (direct problem). As a result, we obtain

$$[H, A(\lambda)] = 0, \qquad [H, B(\lambda)] = -\lambda^2 B(\lambda). \tag{5}$$

The former relation proves that the QNLS model has an infinite number of conserved operators. The latter indicates that the state

$$|k_1, k_2, \ldots, k_n\rangle = B^\dagger(k_1)B^\dagger(k_2)\ldots B^\dagger(k_n)|0\rangle, \tag{6}$$

where $|0\rangle$ is the vacuum state $\phi(x)|0\rangle = 0$, is an eigenstate of the Hamiltonian. Similar to the classical theory, the quantum Gel'fand–Levitan equation can be derived (inverse problem).

The state $|k_1, k_2, \ldots, k_n\rangle$ in (6) is valid irrespective of the sign of κ and describes the continuous state (Bethe ansatz state). For the attractive case ($\kappa < 0$), there appear bound states. A bound state (n-string state) is made of the complex momenta, $k_j = P/n - \mathrm{i}(n-2j+1)\kappa/2$, $j = 1, 2, \ldots, n$ and the energy is $E = \sum_{j=1}^n k_j^2 = P^2/n - \kappa^2 n(n^2-1)/12$. This bound state corresponds to the classical bright soliton in the $n \to \infty$ limit and may be called a quantum soliton.

To make the mathematical structure clear, it is useful to consider an operator version of an auxiliary linear problem defined on a one-dimensional lattice

$$\psi_{m+1} = L_m(\lambda)\psi_m, \qquad \mathrm{d}\psi_m/\mathrm{d}t = M_m\psi_m, \tag{7}$$

where $L_m(\lambda)$ and M_m are $M \times M$ matrix operators, and λ is the spectral parameter. For a quantum integrable system, it is found that direct products of two L_n operators with different spectral parameters satisfy a similarity relation

$$R(\lambda,\mu)[L_n(\lambda)\otimes L_n(\mu)] = [L_n(\mu)\otimes L_n(\lambda)]R(\lambda,\mu). \tag{8}$$

Here, the symbol $\otimes$ denotes the direct product of matrices, and $R(\lambda,\mu)$, called R-matrix, is an $M^2 \times M^2$ c-number matrix. Relation (8) is the Yang–Baxter relation for a quantum system on a lattice. If the $L_n(\lambda)$ operators on different sites commute, (8) leads to

$$R(\lambda,\mu)[\mathcal{T}_N(\lambda)\otimes\mathcal{T}_N(\mu)] = [\mathcal{T}_N(\mu)\otimes\mathcal{T}_N(\lambda)]R(\lambda,\mu), \tag{9}$$

where $\mathcal{T}_N(\lambda) = L_N(\lambda)L_{N-1}(\lambda)\cdots L_1(\lambda)$ is called the transition matrix or monodromy matrix. From (9), the

transfer matrix

$$T_N(\lambda) = \mathrm{Tr}\mathcal{T}_N(\lambda) = \sum_{i=1}^{M} [\mathcal{T}_N(\lambda)]_{ii}, \tag{10}$$

satisfies the commutation relation

$$[T_N(\lambda), T_N(\mu)] = 0. \tag{11}$$

Relation (11) indicates the transition matrix $T_N(\lambda)$ is a generator of conserved operators. The λ (or λ^{-1}) expansion of $T_N(\lambda)$ gives a set of conserved operators $\{I_j\}$, which are involutive, $[I_i, I_j] = 0$. In addition, commutation relations among elements of the monodromy matrix offer an algebraic formulation of the Bethe ansatz method (algebraic Bethe ansatz method).

For quantum field theoretical models, the subscript N of the operator $T_N(\lambda)$ is understood as the system size that is to be sent to infinity. Then relation (11) proves the existence of an infinite number of involutive conserved operators. It is remarkable that we may consider $L_n(\lambda)$ and $R(\lambda, \mu)$ as vertices (local Boltzmann weights) of a vertex model in statistical mechanics. In this context, the Yang–Baxter relation (8) is a sufficient condition for the commutativity of the transfer matrix in statistical mechanics. Thus, quantum integrable models in $(1+1)$-dimension and solvable statistical models in 2-dimensions have a common property, a family of commuting transfer matrices.

Further, the quantum inverse scattering method and the Yang–Baxter relation have produced interesting developments in mathematics. Solutions of the Yang–Baxter relation with the difference property $R(\lambda, \mu) = R(\lambda - \mu)$ are classified into three classes, (i) elliptic, (ii) trigonometric, and (iii) rational functions. The trigonometric (rational) model is the critical case of the elliptic (trigonometric) model. Quantum groups and knot theory are due to the rich mathematical properties of the exactly solvable models at criticality. Extensive studies on the elliptic case are in progress.

MIKI WADATI

See also **Bethe ansatz; Inverse scattering method or transform; Quantum field theory; Solitons**

Further Reading

Faddeev, L.D. 1981. Quantum completely integrable models in field theory. *Soviet Science Review of Mathematics and Physics,* C1: 107–155

Korepin, V.E., Bogoliubov, N.M. & Izergin, A.G. 1993. *Quantum Inverse Scattering Method and Correlation Functions*, Cambridge and New York: Cambridge University Press

Thacker, H.B. 1981. Exact integrability in quantum field theory and statistical systems. *Reviews of Modern Physics*, 53: 253–285

Wadati, M., Deguchi, T. & Akutsu, Y. 1989. Exactly solvable models and knot theory. *Physics Reports*, 180: 247–332

Wadati, M., Kuniba, A. & Konishi, T. 1985. The quantum nonlinear Schrödinger model: Gel'fand–Levitan equation and classical soliton. *Journal of the Physical Society of Japan*, 54: 1710–1723

QUANTUM NONLINEARITY

Although quantum mechanics is a linear theory, it is often used to analyze classical problems that are nonlinear. In the course of such analyses, it is interesting to consider how the nonlinear features of the classical dynamics are represented in the context of linear quantum theory, as is expected from the correspondence principle of Niels Bohr. In this entry, we see how the correspondence principle asserts itself to describe a variety of interesting nonlinear behaviors, including anharmonic oscillation, local modes, soliton binding energy, and soliton pinning.

A Nonlinear Oscillator

Consider the nonlinear mass-spring oscillator shown in Figure 1, where the spring potential is $V(x) = Kx^2/2 - \alpha x^4/4$. Under quantum theory, the oscillator energy (E) is not a continuous variable; it takes only discrete values that are eigenvalues of the time-independent Schrödinger equation

$$\left(\frac{\hbar^2}{2M}\right)\frac{\mathrm{d}^2\psi}{\mathrm{d}x^2} + [E - V(x)]\psi = 0, \tag{1}$$

where M is the oscillating mass and $\hbar$ is Planck's constant divided by 2π (Schiff, 1968). If α is zero, the restoring force of the spring is a linear function of its extension, and the classical oscillator of Figure 1 is linear. In this case, the energy eigenvalues are given by

$$E_n = (n + 1/2)\hbar\omega, \tag{2}$$

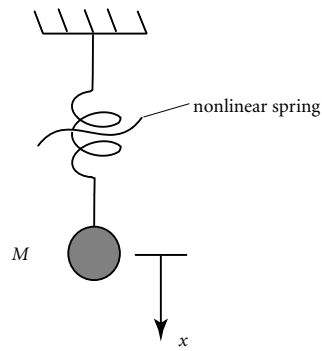

Figure 1. A nonlinear oscillator.

where $n = 0, 1, 2, \ldots$ indicates the number of quanta (called bosons) in the oscillation and $\omega = \sqrt{K/M}$ is the oscillation frequency of the classical oscillator. First derived by Erwin Schrödinger, the corresponding eigenfunctions (ψ_n) in Equation (1) are nth-order Hermite polynomials multiplied by a Gaussian factor—$\exp(-M\omega x^2/2\hbar)$—the first few of which are shown in Figure 2 (Schrödinger, 1926). A restriction of the linear ($\alpha = 0$) case is that transitions are allowed only between adjacent quantum levels. Thus, energy can only enter or leave the oscillator in quantum units of $\hbar\omega$, corresponding to Planck's radiation law.

If $\alpha \neq 0$, the classical oscillator is nonlinear, and two aspects of the quantum picture change. First, the energy eigenvalues are no longer given by the simple expression of Equation (2), and second, energetic transitions are not restricted to jumps between adjacent quantum levels. Both of these new features allow packets of energy to enter and leave the oscillator in amounts that differ from $\hbar\omega$ and, therefore, (according to Planck's law) at frequencies that differ from $\omega = \sqrt{K/M}$, in accord with observations of classical nonlinear oscillators.

In general, Equation (1) must be solved numerically to find its eigenvalues and eigenfunctions in the nonlinear case, but useful results can be obtained if the classical oscillator is considered in the rotating-wave approximation. Under this approximation, the energy eigenvalues are given by Scott (2003)

$$E_n = (\hbar\omega - \gamma/2)(n + 1/2) - \gamma n^2/2, \qquad (3)$$

where $\gamma \equiv 3\alpha\hbar^2/4M^2\omega^2$, and the corresponding eigenfunctions are identical to those of the linear oscillator (as in Figure 2). Equation (3) is an example of the Birge–Sponer relation, which is widely observed for nonlinear interatomic oscillations.

To represent the quantum dynamics of an oscillator, the (linear) superposition theorem allows construction of a wave packet of the form

$$\Psi(x, t) = \sum_{n=1}^{\infty} c_n \psi_n(x) e^{-iE_n t/\hbar}, \qquad (4)$$

where the c_n are complex constants that determine the initial position of the oscillator, $\Psi(x, t)$ is a solution of the linear, time-dependent Schrödinger equation, and the probability density of finding a particular position (x) is $\int |\Psi(x, t)|^2 \, dx$ (Schiff, 1968).

As the mass and spring constant become larger and the total energy of the oscillator is increased, the energy difference between adjacent levels becomes an ever smaller fraction of the total energy, and the discrete energy levels (the E_n) are better approximated as a continuous function. If the c_n in Equation (4) are chosen so that Ψ is a localized wave packet, the center of mass of this packet will follow the classical nonlinear trajectory. Thus the quantum model—which is necessary for describing interatomic oscillations—merges smoothly into the classical description that we use in our daily lives.

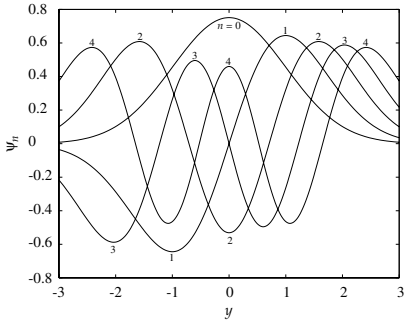

Figure 2. Harmonic oscillator wave functions, where $y = x\sqrt{M\omega/\hbar}$.

Local Modes in Molecules

Although empirical evidence for localization of vibrational energy in molecules has been available since the 1920s, such observations have been questioned because they seem to be at variance with the predictions of quantum theory. The benzene molecule (C_6H_6), for example, is invariant under a 60^0 rotation about its main axis; thus eigenfunctions of the (linear) quantum theory must be similarly invariant, but a local mode of CH-stretching vibration is not (see Figure 3).

This seeming contradiction between theory and experiment can be understood by noting that a local mode is represented not by a single eigenfunction but by a wave packet of them. For a local mode of n quanta, it turns out that the energy levels lie within a range of order (Scott, 2003)

$$\Delta E \sim \frac{n\varepsilon^n}{(n-1)!\gamma^{n-1}},$$

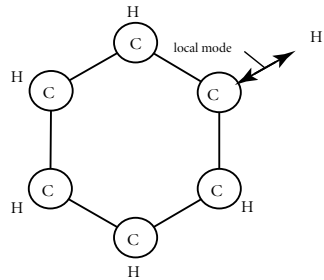

Figure 3. The planar structure of a benzene molecule, showing a local mode of the CH stretching oscillation.

where ε is the coupling energy between CH oscillations and γ is the anharmonicity as defined below Equation (3). For CH-stretching oscillations, $\varepsilon < \gamma$, so this energy range decreases very rapidly with increasing n, making the local-mode wave packet quasidegenerate at moderate quantum levels. This means that the wave packet will remain localized for times of order $\hbar/\Delta E$, which can be much longer than the time required to make an experimental observation.

Quantum Solitons

Consider next a chain (or one-dimensional lattice) of f classical nonlinear oscillators of the form

$$\left(\mathrm{i}\frac{\mathrm{d}}{\mathrm{d}t}-\omega\right) A_j+\varepsilon(A_{j+1}+A_{j-1})+\gamma|A_j|^2A_j = 0, \tag{5}$$

where $A_j = A_{j+f}$ is a complex amplitude and j is an index running over periodic boundary conditions. In this formulation, ω is the oscillation frequency at one of the lattice points, ε is the interaction energy between adjacent oscillators, and γ is the anharmonicity of each oscillator in the rotating wave approximation. (With $f = 6$, Equation (5) provides a model for the benzene oscillations of Figure 3.)

This discrete nonlinear Schrödinger (DNLS) equation has solitary wave solutions that approach solitons of the continuum nonlinear Schrödinger (NLS) equation as $\gamma/\varepsilon \to 0$. (Be careful not to confuse the *linear* Schrödinger equation of quantum theory in Equation (1) with Equation (5), which is a *nonlinear, classical* equation. They are quite different.) Because Equation (5) is in the rotating wave approximation, the corresponding quantum problem can be formulated and solved (Scott et al., 1994).

For two quanta ($n = 2$) in the large f limit, energy eigenvalues are arranged as in Figure 4, where each eigenfunction changes by a factor of $\mathrm{e}^{\mathrm{i}k}$ under translation by one unit of j (lattice spacing); thus k is the "crystal momentum" of an eigenstate, (Haken, 1976). This figure shows both a continuum band (the shaded area) and a soliton band given by

$$\begin{aligned} E_2(k) &= \sqrt{\gamma^2 + 16\varepsilon^2\cos^2(k/2)} \\ &= E_2(0) + k^2/2m^* + \mathrm{O}(k^4), \end{aligned} \tag{6}$$

where m^* is the "effective mass" near the band center. The soliton band is characterized by two features. First, it is displaced below the continuum band by a binding energy $E_\mathrm{b} = \sqrt{\gamma^2 + 16\varepsilon^2} - 4\varepsilon$. Second, inspection of the corresponding eigenfunctions shows that the two quanta are more likely to be on the same site for the soliton band than in the continuum band.

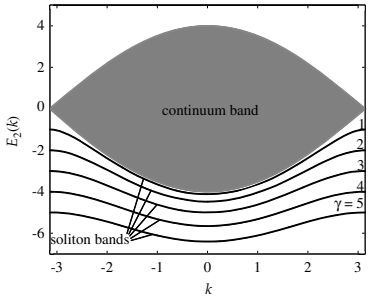

Figure 4. Energy eigenvalues of the DNLS equation at the second ($n = 2$) quantum level with $\varepsilon = 1$. There is one soliton band for each value of γ, which is plotted for several different values of γ.

For arbitrary n, $\gamma \ll \varepsilon$ and sufficiently large f, the quantum binding energy is

$$E_\mathrm{b} = \frac{\gamma^2}{48\varepsilon}n(n^2-1), \tag{7}$$

which corresponds to the binding energy of a classical NLS soliton under the identification $n = \sum |A_j|^2 \gg 1$ (Makhankov, 1990).

In the classical DNLS system with $\gamma \gg \varepsilon$, numerical studies show that the soliton becomes pinned to the lattice. Under quantum theory, this classical, nonlinear phenomenon is reflected by the fact that the effective mass,

$$m^* = \frac{(n-1)!\gamma^{n-1}}{2n\varepsilon^n},$$

becomes very large. Because the classical Ablowitz–Ladik (AL) system is completely integrable for all parameter values, its soliton is not pinned for $\gamma \gg \varepsilon$. This classical fact is reflected by an effective mass that approaches zero under the same conditions. Interestingly, the Salerno equation interpolates between the DNLS and AL limits.

Quantum Representation of a Classical Soliton

Although the quantum formulation can, in principle, be used to represent a classical soliton (on an optical fiber, for example), this is a rather complex dynamical object. The closest quantum representation of a classical soliton is provided by the coherent (or Glauber) state (Makhankov, 1990), which is constructed so that the complex wave amplitude—A_j in Equation (5)—is an eigenfunction of the bosonic lowering operator. This requires a wave packet comprising components with all values of the principal quantum number (n) (Scott, 2003). For a system with f degrees of freedom, a

component at the nth level, in turn, has

$$\frac{(n+f-1)!}{(f-1)!\,n!}$$

terms, each of which is a complex construction of the eigenfunctions shown in Figure 2. (These are all of the different ways that n quanta can be placed on f freedoms.) As the number of terms at each level grows very rapidly with n, it becomes difficult to construct an exact quantum representation.

One way out of this computational dilemma is to go to the continuum approximation ($f \to \infty$) and employ the methods of quantum field theory (Lai & Haus, 1989). Another approach is to use a Hartree approximation (HA), which assumes that each boson feels the same mean-field potential as all of the other bosons (Scott, 2003). When this approximation procedure is carried through, it is found that the binding energy at the nth level is

$$E_{\mathrm{b}}^{\mathrm{HA}} = \frac{\gamma^2}{48\varepsilon} n(n-1)^2, \tag{8}$$

which is less than the exact value by the factor $(n-1)/(n+1)$.

ALWYN SCOTT

See also **Discrete nonlinear Schrödinger equations; Hartree approximation; Local modes in molecules; Quantum field theory; Quantum theory; Rotating wave approximation; Salerno equation**

Further Reading

Haken, H. 1976. *Quantum Field Theory of Solids*, Amsterdam: North-Holland

Lai, Y. & Haus, H. 1989. Quantum theory of solitons in optical fibers. I. Time-dependent Hartree approximation. II. Exact solution. *Physical Review* A, 40: 844–866

Makhankov, V.G. 1990. *Soliton Phenomenology*, Dordrecht: Amsterdam

Schiff, L.I. 1968. *Quantum Mechanics*, 3rd edition, New York: McGraw-Hill

Schrödinger, E. 1926. Quantisierung als Eigenwertproblem. *Annalen der Physik*, 79: 361–376

Scott, A.C. 2003. *Nonlinear Science: Emergence and Dynamics of Coherent Structures*, 2nd edition, Oxford and New York: Oxford University Press

Scott, A.C., Eilbeck, J.C. & Gilhøj, H. 1994. Quantum lattice solitons. *Physica* D, 78: 194–213

QUANTUM THEORY

Quantum theory was born in 1900 with an important paper by Max Planck on black-body radiation. In this paper, he introduced quanta of vibrational energy E which are proportional to their frequency ν, and his famous constant currently known to take the value (Mohr & Taylor, 2000)

$$\frac{E}{\nu} = h = 6.62606876(52)\ 10^{-34}\ \mathrm{J\,s}.$$

Ten years after its formulation, Planck's hypothesis had been extraordinarily successful, explaining the light spectrum of black-body radiation, the photoelectric effect, and the low-temperature reduction of heat capacity in solids.

Using Rutherford's planetary model of atoms, Niels Bohr showed in 1913 that Planck's hypothesis helps to understand the spectral lines of hydrogen by deriving their frequencies in terms of h, and the electron mass and charge. The success of Bohr's atomic model led to the formulation of the Bohr–Sommerfeld quantization rule for classically integrable systems possessing as many invariants of motion as degrees of freedom:

$$\oint p_j\,\mathrm{d}q_j = h\left(n_j + \frac{\mu_j}{4}\right), \qquad j = 1, 2, ..., f,$$

where (q_j, p_j) are the canonically conjugate position-momentum variables in terms of which the system is integrable (also said separable), n_j are integers, μ_j are the so-called Maslov indices that characterize the topology of the motion (e.g., $\mu_j = 0$ for rotation, $\mu_j = 2$ for libration), and f is the number of degrees of freedom.

In 1917, Albert Einstein pointed out that the Bohr–Sommerfeld quantization rule cannot be applied to classically non-integrable systems (such as the helium atom), and it slowly became apparent that radically new ideas were required. In 1923, Louis de Broglie suggested that massive particles should behave as waves and he completed Planck's hypothesis by his famous relation, $p\lambda = h$, between the particle's momentum p and its wavelength λ.

Finally in 1925 and 1926, Werner Heisenberg and Erwin Schrödinger established quantum mechanics in two equivalent formulations. The first represents the observable quantities as matrices and the second is based on the famous Schrödinger equation

$$\mathrm{i}\,\hbar\,\frac{\partial\psi}{\partial t} = -\frac{\hbar^2}{2m}\frac{\partial^2\psi}{\partial \boldsymbol{r}^2} + V(\boldsymbol{r}, t)\ \psi, \tag{1}$$

for the wave function $\psi(\boldsymbol{r}, t)$ of a particle of mass m moving in the energy potential $V(\boldsymbol{r}, t)$, with $\hbar = h/2\pi$ and $\mathrm{i} = \sqrt{-1}$. In 1927, Max Born proposed to interpret the square of the modulus of the wave function, $|\psi(\boldsymbol{r}, t)|^2$, as the probability density to observe the particle at position $\boldsymbol{r}$ and time t if the wave function is normalized to unity over the whole configuration space according to

$$\int |\psi(\boldsymbol{r}, t)|^2\,\mathrm{d}\boldsymbol{r} = 1. \tag{2}$$

In this formulation, physical observables are represented by linear Hermitian operators $\hat{A}$ acting on the wave function. The expectation value of an observable is given by

$$\langle A\rangle = \int \psi^*(\boldsymbol{r}, t)\ \hat{A}\psi(\boldsymbol{r}, t)\ \mathrm{d}\boldsymbol{r},$$

if the particle is in the state described by the normalized wave function ψ. The wave property prevents a quantum particle from having simultaneously well-defined position and momentum as in the classical world. This impossibility (which follows from Fourier transform theory) is expressed by Heisenberg's uncertainty relation between the uncertainties on position Δx and momentum Δp

$$\Delta x \; \Delta p \geq \hbar/2,$$

which finds its origin in the noncommutativity of position and momentum operators.

The normalization condition (2) has the pivotal role of selecting the physically acceptable wave functions among all the possible solutions of the Schrödinger equation (1). In particular, it is the normalization condition that leads to the quantization of energy into well-defined eigenvalues associated with the stationary states. Without the normalization condition, the wave function would present spatial instabilities that are not physically meaningful.

Because of their spatial extension, wave functions are allowed to penetrate into classically forbidden regions where the classical kinetic energy of the particle would be negative. In these regions, the normalization condition (2) forces the wave function to decrease exponentially and precludes its instability. A consequence is the phenomenon of quantum tunneling, which manifests itself in cold electronic emission or α radioactivity and finds technological applications in Leo Esaki's semiconductor tunneling diode, Ivar Giaever's superconducting tunneling diode, and the electron tunneling microscope.

Together with the normalization condition, the Schrödinger equation shares with nonlinear systems the general scheme:

$$\text{instability} \rightarrow \text{saturation} \rightarrow \text{structure}.$$

In quantum mechanics, the instability mechanism is spatial and the saturation is provided by the normalization condition that selects spatially stable wave functions such as the electronic orbitals of atoms, molecules, and solids. The selection of normalizable wave functions generates the molecular structures of stereochemistry.

However, Schrödinger's equation is linear and thus obeys the principle of linear superposition (Dirac, 1930). Accordingly, the linear combination

$$\psi = \sum_n c_n \psi_n$$

(with complex numbers c_n) is a physically acceptable solution of Equation (1). Following studies by Steven Weinberg and others (Weinberg, 1989), extremely stringent limits have been put on hypothetical nonlinear corrections to quantum mechanics. These limits have been obtained by searching for nonlinearly induced detuning of resonant transitions between two atomic levels, putting the following upper bounds on a hypothetical nonlinear term $\Delta E(\psi, \psi^*)\psi$ supposed to correct the right-hand side of Schrödinger Equation (1):

$$|\Delta E| < 2.4\ 10^{-20}\ \text{eV in } {}^9\text{Be}^+ \text{ ion}$$
(Bollinger et al., 1989),
$$|\Delta E| < 1.6\ 10^{-20}\ \text{eV in } {}^{201}\text{Hg atom}$$
(Majumder et al., 1990).

The principle of linear superposition of quantum mechanics has thus been confirmed by these investigations.

Nevertheless, in low-temperature many-body quantum systems, effective nonlinearities may arise if some wave function describing a subset of degrees of freedom has a feedback effect onto itself. Examples of effectively nonlinear quantum equations include the Hartree–Fock equation for fermionic systems, the Ginzburg–Landau equation for superconductors, the Gross–Pitaevskii equation for Bose–Einstein condensates, and the Ginzburg–Landau equation coupled to a Chern–Simon gauge field for the fractional quantum Hall effect.

Another problem where nonlinearities are associated with Schrödinger's equation is the theory of the optimal control of quantum systems by an external electromagnetic field. The optimal external field can be obtained as the solution of coupled nonlinear Schrödinger equations, where nonlinearity arises by a feedback mechanism of the quantum system onto itself through the external field and the desired control. Such feedback mechanisms have been experimentally implemented for laser control of chemical reactions (Rice & Zhao, 2000).

Nonlinear effects also emerge out of wave mechanics in the semiclassical limit, where the motion can be described in terms of classical orbits (solutions of nonlinear Hamiltonian equations). In the 1970s, starting from Schrödinger's equation, Gutzwiller derived a semiclassical trace formula that expresses the density of energy eigenvalues in terms of periodic orbits (Gutzwiller, 1990). The periodic orbits are unstable and proliferate exponentially in chaotic systems, where semiclassical quantization can be performed, thanks to the Gutzwiller trace formula as an alternative to the Bohr–Sommerfeld quantization rule.

In summary, nonlinear effects manifest themselves in quantum systems as phenomena emerging out of the linear wave mechanics in particular limits such as the semiclassical limit or the many-body limit at low temperature.

PIERRE GASPARD

See also **Bose–Einstein condensation; Hartree approximation; Nonlinear Schrödinger equations; Quantum chaos; Superconductivity; Superfluidity**

Further Reading

Bollinger, J.J., Heinzen, D.J., Itano, W.M., Gilbert, S.L., & Wineland, D.J. 1989. Test of the linearity of quantum mechanics by rf spectroscopy of the $^9Be^+$ ground state. *Physical Review Letters*, 63: 1031–1034

Dirac, P.A.M. 1930. *Principles of Quantum Mechanics*, Oxford: Clarendon Press

Gutzwiller, M.C. 1990. *Chaos in Classical and Quantum Mechanics*, New York: Springer

Majumder, P.K., Venema, B.J., Lamoreaux, S.K., Heckel, B.R. & Fortson, E.N. 1990. Test of the linearity of quantum mechanics in optically pumped ^{201}Hg. *Physical Review Letters*, 65: 2931–2934

Mohr, P.J. & Taylor, B.N. 2000. CODATA recommended values of the fundamental physical constants: 1998. *Reviews of Modern Physics*, 72: 351–495

Rice, S.A. & Zhao, M. 2000. *Optical Control of Molecular Dynamics*, New York: Wiley

Weinberg, S. 1989. Precision tests of quantum mechanics. *Physical Review Letters*, 62: 485–488; and references therein

QUASILINEAR ANALYSIS

Analytical methods in the present-day theory of nonlinear oscillations originated in the investigations by Henri Poincaré, George D. Birkhoff, and Aleksandr Lyapunov, who laid the mathematical foundations for this theory. However, it should be noted that direct application of these mathematical methods to oscillation theory as such did not occur till much later, primarily owing to the work of Alexander Andronov (Andronov et al., 1966).

An important contribution to the development of the quantitative theory of nonlinear oscillations, especially of the applied part, was made by Balthasar van der Pol (van der Pol, 1934), who studied the operation of an electronic generator and proposed his own investigative method, namely, the method of slowly time-varying amplitudes. A rigorous justification of this method was later given by Osip Mandelshtam and N. Papaleksi (Mandelshtam & Papaleksi, 1934).

Almost independently of Mandelshtam, Andronov, and other physicists, the mathematical groundwork for nonlinear oscillation theory was laid by Nikolai Krylov, Nikolai Bogolyubov, Yuri Mitropol'sky (Krylov & Bogolyubov, 1947; Bogolyubov, 1950; Bogolyubov & Mitropol'sky, 1961; Mitropol'sky, 1971), and their disciples. They worked out the most important methods for the analysis of quasilinear oscillations: the asymptotic method, the averaging method, and the method of equivalent linearization. The last can serve as a theoretical justification of the heuristic methods of harmonic balance and statistical linearization (Landa, 1980; Pervozvansky, 1962), which are well known in mechanical and electrical engineering. Indeed, in accordance with the method of equivalent linearization, for a nonlinear function $f(x)$, we substitute a linear function λx, where λ is determined from the condition of minimization of the mean-square error $\varepsilon = \overline{\left(f(x) - \lambda x\right)^2}$. Differentiating ε with respect to λ and equating the derivative to zero, we find

$$\lambda = \frac{\overline{f(x)x}}{\overline{x^2}}, \tag{1}$$

where over-line denote the averaging operation. Depending on the averaging technique, we obtain harmonic linearization (harmonic balance) or statistical linearization. The former takes place if we put $x = \cos \omega t$ and average the numerator and denominator of expression (1) over t for the period $T = 2\pi/\omega$. The latter takes place if we suppose x to be distributed according to a certain probability distribution (for example, Gaussian) and find the statistical average.

The van der Pol method, or the method of slowly time-varying amplitudes, is applicable to near-linear, near-conservative self-oscillatory systems. The method was suggested by van der Pol as applied to self-oscillatory systems with one degree of freedom. However, the method may be easily generalized to self-oscillatory systems with n degrees of freedom, which are described by equations of the form

$$\ddot{y}_k + \omega_k^2 y_k = \mu Y_k(t, y, \dot{y}) \quad (k = 1, 2, \ldots, n), \tag{2}$$

where μ is a small parameter, $\boldsymbol{y} = \{y_1, \ldots, y_n\}$, $\dot{\boldsymbol{y}} = \{\dot{y}_1, \ldots, \dot{y}_n\}$. For $\mu = 0$, Equations (2) are the equations of a linear oscillatory system with n degrees of freedom written in terms of normal coordinates.

As mentioned above, a rigorous justification of the van der Pol method was given by Mandelshtam and Papaleksi (Mandelshtam & Papaleksi, 1934). They showed that the truncated van der Pol equations can be found by averaging the initial equations over "fast time" for the period $T = 2\pi/\omega$. By doing so, Mandelshtam and Papaleksi pioneered the averaging method, the rigorous theory of which was worked out by Bogolyubov (1950) and developed by Mitropol'sky (1971). This theory concerns so-called equations in a standard form. By means of a certain change of variables, any equations describing oscillations in near-conservative systems can be reduced to equations in a standard form. More general theory is related to systems incorporating fast and slow variables (Volosov & Morgunov, 1971; Vasilyeva & Butuzov, 1990). In particular, this theory is used for analysis of relaxation oscillators (Mischenko & Rozov, 1975).

The asymptotic Krylov–Bogolyubov method is conceptually a generalization of the van der Pol method that allows us to calculate the higher approximations. The method has two modifications, depending on the form of the original equations and on the problem in question (Landa, 1980). If we are interested in the calculation of multi-frequency oscillations, we conveniently set the equations in the form of (2).

Provided we are interested in the calculation of single-frequency oscillations, we can set the original equations in the following form:

$$\dot{\boldsymbol{y}} + \mathcal{B}\boldsymbol{y} = \mu \boldsymbol{Y}(t, \boldsymbol{y}), \tag{3}$$

where $\boldsymbol{y}$ is a vector with n components, $\mathcal{B}$ is a square matrix with elements b_{jk}, μ is a small parameter, and $\boldsymbol{Y}(t, \boldsymbol{y})$ is a nonlinear vector function of time and of all components of the vector $\boldsymbol{y}$. We assume that for $\mu = 0$, Equations (3) describe a linear conservative system.

First, we consider the case when the original equations of a system are set in the form of (2). For $\mu \neq 0$, let us represent a solution of Equations (2) as a power series in μ:

$$\begin{aligned} y_k &= y_k^{(0)} + \mu u_{1k}(A, \psi, \mu t) \\ &\quad + \mu^2 u_{2k}(A, \psi, \mu t) + \cdots, \end{aligned} \tag{4}$$

where $y_k^{(0)} = A_k \cos \psi_k$, $\psi_k = \omega_k t + \varphi_k$, A_k and φ_k are slowly time-varying functions obeying the equations

$$\begin{aligned} \frac{\mathrm{d}A_k}{\mathrm{d}t} &= \mu f_{1k}(A, \varphi, \mu t) + \mu^2 f_{1k}(A, \varphi, \mu t) + \ldots, \\ \frac{\mathrm{d}\varphi_k}{\mathrm{d}t} &= \mu F_{1k}(A, \varphi, \mu t) + \mu^2 F_{1k}(A, \varphi, \mu t) + \ldots. \end{aligned} \tag{5}$$

Here $u_{1k}(A, \psi, \mu t)$, $u_{2k}(A, \psi, \mu t), \ldots$ and $f_{1k}(A, \psi, \mu t)$, $f_{2k}(A, \psi, \mu t), \ldots$, $F_{1k}(A, \psi, \mu t)$, $F_{2k}(A, \psi, \mu t), \ldots$ are unknown functions, which should be found.

Demanding the absence of resonant constituents in functions u_{1k}, we find the unknown functions f_{1k} and F_{1k}:

$$\begin{aligned} f_{1k} &= -\frac{1}{2\omega_k} X_{1k}(\mu t, A, \varphi), \\ F_{1k} &= -\frac{1}{2\omega_k A_k} Z_{1k}(\mu t, A, \varphi). \end{aligned} \tag{6}$$

Thus, we obtain the equations of the first approximation for the amplitudes and phases:

$$\begin{aligned} \frac{\mathrm{d}A_k}{\mathrm{d}t} &= -\frac{\mu}{2\omega_k} X_{1k}(\mu t, A, \varphi), \\ \frac{\mathrm{d}\varphi_k}{\mathrm{d}t} &= -\frac{\mu}{2\omega_k A_k} Z_{1k}(\mu t, A, \varphi). \end{aligned} \tag{7}$$

These equations coincide with those found by using the van der Pol method. The functions u_{1k} describe the higher harmonics and combination frequencies in the solution of the first approximation.

Using the next terms in the expansions found above, we can obtain the equations of the second and higher approximations.

Let us consider further the case when the original equations of a system are set in the form of (3) and we are interested in finding single-frequency oscillations described by

$$\boldsymbol{y} = A\left(\boldsymbol{V}\mathrm{e}^{\mathrm{i}(\omega t + \varphi)} + \text{c.c.}\right), \tag{8}$$

where ω is one of the system fundamental frequencies, $\boldsymbol{V}$ is the eigenvector of the matrix $\mathcal{B}$ corresponding to the frequency ω, and c.c. means the complex conjugate value.

Using the procedure of the method described, we obtain the equations for the unknown vector functions $\boldsymbol{k}_j$:

$$\begin{aligned} \omega \frac{\partial \boldsymbol{k}_1}{\partial \psi} + \mathcal{B}\boldsymbol{k}_1 &= -f_1\left(\boldsymbol{V}\mathrm{e}^{\mathrm{i}\psi} + \text{c.c.}\right) \\ &\quad -\mathrm{i}AF_1\left(\boldsymbol{V}\mathrm{e}^{\mathrm{i}\psi} - \text{c.c.}\right) + \boldsymbol{Y}_1, \ldots \end{aligned} \tag{9}$$

Let us further expand the vector functions $\boldsymbol{k}_1, \boldsymbol{k}_2, \ldots$, $\boldsymbol{Y}_1, \boldsymbol{Y}_2, \ldots$ into the Fourier series with slowly time-varying coefficients:

$$\begin{aligned} \boldsymbol{k}_j(A, \psi, \mu t) &= \sum_{k=-\infty}^{\infty} \boldsymbol{U}_j^{(k)}(A, \varphi, \mu t)\mathrm{e}^{\mathrm{i}k\psi}, \\ \boldsymbol{Y}_j(A, \psi, \mu t) &= \sum_{k=-\infty}^{\infty} \boldsymbol{Y}_j^{(k)}(A, \varphi, \mu t)\mathrm{e}^{\mathrm{i}k\psi}. \end{aligned} \tag{10}$$

Substituting (10) into (9) and equating the coefficients of the same harmonics, we obtain, for each j, a system of non-uniform equations for the components of the vector functions $\boldsymbol{U}_j^{(k)}$. For $k \neq 1$, the determinant of this system is nonzero, and, hence, all of $\boldsymbol{U}_j^{(k\neq 1)}$ can be determined uniquely. For $k = 1$, the system determinant is zero. In this case we should require, for all j, the fulfillment of the compatibility conditions $\mathcal{A}\boldsymbol{R}_j = 0$, where $\boldsymbol{R}_j$ is the right-hand side of the jth system and $\mathcal{A}$ is the adjoint matrix. These conditions allow us to find $f_1(A, \varphi, \mu t)$, $F_1(A, \varphi, \mu t)$, $f_2(A, \varphi, \mu t)$, $F_2(A, \varphi, \mu t), \ldots$.

Let us consider the first approximation. From (9) and (10) we obtain the following equation for the vector function $\boldsymbol{U}_1^{(k)}$:

$$(\mathrm{i}k\omega\mathcal{E} + \mathcal{B})\boldsymbol{U}_1^{(k)} = -(f_1 + \mathrm{i}AF_1)\delta_{k1}\boldsymbol{V} + \boldsymbol{Y}_1^{(k)}, \tag{11}$$

where $\mathcal{E}$ is an identity matrix and δ_{k1} is the Kronecker delta. For $k = 1$, the compatibility condition of system (11) is

$$-f_1\mathcal{A}\boldsymbol{V} - \mathrm{i}AF_1\mathcal{A}\boldsymbol{V} + \mathcal{A}\boldsymbol{Y}_1^{(1)} = 0. \tag{12}$$

Splitting the real part and the imaginary part in Equation (12) we find

$$\begin{aligned} f_1(A, \varphi, \mu t) &= \mathrm{Re}\left\{\frac{1}{\mathrm{Sp}\,\mathcal{A}} \sum_j \frac{A_{jj}}{V_j} Y_{1j}^{(1)}(A, \varphi, \mu t)\right\}, \\ F_1(A, \varphi, \mu t) &= \frac{1}{A}\,\mathrm{Im}\left\{\frac{1}{\mathrm{Sp}\,\mathcal{A}} \sum_j \frac{A_{jj}}{V_j} Y_{1j}^{(1)}(A, \varphi, \mu t)\right\}, \end{aligned} \tag{13}$$

where $\mathrm{Sp}\,\mathcal{A}$ is the spur of the matrix $\mathcal{A}$.

The second and higher approximations can be found in much the same way.

POLINA LANDA

See also **Averaging methods; Distributed oscillators; Linearization; Perturbation theory; Relaxation oscillators**

Further Reading

Andronov, A.A., Vitt, A.A. & Khaykin, S.E. 1966. *Theory of Oscillations*, Oxford and New York: Pergamon Press (original Russian edition 1959)

Bogolyubov, N.N. 1950. *Teoriya Vozmuscheniy v Nelineynoy Mechanike [Perturbation Theory in Nonlinear Mechanics]*. Sbornik Instituta Stroitel'noy Mekhaniki AN USSR, No 14, 9–34

Bogolyubov, N.N. & Mitropol'sky, Yu.A. 1961. *Asymptotic Methods in the Theory of Nonlinear Oscillations*, New York: Gordon and Breach

Krylov, N.M. & Bogolyubov, N.N. 1947. *Introduction to Nonlinear Mechanics*, Princeton, NJ: Princeton University Press (original Russian edition 1937)

Landa, P.S. 1980. *Avtokolebaniya in Systemakh s Konechnym Chislom Stepeney Svobody [Self-Oscillations in Systems with a Finite Number of Degree of Freedom]*, Moscow: Science

Mandelshtam, L.I. & Papaleksi, N.D. 1934. Obosnovanie metoda priblizhennogo resheniya differentsial'nykh uravneniy [On justification of a method of approximate solving differential equations]. *ZhETF* 4: 117–121

Mischenko, E.F. & Rozov, N.Kh. 1975. *Differentsial'nye Uravneniya s Malym Parametrom i Relaksatsionnye Kolebaniya* [*Differential Equations with a Small Parameter and Relaxation Oscillations*], Moscow: Science

Mitropol'sky, Yu.A. 1971. *Metod Usredneniya v Nelineynoy Mechanike* [*The Averaging Method in Nonlinear Mechanics*], Kiev: Naukova Dumka

Pervozvansky, A.A. 1962. *Sluchaynye Processy v Nelineynykh Upravlyaemykh Sistemakh* [*Random Processes in Nonlinear Control Systems*], Moscow: Fizmatgiz

van der Pol, B. 1934. The nonlinear theory of electric oscillations. *Proceedings of IRE*, 22:1051–1086

Vasilyeva, A.B. & Butuzov, V.F. 1990. *Asimptoticheskie Metody v Teorii Singulyarnykh Vozmuscheniy [Asymptotic Methods in the Theory of Singular Perturbations*, Moscow: High School

Volosov, V.M. & Morgunov, B.I. 1971. *Metod Usredneniya v Teorii Nelineynykh Kolebatel'nykh Sistem [The Averaging Method in the Theory of Nonlinear Oscillatory Systems]*, Moscow: MSU Publ

QUASIPERIODICITY

The term *quasi-periodicity* implies a type of motion that is regular (nonchaotic) but consists of a combination of periodic motions with a trajectory that—after sufficient time—passes arbitrarily close to an earlier value.

For flow systems, a trajectory $x(t) \in \mathbf{R}^n$ is called k-quasi-periodic if it can be written in the form

$$x(t) = f(\omega_1 t, \ldots, \omega_k t).$$

Here f is a smooth nonlinear function of period 2π in each of its k arguments separately. The function f belongs to a class of almost periodic functions

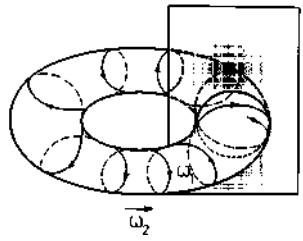

Figure 1. Schematic diagram of motion on the T^2 (two-dimensional) torus and the Poincaré cross section.

if frequencies $\omega_1, \ldots, \omega_k$ are not rationally related (are incommensurate); that is, $\sum_1^k l_i \omega_i \neq 0$ when $l_1, \ldots, l_k \in \mathbf{Z}$ and $\sum_1^k |l_i| > 0$ (Levitan & Zhikov, 1982). In other words, the ratio between two frequencies ω_i and ω_j, $i \neq j$ is irrational:

$$\frac{\omega_i}{\omega_j} \neq \frac{p}{q}, \quad p \in \mathbf{Z}, \quad q \in \mathbf{Z}. \tag{1}$$

A quasi-periodic trajectory lies on a k-dimensional torus (T^k), which can be an attractor, a repeller, or a saddle of a dynamic system. The term *quasi-periodicity* describes motion on the 2-dimensional torus (T^2) whereas *k-quasi-periodicity* is used for motion on tori of larger dimension. A two-dimensional closed surface in phase space corresponds to the two-dimensional torus T^2, and asymptotically (as $t \to \infty$), the trajectory covers its entire surface.

To describe quasi-periodic motion, it is convenient to use a Poincaré cross section (Figure 1) or a map. The T^2 torus is given by a closed invariant curve in Poincaré cross section. Maps are widely used in practice to investigate the properties of quasi-periodic motion. A typical map that serves for this purpose, as well as for investigation of the transition from quasi-periodicity to chaos, is the circle map:

$$\theta_{n+1} = \theta_n + \Omega - \frac{K}{2\pi} \sin 2\pi\theta_n, \quad \text{mod } 1. \tag{2}$$

Here θ is a phase angle defined in the interval [0; 1], while $\Omega \in [0; 1]$ and $K \geq 0$ are parameters of the map. Map (2) for $K < 1$ describes the dynamics of a non-autonomous self-oscillating system, for example, the van der Pol oscillator under external periodic forcing. The variable θ in this case represents the phase difference between the self-oscillations and the external force, the parameter Ω corresponds to the mismatch between the forcing frequency and the natural frequency of the oscillator, and the parameter K corresponds to the forcing amplitude.

A number of problems arise during numerical simulations and experimental investigations of attractors in quasi-periodic systems. First, it is impossible to

simulate an irrational ratio in Equation (1) because each number stored in a computer is limited to a finite set of digits. Second, as a consequence of the measurement error in experimental investigations, it is, in practice, impossible to determinate reliably whether a frequency ratio is rational or irrational. Third, because the presence of noise in real systems leads to a smearing of the system's characteristics, it is possible to interpret experimental results wrongly. Thus, if a calculated invariant curve in a Poincaré cross section is smeared (has a finite width), then a noisy quasi-periodic motion can become entangled with chaos.

To obtain reliable information about the type of motion, it is necessary to use a set of characteristics such as the spectrum of Lyapunov exponents (SLE), a power spectrum, an autocorrelation function (ACF), or the smoothness of the invariant curve in the Poincaré cross section. In quasi-periodic motion, the SLE has no positive values, and the number of zeros is equal to the number of incommensurate base frequencies defined by the quasi-periodic motion. For example, the T^2 torus of a dissipative system is characterized by two Lyapunov exponents that are zero and others that are negative. The SLE of chaotic behavior includes at least one positive value. The power spectrum of quasi-periodic motion is discrete and consists of peaks at frequencies $n\omega_1 \pm m\omega_2$, with n and m taking arbitrary integer values. In reality, the peaks need not be mathematically sharp, but can be instrumentally sharp. The spectrum of a chaotic motion, on the other hand, is continuous and consists of an infinite number of base functions and their combinations. The ACF of a trajectory on a torus is an infinitely oscillating function that does not fall to zero as $t \to \infty$; in contrast, the ACF of a chaotic trajectory tends to zero as $t \to \infty$. In Poincaré cross section, a smooth curve corresponds to a torus, whereas a chaotic regime is characterized by a fractal structure.

Quasi-periodic motion can be observed in conservative and dissipative systems characterized by two or more incommensurate frequencies generated by the system and/or external sources (Glazier & Libchaber, 1988). The transition from a stationary state to quasi-periodic motion is realized as the result of at least two consecutive Hopf bifurcations, which add two incommensurate frequencies to the system, hence giving rise to a T^2 torus. Further Hopf bifurcations lead to a torus of larger dimension. Landau (1965) conjectured that turbulence arises through an infinite series of such Hopf bifurcations, increasing the degree of quasi-periodicity step-by-step up to infinity.

The possibility of such a scenario is problematic because the Kolmogorov–Arnol'd–Moser (KAM) theorem and the results of Newhouse et al. (1979) show that T^k tori can be structurally unstable when $k \geq 3$. This instability is found to increase with nonlinearity, which can lead to synchronization if an irrational frequency ratio becomes rational, or can transform a low-dimensional torus to chaos. However, there are also models (Ott, 2002) and experiments (Gollub & Benson, 1980), which prove that the tori T^k still exist for $k \geq 3$. The flow of blood through the cardiovascular system seems to be an example of dynamics characterized by a hypertorus, with $k \geq 3$ (Stefanovska & Bračič, 1999).

Several scenarios of transition from quasi-periodicity to chaos are known. The transition from T^2 to a strange chaotic attractor has been thoroughly investigated (Afraimovich & Shilnikov, 1991; Anishchenko et al., 2002). First, the torus loses smoothness, and then stable and saddle resonances (cycles corresponding to a rational frequency ratio) arise on the torus. Nonlocal bifurcations (homoclinic tangencies of manifolds) of these saddles lead to chaos later on.

A similar scenario is also observed for the T^3 torus (Anishchenko et al., 2002). The occurrence of torus doublings can precede the appearance of resonances on the torus: a finite number of bifurcations occur, after which the torus is destroyed as described above. The possible reality of an infinite series of torus doubling bifurcations (the Feigenbaum scenario of the transition to chaos) remains an open question, although renormalization group analysis (Feigenbaum et al., 1982) allows such a possibility theoretically.

Newhouse et al. (1979) have shown that small perturbations of the T^3 torus can lead to a strange chaotic attractor on the torus. Bifurcations, which lead from the torus to chaos, have not yet been studied in detail, but investigations indicate that the transition is connected with the appearance and destruction of resonances on the torus. Furthermore, the transition from T^3 to chaos has been observed only in maps, and the possibility of its realization in flow systems remains unclear.

A third scenario is the transition from quasi-periodicity to a nonstrange chaotic attractor (Arnol'd, 1983). If a chaotic attractor on T^3 covers all the surface of the torus, then the capacity of the attractor is integer and the largest Lyapunov exponent is positive.

Another way in which the transition from quasi-periodicity to chaos can occur is through the appearance of a strange nonchaotic attractor (SNA), which has a fractal structure and no positive values in the SLE (Grebogi et al., 1984). Such an evolution is observed in systems under external quasi-periodic forcing that drives the system with an irrational frequency ratio, which does not depend on parameters and properties of the system itself. The bifurcation mechanisms involved in the transition from torus to SNA, and the subsequent transition from SNA to chaos, are subjects of active investigation.

IGOR A. KHOVANOV, NATALYA A. KHOVANOVA, AND ANETA STEFANOVSKA

See also **Attractors; Bifurcations; Cat map; Kolmogorov–Arnol'd–Moser theorem; Lyapunov exponents; One-dimensional maps; Period doubling;**

Phase space; Recurrence; Routes to chaos; Synchronization

Further Reading

Afraimovich, V.S. & Shilnikov, L.P. 1991. Invariant two-dimensional tori, their breakdown and stochasticity. In *American Mathematical Society Translations*, Series 2, 149: 201–212 (original Russian edition 1983)

Anishchenko, V.S. et al. 2002. *Nonlinear Dynamics of Chaotic and Stochastic Systems: Tutorial and Modern Developments*, Berlin and New York: Springer

Arnol'd, V.I. 1983. *Geometrical methods in the Theory of Ordinary Differential Equations*, New York: Springer (original Russian edition 1978)

Feigenbaum, M.J., Kadanoff, L.P & Shenker, S.J. 1982. Quasiperiodicity in dissipative systems: a renormalization group analysis. *Physica* D, 5: 370–386

Glazier, J.A. & Libchaber A. 1988. Quasi-periodicity and dynamical systems: an experimentalist's view. *IEEE Transactions of Circuits and Systems*, 35: 790–318

Gollub, J.P. & Benson, S.M. 1980. Many routes to turbulent convection. *Journal of Fluid Mechanics*, 100: 449–470

Grebogi, C., Ott, E., Pelikan, S. & Yorke, J.A. 1984. Strange attractors that are non chaotic. *Phisica* D, 13: 261–268

Landau, L.D. 1965. On the problem turbulence. In *Collected Papers*, edited by D. ter Haar, Oxford: Pergamon (original Russian edition 1944)

Levitan, B.M. & Zhikov, V.V. 1982. *Almost Periodic Functions and Differential Equations*, Cambridge: Cambridge University Press (original Russian edition 1978)

Newhouse, S., Ruelle, D. & Takens, F. 1979. Occurence of strange Axiom A attractors near quasi-periodic flows on T^m, $m \geq 3$. *Communications in Mathematical Physics*, 64: 35–40

Ott, E. 2002. *Chaos in Dynamical Systems*, 2nd edition, Cambridge and New York: Cambridge University Press

Stefanovska, A. & Bračič, M. 1999. Physics of the human cardiovascular system. *Contemporary Physics*, 40: 31–55

R

RAMAN SOLITONS

See **Rayleigh and Raman scattering and IR absorption**

RANDOM MATRIX THEORY I: ORIGINS AND PHYSICAL APPLICATIONS

The textbook examples of quantum systems typically have a complete set of quantum numbers. For hydrogen-like atoms in a weak magnetic field, the set of radial, angular, and magnetic quantum numbers, together perhaps with the spin state, uniquely determines the energy levels of the atom. Nuclear physicists were among the first to encounter a situation where this is not possible. Scattering protons and neutrons off nuclei revealed a huge number of resonances that could no longer be completely labelled by their quantum numbers. In view of this fact and the uncertainty in the detailed interaction between the neutrons, Eugene Wigner advanced a statistical approach to the observed spectra: instead of trying to characterize each resonance individually, he proposed to look for a statistical description of their distribution and their strengths (see Wigner (1967) for an account of the early developments). Typical quantities of interest are then the mean density of resonances, probabilities for their spacings, the two- or more point correlation functions, and the distribution of transition strengths. The Hamiltonian was modeled as a random matrix, and by ingenious mathematical techniques a complete characterization of the spectral properties of certain ensembles of random matrices could be achieved. Wigner's John von Neumann lecture (Wigner, 1967), and the books by Mehta (1991) and Porter (1965) survey many of the results and methods. These sources also contain references to work in mathematics before the widespread use of random matrices in physics.

The most important ensembles are the Gaussian ones. Consider ensembles of $N \times N$ matrices H with statistically independent real or complex entries and a distribution function

$$P_N(H_{11}, H_{12}, \ldots, H_{NN}) = \prod_{i,j} p_{ij}(H_{ij}). \tag{1}$$

It is natural to demand invariance of the distribution under transformation of bases, since none of them can be singled out a priori. If the allowed transformations are orthogonal, unitary, or symplectic, the Gaussian orthogonal ensemble (GOE), Gaussian unitary ensemble (GUE), or the Gaussian symplectic ensemble (GSE) is obtained, respectively. The distribution functions are

$$P_{N,\beta} = \left(\frac{\beta}{2\pi}\right)^{N/2} \left(\frac{\beta}{\pi}\right)^{\beta N(N-1)/2} \exp\left(-\frac{\beta}{2}\mathrm{tr}\, H^2\right) \tag{2}$$

with the parameters $\beta = 1$ for GOE, $\beta = 2$ for GUE, and $\beta = 4$ for GSE.

Of the many quantities that can be studied and for which in many cases exact results can be obtained, we list only two: the level spacing distribution and the number variance (Figure 1). For others, see Brody et al. (1981), Guhr et al. (1998), Haake (2001), Mehta (1967), and Stöckmann (1999).

The level spacing distribution is the probability density to find two neighboring levels a distance s apart (in units of the mean level spacing). The expression that results from the random matrix ensembles is somewhat involved, but a very good approximation was given by Wigner:

$$P_{\mathrm{GOE}} = \frac{\pi}{2} s \mathrm{e}^{-(\pi/4)s^2}, \tag{3}$$

$$P_{\mathrm{GUE}} = \frac{32}{\pi^2} s^2 \mathrm{e}^{-(4/\pi)s^2}, \tag{4}$$

$$P_{\mathrm{GSE}} = \frac{2^{18}}{3^6\pi^3} s^4 \mathrm{e}^{-(64/9\pi)s^2}. \tag{5}$$

The characteristic feature of these expression is that for small s the distribution increases like s^β, so that small spacings are suppressed.

The number variance measures the deviation between the true and the expected number of eigenvalues in an interval. In units of the mean spacing

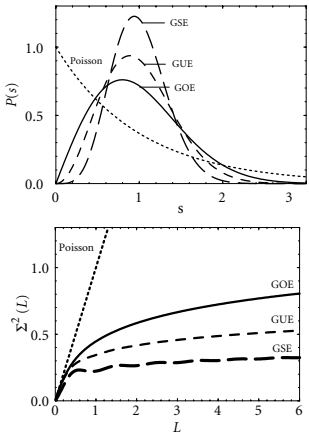

Figure 1. Level spacing distribution and number variance for the different ensembles.

the expected number equals the length L of the interval, and with $N(L)$ the true number, variance is

$$\Sigma^2(L) = \langle (N(L) - L)^2 \rangle = \langle (N(L))^2 \rangle - L^2 . \quad (6)$$

In a Poisson process for uncorrelated levels, the number variance will increase linearly, $\Sigma^2(L) = L$. In the random matrix ensembles, the increase is slower,

$$\Sigma^2(L) \sim \frac{2}{\beta\pi^2} \ln L + c_\beta \quad (7)$$

with constants c_β (for complete expressions, see, for example, Brody et al. (1981)). The slow logarithmic increase reflects the interactions between levels.

Between about 1975 and the mid-1980s, Michael Berry, Oriol Bohigas, and others applied such statistical measures to systems with a chaotic classical limit and observed level distributions and correlators in agreement with random matrix theory. They conjectured that chaotic systems will show random matrix behavior consistent with the global real symmetric, complex Hermitian, or symplectic symmetry of the Hamiltonian. The eigenvalue distribution for integrable systems, as shown earlier by Berry and Tabor, should show Poissonian statistics (Haake, 2001; Stöckmann, 1999). The argument for the two situations is roughly as follows: if the classical system is integrable, the quantum eigenstates are localized on tori and the energies can be approximated by Bohr–Sommerfeld quantization of the appropriate actions. Different tori give independent sequences of quantum eigenvalues, so that the collection of eigenvalues reflects a random appearance of eigenvalues, without correlations. As a result, the distribution of mean level spacings becomes exponential. In a chaotic system the eigenstates are spread over the connected chaotic components. They thus have the same support, but since they have to be orthogonal, they have to interact. This interaction then leads to level repulsion and the observed suppression of small spacings in $P(s)$. The conjecture is supported by semiclassical arguments for the two-point correlation function (Berry, 1985) and a large body of empirical evidence from experimental data for nuclei, atoms, and molecules and from numerical data for various systems (Stöckmann, 1999). The few exceptions (as, for instance, the arithmetical billiards on surfaces of negative curvature (Bogomolny et al., 1997)) have led to clarifications of the necessary requirements. But so far no proof has emerged, neither for integrable nor for chaotic systems.

The connection between random matrices and the chaotic behavior of the underlying wave behavior indicates why random matrix statistics should also appear in many nonquantum situations. Indeed, acoustic resonances in irregularly shaped containers, electromagnetic resonances in cavities, and mechanical vibrations of plates and other solid blocks all show statistical properties in good agreement with random matrix theory expectations when the short wavelength dynamics of wave fronts is chaotic (Stöckmann, 1999).

The statistical measures developed within random matrix theory have propagated into other fields as well, most notably into the theory of the Riemann zeta function. The Riemann zeta function as defined by

$$\zeta_R(s) = \sum_{n=1}^{\infty} n^{-s} \quad (8)$$

can be analytically continued into the complex plane. It then has a pole at $s = 1$ and so-called trivial zeroes at $s = -2, -4, \ldots$. Bernhard Riemann's long-standing conjecture is that all its other zeroes lie along the line $s = \frac{1}{2} + it$. David Hilbert proposed to identify an eigenvalue problem that has these zeroes as eigenvalues. While that system is still elusive, analysis of the statistics suggests that it belongs to the universality class of the Gaussian unitary ensemble (see Berry & Keating (2000) for an account of the fascinating relations between random matrix theory, primes, and the statistics of the Riemann zeroes).

While all previous examples dealt with individual systems having a fixed Hamiltonian, one can also consider disordered systems, where as an additional statistical element, certain variations in the Hamiltonian enter. For instance, in a solid the mean density of impurities can be controlled experimentally, but the detailed positions and their effects on a specific experiment are difficult to fix. It is then possible to again set up random matrix models and to derive measurable quantities that are universal in that they depend on the global symmetry of the system only, see Beenakker (1997), Guhr et al. (1998), and Efetov (1997).

Through the connection to disordered systems, techniques from field theory, Grassmann algebras, and supersymmetry entered random matrix theory (Zirnbauer, 1996). Those tools allow analytical calculations of many quantities both in the extreme quantum limit and in the semiclassical limit. More importantly, they have indicated a link to group theory and homogeneous spaces. The classification into three universality classes (GOE, GUE, and GSE) above has to be extended to a total of 10 cases. The realizations of the other cases require additional symmetries. Three cases can be found by extending the three classical ensembles to Dirac Hamiltonians with a particle-hole symmetry. Examples for the remaining four can be found in certain normal-superconducting systems.

As suggested in the introduction to Guhr et al. (1998), the field of random matrices has opened up a new class of stochastic systems with a wide range of applications in physics and elsewhere and with intriguing mathematical connections. The unifying feature is that stochasticity combined with general symmetries leads to universal laws not based on dynamical principles. Indications are that it can also play a role in the analysis of financial data, in wireless communications, or in extracting correlations in neural signals (see, e.g., Forrester et al., 2003).

BRUNO ECKHARDT

See also **Free probability theory; Periodic orbit theory; Quantum chaos**

Further Reading

Beenakker, C.W.J. 1997. Random-matrix theory of quantum transport. *Reviews of Modern Physics*, 69: 713–808

Berry, M.V. 1985. Semiclassical theory of spectral rigidity. *Proceedings Royal Society of London* A, 400: 229–251

Berry, M.V. & Keating, J.P. 2000. The Riemann zeroes and eigenvalue asymptotics. *SIAM Review*, 41: 236–266

Bogomolny, E.B., Georgeot, B., Giannoni, M.J. & Schmit, C. 1997. Arithmetical chaos. *Physics Reports*, 291: 219–324

Brody, T.A., Floris, T., French, J.B., Mello, P.A., Pandey, A. & Wong, S.S.M. 1981. Random-matrix physics: spectrum and strength fluctuations. *Reviews of Modern Physics*, 53: 385–479

Efetov, K.B. 1997. *Supersymmetry in Disorder and Chaos*, Cambridge and New York: Cambridge University Press

Forrester, P.J., Snaith, N.C. & Verbaarschot, J.J.M. (editors). 2003. Special issue: random matrix theory. *Journal of Physics* A, 36: R1–R10 and 2859–3645

Guhr, T., Müller-Groeling, A. & Weidenmüller, H.A. 1998. Random-matrix theories in quantum physics: common concepts. *Physics Reports*, 299: 190–425

Haake, F. 2001. *Quantum Signatures of Chaos*, 2nd edition, Berlin and New York: Springer

Mehta, M.L. 1967. *Random Matrices and the Statistical Theory of Energy Levels*, New York: Academic Press

Porter, C.E. (editor). 1965. *Statistical Theory of Spectra*, New York: Academic Press

Stöckmann, H.J. 1999. *Quantum Chaos: An Introduction*, Cambridge and New York: Cambridge University Press

Wigner, E.P. 1967. Random matrices in physics. *SIAM Review*, 9: 1–23

Zirnbauer, M.R. 1996. Riemannian symmetric superspaces and their origin in random-matrix theory. *Journal of Mathematical Physics*, 37: 4986–5018

RANDOM MATRIX THEORY II: ALGEBRAIC DEVELOPMENTS

It was hypothesized by Eugene Wigner in the 1950s that the highly excited states of complex nuclei would have the same statistical properties as the eigenvalues of a large random real symmetric matrix. In pure mathematics, one finds a random matrix hypothesis in the theory of the celebrated Riemann hypothesis. Thus the Montgomery–Odlyzko law states that the statistics of the large zeros of the Riemann zeta function on the critical line (Riemann zeros) coincide with the statistics of the eigenvalues of a large complex Hermitian matrix. To test such hypotheses (for definiteness, the Montgomery–Odlyzko law), one computes a large sequence of consecutive Riemann zeros, scales the sequence so that locally the mean spacing is unity, and then empirically computes statistical quantities. A typical example of the latter is the distribution of the spacing between consecutive zeros. This must be compared against the same statistical quantity for the eigenvalues of large random complex Hermitian matrices. How then does one compute the eigenvalue spacing distribution for random matrices?

Hermitian random matrices with real, complex, and quaternion real Gaussian elements form matrix ensembles referred to as the Gaussian orthogonal ensemble (GOE) ($\beta = 1$), the Gaussian unitary ensemble (GUE) ($\beta = 2$), and the Gaussian symplectic ensemble (GSE) ($\beta = 4$), respectively, where β is a convenient label. Consider the bulk eigenvalues of such large matrices, scaled to have unit density. Denote by $p_\beta(k; s)$ the probability density that there are exactly k eigenvalues in between two eigenvalues of spacing s, and denote by $E_\beta(k; s)$ the probability that there are exactly k eigenvalues in an interval of size s. Define the generating functions $p_\beta(s; \xi) = \sum_{k=0}^{\infty}(1-\xi)^k p_\beta(k; s)$ and $E_\beta(s; \xi) = \sum_{k=0}^{\infty}(1-\xi)^k E_\beta(k; s)$. Note from the definitions that these quantities are related by $p_\beta(s; \xi) = \frac{1}{\xi^2}\frac{\mathrm{d}^2}{\mathrm{d}s^2}E_\beta(s; \xi)$.

Gaudin observed that the determinantal form of the correlations in the case $\beta = 2$ allows $E_2(s; \xi)$ to be written as a Fredholm determinant,

$$\begin{aligned} E_2(s; \xi) &= \det(1 - \xi K_2) \\ &= \det(1 - \xi K_2^+)\det(1 - \xi K_2^-), \end{aligned} \quad (1)$$

where K_2, $K_2^\pm$ are integral operators on $(0, s)$ with kernels

$$\frac{\sin \pi(x - y)}{\pi(x - y)},$$

and

$$\frac{1}{2}\left[\frac{\sin\pi(x-y)}{\pi(x-y)} \pm \frac{\sin\pi(x+y)}{\pi(x+y)}\right],$$

respectively. The second equality is noted in (1) because both factors therein are related to E_1. Thus, with $E_1(-1;s)=0$, define

$$E_1^{\pm}(s;\xi) = \sum_{n=0}^{\infty}(1-\xi)^n\Big(E_1(2n;s)+E_1(2n\mp 1;s)\Big).$$

Then an inter-relationship between large GOE and large GUE matrices due to Dyson implies

$$E_2(s;\xi) = E_1^{+}(s;\xi)E_1^{-}(s;\xi).$$

This factorization turns out to be the same as in (1), so one obtains Mehta's result

$$E_1^{\pm}(s;\xi) = \det(1-\xi K_2^{\pm}).$$

For the case $\beta=4$, one uses Mehta's and Dyson's inter-relationship between large GSE matrices and large GOE matrices to conclude

$$E_4(n;s) = E_1(2n;2s)+\tfrac{1}{2}\Big(E_1(2n-1;2s)+E_1(2n+1;2s)\Big).$$

A new line of study of E_β was initiated by Jimbo, Miwa, Môri, and Sato in 1980, which related the Fredholm determinant in (1) to integrable systems theory, resulting in the formula

$$E_2(s;\xi) = \exp\int_0^{\pi s}\sigma(t;\xi)\,\frac{\mathrm{d}t}{t},$$

where σ satisfies a particular example of the σ-form of the Painlevé V equation,

$$(s\sigma'')^2 + 4(s\sigma'-\sigma)\Big(s\sigma'-\sigma+(\sigma')^2\Big) = 0,$$
$$\sigma(s;\xi) \underset{s\to 0}{\sim} -\frac{\xi s}{\pi} - \left(\frac{\xi s}{\pi}\right)^2.$$

The quantities $E_1^{\pm}$ can also be expressed in terms of Painlevé transcendents. Thus, combining results of the present author with results of Tracy and Widom, one has

$$E_1^{\pm}(s;\xi) = \exp\int_0^{(\pi s/2)^2} v(t;\xi;a)\,\frac{\mathrm{d}t}{t}\Big|_{a=\pm 1/2},$$

where $v(t;\xi;a)$ satisfies a particular example of the σ-form of the Painlevé III$'$ equation

$$(tv'')^2 - a^2(v')^2 - v'(4v'+1)(v-tv') = 0,$$
$$v(t;;\xi;a) \underset{t\to 0^+}{\sim} -\frac{\xi t^{a+1}}{2^{2a+2}\Gamma(a+1)\Gamma(a+2)}.$$

Another bulk spacing distribution with a Painlevé type evaluation is the nearest-neighbor spacing between eigenvalues (i.e., the minimum of the distances to the left neighbor and the right neighbor) for large GUE matrices, $nn(t)$ say. Forrester and Odlyzko (1996) have shown that

$$nn(t) = -\frac{y(2\pi t;a)}{t}\exp\int_0^{\pi t}\frac{y(2s;a)}{s}\,\mathrm{d}s\Big|_{a=1},$$

where $y(s;a)$ satisfies the differential equation

$$(sy'')^2 + 4(-a^2+sy'-y)\Big((y')^2-\{a-(a^2-sy'+y)^{1/2}\}^2\Big) = 0$$

subject to the boundary condition

$$y(s;a) \underset{s\to 0^+}{\sim} -\frac{2(s/4)^{2a+1}}{\Gamma(1/2+a)\Gamma(3/2+a)}.$$

Comparison of a plot of this statistic, obtained from the formula in Forrester and Odlyzko (1996), against the same statistic computed, empirically for large sequences of Riemann zeros starting at three different positions along the critical line is given in Figure 1.

P.J. Forrester

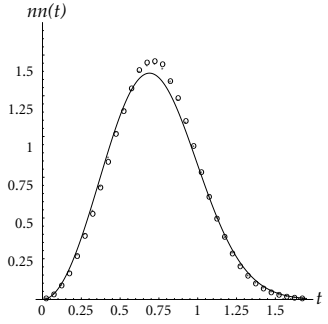

Figure 1. Comparison of $nn(t)$ for the GUE (continuous curve) and for 10^6 consecutive Riemann zeros, starting near zero number 1 (open circles), 10^6 (asterisks), and 10^{20} (filled circles).

See also **Random matrix theory I, III, IV**

Further Reading

Forrester, P.J. Eigenvalue probabilities and Painlevé theory, Chapter 6 of *Log-gases and random matrices*, www.ms.unimelb.edu.au/~matpjf/matpjf.html

Forrester, P.J. & Odlyzko, A.M. 1996. Gaussian unitary ensemble eigenvalues and Riemann ζ function zeros: a non-linear equation for a new statistic, *Physical Review* E, 54: R4493–R4495

Tracy, C.A. & Widom, H. 1993. Introduction to random matrices. In *Geometric and Quantum Aspects of Integrable Systems*, edited by G.F. Helminck, New York: Springer, pp. 407–424

van Moerbeke, P. 2001. Integrable lattices: random matrices and random permutations. In *Random Matrices and Their Applications*, edited by P. Bleher & A. Its, Cambridge and New York: Cambridge University Press, pp. 321–406

RANDOM MATRIX THEORY III: COMBINATORICS

As the two previous entries show, random matrix theory (RMT) is a field of research devoted to the statistical analysis of the eigenvalues of matrices selected at random from a given set of matrices (Mehta, 1991). Recently there have been surprising discoveries that connect RMT to a branch of mathematics called combinatorics.

One fundamental topic within combinatorics is the study of permutations. A permutation is a rearrangement of the elements of a set. The set is usually finite, in which case it may be taken to be the first n positive integers, and a permutation may also be represented as a one-to-one invertible mapping from $\{1, 2, \ldots, n\}$ into itself. For each positive integer n, the number of permutations of length n is $n!$. If permutations of length n are selected at random, and each permutation is equally likely, then the probability of selecting a particular permutation is $1/n!$. In thinking about permutations probabilistically, researchers have discovered new connections to random matrix theory.

Random Matrix Theory: Gaussian Unitary Ensemble

The Gaussian unitary ensemble (GUE) is a fundamental example of a RMT. The collection of matrices is all Hermitian (self-adjoint, complex) matrices of size n. The diagonal matrix entries M_{jj}, $j = 1, 2, \ldots, n$, are independent normal random variables; that is, each has probability measure $\frac{1}{\sqrt{2\pi}} \mathrm{e}^{-m^2/2}\, \mathrm{d}m$. The off-diagonal matrix entries $M_{jk} = M_{jk}^{(\mathrm{R})} + \mathrm{i} M_{jk}^{(\mathrm{I})}$, $1 \le j \ne k \le n$, are complex, and $\left\{ M_{jk}^{(\mathrm{R})}, M_{jk}^{(\mathrm{I})} \right\}_{1 \le j < k \le n}$ is a collection of independent identically distributed Gaussian random variables with probability measure $\frac{1}{\sqrt{\pi}} \mathrm{e}^{-m^2}\, \mathrm{d}m$. The matrix entries below the diagonal are determined by the entries above the diagonal because the matrices satisfy the self-adjointness criterion $M^* = M$, where $(M^*)_{jk} = \overline{M_{jk}}$ and $\overline{(\cdot)}$ represents the complex conjugate of $(\cdot)$. Thus, the GUE of random matrices is merely a probability measure defined on the standard Euclidean space of dimension n^2. In standard probability terminology, the probability of finding a matrix in an "infinitesimal volume element" of matrices centered at a given matrix $M = (M_{jk})_{1 \le j,k \le n}$ is

$$\frac{1}{2^n \pi^{n^2}} \mathrm{e}^{-\frac{1}{2}\sum_{j=1}^{n} M_{jj}^2 - \sum_{j=1}^{n-1}\sum_{k=j+1}^{n} (M_{jk}^{(\mathrm{R})})^2 + (M_{jk}^{(\mathrm{I})})^2} \times \prod_{1}^{n} \mathrm{d}M_{jj} \prod_{1 \le j < k \le n} \mathrm{d}M_{jk}^{\mathrm{R}}\, \mathrm{d}M_{jk}^{\mathrm{I}}.$$

This is often more conveniently written in the form

$$\frac{1}{Z_n} \mathrm{e}^{-\frac{1}{2}\mathrm{Tr}(M^2)}\, \mathrm{d}M, \tag{1}$$

where $Z_n = 2^n \pi^{n^2}$, $\mathrm{d}M = \prod \mathrm{d}M_{jj} \prod \mathrm{d}M_{jk}^{(I)}\, \mathrm{d}M_{jk}^{(\mathrm{R})}$, and $\mathrm{Tr}(A)$ represents the trace of the matrix A, $\mathrm{Tr}(A) = \sum_{j=1}^{n} A_{jj}$.

This is just one example of an RMT. For example, one may replace $\mathrm{Tr}(M^2)$ in (1) by $\mathrm{Tr}(M^r)$, or $\mathrm{Tr}(V(M))$ for any reasonable function $V : \mathbb{R} \to \mathbb{R}$.

The eigenvalues $\lambda_1 \le \lambda_2 \le \ldots \le \lambda_n$ of a matrix M selected at random according to (1) are fundamental random variables, and quite a lot is known about their statistical properties. One example is the largest eigenvalue λ_N. Because of many different applications, their statistical behavior is particularly interesting when n goes to ∞. This random variable's behavior when $n \to \infty$ is as follows:

$$\lim_{n \to \infty} \mathrm{Prob}\left(\lambda_n < \sqrt{2n} + \frac{s}{\sqrt{2} n^{1/6}} \right) = F(s),$$

where

$$F(s) = \exp\left(-\int_s^{\infty} (x - s)^2 q(x) \mathrm{d}x \right) \tag{2}$$

and q is the unique solution to the Painlevé II equation

$$q'' = sq + 2q^3$$

satisfying the condition

$$q(s) \sim \mathrm{Ai}(s) \quad \text{as } s \to \infty.$$

This result is due to Craig Tracy and Harold Widom (1994), and the function F is often referred to as the Tracy–Widom distribution. Surprisingly, the Painlevé equation appears in a fundamental way in random matrix theory. It also appears, in an equally fundamental way, in combinatorics.

Increasing Subsequences of Permutations

A permutation, or an invertible mapping from the set $\{1, 2, \ldots, n\}$ to itself may be represented as a sequence of numbers. For example, the sequence 3,1,2 represents the permutation $\sigma(1) = 3$, $\sigma(2) = 1$, $\sigma(3) = 2$. An increasing subsequence of a permutation is obtained by representing a permutation as a sequence, and then selecting a subsequence in which the elements are increasing. For example, the sequence 1, 2 is an increasing subsequence of the permutation σ considered above.

Each permutation has many increasing subsequences. In combinatorics the length of the largest increasing subsequence of a permutation is an important object of study. For the permutation σ considered above, that length is 2. As another example, if π is

the permutation 1,3,2,4,5, that is, $\pi(1)=1$, $\pi(2)=3$, $\pi(3)=2$, $\pi(4)=4$, $\pi(5)=5$, the length of π's longest increasing subsequence is 4. If σ is a permutation of length n, then $\ell_n(\sigma)$ denotes the length of σ's longest increasing subsequence.

If permutations of length n are selected at random, and each permutation has equal probability $1/n!$, then $\ell_n(\sigma)$ is a natural random variable arising from combinatorics. Its statistical behavior for n large has been an object of study since at least the 1960s. Interest in ℓ_n stems from basic connections between permutations and games of chance, such as "solitaire," also known as "patience sorting." In their mathematical review, Aldous & Diaconis (1999) give a precise description of such a game:

> Take a deck of cards labeled $1, 2, 3, \cdots, n$. The deck is shuffled, cards are turned up one at a time and dealt into piles on the table, according to the rule
>
> - A low card may be placed on a higher card (e.g., 2 may be placed on 7) or may be put into a new pile to the right of the existing piles.
>
> At each stage we see the top card on each pile. If the turned up card is higher than the cards showing then it *must* be put into a new pile to the right of the others. *The object of the game is to finish with as few piles as possible.* (Aldous & Diaconis, 1999, p. 413)

Suppose our deck has 5 cards, numbered 1–5, and that they are shuffled so that they are ordered as 5 3 1 4 2. During the game, the piles might evolve as follows:

		1	1	1
	3	3	3	3 2
5	5	5	5 4	5 4

and at the end of the game, we have two piles. Another (non-optimal) possibility is

			4	4 2
5	5 3	5 3 1	5 3 1	5 3 1

and we wind up with 3 piles. There is a simple algorithm (referred to as the "greedy algorithm") which always yields the minimum number of piles (see Aldous & Diaconis, 1999). The connection between the "solitaire" game described above and longest increasing subsequences is this: for any given shuffle, the minimum number of piles is exactly the longest increasing subsequence of the shuffle (when the shuffle is viewed as a permutation).

Over the past 40 years, mathematicians have studied the statistical behavior of the random variable $\ell_n(\sigma)$ when n, the size of the permutations, tends to infinity. Let $\mathbb{E}(\ell_n)$ denote the mean (or average) value of $\ell_n(\sigma)$, and let $\mathrm{Var}(\ell_n)$ denote its variance, $\mathrm{Var}(\ell_n) = \mathbb{E}(\ell_n^2) - (\mathbb{E}(\ell_n))^2$. Some natural questions are: How does $\mathbb{E}(\ell_n)$ grow with n? How fast does the variance grow? Is there a notion of a central limit theorem, or is there a limiting distribution for ℓ_n that emerges when n tends to ∞? Here are some results, both old and new, which answer these questions, and also demonstrate a striking connection between combinatorial questions and random matrix theory.

Result 1 (Logan & Shepp, 1977, see also Diaconis, 1995, Vershik & Kerov, 1997):

$$\lim_{n\to\infty} \frac{1}{\sqrt{n}} \mathbb{E}(\ell_n) = 2, \tag{3}$$

$$\lim_{n\to\infty} \frac{1}{\sqrt{n}} \mathrm{Var}(\ell_n) = 2. \tag{4}$$

Result 2 (Baik et al., 1999):

$$\lim_{n\to\infty} \mathrm{Prob}\left[\frac{\ell_n(\sigma) - 2n^{1/2}}{n^{1/6}} < x\right] = F(x), \tag{5}$$

where F is the Tracy–Widom distribution function (2). Result 2 was established in 1999. One remarkable aspect of this result is that it provides a mathematically precise connection between random permutations and random matrix theory (and Painlevé equations). There are now several proofs of this result as well as generalizations (see, e.g., Borodin et al. (2002)), and each proof contains different interconnections between areas of mathematics.

Further Developments

There have been a number of recent results that connect combinatorics to random matrix theory. Interesting generalizations of longest increasing subsequence problems have appeared. For example, Baik & Rains (2001) considered only those permutations that are their own inverses (also called involutions) and established results analogous to those mentioned above. Further generalizations to the study of "random words" have appeared (Tracy & Widom, 2001).

The Tracy–Widom distribution F has appeared in a variety of other contexts as well. For example, in the study of random domino tilings of the so-called Aztec diamond, the same distribution function appears in a natural scaling limit (Johansson, 2001). There is a notion of a "frozen region" of a domino tiling, and the boundary of this frozen region may be interpreted as a random variable, which is described, asymptotically, by the Tracy–Widom distribution function. This phenomenon is somewhat universal within random tiling problems as well—it has recently been established (Baik et al., 2004) that the same behavior appears in random rhombi tilings of hexagonal domains.

KENNETH MCLAUGHLIN

See also **Random matrix theory I, II and IV**

Further Reading

Aldous, D.J. & Diaconis, P. 1995. Hammersley's interacting particle process and longest increasing subsequences. *Probability Theory and Related Fields*, 103: 119–213

Aldous, D. & Diaconis, P. 1999. Longest increasing subsequences: from patience sorting to the Baik–Deift–Johansson theorem. *Bulletin of the American Mathematical Society (N.S.)*, 36(4): 413–432

Baik, J., Deift, P. & Johansson, K. 1999. On the distribution of the length of the longest increasing subsequence of random permutations. *Journal of the American Mathematical Society*, 12(4): 1119–1178

Baik, J., Kriecherbauer, McLaughlin, K.D.T.R. & Miller, P. 2004. Uniform asymptotics for polynomials orthogonal with respect to a general class of discrete weights and universality results for associated ensembles. *Annals of Mathematics*, submitted; Preprint CA/0310278

Baik, J. & Rains, E. 2001. The asymptotics of monotone subsequences of involutions. *Duke Mathematical Journal*, 109(2): 205–281

Borodin, A., Okounkov, A. & Olshanski, G. 2000. Asymptotics of Plancherel measures for symmetric groups. *Journal of the American Mathematical Society*, 13(3): 481–515

Johansson, K. 2001. Discrete orthogonal polynomial ensembles and the Plancherel measure. *Annals of Mathematics* (2), 153(1): 259–296

Logan, B.F. & Shepp, L.A. 1977. A variational problem for random Young tableaux. *Advances in Mathematics*, 26: 206–222

Mehta, M.L. 1991. *Random Matrices*, 2nd edition, San Diego: Academic Press

Tracy, C.A. & Widom, H. 1994. Level-spacing distributions and the Airy kernel. *Communications in Mathematical Physics*, 159: 151–174

Tracy, C.A. & Widom, H. 2001. On the distributions of the lengths of the longest monotone subsequences in random words. *Probability Theory and Related Fields*, 119: 350–380

Vershik, A.M. & Kerov, S.V. 1977. Asumptotics of the Plancherel measure of the symmetric group and the limiting form of Young tables. *Soviet Mathematics, Doklady*, 18: 527–531. Translation of *Doklady Academii Nauk, SSSR*, 233(1977): 1024–1027

RANDOM MATRIX THEORY IV: ANALYTIC METHODS

In this article, we address various analytical issues that arise in random matrix theory (RMT) using techniques from the theory of Riemann–Hilbert problems (RHPs). We refer the reader to the previous three entries for more information on the physical applications and various algebraic developments in RMT, and to the entry on Riemann–Hilbert problem for more information on RHPs. The classic text on RMT is Mehta (1991); see also Deift (2000) for a pedagogic presentation of some recent analytical results.

We discuss only the so-called unitary ensembles (UEs), that is, ensembles of $N \times N$ Hermitian matrices $M = M^* = (M_{jk} = M_{jk}^{\mathrm{R}} + \mathrm{i}M_{jk}^{\mathrm{I}})$ with probability distributions

$$P_N(M)\,\mathrm{d}M = \frac{1}{Z_N}\mathrm{e}^{-\operatorname{tr} V(M)}\,\mathrm{d}M = \frac{1}{Z_N}\mathrm{e}^{-\operatorname{tr} V(M)}\prod_{j=1}^{N}\mathrm{d}M_{jj}\prod_{j<k}\mathrm{d}M_{jk}^{\mathrm{R}}\prod_{j<k}\mathrm{d}M_{jk}^{I}, \tag{1}$$

where $V : \mathbb{B} \to \mathbb{R}$ grows sufficiently rapidly at ∞ and Z_N is a normalization constant. The name UE refers to the fact that the distribution is invariant under unitary conjugation $M \to \tilde{M} = UMU^*$, with U unitary, that is, $P(\tilde{M})\,\mathrm{d}\tilde{M} = P(M)\,\mathrm{d}M$. For information on other distributions such as orthogonal ensembles, see Tracy & Widom (1996, 1998) for some additional analytical developments. The special case in which $V(x) = x^2$ is called the Gaussian unitary ensemble (GUE), with $P_N(M)\,\mathrm{d}M = \frac{1}{Z_N}\mathrm{e}^{-\operatorname{tr} M^2}\,\mathrm{d}M$.

Under (1) the eigenvalues $\lambda_1(M) \geq \lambda_2(M) \geq \ldots \geq \lambda_N(M)$ of a matrix M in the ensemble become random variables with distribution given by the Weyl integration formula (see Mehta, 1991)

$$P_N(\lambda)\,\mathrm{d}^N\lambda = \frac{1}{Z_N'}\mathrm{e}^{-\sum_i V(\lambda_i)}\prod_{i<j}(\lambda_i - \lambda_j)^2\chi\,\mathrm{d}^N\lambda, \tag{2}$$

where χ denotes the indicator function on $\mathbb{R}^N$ for the set $\lambda_1 \geq \ldots \geq \lambda_N$. A statistic of basic importance is the *gap probability*

$$P_N(\theta;\, E) = \text{Prob}\ \{\ M \text{ has no eigenvalues in } (E-\theta,\, E+\theta)\} \tag{3}$$

for $E \in \mathbb{R}$, $\theta > 0$. Scaling the eigenvalues in the standard way around the energy E, $\lambda \mapsto \lambda' = \gamma_N(\lambda - E)$, so that the expected number of eigenvalues per unit λ'-interval is 1, one considers the limit

$$P(y;\, E) = \lim_{N\to\infty} P_N(y/\gamma_N;\, E). \tag{4}$$

In the case of GUE, a calculation of Gaudin and Mehta (Mehta, 1991) using classical estimates showed that

$$\gamma_N \sim N^{1/2} \tag{5}$$

and that

$$P(y;\, E = 0) = \det(1 - S_y), \tag{6}$$

where S_y denotes the trace class operator with kernel

$$S_y(\xi,\, \eta) = \frac{\sin \pi(\xi - \eta)}{\pi(\xi - \eta)} \tag{7}$$

acting on $L^2(-y,\, y)$, the space of square integrable functions on the interval $(-y,\, y)$. The *universality conjecture* for the gap probability is the claim that under the correct scaling, (6) is true with the same right-hand side for all suitable V and E. The only thing that depends on V is the scaling parameter γ_N. Universality conjectures for other statistical quantities are discussed briefly below.

In this article we present a sketch of how to prove the universality conjecture for (6) following Deift et al. (1999a,b) in which the authors consider two kinds of potentials V

(i) $V(x) = t_{2m}x^{2m} + \ldots + t_0,\ t_{2m} > 0$,
(ii) $V(x) = NQ(x)$, where

(a) $Q(x)$ is real analytic in a neighborhood of $\mathbb{R}$
(b) $|Q(x)|/|\log x| \to +\infty$ as $|x| \to \infty$.

In order to prove (6), one must choose E in the support of the so-called equilibrium measure for V (see Step 4 Analytical considerations (ii) below).

The universality conjecture was first considered in the physics literature in Brézin & Zee (1993), in the mathematical literature in Pastur and Scherbina (1997), and in the special case $V(x) = x^4 + tx^2$, $t < 0$, in Bleher and Its (1999). The method in Bleher & Its has common elements with Deift et al. (1999a,b), but in addition Bleher & Its uses certain isomonodromy ideas.

Step 1: Representation in terms of orthogonal polynomials

Using an earlier calculation of Gaudin and (2), Gaudin and Mehta (Mehta, 1991) showed that

$$P_N(\theta, E = 0) = \det(1 - K_N), \tag{8}$$

where K_N is the finite rank operator acting on $L^2(E - \theta, E + \theta)$ with kernel

$$K_N(x, y) = \sum_{j=0}^{N-1} \phi_j(x)\phi_j(y), \tag{9}$$

where $\phi_j(x) = \mathrm{e}^{-(1/2)V(x)} p_j(x)$ and $p_j(x) = k_j x^j + \cdots$, $k_j > 0$, $j \geq 0$, are the orthonormal polynomials generated by the measure $\mathrm{e}^{-V(x)}\,\mathrm{d}x$,

$$\int_{\mathbb{R}} p_j(x) p_l(x) \mathrm{e}^{-V(x)}\,\mathrm{d}x = \delta_{jl}. \tag{10}$$

By the Christoffel–Darboux formula (Szegö, 1975), K_N can be expressed in terms of p_N and p_{N-1} and so the proof of (6) reduces to the evaluation of the asymptotics (so-called *Plancherel–Rotach* asymptotics) for $p_N(E + x/\gamma_N)$, $p_{N-1}(E + x/\gamma_N)$ as $N \to \infty$, for polynomials orthonormal with respect to a weight as in (10). For GUE, the p_N's are Hermite polynomials and such asymptotics can be found in the classical literature (Plancherel & Rotach, 1929). This is why Gaudin and Mehta were able to derive (6) for GUE, but for general weights $\mathrm{e}^{-V(x)}\,\mathrm{d}x$ the derivation of Plancherel–Rotach asymptotics is crucial.

Step 2: Introduction of Riemann–Hilbert Problem (RHP)

Write $p_j(x) = k_j \pi_j(x)$, so $\pi_j(x) = x^j + \ldots$. Following Fokas et al. (1991), the orthonormal polynomials p_j can be recovered by solving an RHP. Let the z-plane contour $\Sigma = \mathbb{R}$ be oriented from left to right so that the $(+)$ side (respectively, $(-)$ side) lies to the left (respectively, right) as one traverses Σ in the direction of the orientation. Define the jump matrix

$$v(z) = \begin{pmatrix} 1 & \mathrm{e}^{-V(z)} \\ 0 & 1 \end{pmatrix} \text{ for } z \in \Sigma,$$

and for any nonnegative integer q, let $Y = Y^{(q)} = (Y_{ij})_{1 \leq i,j \leq 2}$ be the (unique) 2×2 solution of the RHP (Σ, v).

(i) $Y(z)$ is analytic in $\mathbb{C} \setminus \Sigma$,
(ii) $Y_+(z) = Y_-(z)v(z)$, $z \in \mathbb{R}$, where $Y_\pm$ denotes the plus/minus boundary values of $Y(z)$, normalized so that
(iii) $Y(z) \begin{pmatrix} z^{-q} & 0 \\ 0 & z^q \end{pmatrix} \to \begin{pmatrix} 1 & 0 \\ 0 & 1 \end{pmatrix}$ as $z \to \infty$.

Then

$$\pi_q(z) = Y_{11}(z),\ \pi_{q-1}(z) = -Y_{21}(z)/2\pi \mathrm{i} k_{q-1}^2 \tag{11}$$

and

$$k_q = \sqrt{-(Y_{21})_1/2\pi \mathrm{i}}, \tag{12}$$

where $Y_{21}(z) = (Y_{21})_1 z^{q-1} \ldots$.

Thus, the evaluation of Plancherel–Rotach asymptotics for p_q, p_{q-1} reduces to the asymptotics of the RHP (Σ, v) as $q = N \to \infty$.

Step 3: Steepest-descent method applied to the RHP

We use the steepest-descent method for the RHPs introduced in Deift & Zhou (1993) and extended in Deift et al. (1997) to include fully nonlinear oscillations (*See* **Riemann–Hilbert problem**). We consider the case where $V(x) = NQ(x)$ with properties (a) and (b) on the left above and as in Deift et al. (1999a). The case where $V(x) = t_{2m}x^{2m} + \ldots + t_0$ can be reduced to this case with lower-order errors by scaling (see Deift et al., 1999b).

Suppose there exists a union of $n+1$ disjoint intervals $J = \cup_{i=0}^{n} (b_i, a_{i+1})$ in $\mathbb{R}$, $b_0 < a_1 < \ldots < b_n < a_{n+1}$, a real number l, and a function $g(z)$ with the following properties:

$$g(z) \text{ is analytic in } \mathbb{C} \setminus \mathbb{R}, \tag{13}$$

$$g(z) = \log z + \mathrm{o}(1) \text{ as } z \to \infty, \tag{14}$$

$$g_+(z) + g_-(z) - V(z) - l \leq 0 \text{ for } z \in \mathbb{R} \setminus \bar{J}, \tag{15}$$

where $\bar{J}$ denotes the closure of J, and where equality holds for at most a finite number of points,

$$g_+(z) - g_-(z) \in \mathrm{i}\mathbb{R}, \tag{16}$$

for all real z and is constant in each component of $\mathbb{R}\setminus\bar{J}$,

$$g_+(z)+g_-(z)-V(z)-l=0 \text{ for } z\in\bar{J}, \quad (17)$$

$$\mathrm{i}(g_+'-g_-')\geq 0 \text{ for } z\in J, \quad (18)$$

where equality holds for at most a finite number of points. As before, $g_\pm$ denotes the boundary values of $g(z)$.

Now define

$$M(z)\equiv \mathrm{e}^{-Nl/2\sigma_3}Y(z)\mathrm{e}^{-(g(z)-l/2)\sigma_3},$$

$$\sigma_3=\begin{pmatrix}1&0\\0&-1\end{pmatrix}. \quad (19)$$

A simple calculation using (13) and (14) shows that $M(z)$ solves a RHP normalized at infinity.

(i) $M(z)$ is analytic in $\mathbb{C}\setminus\mathbb{R}$
(ii) $M_+(z)=M_-(z)v_M(z)$, where $v_M(z)=$

$$\begin{pmatrix}\mathrm{e}^{-N(g_+(z)-g_-(z))}&\mathrm{e}^{N(g_+(z)+g_-(z)-V(z)-l)}\\0&\mathrm{e}^{N(g_+(z)-g_-(z))}\end{pmatrix},$$

$z\in\mathbb{R}$,
(iii) $M(z)\to I$ as $z\to\infty$.

As we now show, the properties of $g(z)$ are chosen carefully so that the jump matrix v_M takes a specific form. By (17)

$$v_M(z)=\begin{pmatrix}\mathrm{e}^{-N(g_+(z)-g_-(z))}&1\\0&\mathrm{e}^{N(g_+(z)-g_-(z))}\end{pmatrix},$$

$$z\in J, \quad (20)$$

and by (16)

$$v_M(z)=\begin{pmatrix}\mathrm{e}^{-\mathrm{i}N\Omega_j}&\mathrm{e}^{N(g_+(z)+g_-(z)-V(z)-l)}\\0&\mathrm{e}^{\mathrm{i}N\Omega_j}\end{pmatrix},$$

$$z\in(a_j,b_j),\ j=1,\dots,n, \quad (21)$$

for some real constants Ω_j. Furthermore, if the inequality in (15) is strict then

$$v_M(z)=\begin{pmatrix}\mathrm{e}^{-\mathrm{i}N\Omega_j}&o(1)\\0&\mathrm{e}^{\mathrm{i}N\Omega_j}\end{pmatrix}, z\in(a_j,b_j)$$

as $N\to\infty$. (22)

By (17), for $z\in J$,

$$G\equiv g_+-g_-=2g_+-V(z)-l=-2g_-+V(z)+l$$

and so has an analytic continuation to a suitable neighborhood U of J. If the inequality in (18) is strict, it follows by the Cauchy–Riemann conditions (make U smaller if necessary) that $\mathrm{Re}\,G(z)\gtrless 0$ for $z\in\{\mathrm{Im}\,z\gtrless 0\}\cap U$, respectively. Extend $\Sigma=\mathbb{R}$ to a new contour $\tilde{\Sigma}$ consisting of $\mathbb{R}$ together with the boundary of $n+1$ lens-shaped regions, one region surrounding each interval (b_{j-1},a_j) in J, as indicated in Figure 1.

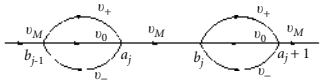

Figure 1. The Riemann–Hilbert problem $(\tilde{\Sigma},\tilde{v})$.

Note the factorization for v_M on J

$$\begin{pmatrix}\mathrm{e}^{-NG}&1\\0&\mathrm{e}^{NG}\end{pmatrix}=\begin{pmatrix}1&0\\\mathrm{e}^{NG}&1\end{pmatrix}\begin{pmatrix}0&1\\-1&0\end{pmatrix}$$

$$\begin{pmatrix}1&0\\\mathrm{e}^{-NG}&1\end{pmatrix}\equiv v_-v_0v_+. \quad (23)$$

The final algebraic step in the procedure is to define

(i) $\tilde{M}(z)\equiv M(z)$ outside the lens-shaped regions,
(ii) $\tilde{M}(z)\equiv M(z)\begin{pmatrix}1&0\\-\mathrm{e}^{-NG}&1\end{pmatrix}$ in the upper lens regions,
(iii) $\tilde{M}(z)\equiv M(z)\begin{pmatrix}1&0\\\mathrm{e}^{NG}&1\end{pmatrix}$ in the lower lens regions.

Then $\tilde{M}$ solves the normalized RHP $(\tilde{\Sigma},\tilde{v})$

(i) $\tilde{M}(z)$ is analytic in $\mathbb{C}\setminus\tilde{\Sigma}$,
(ii) $\tilde{M}_+(z)=\tilde{M}_-(z)\tilde{v}(z),\ z\in\tilde{\Sigma}$,
(iii) $\tilde{M}(z)\to I$ as $z\to\infty$,

where

(i) $\tilde{v}(z)=v_M(z)$ for $z\in\mathbb{R}\setminus\bar{J}$,
(ii) $\tilde{v}(z)=v_\pm(z)$ for $z\in\tilde{\Sigma}\cap\mathbb{C}_\pm$,
(iii) $\tilde{v}(z)=v_0(z)$ for $z\in J$

as indicated in Figure 1.

Now the situation is clear. The above computations show that as $N\to\infty$, $\tilde{v}(z)\to v^\infty(z)$, where

(i) $v^\infty(z)=\begin{pmatrix}\mathrm{e}^{-\mathrm{i}N\Omega_j}&0\\0&\mathrm{e}^{\mathrm{i}N\Omega_j}\end{pmatrix}$ for $z\in(a_j,b_j)$, $j=1,\dots,n$,
(ii) $v^\infty(z)=I$ for $z\in(-\infty,b_0)\cup(a_0,\infty)$,
(iii) $v^\infty(z)=\begin{pmatrix}0&1\\-1&0\end{pmatrix}$ for $z\in J$,
(iv) $v^\infty(z)=I$ for z on the boundary of any of the lens-shaped regions.

Thus, we expect that as $N\to\infty$, $\tilde{M}(z)\to M^\infty(z)$, where $M^\infty(z)$ solves the RHP $(\tilde{\Sigma},v^\infty)$

(i) $M^\infty(z)$ is analytic in $\mathbb{C}\setminus\tilde{\Sigma}$,
(ii) $M^\infty_+(z)=M^\infty_-(z)v^\infty(z).\ z\in\tilde{\Sigma}$,
(iii) $M^\infty(z)\to I$ as $z\to\infty$.

It turns out that the RHP $(\tilde{\Sigma},v^\infty)$ can be solved explicitly in terms of theta functions (Deift et al., 1999a), thus yielding asymptotic formulae for $p_N(E+x/\gamma_N)$, $p_{N-1}(E+x/\gamma_N)$ as $N\to\infty$, which then leads to the proof of the universality conjecture (6) as indicated above.

Step 4: Analytical considerations

In order to make the above schema rigorous, many analytical difficulties must be addressed:

(i) One must show that J, l, and $g(z)$ with properties (13)–(18) actually exist. This can be done by considering the minimization problem

$$E_V = \inf_{\mu\in\mathcal{M}}\left(\int\int \log|s-t|^{-1}\,\mathrm{d}\mu(s)\mathrm{d}\mu(t) + \int V(t)\,\mathrm{d}\mu(t)\right), \tag{24}$$

where $\mathcal{M}$ is the space of probability measure on $\mathbb{R}$. It turns out (Saff & Totik, 1997) that the infinum is achieved at a unique measure $\mu=\mu_V$, the so-called *equilibrium measure* for V. For $V=NQ$ satisfying (i) and (ii) above, a result of Deift, Kriecherbauer and McLaughlin shows that $\mathrm{d}\mu_V(s)=\psi_V(s)\,\mathrm{d}s$ is absolutely continuous with respect to Lebesgue measure and is supported on a finite union of intervals J_V. Then quite remarkably

$$g(z)\equiv\int_{\mathbb{R}}\log(z-s)\,\mathrm{d}\mu_V(s) \tag{25}$$

has the desired properties (13)–(18) on $J=J_V$, provided l is chosen to be the Lagrange multiplier associated with the constraint $\int \mathrm{d}\mu=1$ in the minimization problem E_V.

(ii) The scaling parameter γ_N must be determined. In order to obtain the universality limit (6) one must consider only points E in the support of μ_V, $\psi_V(E)>0$. For such E, one takes $\gamma_N\equiv N\psi_V(E)$. If $\psi_V(E)=0$, the limit in (4) (if it exists!) is *different* from (6). In this connection, see (26) below.

(iii) The convergence of $\tilde{v}(z)$ to $v^\infty(z)$ is not uniform on $\tilde{\Sigma}$ as $N\to\infty$, leading in particular to difficulties at the end points of J.

(iv) The inequalities in (15) and (18) may not be strict.

The analytical heart of the problem lies in addressing the latter three points, and we refer the reader to Deift et al. (1999a) for further details.

The asymptotic behavior of $P(y, E=0)=\det(1-S_y)$ as $y\to\infty$ can itself be evaluated using Riemann–Hilbert techniques (see Deift et al., 1997). The work in Deift et al. (1997) follows on the earlier work of Widom (1994, 1995), who uses more classical techniques. The paper by Deift et al. (1997) is the first application of RHP techniques to random matrix theory.

Universality conjectures for other statistical quantities, such as the k-point correlation function and the nearest-neighbor spacing distribution, can also be proved using the above methods (see Deift et al., 1999a; Deift, 2000). For GUE, Tracy & Widom (1994) proved the beautiful result that if $\lambda_1(M)$ is the largest eigenvalue of a GUE matrix M, then

$$\lim_{N\to\infty}\mathrm{Prob}((\lambda_1(M)-\sqrt{2N})2^{1/2}N^{1/6}\le t) = F(t), \tag{26}$$

where $F(t)$ is the so-called *Tracy–Widom distribution*

$$F(t)=\mathrm{e}^{-\int_t^\infty (s-t)u^2(s)\,\mathrm{d}s},$$

where $u(s)$ is the unique solution (Hastings & McLeod, 1980) of the Painlevé II equation $u''=2u^3+su$ with asymptotics $u(s)\sim\mathrm{Ai}(s)$ as $s\to\infty$. Here Ai(s) is the classical Airy function. As long as $\psi_V(s)$ behaves "generically" near the right end point of J, $\psi_V(s)\sim\sqrt{s-a_{N+1}}$, $s\sim a_{N+1}$, one can use the methods of Deift et al. (1999a) to show that the behavior of $\lambda_1(M)$ is also universal as $N\to\infty$; that is, once the correct scaling parameters at a_{N+1} are inserted, the same limit (26) is true for all UEs. As noted in the entry on Riemann–Hilbert problem, the distribution $F(t)$ arises, in particular, in the solution of Ulam's problem in Baik et al. (1999).

PERCY DEIFT AND XIN ZHOU

See also **Painlevé analysis; Random matrix theory I, II, and III; Riemann–Hilbert problem**

Further Reading

Baik, J., Deift, P. & Johansson, K. 1999. On the distribution of the length of the longest increasing subsequence of random permutations. *Journal of the American Mathematical Society*, 12(4): 1119–1178

Bleher, P. & Its, A.R. 1999. Semiclassical asymptotics of orthogonal polynomials, Riemann–Hilbert problems, and universality in the matrix model. *Annals of Mathematics*, 150(2): 185–266

Brézin, E. & Zee, A. 1993. Universality of the correlations between eigenvalues of large random matrices. *Nuclear Physics* B, 402(3): 613–627

Deift, P. 2000. *Orthogonal Polynomials and Random Matrices: A Riemann–Hilbert Approach*, Providence, RI: American Mathematical Society

Deift, P., Its, A. & Zhou, X. 1997. A Riemann–Hilbert approach to asymptotic problems arising in the theory of random matrix models, and also in the theory of integrable statistical mechanics. *Annals of Mathematics*, 145: 1–88

Deift, P., Kriecherbauer, T., McLaughlin, K., Venakides, S. & Zhou, X. 1999a. Uniform asymptotics for polynomials orthogonal with respect to varying exponential weights and applications to universality questions in random matrix theory. *Communications in Mathematical Physics*, 52: 1335–1425

Deift, P., Kriecherbauer, T., McLaughlin, K., Venakides, S. & Zhou, X. 1999b. Strong asymptotics of orthogonal polynomials with respect to exponential weights. *Communications in Mathematical Physics*, 52: 1491–1552

Deift, P., Venakides, S. & Zhou, X. 1997. New results in small dispersion KdV by and extension of the steepest descent method for Riemann–Hilbert problems, *Internat. Math. Res. Notices*, No. 6, 285–299

Deift, P. & Zhou, X. 1993. A steepest descent method for oscillatory Riemann–Hilbert problems–asymptotics for the MKdV equation. *Annals of Mathematics*, 137: 295–368

Fokas, A.S., Its, A.R. & Kitaev, A.V. 1991. Discrete Painlevé equations and their appearance in quantum gravity. *Communications in Mathematical Physics*, 142(2): 313–344
Hastings, S.P. & McLeod, J.B. 1980. A boundary value problem associated with the second Painlevé transcendent and the Korteweg de Vries equation. *Archive for Rational Mechanics and Analysis*, 73: 31–51
Mehta, M.L. 1991. *Random Matrices*, 2nd edition, San Diego: Academic Press
Pastur, L. & Scherbina, M. 1997. Universality of the local eigenvalue statistics for a class of unitary random matrix ensembles. *Journal of Statistical Physics*, 86(1–2): 109–147
Plancherel, M. & Rotach, W. 1929. Sur les valeurs asymptotiques des polynomes d'Hermite $H_n(x) = (-1)^n e^{x^2/2} d^n(e^{-x^2/2})/dx^n$. *Commentarii Mathematica Helvetica*, 1: 227–254
Saff, E. & Totik, V. 1997. *Logarithmic Potentials and External Fields*, Berlin and New York: Springer
Szegö, G. 1975. *Orthogonal Polynomials*, 4th edition, Providence, RI: American Mathematical Society
Tracy, C.A. & Widom, H. 1994. Level-spacing distributions and the Airy kernel. *Communications in Mathematical Physics*, 159: 151–174
Tracy, C.A. & Widom, H. 1996. On orthogonal and symplectic matrix ensembles. *Communications in Mathematical Physics*, 177: 727–754
Tracy, C.A. & Widom, H. 1998. Correlation functions, cluster functions, and spacing distributions for random matrices. *Journal of Statistical Physics*, 92(5/6): 809–835
Widom, H. 1994. The asymptotics of a continuous analogue of orthogonal polynomials. *Journal of Approximation Theory*, 77: 51–64
Widom, H. 1995. Asymptotics for the Fredholm determinant of the sine kernel on a union of intervals. *Communications in Mathematical Physics*, 171: 159–180

RANDOM PROCESSES

See **Stochastic processes**

RANDOM WALKS

As conceptually simple stochastic processes, random walks have a plethora of practical modeling applications, leading to elegant and sometimes counter-intuitive mathematics. Consider a particle constrained to move in one dimension, moving one unit to the left or right at each unit time step, and with the direction of motion for each time step chosen at random and independently of the particle's position or history. If the particle's position after n time steps is $S(n)$, one can assert

$$S(n) = S(0) + \sum_{i=1}^{n} X_i, \tag{1}$$

where each X_i is an independent identically distributed (IID) random variable taking values $+1$ with probability (say) p and -1 with probability $1-p$. If $p = 1-p = \frac{1}{2}$, then the simple random walk (SRW) has no "preferred direction" and is unbiased. If $p > \frac{1}{2}$, then the particle is more likely to move right than left at each time step; the SRW is biased. The traditional pedagogical example imagines a drunken student's erratic progress along a street, where bias might be caused by the street being inclined or having a pub at one end.

Basic Results

The statistics of Equation (1) are simple and intuitively reasonable; thus

$$\begin{aligned} \mathrm{E}(S(n)) &= S(0) + n(2p-1) \\ \mathrm{Var}(S(n)) &= 4np(1-p), \end{aligned} \tag{2}$$

so the SRW moves with an average speed of $2p-1$ and spreads about the mean as $\sqrt{n}$ (characteristic of diffusive processes). This spread is greatest when the SRW is unbiased.

One can readily prove that the SRW is temporally and spatially homogeneous and Markovian (i.e., it does not matter where one places the origin of time or space, and conditional on the present, the future is independent of the past). Assuming without loss of generality $S(0) = 0$,

$$\begin{aligned} P(S(n) = a) &= C^n_{(n+a)/2} p^{(1/2)(n+a)} \\ &\quad \times (1-p)^{(n-a)/2}, \end{aligned} \tag{3}$$

the particle moves $(n+a)/2$ steps right and $(n-a)/2$ steps left to give a total of n steps and a net right displacement of a, and there are $C^n_{(n+a)/2}$ equally likely paths achieving this. N.B. for a to be attainable in n steps one requires $|a| \le n$ and $(n+a)/2$ to be an integer i.e., only odd positions are attainable at odd times, hence, the mysterious factor of 2 in Equation (5).

Results exploiting symmetries, homogeneities, and combinatorics, and also applications of probability- and moment-generating functions, are summarized in Grimmett & Stirzaker (2001, Chapters 3 and 4). More interesting questions involving absorption or reflection at barriers, dealt with using linear difference equations; where the nature of the barriers, dictates the appropriate boundary conditions, are also addressed therein.

Continuous Limit: Diffusion

For an unbiased SRW, manipulation of Equation (3) reveals, for sufficiently large a and n,

$$P(S(n) = a) \approx \sqrt{\frac{2}{\pi n}} \exp\left(\frac{-a^2}{2n}\right), \tag{4}$$

resembling a normal (Gaussian) probability distribution (Murray, 2002, Chapter 9). Indeed, if one lets the discrete space and time steps have sizes Δx and Δt, respectively, and forces these to zero such that

$$\lim_{\Delta x \to 0, \Delta t \to 0} \frac{(\Delta x)^2}{2\Delta t} = D \tag{5}$$

for some finite constant D (the diffusion coefficient), then one arrives at a diffusion equation,

$$\frac{\partial P}{\partial t} = D\frac{\partial^2 P}{\partial x^2}, \tag{6}$$

where $P(x, t)$ is the probability density function for the particle's position x at time t. Solutions of Equation (6) take the form indicated by Equation (4):

$$P(x, t) = \frac{1}{\sqrt{4\pi Dt}}\exp\left(\frac{-x^2}{4Dt}\right). \tag{7}$$

An alternative derivation, using Taylor series expansions of $P(x, t)$ (Murray, 2002, Chapter 9), lacks beauty and elegance but is more readily generalizable to the nonlinear RWs discussed below (Othmer & Stevens, 1997). If the SRW is biased, then an advection term,

$$v\frac{\partial P}{\partial x}$$

(where v represents the average velocity in the preferred direction) is added to the left-hand side of (6). If one considers $P(x, t)$ to represent a density of particles (rather than a probability density for a single particle), then one can incorporate local dynamics (e.g., chemical reactions or biological reproduction) at each point; a reaction term

$$f(P, x, t)$$

appears on the right-hand side of (6). The description of SRWs using diffusion (or more generally reaction-diffusion-advection) equations allows standard partial differential equation methods to be applied, often elucidating information concerning wave-like and spatially structured solutions (Murray, 2002; Okubo & Levin, 2001).

The extension of the SRW into higher dimensions presents no great conceptual, nor mathematical, challenges. If the processes governing steps in orthogonal directions are mutually independent, then one applies the preceding results to each direction separately. More realistically, suppose that at each time step a unit distance is moved in a direction chosen randomly from the infinite number of possibilities. Again, one can show that the process is, on average, diffusive (Denny & Gaines, 2000, Chapter 6):

$$E(S(n)) = S(0) \text{ and } \mathrm{Var}(S(n)) = n\,. \tag{8}$$

Importantly, motion in more than one spatial dimension allows more realistic random walk models to be developed, some of which are mentioned below.

Random Walks in Biology

Random walks have been widely applied in the life sciences. While ostensibly describing a particle's position, the modeled quantity might equally well refer to the amount of food consumed by an animal, the frequency of an allele in a population, or the contentious notion of "fitness." Crucially, random walk models are developed using local rules of "motion" at the level of the "individual" (organism/cell/molecule, etc.) before any scaling-up to a population level description is undertaken. This encourages the modeller to adhere to realistic assumptions and provides a link between concrete experimental observation and theory.

Several accessible applications are presented in Denny & Gaines (2000, Chapters 5 and 6). For example, Equation (6) can be solved to indicate the rate at which nutrients reach an idealized organism, D being strongly dependent on the organism's environment. Such considerations help to explain relative sizes of aquatic and aerial organisms and underly the varying mechanisms of nutrient transport in plant root systems. More complicated applications deal with the distribution of receptors on cell walls, the random drift to fixation of alleles in finite populations, and the energetics of protein folding. For more mathematically demanding applications involving spatial patterns and reaction-diffusion equations, see Murray (2002) and Okubo & Levin (2001).

Nonlinear Random Walks

The basic concept of a particle "deciding" (using IID random variables) its next direction at every step may be excessively restrictive, particularly in biology. For example, a particle moving in two dimensions may be likely to choose a direction similar to that used during the previous time step or may have some fixed preferred direction toward which its trajectory is biased. The mathematics of such "correlated" RWs is discussed in Othmer et al. (1988).

Alternatively, motion may be influenced by interactions with the local environment (reinforced RWs) leading to nonlinear generalizations of the simple diffusion equation; under reasonable assumptions, Equation (6) may be more properly expressed

$$\frac{\partial P}{\partial t} = D\frac{\partial}{\partial x}\left(\frac{\partial}{\partial x}\left[\ln\frac{P}{\tau(W)}\right]\right), \tag{9}$$

where $\tau(W)$ represents a transition rate dictated by the environment W. Such systems can exhibit properties not found in diffusive SRW formulations; particles may tend to aggregate rather than disperse and may reach locally infinite or zero densities in finite time (Othmer & Stevens, 1997).

Numerical simulation of such systems can be built up from individual-level rules as in Sleeman & Wallis (2002) and Figure 1, where the authors model angiogenesis (the movement of endothelial cells to create a blood supply to an avascular tumor). The cells' motions are dictated by chemical gradients between the tumor and the blood vessel; at first the attractive signal from the tumor is weak and the motion tortuous, but

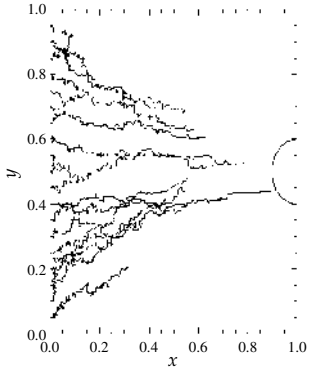

Figure 1. Tumor angiogensis modeled as a reinforced random walk. (Used with kind permission of I.P. Wallis and B.D. Sleeman, Department of Mathematics, University of Leeds, U.K.)

once the tumor's signal is sufficiently strong a more directed motion is observed.

JON PITCHFORD

See also **Brownian motion; Deterministic walks in random environments; Martingales**

Further Reading

Denny, M. & Gaines, S. 2000. *Chance in Biology*, Princeton, NJ: Princeton University Press

Grimmett, G. & Stirzaker, D. 2001. *Probability and Random Processes*, Oxford and New York: Oxford University Press

Murray, J.D. 2002. *Mathematical Biology*, 3rd edition, Berlin and New York: Springer

Okubo, A. & Levin, S.A. 2001. *Diffusion and Ecological Problems*, Berlin and New York: Springer

Othmer, H.G., Dunbar, S.R. & Alt, W. 1988. Models of dispersal in biological systems, *Journal of Mathematical Biology*, 26(3): 263–298

Othmer, H.G. & Stevens, A. 1997. Aggregation, blowup and collapse: the ABC's of taxis in reinforced random walks. *SIAM Journal on Applied Mathematics*, 57(4): 1044–1081

Sleeman, B.D. & Wallis, I.P. 2002. Tumour induced angiogenesis as a reinforced random walk: modelling capillary network formation without endothelial cell proliferation. *Mathematical and Computer Modelling*, 36 (3): 339–358

RATCHETS

An essential and striking feature of living cells is their ability to generate mechanical motion and forces. Important examples are cell motility, muscle contraction, and active mass transport within cells, among other active phenomena in biology. These motions and forces are generated at the molecular level by protein molecules (called molecular motors or pumps) that are driven by chemical reactions in situations far from equilibrium (Astumian, 1997; Jülicher et al., 1997).

Two types of molecular motors are classified as linear (or translational) and rotary (or rotatory). Within the first class, motor proteins are classified into several families: myosins, kinesins, and dyneins. Each of these interacts specifically with a certain type of filament along which it is able to move in the presence of adenosine triphosphate (ATP), which is a chemical fuel. The filaments serve as guides or tracks for the motor motion. Two types of filaments play this role: microtubules and actin filaments. Both are formed by a polymerization process from identical monomers (actin and tubulin monomers, respectively), resulting in a regular and periodic one-dimensional structure. An important feature is their polarity; thus the asymmetry of the monomers that form a polar filament structure is essential for motor operation as it defines the direction of motion.

A typical representative of rotary molecular motors is ATP synthase composed of two coupled rotary engines: a membrane-embedded unit F_0 and a water-surrounded part F_1 (Oster & Wang, 2000) ATP synthase works as a reversible motor-pump machine. Thus, the proton flow through F_0 is believed to generate a mechanical torque driving the F_1 motor to synthesize ATP, and using the hydrolysis energy of ATP, the F_1 motor can drive the F_0 motor in reverse to pump protons. Direct observation of the rotation of the F_1 motor has been demonstrated in fascinating experiments by Japanese scientists (Noji et al., 1997).

Thus, molecular motors are microscopic objects that unidirectionally move along one-dimensional periodic structures. Because the motor operation is considered on the molecular level, the motor must be a Brownian object, subject to random fluctuations. A conversion (rectification) of random fluctuations $F(t)$ into useful work (i.e., a directed motion) is called a "ratchet effect." (The names *thermal ratchet*, *Brownian motor*, *Brownian rectifier*, *mechanical diode*, *stochastic ratchet*, or simply *ratchet* are also in use.) A comprehensive review of the work on ratchets and their practical applications is available in Reimann (2002).

Historically, the problem of converting Brownian motion (in general, unbiased random fluctuations) into useful work and its consistency with the second law of thermodynamics was introduced in a conference talk by Marian Smoluchowski in 1912 (Smoluchowski, 1912) and later popularized and extended by Richard Feynman (Feynman et al., 1963), using a so-called "ratchet and pawl" gadget. A simple stochastic model of this rectifying process (called a Smoluchowski–Feynman's ratchet) can be described using the overdamped Langevin equation for a Brownian particle moving in a one-dimensional viscous medium with

friction coefficient η in the presence of a constant force F:

$$\eta\dot{x}(t) = -V'(x(t)) + F + \xi(t). \tag{1}$$

Here, the overdot and the prime denote differentiation with respect to the time t and the particle coordinate x, respectively. The potential $V(x)$ is a periodic function with period L, $V(x+L) = V(x)$, which has a broken parity symmetry. More precisely, this breaking of symmetry means that there is no Δx such that $V(-x) = V(x+\Delta x)$ for all x. A typical example of such a ratchet potential is a piecewise-linear (saw-tooth) function, consisting of two continuously matched linear pieces per period L, one with negative and one with positive slope, one being steeper than the other. The stochastic force $\xi(t)$ is a Gaussian white noise of zero mean, $\langle\xi(t)\rangle = 0$, satisfying the fluctuation-dissipation relation (Risken, 1989)

$$\langle\xi(t)\xi(s)\rangle = 2\eta k_{\mathrm{B}}T\delta(t-s), \tag{2}$$

where k_{B} is Boltzmann's constant, $2\eta k_{\mathrm{B}}T$ is the noise intensity or strength (T is absolute temperature), and $\delta(t)$ is Dirac's delta function.

The probability densities induced by the above equations obey a Fokker–Planck (FP) equation, which can be written in the form of a conservation law for probability, namely, a continuity equation (Risken, 1989)

$$\partial_t P(x,t) + \partial_x J(x,t) = 0. \tag{3}$$

Here the probability density $P(x,t)$ satisfies the normalization condition

$$\int_{-\infty}^{\infty} P(x,t)\,\mathrm{d}x = 1, \tag{4}$$

whereas the probability current is defined by

$$J(x,t) \doteq -\eta^{-1}[U'(x) + k_{\mathrm{B}}T\partial_x]P(x,t), \tag{5}$$

with the ratchet potential $V(x)$ and the force F being incorporated into a single effective potential

$$U(x) \doteq V(x) - Fx. \tag{6}$$

The quantity of foremost interest in the context of transport in periodic systems is the particle current, defined as the time-dependent ensemble average over the velocities, $\langle\dot{x}(t)\rangle$ (where for convenience the argument t is omitted). From this definition, the general connection between the probability current and the particle current is obtained as

$$\langle\dot{x}\rangle = \int_{-\infty}^{\infty} J(x,t)\,\mathrm{d}x. \tag{7}$$

Instead of solving the FP equation (3) describing the particle transport in periodic systems but with zero boundary conditions at infinity, it is convenient to rewrite it in terms of reduced probabilities (Reimann, 2002):

$$\hat{P}(x,t) \doteq \sum_{n=-\infty}^{\infty} P(x+nL,t), \quad \hat{J}(x,t) \doteq \sum_{n=-\infty}^{\infty} J(x+nL,t), \tag{8}$$

which are evidently periodic functions with period L. Furthermore, Equations (4) and (7) are transformed to

$$\int_0^L \hat{P}(x,t)\,\mathrm{d}x = 1 \tag{9}$$

and

$$\langle\dot{x}\rangle = \int_0^L \hat{J}(x,t)\,\mathrm{d}x, \tag{10}$$

respectively. Indeed, because $V(x)$ is periodic with period L, with $P(x,t)$ being a solution of the FP equation (3), $\hat{P}(x+nL,t)$ is also a solution for any integer n. Next, since the FP equation is linear, Equations (3) and (5) are also satisfied by the reduced quantities (8). Therefore, it is sufficient to solve an FP equation with periodic boundary conditions.

If the reduced dynamics assumes a steady state $\hat{P}^{\mathrm{st}}(x)$ in Equation (3), then the reduced probability current $\hat{J}(x,t) = \hat{J}^{\mathrm{st}}$ becomes independent of x and t. Multiplying this equation by x and integrating both its sides from x to $x+L$, one finds that the particle current takes the form

$$\langle\dot{x}\rangle = L\hat{J}^{\mathrm{st}}, \tag{11}$$

as expected. Moreover, using Equations (3), (5), and (11), it can easily be checked that the steady-state solution is given by (Stratonovich, 1969; Reimann, 2002)

$$\hat{P}^{\mathrm{st}}(x) = \mathcal{N}\frac{\eta}{k_{\mathrm{B}}T}\mathrm{e}^{-U(x)/k_{\mathrm{B}}T}\int_x^{x+L}\mathrm{e}^{U(y)/k_{\mathrm{B}}T}\,\mathrm{d}y, \tag{12}$$

$$\langle\dot{x}\rangle = L\mathcal{N}\left[1 - \mathrm{e}^{[U(L)-U(0)]/k_{\mathrm{B}}T}\right], \tag{13}$$

$$\mathcal{N} \doteq \frac{k_{\mathrm{B}}T}{\eta}\left[\int_0^L \mathrm{d}x\int_x^{x+L}\mathrm{e}^{[U(y)-U(x)]/k_{\mathrm{B}}T}\,\mathrm{d}y\right]^{-1}. \tag{14}$$

This solution is valid for a general potential $U(x)$ provided $U'(x+L) = U'(x)$. For the specific form (6), $U(L) - U(0) = -LF$, and therefore, as expected, the sign of the particle current (13) coincides with the sign of F. The absence of an average particle current ($\langle\dot{x}\rangle = 0$) if $F = 0$, in spite of the broken spatial symmetry, agrees with the second law of thermodynamics, like in the original ratchet and pawl gadget (Feynman et al., 1963). However, if the force

F in Equation (1) depends on time, a rectified motion (ratchet effect) may occur in an asymmetric system.

For the occurrence of the ratchet effect, it is sufficient to show that $\langle \dot{x} \rangle \neq 0$ provided $\langle F(t) \rangle = 0$. If the changes of $F(t)$ are extremely slow, then at any given instant t, the particle current has practically the same value as the steady-state current (13) with a static tilt F. In this adiabatic approximation, the time t plays the role of a parameter and using result (13) for a periodic driving force $F(t+\mathcal{T}) = F(t)$, one finds the time-averaged particle current:

$$\langle \dot{x} \rangle = \frac{1}{\mathcal{T}} \int_0^{\mathcal{T}} \frac{L k_B T \left[1 - e^{-LF(t)/k_B T}\right]}{\eta \int_0^L dx \int_x^{x+L} e^{[V(y)-V(x)-F(t)(y-x)]/k_B T} dy} dt. \quad (15)$$

For general analytical conclusions, the adiabatic expression (15) is still too complicated. Only in simple special cases may one predict the direction of the current. As an example, consider the case of when the tilting force $F(t)$ takes only two possible values $\pm F_0$ with very rare deterministic or random flips for which $\langle F(t) \rangle = 0$, and $V(x)$ is a piecewise linear potential with two continuously matched linear pieces per period L, the slopes of which are different (one steeper and one flatter). Outside this fundamental cell of length L, the potential is periodically continued. In this case, the integrals in Equation (15) can be calculated analytically, yielding an explicit expression (Magnasco, 1993), which is positive if the flatter slopes are arranged in the positive direction. Intuitively, this ratchet effect can be understood as follows. For F_0 within a certain range, one of the two tilted asymmetric potentials $V(x) \mp F_0 x$ does not exhibit any extrema and, therefore, supports a permanent downhill motion (even if $T = 0$), while the other still exhibits extrema acting as motion-blocking barriers. Below this window, both $V(x) \mp F_0 x$ exhibit barriers and, thus, prohibit deterministic motion. Because the barrier induced by the steeper slope of $V(x)$ is higher than that induced by the flatter slope, a weak thermal noise induces the current in the direction of the flatter slope.

Alternatively, the ratchet effect in a spatially periodic system can be achieved under a time-dependent variation (pulsation) of the potential shape without affecting its spatial periodicity. Therefore, Equation (1) can be generalized to include both a pulsating $f(t)$ and tilting $F(t)$ forcing as follows (Jülicher et al., 1997; Reimann, 2002):

$$\eta \dot{x}(t) = -V'[x(t), f(t)] + F(t) + \xi(t), \quad (16)$$

where $V'(x, f) \doteq \partial_x V(x, f)$. Here $F(t)$ may contain a load force or torque, generally depending on time t.

Thus, two fundamental classes of ratchet models arise from Equation (16). The first comprises models with $F(t) \equiv 0$, which are called "pulsating" ratchets. Within these, the first main subclass, called "fluctuating potential" ratchets (Astumian & Bier, 1994; Prost et al., 1994), is obtained when $f(t)$ in Equation (16) is additive, i.e., $V(x, f(t)) = V(x)[1 + f(t)]$. This subclass contains as a special case the "on-off" ratchets (Ajdari & Prost, 1992) when $f(t)$ takes only two values, one of them being -1 (potential "off"). The on-off ratchets are suitable for experimental realizations and have been demonstrated (Rousselet et al., 1994) by means of colloidal polystyrene latex spheres suspended in solution and exposed to a dielectric ratchet potential, created by a series of "Christmas-tree" electrodes, which were turned on and off periodically. A similar experimental setup was used by Faucheux & Libchaber (1995) but with solutions containing *two* different species of particles at a time. As a result, it was demonstrated that they can be separated. A further experimental verification of on-off ratchets has been performed (Faucheux et al., 1995) using polystyrene spheres confined to an effective one-dimensional ratchet potential by laser-optical trapping techniques (optical tweezers). The second subclass of pulsating ratchets, called "traveling potential" ratchets, have potentials of the form $V(x, f(t)) = V(x - f(t))$.

The second class are models with $f(t) \equiv 0$, called "tilting" ratchets (Magnasco, 1993), so that $V(x, f(t)) = V(x)$ in Equation (16). When $V(x)$ is a ratchet potential, then $F(t)$ is mostly considered as a symmetric function. If $F(t)$ is a stochastic process, one speaks of a "fluctuating force" ratchet. The case of a tilting ratchet with a periodic driving $F(t)$ is of particular experimental relevance and carries the obvious name "rocking" ratchet.

Clearly, there are many possible combinations and generalizations of these classes; for example, a simultaneously pulsating and tilting ratchet or the simultaneous breaking of more than one symmetry (Reimann, 2002). For various applications in physics, chemistry, and biology, see Astumian (1997), Jülicher et al. (1997), and Reimann (2002).

ALEXANDER V. ZOLOTARYUK

See also **Brownian motion; Fokker–Planck equation; Nonequilibrium statistical mechanics**

Further Reading

Ajdari, A. & Prost, J. 1992. Mouvement induit par un potentiel périodique de basse symétrie: diélectrophorèse pulsée. *Comptes Rendus de l'Academie des Sciences, Paris, Série II*, 315: 1635–1639

Astumian, R.D. 1997. Thermodynamics and kinetics of a Brownian motor. *Science*, 276: 917–922

Astumian, R.D. & Bier, M. 1994. Fluctuation driven ratchets: molecular motors. *Physical Review Letters*, 72: 1766–1769

Faucheux, L.P., Bourdieu, L.S., Kaplan, P.D. & Libchaber, A. 1995. Optical thermal ratchet. *Physical Review Letters*, 74: 1504–1547

Faucheux, L.P. & Libchaber, A. 1995. Selection of Brownian particles. *Journal of the Chemical Society—Faraday Transactions*, 91: 3163–3170

Feynman, R.P., Leighton, R.B. & Sands, M. 1963. *The Feynman Lectures on Physics*, vol. 1, Reading, MA: Addison-Wesley (Chapter 46)

Jülicher, F., Ajdari, A. & Prost, J. 1997. Modeling molecular motors. *Reviews of Modern Physics*, 69: 1269–1281

Magnasco, M.O. 1993. Forced thermal ratchets. *Physical Review Letters*, 71: 1477–1481

Noji, H., Yasuda, R., Yoshida, M. & Kinosita, K. 1997. Direct observation of the rotation of F_1-ATPase. *Nature*, 386: 299–302

Oster, G. & Wang, H. 2000. Reverse engineering a protein: the mechanochemistry of ATP synthase. *Biochimica et Biphysica Acta*, 1458: 482–510

Prost, J., Chauwin, J.-F., Peliti, L. & Ajdari, A. 1994. Asymmetric pumping of particles. *Physical Review Letters*, 72: 2652–2675

Reimann, P. 2002. Brownian motors: noisy transport far from equilibrium. *Physics Reports*, 361: 57–265

Risken, H. 1989. *The Fokker–Planck Equation: Methods of Solution and Applications*, Berlin: Springer

Rousselet, J., Salome, L., Ajdari, A. & Prost, J. 1994. Directional motion of brownian particles induced by a periodic asymmetric potential. *Nature*, 370: 446–448

Stratonovich, R.L. 1969. *Theory of Random Noise*, London: Gordon and Breach

von Smoluchowski, M. 1912. Experimentell nachweisbare, der üblichen Thermodynamik widersprechende Molekularphänomene. *Physikalische Zeitschrift*, 13: 1069

RAYLEIGH AND RAMAN SCATTERING AND IR ABSORPTION

When an electromagnetic wave, $E = E_0 \cos 2\pi\nu t$, irradiates a molecule, a crystal, or a disordered substance, the energy may be scattered, absorbed, or transmitted. In the scattering process, the irradiated medium becomes polarized and the induced dipole moment (or electric polarization),

$$P = \alpha E + \cdots = \alpha E_0 \cos 2\pi\nu t + \ldots, \qquad (1)$$

oscillates synchronously with the electromagnetic field. The dipole radiates energy (the scattering), and α is the polarizability (usually a second-order tensor).

Irradiating with ultraviolet or visible light of frequency ν induces an electronic polarization that is modulated by the vibrational frequencies (ν_i, ν_j, ν_k, ...) of the substance. Assuming a simple diatomic molecule, vibrating with frequency ν_1, the nuclear displacement is $q = q_0 \cos 2\pi\nu_1 t$, and $\alpha = \alpha_0 + (\partial\alpha/\partial q)_0 q$, then

$$\begin{aligned} P &= \alpha_0 E_0 \cos 2\pi\nu t \\ &\quad + \frac{1}{2}\left(\frac{\partial a}{\partial q}\right)_0 q_0 E_0 \{\cos[2\pi(\nu+\nu_1)t] \\ &\quad + \cos[2\pi(\nu-\nu_1)t]\}. \end{aligned} \qquad (2)$$

The emitted intensity is proportional to the square of the polarization $I \approx P^2$.

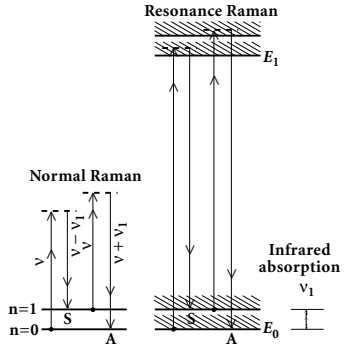

Figure 1. Level schemes for electronic and vibrational transitions involved in Raman scattering, resonance Raman scattering, and infrared absorption.

Rayleigh scattering occurs if the energy, ν, of the scattered photon is equal to that of the incident one (first term of Equation (2)). Rayleigh (1871) demonstrated that the Earth's blue sky was due to scattering of light by atmospheric particles, with a scattering intensity proportional to the inverse fourth power of the wavelength ($I \approx A/\lambda^4$). So, the blue (shorter wavelength) end of the visible spectrum is scattered more strongly, giving the sky its characteristic color.

As shown in Figure 1, the process is called Raman scattering, if the energy of the scattered photon is different from that of the incident one (the process is referred to as Brillouin scattering when the phonon emitted or absorbed is acoustic, and Raman scattering when the phonon is optical) (inelastic scattering, second term of Equation (2)). As a result, light with frequencies $(\nu \pm \nu_i)$, $(\nu \pm \nu_j)$, $(\nu \pm \nu_k)$ ... is emitted. In order that the total energy may be conserved, the vibrational energy of the sample is changed. If the irradiated molecule gains energy, the scattered lines in the Raman spectrum are at $(\nu - \nu_i)$ and are called "Stokes lines." If the sample loses energy, then the scattered lines are at larger frequencies than ν (at $(\nu + \nu_i)$...) and are called "anti-Stokes lines."

Classical theory shows that a vibration is Raman active if the polarizability changes during the vibration, and the Stokes lines are always stronger than the anti-Stokes lines. (This latter fact is explained by quantum theory as a consequence of the Maxwell–Boltzmann distribution law.) In crystals, the photon wave vectors are small compared with the dimensions of the Brillouin zone; thus, the momentum conservation law can be obeyed only if the wave vectors of the scattered phonons are also very small (so only the zone center phonons participate in the Raman scattering). It is difficult to determine which of the phonons are Raman active, as

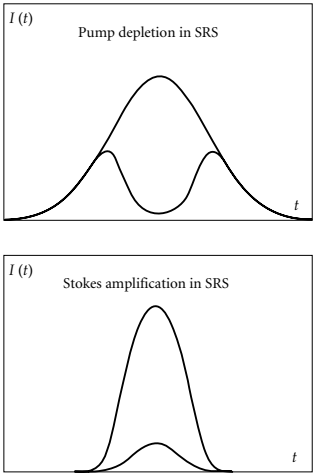

Figure 2. Stimulated Raman scattering: depletion at the pump frequency, and amplification of the Stokes beam.

changes of the components of the polarizability tensor are not obvious from inspection of the normal modes of vibration. Considering the symmetry of the molecule or the crystal and the polarization properties of the Raman lines, application of group theory gives a clear-cut solution to this problem (Poulet & Mathieu, 1970). If the polarization P contains terms of higher order (neglected in Equation (1)), these subsequent terms give hyper-Raman effects.

When the energy of the exciting line coincides with that of an allowed electronic transition of the compound, the intensity of the Raman spectra is enhanced and a series of overtones is observed—this mechanism is referred to as "resonance Raman scattering." This technique has been used in solid state and biophysics studies to identify intrinsic localized modes (Swanson et al., 1999).

Stimulated Raman scattering (SRS) is a nonlinear process in which a medium is irradiated by an intense laser beam at ν_p (pump frequency) and by a weaker beam at ν_s (Stokes frequency). The frequency spacing $\nu_p - \nu_s$ corresponds to a Raman frequency of the medium. In the simpler case, SRS amplifies the weak Stokes beam and depletes the pump beam (Raymer & Walmsley, 1991; see Figure 2).

A Raman soliton has been predicted (Chu & Scott, 1975) as a solution of the equations for transient SRS, and an experimental observation of transient SRS in H_2 gas was reported (Drühl et al., 1983). Recently, a complete interpretation of the above experiment has been given (Claude et al., 1995). The Raman soliton is still to be observed.

Picosecond time-resolved coherent anti-Stokes Raman spectroscopy (CARS) is a method for studying vibrational dephasing in the time domain. It is a special case of four-wave mixing (Levenson, 1982). Two intense simultaneous pulses at ν_p (pump) and ν_s (Stokes) specifically excite each Raman active mode at $\nu_p - \nu_s$. The third beam (probe pulse), also at the frequency ν_p, is delayed by the variable time t and stimulates coherent anti-Stokes emission. This technique is used to study the vibrational lifetime in anharmonic crystals and biomolecules to identify breathers excitations (Kosic et al., 1984).

Infrared (IR) absorption occurs when a compound is irradiated with frequencies that match its natural vibrational (or rotational) modes (Nakamoto, 1986). Absorption spectra in the infrared region originate in transitions between two vibrational levels of a sample in the electronic ground state. The absorption intensity depends on the change in dipole moment that occurs as a result of molecular vibration. If a molecule at equilibrium has a center of symmetry, the vibrations for which the center of symmetry is shared will be infrared inactive. Symmetry selection rules allow prediction of infrared activity when the associated normal coordinate belongs to the same species as one of the components of the dipole moment. When internal vibrations are coupled with phonons, nonlinear characters are observed in the infrared absorption bands: splitting, corresponding to the creation of a vibrational polaron or breather, intensity strongly dependent on the temperature, or an unusual number of overtones (Careri et al., 1984; Barthes et al., 2002). Time-resolved IR spectroscopy is of crucial importance in this field (Hamm et al., 1998; Xie et al., 2000).

MARIETTE BARTHES

See also **Nonlinear optics; Pump-probe measurements; Spectral analysis**

Further Reading

Barthes, M., Vik, A.F., Spire, A., Bordallo, H.N. & Eckert, J. 2002. Breathers or structural instability in solid L-Alanine: a new IR and inelastic neutron scattering vibrational spectroscopic study. *Journal of Physical Chemistry*, A 106(21): 5230–5241

Careri, G., Buontempo, U., Galluzzi, F., Gratton, E., Shyamsunder, E. & Scott, A.C. 1984. Spectrographic evidence for Davydov-like solitons in acetanilide. *Physical Review* B, 30: 4689–4702

Chu, F.Y.F. & Scott, A.C. 1975. Inverse scattering transform for wave-wave scattering. *Physical Review* A, 12: 2060–2064

Claude, C., Ginovart, F. & Léon, J. 1995. Nonlinear theory of transient stimulated Raman scattering and its application to long-pulse experiments. *Physical Review* A, 52: 767–782

Drühl, K., Wenzel, R. & Carlsten, J. 1983. Observation of solitons in stimulated Raman scattering. *Physical Review Letters*, 51: 1171

Hamm, P., Lim, M. & Hochstrasser, R.M. 1998. The structure of the amide I band of peptides measured by femtosecond

nonlinear IR spectroscopy. *Journal of Physical Chemistry* B, 102: 6123–6138

Kosic, T., Cline, R. & Dlott, D. 1984. Picosecond coherent Raman investigation of the relaxation of low frequency vibrational modes in amino acids and peptides. *Journal of Chemical Physics*, 81: 4932

Levenson, M. 1982. *Introduction to Nonlinear Laser Spectroscopy*, New York: Academic Press

Nakamoto, K. 1986. *Infrared and Raman Spectra of Inorganic and Coordination Compounds*, New York: Wiley

Poulet, H. & Mathieu, J.P. 1970. *Spectres de Vibration et Symétrie des Cristaux*, London: Gordon & Breach

Rayleigh, Lord (John William Strutt). 1871. On the light from the sky, its polarization and colour. *Philosophical Magazine*, 41: 107–120, 274–279

Raymer, M. & Walmsley, I.A. 1991. The quantum coherence properties of stimulated Raman scattering. *Progress in Optics*, 28: 216

Swanson, B.I., Brozik, J.A., Love, S.P., Strouse, G.F., Shreve, A.P., Bishop, A.R., Zang, W.-Z. & Salkola, M.I. 1999. Observation of intrinsically localized modes in a discrete low-dimensional material. *Physical Review Letters*, 82: 3288–3291

Xie, A.H., van der Meer, L., Hoff, W. & Austin, R.H. 2000. Long-lived amide I vibrational modes in myoglobin. *Physical Review Letters*, 84: 5435–5438

RAYLEIGH–BÉNARD CONVECTION

See **Thermal convection**

RAYLEIGH–TAYLOR INSTABILITY

The Rayleigh–Taylor instability arises when a layer of heavy fluid is accelerated into a lighter one. This occurs, for instance, if a heavy fluid is put on top of a lighter one in a uniform gravity field. Under these unstable conditions, small disturbances of the interface between the two layers grow, at first exponentially with a growth rate proportional to $\sqrt{k}$ where k is the wave number, as long as the perturbation is small compared with the wavelength. The subsequent nonlinear growth has been mostly investigated numerically or experimentally. The Rayleigh–Taylor instability was first discovered by Lord Rayleigh (John William Strutt) in 1883 for the gravitational case and then extended to the case of any accelerating fluid by Geoffrey Taylor in 1950.

One of Taylor's major observation is related to the Manhattan Project (September 1942 to January 1945), which ultimately led to the successful development of atomic bombs. Indeed, in May 1944, when he was invited to join the project, Taylor pointed out problems due to implosion instabilities (especially of the Rayleigh–Taylor type). This led to a very conservative design to minimize possible instabilities. At the same time, James Tuck brought the idea of explosive lenses for detonation wave shaping, suggesting the use of three-dimensional (3-d) lenses to create a spherical implosion and reduce instabilities.

To study an example of the Rayleigh–Taylor instability, let us look at the interface between a heavy fluid of density ρ_2 on top of a lighter fluid of density ρ_1 subject to gravity. The interface is assumed to be horizontal and both fluids are assumed to be at rest initially. For simplicity, we look at the two-dimensional case. We wish to show that a small disturbance of the interface will grow exponentially fast. Indeed, a small disturbance can engender small potential velocities $v_1 = -\nabla\phi_1$ and $v_2 = -\nabla\phi_2$ in the lower and upper fluid respectively, such that

$$\phi_2 = A\mathrm{e}^{-ky+nt}\cos(kx), \tag{1}$$

$$\phi_1 = -A\mathrm{e}^{ky+nt}\cos(kx). \tag{2}$$

Then the interface that is given by the equation $y = \eta(t, x)$ satisfies $\partial_t\eta = -\partial_y\phi_1(y=0) = -\partial_y\phi_1(y=0)$. Hence,

$$\eta = \frac{Ak}{n}\mathrm{e}^{nt}\cos(kx). \tag{3}$$

Neglecting the nonlinear term, the Euler equation reads $-\rho_2\partial_t\nabla\phi_2 + \nabla p_2 = -\rho_2 g\boldsymbol{j}$, which yields

$$p_2 = p - \rho_2 gy + n\rho_2\phi_2, \tag{4}$$

where p is the mean pressure at the interface. Similarly, the pressure in the lower fluid is given by

$$p_1 = p - \rho_1 gy + n\rho_1\phi_1. \tag{5}$$

At the interface, the pressure should be continuous, namely, $p_1 = p_2$ and, hence,

$$(\rho_2 - \rho_1)g\eta = n(\rho_2 + \rho_1)A\mathrm{e}^{nt}\cos(kx). \tag{6}$$

Combining (3) and (6), we get

$$n^2 = -kg\frac{(\rho_1 - \rho_2)}{(\rho_2 + \rho_1)}. \tag{7}$$

The Atwood number is defined by $At = (\rho_1 - \rho_2)/(\rho_2 + \rho_1)$. In the case $\rho_2 > \rho_1$ (heavy fluid on top of lighter fluid), $-1 < At < 0$, and

$$n = \pm\sqrt{-At\,kg}. \tag{8}$$

The unstable mode corresponds to $n = \sqrt{-At\,kg}$ and yields exponential growth as long as the nonlinear terms can be neglected, namely, as long as η is small compared with the wavelength. In experiments, surface tension and viscosity have a regularizing effect on the motion by damping the waves with large wave numbers. Indeed, for small Weber (and/or) large Reynolds numbers, the Rayleigh–Taylor instability has a short-wave character due to a balance between the exponential growth and the viscous or the surface tension effect, and hence, there exists a wave number that has a maximum growth rate. This is similar to the Rayleigh number, which represents the ratio of the destabilizing effect of buoyancy to the stabilizing effect of viscous force in the Rayleigh–Bénard instability.

Experiments and numerical simulations have given much insight into the different stages of the instability formation. However, they have yielded few quantitative results. Different numerical methods have been used such as the 3-d front tracking and the lattice Boltzmann method. In all cases, the geometric complexity of the interface is a source of difficulties for most of the algorithms. As explained in Sharp (1984), we can divide the growth of the instability into four stages. In the first, we have an exponential growth that can be quantitatively computed using the linear perturbation theory, which is no longer valid if the amplitude is about 20% of its wavelength. During the second stage, the perturbation grows nonlinearly to form bubbles of light fluid rising into the heavy one and spikes of heavy fluid falling into the light one. This stage is strongly influenced by the three-dimensional effects. Experiments and numerical simulations have shown that the bubbles rise at an approximately constant velocity during this stage. The third stage is characterized by the development of additional structures on the spikes. Moreover, the Kelvin–Helmholtz instability begins to develop due to the jump in the tangential velocity at the interface between the two fluids. The heavy fluid begins to roll up along the sides of the spikes to form "mushrooms." This phenomenon is more pronounced when the Atwood number is small and is a 3-d phenomenon. Eventually, the flow evolves into turbulent or chaotic mixing, which dominates the fourth stage.

In engineering applications, the Rayleigh–Taylor instability plays an important role in inertial confinement fusion (ICF). It is also present in the extraction of oil. Indeed, to extract oil from the Earth, water is accelerated into oil, and since oil is lighter, the interface presents the Rayleigh–Taylor instability. Some of the engineering solutions consist in adding polymers to the water. Moreover, there are many astrophysical and geophysical objects that present the Rayleigh–Taylor instability such as the supernova explosions, mantle convection, and deep convection in the ocean.

Another instability that is similar to the Rayleigh–Taylor one is the Ritchtmeyer–Meshkov instability, which arises in the case of an impulsive or instant loading as opposed to a constant acceleration (such as gravity) in the Rayleigh–Taylor case. In many applications the situation is intermediate between these two limiting cases.

NADER MASMOUDI

See also **Kelvin–Helmholtz instability; Wave stability and instability**

Further Reading

Chandrasekhar, S. 1961. *Hydrodynamic and Hydromagnetic Stability*, Oxford: Oxford University Press

Rayleigh, Lord (John William Strutt). 1883. Investigation of the character of the equilibrium of an incompressible heavy fluid of variable density. *Proceedings of the London Mathematical Society*, 14: 170–177

Sharp, D.H. 1984. An overview of Rayleigh–Taylor instability. *Physica* D, 12: 3

Taylor, G.I. 1950. The instability of liquid surfaces when accelerated in a direction perpendicular to their planes. I. *Proceedings of the Royal Society of London, Series* A, 201: 192–196

REACTION-DIFFUSION SYSTEMS

How did life appear and develop on Earth? Although there is not complete agreement, a convincing answer is that given the required conditions (which were almost surely satisfied billions of years ago), life spontaneously emerged through the endless battle of survival of the fittest from a primordial chemical soup. The theory of random catalytic networks (Kauffman, 1995) shows that autocatalytic reactions are likely in this context; thus, the theory of interactions between chemical reactions and molecular diffusion takes center stage in emergence of biological life from atoms and molecules in a system.

Today, reaction-diffusion systems have found many applications ranging from chemical and biological phenomena to medicine (physiology, diseases, etc.), genetics, physics, social science, finance, economics, weather prediction, astrophysics, and so on (Aronson & Weinberger, 1975; Grindrod, 1996; Murray, 2002; Scott, 2003). Even for phenomena that bear no initial resemblance to these processes, it is sometimes useful and productive to use the reaction-diffusion metaphor in order to gain insight into their dynamics.

An important contribution to this subject comes from the theory of pattern formation in nature. Many physical phenomena giving rise to natural patterns can be understood in terms of the interaction of a short-range self-enhancing reaction and a long-range antagonistic reaction. Take a fire, for example. It is a self-enhancing process: more heat is released as more fuel is burned. In the process oxygen and fuel which act as antagonistic factors are consumed and this may lead to a fire's extinction if fuel is not replenished. Also, the heat produced is transported from its local source through diffusion. Thus, we have the two main ingredients for pattern formation, namely, a local antagonistic interaction between two species (or reactions) coupled with a means of transport of their products. Historically, this is also one of the first examples of reaction-diffusion systems studied scientifically, for obvious reasons given the necessity for improved heating and lighting at the beginning of the industrial age. In his "Christmas Lectures" at the Royal Society in London, Michael Faraday discussed the importance

of understanding the candle flame and its analogy with the process of respiration of biological organisms (Faraday, 1861). The flame of the candle is an archetypical nonlinear reaction-diffusion system that today, after decades of research, provides a basis for the science of combustion. In this article, we review the essential topics in the field of reaction-diffusion systems from a theoretical point of view and also consider some of their numerous applications.

Theoretical Aspects

A reaction-diffusion (RD) equation is typically obtained by combining Fick's law of diffusion with the chemical reaction rate law. Although the theory can be made rigorous by using the theory of stochastic differential equations leading to the Fokker–Planck equation (Øksendal, 2003), we present here a heuristic argument. If we consider for simplicity a small domain interval on the line inside which we have a concentration c of some reacting species, then the diffusive flux J_{in} of c into one side of the small region will depend on the concentration gradient, $\partial c/\partial x$, at that boundary and the diffusion coefficient, D, with $J_{\text{in}} = -D(\partial c/\partial x)_{\text{in}}$. The parameter $D > 0$ is called diffusivity with physical units of m^2/s. The diffusive flux out of the region at the other side J_{out} will similarly be given by $J_{\text{out}} = -D(\partial c/\partial x)_{\text{out}}$, where the concentration gradient is now evaluated at the other boundary. The rate at which the concentration grows due to diffusion then depends on the difference between these two fluxes—and so involves the second derivative $\partial^2 c/\partial x^2$. If we add a kinetic reaction rate term $r(c)$, then the reaction-diffusion equation, which gives the rate of change of the concentration c in time at any spatial point, has the general form

$$\frac{\partial c}{\partial t} = D\frac{\partial^2 c}{\partial x^2} + r(c). \tag{1}$$

This can be extended to any number of spatial variables to read

$$\frac{\partial c}{\partial t} = D\Delta c + Q(\boldsymbol{x}, t, c, \ldots), \tag{2}$$

where Δ denotes the n-Laplacian ($1 \le n \le 3$) and Q accounts for other influences including sources or sink terms. Other more complicated formulations for the flux terms are possible in diffusive processes; see Okubo & Levin (2001) for an account of these ideas in biology. In many sciences, the motion of particles or living organisms is subjected to both internal and external effects often acting simultaneously. For example, in biology, bacteria are known to move randomly (akin to diffusion) but are also able to follow a chemical gradient (chemotaxis). Mathematically, this leads to a description involving reaction-diffusion-chemotaxis equations. For example, chemical attractant signaling can give rise to spiral wave pattern formation at a certain life stage in colonies of the slime mold *Dictyostelium discoideum*. Other extensions include advection, electric and/or magnetic field effects, and so on. In many of these cases, the resulting mathematical description is far more complicated than the simple RD systems above and, for many situations, their exact formulation is still an open question.

In writing an equation such as (2), we will consider that c is a vector; thus, Equation (2) will describe a system of RD equations. A simple archetypical example for a RD system is a quadratic autocatalytic reaction between two chemicals according to the rule $\text{A} + \text{B} \to 2\text{B}$ with rate $r = kab$. Denoting by a the concentration of A and by b that of B, the two species satisfy (after suitable scaling) the equations:

$$\begin{aligned} \frac{\partial a}{\partial t} &= D_1\Delta a - ab, \\ \frac{\partial b}{\partial t} &= D_2\Delta b + ab. \end{aligned} \tag{3}$$

From a mathematical point of view, systems of equations such as (3) must be well posed in order to exhibit appropriate solutions. To specify the problem, let the state variables $c(\boldsymbol{x}, t), \ldots$ represent the density or concentration of some substance at time $t \ge 0$ and position $\boldsymbol{x}$ in R^n. Then Δc denotes the Laplacian of c with respect to the space variable $\boldsymbol{x}$, and Equation (1) is an example of a parabolic equation of evolution. If (1) holds for all $\boldsymbol{x}$ in R^n, then the problem is fully specified once appropriate initial conditions

$$c(\boldsymbol{x}, 0) = c_0(\boldsymbol{x}) \tag{4}$$

are known. If (1) holds in a limited domain $\Omega \subset R^n$, then we must impose boundary conditions on c at $\partial\Omega$ (the domain boundary) compatible with the physical situation. Neumann (or no-flux), Dirichlet, or Robin conditions are usually employed in applications. Although these are linear conditions on the variable c, nonlinear conditions could also be applied. The above system of differential equations with specified initial and boundary conditions is called an initial value problem or IVP in short.

For an IVP, one naturally asks whether there are solutions. In the case of reaction-diffusion systems, there are two different aspects to consider; local existence and global existence of the solutions. By local existence we mean the existence of the solutions over a short time interval. Global existence properties are exhibited by the solutions of the IVP when they are known to exist for all positive time. In some applications global existence is precluded because the solution exhibits blow-up in finite time. This means that there is $(\boldsymbol{x}_0, t_0)$ such that $c(\boldsymbol{x}, t) \to \infty$ as $(\boldsymbol{x}, t) \to (\boldsymbol{x}_0, t_0)$. These questions are difficult to deal with in general for RD systems although there is a well-developed body

of results available in the literature (Grindrod, 1996). Moreover, even if the existence of a particular type of solution is established, further important theoretical questions involve the uniqueness of the solution and the stability of this solution to small perturbations. To approach these questions, one usually transforms the given system of RD equations

$$\frac{\partial c}{\partial t} = D\Delta c + f(\boldsymbol{x}, t, c, \nabla c) \tag{5}$$

into a differential equation in an abstract Banach space (for example, $L^2[\Omega]$) as in

$$c_t + Ac = f, \quad t > 0, \quad c = c_0 \quad \text{at } t = 0. \tag{6}$$

Then, the above questions reduce the problem to studying the properties of the (linear) operator A, which are mainly resolved if one knows its spectrum. However, in practice this is a difficult question as A has an infinite-dimensional spectrum.

For many RD systems of interest, in practice, there are several rather specific and powerful analytical methods that give detailed insights into the solutions, including comparison principles, invariant regions, matched asymptotic expansions, nonlinear bifurcation, group invariant symmetries, and so on (Grindrod, 1996).

Applications of Reaction-Diffusion Systems

Historically, some of the first applications of reaction-diffusion equations were in population dynamics, combustion, and nerve impulse conduction. Thus, one of the simplest reaction-diffusion equations is the Fisher–KPP equation

$$\frac{\partial u}{\partial t} = D\Delta u + f(u), \tag{7}$$

which was proposed independently by Ronald Fisher (1937) and Andrei Kolmogorov, Ivan Petrovsky and N. Piscounoff (1937) to explain the spread of genetic influences. In those papers a quadratic function of the form

$$f(u) = ku(1-u) \tag{8}$$

was used with $k > 0$ a parameter. A year later, Yakov Zeldovich and David Frank-Kamenetsky used the same equation but with f being a cubic polynomial as a model that represented flame front propagation (Zeldovich & Frank-Kamenetsky, 1938). Due to its generic form, Equation (7) soon found new interesting applications, for example, as a model of impulse conduction along an active nerve fiber, with the solution $u(x, t)$ representing the voltage across a cell membrane.

An important class of similarity solutions in the form of traveling waves (TW) is common to both the RD system (3) (and many of the type at (5)) and scalar equation (7). A traveling wave is a solution of the form $u(x, t) = u(x - vt) = u(y)$, where $y = x - vt$ is the traveling-wave coordinate with v being the wave speed. The problem is simplified because in the TW coordinate we have now to solve an ordinary differential equation (rather than a partial differential equation). For example, (7) generates the following TW equation to solve

$$\frac{\mathrm{d}^2 u}{\mathrm{d}t^2} + v\frac{\mathrm{d}u}{\mathrm{d}y} + f(u) = 0, \tag{9}$$

which must be supplemented with appropriate boundary conditions as $|y| \to \infty$.

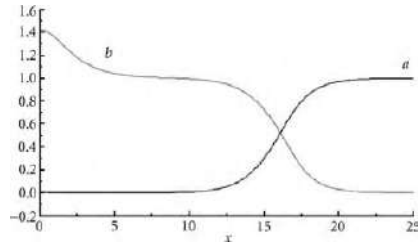

Figure 1. Typical concentration profiles for solutions a, b obtained by numerically solving the RD system (3).

Propagating waves are an important dynamical feature of many physical systems, hence, TW problems have been carefully studied. Key mathematical questions in these cases are the existence and possibly uniqueness of the waves. After the existence of a TW solution is established, it is of physical significance to study its stability under perturbations. Other questions are the influence of the initial conditions on the selection of a particular type of TW solution and the study of the shape of the TW solution. An extensive theory for TW solutions has been developed that deals with many interesting classes of RD systems (see Volpert et al., 1994; Grindrod, 1996; Scott, 2003). One particularly striking property of TW solutions for RD equations such as (3) or (7) is the existence of either a unique speed or a semi-infinite spectrum of speeds with a positive threshold boundary. The first case corresponds to a cubic nonlinearity, as in the nerve conduction application above, whereas the latter applies to a quadratic nonlinearity. These features can be contrasted with the paradox of infinite speed behavior exhibited by the classical diffusion equation. For example, with the quadratic form (8), Equation (7) has a TW solution for all $v \geq v_0 = 2\sqrt{kD}$. A similar property applies to system (3) although in practice only for a limited class of RD equations is an analytical expression known for v_0. In Figure 1, we show a typical profile of a TW solution to system (3) obtained from numerical simulations on a semi-infinite one-dimensional spatial domain via an implicit finite-difference scheme.

One of the oldest but still active fields of application is the modeling of nerve impulse conduction along a

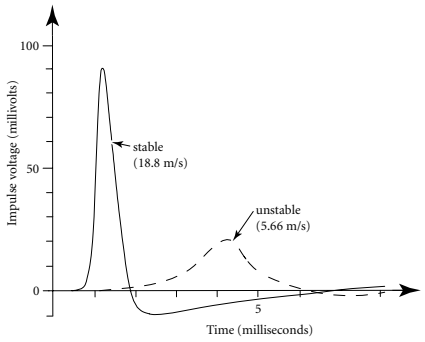

Figure 2. A full-sized action potential and an unstable threshold impulse for the HH axon: (Courtesy of A.C. Scott.)

responsive fiber (Scott, 2003). In 1952, Alan Hodgkin and Andrew Huxley formulated a detailed description of the dynamics of membrane ionic current for a dozen giant squid axons (Hodgkin & Huxley, 1952). They produced the following differential system describing the dynamics of the voltage $V(x,t)$ across the nervous cell (assumed one-dimensional):

$$rc_a \frac{\partial V}{\partial t} = \frac{\partial^2 V}{\partial x^2} + rj_i, \tag{10a}$$

where

$$j_i = 2\pi a J_i\,,\; J_i = G_{\mathrm{K}} n^4 (V - V_{\mathrm{K}}) + G_{\mathrm{Na}} m^3 h (V - V_{\mathrm{Na}}) + G_{\mathrm{L}} (V - V_L). \tag{10b}$$

Here, a is the radius of the fiber, r is the longitudinal resistance per unit length of the fiber, c_a is the membrane capacitance per unit length, and j_i is the total ionic current flowing across the membrane per unit length. The expressions appearing in Equation (10b) are given in terms of differential first-order rate equations describing the concentrations of potassium, sodium "turn-on" and "turn-off" variables (n, m, and h). These equations are determined from experimental data. The RD system (10a,10b) is now known as the Hodgkin–Huxley (HH) system. Using TW theory, one can show that HH is an excitable RD system for parameter ranges of interest that admit traveling pulse solutions called action potentials (see Figure 2).

From a theoretical perspective, the HH system is complicated; thus, simplified theoretical models have been proposed to capture qualitative features. One such model is the system proposed by FitzHugh and Nagumo (FitzHugh, 1961), which reads

$$\frac{\partial V}{\partial t} = \frac{\partial^2 V}{\partial x^2} + F(V) + R\,,\; \frac{\partial R}{\partial t} = \varepsilon (V - c_a - b_a R), \tag{11}$$

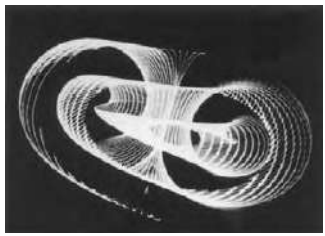

Figure 3. A computer generated scroll wave. (Courtesy of A. Winfree.)

where R is the slowly changing recovery variable and F has a cubic shape. The FitzHugh–Nagumo system admits periodic traveling waves and pulses both stable and unstable. In 2 or 3 spatial dimensions, target (ring) and spiral waves have been numerically produced that today are known to be characteristic types of TW solutions of an excitable system (Scott, 2003).

The most striking illustrations of target and spiral waves can be seen in excitable chemical reactions. Historically, the first such demonstration was produced in the chemical medium proposed by Belousov and Zhabotinsky, now known as the BZ reaction (Zhabotinsky, 1991). A dynamical system is called excitable when it responds in a qualitatively different way to perturbations that are below and above some threshold value, above which it typically amplifies those perturbations. After a pulse has been generated, the system takes some time (refractory state) until it can again support an impulse. In two dimensions, one can find target (ring) and spiral waves as in a typical BZ experiment (*See* photo in **Belousov–Zhabotinsky reaction** and also in color plate section).

To describe these solutions analytically, one can use a simplified model of the BZ reaction, such as the two-species Oregonator model developed by Field and Noyes (1974):

$$\varepsilon \frac{\partial a}{\partial t} = \varepsilon^2 \Delta a + a(1-a) - f\frac{a-q}{a+q} b,$$
$$\frac{\partial b}{\partial t} = \varepsilon \Delta b + b - a, \tag{12}$$

where ε, f, q are kinetics parameters related to the reagents rate reactions and a, b are proportional with the concentrations of $HBrO_2$ and a metal ion. Here the diffusion operator Δ denotes one-, two-, or three-dimensional diffusion. In the latter case, more complicated patterns are found such as toroidal scroll waves and multi-armed spiral waves. Figure 3 shows a computer generated scroll ring obtained in a model of the BZ reaction, which has also been observed experimentally.

To understand such solutions a geometrical theory of traveling waves propagating on arbitrary two- and

three-dimensional manifolds was developed by Tyson, Keener, Grindrod, and others around the mid-1980s, (see Grindrod, 1996). The idea is to compare the problem of three-dimensional wave propagation with that for wave propagation in one dimension. Consider the equation

$$\varepsilon \frac{\partial u}{\partial t} = \varepsilon^2 \Delta u + f(u), \tag{13}$$

which is in the Oregonator model of the BZ reaction (see Equation (12)). Suppose that u_1, u_2 are two solutions to $f(u) = 0$ and that (13) has a TW solution of the form $u = u(y)$ where $y = (x - vt)/\varepsilon$, so that

$$u'' + vu' + f(u) = 0 \tag{14}$$

satisfying $u \to u_1$ as $y \to \infty$ and $u \to u_2$ as $y \to -\infty$ for some speed $v > 0$. For a TW structure to exist in three dimensions, there should be an oriented surface M moving through R^3 such that $u \sim u_1$ ahead of the surface and $u \sim u_2$ behind it. Introducing a normal stretched variable depending on a curvilinear system of coordinates, one can show that a solution $u = \phi(\xi)$ exists subject to $\phi \to u_1$ as $\xi \to \infty$ and $\phi \to u_2$ as $\xi \to -\infty$ if and only if ϕ satisfies the TW equation

$$\phi_{\xi\xi} + (N + \varepsilon K)\phi_\xi + f(\phi) = 0. \tag{15}$$

From (14) and (15) we find that $u = \phi(\xi)$ is the inner solution of the problem when

$$v = N + \varepsilon K, \tag{16}$$

which is called the eikonal equation (Grindrod, 1996). Here N denotes the normal velocity, and K is twice the mean curvature of M. For example for circular waves, the speed of the curved wave v should be smaller than that of the planar wave v_0. The eikonal equation gives $v = v_0 - 2D/r$, where r is the radius and D is the diffusion coefficient. Hence we have a condition for the initiation of circular waves that is purely geometric, namely, $r_{\text{crit}} = 2D/v_0$ for the critical radius of wave initiation. When two circular waves collide, they create cusp-shaped regions with positive curvature. The theory can also be applied to armed spirals and toroidal scroll waves (Grindrod, 1996).

Spiral waves generated by reaction-diffusion processes also occur in surface reactions as tiny spiral waves, visible only through a microscope, that form out of catalytic nitric oxide reduction by hydrogen on rhodium or platinum surfaces. Such pattern formation in surface reactions can be imaged by photoemission electron microscopy (PEEM).

Flames on a spinning disk have been studied at NASA where it is shown that target and spiral waves appear in a mixture of butane in He–O_2. A simple such model is the Salnikov RD system (Scott et al., 1997):

$$a_t = \nabla^2 a + \mu - af(b), \tag{17a}$$

$$b_t = Le\nabla^2 b + \frac{1}{\kappa}(af(b) - b). \tag{17b}$$

Figure 4. A spiral galaxy in Centaurus. VLT, European Southern Observatory.

Here $f(b) = \exp[b/(1 + \gamma b)]$ and $Le, \mu, \kappa, \gamma > 0$ are physical parameters with $\kappa \ll 1$.

Spiral forms are omnipresent throughout the visible and invisible universe in galaxies, accretion disks around black holes, coalescing interstellar clouds, and many other forms of matter and energy (see Figure 4). Lee Smolin (1996) has suggested that the formation of some spiral galaxies can be regarded as an RD process, and he produced a theory of cosmos as a self-sufficient organically developing natural system. In this scenario the galactic spirals (and everything inside them) are gargantuan relatives of the BZ waves.

Waves of spreading depression appear as electrochemical waves associated with the depolarization of the neuronal membrane of the brain as they spiral around lesions of the cortex. There is speculation that this wave activity is linked to epilepsy. Since Art Winfree's pioneering work, scroll waves have been linked quite firmly with cardiac arrhythmias (Keener & Sneyd, 2002). In particular, the onset of fibrillation seems to be connected with the development of scroll type waves (high-frequency waves of electrical activation that recirculate repeatedly, preventing normal function) in the heart muscle. In this case, the heart contractions are much smaller in amplitude than the normal coordinated contraction and also aperiodic, which has potentially fatal consequences.

In early embryo development, circular calcium waves propagate and occasionally annihilate on the surface of a fertilized egg cell as a precursor to cell division. However, in frog eggs they take the form of spiral waves whose purpose is still unclear.

The dynamics of biological populations can self-organize in propagating traveling structures akin to

RD waves (Okubo & Levin, 2001). This is a classical topic in ecology with ramifications for studies in biodiversity. Among the pioneers of the field were Alfred Lotka in 1910 (Lotka, 1925) and Vito Volterra (1926), who have shown that equations similar to those describing reacting chemicals can provide a crude description of interactions between a predator population and its multiplying prey population. Thus, Lotka–Volterra RD type interactions are the heart of modeling in much of ecological dynamics and modeling of epidemics. The spatial spread of epidemics can be usefully approached with a "prey-predator" type dynamics involving the three species: S (the susceptibles), I (infectives), and R (removed individuals) in a population (Kermack & McKendrick 1932; Murray, 2002):

$$S_t = -\beta IS, \quad I_t = \beta IS - \gamma I + D\Delta I, \\ R_t = \gamma I. \tag{18}$$

Equations (18) give a simple model of the spatial spread of rabies by fox, where D is the diffusion coefficient of the infectious foxes and β represents the rate of infection per susceptible per unit density of infectives. More sophisticated versions of such models that are used today to model epidemics (both in humans and in animals) can capture other effects such as secondary outbreaks.

The above discussion has mainly concentrated on the applications of the traveling-wave solutions of the RD systems. However, a much richer solution structure exists in these systems. In fact, the spectrum of possibilities ranges from simple stationary (or time independent) solutions up to complicated spatiotemporal chaotic solutions.

Perhaps one of the most spectacular applications of RD systems is in morphogenesis. The basic question here is to understand how the complicated process of shaping and patterning in an early embryo takes place starting from a uniform structure, the initial egg. In 1952, Alan Turing proposed that this process could be accounted for in terms of the underlying chemical reactions taking place in the embryo. In his paper Turing proposed some hypothetical reactions that could generate spontaneous symmetry breaking, leading to stable spatial patterns (Turing, 1952). Today this mechanism for spatial pattern formation is called Turing instability (or diffusion-driven instability) in recognition of Turing's seminal work. A counterintuitive feature of Turing's prediction is that diffusion can act as a destabilizing force. Murray (1988, 2002) showed that activator-inhibitor RD systems can model the beautiful array of patterns seen on animal skin markings. The idea Murray presented is that at a very early stage, the embryo acquires a "pre-pattern" of chemical morphogens (in Turing's parlance) that is later read out by melanocytes (pigment producing cells). In this way, spotted or striped or a combination of both patterns can be accounted for. Furthermore, Murray showed how the geometrical aspects of the RD domain can considerably alter the final outcome of the patterns. This theory explains why spotted animals (such as cheetah, jaguars, and leopards) can have striped tails, but striped animals (such as zebras and genets) cannot have spotted tails. An equally spectacular application of Turing's theory was proposed by Meinhardt (1998) to account for many patterns seen on seashells.

The book by Murray (2002) contains further references to expanding the above RD framework on modeling crucial processes in morphogenesis, such as feather germs, the initiation of teeth primordia, cartilage and condensation in limb, and epidermis development. Most of them require expansion of the RD framework to incorporate mechanics leading to the study of mechano-chemical models.

With growing evidence of biological morphogens in living tissues, it is now clear that Turing's theory may play a crucial role in explaining biological development. Furthermore, a recent extension of the applications of RD systems in biological pattern formation has strengthened considerably the theoretical arguments in favor of the role of RD systems in biological modeling. Satnoianu et al. (2001) have shown that coupling of diffusion by advection in the presence of autocatalytic reactions can lead to an improved recipe for pattern formation, which is able to account also for biological growth. The new mechanism of patterning, now termed flow and diffusion distributed structures (or FDS), produces both stationary and traveling structures and, thus, can be viewed as an unifying theoretical construct for many of the patterning processes described above (Satnoianu, 2003). The FDS mechanism is a robust patterning process that can explain somitogenesis in vertebrates (Kaern et al., 2001).

Reaction-diffusion-advection equations have been also used in astrophysics, geochemistry, fluid dynamics, and finance, for example. Other applications of RD systems arise in chemotaxis, modeling bacterial growth patterns, the process of wound healing, or the spread of cancer cells in healthy tissue to enumerate only a few such ideas in mathematical biology.

RAZVAN SATNOIANU

See also **Belousov–Zhabotinsky reaction; Brusselator; Cardiac arrhythmias and electrocardiogram; Chemical kinetics; Diffusion; FitzHugh–Nagumo equation; Heat conduction; Morphogenesis, biological; Pattern formation; Population dynamics; Scroll waves; Spiral waves; Turing patterns; Zeldovich–Frank-Kamenetsky equation; Vortex dynamics in excitable media**

Further Reading

Aronson, D.G. & Weinberger, H.F. 1975. Nonlinear diffusion in population genetics, combustion and nerve pulse propagation. In *Partial Differential Equations and Related Topics*, edited by J.A. Goldstein, New York: Springer

Faraday, M. 1861. *A Course of Six Lectures on the Chemical History of a Candle*. Reprinted as *Faraday's Chemical History of a Candle*, Chicago: Chicago Review Press, 1988

Field, R.J. & Noyes, R.M. 1974. Oscillations in chemical systems, IV. Limit cycle behaviour in a model of a real chemical reaction. *Journal of Chemical Physics*, 60: 1877–1884

Fisher, R.A. 1937. The wave of advance of advantageous genes. *Annals of Eugenics*, 7: 353–369

FitzHugh, R. 1961. Impulse and physiological states in theoretical models of nerve membrane. *Biophysical Journal*, 1: 445–466

Grindrod, P. 1996. *The Theory and Applications of Reaction-Diffusion Equations*, Oxford: Clarendon Press

Hodgkin, A.L. & Huxley, A.F. 1952. A quantitative description of membrane current and its application to conduction and excitation in nerve. *Journal of Physiology*, 117: 500–544

Kaern, M., Menzinger, M., Satnoianu, R.A. & Hunding, A. 2001. Chemical waves in open flows of active media: their relevance to axial segmentation in biology. *Faraday Discussions*, 120: 295–312

Kauffman, S.A. 1995. *At Home in the Universe. The Search for the Laws of Self-organization and Complexity*, New York: Oxford University Press

Keener, J. & Sneyd, J. 2002. *Mathematical Physiology*, New York: Springer

Kermack, W.O. & McKendrick, A.G. 1932. Contributions to the mathematical theory of epidemics. *Proceedings of the Royal Society, London*, A 115: 700–721

Kolmogoroff, A., Petrovsky, I. & Piscounoff, N. 1937. Étude de l'équation de la diffusion avec croissance de la quantité de matière et son application à un problème biologique. *Moscow University Bulletin Mathematics*, 1: 1–25

Lotka, A.J. 1925. *Elements of Physical Biology*, Baltimore: Williams and Wilkins

Meinhardt, H. 1998. *The Algorithmic Beauty of Seashells*, Berlin: Springer

Murray, J.D. 1988. How the leopard gets its spots. *Scientific American*, 258: 62

Murray, J.D. 2002, 2003. *Mathematical Biology*, 3rd edition, vols. 1 and 2, Berlin and New York: Springer

Øksendal, B. 2003. *Stochastic Differential Equations*, 6th edition, Berlin and New York: Springer

Okubo, A. & Levin, S.A. 2001. *Diffusion and Ecological Problems: Modern Perspectives*, Berlin and New York: Springer

Satnoianu, R.A. 2003. Coexistence of stationary and traveling waves in reaction-diffusion-advection systems. *Physical Review* E, 68: 032101

Satnoianu, R.A., Maini, P.K. & Menzinger, M. 2001. Parameter space analysis, pattern sensitivity and model comparison for Turing and stationary flow and diffusion distributed structures (FDS). *Physica* D, 160: 79–102

Scott, A. 2003. *Nonlinear Science: Emergence and Dynamics of Coherent Structure*, 2nd edition, Oxford and New York: Oxford University Press

Scott, S.K., Wang, J. & Showalter, K. 1997. Modeling studies of spiral waves and target patterns in premixed flames. *Journal Chemical Society of Faraday Transactions*, 93: 1733–1739

Smolin, L. 1996. Galactic disks as reaction-diffusion systems. eprint arXiv.org astro-ph/9612033, 22 pages

Turing, A. 1952. The chemical basis of morphogenesis. *Philosophical Transactions of the Royal Society of London* B, 327: 37–72

Volpert, A.I. & Volpert, V.A. 1994. *Travelling Wave Solutions of Parabolic Systems*. Translations of mathematical monographs, vol. 140, Providence, RI: American Mathematical Society

Volterra, V. 1926. Variations and fluctuations of a number of individuals in animal species living together. In *Animal Ecology*, New York: McGraw Hill, pp. 409-448, 1931. Translation by R.N. Chapman

Zeldovich, Ya.B. & Frank-Kamenetsky, D.A. 1938. K teorii ravnomernogo rasprostranenia plameni [toward a theory of uniformly propagating flames]. *Doklady Akademii Nauk SSSR*, 19: 693–697

Zhabotinsky, A.M. 1991. A history of chemical oscillations and waves, *Chaos*, 1: 379–386

RECURRENCE

Recurrence means repetition, and this, in turn, implies the presence of two actors: the particular event that is coming back after having occurred in the past and the law prescribing how events unfold in time.

The crossing of the vertical position by a well-serviced pendulum is a recurrent event. Here the event coincides with a particular value of the position coordinate, and the intervening law is Newton's second law in the presence of gravity. We deal here with the simplest version of recurrence, namely, strict periodicity. But one could also say that in a capitalistic economy, economic growth or slow down are recurrent events. The event is now an attribute of a whole succession of outcomes interrupted by irregular periods where this attribute is absent, and the intervening laws are no longer directly reducible to nature's dispassionate fundamental interactions but involve, rather, competing human agents each one of whom wishes to maximize his profit. In a still different vein, the need for survival has made man aware of the repeated appearance (recurrence) of weather patterns associated with different winds and/or precipitation patterns. The Greeks constructed an octagonal structure, the Tower of Winds, which can still be visited in Athens. It depicts the wind from each cardinal point and comprises bas-relief figures representing the typical type of weather associated with such a wind. The event is now a lumped, coarse-grained characterization of the state of the atmosphere that came to be known later on as *Grosswetterlagen* or "atmospheric analogs," and the laws are those of fluid mechanics and thermodynamics as applied to a rotating frame.

In the physical sciences, the description usually adopted views the system of interest as a deterministic dynamical system. At first sight this entails that an event is to be associated with the point that the system occupies in phase space at a given time. But in this view exact recurrence of a state is impossible except for the trivial case of periodic dynamics, because it would

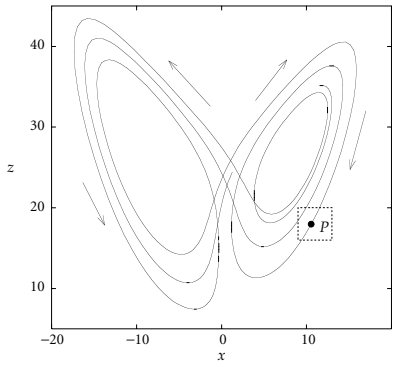

Figure 1. Illustrating recurrence on a two-dimensional projection of the Lorenz chaotic attractor. Recurrence is here reflected by the fact that the trajectory emanating from point P in the dotted square will re-enter this cell (which plays the role of a coarse-grained state) after some time.

violate the basic property of uniqueness of the solutions of the evolution equations. To cope with this limitation, one associates the concept of recurrence with repeated re-entries of the dynamical trajectory in a phase space region possessing finite volume (more technically, "measure") as indicated in Figure 1. This is, precisely, the coarse-grained state referred to earlier, as opposed to the point-like states considered in many (or even most) nonlinear science-related problems. Probabilistic description is a typical instance in which one deals essentially with coarse-grained states.

Poincaré Recurrence

In his celebrated memoir on the three-body problem Henri Poincaré, a founding father of nonlinear science, established a result that may be considered as the first quantitative and rigorous statement concerning recurrence (Poincaré, 1890). He showed that in a system of point particles under the influence of forces depending only on the spatial coordinates, a typical phase space trajectory will visit infinitely often the neighborhood, however small, of a prescribed initial state, provided that the system remains in a bounded region of phase space. The time between two such consecutive visits is referred as a "Poincaré recurrence time."

In modern terms (Kac, 1959), let A be a subset of space Ω within which the system is confined such that $\mu(A) > 0$ where μ designates the measure of A, and T_t a family of one-to-one measure preserving transformations in Ω. Then, for almost every initial point $P \in A$ (i.e., except for a set of Ps of zero μ-measure), there exists a sufficiently large t such that $T_t P \in A$. Using the machinery of the proof, one may derive an expression for the mean recurrence time,

$$\langle \theta_\tau \rangle = \tau / \mu(A), \tag{1}$$

where τ is the time resolution between the successive observations. Actually, as observed by Marian Smoluchowski, this expression needs to be adapted, in the limit of continuous time, to

$$\langle \theta_\tau \rangle = \tau(1 - \mu(A))/(\mu(A) - \mu(P \in A, T_\tau P \in A)), \tag{2}$$

where one has introduced the measure of the intersection of A and its pre-image $T_\tau^{-1} A$.

Part of the historical role of Poincaré's theorem relates to the famous *Wiederkehreinwand*, an early objection by Ernst Zermelo challenging Ludwig Boltzmann's derivation of the second law of thermodynamics on the grounds that since states recur, the H-function (the microscopic analog of entropy) is bound to reverse its course at some stage. Boltzmann made a valiant attempt to respond, based essentially on the enormity of recurrence times in a molecular system (of the order of ten to the power of the Avogadro number). A more pertinent observation is that thermodynamic states are associated with a Gibbs ensemble rather than with single phase space points. Poincaré's theorem does not apply under these conditions; hence, Poincaré recurrences are not necessarily precluding a microscopic interpretation of irreversibility.

From Ehrenfest to Fermi–Pasta–Ulam

A first implementation of the idea that it is indeed possible to reconcile recurrence with irreversible behavior was provided by the, by now famous, "dog flea" model of Paul and Tatiana Ehrenfest. $2N$ numbered balls are distributed in boxes A and B. An integer from 1 to $2N$ is drawn at random and the ball corresponding to that number is moved from the box in which it is found to the other one. The process is then repeated to any desired number of times. One can show (Kac, 1959) that every initial state recurs with probability one, although the system possesses an H-function. Actually, this model belongs to a general class of stochastic processes known as Markov chains, whose theory was developed intensely in the first part of the 20th century (Feller, 1968, 1971). These developments allow one to put the compatibility between recurrence of states and irreversible approach to an asymptotic regime on a firm basis for this very general class of processes amenable to a Markov chain-like description. An important insight is that while recurrence is a property of trajectories (which being now stochastic and thus coarse-grained are not bound to satisfy the uniqueness theorem stated above and can therefore recur as such), the approach to an asymptotic regime is a property of

probability distributions. The theory of stochastic processes has also provided a wealth of further information on recurrence independent of the problem of irreversibility, including connections with the important class of renewal processes.

Despite their power, the above results overlooked the nature of the underlying deterministic dynamics, except that the last had to be complex enough to generate somehow a stochastic game. This shortcoming became clearly recognized in the 1950s, when Poincaré's recurrence was viewed again as a problem of strictly deterministic dynamics, thanks partly to the new possibilities afforded by the availability of electronic computers. From the standpoint of nonlinear science, the most relevant among these early attempts is that by Fermi, Pasta, and Ulam (Fermi et al., 1955) who numerically examined a set of coupled differential equations modeling the motion of a linear chain of equimass particles connected by nonlinear springs

$$\begin{aligned}\frac{d^2x_j}{dt^2} &= \{1+\beta[(x_{j+1}-x_j)^2+(x_j-x_{j-1})^2 \\ &\quad +(x_{j+1}-x_j)(x_j-x_{j-1})]\} \\ &\quad \times(x_{j+1}+x_{j-1}-2x_j), \\ j &= 1,2,\ldots,N-1, x_0=x_N=0. \qquad (3)\end{aligned}$$

Fermi et al. showed that with 64 particles at low energy there was no equipartition of energy among the oscillators (contrary to their expectations). Instead, a beat phenomenon was observed with ongoing recurrences of initial conditions. Recurrence seemed once again to be at odds with the tendency toward thermal equilibrium, to which is associated the stronger property of mixing and equipartition. A closer analysis shows that Fermi–Pasta–Ulam recurrence is not universal: for higher energies a phenomenon of overlap of resonances is taking place, leading to stochasticity in the sense that energy transfer between modes becomes possible. To what extent this stochasticity can invade the entire phase space as N and the energy are increased is still an unsettled question.

Modern Nonlinear Dynamics and Recurrence

The most significant advance on recurrence since the 1960s has been to dissociate the concept from the approach to equilibrium of a many-body system (and, in particular, to realize that the two concepts are not to be opposed), to extend it to cover the class of dissipative dynamical systems, and to establish a link between the deterministic and the stochastic approaches to it.

What made this advance possible is the realization, at the heart of modern nonlinear dynamics, that simple-looking, low-dimensional models may give rise to complex behavior that emulates, to a large extent, the behavior of real world, multivariate systems. Furthermore, in the presence of deterministic chaos, sensitivity to initial conditions raises the problem of long-term prediction and prompts one to adopt a probabilistic approach, perfectly compatible with (and actually induced by) the underlying dynamics, in which quantities of interest are expressed as statistical averages. In this setting, recurrence became a powerful tool providing new insights along two directions.

Recurrence as an Indicator of the Dynamical Complexity

The main point here is that dynamical systems having different ergodic properties show different recurrence patterns. An interesting example is uniform quasi-periodic motion on a two-dimensional torus or its equivalent discrete-time version given by the shift map. It can be shown (Sös, 1958; Theunissen et al., 1999) that, typically, such a system (known to be ergodic) possesses exactly three possible values of recurrence times in any prescribed phase space cell. On the other hand, in a wide class of uniformly hyperbolic systems such as one-dimensional maps, one shows that recurrence times in a sufficiently small phase space cell are generically exponentially distributed, while a sequence of successive recurrences has a Poissonian limit distribution (Collet, 1991). The situation is different in non-uniformly hyperbolic systems. In particular, in systems showing intermittent behavior the above laws are replaced, respectively, by power laws and by Lévy stable distributions (Balakrishnan et al., 1997). Work along similar lines has also led to connections between recurrence patterns and Lyapunov exponents, unstable periodic orbits, or generalized dimensions. There is, however, no firm indication about the universality of these latter results.

Recurrence as a Tool for Prediction

The question whether, and if so how frequently, the future states of a system will come close to a certain initial configuration has a direct bearing on prediction, an issue of central importance in atmospheric sciences, hydrology, and other environment-related disciplines. A dynamical approach to the recurrence of atmospheric analogs, the lumped states of the atmosphere introduced above reveals a strong dependence of recurrence times on the local properties of the attractor and a pronounced variability around their mean (Nicolis, 1998). Of crucial interest is also the recurrence of extreme events such as natural disasters, a problem approached traditionally at the level of a statistical description (Gumbel, 1958). The extension of the statistical theory of extremes and their recurrences to deterministic dynamical systems is still in its infancy.

G. Nicolis and C. Rouvas-Nicolis

See also **Dynamical systems; Fermi–Pasta–Ulam oscillator chain; Intermittancy; Nonequilibrium statistical mechanics**

Further Reading

Balakrishnan, V., Nicolis, G. & Nicolis, C. 1997. Recurrence time statistics in chaotic dynamics I. Discrete time maps. *Journal of Statistical Physics*, 86: 191–212

Collet, P. 1991. Some ergodic properties of maps of the interval, Lectures given at the CIMPA summer school *Dynamical Systems and Frustrated Systems*, edited by J.M. Gambaudo, Temuco

Feller, W. 1968, 1971. *An Introduction to Probability Theory and Its Applications*, 2 vols, 3rd edition, New York: Wiley

Fermi, E., Pasta, J.R. & Ulam, S.M. 1955. Studies of nonlinear problems. Los Alamos Scientific Laboratory Report No. LA-1940

Gumbel, E.J. 1958. *Statistics of Extremes*, New York: Columbia University Press

Kac, M. 1959. *Probability and Related Topics in Physical Sciences*, London and New York:

Nicolis, C. 1998. Atmospheric analogs and recurrence time statistics: toward a dynamical formulation. *Journal of Atmospheric Sciences*, 55: 465–475

Poincaré, H. 1890. Sur le problème des trois corps et les équations de la dynamique. *Acta Matematica*, 13: 1–270

Sös, V.T. 1958. On the distribution mod 1 of the sequence nα. *Annales Universitatis Scientiarum Budapestinensts de Rolando Eotovos Nominatae Sectio Mathematica*, 1: 127–134

Theunissen, M., Nicolis, C. & Nicolis, G. 1999. Recurrence times in quasi-periodic motion: statistical properties, role of cell size, parameter dependence. *Journal of Statistical Physics* 94: 437–467

REGULAR AND CHAOTIC DYNAMICS IN ATOMIC PHYSICS

Many important areas of atomic physics dwell in the intriguing world of semiclassical quantum mechanics, where classical concepts such as orbits and phase space are used to calculate purely quantal quantities such as quantum numbers, wave functions, and ionization thresholds. The past two decades have witnessed renewed interest in classical interpretations of quantum phenomena (Berry & Mount, 1988; Casati et al., 1987; Blümel & Reinhardt, 1997; Jensen, 1992), a view sometimes referred to as postmodern quantum mechanics (Heller & Tomsovic, 1993). This development has led to the much debated term *quantum chaos* (*See* **Quantum chaos**). A central issue is the relevance of chaotic dynamics to the quantum world, where the sensitivity to initial conditions characteristic of classical chaos is obscured by the Heisenberg uncertainty principle. Moreover, the Schrödinger equation is linear and does not normally exhibit extreme sensitivity to initial conditions. Nevertheless, classical dynamics plays an important role in the quantum world, even in chaotic regions. Thus, the ionization of hydrogen by a microwave field is often well described in terms of chaotic diffusion of classical electron orbits, while the quantum mechanical wave function exhibits traces of classical (unstable) periodic orbits, called scarring.

When the classical dynamics are regular, semiclassical quantum numbers can be calculated according to the Einstein–Brillouin–Keller (EBK) prescription (Gutzwiller, 1990),

$$J_i = \oint p_i \mathrm{d}q_i = (n_i + \alpha_i/4)h, \qquad (1)$$

where J_i is the classical action, calculated from the loop integral over coordinate q_i and canonically conjugate momentum p_i, n_i is the corresponding quantum number, h is Planck's constant, and α_i is the Maslov index, an integer that depends on the topology of the invariant torus. In this way, approximate semiclassical wave functions can also be constructed. The semiclassical description is found to work well under two conditions: (i) the quantum numbers are large, and (ii) the number of participating states is also large. Under chaotic conditions (when the classical action does not generally exist), one still has recourse to periodic orbits (Eckhardt, 1988), which can be used to organize energy levels and the form of the wave function (Gutzwiller, 1990). The principal tool under chaotic conditions is the Gutzwiller trace formula, based on the Feynman propagator.

Our unifying theme is the hydrogen atom in an electromagnetic field, for which the motion of the single electron is well described by a Hamiltonian model. We consider first two closely related integrable cases (*See* **Constants of motion and conservation laws; Integrability**), the classical problem of two fixed centers as a model for the hydrogen molecule ion H_2^+, and the H-atom in a homogeneous electrostatic field. In both cases axial symmetry implies the constancy of the azimuthal angular momentum, $p_\phi = m\rho^2\dot{\phi}$ (in cylindrical coordinates ρ, ϕ, z), allowing a reduction in dimensionality from three to two, via an effective potential formed by including the azimuthal part of the kinetic energy with the potential $U(\rho, z)$:

$$U^e(\rho, z) = U + \frac{p_\phi^2}{2m\rho^2}\,. \qquad (2)$$

Thus, in both cases the motion is described by a two degree of freedom autonomous (time-independent) Hamiltonian.

Next we take up the non-integrable case of the H-atom in a homogeneous magnetostatic field, which has been extensively studied, both theoretically and experimentally (Born, 1960; Friedrich & Wintgen, 1989), and which is also described by a two-degree-of-freedom Hamiltonian. Then we describe fruitful experiments on microwave ionization of H-atoms, which have yielded an abundance of information on quantum physics (Blümel & Reinhardt, 1997; Koch & van Leeuwen, 1995). Various Hamiltonian models have been investigated, from one to three degrees of freedom. Here, we shall limit ourselves to a one-dimensional time-periodic model, which captures most

of the relevant physics. Finally, we briefly mention other atomic systems in which a semiclassical treatment sheds light on quantal behavior.

Two Fixed Centers

The two fixed centers model (TC) consists of a test mass orbiting in the gravitational field of two massive bodies rotating about their center of mass at a fixed distance. In atomic physics the attractive force is electrostatic, furnishing a useful model for the hydrogen molecule-ion (Born, 1960; Strand & Reinhardt, 1979; Howard & Wilkerson, 1995). It also enjoys the distinction of being one of the small minority of completely integrable systems, owing to separability in confocal elliptic coordinates. With the two protons fixed at $z = \pm a$, the nonrelativistic motion of the electron is described by the Hamiltonian,

$$H = \frac{1}{2m}(p_\rho^2 + p_z^2) + U^e \tag{3}$$

with effective potential

$$U^e(\rho, z) = \frac{p_\phi^2}{2m\rho^2} - q^2\left(\frac{1}{r_1} + \frac{1}{r_2}\right), \tag{4}$$

where q is the electronic charge,

$$r_1^2 = \rho^2 + (z-a)^2, \quad r_2^2 = \rho^2 + (z+a)^2, \tag{5}$$

and $p_\rho = m\dot{\rho}$, $p_z = m\dot{z}$, and $p_\phi = m\rho^2\dot{\phi}$. All trapped orbits are confined by the two-dimensional effective potential, shown in Figure 1 for two nearby values of the control parameter $\mu = p_\phi^2/a^2$. In the first case, a single well centered on an equatorial critical point of U^e exists, which in the second case has bifurcated into a double well. Quantizable stable circular orbits exist at the elliptic critical points of U^e. Because there is no chaos in this system, it might seem straightforward to construct quantum numbers from the two conserved actions, taking care to get the correct Maslov indices. However, there is a rub: there are two disjoint classes of orbits, a situation referred to as "monodromy," resulting in separate actions, which need to be smoothly joined. This process of "uniform quantization" has been carried out by Strand & Reinhardt (1979), who obtained greatly improved values for energy levels for varying intermolecular separation $R = 2a$.

Hydrogen Atom in a Strong Electric Field

The behavior of the H-atom in a homogeneous electrostatic field is one of the oldest problems of quantum mechanics, the weak-field case giving rise to the Stark effect, traditionally treated using perturbation theory (Born, 1960). For larger fields, ionization occurs (Koch, 1978; Howard, 1995), the ionization threshold field F_c depending on the particle energy as well as a quantity called the Runge–Lenz invariant.

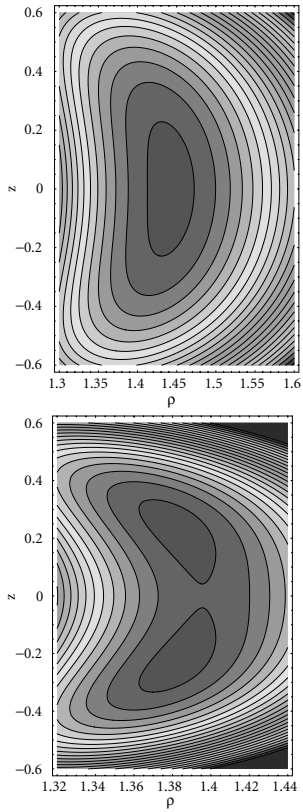

Figure 1. Contour plot of effective potential for the hydrogen molecule-ion before and after pitchfork bifurcation.

This is an interesting problem for two reasons: (i) the required fields are too large for perturbative methods, and (ii) the motion is completely integrable, since the Hamiltonian and the Schrödinger equations both separate in parabolic coordinates. Spectral lines are then conveniently labeled by quantum numbers n, n_1, n_2, and $|m|$, where $n = n_1 + n_2 + |m| + 1$ is the principal quantum number, m is the azimuthal quantum number, and n_1 and n_2 are parabolic quantum numbers.

Field ionization may be treated either classically or via quantum mechanical tunneling (Gallas et al., 1982). With the electric field along the z-axis, the nonrelativistic motion of the electron is again described by Hamiltonian (3), with effective potential

$$U^e(\rho, z) = -\frac{q^2}{\sqrt{\rho^2 + z^2}} + \frac{p_\phi^2}{2m\rho^2} - qFz\,, \tag{6}$$

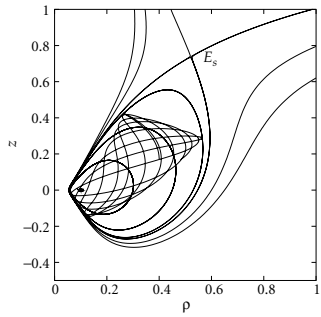

Figure 2. Electron orbit with energy $E < E_S$ trapped in effective potential for the hydrogen atom immersed in a homogeneous electric field.

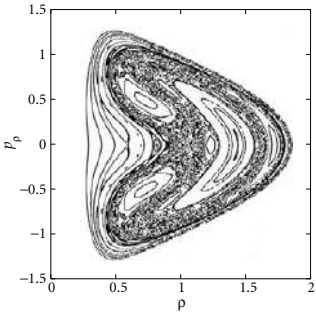

Figure 3. Poincaré section for H-atom in a uniform magnetostatic field.

where p_ϕ gives the azimuthal quantum number $m = p_\phi/\hbar$ and F is the electric field strength. Figure 2 shows an orbit trapped in the two-dimensional potential well formed by the effective potential. All orbits having $E < E_s$, the saddle point energy, are classically trapped. If the system were non-integrable, the condition $E > E_s$ would constitute a necessary and sufficient condition for ionization. However, the existence of the Runge–Lenz invariant allows a subclass of trapped orbits with $E > E_s$. Owing to separability in parabolic coordinates (ξ, η), the actions J_ξ, J_η, and $J_\phi = p_\phi$ always exist so that the EBK formula applies; there is no classical chaos in the Stark problem. In laboratory experiments the electric field is usually gradually increased from zero until ionization occurs. For $m = 0$, the saddle point criterion leads to the ionization threshold $F_c \approx 1/9n^4$, in excellent agreement with experiment.

Hydrogen Atom in a Strong Magnetic field

In contrast to the Stark problem, the electron motion in an H-atom immersed in a homogeneous magnetostatic field can be chaotic, providing a useful testing ground for ideas of quantum chaos (Friedrich & Wintgen, 1989). There are two integrable limits, (i) $B = 0$, for which the orbits are simple Kepler ellipses, and (ii) $B \to \infty$, the helical gyration of a free charged particle in a constant magnetic field. With $\boldsymbol{B} = B_0\hat{\boldsymbol{z}}$, the nonrelativistic motion of a single electron is governed by the effective potential

$$U^e(\rho, z) = \frac{p_\phi^2}{2m\rho^2} - \frac{q^2}{\sqrt{\rho^2 + z^2}} + \frac{1}{8}m\omega_c^2\rho^2 + \frac{1}{2}\omega_c p_\phi, \qquad (7)$$

where $\omega_c = qB_0/mc$ is the cyclotron frequency and now $p_\phi = m\rho^2\dot{\phi} + \frac{1}{2}\rho^2\omega_c$. The constant paramagnetic term may be removed by transforming to a rotating frame. For small magnetic field strength, perturbation theory may be used to calculate energy levels (Zeeman effect); for very large fields, the diamagnetic term proportional to ρ^2 dominates (quadratic Zeeman effect) and the spectrum resembles that of a free electron. In this case, the existence of chaotic trajectories means that a set of classical actions does not always exist, precluding EBK quantization. For small fields, however, canonical perturbation theory can be employed to calculate perturbed actions. This yields useful energy level curves $E_n = E_n(B)$, where the levels are labeled in terms of the unperturbed $(B = 0)$ states. Furthermore, at low fields an approximate constant of the motion exists, facilitating classification of the very complex spectrum and explaining avoided crossings of nearby energy level curves. This recipe fails for larger fields, where the classical motion is mainly chaotic. At very large fields, intriguing regularities persist, called quasi-Landau resonances, close to the spectrum of a free electron in a magnetostatic field. In this case, it is possible to derive a very simple formula for the ionization threshold energy.

The degree of classical chaos is conveniently revealed by the Poincaré section, which is a two-dimensional slice in the four-dimensional phase space, defined by fixing the total energy and recording unidirectional intersections with a coordinate plane (Lichtenberg & Lieberman, 1990). Figure 3 shows a section for a moderately large B-field, generated by calculating particle orbits and recording $(\rho,\ p_\rho)$ each time an orbit crosses the $z = 0$ plane with $p_z > 0$. Regular orbits appear as smooth closed curves, whose centers represent periodic orbits. A single period-one orbit appears near $\rho = 1.45$; all other fixed points are at least period-three. The scattered dots in between represent chaotic orbits (possibly just one), which ergodically fill a connected region of phase space. In this case, classical actions do not exist, and it is

not possible to assign quantum numbers to the very complex spectrum.

Microwave Ionization of Rydberg Atoms

Another fruitful source of information on connections between classical dynamics and quantal behavior is the extensive experimental program on microwave ionization of highly excited Rydberg (hydrogenic) atoms (Blümel & Reinhardt, 1997; Koch & van Leeuwen, 1995). By careful control of experimental conditions, it has been found possible to produce a full range of principal quantum numbers, $n_0 = 34$ to more than 90. Ionization from such excited states can then be readily accomplished using a variety of pulsed or continuous wave sources; linearly polarized, circularly polarized, or elliptically polarized. Remarkably, classical scaling accurately describes much of the experimental results. Thus, the microwave frequency is expressed as a ratio to the Kepler frequency, which according to the Bohr–Sommerfeld model is proportional to n_0^{-3}, giving the dimensionless parameter $\hat{\omega} = n_0^3\omega$. The electric field strength may also be expressed as a ratio to the Coulomb force, giving the dimensionless parameter $\hat{F} = n_0^4 F$. Koch distinguishes several distinct frequency regimes, depending on $\hat{\omega} = n_0^3\omega$; by fixing $\omega/2\pi$ at one of several frequencies between 7 and 36 GHz and varying n_0, a range of scaled frequencies from $\hat{\omega} = 0.02$ to 2.8 can be achieved. For very low $\hat{\omega} \lesssim 0.02$ quantum tunneling dominates, significantly lowering the ionization threshold $\hat{F}_i$. At somewhat higher $\hat{\omega}$ the ionization curves (fraction ionized vs. $\hat{F}$) are primarily classical, with occasional "bumps" deriving from quantum resonances. For $0.1 \lesssim \hat{\omega} \lesssim 1.2$ classical dynamics prevails. Above this value quantum mechanisms increasingly raise the ionization thresholds, by about a factor of two at $\hat{\omega} = 2.8$. As for the Zeeman effect, scarring of the wave function occurs along classical unstable period orbits.

Theoretical and numerical analyses range from crude one-dimensional (1-d) models to elaborate 3-d Monte Carlo simulations. The simplest case to analyze theoretically is linear polarization, in which a simple one-dimensional time-periodic Hamiltonian explains much of the relevant physics,

$$H = H_0 + qFx\sin(\omega t), \tag{8}$$

where

$$H_0 = \begin{cases} \dfrac{p^2}{2m} - \dfrac{q^2}{x}, & x > 0, \\ \infty, & x \le 0. \end{cases} \tag{9}$$

Physically this represents the limiting case of a pencil-thin orbit along the x-axis. In order to compare with experiment, we first transform to action-angle variables $J = \sqrt{a} = \sqrt{-1/2H_0}$, $\theta = u - \sin u$, where a is the semimajor axis and the eccentric anomaly u is defined by $x = a(1 - \cos u)$. The principal quantum number is then given by $J = n_0\hbar$. Poincaré sections can be generated by strobing the orbit at a period $\tau = 2\pi/\omega$ and recording J and θ at $t = \tau, 2\tau, \ldots$. In experiments the microwave field is gradually increased until ionization takes place. For example, for $f_{\mathrm{RF}} = 9.923$ GHz, we obtain the two sections near the $n_0 = 51$ state shown in Figure 4 for $F = 62$ and 66.4 V/cm. At the lower field strength all orbits initialized with $n_0 < 51$ are trapped by invariant circles; at the higher field strength these curves have been destroyed, allowing most of the same orbits to escape. The experimental result for 10% ionization of the $n_0 = 51$ state is about 71 V/cm (Koch & van Leeuwen, 1995), in reasonable agreement with our numerical calculation. Other polarizations have also been investigated (Koch, 1998; Howard, 1992). The most general state is elliptic polarization, which includes circular and linear polarization as special cases. In all cases valuable insight into experiment has been obtained using classical dynamics.

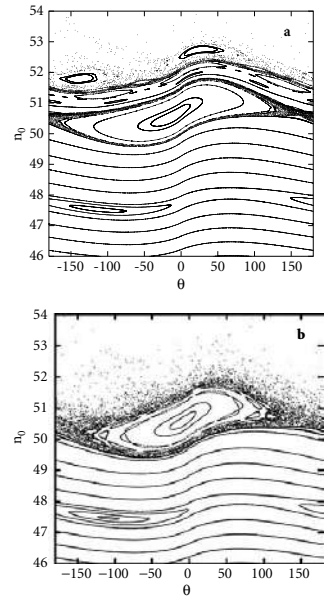

Figure 4. Poincaré section for 1-d H-atom perturbed by a time-periodic microwave field of frequency $f_{\mathrm{RF}} = 9.923$ GHz and strength (a) $F = 62$ V/cm and (b) $F = 66.4$ V/cm.

Discussion

In addition to the above four examples, there are several other systems under active investigation. Combinations

of fields, particularly crossed and parallel fields, $\boldsymbol{E} \times \boldsymbol{B}$ and $\boldsymbol{E} \parallel \boldsymbol{B}$, offer challenging structures that can be partially explained by semiclassical quantization (Farrelly, 1991). Three-body systems, such as the helium atom (Tanner et al., 2000) and the hydrogen negative ion H^-, long considered beyond semiclassical methods, have recently yielded important insights.

JAMES E. HOWARD

See also **Constants of motion and conservation laws; Hamiltonian systems; Quantum chaos**

Further Reading

Berry, M.V. & Mount, K.E. 1972. Semiclassical wave mechanics. *Reports on Progress in Physics*, 35: 315–800

Blümel, R. & Reinhardt, W.P. 1997. *Chaos in Atomic Physics*, Cambridge and New York: Cambridge University Press

Born, M. 1960. *The Mechanics of the Atom*, New York: Unger

Casati, B., Chirikov, B.V., Shepelyansky, D.L. & Guarneri, I. 1987. Relevance of classical chaos in quantum-mechanics—the hydrogen atom in a monochromatic field. *Physics Reports*, 154: 77–123

Eckhardt, B. 1988. Quantum mechanics of classically non-integrable systems. *Physics Reports*, 163: 205–297

Farrelly, D. 1991. Semiclassical mechanics of bounded and unbounded states of atoms and molecules, *Advances in Molecular Vibrations*, 1B, 49–79

Friedrich, H. & Wintgen, D. 1989. The hydrogen atom in a uniform magnetic field—an example of chaos. *Physics Reports*, 183: 37–79

Gallas, J.A.C., Walther, H. & Werner, E. 1982. Simple formula for the ionization rate of Rydberg states in static electric fields. *Physical Review Letters*, 49: 867–891

Gutzwiller, M.C. 1990. *Chaos in Classical and Quantum Mechanics*, New York: Springer

Heller, E.J. & Tomsovic, S. 1993. Postmodern quantum mechanics. *Physics Today*, 46: 38–46

Howard, J.E. 1992. Stochastic ionization of hydrogen atoms in a circularly polarized microwave field. *Physical Review* A, 46: 364–372

Howard, J.E. 1995. Saddle point ionization and the Runge-Lenz invariant. *Physical Review* A, 51: 3934–3946

Howard, J.E. & Wilkerson, T.W. 1995. Problem of two fixed centers and a finite dipole: a unified treatment. *Physical Review A*, 52: 4471–4492

Jensen, R.V. 1992. Quantum chaos. *Nature*, 352: 311–315

Koch, P.M. 1978. Resonant states in the nonperturbative regime: the hydrogen atom in an intense electric field, *Physical Review Letters*, 41: 99–103

Koch, P.M. 1998. Polarization dependence of microwave "ionization" of excited hydrogen atoms. *Acta Physica Polonica*, 93: 105–132

Koch, P.M. & van Leeuwen, K.A.H. 1995. The importance of resonances in microwave "ionization" of excited hydrogen atoms. *Physics Reports*, 255: 289–403

Lichtenberg, A.J. & Lieberman, M.A. 1990. *Regular and Chaotic Dynamics*, 2nd edition, New York: Springer

Strand, M.P. & Reinhardt, W.P. 1979. Semi-classical quantization of the low-lying electronic states of H_2^+. *Journal of Chemical Physics*, 70: 3812–3827

Tanner, G., Richter, K. & Rost, J. 2000. The theory of two-electron atoms: between ground state and complete fragmentation. *Reviews of Modern Physics*, 72: 497–544

RELAXATION OSCILLATORS

The first work related to relaxation oscillators was published by Balthasar van der Pol in 1926 (Van der Pol, 1926). Van der Pol, in collaboration with J. van der Mark, suggested an electrical model of the heart consisting of three relaxation generators (van der Pol & van der Mark, 1928).

An oscillator is said to be of the relaxation type if its period is inversely proportional to a relaxation time and nearly independent of other parameters. Classical examples of relaxation oscillators are a thyratron oscillator (Teodorchik, 1952) and an alternating water source known as Tantal's vessel (Panovko & Gubanova, 1964; Strelkov, 1964). Schematic images of these devices are illustrated in Figures 1a and b. The shape of oscillations of the amount of water in Tantal's vessel and of the voltage across the capacitor C is shown in Figure 1c.

An oscillator described by the Rayleigh equation (Rayleigh, 1877–78)

$$\ddot{x} - \mu(1 - \dot{x}^2)\dot{x} + x = 0 \qquad (1)$$

is also of relaxation type for $\mu \gg 1$. It should be noted that the Rayleigh equation can be obtained from the van der Pol equation

$$\ddot{y} - \mu(1 - y^2)\dot{y} + y = 0 \qquad (2)$$

by the substitution $y = \sqrt{3}\,\dot{x}$.

The phase portrait and the shape of oscillations for Equation (1) are illustrated in Figure 2 for $\mu = 10$. For this value of μ, the equilibrium state is an unstable node and the limit cycle has a shape close to a parallelogram. The time required for the representative point to approach the limit cycle is very short; thus the oscillations are almost discontinuous. For $\mu \ll 1$, the oscillation period is practically independent of μ and approximately equal to the period of free oscillations of the oscillatory circuit $T_0 = 2\pi$. For $\mu \gg 1$, on the other hand, the oscillation period is completely determined by the value of the parameter μ, namely $T \approx 8\mu/3\sqrt{3}$ (see below). As the relaxation time is of the order of $1/\mu$, it follows that for $\mu \gg 1$ the oscillation period is really inversely proportional to the relaxation time.

Introducing the small parameter $\varepsilon = 1/\mu$, we can rewrite Equation (1) in the form of two equations of

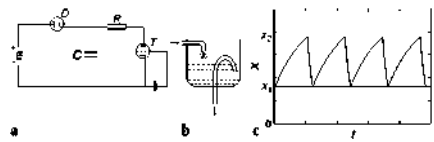

Figure 1. Schematic images (a) of a thyratron oscillator, (b) of Tantal's vessel, and (c) the shape of oscillations of the amount of water in Tantal's vessel and of the voltage across the capacitor C.

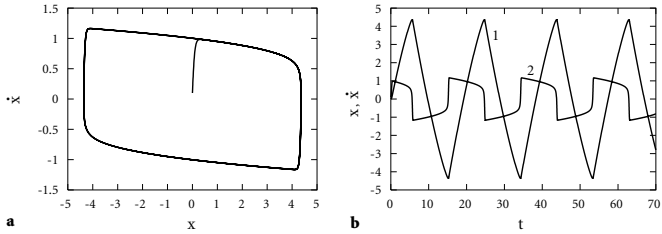

Figure 2. (a) The phase portrait for the Rayleigh equation for $\mu = 10$, and (b) the solution of this equation for $\mu = 10$: curves 1 and 2 show $x(t)$ and $\dot{x}(t)$, respectively.

first order as

$$\dot{x} = y, \tag{3}$$

$$\varepsilon\dot{y} = (1 - y^2)y - \varepsilon x. \tag{4}$$

To find an approximate solution of Equations (3) and (4) we apply the averaging method in systems incorporating fast and slow variables. It follows that the variable x is slow and the variable y is fast. Consequently, in solving Equation (4) the variable x can be considered as a constant. Stationary solutions of Equation (4) under this condition are real roots of the cubic equation

$$y^3 - y + \varepsilon x = 0. \tag{5}$$

Over the range

$$-\frac{2}{3\mu\sqrt{3}} < x < \frac{2}{3\mu\sqrt{3}} \tag{6}$$

Equation (5) has three real roots, whereas outside this range it has only one real root. For $x = \pm 2/(3\mu\sqrt{3})$ Equation (5) has two real roots, $y_1 = \pm 1/\sqrt{3}$, $y2 = \mp 2/\sqrt{3}$. Approximate solutions of Equation (5) can be found analytically under the condition $\varepsilon x \ll 1$. Expanding y sequentially about $y_{10} = 1$, $y_{20} = -1$ and $y_{30} = 0$ we find three solutions:

$$y_1 = 1 - \frac{\mu}{2}x, \quad y_2 = -1 - \frac{\mu}{2}x, \quad y_3 = \mu x. \tag{7}$$

It is seen that the approximate solutions (7) are close to the exact ones over the range (6).

Investigation of the stability of these shows that only those solutions are stable that satisfy the constraint $y_i \geq 1/\sqrt{3}$, which is fulfilled for the upper and the lower parts of the dependence $y(x)$ and is not fulfilled for its middle part.

Substituting $y_{1,2}$ from (7) into Equation (3) and integrating the latter, we find solutions of this equation under the initial condition $x(0) = x_0$:

$$x_{1,2}(t) = x_0 e^{-\varepsilon t/2} \pm \frac{2}{\varepsilon}\left(1 - e^{-\varepsilon t/2}\right). \tag{8}$$

For $\varepsilon t \ll 1$ solutions (8) can be simplified as

$$x_{1,2}(t) = (x_0 \pm t)\,(1 - \varepsilon t/2)\,. \tag{9}$$

Let the initial conditions be $x_0 = -2/(3\varepsilon\sqrt{3})$, $y_0 = y_1(x_0)$. Then, as follows from (9), x will increase with an approximately constant rate, and at the instant $t = 4/(3\varepsilon\sqrt{3})$, it will attain the value $2/(3\varepsilon\sqrt{3})$. At this instant, the solution $y_1(x)$ becomes unstable because it merges with the unstable solution $y_3(x)$. As a result, y will jump to the value $y_2\left(2/(3\varepsilon\sqrt{3})\right)$. Subsequently, x will decrease to the value $-2/(3\varepsilon\sqrt{3})$ and then a jump will occur again; that is, y will take on the value $y_1\left(-2/(3\varepsilon\sqrt{3})\right)$. As the process is repeated, we obtain a limit cycle on the phase plane x, y close to the one calculated numerically (Figure 2).

If $y_0 \neq y_{1,2}(x_0)$, y takes on one of these values very rapidly, practically for a constant x. This means that the corresponding phase trajectories are nearly vertical.

An approximate expression for the oscillation period T can be found on the assumption that the jumps occur instantly and x varies with the constant velocity ± 1. Thus

$$T \approx \frac{8}{3\varepsilon\sqrt{3}} = \frac{4}{3\pi\sqrt{3}}\,\mu T_0, \tag{10}$$

where $T_0 = 2\pi$ is the period of natural oscillations for $\mu = 0$. Thus, in the relaxation regime, the oscillation period is approximately $\mu/4$ times the period of natural oscillations.

Importantly, one of the characteristic features of relaxation oscillators is the ease of frequency synchronization (Landa, 2001). This phenomenon was apparently first studied by Teodorchik (1943, 1945). Relaxation oscillators have long been used in radio and electrical engineering, mainly as multivibrators, but recently interest in these oscillators has quickened in connection with biological and medical applications. As early as 1953, the German physicist Karl Bonhoeffer suggested that a neuron might be modeled by equations similar to the van der Pol equation for a relaxation oscillator. The Bonhoeffer–van der Pol

equations describe oscillations of the voltage across a neural membrane, including refractoriness (difficulty of refiring). These equations are

$$\dot{x} = x - x^3/3 - y + I_0, \quad \dot{y} = \varepsilon(x + a - by), \quad (11)$$

where x is the voltage across the neural membrane; y is a quantity of refractoriness; a, b, ε are membrane radius, specific resistivity of the fluid inside the membrane, and temperature factor, respectively; and I_0 is a direct component of the current across the membrane.

POLINA LANDA

See also **FitzHugh–Nagumo equation; Neurons; Nonlinear electronics; Synchronization; Van der Pol equation**

Further Reading

Bonhoeffer, K.F. 1953. Modelle der Nervenerregung. *Naturwissenschaften*, 40: 301–311

Landa, P.S. 2001. *Regular and Chaotic Oscillations*, Berlin and New York: Springer

Panovko, Ya.G. & Gubanova, I.I. 1964. *Ustoichivost' i Kolebaniya Uprugikh Sistem [Stability and Oscillations of Elastic Systems]*, Moscow: Science

Rayleigh, Lord (Strutt, J.W.) 1877–78. *The Theory of Sound*, 2 vols., London: Macmillan; reprinted New York: Dover, 1877–78

Strelkov, S.P. 1964. *Vvedenie v Teoriyu Kolebanii [Introduction to the Oscillation Theory]*, Moscow: Science

Teodorchik, K.F. 1943. On the theory of synchronization of relaxation generators. *DAN SSSR*, 40: 63–66 (in Russian)

Teodorchik, K.F. 1945. Theory of synchronization of relaxation self-oscillatory systems. *Journal of Physics*, Moscow, 9: 139–146 (in Russian)

Teodorchik, K.F. 1952. *Avtokolebatel'nye Sistemy [Self-Oscillatory Systems]*, Moscow: Gostekhizdat

van der Pol, B. 1926. On relaxation oscillation. *Philosophical Magazine*, 2: 978–992

van der Pol, B. & van der Mark, M. 1928. The heartbeat considered as a relaxation oscillation and an electrical model of the heart. *Philosophical Magazine*, 6: 763–775

RENORMALIZATION GROUPS

Systems undergoing phase transitions at a critical temperature T_c are conveniently described in terms of order parameters and critical exponents. Above T_c, for example, the specific heat is found experimentally to vary as $\varepsilon^{-\alpha}$ where $\varepsilon \equiv (T - T_c)/T_c$, and below T_c, it varies as $(-\varepsilon)^{-\alpha'}$. Thus, α and α' are called critical exponents for specific heat. Similar critical exponents are found for order parameters, isothermal susceptibility, response to an external field, the correlation length ξ, and the pair correlation function $\Gamma(r)$. These are denoted as β, γ, δ, ν, and η, respectively.

Relations among these critical exponents can be derived from scaling assumptions such as the static scaling hypothesis, which asserts that the Gibbs potential $G(T, H)$ for magnetic systems (as an example) is a generalized homogeneous function

$$G(\lambda^{a_\varepsilon}\varepsilon, \lambda^{a_H}H) = \lambda G(\varepsilon, H)\,. \quad (1)$$

With an arbitrary value of λ and selecting a_ε, a_H appropriately, relations among critical exponents are found through thermodynamic identities, for example, $M(\varepsilon, H) = -\,\mathrm{d}G(\varepsilon, H)/\mathrm{d}H$. Thus, Equation (1) leads to the following relations:

$$\beta = \frac{1 - a_H}{a_\varepsilon},\ \delta = \frac{a_H}{1 - a_H},\ \gamma' = \frac{2a_H - 1}{a_\varepsilon},$$
$$\gamma = \frac{2a_H - 1}{a_\varepsilon},\ \alpha' = 2 - \frac{1}{a_\varepsilon}. \quad (2)$$

These can be recast as critical exponent equations:

$$\begin{aligned} \alpha + \beta(\delta + 1) &= 2\,, \\ \alpha' + 2\beta + \gamma' &= 2\,, \\ \gamma(\delta + 1) &= (2 - \alpha)(\delta - 1)\,, \\ \gamma' &= \beta(\delta - 1)\,, \\ \gamma &= \gamma'\,, \\ \alpha &= \alpha'\,, \end{aligned}$$

reducing the number of independent critical exponents to just four (a_ε, a_H, ν, and η).

The two exponents that describe spatial correlations (ν and η) also involve a scaling relationship as was shown through dynamic scaling arguments by Leo Kadanoff and Michael Fisher, among others. In the two-dimensional (2-d) Ising model above T_c, for example, spin-spin correlations show short-range order, whereas below T_c, the system exhibits long-range order. As T tends to T_c from either side, $\Gamma(r - r')$ becomes long ranged and decays slowly as $|r - r'| \gg 1$, with the correlation length diverging. This is typical of most critical systems for which long-range fluctuations accompany the onset of a second-order phase transition. However, in the 2-d XY model, the correlation function exhibits an algebraic fall-off as $\Gamma(r) \sim r^{-\eta(T)}$, demonstrating lack of long-range order in an unusual critical system—the so-called Kosterlitz–Thouless transition whose hallmark is the formation of vortex-antivortex pairs. Mermin and Wagner (1966) proved that any 2-d system with short-range interactions whose ordered phase has a continuous symmetry does *not* support long-range order. This is because at least one branch of collective excitations—called Goldstone bosons—has energy that tends to zero continuously as its wave vector (crystal momentum) vanishes.

With the exception of such unusual systems, spatial scaling applies to criticality, which according to Kadanoff is to be understood as coarse graining. This means that the essential features of the system remain

unchanged as the lattice length scale is increased by a factor λ such that $1 \ll \lambda \ll \xi/a$, where ξ is the correlation length and a is the lattice spacing (see Figure 1).

If N is the number of lattice sites and d the dimensionality of the system, then $m = N/\lambda^d$ is the number of blocks obtained in the first rescaling process. Simultaneously, the lattice variables (e.g., spins) and the interaction parameters are redefined. The effective spins now represent each block and interaction parameters refer to the interacting blocks. Taking the Ising model as an example, the cell Hamiltonian is

$$H_{\text{cell}} = -J \sum_{\langle i,j \rangle}^{N} S_i S_j - h \sum_{i}^{N} S_i. \tag{3}$$

Then the block Hamiltonian becomes

$$H_{\text{block}} = -\tilde{J} \sum_{\langle \alpha,\beta \rangle}^{m} \tilde{S}_\alpha \tilde{S}_\beta - \tilde{h} \sum_{\alpha}^{m} \tilde{S}_\alpha, \tag{4}$$

where the tilde quantities refer to blocks. Crucial assumptions are that thermodynamic potentials scale with block size as

$$F_{\text{block}}(\tilde{\varepsilon}, \tilde{h}) = \lambda^d F_{\text{cell}}(\varepsilon, h), \tag{5}$$

where $\tilde{h} = \lambda^x h$, $\tilde{\varepsilon} = \lambda^y \varepsilon$, and F is a homogeneous function. Hence the exponents x and y are calculated as $y = a_\varepsilon d$ and $x = a_{\text{H}} d$. The Kadanoff construction applied to the pair correlation function,

$$\Gamma(i, j, \varepsilon) = \langle (S_i - \langle S \rangle)(S_j - \langle S \rangle) \rangle, \tag{6}$$

gives $y = \nu^{-1}$, and since $y = d a_\varepsilon$ and $a_\varepsilon = (2 - \alpha')^{-1}$, we find that: $\alpha = \alpha'$ and $d\nu = 2 - \alpha$. Using $x = a_{\text{H}} d$ with $a_{\text{H}} = \delta/(\delta + 1)$ results in $(2 - \mu)\nu = \delta$.

Thus, static and dynamic scaling hypotheses reduce the number of independent critical exponents to just two. The renormalization group (RG) theory was developed to calculate the values of these exponents for particular models by carrying out the scaling procedure up to ξ, and because $\xi \to \infty$ as $T \to T_{\text{c}}$, scaling should continue "ad infinitum" as T approaches T_{c}.

Denoting the cell Hamiltonian by H_0 and the Hamiltonian after the nth step of rescaling as H_n, the chain of scaling transformations R is

$$\begin{aligned} R(H_0) &= H_1,\ R(H_1) = H_2, \ldots, R(H_n) \\ &= H_{n+1}, \ldots, R(H^*) = H^*, \end{aligned} \tag{7}$$

where H^* denotes a fixed point Hamiltonian characteristic of the critical state. Each step in the RG transformation chain reduces the number of degrees of freedom by λ^d. In statistical mechanics, we need to ensure that the partition function retains the same symmetry and ground-state, and hence we must re-scale the coupling constant at each step, for example, $K = J/kT$ in the Ising model. We then develop a recursion relation to compute the partition function.

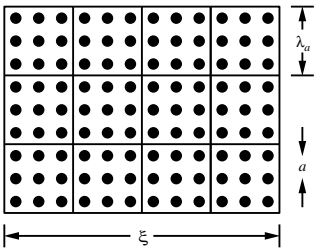

Figure 1. A schematic illustration of the Kadanoff construction.

Model	α	β	γ	ν	δ	η
Classical (MFT)	0 (disc.)	$\frac{1}{2}$	1	—	3	—
Spherical: $d = 3$		$\frac{1}{2}$	2	1	5	0
Spherical: $\varepsilon > 0$	$-\varepsilon/(2-\varepsilon)$	$\frac{1}{2}$	$2/(2-\varepsilon)$	$1/(2-\varepsilon)$	$1 + 4/(2-\varepsilon)$	0
Ising: $d = 2$ (exact)	0 (log)	$\frac{1}{8}$	$\frac{7}{4}$	1	15	$\frac{1}{4}$
Ising: $d = 3$	0.12	0.33	1.25	0.64	4.8	0.04
Heisenberg: $d = 3$	−0.12	0.36	∼1.39	0.71	4.8	0.04
S^4-model: $d > 4$	$\varepsilon/2$	$\frac{1}{2} - \varepsilon/4$	1	$\frac{1}{2}$	$3 + \varepsilon$	0
S^4-model: $d = 4$	0	$\frac{1}{2}$	1	$\frac{1}{2}$	3	0
S^4-model: $d < 4$	$\varepsilon/6$	$\frac{1}{2} - \varepsilon/6$	$1 + \varepsilon/6$	$\frac{1}{2} + \varepsilon/12$	$3 + \varepsilon$	0
S^4-model: $d = 3$	0.17	0.33	1.17	0.58	4	0
XY-model: $d = 3$	0.01	0.34	1.30	0.66	4.8	0.04

Table 1. Summary of critical exponents for key models. Note that $\varepsilon = (4 - d)$.

An iterative solution of this recursion relation for the partition function yields "roots" or fixed points that correspond to resultant critical behaviors in the model. The partition function is preserved in the RG procedure via the condition

$$Z_N(H_n) = Z_m(H_{n+1}), \tag{8}$$

where $m = N/\lambda^d$.

It is conjectured that the values of critical exponents are characteristics not of individual Hamiltonians but their sets, with numerous models leading to the same fixed point. The universality hypothesis states that any two physical systems with the same dimensionality, d, and the same number of order parameter components, n, belong to the same universality class, and each fixed point corresponds to one universality class. Table 1 is a summary of the critical exponent values obtained from RG calculations for key theoretical models.

RG ideas extend into many areas of physics, chemistry, biology, and engineering. Based on the work of Kadanoff, Kenneth Wilson proposed an algorithmic approach to the scaling problem by formulating it in reciprocal space. Although less intuitive than the real-space RG of Kadanoff, it leads to exact results for the removal of divergencies in theories of elementary particles. For this work, Wilson was awarded the 1982 Nobel Prize in Physics.

JACK A. TUSZYŃSKI

See also **Critical phenomena; Ising model; Order parameters; Phase transitions**

Further Reading

Creswick, R.J., Farach, H.A. & Poole, C.P. 1992. *Introduction to Renormalization Group Methods in Physics*, New York: Wiley

Kosterlitz, J.M. & Thouless, D.J. 1973. Ordering, metastability and phase transitions in two-dimensional systems. *Journal of Physics* C, 6: 1181–1203

Ma, S.-K. 1976. *Modern Theory of Critical Phenomena*, New York: Benjamin

Mermin, N.D. & Wagner, H. 1966. Absence of ferromagnetism or antiferromagnetism in one- or two-dimensional isotropic Heisenberg models. *Physics Review Letters*, 17: 1133–1136

Reichl, L.E. 1979. *A Modern Course in Statistical Physics*, Austin: University of Texas Press

Stanley, H.E. 1972. *Introduction to Phase Transitions and Critical Phenomena*, Oxford: Clarendon Press and New York: Oxford University Press

Wilson, K.G. 1972. Feynman-graph expansion for critical exponents. *Physics Review Letters*, 28: 548–551

Wilson, K.G. 1983. The renormalization group and critical phenomena. *Reviews of Modern Physics*, 55: 583–600

Yeomans, J.M. 1992. *Statistical Mechanics of Phase Transitions*, Oxford: Clarendon Press and New York: Oxford University Press

REYNOLDS NUMBER

See **Fluid dynamics**

RHEOLOGY

Rheology is the study of the deformation and flow of materials in general, although most real applications relate to liquids (Barnes, 2000). Deformation and flow processes are linear with respect to extent and rate of deformation only in a limited number of circumstances, and most of the liquids usually considered in practical rheology show strong nonlinear effects in typical deformation and flow situations.

Newtonian Liquids

The simplest flow behavior is that of Newtonian liquids where the viscosity, ν, is a function only of temperature and pressure, and not of the flow conditions (although the dependencies of viscosity on the pressure and temperature are themselves very nonlinear). In simple shear flow (Barnes, 2000), the behavior at any point can be adequately described by the linear equation $\sigma = \nu\dot{\gamma}$, where σ is the shear stress and $\dot{\gamma}$ is the shear rate, or velocity gradient. However, nonlinearities soon set in for the flow of low-viscosity liquids such as water, even at low flow rates. First, smooth, streamline flow is augmented by secondary flows, but these eventually give way to chaotic turbulent flow at higher flow rates. The governing factor for the onset of secondary and turbulent flows is the effect of fluid inertia, arising from the fluid's density. The ratio of inertial to viscous forces is the Reynolds number, Re, and this parameter is important for all fluid flows, whether they are Newtonian or otherwise.

Secondary flows often appear in simple flow geometries such as viscometers and are manifested as an apparent increase in viscosity, due to the extra energy dissipated in the secondary flows cells (Barnes, 2000) (see Figure 1).

The resulting increased couple in the inertial case, T_i, for a cone-and-plate instrument, compared with that for no inertia T, is given for Newtonian liquids by

$$\frac{T_i}{T} \approx 1 + \frac{6}{10^4}\left(\frac{\rho\omega\theta^2 a^2}{\nu}\right)^2, \tag{1}$$

where ρ is the density of the liquid of viscosity ν and a is the cone radius whose angle in radians is θ. From this equation it is easy to see that the correction

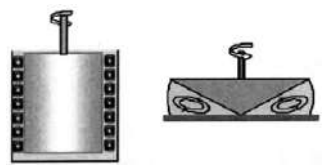

Figure 1. Inertial secondary flow patterns in concentric-cylinder and cone-and-plate geometries.

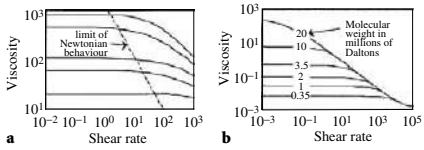

Figure 2. Viscosity (in pascal-seconds) vs. shear rate (1/seconds) for (a) a range of silicone oils, and (b) 3% by weight polystyrene in toluene.

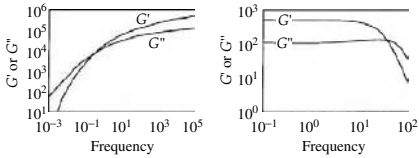

Figure 3. Storage modulus (G') and viscous behavior (G'') (in Pa) vs. Oscillatory frequency (1/s) for (a) low molecular weight polyethylene melt at 150°C, and (b) commercial ketchup.

becomes important when $\rho\omega\theta^2 a^2/\nu$—which is a form of Reynolds number—exceeds 10.

Turbulent flow ensues in pipe flow when the Reynolds number given by $\rho dV/\nu$ (where V is the average velocity in a pipe of diameter d) is well above 2000, and then the pressure drop is no longer a linear function of the flow rate but approaches a quadratic dependence.

Non-Newtonian Liquids

The independence of viscosity to flow conditions is no longer valid for non-Newtonian liquids, but because their microstructure changes with the flow environment, the shear stress shows a nonlinear dependence on the shear rate. The dependence of viscosity on shear rate is such that the typical behavior is a decrease of viscosity with increase in shear rate from a value ν_0 at low shear rates, to a much lower value ν_∞ at much higher shear rates. This can often be described by the nonlinear Cross-type function

$$\frac{\nu - \nu_\infty}{\nu_0 - \nu_\infty} = \frac{1}{1 + (K\dot{\gamma})^m}, \qquad (2)$$

where (written in this particular way) K has the dimensions of time and m is dimensionless. When this model is used to describe non-Newtonian liquids, the degree to which the viscosity decreases with shear rate is dictated by the value of m, with m tending to zero describing more Newtonian liquids, while the most "shear-thinning" liquids have values of m tending to unity. Figure 2 shows the departure from linearity for a number of non-Newtonian liquids.

Viscoelasticity

As well as the nonlinear behavior of viscosity, non-Newtonian liquids also display extra forces. These arise either as time or frequency effects in the linear region of behavior and are manifested, for instance, as an elastic component called the storage modulus G' in oscillatory flow as well as the viscous behavior as G''. In the simplest form of viscoelastic liquid, the parameters G' and G'' are related by a relaxation time, λ, of the liquid. These parameters are only constant over a limited region, but for deformations greater than

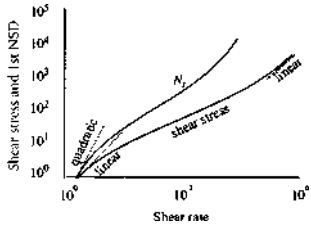

Figure 4. The shear stress (Pa) and first normal-stress difference (1st NSD) N_1(Pa) as a function of shear rate (1/s) for a 0.5% hydroxyethyl cellulose aqueous solution.

a few percent for most non-Newtonian liquids, we enter the nonlinear region. The behavior of these G' and G'' with frequency is shown in Figure 3, along with typical departure from linearity.

For steady flows of viscoelastic liquids, the extra forces that become important are the so-called normal stresses. These arise essentially because the microstructure has a preferred configuration, which can become aligned by the flow. These normal forces manifest themselves in the linear region of slow flow as forces proportional to the square of the shear rate, but they also soon show nonlinear behavior in the region where the viscosity also becomes nonlinear. Figure 4 shows the typical behavior of both the shear stress and the first normal stress difference for a viscoelastic liquid.

Rheology of Polymeric Liquids

The microstructure that dictates the behavior of polymeric liquids is usually the state of entanglement of the polymeric chains. The chains are in incessant motion due to Brownian thermal energy, and their motions among each other give rise to viscous and elastic effects. However, as the shear rate increases, there is a gradual loss of entanglements and development of alignment, so that at high enough shear rates, linear polymer coils are transformed into aligned strings. The consequences of this change in microstructure are some very startling viscoelastic effects (Barnes, 2000).

Rheology of Suspensions

Suspension rheology depends on the relative disposition of particles relative to one another. Sometimes the particles are flocculated, and these flocs break down in size as the shear rate increases. This nonlinear phenomena can give rise to apparent yield stresses, where the viscosity is very high at low shear rates, but drops dramatically over a narrow range of stress.

Theoretical Rheology

The aim of mathematicians working in this area is to capture these complicated, and usually nonlinear, physical phenomena in constitutive equations (CEs). At their best, these describe nonlinear behaviour in viscosity—as above with the Cross-type equations—but also in the viscoelastic areas. CEs are written in the form of either differential or integral equations (see Barnes et al., 1989). A typical example of a nonlinear differential-type equation is the White–Metzner equation, where the rate-dependent viscosity $\nu_s(II_D)$ and the relaxation time $\lambda(II_D)_I I$ are written as

$$\nu_s(II_D) = \frac{\nu_0}{[1 + (K_1 II_D)^n]}$$

and

$$\lambda(II_D) = \frac{\lambda_0}{[1 + K_2 II_D]}, \tag{3}$$

where K_1 and K_2 are parameters with the dimensions of time, n is a numerical constant, and II_D is the second invariant of the deformation tensor (Barnes & Roberts, 1992). Barnes & Roberts (1992) have shown that this type of equation can describe many nonlinear rheological situations.

HOWARD A. BARNES

See also **Cluster coagulation; Fluid dynamics; Granular materials; Liquid crystals; Polymers**

Further Reading

Barnes, H.A. 2000. *A Handbook of Elementary Rheology*, Aberystwyth: The University of Wales Institute of Non-Newtonian Fluid Mechanics

Barnes, H.A., Hutton, J.F. & Walters, K. 1989. *An Introduction to Rheology*, Amsterdam: Elsevier

Barnes, H.A. & Roberts, G.P. 1992. A simple model to describe the steady state shear and extensions viscosity of polymer melts. *Journal of Non-Newtonian Fluid Mechanics*, 44: 113–126

RICCATI EQUATIONS

Count Jacopo Francesco Riccati (1676–1754) was an Italian nobleman who spent most of his life in the little town of Castelfranco, Veneto. Born in Venice and schooled at a Jesuit college in Brescia, he proceeded to the University of Padua where he read law. However, following his natural inclination and talent, he also took mathematical courses at Padua, and befriended Father Stefano degli Angeli, an astronomy lecturer. Angeli introduced him to Newton's *Principia*, which they read and studied together.

Dedicated to intellectual inquiry of every sort, Riccati is mostly remembered for his significant results in mathematics, particularly separation of variables and other solution methods for ordinary differential equations. He wrote extensively on such diverse areas as physics, architecture, and philosophy. Preferring to remain in Castelfranco, where he served as mayor for several years, he turned down numerous academic offers, including an invitation from Peter the Great to become President of the St. Petersburg Academy of Science.

Throughout his life he maintained an active correspondence with Italian scholars such as Agnesi and Rizzetti, as well as with European mathematicians such as the Bernoullis. In a letter of 1720 addressed to Rizzetti, he introduced two new differential equations, which in modern notation would be written

$$\frac{dy}{dx} = ay^2 + bx^m, \quad \frac{dy}{dx} = \alpha y^2 + \beta x + \gamma x^2, \tag{1}$$

where a, b, m and α, β, γ are constants. His first published results on such equations appeared four years later (Riccati, 1724), and this paper is reproduced in Bittanti (1989) along with later related work of Euler and Liouville. Michieli's biographical work (Michieli, 1943) includes a detailed bibliography of Riccati's publications, letters, and manuscripts.

The scalar first order differential equation that today bears Riccati's name takes the general form

$$\frac{dy}{dx} = A(x)y^2 + B(x)y + C(x), \tag{2}$$

where $A \not\equiv 0$, B, C are arbitrary functions of x. Thus, Equations (1) correspond to special cases of the Riccati equation (2) with constant A, zero B, and particular choices of C. There are two main solution methods (Ince, 1926). First, supposing that a particular solution y_1 is known, the general solution of (2) is found by the substitution

$$y = y_1 + \frac{1}{u}, \tag{3}$$

which yields the linear equation

$$\frac{du}{dx} + (2y_1 A + B)u + A = 0$$

for u. Hence u is found by quadratures, and then y is obtained (3) in terms of y_1 and u. The second method involves the substitution

$$y = -\frac{1}{A}\frac{d}{dx}\log\psi, \tag{4}$$

which transforms the Riccati equation to a homogeneous second-order linear equation for ψ, namely,

$$\frac{d^2\psi}{dx^2} + f(x)\frac{d\psi}{dx} + g(x)\psi = 0 \tag{5}$$

with

$$f = -B - \frac{\mathrm{d}}{\mathrm{d}x}\log A, \quad g = AC.$$

The scalar- second order Equation (5) can be converted to a 2×2 matrix linear system of the form

$$\frac{\mathrm{d}}{\mathrm{d}x}\begin{pmatrix} \psi_1 \\ \psi_2 \end{pmatrix} = \begin{pmatrix} M_{11} & M_{12} \\ M_{21} & M_{22} \end{pmatrix}\begin{pmatrix} \psi_1 \\ \psi_2 \end{pmatrix}. \tag{6}$$

Riccati himself considered such a system as describing the trajectory of a point (ψ_1, ψ_2) in the plane. Requesting the equation satisfied by the slope

$$y = \frac{\psi_2}{\psi_1}, \tag{7}$$

he found the answer was precisely (2) with

$$A = -M_{12}, \quad B = M_{22} - M_{11}, \quad C = M_{21}.$$

The left action of the matrix group $SL(2)$ on the linear system (6) induces a corresponding action via Möbius transformations on the projective coordinate y. This generalizes to Nth-order projective Riccati systems with nonlinear superposition principles (Anderson, 1980; Shnider & Winternitz, 1984). The latter are solved in terms of $(N+1)$th-order linear systems, with a projective action of $SL(N+1)$.

Due to this link with linear systems, (coupled) Riccati equations naturally appear in the theory of soliton-bearing integrable partial differential equations (Fordy, 1990). Within the framework of the inverse scattering method, nonlinear soliton equations (in $1+1$ dimensions) arise as the compatibility condition for a pair of matrix linear systems,

$$\Psi_x = U\Psi, \quad \Psi_t = V\Psi. \tag{8}$$

Without loss of generality the matrices U, V are taken as $sl(N+1)$ valued functions of the dependent variables and their derivatives as well as a spectral parameter, λ, say, and subscripts denote partial derivatives.

In the simplest case, $N = 1$, we consider the standard example of the Korteweg–de Vries (KdV) equation, with the first matrix in (8) given by

$$U = \begin{pmatrix} 0 & 1 \\ \lambda - u & 0 \end{pmatrix},$$

and the spatial (x) part of pair (8) is just a 2×2 system (6). The corresponding scalar equation (5) reduces to the Schrödinger equation with potential u and spectral parameter λ; that is,

$$\psi_{xx} + u\psi = \lambda\psi,$$

and in terms of the projective variable y this yields the Riccati equation

$$y_x = -y^2 + \lambda - u. \tag{9}$$

In the special case of zero eigenvalue ($\lambda = 0$), with $y = v$ formula (9) becomes the Miura map

$$u = -v_x - v^2$$

relating a solution u of the KdV equation to a solution v of the modified KdV equation. Riccati equations are further distinguished in the theory of integrable systems by the fact that (for analytic A, B, C) they are the only first- order equations with the Painlevé property (Ince, 1926).

The fundamental problem of the calculus of variations (Gel'fand & Fomin, 1963) is to extremize a functional

$$S[q] = \int_{x_0}^{x_1} L(x, q, \dot{q})\,\mathrm{d}x, \quad \dot{q} \equiv \frac{\mathrm{d}q}{\mathrm{d}x}, \tag{10}$$

subject to $q(x_0) = q_0$, $q(x_1) = q_1$. Under an arbitrary small change $h(x)$ in $q(x)$,

$$q \to q + h,$$

with $h(x_0) = 0 = h(x_1)$, for a scalar function q the requirement $\delta S[h] = 0$ leads to the Euler–Lagrange equation

$$L_q - \frac{\mathrm{d}}{\mathrm{d}x}L_{\dot{q}} \equiv \frac{\partial L}{\partial q} - \frac{\mathrm{d}}{\mathrm{d}x}\frac{\partial L}{\partial \dot{q}} = 0.$$

If we further require to minimize the functional S, then a necessary condition is that the second variation should be nonnegative, that is,

$$\delta^2 S[h] = \frac{1}{2}\int_{x_0}^{x_1}\left(L_{\dot{q}\dot{q}}\dot{h}^2 + 2L_{q\dot{q}}h\dot{h} + L_{qq}h^2\right)\mathrm{d}x \geq 0.$$

After an integration by parts, this takes the form

$$\delta^2 S[h] = \int_{x_0}^{x_1}(P\dot{h}^2 + Qh^2)\,\mathrm{d}x, \tag{11}$$

where

$$P = \frac{1}{2}L_{\dot{q}\dot{q}}, \quad Q = \frac{1}{2}\left(L_{qq} - \frac{\mathrm{d}}{\mathrm{d}x}L_{q\dot{q}}\right).$$

Since h vanishes at the endpoints, there is the freedom to add any function of the form

$$\frac{\mathrm{d}}{\mathrm{d}x}(wh^2)$$

to the integrand in (11). If w is chosen to satisfy the Riccati equation

$$\frac{\mathrm{d}w}{\mathrm{d}x} = \frac{w^2}{P} - Q, \tag{12}$$

then the integrand for the second variation can be written in terms of a perfect square,

$$\delta^2 S[h] = \int_{x_0}^{x_1} P\left(\dot{h} + \frac{wh}{P}\right)^2 \mathrm{d}x.$$

Thus, to ensure nonnegativity of $\delta^2 S$, we arrive at Legendre's necessary condition

$$P(x) \geq 0, \quad x \in [x_0, x_1],$$

for a minimum of the functional $S[q]$. However, some care is needed to make this argument rigorous, since the Riccati equation (12) may not have a solution on the whole interval $[x_0, x_1]$.

In the case where q has n components, $q = (q^1, q^2, \ldots, q^n)$, the analogue of (12) is the matrix Riccati equation

$$\dot{W} = WP^{-1}W - Q,$$

where W, P, Q are symmetric matrices. Matrix Riccati equations are treated extensively in Reid (1972), and together with their discrete versions they find important applications in optimal filtering and control (Bittanti et al., 1991; Zelikin, 2000).

An n-component example is provided by the geodesics on a (pseudo-)Riemannian n-manifold with metric g_{jk} (Hughston & Tod, 1990), derived from the action

$$S[q] = \int_{\tau_0}^{\tau_1} g_{jk}(q)\dot{q}^j \dot{q}^k \, \mathrm{d}\tau$$

with affine parameter τ along the geodesics. The Euler–Lagrange equations for the geodesics, giving the trajectories of free particle motion, are

$$\frac{\mathrm{d}^2 q^j}{\mathrm{d}\tau^2} + \Gamma^j_{kl} \frac{\mathrm{d}q^k}{\mathrm{d}\tau} \frac{\mathrm{d}q^l}{\mathrm{d}\tau} = 0,$$

where Γ^j_{kl} are the Christoffel symbols. In the case of a Riemannian manifold, the metric tensor is positive definite and the Legendre condition is satisfied. The geodesics are the paths of minimum length.

ANDREW HONE

See also **Euler–Lagrange equations; Extremum principles; General relativity; Integrability; Inverse scattering method or transform; Korteweg–de Vries equation; Painlevé analysis**

Further Reading

Anderson, R.L. 1980. A nonlinear superposition principle admitted by coupled Riccati equations of the projective type. *Letters in Mathematical Physics*, 4: 1–7

Bittanti, S. (editor). 1989. *Count Riccati and the Early Days of the Riccati Equation*. Bologna: Pitagora Editrice

Bittanti, S., Laub, A.J. & Willems, J.C. (editors). 1991. *The Riccati Equation*. Berlin: Springer

Fordy, A.P. (editor). 1990. *Soliton Theory: A Survey of Results*. Manchester: Manchester University Press

Gel'fand, I.M. & Fomin, S.V. 1963. *Calculus of Variations*. Englewood Cliffs, NJ: Prentice-Hall

Hughston, L.P. & Tod, K.P. 1990. *An Introduction to General Relativity*. Cambridge and New York: Cambridge University Press

Ince, E.L. 1926. *Ordinary Differential Equations*. 7th edition, Edinburgh: Oliver and Boyd and New York: Interscience, 1959

Michieli, A.A. 1943. Una famiglia di matematici e di poligrafi trivigiani: i Riccati. I. Iacopo Riccati. *Atti del Reale Istituto Veneto di Scienze, Lettere ed Arti*, 102(2): 535–587

Reid, W.T. 1972. *Riccati Differential Equations*. New York: Academic Press

Riccati, J.F. 1724. Animadversiones in aequationes differentiales secundi gradus. *Supplementa Acta Eruditorum Lipsiae*, 8(2): 66–73

Shnider, S. & Winternitz, P. 1984. Classification of nonlinear ordinary differential equations with superposition principles. *Journal of Mathematical Physics*, 25(11): 3155–3165

Zelikin, M.I. 2000. *Control Theory and Optimization I: Homogeneous Spaces and the Riccati Equation in the Calculus of Variations*. Berlin and New York: Springer

RIEMANN INVARIANTS

See **Characteristics**

RIEMANN SURFACES

See **Periodic spectral theory**

RIEMANN WAVE

See **Shock waves**

RIEMANN ZETA FUNCTION

See **Random matrix theory I: Origins and physical applications**

RIEMANN–HILBERT PROBLEM

We begin by defining what is meant by a Riemann–Hilbert problem (RHP). Let Σ be an oriented contour in $\mathbb{C}$.

By convention, if we move along the contour in the direction of the orientation, we say that the $(+/-)$ side lies to the (left/right), as indicated in Figure 1. A map v from Σ to the space of the invertible $k \times k$ matrices with complex entries is called a *jump matrix* for Σ if v and v^{-1} are bounded on Σ. We say that a

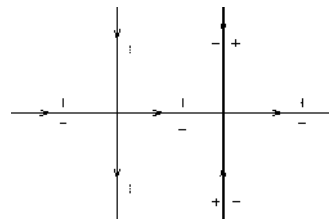

Figure 1. The contour Σ.

$j \times k$ matrix-valued function $m = m(z)$ is a *solution* of the RHP (Σ, v) if

- m is analytic in $\mathbb{C} \setminus \Sigma$,
- $m_+(z) = m_-(z)v(z)$ for $z \in \Sigma$, where $m_\pm(z) = \lim_{\substack{z' \to z \\ z' \in (\pm)\text{–side of } \Sigma}} m(z')$.
  If in addition $j = k$ and
- $m(z) \to I$ as $z \to z_0$ for some $z_0 \in \mathbb{C} \cup \{\infty\}$, we say that the RHP is *normalized* at z_0.

A discussion of technical restrictions on Σ, and the precise sense in which the boundary values, as well as the limit at z_0 in the normalized case, are attained, can be found in many texts (see, e.g., Clancey & Gohberg (1981) and the references therein). Many problems in pure and applied mathematics, and also theoretical physics, can be expressed in terms of an RHP. Riemann–Hilbert problems are closely related to the Wiener–Hopf method. We refer the reader to Clancey & Gohberg (1981) for a history of RHPs and also to the classic text by Muskhelishvili (1946). The goal of this article is to describe some recent developments.

Remark. Included in David Hilbert's famous list of 23 problems, was the following:

> Show that there always exists a linear differential equation of the Fuchsian class with given singularities and a given monodromy group.

A Fuchsian system is an nth-order, linear system of the form

$$\mathrm{d}m/\mathrm{d}z = A(z)m,$$

where A is an $n \times n$ matrix with entries that are analytic except at a finite number of simple poles. Roughly speaking, the monodromy group is the group of transformations of solutions to the above Fuchsian system under analytic continuation about these poles.

The above monodromy problem turns out to be a special case of a Riemann–Hilbert problem with jump matrices that are (essentially) piece-wise constant. In the mathematical literature, the monodromy problem is sometimes identified with the Riemann–Hilbert problem, but this is incorrect. The work of Bernhard Riemann, and later of David Hilbert, on such problems, predates Hilbert's monodromy problem and has very different origins.

Our point of departure here is the observation of Alexey Shabat in 1976 that the inverse scattering method for the Schrödinger operator can be rephrased as a RHP (see Faddeev & Takhtajan, 1987). By way of illustration, we apply Shabat's observation to a simpler case, the self-adjoint ZS–AKNS scattering problem (Zakharov & Shabat, 1971; Ablowitz et al., 1974)

$$\frac{\mathrm{d}\psi}{\mathrm{d}x} = \left(\mathrm{i}z\sigma + \begin{pmatrix} 0 & q(x) \\ \bar{q}(x) & 0 \end{pmatrix}\right)\psi, \qquad (1)$$

where $\sigma = \begin{pmatrix} 1/2 & 0 \\ 0 & -1/2 \end{pmatrix}$ and $q(x)$ is a given function on $\mathbb{R}$, which decays sufficiently fast as $|x| \to \infty$. For fixed $z \in \mathbb{C} \setminus \mathbb{R}$, one seeks so-called Beals–Coifman solutions $\psi = \psi(x, z; q)$ of (1) with the properties

$$\psi \mathrm{e}^{-\mathrm{i}xz\sigma} \to I \text{ as } x \to -\infty, \qquad (2)$$

$$\psi \mathrm{e}^{-\mathrm{i}xz\sigma} \text{ is bounded as } x \to +\infty. \qquad (3)$$

It turns out, conversely, that for fixed $x \in \mathbb{R}$, $m(z) = m(x, z; q) \equiv \psi(x, z; q)\mathrm{e}^{-\mathrm{i}xz\sigma}$ solves the RHP $(\Sigma = \mathbb{R}, v_x)$ normalized at $z_0 = \infty$, where

$$v_x(z) = \begin{pmatrix} 1 - |r(z)|^2 & r(z)\mathrm{e}^{\mathrm{i}xz} \\ -\bar{r}(z)\mathrm{e}^{-\mathrm{i}xz} & 1 \end{pmatrix}, \quad z \in \mathbb{R} \qquad (4)$$

and $r(z) = r(z; q)$ is the *reflection coefficient* for q. Define the *reflection map* $\mathcal{R}$ via $\mathcal{R}(q) \equiv r$. Given q, the direct scattering problem is given by

$$q \mapsto m(x, z; q) \mapsto v_x \mapsto r = \mathcal{R}(q).$$

On the other hand, for a given r and a fixed $x \in \mathbb{R}$, let $m = m(x, z; r)$ be the solution of the RHP $(\mathbb{R}, v_x)$ normalized at ∞. Expand $m(z)$ as $z \to \infty$,

$$m(z) = I + m_1(x; r)/z + O(z^{-2}), \qquad (5)$$

and define

$$(Q(r))(x) \equiv -\mathrm{i}(m_1(x; r))_{12}. \qquad (6)$$

Given r, the inverse scattering problem is given by

$$r \mapsto v_x \mapsto m(x, z; r) \mapsto m_1(x; r) \mapsto Q(r).$$

The basic analytical result in the subject is that $\mathcal{R}$ is bijective from a suitable space of q's onto a suitable space of r's (Beals & Coifman , 1984; Zhou, 1998) and that Q is the inverse of $\mathcal{R}$.

In terms of the classical method of scattering and inverse scattering (Zakharov & Shabat, 1971; Ablowitz et al., 1974), $r \equiv r(z; q)$ is the standard reflection coefficient. Moreover, if m solves the RHP (Σ, v_x), then the Fourier transform of the first row of $m_- \begin{pmatrix} 1 & r\mathrm{e}^{\mathrm{i}xz} \\ 0 & 1 \end{pmatrix} - I$ gives the solution of the Faddeev–Marchenko equation.

In the case of the non-self-adjoint ZS–AKNS scattering problem, the Beals–Coifman solutions $\psi(z)$ may have singularities at points $\{z_j\} \subset \mathbb{C} \setminus \mathbb{R}$, which correspond to eigenvalues with square integrable eigenfunctions. In addition, there may be singularities for $\psi_\pm(z)$ on the contour $\Sigma = \mathbb{R}$. One now associates an RHP to the scattering problem by augmenting the contour $\Sigma \to \Sigma_{\text{aug}}$ so as to enclose these singularities: information about the singularities is then contained in the augmented jump matrix v_{aug} defined on $\Sigma_{\text{aug}} \setminus \Sigma$ (see Zhou, 1989). The above ideas apply to very general first-order systems of size $N \times N$ and also

to differential operators of order M. The underlying contour Σ is now more complicated and may have points of self-intersection, which leads in turn to significant new technical complications. Also, the singularities of ψ in $\mathbb{C}\setminus\Sigma$ need not correspond to eigenvalues with square integrable eigenfunctions.

We now consider the relation of RHPs to the theory of integrable systems. Again by the way of illustration, we consider the normalized RHP $(\mathbb{R}, v_x)$ associated with the self-adjoint ZS–AKNS system. If $q(t)=q(x,t)$ solves the defocusing nonlinear Schrödinger (NLS) equation

$$\begin{aligned} &\mathrm{i}q_t + q_{xx} - 2|q|^2 q = 0,\\ &q(x, t=0) = q_0(x) \to 0 \text{ as } |x| \to \infty, \end{aligned} \tag{7}$$

then by Zakharov & Shabat (1971)

$$r(t,z) = r(z)\mathrm{e}^{-\mathrm{i}tz^2}, \quad z \in \mathbb{R}. \tag{8}$$

This leads to the following solution procedure for NLS. Let $m(x,z;r(\diamondsuit)\mathrm{e}^{-\mathrm{i}t\diamondsuit^2}) = I + m_1(x;r(\diamondsuit)\mathrm{e}^{-\mathrm{i}t\diamondsuit^2})z^{-1} + O(z^{-2})$ be the solution of the normalized RHP $(\mathbb{R}, v_\theta)$, where

$$v_\theta(z) = \begin{pmatrix} 1-|r(z)|^2 & r\mathrm{e}^{\mathrm{i}\theta} \\ -\bar{r}\mathrm{e}^{-\mathrm{i}\theta} & 1 \end{pmatrix}, \quad \theta = xz - tz^2. \tag{9}$$

Then

$$q(x,t) = -\mathrm{i}(m_1(x;r(\diamondsuit)\mathrm{e}^{-\mathrm{i}t\diamondsuit^2}))_{12}. \tag{10}$$

An extraordinarily broad spectrum of problems, both dynamical and nondynamical, can be solved via a RHP as in (10) above. The list includes, in particular, the Painlevé equations (see Flaschka & Newell, 1980; Jimbo et al., 1981) where the underlying contour may be a union of intersecting lines, and also the orthogonal polynomial problem as formulated by Fokas, Its, and Kitaev, and the theory of Hankel and Toeplitz determinants (see e.g., Deift, 1999). In practice, RHPs often arise via associated *integrable operators* (Its et al., 1990; see also Deift, 1999). Let Σ be an oriented contour in $\mathbb{C}$. We say that an operator K acting in $L^p(\Sigma)$, $1<p<\infty$, is integrable if it has a kernel of the form

$$K(z,z') = (z-z')^{-1}\sum_{j=1}^{k} f_j(z)g_j(z'), \quad z, z' \in \Sigma.$$

Special examples of integrable operators began to appear in field theory and in statistical mechanics in the late 1960s and 1970s, particularly in the work of Wu, McCoy, Tracy, and Baruch, and later Sato, Miwa, and Jimbo, but integrable operators as a distinguished class were first identified by Its et al. (1990) and later Sato-Miwa-Jimbo. Some general results on integrable operators were obtained by Lev A. Sakhnovich in the late 1960s, but the full theory of integrable operators is due to Its et al. (1990).

Integrable operators have many remarkable properties, the most important being that if $(1-K)^{-1} = I + R$, then R is also an integrable operator, $R(z,z') = z-z')^{-1}\sum_{j=1}^{k} F(z)G_j(z')$, and F_i, G_j can be constructed by solving an RHP $(\Sigma, v_{f,g})$ naturally associated with f_i, g_j. It turns out that many quantities H of physical interest can be expressed in the form $H = \det(1-K)$, where K is an integrable operator. For example, let K_x be the operator acting on $L^2(0,1)$ with kernel $\frac{\sin\pi x(z-z')}{\pi(z-z')}$, $z, z' \in (0,1)$. Then $H_x = \det(1-K_x)$ is the probability that in the bulk scaling limit, a Hermitian matrix chosen from the Gaussian Unitary Ensemble has no eigenvalues in $[0,x]$. Differentiating with respect to x, one derives an expression for $\frac{\mathrm{d}}{\mathrm{d}x}\log H_x$ in terms of $R_x = (1-K_x)^{-1} - 1$, and hence we see that the analysis of H_x reduces to the analysis of an RHP. Similar examples arise in many different scientific areas, including statistical mechanics, percolation theory, combinatorics, representation theory of large groups, and approximation theory. Relatively recent bibliographies can be found in Deift et al. (1993, 1999).

Returning to the NLS equation, one expects from (9) and (10) that the leading order contribution to the solution $q(x,t)$ as $t\to\infty$ should arise from the stationary phase point $z_0 = x/2t$, $\theta'(z_0) = 0$, as in the classical steepest-descent method for the asymptotic evaluation of (scalar) integrals. In Deift & Zhou (1993), the authors introduce a general noncommutative steepest-descent method to analyze such microlocal problems in the context of RHPs. In the case of NLS, the method proceeds as follows (Deift, Its & Zhou, 1997; Deift & Zhou, 1994). Let δ solve the scalar RHP $((-\infty, z_0), 1-|r|^2)$ normalized at ∞ and set $\tilde{m} = m\delta^{-\sigma_3}$, $\sigma_3 = \begin{pmatrix} 1 & 0 \\ 0 & -1 \end{pmatrix}$. Then $\tilde{m}$ solves the normalized RHP $(\mathbb{R}, \tilde{v}_\theta)$, where $\tilde{v}_\theta$ is as in Figure 2.

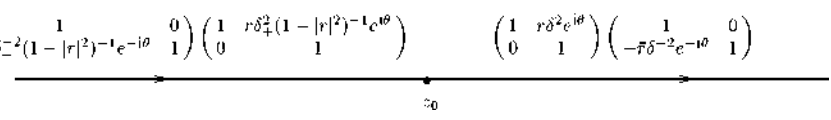

Figure 2. The jump matrix $\tilde{v}_\theta$.

Assuming (as we may, after suitable approximation) that the entries of $\tilde{v}_\theta$ have analytic extensions, define m_θ^d as in Figure 3. Note that, with this definition, m_θ^d solves the normalized RHP $(\Sigma_{z_0}^d, v_\theta^d)$, where v_θ^d is shown in Figure 4.

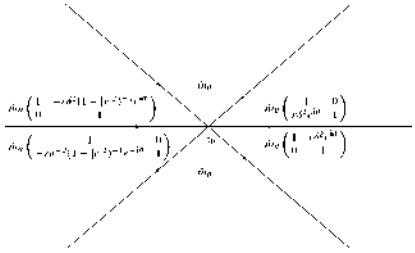

Figure 3. The solution m_θ^d.

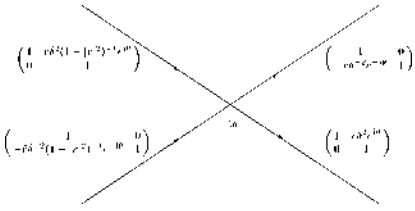

Figure 4. The jump matrix v_θ^d.

Observe that the definition of δ and the choice of the lower/upper and upper/lower factorizations of $\tilde{v}_\theta$, were made precisely to take advantage of the signature table of $\mathrm{Re}, \mathrm{i}\theta = -t\,\mathrm{Re}\,\mathrm{i}\,(z-z_0)^2$ in Figure 5.

As $t \to \infty$, $v_\theta^d \to I$ uniformly on $\Sigma_{z_0}^d \setminus \{|z-z_0| \geq \varepsilon\}$ for any $\varepsilon > 0$, and the RHP localizes at z_0 to an RHP that can be solved explicitly. We obtain as $t \to \infty$

$$q(x,t) = t^{-1/2}\alpha(z_0)\mathrm{e}^{\mathrm{i}[x^2/(4t)-\nu(z_0)\log 2t]} + O(\log t/t), \tag{11}$$

where

$$\nu(z) = -\frac{1}{2\pi}\log(1-|r(z)|^2), \quad |\alpha(z)|^2 = \nu(z)/2 \tag{12}$$

and

$$\arg\alpha(z) = \frac{1}{\pi}\int_{-\infty}^{z}\log(z-s)d\log(1-|r(s)|^2) + \frac{\pi}{4} + \arg\Gamma(\mathrm{i}\nu(z)) + \arg r(z). \tag{13}$$

The above asymptotic form was first obtained by Zakharov and Manakov but without the error estimate. The RHP/steepest-descent method, suitably extended,

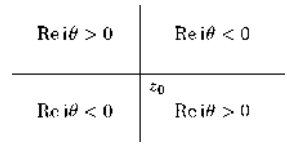

Figure 5. Signature of $\mathrm{Re}, \mathrm{i}\theta$.

has also been used by Deift and Zhou to obtain precise long-time asymptotics of solutions of perturbed NLS equations.

In the above problem, the leading order asymptotic contribution arises from the stationary phase point, as in the classical method of stationary phase for scalar integrals. In many problems, in fact in most problems, the leading order contribution no longer arises from one (or more) critical points, but is given instead by a "critical contour." Such a contour arises, for example, in the asymptotic analysis as $x \to \infty$ of the Painlevé equation by Deift and Zhou, and also in the analysis of the collisionless shock region by Deift, Venakides and Zhou. In Deift, Venakides and Zhou (1997), in the context of the zero-dispersion limit of the Kortweg–de Vries (KdV) equation, the method in Deift & Zhou (1993) was extended significantly to include a prescription for the determination of the critical contour, making it possible in turn to describe the asymptotic development of fully nonlinear oscillations. This extension of Deift & Zhou (1993) made it possible to obtain Plancherel–Rotach-type asymptotics for a general class of orthogonal polynomials, leading in turn to a solution of the so-called universality conjecture for unitary ensembles (see Deift et al., 1999, and **Random Matrix Theory IV: Analytic methods**; see also the work of Pastur and Scherbina for a different approach, and also the work of Bleher and Its for an approach related to Deift et al. (1999), in the special case of a quartic potential). Many other long-standing problems in mathematics and in physics have been solved since the 1990s using RHP techniques and the (extended) steepest-descent method. For example, in combinatorics, Ulam's problem for increasing subsequences in random permutations was solved completely by Baik, Deift, and Johansson in terms of the Tracy–Widom distribution of random matrix theory, giving rise in turn to an explosive growth in applications linking combinatorics, statistical models, and random matrix theory. Many people are contributing to these developments, but there is as yet no adequate review. Fortunately, a comprehensive review, by T. Kriecherbauer, is due to appear in *Nonlinearity* in early 2005. Further extensions of the RHP/steepest-descent method have been given recently in the work of Kamvissis, McLaughlin and Miller on the semiclassical limit for the defocusing nonlinear Schrödinger equation.

Finally, we return to the classical Faddeev–Marchenko approach to inverse scattering theory mentioned earlier and make some comparisons with the RHP method. First, as noted above, the Faddeev–Marchenko equation arises by taking a Fourier transform of objects arising in the RHP theory. This means, in particular, that the classical method only applies in cases where the underlying contour is a group such as a line or a circle; problems such as Painlevé II, for example, cannot be handled in general by the classical method. Second, even in cases where the underlying contour is a group, such as NLS or KdV, the leading order contribution to the solution as $t \to \infty$ arises from the stationary phase points. Taking a Fourier transform "smears out" this feature and the microlocal nature of the problem is obscured.

Beals & Coifman(1984) were the first to use RHPs for the rigorous analysis of scattering and inverse scattering theory.

PERCY DEIFT AND XIN ZHOU

See also **Gel'fand–Levitan theory; Inverse scattering method or transform; Nonlinear Schrödinger equations; Random matrix theory IV: Analytic methods**

Further Reading

Ablowitz, M.J., Kaup, D.J., Newell, A.C. & Segur, H. 1974. The inverse scattering transform-Fourier analysis for nonlinear problems. *Studies in Applied Mathematics*, 53: 249–315

Beals, B. & Coifman, R. 1984. Scattering and inverse scattering for first order systems. *Communications in Pure and Applied Mathematics*, 37, 39–90

Clancey, K. & Gohberg, I.C. 1981. *Factorizations of Matrix Functions and Singular Integral Operators*, Basel and Boston: Birkhäuser

Deift, P. 1999. Integrable operators. *American Mathematical Society Translations*, 2(189): 69–84

Deift, P., Its, A. & Zhou, X. 1993. Long–time asymptotics for integrable nonlinear wave equations. In *Important Developments in Soliton Theory 1980–1990*, edited by A.S. Fokas & V.E. Zakharov, Berlin and New York: Springer, pp.181–204

Deift, P., Kriecherbauer, T., McLaughlin, K., Venakides, S. & Zhou, X. 1999. Uniform asymptotics for polynomials orthogonal with respect to varying exponential weights and applications to universality questions in random matrix theory. *Communications in Pure and Applied Mathematics*, 52: 1335–1425

Deift, P., Venakides, S. & Zhou, X. 1997. New results in small dispersion KdV by an extension of the steepest descent method for Riemann-Hilbert problems, *Internat. Math. Res. Notices*, No. 6, 285–299

Deift, P. & Zhou, X. 1993. A steepest descent method for oscillatory Riemann–Hilbert problems–asymptotics for the MKdV equation. *Annals of Mathematics*, 137: 295–368

Deift, P. & Zhou, X. 1994. *Long-term Behavior of the Non-focusing Nonlinear Schrödinger Equation—A Case Study*, Tokyo: University of Tokyo (Lectures in Mathematical Sciences, vol. 5)

Faddeev, L.D. & Takhtajan, L.A. 1987. *Hamiltonian Methods in the Theory of Solitons*, Berlin and Heidelberg: Springer

Flaschka, H. & Newell, A.C. 1980. Monodromy and spectrum preserving deformations I. *Communications in Pure and Applied Mathematics*, 76: 67–116

Its, A. 2003. The Riemann–Hilbert problem and integrable systems. *Notices of the AMS*, 50: 1389–1400

Its, A.R., Izergin, A.G., Korepin, V.E. & Slavnov, N.A. 1990. Differential equations for quantum correlation functions. *International Journal of Physics* B4: 1003–1037; The quantum correlation function as the τ function of classical differential equations. In *Important Developments in Soliton Theory*, edited by, A.S. Fokas & V. E. Zakharov, Springer, Berlin, pp. 404–417, 1993

Jimbo, M., Miwa, T. & Ueno, K. 1981. Monodromy preserving deformation of linear ordinary differential equations with rational coefficients. I. *Physica* D, 2: 306–352

Muskhelishvili, N.I. 1946. *Singular Integral Equations*, Moscow (in Russian); translation by Groningen. Leiden: P. Noordhoff, 1953

Zakharov, V.E. & Shabat, A.B. 1971. Exact theory of two-dimensional self-focusing and one-dimensional self–modulation of waves in nonlinear media. *Zhurnal Eksperimental'noi Teoreticheskoi Fiziki*, 61: 118–134 [Russian]; translated in *Soviet Physics, JETP*, 34: 62–69 (1972)

Zhou, X. 1989. Direct and inverse scattering transforms with arbitrary spectral singularities. *Communications in Pure and Applied Mathematics*, 42, 895–938

Zhou, X. 1998. The L^2-Sobolev space bijectivity of the scattering and inverse scattering transforms. *Communications in Pure and Applied Mathematics*, 51: 697–731

RING SOLITONS

See **Solitons, types of**

ROBUSTNESS

See **Stability**

ROSSBY WAVES

See **Atmospheric and ocean sciences**

RÖSSLER SYSTEMS

Rössler systems were introduced in the 1970s as prototype equations with the minimum ingredients for continuous-time chaos.

Since the Poincaré–Bendixson theorem precludes the existence of other than steady, periodic, or quasi-periodic attractors in autonomous systems defined in one- or two-dimensional manifolds such as the line, the circle, the plane, the sphere, or the torus (Hartman, 1964), the minimum dimension for chaos is three. On this basis, Otto Rössler came up with a series of prototype systems of ordinary differential equations in three-dimensional phase spaces (Rössler, 1976a,c, 1977a, 1979a). He also proposed four-dimensional systems for hyperchaos, that is, chaos with more than one positive Lyapunov exponent (Rössler, 1979a,b).

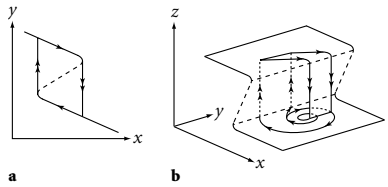

Figure 1. Illustration of the reinjection principle between the two branches of a Z-shaped slow manifold allowing (a) periodic relaxation oscillations in dimension two and (b) higher types of relaxation behavior in dimension three.

Rössler was inspired by the geometry of flows in dimension three and, in particular, by the reinjection principle, which is based on the feature of relaxation-type systems to often present a Z-shaped slow manifold in their phase space. On this manifold, the motion is slow until an edge is reached whereupon the trajectory jumps to the other branch of the manifold, allowing not only for periodic relaxation oscillations in dimension two (see Figure 1a), but also for higher types of relaxation behavior (see Figure 1b) as noted by Rössler (1979a). In dimension three, the reinjection can induce chaotic behavior if the motion is spiraling out on one branch of the slow manifold (see Figure 1b). In this way, Rössler invented a series of systems, the most famous of which is probably (Rössler 1979a):

$$\begin{aligned} \frac{dx}{dt} &= -y - z, \\ \frac{dy}{dt} &= x + ay, \\ \frac{dz}{dt} &= bx - cz + xz. \end{aligned} \tag{1}$$

This system is minimal for continuous chaos for at least three reasons: its phase space has the minimal dimension three, its nonlinearity is minimal because there is a single quadratic term, and it generates a chaotic attractor with a single lobe, in contrast to the Lorenz attractor which has two lobes. In Equation (1), (x, y, z) are the three variables that evolve in the continuous time t, and (a, b, c) are three parameters. The linear terms of the two first equations create oscillations in the variables x and y. These oscillations can be amplified if $a > 0$, which results into a spiraling-out motion. The motion in x and y is then coupled to the z variable ruled by the third equation, which contains the nonlinear term and which induces the reinjection back to the beginning of the spiraling-out motion.

System (1) possesses two steady states: one at the origin $x = y = z = 0$, around which the motion spirals out, and another one at some distance from the origin due to the quadratic nonlinearity. This system presents stationary, periodic, quasi-periodic, and chaotic attractors depending on the value of the parameters (a, b, c). These attractors are interconnected by bifurcations, in particular, a Hopf bifurcation from the stationary to periodic attractors and a period-doubling cascade from periodic to chaotic attractors. The resulting chaotic attractor has a single lobe and is referred to as spiral-type chaos, which mainly manifests itself in irregular amplitudes for the oscillations (see Figure 2a).

A transition occurs to a screw-type chaos in which the oscillations are irregular not only in their amplitudes but also in the reinjection times (see Figure 2b). The

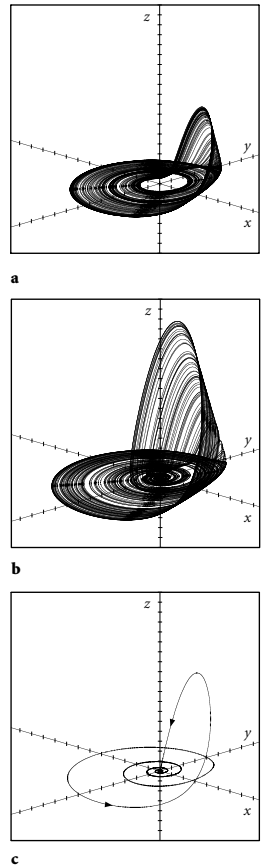

Figure 2. Phase portraits of the Rössler system (1) in the phase space of the variables (x, y, z): (a) spiral-type chaos for $a = 0.32$, $b = 0.3$, and $c = 4.5$; (b) screw-type chaos for $a = 0.38$, $b = 0.3$, and $c = 4.820$, in which case there also exists the Shil'nikov-type homoclinic orbit (c). The ticks are separated by unity. (Adapted from Gaspard & Nicolis, 1983.)

screw-type chaos is closely related to the presence of a Shil'nikov homoclinic orbit (see Figure 2c). This homoclinic orbit is attached to the origin $x = y = z = 0$, which is a saddle-focus with a one-dimensional stable manifold for the reinjection and a two-dimensional unstable manifold where the motion is spiraling out. The Shil'nikov criterion for chaos is that the reinjection is faster than the spiraling-out motion (Shil'nikov, 1965), and it is satisfied in the attractor of Figure 2b. As a consequence, the homoclinic system contains periodic and nonperiodic orbits belonging to multiple horseshoes that can be described in terms of symbolic dynamics. Away from homoclinicity, the system undergoes complex bifurcation cascades generating successive periodic and chaotic attractors.

Chaotic behavior and Shil'nikov homoclinic orbits in the Rössler system (1) can also be understood as originating from an oscillatory-stationary double instability taking place around the origin $x = y = z = 0$ and the parameter values $b = 1$, $-\sqrt{2} < a = c < +\sqrt{2}$.

In his work on continuous chaos, Rössler was motivated by the search for chemical chaos, that is, chaotic behavior in far-from-equilibrium chemical kinetics (Ruelle, 1973; Rössler, 1976b, 1977b; Rössler & Wegmann, 1978). With Willamowski, Rössler proposed the following chemical reaction scheme:

$$
\begin{aligned}
A_1 + X &\underset{k_{-1}}{\overset{k_1}{\rightleftharpoons}} 2X, \\
X + Y &\underset{k_{-2}}{\overset{k_2}{\rightleftharpoons}} 2Y, \\
A_5 + Y &\underset{k_{-3}}{\overset{k_3}{\rightleftharpoons}} A_2, \\
X + Z &\underset{k_{-4}}{\overset{k_4}{\rightleftharpoons}} A_3, \\
A_4 + Z &\underset{k_{-5}}{\overset{k_5}{\rightleftharpoons}} 2Z,
\end{aligned}
\qquad (2)
$$

which features two autocatalytic steps (reactions 1 and 5) involving the species X and Z coupled to another autocatalytic step (reaction 2) involving another species Y and two further steps (reactions 3 and 4) (Willamowski & Rössler, 1980). The concentrations of the species $A_1, \ldots, A_5$ are held fixed by large chemical reservoirs that maintain the system out of thermodynamic equilibrium. The time evolution of the concentrations (x, y, z) of the three intermediate species X, Y, and Z is ruled by a system of three coupled differential equations deriving from the mass action law of chemical kinetics. These equations have quadratic nonlinear terms because of the binary reactive steps and keep the concentrations positive as a consequence of mass action kinetics. The chemical reaction scheme (2) leads to a chaotic attractor very similar to that of the abstract system (1) (see Figure 3), and thus provides a mechanistic understanding of chemical chaos in terms of colliding and reacting particles.

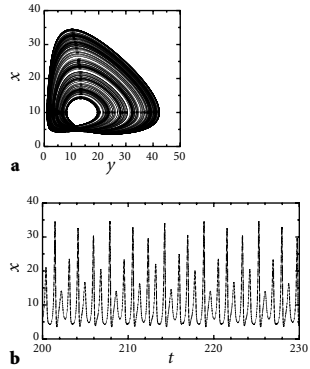

Figure 3. Chaotic time evolution of the concentrations of the Willamowski–Rössler chemical reaction scheme (2) for $k_1 a_1 = 30$, $k_{-1} = 0.5$, $k_2 = 1$, $k_{-2} = 0$, $k_3 a_5 = 10$, $k_{-3} = 0$, $k_4 = 1$, $k_{-4} = 0$, $k_5 a_4 = 16.5$, and $k_{-5} = 0.5$: (a) phase portrait in the plane of the concentrations of species X and Y; (b) concentration of species X versus time t.

In conclusion, Rössler systems are minimal models for continuous-time chaos. The chaotic attractors of Rössler systems are prototypes for a large variety of chaotic behavior, notably, in chemical chaos (Scott, 1991).

P. GASPARD

See also **Attractors; Bifurcations; Brusselator; Chaotic dynamics; Chemical kinetics; Hopf bifurcation; Horseshoes and hyperbolicity in dynamical systems; Invariant manifolds and sets; Period doubling; Phase space; Poincaré theorems; Symbolic dynamics**

Further Reading

Gaspard, P. & Nicolis, G. 1983. What can we learn from homoclinic orbits in chaotic dynamics? *Journal of Statistical Physics*, 31: 499–518

Hartman, P. 1964. *Ordinary Differential Equations*, New York: Wiley

Rössler, O.E. 1976a. An equation for continuous chaos. *Physics Letters* A, 57: 397–398

Rössler, O.E. 1976b. Chaotic behavior in simple reaction systems. *Zeitschrift Naturforschung* A, 31: 259–264

Rössler, O.E. 1976c. Different types of chaos in two simple differential equations. *Zeitschrift für Naturforschung A* 31: 1664–1670

Rössler, O.E. 1977a. Continuous chaos. In *Synergetics: A Workshop*, edited by H. Haken, New York: Springer, pp. 184–199

Rössler, O.E. 1977b. Chaos in abstract kinetics: Two prototypes. *Bulletin of Mathematical Biology*, 39: 275–289

Rössler, O.E. 1979a. Continuous chaos—four prototype equations. *Annals of the New York Academy of Science*, 316: 376–392

Rössler, O.E. 1979b. An equation for hyperchaos. *Physics Letters* A, 71: 155–157
Rössler, O.E. & Wegmann, K. 1978. Chaos in the Zhabotinskii reaction. *Nature*, 271: 89–90
Ruelle, D. 1973. Some comments on chemical oscillators. *Transactions of the New York Academy of Science*, 35: 66–71
Scott, S.K. 1991. *Chemical Chaos*, Oxford: Clarendon Press
Shil'nikov, L.P. 1965. A case of the existence of a countable number of periodic motions. *Soviet Mathematics Doklady*, 6: 163–166
Willamowski, K.-D. & Rössler, O.E. 1980. Irregular oscillations in a realistic abstract quadratic mass action system. *Zeitschrift für Naturforschung* A, 35: 317–318

ROTATING RIGID BODIES

Rigid body motion about a fixed point is a classical mechanics problem associated with the greatest names in 18th-century mathematics. The basic equations of the motion were derived by Leonhard Euler in the 1750s and subsequently solved by him for two special cases (Euler and Lagrange tops). Development of the analytical theory of differential equations in the middle of the 19th century by Augustin Cauchy, Georg Riemann, and Karl Weierstrass inspired Sophia Kovalevsky (1889) to determine all the cases for which the integrals of rigid body dynamics were *single-valued*, *meromorphic* functions in the entire *complex* plane of the time variable. Pursuing this remarkable idea, she obtained a classification of all such (solvable) cases and found a new case, the Kovalevsky top, which she then integrated in quadratures. Considering time as a complex variable and imposing the above conditions upon the integrals of the equations of motion outside the real axis was a revolutionary approach to treating a mechanics problem. It appeared to be a fruitful method that led to a unified theory of (algebraically) completely integrable systems (Adler & van Moerbeke, 1989), a century after it was proposed.

The dynamics of a rigid body rotating about a fixed point can be considered in a fixed (nonmoving) frame of axes or in the moving body frame that has its origin at the fixed point and whose axes are along the principal axes of the ellipsoid of inertia. In 1750, Euler obtained the equations of motion in a fixed frame, but they appeared not to be very useful. In a series of papers during 1758–1765, he introduced the body frame, derived corresponding equations of motion, and also used Eulerian angles to relate the motion of a body frame with respect to a fixed system of coordinates.

Consider first a fixed frame $(\boldsymbol{i}', \boldsymbol{j}', \boldsymbol{k}')$. A fundamental dynamical theorem says that the time derivative of the angular momentum $\boldsymbol{J}$ of a body is equal to the moment $\boldsymbol{L}$ of the forces acting on it,

$$\frac{\mathrm{d}\boldsymbol{J}}{\mathrm{d}t} = \boldsymbol{L}. \tag{1}$$

In the body frame, $(\boldsymbol{i}, \boldsymbol{j}, \boldsymbol{k})$, the tensor of inertia is diagonal, $\boldsymbol{I} = \mathrm{diag}(A, B, C)$, and links the vector of angular velocity $\boldsymbol{\Omega} = p\,\boldsymbol{i} + q\,\boldsymbol{j} + r\,\boldsymbol{k}$ to the angular momentum $\boldsymbol{J}$ through the linear relation

$$\boldsymbol{J} = \boldsymbol{I}\boldsymbol{\Omega} = Ap\,\mathbf{i} + Bq\,\boldsymbol{j} + Cr\,\boldsymbol{k}. \tag{2}$$

The time derivative of vector (2) is

$$\frac{\mathrm{d}\boldsymbol{J}}{\mathrm{d}t} = \frac{\delta \boldsymbol{J}}{\delta t} + \boldsymbol{\Omega} \times \boldsymbol{J}, \tag{3}$$

where $\frac{\delta \boldsymbol{J}}{\delta t}$ is the relative time derivative, evaluated assuming that the frame $(\boldsymbol{i}, \boldsymbol{j}, \boldsymbol{k})$ is stationary. The first three Euler equations, therefore, are

$$\begin{aligned} A\frac{\mathrm{d}p}{\mathrm{d}t} + (C - B)qr &= Mg(y_0\gamma'' - z_0\gamma'), \\ B\frac{\mathrm{d}q}{\mathrm{d}t} + (A - C)rp &= Mg(z_0\gamma - x_0\gamma''), \\ C\frac{\mathrm{d}r}{\mathrm{d}t} + (B - A)pq &= Mg(x_0\gamma' - y_0\gamma), \end{aligned} \tag{4}$$

where $M\boldsymbol{g} = Mg(\gamma\,\boldsymbol{i} + \gamma'\,\boldsymbol{j} + \gamma''\,\boldsymbol{k})$ is the vector of the gravitational force and $\boldsymbol{r}_0 = x_0\,\boldsymbol{i} + y_0\,\boldsymbol{j} + z_0\,\boldsymbol{k}$ is the vector originating in the fixed point and pointing at the center of mass of the body. An extra set of three equations follows from the fact that the vector $M\boldsymbol{g}$ is stationary in the fixed frame; hence, $\frac{\delta M\boldsymbol{g}}{\delta t} = -\,\boldsymbol{\Omega} \times M\boldsymbol{g}$ and

$$\begin{aligned} \frac{\mathrm{d}\gamma}{\mathrm{d}t} &= r\gamma' - q\gamma'', \qquad \frac{\mathrm{d}\gamma'}{\mathrm{d}t} = p\gamma'' - r\gamma, \\ \frac{\mathrm{d}\gamma''}{\mathrm{d}t} &= q\gamma - p\gamma'. \end{aligned} \tag{5}$$

The Eulerian angles, namely, the angle of precession $0 \le \psi < 2\pi$, the angle of nutation $0 \le \vartheta \le \pi$, and the angle of the self rotation $0 \le \varphi < 2\pi$, define the body's position by fixing the moving frame with respect to the fixed one. We have (see Golubev, 1960)

$$\begin{aligned} \gamma &= \sin\varphi\,\sin\vartheta, \qquad \gamma' = \cos\varphi\,\sin\vartheta, \\ \gamma'' &= \cos\vartheta, \end{aligned} \tag{6}$$

$$\begin{aligned} p &= \dot{\psi}\sin\vartheta\,\sin\varphi + \dot{\vartheta}\cos\varphi, \\ q &= \dot{\psi}\sin\vartheta\,\cos\varphi - \dot{\vartheta}\sin\varphi, \quad r = \dot{\psi}\cos\vartheta + \dot{\varphi} \end{aligned} \tag{7}$$

and, therefore,

$$\frac{\mathrm{d}\psi}{\mathrm{d}t} = \frac{p\gamma + q\gamma'}{\gamma^2 + \gamma'^2}. \tag{8}$$

The problem of studying the motion of a rigid body about a fixed point is solved by integration of the system of differential equations (4), (5), and (8).

Conserved Quantities

It is always useful to know a system's first integrals, for instance for controlling numerical calculations or for performing integration in quadratures. There are three important physical integrals for an arbitrary top (an arbitrary set of the six parameters $\{A, B, C, x_0, y_0, z_0\}$ in Equations (4)). They are the following.

(i) Energy integral: $E = \frac{1}{2}\left(Ap^2 + Bq^2 + Cr^2\right) - Mg(x_0\gamma + y_0\gamma' + z_0\gamma'')$.
(ii) Length of the unit vector along $\boldsymbol{Mg}$: $C_1 = \gamma^2 + \gamma'^2 + \gamma''^2 = 1$.
(iii) Projection of the angular momentum $\boldsymbol{J}$ on this vector: $C_2 = Ap\gamma + Bq\gamma' + Cr\gamma''$.

These three first integrals provide three constants of motion (since $C_1 = 1$, there are, in fact, only two arbitrary constants, the third one being the integration constant that appears when integrating (8), that is, the initial value of ψ). In addition, an autonomous system always has an extra constant corresponding to shifting of the time variable t. A remarkable feature of Equations (4) and (5) is that yet another explicit integration can be carried out using the method of Jacobi's last multiplier (Golubev, 1960), bringing in another explicit constant of integration. Therefore, for the case of a complete integration in quadratures of the equations of motion only one first integral is missing. Subsequent analysis showed that an extra algebraic integral exists only in the three special cases of Euler, Lagrange, and Kovalevsky tops. These integrable tops are given by specializing the parameters $\{A, B, C, x_0, y_0, z_0\}$.

Integrable Tops

The simpler cases of the Euler and Lagrange tops were studied, respectively, by Euler and Louis Poinsot and by Joseph-Louis Lagrange and Siméon Poisson, and later on by Gustav Jacobi, who expressed the general integrals for both systems in terms of elliptic functions of time.

Euler Top

In the Euler top $x_0 = y_0 = z_0 = 0$, and the body's center of mass is at the fixed point, so that there is no gravitational effect, meaning a free rotation of an asymmetric top. The fourth integral of motion in this case is the square of the angular momentum $\boldsymbol{J}$:

$$\boldsymbol{J}^2 = A^2p^2 + B^2q^2 + C^2r^2. \tag{9}$$

Poinsot gave a geometric interpretation of the motion based on the intersection of two quadratics: (9) and the energy integral $2E = Ap^2 + Bq^2 + Cr^2$. The vector $\boldsymbol{J}$ is stationary in the fixed frame $(\boldsymbol{i}', \boldsymbol{j}', \boldsymbol{k}')$ and the problem is made simpler if one chooses $\boldsymbol{k}'$ along $\boldsymbol{J}$. Then

$$\cos\vartheta = \frac{Cr}{|\boldsymbol{J}|} \text{ and } \tan\varphi = \frac{Ap}{Bq}. \tag{10}$$

As for time dependence, the variables p, q, and r can be expressed in terms of Jacobi's elliptic functions sn, cn, and dn of time and they are periodic, so are ϑ and φ obtained from (10). The dynamics of the angle of precession ψ is determined by integration of $\dot{\psi} = |\boldsymbol{J}|\,\frac{Ap^2 + Bq^2}{A^2p^2 + B^2q^2} > 0$, derived from (8). It follows that after each period, the value of ψ, in general, changes, so that the body never comes back to its initial orientation, thereby undergoing quasi-periodic motion.

Stationary rotations are those when the vector of angular velocity $\boldsymbol{\Omega}$ is constant. They correspond to uniform rotations about the principal axes of inertia. Rotation around the middle axis is unstable.

A symmetric $(A = B)$ Euler top performs regular precession. The body's symmetry axis draws a circular conic with the axis $\boldsymbol{J}$ and the angle $2\vartheta = \text{const}$. The symmetry axis goes around $\boldsymbol{J}$ with a constant angular velocity while the body rotates with a constant angular velocity around the symmetry axis.

Lagrange Top

This describes the dynamics of a symmetric body, $A = B$, with the fixed point at the symmetry axis and off the center of mass, that is, $x_0 = y_0 = 0$, $z_0 \neq 0$. The fourth constant of motion is simply r. The integration of this top can again be done in terms of elliptic functions, leading to a variety of complicated quasi-periodic motions including pseudo-regular precession, double-asymptotic, and "sleeping" tops. Simpler motions correspond to degenerations of elliptic functions into elementary functions.

The motion of the symmetry axis, described by the angles ϑ and ψ, looks like a perturbation of the corresponding uniform rotation of a symmetric Euler top in the regular precession. Illustrations of this familiar motion are available in many textbooks. Notice that now $\dot{\psi}$ can change sign, thereby giving three kinds of trajectories.

Denote $m = 1 - C/A$ and notice that $m = 0$ for a spherically symmetric body $(A = B = C)$. Consider the Lagrange top with $m \neq 0$ and the variables $(p, q, r, \gamma, \gamma', \gamma'')$ and a fully symmetric Lagrange top with $m = 0$ and the variables $(p_1, q_1, r_1, \gamma_1, \gamma_1', \gamma_1'')$. It is possible to show that the motions of these two bodies coincide when the variables are identified as follows:

$$\begin{aligned} &p_1^2 + q_1^2 = p^2 + q^2, \quad \tan^{-1}\tfrac{q_1}{p_1} = \tan^{-1}\tfrac{q}{p} + mrt, \\ &r_1 = \tfrac{C}{A}\,r, \\ &\varphi_1 = \varphi - mrt, \qquad \vartheta_1 = \vartheta, \\ &\psi_1 = \psi. \end{aligned} \tag{11}$$

See Golubev (1960) for details.

Kovalevsky Top

This is the third general case of complete integrability of the Euler equations (4) and (5), which is characterized by restricting $A = B = 2C$ and $y_0 = z_0 = 0$. Hence, the Kovalevsky top is a special symmetric top whose center of mass lies in the equatorial plane of the ellipsoid of inertia ($x_0 \neq 0$). The fourth constant of motion is of order 4:

$$K = \left(p^2 - q^2 + \frac{Mgx_0}{C}\gamma\right)^2 + \left(2pq + \frac{Mgx_0}{C}\gamma'\right)^2. \tag{12}$$

Kovalevsky found this case (Kovalevsky, 1889) and integrated it in terms of hyper-elliptic functions. Later on, Kötter (1893) simplified the formulae.

There is a great difference in complexity between this top and the other two. This is why there was such a long period between the discovery and integration of Euler and Lagrange tops and that of Kovalevsky. The Paris Academy of Sciences established a special Borden Prize to promote major expansions of the theory. It was finally claimed in 1888 by Sophia Kovalevsky who made major progress toward solution of the problem. Her work required usage of theta-functions in two variables and provided an enormous boost to the creation of the modern theory of completely integrable systems. There is a large body of literature about the Kovalevsky top, of which we mention only three items. In Adler & van Moerbeke (1988), a detailed study of the algebraic geometry of the model is given. In Bobenko et al. (1989), the authors find alternative theta-function formulae by making use of the corresponding Lax matrix and the finite-gap integration technique. In Kuznetsov (2002), connections with a representation of the quadratic r-matrix algebra and with the method of separation of variables are presented.

All other general tops corresponding to other choices of the six parameters (A, B, C, x_0, y_0, z_0) are not integrable, which means that they generally exhibit a chaotic dynamics, and it is impossible to find analytic solutions valid for arbitrary initial conditions.

VADIM B. KUZNETSOV

See also **Constants of motion and conservation laws; Integrability; Newton's laws of motion; Nonlinear toys**

Further Reading

Adler, M. & van Moerbeke, P. 1988. The Kowalevski and Hénon–Heiles motions as Manakov geodesic flows on SO(4)—a two-dimensional family of Lax pairs. *Communications in Mathematical Physics*, 113: 659–700

Adler, M. & van Moerbeke, P. 1989. The complex geometry of the Kowalevski–Painlevé analysis. *Inventiones Mathematicae*, 97: 3–51

Bobenko, A.I., Reyman, A.G. & Semenov-Tian-Shansky, M.A. 1989. The Kowalevski top 99 years later: a Lax pair, generalizations and explicit solutions. *Communications in Mathematical Physics*, 122: 321–354

Golubev, V.V. 1960. *Lectures on Integration of the Equations of Motion of a Rigid Body about a Fixed Point*, Moscow, 1953. Published for the National Science Foundation by the Israel Program for Scientific Translations

Kötter, F. 1893. Sur le cas traité par Mme Kowalevski de rotation d'un corps solide autour d'un point fixe. *Acta Mathematica*, 17(1–2)

Kovalevsky, S. 1889. Sur le problème de la rotation d'un corps solide autour d'un point fixe. *Acta Mathematica*, 12: 177–232

Kuznetsov, V.B. 2002. Kowalevski top revisited. In *The Kowalevski Property*, edited by V.B. Kuznetsov, Providence, RI: American Mathematical Society

ROTATING WAVE APPROXIMATION

Energy conserving oscillators comprise pairs of energetic variables (let us call them P and Q), each being the cause of the other. In a mechanical (spring-mass) oscillator shown in Figure 1, for example, Q would be the displacement of a mass and P its momentum (mass times velocity). For a radio engineer's tank oscillator, Q is the voltage across a capacitor and P is the current through an inductor. In a laser mode, Q is electric field energy and P is magnetic field energy.

Consider the mechanical oscillator of Figure 1, assuming the spring to be linear. From Newton's second law (force equals time derivative of momentum), the dynamic equation describing this system is

$$\frac{\mathrm{d}}{\mathrm{d}t}\left(M\frac{\mathrm{d}x}{\mathrm{d}t}\right) = -Kx, \tag{1}$$

where x is the vertical displacement of the mass from its resting position and M is the oscillator mass. On the right-hand side of this equation is the vertical force acting on the mass caused by extension or compression of the spring, and on the left-hand side is the time derivative of the vertical momentum: $p \equiv M\mathrm{d}x/\mathrm{d}t$. In this case, a solution is evidently $x = a\sin(\omega_0 t)$, where a is an arbitrary amplitude and $\omega_0 = \sqrt{K/M}$ is the frequency of oscillation.

Often the force of a spring is not quite a linear function of its extension but slightly sublinear. (This

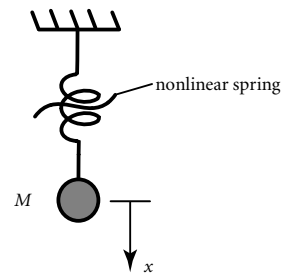

Figure 1. A spring-mass oscillator.

is the case, for example, in molecular vibrations, where the force between a pair of atoms becomes relatively weaker as the distance between them is increased because the electronic contribution to interatomic bonding is lessened.) In such cases, it is convenient to introduce anharmonicity into the formulation through the rotating wave picture (Louisell, 1960; Scott, 2003).

In the rotating wave picture of a linear oscillator, the momentum (p) and extension (x) are combined as real and imaginary parts of a single, complex amplitude

$$A \equiv \frac{(p - \mathrm{i}M\omega_0 x)}{\sqrt{2M\omega_0}}, \tag{2}$$

which obeys the first order equation

$$\mathrm{i}\frac{\mathrm{d}A}{\mathrm{d}t} = \omega_0 A \tag{3}$$

with the solution $A(t) = A(0)\mathrm{e}^{-\mathrm{i}\omega_0 t}$. Under this formulation, the total energy of the oscillator is

$$H = \omega_0 |A|^2 = \frac{1}{2}\left(\frac{p^2}{M} + Kx^2\right), \tag{4}$$

where the first term is the kinetic energy of the moving mass and the second is the potential energy stored in the spring.

If the restoring force of the spring is slightly sublinear, its potential energy may depend upon x as

$$\text{potential energy} = \tfrac{1}{2}Kx^2 - \tfrac{1}{4}\alpha x^4, \tag{5}$$

where $\alpha > 0$ is an anharmonicity parameter. With $\alpha = 0$, $x = \mathrm{i}\,(A - A^*)/\sqrt{2M\omega_0}$, so

$$x^4 = \frac{1}{4M^2\omega_0^2}\left[A^4 - 4A^3A^* + 6|A|^4 - 4A(A^*)^3 + (A^*)^4\right]. \tag{6}$$

Except for the middle ($6|A|^4$) term, each term in Equation (6) varies sinusoidally with time at frequencies $\pm 4\omega_0$ or $\pm 2\omega_0$. Thus, the average of the energy over a cycle of oscillation is

$$\langle H\rangle = \omega_0|A|^2 - \frac{\gamma}{2}|A|^4, \tag{7}$$

where $\gamma = 3\alpha/4M^2\omega_0^2$.

Under the rotating wave approximation (RWA), the energy H is taken as equal to its time average $\langle H\rangle$, whereupon the complex amplitude A is governed by the first order ODE

$$\mathrm{i}\frac{\mathrm{d}A}{\mathrm{d}t} \doteq \omega_0 A - \gamma|A|^2 A. \tag{8}$$

In this expression, the symbol "$\doteq$" indicates that only terms of frequency ω_0 are included. In other words, all nonresonant terms are neglected in the RWA.

Since Equation (8) conserves $N = |A|^2$, a general solution of this equation is

$$A(t) = \sqrt{N}\mathrm{e}^{-\mathrm{i}[(\omega_0 - \gamma N)t + \varphi]}, \tag{9}$$

where φ is an arbitrary phase angle. Equation (9) gives the frequency ($\omega = \omega_0 - \gamma N$) of the nonlinear oscillation as a function of its amplitude in the RWA.

Thus, RWA accounts for all components generated by a weak nonlinearity that resonate with the fundamental oscillator frequency. (As with your radio receiver, those components not in resonance are neglected.) Because the RWA is motivated by a general oscillator formulation, it is widely employed as the initial assumption in a variety of nonlinear analyses (various versions of the nonlinear Schrödinger equation, the discrete self-trapping equation, molecular vibrations, nonlinear optics, etc.). Interestingly, odd terms in the potential function (x^3, x^5, and so on) do not generate resonant components and are, thus, neglected in the RWA.

Finally, the RWA is a convenient formulation because quantum theories are easy to construct and solve for general systems of interacting oscillators, including discrete nonlinear Schrödinger equations and the discrete self-trapping system (Louisell, 1962; Scott et al., 1994; Scott, 2003). This is so for two reasons. First, under quantum theory in the RWA, the complex amplitude (A) becomes the lowering (annihilation) operator for oscillator quanta (bosons), and its complex conjugate (A^*) becomes the raising (creation) operator. Second, the classical fact that $N = \sum |A|^2$ is conserved implies that the corresponding quantum number operator commutes with the energy operator, allowing eigenfunctions of the energy operator to be constructed as sums of linear oscillator eigenfunctions.

ALWYN SCOTT

See also **Damped-driven anharmonic oscillator; Discrete nonlinear Schrödinger equations; Discrete self-trapping system; Quantum nonlinearity; Salerno equation**

Further Reading

Louisell, W.H. 1960. *Coupled Mode and Parametric Electronics*, New York: Wiley

Louisell, W.H. 1962. Correspondence between Pierce's coupled mode amplitudes and quantum oscillators. *Journal of Applied Physics*, 33: 2435–2436

Scott, A.C. 2003. *Nonlinear Science: Emergence and Dynamics of Coherent Structures*, 2nd edition, Oxford and New York: Oxford University Press

Scott, A.C., Eilbeck, J.C. & Gilhøj, H. 1994. Quantum lattice solitons. *Physica* D, 78: 194–213

ROTATION-MODIFIED KORTWEG-DE VRIES EQUATION

See **Korteweg–de Vries equation**

ROUTES TO CHAOS

If a nonlinear systems has chaotic dynamics, then it is natural to ask how this complexity develops as

parameters vary. For example, in the logistic map

$$x_{n+1} = r x_n (1 - x_n), \tag{1}$$

it is easy to show that if $r = \frac{1}{2}$, then there is a fixed point at $x = 0$ that attracts all solutions with initial values x_0 between 0 and 1, while if $r = 4$, the system is chaotic. How, then, does the transition to chaos occur as the parameter r varies? Indeed, is there a clean transition to chaos in any well-defined sense? The identification and description of routes to chaos has had important consequences for the interpretation of experimental and numerical observations of nonlinear systems. If an experimental system appears chaotic, it can be very difficult to determine whether the experimental data comes from a truly chaotic system, or if the results of the experiment are unreliable because there is too much external noise. Chaotic time series analysis provides one approach to this problem, but an understanding of routes to chaos provides another. In many experiments there are parameters (ambient temperature, Raleigh number, etc.) that are fixed in any realization of the experiment, but which can be changed. If recognizable routes to chaos are observed when the experiment is repeated at different values of the parameter, then there is a sense in which the presence of chaotic motion has been explained.

By the early 1980s, three "scenarios" or "routes to chaos" had been identified (e.g., Eckmann, 1981): Ruelle–Takens–Newhouse, period doubling, and intermittency (which has several variants). As we shall see, in their standard forms each of these transitions uses the term "route to chaos" in a different way, so care needs to be taken over the interpretation of experimental or numerical observations of these transitions.

Ruelle–Takens–Newhouse

In 1971, Ruelle and Takens published a mathematical paper with the provocative title "On the Nature of Turbulence." In this paper and a subsequent improvement with Newhouse (1978), they discuss the Landau scenario for the creation of turbulence by the successive addition of new frequencies to the dynamics of the fluid. They show that if the attractor of a system has three independent frequencies (four in the 1971 paper), then a small perturbation of this system has a hyperbolic strange attractor—a Plykin attractor (a solenoid in the 1971 paper). The result became known colloquially as "three frequencies implies chaos," a serious misinterpretation of the mathematical result that has been the cause of a number of misleading statements. First, the result proves the existence of chaos in systems arbitrarily close to the three frequency system in an infinite dimensional function space but gives no indication of the probability of finding chaos in any given example. Second, I know of no experimental situation where a Plykin attractor has been shown to exist even when chaotic behavior has been observed close to systems with three frequency attractors. Numerical experiments suggest that it is much more likely that the system evolves by frequency locking.

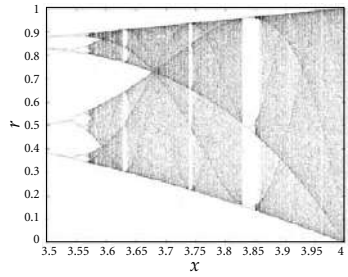

Figure 1. The attractor of the logistic equation as a function of the parameter r.

The Ruelle–Takens–Newhouse route to chaos remains somewhat of an enigma, and more work needs to be done to understand precisely how and when the strange attractors predicted by the theory come into being.

Period Doubling

Figure 1 shows the attractor of the logistic map (1) as a function of the parameter, r, for $3.5 < r < 4$. Thus, the set of points plotted on any vertical line of constant r represents the attractor of the map for that value of r, and if the set is finite, then the (numerically computed) attractor is a periodic orbit that cycles through the finite collection of points. Figure 1 suggests that for small r, the attractor is always periodic and has period 2^n, with n increasing as r increases. Beyond some critical value $r = r_c$, with $r_c \approx 3.569946$, the attractor may be more complicated. There are clearly intervals of r for which the attractor is periodic, and the attractor seems to be contained in 2^n bands that merge as r increases (the final band merging from 2 bands to one band with r just below 3.68 is particularly clear).

As r increases, the periodic orbit of period 2^n is created from the orbit of period 2^{n-1} by a period-doubling bifurcation. If this bifurcation occurs with $r = r_n$, then $r_n \to r_c$ geometrically as $n \to \infty$, with

$$\lim_{n\to\infty} \frac{r_n - r_{n-1}}{r_{n+1} - r_n} = \delta \approx 4.66920, \tag{2}$$
$$\text{i.e.,} \quad r_n \sim r_c - \kappa \delta^{-n}.$$

The really surprising feature of this period-doubling cascade, as shown in Feigenbaum (1978), is that the cascade can be observed in many maps and the accumulation rate δ of the period-doubling cascade (2)

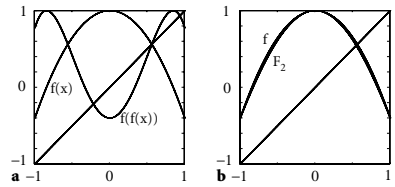

Figure 2. (a) The quadratic map $f(x) = 1 - mx^2$ restricted to the interval $[-1, 1]$ and the second iterate, $f(f(x))$ for $m = 1.40115$ which is just below the critical value m_c. (b) The original map, f, and the rescaled map, $F_2(x) = \mathcal{T}f(x) = -a^{-1}f(f(-ax))$ on $[-1, 1]$ with $a = -f(1) = m - 1$. Note that $a = 0.40115$ is close to the universal value of $\alpha \approx 0.3995$.

is the same although the constants r_c and κ depend on the map. In fact, the universal value of δ depends on the nature of the maximum of the map: $\delta \approx 4.66920$ for maps with quadratic maximum. A complete cascade of band merging from 2^n bands to 2^{n-1} bands occurs at parameter values $\tilde{r}_n$ above r_c, and $\tilde{r}_n \to r_c$ as $n \to \infty$ at the same universal geometric rate δ.

The quantitative universality in parameter space described by the scaling δ has a counterpart in phase space. If x_n denotes the point on the periodic orbit of period 2^{n-1} that is closest to the critical point (or turning point) of the map with $r = r_n$, then

$$\lim_{n\to\infty} \frac{x_{n+1} - \frac{1}{2}}{x_n - \frac{1}{2}} = -\alpha, \tag{3}$$

where α is another universal constant, which, for maps with a quadratic turning point, takes the value $\alpha \approx 0.3995 = 1/2.50\ldots$.

In families of one hump (unimodal) maps this universality can be explained by a renormalization argument. Restrict attention to families of one hump maps with critical point (maximum) at $x = 0$, parametrized by μ and normalized so that $f(0)c = 1$. As shown in Figure 2a, for parameter values near μ_c (the accumulation of period doubling) the second iterate of the map, $f(f(x))$, restricted to an interval about the critical point is a one hump map with a minimum. So, after a rescaling (and flipping) of the coordinates, it is another one hump map with the same normalization as shown in Figure 2b. Mitchell Feigenbaum was able to show (by arguments that have been made rigorous since 1990) that the universal properties described above are due to the structure of the doubling operator $\mathcal{T}$, which is a map on one hump maps $f : [-1, 1] \to [-1, 1]$, with critical point at $x = 0$ and $f(0)c1$, defined by

$$\mathcal{T}f(x) = -a^{-1}f(f(-ax)), \tag{4}$$

where $a = -f(1)$ so that the normalization $\mathcal{T}f(0) = 1$ is preserved. This operator does the rescaling and flipping referred to above. In the appropriate universality class, for example, quadratic critical point together with some further technical conditions, there is a fixed point f_*, of $\mathcal{T}$, so $f_* = \mathcal{T}f_*$, and the universal scaling of phase space is given by $\alpha = -f_*(1)$. Furthermore, the universal accumulation rate δ of (2) is an unstable eigenvalue of the (functional) derivative of $\mathcal{T}$ at f_*.

We can now consider measures of chaos such as the topological entropy or the Lyapunov exponents of the map. If $\{f_\mu\}$ is a family of one hump maps that undergoes period doubling, then the parameter μ can be chosen so that the period-doubling cascade is for $\mu < \mu_c$. Coullet & Tresser (1980) show that the universal structure described above implies that if $H(\mu)$ is either the topological entropy (which can be thought of as the growth rate of the number of periodic orbits) or the Lyapounov exponent of f_μ with $\mu > \mu_c$, then

$$H(\mu) \sim C(\mu - \mu_c)^{(\log 2)/(\log \delta)}. \tag{5}$$

The Lyapunov exponent is a very poorly behaved function of the parameters and this scaling provides only an envelope for the graph of the exponent, but the topological entropy is continuous. Indeed, the proof of Sharkovsky's theorem (*See* **One-dimensional maps**) shows that if a continuous map of the interval has a periodic orbit which is not a power of two, then there is a horseshoe for some iterate of the map, and hence the map has positive topological entropy if $\mu > \mu_c$. The entropy is zero if $\mu < \mu_c$, so if by chaos we mean positive topological entropy, then the period-doubling route is a true route to chaos.

Intermittency

The first stable periodic orbit of each of the windows of periodic motion in $r > r_c$, which can be seen in Figure 1, is created in a saddle-node (or tangent) bifurcation. Throughout the parameter interval for which such orbits are stable, there is a repelling strange invariant set, but most solutions tend to the stable periodic orbit. Just before the creation of the stable periodic orbit, chaotic solutions spend long periods of time near the points at which the stable periodic orbit will be created (the "laminar" phase), then move away and behave erratically before returning to the laminar phase. This behavior is called intermittency by Pomeau & Manneville (1980), who were the first to describe the scaling of the time spent in the laminar phase. They looked at the average time T_A spent by solutions in the laminar phase as a function of the parameter r close to the value r_{sn}, at which the saddlenode bifurcation occurs. A simple argument based on the passage time of a trajectory of a map close to a tangency with the diagonal (the condition for the saddle-node bifurcation) establishes that the average time in the laminar phase diverges as a power law:

$$T_A \sim |r - r_{sn}|^{-1/2}. \tag{6}$$

Other types of intermittency (involving period-doubling bifurcations, etc.) can be analyzed using the same ideas. Note that a strange invariant set exists throughout the parameter regions being considered here, so in this case the term "route to chaos" refers to the stability of the chaotic invariant set, not the creation of a chaotic set. Moreover, in any open neighborhood of r_{sn}, there are parameters for which the map has other stable periodic orbits, so the full description of parameters with stable chaotic motion is much more complicated than the description above suggests.

Other Routes to Chaos

Since the pioneering work of the late 1970s, a number of other routes to chaos have been identified. New routes to chaos are still being identified, and the list provided here is by no means complete. Arnéodo et al. (1981) show that there can be cascades of homoclinic bifurcations to chaos via a mechanism closely related to period doubling. This gives the less standard convergence rates involving nonquadratic turning points immediate relevance. The bifurcation that creates the strange invariant set of the Lorenz model is another type of homoclinic bifurcation, and this strange invariant set becomes stable by a "crisis" in which the strange invariant set collides with a pair of unstable periodic orbits. Ott (2002) contains a good account of such transitions. More complicated transitions involving maps of the circle are detailed in MacKay & Tresser (1986), and Newhouse et al. (1983) give another transition.

PAUL GLENDINNING

See also **Attractors; Bifurcations; Chaotic dynamics; Intermittency; Lorenz equations; One-dimensional maps; Period doubling; Time series analysis**

Further Reading

Arnéodo, A., Coullet, P. & Tresser, C. 1981. A possible new mechanism for the onset of turbulence. *Physics Letters* A, 81: 197–201

Coullet, P. & Tresser, C. 1980. Critical transition to stochasticity for some dynamical systems. *Journal de Physique Lettres*, 41: L255–L258

Eckmann, J.-P. 1981. Roads to turbulence in dissipative dynamical systems, *Reviews of Modern Physics*, 53: 643–654

Feigenbaum, M.J. 1978. Quantitative universality for a class of nonlinear transformations. *Journal of Statistical Physics*, 19: 25–52

MacKay, R.S. & Tresser, C. 1986. Transition to topological chaos for circle maps. *Physica* D, 19: 206–237

Newhouse, S., Palis, J. & Takens, F. 1983. Bifurcations and stability of families of diffeomorphisms. *Publications Mathématiques de l'IHES*, 57: 5–72

Newhouse, S., Ruelle, D. & Takens, F. 1978. Occurrence of strange Axiom A attractors near quasi-periodic flows on $\mathbf{T}^m$, $m \geq 3$. *Communications in Mathematical Physics*, 64: 35–40

Ott, E. 2002. *Chaos in Dynamical Systems*, 2nd edition, Cambridge and New York: Cambridge University Press

Pomeau, Y. & Manneville, P. 1980. Intermittent transition to turbulence in dissipative dynamical systems. *Communications in Mathematical Physics*, 74: 189–197

Ruelle, D. & Takens, F. 1971. On the nature of turbulence. *Communications in Mathematical Physics*, 20: 167–192

RUELLE–TAKENS–NEWHOUSE

See **Routes to chaos**

RUNGE–KUTTA METHOD

See **Numerical methods**

S

SADDLE POINT

See **Phase space**

SAFFMAN–TAYLOR PROBLEM

See **Hele-Shaw cell**

SALERNO EQUATION

The Salerno equation is a q-deformed lattice model that includes, as particular cases, two known discrete versions of the continuous nonlinear Schrödinger equation (NLS): the non-integrable discrete NLS equation (DNLS) with on-site nonlinearity and the integrable Ablowitz–Ladik (AL) equation with intra-site nonlinearity. Here by q-deformed, we mean the existence, both in the Poisson bracket (commutator in the quantum case) and in the Hamiltonian, of a free parameter q that allows "tuning" the nonlinearity (interaction) of the lattice model. From a physical point of view this equation represents a generalization of the tight-binding Schrödinger model

$$\mathrm{i}\frac{\mathrm{d}A_j(t)}{\mathrm{d}t} + \Omega_j A_j(t) + J_j\ (A_{j+1}(t) + A_{j-1}(t)) = 0, \tag{1}$$

for the propagation of a molecular excitation in a crystal. Here A_j denotes the quasi-classical complex mode amplitude of a particular molecular vibration, Ω_j is the on-site frequency of this vibration, and J_j is the next-neighbor resonance interaction energy. Equation (1) was considered by Richard Feynman as a starting point for an alternate formulation of quantum mechanics in terms of coupled probability amplitudes (Feynman, 1965) (also it is equivalent to the Schrödinger equation for the description of the wave function of an electron in a perfect crystal in the tight-binding approximation). By assuming the coupling of the mode amplitudes to low-frequency phonons (lattice distortions), one obtains, in the adiabatic and small field amplitude approximation, a dependence of the local energy and intra-site interaction upon A_j of the type

$$\Omega_j \to \Omega_{0j} + \Omega_{1j}|A_j|^2, \qquad J_j \to J_{0j} + J_{1j}|A_j|^2. \tag{2}$$

The Salerno equation follows by substituting the above relations into Equation (1) and redefining parameters as

$$\varepsilon = \frac{\Omega_1}{J_0}, \eta = \frac{\Omega_1}{J_1}, \omega_j = \frac{2J_0 + \Omega_0}{J_0}, \gamma = \frac{2J_1 + \Omega_1}{J_0},$$

thus giving

$$\mathrm{i}\frac{\mathrm{d}A_j(t)}{\mathrm{d}t} - (2 - \omega_j - \varepsilon|A_j|^2)A_j + (1 + \frac{\varepsilon}{\eta}|A_j|^2)(A_{j+1} + A_{j-1}) = 0, \tag{3}$$

where time has been rescaled by a factor J_0 and equal local energies and intra-site resonance interactions were assumed (note that ω_j can be eliminated from Equation (3) by a rescale of time, so that in the following, we will put $\omega_j = 0$). With the above parametrization the following relationship between ε and η was introduced:

$$q \equiv \frac{\varepsilon}{\eta} = \frac{\gamma - \varepsilon}{2}. \tag{4}$$

This allows interpolatation between the DNLS and the AL lattice as discussed below. To this end, it is worth noting that Equation (3) is a Hamiltonian system with respect to the following q-deformed Poisson bracket:

$$\{f, g\}_q = \sum \left(\frac{\partial f}{\partial A_j}\frac{\partial g}{\partial A_j^*} - \frac{\partial g}{\partial A_j}\frac{\partial f}{\partial A_j^*} \right) \times (1 + q\,|A_j|^2), \tag{5}$$

and with Hamiltonian

$$H = -\sum_j \left\{ A_j^*(A_{j+1} + A_{j-1}) + \eta|A_j|^2 - \frac{(2+\eta)}{\log(1+\frac{\varepsilon}{\eta})}\ \log(1 + \frac{\varepsilon}{\eta}|A_j|^2) \right\}. \tag{6}$$

It is easy to check that Equation (3) is obtained from Equations (5) and (6), as $\mathrm{i}(\mathrm{d}A_j/\mathrm{d}t) = \{A_j, H\}_q$. Two values of the deformation parameter are of particular interest.

Case $q = 0$. This corresponds to the limit $\varepsilon \to \gamma$ for which the Poisson bracket acquires canonical form and Hamiltonian (6) becomes

$$-\sum_j \left\{ A_j^*(A_{j+1} + A_{j-1}) - 2|A_j|^2 - \frac{\gamma}{2}|A_j|^2) \right\}.$$

Equation (3) then reduces to the DNLS equation

$$\mathrm{i}\frac{\mathrm{d}A_j(t)}{\mathrm{d}t} + A_{j+1} - 2A_j + A_{j-1} + \gamma A_j|A_j|^2 = 0, \tag{7}$$

which conserves the number $N = \sum_j |A_j|^2$ and allows solitary wave propagation (Scott, 2003). Although it is non-integrable, the DNLS equation is linked to many physical problems, from propagation of self-trapped modes in biomolecules and in arrays of nonlinear optical fibers, to the tight-binding description of Bose–Einstein condensates in optical lattices.

Case $q = \frac{\gamma}{2}$. This corresponds to the limit $\varepsilon \to 0$ for which Equation (3) reduces to the Ablowitz–Ladik equation

$$\mathrm{i}\frac{\mathrm{d}A_j(t)}{\mathrm{d}t} + A_{j+1} - 2A_j + A_{j-1} + \frac{\gamma}{2} \times (A_{j+1} + A_{j-1})|A_j|^2 = 0, \tag{8}$$

which is known to have exact soliton solutions, being integrable by the Inverse Scattering Method (Scott, 2003).

The property of Salerno's equation to incorporate the above discrete versions of the NLS equation makes it an ideal general model to investigate the interplay between on-site and intra-site nonlinearity, discreteness and continuum, integrability and non-integrability. Studies performed along these lines during the past decade have shown the existence of a rich and wide range of behaviors, ranging from the existence of states localized on few lattice sites (intrinsic localized modes or discrete breathers), to the possibility of shock wave formation (Cai et al., 1994; Kivshar & Salerno, 1994; Konotop & Salerno, 1997; Mackay & Sepulchre, 2002). The existence of an integrable limit of the model also allowed clarification of the relation between intrinsic localized modes and exact discrete solitons of the AL lattice.

Signatures of these classical properties exist in the corresponding quantum model whose Hamiltonian is defined from Equation (6) as

$$\hat{H} = -\sum_j \left\{ \hat{b}_j^\dagger(\hat{b}_{j+1} + \hat{b}_{j-1}) + \eta\, \hat{b}_j^\dagger \hat{b}_j - \frac{2+\eta}{\log(1+\frac{\varepsilon}{\eta})} \log[1 + \frac{\varepsilon}{\eta}\, \hat{b}_j^\dagger \hat{b}_j] \right\}, \tag{9}$$

where complex mode amplitudes A_j, A_j^* were replaced by creation and annihilation operators $\hat{b}_j, \hat{b}_j^\dagger$. Equation (5) implies the following deformed Heisenberg algebra:

$$[\hat{b}_i, \hat{b}_j^\dagger] = \delta_{i,j}(1 + q\, \hat{b}_i^\dagger \hat{b}_i),$$
$$[\hat{b}_i, \hat{b}_j] = [\hat{b}_i^\dagger, \hat{b}_j^\dagger] = 0, \tag{10}$$

with the same q as in Equation (4). Note that the on-site algebra in Equation (10) is the same as the algebra of a q-oscillator (MacFarlane, 1989), thus providing an example of occurrence of a quantum deformation algebra in a physical model. An explicit representation of the q-algebra associated with the Salerno equation can be constructed as (Salerno, 1992; Bogoliubov & Bullough, 1992)

$$b^\dagger |n\rangle = \sqrt{[n+1]_q}\, |n+1\rangle,$$
$$\hat{b}\, |n\rangle = \sqrt{[n]_q}\, |n-1\rangle \tag{11}$$

with $[n]_q = ((1+q)^n - 1)/q$. From this equation, it follows that the number operator is given by

$$\hat{N} = \sum_j \frac{\log(1 + \frac{\varepsilon}{\eta}\hat{b}_j^\dagger \hat{b}_j)}{\log(1+\frac{\varepsilon}{\eta})}. \tag{12}$$

The conservation of $[\hat{N}, \hat{H}] = 0$, and the translational invariance of the system, $[\hat{T}_j, \hat{H}] = 0$ (T_j are translation operators by j sites along the lattice), allows one to block diagonalize the Salerno Hamiltonian into subspaces with fixed $\hat{N}$ eigenvalues and with fixed crystal momentum k. As for the classical model, the two limiting cases $\varepsilon = \gamma$ and $\varepsilon = 0$ correspond to the quantum DNLS lattice and to the quantum Ablowitz–Ladik system, respectively, the latter being integrable by means of the algebraic Bethe ansatz (Scott, 2003). By tuning the deformation parameter, one can get interesting physical behaviors. Thus, for example, for $q = -2$, the first commutator in Equation (10) becomes an anticommutator, so that the model describes a system of bosons with hard-core interactions (no more than one boson on a site). In this case, it was proved that in the mean field approximation (unconstrained hopping) and in the thermodynamic limit, the case $\varepsilon = 0$ displays a Bose–Einstein condensation (Salerno, 1994).

Exact diagonalizations of Equation (9) have been performed mainly for finite size and for finite number of quanta. Figure 1a depicts a typical band structure of Salerno's model in the reduced zone scheme for a chain of 15 sites, $N = 5$, $\gamma = 10$, and $\varepsilon = 5$. For

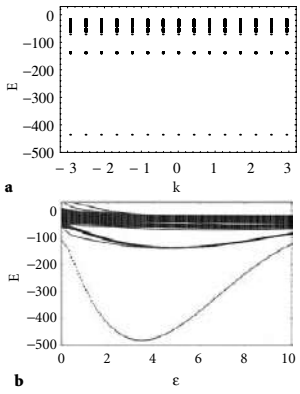

Figure 1. (a) Band structure of Salerno's model in the reduced zone scheme for a chain of 15 sites with $N = 5$, $\gamma = 10$, and $\varepsilon = 5$. (b) Energy of the states with crystal momentum $k = 0$, corresponding to the translational symmetry of the ground state, as a function of ε. Other parameters are fixed as (a).

these parameter values, the lower band corresponds to a bound state in which the five quanta are, with high probability, all on the same site. Figure 1b shows the energy of the states with crystal momentum $k = 0$ (corresponding to the translational symmetry of the ground state) as a function of ε. Note that the minimum ground state energy is achieved for an ε value in between the AL ($\varepsilon = 0$) and the DNLA case ($\varepsilon = 10$).

The presence of an integrable limit of the Salerno model gives the possibility of exploring complicated properties of this quantum many-body system starting from the exact knowledge of its integrable limit. An interesting open problem in this direction is the characterization of the quantum analogue of a discrete breather of the corresponding classical model (discrete quantum breather). Work in this direction is presently under investigation.

MARIO SALERNO

See also **Discrete nonlinear Schrödinger equations; Quantum nonlinearity**

Further Reading

Bogoliubov, N.M. & Bullough, R.K. 1992. A q-deformed completely integrable Bose gas model. *Journal of Physics* A, 25: 4057–4071

Cai, C., Bishop, A.R. & Grønbech-Jensen, N. 1994. *Physical Review Letters*, 72: 591

Feynman, R.P. 1965. *Lectures on Physics*, vol. III, Reading, MA: Addison-Wesley

Kivshar, Yu.S. & Salerno, M. 1994. *Physical Review* E, 49: 3543

Konotop, V.V. & Salerno, M. 1997. *Physical Review* E, 56: 3611

MacKay, R.S. & Sepulchre, J.A. 2002. *Journal of Physics* A, 35: 3985

MacFarlane, A.J. 1989. On q-analogues of the quantum harmonic oscillator and the quantum group $SU(2)_q$. *Journal of Physics* A, 22: 4581

Salerno, M. 1992. Quantum deformations of the discrete nonlinear Schrödinger equation. *Physical Review* A, 46: 6856

Salerno, M. 1994. Bose Einstein condensation in a system of q-bosons. *Physical Review* E, 50: 4528

Scott, A.C. 2003. *Nonlinear Science: Emergence and Dynamics of Coherent Structures*, 2nd edition, Oxford and New York: Oxford University Press, and references therein

SANDPILE MODEL

The concept of self-organized criticality (SOC) was introduced by Bak et al. (1987) using the example of a sandpile. If a sandpile is formed on a horizontal circular base with any arbitrary initial distribution of sand grains, a sandpile of fixed conical shape (steady state) is formed by slowly adding sand grains one after another (external drive). In the steady state, the surface of the sandpile makes on average a constant angle with the horizontal plane, known as the angle of repose. The addition of each sand grain results in some activity on the surface of the pile: an avalanche of sand mass follows, which propagates on the surface of the sandpile. In the stationary regime, avalanches are of many different sizes, and Bak et al. (1987) argued that they would have a power law distribution. If one starts with an initial uncritical state, initially most of the avalanches are small, but the range of sizes of avalanches grows with time. After a long time, the system arrives at a critical state, in which the avalanches extend over all length and time scales (Bak, 1996; Jensen, 1998; Dhar, 1999; Sornette, 2004).

Laboratory experiments on sandpiles, however, have not in general shown evidence of criticality in sandpiles due to the effects of inertia and dilatation (moving grains require more space) (Nagel, 1992), except for small avalanches (Held et al., 1990) or with elongated rice grains (Malte-Sørensen et al., 1999) where these effects are minimized. Small avalanches have small velocities (and thus negligible kinetic energy), and they activate only the first surface layer of the pile. Elongated rice grains slip at or near the surface as a result of their anisotropy (thus minimizing dilatational effects), and they also build up scaffold-like structures, which enhance the threshold nature of the dynamics.

On the theoretical front, a large number of discrete and continuous sandpile models have been studied. Among them, the so-called abelian sandpile model is the simplest and most popular (Dhar, 1999). Other variants include Zhang's model, which has modified rules for sandpile evolution (Zhang, 1989), a model for abelian distributed processors and other stochastic rule models (Dhar, 1999), and the Eulerian Walkers model (Priezzhev et al., 1996).

In the abelian sandpile model, each lattice site is characterized by its height h. Starting from an arbitrary initial distribution of heights, grains are added one at a time at randomly selected sites n: $h_n \to h_n + 1$. The sand column at any arbitrary site i becomes unstable when h_i exceeds a threshold value h_c and topples to reduce its height to $h_i \to h_i - 2d$, where d is the space dimension of the lattice. The $2d$ grains lost from the site i are redistributed on the $2d$ neighboring sites $\{j\}$, which gain a unit sand grain each: $h_j \to h_j + 1$. This toppling may make some of the neighboring sites unstable. Consequently, these sites will topple themselves, possibly making further neighbors unstable. In this way, a cascade of topplings propagates, which finally terminates when all sites in the system become stable. When this avalanche has stopped, the next grain is added on a site chosen randomly. This condition is equivalent to assuming that the rate of adding sand is much slower than the natural rate of relaxation of the system. The large separation of the driving and of the relaxation time scales is usually considered to be a defining characteristic of SOC. Finally, the system must be open to the outside; that is, it must dissipate energy or matter, for instance. An outcoming flux of grains must balance the incoming flux of grains, for a stationary state to occur. Usually, the outcoming flux occurs on the boundary of the system: even if the number of grains is conserved inside the box, it loses some grains at the boundaries. Even in a very large box, the effects of the dissipating boundaries are essential: increasing the box size will have the effect of lengthening the transient regime over which the SOC establishes itself; the SOC state is built from the long-range correlations that establish a delicate balance between internal avalanches and avalanches that touch the boundaries (Middleton & Tang, 1995).

The simplicity of the abelian model is that the final stable height configuration of the system is independent of the sequence in which sand grains are added to the system to reach this stable configuration (hence the name "abelian" referring to the mathematical property of commutativity). On a stable configuration $\mathcal{C}$, if two grains are added, first at i and then at j, the resulting stable configuration $\mathcal{C}'$ is exactly the same as in the case where the grains were added first at j and then at i. In other sandpile models, where the stability of a sand column depends on the local slope or the local curvature, the dynamics is not abelian, since toppling of one unstable site may convert another unstable site to a stable site. Many such rules have been studied in the literature (Manna, 1991; Kadanoff et al., 1989).

An avalanche is a cascade of topplings of a number of sites created by the addition of a sand grain. The strength of an avalanche can be quantified in several ways:

- size (s): the total number of topplings in the avalanche,
- area (a): the number of distinct sites that toppled,
- lifetime (t): the duration of the avalanche, and
- radius (r): the maximum distance of a toppled site from the origin.

These four different quantities are not independent and are related to each other by scaling laws. Between any two such measures x, y belonging to the set $\{s, a, t, r\}$, one can define a mutual dependence by the scaling of the expectation of one quantity y as a function of the other x:

$$\langle y \rangle \sim x^{\gamma_{xy}}, \tag{1}$$

where γ_{xy} is called a critical exponent, index, or dimension. This equation quantifies a nonlinear generalized proportionality between the two observables x and y ($\ln\langle y \rangle$ is proportional to $\ln x$). The exponents γ_{xy} are related to one another, for example,

$$\gamma_{ts} = \gamma_{tr}\gamma_{rs}. \tag{2}$$

For the abelian sandpile model, it can be shown that the avalanche clusters cannot have any holes and in addition that $\gamma_{rs} = 2$ in two dimensions, that is,

$$\langle s \rangle \sim r^2. \tag{3}$$

In words, the size (number of toppling grains) of an avalanche is proportional to its surface. It has also been shown that $\gamma_{rt} = \frac{5}{4}$:

$$\langle t \rangle \sim r^{\frac{5}{4}}; \tag{4}$$

that is, the average duration $\langle t \rangle$ of an avalanche grows with its typical radius r faster than linearly. However, averages reflect only a part of the rich behavior of sandpile models. A significant information is provided by the full distribution function $P(x)$ for any measure $x \in \{s, a, t, r\}$. Associated with the above scaling laws (1) and (2), one often finds the finite size scaling form for $P(x)$:

$$P(x) \sim x^{-\tau_x} f_x\left(\frac{x}{L^{\sigma_x}}\right). \tag{5}$$

The exponent σ_x determines the variation of the cut-off of the tail of the distribution of the quantity x with the system size L. As long as $x < L^{\sigma_x}$, expression (5) describes a power law distribution of x, reflecting a self-similar structure of the set of avalanches. When x becomes comparable with L^{σ_x}, the function f_x ensures a fast fall-off of $P(x)$ describing the impact of the finite size L of the system on the statistics of the fluctuations of x. Scaling relations like $\gamma_{xy} = (\tau_x - 1)/(\tau_y - 1)$ connect any two measures. Scaling assumptions (5) for the avalanche sizes have not been demonstrated and may be open to doubt (Kadanoff et al., 1989). This seems to be due to the effect of rare large avalanches dissipating at the border, which strongly influence the statistics.

Many different sandpile models have been studied. However, the precise classification of various models

into different universality classes in terms of their critical exponents is not yet available. Exact values of all the critical exponents of the most widely studied abelian model are still not known in two dimensions. Some effort has also been made toward the analytical calculation of avalanche size exponents (Ktitarev & Priezzhev, 1998). Blanchard et al. (2000) have developed a dynamical system theory for a certain class of SOC models (like Zhang's model, 1989), for which the whole SOC dynamics can either be described in terms of iterated function systems, or as a piecewise hyperbolic dynamical system of skew-product type where one coordinate encodes the sequence of activations. The product involves activation (corresponding to a kind of Bernouilli shift map) and relaxation (leading to contractive maps).

In summary, the sandpile model of Bak et al. (1987) and its many extensions have helped found the new concept of self-organized criticality, which is now a useful item in the toolbox and set of concepts used to study complex systems involving triggered activities.

DIDIER SORNETTE

See also **Avalanches; Critical phenomena; Granular materials; Fractals; Nonequilibrium statistical mechanics**

Further Reading

Bak, P. 1996. *How Nature Works: The Science of Self-organized Criticality*, Berlin and New York: Springer

Bak, P., Tang, C. & Weisenfeld, K. 1987. Self-organized criticality: an explanation of $1/f$ noise. *Physical Review* A, 38: 364–374

Blanchard, P., Cessac, B. & Kruger, T. 2000. What can one learn about self-organized criticality from dynamical systems theory? *Journal of Statistical Physics*, 98: 375–404

Dhar, D. 1999. The abelian sandpile and related models. *Physica* A, 263: 4–25

Held, G.A., Solina, D.H., Keane, D.T., Haag, W.J., Horn, P.M. & Grinstein, G. 1990. Experimental study of critical-mass fluctuations in an evolving sandpile. *Physical Review Letters*, 65: 1120–1123

Jensen, H.J. 1998. *Self-Organized Criticality*, Cambridge and New York: Cambridge University Press

Kadanoff, L.P., Nagel, S.R., Wu, L. & Zhou, S. 1989. Scaling and universality in avalanches. *Physical Review* A, 39: 6524–6537

Ktitarev, D.V. & Priezzhev, V.B. 1998. Expansion and contraction of avalanches in the two-dimensional abelian sandpile. *Physical Review* E, 58: 2883–2888

Malte-Sørensen, A., Feder, J., Christensen, K., Frette, V., Josang, T. & Meakin, P. 1999. Surface fluctuations and correlations in a pile of rice. *Physical Review Letters*, 83: 764–767

Manna, S.S. 1991. Critical exponents of the sandpile models in two dimensions. *Physica* A, 179: 249–268

Middleton, A.A. & Tang, C. 1995. Self-organized criticality in non-conserved systems. *Physical Review Letters*, 74: 742–745

Nagel, S.R. 1992. Instabilities in a sandpile. *Review of Modern Physics*, 64: 321–325

Priezzhev, V.B., Dhar, A., Krishnamurthy, S. & Dhar, D. 1996. Eulerian Walkers as a model of self-organized criticality. *Physical Review Letters*, 77: 5079–5082

Sornette, D. 2004. *Critical Phenomena in Natural Sciences*, 2nd edition, Berlin and New York: Springer

Zhang, Y.-C. 1989. Scaling theory of self-organized criticality. *Physical Review Letters*, 63: 470–473

SCATTERING OPERATORS

See **Inverse scattering method or transform**

SCHEIBE AGGREGATES

Scheibe aggregates (also called J-aggregates) are a type of Langmuir–Blodgett thin films that were independently discovered in 1936 by Günther Scheibe (Scheibe, 1936) in Germany and E.E. Jelly (Jelly, 1936) in England—hence their names. They comprise compact and regular arrangements of dye molecules composed of chromophores and fatty acids that can be designed to pre-selected specifications. These molecular monolayers exhibit very efficient light capture followed by energy transfer to acceptor molecules present in the film at very low acceptor-to-donor ratios (as low as 1:10,000), giving the efficiency of energy transfer to acceptors as high as 50% (Moebius, 1989).

In the late 1960s and in the 1970s, Kuhn, Moebius and co-workers (Czikkely et al., 1969) studied the effects of irradiation with ultraviolet or visible light and measured the strongly quenched donor fluorescence in these aggregates. An acceptor fluorescence line appeared whose amplitude was almost equal to that of the primary donor spectral line, but its peak was slightly redshifted, which was interpreted as evidence that the aggregate acts as a cooperative molecular array. After absorbing a photon, the energy moves in the form of an exciton traveling laterally over distances of up to 100 nm to a particular acceptor dye in the vicinity. The efficiency of this energy transfer mechanism is strongly linked with the rigidity of the aggregate and its regular order. Surprisingly, the capture of energy by an acceptor molecule improves with the ambient temperature. Optimal efficiency is achieved at fairly low acceptor-to-donor ratios as mentioned above.

Numerous technological applications of these molecular systems have been developed, including photographic and photo-detection processes as well as solar energy cell components (Inoue, 1985).

Several theoretical models of Scheibe aggregates have been developed over the years. The Frenkel exciton picture with the inclusion of diagonal disorder in molecular chains with nearest-neighbor interactions was adopted to describe the pseudo-isocyanine aggregate (Knapp, 1984) and was later extended to account for off-diagonal disorder. Subsequently, linear models of exciton propagation in the presence of shallow impurity potentials at acceptor sites showed (Bartnik et al., 1992) close quantitative agreement with experiment. These impurity potentials were usually assumed to be

of a square-well type, and their depth and spatial extent were parameters subject to optimization schemes. Interestingly, shallow impurity levels gave better capture properties than deep ones.

There have also been a number of theoretical studies advocating a role played by nonlinearity in the propagation of excitonic modes in Scheibe aggregates. The main reason for this claim is due to exciton-phonon coupling whose strength for mero-cyanine was experimentally determined as approximately $\chi = 29$ meV (Inoue, 1985) and theoretically estimated as $\chi = 26$ meV (Spano et al., 1990).

In general, three types of excitonic models can be applied: (a) a nearly free delocalized case, (b) a small polaron limit, and (c) the nonlinear self-trapped exciton state. The applicability criterion for these models involves a phase diagram in terms of two characteristic parameters: $g = \pi \chi^2/\omega J$ and $\gamma = h\omega/2\pi J$, where h is Planck's constant, ω is the phonon frequency, and J is the exciton hopping constant. With the phonon energy approximately 30 meV, J in the range between 50 and 150 meV, and the exciton-phonon coupling constant ranging from 25 to 100 meV, the outcome of this parameter determination is yet inconclusive (Tuszyński et al., 1999).

It is important to stress that these systems should be modeled as two-dimensional structures. Continuous two-dimensional models with nonlinear terms have been developed that treat phonons classically and effectively eliminate them via an adiabatic approximation (Huth et al., 1989), leading to a 2-d radially symmetric cubic nonlinear Schrödinger equation, where the energy transfer takes place through soliton-like ring waves with a characteristic collapse time signifying the exciton lifetime. More recent models involving nonlinear equations of the cubic Schrödinger type also account for the presence of Gaussian impurity potentials (Christiansen et al., 1998).

Finally, it is necessary to include radiative losses in modeling the propagation of an exciton domain. Formally, this can be accomplished by adding an imaginary term to the exciton-phonon part of the Hamiltonian that describes the corresponding loss of energy of excitons as they collide with phonons in the thin-film lattice. Consequently, it has been shown that the rate of excitonic energy loss by a coherent exciton domain covering an area composed of N molecules is proportional to its size, N, and can be expressed as: $k_{\text{rad}} = N$ nanoseconds^{-1}. It has also been demonstrated that the characteristic time for radiative losses is approximately proportional to the absolute temperature T divided by 3000 K, and the result is expressed in nanoseconds (Moebius & Kuhn, 1988). In other words, the radiative decay time in nanoseconds is given by $\tau_{\text{rad}} = (T/3000)$ K. For example, at room temperature, a coherent exciton domain composed of 100 lattice sites has a decay time of 0.1 ns = 100 ps compared with a flight time of only 2 ps, which means that radiative losses will not destroy the coherence of the exciton domain unless it is very large (approximately 10,000 lattice sites). A comprehensive review of the key processes taking place in exciton energy transfer in Scheibe aggregates (time of flight, radiative losses, exciton-phonon interaction, and diffusion on the 2-d lattice) can be found in Tuszyński et al. (1999).

JACK A. TUSZYŃSKI

See also **Excitons; Langmuir–Blodgett films; Nonlinear Schrödinger equations**

Further Reading

Bartnik, E.A., Blinowska, K.J. & Tuszyński, J.A. 1992. Stability of quantum capture in Langmuir–Blodgett monolayers against positional disorder. *Physics Letters* A, 169: 46–50

Christiansen, P.L., Gaididei, Yu.B., Johansson, M., Rasmussen, K.O., Mezentsev, V.K. & Rasmussen, J.J. 1998. Solitary excitations in discrete two-dimensional nonlinear Schrödinger models with dispersive dipole-dipole interactions. *Physical Review* B, 57: 11–303

Czikkely, V., Dreizler, G., Försterling, H., Kuhn, H., Sondermann, J., Tillmann, P. & Wiegand, J. 1969. Lichtabsorption von Farbstoff-Molekülpaaren in Sandwichsystemen aus monomolekularen Schichten. *Zeitschrift für Naturforschung*, 24A: 1823

Czikkely, V., Försterling, H. & Kuhn, H. 1970. Extended dipole model for aggregates of dye molecules. *Chemical Physics Letters*, 6: 207

Huth, G.C., Gutmann, F. & Vitiello, G. 1989. Ring solitonic vibrations in Schiebe aggregates. *Physics Letters* A, 140: 339

Inoue, T. 1985. Optical absorption and luminescence in Langmuir films of merocyanine dye. *Thin Solid Films*, 132: 21

Jelly, E.E. 1936. Spectral absorption and fluorescence of dyes in the molecular state. *Nature*, 138: 1009–1010

Knapp, E.W. 1984. Lineshapes of molecular aggregates—exchange narrowing and intersite correlation. *Chemical Physics*, 85: 73

Kuhn, H. 1979. Synthetic molecular organizates. *Journal of Photochemistry*, 10: 111

Moebius, D. 1989. Monolayer assemblies. *Berichte der Bunsen-Gesellschaft—Physical Chemistry*, 82: 848

Moebius, D. & Kuhn, H. 1988. Energy transfer in monolayers with cyanine dye Scheibe aggregates. *Journal of Applied Physics*, 64: 5138–5141

Scheibe, G. 1936. Variability of the absorption spectra of some sensitizing dyes and its cause. *Angewandte Chemie*, 49: 567

Spano, F.C., Kuklinski, J.R. & Mukamel, S. 1990. Temperature dependent superradiant decay of excitons in small aggregates. *Physical Review Letters*, 65: 211

Tuszyński, J.A., Joergensen, M.F. & Moebius, D. 1999. Mechanisms of exciton energy transfer in Scheibe aggregates. *Physical Review* E, 59: 4374

SCHLESINGER EQUATIONS

See **Monodromy preserving deformations**

SCHOTTKY DIODE

See **Diodes**

SCHRÖDINGER EQUATION, LINEAR

See **Quantum nonlinearity**

SCROLL WAVES

Introduction

Scroll waves, which are observed in excitable media, can be imagined as a continuation of two-dimensional spiral waves to three dimensions. Spiral and scroll waves distribute frequency behavior to the two- and three-dimensional space, respectively, with the exception of a small subset of that space. For spiral waves this subset comprises the vicinity of a point and is called a core, whereas in three dimensions it is formed by the vicinity of a curve and is called a filament. In both cases, this exceptional subset acts as a source of waves that organizes the exhibited periodic or quasi-periodic frequency behavior; therefore, it is often referred to as an organizing center.

The intersection of the three-dimensional excitable medium containing a scroll wave with a plane that is locally perpendicular to the filament corresponds to a sheet in which a spiral wave rotates, showing the close relationship between these two types of excitation waves. But because curves (the filaments) can have complex geometrical and topological properties, the behavior of scroll waves turns out to be much more complicated than that of spirals.

Early work on rotating excitation waves was performed on physical rings of heart tissue (quasi-one-dimensional systems), where an electrical impulse can propagate around a hole without attenuation for days. The importance of this observation lies in the complex anatomy of the heart: in particular, the orifices from arteries make the surface of the heart locally similar to physical rings and, therefore, allow for the so called circus-movement reentry, that is, electrical excitation waves circulating around inhomogeneities. Modeling of this phenomenon was undertaken first by Norbert Wiener and Arturo Rosenblueth in 1946. Periodic excitation was found to be also possible in media without holes, that is, in quasi-two-dimensional media. The electrical excitation wave (see Figure 1) then assumes the shape of a spiral (Tyson & Keener, 1988). The importance of the third dimension was recognized when performing experiments with the excitable Belousov–Zhabotinsky reaction system (*See* **Belousov–Zhabotinsky reaction**), since distortions and other unexpected behavior of spiral waves in presumed two-dimensional shallow layers could be readily explained when assuming a non-uniform excitability along the small but nonnegligible vertical direction (see references in Winfree, 1987).

For the theoretical treatment of scroll waves there are several models that are most commonly used.

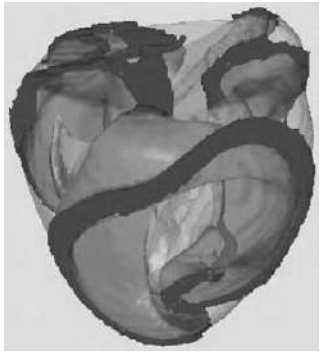

Figure 1. A scroll wave on the surface of a heart. (Image from Panfilov & Pertsov, 2001.)

Since scroll waves are structures appearing in excitable media, it is not surprising that they have been investigated by using three-dimensional FitzHugh–Nagumo equations, that is, a two-variable model designed for the simulation of neural action potentials (*See* **FitzHugh–Nagumo equation**). It was found that scroll waves always undergo twist (see below) when entering inhomogeneous media (Mikhailov et al., 1985).

Another model for the investigation of scroll waves is the Oregonator model derived from the reaction kinetics of the Belousov–Zhabotinsky reaction. The temporal development of a scroll ring, a structure with a closed filament not touching the boundary (see Figure 2, and also Welsh et al., 1983), was investigated by Winfree and Jahnke in 1989. It was found that a scroll ring decreases its size in the course of time and eventually vanishes, showing that scroll waves are topologically distinct from spirals.

A now very popular model is the so-called Barkley model, well known for its computational efficiency. Originally introduced for the investigation of the meander instability of spiral waves (Barkley, 1990), it is also used for investigating scroll waves. With this model it was possible to classify the instabilities of scroll waves in isotropic excitable media (Henry & Hakim, 2002).

While these three models give a description of the full three-dimensional concentration distribution, a fourth one deals with the geometry of an iso-concentration level. Its formulation is based on the eikonal equation, which expresses the relationship between the curvature and the normal velocity of a surface defined by such a level. Thus, the surface is described in specific coordinate systems that reflect the topological situation of the filaments involved in the

Figure 2. A scroll ring in a test tube, inner diameter: 10 mm. (Image from Winfree, 1987.)

wave structure. Investigating this type of model allows one to estimate the stability of complex, linked wave structures (McDermott et al., 2002).

Complexity of Scroll Waves

The complexity of a scroll wave becomes apparent when one imagines such a wave structure extending into a nonhomogenous excitable medium, that is, when in each slice along the filament the rotation period of the spirals is intrinsically different. Without a coupling mechanism, the phase of the spirals in these adjacent slices would evolve independently, and the differences between the phases would diverge. This is not possible, and the wave structure circumvents this inconvenience by tilting the wave fronts emanating from the organizing center. In terms of the rotation phases of the spirals, this corresponds to a phase shift along the filament, which is called twist.

While the twist takes arbitrary values in the case of scroll waves (organized by filaments reaching from one boundary of the medium to another), it has to fulfill quantization conditions for scroll rings. The first limitation is that the twist of a scroll ring along one turn along the filament has to be a multiple of 2π. A further limitation for the possible structures arises from the constraint that the surface must not have any intersections (i.e., it has to be a Seifert-surface, see Figure 3 for an impossible surface). This, for example, excludes single scroll rings of twist 2π. Instead, these always must appear as linked pairs, although in the limiting case one of them may be infinitely large or may reach from one boundary to the other (Winfree, 1987). More elaborate work on the topology and geometry of filaments has been summarized by Tyson and Strogatz (1991).

Although the computational investigation of scroll waves started in the 1980s, about ten years after their discovery, rigorous experimental research on

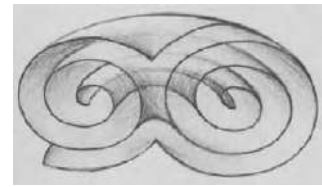

Figure 3. An example of an impossible surface of a wave structure. (Image from Winfree, 1987.)

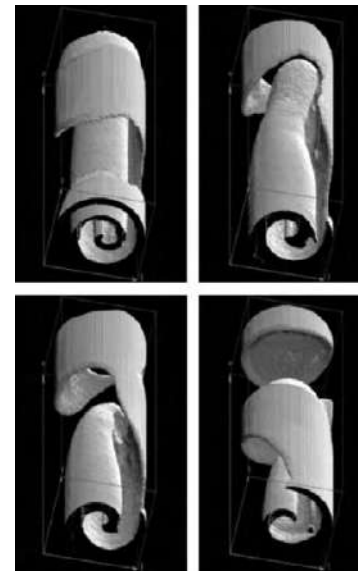

Figure 4. Decomposition of a scroll wave due to a gradient of excitability. (Image from Strob et al., 2003.)

three-dimensional wave structures did not begin before the 1990s. First measuring techniques were restricted to simple projections from one, two, or three pairwise orthogonal directions.

Three-dimensional, fully resolved observations of scroll waves and rings have been performed by optical tomography since about 1995. This technique allows one to record and evaluate time and space resolved data sequences. For instance, the decomposition of a scroll wave due to a gradient of excitability was observed in satisfactory detail (see Figure 4). Thus, experimental and theoretical tools are now available to investigate the complex interaction of the organizing centers of scroll waves.

ULRICH STORB AND STEFAN C. MÜLLER

See also **Belousov–Zhabotinsky reaction; Cardiac arrhythmias and electrocardiogram; Excitability; Geometrical optics, nonlinear; Reaction-diffusion systems; Spiral waves; Vortex dynamics in excitable media**

Further Reading

Barkley, D. 1990. Spiral-wave dynamics in a simple model of excitable media: the transition from simple to compound rotation. *Physical Review* A, 42(4): 2489–2492

Henry, H. & Hakim, V. 2002. Scroll waves in isotropic excitable media: linear instabilities, bifurcations and restabilized states. *Physical Review* E, 65: 046235-1–046235-21

McDermott, S., Mulholland, A.J. & Gomatam, J. 2002. Knotted reaction–diffusion waves. *Proceedings of the Royal Society of London Series A—Mathematical Physical and Engineering Sciences*, 458: 2947–2966

Mikhailov, A.S., Panfilov, A.V. & Rudenko, A.N. 1985. Twisted scroll waves in active three-dimensional media. *Physics Letters* A, 109(5): 246–250

Panfilov, A.V. & Pertsov, A. 2001. Ventricular fibrillation: evolution of the multiple-wavelet hypothesis. *Proceedings of the Royal Society of London Series* A, 359: 1315–1325

Storb, U., Rodrigues Neto, C., Bär, M. & Müller, S.C. 2003. A tomographic study of desynchronization and complex dynamics of scroll waves in an excitable chemical reaction with a gradient. *Physical Chemistry Chemical Physics*, 5: 2344–2353

Tyson, J.J. & Keener, J.P. 1988. Singular perturbation theory of travelling waves in excitable media. *Physica* D, 32: 327–361

Tyson, J.J. & Strogatz, S.H. 1991. The differential geometry of scroll waves. *International Journal of Bifurcation and Chaos*, 1: 723–744

Welsh, B.J., Gomatam, J. & Burgess, A.E. 1983. Three-dimensional chemical waves in the Belousov–Zhabotinskii reaction. *Nature*, 304: 611–614

Wiener, N. & Rosenblueth, A. 1946. The mathematical formulation of the problem of conduction of impulses in a network of connected excitable elements. *Specifically in Cardiac Muscle Archivos del Instituto de Cardiologica de Mexico*, 16: 205–265

Winfree, A.T. 1987. *When Time Breaks Down*, Princeton, NJ: Princeton University Press

Winfree, A.T. & Jahnke, W. 1989. Three-dimensional scroll ring dynamics in the Belousov-Zhabotinsky reagent and in the 2-variable Oregonator model. *Journal of Physical Chemistry*, 93: 2823–2832

SECOND HARMONIC GENERATION

See **Harmonic generation**

SELF-ORGANIZATION

See **Synergetics**

SELF-SIMILARITY

See **Fractals**

SEMICLASSICAL APPROXIMATIONS

See **Quantum theory**

SEMICONDUCTOR LASER

The semiconductor laser is today the most important and widespread type of laser, being a central component in many common household appliances (CD and DVD players) as well as in major industrial areas, such as measurement and sensing, materials manufacturing, and medical surgery. Not least, the semiconductor laser has enabled the rapid evolution of the Internet by providing a means for efficient and cheap conversion of digital electrical signals into optical signals, which can be transmitted at very high data rates and over very long distances in hair-thin optical fibers.

The success of the semiconductor laser to a large degree relies on its many similarities with electronic semiconductor devices such as transistors and diodes. The laser is manufactured by standard semiconductor crystal growth and processing techniques, allowing for small and cheap devices. Furthermore, the semiconductor laser distinguishes itself from other types of lasers by being electrically activated. Thus, the energy needed for pumping the laser to an excited state, from which the energy can be released by emission of photons, is achieved simply by putting direct electrical current through the device. Other kinds of lasers typically need some kind of optical pumping for populating the laser-active states.

Figure 1 shows a schematic of a typical semiconductor laser. The laser is a p-i-n structure; that is, p- and n-doped semiconductor materials sandwich an undoped intrinsic ("i") region. The structure acts as a standard pn-junction diode; when forward biased (with a positive voltage on the metallized p-side relative to the n-side), an electrical current flows. This leads to the build-up of significant electron and hole densities in the intrinsic region, and by recombination of these excited-state (conduction-band) electrons with ground-state (valence-band) holes, photons can be generated. An incoming photon may thus stimulate the emission of a new photon with identical properties. This process of stimulated emission provides optical gain, which is

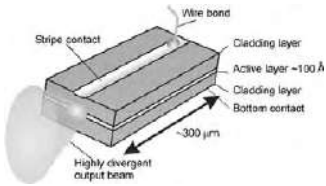

Figure 1. Schematic of a semiconductor laser. Light is confined to a waveguide of transverse dimension typically of the order of $0.2\,\mu\text{m} \times 2\,\mu\text{m}$. For a quantum well structure, stimulated emission occurs in a narrow region of width ~ 100 Å. The laser is pumped electrically by incorporating the active region in a pn-junction.

one of the two key requirements for implementing a laser.

As for any oscillator, the second requirement—besides gain—is the existence of feedback. For a laser, this is usually achieved by incorporating the gain medium in a mirror cavity. In the case of a semiconductor laser, the mirrors are particularly simple since cleaving along one of the crystal planes provides a naturally flat mirror with an intensity reflection coefficient of the order of 30%. Due to the large material gain achievable in semiconductor lasers, a laser-active region length of the order of a few hundred μm is sufficient to compensate for the corresponding 70% outcoupling loss, as well as other losses in the material, thus enabling laser oscillation.

In addition to providing feedback, the laser cavity also must confine the optical laser mode in the transverse plane. This is achieved by establishing a transverse waveguide through index-guiding. The design thus needs to ensure a larger effective index in the active region of the laser as compared with the surrounding regions. In the growth direction, index guiding is provided by use of a so-called semiconductor heterostructure. The intrinsic, "i"-region is thus composed of a material with a smaller bandgap than the surrounding materials, which leads to a larger refractive index. The incorporation of a heterojunction structure was a major achievement in the early development of semiconductor lasers and earned the inventors, Zhores Alferov and Herbert Kroemer, the Nobel Prize in Physics in 2000. Besides providing index confinement, the heterostructure also ensures efficient collection of electrons and holes in the active region.

Index guiding in the plane (lateral direction) of the semiconductor layers is more difficult and is achieved in a number of different ways, the two most important ones employing a ridge waveguide structure and a buried heterostructure. The ridge waveguide structure is obtained by processing a narrow ridge (1–2 μm wide) in the doped semiconductor material topping the active region. The material that is etched away on either side of the ridge is replaced by a material (e.g., polyimide) that is isolating and has an index of refraction less than that of the semiconductor (ca. 3.5). The ridge provides current confinement and leads to an effective refractive index that varies in the lateral direction along the active region, reaching a maximum value right below the high-index ridge, thus imposing lateral waveguiding. The refractive index contrast thus obtained is, however, modest, and ridge waveguide lasers belong to the class of weakly index-guided structures. The other class of strongly index-guided structures is exemplified by the buried heterostructure laser. By employing several growth steps, the active waveguide region can thus be surrounded, in the lateral direction, by materials with higher bandgap and lower refractive index. Furthermore, these regions, adjacent to the active region, are doped to block the current from entering.

By analogy with a standard laser cavity (etalon), a semiconductor laser using cleaved facets to define the laser cavity is denoted a Fabry–Perot laser. Due to the small difference in material gain between the longitudinal modes of such a laser cavity, the laser may oscillate in several closely spaced modes and the single-mode suppression ratio remains modest. By incorporating a grating structure in the laser, either distributed over the entire waveguide length (distributed feedback or DFB laser) or localized close to the facets (distributed Bragg reflector or DBR laser), spectral selection can be achieved, resulting in high-quality single-mode lasers. DFB lasers, in particular, have been successfully applied in optical communications systems. A more recent type of laser is the so-called vertical cavity surface emitting laser (VCSEL), where the laser end mirrors are provided by Bragg gratings parallel to the semiconductor substrate and the laser emits out of the plane of the substrate.

The choice of the materials for the active region determines the wavelength of the output optical beam. Two materials systems are particularly important: GaAlAs lasers, which cover the wavelength range of 700–900 nm, and InGaAsP lasers, which cover the wavelength range of 1000–1600 nm. The latter laser type is the most important for long-distance optical communication systems due to the low loss and/or dispersion of optical fibers in the range of 1300–1550 nm. An additional degree of freedom comes from employing a so-called quantum well structure of the active layer. Thus, by incorporating thin (about 5–10 nm) layers of semiconductor with a bandgap lower than the surrounding (barrier) material in the active region, quantum confinement effects change the allowed energy levels of electrons. This leads to a change in the effective bandgap of the laser (wavelength under lasing), as well as the number of electrons needed to reach population inversion.

Quantum well lasers have achieved low-threshold and high-power operation. Quantum dot lasers, employing three-dimensional quantum confinement of electrons, offer excellent electron control and have led to lasers with record low-threshold current density. However, semiconductor growth technology has not yet (in 2004) matured to the point of offering full control of quantum dot sizes.

The laser threshold condition and the basic features of the laser dynamics are captured by a simple set of rate equations describing the temporal evolution of the photon density, P, and the carrier density, N (Coldren & Corzine, 1995):

$$\frac{\mathrm{d}P}{\mathrm{d}t} = (\Gamma v_g g - \tau_p^{-1})P + \Gamma\beta_{sp}R_{sp}, \quad (1)$$

$$\frac{\mathrm{d}N}{\mathrm{d}t} = \frac{I}{eV} - \frac{N}{\tau_s} - v_g g P. \quad (2)$$

Here, v_g is the group velocity; τ_p is the photon lifetime, its inverse being the rate at which photons are lost from the laser cavity; β_{sp} is the rate of spontaneous emission; ending up in the lasing mode; I is the injected current; e is the electronic charge; V is the active region volume; and τ_s is the carrier lifetime. The confinement factor, Γ, expresses the fraction of the optical mode that overlaps with the active region; it may also be expressed as the ratio between the active region volume, V, and the effective volume of the optical mode, V_{opt}. In the form of the equations stated above, the photon density is normalized with respect to V_{opt}, whereas N is normalized with respect to V. Finally, g is the material gain. When considering a laser operating at the peak of the gain curve, it is, at least for lasers with bulk active regions, a good approximation to parameterize the gain as

$$g \cong g_N(N - N_0) \quad (3)$$

with g_N being the differential gain, and N_0 the carrier density at transparency. For $N = N_0$, we have $g = 0$, corresponding to the case where stimulated emission and absorption exactly balance. For a further increase of the carrier density, population inversion is achieved and the material gain is positive.

The rate equations (1) and (2) are basically book-keeping equations. Equation (2) expresses the effective pumping of electrons from valence to conduction band through the applied current. Due to spontaneous emission as well as nonradiative recombination (Auger processes are particularly important in long-wavelength lasers), the excited carrier density has a lifetime τ_s of the order of a nanosecond or less. Furthermore, stimulated emission, proportional to the product of the gain and the photon density, depletes the population of excited carriers, as expressed by the last term in Equation (2). That same process leads to a generation term in the rate equation for the photon density. Also, a certain fraction, β_{sp}, which may typically be of the order of 10^{-5} of the total rate of spontaneous emission, R_{sp}, ends up in the laser mode and is accounted for by the last term in Equation (1). Finally, the drain term in Equation (1) describes all mechanisms by which photons are lost from the cavity, including output coupling at the mirror facets and internal loss (due to free-carrier absorption, waveguide scattering loss, etc.).

The steady-state solution of the rate equations, with the gain given by Equation (3), yields the light-current characteristics, laser power that is, expressed in terms of the photon density as a function of the applied current. A simple solution, yet accurate except very close to threshold, is obtained by neglecting the rate of spontaneous emission into the lasing mode, that is, the last term in Equation (1). A small-signal analysis shows that the above-threshold solution is a stable focus. The characteristic frequency is the so-called laser relaxation oscillation frequency, which is the natural frequency at which energy is exchanged between the carrier population and the photon population. The relaxation frequency is also a measure of the order of the maximum bit-rate at which a laser can be efficiently current-modulated to produce an intensity-modulated optical output signal. The square of the relaxation oscillation is approximately proportional to the laser output power, although the oscillations become strongly damped as the frequency increases. High-speed lasers have relaxation frequencies of the order of 30 GHz.

From the Kramers–Kronig relations, any change of the gain of a material (proportional to the imaginary part of the susceptibility) implies a change in the refractive index (proportional to the real part of the susceptibility). Due to the asymmetric nature of the gain spectrum of a semiconductor laser—with a transparent region below the bandgap of the material and a strongly absorbing region at large photon energies—the coupling between index and gain is particularly strong for semiconductor lasers, with profound consequences for the dynamics. This coupling is described by the so-called linewidth enhancement factor (or alpha-parameter) α. It was thus realized that the gain-index coupling gives rise to an enhancement of the linewidth of a semiconductor laser by a factor of $1 + \alpha^2$ (Henry, 1983), and also imposes a chirp on the optical signal under current modulation. These effects are not described by the rate equation (1), which only governs the magnitude squared of the electromagnetic (optical) field and is independent of the phase. Rather the dynamics need to be described by an equation for the complex electric field amplitude, E:

$$\frac{\mathrm{d}E}{\mathrm{d}t} = \frac{1}{2}(1 + \mathrm{i}\alpha)\Gamma v_g g_N(N - N_0)E + F_E(t), \quad (4)$$

where $P \propto |E|^2$. The term $F_E(t)$ is a stochastic Langevin noise term accounting for the random nature of spontaneous emission. The amplitude and phase noise properties of single-mode semiconductor lasers can be analyzed based on Equations (3) and (2).

Addition of a feedback term, proportional to $E(t-\tau)$, to the right-hand side of Equation (3) leads to the famous Lang–Kobyashi equations (Lang & Kobyashi, 1980), which govern the dynamics of a semiconductor laser coupled to an external mirror, τ being the roundtrip time in the external cavity. The semiconductor laser with feedback displays very rich dynamics, including mode-hopping, various instabilities and chaos, that to a remarkable degree are explained by Equations (4) and (2) (Mørk et al., 1992).

The rate equation model outlined above is limited to the case of single transverse mode lasers. Wide aperture lasers, in contrast, have an additional degree of freedom in the transverse direction. It has been shown that a complex semiconductor Swift–Hohenberg equation may describe the dynamics of such lasers in a single longitudinal mode mean field limit (Mercier & Moloney, 2002).

JESPER MØRK

See also **Diodes; Lasers; Nonlinear optics; Optical fiber communications**

Further Reading

Coldren, L.A. & Corzine, S.W. 1995. *Diode Lasers and Photonic Integrated Circuits*, New York: Wiley

Henry, C.H. 1983. Theory of the phase noise and power spectrum of a single mode injection laser. *IEEE Journal of Quantum Electronics*, QE-19: 1391–1397

Lang, R. & Kobyashi, K. 1980. External optical feedback effects on semiconductor injection laser properties. *IEEE Journal of Quantum Electronics*, QE-16: 347–355

Mercier, J.-F. & Moloney, J.V. 2002. Derivation of semiconductor laser mean-field and Swift-Hohenberg equations. *Physical Review* E, 66: 036221-1–036221-19

Mørk, J., Tromborg, B. & Mark, J. 1992. Chaos in semiconductor lasers with optical feedback: theory and experiment. *IEEE Journal of Quantum Electronics*, 28: 93–108

SEMICONDUCTOR OSCILLATORS

The electric transport properties of a semiconductor show up most directly in its current-voltage characteristic. It is related to a relationship between the current density j and the electric field E that is determined in a complex way by the microscopic properties of the material. Although a local, static, scalar $j(E)$ relation need not exist, it does in many cases.

Close to thermodynamic equilibrium (at sufficiently low bias voltage), the $j(E)$ relation is linear (Ohm's law), but under practical operating conditions it often becomes nonlinear and may even display a regime of negative differential conductivity (NDC), where $\sigma_{\mathrm{diff}} = \mathrm{d}j/\mathrm{d}E < 0$. The global current-voltage characteristic $I(U)$ of a semiconductor can in principle be calculated from the local $j(E)$ relation by integrating the current density j over the cross section A of the current flow and the electric field E over the length L of the sample. Unlike the $j(E)$ relation, the $I(U)$ characteristic is not only a property of the semiconductor material, but depends also on the geometry, the boundary conditions, and the contacts of the sample. Only for the idealized case of spatially uniform states, are the $j(E)$ and the $I(U)$ characteristics identical, up to re-scaling. The $I(U)$ relation is said to display negative differential conductance if $\mathrm{d}I/\mathrm{d}U < 0$.

In the case of negative differential conductance, the current decreases with increasing voltage, and vice versa, which may lead to instability. The actual electrical response depends upon the attached circuit, which in addition to resistors may comprise capacitors and inductors. These reactive components give rise to additional degrees of freedom that are described by ordinary differential equations for I and U. If a semiconductor element with NDC is operated in such a reactive circuit, oscillatory instabilities may be induced by these reactive components. Self-sustained semiconductor oscillations, where the semiconductor itself introduces an internal unstable temporal degree of freedom, can be distinguished from those circuit-induced oscillations. The self-sustained oscillations under time-independent external bias are discussed here. Examples of internal degrees of freedom are the charge carrier density, the electron temperature, or a junction capacitance within the device.

Two important examples of NDC are described by an N-shaped or an S-shaped $j(E)$ characteristic and denoted by NNDC and SNDC, respectively (Figure 1). However, more complicated forms such as Z-shaped, loop-shaped, or disconnected characteristics are also possible. NNDC and SNDC are associated with voltage or current-controlled instabilities, respectively. In the NNDC case the current density is a single-valued function of the field, but the field is multivalued; in other words, the $E(j)$ relation has three branches in a certain range of j. The SNDC case is complementary in the sense that E and j are interchanged.

In case of NNDC, the NDC branch is often but not always (depending upon external circuit and boundary conditions) unstable against the formation of non-uniform field profiles along the charge transport direction (electric field domains). In the SNDC case, on the other hand, current filamentation generally occurs, in which the current density becomes non-uniform over the cross section of the current flow and forms a conducting channel (Ridley, 1963). These primary self-organized spatial patterns may themselves become unstable, leading to periodically or chaotically breathing, rocking, moving, or spiking filaments or domains, or even solid-state turbulence and spatiotemporal chaos (Schöll, 2001). Alternatively, the spatially uniform steady state may already become unstable with respect to uniform oscillations in a Hopf bifurcation.

Semiconductor oscillators may be classified as dominated by a bulk mechanism (drift instability,

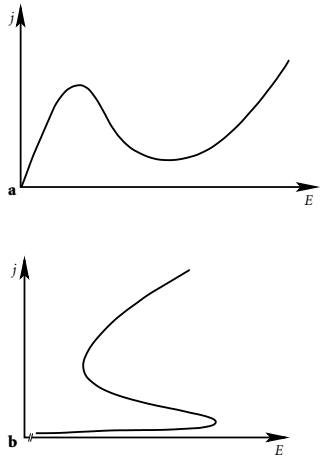

Figure 1. Current density j versus electric field E for two types of negative differential conductivity (NDC): (a) NNDC; (b): SNDC (schematic).

generation-recombination instability) or by heterojunctions and potential barriers and wells (resonant tunneling across, or thermionic emission over, barriers in nanostructures).

The first class of semiconductor oscillators includes drift instability. In the simplest extension of the Drude model, the current density is given by $j(E) = -env(E)$ where $e > 0$ is the electron charge, n is the electron density, and $v(E)$ is the field-dependent drift velocity, which may give rise to negative differential conductivity if $\mathrm{d}|v|/\mathrm{d}|E| < 0$. The best-known example is the Gunn effect, which is based upon intervalley transfer of electrons in k-space from a state of high mobility to a state of low mobility under a strong electric field in direct semiconductors like GaAs or other III–V compounds (Gunn, 1964; Ridley & Watkins, 1961). This phenomenon is used in real devices (Gunn diodes) to generate and amplify microwaves at frequencies typically beyond 1 GHz.

The class of generation-recombination (GR) instabilities is distinguished by a nonlinear dependence of the steady-state carrier concentration n upon the field E that yields a non-monotonic relation $j = en(E)\mu E$ of either NNDC or SNDC type, where μ is the mobility. This dependency is due to a redistribution of electrons between the conduction band and bound states with increasing field. The microscopic transition probabilities of the carriers between different states, and hence the GR coefficients, generally depend upon the electric field. Models of this type are relevant for a variety of materials and in various temperature ranges (Schöll, 1987) and can explain SNDC and current filamentation in the regime of low-temperature impurity breakdown and self-generated current oscillations including chaotic behavior, as observed experimentally (Peinke et al., 1992). Two important devices are also based upon GR-induced bulk negative differential conductivity, but the coupling with junction effects is essential in these cases: p-i-n diodes and impact ionization avalanche transist-time (IMPATT) diodes.

A variety of instabilities can arise due to the specific transport properties of semiconductor heterostructures. One mechanism for NNDC, which is the real space analog of the k-space intervalley transfer in the Gunn effect, uses electron transfer between a high-mobility layer and a low-mobility layer in a modulation-doped semiconductor heterostructure under a time-independent bias applied parallel to the layers (Gribnikov et al., 1995). In the NNDC regime, current oscillations of 2–200 MHz have been experimentally observed and theoretically explained.

Another class of oscillatory instabilities occurs under vertical electrical transport in layered semiconductor structures, for example, in the heterostructure hot-electron diode (HHED) or the double-barrier resonant tunneling diode (DBRT), which are associated with S-shaped and Z-shaped current-voltage characteristics, respectively (Schöll, 2001). A resonant tunneling structure is composed of alternating layers of two different semiconductor materials with different bandgaps. The energy diagram shows a modulation of the conduction band edge on a nanometer scale, forming potential barriers and quantum wells. The current density across the barrier between two wells is due to quantum mechanical tunneling and exhibits a strongly nonlinear dependency upon the electric field. It is maximum if there is maximum overlap between the occupied states in one well and the available unoccupied states in the other (the energies are in resonance). For low-fields, equivalent levels in adjacent wells are approximately in resonance. With increasing field, the energies of the two wells are shifted with respect to each other, and the available states in the collecting well are lowered with respect to the emitting well, and hence the current density drops as the overlap between the energy levels decreases, thereby displaying NDC. Upon further increase of the field, the current density rises again up to a sharp resonance peak when the ground energy level in one quantum well is aligned with the second level in the neighboring well. Thus, resonant tunneling produces NNDC.

The simplest system of this type consists of a double-barrier structure with one embedded quantum well in between, sandwiched between a highly doped emitter and collector region. However, the situation becomes more complicated if the nonlinear feedback between space charges and transport processes is taken

into account. The built-up charge in the well leads to an electrostatic feedback mechanism that increases the energy of the well state supporting resonant tunneling conditions for higher applied voltages. This may result in bistability and hysteresis where a high current and a low current state coexist for the same applied voltage, and the current-voltage characteristic becomes Z-shaped. Switching between the two stable states as well as self-sustained current oscillations may occur under appropriate external circuit conditions. The bistability also provides a basis for lateral pattern formation (current filamentation) and spatiotemporal bifurcation scenarios including chaotic breathing and spiking.

Sequential resonant tunneling in a periodic structure of multiple quantum wells, a semiconductor superlattice, likewise displays NNDC (Esaki & Chang, 1974). Now, along the growth direction, the uniform field distribution may break up into a low-field domain, where the field is near the first peak of the $j(E)$ characteristic, and a high-field domain, where the field is close to the second, resonant-tunneling peak. Depending upon doping, the applied voltage, structural parameters, and the emitter contact conductivity, stationary or traveling domains occur—the latter leading to self-sustained current oscillations ranging from several hundred MHz up to 150 GHz at room temperature (Wacker, 2002).

ECKEHARD SCHÖLL

See also **Avalanche breakdown; Diodes; Drude model; Nonlinear electronics**

Further Reading

Aoki, K. 2000. *Nonlinear Dynamics and Chaos in Semiconductors*, Bristol and Philadelphia: Institute of Physics

Esaki, L. & Chang, L.L. 1974. New transport phenomenon in a semiconductor superlattice. *Physical Review Letters*, 33(8): 495–498

Gribnikov, Z.S., Hess, K. & Kosinovsky, G. 1995. Nonlocal and nonlinear transport in semiconductors: Real-space transfer effects. *Journal of Applied Physics*, 77: 1337–1373

Gunn, J.B. 1964. Instabilities of current in III–V semiconductors. *IBM Journal of Research and Development*, 8: 141–159

Peinke, J., Parisi, J., Rössler, O. & Stoop, R. 1992. *Encounter with Chaos*, Berlin and New York: Springer

Ridley, B.K. 1963. Specific negative resistance in solids. *Proceedings of the Physical Society*, 82: 954

Ridley, B.K. & Watkins, T.B. 1961. The possibility of negative resistance effects in semiconductors. *Proceedings of the Physical Society*, 78: 293–304

Schöll, E. 1987. *Nonequilibrium Phase Transitions in Semiconductors*, Berlin and New York: Springer

Schöll, E. 2001. *Nonlinear Spatio-temporal Dynamics and Chaos in Semiconductors*, Cambridge and New York: Cambridge University Press

Schöll, E., Niedernostheide, F.J., Parisi, J., Prettl, W. & Purwins, H. 1998. Formation of spatio-temporal structures in semiconductors. In *Evolution of Spontaneous Structures in Dissipative Continuous Systems*, edited by F.H. Busse & S.C. Müller, Berlin: Springer, pp. 446–494

Shaw, M.P., Mitin, V.V., Schöll, E. & Grubin, H.L. 1992. *The Physics of Instabilities in Solid State Electron Devices*, New York: Plenum Press

Wacker, A. 2002. Semiconductor superlattices: a model system for nonlinear transport. *Physics Reports*, 357: 1–111

SEMI-LINEAR PDES

See **Quasilinear analysis**

SENSITIVE DEPENDENCE ON INITIAL CONDITIONS

See **Butterfly effect**

SEPARATION OF VARIABLES

Separation of variables is the name of a general method for finding particular solutions of partial differential equations (PDEs) as a product of functions, where each factor depends on only one of the independent variables and satisfies an ordinary differential equation (ODE).

In the study of linear equations, a familiar example of the method is eigenfunction analysis. Using the superposition principle, this approach leads to expansions in products of orthogonal functions. The Fourier transform method is a special limiting case.

For a particular PDE, there may be a family of coordinate systems that admits separation of variables. The problem of finding such coordinate systems is closely connected with the group properties of differential equations. Methods from Lie group theory can be used to describe all the separable solutions of many equations from mathematical physics (Miller, 1977). In Morse and Feshbach (1953), the separable orthogonal coordinate systems for the Laplace, Helmholtz, Schrödinger, heat (diffusion), and wave equations in two and three dimensions are listed.

For example, Laplace's equation

$$u_{xx} + u_{yy} = 0 \tag{1}$$

has product solutions $u(x, y) = X(x)Y(y)$, where X (respectively, Y) is a function of only the independent variable x (respectively, y). Here X and Y satisfy the ordinary differential equations $X'' + \lambda X = 0$ and $Y'' - \lambda Y = 0$, where λ is the separation constant and prime denotes differentiation with respect to the independent variable. X and Y may thus be expressed in terms of trigonometric and exponential functions.

Separability depends on the boundary conditions. As a second example, consider the Helmholtz equation

$$u_{xx} + u_{yy} + k^2 u = 0 \tag{2}$$

in two dimensions with Dirichlet or Neumann boundary conditions ($u = 0$ or $u_n = 0$, where subscript n denotes the derivative in the direction normal to the boundary). This boundary value problem is separable in rectangular, parabolic, polar, and elliptic coordinates.

However, with the mixed (Robin) or impedance boundary condition $u_n + cu = 0$ (where the impedance c is a constant), the problem is only separable in rectangular and polar coordinates.

For nonlinear wave equations a method for separation of variables is sometimes called Lamb's method, stemming from an early analysis of the sine-Gordon (SG) equation (Lamb, 1971)

$$u_{xx} - u_{tt} - \sin u = 0. \tag{3}$$

This equation has solutions of the form $u(x,t) = 4\tan^{-1}(X(x)T(t))$, where $(X')^2 = a_1X^4 + a_2X^2 + a_3$ and $(T')^2 = -a_3T^4 + (a_2 - 1)T^2 - a_1$, and a_1, a_2, and a_3 are separation constants. In general, therefore, X and T are Jacobi elliptic functions.

In special cases simpler SG soliton solutions such as kinks, antikinks, colliding kinks and antikinks, breathers or bions, and plasma waves, are obtained. For example, choosing $a_1 = a_2 = 1/(1 - v^2)$ and $a_3 = 0$ yields colliding kinks, traveling with velocities v and $-v$, respectively, while $a_2 = -a_3 = 1/(1 - v^2)$ and $a_1 = 0$ yields colliding kinks and antikinks. Since the SG equation models long Josephson junctions, fluxons traveling on Josephson junctions of infinite length are obtained as derivatives of the kinks (Scott, 2003), and nonlinear oscillations or standing waves on junctions of finite length can also be found for boundary conditions of Dirichlet or Neumann type (Costabile et al., 1978).

Separation of variables provides solutions to other nonlinear partial differential equations such as the nonlinear Schrödinger equation (NLS)

$$\mathrm{i}u_t + u_{xx} + 2|u|^2u = 0. \tag{4}$$

Writing $u(x,t) = \phi(x,t)\mathrm{e}^{\mathrm{i}\theta(x,t)}$, the amplitude function, $\phi(x,t)$, and the phase function, $\theta(x,t)$, satisfy nonlinear coupled ordinary differential equations that permit traveling wave solutions of the form $\phi(x,t) = \phi(x - vt)$, where v is the velocity. These are the NLS envelope solitons (Scott, 2003).

Standing wave solutions to the so-called improved Boussinesq equation

$$u_{xx} - u_{tt} - (u^2)_{xx} + u_{xxtt} = O \tag{5}$$

of the form $u(x,t) = 1/2 + X(x)T(t)$, where $X(x)$ and $T(t)$ satisfy uncoupled nonlinear ordinary differential equations, have been obtained in Rosenau and Schwarzmeier (1986) and Christiansen et al. (1990).

The Hamilton–Jacobi equation is separable when Hamilton's characteristic function, W, can be written as a sum of functions where each function depends on only one of the independent variables (Goldstein, 1980). Let us look at a particle with mass m moving in central force with potential $V(r)$. Using polar coordinates (r, ϕ) in the plane of the orbit, the Hamiltonian has the form

$$H = \frac{1}{2m}\left(p_r^2 + \frac{p_\phi^2}{r^2}\right) + V(r), \tag{6}$$

and is cyclic in ϕ. Consequently, Hamilton's characteristic function

$$W = W_r(r) + W_\phi(\phi) \equiv W_r(r) + \alpha_\phi\phi, \tag{7}$$

where the momentum conjugated to r is $p_r = \partial W_r(r)/\partial r$ and the angular momentum conjugated to ϕ, $p_\phi = \partial W_\phi(\phi)/\partial\phi = \alpha_\phi$ is a constant. The Hamilton–Jacobi equation now becomes

$$\left(\frac{\partial W_r(r)}{\partial r}\right)^2 + \frac{\alpha_\phi^2}{r^2} + 2mV(r) = 2mE, \tag{8}$$

where E is the total energy of the system. Integrating (8) with respect to r, $W_r(r)$ and thus W given by (7) are obtained. The canonical equations then yield the orbitals in the form $r = r(t)$ or $r = r(\phi)$.

A new approach has been developed by Sklyanin (1995), who argues that separation of variables, understood generally enough, could be a universal tool to solve integrable models of classical and quantum mechanics. Standard construction of the action-angle variables for the poles of the Baker–Akhiezer function can be interpreted as a variant of separation of variables. The new approach has been applied to magnetic chains, the Toda lattice, the nonlinear Schrödinger equation, the sine-Gordon model, and other systems (Skyanin, 1995).

PETER L. CHRISTIANSEN

See also **Boundary value problems; Integral transforms; Long Josephson junctions**

Further Reading

Christiansen, P.L., Lomdahl, P.S. & Muto, V. 1990. On a Toda lattice model with a transversal degree of freedom. *Nonlinearity*, 4: 477–501

Costabile, G., Parmentier, R.D., Savo, B., McLaughlin, D.W. & Scott, A.C. 1978. Exact solutions of the sine-Gordon equation describing oscillations in a long (but) finite Josephson junction. *Applied Physics Letters*, 32: 587–589

Goldstein, H. 1980. *Classical Mechanics*, 2nd edition, Reading, MA: Addison-Wesley

Lamb, G.L., Jr. 1971. Analytical descriptions of ultrashort optical pulse propagation in a resonant medium. *Reviews of Modern Physics*, 43: 99–124

Miller, U. 1977. *Symmetry and Separation of Variables*, Reading, MA: Addison-Wesley

Morse, P.M. & Feshbach, H. 1953. *Methods of Theoretical Physics*, New York and London: McGraw-Hill

Rosenau, P. & Schwarzmeier, J.L. 1986. On similarity solutions of Boussinesq-type equation. *Physics Letters* A, 115: 75–77

Scott, A.C. 2003. *Nonlinear Science: Emergence and Dynamics of Coherent Structures*, 2nd edition, Oxford and New York: Oxford University Press

Sklyanin, E.K. 1995. Separation of variables: new trends. *Progress in Theoretical Physics Supplement*, 118: 35–60

SEPARATRIX

See **Phase space**

SHAPIRO STEPS

See **Josephson junction**

SHARKOVSKY'S THEOREM

See **One-dimensional Maps**

SHEAR FLOWS

Shear flows arise whenever two bodies of fluid move relative to each other, as in a jet of liquid entering a fluid at rest or the flow past a solid obstacle. When the flow speeds become too high, these flows undergo instabilities that are at the root of the vortical structures that dominate turbulent flows. For the Kelvin–Helmholtz; instability of two layers of fluid in relative motion; the instabilities of a fluid sheared between two concentric, rotating cylinders (Taylor–Couette flow); the dynamics of boundary layers; and viscous Hele-Shaw experiments, see the corresponding *Encyclopedia* entries.

Energy balance: The significance of shear as a source of energy for perturbations follows from the analysis of the energy content of a perturbation to a shear flow. Let $\boldsymbol{U}$ be a prescribed stationary flow in a domain V and let $\boldsymbol{u}$ be the perturbation added to $\boldsymbol{U}$. The Reynolds number is defined in terms of the velocity scale U of the reference flow, a length scale L, and the kinematic viscosity ν, that is, $\mathrm{Re} = UL/\nu$. For a divergence free perturbation with boundary conditions $\boldsymbol{u} = 0$ on surfaces, the energy content $E(t) = \int_V \mathrm{d}V(\boldsymbol{u}^2/2)$ satisfies the Orr–Reynolds equation

$$\frac{\mathrm{d}E}{\mathrm{d}t} = -\int_V u_i u_j \frac{\partial U_i}{\partial x_j}\mathrm{d}V - \frac{1}{\mathrm{Re}}\int_V \frac{\partial u_i}{\partial x_j}\frac{\partial u_j}{\partial x_i}\,\mathrm{d}V. \quad (1)$$

Since the last term on the right-hand side is negative semidefinite, all the energy input has to come from the shear $\partial U_i/\partial x_j$. If the shear is too small, then $E(t)$ will decay monotonically. The Reynolds number up to which $\dot{E} \le 0$ for all perturbations defines the energy stability limit Re_E.

Parallel flows: A necessary condition for an instability of parallel inviscid flows was derived by Lord Rayleigh (John William Strutt) in 1880; he found that instability requires an inflection point. If $\boldsymbol{u} = U(y)\boldsymbol{e}_x$ is the unperturbed profile, then instability can occur only if there is a point y_s with $U''(y_s) = 0$. This criterion was later improved by R.Fjørtoft, who found the requirement $U''(y)(U(y) - U(y_s)) < 0$. Necessary and sufficient conditions are more complicated, as discussed in Balmforth & Morrision (1999).

For the viscous stability, it is useful to represent the perturbation with components (u, v, w) in terms of the vertical velocity component v and the vertical vorticity, $\eta = \partial_z u - \partial_x w$, and to expand in terms of Fourier modes,

$$v(x, y, z, t) = \tilde{v}(y)\mathrm{e}^{\mathrm{i}(\alpha x + \beta z - \omega t)}, \quad (2)$$

$$\eta(x, y, z, t) = \tilde{\eta}(y)\mathrm{e}^{\mathrm{i}(\alpha x + \beta z - \omega t)}. \quad (3)$$

Then the amplitudes satisfy

$$\left[(-\mathrm{i}\omega + \mathrm{i}\alpha U)(D^2 - k^2) - \mathrm{i}\alpha U'' - \frac{1}{\mathrm{Re}}(D^2 - k^2)^2\right] \times \tilde{v} = 0, \quad (4)$$

$$\left[(-\mathrm{i}\omega + \mathrm{i}\alpha U) - \frac{1}{\mathrm{Re}}(D^2 - k^2)\right] \times \tilde{\eta} = -\mathrm{i}\beta U'\tilde{v}. \quad (5)$$

The first equation is the Orr–Sommerfeld equation, the second Squire's equation. In 1933, H.B. Squire showed that if there is an instability for a mode with spanwise wave number $\beta \neq 0$, then there is another one with $\beta = 0$ that has a lower Reynolds number, where instabilities set in without spanwise modulations.

The linearized problem can show transient growth: a decaying eigenstate of the Orr–Sommerfeld equation can drive the Squire equation and cause an amplification of the normal vorticity (if $\beta \neq 0$). The most effective modes often have the form of downstream vortices, with only slight modulations in spanwise and downstream direction. They drive spanwise modulations in the downstream velocity component, so-called streaks. Fabian Waleffe (1995, 1997) pointed out that the streaks can undergo an instability themselves, forming normal vortices, which can then be fed back into downstream vortices to close the loop. This self-sustaining regeneration mechanism plays a major role in the turbulence of parallel flows. The results for the transition to turbulence in viscous planar shear flows are summarized in Table 1. The flows are shear flow between parallel plates with a linear profile in the laminar case (plane Couette), pressure-driven flow between parallel plates with a parabolic profile (plane Poiseuille), and pressure-driven flow down a pipe, also with a parabolic profile (Hagen–Poiseuille). The various Reynolds numbers are defined as follows:

- $\mathrm{Re_E}$ *Energy stability*: as above.
- $\mathrm{Re_G}$ *Global stability*: up to this Reynolds number the flow is globally stable, and any perturbation will decay, perhaps after a long transient during which the energy can grow above the initial energy.
- $\mathrm{Re_T}$ Reynolds number near which experiments indicate a transition to turbulence.
- $\mathrm{Re_L}$ Reynolds number for linear instability.

For sufficiently low Re, all flows are linearly stable. For plane Couette flow and pipe flow, we know that the flows cannot be globally stable at Reynolds numbers above the given ones because of the existence of 3-dimensional stationary states or traveling waves

Flow	$\mathrm{Re_E}$	$\mathrm{Re_G}$	$\mathrm{Re_T}$	$\mathrm{Re_L}$
Plane Couette flow	20.7	125	310	∞
Plane Poiseuille flow	49.6	≈ 1000	1000	5772
Hagen–Poiseuille flow	81.5	1250	2250	∞

Table 1. Critical Reynolds numbers for parallel shear flows.

(Nagata, 1990; Ehrenstein & Koch, 1991; Clever & Busse 1997; Faisst & Eckhardt, 2003; Wedin & Kerswell, 2004). Two of the flows do not show a linear instability, and for the third one, it appears at values far above the ones where the transition to turbulence occurs. Incidentally, plane Poiseuille flow provides an example of a flow profile that is inviscidly stable by Rayleigh's criterion but becomes unstable when viscosity is included.

In all three cases, the value for transition to turbulence is somewhat uncertain because of the absence of a sharp transition (Boberg & Brosa, 1988; Darbyshire & Mullin, 1995; Bottin et al., 1998). There is evidence that this is connected with the formation of a chaotic saddle in phase space (Schmiegel & Eckhardt, 1997). Scanning an amplitude–Reynolds number plane for perturbations in a low-dimensional model indeed shows a sensitive dependence on initial conditions and huge variations in lifetimes for neighboring trajectories (see figure in color plate section). The lifetimes of perturbations are exponentially distributed, a clear signature of a chaotic saddle.

Turbulent shear flows: The energy dissipation in a turbulent shear flow can be related to the velocity difference U and the width L of the flow as

$$\varepsilon_V = c_\varepsilon(\mathrm{Re})U^3/L \tag{6}$$

with a dissipation factor $c_\varepsilon(\mathrm{Re})$ that depends on the Reynolds number $\mathrm{Re} = UL/\nu$. For laminar parallel flows, $c_\varepsilon \sim 1/\mathrm{Re}$. For turbulent shear flows, the variational theories of Busse (1970), Doering & Constantin (1992), Kerswell (1997), and Nicodemus et al. (1997) show that in the limit of infinite Reynolds number, $c_\varepsilon(\mathrm{Re})$ can be rigorously bounded from above. The theory bounds c_ε through a variational functional with a background profile $\phi(y)$, with the constraint that the background profile has to be energy stable. The best bound is $c_\varepsilon \leq 0.0109$. Comparing with experiment, one notes that the observed values are lower and that for smooth boundaries, they tend to decrease for increasing Reynolds number.

The presence of a large-scale shear introduces an anisotropy into the flow, which also affects the turbulent statistics. While in an isotropic turbulent flow the odd moments of the normal derivative of the downstream component vanish, this is no longer the case in a turbulent shear flow. Dimensional estimates by Lumley (1967) suggest that the anisotropy should vanish like $1/\mathrm{Re}$, but experimental and numerical evidence indicates that the decay is much slower. Current efforts aim at extracting information about the relevant process from the dynamics of passive scalars: the scalar fields develop characteristic ramps and cliffs that can be related to the asymmetry in the distributions of the gradients (Schumacher & Sreenivasan, 2003).

Other shear flows: In viscoelastic fluids, the interaction between shear and internal degrees of freedom can also give rise to much more complicated instabilities for which Squire's theorem does not hold. The reduction of turbulent drag by small additions of long flexible polymers remains a fascinating phenomenon awaiting explanation (Lumley, 1969).

In astrophysics a combination of differential motion in the plasma and the presence of a magnetic field can give rise to instabilities that are responsible for the transport of angular momentum, thus solving a long-standing puzzle about the angular momentum distribution in galaxies (Balbus & Hawley, 1998).

BRUNO ECKHARDT

See also **Boundary layers; Hele-Shaw cell; Kelvin–Helmholtz instability; Taylor–Couette flow; Turbulence**

Further Reading

Balbus, S.A. & Hawley, J.F. 1998. Instability, turbulence, and enhanced transport in accretion disks. *Reviews of Modern Physics*, 70: 1–52

Balmforth, N.J. & Morrison, P.J. 1999. A necessary and sufficient instability condition for inviscid shear flow. *Studies in Applied Mathematics*, 102: 309–344

Boberg, L. & Brosa, U. 1988. Onset of turbulence in pipe. *Zeitschrift für Naturforschung*, 43a: 697–726

Bottin, S., Daviaud, F., Manneville, P. & Dauchot, O. 1998. Discontinuous transition to spatiotemporal intermittency in plane Couette flow. *Europhysics Letters*, 43: 171–176

Busse, F.H. 1970. Bounds for turbulent shear flow. *Journal of Fluid Mechanics*, 41: 219–240

Clever, R.M. & Busse, F.H. 1997. Tertiary and quaternary solutions for plane Couette flow. *Journal of Fluid Mechanics*, 344: 137–153

Darbyshire, A.G. & Mullin, T. 1995. Transition to turbulence in constant-mass-flux pipe flow. *Journal of Fluid Mechanics*, 289: 83–114

Doering, C.R. & Constantin, P. 1992. Energy dissipation in shear driven turbulence. *Physical Review Letters*, 69: 1648–1651

Drazin, P.G. & Reid, W.H. 1981. *Hydrodynamic Stability*, 2nd edition, Cambridge and New York: University Press, 2004

Ehrenstein, U. & Koch, W. 1991. Three-dimensional wavelike equilibrium states in plane Poiseuille flow. *Journal of Fluid Mechanics*, 228: 111–148

Faisst, H. & Eckhardt, B. 2003. Travelling waves in pipe flow. *Physical Review Letters*, 91: 224502

Grossmann, S. 2000. The onset of shear flow turbulence. *Reviews of Modern Physics*, 72: 603–618

Joseph, D.D. 1976. *Stability of fluid motion*, part I and II, New York: Springer

Kerswell, R.R. 1997. Variational bounds on shear-driven turbulence and turbulent Boussinesq convection. *Physica* D, 100: 355–376
Lumley, J.L. 1967. Similarity and the turbulent energy spectrum. *Physics of Fluids*, 10: 855–858
Lumley, J.L. 1969. Drag reduction by additives. *Annual Reviews of Fluid Mechanics*, 1: 367–384
Nagata, M. 1990. Three-dimensional finite-amplitude solutions in plane Couette flow: bifurcation from infinity. *Journal of Fluid Mechanics*, 217: 519–527
Nicodemus, R., Grossmann, S. & Holthaus, M. 1997. The background flow method, part I and II. *Journal of Fluid Mechanics*, 363: 281–300 and 301–323
Rosenhead, L. (editor). 1963. *Laminar Boundary Layers*, Oxford: Oxford University Press
Schmid, P. & Henningson, D.S. 2001. *Stability and Transition in Shear Flows*, Berlin and New York: Springer
Schmiegel, A. & Eckhardt, B. 1997. Fractal stability border in plane Couette flow. *Physical Review Letters*, 79: 5250–5253
Schumacher, J. & Sreenivasan, K.R. 2003. Geometric features of the mixing of passive scalars at high Schmidt numbers. *Physical Review Letters*, 91: 174501
Waleffe, F. 1995. Transition in shear flows. Nonlinear normality versus non-normal linearity. *Physics of Fluids*, 7: 3060–3066
Waleffe, F. 1997. On a self-sustaining process in shear flows. *Physics of Fluids*, 9: 883–900
Wedin, H. & Kerswell, R.R. 2004. Exact coherent structures in pipe flow: travelling wave solutions. *Journal of Fluid Mechanics*, in press

SHOCK WAVES

In classical gas dynamics, a shock wave is a sharp, stepwise increase of density, pressure, and temperature that propagates at a supersonic speed with respect to the fluid ahead of it while remaining subsonic with respect to the fluid behind it. The fluid entropy increases after passing through the shock. Shock waves can be formed as a result of numerous processes such as supersonic motion of bodies (aircraft, meteors, bullets) in the atmosphere (see Figure 1), explosions in atmosphere and ocean, collapse of bubbles in the course of cavitation, and gas flow out of a nozzle in rockets. Also, the propagation of a nonlinear nondispersive wave (simple wave), in which each point of the profile propagates at its own velocity, generally results in the shock formation.

The changes (jumps) of different physical (thermodynamic) quantities at a shock satisfy specific relations (boundary conditions) following from the conservation of mass, momentum, and energy (mechanical plus thermodynamical). In the reference frame of the shock front, they can be presented in the form

$$[\rho v_n] = 0, \quad \left[p + \rho v_n^2\right] = 0, \left[\frac{v_n^2}{2} + w\right] = 0. \qquad (1)$$

Here the square brackets denote the difference of the corresponding values at the shock; v_n is fluid velocity component normal to the front; w is enthalpy; p and ρ are, respectively, pressure and density. In the reference frame in which the fluid before the shock is immovable, v_n is $-V$ where V is the shock propagation velocity.

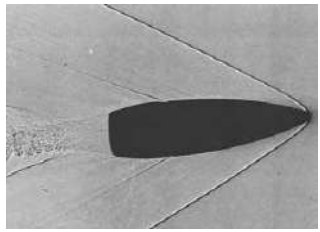

Figure 1. Shadowgraph showing shock waves produced by a Winchester 0.308 caliber bullet traveling through air at about Mach 2.5. (With courtesy from Ruprecht Nennstiel, Wiesbaden, Germany.)

The velocity of tangential fluid motion at the shock is continuous.

Equations (1) give, in particular,

$$w_2 - w_1 = \tfrac{1}{2}(U_2 + U_1)(p_2 - p_1), \qquad (2)$$

where $U = 1/\rho$ is the specific volume, and subscripts 1 and 2 refer to the gas in front of and behind the shock. The enthalpy w can be expressed in terms of p and ρ via the thermodynamic equation of state. As a result, if the gas parameters p_1 and U_1 before the shock are given, Equation (2) determines the dependence between p_2 and U_2 called the Hugoniot adiabat. It differs from the Poisson adiabat that relates p and ρ in a perfect gas in which entropy is constant.

In a stable shock wave the entropy increases due to dissipative processes occurring inside the shock front, which is actually a transient layer of a finite thickness that grows with viscosity and thermal conductivity in the medium. If the transition region remains thin compared with the outer motion scale, it can be considered a discontinuity at which the boundary conditions (1) (which do not depend on the specific dissipation mechanism) remain valid. Note that if only thermal conductivity determines the shock front width (i.e., viscosity is neglected), the shock front can contain a discontinuity (isothermal jump) inside it.

General relations concerning shock waves are simplified in the important case of a polytropic gas in which p is proportional to ρ^γ, where $\gamma = c_p/c_v$, and c_p and c_v are heat capacities at constant pressure and volume, respectively. For example, in a very strong shock when $p_2 \gg p_1$ and the Mach number, $M = V/c \gg 1$ (c is the speed of sound), the ratios of gas densities and temperatures (T) behind and before the shock are

$$\frac{\rho_1}{\rho_2} = \frac{U_2}{U_1} = \frac{\gamma - 1}{\gamma + 1}, \quad \frac{T_2}{T_1} = \frac{\gamma - 1}{\gamma + 1}\frac{p_2}{p_1}. \qquad (3)$$

Note that the maximal gas compression remains finite.

Among the dynamic problems associated with shock waves is that of shock reflection from a hard wall. If the

incidence is normal to the wall, the pressure increases to more than twice that in an incident wave (for a linear wall the pressure is doubled). If a shock of moderate strength is incident obliquely under a sufficiently large grazing angle, the shock is reflected before reaching the wall (Mach stem effect).

Another important problem is a spherical shock from an explosion. For very strong spherical waves, a self-similar solution exists, in which the shock front radius R increases as $t^{2/5}$, whereas the pressure and particle velocity decrease as R^{-3} and $R^{-3/2}$, respectively. For a curved shock front, the solution can be found by an approximation: local shock curvature at each moment is related to the rays normal to the front, and the fluid flows along these ray tubes as in channels of variable width (Whitham, 1974).

A more general description of nonstationary flows containing shocks can be achieved for one-dimensional motions such as the waves in a tube excited by a piston moving at its end. The one-dimensional equations of motion for an ideal gas can be rewritten in terms of two Riemann invariants, $J_\pm$:

$$\left[\frac{\partial}{\partial t} + (v \pm c)\frac{\partial}{\partial x}\right] J_\pm = 0,$$
$$J_\pm = v \pm \int \frac{\mathrm{d}p}{\rho c} = v \pm \frac{2c}{\gamma - 1} \qquad (4)$$

(the latter expressions are written for a polytropic gas). Here $c(\rho) = (\mathrm{d}p/\mathrm{d}\rho)^{1/2} = (\gamma p/\rho)^{1/2}$ is the local speed of sound. Correspondingly, there are two families of trajectories-characteristics, $\mathrm{d}x/\mathrm{d}t = v \pm c$ on the (x, t) plane, along which small perturbations that are linear sound waves propagate. In a particular case when one of the invariants is constant, there is a progressive simple (Riemann) wave that travels at a local velocity $v \pm c$. In such a wave, the variables are related by $v = \pm \int \mathrm{d}p/\rho c$. Each point of the simple wave profile propagates at its own, constant velocity, and if the velocity decreases with x, at some moment the motion becomes multivalued (the wave breaks). In gas dynamics this is physically impossible, which means the formation of a shock wave at which the energy of the continuous part of the wave dissipates.

An important particular case is that of small nonlinearity when $p(\rho) \approx p_0 + c_0^2\rho'$, where p_0 and c_0 refer to the equilibrium state (in the absence of the wave), and ρ' is density variation in the wave. This corresponds to nonlinear acoustics where the velocity of a weak shock wave is approximately the average of the linear sound speeds in front of and behind the shock. In particular, an initially sinusoidal wave transforms into a sawtooth one.

Simple waves may exist in different nondispersive, nonlinear physical systems. One example is a nonlinear surface wave in shallow water when the characteristic wavelength is much larger than the depth of the water layer, h. Such a wave propagates at the local velocity of $c(\eta) = \sqrt{g(h + \eta)}$, where g is gravitational acceleration and $\eta(x, t)$ is the local water surface displacement with respect to its unperturbed level, h. In general, this wave breaks at a finite distance so that the long-wave approximation becomes invalid in the vicinity of the breaking point. The breaking can have different outcomes. Due to dispersion, the wave can generate oscillations that eventually become solitons, or, at larger steepness, the wave crest may break, possibly forming a turbulent front (bore), somewhat similar to a shock.

Magnetohydrodynamic Shock Waves

Shock waves can form in plasma. If the plasma is sufficiently dense, it can be treated as a compressible fluid that has electrical conductivity. When such a fluid moves in a magnetic field, the motion induces electric currents. Interaction between the currents and the magnetic field can significantly affect the fluid motion. Interaction between hydrodynamic and electromagnetic phenomena is the subject of *magnetohydrodynamics*. These phenomena are important in, for example, astrophysics, where at large-scale motions, space plasma typically behaves as a conducting fluid.

In a linear approximation, magnetohydrodynamic (MHD) waves are classified as "slow" and "fast" magnetic sound in which fluid compressibility is significant, and Alfvén waves depending only on magnetic field. In these waves magnetic perturbations are polarized perpendicular to the basic constant magnetic intensity vector $\boldsymbol{H}$ and group velocity is directed along $\boldsymbol{H}$. Finite-amplitude magnetic sound is distorted with a possible formation of MHD shocks.

As in nonmagnetic gas dynamics, parameters of MHD shock waves can be determined from boundary conditions at the discontinuity, which differ from the Rankine–Hugoniot conditions in that they include the magnetic field at both sides of the shock. The corresponding generalization of the Hugoniot adiabat reads (in the CGS system)

$$(\varepsilon_2 - \varepsilon_1) + \frac{1}{2}(p_2 + p_1)(U_2 - U_1) + \frac{1}{16\pi}(U_2 - U_1)(H_{\tau 2} - H_{\tau 1})^2 = 0, \qquad (5)$$

where H_τ is the component tangential to the shock front. In fluids with a positive thermal expansion coefficient, both pressure and density always increase at the shock, as in classical gas dynamics.

The nonshock discontinuities in MHD include tangential discontinuities, in which the vectors of fluid velocity and magnetic field are parallel to the discontinuity plane (in the comoving reference frame), and rotational (Alfvén) discontinuities in which the normal velocity component of velocity is nonzero but

continuous whereas the vector $\boldsymbol{H}$ rotates around the normal with constant absolute value.

In plasma, dispersion can cause an oscillating shock structure and solitary wave formation. If plasma is rarefied so that the free path of electrons exceeds the shock front thickness, the so-called noncollisional shocks may exist.

Electromagnetic Shock Waves

Another class of shock waves occurs in media that can be macroscopically immovable but have nonlinear electromagnetic parameters; for example, the dependence between the vectors of magnetic induction and the magnetic field, $\boldsymbol{B}(\boldsymbol{H})$, or between their electric counterparts, $\boldsymbol{D}(\boldsymbol{E})$, are nonlinear. If the nonlinearity is relatively strong and dispersion effects are small, electromagnetic waves can propagate as simple waves, resulting in the formation of electromagnetic shocks.

Boundary conditions at a shock can be obtained by integrating Maxwell's equations over the shock transition layer, to give

$$[\boldsymbol{n} \times (\boldsymbol{E}_2 - \boldsymbol{E}_1)] = \frac{U_n}{c_0}(\boldsymbol{B}_2 - \boldsymbol{B}_1), \qquad (6)$$

$$[\boldsymbol{n} \times (\boldsymbol{H}_2 - \boldsymbol{H}_1)] = \frac{U_n}{c_0}(\boldsymbol{D}_2 - \boldsymbol{D}_1),$$

$$B_{n2} = B_{n1},\ D_{n2} = D_{n1},$$

where $\boldsymbol{n}$ is a normal to the discontinuity surface, c_0 is the light speed in vacuum, and U_n is the normal component of shock velocity. Typically only either magnetic or electric properties of the medium are nonlinear. In the former case, an expression for the shock velocity is

$$\frac{\varepsilon U_n^2}{c^2} = \frac{H_{\tau 2} - H_{\tau 1}}{B_{\tau 2} - B_{\tau 1}}. \qquad (7)$$

Electromagnetic shock waves are observed in ferrites, ferroelectrics, and semiconductors, and they have been used for construction of powerful impulse generators. In nonlinear dispersive systems, such as nonlinear transmission lines, the shock transition can be oscillating, and as dissipation approaches zero, it becomes a solitary electromagnetic wave.

LEV OSTROVSKY

See also **Alfvén waves; Characterisitics; Cherenkov radiation; Dimensional analysis; Explosions; Jump phenomena; Magnetohydrodynamics; Nonlinear acoustics**

Further Reading

Courant, R. & Friedrichs, K.O. 1948. *Supersonic Flow and Shock Waves*, reprinted New York: Springer, 1992

Gaponov, G., Ostrovsky, L. & Freidman, G. 1967. Electromagnetic shock waves (a review). *Radiophysics and Quantum Electronics*, 10: 9–10

Landau, L. & Lifshitz, E. 1960. *Electrodynamics of Continuous Media*, Oxford and New York, Pergamon Press

Landau, L. & Lifshitz, E. 1987. *Fluid Mechanics*, 2nd edition, Oxford: Pergamon Press

Whitham, G.B. 1974. *Linear and Nonlinear Waves*, New York: Wiley

SHOOTING METHOD

See **Phase plane**

SIERPINSKI GASKET

See **Order from chaos**

SIGNALING PROBLEM

See **Wave stability and instability**

SINAI BILLIARD

See **Billiards**

SINAI–RUELLE–BOWEN MEASURES

What is a natural ivariant measure? In a probabilistic approach to dynamical systems, one seeks to understand average or almost-sure behavior, particularly in the limit as time tends to infinity. In these studies, it is often fruitful to have a stationary process, or equivalently, an *invariant probability measure*. Consider a map f on a bounded domain U of a Euclidean space or a manifold with $f(U) \subset U$. (We will restrict ourselves to the discrete-time case, but the discussion is equally valid for continuous-time.) In general, f admits infinitely many mutually singular invariant probability measures, and the ergodic theory of (f, μ) depends on the choice of μ. The purpose of this entry is to discuss what constitutes a "natural" invariant measure.

Throughout this discussion, we will adopt the view that only properties that hold on positive Lebesgue measure sets are observable. A first attempt to characterize natural invariant measures is to require that they have densities. Thus for a Hamiltonian system, Liouville measure is regarded as natural. This criterion runs into difficulties with dissipative systems. Suppose that f is volume-decreasing with an attractor $\Lambda = \cap_{n \geq 0} f^n(U)$. Since there is no recurrence behavior on $U \setminus \Lambda$, by the Poincaré recurrence theorem, all the invariant probability measures are supported on Λ. Observe that with f decreasing volume, Λ must necessarily have Lebesgue measure zero. Thus f cannot have an invariant density.

For dissipative dynamical systems, then, we must relax the idea of a natural invariant measure from one that has a density to one that reflects the properties of positive Lebesgue measure sets. We discuss below three closely related sets of ideas that go in this direction. In less rigorous discussions, the first two are often confused, even though as we will see, they are different substantively and mathematically.

SRB Measures

Sinai–Ruelle–Bowen measures or *SRB measures* were first introduced for Anosov systems and Axiom A attractors; see Sinai (1972), Bowen (1975), and Ruelle (1978). The idea was later extended to the non-uniform hyperbolic setting (*See* **Horseshoes and hyperbolicity in dynamical systems**), and the name SRB measure was introduced in the review article by Eckmann-Ruelle (1985).

The idea is as follows: SRB measures live on strange attractors. The situation being chaotic, there are positive Lyapunov exponents and unstable manifolds. In the same way that the next best scenario to having a differentiable function is to have partial derivatives, if the dissipative nature of a map prevents it from having an invariant measure that is smooth, then the closest approximation would be one that is smooth in certain directions. The expanding property of a map smoothes out invariant measures along unstable manifolds.

We now give the precise definition. Consider a C^2 invertible map f and an f-invariant Borel probability measure μ. We assume that f has positive Lyapunov exponents and hence unstable manifolds μ-almost everywhere. On each k-dimensional unstable leaf γ, let m_γ denote the k-dimensional Lebesgue measure. Then we say μ is an SRB measure if the conditional measures of μ on unstable leaves have densities with respect to the measures m_γ.

The geometric definition of SRB measures given above turns out to be equivalent to the following "variational principle": SRB measures are exactly those invariant measures for which the Kolmogorov–Sinai entropy of the system is equal to the sum of its positive Lyapunov exponents. (For other invariant measures, entropy is smaller.) If there are no zero Lyapunov exponents, there is a structure theorem that says that SRB measures have at most a countable number of ergodic components, and each ergodic component is mixing up to certain permutations (*See* **Horseshoes and hyperbolicity in dynamical systems**). Relations to other notions of natural invariant measures will be mentioned as we go along.

We explained earlier that SRB measures is a notion associated with strange attractors. This does not mean that every strange attractor necessarily has an SRB measure. In practice, one often assumes that it does, but mathematically, this question is far from resolved. In fact, not many attractors have been rigorously proved to have SRB measures. The main examples are Axiom A attractors and a class of attractors with one direction of instability including certain Hénon attractors (see Young, 2002).

Physical Measures

Let f be a map and μ an invariant probability measure. We say μ is a *physical measure* if there is a positive Lebesgue measure set V in the phase space such that for every continuous observable φ, we have

$$\frac{1}{n}\sum_{i=0}^{n-1}\varphi(f^i x) \;\to\; \int \varphi \, \mathrm{d}\mu$$

for every $x \in V$. Thus, physical measures are those invariant measures that can be *observed*: Suppose we pick an initial condition $x \in V$ and plot the first n points of its trajectory. The resulting picture can be seen as that of a measure giving weight $1/n$ to each one of the points $x, f(x), f^2(x), \cdots, f^{n-1}(x)$. For n large, it is a good approximation of μ.

One of the reasons—some would say the main reason—why SRB measures are important is that all ergodic SRB measures with no zero Lyapunov exponents are physical measures.

Not all physical measures are SRB measures, however. For examples, point masses on attractive fixed points are physical measures. Unlike SRB measures, which are associated with chaotic behavior and have rich, well-defined structures, physical measures have no identifiable characteristics aside from the fact that they are observable.

Zero-noise Limits

If one subscribes to the view that the world is inherently noisy, then the following notion proposed by Kolmogorov is perhaps the most relevant notion of observability. Let f be a map on a bounded domain, and let $P^\varepsilon(\cdot\,|\,\cdot)$, $\varepsilon > 0$ be a family of Markov chains representing random perturbations of f; that is, the transition probabilities $P^\varepsilon(\cdot\,|\,x)$ have the following interpretation: instead of jumping from x to $f(x)$, $P^\varepsilon(\cdot\,|\,x)$ gives the distribution of possible images starting from x. We may think of it as the uniform distribution on an ε-disk centered at $f(x)$ or a Gaussian with ε variance. Let μ_ε be the marginal of the stationary measure of the process defined by $P^\varepsilon(\cdot\,|\,\cdot)$, and let $\varepsilon \to 0$. Limit points of μ_ε are called *zero-noise limits*.

Unlike SRB measures or physical measures, the existence of which leads to unresolved questions, systems defined on compact regions always have zero-noise limits. It is hoped that in most situations, they coincide with the other notions of natural invariant measures. This has been proved for Axiom A attractors and a handful of other examples.

LAI-SANG YOUNG

See also **Cat map; Horseshoes and hyperbolicity in dynamical systems; Measures; Phase space**

Further Reading

Bowen, R. 1975. *Equilibrium States and the Ergodic Theory of Anosov Diffeomorphisms*, Berlin and New York: Springer

Eckmann, J.-P. & Ruelle, D. 1985. Ergodic theory of chaos and strange attractors. *Reviews of Modern Physics*, 57: 617–656

Ruelle, D. 1978. *Thermodynamic Formalism*, Reading, MA: Addison-Wesley

Sinai, Ya. G. 1972. Gibbs measures in ergodic theory. *Russian Mathematical Surveys*, 27: 21–69

Smale, S. 1967. Differentiable dynamical systems. *Bulletin of the American Mathematical Society*, 73: 747–817

Young, L.-S. 1993. Ergodic theory of differentiable dynamical systems. *Proceedings of the NATO Advanced Study Institute* held in Hillerød, June 20–July 2, 1993, edited by B. Branner & P. Hjorth, Dordrecht: Kluwer

Young, L.-S. 2002. What are SRB measures, and which dynamical systems have them? *Journal of Statistical Physics*, 108: 733–754

SINE-GORDON EQUATION

In normalized units, the classical sine-Gordon (SG) equation is the nonlinear partial differential equation

$$\frac{\partial^2\phi}{\partial x^2} - \frac{\partial^2\phi}{\partial t^2} = \sin\phi, \tag{1}$$

where $\phi(x,t)$ is a field in two dimensions—space and time. Since its introduction in 1939 by Yakov Frenkel and Tatiana Kontorova as a model for the dynamics of crystal dislocations (Frenkel & Kontorova, 1939), this equation has found a variety of applications, including Bloch wall dynamics in ferromagnetics and ferroelectrics, fluxon propagation in long Josephson (superconducting) junctions, self-induced transparency in nonlinear optics, spin waves in the A-phase of liquid ^{3}He at temperatures near to 2.6 mK, and a simple, one-dimensional model for elementary particles (Bullough, 1977; Scott, 2003). The name stems from the linear Klein–Gordon equation $\partial^2\phi/\partial x^2 - \partial^2\phi/\mathrm{d}t^2 = \phi$, where the "joke" may be due to Martin Kruskal or it may not (Bullough & Caudrey, 1980).

The SG equation can be physically modeled as a linear array of weakly coupled pendula, suggesting traveling-wave solutions of the form

$$\phi = 4\arctan\exp\left\{\pm(x - vt)/\sqrt{1-v^2}\right\} \tag{2}$$

with $v < 1$. These solutions are called a kink and an antikink, respectively, since at $x = -\infty$, $\phi \to 0$, and at $x = +\infty$, $\phi \to 2\pi$ for the $+$ sign, while at $x = -\infty, \phi \to 2\pi$ and at $x = +\infty$, $\phi \to 0$ for the $-$ sign. In the context of the physical model, ϕ twists from 0 to 2π for the kink and untwists from 2π to 0 for the antikink. Alternatively $\phi/2\pi$ has "topological charge" $+1$ for each kink and -1 for each antikink. Each of these is a one-soliton solution, but there are also N-soliton solutions for the boundary conditions $\phi \to 0 \pmod{2\pi}$ as $x \to \pm\infty$. (In "light-cone coordinates" (see below) the N-soliton solutions were given by Caudrey et al. (1973); see the detailed history in Bullough & Caudrey (1980)).

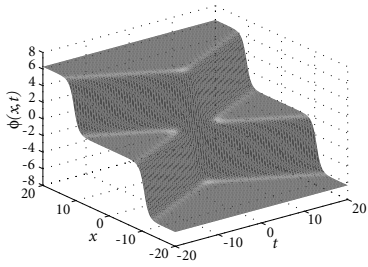

Figure 1. A kink-kink solution of the SG equation plotted from Equation (3) with $v = 0.5$.

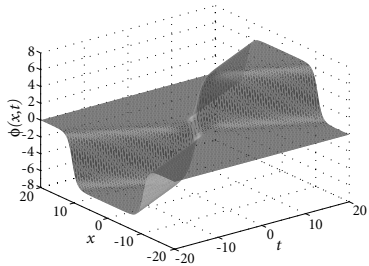

Figure 2. A kink-antikink solution of the SG equation plotted from Equation (4) with $v = 0.5$.

The simplest 2-soliton solution of SG Equation (1) is the kink-kink collision given by Perring & Skyrme (1962) as

$$\phi(x,t) = 4\arctan\left[\frac{v\sinh(x/\sqrt{1-v^2})}{\cosh(vt/\sqrt{1-v^2})}\right] \tag{3}$$

as shown in Figure 1 for $v = 0.5$. Similarly, Figure 2 shows a kink-antikink collision, which is plotted from

$$\phi(x,t) = 4\arctan\left[\frac{\sinh(vt/\sqrt{1-v^2})}{v\cosh(x/\sqrt{1-v^2})}\right] \tag{4}$$

also with $v = 0.5$.

The kink-antikink equation takes an interesting form if the velocity parameter (v) is allowed to be imaginary. For example, setting

$$v = \mathrm{i}\omega/\sqrt{1-\omega^2}\,, \quad \omega < 1,$$

Equation (4) becomes the stationary breather (or "bion")

$$\phi(x,t) = 4\arctan\left[\left(\frac{\sqrt{1-\omega^2}}{\omega}\right)\frac{\sin\omega t}{\cosh\sqrt{1-\omega^2}x}\right], \tag{5}$$

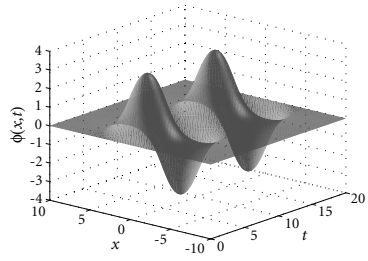

Figure 3. A stationary breather plotted from Equation (5) with $\omega = \pi / 5$.

a localized, oscillating solution that is plotted in Figure 3 for $\omega = \pi/5$. Because Equation (1) is invariant under the Lorentz transformation

$$x' = (x - vt)/\sqrt{1 - v^2}$$

and

$$t' = (t - xv)/\sqrt{1 - v^2}, \tag{6}$$

this stationary breather can be boosted into a moving frame. Thus,

$$\phi(x,t) = 4\arctan\left\{\frac{\sqrt{1-\omega^2}}{\omega}\sin\left[\frac{\omega(t - v_e x)}{\sqrt{1 - v_e^2}}\right] \times \operatorname{sech}\left[\frac{\sqrt{1-\omega^2}(x - v_e t)}{\sqrt{1 - v_e^2}}\right]\right\}$$

is an exact solution of the SG equation moving with an envelope velocity (v_e) that is equal to the reciprocal of its carrier velocity $v_c = 1 / v_e$.

Because $\phi(x,t)$ is defined for each value of x, the Hamiltonian description is infinite dimensional. A standard form of the Hamiltonian (or energy) is (Bullough & Timonen, 1995)

$$H = \int \left[\frac{1}{2}\Pi^2(x,t) + \frac{1}{2}(\partial\phi/\partial x)^2 + (1 - \cos\phi)\right] \mathrm{d}x. \tag{7}$$

Hamilton's equations then take the form

$$\frac{\delta H}{\delta \phi} = -\dot{\Pi} \quad \text{and} \quad \frac{\delta H}{\delta \Pi} = \dot{\phi}, \tag{8}$$

where the δs indicate functional (or Frechêt) derivatives. The second of Equations (8) yields $\dot{\phi} = \Pi$ and the first yields $-\ddot{\phi} = -\dot{\Pi} = -\phi_{xx} + \sin\phi$, which is the SG equation. Computing H in the rest frame, one finds rest masses equal to 8 for both kinks and antikinks, while for stationary breathers the rest masses are $16\sqrt{1-\omega^2}$. Evidently, a stationary breather is a bound pair of a kink and an antikink oscillating at frequency ω.

The SG equation is a completely integrable Hamiltonian system, which means that the number of independent constants of motion is equal to the number of degrees of freedom (Liouville's theorem). As the number of degrees of freedom is infinite (through the labels x), the theorem is not obvious, but an infinite number of commuting and independent constant action variables can be found. Equivalently, solutions of the SG equation can be obtained through a Bäcklund transformation (BT) or by using an inverse scattering method (ISM).

In BT and ISM studies, it is convenient to transform the independent variables as

$$x \to \xi = (x + t)/2 \quad \text{and} \quad t \to \tau = (x - t)/2,$$

whereupon Equation (1) becomes

$$\frac{\partial^2 \phi}{\partial \xi \, \partial \tau} = \sin\phi. \tag{9}$$

These new variables (ξ and τ) are sometimes called "light-cone" coordinates because they point in the directions of characteristics in the (x,t)-plane.

The SG equation first appeared in light-cone coordinates in the mathematical study of surfaces of constant negative Gaussian curvature by Albert Bäcklund (Lamb, 1976). In 1883, he discovered the first BT, which can be written as

$$\begin{aligned} \phi'_x &= \phi_x + 2k\sin(\phi + \phi')/2, \\ \phi'_t &= -\phi_t + 2k^{-1}\sin(\phi - \phi')/2 \end{aligned} \tag{10}$$

for any real value of the parameter k. The integrability condition $\phi'_{xt} = \phi'_{tx}$ implies both $\phi_{xt} = \sin\phi$ and $\phi'_{xt} = \sin\phi'$; thus, Equations (10) transform a known solution ϕ of the SG in light-cone coordinates to a second solution ϕ'. As $\phi = 0$ is a solution, the single-kink solution is found to be $\phi' = 4\arctan\exp(kx - k^{-1}t)$ for this real value of k.

Bullough (1980), for example, shows how the BT Equation (10) becomes the Lax pair for an ISM analysis first written down by Ablowitz et al. (1973) (AKNS). Independently, Takhtajan & Faddeev (1974) gave the corresponding expressions for the covariant SG Equation (1). AKNS's Lax pair is

$$\frac{\partial}{\partial \xi}\begin{bmatrix}\psi_1 \\ \psi_2\end{bmatrix} = \begin{bmatrix}-\mathrm{i}\lambda & -\phi_\xi/2 \\ \phi_\xi/2 & \mathrm{i}\lambda\end{bmatrix}\begin{bmatrix}\psi_1 \\ \psi_2\end{bmatrix},$$

where ψ_1 and ψ_2 are components of the scattering solution and λ is a complex scattering parameter together with the τ-dependence

$$\frac{\partial}{\partial \tau}\begin{bmatrix}\psi_1 \\ \psi_2\end{bmatrix} = \frac{\mathrm{i}}{4\lambda}\begin{bmatrix}\cos\phi & \sin\phi \\ \sin\phi & -\cos\phi\end{bmatrix}\begin{bmatrix}\psi_1 \\ \psi_2\end{bmatrix}. \tag{11}$$

It is readily checked that the cross-derivative condition

$$\frac{\partial}{\partial \tau}\frac{\partial}{\partial \xi}\begin{bmatrix}\psi_1 \\ \psi_2\end{bmatrix} = \frac{\partial}{\partial \xi}\frac{\partial}{\partial \tau}\begin{bmatrix}\psi_1 \\ \psi_2\end{bmatrix}$$

implies Equation (9), thus providing the basis for an ISM analysis.

Assuming that $\phi \to 0 \pmod{2\pi}$ as $\xi \to \pm\infty$, the time evolution matrix defined in Equation (11) takes the simple asymptotic form

$$\frac{\mathrm{i}}{4\lambda}\begin{bmatrix} 1 & 0 \\ 0 & -1 \end{bmatrix};$$

thus the reflection coefficient and the residues r_n of its upper-half-plane-poles (in the λ plane) evolve with time as

$$\begin{aligned} b(\lambda, \tau) &= b(\lambda, 0)\mathrm{e}^{-\mathrm{i}\tau/2\lambda}, \\ r_n(\tau) &= r_n(0)\mathrm{e}^{-\mathrm{i}\tau/2\lambda_n}, \end{aligned}$$

where $b(\lambda, \tau)$ is the reflection coefficient of the solution and n is an index that runs over the number (N) of soliton components.

The evolved solution of Equation (9) turns out to be

$$\frac{\partial\phi}{\partial\xi}(\xi, \tau) = 4K(\xi, \xi; \tau), \tag{12}$$

where $K(\xi, z; \tau)$ is a solution of the (Gel'fand–Levitan–Marchenko) integral equation

$$\begin{aligned} K(\xi, z; \tau) &= B^*(\xi + z; \tau) \\ &\quad - \int_\xi^\infty \int_\xi^\infty K(\xi, y; \tau) B(y + y'; \tau) \\ &\quad \times B^*(z + y'; \tau)\mathrm{d}y\,\mathrm{d}y' \end{aligned} \tag{13}$$

with $z > \xi$, and

$$\begin{aligned} B(\xi + z; \tau) &\equiv \frac{1}{2\pi}\int_{-\infty}^{\infty} b(\lambda, 0)\mathrm{e}^{\mathrm{i}\lambda(\xi+z)-\mathrm{i}\tau/2\lambda}\,\mathrm{d}\lambda \\ &\quad -\mathrm{i}\sum_{n=1}^{N} r_n(0)\mathrm{e}^{\mathrm{i}\lambda_n(\xi+z)-\mathrm{i}\tau/2\lambda_n} \end{aligned} \tag{14}$$

is determined from a scattering analysis of the initial conditions.

The simplest example of this ISM formulation is obtained by assuming that the initial potential is reflectionless ($b(\lambda, \tau) = 0$) and has but one bound state ($N = 1$), corresponding to a single pole at ($\lambda_1 = \mathrm{i}\kappa$) on the imaginary axis of the upper half λ-plane with residue $r_1 = \pm 2\mathrm{i}\kappa$. Thus, from Equation (14)

$$B(\xi + z; \tau) = \pm 2\kappa\mathrm{e}^{-\kappa(\xi+z)-\tau/2\kappa},$$

so Equation (13) takes the form

$$\begin{aligned} K(\xi, z; \tau) &= \pm\, 2\kappa\mathrm{e}^{-\kappa(\xi+z)-\tau/2\kappa} \\ &\quad - 4\kappa^2\mathrm{e}^{-\tau/\kappa}\int_\xi^\infty\int_\xi^\infty K(\xi, y; \tau)\mathrm{e}^{-\kappa(y+y')} \\ &\quad \times\mathrm{e}^{-\kappa(z+y')}\,\mathrm{d}y\,\mathrm{d}y'. \end{aligned}$$

As $K(\xi, z; \tau) \propto \exp(-\kappa z)$, this integral equation is solved for

$$K(\xi, z; \tau) = \pm\frac{2\kappa\exp[-\kappa(\xi + z) - \tau/2\kappa]}{1 + \exp(-4\kappa\xi - \tau/\kappa)}.$$

Thus, from Equation (12)

$$\begin{aligned} \frac{\partial\phi}{\partial\xi} &= \pm 4K(\xi, \xi; \tau) \\ &= \pm 4\kappa\,\mathrm{sech}(2\kappa\xi + \tau/2\kappa), \end{aligned}$$

which integrates to

$$\phi(\xi, \tau) = 4\arctan\{\exp[\pm(2\kappa\xi + \tau/2\kappa)]\}.$$

Finally, one can transform back to the laboratory (x, t) coordinates, whereupon the corresponding solution of Equation (1) is the kink or antikink of Equation (2) with its laboratory velocity identified as

$$v = \frac{1 - 4\kappa^2}{1 + 4\kappa^2} = \frac{1 + 4\lambda_1^2}{1 - 4\lambda_1^2}. \tag{15}$$

With an appropriate choice of the constants c_1 and c_2, the kink-antikink solution of Equation (4) can be generated in a similar manner from the assumption that

$$B(\xi + z; 0) = c_1\mathrm{e}^{-\kappa_1(\xi+z)} + c_2\mathrm{e}^{-\kappa_2(\xi+z)}, \tag{16}$$

where

$$\kappa_1 = \frac{1}{2}\sqrt{\frac{1+v}{1-v}} \quad \text{and} \quad \kappa_2 = \frac{1}{2}\sqrt{\frac{1-v}{1+v}}.$$

These integrable properties of the SG equation are shared by the sinh-Gordon equation and the Liouville equation for which the sine function in Equation (1) is replaced by a hyperbolic-sine function and by an exponential function, respectively—although the Liouville equation has no inverse scattering solution. Perhaps the most striking property of SG solitons, however, is their topological stability, which is evidenced by their nonzero rest masses. This property is carried into three space dimensions by the theory of skyrmions.

Equation (1) can be embedded in a more general framework of inverse-scattering methods, with the Hamiltonian expressed in terms of finite numbers of kinks, antikinks, and breathers, in addition to a continuous spectrum of radiation (Bullough, 1980). In the mid-1970s, Roger Dashen, Brosl Hasslacher, and Andre Neveu used semiclassical quantum methods to study this system, finding the mass (or energy) spectrum of the breather of Equation (5) to be

$$M_n = 16\sin\left(\frac{n}{16}\right),$$

where n is a positive integer less than 8π (Dashen et al., 1975). They correctly conjectured this "DHN spectrum" to be exact—a result of theoretical significance

because it shows that semiclassical analyses of nonlinear field theories can provide useful information about exact mass spectra.

The statistical mechanics of the SG equation is carried out in both the quantum and classical cases in Bullough & Timonen (1995), with a further appraisal of the action-angle variables in one space dimension. Bullough (1977) develops the theory of double and multiple SG equations (with $\sin\phi$ in Equation (1) replaced by $\pm[\sin\phi + (\sin\phi/2)/2]$, $\sin\phi + (\sin\phi/3)/3 + 2(\sin 2\phi/3)/3$, etc.) in connection with models for degenerate self-induced transparency of metal vapors and of spin waves of the B-phase of liquid ^{3}He near 2.6 mK.

ROBIN BULLOUGH

See also **Bäcklund transformations; Hamiltonian systems; Inverse scattering method or transform; Laboratory models of nonlinear waves; Long Josephson junctions; Maxwell–Bloch equations; Pendulum; Skyrmions**

Further Reading

Ablowitz, M.J., Kaup, D.J., Newell, A.C. & Segur, H. 1973. The initial value solution for the sine-Gordon equation. *Physical Review Letters*, 30: 1262–1264

Bullough, R.K. 1977. Solitons. In *Interaction of Radiation with Condensed Matter*, vol.1, Vienna: International Atomic Energy Agency; pp. 381–469

Bullough, R.K. 1980. Solitons: inverse scattering and its applications. Five lectures in the Proceedings of the NATO Advanced Study Institute *Bifurcation phenomena in mathematical physics and related phenomena Cargèse, Corsica, June 1977*, edited by D. Bessis and C. Bardos, Dordrecht: Reidel, pp. 295–349

Bullough, R.K. 2000. The optical solitons of QE1 are the BEC of QE14: has the quantum soliton arrived? Special Foundation Lecture: a personal view. 14th National Quantum Electronics and Photonics Conference, Owens Park, University of Manchester, 8 September 1999. *Journal of Modern Optics*, 47(11): 2029–2065 (Erratum. 2001. *Journal of Modern Optics*, 48(4): 747–748)

Bullough, R.K. & Caudrey, P.J. 1980. The soliton and its history. *Topics in Current Physics*, 17: 1–64

Bullough, R.K. & Timonen, J. 1981. Breather contributions to the dynamical form factors of the sine-Gordon systems $CsNiF_3$ and $(CH_3)_4(NiMnCl)_3$ (TMMC). *Physics Letters*, 82A(82): 182–186

Bullough, R.K. & Timonen, J.T. 1995. Quantum and classical integrable models and statistical mechanics. In *Statistical Mechanics and Field Theory*, edited by V.V. Bazhanov and C.J. Burden, Singapore: World Scientific, pp. 336–414 (Note the 'Solitons' map on pages 358–359)

Caudrey, P.J. 1989. In *Soliton Theory: A Survey of Results*, edited by A.P. Fordy, Manchester: Manchester University Press, and references therein

Caudrey, P.J., Gibbon, J.D., Eilbeck, J.C. & Bullough, R.K. 1973. Exact multi-soliton solutions of the self-induced transparency and sine-Gordon equations. *Physical Review Letters*, 30: 237–238

Dashen, R.F., Hasslacher, B. & Neveu, A. 1975. Semiclassical bound states in an asymptotically free theory. *Physical Review D*, 12: 2443–2458

Dodd, R.K. & Bullough, R.K. 1979. The generalised Marchenko equation and the canonical structure of the AKNS inverse method. *Physica Scripta*, 20: 514–530

Frenkel, J. & Kontorova, T. 1939. On the theory of plastic deformation and twinning. *Journal of Physics (USSR)* 1: 137–149

Lamb, G.L., Jr. 1976. Bäcklund transforms at the turn of the century. In *Bäcklund Transforms*, edited by R.M. Miura, New York: Springer

Perring, J.K. & Skyrme, T.R.H. 1962. A model unified field equation. *Nuclear Physics*, 31: 550–555

Scott, A.C. 2003. *Nonlinear Science: Emergence and Dynamics of Coherent Structures*, 2nd edition, Oxford and New York: Oxford University Press

Takhtajan, L.A. & Faddeev, L.D. 1974. Essentially nonlinear one-dimensional model of classical field theory. *Theoretical and Mathematical Physics*, 47: 1046–1057

SINGULAR PERTURBATION THEORY

See **Perturbation theory**

SINGULAR POINTS

See **Phase space**

SINGULARITY THEORY

Does the view from your window encompass a range of hills or mountains? If you are so blessed, you will see immediately both of the persistent singularities that can be observed generically; they are indicated on the mountains sketched in Figure 1, a section of a remote but important range called the Transversal Alps. The points marked "country" are known as fold singularities. Actually the outline of the mountains, which in reality is a mapping of a surface contour onto the retina of the eye, is composed of an infinite number of fold singularities. The two points marked "western" are known as cusp singularities. They occur where a line of folds along the edge of a mountain meets another line of folds along the gully between the mountains.

If the view from your office is more urban in character—of faces in the street, say—you will probably see many more of these two fundamental singularities. You must search a lot harder to find other types of singularities, or purposefully create one, because all other singularities dissolve under the slightest perturbation into either a fold or a cusp. This remarkable fact was first proved by Whitney (1955) whose fundamental discoveries about singularities of differentiable mappings were developed into catastrophe theory and toolkits for treating bifurcation problems with parameters, by mathematicians such as Mather (in a series of very technical papers from 1968 to 1971), Thom (1972), Martinet (1982), Arnol'd et al. (1985), and Golubitsky & Schaeffer (1985).

Singularity theory is not secret mathematicians' business though, and a more apt name for the whole business would be "theory and applications of

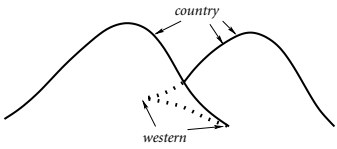

Figure 1. The Transversal Alps.

singularities." It is one of the more accessible entry points both to highly abstract areas of mathematics and to applied fields such as dynamical systems and bifurcations, because singularities can arise in almost any problem. The prerequisites are standard fare in first- and second-year mathematics courses: knowledge of Taylor's formula, the implicit function theorem, the theorem of existence and uniqueness, and some basic group theory, and willingness to learn some terminology.

Naturally, we should begin with a definition of singularity; (after Lu, 1976): Let f be a differentiable mapping from $\mathcal{M}$ to $\mathcal{N}$, where $\mathcal{M}$ and $\mathcal{N}$ are differentiable manifolds. A point $x_0 \in \mathcal{M}$ is a singular point of f if rank $\mathrm{d}f(x_0) < \min\{\dim \mathcal{M}, \dim \mathcal{N}\}$, where $\mathrm{d}f(x_0)$ is the Jacobian matrix of f at x_0. Otherwise x_0 is a regular point of f.

Singularity theory solves three key related problems: Given a mapping f, (i) it determines what types of singularities any good approximation $\bar{f}$ to f must have; (ii) it tells us how can we perturb f slightly to obtain a nicer and simpler, but in some sense equivalent, mapping; and (iii) it provides a taxonomy of singular objects and a binary key to identify them; hence, it is a *classification* science.

At the heart of singularity theory is a concept that is profound and yet somehow ingenuous; it is the concept of transversality. The naive (but not impercipient) version says that two curves intersect transversally if a small deformation of either one would not change the type of intersection. It is transversality that allows us to boil things down to classified normal forms.

Example 1: The mapping f from $\mathbb{R}^2$ into $\mathbb{R}^2$

$$u = x^2, \quad v = y \tag{1}$$

has a fold along $x = 0$ in the xy plane, the set of singular points is $\{(x, y) \in \mathbb{R}^2 \mid y = 2x\}$. Points along the fold remain fixed as y changes, that is, under perturbation. Equations (1) are called the *normal form* for a fold.

Example 2: The equations

$$u = xy - x^3, \quad v = y \tag{2}$$

define a mapping g from $\mathbb{R}^2$ into $\mathbb{R}^2$ for which the set of singular points is $\{(x, y) \in \mathbb{R}^2 \mid y = 3x^2\}$. The arms of the parabola are two lines of folds that come together and disappear at the cusp $(0, 0)$. Equations (2) are the normal form for the cusp, and Whitney proved that any

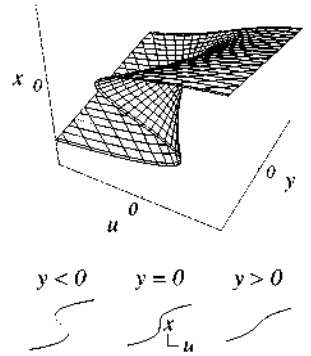

Figure 2. Slices through the cusp manifold (top) yield the three possible bifurcation diagrams (bottom).

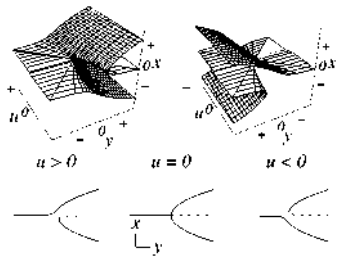

Figure 3. An orthogonal path through that cusp opens into a manifold around the pitchfork.

other mapping containing a regular point satisfying the conditions

$$u_x = u_y = v_x = 0, \quad v_y = 1, u_{xx} = 0,$$
$$u_{xy} \neq 0, u_{xxx} - 3u_{xy}v_{xx} \neq 0 \tag{3}$$

can be transformed by coordinate changes into the normal form (2). In catastrophe theory this normal form becomes the *universal unfolding* $G(x, y, u)$ of the germ $g(x) = x^3$:

$$G(x, y, u) \equiv x^3 - yx + u, \tag{4}$$

where G is the gradient of a governing potential V.

One may understand the cusp by studying the surface $G(x, y, u) = 0$ shown in Figure 2. By taking slices of this surface at constant y we recover the three qualitatively different bifurcation diagrams, as shown. Now visualize a *projection* of this surface onto the (u, y) plane. We find that the two lines of folds meet at a cusp singularity, the very same that we saw in the Transversal Alps in Figure 1.

An instructive and fascinating lesson on the properties and classification of simple singularities is

to parameterize the surface $G(x, y, u) = 0$ differently. In a study of singular surfaces by Ball (2001), it was observed that although the cusp is generic in the sense that all other singularities may be perturbed to either a fold or a cusp, the surface in Figure 2 is not a unique manifold of the cusp. Because all paths through the unfolding (4) are equally valid, we may choose a path in the (x, y) plane. Any such path unfurls laterally into the u-dimension to form a different surface. It is shown from two points of view in Figure 3. Constant-u slices show up the *pitchfork* singularity (center bifurcation diagram) and two of its perturbations. From this point of view Equation (4) is a *partial* unfolding of the pitchfork (but it is not a universal unfolding of the pitchfork).

In applications, the singularity theory approach has been most successful in qualitative studies of the equilibria of dynamical systems dependent on parameters. Given a dynamical system that can be reduced to a set of ordinary differential equations (by a procedure such as Lyapunov–Schmidt reduction), a general approach is to apply defining algebraic criteria systematically to the equilibria until one discovers the highest-order or most degenerate singularity, defined by its normal form. (The binary key given in Golubitsky & Schaeffer (1985, p. 201) is extremely useful for this task.) From a universal unfolding of this *organizing center*, one can "read off" all of the possible qualitatively different bifurcation behavior of the equilibria. A great many dynamical models of physical systems have been given the singularity theory treatment, often yielding results having important implications for the prediction and control of such systems. For a few but varied examples see Ball (1999) (chemical reactions), Ball et al. (2002) (plasma physics), and Broer et al. (2003) (periodic dynamics).

ROWENA BALL

See also **Bifurcations; Catastrophe theory; Development of singularities**

Further Reading

Arnol'd, V.I., Gusein-Zade, S.M. & Varchenko, A.N. 1985. *Singularities of Differentiable Maps*, vol. 1. Boston and Basel: Birkhäuser

Ball, R. 1999. The origins and limits of thermal steady state multiplicity in the continuous stirred tank reactor. *Proceedings of the Royal Society of London Series* A, 455: 141–161

Ball, R. 2001. Understanding critical behaviour through visualisation: a walk around the pitchfork. *Computer Physics Communications*, 142: 71–75

Ball, R., Dewar, R.L. & Sugama, H. 2002. Metamorphosis of plasma shear flow–turbulence dynamics through a transcritical bifurcation. *Physical Review* E, 66: 066408-1–066408-9

Broer, H.W., Golubitsky, M. & Vegter, G. 2003. The geometry of resonance tongues: a singularity theory approach. *Nonlinearity*, 16: 1511–1538

Golubitsky, M. & Schaeffer, D.G. 1985. *Singularities and Groups in Bifurcation Theory*, vol. 1, New York: Springer

Lu, Y.-C. 1976. *Singularity Theory and an Introduction to Catastrophe Theory*, Berlin and New York: Springer

Martinet, J. 1982. *Singularities of Smooth Functions and Maps*, Cambridge and New York: Cambridge University Press

Thom, R. 1972. *Stabilité Structurelle et Morphogénése: Essai d' une Théorie Générale des Modèles*, Reading, MA: W.A. Benjamin

Whitney, H. 1955. On singularities of mappings of Euclidean spaces. I. Mappings of the plane into the plane. *Annals of Mathematics*, 62: 374–410

SINK

See **Attractors**

S-INTEGRABILITY AND C-INTEGRABILITY

See **Integrability**

SKYRMIONS

As described by quantum field theories, elementary particles are associated with the quantization of small fluctuations around the vacuum and have masses that are proportional to Planck's constant, $\hbar$; thus, in the classical limit ($\hbar \to 0$), the mass goes to zero. The properties of a particle follow from the linearization of the field equations and any nonlinear terms are responsible for the interactions between particles, which are often treated perturbatively in the coupling constants. However, the 1960s saw the emergence of a new approach to quantum field theory in which the fully nonlinear classical field equations were investigated. It was found that for certain theories, the classical nonlinear field equations had static solutions that were particle-like, in the sense that they described stable, localized, finite energy field configurations. To describe elementary particles, the field theory must be Lorentz invariant, so such a static solution can simply be Lorentz boosted to describe a particle in uniform motion. These solutions, which are known as topological solitons (or sometimes just solitons for short, though they should not be confused with the solitons of integrable systems), have some novel features in comparison with elementary particles. Because they are classical solutions, then the mass of a soliton, which is identified with the energy of the static solution, is nonzero even in the limit $\hbar = 0$. Also, because the soliton is a solution of the full nonlinear field equation, it is automatically treated nonperturbatively in the coupling constants of the theory. Quantum corrections to the classical properties of a soliton can be addressed, mainly using semiclassical methods, but the important point is that these corrections are often small, so that the classical nonlinear equations largely determine the properties of a soliton. Despite the obvious differences between elementary particles and solitons, impressive research

during the last decade has revealed a great deal of evidence for a remarkable connection between these two kinds of particles, with solitons in some weakly coupled theories appearing to be dual to elementary particles in strongly coupled theories (Olive, 1996). These developments have led to a renewed interest in solitons in field theory, particularly in supersymmetric theories.

As the name suggests, topological solitons arise in theories where there is a topological classification of field configurations, with the soliton being in a different topological sector to the vacuum and, hence, preventing its decay, since time evolution cannot change the conserved topological charge. This is perhaps most easily explained using a simple example. As a toy model we shall consider the static sine-Gordon theory in one space dimension, although our presentation will be slightly unusual in order to make the extension to three spatial dimensions a little more transparent. Consider a two-component unit vector $\boldsymbol{\phi}(x) = (\phi_1, \phi_2)$, so that $\boldsymbol{\phi}$ lies on the circle $\boldsymbol{\phi} \cdot \boldsymbol{\phi} = 1$. If we restrict to static fields, then the sine-Gordon model can be defined by the energy expression

$$E = \int_{-\infty}^{\infty} \left(\frac{1}{2} \frac{\mathrm{d}\boldsymbol{\phi}}{\mathrm{d}x} \cdot \frac{\mathrm{d}\boldsymbol{\phi}}{\mathrm{d}x} + 1 - \phi_2 \right) \mathrm{d}x. \qquad (1)$$

For finite energy the boundary condition is clearly that the field must take the constant vacuum value $\boldsymbol{\phi} = (0, 1)$ at spatial infinity. The fact that the field $\boldsymbol{\phi}$ takes the same value at the two points at spatial infinity implies a compactification of space from $\mathbb{R}$ to S^1, arising from the identification of the points $x = -\infty$ and $x = +\infty$. Therefore, $\boldsymbol{\phi}$ is a map $\boldsymbol{\phi} : S^1 \mapsto S^1$, where the domain is compactified space and the target circle is the set of two-component unit vectors. Such maps have an associated degree, or winding number, N, due to the homotopy group relation $\pi_1(S^1) = \mathbb{Z}$. This integer-valued winding number is simply the number of times (counted with orientation) that the field winds around the target space circle as x ranges over the circle obtained from the compactification of space. The vacuum solution, with energy $E = 0$, is given by $\boldsymbol{\phi}(x) = (0, 1)$ and clearly has $N = 0$. The soliton is the minimal energy field configuration in the $N = 1$ sector and has the explicit expression

$$\boldsymbol{\phi} = (\sin\psi, \cos\psi) \quad \text{with} \quad \psi = 4\tan^{-1}\mathrm{e}^{x-a}, \qquad (2)$$

where a is an arbitrary real constant. The soliton has energy $E = 8$ and the energy density (the integrand in Equation (1)) is a localized lump centered around the point $x = a$, which is the position of the soliton. The full time-dependent sine-Gordon theory follows from the Lorentz invariant Lagrangian associated with the energy (1). The static soliton solution (2) can be Lorentz boosted to provide a moving soliton solution (with any speed less than the speed of light) of the full second-order time-dependent field equations. The antisoliton solution, with $N = -1$, is simply obtained from the soliton solution by making the replacement $(\phi_1, \phi_2) \mapsto (-\phi_1, \phi_2)$. There are no static multisoliton solutions, that is, with $N > 1$, but time-dependent multisoltion solutions can be found in closed form and describe the elastic scattering of several individual solitons (Drazin, 1983). This remarkable fact follows from the integrability property of the time-dependent sine-Gordon equation, a feature which is not shared by more realistic theories with topological solitons in three space dimensions.

The most important aspect of the sine-Gordon model on the line is the topological classification of finite energy field configurations, which follows from the homotopy group relation $\pi_1(S^1) = \mathbb{Z}$. This is the first property that needs to be generalized when searching for a three-dimensional theory with topological solitons. If we consider a theory for which finite energy implies that the field must be constant at spatial infinity, then Euclidean space $\mathbb{R}^3$ becomes compactified to the three-sphere S^3. This is the analogue of the compactification of the line to the circle described above, and hence, we see that the simplest way to obtain a model with topological solitons is to also make the target space S^3. Then the homotopy group relation $\pi_3(S^3) = \mathbb{Z}$ ensures that there is again an integer-valued topological charge, N, which divides finite energy field configurations into distinct topological sectors. To achieve the target space S^3, the field can be taken to be a four-component unit vector, although an equivalent formulation is to take the field to be an $SU(2)$-valued matrix, since S^3 is also the manifold of the group $SU(2)$. The Skyrme model (Skyrme, 1961) is such a theory and has the static energy

$$E = \int \left\{ \mathrm{Tr}(\partial_i U \partial_i U^{-1}) - \frac{1}{8}\mathrm{Tr}\left([(\partial_i U)U^{-1}, (\partial_j U)U^{-1}]^2 \right) \right\} \mathrm{d}^3x, \qquad (3)$$

where $U(\mathbf{x}) \in SU(2)$ is the field of the model and $\partial_i = \partial/\partial x_i$ with x_i $(i = 1, 2, 3)$ is the Cartesian coordinates in Euclidean space, and we have adopted the Einstein summation convention where repeated indices are summed over. Also, the square brackets denote the commutator, $[A, B] = AB - BA$. The first term in (3), called the sigma model energy by physicists and the harmonic map energy by mathematicians, is the higher-dimensional analog of the simple gradient energy given by the first term in (1) for the toy model. In order to provide a finite nonzero scale size for the soliton, the sigma model energy needs to be balanced against an additional term with an appropriate scaling behavior under spatial dilations, as required by the Derrick–Hobart theorem. In one spatial dimension, this requires a term which contains

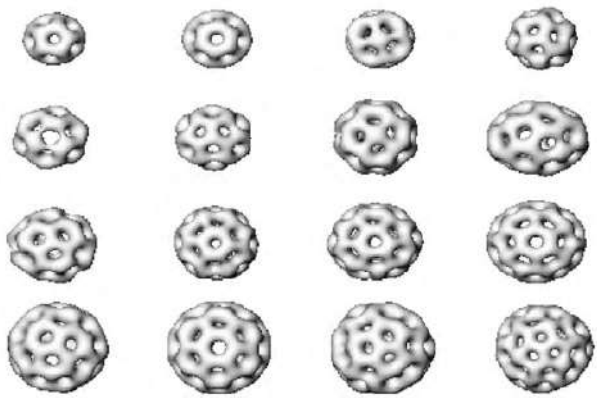

Figure 1. Skyrmions with N from 7 to 22.

no spatial derivatives of the field, such as the final term in (1), but in three spatial dimensions, the appropriate term must be at least fourth-order in the spatial derivatives. The final term in (3), known as the Skyrme term, is the unique order-four expression whose relativistic extension provides a Lagrangian in $(3+1)$-dimensions, which yields a nonlinear field equation that is only second order in time derivatives. The Skyrme model has a stable topological soliton, the solution with minimal energy in the $N=1$ sector, and this is known as a skyrmion. The solution is spherically symmetric but cannot be written in closed form and is only known numerically. Unlike the sine-Gordon toy model, the Skyrme model has static stable bound-state multi-solitons for all $N>0$. These multi-skyrmions are not spherically symmetric but often have surprising discrete symmetries, including the symmetries of the Platonic solids (Battye & Sutcliffe, 2002). Figure 1 displays skyrmions with $7 \leq N \leq 22$ by plotting surfaces around which the topological charge density is concentrated.

The Skyrme model was originally introduced (Skyrme, 1961) in the early 1960s as a model for the strong interactions of hadrons. It is a nonlinear theory of pions, with the pion particles being described in the usual quantum field theory approach by the quantization of the three degrees of freedom associated with the small fluctuations of the field around the vacuum, where U is the identity matrix, with $N=0$. Skyrme identified the conserved topological charge N with baryon number and, hence, within the nonlinear pion theory baryons appear for free as the classical soliton solutions. The Skyrme model was set aside after the advent of quantum chromodynamics (QCD), but much later it was revived by Witten (1983), who showed that it could arise from QCD as a low energy effective description in the limit in which the number of quark colors is large. Semiclassical quantization of the $N=1$ skyrmion reproduces the properties of the nucleon to within an accuracy of around 30% (Adkins et al., 1983), which is quite an achievement. There has been considerable recent progress in computing classical multi-skyrmion solutions, but it still remains to be seen whether their quantization provides a good description of nuclei.

Finally, it should be noted that in Yang–Mills–Higgs gauge theories the topological classification of field configurations arises in a slightly different way than described above for skyrmions and other modified sigma models. In gauged theories, the Higgs field is not required to be constant at infinity, and indeed, it is a nontrivial winding at infinity that provides the topological charge. In two spatial dimensions this yields vortices, and in three-dimensional space it leads to magnetic monopoles. When the Higgs field is massless, which is the situation that arises in interesting supersymmetric theories with monopoles, then the classical field equations have a particularly rich mathematical structure, and many exact results on monopole solutions are known (for a review see, e.g., Sutcliffe, 1997).

PAUL SUTCLIFFE

See also **Derrick–Hobart theorem; Quantum field theory; Sine-Gordon equation; Solitons, types of; Yang–Mills theory**

Further Reading

Adkins, G.S., Nappi, C.R. & Witten, E. 1983. Static properties of nucleons in the Skyrme model. *Nuclear Physics* B, 228: 552–566

Battye, R.A. & Sutcliffe, P.M. 2002. Skyrmions, fullerenes and rational maps. *Reviews in Mathematical Physics*, 14: 29–85
Drazin, P.G. 1983. *Solitons*, Cambridge and New York: Cambridge University Press
Olive, D.I. 1996. Exact electromagnetic duality. *Nuclear Physics Proceedings Supplement* 45A: 88–102
Skyrme, T.H.R. 1961. A nonlinear field theory. *Proceedings of the Royal Society* A, 260: 127–138
Sutcliffe, P.M. 1997. BPS monopoles. *International Journal of Modern Physics* A, 12: 4663–4705
Witten, E. 1983. Current-algebra, baryons, and quark confinement. *Nuclear Physics* B, 223: 433–444

SLAVING PRINCIPLE

See **Synergetics**

SMALE HORSESHOE

See **Horseshoes and hyperbolicity**

SNOWFLAKES

See **Pattern formation**

SOLAR SYSTEM

The solar system shows a multitude of periodic phenomena: from the daily rotations of the Earth, to the monthly phases of the Moon, the seasonal changes during the course of a year, the phases of Venus and other planets, the regular recurrences of comets such as Halley's (every 76 years), the 25,700 year precession of the Earth's rotation axis, all the way up to changes in the parameters of the Earth's orbit, with periods of 40,000 years and more. Closer inspection reveals small modulations on top of these periods, but it is tempting to describe these by additional periods, as in the Ptolemaic theory of cycles, epicycles, and equants. However, the dynamics of the planets is governed by gravitational forces that vary as the inverse square of the distance and, hence, are strongly nonlinear. The question arises whether this nonlinearity results in some chaos.

Johannes Kepler concluded in the early 17th century that an isolated planet would move along a Kepler ellipse (such that a line joining the planet to the Sun sweeps out equal areas in equal times). For several planets their mutual perturbations leads to perihelion precessions and other variations of orbital parameters. Taking such perturbations into account was a major issue in solar mechanics in the following centuries and led to remarkable achievements. For instance, observations of the orbit of Uranus (discovered in 1781 by William Herschel) revealed significant differences to the orbit calculated in the presence of the known planets. When interpreted as due to the influence of another planet, the position of the missing planet could be predicted, and soon thereafter the efforts of Urbain V. LeVerrier, James C. Adams, and Johannes G. Galle were rewarded with the discovery of Neptune in 1846.

These results were obtained using perturbation theory. But does it actually converge? Advances in analytical mechanics in the 19th century suggested that an answer could be found and Gösta Mittag-Leffler included the issue of the stability of the solar system among the list of problems for a prize to be awarded in 1889 by King Oskar II of Sweden and Norway. Henri Poincaré was awarded the prize for his announcement that he could prove convergence, but in the course of revising his paper he noticed that there was a gap in the proof which he could not patch up. Instead, he discovered the intricate motions near a weakly perturbed hyperbolic fixed point, the so-called hyperbolic tangle, which effectively prevents quantitative continuation of trajectories that pass near a hyperbolic fixed point. Barrow-Green (1996) and Diacu & Holmes (1996) give vivid accounts of the events surrounding the prize.

A practical answer to the question of the stability of the solar system emerged in the late 20th century with the advent of powerful computers that allow integration of the equations of motions for several million years. It was then discovered that the inner planets are most susceptible to chaos, and that the Lyapunov time (inverse of the Lyapunov exponent) is about 5 million years. To illustrate the consequences of that, we quote from Laskar (1995):

> A 15 m uncertainty in the position of the Earth will grow to about 150 m in a time of 10 million years. But it will increase to 150 million km or the mean distance of Earth from the Sun within 100 million years.

As a consequence, we have difficulty predicting the Earth's orbit for times much larger than a few tens of millions of years. The consequences such an uncertainty can have are illustrated by numerical simulations for Mercury: by suitably selecting continuations, it is argued in Laskar (1995) that over a time of about 10^9 years the orbit of Mercury could change so that the planet collides with Venus and/or escapes from the solar system. It should be noted that this trajectory was especially tailored in order to show that escape is possible in principle; it does not give a clue as to how likely such an event may be.

The issue of the orbital parameters of the Earth is interesting because variations in the major rotation axis and the distance to the Sun influence our climate. In 1920, Milutin Milankovich calculated insolation data (incident solar radiation) for the Earth for long-term variations in the Earth's orbit and suggested some relationship to the appearance of past ice ages. The uncertainty in orbital parameters over periods of more than 40 million years thus indicate that reconstructing paleoclimates will be problematic (Laskar, 1999).

Besides planets there are many other objects in the solar system. Direct evidence for a chaotic trajectory has been found, for example, for the tumbling motion of Phobos and Deimos (moons of Mars) and for Saturn's moon Hyperion (Wisdom, 1987). Similarly, efforts to retrace the trajectory of Halley's comet back to its earliest recorded sighting in 163 BC gave wildly diverging results. As explained by Chirikov and Vecheslavov (1989), the orbit of Halley is chaotic with an inverse Lyapunov time of about 29 returns, so that the earliest observation is just beyond predictability. The distribution of asteroids between Mars and Jupiter shows conspicuous gaps (named after the astronomer Daniel Kirkwood) near orbits with rotation periods rationally related to the 11.9 year period of Jupiter. Such resonant interactions have strong effects on the orbits and can easily lead to collisions and escape from the resonance (Laskar, 1995; Wisdom, 1987).

The relation between the Moon, the Earth, and the Sun also holds surprises. The history of the problem, and the contributions of Babylonian, Greek, and modern astronomers to the observations and mathematical tools, is reviewed in Gutzwiller (1998). Gutzwiller also gives a quantitative example for the significance of small denominators: in order to calculate the distance between the Earth and Moon with the accuracy of 10^{-10} achievable within the Lunar Laser Ranging project, amplitudes as small as 10^{-17} have to be kept because of a significant resonance. While this does not result in positive Lyapunov exponents, it is a precursor to it, a mild form of chaos, as Gutzwiller calls it.

More surprisingly, the presence of the Moon is very important for the stability of the rotation axis of Earth: with the Moon the obliquity stays within about $\pm 1.3°$ of $23.3°$. Without it, the obliquity ends up in a resonance and can become as large as $60°$ to $90°$, with catastrophic consequences for our climate and the evolution of life (Laskar et al., 1993).

Finally, it is worthwhile to point out that the presence of hyperbolic orbits in the solar system was used in connection with the satellite GENESIS (launched in August 2001) to bring it along a stable orbit close to a Lagrange point, where it will remain for a few years to collect particles in the solar wind, before being brought back to Earth along an unstable manifold (Koon et al., 2000). Exploiting trajectories that exist in the dynamical system allows the mission to be completed with minimal requirements on fuel. This mission may thus also be considered an example of chaos control, where similar ideas are being investigated.

BRUNO ECKHARDT

See also **Celestial mechanics; Controlling chaos; Hénon–Heiles system; *N*-body problem**

Further Reading

Barrow-Green, J. 1996. *Poincaré and the Three-body Problem*, Providence, RI: American Mathematical Society

Chirikov, B.V. & Vecheslavov, V.V. 1989. Chaotic dynamics of comet Halley. *Astronomy and Astrophysics*, 221: 146–154

Diacu, F. & Holmes, P. 1996. *Celestial Encounters*, Princeton, NJ: Princeton University Press

Gutzwiller, M.C. 1998. Moon–Earth–Sun: the oldest three-body problem. *Reviews of Modern Physics*, 70: 589–639

Koon, W.S., Lo, M.W., Marsden, J.E. & Ross, S.D. 2000. Heteroclinic connections between periodic orbits and resonance transitions in celestial mechanics. *Chaos*, 10: 427–469

Laskar, J. 1995. Large scale chaos and marginal stability in the solar system. In *Constructive Methods and Results*, Proceedings of the XIth ICMP Conference, edited by D. Iagolnitzer, Boston: International Press, pp. 75–120

Laskar, J. 1999. The limits of Earth orbital calculations for geolocical time-scale use. *Philosophical Transactions Royal Society of London*, Series A, 357: 1735–1759

Laskar, J., Joutel, F. & Robutel, P. 1993. Stabilization of the Earth's obliquity by the moon. *Nature*, 361: 615–617

Wisdom, J. 1987. Chaotic motion in the solar system. *Icarus*, 72: 241–275

SOLIDIFICATION PATTERNS

See **Growth patterns**

SOLITON WAVE PACKET

See **Quantum nonlinearity**

SOLITONS

A *soliton* is a localized nonlinear wave that maintains its shape and speed as it travels, even through interaction with other waves. Another name for a localized traveling wave is a *solitary wave*. The term *soliton* was coined (by Zabusky & Kruskal, 1965) to reflect both the solitary-wave-like character and the particle-like interaction properties. Their surprising discovery has had an enormous impact on the field of nonlinear mathematics and science.

In many physical applications, however, the use of the word *soliton* has come to rely on observation of long-lived solitary waves, with little emphasis placed on interaction properties. Jupiter's Great Red Spot is often described as a soliton due to its long-lived identity (observed over hundreds of years) and the fact that it appears to maintain its identity through interaction with other disturbances. However, recent studies indicate that such Jovian vortices do not keep their identity through intrazonal interactions. In nonlinear optics, the deduction of stable, long-lived solitary waves is of great physical interest for their application as coherent light signals propagating through optical fibers, while their interaction properties are secondary. The definition of the word *soliton* in some dictionaries has come to reflect such usage by physicists, omitting the requirement of interaction. However, for mathematicians, the many surprising and miraculous discoveries of soliton theory are tied

fundamentally to the special interaction properties so its definition always contains elastic interaction as an essential requirement.

The preservation of identity through interaction would not be surprising if we were describing solutions of linear nondispersive wave equations. A simple example is the linear wave equation $u_{tt} + c^2 u_{xx} = 0$, where c is a constant (assumed positive). The general solution is given by $u(x,t) = f(x - c\,t) + g(x + c\,t)$, where f and g are determined by initial conditions. The first part, $f(x - c\,t)$, is a wave traveling to the right with speed c, while the second part, $g(x + c\,t)$, is a wave traveling to the left with speed c. Two such wave profiles interact when they meet head-on but they both come out of the interaction with the same shape and speed.

However, until the discovery of solitons, it was generally believed that no such property could hold for nonlinear equations. Common understanding in mathematics and physics in the 1950s suggested that nonlinear wave solutions either break, dissipate, or thermalize, that is, distribute initial energy between different solutions over time, and, therefore, lose their identities with time. Much of this understanding was based on prototypical examples, such as the inviscid Burgers equation

$$\frac{\partial u}{\partial t} + u\frac{\partial u}{\partial x} = 0, \tag{1}$$

which describes the one-dimensional propagation of compression waves in gas or dust or automoblie traffic. For the initial condition $u(x,0) = u_0(x)$, the solution is a wave, given implicitly by $u(x,t) = u_0\big(x - t\,u(x,t)\big)$. If the initial wave profile $u_0(x)$ has a part with negative slope, the wave front steepens and eventually breaks in finite time, just like ocean waves do at a beach. (The break up time is easy to find by differentiating the solution with respect to x.)

In 1965, Zabusky and Kruskal published numerical studies of the solutions of the Korteweg–de Vries (KdV) equation

$$\frac{\partial u}{\partial t} + u\frac{\partial u}{\partial x} + \delta^2\frac{\partial^3 u}{\partial x^3} = 0, \tag{2}$$

which changed the above-described common beliefs about nonlinear waves forever (*See* **Solitons, a brief history**). If $\delta \to 0$, the limiting equation is the inviscid Burgers equation. Zabusky and Kruskal labeled Equation (2) as (1), chose $\delta = 0.022$ and the initial condition $u(x,0) = \cos(\pi x)$ and studied its periodic solutions numerically. The word *soliton* was used for the first time in their paper of 1965, in the following extract.

> (I) Initially, the first two terms of Eq. (1) dominate and the classical overtaking phenomenon occurs; that is, u steepens in regions where it has negative slope. (II) Second, after u has steepened sufficiently, the third term becomes important and serves to prevent the formation of a discontinuity. Instead, oscillations of small wavelength (of order δ) develop on the left of the front. The amplitudes of the oscillations grow, and finally *each* oscillation achieves an almost steady amplitude (that increases linearly from left to right) and has the shape of an individual solitary-wave of (1). (III) Finally, each "solitary wave pulse" or *soliton* begins to move uniformly at a rate (relative to the background value of u from which the pulse rises) that is linearly proportional to its amplitude. Thus, the solitons spread apart. Because of the periodicity, two or more solitons eventually overlap spatially and interact nonlinearly. Shortly after the interaction they reappear virtually unaffected in size or shape. In other words, solitons "pass through" one another without losing their identity.

A standard form of the KdV equation is

$$\frac{\partial u}{\partial t} + 6\,u\frac{\partial u}{\partial x} + \frac{\partial^3 u}{\partial x^3} = 0. \tag{3}$$

This is equivalent to Equation (2) under a scaling transformation; that is, $u(x,t) \mapsto 6\delta^{2/3}\,u\big(x\,\delta^{-2/3},\ t\big)$ maps any solution of (2) to one of (3). If we consider the initial value problem for the KdV equation on the whole real x-line and look for solutions that vanish at infinity, then solitons are characterized by the initial condition

$$u(x,0) = N(N+1)\,k^2\,\mathrm{sech}^2\big(k\,x\big), \tag{4}$$

where N is any nonnegative integer. The corresponding solutions are called N-soliton or multisoliton solutions. The case $N = 1$ gives the traveling wave solution

$$u(x,t) = 2\,k^2\,\mathrm{sech}^2\big(k\,(x - 4\,k^2\,t)\big), \tag{5}$$

often called the one-soliton solution of the KdV equation. It is equivalent to the solitary wave observed by John Scott Russell in 1834 and deduced mathematically by Diederik Korteweg and Hendrik de Vries in 1895 (*See* **Solitons, a brief history**).

When $N \geq 2$ and time t is considered to be large negative (a long time into the past) or large positive (a long time into the future), the solution separates into a chain of N distinct, localized one-soliton solutions each having the form (5) for some value of k. The chain is positioned far to the left if t is negative or far to the right if t is positive. Each wave in the chain has a distinct height related to its speed. If their phases are arranged so that a taller soliton is to the left of a shorter one at some time in the past, then the taller one overtakes the shorter one, and reappears to the right with its distinctive height, shape, and speed unchanged. The only explicit sign that interaction has occurred is a phase shift, visible asymptotically as x and t become large, in each soliton. As in the one-soliton case, explicit formulae can be found for the N-soliton solution for all x and t. Moreover, the phase shifts due to pairwise interactions can be calculated exactly (*See* ***N*-soliton formulas**).

The soliton solutions of the KdV equation can be obtained explicitly by using the inverse scattering method. This method associates each solution $u(x,t)$ of Equation (3), that vanishes (faster than $1/x$) as $x \to \pm\infty$, to the stationary Schrödinger equation

$$\psi_{xx} + \big(u(x,t) + \lambda\big)\psi = 0, \tag{6}$$

where $u(x,\cdot)$ plays the role of the potential function and λ is a parameter. If we let $\lambda = \zeta^2$, we can characterize the space of solutions $\psi(x;\zeta)$ near infinity (in x) in terms of linear combinations of $\exp(\pm \mathrm{i}\,\zeta\,x)$. (Since u vanishes there, the equation becomes simply $\psi_{xx} - \zeta^2\,\psi = 0$, which has such exponentials as solutions.) Quantum mechanical convention regards the solution with behavior $\exp(\mathrm{i}\,\zeta\,x)$ at $x = +\infty$ as an *incoming wave* from $+\infty$. Part of this incoming wave reflects off the potential barrier u while part of it is transmitted through to the other side. Not all boundary conditions at infinity can be satisfied without imposing conditions on ζ. A discrete set of eigenvalues $\{\zeta_i\}$ arises when we demand that the solutions vanish at infinity. The corresponding solutions are called bound states and their amplitudes are usually normalized. The collected information about discrete eigenvalues, the normalization constants, the reflection coefficient, and the transmission coefficient is called the set of spectral or scattering data. A beautiful and fundamental result of soliton theory is that the time evolution of the spectral data can be obtained explicitly as the potential evolves according to the KdV equation. Another fundamental result is that such evolved spectral data can be inverted to give the solution $u(x,t)$ of the KdV equation at a later time.

If all waves ψ are transmitted, with none being reflected, the potential u is called a *reflectionless* potential. It is an amazing fact that the N-soliton solutions of the KdV equation are precisely the reflectionless potentials of Equation (6).

Another way to find the N-soliton solutions of the KdV is through its Bäcklund transform (*See* **Bäcklund transformations**) or equivalently the Darboux transform of the Schrödinger equation (6). The latter was introduced by Gaston Darboux in 1882, and expanded in his four-volume lecture notes on the geometry of surfaces (Darboux, 1915). The Darboux transform relates the potentials of two copies of the Schrödinger equation whose solutions are related linearly. His method shows how to change a potential so that a new discrete eigenvalue is added to those of the old potential (*See* **Darboux transformation**).

Many other nonlinear PDEs are now known to have soliton solutions. Solitons come in different shapes and many flavors (*See* **Solitons, types of**). The sine-Gordon equation

$$\frac{\partial^2 u}{\partial x^2} - \frac{\partial^2 u}{\partial t^2} = \sin u \tag{7}$$

has N-soliton solutions that asymptote to constants as $x \to \pm\infty$. One-soliton solutions can be one of two types, called a "kink" or an "anti-kink," according to whether it decays to zero to the left or the right, respectively. The explicit expression for such solutions is

$$u(x,t) = 4\arctan\left(\exp\left(\pm\frac{x - \eta\,t - x_0}{\sqrt{1-\eta^2}}\right)\right). \tag{8}$$

The "+" choice gives a kink and the "−" choice an antikink. Multisoliton solutions decompose into a sequence of kinks and antikinks as x and t approach $\pm\infty$.

There is another type of soliton admitted by the SG equation, which appears to make it unique within the class of nonlinear Klein–Gordon equations: $u_{xx} - u_{tt} = F(u)$. This is the "breather" solution:

$$u(x,t) = 4\arctan\left(\frac{\sqrt{1-\omega^2}}{\omega}\,\frac{\sin(\omega\,t)}{\cosh(\sqrt{1-\omega^2}\,(x - x_0))}\right). \tag{9}$$

This solution oscillates (or "breathes") while staying in the same location as time evolves. However, because SG is invariant under the Lorentz transform: $(x,t) \mapsto (X,T)$, $X = (x - c\,t)/\sqrt{1-c^2}$, $T = (t - c\,x)/\sqrt{1-c^2}$, where c is constant, the breather can be transformed to one that moves with speed $|c| < 1$. The existence of such spatially localized, temporally periodic solutions is rare for nonlinear wave equations.

The nonlinear Schrödinger (NLS) equation

$$\mathrm{i}\,\frac{\partial u}{\partial t} + \frac{\partial^2 u}{\partial x^2} + 2\,|u|^2 u = 0 \tag{10}$$

provides a third example of a nonlinear PDE with N-soliton solutions. Its one-soliton solution is given by

$$u(x,t) = a\,\exp\big(\mathrm{i}\,\eta x + (a^2 - \eta^2)t\big) \times \operatorname{sech}\Big(a\,(x - 2\eta\,t - x_0)\Big). \tag{11}$$

Solitons are not confined to partial differential equations. A differential-difference equation such as the Toda equation

$$\frac{\partial^2 u_n}{\partial t^2} = \exp\,(-(u_n - u_{n-1})) - \exp\,(-(u_{n+1} - u_n)), \tag{12}$$

also has N-soliton solutions for arbitrary positive integers N. See Ablowitz & Segur (1981) for inverse scattering theory extended to such discrete evolution equations.

There also exist nonlinear PDEs that have solutions that can be interpreted as 2-soliton solutions, but which

do *not* have N-soliton solutions for integer $N > 2$. Hirota pointed this out after inventing a method of calculating solitons explicitly and directly without using the inverse scattering method or Bäcklund transformations. (For details, *see* Ablowitz & Segur (1981) and **Hirota's method**.) An example is the two-dimensional version of the SG equation

$$\frac{\partial^2 u}{\partial x^2} + \frac{\partial^2 u}{\partial y^2} - \frac{\partial^2 u}{\partial t^2} = \sin u\,. \tag{13}$$

Hirota's method shows that there is a traveling wave solution that can be interpreted as a two-soliton. However, no N-soliton solution with higher N appears to exist.

There are many more equations with solitary waves than those with N-soliton solutions. Traveling waves may also be known to exist without having an exact expression. An example is provided by the reduced model of nerve transmission given by the Fitzhugh–Nagumo equation (*See* **FitzHugh–Nagumo equation**).

It can be shown that (for a certain range of parameter values) this equation admits traveling waves that are solitary waves. However, energy is not conserved for nerve impulses while it is for solitons.

Despite their rarity in the class of differential equations, soliton equations arise ubiquitously as models of nature. The KdV equation arises as a canonical model of water waves, under certain constraints. Consider the motion of surface waves in a fluid that is inviscid and nondispersive to leading order. Assume that the height of the waves is small compared with the depth of fluid, which in turn is much smaller than the length scale in one direction (x, say) and, moreover, that these two small ratios of scales balance. Then the resulting model is always given by the KdV equation (or its relations, such as the modified KdV equation). See Ablowitz & Segur (1981) for a detailed derivation. The soliton solutions, in the case when dimensionless surface tension is less than $\frac{1}{3}$, are the waves that travel on and raise the free surface. The general solutions are composed of N-solitons and a part called *radiation* that decays in amplitude as it moves away to infinity. When the water waves are nearly two-dimensional, the model equation becomes the Kadomtsev–Petviashvili equation

$$\frac{\partial}{\partial x}\left(\frac{\partial u}{\partial t} + 6\,u\frac{\partial u}{\partial x} + \frac{\partial^3 u}{\partial x^3}\right) + \frac{\partial^2 u}{\partial y^2} = 0\,, \tag{14}$$

which also possesses N-soliton solutions. Since such models always arise in an asymptotic sense (e.g., the balance of small wave height to depth of fluid), stability of solutions under perturbation is important. Solitons are stable under perturbations.

Stratified fluids are another context in which the KdV equation arises as a universal model. Consider a situation where a lower, heavier fluid rests on an impermeable solid with a lighter fluid on top that has a free surface above. A common example is the stratified ocean where colder, denser water lies underneath a warmer, lighter layer. If the sea is contained by a boundary that restricts the colder layer but there are forces present, such as tides, that force the lighter layer, interface waves appear between the two layers. Such waves are also governed by the KdV equation under appropriate assumptions. The soliton solutions are then interface waves that thicken the upper layer. The KdV and its solitons also arise in collision-free hydromagnetic waves, ion-acoustic waves, plasma physics, and lattice dynamics.

Like the KdV equation, the SG and NLS equations also arise as universal models in certain contexts. Some of the applications of the SG equation include the study of propagation of crystal defects, that of domain walls in ferromagnetic and ferroelectric materials, as a one-dimensional model for elementary particles, self-induced transparency of short optical pulses, and propagation of quantum units of magnetic flux on long Josephson (superconducting) transmission lines. See Scott (2003) for detailed descriptions. The NLS equation appears as a model of the propagation of packets of hydrodynamic waves on deep water, nonlinear pulses of light in an optical fibre, two-dimensional self-focusing of a plane wave, one-dimensional self-modulation of a monochromatic wave, propagation of a heat pulse in a solid, and Langmuir waves in plasmas.

NALINI JOSHI

See also **Bäcklund transformations; Inverse scattering method or transform; Solitons, types of; Zero-dispersion limit**

Further Reading

Ablowitz, M. & Segur, H. 1981. *Solitons and the Inverse Scattering Transform*, Philadelphia: SIAM

Darboux, G. 1915. *Leĉons sur la théorie générale des surfaces et les applications géometriques du calcul infinitésimal*, vol. 2, 2nd edition, Paris: Gauthier-Villars

Scott, A. 2003. *Nonlinear Science: Emergence and Dynamics of Coherent Structures*, 2nd edition, Oxford and New York: Oxford University Press

Zabusky, N.J. & Kruskal, M.D. 1965. Interactions of solitons in a collisionless plasma and the recurrence of initial states. *Physical Review Letters*, 15: 240–243

SOLITONS, A BRIEF HISTORY

In 1834, a young engineer named John Scott Russell was conducting experiments on the Union Canal (near Edinburgh, Scotland) to measure the relationship between the speed of a canal boat and its propelling force, with the aim of finding design parameters for conversion from horse power to steam. One August day, a rope parted in his apparatus and (Russell, 1844)

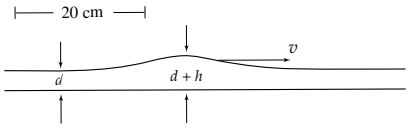

Figure 1. A hydrodynamic solitary wave (or soliton) in a tank similar to that described by John Scott Russell (1844). The wave is generated by suddenly releasing (or displacing) a mass of water at the left-hand side of the tank.

> the boat suddenly stopped—not so the mass of water in the channel which it had put in motion; it accumulated round the prow of the vessel in a state of violent agitation, then suddenly leaving it behind, rolled forward with great velocity, assuming the form of a large solitary elevation, a rounded, smooth and well-defined heap of water, which continued its course along the channel without change of form or diminution of speed.

Russell did not ignore this serendipitous phenomenon, but "followed it on horseback, and overtook it still rolling on at a rate of some eight or nine miles an hour, preserving its original figure some thirty feet long and a foot to a foot and a half in height" until the wave became lost in the windings of the channel. He continued to study the solitary wave in tanks and canals over the following decade, finding it to be an independent dynamic entity moving with constant shape and speed.

Using a wave tank, he demonstrated four facts Russell (1844). First, solitary waves have a hyperbolic secant shape. Second, a sufficiently large initial mass of water produces two or more independent solitary waves. Third, solitary waves cross each other "without change of any kind." Finally, a wave of height h and traveling in a channel of depth d has a velocity given by the expression $\sqrt{g(d+h)}$ (where g is the acceleration of gravity), implying that a large amplitude solitary wave travels faster than one of low amplitude.

Although soon confirmed by observations on the Canal de Bourgogne near Dijon, most subsequent discussions of the hydrodynamic solitary wave missed the physical significance of Russell's observations. Evidence that Russell maintained a deeper appreciation of the importance of his discovery is provided by a posthumous work where—among several provocative ideas—he correctly estimated the height of the Earth's atmosphere from the fact (well known to military engineers of the time) that "the sound of a cannon travels faster than the command to fire it" (Russell, 1885).

In 1895, Diederik Korteweg and Hendrik de Vries published a theory of shallow water waves that reduced Russell's problem to its essential features. One of their results was the nonlinear partial differential equation (PDE)

$$\frac{\partial u}{\partial t} + c\frac{\partial u}{\partial x} + \varepsilon\frac{\partial^3 u}{\partial x^3} + \gamma u\frac{\partial u}{\partial x} = 0, \tag{1}$$

which would play a key role in soliton theory (Korteweg & de Vries, 1895). In this equation, $u(x,t)$ is the wave amplitude, $c = \sqrt{gd}$ is the speed of small amplitude waves, $\varepsilon \equiv c(d^2/6 - T/2\rho g)$ is a dispersive parameter, $\gamma \equiv 3c/2d$ is a nonlinear parameter, and T and ρ are, respectively, the surface tension and the density of water. In general, Equation (1) is nonlinear with exact traveling-wave solutions

$$u(x,t) = h\,\mathrm{sech}^2[k(x - vt)], \tag{2}$$

where $k \propto \sqrt{h}$ implying that higher amplitude waves are more narrow. With this shape, the effects of dispersion balance those of nonlinearity at an adjustable value of the pulse speed; thus, the hydrodynamic solitary wave is seen to be an independent dynamic entity.

Bäcklund Transformations

Although unrecognized at the time, such an energy conserving solitary wave is related to the existence of a transform technique that was proposed by Albert Bäcklund in 1855 (Lamb, 1976). Under this Bäcklund transformation (BT), a known solution generates a new solution through an integration, after which the new solution can be used to generate yet another new solution, and so on. It is straightforward to find a BT for any linear PDE, which introduces a new eigenfunction into the total solution with each application of the transformation. Only special nonlinear PDEs have BTs, but 19th century mathematicians knew that these include

$$\frac{\partial^2 u}{\partial \xi\,\partial \tau} = \sin u, \tag{3}$$

which arose in research on the geometry of curved surfaces (Steuerwald, 1936).

In 1939, Yakov Frenkel and Tatiana Kontorova introduced a seemingly unrelated problem arising in solid state physics to model dislocation dynamics in a crystal (Frenkel & Kontorova, 1939). From this study, an equation describing dislocation motion is

$$\frac{\partial^2 u}{\partial x^2} - \frac{\partial^2 u}{\partial t^2} = \sin u, \tag{4}$$

where $u(x,t)$ is atomic displacement in the x-direction and the sine function represents periodicity of the crystal lattice. A traveling-wave solution of Equation (4), corresponding to the propagation of a dislocation, is

$$u(x,t) = 4\arctan\left[\exp\left(\frac{x - vt}{\sqrt{1 - v^2}}\right)\right], \tag{5}$$

with velocity v in the range $(-1, +1)$. Because Equation (4) is identical to Equation (3) after an

independent variable transformation, exact solutions involving arbitrary numbers of dislocation components as in Equation (5) can be generated through a succession of Bäcklund transformations, but this was not known to Frenkel and Kontorova.

Numerical Discoveries of the Soliton

In the late 1940s, Enrico Fermi, John Pasta, and Stan Ulam (FPU) suggested one of the first scientific problems to be assigned to the Los Alamos MANIAC computing machine: the dynamics of energy equipartition in a slightly nonlinear crystal lattice, which is related to thermal conductivity. The system they chose was a chain of equal mass particles connected by slightly nonlinear springs, and it was expected that if all the initial energy were put into a single vibrational mode, the small nonlinearity would cause a gradual progress toward equal distribution of the energy among all modes (thermalization). But the numerical results were surprising. If all the energy is originally in the mode of lowest frequency, it returns almost entirely to that mode after a period of interaction among a few other low frequency modes. In the course of several numerical refinements, no thermalization was observed (Fermi et al., 1955).

Pursuit of an explanation for this "FPU recurrence" led Zabusky and Kruskal to approximate the nonlinear spring-mass system by the KdV equation. In 1965, they reported numerical observations that KdV solitary waves pass through each other with no change in shape or speed, and coined the term *soliton* to suggest this particle-like property (Zabusky & Kruskal, 1965).

Zabusky and Kruskal were not the first to observe nondestructive interactions of energy conserving solitary waves. Apart from Russell's tank measurements, Perring and Skyrme had studied solutions of Equation (4) comprising two solutions as in Equation (5) undergoing a collision. In 1962, they published numerical results showing perfect recovery of shapes and speeds after a collision and went on to discover an exact analytical description of this phenomenon (Perring & Skyrme, 1962).

This result would not have surprised 19th-century mathematicians; it is merely the second member of the hierarchy of solutions generated by a BT. Nor would it have been unexpected by Seeger and his colleagues, who had noted in 1953 the connections between the 19th-century work (Steuerwald, 1936) and the studies of Frenkel and Kontorova (Seeger et al., 1953). Because Perring and Skyrme were interested in Equation (4) as a nonlinear model for elementary particles of matter, however, the complete absence of scattering may have been disappointing.

Throughout the 1960s, Equation (4) arose in a variety of problems, including the propagation of ferromagnetic domain walls, self-induced transparency in nonlinear optics, and the propagation of magnetic flux quanta in long Josephson transmission lines. Eventually it became known as the "sine-Gordon" (SG) equation—a nonlinear version of the Klein–Gordon equation: $(u_{xx} - u_{tt} = u)$.

Perhaps the most important contribution made by Zabusky and Kruskal in their 1965 paper was to recognize the relation between nondestructive soliton collisions and the riddle of FPU recurrence. Viewing KdV solitons as independent and localized dynamic entities, they explained the FPU observations as follows. The initial condition generates a family of solitons with different speeds, moving apart in the x–t plane. Since the system studied was of finite length with perfect reflections at both ends, the solitons could not move infinitely far apart; instead, they eventually reassembled in the x–t plane, approximately recreating the initial condition after a surprisingly short "recurrence time."

By 1967, this insight had led Gardner, Greene, Kruskal, and Miura (GGKM) to devise a nonlinear generalization of the Fourier transform method for constructing solutions of the KdV emerging from arbitrary initial conditions (Gardner et al., 1967). Called the inverse scattering method (ISM), this approach proceeds in three steps. First, the nonlinear KdV dynamics are mapped onto an associated linear scattering problem, where each eigenvalue of the linear problem corresponds to the speed of a particular KdV soliton. Second, the time evolution of the associated linear scattering data is computed. Finally, an inverse scattering calculation determines the time evolved KdV dynamics from the evolved scattering data. Thus, the solution of a nonlinear problem is found from a series of linear computations.

Toda Lattice Solitons

Another development of the 1960s was Morikazu Toda's discovery of exact two-soliton interactions on a nonlinear spring-mass system (Toda, 1967). As in the FPU system, equal masses were assumed to be interconnected with nonlinear springs, but Toda chose the potential

$$\left(\frac{a}{b}\right)[\mathrm{e}^{-bu_j} - 1] + au_j, \tag{6}$$

where $u_j(t)$ is the longitudinal extension of the jth spring from its equilibrium value and both a and b are adjustable parameters. (In the limit $a \to \infty$ and $b \to 0$ with ab finite, this reduces to the quadratic potential of a linear spring. In the limit $a \to 0$ and $b \to \infty$ with ab finite, it describes the interaction between hard spheres.) Thus by the late 1960s, it was established that solitons were not limited to PDEs; local solutions of difference-differential equations could also exhibit the unexpected properties of unchanging shapes and speeds after collisions.

A Seminal Workshop

These events are only the salient features of a growing panorama of nonlinear wave activities that became gradually less parochial during the 1960s. Solid state physicists began to see relationships between their solitary waves (magnetic domain walls, self-shaping pulses of light, quanta of magnetic flux, polarons, etc.), and those from classical hydrodynamics and oceanography, while applied mathematicians began to suspect that the ISM (originally formulated by GGKM for the KdV equation) might be used for a broader class of nonlinear wave equations. It was amid this intellectual ferment that the first soliton research workshop was organized during the summer of 1972 (Newell, 1974). Interestingly, one of the most significant contributions to this conference came by post. From the Soviet Union arrived a paper by Vladimir Zakharov and Alexey Shabat formulating the ISM for the nonlinear PDE Zakharov & Shabat (1972)

$$\mathrm{i}\frac{\partial u}{\partial t} + \frac{\partial^2 u}{\partial x^2} + 2|u|^2 u = 0. \qquad (7)$$

In contrast to KdV, SG, and the Toda lattice, the dependent variable in this equation is complex rather than real, so the evolutions of two quantities (magnitude and phase of u) are governed by the equation. This reflects the fact that Equation (7) is a nonlinear generalization of a linear equation $\mathrm{i}u_t + u_{xx} + u = 0$, solutions of which comprise both an envelope and a carrier wave. As this linear equation is a Schrödinger equation for the quantum mechanical probability amplitude of a particle (like an electron) moving through a region of uniform potential, it is natural to call Equation (7) the nonlinear Schrödinger (NLS) equation. When the NLS equation is used to model classical wave packets in such fields as hydrodynamics, nonlinear acoustics, and plasma waves, however, its solutions are devoid of quantum character.

Upon appreciating the Zakharov and Shabat paper, participants left the 1972 workshop aware that four nonlinear equations (KdV, SG, NLS, and the Toda lattice) display solitary wave behavior with the special properties that led Zabusky and Kruskal to coin the term *soliton* (Newell, 1974). Within two years, ISM formulations had been constructed for the SG equation and also for the Toda lattice.

Since the mid-1970s, the soliton concept has become established in several areas of applied science, and dozens of nonlinear systems are now known to be integrable through the ISM. Thus, one is no longer surprised to find stable spatially localized regions of energy, balancing the opposing effects of nonlinearity and dispersion and displaying the essential properties of objects.

ALWYN SCOTT

See also **Bäcklund transformations; Fermi–Pasta–Ulam oscillator chain; Inverse scattering method or transform; Laboratory models of nonlinear waves; Solitons**

Further Reading

Fermi, E., Pasta, J.R. & Ulam, S.M. 1955. Studies of nonlinear problems, Los Alamos Scientific Laboratory Report No. LA–1940 (Reprinted in Newell, 1974.)

Frenkel, J. & Kontorova, T. 1939. On the theory of plastic deformation and twinning. *Journal Physics (USSR)* 1: 137–149

Gardner, C.S., Greene, J.M., Kruskal, M.D. & Miura, R.M. 1967. Method for solving the Korteweg–de Vries equation. *Physical Review Letters*, 19: 1095–97

Korteweg, D.J. & de Vries, H. 1895. On the change of form of long waves advancing in a rectangular canal, and on a new type of long stationary waves. *Philosophical Magazine*, 39: 422–443

Lamb, G.L., Jr. 1976. Bäcklund transforms at the turn of the century. In *Bäcklund Transforms*, edited by R.M. Miura, Berlin and New York: Springer

Newell, A.C. (editor). 1974. *Nonlinear Wave Motion*, Providence, R.I: American Mathematical Society

Perring, J.K. & Skyrme, T.R.H. 1962. A model unified field equation. *Nuclear Physics*, 31: 550–555

Russell, J.S. 1844. *Report on Waves*, 14th meeting of the British Association for the Advancement of Science, London: BAAS, 311–339

Russell, J.S. 1885. *The Wave of Translation in the Oceans of Water, Air and Ether*, London: Trübner

Scott, A.C. 2003. *Nonlinear Science: Emergence and Dynamics of Coherent Structures*, 2nd edition, Oxford and New York: Oxford University Press

Seeger, A., Donth, H. & Kochendörfer, A. 1953. Theorie der Versetzungen in eindimensionalen Atomreihen. *Zeitschrift für Physik*, 134: 173–193

Steuerwald, R. 1936. Über Enneper'sche Flächen und Bäcklund'sche Transformation. *Abhandlungen der Bayerischen Akademie der Wissenschaften* München, pp. 1–105

Toda, M. 1967. Vibration of a chain with nonlinear interactions. *Journal of the Physical Society of Japan*, 22: 431–436; Wave propagation in anharmonic lattices. *Journal of the Physical Society of Japan*, 23: 501–506

Zabusky, N.J. & Kruskal, M.D. 1965. Interactions of solitons in a collisionless plasma and the recurrence of initial states. *Physical Review Letters*, 15: 240–243

Zakharov, V.E. & Shabat, A.B. 1972. Exact theory of two-dimensional self-focusing and one-dimensional self-modulation of waves in nonlinear media. *Soviet Physics, JETP*, 34: 62–69

SOLITONS, TYPES OF

Solitons are localized solutions of nonlinear partial or difference-differential equations that preserve their integrity under collisions with other such solutions. In general, energy is conserved for soliton systems; thus, they are a special class of Hamiltonian systems. Localization may result from a dynamic balance between the effects of nonlinear and dispersion (nontopological solitons) or from a topological constraint.

Nontopological Solitons

Perhaps the most famous example among equations admitting solitary wave solution is the Korteweg–de Vries (KdV) equation

$$u_t + \alpha u u_x + u_{xxx} = 0, \tag{1}$$

which has the solitary-wave solution

$$u = a\,\mathrm{sech}^2\left\{\sqrt{a\alpha/12}[x - (a\alpha/3)t]\right\}, \tag{2}$$

where a is the wave amplitude. The quadratic nonlinear term ($\alpha u u_x$) is balanced by the dispersive term (u_{xxx}) in the solution of Equation (2). A feature of such solitary waves of this type is that they preserve their shapes and speeds under collisions (act as particles); thus they are called "solitons."

In general, Equation (1) approximates a more detailed physical description. When the quadratic nonlinear term is small, the cubic nonlinear term may be taken into account, leading to the following equation.

$$u_t + \alpha u u_x + \beta u^2 u_x + u_{xxx} = 0, \tag{3}$$

which is known as the extended Korteweg-de Vries (eKdV) equation. With $\alpha = 0$ and $\beta = 6$, Equation (3) is known as the modified Korteweg–de Vries (mKdV) equation with negative dispersion,

$$u_t + 6u^2 u_x + u_{xxx} = 0. \tag{4}$$

Equation (4) admits solitary wave solutions tending to u_0 at infinity (Grimshaw et al., 1999),

$$u(x,t) = u_0 + \frac{2\nu^2}{u_0 + \sigma\lambda\cosh[2\nu(x - \mu t)]}, \tag{5}$$

where $\lambda > |u_0|, \nu = \sqrt{\lambda^2 - u_0^2}, \sigma = \pm 1, \mu = 2u_0^2 + 4\lambda^2$, and

$$u(x,t) = u_0 - \frac{4u_0}{1 + 4u_0^2(x - 6u_0^2 t)^2}. \tag{6}$$

Equation (5) reduces to a soliton solution as $u_0 \to 0$,

$$u = 2\sigma\lambda\,\mathrm{sech}\{2\lambda(x - 4\lambda^2 t)\}, \tag{7}$$

which is different from the KdV soliton solution (2). Equation (6) shows that the wave shape $(u - u_0)$ vanishes algebraically as $|x| \to \infty$. We call it an *algebraic soliton* or *rational soliton*.

The eKdV equation (3) has the following solitary-wave solution ((Grimshaw et al., 1999),

$$u(x,t) = \frac{(6\gamma^2/\alpha)}{1 + B\cosh\{\gamma(x - \gamma^2 t)\}}, \tag{8}$$

where $B^2 = 1 + (6\beta\gamma^2/\alpha^2)$ and γ is an arbitrary parameter, characterizing the inverse width of the solitary wave. In the case $\beta < 0$ $(0 < B < 1)$, at small wave amplitudes $(B \to 1)$, Equation (8) transforms into the KdV soliton solution. On the other hand, as the wave amplitude increases $(B \to 0)$, it approaches the critical value $a_{cr} = \alpha/|\beta|$. In the limit $(B \to 0)$, the width of the solitary wave increases to infinity and it becomes the so-called *thick soliton*. The thick soliton can be viewed as a kink-antikink combination.

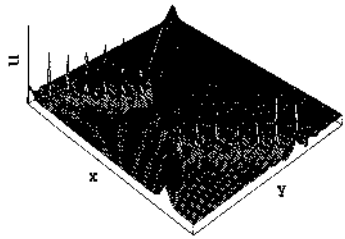

Figure 1. Interaction between line soliton and periodic soliton.

An extension of the KdV equation to motion in two space dimensions was given by Kadomtsev and Petviashvili in order to discuss the stability of the KdV soliton (line soliton in two-dimensional space) against a long transverse disturbance. This two-dimensional extension is known as the Kadomtsev–Petviashvili (KP) equation,

$$(u_t + 6uu_x + u_{xxx})_x + 3su_{yy} = 0, \tag{9}$$

which corresponds to the case of negative and positive dispersion when $s = +1$ and $s = -1$, respectively (Kadomtsev & Petviashvili, 1970). They have shown that the line soliton is stable in the case of negative dispersion and is unstable for the positive dispersion. This leads to the conjecture that a localized soliton in two-dimensional space should be formed in the positive dispersion case, since the line soliton is unstable. Such a soliton solution has been found by Manakov et al. (1977) and Ablowitz & Satsuma (1978), which is no longer exponential in character, but a rational function of space variables,

$$u = 4\frac{(L + L^*)^{-2} - \xi^2 + \eta^2}{\left[(L + L^*)^{-2} + \xi^2 + \eta^2\right]^2}, \tag{10}$$

with

$$\xi = \mathrm{Re}\{x - 2\mathrm{i}Ly - 12L^2 t\} + \xi_0,$$
$$\eta = \mathrm{Im}\{x - 2\mathrm{i}Ly - 12L^2 t\} + \eta_0,$$

where ξ_0 and η_0 are arbitrary constants and $*$ indicates the complex conjugate. This solution decays like $(x^2 + y^2)^{-1}$ as $(x^2 + y^2)^{1/2} \to \infty$; thus, it is also called an *algebraic soliton* or *rational soliton* or *lump*. Another type of localized soliton appears in the positive dispersion case as a sequence of infinite algebraic solitons, called a *periodic soliton* or *soliton chain* (Tajiri & Murakami, 1989). Figure 1 shows a typical interaction between line soliton and periodic soliton.

The Benjamin–Ono (BO) equation,

$$u_t + 4uu_x + \frac{1}{\pi} P \int_{-\infty}^{\infty} \frac{u_{\xi\xi}(\xi, t)}{\xi - x} \mathrm{d}\xi = 0, \qquad (11)$$

describes a weakly nonlinear, long internal wave in a stratified fluid of great depth, where P stands for the principal value of the integration and the third term is dispersive (Ono, 1975). The BO equation has an algebraic soliton solution,

$$u = \frac{a}{a^2(x - at - x_0)^2 + 1}, \qquad (12)$$

which is called a *Benjamin–Ono soliton*.

Envelope solitons

Consider next the propagation of a modulated plane wave in a nonlinear and dispersive medium where the dispersion relation is amplitude dependent, $\omega = \omega(k, |u|^2)$. Expanding around the carrier wave number k_0 and frequency ω_0, we have

$$\omega - \omega_0 = \left(\frac{\partial \omega}{\partial k}\right)_0 (k - k_0) + \frac{1}{2}\left(\frac{\partial^2 \omega}{\partial k^2}\right)_0 (k - k_0)^2 + \left(\frac{\partial \omega}{\partial |u|^2}\right)_0 |u|^2 ... \qquad (13)$$

Replacing $\omega - \omega_0$ by $\mathrm{i}\partial/\partial t$ and $k - k_0$ by $-\mathrm{i}\partial/\partial x$ and operating on u gives

$$\mathrm{i}\left\{\frac{\partial u}{\partial t} + \left(\frac{\partial \omega}{\partial k}\right)_0 \frac{\partial u}{\partial x}\right\} + \frac{1}{2}\left(\frac{\partial^2 \omega}{\partial k^2}\right)_0 \frac{\partial^2 u}{\partial x^2} - \left(\frac{\partial \omega}{\partial |u|^2}\right)_0 |u|^2 u = 0, \qquad (14)$$

which is the nonlinear Schrödinger (NLS) equation. If

$$(\partial^2 \omega/\partial k^2)_0 (\partial \omega/\partial |u|^2)_0 < 0,$$

the plane wave is unstable for the modulation, otherwise it is stable.

Under appropriate scaling and variable transformations, Equation (14) takes the standard form

$$\mathrm{i}u_t + u_{xx} + 2\varepsilon |u|^2 u = 0, \ (\varepsilon = \pm 1). \qquad (15)$$

With $\varepsilon = 1$, this is called the focusing NLS (FNLS) equation and has an *envelope soliton* solution,

$$u = K \mathrm{e}^{\mathrm{i}(\tilde{k}x - \tilde{\omega}t + \theta)} \mathrm{sech}(Kx - \Omega t + \sigma), \qquad (16)$$

where $-(\Omega + \mathrm{i}\tilde{\omega}) + (K + \mathrm{i}\tilde{k})^2 = 0$ and θ and σ are arbitrary constants. This is called a *bright soliton* in nonlinear optics (see Figure 2a). If the phase velocity decreases (increases) with increased amplitude, nonlinear effect results in a decrease (increase) of the wave number in the leading half of the envelope and a increase (decrease) in wave number in the trailing half. Thus, the envelope is compressed, and a soliton finds a balance between the effect of compression caused by nonlinearity and broadening caused by dispersion.

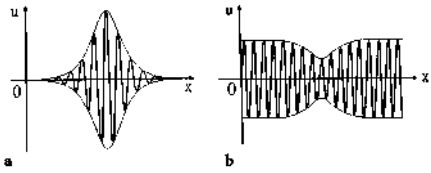

Figure 2. (a) Bright soliton and (b) dark soliton.

The defocusing NLS (DNLS) equation (with $\varepsilon = -1$) has a *dark soliton* solution (shown in Figure 2b)

$$|u|^2 = u_0^2[1 - a^2 \mathrm{sech}^2\{u_0 a(x - vt)\}], \qquad (17)$$

which appears as an intensity dip in an infinitely extended constant background. The dark soliton solution with $a = 1$

$$|u|^2 = u_0^2 \tanh^2 u_0(x - vt), \qquad (18)$$

is called a *black soliton* and the solution with $a < 1$ is sometimes referred to as a *gray soliton*.

Optical communication systems are degraded by the spreading out of pulses as they travel along a fiber, which is caused by dispersion. Hasagawa and Tappert proposed using the nonlinear change of dielectric constant of the fiber to compensate for this dispersive effect (Hasagawa & Tappert, 1973). The optical pulse was shown to form a bright soliton in the case of anomalous dispersion ($\partial^2 \omega/\partial k^2 > 0$), a prediction that was verified by Mollenauer et al. (1980).

Writing $k = k(\omega, |u|^2)$ as the solution of the dispersion relation again leads to the NLS equation but with different variables (ω and k interchanged). The NLS equation in these variables is important in nonlinear optics.

More Space Dimensions

Spatial dark-soliton stripes are experimentally found in the transverse cross section of a continuous-wave (cw) optical beam propagating through material with a self-defocusing nonlinearity. The spatial evolution of a monochromatic transverse electric field $E(x, y, z)$ in a self-defocusing medium with Kerr nonlinearity (the intensity-dependent refractive index $n = n_0 - n_2|E|^2$) is described by the NLS equation

$$\mathrm{i}u_z + \tfrac{1}{2}\triangle_\perp u - |u|^2 u = 0, \qquad (19)$$

where $\triangle_\perp = \partial_x^2 + \partial_y^2$ is the transverse diffraction operator and z is the propagation coordinate. Although dark-soliton stripes are unstable to transverse long-wavelength modulation, linear analysis predicts stability to transverse modulation having a short period.

Kivshar & Yang (1994) showed that self-defocusing nonlinear media can support a *ring soliton*, which is a dark-solitary wave with ring symmetry. If the ring radius is small enough, it is not subject to the transverse instability characteristic of dark-stripe solitons. It has also been demonstrated that in the small-amplitude limit such solitons are governed by a cylindrical KdV equation. Frantzeskakis and Malomed also showed that *anti-dark ring solitons* (humps on top of the cw background rather than dips) can exist too but only for non-Kerr saturable nonlinearities (Frantzeskakis & Malomed, 1999).

Spatial solitons are optical beams that are self-trapped in space due to a balance between the Kerr nonlinearity and diffraction, a well-studied phenomenon. A new type of spatial soliton, which was proposed by Segev et al. (1992), occurs in a photorefractive (PR) crystal biased with an external dc electric field. The presence of optical beams in a crystal leads to photoexcitation of electric charges. The space charge screens the externally applied electric field in the illuminated area of the crystal. The non-uniform screening of the electric field modifies the refractive index in such a way that the beam becomes self-trapped and propagates in a form of a *PR spatial soliton*. PR spatial solitons can occur at microwatt power levels, whereas the observation of Kerr solitons requires much higher power. Steady solitons in PR crystals are called *screening solitons*.

With the application of a slightly detuned driving field, a slightly lossy Kerr medium supports *cavity solitons*, which are then induced by writing pulses (Firth et al., 2002). This provides an optical means for writing patterns of light onto the cavity cross section and subsequently erasing them, in other words an optical memory.

It is known that the diffusion effect of photoexcited charges leads to a bending of the trajectories of PR solitons. Królikowski et al. (1996) showed by using numerical simulations that *self-bending solitons* in the presence of the diffusion processes are stable and withstand relatively large perturbations. They also showed that even a small contribution of diffusion effect leads to strong energy exchange between colliding PR solitons. In general, spatial solitons in PR media do not satisfy the mathematical definition of solitons, even when they propagate as solitary waves with an unchanging beam profile.

Self-trapping has been studied in Kerr-type, PR, quadratic, and resonant atomic nonlinear media. All of these studies have investigated self-trapping of spatially coherent light beams only. Diffraction of a spatially incoherent beam is larger than that of a coherent beam of the same width. Therefore, a spatially incoherent beam diverges much faster than a coherent beam, and self-trapping of an incoherent beam requires stronger optical nonlinearities than self-trapping a coherent beam. Recently, self-trapping of incoherent light beams has been demonstrated experimentally (Mitchell et al., 1996) and theoretically (Mitchell et al., 1997). In general, spatial *incoherent solitons* are multimode, self-trapped entities, found only in materials with non-instantaneous (internal) nonlinearity (Mitchell et al., 1997).

Another interesting phenomena is the formation of solitons by the mutual trapping of the interacting waves. Torner et al. (1996) showed that soliton-like propagation occurs in the presence of walk-off between the interacting waves. The solitons in the presence of walk-off are called *walking solitons*. Temporal walk-off is due to different group velocities of the waves forming the soliton, while spatial walk-off is due to different propagation directions of energy and phase fronts in anisotropic media.

The possibility of creating three-dimensional (3-d) localized pulses in a self-focusing medium with anomalous group-dispersion was demonstrated by Silberberg (1990), who showed that they pulses are robust in the sense that remain as separate solitary formations even after collisions. These 3-d-pulses propagating without changes in space or time are called *light bullets*.

Topological Solitons

Another mechanism leading to the emergence of solitons is a topological constraint, exemplified by the sine-Gordon (SG) equation

$$u_{tt} - u_{xx} + m^2 \sin u = 0. \tag{20}$$

The SG equation is characterized by two properties: Lorentz invariance and multiple ground states of the energy. The presence of multiple ground states aids soliton formation because the field takes different asymptotic values on both sides of the isolated wave, so the wave is unable to disperse. (It cannot decay by spreading out for the same reason a twist sealed in the boundary condition at the end of a band cannot be removed.) Thus, wave fields can incorporate *topological solitons* if there are multiple ground states with an appropriate topology. Such a soliton of the SG equation is given by

$$u = 4 \arctan\left[\exp\left(\pm m \frac{x - vt - x_0}{\sqrt{1 - v^2}}\right)\right]. \tag{21}$$

The solution represents a twist in the configuration of the field connecting one ground state $2n\pi$ to the another ground state $(2n \pm 2)\pi$. The $+$ sign and $-$ sign solutions are called a *kink* and an *antikink*, respectively, as shown in Figure 3. They are often termed *soliton* and *antisoliton* instead of kink and antikink. The energy of the SG kink solution is given by $8m/\sqrt{1 - v^2}$,

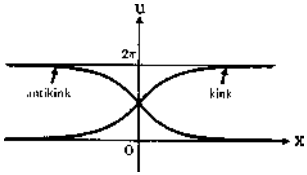

Figure 3. Kink and antikink.

which has relativistic dependence on the velocity v. There is an analogy between kink/antikink and positively/negatively charged elementary particles. The time evolution of an initial state consisting of two kinks shows that the two kinks move away from each other. On the other hand, the kink and antikink move toward each other. The twist (Q) of a kink ($+2\pi$) or antikink (-2π) is known as its *topological charge*.

Perring and Skyrme were interested in the SG equation as a model equation for physical elementary particles (Perring & Skyrme, 1962). They regarded the kink as nucleon and the linear wave (with $Q=0$) as a meson. The soliton solution of a nuclear model for which topological charge is the baryon number is called a *skyrmion*. Topological charge is a conserved quantity stemming from the geometric configuration of the field—an important feature of many field theories that admit kink solutions.

Numerous attempts were made to find particle-like solutions of relativistically invariant nonlinear field equations in higher dimensions. Under radial symmetry, ring and spherical solitons to the SG and Higgs field equations have been studied numerically by Bogolyubskii and Makhan'kov who called such waves *pulsons* due to their pulsating behavior (Bogolyubskii & Makhan'kov, 1976).

Lattice-solitons

Solitons and kinks in discrete systems are sometimes called *lattice-solitons* and *lattice-kinks*, respectively. The Toda lattice is a one-dimensional lattice of equal masses, interconnected by exponetial interaction potentials of the form (Toda, 1981)

$$\phi(r) = \frac{a}{b}\exp(-br) + ar + \text{const.}, \qquad (22)$$

where $a, b > 0$ and r is the change of a distance between adjacent masses from its equilibrium value. The equation of motion for Toda lattice is an integrable system, admitting exact N-soliton solutions, whose form for $N=1$ is given by

$$\exp(-br_n) - 1 = \sinh^2(\kappa)\operatorname{sech}^2\left(\kappa n \pm t\sqrt{ab/m}\sinh\kappa\right), \qquad (23)$$

where κ is an amplitude parameter and m is the mass of the particles.

The theory of wave propagation in periodic structures shows the existence of forbidden frequency bands or band gaps, located around the (Bragg) reflection frequencies. A wave with overtone frequencies within the forbidden frequency bands will have little means of interaction with the periodic structure. The solitons that emerge from a balance between nonlinear self-phase modulation and dispersion associated with the periodic structure are called *gap solitons*.

Other Types of Solitons

A variable coefficient KdV equation arises in the study of a solitary water waves as it enters a region where the bottom is no longer level (Johnson, 1980). A soliton on non-uniform background generally moves with variable speed. When a soliton comes from left (or right) and goes back to left (or right) with opposite velocity—sailing back like an Australian boomerang—it is called a *boomeron*. When a soliton oscillates without ever escaping to infinity, the soliton is referred to as a *trappon* (Calogero & Degasperis, 1982).

The *Dym* equation ($r_t = r^3 r_{xxx}$) was discovered in unpublished work by Harry Dym and rediscovered in a more general form by Sabatier within the classical string problem. This equation belongs to a wide class of nonlinear equations (WKI equations) found by Wadati, Konno, and Ichikawa to be completely integrable (Wadati et al., 1979). Reciprocal links between the Dym and KdV and MKdV equations provide implicit solutions, since they include the simultaneous change of both dependent and independent variables (Kawamoto, 1985). The Dym equation has *cusp soliton* solutions. Some new approaches, which allow construction of multisoliton solutions almost explicitly have been developed for the Dym equation by (Dmitrieva, 1993). Recently, it was shown that the Dym equation on the complex plane is relevant to such physical problems as the Hele-Shaw problem and the Saffman–Taylor problem (Constantin & Kadanoff, 1991).

The nonlinear transverse oscillation of an elastic beam subject to an end-thrust is described by one of the WKI equations. If the beam is flexible enough, it deforms into a loop, with the upper half portion having negative curvature. In this case, the nonlinear oscillation can be described by an equation of the following form (Konno et al., 1981):

$$y_{xt} + \operatorname{sgn}\left(\frac{\mathrm{d}s}{\mathrm{d}x}\right)\left(\frac{y_{xx}}{(1+y_x^2)^{3/2}}\right)_{xx} = 0, \qquad (24)$$

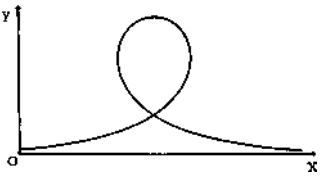

Figure 4. Loop soliton.

where s denotes arc length measured around the loop. Konno et al. showed that such a *loop soliton* (shown in Figure 4) propagating along a stretched rope can be obtained as a one soliton solution to Equation (24).

Solitary waves with finitely extended (compact) support were recently studied in various equations with nonlinear dispersion. Rosenau and Hyman showed that solitary-wave solutions may have compact support under the influence of nonlinear dispersion in various generalizations of the KdV equations with nonlinear dispersion (Rosenau & Hyman, 1993). The nonlinear dispersion is weaker for small amplitude than the linear dispersion in the KdV equation, leading to compactification. Such robust soliton-like pulses—characterized by the absence of the infinite tail—are called *compactons*.

MASAYOSHI TAJIRI

See also **Korteweg–de Vries equation; Multidimensional solitons; Nonlinear optics; Nonlinear Schrödinger equations; Sine-Gordon equation; Skyrmions; Solitons; Toda lattice**

Further Reading

Ablowitz, M.J. & Satsuma, J. 1978. Solitons and rational solutions of nonlinear evolution equations. *Journal of Mathematical Physics*, 19: 2180–2186

Bogolyubskii, I.L. 1976. Oscillating particle-like solutions of the nonlinear Klein–Gordon equation. *Soviet Physics JETP Letters*, 24: 535–538

Bogolyubskii, I.L. & Makhan'kov, V.G. 1976. Lifetime of pulsating solitons in certain classical models. *Soviet Physics JETP Letters*, 24: 12–14

Calogero, F. & Degasperis, A. 1982. *Spectral Taransform and Solitons I*, North-Holland, Amsterdam

Constantin, P. & Kadanoff, L. 1991. Dynamics of a complex interface. *Physica* D, 47: 450–460

Dmitrieva, L.A. 1993. Finite-gap solutions of the Harry Dym equation. *Physics Letters* A, 182: 65–70

Firth, W.J., Harkness, G.K., Lord, A., McSloy, J.M., Gomila, D. & Colet, P. 2002. Dynamical properties of two-dimensional Kerr cavity solitons. *Journal of Optical Society of America* B, 19(4): 747–752

Frantzeskakis, D.J. & Malomed, B.A. 1999. Multiscale expansions for a generalized cylindrical nonlinear Schrödinger equation. *Physics Letters* A, 264: 179–185

Grimshaw, R., Pelinovsky, E. & Talipova, T. 1999. Solitary wave transformation in a medium with sign-variable quadratic nonlinearity and cubic nonlinearity. *Physica* D, 132: 40–62

Hasagawa, A. & Tappert, F. 1973. Taransmission of stationary nonlinear optical pulses in dispersive dielectric fibers. I. Anomalous dispersion, II. Normal dispersion. *Applied Physics Letters*, 23: 142–144, 171–172

Johnson, R.S. 1980. Water waves and Korteweg–de Vries equations. *Journal of Fluid Mechanics*, 97: 701–719

Kadomtsev, B.B. & Petviashvili, V.I. 1970. On the stability of solitary waves in weakly dispersing media. *Soviet Physics-Doklady*, 15: 539–541

Kawamoto, S. 1985. An exact transformation from the Harry Dym equation to the modified K-dV equation. *Journal of the Physical Society of Japan*, 54: 2055–2056

Kivshar, Y.S. & Yang, X. 1994. Ring dark solitons. *Physical Review* E, 50: R40–R43

Konno, K., Ichikawa, Y.H. & Wadati, M. 1981. A loop soliton propagating along a stretched rope. *Journal of the Physical Society of Japan*, 50: 1025–1026

Królikowski, W., Akhmediev, N., Luther-Davies, B. & Gronin-Golomb, M. 1996. Self-bending photorefractive solitons. *Physical Review* E, 54: 5761–5765

Manakov, S.V., Zakharov, V.E., Bordag, L.A., Its, A.R. & Matveev, V.B. 1977. Two-dimensional solitons of the Kadomtsev–Petviashvili equation and their interaction. *Physics Letters*, 63A: 205–206

Mitchell, M., Chen, Z., Shih, M. & Segev, M. 1996. Self-trapping of partially spatially incoherent light. *Physical Review Letters*, 77: 490–493

Mitchell, M., Segev, M., Coskun, T.H. & Christodoulides, D.N. 1997. Theory of self-trapping spatially incoherent light beams. *Physical Review Letters*, 79: 4990–4993

Mollenauer, L.F., Stolen, R.H. & Gordon, J.P. 1980. Experimental observation of picosecond pulse narrowing and solitons in optical fibers. *Physical Review Letters*, 45: 1095–1098

Ono, H. 1975. Algebraic solitary waves in stratified fluids. *Journal of the Physical Society of Japan*, 39: 1082–1091

Perring, J.K. & Skyrme, T.H.R. 1962. A model unified field equation. *Nuclear Physics*, 31: 550–555

Rosenau, P. & Hyman, J. M. 1993. Compactons: solutions with finite wavelength. *Physical Review Letters*, 70: 564–567

Segev, M., Crosignani, B., Yariv, A. & Fischer, B. 1992. Spatial solitons in photorefractive media. *Physical Review Letters*, 68: 923–936

Silberberg, Y. 1990. Collapse of optical pulses. *Optics Letters*, 15: 1282–1284

Tajiri, M. & Murakami, Y. 1989. The periodic soliton resonance: solutions to the Kadomtsev–Petviashvili equation with positive dispersion. *Physics Letters* A, 143: 217–220

Toda, M. 1981. *Theory of Nonlinear Lattices*, Springer-Verlag, Berlin

Torner, L., Mazilu, D. & Mihalache, D. 1996. Walking solitons in quadratic nonlinear media. *Physical Review Letters*, 77: 2455–2458

Wadati, M., Konno, K. & Ichikawa, Y. H. 1979. New integrable nonlinear evolution equations. *Journal of the Physical Society of Japan*, 47: 1698–1700

SOLUTION TRAJECTORY

See **Phase space**

SPATIOTEMPORAL CHAOS

Spatiotemporal chaos is a dynamical regime developing in spatially distributed systems lacking long-time, large-distance coherence in spite of an organized regular behavior at the local scale. It is, so to speak, located in the middle of a triangle, the corners of which are temporal chaos, which is prevalent for a few

spatially frozen degrees of freedom, spatial chaos, in disordered time-independent patterns, and turbulence, with cascading processes over a wide range of space and time scales.

Short-term local coherence is usually the result of some instability mechanism that generates dissipative structures of different kinds depending on whether or not a specific frequency ($\omega_c = 0$ or $\neq 0$) and/or a spatial periodicity ($k_c = 0$ or $\neq 0$) is introduced in the system (Cross & Hohenberg, 1993). Examples of spatiotemporal chaos may be found in every combination of these elementary cases: Rayleigh–Bénard convection produces a time-independent cellular pattern ($\omega_c = 0, k_c \neq 0$), the Belousov–Zhabotinsky (BZ) reaction-diffusion system is unstable against a homogeneous oscillatory mode ($\omega_c \neq 0, k_c = 0$), convection in binary fluid mixtures develops in the form of dissipative waves ($\omega_c \neq 0, k_c \neq 0$), and the same holds for hydrothermal waves. Transitions to spatiotemporal chaos have been observed and studied in many experimental systems, including parametrically excited surface waves, electro-hydrodynamic instabilities in nematic liquid crystals (Kramer & Pesch, 1996), and liquid films flowing down inclines (Chang, 1994). Figure 1 (left) illustrates the case of spiral defect chaos in convection.

In practice, confinement effects enter and compete with instability mechanisms in the ordering process. Their intensity can be appreciated through aspect ratios, measuring the physical size of the system in units of the instability wavelength. In small aspect-ratio experiments, confinement effects are effective in the three space directions and chaos is purely temporal. Spatiotemporal chaos develops when confinement is partially relaxed. Accordingly, phenomena developing at surfaces or in thin layers can be understood as (quasi-)two-dimensional (Gollub, 1994). In the same way, narrow channels or oriented media along a specific direction exemplify the case of (quasi-)one-dimensional systems (Daviaud, 1994).

A second important classification results from the nature of the bifurcation, either supercritical or subcritical (continuous or discontinuous), which implies either substitution or coexistence of bifurcating and bifurcated states. To a large extent, this feature dictates the type of theory most appropriate to understand the growth of spatiotemporal chaos.

Consider first the supercritical case. When confinement effects are unable to maintain order everywhere, reduced universal descriptions are generically obtained as "envelope equations" (Newell, 1974). Standing as a paradigm, the cubic complex Ginzburg–Landau (CGL3), reviewed by Aranson & Kramer (2002), spatially unfolds a local supercritical Hopf bifurcation signalling the emergence of uniform oscillations ($\omega_c \neq 0$, $k_c = 0$). In one dimension (1-d), this equation reads

$$\partial_t A = A + (1 + \mathrm{i}\alpha)\partial_{xx} A - (1 + \mathrm{i}\beta)|A|^2 A, \qquad (1)$$

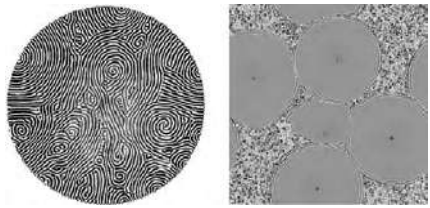

Figure 1. Left: Spiral defect chaos near threshold in Rayleigh–Bénard convection at $\mathcal{O}(1)$ Prandtl number. (Courtesy Ahlers, 1998). Right: Coexistence of spirals and defect mediated chaos in the 2-d CGL equation for $\alpha = -2$ and $\beta \simeq 0.75$ (Manneville, unpublished).

where the parameters α and β measure linear and nonlinear dispersion effects, respectively. The CGL3 equation admits trivial exact solutions in the form of plane waves $A = A_q \exp[\mathrm{i}(qx - \omega_q t)]$, with amplitude $A_q = (1 - q^2)^{1/2}$ and angular frequency $\omega_q = \alpha q^2 + \beta(1 - q^2)$, which are stable or unstable depending on the values of α, β, and q. Other nonlinear solutions can exist; in one dimension, solitary waves called Bekki–Nozaki holes are the best known. In two dimensions (2-d) they take the form of spiral waves that are topological defects of the complex order parameter A. Figure 1 (right) illustrates the coexistence of spirals and defect-mediated chaos (see below) in the 2-d CGL equation. Figure 2 displays the different possible steady-state regimes of the 1-d CGL equation in the $(1/\beta, -\alpha)$ plane. In region I, plane waves attract most initial conditions. Phase turbulence is present in region IV slightly beyond the Benjamin–Feir instability (BF) line, as given by Newell's criterion for "$q = 0$" oscillations (Newell, 1974). In the vicinity of this line, the solution can be written as $A(x, t) = (1 + \varrho(x, t)) \exp(\mathrm{i}\theta(x, t))$. The amplitude modulation ϱ, enslaved to the gradient of the phase perturbation θ, remains small, while θ is governed at lowest order by the Kuramoto–Sivashinsky equation (Kuramoto, 1978)

$$\partial_t \theta = D\partial_{xx}\theta - K\partial_{xxxx}\theta + g(\partial_x \theta)^2, \qquad (2)$$

where $D = 1 + \alpha\beta$ is an effective diffusion coefficient that is negative in the unstable range (Chaté & Manneville, 1994a). Deeper in the unstable domain, in region V, a "revolt" of $|A|$ ends in the formation of defects (phase singularities at zeroes of $|A|$) and amplitude turbulence or defect-mediated turbulence sets in (Coullet et al., 1989). Defects analogous to Bekki–Nozaki holes are observed to evolve in a spatiotemporal intermittent fashion in region II. As suggested by its position in the diagram, the "bi-chaos" regime in region III presents itself as a fluctuating mixture of states in regions IV and V.

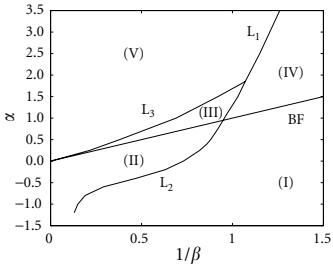

Figure 2. Bifurcation diagram of the 1-d CGL equation. (Data from Chaté, 1994.)

By contrast, subcritical instabilities are characterized by the possibility of finding the system in one of several (usually two) states at a given point in space. Short-range coherence then implies the formation of homogeneous domains of each state, separated by fronts (Pomeau, 1986). In gradient systems, these fronts move regularly so as to decrease the potential, but in nongradient systems, they may have more complicated behaviors. A particularly interesting scenario develops when one of the competing local states is a chaotic transient while the other is regular. At a given time, the whole system can be divided into so-called laminar and turbulent domains, and at a given point in space, the system is alternatively laminar or turbulent, hence the name "spatiotemporal intermittency" (STI). According to Pomeau (1986), front propagation is then akin to a time-oriented stochastic process known as "directed percolation" (DP) used to model epidemic processes (Kinzel, 1983). Directed percolation defines a critical phenomenon, with an associated universality class (a specific set of scaling exponents governing the statistical behavior of the system as a function of the distance to threshold).

The existence of separated domains and sharp fronts supports the idea of modeling extended systems in terms of identical subsystems arranged on a regular lattice, each with its own phase space, and coupled to its neighbors. In addition to space discretization, time discretization leads to the definition of coupled map lattices that have served to illustrate several transition scenarios such as cascades of spatial period doublings, defect-mediated regimes (Kaneko, 1993), or STI (Chaté & Manneville 1994b) that make explicit how local transient temporal chaos is converted into sustained spatiotemporal chaos. A last step can be taken by also discretizing the local phase space, which yields cellular automata (Wolfram, 1986). Further randomization of the dynamics then points towards an understanding of the transition to turbulence in statistical physics terms (Kinzel, 1983). Such approaches should help in understanding plane Couette flow, the simplest shear flow produced by two parallel plates sliding in opposite directions. This configuration is a particularly intriguing example of a subcritical hydrodynamic system where domains of laminar flow, known to be stable for all flow conditions, coexist in a wide range of Reynolds numbers and in continuously varying proportions with domains of small-scale turbulence.

Spatio-temporal chaos definitely relates to the process of transition to turbulence when confinement effects are weak. It appears to occupy a central position at the crossroads of nonlinear dynamics, mathematical stability theory, and statistical physics of many-body systems and non-equilibrium processes, with a wide potential for applications (Rabinovich et al., 2000).

PAUL MANNEVILLE

See also **Cellular automata; Chaos vs. turbulence; Coherence phenomena; Coupled map lattice; Development of singularities; Gradient system; Hydrothermal waves; Kuramoto–Sivashinsky equation; Modulated waves; Multiple scale analysis; Navier–Stokes equation; Nonequilibrium statistical mechanics; Order parameters; Pattern formation; Phase dynamics; Reaction-diffusion systems; Spiral waves; Surface waves; Topological defects; Turbulence**

Further Reading

Ahlers, G. 1998. Experiments on spatio-temporal chaos. *Physica* A, 249: 18–26

Aranson, I.S. and Kramer, L. 2002. The world of the complex Ginzburg–Landau equation. *Reviews of Modern Physics*, 74: 99–143

Chang, H.-C. 1994. Wave evolution on a falling film. *Annual Reviews of Fluid Mechanics*, 26: 103–136

Chaté, H. 1994. Spatiotemporal intermittency regimes of the one-dimensional complex Ginzburg–Landau equation. *Nonlinearity* 7: 185–204

Chaté, H. & Manneville, P. 1994a. Phase turbulence. In *Turbulence, A Tentative Dictionary*, edited by P. Jabeling & O. Cardoso, NewYork: Plenum press

Chaté, H. & Manneville, P. 1994b. Spatiotemporal intermittency. In *Turbulence A Tentative Dictionary*, edited by P. Jabeling & O. Cardoso, NewYork: Plenum press

Cross, M.C. & Hohenberg, P.C. 1993. Pattern formation outside equilibrium. *Reviews of Modern Physics*, 65: 851–1112

Coullet, P., Gil, L. & Lega, J. 1989. Defect-mediated turbulence. *Physical Review Letters*, 62: 1619–1622

Daviaud, F. 1994. Experiments in 1D turbulence. In *Turbulence A Tentative Dictionary*, edited by P. Jabeling & O. Cardoso, NewYork: Plenum press

Gollub, J.P. 1994. Experiments on spatiotemporal chaos (in two dimensions). In *Turbulence A Tentative Dictionary*, edited by P. Jabeling & O. Cardoso, NewYork: Plenum press

Kaneko, K. (editor). 1993. *Theory and Application of Coupled Map Lattices*. Chichester and New York: Wiley

Kinzel, W. 1983. Directed percolation. In *Percolation Structures and Processes*, edited by G. Deutscher, R. Zallen & J. Adler, Annals of the Israel Physics Society, 5: 425–445

Kramer, L. & Pesch, W. 1996. Electrohydrodynamic instabilities in nematic liquid crystals. In *Pattern Formation in Liquid*

Crystals, edited by A. Buka & K. Kramer, New York: Springer
Kuramoto, Y. 1978. Diffusion-induced chaos in reaction systems. *Suppl. Progress in Theoretical Physics*, 64: 346–367
Newell, A.C. 1974. Envelope equations *Lectures in Applied Mathematics*, 15: 157–163
Pomeau, Y. 1986. Front motion, metastability and subcritical bifurcations in hydrodynamics. *Physica* D, 23: 3–11
Rabinovich, M.I., Ezersky, A.B. & Weidman, P.D. 2000. *The Dynamics of Patterns*. Singapore: World Scientific
Tabeling, P. & Cardoso, O. (editors). 1994. *Turbulence: A Tentative Dictionary*. New York: Plenum Press
Wolfram, S. (editor). 1986. *Theory and Applications of Cellular Automata*. Singapore: World Scientific

SPECTRAL ANALYSIS

Spectral analysis is a central method in studies of linear systems (which obey the superposition principle), and spectral representations are widely used in acoustics, quantum mechanics, wave propagation, optical spectroscopy, harmonic analysis, and signal processing. If $f(x)$ is a square integrable function on real line, it can be represented in a dual (spectral) space k with the integral transforms (Hildebrand, 1976)

$$f(x) = \frac{1}{2\pi}\int_{-\infty}^{\infty} \hat{f}(k)\mathrm{e}^{\mathrm{i}kx}\mathrm{d}k \tag{1}$$

and

$$\hat{f}(k) = \int_{-\infty}^{\infty} f(x)\mathrm{e}^{-\mathrm{i}kx}\mathrm{d}x. \tag{2}$$

The Fourier transform $\hat{f}(k)$ gives the spectral density of harmonic oscillations $\mathrm{e}^{\mathrm{i}kx}$ between the wave numbers k and $k+dk$. The inverse Fourier transform $f(x)$ corresponds to a spectral decomposition of a function $f(x)$ over a continuous linear combination of the harmonic oscillations $\mathrm{e}^{\mathrm{i}kx}$.

For periodic functions with a period L, such that $f(x+L)=f(x)$, the spectral density has peaks at wave numbers $k=k_n=2\pi n/L$; that is, the spectral decomposition of a function $f(x)$ becomes a discrete sum of the harmonic oscillations $\mathrm{e}^{\mathrm{i}k_n x}$:

$$f(x) = \sum_{n=-\infty}^{\infty} \hat{f}_n \mathrm{e}^{\mathrm{i}k_n x} \tag{3}$$

and

$$\hat{f}_n = \frac{1}{2L}\int_{-L}^{L} f(x)\mathrm{e}^{-\mathrm{i}k_n x}\mathrm{d}x, \tag{4}$$

where $\hat{f}_n$ are Fourier coefficients of the complex Fourier series for $f(x)$. Thus, depending on properties of a function $f(x)$, it can be decomposed over continuous or discrete spectrum in the Fourier spectral representation.

As an example, the rectangular wave defined as

$$\Delta_\varepsilon(x) = \begin{cases} 1/2\varepsilon, & |x| < \varepsilon, \\ 0, & |x| > \varepsilon \end{cases} \tag{5}$$

can be expressed in the continuous spectral representation with the Fourier transform:

$$\hat{\Delta}_\varepsilon(k) = \frac{1}{2\varepsilon}\int_{-\varepsilon}^{\varepsilon} \mathrm{e}^{-\mathrm{i}kx}\mathrm{d}x = \frac{\sin\varepsilon k}{\varepsilon k}. \tag{6}$$

The power spectrum of a signal is defined as the squared amplitude of its Fourier spectrum: $\hat{R}(k)=|\hat{f}(k)|^2$. Equivalently, the power spectrum is the Fourier spectrum of the autocorrelation function $R(x)$ defined as

$$\begin{aligned} R(x) &= \int_{-\infty}^{\infty} f(x')f(x'-x)\,\mathrm{d}x' \\ &= \frac{1}{2\pi}\int_{-\infty}^{\infty} |\hat{f}(k)|^2 \mathrm{e}^{\mathrm{i}kx}\,\mathrm{d}k \\ &= \frac{1}{2\pi}\int_{-\infty}^{\infty} \hat{R}(k)\mathrm{e}^{\mathrm{i}kx}\,\mathrm{d}k. \end{aligned} \tag{7}$$

The autocorrelation function $R(x)$ represents similarities between the function $f(x)$ and itself, and its Fourier transform can be really measured in applications.

A power spectrum measures the energy of a signal between the wave numbers k and $k+\mathrm{d}k$. The total energy of a signal is related to the power spectrum by the Parseval formula:

$$E = \int_{-\infty}^{\infty} f^2(x)\,\mathrm{d}x = \frac{1}{2\pi}\int_{-\infty}^{\infty} |\hat{f}(k)|^2\,\mathrm{d}k = R(0). \tag{8}$$

As a result, the autocorrelation function is bounded as $|R(x)| \le R(0) = E$.

Linear differential equations, especially initial-value problems for wave equations, can be easily solved with the use of spectral decompositions such as Fourier transforms. In the linear limit, for example, small-amplitude long water waves are described by the linearized KdV equation:

$$\frac{\partial u}{\partial t} + \frac{\partial^3 u}{\partial x^3} = 0, \tag{9}$$

with initial data: $u(x,0)=f(x)$. The Fourier transform method represents the solution to this problem as (Ablowitz & Fokas, 1997)

$$u(x,t) = \frac{1}{2\pi}\int_{-\infty}^{\infty} \hat{u}(k,t)\mathrm{e}^{\mathrm{i}kx}\mathrm{d}k, \tag{10}$$

where $\hat{u}(k,0)=\hat{f}(k)$. Since the Fourier transform $\hat{f}(k)$ has the property $\hat{f}'(k)=\mathrm{i}k\hat{f}(k)$, the time evolution of the spectral density $\hat{u}(k,t)$ is trivial,

$$\frac{\partial \hat{u}}{\partial t} - \mathrm{i}k^3\hat{u}(k,t) = 0, \tag{11}$$

with the solution $\hat{u}(k,t)=\hat{f}(k)\mathrm{e}^{\mathrm{i}k^3 t}$. As a result, the exact solution $u(x,t)$ of the initial-value problem for the linearized KdV equation is a spectral superposition with density $\hat{f}(k)$ of waves $\mathrm{e}^{\mathrm{i}(kx-\omega(k)t)}$, where

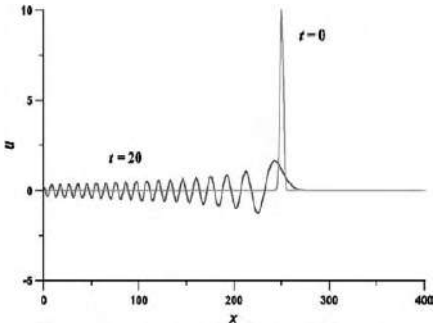

Figure 1. Exact solution $u(x, t)$ of the linear KdV equation in the Fourier spectral representation for $t > 0$, compared with the initial (Gaussian) form $u(x, 0) = e^{-x^2}$.

$\omega(k) = -k^3$ is the dispersion relation. Figure 1 shows the exact solution $u(x, t)$ at a time $t > 0$, which evolves from the initial (Gaussian) form $u(x, 0) = f(x) = e^{-x^2}$.

The inverse scattering transform (IST) extends spectral analysis for solutions of initial-value problems for nonlinear differential equations. For example, a solution of the nonlinear KdV equation

$$\frac{\partial u}{\partial t} + \frac{\partial^3 u}{\partial x^3} - u\frac{\partial u}{\partial x} = 0, \tag{12}$$

such that $u(x, 0) = f(x)$ is related to the spectrum of the stationary Schrödinger equation on a real line of x with a t-dependent potential $u(x; t)$ (Ablowitz et al., 1974)

$$-\psi_\lambda''(x) + u(x; t)\psi_\lambda(x) = \lambda\psi_\lambda(x). \tag{13}$$

If $f(x)$ is a square integrable function on real line, the spectral data consists of the continuous spectrum at $\lambda = k^2 \geq 0$ with eigenfunctions $\psi_\lambda = \Psi(x; k)$ and a finite discrete spectrum at $\lambda = -p_n^2 < 0$ with eigenfunctions $\psi_\lambda = \Psi_n(x)$. The spectral decomposition of the potential $u(x; t)$ over eigenfunctions of the continuous and discrete spectrum takes the form (Pelinovsky & Sulem, 2000)

$$u(x; t) = \frac{1}{2\pi}\int_{-\infty}^{\infty} \rho(k, t)\Psi(x; k)\,\mathrm{d}k + \sum_n \rho_n(t)\Psi_n(x), \tag{14}$$

where $\rho(k, t)$ and $\rho_n(t)$ are coefficients of the spectral decomposition. The time-evolution of the spectral data has the simple solution

$$\rho(k, t) = \rho(k, 0)e^{ik^3 t}, \quad \rho_n(t) = \rho_n(0)e^{p_n^3 t}. \tag{15}$$

The initial values for the spectral data are found from spectral analysis of the stationary Schrödinger equation with the initial potential $u(x; 0) = f(x)$.

DMITRY PELINOVSKY

See also **Generalized functions; Integral transforms; Inverse scattering method or transform; Quantum theory**

Further Reading

Ablowitz, M.J. & Fokas, A.S. 1997. *Complex Variables: Introduction and Applications*, Cambridge and New York: Cambridge University Press

Ablowitz, M.J., Kaup, D.J., Newell, A.C. & Segur, H. 1974. The inverse scattering transform-Fourier analysis for nonlinear problems. *Studies in Applied Mathematics*, 53: 249–315

Hildebrand, F.B. 1976. *Advanced Calculus for Applications*, 2nd edition, Englewood Cliffs, NJ: Prentice-Hall

Pelinovsky, D.E. & Sulem, C. 2000. Eigenfunctions and eigenvalues for a scalar Riemann–Hilbert problem associated to inverse scattering. *Communications in Mathematical Physics*, 208: 713–760

SPIN SYSTEMS

Spin systems generally refer to ordered magnetic systems. A feel for how spins behave can be obtained by observing the behavior of two or more small compasses or magnetic needles pinned close to each other but free to rotate in a plane (perpendicular to the north–south direction), so that they align in parallel corresponding to a minimum energy configuration.

Even though magnetism is one of the oldest natural phenomena known, it took many centuries to identify its origin. In 1820, the Danish physicist Hans Oersted observed that electric current flowing through a wire affects a nearby magnet, and it is now known that the motion of an electron in an orbit around the nucleus of an atom is equivalent to a small electric current loop that behaves as an atomic magnet called a magnetic dipole moment. Each electron also possesses a rotation about its own axis, which is identified as electron spin, and is equivalent to a circulating electric current with its own dipole magnetic moment.

More generally, spin angular momentum or spin is an intrinsic property, associated with quantum particles, which does not have a classical counterpart. The magnetic dipole moment due to the spinning motion with spin angular momentum operator $\boldsymbol{S}$ is given by $\boldsymbol{m}_S = -(g\mu_B/\hbar)\boldsymbol{S}$, where g is the gyromagnetic ratio, μ_B is the Bohr magneton and $\hbar = h/2\pi$ is Planck's constant.

Macroscopically, all substances are magnetic to some extent and every material when placed in a magnetic field acquires a magnetic moment. Magnetic materials can be classified in terms of magnetic moment in the absence of an applied field. The magnetic moment is zero for each atom in diamagnetic materials. In the case of paramagnetic materials, for each atom the moment is nonzero but still averages to zero over many atoms. In ferromagnetic materials, the moment of each atom and even the average is not zero (Mattis, 1988).

Model	Directional Coefficient
Ising/Potts	$a = b = 0$
XY	$c = 0$
Easy axis exchange anisotropy	$c > a = b$
Easy plane exchange anisotropy	$c < a = b$
Heisenberg	$a = b = c = 1$
XYZ	$a \neq b \neq c$

Table 1. Ferromagnetic models.

Ferromagnetic materials, which are made up of domains, exhibit long-range ordering that causes the spins of the atomic ions to line up parallel to each other in a domain. The underlying interaction originates from an exchange interaction that is caused by the overlapping of electronic wave functions that has no classical analog. The exchange interaction is a quantum phenomenon of electrostatic origin first proposed by Heisenberg, and the Hamiltonian representing spin-spin exchange interaction is given by

$$H_{\text{ex}} = -\sum_{\langle ij \rangle} J_{ij} \boldsymbol{S}_i \cdot \boldsymbol{S}_j. \tag{1}$$

Here $\boldsymbol{S}_i$ is the total spin of all the electrons bound to the atom or ion at the lattice site i. J_{ij} is the phenomenological exchange constant and is positive for ferromagnetic coupling. It is often sufficient to consider only interaction of nearest neighbors, represented by the bracket $\langle ij \rangle$. In the isotropic case J_{ij} is treated as a constant, J.

Different magnetic spin models can be identified by generalizing the Heisenberg Hamiltonian by introducing directional coefficients,

$$H_{\text{ex}} = -\sum_{\langle ij \rangle} \left[a S_{ix} S_{jx} + b S_{iy} S_{jy} + c S_{iz} S_{jz} \right]. \tag{2}$$

The underlying models are indicated in Table 1. Among these, the Ising model is the simplest, where the interacting spins can be either parallel or antiparallel. The Potts model is a generalization of the Ising model where the number of spin states is extended to k equally spaced directions in a plane.

Other models involve additional interactions: (i) *magnetocrystalline anisotropy* is due to interaction between the crystal field and the spin-orbit coupling, either of easy axis or of easy plane. (ii) *Zeeman energy*: When a strong external magnetic field $\boldsymbol{H}$ is applied, the Hamiltonian is modified with the addition of a term $H_Z = -g\mu_B \sum_i \boldsymbol{S}_i \cdot \boldsymbol{H}$. (iii) One can also consider interactions such as biquadratic exchange, or weak interactions such as Dzyaloshinski–Moriya type.

There are certain materials for which the exchange integrals J_{ij} become negative. Consequently, the spins align antiparallel to each other so that the net magnetization is zero. These materials are called antiferromagnets and are normally modeled to be made up of two sublattices. However, if the resulting total magnetization, which is the difference between that of the two sublattices, is nonzero, the material is a ferrimagnet.

A spin glass is another state of magnetism that is different from the long-range ordered ferro- and antiferromagnetic phases. A spin glass phase can be considered as consisting of randomly interacting spins with ferro- or antiferromagnetic coupling between them. The combination of the randomness with the competing or mixed interactions causes frustration. Consequently, the exchange integrals J_{ij} are normally distributed random variables corresponding to the so-called Ruderman, Kittel, Kasuya, and Yoshida (RRKY) interaction. The two famous models that describe spin glass are the Edwards–Anderson (EA) model and the Sherrington–Kirkpatrick (SK) mean field model.

The spin glass theory can also be considered as a statistical model of neural networks. The simple spin glass theory based on the SK model provides a qualitative description of memory. In a neural network, the minimal structure element is a neuron whose state can be described by one real variable, and a simple Ising representation $\boldsymbol{S}_i = \pm 1$ is often used. The problem of neural network systems can be formulated by writing the Hamiltonian in Ising form with the so-called Hebbian learning rule for J_{ij}, which is the Hopfield model (Dotsenko, 1994).

The Bethe ansatz is extremely useful in solving quantum spin chain models and to obtain exact results including ground state and excited states. A chain of spin one-half with spin-spin coupling has been solved using the Bethe ansatz method. However, the quantum mechanical description corresponding to the spin Hamiltonian with higher spin values is extremely complicated because it is difficult to know in which particular state one of the individual spins finds itself. Even in the ground state this is impossible. Hence in these cases, one looks for limiting procedures, either classical or semiclassical.

Owing to the presence of the exchange interaction, a small disturbance in one of the spins will be propagated in the form of spin waves. It can also be regarded as oscillations in the magnetic moment density, propagating through a magnetically ordered crystal. The spin wave energy must be equal to the excitation energy of the crystal required to cause a change in the orientation of the spin. The basic entity of the quantized form of the spin wave is called a magnon.

In semiclassical theories of magnetism it is common to approximate the unwieldy spin operators or matrices (which obey the standard spin commutation relations) by the analogous harmonic oscillator operators. Among the machineries established to handle the spin operators, namely, (i) Holstein–Primakoff (H–P) transformation, (ii) Schwinger–Boson representation, (iii) Dyson–Maleev transformation, and (iv) Jordon–

Wigner transformation. The H–P transformation is the most useful one.

Just like photons and phonons, spin waves are bosons describing collective excitations that involve all the spins to the same degree. The operators $S_n^{\pm} = S_{nx} \pm iS_{ny}$ act on the ground state as field theoretical creation and annihilation operators. It is, thus, reasonable to change by means of a unitary transformation to operators a and a^+ that satisfy the Bose commutation relation $[a_i, a_j^+] = \delta_{ij}$. In this way, one can obtain the H–P transformation of spin operators, which transforms the quantum mechanical spin operators into standard boson operators. In the low-temperature limit, one can use semiclassical expansion for S_n^+ and S_n^-. The Heisenberg equation of motion for the boson operator $i\hbar da_j/dt = [a_j, H]$ when combined with Glauber's coherent state representation for Bose operators in the long wavelength, low temperature limit (continuum limit) leads to nonlinear evolution (partial differential) equations. Specific one-dimensional cases correspond to integrable spin models exhibiting soliton type spin excitations in addition to linear magnons (Kosevich et al., 1991).

Alternatively, in the large spin limit, the quantum description goes over to the classical vector model for spin, so that the spin operator can be replaced by an ordinary vector of length $s(s+1) > s$, which can be treated as a dynamical/canonical variable. For a ferromagnet described by Heisenberg Hamiltonian (Equation (1)) or its generalization, the classical canonical equations for the spins can be obtained in analogy with a spinless nonrelativistic particle, which is a typical nonlinear dynamical system. The resultant equation of motion $d\boldsymbol{S}_n/dt = \{\boldsymbol{S}_n, H\}$, where $\{\ \}$ represents spin Poisson bracket defined for functions of spins under continuum approximation, reduces to the appropriate Landau–Lifshitz (LL) equation. In real magnets, dissipative effects also play an important role, which is included in the LL equation via Gilbert damping. Thus, the LL equation with Gilbert damping (originally derived phenomenologically) is written as

$$\frac{\partial}{\partial t}\boldsymbol{S}(\boldsymbol{r}, t) = \boldsymbol{S} \times \boldsymbol{F} + \lambda \boldsymbol{S} \times (\boldsymbol{S} \times \boldsymbol{F}),$$
$$\boldsymbol{S} = (S_x, S_y, S_z), \quad \boldsymbol{S}^2 = 1, \qquad (3)$$

where $\boldsymbol{F}$ is the effective field and λ is the Gilbert damping parameter. A typical form for $\boldsymbol{F}$ is $\boldsymbol{F} = J\nabla^2\boldsymbol{S} + 2A(\boldsymbol{S} \cdot \boldsymbol{n})\boldsymbol{n} + \mu\boldsymbol{H}$, where A is the anisotropy parameter, $\boldsymbol{H}$ is the external magnetic field, and $\boldsymbol{n}$ is a unit vector.

The Landau–Lifshitz equation is a highly non-trivial vector nonlinear partial differential equation in three spatial dimensions. Several one-dimensional cases (without damping) corresponding to quasi-one-dimensional ferromagnetic spin chains (Mikeskса & Steiner, 1991; Kosevich et al., 1991) have been found to be completely integrable soliton systems. These include the isotropic case, uniaxial, and biaxial as well as circularly symmetric cases and are related to the nonlinear Schrödinger equation (Lakshmanan, 1977), (Lakshmanan et al., 1990) and its generalizations. In two dimensions, instanton and vortex-type structures have been identified. Magnetic spatiotemporal patterns have also been identified in the presence of damping and external oscillating fields.

The study of spin excitations in magnetic systems has numerous potential applications. These include (i) magnetic storage devices such as magnetic disks in computers, (ii) spintronics or spin electronics (microelectronic devices that function using the spin of the electrons), (iii) magnetic microchips (magnetic dots, magnetic waves, and magnetic computers), and (iv) magneto-optical recording. (For details, refer to the special issue on Magneto-electronics, *Physics Today*, April 1995).

MUTHUSAMY LAKSHMANAN

See also **Attractor neural network; Bethe ansatz; Ferromagnetism and ferroelectricity; Ising model; Landau–Lifshitz equation; Poisson brackets; Solitons**

Further Reading

Dotsenko, V. 1994. *An Introduction to the Theory of Spin Glasses and Neural Networks*, Singapore: World Scientific

Kosevich, A.M. Ivanov, B.A. & Kovalev, A.S. 1991. Magnetic Solitons. *Physics Reports*, 194: 117–238

Lakshmanan, M. 1977. Continuum spin systems as an exactly solvable dynamical system. *Physics Letters* A, 61: 53–54

Lakshmanan, M., Porsezian, K. & Daniel, M. 1990. On the nonlinear dynamics of the one-dimensional classical Heisenberg ferromagnetic spin chain. In *Nonlinear Evolution Equations: Integrability and Spectral Methods*, edited by A. Degasperis, A.P. Fordy & M. Lakshmanan, Manchester: Manchester University Press

Mattis, D.C. 1988. *Theory of Magnetism I: Statics and Dynamics*, Berlin and New York: Springer

Mikeska, H.J. & Steiner, M. 1991. Solitary excitations in one-dimensional magnets. *Advances in Physics*, 40: 191

SPIRAL WAVES

Rotating spiral waves occur in a wide range of chemical, biological, and physical systems that can be considered as effectively two-dimensional excitable or oscillatory media in which the local nonlinear dynamics exhibits threshold behavior, separating an excited state from a recovered state (Holden et al., 1991). In such a medium, waves of excitation spread without decrement through the stationary medium, with diffusive spread of the excitation from a region triggering excitation of neighboring regions.

A single spiral wave in a large homogeneous medium acts as an organizing center, imposing its pattern throughout the medium. It has the characteristics of

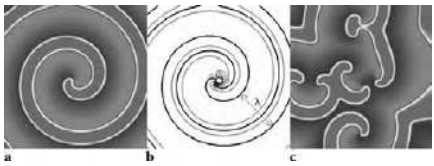

Figure 1. Spiral wave solutions of the FitzHugh–Nagumo equations for an excitable medium: (a) snapshot of solitary spiral wave; (b) intersection of excitation and recovery isolines defining the tip (solid circle), which meanders biperiodically around the central corel; and (c) evolving field of wavebreaks.

a field, in that it fills the medium, but it also has a location. The location of a spiral wave is that of its center, variously defined as the central core that is not invaded by the propagating wave, and around which the spiral rotates; or as a phase singularity; or by the tip, defined by where the wave front meets the wave back; or by the intersection of two isolines. For a rigidly rotating spiral in an isotropic medium, the tip encloses a circular core, but even in a homogeneous medium, the tip motion can be complex, meandering quasi-periodically within a bounded region, or hypermeandering in an unbounded region, and any inhomogeneities and boundaries interactions can produce drift (Barkley, 1994). Along any radius far from the core, activity appears as a periodic wave train with a temporal frequency ω (for a rigidly rotating spiral equal to the rotation frequency of the spiral) and spatial wavelength λ. These are generally single-valued functions of the medium parameters. The wave front (or any other isoline) approximates an Archimedean spiral (the involute of a circle) with a pitch λ, as illustrated in Figure 1b. The simple (one-armed) Archimedean rotating spiral in polar coordinates (θ, r) is a periodic function of phase ϕ

$$\phi = \omega t \pm \theta + a(r - r_0) \qquad (1)$$

with $a > 0$ giving the wavelength λ and pitch $\mathrm{d}r / \mathrm{d}\theta|_{\phi = \mathrm{const}}$ equals to $1 / a$.

If a stable spiral wave is subject to a parametric perturbation, the form of the spiral will be restored, but its location and phase may be changed: this allows periodic perturbations, at the same frequency as the rotation frequency of the spiral, to produce a directed, resonant drift. A single spiral need not be stable—even in a parametrically homogeneous medium, dynamical heterogeneities produced by the rotating spiral wave can lead to wave breaks, resulting in pairs of new phase singularities that may develop into new spirals, collapse, or be extinguished, giving a spiral wave turbulence as illustrated in Figure 1c. In such an evolving field of wave breaks, the singularities may be considered as defects; are born and annihilate on collision, in pairs with opposite chirality; or exit the medium at boundaries.

The best studied laboratory example of spiral waves is the Belousov–Zhabotinsky reaction, a chemical excitable or oscillatory reaction originally constructed as an organic chemical analogue for oscillatory reactions in a biochemical system, in which the phase of the redox oscillation is monitored by color changes. In a shallow layer of solution in a Petri dish, spirals and interacting spirals can be initiated (Winfree, 1972), and spatiotemporal changes in activity can be monitored optically and quantified (Müller et al., 1987). Winfree's experimental and numerical modeling of simplified models and caricatures (Winfree, 1991) of two- and three-dimensional excitable systems established much of the phenomenology of spiral wave behavior.

Spiral waves occur in several biological systems. In many cell types there are intracellular waves of calcium, where calcium-induced calcium release provides the positive feedback necessary for excitability. In the slime mold, where the intercellular relaying of a chemotactic signal—cyclic AMP—between individual amoebae by cAMP-induced cAMP release provides the excitability, the social amoebae collect together in a rotating spiral wave and aggregate into a slug, which can then metamorphose into a fruiting body. An important example is from cardiac patho-physiology, where the three-dimensional analogue of a spiral, the scroll, provides the re-entrant propagation that produces high frequency arrhythmias in cardiac muscle and provides the route to ventricular fibrillation and sudden cardiac death.

In physics, spiral waves are found in surface catalysis, nonlinear optical media, and it has been suggested that spiral galaxies represent a rotating spiral wave of star formation and death.

In all these examples, the excitable medium can be modeled by a reaction-diffusion equation, in which only the excitatory variable (as in most biological examples) or both excitatory and recovery variables (as in most chemical examples) have nonzero diffusion coefficients. Spiral wave solutions of mechanistically detailed, high order models, or simplifications, can be obtained by initiation from artificial initial conditions, or by imposing a wave break or wavebreaking dynamical or parametric heterogeneity. Much of the phenomenology can be seen in the simple, two-variable FitzHugh–Nagumo system, or computationally faster simplifications (Zykov, 1987), and reproduced by eikonal equations that describe the dependence of the propagation velocity of the wave front on its curvature (Mikhailov et al., 1994).

ARUN V. HOLDEN

See also **Belousov–Zhabotinsky reaction; Excitability; FitzHugh–Nagumo equation; Geometrical optics, nonlinear; Reaction-diffusion systems; Vortex dynamics in excitable media**

Further Reading

Barkley, D. 1994. Spiral meandering. In *Chemical Waves and Patterns*, edited by R. Kapral & K. Showalter. Dordrecht: Kluwer, pp. 163–194

Holden, A.V., Markus, M. & Othmer, H.G. 1991. *Nonlinear Wave Processes in Excitable Media*, New York: Plenum Press

Mikhailov, A.S., Davydov, V.A. & Zykov, V.S. 1994. Complex dynamics of spiral waves and motion of curves. *Physica* D, 70: 1–39

Müller, S.C., Plesser, T. & Hess, B. 1987. Two-dimensional spectrophotometry of spiral wave propagation in the Belousov–Zhabotinskii reaction. *Physica* D, 24: 71–96

Winfree, A.T. 1972. Spiral waves of chemical reaction. *Science*, 175: 634–636

Winfree, A.T. 1991. Varieties of spiral wave behavior: an experimentalist's approach to the theory of excitable media. *Chaos* 1: 303–334

Zykov, V.S. 1987. *Simulation of Wave Processes in Excitable Media*, Manchester: Manchester University Press

STABILITY

The concept of stability lies at the heart of mathematical physics. Although in a perfect environment it might be thought possible to balance a pencil on its point, this is not possible in the real, noisy world—a pencil standing on its point is unstable. Meanwhile a hexagonal pencil lies easily on its side in a stable equilibrium. Intermediate is the pencil standing on its flat end, which can be achieved, albeit with difficulty, because this configuration is metastable, meaning stable against infinitesimally small disturbances, $\boldsymbol{D}_{\mathrm{S}}$, and unstable against large disturbances, $\boldsymbol{D}_{\mathrm{L}}$. Notice that under $\boldsymbol{D}_{\mathrm{S}}$, the pencil has more than one stable equilibrium (multistability). A special case is a circular pencil on its side: if it rolls a little, and it will not come back and so is marginally stable. Generalizing these experiences, a state is declared stable if it is physically observable under $\boldsymbol{D}_{\mathrm{S}}$: otherwise, it is unstable.

In 1892, Aleksandr Lyapunov formalized this intuitive idea of stability against $\boldsymbol{D}_{\mathrm{S}}$ by considering free motions of a dynamical system in phase space. Although this ignores external noise, the results agree with more realistic stochastic criteria. Consider a system of n first-order differential equations, $\dot{\boldsymbol{x}} = \boldsymbol{f}(\boldsymbol{x})$, giving a stationary vector field in the phase space spanned by the n components of vector $\boldsymbol{x}$. Trajectories fill this space with a fluid-like flow. A driven oscillator is put into this form by identifying velocity as a second phase coordinate and time as a third (with $\dot{t} = 1$).

A fixed (equilibrium) point with $\boldsymbol{f}(\boldsymbol{x}) = \boldsymbol{0}$ is asymptotically stable if all local trajectories flow into it (Figure 1). This point attractor is exemplified by the hanging state of a damped pendulum. The equilibrium of a Hamiltonian system (undamped pendulum) can be at most neutrally stable with all trajectories staying close, though not converging. A point is unstable if any single adjacent motion moves out of the neighborhood (inverted pendulum).

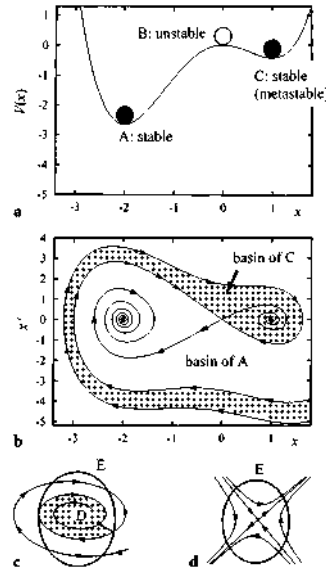

Figure 1. Potential well (a), and phase portrait (b), for $\ddot{x} + 0.4\dot{x} + \mathrm{d}V(x)/\mathrm{d}x = 0$, where $V(x) = x^4/4 + x^3/3 - x^2$, showing two asymptotically stable minima and an unstable maximum. In the enlarged focus (c), representing either minimum, we can devise a region D from which no trajectories leave the small region E, guaranteeing stability; in (d) we cannot construct a closed neighborhood around the saddle from which no trajectories leave E, proving instability.

Linear Stability

Stability analysis starts with the linearized equations describing small variations about the state. For a fixed point of a flow, stability hinges on the real parts, α_i, of the eigenvalues. Typically, the point will be hyperbolic (noncritical) with no $\alpha_i = 0$, and we then have (asymptotic) stability if and only if (*iff*) all $\alpha_i < 0$. Any one $\alpha_i > 0$ gives instability.

For a cycle we use an $(n-1)$-dimensional Poincaré mapping, $\boldsymbol{x}_{i+1} = \boldsymbol{F}(\boldsymbol{x}_i)$, where the cycle is a fixed point with $\boldsymbol{x}_{i+1} = \boldsymbol{x}_i$. Stability hinges on the moduli, ρ_i, of the eigenvalues. Stability of a (hyperbolic) periodic orbit requires all $\rho_i < 1$.

An unstable state, attracting in some directions, repelling in others, is a saddle. The instability index (degree of instability) is the number of $\alpha_i > 0$ (or $\rho_i > 1$). In nonlinear dissipative systems, saddles with index 1 play an important role organizing basin boundaries.

Nonlinear Stability

A conservative system has zero divergence in phase space (Liouville's theorem), like an incompressible

fluid. With dissipation, the negative divergence ensures that an ensemble of starts will shrink onto an attracting set of zero volume. Such a post-transient can be a point, periodic, quasi-periodic, or chaotic attractor. Generically, each attractor is surrounded by its own basin of attraction. All transients from a vanishingly small neighborhood move asymptotically back to it, making it asymptotically stable.

To assess how stable an attractor is against finite disturbances, we estimate the size of its basin. A brute-force method is to make computer simulations from a grid of starts; more efficient is cell-to-cell mapping (Hsu, 1980). A refined approach is to locate a governing saddle and run simulations backwards in time to trace out the boundary formed by its stable manifold (inset). Boundaries can, however, be fractal, making their detailed location impossible (McDonald et al., 1985; Thompson & Stewart, 2002). Analytical techniques, notably Lyapunov's second (direct) method (La Salle & Lefschetz, 1961), can identify contracting (trapping) regimes of guaranteed return, but they may be excessively conservative.

Local nonlinear analysis is necessary to test the Lyapunov stability of a nonhyperbolic state at which a system is about to lose its stability. An oscillator with exclusively nonlinear negative damping is, for example, linearly (non-asymptotically) stable but nonlinearly unstable. In contrast to Lyapunov's local concept, a point is globally stable if every trajectory tends to it.

Loss of Stability

When linear theory indicates a loss of stability, the nonlinear system exhibits a bifurcation. Consider first an α_i passing through zero along a path. If a real eigenvalue becomes zero, we have a saddle-node bifurcation. Typically this gives a fold, at which the path folds smoothly back at a maximum of the control parameter, μ. A saddle-node coalescence at $\mu = \mu^{\mathrm{C}}$ leaves no local solution; the system jumps to a distant, unrelated attractor (Figure 2). With symmetry the saddle-node manifests itself as a pitchfork (Figure 3). Two α_i of a complex conjugate pair passing through zero give the Hopf bifurcation generating stable or unstable cycles.

A mapping loses stability when a ρ_i reaches one. If a real eigenvalue equals $+1$, we have a saddle-node bifurcation, typically a cyclic fold. If it equals -1, we have a flip (period-doubling) bifurcation. If a complex conjugate pair penetrates the unit circle, we have the Neimark–Sacker (secondary Hopf) bifurcation.

Structural Stability

Because parameters of a physical system are never known precisely and may vary, a mathematical model should ideally have a phase portrait that is robust against small changes in the model itself. Small changes of parameters and functions should not qualitatively change the topology. A portrait having this robustness is structurally stable. Structurally unstable portraits encountered under variation of μ signal a bifurcation.

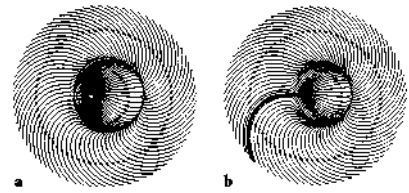

Figure 2. Two phase portraits illustrating the ABC of nonlinear dynamics. Here A stands for attractor, an example of which we see in the center of (a). B stands for basin, and we see the circular basin of attraction in (a); its boundary defined by the flow into an unstable saddle point. C stands for catastrophe, conveniently used here to mean bifurcation. Under variation of a control, (a) has changed qualitatively to become the portrait (b); the central stable node has collided with the saddle in a fold bifurcation, leaving no attractor and all trajectories flowing out to infinity. (Figure reproduced with permission of John Wiley from Thompson & Stewart 2002.)

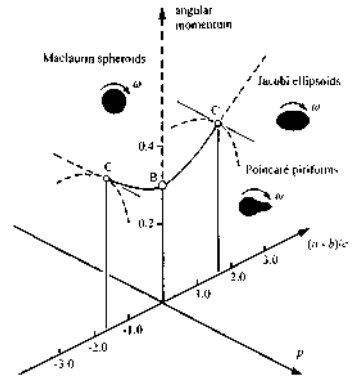

Figure 3. Stability of a rotating mass of a self-gravitating liquid is a classical problem in astrophysics, relevant to planetary evolution and the origin of satellites. It dates back to Poincaré (1899), and following the buckling studies of Euler, it gave fresh impetus to the development of stability and bifurcation theory. Stable (unstable) paths are denoted by solid (broken) lines. As the angular momentum parameter is slowly increased, the rotationally symmetric spheroids become unstable at the supercritical pitchfork at B. Emerging from B is a rising path of stable ellipsoids (with semi-axes a, b, c), which then exhibit a secondary instability at the subcritical pitchforks at C, from which unstable pear-shaped forms of "amplitude" p descend. (Figure reproduced with permission of John Wiley from Thompson, 1982.)

If we have m controls, μ_i, bifurcations observed under variation of one μ_i will lie in control space on surfaces of dimension $m-1$. A bifurcation in phase-control space is structurally stable if the whole event is topologically robust. Catastrophe theory (Poston & Stewart, 1978) shows how bifurcations of equilibria that are structurally unstable under one μ_i can be made structurally stable (unfolded) by embedding in a higher-dimensional control space. The codimension is the number of μ_i needed to achieve this. An example is the symmetry-breaking imperfection needed to unfold a pitchfork into the codimension-two cusp. The resulting saddle-node locus gives the imperfection-sensitivity of elastic stability theory (Thompson & Hunt, 1973).

MICHAEL THOMPSON

See also **Attractors; Equilibrium; Phase space; Wave stability and instability**

Further Reading

Hsu, C.S. 1980. A theory of cell-to-cell mapping for nonlinear dynamical systems. *ASME Journal of Applied Mechanics*, 47: 931–939

La Salle, J. & Lefschetz, S. 1961. *Stability by Liapunov's Direct Method with Applications*, New York: Academic Press

Lyapunov, A. 1892. *Problème général de la stabilité du mouvement*, Kharkov (in Russian); French translation in *Annals of the Faculty of Science, University of Toulouse*, vol. 9 (1907); reprinted, Princeton, NJ: Princeton, University Press (1949)

McDonald, S.W., Grebogi, C., Ott, E. & Yorke, J.A. 1985. Fractal basin boundaries. *Physica* D, 17: 125–153

Poincaré, H. 1899. *Les Méthodes nouvelles de la mécanique céleste*, vols. 1–3, Paris: Gauthier-Villars; as *New methods of celestial mechanics*, 3 vols., Woodbury, NY: American Institute of Physics, 1991

Poston, T. & Stewart, I. 1978. *Catastrophe Theory and Its Applications*, London: Pitman

Thompson, J.M.T. 1982. *Instabilities and Catastrophes in Science and Engineering*, Chichester: Wiley

Thompson, J.M.T. & Hunt, G.W. 1973. *A General Theory of Elastic Stability*, London: Wiley

Thompson, J.M.T. & Stewart, H.B. 2002. *Nonlinear Dynamics and Chaos*, 2nd edition, Chichester and New York: Wiley

STABLE AND UNSTABLE MAINFOLDS

See **Phase space**

STANDARD MAP

The standard or Taylor–Chirikov map is a family of area-preserving maps: $z' = f(z)$ where $z = (x, y)$ is the original position and $z' = (x', y')$ the new position after application of the map, which is defined by

$$x' = x + y - \frac{k}{2\pi}\sin(2\pi x),$$
$$y' = y - \frac{k}{2\pi}\sin(2\pi x). \qquad (1)$$

Here x is a periodic configuration variable (usually computed modulo 1), $y \in \mathbb{R}$ is the momentum variable, and the parameter k represents the strength of a nonlinear kick. This map was first proposed in 1968 by Bryan Taylor and then independently obtained by Boris Chirikov to describe the dynamics of magnetic field lines. The standard map and Hénon's area-preserving quadratic map are extensively studied paradigms for chaotic Hamiltonian dynamics.

The standard map is an "exact symplectic" map of the cylinder. Because $x'(x, y)$ is a monotone function of y for each x, it is also an example of a monotone twist map (*See* **Aubry–Mather theory**). Every twist map has a Lagrangian generating function, and the standard map is generated by $F(x, x') = \frac{1}{2}(x' - x)^2 + (k/4\pi^2)\cos(2\pi x)$, so that $y = -\partial F/\partial x$ and $y' = \partial F/\partial x'$. The map can also be obtained from a discrete Lagrangian variational principle as follows. Define the discrete action for any configuration sequence $\ldots, x_{t-1}, x_t, x_{t+1}, \ldots$ as the formal sum

$$A[\ldots, x_{t-1}, x_t, x_{t+1}, \ldots] = \sum_t F(x_t, x_{t+1}). \qquad (2)$$

Then an orbit is a sequence that is a critical point of A. This gives the discrete Euler–Lagrange equation

$$x_{t+1} - 2x_t + x_{t-1} = -\frac{k}{2\pi}\sin(2\pi x_t). \qquad (3)$$

This second difference equation is equivalent to (1) upon defining $y_t = x_t - x_{t-1}$.

The standard map is an exact or approximate description of many physical systems, including the "kicked rotor." Consider a rigid body with moment of inertia I that is free to rotate in a horizontal plane about its center of mass. Suppose that an impulsive torque $\Gamma(\theta) = -A\sin(\theta)$ is applied to the rotor at times nT, $n \in \mathbb{Z}$. Let (θ_j, L_j) be angular position and angular momentum at time $jT - \varepsilon$ for $\varepsilon \to 0^+$. At time T later, these become $(\theta_{j+1}, L_{j+1}) = (\theta_j + (T/I)L_{j+1}, L_j + \Gamma(\theta_j))$. Scaling variables appropriately gives (1).

The standard map also describes the relativistic cyclotron and is the equilibrium condition for a chain of masses connected by harmonic springs in a periodic potential—the Frenkel–Kontorova model introduced in 1938 (Meiss, 1992). Similar maps include Chirikov's separatrix map (valid near the separatrix of a resonance), the Kepler map (describing the motion of comets under the influence of Jupiter as well as a classical hydrogen atom in a microwave field), and the Fermi map (for a ball bouncing between oscillating walls) (Lichtenberg & Lieberman, 1992). The higher-dimensional version is the Froeshlé map (*See* **Symplectic maps**).

Symmetries

The standard map f has a number of symmetries that lead to special dynamical behavior. To see these, it is convenient to lift the map from the cylinder to the plane by extending the angle variable x to $\mathbb{R}$.

Let $T_{m,n}(x, y) = (x+m, y+n)$ be the translation by an integer vector (m, n). As f is periodic, its lift has a discrete translation symmetry $f \circ T_{m,0} = T_{m,0} \circ f$. More unusually, the standard map also has a discrete vertical translation symmetry $f \circ T_{0,n} = T_{0,n} \circ f$. Identifying orbits equivalent under these symmetries implies that standard map can be thought of as acting on the torus $\mathcal{T} = \{-\frac{1}{2} \le x, y < \frac{1}{2}\}$.

The standard map also commutes with the reflection $S(x, y) = (-x, -y)$. This can be used to identify the lower half plane with the upper one and to restrict the map to the space $\mathcal{S} = \{(x, y) : -\frac{1}{2} \le x < \frac{1}{2},\ 0 \le y \le \frac{1}{2}\}$ identifying $(-\frac{1}{2}, y) \equiv (\frac{1}{2}, y)$ and each half of the upper and lower boundaries: $(x, 0) \equiv (-x, 0)$, $(x, \frac{1}{2}) \equiv (-x, \frac{1}{2})$. The map on the two sphere $\mathcal{S}$ is singular at the corners $(\pm\frac{1}{2}, 0)$ and $(\pm\frac{1}{2}, \frac{1}{2})$.

The standard map is also reversible; it is conjugate to its inverse $RfR^{-1} = f^{-1}$ (Lamb & Roberts, 1998). One reversor is $R_1(x, y) = (-x, y - (k/2\pi)\sin(2\pi x))$; this generates a family of reversors $R = f^n \circ R_1$. These reversors are involutions, $R^2 = id$, thus f can be written as the composition of two involutions $f = (f \circ R) \circ R$. Finally, the composition of a symmetry and a reversor is also a reversor, so that, for example, $R_2 = SR$ is also a reversor.

Symmetric orbits are invariant under a symmetry or a reversor. This is particularly interesting since symmetric orbits must have points on the fixed sets of the reversor, $\mathrm{Fix}(R) = \{z : z = R(z)\}$, or on $\mathrm{Fix}(fR)$. Because these fixed sets are curves, symmetric orbits are particularly easy to find. Rimmer showed that the bifurcations of symmetric orbits are special; for example, they undergo pitchfork bifurcations (*See* **Bifurcations**).

Dynamics

When $k = 0$, the dynamics of the standard map are integrable: the momentum y is an invariant. On each invariant circle $\mathcal{C}^0_\omega = \{(x, y) : y = \omega\}$, the angle after t iterates is given by $x_t = x_0 + \omega t \mod 1$; thus, the dynamics are that of the constant rotation, $R_\omega(\theta) = \theta + \omega$, on the circle with rotation number ω. When ω is rational, every orbit on $\mathcal{C}^0_\omega$ is periodic; otherwise, they are quasi-periodic and densely cover the circle.

When $|k| \ll 1$, Moser's version of the KAM theorem implies that most of these invariant circles persist; that is, there is a rotational invariant circle $\mathcal{C}_\omega$ on which the dynamics is conjugate to the rotation R_ω (*See* **Hamiltonian systems**). KAM theory applies to circles with Diophantine rotation number, that is, $\omega \in \{\Omega : |n\Omega - m| > c/n^\tau;\ \forall m, n \in \mathbb{Z}, n \neq 0\}$ for some $\tau \ge 1$ and $c > 0$. This excludes, of course, all of the rational rotation numbers as well as intervals about each rational, but still leaves a positive measure set. While it is difficult to obtain reasonable estimates for the interval of k for which all Diophantine circles (with given c and τ) persist, in 1985 Herman showed analytically that there is at least one invariant circle when $|k| \le 0.029$, and de la Llave & Rana (1990) used a computer-assisted proof to extend this result up to 0.91.

Some of the periodic orbits on the rational circles $\mathcal{C}^0_{m/n}$ also persist for nonzero k. Indeed, the Poincaré–Birkhoff theorem implies that there are at least two period n orbits (with positive and negative Poincaré indices). Aubry–Mather theory implies that orbits with rotation number m/n can be found variationally; one is a global minimum of the action (2), and the other is a minimax point (a saddle of A with one downward direction). For example, when $k > 0$, $(\frac{1}{2}, 0)$ is a minimizing fixed point, and $(0, 0)$ is a minimax fixed point. The reversibility of the standard map implies that there must be symmetric periodic orbits for each $\omega = m/n$ as well. Indeed, it is observed that the minimax periodic orbits always have a point on the line $\mathrm{Fix}(R) = \{y = 0\}$, the "dominant" symmetry line.

The minimax orbits are elliptic when k is small enough. A convenient measure of stability of a period-n orbit is Greene's residue

$$R = \frac{1}{4}(2 - Tr(M)), \quad M = \prod_{t=0}^{n-1} Df(z_t).$$

An orbit is elliptic when $0 < R < 1$. For example, the fixed point $(0, 0)$ has residue $k/4$. Perturbation theory shows that the residues of the minimizing and minimax orbits are $\mathcal{O}(k^n)$.

Each nondegenerate minimum of the action (2) is a hyperbolic orbit and has unstable and stable manifolds. For each minimizing m/n orbit, these intersect and enclose the minimax orbit, forming an island chain or resonance. The intersection of the manifolds is transverse, though the angle between them is exponentially small in k (Gelfreich & Lazutkin, 2001).

A number of island chains are easily visible in computer simulations. In the color figure (*See* **Standard map**: on page 8 of color plate section), we show a number of orbits of the standard map for $k = 0.6$ on the torus $\mathcal{T}$. In the figure, each of the blue curves is formed from many iterates on a rotational invariant circle like those predicted by the KAM theorem. The green orbits are secondary and tertiary circles arising from resonances.

When stable and unstable manifolds intersect transversely, some iterate of the map has a Smale horseshoe. This implies that there is, at least, a Cantor set of chaotic orbits. Umberger & Farmer (1985)

showed numerically that there is a fat fractal set on which the dynamics has a positive Lyapunov exponent. The proof of this statement is still illusive. The regions occupied by chaotic orbits appear to grow in measure as k increases. Numerically, it appears that a single initial condition densely covers each "zone of instability," a chaotic zone bounded by invariant circles. Chaotic trajectories that were only slightly visible in the previous color figure (gold orbits near the stable and unstable manifolds of the resonances) dominate the dynamics when $k = 2.0$ (*See* **Standard map**: page 8 in the color plate section). At this value of k, there are no rotational invariant circles. In the figure, the gold region is filled by a single trajectory with 1.5×10^6 iterates. It appears to densely cover most of phase space, though there are still a number of secondary and tertiary islands visible.

There are also many elliptic periodic orbits that are created for nonzero k. For example, the $(0, 0)$ fixed point undergoes a period-doubling bifurcation at $k = 4$, creating a period-two orbit. More generally, when the eigenvalues of any elliptic period-n orbit are $\lambda_\pm = e^{\pm 2\pi i\omega}$, then new orbits are born that encircle the original orbit and have relative rotation number ω. When $\omega = m'/n'$, these correspond to a chain of nn' islands. The color figure (*See* **Standard Map**: page 8 in the color plate section) shows red and blue island chains that encircle the fixed point with rotation number $\frac{1}{5}$; that there are two such chains is due to the reflection symmetry S. As Birkhoff realized, the newly created elliptic orbit also will undergo similar bifurcations, so that the phase space shows a structure of islands-around-islands, ad infinitum. This structure can even exhibit self-similarity (Meiss, 1992) just like the Feigenbaum period-doubling sequence for dissipative systems.

The Last Invariant Circle

In 1968, John Greene began studying the destruction of invariant circles in the standard map. He showed that sequences of periodic orbits, namely, the minimizing and minimax m/n orbits, whose rotation numbers converge on a given irrational, can be used to determine the existence of a circle with that frequency. Suppose that ω has a continued fraction expansion $[a_0, a_1, \ldots]$, $a_j \in \mathbb{Z}^+$, and let $m_j/n_j = [a_0, a_1, \ldots, a_j]$ be the jth convergent of ω. Greene conjectured that when the residues of these orbits $R_j \to 0$, as $j \to \infty$, then the invariant circle $\mathcal{C}_\omega$ exists—MacKay (1992) gives a proof of much of this.

For the standard map, it appears that each rotational invariant circle exists only up to a critical value, $k = k_{\rm cr}(\omega)$; this graph was called the "fractal diagram" by Schmidt and Bialek in 1982. The critical k vanishes at every rational and appears to have local maxima for each *noble* irrational ω. Percival called a number noble if its continued fraction expansion has a tail that is eventually all ones. By this criterion the "most irrational" number is the golden mean $\gamma = (1 + \sqrt{5})/2 = [1, 1, 1, \ldots]$. Indeed for the standard map, Greene discovered that the invariant circles with rotation numbers $\gamma \pm m$, $m \in \mathbb{Z}$ appear to be the last circles destroyed (all such circles are destroyed simultaneously due the symmetries). Numerically it is known that the golden circle is destroyed at $k_{\rm cr}(\gamma) \approx 0.971635406$.

This value is most efficiently computed by renormalization theory (MacKay, 1993). At the critical parameter for the destruction of a noble invariant circle, the phase space exhibits a self-similar structure. The geometric scaling of this self-similarity can be used to compute $k_{\rm cr}$ from the residues of the m_j/n_j orbits. This is more accurate than iteration methods—pioneered by Chirikov—which rely on finding an orbit that crosses the region containing the circle, and frequency methods—developed by Laskar—which rely on the irregularity of the numerically computed rotation number. While none of these methods proves that $k_{\rm cr}$ corresponds to the last invariant circle, "converse KAM theory" leads to a computer proof that there are no rotational circles for $k > \frac{63}{64}$ (MacKay & Percival, 1985). This is based on Birkhoff's theorem that every rotational invariant circle is a Lipschitz graph (Meiss, 1992). The color figure (*See* **Standard map**: page 8 in the color plate section) shows the dynamics on the sphere $\mathcal{S}$ at $k_{\rm cr}(\gamma)$. Here the the golden circle (purple) is on the threshold of destruction. Also shown in the figure are 1.5×10^6 iterates of two chaotic trajectories (light blue and light green); the stable (blue) and unstable (red) manifolds of the $(m, n) = (0, 1)$, $(1, 2)$, and (1.3) orbits; and a number of orbits trapped in these island chains as well as the $(2, 5)$ and $(3, 8)$ chains.

Transport

Transport theory studies the motion of ensembles of trajectories from one region of phase space to another. When there are invariant circles separating the regions, then there is no transport. A Birkhoff "zone of instability" is an annular region bounded by, but otherwise not containing any, rotational invariant circles. Birkhoff showed there are orbits that traverse each zone of instability, and Mather (1991) extended this to show that there are orbits future and past asymptotic to the upper and lower bounding rotational invariant circles, respectively.

Aubry–Mather theory implies that for each irrational rotation number there is a minimizing trajectory that is dense on a circle or a cantor set. Percival proposed calling the latter sets "cantori." Thus, for $k > \frac{63}{64}$, every rotational invariant circle has become a cantorus, and vertical transport between any two momentum levels occurs. The color figure (in the color plate section)

shows two such cantori (brown) with rotation numbers $(1+\gamma)/(3+4\gamma)$ and $(1+2\gamma)/(2+5\gamma)$. The rate of transport is locally governed by the flux, the area that crosses a closed loop upon iteration. The flux across a cantorus or a separatrix is given by Mather's ΔW, the difference in action between the corresponding minimax and minimizing orbits (MacKay et al., 1984). Renormalization theory shows that the flux through a noble cantorus goes to zero as $(k-k_{\rm cr})^{3.01}$; this can be very small, well beyond $k_{\rm cr}$. For example in the color figure 3 (page 8 in the plate color section), the blue chaotic trajectory is bounded below by a low flux cantorus even for tens of millions of iterates. Geometrically, the flux is the area contained in a "lobe" bounded by pieces of stable and unstable manifolds. All transport occurs through lobes in two-dimensional maps (Wiggins, 1992); unfortunately, the higher-dimensional generalization is not clear.

JAMES D. MEISS

See also **Aubry–Mather theory; Cat map; Chaotic dynamics; Ergodic theory; Fermi acceleration and Fermi map; Hamiltonian systems; Hénon map; Horseshoes and hyperbolicity in dynamical systems; Lyapunov exponents; Maps; Measures; Mel'nikov method; Phase space; Symplectic maps**

Further Reading

Gelfreich, V.G. & Lazutkin, V.F. 2001. Separatrix splitting: perturbation theory and exponential smallness. *Russian Mathematical Surveys*, 56(3): 499–558

de la Llave, R. & Rana, D. 1990. Accurate strategies for small divisor problems. *Bulletin of the American Mathematical Society*, 22: 85–90

Lamb, J.W.S. & Roberts, J.A.G. 1998. Time-reversal symmetry in dynamical systems: a survey. *Physica* D, 112: 1–39

Lichtenberg, A. & Lieberman, M. 1992. *Regular and Chaotic Motion*, *Applied Mathematical Sciences*, vol. 38, 2nd edition, New York: Springer-Verlag

MacKay, R., Meiss, J. & Percival, I. 1984. Stochasticity and transport in Hamiltonian systems. *Physical Review Letters*, 52: 697–700

MacKay, R.S. 1992. Greene's residue criterion. *Nonlinearity*, 5: 161–187

MacKay, R.S. 1993. *Renormalisation in Area-Preserving Maps*, *Advanced Series in Nonlinear Dynamics*, vol. 6, Singapore: World Scientific

MacKay, R.S. & Percival, I.C. 1985. Converse KAM: theory and practice. *Communications in Mathematical Physics*, 98: 469–512

Mather, J.N. 1991. Variational construction of orbits of twist diffeomorphisms. *Journal of the American Mathematical Society*, 4(2): 207–263

Meiss, J.D. 1992. Symplectic maps, variational principles, and transport. *Reviews of Modern Physics*, 64(3): 795–848

Umberger, D.K. & Farmer, J.D. 1985. Fat fractals on the energy surface. *Physical Review Letters*, 55: 661–664

Wiggins, S. 1992. *Chaotic Transport in Dynamical Systems*, *Interdisciplinary Applied Mathematics*, vol. 2, New York: Springer

STATE DIAGRAMS

Consider a system comprising N elements, each of which can be set at one or the other of two values. Thinking of the elements as switches, the values (positions or settings) can be defined as one of the two Boolean variables: off (0) and on (1) (Birkhoff & MacLane, 1953). Now suppose that time progresses in discrete units and the values of the switches at time t_{n+1} depend on their values at t_n. In addition to being a rather general computer model (Fowler, 2004), such a system describes certain relay and electronic switching circuits used by electrical engineers, and it provides an approximate description of biological brains (Scott, 2002), including the "nets with circles" of Warren McCulloch and Walter Pitts (McCulloch & Pitts, 1943). If the elements are placed in a geometrical pattern (e.g., a square array), one has a cellular automaton, such as John Conway's famous "Game of life" (Gardner, 1970).

To understand how the model evolves in time, it is sometimes instructive to sketch a state diagram, which displays all states of the system and shows how these states change from one time increment to the next.

In Figure 1(a), for example, this is done for a system comprising a single switch ($N=1$), where the arrows indicate what will happen in the next increment of time. Reading from left to right, the first diagram shows a system in which the switch turns on if it is off and stays on if it is on. The second diagram shows a system that turns off if it is on and stays off if it is off. In the third diagram, the system stays off if it is off and stays on if it is on. (This corresponds to a typical wall switch.) Finally, the last diagram represents a system that turns off if it is on and turns on if it is off. (This models a "blocking oscillator" in electronic engineering.)

The number of possible state diagrams increases very rapidly with the number of elements (N) in a system. To see this, note that the number of states of the system is 2^N, and from each of these states we must choose an arrow that goes to (possibly) another state. Thus, the total number of diagrams $\mathcal{N}$ is 2^N raised to the 2^Nth power, or

$$\mathcal{N} = 2^{N2^N}. \tag{1}$$

A few calculations from this formula are given in Table 1, demonstrating a growth of $\mathcal{N}$ with N, which mathematicians term "combinatorial."

For a system comprising only six switches, the total number of state diagrams is greater than 10^{110}, which in turn equals the atomic mass of the universe (the mass of the universe measured in units of the hydrogen atom) times the age of the universe in picoseconds. In his analysis of biological organisms, the physicist Walter Elsasser has called such a finite number "immense," which implies that (although the number of them is finite) it is not—and never will be—physically possible to examine all possible diagrams (Elsasser, 1998).

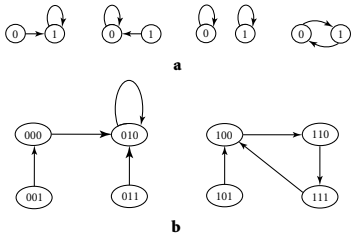

Figure 1. (a) The four Boolean state diagrams that can be constructed from a single switch. (b) One of the more than sixteen million state diagrams that can be constructed from three switches. Note that several arrows can converge on each state, but only one arrow leaves any one state.

N	$\mathcal{N} = 2^{N2^N}$
1	$2^2 = 4$
2	$4^4 = 256$
3	$8^8 \doteq 1.7 \times 10^7$
4	$16^{16} \doteq 1.8 \times 10^{19}$
5	$32^{32} \doteq 1.5 \times 10^{48}$
6	$64^{64} \doteq 3.9 \times 10^{115}$

Table 1. The number of state diagrams ($\mathcal{N}$) that can be constructed for various numbers (N) of Boolean switches.

In Figure 1(b) is shown one of the more than sixteen million state diagrams for a system of three switches. Here we find the following behaviors.

- *Transients:* (001) → (000) → (010), (011) → (010), and (101) → (100).
- *Periodicities:* (010) → (010) and (100) → (110) → (111) → (100).
- *Disjoint dynamics:* States (000), (010), (011), and (001) are dynamically disjoint from states (100), (110), (111), and (101).

The shortest transient or period is a single time unit, whereas the longest is 2^N time units, but this is unlikely for larger values of N.

Consider how the number of state diagrams depends on the way that the state of a system in the next time increment is computed. If each switch responds to the present positions of all N switches (including itself), there are

$$2^{2^N}$$

possible Boolean functions that can perform the computations. In the most general case, any one of the N switches can be assigned one of these Boolean functions. Thus, the number of possible diagrams is equal to

$$\left(2^{2^N}\right)^N = 2^{N2^N},$$

just as in Equation (1). In choosing the arrows for a particular diagram—as in Figure 1(b)—one defines a particular Boolean function.

When state diagrams are used to model biological brains, we may wish to limit the computations to threshold functions rather than Boolean functions. The total number of threshold functions of n inputs is

$$2^{kn^2},$$

where k lies between $\frac{1}{2}$ and 1 (Yajima et al., 1968). In a brain model, furthermore, it is unrealistic to assume that each neuron receives inputs from all other neurons. If each of N neurons receives inputs from n neurons, then the total number of state diagrams is

$$\mathcal{N}_{\text{th}} \geq \left(2^{n^2/2}\right)^N = 2^{n^2N/2}. \qquad (2)$$

Taking $N = 10^{10}$ as a conservative estimate for the number of neurons in the human neocortex and $n = 10^4$ as an estimate for the number of synaptic inputs to each neuron, implies that the number of possible brains is about $10^{10^{17}}$.

ALWYN SCOTT

See also **Attractor neural network; Cellular automata; Game of life; McCulloch–Pitts network; Neural network models**

Further Reading

Birkhoff, G. & MacLane, S. 1953. *A Survey of Modern Algebra*, New York: Macmillan

Elsasser, W.M. 1998. *Reflections on a Theory of Biology: Holism in Biology*, Baltimore: Johns Hopkins University Press (first published in 1987)

Fowler, M. 2004. *UML Distilled: A Brief Guide to the Standard Object Modeling*, Boston: Addison-Wesley

Gardner, M. 1970. Mathematical games. *Scientific American*, 223 (October): 120–123

McCulloch, W.S. & Pitts, W.H. 1943. A logical calculus of the ideas immanent in nervous activity. *Bulletin of Mathematical Biology*, 5: 115–133

Scott, A.C. 2002. *Neuroscience: A Mathematical Primer*, Berlin and New York: Springer

Yajima, S., Ibaraki, T. & Kawano, I. 1968. On autonomous logic nets of threshold computers. *Transactions on IEEE Computers*, 17: 385–391

STATIONARY SOLUTIONS

See **Discrete self-trapping system; Equilibria**

STEADY STATE

See **Equipartition of energy**

STEREOSCOPIC VISION AND BINOCULAR RIVALRY

Most vertebrate predators, including humans, have their two eyes positioned in the front of the head

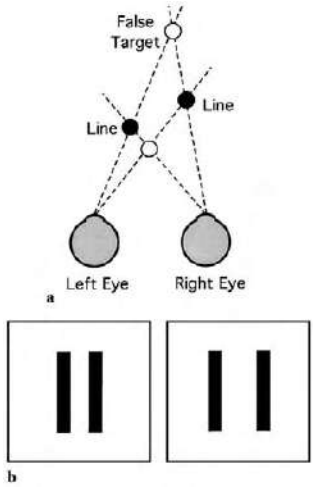

Figure 1. (a) The geometry of stereopsis. (b) The simplest two line stereogram.

looking forward. In contrast, most prey species, such as rabbits, have eyes positioned on the sides of the head. This confers on prey almost panoramic vision, thus enabling them to see predators creeping up behind them. In contrast, predators receive two slightly different views of the scene in front of them due to the horizontal offset between the two eyes (approximately 6.7 cm in humans), which confers depth information. Stereoscopic vision may be defined as the perception of depth that arises when the brain compares the images falling on the two retinas. Indeed, there are neurons in the visual cortex that receive stimulation from both eyes and consequently are sensitive to the depth of lines and contours in the world.

The geometry of stereopsis is illustrated in Figure 1a, which provides a horizontal view of two eyes viewing a scene containing two vertical rods at different depths relative to the eyes. As shown by the dashed sight lines, the retinal images of these two lines will be closer together in one eye's view than in the other. Figure 1b contains a simple two line stereogram, namely a pair of views, one for each eye, with vertical lines closer together in one view than in the other. If the viewer can either cross or diverge their eyes so that each eye fixates a different one of these views, the percept will be one in which one line lies closer to the viewer than the other line. (It should be noted that several percent of humans lack stereoscopic ability, usually due to amblyopia or "lazy eye" during early childhood.) Rather than requiring viewers to cross or diverge their eyes, laboratory research into stereopsis utilizes some version of a stereoscope, which was

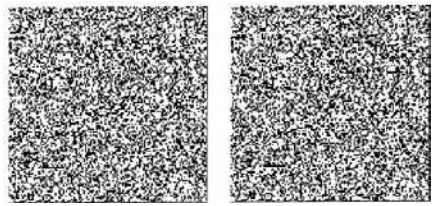

Figure 2. Random dot stereogram.

invented by Charles Wheatstone in 1838. A stereoscope utilizes either prisms or mirrors in front of each eye to optically diverge the views so that each eye views a different visual stimulus. Indeed, stereoscopes and stereoscopic photographs were a Victorian fascination, and many excellent stereoscopes may still be found in antique shops.

The two line stereogram in Figure 1b is the simplest possible, as two objects are the minimum for which different depths can be defined. A much more complex example is the random dot stereogram (RDS), which was developed by Bela Julesz (1971) as a tool for the study of stereopsis. To make an RDS, a computer first generates a completely random pattern of black and white dots (little squares), such as that depicted in Figure 2. This will be the stimulus for one eye. An exact copy of this is then made as the basis for the other eye's view. To generate a stimulus for depth, a rectangular (or other shaped) region of dots in the middle of this second random pattern is now shifted horizontally left or right by a distance of several dots. The space vacated by shifting this rectangular region is then filled in with random black and white dots. When each eye views one of the two random dot patterns in an RDS, the brain extracts depth information and produces a percept of a rectangular region of random dots floating in depth in front of (or behind, depending on which eye views which half of the stereogram) a random dot background. Readers who can converge or diverge their eyes while viewing Figure 2 can experience this.

Neural Basis of Stereopsis

Information originating in the two retinas remains segregated until it reaches primary visual cortex at the back of the brain. In the cortex, many individual neurons respond best when they are stimulated through both eyes at once. However, each cortical neuron receives stimulation only from a very small area on each retina, which is known as a "receptive field." If one imagines there being a coordinate system affixed to each retina with the center of the retina (the fovea) being the origin, then each cortical cell receives information from a pair of receptive fields, one from each retina, whose coordinates may be the same or different. If a cortical neuron receives stimulation from receptive fields with

the same relative coordinates in each retina, it will be sensitive to lines and edges that lie in the plane on which the eyes are converged. Therefore, such a neuron will be sensitive to objects with zero depth relative to fixation. Other neurons, however, have their receptive fields at different points on the two retinas. For most of these cells, this means that the receptive field in one eye is shifted a short distance horizontally left or right relative to its receptive field in the other eye. Such a difference in receptive field coordinates on the two retinas is termed a horizontal disparity. Neurons with a particular horizontal disparity will respond to objects at a particular depth relative to the fixation plane. For example, if a cortical neurons has its receptive field in the left eye shifted left relative to that in the right eye, its disparity will correspond to lines and edges nearer than fixation. Conversely, a neuron with a left eye receptive field shifted to the right relative to the other eye will be sensitive to disparities corresponding to lines and edges farther away than the plane of fixation. Thus, different cortical neurons, in virtue of the relative placement of their two retinal receptive fields, signal the location of lines and edges in three-dimensional space, including their depth relative to the fixation plane. Although only horizontal disparities are discussed here, vertical disparities are now known to play a role in stereopsis as well, and details can be found in Howard & Rogers (2002).

The RDS demonstrates dramatically the computational problems confronted by cortical neurons in comparing the two retinal images to extract depth information. To make the point, consider a single black dot in one horizontal line of the pattern in one eye's view. The corresponding horizontal line of dots in the other eye's view will contain roughly 50% black dots, any one of which might be the appropriate match for the black dot in question. Thus, the problem has an extremely large number of potential depth solutions, only one of which is actually perceived. In other words, the existence of neurons sensitive to different disparities and, therefore, different depths only represents the initial part of the solution to the problem of extracting depth information from two retinal images.

The types of interactions among disparity-tuned cortical neurons that must be involved in the extraction of accurate depth information may be appreciated by reconsidering the simple two line stereogram in Figure 1. As shown by the dashed lines in Figure 1a, sight lines from the two eyes intersect not only at the locations of the two targets (black circles) but also at two other points in depth (open circles). These are known as "false targets," and neural interactions in the cortex are required to eliminate them. The types of interactions believed to occur include facilitation between neurons tuned to similar disparities in neighboring regions plus inhibition between neurons tuned to very different disparities at adjacent points. Examination of Figure 1a shows that if the neurons tuned to the disparities or depths represented by the black circles were mutually excitatory, whereas both of these inhibited neurons tuned to the much more extreme disparities indicated by the open circles, the neurons representing the black circles would win the competition and suppress the responses to the false targets. Many variations on this theme of facilitation between neurons tuned to similar disparities and inhibition between neurons tuned to radically different disparities have been proposed, and these have been summarized elsewhere (Blake & Wilson, 1991). Such interactions may be conceptualized as implementing an evolutionary constraint that most real world objects are bounded by surfaces that vary smoothly in depth except at their edges.

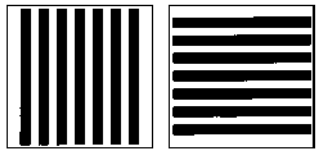

Figure 3. Stereogram illustrating binocular rivalry. Try viewing and perceiving both images simultaneously.

Binocular Rivalry

The preceding discussion assumes that the two eyes are looking ahead and viewing the same scene, albeit from slightly different viewpoints that give rise to disparities. In the laboratory, however, it is possible to generate stereograms that present radically different views to the two eyes. A simple example of this is depicted in Figure 3, where one eye is presented with horizontal lines, while the other is presented with vertical lines. Readers who can converge or diverge their eyes will discover that these lines cannot be fused to produce a depth percept. Rather, one perceives an alternation between horizontal and vertical lines such that the two are almost never seen at the same point at the same time. This perceptual alternation, which occurs at a rate of about one alternation every 2–4 s, is known as binocular rivalry. Rivalry results when the two eyes view images that could not have arisen from a real three-dimensional world in the absence of mirrors or other optical devices. It appears, therefore, that rivalry must reflect neural interactions that evolved to process depth information but that default into a perceptual oscillation when the depth task is impossible.

The neural basis of binocular rivalry requires two components. First, the different groups of rivaling neurons responding to orthogonal stimuli must be strongly and mutually inhibitory. This guarantees that only one set of these neurons can be active at any given

place and time. The second ingredient is fatigue or self-adaptation. Self-adaptation, which is well documented among excitatory cortical neurons, causes neurons that are firing rapidly to slowly decrease their response rate over the course of a second or more. As they adapt, their ability to inhibit other neurons weakens. Eventually, these previously inhibited neurons overcome the inhibition and begin to respond, and they then inhibit the adapted neurons so that the percept switches. This neural mechanism has been developed into nonlinear dynamical models that accurately explain many aspects of binocular rivalry (Wilson, 2004).

A further aspect of binocular rivalry is that the reversals are not precisely periodic. Scientists have measured the duration of intervals during which the pattern presented to one eye is visible (e.g., the vertical stripes in Figure 3). The results are well described by a gamma distribution in which both short and long intervals recur in a seemingly random sequence. Recent research using neural network modeling suggests that this gamma distribution results from chaotic dynamics among cortical neurons (see Wilson, 2004).

The final and most important question concerning binocular rivalry is how the inhibitory neural interactions underlying rivalry change their role when stimuli permitting depth perception are viewed. This remains unanswered, but it is at least clear from the discussion of depth perception that inhibition is a necessary neural component. Perhaps, future research will show that the inhibition involved in elimination of false targets during depth perception is related to the inhibition causing perceptual alternations in binocular rivalry.

HUGH R. WILSON

See also **Attractor neural network; Cell assemblies; Gestalt phenomena; Neural network models; Perceptron; Synergetics**

Further Reading

Alais, D. & Blake, R. (editors). 2003. In *Binocular Rivalry and Perceptual Oscillations*, Cambridge, MA: MIT Press

Blake, R. & Wilson, H.R. 1991. Neural models of stereoscopic vision. *TINS*, 14: 445–452

Howard, I. & Rogers, B. 2002. *Seeing in Depth*, Toronto: I. Porteous

Julesz, B. 1971. *Foundations of Cyclopean Perception*, Chicago: University of Chicago Press

Wilson, H.R. 2004. Rivalry and perceptual oscillations: a dynamical synthesis. In *Binocular Rivalry and Perceptual Oscillations*, edited by D. Alais & R. Blake, Cambridge, MA: MIT Press

STIMULATED BRILLOUIN AND RAMAN SCATTERING

See **Rayleigh and Raman scattering and IR absorption**

STOCHASTIC ANALYSIS OF NEURAL SYSTEMS

Oscillatory activity abounds in the central nervous systems of animals and humans (Freeman, 1975; Steriade et al., 1990). Single neurons may act as oscillators by rhythmically generating action potentials or bursts. Central pattern generators (Cohen et al., 1988) are networks of neurons located in the spinal cord and the brain stem, which produce oscillatory activity intrinsically (Sherrington, 1947; von Holst, 1954; Cohen et al., 1988). Central pattern generators are essential for repetitive motor behavior like walking, running, flying, swimming, and chewing (Sherrington, 1947; von Holst, 1954; Cohen et al., 1988). Phase synchronization (PS) between different central pattern generators is the mechanism that controls the different types of locomotion such as walk, trot, or gallop (von Holst, 1954; Cohen et al., 1988).

In the cortex, the well-coordinated action of neural oscillations is indispensable to physiological information processing (Freeman, 1975; Steriade et al., 1990; Haken, 1996). In-phase synchronization might be one aspect of such processes (Singer & Gray, 1995).

In several neurological diseases, brain function is severely perturbed by pathologically enhanced synchronization. Resting tremor in Parkinson's disease (PD) appears to be caused by a cluster of neurons located in the thalamus and the basal ganglia, which fires synchronously at a frequency similar to that of the tremor (3–6 Hz). While under physiological conditions these neurons fire incoherently (Nini et al., 1995); in patients with PD, this cluster acts like a pacemaker and activates cortical areas, which causes the peripheral shaking.

In patients with advanced Parkinson's disease or with essential tremors that do not respond to drug therapy, depth electrodes are chronically implanted in target areas like the thalamic ventralis intermedius nucleus or the subthalamic nucleus (Benabid et al., 1991). Electrical deep brain stimulation (DBS) is performed by administering a permanent high-frequency (>100 Hz) periodic pulse train via the depth electrodes. DBS suppresses the activity of the pacemaker-like cluster, which, in turn, suppresses the peripheral tremor (Benabid et al., 1991). DBS has been developed empirically, mainly based on observations during stereotaxic neurosurgery. The advent of nonlinear dynamics and statistical physics in the field of clinically oriented neuroscience has led to an improvement of data analysis as well as a model-based development of stimulation techniques.

Stochastic Synchronization

Phase synchronization is a type of synchronization where two oscillators adjust their phases, while their amplitudes need not be correlated. Phase

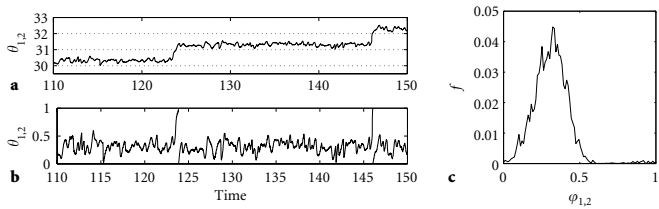

Figure 1. 1 : 2 phase difference $\theta_{1,2}$ (a) and its cyclic version $\varphi_{1,2}$ (b) from Equation (1) between the activity of the right flexor muscle of a patient with Parkinsonian resting tremor and the magnetic field measured above the corresponding left sensorimotor cortex. Corresponding distribution of $\varphi_{1,2}$ (c). (Adapted from Tass et al., 1998).

synchronization is observed in many physical, chemical, and neural systems (von Holst, 1954; Haken, 1996; Tass et al., 1998; Pikovsky et al., 2001; Tass et al., 2003). As neural systems are noisy, it is convenient to use the general concept of PS, which is valid in noisy periodic oscillators as well as in chaotic oscillators (Pikovsky et al., 2001).

To study $n : m$ phase synchronization (PS) we introduce the $n : m$ phase difference $\theta_{n,m}$ and the cyclic $n : m$ phase difference $\varphi_{n,m}$ with

$$\theta_{n,m}(t) = \frac{n\phi_1(t) - m\phi_2(t)}{2\pi},$$

$$\varphi_{n,m}(t) = \frac{n\phi_1(t) - m\phi_2(t)}{2\pi} \mod 1, \qquad (1)$$

where ϕ_1 and ϕ_2 are the phases of the two oscillators. The time course of $\theta_{n,m}$ typically exhibits horizontal periods intersected by 2π jumps (Figure 1a), that vanish when the coupling is sufficiently strong compared to the noise. By $n : m$ PS is meant that the two oscillators maintain a stable relationship of $\varphi_{n,m}$ in a statistical sense (Figure 1b), and thus it is characterized by the appearance of one or more distinct peaks in the distribution of $\varphi_{n,m}$ (Figure 1c). Absence of $n : m$ PS corresponds to a uniform distribution of $\varphi_{n,m}$, whereas perfect $n : m$ PS is related to a Dirac-type distribution of $\varphi_{n,m}$. To quantify the strength of $n : m$ PS, the actual distribution is compared to a uniform distribution with synchronization indices that are based on the Shannon entropy or the Fourier transformation (Tass et al., 1998; Pikovsky et al., 2001). The phase of an oscillatory signal is determined with the Hilbert transform or the wavelet transform (Tass et al., 1998; Pikovsky et al., 2001). Already by the 1930s, PS was studied in coordinated movements using a similar, Poincaré-like approach, but limited phase estimation (von Holst, 1954).

In Parkinsonian patients with resting tremor, a 1 : 2 PS was found between the activity of the shaking muscles and brain areas such as the sensorimotor cortex and premotor areas (Tass et al., 1998) (Figure 1). The dominant frequency of the activity in the brain areas is approximately twice as large as that of the peripheral tremor.

Compared to PS analysis, the cross coherence method cannot distinguish between PS and amplitude modulation as well as between PS and simple linear superposition. Furthermore, cross coherence is not appropriate for the detection of $n : m$ PS with $n/m \neq 1$ (Tass et al., 1998; Pikovsky et al., 2001, 2003).

Stochastic Phase Resetting

In both single neurons and neural populations, the effect of a stimulus depends on the phase of the neural oscillation at which the stimulus is administered. To study phase-dependent effects of pulsing stimuli on neural populations and, in particular, to analyze desynchronizing effects of such stimuli, the concept of phase resetting (Winfree, 1980) has been extended to populations of non-interacting and interacting oscillators in the presence of random forces (Tass, 1999). The single neuron is modeled by a phase oscillator (Kuramoto, 1984). The dynamics of a cluster of N interacting phase oscillators subject to a stimulus S and to random forces F_j is governed by

$$\dot{\psi}_j = \omega_j + \frac{1}{N}\sum_{k=1}^{N}\Gamma(\psi_j - \psi_k) + X(t)\,S(\psi_j) + F_j(t), \qquad (2)$$

where ψ_j is the phase of the jth phase oscillator, Γ is a 2π-periodic global coupling, and S is a 2π-periodic, time-independent function modeling the stimulus, where $X(t) = 1$ during stimulation and $X(t) = 0$ without stimulation (Tass, 1999). The random forces $F_j(t)$ are modeled by Gaussian white noise fulfilling $\langle F_j(t)\rangle = 0$, $\langle F_j(t)\ F_k(t')\rangle = D\delta_{jk}\delta(t - t')$ with constant noise amplitude D.

Via the Fokker–Planck equation, one obtains an evolution equation for the average number density $n(\psi, t) = \int_0^{2\pi}\ldots\int_0^{2\pi} \mathrm{d}\psi_1\cdots\mathrm{d}\psi_N\ \tilde{n}(\Psi;\psi) f(\Psi; t)$, where $f(\Psi, t)$ is the the probability density with $\Psi = (\psi_1, \ldots, \psi_N)$ and $\tilde{n}(\Psi;\psi) = N^{-1}\sum_{j=1}^{N}\delta(\psi - \psi_j)$. $n(\psi, t)$ tells us how many oscillators most probably have phase ψ at time t. Detailed analytical studies of

that equation were performed for $X = 0$ (Kuramoto, 1984; Tass, 1999), whereas the transient stimulation-induced dynamics was analyzed numerically, mainly for the case when all oscillators have the same eigenfrequency (Tass, 1999). Since the single model neuron fires whenever its phase equals 0 (modulo 2π) the average number density of firing neurons is given by the firing density

$$p(t) = n(0, t) . \tag{3}$$

It is possible to desynchronize a synchronized cluster of oscillators with a single pulse of the right intensity and duration. To this end, however, the pulse has to hit the cluster in a vulnerable phase range, which corresponds to only a small fraction (5% or even less) of a period of the oscillation. To compound matters, different stimulation parameters have to be used to desynchronize a cluster that is not in its fully synchronized state (Tass, 1999). Hence, complex stimulation techniques have been developed that make it possible to effectively desynchronize a cluster of phase oscillators independently of the cluster's dynamical state at the beginning of the stimulation (Tass, 2002). These methods share one particular feature: the stimulus consists of two qualitatively different stimuli. The first stimulus is stronger and resets (restarts) the cluster, whereas the second, weaker stimulus is a single pulse that is administered after a constant time delay and desynchronizes by hitting the cluster in a vulnerable state. The goal of the reset is to control the dynamics of the cluster by restarting the cluster in a stereotypical way. The reset may be achieved by means of a strong single pulse, a high-frequency pulse train (HFPT) (with a pulse rate 20 times larger than the mean eigenfrequency $\bar{\omega}$) or a low-frequency pulse train (LFPT) (with a pulse rate similar to $\bar{\omega}$) (Tass, 2002). A strong pulse and an HFPT cause a hard (abrupt) reset within less than one period, whereas an LFPT causes a soft (slow) reset, where in the course of an entrainment the influence of the initial dynamic state fades away.

Since the desynchronizing effect of these stimulation techniques does not depend on the initial dynamical state of the neural population, resynchronization can effectively be blocked by administering a desynchronizing stimulus whenever the population tends to resynchronize (Figure 2a). In contrast, high-frequency stimulation not combined with a desynchronizing single pulse causes only a suppression of the firing during stimulation but no desynchronization (Figure 2b). After a simple HFPT, the extent of synchronization is particularly high, and the cluster restarts in a rebound-like manner.

Transient stimulus-induced responses of coupled neural oscillators are a key approach not only for manipulating synchronization processes, but also for studying neural information processing in basic

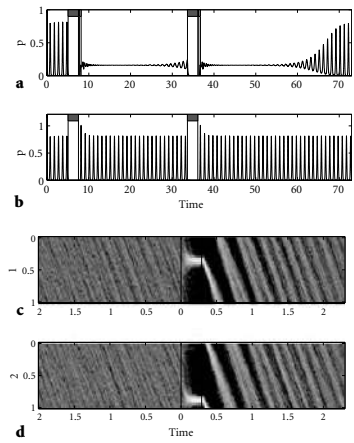

Figure 2. (a) Firing density p from Equation (3) of a neural population stimulated with two subsequent identical composite stimuli consisting of a high-frequency pulse train followed by a single pulse. (b) Two successively administered identical high-frequency pulse trains with parameters as in (a) but without following single pulses. Begin and end of a single pulse are indicated with vertical lines connected by a shaded region ((a) and (b) from Tass, 2001). CT distributions from Equation (5) of ϕ_1 (c) and ϕ_2 (d) show that the post-stimulus responses of each oscillator split into two antiphase ensembles (0 is black and maximal values are white). Begin (at $t = 0$) and end of stimulation are indicated by vertical lines. ((c) and (d) from Tass, 2003).

research as well as in diagnosis (Dawson, 1954; Steriade et al., 1990). To improve the signal-to-noise ratio, one typically averages across an ensemble of responses to reveal what is supposed to be the actual response to a stimulus (Dawson, 1954). But noise inherent in the neural dynamics makes coupled neural oscillators react to a stimulus in more than one way, which may be essential for sensory short-term adaptation (Tass, 2003). In this case, averaging causes severe artifacts.

For illustration we consider Equation (2) for two coupled oscillators ($N = 2$) undergoing an antiphase reset caused by stimuli $S_1(\psi_1) = I \cos(\psi_1)$ and $S_2(\psi_2) = I \cos(\psi_2 + \pi)$. We use the normalized cyclic phases

$$\phi_j(t) = \frac{\psi_j(t)}{2\pi} \bmod 1 \quad (j = 1, 2) \tag{4}$$

and the normalized cyclic $n : m$ phase difference $\varphi_{n,m}$ from Equation (1). To detect whether, in an ensemble of responses, there are epochs during which the phases ϕ_j and/or the phase difference $\varphi_{n,m}$ display, a stereotypical, tightly stimulus-locked time course; the stimuli S_1 and S_2 are simultaneously administered at l random times $\tau_1, \tau_2, \ldots, \tau_l$. Time-dependent

cross-trial (CT) distributions of ϕ_j and $\varphi_{n,m}$ are calculated across trials for each time t relative to stimulus onset with

$$\{\phi_j(t+\tau_k)\}_{k=1,\ldots,l}\,,\,\{\varphi_{n,m}(t+\tau_k)\}_{k=1,\ldots,l}\,. \quad (5)$$

The time course of ϕ_j and $\varphi_{n,m}$ is perfectly stimulus-locked at time t if the corresponding CT distributions are Dirac-type distributions, whereas these distributions are uniform if ϕ_j and $\varphi_{n,m}$ are not stimulus-locked at all at time t. The extent of stimulus locking is quantified for each time t with indices characterizing the corresponding CT distributions with Shannon entropy or Fourier transformation (Tass, 1999, 2003). In this way, it is possible to detect stimulus-locked transient synchronization/desynchronization ($\varphi_{n,m}$) as well as transient cross-trial response clustering (ϕ_j). The latter is illustrated in Figures 2c and d, where the pre-stimulus CT distribution of ϕ_j is nearly uniform because of the randomized stimulus application. In all of the $l = 200$ trials, the stimuli S_1 and S_2 reset the oscillators to the phases $\phi_1^{\mathrm{res}} \approx 0.36$ and $\phi_2^{\mathrm{res}} = \phi_1^{\mathrm{res}} + 0.5$, so that Dirac-like CT distributions evolve. Each oscillator reacts in two qualitatively different ways: The ensemble of post-stimulus responses starts at ϕ_j^{res} and splits into two antiphase ensembles, so that two antiphase peaks of the corresponding CT distribution emerge. The mechanism that induces cross-trial response clustering is a stochastic resonance (Tass, 2003).

Coordinated transient responses of neural oscillators such as antiphase cross-trial response clustering typically escape detection with standard methods like cross-trial averaging (Tass, 2003).

Deep Brain Stimulation Techniques

Permanent high-frequency DBS is an unphysiological type of stimulation, which in a number of patients leads to side effects like dysarthria and psychiatric sympotms. Furthermore, the therapeutic effect of DBS may vanish in the course of the treatment, possibly due to adaptation.

Demand-controlled DBS with the stimulation techniques explained in the former section has been suggested as an alternative and milder therapeutic approach (Tass, 2002). Instead of simply suppressing the neural firing of the pacemaker-like cluster, these novel stimulation techniques aim at desynchronizing the pacemaker's pathologically synchronized firing in a demand-controlled way (Tass, 2002). For this, either the depth electrode or an epicortical electrode measures the feedback signal, that is, the local field potential of the pacemaker population or the electrical activity of a cortical area that is strongly coupled to it. A desynchronizing stimulus is administered only whenever the pacemaker-like cluster becomes synchronized (Figure 2a). Repeated administration of desynchronizing stimuli may effectively maintain an uncorrelated firing. Demand-controlled DBS should, in principle, be less aggressive to the brain tissue stimulated and is currently evaluated for clinical use.

PETER A. TASS

See also **Attractor neural network; Cell assemblies; Coupled oscillators; Electroencephalogram at large scales; Electroencephalogram at mesoscopic scales; Stochastic processes; Synchronization**

Further Reading

Benabid, A.L., Pollak, P., Gervason, C., Hoffmann, D., Gao, D.M., Hommel, M., Perret, J.E. & De Rougemont, J. 1991. Long-term suppression of tremor by chronic stimulation of the ventral intermediate thalamic nucleus. *The Lancet*, 337: 403–406

Cohen, A.H., Rossignol, S. & Grillner, S. (editors). 1988. *Neural Control of Rhythmic Movements in Vertebrates*, New York: Wiley

Dawson, G.D. 1954. Summation technique for the detection of small evoked potentials. Electroencephalography and Clinical Neurophysiology, 44: 153–154.

Freeman, W.J. 1975. *Mass Action in the Nervous System*, New York: Academic Press

Haken, H. 1996. *Principles of Brain Functioning. A Synergetic Approach to Brain Activity, Behavior and Cognition*, Berlin and New York: Springer

Kuramoto, Y. 1984. *Chemical Oscillations, Waves, and Turbulence*, Berlin and New York: Springer

Nini, A., Feingold, A., Solvin, H. & Bergman, H. 1995. Neurons in the globus pallidus do not show correlated activity in the normal monkey, but phase-locked oscillations appear in the MPTP model of parkinsonism. *Journal of Neurophysiology*, 74: 1800–1805

Pikovsky, A., Rosenblum, M. & Kurths, J. 2001. *Synchronization: A Universal Concept in Nonlinear Sciences*, Cambridge and New York: Cambridge University Press

Sherrington, C. 1947. *The Integrative Action of the Nervous System*, 2nd edition, New Haven, CT: Yale University Press

Singer, W. & Gray, C.M. 1995. Visual feature integration and the temporal correlation hypothesis. *Annual Reviews of Neuroscience*, 18: 555–586

Steriade, H., Jones, E.G. & Llinás, R. 1990. *Thalamic Oscillations and Signaling*, New York: Wiley

Tass, P.A. 1999. *Phase Resetting in Medicine and Biology: Stochastic Modelling and Data Analysis*, Berlin: Springer

Tass, P.A. 2002. Effective desynchronization with bipolar double pulse stimulation. *Physical Review* E, 66: 036226

Tass, P.A. 2003. Stochastic phase resetting of two coupled phase oscillators stimulated at different times. *Physical Review* E, 67: 051902

Tass, P.A., Fieseler, T., Dammers, J., Dolan, K., Morosan, P., Majtanik, M., Boers, F., Muren, A., Zilles, K. & Fink, G.R. 2003. Synchronization tomography: a method for three-dimensional localization of phase synchronized neuronal populations in the human brain using magnetoencephalography. *Physical Review Letters*, 90: 088101

Tass, P.A., Rosenblum, M.G., Weule, J., Kurths, J., Pikovsky, A., Volkmann, J., Schnitzler, A. & Freund, H.-J. 1998. Detection of $n : m$ phase locking from noisy data: application

to magnetoencephalography. *Physical Review Letters*, 81: 3291–3294
von Holst, E. 1954. Relations between the central nervous system and the peripheral organs. *British Journal of Animal Behavior*, 2: 89–94
Winfree, A.T. 1980. *The Geometry of Biological Time*, Berlin: Springer

STOCHASTIC PROCESSES

Complex processes in physics, chemistry, biology, engineering, and finance often exhibit uncertainties, fluctuations, or noises in their structures as a rule rather than as an exception. It is known that low-dimensional nonlinear dynamical systems can exhibit chaotic phenomena that appear random in nature. Nevertheless, stochastic processes involve an unmanageably large number of variables and their temporal fractal dimensions approach infinity. To interpret, analyze, model, and simulate these noises, several stochastic algorithms developed in the last century yield not only the structure or pattern of these processes, but also the statistical characteristics of the underlying uncertainties that the conventional deterministic models cannot offer.

Analysis of a stochastic process usually starts with the assumption of a Markov property. A Markov process, $X(t)$, is a stochastic process with the property that, given the value of $X(t = t_r)$, the values of $X(t = t_s)$ for $t_s > t_r$ are not influenced by the values of $X(t = t_q)$ for $t_q < t_r$. Depending on the nature of the process and the method of analysis, the random variable, $X(t)$, may assume continuous values or only discrete values. Moreover, the random variable can be analyzed with a continuous or a discrete time scale.

Algorithms have been developed for analyzing two distinct types of noise, internal and external. Internal noise is caused by the fact that the system itself consists of discrete particles and many variables associated with the particles are ignored; it is inherent in the very mechanism by which the process evolves. Small discrete systems governed by a large number of variables often exhibit notable internal fluctuations. The energy state of an electron in a molecule, the spread of an epidemic within a population, the mutation of a gene, and diffusion of a molecule into a medium cannot be predicted precisely due to their inherent complexities; thus, these processes exert internal fluctuations. The discrete state, continuous-time stochastic processes can be analyzed by the master equation in the following general form (Oppenheim et al., 1977; Gardiner, 1985; van Kampen, 2001):

$$\frac{\mathrm{d}p_n(t)}{\mathrm{d}t} = \sum_{n'} \{W_{nn'}p_{n'}(t) - W_{n'n}p_n(t)\}, \qquad (1)$$

where $p_n(t)$ denotes the probability of the system to be in state n at time t, and $W_{nn'}$ the transition probability per unit time from state n' to state n. The master equation is a gain-loss equation for the probabilities of the separate state n. The first term is the gain of state n due to transitions from other states n', and the second term is the loss due to transition from n into other states. For a system involving a set of random variables or a random vector, n is a vector and $W_{n'n}$ is a matrix.

When all elements of the transition intensity functions $W_{n'n}$ are either constant or linear functions of n, Equation (1) is considered a linear master equation; otherwise, it is considered nonlinear. Simple linear master equations such as the Poisson equation and birth and death processes can be solved by induction (see, e.g., Karlin & Taylor, 1975). For processes involving large numbers of random variables, full solutions of their joint probability distribution function are usually difficult, if not impossible, and it often suffices to determine only the first and second moments of the resultant probability distribution. These moments can be found by taking the averages of the master equations or by the method of joint probability generating function (Karlin & Taylor, 1975, 1981; Chiang, 1980). For nonlinear master equations, solutions can be approximated by resorting to the system-size expansion, a rational linearization approximation technique based on the power-series expansion (van Kampen, 1976, 2001). The system size, Ω, has been proposed as an expansion parameter because it measures the relative importance of the noises. For a linear system, fluctuations or variances are of the order of $\Omega^{1/2}$ in a collection of Ω entities. As a result, their effect on the macroscopic properties is of the order of $\Omega^{1/2}$. It is expected that the joint probability for the nonlinear system, $p_n(t)$, will have a sharp maximum around the macroscopic value with a noise of width of the order of $\Omega^{1/2}$. Thus, when the higher-order moments are ignored, the approximated joint probability becomes a time-dependent Gaussian distribution. The technique gives rise to the deterministic macroscopic equations and the equations of noises for the master equation; the latter is a set of linear Fokker–Planck equations whose characteristics and solutions will be discussed below.

For the interpretation of its relation with other stochastic algorithms, the master equation has been expressed in terms of a continuous random variable $Y(t)$ with its realization $y(t)$

$$\frac{\partial P(y,t)}{\partial t} = \int \{W(y \mid y')P(y',t) - W(y' \mid y)P(y,t)\}\,\mathrm{d}y'. \qquad (2)$$

Taylor expansion of the above master equation yields the Kramers–Moyal expansion

$$\frac{\partial P(y,t)}{\partial t} = \sum_{v=1}^{\infty} \frac{(-1)^v}{v!} \left(\frac{\partial}{\partial y}\right)^v \{a_v(y)P(y,t)\}, \qquad (3)$$

where $a_v(y)$ denotes the jump moments:

$$a_v(y) = \int_{-\infty}^{\infty} r^v W(y, r)\, \mathrm{d}r \tag{4}$$

and

$$W(y \mid y') = W(y', r), \quad r = y - y'. \tag{5}$$

A particular important class of continuous Markov processes is that for which $a_v(y) = 0$ for $v \geq 3$ in Equation (3). It is called the Fokker–Planck equation or the diffusion process (Risken, 1996):

$$\frac{\partial P(y,t)}{\partial t} = -\frac{\partial}{\partial y} a_1(y) P(y,t) + \frac{1}{2}\frac{\partial^2}{\partial y^2} a_2(y) P(y,t), \tag{6}$$

where a_1 and $a_2/2$ are called the drift and diffusion coefficients, respectively. Thus, the Fokker–Planck equation is a truncated master equation. If a_1 is a linear function of y and a_2 is constant, Equation (6) is called a linear Fokker–Planck equation, a linearity definition consistent with that of the master equation. Linear Fokker–Planck equations have been used by Rayleigh, Einstein, Smoluchowski, and Fokker for special cases. Taking the moments of Equation (6) yields the equations governing the mean trajectory and the noise around the mean. The solutions of these equations are sufficient in the construction of the macroscopic trajectory and its time-dependent Gaussian noise. An Ornstein–Uhlenbeck process is characterized by the jump coefficients, $a_1(y) = -ky$, and $a_2(y) = D$ where the constants satisfy $k > 0$ and $D \geq 0$ (Gillespie, 1992). For an Ornstein–Uhlenbeck process with the initial condition $P(y, t = 0) = \delta(y - y_0)$, where δ denotes Dirac's delta function, its evolution of the probability distribution function can be written as

$$P(y,t) = \frac{1}{[\pi \frac{D}{k}(1 - \exp[-2kt])]^{0.5}} \times \exp\left\{ -\frac{(y - y_0 \exp[-2kt])^2}{\frac{D}{k}(1 - \exp[-2kt])} \right\}. \tag{7}$$

The evolution of an Ornstein–Uhlenbeck process and its statistical features are illustrated in Figure 1.

A discrete state, discrete time stochastic process can be designated by X_i, where $X_i = X(t = t_i)$ and $i = 0, 1, 2, \ldots$. X_i is called a Markov chain if it follows the Markov property. Examples of these processes include a random walk on a line, the number of persons in a waiting line at 1 minute intervals, and the number of catalyst particles of different sizes during attrition. The propagation of a Markov chain can be expressed in the following matrix form (Taylor & Karlin, 1998):

$$p(X_n) = p(X_0) P^n, \tag{8}$$

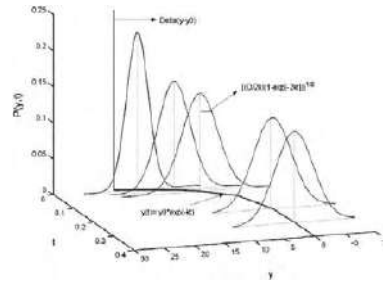

Figure 1. The evolution of an Ornstein–Uhlenbeck process, and its statistical features. The process starts with a given deterministic, initial condition, $P(y, t = 0) = \delta(y - y_0)$, and its fluctuations grow over time and eventually stabilize. The plot is drawn for $y_0 = 20$, $k = 20$, and $D = 1$. The solid line on the (y, t)-plane, $y(t) = y_0 \exp(kt)$, denotes the macroscopic trajectory and its limiting distribution when $t \to \infty$ depicts the Brownian motion.

where $p(X_k)$ is a row vector representing the probability distribution at t_k and P is the one-step transition probability matrix with the following elements:

$$P_{ij} \equiv Pr\{X_{k+1} = j \mid X_k = i\}. \tag{9}$$

Equation (9) suggests that the probability distribution at a given time t_k can be estimated by successive matrix multiplication.

External noises are the fluctuations created in an otherwise deterministic system by the application of an external random force, whose stochastic properties are supposed to be known. The displacement of a mass attached to a spring with a fluctuating external force, an animal population under the influence of a fluctuating environment, the response of an electronic circuit equipped with a noise generator, the random loading of a bridge, and the yield from a chemical reactor with a fluctuating feed rate are examples of external noises. The Langevin approach is widely used for the purpose of finding the effect of noise in macroscopically known systems. The noise is introduced by adding a random term, $L(t)$, to the deterministic equation (Karlin & Taylor, 1981; van Kampen, 2001; Øksendal, 2003)

$$\frac{\mathrm{d}y}{\mathrm{d}t} = A(y) + C(y) L(t), \tag{10}$$

where $A(y)$ denotes the macroscopic characteristics of the system and $C(y)$ characterizes the interaction of the noise and the system. When $A(y)$ is a linear function of y and $C(y)$ a constant, Equation (10) is called a linear Langevin equation. When $A(y)$ is a nonlinear function of y and $C(y)$ a constant, Equation (10) is called a quasilinear Langevin equation. When $C(y)$ is a function of y, Equation (10) is called a nonlinear Langevin

equation. These linearity definitions are consistent with those for the master and the Fokker–Planck equations after transformations. This consistency is important because some difficulties emerge during the integration of a Langevin equation that yields the Fokker–Planck equation (van Kampen, 2001). The treatment of the discontinuous stochastic noise, $L(t)$, is the source of the complexity. The added external noise, or the Langevin force, $L(t)$, is irregular and unpredictable, but its averaged properties over an ensemble of similar systems are simple. White noise is a commonly adopted simplification, which satisfies two averaged properties. Its ensemble has zero; that is,

$$E[L(t)] = 0\,. \tag{11}$$

Moreover, the individual noise takes place instantaneously with strength $\sqrt{\Gamma}$, and two successive noises arrive uncorrelated; that is,

$$E[L(t)L(t')] = \Gamma\delta(t - t'). \tag{12}$$

The spectral distribution of white noise, or the Fourier transform of Equation (12), is independent of the frequency ω. If the noise $L(t)$ is not δ correlated, the spectral density depends on the frequency and one uses the term *colored noise*.

Taking the first and second moments of Δy associated with a Langevin equation yields the jump moments of the Fokker–Planck equation. For a linear Langevin equation with $C(y) = 1$, the averaging process give rise to a linear Fokker–Planck equation (see, e.g., van Kampen, 2001)

$$\frac{\partial P(y,t)}{\partial t} = -\frac{\partial}{\partial y}A(y)P(y,t) + \frac{\Gamma}{2}\frac{\partial^2}{\partial y^2}P(y,t), \tag{13}$$

and it represents an Ornstein–Uhlenbeck process. For a quasilinear Langevin equation, the process gives rise to an expression identical to Equation (13). Nevertheless, the nonlinear nature of $A(y)$ suggests its Fokker–Planck equation is also nonlinear. Analytical solutions of the nonlinear Fokker–Planck equation are discussed by Risken (1996) and Grasman and van Herwaarden (1999).

Due to the discontinuous nature of $L(t)$, integrating $C(t)L(t)$ of a nonlinear Langevin equation in the averaging process, however, results in two different interpretations. If the averaged value of $C(y)$ during $(t, t + \Delta t)$ is used, the averaging process yields

$$\frac{\partial P(y,t)}{\partial t} = -\frac{\partial}{\partial y}[A(y)P(y,t)] + \frac{\Gamma}{2}\frac{\partial}{\partial y}\left[C(y)\frac{\partial}{\partial y}[C(y)P(y,t)]\right] \tag{14}$$

and the integration procedure is called the Stratonovich calculus. If the value of $C(y)$ before the arrival of the delta peak during $(t, t + \Delta t)$ is used, the averaging process yields

$$\frac{\partial P(y,t)}{\partial t} = -\frac{\partial}{\partial y}[A(y)P(y,t)] + \frac{\Gamma}{2}\frac{\partial^2}{\partial y^2}[C^2(y)P(y,t)] \tag{15}$$

and the integration procedure is called the Ito calculus. For practical processes experiencing external noise, the noise $L(t)$ is never infinitely sharp, and it lasts for a finite period of time; this consideration suggests that the Stratonovich interpretation is appropriate (van Kampen, 2001).

WEI-YIN CHEN

See also **Averaging methods; Deterministic walks in random environments; Ergodic theory; Fokker–Planck equation; Lévy flights; Martingales; Monte Carlo methods; Nonlinearity, definition of; Random walks; Stochastic analyses of neural systems; Time series analysis**

Further Reading

Chiang, C.L. 1980. *An Introduction to Stochastic Processes and Their Applications*, Huntington, NY: Krieger

Gardiner, C.W. 1985. *Handbook of Stochastic Methods for Physics, Chemistry, and Natural Sciences*, 2nd edition, Berlin: Springer

Gillespie, D.T. 1992. *Markov Processes*, San Diego: Academic Press

Grasman, J. & van Herwaarden, O.A. 1999. *Asymptotic Methods for the Fokker–Planck Equation and the Exit Problem in Applications*, Berlin: Springer

Karlin, S. & Taylor, H.M. 1975. *A First Course in Stochastic Processes*, 2nd edition, New York: Academic Press

Karlin, S. & Taylor, H.M. 1981. *A Second Course in Stochastic Processes*, New York: Academic Press

Oppenheim, I., Shuler, K.E. & Weiss, G.H. 1977. *Stochastic Processes in Chemical Physics: The Master Equation*, Cambridge, MA: MIT Press

Øksendal, B. 2003. *Stochastic Differential Equations: An Introduction with Applications*, 6th edition, Berlin: Springer

Risken, H. 1996. *The Fokker–Planck Equation: Methods of Solution and Applications*, 2nd edition, Berlin: Springer

Taylor, H.M. & Karlin, S. 1998. *An Introduction to Stochastic Modeling*, 3rd edition, San Diego: Academic Press

van Kampen, N.G. 1976. The expansion of the master equation. *Advances in Chemical Physics*, 34: 245–309

van Kampen, N.G. 2001. *Stochastic Processes in Physics and Chemistry*, revised edition, Amsterdam: Elsevier

STOKES SCATTERING

See **Rayleigh and Raman scattering and IR absorption**

STRANGE ATTRACTORS

See **Chaotic dynamics**

STRING THEORY

String theories (Green et al., 1987; Davies & Brown, 1988; Polchinski, 1998; Gauntlett, 1998; Kaku, 1999) were developed in the 1980s and 1990s in the hope of finding a unified description of all forces in nature. The aim is to combine electroweak, strong, and gravitational interactions into one consistent theory. The basic idea is that subatomic particles are not point-like but one-dimensional extended objects: strings. These vibrate (similarly to a violin string) in various modes and can move in space-time. The various particle states that we observe in nature should then all be explained as suitable excitations of suitable strings. Interaction processes between particles are described by splitting and merging of strings. Due to the finite size of strings, many of the divergences that occur for point-like particles can be avoided. The size of the string is very small, typically of the order of a few Planck lengths (1.6×10^{-35} m), so that on large scales string-like particles look like point particles.

Different types of boundary conditions are possible; there are open strings and closed strings. The simplest example is a bosonic string. In suitable coordinates, the equation of motion is simply a wave equation of the form

$$\frac{\partial^2 X^\mu(\sigma,\tau)}{\partial \tau^2} = C^2 \frac{\partial^2 X^\mu(\sigma,\tau)}{\partial \sigma^2}. \qquad (1)$$

Here X^μ is the coordinate of the string-like particle in d-dimensional space-time ($\mu = 0, 1, \ldots, d-1$), σ and τ denote an internal position and time variable parametrizing the string, and C is a constant.

The general solution can be written as a mode expansion of the form

$$X^\mu(\sigma,\tau) = x^\mu + \dot{x^\mu}\tau + \mathrm{i}\sqrt{2\alpha'}\sum_{n\neq 0}\frac{1}{n}\alpha_n^\mu \mathrm{e}^{-\mathrm{i}\frac{n\pi C\tau}{L}}\cos\frac{n\pi\sigma}{L}. \qquad (2)$$

Here x^μ and $\dot{x}^\mu$ are constants independent of σ and τ that essentially represent the position and velocity components of a constantly moving point particle, whereas the sum over n describes the oscillating part of the dynamics. The string parameter $\sqrt{\alpha'}$ describes the approximate scale where string effects become relevant, and L is the length of the string. Unlike a violin string, this string is not tied down at the end points but it can move freely through space-time while it oscillates.

So far this is a classical string. First quantization is done by letting the coefficients α_n^μ of the above normal mode expansion satisfy suitable commutator relations. Second, quantization of strings, up to now, is still an active area of research with many open questions (Kaku, 1999).

The quantization of bosonic strings yields unpleasant surprises, so-called ghosts. These are quantum states with negative norm. One wants to avoid these unphysical states, which is only possible if the dimension of space-time is $d = 26$. Consequently, it has been necessary to assume that the 22 extra dimensions are "compactified," that is, curled up on small circles that are so small that we do not notice them in daily life.

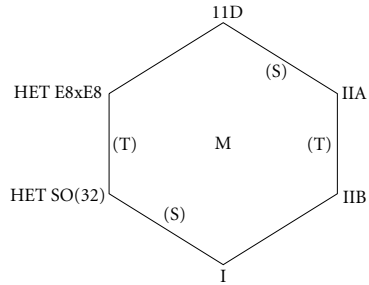

Figure 1. A schematic diagram of M-theory with its known string theory limits and the 11-dimensional theory. Some of the dualities are also shown.

But bosonic string theories have another problem. The lowest excitation mode (the ground state) is a so-called "tachyon," a state for which the mass squared is negative. To avoid this unphysical (unstable) ground state, one proceeds to supersymmetric string theories, in short "superstring theories." In these theories, for each boson there is a corresponding fermionic partner and vice versa. Technically, one introduces anti-commuting coordinates in addition to commuting ones. For supersymmetric theories, ghost states occur as well, but can now be avoided if the number of space-time dimensions is $d = 10$. So to describe low-energy physics, again six extra dimensions have to be compactified. Five different superstring theories have been found, which are denoted as type I, IIA, IIB, HET $E_8 \times E_8$, and HET SO(32). They differ in the degree of supersymmetry, the underlying gauge symmetry (if any), and whether the strings are closed or open.

Nowadays the five superstring theories are regarded as special limit cases of a more fundamental theory, called M-theory. This contains the five superstring theories and an 11-dimensional theory as special cases. These special cases are marked as the edge points of the diagram in Figure 1. Unfortunately, it is not known how M-theory should be formulated in full generality and how it should be second quantized. It is not even clear what the fundamental objects are that this theory describes. Much work needs to be done.

Some of the string theories contained in M-theory are connected by the so-called duality transformations. S-duality essentially means that a string theory with a small coupling constant α describes the same physics as another string theory with a large coupling given by $1/\alpha$. T-duality means invariance of the physics if

a compactified dimension of radius R is replaced by another one of radius $1/R$.

In recent years, much research emphasis has concentrated on higher-dimensional objects contained in string and M-theory, so-called D-branes. Open strings can end and start on D-branes. Remember that in electromagnetism there are point charges, which are the sources of the electromagnetic field. D-branes are in a sense higher-dimensional generalizations of these point charges.

As already mentioned, to proceed to our four-dimensional world, six of the dimensions of superstring theory (or 7 of those of M-theory) have to be compactified. The way this should be done is unclear. One needs to compactify on special types of compact manifolds, so-called Calabi–Yau manifolds, to preserve what is generally believed to be the right amount of supersymmetry. The compactification step is clearly necessary for string theory to make contact with the real world, but almost all relevant low energy predictions depend on the numerous possibilities of how to compactify. This severely undermines the predictive power of string theories.

In principle, the ultimate theory should predict everything we want to know about particle physics, such as the values of the coupling constants of the four different forces or the masses of all fermions and bosons. In string theories, the numerical values of gauge couplings (e.g. the fine structure constant α_{el}, which is about $\frac{1}{137}$ at low energies) can be related to vacuum expectations of a scalar field contained in string theories, the dilaton field. But this vacuum expectation depends in an unknown way on second quantization effects and has not been predicted so far. As 't Hooft puts it in his book ('t Hooft, 1997), string theory, at least in its present stage, has similarities with a very uncomplete piece of furniture: "Imagine that I give you a chair while explaining that the legs are still missing, and that the seat, back, and armrest will perhaps be delivered soon; whatever I did give you, can I still call it a chair?"

While typical equations for (free) strings, such as Equation (1), are linear, a recent proposal is to amend ordinary strings (evolving in a regular way) by nonlinear versions of strings, so-called chaotic strings (Beck, 2002). These evolve in a deterministic chaotic way. In this approach, each ordinary string is shadowed by a chaotic string, which yields the "noise" for second quantization via the so-called stochastic quantization method. Mathematically, chaotic strings consist of one-dimensionally coupled Tchebyscheff maps, a very nonlinear and strongly self-interacting theory, which describes a kind of "turbulent quantum state" on a small (quantum gravity) scale. It turns out that the vacuum energy of chaotic strings is minimized for observed standard model parameters; that is, in this extended approach to second quantization, concrete predictions for vacuum expectations of dilaton-like fields and hence on masses and coupling constants can be given.

CHRISTIAN BECK

See also **General relativity; Particles and antiparticles; Quantum field theory**

Further Reading

Beck, C. 2002. *Spatio-temporal Chaos and Vacuum Fluctuations of Quantized Fields*, Singapore: World Scientific

Davies, P.C.W. & Brown, J. 1988. *Superstrings: A Theory of Everything?* Cambridge and New York: Cambridge University Press

Gauntlett, J.P. 1998. M-theory: strings, duality and branes. *Contemporary Physics*, 39: 317–328

Green, M.B., Schwarz, J.H. & Witten, E. 1987. *Superstring Theory*, 2 vols, Cambridge and New York: Cambridge University Press

't Hooft, G. 1997. *In Search of the Ultimate Building Blocks*, Cambridge and New York: Cambridge University Press

Kaku, M. 1999. *Introduction to Superstrings and M-theory*, Berlin and New York: Springer

Polchinski, J. 1998. *String Theory*, 2 vols, Cambridge and New York: Cambridge University Press

STRONG COLLAPSE

See **Development of singularities**

STRUCTURAL COMPLEXITY

By *structural complexity* we mean the study of morphologically complex patterns associated with many physical entities of dynamical systems, using methods based on algebraic, geometric, and topological information (Ricca, 2001). In this respect, structural complexity offers an alternative and complementary route to study complex systems, based on morphological characteristics rather than the governing rules generating complexity. Structural complexity arises from spontaneous growth and self-organization of interacting components present in the bulk of physical systems, such as in turbulence, in biological and chemical reactions, in growth phenomena, across scales of space, time, and organizational complexity (Badii & Politi, 1997). Much of our understanding comes from observations of natural phenomena, from simulations and computational visualizations. Mathematical methods are used to extract and synthesize the relevant information, and to explore possible relationships between morphological complexity, energy localization, and other physical properties.

Dynamical systems are often characterized by the emergence and interaction of *coherent structures* (Nicolis & Prigogine, 1998; Scott, 2003). These latter are produced through filamentation mechanisms and space-time localization of characteristic physical properties. Examples of coherent filamentary structures may be as disparate as DNA macromolecules, synthetic polymer chains, nerve fibers, actin filaments, vortex filaments, magnetic flux tubes, or massive cosmic

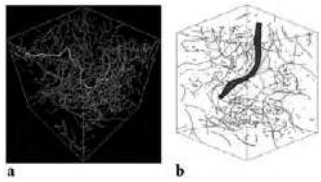

Figure 1. Computational field visualization of a pattern of vortex filaments produced by turbulent flow in a numerical box: (a) low-pressure line and (b) iso-pressure surface, obtained by numerical extraction techniques (Courtesy of S. Kida, Theoretical Division, National Center for Fusion Research, Toki, Japan).

strings. Dislocations and discontinuities in mesoscopic and solid-state physics, fronts and cell membranes in chemistry, fluid dynamics, and biology provide other examples of complex structuring. The formation and continuous re-arrangement of coherent structures are due to local interactions and recombination, governed by specific dynamics given by nonlinear differential equations $\dot{\boldsymbol{x}} = F(\mathbf{x}, \lambda)$, with a nonlinear function F of the vector $\boldsymbol{x} = (x_1, \ldots, x_n)$, which depends on an external control parameter λ. At certain critical values, this parameter causes phase transitions and pattern changes (Levin, 2002). *Pattern recognition* techniques aim at providing mathematical methods for diagnostics of the morphological complexity of the emerging pattern, regardless of the governing fundamental physical mechanism that is responsible for complexity.

One of the great benefits of modern capability to perform complex three-dimensional simulations is the possibility to effectively analyze and visualize huge sets of three-dimensional data. Direct volume rendering, iso-surface extraction, integral convolution, and many other computational techniques allow sophisticated multi-field visualizations of complex physical patterns (Johnson et al., 2001). Progress in *visiometrics*, based on the exploitation of such techniques for an accurate identification and representation of complex three-dimensional structures, provides powerful tools and an almost inexhaustible source of information for analysis of structural complexity (see Figure 1; also see **Visiometrics**).

Physical as well as computational domains are decomposed into *tropicity* domains, defined by the characterizing properties of nulls, tubes, sheets, and blobs. These are reference sets defined by the reference physical field distribution, that allow direct measurement of the degree of *tubeness*, *sheetness*, and *bulkiness* of the coherent set by analyzing the aspect ratio of the distribution.

Algebraic, geometric, and topological measures are used to quantify structural complexity. In case of high filamentation, the original network of filaments is

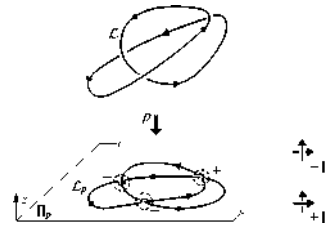

Figure 2. Example of analysis of an oriented space curve $\mathcal{L}$, based on crossing number information of the projected curve $\mathcal{L}_p$: we can calculate the total number of un-signed crossings (3, in the example shown in the figure) and, according to the sign convention shown on the right-hand side of the diagram, the algebraic sum of the $\pm$ signs ($-1-1+1=-1$, in the example shown). By averaging these two quantities over all directions p of projections, we obtain estimates of, respectively, the average crossing number and the writhing number of $\mathcal{L}$.

reduced (by appropriate threshold filtering) to a tangle $\mathcal{T}$ of space curves (representing the filament axes), hence reducing the problem to the analysis of the mutual positioning of the system of curves in space. By using methods based on crossing number information, we can evaluate the *average crossing number* $\bar{C}$ of the tangle that provides a fundamental algebraic measure of structural complexity. This quantity is defined by the formula

$$\bar{C} = \sum_{\mathcal{L}_i, \mathcal{L}_j \in \mathcal{T}} \bar{C}_{ij}, \tag{1}$$

where

$$\bar{C}_{ij} = \left\langle \sum_{r \in \mathcal{L}_i \sqcap \mathcal{L}_j} |\varepsilon_r| \right\rangle, \quad \varepsilon_r = \pm 1 \tag{2}$$

denotes the un-signed crossings between the curve $\mathcal{L}_i$ and $\mathcal{L}_j$ of the tangle $\mathcal{T}$, and summation is made over all the crossings resulting from $\mathcal{L}_i \sqcap \mathcal{L}_j$; the average number of crossings is then evaluated by projecting the tangle onto projection planes; here the angular brackets denote averaging over all directions of projections (in the simple case of one oriented space curve, Figure 2 shows an application of this analysis). Geometric measures are based on integral measures of curvature and torsion of the reference curves and surfaces; for tangles of curves, these include *total curvature*, *average twist*, and *writhing number* which give information on the amount of coiling and entwinement of the corresponding filaments. Topological information comes from different types of measures: number of *nulls* (zero-value field singularities), *linking numbers* for open or closed curves, winding numbers and invariants associated with handle-body decomposition of reference sets are all calculable quantities. Further information may come from analysis of cell-decomposition of the network. In particular situations, when a prevailing type of

geometry emerges, ad hoc analysis is used; for example, spiral spectrum analysis can be employed for scroll-wave reactions in Belousov–Zhabotinsky-type chemical systems and braid theory can be applied to study dynamics of particulates, fluid mixing, trailing vortices, astrophysical plasma loops, and tangle diagrams for polymers. Other information may come from study of dynamical systems, where we have information, for example, on Lyapunov exponents, topological entropy, multifractal properties, and topological scaling (see, for example, de Gennes, 1979; Jensen, 1998), whereas artificial intelligence provides us tools based on algorithmic complexity for neural-type networks. Measures of structural complexity are implemented computationally as time-dependent variables that change with the evolution of the physical system.

Collected information on structural complexity is analyzed against physical information. Since the evolution of any physical system is driven by variational principles that take account of energy and entropy redistributions, information on structural complexity may disclose some useful information on the physics and dynamics of the process. It is known that geometric properties strongly influence the dynamics: curvature forces (such as bending force in elastic rods or surface tension in liquid films) cause telephone cords to coil-up and foam bubbles to coalesce. We, therefore, expect relationships between geometry, dynamics, and ultimately, energy. Possible relationships between energy, entropy, and structural complexity in terms of algebraic information have, however, a more subtle rationale: network restructuring is due to local interactions and recombinations that are induced by acting potentials. These are associated with localized coherent structures, acting either on the strands of neighboring filaments (as in the case of reconnection of vortex tubes) or on the surface elements of sheet discontinuities (as in the formation of elastic films). In this context, local interaction of neighboring structures, resulting in the emergence of apparent crossings (possibly weighted by some distribution function) is a measure of the localization of internal energy. Hence, the resulting growth rate of the average crossing number provides an estimate of energy and entropy variations in the system. In absence of dissipation, topology is conserved; however, even in fully dissipative systems, topological information provides indications to detect preferred paths of energy depletion. In general, if χ denotes a measure (or a family of measures) of structural complexity, and E the energy of the system, we may expect *energy-complexity relations* of type $E = G(\chi)$, where G is a nonlinear function, where the nonlinearity is prescribed by the growth rate exponents of the physical process (see, e.g., Barenghi et al., 2001). Algebraic, geometric, and topological measures of structural complexity are, therefore, not only useful for computational implementation of diagnostics and pattern recognition, but they can also provide new tools to investigate localization and transfer of energy in complex physical systems.

RENZO L. RICCA

See also **Algorithmic complexity; Filamentation; Knot theory; Pattern formation; Topological defects; Vortex dynamics of fluids**

Further Reading

Badii, R. & Politi, A. 1997. *Complexity*, Cambridge and New York: Cambridge University Press

Barenghi, C., Ricca, R.L. & Samuels, D.C. 2001. How tangled is a tangle? *Physica* D, 157: 197–206

de Gennes, P.G. 1979. *Scaling Concepts in Polymer Physics*, Ithaca, New York: Cornell University Press

Jensen, M.H. 1998. *Self-Organized Criticality*, Cambridge and New York: Cambridge University Press

Johnson, C.R., Livnat, Y., Zhukov, L., Hart, D. & Kindlmann, G. 2001. Computational field visualization. In *Mathematics Unlimited – 2001 and Beyond*, edited by B. Engquist & W. Schmid, New York: Springer

Levin, S.A. 2002. Complex adaptive systems: exploring the known, the unknown and the unknowable. *Bulletin of the American Mathematical Society*, 40(1): 3–19

Nicolis, G. & Prigogine, I. 1998. *Exploring Complexity*, New York: W.H. Freeman

Ricca, R.L. (editor) 2001. *An Introduction to the Geometry and Topology of Fluid Flows*, Dordrecht: Kluwer

Scott, A. 2003. *Nonlinear Science: Emergence and Dynamics of Coherent Structures*, Oxford and New York: Oxford University Press

SUBHARMONIC GENERATION

See **Harmonic generation**

SUPERCONDUCTING QUANTUM INTERFERENCE DEVICE

The Superconducting QUantum Interference Device (SQUID) is the most sensitive detector for magnetic flux, Φ. It relies on the fundamental concept of flux quantization in a multiply connected superconductor, for example, a ring (torus). Flux quantization is a clear demonstration of the quantum mechanical properties of a superconductor in which the conduction electrons form (Cooper) pairs and condense in the ground state: the so-called "Bose condensation." Below the transition temperature, T_c, all the bosonic pairs can be described by a single macroscopic many-body wave function

$$\Psi(\mathbf{r}) = [n_s(\mathbf{r})]^{1/2} e^{i\theta(\mathbf{r})}, \qquad (1)$$

where n_s is the density of Cooper pairs. The phase $\theta(\mathbf{r})$ is a scalar function of the position. For small fields one may ignore the spatial dependence of n_s.

A direct consequence of the condensation is that for $T < T_c$ a superconductor exhibits zero electrical resistance and that magnetic fields are expelled from its interior. However, this diamagnetism (Meissner effect)

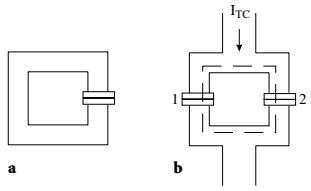

Figure 1. (a) The RF-SQUID and (b) the DC-SQUID. Dashed line is an integration contour deep inside the superconductor.

is not perfect as currents may penetrate into a thin surface layer (about 50 nm) called the London penetration depth (λ_L).

Early superconductors were metals (Hg, Al, Sn, Pb, Nb) or alloys (NbTi, Nb_3Sn) with T_c below ≈ 20 K. Since 1986, a new class of ceramic materials has been discovered with transition temperatures in the range 50–135 K, meaning that instead of requiring cooling by liquid helium (4 K), they only need cooling with liquid nitrogen (77 K) or by traditional cryocoolers. The terms low-T_c (LTS) and high-T_c (HTS) are used for these two types of superconducting materials.

The gradient of the phase θ of the macroscopic wave function describing all Cooper pairs depends on the pair-current density, $\boldsymbol{J_s}$, and the magnetic vector potential, $\boldsymbol{A}$, as

$$\hbar\nabla\theta = 2e(\Lambda\vec{\boldsymbol{J}}_{\boldsymbol{s}} + \vec{\boldsymbol{A}}), \tag{2}$$

where the pre-factor, $\Lambda = 2m/n_s(2e)^2$, reflects the double electron charge $2e$ and mass $2m$ of the Cooper pair. If Equation (2) is integrated along a closed contour deep inside the superconducting ring where $J_s = 0$, the fact that the wave function has to be single-valued with phase (modulo 2π) leads to quantization of the magnetic flux contained in the ring so that

$$\Phi_{\text{encl}} = n\Phi_0\,, \tag{3}$$

where $n = 0, 1, 2, 3, \ldots$ is an integer and $\Phi_0 = h/(2e)$ $= 2.07 \times 10^{-15}$ Wb is the "flux quantum." Φ_0 is very small, corresponding to the flux generated by the Earth's magnetic field ($\approx 40\,\mu$T) in a circular loop with radius $\approx 4\,\mu$m.

A SQUID is a superconducting ring including either one or two Josephson junctions as shown in Figure 1. Named after their operational modes, these are called the RF-SQUID and the DC-SQUID. In both configurations, the response to an external magnetic flux is periodic in the flux quantum Φ_0. For simplicity, we consider only the two-junction DC-SQUID shown in Figure 1b.

Upon integrating Equation (2) along the closed contour, one may show that the difference between the phases, φ_1 and φ_2, of the macroscopic wave functions of the two Josephson junctions varies periodically with

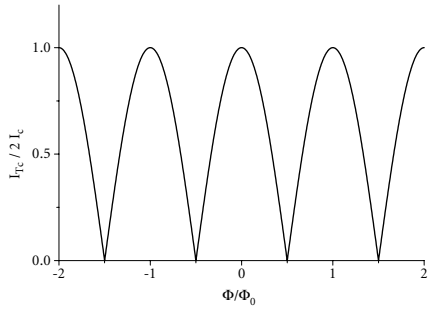

Figure 2. Magnetic interference pattern of symmetric DC-SQUID. Total critical current versus applied magnetic flux, $\beta_L = 0$.

the applied flux Φ as

$$\varphi_1 - \varphi_2 = 2\pi\,\Phi/\Phi_0, \tag{4}$$

giving a total critical (super-)current, I_{Tc}, of the SQUID

$$I_{Tc}(\Phi) = I_{c1}\sin\varphi_1 + I_{c2}\sin(\varphi_1 - 2\pi\,\Phi/\Phi_0)\,. \tag{5}$$

For two identical ($I_c = I_{c1} = I_{c2}$) junctions, $I_{Tc}(\Phi)$ varies from $2I_c$ to zero with a period of Φ_0 (see Figure 2). The first zero is at $\Phi = \Phi_0/2$. We say that the depth of modulation, $M = I_{Tc,max}/I_{Tc,min} = I_{Tc}/2I_c$, is 100%. M is reduced if the two junctions are different.

The variation in $I_{Tc}(\Phi)$ reflects the fact that the applied flux generates a circulating shielding supercurrent, $I_{circ}(\Phi)$ in the SQUID ring. Given the loop inductance, L, it generates a self-flux $\Phi_{self} = L\,I_{circ}$, which counteracts the applied flux. The effective flux in the ring is only $\Phi = \Phi_{appl} - \Phi_{self}$ leading to a reduced depth of modulation. A practical measure for a symmetric SQUID is the inductance parameter $\beta_L = \pi\,L\,I_c/\Phi_0$. For $\beta_L = 0$, $M = 100\%$ (as above) while for $\beta_L \to \infty$, $M \to 0$. Practical DC-SQUIDs are optimized with $M \approx 50\%$ corresponding to $\beta_L \approx 1$.

In order to avoid complications caused by hysteresis and flux contained in finite size junctions, one usually keeps junctions small and nonhysteretic (i.e., with relatively large damping and small capacitance). DC-SQUIDs with such junctions can be stably biased in the voltage state using a fixed DC current $I_b > I_{Tc}$. When an external flux is applied, the I-V curve is shifted following $I_{Tc}(\Phi)$, given in Equation (5), and a sensitive measurement of the oscillating voltage, $V(\Phi)|_{I_b}$, across the SQUID enables determination of Φ to a small fraction of Φ_0. Generally, the flux resolution is limited by thermal noise.

The use of a SQUID as a detector is complicated by the highly nonlinear dependence of the voltage response on the applied flux (see Figure 2). This may be overcome by operating the SQUID in the so-called

"flux locked mode," where the SQUID output voltage via a feedback loop is returned as a current in a coil placed near the SQUID ring. By proper design, the coil produces a flux that exactly compensates the applied flux in the ring. The SQUID now acts as a null detector where the feedback current is a linear function of Φ over a very large range of magnetic flux.

Its impressive flux resolution does not imply that the SQUID can resolve such small magnetic fields, because the area of the SQUID ring is normally very small. An ingenious way to effectively increase the loop area without increasing L (keeping $\beta_L \leq 1$) is to use a superconducting flux transformer. This is a closed superconducting loop consisting of a series connection of a pickup coil placed in the ambient magnetic field and an *input coil* inductively coupled to the SQUID ring. When an external magnetic field is applied to the pickup coils, a shielding current is set up in the loop so that the total flux in the flux transformer is conserved (flux quantization). The current generates a flux in the input coil, which in turn couples the flux into the SQUID. To increase sensitivity, the input coil often is a multiturn thin-film coil (Washer type) placed on top of the SQUID ring. Usually, the input coil and the SQUID are enclosed in a magnetic shield to suppress external noise.

A well-designed LTS DC-SQUID magnetometer with proper pickup coil has an unsurpassed magnetic field sensitivity of $\approx 10\,\mathrm{fT}$ ($10^{-14}\,\mathrm{T}$), about one billionth (10^{-9}) of the Earth's magnetic field. LTS RF-SQUIDs and HTS DC-SQUIDs reach 100 fT. Most field measurements, therefore, are limited by magnetic noise from the environment and not from the magnetometer itself. Magnetic noise may be dramatically reduced by shaping the pickup coil as two matched counter-wound coils, so that a uniform magnetic field (e.g., from a distant source) generates zero net flux in the flux transformer. Effectively it measures the gradient of the magnetic field working as a first-order gradiometer with baseline equal to the distance between two counter-wound coils. Higher order gradiometers with three (or more) balanced coils have also been constructed. Modern multi-SQUID magnetometers use first-order gradiometers with advanced digital noise reduction and background field nulling.

Because of their high sensitivity, SQUIDs are now used as transducers for virtually any response that can be converted to magnetic flux, including magnetic fields, field gradients, currents, voltages, electromechanical positioning, and movements. A prominent biomedical application is three-dimensional magnetic source imaging, where an array of several hundred SQUIDs placed in a helmet fitted around the head can localize magnetic sources in the human brain to about a millimeter. This is important for precise location before or during brain surgery and for diagnosis of mental disorders. Many hospitals already use commercial SQUID instruments to record the very weak fields generated by nerve pulses in the brain (MEG, magnetoencephalogram) and heart, even the fetal heart beat (MCG, magnetocardiogram), as supplements or improved alternatives to the established electrical counterparts, EEG (electroencephalogram) and ECG (electrocardiogram) using electrodes placed on the skin.

Dedicated SQUID magnetometers are also used in geomagnetic surveying as well as for nondestructive testing (NDT), where defects in conducting samples can de detected by monitoring magnetic fields of induced eddy currents. For detection of the Earth's magnetic field, signal frequencies are typically a few millihertz, but SQUIDs may also be used for ultra-low noise microwave amplifiers as well as picosecond electronics and terahertz oscillators based on propagation at high speed of single quanta of magnetic flux in SQUID arrays.

JESPER MYGIND

See also **Josephson junctions; Superconductivity**

Further Reading

Duzer, T. Van & Turner, C.W. 1998. *Principles of Superconductive Devices and Circuits*, Upper Saddle River, NJ: Prentice-Hall, pp. 256–283

Kadin, A.M. 1999. *Introduction to Superconducting Circuits*, New York: Wiley, pp. 207–225

Orlando, T.P. & Delin, K.A. 1990. *Foundations of Applied Superconductivity*, New York: Addison-Wesley, pp. 244–251 and 410–420

SUPERCONDUCTIVITY

The phenomenon of superconductivity was discovered in 1911 by the Dutch scientist Heike Kamerlingh Onnes. In connection with work on the liquefaction of helium (normal boiling point at 4.2 K), he measured the resistance of mercury and noticed that the resistance dropped gradually with temperature as was expected. However, near 4.2 K, the resistance apparently dropped to a very small value consistent with zero. This, of course, must have been a very dramatic discovery, changing completely the general picture of the properties of solid-state matter. Today, the simple and direct consequence of zero resistance—that a large current can run indefinitely in a closed wire without energy input—intrigues many people. Even though zero resistance may be counter-intuitive, it is not forbidden by the laws of nature, and it does not imply a "perpetuum mobile." The second important property of a superconductor is that it is a perfect diamagnet. This property also has a feature that at first may seem quite unnatural. If a magnet is lowered towards a superconductor, the magnetic field of the magnet cannot penetrate into the superconductor. The magnetic field lines become compressed between the magnet and the superconductor, and eventually the magnet will levitate. This exclusion of the magnetic field is not a consequence of the

Figure 1. A levitated HTS superconductor.

induction law in connection with zero resistance of the superconductor, but an independent phenomenon. The phenomenon was discovered in 1933 by Walter Meissner and Robert Ochsenfeld long after the discovery of zero resistance. It is called the Meissner effect.

Superconductivity as discussed above occurs in many ordinary metallic elements from the periodic table. Examples are mercury, lead, tin, and niobium. The transition temperatures T_c (i.e., the highest temperature where superconductivity occur) are typically below 10 K. If the external magnetic field is too high, it will quench the superconductivity completely. This field is called the critical field H_c, and it is typically of order some hundreds of Gauss, too low for practical applications in electric machinery. The type of superconductor described above is called a type I superconductor.

Type II superconductors were discovered much later—in the 1950s. They are typically alloys of metals such as NbTi or Nb_3Sn and have transition temperatures typically in the 10–20 K range up to 23 K. They can carry much higher currents and can withstand much higher magnetic fields, thus, being much more useful for applications. A major difference from type I superconductors is the way they behave in a magnetic field. The Meissner effect as described above exists up to a so-called lower critical field H_{c_1}. At H_{c_1}, the magnetic field in the form of magnetic flux lines starts to penetrate the superconductor. As the external field is increased up to the upper critical field H_{c_2}, more and more flux lines penetrate the superconductor until at H_{c_2}, the flux lines completely fill the superconductor, which then becomes normally conducting.

In 1986, a new type of superconductor was found with a complicated structure. These superconductors are called High Temperature Superconductors (HTS, see below) and may, for lack of better understanding, be described as extreme type II. Examples are $YBa_2Cu_3O_7$ (known as YBCO) and $Bi_2Sr_2Ca_1Cu_2O_8$ (BSCCO), both of which have transition temperatures above the boiling point of liquid nitrogen at 77 K. These materials are quite useful for applications since liquid nitrogen—a cheap industrial product—may be used as a coolant. These important superconductors will be discussed separately below.

Figure 1 shows a levitated HTS superconductor. Since it is an extreme type II superconductor, magnetic flux lines penetrate the superconductor. These flux lines are "pinned" on imperfections of the crystal lattice, such as dislocations, and provide a stability not seen in type I superconductors. Thus, the HTS superconductors may even "levitate" below the magnet—hanging on the flux lines from the magnet. By symmetry a magnet can alsobe levitated over a superconductor.

Ginzburg–Landau Theory

Superconductivity is a complicated quantum mechanical phenomenon. The particles giving rise to the supercurrents may be described by a quantum mechanical wave function $\psi(r) = |\psi(r)|\exp(i\Theta)$. In a normal metal, the phases of all the electrons are different. In the superconducting state, all carriers have the same quantum mechanical phase of the wave function. This is referred to as macroscopic phase coherence. Thus, a simply connected macroscopic superconductor is characterized by a single-phase angle. The difference between a normal metal and a superconductor has some similarity to the difference between the coherent light of a laser, where all the atomic oscillators oscillate in phase and the "white" light of an ordinary bulb, where all the exited atoms are incoherent.

The interpretation of superconductivity as a macroscopic quantum phenomena and the first useful theory of superconductivity were due to Fritz and Heinz London in 1935.

A real breakthrough for applications is the still very often-used phenomenological theory published by the Russian scientists Vitaly Ginzburg and Lev Landau in 1950. Ginzburg and Landau introduced a position-dependent order parameter with a conceptual similarity to a quantum mechanical wave function. The Ginzburg–Landau theory is a masterpiece of intuition. It postulates that as the temperature is lowered and T_c is crossed from above, a (complex) order parameter $(\psi(r))$ for an ordered, superconducting phase appears—increasing from the value zero at T_c. Gibbs free energy is then expressed as a series expansion in terms of this order parameter $(\psi(r))$. Finding the equilibrium value of the Gibbs free energy leads to two coupled differential equations that connect the order parameter and the electromagnetic fields.

Variational methods are used and the Ginzburg–Landau equation is derived. It may be written

$$\alpha\psi(\boldsymbol{r}) + \beta|\psi(\boldsymbol{r})|^2\psi(\boldsymbol{r}) + 1/2m((h/2\pi i)\nabla - q\boldsymbol{A})2\psi(\boldsymbol{r}) = 0$$

Here α and β are coefficients to be determined by the particular system, $\boldsymbol{A}$ is the vector potential and m is a particle mass. The last term on the left side has the appearance of a kinetic energy, and we note the similarity to the Schrödinger equation (*See* **Nonlinear Schrödinger equations**).

As mentioned above, the nonlinear Ginzburg–Landau equation can be applied to other systems with an order parameter characterizing a phase transition. Examples are magnetic materials, liquid helium, and liquid crystals. Because of the series expansion, which is only good when the expansion parameter is small, the theory is formally only valid near the transition temperature.

BCS Theory

Although rather successful, the above theories are phenomenological in nature. They do not specify the nature of the physical system or why superconductivity occurs. For this, a full microscopic quantum mechanical theory must be derived. This was done by John Bardeen, Leon Cooper, and Robert Schrieffer in 1957, and their theory carries the name BCS theory. The derivation of the BCS theory is too complicated to be described here, but we note that in most practical cases a full understanding is not needed. Close to T_c the BCS theory approaches the phenomenological Ginzburg–Landau theory as it should. Central to BCS theory is the notion that there are two types of currents. Normal currents are carried by normal electrons, and supercurrents are carried by so-called "superelectrons." Just below T_c, there are only a few superelectrons and many normal electrons. At $T = 0$, all charge carriers are superelectrons. These "superelectrons" are bound pairs of normal electrons called Cooper pairs. Accordingly they have two electron masses and two electron charges. Intuitively, one would think that two electrons could not form a pair since Coulomb repulsion would rip them apart. However, the pairing mechanism has its origin in the electron-phonon interaction, which is responsible for overwhelming the Coulomb repulsion and providing the attractive potential binding the two electrons together.

The binding energy of the pair, Δ, is of order a few meV and is related to the energy scale of the phonons involved in the pairing process. Naturally in the BCS theory, there is a direct proportionality between the transition temperature T_c and the pair binding energy Δ. In fact, this way it has been suggested that T_cs cannot exceed about 30 K. Until recently the highest T_c observed experimentally was 23 K in general agreement. This is not true any more as will be described in the next section.

High T_c Superconductors

In 1986, K. Alex Muller and J. Georg Bednorz from the IBM Zurich research laboratory discovered superconductivity in a new class of materials involving typically the so-called rare earths. Within a few months after the discovery was known, researchers found a T_c of 92 K in the material $YBa_2Cu_3O_7$ and related compounds. YBCO is typical of the so-called HTS although now many other families are known, including the widely used $Bi_2Sr_2Ca_2Cu_3O_8$ compounds. To become superconducting, these materials must undergo a heat treatment at about 1000 K in an oxygen atmosphere. After this baking, the materials appear as a ceramic and are thus hard and brittle—which causes some engineering problems for making the superconductors into wires and coils. Now, many more HTSs are known and the highest T_c found so far is about 150 K. New HTS materials are found regularly, and it cannot be predicted what the limit to higher T_c will be. Maybe we will one day have room-temperature superconductors.

The theory for HTSs is not known, in spite of the efforts of many theoreticians. Obviously, the BCS theory is not directly applicable since it predicts a maximum T_c of about 30 K. An HTS typically has a layered structure with copper-oxide planes separated by isolating atoms at atomic distances, and it is speculated that the superconductivity somehow has its explanation in this structure.

Particularly following the discovery of HTS, the potential for useful applications of superconductivity is quite large. A significant benefit of the high transition temperatures is that liquid nitrogen at 77 K can be used as the coolant. Applications are both small scale (electronics, sensors, and communications) and large scale (power cables, motors, transformers, and large magnets.)

Starting with small scale, we note that Josephson junctions (*See* **Josephson junctions**) are the main component in superconducting electronics. The general advantage over semiconductors is higher speed and lower dissipation. Computers can be constructed that are much faster and much smaller than conventional computers. Sensors, in general, can be made much more sensitive with superconductor technology. This is because of the quantum mechanical nature of superconductivity and, of course, the low temperatures where thermal noise is reduced. A so-called super conducting quantum interference device (SQUID) is a commercial superconducting magnetic field sensor that is so sensitive that it can measure the magnetic field from nerve impulses in the brain. It can also be used to detect internal cracks in the aluminum-alloy plates of aircraft wings. Superconducting photon detectors can detect single photons from space. High-frequency microwave detectors can detect signals down to the quantum limit and in some spectacular cases even lower. Filters for mobile telephone ground stations can be made much sharper than conventional ones, implying more telephones, improved quality, and lower prices.

Large-scale applications include large magnets, levitated trains, power cables, motors, energy storage, and fault current limiters. Large magnets are, for example, used in the Magnetic Resonance Imaging

(MRI) systems at hospitals where a patient's whole body is introduced into the magnet. This is a very large market, and it is only feasible with superconducting magnets. A levitated train with superconducting magnets has already been built in Japan (Maglev). Superconducting (HTS) power cables have already been built in several countries. In Denmark, a 35 m section has already been installed in the Copenhagen grid. In general, the benefits of the superconducting systems is that energy savings can be obtained because there is no—or at least very low—dissipation. Thus superconducting machinery can be made much smaller than similar conventional machinery, which is important in many cases in the automotive industry. Energy can be stored in large superconducting coils or friction-free flywheels. A fault current limiter is an important protection device for the utility grid that can be made using only superconducting technology.

In the coming generation, superconductivity may play the revolutionary role that semiconductors did in the previous generation.

NIELS FALSIG PEDERSEN

See also **Bose–Einstein condensation; Josephson junctions; Nonlinear Schrödinger equations; Superconducting quantum interference device**

Further Reading

Barone, A. & Paterno, G. 1982. *Physics and Applications of the Josephson Effect*, New York: Wiley

Seeber, B. (editor). 1998. *Handbook of Applied Superconductivity*, 2 vols, Bristol and Philadelphia: Institute of Physics Publishing

Sheahen, T.B. 1994. *Introduction to High Temperature Superconductivity*, New York: Plenum Press

Tinkham, M. 1996. *Introduction to Superconductivity*, 2nd edition, New York: McGraw-Hill

SUPERFLUIDITY

Superfluidity is the state of a quantum liquid in which the liquid has the ability to flow through fine slits and capillaries without friction or production of a pressure gradient. The superfluidity of liquid helium He^4 (called "He-II") at temperatures below $T_\lambda = 2.17$ K was discovered by Peter Kapitza in 1938. The transformation of normal liquid helium into the superfluid state is a phase transition of the second order. Nevertheless, the superfluid He-II cannot be considered as a liquid without viscosity. Experiments on rotational vibrations of a disk suspended in He-II show that damping is observed at temperatures below ($T < T_\lambda$), decreasing as the temperature is lowered.

The first qualitative explanation of superfluidity phenomena was proposed by Lazlo Tisza (1938), who introduced a two-fluid model of superfluidity. Lev Landau (1941) later formulated a so-called two-fluid hydrodynamics of He-II. According to this explanation, He-II consists of two interpenetrating fluids, a normal fluid with viscosity and a superfluid fluid with zero viscosity. It is the superfluid that flows without friction through the finest of channels, while the finite viscosity of the normal component is responsible for the observed damping of the oscillating disk. Each component is assigned a density ρ_n and ρ_s, whose sum is the total density $\rho = \rho_n + \rho_s$, and each is assigned its velocity field v_n and v_s.

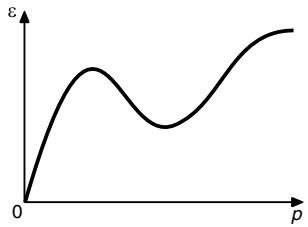

Figure 1. Dependance of the energy of elementary excitations on momentum.

Landau's theory is based on the idea of a possible description of physical properties of a weakly excited macroscopic system at low temperatures by means of elementary excitations or "quasiparticles." The elementary excitations have energy $\varepsilon(p)$ and are regarded as particles of momentum p. The normal component represents a gas of elementary quasiparticles with a dispersion curve as sketched in Figure 1. There are two types of the quasiparticles at low temperatures: sound quanta or phonons of long wavelength (with dispersion relation $\varepsilon = sp$, where s is the sound velocity) and excitations of short wavelength called "rotons" (near the minimum of the curve in Figure 1 their energy is $\varepsilon = \Delta + \frac{1}{2}(p - p_0)^2/\mu$), where μ is the effective mass of the roton). Interactions of quasiparticles with each other and with the vessel's walls cause the viscosity of the normal component. At zero temperature, the normal density $\rho_n = 0$ and the system is in the ground state.

The remaining part of He-II is the superfluid component. It has zero viscosity and can move without friction through narrow slits and capillaries if the energy spectrum of the quasiparticles satisfies the following condition: $\varepsilon(p)/p > 0$. At $T = 0$, the superfluid density $\rho_s = \rho$. The quasiparticle concentration grows when the temperature increases and ρ_s decreases turning into zero at $T = T_\lambda$. According to the Landau theory, the liquid loses the superfluidity property if the velocity of its flux exceeds a critical velocity,

$$v_c = \min(\varepsilon(p)/p); \qquad (1)$$

this condition is called the "Landau criterion." Real critical velocities are much less than (1) because

the superfluidity is broken by vortices arising in the superfluid liquid at even smaller velocities. Quantum vortices have been observed during experiments on the motion of the He-II in a rotating cylindrical container.

In a quantum Bose gas and He-II at low temperatures, a large number of particles (a finite proportion of all particles) turns into one coherent state called a "condensate," which can have a stationary velocity different from zero. Such a phenomenon is called "Bose–Einstein condensation," and superfluidity is often connected with it. When the superfluidity component is a correlated many-particle quantum state; however, it may not be connected directly with Bose–Einstein condensation.

The energy spectrum of excitations in a weakly non-ideal Bose gas with repulsive interactions between particles was first derived by Nikolai Bogolubov (1947) assuming existence of the condensate

$$\varepsilon(p) = [(p^2/m)\rho_0 v(p) + p^4/(4m^2)]^{1/2}, \qquad (2)$$

where ρ_0 is the density of particles in the state $\boldsymbol{p} = 0$, $v(p)$ is the Fourier component of the potential of interparticle interaction ($v(0) > 0$), and m is the mass of the particle. Equation (2) determines a spectrum of small vibrations of the condensate in the non-ideal Bose gas. This dispersion relation is of the phonon type at small p, where the Landau criterion is satisfied. Therefore, even the weakly non-ideal Bose gas possesses the superfluid property.

A macroscopic theory of the superfluid dynamics of the weakly non-ideal Bose gas was developed by Gross (1961) and Pitaevskii (1961). In this theory, a condensate wave function Ψ is described by the nonlinear Schrödinger equation ($\hbar = 1$):

$$\mathrm{i}\frac{\partial \Psi}{\partial t} = -\frac{1}{2m}\Delta\Psi + v(0)\left(|\Psi|^2 - \rho\right)\Psi. \qquad (3)$$

A solution of the linearized Equation (3) has a form of harmonic vibrations whose frequency spectrum is determined by Equation (2). Thus, Equation (3) in a total form possesses a solution in the form of the straight-line vortex

$$\Psi = \sqrt{n}\, f\left(\frac{r}{r_0}\right)\mathrm{e}^{\mathrm{i}\phi}, \quad r_0^2 = \frac{h^2}{2m v(0) n}, \qquad (4)$$

where r and ϕ are the distance from the vortex axis and the polar angle with respect to it, and the function $f(r)$ has a shape sketched in Figure 2.

Superfluidity is also possible in quantum Fermi liquids both in neutral (e.g., liquid He^3) and charged (conducting electrons in metals) liquids. Then a generation of pairs of coupled fermions is necessary (pairs of He^3 atoms or electrons with an integer spin) to create bosons. Such pairing is a result of any attraction (either van der Waals interactions between the atoms or interaction of the electrons with vibrations of the crystal lattice). Being bosons, these "Cooper pairs" can form coherent superfluid condensates. The attractive forces between He^3 atoms are very small; therefore, conditions for generation of the Cooper pairs of quasiparticles and origin of the superfluidity of He^3 appear only at superlow temperatures of the order of 10^{-6}K. Interestingly, there are two superfluid phases (A and B) of the He^3 at superlow temperatures.

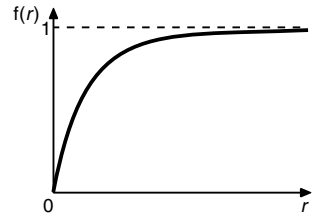

Figure 2. Distribution of the condensate near the vortex.

The emergence of electron Cooper pairs in a metal corresponds to the appearance of superconductivity. Concepts from superfluidity theory have influenced the theory of superconductivity in metals and also the development of models of the superfluidity of the atomic nucleus. As the atomic nucleus presents a Fermi system with strong interparticle interaction, both the pair correlation effects and also manifestations of some superfluid properties of Bose systems should take place.

Superfluid liquids possess several unusual properties. Besides ordinary sound (i.e., vibrations of the liquid's density), a so-called "second sound" can propagate in such a liquid. The second sound represents sound propagation in the quasiparticle gas (vibrations of the quasiparticle density and, therefore, vibrations of the temperature). Also, a thin film of superfluid He-II forms on a solid wall, rising easily up to a large height. This film can equalize liquid levels of the helium in vessels having a common wall.

ARNOLD KOSEVICH

See also **Bose–Einstein condensation; Nonlinear Schrödinger equations; Superconductivity**

Further Reading

Bogolubov, N.N. 1947. On the theory of superfluidity. *Izvestia Akademii Nauk SSSR*, Seriya Fiziko, 11: 77

Donnelly, R.J. 1967. *Experimental Superfluidity*, Chicago: University of Chicago Press

Feynman, R.P. 1957. Appliction of quantum mechanics to liquid helium. In *Progress in Low Temperature Physics*, edited by C.J. Gorter, vol. I: pp. 17–53

Gross, E.P. 1961. Structure of a quantized vortex in boson systems. *Nuovo Cimento*, 20: 454

Kapitza, P.L. 1938. Viscosity of liquid helium at temperatures below the lambda point. *Doklady Akademii Nauk SSSR*, 18: 21 (in Russian); translated in *Nature*, 141: 74

Kapitza, P.L. 1977. *Experiment. Theoriya. Practika*, Moscow: Nauka (in Russian)
Khalatnikov, I.M. 1971. *Teoriya Sverkhprovodimosti*, Moscow: Nauka (in Russian)
Landau, L.D. 1941. Theory of superfluidity of helium II. *Zhurnal Experimental'noj i Teoreticheskoj Fiziki*, 11: 592 (in Russian)
Landau, L.D. 1947. On the theory of superfluidity in helium II. *Journal of Physics of the USSR*, 11: 91
Lifshitz, E.M. & Pitajevski, L.P. 1978. *Statisticheskaya Fizika*, p.2 Moscow: Nauka (in Russian)
Pitaevskii, L.P. 1961. Vortex lines in an imperfect Bose gas. *Zhurnal Experimental'noj i Teoreticheskoj Fiziki*, 40: 646 (in Russian); translation in *Soviet Physics JETP*, 13: 451
Tisza, L. 1938. Transport phenomena in helium II. *Nature*, 141: 913
Tisza, L. 1940. On the theory of quantum liquids. Application to liquid helium. *Journal de Physic et Radium*, 1: 350 (in French)

SUPERLATTICES

Superlattices (SLs) are solid periodic structures usually made artificially and having a period much larger than the interatomic distance. The SL is called one-dimensional (1-d) if it is periodic along one axis. In such a case, the SL has the form of alternating plane-parallel layers of two or several materials differing in their physical properties (dielectric, elastic, magnetic, etc., depending on the implementation of interest) (see Figure 1). Modern techniques of crystal growth allow the creation of artificial crystals with atomic smooth boundaries between layers, which can be arranged in any order. A two-dimensional SL is periodic in two directions and homogeneous in the third, and a three-dimensional SL is periodic along three axes. There are many types of SLs, including semiconducting and superconducting SLs, dielectric or optical SLs (called photonic crystals), and elastic or acoustic SLs (called phononic crystals).

The main physical property of an SL important for applications is a band structure of the energy or frequency spectrum caused by the macroscopic periodicity analogous to the structure of electron energy or phonon frequency spectra in monocrystals.

The physical origin of the band structure can be understood by analyzing a one-dimensional SL constructed from two types of materials, where the alternating layers have thicknesses d_1 and d_2 (see Figure 1). The SL period equals $d = d_1 + d_2$, and the electromagnetic or elastic fields inside each layer are described by wave equations with phase velocities c_1 and c_2. Thus, eigenfunctions of the wave equations are characterized by a quasiwave number k, and the energy or frequency of any excitation is a periodic function of k with the period $2\pi/d$, so values of k can be restricted to the one-dimensional Brillouin zone $-\pi/d < k < \pi/d$.

If the velocities c_1 and c_2 are close, one can assume $c_1 = c_2 = c$ in the first approximation, so the dispersion relation for the wave solution is that for

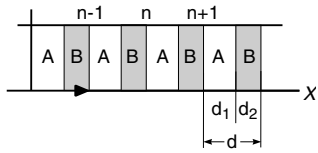

Figure 1. 1D SL made of substances of two types A and B.

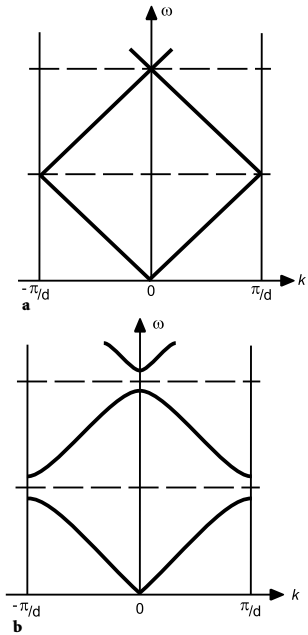

Figure 2. Dispersion relations for the SL (a) in the limiting case $c_1 = c_2$ and (b) in the case $|c_1 - c_2| \ll c_1 \approx c_2$.

a homogeneous material. In the case of an elastic medium or a dielectric transparent for electromagnetic waves, $\omega(k) = ck$ where ω is the frequency and c is either the sound or light velocity (the straight lines in Figure 2a). Because the function $\omega(k)$ repeats itself outside the Brillouin zone, the lines fold back into the zone when they reach edges. A small perturbation provided by the small difference between c_1 and c_2 takes off the degenerations at the points $k = 0, \pm\pi/d$ and as a result, a small frequency gap appears between the upper and lower branches of the lines (Figure 2b). This is called a forbidden gap as no excitation mode of the SL can exist in the gap. As the difference $c_1 - c_2$ is increased, the forbidden gap widens considerably.

Dispersion equations for the frequencies of arbitrary one-dimensional SLs made of two dielectric or elastic materials were obtained by the Soviet scientist Sergei Rytov (1955, 1956) using the standard boundary conditions at the layer boundaries

$$\cos kd = \cos k_1 d_1 \cos k_2 d_2 - \frac{1}{2}\left(\frac{k_1}{k_2} + \frac{k_2}{k_1}\right) \sin k_1 d_1 \sin k_2 d_2, \quad (1)$$

where $k_1 = \omega / c_1$ and $k_2 = \omega / c_2$. When the right-hand side of Equation (1) has values from -1 to $+1$, the equation has real roots, which give the values of ω.

If one of the alternating layers is opaque for electromagnetic waves, the corresponding wave vector is imaginary: $k_2 = \mathrm{i}\kappa_2$ and Equation (1) transforms to

$$\cos kd = \cos k_1 d_1 \cosh \kappa_2 d_2 - \frac{1}{2}\left(\frac{k_1}{\kappa_2} - \frac{\kappa_2}{k_1}\right) \sin k_1 d_1 \sinh \kappa_2 d_2. \quad (2)$$

There are two limiting cases of Equations (1) and (2) when the roots of interest can be easily obtained either graphically or analytically. The first one concerns (2) and assumes $\kappa_2 = \text{constant} \to \infty$ and $d_2 \to 0$ at $\kappa_2 d_2 \to 0$ under the condition $\kappa_2^2 d_2 = \text{constant} = q$ (Kronig & Penny, 1931). The simplified version of Equation (2) has the form

$$\cos kd = \cos kd + M \frac{\sin k_1 d}{k_1 d}, \quad M = \frac{1}{2} q d, \quad (3)$$

which can be solved graphically. In Figure 3a, $z = k_1 d$ and the roots of the equation run over values within intervals marked off on the abscissa axis. These intervals become wider and the forbidden gaps become more narrow when the frequency increases.

The second limiting case concerns Equation (1) and corresponds to the limit $d_2 \to 0$, $c_2 \to 0$ under the conditions $d_2 / c_2 = 0$ and $d_2 / c_2^2 = P = \text{constant}$, leading to (Kosevich, 2001)

$$\cos kd = \cos k_1 d - Q k_1 d \sin k_1 d, \quad Q = c_1^2 P / (2d). \quad (4)$$

Equation (4) can also be solved graphically (see Figure 3b), and a set of permitted intervals contracting with increasing frequency can be obtained. However, there is an analytical expression for frequencies at large numbers m of these intervals ($m^2 Q \gg 1$)

$$\omega = \frac{m\pi c}{d} + \frac{2\Omega}{m} \begin{cases} \sin^2(kd/2), & m = 2p; \\ \cos^2(kd/2), & m = 2p+1, \end{cases} \quad (5)$$

where $\Omega = c/(\pi Qd)$ and p is an integer.

The frequencies of forbidden bands correspond to a solution of the wave equation inside n-th layer of the type $\exp \pm \kappa nd$ (when $k = \mathrm{i}\kappa$) or $(-1)^n \exp(\pm \kappa nd)$ (when $k = \mathrm{i}\kappa + \pi$), which decrease (grow) with increasing n. The frequency dependence of the parameter κ for solutions of the first (second) type is found from Equation (1) when its right-hand side is larger then $+1$ (then $\cos kd = \cosh \kappa d$ in the left-hand side) or less than -1 (then $\cos kd = -\cosh \kappa d$). Such solutions have a physical meaning only in the x semiaxis under the condition that a solution vanishing at infinity and corresponding to certain boundary conditions at the origin is selected. The necessity of using exponentially decreasing solutions arises in describing localized states of fields under consideration in the vicinity of a local SL defect. Of course, a one-dimensional SL can have only localized states near a given plane. In certain circumstances, a localized mode can exist at the face of the SL (called a surface state).

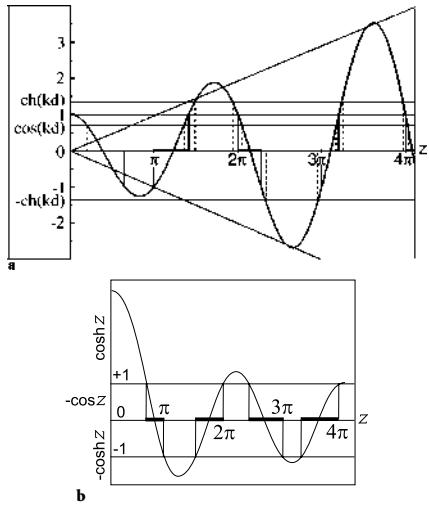

Figure 3. Graphical solutions of (a) Equation (3) and (b) Equation (4). Eigenfrequency bands are shown in heavy lines on the z-axis ($z = k_1 d$).

In the general case, the spectrum of an SL is complicated and contains a system of a great number of both eigenfrequency bands and gaps corresponding to forbidden frequencies of eigenmodes. No extended states are allowed in the gap, but there exist evanescent modes, decaying exponentially with increasing the distance from the defect. In a three-dimensional SL, they are localized states.

Dependence of the physical parameters of materials (the velocities c_1 and c_2, or the parameters Q and M in the above equations) on the field strength leads to nonlinear effects in SLs. In optical SLs, a source of nonlinear effects is the dependence of the refraction coefficient on the electric field of a light wave. In the simplest case, which corresponds to the

dispersion relations (5) in the linear approximation, an electromagnetic wave Ψ_n in the nth layer of the SL is governed by the discrete NLS equations for $m = 2p$

$$i\frac{\partial \Psi_n}{\partial t} = \frac{m\pi c}{d}\Psi_n - U_0|\Psi_n|^2\Psi_n - \frac{2\Omega}{m}(2\Psi_n - \Psi_{n+1} - \Psi_{n-1}) \qquad (6)$$

and for $m = 2p + 1$

$$i\frac{\partial \Psi_n}{\partial t} = \frac{m\pi c}{d}\Psi_n - U_0|\Psi_n|^2\Psi_n + \frac{2\Omega}{m}(2\Psi_n + \Psi_{n+1} + \Psi_{n-1}), \qquad (7)$$

where U_0 is a parameter of the nonlinearity. Actually, Equations (6) and (7) are equations for the envelope curve of SL vibrations taken in discrete points. Such equations can be used for describing nonlinear effects and particularly dynamics of solitons in the optical SL.

ARNOLD KOSEVICH

See also **Discrete nonlinear Schrödinger equations; Nonlinear optics; Photonic crystals; Solitons**

Further Reading

Hasegawa, A. 2003. *Optical Solitons in Fibers*, 3rd edition, Berlin and New York: Springer

Jin, B.Y. & Ketterson, J.B. 1989. Artificial metallic superlattices. *Advances in Physics*, 38: 189–366

Joannopoulos, J.D., Meade, R.D. & Winn, J.N. 1995. *Photonic Crystals*, Princeton, NJ: Princeton University Press

Kivshar, Y. & Agrawal, G. 2003. *Optical Solitons: From Fibers to Photonic Crystals*, Amsterdam and New York: Academic Press

Kosevich, A.M. 2001. On a simple model of the photonic or phononic crystal. *JETP Letters*, 74: 559–563

Kronig, R. de L. & Penny, W.G. 1931. Quantum mechanics of electrons in crystal lattices. *Proceedings of the Royal Society, London, Series* A, 130: 499–513

Rytov, S.M. 1955. Electromagnetic properties of laminated media. *Zhurnal Experimental'noj i Teoreticheskoj Fiziki*, 29: 605–616; *Soviet Physics, JETP*, (1956), 2: 66

Rytov, S.M. 1956. Properties of laminated medium. *Soviet Physics-Acoustics*, 2: 68

Yeh, P. 1988. *Optical Waves in Layered Media*, New York: Wiley

SUPERSYMMETRY

See **String theory**

SURFACE WAVES

The surface of a fluid such as water lends itself most easily to the demonstration of wave phenomena. At the same time, waves on the surface of shallow water have played a very important role in the development of nonlinear science. The entries in this encyclopedia on water waves and solitons cover this aspect. Following narrower definitions, the term *surface waves* is often used for standing waves that form on the surface of a vessel filled with a liquid and moved up and down periodically in the direction normal to the liquid's surface. When adding the adjective *acoustic* (surface acoustic waves, SAW), one thinks of waves propagating on the surface of a solid elastic medium. These two types of surface waves will be discussed here. The former are called Faraday waves, and the most common species of the latter is named after Lord Rayleigh (John William Strutt).

Faraday Waves

In 1831, Michael Faraday reported on a series of experiments with various liquids that he made oscillate on glass plates and in a basin attached to a vibrating strip of wood (or lath) (Faraday, 1831). On the surface of the vibrating liquids, he observed the formation of standing wave patterns. With increasing amplitude of vibration, he found these standing waves to evolve into a regular square pattern (Figure 1). Faraday also noticed that the frequency of the surface waves was half of that of the driving force.

A proper mathematical explanation for the instability of the flat fluid surface, when being accelerated periodically, was given more than a century later, in 1954, by T.B. Benjamin and F. Ursell. They considered a sinusoidal acceleration with frequency ω. Let the initially planar surface be parallel to the x, y-plane and define the two-dimensional position vector $\boldsymbol{R} = (x, y)$. Benjamin and Ursell expanded the local excursion $\zeta(\boldsymbol{R}, t)$ of the surface from the planar initial position in real eigenfunctions S_m, $m = 1, 2, \ldots$, of the two-dimensional Laplace operator, satisfying Neumann boundary conditions at the boundary of the fluid surface with vanishing normal derivative,

$$\zeta(\boldsymbol{R}, t) = \sum_m a_m(t) S_m(\boldsymbol{R}). \qquad (1)$$

Linearizing the equations of hydrodynamics, they arrived at the Mathieu equation for the amplitudes a_m,

$$\frac{\partial^2 a_m}{\partial t^2} = [p_m + q_m \cos(\omega t)]a_m \qquad (2)$$

with coefficients q_m and p_m that depend on the corresponding eigenvalue of the Laplace operator and, hence, on the shape of the surface, on the depth of the liquid, as well as on gravity and surface tension. In addition, q_m is proportional to the amplitude of the periodic driver. The exponentially increasing solutions of the Mathieu equation that occur for certain combinations of system parameters, correspond to the instability. In particular, it becomes clear from (2) why the dominant instability is subharmonic.

The Faraday instability can thus be understood within linear theory. However, linear theory is not

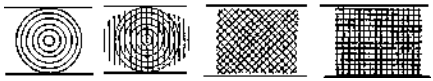

Figure 1. Sequence of surface wave patterns observed by Faraday on a quadrangular pool (Faraday, 1831).

sufficient to decide on which pattern will actually form after the instability has occurred. This can be determined by application of the modern theory of pattern formation to this damped-driven system (Miles & Henderson, 1990; Zhang & Viñals, 1997). Here, the nonlinearity comes into play. For sufficiently large spatial extension of the surface, boundary conditions at the edge of the surface become unimportant, and we may expand ζ in plane waves. Near the onset of the subharmonic instability, one may write

$$\zeta(\boldsymbol{R}, t) = \cos(\omega t/2) \sum_{j=1}^{N} \exp(\boldsymbol{k}_j \cdot \mathbf{R}) A_j(t) + \text{c.c.} \quad (3)$$

to a good approximation. (In (3) c.c. stands for the complex conjugate and a finite number N of wave vectors has been considered.) The modulus of the wave vectors $\boldsymbol{k}_j$ is fixed by the dispersion relation of linear surface waves at frequency $\omega/2$. Viñals and his coworkers have shown that the slow variations of the amplitudes A_j are governed by a nonlinear equation of the form (Zhang & Viñals, 1997)

$$\frac{\partial A_j}{\partial \tau} = -\partial \mathcal{F}/\partial A_j^* \quad (4)$$

with the Lyapunov function

$$\mathcal{F} = \sum_{j=1}^{N} |A_j|^2 + \frac{1}{2} \sum_{j,j'=1}^{N} g(c_{jj'}) |A_j|^2 |A_{j'}|^2. \quad (5)$$

Here, τ is a stretched time, $c_{jj'}$ is the cosine of the angle between wave vectors $\boldsymbol{k}_j$ and $\boldsymbol{k}_{j'}$, and the function g depends on the system parameters. Stable stationary wave patterns correspond to minima of the Lyapunov function. For given system parameters, the pattern corresponding to the lowest value of $\mathcal{F}$ should be attained. Zhang and Viñals tested configurations with amplitudes A_j, 1, ..., M nonzero and $|A_j|$ independent of j, while the remaining $N - M$ amplitudes are zero. If the amplitudes corresponding to three or fewer different wave vectors are nonzero ($M \leq 3$), regular periodic patterns are obtained. The square pattern, already observed by Faraday, corresponds to two orthogonal wave vectors. With amplitudes of three different wave vectors nonzero, hexagonal or triangular patterns are generated. Interestingly, the theory of Zhang and Viñals also predicts patterns with more than three different wave vectors to be stable for certain system parameters. These correspond to quasi-periodic structures analogous to two-dimensional quasicrystals

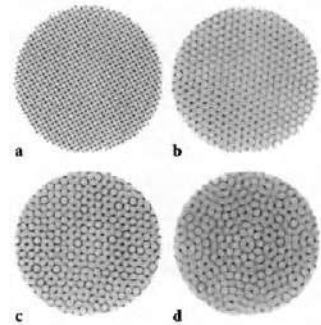

Figure 2. Faraday wave patterns of square (a), hexagonal (b), eight-fold quasi-periodic (c), and ten-fold quasi-periodic (d) symmetry observed by Binks & van de Water (1997).

such as the Penrose tiling, for example. It has been a remarkable success of this nonlinear theory of pattern selection to predict the appearance of such quasi-periodic patterns of eight-fold (four wave vectors) and ten-fold (five wave vectors) symmetry, which have subsequently been found in experiments (Binks & van de Water, 1997) (see Figure 2).

In systems with length scales such that the boundary of the fluid's surface is relevant for the pattern formed, one has to consider the eigenfunctions $S_m(\boldsymbol{R})$ of the Laplace operator satisfying the correct conditions at the boundary and, hence, depending on the shape of the surface. This opens up the possibility of using Faraday waves to visualize wave-mechanical modes of stadium billiards and relating them to classical trajectories (Kudrolli et. al., 2001). At high values of the periodic acceleration of the fluid, spatiotemporal chaos has been observed.

In addition to the wave patterns arising on the surface of a moving liquid, Faraday, in his 1831 report, describes two other types of standing waves on the surfaces of liquids. The first one concerns patterns that he observed when a wave-maker was oscillating right on top of the surface or partly immersed in the liquid. Ridges are formed that are directed away from the wave-maker. The second type of standing waves occurs on a sloping beach when wind is blowing along the surface against the beach. Here, the ridges are parallel to the direction of the wind. These waves have been studied in detail in theory and by further experiments (Miles & Henderson, 1990). They are relevant in the context of oceanography.

Surface Acoustic Waves

In his landmark paper of 1885, Lord Rayleigh showed that the equations of linear elasticity theory for an isotropic homogeneous elastic half-space with a planar

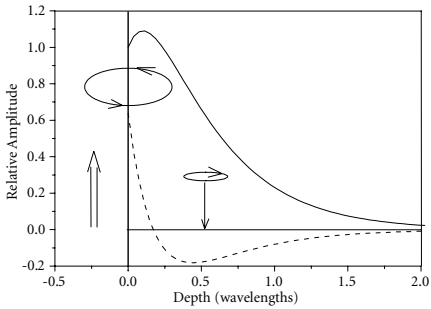

Figure 3. Displacements associated with a Rayleigh wave as function of depth. The surface wave is propagating in the direction of the double arrow. Displacement component normal (solid) and parallel (dashed) to the surface.

stress-free surface admit solutions that correspond to straight-crested waves propagating along the surface (Rayleigh, 1885). The deformations associated with these waves decay exponentially with depth. Such a Rayleigh wave is polarized in the plane spanned by the propagation direction and the surface normal (sagittal plane). It causes the mass elements of the solid to move on ellipses. This motion is retrograde near the surface and changes to prograde at greater depth (Figure 3).

Rayleigh himself thought of these waves in connection with earthquakes and their consequences, pointing out that surface wave amplitudes decrease more slowly with distance from the epicenter than those of bulk waves.

Since then, surface acoustic waves have found important applications in many branches of science and technology with wavelengths ranging from the kilometer scale in geophysics down to micrometers in ultrasonic nondestructive testing, acoustic microscopy, sensors, and micro-electronics. They are also used for basic research in solid-state physics with wavelengths down to the nanometer scale. The advent of the interdigital transducer on surfaces of piezoelectric media led to a number of signal processing devices based on SAW, especially frequency filters that are nowadays used in television sets and cell phones.

A distinctive feature of surface waves on solids as compared with ordinary liquids is the possibility of the medium to be anisotropic. For a long time it had not been known whether surface acoustic waves exist at all on surfaces of anisotropic media apart from special highly symmetric geometries. In the meantime, a mathematical theorem was established by Lothe and Barnett that guarantees their existence in most cases. However, generalized Rayleigh waves that occur in anisotropic media need no longer be polarized in the sagittal plane and may have more complicated depth profiles than the one shown in Figure 3. Their associated displacement field $\boldsymbol{u}$ is a superposition of generalized plane waves,

$$\boldsymbol{u}(x,z,t) = \sum_{j=1}^{n} \boldsymbol{W}_j \exp[\mathrm{i}k(x - vt) - |k|\alpha_j z] + \text{c.c.}\,, \qquad (6)$$

when the wave vector $\boldsymbol{k} = k\hat{\boldsymbol{x}}$ is along the x-direction and the elastic medium fills the half-space $z > 0$. (v is the phase velocity.) The (often complex) coefficients α_j have positive real part. In isotropic media, $n = 2$; in nonpiezoelectric media, $n \leq 3$. In very special circumstances, n may even be 1. In piezoelectric substrates, $n \leq 4$.

In anisotropic media, the group velocity of a surface acoustic wave need no longer be parallel to its wave vector. This can lead to focusing of acoustic energy propagating away from a local excitation of the surface. This effect, which is well known for acoustic bulk waves, has been demonstrated for surface waves in a comparatively simple and efficient way by Kolomenskii and Maznev. Anisotropy also gives rise to leaky waves (pseudo-surface waves) with a very high degree of localization at the surface.

When accounting for piezoelectricity and/or considering an elastic substrate in contact with other media, a whole zoo of various species of surface waves is found (Maradudin, 1985; Auld, 1990), including waves

- of shear-horizontal polarization in homogeneous piezoelectric substrates with or without metal coating (Bleustein–Gulyaev waves),
- in layered structures with shear-horizontal (Love waves) or sagittal polarization (generalized Lamb waves, Sezawa waves),
- at the interface of a solid and a liquid (Scholte waves),
- at the interface between two different solids (Stoneley waves).

The power flow associated with a Rayleigh wave is localized at the surface within a layer of approximately a wavelength. The high spatial localization favors effects generated by the elastic nonlinearity of the medium. In particular, higher harmonics are easily observed. Because neither the equations of nonlinear elasticity nor the geometry of a homogeneous half-space with a planar surface define a length scale, surface acoustic waves are nondispersive in this system. Therefore, shock formation can be observed. Theoretically, the evolution of nonlinear wave forms is studied on the basis of the following equation which follows from derivations by Lardner and Parker (Parker, 1988):

$$\mathrm{i}\frac{\partial}{\partial\tau}B(k) = k\int_0^k F(q/k)\,B(q)\,B(k-q)\,\mathrm{d}q + 2k\int_k^\infty (k/q)\,F^*(k/q)\,B(q)\,B^*(q-k)\,\mathrm{d}q. \qquad (7)$$

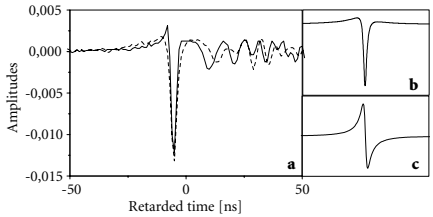

Figure 4. Solitary pulse shapes on the coated Si(111) surface (propagation along the $[\bar{1}\bar{1}2]$ direction) (a,b) and on a coated surface of isotropic quartz (c). Left: Experimental results by Lomonosov and Hess (solid) and numerical simulation (dashed). Right: Stationary pulse shapes. The local slope of the surface is shown as function of arrival time. (Compiled from data published in Lomonosov et al., 2002).

Here, τ is a stretched time and the function B is the Fourier transform of the local surface slope,

$$\frac{\partial}{\partial x}u_3(x,0,t) = \int_0^\infty B(k,\tau)\exp[\mathrm{i}k(x-vt)]\,\mathrm{d}k + \text{c.c.} \quad (8)$$

The complex function F depends on the second-order and third-order elastic moduli of the medium and may often be well approximated by its value at the argument 1 / 2. When transforming (7) into real space, the nonlinearity turns out to be strongly nonlocal. This is the price one has to pay for eliminating the depth dependence of the displacement field from the evolution equation.

On the surface of homogeneous isotropic media, the velocity component of mass elements normal to the surface develops a cusp, while the component parallel to the surface steepens in a way similar to the pressure in the formation of shocks in gases and liquids. This behavior has been found in simulations starting with a sinusoidal wave form and in experiments with pulsed laser excitation. In order to generate acoustic pulses of high intensity at solid surfaces, this experimental technique has proven to be most effective (Lomonosov et al., 2001). A laser pulse focused on a line on the surface leads to rapid local heating and generates an explosive evaporation of a highly absorbing coating. Similar to the epicenter of an earthquake in the macroscopic world, the explosion leads to an acoustic pulse that is localized at the surface after having propagated some distance from the line of excitation.

Depositing on the substrate surface a thin film of a material different from that of the substrate leads to a linear dispersion term in (7). The evolution equation then has solitary wave solutions that may be regarded as solid state analogs of the solitons on shallow water. They have shapes strongly influenced by the anisotropy of the substrate, as demonstrated by the examples in Figure 4. The existence of solitary surface acoustic pulses has been verified by Lomonosov and Hess using laser excitation to generate an initial pulse that subsequently evolves into a solitary pulse and a quasilinear background (Figure 4).

ANDREAS MAYER

See also **Billiards; Nonlinear acoustics; Pattern formation; Shock waves; Solitons; Tessellation; Water waves**

Further Reading

Auld, B.A. 1990. *Acoustic Fields and Waves in Solids*. 2nd edn., Malabar, Florida: Krieger

Binks, D. & van de Water, W. 1997. Nonlinear pattern formation of Faraday waves. *Physical Review Letters*, 78: 4043–4046

Faraday, M. 1831. On a peculiar class of acoustical figures; and on certain forms assumed by groups of particles upon vibrating elastic surfaces. *Philosophical Transactions of the Royal Society of London*, 121: 299–340

Kudrolli, A., Abraham, M.C., & Gollub, J.P. 2001. Scarred patterns in surface waves. *Physical Review* E, 63: 026208/1–8

Lomonosov, A., Mayer, A.P. & Hess, P. 2001. Laser-based surface acoustic waves in materials science. In *Experimental Methods in the Physical Sciences*, vol. 3: *Modern Acoustical Techniques for the Measurement of Mechanical Properties*, edited by M. Levy, H.E. Bass, & R. Stern, San Diego: Academic, pp. 65–134

Lomonosov, A., Hess, P. & Mayer, A.P. 2002. Observation of solitary elastic surface pulses. *Physical Review Letters* 88: 076104/1–4

Maradudin, A.A. 1985. Surface acoustic waves. In *Nonequilibrium Phonon Dynamics*, edited by W.E. Bron, New York: Plenum, pp. 395–599

Miles, J. & Henderson, D. 1990. Parametrically forced surface waves. *Annual Review of Fluid Mechanics*, 22: 143–165

Parker, D.F. 1988. Waveform evolution for nonlinear surface acoustic waves. *International Journal of Engineering Science*, 26: 59–75

Rayleigh, Lord (John William Strutt). 1885. On waves propagating along the plane surface of an elastic solid. *Proceedings of the London Mathematical Society*, 17: 4–11

Zhang, W. & Viñals, J. 1997. Pattern formation in weakly damped parametric surface waves. *Journal of Fluid Mechanics*, 336: 301–330

SYMBOLIC DYNAMICS

Dynamical systems on manifolds are usually described by equations using local Euclidean variables. Symbolic dynamics has its origins in an alternative description of the orbits of a dynamical system by Jacques Hadamard at the end of the 19th century and later by Marston Morse, where it was shown that complex orbital behavior of a dynamical system could be described using sequences of symbols (Hadamard, 1898; Morse, 1921).

A simple example that shows the usefulness of this approach is the iteration $x_{n+1} = f(x_n)$ on the interval of real numbers $\mathbb{I} = [0, 1]$ defined by a piecewise linear map

$$x_{n+1} = \begin{cases} 2x_n, & x_n < 0.5, \\ 2x_n - 1, & x_n \geq 0.5. \end{cases}$$

This map can also be described by

$$x_{n+1} = 2x_n \bmod 1$$

for $x_n \in [0, 1)$ together with $f(1) = 1$. It is easy to *solve* the modular equation formally for the orbital sequence $x_n = f^n(x_0)$, $0 \le q x_0 < 1$, as

$$x_n = 2^n x_0 \bmod 1.$$

However, the formal solution is no more illuminating than the defining iteration, because it is not at all clear how the repeated exponentiation of the solution interacts with the process of reducing mod 1. To overcome this problem and unlock the dynamical secrets held within the formula, note that any real number $x \in \mathbb{I}$ can be written in the form

$$x = \sum_{n=1}^{\infty} \frac{b_n}{2^n},$$

where $b_n = 0$ or 1. Let Σ_2 denote the set of all such binary sequences. Thus, every binary sequence $\mathbf{b} = \{b_n\}_{n=1}^{\infty} \in \Sigma_2$ represents a point $\pi(\mathbf{b}) = x \in \mathbb{I}$ by a map $\pi : \Sigma_2 \to \mathbb{I}$.

Relative to this new representation of points in $\mathbb{I}$ the map f takes the form of a shift $\sigma : \Sigma_2 \to \Sigma_2$ on binary sequences as

$$\{b_1, b_2, \ldots, b_n, \ldots\} \longmapsto \{b_2, b_3, \ldots, b_{n-1}, \ldots\},$$

that is,

$$\sigma(\{b_n\}_{n=1}^{\infty}) = \{b_{n+1}\}_{n=1}^{\infty}$$

simply because

$$2\left(\sum_{n=1}^{\infty} \frac{b_n}{2^n}\right) \bmod 1 \; = \sum_{n=1}^{\infty} \frac{b_{n+1}}{2^n}.$$

It is easy to check that the map π provides a *semi-conjugacy* $f\pi = \pi\sigma$ for f and σ. The map π is not a conjugacy because of the redundancy in the binary representation of the reals. This can be resolved by always choosing binary sequences representing reals in [0,1] that *do not* have infinite sequences of 1s. So, for example, 0.25 has the infinite binary representations $\{01\overline{0}\}$ and $\{00\overline{1}\}$, but we choose the former. Nevertheless, the semi-conjugacy implies that for every positive integer m, $f^m\pi = \pi\sigma^m$. In particular, if $\mathbf{b} = \{b_n\} \in \Sigma_2$ is a period-m orbit of σ, then

$$f^m(\pi(\mathbf{b})) = \pi\sigma^m(\mathbf{b}) = \pi(\mathbf{b}),$$

and so π maps the σ-periodic point $\mathbf{b}$ to an f-periodic point $\pi(\mathbf{b})$. Thus, we can obtain the periodic orbits of f by investigating the periodic orbit structure of σ. But this is straightforward because the period-m periodic points of σ in Σ_2 are precisely those binary sequences that repeat after m-digits and no fewer. Thus, period-1 points of σ are given by the repeating expansions

$$\mathbf{b} = \{\overline{0}\ldots\} = \{00000\ldots\}$$

and

$$\mathbf{b} = \{\overline{1}\ldots\} = \{11111\ldots\},$$

which both correspond by π to the fixed points $x = 0$ and $x = 1$, respectively, of the map f.

Period-2 points of σ are given by

$$\mathbf{b}_1 = \{\overline{01}\ldots\}, \qquad \mathbf{b}_2 = \{\overline{10}\ldots\}.$$

Note that $\pi(\mathbf{b}_1) = \frac{1}{3}$ and $\pi(\mathbf{b}_2) = \frac{2}{3}$ and $\left\{\frac{1}{3}, \frac{2}{3}\right\}$ is the only period-2 orbit of f. We can immediately see that periodic points of all orders can be constructed for σ, and thus also for f, in this way. Points that are on *eventually* periodic orbits of f can also be obtained by delaying the introduction of the binary recurrences in the symbol sequences. Thus, any map f defined on $\mathbb{I}$ that is described by a shift on symbol sequences has a rich periodic structure. We can extract further properties about orbits of f when we observe that π can be seen as a continuous function by taking the usual Euclidean metric on $\mathbb{I}$ and the metric

$$d(\mathbf{b}, \mathbf{b}') = \sum_{n=1}^{\infty} \frac{(b_n - b'_n)}{2^n},$$

where $\mathbf{b} = \{b_n\}_{n=1}^{\infty}$ and $\mathbf{b}' = \{b'_n\}_{n=1}^{\infty}$ are elements of Σ_2. It is now possible to consider a *topology* on Σ_2.

A key feature of chaos is the requirement that the orbits of the map f should in some sense be bound together, thus, making the dynamics indecomposable. This can be achieved by finding an orbit of f that *densely* fills out the set $\mathbb{I}$. Such an orbit is given by constructing a sequence $\mathbf{b}$ obtained by listing all symbol sequences of length 1, then of length 2, and so on for all positive integers. Let $\mathbf{b}'$ be any prescribed binary sequence. Given any positive integer n, by construction $\mathbf{b}$ has within it the symbol block $\mathbf{b}'^{(n)}$ consisting of the first n symbols of $\mathbf{b}'$. Suppose this block commences at the point b_{k+1} of $\mathbf{b}$. Then $\mathbf{b}'$ and $\sigma^k(\mathbf{b})$ have the same first n entries and thus $d(\mathbf{b}', \sigma^k(\mathbf{b})) < 2^{-n}$. The positive integer n was chosen arbitrarily, and so the orbit of $\mathbf{b}$ approaches arbitrarily close to $\mathbf{b}'$. Thus, the orbit of $\mathbf{b}$ is *dense* on $\mathbb{I}$ and binds the dynamical behavior together preventing a decomposition into closed subsets with simpler dynamical behavior.

The dense orbit was, of course, produced to a special recipe. Obviously, the orbit is not unique as other dense orbits in Σ_2 can be constructed by simple permutations of the ordering of the blocks used to construct the sequence $\mathbf{b}$. What is astonishing is that "almost all" orbits are dense. This follows from a classical result of Emil Borel around 1900 (Hardy, 1983), which, when paraphrased, says that the set of real numbers in $\mathbb{I}$, which

have all possible finite sequences of "0"s and "1"s in their binary expansions, called *normal* numbers, has full measure.

Thus, the doubling map can be described by a shift map σ on the space of symbolic sequences on two symbols, Σ_2. The simple ideas discussed here can be extended to provide symbolic dynamics for various types of maps. The *coding* involving two or more symbols has to be carried out so that each point x of the map domain is given by a symbol string that provides the orbit of x by merely shifting the symbols (Devaney, 2003). Note that the binary sequence gives the itinerary of an orbit where if "0" represents the interval $[0, \frac{1}{2}]$ and "1" represents $[\frac{1}{2}, 1]$, the sequence gives the sequence of intervals visited by the orbit of the map f. This approach can be applied to a wide class of one-dimensional maps (Guckenheimer, 1979; Guckenheimer et al., 1977), but it also has much greater importance in dynamical systems.

A key dynamical construction is the *Smale Horseshoe* (Smale, 1967). The simplest example is a diffeomorphism h of the square $Q \in \mathbf{R}^2$ whose image in $\mathbf{R}^2$ is folded in the shape of a horseshoe to overlay the square. The map h has an invariant Cantor set $\Lambda \subset Q$ such that $h|\Lambda$ can also be coded with *bi-infinite* binary sequences together with a shift map. This results in a complex periodic orbit structure and dense orbits within Λ, which gives some of the ingredients of chaos. The key components of the set Λ are the *homoclinic* points, that is, those points that asymptotically approach a periodic orbit of h in both forward and reverse iterations.

The Smale–Birkhoff Theorem proves that "folding maps" of this type, and the associated complex dynamical behavior, exist in the neighborhood of such homoclinic points. This is precisely stated as follows (Smale, 1967).

Theorem. Let $\mathbf{f}$ be a Kupka–Smale diffeomorphism of a compact manifold M and $x^\dagger$ be a transverse homoclinic point of a periodic point x^* of $\mathbf{f}$. Then there is a closed subset Λ containing $x^\dagger$, such that (i) Λ is a Cantor set; (ii) $\mathbf{f}^p(\Lambda) = \Lambda$ for some $p \in \mathbf{Z}^+$; and (iii) $\mathbf{f}^p|\Lambda$ is topologically conjugate to a shift on a symbol space.

Note that all possible binary sequences are allowed in the above symbol spaces and, thus, we have been considering *full* shifts. In many practical applications of data storage, there are practical restrictions on the stored patterns of sequences. The problem of transferring codes that satisfy one set of constraints into other restricted symbol sets involve *sub-shifts of finite type* and allow applications to communications coding and algebra (Coornaert & Papadopoulos, 1993; Lind & Marcus, 1996; Kitchens, 1997). Symbolic coding has been directly useful in modeling in engineering and biology, see (Daw et al., 1997) and (Voss et al., 2000).

DAVID D. ARROWSMITH

See also **Chaotic dynamics; Horseshoes and Hyperbolicity in dynamical systems; Maps; One-dimensional maps; Topology**

Further Reading

Coornaert, M. & Papadopoulos, A. 1993. *Symbolic Dynamics and Hyperbolic Groups*, Berlin & New York: Springer

Crutchfield, J.P. & Packard, N. 1982. Symbolic dynamics of one-dimensional maps: entropies, finite precision, and noise. *International Journal of Theoretical Physics*, 21: 433–466

Daw, C.S., Finney, C.E.A., Kennel, M.B. & Connolly, F.T. 1997. Cycle-by-cycle combustion variations in spark-ignited engines. *Proceedings of the Fourth Experimental Chaos Conference*, Boca Raton, FL, Singapore: World Scientific

Devaney, R.L. 2003. *An Introduction to Chaotic Dynamical Systems*, 2nd edition, Boulder, CO: Westview Press

Guckenheimer, J. 1979. Sensitive dependence to initial conditions for one-dimensional maps. *Communications in Mathematical Physics*, 70: 133–160

Guckenheimer, J., Oster, G. & Ipatchki, A. 1977. The dynamics of density dependent population models. *Journal of Mathematical Biology*, 4: 101–147

Hadamard, J. 1898. Les surfaces á courbures opposeés et leur lignes géodesiques. *Journal de Mathématiques Pures et Appliquées*, 4: 27–73

Hao, B.-L. 1986. *Elementary Symbolic Dynamics and Chaos in Dissipative Systems*, Singapore: World Scientific

Hao, B.-L. & Zheng, W.-M. 1998. *Applied Symbolic Dynamics and Chaos*, Singapore: World Scientific

Hardy, G.H. 1983. *An Introduction to the Theory of Numbers*, 5th edition, Oxford and New York: Oxford University Press (first published, 1938)

Kitchens, B.P. 1997. *Symbolic Dynamics: One-Sided, Two-Sided, and Countable State Markov Shifts*, Berlin and New York: Springer

Lind, D. & Marcus, B. 1996. *An Introduction to Symbolic Dynamics and Coding*, Cambridge and New York: Cambridge University Press

Milnor, J. & Thurston, W. 1988. On iterated maps of the interval. In *Dynamical Systems Proceedings, University of Maryland 1986–87*, edited by J.C. Alexander, Berlin and New York: Springer, pp. 425–563

Morse, M. 1921. A one-to-one representation of geodesics on a surface of negative curvature. *American Journal of Mathematics*, 43: 33–51

Smale, S. 1967. Differentiable dynamical systems. *Bulletin American Mathematical Society*, 73(6): 747–817.

Voss, A., Wessel, N., Kurths, J., Schirdewan, A., Osterziel, K.J., Malik, M. & Dietz, R. 2000. Symbolic dynamics—a powerful tool in non-invasive biomedical signal processing. In *Advances in Noninvasive Electrocardiographic Monitoring Techniques*, edited by H.H. Osterhues, V. Mombach & A.J. Moss, Dordrecht and Boston: Kluwer, pp. 429–437

SYMMETRY BREAKING

See **Bifurcations**

SYMMETRY GROUPS

Mathematically, a group is a set G together with a pair-wise "group multiplication" on elements of G that satisfies the following axioms. (i) Multiplication is associative, meaning that $xy(z) = x(yz)$ for x,

y, and z any elements of G. (ii) G contains an identity element e for which $ex = x = xe$ where x is any element of G. (iii) Each element of G has an inverse (x^{-1}), satisfying $x^{-1}x = e = xx^{-1}$ (Armstrong, 1988; Birkhoff & MacLane, 1953). Groups for which all of the multiplications commute are said to be abelian.

Easily visualized examples of finite symmetry groups are provided by operations on familiar geometrical objects, such as squares, hexagons, cubes, and tetrahedrons, which carry vertices into themselves. In general, there will be a finite set of f linearly independent functions (in the space of the geometrical object) that are carried into linear combinations of themselves by the group operations. Thus, each group element corresponds to a matrix, and the corresponding set of $f \times f$ matrices is called a representation of the group (Landau & Lifschitz, 1958).

For a square that is lying on the plane with its center at the origin, group elements are rotations about the origin (by 90°, 180°, and 270°) and reflections (in horizontal and vertical axes and in the two diagonals). Group multiplication is defined as performing two operations in order, and the identity element leaves all vertices unchanged. The reader may find it helpful to cut out a square of cardboard, number the four corners, and construct a group multiplication table for these eight elements, noting that it is not abelian.

It has long been known that symmetries of a dynamic system influence the nature of possible characteristic solutions or natural modes of behavior (*See* **Symmetry: equations vs. solutions**). To appreciate this restriction, consider a system with reflection symmetry, and note that any solution can be resolved into two components that are respectively symmetric and antisymmetric about the plane of symmetry. In a linear system, the symmetric and antisymmetric components do not interact; thus, modes must be either symmetric or antisymmetric about the plane. In a nonlinear system, however, there can also be natural modes of behavior that are neither symmetric nor antisymmetric. Such symmetry breaking is a fundamental feature of nonlinear dynamic systems, leading to the formation of solitons on optical fibers, impulses on nerve axons, and local modes in chemical molecules and molecular crystals.

Applications to Physical Chemistry

A typical chemical molecule is a simple geometric structure for which a symmetry group multiplication table has a finite number of entries (Herzberg, 1991; Wilson et al., 1980). Thus, the water molecule (H_2O) has a single reflection plane; methane (CH_4) is described by the same symmetry group as the regular tetrahedron, benzene (C_6H_6) by a planar hexagon, and so on. The physical chemist uses these finite symmetry groups to organize measurements of electronic and vibrational spectra, using the following notations: reflection group (σ), n-fold rotation symmetry (C_n), inversion symmetry (I), tetrahedral symmetry (T), and so on. A particularly lucid introduction to point symmetry notations is given by Landau & Lifschitz (1958).

Because quantum theory is linear, vibrational and electronic wave functions have the following property. If n successive applications of a symmetry operation return a molecule to its original orientation, the amplitude of the corresponding quantum wave function must change by an nth root of unity under the same operation. Under reflections, in other words, amplitudes change by factors of either $+1$ or -1 (symmetric or antisymmetric), whereas CH-stretching modes of benzene (C_6) change under rotations of 60° by factors of $\exp(\pm im\pi/3)$, where $m = 0, \pm 1, \pm 2, \pm 3, \pm 4$, or ± 5. Physical chemists label their spectral lines with notations that correspond to these factors (Landau & Lifschitz, 1958).

Although molecular vibrations can be quite nonlinear (especially those involving hydrogen atoms), this nonlinearity does not play a role in transitions from the ground state to first quantum levels of small molecules. (This is because the nonlinear operator of lowest order contains a product of two lowering operators, which annihilates first quantum states.) Thus, the excitations to the first quantum level are governed by linear symmetry considerations, and local modes in molecules are observed only for transitions to higher quantum levels.

The linear modes of a molecule with a center of inversion (I) appear either in infrared absorption or Raman scattering measurements, but not both. This "principle of mutual exclusion" helps to sort out the components of linear vibrational spectra. Local modes, which are nonlinear, can appear in both infrared and Raman measurements.

A periodic solid (or molecular crystal) with periodic boundary conditions can be viewed as a very large molecule, for which the number of elements of the corresponding symmetry group is also very large. Of particular interest are translations by lattice constants (a, b, and c) along the crystal axes, which bring the crystal back to its original configuration. The phase shift of an electronic or vibrational wave function under such a translation is $\exp(i\boldsymbol{k})$, where $\boldsymbol{k}$ is called the crystal momentum. As the number of unit cells in the model approaches infinity, the three components of $\boldsymbol{k}$ vary, respectively, from $-\pi/a$ to π/a, $-\pi/b$ to π/b, and $-\pi/c$ to π/c. In vibrational modes of such systems, nonlinearity can arise from local lattice distortion, which allows symmetry breaking (local mode formation) to be observed at the first quantum level.

Applications to Field Theories

The above definition of a group does not require the number of group elements to be finite, and many partial

differential equations provide examples of infinite-order symmetry groups.

The sine-Gordon (SG) equation, for example, is invariant under the independent variable transformation $(x, t) \to (\xi, \tau)$, where $\xi = (x - vt) / \sqrt{1 - v^2}$ and $\tau = (t - vx) / \sqrt{1 - v^2}$. Taking this invariance as the property defining elements of the group, a symmetry group comprises all such transformations, parameterized by the continuous variable v with $|v| < 1$. This is a one-dimensional version of the Lorentz transformation, which is shared by Maxwell's equations. Interestingly, if $u(x)$ is a time-independent solution of SG, then $u\left[(x - vt) / \sqrt{1 - v^2}\right]$ is also a solution that demonstrates Lorentz contraction (becomes smaller as $v \to 1$).

In 1915, Emmy Noether established the following important result on the application of symmetry groups to field theories (José & Saletan, 1998).

> **Noether's theorem.** *If a system is described by a Lagrangian that remains invariant under some continuous symmetry transformation, then there is a corresponding conservation law and constant of the motion.*

This theorem has immediate implications. As fundamental descriptions of nature are assumed to be Lagrangian and independent of time displacements (the science of today is the same as it was yesterday), the corresponding conserved quantity is energy. In other words, the law of energy conservation stems from time invariance of scientific laws. Similarly, conservation of momentum and conservation of angular momentum arise, respectively, from the assumptions that scientific laws are independent of spatial displacements and angles of rotation.

Nowadays, it is widely assumed that the fundamental fields of nature are derived from a Lorentz invariant Lagrangian density or more generally based on the Poincaré group, which incorporates independence with respect to displacements in time and space (Kim & Noz, 1986). As physicists attempt to formulate a fundamental description of nature, they use Noether's theorem to build in additional constants (charge, spin, rest mass, etc.) that have been empirically observed.

The pure soliton equations (Korteweg–de Vries, nonlinear Schrödinger, sine-Gordon, and so on) are Lagrangian systems that each have a countably infinite number of conservation laws and constants of the motion. It would be interesting to better understand the corresponding symmetries.

ALWYN SCOTT

See also **Bäcklund transformations; Dimensional analysis; Lie algebras and Lie groups; Local modes in molecules; Symmetry: equations vs. solutions**

Further Reading

Armstrong, M.A. 1988. *Groups and Symmetry*, New York: Springer

Birkhoff, G. & MacLane, S. 1953. *A Survey of Modern Algebra*, New York: Macmillan

Herzberg, G. 1991. *Molecular Spectra and Molecular Structure: Infrared and Raman of Polyatomic Molecules*, Melbourne, FL: Krieger Publishing Company

José, J.V. & Saletan, E. 1998. *Classical Dynamics: A Contemporary Approach*, Cambridge: Cambridge University Press

Kim, Y.S. & Noz, M.E. 1986. *Theory and Applications of the Poincaré Group*, Dordrecht: Reidel

Landau, L.D. & Lifshitz, E.M. 1958. *Quantum Mechanics: Non-relativistic Theory*, Reading, MA: Addison-Wesley

Weyl, H. 1952. *Symmetry*, Princeton, NJ: Princeton University Press

Wilson, E.B., Jr., Decius, J.C. & Cross, P.C. 1980. *Molecular Vibrations: The Theory of Infrared and Raman Vibrational Spectra*, New York: Dover

SYMMETRY: EQUATIONS VS. SOLUTIONS

The importance of symmetries in various fields of science is well appreciated, much beyond the scope of this entry. Here we focus on one particular aspect—how knowledge about discrete symmetry operations allows one to conclude certain properties of solutions of differential equations.

Let us start with one of the simplest examples: one oscillator that is governed by the equation

$$\frac{d^2x}{dt^2} = -\frac{dV(x)}{dx}, \tag{1}$$

where t is time, x the coordinate of the oscillator, and $V(x)$ its nonnegative potential with $V(0) = 0$. All solutions to this equation are time-periodic. If an equation is invariant under a certain symmetry operation, then the same symmetry operation applied to a solution of the equation either generates a new solution or reproduces the same old solution it is then said that the solution is also invariant.

All symmetries considered below, in fact, do not change the energy of the oscillator; thus, the solution is always invariant up to a trivial shift of the origin of time $t \to t + t_0$. One symmetry that leaves Equation (1) invariant is time reversal $t \to -t$, which implies that for each solution the origin of time can be chosen in such a way that the solution is also invariant under time reversal, that is, $x_s(t) = x_s(-t)$. For practical purposes, it means that numerical expansions of solutions into Fourier series may be restricted to cosine Fourier series. Another symmetry may hold if $V_s(x) = V_s(-x)$. Then the equation is invariant under space reflection $x \to -x$.

In order to invert the sign of a periodic function $x(t)$, we may assume either antisymmetry $x_a(t) = -x_a(-t)$ or shift symmetry $x_{sh}(t) = -x_{sh}(t + T/2)$ where T

is the period. Thus, for symmetric potentials, $x(t)$ is symmetric in time, antisymmetric in time (around a different origin), and shift symmetric. In particular, this implies that all even components of the Fourier expansion of this function vanish, including the dc component.

Consider next a more sophisticated model of a particle subject to a space-periodic force $f(x) = -\mathrm{d}V/\mathrm{d}x$ (period λ) and a time-periodic field $E(t)$ (period T) with zero mean:

$$\frac{\mathrm{d}^2x}{\mathrm{d}t^2} = f(x) + E(t)\,. \tag{2}$$

Equation (2) corresponds to a non-integrable system with 1.5 degrees of freedom (a three-dimensional phase space). The more complicated the equations become, the more symmetries one might consider. Assume symmetry operations that change the sign of the velocity $v = \mathrm{d}x/\mathrm{d}t$. There are two symmetries: time reversal $t \to -t$ if $E(t) \equiv E_\mathrm{s}(t)$ and a combined space reflection with time shift one $x \to -x,\ \ t \to t + T/2$ if $f(x) \equiv f_\mathrm{a}(x),\ \ E(t) \equiv E_\mathrm{sh}(t)$. For both symmetries to be valid, certain properties of the functions f and E are required. In particular, the time-periodic field $E(t)$ (e.g., an ac electric field) enters both symmetry requirements. That means that by choosing an $E(t)$ dependence that is neither symmetric nor shift symmetric, we lose both symmetries. What are the consequences?

Note first that due to the non-integrability of (2), the separatrix for $E = 0$ is replaced by a chaotic or stochastic layer in the phase space. Ergodicity inside the layer implies that the time average of a certain quantity over a trajectory, if existing, does not depend on the concrete trajectory choice. Returning to the above symmetries and choosing the time average of the velocity of the particle, we conclude that (i) the velocity average exists because the stochastic layer is bounded, and (ii) if the average velocity is nonzero for one trajectory from the stochastic layer and if any of the above symmetries apply, the velocity average will be opposite for a corresponding symmetry related trajectory from the same stochastic layer—with the only consequence that the average velocity vanishes exactly. However, choosing an $E(t)$ dependence that violates both symmetry requirements, we may expect that the average velocity of any trajectory inside the stochastic layer will become nonzero. In other words, we can predict how to generate a dc current of many non-interacting particles by a symmetry breaking choice of the field $E(t)$. This has been, indeed, predicted and demonstrated theoretically and numerically (Flach et al., 2000) and verified experimentally for directed diffusion of ultracold rubidium atoms in symmetric optical lattices (Schiavoni et al., 2003).

Next, consider applications of the above concepts to systems that are characterized by the presence of dissipation and fluctuations. Usual additive Gaussian white noise terms possess all symmetries of periodic functions; that is, if $\xi(t)$ is a realization of a stochastic process, so is $\xi(-t),\ \ \xi(t+\tau),\ \ -\xi(t)$, and so on. When starting with a corresponding Langevin type equation

$$\frac{\mathrm{d}^2x}{\mathrm{d}t^2} = f(x) + E(t) - \gamma\frac{\mathrm{d}x}{\mathrm{d}t} + \xi(t), \tag{3}$$

it is then possible to drop the noise term and study the symmetries of the deterministic yet dissipative equation

$$\frac{\mathrm{d}^2x}{\mathrm{d}t^2} = f(x) + E(t) - \gamma\frac{\mathrm{d}x}{\mathrm{d}t}. \tag{4}$$

While the strategy of the analysis is similar to the one outlined above, for the case of zero dissipation $\gamma = 0$, the phase space of Equation (4) is again three-dimensional, but is now composed of basins of attraction with each basin corresponding to a certain attractor. Existing symmetries of the equation imply symmetry relationships between attractors and their basins of attraction. Violation of symmetries of the equations implies desymmetrization of basins of attraction of (previously symmetry related) attractors. Thus, adding again the stochastic noise to return to the starting Equation (3), intuition suggests that the noise when leading to an average over various basins of attraction will either make certain averages vanish (in the presence of symmetries) or not vanish (in the absence of symmetries). Special care is required due to the fact that some symmetries of (4) may relate attractors with repellors. Another approach is to consider partial differential equations for the probability distributions and their symmetry properties (see Denisov et al., 2002).

The above approach has been successfully used to predict such diverse phenomena as rectification of heat currents (Flach et al., 2002) and induction of magnetizations (Flach & Ovchinnikov, 2000). Finally, note that it is easier to predict a nonzero average by breaking symmetries than to obtain an understanding for the concrete microscopic mechanisms of symmetry breaking and thus to obtain reliable estimates for the expected quantity of rectification and its dependence on essential parameters of the system (Reimann, 2002).

SERGEJ FLACH

See also **Ratchets; Symmetry groups; Stochastic processes**

Further Reading

Denisov, S., Flach, S., Ovchinnikov, A.A., Yevtushenko, O. & Zolotaryuk, Y. 2002. Broken space-time symmetries and mechanisms of rectification of ac fields by nonlinear (non)adiabatic response. *Physical Review* E, 66: 041104

Flach, S. & Ovchinnikov, A.A. 2000. Static magnetization induced by time-periodic fields with zero mean. *Physica* A, 292: 268–276

Flach, S., Yevtushenko, O. & Zolotaryuk, Y. 2000. Directed current due to broken time-space symmetry. *Physical Review Letters*, 84: 2358–2361

Flach, S., Zolotaryuk, Y., Miroshnichenko, A.E. & Fistul, M.V. 2002. Broken symmetries and directed collective energy transport. *Physical Review Letters*, 88: 184101

Reimann, P. 2002. Brownian motors: noisy transport far from equilibrium. *Physics Reports*, 361: 57–265

Schiavoni, M., Sanchez-Palencia, L., Renzoni, F. & Grynberg, G. 2003. Phase control of directed diffusion in a symmetric optical lattice. *Physical Review Letters*, 90: 094101

SYMPLECTIC MAPS

First used mathematically by Hermann Weyl, the term *symplectic* arises from a Greek word that means "twining or plaiting together." This is apt, as symplectic systems always involve a pair of n-dimensional variables, the configuration q, and momentum p, which are intertwined by the symplectic two form

$$\omega = \mathrm{d}p \wedge \mathrm{d}q. \tag{1}$$

This antisymmetric, bilinear form acts on a pair of tangent vectors and computes the sum of the areas of the parallelograms formed by projecting the vectors onto the planes defined by each canonical pair (q_i, p_i), $i = 1, \ldots, n$, giving

$$\omega(v, w) = \sum_{i=1}^{n} (v_{p_i} w_{q_i} - v_{q_i} w_{p_i}).$$

A diffeomorphism $f : X \to X$ on a $2n$-dimensional manifold X with coordinates $z = (q, p)$ is symplectic if it preserves the symplectic form, that is, if $f^*\omega = \omega$ (Arnol'd, 1989; McDuff & Salamon, 1995). If we write $z' = (q', p') = f(q, p)$, the symplectic condition becomes

$$Df^t J Df = J, \quad \text{where} \quad J = \begin{pmatrix} 0 & I \\ -I & 0 \end{pmatrix}. \tag{2}$$

Here $Df_{ij} = \partial f_i / \partial z_j$ is the Jacobian matrix of f, J is the Poisson matrix, and I is the $n \times n$ identity matrix. Equivalently, Stokes' theorem can be used to show that the loop action, $A[\gamma] = \oint_\gamma p\mathrm{d}q$, is preserved by f for any contractible loop γ on X. If f preserves the loop action for all loops, even those that are not contractible, then it is *exact symplectic*.

When $n = 1$, the symplectic condition is equivalent to $\det(Df) = 1$, so that the map is area- and orientation-preserving. Examples include the much studied *standard map* and the area-preserving Hénon quadratic map $f(q, p) = (p + a - q^2, -q)$ (Meiss, 1992). When $n > 1$, the symplectic condition implies volume and orientation preservation, but as we will see, it is stronger than this. A generalization of the standard map to higher dimensions is the map

$$\begin{aligned} q' &= q + p - \nabla V(q), \\ p' &= p - \nabla V(q)\,, \end{aligned} \tag{3}$$

where $q \in \mathbb{T}^n$ is an angle, $p \in \mathbb{R}^n$ is its conjugate momentum, and $V(q)$ is a periodic potential. This map is exact symplectic for any V. Beginning in 1972, Claude Froeschlé studied the case $n = 2$ and $V(q) = a \cos q_1 + b \cos q_2 + c \cos(q_1 + q_2)$. Similarly, the natural generalization of the Hénon map is the quadratic symplectic map whose normal form has been given by Moser (1994).

Applications

Symplectic maps arise from Hamiltonian dynamics, because these preserve the loop action. Thus, for example, the time t map of any Hamiltonian flow is symplectic, as is a Poincaré return map defined on a cross section. It is often easier to study the Poincaré map instead of the flow, because the dimension is reduced. Even though explicit construction of the map is typically impossible, approximation methods often suffice.

For example, the time T map of a periodically forced system $H(q, p, t) = H(q, p, t + T)$, such as a pendulum with an oscillating support, is symplectic (*See* **Hamiltonian systems**). An extreme example is $H = \frac{1}{2}p^2 - k \cos(q)\bar{\delta}(t)$, where $\bar{\delta}$ is the periodic Dirac delta function; the corresponding map is the standard map.

As Birkhoff showed, an ideal billiard (a free particle moving inside a rigid, convex table) is naturally written as a symplectic map. The canonical coordinates are the position and the tangential momentum at a collision point. Symplectic maps also arise naturally in systems where the forces are localized in time or space. For example, a circular particle accelerator or storage ring has a sequence of accelerating and focusing elements that can be modeled by a composition of symplectic maps, providing the damping effects of radiation can be neglected (Forest, 1998).

Area-preserving maps also arise in the study of the motion of Lagrangian tracers in incompressible fluids or of particles tightly gyrating around magnetic field lines. In particular, when one component of the field is particularly strong, such as in the plasma device called a tokamak, the transverse dynamics reduces to an area-preserving map.

Autonomous canonical transformations are symplectic maps. For example, if $F(q, q')$ is a generating function for a canonical transformation, then it generates a symplectic map. In particular, the Froeschlé map (3) is generated by $F(q, q') = \frac{1}{2}(q' - q)^2 - V(q)$.

An algorithm that respects the symplectic nature of Hamiltonian dynamics is called a symplectic integrator. A first-order symplectic algorithm with time step Δt for the Hamiltonian $H(q, p)$ is generated by $F(q, p') = qp' + \Delta t H(q, p')$, where

$\mathrm{d}F = q'\mathrm{d}p' + p\mathrm{d}q$, giving the map

$$q' = q + \Delta t \frac{\partial H}{\partial p'}(q, p'), \quad p' = p - \Delta t \frac{\partial H}{\partial q}(q, p'). \quad (4)$$

Note that the map is implicit because H is evaluated at p'. However, for the case that $H = K(p) + V(q)$ this becomes a leap-frog Euler scheme, an example of a "splitting" method. Symplectic versions of many standard algorithms—such as Runge–Kutta—can be obtained (Marsden et al., 1996). While there is still some controversy on the utility of symplectic methods versus methods that, for example, conserve energy and other invariants or have variable time-stepping, they are superior for stability properties because they respect the spectral properties of the symplectic group.

The Symplectic Group

The stability of an orbit $\{...z_t, z_{t+1}, ...\}$, where $z_{t+1} = f(z_t)$, is governed by the Jacobian matrix of f evaluated along the orbit, $M = \prod_t Df(z_t)$. When f is symplectic, M obeys (2), $M^T J M = J$. The set of all such $2n \times 2n$ matrices form the symplectic group $Sp(2n)$. This group is an $n(2n+1)$-dimensional Lie group, whose Lie algebra is the set of Hamiltonian matrices—matrices of the form JS where S is symmetric. Thus, every near-identity symplectic matrix can be obtained as the exponential of a Hamiltonian matrix and corresponds to the time t-map of a linear Hamiltonian flow. There are symplectic matrices, however, that are not the exponentials of Hamiltonian matrices; for example, $-I$. As a manifold, the symplectic group has a single nontrivial loop (its fundamental group is the integers). The winding number of a loop in the symplectic group is called the Maslov index (McDuff & Salamon, 1995); it is especially important for semi-classical quantization.

If M is a symplectic matrix and λ is an eigenvalue of M with multiplicity k, then so is λ^{-1}. Moreover $\det(M) = 1$, so M is volume and orientation preserving. A consequence of this spectral theorem is that orbits of a symplectic map cannot be asymptotically stable. There are four basic stability types for symplectic maps: an eigenvalue pair (λ, λ^{-1}) is

- *hyperbolic*, if λ is real and larger than one;
- *hyperbolic with reflection*, if λ is real and less than minus one;
- *elliptic*, if $\lambda = \mathrm{e}^{2\pi \mathrm{i}\omega}$ has magnitude one;
- part of a *Krein quartet*, if λ is complex and has magnitude different from one, for then there is a quartet of related eigenvalues $(\lambda, \lambda^{-1}, \bar{\lambda}, \bar{\lambda}^{-1})$.

Thus, a periodic orbit can be linearly stable only when all of its eigenvalue pairs are elliptic. For this case, the linearized motion corresponds to rotation with n rotation numbers ω_i.

Symplectic Geometry

Every symplectic map is volume- and orientation-preserving, but the group $\mathrm{Symp}(X)$ of symplectic diffeomorphisms on X is significantly smaller than that of the volume-preserving ones. This was first shown in 1985 by Gromov in his celebrated "nonsqueezing" (or symplectic camel) theorem. Let $B(r)$ be the closed ball of radius r in $\mathbb{R}^{2n}$ and $C_1(R) = \{(q, p) : q_1^2 + p_1^2 \leq R^2\}$ be a cylinder of radius R whose circular cross section is a symplectic plane. Because the volume of C_1 is infinite, it is easy to construct a volume-preserving map that takes $B(r)$ into $C_1(R)$ regardless of their radii. What Gromov showed is that it is impossible to do this symplectically whenever $r > R$. This is one example of a *symplectic capacity*, leading to a theory of symplectic topology (McDuff & Salamon, 1995).

Another focus of this theory is to characterize the number of fixed points of a symplectic map, that is, to generalize the classical Poincaré–Birkhoff theorem for area-preserving maps on an annulus. Arnol'd conjectured in the 1960s that any Hamiltonian diffeomorphism on a compact manifold X must have at least as many fixed points as a function on X must have critical points. A Hamiltonian map is a symplectic map that can be written as a composition of maps of the form (4). Conley and Zender proved this in 1985 for the case that X is the $2n$-torus: f must have at least $2n+1$ fixed points (at least 2^{2n} if they are all nondegenerate) (Golé, 2001).

Dynamics

In general, the dynamics of a symplectic map consists of a complicated mixture of regular and chaotic motion (Meiss, 1992). Numerical studies indicate that the chaotic orbits have positive Lyapunov exponents and fill sets of positive measure that are fractal in nature. Regular orbits include periodic and quasi-periodic orbits. The latter densely cover invariant tori whose dimensions range from 1 to n. Near elliptic periodic orbits, the phase space is foliated by a positive-measure cantor set of n-dimensional invariant tori. There are chaotic regions in the *resonant* gaps between the tori, but the chaos becomes exponentially slow and exponentially small close to the periodic orbit. Some of these observations, but not all, can be proved.

The simplest case is that of an integrable symplectic map, which can be written in Birkhoff normal form: $f(\theta, J) = (\theta + \nabla S(J), J)$. Here (θ, J) are angle-action coordinates (each n-dimensional) and $\Omega = \nabla S$ is the rotation vector. Orbits for this system lie on invariant tori; thus, the structure is identical to that for integrable Hamiltonian systems.

The Birkhoff normal form is also an asymptotically valid description of the dynamics in the neighborhood of a nonresonant elliptic fixed point, one for which

$m \cdot \Omega(0) \neq n$ for any integer vector m and integer n. However, the series for the normal form is not generally convergent. Nevertheless, KAM theory implies that tori with Diophantine rotation vectors do exist near enough to the elliptic point, providing the map is more than C^3 and that the twist, $\det D\Omega(0)$, is nonzero. Each of these tori is also a Lagrangian submanifold (an n-dimensional surface on which the restriction of the symplectic form (1) vanishes). The relative measure of these tori approaches one at the fixed point.

Nevertheless, the stability of a generic, elliptic fixed point is an open question. Arnol'd showed by example in 1963 that lower-dimensional tori can have unstable manifolds that intersect the stable manifolds of nearby tori and thereby allow nearby trajectories to drift "around" the n-dimensional tori; this phenomenon is called Arnol'd diffusion (Lochak, 1993). When the map is analytic, the intersection angles become exponentially small in the neighborhood of the fixed point, and the existence of connections becomes a problem in perturbation theory *beyond all orders*.

Aubry–Mather theory gives a nonperturbative generalization of KAM theory for the case of monotone twist maps when $n = 1$. These are symplectic diffeomorphisms on the cylinder $\mathbb{S} \times \mathbb{R}$ (or on the annulus) such that $\partial q'/\partial p \geq c > 0$. For this case, Aubry–Mather theory implies that there exist orbits for all rotation numbers ω. When ω is irrational, these orbits lie on a *Lipschitz graph*, $p = P(q)$, and their iterates are ordered on the graph just as the iterates of the uniform rotation by ω. They are either dense on an invariant circle or an invariant Cantor set (called a *cantorus* when discovered by Percival). These orbits are found using a Lagrangian variational principle and turn out to be global minima of the action.

Aubry–Mather theory can be partially generalized to higher dimensions, for example, to the case of rational rotation vectors, where the orbit is periodic (Golé, 2001). Moreover, Mather (1991) has shown that action-minimizing invariant measures exist for each rotation vector, though they are not necessarily dynamically minimal. The existence of invariant cantor sets with any incommensurate rotation vector can also be proven for symplectic maps near an anti-integrable limit (MacKay & Meiss, 1992). Finally, converse KAM theory, which gives parameter domains where there are no invariant circles for the standard map, implies that, for example, the Froeschlé map has no Lagrangian invariant tori outside a closed ball in the space of its parameters (a, b, c) (MacKay et al., 1989).

JAMES D MEISS

See also **Aubry–Mather theory; Cat map; Chaotic dynamics; Constants of motion and conservation laws; Ergodic theory; Fermi acceleration and Fermi map; Hamiltonian systems; Hénon map; Horseshoes and hyperbolicity in dynamical systems; Lyapunov exponents; Maps; Measures; Mel'nikov method; Phase space; Standard map**

Further Reading

Arnol'd, V.I. 1989. *Mathematical Methods of Classical Mechanics*, New York: Springer

Forest, E. 1998. *Beam Dynamics: A New Attitude and Framework (The Physics and Technology of Particle and Photon Beams)*, Amsterdam: Harwood Academic

Golé, C. 2001. *Symplectic Twist Maps: Global Variational Techniques*, Singapore: World Scientific

Lochak, P. 1993. Hamiltonian perturbation theory: periodic orbits, resonances and intermittancy. *Nonlinearity*, 6: 885–904

MacKay, R.S. & Meiss, J.D. 1992. Cantori for symplectic maps near the anti-integrable limit. *Nonlinearity*, 5: 149–160

MacKay, R.S., Meiss, J.D. & Stark, J. 1989. Converse KAM theory for symplectic twist maps. *Nonlinearity*, 2: 555–570

Marsden, J.E., Patrick, G.W. & Shadwick, W.F. (editiors). 1996. *Integration Algorithms and Classical Mechanics*, Providence, RI: American Mathematical Society

Mather, J.N. 1991. Action minimizing invariant measures for positive definite Lagrangian systems. *Mathematische Zeitschrift*, 207: 169–207

McDuff, D. & Salamon, D. 1995. *Introduction to Symplectic Topology*, Oxford: Clarendon Press

Meiss, J.D. 1992. Symplectic maps, variational principles, and transport. *Reviews of Modern Physics*, 64(3): 795–848

Moser, J.K. 1994. On quadratic symplectic mappings. *Mathematische Zeitschrift*, 216: 417–430

SYNAPSES

See **Neurons**

SYNCHRONIZATION

In a classical context, synchronization means adjustment of rhythms of self-sustained periodic oscillators due to their weak interaction, which can be described in terms of phase locking and frequency entrainment. The modern concept also covers such objects as rotators and chaotic systems, in which one distinguishes between different forms of synchronization, including complete, phase, and master–slave.

The history of synchronization goes back to the 17th century when the Dutch scientist Christiaan Huygens reported on his observation of synchronization of two pendulum clocks, which he had invented shortly before (Hugenii, 1673).

> ... It is quite worth noting that when we suspended two clocks so constructed from two hooks imbedded in the same wooden beam, the motions of each pendulum in opposite swings were so much in agreement that they never receded the least bit from each other and the sound of each was always heard simultaneously. Further, if this agreement was disturbed by some interference, it reestablished itself in a short time. For a long time I was amazed at this unexpected result, but after a careful examination finally found that the cause of this is due to the motion of the beam, even though this is hardly perceptible. The cause is that the oscillations of the pendula, in

proportion to their weight, communicate some motion to the clocks. This motion, impressed onto the beam, necessarily has the effect of making the pendula come to a state of exactly contrary swings if it happened that they moved otherwise at first, and from this finally the motion of the beam completely ceases. But this cause is not sufficiently powerful unless the opposite motions of the clocks are exactly equal and uniform.

Despite being among the oldest scientifically studied nonlinear effects, synchronization was understood only in the 1920s when Edward Appleton and Balthasar van der Pol theoretically and experimentally studied synchronization of triode oscillators.

The synchronization properties of periodic self-sustained oscillators are based on the existence of a special variable, phase ϕ. Mathematically, ϕ can be introduced as the variable parametrizing motion along the stable limit cycle in the state space of an autonomous continuous-time dynamical system. One can always choose phase in a way that it grows uniformly in time,

$$\frac{\mathrm{d}\phi}{\mathrm{d}t} = \omega_0, \tag{1}$$

where ω_0 is the natural frequency of oscillations. The phase is neutrally stable, meaning that its perturbations neither grow nor decay. This corresponds to the invariance of solutions of autonomous dynamical systems with respect to time shifts. Thus, a small perturbation (for example, an external periodic forcing or coupling to another system) can cause large deviations of the phase—contrary to the amplitude, which is only slightly perturbed due to the transversal stability of the cycle. This property allows description of the effect of small forcing/coupling via the phase approximation.

Considering the simplest case of a limit cycle oscillator driven by a periodic force with frequency ω and amplitude ε, one can write the equation for the perturbed phase dynamics in the form

$$\frac{\mathrm{d}\phi}{\mathrm{d}t} = \omega_0 + \varepsilon Q(\phi, \omega t), \tag{2}$$

where the coupling function Q is 2π-periodic in both its arguments and depends on the form of the limit cycle and the forcing. Close to the resonance $\omega \approx \omega_0$, the function Q contains fast oscillating and slow varying terms, the latter can be written as $q(\phi - \omega t)$. Upon averaging over a cycle, one obtains the following basic equation for the phase dynamics

$$\frac{\mathrm{d}\Delta\phi}{\mathrm{d}t} = -(\omega - \omega_0) + \varepsilon q(\Delta\phi), \tag{3}$$

where $\Delta\phi = \phi - \omega t$ is the difference between the phases of the oscillations and of the forcing. The function q is 2π-periodic, and in the simplest case $q(\cdot) = \sin(\cdot)$ Equation (3) is called the Adler equation.

One can see that on the plane of parameters of the external forcing, there is a region

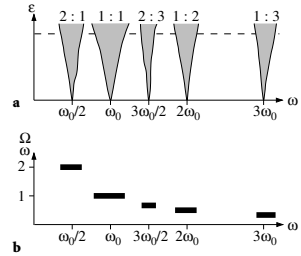

Figure 1. (a) A sketch of Arnol'd tongues. (b) Devil's staircase for a fixed amplitude of the forcing (dashed line in (a)).

($\varepsilon q_{\min} < \omega - \omega_0 < \varepsilon q_{\max}$) where Equation (3) has a stable stationary solution that exactly corresponds to phase locking (the phase ϕ just follows the phase of the forcing, so $\phi = \omega t + \text{constant}$) and frequency entrainment (the observed frequency of the oscillator $\Omega = \langle\dot{\phi}\rangle$ exactly coincides with the forcing frequency ω). Everyday examples of synchronization by external forcing are radio-controlled clocks, cardiac pacemakers, and circadian systems (the internal clocks of living objects that are synchronized to the exact 24-h periodic rhythm of sunlight).

Generally, synchronization is also observed for higher-order resonances $n\omega \approx m\omega_0$. In this case, the dynamics of the generalized phase difference $\Delta\phi = m\phi - n\omega t$ is described by an equation similar to Equation (3), namely, by $\mathrm{d}(\Delta\phi)/\mathrm{d}t = -(n\omega - m\omega_0) + \varepsilon\tilde{q}(\Delta\phi)$. The term *synchronous regime* then means perfect entrainment of the oscillator frequency at the rational multiple of the forcing frequency, $\Omega = n\omega/m$, as well as phase locking $m\phi = n\omega t + \text{constant}$. The overall picture can be shown on the (ω,ε) plane, where a family of triangular-shaped synchronization regions exists touching the ω-axis at the rationals of the natural frequency $m\omega_0/n$. These regions are called "Arnol'd tongues" (see Figure 1a). This picture is preserved for moderate forcing, although now the shape of the tongues generally differs from being exactly triangular.

For a fixed amplitude of the forcing ε and variable driving frequency ω, one observes different phase locking intervals where the motion is periodic, whereas in between them it is quasi-periodic. The curve Ω vs. ω, thus, consists of horizontal plateaus at all possible rational frequency ratios; this fractal curve is called a "devil's staircase" (Figure 1b).

An experimental example of such a curve is the voltage–current plot for a Josephson junction in an ac electromagnetic field, where synchronization plateaus are called Shapiro steps. As a junction can be considered as a rotator (rotations are maintained by a dc current), this example demonstrates that synchronization properties of rotators are very close to those of oscillators.

Synchronization of two coupled self-sustained oscillators can be described in a similar way. A weak interaction affects only the phases of two oscillators ϕ_1 and ϕ_2, and Equation (1) generalizes to

$$\frac{d\phi_1}{dt} = \omega_1 + \varepsilon Q_1(\phi_1, \phi_2),$$
$$\frac{d\phi_2}{dt} = \omega_2 + \varepsilon Q_2(\phi_2, \phi_1). \quad (4)$$

For the phase difference $\Delta\phi = \phi_2 - \phi_1$, one obtains after averaging an equation of the type of (3). Synchronization now means that two non-identical oscillators start to oscillate with the same frequency (or, more generally, with rationally related frequencies). This common frequency usually lies between ω_1 and ω_2. Note that locking of the phases and frequencies implies no restrictions on the amplitudes, in fact, the synchronized oscillators may have very different amplitudes and wave forms; for example, oscillations may be relaxation (integrate-and-fire) or quasiharmonic.

The mutual synchronization in a large population of oscillators (the Kuramoto transition in a population of globally coupled phase oscillators, for example) can be treated as a nonequilibrium phase transition—the mean oscillating field serving as an order parameter. Examples of synchronization in large ensembles include rhythmic applause and simultaneous flashing of fireflies, adjustment of menstrual cycles in women's dormitories, and so on. Synchronization in lattices of coupled self-sustained oscillators usually sets in via formation of clusters, that is, groups of oscillators (neighbors in a lattice) having the same frequency, and with increase of coupling the clusters grow and merge.

The concept of synchronization has been extended to include chaotic systems. One effect, called phase synchronization, is mostly close to the classical locking phenomena. Indeed, many chaotic self-sustained oscillators admit determination of the instantaneous phase and the corresponding mean frequency. Often one can find a projection of the strange attractor that looks like a smeared limit cycle, so phase is then introduced as a variable that gains 2π with each rotation. These rotations are non-uniform due to chaos, which can be modeled by an effective noise in phase dynamics. If this noise is small (i.e., the rotations are rather uniform), the mean frequency of the system can be entrained by a periodic forcing while the chaos is preserved. If two or more chaotic oscillators with different natural frequencies interact, their mean frequencies can be adjusted while the amplitudes remain chaotic and only weakly correlated.

Another type of chaotic synchronization—complete synchronization—can be observed for identical chaotic systems of any type (maps, autonomous or driven time-continuous systems). In the simplest case of two diffusively coupled in all variables systems, the dynamics is described by

$$\frac{d\boldsymbol{x}}{dt} = \boldsymbol{F}(\boldsymbol{x}) + \varepsilon(\boldsymbol{y} - \boldsymbol{x}),$$
$$\frac{d\boldsymbol{y}}{dt} = \boldsymbol{F}(\boldsymbol{y}) + \varepsilon(\boldsymbol{x} - \boldsymbol{y}), \quad (5)$$

where ε is the coupling parameter. The regime when $\boldsymbol{x}(t) = \boldsymbol{y}(t)$ for all t is called complete synchronization; because in this state the diffusive coupling vanishes, the dynamics is the same as if the systems were uncoupled. Although such symmetric solution exists for all ε, it is stable only if the coupling is sufficiently strong. To find the critical value of the coupling, one linearizes Equations (5) near the synchronized state and obtains for the mismatch $\boldsymbol{v}(t) = \boldsymbol{y}(t) - \boldsymbol{x}(t)$, the linearized system

$$\frac{d\boldsymbol{v}}{dt} = J(t)\boldsymbol{v} - 2\varepsilon\boldsymbol{v}, \quad (6)$$

where $J(t)$ is the Jacobian at the chaotic solution $\boldsymbol{x}(t)$. The ansatz $\boldsymbol{v} = e^{-2\varepsilon t}\boldsymbol{u}$ removes the last term on the right-hand side of (6), and the resulting equation coincides with the linearized equation for small perturbations of the solutions of an individual chaotic oscillator. Thus, $\boldsymbol{u}$ grows in proportion to the maximum Lyapunov exponent λ of a single system, and the critical coupling is $\varepsilon_c = \lambda / 2$. Complete synchronization occurs if $\varepsilon > \varepsilon_c$, that is, when the divergence of trajectories of interacting systems due to chaos is suppressed by the diffusive coupling. For weak coupling $\varepsilon < \varepsilon_c$, the states of two systems are different, $\boldsymbol{x}(t) \neq \boldsymbol{y}(t)$. Some other forms of synchronization in chaotic systems (generalized, master–slave) are similar to the complete one, and in all these cases synchronization appears if the coupling is strong enough.

MICHAEL ROSENBLUM AND ARKADY PIKOVSKY

See also **Commensurate-incommensurate transition; Coupled oscillators; Phase dynamics; Van der Pol equation**

Further Reading

Blekhman, I.I. 1988. *Synchronization in Science and Technology*, New York: ASME Press

Glass, L. 2001. Synchronization and rhythmic processes in physiology. *Nature*, 410: 277–284

Huygens (Hugenii), Ch. 1673. *Horologium Oscillatorium*, Paris: Apud F. Muguet; as *The Pendulum Clock*, Ames: Iowa State University Press, 1986

Kuramoto, Y. 1984. *Chemical Oscillations, Waves and Turbulence*, Berlin: Springer

Mosekilde, E., Maistrenko, Yu. & Postnov D. 2002. *Chaotic Synchronization: Applications to Living Systems*, Singapore: World Scientific

Pikovsky, A., Rosenblum, M. & Kurths, J. 2001. *Synchronization: A Universal Concept in Nonlinear Sciences*, Cambridge and New York: Cambridge University Press

SYNERGETICS

Synergetics deals with the spontaneous formation of spatiotemporal or functional structures in complex open systems by means of self-organization. The word *synergetics* is taken from Greek and means "science of cooperation." The central aim of synergetics, comprising both theoretical and experimental studies, is the search for basic principles that govern self-organization in both the physical and life sciences. To this end, a comprehensive mathematical theory has been developed that comprises both deterministic and stochastic processes.

Historical Background

Synergetics was initiated by Hermann Haken in 1969 in lectures at Stuttgart University (see also Haken & Graham, 1971). It originated from laser physics, where a pronounced transition from the disordered light of a lamp to the highly ordered light of a laser takes place. This transition can be interpreted as a nonequilibrium phase transition, on the one hand (Graham & Haken, 1968, 1970), and as a typical event of self-organization, on the other. Synergetics shows common features with and differences from a variety of interdisciplinary research fields:

1. In common with cybernetics as introduced by Norbert Wiener (1948), synergetics looks for general laws common to physical and biological systems. While cybernetics focuses on the control of a system in order to achieve its specific performance, synergetics studies the various dynamical structures a complex system can acquire.

2. Synergetics shares with general system theory as introduced by Ludwig von Bertalanffy (1968) the aim of finding general laws, in particular by seeking analogies. But while von Bertalanffy was seeking such analogies between otherwise different systems at the level of their individual elements, synergetics establishes close analogies at the level of order parameters (macroscopic field variables; see below).

3. Synergetics has used and developed methods belonging to dynamical systems theory (see, e.g., Guckenheimer & Holmes, 1983; Haken, 1983). Here in particular, emphasis is laid on the qualitative changes of the behavior of dynamical systems close to their points of instability (singular points, bifurcation points). In contrast to, for example, bifurcation theory, synergetics takes into account the pivotal role of random processes (Haken, 1983).

4. Synergetics has used and developed methods from statistical physics, such as various types of (generalized) Fokker–Planck equations, Langevin equations, and master equations (see, e.g., Stratonovich, 1963, 1967).

5. Synergetics shares with the theory of dissipative structures as introduced by Ilya Prigogine the goal of general laws (Nicolis & Prigogine, 1977). But while Prigogine's theory of dissipative structures is mainly based on thermodynamic principles, such as the entropy production principle or excess entropy production principle, synergetics is based on an approach that is close to statistical physics.

6. The concepts of synergetics have similarities with ideas developed in Gestalt theory founded by Max Wertheimer and Wolfgang Köhler (1924, 1969).

Theoretical Approach

All systems are considered subject to fixed internal or external conditions that are described by control parameters α. At particular values of α the behavior of the system may change macroscopically and qualitatively ("instability" of the previous state). As synergetics shows, close to such instability points the behavior of the system is determined by a small number of dynamical quantities, the order parameters. According to the "slaving principle" of synergetics, the order parameters determine the behavior of the individual parts of the system. In turn, the individual parts generate the order parameters by their cooperation (circular causality). Close to the instability points, nonequilibrium phase transitions occur that are characterized by symmetry breaking, critical fluctuations, and critical slowing down of the order parameters. This approach requires knowledge of the microscopic dynamics (*microscopic synergetics*). If this knowledge is absent, in *phenomenological synergetics* an order parameter dynamics is postulated.

Outline of Micoscopic Synergetics

The multi-component system is described by its state vector $\boldsymbol{q}$, whose components are labeled by the subsystem ℓ and the state or component j of each of them, $q_{\ell j}$, $\ell = 1, ..., N$; $j = 1, ..., J$. In continuous media, $\boldsymbol{q}$ becomes a function of a spatial coordinate $\boldsymbol{x}$, $\boldsymbol{q}(\boldsymbol{x})$. The state vector obeys an evolution equation

$$\mathrm{d}\boldsymbol{q}(t)/\mathrm{d}t = \boldsymbol{N}(\boldsymbol{q}(t), \nabla, \boldsymbol{x}, \alpha) + \boldsymbol{F}(\boldsymbol{q}, \boldsymbol{x}, t). \quad (1)$$

$\boldsymbol{N}$ is a nonlinear vector-valued, nonlinear function of $\boldsymbol{q}$, ∇ indicates spatial derivatives, α control parameters, and $\boldsymbol{F}$ fluctuating forces. $\boldsymbol{F}$ is mostly assumed to be δ-correlated in time ("white noise").

It is assumed that for a value $\alpha = \alpha_0$, the solution to (1) is known and the stability of $\alpha_0 : \boldsymbol{q}_0(t)$ is studied by *linear stability analysis*, putting $\boldsymbol{q}(t) = \boldsymbol{q}_0(t) + \boldsymbol{\xi}(t)$ and $\boldsymbol{F} = 0$. This leads to

$$\mathrm{d}\boldsymbol{\xi}(t)/\mathrm{d}t = L(\boldsymbol{q}_0(t), \alpha)\boldsymbol{\xi}, \quad (2)$$

where the linear operator L depends on $\boldsymbol{q}_0(t)$. The solutions to (2) are of the form

$$\boldsymbol{\xi}_k(t) = \exp(\lambda_k t)\boldsymbol{v}_k(t), \quad k = 1, ... \quad (3)$$

If λ_k has a discrete spectrum, then (Haken, 1983):

(a) $\boldsymbol{q}_0$ is time-independent (fixed point); $\boldsymbol{v}_k$ is time-independent and contains powers of t if λ_k is degenerate;

(b) $\boldsymbol{q}_0$ is time-periodic (limit cycle); $\boldsymbol{v}_k$ is time-periodic with the same period and contains powers of t if λ_k is degenerate and

(c) $\boldsymbol{q}_0(t)$ is on torus, or arbitrary; $|\boldsymbol{v}_k(t)|$ increases in time more slowly than exponential.

Close to instability points, where $\mathrm{Re}\lambda_k \geq 0$ for some k, we distinguish between unstable modes, $\boldsymbol{v}_u$, and stable modes, $\boldsymbol{v}_s$. In the case of (a), the wanted solution is assumed in the form

$$\boldsymbol{q}(t) = \boldsymbol{q}_0 + \sum_u \xi_u(t)\boldsymbol{v}_u + \sum_s \xi_s(t)\boldsymbol{v}_s, \qquad (4)$$

where the amplitudes ξ_u and ξ_s are still to be determined by inserting (4) into the complete Equations (1) and projecting onto the modes $\boldsymbol{v}_k$. This yields the equations

$$\mathrm{d}\boldsymbol{\xi}_u/\mathrm{d}t = \Lambda_u\boldsymbol{\xi}_u + \hat{\boldsymbol{N}}_u(\boldsymbol{\xi}_u, \boldsymbol{\xi}_s) + \boldsymbol{F}_u, \qquad (5)$$

$$\mathrm{d}\boldsymbol{\xi}_s/\mathrm{d}t = \Lambda_s\boldsymbol{\xi}_s + \hat{\boldsymbol{N}}_s(\boldsymbol{\xi}_u, \boldsymbol{\xi}_s) + \boldsymbol{F}_s. \qquad (6)$$

In the cases, (b) and (c), the hypothesis (4) must be extended to include phase angles, $\boldsymbol{\phi}$. In such a case, Equations (5) and (6) must be supplemented by equations for $\boldsymbol{\phi}$

$$\mathrm{d}\boldsymbol{\phi}/\mathrm{d}t = \hat{\mathbf{N}}_\phi(\boldsymbol{\xi}_u, \boldsymbol{\xi}_s, \boldsymbol{\phi}) + \boldsymbol{F}_\phi, \qquad (7)$$

where $\hat{\boldsymbol{N}}_\phi$ is 2π-periodic in $\boldsymbol{\phi}$. In this case, the nonlinear functions on the right-hand side of (5) and (6) become also $\boldsymbol{\phi}$-dependent with periodicity 2π. The slaving principle of synergetics allows us to express the enslaved amplitudes $\boldsymbol{\xi}_s$ by means of the order parameters $\boldsymbol{\xi}_u, \boldsymbol{\phi}$ at the same time

$$\boldsymbol{\xi}_s(t) = \mathbf{f}(\boldsymbol{\xi}_u(t), \boldsymbol{\phi}(t), t). \qquad (8)$$

The explicit time dependence stems from the action of the fluctuating forces $\boldsymbol{F}$. By means of (8), the originally high-dimensional system (5)–(7) can be reduced to a low-dimensional system

$$\mathrm{d}\tilde{\boldsymbol{\xi}}_u/\mathrm{d}t = \tilde{\boldsymbol{N}}(\tilde{\boldsymbol{\xi}}_u) + \tilde{\boldsymbol{F}}_u, \qquad (9)$$

where $\tilde{\boldsymbol{\xi}}_u$ comprises both $\boldsymbol{\xi}_u, \boldsymbol{\phi}$. In continuous media, where

$$\boldsymbol{\xi}_u(t) \to \boldsymbol{\xi}_u(\mathbf{x}, t), \qquad (10)$$

the order parameter equations (9) are replaced by generalized Ginzburg–Landau equations

$$\mathrm{d}\boldsymbol{\xi}_u(\mathbf{x}, t)/\mathrm{d}t = \Lambda_u(\nabla)\boldsymbol{\xi}_u(\boldsymbol{x}, t) + \tilde{\boldsymbol{N}}(\boldsymbol{\xi}_u(\boldsymbol{x}, t)) + \boldsymbol{F}_u, \qquad (11)$$

where the matrix of eigenvalues Λ_u depends on differential operators. In higher approximation, $\tilde{\boldsymbol{N}}$ also depends on differential operators, $\tilde{\boldsymbol{N}}(\boldsymbol{\xi}_u, \nabla)$.

While Equations (1), (9), and (11) are of Langevin type, the stochastic problems can also be formulated by means of the Fokker–Planck equation, where the distribution function depends on the vector $[\boldsymbol{\xi}, f(\boldsymbol{\xi}, t)]$ and f obeys the Fokker–Planck equation

$$\partial f/\partial t = Lf,$$
$$L = -\sum_j \frac{\partial}{\partial \xi_j}(\tilde{N}_j f) + \sum_{ij} Q_{ij}\partial^2/\partial\xi_i\partial\xi_j f. \qquad (12)$$

Furthermore, another approach is based on the master equation for the distribution function P obeying

$$\mathrm{d}P(\boldsymbol{m}, t)/\mathrm{d}t = \sum_{\boldsymbol{m}'} w(\boldsymbol{m}, \boldsymbol{m}')P(\boldsymbol{m}', t) - P(\boldsymbol{m}, t)\sum_{\boldsymbol{m}'} w(\boldsymbol{m}', \boldsymbol{m}), \qquad (13)$$

where $\boldsymbol{w}(\boldsymbol{m}, \boldsymbol{m}')$ are the transition probabilities from state $\boldsymbol{m}' \to \boldsymbol{m}$.

Phenomenological Synergetics

In the case where microscopic dynamics of the system are not known, the analysis is based on phenomenological equations of the type (9), where the order parameters are characterized by those experimentally determined macroscopic quantities that change qualitatively when the control parameters are changed.

Applications of Concepts and Methods of Synergetics

Physics and Chemistry

Synergetics approaches are used to study stochastic properties and spatiotemporal patterns of laser light and of fluids and plasmas, current distributions in semiconductors, crystal growth, and meteorological structures, for example, baroclinic instability.

Synergetics is also used to study the formation of spatiotemporal patterns at macroscopic scales in chemical reactions, for example the Belousov–Zhabotinsky reaction.

Biology

Based on Turing's ideas of morphogenesis, synergetics calculates spatial density distributions, in particular gradients, stripes, hexagons, etc., in dependence on boundary and initial conditions. In initially undifferentiated omnipotent cells, molecules are produced as activators or inhibitors that diffuse between cells and react with each other and thus can be transformed. At places of high concentration, the activator molecules switch on genes that, eventually, lead to cell differentiation.

By means of synergetics, new kinds of analogies between evolution in biological and physical systems

have been unearthed. For instance, the equations established by Manfred Eigen (1971) for prebiotic, that is, molecular evolution, turn out to be isomorphic to specific rate equations for laser light (photons), where a specific kind of photon wins the competition between different kinds.

In population dynamics, the resources, such as food, nesting places for birds, or light intensity for plants, serve as control parameters for synergetic analyses of self-organization. The numbers or densities of the individuals of species serve as order parameters. Specific examples are provided by the Verhulst equation or the predator-prey relation of the Lotka–Volterra equations. Of particular interest are dramatic changes, for instance the dying out of species under specific control parameter values. This has influences on environmental policy. If specific control parameters exceed critical values, the system's behavior can change dramatically. For instance, beyond a specific degree of evolution, the fish population of a lake may die out.

Nearly all biological systems show more or less regular rhythms—periodic oscillations or fluctuations. These can be imposed on the system from the outside, for instance, by the day/night cycle or seasons (exogen), or produced by the system itself (endogen). Endogenous rhythms that may proceed on quite different spatial and temporal scales are widely researched in synergetics. Examples are cell metabolism, circadian rhythms, brain waves in different frequency bands (see below), menstrual cycles, and cardiovascular rhythms. For instance, in the last, Stefanovska et al. (2000) were able to identify five order parameters. For certain time intervals, these order parameters can show phase and frequency couplings.

Rhythmical movements of humans and animals show well-defined patterns of coordination of the limbs, for instance, walking or running in humans or gaits of quadrupeds. Synergetics studies especially transitions between movement patterns, for instance the paradigmatic experiment by Kelso (1995). If subjects move their index fingers in parallel at a low frequency; increasing the frequency results in an abrupt involuntary transition to a new symmetric movement. The control parameter is the prescribed finger movement frequency, the order parameter is the relative phase between the index fingers. The experimentally proven properties of a nonequilibrium phase transition (critical fluctuations, critical slowing down, hysteresis) substantiate the concept of self-organization and exclude that of a fixed motor program. Numerous further coordination experiments between different limbs can be represented by the Haken–Kelso–Bunz model (Haken et al., 1985). Gaits of quadrupeds and transitions between them have been modeled in detail (Schöner et al., 1990).

In visual perception, the recognition of patterns, for example, faces, is interpreted as the action of an associative memory in accordance with usual approaches. Here incomplete data (features) with which the system is provided from the outside are complemented by means of data stored in the memory. A particular aspect of the synergetic approach is the idea that pattern recognition can be conceived as pattern formation. This is not only meant as a metaphor, but means also that specific activity patterns in the brain are established. In pattern formation, a partly ordered pattern is provided to ths system whereby several order parameters are evoked that compete with each other dynamically. The control parameters are so-called attention parameters that in cases without bias are assumed to be equal. The winning order parameter imposes a total pattern on the system according to the slaving principle. This process is the basis of the synergetic computer for pattern recognition (Haken, 1991). By means of appropriate preprocessing an invariance of the recognition process against scales, displacements and rotations, and even deformations can be achieved.

Gestalt Psychology

As is shown in Gestalt psychology (Wertheimer, Köhler), *Gestalt* is conceived as a specific organized entity to which in synergetics an order parameter with its synergetic properties (slaving principle) can be attached. The cognition or perception process of Gestalt proceeds in principle according to the synergetic process of pattern recognition. The winning order parameter generates, according to the slaving principle, an ideal percept that is the corresponding Gestalt. In ambiguous patterns, an order parameter is attached to each percept of an object. Because in ambiguous figures two or more possible interpretations are contained, several order parameters participate in the dynamics whereby the attention parameters become dynamical quantities. As already assumed by Köhler and as is shown by the synergetic equations, the corresponding attention parameter saturates; that is, it becomes zero if the corresponding object has been recognized and the other interpretation now becomes possible, where again the corresponding saturation process starts, etc. The model equations allow us also to take into account bias. (*See* the article on **Gestalt phenomena**.)

Psychology

According to the concept of synergetics, psychological behavioral patterns are generated by self-organization of neuronal activities under specific control parameter conditions and are represented by order parameters. In important special cases, the order parameter dynamic can be represented as the overdamped motion of a ball in mountainous terrain. By means of changes in the control parameters, this landscape is deformed and allows new equilibrium positions (stable behavioral patterns). This leads to new approaches to

psychotherapy: destabilization of unwanted behavioral patterns by means, for example, of new external conditions or new cognitive influences and measures that support the self-organization of desired behavioral patterns. The insights of synergetics have been applied in the new field of psychosynergetics with essential contributions by Schiepek, Tschacher, Hansch, and others (Tschacher et al., 1992; Hansch, 1997; Ciompi, 1998, 1999).

Brain Theory

According to a proposal by Haken (1983), the brain of humans and animals is conceived as a synergetic, that is, a self-organizing system. This concept is supported by experiments and models on movement coordination, visual perception, and Gestalt psychology and by EEG and MEG analysis (see below). The human brain with its 10^{11} neurons (and glia cells) is a highly interconnected system with numerous feedback loops. In order to treat it as a synergetic system, control parameters and order parameters must be identified. While in synergetic systems of physics, chemistry, and partly biology the control parameters are fixed from the outside, for instance, by the experimenter, in the brain and in other biological systems, the control parameters can be fixed by the system itself. In modeling them it is assumed, however, that they are practically time-independent during the self-organization process. Such control parameters can be, among others, the synaptic strengths between neurons that can be changed by learning according to Hebb (1949), neurotransmitters, such as Dopamin, Serotonin, and drugs that block the corresponding receptors (e.g., Haloperidol, Coffein), and hormones (influencing the attention parameters). Furthermore, the control parameters may be more or less permanent external or internal stimuli.

In the frame of the given control parameters, self-organization takes place in neuronal activity whereby the activity patterns are connected with the corresponding order parameters by means of circular causality. The order parameters move for a short time in an attractor landscape whereby the attractor and also the order parameter disappear (concept of quasi-attractors). An example is the disappearance of a percept in watching ambiguous figures. The origin and disappearance of quasi-attractors and the corresponding order parameters can happen on quite different time scales, so that some of them can act as attractors practically all the time or are hard to be removed (psychotherapy in the case of behavioral disturbances). The activity patterns can be stimulated by external stimuli (exogenous activity) but can also be created spontaneously (endogenous activity), for instance in dreams, hallucinations, and, of course, thinking.

Synergetics throws a new light on the mind–body problem, for instance the percepts are conceived as order parameters, whereas the parts of a system are represented by electrochemical activities of the individual neurons. Because of circular causality, the percepts as order parameters and the neural activity (the "enslaved parts") condition each other. Beyond that, the behavior of a system can be described at the level of order parameters (information compression) or at the level of the activities of individual parts (large amount of information).

Analysis of Electroencephalograms (EEG) and Magnetoencephalograms (MEG)

Neuronal activity is accompanied by electromagnetic brain waves that cover the brain over large areas. The corresponding electric and magnetic fields are measured by the EEG and MEG, respectively. According to the ideas of synergetics, at least in situations where the macroscopic behavior changes qualitatively, the activity patterns should be connected with few order parameters. Typical experiments are the above-described finger coordination experiments by Kelso and closely related experiments, for instance, the coordination between the movement of a finger and a sequence of acoustic signals. In a typical experiment, parts of the brain or the whole brain are measured by an array of SQUIDS (superconducting quantum interference devices) that allows the determination of spatiotemporal field patterns. By means of appropriate procedures, these patterns are decomposed into fundamental patterns. As the analysis shows, two dominant basic patterns appear, whose amplitudes are the order parameters. If the coordination between finger movement and the acoustic signal changes dramatically, the dynamics of the order parameters also does so.

Sociology

Here we may distinguish between the more psychological and the more systems theoretical schools, where synergtics belongs to the second approach. We can distinguish between a qualitative and a quantitative synergetics (for a quantitative approach, see Weidlich, 2000). In the latter case, a number of sociologically relevant order parameters are identified. One example is the language of a nation. After his/her birth, a baby is exposed to the corresponding language and learns it (in technical terms of synergetics: the baby is enslaved) and then carries on this language as an adult (circular causality). These language order parameters may compete, where one wins (e.g., in the United States, the English language), they may coexist (e.g., in Switzerland), or they may cooperate (for instance, popular language and technical language). Whereas in this case the action of the slaving principle is evident, in the following examples its applicability is critically discussed by sociologists so that instead of slaving, some sociologists like to speak of binding or consensualization. Corresponding

order parameters are type of state (e.g., democracy, dictatorship), public law, rituals, corporate identity, social climate in a company, and ethics. The latter example is particularly interesting, because order parameters are not prescribed from the outside or ab initio, but originate through self-organization and need not be uniquely determined.

Ethics

Conceived as order parameter means that it originates from the formation of a consensus so that the slaving principle becomes valid and also that there may exist several ethics.

Epistemology

An example for order parameters is provided by the scientific paradigms in the sense of Thomas S. Kuhn (1970), where a change of paradigms has the properties of a nonequilibrium phase transition, such as critical fluctuations and critical slowing down. Synergetics as a new scientific paradigm is evidently self-referential. It explains its own origin.

Management

The concept of self-organization is increasingly used in management theory and management praxis. Instead of fixed order structures with many hierarchical levels, now flat organizational structures with new hierarchical levels are introduced. In the latter case, a hierarchical level makes its decisions by means of its distributed intelligence. For an indirect steering of these levels by means of a higher level, specific control parameters in the sense of synergetics must be fixed, for instance, by fixing special conditions and goals. The order parameters are, for instance, the self-organized collective labor processes. In this context, the slaving principle—according to which the order parameters change slowly, whereas the enslaved parts react quickly (adaptability)—gains a new interpretation. For instance, the employees that are employed for a longer time determine the climate of labor and the style of work whereby it can also be possible that undesired cliques are established. This trend can be counteracted by job rotation.

Development of Cities

So far the development of cities was based on the concept of city planning with detailed plans for areas, but new approaches use concepts of self-organization according to synergetic principles. Instead of a detailed plan, now specific control parameters, such as a general infrastructure (streets, communication centers, and so on), are fixed. For details consider the book by Portugali (1999).

HERMANN HAKEN

See also **Dynamical systems; Emergence; Gestalt phenomena; Lasers; Turing patterns**

Further Reading

von Bertalanffy, L. 1968. *General System Theory*, New York: Braziller and London: Allen Lane, 1971

Ciompi, L. 1999. *Emotionale Grundlagen des Denkens*, Göttingen: Van den Hoeck; 1998. *Affektlogik*. Stuttgart: Klett-Cotta

Eigen, M. 1971. Molekulare Selbstorganisation und Evolution (Self-organization of matter and the evolution of biological macro molecules). *Naturwissenschaften*, 58: 465–523

Graham, R. & Haken, H. 1968. Quantum theory of light propagation in a fluctuating laser-active medium. *Zeitschrift für Physik*, 213: 420–450

Graham, R. & Haken, H. 1970. Laser light—first example of a second-order phase transition far away from thermal equilibrium. *Zeitschrift für Physik*, 237: 31–46

Guckenheimer, J. & Holmes, P.J. 1983. *Nonlinear Oscillations, Dynamical Systems, and Bifurcations of Vector Fields*, Berlin: Springer

Haken, H. 1983. Synopsis and introduction. In *Synergetics of the Brain*, edited by, E. Başar, H. Flohr, H. Haken & A.J. Mandell, Berlin: Springer, pp. 3–25

Haken, H. 1991. *Synergetic Computers and Cognition*, Berlin: Springer

Haken, H. 1993. *Advanced Synergetics*, 3rd edition, Berlin: Springer

Haken, H. & Graham, R. 1971. Synergetik—Die Lehre vom Zusammenwirken. *Umschau*, 6: 191

Haken, H., Kelso, J.A.S. & Bunz, H. 1985. A theoretical model of phase transitions in human hand movements. *Biological Cybernetics*, 51: 347–356

Hansch, D. 1997. *Psychosynergetik*, Wiesbaden: Westdeutscher Verlag

Hebb, D.O. 1949. *The Organization of Behavior*, New York: Wiley

Kelso, J.A.S. 1995. *Dynamic Patterns: The Self-organization of Brain and Behavior*, Boston: MIT Press

Köhler, W. 1924. *Die physischen Gestalten in Ruhe und im stationären Zustand*, Erlangen: Philosophische Akademie

Köhler, W. 1969. *The Task of Gestalt Psychology*, Princeton, NJ: Princeton University Press

Kuhn, T.S. 1970. *The Structure of Scientific Revolutions*, Chicago: University of Chicago Press

Nicolis, G. & Prigogine, I. 1977. *Self-organization in Non-equilibrium Systems*, New York: Wiley

Portugali, J. 1999. *Self-organization in the City*, Berlin: Springer

Schöner, G., Yiang, W.Y. & Kelso, J.A.S. 1990. A synergetic theory of quadrupedal gaits and gait transitions. *Journal of Theoretical Biology*, 142: 359–391

Scott, A.C. 2003. *Nonlinear Science: Emergence and Dynamics of Coherent Structures*, 2nd edition, Oxford and New York: Oxford University Press

Stefanovska, A., Haken, H., McClintock, P.V.E., Hožič, M., Bajrović, F. & Rivarič, S. 2000. Reversible transitions between synchronization states of the cardiorespiratory system. *Physical Review Letters*, 85(22): 4831–4834

Stratonovich, R.L. 1963, 1967. *Topics in the Theory of Random Noise*, vols. 1, 2, New York: Gordon and Breach

Tschacher, W., Schiepek, G. & Brunner, E.J. 1992. *Self-organization and Clinical Psychology*, Berlin: Springer

Weidlich, W. 2000. *Sociodynamics. A Systematic Approach to Mathematical Modelling in the Social Sciences*, Amsterdam: Harwood Academic Publishers

Wiener, N. 1948. *Cybernetics, or Control and Communication in the Animal and the Machine*, Cambridge, MA: MIT Press

T

TACHYONS AND SUPERLUMINAL MOTION

With a name derived from the Greek *tachys* (for swift), the tachyon is a hypothetical elementary particle that travels at speeds exceeding that of light (superluminal speed). In his 1905 paper on special relativity, Albert Einstein showed that the light speed in vacuum (c) is invariant with respect to all inertial observers, constituting a limiting value for the speed (v) of a moving mass. Consequently, tachyon research was delayed until the 1950s and 1960s, in particular till the appearance of the papers by Sudarshan and coworkers (Bilaniuk et al., 1962), and later by Recami and coworkers, among others.

If the special relativity theory is not a priori restricted to subluminal speeds, however, it seems able to accommodate tachyons. Such an extended relativity (ER) is based on the ordinary postulates of special relativity, and, therefore, does not appear to imply violations of causality (Recami, 1986). Just as photons are born, live, and die, always at the speed of light (without any need of accelerating from rest to the light speed), particles or waves may exist endowed always with speeds v larger than c.

Several areas of experimental physics suggest superluminal group velocities and energy propagation although it is not yet clear whether these phenomena imply signal and information transmissions with faster-than-light speeds (Recami, 2001).

Evanescent Waves and Tunneling Photons

In quantum mechanics, the tunneling time does not depend on the potential barrier width, implying arbitrarily large group velocities inside long barriers (Olkhovsky et al., 1992). Analogously, evanescent electromagnetic waves that travel with superluminal speeds have been predicted by extended relativity, confirmed by computer simulations based on Maxwell equations, and empirically observed (Chiao et al., 1993).

The most interesting experiment of this series was performed in 1994 by Günter Nimtz and his colleagues using two classical barriers separated by an intermediate region of width R. For nonresonant tunneling of microwaves, it was claimed that the total crossing time did not depend on R, implying the speed of transmission to be therein practically infinite. This result agrees with theoretical predictions for nonresonant tunneling through two successive opaque barriers (Olkhovsky et al., 2002) that were experimentally confirmed and have been verified by an experiment with two gratings in an optical fiber, suggesting potentially important applications.

Superluminal Localized Solutions (SLS) to the Wave Equation

Although the simplest subluminal object is a small sphere (or a point), a result of ER is that the simplest superluminal objects appear as "X-shaped" waves (double cones), rigidly moving in a homogeneous medium. Beams of this sort have been constructed (as superpositions of Bessel beams) in experiments with acoustic waves (Lu and Greenleaf, 1992), electromagnetic waves, and visible light (Saari & Reivelt, 1997). A single Bessel beam is the following solution of the

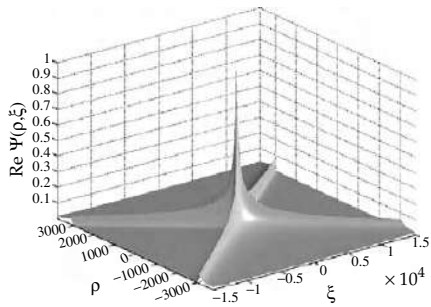

Figure 1. Illustration of the real part of a classical X-shaped wave (as a function of $\zeta \equiv z - vt$ and the radial coordinate ρ), evaluated for $v = 5\,c$ and $a = 5 \times 10^{-7}$ m, plotted from Equation (3).

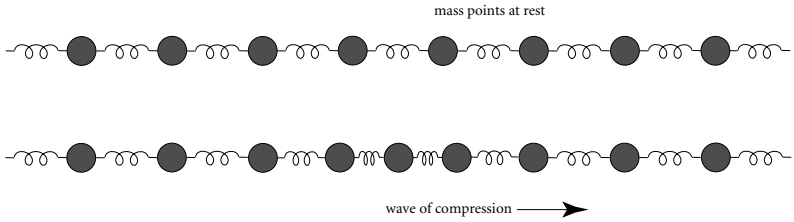

Figure 2. A spring–mass system with nonlinear springs. (Upper) Masses at rest. (Lower) A supersonic compression wave.

Maxwell equations in vacuum:

$$\psi(\rho, \zeta) = J_0[(\omega\rho/c)\sin\theta]\ \exp[\mathrm{i}(\omega\zeta/c)\cos\theta], \tag{1}$$

where J_0 is a Bessel function of the first kind of order zero, $\zeta \equiv z - vt$, $v = c/\cos\theta$, and θ is the axicone angle (angle between the direction of propagation and the propagating cone). This solution depends on z and t only through the quantity ζ; thus, it propagates without dispersion along the z-axis with speed $v > c$. By superposition of Bessel beams, for example, with variable angular frequency ω but constant θ and, therefore, constant v, one can obtain additional solutions to the Maxwell equations with any degree of transverse and longitudinal localization and centered at the desired angular frequency ω with the desired bandwidth (Zamboni-Rached et al., 2002); thus

$$\Psi(\rho, \zeta) = \int_0^\infty S(\omega) J_0[(\omega\rho/c)\sin\theta] \times \exp[\mathrm{i}(\omega\zeta/c)\cos\theta]\,\mathrm{d}\omega. \tag{2}$$

By choosing the exponential spectrum $S(\omega) = \exp[-a\omega]$, one gets the ordinary X-wave (with $v \equiv c/\cos\theta > c$)

$$\Psi(\rho, \zeta) = v\left[\sqrt{(av - \mathrm{i}\zeta)^2 + \rho^2(v^2/c^2 - 1)}\right]^{-1}, \tag{3}$$

which is a superluminal localized solution (SLS) to the wave equation. The plot of Equation (3) in Figure 1 can be understood as follows. For $\zeta < 0$, one has the familiar bow wave of a moving boat or shock wave of a supersonic aircraft. The branches for $\zeta > 0$, on the other hand, prepare the medium for the superluminal disturbance.

SLSs have also been constructed which travel without distortion along cylindrical waveguides and coaxial cables (Zamboni et al., 2002). X-shaped waves keep their localization and superluminality properties only to a certain depth of field (whose length can be determined a priori), decaying abruptly thereafter. As suggested by extended relativity, the simplest means for experimentally producing SLSs employs dynamic antennas consisting of a set of circular rings (or axicons or holographic elements). Acoustic localized supersonic beams have been used in a 3-dimensional ultrasound scanner for medical purposes: high-resolution scanning of the heart (Lu & Greenleaf, 1992).

Tachyons and SLSs in Nonlinear Media

Localized solutions for nonlinear partial differential equations that travel faster than the limiting speed for small amplitude waves are not uncommon (Conti et al., 2003). The sine-Gordon equation, for example, is Lorentz invariant and has tachyonic soliton solutions (Scott, 2003). Although dynamically unstable over long distances, these solutions may influence dynamics over shorter spans.

Another well-known example of a SLS goes back to the birth of nonlinear science, when John Scott Russell measured the speed of a hydrodynamic solitary wave in a wave tank to be $\sqrt{g(d+h)}$, where g is the acceleration of gravity, d the depth of the channel, and h the wave height. Clearly, the solitary wave speed is larger than the speed $\sqrt{gd}$ of low-amplitude waves.

Similar phenomena are observed for lattice solitary waves on spring-mass ladders (see Figure 2), which include the Fermi–Pasta–Ulam system, the Toda lattice, and various generalizations: Existence of supersonic compression-wave solutions has been mathematically proven for a general class of nonlinear intermass potentials (Friesecke & Wattis, 1994). As an example of superluminal propagation that was well known to military engineers in the early 19th century, Russell cited the fact that "the sound of a cannon travels faster than the command to fire it".

ERASMO RECAMI AND ALWYN SCOTT

See also **Cherenkov radiation; Sine-Gordon equation; Skyrmions; Solitons, a brief history**

Further Reading

Bilaniuk, O.M, Deshpande, V.K. & Sudarshan, E.C.G. 1962. Meta relativity. *American Journal of Physics*, 30: 718

Chiao, R.Y., Kwiat, P.G. & Steinberg, A.M. 1993. Faster than light. *Scientific American*, 269(2): 52–60
Conti, C., Trillo, S., Di Trapani, P., Valiulis, G., Piskarskas, A., Jedrkiewicz, O. & Trull, J. 2003. Nonlinear electromagnetic X-waves. *Physical Review Letters*, 90: no.170406
Friesecke, G. & Wattis, J.A.D. 1994. Existence theorem for travelling waves on lattices. *Communications in Mathematical Physics*, 161: 391–418
Lu, J.-Y. & Greenleaf, J.F. 1992. Experimental verification of nondiffracting X-waves. *IEEE Transactions on Ultrasonic Ferroelectric Frequency Control*, 39: 441–446
Olkhovsky, V.S. et al. 1992. Recent developments in the time analysis of tunneling processes. *Physics Reports*, 214: 339–356 and references therein
Olkhovsky, V.S. et al. 2002. Superluminal tunneling through two successive barriers. *Europhysics Letters*, 57: 879–884
Recami, E. 1986. Classical tachyons and possible applications. *Rivista del Nuovo Cimento*, 9(6): 1–178 and references therein
Recami, E. 2001. Superluminal motions? A bird's-eye view of the experimental situation. *Foundations of Physics*, 31: 1119–1135
Saari, P. & Reivelt, K. 1997. Evidence of X-shaped propagation-invariant localized light waves. *Physical Review Letters*, 79: 4135–4138
Scott, A.C. 2003. *Nonlinear Science: Emergence and Dynamics of Coherent Structures.*, 2nd edition, Oxford and New York: Oxford University Press
Zamboni-Rached, M. et al. 2002. New localized superluminal solutions to the wave equations with finite total energies and arbitrary frequencies. *European Physical Journal D*, 21: 217–228
Zamboni, M. et al. 2002. Superluminal X-shaped beams propagating without distortion along a coaxial guide. *Physical Review* E, 66: no. 046617

TACOMA NARROWS BRIDGE COLLAPSE

The Tacoma Narrows suspension bridge in Washington state was opened to traffic on July 1, 1940. At the time, it was the latest in a trend in suspension bridge design toward building ever longer, lighter, and more flexible bridges. At least two other suspension bridges in America, the Golden Gate bridge in San Francisco and the Bronx–Whitestone bridge in New York, had at that time, already experienced some problems with unwanted oscillations; these bridges were stabilized by adding dampers, stiffening girders, and additional cables. The Tacoma Narrows bridge was far lighter and more flexible than its predecessors.

From its opening, the bridge experienced relatively small vertical oscillations. These were observed, and carefully recorded and the record survives in Amann et al. (1941), which is our primary source for what follows.

These oscillations were purely vertical, with no torsional component. They could be anything from no-noded (with a comparatively low frequency of about 8 cycles/min) to as many as seven-noded (with a frequency of 30 cycles/min). Amplitudes were as much as 5 f from top to bottom. Motions as large as 4 f with a frequency of 16 min^{-1} were observed

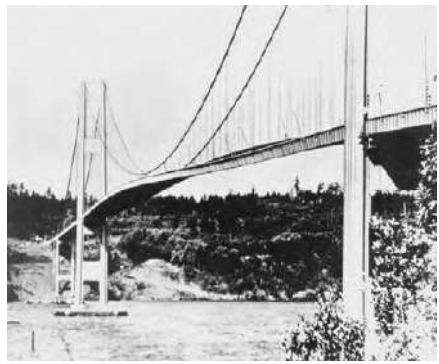

Figure 1. The Tacoma Narrows Bridge twisting, November 7, 1940. (Courtesy, Manuscripts, Special Collections, University Archives, University of Washington Libraries, UW2143.)

in winds of 3 mi/h, while at other times, the bridge remained stationary in winds of 35 mi/h. The structure had already survived winds of 48 mi/h.

These motions were not considered grounds for alarm, and it was apparently expected that with some modifications, they would eventually be eliminated. By October, hold-down cables had been installed in the side-spans, and these had effectively stopped the oscillations in these spans although, of course, they did not effect the center span. Hold-down cables for the center span had already been ordered.

On the morning of November 7, 1940, a qualitatively different phenomenon occurred. The wind was about 42 mi/h. The bridge began oscillating with somewhat more violence than usual in the vertical direction. The motion appears to have been eight- or nine-noded, with an amplitude of 4–5 f and a frequency of about 36–38 cycles/min. Although this seems rather violent, it was not initially viewed as cause for alarm. People and cars were on the bridge.

Suddenly, without warning, and virtually instantaneously, the bridge switched from the vertical motion to the famous torsional motion most often associated with the bridge (see Figure 1).

This new motion was one-noded, with an angle of rotation of nearly 45° each way, and a frequency of about 14/min. The sides of the bridge were moving with a double amplitude of 28 f, with accelerations in excess of gravity. Amazingly, this motion continued for about 45 min, after which the bridge finally began to break up. Occasionally, it would switch from one-noded to no-noded and back, but it remained primarily one-noded. The side-spans remained motionless, until the collapse of the center span, after which a torsional oscillation built up and then died down.

Thus, we are presented with at least three distinct nonlinear phenomena.

(i) The vertical oscillations: why so many and under such widely different wind conditions?
(ii) The instantaneous transition from vertical to torsional motion.
(iii) The persistence of large torsional periodic oscillation for 45 min under comparatively small aerodynamic forcing.
(iv) The peculiar shifting from one-noded torsional motion to no-noded and back.

A commission, including Othmar Amann and Theodore von Karman, tried to investigate the cause of the collapse. They made some preliminary conclusions, including "it is very improbable that resonance with alternating vortices plays an important role in the oscillations of suspension bridges." However, the main recommendation was simply to avoid designs that were light and flexible, This advice has largely been followed since that time, with the notable exception of the Millennium Bridge over the Thames in London. Moreover, other light, flexible, long-span bridges such as the Golden Gate were substantially re-engineered at great cost in the 1950s to eliminate similar unwanted oscillations.

Recent advances in nonlinear science have cast light on some of the phenomena mentioned above. The vertical oscillations may have been the result of the existence of multiple periodic solutions of a nonlinearly supported beam equation (Lazer & McKenna, 1990). They may also have been the result of some sort of negative damping induced by the aerodynamic interaction of the wind and the structure. Wind tunnel experiments on scale models (Scanlan & Tomko, 1971), predict the existence of small torsional oscillations (e.g., in torsion $0 \leq \alpha \leq \pm 3°$). However, this type of motion was never observed on the Tacoma Narrows.

The violent transition from vertical to torsional motion is now well understood. In McKenna (1999), a two-degree-of-freedom oscillator with physical constants chosen to match the bridge exhibits exactly this type of instability, as soon as the cables start alternately slackening. Also in McKenna (1999), this oscillator shows how small torsional forcing can induce large torsional periodic solutions, once one takes into account the pendulum-like nonlinearity of the torsional oscillator. The solutions are remarkably similar, in terms of amplitude and frequency, to the behavior observed on the Tacoma Narrows.

The transition from one-noded to no-noded and back has been observed in Moore (2002), where the torsional oscillations in a nonlinear beam are shown to obey a sine-Gordon equation whose long-term solutions are investigated. One can also see a numerical simulation of the bridge at www.math.lsa.umich.edu/ksmoore.

A good source of interesting behavior of early suspension bridges is Bleich et al. (1950).

JOE MCKENNA

See also **Bifurcations; Distributed oscillators; Stability**

Further Reading

Amann, O.H., von Karman, T. & Woodruff, G.B. 1941. *The Failure of the Tacoma Narrows Bridge*, Federal Works Agency Washington, D.C.

Bleich, F., McCullough, C.B., Rosecrans, R. & Vincent, G.S. 1950. *The Mathematical Theory of Suspension Bridges*, U.S. Dept. of Commerce, Bureau of Public Roads Washington, D.C.

Lazer, A.C. & McKenna, P.J. 1990. Large amplitude periodic oscillations in suspension bridges: some new connections with nonlinear analysis. *SIAM Review*, 32: 537–578

McKenna, P.J. 1999. Large torsional oscillations in suspension bridges revisited: fixing an old approximation. *American Mathematics Monthly*, 106: 1–18

Moore, K.S. 2002. Large torsional oscillations in a suspension bridge: multiple periodic solutions to a nonlinear wave equation. *SIAM Journal of Mathematical Analysis* 33(6): 1411–1429

Scanlan, R.H. & Tomko, J.J. 1971. Airfoil and bridge deck flutter derivatives. *ASCE, Journal of the Engineering Mechanics Division*, EM6: 1717–1737

TANGENT SPACE

See **Differential geometry**

TAYLOR–COUETTE FLOW

Taylor–Couette flow is generated in the gap between a pair of concentric cylinders by the rotary motion of one or both of the cylinders. If the outer cylinder alone is rotated, the torque induced by viscous drag on the inner one can be used to measure the viscosity of the fluid in the gap. This technique (studied by Arnulph Mallock in 1888 and independently by M.M. Couette in 1890) is still in use today as the basis of some commercial viscometers.

In 1916, Lord Rayleigh (John William Strutt) proposed general arguments on the stability of rotating fluids, showing that when the centrifugal force gradient decreases outwards in a rotating body of fluid, this will be an unstable situation for an inviscid fluid. In the case of Mallock's viscometer, the flow will be stable. But suppose the inner cylinder is rotated and the outer is held fixed. Here the flow will be unstable according to Rayleigh's criterion, and this question intrigued Geoffrey Taylor. In 1923, he published a brilliant theoretical and experimental investigation of a viscous version of the Rayleigh criterion, using rotating cylinders to generate what has come to be called Taylor–Couette flow. Taylor's work forms the cornerstone of much modern research on hydrodynamic stability

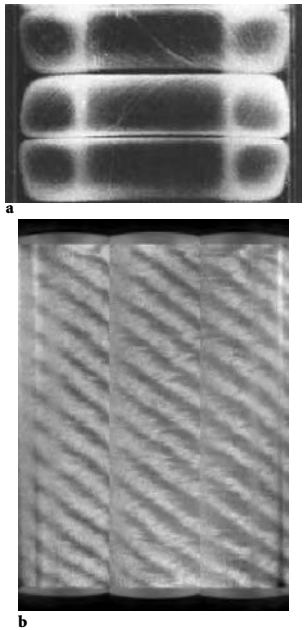

Figure 1. (a) Front view of steady Taylor–Couette cells (G. Pfister). (b) Front view of turbulent spiral flow (O. Dauchot).

and contains important ideas such as the exchange of stability between states.

In the simplest case, the outer cylinder is stationary and the inner cylinder alone rotates. When a critical Reynolds number is exceeded, the initially featureless rotary Couette flow has secondary vortices superposed on it. An example of such a Taylor vortex state is shown in Figure 1(a) where a front view of a Taylor vortex state is shown. The pattern is repeated along the length of the cylinder and has the appearance of a set of doughnuts stacked along the length the inner cylinder.

Increasing the speed of the inner cylinder leads to an instability (Davey et al., 1968) in the form of traveling waves that move at a fixed fraction of the speed of the inner cylinder (Coles, 1965). Yet, further increases in rotation rate give rise to more complicated quasi-periodic motion until low-dimensional temporal chaos ensues within each Taylor cell (Gollub & Swinney, 1975). Nowadays, it is recognized that many routes to chaos exist within this flow (Tagg, 1994), which has proved to be a rich research field for dynamical systems and bifurcation theory.

Taylor considered the general case with both cylinders rotating in co- and counter-directions, obtaining remarkable agreement between theory and experiment for the stability boundary. When the cylinders are rotated in opposite directions, new states of spiraling turbulence are sometimes found (Coles, 1965). An example of such a flow from a more recent study (Prigent et al., 2002) is shown in Figure 1(b). The general case of co- and counter-rotation produces a plethora of interesting dynamical states (Andereck et al., 1986) that can now be classified in terms of equivariant bifurcation theory (Tagg, 1994).

Coles also demonstrated dynamical non-uniqueness when the outer cylinder is stationary, finding more than 20 states at a particular Reynolds number. This multiplicity of solutions has also been observed in the steady vortex states (Burkhalter & Koschmieder, 1973; Benjamin & Mullin, 1982) where evidence was found for 42 different solutions at a single point in parameter space in the latter study.

Most of the above work is based on the notion of a theoretical model where the cylinders are considered to be infinitely long. This permits the use of periodic boundary conditions which allows analytical and numerical progress to be made in the nonlinear regime. However, the importance of end effects and their influence on global aspects of the steady flows was first recognized by Benjamin in 1978. He showed their importance in the selection process for steady flows and discovered the so called "anomalous modes" where all cells rotate in the opposite direction. These modes form an essential part of the solution set. The ideas have been developed and the role of end effects in determining the dynamics is now understood in some detail (Abshagen et al., 2001).

One clear advantage of studying fluid dynamical systems such as Taylor–Couette flow is that quantitative comparisons can be made between the results of controlled laboratory experiments and numerical calculations of the governing equations of motion—the Navier–Stokes equations (Cliffe et al., 2000). This is so not only for steady flows but also for time-dependent states, although disordered motion remains an outstanding challenge.

TOM MULLIN

See also **Bifurcations; Catastrophe theory; Chaos vs. turbulence; Hopf bifurcation; Stability**

Further Reading

Abshagen, J., Pfister, G. & Mullin, T. 2001. Gluing bifurcations in a dynamically complicated extended fluid flow. *Physical Review Letters*, 87: 4501–4505

Andereck, C.D., Liu, S.S. & Swinney, H.L. 1986. Flow regimes in a circular Couette system with independently rotating cylinders. *Journal of Fluid Mechanics*, 164: 155–183

Benjamin, T.B. & Mullin, T. 1982. Notes on the multiplicity of flows in the Taylor experiment. *Journal of Fluid Mechanics*, 121: 219–230

Benjamin, T.B. 1978. Bifurcation phenomena in steady flows of a viscous fluid. *Proceedings of the Royal Society of London*, A359, 1–43

Burkhalter, J.E. & Koschmieder, E.L. 1973. Steady supercritical Taylor vortex flow. *Journal of Fluid Mechanics*, 58: 547–560
Cliffe, K.A., Spence, A. & Tavener, S.J. 2000. The numerical analysis of bifurcation problems with application to fluid mechanics. *Acta Numerica*, 9: 39–131
Coles, D. 1965. Transition in circular Couette flow. *Journal of Fluid Mechanics*, 21: 385–425
Couette, M.M. 1890. Etudes sur le frottement des liquides. *Annales de Chimie et de Physique*, 6: 433–510
Davey, A., diPrima, R.C. & Stuart, J.T. 1968. On the instability of Taylor vortices. *Journal of Fluid Mechanics*, 31: 17–52
Gollub, J. & Swinney, H.L. 1975. Onset of turbulence in a rotating fluid. *Physical Review Letters*, 35: 927–930
Mallock, A. 1888. Determination of the viscosity of water. *Proceedings of the Royal Society of London*, A45: 126–132
Prigent, A., Gregoire, G., Chate, H., Dauchot, O. & van Saarloos, W. 2002. Large-scale finite-wavelength modulation within turbulent shear flows. *Physical Review Letters*, 89: 1501–1504
Rayleigh, Lord. 1916. On the dynamics of revolving fluids. *Proceedings of the Royal Society of London*, A93: 148–154
Tagg, R. 1994. The Couette–Taylor problem. *Nonlinear Science Today*, 4: 2–25
Taylor, G.I. 1923. Stability of a viscous liquid contained between two rotating cylinders. *Philosophical Transactions of the Royal Society of London*, 223: 289–343

TENSORS

Tensors are mathematical representations of objects that have intrinsic, geometric significances. This is a rather wider definition than many which can be found in textbooks, often referring to "sets of quantities" that "transform according to hideous formulae." The best way to understanding is likely to follow a few examples.

Readers interested in learning more will find the books of Simmon (1994) and Dodson & Poston (1991) helpful, as well as that of Bishop & Goldberg (1968). The main caveat, at the risk of repetition, is to beware of books that define tensors as some set of quantities tied to a coordinate system and then describe how they transform—tensors are there whether or not you have coordinates.

Suppose you have some apples on a table. The quantity of apples present is described completely by one number, and that number is well defined and meaningful no matter how you might orient any coordinate axes in the room. The fact that it is meaningful independent of the coordinates makes it a tensor, and the fact that it is the same no matter what coordinates might be introduced makes it a *scalar* or zeroth-rank tensor—the simplest kind of tensor.

Now, consider the weight of one of the apples. This weight is a force, equal to the mass of the apple, m, times the gravitational acceleration ($g = 9.8\ \mathrm{m/s^2}$), and it is directed downwards. That is, its weight is mg directed downwards towards the table top. Let us call this weight $\boldsymbol{W}$, which has a clear physical meaning independent of coordinates, although it is helpful to describe its direction as "downwards." The fact that $\boldsymbol{W}$ is well defined even in the absence of coordinates makes it a tensor, and because it has a direction, it is called a *vector*, or first-rank tensor. If I introduce a set of coordinates x, y, z, I may place these axes in any way I choose. If I put the z-axis pointing downwards, the vector will have components relative to that coordinate system, with only the z component nonzero, and I might describe it as "the vector $(0, 0, mg)$." This (old) point of view is legitimate but carries with it the need to understand that the *components* are referred to as a coordinate system and as such have no intrinsic meaning.

More complicated objects can be easily imagined. For example, there could be a wind blowing across the table, and that could be described by another vector $\boldsymbol{V}$ describing its velocity. Referred to a coordinate system, it would be described by three components, and the presence of these two vectors is clearly something of intrinsic geometric significance. We can think of a product of the two vectors, meaning simply all the information needed to describe them. In terms of coordinates, if the weight is described by components w_i with i ranging from 1 to 3 and the wind velocity by v_j with j ranging from 1 to 3, we can think of a single geometric object $\boldsymbol{V} \bigotimes \boldsymbol{W}$ called the *tensor product* of $\boldsymbol{V}$ and $\boldsymbol{W}$ with 9 components $(\boldsymbol{V} \bigotimes \boldsymbol{W})^{ij} = v^i w^j$. The object $(\boldsymbol{V} \bigotimes \boldsymbol{W})$ is called a second-rank tensor, and this construction can be repeated to create more and more complex objects. (The reason for the upper placement of indices will be made clear shortly.)

The example given above was chosen to make it clear that tensors can turn up anytime one has vectors, but it is easy to find more physically motivated examples. Suppose one has a perfect fluid of density ρ moving with velocity $\boldsymbol{V}$ with components v^i. Density is a scalar if we allow only "proper" rotations which cannot change the signs of volumes. The flux or mass per unit volume per unit area perpendicular to direction i flows has components ρv^i. The flux of momentum in direction j is $\rho v^i v^j$. This motivates defining the second-rank "momentum tensor" tensor $\boldsymbol{T} = \rho \boldsymbol{V} \bigotimes \boldsymbol{V}$ with components $T^{ij} = \rho v^i v^j$.

All the tensors of a given rank have the structure of a vector space which they inherit from the operations allowed on vectors: they can be added, or multiplied by scalars. In fact, all the machinery of linear algebra carries over directly to them.

There has been an implicit indication that tensors here have something to do with symmetry or a concept of allowed transformation of the coordinates. The class of acceptable coordinate systems defines the geometry in any given situation, and we can speak then of tensors with respect to a symmetry group. For example, if we allow arbitrary rotations of a given orthogonal coordinate system, we can speak of "Cartesian tensors" or tensors under the group of orthogonal transformations in three dimensions. This means that one can pass from a representation of a tensor in terms of components with respect to one coordinate system to another by making the coordinates

transform according to a matrix which represents that coordinate change.

This final step in thinking clarifies the notion of what a tensor must be. Given some space, one considers the geometry to be defined by the group of transformations which leave it invariant. For example, in flat Euclidean three-dimensional space, one might take the group of rotations, which are orthogonal matrices of determinant one, or SO(3). The vectors and tensors we have been talking about so far are then elements of spaces in which SO(3) acts linearly, i.e., they lie in representation spaces of SO(3).

Depending on the space in question and the structures imposed upon it, special tensors and operations can be defined. For example, in three-dimensional flat space, we have an operation that takes two vectors and produces from them a (coordinate-independent!) scalar called the "dot product," "inner product," or "scalar product." This is defined using the Kronecker delta δ_{ij} which is defined to have the value 1 when $i = j$ and 0 otherwise. It is a geometric object with a well-defined meaning independent of coordinates and is, thus, a tensor but of a different kind. One says that while $v^i w^j$ are components of a "contravariant tensor," δ_{ij} are the components of a "covariant tensor." The expression $\sum_i \sum_j \delta_{ij} v^i w^j$ is the scalar product of $\boldsymbol{v}$ and $\boldsymbol{w}$ and is a scalar. The terms *covariant* and *contravariant* are historical and come from the idea that for a quantity such as $\sum_i \sum_j \delta_{ij} v^i w^j$ to be invariant, the components with upper and lower indices should transform differently under a change of coordinates. The summation signs are often omitted, with a summation over repeated indices implied following the so-called "Einstein summation convention." An inner product automatically provides a dual space to that of the tensors, and one can write $v_i = \delta_{ij} v^j$ and speak of "covariant" as opposed to "contravariant" components of $\boldsymbol{v}$, and of the use of δ_{ij} to "lower indices."

The concept of a tensor is independent of any notion of a dot product, but many spaces of interest have such a product naturally present. In special relativity, for example, we consider "four-vectors" labeling differences in space and time and requiring four components. In units where the speed of light is unity, the dot product is provided by the Minkowski metric tensor η_{ab}: (a, b running from 0 to 3) where η_{ab} is 1 when $a = b = 0$, -1 when $a = b \neq 0$, and zero otherwise. This dot product is preserved by a larger group than just rotations, and this group is the Lorentz group of rotations and boosts, also called SO(3,1). Note that it is not positive-definite, so it is not an inner product in the strict sense of the word, and it defines a pseudo-Euclidean metric. In this case, we have SO(3,1) vectors as opposed to SO(3) vectors.

The most general (pseudo-)Riemannian geometry provides a dot product in terms of a metric tensor g_{ab} which is similar to η_{ab} but unrestricted other than to be nonsingular. In general relativity, we allow all invertible linear transformations in four dimensions, the symmetry group is GL(4), and we have GL(4) tensors for physical quantities.

JOHN DAVID SWAIN

See also **Einstein equations; Symmetry groups**

Further Reading

Bishop, R.L. & Goldberg, S.I. 1968. *Tensor Analysis on Manifolds*, New York: Macmillan

Dodson, C.T.J. & Poston, T. 1991. *Tensor Geometry*, 2nd edition, Berlin and New York: Springer

Simmon, J.G. 1994. *A Brief on Tensor Analysis*, 2nd edition, New York: Springer

TESSELLATION

A tessellation (or tiling) is a covering of a surface with tiles so that there are no gaps or overlaps. The tile shapes can be all different, as in the chips used to produce a complex Byzantine mosaic, or they may consist of a limited number of shapes, each congruent to one or more "prototiles" which serve as templates. Since ancient times, almost every culture has produced tessellations for utilitarian or decorative purposes—on walls, ceilings, and roofs of buildings, for pavements and plazas, and for designs to be woven, painted, printed, incised, or inlaid on every variety of surface. Tessellations adorn many churches, temples, palaces, and mosques; perhaps the most celebrated geometric tessellations are found in the Alhambra, in Granada, Spain. Tessellations also occur in nature, in the designs formed by scales or packed cells on a living surface.

Although artisans have produced tessellations for thousands of years, only recently have mathematicians undertaken a methodical study of the subject. Grünbaum and Shephard's book is the most complete reference. Intuitively, a shape "tiles" (is a prototile for a tessellation) if congruent copies of that shape can be fitted together exactly to fill a surface. Every triangle and every quadrilateral can tile the plane, and convex polygons with seven or more sides can never tile the plane. All convex hexagons that tile the plane have been determined, and 14 classes of convex pentagons that tile have been discovered, but it is not known if there are others. Tessellations by regular polygons appear frequently; those known as Archimedean tessellations are composed of regular polygons with edges matched, and have the same arrangement of tiles occurring at every vertex of the tiling (Figure 1).

An infinite variety of shapes tile the plane, many of them classified by special properties. Given an arbitrary set of shapes, many tests can attempt to answer the question: Will these tile the plane? But there is no guarantee of an answer. The question is mathematically

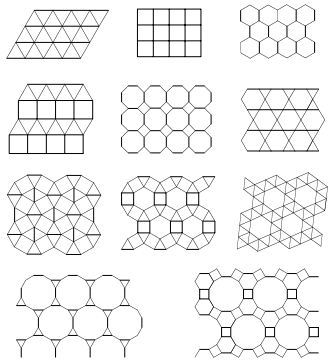

Figure 1. The 11 Archimedean tessellations. The three with only one prototile are called regular tessellations; the others are often called semiregular.

undecidable; that is, there is no algorithm that can deliver an answer of yes or no for every possible set of shapes.

M.C. Escher, a Dutch graphic artist (1898–1972), is the best-known creator of tessellations using whimsical figures as tiles (Figure 2). Inspired by the geometric tessellations in the Alhambra, he sought to answer the question: What shapes can tile the plane so that every tile is surrounded in the same way? As he discovered some answers, he developed a system of tile types that enabled him to create imaginative shapes that fit together in a prescribed manner. In his lifetime, he produced more than 150 finished tessellations; many have been used by scientists, particularly crystallographers, to illustrate their theories.

Almost all tessellations with repetition (including those in Figures 1 and 2) are periodic, that is, there is a smallest patch of the tiling that can be translated repeatedly by two independent vectors to fill out the whole tiling. It is natural to want repetition in a predictable manner to lay tile, to print, or to weave a pattern. Symmetry groups of periodic tilings are known as two-dimensional crystallographic groups, because crystals, by definition (until very recently), were defined by their periodic molecular structure. These groups consist of the translations, rotations, reflections, and glide-reflections that can act on the tiling in such a way that each tile moves to fit exactly onto another, leaving the tiling invariant. There are only 17 distinct symmetry groups for periodic tilings in the Euclidean plane; these are frequently used to classify tilings. Colored tilings (such as an extended checkerboard or Escher's tilings) can be analyzed according to color symmetries, which permute colors of tiles as well as positions of tiles in the tiling.

Nonperiodic tessellations have no translation symmetry. Although a regular tiling by squares can be made

Figure 2. An Escher tessellation covers a column in a school in Baarn, Holland. (All M.C. Escher works © Cordon Art B.V., Baarn, The Netherlands.)

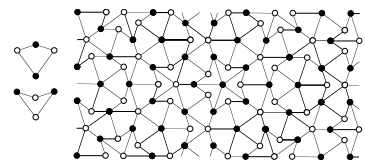

Figure 3. A Penrose tiling by kites and darts requires matching vertices of the same color.

nonperiodic by shifting a few rows a small distance, the most interesting nonperiodic tessellations are produced by an aperiodic set of prototiles—every tiling formed by such a set is nonperiodic. It is not known if there is a single aperiodic tile, but there are several known aperiodic sets of two or more prototiles. The most well-known pairs were discovered by Roger Penrose in the 1970s: a kite and a dart (or a thick and a thin rhombus). In each Penrose tiling formed by these pairs (Figure 3), every patch of the tiling repeats infinitely often, but never by a translation that leaves the tiling invariant. Some properties of Penrose tilings are similar to those exhibited by unusual alloys discovered in the 1980s. These were named quasicrystals because their X-ray diffraction patterns displayed a crystal-like orderly repetition of bright spots, but also exhibited rotation symmetry forbidden in a periodic structure. Many unusual properties of Penrose and other aperiodic tilings have been discovered, and various techniques have been developed to study their structure (Senechal, 1995). Yet the study of aperiodic tilings and of quasicrystals is in its infancy, and it remains to be seen if the connections between them are more than superficial.

A Voronoï (or Dirichlet) tessellation is determined by a given discrete set S of points in a surface. Each point x of S is surrounded by the region of points that are closer to x than to any others in S. The boundaries of these regions consist of those points that lie equidistant between at least two points of S. These regions with their boundaries (called Voronoï polygons or Dirichlet domains) are the tiles of the Voronoï tessellation determined by S. Such tessellations arise naturally in a wide variety of applications in physics (Wigner–Seitz regions); crystallography (Wirkungsbereich); physiology (capillary domains); urban planning (regions of service for schools or fire stations); biology (modeling cell arrangement); statistical spatial data analysis; and many other areas. Such tilings are almost always nonperiodic with many differently shaped tiles. Mathematical properties of such tilings and various algorithms to construct them are vigorous areas of research (Okabe et al., 1992).

Tessellations on surfaces such as spheres or the hyperbolic plane and tessellations of space of three or higher dimensions are equally important. Which shapes can fill space, and in what manner, is of great interest to scientists (and manufacturers). Little is known in this area; there is not even a complete list of space-filling tetrahedra. Other topics of investigation are tessellations with special tiles (e.g., polyominoes, or fractal tiles), relationships between local and global properties, classification, and construction of tessellations with special properties.

DORIS SCHATTSCHNEIDER

See also **Symmetry groups**

Further Reading

Bezdek, K. 2000. Space filling. In *Handbook of Discrete and Combinatorial Mathematics*, edited by K.H. Rosen, Boca Raton: CRC Press, pp. 824–830

Goodman, J.E. & O'Rourke, J. (editors). 2004. *Handbook of Discrete and Computational Geometry*, 2nd edition, Boca Raton: CRC Press (Relevant chapters: Tiling, D. Schattschneider & M. Senechal; Polyominoes, D. Klarner & S.W. Golomb; Voronoï diagrams and Delaunay triangulations, S. Fortune; Crystals and Quasicrystals, M. Senechal)

Gruber, P.M. & Wills, J.M. (editors). 1993. *Handbook of Convex Geometry*, Amsterdam: North-Holland (Relevant chapters: Geometric algorithms, H. Edelsbrunner, vol. A, pp. 699–735; Tilings, E. Schulte, vol. B, pp. 899–932); Geometric crystallography, P. Engel, vol. B, pp. 989–1041)

Grünbaum, B. & Shephard, G.C. 1987. *Tilings and Patterns*, New York: Freeman

Okabe, A., Boots, B. & Sugihara, K. 1992. *Spatial Tessellations: Concepts and Applications of Voronoï Diagrams*, 2nd edition, New York: Wiley (Okabe, A., Boots, B., Sugihara, K. & Chiu, S.N. 2000)

Patera, J. (editor). 1998. *Quasicrystals and Discrete Geometry*, Providence, RI: American Mathematical Society

Schattschneider, D. 2004. *M.C. Escher: Visions of Symmetry*, new edition, New York: Abrams

Schulte, E. 2002. Tilings. In *Encyclopedia of Physical Science and Technology*, 3rd edition, vol. 16, New York: Academic Press, pp. 763–782

Senechal, M. 1995. *Quasicrystals and Geometry*, Cambridge and New York: Cambridge University Press

Washburn, D.K. & Crowe, D.W. 1988. *Symmetries of Culture: Symmetry and Practice of Plane Pattern Analysis*, Seattle: University of Washington Press

THERMAL CONVECTION

Thermal convection is the transfer of heat by flow. In general, heat can be transported by convection, conduction, or radiation. In all cases, heat transfer requires the presence of a temperature gradient, and heat is transported from high to low temperature. Conduction is a diffusive process that involves the exchange of energy via collisions between molecules in a gas or a liquid, or interactions between lattice waves or electrons in a solid. Heat transport by radiation results from the emission and absorption of electromagnetic waves. Convection, finally, involves the transport of heat by the bulk physical motion of a fluid medium. The flow can arise naturally, due to thermal expansion—hot fluid is less dense than cold fluid and so tends to rise, while cold fluid is more dense and tends to fall—or it can be forced by some externally applied means.

In a layer of fluid heated from below, thermal convection is known as Rayleigh–Bénard convection, which is one of the most important systems for the study of pattern formation. This is because precise, well-controlled experiments are possible and because the equations describing the system (the Navier–Stokes equations coupled with an equation for heat transport and the appropriate boundary conditions) are well known, allowing close contact among experiment, theory, and simulations.

Figure 1(a) shows schematically an experiment for the study of Rayleigh–Bénard convection. The top plate is maintained at a temperature T_t, while the bottom plate is at a higher temperature $T_b = T_t + \Delta T$. The separation between the plates is d. For ΔT small, there is no flow and heat transport across the fluid layer is by conduction. Because of thermal expansion, however, the hotter fluid near the bottom plate is less dense than the cooler fluid above it. This is gravitationally unstable, but initiating flow costs energy due to viscous dissipation. As a result, convection does not begin until ΔT is large enough that the energy gained by starting flow offsets the cost due to dissipation. It is convenient to write ΔT in dimensionless form as the Rayleigh number, given by $\mathrm{Ra} = g\alpha d^3 \Delta T/\nu\kappa$, where g is the acceleration due to gravity, α is the thermal expansion coefficient of the fluid, ν is the fluid's viscosity, and κ is its thermal diffusivity. The onset of convection occurs when Ra reaches a critical value $\mathrm{Ra_c}$ which depends on the nature of the top and bottom boundaries. For rigid, isothermal boundaries, $\mathrm{Ra_c} = 1708$. For a rectangular cell with the same boundaries, the flow appears as a pattern of straight convection rolls oriented parallel to the short side of the cell, with a

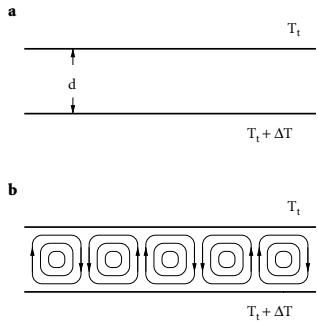

Figure 1. A schematic illustration of Rayleigh–Bénard convection. A fluid layer is bounded above and below by plates separated by a distance d, with the bottom plate at a temperature higher by ΔT than the top plate. When ΔT is below a critical value, there is no flow (a), but when ΔT is higher than the critical value, convective flow develops in the form of parallel, counter-rotating convection rolls (b).

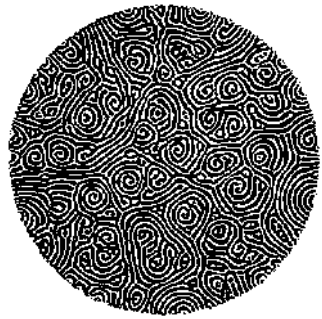

Figure 2. Spiral defect chaos visualized in a convection experiment in a pressurized gas. Spiral defect chaos is a time-dependent steady state that appears near onset at low Prandtl number. Here dark regions indicate upflow and light regions indicate downflow. (Image courtesy of S.W. Morris.)

wavelength equal to $2.016d$. This situation is shown in Figure 1(b).

Heat transport in a convecting fluid is measured by the Nusselt number Nu, defined as $\mathrm{Nu} = \lambda_{\mathrm{eff}}/\lambda$, where λ is the thermal conductivity of the fluid and λ_{eff} is the effective thermal conductivity taking into account the heat transported by the flow. The Prandtl number, $\mathrm{Pr} = \nu/\kappa$, affects the dynamics of the flow pattern above onset.

The onset of Rayleigh–Bénard convection is an example of a bifurcation from a uniform (no-flow) state to one characterized by a spatial pattern. It can be described by the Ginzburg–Landau equation, which can be derived from the full equations describing the system. For the case of two rigid, isothermal boundaries, the system is up-down symmetric and the bifurcation is a supercritical pitchfork bifurcation. If we define $\varepsilon = (\mathrm{Ra} - \mathrm{Ra_c})/\mathrm{Ra_c}$, then the bifurcation occurs at $\varepsilon = 0$. The Ginzburg–Landau equation predicts that close to onset, the amplitude of the convective flow field will grow as $\varepsilon^{1/2}$, while the correlation length of the pattern (the length scale over which the amplitude changes) behaves as $\varepsilon^{-1/2}$. These predictions have been confirmed experimentally.

If the up-down symmetry of the system is broken, either by making top and bottom boundaries different or due to a variation in the fluid properties with temperature across the cell (non-Boussinesq effects), then the symmetry of the bifurcation is also broken and convection appears via a subcritical bifurcation. In this case, the convection pattern at onset takes the form of an array of hexagonal cells (see photo of atmospheric hexagonal convection cells on page 3 of color plate section).

Above onset, the straight-roll pattern is stable within a range of wave numbers and Rayleigh numbers. The range of stability (known as the "Busse balloon") is limited by a variety of secondary instabilities which depend on Pr. The original straight–roll pattern becomes unstable to perturbations in phase or amplitude which lead to new flow patterns, which can have different wave numbers, orientations, and symmetries. Certain of these secondary instabilities can make the flow pattern two- or three-dimensional or time dependent.

In larger systems, when the size of the system becomes much greater than the correlation length of the pattern, the convection patterns are more complex than ideal straight rolls. The tendency of the rolls to orient perpendicular to the sidewalls results in patterns with curved rolls and a spatially varying wave number. Even close to onset, defects and localized instabilities can lead to time-dependent patterns. At low Pr, a transition to a complex, spatiotemporally chaotic state known as spiral defect chaos occurs (Figure 2). Interestingly, spiral defect chaos exists in exactly the regime where ideal straight rolls are expected to be stable, and experiments have shown that the two states can coexist. This suggests that there are two stable states in this regime, with different basins of attraction. Spiral defect chaos is obtained for most conditions, while specially chosen initial or boundary conditions are required to obtain ideal straight rolls.

At high Ra, the convective flow becomes turbulent. In this case, most of the temperature drop occurs in boundary layers near the top and bottom plates of the cell. Coherent plumes of hot and cold fluid can form at the lower and upper boundary layers, respectively, and a coherent large scale flow can exist in the convection cell. Simple theories based on the stability of the boundary layers predict that heat flow for turbulent convection should scale as $\mathrm{Nu} \sim \mathrm{Ra}^{1/3}$, while more sophisticated models give different values of the

exponent. Recent research indicates that the exponent is itself a function of Ra.

There are many variants of Rayleigh–Bénard convection that have been studied in an effort to elucidate particular aspects of nonlinear dynamics. In appropriately chosen binary mixtures, one can obtain traveling-wave convection patterns. Thermal convection in anisotropic materials (e.g., liquid crystals) also leads to complex dynamics. Convection with an imposed mean flow has been used to study the transition from convective to absolute instability. Convection with rotation exhibits spatiotemporally chaotic patterns close to onset.

JOHN R. DE BRUYN

See also **Bifurcations; Pattern formation; Turbulence**

Further Reading

Bodenschatz, E., Pesch, W. & Ahlers, G. 2000. Recent developments in Rayleigh–Bénard convection. *Annual Review of Fluid Mechanics*, 32: 709–778

Busse, F. 1981. Transition to turbulence in Rayleigh–Bénard convection. In *Hydrodynamic Instabilities and the Transition to Turbulence*, edited by H.L. Swinney & J.P. Gollub, Berlin: Springer

Cross, M.C. & Hohenberg, P.C. 1993. Pattern formation outside of equilibrium. *Reviews of Modern Physics*, 65: 851–1112

de Bruyn, J.R, Bodenschatz, E., Morris, S.W., Trainoff, S.P., Hu, Y., Cannell, D.S. & Ahlers, G. 1996. Apparatus for the study of Rayleigh–Bénard convection in gases under pressure. *Review of Scientific Instruments*, 67: 2043–2067

Manneville, P. 1990. *Dissipative Structures and Weak Turbulence*, London: Academic Press

Siggia, E. 1994. High Rayleigh number convection. *Annual Review of Fluid Mechanics*, 26: 137–168

THERMO-DIFFUSION EFFECTS

In fluid mixtures, a temperature gradient can drive a concentration current or generate a concentration gradient depending on boundary conditions. This thermo-diffusion effect—nowadays referred to as the Soret effect or Ludwig–Soret effect—was first reported by Carl Ludwig in 1856 and by Charles Soret in 1879. They observed an increase (decrease) of salt concentration at the cold (hot) end of a tube filled with salty water (Ludwig, 1856; Soret, 1879). The reciprocal effect that a concentration gradient drives a heat flow or generates a temperature gradient was first reported by Louis Dufour in 1872 for gas mixtures in a porous medium. Theoretically, these and similar effects are most conveniently captured within the Onsager theory of irreversible macroscopic processes, in which generalized thermodynamic forces and resulting fluxes are linearly related to each other (de Groot & Mazur, 1962; Landau & Lifshitz, 1959).

In the last 20 years or so, it has become clear that the linear Soret effect plays a dominant role in the nonlinear behavior of convective pattern formation in binary fluid mixtures (Platten & Legros, 1984; Cross & Hohenberg, 1993; Lücke et al., 1998). Consider the typical Bénard configuration of a horizontal fluid layer of height d that is heated from below in a homogeneous gravitational field, $\boldsymbol{g} = -g\,\boldsymbol{e}_z$. Strongly heat-conducting impermeable horizontal plates impose a vertical temperature difference ($\Delta T > 0$) such that $T = T_0 \pm \Delta T/2$ at $z = \mp d/2$. T_0 is the mean temperature of the fluid layer. At small ΔT, the laterally homogeneous quiescent conductive state is stable with the linear temperature profile $T_{\rm cond}(z) = T_0 - \Delta T z/d$. In a mixture like, for example, ethanol dissolved in water, this conductive temperature gradient generates as a consequence of the Soret effect a concentration gradient, so that

$$C_{\rm cond}(z) = C_0 + S_T C_0(1 - C_0)\Delta T z/d. \qquad (1)$$

Here, $C = \rho_1/(\rho_1 + \rho_2)$ is the mass concentration of the solute which is in our example the lighter component. C_0 is its mean, S_T the Soret coefficient, and $k_T = T_0 C_0(1 - C_0)S_T$ the thermo-diffusion ratio. The Soret coupling between temperature and concentration fields (cf. below) is most conveniently measured in terms of the separation ratio $\psi = -S_T C_0(1 - C_0)\beta/\alpha = -(k_T/T_0)\beta/\alpha$. Here, α and β are the thermal and solutal expansion coefficients of the total mass density $\rho_1 + \rho_2 = \rho = \rho_0[1 - \alpha(T - T_0) - \beta(C - C_0)]$ of the mixture for small deviations of T and C from their means. Positive S_T corresponding to negative ψ (for mixtures such as ethanol-water where α and β are positive) implies a concentration increase (of the lighter component) near the cold upper plate and a decrease near the warmer lower plate and vice versa for $S_T < 0$ ($\psi > 0$). Note that in experiments, ψ can easily be varied, say, between -0.6 and 0.25, by varying T_0 and C_0.

Convection is described by the balance equations

$$\boldsymbol{\nabla}\cdot\boldsymbol{u} = 0, \qquad (2a)$$

$$(\partial_t + \boldsymbol{u}\cdot\boldsymbol{\nabla})\boldsymbol{u} = \sigma\nabla^2\boldsymbol{u} + R\sigma\,(\delta T + \delta C)\,\boldsymbol{e}_z - \boldsymbol{\nabla}p, \qquad (2b)$$

$$(\partial_t + \boldsymbol{u}\cdot\boldsymbol{\nabla})T = \nabla^2 T, \qquad (2c)$$

$$(\partial_t + \boldsymbol{u}\cdot\boldsymbol{\nabla})C = L\nabla^2 C - L\psi\nabla^2 T \qquad (2d)$$

for mass (2a), momentum (2b), heat (2c), and concentration (2d) in the Oberbeck–Boussinesq approximation. δT and δC in (2b) denote deviations from the mean T_0 and C_0, respectively. Lengths are scaled with d, time with the vertical thermal diffusion time d^2/κ, and the velocity field $\boldsymbol{u} = (u, v, w)$ with κ/d, where κ is the thermal diffusivity of the mixture. Temperatures are reduced by ΔT, concentration by $\Delta T\alpha/\beta$, and pressure p by $\rho_0(\kappa/d)^2$.

The Dufour effect that provides a coupling of concentration gradients into the heat balance is discarded because it is relevant only in a few gas

mixtures and possibly in liquid mixtures near the liquid–vapor critical point.

Besides the Rayleigh number $R = (\alpha g d^3/\nu\kappa)\Delta T$ measuring the thermal driving force, three additional numbers enter into the field equations: the Prandtl number $\sigma = \nu/\kappa$, which is of order 10 for ethanol–water mixtures at room temperature, the Lewis number $L = D/\kappa \simeq 0.01$, and the separation ratio ψ. Here, ν denotes the kinematic viscosity and D the concentration diffusivity.

The concentration field is responsible for the significantly larger complexity of binary mixture convection compared with pure fluids. It causes the richness of spatiotemporal properties of the convective structures, of the bifurcation behavior, and of the transient growth of convection. The Soret-generated concentration variations δC influence the buoyancy, that is, the driving force for convective flow in (2b). The flow in turn mixes by advectively redistributing concentration. This nonlinear advective mixing in developed convective flow is typically much larger than the smoothing by linear diffusion—the Péclet number measuring the strength of advective concentration transport relative to diffusion is easily of the order of a few thousand. Thus, the concentration balance is strongly nonlinear giving rise to boundary layer behavior and strongly anharmonic concentration field profiles in the horizontal direction, as in Figure 1. In contrast, the momentum and heat balances remain weakly nonlinear close to onset as in pure fluids, implying only smooth and basically harmonic variations, $\sim e^{i\boldsymbol{k}\cdot\boldsymbol{x}}$, as the critical modes (cf. Figure 1).

To summarize, the feedback interplay among (i) the Soret-generated concentration variations that are sustained against mixing and diffusion by externally imposed and internal temperature gradients, (ii) the resulting changes in the buoyancy, and (iii) the strongly nonlinear advective transport and mixing causes binary mixture convection to be rather complex not only with respect to its spatiotemporal properties but also concerning its bifurcation behavior.

Take, for example, $\psi < 0$, where the Soret-induced separation requires higher heating to destabilize the conductive state than for a pure fluid characterized by $\psi = 0$ (for a review of the multitude of convection states appearing for destabilizing positive ψ see, for example, Huke et al., 2000). Then the off-diagonal coupling between solutal buoyancy and advection of Soret-induced concentration variations described above generates oscillations—traveling waves (TWs) of horizontally propagating rolls occur via a subcritical Hopf bifurcation whenever ψ is sufficiently negative. The bifurcation properties of such oscillatory TW states are shown in Figure 2 for different ψ as a function of the reduced Rayleigh number $r = R/R_c^0$, where $R_c^0 = 1707.76$ marks the convective onset in pure fluids. With increasing flow intensity (Figure 2a), the fluid gets

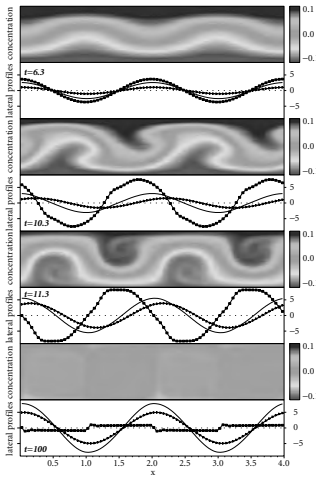

Figure 1. Evolution of convection after perturbing the quiescent conductive state. The concentration distribution in a vertical cross section of the fluid layer is displayed by color-coded plots where highest concentration was initially at the top, and lowest at the bottom. Wave profiles at midheight, $z = 0$, are shown for the fields of vertical velocity w (thin lines), $40\delta T$ (lines with triangles), and $400\delta C$ (lines with squares). The final TW propagates to the left. Parameters are $L = 0.01$, $\sigma = 10$, $\psi = -0.25$, $r = 1.42$, and wavelength $\lambda = 2$. For better visibility two wavelengths are shown. (This figure is also reproduced on page 3 of the color plate section.)

more mixed while simultaneously the TW frequency decreases (Figure 2b) as the flow intensity and the Nusselt number (Figure 2d) approach the pure fluid reference values. Here the mixing is measured by the reduced spatial variance $M = \sqrt{\langle \delta C^2 \rangle / \langle \delta C_{\mathrm{cond}}^2 \rangle}$ of the concentration.

Figure 1 shows the complex spatiotemporal concentration redistribution during the growth of oscillatory convection at slightly supercritical heating. The growth starts generically from perturbations of the conductive state that contain the two critical Hopf modes for counterpropagating TWs with roughly equal amplitudes. First, they linearly superimpose to form SW-like oscillations of growing amplitude with the large Hopf frequency. But then they compete via nonlinear advection with each other; at a critical SW amplitude, advective breaking of the concentration wave triggers a very fast flow-induced transition from SW to TW convection with anharmonic profile, large phase velocity, and large amplitude of the concentration wave. Finally, advective mixing and diffusive homogenization slow down the TW as the concentration differences between left and right turning rolls slowly decrease.

In mixtures with sufficiently negative ψ, there are also uniquely selected stable LTW states of

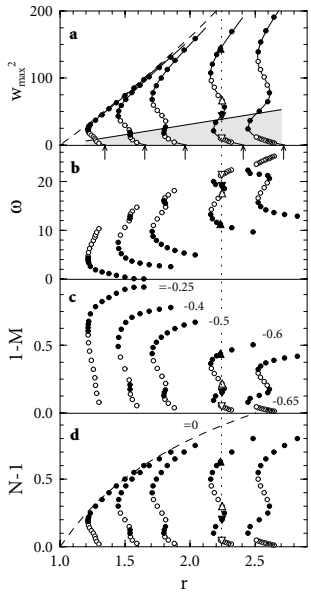

Figure 2. TW–bifurcation diagrams for different Soret coupling strength ψ: (a) squared maximal vertical flow $w_{\max}^2$, (b) frequency ω, (c) degree of mixing $1-M$, and (d) convective contribution to the Nusselt number $N-1$ vs reduced Rayleigh number r. Stable (unstable) TW states are marked by filled (open) symbols. Arrows mark Hopf thresholds $r_{\rm osc}$ for onset of TW convection. The $\psi=0$ pure fluid limit is included in (a) and (d) by the dashed line. TW states on the vertical line are discussed in more detail in Hollinger et al. (1997). Only states in the shaded region of (a) are weakly nonlinear. Parameters are $L=0.01$, $\sigma=10$, and $\lambda=2$.

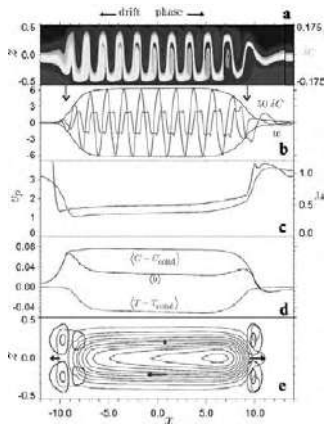

Figure 3. Broad LTW of length $l=17.4$: (a) Concentration deviation δC from global mean (pale gray) in a vertical cross section of the layer. (b) Lateral wave profiles at midheight, $z=0$, of δC (gray), vertical velocity w (black), and its envelope. At the arrows, $w_{\max}=v_{\rm p}$. (c) Mixing number M (gray) and phase velocity $v_{\rm p}$ (black). The variation of the wavelength $\lambda(x)=2\pi\, v_{\rm p}(x)/\omega$ is the same because the LTW frequency ω is a *global* constant. (d) Time averaged deviations from the conductive state at $z=-0.25$ for concentration (upper), temperature (lower), and their sum $(\langle b\rangle)$ measuring the convective contribution to the buoyancy. (e) Streamlines of time averaged concentration current $\langle \boldsymbol{J}\rangle = \langle \boldsymbol{u}\delta C - L\boldsymbol{\nabla}(\delta C - \psi\delta T)\rangle$ (gray) and velocity field $\langle \boldsymbol{u}\rangle$ (black). The latter results from $\langle b\rangle$ and documents roll shaped contributions of $\langle \boldsymbol{u}\rangle\langle\delta C\rangle$ to $\langle \boldsymbol{J}\rangle$ under the fronts and the associated $\langle\delta C\rangle$ redistribution. Thick black and gray arrows indicate $\langle \boldsymbol{u}\rangle$ and transport of positive δC (alcohol surplus), respectively. Thus, in the lower half of the layer, negative δC (water surplus) is transported to the right. Parameters are $L=0.01$, $\sigma=10$, $\psi=-0.35$, $r=1.346$. (This figure is also reproduced on page 3 of the color plate section.)

localized, that is, spatially confined, TWs. They occur at small subcritical heating where extended TWs cannot exist and where the conductive state is strongly stabilized by the Soret effect. Such a strongly nonlinear LTW (Figure 3) is robustly sustained by a complex concentration redistribution process. Therein flow-induced mixing locally reduces the Soret separation and thereby increases the buoyancy to levels that suffice to drive well-mixed fluid flow there. In Figure 3, positive (negative) δC is sucked from the top (bottom) boundary layer into right (left) turning rolls as soon as they become nonlinear under the trailing LTW front. This happens when the vertical velocity w roughly exceeds the local phase velocity v_p (left arrow in Figure 3b) so that regions with closed streamlines appear (Hollinger et al., 1997; Lücke et al., 1998). Within them "dark" ("gray") concentration is transported predominantly in the upper (lower) part of the layer to the right. Mean concentration, on the other hand, migrates mostly to the left along open streamlines that meander between the closed roll regions and that follow the global mean in Figure 3a. The *time-averaged* current of δC (gray lines in Figure 3e) reflects the mean properties of this transport. Since positive and negative (zero) δC is transported away from (towards) the left trailing front, mean concentration accumulates there and causes a strong drop of $M(x)$. In the same way, the leading front's concentration varies and with it, $M(x)$ are strongly increased even beyond the conductive state's values. Thus, unlike TWs, LTWs do not reach a balance among δC injection, advective mixing, and diffusive homogenization on a constant level of small M. Rather LTW rolls collapse under the leading front when $v_{\rm p}$ has grown up to w (right arrow in Figure 3b). Thereafter, concentration is discharged and sustains ahead of the leading front a barrier of $\langle\delta C\rangle$ that prevents the expansion of the conductive state into the LTW.

M. LÜCKE

See also **Thermal convection**

Further Reading

Cross, M.C. & Hohenberg, P.C. 1993. Pattern formation outside of equilibrium. *Reviews of Modern Physics*, 65: 851

de Groot, S.R. & Mazur, P. 1962. *Non-equilibrium Thermodynamics*, Amsterdam: North-Holland

Hollinger, St., Büchel, P. & Lücke, M. 1997. Bistability of slow and fast traveling waves in fluid mixtures. *Physical Review Letters*, 78: 235

Huke, B., Lücke, M., Büchel, P. & Jung, Ch. 2000. Stability boundaries of roll and square convection in binary fluid mixtures with positive separation ratio. *Journal of Fluid Mechanics*, 408: 121

Jung, D. & Lücke, M. 2002. Localized waves without the existence of extended waves: Oscillatory convection of binary mixtures with a strong Soret effect. *Physical Review Letters*, 89: 054502

Köhler, W. & Wiegand, S. (editors). 2002. *Thermal Nonequilibrium Phenomena in Fluid Mixtures*, Berlin and New York: Springer

Landau, L.D. & Lifshitz, E.M. 1959. *Fluid Mechanics*, Oxford: Pergamon Press and Reading, MA: Addison-Wesley (originally published in Russian)

Lücke, M., Barten, W., Büchel, P., Fütterer, C., Hollinger, St. & Jung, Ch. 1998. Pattern formation in binary fluid convection and in systems with throughflow. In *Evolution of Structures in Dissipative Continuous Systems*, edited by F.H. Busse & S.C. Müller, Berlin and New York: Springer, p. 127

Ludwig, C. 1856. Diffusion zwichen ungleich erwärmten Orten gleich zusammengesetzter Lösungen. *Sitzungsberichte der Kaiserliche. Akademie der Wissenschaften (Mathematisch-Naturwissenschaftlicheclasse), Wien*, 65: 539

Platten, J.K. & Legros, J.C. 1984. *Convection in Liquids*, Berlin: Springer

Soret, C. 1879. Sur l'état d'équilibre que prend, au point de vue de sa concentration, une dissolution saline primitivement homogène, dont deux parties sont portées à des températures différentes. *Archives des Sciences: Physiques et Naturelles, Genève*, 2: 48–61

THETA FUNCTIONS

The n-dimensional *theta function* is a function of $n+n(n+1)/2$ complex variables, $\theta(z|\tau)$. The first n coordinates form a vector in an n-dimensional complex space $z=(z_1,\ldots,z_n)$ while the remaining $n(n+1)/2$ variables are entries in a symmetric n-dimensional matrix τ_{ik}; $(i,k=1,\ldots,n)$. The theta function is defined by a Fourier series as

$$\theta(z|\tau)=\sum_{\boldsymbol{m}\in\mathbb{Z}^n}\mathrm{e}^{\{i\pi\boldsymbol{m}\tau\boldsymbol{m}^t+2i\pi z\boldsymbol{m}^t\}},$$

where the n-tuple summation runs over the whole n-dimensional set of integers $\mathbb{Z}^n$, and the imaginary part of the matrix τ is supposed to be positive definite to provide convergence of the series. The defining properties of the theta function are its periodicity and modular properties. The periodicity property is given by the relation

$$\begin{aligned}\theta(z+\boldsymbol{e}_k|\tau)&=\theta(z|\tau),\quad \theta(z+\boldsymbol{e}_k\tau|\tau)\\&=\mathrm{e}^{-i\pi\tau_{kk}-2i\pi z_k}\theta(z|\tau),\quad k=1,\ldots,n,\end{aligned}$$

where only the kth component of the vector $\boldsymbol{e}_k$ is nonzero and equal to unity.

Consider the modular group Γ the group of all $2n\times 2n$ integer matrices γ such that $\gamma J\gamma^t=J$ where

$$J=\begin{pmatrix}0 & -1_n\\ 1_n & 0\end{pmatrix},$$

and 1_n is the unit n-dimensional matrix. Under the action of the modular group, the theta-function transforms as

$$\theta(z|\tau)=\frac{\varepsilon}{\sqrt{\det M(\tau)}}\exp\left\{\frac{1}{2}\sum_{i,k=1}^{n}z_iz_k\frac{\partial}{\partial\tau_{ik}}\det M(\tau)\right\}\theta\left(z'|\tau'\right),$$

where

$$\begin{aligned}M(\tau)&=c\tau+d,z'=(a\tau+d)^{-1}z,\\ \gamma&=\begin{pmatrix}a & b\\ c & d\end{pmatrix},\\ \tau'&=(a\tau+b)(c\tau+d)^{-1},\end{aligned}$$

a,b,c,d are $n\times n$ matrices and $\varepsilon^8=1$.

The theta functions are introduced to construct modular functions in τ-variables of order k defined to satisfy $f(\gamma\circ\tau)=\det(c\tau+d)^kf(\tau)$ and abelian functions in z-variables. Abelian functions $F(z)$ are functions of n complex variables with $2n$ complex periods, $\boldsymbol{T}_i$, $i=1,\ldots,2n$, $F(z+\boldsymbol{T}_i)=F(z)$. The advantage of using theta functions to define modular and abelian functions comes from the rapid convergence of the *theta*-series.

The most important class of abelian functions are abelian functions whose τ-variables are constructed from an algebraic curve X of genus n, given by a polynomial equation $P(\lambda,\mu)=0$. The introduction of local coordinates turns X into a one-dimensional complex analytical variety called the Riemann surface of the curve X. The Riemann surface of genus n can be topologically described as a sphere with n handles. It is always possible to draw, on such a torus, a basis of $2n$-cycles $a_1,\ldots,a_n;b_1,\ldots,b_n$ with intersection numbers $a_i\circ a_j=b_i\circ b_j=0$ and $a_i\circ b_j=-b_j\circ a_i=\delta_{ij}$, where $\circ$ means intersection of corresponding cycles.

Differential and integral calculus can also be developed on X. In contrast to the case of an extended complex plane, or Riemann sphere, which can be considered as a Riemann surface of genus zero, there exists n linearly independent holomorphic differentials $\mathrm{d}w_1,\ldots,\mathrm{d}w_n$ which can be normalized by the conditions $\oint_{a_k}\mathrm{d}w_i=\delta_{ik}$. The period matrix τ of the curve is then given by $\tau_{ik}=\oint_{b_k}\mathrm{d}w_i$. Meromorphic differentials $\mathrm{d}\omega_k$, that is, differentials with poles of order k,

can be also defined on X; usually these differentials are normalized by the condition $\oint_{a_l} \mathrm{d}\omega_k = 0, l = 1, \ldots, n$.

The abelian function $u(\boldsymbol{t}) = u(t_1, \ldots, t_n)$ of n complex variables associated with the curve X of genus n is then defined as

$$u(t_1, \ldots, t_n) = -2\frac{\partial^2}{\partial t_1^2} \log\theta \left(\sum_{k=1}^{n} \boldsymbol{U}_k t_k + \boldsymbol{U}_0 | \tau \right) + c, \tag{1}$$

where the vector $\boldsymbol{U}_k$ is the vector of b-periods of the normalized meromorphic differential $\mathrm{d}\omega_k$, $\boldsymbol{U}_0$ is a vector through which initial data are introduced and c is a constant.

The most developed case is the case of hyperelliptic curves, when the polynomial P is given by

$$P(\lambda, \mu) = \mu^2 - \prod_{k=1}^{2n+1} (\lambda - \lambda_k),$$

where n is the genus and the branching points λ_k, $k = 1, \ldots, 2n+1$ are supposed to be distinct. The holomorphic differentials described above are given in this case by the formula $\mathrm{d}w_k = \lambda^{k-1}\mathrm{d}\lambda/\mu$, $k = 1, \ldots, n$. In the case $n = 1$, the abelian function of the curve is the well-known elliptic function.

The remarkable role of θ functions in the spectral theory of the Schrödinger equation was discovered by Its & Matveev (1975). Consider the spectral problem

$$\left\{ \frac{\partial^2}{\partial x^2} - u(x) \right\} \Psi(x; \lambda, \mu) = \lambda \Psi(x; \lambda, \mu),$$

where $u(x)$ is smooth and real potential, $\Psi(x; \lambda, \mu)$ is an eigenfunction, and λ is the spectral parameter. Suppose that the spectrum consists of $n+1$ continuous segments $[\lambda_1, \lambda_2], \ldots, [\lambda_{2n+1}, \infty]$. Then the potential is given by the formula (1) with $t_1 = x$ and $t_k = \text{const}$ for $k > 1$, while the eigenfunction $\Psi(x; \lambda, \mu)$ is given by the formula

$$\Psi(x; \lambda, \mu) = C \frac{\theta\left(\int_{(\infty,\infty)}^{(\lambda,\mu)} \mathrm{d}\boldsymbol{w} + \boldsymbol{U}_2 x + \boldsymbol{U}_0 | \tau \right)}{\theta\left(\boldsymbol{U}_2 x + \boldsymbol{U}_0 | \tau \right)} \times \exp\left\{ x \int_{(\lambda_0,\mu_0)}^{(\lambda,\mu)} \mathrm{d}\omega_2(\lambda, \mu) \right\}, \tag{2}$$

where C is a normalizing constant, $\mathrm{d}\omega_2(\lambda, \mu)$ is the second kind abelian differential with second-order pole at infinity and zero a_i-periods, $\boldsymbol{U}_2$ is a vector of b_i-periods of $\mathrm{d}\omega_2(\lambda, \mu)$, and the constant vector $\boldsymbol{U}_0$ and point (λ_0, μ_0) are defined by initial conditions. The isospectral deformation of the potential $u(x)$ when the second variable $t_2 = t$ in formula (1) is switched on, while other variables $t_k, k > 2$ remain constant, turns the function $u(x, t)$ into the n-gap solution of the Korteweg–de Vries equation. Equations (1) and (2) form the foundation of the theory of finite-gap solutions of soliton equations. In the limit when the branch points collide in pairs, $\lambda_{2k-1} \to \lambda_{2k}$ $k = 1, \ldots, n$, these formulae become N-soliton formulae. Krichever (1977) generalized the whole theory to other soliton equations and nonhyperelliptic curves.

Introductions to the subject are given in Farkas & Kra (1998) for the theory of Riemann surfaces, Novikov, Chapter 11 in Zakharov et al. (1980), Dubrovin (1981). Mumford (1983, 1984) for theta functions and completely integrable equations, and Belokolos et al. (1994) for algebro-geometric methods of integration of nonlinear equations.

VICTOR ENOLSKII

See also **Elliptic functions; Inverse scattering method or transform; *N*-soliton formulas**

Further Reading

Belokolos, E.D., Bobenko, A.I., Enolskii, V.Z., Its, A.R. & Matveev, V.B. 1994. *Algebro-geometric Approach to Nonlinear Integrable Equations*, Berlin and New York: Springer

Dubrovin, B.A. 1981. Theta functions and nonlinear equations. Russian Mathematical Surveys, 36: 11–80

Farkas, H. & Kra, I. 1998. *Riemann Surfaces*, New York: Springer

Its, A.R. & Matveev, V.B. 1975. Sohrödinger operators with a finite-band spectrum and the N-soliton solutions of the Korteveg–de Vries equation. *Teoreticheskaya i Matematicheskaya Fizika*, 23: 51–68

Krichever, I.M. 1977. The method of algebraic geometry in the theory of nonlinear equations. *Russian Mathematical Surveys*, 32: 180–208

Mumford, D. 1983, 1984. *Tata Lectures on Theta*, vols. 1, 2, Boston: Birkhäuser

Zakharov, V.E., Manakov, S.V., Novikov, S.P. & Pitaevskii, L.P. 1980. *Soliton Theory: Inverse Scattering Method*, Moscow: Nauka (in Russian)

THREE-BODY PROBLEM

See ***N*-body problem**

THREE-WAVE INTERACTION

See ***N*-wave interactions**

THRESHOLD PHENOMENA

Defined in the dictionary as an "intensity below which a mental or physical stimulus cannot be perceived and can produce no response," the term *threshold* has deep roots in our language, representing a collective awareness of strong nonlinearity. Above threshold, the effect of a stimulus changes dramatically from that below, as is indicated by such common phrases as the "tipping point" and the "last straw." Examples of threshold phenomena abound in physics, engineering, nonlinear mathematics, chemistry, biology, and neuroscience.

Applications of the Threshold Concept

In nonlinear optics, the threshold for laser oscillation specifies a level of pump power below which only a small amount of incoherent light is emitted from the laser, while above threshold a brilliant, highly directed beam of output light is observed. Beginning with the wall switch, electrical engineers have devised many varieties of threshold circuits that change rapidly from one voltage level to another when an input variable exceeds a certain value; indeed, a digital computer can be viewed as a large collection of interacting threshold devices. Also the threshold logic unit (TLU), comprising a switch with input channels having adjustable weights, is a useful component of learning systems for pattern recognition (Nilsson, 1990).

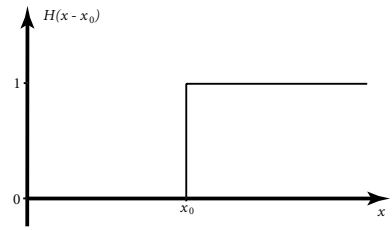

Figure 1. A Heaviside step function.

Mathematical representations of switching devices often involve the Heaviside step function,

$$H(x - x_0),$$

a generalized function that is zero for $x < x_0$ and one for $x > x_0$, where x_0 is the threshold as shown in Figure 1. In phase space models of nonlinear dynamic systems, one often finds a *separatrix*, or critical surface across which solution trajectories have very different behaviors. Noting this, mathematician cum meteorologist Edward Lorenz famously asked: "Does the flap of a butterfly's wings in Brazil set off a tornado in Texas?"—not only coining a dramatic metaphor for threshold phenomena and launching modern studies of chaos, but also leading philosophers to examine what is meant by causality. Is it only the *last* straw that should be blamed for breaking the camel's back? Or are *all* the straws that were loaded onto the beast to some degree complicit?

In the realms of physical chemistry, a reaction-diffusion (excitable) system rests quietly until stimulated above its threshold for self-supporting activity, whereupon traveling waves, spirals, and scroll waves are typically observed to emerge. In biology, examples of threshold phenomena include the germination of a seed at a critical (threshold) level of ambient moisture and the insemination of an ovum, in addition to the birth of life itself from the chemical components of the Hadean oceans some 3.5 billion years ago.

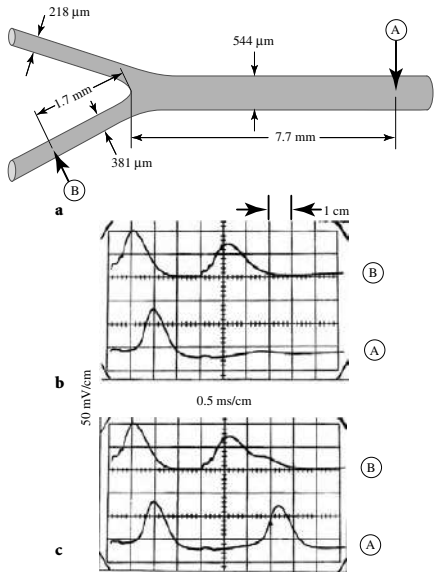

Figure 2. Threshold action in a branching region of a squid giant axon. The interpulse interval is slightly longer in (c) than in (b).

Threshold Effects in Neuroscience

As one would suppose from introspection, the field of neuroscience offers many examples of threshold phenomena which have become known since the observation of "all-or-none" response of a neuron was proposed by Edgar Adrian in 1914 (Adrian, 1914). This threshold behavior of a neuron was used by psychiatrist Warren McCulloch and mathematician Walter Pitts in 1943 to formulate the first computer model of the human brain McCulloch & Pitts (1943). Their model assumes each neuron to be represented by a single Heaviside step function, which jumps from the off (zero) to the on (one) state when a linear sum of input (dendritic) signals exceeds a threshold value. In 1958, Frank Rosenblatt introduced the "perceptron" which employs TLUs as the basic emenents of a brain model (Rosenblatt, 1958).

Recent studies of dendritic dynamics suggest far greater complexity, with the possibility of threshold effects occurring at the branching regions of incoming fibers (Stuart et al., 1999). In Figure 2 are displayed some experimental measurements of nerve impulse transmission through a branching region in the giant axon of a squid (Scott, 2002). Figure 2(a) shows the geometry of the preparation (not to scale), indicating the electrode positions where upstream (B) and downstream (A) recordings were made. The preparation was stimulated with two pulses, which are seen in the upper traces of both Figures 2(b) and 2(c). In these experiments, the spacing between the two incoming impulses was under experimental control, and below a certain threshold value of this impulse interval—that shown in Figures 2(b) and 2(c)—it is seen that the second impulse no longer makes it through. Besides interpulse interval, several other neural parameters can result in such a threshold effect, including branch geometry, ionic concentrations, fatigue, and narcotization level.

As the dendrites of many neurons are known to carry active impulses (action potentials) (Stuart et al., 1999), it appears that the branching regions of dendrites can act as threshold devices (switches), greatly increasing our estimates of the ability of a neuron to process information (Scott, 2002).

ALWYN SCOTT

See also **Butterfly effect; Excitability; Flip-flop circuit; Lasers; McCulloch–Pitts network; Multiplex neuron; Nerve impulses; Phase space; Reaction-diffusion systems**

Further Reading

Adrian, E.D. 1914. The all-or-none principle in nerve. *Journal of Physiology (London)* 47: 460–474

McCulloch, W.S. & Pitts, W.H. 1943. A logical calculus of the ideas immanent in nervous activity. *Bulletin of Mathematical Biology* 5: 115–133

Nilsson, N.J. 1990. *Learning Machines*, 2nd edition, San Mateo, CA: Morgan Kaufmann

Rosenblatt, F. 1958. A probabilistic model for information storage and organization in the brain. *Psychology Review* 65: 386–408

Scott, A.C. 2002. *Neuroscience: A Mathematical Primer*, New York: Springer-Verlag

Stuart, G., Spruston, N. & Häusser, M. 1999. *Dendrites*, Oxford: Oxford University Press

TIME-SERIES ANALYSIS

Predicting total eclipses of the moon or the sun is an art that dates back to mankind's oldest civilizations. Nonetheless, it represents a class of very modern analytic tools: the analysis of time-series data. A time-series is a set of measurements s_n, $n = 1, \ldots, T$, whose index n refers to the time t when the measurement is recorded by $n\tau = t$, τ is the sampling interval. For time-dependent phenomena, this index carries part of the information which is destroyed, for example, by a random reshuffling of the temporal order of the measurements. If one wishes to make use of this property in data analysis, particular statistical methods are required which are able to characterize temporal correlations inside the data. Typical goals in time-series analysis are predictions, data classification, signal manipulation, and system identification.

Today's technical facilities for data acquisition and data storage call for efficient time-series tools. To mention a few examples, in medicine (particularly cardiology and neurology), there is a need for automated diagnostics (i.e., data classification). In finance or weather and climate research, data-driven prediction methods are relevant, since model equations are either lacking (economy) or expensive to solve (weather). In modern telecommunications and automatic speech recognition, noise reduction is an essential issue, where time-series analysis should supply the background for signal separation.

The above examples show that unlike data of the positions of the planets, whose analysis enabled Johannes Kepler to derive the laws of planetary motion, modern time-series problems are concerned with data that have a complicated, strong aperiodic component. All data analysis methods start from some paradigm about the origin of the observed signatures and irregularities. This background is indispensable for a sound interpretation of the statistical quantities thus obtained, or for an estimate of the validity of the consequences drawn from the results. However, the large number of different approaches in time-series modeling supplies a corresponding diverse set of time-series analysis methods. We focus here on the two most general approaches, both of which represent a whole theoretical framework and not just a particular aspect.

Linear stochastic models are a well-developed class of time-series models. Being linear, their properties

can be fully and rigorously derived from their model equations. However, in order to generate aperiodic time-series data, such models require stochastic inputs. Auto regressive models AR(M),

$$s_{n+1} = \sum_{k=0}^{M-1} a_k s_{n-k} + \xi_n,$$

where ξ_n is Gaussian distributed white noise ($\langle \xi_l \xi m \rangle = \delta_{l,m}$) with unit variance, represent the time discretized motion of the superposition of $M/2$ damped harmonic oscillators driven by noise, if the coefficients a_k fulfill certain stability conditions. The output is therefore characterized by $M/2$ frequencies and the corresponding damping coefficients, such that a spectral analysis is the most suitable analysis tool (*See* **Spectral analysis**). Thus, AR-models are suitable for data sets that have a few pronounced peaks in their power spectrum. If the observed power spectrum instead is broad band, another linear model, the moving average model MA(N), can be more reasonable:

$$s_{n+1} = \sum_{k=0}^{N-1} b_k \xi_{n-k},$$

where ξ_n is again white Gaussian noise. Notice that there is no feedback of the observable s, so that this model just averages over the independent noise inputs and hence creates colored noise. In the limits $N, M \to \infty$, both model classes are equivalent. For practical purposes where a small number of coefficients is desirable, a combination of both, the ARMA(M,N)-model, is often used. The coefficients of such models can be fit to observed data, for example, by solving least-squares problems (Box & Jenkins, 1976).

The well-known sunspot number time series of solar activity with its pronounced 11-year period can be well captured by an AR-model. ARMA models are also rather suited to describe many noise-dominated signals such as sound emission signals in technical environments, and they are used to model single phonemes of human speech in automatic speech recognition systems. ARMA-models are hence employed for data-driven predictions and signal classification tasks. They are often useful if the signal is either dominated by some few frequencies or when it is really noisy. However, the linearity of the model behind translates into the fact that the observables should be Gaussian random variables themselves, and that all higher-order statistics beyond the power spectrum and the auto-correlation function are fully determined by either of these two.

From many model systems and physical laboratory experiments arises a different class of sources for aperiodic time-series data: so-called chaotic dynamical systems. Aperiodicity here comes from intrinsic instabilities without random inputs, and nonlinearity

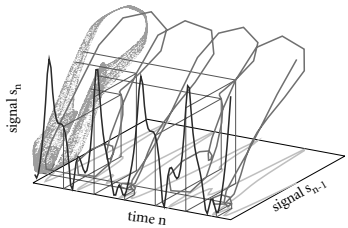

Figure 1. Sketch of the time-delay embedding procedure: The time series s_n (plotted in the frontal plane) combined with its time shifted version (in the bottom plane) forms a sequence of vectors (the curve in space), whose projection along the time axis accumulates to a set of points representing (in this particular case) a strange attractor together with an invariant measure on it. The data are voltages measured in a chaotic electric resonance circuit.

destroys the superposition principle, such that a Fourier decomposition of the signal is not useful. Higher-order statistics is not trivially related to second-order statistics. Instead of a statistical characterization, one would here try to reconstruct the deterministic and dynamic origin of the signal.

If one assumes that a given experimental observable represents the deterministic dynamics in some non-observed and even unknown phase space, the concept of phase space reconstruction by embedding is needed: As proven by Takens (1981), the set of delay vectors obtained from a scalar time series by joining successive observations, $\boldsymbol{s}_n = (s_n, s_{n-1}, s_{n-2}, \ldots, s_{n-m+1})$, is equivalent to a set of phase space vectors of the underlying dynamical system, provided that the embedding dimension m fulfills $m > 2D_f$ (see Figure 1). Here, D_f is the attractor dimension of the underlying dynamical system (*See* **Attractors; Dimensions; Fractals**). Hence, successive vectors $\boldsymbol{s}_n$ are deterministically related to each other by an unknown function $\boldsymbol{s}_{n+1} = \boldsymbol{F}(\boldsymbol{s}_n)$, which reduces to an unknown scalar function $s_{n+1} = f(\boldsymbol{s}_n)$, since the other components of $\boldsymbol{s}_{n+1}$ are just copied from $\boldsymbol{s}_n$.

In a practical analysis, one represents the time-series data in embedding spaces with increasing dimension m and searches for signatures of determinism. One model free approach for this is the estimation of the fractal dimension of the set of delay vectors in the embedding space, which should saturate at the value D_f for $m > D_f$. Of interest is predictability: one can try to extract the unknown function $f(\boldsymbol{s}_n)$ from the time series, by selecting a suitable model for f and then solving the least-squares problem $\sum (s_{n+1} - f(\boldsymbol{s}_n))^2 = \min$, where the minimization is done with respect to parameters in f. In the simplest case, f is approximated by a constant in a neighborhood of the actual observation $\boldsymbol{s}_n$. Then, the predictor is the average over the future values of all neighboring vectors

s_k of s_n, $\hat{s}_{n+1} = \langle s_{k+1} \rangle$, where $||s_k - s_n|| < \varepsilon$ with some suitable norm and some suitably small ε (also called the "Lorenz method of analogues"). Regardless of how the function f is represented, the relation $\hat{s}_{n+1} = f(s_n)$ will yield only good predictions for s_{n+1} if the embedding dimension m is large enough for the delay vectors to be equivalent to the unknown phase space vectors of the underlying dynamical system. In such an embedding space, the delay vectors form a finite sample according to the underlying invariant measure of the dynamical system, so that, in principle, all characteristics of the latter (Lyapunov exponents, entropies) can be determined (*See* **Chaotic dynamics**).

Such methods have been successfully applied to many physical laboratory experiments, but more recently successful applications to real-world data have been reported, such as noise reduction for human voice, wind speed prediction for wind farms, diagnostics on human heart rate data, epilepsy prediction, and machine wear detection in technical production systems. The extension of the theory to noise-driven nonlinear systems and to nonstationary data has recently been tackled, but highly nonrecurrent data such as economics data will probably remain untractable.

HOLGER KANTZ

See also **Attractors; Chaotic dynamics; Dimensions; Fractals; Spectral analysis**

Further Reading

Abarbanel, H.D.I. 1996. *Analysis of Observed Chaotic Data*, New York: Springer

Box, G.E.P. & Jenkins, G.M. 1976. *Time Series Analysis*, San Francisco: Holden-Day

Farmer, J.D. & Sidorowich, J.J. 1987. Predicting chaotic time series. *Physical Review Letters*, 59: 845

Kantz, H. & Schreiber, T. 1997. *Nonlinear Time Series Analysis*, Cambridge and New York: Cambridge University Press

Lorenz, E.N. 1969. Atmospheric predictability as revealed by naturally occuring analogues. *Journal of Atmospheric Sciences*, 26: 636

Takens, F. 1981. Detecting strange attractors in turbulence. In *Dynamical Systems and Turbulence*, edited by, D.A. Rand & L.S. Young Berlin and New York: Springer, p. 366

TODA LATTICE

The Hamiltonian system governing the longitudinal oscillations of a chain of unit point masses connected by identical springs is

$$\begin{aligned} \dot{q}_n &= \dot{p}_n, \\ \dot{p}_n &= V'(q_{n+1} - q_n) - V'(q_n - q_{n-1}), \end{aligned} \tag{1}$$

where $-V'$ is the restoring force of the springs and q_n is the displacement of the nth mass from equilibrium. Morikazu Toda (Toda, 1981) introduced the potential (scaled here so that two physical parameters disappear)

$$V(r) = e^{-r} + r - 1, \tag{2}$$

and discovered explicit solutions of (1). He obtained periodic traveling waves, in terms of elliptic functions, and two-soliton solutions in terms of sech^2. (The term $(r-1)$ makes $V(r) \sim r^2/2$ for small r; it cancels out in the problems considered below.)

This mass-spring chain is the Toda lattice. It is valuable as a solvable model of one-dimensional lattice dynamics; it is frequently used to illustrate fundamental constructions common to many integrable systems; and it appears, sometimes in surprising ways, in a variety of physical and mathematical problems.

The Infinite and Periodic Lattices

All the special properties of the Toda lattice flow from a Lax representation, $\dot{\mathsf{L}} = [\mathsf{B}, \mathsf{L}]$, which implies that eigenvalues and certain other spectral data of L are independent of time. For many purposes, it is convenient to write L and B in new coordinates. With the definition

$$a_n = \tfrac{1}{2}\, \mathrm{e}^{-(q_{n+1} - q_n)/2}, \quad b_n = \tfrac{1}{2}\, p_n, \tag{3}$$

the exponential nonlinearity in (2) becomes polynomial:

$$\dot{a}_n = a_n(b_n - b_{n+1}), \quad \dot{b}_n = 2\,(a_{n-1}^2 - a_n^2). \tag{4}$$

The standard Poisson bracket on q_n, p_n induces a (nonstandard) Poisson bracket on a_n, b_n, in which the only nonzero relations are

$$\{a_n, b_n\} = -\frac{1}{4} a_n, \quad \{a_n, b_{n+1}\} = \frac{1}{4} a_n. \tag{5}$$

The Lax operators are discretized Schrödinger operators with potentials a_n, b_n, acting on sequences $\mathbf{y} = (\ldots, y_{-1}, y_0, y_1, \ldots)$:

$$\begin{aligned} (\mathsf{L}\mathbf{y})_n &= a_{n-1} y_{n-1} + b_n y_n + a_n y_{n+1}, \\ (\mathsf{B}\mathbf{y})_n &= a_{n-1} y_{n-1} - a_n y_{n+1}. \end{aligned} \tag{6}$$

A (finite or infinite) tridiagonal symmetric matrix, such as L, is called a "Jacobi matrix." In terms of the shift operator $\Delta z_n = z_{n+1}$, which is a convenient abbreviation,

$$\mathsf{L} = \Delta^{-1} a + b + a\Delta, \tag{7}$$

where a and b are the diagonal matrices $\mathrm{diag}(a_n)$, $\mathrm{diag}(b_n)$. Constants of motion derived from the Jacobi operator L will be in involution, that is, they have zero Poisson bracket.

Thanks to its Lax representation, methods used in the study of other soliton equations also apply to the Toda lattice.

The Bi-infinite Lattice with Decaying Initial Condition (Toda, 1981)

According to (3), $(q_{n+1} - q_n) \to 0$ and $p_n \to 0$ translates to $a_n \to \frac{1}{2}$, $b_n \to 0$. The initial value problem is studied by a discrete version of the inverse scattering method. The unperturbed eigenvalue operator at $n = \pm\infty$ is $\mathsf{L}_0 = \frac{1}{2}(\Delta^{-1} + \Delta)$, which has the bounded "plane wave" eigenfunctions $y_n = z^{\pm n}$, $|z| = 1$, for $\lambda = (z + z^{-1})/2 \in [-1, 1]$. This relation between "energy" λ and "momentum" z is the analog of $\lambda = k^2$ in the Schrödinger equation. The scattering matrix is a function of momentum and is defined on $|z| = 1$. Bound states may occur for $\lambda < -1$ and $\lambda > 1$; these correspond to solitons moving to the left and to the right, respectively. In the absence of solitons (and with a certain condition on the reflection coefficient), the large-time behavior consists of a decaying wave train for $|n/t| < 1$, vanishingly small motion when $|n/t| > 1$, and a connecting regime described by a Painlevé transcendent (Kamvissis, 1993).

Constants of motion of the infinite lattice can be computed explicitly as $I_k := \mathrm{Trace}\,\frac{1}{k}(\mathsf{L}^k - \mathsf{L}_0^k)$ (L_0^k removes a divergent term). The Hamiltonian equations generated by the I_k are found by use of the Poisson bracket (5).

The Periodic Lattice (Toda, 1981)

The potential in the Lax operator is periodic, say, period N. As in the theory of Hill's equation, one introduces a Floquet multiplier and Floquet solutions by imposing the condition

$$y_{N+n} = \rho y_n. \tag{8}$$

L and B then reduce to matrices:

$$\mathsf{L}(\rho) = \begin{pmatrix} b_1 & a_1 & 0 & \dots & \rho^{-1} a_N \\ a_1 & b_2 & a_2 & \dots & 0 \\ 0 & a_2 & \ddots & \ddots & \vdots \\ \vdots & & \ddots & \ddots & a_{N-1} \\ \rho\, a_N & \dots & \dots & a_{N-1} & b_N \end{pmatrix}, \tag{9}$$

$$\mathsf{B}(\rho) = \begin{pmatrix} 0 & -a_1 & 0 & \dots & \rho^{-1} a_N \\ a_1 & 0 & -a_2 & \dots & 0 \\ 0 & a_2 & \ddots & \ddots & \vdots \\ \vdots & & \ddots & \ddots & -a_{N-1} \\ -\rho\, a_N & \dots & \dots & a_{N-1} & 0 \end{pmatrix}. \tag{10}$$

The parameter ρ cancels from the Lax equation. The characteristic polynomial $\det(\mathsf{L}(\rho) - \lambda\mathbb{I})$ is a rational function whose coefficients are independent of time. The function $\rho(\lambda)$ obtained by solving the characteristic equation for ρ is defined on the λ–plane with branch cuts, and determines a compact Riemann surface. For Toda's traveling wave, there are only two branch cuts; this fact is responsible for the occurrence of elliptic functions in his solution formula.

Every energy surface is compact, so that the solution curves lie on tori; abstractly, these are the (real) Jacobian varieties associated with the Riemann surface. Action variables can be written explicitly as loop integrals. The solution of the periodic Toda lattice is expressed in terms of theta functions.

The Free Toda Lattice and Lie Theory

Many features common to integrable systems are illustrated by an example due to Jürgen Moser.

The Free Toda Lattice (Toda, 1981)

Particles number 0 and $(N + 1)$ are pulled to $-\infty$ and $+\infty$, respectively. (3) implies that $a_0 = a_N = 0$, and the corner entries in $\mathsf{L}(\rho)$ and $\mathsf{B}(\rho)$ disappear. The resulting matrices will be written simply as L, B.

Springs governed by potential (2) resist compression and are encouraged to expand. Therefore, there will now be no confining force on the remaining springs. The masses move apart as $t \to \pm\infty$, and behave asymptotically like free particles. As $t \to \pm\infty$, $(q_{n+1} - q_n) \to \infty$, whence $a_n \to 0$, the matrix $\mathsf{L}(t)$ becomes diagonal, and the entries $b_n = p_n/2$ approach the eigenvalues of $\mathsf{L}(0)$. Thus, the eigenvalues are the momenta of the free particles. As $t \to -\infty$, these are arranged with the slowest particle farthest to the right; after interaction and a phase shift, the particles emerge as $t \to +\infty$ with the fastest to the right. This is soliton interaction reduced to bare essentials. The diagonalization of $\mathsf{L}(t)$ as $t \to +\infty$, with the eigenvalues (momenta) ordered, is called the "sorting property," and points to a connection between isospectral flows and numerical linear algebra.

For tridiagonal L, the number of eigenvalues is exactly half the number of entries, and they suffice for integrability. Remarkably, the Lax equation $\dot{\mathsf{L}} = [\mathsf{B}, \mathsf{L}]$ (with appropriate B), is completely integrable even when L is a generic symmetric matrix. The additional constants of motion required are constructed in Deift et al. (1986). The sorting property again holds; it is related to the QR diagonalization algorithm in numerical linear algebra.

The free Toda lattice is perhaps the simplest integrable system with a clear Lie-algebraic generalization. If one sets $\mathrm{Trace}\,\mathsf{L} = 0$ in (9), that is, total momentum $= 0$, then L belongs to $\mathfrak{sl}_N$, the Lie algebra of $N \times N$ matrices with trace zero. Let $\{h_i\}$ be a basis for the diagonal matrices in $\mathfrak{sl}_N$. The matrices $e_{\pm i}$ with a single 1 in the $(i, i+1)$, resp, $(i+1, i)$ entry, and zeros elsewhere, are called "raising and lowering operators." There are analogs of $e_{\pm i}$, h_i in the class of split real semisimple Lie algebras, such as the algebra

of symplectic matrices. The Lax pair, written as

$$\mathsf{L} = \sum_{i=1}^{N-1} [\beta_i h_i + a_i(e_i + e_{-i})],$$
$$\mathsf{B} = \sum_{i=1}^{N-1} a_i(-e_i + e_{-i}),$$

makes sense in those algebras. In the corresponding generalized mass–spring systems, some particles will be governed by modifications of (2) (Olshanetsky & Perelomov, 1994; Guest, 1997; Reyman & Semenov-Tyan-Shansky, 1994; Semenov-Tyan-Shansky, 1994 a,b).

The extension to Lie algebras is not just generalization for sake of generalization. It illuminates concrete matrix calculations. There is an abstractly defined Poisson bracket, the Kostant–Kirillov bracket, of which (5) is a special case. Hamiltonian equations with respect to this Poisson bracket always have the Lax form, $\dot{\mathsf{X}} = [\mathsf{Y}, \mathsf{X}]$. One of the fundamental properties of Lax equations, the representation of the solution by means of a factorization in the Lie group, is a general Lie-theoretic phenomenon that specializes to many different integrable systems and, in particular, yields involutivity of the constants of motion $\mathrm{Trace}\mathsf{L}^k$ (Guest, 1997; Semenov-Tyan-Shansky, 1994 a,b)

For the free Toda lattice, the factorization method is simple linear algebra, but it already conveys the basic idea.

Here, as well as later, it is convenient to redefine

$$a_n = \exp(q_n - q_{n+1}),\ b_n = -p_n. \tag{11}$$

In terms of the shift operator (7), L and B then become

$$\mathsf{L} = \Delta^{-1}a + b + \Delta, \quad \mathsf{B} = -\Delta^{-1}a. \tag{12}$$

($\mathsf{L} = b + \Delta$ or $\mathsf{B} = b + \Delta$ will give the same $\dot{\mathsf{L}}$.) Given the initial value $\mathsf{L}(0)$, write

$$\exp(t\mathsf{L}(0)) = n_-(t)^{-1}d(t)n_+(t) := n_-(t)^{-1}b_+(t) \tag{13}$$

with $n_{\pm(t)}$ upper/lower triangular having 1's on the diagonal and $d(t)$ diagonal; this is just Gaussian elimination. Then

$$\mathsf{L}(t) = b(t)\mathsf{L}(0)b(t)^{-1} \text{ satisfies } \dot{\mathsf{L}}(t) = [B(t), \mathsf{L}(t)], \tag{14}$$

where $\mathsf{B}(t) = \mathsf{L}(t)_+$ is the upper triangular part of $\mathsf{L}(t)$.

Similarly, one finds the solutions of the Hamiltonian equations generated by the constants of motion I_{k+1} (referred to as "higher Toda flows"). One introduces a separate time variable t_k for each of these systems and now factors $\exp(t_k\mathsf{L}(0)^k)$. The resulting $\mathsf{L}(t_k)$ satisfies

$$\frac{\partial \mathsf{L}}{\partial t_k} = [\mathsf{B}_k, \mathsf{L}], \quad \text{with } \mathsf{B}_k = (\mathsf{L}^k)_+. \tag{15}$$

(L^k arises because $\nabla I_{k+1} = \mathsf{L}^k$). The simultaneous solution of (15) is a multi-parameter flow, $\mathsf{L}(t_1, \ldots, t_{N-1})$, on phase space ($t_1$ is the original t). Compatibility of these equations, that is, equality of mixed partial derivatives of L, is equivalent to the involutivity of the I_k. For an infinite lattice, there are infinitely many equations (15), and infinitely many time variables $\mathbf{t} = (t_1, t_2, \ldots)$. Many soliton hierarchies have the same general form; for the higher KdV equations, for example, $\mathsf{L} = \mathrm{d}^2/\mathrm{d}x^2 + u(x)$ and $\mathsf{B}_k = (\mathsf{L}^{(2k+1)/2})_+$.

In Gaussian elimination, as in (13), d_{nn} is known to be τ_n/τ_{n-1}, where τ_n is the upper left $n \times n$ minor determinant of $\exp[t\mathsf{L}(0)]$. Tracing through the factorization steps, one finds the Hirota formula

$$a_n(t) = a_n(0)\frac{\tau_{n+1}(t)\tau_{n-1}(t)}{\tau_n(t)^2}, \tag{16}$$

which implies

$$a_n = \frac{\mathrm{d}^2}{\mathrm{d}t^2}\ln\tau_n, \quad b_n = \frac{\mathrm{d}}{\mathrm{d}t}\ln\frac{\tau_n}{\tau_{n-1}}.$$

These τ_n are prototypes of a fundamental object in the theory of soliton hierarchies, the "τ-function," which elsewhere occurs in far more complex settings.

The τ-functions have a representation-theoretic meaning. They are the matrix elements

$$\tau_n(t) = \langle \exp(t\mathsf{L}(0))\, \mathbf{e}_1 \wedge \mathbf{e}_2 \wedge \cdots \wedge \mathbf{e}_n \mid \mathbf{e}_1 \wedge \mathbf{e}_2 \wedge \cdots \wedge \mathbf{e}_n \rangle \tag{17}$$

in the representation of the Lie group SL_N on the n^{th} exterior power of $\mathbb{R}^N$ (totally antisymmetric covariant tensors of order n). This formula gives precisely the $n \times n$ minor determinant of $\exp(t(0))$. The skew-vector $\mathbf{e}_1 \wedge \ldots \wedge \mathbf{e}_n$ is the highest weight vector of the representation; it is annihilated by all raising operators. One may think of it as a vacuum vector and of (17) as a vacuum expectation value.

Loop Algebras and Affine Lie Algebras

The lower/upper factorization (13), solution (14), the τ-functions arising from the diagonal part in this factorization, and their interpretation in terms of group representations are fundamental features of integrable systems. The free Toda lattice affords a transparent illustration; more sophisticated versions of these ideas, set in other Lie algebras and groups, apply to a wide variety of equations. "Loop algebras" and "affine Lie algebras" are particularly useful in the theory of the periodic Toda lattice.

The loop algebra, $\widetilde{\mathfrak{sl}_N}$, is an infinite-dimensional Lie algebra whose elements are trace zero matrices $\mathsf{X}(\rho)$ with entries that are polynomials in ρ and ρ^{-1}. Such $\mathsf{X}(\rho)$ are called "loops," because the mapping $\mathsf{X} : \{|\rho| = 1\} \mapsto \mathfrak{sl}_N$ gives a closed curve, that is, "loop," of matrices. The Lie bracket is still the matrix commutator.

The Lax operators (9) and (10), for the periodic Toda lattice, belong to $\widehat{sl}_N$. To solve the periodic Toda lattice by factorization, one prescribes the initial value $\mathsf{A}(\rho)$ of $\mathsf{L}(\rho)$ and seeks matrix functions $g_\pm(t,\rho)$ for which

$$\exp(t\mathsf{A}(\rho)) = g_-(t,\rho)^{-1} g_+(t,\rho). \tag{18}$$

These $g_\pm(\cdot,\rho)$ are required to be analytic inside (resp. outside) the circle $|\rho|=1$; this is the analog of lower/upper in (13). The eigenvector $v(\lambda,\rho(\lambda))$ of $\mathsf{A}(\rho)$, which is a function on the Riemann surface $\det(\mathsf{A}(\rho)-\lambda\mathbb{I})=0$, determines $g_\pm(t,\rho)$. The former is expressed in terms of theta functions; hence, so are $g_\pm$ and also $\mathsf{L}=g_+\mathsf{A}g_+^{-1}$ (Reyman & Semenov-Tyan-Shansky, 1994).

To obtain the τ-functions from a Lie algebra representation, one must introduce an extension of the loop algebra, the "affine" Lie algebra $\widehat{sl}_N$. (Affine Lie algebras give the name to affine Toda field theory, described below.)

The affine algebra has one extra element $\hbar$, which, in some respects, acts like an identity matrix. It has zero bracket with all loops; however, the ordinary matrix commutator in $\widehat{sl}_N$ is modified so that $\hbar$ can arise as a Lie bracket of loops. This would not be possible if $\hbar$ were truly the identity, since a matrix commutator $[\mathsf{X}(\rho),\mathsf{Y}(\rho)]$ must have trace zero. The extended algebra contains loops that behave as annihilation and creation operators: they satisfy $[a_k^*, a_k]=\hbar$. Thanks to this modification, the familiar realization of the Heisenberg commutation relations by multiplication and differentiation operators becomes available in the study of representations of $\widehat{sl}_N$.

The τ-functions for the periodic Toda lattice are obtained as vacuum expectation values, analogous to (17), in certain representations of the affine Lie algebra; they turn out to be theta functions and again satisfy the Hirota equations (16). For the free Toda lattice, τ-functions also arose from the diagonal factor in n_-dn_+. There is a similar factorization in the affine group $\widehat{SL}_N$. This group and the diagonal factor in the lower/upper factorization are rather complicated objects. In particular, the determinant of d will be an infinite determinant.

The matrices e_0 (resp. f_0) with the corner elements $\rho\, e_{N1}$, resp. $\rho^{-1} e_{1N}$ in (9), (10) have an intrinsic meaning (they are raising resp. lowering operators in $\widehat{sl}_N$). Therefore, the periodic Toda lattice will generalize to the algebra of loops with values in a semisimple Lie algebra.

An affine Lie algebra also provides the setting for a remarkable unification of two of the most important soliton systems, the Toda lattice and the Ablowitz–Kaup–Newell–Segur (AKNS) equations. From the solution $a_n(\mathbf{t}), b_n(\mathbf{t})$ of the Lax equations (15) for the infinite lattice, one can build functions $q_n(\mathbf{t}), r_n(\mathbf{t})$, which, for every n, satisfy the general AKNS hierarchy, with t_1 playing the role of x. For example, the simultaneous solution $a_n(t_1,t_3), b_n(t_1,t_3)$ of the Toda equations and the higher Toda flow generated by Trace L^4 will be transformed into solutions $q_n(x,t_3), r_n(x,t_3)$ of the modified KdV (MKdV) equation. A kind of Bäcklund transformation (precisely, a Schlesinger transformation) connects q_n, r_n and $q_{n\pm1}, p_{n\pm1}$. As a special case, solutions of the free Toda lattice correspond to soliton-like potentials for AKNS.

This result can be obtained by operations on formal series, but the Lie-theoretic explanation is more illuminating (Bergvelt & ten Kroode, 1988). The 2×2 matrix in the AKNS scattering problem depends on a (spectral) parameter and so belongs to the loop algebra $\widehat{sl}_2$. There is a representation of the affine extension $\widehat{sl}_2$ in which the Heisenberg subalgebra, mentioned above, has infinitely many vacuum vectors killed by the a_k^*. The vacuum expectation values are the Toda τ-functions τ_n, and the AKNS variables are determined by $q_n = -\tau_{n+1}/\tau_n$, $r_n=\tau_{n-1}/\tau_n$.

The Two-dimensional Toda Lattice

The Toda-AKNS family has a sweeping generalization related to the Kadomtsev–Petviashvili equation (KP). It consists of four Lax equations which involve two infinite families of time variables, t_k, x_k. A continuum limit of this system was encountered in the study of deformations of a two-dimensional oil–water interface (Hele-Shaw flow) and has revealed an integrable structure of conformal mappings. This is sketched in the next section.

The operator L in (12) is replaced by a formal series, and a second operator M is introduced:

$$\mathsf{L} = \Delta + u_0 + u_1\Delta^{-1} + u_2\Delta^{-2} + \cdots, \tag{19}$$

$$\mathsf{M} = \Delta^{-1} + v_0 + \Delta v_1 + \Delta v_2 + \cdots. \tag{20}$$

The u_k, v_k are infinite diagonal matrices. Two of the Lax equations are

$$\frac{\partial \mathsf{L}}{\partial t_k} = [\mathsf{B}_k, \mathsf{L}],\ \mathsf{B}_k = (\mathsf{L}^k)_+,$$

$$\frac{\partial \mathsf{L}}{\partial x_k} = [\mathsf{C}_k, \mathsf{L}],\ \mathsf{C}_k = (\mathsf{M}^k)_-. \tag{21}$$

The subscripts $\pm$ denote projections on the positive/negative powers of Δ (analog of upper/lower triangular). In the other two equations, L is replaced by M (Ueno & Takasaki, 1984).

Equations (21) specialize to the usual Toda lattice, the equations $\dot{\mathsf{L}}=[\mathsf{B},\mathsf{L}]$ for banded matrices L, and an extension of the Toda lattice in which the q_n depend on two variables. This is the "two–dimensional Toda lattice" (2DTL).

The 2DTL is obtained as follows. The compatibility conditions of the two systems in (21) are "zero curvature equations." With the abbreviations $x_1=x, t_1=t$,

the first of these is

$$\frac{\partial \mathsf{B}}{\partial x} - \frac{\partial \mathsf{C}}{\partial t} + [\mathsf{B}, \mathsf{C}] = 0. \tag{22}$$

Following the one-dimensional case (12), let $\mathsf{B} = -\Delta^{-1}a$ and $\mathsf{C} = b + \Delta$. a_n, b_n, still given by (11), are now functions of t and x. (22) becomes

$$(a_n)_x = a_n(b_{n+1} - b_n),\ (b_n)_t = a_n - a_{n-1}$$

or

$$(q_n)_{xt} = \exp(q_{n-1} - q_n) - \exp(q_n - q_{n+1}). \tag{23}$$

A standard change of variables converts $(q_n)_{xt}$ to the wave operator $(q_n)_{\xi\xi} - (q_n)_{\tau\tau}$.

The free and periodic boundary conditions on the 2DTL are of primary interest. The free boundary condition for 2×2 matrices B, C yields the Liouville equation

$$q_{xt} + \exp q = 0. \tag{24}$$

Under the periodic boundary condition $q_0 = q_2$, $q_1 = q_3$, system (23) becomes the sinh-Gordon equation for $\Theta = q_2 - q_1$,

$$\Theta_{xt} = -4 \sinh \Theta,$$

or, if q_1, q_2 are taken to be imaginary, the sine-Gordon equation

$$\Theta_{xt} = -4 \sin \Theta.$$

Since the sine-Gordon equation is solved by the inverse scattering method, it is natural to introduce a spectral parameter ζ and an eigenvalue problem for the N-component free 2DTL:

$$\Psi_t = \mathsf{B}(\zeta)\Psi, \quad \Psi_x = \mathsf{C}(\zeta)\Psi. \tag{25}$$

Sine-Gordon theory, in which ζ^{-1} appears, further suggests that for the free 2DTL

$$\mathsf{B}(\zeta) = -\zeta^{-1}\Delta^{-1}a, \quad \mathsf{C}(\zeta) = b + \zeta\Delta. \tag{26}$$

Compatibility of the two equations in (25) implies (22). The free 2DTL is referred to as "Toda field theory."

Periodic boundary conditions are handled by an adaptation of (26). ζ is put in the lower left corner of $\mathsf{C}(\zeta)$ and $-\zeta^{-1}a_N$ in the upper right corner of $\mathsf{B}(\zeta)$. The inverse scattering method can be applied to (25). Indeed, under two-periodic boundary condition, (25) is precisely the AKNS system used to solve the sine-Gordon equation.

The periodic 2DTL is called "affine Toda field theory" (ATFT), because, as is the case for the one-dimensional periodic lattice, it is set in the context of loop and affine Lie algebras and groups. The structure of ATFT, however, is richer because of the new x–dependence.

In complex coordinates $t = w, x = \overline{w}$, ATFT is a system of elliptic partial differential equations which is encountered in the theory of harmonic maps. Solutions of the sinh-Gordon equation define Riemannian metrics on surfaces $z = f(x, y)$, $(x, y) \in U$, of constant mean curvature 2. The Gauss map, which sends the unit normal vector to the unit sphere S^2, is a harmonic map, meaning that it is a critical point of the "energy" $\frac{1}{2}\int_U \|\nabla\phi\|^2 \,\mathrm{d}x\,\mathrm{d}y$ of maps $\phi : U \to S^2$. (For real–valued maps, a critical ϕ is an ordinary harmonic function.) Solutions of the multi-component elliptic ATFT define harmonic maps into other symmetric spaces. A certain group of loops is the infinite–dimensional symmetry group of this 2DTL: given a solution of 2DTL and a loop, one can construct a new solution via a factorization problem (Guest, 1997; Fordy & Woods, 1994).

In wave equation form, $(q_n)_{\xi\xi} - (q_n)_{\tau\tau}$, the 2DTL equations are hyperbolic; they describe fields on two-dimensional Minkowski space. As a first step toward a quantum theory of these fields, one can ask whether they are conformally invariant. Conformal transformations scale the (indefinite) metric. In light cone coordinates $x_\pm = \xi \pm \tau$, they are given by $(x_+, x_-) \mapsto (f_+(x_+), f_-(x_-)) = (\bar{x}_+, \bar{x}_-)$. Then $(q_n)_{x_+x_-}$, the left side of (23), becomes

$$\frac{\partial x_+}{\partial \bar{x}_+}\frac{\partial x_-}{\partial \bar{x}_-}(q_n)_{\bar{x}_+\bar{x}_-}\text{, abbreviated} \quad J \cdot (q_n)_{\bar{x}_+\bar{x}_-}. \tag{27}$$

The 2DTL equations will be conformally invariant under a transformation of the fields, $q_n(x_\pm) \mapsto \bar{q}_n(\bar{x}_\pm)$, for which the right-hand side of (23) is also multiplied by J.

The Liouville equation (24) is conformally invariant if q transforms according to $q \mapsto \bar{q} + \ln J$. The sinh-Gordon equation, whose right side is $-2(\exp(\Theta) + \exp(-\Theta))$, admits no such transformation of Θ and is not conformally invariant. A particle described by sinh-Gordon theory has "mass": if $\sinh\Theta$ is linearized about the vaccuum state $\Theta = 0$, one obtains $\Theta_{x_+x_-} = -4\Theta$; the mass is $\sqrt{4}$. The sinh-Gordon equation is a perturbation of the conformal Liouville field equation. For example, under the change of variables $q \mapsto \Theta + \ln\varepsilon$, the equation

$$q_{x_+x_-} = -\mathrm{e}^q + \varepsilon^2\mathrm{e}^{-q},$$

becomes the sinh-Gordon equation with mass $\sqrt{2\varepsilon}$. As $\varepsilon \to 0$, which recovers the Liouville equation, the mass tends to zero. Similarly, Toda field theory is conformally invariant, while affine Toda field theory is not. Affine Toda field theory is massive in the sense described. The actual fields of interest are linear combinations of the q_n that are suitable for generalization to affine Lie algebras. This generalization is important, because the quantizations of ATFTs associated to different types of affine Lie algebras can have very different properties (Corrigan, 1999).

Continuum Limits

There are two natural continuum limits of the Toda mass–spring chain. Keeping both nonlinearity and dispersion to first order, one gets the KdV equation. The "zero dispersion limit" results in a hyperbolic system, called the "dispersionless Toda lattice."

The approximation leading to the KdV equation is taken in a right-moving coordinate system, so that the left-moving solitons of the Toda lattice disappear. The difference operator (6) becomes the Schrödinger operator, and the discrete Gel'fand–Levitan–Marchenko inverse theory limits to the inverse scattering formalism for KdV (Toda, 1981).

The zero dispersion limit retains only the quadratic nonlinearity. In the Toda equations $\dot{a}_n = a_n(b_n - b_{n+1})$, $\dot{b}_n = 2\,(a_{n-1}^2 - a_n^2)$, take $q = n\varepsilon$ and $T = t\varepsilon$. These are slow scales. With $b_n(T) \sim b(q, T)$, the difference $(b_n - b_{n+1})$ is approximately $-\varepsilon\, b_q$. The inconvenient minus signs are removed by redefining a_n, b_n. One then finds the DTL equations

$$a_T = a b_q, \quad b_T = 2(a^2)_q. \tag{28}$$

There are again Lax equations. In the Toda eigenvalue problem (6), write $\exp(\pm\varepsilon\partial/\partial n)$ for the shift by $\pm\varepsilon$, and assume a WKB ansatz for $y_n(T) \sim y(q, T)$,

$$y(q, T) = \exp[\varepsilon^{-1} S(q, T)].$$

In the WKB approximation to the Schrödinger wave function, S_q is the inverse wavelength, which is proportional to momentum, by the deBroglie relation. Set $p = S_q$. Thus, p and q are canonically conjugate variables. As $\varepsilon \to 0$, the eigenvalue problem $\mathsf{L}\mathbf{y} = \lambda\mathbf{y}$ reduces to an eikonal equation, and $\mathbf{y}_t = \mathsf{B}\mathbf{y}$ becomes the time-evolution of the momentum S_q:

$$\begin{aligned} \mathfrak{L}(p, q) :&= a\,(\mathrm{e}^{p} + \mathrm{e}^{-p}) + b = \lambda, \\ p_T &= \frac{\partial}{\partial q}\,[a(\mathrm{e}^{p} - \mathrm{e}^{-p})] := \frac{\partial}{\partial q}\,\mathfrak{B}(p, q). \end{aligned} \tag{29}$$

The commutator $[\mathsf{L}, \mathsf{B}]$ is replaced by the Poisson bracket with respect to p and q, and then

$$\dot{\mathcal{L}} = \{\mathcal{B}, \mathcal{L}\}$$

yields Equations (28). Their solutions may develop shocks, but as long as they are smooth, the dispersionless limits of the Toda lattice constants of motion, I_k, are constants of motion, say H_k, for (28). For example, $\sum(2a_n^2 + b_n^2) \to H_2(a, b) = \int(2a^2 + b^2)\,\mathrm{d}q$.

For smooth solutions, the eigenvalue sorting property of the free Toda lattice remains valid. The "free" boundary conditions are $a(q, T) = 0$ for $q = 0, q = 1$. Let $a_0(q), b_0(q)$ be the initial values. As $T \to \infty$, $a(q, T) \to 0$, while $b(q, T)$ tends to a decreasing function $b^*(q)$. The conserved quantities H_k have the same values for b^* as for a_0, b_0, for example, $H_2(a_0, b_0) = H_2(0, b^*)$. In this sense, the initial "matrix" a_0, b_0 becomes diagonal, and the "eigenvalues" are sorted (Brockett & Bloch, 1990).

The two-dimensional dispersionless Toda lattice hierarchy arises in an idealized model of viscous fingering in a Hele-Shaw cell. This sketch follows Kostov et al. 2001 and references therein. Two plates confine water (zero viscosity) and oil (viscous) in the complex z-plane. The water occupies a bounded region D_+, which is surrounded by oil in the exterior domain D_-. There is a source of water at $z = 0$ and a compensating sink for the oil at $z = \infty$. The object is to find the motion of the interface $\Gamma(t)$. Under some simplifying assumptions, the time development of Γ is governed by the "Laplacean growth equation" (LGE), so called because the velocity potential satisfies $\triangle\phi = 0$.

The shape of Γ is determined by the harmonic moments

$$\begin{aligned} t_k &= -\frac{1}{k\pi}\int_{D_-} z^{-k}\,\mathrm{d}x\mathrm{d}y,\ k \geq 1, \\ t_0 &= \frac{1}{\pi} \times \text{area of } D_+. \end{aligned} \tag{30}$$

It is known that the t_k are constant under the LGE, while the area t_0 changes linearly. One, therefore, takes t_0 as time variable. Finding $\Gamma(t_0)$ amounts to finding the time-dependent conformal map $\mathfrak{L}(t_0)$ from $\{w \mid |w| > 1\}$ to $\{z \mid z \in D_-\}$. The dispersionless limit of the two-dimensional Toda hierarchy (21) enters when one allows the moments $\boldsymbol{t} = (t_1, \ldots)$ to vary and considers a family $\mathfrak{L}(t_0, \boldsymbol{t})$ of conformal maps; the LGE is then recovered as a constraint on this family.

The time-like variables t_k, x_k in (21) are taken to be the moments t_k and their conjugates $\bar{t}_k$. The area t_0 plays the role of the spatial coordinate q in (28); also set $w = \exp p$. The conformal map $\mathfrak{L}(w, \boldsymbol{t})$ and its conjugate $\bar{\mathfrak{L}}(w^{-1}, \bar{\boldsymbol{t}})$ are the dispersionless limits of L and M. The expansion of L in powers of Δ^{-1} becomes the Laurent expansion $\mathfrak{L}(w) = \text{const} \cdot w + u_0 + u_1 w^{-1} + \ldots$. The dependence of $\mathfrak{L}$, $\bar{\mathfrak{L}}$ on the deformation parameters $\boldsymbol{t}$, $\bar{\boldsymbol{t}}$ is given by

$$\frac{\partial\mathfrak{L}}{\partial t_k} = \{\mathfrak{B}_k, \mathfrak{L}\}, \quad \frac{\partial\mathfrak{L}}{\partial\bar{t}_k} = -\{\bar{\mathfrak{B}}_k, \mathfrak{L}\}, \tag{31}$$

plus similar equations for $\bar{\mathfrak{L}}$. As in (21), $\mathfrak{B}_k$ is $(\mathfrak{L}^k)_+$. The Poisson bracket is still $\{p, q\} = 1$ or in the new notation, $\{\ln w, t_0\} = 1$. The Laplacean growth equation can be written in the form

$$\{\mathfrak{L}(w, t_0), \bar{\mathfrak{L}}(w^{-1}, t_0)\} = 1,$$

with all $t_k, \bar{t}_k$ fixed. The constraint $\{\cdot, \cdot\} = 1$ is known as the "dispersionless string equation."

Other Topics

The topics chosen give only a hint of the importance of the Toda lattice and its generalizations. Other aspects and applications that deserve an expanded description include the following.

The Toda mass-spring chain can model dispersive lattice shocks. Two unstretched halves of the lattice move toward each other at constant speed $2c$. In the scattering problem, the boundary condition is not $b_{|n|} \to 0$, but $b_n \to \mp c$ for $n \gtrless 0$. The spectrum changes with c, and this is reflected in the shockwave behavior, which is analyzed by means of the powerful steepest descent method for Riemann–Hilbert problems (Deift et al., 1995).

The quantized Toda lattice is solvable; the eigenstates of the multi-particle Toda Hamiltonian are matrix elements of infinite-dimensional group representations. The construction generalizes the one-dimensional case, $-\mathrm{d}^2/\mathrm{d}q^2 + \exp(-2q)$, whose eigenfunctions are Whittaker functions (Semenov-Tyan-Shansky, 1994a).

Orthogonal polynomials satisfy a three-term recurrence relation such as (6). For this reason, the Toda lattice arises in random matrix theory. A probability measure

$$\mathrm{d}\mu_N(H) = Z_N^{-1} \mathrm{e}^{-N \mathrm{Trace} V(H)}\, \mathrm{d}H$$

on Hermitean matrices is given. It determines a family $p_j(x)$ of orthogonal monic polynomials, $\int p_i(x) p_j(x)\, \mathrm{d}\mu_N(x) = 0$ if $i \neq j$. In this basis, the shift operator $Lp(x) = xp(x)$ acting on polynomials $p(x)$ has the Jacobi form (12). If $V(x)$ depends on parameters t_k, for example, $V(x) = x^2 + t_4 x^4$, then $\mathrm{d}\mu_N$ and the p_j depend on the t_k. The change of L in the moving basis $\{p_j\}$ is described by a Lax equation (Witten, 1991).

HERMANN FLASCHKA

See also **Hele-shaw cell; Integrable lattices; Lie algebras and lie groups; Zero-dispersion limits**

Further Reading

Bergvelt, M. & ten Kroode, F. 1988. τ-functions and zero curvature equations. *Journal of Mathematical Physics*, 29: 1308–1320

Brockett, R. & Bloch, A. 1990. Sorting with the dispersionless limit of the Toda lattice. In *Proceedings of the Conference on Hamiltonian Systems, Transformation Groups and Spectral Transform Methods*, edited by J. Harnad & J. Marsden, Montréal: Publications CRM

Corrigan, E. 1999. Recent developments in affine Toda field theory. In *Particles and Fields*, edited by G.E. Semenoff & L. Vinet, New York: Springer

Deift, P., Kriecherbauer, T. & Venakides, S. 1995. Forced lattice vibrations, I, II, *Communications in Pure and Applied Mathematics*, 48: 1187–1249, 1251–1298

Deift, P., Li, L.-C., Nanda, T. & Tomei, C., 1986. The Toda lattice on a generic orbit is integrable, *Communications in Pure and Applied Mathematics*, 39: 183–232

Fordy, A. & Woods, J.C. (editors). 1994. *Harmonic Maps and Integrable Systems*. Braunschweig/Wiesbaden: Viehweg

Guest, M.A. 1997. *Harmonic Maps, Loop Groups, and Integrable Systems*, Cambridge and New York: Cambridge University Press

Kamvissis, S. 1993. On the long time behavior of the doubly infinite Toda lattice. *Communications in Mathematical Physics*, 153: 479–519

Kostov, I.K., Krichever, I., Mineev-Weinstein, M., Wiegmann, P.B. & Zabrodin, A. 2001. τ-function for analytic curves. In *Random Matrix Models and Their Applications*, edited by P. Bleher & A. Its, Mathematical Sciences Research Institute Publications, Cambridge University Press

Olshanetsky, M.A. & Perelomov, A.M. 1994. Integrable systems and finite-dimensional Lie algebras. In *Encyclopaedia of Mathematics, Dynamical Systems VII*, edited by V.I. Arnol'd & S. P. Novikov, New York: Springer (original Russian edition 1987)

Reyman, A.G. & Semenov-Tyan-Shansky, M.A. 1994. Group theoretical methods in the theory of finite dimensional integrable systems. In *Encyclopaedia of Mathematics, Dynamical Systems VII*, edited by V.I. Arnol'd & S.P. Novikov, New York: Springer (original Russian edition 1987)

Semenov-Tyan-Shansky, M.A. 1994a. Lectures on R–matrices, Poisson–Lie groups, and integrable systems. In *Lectures on Integrable Systems, In Memory of Jean-Louis Verdier*, edited by O. Babelon, P. Cartier & Y. Kosmann-Schwarzbach, Singapore: World Scientific

Semenov-Tyan-Shansky, M.A. 1994b. Quantization of open Toda lattices. In *Encyclopaedia of Mathematics, Dynamical Systems VII*, edited by V.I. Arnol'd & S.P. Novikov, New York: Springer (original Russian edition 1987)

Takasaki, K. & Takebe, T. 1995. Integrable hierarchies and dispersionless limits. *Reviews in Modern Physics*, 7: 743–808

Toda, M. 1981. *Theory of Nonlinear Lattices*, Berlin and Heidelberg: Springer (original Japanese edition 1978)

Ueno, K. & Takasaki, K. 1984. Toda lattice hierarchy. In *Group Representations and Systems of Differential Equations*, edited by K. Okamoto, Tokyo: Kinokuniya

Witten, E. 1991. Two-dimensional gravity and intersection theory on moduli space. In *Surveys in Differential Geometry*, Bethlehem, PA; Lehigh University

TOPOLOGICAL CHARGE

See **Sine-Gordon equation**

TOPOLOGICAL CONJUGACY

See **Maps**

TOPOLOGICAL DEFECTS

A *topological defect* (or *topological soliton*) represents a spatially non-uniform configuration of an order parameter field that offers topological stability and cannot be transformed into the ground state of a system under finite deformation of a field (Mermin, 1979). The structure and properties of a topological defect (TD) depend essentially on the dimensionality of a system, its symmetry, and degeneration of the ground state. Historically, vortices in liquid were the first example of a TD to be investigated (Lugt, 1996). In a two-dimensional (2-d) incompressible liquid, the equation

$\Delta\varphi = 0$ for the velocity potential φ (velocity $\boldsymbol{v} = \nabla\varphi$) has the evident solution $\varphi = \kappa\chi$ for the vortex, where κ is an arbitrary parameter and χ is the azimuthal angle in cylindrical coordinates (ρ, χ) in the x, y plane with its origin in the vortex center.

Pitaevskii vortices in superfluidity theory (Lifshitz & Pitaevskii, 1980), *magnetic vortices* in easy-plane ferro- and anti-ferromagnets (FMs and AFMS) (Mertens & Bishop, 2000), magnetic *disclinations*, and disclinations in nematic liquid crystals (de Gennes, 1974) exemplify the similar one-dimensional TD in 3-d continuous media with continuous degeneration of the ground state. The order parameters in the above examples are of the two-component type: the complex thermodynamical wave function $\psi(\boldsymbol{r}, t) = \psi_0 \exp(\mathrm{i}\phi)$ of a Bose condensate for the superfluid liquid, which, within the approach of a weakly nonideal Bose gas, satisfies the Gross–Pitaevskii equation

$$\mathrm{i}\hbar\frac{\partial\psi}{\partial t} + \frac{\hbar^2}{2m}\triangle\psi + U\{\psi - |\psi|^2\psi\} = 0, \qquad (1)$$

and two angle variables (θ, ϕ) in polar coordinates in magnetic space (associated with the hard axis z) of a magnetization vector $\boldsymbol{M} = M_0(\sin\theta\cos\phi, \sin\theta\sin\phi, \cos\theta)$, which satisfies the Landau–Lifshitz equation (similar in structure to (1)), or the director vector $\boldsymbol{L}$ in antiferromagnets and liquid crystals. These parameters are continuously degenerate in the phase of wave function ψ or in the direction of spins (or elongated molecules), defined by the angle ϕ in the easy-plane.

The solutions for the discussed TD map a plane (x, y), perpendicular to the defect line in coordinate space, onto the 2-d manifold of the order parameter (complex plane of ψ, half-sphere of radius $|\boldsymbol{M}|$, or sphere of radius $|\boldsymbol{L}|$). For example, the solution of (1) has the form $\psi = \psi_0(\rho)\exp(in\chi)$, where $n = \pm 1, \pm 2, \cdots$ and $(\pm)$ correspond to the vortex and antivortex. The density of a Bose gas tends to zero in the center of the vortex, $\psi^2(0) = 0$, and the solution has no singularity. A magnetic vortex has the same properties: $\phi = n\chi (n = \pm 1, \pm 2\cdots)$, $\theta(\rho = 0) = 0$ or $\pi, \theta(\rho \to \infty) \to \pi/2$ (Kosevich et al., 1990). In AFM- and nematic disclinations $\phi = k\chi/2$, where $k = \pm 1, \pm 2\cdots$, is called the Frank index. The mapping degree of TD is usually characterized by some integral *topological invariant* (or *topological charge*) related to the solution under consideration. The hydrodynamic vortex in an incompressible liquid is defined by its total vorticity $(1/2\pi)\oint \boldsymbol{v}\,\mathrm{d}\boldsymbol{l}$, where integration is performed over the contour enclosing the vortex center. This value coincides with κ and can be arbitrary. Other types of vortices can be characterized by the same integral $\oint \nabla\phi\,\mathrm{d}\boldsymbol{l}$. (Since a contour can be chosen with an infinite radius, these topological solitons are nonlocalized.) But in some cases, the topological charge is more conveniently defined as the 2-d integral over the coordinate plane. For example, in a ferromagnet, this invariant is

$$Q = \frac{1}{4\pi}\int m\left(\frac{\partial m}{\partial x_\alpha} \times \frac{\partial m}{\partial x_\beta}\right)\varepsilon_{\alpha\beta}\,\mathrm{d}^2x = \frac{1}{2\pi}\int \sin\theta\,\mathrm{d}\theta\,\mathrm{d}\phi, \qquad (2)$$

where $m = \boldsymbol{M}/M_0$. For a magnetic vortex $Q = pn$, where $p = m_z(\rho = 0)$, is the polarity of the vortex.

Another situation appears in systems with discrete degeneracy of the ground state. For instance, a localized magnetic 2-d topological soliton (TS) (*magnetic skyrmion*) of the type $\phi = n\chi$, $\theta = \theta(\rho)$, and $\theta(0) = 0$, $\theta(\infty) = \pi$ can exist in the easy-axis ferromagnet with two equivalent ground states $m_z = \pm 1$. At fixed n, the topological charge for this skyrmion is twice that for the vortex. Moreover, in such a system, TDs can exist in the 1-d and 3-d cases. In 3-d easy-axis FM, the TS, localized in all 3 dimensions, corresponds to the solution with the nonzero integer Hopf invariant. The 1-d TS can exist in 1-d and quasi-1-d systems or in 2-d and 3-d media as solutions depending on one spatial coordinate. Such a TD describes the *domain wall* in ferromagnets. In the framework of the Landau–Lifshitz equation, the corresponding *kink* solution is written as

$$\theta(x) = \arccos(\tanh(x/l_0)), \quad \phi = \text{const.}, \qquad (3)$$

where l_0 is the magnetic length. The domain boundary (kink) separates two half-spaces in different ground states. The topological charge, analogous to (2), can be defined in this case as follows: $Q = (1/2\pi)\int \sin\theta(x)\,\mathrm{d}\theta(x)\,\mathrm{d}\phi(x)$. If an additional anisotropy in the plane perpendicular to the easy axis is taken into account (in orthorhombic ferromagnets), more complicated TDs can exist inside the domain walls: *Bloch lines* and *Bloch points*. Similar to (3), the kink-like TD can exist in other systems with discrete degenerate ground states: kinks in antiferromagnets, kinks of incommensurate surface structures, fluxons in a long Josephson junction, phase boundaries in the problem of structural phase transitions, solitons in polyacetylene, in 1-d metals in the Peierls–Fröhlich phase, and so on. Usually these TDs are investigated within the framework of the φ^4-model or sine-Gordon equation

$$\frac{\partial^2 w}{\partial t^2} - s^2\frac{\partial^2 w}{\partial x^2} + \omega_0^2\sin w = 0, \qquad (4)$$

where the field variable w and coefficients have different physical meanings for various systems. The topological solution to this equation is well known: $w = 4\arctan\exp((x - vt)/l\sqrt{1 - v^2/s^2})$ with $l = s/\omega_0$.

A crystal *dislocation* represents one of the most important examples of a TD in a crystal lattice. Dislocations exist due to the translational symmetry

of the lattice: it transforms into itself under the translation by the interatomic distance a. (Rotational symmetry of the crystal lattice leads to the existence of another TD—crystal *disclination*.) A dislocation represents a one-dimensional TD with the following properties: the regular lattice structure is distorted only in the core of the dislocation line and the total displacement, as a closed contour goes around the dislocation line, is equal to the translation period. (In two-sublattice antiferromagnets, this translation period is twice as small as that for a magnetic lattice.) This fact leads to the appearance of the magnetic disclination and formation of the complex magnet-structural TD (Kovalev & Kosevich, 1977). In the simplest case of a screw dislocation or in a scalar model, the deformation is characterized solely by one component of displacement, u. Then, within the elasticity theory approximation, the deformation of a crystal is governed by the equation $\triangle u = 0$ with the dislocation solution $u = a\chi/2\pi$. (Here, a plays the role of the topological charge of the dislocation: $\oint du = a$.) The above solution is singular and does not describe the discrete structure of the dislocation core. It can be investigated in the simple one-dimensional model proposed by Yakov Frenkel and Tatiana Kontorova (1938) (*See also* **Frenkel–Kontorova model**). The FK model was the first 1-d model for 2-d topological defects. Within this model, the relative displacements u of the atoms from two atomic rows above and below the dislocation center are described by Equation (4), where $w = 2\pi u/a$, $\omega_0 = (2\pi/a)\sqrt{U/m}$, m is the atomic mass, s is the velocity of sound, U is the energy of the interaction between the rows, and l is the width of the dislocation core. The energy of a stationary dislocation (kink) is $E_0 = (4/\pi)\sqrt{ms^2U}$. The integral $\int \partial u/\partial x \, dx$ now plays the role of the topological charge. The FK model describes more adequately other TDs in the crystal lattice: *crowdions*, kinks of incommensurate surface structures, and dislocation kinks.

The dynamics of TDs are of great variety and depend strongly on the nature of the TD. The dynamics of dislocations, dislocation kinks, crowdions, domain walls, and phase boundaries are very simple within the framework of the Lorentz-invariant 1-d FK model: the kink can move with velocities below the velocity of sound in a system and its effective mass can be considerably smaller than the atomic mass. Actually, the dynamics of TDs in a lattice is much more complicated. Dislocations move mainly in some preferred direction (in slip planes), and crowdions propagate in closely packed atomic rows in a "relay race" manner. The discreteness of a lattice gives rise to Peierls relief for TP, and its dynamics assume diffusive features. Dislocation creeps over this relief, producing the dislocation kinks. The dynamics of vortices in media with distributed parameters has some interesting peculiarities. An isolated vortex in an infinite ideal medium cannot move: it is frozen in a liquid or superfluid flow or spin flux. The vortex can move in a bounded area or in the presence of other defects but these dynamics are non-Newtonian. Within the collective coordinates approach, the effective equation of motion for the center of a vortex $\boldsymbol{X}(t)$ is (Thiele, 1973)

$$\frac{d\boldsymbol{X}}{dt} \times \boldsymbol{G} = \boldsymbol{F}_G, \tag{5}$$

where the force $\boldsymbol{F}_G$ is formally equivalent to the Magnus force in fluid dynamics and the gyrocoupling vector $\boldsymbol{G}$ is parallel to the line of a vortex and depends on its topological charge.

In all the examples above, topological defects with the opposite sign of the topological charge exist (vortex-antivortex, kink-antikink, dislocations with opposite signs, etc). This implies that TDs can emerge from the ground state of a medium in pairs with zero total topological charge. At a nonzero temperature, these pairs dissociate and the finite density of TDs can be observed. Seeger & Schiller (1966) were the first to develop the thermodynamics of topological solitons in the framework of the 1-d FK model. As they showed, the equilibrium density of kinks and antikinks at a temperature T is

$$n \approx \frac{a}{l}\sqrt{\frac{2}{\pi\tau}} \exp\left(-\frac{1}{\tau}\right), \tag{6}$$

where $\tau = k_B/E_0$, E_0 is the soliton energy, and l is the width of this kink. The situation with a TD in the 2-d case (vortices and 2-d dislocations) is essentially different. The energy of vortices and dislocations in infinite 2-d systems is infinite, but in systems of size R, it is of the order of $E_v \sim E_* \ln(R/a)$, where E_* is a characteristic energy, being specific for different TDs. The contribution from a vortex or dislocation to configuration entropy in a 2-d crystal is $\delta S = \ln(R/a)^2$, and hence, the change in free energy, if one TD is added, is $\delta F = (E_* - 2T)\ln(R/a)$. At the temperature $T_c = E_*/2$, the value δF becomes negative and a Berezinskii–Kosterlitz–Thouless phase transition takes place: the crystal melts or magnetic ordering is broken (Berezinskii, 1971).

As indicated above, topological defects play an important role in the kinetic and thermodynamic properties of condensed matter. Dislocations and dislocation kinks cause plasticity and strengthening of a crystal, and their behavior under radiation depends to a large extent on the crowdions. Recently, the influence of dislocations on the concentration and mobility of current carriers has been widely studied experimentally in pure semiconductor and alkali-halide crystals (Osip'yan et al., 2000). Topological defects (charge-density-wave solitons) make an essential contribution to the conductivity and electrodynamics of

quasi-1-d conductors such as $(CH)_x$, TaS_2, and $NbSe_2$ (Krive et al., 1986).

ALEXANDER S. KOVALEV

See also **Collective coordinates; Dislocations in crystals; Domain walls; Frenkel–Kontorova model; Landau–Lifshitz equation; Liquid crystals; Long Josephson junctions; Multidimensional solitons; Nonlinear Schrödinger equations; Sine-Gordon equation; Spin systems; Superfluidity; Topology; Vortex dynamics of fluids**

Further Reading

Berezinskii, V.L. 1971. Violation of long range order in one-dimensional and two-dimensional systems with a continuous symmetry group. I. Classical systems. *Soviet Physics-JETP*, 34: 610

de Gennes, P.G. 1974. *The Physics of Liquid Crystals*, Oxford: Clarendon Press

Frenkel, J. & Kontorova, T. 1938. On the theory of plastic deformation and twinning. *Physikalishe Zeitschrift der Sowjetunion*, 13: 1–12

Kosevich, A.M., Ivanov, B.A. & Kovalev, A.S. 1990. Magnetic solitons. *Physics Reports*, 194: 117–238

Kovalev, A.S. & Kosevich, A.M. 1977. Dislocation and domains in an antiferromagnet. *Soviet Journal of Low Temperature Physics*, 3: 125–126

Krive, I.V., Rozhavsky, A.S. & Kulik, I.O. 1986. Nonlinear conductivity mechanisms and electrodynamics of quasi-1D conductors in Peierls dielectric phase. *Soviet Journal of Low Temperature Physics*, 12: 635

Lifshitz, E.M. & Pitaevskii, L.P. 1980. *Statistical Physics*, part 2, Oxford: Pergamon Press

Lugt, H.J. 1996. *Introduction to Vortex Theory*, Potomac, MD: Vortex Flow Press

Mermin, N.D. 1979. The topological theory of defects in ordered media. *Review of Modern Physics*, 51: 591–648

Mertens, F.G. & Bishop, A.R. 2000. Dynamics of vortices in two-dimensional magnets. In *Nonlinear Science at the Dawn of the 21st Century*, Berlin and New York: Springer

Osip'yan, Yu.A. et al. 2000. *Electronic Properties of Dislocations in Semicondactors*. Moscow: Editorial USSR (in Russian)

Seeger, A. & Schiller, P. 1966. *Physical Acoustics*, New York: Academic Press

Thiele, A.A. 1973. Steady-state motion of magnetic domains. *Physical Review Letters*, 30: 239–233

TOPOLOGICAL ENTROPY

See **Entropy**

TOPOLOGICAL SOLITONS

See **Solitons, types of**

TOPOLOGY

Continuity is conventionally associated with functions defined on the real line or higher-dimensional Euclidean spaces. Topology is concerned with the abstraction of continuity to maps between more general sets. The subject is vast and its study can take many forms depending on the nature of the structures considered. They include the areas of point-set, combinatorial, algebraic, and differential topology.

A topological space has a distinguished collection of subsets known as *open sets*. An open subset U of the real line $\mathbb{R}$ is one for which every point of U is a subset of some real interval wholly contained in U. Thus, every point of U is the *interior* of U. Openness of a set U can also be expressed using the Euclidean distance, or *metric*, by saying that for every point $x \in U$, all points within a sufficiently small distance of x also lie in U. Thus, metrics can be used to create open sets. Complements of open sets are said to be *closed*. The simplest examples of open and closed sets in $\mathbb{R}$ are, respectively, the "open interval" (a, b) of all points between the numbers a and b excluding the end points, and the "closed interval" $[a, b] = (a, b) \cup \{a, b\}$. Also, sets can be neither open nor closed, for example $[a, b) = (a, b) \cup \{a\}$.

A *topology* on a set X is defined by its collection of open subsets, τ, which then makes X a *topological space* (X, τ). The collection of open subsets must include both X and the empty set ϕ, any union of elements of τ, and the intersection of any finite collection of elements of τ. The conditions for a topology can equally well be cast in terms of closed sets. Also, a set can have many different topologies.

In any sophisticated mathematical structure, there is usually a way of relating two objects. For example, if we are only considering sets, say X and Y, we consider maps $f : X \to Y$. The natural equivalence for sets X,Y would be the existence of a map $f : X \to Y$ which is both one–one and onto, that is, a bijection. When topologies are placed on X and Y, it is natural to consider maps $f : X \to Y$ that are continuous. The metric definition of continuity for maps $f : \mathbb{R} \to \mathbb{R}$, or more generally $f : \mathbb{R}^m \to \mathbb{R}^n$, can be shown to be equivalent to the topological definition: $f : X \to Y$ is continuous if V is an open subset of Y; the set $f^{-1}(V)$ is an open subset of X.

This alternative definition of continuity is the one that makes topology a key mathematical discipline of widespread importance.

The corresponding equivalence for topological spaces X and Y requires a map $h : X \to Y$, which is both (i) a bijection, and (ii) bicontinuous; that is, both h and its inverse h^{-1} are continuous. Such a map is called a *homeomorphism*. The spaces X and Y are said to be topologically equivalent or homeomorphs. Any subset S of a topological space X can be made into a topological space by declaring the intersections of open sets of X with S to be open sets of S. In fact, this collection of subsets of S forms a topology on S, called the *subspace topology*. Thus, important geometrical objects which are subsets of Euclidean spaces such as the circle, the sphere (and therefore all classical

polyhedra), the torus, the pretzel, and the Klein bottle (see Figure 1) can all be seen as topological spaces when endowed with the subspace topology.

An important property of continuous functions defined on the real numbers is that a continuous function defined on a bounded closed interval attains its bounds; that is, there exist points at which the function takes its maximum and minimum value. This is not true if the "closed, bounded" condition is relaxed. For example, $f(x) = x$ is not bounded on the real line $\mathbb{R}$ which is a closed (but not bounded) set. Also, $f(x) = x$ does not attain its bounds on the bounded (but not closed) set $(0, 1)$. The bounded closed interval on $\mathbb{R}$ is called a *compact* set. Again, such a set can be defined solely in terms of open sets, and so we can define the concept of a *compact topological space* (Munkres, 2000).

Another key result in elementary analysis is that the continuous image of an interval of real numbers is also an interval. This property is often used to find roots of a continuous function $f : \mathbb{R} \to \mathbb{R}$ by finding values $a, b \in \mathbb{R}$ for which $f(a) \cdot f(b) < 0$, the so-called "intermediate value" theorem. In the generalization of this result to topological spaces, the key property of the interval is its *connectedness*. The analogous result for topological spaces is that the continuous image of a connected set is also a connected set. The characterization of connectedness in the real numbers can be described purely in terms of the properties of the open sets on the real line, that is, in terms of the Euclidean topology on $\mathbb{R}$.

Thus, both compactness and connectedness are topological properties in the sense that they can be described purely in terms of properties of the open sets of a topological space (Munkres, 2000).

In some areas of topology, the importance of the open sets is not so apparent and other features of the topological space are considered. For example, polyhedra such as the cube, tetrahedron, and dodecahedron are finite ways of building homeomorphic images of the standard sphere. We note that for all such constructs, the number of vertices (V), edges (E), and faces (F) satisfy the condition $V - E + F = 2$, the *Euler characteristic* of the sphere. The torus, when built up in terms of faces, edges, and vertices, has the property that its Euler characteristic is zero. Given that the numbers V, E, and F are conserved by homeomorphism, we see that the torus and sphere having different Euler characteristics not only makes them look "different," but ensures that they are not homeomorphic; that is, they are topologically distinct.

Note that not all spaces can be easily distinguished using topology. For example, the subsets of rational numbers, $\mathbb{Q}$, and the irrationals, I, of the real line $\mathbb{R}$, are both topologically *dense* sets in $\mathbb{R}$; that is, for both sets, the smallest closed superset is the whole interval $\mathbb{R}$. Also, both are neither open nor closed. However, note that there is no bijection between the sets $\mathbb{Q}$ and I because they have different cardinalities and, thus, cannot be homeomorphs.

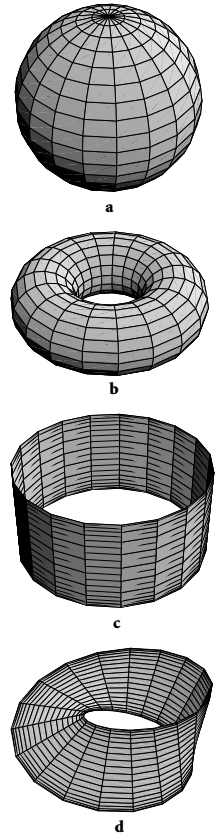

Figure 1. Four distinct topological spaces: (a) sphere; (b) torus; (c) cylinder; (d) Möbius band. See http://library.wolfram.com/graphics/

The topological spaces mentioned above, such as the torus, sphere, and pretzel, can be easily visualized within the three-dimensional Euclidean space $\mathbb{R}^3$ in which we locally live. However, it is not difficult to see how we can start to construct spaces in $\mathbb{R}^3$ which are more geometrically demanding. The simplest is the Möbius strip, M, which is derived from the rectangle by pasting together one opposite pair of edges of a band with a half-twist, see Figure 1(d). Note that the Möbius band has only one "side"; just draw a pen line along the spine of the band and the line arrives on the opposite side of the paper from its initial point. Continuing the

line brings a return to the initial point of the curve. By comparison, one cannot get from one side of a cylinder to the other without passing across one of its edges. The Möbius band is topologically different from the cylinder for several reasons. For instance, the boundary of the cylinder consists of two disjoint circles whereas that of the Möbius band is a single circle.

DAVID ARROWSMITH

Further Reading

Dieudonné, J. 1985. The beginnings of topology from 1850 to 1914. *Proceedings of the Conference on Mathematical Logic 2 (Siena, 1985)*, 585–600

Dieudonné, J. 1989. *A History of Algebraic and Differential Topology, 1900–1960*, Boston: Birkhäuser

Lefschetz, S. 1970. The early development of algebraic topology. *Boletim da Sociedade Brasileira de Matematica*, 1(1): 1–48

Mendelson, B. 1990. *Introduction to Topology*, New York: Dover

Munkres, J.R. 2000. *Topology*, Upper Saddle River, NJ: Prentice-Hall

Stillwell, J.C. 1993. *Classical Topology and Combinatorial Group Theory*, 2nd edition, New York: Springer

Weil, A. 1979. Riemann, Betti and the birth of topology. *Archive for the History of Exact Sciences*, 20(2): 91–96

MATHEMATICA (http://library.wolfram.com/graphics/) Graphics of various surfaces

TRAFFIC FLOW

Most automobile drivers have encountered the widespread phenomenon of so-called "phantom traffic jams," for which there is no visible reason such as an accident or a bottleneck. Why are vehicles sometimes stopped although everyone likes to drive fast? Due to the finite adaptation time (= reaction time + acceleration time), a small disturbance in the traffic flow Q_* can cause an overreaction (overbraking) of a driver, if the safe vehicle speed $V_*(\rho)$ drops too rapidly with increasing vehicle density ρ. At high enough densities ρ, this will give rise to a chain reaction of the followers, as other vehicles will have approached before the original speed can be regained. This feedback can eventually cause the unexpected standstill of vehicles known as traffic jam.

Lighthill & Whitham (1955) described traffic flow as a function of space x and time t by means of a fluid-dynamic conservation law of vehicles, reflecting the fact that vehicles are not generated or lost in the absence of ramps, intersections, or accidents. The traffic flow $Q(x,t)$ (= vehicle density $\rho(x,t) \times$ average velocity $V(x,t)$) was specified as a function of the density $\rho(x,t)$. The corresponding "fundamental diagram" $Q_*(\rho) = \rho V_*(\rho)$ is obtained as a fit to empirical data. The conservation law $\partial\rho/\partial t + \partial Q/\partial x = 0$ leads to the nonlinear wave equation

$$\frac{\partial \rho}{\partial t} + C(\rho)\frac{\partial \rho}{\partial x} = 0\,, \qquad (1)$$

according to which the propagation velocity

$$C(\rho) = V_*(\rho) + \rho\frac{\mathrm{d}V_*(\rho)}{\mathrm{d}\rho} \le V_*(\rho) \qquad (2)$$

of kinematic waves depends on the vehicle density. Thus, while a density profile on a ring road keeps its amplitude, its shape is changing until shock waves (i.e., discontinuous changes in the density) have developed. The densities ρ_+ and ρ_- immediately upstream and downstream of a shock front determine its propagation speed

$$S(\rho_+, \rho_-) = \frac{Q_*(\rho_+) - Q_*(\rho_-)}{\rho_+ - \rho_-}\,. \qquad (3)$$

As discontinuous density changes are not fully consistent with empirical observations and a problem for efficient numerical integration, Whitham (1974) has suggested adding a diffusion term $D\,\partial^2\rho/\partial x^2$ with $D > 0$ to the right-hand side of the Lighthill–Whitham equation. For the linear velocity-density relation $V_*(\rho)$ suggested by Greenshields (1935), the resulting equation is equivalent with the Burgers equation and can be transformed into the linear heat or diffusion equation; that is, it is analytically solvable.

Experimental observations of traffic patterns show some additional features that cannot be reproduced by the above models. While traffic flow appears to be stable with respect to perturbations at small and large densities, there is a linearly unstable range at medium densities, where already small disturbances of uniform traffic flow give rise to traffic jams. Between these three density ranges, one finds meta- or multistable ranges, since there exists a density-dependent, critical amplitude $A(\rho)$, so that the resulting traffic pattern is path- or history-dependent (Kerner et al., 1994–1997). While subcritical perturbations fade away, supercritical perturbations cause a breakdown of traffic flow (nucleation effect). Consequently, traffic flows display critical points, nonequilibrium phase transitions, noise-induced transitions, and fluctuation-induced ordering phenomena.

One may view this situation as nonequilibrium analogue of the phase transitions between vapor, water, and ice. However, the breakdown and structure formation phenomena, when the "temperature" (i.e., the fluctuation strength) is increased, are sometimes counterintuitive due to the repulsive nature of vehicular interactions. From classical many-particle systems with attractive interactions, we are rather used to the idea that increasing temperature breaks up structures and destroys patterns (fluid structures are replaced by gaseous ones, not by solid ones).

The above observations in freeway traffic can be described by microscopic, mesoscopic, or macroscopic models, which are theoretically connected by means of a micro-macro link. Microscopic models are usually

follow-the-leader models specifying the acceleration $\mathrm{d}v_i/\mathrm{d}t$ of the single vehicles i as a function of their distance headway $d_i = x_{i-1} - x_i$, their speed v_i, and/or their relative velocity $\Delta v_i = v_i - v_{i-1}$:

$$\frac{\mathrm{d}v_i}{\mathrm{d}t} = f(d_i, v_i, \Delta v_i)\,. \tag{4}$$

A typical example is the non-integer car-following model:

$$\frac{\mathrm{d}v_i(t+\Delta t)}{\mathrm{d}t} = -\frac{\Delta v_i(t)}{T}\frac{[v_i(t+\Delta t)]^m}{[d_i(t)]^l} \tag{5}$$

with the reaction time $\Delta t \approx 1.3$ s and the parameters $T \approx \Delta t/0.55$, $m \approx 0.8$, and $l \approx 2.8$ (Gazis et al., 1961). It has a linearly unstable range for $\Delta t/T > \frac{1}{2}$. A simpler model is the optimal velocity model

$$\frac{\mathrm{d}v_i(t)}{\mathrm{d}t} = \frac{1}{\tau}\Big[v\big(d_i(t)\big) - v_i(t)\Big], \tag{6}$$

where $v(d_i)$ is the "optimal" velocity-distance relation and τ the adaptation time (Bando et al., 1994, 1995). This model has an unstable range for $\mathrm{d}v(d_i)/\mathrm{d}d_i > 1/(2\tau)$. The respective nonlinearly coupled differential equations (or stochastic differential equations, if fluctuations are taken into account) are numerically solved as in molecular dynamics. An alternative approach is rule-based cellular automata, which discretize space and time in favor of numerical efficiency: $t = i\,\Delta t, x = j\,\Delta x, d = \hat{d}\Delta x, v = \hat{v}\,\Delta x/\Delta t$. The Nagel–Schreckenberg model (1992), for example, can be written in the form

$$\hat{v}_{i+1} = \max\Big(0, \min(\hat{v}_{\max}, \hat{d}_i - 1, \hat{v}_i + 1) - \xi_i^{(p)}\Big), \tag{7}$$

where $\hat{v}_{\max}\Delta x/\Delta t$ is the maximum velocity and $\xi_i^{(p)}$ a Boolean random variable which is 1 with probability p and 0 otherwise. Typical parameters are $\Delta t = 1$ s, $\Delta x = 7.5$ m, $\hat{v}_{\max} = 5$, and $0.2 < p \leq 0.5$.

Mesoscopic models describe the spatiotemporal change of the phase space density (= vehicle density $\times$ velocity distribution). This approach has been introduced by Prigogine et al. (1960, 1961, 1971) and is inspired by kinetic gas theory. The related equations are either of Boltzmann type (for point-like vehicles or low densities) or of Enskog type, if vehicular space requirements at moderate and high densities are taken into account (Helbing et al., 1995–1999). The equations allow a systematic derivation of a hierarchy of macroscopic equations for the vehicle density $\rho(x,t)$, the average velocity $V(x,t)$, the velocity variance $\Theta(x)$, etc. This hierarchy is usually closed after the velocity or variance equation, although the separation of time scales assumed by the underlying approximations is weak. Nevertheless, the observed traffic dynamics are rather well reproduced by the resulting coupled partial differential equations. The density equation is just the continuity equation

$$\frac{\partial\rho}{\partial t} + \frac{\partial(\rho V)}{\partial x} = \nu_+ - \nu_-\,, \tag{8}$$

where ν_+ and ν_- denote on- and off-ramp flows, respectively. The velocity equation can be cast into the form

$$\frac{\partial V}{\partial t} + V\frac{\partial V}{\partial x} = -\frac{1}{\rho}\frac{\partial P}{\partial x} + \frac{1}{\tau}(V^* - V). \tag{9}$$

In theoretically consistent macroscopic traffic models such as the gas-kinetic-based traffic model, the "traffic pressure" P and the velocity V^* are nonlocal functions of the density ρ, the average velocity V, and the variance Θ (Helbing et al., 1998, 1999). The Lighthill–Whitham model (1955) results in the unrealistic limit $\tau \to 0$ of vanishing adaptation times τ. Payne's macroscopic traffic model (1971, 1979) is obtained for $P(\rho) = [V_0 - V_*(\rho)]/(2\tau)$ and $V^* = V_*(\rho)$, where V_0 denotes the (average) desired velocity (the average velocity at very low densities). Kerner and Konhäuser's model (1993) is a variant of Kühne's model (1984) and corresponds to the specifications $P = \rho\Theta_0 - \eta_0\partial V/\partial x$, and $V^* = V_*(\rho)$, where Θ_0 and η_0 are positive constants. The corresponding equation is a Navier–Stokes equation with a viscosity term $\eta_0\partial^2 V/\partial x^2$ and an additional relaxation term $[V_*(\rho) - V]/\tau$ describing the delayed adaptation to the velocity–density relation $V_*(\rho)$. The condition for linear instability reads

$$\rho\left|\frac{\mathrm{d}V_*(\rho)}{\mathrm{d}\rho}\right| > \sqrt{\frac{\mathrm{d}P(\rho)}{\mathrm{d}\rho}}\,; \tag{10}$$

that is, the Payne model and the Kerner–Konhäuser model have linearly unstable ranges, if $\mathrm{d}V_*(\rho)/\mathrm{d}\rho$ is large, while the Lighthill–Whitham model is marginally stable. The Burgers equation, by the way, is always stable.

According to Krauß (1998), traffic models show the observed hysteretic phase transition related with metastable traffic and high flows only, if the typical maximal acceleration is not too large and the deceleration strength is moderate. In such models, the outflow Q_{out} from traffic jams is a self-organized constant of traffic flow (Kerner et al., 1994, 1996). It corresponds approximately to the intersection point of the linear jam line

$$J(\rho) = \frac{1}{T}\left(1 - \frac{\rho}{\rho_{\mathrm{jam}}}\right) \tag{11}$$

with the free branch of the flow-density diagram, where T denotes the time headway in congested traffic and

ρ_{jam} the density inside traffic jams. The jam line corresponds to the flow-density relation for moving traffic patterns with a self-organized, stationary profile (Kerner & Konhäuser, 1994). These propagate with the velocity $C = -1/(T\rho_{\text{jam}}) \approx -15$ km/h, which is another traffic constant. (Once a traffic jam is fully developed, it moves upstream with constant velocity, as vehicles leave the downstream jam front at a constant rate, while new ones join it at the upstream front.)

With this knowledge, one can understand the various congested traffic states observed on freeway sections with bottlenecks (Helbing et al., 1998–2002). Let us assume a bottleneck due to ramp flows $v_+ = Q_{\text{rmp}}/(nL)$, where L is the used length of the on-ramp and n the number of freeway lanes. The corresponding bottleneck strength is, then, $\Delta Q = Q_{\text{rmp}}/n$. If Q_{up} denotes the traffic flow upstream of the bottleneck and $Q_{\text{tot}} = (Q_{\text{up}} + \Delta Q)$ is the total capacity required downstream of the ramp, we will eventually find a growing vehicle queue upstream of the bottleneck, if Q_{tot} is greater than the dynamic capacity Q_{out}. The traffic flow Q_{cong} resulting in the congested area plus the inflow or bottleneck; strength ΔQ are normally given by the outflow Q_{out}; that is,

$$Q_{\text{cong}} = Q_{\text{out}} - \Delta Q \tag{12}$$

(if vehicles cannot enter the freeway downstream of the congestion front). One can distinguish the following cases: If the density ρ_{cong} associated with the congested flow

$$Q_{\text{cong}} = Q_*(\rho_{\text{cong}}) \tag{13}$$

lies in the stable range, we find homogeneous congested traffic (HCT) such as typical traffic jams during holiday seasons or after serious accidents. For a smaller on-ramp flow or bottleneck strength ΔQ, the congested flow Q_{cong} is linearly unstable, and we either find oscillating congested traffic (OCT) or triggered stop-and-go traffic (TSG). In contrast to OCT, stop-and-go traffic is characterized by a sequence of moving jams, between which traffic flows freely. This state can either emerge from a spatial sequence of homogeneous and oscillating congested traffic (Koshi et al., 1983; called "pinch effect" by Kerner, 1998), or it can be caused by the inhomogeneity at the ramp. In the latter case, each traffic jam triggers another one by inducing a small

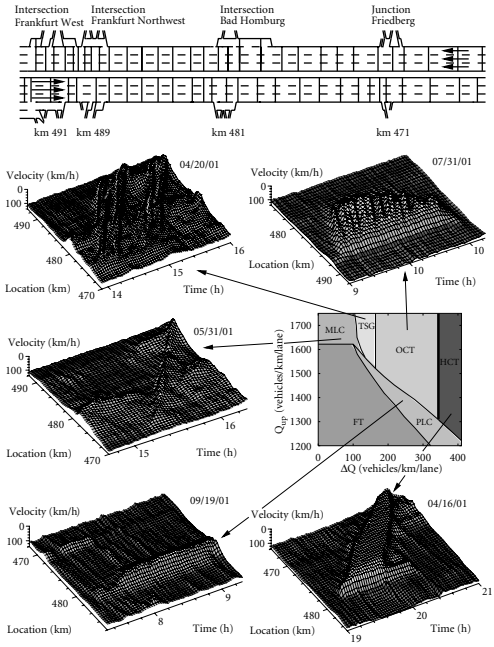

Figure 1. Numericlly determined phase diagram of traffic states in the presence of one bottleneck as a function of the upstream flow Q_{up} and the bottleneck strength ΔQ (center right), and empirical representatives for the related kinds of congested traffic (by Martin Schönhof and D. Helbing. Note that the outflow Q_{out} in the applied simulation model depends on the bottleneck strength ΔQ.

perturbation in the inhomogeneous freeway section (see Figure 1), which propagates downstream as long as it is small, but turns back when it has grown large enough (boomerang effect). This, however, requires the downstream traffic flow to be linearly unstable. If it is (meta-)stable instead (when the traffic volume Q_{tot} is further reduced), a traffic jam will usually not trigger a growing perturbation. In that case, one finds either a single moving localized cluster (MLC) or a pinned localized cluster (PLC) at the location of the ramp. The latter requires the traffic flow in the upstream section to be stable, so that no traffic jam can survive there. Finally, for sufficiently small traffic volumes Q_{tot}, we find free traffic (FT), as expected. For freeways with a single bottleneck and a large perturbation of traffic flow, these facts can be summarized by the phase diagram in Figure 1, which is universal for all microscopic and macroscopic, stochastic and deterministic traffic models with the same instability diagram (stable, metastable, and unstable density ranges). Results for more complex freeway geometries, other initial or boundary conditions, and other instability diagrams are available as well.

Current research focuses on the following open questions: Are fluctuations and psychological concepts necessary to understand the empirical observations in traffic flows? Can the large individual variation of time headways fully account for the large scattering of flow-density data in synchronized flow? (In congested traffic flow, the velocities in neighboring lanes are usually synchronized, as different speeds are balanced by lane changes.) What are the site- and country-dependent differences in traffic dynamics, and can they be adequately reflected by different model parameters for the driver-vehicle units? How can the insights regarding the laws of traffic dynamics be used for traffic optimization by variable speed limits, intelligent on-ramp controls, dynamic re-routing, and driver assistance systems? How can they be transferred to the explanation of breakdown and obstruction phenomena in socioeconomic systems?

DIRK HELBING

See also **Burgers equation; Constants of motion and conservation laws; Phase transitions; Shock waves**

Further Reading

Helbing, D. 2001. Traffic and related self-driven many-particle systems. *Reviews of Modern Physics*, 73(4): 1067–1141 [All the authors mentioned in the text above are found as references in this article.]

Lighthill, M.J. & Whitham, G.B. 1955. On kinematic waves: II. A theory of traffic on long crowded roads. *Proceedings of the Royal Society, London* A, 229: 317–345

Whitham, G.B. 1974. *Linear and Nonlinear Waves*, New York: Wiley

TRAJECTORIES

See **Phase space**

TRANSITION TO CHAOS

See **Chaotic dynamics**

TRAVELING WAVE

See **Wave of translation**

TRIAD INTERACTION

See ***N*-wave interactions**

TUNNEL DIODE ARRAYS

See **Distributed oscillators**

TURBULENCE

Turbulence is a state of a nonlinear physical system that has energy distribution over many degrees of freedom strongly deviated from equilibrium. Turbulence is irregular both in time and in space. Turbulence can be maintained by some external influence or it can decay on the way to relaxation to equilibrium. The term first appeared in fluid mechanics and was later generalized to include far-from-equilibrium states in solids and plasmas.

If an obstacle of size L is placed in a fluid of viscosity ν that is moving with velocity V, a turbulent wake emerges for sufficiently large values of the Reynolds number

$$\text{Re} \equiv VL/\nu.$$

At large Re, flow perturbations produced at scale L experience a viscous dissipation that is small compared with nonlinear effects. Nonlinearity then induces motions at smaller and smaller scales until viscous dissipation terminates the process at a scale much smaller than L, leading to a wide (so-called inertial) interval of scales where viscosity is negligible and nonlinearity plays a dominant role.

Examples of this phenomenon include waves excited on a fluid surface by wind or moving bodies and waves in plasmas and solids that are excited by external electromagnetic fields. The state of such a system is called turbulent when the wavelength of the waves excited greatly differs from the wavelength of the waves that dissipate. Nonlinear interactions excite waves in the interval of wavelengths (called the transparency window or inertial interval as in fluid turbulence) between the injection and dissipation scales.

The ensuing complicated and irregular dynamics require a statistical description based on averaging over regions of space or intervals of time. Because

nonlinearity dominates in the inertial interval, it is natural to ask to what extent the statistics are universal, in the sense of being independent of the details of excitation and dissipation. The answer to this question is far from evident for nonequilibrium systems. A fundamental physical problem is to establish which statistical properties are universal in the inertial interval of scales and which are features of different turbulent systems.

Constraints on dynamics are imposed by conservation laws, and therefore, conserved quantities must play an essential role in turbulence. Although the conservation laws are broken by pumping and dissipation, these factors do not act in the inertial interval. Under incompressible turbulence, for example, the kinetic energy is pumped by external forcing and is dissipated by viscosity. As suggested by Lewis Fry Richardson in 1921, kinetic energy flows throughout the inertial interval of scales in a cascade-like process. The cascade idea explains the basic macroscopic manifestation of turbulence: the rate of dissipation of the dynamical integral of motion has a finite limit when the dissipation coefficient tends to zero. In other words, the mean rate of the viscous energy dissipation does not depend on viscosity at large Reynolds numbers. That means that symmetry of the inviscid equation (here, time-reversal invariance) is broken by the presence of the viscous term, even though the latter might have been expected to become negligible in the limit $\mathrm{Re} \to \infty$.

The cascade idea fixes only the mean flux of the respective integral of motion, requiring it to be constant across the inertial interval of scales. To describe an entire turbulence statistics, one has to solve problems on a case-by-case basis with most cases still unsolved.

Weak Wave Turbulence

From a theoretical point of view, the simplest case is the turbulence of weakly interacting waves. Examples include waves on the water surface, waves in plasma with and without a magnetic field, and spin waves in magnetics. We assume spatial homogeneity and denote by a_k the amplitude of the wave with the wave vector $\boldsymbol{k}$. When the amplitude is small, it satisfies the linear equation

$$\frac{\partial a_k}{\partial t} = -\mathrm{i}\omega_k a_k + f_k(t) - \gamma_k a_k. \tag{1}$$

Here, the dispersion law ω_k describes wave propagation, γ_k is the decrement of linear damping, and f_k describes pumping. For the linear system, a_k is different from zero only in the regions of $\boldsymbol{k}$-space where f_k is nonzero. To describe wave turbulence that involves wave numbers outside the pumping region, one must account for the interactions among different waves. Considering the wave system to be closed (no external pumping or dissipation), one can describe it as a Hamiltonian system using wave amplitudes as normal canonical variables (Zakharov et al., 1992). At small amplitudes, the Hamiltonian can be written as an expansion over a_k, where the second-order term describes noninteracting waves and high-order terms determine the interaction

$$H = \int \omega_k |a_k|^2 \,\mathrm{d}\boldsymbol{k} + \int \left(V_{123} a_1 a_2^* a_3^* + \text{c.c.} \right) \delta(\boldsymbol{k}_1 - \boldsymbol{k}_2 - \boldsymbol{k}_3)\, \mathrm{d}\boldsymbol{k}_1\, \mathrm{d}\boldsymbol{k}_2\, \mathrm{d}\boldsymbol{k}_3 + \mathrm{O}(a^4). \tag{2}$$

Here, $V_{123} = V(\boldsymbol{k}_1, \boldsymbol{k}_2, \boldsymbol{k}_3)$ is the interaction vertex, and c.c. denotes complex conjugate. In this expansion, we presume every subsequent term smaller than the previous one, in particular, $\xi_k = |V_{kkk} a_k| k^d / \omega_k \ll 1$. Wave turbulence that satisfies that condition is called weak turbulence. Also, space dimensionality d can be 1, 2, or 3.

A dynamic equation that accounts for pumping, damping, wave propagation, and interaction thus has the following form:

$$\frac{\partial a_k}{\partial t} = -\mathrm{i}\frac{\delta H}{\delta a_k^*} + f_k(t) - \gamma_k a_k. \tag{3}$$

It is likely that the statistics of the weak turbulence at $k \gg k_f$ is close to Gaussian for wide classes of pumping statistics (this has not been shown rigorously). It is definitely the case for a random force with the statistics close to Gaussian. We consider here and below a pumping by a Gaussian random force statistically isotropic and homogeneous in space and white in time. Thus,

$$\langle f_k(t) f_{k'}^*(t') \rangle = F(k) \delta(\boldsymbol{k} + \boldsymbol{k}') \delta(t - t'), \tag{4}$$

where angular brackets imply spatial averages, and $F(k)$ is assumed nonzero only around some k_f. For waves to be well defined, we assume $\gamma_k \ll \omega_k$.

Because the dynamic equation (3) contains a quadratic nonlinearity, the statistical description in terms of moments encounters the closure problem: the time derivative of the second moment is expressed via the third one, the time derivative of the third moment is expressed via the fourth one, and so on. Fortunately, weak turbulence in the inertial interval is expected to have the statistics close to Gaussian, so one can express the fourth moment as the product of two second ones. As a result, one gets a closed kinetic equation for the single-time pair correlation function $\langle a_k a_{k'} \rangle = n_k \delta(\boldsymbol{k} + \boldsymbol{k}')$ (Zakharov et al., 1992):

$$\begin{aligned} &\frac{\partial n_k}{\partial t} = F_k - \gamma_k n_k + I_k^{(3)}, \\ &I_k^{(3)} = \int \left(U_{k12} - U_{1k2} - U_{2k1} \right) \mathrm{d}\boldsymbol{k}_1\, \mathrm{d}\boldsymbol{k}_2, \\ &U_{123} = \pi \left[n_2 n_3 - n_1 (n_2 + n_3) \right] |V_{123}|^2 \\ &\qquad \times \delta(\boldsymbol{k}_1 - \boldsymbol{k}_2 - \boldsymbol{k}_3) \delta(\omega_1 - \omega_2 - \omega_3). \end{aligned} \tag{5}$$

This is called the kinetic equation for waves. The collision integral $I_k^{(3)}$ describes three-wave interactions: the first term in the integral corresponds to a decay of a given wave while the second and third terms correspond to a confluence with other waves.

One can estimate from (5) the inverse time of nonlinear interaction at a given k as $|V(k,k,k)|^2 n(k) k^d/\omega(k)$. We define k_d as the wave number where this inverse time is comparable with $\gamma(k)$ and assume nonlinearity to dominate over dissipation at $k \ll k_d$. As has been noted, wave turbulence appears when there is a wide (inertial) interval of scales where both pumping and damping are negligible, which requires $k_d \gg k_f$, the condition analogous to $\mathrm{Re} \gg 1$.

The presence of the frequency delta-function in $I_k^{(3)}$ means that wave interaction conserves the quadratic part of the energy $E = \int \omega_k n_k \, \mathrm{d}\boldsymbol{k} = \int E_k \, \mathrm{d}k$. For the cascade picture to be valid, the collision integral has to converge in the inertial interval which means that energy exchange is small between motions of vastly different scales, a property called interaction locality in k-space. Consider now a statistical steady state established under the action of pumping and dissipation. Let us multiply (5) by ω_k and integrate it over either interior or exterior of the ball with radius k. Taking $k_f \ll k \ll k_d$, one sees that the energy flux through any spherical surface (Ω is a solid angle),

$$P_k = \int_0^k k^{\mathrm{d}-1} \mathrm{d}k \int \mathrm{d}\Omega \, \omega_k I_k^{(3)},$$

is constant in the inertial interval and is equal to the energy production/dissipation rate:

$$P_k = \varepsilon = \int \omega_k F_k \, \mathrm{d}\boldsymbol{k} = \int \gamma_k E_k \, \mathrm{d}k. \qquad (6)$$

Let us assume now that the medium (characterized by ω_k and V_{123}) can be considered isotropic at the scales in the inertial interval. In addition, for scales much larger or much smaller than a typical scale in the medium (like the Debye radius in plasma or the depth of the water), the Hamiltonian coefficients are usually scale invariant: $\omega(k) = ck^\alpha$ and $|V(\boldsymbol{k}, \boldsymbol{k}_1, \boldsymbol{k}_2)|^2 = V_0^2 k^{2m} \chi(\boldsymbol{k}_1/k, \boldsymbol{k}_2/k)$ with $\chi \simeq 1$. Remember that we presumed statistically isotropic force. In this case, the pair correlation function that describes a steady cascade is also isotropic and scale invariant:

$$n_k \simeq \varepsilon^{1/2} V_0^{-1} k^{-m-d}. \qquad (7)$$

One can show that (7) reduces $I_k^{(3)}$ to zero (see Zakharov et al., 1992).

If the dispersion relation $\omega(k)$ does not allow for the resonance condition $\omega(k_1)+\omega(k_2) = \omega(|\boldsymbol{k}_1 + \boldsymbol{k}_2|)$, then the three-wave collision integral is zero and one has to account for four-wave scattering which is always resonant; that is, whatever $\omega(k)$ one can always find four wave vectors that satisfy $\omega(k_1) + \omega(k_2) = \omega(k_3) + \omega(k_4)$ and $\boldsymbol{k}_1 + \boldsymbol{k}_2 = \boldsymbol{k}_3 + \boldsymbol{k}_4$. The collision integral that describes scattering,

$$I_k^{(4)} = \frac{\pi}{2} \int |T_{k123}|^2 \big[n_2 n_3 (n_1 + n_k) - n_1 n_k (n_2 + n_3) \big] \delta(\boldsymbol{k} + \boldsymbol{k}_1 - \boldsymbol{k}_2 - \boldsymbol{k}_3) \times \delta(\omega_k + \omega_1 - \omega_2 - \omega_2) \, \mathrm{d}\boldsymbol{k}_1 \, \mathrm{d}\boldsymbol{k}_2 \, \mathrm{d}\boldsymbol{k}_3, \qquad (8)$$

conserves the energy and also the wave action $N = \int n_k \, \mathrm{d}\boldsymbol{k}$ (which can also be called the number of waves). Pumping generally provides for an input of both E and N. If there are two inertial intervals (at $k \gg k_f$ and $k \ll k_f$), then there should be two cascades. Indeed, if $\omega(k)$ grows with k, then absorbing finite amount of E at $k_d \to \infty$ corresponds to an absorption of an infinitely small N. It is thus clear that the flux of N has to go in the opposite direction, that is, to small wave numbers. A so-called inverse cascade with a constant flux of N can thus be realized at $k \ll k_f$. A sink at small k can be provided by wall friction in the container or by long waves leaving the turbulent region in open spaces (as in sea storms).

The collision integral $I_k^{(3)}$ involves products of two n_k, so that flux constancy requires $E_k \propto \varepsilon^{1/2}$ while for the four-wave case, one has $E_k \propto \varepsilon^{1/3}$. In many cases (when there is complete self-similarity), that knowledge is sufficient to obtain the scaling of E_k from a dimensional reasoning without actually calculating V and T. For example, short waves in deep water are characterized by the surface tension σ and density ρ, so the dispersion relation must be $\omega_k \sim \sqrt{\sigma k^3/\rho}$, which allows for the three-wave resonance and thus $E_k \sim \varepsilon^{1/2} (\rho\sigma)^{1/4} k^{-7/4}$. For long waves in deep water, the surface-restoring force is dominated by gravity, so that the gravitational acceleration g replaces σ as a defining parameter and $\omega_k \sim \sqrt{gk}$. Such a dispersion law does not allow for three-wave resonance, so that the dominant interaction is four-wave scattering which permits two cascades. The direct energy cascade corresponds to $E_k \sim \varepsilon^{1/3} \rho^{2/3} g^{1/2} k^{-5/2}$. The inverse cascade carries the flux of N which we denote Q; it has the dimensionality $[Q] = [\varepsilon]/[\omega_k]$ and corresponds to $E_k \sim Q^{1/3} \rho^{2/3} g^{2/3} k^{-7/3}$.

Because the statistics of weak turbulence is near Gaussian, it is completely determined by the pair correlation function, which is in turn determined by the respective flux. We thus conclude that weak turbulence is universal in the inertial interval.

Strong Wave Turbulence

One cannot treat wave turbulence as a set of weakly interacting waves when the wave amplitudes are large ($\xi_k \geq 1$) and also in the particular case of linear

(acoustic) dispersion where $\omega(k) = ck$ for arbitrarily small amplitudes. Indeed, there is no dispersion of wave velocity for acoustic waves, so waves moving in the same direction interact strongly and produce shock waves when viscosity is small. Formally, there is a singularity due to the coinciding arguments of delta-functions in (5) (and in the higher terms of perturbation expansion for $\partial n_k/\partial t$), which is thus invalid at however small amplitudes. Still, some features of the statistics of acoustic turbulence can be understood even without a closed description.

Consider a one-dimensional case which pertains, for instance, to sound propagating in long pipes. Because weak shocks are stable with respect to transverse perturbations (Landau & Lifshitz, 1987), quasi-one-dimensional perturbations may propagate in two and three dimensions as well. In a reference frame that moves with the sound velocity, weakly compressible 1-d flows ($u \ll c$) are described by the Burgers equation (Landau & Lifshitz, 1987)

$$u_t + uu_x - \nu u_{xx} = 0. \tag{9}$$

The Burgers equation has a propagating shock-wave solution $u = 2v\{1 + \exp[v(x - vt)/\nu]\}^{-1}$ with the energy dissipation rate $\nu \int u_x^2 \, \mathrm{d}x$ independent of ν. The shock width ν/v is a dissipative scale, and we consider acoustic turbulence produced by a pumping correlated on much larger scales (i.e., pumping a pipe from one end by frequencies much less than cv/ν). After some time, the system will develop shocks at random positions. Here we consider the single-time statistics of the Galilean invariant velocity difference $\delta u(x, t) = u(x, t) - u(0, t)$. The moments of δu are called structure functions $S_n(x, t) = \langle [u(x, t) - u(0, t)]^n \rangle$. Quadratic nonlinearity allows the time derivative of the second moment to be expressed via the third one:

$$\frac{\partial S_2}{\partial t} = -\frac{\partial S_3}{3\partial x} - 4\varepsilon + \nu \frac{\partial^2 S_2}{\partial x^2}. \tag{10}$$

Here $\varepsilon = \nu \langle u_x^2 \rangle$ is the mean energy dissipation rate. Equation (10) describes both a free decay (then ε depends on t) and the case of a permanently acting pumping which generates turbulence statistically steady at scales less than the pumping length.

In the first case, $\partial S_2/\partial t \simeq S_2 u/L \ll \varepsilon \simeq u^3/L$ (where L is a typical distance between shocks); while in the second case, $\partial S_2/\partial t = 0$ so that $S_3 = 12\varepsilon x + \nu \partial S_2/\partial x$. Consider now the limit $\nu \to 0$ at fixed x (and t for decaying turbulence). Shock dissipation provides for a finite limit of ε at $\nu \to 0$, then

$$S_3 = -12\varepsilon x. \tag{11}$$

This formula is a direct analog of (6). Indeed, the Fourier transform of (10) describes the energy density $E_k = \langle |u_k|^2 \rangle /2$: $(\partial_t - \nu k^2) E_k = -\partial P_k/\partial k$ where the k-space flux

$$P_k = \int_0^k \mathrm{d}k' \int_{-\infty}^{\infty} \mathrm{d}x \, S_3(x) k' \sin(k'x)/24.$$

It is thus the flux constancy that fixes $S_3(x)$ which is universal (determined solely by ε) and depends neither on the initial statistics for decay nor on the pumping for steady turbulence. On the contrary, other structure functions $S_n(x)$ are not given by $(\varepsilon x)^{n/3}$. Indeed, the scaling of the structure functions can be readily understood for any dilute set of shocks (that is, when shocks do not cluster in space) which seems to be the case for both smooth initial conditions and large-scale pumping in Burgers turbulence. In this case, $S_n(x) \sim C_n|x|^n + C_n'|x|$, where the first term comes from the regular (smooth) parts of the velocity while the second comes from $O(x)$ probability to have a shock in the interval x. The scaling exponents, $\xi_n = \mathrm{d} \ln S_n/\mathrm{d} \ln x$, thus behave as follows: $\xi_n = n$ for $n \leq 1$ and $\xi_n = 1$ for $n > 1$. That means that the probability density function (PDF) of the velocity difference in the inertial interval $P(\delta u, x)$ is not scale-invariant; that is, the function of the rescaled velocity difference $\delta u/x^a$ cannot be made scale-independent for any a. As one goes to smaller scales, the lower-order moments decrease faster than the higher-order ones, that means that the smaller the scale the more probable are large fluctuations. In other words, the level of fluctuations increases with the resolution. When the scaling exponents ξ_n do not lie on a straight line, this is called an anomalous scaling since it is related again to the symmetry (scale invariance) of the PDF broken by pumping and not restored even when $x/L \to 0$. As an alternative to the description in terms of structures (shocks), one can relate the anomalous scaling in Burgers turbulence to the additional integrals of motion. Indeed, the integrals $E_n = \int u^{2n} \, \mathrm{d}x/2$ are all conserved by the inviscid Burgers equation. Any shock dissipates the finite amount of E_n at the limit $\nu \to 0$, so that similar to (11), one denotes $\langle \dot{E}_n \rangle = \varepsilon_n$ and obtains $S_{2n+1} = -4(2n + 1)\varepsilon_n x/(2n - 1)$ for integer n.

Note that $S_2(x) \propto |x|$ corresponds to $E(k) \propto k^{-2}$, which is natural since every shock gives $u_k \propto 1/k$ at $k \ll v/\nu$; that is, the energy spectrum is determined by the type of structures (shocks) rather than by energy flux constancy. Similar ideas were suggested for other types of strong wave turbulence assuming them to be dominated by different structures. Weak wave turbulence, being a set of weakly interacting plane waves, can be studied uniformly for different systems (Zakharov et al., 1992). On the contrary, when nonlinearity is comparable with or exceeds dispersion, different structures appear in different systems. Identifying structures and the role they play in determining different statistical characteristics of strong wave turbulence remains to be investigated for most cases. Broadly, one distinguishes conservative

structures (like solitons and vortices) from dissipative structures which usually appear as a result of finite-time singularity of the nondissipative equations (like shocks, light self-focusing, or wave collapse). For example, nonlinear wave packets are described by the nonlinear Schrödinger equation,

$$i\Psi_t + \Delta\Psi + T|\Psi|^2\Psi = 0. \qquad (12)$$

Weak wave turbulence is determined by $|T|^2$ and is the same for both $T < 0$ (wave repulsion) and $T > 0$ (wave attraction). At high levels of nonlinearity, different signs of T correspond to dramatically different physics: At $T < 0$, one has a stable condensate, solitons, and vortices, while at $T > 0$, instabilities dominate and wave collapse is possible at $d = 2, 3$. No analytic theory is yet available for strong turbulence described by (12).

Because the parameter of nonlinearity $\xi(k)$ generally depends on k, then there may exist a weakly turbulent cascade until some k_* where $\xi(k_*) \sim 1$, and strong turbulence beyond this, wave number; thus weak and strong turbulence can coexist in the same system. Presuming that some mechanism (for instance, wave breaking) prevents the appearance of wave amplitudes that correspond to $\xi_k \gg 1$, one may hypothetize that some cases of strong turbulence correspond to the balance between dispersion and nonlinearity local in k-space so that $\xi(k)$ is constant throughout its domain in k-space. That would correspond to the spectrum $E_k \sim \omega_k^3 k^{-d}/|V_{kkk}|^2$ which is ultimately universal, that is, independent even of the flux (only the boundary k_* depends on the flux). For gravity waves, this gives $E_k = \rho g k^{-3}$, the same spectrum one obtains presuming the wave profile to have cusps (another type of dissipative structure leading to whitecaps in stormy seas—see Phillips, 1977). It is unclear if such flux-independent spectra are realized.

Incompressible Turbulence

Incompressible fluid flow is described by the Navier–Stokes equation

$$\partial_t \boldsymbol{v}(\boldsymbol{r}, t) + \boldsymbol{v}(\boldsymbol{r}, t) \cdot \nabla \boldsymbol{v}(\boldsymbol{r}, t) - \nu \nabla^2 \boldsymbol{v}(\boldsymbol{r}, t) = -\nabla p(\boldsymbol{r}, t), \quad \operatorname{div} \boldsymbol{v} = 0.$$

We are again interested in the structure functions $S_n(\boldsymbol{r}, t) = \langle [(\boldsymbol{v}(\boldsymbol{r}, t) - \boldsymbol{v}(0, t)) \cdot \boldsymbol{r}/r]^n \rangle$ and treat first the three-dimensional case. Similar to (10), one considers distance r smaller than the force correlation scale for a steady case and smaller than the size of the turbulent region for a decay case. For such r, one can derive the Karman–Howarth relation between S_2 and S_3 (see Landau & Lifshitz, 1987):

$$\frac{\partial S_2}{\partial t} = -\frac{1}{3r^4}\frac{\partial}{\partial r}(r^4 S_3) + \frac{4\varepsilon}{3} + \frac{2\nu}{r^4}\frac{\partial}{\partial r}\left(r^4 \frac{\partial S_2}{\partial r}\right). \qquad (13)$$

Here $\varepsilon = \nu \langle (\nabla \boldsymbol{v})^2 \rangle$ is the mean energy dissipation rate. Neglecting the time derivative (which is zero in a steady state and small compared with ε for decaying turbulence), one can multiply (13) by r^4 and integrate $S_3(r) = -4\varepsilon r/5 + 6\nu\, \mathrm{d}S_2(r)/\mathrm{d}r$. Andrei Kolmogorov in 1941 considered the limit $\nu \to 0$ for fixed r and *assumed* nonzero limit for ε, which gives the so-called $\frac{4}{5}$ law (see Landau & Lifshitz, 1987; Frisch, 1995):

$$S_3 = -\tfrac{4}{5}\,\varepsilon\, r. \qquad (14)$$

This relation is a direct analog of (6) and (11). It also means that the kinetic energy has a constant flux in the inertial interval of scales (the viscous scale η is defined by $\nu S_2(\eta) \simeq \varepsilon \eta^2$). Law (14) implies that the third-order moment is universal; that is, it does not depend on the details of the turbulence production but is determined solely by the mean energy dissipation rate. The rest of the structure functions have not yet been derived. Kolmogorov (and also Werner Heisenberg, Karl von Weizsacker, and Lars Onsager) presumed the pair correlation function to be determined only by ε and r which would give $S_2(r) \sim (\varepsilon r)^{2/3}$ and the energy spectrum $E_k \sim \varepsilon^{2/3} k^{-5/3}$. Experiments suggest that $\zeta_n = \mathrm{d} \ln S_n / \mathrm{d} \ln r$ lie on a smooth concave curve sketched in Figure 1. While ζ_2 is close to $2/3$, it has to be a bit larger because experiments show that the slope at zero $\mathrm{d}\zeta_n/\mathrm{d}n$ is larger than $\frac{1}{3}$ while $\zeta(3) = 1$ in agreement with (14). As in Burgers turbulence, the PDF of velocity differences in the inertial interval is not scale-invariant in 3-d incompressible turbulence. No one has yet found an explicit relation between the anomalous scaling for 3-d Navier–Stokes turbulence and either structures or additional integrals of motion.

While not exact, the Kolomogorov approximation $S_2(\eta) \simeq (\varepsilon\eta)^{2/3}$ can be used to estimate the viscous scale: $\eta \simeq L\mathrm{Re}^{-3/4}$. The number of degrees of freedom involved in 3-d incompressible turbulence can thus be roughly estimated as $N \sim (L/\eta)^3 \sim \mathrm{Re}^{9/4}$. That means, in particular, that detailed computer simulation of water or oil pipe flows ($\mathrm{Re} \sim 10^4 - 10^7$) or turbulent clouds ($\mathrm{Re} \sim 10^6 - 10^9$) is out of question for the foreseeable future. To calculate correctly at least the large-scale part of the flow, it is desirable to have some theoretical model to parametrize the small-scale motions, the main obstacle being our lack of qualitative understanding and quantitative description of how turbulence statistics changes as one goes downscale.

Large-scale motions in a shallow fluid can be approximately considered two dimensional. When the velocities of such motions are much smaller than the velocities of the surface waves and the velocity of sound, such flows can be considered incompressible. Their description is important for understanding atmospheric and oceanic turbulence at the scales larger than atmosphere height and ocean depth.

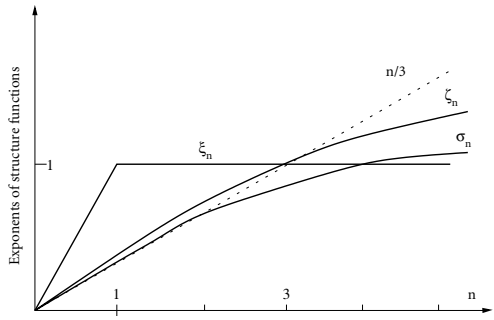

Figure 1. The scaling, exponents of the structure functions ξ_n for Burgers, ζ_n for Navier–Stokes, and σ_n for the passive scalar. The dotted straight line is the Kolmogorov hypothesis $n/3$.

Vorticity $\omega = \operatorname{curl} \boldsymbol{v}$ is a scalar in a two-dimensional flow. It is advected by the velocity field and dissipated by viscosity. Taking the curl of the Navier–Stokes equation, one gets

$$\partial_t \omega + (\boldsymbol{v} \cdot \boldsymbol{\nabla})\omega = \nu \nabla^2 \omega. \tag{15}$$

Two-dimensional incompressible inviscid flow just transports vorticity from place to place and thus conserves spatial averages of any function of vorticity. In particular, we now have the second quadratic inviscid invariant (in addition to energy) which is called enstrophy: $\int \omega^2 \, \mathrm{d}\boldsymbol{r}$. Since the spectral density of the energy is $|\boldsymbol{v}_k|^2/2$ while that of the enstrophy is $|\boldsymbol{k} \times \boldsymbol{v}_k|^2$, Robert Kraichnan suggested in 1967 that the direct cascade (towards large k) is that of enstrophy while the inverse cascade is that of energy. Again, for the inverse energy cascade, there is no consistent theory except for the flux relation that can be derived similar to (14):

$$S_3(r) = 4\varepsilon r/3. \tag{16}$$

The inverse cascade is observed in the atmosphere (at scales of 30–500 km) and in laboratory experiments. Experimental data suggest that there is no anomalous scaling; thus, $S_n \propto r^{n/3}$. In particular, $S_2 \propto r^{2/3}$ which corresponds to $E_k \propto k^{-5/3}$. It is ironic that probably the most widely known statement on turbulence, the $\frac{5}{3}$ spectrum suggested by Kolmogorov for the 3-d case, is not correct in this case (even though the true scaling is close), while it is probably exact in Kraichnan's inverse 2-d cascade. Qualitatively, it is likely that the absence of anomalous scaling in the inverse cascade is associated with the growth of the typical turnover time (estimated, say, as $r/\sqrt{S_2}$) with the scale. As the inverse cascade proceeds, the fluctuations have enough time to get smoothed out as opposed to the direct cascade in three dimensions, where the turnover time decreases in the direction of the cascade.

Before discussing the direct (enstrophy) cascade, we describe a similar yet somewhat simpler problem of passive scalar turbulence, which allows one to introduce the necessary notions of Lagrangian description of the fluid flow. Consider a scalar quantity $\theta(\boldsymbol{r}, t)$ that is subject to molecular diffusion and advection by the fluid flow but has no back influence on the velocity (i.e., is passive):

$$\partial_t \theta + (\boldsymbol{v} \cdot \boldsymbol{\nabla})\theta = \kappa \nabla^2 \theta + \varphi. \tag{17}$$

Here κ is molecular diffusivity. In the same 2-d flow, ω and θ behave in the same way, but vorticity is related to velocity while the passive scalar is not. Examples of passive scalar are smoke in air, salinity in water, and temperature when one neglects thermal convection. If the source φ produces fluctuations of θ on some scale L, then the inhomogeneous velocity field stretches, contracts, and folds the field θ producing progressively smaller and smaller scales. If the rms velocity gradient is Λ, then molecular diffusion is substantial at scales less than the diffusion scale $r_d = \sqrt{\kappa/\Lambda}$. The ratio

$$\mathrm{Pe} = L/r_d$$

is called the Péclet number. It is an analog of the Reynolds number for passive scalar turbulence. When $\mathrm{Pe} \gg 1$, there is a long inertial interval where the flux constancy relation derived by A.M. Yaglom in 1949 holds,

$$\langle (\boldsymbol{v}_1 \cdot \boldsymbol{\nabla}_1 + \boldsymbol{v}_2 \cdot \boldsymbol{\nabla}_2)\theta_1\theta_2 \rangle = 2P, \tag{18}$$

where $P = \kappa \, \langle \, (\nabla\theta)^2 \, \rangle$ and subscripts denote the spatial points. In considering the passive scalar problem, the velocity statistics is presumed to be given. Still, the correlation function (18) mixes $\boldsymbol{v}$ and θ and does not generally allow one to make a statement on any correlation function of θ. The proper way to describe the correlation functions of the scalar at scales much larger

than the diffusion scale is to employ the Lagrangian description, that is, to follow fluid trajectories. Indeed, if we neglect diffusion, then Equation (17) can be solved along the characteristics $\boldsymbol{R}(t)$ which are called Lagrangian trajectories and satisfy $\mathrm{d}\boldsymbol{R}/\mathrm{d}t = \boldsymbol{v}(\boldsymbol{R}, t)$. Presuming zero initial conditions at $t \to -\infty$, we write

$$\theta\Big(\boldsymbol{R}(t), t\Big) = \int_{-\infty}^{t} \varphi\Big(\boldsymbol{R}(t'), t'\Big)\, \mathrm{d}t'. \qquad (19)$$

In that way, the correlation functions of the scalar $F_n = \langle\, \theta(\boldsymbol{r}_1, t) \ldots \theta(\boldsymbol{r}_n, t)\,\rangle$ can be obtained by integrating the correlation functions of the pumping along the trajectories that satisfy the final conditions $\boldsymbol{R}_i(t) = \boldsymbol{r}_i$.

Consider first, the case of pumping which is Gaussian, statistically homogeneous, and isotropic in space and white in time: $\langle\, \varphi(\boldsymbol{r}_1, t_1)\varphi(\boldsymbol{r}_2, t_2)\,\rangle = \Phi(|\boldsymbol{r}_1 - \boldsymbol{r}_2|)\, \delta(t_1 - t_2)$ where the function Φ is constant at $r \ll L$ and goes to zero at $r \gg L$. The pumping provides for symmetry $\theta \to -\theta$ which makes only even correlation functions F_{2n} nonzero. The pair correlation function is

$$F_2(r, t) = \int_{-\infty}^{t} \Phi\Big(R_{12}(t')\Big)\, \mathrm{d}t'. \qquad (20)$$

Here $R_{12}(t') = |\boldsymbol{R}_1(t') - \boldsymbol{R}_2(t')|$ is the distance between two trajectories and $R_{12}(t) = r$. The function Φ essentially restricts the integration to the time interval when the distance $R_{12}(t') \le L$. Simply speaking, the stationary pair correlation function of a tracer is $\Phi(0)$ (which is twice the injection rate of θ^2) times the average time $T_2(r, L)$ that two fluid particles spend within the correlation scale of the pumping. The larger r, the less time it takes for the particles to separate from r to L and the smaller is $F_2(r)$. Of course, $T_{12}(r, L)$ depends on the properties of the velocity field. A general theory is available only when the velocity field is spatially smooth at the scale of scalar pumping L. This so-called Batchelor regime happens, in particular, when the scalar cascade occurs at the scales less than the viscous scale of fluid turbulence. This requires the Schmidt number ν/κ (called the Prandtl number when θ is temperature) to be large, which is the case for very viscous liquids. In this case, one can approximate the velocity difference $\boldsymbol{v}(\boldsymbol{R}_1, t) - \boldsymbol{v}(\boldsymbol{R}_2, t) \approx \hat{\sigma}(t)\boldsymbol{R}_{12}(t)$ with the Lagrangian strain matrix $\sigma_{ij}(t) = \nabla_j v_i$. In this regime, the distance obeys the linear differential equation

$$\dot{\boldsymbol{R}}_{12}(t) = \hat{\sigma}(t)\boldsymbol{R}_{12}(t). \qquad (21)$$

The theory of such equations is well developed and related to what is called Lagrangian chaos, as fluid trajectories separate exponentially as is typical for systems with dynamical chaos (see, e.g., Falkovich et al., 2001): At t much larger than the correlation time of the random process $\hat{\sigma}(t)$, all moments of R_{12} grow exponentially with time and $\langle\, \ln[R_{12}(t)R_{12}(0)]\,\rangle = \lambda t$, where λ is called a senior Lyapunov exponent of the flow (note that for the description of the scalar we need the flow taken backwards in time which is different from that taken forward because turbulence is irreversible). Dimensionally, $\lambda = \Lambda f(\mathrm{Re})$ where the limit of the function f at $\mathrm{Re} \to \infty$ is unknown. We thus obtain

$$F_2(r) = \Phi(0)\lambda^{-1} \ln(L/r) = 2P\lambda^{-1} \ln(L/r). \quad (22)$$

In a similar way, one shows that for $n \ll \ln(L/r)$, all F_n are expressed via F_2 and the structure functions $S_{2n} = \langle\, [\theta(\boldsymbol{r}, t) - \theta(0, t)]^{2n}\,\rangle \propto \ln^n(r/r_d)$ for $n \ll \ln(r/r_d)$. This can be generalized for an arbitrary statistics of pumping as long as it is finite-correlated in time (Falkovich et al., 2001).

One can use the analogy between passive scalar and vorticity in two dimensions as has been shown by Falkovich and Lebedev in 1994 following the line suggested by Kraichnan in 1967. For the enstrophy cascade, one derives the flux relation analogous to (18):

$$\langle(\boldsymbol{v}_1 \cdot \boldsymbol{\nabla}_1 + \boldsymbol{v}_2 \cdot \boldsymbol{\nabla}_2)\omega_1\omega_2\rangle = 2D, \qquad (23)$$

where $D = \langle\, \nu(\nabla\omega)^2\,\rangle$. The flux relation along with $\omega = \mathrm{curl}\, \boldsymbol{v}$ suggests the scaling $\delta v(r) \propto r$, that is, velocity being close to spatially smooth (of course, it cannot be perfectly smooth to provide for a nonzero vorticity dissipation in the inviscid limit, but the possible singularitites are indeed shown to be no stronger than logarithmic). That makes the vorticity cascade similar to the Batchelor regime of passive scalar cascade with a notable change in that the rate of stretching λ acting on a given scale is not a constant but is logarithmically growing when the scale decreases. Since λ scales as vorticity, the law of renormalization can be established from dimensional reasoning, and one gets $\langle\omega(\boldsymbol{r}, t)\omega(0, t)\,\rangle \sim [D \ln(L/r)]^{2/3}$ which corresponds to the energy spectrum $E_k \propto D^{2/3}k^{-3} \ln^{-1/3}(kL)$. Higher-order correlation functions of vorticity are also logarithmic, for instance, $\langle\, \omega^n(\boldsymbol{r}, t)\omega^n(0, t)\,\rangle \sim [D \ln(L/r)]^{2n/3}$. Note that both passive scalar in the Batchelor regime and vorticity cascade in two dimensions are universal, that is, determined by the single flux (P and D, respectively) despite the existence of higher-order conserved quantities. Experimental data and numeric simulations support these conclusions.

Zero Modes and Anomalous Scaling

Let us now return to the Lagrangian description and discuss it when velocity is not spatially smooth, for example, that of the energy cascades in the inertial interval. One can assume that it is Lagrangian statistics that are determined by the energy flux when the distances between fluid trajectories are in the inertial interval. That assumption leads, in particular, to the Richardson law for the asymptotic growth of the

interparticle distance:

$$\langle R_{12}^2(t)\rangle \sim \varepsilon t^3, \tag{24}$$

which was first established from atmospheric observations (in 1926) and later confirmed experimentally for energy cascades both in 3-d and in 2-d. There is no consistent theoretical derivation of (24), and it is unclear whether it is exact (likely to be in 2-d) or just approximate (possible in 3-d). The semi-heuristic argument usually presented in textbooks is based on the mean-field estimate: $\dot{\boldsymbol{R}}_{12} = \delta\boldsymbol{v}(\boldsymbol{R}_{12}, t) \sim (\varepsilon R_{12})^{1/3}$, which upon integration gives $R_{12}^{2/3}(t) - R_{12}^{2/3}(0) \sim \varepsilon^{1/3} t$. For the passive scalar it gives, by virtue of (20), $F_2(r) \sim \Phi(0)\varepsilon^{-1/3}[L^{2/3} - r^{2/3}]$ which was suggested by S. Corrsin and A.M. Oboukhov. The structure function is then $S_2(r) \sim \Phi(0)\varepsilon^{-1/3} r^{2/3}$. Experiments measuring the scaling exponents $\sigma_n = \mathrm{d}\ln S_n(r)/\mathrm{d}\ln r$ generally give σ_2 close to $2/3$ but higher exponents deviating from the straight line are even stronger than the exponents of the velocity in 3-d. Moreover, the scalar exponents σ_n are anomalous even when advecting velocity has a normal scaling like in the 2-d energy cascade.

To better understand the Lagrangian dynamics (and passive scalar statistics) in a spatially nonsmooth velocity, Kraichnan suggested considering the model of a velocity field as having the simplest statistical and temporal properties, namely Gaussian velocity which is white in time:

$$\langle v^i(\boldsymbol{r}, t) v^j(0, 0)\rangle = \delta(t)\Big[D_0\delta_{ij} - d_{ij}(\boldsymbol{r})\Big],$$
$$d_{ij} = D_1 r^{2-\gamma}\Big[(d + 1 - \gamma)\,\delta^{ij} + (\gamma - 2) r^i r^j r^{-2}\Big]. \tag{25}$$

Here the exponent $\gamma \in [0, 2]$ is a measure of the velocity nonsmoothness with $\gamma = 0$ corresponding to a smooth velocity and $\gamma = 2$ corresponding to a velocity very rough in space (distributional). Richardson–Kolmogorov scaling of the energy cascade corresponds to $\gamma = 2/3$. Lagrangian flow is a Markov random process for the Kraichnan ensemble (25). Every fluid particle undergoes a Brownian random walk with the so-called eddy diffusivity D_0. The PDF for two particles to be separated by r after time t satisfies the diffusion equation (see, e.g., Falkovich et al., 2001)

$$\partial_t P(r, t) = L_2 P(r, t)\,,$$
$$L_2 = d_{ij}(\boldsymbol{r})\nabla^i\nabla^j = D_1(d - 1) r^{1-d}\partial_r r^{d+1-\gamma}\partial_r, \tag{26}$$

with the scale-dependent diffusivity $D_1(d-1)r^{2-\gamma}$. The asymptotic solution of (26) is lognormal for the Batchelor case while for $\gamma > 0$

$$P(r, t) = r^{d-1} t^{d/\gamma} \exp\Big(-\mathrm{const}\, r^\gamma / t\Big). \tag{27}$$

For $\gamma = 2/3$, it reproduces, in particular, the Richardson law. Multiparticle probability distributions also satisfy diffusion equations in the Kraichnan model as well as all the correlation functions of θ. Multiplying equation (17) by $\theta_2 \ldots \theta_{2n}$ and averaging over the Gaussian statistics of $\boldsymbol{v}$ and φ, one derives

$$\partial_t F_{2n} = L_{2n} F_{2n} + \sum_{l,m} F_{2n-2}\Phi(\boldsymbol{r}_{lm})\,,$$
$$L_{2n} = \sum d_{ij}(\boldsymbol{r}_{lm})\nabla_l^i \nabla_m^j. \tag{28}$$

This equation enables one, in principle, to derive inductively all steady-state F_{2n} starting from F_2. The equation $\partial_t F_2(r, t) = L_2 F_2(r, t) + \Phi(r)$ has a steady solution $F_2(r) = 2[\Phi(0)/\gamma d(d-1)D_1][dL^\gamma/(d-\gamma) - r^\gamma]$, which has the Corrsin–Oboukhov form for $\gamma = 2/3$. Further, F_4 contains the so-called forced solution having the normal scaling 2γ but also, remarkably, a zero mode Z_4 of the operator L_4: $L_4 Z_4 = 0$. Such zero modes necessarily appear (to satisfy the boundary conditions at $r \simeq L$) for all $n > 1$, and the scaling exponents of Z_{2n} are generally different from $n\gamma$ that is anomalous. In calculating the scalar structure functions, all terms cancel out except a single zero mode (called irreducible because it involves all distances between $2n$ points). Calculations of Z_n and their scaling exponents σ_n were carried out analytically at $\gamma \ll 1$, $2 - \gamma \ll 1$ and $d \gg 1$, and numerically for all γ and $d = 2, 3$ (Falkovich et al., 2001).

That gives σ_n lying on a convex curve (as in Figure 1) which saturates to a constant at large n. Such saturation (confirmed by experiments) is a signature that most singular structures in a scalar field are shocks (as in Burgers turbulence), the value σ_n at $n \to \infty$ is the fractal codimension of fronts in space. Interestingly, the Kraichnan model enables one to establish the relation between the anomalous scaling and conservation laws of a new type. Thus, the combinations of distances between points that constitute zero modes are the statistical integrals of Lagrangian evolution. To give a simple example, in a Brownian walk, the mean distance between every two particles grows with time, $\langle R_{lm}^2(t)\rangle = R_{lm}^2(0) + \kappa t$, while $\langle R_{lm}^2 - R_{pq}^2\rangle$ and $\langle 2(d+2)R_{lm}^2 R_{pq}^2 - d(R_{lm}^4 + R_{pq}^4)\rangle$ (and an infinity of similarly built harmonic polynomials) are conserved. Note that the integrals are not dynamical, they are conserved only in average. In a turbulent flow, the form of such conserved quantities is more complicated, but the essence is the same: the increase of averaged distances between fluid particles is compensated by the decrease in shape fluctuations. The existence of statistical conserved quantities breaks the scale invariance of scalar statistics in the inertial interval and explains why scalar turbulence knows more about pumping than just the value of the flux. Note that both symmetries, one broken by pumping (scale invariance) and another by damping (time reversibility) are not restored even when $r/L \to 0$ and $r_d/r \to 0$.

For the vector field (like velocity or magnetic field in magnetohydrodynamics), the Lagrangian statistical integrals of motion may involve both the coordinate of the fluid particle and the vector it carries. Such integrals of motion were built explicitly and related to the anomalous scaling for the passively advected magnetic field in the Kraichnan ensemble of velocities (Falkovich et al., 2001). Doing the same for velocity that satisfies the Navier–Stokes equation remains a task for the future.

GREGORY FALKOVICH

See also **Burgers equation; Chaos vs. turbulence; Development of singularities; Intermittency; Kolmogorov cascade; Lagrangian chaos; Magnetohydrodynamics; Mixing; Navier–Stokes equation; Nonlinear Schrödinger equations; Water waves; Wave packets, linear and nonlinear**

Further Reading

Falkovich, G., Gawędzki, K. & Vergassola, M. 2001. Particles and fields in fluid turbulence, *Reviews of Modern Physics*, 73: 913–975

Frisch, U. 1995. *Turbulence: The Legacy of A.N. Kolmogorov*, Cambridge and New York: Cambridge University Press

Landau, L. & Lifshitz, E. 1987. *Fluid Mechanics*, 2nd edition, Oxford and New York: Pergamon Press

Phillips, O. 1977. *The Dynamics of the Upper Ocean*, 2nd edition, Cambridge and New York: Cambridge University Press

Zakharov, V., L'vov, V. & Falkovich, G. 1992. *Kolmogorov Spectra of Turbulence*, Berlin and New York: Springer

TURBULENCE, IDEAL

Ideal turbulence (IT) is a mathematical phenomenon that occurs in certain infinite-dimensional deterministic dynamical systems. The attractor of an IT system lies off the phase space, and among the attractor points there are fractal or even random functions. IT is observed in various idealized models of real distributed systems (electrodynamics, acoustics, radiophysics, etc.), and it helps to understand the mathematical scenarios for features of real turbulence. Cascade processes in IT are capable of giving birth to structures of arbitrarily small scale and even causing stochastization of the systems.

A mathematically rigorous definition of ideal turbulence is based on notions of dynamical systems theory and chaos theory. Spatiotemporal chaotization in dynamical systems on spaces of smooth or piecewise smooth functions is perceived as a cascading evolution of such functions with the result that their behavior becomes more and more intricate (see Figure 1), whereupon the limiting states cannot be described with smooth functions. This implies that the attractor of the dynamical system is not contained entirely in the phase space; thus, the dynamical system needs to be extended on a wider functional space so that this new space contains whole "ω-limit" sets of all or almost all

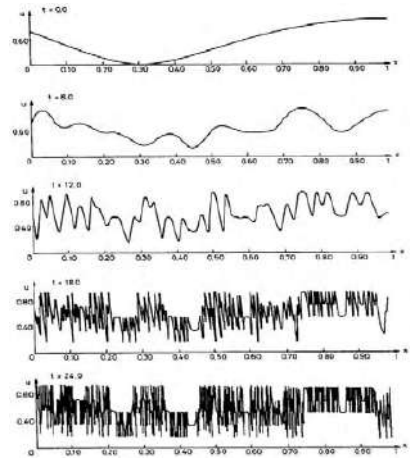

Figure 1. Start of ideal turbulence: Typical instantaneous distributions of current in a lossless transmission line described by the boundary-value problem $i_x = -Cv_t$, $v_x = -Li_t$, and $v(0,t) = 0$, $i(1,t) = G(v(1,t))$, where i and v are the current and voltage along the line, and G specifies the v-i characteristic of an Esaki (tunnel) diode fixing the boundary condition at $x = 1$.

trajectories. (The ω-limit set of a trajectory is defined as the attractor of the trajectory or, more precisely, as the set of limit points of the trajectory.) The spaces of fractal and random functions are particularly appealing for use as a wider space.

If, with such an extension, the ω-limit set of the trajectory corresponding to some initial state contains a "point" that is a fractal function, then this initial state is said to generate IT. Similarly, if a dynamical system can be extended on a space containing both deterministic and random functions and for some initial state its associated ω-limit set contains a "point" that is a random function, then this initial state is said to generate stochastic ideal turbulence (SIT). If initial states generate IT or SIT, then IT or SIT is said to occur in the dynamical system.

For a space containing fractal functions, one may take the space of multivalued functions with the metric $\rho(\zeta_1, \zeta_2) = \mathrm{dist}_H(\mathrm{gr}\,\zeta_1, \mathrm{gr}\,\zeta_2)$, where $\mathrm{dist}_H(\cdot,\cdot)$ is the Hausdorff distance between sets and $\mathrm{gr}\,\zeta$ denotes the graph of ζ. As any function (deterministic or random) can be interpreted as the collection of all its finite-dimensional distributions, a metric for spaces containing random and deterministic functions is conveniently chosen to compare the distributions of functions (Sharkovsky & Romanenko, 1992).

This classification can be deepened. For instance, an initial state is said to generate weak ideal turbulence (WIT) if it does not generate IT but its associated

ω-limit set contains a function that is multivalued at an infinite number of points.

A simple example of a system with turbulence is the discrete dynamical system acting on the space of smooth functions $\varphi : D \to E$ according to the rule

$$S : \varphi(x) \mapsto f(\varphi(x)), \tag{1}$$

where $f : E \to E$ is a smooth function, and D and E are regions of Euclidean spaces. The trajectory through a point φ is the sequence $f^n(\varphi(x))$, $n = 0, 1, 2, \ldots$, where the superscript n denotes the nth iteration. Thus, the dynamics of the trajectory can be treated as the dynamics of a continuum of uncoupled oscillators. At every point $x \in D$, there is a "pendulum," oscillating under the law $z_n \mapsto z_{n+1} = f(z_n)$ with $z_0 = \varphi(x)$ and independently of the pendula at other points of D. The independence of the oscillators causes IT in the dynamical systems (1), and moreover, when f has the property of sensitive dependence on initial data on some open set $E' \subset E$, those φ such that $\varphi(D) \supset E'$ often generate SIT. In more general situations that occur in applied problems, the oscillation law depends on initial data φ and/or a point $x \in D$; it can also be time-dependent.

A description of long-term properties for the dynamical systems (1) is most advantageous when f is a one-dimensional map, and D and E are intervals, whereupon one has the following result:

Theorem. *There occur (i) weak ideal turbulence, if f has periodic trajectories of periods $2^i, 0 \le i \le l$, with some $l > 1$, and no other periodic trajectories; (ii) ideal turbulence, if f has a periodic trajectory of period $\ne 2^i, i = 0, 1, \ldots$; and (iii) stochastic turbulence, if f possesses an ergodic smooth invariant measure.*

The map $f : z \mapsto 4z(1-z)$, $z \in [0, 1]$, has an invariant measure with the density $p(z) = 1/\pi\sqrt{z(1-z)}$, and almost each $\varphi : [0, 1] \to (0, 1)$ generates SIT. Its associated ω-limit set consists of a single point which is the random function with the distribution $F(x, z) = \int_0^z p(z)\,dz = (2/\pi)\arcsin\sqrt{z}$. Thus the attractor of the dynamical system (1) consists of just this one point. For $f = f_\lambda : z \mapsto \lambda z(1-z)$, $0 < \lambda \le 4$, there exists a set of positive Lebesgue measure $\Lambda \subset (3, 4]$ such that f_λ with $\lambda \in \Lambda$ has an ergodic smooth invariant measure on $[0, 1]$; hence SIT in the dynamical systems (1) is a non-exclusive phenomenon.

Many evolutionary boundary-value problems (BVPs) for partial differential equations induce dynamical systems of shifts along solutions. It is natural to say that there arises IT or SIT in a BVP if such turbulence occurs in the corresponding dynamical system. The simplest example is the BVP

$$w_t - w_x = 0,\ 0 \le x \le 1,\ t \ge 0, \tag{2}$$

$$w(1, t) = f(w(0, t)), \tag{3}$$

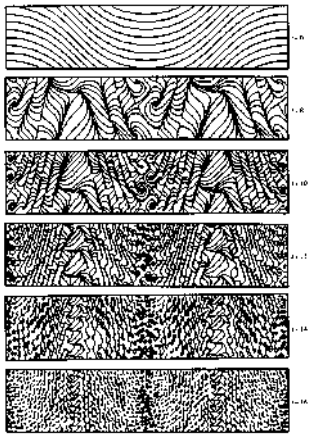

Figure 2. Towards stochastic turbulence: Typical evolution of flow lines for the vector field (w^1, w^2) given by $w^1_t = w^1_x + w^1_y$, $w^2_t = -w^2_x - w^2_y$, $-\infty < x < +\infty$, $0 \le y \le 1$, and $w^1 = w^2|_{y=0}$, $w^1 = f(w^2)|_{y=1}$ with $f(z) = 1 - 2z^2$. The attractor of the BVP consists of one point—the random vector field $(\hat{w}^1, \hat{w}^2)$ whose components have the same (x, y)-independent distribution density $1/2\pi\sqrt{1-z^2}$, $-1 < z < 1$.

where f is a smooth function from some interval E into itself. On the space of smooth functions $\varphi : [0, 1] \to E$, the BVP induces the dynamical system of shifts $S^t : \varphi(x) \mapsto w_\varphi(x, t)$, $t \ge 0$, where $w_\varphi(x, t)$ is the solution meeting the initial condition $w(x, 0) = \varphi(x)$. For the BVP considered, the shift operator S^t is represented as

$$S^t : \varphi(x) \mapsto f^{\langle x+t \rangle}(\varphi(\{x + t\})) \tag{4}$$

with $\langle \cdot \rangle$ and $\{\cdot\}$ being the integer and fractional part of a number, respectively. Thus the dynamical system (4) is a continuous analog of the dynamical system (1), and one can formulate conditions for turbulence in the BVP according to the above theorem.

Replacing (3) with $w_t(1, t) = g(w(0, t))\, w_t(0, t))$ leads to the dynamical system (4) where f is replaced with $f_{\gamma[\varphi]} = f + \gamma[\varphi]$, f is an antiderivative of g and $\gamma[\varphi] = f(\varphi(0)) - \varphi(1)$. The type of the turbulence arising in a solution $w_\varphi(x, t)$ follows the theorem, as applied to $f_{\gamma[\varphi]}$.

BVPs for the wave equation (and related systems) provide examples of ideal turbulence. For the BVP

$$w_{tt} - w_{xx} = 0, \quad 0 \le x \le 1, \tag{5}$$

$$w(0, t) = 0, \quad w_t(1, t) = h(w_x(1, t)), \tag{6}$$

its associated shift operator S^t is expressed through a one-dimensional map $f : z_n \mapsto z_{n+1}$, defined implicitly by $z_{n+1} - z_n = h(z_n + z_{n+1})$. This allows one to find conditions for IT or SIT for particular functions h (Sharkovsky, 1994; Sharkovsky et al., 1995). When the conditions of (6) are replaced with $w(0,t) = 0, \quad w_x(1,t) = h(w_x(0,t))$, there arises a two-dimensional map defined by $z_{n+1} - z_{n-1} = h(z_n)$.

There are many other one- and many-dimensional BVPs whose dynamics are described in terms of low-dimensional maps, as in the above examples. In these cases, the theory of maps suggests why and how turbulence occurs in the BVP and presents scenarios for self-structuring and self-stochastization. Of importance here are the following properties of maps: the intricate dynamical structure of the basins of attracting cycles, the local self-similarity of the set of points with unstable trajectories, and the occurrence of a smooth invariant measure. Figure 2 is an example of how processes of self-structuring lead to stochastic turbulence.

A.N. SHARKOVSKY AND E.YU. ROMANENKO

See also **Attractors; Butterfly effect; Chaotic dynamics; Dimensions; Dynamical systems; Ergodic theory; Maps; Measures; Mixing; One-dimensional maps; Phase space; Routes to chaos; Sinai–Ruelle–Bowen measures; Turbulence**

Further Reading

Romanenko, E.Yu. & Sharkovsky, A.N. 1996. From one-dimensional to infinite-dimensional dynamical systems: ideal turbulence. *Ukrainian Mathematical Journal*, 48(12): 1817–1842

Romanenko, E.Yu., Sharkovsky, A.N. & Vereikina, M.B. 1995. Self-structuring and self-similarity in boundary value problems. *International Journal of Bifurcation and Chaos*, 5(5): 145–156

Sharkovsky, A.N. 1994. Ideal turbulence in an idealized time-delayed Chua's circuit. *International Journal of Bifurcation and Chaos*, 4(2): 303–309

Sharkovsky, A.N., Deregel, Ph. & Chua, L.O. 1995. Dry turbulence and period-adding phenomena from a 1-D map. *International Journal of Bifurcation and Chaos*, 5(5): 1283–1302

Sharkovsky, A.N. & Romanenko, E.Yu. 1992. Ideal turbulence: attractors of deterministic systems may lie in the space of random fields. *International Journal of Bifurcation and Chaos*, 2(1): 31–36

TURING PATTERNS

As noted by D'Arcy Wentworth Thompson (1917) people in the early 1900s (when the study of symmetry-breaking instabilities was still in its infancy) had already considered the possibility of generating stationary regular concentration patterns through the interplay of diffusion and chemistry. At mid-century, the British mathematician and computing pioneer, Alan Turing, was the first to formulate necessary conditions for the occurrence of space symmetry breaking in the context of biological morphogenesis (Turing, 1952). Following the emergence of the self-oscillating Belousov–Zhabotinsky reaction (Epstein & Pojman, 1998) in the mid-1960s, Ilya Prigogine and coworkers revived Turing's concept, put it on sound thermodynamic and kinetic grounds, and showed that it could only be sustained in continuously fed reactors at a finite distance from equilibrium (Nicolis & Prigogine, 1977).

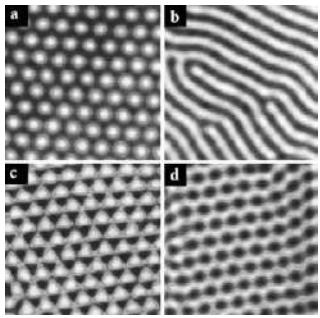

Figure 1. (a)–(d) Turing structures of different symmetries obtained with the chlorite-iodide-malonic acid reaction. Dark and light regions, respectively, correspond to high and low iodide concentration. The wavelength, a function of kinetic parameters and diffusion coefficients, is of the order of 0.2 mm. All patterns are at the same scale: view size 1.7mm × 1.7mm (Courtesy P. De Kepper, CRPP).

This work opened up a whole new field of physical chemistry. Many theoretical studies followed, and the diffusive instability that generates such dissipative structures has popped up in other domains of physics and chemistry (Ball, 1999). However, experiments in the chemical realm lagged behind, and it was only in 1989 that the first experimental evidence was obtained by De Kepper and his group (Castets et al., 1990) using the chlorite-iodide-malonic acid reactive system in so-called gel reactors. A recent detailed status of Turing patterns and other symmetry-breaking instabilities in solution chemistry is presented in Borckmans et al. (2002).

The Turing–Prigogine mechanism consists in the spontaneous instability of a homogeneous mixture of chemically reacting species, when some parameter threshold is crossed as one moves away from equilibrium conditions. It leads to stationary, space-periodic patterns for the concentrations of reactants (see Figure 1). In its minimal form, the description of all the systems that exhibit such diffusive instability can formally be cast in the common language of reaction-diffusion systems governed by the set of equations

$$\frac{\partial \boldsymbol{c}(\boldsymbol{r},t)}{\partial t} = \boldsymbol{f}(\boldsymbol{c},b) + \nabla \cdot D\nabla \boldsymbol{c}(\boldsymbol{r},t), \qquad (1)$$

where $\boldsymbol{c}(\boldsymbol{r}, t) \equiv (\ldots, c_i, \ldots)$ is the local concentration vector, $\boldsymbol{f}(\boldsymbol{c}, b)$ is a vector function representing the reaction kinetics wherein lies the source of nonlinearity, b stands for a set of control parameters, and D is the matrix of diffusive transport coefficients. Appropriate initial and boundary conditions, in relation with the experimental setup are added to complete the mathematical formulation.

To support such symmetry-breaking instability, the chemical kinetics must involve some type of positive feedback loop controlled at least by an activator species that reinforces its own changes, the latter being counterbalanced by an inhibitory process. Spatial structures can form when the inhibitory effects are transported by diffusion over a larger space range than that of the activating mechanism. An intuitive picture may be obtained when a single activator (A) and inhibitor (H) are present. A autocatalytically promotes its own production and that of H, while the latter opposes the production of A. Consider such system in a nonequilibrium homogeneous steady state (hss) and quench it beyond the instability threshold. The hss then becomes very sensitive. A slight local fluctuation of the concentration of A will increase while it also spreads to the surroundings through diffusion. It will also start producing some H that, however, will diffuse away much faster from the point where the fluctuation occurred as $D_{\mathrm{H}} > D_{\mathrm{A}}$. H thereby hinders the propagation of A. A localized peak of activator surrounded by a barrier of H is thus created. In extended systems, such peaks tend to emerge everywhere, randomly distributed, and their interactions lead to the periodic concentration patterns. The beauty of Turing's idea lies in the counterintuitive organization role of diffusive processes when they compete with the proper autocatalytic chemistry, while diffusion still locally strives to erase any concentration of inhomogeneity.

Theoretical work uses nonlinear kinetic models for $\boldsymbol{f}(\boldsymbol{c}, b)$ with a limited number of chemical species, typically two or three (Brusselator, Oregonator, CDIMA, etc.). These models stand as a compromise between a minimum of chemical realism and mathematical tractability. For their part, the experimental kinetic schemes usually involve many species, often not fully determined (Epstein & Pojman, 1998).

Analytical work that relies heavily on bifurcation theory (Nicolis & Prigogine, 1977; Manneville, 1990) allows one to determine, through the solution of amplitude equations, which structures of given symmetry are stable for specific conditions (pattern selection). The calculated bifurcation diagrams help to organize the results obtained by straightforward numerical integration of the reaction-diffusion equations. Both types of information may be used to interpret the experimental results. This pattern selection problem was already on Turing's mind when he stated (Turing, 1952): "Most of an organism, most of the time, is developing from one pattern into another, rather than from homogeneity into a pattern. One would like to be able to follow this more general process mathematically also."

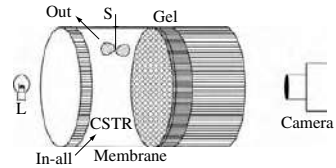

Figure 2. Schematic representation of a disc-shaped one side fed reactor (OSFR): CSTR (continuous stirred tank reactor), Membrane (mineral disc, pore size 0.02 mm) often placed to protect the gel from mechanical stress produced by the stirrer of the CSTR, Gel, In and Out (input and output ports of chemicals), L (light source), CCD camera.

The experimental work takes place in so-called open spatial reactors (Borckmans et al., 2002) which are specifically designed to control the reaction and the structures that eventually develop at a fixed distance from equilibrium and allow probing of the true asymptotic states of the reaction-diffusion systems. Experiments are now usually performed in a one-side fed reactor (OSFR) sketched in Figure 2. The core consists of a piece of soft hydrogel fed by diffusion through one of its faces with chemicals contained in a continuous stirred tank reactor (CSTR), the contents of which are continuously renewed by pumps. The other faces of the gel are pressed against impermeable transparent walls (Plexiglas). Viewing can be practiced both along the feeding axis or orthogonal to it (Ball, 1999; Ouyang & Swinney, 1991). The gel is used to avoid all perturbations induced by the hydrodynamic flows as those associated with the constant supply of fresh reactants, so that only reactive and diffusive processes compete. The necessary diffusion differential between activator and inhibitor species is obtained through the reversible binding of the activator molecules to the large molecular weight color indicator species that is included for visualization purposes. An advantage of such reactors is that they allow for direct correlations to be made between the dynamics of the CSTR, the bifurcation behaviors of which have been extensively studied in the past (Epstein & Pojman, 1998), and that of the gel.

Although scores of papers have been devoted to the application of Turing's idea to biological problems, this speculation remains to be confirmed (Epstein & Pojman, 1998; Borckmans et al., 2002).

PIERRE BORCKMANS AND GUY DEWEL

See also **Belousov–Zhabotinsky reaction; Brusselator; Morphogenesis, biological; Pattern formation; Reaction-diffusion systems**

Further Reading

Ball, P. 1999. *The Self-made Tapestry*, Oxford and New York: Oxford University Press
Borckmans, P., Dewel, G., De Wit, A., Dulos, E., Boissonade, J., Gauffre, F. & De Kepper, P. 2002. Diffusive instabilities and chemical reactions. *International Journal of Bifurcation and Chaos*, 12: 2307–2332
Castets, V., Dulos, E., Boissonade, J. & De Kepper, P. 1990. Experimental evidence of a sustained standing Turing-type nonequilibrium chemical pattern. *Physical Review Letters*, 64: 2953–2956
Cross, M.C. & Hohenberg, P.C. 1993. Pattern formation outside of equilibrium. *Reviews of Modern Physics*, 65: 851–1112
Epstein, I.R. & Pojman, J.A. 1998. *An Introduction to Nonlinear Chemical Dynamics*, Oxford and New York: Oxford University Press
Manneville, P. 1990. *Dissipative Structures and Weak Turbulence*, New York: Academic Press
Nicolis, G. & Prigogine, I. 1977. *Self-Organization in Nonequilibrium Systems*, New York: Wiley
Ouyang, Q. & Swinney, H.L. 1991. Transition from a uniform state of hexagonal and striped Turing patterns. *Nature*, 352: 610–612
Thompson, D'A.W. 1917. *On Growth and Form*, 2nd edition, Cambridge: Cambridge University Press (2nd edition, 1942); see quotes to S. Leduc
Turing, A. 1952. The chemical basis of morphogenesis *Philosophical Transactions of the Royal Society*, B 237: 37–42
Turing, A. 1992. *Morphogenesis*, Collected works of A. Turing, vol. 3, edited by P.T. Saunders, Amsterdam: Elsevier
http://www.turing.org.uk/, Alan Hodges's pages on Alan Turing
http://data.archives.ecs.soton.ac.uk/turing/, the Turing digital archive
http://www.swintons.net/jonathan/turing.htm, Alan Turing and morphogenesis

TWIST MAP

See **Nontwist maps**

TWISTOR THEORY

Introduced by Roger Penrose as a geometrical framework for the unification of quantum theory and general relativity (gravity), twistor theory brings out the complex (holomorphic) geometry that underlies real space-time. In general relativity, space-time is a four manifold with metric g. When $g = \mathrm{d}t^2 - \mathrm{d}x^2 - \mathrm{d}y^2 - \mathrm{d}z^2$, where (t, x, y, z) are coordinates on $\mathbb{R}^4$, g is said to be flat with signature (1,3) and is called Minkowski space.

The first appearance of a complex structure arises from the fact that at a given event, the celestial sphere of light rays (null directions with respect to g) naturally has the structure of the Riemann sphere, $\mathbb{CP}^1$, in such a way that Lorentz transformations (linear transformations of the tangent space preserving the metric) act on this sphere by Möbius transformations. Twistor space extends this idea to the whole of Minkowski space. Denoted $\mathbb{PT}$, the twistor space for Minkowski space is complex projective three space, $\mathbb{CP}^3$, the space of one-dimensional subspaces of $\mathbb{C}^4$; it is a three-dimensional complex manifold obtained by adding a "plane at infinity" to $\mathbb{C}^3$. Physically, points of twistor space correspond to spinning massless particles in Minkowski space. Mathematically, the correspondence can be understood as the Klein correspondence.

The Klein Correspondence

The correspondence between $\mathbb{PT}$ and Minkowski space can be extended first to complexified Minkowski space, so that the coordinates are allowed to take on values in $\mathbb{C}$, and then to its conformal compactification by including some points at infinity. It then coincides with the classical complex Klein correspondence. The Klein correspondence is the one-to-one correspondence between lines in $\mathbb{CP}^3$ and points of a four complex-dimensional quadric, $\mathbb{CM}$, in $\mathbb{CP}^5$. The four-quadric $\mathbb{CM}$ can be understood as conformally compactified complexified Minkowski space. Introducing affine coordinates (λ, z_1, z_2) on $\mathbb{PT}$, we find that a line in $\mathbb{PT}$ corresponds to a point (t, x, y, z) by

$$\begin{pmatrix} z_1 \\ z_2 \end{pmatrix} = \begin{pmatrix} t - z & x + \mathrm{i}y \\ x - \mathrm{i}y & t + z \end{pmatrix} \begin{pmatrix} 1 \\ \lambda \end{pmatrix}.$$

Alternatively, fixing (λ, z_1, z_2) in these equations gives a two-plane in complex Minkowski space corresponding to all the lines in $\mathbb{PT}$ through (λ, z_1, z_2). Such two-planes are called α-planes. They are totally null (i.e., the tangent vectors not only have zero length but are also mutually orthogonal) and also self-dual (under the differential geometer's notion of Hodge duality).

This complex correspondence can also be restricted to give correspondences for $\mathbb{R}^4$ with metrics of positive definite signature or ultra-hyperbolic (2, 2) signature.

The Penrose Transform

A basic task of twistor theory is to transform solutions to the field equations of mathematical physics into objects on twistor space. This works well for linear massless fields such as the Weyl neutrino equation, Maxwell's equations for electromagnetism, and linearized gravity. In its general form, this transform has become known as the Penrose transform. Such fields correspond to freely prescribable holomorphic functions $f(\lambda, z_1, z_2)$ (or, more precisely, analytic cohomology classes) on regions of twistor space. The field can be obtained from this function by means of a contour integral. The simplest of these integral formulae is

$$\phi(x^a) = \oint f\,(\lambda, t - z + \lambda(x + \mathrm{i}y), x - \mathrm{i}y + \lambda(t + z))\,\mathrm{d}\lambda, \tag{1}$$

and differentiation under the integral sign leads to the fact that ϕ satisfies the wave equation

$$\frac{\partial^2\phi}{\partial t^2} - \frac{\partial^2\phi}{\partial x^2} - \frac{\partial^2\phi}{\partial y^2} - \frac{\partial^2\phi}{\partial z^2} = 0\,.$$

Equation (1) was originally discovered by Bateman (1910).

The Penrose transform has found important applications in representation theory and integral geometry. For a review, the reader is referred to Baston and Eastwood (1989), the relevant survey articles in Bailey & Baston (1990) or Chapter 1 of Mason et al. (1990).

Twistor Theory and Nonlinear Equations

The Penrose transform for the Maxwell equations and linearized gravity turns out to be linearizations of correspondences for nonlinear versions of these equations, the Einstein vacuum equations and the Yang–Mills equations, but only in the case that these fields are anti-self-dual. This is the condition that the curvature two-forms satisfy $F^* = -\mathrm{i}F$ where $*$ denotes the Hodge dual (which, up to a change of sign, has the effect of interchanging electric and magnetic fields); it is a nonlinear generalization of the right-handed circular polarization condition. In Minkowski signature, the i factor in the anti-self-duality condition implies that real fields cannot be anti-self-dual. Thus, these extensions are not sufficient to fulfill twistor theory's aim of incorporating real basic physics in Minkowski space. However, the factor of i is not present in Euclidean and ultrahyperbolic signature, so the anti-self-duality condition *is* consistent with real fields in these signatures, and this is where the main applications of these constructions have been.

The Nonlinear Graviton Construction and Its Generalizations

The first nonlinear twistor construction was due to Penrose (1976) and was inspired by Newman's construction of "heavens" from the infinities of asymptotically flat space-times in general relativity (Newman, 1976).

The nonlinear graviton construction proceeds from the definition of twistors in flat space-time as α-planes in complexified Minkowski space. It is natural to ask which complexified metrics admit a full family of α-surfaces, that is, two surfaces that are totally null and self-dual. The answer is that a full family of α-surfaces exists if and only if the conformally invariant part of the curvature tensor, the Weyl tensor, is anti-self-dual. In this case, twistor space can be defined to be the (necessarily three-dimensional) space of such α-surfaces. A remarkable fact is that the twistor space (together with its complex structure) is sufficient to determine the original space-time, and that the data defining the twistor space is effectively freely prescribable, see Penrose (1976) or Atiyah et al. (1978), for a discussion specialized to Euclidean signature.

There are now large families of extensions, generalizations and reductions of this construction. They are all based on the idea of realizing a space with a given complexified geometric structure as the parameter space of a family of holomorphically embedded submanifolds inside a twistor space. In general, the most useful of these constructions are those in which the "space-time" is obtained as the space of rational curves in a twistor space. This is because the equations that are solved on the corresponding space-time can be thought of as a completely integrable system. See Chapter 13 of Mason & Woodhouse (1996) for a more detailed discussion from this point of view.

The Anti-self-dual Yang–Mills Equations and Its Twistor Correspondence

The anti-self-dual Yang–Mills equations extend Maxwell's equations for electromagnetism in the right circularly polarized case. They are really a family of equations depending on a choice of Lie group G, usually taken to be a group of complex matrices, and Maxwell's equations arise from the case in which $G = U(1)$.

Introduce coordinates x^a, $a = 0, 1, 2, 3$, on $\mathbb{R}^4$ with metric $\mathrm{d}s^2 = \mathrm{d}x^0\,\mathrm{d}x^3 + \mathrm{d}x^1\,\mathrm{d}x^2$. The dependent variables are the components A_a of a connection $D_a = \partial_a - A_a$, where $\partial_a = \partial/\partial x^a$ and $A_a = A_a(x^b) \in$ Lie G, the Lie algebra of G. This connection defines a method of differentiating vector valued functions s in some representation of G. The freedom in changing bases for the vector bundle induce the gauge transformations $A_a \to g^{-1}A_a g - g^{-1}\partial_a g$, $g(x) \in G$ on A_a, and two connections that are related by a gauge transformation are deemed to be the same.

The self-dual Yang–Mills equations are the condition

$$[D_0, D_2] = [D_1, D_3] = [D_0, D_3] + [D_1, D_2] = 0\,.$$

They are the compatibility conditions $[D_0 + \lambda D_1, D_2 + \lambda D_3] = 0$ for the linear system of equations

$$(D_0 + \lambda D_1)s = (D_2 + \lambda D_3)s = 0, \qquad (2)$$

where $\lambda \in \mathbf{C}$ and s is an n-component column vector. These last equations form a Lax pair for the system.

The Ward construction (Ward, 1977) provides a one-to-one correspondence between gauge equivalence classes of solutions of the self-dual Yang–Mills equations and holomorphic vector bundles on regions in twistor space. The key point here is that Equation (2) defines parallel propagation along α-planes. To each point Z in twistor space, we can associate the vector space E_Z of solutions to Equation (2) along

the corresponding α-plane. These vector spaces vary holomorphically with Z, and that is what one means by a vector bundle $E \to \mathbb{PT}$. A remarkable fact is that the anti-self-dual Yang–Mills field can be reconstructed up to gauge from E, and E is effectively freely prescribable. See Penrose (1984, 1986); Ward & Wells (1990), or Mason & Woodhouse (1996) for a full discussion, and Atiyah (1979) for a discussion in Euclidean signature.

The Connection with Completely Integrable Systems

In effect, the twistor constructions amount to providing a geometric general local solution to the anti-self-duality equations in the sense that the twistor data is (for a local solution) freely prescribable. Thus, they demonstrate complete integrability of the anti-self-duality equations. The reconstruction of a solution on space-time from twistor data can be hard. In the anti-self-dual Yang–Mills case, it involves the solutions of a Riemann–Hilbert problem, and in the case of the anti-self-dual Einstein equations, the construction of a family of rational curves inside a complex manifold. Nevertheless, such constructions are a familiar part of the apparatus of the theory of integrable systems.

In Ward (1985), this connection with integrable systems was developed further, and the anti-self-dual Yang–Mills equations were shown to yield many important integrable systems under symmetry reduction. Ward's list has been extended and now includes many of the most famous examples of integrable systems such as the Painlevé equations, the Korteweg–de Vries equation, the nonlinear Schrödinger equation, the N-wave equations, among others (see Ablowitz & Clarkson (1992) and Mason & Woodhouse (1996) for a review). There are some notable omissions from the list such as the Kadomtsev–Petviashvili and Davey–Stewartson equations (at least if one restricts oneself to finite-dimensional gauge groups), but the list remains impressive.

One can impose symmetries on the twistor constructions for the anti-self-duality equations to obtain a reduced twistor correspondence for solutions to any of these integrable equations (see Mason & Woodhouse (1996) and Chapter 1 of Mason et al. (1995)), so there are many many twistor correspondences.

Applications

Twistor constructions have the effect of reducing problems in nonlinear differential equations to problems in complex holomorphic geometry, where there are many powerful tools. Twistor theory underlies the many appearances of algebraic geometry, loop groups, and Riemann–Hilbert problems in the theory of integrable systems, even though these structures were, for systems in one and two dimensions, usually discovered without knowledge of the twistor theory, see Mason & Woodhouse (1996). The most impressive applications of twistor theory have been in three and four dimensions, where it is difficult to imagine making such significant progress without the twistor theory.

The Ward construction was used by Atiyah, Drinfeld, Hitchin, and Manin to construct the Yang–Mills instantons on S^4; see Atiyah (1979). Its symmetry reduction was also used by both to obtain monopoles on $\mathbb{R}^3$ and to study the hyperkähler metric on their moduli spaces, see Ward & Wells (1990) and Atiyah and Hitchin (1988) (see Mason & Woodhouse (1996) for further applications).

The nonlinear graviton construction and its generalizations have been used for many constructions of Einstein manifolds and more general anti-self-dual manifolds (see Hitchin (1979) for the construction of asymptotically locally Euclidean hyperkähler spaces in four dimensions). The twistor constructions have also been an important tool in studying general properties, for a twistor construction of an anti-self-dual conformal structure on any manifold that is a connected sum of two other such manifolds (Donaldson & Friedman, 1989). Further applications and developments can be found in Mason et al. (2001).

An application that goes beyond complete integrability is the twistor framework of Merkulov for studying arbitrary geometric structures. This has led to the remarkable classification of all possible irreducible holonomies of torsion-free affine connections (Merkulov & Schwachhöfer, 1999).

It is to be hoped that these many applications will one day feed back into Penrose's original program and provide a unification between quantum theory and gravity.

LIONEL MASON

See also **Einstein equations; General relativity; Instantons; Integrability; Integral transforms; Inverse scattering method or transform; Riemann–Hilbert problem; Yang–Mills theory**

Further Reading

Ablowitz, M.J. & Clarkson, P.A. 1992. *Solitons, Nonlinear Evolution Equations and Inverse Scattering*, Cambridge and New York: Cambridge University Press

Atiyah, M.F. 1979. *Geometry of Yang-Mills Fields*, Pisa: Accademia Nazionale dei Lincei Scuola Normale Superiore

Atiyah, M.F. & Hitchin, N.J. 1988. *The Geometry and Dynamics of Monopoles*, Princeton, NJ: Princeton University Press

Atiyah, M.F., Hitchin, N.J. & Singer, I.M. 1978. Self-duality in four-dimensional Riemannian geometry. *Proceedings of the Royal Society* A, 362: 425

Bailey, T.N. & Baston, R. (editors). 1990. *Twistors in Mathematics and Physics*, Cambridge and New York: Cambridge University Press

Baston, R.J. & Eastwood, M.G. 1989. *The Penrose Transform: Its Interaction with Representation Theory*, Oxford and New York: Oxford University Press

Bateman, H. 1910. *Partial Differential Equations of Mathematical Physics*, New York: Dover
Donaldson, S. & Friedman, R. 1989. Connected sums of self-dual manifolds and deformations of singular spaces. *Nonlinearity*, 2(2): 197–239
Hitchin, N. 1979. Polygons and gravitons. *Mathematical Proceedings of the Cambridge Philosophical Society*, 85: 456–476
Mason, L.J. & Hughston, L.P. (editors). 1990. *Further Advances in Twistor Theory, Vol. I: The Penrose Transform and Its Applications*, Harlow: Longman
Mason, L.J., Hughston, L.P. & Kobak, P.Z. 1995. *Further Advances in Twistor Theory, Vol. II: Integrable Systems, Conformal Geometry and Gravitation*, Harlow: Longman
Mason, L.J., Hughston, L.P., Kobak, P.Z. & Pulverer, K. (editors). 2001. *Further Advances in Twistor Theory, Vol. III: Curved Twistor Spaces*, Boca Raton, FL: Chapman & Hall
Mason, L.J. & Woodhouse, N.M.J. 1996. *Twistor Theory, Self-duality and Twistor Theory*, Oxford and New York: Oxford University Press
Merkulov, S., & Schwachhöfer, L. 1999. Classification of irreducible holonomies of torsion-free affine connections. *Annals of Mathematics*, (2), 150(1): 77–149
Newman, E.T. 1976. Heaven and its properties. *General Relativity and Gravitation*, 7(1): 107–111
Penrose, R. 1976. Nonlinear gravitons and curved twistor theory. *General Relativity and Gravitation*, 7: 31–52
Penrose, R. 1984, 1986. *Spinors and Space-time*, 2 vols., Cambridge and New York: Cambridge University Press
Ward, R.S. 1977. On self-dual gauge fields. *Physics Letters*, 61A: 81–82
Ward, R.S. 1985. Integrable and solvable systems and relations among them. *Philosophical Transactions of the Royal Society* A, 315: 451–457
Ward, R.S. & Wells, R.O. 1990. *Twistor Geometry and Field Theory*, Cambridge and New York: Cambridge University Press

TWO SOLITON COLLISION

See ***N*-soliton formulas**

U

UEDA EQUATION

See **Duffing equation**

UNIVERSALITY

The concept of universality serves to emphasize like behavior in seemingly unrelated systems. It became popular in the context of phase transitions when it was noted that after a suitable mapping between the thermodynamic variables, the scaling behavior of spin systems near the critical point depends on the number of spin directions, the dimensionality of the system, and the type and range of interactions only (Griffiths, 1970; Binney et al., 1992). Thus, there is no "universal" universality, but only a restricted one among systems that belong to the same universality class.

A deeper understanding of the empirically established relations emerged within the renormalization group treatment of phase transitions, which allowed identification of the parts of the interactions that are relevant for an assignment to a universality class (Wilson, 1983; Binney et al., 1992).

An elementary example of thermodynamic universality is provided by the law of corresponding states for interacting gases. They can be described over a wide range of temperature T, pressure p, and volume V by the van der Waals equation of state. For one mole of the gas it is

$$(p + a/V^2)(V - b) = RT \tag{1}$$

with R being the gas constant and a and b parameters characteristic of the gas. This equation of state has a critical point where both $\partial p/\partial V = 0$ and $\partial^2 p/\partial V^2 = 0$, given by

$$RT_c = \frac{8a}{27b}, \qquad p_c = \frac{a}{27b^2} \text{ and } V_c = 3b. \tag{2}$$

Because of the dependence on the material parameters a and b, these quantities differ from gas to gas. However, when p, T, and V are expressed in terms of the critical values, the material constants disappear. With $\tilde{p} = p/P_c$, $\tilde{V} = V/V_c$, and $\tilde{T} = T/T_c$ the reduced quantities, the van der Waals equation of state becomes

$$(\tilde{p} + 3/\tilde{V}^2)(3\tilde{V} - 1) = 8\tilde{T}. \tag{3}$$

Interestingly, this mapping between states of different gases remains useful even when the gases do not follow the predictions from van der Waals theory, for example, near the critical point and in the liquid-gas coexistence region (Stanley, 1971; Binney et al., 1992).

Universality in thermodynamic systems is often characterized quantitatively by the exponents in the power laws with which quantities, such as the specific heats, susceptibilities, and spatial or temporal correlation functions, diverge near a critical point (if the exponent vanishes, then there can be logarithmic variations or discontinuities). The ideal behavior in the thermodynamic limit is often clouded by corrections because of the finite size of the sample, and these very often show power law dependencies too. The search for universality in other systems and situations is, hence, often accompanied by investigations of scaling laws and comparisons of exponents.

The success of universality considerations in thermodynamics has triggered many investigations in nonlinear dynamical systems. Universality arguments can help to link behavior in one-dimensional maps, in chemical reactions, in electrical circuits, or in hydrodynamic systems, for instance. Here are some situations where universality and scaling appear in nonlinear systems.

Period-doubling cascade. Grossmann & Thomae (1977), Feigenbaum (1978), and Coullet & Tresser (1978) noted that the sequence of parameters λ_n in quadratic maps, like $x_{i+1} = \lambda_n(1 - 2x_i^2)$ where bifurcations from orbits of period 2^n to 2^{n+1} occur, that is, $\lambda_1 = 0.70716$, $\lambda_2 = 0.80953$, $\lambda_3 = 0.83112$, $\lambda_4 = 0.83574$, etc., form a geometric sequence, $\lambda_n = \lambda_\infty - a\delta^{-n}$ (a is a constant). The ratio

$$\delta = \frac{\lambda_n - \lambda_{n-1}}{\lambda_{n+1} - \lambda_n} \tag{4}$$

converges to a value

$$\delta = 4.669201609\ldots\ . \tag{5}$$

This values appears for all maps with a single quadratic maximum and negative Schwartzian derivative $(f'''/f' - (\frac{3}{2})(f''/f')^2) < 0)$, as a renormalization of the map due to Cvitanovic (1984), Feigenbaum (1979), Coullet & Tresser (1978), and Lanford (1982) shows. It also appears in higher-dimensional dissipative maps, in continuous differential equations, and even in partial differential equations. Experimental evidence was first found in experiments on thermal convection (Libchaber & Maurer, 1980) and in acoustical, electrical, chemical, and many other cases since. Examples are given in Schuster (1988) and Cvitanovic (1984).

Further universal scaling laws have been established for period n-tupling, for period doubling with other forms of the maximum, for the scaling of the splitting of iterates in period doubling, for the amplitudes of higher harmonics in Fourier spectra, and for the influence of noise on period-doubling bifurcations (Cvitanovic, 1984; Schuster, 1988). Period-doubling in conservative systems has different scaling exponents (MacKay & Meiss, 1987).

Other situations with universal scaling laws arise in the case of intermittency (saddle-node bifurcations) and near the break-up of tori in conservative systems (Cvitanovic, 1984; Schuster, 1988).

Pattern formation. In many pattern forming systems, the equation for the amplitude of the pattern is of Ginzburg–Landau type, with the interactions dictated by continuous and discrete symmetries of the system (Golubitsky & Schaeffer, 1985; Golubitsky et al., 1988). A simple example for a system with a real amplitude A and invariance under $A \to -A$ is

$$\partial_t A = \varepsilon A - A^3 + \Delta A\,, \tag{6}$$

If the control parameter ε is negative, there is no pattern. For positive ε the amplitude increases like $\varepsilon^{1/2}$. This behavior is widely observed (Cross & Hohenberg, 1993).

Singularity formation. The final stages during the formation of singularities often show asymptotic scaling behavior. For instance, two gravitating bodies starting at rest will collide with distance vanishing like $t^{2/3}$ and velocities diverging like $t^{-1/3}$. The formation of the pinching off of a cylindrical column of liquid is an example of a process that is universal not only in its scaling behavior but also in the prefactors. The formation of the pinch is due to surface tension and is counteracted by viscous effects. From the relevant material parameters surface tension γ (of dimension kg/s^2), viscosity η (kg/(m s)), and density ρ (kg/m^3), one can form a scale of length $l_p = \eta/(\rho\gamma)$ and one of time $t_p = \eta^3/(\gamma^2\rho)$. The behavior of an axisymmetric column is universal in the sense that the minimal diameter $d_{\min}(t)$ and the maximal velocity $v_{\max}(t)$ at a time t before pinch off are given by (Eggers, 1993)

$$\frac{d_{\min}(t)}{l_p} = 0.0608\left(\frac{t}{t_p}\right),$$

$$\frac{v_{\max}(t)}{l_p/t_p} = 3.07\left(\frac{t}{t_p}\right)^{-1/2}. \tag{7}$$

Random matrix theories. The Hamiltonian operator that describes a given quantum system has a specific form that may be poorly known, as in the case of impurities in a solid or the interactions between nucleons in an atomic nucleus, but it certainly is not arbitrary or random. Nevertheless, for very many systems, the statistical properties of eigenvectors or the statistics of neighboring eigenvalues behave in a universal way that does not depend on the specific system anymore. When rescaled by the mean distance, neighboring energy eigenvalues of hydrogen in strong magnetic fields, electrons in quantum dots, scattering resonances in nuclei such as ^{26}Al, resonance frequencies in microwave resonators, and vibrating quartz blocks can all show the same spacing distribution (Stöckmann, 1999). The only requirement is that the systems are disordered or classically chaotic. The specific form of the distributions then depends on the global symmetry properties of the Hamiltonian, that is, on whether it is real symmetric, complex Hermitian, or symplectic (Guhr et al., 1998; Stöckmann, 1999). System-specific properties appear on much larger scales of separation between eigenvalues; they can be understood within semiclassical periodic orbit theory.

Universality in turbulence. Lewis Fry Richardson described a turbulent flow as a hierarchical arrangement of vortices of different sizes that appear and disappear in an unpredictable fashion. The famous scaling laws of Kolmogorov, Obhukov, Weizäcker, and Onsager hold that in homogeneous, isotropic turbulence, the square of the velocity difference between two points a distance r apart scales like $(\varepsilon r)^{2/3}$, where ε is now the energy dissipation (Frisch, 1995). The expectation is that this is independent of the precise mechanism of stirring, as long as it is confined to large scales and becomes exact as the Reynolds number of the flow approaches infinity. Turbulent fluctuations behind grids in wind or water tunnels or in turbulent jets support this observation.

BRUNO ECKHARDT

See also **Critical phenomena; Dimensional analysis; Fractals; Free probability theory; Kolmogorov cascade; Period doubling; Periodic orbit theory; Random matrix theories: I, II, III, IV; Renormalization groups; Turbulence**

Further Reading

Binney, J.J., Dowrick, N.J., Fisher, A.J. & Newman, M.E.J. 1992. *The Theory of Critical Phenomena: An Introduction to the Renormalization Group*, Oxford: Clarendon Press

Coullet, P. & Tresser, C. 1978. Iterations d'endomorphismes et groupe de renormalization. *Journale de Physique* 39: Colloque C5–C25

Cross, M.C. & Hohenberg, P.C. 1993. Pattern formation outside of equilibrium. *Reviews of Modern Physics*, 65: 851–1112
Cvitanovic, P. 1984. *Universality in Chaos*, Bristol: Adam Hilger
Eggers, J. 1993. Universal pinching of 3D axisymmetric free-surface flow. *Physical Review Letters*, 71: 3458–3460
Feigenbaum, M.J. 1978. Quantitative universality for a class of nonlinear transformations. *Journal of Statistical Physics*, 19: 25–52
Feigenbaum, M.J. 1979. The universal metric properties of nonlinear transformations. *Journal of Statistical Physics*, 21: 669–706
Frisch, U. 1995. *Turbulence: The Legacy of A.N. Komlogorov*, Cambridge and New York: Cambridge University Press
Griffiths, R.B. 1970. Dependence of critical indices on a parameter. *Physical Review Letters*, 24: 1479–1482
Golubitsky, M. & Schaeffer, D.G. 1985. *Singularities and Groups in Bifurcation Theory*, vol. 1, New York: Springer
Golubitsky, M., Stewart, I.N. & Schaeffer, D.G. 1988. *Singularities and Groups in Bifurcation Theory*, vol. 2, New York: Springer
Grossmann, S. & Thomae, S. 1977. Invariant distributions and stationary correlation functions of the one-dimensional discrete processes. *Zeitschrift für Naturforschung*, 32a: 1353–1363
Guckenheimer, J. & Holmes, P. 1983. *Nonlinear Oscillations, Dynamical Systems and Bifurcations of Vector Fields*, New York: Springer
Guhr, T., Müller-Groeling, A., & Weidenmüller, H.A. 1998. Random-matrix theories in quantum physics: common concepts. *Physics Reports*, 299: 190–425
Lanford, O.E. 1982. A computer assisted proof of the Feigenbaum conjectures. *Bulletin of the American Mathematical Society*, 6: 427–434
Libchaber, A. & Maurer, J. 1980. Une experience de Rayleigh-Bénard de geometrie reduite: multiplication, acchroage, et demultiplication de frequences. *Journal de Physique*, 41: Colloque C3–51
MacKay, R.S. & Meiss, J.D. (editors). 1987. *Hamiltonian Dynamical Systems: A Reprint Collection*, Bristol: Adam Hilger
Schuster, H.G. 1988. *Deterministic Chaos*, 2nd edition, Weinheim: Physik-Verlag and New York: VCH
Stanley, H.E. 1971. *Introduction to Phase Transitions and Critical Phenomena*, Oxford: Clarendon Press and New York: Oxford University Press
Stöckmann, H.J. 1999. *Quantum Chaos: An Introduction*, Cambridge and New York: Cambridge University Press
Wilson, K.G. 1983. The renormalization group and critical phenomena. *Reviews of Modern Physics*, 55: 583–600

UNSTABLE MANIFOLD

See **Phase space**

V

VAN DER POL EQUATION

In 1926, Balthasar van der Pol derived the equation (now named after him) to describe self-sustained oscillations in a triode circuit. To solve the equation, he developed a method that is based on the separation of fast and slow time dependencies and on averaging, an idea that provides the basis of various analytic approaches to nonlinear problems (van der Pol, 1926).

In dimensionless variables, the van der Pol (VDP) equation reads

$$\frac{\mathrm{d}^2x}{\mathrm{d}t^2} - \mu(1-x^2)\frac{\mathrm{d}x}{\mathrm{d}t} + x = 0. \tag{1}$$

The variable x represents the triode plate voltage in the oscillating circuit, and the frequency of the circuit is normalized to 1 by the appropriate change of the time scale. The parameter $\mu > 0$ gives the growth rate of small linear oscillatory perturbations, and the nonlinear term, approximating the nonlinear current-voltage characteristic of the triode, is normalized by scaling x. Physically, the VDP equation describes growth and saturation of oscillatory perturbations with eventual onset of periodic self-sustained oscillations. With a change of variables $x = \mathrm{d}y/\mathrm{d}t$, the VDP equation transforms to the Rayleigh equation

$$\frac{\mathrm{d}^2y}{\mathrm{d}t^2} - \mu\left[1 - \frac{1}{3}\left(\frac{\mathrm{d}y}{\mathrm{d}t}\right)^2\right]\frac{\mathrm{d}y}{\mathrm{d}t} + y = 0.$$

In the case of weak instability and nonlinearity ($\mu \ll 1$), the VDP equation can be treated analytically. Here the oscillations are nearly sinusoidal with slowly (on the time scale of order $1/\mu$) varying amplitude and phase. This key observation constitutes the essence of the method of averaging developed by van der Pol.

The first step in the solution is a transformation from $(x, \dot{x})$ to new variables: the amplitudes A, B; thus,

$$\begin{aligned} x(t) &= A(t)\cos t + B(t)\sin t, \\ \dot{x}(t) &= -A(t)\sin t + B(t)\cos t. \end{aligned} \tag{2}$$

In these variables, Equation (1) reads

$$\begin{aligned} \frac{\mathrm{d}A}{\mathrm{d}t} &= -\mu\dot{x}(1-x^2)\sin t, \\ \frac{\mathrm{d}B}{\mathrm{d}t} &= \mu\dot{x}(1-x^2)\cos t, \end{aligned} \tag{3}$$

where $\dot{x}, x$ on the right-hand side are to be expressed through A, B. One can see that the time variations of A, B are slow, and the major contribution to them is given by non-oscillating terms on the right-hand side of (3). Keeping only the non-oscillating terms is equivalent to averaging over the oscillation period 2π, and under the averaging procedure, the slowly varying amplitudes $A(t)$ and $B(t)$ are considered as constants. Having performed the averaging, van der Pol obtained the approximate equations in the form

$$\begin{aligned} \frac{\mathrm{d}A}{\mathrm{d}t} &= \frac{\mu}{2}A\left(1 - \frac{A^2+B^2}{4}\right), \\ \frac{\mathrm{d}B}{\mathrm{d}t} &= \frac{\mu}{2}B\left(1 - \frac{A^2+B^2}{4}\right). \end{aligned} \tag{4}$$

This equation can be readily solved by means of a transformation to the slow amplitude and phase $A = R\cos\phi$, $B = R\sin\phi$:

$$\frac{\mathrm{d}R}{\mathrm{d}t} = \frac{\mu}{2}R\left(1 - \frac{R^2}{4}\right), \quad \frac{\mathrm{d}\phi}{\mathrm{d}t} = 0.$$

For any initial condition $R \neq 0$, the stationary amplitude $R_0 = 2$ is established as $t \to \infty$. In the original variables of Equation (1), the corresponding periodic solution reads $x(t) = 2\cos(t - \phi)$ (see Figure 1). In terms of the dynamical systems theory, the van der Pol equation (1) possesses a limit cycle; for small μ, the cycle is approximately circular with radius 2. Physically, it corresponds to periodic weakly nonlinear, self-sustained oscillations.

The solution of the VDP equation can be treated analytically also in the limiting case $\mu \gg 1$, when the equation describes relaxation oscillations. Introducing new time $\tau = t/\mu$, we can rewrite Equation (1) as a

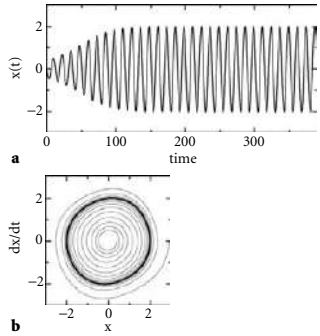

Figure 1. A solution of the van der Pol equation for $\mu = 0.1$. (a) The time dependence of x. (b) The limit cycle on the phase plane $(x, \mathrm{d}x/\mathrm{d}t)$ attracts other trajectories; its form for this small value of μ is nearly circular.

system

$$\mu^{-2}\frac{\mathrm{d}x}{\mathrm{d}\tau} = -y + x - \frac{x^3}{3}, \tag{5}$$

$$\frac{\mathrm{d}y}{\mathrm{d}\tau} = x. \tag{6}$$

This system has a small parameter μ^{-2} at the derivative, and it belongs to the class of singularly perturbed equations. All motions in the phase space (x, y) are divided into fast motions, when variable x jumps with the rate $\sim\mu^2$ while variable y remains nearly constant, and slow motions, when both variables x and y vary with rates of ~ 1. The slow motions are restricted to the slow manifold, where the right-hand side of Equation (5) vanishes (the curve $y = x - x^3/3$ shown as a dotted line in Figure 2b). More precisely, they are restricted to the stable branches of the curve, where $\mathrm{d}(x - x^3/3)/\mathrm{d}x < 0$. The direction of motion on these stable branches is determined by Equation (6) and is depicted in Figure 2b by arrows. When the phase point moving along a stable branch arrives at its border, it jumps to the other branch. Thus, the limit cycle consists of two pieces of slow motion connected by two pieces of fast motion (solid line in Figure 2b).

The VDP equation serves as a prototype for different dynamical models with a limit cycle. For example, an equation with a more complex nonlinearity and $\mu > 0$,

$$\frac{\mathrm{d}^2x}{\mathrm{d}t^2} - \mu(-1 + x^2 - \beta x^4)\frac{\mathrm{d}x}{\mathrm{d}t} + x = 0,$$

describes the so-called "hard excitation" of self-sustained oscillations. (This equation was derived by van der Pol and Appleton for the description of a triode generator, whose operating point is shifted from the inflection point of the current-voltage characteristics of the triode.) In this case, the averaging method above described leads to the following amplitude equation:

$$\frac{\mathrm{d}R}{\mathrm{d}t} = \frac{\mu}{2}R\left(-1 + \frac{R^2}{4} - \beta\frac{R^4}{8}\right), \quad \frac{\mathrm{d}\phi}{\mathrm{d}t} = 0.$$

For $\mu > 0$ and $0 < \beta < \frac{1}{8}$, this equation possesses coexisting stable steady state $R = 0$, an unstable limit cycle at $R_{\mathrm{un}} = \beta^{-1/2}(1 - \sqrt{1 - 8\beta})^{1/2}$, and a stable limit cycle at $R_{\mathrm{st}} = \beta^{-1/2}(1 + \sqrt{1 - 8\beta})^{1/2}$. The basin of attraction of the stable limit cycle is $R > R_{\mathrm{un}}$, while the circle $R < R_{\mathrm{un}}$ is the basin of the stable fixed point. For the triode generator this means that self-sustained oscillations cannot develop from small fluctuations, but appear only if a relatively large (larger than R_{un}) perturbation is applied.

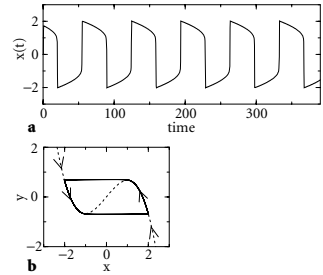

Figure 2. A solution of the van der Pol equation for $\mu = 20$. (a) The time dependence of x. (b) The limit cycle on the phase plane (x, y) consists of pieces of the slow manifold (shown with a dotted line) and fast jumps of x.

Another generalization of the van der Pol equation is often called the van der Pol–Duffing oscillator:

$$\frac{\mathrm{d}^2x}{\mathrm{d}t^2} - \mu(1 - x^2)\frac{\mathrm{d}x}{\mathrm{d}t} + x + \gamma x^3 = 0. \tag{7}$$

This model combines the dissipative nonlinearity of the van der Pol equation (term proportional to μ) with the conservative nonlinearity of the Duffing equation (term proportional to γ). For $\mu \ll 1$ and $\gamma \ll 1$, the equations for the slowly varying amplitude and phase can be obtained by the method of averaging as

$$\frac{\mathrm{d}R}{\mathrm{d}t} = \frac{\mu}{2}R\left(1 - \frac{R^2}{4}\right), \quad \frac{\mathrm{d}\phi}{\mathrm{d}t} = \frac{3\gamma}{4}R^2.$$

The difference to the van der Pol case is in the phase dynamics. Now the oscillations are non-isochronous, because the dynamics of the slow phase depends on the amplitude. In particular, the frequency of the self-sustained oscillations differs from the frequency of linear oscillations by 3γ. In the VDP equation (1), such a frequency shift appears only in the second approximation (by taking into account the terms $\sim\mu^2$).

Another model related to Equation (1) is the Bonhoeffer–van der Pol (BVDP) oscillator, with equations

$$\frac{dx}{dt} = -y + x - \frac{x^3}{3} + I_0,$$
$$\frac{dy}{dt} = c(x + a - by).$$

Writing this system as one second-order equation, one gets a model similar to Equation (7), but with additional terms; thus,

$$\frac{d^2x}{dt^2} - (1 - bc - x^2)\frac{dx}{dt} + c(1 - b)x + \frac{bc}{3}x^3 + c(a - bI_0) = 0\ . \quad (8)$$

In the case $b = I_0 = 0$, the BVDP model reduces to the FitzHugh–Nagumo model of neuron spiking. Depending on the parameters, both these models demonstrate self-sustained oscillations, excitability (a stable steady state that responses to a finite perturbation by generating a spike), or bistability.

A periodically forced VDP equation,

$$\frac{d^2x}{dt^2} - \mu(1 - x^2)\frac{dx}{dt} + \omega_0^2 x = E\sin\omega t,$$

displays the phenomenon of frequency locking. For ω close to the natural frequency of the autonomous system ω_0, the forced systems starts to oscillate with the frequency of the forcing term or becomes entrained. Entrainment occurs even for relatively small E, especially when $\mu \gg 1$. For large E, the forced VDP equation can demonstrate chaotic regimes.

ARKADY PIKOVSKY AND MICHAEL ROSENBLUM

See also **Attractors; Averaging methods; Duffing equation; FitzHugh–Nagumo equation; Nonlinear electronics; Relaxation oscillators; Synchronization**

Further Reading

Andronov, A.A., Vitt, A.A. & Khaykin, S.E. 1966. *Theory of Oscillators*, Oxford and New York: Pergamon Press (original Russian edition, 1937)

Bogoliubov, N.N. & Mitropolsky, Yu.A. 1961. *Asymptotic Methods in the Theory of Nonlinear Oscillations*, New York: Gordon and Breach

van der Pol, B. 1926. On "relaxation oscillations." *Philosophical Magazine*, 2: 978–992

VECTOR FIELD

See **Phase space**

VERHULST EQUATION

See **Population dynamics**

VIRIAL THEOREM

First established by Rudolf Clausius in 1870, the virial theorem relates the average potential energy $\langle V\rangle$ to the average kinetic energy $\langle T\rangle$ of a system of particles. The particles can have arbitrary potential interactions, and the theorem holds both in classical and quantum mechanics.

For a single classical nonrelativistic particle, the theorem can be derived as a consequence of Newton's second law: $\boldsymbol{F} = m\mathrm{d}^2\boldsymbol{x}/\mathrm{d}t^2$. Thus,

$$\frac{\mathrm{d}(m\boldsymbol{x}\cdot\mathrm{d}\boldsymbol{x}/\mathrm{d}t)}{\mathrm{d}t} = \boldsymbol{x}\cdot\boldsymbol{F} + m\left(\frac{\mathrm{d}\boldsymbol{x}}{\mathrm{d}t}\right)\cdot\left(\frac{\mathrm{d}\boldsymbol{x}}{\mathrm{d}t}\right), \quad (1)$$

which in terms of the momentum $\boldsymbol{p} = m(\mathrm{d}\boldsymbol{x}/\mathrm{d}t)$ and the kinetic energy $T = m(\mathrm{d}\boldsymbol{x}/\mathrm{d}t)^2/2$ reads

$$-\boldsymbol{x}\cdot\boldsymbol{F} = -\frac{\mathrm{d}(\boldsymbol{x}\cdot\boldsymbol{p})}{\mathrm{d}t} + 2T. \quad (2)$$

In taking the average over time, the first term on the right-hand side of the equation does not contribute; thus, one obtains

$$-\langle\tfrac{1}{2}\boldsymbol{x}\cdot\boldsymbol{F}\rangle_{\mathrm{av}} = \langle T\rangle_{\mathrm{av}}, \quad (3)$$

which is the classical virial theorem. The expression on the left-hand side of this equation (called the virial by Clausius) is a measure of the net attractiveness of a system.

In the special case when the force is derivable from a potential $\boldsymbol{F} = -\nabla V$ and the potential varies as the nth power of the distance to the origin $V = C|\boldsymbol{x}|^n$, the term $\boldsymbol{x}\cdot\boldsymbol{F} = -nV$, and the virial theorem reduces to

$$n\langle V\rangle_{\mathrm{av}} = 2\langle T\rangle_{\mathrm{av}}\ . \quad (4)$$

The theorem can also be obtained from a variational derivation.

Applications

- For the harmonic oscillator, $V(\boldsymbol{x}) = \frac{1}{2}mw^2|\boldsymbol{x}|^2$ then $n = 2$ and $E \equiv \langle V\rangle + \langle T\rangle = 2\langle T\rangle = 2\langle V\rangle$.
- For a bouncing ball, $V(\boldsymbol{x}) = mg|\boldsymbol{x}|$ and $n = 1$, then $E = 3\langle T\rangle = 3/2\langle V\rangle$.
- If the forces vary inversely as the square of the distance (as in atomic and planetary systems), then $V(\boldsymbol{x}) = e^2/|\boldsymbol{x}|$ and $n = -1$. The average kinetic energy is then numerically equal to the total energy $E = -\langle T\rangle$ but of opposite sign.
- In astrophysics, the virial theorem is a valuable tool for studying static, non-evolving (relaxed) systems such as stars (systems of gas particles), gas clouds, star clusters, galaxies, and galaxy clusters. This theorem can be used to estimate the mass of a given system since for the gravitational case $\langle T\rangle = -\frac{1}{2}\langle V\rangle$ and

$$\frac{1}{2}M_{\mathrm{tot}}\left\langle\left(\frac{\mathrm{d}\boldsymbol{x}}{\mathrm{d}t}\right)^2\right\rangle = +\frac{1}{4}\frac{GM_{\mathrm{tot}}^2}{\langle R_{\mathrm{tot}}\rangle}\ .$$

Thus, the virial mass of the system can be estimated as

$$M_{\rm tot} \approx 2\frac{\langle R_{\rm tot}\rangle\langle {\rm d}\boldsymbol{x}/{\rm d}t\rangle^2}{G}.$$

- Another application of this theorem is in the classical calculation of the state equation of gases. The system considered is that of a large number N of particles with coordinates $\boldsymbol{x}_i$ acted on by external and internal forces $\boldsymbol{F}_i = \boldsymbol{F}_{i,\rm ext} + \boldsymbol{F}_{i,\rm int}$ and confined within a box of volume $\mathcal{V}$. As the contribution from the external forces can be related to the pressure of the gas on the walls of the box, the virial theorem takes the form

$$P\mathcal{V} = Nk_{\rm B}T + \frac{1}{3}\left\langle \sum_i^N \boldsymbol{x}_i \cdot \boldsymbol{F}_{i,\rm int}\right\rangle_{\rm av},$$

where $k_{\rm B}$ is the Boltzmann constant. This was the application originally considered by Clausius.

- The virial theorem can be extended to a quantum system described by the linear dimensionless Schrödinger equation

$$\mathrm{i}\psi_t = -\Delta\psi + V(\boldsymbol{x})\psi\,.$$

In this case, $2T_m = nV_m$, where T_m and V_m are the kinetic and potential energy of the mth eigenstate, respectively.

- The virial theorem can also be applied to the study of the solitary waves. As an illustration, consider the one-dimensional nonlinear Schrödinger (NLS) equation

$$\mathrm{i}u_t + u_{xx} + 2(u^*u)u = 0\,, \tag{5}$$

which has solitary wave solutions that preserve their shape after collision with other solitary waves. The general form of a solitary wave is

$$u(x,t) = a\exp\mathrm{i}\left[\frac{v_{\rm e}}{2}x + \left(a^2 - \left(\frac{v_{\rm e}}{2}\right)^2\right)t - \phi_0\right] \times \mathrm{sech}\left[a(x - v_e t - x_0)\right], \tag{6}$$

where a is the wave amplitude and $v_{\rm e}$ the envelope velocity, while ϕ_0 and x_0 are the initial phase and position.

One of the infinite conservation laws associated to (5) is the energy

$$E = \int u_x^* u_x\,{\rm d}x + \int -(u^*u)^2\,{\rm d}x,$$

where the first term is the kinetic energy (T) and the second term is the potential energy (V).

The NLS equation is derived from the Lagrangian density $\mathcal{L} = \frac{1}{2}(uu_t^* - u_t u^*) + u_x^* u_x - (u^*u)^2$ and the corresponding action is $\mathcal{S} = \int {\rm d}t\,{\rm d}x\,\mathcal{L}$. Consider a stationary localized solution $u = \exp(\mathrm{i}\Omega t)\ u(x)$, which is the case of solution (6) with $v_{\rm e} = 0$ and $\Omega = a^2$. As the Lagrangian density is static, we can apply a dilation transformation to get the global condition $\int |u_x|^2\,{\rm d}x = \int(\Omega|u|^2 - |u|^4)\,{\rm d}x$. From Equation (5), $\int(\Omega|u|^2 + |u_x|^2 - 2|u|^4)\,{\rm d}x = 0$, which in turn implies that $\int |u_x|^2\,{\rm d}x = \frac{1}{2}\int |u|^4\,{\rm d}x$. Thus the total energy is $E = -T = \frac{1}{2}V$, and in the case of the stationary soliton, $E = -2a^3/3$.

Thus, the virial theorem provides nontrivial relations between quantities of physical interest, which can be used to test the accuracy of numerical simulations and to find variational solutions.

Luis Vazquez and M.P. Zorzano

See also **Damped-driven anharmonic oscillator; Nonlinear Schrödinger equations; Rotating wave approximation**

Further Reading

Goldstein, H. 1980. *Classical Mechanics*, 2nd edition, Reading, MA: Addison-Wesley

Saslaw, W.C. 1985. *Gravitational Physics of Stellar and Galactic Systems*, Cambridge and New York: Cambridge University Press

Scott, A. 2003. *Nonlinear Science: Emergence and Dynamics of Coherent Structures*, 2nd edition, Oxford and New York: Oxford University Press

VISIOMETRICS

With the advent of robust and rapid sensing devices and increasing computer speeds, memories and transfer rates, the technology for observation, measurement, and computer simulation of nonlinear processes in physical and biological systems has improved rapidly, allowing massive experimental and simulated data sets to be produced. In order to gain physical insight into the evolving phenomena and construct reduced mathematical models, the mathematical essences in this sea of data need to be determined.

This can be accomplished through the process of visiometrics, which involves visualization, projection, identification and classification, extraction, tracking, quantification, and juxtaposition of evolving amorphous coherent structures and statistical backgrounds in massive multidimensional data sets. The goal is to produce cogent images and specific, parameter-scaled (normalized) graphs for intuitive understanding and mathematical analyses (Bitz & Zabusky, 1990; Zabusky et al., 1993; Feher & Zabusky, 1996; Fernandez et al., 1996; Zabusky, 1999).

Consider the process of dealing with evolving simulation data. Most simulations use continuum partial or integro-differential equations or discrete particle descriptions and produce numerous fields, particle locations, and trajectories. (In hybrid codes both are present.) Examples of continuum fields mainly from the compressible Euler equations of fluid motion are presented here. For particle data (e.g., from Monte Carlo

or plasma simulations), appropriate local averages can be used to convert to continuum quantities.

In fluid flows, we deal with scalars such as density, pressure, and temperature, vectors such as velocity $\boldsymbol{u}$ and vorticity $\boldsymbol{\omega}$, and tensors such as the rate of strain tensor $\nabla\boldsymbol{u}$. Very thin high-gradient regions such as shock waves and diffusing interfacial transition layers (ITLs) (Zabusky et al., 2003) between species with different properties may be embedded in the flows. To quantify the ITLs, we may extract a medial axis (i.e., some center line) or surface, so we can determine tangents and normals to these curves in two-dimensions (2-d) and surfaces (in 3-d), respectively. In 3-d, the curvatures of these medial surfaces may be important tensors. The visiometrics operations of visualization, projection, identification and classification, extraction, tracking, quantification, and juxtaposition are each considered below.

Visualization: Numerical fields are displayed in a variety of 2-d and 3-d images. The data are first preprocessed or filtered to make them more accessible visually. High wave number incoherent modes are removed with a filter (e.g., the wavelet process of Farge et al., 2001). The choice of appropriate color maps (palettes) (Farge, 2000) is a nontrivial operation. Farge (1992) represented the vorticity scalar with a grayscale format for lower magnitudes, a yellow intermediate contour for the region near zero, and a few graded colors for the higher magnitudes. In DAVID (see http://www.caip.rutgers.edu/~nzabusky/vizlab_cfd/david/david.html), an interactive color domain system has been developed with colors chosen, for example, with hue, saturation, and value (HSV), and with optional black/white grading superimposed in each color domain. The user sees the image automatically colored as the color map is modified. Simultaneously, at each color transition, the numerical value of the function and between neighboring color transitions, the integrated content, and the corresponding underlying pixel-area of the image are seen. (This gives the user a qualitative feeling about the magnitudes of the objects that the color renders.)

Standard visualization techniques include continuous or discrete contour maps in 2-d; volume rendering a function in 3-d as it would appear when radiating or reflecting light from various sources (Upson & Keeler, 1988); and displaying isosurfaces (contours) from connected polygons that bound regions of functions extracted by thresholding (Lorensen & Cline, 1987). There are many excellent computer vision and scientific visualization contemporary texts in the literature (both web and printed).

Projection: A general process produces abstract images and graphical information in lower dimensions, for example, the projection to 2-d from 3-d by integration with respect to a kernel. If it is a planar delta function, one extracts 2-d surfaces or curves from 3-d or 2-d spatial data, respectively. Also, integration of an appropriately weighted field variable transverse to some initial axis or flow direction (like that behind a planar shock in a shock tube) will produce a space–time diagram from a 2d+1 data set (see color plate section; Figure 2 of Hawley & Zabusky, 1989; see also Zabusky, 1999).

Identification and classification: The geometry, topology, content, moments, and distribution functions of an extracted region are examined. Are the domains in 3-d layer-like or tube-like? Are the tube-like domains right- or left- handed helices?

Extraction and setting of thresholds: Complex data sets may have a hierarchy of embedded coherent structures in a sea of incoherent very small-scale structures. Farge and colleagues (Farge et al., 2001) have applied a threshold prescription to wavelet amplitude coefficients and have developed high-compression techniques to systematically extract coherent vortex objects. Samtaney and Zabusky (2000) have examined the extraction of shocks and species ITLs in 2-d. For ITLs, one looks at absolute values of gradients and Laplacians of the density, temperature, and so on. Various heuristic and analytical methodologies have been presented by Villasenor & Vincent (1992), Melander & Hussain (1994), Jeong & Hussain (1995), Kida & Miura (1998), and Miura (2002). The results of Melander, Jeong, and Hussain are particularly noteworthy.

Tracking: Structures in space-time that have been extracted and identified are followed. One must allow for objects to collide and amalgamate, split, be created, and disappear (Samtaney et al., 1994). Post et al. (2002) and colleagues (e.g., Vrolijk et al., 2003) have carried this work further. With this information, we may be able to formulate kinematic and dynamical models.

Quantification: Graphs of projected and tracked structures are plotted and underlying physical, mathematical, and numerical parameters are varied. In the vicinity of extrema (e.g., magnitude of vorticity $\boldsymbol{\omega}$), second- and third-order moments are useful (e.g., ellipsoids in 3-d). Distribution functions of one or more variables are evaluated, and statistical characterizations of incoherent domains, after structures have been extracted, are examined.

Juxtaposition: These comparisons are of similar or different functions at the same or different times from simulations of the same or linked mathematical models in a relevant domain of parameters. Coherent structures of different functions (e.g., density or vorticity) and their quantifications with runs from different resolutions (validation) and parameters (scaling physical behavior) are compared. One often has to remove a background translation or rotation.

As nonlinear phenomena are simulated at increasingly high resolution and for longer times on adaptive meshes across parallel processors, the validity of results becomes an important issue. Numerical errors accumulate from round-off, truncation (e.g., higher-order and nonlinear dissipative and dispersive regularizations),

spatially and temporally adjusting meshes, and ad-hoc filters. The visiometric process will help find these defects and provide a more rigorous basis for model building and prediction. Visiometrics will also produce new art forms (Zabusky, 2000).

N.J. ZABUSKY

See also **Contour dynamics; Fluid dynamics; Vortex dynamics of fluids; Wavelets**

Further Reading

Bitz, F. & Zabusky, N. 1990. DAVID and "Visiometrics": visualizing and quantifying evolving amorphous objects. *Computers in Physics*, 4: 603–14

Farge, M. 1992. Wavelet transforms and their application to turbulence. *Annual Reviews of Fluid Mechanics*, 24: 395–457

Farge, M. 2000. Choice of representation modes and color scales for visualization in computational fluid dynamics. In *Proceedings of the Science and Art Symposium*, edited by A. Gyr, P.D. Koumoutsakos & U. Burr, Dordrecht: Kluwer, pp. 91–100

Farge, M.G., Pellegrino, G. & Schneider, K. 2001. Coherent vortex extraction in 3D turbulent flows using orthogonal wavelets. *Physical Review Letters*, 87(5): 054501-1–054501-4

Feher, A. & Zabusky, N. 1996. An interactive imaging environment for scientific visualization and quantification. *International Journal of Imaging System Technology*, 7: 121–30

Fernandez, V.M., Silver, D. & Zabusky, N.J. 1996. Visiometrics of complex physical processes: diagnosing vortex-dominated flows. *Computers in Physics*, 10: 463–470

Hawley, J. & Zabusky, N. 1989. Vortex paradigm for shock accelerated density stratified interfaces. *Physical Review Letters*, 63: 1241–44

Jeong, J. & Hussain, F. 1995. On the identification of a vortex. *Journal of Fluid Mechanics*, 285: 69–94

Kida, S. & Miura, H. 1998. Identification and analysis of vortical structures. *European Journal of Mechanics*, B/Fluids, 17(4): 471–488

Lorensen, W.E. & Cline, H.E. 1987. Marching cubes: A high resolution 3D surface construction algorithm. *Computer Graphics*, 21(3): 163–169

Melander, M.V. & Hussain, F. 1994. Topological vortex dynamics in axisymmetric viscous flows. *Journal of Fluid Mechanics*, 260: 57–80

Miura, H. 2002. Analysis of vortex structures in compressible isotropic turbulence. *Computer and Physics Communications*, 147: 552–554

Post, F.H., Vrolijk, B., Hauser, H., Laramee, R.S. & Doleisch, H. 2002. Feature extraction and visualization of flow fields. In *Eurographics* 2002 *State-of-the-Art Reports*, edited by D. Fellner, & R. Scopigno, pp. 69–100. See also http://visualization.tudelft.nl/

Samtaney, R., Silver, D., Zabusky, N. & Cao, J. 1994. Visualizing features and tracking their evolution. *IEEE Computer*, 27(7): 20–27

Samtaney, R. & Zabusky, N.J. 2000. Visualization, feature extraction and quantification of numerical visualizations of high-gradient compressible flows. In *Flow Visualization, Techniques and Examples*, edited by A. Smits & T.T. Lim, London: Imperial College Press, pp. 317–344

Upson, C. & Keeler, M. 1988. V-BUFFER: visible volume rendering. *Computer Graphics*, 22(4): 59–64

Villasenor, J. & Vincent, A. 1992. An algorithm for space recognition and time tracking of vorticity tubes in turbulence. *CVGIP: Image Understanding*, 55: 27–35

Vrolijk, B., Reinders, F. & Post, F.H. 2003. Feature tracking with skeleton graphs. In *Data Visualization: The State of the Art*, edited by F.H. Post, G.M. Nielson & G.P. Bonneau, Boston: Kluwer, pp. 37–52

Zabusky, N.J. 1999. Vortex paradigm for accelerated inhomogeneous flows: visiometrics for the Rayleigh–Taylor and Richtmyer–Meshkov environments. *Annual Review of Fluid Mechanics*, 31: 495

Zabusky, N.J. 2000. Scientific computing visualization—a new venue in the arts. In *Proceedings of the Science and Art Symposium*, edited by A. Gyr, P.D. Koumoutsakos & U. Burr, Dordrecht: Kluwer, pp. 1–11

Zabusky, N.J., Gupta, S. & Gulak, Y. 2003. Localization and spreading of contact discontinuity layers in simulations of compressible dissipationless flows. *Journal of Computational Physics*, 188: 347—363

Zabusky, N.J., Silver, D. & Pelz, R. 1993. Vizgroup '93. Visiometrics, juxtaposition and modeling. *Physics Today*, 46(3): 24-31

VOLCANOS

See **Geomorphology and tectonics**

VOLTERRA SERIES AND OPERATORS

In addition to playing an important role in the development of theoretical biology, the Italian mathematician Vito Volterra (1860–1940) also strongly influenced the development of modern calculus. We deal here with the Volterra functional series (VFS) and associated Volterra differential operators (VDO) which provide a consistent mathematical framework for stating material properties in nonlinear wave propagation systems, for example, in nonlinear optics (Censor & Melamed, 2002; Censor, 2000; Sonnenschein & Censor, 1998). For simplicity, the present introduction is restricted to the temporal domain, adequate for time signals. Waves require a spatiotemporal domain.

Linear Systems

Modeling of physical systems requires material (or constitutive) relations. In electromagnetics, we have relations like $D = \varepsilon E$, $B = \mu H$; in acoustics, the compressibility (relation of pressure to volume) is needed; in elastodynamics, we include Hooke's law (relation of stress to strain). Here $D = \varepsilon E$ and its nonlinear extensions are treated as prototypes.

Materials are dispersive, depending (in the restricted sense of temporal dispersion discussed here) on frequency f. Consider the linear case first:

$$D(\omega) = \varepsilon(-\mathrm{i}\omega)E(\omega), \quad \omega = 2\pi f, \tag{1}$$

where ω is the angular frequency, and defining $\varepsilon(-\mathrm{i}\omega)$ instead of $\varepsilon(\omega)$ is convenient for subsequent applications.

The Fourier transform pair

$$F(t) = \frac{1}{2\pi}\int_{-\infty}^{\infty} \mathrm{d}\omega F(\omega)\mathrm{e}^{-\mathrm{i}\omega t},$$
$$F(\omega) = \int_{-\infty}^{\infty} \mathrm{d}t\, F(t)\mathrm{e}^{\mathrm{i}\omega t} \qquad (2)$$

relates the spectral and temporal domains. We use the same symbol F, although $F(t)$ and $F(\omega)$ are different functions. Accordingly, (1) becomes a convolution integral

$$D(t) = \int_{-\infty}^{\infty} \mathrm{d}t_1 \varepsilon(t_1)E(t-t_1), \qquad (3)$$

where $D(t)$, $\varepsilon(t)$, $E(t)$, are related to $D(\omega)$, $\varepsilon(-\mathrm{i}\omega)$, $E(\omega)$, respectively, according to (2). Note that (3) can be viewed as an integral operation, acting on $E(t)$. Also (3) is the simplest form of a VFS.

Formally we can start with (1), transform according to (2), and note that in the integral $E(-\mathrm{i}\omega)$ (if it can be represented or approximated by a polynomial in $-\mathrm{i}\omega$) can be considered as a polynomial operator $\varepsilon(\partial_t)$ acting on the exponential, in which every time derivative ∂_t replaces a term $-\mathrm{i}\omega$ in $\varepsilon(-\mathrm{i}\omega)$. Note that $\varepsilon(t)$ and $\varepsilon(\partial_t)$ are different functions, but $\varepsilon(-\mathrm{i}\omega)$ and $\varepsilon(\partial_t)$ possess the same functional structure. Thus, instead of (3), we now have the VDO representation

$$D(t) = \varepsilon(\partial_t)E(t) = \varepsilon(\partial_\tau)E(\tau)\mid_{\tau\to t}. \qquad (4)$$

The last expression in (4) with the instruction $\tau \to t$ is superfluous here but will be important for the nonlinear case below. The possibility of using this technique for $\varepsilon(\partial_t)$ a rational function (ratio of polynomials) is discussed elsewhere (Censor, 2001).

As a trivial example for (3) and (4), consider a harmonic signal

$$\begin{aligned} E(t) &= E_0\mathrm{e}^{-\mathrm{i}\omega t}, \\ D(t) &= E_0\mathrm{e}^{-\mathrm{i}\omega t}\int_{-\infty}^{\infty} \mathrm{d}t_1\, \varepsilon(t_1)\mathrm{e}^{\mathrm{i}\omega t_1} \\ &= \varepsilon(-\mathrm{i}\omega)E_0\mathrm{e}^{-\mathrm{i}\omega t} = \varepsilon(\partial_t)E_0\mathrm{e}^{-\mathrm{i}\omega t} \end{aligned} \qquad (5)$$

clarifying the role of the VDO in (4).

Nonlinear Systems and the Volterra Series and Operators

In nonlinear systems, the material relations involve powers and products of fields. Can we simply replace (1) by a series involving powers of $E(\omega)$? A cursory analysis reveals that this leads to inconsistencies. Instead, we ask if (3) can be replaced by a "super convolution" and what form that should take. Indeed, the Volterra series provides a consistent mathematical answer to these questions. It is given by

$$\begin{aligned} D(t) &= \sum_m D^{(m)}(t), \\ D^{(m)}(t) &= \int_{-\infty}^{\infty}\mathrm{d}t_1 \ldots \int_{-\infty}^{\infty}\mathrm{d}t_m \\ &\quad \times\varepsilon^{(m)}(t_1,\ldots,t_m)E(t-t_1)\ldots E(t-t_m). \end{aligned} \qquad (6)$$

Typically, the VFS (6) contains the products of fields expected for nonlinear systems, combined with the convolution structure (3). Various orders of nonlinear interaction are indicated by m.

Theoretically, all the orders co-exist (in practice, the series will have to be truncated within some approximation), and therefore, we cannot inject a time harmonic signal as in (5). If instead, we start with a periodic signal, $E(t) = \sum_n E_n\mathrm{e}^{-\mathrm{i}n\omega t}$ and substitute in (6), we find

$$\begin{aligned} D^{(m)}(t) &= \sum_{n_1,\ldots,n_m} \varepsilon^{(m)}(-\mathrm{i}n_1\omega,\ldots,-\mathrm{i}n_m\omega) \\ &\quad \times E_{n_1}\ldots E_{n_m}\mathrm{e}^{-\mathrm{i}N\omega t} = \sum_N D_N\mathrm{e}^{-\mathrm{i}N\omega t}, \\ N &= n_1+\ldots+n_m, \end{aligned} \qquad (7)$$

with (7) displaying the essential features of a nonlinear system, namely, the dependence on a product of amplitudes, and the creation of new frequencies as sums (including differences and harmonic multiples) of the interacting signals frequencies. In addition, (7) contains the weighting function $\varepsilon^{(m)}(-\mathrm{i}n_1\omega,\ldots,-\mathrm{i}n_m\omega)$ for each interaction mode.

The extension of (4) to the nonlinear VDO is given by

$$\begin{aligned} D^{(m)}(t) &= \varepsilon^{(m)}(\partial_{t_1},\ldots,\partial_{t_m}) \\ &\quad \times E(t_1)\ldots E(t_m)\mid_{t_1,\ldots,t_m\to t}. \end{aligned} \qquad (8)$$

In (8), the instruction $t_1,\ldots,t_m \to t$ guarantees the separation of the differential operators, and finally renders both sides of the equation to become functions of t.

The VFS (6), including the convolution integral (3), is a global expression describing $D(t)$ as affected by integration times extending from $-\infty$ to ∞. Physically, this raises questions about causality, that is, how future times can affect past events. In the full-fledged four-dimensional generalization, causality is associated with the so-called "light cone" (Bohm, 1965). It is noted that the VDO representation (4, 8) is local, with the various time variables just serving for bookkeeping of the operators, and where this representation is justified, causality problems are not invoked.

In general, the frequency constraint of (7) is obtained from the Fourier transform of (6), having the form

$$D^{(m)}(\omega) = \frac{1}{(2\pi)^{m-1}} \int_{-\infty}^{\infty} \mathrm{d}\omega_1 \ldots \int_{-\infty}^{\infty} \mathrm{d}\omega_{m-1} \times \varepsilon^{(m)}(-\mathrm{i}\omega_1, \ldots, -\mathrm{i}\omega_m) E(\omega_1) \ldots E(\omega_m), \quad \omega = \omega_1 + \ldots + \omega_m. \tag{9}$$

It is noted that in (9), we have $m-1$ integrations, one less than in (6). This tallies with the linear case where (1) and (3) involve zero and one integration, respectively. Consequently, the left- and right-hand sides of (9) are functions of ω and ω_m, respectively. The additional constraint $\omega = \omega_1 + \cdots + \omega_m$ completes the equation and renders (9) self-consistent.

Summary

The modeling of nonlinear media using the VFS and VDO provides a mathematically consistent framework which includes linear media as a limiting case. The model displays the typical ingredients of nonlinear circuits and wave systems, where the nonlinear terms are proportional to the product of the amplitudes of the interacting fields, and the newly created frequencies are sums (or differences, or harmonic multiples) of the interaction frequencies, given by $\omega = \omega_1 + \cdots + \omega_m$. In the quantum-mechanical context this is an expression of the conservation of energy. Not shown here is the associated wave propagation vector constraint $\boldsymbol{k} = \boldsymbol{k_1} + \cdots + \boldsymbol{k_m}$, which in the quantum-mechanical context expresses conservation of momentum. Schetzen (1980) is an excellent source of further reading on VFS in nonlinear systems and has many early references.

DAN CENSOR

See also **Harmonic generation; Manley–Rowe relations; Nonlinear acoustics; Nonlinear optics**

Further Reading

Bohm, D. 1965. *The Special Theory of Relativity*, New York: Benjamin

Censor, D. 2000, A quest for systematic constitutive formulations for general field and wave systems based on the Volterra differential operators. *Progress in Electromagnetics Research*, 25: 261–284

Censor, D. 2001, Constitutive relations in inhomogeneous systems and the particle–field conundrum. *Progress in Electromagnetics Research*, 30: 305–335

Censor, D. & Melamed, T. 2002. Volterra differential constitutive operators and locality considerations in electromagnetic theory. *Progress in Electromagnetic Research*, 36: 121–137

Schetzen, M. 1980. *The Volterra and Wiener Theorems of Nonlinear Systems*, Chichester and New York: Wiley

Sonnenschein, M. & Censor, D. 1998. Simulation of Hamiltonian light beam propagation in nonlinear media. *Journal of the Optical Society of America* B, 15: 1335–1345

VOLTERRA–LOTKA EQUATIONS

See **Population dynamics**

VOLUME-PRESERVING MAPS

See **Measures**

VORONOÏ DIAGRAMS

See **Tessellation**

VORTEX DYNAMICS IN EXCITABLE MEDIA

Vortices in excitable media include spiral waves in two spatial dimensions and scroll waves in three spatial dimensions. They are described by reaction-diffusion systems of equations,

$$\partial_t \boldsymbol{u} = \boldsymbol{f}(\boldsymbol{u}) + \mathbf{D}\nabla^2 \boldsymbol{u} + \varepsilon \boldsymbol{h}, \quad \boldsymbol{u}, \boldsymbol{f}, \boldsymbol{h} \in \mathbb{R}^{\ell},\ \mathbf{D} \in \mathbb{R}^{\ell \times \ell},\ \ell \geq 2, \tag{1}$$

where $\boldsymbol{u}(\boldsymbol{r}, t) = (u_1, u_2, \ldots)^{\mathrm{T}}$, is a column-vector of the reagent concentrations, $\boldsymbol{f}(\boldsymbol{u})$ is a column vector of the reaction rates, $\mathbf{D}$ is the matrix of diffusion coefficients, $\varepsilon \boldsymbol{h}(\boldsymbol{u}, \boldsymbol{r}, t)$ is some small perturbation, and $\boldsymbol{r} \in \mathbb{R}^2$ or $\mathbb{R}^3$ is the vector of coordinates on the plane or in space.

In an unbounded two-dimensional medium with $\varepsilon \boldsymbol{h} = 0$, a spiral wave solution rotating with angular velocity ω has the form

$$\boldsymbol{u} = \boldsymbol{U}(\boldsymbol{r}, t) = \boldsymbol{U}[\rho(\boldsymbol{r}), \vartheta(\boldsymbol{r}) + \omega t] \approx \boldsymbol{P}[\rho(\boldsymbol{r}) - \frac{\lambda}{2\pi}(\vartheta(\boldsymbol{r}) + \omega t)]\Big|_{\rho \to +\infty}, \tag{2}$$

where $\rho(\boldsymbol{r})$ and $\vartheta(\boldsymbol{r})$ are the polar coordinates corresponding to the cartesian coordinates $\boldsymbol{r}$. $\boldsymbol{P}(\xi; \omega, \lambda)$ is a periodic wave solution with frequency ω and spatial period λ, so the $\rho \to +\infty$ asymptotic means that isolines are approximately Archimedian spirals with pitch λ. Solutions (2) are typically possible for isolated values of ω and corresponding λ.

Note that system (1) with $\varepsilon \boldsymbol{h} = 0$ is invariant with respect to the Euclidean group of motions of the plane $\{\boldsymbol{r}\}$. Solution (2) is a relative equilibrium, meaning that the states of the wave at all moments of time are equivalent to each other up to a Euclidean motion, namely, a rotation around the origin. If (2) is a solution, then from symmetry

$$\tilde{\boldsymbol{U}} = \boldsymbol{U}(\rho(\boldsymbol{r} - \boldsymbol{R}_{\odot}), \vartheta(\boldsymbol{r} - \boldsymbol{R}_{\odot}) + \omega t - \Phi_{\odot}) \tag{3}$$

is another solution for any constant displacement vector $\boldsymbol{R}_{\odot} = (X_{\odot}, Y_{\odot})^{\mathrm{T}}$ and initial rotation phase $\Phi_{\odot}$. Thus, we have a three-dimensional manifold, parameterized by coordinates $X_{\odot}, Y_{\odot}, \Phi_{\odot}$, of spiral wave solutions

neutrally stable with respect to each other. By "dynamics" of the vortices, we understand any deviation of the solutions from the stationary rotation (2).

Meander

A nonstationary rotation of a spiral wave accompanied by constant change of its shape is called meander. It is convenient to describe this phenomenon in terms of the spiral tip, which can be defined as an intersection of selected isolines of two components of the nonlinear field $\boldsymbol{u}$,

$$u_{j_1}(X_\bullet, Y_\bullet, t) = v_1, \quad u_{j_2}(X_\bullet, Y_\bullet, t) = v_2,$$
$$\Phi_\bullet = \arg(\partial_x + \mathrm{i}\partial_y) u_{j_3}(X_\bullet, Y_\bullet, t), \tag{4}$$

$j_1 \neq j_2$, where $X_\bullet(t)$, $Y_\bullet(t)$ are the coordinates of the tip and $\Phi_\bullet(t)$ is its orientation angle. Typically, a spiral wave in a given system develops the same kind of meander pattern $X_\bullet(t)$, $Y_\bullet(t)$ independent of the initial conditions. Changes of parameters in the same system change the meander pattern, and types of patterns can be qualitatively similar in very different excitable media models.

Possible types of meander can be classified using an orbit manifold decomposition of (1) by the Euclidean group. Evolution of the shape of the wave can be described in coordinates (ξ, η) in a moving frame of reference attached to the spiral tip,

$$\partial_t \boldsymbol{u} = \mathbf{D}(\partial_\xi^2 + \partial_\eta^2)\boldsymbol{u} + \big[C_1(t)\partial_\xi + C_2(t)\partial_\eta + \omega(t)\left(\xi\partial_\eta - \eta\partial_\xi\right)\big]\boldsymbol{u} + \boldsymbol{f}(\boldsymbol{u})$$
$$u_{j_{1,2}}(0,0) = 0, \quad \partial_\eta u_{j_3} = 0, \tag{5}$$

and the movement of the tip is described by ordinary differential equations

$$\frac{\mathrm{d}\Phi_\bullet}{\mathrm{d}t} = \omega(t),$$
$$\frac{\mathrm{d}X_\bullet}{\mathrm{d}t} + \mathrm{i}\frac{\mathrm{d}Y_\bullet}{\mathrm{d}t} = (C_1(t) + \mathrm{i}C_2(t))\mathrm{e}^{\mathrm{i}\Phi_\bullet}. \tag{6}$$

Equations (5) define a dynamic system with the phase space $\{(\boldsymbol{u}(\xi,\eta), C_1, C_2, \omega)\}$, devoid of the Euclidean symmetry of the original system (1). Knowing the attractor in (5), one can deduce the properties of the meander patterns by integrating the ODE system (6) (see Figure 1).

Forced Drift

Another kind of deviation from (2) is drift of spirals due to perturbations $\varepsilon\boldsymbol{h} \neq 0$. As solutions of family (3) are neutrally stable with respect to each other, a small perturbation of a spiral wave caused by an $\varepsilon\boldsymbol{h}$ limited in time will die out, but it will typically result in a small change in the spiral wave coordinates $X_\odot$, $Y_\odot$ and $\Phi_\odot$.

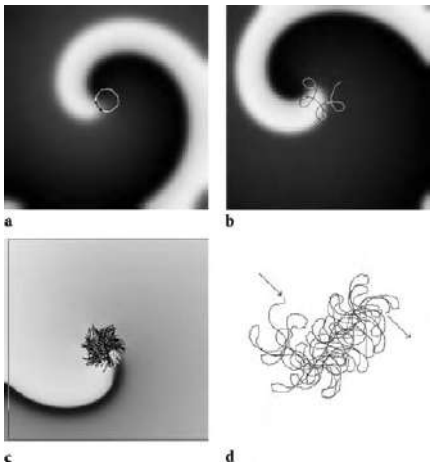

Figure 1. Typical meander patterns. Shown are snapshots of the excitation field with pieces of preceding tip paths superimposed. (a) Stationary (rigid) rotation: equilibrium in the base system (5). (b) Classical biperiodic "flower" meander: limit cycle in the base system (5). (c) Quasi-periodic hypermeander: invariant torus in the base system (5). (d) Pseudorandom walk hypermeander: chaotic attractor in the base system (5) (only the tip path shown).

If similar perturbations are applied repeatedly with a period equal to the period of the spiral, then small shifts of $X_\odot$ and $Y_\odot$ accumulate, which is called a resonant drift. Another type of slow drift is inhomogeneity-induced drift, occurring when $\varepsilon\boldsymbol{h}$ depends explicitly on spatial coordinates (medium properties are slightly inhomogeneous, as in Figure 2(b)). In the first order of perturbation theory, this is equivalent to a time-dependent perturbation synchronized with the spiral rotation and is therefore resonant. A third type of drift occurs if the medium is bounded, and the boundary influence on the spiral wave is not negligible. Although a boundary is not a slight perturbation, the effects of passive (nonflux) on the spiral wave can be small and similar to that of small spatial inhomogeneity (Figure 2(c)). Other kinds of perturbations breaking the Euclidean symmetry of (1) can also cause drift.

Being a first-order effect, the slow drift of a spiral due to small forces of different types obeys a superposition principle. It leads to motion equations

$$\partial_t(X_\odot + \mathrm{i}Y_\odot) = C(X_\odot, Y_\odot) + v(X_\odot, Y_\odot)\mathrm{e}^{\mathrm{i}\Theta},$$
$$\partial_t\Theta = \Omega(t) - \omega(X_\odot, Y_\odot), \tag{7}$$

where $C(X_\odot, Y_\odot)$ is the velocity of the inhomogeneity and boundary induced drift, $v(X_\odot, Y_\odot)$ is the velocity of the resonant drift, Θ is the phase difference between the spiral and the resonant forcing, $\Omega(t)$ is the

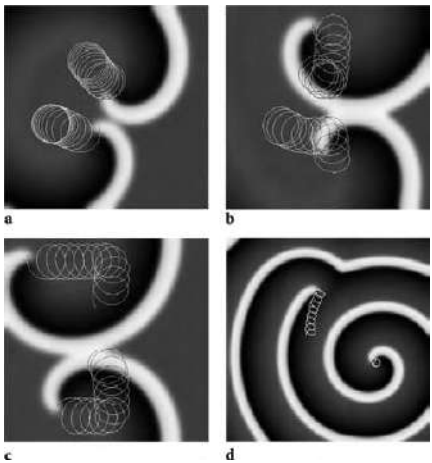

Figure 2. Different drifts of spiral waves. Shown are snapshots of the excitation field with pieces of preceding tip paths superimposed. The right half of the medium is slightly "stronger" than the left half; (a)–(c) are consecutive stages of the same numeric experiment. (a) Two close oppositely charged spirals attract with each other and form a pair drifting in SE direction. (b) The spirals have reached the inhomogeneity and are being driven apart by it. (c) The spirals have reached the medium boundary and now drift along it. (d) In a bigger medium: the right spiral has subdued the left spiral into an induced drift.

perturbation frequency, and $\omega(X_\odot, Y_\odot)$ is the own spiral angular frequency possibly depending on the current spiral location.

These are motion equations for rigidly rotating spirals, and $X_\odot$ and $Y_\odot$ are sliding period averages of $X_\bullet$, $Y_\bullet$. Dynamics of forced meandering spirals are more complicated because of possible resonances.

Spiral Waves as Particles

Motion equations (7) are obtained by summation of the effects of elementary perturbations of different modalities localized in different sites and occurring at different moments of time, onto the spiral's location and phase. These elementary responses are described by response functions, which are critical eigenfunctions of the adjoint linearized operator. An interesting property of the response function is their localization in the vicinity of the spiral core (see Figure 3). The spiral will only drift if the perturbation is applied not too far from its core.

A paradox is thus created. Although a spiral wave appears as a significantly nonlocal process, involving in its rhythm all of the excitable medium, it behaves as a localized, particle-like object in its response to perturbations.

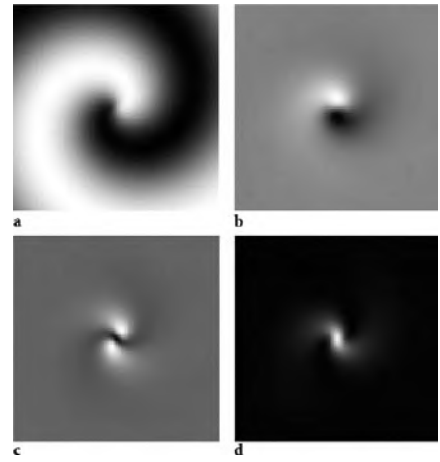

Figure 3. A spiral wave solution (a) and its temporal (b) and spatial (c,d) response functions, as density plots. Monotone gray periphery on (b–d) corresponds to zero. Thus the spiral wave is a non-local process, but its response functions are well localized.

A spatial response function, defining the proportionality between drift velocity and inhomogeneity magnitude, typically has scalar (drift along the parameter gradient or toward the boundary) and pseudo-scalar (across the parameter gradient or along the boundary) components. The sign of the latter depends on the direction of the spiral rotation.

Bending and Twisting of Scroll Waves

As a scroll wave is a three-dimensional analogue of a spiral wave, all comments about spiral wave dynamics remain valid for the scrolls, but there are new aspects arising from the third dimension. The simplest 3-d vortex is the straight scroll wave, a spiral wave continued unchanged in the third dimension. The spiral tip, a point in the plane, becomes the edge of the scroll, a line in space, and the spiral core, a circle in the plane, becomes the scroll filament, a tube. The term *filament* also sometimes denotes the center line of the tube filament.

More interesting regimes are scrolls with bent filaments (Figure 4(a)), and with rotation phase varying along the filament (twisted scrolls, as in Figure 4(b)). Both bending and twist of scrolls are factors of their dynamics. A vortex ring will collapse or expand and, at the same time, drift along its symmetry axis, and twisted vortex will usually spread the twist evenly along its filament or, if possible, untwist.

The asymptotic motion equation for the scroll waves can be derived using response functions. If the twist is

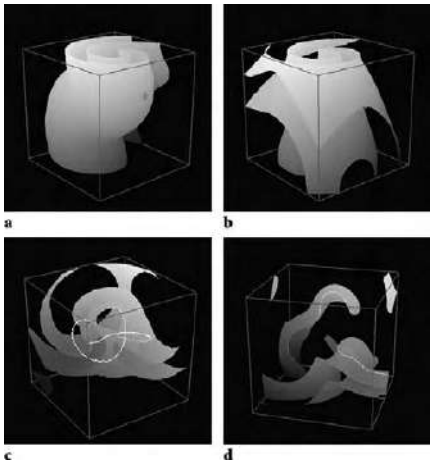

Figure 4. Scroll waves. (a) Scroll with a curved filament. (b) Twisted scroll with straight filament. (c) Scroll with a knotted filament. (d) "Turbulent regime": many scrolls developed from one via negative filament tension multiplication mechanism. On panels (c) and (d), part of the wavefronts is cut out, to make the filaments (white lines) visible.

not too strong, then the dynamics of the scroll due to bending and due to twist are decoupled. The motion equation of the filament is

$$\partial_t \boldsymbol{R}_\mathrm{f} = b_2 \partial_\mathrm{s}^2 \boldsymbol{R}_\mathrm{f} + c_3 \left[\partial_\mathrm{s} \boldsymbol{R}_\mathrm{f} \times \partial_\mathrm{s}^2 \boldsymbol{R}_\mathrm{f}\right], \qquad (8)$$

where $\boldsymbol{R}_\mathrm{f} = \boldsymbol{R}_\mathrm{f}(p,t) \in \mathbb{R}^3$ is the position of the filament as function of a length parameter p and time, and ∂_s is arclength differentiation, $\partial_\mathrm{s} \equiv \left|\partial_p \boldsymbol{R}_\mathrm{f}\right|^{-1} \partial_p$. At $b_2 = 0$, Equation (8) is completely integrable; in particular, the total length of the filament is conserved. Otherwise, the total filament length decreases if $b_2 > 0$ and increases if $b_2 < 0$, and in the latter case, a straight filament is unstable.

If twist is high, it changes the filament tension and may make it negative. This causes an instability of the straight filament shape, leading to "sproing": a sudden transition from a strongly twisted scroll with straight filament to a less twisted scroll with a helical filament.

Competition and Interaction *(Divide et impera)*

Normally, two colliding excitation waves annihilate each other. Thus, if there are many periodic sources of waves (e.g., vortices), then the medium splits into domains, or regions of influence, each domain receiving waves from its source. The domains are separated by shock structures where the waves collide (see Figure 2(a–c)).

The domain boundaries work like non-flux boundaries. Thus, two spiral waves can interact with each other (cause each other's drift and frequency shift), whereas each of them actually interacts with the boundary between their domains. Such interaction between spirals may lead to the formation of linked pairs (see Figure 2(a)).

Different scroll filaments or different parts of the same filament can also interact with each other. If this interaction is repulsive, it may compensate positive tension normally causing closed filaments to contract and collapse, leading to stable "particle-like" 3-d scrolls with compact filaments (see Figure 4(c)).

Induced Drift

If colliding waves annihilate in a ratio of one-to-one, continuity of phase applies. If two vortices have different frequencies (e.g., because of a spatial inhomogeneity of the medium), then by continuity of phase the domain boundary between them moves toward the slower vortex. When it reaches its core, the slower vortex loses its identity and turns into a dislocation in the wave field emitted by the faster vortex. This dislocation, appearing as a free end of an excitation wave, periodically rejoins from one wave to another with some overall drift depending on the frequency and direction of the incident waves (see Figure 2(d)). If the incident wave packet ceases, the dislocation can develop into a vortex again.

As a dislocation is very different from a vortex, this induced drift is an example of hard, non-perturbative dynamics.

Hard Dynamics: Births, Deaths, and Multiplication of Vortices

Another kind of hard dynamics involves complete elimination of a vortex. This may happen if the wave propagation around the vortex becomes impossible, for example, if the vortex has been driven too close to a medium boundary. Alternatively, two spiral waves with opposite topological charges may annihilate if driven too close to each other. For a scroll wave, annihilation may happen to a piece of its filament, which then appears as splitting of a scroll wave into two.

Birth of a vortex may occur as a result of a temporary local block of excitation propagation. Unless this happens near the medium boundary, this means birth of a pair of oppositely rotating spirals in the plane, or a scroll with a closed filament around the perimeter of the propagation block. The block may occur as a result of external forcing or special initial conditions, or develop as a result of an instability of an existing vortex. Such instability can underlie a chain reaction of the vortex multiplication, which may lead to a turbulence of excitation vortices—a spatiotemporal chaotic state

where generation of new vortices is balanced by their annihilation when they get close to each other due to overcrowding.

Several mechanisms of such instabilities have been identified, including those working in two or three dimensions, such as Eckhaus instability, zigzag/lateral instability or imposed mechanical movement of the medium, and those possible only in three dimensions. The latter include instability due to the negative "tension" b_2 of the vortex filament (see Figure 4(d)), or caused by spatially inhomogeneous anisotropy of the medium such as that observed heart ventricular muscle. Some of these types of instabilities may be responsible for the phenomenon of fibrillation of the heart (*See* **Cardiac arrhythmias**).

VADIM N. BIKTASHEV

See also **Complex Ginzburg–Landau equation; Framed space curves; Reaction-diffusion systems; Scroll waves; Spiral waves**

Further Reading

Gaponov-Grekhov, A.V., Rabinovich, M.I. & Engelbrecht, J. (editors). 1989. *Nonlinear Waves II. Dynamics and Evolution*, Berlin and New York: Springer

Holden, A.V. & El Naschie, M.S. (editors). 1985. *Nonlinear Phenomena in Excitable Physiological Systems*. Special issue: *Chaos Solitons & Fractals*, 5(3/4)

Holden, A.V., Markus, M. & Othmer, H.G. (editors). 1989. *Nonlinear Wave Processes in Excitable Media*, New York and London: Plenum Press

Kapral, R. & Showalter, K. (editors). 1995. *Chemical Waves and Patterns*, Dordrecht and Boston: Kluwer

Panfilov, A.V. & Holden, A.V. (editors). 1997. *Computational Biology of the Heart*, Chichester and New York: Wiley

Panfilov, A. & Pertsov, A. 2001. Ventricular fibrillation: evolution of the multiple wavelet hypothesis. *Philosophical Transactions of the Royal Society of London* A, 359: 1315–1325

Swinney, H.L. & Krinsky, V.I. (editors). 1991. *Waves and Patterns in Chemical and Biological Media*, Cambridge, MA: MIT Press

Winfree, A.T. (editor). 1998. *Fibrillation in normal ventricular myocardium*. Focus issue. *Chaos*, 8(1)

Winfree, A.T. 1991. Varieties of spiral wave behavior in excitable media. *Chaos*, 1(3): 303–334

Zykov, V.S. 1987. *Modelling of Wave Processes in Excitable Media*, Manchester: Manchester University Press

VORTEX DYNAMICS OF FLUIDS

The swirling and chaotic behavior of vortex-dominated fluid flows has inspired philosophers, poets, and artists from antiquity to the present, including Leonardo da Vinci, the 15th-century artist, scientist, and engineer who captured complex fluid motions as part of his applied and creative work (van Dyke, 1982; Lugt, 1983; Minahen, 1992). The traditional woodblock prints (*Ukioy-e*) of Hiroshige and Hokusai also show spiral motion produced by a vortex and "curls" on breaking ocean waves in various locations around Japan (Zabusky, 2000).

Vorticity is a measure of the "spin" or rotation of the fluid and is usually represented by a continuous vector variable $\boldsymbol{\omega}(\boldsymbol{x}, t)$. Regions of flow that do not contain vorticity are called irrotational. Vorticity can be defined in two equivalent ways. First, as the curl of the velocity $\boldsymbol{u}$, $\boldsymbol{\omega} = \nabla \times \boldsymbol{u}$. Second, and more geometrically, as a limit (when it is finite) of a closed circuit integral over a domain boundary D' (or equivalently the integral over domain D within boundary D') whose enclosed area $A \to 0$, or $\boldsymbol{\omega} = \boldsymbol{e}_{\tan}[\lim |_{A \to 0} (\Gamma/A)]$ where for finite A, Γ is the circulation or line integral of velocity around the domain,

$$\Gamma = \int_{D'} \boldsymbol{u} \cdot \mathbf{d}s = \int_{D} \boldsymbol{\omega} \cdot \mathbf{d}A \qquad (1)$$

and $\boldsymbol{e}_{\tan}$ is the tangent to the vorticity vector at the point where $A \to 0$. Note that the scalars $\frac{1}{2}\boldsymbol{\omega} \cdot \boldsymbol{\omega}$ (enstrophy) and $\boldsymbol{\omega} \cdot \boldsymbol{u}$ (helicity) arise frequently in discussions of turbulence.

Leonhard Euler derived continuum mathematical equations for an ideal (non-dissipative) fluid. In the 19th century, Claude Navier, George Stokes, and others included dissipative processes for a realistic viscous fluid (Lamb, 1932; Batchelor, 1967; Kiselev et al., 1999). These equations provide models of fluids under usual (for example nonrelativistic) conditions. Asymptotic (reduced) mathematical equations, particularly those emphasizing inviscid vortex-dominated flows (Saffman, 1992) were derived in the 19th century with works of William Thomson (Lord Kelvin) and Hermann von Helmholtz, among others (*See* **Kelvin–Helmholtz instability**). Vortex models are used today to predict the behavior of geophysical and astrophysical fluids (Nezlin, 1993), and in engineering applications (Green, 1995).

If $\boldsymbol{\omega}(\boldsymbol{x}, t)$ is modeled by one or more line filaments in three dimensions (3-d) on which the vorticity is concentrated, then the velocity produced by this vorticity can be calculated from a (Biot–Savart) line integral over the filaments. With this velocity, one can obtain the trajectories of points in the fluid merely by solving $\mathrm{d}\boldsymbol{x}/\mathrm{d}t = \boldsymbol{u}(\boldsymbol{x}, t)$. In 2-d planar flows, the vorticity vector has one component perpendicular to the plane, $(\omega = \partial_x v - \partial_y u)$, and it may be modeled by one or more points of strength Γ_i.

With these definitions, one can prove some fundamental theorems, including the following (Kiselev et al., 1999):

- *Thomson's theorem*: In an ideal barotropic moving fluid, Γ for any closed contour does not depend on time.
- *Helmholtz's theorem*: If the particles of a liquid satisfy Thomson's theorem and form a vortex filament at some moment of time, then these particles form a vortex filament at all subsequent and previous

moments of time and the vortex tube of circulation Γ will be time invariant and constant along its length.

For 2-d, the simplicity of the kinematic description for homogeneous incompressible fluids allows for simple computer models and valuable insights into the motion of ideal fluids. For example, point circulations Γ_i are usually positive and negative constants; vortex sheets along a line described by the circulation per unit length $\gamma(\boldsymbol{s}, t)$; or vorticity $\omega(\boldsymbol{x}, t)$ is constant in a domain (*See* **Contour dynamics**). (Note that for points and sheets, the equations are ill-posed mathematically, and regularization techniques must be used when computing numerically long times.) Interesting effects observed in 2-d include the merger of like-signed vortex domains if initially placed sufficiently close, binding of opposite-signed domains into "vortex projectiles" (a generic translating form whose simplest example is the dipole composed of two opposite-signed points). For vortex sheets, a linear (Kelvin–Helmholtz) stability analysis shows growth of a perturbation for all wavelengths of the disturbance. These evolve into finite-amplitude rolls with a characteristic spiral depending on their sign (see photo of an atmospheric vortex sheet on page 1 of color plate section). If one relaxes the sheet to a very thin layer then small wavelength perturbations are stabilized whereas wavelengths larger than the initial thickness remain unstable. Placing more than one harmonic perturbation on the thin layer, one observes roll-up and merger (energy cascade to large scales) as well as entrophy cascade to smaller scales; that is, the process becomes turbulent. Many details are found in the references below.

In 3-d, $\boldsymbol{\omega}$ may be concentrated on one or more filamentary lines or in finite area tubes, for example, the well-known vortex ring which translates at uniform speed and is unstable (Shariff & Leonard, 1992). If the ring is perturbed, this can lead to collapse and reconnection (Kida & Takaoka, 1994; Fernandez et al., 1995). In a dramatic experiment, Lim and Nickels (1992, 1995) fired a blue and red vortex ring toward each other in water and observed them interact and split into many blue-red smaller vortex ringlets.

The vorticity evolution equation is obtained if one applies the curl operation to the fluid momentum equation. This shows clearly many fundamental and interesting results on vorticity creation, modification, and dissipation. For the zero viscosity (ideal or Euler equation) limit, we have

$$\frac{\partial \boldsymbol{\omega}}{\partial t} + \boldsymbol{u} \cdot \nabla \boldsymbol{\omega} + \boldsymbol{\omega}(\nabla \cdot \boldsymbol{u}) = \boldsymbol{\omega} \cdot \nabla \boldsymbol{u} + \rho^{-2}(\nabla \rho \times \nabla p). \qquad (2)$$

On the right-hand side the terms are: (1) vorticity "stretching" by the rate of strain tensor, which is only present in 2-d-axisymmetric and 3-d motions and is essential for turbulence seen in 3-d; and (2) baroclinic terms, which stem from the misalignment between the gradient of density and either the gravitation vector or the gradient of pressure. Both are important in incompressible inhomogeneous multispecies fluids (e.g., the Rayleigh–Taylor instability) and the latter term is important when shock waves interact with density inhomogeneities in compressible fluids (known as the Richtmyer–Meshkov (RM) instability environment). Recently, Ghoneim and colleagues (e.g., Soteriu & Ghoneim, 1995; Reinaud et al., 2000) used a point vortex model to represent inhomogeneous fluids where Γ_i and $\nabla\rho$ vary in time and Zabusky and colleagues have quantified the vortex-accelerated vorticity deposition in the compressible RM environment (Peng et al., 2003) relevant to laser fusion and supersonic combustion.

For real fluids with small dissipation or at high Reynolds number,

$$\mathrm{Re} = \frac{UL}{\nu} = \frac{\text{velocity} \times \text{length}}{\text{kinematic viscosity}}, \qquad (3)$$

these insights are for short times. Vorticity is generated in a thin boundary layer in the vicinity of rigid or compliant objects in the flow—for example, cylinders (Williamson, 1996), spheres, or airfoils—or within channels because of viscosity (non-slip boundaries). Note, that the larger the Reynolds number, the more "unstable" is the fluid motion and the more likely that one finds it in a turbulent state. Cogent discussions of realistic turbulent effects including vortex phenomena are given in recent books (Pope, 2000; Tsinober, 2001).

Vortices are audible. When we hear the wind howling or the crack of a whip, we are sensing vortices in action. Aeroacoustics, the branch of fluid dynamics concerned with sound generated from vortices, is being applied to noise from jet engines, sounds in music and speech, and so on.

Currently, active fields of study include separating turbulent flows into their coherent and incoherent vortex structures (thereby simplifying prediction and control of flows) (*See* **Visiometrics**). These studies arise in geophysics (e.g., hurricanes, the Gulf stream, and Jupiter's red spot) and astrophysics (planetary nebulae, supernova, and galaxy collisions).

N.J. Zabusky

See also **Chaotic advection; Contour dynamics; Fluid dynamics; Turbulence; Visiometrics; Vortex dynamics in excitable media**

Further Reading

Batchelor, G. 1967. *An Introduction to Fluid Dynamics*, Cambridge: Cambridge University Press

Fernandez, V.M., Zabusky, N.J. & Gryanik, V.M. 1995. Vortex intensification and collapse of the Lissajous-elliptic ring: single and multiple-filament Biot–Savart simulations and visiometrics. *Journal of Fluid Mechanics*, 299: 289–331

Green, S.I. 1995. (editor). *Fluid Vortices*, Boston: Kluwer

Kida, S. & Takaoka, M. 1994. Vortex reconnection. *Annual Reviews of Fluid Mechanics*, 26: 169–189

Kiselev, S.P, Vorozhtsov, E.V. & Fomin, V.M. 1999. *Foundations of Fluid Mechanics with Applications*, Boston: Birkhauser

Lamb, H. 1932. *Hydrodynamics*, 6th edition, Cambridge: Cambridge University Press

Leonard, A. 1985. Computing three-dimensional incompressible flows with vortex elements. *Annual Reviews of Fluid Mechanics*, 17: 523–559

Lim, T.T. & Nickels, T.B. 1992. Instability and reconnection in the head-on collision of two vortex rings. *Nature*, 357: 225

Lim, T.T. & Nickels, T.B. 1995. Vortex rings. In *Fluid Vortices*, edited by S.I. Green, Boston: Kluwer, pp. 95–153

Lugt, H.J. 1983. *Vortex Flow in Nature and Technology*, New York: Wiley

Minahen, C. 1992. *Vortex/t: The Poetics of Turbulence*, University Park: Pennsylvania State University Press

Nezlin, M.V. 1993. *Rossby Vortices, Spiral Structures and Solitons: Astrophysics and Plasma Physics in Shallow Water Experiments*, New York: Springer

Peng, G., Zabusky, N.J. & Zhang, S. 2003. Vortex-accelerated secondary baroclinic vorticity deposition and late-intermediate times of a two-dimensional Richtmyer–Meshkov interface. *Physics of Fluids*, 15: 3730–3744

Pope, S.B. 2000. *Turbulent Flows*, Cambridge and New York: Cambridge University Press

Reinaud, J., Joly, L. & Chassaing, P. 2000. The baroclinic secondary instability of the two-dimensional shear layer. *Physics of Fluids*, 12(10): 2489–2505

Saffman, P.G. 1992. *Vortex Dynamics*, Cambridge and New York: Cambridge University Press

Shariff, K. & Leonard, A. 1992. Vortex rings. *Annual Reviews of Fluid Mechanics*, 24: 235-279

Soteriu, M.C. & Ghoneim, A. 1995. Effects of the free-stream density ratio on free and forced spatially developing shear layers. *Physics of Fluids*, 7: 2036–2051

Tsinober, A. 2001. *An Informal Introduction to Turbulence*, Boston: Kluwer

van Dyke, M. 1982. *An Album of Fluid Motion*, Stanford, CA: Parabolic Press

Williamson, C.H.K. 1996. Vortex dynamics in the cylinder wake. *Annual Reviews of Fluid Mechanics*, 28: 477–539

Zabusky, N.J. 1999 Vortex paradigm for accelerated inhomogeneous flows: visiometrics for the Rayleigh–Taylor and Richtmyer–Meshkov environments. *Annual Reviews of Fluid Mechanics*, 31: 495–536

Zabusky, N.J. 2000. Scientific computing visualization—a new venue in the arts. In *Science and Art Symposium 2000*, edited by A. Gyr, P.D. Koumoutsakos & U. Burr, Boston: Kluwer

W

WATER WAVES

Water waves have attracted the attention of scientists for many centuries. Although much is now understood, they are a continuing source of fascination, as many aspects of their often-complicated nonlinear behavior remain to be fully elucidated. We describe first the linear theory, much of which was developed in the 19th century, before discussing the more modern developments concerning weakly nonlinear waves. Throughout, the theory is based on the traditional assumptions that water is inviscid, incompressible with a constant density ρ, and in irrotational flow; that is, it has zero vorticity. It follows that for water waves, the governing equation is Laplace's equation, which is linear, and so all the nonlinearity in the problem resides in the free-surface boundary conditions. There is the kinematic condition that the free surface is a material surface at all times and the dynamic condition that the free surface has constant pressure at all times. The weakly nonlinear theory for water waves is described, which employs some of the basic paradigms for nonlinear waves. The special features that emerge when one considers finite-amplitude water waves are described in the review articles of Schwarz & Fenton (1982) and Dias & Kharif (1999).

Linear Waves

When the governing equations of motion are linearized about the rest state, it is customary to make a Fourier decomposition and seek solutions in which the wave elevation (deviation of the water surface from its rest position) is given by

$$\zeta = a \exp(\mathrm{i}(\boldsymbol{k}\cdot\boldsymbol{x} - \omega t)) + \text{c.c.}, \tag{1}$$

where $\boldsymbol{x} = (x, y)$ denotes the horizontal coordinates, and t is the time variable, while $\boldsymbol{k} = (k, l)$ is the wave number, ω is the wave frequency, and a is the wave amplitude. Here, c.c. denotes the complex conjugate. This elementary disturbance represents a sinusoidal wave propagating in the direction $\boldsymbol{k}/\kappa$ where $\kappa = |\boldsymbol{k}| = \sqrt{k^2 + l^2}$, with a phase speed $c = \omega/\kappa$, a wavelength $\lambda = 2\pi/\kappa$, and a period $T = 2\pi/\omega$. The corresponding fluid velocity is $\boldsymbol{u} = (u, v)$ and is obtained from a velocity potential (so that $\boldsymbol{u} = \mathrm{grad}\,\phi$), where

$$\phi = -\mathrm{i}ca\frac{\cosh\kappa(z+h)}{\sinh\kappa h}\exp(\mathrm{i}(\boldsymbol{k}\cdot\boldsymbol{x} - \omega t)) + \text{c.c.} \tag{2}$$

Here, z is the vertical coordinate, and h is the total depth of water in the rest state (that is, the water occupies the region $-h < z < 0$). Note that the horizontal velocity $\boldsymbol{u}$ is then in phase with the surface elevation, but that the vertical velocity w is $\pi/2$ out of phase, while both velocity components decrease with depth away from the free surface.

Equations (1) and (2) provide a kinematic description of water waves, which to this point means that the conditions of incompressibility and irrotational flow have been satisfied, that the vertical velocity is zero at the bottom, and that the (linearized) kinematic boundary condition that the free surface remains a material surface for all time has been satisfied. To obtain the dynamics, these expressions are substituted into the remaining boundary condition that the free surface is one of constant pressure. This linearized formulation then yields the dispersion relation determining the wave frequency in terms of the wave number,

$$\omega^2 = (g\kappa + \sigma\kappa^3)\tanh(\kappa h), \tag{3}$$

where $\rho\sigma$ is the coefficient of surface tension, which has a value of 74 dyn/cm at 20°C (*See* **Dispersion relations**). Detailed derivations of (3) and discussions of the consequences for the properties of water waves can be found in many classical and modern texts, see for instance, Lamb (1932), Whitham (1974), Lighthill (1978), or Mei (1983). Indeed, water waves have formed the paradigm for much of our present-day understanding of linear dispersive waves.

There are two branches of the dispersion relation (3), corresponding to waves running to either the right or the left. Note that (3) is isotropic, in that the wave frequency, and hence the phase speed, depend only on the magnitude of the wave number and not its direction. It is apparent from (3) that the effect of surface tension

is significant only when $\kappa > (g/\sigma)^{1/2}$; using the above value for σ this corresponds to $\lambda < 1.73$ cm. Such waves are then usually called capillary waves, while waves with $\kappa < (g/\sigma)^{1/2}$ are called gravity waves. Another useful measure of the effect of surface tension is the Bond number $B = \sigma/gh^2$. When $B < 1/3$, the phase speed $c = \omega/\kappa$ decreases from its long wave value $c_0 = (gh)^{1/2}$, achieved at $\kappa = 0$, to a minimum value of c_m at a wave number $\kappa = \kappa_m$, and then increases without limit as κ increases to infinity. For the case when the Bond number $B > 1/3$, the phase speed increases monotonically from the long wave value c_0 as κ increases from zero. However, the critical depth below which this regime is realized occurs when the Bond number $B = 1/3$, which corresponds to $h = 0.48$ cm. In practice, this is too shallow to ignore the effects of friction and, hence, is usually not regarded as being of any practical interest.

From expressions (2) for the velocity potential and the dispersion relation (3), we see that water waves do not feel the effect of the bottom if $\kappa h \gg 1$. More precisely, if $\kappa h > 2.65$ (or $\lambda/h < 2.37$), then there is less than 1% error in supposing that $h \to \infty$ and that $\tanh(\kappa h) \to 1$. This case describes deep water waves, for which the dispersion relation (3) collapses to

$$\omega^2 = g\kappa + \sigma\kappa^3. \tag{4}$$

In this deep water limit, the Bond number $B \to 0$ ($<1/3$), so that the dispersion relation for the phase speed $c = \omega/\kappa$ has a minimum value at $\kappa = \kappa_m$ ($= (g/\sigma)^{1/2}$ here) or $c_m = (4g\sigma)^{1/4} = 23.2$ cm/s. There are no sinusoidal waves of the form (1) for any phase speed $c < c_m$, while for any $c > c_m$ there are two classes of deep water waves, gravity waves with $\kappa < \kappa_m$ and capillary waves with $\kappa > \kappa_m$.

Long waves are characterized by the limit $\kappa h \to 0$, that is, the limit when $\lambda/h \to \infty$. In this limit, the wave frequency tends to zero, and the wave phase speed tends to $c_0 = (gh)^{1/2}$. In this case, for the reasons discussed above, it is customary to ignore the effects of surface tension, so that there is only one class of waves, namely, gravity waves, which in this limit of $\kappa h \to 0$ are often referred to as shallow water waves. The fluid velocity is then approximately horizontal and independent of the vertical coordinate z, while at $O(\kappa h)$, the vertical component of the fluid velocity is a linear function of $(z + h)$.

In this linearized system, more general solutions can be built up by Fourier superposition of the elementary solutions (1) over the wave number $\boldsymbol{k}$ in which the dispersion relation (3) is satisfied and the wave amplitude a is allowed to be a function of $\boldsymbol{k}$. From this process, it can readily be established that a localized initial state will typically evolve into wave packets, with a dominant wave number $\boldsymbol{k}$ and corresponding frequency ω given by (3), within which each wave phase propagates with the phase speed c, but whose envelope propagates with the group velocity, given by

$$\boldsymbol{c}_g = \nabla_{\boldsymbol{k}}\omega. \tag{5}$$

The group velocity is the velocity of energy propagation, where the wave energy density is $2\rho(g + \sigma\kappa^2)|a|^2$, being composed of equal parts of potential and kinetic energy. Because water waves are isotropic, the group velocity is in the direction of the wave number $\boldsymbol{k}$, and has a magnitude

$$c_g = \partial\omega/\partial\kappa = \frac{c}{2}\left\{\frac{g + 3\sigma\kappa^2}{g + \sigma\kappa^2} + \frac{2\kappa h}{\sinh 2\kappa h}\right\}. \tag{6}$$

Assuming that the Bond number $B < \frac{1}{3}$, it can be shown for gravity waves (defined by the wave number range $0 < \kappa < \kappa_m$) that $c_g < c$, with equality in the long wave limit, $\kappa \to 0$ when c_g and c tend to c_0, and at the value $\kappa = \kappa_m$, $c_g = c = c_m$. For capillary waves (defined by the wave number range $\kappa > \kappa_m$), on the other hand, $c_g > c$. In the absence of surface tension (i.e., $B \to 0$), $c_g < c$ for all wave numbers $\kappa > 0$, and in the deep water limit $c_g \approx c/2$.

Weakly Nonlinear Waves

The theory of linearized waves described in the previous section is valid when initial conditions are such that the waves have sufficiently small amplitudes. However, after a sufficiently long time (or if the initial conditions describe waves of moderate or large amplitudes), the effects of the nonlinear terms in the free surface boundary conditions need to be taken into account. There are three different areas where weak nonlinearity needs to be taken into account, namely, long waves, wave packets, and wave resonances.

Long Waves: Korteweg–de Vries Equation

Initially, we consider unidirectional waves propagating in the positive x-direction, so that the wave number is $\boldsymbol{k} = (k, 0)$. In the long wave limit, $kh \to 0$, the dispersion relation (3) can be approximated by

$$\omega = c_0 k - \frac{c_0 h^2}{6}\delta k^3 + \dots, \qquad \delta = 1 - 3B,$$

where we recall that B is the Bond number measuring the effect of surface tension. To leading order, the waves propagate with the linear long wave phase speed $c_0 = (gh)^{1/2}$. But, after a long time the cumulative effects of weak nonlinearity must be taken into account. When these are balanced against the leading order linear dispersive terms (the $O(k^3h^3)$ terms above), the result is the well-known Korteweg–de Vries (KdV) equation for the wave elevation

$$\zeta_t + c_0\zeta_x + \frac{3c_0}{2h}\zeta\zeta_x + \frac{c_0 h^2}{6}\delta\zeta_{xxx} = 0. \tag{7}$$

This equation was derived by Diederik Korteweg and Hendrik de Vries in a now very famous paper published

in 1895 (Korteweg & de Vries, 1895), although in fact Joseph Boussinesq had obtained it earlier in 1877 (Boussinesq, 1877; *See* **Korteweg–de Vries equation**). Relative to the leading order propagation with the speed c_0, the time evolution occurs on the nondimensional scale ε^{-3}, where the wave amplitude ζ/h scales with ε^2 and the wave dispersion kh scales with ε (that is, spatial derivatives scale with ε).

Korteweg and de Vries found a family of traveling-wave solutions, periodic waves described by elliptic functions and commonly called cnoidal waves, and the solitary wave solution

$$\zeta = a\,\mathrm{sech}^2(\gamma(x - Vt)),$$
$$\text{where} \quad V - c_0 = \frac{c_0 a}{2h} = \delta\frac{2c_0h^2}{3}\gamma^2. \qquad (8)$$

The solitary wave has a free parameter, for instance, the amplitude a. When $\delta > 0$ (that is, $B < 1/3$), then the amplitude a is always positive and $V > c_0$. Further, as a increases, the wave speed V and the wave number γ also increase. Although the case when $B > \frac{1}{3}$ has little practical application, it is interesting to note that these conclusions are all reversed as then $\delta < 0$, now, $a < 0$ and $V < c_0$. This solitary wave had earlier been obtained directly from the governing equations independently by Boussinesq (1871) and Rayleigh (1876), who were motivated to explain the now very well-known observations and experiments of John Scott Russell (1844). Curiously, it was not until quite recently that it was recognized that the KdV equation is not strictly valid if surface tension is taken into account and $0 < B < \frac{1}{3}$, as there is then a resonance between the solitary wave and very short capillary waves.

After this ground-breaking work of Korteweg and de Vries, interest in solitary water waves declined until the dramatic discovery of the "soliton" by Zabusky and Kruskal in 1965 (*See* **Solitons, a brief history**). Through numerical integrations of the KdV equation, they demonstrated that the solitary wave (8) could be generated from quite general initial conditions, and could survive intact collisions with other solitary waves, leading them to coin the term *soliton*. Their remarkable discovery, followed almost immediately by the theoretical work of Gardner, Greene, Kruskal, and Miura (Gardener et al., 1967) showing that the KdV equation was integrable through an inverse scattering transform, led to many other startling discoveries and marked the birth of the soliton theory as we know it today. The implication for water waves is that the solitary wave is the key component needed to describe the behavior of long, weakly nonlinear waves.

An alternative to the KdV equation is the Benjamin–Bona–Mahony (BBM) equation in which the linear dispersive term $c_0\zeta_{xxx}$ in (7) is replaced by $-\zeta_{xxt}$. It has the same asymptotic validity as the KdV equation and, since it has rather better high wave number properties, is somewhat easier to solve numerically. However, it is not integrable and, consequently, has not attracted the same interest as the KdV equation.

Both the KdV and BBM equations are unidirectional. A two-dimensional version of the KdV equation is the KP equation (Kadomtsev & Petviashvili, 1970; *See* also **Kadomtsev–Petviashvili equation**),

$$\left(\zeta_t + c_0\zeta_x + \frac{3c_0}{2h}\zeta\zeta_x + \frac{c_0h^2}{6}\delta\zeta_{xxx}\right)_x + \frac{c_0}{2}\zeta_{yy} = 0. \qquad (9)$$

This equation includes the effects of weak diffraction in the y-direction, in that y-derivatives scale as ε^2 whereas x-derivatives scale as ε. When $\delta > 0$ ($0 \le B < \frac{1}{3}$), this is the KPII equation, and it can be shown that then the solitary wave is stable to transverse disturbances. On the other hand, if $\delta < 0$ ($B > \frac{1}{3}$), this is the KPI equation for which the solitary wave (8) is unstable; instead this equation supports "lump" solitons. Both KPI and KPII are integrable equations. To take account of stronger transverse effects and/or to allow for bi-directional propagation in the x-direction, it is customary to replace the KdV equation with a Boussinesq system of equations. These combine the long wave approximation to the dispersion relation with the leading order nonlinear terms and occur in several asymptotically equivalent forms.

Wave Packets: Nonlinear Schrödinger Equation

The linear theory of water waves predicts that a localized initial state will typically evolve into wave packets, with a dominant wave number $\boldsymbol{k}$ and corresponding frequency ω given by (3), within which each wave phase propagates with the phase speed c, but whose envelope propagates with the group velocity c_g (5, 6). After a long time, the packet tends to disperse around the dominant wave number, which tendency may be opposed by cumulative nonlinear effects. In the absence of surface tension, the outcome for unidirectional waves is described by the nonlinear Schrödinger (NLS) equation, for the wave amplitude $A(x, t)$; that is, the wave elevation is $\zeta = A\exp\mathrm{i}(kx - \omega t) +$ c.c. to leading order,

$$\mathrm{i}(A_t + c_gA_x) + \tfrac{1}{2}\lambda A_{xx} + \mu|A|^2A = 0, \qquad (10)$$

and the coefficients are given by

$$\lambda = \frac{\partial^2\omega}{\partial k^2},$$
$$\mu = -\frac{\omega k^2}{16S^4}(8C^2S^2 + 9 - 2T^2) + \frac{\omega}{8C^2S^2}\frac{(2\omega C^2 + kc_g)^2}{gh - c_g^2},$$

where

$$C = \cosh(kh)\,,\ S = \sinh(kh)\,,\ T = \tanh(kh).$$

For water waves, the NLS equation was first derived by Zakharov (1968) for the case of deep water, and

then by Hasimoto and Ono (1972) for finite depth. An analogous equation can be derived for nonzero surface tension in which the nonlinear coefficient μ will take a different value, but for reasons discussed below, it is not so useful in that case. In deep water ($kh \to \infty$) the coefficient $\mu \to -\omega k^2/2 < 0$. In general, $\mu < 0 (> 0)$ according as $kh > (<) 1.36$.

Like the KdV equation, the NLS equation is integrable with an associated inverse scattering transform, a result first shown by Zakharov and Shabat (1972). There are two cases, the so-called focusing NLS equation when $\lambda\mu > 0$ and the defocusing NLS equation when $\lambda\mu < 0$. For water waves, $\lambda = \partial c_g/\partial k < 0$, and so we have the focusing (defocusing) NLS equation according as $kh > (<) 1.36$. The focusing NLS equation has solitary wave solutions (bright solitons), given by

$$A = a\,\mathrm{sech}(\gamma(x - c_g t))\exp(-\mathrm{i}\Omega t),$$
$$\text{where } \mu a^2 = \lambda\gamma^2,\ \Omega = -\tfrac{1}{2}\mu a^2. \qquad (11)$$

On the other hand, the defocusing NLS equation has no such solitary wave solutions which decay to zero at infinity. Instead, it has solitary waves riding on a nonzero background (dark solitons). A key property of the NLS equations is that plane waves are modulationally unstable (stable) in the focusing (defocusing) case. That is, the NLS equation has the exact plane wave solution,

$$A = A_0 \exp(\mathrm{i}\mu|A|^2 t), \qquad (12)$$

which is then perturbed with a small-amplitude modulation proportional to $\exp(\mathrm{i}Kx - \sigma t)$. It is readily found that the growth rate σ is given by

$$\sigma = K^2\left(\lambda\mu A_0^2 - \frac{\lambda^2 K^2}{4}\right). \qquad (13)$$

Thus, in the focusing NLS case when $\lambda\mu > 0$, there is a positive growth rate for modulation wave numbers K such that $K < 2(\lambda/\mu)^{1/2}|A_0|$. On the other hand, σ is purely imaginary for all K in the defocusing case when $\lambda\mu < 0$. The implication for water waves is that plane Stokes waves in deep water ($kh > 1.36$) are unstable. This remarkable result was first discovered by Benjamin and Feir in 1967, by a different theoretical approach, and has since been confirmed in experiments. The maximum growth rate occurs for $K = K_m = (\lambda/\mu)^{1/2}|A_0|$, and the instability is due to the generation of side bands with wave numbers $k \pm K_m$. As the instability grows, the full NLS equation (10) is needed to describe the long-time outcome of the collapse of the uniform plane wave into several soliton wave packets, each described by (11).

When the effects of modulation in the transverse y-direction are taken into account, so that the wave amplitude is now given by $A(x, y, t)$, the NLS equation is replaced by the Benney–Roskes system (Benney & Roskes, 1969), also widely known as the Davey–Stewartson equations (Davey & Stewartson, 1974),

$$\mathrm{i}(A_t + c_g A_x) + \tfrac{1}{2}\lambda A_{xx} + \tfrac{1}{2}\delta A_{yy} + \mu|A|^2 A + UA = 0, \qquad (14)$$
$$\alpha U_{xx} + U_{yy} + \beta(|A|^2)_{yy} = 0, \qquad (15)$$

where the coefficients μ and λ are those defined in (10), while

$$\delta = \frac{c_g}{k},\ \alpha = 1 - \frac{c_g^2}{gh},$$
$$gh\beta = \frac{\omega}{8C^2S^2}(2\omega C^2 + kc_g)^2.$$

Here, the surface tension has been set to zero. If surface tension effects are included, a similar equation holds but with different values for the coefficients (Djordjevic & Redekopp, 1977). Note that $\lambda\delta < 0$ and $\alpha > 0$, so that the equation for A is hyperbolic, but that for U it is parabolic. The variable U which appears here is a wave-induced mean flow, which tends to zero in the limit of deep-water waves, $kh \to \infty$. This system (14) again has the plane wave solution (12), whose stability can be analyzed in a manner similar to that described above in the context of the NLS equation. The outcome is that now instability can occur for all values of kh and occurs in a band in the $k - l$ plane where k and l are the modulation wave numbers. The instability is purely two-dimensional when $kh < 1.36$, and the band becomes narrower and the growth rate weaker as $kh \to 0$. For more details, see Benney and Roskes (1969) or Mei (1983).

Wave Resonant Interactions

A superposition of weakly nonlinear waves, each of which is given by (1) with a wave number $\boldsymbol{k}_n, n = 1, 2, \ldots, N$, and a corresponding frequency $\omega_n(\boldsymbol{k}), n = 1, 2, \ldots, N$, each satisfying the dispersion relation (3), interact resonantly whenever

$$\boldsymbol{k}_1 + \boldsymbol{k}_2 + \cdots + \boldsymbol{k}_N = 0,$$

and

$$\omega_1 + \omega_2 + \cdots + \omega_N = \Omega.$$

Here, Ω is a detuning term, so that exact resonance is achieved whenever $\Omega = 0$. The most prominent interactions are triad interactions; that is, $N = 3$, followed by the quartet interactions when $N = 4$, and so on. In a resonant interaction, energy is exchanged between the Fourier components in a periodic manner, assuming that dissipation is absent. For instance, the set of equations describing a triad interaction is (Craik, 1985)

$$A_{1t} + \boldsymbol{c}_{g1} \cdot \nabla A_1 = \frac{\partial D}{\partial \omega_1}\mu A_2^* A_3^* \exp(-\mathrm{i}\Omega t), \ldots,$$

where $A_n(\boldsymbol{x}, t)$ is the amplitude of the nth mode, $D(\omega, \boldsymbol{k}) = 0$ is the dispersion relation, μ is a coefficient, and the superscript "*" denotes the complex conjugate. Remarkably, these equations are integrable for exact resonance ($\Omega = 0$) (Zakharov & Manakov, 1973).

For water waves in the absence of surface tension, the dispersion relation does not allow for triad interactions. Hence, the dominant resonance is a quartet interaction, as first shown by Phillips (1960). The four wave numbers making up the quartet are two-dimensional (i.e., the y-wave number components are generally not zero), and the allowed wave number vectors can be determined graphically from Phillips' "figure-of-eight" diagram. The interaction equations for a discrete quartet of waves is analogous to that displayed above for a triad interaction. Further, in deep water ($kh \to \infty$), Craig and Worfolk (1995) have shown that in the Birkhoff normal form for these interaction equations, the coefficients vanish for all nongeneric resonant terms and the remaining system is then integrable. However, the same is not the case for quintet interactions.

When considering a continuous spectrum of gravity waves, the resulting evolution of a spectral component is described by Zakharov's integral equation, first derived in the deep water limit by Zakharov (1968). Krasistskii (1994) later employed canonical transformations to obtain a more desirable Hamiltonian form (see also the review by Dias & Kharif, 1999). In this equation, usually truncated at the third order in wave amplitude, the evolution of the spectral component $A(\boldsymbol{k}, t)$, which is the spatial Fourier transform of $\eta(\boldsymbol{x}, t)$, is determined essentially by quartet interactions, since the nonresonant triad interactions are removed by a canonical transformation. This integral evolution equation contains much of the previous weakly nonlinear theory, in that the discrete interaction equations and the NLS equation can be derived from it. It also forms the basis for a statistical description of water waves and can then be used to describe the ocean wave spectrum.

When surface tension is taken into account, then triad interactions are possible (i.e., $N = 3$ in (**??**)). The most well-known example occurs when $\boldsymbol{k}_1 = \boldsymbol{k}_2 = -\boldsymbol{k}_3/2$, and is a second harmonic resonance in that then $\omega_1 = \omega_2 = -\omega_3/2$. It was first noted by Wilton (1915) and leads to a phenomenon known as Wilton's ripples. In general, the existence of triad resonances implies that capillary-gravity waves undergo wave–wave interactions on a faster time scale than pure gravity waves.

ROGER GRIMSHAW

See also **Dispersion relations; Group velocity; Korteweg–de Vries equation; Modulated waves; Nonlinear Schrödinger equations; Solitons, a brief history; Wave packets, linear and nonlinear**

Further Reading

Benjamin, T.B. & Feir, J.E. 1967. The disintegration of wave trains on deep water. *Journal of Fluid Mechanics*, 27: 417–430

Benney, D.J. & Roskes, G. 1969. Wave instabilities. *Studies in Applied Mathematics*, 48: 377–385

Boussinesq, M.J. 1871. Theórie de l'intumescence liquid appellée onde solitaire ou de translation, se propageant dans un canal rectangulaire. *Comptes Rendus de l'Académie des Sciences (Paris)*, 72: 755–759

Boussinesq, M.J. 1877. Essai sur la theorie des eaux courantes, *Memoires presentees par diverse savants a l'Academie des Sciences Inst. France (Series 2)*, 23: 1–680

Craig, W. & Worfolk, P.A. 1995. An integrable normal form for water waves in infinite depth. *Physia* D, 84: 513–531

Craik, A.D.D. 1985. *Wave Interactions and Fluid Flows*, Cambridge and New York: Cambridge University Press

Davey, A. & Stewartson, K. 1974. On three-dimensional packets of surface waves. *Proceedings of the Royal Society of London* A, 338: 101–110

Dias, F. & Kharif, C. 1999. Nonlinear gravity and capillary-gravity waves. *Annual Reviews of Fluid Mechanics*, 31: 301–346

Djordjevic, V.D. & Redekopp, L.G. 1977. On two-dimensional packets of capillary-gravity waves. *Journal of Fluid Mechanics*, 79: 703–714

Gardner, C.S., Greene, J.M., Kruskal, M.D. & Miura, R.M. 1967. Method for solving the Korteweg–de Vries equation. *Physical Review Letters*, 19: 1095–1097.

Hasimoto, H. & Ono, H. 1972. Nonlinear modulation of gravity waves. *Journal of the Physical Society of Japan*, 33: 805–811

Kadomtsev, B.B. & Petviashvili, V.I. 1970. On the stability of solitary waves in weakly dispersive media. *Soviet Physics Doklady*, 15: 539–541

Korteweg, D.J. & de Vries, H. 1895. On the change of form of long waves advancing in a rectangular canal, and on a new type of long stationary waves. *Philosophical Magazine*, 39: 422–443

Krasitskii, V.P. 1994. On reduced equations in the Hamiltonian theory of weakly nonlinear surface waves. *Journal of Fluid Mechanics*, 272: 1–30

Lamb, H. 1932. *Hydrodynamics*, Cambridge and New York: Cambridge University Press; 6th edition, Cambridge and New York, Cambridge University Press, 1993

Lighthill, M.J. 1978. *Waves in Fluids*, Cambridge and New York: Cambridge University Press

Mei, C.C. 1983. *The Applied Dynamics of Ocean Surface Waves*, New York: Wiley

Phillips, O.M. 1960. On the dynamics of unsteady gravity waves of finite amplitude. Part 1. The elementary interactions. *Journal of Fluid Mechanics*, 9: 193–217

Rayleigh, Lord (Strutt, W.J.) 1876. On waves. *Philosophical Magazine*, 1: 257–279

Russell, J.S. 1844. Report on Waves, *14th meeting of the British Association for the Advancement of Science*, London: BAAS, 311–390

Schwarz, L.W. & Fenton, J.D. 1982. Strongly nonlinear waves. *Annual Reviews of Fluid Mechanics*, 14: 39–60

Wilton, J.R. 1915. On ripples. *Philosophical magazine*, 29: 688–700

Whitham, G.B. 1974. *Linear and Nonlinear Waves*, New York: Wiley

Zabusky, N.J. & Kruskal, M.D. 1965. Interactions of solitons in a collisionless plasma and the recurrence of initial states. *Physical Review Letters*, 15: 240–243

Zakharov, V.E. 1968. Stability of periodic waves of finite amplitude on the surface of a deep fluid. *Journal of Applied Mechanics and Technical Physics*, 2: 190–194

Zakharov, V.E. & Manakov, S.V. 1973. Resonant interactions of wave packets in nonlinear media. *Soviet Physics, JETP*, 18: 243–247

Zakharov, V.E. & Shabat, A.B. 1972. Exact theory of two-dimensional self-focusing and one-dimensional self-modulation of waves in nonlinear media. *Soviet Physics, JETP*, 34: 62–69

WAVE OF TRANSLATION

Translational invariance is one of the fundamental symmetries of continuum nonlinear partial differential equations (PDEs). Such a symmetry is present when the equation of interest remains unchanged under the transformation $x \to x + \varepsilon$. Typically, partial differential equations that contain only derivatives with respect to the spatial variable x (but no explicit dependence on x) possess this symmetry.

The topic of symmetries and their role in bifurcation theory is a very large subject, a detailed discussion of which can be found, for example in Golubitsky & Schaeffer (1995) and Golubitsky (1988). Here, our scope is much narrower in giving a perspective of translational symmetry and its role in the existence, bifurcation, or absence of traveling wave solutions in some Hamiltonian and dissipative classes of PDEs.

To make our discussion of this subject more definitive, we will introduce a rather general class of dissipative or Hamiltonian PDEs of the form

$$\{u_t, u_{tt}\} = u_{xx} + f(u). \tag{1}$$

The paradigm of Equation (1) is dissipative (that is, of the reaction-diffusion type), if a one-time derivative of the field u is used in the left-hand side. On the other hand, the model is Hamiltonian if the second time derivative is used on the left-hand side. While the model is written as a single component model in a one-dimensional setting, it can be easily generalized in multiple components/dimensions. In the former case, u becomes a vector, while in the latter, the spatial second partial derivative is substituted by the Laplacian operator. We should note in passing that while here we consider the Hamiltonian and dissipative cases, there are many models which lie between the conservative and diffusion limits. Numerous examples of this type can be found in Kivshar & Malomed (1989).

It can be immediately observed that the translational symmetry mentioned above is present in the model of Equation (1). A straightforward example of its absence would be the case of a "reaction term" $f(u, x)$, i.e., one explicitly dependent on x. Let us now explore the implications of this symmetry for the static problem of Equation (1) and then for the corresponding dynamic problem.

For the static problem (i.e., for solutions $u = g(x)$ that satisfy $u_{xx} + f(u) = 0$), the presence of the invariant direction signifies that the solution can be translated along the group orbit of this invariance. Otherwise stated, there is a one parameter infinity of solutions (alternatively, a degeneracy of solutions) due to the available freedom to select solutions along the symmetry direction. In practical terms, this means that if $u = g(x)$ is a solution, then $u = g(x - x_0)$ is also a solution and arbitrary translations of the solution satisfy the original equation. Furthermore, this feature bears consequences on the linear stability around the solution. In particular, looking for the linear stability of the solution $u = g(x)$, we use the linearization $u = g(x) + \varepsilon \exp(\lambda t) w(x)$, which to $O(\varepsilon)$, yields the eigenvalue problem:

$$\{\lambda, \lambda^2\} w = w_{xx} + f'(g(x)) w. \tag{2}$$

Given that $g(x)$ satisfies the $u_{xx} + f(u) = 0$, differentiation of the latter immediately yields that (due to the absence of the explicit spatial dependence and hence due to the symmetry) $w = u_x \equiv g'(x)$ satisfies Equation (2), with $\lambda = 0$ (for the dissipative system) or $\lambda^2 = 0$ (for the Hamiltonian system). Hence, the existence of the symmetry generates a single (for the dissipative) or a pair (for the Hamiltonian) of eigenvalues at the origin of the spectral plane (i.e., with $\lambda = 0$). This is the neutral eigendirection connected with the symmetry that is often referred to as a Goldstone mode.

Furthermore, in the Hamiltonian version of the system, the presence of such eigenmodes, and of their corresponding symmetries, is intimately connected with conservation laws (through Noether's theorem; see for example the discussion in Arnol'd (1989); Sulem & Sulem (1999)). The invariance with respect to translations is directly related with the conservation of linear momentum, which in the case of Equation (1) is of the form

$$P = \int_{-\infty}^{\infty} u_t u_x \, \mathrm{d}x. \tag{3}$$

We now turn to the dynamic consequences of the symmetry. The translational symmetry is directly related to the traveling of solutions. In the case of Hamiltonian (especially continuum) systems, there may be extra symmetries that may allow the construction of traveling solutions from stationary ones. In the case of Equation (1), such a symmetry is the Lorentz invariance $[x \to x' = \gamma(x - vt), t \to t' = \gamma(t - vx/c^2)$, $\gamma = 1/\sqrt{1 - v^2/c^2}]$, which allows one to boost the solutions to any "subsonic" speed. In other cases, such as the one of the nonlinear Schrödinger equation, the corresponding symmetry, is the Galilean invariance. Hence, in Hamiltonian systems, due to the additional symmetry, traveling and standing solutions are often, in some sense, equivalent. On the other hand, for dissipative systems, such equivalence is typically absent. In the latter case, we look for traveling wave solutions in the form $u = u(\xi)$, where $\xi = x - ct$ is the traveling wave variable. This transformation leads to the so-called traveling wave frame (TWF) equation of

motion (i.e., we travel together with the solution and, hence, observe it as a steady one) of the form

$$u_t = u_{\xi\xi} + cu_\xi + f(u). \tag{4}$$

By solving the steady-state problem of Equation (4) (notice: an ordinary differential equation (ODE) problem to find special solutions of the PDE), we can identify the traveling-wave solutions of Equation (1). In dissipative systems, the absence of additional symmetries typically allows for isolated solutions of the TWF ODE rather than monoparametric families of such solutions. Notice that here we have in mind fixed model parameter values (but not fixed initial condition parameters, such as, for example, energy). Furthermore, we do not discuss the mechanisms (in dissipative systems) of selection of a given speed (which is related to issues of stability). Such examples and a detailed discussion can be found in Xin (2000). A typical example is the bistable nonlinearity where $f(u) = 2u(u-1)(\mu - u)$, for which a front solution of the form

$$u(x,t) = \frac{1}{2}\left[1 - \tanh\left(\frac{x - x_c(t)}{2}\right)\right], \tag{5}$$

exists, where $x_c = x_c^{\text{in}} + ct$ and x_c^{in} is the original position of the center, while the speed c is connected to the parameter μ through

$$c = 1 - 2\mu. \tag{6}$$

In view of the above comments, in energy conserving systems, typically standing and traveling solutions coexist, while in dissipative systems one can (locally) have solutions either of the former or of the latter type. In fact, as parameters are varied in dissipative settings, traveling solutions may bifurcate from standing ones, through the so-called drift pitchfork bifurcation (Kness et al., 1992, see also Malomed & Tribelsky (1984) and Coullet & Iooss, 1990). It is worth noting that recently, a template-based technique has been proposed that dynamically factors out translational invariance (and other continuous symmetries) (Rowley & Marsden, 2000; Rowley et al., 2003).

Discrete Systems and Symmetry Breaking

An interesting variation of the above presented scenario occurs in (spatially) discrete systems. In this case, generic discretizations of the original problem of Equation (1) no longer preserve the symmetry with respect to continuum translations. Instead, only an integer shift invariance persists in this discrete limit of the equation:

$$\{\dot{u}_n, \ddot{u}_n\} = \Delta_2 u_n + f(u_n), \tag{7}$$

where $\Delta_2 u_n = (u_{n+1} + u_{n-1} - 2u_n)/h^2$ is the discrete Laplacian for a lattice of spacing h. In this case, from the informative Taylor expansion of the form

$$\Delta_2 u_n = \sum \frac{2h^{2j-2}}{(2j)!}\frac{\mathrm{d}^{2j}u}{\mathrm{d}x^{2j}}, \tag{8}$$

we deduce the following conclusions:

- discreteness is a singular higher-order derivative perturbation to the continuum limit;
- to all orders in this asymptotic expansion, the right-hand side is translationally invariant. Hence, the breaking of the translational symmetry can only occur beyond all algebraic orders and thus has to be an exponentially small effect.

A manifestation of this exponentially small symmetry breaking effect is given by the fact that there are now two (lattice shift invariant) stationary wave states in the lattice context. One of these solutions is centered on a lattice site and one is centered between two consecutive lattice sites (instead of a single translationally invariant steady state in the continuum limit). One of these solutions is stable and one is unstable. The energy difference between the two (which mirrors the amount of symmetry breaking and hence should be exponentially small, that is, $\Delta E \sim \exp(-\pi^2/h)$) is the celebrated Peierls–Nabarro barrier. For a detailed discussion of these issues, see, for example, the review by Kevrekidis et al. (2001).

From the above, we can infer that the generic effect of discreteness in breaking translational invariance is to generate an exponentially small (in the natural lattice spacing parameter) shift periodic (in fact approximately trigonometric) potential. The center of mass of the waves propagates inside the Peierls–Nabarro barrier. There is considerable interest in shearing this potential with an external (constant) field.

A constant external force F introduces a term in the potential energy $\sim Fu$, generating a washboard potential for the motion of the wave. If the external field becomes sufficiently strong, then one can infer that a saddle-node (in fact, infinite period; the so-called SNIPER) bifurcation will occur in which the stationary states (the maxima and minima of the potential, that is, the saddles and nodes) will disappear and traveling waves will arise. Scaling analysis predicts and numerical results verify (Kaldko et al., 2000; Keverkidis et al., 2001; Carpio & Bonilla, 2001) that the relevant bifurcation will yield waves of speed

$$c \sim (F - F_{\text{c}})^{1/2}, \tag{9}$$

where F is the constant external field and F_{c} is its critical value. The energy landscapes for the cases of $F = 0$, $F < F_{\text{c}}$, and $F > F_{\text{c}}$ are shown in Figure 1. This scenario happens in the dissipative case, but one can also analyze the Hamiltonian case in the same manner.

Finally, it should be noted that while the above scenario will be the generically relevant one, there

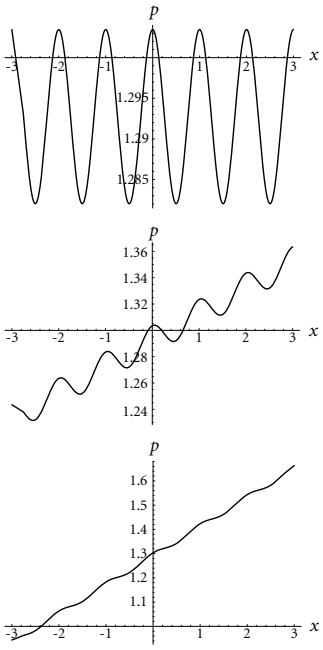

Figure 1. The (potential) energy (P) landscape for generic DDE models in the case of $F = 0$ (top panel), $F < F_c$ (middle panel) and $F > F_c$ (bottom panel), as a function of the position of the kink center.

are exceptions to the rule of absence of a continuum-like symmetry in the lattice setting. Let us consider, for example, the discretization of the Hamiltonian PDE:

$$\ddot{u}_n = \Delta_2 u_n + \frac{F(u_{n+1}) - F(u_{n-1})}{u_{n+1} - u_{n-1}}. \qquad (10)$$

It can be seen that the equation of motion has a conservation law of the form

$$P = \sum \dot{u}_n (u_{n+1} - u_{n-1}) \qquad (11)$$

which is the discrete analog of Equation (3). In this case, the discrete equation preserves a "ghost" of the continuum symmetry and maintains the multiplicity of Goldstone modes of the continuum problem (Kevrekidis, 2003).

In conclusion, translational invariance is a symmetry that plays a significant role in the context of both partial-differential as well as differential-difference (i.e., lattice) equations. In the former, it is typically present (unless an explicit spatial dependence occurs) and has both static as well as kinematic consequences on the solutions of the problem and their stability. In the discrete setting, the symmetry is generically absent and its absence plays a critical role in diversifying kinematic and dynamic phenomena on the lattice (see, for example, Kevrekidis, et al. (2001)) from their continuum siblings. However, it is possible to construct discretizations that respect a discrete conservation law reminiscent of the one imposed by the continuum symmetry group. In the nongeneric case, the lattice dynamics can be significantly closer to their continuum counterparts.

P.G. KEVREKIDIS AND I.G. KEVREKIDIS

See also **Partial differential equations, nonlinear; Peierls barrier; Sine-Gordon equation; Zeldovich–Frank-Kamenetsky equation**

Further Reading

Arnol'd, V.I. 1989. *Mathematical Methods in Classical Mechanics*, New York: Springer

Carpio, A. & Bonilla, L.L. 2001. Wave front depinning transition in discrete one-dimensional reaction–diffusion systems. *Physical Review Letters*, 86: 6034–6037

Coullet, P. & Iooss, G. 1990. Instabilities of one-dimensional cellular patterns. *Physical Review Letters*, 64: 866–869

Dodd, R.K., Eilbeck, J.C., Gibbon, J.D. & Morris, H.C. 1982. *Solitons and Nonlinear Wave Equations*, London and New York: Academic Press

Golubitsky, M. & Schaeffer, D.G. 1985. *Singularities and Groups in Bifurcation Theory*, vol. I, New York: Springer

Golubitsky, M., Stewart, I.N. & Schaeffer, D.G. 1988. *Singularities and Groups in Bifurcation Theory*, vol. II, New York: Springer

Kevrekidis, P.G. 2003. On a class of discretizations of Hamiltonian nonlinear partial differential equations. *Physica* D, 183: 68–86

Kevrekidis, P.G., Kevrekidis, I.G. & Bishop, A.R. 2001a. Propagation failure, universal scalings and Goldstone modes. *Physics Letters* A, 279: 361–369

Kevrekidis, P.G., Rasmussen, K.Ø. & Bishop, A.R. 2001b. The discrete nonlinear Schrodinger equation: a survey of recent results. *International Journal of Modern Physics* B, 15: 2833–2900

Kivshar, Yu.S. & Malomed, B.A. 1989. Dynamics of solitons in nearly integrable systems. *Reviews of Modern Physics*, 61: 763–915

Kladko, K., Mitkov, I. & Bishop, A.R. 2000. Universal scaling of wave propagation failure in arrays of coupled nonlinear cells. *Physical Review Letters*, 84: 4505–4508

Kness, M., Tuckerman, L.S. & Barkley, D. 1992. Symmetry-breaking bifurcations in one-dimensional excitable media. *Physical Review* A, 46: 5054–5062

Malomed, B.A. & Tribelsky, M.I. 1984. Bifurcations in distributed kinetic systems with aperiodic instability. *Physica* D, 14: 67–87

Rowley, C.W. & Marsden, J.E. 2000. Reconstruction equations and the Karhunen-Loeve expansion for systems with symmetry. *Physica* D, 142: 1–19

Rowley, C.W., Kevrekidis, I.G., Marsden, J.E. & Lust, K. 2003. Reduction and reconstruction for self-similar dynamical systems. *Nonlinearity*, 16: 1257–1275

Sulem, C. & Sulem, P.L. 1999. *The Nonlinear Schrödinger Equation*, New York: Springer
Xin, J. 2000. Front propagation in heterogeneous media. *SIAM Review*, 42: 161–230

WAVE PACKETS, LINEAR AND NONLINEAR

Because linear wave systems have elementary solutions of the form $e^{i(kx-\omega t)}$, it is often convenient to write the general solution of an initial value problem as an integral of Fourier components. Thus,

$$u(x,t) = \frac{1}{2\pi}\int_{-\infty}^{\infty} F(k)e^{i(kx-\omega t)}\,dk, \tag{1}$$

where $F(k)$ is the Fourier transform of $u(x,0)$. Initial conditions thus determine the Fourier transform, each component of which evolves independently with frequency ω related to wave number k through the dispersion relation

$$\omega = \omega(k). \tag{2}$$

Unless $\omega = k$, different components in Equation (1) travel at different speeds (ω/k), and an initially localized wave spreads out or "disperses," hence the name.

A wave packet is a special form of Equation (1) with the largest Fourier components lying close to some wave number (k_0) and the corresponding frequency (ω_0). In other words, the initial conditions $u(x,0)$ are selected so that $F(k)$ has its maximum value at $k = k_0$, falling rapidly with increasing $|k - k_0|$. This suggests writing the dispersion relation as a power series about k_0. With the notation

$$\omega = \omega_0 + b_1(k-k_0) + b_2(k-k_0)^2 \tag{3}$$

(which assumes that the system has no higher than second derivatives with respect to x), Equation (1) becomes

$$u(x,t) = e^{i(k_0x-\omega_0t)}\frac{1}{2\pi} \times \int_{-\infty}^{\infty} F(k)e^{i[(k-k_0)x-b_1(k-k_0)t-b_2(k-k_0)^2t]}dk, \tag{4}$$

where the factor $e^{i(k_0x-\omega_0t)}$ is a carrier wave with a velocity $v_c = \omega_0/k_0$, shown in Figure 1(a). Riding over (or multiplying) the carrier is an envelope wave

$$\phi(x,t) = \frac{1}{2\pi}\int_{-\infty}^{\infty} F(\kappa+k_0)e^{i(\kappa x-b_1\kappa t-b_2\kappa^2 t)}\,d\kappa, \tag{5}$$

where the variable of integration has been changed from k to $\kappa \equiv k - k_0$.

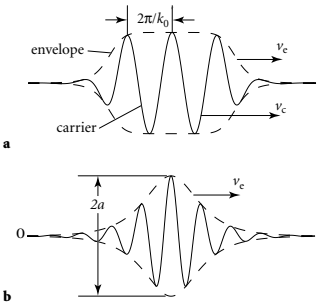

Figure 1. (a) The real part of a linear wave packet, showing the envelope (dashed lines) and the carrier (full line), as in Equation (4). (b) The real part of a soliton solution of Equation (7).

Taking the time derivative of Equation (5), one finds

$$\frac{\partial\phi}{\partial t} = \frac{1}{2\pi}\int_{-\infty}^{\infty} -i(b_1\kappa + b_2\kappa^2)F(\kappa+k_0) \times e^{i(\kappa x-b_1\kappa t-b_2\kappa^2 t)}\,d\kappa = -b_1\frac{\partial\phi}{\partial x} + ib_2\frac{\partial^2\phi}{\partial x^2},$$

which can be written as

$$i\left(\frac{\partial\phi}{\partial t} + b_1\frac{\partial\phi}{\partial x}\right) + b_2\frac{\partial^2\phi}{\partial x^2} = 0. \tag{6}$$

Equation (6) is a partial differential equation that governs time evolution of the envelope for a linear wave packet solution of a second-order equation. Assuming b_2 is not too large (weak dispersion), the envelope moves with the velocity $v_e \doteq b_1 = d\omega/dk|_{k=k_0}$, as in Figure 1(a).

Up to this point, the discussion has remained within the realm of linear theory, but now assume that nonlinear effects alter Equation (6) to

$$i\left(\frac{\partial\phi}{\partial t} + b_1\frac{\partial\phi}{\partial x}\right) + b_2\frac{\partial^2\phi}{\partial x^2} + \alpha|\phi|^2\phi = 0, \tag{7}$$

with the nonlinear (amplitude-dependent) dispersion relation $\omega = b_1\kappa + b_2\kappa^2 - \alpha|\phi|^2$. Equation (7) is the nonlinear Schrödinger (NLS) equation, for which the following comments are relevant:

- If ϕ is assumed independent of x, Equation (7) has the plane wave solution

$$\phi = \phi_0 e^{i\alpha|\phi_0|^2 t}, \tag{8}$$

  which may or may not be stable.
- With $\alpha b_2 < 0$, this plane wave is stable (Whitham, 1974). If $\alpha b_2 > 0$, on the other hand, the plane wave experiences Benjamin–Feir instability, out of which emerge stable NLS solitons (Benjamin & Feir, 1967; Ostrovsky, 1967).

- The term $b_2(\partial^2\phi/\partial x^2)$ introduces wave dispersion into the problem at the lowest order of approximation. Similarly, the term $\alpha|\phi|^2\phi$ introduces nonlinearity at the lowest order of approximation. Thus, the NLS equation is generic, arising whenever one wishes to consider lowest order effects of dispersion and nonlinearity on a wave packet, including nonlinear optics (Kelley, 1965), deep water waves (Benney & Newell, 1967), and acoustics (Ostrovsky & Potapov, 1999).
- Unstable NLS wave packets decay into one or more solitons. Choosing $b_1 = 0$, $b_2 = 1$, and $\alpha = 2$ in Equation (7), for example, a family of NLS solitons is (Zakharov & Shabat, 1972)

$$u(x,t) = a\exp\left[\mathrm{i}\frac{v_e}{2}x + \mathrm{i}\left(a^2 - \frac{v_e^2}{4}\right)t\right] \times \mathrm{sech}\,[a(x - v_e t - x_0)], \qquad (9)$$

one of which is sketched in Figure 1(b).

Beyond the superficial similarities between Figures 1(a) and (b), the differences are profound. In the linear wave packet of Figure 1(a), the shape of the envelope is determined by initial conditions and their subsequent time evolution, as in Equation (6). In the NLS soliton of Figure 1(b), on the other hand, the envelope shape is determined through a dynamic balance between the influences of dispersion and nonlinearity, as expressed by the last two terms of Equation (7).

ALWYN SCOTT

See also **Dispersion relations; Modulated waves; Nonlinear Schrödinger equations; Wave stability and instability**

Further Reading

Benjamin, T.B. & Feir, J.E. 1967. The disintegration of wave trains in deep water. *Journal of Fluid Mechanics*, 27: 417–430

Benney, D.J. & Newell, A.C. 1967. The propagation of nonlinear wave envelopes. *Journal of Mathematical Physics*, 46: 133–139

Kelley, P.L. 1965. Self-focusing of optic beams. *Physical Review Letters*, 15: 1005–1008

Ostrovsky, L.A. 1967. Propagation of wave packets and space-time self-focusing in a nonlinear medium. *Soviet Physics, JETP*, 24: 797–800

Ostrovsky, L.A. & Potapov, A.I. 1999. *Modulated Waves: Theory and Applications*, Baltimore: Johns Hopkins University Press

Whitham, G.B. 1974. *Linear and Nonlinear Waves*, New York: Wiley

Zakharov, V.E. & Shabat, A.B. 1972. Exact theory of two-dimensional self-focusing and one-dimensional self-modulation of waves in nonlinear media. *Soviet Physics, JETP*, 34: 62–69

WAVE PROPAGATION IN DISORDERED MEDIA

Although nonlinear partial differential equations with constant coefficients well describe main features of numerous nonlinear systems, understanding of many natural phenomena or experimental data requires taking into account the imperfectness of media which often have random character of two main types: time-dependent fluctuations and random spatial inhomogeneities (both may appear simultaneously). A thermal bath and quantum laser fluctuations are examples of the first type while impurities in crystal lattices, irregular variations of dielectric permittivity, and imperfectness of optical fibers are of the second type. Modeling of such phenomena requires nonlinear evolution equations with stochastic terms.

If a physical process is described by a field $u(t, \boldsymbol{r})$ that in an idealized situation is governed by a nonlinear equation $N[u] = 0$, then including irregularities (fluctuations) of the medium in the consideration will result in an equation of the type $N[u] = \varepsilon(t, \boldsymbol{r})R[u]$, where $\varepsilon(t, \boldsymbol{r})$ is a random field and a (possibly nonlinear) operator $R[u]$ depends on physical nature of randomness. Such problems are difficult and still not well understood. The main difficulty arises because nonlinearity invalidates powerful methods of the linear theory (such as the Fourier transform) which allow one to relate stationary and nonstationary problems or introduce a Gaussian approach, allowing decoupling of high-order moments.

From the physical point of view, we can distinguish several important factors that must be taken into account, including generation of high harmonics resulting in nontrivial changes of the field statistics, creation of rather stable localized excitations (which have no analogy in the linear theory), and the multistability phenomenon.

Let us illustrate these issues with two examples: the nonlinear Schrödinger equation for a complex field $u(t, x)$:

$$\mathrm{i}\frac{\partial u}{\partial t} + \frac{\partial^2 u}{\partial x^2} + 2|u|^2 u = \varepsilon(t,x)R[u] \qquad (1)$$

and the nonlinear Klein–Gordon equation for a real scalar field $u(t, x)$

$$\frac{\partial^2 u}{\partial t^2} - \frac{\partial^2 u}{\partial x^2} + u - u^3 = \varepsilon(t,x)R[u]. \qquad (2)$$

These models represent some essential differences. First, at $\varepsilon = 0$ Equations (1) and (2) are, respectively, integrable and nonintegrable. Second, the former model allows a solution in a form of a monochromatic wave and hence admits formulation of a stationary problem while harmonic generation is an indispensable property of the second model. Finally, their solitary wave solutions at $\varepsilon(t, x) = 0$ are of different types: a dynamical soliton (in the restricted mathematical sense) in case (1) and a topological kink in case (2).

The random field $u(t, x)$, being a functional of $\varepsilon(t, x)$, is completely determined by a set of all $(n + m)$-

order moments

$$\langle u(t_1, x_1) \cdots u(t_n, x_n)\bar{u}(t_{n+1}, x_{n+1}) \cdots \bar{u}(t_{n+m}, x_{n+m})\rangle, \quad (3)$$

where averaging is designated by the angular brackets and is provided over all realizations of $\varepsilon(t, x)$, when they are known. Because a Gaussian approximation is not applicable in nonlinear theory, the generic situation is that an $(n + m)$-order momentum cannot be expressed only through lower-order correlation functions. Moreover, temporal evolution of the mean field may drastically differ from the evolution of the field itself.

This is illustrated by Equation (1) with $\varepsilon(t, x)R[u] \equiv -f(t)xu(t, x)$, $f(t)$ being a Gaussian random process with

$$\langle f(t)\rangle = 0 \quad \text{and} \quad \langle f(t)f(t')\rangle = \sigma^2\delta(t - t'), \quad (4)$$

where σ is the dispersion of the fluctuations (Besieris, 1980). This equation is exactly solvable with the one-soliton solution

$$u(t, x) = \eta\frac{\exp\left\{\mathrm{i}\left[\mu(t)x + \eta^2 t - \beta(t)\right]\right\}}{\cosh\{\eta[x - 2\xi(t)]\}}, \quad (5)$$

where $\dot{\mu}(t) = f(t)$, $\mu(t) = \dot{\xi}(t)$, and $\dot{\beta} = \mu^2$ (a dot indicates a time derivative). Being interested in the evolution of the soliton intensity, which depends on $\xi(t)$ only, one can calculate the distribution

$$P(\xi, t) = \int_{-\infty}^{\infty}\langle\delta(v - \dot{\xi}(t))\delta(\xi - \xi(t))\rangle\,\mathrm{d}v = \sqrt{\frac{3}{2\sigma^2 t^3}}\exp\left(-\frac{3\xi^2}{2\sigma^2 t^3}\right). \quad (6)$$

Although the solution undergoes Brownian motion without any distortion, it follows from Equations (5) and (6) that its mean intensity is described by the Gaussian asymptotics

$$\langle u(t, x)\bar{u}(t, x)\rangle \approx \eta\sqrt{\frac{3}{2Dt^3}}\exp\left(-\frac{3x^2}{8\sigma^2 t^3}\right) \quad \text{at} \quad t \gg \frac{1}{(\sigma\eta)^{2/3}}.$$

In a general situation when exact solutions are not available, the problem becomes dependent on its statement and on the physical characteristics to be determined. The main statements of the problem are listed below.

Stationary Wave Scattering

This is a generalization of the problem of a wave transmission through a random slab to the nonlinear case. In the linear theory, the wave intensity decays exponentially with the slab width (Anderson localization). In the nonlinear case, one considers a monochromatic solution of Equation (1): $u(t, x) = (k/\sqrt{2})\exp(-\mathrm{i}k^2 t)\phi(x)$, where $\varepsilon(t, x) \equiv k^2\varepsilon_0(x)$, $\varepsilon_0(x)$ being a random function in the interval $0 < x < L$ and zero outside this interval, and $R[u] \equiv u(t, x)$. Then $\phi(x)$ satisfies the equation

$$\frac{\mathrm{d}^2\phi}{\mathrm{d}x^2} + k^2(1 + \varepsilon_0(x) + |\phi|^2)\phi = 0. \quad (7)$$

In order to describe an incidence of a plane wave on the random layer from the right, one imposes

$$\phi(x) = \begin{cases} a\left[\mathrm{e}^{\mathrm{i}k(L-x)} + R(L, w)\mathrm{e}^{\mathrm{i}k(x-L)}\right], & x \geq L, \\ T(L, w)\mathrm{e}^{-\mathrm{i}kx}, & x \leq 0 \end{cases} \quad (8)$$

and the conditions of the continuity of the field $\phi(x)$ and of its derivative $\mathrm{d}\phi(x)/\mathrm{d}x$ at the boundaries of the layer, $x = 0$ and $x = L$ (see Figure 1).

The coefficients a, $R(L, w)$ and $T(L, w)$ are amplitudes of the incident wave, reflection and transmission coefficients. The last two quantities depend on the slab width L and on the intensity of the incident wave $w = a^2$. Using the imbedding method (Klyatskin, 1988), one can obtain a nonlinear partial differential equation for the reflection coefficient as a function of L and w, which (upon applying the method of characteristics) results in a system (Doucot & Rammal, 1987)

$$\frac{\mathrm{d}R_1}{\mathrm{d}L} = -2kR_2 - kR_2(1+R_1)(\varepsilon(L)+w|1+R|^2), \quad (9)$$

$$\frac{\mathrm{d}R_2}{\mathrm{d}L} = 2kR_1 + \frac{k}{2}\left[(1 + R_1)^2 - R_2^2\right] \times(\varepsilon(L) + w|1 + R|^2), \quad (10)$$

where $R_1(L) = \Re(R(L, w))$, $R_2(L) = \Im(R(L, w))$,

$$w(L) = \frac{w(0)}{1 - |R(L, w)|}, \quad (11)$$

and the initial conditions are $R_1(0) = R_2(0) = 0$. Formula (11) allows us to understand two essentially different statements of the scattering problem. Indeed, (9) and (10) are dynamical equations for the characteristics that pass either through the point $(L = 0, w(0) = w_0)$, if the output intensity of the wave w_0, is given, or through the point $(L, w(L))$ if the input intensity is given (called fixed input and fixed output problems). In the former case, while increasing L, one follows the characteristic starting with its initial position. To solve a fixed output problem, one must determine a characteristic or characteristics which cross the point $(L, w(L))$ (having different starting points). As there may be more than one characteristic, multistability occurs (for another way of understanding the multistability phenomenon, see Knapp et al. (1991)).

Consider the fixed output problem (w_0 is given) in the case of weak Gaussian fluctuations, when

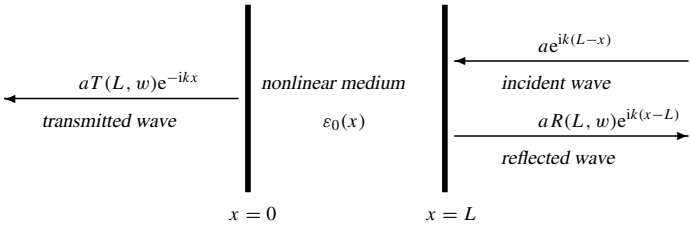

Figure 1. To the statement of the stationary scattering problem.

$\langle\varepsilon_0(x)\rangle = 0$, $\langle\varepsilon_0(x)\varepsilon_0(x')\rangle = D\delta(x - x')$, and $L_{\rm loc} \gg \lambda, L_{\rm nl}$ where $L_{\rm loc} = 1/(Dk^2)$ is the Anderson localization length of the underlying linear system, $\lambda = 2\pi/k$ is the incident wavelength, and $L_{\rm nl} = 1/(w_0 k)$ is the effective nonlinear length characterizing change of the reflection coefficient due to the nonlinearity. Starting with the region of a relatively strong nonlinearity, $L_{\rm nl} \ll \lambda$, one can define a period of motion $L_{\rm p} = \int_0^{2\pi} (\mathrm{d}\theta/\mathrm{d}L)^{-1}\mathrm{d}\theta \approx L_{\rm nl}$ (here $\theta = \arg R$) and study weak drift of trajectories of "dynamical system" (9), (10) due to the random perturbations over one period $L_{\rm p}$ (providing averaging over θ). The main result can be formulated as $\langle 1/T^2\rangle = O(L^2)$ and decay of the fluctuations of $\langle \ln T^2\rangle$ at $L \to \infty$ (Doucot & Rammal, 1987). Similar results, obtained for a step-like random function $\varepsilon_0(x)$ (Fröhlich et al., 1986). Thus, compared with the linear theory, the nonlinearity does not change the property of $\ln T^2$ to be a self-averaging value, but results in change of the decay law for the decay of the transmission coefficient from the exponential one to a power one. However, when the intensity of the wave becomes small enough and the effect of back-scattering becomes dominating, one can recover the exponential decay law $T \sim \exp(-L/L_{\rm loc})$. The transition between two regions with the different laws of the decay of the reflection coefficient happens at $L_0 \sim L_{\rm loc} \ln(1/w_0)$: the law is power at $L > L_0$ and is exponential at $L < L_0$.

Interaction of a Wave Packet with a Random Layer

As this case cannot be reduced to the study of a stationary problem, the statement of the problem and physical characteristics describing wave scattering must be redefined (compared with the previous case of stationary scattering). Consider the Cauchy problem with a given initial field distribution that decays sufficiently rapidly at infinity. The main task can be formulated as a description of the evolution of the wave-packet characteristics during its propagation. Such a statement acquires a special meaning in systems that possess stable solitary wave solutions in the unperturbed ($\varepsilon = 0$) limit and in which the randomness is weak enough. For relatively large temporal intervals, the nonlinear field can be represented in the form $u(t, x) \approx u_{\rm ad}(t, x) + u_{\rm rad}(t, x)$, where $u_{\rm ab}(t, x)$ is a function having the same form as the unperturbed solitary wave but now with slowly varying parameters (adiabatic approximation) and $u_{\rm rad}(t, x)$ is a small component compared with $u_{\rm ab}(t, x)$ describing deformation of the soliton shape and radiative losses.

An advantage of the adiabatic approximation is that it reduces a stochastic partial differential equation to a system of ordinary differential equations for the soliton parameters. For Equation (1), the adiabatic approximation corresponds to the substitution (5) with time-dependent coefficients $\eta(t)$, $\xi(t)$, $\mu(t)$, and $\beta(t)$. If $R[u] \equiv u(t, x)$, the standard perturbation theory for solitons shows that (Karpman, 1979)

$$\frac{\mathrm{d}\mu}{\mathrm{d}t} = \eta \int_{-\infty}^{\infty} \frac{\tanh z}{\cosh^2 z}\, \varepsilon\left(t, \frac{z}{\eta} + 2\xi\right) \mathrm{d}z, \tag{12}$$

$$\frac{\mathrm{d}\xi}{\mathrm{d}t} = 2\mu, \qquad \eta = \text{ const}, \tag{13}$$

$$\frac{\mathrm{d}\beta}{\mathrm{d}t} = \mu^2 + \eta \int_{-\infty}^{\infty} \frac{1 - z\tanh z}{\cosh^2 z}\, \varepsilon\left(t, \frac{z}{\eta} + 2\xi\right) \mathrm{d}z. \tag{14}$$

If $\varepsilon(t, x) = f(t)x$, one recovers the exact solution. As the perturbation is random, this is a system of stochastic equations; it allows rather complete analysis when $\varepsilon(t, x) \equiv V_\varepsilon(x)$ is an ergodic process with a finite support localized on the interval $[0, L/\varepsilon^2]$ (Garnier, 1998). The soliton dynamics are then governed by deterministic equations for almost every realization of $V_\varepsilon(x)$. For a soliton of small amplitude (weak nonlinearity), one can define $\nu_0 \ll \mu$ such that decay of the soliton amplitude follows either an exponential, for $\nu < \nu_0$, or a power, for $\nu_0 \nu \ll \mu$, law. When the soliton has large amplitude and small velocity, $\mu \ll \nu$, its amplitude experiences rather weak changes, while the velocity decreases.

Solitary Wave Propagation in Media with Fluctuating Parameters

Consider $\varepsilon(t, x) \equiv f(t)$ to be a stationary Gaussian process (4). Then the adiabatic approximation allows us to obtain a Fokker–Planck equation for the distribution function of the soliton parameters, similar to Equation (6), where typical behavior is a kind of Brownian motion (Konotop & Vazquez, 1994). At large times, the adiabatic approximation fails and fluctuations of the medium may result in resonant parametrical processes. Such processes are especially interesting in systems having topological solitons which cannot be destroyed by fluctuations. If, for example, $R[u] \equiv u - u^3$ in Equation (2), long-time numerical simulations of the kink dynamics show anomalous diffusion, and the dispersion of the fluctuation of its center grows as $t^{2.087}$ while the energy of the system increases exponentially. This phenomenon is a manifestation of the stochastic parametrical resonance of linear modes.

VLADIMIR V. KONOTOP AND LUIS VÁZQUEZ

See also **Brownian motion; Characteristics; Nonlinear Schrödinger equations; Stochastic processes**

Further Reading

Besieris, I.M. 1980. Solitons in randomly inhomogeneous media. In *Nonlinear Electromagnetics*, edited by P.L.E. Uslenghi, London and New York: Academic Press, pp. 87–116

Doucot, B. & Rammal, R. 1987. On Anderson localization in nonlinear random media. *Europhysics Letters*, 3: 969–974

Fröhlich, J., Spencer, Th. & Wayne, C.E. 1986. Localization in disordered, nonlinear dynamical systems. *Journal of Statistical Physics*, 42: 247–274

Garnier, 1998. Asymptotic transmission of solitons through random media. *SIAM Journal of Applied Mathematics*, 58: 1969–1995

Karpman, V.I. 1979. Soliton evolution in the presence of perturbations. *Physica Scripta*, 20: 462–478

Klyatskin, V.I. 1988. *Imbedding Approach in the Theory of Wave Propagation*, Moscow: Nauka (in Russian)

Knapp, R., Papanicolaou, G. & White, B. 1991. Transmission of waves by a nonlinear random medium. *Journal of Statistical Physics*, 63: 567–583

Konotop, V.V. & Vázquez, L. 1994. *Nonlinear Random Waves*, Singapore: World Scientific

WAVE STABILITY AND INSTABILITY

As with other dynamic entities, a solution of a wave system is considered to be stable if it does not deviate greatly under small perturbations, and unstable if it does.

Consider first the stability of the null solution of a partial differential equation (PDE) system in an infinite and uniform medium. Small perturbations of the null solution can be taken in the form $A\exp[\mathrm{i}(kx - \omega t)]$. To satisfy the PDE, k and ω are related by a dispersion relation, which is denoted as $D(k, \omega) = 0$. The dispersion relation may be solved in the form

$$\omega = \omega_n(k), \quad (n = 1, 2, \ldots). \tag{1}$$

Thus, there may be several solutions (or modes), with different functions $\omega_n(k)$, which are referred to as different modes. In general, ω may be complex for real k, leading to real solutions of the form

$$\begin{aligned} &A\exp[\mathrm{i}(kx - \omega t)] + \text{c.c.} \\ &\quad = \{A\exp[\mathrm{i}(kx - \omega_r t)] + \text{c.c.}\}\exp(\omega_i t), \end{aligned} \tag{2}$$

where $\omega = \omega_r + \mathrm{i}\omega_i$. Therefore, if $\omega_i > 0$ for any mode, that mode will grow with time, indicating instability. If all ω_i are negative, all modes damp away, indicating stability.

Convective and Absolute Instability

In practice, an initial perturbation is often localized and can be represented as a (Fourier) wave packet of various normal modes, in which each component propagates with its own phase velocity ($v_\mathrm{p} = \omega/k$). The collective motion of a wave packet, on the other hand, is governed by its group velocity ($v_\mathrm{g} = \mathrm{d}\omega/\mathrm{d}k$). If a perturbative wave packet is localized and moving with a certain group velocity, its amplitude at a certain point will at first begin to rise and then eventually fall back to zero. This leads to two distinct concepts: convective and absolute instability, which originally arose in studies of wave instabilities in plasmas (Briggs, 1964).

A wave system is convectively unstable if the maximum amplitude of a perturbing wave packet grows without bound, but at any fixed point of the system, the disturbance eventually relaxes back to zero as the wave packet propagates away. Such behavior is useful for the design of distributed amplifiers, such as the traveling-wave tube or optical (laser) amplifiers.

If the dispersion equation contains unstable modes with zero group velocity, however, a more robust instability arises. In this case, called absolute instability, perturbations grow without bound at every point of the system. Absolutely unstable dynamics can be employed for the design of distributed oscillators (backward-wave oscillators, for example) but not distributed amplifiers.

Modulational Instability

Consider next the stability of a small amplitude component of a wave system, which is stable at infinitesimal amplitude. At finite amplitude, however, the wave is not necessarily stable against wave modulation, because the finite intensity of wave modifies the propagation properties of medium. In this case, a nonlinear dispersion relation that takes into account the finite intensity of wave may be written as $\omega = \omega(k, a)$, where a is the amplitude of wave. For a slowly modulated plane wave having a small but

finite amplitude, the frequency ω may be expressed approximately as

$$\omega(k, a) = \omega_0(k) + \alpha(k)a^2 + \mathrm{O}(a^4). \tag{3}$$

(Odd terms in a are excluded from this formulation because they would imply different values of ω when a merely changes its algebraic sign.) Modulations on a linear and weakly nonlinear wave train can be described by the equations (Whitham, 1974)

$$\frac{\partial k}{\partial t} + \frac{\partial \omega}{\partial x} \doteq 0, \tag{4}$$

$$\frac{\partial a^2}{\partial t} + \frac{\partial}{\partial x}\left(\frac{\partial \omega}{\partial k}a^2\right) \doteq 0. \tag{5}$$

Equation (4) follows from the relations $\omega = -\partial\theta/\partial t$ and $k = \partial\theta/\partial x$, where $\theta(x, t)$ is the phase. (This equation can also be viewed as a conservation law for wave crests.) As a^2 is proportional to energy density and $a^2\partial\omega/\partial k = a^2 v_g$ is proportional to power flow, Equation (5) is the law of energy conservation.

Substituting Equation (3) into these equations and assuming a to be sufficiently small leads to the following equations:

$$\frac{\partial k}{\partial t} + v_g\frac{\partial k}{\partial x} + \alpha(k_0)\frac{\partial a^2}{\partial x} \doteq 0, \tag{6}$$

$$\frac{\partial a^2}{\partial t} + v_g' a^2\frac{\partial k}{\partial x} + v_g\frac{\partial a^2}{\partial x} \doteq 0. \tag{7}$$

Here $v_g = \mathrm{d}\omega_0(k_0)/\mathrm{d}k_0$, the group velocity of the linear wave with wave number k_0, and $v_g' = \mathrm{d}^2\omega_0(k_0)/\mathrm{d}k_0^2$. Linearizing k and a by

$$k = k_0 + \bar{k}\exp\{\mathrm{i}(Kx - \nu t)\},$$
$$a = a_0 + \bar{a}\exp\{\mathrm{i}(Kx - \nu t)\},$$

yields the modulational dispersion relation

$$\nu = K\left(v_g \pm \sqrt{\alpha a_0^2 v_g'}\right). \tag{8}$$

If $\alpha v_g' < 0$, ν becomes complex, which implies that the modulation becomes unstable and grows (Lighthill, 1965; Whitham, 1974). Equation (8) is called Lighthill's theorem, and the corresponding modulational instability (which has been studied analytically and experimentally in the context of deep water waves by Benjamin & Feir (1967)) is called the Benjamin–Feir (BF) instability. The nonlinear evolution of modulated envelopes is described by the nonlinear Schrödinger equation. Interestingly, the BF instability can lead to formation of stable traveling waves of modulation—envelope solitons. For further discussions, see Whitham (1974), Infeld & Rowlands (2000), Longuet-Higgins (1978), and McLean (1982).

Soliton Stability

The stability problem of traveling-wave solutions with respect to small perturbations has been studied by various methods, including the normal-mode approach (Infeld and Rowlands, 2000). Consider the solution $u(x, t)$ of a nonlinear PDE to be the stationary traveling wave $u_s(\xi)$ plus a small perturbation $p(\xi, t)$

$$u(x, t) = u_s(\xi) + p(\xi, t), \tag{9}$$

where $\xi = x - v_s t$ and v_s is a propagation velocity. Transforming the original nonlinear PDE to a coordinate system moving at v_s and linearizing, the resulting equation has parameters that are functions of ξ. This equation can then be solved for the time development of the perturbation subject to an appropriate boundary condition.

When such problems are uniform in time (as they often are), it is convenient to express $p(\xi, t)$ as product solution in the form $p(\xi, t) = f(\xi)\exp(\sigma t)$ (separation of variables). Traveling-wave solutions are linearly unstable if any product solution has $\mathrm{Re}(\sigma) > 0$ and asymptotically stable if all product solutions have $\mathrm{Re}(\sigma) < 0$. A stationary solution that is neither unstable nor asymptotically stable is said to be neutrally stable, and there is always such a case because $\sigma = 0$ corresponds to a simple displacement of the traveling wave in the direction of propagation.

As examples, consider the stability of solitons of the Korteweg–de Vries (KdV) and its two-dimensional generalization. Writing the KdV equation as $u_t + 6(u^2)_x + u_{xxx} = 0$, a solitary wave solution is given by

$$u_s = A + k^2\mathrm{sech}^2\{k(x - v_s t) + \delta\} = 0, \tag{10}$$

where $v_s = 4k^2 + 12A$ and A and k are both arbitrary. Using the method of normal modes, Jeffrey and Kakutani (1972) and also Berryman (1976) have investigated the stability of this soliton, showing that small localized perturbations do not grow without bound; thus, the KdV soliton is linearly stable. Benjamin formulated a nonlinear stability theory for the KdV soliton and also showed that the KdV soliton is stable against small but finite perturbations (Benjamin, 1972).

A soliton in a two-dimensional (2-d) space often appears as a line soliton (LS). Kadomtsev and Petviashvili studied a 2-d-generalization of the KdV equation in order to discuss the stability of the line soliton with respect to long and small transverse perturbations. They obtained the KP equation (Kadomtsev & Petviashvili, 1970)

$$(u_t + 6(u^2)_x + u_{xxx})_x + su_{yy} = 0, (s = \pm 1), \tag{11}$$

which corresponds to the case of negative and positive dispersion when $s = +1$ and -1, respectively. The line soliton is unstable in the case of positive dispersion and is stable for negative dispersion. The KP equation with positive dispersion also has a periodic soliton (PS) solution. A spatially periodic resonance exist between the LS and PS solutions, as indicated in Figure 1. From this

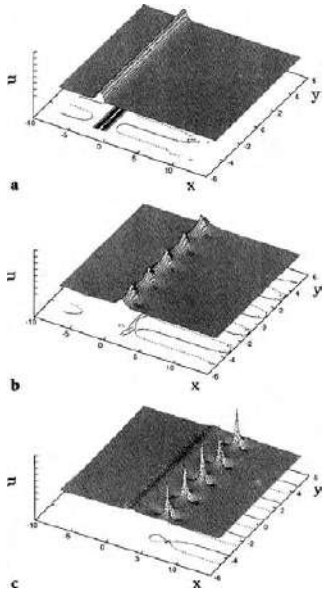

Figure 1. The sequence of snapshots of quasiresonant solution.

figure, we see how a transversely perturbed LS decays into a small LS and a PS, where the instability of the LS may be relaxed by the emission of a PS (Infeld and Rowlands, 2000, Chapter 10). Importantly, the nonlinear stage of instability of soliton is, in general, different from the conclusion of the linear stability theory. For more detailed studies of 2-d soliton stability, see Infeld & Rowlands (2000) and Zakharov et al. (1986).

Eckhaus Instability

In the neighborhood of a bifurcation (the appearance of a new solution as a parameter λ is changed), the description of a dynamical system can be greatly reduced, where the only relevant variable is a complex normalized amplitude: Z. Studies of the dissipative structures that emerge beyond the instability is often facilitated by using amplitude equations, such as the Newell–Whitehead (NW) equation (Newell & Whitehead, 1969)

$$\frac{\partial Z}{\partial t} = (\lambda - \lambda_c)Z + \left(\frac{\partial}{\partial x} - \frac{\mathrm{i}}{2k_c}\frac{\partial^2}{\partial y^2}\right)^2 Z - |Z|^2 Z. \tag{12}$$

This is the normal form of a symmetry-breaking bifurcation leading to roll or stripe patterns with wave vector parallel to the x-axis, where λ_c is the critical control parameter and k_c is the critical wave number. In the supercritical region, $(\lambda - \lambda_c) > 0$, the NW equation has the two parameter $(\delta k, \theta_0)$ family of solutions:

$$Z_k = A_k \mathrm{e}^{\mathrm{i}(\delta k x + \theta_0)}, \tag{13}$$

where $A_k = \sqrt{(\lambda - \lambda_c) - (\delta k)^2}$, δk is a small wave number describing the modulation of the basic dissipative structure at the critical wave number k_c, and θ_0 is an arbitrary phase. This solution expresses a stationary roll pattern with wave number $k = k_c + \delta k$.

Introducing a solution that is perturbed by small changes in amplitude and phase leads to the instability criterion (Eckhaus, 1965)

$$|\delta k| > \sqrt{\frac{\lambda - \lambda_c}{3}}. \tag{14}$$

If perturbations transverse to the basic structure are allowed, a zig-zag instability emerges (Nicolis, 1995; Mori & Kuramoto, 1998).

Nerve Impulse Stability

The stability of nerve impulses can be studied by the reduced version of the Hodgkin–Huxley system called the FitzHugh–Nagumo (FN) equation (FitzHugh, 1961; Nagumo et al., 1962):

$$\frac{\partial V}{\partial t} = \frac{\partial^2 V}{\partial x^2} - f(V) - R,$$
$$\frac{\partial R}{\partial t} = \varepsilon(V - bR),$$

where V is the nerve membrane potential, $f(V) = V(V-1)(V-a)$, and ε is a temperature parameter which controls the rate of change of the recovery variable R.

If $0 < \varepsilon < \varepsilon_c$, the FN equation has slow and fast impulse solutions with propagation speeds $c_s(\varepsilon)$ and $c_f(\varepsilon)$: $0 < c_s < c_f$. The relation between these two speeds and the temperature parameter is sketched in Figure 2, where the fast solution is stable and the slow solution is unstable (Rinzel & Keller, 1973). Thus, small positive perturbations of the slow solution will eventually grow into the fast solution, whereas small negative perturbations will cause the slow solution to collapse to zero (Scott, 2003).

At each value of ε, the FN equation has also two periodic traveling-wave solutions with the same wavelength but different propagation speeds. Viewed as a traveling wave, the fast periodic solution is stable and the slow solution is unstable, just as for a single impulse.

Suppose that a time-periodic boundary condition is imposed at $x = 0$ (where $V(0,t) = V(0,t+T)$) and periodic solutions are sought (for $x > 0$) of the form $V(x,t) = V(x+\lambda,t) = V(x,t+T)$. In this "signaling problem," an important question is whether (or not)

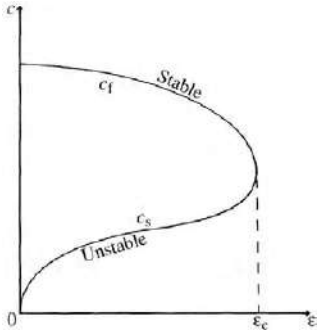

Figure 2. The typical relation between the pulse speed c and the temperature parameter ε.

small perturbations grow with x. Because $c(\lambda) = \lambda/T$, the dependence of the nonlinear frequency $(1/T)$ upon the nonlinear wave number $(1/\lambda)$ is readily calculated, and Rinzel has shown that the condition for solutions not to grow with increasing x is (Rinzel, 1975)

$$\frac{\mathrm{d}(1/T)}{\mathrm{d}(1/\lambda)} > 0.$$

MASAYOSHI TAJIRI

See also **Equilibrium; Kelvin–Helmholtz instability; Modulated waves; Rayleigh–Taylor instability; Stability**

Further Reading

Benjamin, T.B. 1972. The stability of solitary waves. *Proceedings of the Royal Society of London*, 328A: 153–183

Benjamin, T.B. & Feir, J.E. 1967. The disintegration of wave trains in deep water, I. *Journal of Fluid Mechanics*, 27: 417–430

Berryman, J.G. 1976. Stability of solitary waves in shallow water. *Physics of Fluids*, 19: 771–777

Briggs, R.G. 1964. *Electron-Stream Interaction with Plasmas*, Cambrige, MA: MIT Press

Eckhaus, W. 1965. *Studies in Nonlinear Stability Theory*, Berlin: Springer

FitzHugh, R. 1961. Impulses and physiological states in theoretical models of nerve membranes. *Biophysical Journal*, 1: 445–466

Infeld, E. & Rowlands, G. 2000. *Nonlinear Waves, Solitons and Chaos*, Cambridge and New York: Cambridge University Press

Jeffrey, A. & Kakutani, T. 1972. Weakly nonlinear dispersive waves: a discussion centered around the Korteweg–de Vries equation. *SIAM Review*, 14: 582–643

Kadomtsev, B.B. & Petviasvili, V.I. 1970. On the stability of solitary waves in weakly dispersive media. *Soviet Physics-Doklady*, 15: 539–541

Lighthill, J. 1965. Contributions to the theory of waves in nonlinear dispersive system. *Journal of the Institute of Mathematics and Its Applications*, 1: 269–306

Longuet-Higgins, M.S. 1978. The instabilities of gravity waves of finite amplitude. *Proceeding of Royal Society of London, I Superhamonics*, A360: 471–488; *II Subharmonics*, A360: 489–505

McLean, J.W. 1982. Instabilities of finite-amplitude water waves, *Journal of Fluid Mechamics*, 114: 315–330

Mori, H. & Kuramoto, Y. 1998. *Dissipative Structures and Chaos*, Berlin: Springer

Nagumo, J., Arimoto, S. & Yoshizawa, S. 1962. An active pulse transmission line simulating nerve axon. *Proceedings of the Institute of Radio Engineering*, 50: 2061–2070

Newell, A.C. & Whitehead, J.A. 1969. Finite bandwidth, finite amplitude convection. *Journal of Fluid Mechanics*, 38: 279–303

Nicolis, G. 1995. *Introduction to Nonlinear Science*, Cambridge and New York: Cambridge University Press

Rinzel, J. 1975. Spatial stability of traveling-wave solutions of a nerve conduction equation. *Biophysical Journal*, 15: 975–988

Rinzel, J. & Keller, J.B. 1973. Traveling-wave solutions of nerve conduction equation. *Biophysical Journal*, 13: 1313–1337

Scott, A.C. 2003. *Nonlinear Science: Emergence and Dynamics of Coherent Structures*, 2nd edition, Oxford and New York: Oxford University Press

Whitham, G.B. 1974. *Linear and Nonlinear Waves*, New York: Wiley

Zakharov, V.E., Kuznetsov, E.A. & Rubenchik, A.M. 1986. Soliton stability. In *Solitons*, edited by S.E. Trullinger, V.E. Zakharov & V.L. Pokrovsky, Amsterdam and New York: North-Holland, pp. 503–554

WAVE TANKS

See **Laboratory models of nonlinear waves**

WAVELETS

The wavelet transform is a tool that divides up data, functions, or operators into different frequency components and then studies each component with a resolution matched to its scale. The idea emerged independently in many different fields, including mathematics, quantum physics, electrical engineering, and seismology. By the end of the 1980s, French researchers Grossmann & Morlet (1984), Meyer (1990), and later Daubeschies (1992) had laid the mathematical foundations of the wavelet transform technique. Their work was motivated by the problem Morlet (a geophysicist) was facing while analyzing seismic data which comprised different features in time and frequency.

The frequency content of a signal can be obtained by taking its Fourier transform. However, in transforming to the frequency domain, time information is lost and it is impossible to tell when a particular event took place. To correct this deficiency, the Fourier transform was adapted to analyze only a small section (or window) of the signal at a time. Such a short-time Fourier transform (STFT) maps a signal into a two-dimensional function of time and frequency and provides information about both when and at what frequencies a signal event occurs. This information can only be obtained with limited precision, and that precision is determined by

the size of the time window. The main drawback of STFT is that once a particular size for the time window is chosen, that window is the same for all frequencies. With Morlet's data, this approach failed either to follow the time evolution of rapid events or to estimate the frequency content in the low-frequency band.

Wavelet analysis represents the next logical step: signal cutting is performed by a window of variable length. Short windows are used at high frequencies and long windows at low frequencies. Thus, the time-frequency resolution is no longer constant but changes with frequency, allowing good time resolution for high frequencies and good frequency resolution for low frequencies to be achieved.

In Fourier analysis, the signal is decomposed into sine waves of various frequencies. Similarly, wavelet analysis is a decomposition of a signal into a set of basis functions $\Psi_{s,\tau}(t)$ called wavelets

$$\hat{f}(s,\tau) = \int f(t)\Psi^*_{s,\tau}\,\mathrm{d}t, \tag{1}$$

where $\hat{f}(s,\tau)$ is the wavelet transform of $f(t)$ and * denotes complex conjugation. The wavelets are generated from a single basic wavelet $\psi(t)$ called the mother wavelet, by scaling and translation:

$$\Psi_{s,\tau} = \sqrt{|s|}\,\psi\Big(\frac{t-\tau}{s}\Big). \tag{2}$$

As the scaling parameter s changes, the wavelets cover different frequency ranges: large values of s correspond to low frequencies, small values of s correspond to high frequencies. Changing the translation parameter τ allows the time localization center to be moved: each $\Psi_{s,\tau}(t)$ is localized around $t=\tau$. The factor $\sqrt{|s|}$ is for energy normalization across different scales.

An important difference between wavelet and Fourier transforms is that wavelet basis functions are not specified. The theory deals with general properties of wavelets and defines a framework within which different wavelets can be designed. Numerous families of wavelets have been proposed and proven to be useful in different applications. In order for a function to be used as the mother wavelet, it must allow for analysis and reconstruction of the signal without loss of information. This so-called admissibility condition implies that the average value of a wavelet in the time domain must be zero and it must, therefore, be oscillatory, a wave. The other important property of wavelets (the regularity condition) states that wavelets are smooth and concentrated both in time and frequency. This makes them suitable for capturing local features of a signal. Figure 1 presents an example of a wavelet, the Morlet wavelet, in time and frequency domains for two scales.

We can distinguish between the continuous and discrete wavelet transform. In a continuous transform, the parameters s and τ vary continuously. It maps a one-dimensional signal to a two-dimensional time-scale joint representation that is highly redundant. This redundancy can be either exploited or removed. To reduce the redundancy, discrete wavelets have been introduced, which can only be scaled and translated in discrete steps. For the scale, we choose integer powers of fixed dilation parameter $s_0 > 1$, $s = s_0^j$, and j is an integer. The discretization of the translation parameter τ depends on j: narrow wavelets are translated by small steps, while wider wavelets are translated by larger steps, $\tau = n\tau_0 s_0^j$, with j and n integers and $\tau_0 > 0$ is fixed. For some special choices of mother wavelets, the discrete wavelets can be made orthogonal to their own translations and dilations. In this case, they behave exactly like an orthonormal basis and redundancy is removed.

Wavelets have a bandpass-like spectrum and can be viewed as bandpass filters. Compression in time stretches the spectrum and shifts it upwards, while stretching in time compresses the bandwidth and shifts it toward zero (Figure 1). The series of dilated wavelets can be used to cover the spectrum of a signal. However, an infinite number of wavelets is needed to reach zero frequency. This problem was solved by introducing a low-pass or averaging filter with a spectrum that belongs to the scaling function $\phi(t)$. If we analyze the signal using a combination of scaling functions and wavelets, the scaling function takes care of the spectrum otherwise covered by all the wavelets up to a chosen scale, while the rest is done by wavelets. The family of scaling functions and wavelets allows for wavelet multiresolution analysis. In multiresolution analysis, the signal is split into an approximation on a coarser scale, obtained using the scaling function, and details on a current scale, obtained by wavelets. This process is repeated, giving a sequence of approximations and details removed at every scale. After N iterations, the original signal can be reconstructed by summing up the last approximations and details on all previous scales.

Interactions between the fields where wavelets were first introduced have led to many wavelet applications. Wavelets are of particular interest for the analysis of nonstationary signals with broad spectra because they permit time-frequency presentation with logarithmic resolution. Wavelet analysis is capable of revealing aspects of signals that other signal analysis techniques miss, such as trends, breakdown points, discontinuities in higher derivatives, and self-similarity. Furthermore, wavelet analysis can often compress (or reduce noise in) a signal without appreciable degradation. The above-described one-dimensional aspect can be generalized to more dimensions, for example, to handle image analysis. Wavelets are a very powerful tool for image compression, since wavelet transform clearly separates high-pass and low-pass information on a pixel-by-pixel

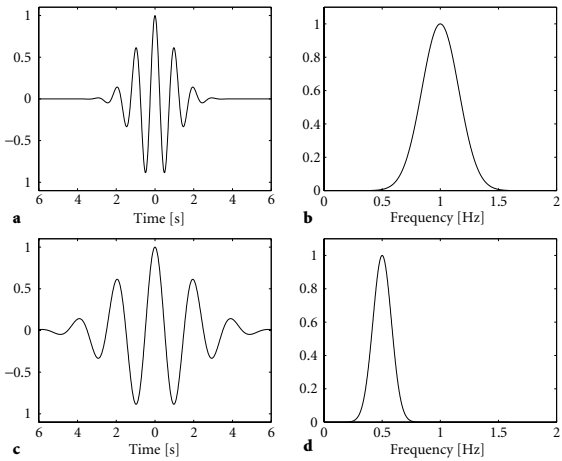

Figure 1. Morlet wavelet in time and frequency domain for scales $s = 1$ (a,b) and $s = 2$ (c,d).

basis. Among the successes of wavelet representation are the compression of digitized fingerprints by the US Federal Bureau of Investigation and image compression using the JPEG 2000 standard (the older JPEG standard uses a non-wavelet compression).

MAJA BRAČIČ LOTRIČ AND ANETA STEFANOVSKA

See also **Integral transforms; Nonlinear signal processing**

Further Reading

Daubeschies, I. 1992. *Ten Lectures on Wavelets*, Philadelphia, PA: Society for Industrial and Applied Mathematics

Grossmann, A. & Morlet, J. 1984. Decomposition of Hardy functions into square integrable wavelets of constant shape. *SIAM Journal of Mathematical Physics*, 27: 2437–2479

Meyer, Y. 1990. *Ondelettes et Operateurs*, 3 vols, Paris: Herrmann; vol. 1 as *Wavelets and Operators*, Cambridge and New York: Cambridge University Press, 1992 and vols. 2 and 3 as *Wavelets: Calderón-Zygmund and Multilinear Operators*, Cambridge and New York: Cambridge University Press, 1997

WAVE NUMBER SELECTION

See **Pattern formation**

WEAK COLLAPSE

See **Development of singularities**

WEAK TURBULENCE

See **Turbulence**

WEAKLY NONLINEAR ANALYSIS

See **Quasilinear analysis**

WEATHER FRONTS

See **Atmospheric and ocean sciences**

WEIERSTRASS ELLIPTIC FUNCTIONS

See **Elliptic functions**

WESTERVELT EQUATION

See **Nonlinear acoustics**

WHISTLERS

See **Nonlinear plasma waves**

WHITHAM'S METHOD

See **Modulated waves**

WIGNER STATISTICS

See **Random matrix theory I, II**

WINDING NUMBERS

If you wrap a rubber ring (rubber band) around a pencil, the intuitive idea of an integer invariant for the wrapping process arises. The number of oriented turns around the

pencil is an integer, and it is independent of how tight or creased the ring is. The only way to change this integer is to wrap/unwrap one loop of the ring at the endpoints of the pencil. Using a rubber string, the number of turns could be some real number instead.

How does this fact connect with dynamics? Consider a three-dimensional (3-d) dynamical system having a torus as phase space. Let the hole in the torus represent the pencil and the rubber ring represent a closed trajectory within the torus. Small modifications to the trajectory will not alter the wrapping property.

The underlying feature in the above examples is the forbidden region given by the pencil or the hole of the torus. To further analyze its structure, decompose 3-d space ($\mathbb{R}^3$) as the product of the pencil direction times a perpendicular plane (equivalent to $\mathbb{R}^2$). The role of the pencil is to identify a special point on that plane given by the projection along the pencil direction.

Similarly, consider a periodic orbit in $\mathbb{R}^3$, as the forbidden region. Since the points in the periodic orbit are regular points in a small tube around the periodic orbit, the flow can be decomposed in a component parallel to the periodic orbit and a projected flow onto a perpendicular section. Hence, any other closed trajectory sufficiently near to the orbit will wind around it. A similar situation arises around a period-one orbit of a periodically forced flow in $\mathbb{R}^2$.

The winding number characterizes the topological properties of "the plane minus one point." Moreover, the topology of the plane minus n points gives a deeper characterization of the periodic orbit structure of 3-d dynamical systems admitting a Poincaré section.

Definition

Consider a simple continuous closed curve γ in the complex plane ($\mathbb{C}$) and a point $z_0 \in \mathbb{C} - \gamma$. The winding number n is defined as

$$n(\gamma, z_0) = \frac{1}{2\pi \mathrm{i}} \int_\gamma \frac{\mathrm{d}z}{z - z_0}. \tag{1}$$

We may regard our wrapped rubber ring as a suitable complex function γ of the unit circle, thus connecting our motivating idea with the formal definition (similarly for the second example if we project the torus along the direction perpendicular to the hole when seen as a disc). Where appropriate in the sequel, we will let $z_0 = 0$ for simplicity and recast γ as a map of the unit circle $\gamma : \mathbb{S}^1 \to \mathbb{S}^1$. It follows from Equation (1) that $n(\gamma, 0)$ is a real integer given by

$$n(\gamma, 0) = \int_{\mathbb{S}^1} \frac{\gamma'(\theta)}{\gamma(\theta)} \, \mathrm{d}\theta, \tag{2}$$

which is called the degree of γ (Rotman, 1988, p. 50).

Applications

Homotopy classes of the circle. A loop is a continuous map g of the circle to itself such that $g(0) = g(2\pi) = 2\pi$. Two loops α and β are homotopic if there exists a continuous map $H : \mathbb{S}^1 \times [0, 1] \to \mathbb{S}^1$ such that $H(\cdot, 0) = \alpha$, $H(\cdot, 1) = \beta$ and for each t, $H(\cdot, t)$ is a loop. In other words, two loops are homotopic if one can continuously deform one of them into the other, keeping it as a loop all the way throughout the deformation. The winding number classifies the homotopy classes of loops, namely, if σ is homotopic to γ, then $n(\sigma, 0) = n(\gamma, 0)$ (Rotman, 1988, p. 52).

Braids and periodic orbits. While the plane minus one point produces the winding number as a class invariant under homotopies, the homotopy classes of the plane with n special points requires a more elaborated structure which connects nicely with the dynamical properties of 3-d flows admitting a Poincaré section. In fact, periodic orbits of such flows can be regarded as imbeddings of the unit disk in phase space parametrized with time in units of $2\pi/T$ where T is the minimal period. On the Poincaré section, these special trajectories appear as an invariant set of n periodic points. The homotopy classes of loops on the plane with an invariant set of n points are classified by elements of the *Braid group on n strands* (Thurston, 1988; Hall, 1994; Natiello & Solari; 1994).

Linking number. In the same lines, given a pair of periodic orbits in phase space, we may think of the number of turns that one orbit does around the other when completing one excursion along itself. Such number is a link invariant which has a natural interpretation in terms of winding number, and it is called *linking number* (Uezu & Aizawa, 1982; Solari et al., 1996).

For 3-d flows admitting a Poincaré section, the periods of the orbits are commensurate and one may compute the average rotation per period of one orbit around another. This is called the *relative rotation rate* (Solari et al., 1996) and helps in understanding the orbit organization of such flows.

Poincaré index (PI). Consider a planar dynamical system $\dot{x} = f(x, y)$, $\dot{y} = g(x, y)$ and a simple closed counterclockwise curve C not passing through any equilibrium points. The PI k computed along C is defined as

$$\begin{aligned} k &= \frac{1}{2\pi} \int_C \mathrm{d} \left\{ \arctan\left(\frac{\mathrm{d}y}{\mathrm{d}x} \right) \right\} \\ &= \frac{1}{2\pi} \int_C \frac{f \, \mathrm{d}g - g \, \mathrm{d}f}{f^2 + g^2}. \end{aligned} \tag{3}$$

(See below for a discussion of the PI in terms of complex analysis and winding number.)

In the context of planar dynamics, the PI of a node or a center is $+1$, of a hyperbolic saddle point is -1, and of a closed orbit is $+1$. Also the PI of a closed

curve not containing fixed points is zero, and the PI of a closed curve equals the sum of the indices of the fixed points within (Guckenheimer & Holmes, 1983, p. 51).

Fixed point theorems. The degree of a map can be generalized to higher dimensions. In fact, this property (or the winding number when adequate) is a basic ingredient in the proof of Brouwer's fixed point theorem. An interesting discussion of this fact along with some philosophical considerations can be found in www.mathpages.com.

Complex analysis. The computation of the winding number is a standard tool in the proof of the Fundamental Theorem of Algebra.

Also, let C be a closed contour on the complex plane not passing through any singularities or zeroes of the complex function f, which is analytic inside C except at most at a finite number of poles. Then

$$\frac{1}{2\pi \mathrm{i}} \int_C \frac{f'(z)}{f(z)} \, \mathrm{d}z = N - P, \tag{4}$$

where N is the number of zeroes of f and P the number of poles inside C. This is called the Principle of the Argument in standard textbooks (Wunsch, 1994, p. 458).

This result is related to Equation 2 and to the PI. Concerning Equation (2), taking the special point of the plane to be the origin (or any point inside the unit circle), n counts how many turns γ performs around this point when running along the unit circle. Assume now that f has only one zero inside C with multiplicity n and no poles. Then f restricted to C is exactly the same as γ with a suitable choice of parametrization for C and $\mathbb{S}^1$. Concerning the PI, let $z = x + \mathrm{i}y$ and $F(z) = f(x, y) + \mathrm{i}g(x, y)$, regarding the xy-plane as the complex plane. If the vector field (f, g) is continuous, F will not have poles within C and the Poincaré index reduces to the Principle of the Argument calculation for F.

MARIO NATIELLO AND HERNÁN SOLARI

See also **Conley index; Phase space; Poincaré theorems**

Further Reading

Guckenheimer, J. & Holmes, P.J. 1983. *Nonlinear Oscillators, Dynamical Systems and Bifurcations of Vector Fields*, New York and London: Springer

Hall, T. 1994. Fat one-dimensional representatives of pseudo-Anosov isotopy classes with minimal periodic orbit structure. *Nonlinearity*, 7: 367–384

Natiello, M.A. & Solari, H.G. 1994. Remarks on braid theory and the characterisation of periodic orbits. *Journal of Knot Theory and Its Ramifications*, 3: 511–539

Rotman, J.J. 1988 *An Introduction to Algebraic Topology*. New York: Springer

Solari, H.G. & R. Gilmore. 1988. Relative rotation rates for driven dynamical systems. *Physical Review* A, 37: 3096

Solari, H.G., Natiello, M.A. & Mindlin, B.G. 1996. *Nonlinear Dynamics: A Two-way Trip from Physics to Math*, Bristol: Institute of Physics Publishing

Thurston, W.P. 1988. On the geometry and dynamics of diffeomorphisms of surfaces. *Bulletin of American Mathematical Society*, 19: 417

Uezu, T. & Aizawa, Y. 1982. Topological character of a periodic solution in three-dimensional ordinary differential equation system. *Progress of Theoretical Physics*, 68: 1907

Wunsch, A.D. 1994. *Complex Variables with Applications*, Reading, MA: Addison-Wesley

www.mathpages.com see http://www.mathpages.com/home/kmath262/kmath262.htm or do a search for "Brouwer" on http://www.mathpages.com

Y

YANG–BAXTER EQUATION

See **Quantum inverse scattering method**

YANG–MILLS THEORY

Modern particle theories, such as the Standard Model, are quantum Yang–Mills theories. In a quantum field theory, space-time fields with relativistic field equations are quantized and, in many calculations, the quanta of the fields are interpreted as particles. In a Yang–Mills theory, these fields have an internal symmetry: they are acted on by space-time-dependent non-abelian group transformations in a way that leaves physical quantities, such as the action, invariant. These transformations are known as local gauge transformations, and Yang–Mills theories are also known as non-abelian gauge theories.

Yang–Mills theories, and especially quantum Yang–Mills theories, have many subtle and surprising properties and are still not fully understood, either in terms of their mathematical foundations or in terms of their physical predictions. However, the importance of Yang–Mills theory is clear; the Standard Model has produced calculations of amazing accuracy in particle physics, and in mathematics, ideas arising from Yang–Mills theory and from quantum field theory are increasingly important in geometry, algebra, and analysis.

Consider a complex doublet scalar field ϕ_a; a scalar field is one that has no Lorentz index, but, as a doublet, ϕ_a transforms under a representation of SU(2), the group represented by special unitary 2×2 matrices:

$$\phi_a(x) \to g_{ab}\phi_b(x), \tag{1}$$

where $g \in \mathrm{SU}(2)$ and the repeated index are summed over. If this is a global transformation; that is, if g is independent of x, then derivatives of ϕ_a have the same transformation property as ϕ_a itself:

$$\frac{\partial \phi_a}{\partial x_\mu} \to \frac{\partial g_{ab}\phi_b}{\partial x_\mu} = g_{ab}\frac{\partial \phi_b}{\partial x_\mu} \tag{2}$$

However, this is not true for a local, or space-time-dependent, transformations where

$$\frac{\partial \phi_a}{\partial x_\mu} \to \frac{\partial g_{ab}\phi_b}{\partial x_\mu} = g_{ab}\frac{\partial \phi_b}{\partial x_\mu} + \frac{\partial g_{ab}}{\partial x_\mu}\phi_b. \tag{3}$$

In order to construct an action that includes derivatives and that is invariant under local transformations, a new derivative is defined that transforms the same way as ϕ_a:

$$D_\mu \phi_a = \frac{\partial \phi_a}{\partial x_\mu} + (A_\mu)_{ab}\phi_b, \tag{4}$$

where A_μ is a new two-indexed space-time field, called a gauge field or gauge potential, defined to have the transformation property

$$(A_\mu)_{ab} \to g_{ac}(A_\mu)_{cd}g^{-1}_{db} - \frac{\partial g_{ac}}{\partial x_\mu}g^{-1}_{cb}. \tag{5}$$

Now, under a local transformation

$$D_\mu \phi_a \to g_{ab} D_\mu \phi_b \tag{6}$$

and so, $D_\mu \phi_a$ transforms in the same way as ϕ_a. This derivative is called a covariant derivative.

A physical theory that includes the gauge field A_μ should treat A_μ as a dynamical field, and so the action should have a kinetic term for A_μ. In other words, the action should include derivative terms for A_μ. These terms are found in the field strength

$$F_{\mu\nu} = \frac{\partial A_\nu}{\partial x^\mu} - \frac{\partial A_\mu}{\partial x^\nu} + [A_\mu, A_\nu] \tag{7}$$

that has the covariant transformation property

$$(F_{\mu\nu})_{ab} \to g_{ac}(F_{\mu\nu})_{cd}g^{-1}_{db}, \tag{8}$$

where $[A_\mu, A_\mu]$ is the normal matrix commutator. In fact, the simplest Yang–Mills theory is pure Yang–Mills theory with action

$$S[A] = -\frac{1}{2}\int \mathrm{d}^4x \,\mathrm{trace}\, F_{\mu\nu}F^{\mu\nu} \tag{9}$$

and corresponding field equation

$$\frac{\partial F_{\mu\nu}}{\partial x_\mu} = 0. \tag{10}$$

Solutions to this equation are known as instantons (*See* **Instantons**).

More generally, Yang–Mills theories contain gauge fields and matter fields like ϕ and fields with both group and Lorentz or spinor indices. Also, the group action described here can be generalized to other groups and to other representations. In the case of the Standard Model of particle physics, the gauge group is $SU(3) \times SU(2) \times U(1)$, and the group representation structure is quite intricate.

Yang–Mills theory was first discovered in the 1950s. At that time, quantum electrodynamics (QED) was known to describe electromagnetism. Quantum electrodynamics is a local gauge theory but with an abelian gauge group. It was also known that there is an approximate global non-abelian symmetry called isospin symmetry that acts on the proton and neutron fields as a doublet and on the pion fields as a triplet. This suggested that a local version of the isospin symmetry might give a quantum field theory for the strong force with the pion's fields as gauge fields (O'Raifeartaigh, 1997). This did not work because pion fields are massive whereas gauge fields are massless, and the main thrust of theoretical effort in the 1950s and 1960s was directed at other models of particle physics.

However, it is now known that the proton, neutron, and pion are not fundamental particles, but are composed of quarks and that there is, in fact, a quantum Yang–Mills theory of the strong force with quark fields and gauge particles called gluons. Furthermore, it is now known that it is possible to introduce a particle, called a Higgs boson, to break the non-abelian gauge symmetry in the physics of a symmetric action and give mass terms for gauge fields. This mechanism is part of the Weinberg–Salam model, a quantum Yang–Mills theory of the electroweak force, that is a component of the Standard Model and that includes both massive and massless gauge particles.

These theories were only discovered after several key experimental and theoretical breakthroughs in the late 1960s and early 1970s. After it became clear from collider experiments that protons have a substructure, theoretical study of the distance-dependent properties of quantum Yang–Mills theory led to the discovery that Yang–Mills fields are asymptotically free (Gross, 1999). This means that the high-energy behavior of Yang–Mills fields includes the particle-like properties seen in experiments, but the low-energy behavior may be quite different, and in fact, the quantum behavior might not be easily deduced from the classical action. Confinement and the mass gap are examples of this. The strong force is a local gauge theory with quark fields. The quark structure of particles is observed in collider experiments; but free quarks are never detected, instead, at low energies, they appear to bind together to form composite particles, such as neutrons, protons, and pions. This is called confinement. It is possible to observe this behavior in simulations of the quantum gauge theory of the strong force, but it has not been possible to prove mathematically that confinement is a consequence of the theory. The same is true of the mass gap; it is known that particles have nonzero mass, and this is observed in simulations, but there is no known way of deriving the mass gap mathematically from the original theory (Clay, 2002).

The symmetries of Yang–Mills theory can be extended to include a global symmetry between the bosonic and fermionic fields called supersymmetry. While there is no direct evidence for supersymmetry in physics, the indirect case is very persuasive, and it is commonly believed that direct evidence will be found in the future. Often, supersymmetric theories are more tractable; for example, Seiberg and Witten have found an exact formula for many quantum properties in $N = 2$ super-Yang–Mills theory (Seiberg & Witten, 1994). It is also commonly believed by theoretical physicists that the quantum Yang–Mills theories in particle physics are in fact a limit of a more fundamental string theory.

CONOR HOUGHTON

See also **Higgs boson; Instantons; Matter, nonlinear theory of; Particles and antiparticles; Quantum field theory; String theory; Tensors**

Further Reading

Clay Mathematics Institute, Millennium Prize, 2002. The Clay Institute has offered a prize for a rigorous formulation of a quantum Yang–Mills theory in which there is a mass gap. The Clay Institute web site has a description of the problem along with an essay by A. Jaffe & E. Witten http://www.claymath.org/Millennium_Prize_Problems

Davies, C. 2002. *Lattice QCD*, Bristol: Institute of Physics Publishing

Gross, D. 1999. Twenty-five years of asymptotic freedom. *Nuclear Physics Proceedings Supplements*, 74: 426–446

O'Raifeartaigh, L. 1997. *The Dawning of Gauge Theory*, Princeton, NJ: Princeton University Press

Seiberg, N. & Witten, E. 1994. Electric-magnetic duality, monopole condensation and confinement in $N = 2$ supersymmetric Yang–Mills theory. *Nuclear Physics* B, 426: 19–52, Erratum-ibid 430: 485–486 and Monopoles, duality and chiral symmetry breaking in $N = 2$ supersymmetric QCD. *Nuclear Physics* B, 431: 484–558

Weinberg, S. 1996. *Quantum Field Theory*, vol. 2, Cambridge and New York: Cambridge University Press

Z

ZAKHAROV–SHABAT EQUATION

See **Nonlinear Schrödinger equations**

ZELDOVICH–FRANK-KAMENETSKY EQUATION

In 1938, Yakov Zeldovich and David Frank-Kamenetsky published a brief theoretical paper devoted to flame propagation, presenting one of the first nonlinear traveling-wave front solutions (Zeldovich & Frank-Kamenetsky, 1938). Although both scientists later played outstanding roles in Soviet H-bomb and nuclear projects (and then both performed remarkable works in different fields of physics, including the theory of elementary particles, plasma physics, astrophysics, and cosmology), in the third decade of the last century, they were engaged with the theory of combustion and detonation and attendant problems of chemical kinetics. Their paper was intended for experts and had a rather specialized character, but one of the problems that they examined can be presented as follows.

Consider the autocatalytic production, destruction, and diffusion transfer of a substance proceeding in a homogeneous active chemical medium that occupies some region of physical space. Such processes obey two fundamental macroscopic relationships, the continuity equation

$$u_t + \operatorname{div} \boldsymbol{J} = f(u)$$

and the phenomenological Fick diffusion law

$$\boldsymbol{J} = -D \operatorname{grad} u \qquad (D = \text{const}).$$

Here, $u = u(\boldsymbol{r}, t)$ is the concentration of the substance at the point $\boldsymbol{r} = \{x, y, z\}$ and moment of time t; the literal subscripts symbolize the derivatives with respect to the corresponding variables; the symbols div and *grad* designate the spatial divergence and gradient operators; $\boldsymbol{J} = \boldsymbol{J}(\boldsymbol{r}, t)$ is the vector of diffusion flux density of the substance; the function $f(u)$ is the kinetic function of th active medium, which determines the dependence of the production/destruction rate of substance per unit volume on the concentration u; and D is diffusivity.

Generally speaking, in a medium of this type, self-sustaining nonlinear concentration waves can propagate, and their velocities will not be arbitrary but will be determined by the balance between two types of processes: the active processes of production/destruction of a substance at each local patch of medium and the passive processes of diffusion transfer between the patches. With the diffusivity taken as unity (this can always be achieved by a proper choice of units of measurements), the wave velocity will depend only on the parameters of the function $f(u)$. The problem consists in finding both the profile of a propagating wave and the wave velocity.

Zeldovich and Frank-Kamenetsky solved the last problem for the case of a one-dimensional infinite medium extending along the x-axis, whose kinetic function is described by a cubic polynomial with three zeros (see below). In this case, the diffusion flux density $\boldsymbol{J}$ has only one nonzero component, the x-component J, and the two equations written above look (at $D = 1$) like

$$u_t + J_x = f(u),$$

$$J = -u_x,$$

or, equivalently,

$$u_t = u_{xx} + f(u), \tag{1}$$

where $f(u)$ is given as

$$f(u) = -Ku(u - b)(u - 1), \tag{2}$$

where K is a positive constant and b is a constant ($0 < b < 1$). The reaction-diffusion equation (1) endowed with the kinetic function (2) is referred today to as the Zeldovich–Frank-Kamenetsky (ZF) equation. As its authors have noted, the cubic polynomial structure of (2) corresponds to autocatalysis of the second order.

The active chemical medium described by the ZF equation is bistable: it has two homogeneous stable

states described by two trivial solutions $u(x,t)\equiv 0$, $u(x,t)\equiv 1$ of Equation (1), which are determined by zeros $u=0, 1$ of the kinetic function (2). Its third homogeneous state $u(x,t)\equiv b$, which is determined by intermediate zero b of $f(u)$ and located between 0 and 1, is unstable; it plays the role of a threshold. Testing the stability of these states proceeds as follows.

Let $u=u_*$, $u_*\in\{0, b, 1\}$ be a coordinate of one of three zeros of the kinetic function, and $k_*=f_u(u_*)$, $k_*\in\{k_0, k_b, k_1\}$ be the slope of the kinetic function at this zero; note that the values of k_* satisfy the inequalities

$k_0 = f_u(0) = -Kb < 0,$
$k_b = f_u(b) = Kb(1-b) > 0,$
$k_1 = f_u(1) = -K(1-b) < 0.$

Next, find the solution to Equation (1) in form of $u(x,t)=u_*+w(x,t)$, where

$$w(x,t)=\omega(x,t)\exp(k_*t)$$
$$w(x,0)=\omega(x,0)=w_0(x),$$
$$|w_0(x)|\ll 1$$

is the perturbation, supposed to be small at moments of time close to $t=0$. Substituting these expressions into (1) and linearizing the kinetic function, one comes to the usual diffusion equation $\omega_t=\omega_{xx}$. The solution of the latter, defining on the infinite x-axis and satisfying the initial condition $\omega(x,0)=w_0(x)$ is well known to be given by Poisson's formula. Recopying this solution and multiplying it by the factor $\exp(k_*t)$ yields the expression

$$w(x,t) = 2^{-1}(\pi t)^{-1/2}\exp(k_*t) \times\int_{-\infty}^{+\infty}\exp\left[-(x-x')^2/4t\right]w_0(x')\,dx',$$

which describes the time evolution of perturbation. Examination of this expression indicates that $w(x,t)$ decreases with time at the values $k_*=k_0<0$ and $k_*=k_1<0$, that is, near the states determined by zeros 0, 1 of function $f(u)$. At $k_*=k_b>0$ (near the state determined by intermediate zero b of function $f(u)$), the perturbation increases because the exponent before the integral rises with time faster than the preexponential factor $2^{-1}(\pi t)^{-1/2}$ falls.

For physical reasons, a bistable medium obeying the ZF equation must maintain the propagation of nonlinear wave fronts, which switch the medium from one of its two stable states to the other. For example, a wave of this type can be obtained numerically by setting the initial conditions $u(x,0)=1$ at $x<0$, $u(x,0)=0$ at $x>0$. In the steady-state regime, which is established after some transition time, the switching wave moves along x with constant velocity v and possesses a steady spatial profile, which is described by the traveling-wave front solution of a ZF equation of the kind

$$u=u(\xi),\quad \xi=x-vt, \tag{3}$$

$$u(-\infty)=1,\quad u(+\infty)=0, \tag{4}$$

$$|u(\xi)|<\infty. \tag{5}$$

Obtaining this solution is a principal goal of the ZF analysis. It includes both the problem of derivation of $u(\xi)$ and the relevant problem of determination of v. Of course, the latter problem is a central one: as a rule, it appears every time when one deals with wave propagation in nonlinear reaction-diffusion systems. Zeldovich and Frank-Kamenetsky found the expression for v in the case of (1), (2) to be

$$v=\sqrt{K/2}(1-2b)=\sqrt{2K}\,(1/2-b)\,. \tag{6}$$

This beautiful formula connects the wave front velocity v with the position b of intermediate zero of the cubic kinetic function. In particular, it indicates that v is proportional to the deviation of b from the middle value of u, which is equal to $1/2$. If $b<1/2$ ($b>1/2$), then v is positive (negative), and the wave front, which obeys the boundary conditions (4), (5), moves in the positive (negative) direction of the x-axis. If b is exactly equal to $1/2$, then the front does not move: it is stationary.

A short derivation of (6) along with the expression for $u(\xi)$ proceeds as follows. First, substituting (3) directly into two equations written immediately before (1) (they are evidently equivalent to (1)) and allowing for the relations $\partial/\partial t=-v\,(\mathrm{d}/\mathrm{d}\xi)$, $\partial/\partial x=\mathrm{d}/\mathrm{d}\xi$, which follow from (3), one obtains

$$u_\xi=-J, \tag{7a}$$

$$J_\xi=-vJ+f(u). \tag{7b}$$

Second, dividing (7b) by (7a), one excludes the independent variable (thereupon, the evident equality $J_\xi/u_\xi=J_u$ is used) and reduces Equation (7) to the single equation

$$JJ_u=vJ-f(u). \tag{8}$$

To be integrated correctly, this differential equation must be provided with the proper boundary conditions at the points $u=0$, 1, that is, in the equilibrium states that are achieved by the traveling wave front solution at $\xi\longrightarrow\pm\infty$. To set these conditions, one should know the asymptotic behavior of diffusion flux $J=u_\xi(\xi)$ generated by the traveling wave near the states $u=0$, 1. To recognize it, one represents the unknown solution near these states in the form of $u(\xi)=u_*+w(\xi)$, $u_*\in\{0,1\}$, where $w(\xi)$ is a small perturbation necessarily satisfying the conditions $w(\pm\infty)=0$. Substituting this expression directly into (1) and linearizing the kinetic function yields

$$w_{\xi\xi}+vw_\xi-|k_*|w=0,\quad (k_*=f_u(u_*),$$
$$k_*\in\{k_0,k_1\},\ k_0<0,\ k_1<0),$$

where the negative parameter k_* is presented as the positive constant $|k_*|$ taken with the sign "minus." The

solutions of the last linear ordinary equation, singled out by the conditions $w(\pm\infty) = 0$ look like

$$w = A_1 \exp(\lambda_1 \xi), \quad A_1 = \text{const},$$
$$\lambda_1 = -(v/2) + \sqrt{(v/2)^2 + |k_*|} > 0 \quad (\text{at } \xi \longrightarrow -\infty),$$

$$w = A_2 \exp(\lambda_2 \xi), \quad A_2 = \text{const},$$
$$\lambda_2 = -(v/2) - \sqrt{(v/2)^2 + |k_*|} < 0 \quad (\text{at } \xi \longrightarrow +\infty).$$

Thus, irrespective of the unknown value of velocity v, the traveling-wave front solution $u(\xi)$ approaches its limit values 0, 1 exponentially and therefore, the diffusion flux $J = -u_\xi = -w_\xi$ tends to zero near these values. Hence, the correct boundary conditions to the solution $J(u)$ of Equation (8), which are compatible with the desired traveling wave front solution (3)–(5), look like

$$J(0) = J(1) = 0. \tag{9}$$

Next, Zeldovich and Frank-Kamenetsky assumed the solution to Equation (8) to have the form of a quadratic parabola $J = -\alpha u(u-1)$ (α is a positive constant to be determined), which satisfies conditions (9) automatically. Substituting this expression into (8) and performing the cancellation yields an equation of the sort $P(\alpha, v)u + Q(\alpha, v) = 0$, where $P(\alpha, v)$ and $Q(\alpha, v)$ are set by calculations. Here, u can take any value belonging to the segment $[0, 1]$. Fixing the variable u on its limit value $u = 0$ yields the equation $Q(\alpha, v) = 0$; taking into account the latter and setting $u = 1$ yields the equation $P(\alpha, v) = 0$. Solving these two equations with respect to α and v leads directly to Equation (6) and to the desired expression $J = -\sqrt{K/2}u(u-1)$. Substituting the latter into (7a) and taking the integral (at the condition $u(0) = \frac{1}{2}$) yields the desired profile of the traveling-wave front:

$$u = 1/\left[1 + \exp\left(\sqrt{K/2}\xi\right)\right] = (1/2)\left[1 - \tanh\left(\sqrt{K/8}\xi\right)\right]. \tag{10}$$

To appreciate the significance of this result in the context of current knowledge, we should stress that the problem of finding a traveling-wave solution to the parabolic reaction-diffusion equations dramatically differs from that arising in the case of nonlinear hyperbolic equations. The latter correspond to conservative physical systems and usually possess the first integrals of the kind of integrals describing energy conservation. Such equations have a Hamiltonian structure, which helps to integrate them analytically using different powerful methods (for example, by methods based on the inverse scattering problem). But the ZF equation is dissipative rather than conservative. Thus it is not Hamiltonian: it describes a gradient physical system that shows the dissipation of its free energy during its time evolution. In these circumstances, the analytical integration of reaction-diffusion equation (1) with the arbitrary kinetic function was a challenge. Zeldovich and Frank-Kamenetsky were the first to have recognized the integrable case of this equation and presented its nontrivial solution.

We should emphasize a distinction of the ZF equation from Fisher's equation, which was investigated in 1937, one year before Zeldovich and Frank-Kamenetsky's work.

The form of the Fisher equation is identical to (1), but the corresponding kinetic function is a quadratic polynomial, which possesses only two zeros. Of course, these zeros correspond to two stationary states of an active medium, but only one of them is a stable one, whereas the second is unstable. As a consequence, the Fisher equation admits not only one traveling-wave front solution, but also a continuum of such waves, and either of them is very responsive to the initial conditions. This equation is applicable only to those media in which the processes of spontaneous production of substances occur against the unstable background state.

In contrast to the Fisher equation, the ZF equation describes active media, which possess two stable states, separated by a third, unstable, state playing the role of a threshold of excitation. The natural field of application of the ZF equation covers the class of bistable active media displaying threshold properties. The linear stability analysis, which was first carried out by Zeldovich and Barenblatt in 1959, and subsequent nonlinear stability analyses performed independently by Lingren and Buratti and by Maginu show that traveling-wave fronts propagating in such media are stable (Scott, 2002).

After Zeldovich and Frank-Kamenetsky's work, decades passed before new analytical traveling-wave front solutions to the ZF-like reaction-diffusion equations appeared. They were constructed with the use of different representations of three-zero kinetic function including the piecewise linear and sinusoidal approximations (Scott, 2002, 2003). The significance of these solutions is predetermined by the fact that all of them describe various physical, chemical, and biological phenomena, which, at first glance, have no common ground. Among these are:

- Electric signals propagating along bistable transmission lines of nerve fibers and neuristors (Scott, 2002, 2003);
- Thermal waves switching boiling regimes from nucleate to film boiling near one-dimensional fuel elements (Zhukov et al., 1980);

- Waves of resistance modification in normal metals (Barelko et al., 1983) and superconductors (Gurevich & Mints, 1984), caused by thermal change;
- Gene flows and population waves in spatially distributed biological populations (Svirezev & Pasekov, 1990) and
- Nonlinear processes arising in synergetics (Loskutov & Mikhailov, 1996).

In view of these applications, the importance of Zeldovich and Frank-Kamenetsky's result is established, yet the destiny of their paper of 1938 is strange. The result obtained in it was used in the Soviet Union for processing experimental data on chemical kinetics even before World War II. After the war, when rapid development of research in the field of physiology of nervous impulses and nonlinear physical chemistry took place, Equation (6) for the velocity of a traveling-wave front became familiar to a broad audience of researchers and appeared frequently in papers and monographs. But the manuscript from which this formula was derived for the first time seemed to have been forgotten: the paper has not been cited until recently! Surprisingly, it is absent even in the two-volume edition of Zeldovich's selected works issued in Russia in 1984, in the lifetime of their author. However, as Mikhail Bulgakov has written (in his classic *Master and Margarita*): "manuscripts do not burn." One could add: even if they are devoted to the theory of combustion.

O.A. MORNEV

See also **Diffusion; Flame front; Gradient system; Nerve impulses; Reaction-diffusion systems**

Further Reading

Barelko, V.V., Beibutian, V.M., Volodin, Yu.E. & Zeldovich, Ya.B. 1983. Thermal waves and non-uniform steady states in a $Fe + H_2$ system. *Chemical Engineering Science*, 38(11): 1775–1780

Frank-Kamenetskii, D.A. 1969. *Diffusion and Heat Transfer in Chemical Kinetics*, New York: Plenum Press (original Russian editions, 1947, 1967, 1987)

Gurevich, A.V. & Mints, R.G. 1984. Localized waves in inhomogeneous media. *Soviet Physics – Uspekhi,* 27(1): 19–41

Loskutov, A.Yu. & Mikhailov, A.S. 1996. *Foundations of Synergetics*, 2nd edition, Berlin: Springer (original Russian edition 1990)

Scott, A.C. 2002. *Neuroscience: A Mathematical Primer*, Berlin and New York: Springer

Scott, A.C. 2003. *Nonlinear Science: Emergence and Dynamics of Coherent Structures*, 2nd edition, Oxford and New York: Oxford University Press

Svirezhev, Yu.M. & Pasekov, V.P. 1990. *Fundamentals of Mathematical Evolutionary Genetics*, Dordrecht: Kluwer (original Russian edition 1982)

Zeldovich, Ya.B. & Frank-Kamenetsky, D.A. 1938. K teorii ravnomernogo rasprostraneniya plameni [On the theory of uniform propagation of flame]. *Doklady Akademii Nauk SSSR*, 19(9):693–697

Zhukov, S.A., Barelko, V.V. & Merzhanov, A.G. 1980. Wave processes on heat generating surfaces in pool boiling. *International Journal of Heat Mass Transfer*, 24: 47–55

ZENER DIODE

See **Diodes**

ZERO FIELD STEPS

See **Josephson junctions**

ZERO-DISPERSION LIMITS

The Korteweg–de Vries (KdV) equation with small dispersion

$$\begin{cases} u_t - uu_x + \varepsilon^2 u_{xxx} = 0, \quad t, x \in R, \\ u(x, t = 0; \varepsilon) = u_0(x), \end{cases} \tag{1}$$

is a model for the formation and propagation of dispersive shock waves in one dimension. Let $u(x, t; \varepsilon)$ denote the solution of Cauchy problem (1), where the initial data $u_0(x)$ is smooth and decreases at infinity sufficiently fast. It is known that for $\varepsilon > 0$, no matter how small, the solution of (1) remains smooth for all $t > 0$. For $\varepsilon = 0$, (1) becomes the Cauchy problem for the Hopf equation

$$\begin{cases} u_t - uu_x = 0, \\ u(x, t = 0) = u_0(x). \end{cases} \tag{2}$$

The solution of the Hopf equation can be obtained by the method of characteristics. If the initial data $u_0(x)$ is somewhere increasing, the solution $u(x, t)$ of Equation (2) always has a point (x_c, t_c) of gradient catastrophe where an infinite derivative develops.

After the time of gradient catastrophe t_c, the solution $u(x, t, \varepsilon)$ of (1) develops in the neighborhood of x_c an expanding region filled with rapid modulated oscillations of wavelength of order $1/\varepsilon$. These oscillations are called dispersive shock waves.

Lax and Levermore (1998), performing the zero-dispersion asymptotics for the inverse-scattering problem for the KdV equation, showed that as ε tends to zero, $u(x, t; \varepsilon)$ tends uniformly to the smooth solution $u(x, t)$ of (2) as long as $t < t_c$. For $t > t_c$, the solution $u(x, t; \varepsilon)$ converges weakly in the oscillation region to a limit $\bar{u}(x, t)$ that is not a solution of conservation law (2).

The first example describing dispersive shock waves was proposed by Gurevich and Pitaevski (1973). Their description was rigorously proved by Venakides (1990) who derived the general form of the rapid oscillations. The oscillation zone is approximately described for a short time $t > t_c$ by a modulated periodic wave solution

of the KdV equation:

$$u(x,t,\varepsilon) \simeq V(x,t) + \frac{1}{3}\alpha(x,t) + \Theta\left(\frac{x - Vt + \phi}{\varepsilon}\right), \tag{3}$$

$$V(x,t) = \tfrac{1}{6}(u_1(x,t) + u_2(x,t) + u_3(x,t)) .$$

In the above formula, the term $V(x,t) + \frac{1}{3}\alpha(x,t)$ is the weak limit $\bar{u}(x,t)$ of $u(x,t,\varepsilon)$ as $\varepsilon \to 0$, while the remaining term describes the rapid oscillations. The function Θ is 2π-periodic with zero average, and it can be expressed in terms of elliptic functions. The quantity α defined below and the phase ϕ depend on some functions $u_i(x,t)$, $i = 1, 2, 3$. The functions $u_1(x,t) > u_2(x,t) > u_3(x,t)$ solve the Whitham (1974) modulation equations

$$\partial_t u_i(x,t) - \lambda_i(u_1,u_2,u_3)\partial_x u_i(x,t) = 0, \quad i = 1,2,3, \tag{4}$$

where

$$\lambda_i(u_1,u_2,u_3) = \frac{1}{3}(u_1+u_2+u_3) + \frac{2}{3}\frac{\prod_{j\neq i, j=1}^{3}(u_i - u_j)}{u_i + \alpha}, \tag{5}$$

$$\alpha = -u_3 + (u_3 - u_1)\frac{E(s)}{K(s)} \tag{6}$$

and $K(s)$ and $E(s)$ are the complete elliptic integrals of the first and second kind with modulus $s = (u_2 - u_1)/(u_3 - u_1)$.

The solution $u_1(x,t) > u_2(x,t) > u_3(x,t)$ of the Whitham equations can be plotted in the (x,u) plane as branches of a multivalued function. The solutions of the Hopf equation and the Whitham equations are connected to one another as illustrated in Figure 1(a). The function $u_2(x,t)$ can vary from $u_3(x,t)$ to $u_1(x,t)$. On the $(x, t \geq 0)$ plane, the oscillation region is bounded on one side by the curve $x^-(t)$ where $u_2(x,t) = u_1(x,t)$, and on the other side by the curve $x^+(t)$ where $u_2(x,t) = u_3(x,t)$ (see Figure 1(a)). For $x^-(t) < x < x^+(t)$, the solution of (1) for small ε is approximately given by (3) while outside the interval $[x^-(t), x^+(t)]$ is given by the solution $u(x,t)$ of the Hopf equation (2). At edge $x = x^-(t)$ of the oscillation region, the amplitude of the oscillations vanishes and (3) goes to $u(x,t,\varepsilon)|_{u_1=u_2} \simeq u_3(x,t)$. When $x = x^+(t)$, solution (3) goes to the one-soliton solution of the KdV equation. In general, the oscillation zone grows with time. For generic analytic initial data with a cubic inflection point, the growth in the (x,t) plane of the oscillation zone near the point of gradient catastrophe (x_c, t_c) is described, up to shifts and rescaling, by the semi-cubic law

$$x^{\pm}(t) = x_c \pm a^{\pm}(t - t_c)^{3/2},$$

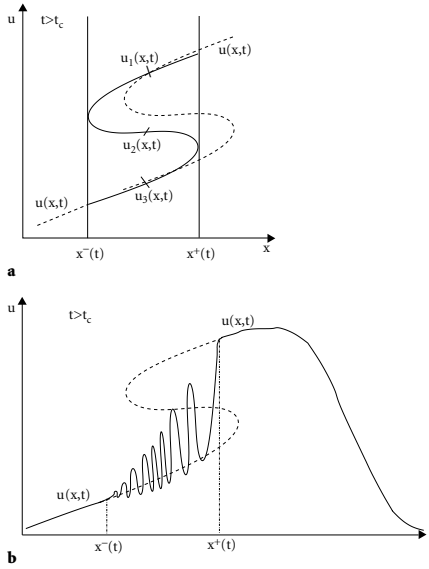

Figure 1. (a) The dashed line represents the formal solution of the Hopf equation; the continuous line represents the solution of the Whitham equations. The solution $(u_1(x,t), u_2(x,t), u_3(x,t))$ of the Whitham equations and the position of the boundaries $x^-(t)$ and $x^+(t)$ are to be determined from the conditions $u(x^-(t),t) = u_3(x^-(t),t)$, $u(x^+(t),t) = u_1(x^+(t),t)$, where $u(x,t)$ is the solution of the Hopf equation. (b) The oscillations in the region $x^-(t_1) < x < x^+(t_1)$.

where $a^{\pm}$ are two positive numbers. A completely different behavior appears in the zero-diffusion case. The simplest equation that combines nonlinearity and diffusion is the Burgers equation

$$u_t - uu_x = \varepsilon u_{xx} , \tag{7}$$

where $\varepsilon > 0$. For smooth initial data $u_0(x)$, the Burgers equation can be integrated through the Cole–Hopf transformation to

$$u(x,t,\varepsilon) = -\frac{\int_{-\infty}^{\infty} \frac{x-\xi}{t} e^{-\frac{G(\xi)}{2\varepsilon}} \, d\xi}{\int_{-\infty}^{\infty} e^{-\frac{G(\xi)}{2\varepsilon}} \, d\xi}, \tag{8}$$

where

$$G(\xi) = -\int_0^{\xi} u_0(\eta)\, d\eta + \frac{(x-\xi)^2}{2t}.$$

The behavior of the exact solution (8) as $\varepsilon \to 0$ can be obtained by observing that the dominant contributions

to the integrals in (8) come from the neighborhood of the stationary points of G where

$$\frac{\partial G}{\partial \xi} = -u_0(\xi) - \frac{x-\xi}{t} = 0. \tag{9}$$

If (9) has only one stationary point, by the application of the steepest descent method, the asymptotic solution $u(x,t;\varepsilon)$ as $\varepsilon \to 0^+$ converges strongly to

$$u(x,t) = u_0(\xi), \quad x = \xi - u_0(\xi)t. \tag{10}$$

The above is exactly the solution of the Cauchy problem for the Hopf equation (2). The stationary point $\xi(x,t)$ of (9) becomes the characteristic variable in (10). For bump-like initial data the solution of the Hopf equation (2) has a point of gradient catastrophe (x_c, t_c). After the time $t = t_c$ of gradient catastrophe, (10) gives a multivalued solution: the characteristics of the Hopf equation begin to intersect. For a typical initial pulse, there are usually three characteristics that intersect at each point of the multivalued region; that is, (9) has three solutions $\xi_1(x,t), \xi_2(x,t), \xi_3(x,t), \xi_1 > \xi_2 > \xi_3$. The dominant behavior of the solution of the Burgers equation will be given by the following contributions:

$$u \simeq -\frac{\sum_{i=1}^{3} \frac{x-\xi_i}{t} |G''(\xi_i)|^{-\frac{1}{2}} \mathrm{e}^{-\frac{G(\xi_i)}{2\varepsilon}}}{\sum_{i=1}^{3} |G''(\xi_i)|^{-\frac{1}{2}} \mathrm{e}^{-\frac{G(\xi_i)}{2\varepsilon}}}. \tag{11}$$

Let us suppose that for $x_c < x < x_s$ and $t > t_c$, the function $G(\xi_1(x,t))$ is less than $G(\xi_2(x,t))$ and $G(\xi_3(x,t))$. Then the above expression for u in the limit $\varepsilon \to 0$ reads

$$u \simeq -\frac{x-\xi_1}{t}, \quad x_c < x < x_s, \tag{12}$$

while assuming that for $x > x_s$ $G(\xi_2(x,t)) < G(\xi_1(x,t)), G(\xi_3(x,t))$, we have

$$u \simeq -\frac{x-\xi_2}{t}. \tag{13}$$

In each case, (10) applies to both ξ_1 and ξ_2. Therefore, the solution of the Burgers equation converges as $\varepsilon \to 0^+$ to the solution of the Hopf equation (2) almost everywhere except at the points (x,t) where $G(\xi_i(x,t)) = G(\xi_j(x,t))$, $i \neq j$, $i, j = 1, 2, 3$. For example, in the case treated above, the change over from ξ_1 to ξ_2 occurs when $x = x_s$ where $G(\xi_1) = G(\xi_2)$. Near $x = x_s$ the solution of the Burgers equation as $\varepsilon \to 0^+$ has a transition from (12) to (13) which is called a shock wave. In other words, the solution of the Burgers equation in the zero viscosity limit is given by two different branches of the solution of the Hopf equation joined by a jump at the point x_s. The condition $G(\xi_1) = G(\xi_2)$ reads

$$-\int_0^{\xi_1} u_0(\eta)\,\mathrm{d}\eta + \frac{(x-\xi_1)^2}{2t} = -\int_0^{\xi_2} u_0(\eta)\,\mathrm{d}\eta + \frac{(x-\xi_2)^2}{2t}.$$

Because of (10), the above relation is equivalent to

$$\frac{1}{2}(u_0(\xi_1) + u_0(\xi_2)) = \frac{1}{\xi_1 - \xi_2} \int_{\xi_2}^{\xi_1} u_0(\eta)\,\mathrm{d}\eta, \tag{14}$$

which describes the shock wave. Since the shock occurs at $x = x_s(t)$, $t > t_c$, we also have

$$x_s(t) = \xi_1 - u_0(\xi_1)t, \quad x_s(t) = \xi_2 - u_0(\xi_2)t.$$

The above three equations determine the functions $x_s(t)$, $\xi_1(t)$, and $\xi_2(t)$. The values of $u(x,t)$ on the two sides of the shock are $u^-(x,t) = u_0(\xi_1(x,t))$ and $u^+(x,t) = u_0(\xi_2(x,t))$. The shock speed can be derived by taking the time derivative of the above two equations and reads

$$\frac{\mathrm{d}x_s(t)}{\mathrm{d}t} = -\frac{1}{2}(u_0(\xi_1) + u_0(\xi_2)).$$

Comparison of the above relation with (14) shows that the modulus of the shock speed is equal to the average value of the characteristics velocity $u_0(\eta)$ over the interval $[\xi_1, \xi_2]$.

While the zero-dispersion limits have been studied only for integrable equations such as the KdV or the nonlinear Schrödinger equation, the zero-viscosity limits have been studied for the parabolic equation of the form

$$u_t + [f(u)]_x = \varepsilon u_{xx}, \quad u \in R^n, \ (t,x) \in R \times R^m.$$

The scalar case in several spatial dimensions was investigated by Kruzhkov (1970). The two-component case in one spatial dimension has been studied by DiPerna (1983), while the n-component case in one spatial dimension has been investigated by Bressan (2002).

TAMARA GRAVA

See also **Burgers equation; Constants of motion and conservation laws; Inverse scattering method or transform; Jump phenomena; Modulated waves; Shock waves**

Further Reading

Bressan, A. 2002. Hyperbolic systems of conservation laws in one space dimension. In *Proceedings of the International Congress of Mathematicians,* Beijing, vol. I, Beijing: Higher Education Press, pp. 159–178

DiPerna, R. 1983. Convergence of approximate solutions to conservation laws. *Archive for Rational Mechanics and Analysis*, 82: 27–70

Gurevich, A.G. & Pitaevskii, L.P. 1973. Non-stationary structure of a collisionless shock waves. *JEPT Letters*, 17: 193–195

Kamvissis, S., McLaughlin, K.D.T.-R. & Miller, P.D. 2003. *Semiclassical Soliton Ensembles for the Focusing Nonlinear Schrödinger Equation*, Princeton, NJ: Princeton University Press

Kruzhkov, S. 1970. First order quasi-linear equations with several space variables. *Mathematics of the USSR Sbornik*, 10: 217–243

Lax, P.D. & Levermore, C.D. 1983. The small dispersion limit of the Korteweg de Vries equation, I, II, III. *Communications in Pure and Applied Mathematics*, 36: 253–290, 571-593, 809–830
Novikov, S., Manakov, S.V., Pitaevski, L.P. & Zakharov, V.E. 1984. *Theory of Solitons: The Inverse Scattering Method*, New York: Consultants Bureau
Venakides, S. 1990. The Korteweg–de Vries equations with small dispersion: higher order Lax–Levermore theory. *Communications in Pure and Applied Mathematics*, 43: 335–361
Whitham, G.B. 1974. *Linear and Nonlinear Waves*, New York: Wiley

ZETA FUNCTIONS

See **Randum matrix theory II**

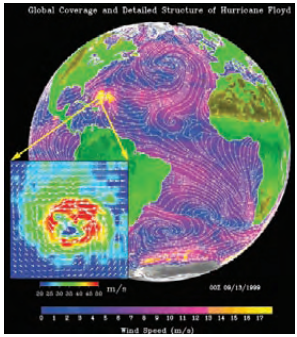

Synoptic view of surface winds over the Atlantic Ocean on September 13, 1999. The background colors indicate wind speeds and the white arrows show the direction of the wind. The high winds of Hurricane Floyd can be seen east of the Bahamas. The images are obtained from the NASA/NOAA sponsored data system Seaflux, at JPL through the courtesy of W. Timothy Liu and Wenqing Tang. (*See* **Atmospheric and ocean sciences; Hurricanes and tornadoes; Vortex dynamics in fluids**.)

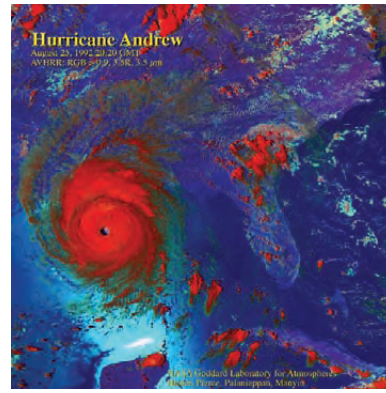

Overhead view of Hurricane Andrew on 25 August 1992 at 20:20 Universal Time (UT). Different wavelengths are assigned to the red, green, and blue channels to make the hurricane appear red. Courtesy of National Oceanic and Atmospheric Administration. (*See* **Atmospheric and ocean sciences; Hurricanes and tornadoes; Vortex dynamics of fluids**.)

Aircraft wake vortex visualized by colored smoke. NASA's Wake Vortex Study at Wallops Island, 1990. Courtesy of NASA Langley Research Center. (*See* **Fluid dynamics; Vortex dynamics in fluids.**)

The planet Jupiter showing the Great Red spot, photographed by the NASA Cassini satellite on December 29, 2000. Courtesy NASA/JPL/ Space Science Institute. (*See* **Fluid dynamics; Jupiter's Great Red spot; Vortex dynamics of fluids.**)

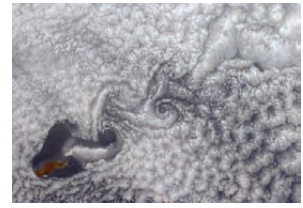

An atmospheric flow pattern known as the von Karman vortex street—a linear chain of spiral eddies. The vortex pattern is made visible by the marine stratocumulus clouds around Guadalupe Island, which is about 22 miles long and lies about 250 miles southwest of San Diego. Multi-angle Imaging Spectroradiometer (MISR) images from June 11, 2000: NASA/ GSFC/JPL, MISR Team. (*See* **Fluid dynamics; Turbulence; Vortex dynamics of fluids**.)

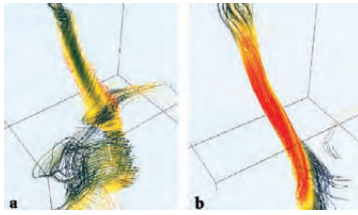

Close-up view of coherent vortex structure from direct numerical simulation of homogeneous isotropic turbulence: (a) streamlines, and (b) vortex lines—color-coded according to intensity—forming a tangle of space curves in a reference box (tropicity domain). Courtesy of Z.-S. She, E. Jackson and S.A. Orszag, Princeton University, Princeton, NJ, USA. (*See* **Structural complexity; Turbulence**.)

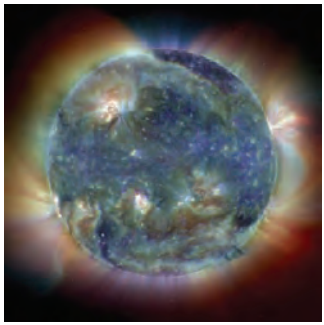

The Sun, imaged in three color-coded wavelengths (171, 195 and 284 angstrom), showing solar flares (sun spots) comprising coronal mass ejections which launch solar winds. Courtesy of SOHO/Extreme Ultraviolet Imaging Telescope (EIT) consortium. SOHO is a project of international cooperation between ESA and NASA. (*See* **Alfvén waves; Nonlinear plasma waves**.)

Pumice and ash erupting from Mount St. Helens on May 18, 1980 is a powerful example of turbulent dispersion of small particles. The plume eventually reached 12 to 15 miles (20–25 km) above sea level. Photograph by Donald A. Swanson, USGS/CVO. (*See* **Evaporation waves; Plume dynamics**.)

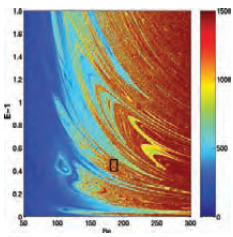

Lifetimes of perturbations in a planar shear flow for different values of initial energy (E) and Reynolds number (Re). In the transition region the lifetimes show a sensitive dependence on initial conditions and huge fluctuations. Similar behavior has been observed in plane Couette flow and in pipe flow. (*See* **Fluid dynamics; Shear flow**.)

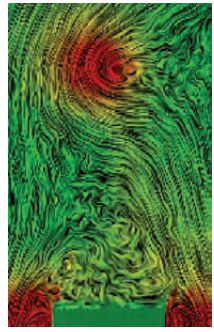

Red and green colors predominate in this view of the Aurora Australis photographed from the Space Shuttle in May 1991. Long a source of myth, auroras are known from late nineteenth-century studies by Kristian Birkeland to be driven by solar wind and stabilized by Earth's magnetosphere. Photograph by the STS-39 Crew, courtesy of Earth Sciences and Image Analysis Laboratory, NASA Johnson Space Center. (*See* **Alfvén waves; Nonlinear plasma waves**.)

Turbulent clouds of hydrogen gas mix with small amounts of oxygen, sulfur, and other elements in this Hubble Space Telescope image of a region of M17, a nebula about 5,500 light-years away that is giving birth to new stars. Ultraviolet energy from hot, young stars in the nebula causes the gas to glow, and the intense heat and pressure cause turbulence. The different colors represent different gases. Courtesy of NASA/ESA/J. Hester (ASU). (*See* **Galaxies**.)

A slice from a three-dimensional numerical simulation of turbulent flow around a square cylinder (visible at the bottom of the image). The data is visualized using the spot noise technique to show flow structure, color shows the pressure. Simulation by R. Verstappen and A. Veldman of the University of Groningen in the Netherlands, and visualization by W. de Leeuw and R. van Liere of the Center of Mathematics and Computer Science in Amsterdam. (*See* **Fluid dynamics; Turbulence**.)

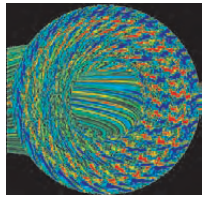

Snapshot of the results of a simulation for a toroidal magnetic confinement system called a tokamak. Contours of **E**×**B** reveal ballooning turbulence. Turbulence is on a relatively short scale perpendicular to the magnetic field and very extended along the magnetic field lines. The eddies tend to point preferentially in the direction of positive (bad) magnetic curvature. Photograph courtesy of Gary Kerbel, National Energy Research Supercomputer Center. (*See* **Nonlinear plasma waves**.)

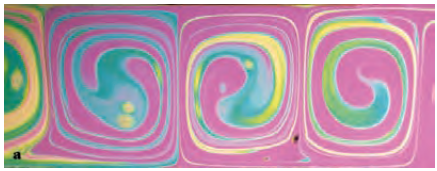

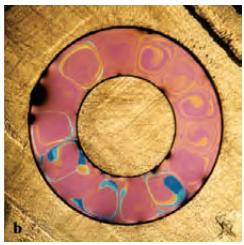

Electrically driven convection in a smectic (the most ordered phase) liquid crystal film. (a) A nonuniformly thick film is freely suspended between two wires about 1mm apart. The film itself is less than 1 micron thick, and shows bright interference colors under reflected white light, like a soap bubble. The film convects when a DC voltage of a few volts is applied to the wires. The vortex flow is visualized as it advects the thickness variations. The driving mechanism involves the field coupling to the surface charge which develops on the film's two free surfaces. This system forms a simple one-dimensional nonlinear pattern which has been quantitatively studied in films with perfectly uniform thickness, for which no color variation is visible. (b) As in the previous figure, now with annular electrodes and a radial driving force. One can also rotate the inner electrode and thus study convection superposed on a two-dimensional circular Couette flow. Images courtesy of Stephen W. Morris, University of Toronto. (*See* **Liquid crystals; Spatiotemporal chaos; Thermal convection**.)

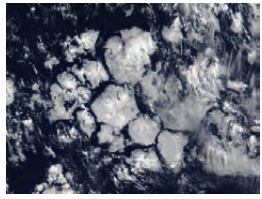

Closed Rayleigh–Bénard convection cells in clouds over the South Atlantic Ocean. NASA/GSFC. (*See* **Atmospheric and ocean sciences; Fluid dynamics; Pattern formation; Thermal convection**.)

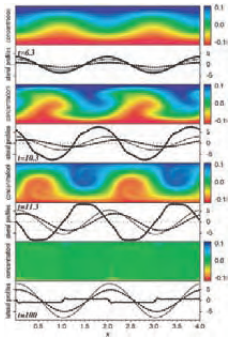

Evolution of oscillatory convection in a binary fluid layer heated from below. The concentration distribution in a vertical cross section of the fluid layer is displayed by color coded plots with blue and red denoting high and low concentration, respectively. Wave profiles at midheight are shown for the fields of vertical velocity (thin lines), temperature (lines with triangles), and concentration (lines with squares). Initially a standing wave grows ($t = 6.3$). It breaks at $t = 10.3$ and is thereby transformed into a fast traveling wave propagating to the left which then slows down. For better visibility two wavelengths are shown. (*See* **Fluid dynamics; Rayleigh–Taylor instability; Thermo-diffusion effects**.)

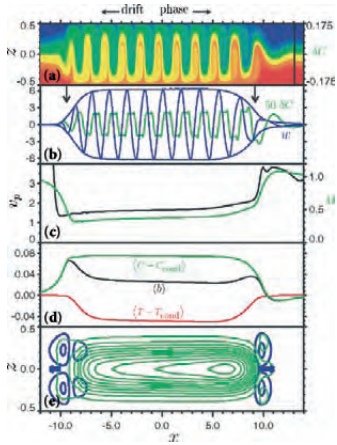

Spatially confined convection in binary fluid mixtures in the form of a localized traveling wave. (a) Concentration deviation (δC) from global mean (light green/yellow) in a vertical cross section of the layer. (b) Lateral wave profiles at midheight, $z = 0$, of δC (green), vertical velocity w (blue), and its envelope. (c) Phase velocity v_p (black) and mixing number M (green) measuring rms deviations of concentration. (d) Time averaged deviations from the conductive state at $z = -0.25$ for concentration (green), temperature (red), and their sum ($\langle b \rangle$) measuring the convective contribution to the buoyancy. (e) Streamlines of time averaged concentration current $\langle \boldsymbol{J} \rangle$ (green) and velocity field $\langle \boldsymbol{u} \rangle$ (blue). Thick blue and green arrows indicate $\langle \boldsymbol{u} \rangle$ and transport of positive δC (alcohol surplus), respectively. Thus, in the lower half of the layer negative δC (water surplus) is transported to the right. (*See* **Fluid dynamics; Thermo-diffusion effects**.)

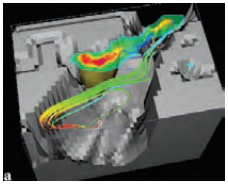

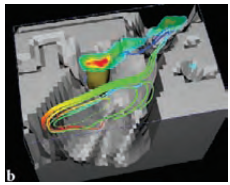

Numerical results from a coupled atmosphere-ocean model of the North Atlantic circulation including bottom topography (a) now and (b) the prediction for 100 years from now. Noticeable are the divergence of the Gulf Stream in the North Atlantic, reduction in the production of deep cold water masses near Greenland, and slowing of part of the global conveyor belt. Relevant streamlines of the general circulation are colored according to their temperature (red=warm, blue=cold). Courtesy of the Deutsches Klimarechenzentrum (Michael Böttinger, DKRZ, Hamburg, Germany). (*See* **Atmospheric and ocean sciences**.)

Snowflakes on a window pane. Ice crystals are now recognized as examples of nonlinear pattern formation. (*See* **Growth patterns; Pattern formation**.)

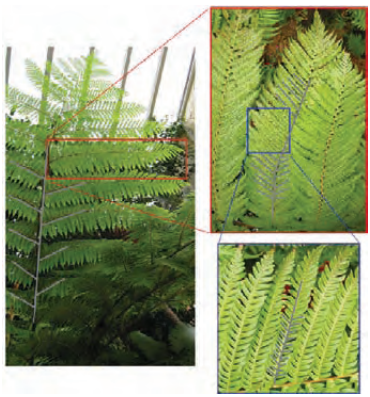

Self similarity of a fern frond. There is a limit to the range of scales at which the self similarity is maintained, and it occurs at only a few discrete scales. Courtesy of Paul Bourke. (*See* **Fractals; Turing patterns**.)

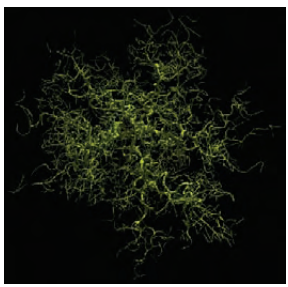

Computer simulation of growth in three dimensions by diffusion-limited aggregation. Such growth patterns are natural fractals. Courtesy of Paul Bourke. (*See* **Cluster coagulation; Fractals; Growth patterns**.)

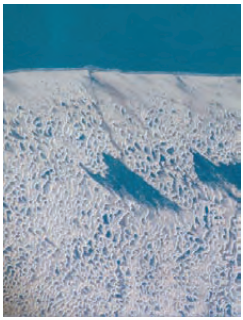

Dune fields with a regular pattern, Lençóis Maranhenses National Park, on Brazil's north coast. Image courtesy of Earth Sciences and Image Analysis Laboratory, NASA Johnson Space Center, ISS007-E-15177. (*See* **Dune Formation; Geomorphology and tectonics; Pattern formation**.)

Bacterial colonies develop complex spatiotemporal patterns in response to adverse conditions such as nutrient starvation. (a) Branching pattern in a Petri dish of *Paenibacillus dendritiformis*. Growth rate is limited by diffusion of nutrients towards the colony, giving a branching or fractal pattern. (b) Vortex branching exhibited by *Paenibacillus vortex* bacteria. At the dark dot at the tip of each of the branches, millions of bacteria rotate in a highly organized vortex. Chemorepellents push the vortices outwards, allowing the colony to expand. Images courtesy of Eshel Ben Jacob, Tel Aviv University. (*See* **Cluster coagulation**; **Growth patterns**.)

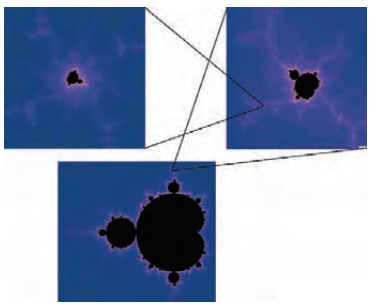

Approximate self similarity in the Mandelbrot set. The Mandelbrot set is the set of all c for which the iteration $z \rightarrow z^2+c$, starting from $z=0$, does not diverge to infinity. This set is named after the mathematician Benoit Mandelbrot, who discovered their fractal and self replicating structure. Three successive magnifications are shown, and at each level a structure similar, but not exactly the same, as the entire set is observed. Courtesy of Paul Bourke. (*See* **Fractals; Multifractal analysis**.)

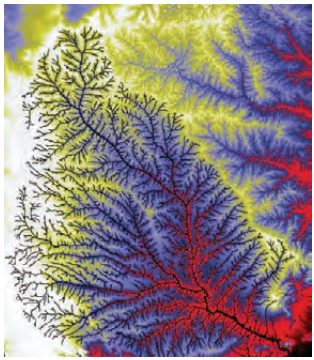

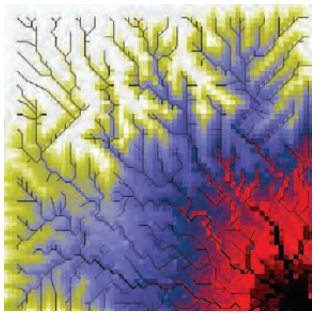

Drainage networks have scale-invariant (fractal) symmetry. Top: Color image of elevation (white/yellow = high elevation black/red = low elevation) and drainage network (black lines) for a river basin in the Loess Plateau region of the Shanxi Province, P.R.C. River basins in homogeneous material such as loess (a silty soil deposited by wind storms) form particularly symmetric and ordered networks. Bottom: Color image of elevation for a fluvial landscape evolution simulation. Courtesy of Jon Pelletier, University of Arizona. (*See* **Geomorphology and tectonics**.)

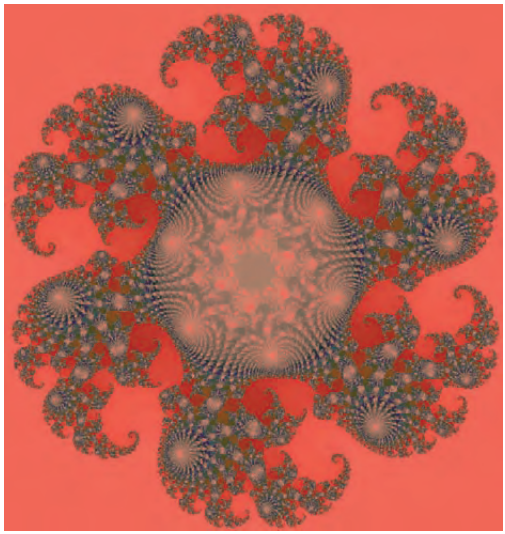

The elephants image is a Julia set with an unusual initialization scheme. The image plane is mapped to the 3rd power of the pixel coordinate. This has the effect of increasing symmetrical order. Maximim iterations/ pixel = 1024, center coordinates = $(+3.4861\times10^{-14}, -4.88498\times10^{-15})$, magnification = 0.9662319. The Julia set coordinate, p1 = (0.28767393, 0.01500042), $z = \text{pixel}^3$: $z = z^2 + p1$, ($|z| \leq 4$.) Image courtesy of Noel Giffin. (*See* **Maps in the complex plane.**)

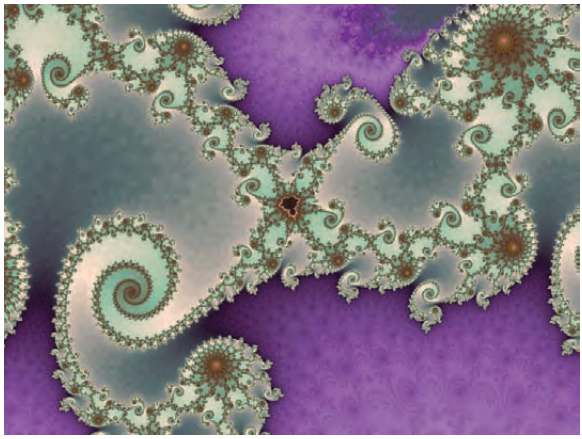

A classic Mandelbrot image created with high iteration limits. Maximum iterations/pixel = 300,000, minimum iterations/pixel = 9587, center coordinates = (+0.37873904887513700, +0.22838619041160610), magnification = 8.279722×10^{10}. High iteration fractals can reveal striking fractal detail as the iteration count and zoom depth increase. A logarithmic coloring algorithm is used to distribute the color pallette over the large iterative range. Image courtesy of Noel Giffin. (*See* **Maps in the complex plane.**)

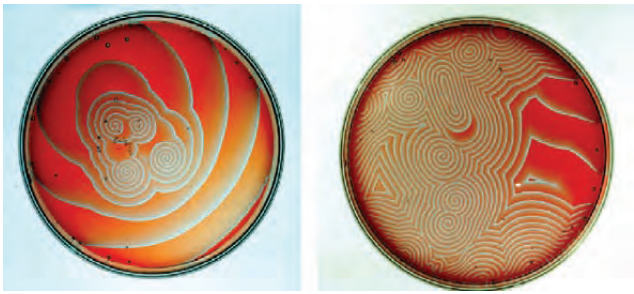

Spiral wave patterns in a BZ reaction, confined to a thin layer in a petri dish. Early on in the reaction, the fronts of the target pattern are far apart, but as the reaction proceeds they become closer and additional wave sources appear, producing a complicated pattern. Courtesy of S.K. Scott, University of Leeds. (*See* **Belousov–Zhabotinsky reaction; Chaotic dynamics; Reaction-diffusion systems**.)

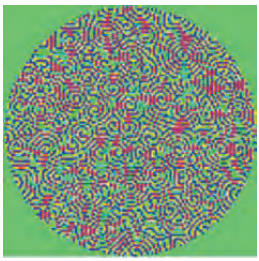

Simulation of spiral defect chaos in Rayleigh–Bénard convection. Color corresponds to temperature, increasing from violet to red. Local spirals are erratic in time—changing position and size. Courtesy of James D. Gunton, Lehigh University. (*See* **Spatiotemporal chaos; Spiral waves; Thermal convection**.)

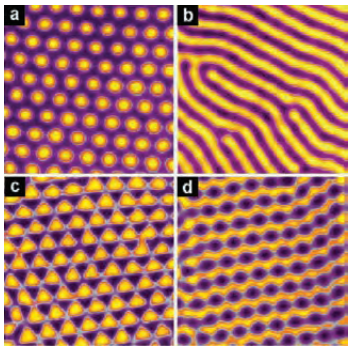

Turing structures of different symmetries obtained with the chlorite-iodide-malonic acid reaction. Dark and light regions respectively correspond to high and low iodide concentration. The wavelength (a function of kinetic parameters and diffusion coefficients) is of the order of 0.2 mm. All patterns in (a)–(d) are at the same scale: view size 1.7 mm × 1.7 mm. Courtesy P. De Kepper, CRPP. (*See* **Turing patterns**.)

A montage of planetary images taken by spacecraft managed by the Jet Propulsion Laboratory in Pasadena, CA. (Pluto is not shown.) The emergence of our planets from a cloud of gas and dust about 4.5 billion years ago was a highly nonlinear event. In his work to solve the three-body problem of planetary motion, Henri Poincaré first formulated the basic concepts of chaotic dynamics. Courtesy of NASA. (*See* ***N*-body problem; Solar system**.)

Re-creation of the famous 1834 first sighting of a soliton or solitary wave on the Union Canal near Edinburgh, 12 July 1995. Copyright Heriot-Watt University, used with permission. (*See* **Solitons, a brief history.)**

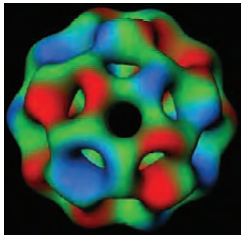

The baryon density isosurface of a 17-Skyrmion (topological charge of 17). The color represents the value of the third component of the pion field. (*See* **Skyrmions**.)

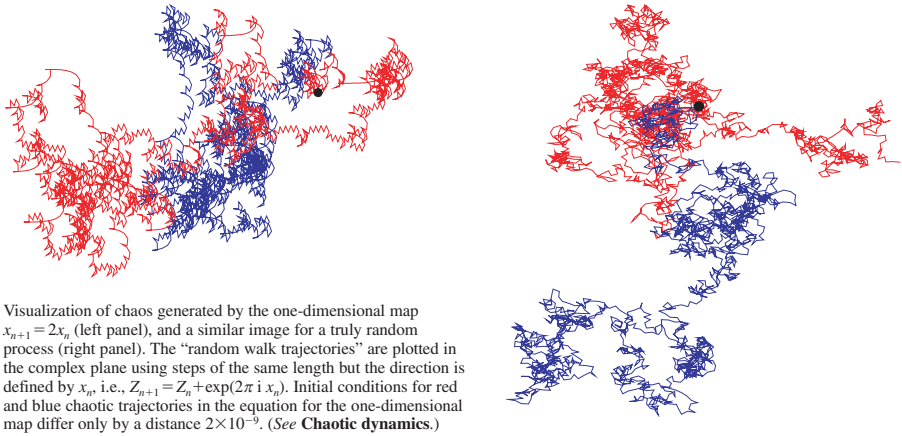

Visualization of chaos generated by the one-dimensional map $x_{n+1} = 2x_n$ (left panel), and a similar image for a truly random process (right panel). The "random walk trajectories" are plotted in the complex plane using steps of the same length but the direction is defined by x_n, i.e., $Z_{n+1} = Z_n + \exp(2\pi\, i\, x_n)$. Initial conditions for red and blue chaotic trajectories in the equation for the one-dimensional map differ only by a distance 2×10^{-9}. (*See* **Chaotic dynamics**.)

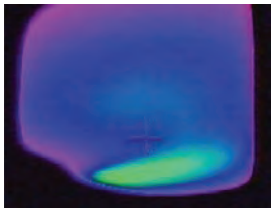

Infrared image of a spin mode in the free-radical-frontal polymerization of an acrylate in a 1.5 cm diameter tube. Image courtesy of J. Pojman. (*See* **Polymerization**.)

Numerical simulations of a dripping water faucet. The dripping faucet is a familiar example of chaotic dynamics. (*See* **Chaotic dynamics; Dripping faucet**.)

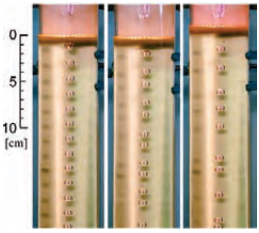

Dripping patterns of water drops falling from a nozzle (7 mm inner diameter and 10 mm outer diameter) into a transparent cylindrical container of salad oil, which sensitively depends on the flow rate. The salad oil was used only to decrease the acceleration of the drops to obtain successive pictures. Examples of period-one (left), period-two (middle) and chaos (right) are presented. (*See* **Dripping faucet**.)

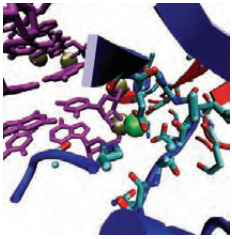

RNA polymerase active site. The DNA template and growing RNA strands are shown in purple with gold phosphorous atoms; the protein backbone is shown in blue; protein atoms are colored red for oxygen, blue-green for carbon, and blue for nitrogen. The green sphere is a magnesium ion, which coordinates both the protein and the nucleotide tri-phosphate which is being added to the growing DNA strand. Atomic coordinates are available using the protein data bank accession code 1I6H. Produced with VMD. (*See* **Protein structure**.)

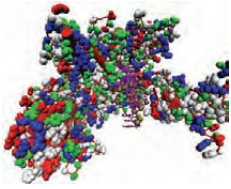

RNA polymerase catalytic subunit with DNA bound at the catalytic site. The nucleic acids are shown in purple, as in active site figure. The protein backbone is shown in red, with amino acid side chains colored according to charge and polarity; negatively charged amino acids are red, positively charged amino acids are blue, non-polar amino acids are white, and polar but uncharged amino acids are green. The patterns of charge, hydrogen bonds, and shape are recognized by other proteins in order to regulate activity of this protein. (*See* **Protein dynamics**.)

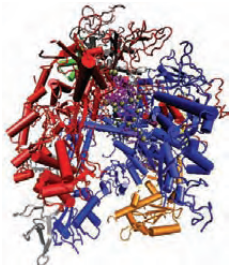

RNA polymerase transcription initiation complex, shown with several of the additional proteins necessary for it to function. Different colors represent different proteins interacting with the catalytic subunit. The interactions are quite specific. (*See* **Protein dynamics**.)

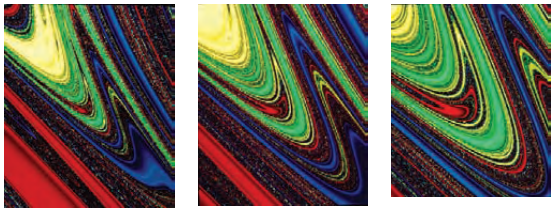

A periodically forced damped pendulum has complex behavior. These computer-generated images show initial positions that map to one of several different behaviors (one color for each). For example, orbits starting at points in the blue region would yield a different type of asymptotic motion than orbits starting in the red region. The brighter the shade of color, the longer it takes to settle into the corresponding motion. The different regions are separated by fractal basin boundaries. The pictures are made at increasing magnification levels. Courtesy, University of Maryland Chaos Group. (*See* **Attractors; Damped-driven anharmonic oscillator; Pendulum**.)

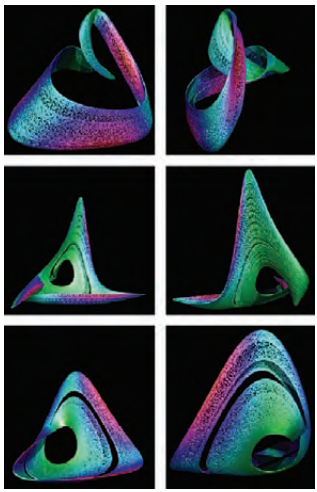

Three chaotic attractors arising from numerical solutions of a spatially homogeneous model of the mammalian electroencephalogram. Each attractor was constructed by delay-embedding a single state variable corresponding to the electroencephalographic observable. Attractors were rendered from two different viewpoints (left and right images), from 100,000 point time series of 10 seconds total duration and colored by velocity. All attractors have a dominant frequency of oscillation in the electroencephalographic alpha band (8–13 Hz). The top attractor has a Lyapunov dimension of 2.086 ± 0.003, representing an upper bound for the correlation (D_2) dimension. Graphics by Paul Bourke, Centre for Astronomy and Supercomputing, Swinburne University of Technology, Melbourne, Australia. (*See* **Electroencephalogram at mesoscopic scales**.)

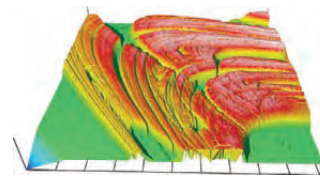

Chaos in a spatially homogeneous version of Liley et al.'s theory of the mammalian electroencephalogram. The two independent axes represent neuronal population input parameters, whereas the dependent variable (indicated by height and color) represents the largest Lyapunov exponent (LLE) of the system dynamics. Each point in this plane can be thought of as indexing a particular attractor (see previous figure). Green represents limit cycle ($LLE = 0$) activity, whereas points above and below this plane correspond to chaos ($LLE > 0$) and point attractor dynamics ($LLE < 0$) respectively. (*See* **Electroencephalogram at mesoscopic scales**.)

Standard Map (a): Dynamics of the standard map for $k = 0.6$; (b). Dynamics of the standard map for $k = 2.0$; (c). Dynamics of the standard map for $k = k_{cr}(\gamma) = 0.971635406$. (*See* **Standard map.**)

Smale's solenoid, an Axiom-A attractor. At each iteration, the fat torus is mapped into a long, thin torus which is then put back into the original torus, winding around twice. Reprinted from *A First Course in Dynamics*, Hasselblatt & Katok with the permission of Cambridge University Press. (*See* **Anosov and Axiom A systems**.)

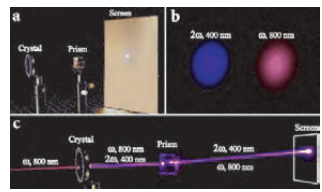

Second harmonic generation in lithium niobate: (a) Experimental setup; (b) Closeup view of the observation screen showing the fundamental and second-harmonic light; (c) Side view showing the partial conversion of the red 800-nm incident beam into the blue 400-nm beam; the separation of the colors by the prism is relatively small in the plane of this photograph. (*See* **Frequency doubling.**)

The Universal Book of Mathematics

From **A**bracadabra to **Z**eno's Paradoxes

David Darling

WILEY
John Wiley & Sons, Inc.

The Universal Book of Mathematics

The Universal Book of Mathematics

From **A**bracadabra to **Z**eno's Paradoxes

David Darling

WILEY
John Wiley & Sons, Inc.

This book is printed on acid-free paper. ♾

Copyright © 2004 by David Darling. All rights reserved

Published by John Wiley & Sons, Inc., Hoboken, New Jersey
Published simultaneously in Canada

No part of this publication may be reproduced, stored in a retrieval system, or transmitted in any form or by any means, electronic, mechanical, photocopying, recording, scanning, or otherwise, except as permitted under Section 107 or 108 of the 1976 United States Copyright Act, without either the prior written permission of the Publisher, or authorization through payment of the appropriate per-copy fee to the Copyright Clearance Center, 222 Rosewood Drive, Danvers, MA 01923, (978) 750-8400, fax (978) 646-8600, or on the web at www.copyright.com. Requests to the Publisher for permission should be addressed to the Permissions Department, John Wiley & Sons, Inc., 111 River Street, Hoboken, NJ 07030, (201) 748-6011, fax (201) 748-6008.

Limit of Liability/Disclaimer of Warranty: While the publisher and the author have used their best efforts in preparing this book, they make no representations or warranties with respect to the accuracy or completeness of the contents of this book and specifically disclaim any implied warranties of merchantability or fitness for a particular purpose. No warranty may be created or extended by sales representatives or written sales materials. The advice and strategies contained herein may not be suitable for your situation. You should consult with a professional where appropriate. Neither the publisher nor the author shall be liable for any loss of profit or any other commercial damages, including but not limited to special, incidental, consequential, or other damages.

For general information about our other products and services, please contact our Customer Care Department within the United States at (800) 762-2974, outside the United States at (317) 572-3993 or fax (317) 572-4002.

Wiley also publishes its books in a variety of electronic formats. Some content that appears in print may not be available in electronic books. For more information about Wiley products, visit our web site at www.wiley.com.

Library of Congress Cataloging-in-Publication Data:

Darling, David J.
The universal book of mathematics : from abracadabra to Zeno's paradoxes / David Darling.
p. cm.
Includes bibliographical references and index.
ISBN 0-471-27047-4 (cloth: alk. paper)
1. Mathematics–Encyclopedias. I. Title.
QA5 .D27 2004
510'.3–dc22 2003024670
Printed in the United States of America

10 9 8 7 6 5 4 3 2 1

Mathematics is not a careful march down a well-cleared highway, but a journey into a strange wilderness, where the explorers often get lost. Rigor should be a signal to the historian that the maps have been made, and the real explorers have gone elsewhere.

–William S. Anglin

But leaving those of the Body, I shall proceed to such Recreation as adorn the Mind; of which those of the Mathematicks are inferior to none.

–William Leybourn (1626–1700)

The last thing one knows when writing a book is what to put first.

–Blaise Pascal (1623–1662)

Contents

Acknowledgments	ix
Introduction	1
Mathematics Entries A to Z	3
References	359
Solutions to Puzzles	369
Category Index	373

Acknowledgments

Many people have helped me enormously in assembling this collection of mathematical oddities, delights, whimsies, and profundities. Thanks especially go to Jan Wassenaar (www.2dcurves.com) for drawing many of the plane curves that are featured in the book; Robert Webb (www.software3d.com) for numerous photos of his wonderful, homemade polyhedra; Jos Leys (www.josleys.com) for his mesmerizing fractal artwork; Xah Lee (www.xahlee.org) for a variety of ingenious digital imagery; Sue and Brian Young at Mr. Puzzle Australia (www.mrpuzzle.com.au) and Kate and Dick Jones at Kadon Enterprises (www.gamepuzzles.com) for their advice and photos of puzzles from their product lines and personal collections; Gideon Weisz (www.gideonweisz.com) and Istvan Orosz for stunning recursive and anamorphic art images; my good friend Andrew "Dogs" Barker for stimulating discussions and the solution to one of the problems; William Waite for pictures from his antique math collection; and Peter Cromwell, Lord & Lady Dunsany, Peter Knoppers, John Lienhard, John Mainstone, David Nicholls, Paul and Colin Roberts, Anders Sandberg, John Sullivan, and others for their valuable contributions.

I'm greatly indebted to Stephen Power, senior editor, and to Lisa Burstiner, senior production editor, at John Wiley & Sons, for their encouragement and unfailing attention to detail, and even proffering of alternative, clever solutions to some of the problems in the book. Any errors that remain are entirely my own responsibility. Thanks also to my marvelous agent, Patricia Van der Leun. And last but most of all, thanks to my family for letting me pursue a career that is really a fantasy.

Introduction

You are lost in a maze: How do you find your way out? You want to build a time machine, but is time travel logically possible? How can one infinity be bigger than another? Why can't you drink from a Klein bottle? What is the biggest number in the world to have a proper name, and how can you write it? Who claimed he could see in the fourth dimension? And what does "iteration" mean? And what does "iteration" mean?

Mathematics was never my strong point in school, but because I wanted to become an astronomer, I was told to stick with it. Fortunately, in my last two years before heading off to university, I had a wonderful old-fashioned, eccentric teacher (he actually wore a black gown when teaching), called Mr. Kay (known to one and all as "Danny"), who would suddenly divert from the chalk and blackboard to ask, "But how did the universe come to be *asymmetric*–that's what I want to know," or "These imaginary numbers are *very* interesting; in part, because they are so remarkably real." During lunch-break, Danny and the senior chemistry teacher, Mr. Erp (whose nickname I need hardly spell out), would always meet in the chemistry prep room for a game of chess. They looked and acted very much like characters from a Wellsian science fiction tale, and I sometimes imagined them musing on formulas for invisibility or doorways to higher dimensions. At any rate, though I was never a shining student, I realize what a profound effect those two deeply imaginative, thoughtful men had on my future career. I did become an astronomer. I did persevere with math to a certain level of competence. But, much more than that, my curiosity was fired by the wonderful and weird possibilities of these subjects: curved space, Möbius bands, parallel universes, patterns in the heart of chaos, alternative realities. These strange possibilities, and a thousand others, make up the stuffing of this book. If you want a comprehensive, academic dictionary of mathematics, look elsewhere. If you want rigor and proof, try the next shelf. Herein you will find only the unusual and the outrageous, the fanciful and the fantastic: a compendium of the mathematics they *didn't* teach you in school.

Entries range from short definitions to lengthy articles on topics of major importance or unusual interest. These are arranged alphabetically according to the first word of the entry name and are extensively cross-referenced. Terms that appear in **bold** type have their own entries. A number of puzzles are included for the reader to try; the answers to these can be found at the back of the book. Also at the back are a comprehensive list of references and a category index. Readers are invited to visit the author's Web site at www.daviddarling.info for the latest news in mathematics and related subjects.

A

abacus

A counting frame that started out, several thousand years ago, as rows of pebbles in the desert sands of the Middle East. The word appears to come from the Hebrew *âbâq* (dust) or the Phoenician *abak* (sand) via the Greek *abax*, which refers to a small tray covered with sand to hold the pebbles steady. The familiar frame-supporting rods or wires, threaded with smoothly running beads, gradually emerged in a variety of places and mathematical forms.

In Europe, there was a strange state of affairs for more than 1,500 years. The Greeks and the Romans, and then the medieval Europeans, calculated on devices with a **place-value system** in which **zero** was represented by an empty line or wire. Yet the written notations didn't have a symbol for zero until it was introduced in Europe in 1202 by **Fibonacci**, via the Arabs and the Hindus.

abacus A special form of the Chinese abacus (c. 1958) consisting of two abaci stacked one on top of the other. *Luis Fernandes*

The Chinese *suan pan* differs from the European abacus in that the board is split into two decks, with two beads on each rod in the upper deck and five beads, representing the digits 0 through 4, on each rod in the bottom. When all five beads on a rod in the lower deck are moved up, they're reset to the original position, and one bead in the top deck is moved down as a carry. When both beads in the upper deck are moved down, they're reset and a bead on the adjacent rod on the left is moved up as a carry. The result of the computation is read off from the beads clustered near the separator beam between the upper and lower decks. In a sense, the abacus works as a 5-2-5-2-5-2 . . . –based number system in which carries and shifts are similar to those in the decimal system. Since each rod represents a digit in a decimal number, the capacity of the abacus is limited only by the number of rods on the abacus. When a user runs out of rods, she simply adds another abacus to the left of the row.

The Japanese *soroban* does away with the dual representations of fives and tens by having only four counters in the lower portion, known as "earth," and only one counter in the upper portion, known as "heaven." The world's largest abacus is in the Science Museum in London and measures 4.7 meters by 2.2 meters.

Abbott, Edwin Abbott (1838–1926)

An English clergyman and author who wrote several theological works and a biography (1885) of Francis Bacon, but is best known for his standard *Shakespearian Grammar* (1870) and the pseudonymously written ***Flatland: A Romance of Many Dimensions*** (by A Square, 1884).[1]

ABC conjecture

A remarkable **conjecture**, first put forward in 1980 by Joseph Oesterle of the University of Paris and David Masser of the Mathematics Institute of the University of Basel in Switzerland, that is now considered one of the most important unsolved problems in **number theory**. If it were proved correct, the proofs of many other famous conjectures and theorems would follow immediately–in some cases in just a few lines. The vastly complex current proof of **Fermat's last theorem**, for example, would reduce to less than a page of mathematical reasoning. The ABC conjecture is disarmingly simple compared to most of the deep questions in number theory and,

moreover, turns out to be equivalent to all the main problems that involve **Diophantine equation**s (equations with integer coefficients and integer solutions).

Only a couple of concepts need to be understood to grasp the ABC conjecture. A *square-free number* is an integer that isn't divisible by the square of any number. For example, 15 and 17 are square-free, but 16 (divisible by 4^2) and 18 (divisible by 3^2) are not. The *square-free part* of an integer *n,* denoted sqp(*n*), is the largest square-free number that can be formed by multiplying the prime factors of *n.* For $n = 15$, the prime factors are 5 and 3, and $3 \times 5 = 15$, a square-free number, so that sqp(15) = 15. On the other hand, for $n = 16$, the prime factors are all 2, which means that sqp(16) = 2. In general, if *n* is square-free, the square-free part of *n* is just *n;* otherwise, sqp(*n*) represents what is left over after all the factors that create a square have been eliminated. In other words, sqp(*n*) is the product of the distinct **prime number**s that divide *n.* For example, sqp(9) = sqp(3×3) = 3 and sqp(1,400) = sqp($2 \times 2 \times 2 \times 5 \times 5 \times 7$) = $2 \times 5 \times 7 = 70$.

The ABC conjecture deals with pairs of numbers that have no common factors. Suppose *A* and *B* are two such numbers that add to give *C.* For example, if $A = 3$ and $B = 7$, then $C = 3 + 7 = 10$. Now, consider the square-free part of the product $A \times B \times C$: sqp(ABC) = sqp($3 \times 7 \times 10$) = 210. For most values of *A* and *B,* sqp(ABC) > *C,* as in the prior example. In other words, sqp(ABC)/$C > 1$. Occasionally, however, this isn't true. For instance, if $A = 1$ and $B = 8$, then $C = 1 + 8 = 9$, sqp(ABC) = sqp($1 \times 8 \times 9$) = sqp($1 \times 2 \times 2 \times 2 \times 3 \times 3$) = $1 \times 2 \times 3 = 6$, and sqp(ABC)/C = $^6/_9$ = $^2/_3$. Similarly, if $A = 3$ and $B = 125$, the ratio is $^{15}/_{64}$.

David Masser proved that the ratio sqp(ABC)/C can get arbitrarily small. In other words, given any number greater than zero, no matter how small, it's possible to find integers *A* and *B* for which sqp(ABC)/C is smaller than this number. In contrast, the ABC conjecture says that [sqp(ABC)]^n/C reaches a minimum value if *n* is any number greater than 1—even a number such as 1.0000000001, which is only barely larger than 1. The tiny change in the expression results in a huge difference in its mathematical behavior. The ABC conjecture in effect translates an infinite number of Diophantine equations (including the equation of Fermat's last theorem) into a single mathematical statement.[144]

Abel, Niels Henrik (1802–1829)

> *The divergent series are the invention of the devil, and it is a shame to base on them any demonstration whatsoever. By using them, one may draw any conclusion he pleases and that is why these series have produced so many fallacies and so many paradoxes.*

A Norwegian mathematician who, independently of his contemporary Évariste **Galois**, pioneered **group** theory and proved that there are no algebraic solutions of the general **quintic** equation. Both Abel and Galois died tragically young—Abel of tuberculosis, Galois in a sword fight.

While a student in Christiania (now Oslo), Abel thought he had discovered how to solve the general quintic algebraically, but soon corrected himself in a famous pamphlet published in 1824. In this early paper, Abel showed the impossibility of solving the general quintic by means of radicals, thus laying to rest a problem that had perplexed mathematicians since the mid-sixteenth century. Abel, chronically poor throughout his life, was granted a small stipend by the Norwegian government that allowed him to go on a mathematical tour of Germany and France. In Berlin he met Leopold Crelle (1780–1856) and in 1826 helped him found the first journal in the world devoted to mathematical research. Its first three volumes contained 22 of Abel's papers, ensuring lasting fame for both Abel and Crelle. Abel revolutionized the important area of elliptic integrals with his theory of **elliptic function**s, contributed to the theory of **infinite series**, and founded the theory of commutative groups, known today as **Abelian group**s. Yet his work was never properly appreciated during his life, and, impoverished and ill, he returned to Norway unable to obtain a teaching position. Two days after his death, a delayed letter was delivered in which Abel was offered a post at the University of Berlin.

Abelian group

A **group** that is **commutative**, that is, in which the result of multiplying one member of the group by another is independent of the order of multiplication. Abelian groups, named after Niels **Abel**, are of central importance in modern mathematics, most notably in **algebraic topology**. Examples of Abelian groups include the **real number**s (with addition), the nonzero real numbers (with multiplication), and all cyclic groups, such as the **integer**s (with addition).

abracadabra

A word famously used by magicians but which started out as a cabalistic or mystical charm for curing various ailments, including toothache and fever. It was first mentioned in a poem called "Praecepta de Medicina" by the Gnostic physician Quintus Severus Sammonicus in the second century A.D. Sammonicus instructed that the letters be written on parchment in the form of a triangle:

A B R A C A D A B R A
A B R A C A D A B R
A B R A C A D A B
A B R A C A D A
A B R A C A D
A B R A C A
A B R A C
A B R A
A B R
A B
A

This was to be folded into the shape of a cross, worn for nine days suspended from the neck, and, before sunrise, cast behind the patient into a stream running eastward. It was also a popular remedy in the Middle Ages. During the Great Plague, around 1665, large numbers of these amulets were worn as safeguards against infection. The origin of the word itself is uncertain. One theory is that it is based on Abrasax, the name of an Egyptian deity.

PUZZLE

A well-known puzzle, proposed by George Polya (1887–1985), asks how many different ways there are to spell abracadabra in this diamond-shaped arrangement of letters:

A
B B
R R R
A A A A
C C C C C
A A A A A A
D D D D D
A A A A
B B B
R R
A

Solutions begin on page 369.

abscissa

The *x*-coordinate, or horizontal distance from the *y*-axis, in a system of **Cartesian coordinates**. Compare with **ordinate**.

absolute

Not limited by exceptions or conditions. The term is used in many different ways in mathematics, physics, philosophy, and everyday speech. Absolute space and absolute time, which, in Newton's universe, form a unique, immutable frame of reference, blend and become deformable in the **space-time** of Einstein. See also **absolute zero**. In some philosophies, the absolute stands behind the reality we see–independent, transcendent, unconditional, and all-encompassing. The American philosopher Josiah Royce (1855–1916) took the absolute to be a spiritual entity whose self-consciousness is imperfectly reflected in the totality of human thought. Mathematics, too, reaches beyond imagination with its absolute **infinity**. See also **absolute value**.

absolute value

The value of a number without regard to its sign. The absolute value, or *modulus,* of a **real number**, *r,* is the distance of the number from zero measured along the real **number line**, and is denoted $|r|$. Being a distance, it can't be negative; so, for example, $|3| = |-3| = 3$. The same idea applies to the absolute value of a **complex number** $a + ib$, except that, in this case, the complex number is represented by a point on an **Argand diagram**. The absolute value, $|a + ib|$, is the length of the line from the origin to the given point, and is equal to $\sqrt{(a^2 + b^2)}$.

absolute zero

The lowest possible temperature of a substance, equal to 0 Kelvin (K), –273.15°C, or –459.67°F. In classical physics, it is the temperature at which all molecular motion ceases. However, in the "real" world of **quantum mechanics** it isn't possible to stop all motion of the particles making up a substance as this would violate the Heisenberg uncertainty principle. So, at 0 K, particles would still vibrate with a certain small but nonzero energy known as the *zero-point energy.* Temperatures within a few billionths of a degree of absolute zero have been achieved in the laboratory. At such low temperatures, substances have been seen to enter a peculiar state, known as the *Bose-Einstein condensate,* in which their quantum wave functions merge and particles lose their individual identities. Although it is possible to approach ever closer to absolute zero, the third law of thermodynamics asserts that it's impossible to ever attain it. In a deep sense, absolute zero lies at the asymptotic limit of low energy just as the speed of light lies, for particles with mass, at the asymptotic limit of high energy. In both cases, energy of motion (kinetic energy) is the key quantity involved. At the high energy end, as the average speed of the particles of a substance approaches the speed of light, the temperature rises without limit, heading for an unreachable ∞ K.

abstract algebra

To a mathematician, real life is a special case.

–Anonymous

Algebra that is not confined to familiar number systems, such as the **real number**s, but seeks to solve equations

that may involve many other kinds of systems. One of its aims, in fact, is to ask: What other number systems are there? The term *abstract* refers to the perspective taken on the subject, which is very different from that of high school algebra. Rather than looking for the solutions to a particular problem, abstract algebra is interested in such questions as: When does a solution exist? If a solution does exist, is it unique? What general properties does a solution possess? Among the structures it deals with are **group**s, **ring**s, and **field**s. Historically, examples of such structures often arose first in some other field of mathematics, were specified rigorously (axiomatically), and were then studied in their own right in abstract algebra.

Abu'l Wafa (A.D. 940–998)

A Persian mathematician and astronomer who was the first to describe geometrical constructions (see **constructible**) possible only with a straightedge and a fixed compass, later dubbed a "rusty compass," that never alters its radius. He pioneered the use of the tangent function (see **trigonometric function**), apparently discovered the secant and cosecant functions, and compiled tables of sines and tangents at 15′ intervals–work done as part of an investigation into the orbit of the Moon.

abundant number

A number that is smaller than the sum of its **aliquot part**s (proper divisors). Twelve is the smallest abundant number; the sum of its aliquot parts is $1 + 2 + 3 + 4 + 6 = 16$, followed by 18, 20, 24, and 30. A *weird number* is an abundant number that is not *semiperfect;* in other words, n is weird if the sum of its divisors is greater than n, but n is not equal to the sum of any subset of its divisors. The first few weird numbers are 70, 836, 4,030, 5,830, and 7,192. It isn't known if there are any odd weird numbers. A *deficient number* is one that is greater than the sum of its aliquot parts. The first few deficient numbers are 1, 2, 3, 4, 5, 8, and 9. Any divisor of a deficient (or perfect) number is deficient. A number that is not abundant or deficient is known as a **perfect number**.

Achilles and the Tortoise paradox

See **Zeno's paradoxes**.

Ackermann function

One of the most important **function**s in computer science. Its most outstanding property is that it grows astonishingly fast. In fact, it gives rise to **large numbers** so quickly that these numbers, called *Ackermann numbers,* are written in a special way known as **Knuth's up-arrow notation**. The Ackermann function was discovered and studied by Wilhelm Ackermann (1896–1962) in 1928. Ackermann worked as a high school teacher from 1927 to 1961 but was also a student of the great mathematician David **Hilbert** in Göttingen and, from 1953, served as an honorary professor in the university there. Together with Hilbert he published the first modern textbook on mathematical logic. The function he discovered, and that now bears his name, is the simplest example of a well-defined and total function that is also computable but not primitive recursive (PR). "Well-defined and total" means that the function is internally consistent and doesn't break any of the rules laid down to define it. "Computable" means that it can, in principle, be evaluated for all possible input values of its variables. "Primitive recursive" means that it can be computed using only *for loops*–repeated application of a single operation a predetermined number of times. The recursion, or feedback loop, in the Ackermann function overruns the capacity of any *for loop* because the number of loop repetitions isn't known in advance. Instead, this number is itself part of the computation, and grows as the calculation proceeds. The Ackermann function can only be calculated using a *while loop,* which keeps repeating an action until an associated test returns false. Such loops are essential when the programmer doesn't know at the outset how many times the loop will be traversed. (It's now known that everything computable can be programmed using while loops.)

The Ackermann function can be defined as follows:

$$A(0, n) = n + 1 \text{ for } n = 0$$
$$A(m, 0) = A(m - 1, 1) \text{ for } m = 1$$
$$A(m, n) = A(m - 1, A(m, n - 1)) \text{ for } m, n = 1.$$

Two positive integers, m and n, are the input and $A(m, n)$ is the output in the form of another positive integer. The function can be programmed easily in just a few lines of code. The problem isn't the complexity of the function but the awesome rate at which it grows. For example, the innocuous-looking $A(4,2)$ already has 19,729 digits! The use of a powerful large-number shorthand system, such as the up-arrow notation, is indispensable as the following examples show:

$$A(1, n) = 2 + (n + 3) - 3$$
$$A(2, n) = 2 \times (n + 3) - 3$$
$$A(3, n) = 2\uparrow(n + 3) - 3$$
$$A(4, n) = 2\uparrow(2\uparrow(2\uparrow\ (\ldots\uparrow 2))) - 3 \ (n + 3 \text{ twos})$$
$$= 2\uparrow\uparrow(n + 3) - 3$$
$$A(5, n) = 2\uparrow\uparrow\uparrow(n + 3) - 3, \text{ etc.}$$

Intuitively, the Ackermann function defines generalizations of multiplication by 2 (iterated additions) and exponentiation with base 2 (iterated multiplications) to iterated exponentiation, iteration of this operation, and so on.[84]

acre
An old unit of **area**, equal to 160 square rods, 4,840 square yards, 43,560 square feet, or 4,046.856 square meters.

acute
From the Latin *acus* for "needle" (which also forms the root for *acid*, *acupuncture*, and *acumen*). An acute **angle** is less than 90°. An acute **triangle** is one in which all three angles are acute. Compare with **obtuse**.

adjacent
Next to. *Adjacent angles* are next to each other, and thus share one side. *Adjacent sides* of a **polygon** share a vertex.

affine geometry
The study of properties of geometric objects that remain unchanged after parallel projection from one plane to another. During such a projection, first studied by Leonhard **Euler**, each point (x, y) is mapped to a new point $(ax + cy + e, bx + dy + f)$. Circles, angles, and distances are altered by affine transformations and so are of no interest in affine geometry. Affine transformations do, however, preserve collinearity of points: if three points belong to the same straight line, their images (the points that correspond to them) under affine transformations also belong to the same line and, in addition, the middle point remains between the other two points. Similarly, under affine transformations, parallel lines remain parallel; concurrent lines remain concurrent (images of intersecting lines intersect); the ratio of lengths of line segments of a given line remains constant; the ratio of areas of two triangles remains constant; and ellipses, parabolas, and hyperbolas continue to be ellipses, parabolas, and hyperbolas.

age puzzles and tricks
Problems that ask for a person's age or, alternatively, when a person was a certain age, given several roundabout facts. They go back at least 1,500 years to the time of Metrodorus and **Diophantus's riddle**. A number of distinct types of age puzzles sprang up between the sixteenth and early twentieth centuries, in most cases best solved by a little algebra. One form asks: if X is now a years old and Y is now b years old, when will X be c times as old as Y? The single unknown, call it x, can be found from the equation $a + x = c(b + x)$. Another type of problem takes the form: if X is now a times as old as Y and after b years X will be c times as old as Y, how old are X and Y now? In this case the trick is to set up and solve two simultaneous equations: $X = aY$ and $X + b = c(Y + b)$.

PUZZLES

Around 1900, two more variants on the age puzzle became popular. Here is an example of each for the reader to try.

1. Bob is 24. He is twice as old as Alice was when Bob was as old as Alice is now. How old is Alice?
2. The combined ages of Mary and Ann are 44 years. Mary is twice as old as Ann was when Mary was half as old as Ann will be when Ann is three times as old as Mary was when Mary was three times as old as Ann. How old is Ann?"

Solutions begin on page 369.

Various mathematical sleights of hand can seem to conjure up a person's age as if by magic. For example, ask a person to multiply the first number of his or her age by 5, add 3, double this figure, add the second number of his or her age to the figure, and tell you the answer. Deduct 6 from this and you will have their age.

Alternatively, ask the person to pick a number, multiply this by 2, add 5, and multiply by 50. If the person has already had a birthday this year and it's the year 2004, she should add 1,754, otherwise she should add 1,753. Each year after 2004 these numbers need to be increased by 1. Finally, the person should subtract the year they were born. The first digits of the answer are the original number, while the last two digits are the person's age.

Here is one more trick. Take your age, multiply it by 7, then multiply again by 1,443. The result is your age repeated three times. (What you have actually done is multiplied by 10,101; if you multiply by 1,010,101, the repetition is fourfold, and so on.)

Agnesi, Maria Gaetana (1718–1799)
An Italian mathematician and scholar whose name is associated with the curve known as the *Witch of Agnesi.* Born in Milan, Maria was one of 24 children of a professor of mathematics at the University of Bologna. A child prodigy, she could speak seven languages, including Latin, Greek, and Hebrew, by the age of 11 and was solving difficult problems in geometry and ballistics by her early teens. Her father encouraged her studies and her appearance at public debates. However, Maria developed a chronic illness, marked by convulsions and headaches, and, from the age of about 20, withdrew socially and devoted herself to mathematics. Her *Instituzioni analitiche ad uso della gioventu italiana,* published in 1748, became a standard teaching manual, and in 1750, she was appointed to the chair of mathematics and natural philosophy at Bologna. Yet she never fulfilled her early promise in terms of making new

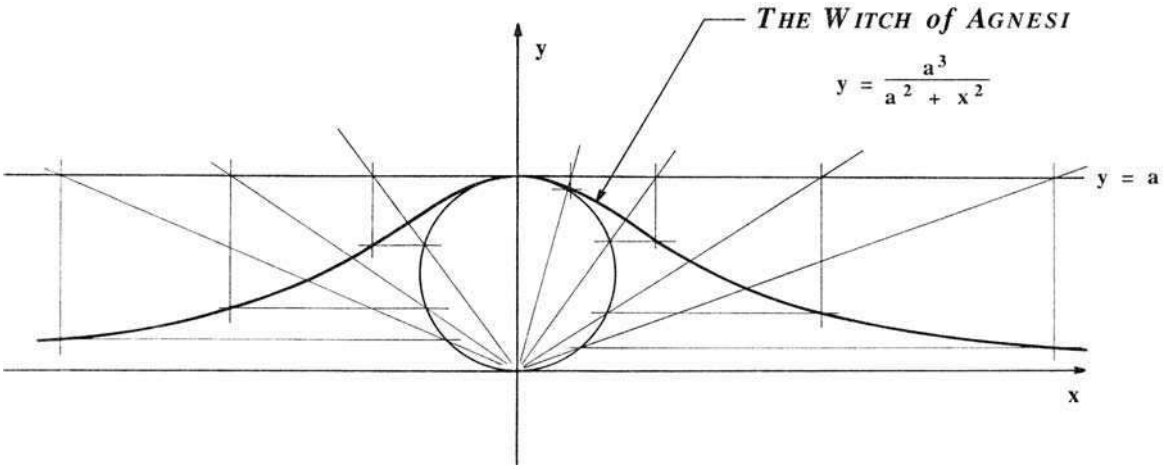

Agnesi, Maria Gaetana The Witch of Agnesi curve. *John H. Lienhard*

breakthroughs. After the death of her father in 1752, she moved into theology and, after serving for some years as the directress of the Hospice Trivulzio for Blue Nuns at Milan, joined the sisterhood herself and ended her days in this austere order.

The famous curve that bears her name had been studied earlier, in 1703, by Pierre de **Fermat** and the Italian mathematician Guido Grandi (1671–1742). Maria wrote about it in her teaching manual and referred to it as the *aversiera,* which simply means "to turn." But in translating this, the British mathematician John Colson (1680–1760), the fifth Lucasian professor of mathematics at Cambridge University, confused *aversiera* with *avversiere* which means "witch," or "wife of the devil." And so the name of the curve came down to us as the Witch of Agnesi. To draw it, start with a circle of diameter *a,* centered at the point (0, *a*/2) on the *y*-axis. Choose a point *A* on the line $y = a$ and connect it to the origin with a line segment. Call the point where the segment crosses the circle *B*. Let *P* be the point where the vertical line through *A* crosses the horizontal line through *B*. The Witch is the curve traced by *P* as *A* moves along the line $y = a$. By a happy coincidence, it does look a bit like a witch's hat! In Cartesian coordinates, its equation is

$$y = a^3/(x^2 + a^2).$$

Ahmes papyrus

See **Rhind papyrus**.

Ahrens, Wilhelm Ernst Martin Georg (1872–1927)

A great German exponent of recreational mathematics whose *Mathematische Unterhaltungen und Spiele*[6] is one of the most scholarly of all books on the subject.

Alcuin (735–804)

A leading intellectual of his time and the probable compiler of *Propositiones ad Acuendos Juvenes* (Problems to sharpen the young), one of the earliest collections of recreational math problems. According to David **Singmaster** and John Hadley: "The text contains 56 problems, including 9 to 11 major types of problem which appear for the first time, 2 major types which appear in the West for the first time and 3 novel variations of known problems. . . . It has recently been realized that the **river-crossing problems** and the crossing-a-desert problem, which appear here for the first time, are probably the earliest known combinatorial problems."

Alcuin was born into a prominent family near the east coast of England. He was sent to York, where he became a pupil and, eventually, in 778, the headmaster, of Archbishop Ecgberht's School. (Ecgberht was the last person to have known the Venerable Bede.) Alcuin built up a superb library and made the school one of the chief centers of learning in Europe. Its reputation became such that, in 781, Alcuin was invited to become master of Charlemagne's Palace School at Aachen and, effectively, minister of education for Charlemagne's empire. He accepted and traveled to Aachen to a meeting of the leading scholars. Subsequently, he was made head of Charlemagne's Palace School and there developed the Carolingian minuscule, a clear, legible script that became the basis of how letters of the present Roman alphabet are written.

Before leaving Aachen, Alcuin was responsible for the most prized of the Carolingian codices, now called the

Golden Gospels: a series of illuminated masterpieces written largely in gold, on white or purple vellum. The development of Carolingian minuscule had, indirectly, a major impact on the history of mathematics. Because it was a far more easily readable script than the older unspaced capital, it led to many mathematical works being newly copied into this new style in the ninth century. Most of the works of the ancient Greek mathematicians that have survived did so because of this transcription. Alcuin lived in Aachen from 782 to 790 and again from 793 to 796. In 796, he retired from Charlemagne's Palace School and became abbot of the Abbey of St. Martin at Tours, where he and his monks continued to work with the Carolingian minuscule script.

aleph

The first letter of the Hebrew alphabet, ℵ. It was first used in mathematics by Georg **Cantor** to denote the various orders, or sizes, of **infinity**: $\aleph_0$ (aleph-null), $\aleph_1$ (aleph-one), etc. An earlier (and still used) symbol for infinity, ∞, was introduced in 1655 by John **Wallis** in his *Arithmetica infinitorum* but didn't appear in print until the *Ars conjectandi* by Jakob Bernoulli, published posthumously in 1713 by his nephew Nikolaus Bernoulli (see **Bernoulli Family**).

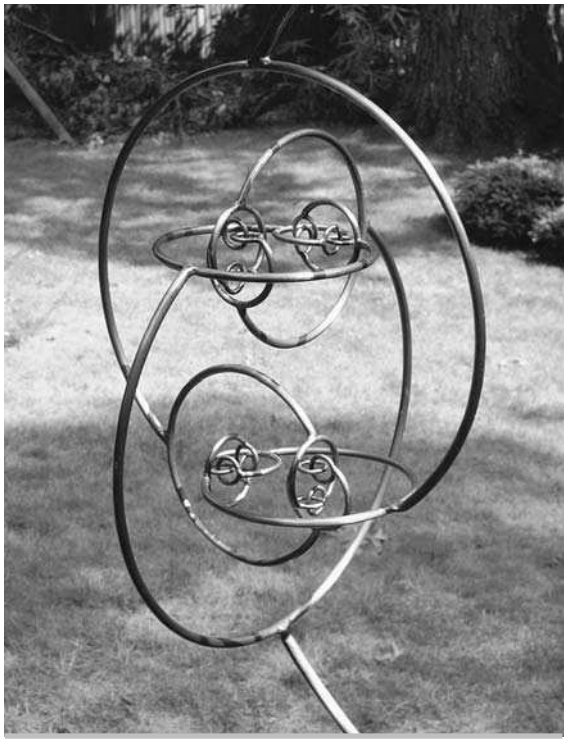

Alexander's horned sphere A sculpture of a five-level Alexander's horned sphere. *Gideon Weisz, www.gideonweisz.com*

Alexander's horned sphere

In **topology,** an example of what is called a "wild" structure; it is named after the Princeton mathematician James Waddell Alexander (1888–1971) who first described it in the early 1920s. The horned sphere is topologically equivalent to the **simply connected** surface of an ordinary hollow **sphere** but bounds a region that is not simply connected. The horns-within-horns consist of a recursive set–a **fractal**–of interlocking pairs of orthogonal rings (rings set at right angles) of decreasing radius. A rubber band around the base of any horn couldn't be removed from the structure even after infinitely many steps. The horned sphere can be embedded in the plane by reducing the interlock angle between ring pairs from 90° to 0°, then weaving the rings together in an over-under pattern. The sculptor Gideon Weisz has modeled a number of approximations to the structure, one of which is shown in the photograph.

algebra

A major branch of mathematics that, at an elementary level, involves applying the rules of arithmetic to numbers, and to letters that stand for unknown numbers, with the main aim of solving equations. Beyond the algebra learned in high school is the much vaster and more profound subject of **abstract algebra**. The word itself comes from the Arabic *al-jebr,* meaning "the reunion of broken parts." It first appeared in the title of a book, *Al-jebr w'al-mugabalah* (The science of reduction and comparison), by the ninth-century Persian scholar **al-Khowarizmi**–probably the greatest mathematician of his age, and as famous among Arabs as Euclid and Aristotle are to the Western world.

algebraic curve

A curve whose equation involves only *algebraic functions.* These are functions that, in their most general form, can be written as a sum of **polynomial**s in x multiplied by powers of y, equal to zero. Among the simplest examples are straight lines and **conic section**s.

algebraic fallacies

Misuse of **algebra** can have some surprising and absurd results. Here, for example, is a famous "proof" that $1 = 2$:

$$
\begin{aligned}
\text{Let } a &= b.\\
\text{Then } a^2 &= ab\\
a^2 + a^2 &= a^2 + ab\\
2a^2 &= a^2 + ab\\
2a^2 - 2ab &= a^2 + ab - 2ab\\
2a^2 - 2ab &= a^2 - ab\\
2(a^2 - ab) &= 1(a^2 - ab).\\
\text{Dividing both sides by } a^2 - ab&\\
2 &= 1.
\end{aligned}
$$

Where's the mistake? The problem lies with the seemingly innocuous final division. Since $a = b$, dividing by $a^2 - ab$ is the same as dividing by **zero**–the great taboo of mathematics.

Another false argument runs as follows:

$$(n+1)^2 = n^2 + 2n + 1$$
$$(n+1)^2 - (2n+1) = n^2.$$

Subtracting $n(2n+1)$ from both sides and factorizing gives

$$(n+1)^2 - (n+1)(2n+1) = n^2 - n(2n+1).$$

Adding $\frac{1}{4}(2n+1)^2$ to both sides yields

$$(n+1)^2 - (n+1)(2n+1) + \tfrac{1}{4}(2n+1)^2 = n^2 - n(2n+1) + \tfrac{1}{4}(2n+1)^2.$$

This may be written:

$$[(n+1) - \tfrac{1}{2}(2n+1)]^2 = [(n - \tfrac{1}{2}(2n+1)]^2.$$

Taking square roots of both sides,

$$n + 1 - \tfrac{1}{2}(2n+1) = n - \tfrac{1}{2}(2n+1).$$

Therefore,

$$n = n + 1.$$

The problem here is that there are *two* square roots for any positive number, one positive and one negative: the square roots of 4 are 2 and –2, which can be written as ± 2. So the penultimate step should properly read:

$$\pm(n + 1 - \tfrac{1}{2}(2n+1)) = \pm(n - \tfrac{1}{2}(2n+1))$$

algebraic geometry

Originally, the geometry of **complex number** solutions to **polynomial** equations. Modern algebraic geometry is also concerned with algebraic varieties, which are a generalization of the solution sets found in the traditional subject, as well as solutions in fields other than complex numbers, for example *finite fields*.

algebraic number

A **real number** that is a **root** of a **polynomial** equation with integer coefficients. For example, any **rational number** a/b, where a and b are nonzero integers, is an algebraic number of degree one, because it is a root of the linear equation $bx - a = 0$. The **square root of two** is an algebraic number of degree two because it is a root of the quadratic equation $x^2 - 2 = 0$. If a real number is not algebraic, then it is a **transcendental number**. Almost all real numbers are transcendental because, whereas the set of algebraic numbers is countably infinite (see **countable set**), the set of transcendental numbers is uncountably infinite.

algebraic number theory

The branch of **number theory** that is studied without using methods such as **infinite series** and **convergence** taken from **analysis.** It contrasts with **analytical number theory**.

algebraic topology

A branch of **topology** that deals with invariants of a topological space that are algebraic structures, often **group**s.

algorithm

A systematic method for solving a problem. The word comes from the name of the Persian mathematician, **al-Khowarizmi**, and may have been first used by Gottfried **Liebniz** in the late 1600s. It remained little known in Western mathematics, however, until the Russian mathematician Andrei Markov (1903–1987) reintroduced it. The term became especially popular in the areas of math focused on computing and computation.

algorithmic complexity

A measure of **complexity** developed by Gregory **Chaitin** and others, based on Claude **Shannon**'s **information theory** and earlier work by the Russian mathematicians Andrei **Kolmogorov** and Ray Solomonoff. Algorithmic complexity quantifies how complex a system is in terms of the shortest computer program, or set of **algorithm**s, needed to completely describe the system. In other words, it is the smallest model of a given system that is necessary and sufficient to capture the essential patterns of that system. Algorithmic complexity has to do with the mixture of repetition and innovation in a complex system. At one extreme, a highly regular system can be described by a very short program or algorithm. For example, the bit string 01010101010101010101 . . . follows from just three commands: print a zero, print a one, and repeat the last two commands indefinitely. The complexity of such a system is very low. At the other extreme, a totally **random** system has a very high algorithmic complexity since the random patterns can't be condensed into a smaller set of algorithms: the program is effectively as large as the system itself. See also **compressible**.

Alhambra

The former palace and citadel of the Moorish kings of Granada, and perhaps the greatest monument to Islamic mathematical art on Earth. Because the Qur'an consid-

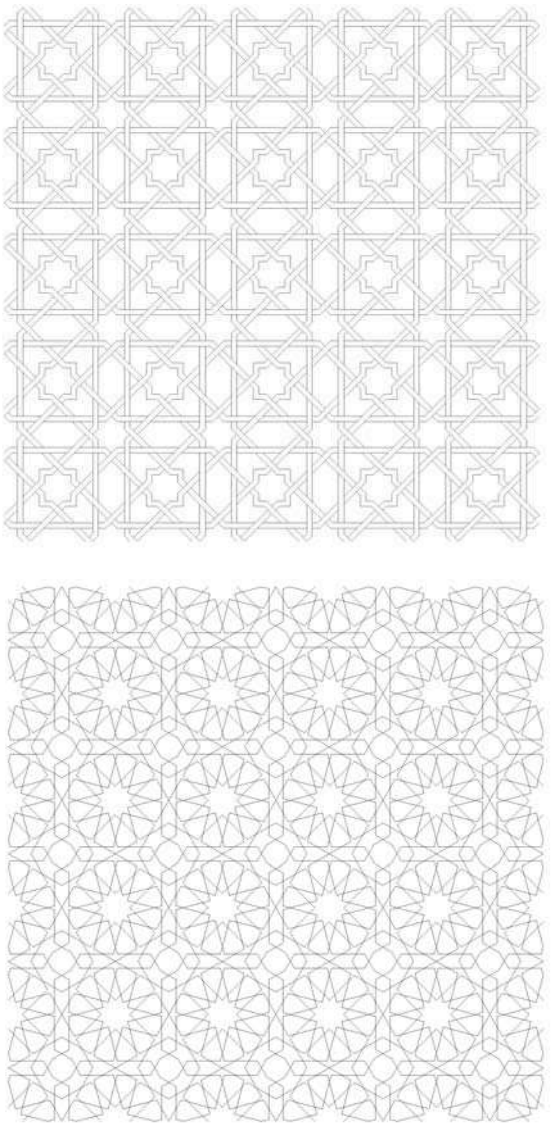

Alhambra Computer-generated tilings based on Islamic tile designs such as those found in the Alhambra. *Xah Lee, www.xahlee.org*

ers the depiction of living beings in religious settings blasphemous, Islamic artists created intricate patterns to symbolize the wonders of creation: the repetitive nature of these complex geometric designs suggests the limitless power of God. The sprawling citadel, looming high above the Andalusian plain, boasts a remarkable array of mosaics with tiles arranged in intricate patterns. The Alhambra **tiling**s are *periodic;* in other words, they consist of some basic unit that is repeated in all directions to fill up the available space. All 17 different groups of isometries–the possible ways of repeatedly tiling the plane–are used at the palace. The designs left a deep impression on Maurits **Escher**, who came here in 1936. Subsequently, Escher's art took on a much more mathematical nature, and over the next six years he produced 43 colored drawings of periodic tilings with a wide variety of symmetry types.

aliquot part

Also known as a *proper divisor,* any divisor of a number that isn't equal to the number itself. For instance, the aliquot parts of 12 are 1, 2, 3, 4, and 6. The word comes from the Latin *ali* ("other") and *quot* ("how many"). An *aliquot sequence* is formed by taking the sum of the aliquot parts of a number, adding them to form a new number, then repeating this process on the next number and so on. For example, starting with 20, we get $1 + 2 + 4 + 5 + 10 = 22$, then $1 + 2 + 11 = 14$, then $1 + 2 + 7 = 10$, then $1 + 2 + 5 = 8$, then $1 + 2 + 4 = 7$, then 1, after which the sequence doesn't change. For some numbers, the result loops back immediately to the original number; in such cases the two numbers are called **amicable numbers.** In other cases, where a sequence repeats a pattern after more than one step, the result is known as an *aliquot cycle* or a *sociable chain.* An example of this is the sequence 12496, 14288, 15472, 14536, 14264, . . . The aliquot parts of 14264 add to give 12496, so that the whole cycle begins again. Do all aliquot sequences end either in 1 or in an aliquot cycle (of which amicable numbers are a special case)? In 1888, the Belgian mathematician Eugène Catalan (1814–1894) conjectured that they do, but this remains an open question.

al-Khowarizmi (c. 780–850)

An Arabic mathematician, born in Baghdad, who is widely considered to be the founder of modern day **algebra**. He believed that any math problem, no matter how difficult, could be solved if broken down into a series of smaller steps. The word ***algorithm*** may have derived from his name.

Allais paradox

A **paradox** that stems from questions asked in 1951 by the French economist Maurice Allais (1911–).[8] Which of these would you choose: (A) an 89% chance of receiving an unknown amount and 11% chance of $1 million; or (B) an 89% chance of an unknown amount (the same amount as in A), a 10% chance of $2.5 million, and a 1% chance of nothing? Would your choice be the same if the

unknown amount was $1 million? What if the unknown amount was zero?

Most people don't like risk and so prefer the better chance of winning $1 million in option A. This choice is firm when the unknown amount is $1 million, but seems to waver as the amount falls to nothing. In the latter case, the risk-averse person favors B because there isn't much difference between 10% and 11%, but there's a big difference between $1 million and $2.5 million. Thus the choice between A and B depends on the unknown amount, even though it is the same unknown amount independent of the choice. This flies in the face of the so-called *independence axiom,* that rational choice between two alternatives should depend only on how those two alternatives differ. Yet, if the amounts involved in the problem are reduced to tens of dollars instead of millions of dollars, people's behavior tends to fall back in line with the axioms of rational choice. In this case, people tend to choose option B regardless of the unknown amount. Perhaps when presented with such huge numbers, people begin to calculate qualitatively. For example, if the unknown amount is $1 million the options are essentially (A) a fortune guaranteed or (B) a fortune almost guaranteed with a small chance of a bigger fortune and a tiny chance of nothing. Choice A is then rational. However, if the unknown amount is nothing, the options are (A) a small chance of a fortune ($1 million) and a large chance of nothing, and (B) a small chance of a larger fortune ($2.5 million) and a large chance of nothing. In this case, the choice of B is rational. Thus, the Allais paradox stems from our limited ability to calculate rationally with such unusual quantities.

almost perfect number

A description sometimes applied to the powers of 2 because the **aliquot part**s (proper divisors) of 2^n sum to $2^n - 1$. So a power of 2 is a deficient number (one that is less than the sum of its proper divisors), but only just. It isn't known whether there is an odd number n whose divisors (excluding itself) sum to $n - 1$.

alphamagic square

A form of **magic square**, introduced by Lee **Sallows**,[278–280] in which the number of letters in the word for each number, in whatever language is being used, gives rise to another magic square. In English, for example, the alphamagic square:

5 (five)	22 (twenty-two)	18 (eighteen)
28 (twenty-eight)	15 (fifteen)	2 (two)
12 (twelve)	8 (eight)	25 (twenty-five)

generates the square:

4	9	8
11	7	3
6	5	10

A surprisingly large number of 3×3 alphamagic squares exist–in English and in other languages. French allows just one 3×3 alphamagic square involving numbers up to 200, but a further 255 squares if the size of the entries is increased to 300. For entries less than 100, none occurs in Danish or in Latin, but there are 6 in Dutch, 13 in Finnish, and an incredible 221 in German. Yet to be determined is whether a 3×3 square exists from which a magic square can be derived that, in turn, yields a third magic square–a magic triplet. Also unknown is the number of 4×4 and 5×5 language-dependent alphamagic squares. Here, for example, is a four-by-four English alphamagic square:

26	37	48	59
49	58	27	36
57	46	39	28
38	29	56	47

alphametic

A type of **cryptarithm** in which a set of words is written down in the form of a long addition sum or some other mathematical problem. The object is to replace the letters of the alphabet with decimal digits to make a valid arithmetic sum. The word *alphametic* was coined in 1955 by James **Hunter**. However, the first modern alphametic, published by Henry **Dudeney** in the July 1924 issue of *Strand Magazine,* was "Send more money," or, setting it out in the form of a long addition:

```
  SEND
 MORE
------
MONEY
```

and has the (unique) solution:

```
  9567
 1085
------
10652
```

PUZZLES

The reader is invited to try to solve the following elegant examples:

1. Earth, air, fire, water: nature. (Herman Nijon)
2. Saturn, Uranus, Neptune, Pluto: planets. (Peter J. Martin)
3. Martin Gardner retires. (H. Everett Moore)

Solutions begin on page 369.

Two rules are obeyed by every alphametic. First, the mapping of letters to numbers is one-to-one; that is, the same letter always stands for the same digit, and the same digit is always represented by the same letter. Second, the digit zero isn't allowed as the left-most digit in any of the numbers being added or in their sum. The best alphametics are reckoned to be those with only one correct answer.

Altekruse puzzle

A symmetrical 12-piece **burr puzzle** for which a patent was granted to William Altekruse in 1890. The Altekruse family is of Austrian-German origin and, curiously, the name means "old cross" in German, which has led some authors to incorrectly assume that it was a pseudonym. William Altekruse came to the United States as a young man in 1844 with his three brothers to escape being drafted into the German army. The Altekruse puzzle has an unusual mechanical action in the first step of disassembly by which two halves move in opposition to each other, unlike the more familiar burr types that have a key piece or pieces. Depending on how it is assembled, this action can take place along one, two, or all three axes independently but not simultaneously.

alternate

A mathematical term with several different meanings: (1) *Alternate angles* are angles on opposite sides and opposite ends of a line that cuts two parallel lines. (2) A well-known theorem called the *alternate segment theorem* involves the segment on the opposite side of a given chord of a circle. (3) An *alternate hypothesis* in statistics is the alternative offered to the **null hypothesis**. (4) To alternate is to cycle backward and forward between two different values, for example, 0, 1, 0, 1, 0, 1, ...

altitude

A perpendicular line segment from one **vertex** of a figure or solid to an edge or face opposite to that vertex. Also the length of such a line segment.

ambiguous figure

An **optical illusion** in which the subject or the perspective of a picture or shape may suddenly switch in the mind of the observer to another, equally valid possibility. Often the ambiguity stems from the fact that the figure and ground can be reversed. An example of this is the vase/profile illusion, made famous by the Danish psychologist Edgar John Rubin (1886–1951) in 1915, though earlier versions of the same illusion can be found in many eighteenth-century French prints depicting a variety of vases, usually in a naturalistic setting, and profiles of particular people. The same effect can be created in three dimensions with a suitably shaped solid vase. In some ambiguous figures, the features of a person or of an animal can suddenly be seen as different features of another individual. Classic examples include the old woman–young woman illusion and the duck–rabbit illusion. **Upside-down picture**s involve a special case of dual-purpose features in which the reversal is accomplished not mentally, by suddenly "seeing" the alternative, but physically, by turning the picture 180°. Ambiguity can also occur, particularly in some geometric drawings, when there is confusion as to which are the front and the back faces of a figure, as in the **Necker cube**, the **Thiery figure**, and **Schröder's reversible staircase**.

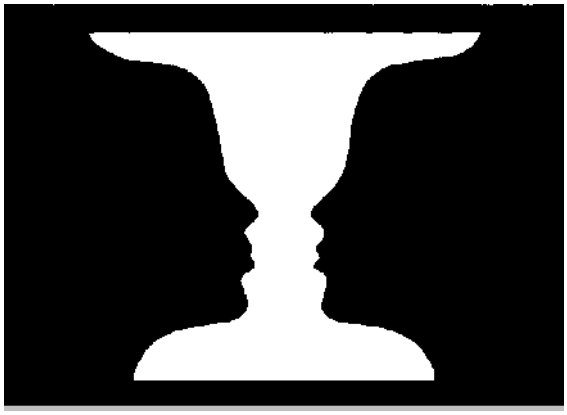

ambiguous figure The Rubin vase illusion: one moment a vase, the next two people face to face.

ambiguous connectivity

See **impossible figure**.

Ames room

The famous distorted room illusion, named after the American ophthalmologist Adelbert Ames Jr. (1880–1955), who first constructed such a room in 1946 based on a concept by the German physicist Hermann Helmholtz in the late nineteenth century. The Ames room looks cubic when seen with one eye through a specially positioned peephole; however, the room's true shape is trapezoidal. The floor, ceiling, some walls, and the far windows are trapezoidal surfaces; the floor appears level but is actually at an incline (one of the far corners being

Ames room Misleading geometry makes these identical twins appear totally different in size. *Technische Universitat, Dresden*

much lower than the other); and the walls are slanted outward, though they seem perpendicular to the floor. This shape makes it look as if people or objects grow or shrink as they move from one corner of the room to another. See also **distortion illusion**.[142, 178]

amicable numbers

A pair of numbers, also known as *friendly numbers,* each of whose **aliquot part**s add to give the other number. (An aliquot part is any divisor that doesn't include the number itself.) The smallest amicable numbers are 220 (aliquot parts 1, 2, 4, 5, 10, 11, 20, 22, 44, 55, and 110, with a sum of 284) and 284 (aliquot parts 1, 2, 4, 71, and 142, with a sum of 220). This pair was known to the ancient Greeks, and the Arabs found several more. In 1636, Pierre de **Fermat** rediscovered the amicable pair 17,296 and 18,416; two years later René **Descartes** rediscovered a third pair, 9,363,584 and 9,437,056. In the eighteenth century, Leonhard **Euler** drew up a list of more than 60. Then, in 1866, B. Nicolò Paganini (not the violinist), a 16-year-old Italian, startled the mathematical world by announcing that the numbers 1,184 and 1,210 were amicable. This second-lowest pair of all had been completely overlooked! Today, the tally of known amicable numbers has grown to about 2.5 million. No amicable pair is known in which one of the two numbers is a square. An unusually high proportion of the numbers in amicable pairs ends in either 0 or 5. A *happy amicable pair* is an amicable pair in which both numbers are **happy number**s; an example is 10,572,550 and 10,854,650. See also **Harshad number**.

amplitude

Size or magnitude. The origin of the word is the same Indo-European *ple* root that gives us *plus* and *complement.* The more immediate Latin source is *amplus* for "wide." Today, **amplitude** is used to describe, among other things, the distance a **periodic** function varies from its central value, and the magnitude of a **complex number**.

anagram

The rearrangement of the letters of a word or phrase into another word or phrase, using all the letters only once. The best anagrams are meaningful and relate in some way to the original subject; for example, "stone age" and "stage one." There are also many remarkable examples of long anagrams. " 'That's one small step for a man; one giant leap for mankind.' Neil Armstrong" becomes "An 'Eagle' lands on Earth's Moon, making a first small permanent footprint."

PUZZLES

The reader is invited to untangle the following anagrams that give clues to famous people:

1. A famous German waltz god.
2. Aha! Ions made volts!
3. I'll make a wise phrase.

Solutions begin on page 369.

An *antonymous anagram,* or *antigram,* has a meaning opposite to that of the subject text; for example, "within earshot" and "I won't hear this." *Transposed couplets,* or *pairagrams,* are single word anagrams that, when placed together, create a short meaningful phrase, such as "best bets" and "lovely volley." A rare *transposed triplet,* or *trianagram,* is "discounter introduces reductions." See also **pangram**.

anallagmatic curve

A curve that is invariant under inversion (see **inverse**). Examples include the **cardioid**, **Cassinian ovals**, **limaçon of Pascal**, **strophoid**, and **Maclaurin trisectrix**.

analysis

A major branch of mathematics that has to do with *approximating* certain mathematical objects, such as numbers or **function**s, in terms of other objects that are easier to understand or to handle. A simple example of analysis is the calculation of the first few decimal places

of **pi** by writing it as the **limit** of an **infinite series**. The origins of analysis go back to the seventeenth century, when people such as Isaac **Newton** began investigating how to approximate locally–in the neighborhood of a point–the behavior of quantities that vary continuously. This led to an intense study of limits, which form the basis of understanding infinite series, differentiation, and integration.

Modern analysis is subdivided into several areas: real analysis (the study of derivatives and integrals of real-valued functions); functional analysis (the study of spaces of functions); **harmonic analysis** (the study of **Fourier series** and their abstractions); **complex analysis** (the study of functions from the complex plane to the complex plane that are complex differentiable); and **nonstandard analysis** (the study of **hyperreal number**s and their functions, which leads to a rigorous treatment of infinitesimals and of infinitely large numbers).

analytical geometry

Also known as *coordinate geometry* or *Cartesian geometry*, the type of geometry that describes points, lines, and shapes in terms of **coordinate**s, and that uses **algebra** to prove things about these objects by considering their coordinates. René **Descartes** laid down the foundations for analytical geometry in 1637 in his *Discourse on the Method of Rightly Conducting the Reason in the Search for Truth in the Sciences,* commonly referred to as *Discourse on Method.* This work provided the basis for **calculus**, which was introduced later by Isaac **Newton** and Gottfried **Leibniz**.

analytical number theory

The branch of **number theory** that uses methods taken from **analysis**, especially **complex analysis**. It contrasts with **algebraic number theory**.

anamorphosis

The process of distorting the perspective of an image to such an extent that its normal appearance can only be restored by the observer completely changing the way he looks at the image. In *catoptric anamorphosis,* a curved mirror, usually of cylindrical or conical shape, is used to restore an anamorphic picture to its undistorted form. In other kinds of anamorphism, the observer has to change her viewing position–for example, by looking at the picture almost along its surface. Some anamorphic art adds deception by concealing the distorted image in an

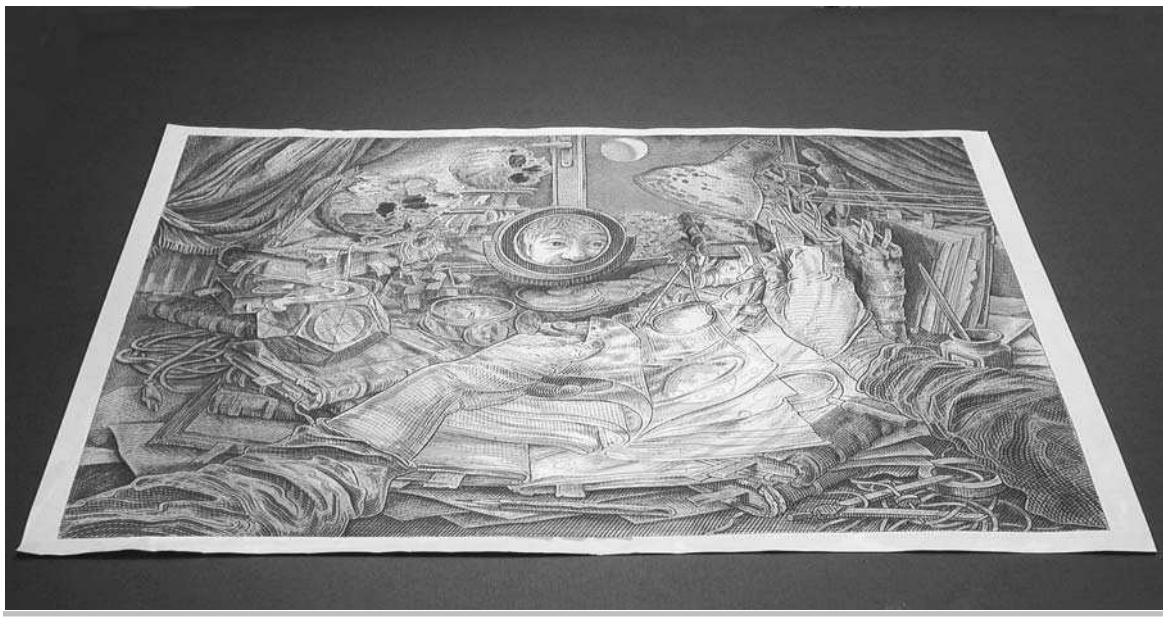

anamorphosis "Self-portrait with Albert" is a clever example of anamorphic art by the Hungarian artist Istvan Orosz. The artist's hands over his desk and a small round mirror in which the artist's face is reflected can be seen in the etching. *Istvan Orosz*

(continued)

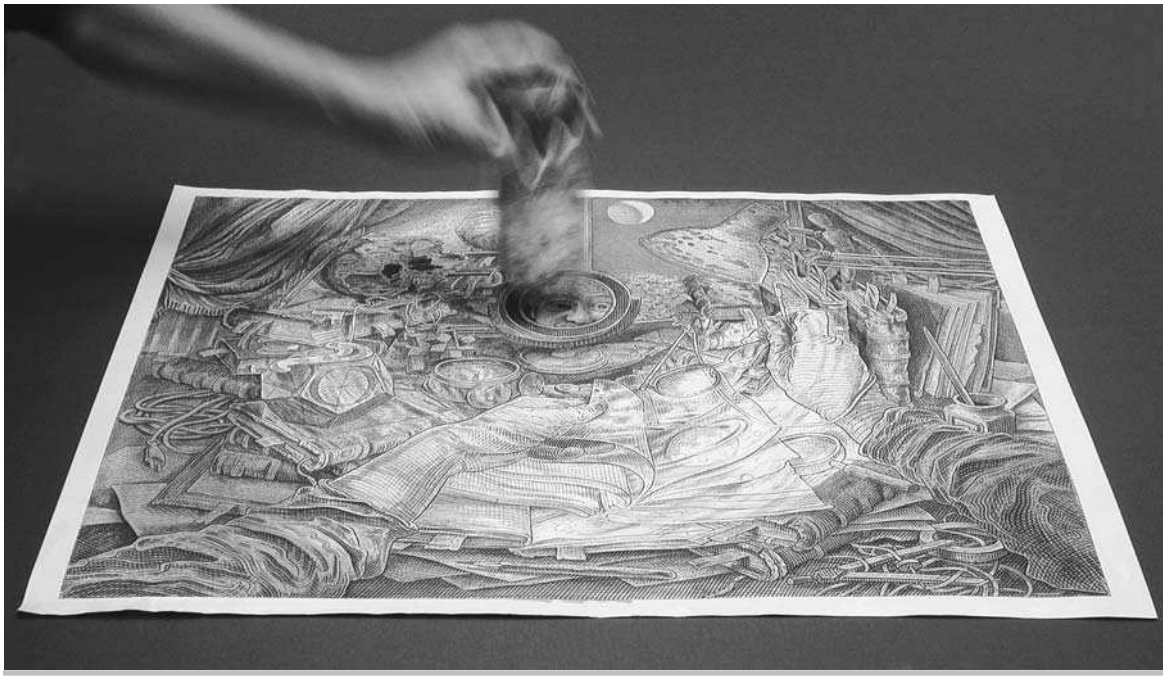

anamorphosis *(continued)* A cylindrical mirror is placed over the circle. *Istvan Orosz*

The mirror reveals a previously unsuspected aspect of the picture. The distorting effect of the curved mirror is to undistort a face hidden amid the shapes on the desk: the face of Albert Einstein. Orosz created this etching for an exhibition in Princeton, where the great scientist lived. *Istvan Orosz*

otherwise normal looking picture. At one time, artists who had the mathematical knowledge to create anamorphic pictures kept their calculations and grids well-guarded secrets. Now it is relatively easy to create such images by computer.

angle

> *My geometry teacher was sometimes acute, and sometimes obtuse, but he was always right.*
>
> –Anonymous

The opening between two lines or two planes that meet; the word comes from the Latin *angulus* for "sharp bend." Angles are measured in **degree**s. A right angle has 90°, an **acute** angle less than 90°, and an **obtuse** angle has between 90° and 180°. If an angle exceeds the straight angle of 180°, it is said to be convex. *Complementary angles* add to 90°, and *supplementary angles* make a total of 180°.

angle bisection

See **bisecting an angle**.

angle trisection

See **trisecting an angle**.

animals' mathematical ability

Many different species, including rats, parrots, pigeons, raccoons, and chimpanzees, are capable of doing simple calculations. Tests on dogs have shown that they have a basic grasp of cardinality–the number of things on offer. If they're shown a pile of treats and then shown the pile again after it has been concealed and the number of treats changed slightly, they will react differently than if there's been no change. However, not all purported animal math talents stand the test of time. At the turn of the century, a horse named Clever Hans wowed audiences with his counting skills. His trainer would pose a problem, and the horse would tap out the answer. In the end, though, it was found that Hans couldn't really add or subtract but was instead responding to subtle, unintended clues from its trainer, who would visibly relax when the horse reached the correct number.

annulus

The region between the smaller and the larger of two circles that share a common center.

antigravity houses and hills

The House of Mystery in the Oregon Vortex, Gold Hill, Oregon, built during the Great Depression in the 1930s, can claim to be the first "antigravity house." It spawned many imitators around the United States and in other parts of the world. Such buildings give rise to some spectacular visual effects, which seem bewildering until the underlying cause is revealed. Of course, the visitor guides are not forthcoming about what is really going on and make fantastic claims about magnetic or gravitational anomalies, UFOs, or other weird and wonderful phenomena. The fact is that all the stunning effects stem from clever construction and concealment that make an incline seem like a horizontal in the mind of the visitor. All antigravity houses are built on hills, with a typical incline of about 25°. But unlike a normal house on the side of a hill, an antigravity house is built so that its walls are perpendicular to the (inclined) ground. In addition, the area around the house is surrounded by a tall fence that prevents the visitor from establishing a true horizontal. Thus compelled to fall back on experience, the visitor assumes that the floor of the house is horizontal and that the walls are vertical with respect to Earth's gravity. All the stunning visual shenanigans follow from this.

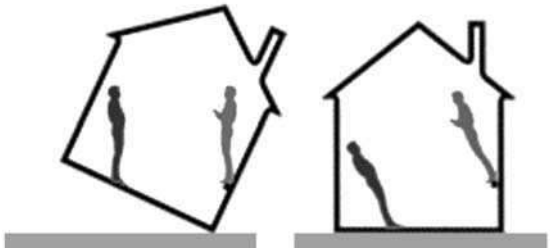

antigravity houses and hills Visitors to a "house of mystery," believing that the floor of the house is horizontal, may be astonished by the apparent gravity-defying effects (right). All these effects are easily understood, however, when it is realized that the entire house tilts at the same angle as a hill on which it is built.

In addition to man-made antigravity illusions, there are also a number of remarkable natural locations around the world where gravity seems to be out of kilter. One example is the "Electric Brae," known locally as Croy Brae, in Ayrshire, Scotland. This runs the quarter-mile from the bend overlooking the Croy railway viaduct in the west (86 meters above sea level) to the wooded Craigencroy Glen (92 meters above sea level) to the east. While there is actually a slope of 1 in 86 (a rise of 1 meter for every 86 meters horizontally) upward from the bend at the Glen, the configuration of the land on either side of the road creates the illusion that the slope runs the other way. The author is among countless folk who have parked their cars with the brakes off on

this stretch of road and been amazed to see it roll apparently uphill. See also **distortion illusion**.

antimagic square

An $n \times n$ square arrangement of the numbers 1 to n^2 such that the totals of the n rows and n columns and two long diagonals form a sequence of $(2n + 2)$ consecutive integers. There are no antimagic squares of size 2×2 and 3×3 but plenty of them for larger sizes. Here is a 4×4 example:

1	13	3	12
15	9	4	10
7	2	16	8
14	6	11	5

See also **magic square**.

antiprism

A **semi-regular polyhedron** constructed from two *n-sided* **polygon**s and $2n$ triangles. An antiprism is like a **prism** in that it contains two copies of any chosen regular polygon, but is unlike a prism in that one of the copies is given a slight twist relative to the other. The polygons are connected by a band of triangles pointing alternately up and down. At each vertex, three triangles and one of the chosen polygons meet. By spacing the two polygons at the proper distance, all the triangles become equilateral. Antiprisms are named square antiprisms, pentagonal antiprisms, and so on. The simplest, the triangular antiprism, is better known as the **octahedron**.

aperiodic tiling

A **tiling** made from the same basic elements or tiles that can cover an arbitrarily large surface without ever exactly repeating itself. For a long time it was thought that whenever tiles could be used to make an aperiodic tiling, those same tiles could also be fitted together in a different way to make a **periodic tiling**. Then, in the 1960s, mathematicians began finding sets of tiles that were uniquely aperiodic. In 1966, Robert Berger produced the first set of 20,426 aperiodic tiles, and soon lowered this number to 104. Over the next few years, other mathematicians reduced the number still further.

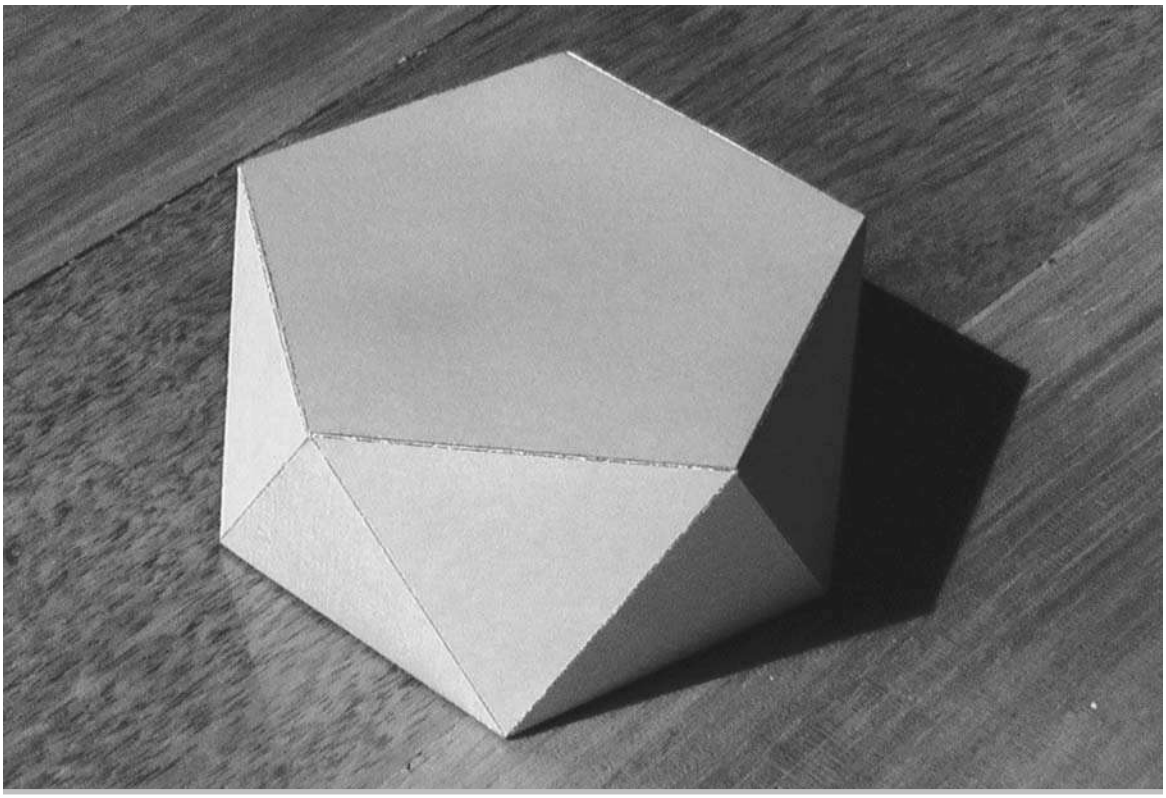

antiprism A pentagonal antiprism. *Robert Webb, www.software3d.com; created using Webb's Stella program*

In 1971, Raphael Robinson found a set of six aperiodic tiles based on notched squares; then, in 1974, Roger **Penrose** found a set of two colored aperiodic tiles (see **Penrose tilings**). The coloring can be dispensed with if the pieces are notched. There is a set of three convex (meaning no notches) aperiodic tiles, but it isn't known if there is a set of two such tiles or even a single tile (see **Einstein problem**). In three dimensions, Robert Ammann found two aperiodic polyhedra, and Ludwig Danzer found four aperiodic tetrahedra.

Apéry's constant

The number defined by the formula $\zeta(3) = \sum_{n=1}^{\infty} 1/n^3$, where ζ is the **Riemann zeta function**: It has the value 1.202056 . . . and gives the odds (1 in 1.202056 . . .) of any three positive integers, picked at random, having no common divisor. In 1979, the French mathematician Roger Apéry (1916–1994) stunned the mathematical world with a proof that this number is irrational.[11] Whether it is a **transcendental number** remains an open question.

apex

The **vertex** of a cone or a pyramid.

apocalypse number

See **beast number**.

Apollonius of Perga (c. 255–170 B.C.)

A highly influential Greek mathematician (born in a region of what is now Turkey), known as the "Great Geometer," whose eight-part work *On Conics* introduced such terms as *ellipse, parabola,* and *hyperbola.* **Euclid** and others had written earlier about the basic properties of **conic section**s but Apollonius added many new results, particularly related to **normal**s and **tangent**s to the various conic curves. One of the most famous questions he raised is known as the **Apollonius problem**. He also wrote widely on other subjects including science, medicine, and philosophy. In *On the Burning Mirror* he showed that parallel rays of light are not brought to a focus by a spherical mirror (as had been previously thought), and he discussed the focal properties of a parabolic mirror. A few decades after his death, Emperor Hadrian collected Apollonius's works and ensured their publication throughout his realm.

Apollonius problem

A problem first recorded in *Tangencies,* written around 200 B.C. by **Apollonius of Perga**. Given three objects in the plane, each of which may be a circle *C,* a point *P* (a degenerate circle), or a line *L* (part of a circle with infinite radius), find another circle that is tangent to (just touches) each of the three. There are ten cases: *PPP, PPL, PLL, LLL, PPC, PLC, LLC, LCC, PCC, CCC.* The two easiest involve three points or three straight lines and were first solved by **Euclid**. Solutions to the eight other cases, with the exception of the three-circle problem, appeared in *Tangencies;* however, this work was lost. The most difficult case, to find a tangent circle to any three other circles, was first solved by the French mathematician François Viète (1540–1603) and involves the simultaneous solution of three **quadratic** equations, although, in principle, a solution could be found using just a compass and a straightedge. Any of the eight circles that is a solution to the general three-circle problem is called an *Apollonius circle.* If the three circles are mutually tangent then the eight solutions collapse to just two, which are known as **Soddy circle**s. A **fractal** is produced by starting with three mutually tangent circles and creating a fourth–the inner Soddy circle–that is nested between the original three. The process is repeated to yield three more circles nested between sets of three of these, and then repeated again indefinitely. The points that are never inside a circle form a fractal set called the *Apollonian gasket,* which has a fractional dimension of about 1.30568.

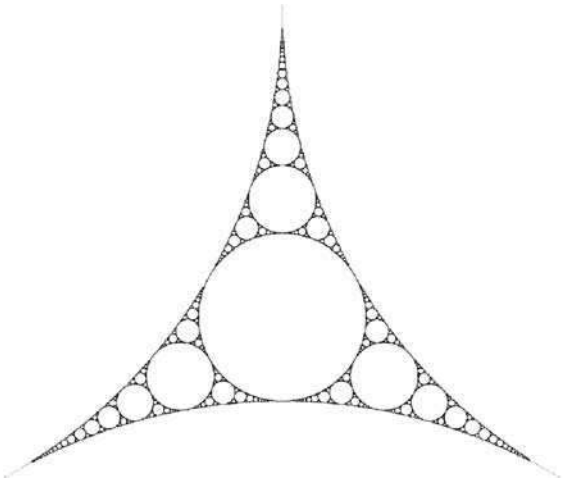

Apollonius problem The Apollonian gasket.

apothem

Also known as a *short radius,* the perpendicular distance from the center of a **regular polygon** to one of its sides. It is the same as the radius of a circle inscribed in the polygon.

apotome
One of Euclid's categories of **irrational number**s. An apotome has the form $\sqrt{(\sqrt{A} - \sqrt{B})}$. The corresponding number with a "+" sign is called a *binomial* in Euclid's scheme.

applied mathematics
Mathematics for the sake of its use to science or society.

Arabic numeral
A **numeral** written with an Arabic digit alone: 0, 1, 2, 3, 4, 5, 6, 7, 8, 9, or in combination: 10, 11, 12, . . . 594, ...

arbelos
A figure bounded by three semicircles *AB*, *BC*, and *AC*, where *ABC* is a straight line. Archimedes (about 250 B.C.) called it an *arbelos*–the Greek word for a knife of the same shape used by shoemakers to cut and trim leather–and wrote about it in his *Liber assumptorum* (Book of lemmas). Among its properties are that the sum of the two smaller arc lengths is equal to the larger; the area of the arbelos is $\pi/4$ times the product of the two smaller diameters (*AB* and *BC*); and the area of the arbelos is equal to the area of a circle whose diameter is the length of a perpendicular segment drawn from the tangent point *B* of the two smaller semicircles to the point *D*, where it meets the larger semicircle. The circles inscribed on each half of *BD* of the arbelos (called *Archimedes's circles*) each have a diameter of $(AB)(BC)/(AC)$. Furthermore, the smallest circumcircle of these two circles has an area equal to that of the arbelos. **Pappus of Alexandria** wrote on the relations of the chain of circles, C_1, C_2, C_3, . . . (called a *Pappus chain* or an *arbelos train*) that are mutually tangent to the two largest semicircles and to each other. The centers of these circles lie on an ellipse and the diameter of the *n*th circle is $(1/n)$ times the base of the perpendicular distance to the base of the semicircle.

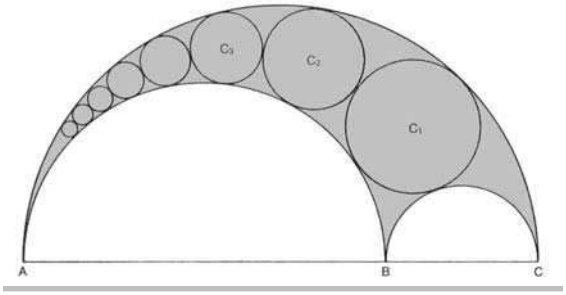

arbelos A Pappus chain of circles, C_1, C_2, C_3, . . . , inside an arbelos (shaded region).

arc
Any part of a curved line or part of the circumference of a circle; the word comes from the Latin *arcus* for a bow, which also gives rise to *arch*. *Arc length* is the distance along part of a curve.

arch
A strong, curved structure, traditionally made from wedge-shaped elements, that may take many different forms and that provides both an opening and a support for overlying material. Two common forms are the semicircular arch, first used by the Romans, and the pointed Gothic arch. The semicircular arch is the weaker of the two because it supports all the weight on the top and tends to flatten at its midpoint. It also requires massive supporting walls since all the stress on the arch acts purely downward. The pointed arch, by contrast, directs stresses both vertically and horizontally, so that the walls can be thinner, though buttressing may be required to prevent the walls from collapsing sideways. See also **Vesica Piscis**.

Archimedean dual
See **Catalan solid**.

Archimedean solid
A convex **semi-regular polyhedron**; a solid made from regular polygonal sides of two or more types that meet in a uniform pattern around each corner. (A regular polyhedron, or **Platonic solid**, has only one type of polygonal side.) There are 13 Archimedean solids (see table "Archimedian Solids"). Although they are named after their discoverer, the first surviving record of them is in the fifth book of the *Mathematical Collection* of **Pappus of Alexandria**. The **dual**s of the Archimedean solids (made by replacing each face with a vertex, and each vertex with a face) are commonly known as **Catalan solid**s. Apart from the Platonic and Archimedean solids, the only other convex uniform polyhedra with regular faces are **prism**s and **antiprism**s. This was shown by Johannes **Kepler**, who also gave the names generally used for the Archimedean solids. See also **Johnson solid**.

Archimedean spiral
A **spiral**, like that of the groove in a phonograph record, in which the distance between adjacent coils, measured radially out from the center, is constant. **Archimedes** was the first to study it and it was the main subject of his treatise *On Spirals*. The Archimedean spiral has a very simple equation in **polar coordinates** (r, θ):

$$r = a + b\theta$$

where *a* and *b* can be any real numbers. Changing the parameter *a* turns the spiral, while *b* controls the distance

Archimedean Solids

		Number of	
Name	**Vertices**	**Faces**	**Edges**
Truncated tetrahedron	8 = 4 + 4	12	18
Truncated cube	14 = 8 + 6	24	36
Truncated octahedron	14 = 6 + 8	24	36
Truncated dodecahedron	32 = 20 + 12	60	90
Truncated icosahedron	32 = 12 + 20	60	90
Cuboctahedron	14 = 8 + 6	12	24
Icosidodecahedron	32 = 20 + 12	30	60
Snub dodecahedron	92 = 80 + 12	60	150
Rhombicuboctahedron	26 = 8 + 18	24	48
Great rhombicosidodecahedron	62 = 30 + 20 + 12	120	180
Rhombicosidodecahedron	62 = 20 + 30 + 12	60	120
Great rhombicuboctahedron	26 = 8 + 12 + 6	48	72
Snub cube	38 = 32 + 6	24	60

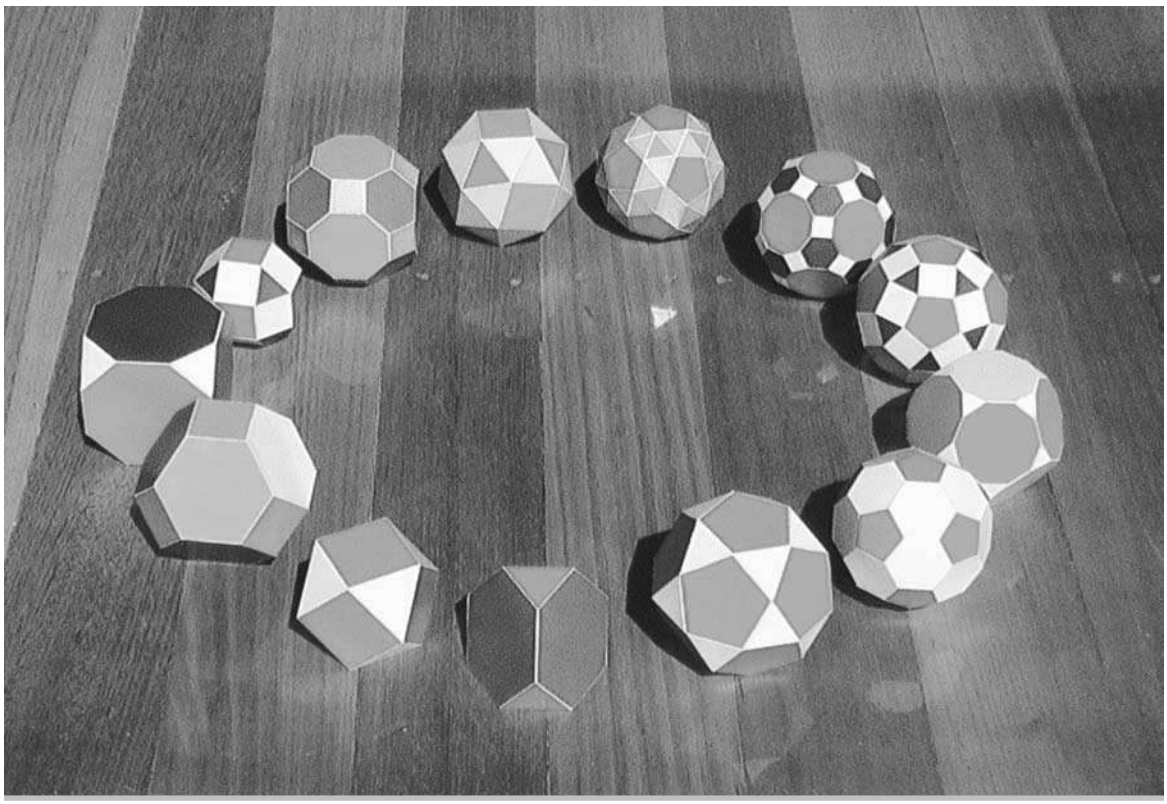

Archimedean solid The complete set of Archimedean solids, starting far left and going clockwise: truncated cube, small rhombicuboctahedron, great rhombicuboctahedron, snub cube, snub dodecahedron, great rhombicosidodecahedron, small rhombicosidodecahedron, truncated dodecahedron, truncated icosahedron (soccer ball), icosidodecahedron, truncated tetrahedron, cuboctahedron, and truncated octahedron. *Robert Webb, www.software3d.com; created using Webb's Stella program*

between the arms. The Archimedean spiral is distinguished from the **logarithmic spiral** by the fact that successive arms have a fixed distance (equal to $2\pi b$ if θ is measured in radians), whereas in a logarithmic spiral these distances form a **geometric sequence**. Note that the Archimedean spiral has two possible arms that coil in opposite directions, one for $\theta > 0$ and the other for $\theta < 0$. Many examples of spirals in the man-made world, such as a watch spring or the end of a rolled carpet, are either Archimedean spirals or another curve that is very much like it, the **circle involute**.

Archimedean tessellation

Also known as a *semiregular tessellation,* a **tiling** that uses only regular **polygon**s arranged so that two or more different polygons are around each vertex and each vertex involves the same pattern of polygons. There are eight such tessellations, two involving triangles and squares, two involving triangles and hexagons, and one each involving squares and octagons; triangles and dodecagons; squares, hexagons, and dodecagons; and triangles, squares, and hexagons.

Archimedes of Syracuse (c. 287–212 B.C.)

One of the greatest mathematicians and scientists of all time. He became a popular figure because of his involvement in the defense of Syracuse against the Roman siege in the first and second Punic Wars when his war machines helped keep the Romans at bay. He also devised a scheme to move a full-size ship, complete with crew and cargo, by pulling a single rope, and invented the irrigation device known as the Archimedean screw. According to one of many legends about him, he is said to have discovered the principle of buoyancy while taking a bath and then ran into the street naked shouting "eureka" ("I found it!").

In his book *The Sand-Reckoner,* he described a positional **number system** and used it to write the equivalent of numbers up to 8×10^{64}–the number of grains of sand he thought it would take to fill the universe. He devised a rule-of-thumb method to do private calculations that closely resembles integral calculus (2,000 years before its "discovery"), but then switched to geometric proof for his results. He demonstrated that the ratio of a circle's perimeter to its diameter is the same as the ratio of the circle's area to the square of the radius. Although he didn't call this ratio "**pi**," he showed how to work it out to arbitrary accuracy and gave an approximation of it as "exceeding 3 in less than $1/7$ but more than $10/71$."

Archimedes was the first, and possibly the only, Greek mathematician to introduce mechanical curves (those traced by a moving point) as legitimate objects of study, and he used the **Archimedean spiral** to square the circle. He proved that the area and volume of the **sphere** are in the same ratio to the area and volume of a circumscribed straight cylinder, a result that pleased him so much that he made it his epitaph. Archimedes is probably also the first mathematical physicist on record, and the best before Galileo and Isaac **Newton**. He invented the field of statics, enunciated the law of the lever, the law of equilibrium of fluids, and the law of buoyancy, and was the first to identify the concept of center of gravity. He is also, perhaps erroneously, credited with the invention of a square **dissection** puzzle known as the **loculus of Archimedes**. Many of his original works were lost when the library at Alexandria burned down and they survive only in Latin or Arabic translations. Plutarch wrote of him: "Being perpetually charmed by his familiar siren, that is, by his geometry, he neglected to eat and drink and took no care of his person; that he was often carried by force to the baths, and when there he would trace geometrical figures in the ashes of the fire, and with his finger draws lines upon his body when it was anointed with oil, being in a state of great ecstasy and divinely possessed by his science."

Archimedes's cattle problem

A fiendishly hard problem involving very **large numbers** that **Archimedes** presented in a 44-line letter to **Eratosthenes,** the chief librarian at Alexandria. It ran as follows:

> If thou art diligent and wise, O stranger, compute the number of cattle of the Sun, who once upon a time grazed on the fields of the Thrinacian isle of Sicily, divided into four herds of different colors, one milk white, another a glossy black, a third yellow and the last dappled. In each herd were bulls, mighty in number according to these proportions: Understand, stranger, that the white bulls were equal to a half and a third of the black together with the whole of the yellow, while the black were equal to the fourth part of the dappled and a fifth, together with, once more, the whole of the yellow. Observe further that the remaining bulls, the dappled, were equal to a sixth part of the white and a seventh, together with all of the yellow. These were the proportions of the cows: The white were precisely equal to the third part and a fourth of the whole herd of the black; while the black were equal to the fourth part once more of the dappled and with it a fifth part, when all, including the bulls,

went to pasture together. Now the dappled in four parts were equal in number to a fifth part and a sixth of the yellow herd. Finally the yellow were in number equal to a sixth part and a seventh of the white herd. If thou canst accurately tell, O stranger, the number of cattle of the Sun, giving separately the number of well-fed bulls and again the number of females according to each color, thou wouldst not be called unskilled or ignorant of numbers, but not yet shalt thou be numbered among the wise.

But come, understand also all these conditions regarding the cattle of the Sun. When the white bulls mingled their number with the black, they stood firm, equal in depth and breadth, and the plains of Thrinacia, stretching far in all ways, were filled with their multitude. Again, when the yellow and the dappled bulls were gathered into one herd they stood in such a manner that their number, beginning from one, grew slowly greater till it completed a triangular figure, there being no bulls of other colors in their midst nor none of them lacking. If thou art able, O stranger, to find out all these things and gather them together in your mind, giving all the relations, thou shalt depart crowned with glory and knowing that thou hast been adjudged perfect in this species of wisdom.

The answer to the first part of the problem—the smallest solution for the total number of cattle—turns out to be 50,389,082. But when the extra two constraints in the second part are factored in, the solution is vastly larger. The approximate answer of 7.76×10^{202544} was found in 1880 by A. Amthor, having reduced the problem to a form called a **Pell equation**.[9] His calculations were continued by an ad hoc group called the Hillsboro Mathematical Club, of Hillsboro, Illinois, between 1889 and 1893. The club's three members (Edmund Fish, George Richards, and A. H. Bell) calculated the first 31 digits and the last 12 digits of the smallest total number of cattle to be

776027140648681826953023283**209 . . .** 719455081800

though the two digits in bold should be 13.[31] In 1931, a correspondent to the *New York Times* wrote: "Since it has been calculated that it would take the work of a thousand men for a thousand years to determine the complete [exact] number [of cattle], it is obvious that the world will never have a complete solution." But *obvious* and *never* are words designed to make fools of prognosticators. Enter the computer. In 1965, with the help of an IBM 7040, H. C. Williams, R. A. German, and C. R. Zarnke reported a complete solution to the cattle problem, though it was 1981 before all 202,545 digits were published, by Harry Nelson, who used a Cray-1 supercomputer to generate the answer, which begins: $7.760271406486818269530232833213 \ldots \times 10^{202544}$.[341]

Archimedes's square

See **loculus of Archimedes**.

area

A measure of surface extension in two-dimensional space. *Area* is the Latin word for a vacant piece of level ground and still carries this common meaning. The French shortened form *are* denotes a square of land with a side length of 10 meters, that is, an area of 100 square meters. A *hectare* is a hundred are.

area codes

North American telephone area codes seem to have been chosen at random. But there was a method to their selection. In the mid-1950s when direct dialing of long-distance calls first became possible, it made sense to assign area codes that took the shortest time to dial to the larger cities. Almost all calls were from rotary dials. Area codes such as 212, 213, 312, and 313 took very little time for the dial to return to its starting position compared, for example, to numbers such as 809, 908, 709. The quickest-to-dial area codes were assigned to the places expected to receive the most direct-dialed calls. New York City got 212, Chicago 312, Los Angeles 213, and Washington, D.C., 202, which is a little longer to dial than 212, but much shorter than others. In order of decreasing size and estimated amount of telephone traffic, the numbers grew larger: San Francisco got 415, Miami 305, and so on. At the other end of the spectrum came places like Hawaii (the last state annexed in 1959) with 808, Puerto Rico with 809, and Newfoundland with 709. The original plan (still in use until about 1993) was that area codes had a certain construction to the numbers: the first digit is 2 through 9, the second digit is 0 or 1, and the third digit is 1 through 9. Three-digit numbers with two zeros are special codes, that is, 700, 800, or 900. Three-digit numbers with two ones are for special local codes such as 411 for local directory assistance, 611 for repairs, and so forth.

Argand diagram

A way of representing **complex number**s as points on a coordinate plane, also known as the *Argand plane* or the *complex plane,* using the *x*-axis as the real axis and the *y*-axis as the imaginary axis. It is named for the French amateur mathematician Jean Robert Argand

(1768–1822) who described it in a paper in 1806.[14] John **Wallis** suggested a similar method 120 years earlier and Casper **Wessel** extensively developed it. But Wessel's paper was published in Danish and wasn't circulated in the languages more common to mathematics at that time. In fact, it wasn't until 1895 that his paper came to the attention of the mathematical community–long after the name "Argand diagram" had stuck.

argument
(1) The input for a **function**. (2) The angle between ZO, where Z is the point representing a complex number on an **Argand diagram** and O is the origin, and the real axis. (3) A mathematical proof, possibly an informal one.

Aristotle's wheel
A **paradox** mentioned in the ancient Greek text *Mechanica*, whose author is unknown but is suspected by some to have been Aristotle. The paradox concerns two concentric circles on a wheel, as shown in the diagram. A **one-to-one** correspondence exists between points on the larger circle and those on the smaller circle. Therefore, the wheel should travel the same distance regardless of whether it is rolled from left to right on the top straight line or on the bottom one. This seems to imply that the two circumferences of the different-sized circles are equal, which is impossible. How can this apparent contradiction be resolved? The key lies in the (false) assumption that a one-to-one correspondence of points means that two curves must have the same length. In fact, the cardinalities of points in a line segment of any length (or even an infinitely long line or an infinitely large n-dimensional Euclidean space) are all the same. See also **infinity**.

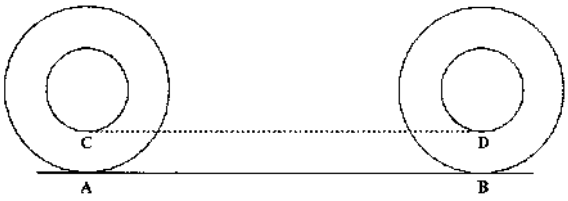

Aristotle's wheel The outer circle turns once when going from A to B, as does the inner circle when going from C to D. Yet AB is the same length as CD. How can this be, since the circles are a different size?

arithmetic
A branch of mathematics concerned with doing calculations with numbers using addition, subtraction, multiplication, and division.

arithmetic mean
The sum of n given numbers divided by n. See also **geometric mean** and **harmonic mean**.

arithmetic sequence
Also known as an *arithmetic progression,* a finite **sequence** of at least three numbers, or an infinite sequence, whose terms differ by a constant, known as the *common difference.* For example, starting with 1 and using a common difference of 4 we can get the finite arithmetic sequence: 1, 5, 9, 13, 17, 21, and also the infinite sequence 1, 5, 9, 13, 17, 21, 25, 29, . . . , $4n + 1$, ... In general, the terms of an arithmetic sequence with the first term a_0 and common difference d, have the form $a_n = dn + a_0$ ($n = 1, 2, 3, \ldots$). Does every increasing sequence of integers have to contain an arithmetic progression? Surprisingly, the answer is no. To construct a counterexample, start with 0. Then for the next term in the sequence, take the *smallest possible integer* that doesn't cause an arithmetic progression to form in the sequence constructed thus far. (There must be such an integer because there are infinitely many integers beyond the last term, and only finitely many possible progressions that the new term could complete.) This gives the nonarithmetic sequence 0, 1, 3, 4, 9, 10, 12, 13, 27, 28, ...

If the terms of an arithmetic sequence are added together the result is an *arithmetic series,* $a_0 + (a_0 + d) + \ldots + (a_0 + (n-1)d)$, the sum of which is given by:

$$S_n = n/2\ (2a_0 + (n-1)d) = n/2\ (a_0 + a_n).$$

See also **geometric sequence**.

around the world game
See **Icosian game**.

array
A set of numbers presented in a particular pattern, usually a grid. Matrices (see **matrix**) and **vector**s are examples of arrays.

Arrow paradox
The oldest and best-known **paradox** related to voting. The American economist Kenneth Arrow (1921–) showed that it is impossible to devise a perfect democratic voting system. In his book *Social Choice and Individual Values,*[16] Arrow identified five conditions that are universally regarded as essential for any system in

which social decisions are based on individual voting preferences. The Arrow paradox is that these five conditions are logically inconsistent: under certain conditions, at least one of the essential conditions will be violated.

arrowhead

See **dart**.

artificial intelligence (AI)

The subject of "making a machine behave in ways that would be called intelligent if a human were so behaving," according John McCarthy, who coined the term in 1955. How can we tell if a computer has acquired AI at a human level? One way would be to apply the **Turing test**, though not everyone agrees that this test is foolproof (see **Chinese room**). Certainly, AI has not developed at nearly the rate many of its pioneers expected back in the 1950s and 1960s. Meanwhile, progress in fields such as **neural network**s and **fuzzy logic** continues to be made, and most computer scientists have no doubt that it is only a matter of time before computers are outperforming their biological masters in a wide variety of tasks beyond those that call for mere number-crunching ability.

artificial life

A lifelike pattern that may emerge from a **cellular automaton** and appear organic in the way it moves, grows, changes shape, reproduces, aggregates, and dies. Artificial life was pioneered by the computer scientist Chris Langton, and has been researched extensively at the Santa Fe Institute. It is being used to model various **complex system**s such as ecosystems, the economy, societies and cultures, and the immune system. The study of artificial life, though controversial, promises insights into natural processes that lead to the buildup of structure in self-organizing (see **self-organization**) systems.

associative

Three numbers, x, y, and z, are said to be *associative under addition* if

$$x + (y + z) = (x + y) + z,$$

and to be *associative under multiplication* if

$$x \times (y \times z) = (x \times y) \times z.$$

In general, three elements a, b, and c of a set S are associative under the binary operation (an operation that works on two elements at a time) $*$ if

$$a * (b * c) = (a * b) * c.$$

The word incorporates the Greek root *soci*, from which we also get *social*, and may have been first used in the modern mathematical sense by William **Hamilton** around 1850. Compare with **distributive** and **commutative**.

astroid

A **hypocycloid**–the path of a point on a circle rolling inside another circle–for which the radius of the inner circle is four times smaller than that of the larger circle; this ratio results in the astroid having four cusps. The astroid was first studied by the Danish astronomer Ole Römer in 1674, in his search for better shapes for gear teeth, and later by Johann Bernoulli (1691) (see **Bernoulli family**), Gottfried **Leibniz** (1715), and Jean **d'Alembert** (1748). Its modern name comes from the Greek *aster* for "star" and was introduced in a book by Karl Ludwig von Littrow published in Vienna in 1836; before this, the curve had a variety of names, including tetracuspid (still used), cubocycloid, and paracycle. The astroid has the Cartesian equation

$$x^{2/3} + y^{2/3} = r^{2/3}$$

where r is the radius of the fixed outer circle, and $r/4$ is the radius of the rolling circle. Its area is $3\pi r^2/8$, or $^3/_2$ times that of the rolling circle, and its length is $6r$. The astroid is a sextic curve and also a special form of a **Lamé curve**. It has a remarkable relationship with the quadrifolium (see **rose curve**): the radial, pedal, and orthoptic of the astroid are the quadrifolium, while the cata**caustic** of the quadrifolium is the astroid. The

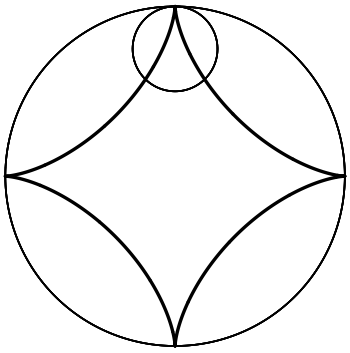

astroid As a small circle rolls around the inside of a larger one with exactly four times its circumference, a point on the rim of the small circle traces out an astroid. © *Jan Wassenaar, www.2dcurves.com*

astroid is also the catacaustic of the **deltoid** and the **evolute** of the ellipse.

asymptote

A curve that gets closer and closer to a fixed straight line without ever actually touching it. Imagine facing along the direction of a great wall that is just a meter to your left. Every second, you walk forward a meter and at the same time move sideways slightly so that you halve the distance between you and the wall. The path you follow is an asymptote. The word comes from the Greek roots *a* (not), *sum* (together), and *piptein* (to fall), so that it literally means "not falling together" and was originally used in a wider sense to describe any two curves that don't intersect. **Proclus** writes about both asymptotic lines and symptotic lines (those that do cross). Nowadays, "symptotic" is almost never heard, and "asymptote" is used mainly to denote lines that serve as a limiting barrier for some curve as one of its parameters approaches plus or minus infinity. The "~" symbol is often used to show that one **function** is asymptotic to another. For example, $f(x) \sim g(x)$ indicates that the ratio of the functions $f(x)$ to $g(x)$ approaches 1 as x tends to infinity. Asymptotes are not always parallel to the x- and y-axes, as shown by the graph of $x + 1/x$, which is asymptotic to both the y-axis and the diagonal line $y = x$.

Atiyah, Michael Francis (1929–)

An English mathematician who has contributed to many topics in mathematics, notably dealing with the relationships between geometry and **analysis**. In **topology**, he developed *K-theory.* He proved the *index theorem* on the number of solutions of elliptic differential equations, linking **differential geometry**, topology, and analysis–a theorem that has been usefully applied to quantum theory. Atiyah was influential in initiating work on gauge theories and applications to nonlinear differential equations, and in making links between topology and quantum field theory. Theories of superspace and supergravity, and string theory, were all developed using ideas introduced by him.

Atomium, the

A giant steel monument in Heysel Park, Brussels, Belgium, consisting of 9 spheres that represent the body-centered cubic structure of an iron crystal magnified 150 billion times. Designed by the architect André Waterkeyn and built for the 1958 World's Fair, the 103-meter-high Atomium was originally meant to stand for only 6 months. It may be the world's largest cube. Each of its spheres have a diameter of 18 meters and are connected by escalators. Three of the upper spheres have no vertical support, and so for safety reasons are not open to the public. However, the top sphere offers a panoramic view of Brussels through its windows, and the lower spheres contain various exhibitions.

attractor

A trajectory, or set of points in **phase space**, toward which nearby orbits converge, and which is stable. Specific types of attractor include **fixed-point attractor**, **periodic attractor**, and **chaotic attractor**.

Aubel's theorem

Given a quadrilateral and a square drawn on each side of it, the two lines connecting the centers of the squares on opposite sides are perpendicular and of equal length.

autogram

See **self-enumerating sentence**.

automorphic number

Also known as an *automorph,* a number n whose square ends in n. For instance 5 is automorphic, because $5^2 = 25$, which ends in 5. A number n is called *trimorphic* if n^3 ends in n. For example $49^3 = 117{,}649$, is trimorphic. Not all trimorphic numbers are automorphic. A number n is called *tri-automorphic* if $3n^2$ ends in n; for example 6,667 is tri-automorphic because $3 \times 667^2 = 133{,}346{,}667$ ends in 7.

automorphism

An **isomorphism** from a **set** onto itself. An *automorphism group* of a **group** G is the group formed by the automorphisms of G (bijections from G to itself that preserve the multiplication). Similarly, one can consider the automorphism groups of other structures such as **ring**s and **graph**s, by looking at bijections that preserve their mathematical structure.

Avagadro constant

One of the best known examples of a **large number** in science. It is named after the Italian physicist Amedio Avagadro (1776–1856) and is defined as the number of carbon atoms in 12 grams of pure carbon, or, more generally as the number of atoms of n grams in an element with atomic weight n. It has the value $6.02214199 \times 10^{23}$.

average

A vague term that usually refers to the **arithmetic mean** but can also signify the **median**, **mode**, **geometric mean**, or weighted mean. The word stems from a commercial practice of the shipping age. The root *aver* means to declare, and the shippers of goods would declare the

value of their goods. When the goods were sold, a deduction was made from each person's share, based on their declared value, for a portion of the loss or "average."

axiom

A statement that is considered to be true without need of **proof**. The term *axiom* comes from the Greek *axios* meaning "worthy" and was used by many Greek philosophers and mathematicians, including **Aristotle**. Curiously, **Euclid**, whose axioms are best known of all, seems to have favored a more general phrase meaning "common notion."

axiom of choice

An **axiom** in **set theory** that is one of the most controversial axioms in mathematics; it was formulated in 1904 by the German mathematician Ernst Zermelo (1871–1953) and, at first, seems obvious and trivial. Imagine there are many–possibly an unlimited number of–boxes in front of you, each of which has at least one thing in it. The axiom of choice (AC) says simply that you can always choose one item out of each box. More formally, if $\boldsymbol{S}$ is a collection of nonempty sets, then there exists a set that has exactly one element in common with every set S of $\boldsymbol{S}$. Put another way, there exists a function f with the property that, for each set S in the collection, $f(S)$ is a member of S. Bertrand **Russell** summed it up neatly: "To choose one sock from each of infinitely many pairs of socks requires the Axiom of Choice, but for shoes the Axiom is not needed." His point is that the two socks in a pair are identical in appearance, so, to pick one of them, we have to make an arbitrary choice. For shoes, we can use an explicit rule, such as "always choose the left shoe." Russell specifically mentions *infinitely many* pairs, because if the number is finite then AC is superfluous: we can pick one member of each pair using the definition of "nonempty" and then repeat the operation finitely many times using the rules of formal logic.

AC lies at the heart of a number of important mathematical arguments and results. For example, it is equivalent to the *well-ordering principle,* to the statement that for any two **cardinal number**s m and n, then $m < n$ or $m = n$ or $m > n$, and to *Tychonoff's theorem* (the product of any collection of compact spaces in topology is compact). Other results hinge upon it, such as the assertion that every infinite set has a denumerable subset. Yet AC was strongly attacked when it was first suggested, and still makes some mathematicians uneasy. The central issue is what it means to *choose* something from the sets in question and what it means for the choosing function to *exist.* This problem is brought into sharp focus when $\boldsymbol{S}$ happens to be the collection of all nonempty subsets of the **real number**s. No one has ever found a suitable choosing function for this collection, and there are good reasons to suspect that no one ever will. AC just mandates that there *is* such function. Because AC conjures up sets without offering workable procedures, it is said to be *nonconstructive,* as are any theorems whose proofs involve AC. Another reason that some mathematicians aren't greatly enamored with AC is that it implies the existence of some bizarre counterintuitive objects, the most famous and notorious example of which is the **Banach-Tarski paradox**. The main reason for accepting AC, as the majority of mathematicians do (albeit often reluctantly), is that it is useful. However, as a result of work by Kurt **Gödel** and, later, by Paul Cohen, it has been proven to be independent of the remaining axioms of set theory. Thus there are no contradictions in choosing to reject it; among the alternatives are to adopt a contradictory axiom or to use a completely different framework for mathematics, such as **category theory**.

axis

A line with respect to which a curve or figure is drawn, measured, rotated, and so forth. The word comes from the Greek root *aks* for a point of turning or rotation and seems to have first been used in English by Thomas Digges around 1570 in reference to the rotational axis of a right circular cone.

B

Babbage, Charles (1791–1871)

> *On two occasions I have been asked [by members of Parliament], "Pray, Mr. Babbage, if you put into the machine wrong figures, will the right answers come out?" I am not able rightly to apprehend the kind of confusion of ideas that could provoke such a question.*

An English mathematician who served as Lucasian Professor of Mathematics at Cambridge (1828–1839) and became the most important figure in the prehistory of computers. Babbage noted that astronomical and other mathematical tables of the period were riddled with errors because all the calculations had to be done by hand. This gave him the idea of building a machine that would do the tedious work of computation more accurately, faster, and without ever getting tired.

In 1822, Babbage wrote a letter to one of the top British scientists of the day, Humphrey Davy, in which he talked about the design of an automatic calculator. Shortly after, he was given a grant by the British government to build this device–an elaborate symphony of rods and interlocking gear teeth–which Babbage called the Difference Engine. Construction started but never finished. Despite heroic efforts to construct a working model, the critical tolerances were beyond what engineers could provide in the first half of the eighteenth century (though the resultant gear-making skills gave Britain an edge in precision machinery for several decades and even contributed to the qualitative superiority of the British navy in World War I). The government had spent £17,000, and Babbage contributed a similar amount of his own money, on the project, when Babbage set his sights on something even more ambitious. He grasped

Babbage, Charles The realization of Babbage's dream: the Manchester Mark 1 computer at Manchester University, England, in 1948. This was the first computer that could store both data and programs electronically. *Ferranti Electronics Ltd.*

that the basic mechanisms of the Difference Engine could be generalized to an all-purpose calculating machine, programmable by a punched-card mechanism like that of a Jacquard loom. This vastly more powerful machine was called the Analytical Engine and would have been the world's first true computer. But it never got off the ground. "He was ill-judged enough," wrote the secretary of the Royal Astronomical Society, "to press the consideration of this new machine upon the members of Government, who were already sick of the old one." Prime Minister Robert Peel was less than enthusiastic: "I would like a little previous consideration before I move in a thin house of country gentlemen a large vote for the creation of a wooden man to calculate tables from the formula $x^2 + x + 41$." The government's eventual withdrawal of support for his schemes left Babbage a disappointed and embittered man. However, his ideas survived and proved to be the forerunner of modern computers. Parts of his uncompleted mechanisms are on display in the London Science Museum. In 1991, working from Babbage's original plans, a Difference Engine was completed–and functioned perfectly. Among Babbage's many lesser known accomplishments was his cracking of the Vigenère cipher, a discovery that helped English military campaigns but wasn't published for several years, by which time the credit had gone instead to Friedrich Kasiski, who broke the code some years after Babbage.[329] See also **Byron, Ada**.

Bachet de Méziriac, Claude-Gaspar (1581–1638)

A poet and early mathematician of the French Academy, best known for his 1621 translation of **Diophantus**'s *Arithmetica,* the book that Pierre de **Fermat** was reading when he inscribed the margin with his famous last theorem. Bachet is also remembered as a collector of mathematical puzzles, many of which he published in *Problèmes plaisans et délectables qui font par les nombres* (1612) (Pleasant and delightful problems that involve numbers), including **river-crossing problem**s, **measuring and weighing puzzle**s, number tricks, and **magic square**s. One of the puzzles is to find the least number of weights that can be used on a scale pan to weigh any integral number of pounds from 1 to 40 inclusive, if the weights can be placed in either of the scale pans. The answer is four: 1, 3, 9, and 27 pounds. On a slightly more serious note, Bachet observed that apparently every positive number can be expressed as a sum of at most four squares; for example, $5 = 2^2 + 1^2$, $6 = 2^2 + 1^2 + 1^2$, $7 = 2^2 + 1^2 + 1^2 + 1^2$, $8 = 2^2 + 2^2$, and $9 = 3^2$. The case of 7 shows that sometimes three squares wouldn't be enough. Bachet said he had checked this for more than 300 numbers but didn't know how to prove it. It wasn't until the late eighteenth century that Joseph **Lagrange** supplied a complete proof.[339]

backgammon

A gambling game for two in which each player seeks to get a set of pieces from one side of the board to the other, while trying to prevent the other player from doing the same. The distance that a piece can be moved at each turn is determined by the throw of dice.

Backgammon has roots stretching back 5,000 years. From Mesopotamia, versions of it spread to Greece and Rome as well as to India and China. The rules of the modern form of the game were largely established in England in 1743 by Edmond Hoyle but benefited from a crucial modification that emerged in American gambling clubs in the 1920s. This final innovation, which added a new level of subtlety, is known as the *doubling cube.*

Backgammon is played with two sets of 15 checkers: one player has black, the other white. The players' checkers move in opposite directions on a board with 24 spaces or *points.* Each player's goal is to be the first to bring all their own checkers "home" (into their own quarter of the board) and then "bear them off" (remove them from the board altogether). The movement of the checkers follows the outcome of a roll of two dice, the numbers on the two dice constituting separate moves.

The actual amount that changes hands at the end of the game can be more than the initial stake. For instance, in certain winning positions called *gammon* and *backgammon,* the stake is doubled or trebled, respectively. The other way the stake can change is by means of the doubling cube. If one of the players thinks that she is in a winning position, she can turn the doubling cube and *announce a double,* which means that the total stake will be doubled. If her opponent *refuses the double,* he immediately loses his (undoubled) stake and the game is finished. If he *accepts the double,* the stakes are doubled and, as a compensation, the doubling cube is handed over to him and he gets the exclusive right to announce the next double. (He is now said to *own the cube.*) If the luck of the game changes so that he later judges that he is now winning, he'll be in a position to announce a *redouble,* which means that the stake is doubled again. If the first player refuses the double, she now loses the doubled stake; if she accepts, the game goes on with a redoubled stake, four times the original value. There's no limit to how many times the stake can be doubled, but the right to announce a double switches from one player to the other every time it's exercised. (Initially either player can double–no one owns the cube.) This aspect of the game adds greatly to the variety of tactical possibilities and problems.

baker's dozen

See **thirteen**.

Bakhshali manuscript

An early mathematical manuscript, written on birch bark and found in the summer of 1881 near the village of Bakhshali in the Yusufzai subdivision of the Peshawar district (now in Pakistan). A large part of the manuscript had been destroyed and only about 70 leaves of birch bark, of which a few were mere scraps, survived to the time of its discovery. Although its date is uncertain, it is most commonly put at about the third or fourth century A.D. and appears to be a commentary on an earlier mathematical work. Among the rules and techniques it sets out for solving problems, mostly in arithmetic and algebra, but also to a lesser extent in geometry and mensuration, is this formula (stated here in modern terms) for calculating the square root of a nonsquare number Q:

$$\sqrt{Q} = \sqrt{(A^2 + b)} = A + b/2A - (b/2A)^2/[2(A + b/2A)]$$

If $Q = 41$ (so that $A = 6$ and $b = 5$) this gives $\sqrt{Q} = 6.403138528$, which compares very favorably with the correct result of 6.403124237.

ball

Mathematicians, unlike the rest of the human race, draw a sharp distinction between a **sphere** and a ball. A sphere (in mathematics) is only a surface, whereas a ball is everything inside, and possibly including, that surface–the filling of the sphere. An *open ball* consists of all the points that are less than a given distance (the radius) away from a given point (the center); a *closed ball* consists of all the points that are less than or equal to the radius.

Mathematical balls can also exist in any number of dimensions. A one-dimensional ball of radius r is just a line segment. It consists of all the points on a line between $-r$ and r, or, in the case of a one-dimensional *unit ball* (a ball with a radius of 1), between –1 and 1. A 1 – d unit ball thus has a length, or "1 – d volume," of 2. A 2 – d unit ball, which is the filling of a unit circle, has an area, or 2 – d volume, of π. The volume of a unit ball in 3 – d is $4/3\pi$. In 4 – d it is $\pi^2/2$. Apparently, as the number of dimensions increases, so does the volume of the unit ball. What does this volume tend to do as the dimension tends to infinity? Intuitively, it might seem that in higher and higher dimensions there's more and more "room" in the unit ball, allowing its volume to become larger and larger. Does the volume become infinite, or does it approach a sufficiently large constant as the dimension increases? The answer is surprising and shows how our intuition is often misleading. Using a technique called *multivariable calculus* the volume of the unit ball in n dimensions, $V(n)$, can be shown to be $\pi^{n/2}/\ \Gamma(n/2 + 1)$, where Γ is the **gamma function** that generalizes the factorial function (i.e., $\Gamma(z + 1) = z!$). For n even, say $n = 2k$, the volume of the unit ball is thus given by $V(n) = \pi^k / k!$.

Ball, Walter William Rouse (1850–1925)

A British mathematician who lectured at Trinity College, Cambridge University, from 1878 to 1905, but is best known as a historian and as the author of the timeless classic *Mathematical Recreations and Essays*.[24] It was first published in 1892 and ran to fourteen editions, the last four with revisions by the great geometer Harold **Coxeter**.

Banach, Stefan (1892–1945)

A great Polish mathematician who founded functional **analysis** and also made important contributions to the understanding of **vector space**s, **measure theory**, and **set theory**. His name is associated with *Banach space, Banach algebra,* the *Hahn-Banach theorem,* and the remarkable **Banach-Tarski paradox**. Largely self-taught in mathematics, Banach was "discovered" by Hugo **Steinhaus** and when World War II began was president of the Polish Mathematical Society and a full professor at Lvov University. Being on good terms with Soviet mathematicians, he was allowed to hold his chair during the Soviet occupation of Lvov. The German occupation of the city in 1941 resulted in the mass murder of Polish academics. Banach survived, but the only way he could earn a living was by feeding lice with his blood in a German institute where typhoid fever research was conducted. His health declined during the occupation, and Banach died before he could be repatriated from Lvov, which was incorporated into the Soviet Union and returned to Poland after the war. *Théorie des opérations linéaires* (The theory of linear operations) is regarded as his most influential work.

Banach-Tarski paradox

> *There are more things in heaven and earth, Horatio, than are dreamt of in your philosophy.*
>
> –William Shakespeare

A seemingly bizarre and outrageous claim that it is possible to take a ball, break it into a number of pieces, and then reassemble those pieces to make two identical copies of the ball. The claim can be made even stronger: it is possible to decompose a ball the size of a marble and then reassemble the pieces to make another ball the size of Earth, or, indeed, the size of the known universe!

Before writing off Banach and Tarski as being either very bad mathematicians or very good practical jokers, it's important to understand that this is not a claim about what can actually be done with a real ball, a sharp knife, and some dabs of glue. Nor is there any chance of some entrepreneur being able to slice up a gold ingot and assemble in its place two new ones like the original. The Banach-Tarski paradox tells us nothing new about the physics of the world around us but a great deal about how volume, space, and other familiar-sounding things can

assume unfamiliar guises in the strange abstract world of mathematics.

Stefan **Banach** and Alfred **Tarski** announced their startling conclusion in 1924, having built on earlier work by Felix **Hausdorff**, who proved that it's possible to chop up the unit interval (the line segment from 0 to 1) into countably many pieces, slide these bits around, and fit them together to make an interval of length 2. The Banach-Tarski paradox, which mathematicians often refer to as the *Banach-Tarski decomposition* because it's really a proof not a paradox, highlights the fact that among the infinite **set** of points that make up a mathematical **ball**, the concepts of volume and measure can't be defined for all possible subsets. What this boils down to is that quantities that can be measured in any familiar sense are not necessarily preserved when a ball is broken down into subsets and then those subsets reassembled in a different way using just translations (slides) and rotations (turns). These unmeasurable subsets are extremely complex, lacking reasonable boundaries and volume in the ordinary sense, and thus are not attainable in the real world of matter and energy. In any case, the Banach-Tarski paradox doesn't give a prescription for *how* to produce the subsets: it only proves their *existence* and that there must be at least five of them to produce a second copy of the original ball. The fact that the Banach-Tarski paradox depends on the **axiom of choice** (AC), yet is so strongly counterintuitive, has been used by some mathematics to suggest that the AC must be wrong; however, the benefits of adopting the AC are so great that such black sheep of the mathematical family as the paradox are generally tolerated.[324, 340]

Bang's theorem

If all the faces of a **tetrahedron** have the same perimeter, then the faces are all **congruent** triangles.

banker's rounding

For banking or scientific purposes it's often considered correct to round something 0.5 to the nearest *even* number (not always upward). For instance, 5.5 rounds to 6, but 12.5 rounds to 12. This method avoids introducing a bias to a large set of numbers, by rounding up more or less as often as rounding down. Unfortunately, at a lower level, it is often taught to round something 0.5 upward all the time. See also **round-off error**.

Barbaro, Daniele (1513–1570)

A Venetian geometer whose book, *La Practica della Perspectiva* (1568–9), presents the techniques of perspective, illustrated in part with a range of **polyhedra**. Partly based on the methods and writings of the great artist Piero della Francesca (1416–1492), but written in a more readable and humanistic style, it includes the earliest drawing of the *truncated icosidodecahedron* and one of the earliest representations, along with that of the German goldsmith Wenzel Jamnitzer (1508–1585), of a *rhombicosidodecahedron*. *La Practica* was one of the most respected texts on perspective in the sixteenth century, comparable to Albrecht **Dürer**'s *Painter's Manual.*

barber paradox

See **Russell's paradox**.

Barbier's theorem

See **curve of constant width**.

Barlow, Peter (1776–1862)

A self-educated English mathematician who wrote several important books on the subject but is best known for *New Mathematical Tables* (generally known as *Barlow's Tables*), a compendium of factors, squares, cubes, square roots, reciprocals, and hyperbolic logarithms of all numbers from 1 to 10,000, and his invention of a special telescope lens. "Barlows" are popularly used by amateur astronomers to this day to multiply the power of other lenses. Barlow also worked on the design of bridges and was appointed as royal commissioner for railways, conducting experiments to see if the limitation on gradients and radius of curvature proposed by George Stephenson was correct.

Barnsley's fern

A **fractal** shape, first explored by Michael F. Barnsley at the Georgia Institute of Technology in the 1980s, that has many geometric features in common with a natural fern,

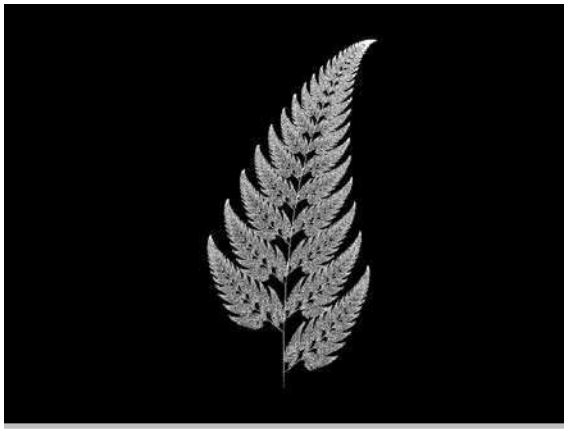

Barnsley's fern *David Nicholls*

most notably the appearance of frondlike forms at different scales. As in the case of real ferns, Barnsley's fern reveals smaller prominences along the edge of each frond that are miniature versions of the overall figure. Along these small prominences are still smaller protuberances, and so on. Barnsley's fern is created by the repetitive application of four relatively simple mathematical rules and is a type of fractal, introduced by Barnsley, known as an *iterated function system* (IFS).[26]

base

(1) The flat plane or straight line upon which a shape or a solid rests. (2) The number upon which a **number system** is based; this is also the number of different characters or figures needed by the number system. The base, or *radix,* of our familiar decimal system is 10. Thus, there are ten symbols, 0, 1, 2, 3, 4, 5, 6, 7, 8, and 9, and a decimal number is written right to left in terms of units, tens, hundreds, and so on. Each move to the left represents a jump by a **power** of 10. The decimal number 375, for example, equals $(3 \times 10^2) + (7 \times 10) + (5 \times 1)$. This can easily be written to another base. Decimal 375_{10} becomes in octal (base 8) $567_8 = (5 \times 8^2) + (6 \times 8) + (7 \times 1)$, or in binary (base 2) 101111001_2.

basin of attraction

The set of all points in **phase space** that are under the influence of an **attractor**, or, more generally, the initial conditions of a system that evolve into the range of behavior allowed by the attractor. If one imagines a **complex system** as a sink, then the attractor can be considered the drain at the bottom, and the basin of attraction is the sink's basin.

basis

In mathematics, usually associated with linear algebra; a minimal set of **vector**s that spans a **vector space**.

Bayes, Thomas (1702–1761)

An English mathematician and theologian, remembered chiefly for the theorem named after him (see **Bayes's theorem**), and the technique of **Bayesian inference** that arises from it. Bayes wrote on probability theory, the logical basis of calculus, and asymptotic series.

Bayesian inference

Statistical inference in which probabilities are interpreted not as frequencies or proportions, but rather as degrees of belief. A prior distribution for a certain random variable is assumed; then this is modified, in the light of experimentation, using **Bayes's theorem**. Pierre **Laplace** applied Bayesian inference to estimate the mass of Saturn and in a variety of other problems.

Bayes's theorem

Also known as *Bayes's rule,* a result in **probability theory**, named after Thomas **Bayes**, who proved a special case of it. It is used in statistical inference to update estimates of the probability that different hypotheses are true, based on observations and a knowledge of how likely those observations are, given each hypothesis. In fact, it is habitually used by scientists in preference to the principle of **induction**. Bayes's theorem says that if an instance X is actually observed, then the probability of a hypothesis H must be multiplied by the following ratio:

$$\frac{\text{probability of observing } X \text{ if } H \text{ is true}}{\text{probability of observing } X}$$

In other words, the probability of a hypothesis H conditional on a given body of data X is equal to the ratio of the unconditional probability of the conjunction of the hypothesis with the data to the unconditional probability of the data alone.

Beale cipher

One of the greatest unsolved puzzles in **cryptography**—or a mere hoax. About a century ago, a fellow by the name of Thomas Beale supposedly buried two wagonloads of pots filled with silver coins in Bedford County, near Roanoke, Virginia. Local rumors claim the treasure was buried near Bedford Lake. Beale wrote three encoded letters telling what was buried, where it was buried, and to whom it belonged. He entrusted these three letters to a friend, went west, and was never heard from again. Several years later, someone examined the letters and was able to crack the code in the second one, which turned out to be based on the text from the Declaration of Independence. A number in the letter indicated which word in the document was to be used. The first letter of that word replaced the number. For example, if the first four words of the document were "We hold these truths," the number 3 in the letter would represent the letter *t.* The second letter translated as follows:

> I have deposited in the county of Bedford about four miles from Bufords in an excavation or vault six feet below the surface of the ground the following articles belonging jointly to the parties whose names are given in number three herewith. The first deposit consisted of ten hundred and fourteen pounds of gold and thirty eight hundred and twelve pounds of silver deposited Nov eighteen nineteen. The second was made Dec eighteen twenty one and consisted of nineteen hundred and seven pounds of gold and twelve hundred and eighty eight of silver, also jewels obtained in St. Louis in exchange to save transportation and valued at thirteen [t]housand dollars. The above is securely

> packed i[n] [i]ron pots with iron cov[e]rs. Th[e] vault is roughly lined with stone and the vessels rest on solid stone and are covered [w]ith others. Paper number one describes th[e] exact locality of the va[u]lt so that no difficulty will be had in finding it.

One of the remaining letters supposedly contains directions on how to find the treasure but, to date, no one has solved the code. One theory is that both the remaining letters are encoded using either the same document in a different way, or another very public document. Or, of course, this could all be an elaborate, but entertaining, wheeze. Those interested may wish to contact the Beale Cypher Association, P.O. Box 975, Beaver Falls, PA 15010.

Beal's conjecture

In 1997, the Texan financier Andrew Beal offered $75,000, later increased to $100,000, to the first person who could prove or provide a counterexample to the following conjecture:

> If $x^m + y^n = z^r$, where x, y, z $m, n,$ and r are all positive integers, and m, n and r are greater than two, then $x, y,$ and z have a common factor (greater than one).

Fermat's last theorem, which was proved in 1994, is a special case of Beal's conjecture. However, no one has yet been able to use this fact to prove or disprove the conjecture, nor has anyone been able to come up with a counterexample as a disproof. It is known that for any set of three exponents $m, n,$ and $r,$ each greater than two, there can be at most finitely many solutions. But is this finite number zero? The prize remains unclaimed.

beast number (666)

Also known as the *Apocalypse number,* the "number of the beast" mentioned in the Bible's book of Revelation, the relevant verse of which (Rev. 13:18) is often quoted as:

> Here is wisdom. Let him that hath understanding count the number of the beast: for it is the number of a man; and his number is six hundred threescore and six.

Leaving aside the thorny issue of what this actually means, the number 666 does have some interesting mathematical properties. Most notably, it is the sum of the first 36 natural numbers (all the numbers on a roulette wheel): $1 + 2 + 3 + \ldots + 36$, which makes it the thirty-sixth **triangular number**. It is also the sum of the squares of the first seven **prime numbers**, $2^2 + 3^2 + 5^2 + 7^2 + 11^2 + 13^2 + 17^2$. Other curious representations of "the beast" include:

$$1^3 + 2^3 + 3^3 + 4^3 + 5^3 + 6^3 + 5^3 + 4^3 + 3^3 + 2^3 + 1^3$$
$$3^6 - 2^6 + 1^6$$
$$6 + 6 + 6 + 6^3 + 6^3 + 6^3.$$

Furthermore, 666 is one member of a **Pythagorean triplet** (216, 630, 666), which can be written in the remarkable form:

$$(6 \times 6 \times 6)^2 + (666 - 6 \times 6)^2 = 666^2.$$

In Roman numerals, 666 represents all the numbers from 500 in descending order, namely D (500) + C (100) + L (50) + X (10) + V (5) + I (1), or DCLXVI. In fact, it's been suggested that the Roman representation of 666 may have something to do with the biblical reference. DCLXVI was often used as a generic way of referring to any unspecified or unknown large number–the Roman equivalent of our "zillion." Thus, the writer of Revelation might simply have been using "666" to mean "big but unspecified."

Beatty sequences

Suppose R is an **irrational number** greater than 1, and let S be the number satisfying the equation $1/R + 1/S = 1$. Let $[x]$ denote the *floor function* of $x,$ that is, the greatest integer less than or equal to $x.$ Then the sequences $[nR]$ and $[nS]$, where n ranges through the set N of positive integers, are the Beatty sequences determined by $R.$ The interesting thing about them is that they partition $N;$ in other words, every positive integer occurs exactly once in one sequence or the other. For example, when R is the **golden ratio** (about 1.618), the two sequences begin with

1, 3, 4, 6, 8, 9, 11, 12, 14, 16, 17, 19, 21, . . . , and
2, 5, 7, 10, 13, 15, 18, 20, 23, 26, 28, 31, 34 . . . .

Beatty sequences are named after the American mathematician Samuel Beatty (1881–1970), who introduced them in 1926 in a problem in the *American Mathematical Monthly.* Beatty was the first person to receive a Ph.D. in mathematics from a Canadian university, and later became the chairman of the mathematics department and chancellor of the University of Toronto.

beauty and mathematics

Many mathematicians and scientists have commented on the beauty they find in the structure and symmetry of the equations that underpin their work, and that beauty is often the first sign of truth. In *A Mathematician's Apology,*[151] G. H. **Hardy** wrote:

> The mathematician's patterns, like the painter's or the poet's must be beautiful; the ideas, like the colors or the words must fit together in a harmonious way. Beauty is the first test: there is no permanent place in this world for ugly mathematics.

The physicist Paul **Dirac** went even further:

> I think that there is a moral to this story, namely that it is more important to have beauty in one's

> equations than to have them fit experiment. If [Erwin] Schrödinger had been more confident of his work, he could have published it some months earlier, and he could have published a more accurate equation. It seems that if one is working from the point of view of getting beauty in one's equations, and if one has really a sound insight, one is on a sure line of progress. If there is not complete agreement between the results of one's work and experiment, one should not allow oneself to be too discouraged, because the discrepancy may well be due to minor features that are not properly taken into account and that will get cleared up with further development of the theory.[176]

The architect Richard Buckminster Fuller also saw beauty as an acid test of truth: "When I'm working on a problem, I never think about beauty. I think only how to solve the problem. But when I have finished, if the solution is not beautiful, I know it is wrong."

Bell, Eric Temple (1883–1960)

A Scottish-born mathematician and writer who, from 1903, spent most of his life in the United States, teaching at the University of Washington from 1912 until 1926, then serving as professor of mathematics at the California Institute of Technology. He did work in **number theory** but is best remembered for his books, including *Algebraic Arithmetic* (1927) and *The Development of Mathematics* (1940), which became classics, and, at a more popular level, *Men of Mathematics* (1937)[32] and *Mathematics, Queen and Servant of Science* (1951). He was also a prolific writer of science fiction under the penname John Taine.

bell curve

The characteristic shape of the graph of a normal (Gaussian) distribution.

Bell number

Named after Eric **Bell,** one of the first to analyze them in depth, the number of ways that n distinguishable objects (such as differently colored balls) can be grouped into sets (such as buckets) if no set can be empty. For example, if there are three balls, colored red (R), green (G), and blue (B), they can be grouped in five different ways: (RGB), (RG)(B), (RB)(G), (BG)(R), and (R)(G)(B), so that the third Bell number is 5. The sequence of Bell numbers, 1, 2, 5, 15, 52, 203, 877, 4,140, 21,147, . . . , can be built up in the form of a triangle, as follows. The first row has just the number one. Each successive row begins with the last number of the previous row and continues by adding the number just written down to the number immediately above and to the right of it.

```
                1
              1   2
            2   3   5
          5   7   10   15
       15   20   27   37   52
    52 . . .
```

The Bell numbers appear down the left-hand side of the triangle. These normal Bell numbers contrast with *ordered Bell numbers,* which count the number of ways of placing n distinguishable objects (balls) into one or more *distinguishable* sets (buckets). The ordered Bell numbers are 1, 3, 13, 75, 541, 4,683, 47,293, 545,835, ... Bell numbers are related to the **Catalan number**s.

Benford's law

If a number is chosen at random from a large table of data or statistics, such as stock quotations, populations of towns in Germany, or half-lives of radioactive atoms, the chance that the first digit is 1 is about 30.1%, that the first digit is 2 is about 17.6%, that it is 3 is 12.4%, . . . , and that it is 9 is 4.5%. These figures fit the rule that the probability that the first digit is d is $\log_{10}(1 + 1/d)$. This rule is called Benford's law after the American physicist Frank Benford, who publicized his findings in 1938.[34] The same discovery had been made 57 years earlier by the astronomer and mathematician Simon Newcomb, who noticed that the front pages of logarithm tables tended to be more dog-eared than pages later on.[232]

Benford tested thousands of different collections of data, including the surface areas of 335 rivers, specific heats and molecular weights of thousands of chemicals, baseball statistics, and the street addresses of the first 342 people listed in the book *American Men of Science.* All these seemingly unrelated sets of numbers followed the same first-digit probability pattern as the worn pages of logarithm tables suggested. In all cases, the number 1 showed up as the first digit about 30% of the time, more often than any other, and seven times more often than the number 9.

It seems extraordinary. Why shouldn't the numbers 1 to 9 take equal turns to be the first digit? Benford's findings have been verified by other researchers. The larger and more varied the sampling of numbers from different data sets, it has been found, the more closely the distribution of numbers approaches what Benford's law predicts. Moreover these probabilities are *scale invariant* and *base invariant.* For example, it doesn't matter whether the numbers are based on the dollar prices of stocks or their prices in yen or euros, nor does it matter if the numbers are in terms of stocks per dollar; provided there are enough numbers in the sample, Benford's law will hold.[164, 263]

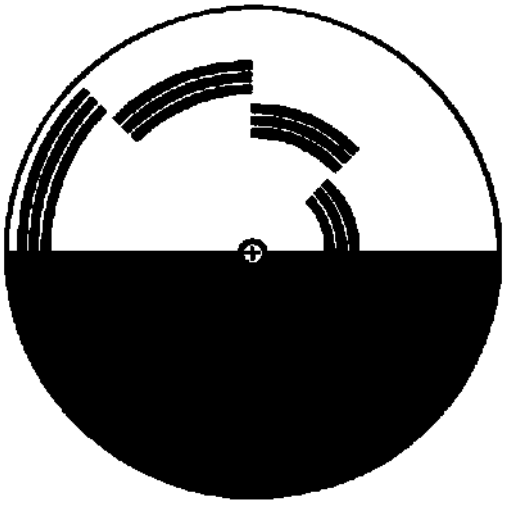

Benham's disk

Benham's disk

A disk, marked with a black and white pattern, which, when spun around, causes people to see colors. Benham's disk, also known as *Benham's wheel* and *Benham's top*, was invented in 1894 by the toy maker C. E. Benham and originally sold through Messrs. Newton and Co. as the Artificial Spectrum Top. It is one of a number of spinning disk color illusions first described by Gustav **Fechner** in 1838. For this reason, the illusory colors are known as *Fechner colors*. From the beginning, it was realized that the root of the illusion probably lay in the variation of retinal response time with wavelength. An online animated version of the disk can be seen at http://www.michaelbach.de/ot/col_benham/index.html.

Bernoulli family

An extraordinary Swiss family from Basle that produced eight outstanding mathematicians within three generations. Together with Isaac **Newton**, Gottfried **Leibniz**, Leonhard **Euler**, and Joseph **Lagrange**, the Bernoulli family dominated mathematics and physics in the seventeenth and eighteenth centuries, making important contributions to differential calculus, geometry, mechanics, ballistics, thermodynamics, hydrodynamics, optics, elasticity, magnetism, astronomy, and probability theory. Unfortunately, the Bernoullis were as conceited and arrogant as they were brilliant, and engaged in bitter rivalries and rows with one another.

The patriarchs of this mathematical dynasty were Jakob I (1654–1705) and his brother Johann I (1667–1748). (The Roman numerals are used to tell fathers, brothers, sons, and cousins apart, as the same Christian names were used repeatedly.) Next came Jakob's son, Nikolaus I, and Johann's three sons, Nikolaus II, Daniel (1700–1772), and Johann II. Finally, came Johann II's mathematical offspring, Johann III and Jakob II.

Jakob I developed a passion for science and mathematics after meeting Robert Boyle during a trip to England in 1676. He largely taught himself in these subjects and went on to lecture in experimental physics at the University of Basle. He also secretly introduced his younger brother to mathematics, against the wishes of his parents who wanted the younger brother to go into commerce. The cooperation between the two brothers soon degenerated, however, into vitriolic argument. Irked by Johann's bragging, Jakob publicly claimed that his younger brother had copied his own results. Later, having been appointed to the chair of mathematics at Basle, Jakob succeeded in blocking his brother's appointment to the same department, forcing Johann to take a teaching job at the University of Groningen instead. Johann proposed the so-called **brachistrochrone problem** and, along with Newton, Leibniz, l'Hospital, and Jakob, managed to solve it–but only after he first came up with a faulty proof and then tried to substitute one of Jakob's in its place! Eventually, Johann was offered a post at Basle as, of all things, the department head of Ancient Greek. But, en route to Basle, Johann learned that Jakob had died of tuberculosis. Upon his arrival he set about lobbying for the vacant position and, in less than two months, got his way. Jakob's most important work, his *Ars Conjectandi* (The art of conjecture), was published posthumously and formed the basis of **probability theory**.

Sadly, Johann I repeated his father's mistake and tried to force the most mathematically talented of his three sons, Daniel, into an unwanted career as a merchant. When the attempt failed, Johann let Daniel study medicine, in order to prevent his son from becoming a competitor. But all three sons followed their father's path, and Daniel, while studying medicine, was tutored in math by his older brother Nikolaus II. In 1720, Daniel went to Venice to work as a physician but won such a big reputation for his work in physics and mathematics that Peter the Great of Russia offered him a chair at the Academy of Science in St. Petersburg. Daniel went, along with Nikolaus II, who was also offered a position at the Academy. However, after just eight months, Nikolaus came down with a fever and died. Upset, Daniel wanted to return to Basle, but Johann I didn't want his son–a potential rival–back home. Instead he sent one of his pupils, none other than the great Leonhard **Euler**, to St. Petersburg to keep Daniel company. The two Swiss

mathematicians became good friends, and the six years they spent together in St. Petersburg were the most productive of Daniel's life.

When Daniel finally returned to Basle, quarrels within the family flared up again after he won the prize of the Parisian Academy of Science with a paper, coauthored with his father, on astronomy. Jealous of Daniel's success, Johann threw him out of the family house. And worse was to come. In 1738 Daniel published his magnum opus, *Hydrodynamica.* Johann I read the book, hastily wrote one of his own called *Hydraulica,* back-dated it to 1732, and claimed to be the inventor of fluid dynamics! The plagiarism was soon uncovered, and Johann was ridiculed by his colleagues, but his son never recovered from the blow. See also **St. Petersburg paradox**.

Bernoulli number

A number of the type defined by Jakob **Bernoulli** in connection with evaluating sums of the form $\sum i^k$. The sequence B_0, B_1, B_2, . . . can be generated using the formula

$$x/(e^x - 1) = \sum (B_n x^n)/n!$$

though various different notations are used for them. The first few Bernoulli numbers are: $B_0 = 1$, $B_1 = -\frac{1}{2}$, $B_2 = \frac{1}{6}$, $B_4 = -\frac{1}{30}$, $B_6 = \frac{1}{42}$, ... They crop up in many diverse areas of mathematics including the series expansions of $\tan(x)$ and **Fermat's last theorem**.

Berry's paradox

A **paradox**, devised by G. G. Berry of the Bodleian Library at Oxford University in 1906, that involves statements of the form: "The smallest number not nameable in under ten words." At first sight, there doesn't seem anything particularly mysterious about this sentence. After all, there are only so many sentences that have less than ten words, and only a set **S** of these specify unique numbers; so there is clearly some number N that is the smallest integer not in **S**. The trouble is, the Berry sentence itself is a specification for that number *in only nine words!* Berry's paradox shows that the concept of nameability is inherently ambiguous and a dangerous concept to be used without qualification. A similar air of the paradoxical swirls around the notion of **interesting numbers.**[60]

Bertrand's box paradox

A problem, similar to the **Monty Hall problem**, that was published by the French mathematician Joseph Bertrand (1822–1900) in his 1889 text *Calcul des Probabitités.* Suppose there are three desks, each with two drawers. One desk contains a gold medal in each drawer, one contains a silver medal in each drawer, and one contains one of each, but you don't know which desk is which. If you open a drawer and find a gold medal, what are the chances that the other drawer in that desk also contains gold? This comes down, then, to figuring out the probability that you've picked the gold-gold desk instead of the gold-silver desk. Many people quickly jump to the conclusion that there are two possibilities, and since the selection was random, it must be 50-50. But this is wrong. Think of the initial selection as picking from among six drawers:

Before			After		
S	S	G		G	G
S	G	G			G
1	2	3	1	2	3

So, we have it narrowed down to three drawers, with an equal probability of each one being the one that was picked. One of the drawers is in desk 2, so there's a one-third chance that desk 2 was picked. Two of the drawers are in desk 3, so there are two one-third chances (i.e., a two-third chance) that desk 3 was picked.

Bertrand's postulate

Also known as *Betrand's conjecture,* if n is an integer greater than 3, then there is at least one **prime number** between n and $2n - 2$. This postulate (which should now be called a theorem) is named after the French mathematician Joseph Bertrand (1822–1900) who, in 1845, showed it was true for values of n up to 3 million. The Russian Pafnuty Chebyshev (1821–1894) gave the first complete proof in 1850, so that it is sometimes called *Chebyshev's theorem* (although another theorem also goes by this name). In 1932, Paul **Erdös** gave a more elegant proof, using the **binomial coefficient**s, which is the one that appears in most modern textbooks. Bertrand's postulate implies that the nth prime p_n is at most 2^n.

Bessel, Friedrich Wilhelm (1784–1846)

A German astronomer and mathematician who became director of the observatory at Königsberg (see **bridges of Königsberg**). Much of Bessel's work dealt with **perturbation**s (wobbles) in the motion of planets and stars caused by the gravitational influence of other bodies. To help analyze these perturbations he developed certain mathematical **function**s that are now known as *Bessel functions* and are used widely in physics.

beta function

The function

$$B(m, n) = \int_0^1 x^{m-1} (1 - x)^{n-1} \, dx.$$

It can be defined in terms of the **gamma function** by

$$B(m, n) = \frac{\Gamma(m)\Gamma(n)}{\Gamma(m+n)}.$$

Many integrals can be reduced to the evaluation of beta functions.

Betti number

An important topological property of a surface, named after the Italian mathematician Enrico Betti (1823–1892). The Betti number is the maximum number of cuts that can be made without dividing the surface into two separate pieces. If the surface has edges, each cut must be a "crosscut," one that goes from a point on an edge to another point on an edge. If the surface is closed, like a sphere, so that it has no edges, each cut must be a "loop cut," a cut in the form of a simple closed curve. The Betti number of a square is 0 because it is impossible to crosscut without leaving two pieces. However, if the square is folded into a tube, its topology changes–it now has two disconnected edges–and its Betti number changes to 1. A **torus**, or donut shape, has a Betti number of 2. See also **chromatic number**.

bicorn

Also known as the *cocked-hat,* any of a collection of **quartic** curves studied by James **Sylvester** in 1864 and by Arthur **Cayley** in 1867. The bicorn has the Cartesian equation

$$y^2(a^2 - x^2) = (x^2 + 2ay - a)^2.$$

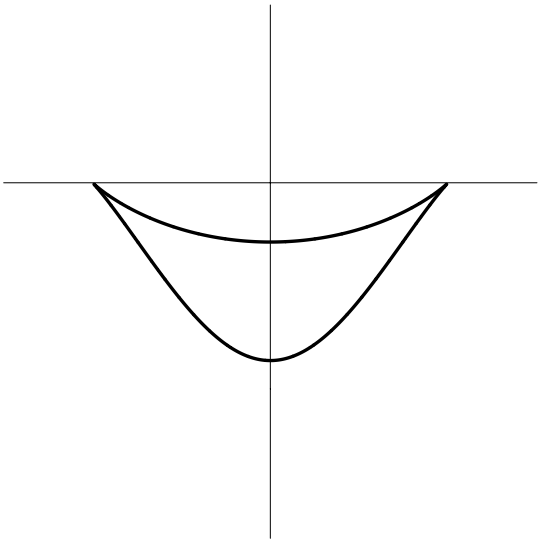

bicorn The bicorn curve © *Jan Wassenaar, www.2dcurves.com*

bicuspid curve

The **quartic** curve given by the equation

$$(x^2 - a^2)(x - a)^2 + (y^2 - a^2)^2 = 0.$$

Bieberbach conjecture

A celebrated conjecture made by the German mathematician Ludwig Bieberbach (1886–1982) in 1916, that was finally proved, after many partial results by others, by Louis de Branges of Purdue University in 1984.[54] Bierberbach is infamous in the history of mathematics because of his outspoken anti-Semitism during the Nazi era. Following the dismissal of Edmund Landau (1877–1938) from the University of Göttingen, Bierberbach wrote: "This should be seen as a prime example of the fact that representatives of overly different races do not mix as students and teachers. . . . The instincts of the Göttingen students felt that Landau was a type who handled things in an un-German manner."

Bieberbach's conjecture (BC) stemmed from the Riemann mapping theorem (RMT), which makes a claim about any region of a plane that is simply connected (in other words, any region, however complicated, that doesn't have any holes). The RMT says there must be some function, or mapping, such that every point in the arbitrary region is associated with one and only one point inside a circle with unit radius. Complex functions are best suited to plane-to-plane mappings and are often easier to work with if they can be represented as a power series. For example, given the complex number z, the function e^z can be expressed as the infinite series $1 + z + z^2/2! + z^3/3! + \ldots$. Bieberbach guessed that there is a link between the conditions imposed on a function by RMT and the numerical coefficients of the terms in a power series that represents the function. The BC says that if a function gives a one-to-one association between points in the unit circle and points in a simply connected region of the plane, the coefficients of the power series that represents the function are never larger than the corresponding power. In other words, given that $f(z) = a_0 + a_1z + a_2z^2 + a_3z^3 + \ldots$, then $|a_n| \leq n|a_1|$ for each n.

bifurcation

The value of a smoothly varying control parameter, or the point in *parameter space,* at which the behavior of a **dynamical system** undergoes a qualitative change. For example, a simple equilibrium, or a **fixed-point attractor**, might give way to a periodic oscillation as the stress on a system increases. Similarly, a **periodic attractor** might become unstable and be replaced by a **chaotic attractor**. To give a real-world example, drops fall individually at equal intervals, from a dripping faucet at low pressure. As the pressure is increased, however, the

pattern of dripping abruptly changes so that two drops fall close together, with a longer interval before the next pair fall. In this case, a simple periodic process has given way to a periodic process with twice the period, a process described as "period doubling." If the flow rate of water through the faucet is increased still further, beyond the bifurcation point, often an irregular dripping is found and the behavior can become chaotic. See also **chaos**.

bilateral

Having two sides, or relating to the right and left sides of an object. *Bilateral symmetry* is a symmetrical arrangement, as of an organism or a body part, along a central axis, so that the body is divided into equivalent right and left halves by only one plane. See also **mirror reversal problem**.

bilateral diagram

A device invented by Lewis **Carroll** to represent the different logical states that two objects with two properties can take. Each cell in a four-square array represents one of the four possible object/property states and is covered by a red counter if the state is present and by a gray counter if it is absent.

billion

See **large number**s.

bimagic square

A **magic square** that becomes a new magic square when each integer is squared. If, in addition to being bimagic, the integers in the square can be cubed and the resulting square is still magic, the square is said to be *trimagic.* To date the smallest bimagic square seems to be of order 8, while the smallest trimagic square is of order 32.

binary

> *There are 10 kinds of people in the world, those who understand binary math, and those who don't.*
>
> –Anonymous

The simplest positional **number system** and the natural one to use when dealing with computers; it employs just two symbols, 0 and 1, which correspond to the possible states of an off-on switch. Each place to the left in a binary number represents the next highest power of two. The binary number 10110_2, for example, means $1 \times 2^4 + 0 \times 2^3 + 1 \times 2^2 + 1 \times 2^1 + 0 \times 2^0$, or 22_{10} in the familiar decimal notation. Nonintegers can be represented by using negative powers, which are set off from the other digits by means of a *radix point* (called a *decimal point* in base 10). The binary number 11.01_2 thus means $1 \times 2^1 + 1 \times 2^0 + 0 \times 2^{-1} + 1 \times 2^{-2}$ which equals 3.25_{10}. A number that terminates in a decimal doesn't necessarily do so in binary (e.g., $0.3_{10} = 0.0100110011001\ldots_2$), and vice versa. An irrational number, however, is nonperiodic in both systems (e.g., **pi**, $= 3.1415926\ldots_{10} = 11.001001000011111\ldots_2$). Binary arithmetic was first investigated by Gottfried **Leibniz** in 1672, though he didn't publish anything about it until 1701.

binary operation

An operation that involves two operands. For example, addition and subtraction are binary operations.

binomial

An expression containing two terms, joined by + or –. The **binomial theorem** gives the result of raising a binomial expression to a power; the expansion and the series it leads to are called the *binomial expansion* and the *binomial series.* A *binomial distribution* is described by a formula related to the binomial expansion. A binomial equation is a particular kind of equation that contains two terms.

binomial coefficient

A **coefficient** of x in the expansion of $(x + y)^n$. The binomial coefficient ${}_nC_m$ or $\binom{m}{n}$ gives the number of ways of picking m unordered outcomes from n possibilities, and is also known as a **combination**. It has the value $n!/(n - m)!m!$ The binomial coefficients form the rows of **Pascal's triangle**.

binomial theorem

The result that allows the expansion of a **binomial** expression:

$$(x+y)^n = x^n + a_{n-1}x^{n-1}y + a_{n-2}x^{n-2}y^2 + \ldots + y^n$$

where the coefficients a_i are called **binomial coefficient**s.

Birkhoff, George David (1884–1944)

The foremost American mathematician of the early twentieth century and the first prominent dynamicist in the New World. He is known for his work on linear **differential equation**s and **difference equation**s, and was also deeply interested in and made contributions to the analysis of **dynamical system**s, celestial mechanics, the **four-color map problem**, and function spaces. Although a geometer at heart, he discovered new symbolic solution methods. He saw beyond the theory of oscillations, created a rigorous theory of **ergodic** behavior, and foresaw dynamical models for **chaos**. In addition he wrote on the foundations of relativity and quantum mechanics and, in *Aesthetic Measure* (1933), on art and music.

birthday paradox

The fact–not really a **paradox**–that you need a group of only 23 people for there to be a better than 50/50

chance that two of these people will have the same birthday. This seems surprising because we are used to comparing our particular birthday with others and only rarely finding a perfect match. The probability of any two individuals having the same birthday is just $1/365$. Even if you were to ask 20 people, the probability of finding someone with your birthday is still less than $1/20$. But the odds improve dramatically when a group of people *ask each other* about their birthdays because then there are many more opportunities for a matchup. One way to calculate the probability of a birthday match is to count the pairs of people involved. In a room of 23 people, there are $(23 \times 22)/2$, or 253, possible pairs. Each pair has a probability of success of $1/365 = 0.00274$ (0.274%), and thus a probability of failure of $(1 - 0.00274) = 0.99726$ (99.726%). The probability of no match among any of the pairs of people is 0.99726 to the 253rd power, which is 0.499 (49.9%). So the probability of a successful match is (1 – 0.499), or slightly better than even (50/50). With 42 people, the probability of a birthday match climbs to 90%.

birthday surprise

Here is a way to learn someone's birthday by doing a little simple math. Ask a person to take the month number (January = 1, February = 2, and so forth) of their birthday, multiply by 5, add 6, multiply the total by 4, add 9, and multiply the new total by 5 again. Finally, have her add the number of the day on which she was born and give you the total. In your head, subtract 165 and you will have the month and day of her birth. How does this work? If M is the month number and D the day number, then after the seven steps the expression for their calculation is: $5(4(5M + 6) + 9) + D = 100M + D + 165$. Thus, if you subtract the 165, what will remain will be the month in hundreds plus the day.

bisect

To cut in half.

bisecting an angle

Splitting an angle exactly in two. The ancient Greeks knew how to easily do it using only a pair of compasses and a straightedge. Here's how: Put the point of the compass at a point O and draw a circle so that it cuts the two lines coming out from the angle. Call these intersection points A and B. Now put the point of the compass at A and draw an arc that follows within the opening of the angle. Without changing the radius at which the compass is set, move its point to B and draw another arc. Join the point where the two arcs cross, P, to O using the straight edge: angle POB is half of angle AOB. See also **trisecting an angle**.

bishops problem

To find the maximum number of bishops (chess pieces capable of moving any number of spaces along diagonals of their own color) that can be placed on an $n \times n$ chessboard in such a way that no two are attacking each other. The answer is $2n - 2$, which gives the solution 14 for a standard (8×8) chessboard. The numbers of distinct maximal arrangements for $n = 1, 2, \ldots$ bishops are 1, 4, 26, 260, 3,368, ...

bistromathics

The revolutionary new (and totally fictitious) field of mathematics in restaurants, as described by Douglas Adams in his book *Life, the Universe and Everything*:[4]

> Numbers written on restaurant bills within the confines of restaurants do not follow the same mathematical laws as numbers written on any other pieces of paper in any other parts of the Universe. This single statement took the scientific world by storm. . . . So many mathematical conferences got held in such good restaurants that many of the finest minds of a generation died of obesity and heart failure and the science of math was put back by years.

Adams explains that just as Einstein found that space and time are not an absolute but depend on the observer's movement, so numbers are not absolute, but depend on the observer's movement in restaurants:

> The first non-absolute number is the number of people for whom the table is reserved. This will vary during the course of the first three telephone calls to the restaurant, and then bear no apparent relation to the number of people who actually turn up, or to the number of people who subsequently join them after the show/match/party/gig, or to the number of people who leave when they see who else has turned up. The second non-absolute number is the given time of arrival, which is now known to be one of the most bizarre of mathematical concepts, a reciprivers-excluson, a number whose existence can only be defined as being anything other than itself. In other words, the given time of arrival is the one moment of time at which it is impossible that any member of the party will arrive. . . . The third and most mysterious piece of nonabsoluteness of all lies in the relationship between the number of items on the bill, the cost of each item, the number of people at the table and what they are each prepared to pay for.

See also **large numbers**.

bit

A **binary** digit, either 0 or 1. See also **byte**.

blackjack

Also known as *twenty-one,* the most popular casino game in the world and the only such game with a *fluctuating* probability: the odds of winning change with the makeup of the deck. The cards two to nine have a numerical value equal to the number printed on the card. Tens and all face cards (jack [J], queen [Q], and king [K]) have the value of 10. Aces may be counted as either 11 or one. A dealer plays against one to seven players. Every player and the dealer initially receive two cards each, dealt by the dealer. Each player's hand is played against the dealer's hand only. If a player's hand has a value closer to 21 (without going over) than the dealer's hand, the player wins. The best possible hand is known as a *blackjack* (21 in the first two cards) and consists of an ace and a ten-valued card (10, J, Q, K). The payout for a blackjack is 3-to-2: the player is paid three chips for every two chips bet. When both the player and the dealer have blackjacks, it is a normal *tie* (*push*) situation and the player retains the initial bet. The player has several choices after receiving the first two cards: (1) *Hit* or *draw:* take one or more cards to add-up to a better hand. (2) *Stand:* stop taking more cards. (3) *Double down:* double the initial amount (in cases considered more favorable). (4) *Split pairs:* if the two cards are equal in value they may be played in two separate hands. The dealer must draw until his hand adds up to 17 or more. Both the player and the dealer can go over 21, a situation known as *bust;* the player loses the bet immediately. The dealer plays his hand last, after all the players at the table. This rule creates the so-called *house edge.* John Scarne[282] was the first to calculate the house advantage at blackjack as 5.9%. However, the house edge can be cut to around 1% if the player follows certain rules. The set of rules known as *basic strategy* make blackjack one of the fairest games of any kind, almost as fair as coin tossing.

In 1962 Edward O. Thorp, an IBM computer scientist, published *Beat the Dealer,*[333] which introduced a winning method called *card counting.* This method considered the 10-valued cards and the aces as positive, and the cards 2 to 6 as negative. If the net value of the remaining deck was positive, the player must increase the bet accordingly. The method had visible results when only one deck was used and very few cards remained in the deck. Casinos responded by changing the rules dramatically. The *penetration* was introduced: not all the cards in the deck are played. Shuffling is done unexpectedly. Also, most casinos introduced *multiple-deck blackjack.*

Blanche's dissection

The simplest **dissection** of a square into rectangles of the same areas but different shapes. It is composed of seven pieces; the square is 210 units on a side, and each rectangle has area of $210^2/7 = 6{,}300$.

Bólyai, János (1802–1860)

A Hungarian mathematician who was one of the founders of **non-Euclidean geometry**, independently coming to almost the same conclusions as Nikolai **Lobachevsky**. He was initially taught by his father, Farkas, also a mathematician, then he studied at the Royal Engineering College in Vienna from 1818 to 1822. Between 1820 and 1823 he prepared his treatise on a complete system of non-Euclidean geometry, commenting, "Out of nothing I have created a strange new universe." It was published in 1832 as an appendix to an essay by his father. Carl **Gauss**, on reading the appendix, wrote to a friend saying, "I regard this young geometer Bólyai as a genius of the first order." It was not until 1848 that Bólyai learned that Lobachevsky had produced a similar piece of work in 1829. Although he never published more than the 24 pages of the appendix, Bólyai left more than 20,000 pages of manuscript of mathematical work when he died. He was an accomplished linguist, speaking nine foreign languages including Chinese and Tibetan.

book-stacking problem

How much of an overhang can be achieved by stacking books on a table before the books overbalance and fall off? Assume each book is one unit long. To balance one book on a table, the center of gravity of the book must be somewhere over the table; to achieve the maximum overhang, the center of gravity should be just over the table's edge. The maximum overhang with one book is

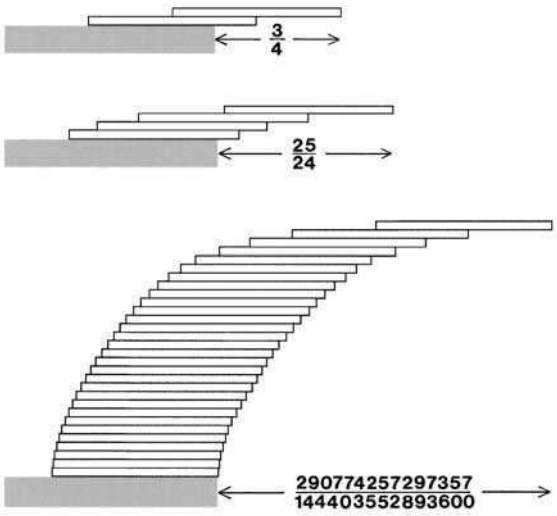

book-stacking problem The solution to the book-stacking problem.

obviously ½ unit. For two books, the center of gravity of the first should be directly over the edge of the second, and the center of gravity of the stack of two books should be directly above the edge of the table. The center of gravity of the stack of two books is at the midpoint of the books' overlap, or $(1 + ½)/2$, which is ¾ unit from the far end of the top book. It turns out that the overhangs are related to the harmonic numbers H_n, (see **harmonic sequence**), which are defined as $1 + ½ + ⅓ + \ldots + 1/n$: the maximum overhang possible for n books is $H_n/2$. With four books, the overhang $(1 + ½ + ⅓ + ¼)/2$ exceeds 1, so that no part of the top book is directly over the table. With 31 books, the overhang is 2.0136 book lengths.

Boole (Stott), Alicia (1860–1940)

The third daughter of George **Boole** and an important mathematician in her own right. At the age of 18, she was introduced to a set of wooden cubes devised by her brother-in-law Charles **Hinton** as an aid to visualization of the **fourth dimension**. Despite having had no formal education, she surprised everyone by becoming adept with the cubes and developing an amazing feel for four-dimensional geometry. She introduced the word ***polytope*** to describe a four-dimensional convex solid, and went on to explore the properties of the six regular polytopes and to make 12 beautiful card models of their three-dimensional central cross sections. She sent photographs of these models to the Dutch mathematician Pieter Schoute (1846–1923), who had done similar work and with whom she subsequently published two papers. The models themselves are now housed in the Department of Pure Mathematics and Mathematical Statistics at Cambridge University.

Boole, George (1815–1864)

An English mathematician and philosopher who is regarded as one of the founders of computer science. His great contribution was to approach logic in a new way, reducing it to a simple algebra and thus incorporating logic into mathematics. He pointed out the analogy between algebraic symbols and those that represent logical forms; his algebra of logic became known as **Boolean algebra** and is now used in designing computers and analyzing logic circuits. Although he never studied for a degree, Boole was appointed to the chair of mathematics at Queens College, Cork, Ireland, in 1849. One day in 1864 he walked the two miles in pouring rain from his home to the college and then lectured in wet clothes. A fever followed but whether this alone would have caused his demise is unknown. Certainly his condition wasn't helped by his wife, Mary (a niece of Sir George Everest, after whom the mountain is named), who, following the principle that remedy should resemble cause, put Boole to bed and threw buckets of water over him. He expired shortly after. See also **Boole** (**Stott**), **Alicia**.

Boolean

Taking only 0/1, true/false, yes/no values.

Boolean algebra

An **algebra** in which the **binary** operations are chosen to model the **union** and **intersection** operations in **set theory**. For any set A, the subsets of A form a Boolean algebra under the operations of union, intersection, and complement.

Borel, Emile (1871–1956)

A French mathematician who worked on divergent series, the theory of functions, probability, and **game theory**, and was the first to define games of strategy. He also founded **measure theory**, which applies the theory of sets to the theory of functions, and thus became an originator, with Henri **Lebesgue** and René Louis Baire (1874–1932), of the modern theory of functions of a real variable.

Borges, Jorge Luis (1899–1986)

An Argentinian author, essayist, and poet, many of whose short stories explore paradoxes and other strange avenues of mathematics, logic, philosophy, and **time**. For example, the possibility of branches in time is dealt with in "The Garden of Forking Paths," while the strange notion of the **Universal Library** is the subject of "The Library of Babel." Borges was profoundly influenced by European culture, English literature, and such thinkers as George Berkeley.

Borromean rings

Three rings linked in such a way that although they can't be separated, no two rings are linked; remove any one ring, however, and the other two fall apart. Named after the Italian family of Borromeo whose family crest has borne the rings since the fifteenth century, the design has been used in many places and times as a symbol of strength in unity. A form of the Borromean link known as Odin's triangle or the walknot ("knot of the slain") was used by the Norse folk of Scandinavia in two variants: a set of Borromean triangles and a unicursal curve that makes a trefoil knot. A motif of three interlaced crescent moons, similar to the Borromean rings, can be seen at the Palace of Fontainebleau. Designed by the architect Philibert de l'Orme, it is based on the moon emblem used by Diane de Poitiers (1499–1566), mistress of King Henry II of France. A similar pattern, but with three

Borromean rings A flowerpot on Isola Bella, an island on Lake Maggiore, near Arona in northern Italy, that bears the Borromeo family crest. *Peter Cromwell*

interlaced snakes in place of the crescent moons, occurs at various sites in Wales, including Bangor Cathedral. The Borromean rings are commonly used to symbolize the Christianity Trinity. An early source for this was a thirteenth-century French manuscript, now lost, in which the word *unitas* appears in the center, inside all the circles, and the three syllables of "tri-ni-tas" are distributed in the outer sectors. Borromean rings can also be found on Japanese family emblems, at a Japanese Shinto shrine north of Sakurai in the province of Nara, and in the sculptures of the Australian artist John Robinson. In North America, the design is known as the Ballantine rings after the New Jersey brewing company P. Ballantine and Sons who use it as a trademark with the rings labeled Purity, Body, and Flavor.

The rings first appeared in mathematics in the earliest work on knots by Peter **Tait** in 1876. The pattern of circles can be interlaced by replacing each of the six vertices by a crossing that shows how the circles pass over and under one another. Since there are two choices for each crossing, there are $2^6 = 64$ possible interlaced patterns. However, after taking symmetry into account, these 64 reduce to only 10 geometrically distinct patterns. Two patterns are considered to be the same if one can be obtained from the other by applying one or more of the following operations: rotation by 120°, reflection, and reflection in the plane of the pattern. The last symmetry operation means that the sense of all the crossings is switched. The rings can also be analyzed from the viewpoint of **topology**, which means that the designs are thought of as links made from a flexible and elastic material. If two links can be manipulated and deformed to look like one another (without breaking and joining the rings) then they are topologically equivalent. The 10 geometrically distinct patterns boil down to only five distinct topological types.

Borromean rings Three alternating rings carved in a panel in a walnut door of the church of San Sigismondo in Cremona, Italy. The emblem is one of several belonging to the Sforza family. *Peter Cromwell*

Borsuk-Ulam theorem

One of the most important and profound statements in **topology**: if there are n regions in n-dimensional space, then there is some hyperplane that cuts each region exactly in half, measured by volume. All kinds of interesting results follow from this. For example, at any given moment on Earth's surface, there must exist two antipodal points–points on exactly opposite sides of Earth–with the same temperature and barometric pressure! One way to see that this must be true is to think of two opposite points A and B on the equator. Suppose A starts out warmer than B. Now move A and B together around the equator until A moves into B's original position, and simultaneously B into A's original position. A is now cooler than B, so somewhere in between they must have been the same temperature. The Borsuk-Ulam theorem implies the **Brouwer fixed-point theorem** and also the **ham sandwich theorem**.

bottle sizes

Wine and champagne come in various standard bottle sizes, as shown in the table "Wine Bottle Sizes." These follow a **geometric sequence**, doubling in size with each step, up to the double-magnum, but thereafter increase in a more complicated way. There are also regional variations (for example, a Nebuchadnezzar may hold from 12 to 15 liters) and differences depending on the type of drink held.

Wine Bottle Sizes

Name of Size	Region	Capacity (liters)	Standard Bottle Equivalents
Baby/split	All	0.1875	0.25
Half-bottle	All	0.375	0.5
Bottle	All	0.75	1
Magnum	All	1.5	2
Double-magnum	All	3	4
Jeroboam	Burgundy, Champagne	5	6.67
Jeroboam	Bordeaux, Cabernet S.	4.5	6
Rehoboam	Burgundy, Champagne	4.5	6
Imperial	Bordeaux, Cabernet S.	6	8
Methuselah	Burgundy, Champagne	6	8
Salmanazar	Burgundy, Champagne	9	12
Balthazar	Burgundy, Champagne	12	16
Nebuchadnezzar	Burgundy, Champagne	15	20

boundary condition
The value of a **function** at the edge of the range of some of its variables. Recognizing the boundary conditions of an unknown function helps in its identification since other unknowns, such as variables in integrations, can then be eliminated.

boundary value problem
An **ordinary differential equation** or a **partial differential equation** given together with **boundary condition**s to ensure a unique solution.

Bourbaki, Nicholas
Not an individual but a collective mathematician. In the 1930s, the Bourbaki group, made up of some of the brightest mathematicians in France, began as a club, holding secret meetings in Strasbourg to update university lectures and texts in the wake of World War I, which had essentially wiped out a generation of young talent. In time, Bourbaki authored encyclopedic accounts of all areas of mathematics, and its influence became widespread.

Its origins can be traced to 1934 and to André Weil and Henri Cartan who were maîtres de conférences (the equivalent of assistant professors) at the University of Strasbourg. One of their duties was to teach differential and integral calculus but they found the standard text on this subject, *Traité d'Analyse* by E. Goursat, wanting. Following a suggestion by Weil to write a new "Treatise on Analysis," a group of about 10 mathematicians began to meet regularly to plan the new work. Quickly, it was decided that the work should be collective, without any acknowledgment of individual contributions, and this became a feature of Bourbaki's output. In the summer of 1935, the pen name Nicholas Bourbaki was chosen, and the initial membership consisted of Weil, Cartan, Claude Chevalley, Jean Delsarte, and Jean Dieudonné–all former students at the École Normale Supérieure in Paris. Over the years, the membership varied; some people in the first group dropped out quickly, others were added, and later there was a regular process of addition and retirement (mandatory by the age of 50).

Bourbaki adopted rules and procedures that to outsiders often seemed eccentric and even bizarre. For example, during meetings to review and revise drafts for the various books the group developed, anyone could express his opinion as loudly as he wanted at any time, so it was not uncommon for several distinguished mathematicians to be on their feet at the same time shouting monologues at the top of their voices. Somehow out of this mayhem emerged work of extreme precision, to the point of pedantry and dryness. Bourbaki would have nothing to do with geometry or any attempt at visualization, and believed that mathematics should distance itself from the sciences. However, despite its tendency to be boring and long-winded, Bourbaki did achieve its goal: to set down in writing what was no longer in doubt in modern mathematics.

brachistochrone problem
A problem with which Johann Bernoulli (see **Bernoulli Family**) challenged his contemporaries in *Acta Eruditorum* in June 1696:

> Following the example set by Pascal, Fermat, etc., I hope to gain the gratitude of the whole scientific community by placing before the finest mathematicians of our time a problem which will test their methods and the strength of their intellect. If someone communicates to me the solution of the proposed problem, I shall publicly declare him worthy of praise. . . . Given two points A and B in a vertical plane, what is the curve traced out by a point acted on only by gravity, which starts at A and reaches B in the shortest time?

Isaac **Newton** reportedly solved the problem between four in the evening and four in the morning after a hard day at the Royal Mint, later commenting: "I do not love to be dunned [pestered] and teased by foreigners about mathematical things. . . ." Other correct solutions came from Gottfried **Leibniz**, the Frenchman Guillaume **de L'Hôpital**, and Johann's brother Jakob. They, like Johann, realized that the solution to the brachistochrone problem, as it was also to the **tautochrone problem**, was a curve known as the **cycloid**.

Brahmagupta (A.D. 598–after 665)
A Hindu astronomer and mathematician who became the head of the observatory at Ujjain–the foremost mathematical center of ancient India. His main work, *Brahmasphutasiddhanta* (The opening of the universe), written in 628, contains some remarkably advanced ideas, including a good understanding of the mathematical role of **zero**, rules for manipulating both positive and **negative number**s, a method for computing square roots, methods of solving linear and some **quadratic** equations, and rules for summing series. His contributions to astronomy were equally ahead of their time. *Brahmagupta's theorem* states that in a cyclic quadrilateral (a four-sided shape whose corners lie on a circle) having perpendicular diagonals, the perpendicular to a side from the point of intersection of the diagonals always bisects the opposite side. **Brahmagupta's formula** for the area of a cyclic quadrilateral with sides of length a, b, c, and d is $\sqrt{(S-a)(S-b)(S-c)(S-d)}$, where $S=(a+b+c+d)/2$. As d goes to zero, this reduces to **Heron's formula**.

braid
A collection of lines or strings that are plaited together and whose ends are attached to two parallel straight lines.

Braid theory was pioneered by the Austrian mathematician Emil Artin (1898–1962) and is related to **knot** theory. It also has other applications: for instance, if we consider the way the roots of a **polynomial** move as one of the polynomial's coefficients changes, this motion can be thought of as a braid.

Brianchon's theorem

Given a **conic section**, if we circumscribe a hexagon about it, then the major diagonals of the hexagon are concurrent.

bridges of Königsberg

A famous routing problem that was analyzed and solved by Leonhard **Euler** in 1736, and that helped spur the development of **graph** theory. The old city of Königsberg, once the capital of East Prussia, is now called Kaliningrad. It falls within a tiny part of Russia known as the Western Russian Enclave, between Poland and Lithuania, which (to the surprise even of many modern Russians) is not connected with the rest of the country! Königsberg lay some four miles from the Baltic Sea on rising ground on both sides of the river Pregel (now the Pregolya), which flowed through the town in two branches before uniting below the Grune Brocke (Green Bridge). Seven bridges (numbered in the diagram) crossed the Pregel and connected various parts of the city (letters A to D), including Kneiphof Island (B), the site of Königsberg University and the grave of its most famous son, the great philosopher Emmanuel Kant (1724–1804).

A question arose among the town's curious citizens: Was it possible to make a journey across all seven bridges *without having to cross any bridge more than once*? No one had been able to do it, but was there a solution? Euler, who was in St. Petersburg, Russia, at the time, heard about this puzzle and looked into it. In 1736, he published a paper called *Solutio problematis ad geometriam situs pertinentis* (The solution of a problem relating to the geometry of position) in which he gave his answer. Euler reasoned that, for such a journey to be possible, each land mass would need to have an even number of bridges connected to it, or, if the journey began at one land mass and ended at another then those two land masses alone could have an odd number of connecting bridges while all the other land masses would have to have an even number of connecting bridges. Since the Königsberg bridges violated this layout, a grand tour that involved only one crossing per bridge was impossible. Euler's paper was important because it solved not just the Königsberg conundrum but the much more general case of any network of points, or *vertices,* that are connected by lines, or *arcs*. What is more, the words *geometry of position* in the title show that Euler realized that he was dealing with a different type of geometry where distance is irrelevant. So this work can be seen as a prelude to the subject of **topology**. See also **Euler path**.

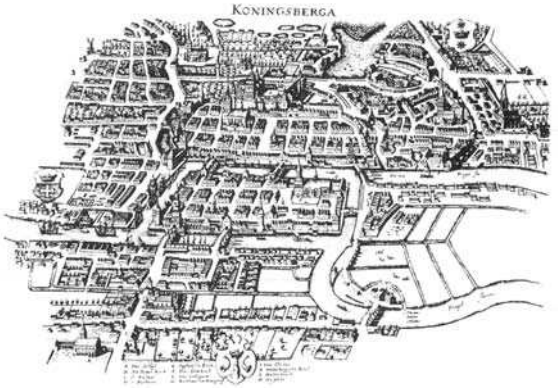

bridges of Königsberg An old map of the city showing the seven bridges.

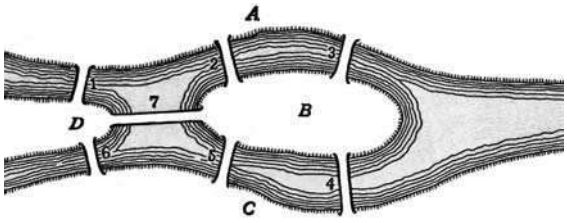

bridges of Königsberg The essential layout of the bridges. *B* represents Kneiphof Island.

Briggs, Henry (1561–1630)

An English mathematician who introduced common **logarithms** (to base 10) and was largely responsible for getting scientists to use them. Although a well-regarded mathematician in his own right, holding the Savilian chair of geometry at Oxford, Briggs was most important as a contact and as a public relations man for his field.

Brocard problem

The problem of finding the integer solutions of the equation

$$n! + 1 = m^2.$$

These solutions are called *Brown numbers,* and only three of them are known: (5, 4), (11, 5), and (71, 7). Paul **Erdös** conjectured that there are no others.

broken chessboard

See **polyomino**.

Bronowski, Jacob (1908–1974)
A Polish mathematician who worked first on operation theory and its application to military strategy, but later on the ethics of science. He is remembered for writing and narrating the television series *The Ascent of Man* in 1973.

Brouwer, Luitzen Egbertus Jan (1881–1966)
A Dutch mathematician who opposed the logicist school of Bertrand **Russell** and established the intuitionist school of mathematical thought. He was also one of the founders of **topology**, doing most of his work in this field between 1909 and 1913.

Brouwer fixed-point theorem
An amazing result in **topology** and one of the most useful theorems in mathematics. Suppose there are two sheets of paper, one lying directly on top of the other. Take the top sheet, crumple it up, and put it back on top of the other sheet. Brouwer's theorem says that there must be at least one point on the top sheet that is in exactly the same position relative to the bottom sheet as it was originally. The same idea works in three dimensions. Take a cup of coffee and stir it as much as you like. Brouwer's theorem insists that there must be some point in the coffee that is in exactly the same spot as it was before you started stirring (though it might have moved around in between). Moreover, if you stir again to move that point out of its original position, you can't help but move another point back into its original position! Not surprisingly, the formal definition of Brouwer's theorem makes no mention of sheets of paper or cups of coffee. It states that a continuous function from an *n*-**ball** into an *n*-ball (that is, any way of mapping points in one object that is topologically the same as the filling of an *n*-dimensional sphere to another such object) must have a fixed point. Continuity of the function is essential: for example, if you rip the paper in the previous example then there may not be a fixed point.

Brownian motion
The most common type of continuous **random** motion of a particle, one in which the particle's vibrations have more energy at short length and time scales. It models the motion of a particle in a fluid, fluctuation of stock prices, and many other processes. Brownian motion is named after the Scottish botanist Robert Brown (1773–1858) who first studied it.

Brun's constant
See **twin primes**.

bubbles
Whether alone or in groups joined together, bubbles get their shape by following one simple rule: soap film always tries to form a **minimal surface**. The mathematical study of bubbles and films began in earnest in the 1830s with the experiments of Joseph **Plateau**. A single bubble will always try to form a sphere because this shape, as proposed by **Archimedes** and proved by Hermann Amandus Schwarz (1843–1921) in 1884, is the minimal surface enclosing a single volume. For a long time, mathematicians believed that the minimal surface for enclosing two separate volumes of air is a double bubble separated by a third surface, which meets the other two along a circle at 120° and is flat if the bubbles enclose the same volume and, otherwise, is a spherical surface that bulges a little into the larger of the two. The *double bubble conjecture* was finally confirmed by a team of four mathematicians in 2000.

Another great bubble mystery that has recently been solved is why the bubbles in a glass of Guinness appear to sink rather than rise. Bubbles that rise, like those in a saucepan or those breathed out by a diver, are a familiar sight and easy to explain: gas bubbles are lighter than liquid and experience a buoyancy force that drives them up toward the liquid surface. But many of the bubbles in a glass of Guinness can be seen heading downward. Researchers have found that large bubbles in the center of the glass move upward relatively quickly and drag liquid with them. Since the amount of liquid in the glass stays the same (unless someone drinks it!) the liquid moving upward near the center must eventually move back down near the walls of the glass. This downward-

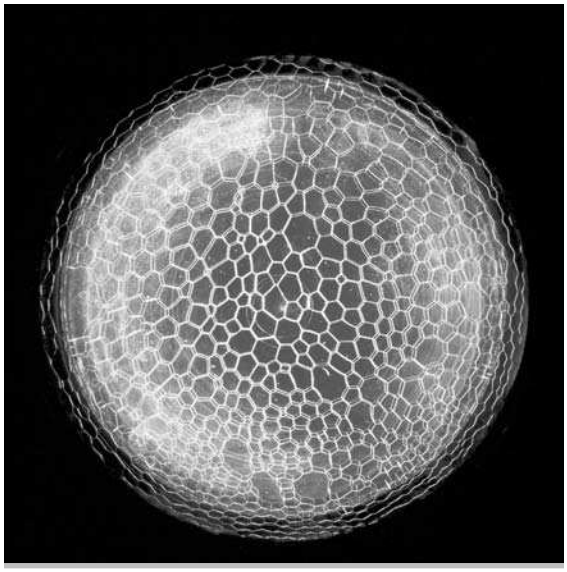

bubbles A honeycomb-like arrangement of tightly packed bubbles.
Australian National University

moving liquid has a dragging effect on the bubbles. Larger bubbles are more buoyant than smaller bubbles, and continue to move upward. Smaller bubbles (less than 0.05 mm in diameter) aren't buoyant enough to resist this drag force, and move downward with the liquid near the sides of the glass. Since Guinness is quite opaque, and these downward-moving small bubbles are close to the side of the glass, it often looks as if almost all the bubbles are moving down. See also **Plateau problem**.

buckyball

Also known as a *fullerene,* a large molecule made of carbon atoms arranged in the form of a convex polyhedral cage. Buckyballs are named after the architect Richard Buckminster Fuller because they look like the geodesic domes that he invented. The first buckyball to be discovered (by accident) was C_{60}, in which 60 carbon atoms are arranged at each of the vertices of a truncated **icosahedron**. This shape, which looks like a soccer ball, has 32 faces, of which 20 are regular hexagons and 12 are regular pentagons. Many

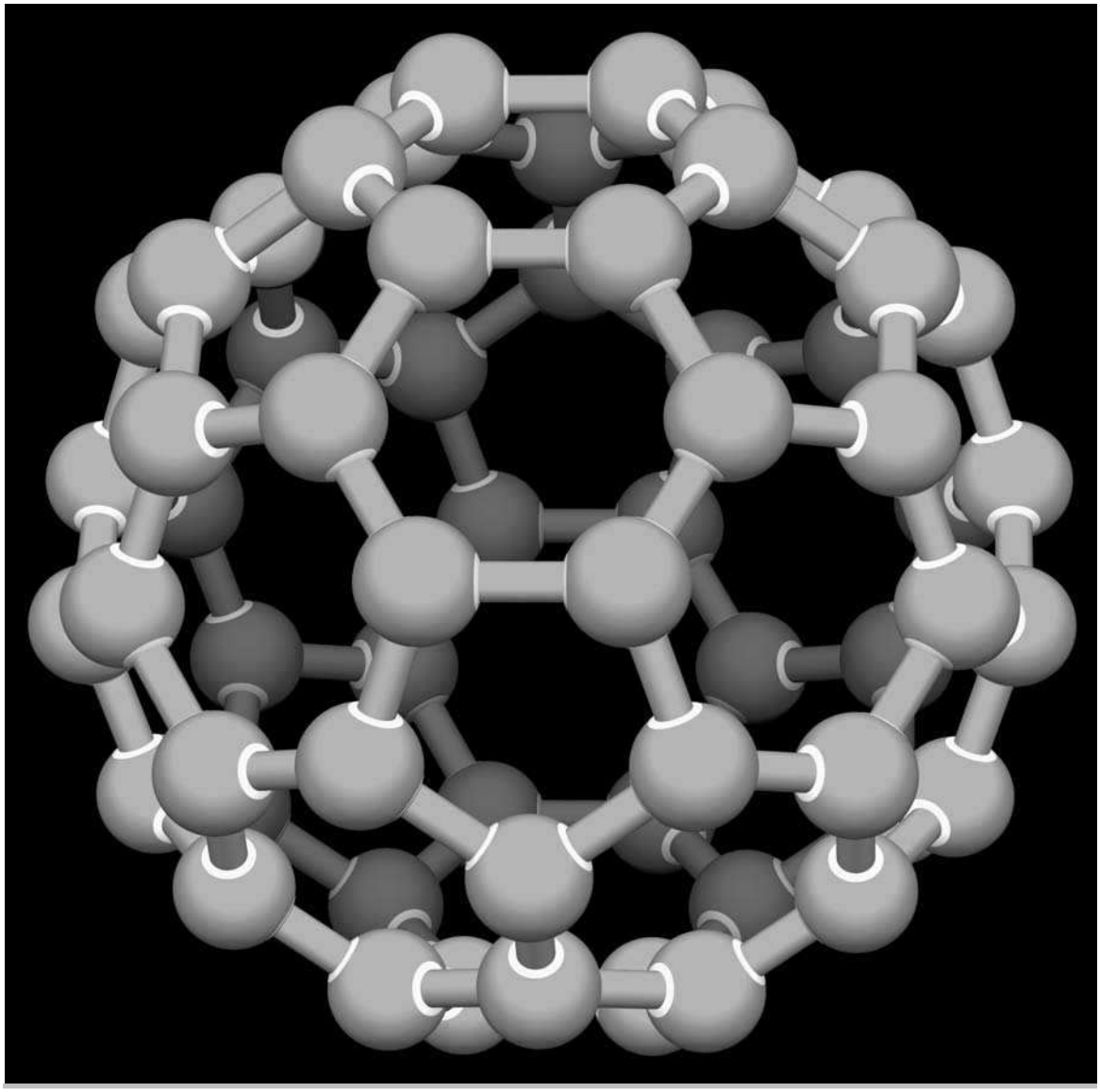

buckyball A molecule of Buckminster fullerene—a buckyball. *Nick Wilson*

different types of buckyballs are known. Common ones have 70, 76, and 84 carbon atoms, but all are built up exclusively from hexagonal and pentagonal faces in arrangements that follow **Euler's formula**. This formula ensures that while the number of hexagons can vary from one type of fullerene to another, every fullerene has exactly 12 pentagons. (In fact, buckyballs with heptagonal faces have been seen, but these faces are concave and are regarded as defects.)

Buffon's needle

An early problem in geometrical probability (see **probability theory**) that was investigated experimentally in 1777 by the French naturalist and mathematician Comte Georges Louis de Buffon (1707–1788). It involves dropping a needle repeatedly onto a lined sheet of paper and finding the probability of the needle crossing one of the lines on the page. The result, surprisingly, is directly related to the value of **pi**.

Consider a simple case in which the lines are 1 cm apart and the needle is 1 cm in length. After many drops the probability of the needle lying across a line is found to be very close to $2/\pi$. Why? There are two variables: the distance from the center of the needle to the closest line, d, which can vary between 0 and 0.5 cm, and the angle, θ, at which the needle falls with respect to the lines, which can vary between 0 and 180°. The needle will hit a line if $d \leq \frac{1}{2} \sin\theta$. In a plot of d against $\frac{1}{2} \sin\theta$, the values on or below the curve represent a hit; thus, the probability of a success is the ratio of the area below the curve to the area of entire rectangle. The area below the curve is given by the integral of $\frac{1}{2} \sin\theta$ from 0 to π, which is 1. The area of the rectangle is $\pi/2$. So, the probability of a hit is $1/(\pi/2)$ or $2/\pi$ (about 0.637). Dropping a needle many times onto lined paper gives an interesting (but slow) way to find π. This kind of probabilistic means of performing calculations is the basis of a technique known as the **Monte Carlo method**.

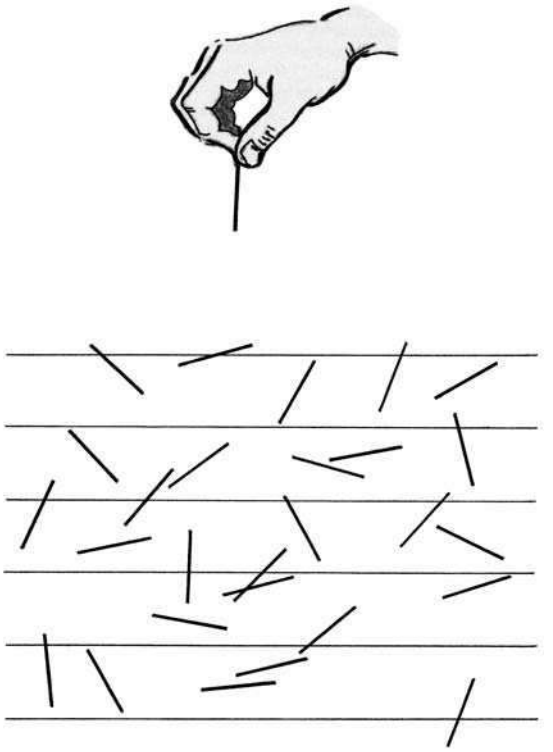

Buffon's needle Needles are dropped randomly onto a lined surface.

bundle

A map between two **topological space**s A and B, where the sets $f^{-1}(b)$ for elements b of B (known as fibers), are all **homeomorphic** to a single space. The simplest example is the **Möbius band**, for which A is the Möbius band, B is a circle, and the fibers are homeomorphic to an interval on the real number line.

Burali-Forti paradox

An argument that shows that the collection of **ordinal number**s (numbers that give the position of objects) do not, unlike the **natural number**s, form a **set**. Each ordinal number can be defined as the set of all its predecessors. Thus:

0 is defined as {}, the **empty set**

1 is defined as {0} which can be written as {{}}

2 is defined as {0, 1} which can be written as {{}, {{}}}

3 is defined as {0, 1, 2} which can be written as {{}, {{}}, {{}, {{}}}} . . .

in general, n is defined as $\{0, 1, 2, \ldots n-1\}$

If the ordinal numbers formed a set, this set would then be an ordinal number greater than any number in the set. This contradicts the assertion that the set contains all ordinal numbers. Although the ordinal numbers don't form a set, they can be regarded as a collection called a class.

Buridan's ass

A paradox of medieval logic concerning the behavior of an ass that is placed equidistantly from two piles of food of equal size and quality. Assuming that the behavior of the ass is entirely rational, it has no reason to prefer one pile to the other. Thus lacking a basis to decide which pile to eat first, it remains in its original position and starves. With one pile it would have lived; having two identical piles it dies. How can this make sense? The paradox is named after the French philosopher Jean Buridan (c. 1295–1356).

burr puzzle

An interlocking wooden puzzle that, when put together, typically looks like three rectangular blocks crossing one another at right-angles. Little is known about its early history, but it was certainly produced both in Asia and Europe in the eighteenth century. It acquired the name *Chinese puzzle*, probably because so many were produced in the Orient from the early 1900s. In 1928, Edwin Wyatt published *Puzzles in Wood*,[355] the first book devoted to the subject, and introduced the term *burr puzzle* because of the likeness of the assembled toy to a seed burr.

Burr puzzles consist of three (the smallest number), six (the most common number), twelve, or other numbers of pieces that are notched in various ways so as to pose a challenge to the would-be assembler. The earliest known reference to the popular six-piece burr appears in a Berlin catalog of 1790, but not until 1917 was a patent taken out on a particular design. In 1977, William **Cutler** proved that 25 possible notchable pieces can be used to make solid six-piece burrs and that they can be put together in 314 ways. (Pieces are considered notchable if they can be made by a sequence of notches that are produced by chiseling out the space between two saw cuts.) Cutler also proved there are 369 general pieces from which solid burrs can be made and that these can be assembled in 119,979 ways. One particular form of burr has six identical pieces, all of which move outward or inward together. Another form, with flat notched pieces, has one piece with an extra notch or an extended notch that allows it to fit in last, either by sliding or twisting, although this isn't initially obvious. This form is sometimes made with equal pieces so that it can only be assembled by force, perhaps after steaming.

butterfly effect

One of the more sensational and loudly touted claims of **chaos** theory: a butterfly beating its wings could, by an intricate chain of causes and effects, give rise to a hurricane. The gist of the argument is that minuscule disturbances can be amplified unpredictably into major phenomena. However, the overwhelming likelihood is that any effect as small as the beating of a butterfly's wing would be quickly dampened out and play no significant part in future events. See also **causality**.

butterfly theorem

Let M be the midpoint of a **chord** PQ of a circle, through which two other chords AB and CD are drawn. If AD intersects PQ at X and CB intersects PQ at Y, then M is also the midpoint of XY. The theorem gets its name from the shape of the resulting figure.

Byron, (Augusta) Ada (1815–1852)

Also known as Lady Lovelace, the daughter of Lord Byron and one of the most picturesque characters in computer prehistory. Her parents separated five weeks after her birth and she was raised by her mother (neé Annabella Milbanke), whom Lord Byron had called his "Princess of Parallelograms" because of her interest in mathematics. She was determined that Ada would become a mathematician and scientist, not a poet like her father. Ada, however, managed to combine both worlds, blending her science with poetical vision and her mathematics with metaphor.

At the age of 17 she was introduced to Mary Somerville, a remarkable woman who translated **Laplace**'s works into English, and whose texts were used at Cambridge (where a

burr puzzle A difficult six-piece burr with 19 false assemblies and a final piece that requires 10 directional moves. *Mr. Puzzle Australia/William Cutler*

women's college is now named after her). It was at one of Mary Somerville's dinner parties, in November 1834, that Ada first heard of Charles **Babbage**'s ideas for a new calculating machine, the Analytical Engine, and was immediately intrigued. In 1843, Ada, married and the mother of three children, translated a French article about the Engine and showed it to Babbage. He suggested that she add her own notes, which turned out to be three times the length of the original piece and included prescient comments about how such a machine might be used to compose complex music, produce graphics, and solve scientific problems. A regular correspondence ensued between Ada and Babbage, during which Ada suggested to Babbage a plan for how the engine might calculate **Bernoulli numbers**—a plan now regarded as the first computer program. In recognition of this, a software language developed by the U.S. Department of Defense was named "Ada" in 1979. Like her father, she died at the age of 36, following a series of illnesses.[335]

byte

A string of 8 **bit**s, used to represent a character.

C

caduceus

In mathematics, a pair of curves in space, each of which is a **helix** and which twist in opposite directions around one another. In mythology, the caduceus is the wing-topped staff, wound about by two snakes, carried by Hermes, the Greek messenger of the gods. The snakes became entwined after Hermes threw his staff at them to stop their fighting. A caduceus was carried by Greek officials and became a Roman symbol for truce and neutrality. Since the sixteenth century it has also served as a symbol of medicine. Before modern medicine, people infected by parasitic worms were treated by physicians using a stick and a knife. A slit would be cut in the patient's skin in front of the worm, and as the parasite crawled out of the incision, the worm would be wound around a stick until it was totally removed. The medical treatment of parasitic worm infection by knife and stick is believed to be the inspiration for the original caduceus. It was used as a promotional sign for physicians of that period.

caduceus *Auckland Medical Research Foundation*

Cage, John (1912–1992)

The American avant-garde composer perhaps best known for the quietest piece of music ever written. His piano composition *4′33″* calls for the player to sit in silence for 273 seconds–this being the number of degrees below zero on the centigrade scale of **absolute zero** at which molecular motion stops. *4′33″* was inspired by Cage's visit to Harvard University's anechoic chamber about which he wrote:

> There is no such thing as empty space or empty time. There is always something to hear or something to see. In fact, try as we might to make a silence, we cannot. For certain engineering purposes, it is desirable to have as silent a situation as possible. Such a room is called an anechoic chamber, its walls made of special materials, a room without echoes. I entered one at Harvard University . . . and heard two sounds, one a high and one a low. When I described them to the engineer in charge, he informed me that the high one was my nervous system and the low one was my blood circulation.

Cage's *4′33″* breaks traditional boundaries by shifting attention from the stage to the audience and even beyond the concert hall. The listener becomes aware of all sorts of sound, from the mundane to the profound, from the expected to the surprising, from the intimate to the cosmic: shifting in seats, riffling programs, breathing, a creaking door, passing traffic, a recaptured memory. Is sitting quietly alone for 273 seconds equivalent to a private performance (and audience) of the piece? Or, in the final analysis, is it all pretentious nonsense? In his essay on "Nothing" Martin Gardner wrote: "I have not heard *4′33″* performed, but friends who have tell me it is Cage's finest composition."

Caesar cipher

The simplest and oldest known type of **substitution cipher**, attributed to Julius Caesar, who used it to send government messages. In it, each letter in the alphabet is replaced by another letter using a predefined rule that shifts the alphabet a uniform amount to the right or left. For example, a shift of three units to the right, would turn the "This is secret" into "Wklv lv vhfuhw."

cake-cutting

How can a group of people cut up a cake so that each gets what they consider to be a fair share? In its modern mathematical form, this classic problem of *fair division* dates from World War II, when Hugo **Steinhaus** tackled it using a **game theory** approach.[315] Any number of "players" are allowed. They agree on rules for dividing the cake, and

then everyone follows those rules. In the end, each player must get what he or she perceives to be a fair share. In the simplest case, involving just two people, there is an easy, well-known strategy: one cuts, the other chooses. Can this method be extended to three people? Can it be extended so that each person, according to his own judgment, receives the *biggest* piece? Steinhaus was able to prove that a so-called *envy-free division,* where everyone believes they got the best deal exists in every case, for any number of players. However, it was left for others to find actual algorithms that worked for three or more players.

A three-person envy-free method was first devised by John Selfridge and John **Conway**. Suppose the players are called Alice, Bob, and Carol. The method goes like this: (1) Alice cuts the cake into what she thinks are thirds. (2) Bob trims one piece to create a two-way tie for largest, and sets the trimmings aside. (3) Carol picks a piece, then Bob, then Alice. Bob has to take a trimmed piece if Carol does not. Call the person who took the trimmed piece T, and the other (of Bob and Carol) NT. (4) To deal with the trimmings, NT cuts them into what she thinks are thirds. (5) The players pick pieces in this order: T, Alice, NT. The key to the success of the Selfridge-Conway strategy is that for the trimmings, Alice has an "irrevocable advantage" with respect to T, since Alice will never envy T even if T gets all the trimmings. Thus Alice can pick after T and allow the method to end in a finite number of steps.

For four or more cake-cutters, envy-free solutions are very complex and can take arbitrarily long to resolve. However, a general solution of the problem of fair, envy-free division was eventually found in 1992 by the Americans Steven Brams, a political scientist at New York University, and Alan Taylor, a mathematician at Union College in Schenectady, New York.[51, 52] With two players, the first player cuts the cake in half. With three players, the first player cuts the cake into thirds. With four players, Brams and Taylor showed, the first player, say Bob, cuts the cake into five equal-looking pieces. He passes them to Carol, who trims two at most to create a three-way tie for largest in her eyes. She sets the trimmings aside and gives the five pieces to Don, who trims one at most to create a two-way tie for largest in his eyes. Alice, the fourth player, now selects the piece she likes best. Choosing proceeds in the reverse order from cutting, with the proviso that anyone who trimmed one or more pieces must take one of them if any are still available when it's his or her turn to choose. The extra piece to begin with assures that no player gets second-best. If someone takes a piece she likes before it's her turn to choose, an equivalent piece or better always remains on the table. According to a formula Brams and Taylor developed, Bob must cut the cake into at least $2^{(n-2)+1}$ pieces at the start. This amounts to nine pieces for five players, 17 pieces for six, and so on. Bob has to cut all these extra pieces to make sure that, when he finally gets to choose at the end, there will be a piece left that hasn't been either trimmed or chosen by one of the many other players. With 22 players, Bob has to divide the cake into over a million pieces–small crumbs of comfort in the quest for a fairer world.[268]

Calabi-Yau space

A type of mathematical space that enters into **string theory**, where the geometry of the universe is held to consist of at least 10 dimensions–the four familiar dimensions of **space-time** and six compact dimensions of Calabi-Yau space. These extra dimensions are so tightly curled up that they aren't noticed. Although the main application of Calabi-Yau spaces is in theoretical physics, they are also interesting from a purely mathematical standpoint.

calculus

> *The calculus is the greatest aid we have to the application of physical truth in the broadest sense of the word.*
> –William Fogg Osgood (1864–1943)

The branch of mathematics that deals with (1) the rate of change of quantities (which can be interpreted as the slopes of curves), known as *differential calculus,* and (2) the length, area, and volume of objects, known as *integral calculus.* Calculus was one of the most important developments in mathematics and also in physics, much of which involves studying how quickly one quantity changes with respect to another. It is no coincidence that one of the founders of calculus was the brilliant English physicist Isaac **Newton**; another was Gottfried **Leibniz**. Although students nowadays learn differential calculus first, integral calculus has older roots.

calculus of variations

Calculus problems, especially **differentiation** and *maximization,* that involve **function**s on a set of functions of a real variable. An example is to find the shape of a cable suspended from both ends.

calendar curiosities

The earliest event in human history for which a definite date is known is a battle between the Lydians (allies of the Greek Spartans) and the Medes (ruled by the Persian king Cyrus) who had been locked in a war for five years. As the two sides faced each other for a crucial daytime confrontation, a solar eclipse occurred. This was taken as a sign of the gods' disapproval and the Lydians and Medes agreed to end the fighting then and there. The dates of solar eclipses can be figured out with great accuracy, and this one is known to have taken place on May 28, 586 B.C.

Much less certain is the birth date of Christ. It was not until A.D. 440 that Christmas was celebrated on Decem-

ber 25. This date was chosen because it coincided with the birth date of Mithras, the Persian sun-god, and was close to the pagan festival of Yule. In A.D. 534, Dionysius Exiguus (also known as Dennis the Little) created the system, still used today, of counting the years from the birth of Christ. Unfortunately, he slipped up in his calculations. No one knows exactly when Jesus was born, but it was probably around 6 B.C. and certainly before the death of Herod the Great in 4 B.C.

As for the future, there's no shortage of predictions about the end of the world. According to the Mayan "long count" linear calendar, it will happen on June 5, 2012. Other calendric curiosities: February 1865 is the only month in recorded history not to have a full moon, and months that begin on a Sunday will always have a Friday the 13th.

Caliban

A pseudonym of Hubert **Phillips**.

Caliban puzzle

A logic puzzle in which one is asked to infer one or more facts from a set of given facts.

cannonball problem

The mathematical analysis of stacks of cannonballs (or of spheres in general) that has its roots in a question posed by Sir Walter Raleigh, explorer, introducer of the potato and tobacco to Britain, and part-time pirate on the high seas. Raleigh asked his mathematical assistant, Thomas Harriot, how he could quickly figure out the number of cannonballs in a square pyramidal stack without having to count them individually. Harriot solved this problem without difficulty. If k is the number of cannonballs along the side of the bottom layer, the number of cannonballs in the pyramid n is equal to $\frac{1}{6}\, k(1 + k)(1 + 2k)$. For example, if $k = 7$, $n = 420$. A more specific form of the cannonball problem asks what is the smallest number of balls that can first be laid out on the ground as an $n \times n$

cannonball problem Cannonballs stacked in Narbonne, France. *Australia National University*

square, then piled into a square pyramid k balls high? In other words, what is the smallest square number that is also a square pyramidal number? This answer is the smallest solution to the **Diophantine equation**

$$\tfrac{1}{6}\, k(1 + k)(1 + 2k) = n^2$$

and turns out to be $k = 24$, $n = 70$, corresponding to 4,900 cannonballs. The ultimate form of the cannonball problem is to ask if there are any other, larger solutions. In 1875 Edouard **Lucas** conjectured that there weren't, and in 1918 G. N. Watson proved that Lucas was right.[345]

Returning to Elizabethan times, Thomas Harriot's interest in spheres extended far beyond piles of cannonballs. Harriot was an atomist, in the classical Greek sense, and believed that understanding how spheres pack together was crucial to understanding how the basic constituents of nature are arranged. Harriot also carried out numerous experiments in optics and was far ahead of his time in this field. So when, in 1909, Johannes **Kepler** wanted some advice on how to give his own theories on optics a stronger scientific underpinning who better to turn to than the Englishman? Harriot supplied Kepler with important data on the behavior of light rays passing through glass, but he also stimulated the German's interest in the sphere-packing problem. In response, Kepler published a little booklet titled *The Six-Cornered Snowflake* (1611) that would influence the science of crystallography for the next two centuries and that contained what has come to be known as **Kepler's conjecture** about the most efficient way to pack spheres.

canonical form

A form of any given **polyhedron** distorted so that every edge is **tangent** to the unit sphere and the center of gravity of the tangent points is the origin.

Cantor, Georg Ferdinand Ludwig Philipp (1845–1918)

A Russian-born German mathematician who founded **set theory** and introduced the concept of **transfinite number**s. His shocking and counterintuitive ideas about **infinity** drew widespread criticism before being accepted as a cornerstone of modern mathematical theory.

Cantor was 11 when his family moved from St. Petersburg to Germany. Despite attempts to push him into the more lucrative field of engineering, he eventually won his father's approval to study math at the Polytechnic of Zurich. The following year, 1863, his father died and Cantor switched to the University of Berlin where he studied under some of the greats of the day, including Karl **Weierstrass** and Leopold **Kronecker**. After receiving his doctorate in 1867, he had trouble finding a good job and was forced to accept a position as an unpaid lecturer and later as an assistant professor at the backwater University of Halle. In 1872, he achieved his first breakthrough–and a promotion–by proving that if a **function** is continuous (in other words, its graph is smooth) throughout an interval, it can be represented by a unique trigonometric series. This work, suggested to him by his colleague Heinrich Heine, was crucial because it led Cantor to think about the relations between points, represented by **real number**s, that make up an unbroken line–the so-called *continuum.* Cantor realized that **irrational number**s can be represented as infinite sequences of **rational number**s, so that they can be understood as geometric points on the real-number line, just as rational numbers can. He was now in uncharted territory and at odds with mathematical orthodoxy, which frowned on the idea of actual **infinity**; however, he found like-minded friends in Richard **Dedekind** and, later, Gösta **Mittag-Leffler**.

In 1873 to 1874 Cantor proved that the rational numbers could be paired off, one by one, with the natural numbers and were therefore countable, but that there was no such one-to-one correspondence with the real numbers. He then went on to show, incredibly, that there are exactly the same number of points on a short line as there are on an indefinitely long line, or on a plane, or in any mathematical space of higher dimensions. On this, he wrote to Dedekind: "I see it, but I don't believe it!"

By 1883, Cantor had abandoned his earlier reticence about dealing with irrationals only as sequences of rationals and started to think in terms of a new type of number–the **transfinite number**s. The sets of natural numbers and of real numbers were, he reasoned, just two elements of a series of different kinds of infinity. This dramatic extension of the number system to allow for legitimate mathematics of the infinite was violently opposed. Henri **Poincaré** said that Cantor's theory of infinite sets would be regarded by future generations as "a disease from which one has recovered." Kronecker went further and did all he could to ridicule Cantor's ideas, suppress publication of his results, and block Cantor's ambition of gaining a position at the prestigious University of Berlin. In the spring of 1884 Cantor suffered the first of several attacks of depression, exacerbated if not induced by the negative reaction of his contemporaries. In between these attacks, he published further results but was increasingly troubled by his failure to prove the **continuum hypothesis**–his belief that the order of infinity of the real numbers came next after that of the natural numbers. Although his later years were spent in and out of a sanatoria, he lived long enough to see his ideas on set theory vindicated and be described by David **Hilbert** as "the finest product of mathematical genius and one of the supreme achievements of purely intellectual human activity."

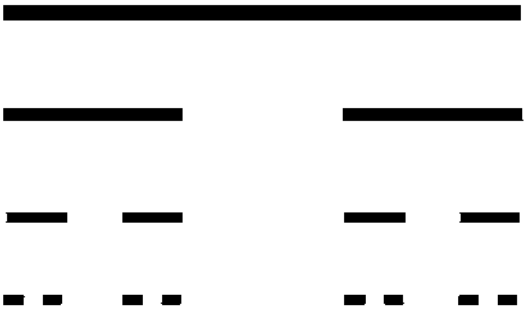

Cantor dust.

Cantor dust

Also known as the *Cantor set,* possibly the first pure **fractal** ever found. It was detected by Georg **Cantor** around 1872. To produce Cantor dust, start with a line segment, divide it in three equal smaller segments, take out the middle one, and repeat this process indefinitely. Although Cantor dust is riddled with infinitely many gaps, it still contains uncountably many points. It has a **fractal dimension** of log 2/log 3, or approximately 0.631. See also **Sierpinski carpet**.

cap

The symbol ∩ used to denote the **union** between two **set**s.

Cardano, Girolamo (1501–1570)

A celebrated Renaissance mathematician, physician, astrologer, and gambler, whose writings on the use of **negative number**s are the earliest known in Europe. As a physician, he gave one of the first clinical descriptions of typhoid fever. The illegitimate child of a mathematically gifted lawyer who was a friend of Leonardo da Vinci, he entered the University of Pavia in 1520 and later studied medicine at Padua. His eccentric and confrontational style earned him few friends, and he had trouble finding work. Eventually, he won a reputation as a physician and his services were highly valued at the courts.

Today, Cardano is remembered mostly for his achievements in algebra. He published the solutions to the **quartic** and **cubic equations** in his book *Ars magna* (1545). The solution to the cubic was communicated to him by Niccoló **Tartaglia** (who later claimed that Cardano had sworn not to reveal it, and became embroiled with Cardano in a decade-long fight), and the quartic was solved by Cardano's student Lodovico Ferrari. Both were acknowledged in the foreword of the book. Cardano was notoriously short of money and kept himself afloat by being an accomplished gambler and chess player. A book by him about games of chance, *Liber de Ludo Aleae* (Book on games of chance), written in the 1560s but published posthumously in 1663, contains the first systematic treatment of **probability theory**, as well as a section on effective cheating methods. Cardano invented several mechanical devices including the combination lock, the *Cardano suspension* (consisting of three concentric circles that allow a supported compass to rotate freely), and the *Cardan shaft,* which allows the transmission of rotary motion at various angles and is used in vehicles to this day. He made several contributions to hydrodynamics and claimed that perpetual motion is impossible, except in celestial bodies. He published two encyclopedias of natural science that contain a wide variety of inventions, facts, and occult superstitions.

Cardano led a beleaguered life. His elder and favorite son was executed in 1560 after he confessed to having poisoned his mercenary, cuckolding wife. Cardano's daughter was allegedly a prostitute who died from syphilis, prompting him to write a treatise about the disease. His younger son was a gambler who stole money from him. And Cardano himself was accused of heresy in 1570 because he computed the horoscope of Jesus Christ. Apparently, his own son contributed to the prosecution. Cardano was arrested and had to spend several months in prison, then was forced to abjure and had to give up his professorship. He moved to Rome, received a lifetime annuity from Pope Gregory XIII, and finished his not-uneventful autobiography. He died on the day he had (supposedly) astrologically predicted. See also **Chinese rings**.

Cardan's rings

See **Chinese rings**.

cardinal number

A number, often called simply a *cardinal,* that is used to count the objects or ideas in a **set** or collection: 0, 1, 2, . . . , 83, and so on. The *cardinality* of a set is just the number of elements the set contains. For finite sets this is always a **natural number**. To compare the sizes of two sets, X and Y, all that's necessary is to pair off the elements of X with those of Y and see if there are any left over. This concept is obvious in the case of finite sets but leads to some strange conclusions when dealing with infinite sets (see **infinity**). For example, it is possible to pair off all the natural numbers with all the even numbers, with none left over; thus the set of natural numbers and the set of even numbers have the same cardinality. In fact, an infinite set can be *defined* as any set that has a proper subset of the same cardinality. Every **countable set** that is infinite has a cardinality of **aleph**-null; the set of **real number**s has cardinality aleph-one. See also **ordinal number**.

cardioid

A heart-shaped curve first studied in 1674 by the Danish astronomer Ole Römer who was trying to find the

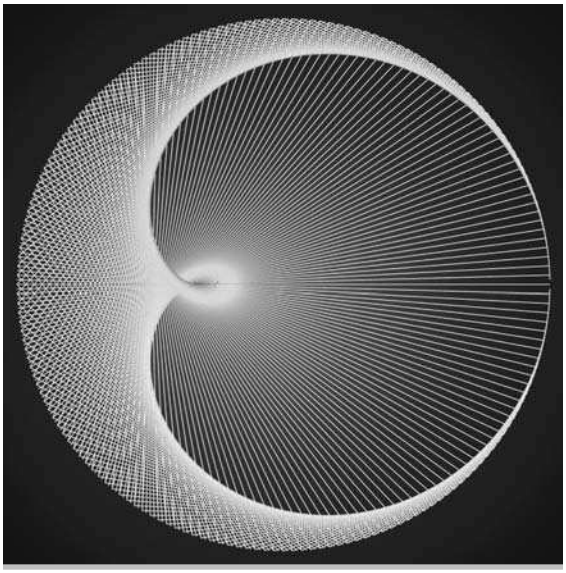

cardioid A cardioid curve spun by thread on a computer loom. *Jos Leys www.josleys.com*

best shape for gear teeth; the curve appears to have been named by Giovanni Salvemini de Castillon (1708–1791). When a circle rolls around another circle of the same size, any point on the moving circle traces out a cardioid. The Greeks used this fact when attempting to describe the motions of the planets. The cardioid is also the envelope of all circles with centers on a fixed circle, passing through one point on the fixed circle. In polar coordinates, it has the equation $r = 2a(1 - \cos\theta)$. It can also be described as an **epicycloid** with one cusp.

cards

The standard deck of 52 cards can be ordered in 52! (see **factorial**), or $8.065817517094 \times 10^{67}$ ways. There are various ways to **shuffle** cards in order to randomize them or to perform tricks with them. Each of the four kings in a deck represents a great leader from history: Charlemagne (hearts), Alexander the Great (clubs), Julius Caesar (diamonds), King David (spades). The king of hearts is the only one without a moustache. See also **blackjack**.

Carmichael number

Also known as an *absolute pseudoprime*, a number n that is a Fermat **pseudoprime** to any **base**, that is, it divides $(a^n - a)$ for any a. Another way of saying this is that a Carmichael number is actually a **composite number** even though **Fermat's little theorem** suggests it is probably a **prime number**. (Fermat's little theorem says that if P is a prime number, then for any number a, $(a^P - a)$ must be divisible by P. Carmichael numbers satisfy this condition to any base despite being composite.) There are only seven Carmichael numbers under 10,000 (they are 561, 1,105, 1,729, 2,465, 2,821, 6,601, and 8,911), and less than a quarter of a million of them under 10^{16}. Nevertheless, in 1994 it was proved that there are infinitely many of them. All Carmichael numbers are the product of at least three distinct primes, for example, $561 = 3 \times 11 \times 17$.

Carroll, Lewis (1832–1898)

The pen name of Charles Lutwidge Dodgson (obtained by anglicizing the Latin translation, "Carolus Lodovicus," of his first two names), an English mathematician, logician, and writer. Carroll was born at the Old Parsonage, Newton-by-Daresbury, Cheshire, his father being the vicar of All Saints Church, Daresbury. There is a commemorative window in the church, and a "Wonderland" weathervane, showing the Mad Hatter, the White Rabbit, and Alice, on the local primary school. Carroll was educated at Rugby School (the student mathematics society there is still called the Dodgson Society in his honor) and then at Christ Church, Oxford, at which college he was to spend the rest of his life, employed mainly as a lecturer.

Carroll's most famous book, *Alice's Adventures in Wonderland* (1865), grew out of a story he told on the

Carroll, Lewis Lewis Carroll's Chess Wordgame, a game based on notation in Carroll's diaries with rules devised by Martin Gardner. *Kadon Enterprises, Inc., www.gamepuzzles.com*

hot summer afternoon of July 4, 1862, when out rowing with the three young daughters of the Greek scholar H. G. Liddell, dean of Christ Church. Alice, named after Alice Liddell (later Hargreaves, 1852–1934), continued her adventures in *Through the Looking-Glass* (1871). Carroll wrote other books for children, including a long poem, "The Hunting of the Snark" (1876) and published several mathematical works, but was not distinguished academically. He stammered badly, never married, and seemed to find greatest pleasure in the company of little girls, with whom he lost his shyness. He was also an amateur pioneer in photography and an inventor of puzzles, games, ciphers, and mnemonics.[57–59] Carroll was a master of fantasy and his stories have their own logic. Carroll used puns and coined neologisms, including what he called "portmanteau words" like chortle (combining chuckle and snort). He played games with idioms, using such expressions as "beating time" (to music) in a literal sense. He reshaped such animals of fable or rhetoric as the Gryphon, the March Hare (said to have been inspired by a carved hare carrying a satchel located at St. Mary's Church, Beverly, Humberside, where Carroll visited), and the Cheshire Cat, and invented new ones, including the Bandersnatch and the Boojum.

PUZZLES

Here are a few examples of puzzles invented by Carroll:

1. You are given two glasses. One contains 50 tablespoons of milk, the other 50 tablespoons of water. Take one tablespoon of milk and mix it with the water. Now take one tablespoon of the water/milk mixture and mix it with the pure milk to obtain a milk/water mixture. Is there more water in the milk/water mixture or more milk in the water/milk mixture?
2. If you paint the faces of a cube with six different colors, how many ways are there to do this if each face is painted a different color and two colorings of the cube are considered equivalent if you can rotate one to get the other? What if we drop the restriction that the faces be painted different colors?
3. Make a word-ladder from FOUR to FIVE. (Every step in a word ladder differs from the previous step in exactly one letter and each step in the ladder is an English word.)
4. Why is a raven like a writing desk?

Solutions begin on page 369.

CARROLLIAN QUOTES

From *Alice's Adventures in Wonderland:*

- "The different branches of Arithmetic—Ambition, Distraction, Uglification, and Derision."
- "Then you should say what you mean," the March Hare went on.

  "I do," Alice hastily replied; "at least I mean what I say, that's the same thing, you know."

  "Not the same thing a bit!" said the Hatter. "Why, you might just as well say that 'I see what I eat' is the same thing as 'I eat what I see!' "
- "Take some more tea," the March Hare said to Alice, very earnestly.

  "I've had nothing yet," Alice replied in an offended tone, "so I can't take more."

  "You mean you can't take *less,*" said the Hatter. "It's very easy to take *more* than nothing."

From *The Hunting of the Snark:*

- "What I tell you three times is true."

From *Alice through the Looking Glass*

- "Can you do addition?" the White Queen asked.

  "What's one and one and one and one and one and one and one and one and one and one?"

  "I don't know," said Alice. "I lost count."
- "It's very good jam," said the Queen.

  "Well, I don't want any to-day, at any rate."

  "You couldn't have it if you did want it," the Queen said. "The rule is jam tomorrow and jam yesterday but never jam to-day."

  "It must come sometimes to "jam to-day," Alice objected.

  "No it can't," said the Queen. "It's jam every other day; to-day isn't any other day, you know."

  "I don't understand you," said Alice. "It's dreadfully confusing."
- "When I use a word," Humpty Dumpty said, in a rather scornful tone, "it means just what I choose it to mean—neither more nor less."

  "The question is," said Alice, "whether you can make words mean so many different things."

  "The question is," said Humpty Dumpty, "which is to be master—that's all."

Cartesian geometry

See **analytical geometry**.

Cartesian coordinates

An ordered set of **real number**s that defines the position of a point in terms of its projection onto mutually perpendicular number lines. In the plane, each point is defined by two such projections, one onto the *x*-axis and

one onto the *y*-axis, and is written as an **ordered pair** of real numbers (x, y). The same system works equally in spaces of three or more dimensions.

Cartesian oval

A curve that actually consists of two ovals, one inside the other. It is the locus of a point whose distances *s* and *t* from two fixed points *S* and *T* satisfy the equation $s + mt = a$. When *c* is the distance between *S* and *T* then the curve can be expressed in the form:

$$((1 - m^2)(x^2 + y^2) + 2m^2cx + a^2 - m^2c^2)^2 = 4a^2(x^2 + y^2)$$

The curves were first studied by René **Descartes** in 1637 and are sometimes called the *ovals of Descartes;* they were also investigated by Isaac **Newton** in his classification of **cubic curve**s. If $m = \pm 1$, then the Cartesian oval is a central conic. If $m = a/c$, then it becomes a **limaçon of Pascal**, in which case the inside oval touches the outside one. Cartesian ovals are **anallagmatic curve**s.

Cassinian ovals

Also known as *Cassini's ovals,* a family of curves, each member of which is defined as follows: given two points *A* and *B* and a constant c^2, the locus of points *P* with $PA \times PB = c^2$. The locus has the equation $(x^2 + y^2)^2 - 2a^2(x^2 - y^2)^2 - a^4 + c^4 = 0$, where $a = AB$. Equivalently, Cassinian ovals can be thought of as the set of curves produced when a circular **torus** is sliced at every possible point parallel to its axis. If $c = a$, then the curve is a special case known as the **lemniscate of Bernoulli** (a figure-eight type curve). The ovals are named after the Italian-born astronomer Giovanni Cassini (1625–1712) who first investigated them in 1680 while studying the relative motions of Earth and the Sun. Cassini thought that the Sun traveled round Earth on one of these curves (rather than the **ellipse**, as correctly proposed in Kepler's heliocentric scheme), with Earth at one focus.

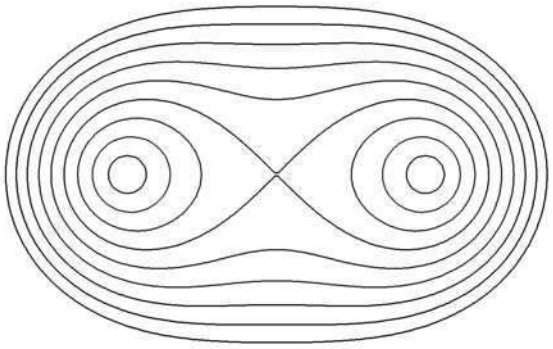

Cassinian ovals The many different ways to slice a doughnut. *Xah Lee, www.xahlee.org*

casting out nines

A method for checking arithmetic that uses the idea of the **digital root** of a number. Let the digital root of a number *n* be $r(n)$; for example, $r(7{,}586) = 8$. For any two numbers *a* and *b:* $r(a + b) = r(r(a) + r(b))$ and $r(a \times b) = r(r(a) \times r(b))$. These rules allow checks on addition and multiplication as the following examples show. Does $7{,}586 + 9{,}492 = 16{,}978$? $r(r(7{,}586) + r(9{,}492)) = r(8 + 6) = 5$; $r(16{,}978) = 4$; so the sum given is incorrect. Does $7{,}586 \times 9{,}492 = 72{,}006{,}312$. $r(r(7{,}586) \times r(9{,}492)) = r(8 \times 6) = r(48) = 3$; $r(72{,}006{,}312) = r(21) = 3$; which suggests that the product given is likely to be correct. The name "casting out nines" comes from the fact that nines need not be included in the calculation of the digital roots, since they have no effect on the final result. This a direct outcome of the fact that we use a **decimal** number system. If we calculated instead in octal (base eight), say, then the process would be one of "casting out sevens." This kind of checking will pick up most errors, but not all. For example, an interchange of two digits will not be detected, nor will replacing a nine by a zero or vice versa. The method appears in the work of ninth-century Arab mathematicians but may have originated earlier with the Greeks and, possibly, the Hindus.

Catalan number

Any number, u_n, from the *Catalan sequence* defined by

$$u_n = (2n)! \,/\, (n + 1)!n!.$$

It begins: 1, 2, 5, 14, 42, 132, 429, 1,430, 4,862, 16,796, 58,786, 208,012, 742,900, ... The values of u_n represent the number of ways a **polygon** with $n + 2$ sides can be cut into *n* triangles using straight lines joining vertices (see **vertex**). Catalan numbers are named after the Belgian mathematician Eugène Catalan (1814–1894). They also arise in other counting problems, for example in determining how many ways $2n$ beans can be divided into two containers if one container can never have less than the second.

Catalan solid

A **polyhedron** that is a dual of an **Archimedean solid**. (A dual of a polyhedron is obtained by replacing each face with a vertex, and each vertex with a face.) Catalan solids are named after the Belgian mathematician Eugène Catalan (1814–1894) who first described them in 1865. See also **Platonic solid** and **Johnson solid**. (See table, "Catalan solids.")

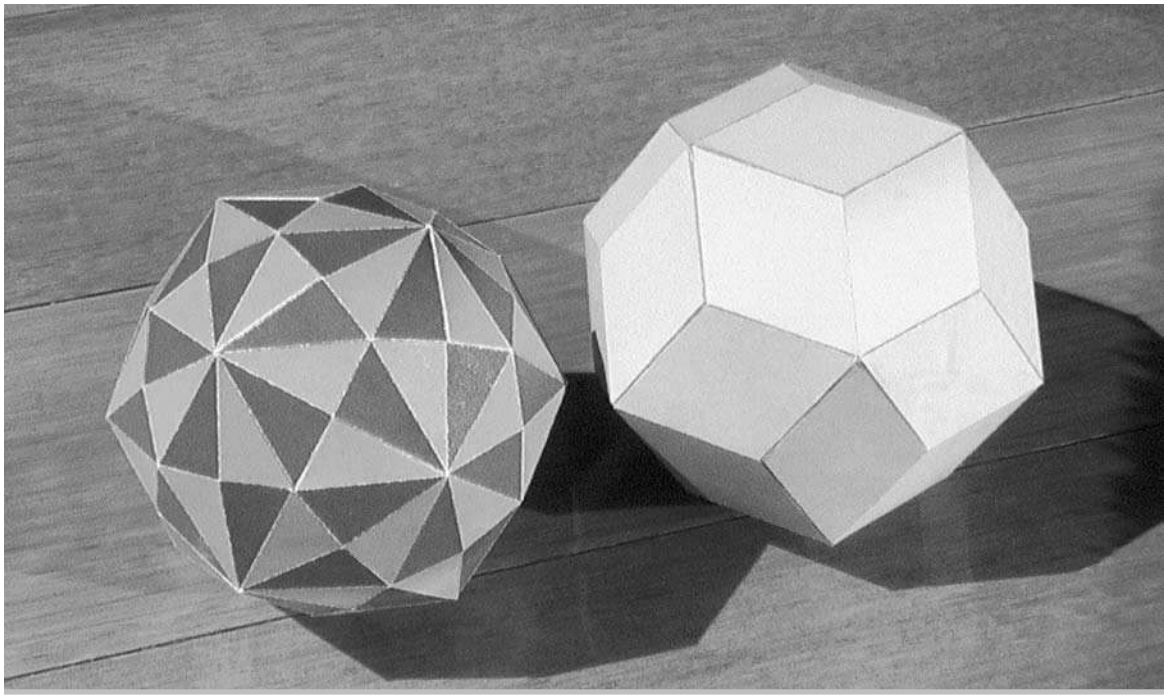

Catalan solid Two of the Catalan solids: the rhombic tricontahedron (right) and the disdyakistriacontahedron (left). *Robert Webb, www.software3d.com; created using Webb's Stella program*

Catalan Solids

Name	Corresponding Archimedean Solid
Triakis tetrahedron	Truncated tetrahedron
Rhombic dodecahedron	Cuboctahedron
Triakis octahedron	Truncated cube
Tetrakis hexahedron	Truncated octahedron
Deltoidal icositetrahedron	Small rhombicubocta-hedron
Disdyakis dodecahedron	Great rhombicubocta-hedron
Pentagonal icositetrahedron	Snub cube
Rhombic triacontahedron	Icosidodecahedron
Triakis icosahedron	Truncated dodecahedron
Pentakis dodecahedron	Truncated icosahedron
Deltoidal hexecontahedron	Rhombicosidodeca-hedron
Disdyakis triacontahedron	Great rhombicosidodeca-hedron
Pentagonal hexecontahedron	Snub dodecahedron

Catalan's conjecture

The hypothesis, put forward by the Belgian mathematician Eugène Catalan (1814–1894) in 1844, that 8 (= 2^3) and 9 (= 3^2) are the only pair of consecutive powers. In other words, the *Catalan equation* for **prime number**s p and q and positive integers x and y

$$x^p - y^q = 1$$

has only the one solution

$$3^2 - 2^3 = 1.$$

In 1976 R. Tijdeman took the first major step toward showing this is true by proving that for any solution, y^q is less than **e** to the power e to the power e to the power e to the power 730 (a huge number!). Since then, this bound has been reduced many times, and it is now know that the larger of p and q is at most 7.78×10^{16} and the smaller is at least 10^7. On April 18, 2002, the Romanian number theorist Preda Mihailescu sent a manuscript to several mathematicians with a proof of the entire conjecture together with an analysis by Yuri Bilu. It is expected that as soon as this work is completely reviewed by other mathematicians that Catalan's conjecture will have been proved.[266]

Solutions to Catalan's conjecture and **Fermat's last theorem** are special cases of the *Fermat-Catalan equation:*

$$x^p + y^q = z^r,$$

where x, y, and z are positive, **coprime** integers and the exponents are all primes with

$$1/p + 1/q + 1/r \leq 1.$$

The *Fermat-Catalan conjecture* is that there are only finitely many solutions to this system. These solutions include:

$1^p + 2^3 = 3^2$ ($p \geq 2$); $2^5 + 7^2 = 3^4$
$13^2 + 7^3 = 2^9$;
$33^8 + 1{,}549{,}034^2 = 15{,}613^3$
and $43^8 + 96{,}222^3 = 30{,}042{,}907^2$.

Catalan's constant

A constant that crops up regularly in combinatorial problems, especially in the evaluation of certain infinite series and integrals. For example, it is equal to

$\int_0^1 \arctan(x) / x \, dx$, and
$1 - 1/3^2 + 1/5^2 - 1/7^2 + 1/9^2 - \ldots$

It is also the solution to the following problem as n becomes arbitrarily large: If you have a $2n \times 2n$ checkerboard and a supply of $2n^2$ dominoes that are just large enough to cover two squares of the checkerboard, how many ways are there to cover the whole board with the dominoes? Catalan's constant has the value 0.915965 . . . ; it is not known if it's an **irrational number**.

catastrophe theory

A theory, developed by the French mathematician René Thom (1923–2003), that attempts to explain the behavior of complex **dynamical system**s by relating it to **topology**. The evolution of such systems consists of steady continuous change interspersed with sudden major jumps, or "catastrophes," when the topology of the set changes. Catastrophe theory has been applied, with varying degrees of success, to phenomena as diverse as earthquakes, stock market crashes, prison riots, and human conflicts, at the personal, group, and societal level. The theory was first developed by Thom in a paper published in 1968 but became well known through his book *Structural Stability and Morphogenesis* (1972).[331] Many mathematicians took up the study of catastrophe theory and it was in tremendous vogue for a while, yet it never achieved the success that its younger cousin **chaos** theory has because it failed to live up to its promise of useful predictions. Late in his career, the surrealist Salvador Dali painted *Topological Abduction of Europe: Homage to René Thom* (1983), an aerial view of a seismically fractured landscape juxtaposed with the equation that strives to explain it.

catch-22

A situation in which a person is frustrated by a paradoxical rule or set of circumstances that preclude any attempt to escape from them. The name comes from the title of a novel by Joseph Heller (1923–1999), based on his personal experiences, about an American airman's attempts to survive the madness of World War II. Heller wrote:

> There was only one catch and that was Catch-22, which specified that concern for one's own safety in the face of dangers that were real and immediate was the process of a rational mind. Orr was crazy and could be grounded. All he had to do was ask; and as soon as he did, he would no longer be crazy and would have to fly more missions. Orr would be crazy to fly more missions and sane if he didn't, but if he was sane he had to fly them. If he flew them he was crazy and didn't have to; but if he didn't want to he was sane and had to.

category theory

The study of abstracted collections of mathematical objects, such as the category of **set**s or the category of **vector space**s, together with abstracted operations sending one object to another, such as the collection of **function**s from one set to another or linear **transformation**s from one vector space to another.

catenary

The shape that a rope or telephone cable makes, under the influence of gravity, when suspended between two points. The word comes from the Latin *catena*, meaning "chain," and was first used by Christiaan **Huygens** while studying the form of suspended chains. Galileo thought the shape would be a **parabola**. In fact, near the **vertex**, a parabola and a catenary do look very similar. When x is slightly greater than three, however, the catenary begins to rapidly outgrow the value of the parabola. The two shapes are related in another way. If a parabola is rolled along a straight line, the **focus** of the parabola moves along a catenary curve. Surprisingly, too, if a bicycle with square (or any polygon-shaped) wheels is ridden along a road made of upturned catenaries the wheels will roll smoothly and the rider will stay at the same height! The St. Louis Arch, which is 192 meters wide at the base and 192 meters tall, follows the form of a catenary, the exact formula for which is displayed inside the arch: $y = 68.8 \cosh(0.01x - 1)$, where cosh is the hyperbolic cosine function.

The general equation of a catenary can be written

$$y = k \cosh(x/k),$$

where k is a constant, or, in terms of the **exponential** function,

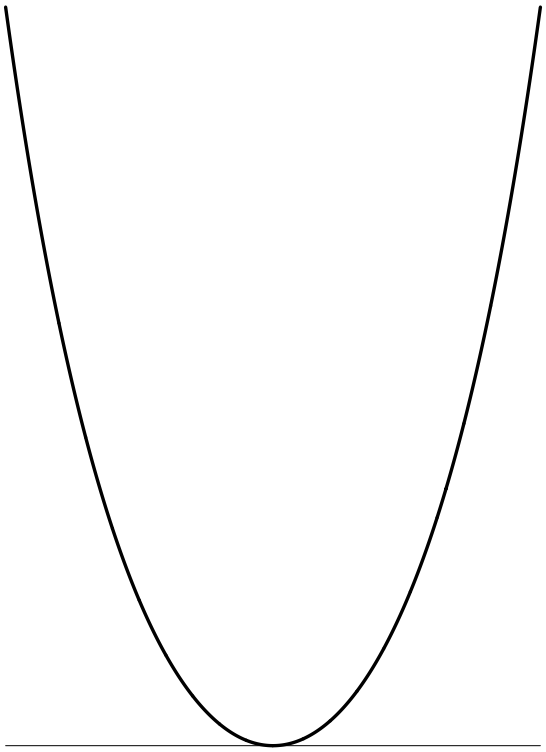

catenary The catenary curve. © *Jan Wassenaar, www.2dcurves.com*

$$y = k(e^{x/k} + e^{-x/k})/2.$$

In the special case where $k = 1$, these reduce to

$$y = \cosh(x) = (e^{x} + e^{-x})/2.$$

In terms of a polynomial series

$$\begin{aligned} y = 0.5\ (1 + x + x^2/2! + x^3/3! + x^4/4! + \ldots + 1 - x + x^2/2! \\ - x^3/3! + x^4/4! - \ldots) \\ = 1 + x^2/2! + x^4/4! + x^6/6! + \ldots . \end{aligned}$$

For small values of x the terms beyond $x^2/2!$ are very small, so that the equation closely approximates that of a parabola, as we have already seen.

catenoid

The **surface of revolution** produced when a **catenary** rotates about its central axis. The catenoid was first described by Leonhard **Euler** in 1740 and is the oldest known **minimal surface** (a shape of least area when bounded by a given closed space). It is the minimal surface connecting two parallel circles of unequal diameter on the same axis; soap film between two circular rings takes this form (see also **bubbles**). The catenoid is the only known minimal surface that is also a surface of revolution, and is one of only four minimal surfaces that have the topological properties of being unbounded, embedded, and non-periodic; the others are the simple plane, the **helicoid**, and *Costa's surface*.

cathetus

A line that is perpendicular to another line. Usually, it refers to one of the lines in a right triangle that is not the **hypotenuse**.

Cauchy, Augustin Louis, Baron (1789–1857)

A French mathematician who founded **complex analysis** by discovering the *Cauchy-Riemann equations* and wrote 789 papers–an output surpassed only by Leonhard **Euler**, George **Cayley**, and Paul **Erdös**. He coined the name for the **determinant** and systematized its study and gave nearly modern definitions of **limit**, **continuity**, and **convergence**.

causality

The relationship between causes and effects. An event or state of affairs A is the cause of an event B if A is the reason that brings about the effect B. For instance, one might say, "my pushing the gas pedal *caused* the car to go faster." An important question in philosophy and other fields is how (and if) causes can bring about effects. In a strict reading, if A causes B, then A must *always* be followed by B. In this sense, for example, smoking doesn't cause cancer. In everyday usage, we therefore often take "A causes B" to mean "A causes an increase in the probability of B." The establishment of cause and effect, even with this relaxed reading, is notoriously difficult. The Scottish philosopher David Hume held that causes and effects are not real, but instead are imagined by our minds to make sense of the observation that A often occurs together with or slightly before B. All we can actually observe are *correlations,* not causations. This is also expressed in the logical fallacy, "correlation implies causation." For instance, the observation that smokers have a dramatically increased lung cancer rate doesn't establish that smoking must be the *cause* of that increased cancer rate: maybe there exists a certain genetic defect which both causes cancer and a yearning for nicotine.[194]

caustic

The envelope of rays of light reflected (or refracted) by a given curve from a given point source of light; a *catacaustic* results from reflection, a *diacaustic* from refraction. Among the caustic curves of a circle are a lima, if the light source is nearby, a **nephroid**, if the source is at infinity, and a **cardioid**, if the source is on the circle.

Cavalieri's principle
If two solids have the same height and the same cross-sectional area at every level, then they have the same volume. This principle is named after the Italian mathematician Bonaventura Cavalieri (1598–1647).

Cayley, Arthur (1821–1895)
A British mathematician who made important contributions to **non-Euclidean geometry** and the algebra of matrices (see **matrix**). The former eventually found its way into the study of the **space-time** continuum, the latter into a formulation of **quantum mechanics** by the German physicist Werner Heisenberg. Cayley was also far ahead of his time in pioneering the idea of abstract **group**s.

Cayley number
See **octonion**.

Cayley's mousetrap
A **permutation** problem invented by Arthur **Cayley**. Write the numbers 1, 2, . . . , n on a set of cards and shuffle the deck. Start counting using the top card. If the card chosen does not equal the count, move it to the bottom of the deck and continue counting forward. If the card chosen *does* equal the count, discard the chosen card and begin counting again at 1. The game is won if all cards are discarded, and lost if the count reaches $n + 1$. The number of ways the cards can be arranged such that at least one card is in the proper place for $n = 1, 2, \ldots$, are 1, 1, 4, 15, 76, 455, ...

Cayley's sextic
A sinusoidal spiral curve described by the Cartesian equation

$$4(x^2 + y^2 - ax)^3 = 27a^2(x^2 + y^2)^2.$$

It was discovered by Colin **Maclaurin** but was first studied in detail by Arthur **Cayley** and named after him by R. C. Archibald in 1900.

ceiling
The largest value that something can take. The *ceiling function* of a number x is the smallest integer that is not smaller than x.

cell
(1) A three-dimensional object that is part of a higher-dimensional object, such as a **polychoron**. A cell is related to higher-dimensional objects in the way that a face, or (two-dimensional) **polygon**, is related to higher-dimensional objects. For example, a cell is to a Four-dimensional polytope, or polychoron, what a face is to a three-dimensional polytope, or **polyhedron**. Often polytopes are classified simply by how many cells they have. For example, the **tesseract** has eight cells, each one of which is a cube. (2) The fundamental spatial unit operated on by the rules of a **cellular automaton** during one generation.

cellular automaton
An array of cells that evolves according to a set of rules based on the states of surrounding cells; for example, a cell might be "on" if its four neighbor cells (east, west, north, and south) are also on. The entire array can self-organize into global patterns that may move around the screen. These patterns can be quite complex even though they emerge from just a few very simple rules governing the connections among the cells. Cellular automata are the simplest models of spatially distributed processes. They were first investigated by John **von Neumann** in about 1952. Von Neumann incorporated a cellular model into his "universal constructor" and also proved that an automaton consisting of cells with four orthogonal neighbors and 29 possible states would be capable of simulating a **Turing machine** for some configuration of about 200,000 cells. The best-known cellular automaton is Life (see **Life, Conway's game of**). Another example is **Langton's ant**. The study of cellular automata and their patterns has led to insights into the way structure is built up in biological and other complex systems, and for this reason forms part of the subject of **artificial life**.

celt
Also known as a *rattleback*, a simple ancient toy that behaves in a very counterintuitive way. When spun one way about its vertical axis, the celt spins for a long time. When spun the other way, however, a wobble quickly sets in that halts the rotation and then, incredibly, reverses it. In his 1986 paper on the subject, the British physicist Hermann Bondi wrote: "Many people, even trained scientists, find it hard to understand that the behaviour of the toy doesn't violate the principle of conservation of angular momentum."[47] The celt's remarkable antics stem from three factors: a curved base that has two different radii–one long radius for the lengthwise curve and one shorter radius for the tighter curve across the width; axes of symmetry that are skewed slightly from the principal axes of inertia; and a different distribution of mass about each of the two horizontal axes of inertia. To understand how the celt can switch direction halfway through its performance, think of the frictional force that acts at the point of contact between the celt and the surface. One component of the friction creates a torque (twisting force) that tends to rotate the celt about its vertical axis. The point of contact is moving all the time and the torque changes. If the inertial and symmetrical axes coin-

cided, the average torque over a single oscillation would be zero. But for the celt, there's a net torque in one direction, which reverses the angular momentum. See also **Tippee Top**.

center of perspective
The point where the lines joining corresponding points of two figures that are in perspective meet.

centillion
See **large number**.

central angle
The angle subtended at the center of a **circle** by an **arc** or a **chord**; in other words, the angle between two radii.

centroid
For a **triangle**, the point of intersection of the **median**s. For any other shape, the point where coordinates are the average of the coordinates of the shape's vertices (see **vertex**). The centroid is the *center of mass* of a figure.

century
A period of 100 years. The original Latin *centuria* means simply "one hundred" and was used to describe any collection of 100 items. In the Roman army, a century was a group of 100 men, each known as a *centurion.* One of the few modern examples of "century" being used other than to denote a period of time is in the game of cricket where a batsman who scores 100 runs in an inning is said to have "made a century."

Ceva, Giovanni (1647–1734)
A Jesuit-trained Italian mathematician who specialized in **geometry**. His greatest discovery, now known as *Ceva's theorem,* can be stated as follows. Given a triangle with vertices (corners), *A, B,* and *C* and points *D, E,* and *F* on the opposite sides, the lines *AD, BE,* and *CF* will intersect at a single point if $BD \times CE \times AF = DC \times EA \times FB$. The term *cevian line* was coined by French geometers around the end of the eighteenth century to honor Ceva. It is defined as any line joining a vertex of a triangle to a point on the opposite side. The **median**, **altitude**, and angle **bisect**or are all examples of cevians. The perpendicular bisector, however, in most cases, is not a cevian because it doesn't usually pass through a vertex.

chained arrow notation
See **Conway's chained arrow notation**.

Chaitin, Gregory (1947–)
An American mathematician and computer scientist at IBM's T. J. Watson Research Center who is the chief architect of a new subject known as *algorithmic information theory,* which has profound consequences for our ideas about **random**ness. In particular, because of the limitations of computers and the programs they run, Chaitin has shown that there is an inherent uncertainty or unknowability in mathematics that is similar to the uncertainty principle in physics. Although there are an infinite number of mathematical facts, they are, for the most part, unrelated to each other and impossible to tie together with unifying theorems. His powerful message is that most of mathematics is true for no particular reason; math is true by accident. See **Chaitin's constant**.

Chaitin's constant
A **real number**, represented by capital omega (Ω) and also known as the *Halting probability,* whose digits are distributed so **random**ly that no rule can be found to predict them. Discovered by Gregory **Chaitin**, Ω is definable but not computable. It has no pattern or structure to it whatsoever, but consists instead of an infinitely long string of zeros and ones in which each digit is as unrelated to its predecessor as one coin toss is to the next. Although called a constant, it is not a constant in the sense that, for example, **pi** is, since its definition depends on the arbitrary choice of computation model and programming language. For each such model or language, Ω is the probability that a randomly produced string will represent a program that, when run, will eventually halt. To derive it, Chaitin considered all the possible programs that a hypothetical computer known as a **Turing machine** could run, and then looked for the probability that a program, chosen at random from among all the possible programs, will halt. He eventually showed that this halting probability turns Turing's question of whether a program ever stops into a real number, somewhere between zero and one. He further showed that, just as there are no computable instructions for deciding in advance whether a computer will halt, there are also no instructions for determining the digits of Ω. Omega is uncomputable and unknowable: we don't know its value for any programming language and we never will. This is extraordinary enough in itself, but Chaitin has found that Ω permeates the whole of mathematics, placing fundamental limits on what we can know.

And Ω is just the beginning. There are more disturbing numbers called Super-Omegas, whose degree of randomness is vastly greater even than that of Ω. If there were an omnipotent computer that could solve the halting problem and evaluate Ω, this mega-brain would have its own unknowable halting probability called Ω′. And if there were a still more godlike machine that could find Ω′, its halting probability would be Ω″. These higher Omegas, it has been recently discovered, are not meaningless abstractions. Ω′, for instance, gives the probability that

an infinite computation produces only a finite amount of output. Ω″ is equivalent to the probability that, during an infinite computation, a computer will fail to produce an output–for example, get no result from a computation and move on to the next one–and that it will do this only a finite number of times. Omega and the Omega hierarchy are revealing to mathematicians an unsettling truth: the problems that we can hope ever to solve form a tiny archipelago in a vast ocean of undecidability.[130]

Champernowne's number

The first known **normal number**. It was discovered in 1933 by the English mathematician David G. Champernowne and consists of a decimal fraction in which the decimal integers are written down in increasing order: 0.12345678910111213 . . . . Champernowne's number has been proven to be a normal number in base 10 and also to be an **irrational number**. However, although its digits appear with equal frequency, the sequence of its digits are not unpredictable. An example of a number whose sequence of digits *is* unpredictable is **Chaitin's constant**.

chance

See **probability theory**.

change ringing

> *The art of change ringing is peculiar to the English, and, like most English peculiarities, unintelligible to the rest of the world. To the musical Belgian, for example, it appears that the proper thing to do with a carefully tuned ring of bells is to play a tune upon it. By the English campanologist . . . the proper use of the bells is to work out mathematical permutations and combinations.*
>
> –Dorothy L. Sayers, *The Nine Tailors*

The ringing of a set of bells in a precise relationship to one another to produce a pleasing sound. Bells are numbered 1, 2, 3, 4, 5 . . . from lightest (highest-pitched) to heaviest. After each sequence, or *round*, the order of the bells is changed slightly in a predetermined way. With 5 bells, there are $5 \times 4 \times 3 \times 2 \times 1$, or 120, possible changes, which take about 4 minutes to ring. With 6, 7, or 8 bells, the number of unique changes is 720, 5,040, and 40,320, respectively. To produce pleasing variations in the sound, bells are made to change places with adjacent bells in the row, for example:

1	2	3	4	5	6	7	8
2	1	4	3	6	5	8	7

These rows are the musical notation of change ringing. No bell moves more than one place in the row at a time, although more than one pair may change in the same row. In order to ring a different row with each pull of the rope, ringers have devised methods for changing pairs in orderly ways. In ringing a method, the bells begin in rounds, ring changes according to the method, and return to rounds without repeating any row along the way. These place changes produce musical patterns, with the sounds of the bells weaving in and out. For example, a "Plain Hunt Minimus" with four bells is rung as shown in the diagram.

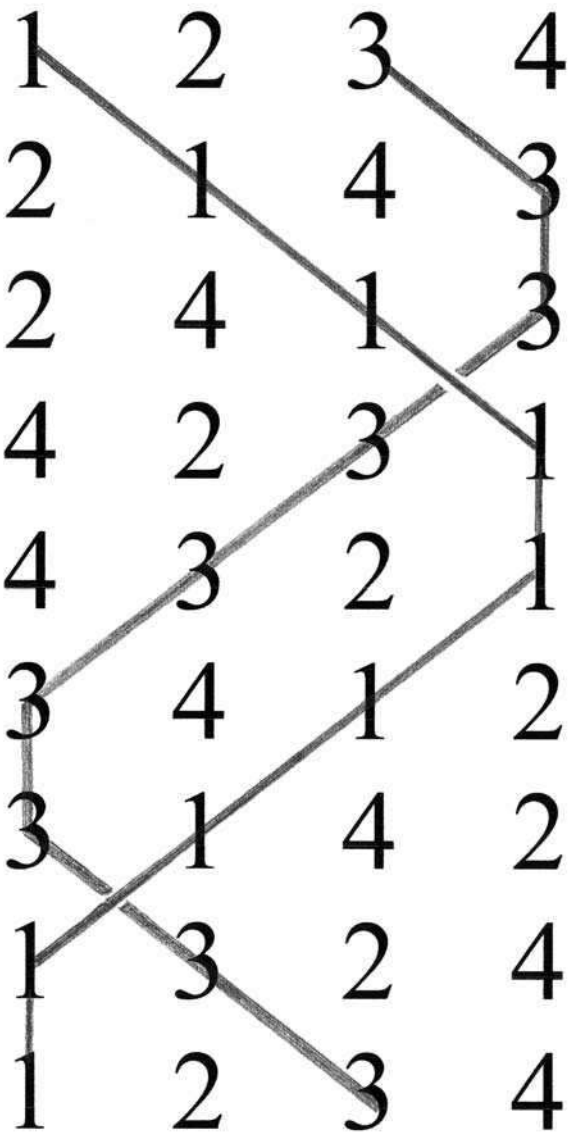

change ringing The "Plain Hunt Minimus" for four bells. The sequences for bells 1 and 3 are shown by lines.

Experienced ringers test and extend their abilities by ringing peals: 5,000 or more changes without breaks or repeating a row. Peals customarily last about three hours. The first peal was rung in England in 1715. Chiming bells (swinging them through a short arc using a rope and a lever) goes well back into the Middle Ages, but it wasn't until the seventeenth century that ringers developed the full wheel, which allowed enough control for orderly ringing. In 1668 Fabian Stedman published *Tintinnalogia* (The art of change ringing), containing all the available information on systematic ringing. The theory of change ringing set forth by Stedman has been refined in later years but remains essentially unchanged today. Bells for change ringing are hung in stout frames that allow the bells to swing through 360°. Each bell is attached to a wooden wheel with a handmade rope running around it and takes about 2 seconds to rotate. The bells are arranged in the frame so their ropes hang in a circle in the ringing chamber below. Into each rope is woven a tuft of brightly colored wool (a *sally*), which marks where the ringer must catch the rope while ringing. Bells are rung from the "mouth up" position. With a pull of the rope, the bell swings through a full circle to the up position again. With the next pull it swings back in the other direction. The plot of Dorothy Sayers's *The Nine Tailors* (1934), considered one of her best works, revolves around the art of change ringing.

chaos

We adore chaos because we love to produce order.
–M. C. Escher

A phenomenon shown by some **dynamical system**s, which consists of a curious, infinitely complex pattern of behavior that lies just beyond the edge of total order. A system is chaotic if it is predictable in principle and yet is unpredictable in practice over long periods because its behavior depends very sensitively on initial conditions. Despite this unpredictability, however, there are certain constants, such as **Feigenbaum's constant**, and certain structures, such as **chaotic attractor**s, that are fixed and susceptible to analysis. The weather, the movements of a metal pendulum moving over fixed magnets, and the orbits of closely spaced moons are all examples of chaotic systems. Although the ideas behind modern chaos theory were actively studied at some level throughout most of the twentieth century, the word as a mathematical term dates only from an article in *American Mathematical Monthly* in 1975 called "Period Three Implies Chaos."

In everyday language, chaos has come to mean the exact opposite of order. But the Greek root *khaox* means "empty space" and this meaning still persists in archaic usage where it refers to a canyon or abyss. The evolution of the word to mean disorder seems to come from reference to the time before God created the universe. Empty space was formless and the creation filled the emptiness and established order. Mathematical chaos represents an unexpected third state: a deterministic system subject to simple rules that nevertheless displays infinitely complex behavior.[135]

chaos tiles

See **Penrose tiling**.

chaotic attractor

Also known as a *strange attractor,* a type of **attractor** (i.e., an attracting set of states) in a complex **dynamical system**'s **phase space** that shows **sensitivity** to initial conditions. Because of this property, once the system is on the attractor, nearby states diverge from each other exponentially fast. Consequently, small amounts of noise are amplified. Once sufficiently amplified the noise determines the system's large-scale behavior and the system is then unpredictable. Chaotic attractors themselves are markedly patterned, often having elegant, fixed geometric structures, despite the fact that the trajectories moving within them appear unpredictable. The chaotic attractor's geometric shape is the order underlying the apparent chaos. It functions in much the same way as someone kneading dough. The local separation of trajectories corresponds to stretching the dough and the global attraction property corresponds to folding the stretched dough back onto itself. One result of the stretch-and-fold aspect of chaotic attractors is that they are **fractal**s; that is, some cross section of them reveals similar structure on all scales.

character theory

The study of the traces (sums of the diagonal elements) of the **matrix** representations of a **group**. The information gained is listed in *character tables,* the properties of which give insight into the group's properties.

chess

A game of strategy for two players that probably originated in India, though the earliest documentary references are in Chinese and Persian texts in about A.D. 600. Each player has 16 pieces, either black or white, consisting of eight pawns, two rooks (also known as castles), two knights, two bishops, a queen, and a king. The object is to lay siege to the opposing king in such a way that it cannot escape attack–a position known as *checkmate* (from the Persian phrase *Shah Mat,* meaning "the king is dead"). There are 400 first-move combinations–20 for white × 20 for black (though only 64 of these are regarded as strong), 318,979,564,000 ways of playing the first four moves, and 169,518,829,100,544,000 trillion ways of playing the first

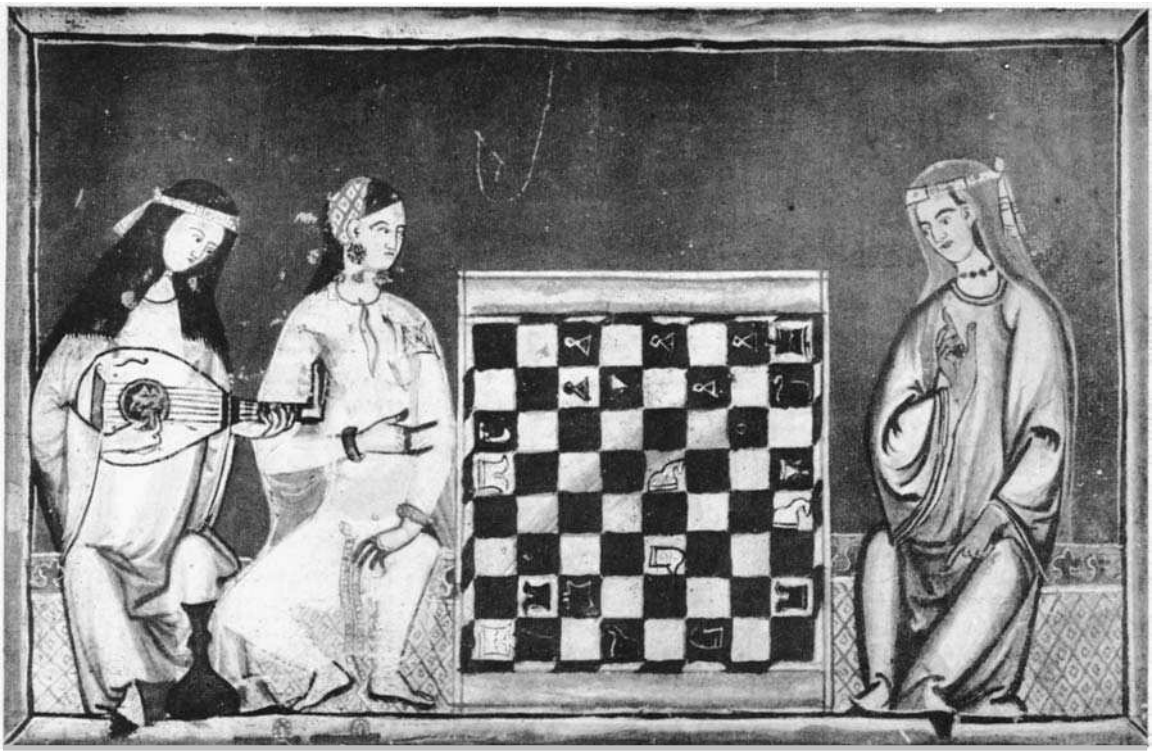

chess An illumination from the *Cantigas de Santa Maria* (a thirteenth-century collection of songs) showing a chess game in progress.

10 moves. The total number of possible board configurations is estimated at 10^{120}; for comparison, that of **Go** is generally put at about 10^{174}.

A standard chessboard is a square plane divided into 64 smaller squares by straight lines at right angles. Originally, it wasn't checkered (that is, made with its rows and columns alternately of dark and light colors), and this feature was introduced merely to help the eye in actual play. In many puzzles based on chess the utility of checkering is questionable, and the board may be generalized to any $n \times n$ size.

One of the first puzzles to use a chessboard was the **wheat and chessboard problem**, posed in 1256 by the Arabic mathematician Ibn Kallikan. Among the earliest problems to involve chess *pieces,* proposed by Guarini di Forli in 1512, asks how two white and two black knights can be interchanged, using normal knight's moves, if they are placed at the corners of a 3×3 board. The unusual L-shaped movement of the knight is what makes one of the best known chess puzzles, the **knight's tour**, such a challenge. Other standard puzzles, often called simply the **kings problem**, the **queens puzzle**, the **rooks problem**, the **bishops problem**, and the **knights problem**, ask for the greatest number of each of these pieces that can be placed on an 8×8 board or on a generalized $n \times n$ board without attacking each other, and/or the smallest number of each of these pieces that are needed to occupy or attack every square. *Fairy chess* is any variant on the standard game, which may involve a change in the form of the board, the rules of play, or the pieces used. For example, the normal rules of chess can be used but with a cylindrical or **Möbius band** connection of the edges.

Chinese cross

See **burr puzzle**.

Chinese remainder theorem

If there are n numbers, a_1 to a_n, that have no **factor**s in common (i.e., are pairwise relatively prime), then any integer greater than or equal to 0 and less than the product of all the numbers n can be uniquely represented by a series consisting of the remainders of division by the numbers n. For example, if $a_1 = 3$ and $a_2 = 5$, the Chinese remainder theorem (CRT) says that every integer from 0

to 14 will have a unique set of remainders when divided separately by (**modulo**) 3 and 5. Listing out all the possibilities shows that this is true:

0 has a remainder of 0 modulo 3 and a remainder of 0 modulo 5.

1 has a remainder of 1 modulo 3 and a remainder of 1 modulo 5.

2 has a remainder of 2 modulo 3 and a remainder of 2 modulo 5.

3 has a remainder of 0 modulo 3 and a remainder of 3 modulo 5.

4 has a remainder of 1 modulo 3 and a remainder of 4 modulo 5.

5 has a remainder of 2 modulo 3 and a remainder of 0 modulo 5.

6 has a remainder of 0 modulo 3 and a remainder of 1 modulo 5.

7 has a remainder of 1 modulo 3 and a remainder of 2 modulo 5.

8 has a remainder of 2 modulo 3 and a remainder of 3 modulo 5.

9 has a remainder of 0 modulo 3 and a remainder of 4 modulo 5.

10 has a remainder of 1 modulo 3 and a remainder of 0 modulo 5.

11 has a remainder of 2 modulo 3 and a remainder of 1 modulo 5.

12 has a remainder of 0 modulo 3 and a remainder of 2 modulo 5.

13 has a remainder of 1 modulo 3 and a remainder of 3 modulo 5.

14 has a remainder of 2 modulo 3 and a remainder of 4 modulo 5.

CRT enables problems such as the following to be solved: Find the two smallest counting numbers that will each have the remainders 2, 3, and 2 when divided by 3, 5, and 7, respectively. It is said that the ancient Chinese used a variant of this theorem to count their soldiers by having them line up in rectangles of 7 by 7, 11 by 11, and so forth. After counting only the remainders, they solved the associated system of equations for the smallest positive solution.

Chinese rings

One of the oldest known **mechanical puzzle**s, the object of which is to remove all n rings from a horizontal loop of stiff wire, and/or put them back on the loop. On the first move it is possible to take up to two rings off the left end of the wire. One or both of those can then be slipped through the wire loop (from top to bottom). If both are removed then the fourth ring can be slipped over the end. If just one of the first two is removed, then the next step is to slip the third ring over the end. Subsequently, rings must be put back on to the wire loop in order to remove other rings, and this procedure is repeated over and over again. In general, the minimum number of moves needed is $(2^{n+1} - 2)/3$ if n is even and $(2^{n+1} - 1)/3$ if n is odd. For example, with seven rings the solution takes 85 moves. Most of the solution is easy, as each move normally involves going forward or back to the previous state. The key to a correct solution is the first step: if n is even, you must remove two rings; if n is odd, you must remove only one. The solution is similar to that of the **Tower of Hanoi**. In fact, Edouard **Lucas**, who invented the Tower of Hanoi, gave an elegant solution to the Chinese rings that uses **binary** arithmetic.

Stewart Cullin, the noted nineteenth-century ethnologist, relates that the puzzle was invented by the famous Chinese general Chu-ko Liang (A.D. 181–234), in the second century, as a present to his wife so that, in trying to solve it, she would have something to do while he was away at the wars. However, this is anecdotal and its origins remain obscure. The earliest reference to it in Europe may be in about 1500 in the form of Problem 107 of the manuscript *De Viribus Quantitatis* by Luca **Pacioli** in which the description appears: "*Do Cavare et Mettere una Strenghetta Salda in al Quanti Anelli Saldi, Difficil Caso*" (Remove and put a little bar joined in some joined rings,

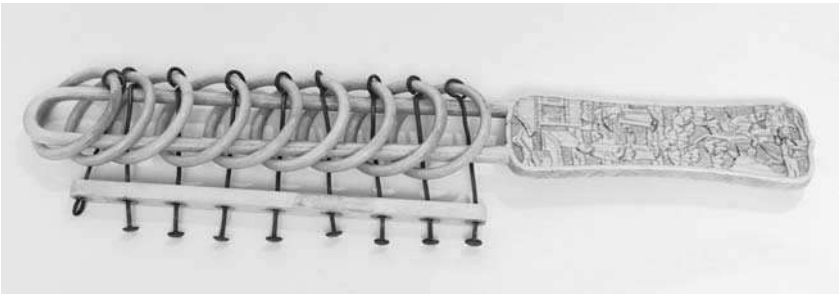

Chinese rings An unusual example of Chinese rings in ivory, dating from the mid-nineteenth century. *Sue & Brian Young/Mr. Puzzle Australia, www.mrpuzzle.com.au*

difficult case). It was also mentioned by Girolamo **Cardan** in the 1550 edition of his book *De Subtililate* from which comes the name *Cardan's rings,* and was treated at length in mathematical terms by John **Wallis** in about 1685. By the end of the seventeenth century, it had become popular in many European countries. French peasants used it to lock chests and called it *baguenaudier,* or "time-waster."

Chinese room

An argument first put forward by the American philosopher John Searle (1932–) in 1980 in an attempt to show that the human mind is not a computer and that the **Turing test** is not adequate to prove that a machine can have strong **artificial intelligence** (strong AI)–in other words, can think in a humanlike way.[292] In the Chinese room scenario, a person who understands no Chinese sits in a room into which written Chinese characters are passed. The person uses a complex set of rules, established ahead of time, to manipulate these characters, and pass other characters out of the room. The idea is that a Chinese-speaking interviewer would pass questions written in Chinese into the room, and the corresponding answers would come out of the room in Chinese. Searle maintains that if such a system could indeed pass a Turing test, the person who manipulated the symbols would obviously not understand Chinese any better than he did before entering the room.

Searle proceeds systematically to refute the claims of strong AI by positioning himself as the one who manipulates the Chinese symbols. The first claim is that a system able to pass the Turing test understands the input and output. Searle replies that as the "computer" in the Chinese room, he gains no understanding of Chinese by simply manipulating the symbols according to the formal program (the complex translation rules). The operator in the room need not have any understanding of what the interviewer is asking, or of the replies that he is producing. He may not even know that there is a question-and-answer session going on outside the room.

The second claim of strong AI to which Searle objects is the claim that the system explains human understanding. Searle asserts that since the system is functioning–in this case passing the Turing Test–and yet there is no understanding on the part of the operator, then the system does not understand and therefore could not explain human understanding.

chiral

Having different left-hand and right-hand forms; not mirror symmetric. For example, the *snub cube* (one of the **Archimedean solid**s) is chiral, where as the ordinary **cube** is not.

Chladni, Ernst Florens Friedrich (1756–1827)

A German lawyer, musician (he was born in Leipzig in the same year as Mozart and died in the same year as Beethoven), and amateur scientist who founded the science of acoustics. While investigating musical tones, he had the inspired idea of making the sounds visible in a solid material. He spread fine sand over a glass or metal plate and set it into vibration with the bow of a violin by scraping the bow along one edge of the plate. The bow alternately stuck and slipped in rapid succession on the edge of the plate creating waves that moved across the plate and were reflected from the edges. These reflected waves became superimposed on the new waves coming from the bow edge, resulting in symmetrical patterns of nodal lines where the plate wasn't moving. The type of pattern produced on a Chladni plate depends on a variety of factors, including the point or points of support and their location; the point where the bow touches the plate; the frequency of the vibration, which is influenced by the speed the bow; and the shape and other properties of the plate itself.

chord

A straight line that joins two points on a curve. Most commonly, *chord* is used to mean a straight line segment joining, and included between, two points on a **circle**. In this more restricted sense it first appears in English in 1551 in Robert **Recorde**'s *The Pathwaie to Knowledge:* "*Defin.,* If the line goe crosse the circle, and passe beside the centre, then is it called a corde, or a stryngline."

Some surprising results emerge from moving chords. For example, take a chord in a circle C, and slide the chord around the circle so that the midpoint of the chord traces out a smaller concentric circle. Call the area between the two circles $A(C)$. Now do the same thing with a larger circle C' but with the same length chord. Is $A(C')$ larger or smaller than $A(C)$? Surprisingly, they are the same. In other words $A(C)$ doesn't depend on what circle you start with, only the length of the chord. An even more amazing fact is that if you slide a chord of fixed length around *any convex shape C* so that the chord's midpoint traces out another figure D, the area between C and D doesn't depend on what shape you started with.

chromatic number

(1) In **graph theory**, the minimum number of colors needed to color (the vertices of) a **connected graph** so that no two adjacent vertices are colored the same. In the case of simple graphs, this so-called *coloring problem* can be solved by inspection. In general, however, finding the chromatic number of a large graph (and, similarly, an optimal coloring) is an **NP-hard problem**. (2) In **topology**, the maximum number of regions that can be drawn

on a surface in such a way that each region has a border in common with every other region. If each region is given a different color, each color will border on every other color. The chromatic number of a square, tube, or sphere, for example, is 4; in other words, it is impossible to place more than four differently colored regions on one of these figures so that any pair has a common boundary. "Chromatic number" also indicates the least number of colors needed to color any finite map on a given surface. Again, this is 4 in the case of the plane, tube, and sphere, as was proved quite recently in the solution to the **four-color map problem**. The chromatic number, in both senses just described, is 7 for the **torus**, 6 for the **Möbius band**, and 2 for the **Klein bottle**. See also **Betti number**.

chronogram

A phrase or sentence in which certain letters represent, cryptically, a date, epoch, or, in rare cases, a non-date number. For example, the chronogram "My Day Is Closed In Immortality" commemorates the death of Queen Elizabeth the First of England: the capital letters can be rearranged to give MDCIII, or 1603, the year in which she died.

Church, Alonzo (1903–1995)

An American logician and professor at Princeton University who was an early pioneer of theoretical computer science. He is best known for his development, in 1934, of the so-called **lambda calculus**, a model of computation, and his discovery, in 1936, of an "undecidable problem" within it. This result preceded Alan **Turing**'s famous work on the **halting problem**, which also pointed out the existence of a problem unsolvable by mechanical means. Church and Turing then showed that the lambda calculus and the **Turing machine**, which is used in the halting problem, are equivalent in capability. They also demonstrated a variety of alternative "mechanical processes for computation" with equivalent computational abilities. See also **Church-Turing thesis**.

Church-Turing thesis

A logical/mathematical postulate, independently arrived at by Alan **Turing** and Alonzo **Church**, which asserts that as long as a procedure is sufficiently clear-cut and mechanical, there is some **algorithm**ic way of solving it (such as via computation on a **Turing machine**). Thus, there are some processes or problems that are computable according to some set of algorithms, and other processes or problems that are not. A strong form of the Church-Turing thesis claims that all neural and psychological processes can be simulated as computational processes on a computer.

cipher

(1) A cryptographic system (see **cryptography**) in which units of plain text of regular length, usually letters, are arbitrarily transposed (see **transposition cipher**) or substituted (see **substitution cipher**) according to a predetermined code, or a message written or transmitted in such a system. See also **Caesar cipher** and **Beal cipher**. (2) The mathematical symbol (0) for **zero**.

circle

The set of all points in a plane at a given distance, called the *radius,* from a fixed point, called the *center.* A circle is a simple **closed** curve that divides the plane into an interior and exterior. It has a perimeter, called a *circumference,* of length $2\pi r$ and encloses an area of πr^2. In coordinate geometry a circle with center (x_0, y_0) and radius r is the set of all points (x, y) such that:

$$(x - x_0)^2 + (y - y_0)^2 = r^2$$

"Circle" comes from the Latin *circus,* which refers to a large round or rounded oblong enclosure in which the famous Roman chariot races were held.

A line cutting a circle in two places is called a *secant.* The *segment* of a secant bound by the circle is called a *chord,* and the longest chord is that which passes through the center and is known as a *diameter.* The ratio of the circumference to the diameter of a circle is **pi**. The length of a circle between two radii is called an *arc;* the ratio between the length of an arc and the radius defines the *angle* between two radii in *radians.* The area bounded by two radii and an arc is known as a *sector.* A line touching a circle in one place is called a *tangent.* Tangent lines are perpendicular to radii. In **affine geometry** all circles and ellipses become **congruent**, and in **projective geometry** the other **conic section**s join them. A circle is a conic section with eccentricity zero. In **topology** all simple closed curves are **homeomorphic** to circles, and the word *circle* is often applied to them as a result. The three-dimensional analog of the circle is the **sphere,** and the four-dimensional analog is the **hypersphere**.

circle involute

The simplest kind of **spiral** to draw and understand. It is the path that a goat, tethered to a post, would follow if it walked around and around in the same direction, keeping its tether taught until it wound its way to the center. The radial distance between adjacent loops of the spiral is equal to the circumference of the central circle. Except for the innermost loop, the circle involute is hard to distinguish from the **Archimedean spiral**, though the two curves are never identical.

circular cone

A **cone** whose base is a **circle**.

circular helix
See **helix**.

circular prime
A **prime number** that remains prime on any cyclic rotation of its digits. An example (in the decimal system) is 1,193 because 1,931, 9,311, and 3,119 are also prime. Any one-digit prime is circular by default. In base ten, any circular prime with two or more digits can only contain the digits 1, 3, 7, and 9; otherwise when 0, 2, 4, 5, 6, or 8 is rotated into the units place, the result can be divided by 2 or 5. The only circular primes known, listing just the smallest representative from each cycle, are: 2, 3, 5, 7, 11, 13, 17, 37, 79, 113, 197, 199, 337, 1,193, 3,779, 11,939, 19,937, 193,939, 199,933, R_{19}, R_{23}, R_{317}, R_{1031} and possibly R_{49081}. These last five are the known **rep-unit** primes and probable primes. It's generally believed that there are infinitely many rep-unit primes, so there should be infinitely many circular primes. But it's very likely that all circular primes not on the list above are rep-units.

circumcenter
The center of a **circle** that passes through the vertices (see **vertex**) of a given **polygon**, usually a triangle. For a triangle, it is the same as the point of intersection of the perpendicular **bisect**ors of the three sides.

circumcircle
The **circle** that passes through all three vertices (see **vertex**) of a given triangle. It is said to *circumscribe* the triangle.

circumference
The distance around the outside of a **circle**. The word comes the Latin *circus* ("circle") and *ferre* ("to carry"), thus means "to carry around."

cissoid
Given a fixed point A and two curves C and D, the cissoid of the two curves with respect to A is constructed as follows: pick a point P on C, and draw a line l through P and A. This cuts D at Q. Let R be the point on l such that $AP = QR$. The **locus** of R as P moves on C is the cissoid. The name *cissoid*, meaning "ivy-shaped," first appears in the work of Geminus in the first century B.C.

A special case of this curve, now known as the *cissoid of Diocles*, was first explored by **Diocles** in his attempt to solve the classical problem of **duplicating the cube**. Later investigators of the same curve include Pierre de **Fermat**, Christiaan **Huygens**, John **Wallis**, and Isaac **Newton**. The cissoid of Diocles is traced out by the **vertex** of a **parabola** as it rolls, without slipping, on a second parabola of the same size. It has the Cartesian equation

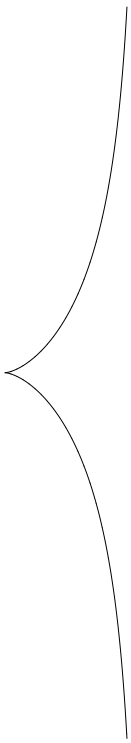

cissoid The cissoid of Diocles. © *Jan Wassenaar, www.2dcurves.com*

$$y^2 = x^3/(2a - x).$$

Interestingly, Diocles investigated the properties of the focal point of a parabola in *On Burning Mirrors* (a similar title appears in the works of Archimedes). The problem, then as now, is to find a mirror surface such that when it is placed facing the Sun, it focuses the maximum amount of heat.

classification
The goal in a branch of mathematics of providing an exhaustive list of some type of mathematical object with no repetitions. For example, the classification of 3-**manifold**s is one of the outstanding problems in **topology**. With the advent of computers, one weak but precise way to state a classification problem is to ask whether there is an **algorithm** to determine whether two given objects are equivalent.

clelia
Also known as a *clelie curve*, the **locus** of a point P that moves on the surface of a **sphere** in such a way that ϕ/θ is constant, where ϕ and θ are the longitude and colatitude (the angular distance from a pole).

Clifford, William Kingdon (1845–1879)

An English mathematician who studied **non-Euclidean geometry** and **topology**. In 1870, he wrote *On the Space Theory of Matter* in which he argued that energy and matter are simply different types of curvature of space–a remarkably advanced idea that would come to fruition in Einstein's general **relativity theory**. Although small of build Clifford was remarkably strong and able to do one-armed chin-ups. His death at an early age was the result of overwork and exhaustion.

clock puzzles

The earliest known clock problem was posed in 1694 by Jacques **Ozanam** in his *Récréations mathématiques et physiques*.

PUZZLES

Here are two clock puzzles invented by Lewis **Carroll**:

1. A clock has hour and minute hands of the same length and no numerals on its face. At what time between 6 and 7 o'clock will the time on the clock appear to be the same as the time read on the reflection of the clock in a mirror?
2. Which has a better chance of giving the right time: a clock that has stopped or one that loses a minute every day?

And here is another from Henry **Dudeney**'s *Amusements in Mathematics* called "The Club Clock":

3. One of the big clocks in the Cogitators' Club was found the other night to have stopped just when the second hand was exactly midway between the other two hands. One of the members proposed to some of his friends that they should tell him the exact time when (if the clock had not stopped) the second hand would next again have been midway between the minute hand and the hour hand. Can you find the correct time that it would happen?

Solutions begin on page 369.

closed

A *closed curve* is one that has no endpoints so that it completely encloses a certain area. A *closed interval*, which corresponds to a *closed set*, is an interval that includes its endpoints.

cochleoid

A **spiral** curve that was first studied by J. Peck in 1700 and Bernoulli in 1726. Its name, meaning "snail-form" (*kochlias* is Greek for "snail"), was coined by Benthan and Falkenburg in 1884. It can be constructed starting from a point O on the y-axis. For all circles through O (tangent to the y-axis), pace a constant distance on the circle. The collection of those points is the cochleoid. In Cartesian coordinates, it is given by the formula

$$(x^2 + y^2)\tan^{-1}(y/x) = ay$$

and in polar coordinates by

$$r = a\sin\theta / \theta.$$

The points of contact of parallel tangents to the cochleoid lie on a **strophoid**.

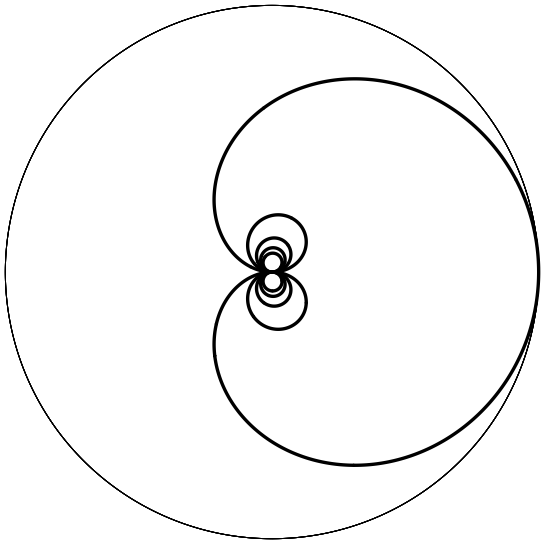

cochleoid A cochleoid inside the circle used to construct it.
© Jan Wassenaar, www.2dcurves.com

code

See **cipher**.

codimension

In general, if a mathematical object sits inside or is associated with another object of **dimension** n, then it is said to have codimension k if it has dimension $n - k$.

coding theory

The branch of mathematics concerned with sending data across noisy channels and recovering the message. Whereas **cryptography** is about making messages *hard* to read, coding theory focuses on making messages *easy* to read. The basic problem is that messages, in the form of binary digits or *bits* (strings of 0 or 1) have to be sent along a channel (such as a phone line) in which errors occur randomly, but at a predictable overall rate. To compensate for the errors, more bits have to be sent than are contained in the original message. The easiest way to detect errors in binary data is

the **parity** code, which inserts an extra parity bit after every 7 bits from the source message. To correct as well as detect errors, the data has to be retransmitted. A simple way to do this is to repeat each bit a set number of times. The recipient sees which value, 0 or 1, occurs more often and assumes that to be the intended bit. This method can cope with error rates up to 1 error in every 2 bits transmitted but it means that an awful lot of extra bits have to be sent.

In 1948, Claude **Shannon** at Bell Labs began the subject of coding theory by proving the minimum number of extra bits that had to be transmitted to encode messages but without showing ways to find these optimal codes. Two years later, Richard Hamming, also at Bell Labs, gave details of error-correcting codes with information transmission rates more efficient than simple repetition. His first code, in which four data bits were followed by three check bits, allowed not only the detection but the correction of a single error.

While Shannon and Hamming were involved with information transmission in the United States, John Leech devised similar codes while working on **group** theory at Cambridge University. This research also took in the sphere **packing** problem and culminated in the amazing, 24-dimensional *Leech lattice,* the study of which proved crucial to understanding and classifying finite symmetry groups. The value of error-correcting codes for information transmission, both on Earth and from space, was immediately grasped, and a variety of codes were constructed that boosted both economy of transmission and error-correction capacity. Between 1969 and 1973 the NASA Mariner probes used a powerful *Reed-Muller code* capable of correcting 7 errors out of 32 bits transmitted. A less obvious application of error-correcting codes came with the development of the compact disk on which the signal is encoded digitally. To guard against scratches and other damage, two interleaved codes that can correct up to 4,000 consecutive errors are used. By the late 1990s the goal of finding explicit codes that reach the limits predicted by Shannon's original work had been achieved.

codomain

For a given **function** or mapping, a **set** within which the values of the function lie. This is different from the set of values, known as the **range**, that the function actually takes.

coefficient

A number or other factor that multiplies a variable. For example, in the equation $3x - 4ky = 8$, the 3 and $4k$ are coefficients of the variables x and y. The word combines three elements, the Latin *facere* ("to do"), and the prefixes *ex* ("out") and *co* ("with"), to give the overall meaning of joining two things together to bring about a result. The sixteenth-century mathematician Francois Vieta may have coined the word, but it was not commonly used until around the beginning of the eighteenth century.

Coffin, Stewart T.

A leading designer of mechanical puzzles. He is also the author of *The Puzzling World of Polyhedral Dissections,*[64] one of the most significant works produced on this subject.

cohomology

A subject that involves calculating algebraic **invariant**s of **topological space**s that are formally dual to **homology**. The invariants obtained are in general more powerful than those given by homology and usually have more algebraic structure. *Generalized cohomology theories,* both for topological spaces and for purely algebraic structures, have been developed that have some of the formal properties of cohomology but which don't have the same geometric background.

coin paradox

Consider two round coins of equal size. Imagine holding one still and then rolling the other coin around it, making sure that it doesn't slip and that the rims are touching at all times. How many times will the moving coin have rotated after it has completed one revolution of the stationary coin? Most people believe that the answer will be once and are therefore surprised to discover that the truth is in fact *twice.*

coincidence

What an amazing coincidence! Well, not really. Coincidences are bound to happen. In a world where there are a great many potential coincidences each with a small probability of happening, someone, somewhere is going to see one–and be amazed by it. The fact that there are countless numbers of noncoincidences and many people who don't see a significant coincidence in the same period of time is overlooked. Also, we tend to underestimate the probabilities of coincidences in certain situations and are therefore more surprised than we should be when coincidences happen. A classic example of this is the **birthday paradox**.

Obviously some things are extraordinarily unlikely. What are the chances, for example, of a meteorite hitting your car? Next to nothing, but not quite nothing. There are a lot of cars and there are dozens of meteorites that strike Earth every day. Sooner or later, it's bound to happen. In fact, it did happen to Michelle Knapp's Chevy Malibu parked outside her home in Peekskill, New York, on the evening of October 9, 1992. A 12-kilogram space rock smashed through the car's trunk and ended up on the driveway below.

Does coincidence completely explain away all events that might otherwise be put down to precognition? On April 15, 1912, the SS *Titanic* sunk on her maiden voyage, having been holed by an iceberg, and over 1,500 people died. Fourteen years earlier a novel had been published by Morgan Robertson that seemed to foretell the disaster. The book described a ship the same size as *Titanic* that struck an iceberg on its maiden voyage on a misty April night. The name of Robertson's fictional ship was the *Titan*. Mere happenstance or evidence of something deeper? Numerologists often spot matchups that would go unnoticed by the rest of us. Is it so strange that there are almost exactly 500 million inches in the pole-to-pole diameter of Earth? Not if you work in centimeters. And should we make such a fuss over the fact that the speed of light is within 0.1% of 300,000 kilometers per second when we give no attention to the miles-per-second value of 186,282? Yet, surely, there can be no doubt that Shakespeare wrote the Bible. The King James Version was published in 1611, when Shakespeare was 46 years old. Look up Psalm 46. Count 46 words from the beginning of the Psalm. You will find the word "Shake." Count 46 words from the end of the Psalm. You will find the word "Spear." To some, an obvious coded message. See also **thirteen**.

Collatz problem

A problem first posed by the German mathematician Lothar Collatz (1910–1990) in 1937, that is also known variously as the *3n + 1 problem, Kakutani's problem,* the *Syracuse problem, Thwaites' conjecture,* and *Ulam's conjecture*. It runs as follows. Let n be any integer. (1) If n is odd, put n equal to $3n + 1$; otherwise, put n equal to $n/2$. (2) If $n = 1$, stop; otherwise go back to step 1. Does this process always terminate (i.e., end in 1) for any value of n? To date, this question remains unanswered, though the process has been found to stop for all n up to 5.6×10^{13}. British mathematician Bryan Thwaites (1996) has offered a £1,000 reward for a resolution of the problem. However, John **Conway** has shown that Collatz-type problems can be formally undecidable, so it not known if a solution is even possible. The members of sequences produced by the Collatz problem are sometimes known as **hailstone sequences**.[144]

combination

A set of objects selected without reference to the order in which they are arranged. Compare with **permutation**. See also **binomial coefficient**.

combinatorics

The study of the ways of choosing and arranging objects from given collections and the study of other kinds of problems relating to counting the number of ways to do something.

commensurable

Two lines or distances are commensurable if the ratio of their lengths is a **rational number**. If the ratio is an **irrational number**, they are called *incommensurable.*

common fraction

A **fraction** that consists of the **quotient** of two **integer**s.

communication theory

See **information theory**.

commutative

Two numbers, x and z, are said to be *commutative under addition* if

$$x + y = y + x$$

and to be *commutative under multiplication* if

$$x \times y = y \times y.$$

In general, two elements a and b of a **set** S are commutative under the binary operation (an operation that works on two elements at a time) $*$ if

$$a * b = b * b.$$

Compare with **associative** and **distributive**.

complement

That which is needed to complete something. For instance, the complement of a number is what needs to be added to it to make a specified value; the complement of an angle is the angle required to turn it into a right angle. The complement of a **set** is composed of all the elements that are not members of that set.

complete

Describes a **formal system** in which all statements can be proved as being true or false. Most interesting formal systems are not complete, as demonstrated by **Gödel's incompleteness theorem**.

complete graph

A **connected graph** in which exactly one **edge** connects each pair of vertices (see **vertex**). A complete graph with n vertices, denoted K_n, has $n(n - 1)/2$ edges (i.e., the nth **triangular number**), $(n - 1)!$ **Hamilton circuit**s, and a **chromatic number** of n. Every vertex in K_n has **degree** $n - 1$; therefore K_n has an **Euler circuit** if and only if n is odd. In a *weighted complete graph,* each edge has a number called a *weight* attached to it. Each path then has a total weight, which is the sum of the weights of the edges in the path. See also **traveling salesman problem**.

complex adaptive system (CAS)

A nonlinear, interactive, **complex system** with the ability to adapt to a changing environment. CASs evolve by random mutation, **self-organization**, the transformation of their internal models of the environment, and natural selection. Examples include living organisms, the nervous system, the immune system, the economy, corporations, and societies. In a CAS, semiautonomous agents interact according to certain rules of interaction, evolving to maximize some measure like fitness. The agents are diverse in form and capability and they adapt by changing their rules and, hence, behavior, as they gain experience. CASs evolve historically–their experience determines their future trajectory. Their adaptability can either be increased or decreased by the rules shaping their interaction. Moreover, unanticipated, emergent structures can play a determining role in the evolution of such systems, which is why they are highly unpredictable. On the other hand, CASs have the potential of a great deal of creativity that was not programmed into them from the beginning.

complex analysis

The study of **function**s of a complex variable. Often, the most natural proofs for statements in real **analysis** or even **number theory** use techniques from complex analysis. Unlike real functions, which are commonly represented as two-dimensional graphs, complex functions have four-dimensional graphs and may usefully be illustrated by color-coding a three-dimensional graph to suggest four dimensions.

complex number

A **real number** plus a real number times the square root of –1; in other words, a number of the form $z = a + ib$, where a and b are real and $i = \sqrt{-1}$. The term ib is known as an **imaginary number** or the *imaginary part* of the complex number $a + ib$; a is called the real part. The names "complex," "real," and "imaginary," which came about historically, are totally misleading because complex numbers are not particularly complex and imaginary numbers are no less real than real numbers! Another way to represent a complex number is as an **ordered pair** of real numbers (a, b) together with the operations: $(a, b) + (c, d) = (a + c, b + d)$ and $(a, b) \times (c, d) = (ac - bd, bc + ad)$. Alternatively, complex numbers can be shown as points on an **Argand diagram** (a representation of the *complex plane*) in which the horizontal axis is the real number line and the vertical axis represents all possible purely imaginary numbers. Any point that appears on the complex plane off-axis has both real and imaginary parts. On an Argand diagram a complex number can also be shown as a **vector**, or directed line segment (a line of a certain length with an arrow), extending from the origin $(0 + 0i)$ to the number $(a + bi)$. The *absolute value* or *magnitude* of a complex number z, thought of as a point on a plane, is its Euclidean distance from the origin, and is denoted $|z|$; this is always a nonnegative real number. Algebraically, if $z = a + ib$, we can define $|z| = \sqrt{(a^2 + b^2)}$. If the complex number z is written in polar coordinates $z = r e^{i\varphi}$, then $|z| = r$.

Complex numbers are a natural extension of real numbers and form what is called an *algebraically closed field*. Because of this, mathematicians sometimes consider the complex numbers to be more "natural" than the real numbers: all **polynomial** equations have solutions among the complex numbers, which is not true for the real numbers. Complex numbers are used in electrical engineering and other branches of physics as a convenient description for periodically varying signals. In an expression $z = re^{i\varphi}$ one may think of r as the amplitude and ϕ as the phase of a sine wave of given frequency. In special and general **relativity theory**, some formulas for the metric on **space-time** become simpler if the time variable is taken to be imaginary.

complex plane

See **Argand diagram**.

complex system

A collection of many simple nonlinear units that operate in parallel and interact locally with each other so as to produce emergent (see **emergence**) behavior.

complexity

A phenomenon that has two distinct and almost opposite meanings. The first, and probably the oldest mathematically, goes back to Andrei **Kolmogorov**'s attempt to give an **algorithm**ic foundation to notions of **random**ness and probability and to Claude **Shannon**'s study of communication channels via his notion of information. In both cases, complexity is synonymous with *disorder* and a lack of structure. The more random a process, the greater its complexity. An ideal gas, for example, with its numerous molecules bouncing around in complete disarray, is complex as far as Kolmogorov and Shannon are concerned. Thus, in this sense, complexity equates to the degree of complication.

The second, and more recent notion of complexity refers instead to how structured, intricate, hierarchical, and sophisticated a natural process is. In particular, it's a property associated with **dynamical system**s in which new, unpredictable behavior arises on scales above the level of the constituent components. The distinction between these two meanings can be revealed by answering a simple question about a system: Is it complex or is it merely complicated? Measures of complexity include **algorithmic complexity**, **fractal dimension**ality; **Lyapunov fractal**s, and **logical depth**.

complexity theory

A part of the theory of computation that has to do with the resources needed to solve a given problem. The most common resources are *time* (how many steps it takes to solve a problem) and *space* (how much memory it takes to solve a problem). Complexity theory differs from **computability theory**, which deals with whether a problem can be solved at all, regardless of the resources required.

composite number

A positive integer that can be factored into smaller positive integers, neither of which is one. If a positive integer is not composite (4, 6, 8, 9, 10, 12, . . .) or one, then it is a **prime number** (2, 3, 5, 7, 11, 13, 17, . . .). As Karl **Gauss** put it in his *Disquisitiones Arithmeticae* (1801): "The problem of distinguishing prime numbers from composite numbers and of resolving the latter into their prime factors is known to be one of the most important and useful in arithmetic." One reason for its importance today is that many secret codes and much of the security of the Internet depends in part on the relative difficulty of factoring large numbers. But more basic to a mathematician is that this problem has always been central to **number theory**. Numbers that, for their size, have a lot of factors are sometimes referred to as *highly composite numbers*. Examples include 12, 24, 36, 48, 60, and 120.

compound polyhedron

An assemblage of two or more polyhedra, usually interpenetrating and having a common center. There are two types: a combination of a solid with its **dual** and an interpenetrating set of several copies of the same **polyhedron**. The simplest example of a compound polyhedron is the compound of two tetrahedra, known as the *stella octangula* and first described by Johannes **Kepler**. This shape is unique in that it falls under both of the above classes, because the **tetrahedron** is the only self-dual **uniform polyhedron**; the edges of the two tetrahedra form the diagonals of the faces of a **cube** in which the stella octangula can be inscribed.

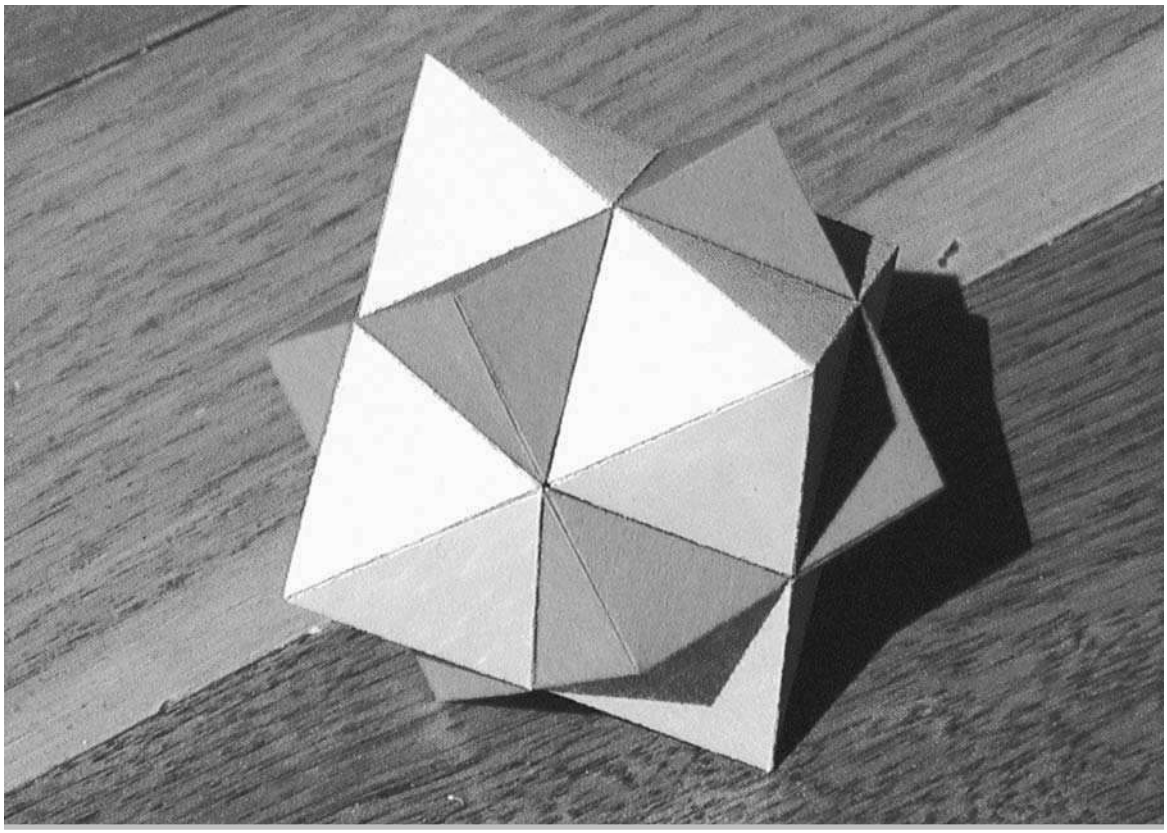

compound polyhedron A compound of duals: the cube and the octahedron. *Robert Webb, www.software3d.com; created using Webb's Stella program*

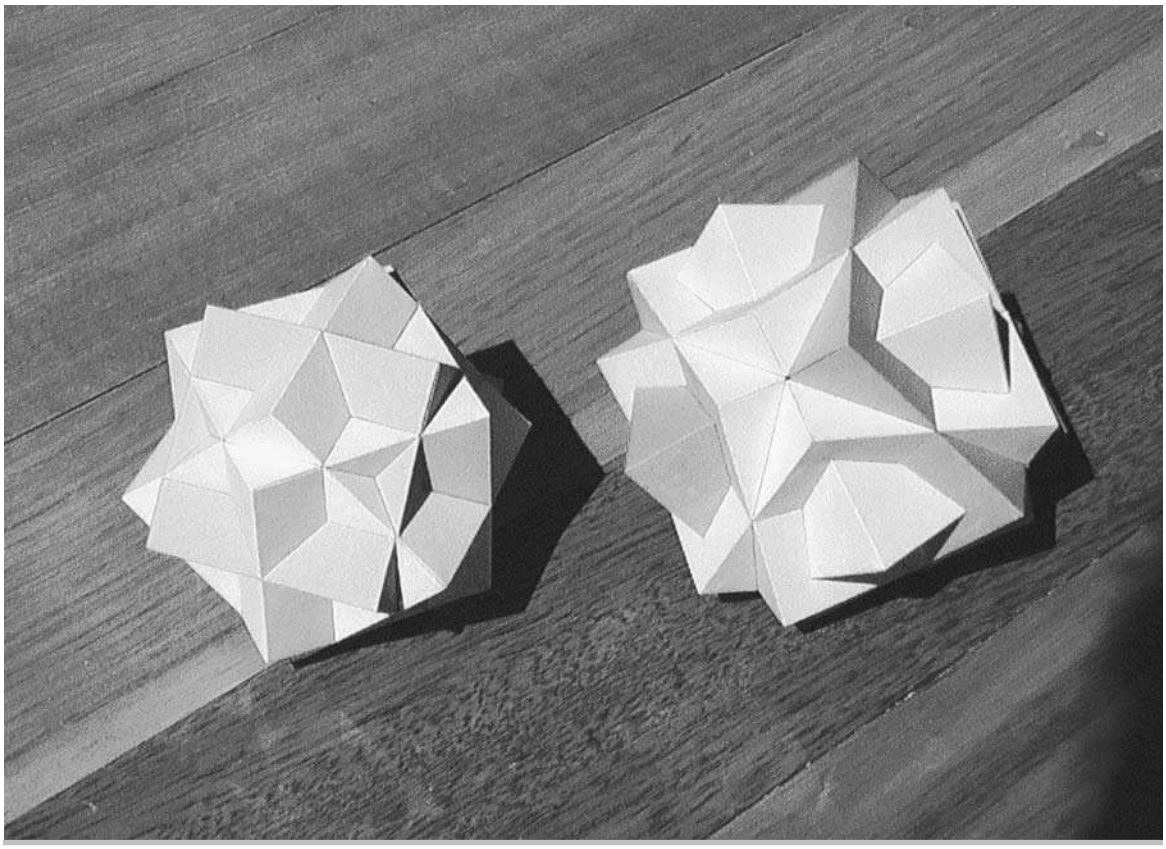

compound polyhedron A compound polyhedron of three cubes (left), such as that used in Escher's picture "Waterfall." The compound of four cubes (right) is also known as Bakos's compound. *Robert Webb, www.software3d.com; created using Webb's Stella program*

Another example of a compound follows from an important Platonic relationship: a cube can be inscribed within a **dodecahedron**. There are five different positions for a cube within a dodecahedron; superimposing all five gives the compound known as the *rhombic triacontahedron*.

compressible

Having a description that is smaller than itself; not **random**; possessing regularity.

computability theory

The part of the theory of computation that deals with problems that are solvable by **algorithms** or–what amounts to the same thing–by **Turing machine**s. Computability theory is concerned with four main questions: What problems can Turing machines solve? What other systems are equivalent to Turing machines? What problems require more powerful machines? What problems can be solved by less powerful machines? Not all problems can be solved computationally. An *undecidable problem* is one that can't be solved by any algorithm, no matter how much time, processing speed, or memory is available. Many examples are known, one of the most famous of which is the **Halting problem**. See also **cellular automaton**.

computable number

A **real number** for which there is an **algorithm** that, given n, calculates the nth digit. Alan **Turing** was the first to define a computable number and the first to prove that almost all numbers are uncomputable. An example of a number that, even though well-defined, is uncomputable is **Chaitin's constant**.

concave

Curved inward, like the inner surface of a sphere; the word comes from the Latin *concavus* for "hollow." A figure, such as a **polygon** or **polyhedron**, is said to be concave if a line

segment joining any points inside the figure goes outside the figure. Similarly, a **set** is concave if it doesn't contain all the line segments connecting any pair of its points.

conchoid

A shell-shaped curve. Given a point A and a curve C, if we pick a point Q on C and draw a line L through A and Q and mark points P and P' on L at some fixed distance in either direction from Q, then the locus of P and P' as Q moves on C is a conchoid. The *conchoid of Nichomedes* is a conchoid in which the given line is a straight line; that is, given a line C and a point A we pick a point Q on C, draw a line L through A and Q, and mark P and P' on L at some fixed distance from Q. The conchoid of Nicomedes is the locus of P and P' as Q moves along C. It has the polar equation $R = a\sec\theta + k$. The *conchoid of de Sluze* is the curve with the Cartesian equation $a(x-a)(x^2+y^2) = k^2x^2$.

cone

A shape (its name comes from the Greek *konos* for pinecone) that has a circular or elliptical base and a **vertex**, also known as an *apex*, lying outside the plane of the base and that is formed from all the line segments joining points on the edge of the base to the vertex. If the base is a circle, the shape is a *circular cone;* if the line, or *axis,* from the center of the base to the vertex is perpendicular to the base, then it is a *right cone* (an ice-cream cone is a right circular cone); otherwise it's an *oblique cone.* The curved lateral surface of the cone is called a *nappe.* If the cone is extended in both directions from the vertex, the result is a *double cone* or *bicone.* A section through a double cone that has been extended indefinitely in both directions to form a *conic surface* is known as a **conic section**. Another way to think of a cone is as a **surface of revolution** generated by a line that rotates around a fixed point, at a fixed angle from another line (the axis), both lines passing through that fixed point. The volume of a cone, of perpendicular height h and circular base of radius r, is $\frac{1}{3}\pi r^2 h$.

Take a solid cylinder of radius r and height $2r$. Remove the right double cone that passes through the center of the cylinder and extends to meet the circular disks on the cylinder's top and bottom. Interestingly, the volume of the remaining object and the volume of a sphere of radius r are the same.

PUZZLE

The *Cone Puzzle* (no. 202) from Henry **Dudeney**'s *Amusements in Mathematics*[88] runs as follows: "I have a wooden cone. How am I to cut out of it the greatest possible cylinder?"

Solutions begin on page 369.

conformal mapping

A map from the plane to itself that preserves angles. Conformal mapping results in the angle between any two curves being the same as the angle between their images. The Mercator map is a conformal map of Earth's surface.

congruent

In the case of geometric figures, having exactly the same shape and size.

congruum problem

Find a **square** number x^2 such that, when a given number h is added or subtracted, new square numbers are obtained, so that $x^2 + h = a^2$ and $x^2 - h = b^2$. This problem was posed by the mathematicians Théodore and Jean de Palerma in a mathematical tournament organized by Frederick II in Pisa in 1225. The solution is $x = m^2 + n^2$ and $h = 4mn(m^2 - n^2)$, where m and n are integers.

conic section

An important, familiar, and ubiquitous family of curves obtained by slicing a right circular double **cone**, extended indefinitely in both directions, with a plane. Depending on the angle of the slice to the axis of the cone, the resulting curve may be a **circle**, an **ellipse**, a **parabola**, or a **hyperbola**. The circle is a limiting case of the ellipse, when the slice is made at right angles to the axis, while the parabola is the limiting case of both the ellipse and the hyperbola, when the slice is made parallel to the side of the cone. The name *conic sections* comes from the eight-volume work *Conics* (Κωνικα) by **Apollonius**, who also gave us the names *ellipse*, *parabola,* and *hyperbola.*

Another geometric way to define the conics is as the **locus** of all points in the plane whose distances, r, from a fixed point called the *focus,* and a, from a given straight line called the **directrix**, have a constant ratio. This ratio, r/a, is known as the *eccentricity, e.* The circle has an eccentricity of zero. As the eccentricity increases from near zero, corresponding to a nearly circular ellipse, the ellipse stretches until the right-hand side of it disappears to infinity, e becomes 1, and the ellipse turns into a parabola, with just one open branch. Like the circle, the parabola has only one shape, though it may look different depending on how much it is enlarged or diminished. As the eccentricity increases beyond 1, the "lost" right-hand end of the ellipse reappears from the other side of infinity, so to speak, and turns into the left-hand branch of a hyperbola.

Because a hyperbola is effectively an ellipse split in two by infinity, it comes as no surprise that these curves are related in an inverse way. An ellipse consists of all points whose distances from two foci have a constant sum, while a hyperbola is made from all points whose

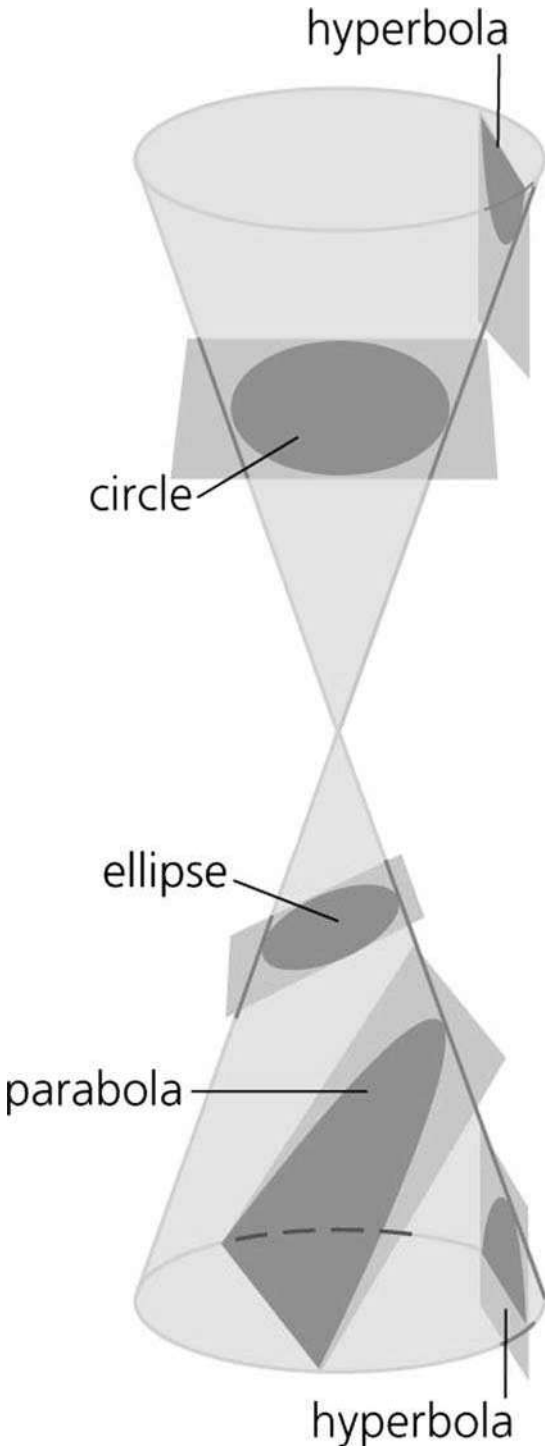

conic section The circle, ellipse, parabola, and hyperbola, obtained by slicing a right double cone in various ways.

distances from two foci have a constant difference. These definitions also apply to the circle and the parabola, if the two foci are considered to coincide in the case of the circle and to be separated by an infinite distance in the case of the parabola.

In terms of algebra, the family of conics represents all the possible **real number** solutions to the general **quadratic** equation $ax^2 + bxy + cy^2 + dx + ey + f = 0$. In other words, the graph of any quadratic with real solutions is always a conic section. The key quantity is the difference $b^2 - 4ac$. If this is less than zero, the graph is an ellipse, a circle, a point, or no curve. If $b^2 - 4ac = 0$, the graph is a parabola, two parallel lines, one line, or no curve; if it is greater than zero, the graph is a hyperbola or two intersecting lines.

conical helix
See **helix**.

conjecture
A mathematical statement that has been put forward as a true statement, but that no one has yet been able to prove or disprove; in mathematics, a conjecture and a hypothesis are essentially the same thing. When a conjecture has been proven to be true, it becomes known as a **theorem**. Famous conjectures include the **Riemann hypothesis**, the **Poincaré conjecture**, the **Goldbach conjecture**, and the **twin primes** conjecture. Just to show how terminology can be used inconsistently, however, the most famous of all conjectures, for centuries before its proof in 1995, was always known as **Fermat's last theorem**!

conjugate
(1) *Conjugate angles* add up to 360°. (2) The *complex conjugate* of a **complex number** $a + bi$ is $a - bi$. (3) *Conjugate lines* of a **conic section** have the property that each contains the pole point of the other, while *conjugate points* of a conic have the property that each lies on the polar line of the other. In general, conjugate indicates that there is a symmetrical relationship between two objects A and B; in other words, there is an operation that will turn A into B and B into A.

connected
A space S is said to be connected if any two points in S can be connected by a curve lying wholly within S. Two spaces can be added by what is called a *connected sum*. Roughly speaking, this involves pulling out a disk from each surface, creating **hole**s, and then sewing the two surfaces together along the boundaries of the holes. In this way, a one-holed **torus** can be added to a two-holed torus to give a three-holed torus; alternatively, a **projective**

plane can be added to a projective plane to give a **Klein bottle**. The operation is **commutative** and **associative** and there is even an **identity** element: for example, adding a sphere to any surface simply returns the same surface. See also **simply connected**.

connected graph

A **graph** in which a path exists between all pairs of vertices (see **vertex**). If the graph is also a **directed graph**, and there exists a path from each vertex to every other vertex, then it is a *strongly connected graph*. If a connected graph is such that exactly one edge connects each pair of vertices, then it is said to be a **complete graph**. See also **Euler path** and **Hamilton path**.

connectionism

A computational approach to modeling the brain that relies on the interconnection of many simple units to produce complex behavior.

connectivity

The amount of interaction in a system, the structure of the weights in a **neural network**, or the relative number of edges in a **graph**.

consistency

An **axiom**atic theory is said to be consistent if it's impossible (within the confines of the theory) to prove simultaneously a statement and its negation. **Godel's incompleteness theorem** states that any (sufficiently powerful) consistent axiomatic theory is incomplete.

constructible

In classical geometry, a figure or length that can be drawn using only an unmarked straightedge and a compass. The Greeks were adept at constructing **polygon**s, but the question of proving which **regular polygons** are constructible and which are not had to wait for the genius of Carl **Gauss**. At the age of only 19, Gauss found that a regular polygon with n sides is constructible if and only if n is a prime **Fermat number**. The only known such primes are 3, 5, 17, 257, 65,537. It is also possible to construct certain numbers, known as *constructible numbers*, that correspond to line segments, including **rational number**s and some **irrational number**s, but no **transcendental number**s. It turns out that all constructions possible with a compass and straightedge can be done with a compass alone, as long as a line is considered constructed when its two endpoints are located. The reverse is also true, since Jakob **Steiner** showed that all constructions possible with straightedge and compass can be done using only a straightedge, as long as a fixed circle and its center (or two intersecting circles without their centers, or three nonintersecting circles) have been drawn beforehand. Such a construction is known as a *Steiner construction*. The Greeks were unable to achieve certain constructions, such as **squaring the circle**, **duplicating the cube**, and **trisecting an angle**, despite numerous attempts, but it wasn't until hundreds of years later that the problems were proved to be actually impossible under the limitations imposed.

continued fraction

A representation of a **real number** in the form

$$x = a_0 + \cfrac{1}{a_1 + \cfrac{1}{a_2 + \cfrac{1}{a_3 + \ldots}}}$$

which, mercifully for typesetters, can be written in compact notation as

$$x = [a_0; a_1, a_2, a_3, \ldots],$$

where the integers a_i are called *partial quotients*. Although rarely encountered in school and even college math courses, continued fractions (CFs) provide one of the most powerful and revealing forms of numerical expression. Numbers whose decimal expansions look unremarkable turn out, when unfolded as CFs, to have extraordinary symmetries and patterns. CFs also offer a way of constructing rational approximations to **irrational numbers** and of discovering the most irrational numbers.

CFs first appeared in the sixth century in the works of the Indian mathematician Aryabhata, who used them to solve linear equations. They surfaced in Europe in the fifteenth and sixteenth centuries and **Fibonacci** attempted to define them in a general way. The term "continued fraction" first appeared in 1653 in an edition of *Arithmetica Infinitorum* by John **Wallis**. Their properties were also studied by one of Wallis's English contemporaries, William Brouncker, who, along with Wallis, was one of the founders of the Royal Society. At about the same time, in Holland, Christiaan **Huygens** made practical use of CFs in his designs of scientific instruments. Later, in the eighteenth and early nineteenth centuries, Carl **Gauss** and Leonhard **Euler** delved into many of their deeper properties.

CFs can be finite or infinite in length. Finite CFs can be evaluated level by level (starting at the bottom) and will always reduce to a rational fraction; for example, the

CF [1; 3, 2, 4] = 40/31. By contrast, infinitely long CFs produce representations of irrational numbers. Here are the leading terms from a few notable examples of infinite CFs:

e = [2; 1, 2, 1, 1, 4, 1, 1, 6, 1, 1, 8, 1, 1, 10, . . .]

$\sqrt{2}$ = [1; 2, 2, 2, 2, 2, 2, 2, 2, 2, 2, 2, 2, 2, 2, . . .]

$\sqrt{2}$ = [1; 2, 1, 2, 1, 2, 1, 2, 1, 2, 1, 2, 1, 2, 1, . . .]

π = [3; 7, 15, 1, 292, 1, 1, 1, 2, 1, 3, 1, 14, 2, 1, 1, 2, 2, 2, 2, 1, 84, 2, . . .]

Each of these expansions has a simple pattern except that for π (see **pi**), which has no obvious pattern at all. There's also a preference for the quotients to be small numbers.

If an infinite CF is truncated after a finite number of steps, the result is a *rational approximation* to the original irrational. In the case of π, chopping the CF at [3; 7] gives the familiar approximation for π of 22/7 = 3.1428571 . . . . Keeping two more terms leads to [3; 7, 15, 1] = 353/113 = 3.1415929 . . . , which is an even better approximation to the true value of π (3.14159265 . . .). The more terms retained in the CF, the better the rational approximation becomes. In fact, the CF gives yields the best possible rational approximations to a general irrational number. Notice also that if a large number occurs in the expansion of quotients, then truncating the CF after that will produce an especially good rational approximation. Most CF quotients are small numbers (1 or 2), so the appearance in the CF of π of a number as large as 292 so early in the expansion is unusual. It also leads to an extremely good rational approximation to π = [3; 7, 15, 1, 292] = 103,993/33,102.

continuity

A mathematical property that has to do with how smooth or "well-behaved" a **function** or curve is. If two adjacent points on a graph, for example, are not connected or are separated by a jump, this marks a breakdown of continuity. At such a discontinuity it is impossible to obtain a **derivative**, or slope, of the curve. Usually if a curve does misbehave like this, it is only at one or two isolated places; elsewhere the curve is likely to be both continuous and differentiable. However, it is possible to construct a continuous function that has "problem points" everywhere and, therefore, is nowhere differentiable! The first example was found by Karl **Weierstrass** in 1872 and came as a total surprise. It is defined as an infinite series

$$f(x) = \sum_{n=0}^{\infty} B^n \cos(A^n \pi x),$$

where A and B can be any numbers such that B is between 0 and 1, and $A \times B$ is bigger than $1 + (3\pi/2)$.

continuum

Any **set** that can be brought into **one-to-one** correspondence with the set of **real number**s. Examples include a finite line segment, a square, a circle, and a disk.

continuum hypothesis

In 1874 Georg **Cantor** discovered that there is more than one level of **infinity**. The lowest level is called *countable infinity;* higher levels are known as *uncountable infinities.* The **natural number**s are an example of a countably infinite set and the **real number**s are an example of an uncountably infinite set. The continuum hypothesis, put forward by Cantor in 1877, says that the number of real numbers is the *next* level of infinity above countable infinity. It is called the continuum hypothesis (CH) because the real numbers are used to represent a linear continuum. Let c be the cardinality of (i.e., number of points in) a continuum, **aleph**-null (χ_0) be the cardinality of any countably infinite set, and χ_1 be the next level of infinity above χ_0. CH is equivalent to saying that there is no **cardinal number** between χ_0 and c, and that $c = \chi_1$. CH has been, and continues to be, one of the most hotly pursued problems in mathematics.

convergence

A property of some **sequence**s. A sequence u_i is said to be convergent if there exists a value u with the property that by choosing a large enough value of i, we can make u_i as close as we wish to u.

convex

Curved outward, like the exterior surface of a sphere; the word comes from the Latin *convexus* for "vaulted." A figure, such as a **polygon** or a **polyhedron**, is said to be convex if every line segment that joins two interior points remains inside the figure. Similarly, a **set** is convex if it contains all the line segments connecting any pair of its points.

Conway, John Horton (1937–)

A British-born (Liverpool) mathematician, who studied and taught at Cambridge University and is now a professor at Princeton University. Conway has been an extraordinarily fertile source of new ideas in mathematics and of mathematical games. His most significant contribution was the discovery of **surreal number**s, to which he was led after watching the British **Go** champion play at Cambridge. In 1967, he found a cluster of three new sporadic **group**s, now sometimes called *Conway's constellation,* building on an earlier discovery by John Leech of an extremely dense **packing** of unit spheres in a space of 24 dimensions. He has also been active in the field of **knot**s and in **coding theory**. Among amateur mathematicians, Conway is best known as the inventor of the games of **Life**, **Sprouts**, and **Phutball**,

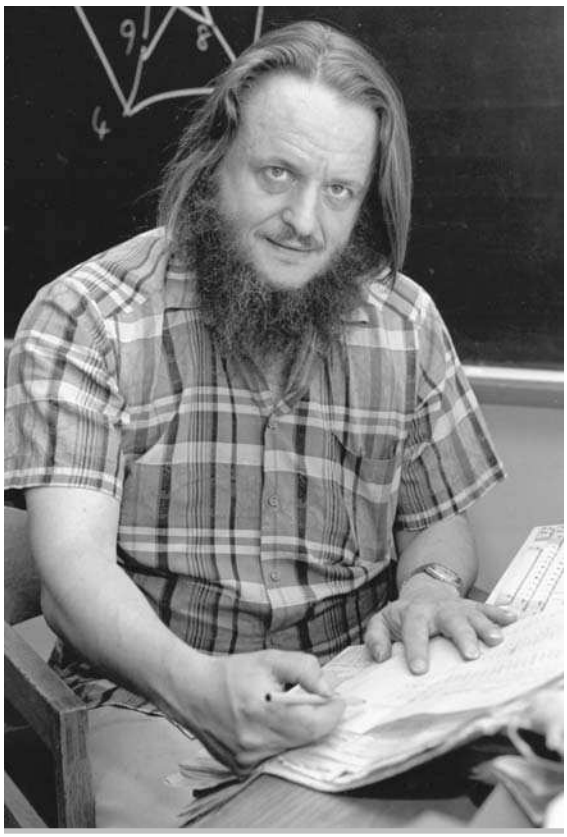

Conway, John Horton *Princeton University*

as well as for his detailed analyses of many other games and puzzles, such as the **Soma Cube**.

Conway's chained-arrow notation

One of various methods that have been devised recently for representing extremely **large number**s. Developed by John **Conway**, it is based on **Knuth's up-arrow notation** but is even more powerful. The two systems are related thus:

$a \to b \to 1 = a \uparrow b$
$a \to b \to 2 = a \uparrow\uparrow b$
$a \to b \to 3 = a \uparrow\uparrow\uparrow b$
$a \to b \to c = a \uparrow\uparrow \ldots \uparrow\uparrow b$ (c up arrows)

Longer chains are evaluated by the following general rules:

$$a \to \ldots \to b \to c \to 1 = a \to \ldots \to b \to c$$
$$a \to \ldots \to b \to 1 \to d + 1 = a \to \ldots \to b$$

and
$$a \to \ldots \to b \to c + 1 \to d + 1$$
$$= a \to \ldots \to b \to (a \to \ldots \to b \to c \to d) \to d$$

It's important to recognize that the Conway arrow isn't an ordinary *dyadic* operator. Where three or more numbers are joined by arrows, the arrows don't act separately but rather the whole chain has to be considered as a unit. The chain might be thought of as a **function** with a variable number of arguments, or as a function whose single argument is an ordered list or **vector**. The **Ackermann function** is equivalent to a three-element chain: $A(m, n) = (2 \to (n + 3) \to (m - 2)) - 3$. It can also be shown that **Graham's number** is bigger than $3 \to 3 \to 64 \to 2$ and smaller than $3 \to 3 \to 65 \to 2$.

coordinate

One of a set of variables that specifies the location of a point in space. If the coordinates are distances measured along perpendicular axes, they are known as **Cartesian coordinates**. See also **polar coordinates**.

coordinate geometry

See **analytical geometry**.

coprime

Two or more numbers are coprime if they have no **factor**s in common other than 1.

cosine

See **trigonometric function**.

countable set

A **set** that is either finite or *countably infinite*. A countably infinite set is one that can be put in **one-to-one** correspondence with the **natural number**s and thus has a **cardinal number** ("size") of **aleph**-null ($\aleph_0$). Examples of countable sets include the set of all people on Earth and the set of all fractions. See also **infinity**.

counterfeit coin problem

Among n coins, identical in size, shape, and appearance, one is a counterfeit and has a slightly different weight than the others. Using only a two-pan balance, what is the smallest number of weighings that would guarantee finding the fake coin? The problem of the counterfeit coin (or some other object), especially involving 8, 10, 12, or 13 coins, has cropped up in many guises over the years. Typically, the problem also involves finding whether the counterfeit coin is lighter or heavier than the rest. The answer depends on the specific problem and can involve quite a number of steps.

covariance

The tendency of two **random** variables to move in tandem. This is important in applications such as survey-taking and sociology, as well as in many branches of science, because if

two things tend to vary together, there is a good chance they may be causally linked. See also **causality**.

Coxeter, Harold Scott MacDonald (1907–2003)

A British-born, Cambridge-educated mathematician who spent most of his career (from 1936 on) at the University of Toronto and was regarded as the greatest classical geometer of his generation. Always known as "Donald," he is best known for his work on hyperdimensional geometries and regular **polytope**s.

In 1926, at the age of 19, Coxeter discovered a new regular polyhedron, having six hexagonal faces at each vertex. He went on to study the mathematics of kaleidoscopes and, by 1933, had enumerated the *n*-dimensional kaleidoscopes. His algebraic equations expressing how many images of an object may be seen in a kaleidoscope are now known as *Coxeter groups*. His research on icosahedral symmetries played an important role in the discovery by scientists at Rice University, Texas, of the carbon-60 molecule (see **buckyball**), for which they won the 1996 Nobel Prize in Chemistry.

Coxeter was a close friend of the artist M. C. **Escher**, whom he met in 1954, and also of Buckminster Fuller, who used Coxeter's ideas in his architecture. Indeed Coxeter's work was motivated by a strong artistic temperament and a sense of what is beautiful. He had originally intended to be a composer but fascination for symmetry took him toward mathematics and a career about which he said "I am extremely fortunate for being paid for what I would have done anyway."

Several of Coxeter's books are considered classics, including *The Real Projective Plane* (1955), *Introduction to Geometry* (1961),[74] *Regular Polytopes* (1963),[75] *Non-Euclidean Geometry* (1965)[72] and, written jointly with S. L. Greitzer, *Geometry Revisited* (1967). In 1938, he revised and updated Rouse **Ball**'s *Mathematical Recreations and Essays*.[24]

cross

A shape that consists in its most basic form of an upright section and a transverse section. The *Latin cross* has the shape of an irregular **dodecahedron** with a single (vertical) line of symmetry, and can be folded up to make a cube. The *Greek cross* has the shape of a plus sign, has four lines of symmetry, and is used as the emblem of the Red Cross organization. A version of the Greek cross that has flared ends is also known as the *crux immissa* or *cross patée*. A cross of Saint Andrew is an ordinary Greek cross rotated through 45°, and is also called the *crux decussata;* it served as the basis for the multiplication sign. A cross of Saint Anthony takes the form of a capital T. The *Maltese cross* is an irregular dodecahedron whose cross pieces flange out from the center.

crunode

A point where a curve intersects itself so that two branches of the curve have distinct **tangent** lines.

cryptarithm

A number puzzle in which a group of arithmetical operations has some or all of its digits replaced by letters or symbols, and where the original digits must be found. In such a puzzle, each letter or symbol represents a unique digit. The first example appeared in *American Agriculturist* in 1864. Specific types of cryptarithm include the **alphametic**, the **digimetic**, and the **skeletal division**.

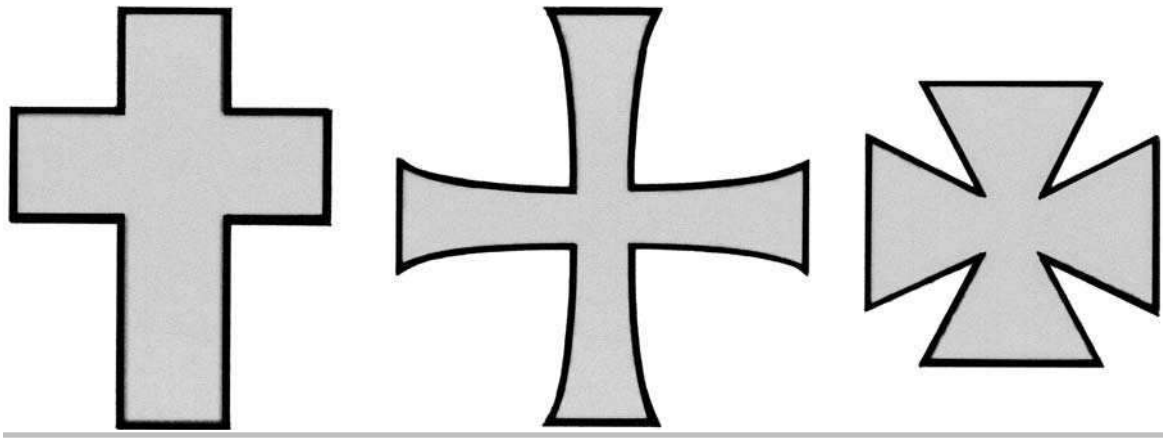

cross From left to right: a Latin cross; a *crux immissa* (a Greek cross with flared ends), also sometimes called a Latin cross; and a Maltese cross.

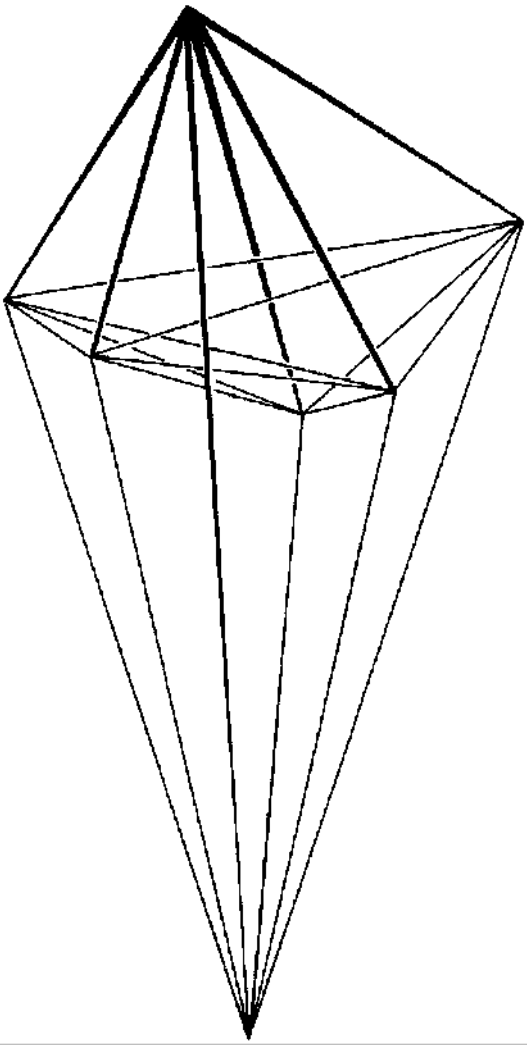

Császár polyhedron

cryptography

The science and mathematics of encoding and decoding information. See also **cipher** and **cryptarithm**.

Császár polyhedron

A **polyhedron**, first described in 1949 by the Hungarian mathematician Ákos Császár,[79] that is a solution to an interesting problem, namely: How many polyhedra exist such that every pair of vertices is joined by an edge? The first clear example is the well known **tetrahedron** (triangular pyramid). Some simple **combinatorics** specify how many vertices, edges, faces, and holes such polyhedra must have. It turns out that, other than the tetrahedron, any such polyhedron must have at least one hole. The first possible polyhedron beyond the tetrahedron has exactly one hole; this is the Császár polyhedron, which is thus topologically equivalent to a **torus** (donut). The Császár polyhedron has 7 vertices, 14 faces, and 21 edges, and is the **dual** of the **Szilassi polyhedron**. It isn't known if there are any other polyhedra in which every pair of vertices is joined by an edge. The next possible figure would have 12 faces, 66 edges, 44 vertices, and 6 holes, but this seems an unlikely configuration–as, indeed, to an even greater extent, does any more complex member of this curious family.

cube

(1) The **Platonic solid** that has a square for every one of its 6 faces; it also has 12 edges and 8 vertices (corners). The $60' \times 30' \times 30'$ Double Cube Room of Wilton House (the seat of the Earl of Pembroke), near Salisbury, is considered, together with the Single Cube Room of the same domicile, among the finest surviving rooms in England from the mid-seventeenth century. A favorite with filmmakers, it has provided locations for *Barry Lyndon* by Stanley Kubrick, *The Madness of King George,* and *Sense and Sensibility.* See also **Atomium, the**. (2) To cube something is to raise it to the power of three. The result of cubing is a *cube number:* $1^3 = 1$, $2^3 = 8$, $3^3 = 27$, and so on. To take the *cube root* is the reverse process; thus, 4 cubed (4^3) is 64 and the cube root of 64 ($\sqrt[3]{64}$) is 4. For cube **dissection** problems, see **Hadwiger problem**, **Slothouber-Graatsma puzzle** and **Soma cube**. See also **tesseract** and **Prince Rupert's problem**.

cubic curve

An **algebraic curve** described by a **polynomial** equation of the general form

$$ax^3 + bx^2y + cxy^2 + dy^3 + ex^2 + fxy + gy^2 + hx + iy + j = 0,$$

where *a, b, c, d, e, f, g, h, i,* and *j* are constants, such that at least one of *a, b, c,* and *d* is nonzero, and *x* and *y* are variables. One of Isaac **Newton**'s many accomplishments was the classification of the cubic curves. Newton found 72 different species of curve; later investigators found six more, and it is now known that there are precisely 78 different types of cubic curves. Interesting examples include the **folium** of Decartes and the Witch of **Agnesi**.

cubic equation

A **polynomial** equation of the third degree, the general form of which is

$$ax^3 + bx^2 + cx + d = 0,$$

where *a, b, c,* and *d* are constants. There was a great controversy in sixteenth-century Italy between Girolamo **Cardano** and Niccoló **Tartaglia** about who should get credit for solving the cubic. At this time symbolic algebra

hadn't been developed, so all the equations were written in words instead of symbols. Early studies of cubics helped legitimize **negative number**s, give a deeper insight into equations in general, and stimulate work that eventually led to the discovery and acceptance of **complex number**s. Cardano, in his *Ars Magna,* found negative solutions to equations, but called them "fictitious." He also noted an important fact connecting solutions of a cubic equation to its **coefficient**s, namely, that the sum of the solutions is the negation of *b,* the coefficient of the x^2 term. At one other point, he mentions that the problem of dividing 10 into two parts so that their product is 40 would have to be $5 + v(-15)$ and $5 - v(-15)$. Cardano didn't go further than this observation of what later came to be called complex numbers, but a few years later Rafael Bombelli (1526–1672) gave several examples that involved these strange new mathematical beasts.

cubit

A measure of length used in the ancient world. It is approximately equal to the length of a person's forearm, that is, the part of the arm from the elbow to the fingers. The Romans used a cubit equal to 17.4 modern inches; the Egyptians used one of 20.64 inches.

cuboctahedron

A **polygon** obtained by cutting the corners off a cube or an **octahedron**. It has eight faces that are equilateral triangles and six faces that are squares.

cuboid

Also called a *rectangular prism,* a **hexahedron** of which all of the faces are rectangles and all of the opposite faces are identical. It is not known whether a *perfect cuboid,* whose sides, face diagonals, and space diagonals are all integers, exists. The general suspicion is that it doesn't, although several near misses have been found, including one in which $a = 240$, $b = 117$, $c = 44$, $dab = 267$, $dac = 244$, and $dbc = 125$. If there is a perfect cuboid, it has been shown that the smallest side must be at least $2^{32} = 4{,}294{,}967{,}296$.

Cullen number

A number of the form $(n \times 2^n) + 1$, denoted C_n, and named after the Reverend James Cullen (1867–1933), an Irish Jesuit priest and schoolmaster. Cullen noticed that the first, $C_1 = 3$, was a **prime number**, but with the possible exception of the fifty-third, the next 99 were all composite. Soon afterward, Cunningham discovered that 5,591 divides C_{53}, and noted that all the Cullen numbers are **composite number**s for n in the range $2 \le n \le 200$, with the possible exception of 141. Five decades later Robinson showed that C_{141} is a prime. Currently, the only known Cullen primes are those with n = 1, 141, 4,713, 5,795, 6,611, 18,496, 32,292, 32,469, 59,656, 90,825, 262,419, 361,275, and 481,899. Although the vast majority of Cullen numbers are composite, it has been conjectured that there are infinitely many Cullen primes. Whether n and C_n can simultaneously be prime isn't known. Sometimes, the name "Cullen number" is extended to include the Woodall numbers, $W_n = (n \times 2^n) - 1$. Finally, a few authors have defined a number of the form $(n \times b^n) + 1$, with $n + 2 > b$, to be a *generalized Cullen number.*

Cunningham chain

A sequence of **prime number**s in which each member is twice the previous one plus one. For example, {2, 5, 11, 23, 47} is the first Cunningham chain of length 5 and {89, 179, 359, 719, 1,439, 2,879} is the first of length 6. In general, a *Cunningham chain of length k of the first kind* is a sequence of k prime numbers, each of which is twice the preceding one plus one. A *Cunningham chain of length k of the second kind* is a sequence of k primes, each of which is twice the preceding one minus one. For example, {2, 3, 5} is a Cunningham chain of length 3 of the second kind and {1,531, 3,061, 6,121, 12,241, 24,481} is a Cunningham chain of length 5 of the second kind. Prime chains of both these forms are said to be complete if they can't be extended by adding either the next larger or the next smaller terms. See also **Sophie Germain prime**.

cup

The symbol ∪, which is used to denote the **union** of two **set**s.

curvature

A measure of the amount by which a curve, a surface, or any other **manifold** deviates from a straight line, a plane, or a hyperplane (the multidimensional equivalent of a plane). For a plane curve, the curvature at a given point has a magnitude equal to one over the radius of an *osculating* circle (a circle that "kisses," or just touches, the curve at the given point) and is a **vector** pointing in the direction of that circle's center. The smaller the radius r of the osculating circle, the greater the magnitude of the curvature $(1/r)$ will be. A straight line has zero curvature everywhere; a circle of radius r has a curvature of magnitude $1/r$ everywhere.

For a two-dimensional surface, there are two kinds of curvature: a *Gaussian* (or *scalar*) *curvature* and a *mean curvature.* To compute these at a given point, consider the intersection of the surface with a plane containing a fixed normal vector (an arrow sticking out perpendicularly) at the point. This intersection is a plane and has a curvature; if the plane is varied, this curvature also changes, and there are two extreme values–the maximal and the minimal curvature–which are known as the *main curva-*

tures, $1/R_1$ and $1/R_2$. (By convention, a curvature is taken to be positive if its vector points in the same direction as the surface's chosen normal, otherwise it is negative.) The Gaussian curvature is equal to the product $1/R_1R_2$. It is everywhere positive for a **sphere**, everywhere negative for a **hyperboloid** and **pseudosphere**, and everywhere zero for a plane. It determines whether a surface has elliptic (when it is positive) or hyperbolic (when it is negative) geometry at a point. The integral of the Gaussian curvature over the whole surface is closely related to the surface's **Euler characteristic**. The mean curvature is equal to the sum of the main curvatures, $1/R_1 + 1/R_2$.

A **minimal surface**, like that of a soap film, has a mean curvature of zero. In the case of higher-dimensional manifolds, curvature is defined in terms of a curvature **tensor**, which describes what happens to a vector that is transported around a small loop of the manifold.

curve

A continuous mapping from a one-dimensional space to an *n*-dimensional space. The most familiar mathematical curves are two- and three-dimensional **graph**s. A curve, such as a circle, that lies entirely in a plane is called a *plane curve;* by contrast, a curve that may pass through any region of three-dimensional space is called a *space curve.* See also **space-filling curve**.

curve of constant width

A curve that, when rotated in a square, makes continuous contact with all four sides. It may seem, at first sight, as if there is only one such curve–a circle. But, in fact, there are infinitely many different curves of constant width. The circle is the one with the largest area. The simplest noncircular one, and the one with the smallest area, is the **Reuleaux triangle**. Others can be constructed starting with equilateral (but not necessarily equiangular) stars. Every curve of constant width is **convex**. Moreover, *Barbier's theorem* states that every curve of constant width w has the same perimeter, πw. (The width of a convex figure is defined as the distance between parallel lines–known as *supporting lines*–that bound it.) A curve of constant width can be used in a special drill chuck to cut square holes. A generalization gives solids of constant width. These do not have the same surface area for a given width, but their shadows are curves of constant width with the *same* width.

cusp

In mathematics, a point on a curve where two branches, coming from different directions, meet and have a common **tangent**. If the two branches of the curve approach the tangent from opposite sides the cusp is called a *keratoid* (from the Greek *kera* for "horn") or *first-order cusp.* This is the case, for example, with the curve given by the equation $y^2 = x^2y + x^5$. If the two branches of the curve approach the tangent from the same side the result is a *ramphoid* or *second-order cusp.* "Cusp" derives from the Latin *cuspis* for "sharp." Outside of mathematics, the points of a crescent moon are called cusps and the sharp pointed premolar teeth of children are known as bicuspids.

cute number

A number n such that a square can be cut into n squares of, at most, two different sizes. For example, 4 and 10 are cute numbers.

Cutler, William (Bill)

An Australian puzzle maker and solver who, in 1977, became the first to completely analyze, using a computer, six-piece burrs used to make solid six-piece **burr puzzle**s. Martin Gardner devoted his January 1978 "Mathematical Games" column in *Scientific American* to this and other of Cutler's discoveries. In 2003, Cutler used a computer to enumerate all solutions of the **Loculus of Archimedes**.

cybernetics

The theoretical study of communication and control processes in biological, mechanical, and electronic systems, especially the comparison of these processes in biological and artificial systems. It was pioneered by Norbert **Wiener**.

cyclic number

A number with n digits, which, when multiplied by 1, 2, 3, . . . , n produces the same digits in a different order. For example, 142,857 is a cyclic number: $142{,}857 \times 2 = 285{,}714$; $142{,}857 \times 3 = 428{,}571$; $142{,}857 \times 4 = 571{,}428$; $142{,}857 \times 5 = 714{,}285$; $142{,}857 \times 6 = 857{,}142$, and so on. It has been conjectured, but not yet proven, that an infinite number of cyclic numbers exist.

cyclic polygon

A **polygon** with vertices (see **vertex**) that all lie on the same circle. All triangles are cyclic (but not all of any other kind of polygon) because any set of three points, not lying on a single line, can have a circle drawn through it.

cycloid

The shape defined by a fixed point on a wheel as it rolls; more precisely, it is the **locus** of a point on the rim of a circle rolling along a perfectly straight line. The cycloid was named by Galileo in 1599. It is the solution to both the **tautochrone problem** and the **brachistochrone problem**. In 1634, the French mathematician Gilles de Roberval (1610–1675) showed that the area under a cycloid is three times the area of its generating circle. In 1658, the English architect Christopher Wren showed

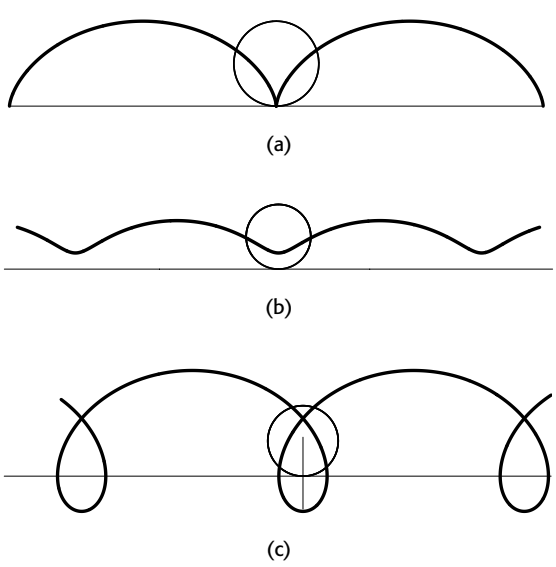

cycloid An ordinary cycloid is traced out by a point on a wheel as it rolls along a flat surface (a). A curtate cycloid is traveled by a point on the wheel that is inside the circumference (b). If the point lies outside the circumference of the wheel, the result is a prolate cycloid (c).

that the length of a cycloid is four times the diameter of its generating circle. But there was a lot of bickering and a lack of public sharing of information around this time that led to much duplication of effort, particularly over questions related to the cycloid. In fact, the confusion was so bad that the curve was nicknamed the Helen of Geometers, and Jean Montucla referred to it as "*la pomme de discorde*" (the apple of discord).

As well as the ordinary cycloid there is the *curtate cycloid,* which is the path traced out by a point on the inside of a rolling circle, and the *prolate cycloid,* which is followed by a point on the outside of the circle. A prolate cycloid is traced out, for example, by points on the flange of the wheels of a locomotive, which extends below the top of the tracks. This leads to the surprising conclusion that even as the locomotive is moving forward there are always parts of its wheels that are going backward for a moment before moving forward again. See also **epicycloid** and **hypocycloid**.

cylinder

A three-dimensional surface described by the Cartesian equation $(x/a)^2 + (y/b)^2 = 1$. If $a = b$ then the surface is a *circular cylinder,* otherwise it is an *elliptic cylinder.* The cylinder is a *degenerate quadric* because at least one of the coordinates (in this case z) doesn't appear in the equation, though by some definitions the cylinder isn't considered to be a quadric at all. In common usage, a *cylinder* is taken to mean a finite section of a right circular cylinder with its ends closed to form two circular surfaces. If the cylinder has a radius r and a length h, then its volume is $V = \pi r^2 h$ and its surface area is $A = 2\pi r^2 + 2\pi rh$. For a given volume, the cylinder with the smallest surface area has $h = 2r$. For a given surface area, the cylinder with the largest volume has $h = 2r$. More unusual types of cylinder include the *imaginary elliptic cylinder:* $(x/a)^2 + (y/b)^2 = -1$, the *hyperbolic cylinder:* $(x/a)^2 - (y/b)^2 = 1$, and the *parabolic cylinder:* $x^2 + 2y = 0$.

D

d'Alembert, Jean Le Rond (1717–1783)
A French mathematician named for the church of St. Jean Baptiste de Rond upon whose steps he was abandoned as a baby, the illegitimate son of a Parisian society hostess. He clarified the concept of a **limit** in calculus, discovered the *Cauchy-Riemann equations* decades before Augustin **Cauchy** or Bernhard **Riemann**, was the first to find and solve the wave equation, and recast **Newton**'s third law in a new and powerful form through what has become known as *d'Alembert's principle*.

Dandelin spheres
If a **cone** is sliced through by a plane, the two spheres that just fit inside the cone, one on each side of the plane and both tangent to it and touching the cone, are known as Dandelin spheres. They are named after the Belgian mathematician and military engineer Germinal Pierre Dandelin (1794–1847) who gave an elegant proof that the two spheres touch the **conic section** at its foci. In 1826, Dandelin showed that the same result applies to the plane sections of a **hyperboloid** of revolution.

dart
Also known as an *arrowhead*, a special kind of quadrilateral that has one **reflex angle**. See also **Penrose tiling**.

de L'Hôpital, Guillaume François Antoine, Marquis de (1661–1704)
A French mathematician who wrote the first textbook on differential calculus, *Analyse des infiniment petits pour l'intelligence des lignes courbes* (1696). This contains the rule, now known as *L'Hôpital's rule*, for finding the limit of a rational function whose numerator and denominator tend to zero at a point. Along with Isaac **Newton**, Gottfried **Leibniz**, and Jacob Bernoulli (see **Bernoulli family**), de L'Hôpital was among the first to solve the **brachistochrone problem**.

de L'Hôpital's cubic
See **Tschirnhaus's cubic**.

de Malves's theorem
Given a **tetrahedron** in which the edges meeting at one **vertex**, *X*, form three right angles (i.e., the tetrahedron is the result of chopping off the corner of a **cuboid**), the square of the face opposite *X* is equal to the sum of the squares of the other three faces.

de Méré's problem
A question posed in the mid-seventeenth century to Blaise **Pascal** by a French nobleman and inveterate gambler, the Chevalier de Méré, which marked the birth of **probability theory**. One of de Méré's favorite bets was that at least one six would appear during a total of four rolls of a die. From past experience, he knew that this gamble paid off more often than not. Then, for a change, he started betting that he would get a double-six on 24 rolls of two dice. However, he soon realized that his old approach to the game was more profitable. He asked his friend Pascal why. Pascal showed that the probability of getting at least one six in four rolls of a die is $1 - (5/6)^4 \approx 0.5177$, which is slightly higher than the probability of at least one double-six in 24 throws of two dice, $1 - (35/36)^{24} \approx 0.4914$. This problem and others posed by de Méré are thought to have been the original inspiration for a fruitful exchange of letters on probability between Pascal and Pierre de **Fermat**. To tackle these problems, Fermat used combinatorial analysis (finding the number of possible outcomes in ideal games of chance by computing permutation and combination numbers), while Pascal reasoned by recursion (an iterative process that determines the result of the next case by the present case). Their combined work laid the foundations for probability theory as we know it today.

de Moivre, Abraham (1667–1754)
A French-British mathematician who founded analytical trigonometry and stated what has become known as **de Moivre's theorem**. He also worked on probability theory and the normal distribution, and was a good friend of Isaac **Newton**. In 1698 he wrote that the theorem had been known to Newton as early as 1676.

de Moivre's theorem
A theorem, named after Abraham **de Moivre**, that links **complex number**s and trigonometry. It states that for any real number x and any integer n,

$$(\cos x + i\sin x)^n = \cos(nx) + i\sin(nx).$$

By expanding the left-hand side and then comparing real and imaginary parts, it is possible to derive useful

expressions for $\cos(nx)$ and $\sin(nx)$ in terms of $\sin(x)$ and $\cos(x)$. Furthermore, the formula can be used to find explicit expressions for the nth **root of unity**: complex numbers z such that $z^n = 1$. It can be derived from (but historically preceded) **Euler's formula** $e^{ix} = \cos x + i \sin x$ and the exponential law $(e^{ix})^n = e^{inx}$.

de Morgan, Augustus (1806–1871)

A British mathematician, born in India, who was an important innovator in the field of mathematical logic. The system he devised to express such notions as the contradictory, the converse, and the transitivity of a relation, as well as the union of two relations, laid some of the groundwork for his friend George **Boole**. De Morgan lost the sight of his right eye shortly after birth, entered Trinity College, Cambridge, at the age of 16, and received his B.A. However, he objected to a theological test required for the M.A. and returned to London to study for the bar. In 1827, he applied for the chair of mathematics in the newly founded University College, London and, despite having no mathematical publications, he was appointed. In 1831, he resigned on principle (after another professor was fired without explanation) but regained his job five years later when his replacement died in an accident. He resigned again in 1861.

His most important published work, *Formal Logic,* included the concept of the *quantification of the predicate,* an idea that solved problems that were impossible under the classic Aristotelian logic. De Morgan coined the phrase "**universe of discourse**," was the first person to define and name mathematical **induction**, and developed a set of rules to determine the **convergence** of a mathematical series. In addition, he devised a decimal coinage system, an almanac of all full moons from 2000 B.C. to A.D. 2000, and a theory on the probability of life events that is still used by insurance companies. De Morgan was also deeply interested in the history of mathematics. In *Arithmetical Books* (1847) he describes the work of over fifteen hundred mathematicians and discusses subjects such as the history of the length of a foot, while in *A Budget of Paradoxes* he gives a marvelous compendium of eccentric mathematics including the poem

> Great fleas have little fleas upon their backs to bite 'em,
> And little fleas have lesser fleas, and so ad infinitum,
> And the great fleas themselves, in turn, have greater fleas to go on,
> While these again have greater still, and greater still, and so on.

The first lines of this poem paraphrase a similar rhyme by Jonathan Swift.

PUZZLE

On one occasion, when asked his age, de Morgan replied: "I was x years old in the year x^2." How old must he have been at the time?

Solutions begin on page 369.

decagon

A **polygon** with 10 sides.

decimal

The commonly used **number system**, also known as *denary,* in which each place has a value 10 times the value of the place at its right. For example, 4,327 in the decimal (base 10) system is shorthand for $(4 \times 10^3) + (3 \times 10^2) + (2 \times 10^1) + (7 \times 10^0)$, where $10^0 = 1$. "Decimal" comes from the Latin *decimus* for "tenth." The verb *decimare,* literally "to take a tenth of," was used to describe a form of punishment applied to mutinous units in the Roman army. The men were lined up and every tenth soldier was killed as a lesson to the rest. From this custom comes our word *decimate,* which we use more loosely—in fact, incorrectly—to indicate near-total destruction. The Latin *decimare* was also used in a less ferocious sense to mean "to tax to the amount of one tenth." However, the usual word describing a one-tenth tax in English is *tithe,* which comes from the Old English *teogotha,* a form of *tenth.*

decimal fraction

A number consisting of an **integer** part, which may be zero, and a decimal part less than unity that follows the decimal marker (which may be a point or a comma). A *finite* or *terminating decimal fraction* has a sequence of decimals with a definite break-off point after which all the places are zeros. Other fractions produce endless sequences of decimals that are *periodic nonterminating.*

Dedekind, (Julius Wilhelm) Richard (1831–1916)

A German mathematician whose most important contribution was the discovery of what became known as the *Dedekind cut.* He realized that every **real number** r divides the **rational number**s into two subsets: those greater than r and those less than r. Dedekind's brilliant idea was to represent the real numbers by such divisions of the rationals. He also provided important support for Georg **Cantor**'s set theory, which was highly controversial at the time.

Dee, John (1527–1609)

A notable English alchemist, mathematician, and astronomer, sometimes referred to as the "last magician" because of his astrological services to Queen Elizabeth I; Dee may also have influenced the writings of Shake-

speare. He enrolled at St. Johns College, Cambridge, at age 15, but found the atmosphere there stifling and later went to the Continent to study and lecture. Upon his return to England, Dee cast the horoscope for Queen Mary and later visited Mary's half-sister Elizabeth in jail to determine when Mary would die. Accused of black magic, he was jailed and then released in 1555, three years before Mary's death. When Elizabeth came to the throne she consulted Dee on many matters, including the geography of newly discovered lands, and paid him well. Some of his income he spent on extensive traveling, which may have involved some spying on behalf of his sponsor.

Dee had a large library of books on witchcraft, the occult, and magic, and he wrote 79 manuscripts, only a few of which were published. He married three times and fathered eight children. He also struck up an uneasy partnership with Edward Kelly, a bad-tempered Irishman who claimed to have discovered the alchemical secret of transmuting base metal into gold but had lost his ears for forgery. In 1585 Dee and Kelly went on a four-year trek across the Continent conducting astrological readings for nobility and royalty. But Dee and Kelly had many arguments and eventually parted company. Back in England Dee found his house ransacked and many of his possessions stolen or destroyed. Elizabeth helped pay for the damage and made him warden of Christ's College in Manchester in 1595. However, Elizabeth died in 1603 and her successor James I opposed magic. Dee was forced to retire, his life ending in poverty.

deficient number
See **abundant number**.

degree
(1) The unit of measurement for angles; one degree is $^1/_{360}$ of a circle. (2) The **exponent** of a variable. For example, the degree of $7x^5$ is 5. See also **degree of freedom**.

degree of freedom
A positive integer that gives the number of pieces of data that are independent.

deletable prime
See **truncatable prime**.

delta curve
A curve that can be turned inside an equilateral **triangle** while continuously making contact with all three sides. There are an infinite number of delta curves, but the simplest are the **circle** and lens-shaped delta-biangle. All the delta curves of height h have the same perimeter $2\pi h/3$. See also **Reuleaux triangle** and **rotor**.

deltahedron
A **polyhedron** whose faces consist of equilateral triangles that are all the same size. Although there are an infinite number of different deltahedra, only eight of them are convex, as O. Rausenberger first showed in 1915. Among this group of eight, faces made of coplanar equilateral triangles sharing an edge (such as the rhombic dodecahedron) aren't allowed. The eight convex deltahedra have 4, 6, 8, 10, 12, 14, 16, and 20 faces.

deltoid
A **hypocycloid** with three cusps, also known as a *tricuspoid* or *Steiner's hypocycloid* after the Swiss mathematician Jakob **Steiner** who investigated the curve in 1856. The deltoid, so-named because it looks like an uppercase Greek delta, Δ, is formed by a point on the circumference of a circle rolling inside another circle with a radius three times as large. While working on a problem in optics in 1745, Leonhard **Euler** was among the first to study its properties. The parametric equations of the cycloid with inner circle of radius r are:

$$x(t) = 2r\cos t + r\cos 2t$$
$$y(t) = 2r\sin t - r\sin 2t$$

The length of the path of the deltoid is $16r/3$, and the area inside the deltoid is $2\pi r^2$. If a tangent is drawn to the deltoid at some point, P, and the points where the tangent crosses the deltoids other two branches are called points A and B, then the length of AB equals $4r$. If the deltoid's tangents are drawn at points A and B, they will

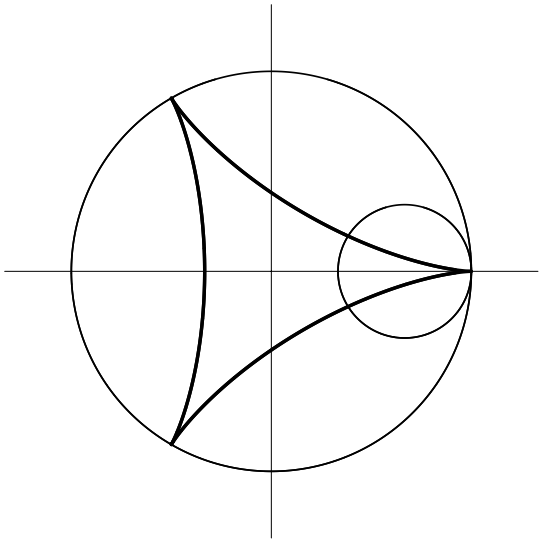

deltoid The deltoid curve. © *Jan Wassenaar, www.2dcurves.com*

be perpendicular, and they will intersect at a point inside the deltoid that is the 180° rotation of point P about the center of the fixed circle.

denominator

In a **rational number**, the number below the fraction bar; it indicates into how many parts the whole is divided.

derivative

The result of differentiating a **function**; that is, the infinitesimal change in a function caused by an infinitesimal change in the variable(s) upon which it depends. The derivative gives the rate of change of a function (the slope of its curve) at a particular point. Second and third derivatives give the rate at which the rate of change is changing and the rate at which the rate of rate of change is changing, respectively. In an article in 1996, Hugo Rossi wrote: "In the fall of 1972 President Nixon announced that the rate of increase of inflation was decreasing. This was the first time a sitting president used the third derivative to advance his case for reelection."[269]

Here is a fallacious "proof" that $x = 2x$ based on derivatives. Consider the function $f(x) = x^2$, the derivative of which is $2x$. What is wrong with the following?

$$x^2 = x + x + \ldots + x \text{ (repeated } x \text{ times)}$$

Taking the derivative of both sides gives

$$(x^2)' = 1 + 1 + \ldots + 1 = x.$$

But we have already said that the derivative of x^2 is $2x$. Therefore, $x = 2x$. The error stems from taking the derivative of x different x's. Each of the terms depends not only on x, which was accounted for in taking the derivative, but also on the *number* of terms (which could be fractional) which depends on x, too, and this was not accounted for. Put another way, the derivative measures the rate of change of x^2 as x changes, but as x changes, the number of terms on the right, as well as the terms themselves, increases. For positive x, the correct answer must be larger than x–as indeed it is.

Desargues, Girard (1591–1661)

A French mathematician who is regarded as the chief founder of perspective geometry. His 12-page treatise *La perspective* (1636) consists of a single worked example in which Desargues sets out a method for constructing a perspective image without using any point lying outside the picture field. He considers the representation in the picture of a plane of lines that meet at a point and also of lines that are parallel to each another. In the last paragraph of the work he considers the problem of finding the perspective image of a conic section. Three years later, he wrote his treatise on projective geometry *Brouillon project d'une atteinte aux evenemens des rencontres du cone avec un plan* (Rough draft for an essay on the results of taking plane sections of a cone). The first part of this deals with the properties of sets of straight lines meeting at a point and of ranges of points lying on a straight line. In the second part, the properties of conics are investigated in terms of properties of ranges of points on straight lines and the modern term "point at infinity" appears for the first time. Desargues shows that he has completely grasped the connection between conics and perspective; in fact he treats the fact that any conic can be projected into any other conic as obvious. Given such innovative work it may seem surprising that the subject didn't develop rapidly in the following years. That may be partly due to mathematicians failing to recognize the power of what had been put forward. On the other hand, the algebraic approach to geometry put forward by René **Descartes** at almost exactly the same time (1637) may have diverted attention from Desargues's projective methods.

Descartes, René (1596–1650)

> *If you would be a real seeker after truth, it is necessary that at least once in your life you doubt, as far as possible, all things.*

A hugely influential philosopher and mathematician, born in La Haye (now named Descartes after its most famous son), Indre-et-Loire, France, who is often referred to as the father of modern philosophy and one of the founders of modern mathematics. He studied law at the University of Poitiers but never practiced it, served in the military for a while, and then lived in Holland for 20 years where he did the bulk of his great work. In his *Meditations on First Philosophy,* he tried to establish what can be known as true beyond doubt. His tool was methodological skepticism: the assumption that any idea that can be doubted is false. He gives the example of dreaming: in a dream, one senses things that seem to be real, but that don't actually exist. Thus, the data of the senses can't be fully trusted. Then again, he mused, perhaps there is an "evil genius"–a supremely powerful and devious being who sets out to prevent anyone from knowing the true nature of reality. Given these possibilities, what is it that one can know for certain? Descartes argues that if "I" am being deceived, then surely "I" must exist–the statement famously referred to as *cogito ergo sum* ("I think, therefore I am"), though these words don't actually appear anywhere in the *Meditations.* Descartes concludes that he can be certain that he exists. But in what form? If the senses are unreliable, Descartes reasons, all he can say for sure is that he is a *thinking thing.* He then proceeds to build a system of knowledge, discarding perception as

unreliable and instead admitting only deduction as a method. Halfway through the *Meditations* he also claims to prove the existence of a benevolent **God** who has provided him with a working mind and sensory system, and who cannot desire to deceive him, and thus, finally, he establishes the possibility of acquiring knowledge about the world based on deduction *and* perception.

In mathematics, Descartes is important for his discovery of **analytical geometry**. Up to Descartes's time, **geometry**, dealing with lines and shapes, and **algebra**, dealing with numbers, were regarded as completely independent aspects of mathematics. Descartes showed how almost all problems in geometry can be translated into problems in algebra, by regarding them as questions asking for the length of a line segment, and using a coordinate system to describe the problem. Descartes's theory provided the basis for **calculus**, developed by Isaac **Newton** and Gottfried **Leibniz**, and thus for much of modern mathematics. This is particularly amazing when you consider that Descartes intended it merely as an example to support his *Discours de la méthode pour bien conduire sa raison, et chercher la verité dans les sciences* (Discourse on the method to rightly conduct the reason and search for the truth in sciences), better known under the shortened title *Discours de la méthode.*

Descartes died of pneumonia in Stockholm, where he had been invited to serve as tutor to the energetic 19-year-old Queen Christina of Sweden. Accustomed to working in a warm bed till noon, he was shocked into a rapid decline by having to teach philosophy at 5 A.M. in a freezing library. Seventeen years after his death, the Roman Catholic Church placed his works on the Index of Prohibited Books.

Descartes's circle theorem

See **Soddy's formula**.

determinant

A quantity obtained from a square ($n \times n$) array of numbers that can be useful, among other things, in solving systems of **linear** equations (equations in which the unknowns are raised to at most the first power). More generally, a determinant transforms a square **matrix** into a **scalar**–an operation that has many important properties. Two-by-two determinants were considered by Girolamo **Cardano** at the end of the sixteenth century and ones of arbitrary size by Gottfried **Leibniz** about a century later. Determinants are so named because, when applied to systems of linear equations, they "determine" if the systems are singular–that is, have multiple solutions. They also have important geometric applications, because they describe the area of a **parallelogram** and, more generally, the volume of a **parallelepiped**. A three-rowed determinant is defined by:

$$\begin{vmatrix} a_{11} & a_{12} & a_{13} \\ a_{21} & a_{22} & a_{23} \\ a_{31} & a_{32} & a_{33} \end{vmatrix} = \begin{array}{r} a_{11} \times a_{22} \times a_{33} + a_{12} \times a_{23} \times a_{31} \\ + a_{13} \times a_{21} \times a_{32} - a_{13} \times a_{22} \times a_{31} \\ - a_{12} \times a_{21} \times a_{33} - a_{11} \times a_{23} \times a_{32} . \end{array}$$

deterministic system

A system in which the later states of the system follow from, or are determined by, the earlier ones. Such a system contrasts with a *stochastic* or *random system* in which future states are not determined from previous ones. An example of a stochastic system would be the sequence of heads or tails of an unbiased coin, or radioactive decay.

If a system is deterministic, this doesn't necessarily imply that later states of the system are predictable from a knowledge of the earlier ones. In this way, **chaos** is similar to a random system. Chaos has been termed "deterministic chaos" since, although it is determined by simple rules, its property of sensitive dependence on initial conditions makes a chaotic system, in practice, largely unpredictable.

devil's curve

Also known as the *devil on two sticks*, a curve with the Cartesian equation

$$y^4 - a^2y^2 = x^4 - b^2x^2$$

and the polar equation

$$r^2 (\sin^2\Theta - \cos^2\Theta) = a^2\sin^2\Theta - b^2\cos^2\Theta).$$

Early studies of it were carried out in 1750 by the Swiss mathematician Gabriel Cramer (1704–1752), who is

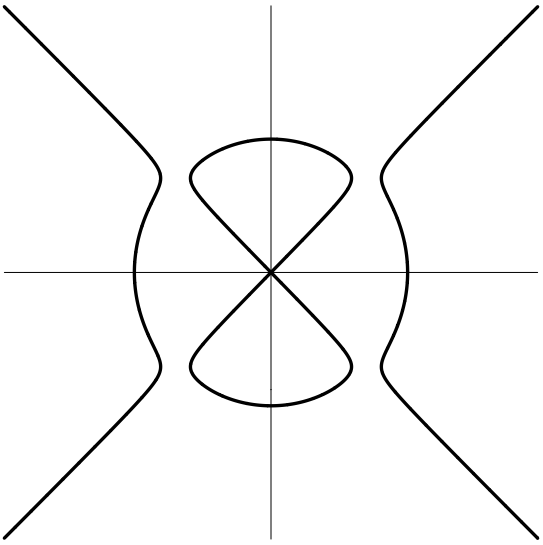

devil's curve *© Jan Wassenaar, www.2dcurves.com*

most famous for his work on **determinant**s, and in 1810 by Lacroix. For $a = {}^{25}/_{24}$, the curve is called the *electric motor curve*.

Dewdney, Alexander Keewatin (1941–)

A Canadian computer scientist and mathematician at the University of Western Ontario, Canada, best known for his popular books and articles, most notably *The Planiverse: Computer Contact with a Two-dimensional World*, first published in 1984.[81] For several years, Dewdney wrote the "Mathematical Recreations" column for *Scientific American*.

diagonal

A line that joins any two vertices of a **polygon**, if the vertices are not next to each other; or a line that joins two vertices of a **polyhedron** that are not on the same face.

diagonal matrix

A **matrix** that has zero entries along all nondiagonal entries, that is, only the main diagonal may have nonzero values.

diameter

The distance across a **circle** through the center.

dice

Small polyhedra (see **polyhedron**), usually cubes, whose faces are numbered from one to six by patterns of dots, with opposite sides totaling seven. They are thrown, singly or in groups, from the hand or from a cup, onto a flat surface, to provide **random** numbers for gambling and other games. The face of each die that is uppermost when it comes to rest provides the value of the throw. Typical of their use today is the game of craps, in which two dice are thrown together, and bets placed on the total face-up value. Dice probably evolved from knucklebones, which are approximately tetrahedral. Even today, dice are sometimes colloquially referred to as "bones." Ivory, bone, wood, metal, and stone materials have been commonly used to make dice, though the use of plastics is now nearly universal.

Dice found in ancient tombs in the Orient point to an Asiatic origin and dicing is mentioned as an Indian game in the Rig-veda. In its primitive form, knucklebones was essentially a game of skill, played by women and children; gradually, a derivative form evolved for gambling in which four sides of the bones received different values and were counted like dice. Gambling with three, sometimes two, dice was a popular form of amusement in Greece, especially with the upper classes, and was an almost invariable accompaniment to the symposium, or drinking banquet. The Romans were passionate gamblers, and dicing was a favorite form, though it was forbidden except during the festival of Saturnalia (December 17). Throwing dice for money led to many special laws in Rome, one of which decreed that no suit could be brought by a person who allowed gambling in his house, even if he'd been cheated or assaulted! Professional gamblers were common, and some of their loaded dice are preserved in museums.

The Roman historian Tacitus states that the Germans also were passionately fond of dicing–so much so, that, having lost everything, they would even stake their personal liberty. Centuries later, in medieval times, dicing became the favorite pastime of knights, and both dicing schools and guilds of dicers flourished.

Dice are frequently used to randomize allowable moves in board games such as **backgammon**. Loaded dice can be made in many ways to cheat at such games. Weights can be added, or some edges made round while others are sharp, or some faces made slightly off-square, to make some outcomes more likely than would be predicted by pure chance. Dice with non-cubical shapes were once almost exclusively used by fortune-tellers and in other occult practices, but they have become popular lately among players of role-playing and war-games.

difference equation

An equation that describes how something changes in discrete time steps. Numerical solutions to **integral**s are usually realized as difference equations.

differential

A term such as dx used in an expression such as $y\,dx - x\,dy$ to denote first-order small changes in the variable. *Differentiation* is the method by which a differential is found.

differential equation

A description of how something continuously changes over time (see **continuity**). Some differential equations have an exact *analytical solution* such that all future states can be known without simulating the time evolution of the system. However, most have a *numerical solution* with only limited accuracy. A differential equation involves the first or higher derivatives of the **function** to be solved for. If the equation only involves first derivatives, it is known as an equation of *order* one, and so on. If only nth powers of the derivatives are involved, the equation is said to have *degree n*. Equations of degree one are called *linear*. Equations in only one variable are called **ordinary differential equation**s to distinguish them from **partial differential equation**s, which have two or more.

differential geometry

The study of geometry using **calculus**; it has many applications in physics, especially in **relativity theory**. The

objects studied by differential geometry are known as *Riemannian **manifold**s*. These are geometrical objects, such as surfaces, that locally look like **Euclidean space** and therefore allow the definition of analytical concepts such as tangent **vector**s and tangent space, differentiability (see **differential**), and vector and **tensor** fields. Riemannian manifolds have a **metric**, which opens the door to measurement because it allows distances and angles to be evaluated locally and concepts such as **geodesic**s, **curvature**, and torsion to be defined.

differential topology
A branch of **topology** concerned with those properties of **differential geometry** that are preserved by continuous transformation.

differentiation
The method by which the **derivative** of a **function** is found.

digimetic
A **cryptarithm** in which digits are used to represent other digits.

digit
A symbol or numeral that is used to represent an **integer** in a positional **number system**. Examples of digits include the decimal characters 0 through 9, the binary characters 0 or 1, and the hexadecimal digits 0 . . . 9, A . . . F. The word comes from the Latin *digitus* for "finger" or "toe," and retains this meaning, reminding us of the origins of our base 10 number system. The earlier Indo-European root *deik* is related to many other words that hark back to the use of the hands and fingers to "point" out objects, including index, indicate, token, and teach.

digital root
Take a number, *n,* add its digits, then add the digits of numbers derived from it, and so on, until the remaining number has only one digit. This single digit result is called the digital root of *n*. For example, in the case of 5381: 5 + 3 + 8 + 1 = 19; 1 + 9 = 10; 1 + 0 = 1; thus, the digital root of 5381 is 1. See also **casting out nines**.

digraph
A **graph** in which each edge has a direction associated with it.

dihedral angle
The angle defined by two given faces meeting at an edge; for example, all the dihedral angles of a cube are 90°. An almost-spherical **polyhedron** (with many faces) has small dihedral angles.

dimension
An extension in some unique direction or sense; the word comes from the Latin *dimetiri* for "measured out." The most common way to think of a dimension is as one of the three spatial dimensions (up-down, left-right, back-forth) in which we live. Mathematicians and science fiction writers alike have long imagined what it would be like in a world with a different number of spatial dimensions. Speculation has particularly focused on **two-dimensional worlds** and, to an even greater extent, on the **fourth dimension**. **Time** is also thought of as a dimension; indeed, in **relativity theory** and as a component of **space-time**, it is treated almost exactly the same as a dimension of space. The universe may have additional spatial dimensions–a total of 10, 11, or 26 are especially favored–according to some theories of the subatomic world (see **string theory** and **Kaluza-Klein theory**), though the additional ones are "curled up" incredibly small and only become important at scales far smaller than those that can be experimentally probed today.

In mathematics, the term *dimension* is used in many different ways. Some of these correspond to the everyday idea of an extension in physical space or to some of the more esoteric meanings in physics. Others are purely abstract and exist only in certain types of theoretical, mathematical space. There are, for example, *Hamel dimensions, Lebesgue covering dimensions,* and **Hilbert space**s. So-called **Hausdorff dimension**s are used to characterize **fractal**s–mathematical objects that have fractional dimensions–by giving a precise meaning to the idea of how well something, such as an extremely "wriggly" curve or surface, fills up the space in which it is embedded.

dinner party problem
See **Ramsey theory**.

Diocles (c. 240–c. 180 B.C.)
A Greek mathematician and contemporary of **Apollonius** who studied the **cissoid** as part of an attempt to duplicate the cube and also was the first to prove the focal property of a parabolic mirror.

Diophantine approximation
The approximation of a **real number** by a **rational number**.

Diophantine equation
An equation that has integer **coefficient**s and for which integer solutions are required. Such equations are named after **Diophantus**. The best known examples are those from **Pythagoras's theorem**, $a^2 = b^2 + c^2$, when a, b, and c are all required to be whole numbers–a **Pythagorean triplet**. Despite their simple appearance Diophantine

equations can be fantastically difficult to solve. A notorious example comes from **Fermat's last theorem** (recently solved), $a^n = b^n + c^n$ for $n > 2$. To give a specific example, suppose we want to find integer values for x and y such that

$$x^2 = 1620y^2 + 1.$$

A trial-and-error approach using a computer would quickly find the solution: $y = 4$, $x = 161$. However, just a slight change to the equation to make it

$$x^2 = 1621y^2 + 1$$

would leave the trial-and-error method floundering, even with the resources of the most powerful computers on Earth. The smallest integer solution to this innocent looking formula involves a y-value that is on the order of a thousand trillion trillion trillion trillion trillion trillion! One of the challenges (the tenth one) that David **Hilbert** threw down to twentieth-century mathematicians in his famous list was to find a general method for solving equations of this type. In 1970, however, the Russian mathematician Yu Matijasevic showed that there is no general algorithm for determining whether a particular Diophantine equation is soluble: the problem is undecidable.[217, 218]

Diophantus of Alexandria (A.D. c. 200–c. 284)

A Greek mathematician who developed his own algebraic notation and is sometimes called "the father of algebra." His works were preserved by the Arabs and translated into Latin in the sixteenth century, when they served to inspire momentous new advances. **Diophantine equation**s are named in his honor. It was in the margin of a French translation of Diophantus's work *Aritmetike* from c. 250 that Pierre de **Fermat** scribbled his famous comment that became known as **Fermat's last theorem**.

Diophantus's riddle

One of the oldest known age problems (see **age puzzles and tricks**). It comes from the *Greek Anthology,* a collection of puzzles compiled by Metrodorus in about A.D. 500, and purports to tell how long **Diophantus** lived in the form of a riddle engraved on his tombstone:

> God vouchsafed that he should be a boy for the sixth part of his life; when a twelfth was added, his cheeks acquired a beard; He kindled for him the light of marriage after a seventh, and in the fifth year after his marriage He granted him a son. Alas! late-begotten and miserable child, when he had reached the measure of half his father's life, the chill grave took him. After consoling his grief by this science of numbers for four years, he reached the end of his life.

If d and s are the ages of Diophantus and his son when they died, then the epitaph boils down to these two equations,

$$d = (\tfrac{1}{6} + \tfrac{1}{12} + \tfrac{1}{7})d + 5 + s + 4$$
$$s = \tfrac{1}{2}\, d,$$

which can be solved simultaneously to give $s = 42$ years and $d = 84$ years.

Dirac, Paul Adrien Maurice (1902–1984)

A British theoretical physicist who played a major role in the development of **quantum mechanics** and predicted the existence of antiparticles. He made his first great breakthrough at Cambridge University in 1928, when he found a wave equation for the electron. This explained aspects of the electron that had previously been observed but not understood, and, incidentally, is the only equation to appear in Westminster Abbey, where it is engraved on Dirac's commemorative plaque. Dirac's electron equation also made the remarkable prediction that there exists a previously unseen type of matter–a particle like the electron, but with the opposite charge. This was startling at the time because only two subatomic particles, the electron and the proton, were known, and there was no suspicion that others might be waiting in the wings. The prediction was fulfilled four years later when the *positron,* as it is now called, was first seen. A central theme of Dirac's work was his belief that **beauty and mathematics** go hand in hand. When a journalist once asked him to explain the concept of mathematical beauty, Dirac asked the journalist "Do you know mathematics?" and when the journalist replied "No," Dirac said, "Then you can't understand the concept of mathematical beauty." A shy, retiring person, Dirac is not as famous as his achievements warrant.

Dirac string trick

Take a cardboard square and tie the four corners to another larger square by loose string. Rotate the small square by 360° about a vertical axis, that is, in a horizontal plane. The strings will become somewhat tangled, and it is not possible to untangle them without rotating the square. Turn the square through another 360°, for a total of 720°. Contrary to all expectations, it is now possible to untangle the string, without further rotation of the square, simply by allowing enough space for the strings to be looped over the top of the square!

Another version of the Dirac string trick has been called the Philippine wineglass trick. A glass of water held in the hand can be rotated continuously through 720° without spilling any water. Surprisingly, these geometrical demonstrations are related to the physical fact that an

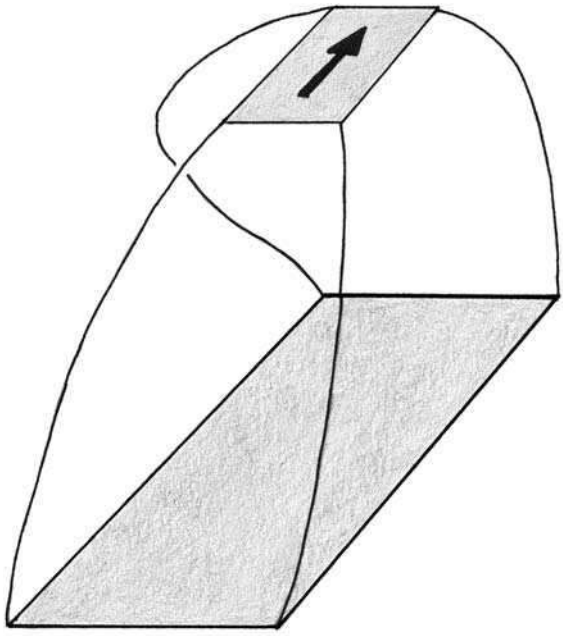

Dirac string trick The equipment needed to simulate an electron's spin property.

electron has spin ½. A particle with spin ½ is something like a ball attached to its surroundings with string. Its amplitude changes under a 360° (2π) rotation and is restored on rotation to 720° (4π).

direct proportion
The relationship two quantities have if the graph of one against the other is a straight line through the origin; so if one doubles then the other doubles, and so forth.

directed graph
Also known as a *digraph*, a **graph** in which each edge is replaced by a directed edge, indicated by an arrow. A directed graph having no multiple edges or loops is called a *simple directed graph*. A **complete graph** in which each edge is bidirected is called a complete directed graph. A directed graph having no symmetric pair of directed edges (i.e., no bidirected edges) is known as an *oriented graph*. A complete oriented graph (i.e., a directed graph in which each pair of vertices is joined by a single edge having a unique direction) is called a *tournament*.

directrix
The line that, together with a point called the **focus**, serves to define a **conic section** as the **locus** of points whose distance from the focus is proportional to the horizontal distance from the directrix. If the ratio $r = 1$, the conic is a **parabola**, if $r < 1$, it is an **ellipse**, and if $r > 1$, it is a **hyperbola**.

Dirichlet, Peter Gustav Lejeune (1805–1859)
A German mathematician who made significant contributions to **number theory**, **analysis**, and mechanics, and who is credited with the modern formal definition of a **function**. He taught at the universities of Breslau (1827) and Berlin (1828–1855) and in 1855 succeeded Carl **Gauss** at the University of Göttingen but died of a heart attack only three years later. Dirichlet continued Gauss's great work on number theory, publishing on **Diophantine equation**s of the form $x^5 + y^5 = kz^5$. His book *Lectures on Number Theory* (published posthumously in 1863) is similar in stature to Gauss's earlier *Disquisitiones* and founded modern **algebraic number theory**. In 1829 he gave the conditions sufficient for a **Fourier series** to converge (though the conditions *necessary* for it to converge are still undiscovered).

Dirichlet's theorem
For any two positive **coprime** integers, a and b, there are infinitely many **prime number**s of the form $an + b$, where $n > 0$. This theorem was first conjectured by Karl **Gauss** and proved by Peter **Dirichlet** in 1835.

discontinuity
Also called a *jump*, a point at which a **function** is not **continuous**.

discrete
Taking only non**continuous** values, for example, **Boolean** or **natural number**s.

discriminant
A quantity that gives valuable information about the solutions of an equation. In the case of the **quadratic** equation $ax^2 + bx + c = 0$, the discriminant is given by $d = b^2 - 4ac$. If $d > 0$, the roots of the equation are two different **real number**s; if $d = 0$, the roots are real and equal; if $d < 0$, the roots are **complex number**s. The concept of discriminant can also be applied in the case of **polynomial**s, **elliptic curve**s, and **metric**s.

disk
Roughly speaking, the "filling" of a **circle**. A flat (two-dimensional) disk of radius r consists of all the points that are at a distance $\leq r$ (*closed disk*) or $< r$ (*open disk*) from a fixed point in the plane. More generally, an n dimensional disk of radius r is the set of all points at a distance $\leq r$ (*closed*) or $< r$ (*open*) from a fixed point in

Euclidean *n*-space. A disk is the two-dimensional analog of a **ball**.

disme
An old word for "tenth." A notation for **decimal** fractions was introduced for the first time in 1585 in a pamphlet called *La Disme* by Simon Stevin of Holland.

dissection
Cutting apart one or more figures and rearranging the pieces to make another figure. Dissection puzzles have been around for thousands of years. The problem of dissecting two equal squares to form one larger square using four pieces dates back to at least the time of Plato (427–347 B.C.). In the tenth century, Arabian mathematicians described several dissections in their commentaries on Euclid's *Elements*. The eighteenth-century Chinese scholar Tai Chen presented an elegant dissection for approximating the value of **pi**. Others worked out dissection proofs of the **Pythagoras's theorem**. In the nineteenth century, dissection puzzles by Sam **Loyd**, Henry **Dudeney**, and others became tremendously popular in magazine and newspaper columns. A classic example is the **Haberdasher's puzzle**. Dissections can get quite elaborate: an eight-piece octahedron becomes a hexagon, a nine-piece five-pointed star becomes a pentagon, and so on. See also **tangrams** and **Loculus of Archimedes**.[201, 202]

dissipative system
A **dynamical system** that contains internal friction that deforms the structure of its **attractor**. Dissipative systems often have internal structure despite being far from **equilibrium**, like a whirlpool that preserves its basic form despite being in the midst of constant change.

distortion illusion
An illusion that distorts an image's shape and/or size. Famous examples include **Poggendorff illusion**, **Zöllner illusion**, **Titchener illusion**, **irradiation illusion**, **Fraser spiral**, **Müller-Lyer illusion**, **Orbison's illusion**, **vertical-horizontal illusion**, and **Ames room**.

distributive
Three numbers *x, y,* and *z* are said to be distributive over the operation + if they obey the identity

$$x(y+z) = xy + xz.$$

Compare with **associative** and **commutative**.

diverge
If a **sequence** doesn't converge it is said to diverge (see **convergence**). This can be if it goes to infinity, or if it simply cycles between two or more values without ever staying on one of them. For example, the sequences: 1, 2, 4, 8, 16, 32, . . . and 1, 0, 1, 0, 1, 0, . . . are both divergent.

division
A counterpart to **multiplication** defined so that if

$$a \times b = c$$

where b is nonzero, then

$$a = c/b.$$

In this equation, *a* is the *quotient, b* is the *divisor,* and *c* is the *dividend.* A **skeletal division** is a long division in which most or all of the digits are replaced by a symbol (usually asterisks) to form a **cryptarithm**.

dodecagon
A **polygon** with 12 sides.

dodecahedron
A **polyhedron** with 12 faces. A *regular dodecahedron* is made from faces that are identical regular **pentagon**s and is one of the **Platonic solid**s.

dodecahedron A mechanical puzzle in the form of a dodecahedron. *Mr. Puzzle Australia, www.mrpuzzle.com.au*

Dodgson, Charles Lutwidge
See **Carroll, Lewis**.

dollar
The elaborate designs on the various denominations of American dollar bills can be used for some amusing games of the "Can you find . . . ?" variety. On a $1 bill, there is an owl in the upper left-hand corner of the "1" encased in the shield, and a spider hidden in the front upper right-hand corner. There are also at least nine occurrences of **thirteen** things: 13 steps on the pyramid, 13 letters in the Latin above the pyramid, 13 letters in "E Pluribus Unum," 13 stars above the eagle, 13 plumes of feathers on each span of the eagle's wing, 13 bars on the shield, 13 leaves on the olive branch, 13 fruits, and 13 arrows. On the back of a $5 bill the number 172 can be found in the bushes at the base of the Lincoln Memorial, while on the back of the old $10 bill are four cars and eleven light posts. On the new $100 dollar bill the time on the clock tower of Independence Hall reads 4:10.

domain
The set of numbers x for which the **function** $f(x)$ is defined. See also **codomain** and **range**.

domino
A small rectangular tile, marked with spots, that is used to play games. There are many varieties of dominoes and games based on them. Most domino tiles, however, have roughly 2-to-1 proportions and each half of each domino has spots arranged as on a six-sided die; the set generally contains tiles with all possible combinations of two numbers. A tile is identified by the number of spots on each half: for example, "1-6" or "3-3." English/American dominoes include blank sides; Chinese dominoes don't but do duplicate some whole tiles. English/American dominoes can also be bought in larger sets with numbers of spots up to nine or twelve per side. Other than games of strategy, there are many mathematical puzzles that involve dominoes. Some of these puzzles involve tiling variations on the standard 8×8 chessboard.

PUZZLE

A standard chessboard can easily be tiled by using four dominos in each row. But what if two squares are removed, one each from diagonally opposite corners of the chessboard? Can this reduced board be completely tiled by nonoverlapping dominoes?

Solutions begin on page 369.

Another common pastime using domino tiles is to stand them on edge in long lines, then topple the first tile, which falls on and topples the second, and so forth, resulting in all of the tiles falling. Arrangements of thousands of tiles have been made that take several minutes to fall. By analogy, phenomena of chains of small events each causing similar events leading to eventual catastrophe are called *domino effects*. The word *domino* was first used to refer to the hooded black cape worn by priests, and later to black masks (of the Lone Ranger type) worn at masquerade balls. The domino is the simplest form of **polyomino**.

domino problem
Is there an algorithm (a set of instructions) that, when given a particular shape as an input, decides if the shape can be used to tile the entire plane? The solution to this unresolved problem is tied up with **Heesch number**s. The domino problem in turn has a deep connection with the **Einstein problem**.

dozen
See **twelve**.

dragon curve
A classic example of a recursively generated **fractal** shape. Benoit **Mandelbrot** called it the "Harter-Heighway" dragon curve and it formed the subject of one of Martin

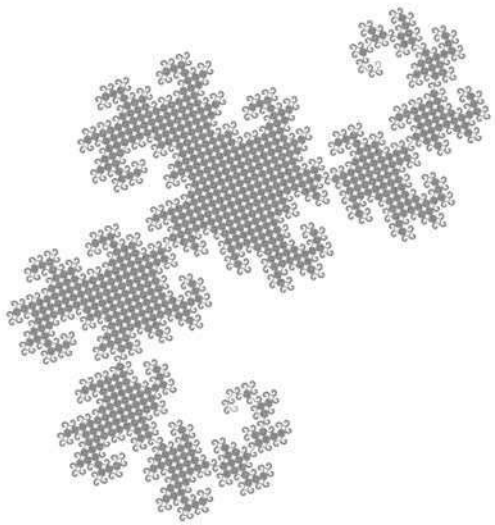

dragon curve *Jos Leys, www.josleys.com*

Gardner's *Mathematical Games* columns in *Scientific American* in 1967.[116] The dragon curve fills out an "island" of positive area with a fractal boundary.

dual

(1) The *dual of a solid* is formed by joining the centers of adjacent faces with straight lines. In the resulting dual solid, each **vertex** of the dual corresponds to a face on the original, each face on the dual to an original vertex, while the edges match, one for one. (2) The *dual of a* ***tessellation*** is obtained by replacing each tile with a point at its center, and each edge between tiles with an edge joining vertices. The dual of a regular tessellation is a regular tessellation; the dual of a semi-regular tessellation is not semi-regular.

Dudeney, Henry Ernest (1857–1930)

An English writer and puzzle-maker who became one of the greatest exponents of recreational mathematics of his time. **Chess** and chess problems captivated him from an early age and he was only 9 when he started contributing puzzles to a local newspaper. His education was limited and he started work as a clerk in the civil service at the age of 13. However, he kept up his interest in math and chess, wrote articles for magazines under the pseudonym "Sphinx," and joined a literary circle that included Arthur Conan Doyle. In 1893 he struck up a correspondence with the American puzzle-maker Sam **Loyd**, the other leading mathematical recreationist of the day, and the two shared many ideas. However, a rift developed after Dudeney accused Loyd of publishing many of Dudeney's puzzles under his own name. One of Dudeney's daughters "recalled her father raging and seething with anger to such an extent that she was very frightened and, thereafter, equated Sam Loyd with the devil." Dudeney was a columnist for the *Strand Magazine* for over 30 years and wrote six books. The first of these, *The Canterbury Puzzles,*[87] published in 1907, purports to include a collection of problems posed by the characters in Chaucer's *The Canterbury Tales*. The answer to the so-called **Haberdasher's puzzle** is Dudeney's best known geometrical discovery. His other books include *Amusements in Mathematics* (1917)[88] and *The World's Best Word Puzzles* (1929). See also **spider-and-fly problem** and **polyomino**.[233]

Dunsany, Lord Edward Plunkett (1878–1957)

An Irish writer who was one of the founders of the fantasy genre of literature. Edward John Moreton Drax Plunkett was born in London to a family whose roots in Ireland predate the Norman invasion. He inherited his father's title in 1899, fought in the Boer War, and returned to the ancestral home, Dunsany Castle, in 1901. Lord Dunsany was a keen marksman and hunter, a fine player of cricket (Dunsany had its own cricket ground near the village), tennis (there is a court beside the Castle), and **chess** (he was an amateur champion and once drew with Grand Master Capablanca. He also wrote chess puzzles for the *Times* over many years and invented his own variant of the game. His first of many books, *The Gods of Pegana,* was published in 1905. In writings that spanned fantasy, drama, poetry, and science fiction, he was an early explorer of such ideas as chess-playing computers (in "The Three Sailors' Gambit" from *The Last Book of Wonder* and, again, in his 1951 novel *The Last Revolution*) and paradoxes in **time travel** (e.g., in "Lost" from *The Fourth Book of Jorkens* and "The King That Was Not" from *Time and the Gods*).

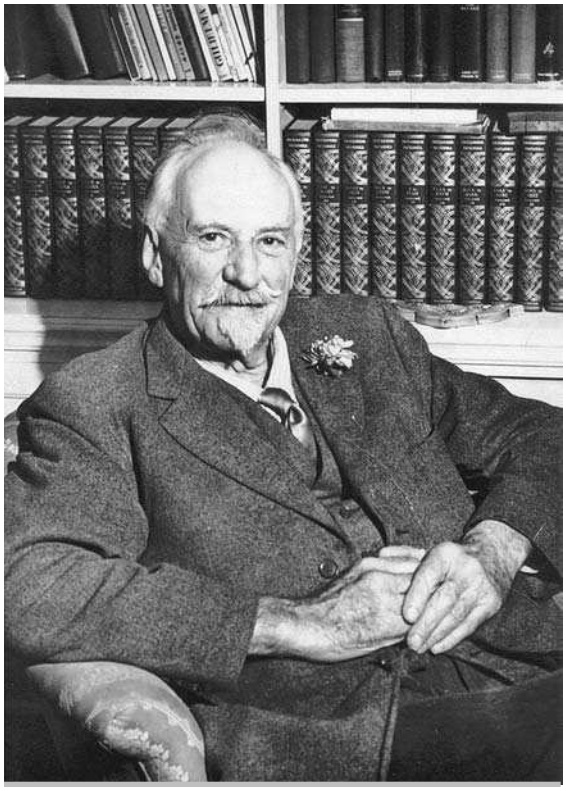

Dunsany, Lord Edward Plunkett *The Dunsany Estate*

Dupin cyclide

The envelope of all **sphere**s touching three given fixed spheres. (Each of the fixed spheres is to be touched in an assigned manner, either externally or internally.) Equivalently, the envelope of all spheres whose centers lie on a

given **conic section** and which touch a given sphere. Also equivalently, the inverse of a **torus**.

duplicating the cube

A classical mathematical challenge of antiquity: using only a straightedge and compass, construct a **cube** whose volume is exactly twice that of a given cube. It is often called the "Delian" problem because of a legend that surrounds its origin. The citizens of Athens were being devastated by a plague so that, in 430 B.C., they sought advice from the oracle at Delos on how to rid their community of this pestilence. The oracle replied that the altar of Apollo, which was in the form of a cube, had to be doubled in size. Thoughtless builders merely doubled the edges of the cube, failing to appreciate that this increased the volume of the altar eightfold. The oracle said the gods had been angered; the plague grew worse. Other delegations consulted Plato. When informed of the oracle's admonition, Plato told the citizens "the god has given this oracle, not because he wanted an altar of double the size, but because he wished in setting this task before them, to reproach the Greeks for their neglect of mathematics and their contempt of geometry." Many Greek mathematicians attacked the problem. All failed, because the so-called *Delian constant,* $\sqrt[3]{2}$ (the required ratio of sides of the original cube and that to be constructed), needed for the duplication can't be constructed as prescribed. Cube duplication is possible, however, using a **Neusis construction**. See also **cissoid** of Diocles.

Dürer, Albrecht (1471–1528)

> *Sane judgment abhors nothing so much as a picture perpetrated with no technical knowledge, although with plenty of care and diligence. Now the sole reason why painters of this sort are not aware of their own error is that they have not learnt Geometry, without which no one can either be or become an absolute artist.*
>
> –from *The Art of Measurement,* 1525

A German printmaker who, through applying mathematics to art, brought important ideas to mathematics itself especially in the area of perspective geometry. Dürer was born in Nüremberg, one of 18 children, and showed an early talent for art. After a four-year apprenticeship in painting and woodcutting, he began traveling Europe, especially Italy, in search of new styles and ideas. Back in Nüremberg, he began a serious study of mathematics, absorbing *Elements* by **Euclid** and *De architectura* by the great Roman architect Vitrivius, and studying the work of Leone Alberti (1404–1472) and Luca **Pacioli** on mathematics and art, in particular their work on proportion. His mastery of perspective is clear in woodcuts *Life of a Virgin* (1502–1505). In about 1508, Dürer began to collect material for a major work on mathematics and its applications to the arts. This work was never finished but Dürer did use parts of the material in later published work. One of his most famous engravings *Melancholia,* produced in 1514, contains the first **magic square** to be seen in Europe, cleverly including the date 1514 as two entries in the middle of the bottom row. Also of mathematical interest in *Melancholia* is the **polyhedron** in the picture, the faces of which appear to consist of two equilateral triangles and six somewhat irregular pentagons. In 1825 Dürer published a four-volume treatise, *Underweysung der Messung* (available in English translation as *Painter's Manual*), which dealt with, among other things, the construction of various curves, polygons, and other solid bodies. One of the first books to teach the methods of perspective, it was highly regarded throughout the sixteenth century and presents the earliest known examples of polyhedral **net**s, that is, polyhedra unfolded to lie flat for printing.

Dürer traveled to Italy to learn about perspective and was keen to publish the methods so they weren't kept secret among a few artists. Who he learned from is not known, but Luca Pacioli is a likely possibility. Some of

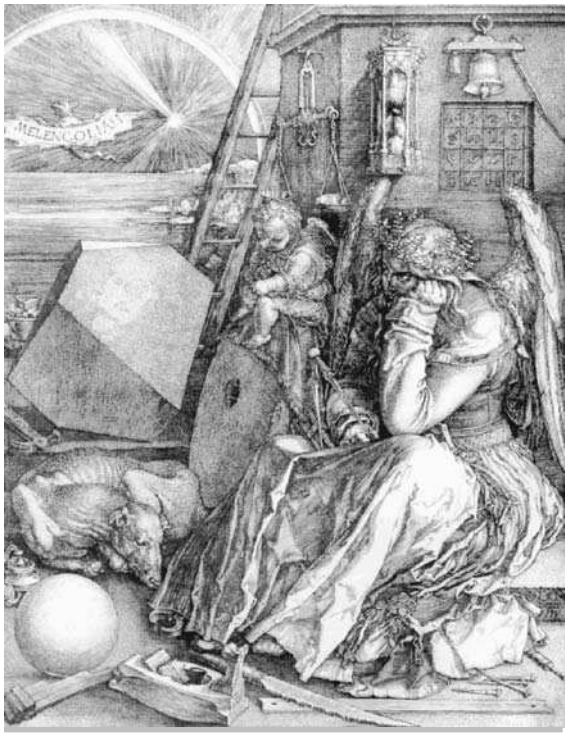

Dürer, Albrecht The famous woodcut *Melancholia,* by Albrecht Dürer, features a magic square and an unusual polyhedron.

the techniques and illustrations also follow closely the work of Piero della Francesca.

Dürer's final work, his *Treatise on Proportion*, was published posthumously and laid the groundwork for descriptive geometry and its rigorous mathematical treatment by Gaspard **Monge**.

Dürer's shell curve

Given a **parabola** and a line that is **tangent** to the parabola, the **glissette** of a point on a line sliding between the parabola and the tangent. It has the equation $(x^2 + xy + ax - b^2) = (b^2 - x^2)(x - y + a)^2$.

dynamical system

A **nonlinear**, interactive system that evolves over time, showing transformations of behavior and an increase in **complexity**. Key to this evolution is the presence and emergence of **attractor**s, most notably **chaotic attractor**s. The changes in the system's organization and behavior are known as **bifurcation**s. Dynamical systems are **deterministic system**s, although they can be influenced by random events. Times series data of dynamical systems can be graphed as phase portraits in **phase space** in order to indicate the qualitative or topological properties of the system and its attractors. For example, various physiological systems, such as the heart, can be conceptualized as dynamical systems. Seeing physiological systems as dynamical systems opens up the possibility of studying various attractor regimes. Moreover, certain diseases can be understood now as "dynamical diseases," meaning that their temporal phasing can be a key to understanding pathological conditions.

dynamics

Pertaining to the change in behavior of a system over time.

E

e

Pi goes on and on and on . . .
And e is just as cursed.
I wonder: Which is larger
When their digits are reversed?

–Martin Gardner

Possibly the most important number in mathematics. Although **pi** is more familiar to the layperson, *e* is far more significant and ubiquitous in the higher reaches of the subject. One way to think of *e* is as the number of dollars you would have in the bank at the end of a year if you invested $1 at the start of the year and the bank paid an annual interest rate of 100% compounded *continuously*. Compound interest doesn't behave in quite the way intuition suggests. Because more frequent compounding causes the principal to grow faster, it might seem that continuous compounding would make the investor very rich in short order. But the effect tails off. At the end of one year, the $1 would have grown to a mere $2.72, rounded to the nearest cent. To a better approximation, *e* is 2.718281828459045 . . . , its decimal expansion stretching out forever, never repeating in any permanent pattern, because *e* is a **transcendental number**. It is the base of natural **logarithm**s, which is equivalent to the fact that the area under the curve (the integral of) $y = 1/x$ between $x = 1$ and $x = e$ is exactly equal to one unit. It also features in the **exponential** function $y = e^x$, which is unique in that its value (y) is exactly equal to its growth rate (dy/dx in calculus notation) at every point. As well as showing up in problems involving growth or decay (including compound interest) or in calculus, whenever logarithmic or exponential functions are involved, *e* is at the heart of the statistical **bell curve**; the shape of a hanging cable, known as a **catenary**; the study of the distribution of **prime number**s; and Stirling's formula for approximating **factorial**s.

Like π, *e* pops up as the limit of many **continued fraction**s and **infinite series**. Leonhard **Euler**, who was the first to study and to use the symbol *e* (in 1727), found it could be expressed as the curious fraction:

$$\cfrac{1+1}{0+\cfrac{1+1}{1+\cfrac{1+1}{1+\cfrac{1+1}{2+\cfrac{1+1}{1+\cfrac{1+1}{1+\cfrac{1+1}{4+\cfrac{1+1}{1+\cfrac{1+1}{1+\cfrac{1+1}{6+\ldots}}}}}}}}}}$$

No less remarkable is this infinite series of which *e* is the sum:

$$1 + 1/1! + 1/2! + 1/3! + 1/4! + \ldots$$

But of all the places that *e* appears in mathematics none is more extraordinary than **Euler's formula** from which comes the most profound relationship in mathematics: $e^{i\pi} + 1 = 0$, linking *e* and π with **complex number**s.[215]

Earthshapes

A series of 12 hypothetical Earths as conceived by American airman Joseph Portney in 1968 during a flight to the North Pole onboard a U.S. Air Force KC-135. As the North Pole was reached, Portney looked on the icy terrain below and asked himself, "What if the Earth were . . . ?" The hypothetical Earths, cylindrical, conic, donut-shaped, and so forth, were sketched and captioned by Portney and given to the Litton Guidance & Control Systems graphic arts group to create models. These models were then photographed and became the theme of a Litton publication entitled *Pilots and*

Navigators Calendar for 1969. Each month was introduced with a different one of the 12 hypothetical Earths. The result was an international sensation, attracting awards and heavy fan mail.

eccentricity

See **conic section**.

economical number

A number that has no more digits than there are digits in its prime factorization (including powers). If a number has fewer digits than are in its prime factorization it is known as a *frugal number*. The smallest frugal is 125, which has three digits, but can be written as 5^3, which has only two. The next few frugals are 128 (2^7), 243 (3^5), 256 (2^8), 343 (7^3), 512 (2^9), 625 (5^4), and 729 (3^6). An *equidigital number* is an economical number that has the same number of digits as make up its prime factorization. The smallest equidigitals are 1, 2, 3, 5, 7, and 10 ($= 2 \times 5$). All **prime number**s are equidigital. An *extravagant number* is one that has fewer digits than are in its prime factorization. The smallest extravagant number is 4 ($= 2^2$), followed by 6, 8, and 9. There are infinitely many of each of these kinds of numbers. Are there also arbitrarily long sequences of consecutive ones? Seven-member strings of consecutive economical numbers start at each of 157; 108,749; 109,997; 121,981; and 143,421. On the other hand, the longest string of consecutive frugal numbers up to 1 million is just two (for example, 4374 and 4375). Even so, it has been proved that if a certain conjecture about prime numbers known as *Dickson's conjecture* is true, then there are arbitrarily long strings of frugals.

Eddington number

"I believe there are 15,747,724,136,275,002,577,605,653,961,181,555,468,044,717,914,527,116,709,366,231,425,076,185,631,031,296 protons in the universe and the same number of electrons." So wrote the English astrophysicist Sir Arthur Eddington (1882–1944) in his book *Mathematical Theory of Relativity* (1923). Eddington arrived at this outrageous conclusion after a series of convoluted (and wrong!) calculations in which he first "proved" that the value of the so-called fine-structure constant was exactly $1/136$. This value appears as a factor in his prescription for the number of particles (protons + electrons; neutrons were not discovered until 1930) in the universe: $2 \times 136 \times 2^{256} = 17 \times 2^{260} \cong 3.149544 \ldots \times 10^{79}$ (double the number written out in full in the quote above). This is the Eddington number, notable for being the largest *specific* integer (as opposed to an estimate or approximation) ever thought to have a unique and tangible relationship to the physical world. Unfortunately, experimental data gave a slightly lower value for the fine-structure constant, closer to $1/137$. Unfazed, Eddington simply amended his "proof" to show that the value had to be exactly $1/137$, prompting the satirical magazine *Punch* to dub him "Sir Arthur Adding-One." See also **large number**.

edge

A line segment where two faces meet. A **cube**, for example, has 12 edges.

edge coloring theorem

See **Tait's conjecture**.

edge of chaos

The hypothesis that many natural systems tend toward dynamical behavior that borders static patterns and the chaotic regime. See also **chaos**.

egg

Specifically, a chicken's egg and its mathematical equivalent. Eggs are often described as being **oval** in shape, which is effectively tautological since "oval" comes from the Latin *ovus* for "egg." Strictly speaking, an oval is a flat two-dimensional curve, so it is more accurate to say that an egg is shaped like the **surface of revolution** of an oval. In real life, eggs, like ovals, come in a variety of forms all of which can be loosely described as "like an **ellipsoid** but with one end more pointed than the other." Because eggs vary in shape, so too do their mathematical descriptions. Having said this, there are a variety of ways to approximate the shape of a hen's egg by modifying the equation of an ellipsoid, $x^2/a^2 + y^2/b^2 + z^2/c^2 = 1$, so as to

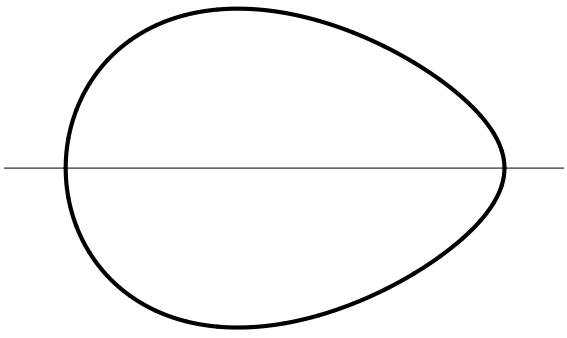

egg A good egg shape is obtained by drawing four circle arcs of different radii. © *Jan Wassenaar, www.2dcurves.com*

introduce an asymmetry about the long (say, *z*-) axis. These involve multiplying z^2/c^2 by a suitable term, so that *y* becomes larger on the right side of the *y*-axis and smaller on the left side. For example, $x^2/a^2 + y^2/b^2 + z^2/c^2 (1 - kx) = 1$ gives a good egg. Other useful egg approximations come from surfaces of revolution of **Cartesian ovals**, **Cassinian ovals**, and sections through cones and cylinders. In France, where tennis first became popular, a zero on the scoreboard looked like an egg and was called *l'oeuf,* which is French for "egg." When tennis was introduced in the United States, Americans pronounced it "love."

Why is a hen's, or other bird's, egg shaped as it is? Because it gives strength even though the eggshell is thin enough to allow the young bird to peck its way out when ready. To demonstrate this strength, try balancing a pile of books on four half egg shells. It is even possible for a person's weight to be supported in this way.

Another trick with eggs is to distinguish between a raw egg and a hardboiled one without cracking them open to see which is which. Lay both eggs on their sides on a table, and spin them as you would a spinning top. With a bit of practice, the cooked egg will be made to rise up for a few seconds, while the raw one will remain on its side. The physics of this odd behavior was finally cracked by two mathematicians, Keith Moffat of Cambridge University and Yutaka Shimomura of Keio University, who reported their findings in 2002. They concluded that friction between the egg and the surface produces a gyroscopic effect, which causes some of the kinetic energy of the object to be translated into potential energy, raising its center of gravity (see also **Tippee Top**). As the hardboiled egg spins, its curved surface causes it to touch the tabletop at only one point. The contact point changes and traces out a little circle. If the texture of the tabletop is just right (neither too slippery nor too sticky) the egg will slide a bit as it spins. This sliding slows the spin a bit and causes a wobble. This in turn tilts the egg, lifting one end off the table more than the other, at which point the gyroscopic effect kicks in and swaps some of the kinetic energy of the spinning egg into potential energy and raises its center of gravity in a seemingly paradoxical way. This effect is heightened by the fact that as the end of the egg rises, the egg draws in closer to the axis of spin, causing it to spin more quickly–just as figure-skaters can make themselves pirouette faster by raising their arms above their heads. Why doesn't the effect occur with a raw egg? Because the inside of the egg is runny and it lags behind the shell. This lag serves as a drag, which reduces the spin rate and dissipates the egg's kinetic energy. This in turn reduces the friction between the egg and tabletop, and means that not enough energy is available to be turned into potential energy to raise the egg's center of gravity. As well as solving the mystery of the balancing egg, Moffat also found time to write a limerick to commemorate the event:

Place a hard-boiled egg on a table,
And spin it as fast as you're able;
It will stand on one end
With vectorial blend
Of precession and spin that's quite stable.

See also **superegg**.

Egyptian fraction

A unit **fraction**; in other words, a fraction in which the numerator (the number on top) is one. This type of fraction was the only kind used by the ancient Egyptians and appears extensively in the **Rhind papyrus**. Other fractions can be obtained by adding Egyptian fractions together; for example, $\frac{5}{7} = \frac{1}{2} + \frac{1}{6} + \frac{1}{21}$. In 1201 **Fibonacci** proved that every **rational number** can be written as a sum of Egyptian fractions.

eigenvalue

A **complex number**, λ, that satisfies the equation $Ax = \lambda x$, where A is an $n \times n$ **matrix** and x is some **vector**. In this case, x is called an *eigenvector.*

eight

The second smallest cube number (after 1^3): $8 = 2^3 = 2 \times 2 \times 2$. A queen or king in **chess** can move in eight different directions, in the same way that a compass has eight principal points: north, northeast, east, southeast, south, southwest, west, and northwest. In three dimensions, there are eight diagonal ways to move, corresponding to the eight *octants* into which three-dimensional space is divided by three mutually perpendicular planes. Add a **fourth dimension** and movement becomes possible back and forth along four directions at right angles to each other: up and down, left and right, forward and back, and to one other! The Spanish dollar was a gold coin with a value of eight reales, and was sometimes actually cut into eight wedge-shaped pieces–"pieces of eight"–to make change.

eight curve

A curve, also known as the *lemniscate of Gerono,* that has the Cartesian equation

$$x^4 = a^2(x^2 - y^2)$$

and the appearance of a figure eight lying on its side.

Einstein problem

(1) Is there a single shape that will tile a plane aperiodically (see **aperiodic tiling**)? An answer of "no" would imply the existence of a decision method for the **domino problem**. This problem, which is named because of the German translation (*ein* = "one," *stein* = "stone") and was not an invention of the famous scientist, remains unsolved. (2) A logic problem, invented by Albert Einstein, who claimed that 98% of the people in the world couldn't solve it.

PUZZLES

1. There are 5 houses (along a street) in 5 different colors: blue, green, red, white, and yellow.
2. In each house lives a person of a different nationality: Briton, Dane, German, Norwegian, and Swede.
3. These 5 owners drink a certain beverage: beer, coffee, milk, tea, or water; smoke a certain brand of cigar: Blue Master, Dunhill, Pall Mall, Prince, or blend; and keep a certain type of pet: cat, bird, dog, fish, or horse.
4. No owners have the same pet, smoke the same brand of cigar, or drink the same beverage.
5. The Briton lives in a red house. The Swede keeps dogs as pets. The Dane drinks tea. The green house is on the left of the white house (next to it). The green house owner drinks coffee. The person who smokes Pall Mall rears birds. The owner of the yellow house smokes Dunhill. The man living in the house right in the center drinks milk. The Norwegian lives in the first house. The man who smokes blend lives next to the one who keeps cats. The man who keeps horses lives next to the man who smokes Dunhill. The owner who smokes Blue Master drinks beer. The German smokes Prince. The Norwegian lives next to the blue house. The man who smokes blend has a neighbor who drinks water.

The question is: Who keeps the fish?

Solutions begin on page 369.

elementary function

Any real-value algebraic function or transcendental function (trigonometric, hyperbolic, exponential, logarithmic).

eleven

A **palindromic number**, the smallest integer that is not a **Harshad number**, a **prime number** that is a member of a **twin prime** (11 and 13), and the largest integer that is not the sum of two or more distinct primes. There are 11 players on a soccer team and on a cricket team. Strange but true: the youngest pope was 11 years old.

ellipse

A shape that looks like a squashed circle. It is one of the **conic section**s and can be defined as the **locus** of all points in a plane that have the same sum of distances from two given fixed points known as *foci*. If the two foci coincide then the ellipse is a **circle**. The line segment connecting the foci is called the *major axis* of the ellipse; half this is the *semimajor axis, a*. The line passing through the center of the ellipse (the midpoint of the foci) at right angles to the major axis is called the *minor axis*, half of which is the *semiminor axis, b*. An ellipse centered at the origin of an *x*-*y* coordinate system with its major axis along the *x*-axis is defined by the equation

$$x^2/a^2 + y^2/b^2 = 1.$$

The shape of an ellipse is expressed by a number called the *eccentricity, e*, which is related to *a* and *b* by the formula $b^2 = a^2(1 - e^2)$. The eccentricity is a positive number less than 1, or 0 in the case of a circle. The greater the eccentricity, the larger the ratio of *a* to *b*, and therefore the more elongated the ellipse. The distance between the foci is $2ae$. The area enclosed by an ellipse is πab. The circumference of an ellipse is $4aE(e)$, where the function E is the complete elliptical integral of the second kind.

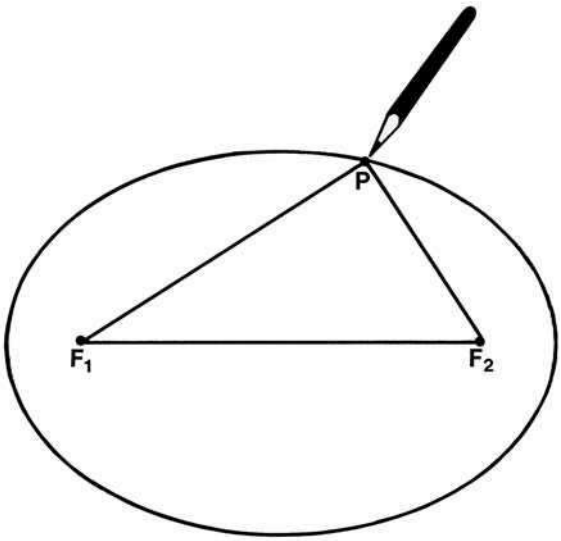

ellipse Nails mark the foci, F_1 and F_2, of an ellipse that is drawn by pencil whose moving tip, *P*, keeps the string threaded around the nails taut.

ellipsoid

A **quadratic** surface that is the three-dimensional analog of an **ellipse**. The general equation of an ellipsoid in Cartesian coordinates is

$$x^2/a^2 + y^2/b^2 + z^2/c^2 = 1,$$

where *a, b,* and *c* are positive real numbers determining the shape. If two of these numbers are equal, the ellipsoid is a **spheroid**; if all three are equal, it is a **sphere**. The intersection of an ellipsoid with a plane is a single point or an ellipse. Ellipsoids can also be defined in higher dimensions.

elliptic curve

The set of solutions to a type of **cubic equation** whose solutions lie on a **torus** (a donut-shaped surface). The particular type of cubic equation whose solutions lead to elliptic curves takes the form

$$y^2 + axy + by = x^3 + cx^2 + dx + e.$$

Elliptic curves, which are said to have a **genus** of 1, have an unusually rich theory and structure, and their study is linked to many other important areas of mathematics and their applications. For example, it was work done on elliptic curves by Andrew **Wiles** that finally led to a proof of **Fermat's last theorem**.

elliptic function

In **complex analysis**, a **function** defined on the complex plane that is **periodic** in two directions. The elliptic functions can be thought of as analogs of the **trigonometric functions** (which have only a single period). Leading eighteenth-century mathematicians, including Leonhard **Euler** and Joseph **Lagrange**, had studied elliptic integrals, such as the integral that gives the arc length of an ellipse; however, these cannot be expressed in terms of the elementary functions (polynomials, exponentials, and trigonometric functions). It was the insight of Karl **Jacobi**, and also of Karl **Gauss** and Niels **Abel**, that the *inverse* functions of elliptic integrals are much easier to study. They turn out to be doubly periodic functions of a complex variable. While a singly periodic function like sine has a number *a* (specifically $a = 2\pi$) so that $\sin(x + a) = \sin(x)$, a doubly periodic function *f* has the property that there are two numbers *a, b,* not rational multiples of each other, so that $f(x + a) = f(x + b) = f(x)$. As Jacobi proved in 1834, the ratio *a/b* is necessarily an imaginary number.

elliptical geometry

One of the two most important types of **non-Euclidean geometry**: the other is **hyperbolic geometry**. In elliptical geometry, Euclid's **parallel postulate** is broken because no line is parallel to any other line. The original form of elliptical geometry, known as *spherical geometry* or *Riemannian geometry,* was pioneered by Bernhard **Riemann** and Ludwig **Schläfli** and treats lines as **great circle**s on the surface of a sphere. The most familiar example of such circles, which are **geodesic**s (shortest routes) on a spherical surface, are the lines of longitude on Earth. In spherical geometry any two great circles always intersect at exactly two points. Two lines of longitude, for example, meet at the North and South Poles. Working in spherical geometry produces some surprising, nonintuitive results. For instance, it turns out that the shortest flying distance from Florida to the Philippine Islands is a path across Alaska–even though the Philippines are at a more southerly latitude than Florida! The reason is that Florida, Alaska, and the Philippines lie on the same great circle and so are collinear in spherical geometry. Another odd property of spherical geometry is that the sum of the angles of a triangle is greater than 180°. This is always the case on a surface that bulges out or, in mathematical parlance, has positive **curvature**. It was Felix **Klein** who first saw clearly how to rid spherical geometry of its one blemish: the fact that two lines have not one but two common points. He redefined the notion of a point as a **set** of antipodal points. With this definition, any two points determine a unique line so that the traditional form of Euclid's first postulate is restored. Thus modified, spherical geometry became what Klein called elliptical geometry.

embedding

Putting one mathematical object inside another, such as a subgroup within a group or one topological space inside another, while preserving all topological properties.

emergence

The arising of new, unexpected structures, patterns, or processes in a self-organizing system (see **self-organization**). These *emergents* have their own rules, laws, and possibilities, and can be understood as existing on a higher level than that of the components from which they came. The term was first used by the nineteenth-century philosopher G. H. Lewes and came into greater currency in the scientific and philosophical movement known as *emergent evolutionism* in the 1920s and 1930s.

emirp

A **prime number** that becomes a different prime number when its digits are reversed ("emirp" is "prime" spelled backward). The first twenty emirps are 13, 17, 31, 37, 71, 73, 79, 97, 107, 113, 149, 157, 167, 179, 199, 311, 337, 347,

359, and 389. Compare with a *palindromic prime* (see **palindromic number**), which gives the same prime when reversed.

empty set

The **set**, denoted by ∅ or {}, that has no members; also known as the *null set*. This is not the same as **zero**, which is the number of members of ∅. Nor is ∅ the same as **nothing** because a set with nothing in it is still a set, and a set is something. The empty set, for example, is the set of all triangles with four sides, the set of all numbers that are bigger than nine but smaller than eight, and the set of all opening moves in chess that involve a king. Applying the concept of the empty set helps distinguish between the different ways that "nothing" is used in everyday language. In his book *What Is the Name of This Book?* (1978), Raymond **Smullyan** wrote:[304] "Which is better, eternal happiness or a ham sandwich? It would appear that eternal happiness is better, but this is really not so! After all, nothing is better than eternal happiness, and a ham sandwich is certainly better than nothing. Therefore a ham sandwich is better than eternal happiness."

What is wrong with this declaration? The first statement is equivalent to "The set of things that are better than eternal happiness is ∅." The second statement is equivalent to "The set {ham sandwich} is better than the set ∅." The confusion arises because the first is comparing individual things, while the second is comparing sets of things, and ∅ plays a different role in each.

enantiomorph

The mirror image of a given **chiral** polyhedron or other figure.

enormous theorem

The largest theorem in mathematics; it concerns the classification of finite **simple group**s and encapsulates the work of hundreds of mathematicians over many years.

entropy

A measure of a system's degree of **random**ness or disorder.

envelope

A curve or a surface that touches every member of a family of lines, curves, planes, or surfaces.

epicycloid

The path traced out by a point on the circumference of a circle of radius b rolling on the outside of a **circle** of radius a. It is described by the parametric equations:

$$x = (a + b)\cos(t) - b\cos((a/b + 1)t)$$
$$y = (a + b)\sin(t) - b\sin((a/b + 1)t).$$

An epicycloid is like a **cycloid** on the circumference of a circle and is closely related to the **epitrochoid**, **hypocycloid**, and **hypotrochoid**. An epicycloid with one cusp is called a **cardioid**, one with two cusps is called a **nephroid**, and one with five cusps is called a **ranunculoid** (after the buttercup genus *Ranunculus*).

Epimenides paradox

See **liar paradox**.

epitrochoid

A curve traced out by a point that is a distance c from the center of a circle of radius b, where $c < b$, that is rolling around the outside of another circle of radius a. It is described by the parametric equations

$$x = (a + b)\cos(t) - c\cos((a/b - 1)t)$$
$$y = (a + b)\sin(t) - c\sin((a/b + 1)t).$$

Closely related to the epitrochoid are the **epicycloid**, **hypocycloid**, and the **hypotrochoid**. An example of an epitrochoid appears in Albrecht **Dürer**'s work *Instruction in Measurement with Compasses and Straightedge* (1525).

EPORN

An equal product of reversible numbers; defined by the Indian recreational mathematician Shyam Sunder Gupta as a number that can be expressed as the product of two reversible numbers (numbers whose digits are reversed) in two different ways. For example: 4,030 = 130 × 031 = 310 × 013 and 144,648 = 861 × 168 = 492 × 294. The smallest EPORN, 2,520 = 120 × 021 = 210 × 012, is also the least common multiple of all single digit natural numbers in decimal system. The **digital root**, i.e. the ultimate sum of digits, of all EPORNs is always 1, 4, 7, or 9. For example, 2,520 = 2 + 5 + 2 + 0 = 9; 4,030 = 4 + 0 + 3 + 0 = 7; 9,949,716 = 9 + 9 + 4 + 9 + 7 + 1 + 6 = 36 and 3 + 6 = 9.

equichordal point

A point inside a closed **convex** curve in the plane, all the **chord**s through which have the same length.

equilateral

Having sides of equal length, as in the case of an equilateral **polygon**. The equilateral **triangle**, with its three equal angles of 60°, is widely found in historic buildings and structures across Europe. See **Triangular Lodge**.

equilibrium

A term indicating a rest state of a system, for example, when a **dynamical system** is under the sway of a **fixed-point attractor** or **periodic attractor**. The concept originated in ancient Greece when **Archimedes** experimented with levers in balance, literally "equilibrium." The idea was elaborated through the Middle Ages, the Renaissance, and the birth of modern mathematics and physics in the seventeenth and eighteenth centuries. "Equilibrium" has come to mean pretty much the same thing as *stability,* that is, a system that is largely unaffected by internal or external changes since it easily returns to its original condition after being perturbed.

equivalent numbers

Numbers such that the sums of their **aliquot part**s (proper divisors) are the same. For example, 159, 559, and 703 are equivalent numbers because their aliquot parts all sum to 57.

Eratosthenes of Cyrene (c. 276–194 B.C.)

A Greek mathematician, astronomer, and geographer who was born in Cyrene, a Greek colony to the west of Egypt. He studied at Plato's school in Athens and eventually became the chief librarian of the great Library at Alexandria. He wrote works on geography, philosophy, history, astronomy, mathematics, and literary criticism. One of Eratosthenes' contributions to mathematics was his measurement of Earth's circumference, which he calculated to be about 252,000 stadii, or 24,700 miles (about one-tenth the actual value, but still a big improvement on earlier estimates). Eratosthenes is also known in number theory for his **sieve of Eratosthenes**, which finds all **prime number**s less than a given integer *n*.

Eratosthenes's sieve

See **sieve of Eratosthenes**.

Erdös, Paul (1913–1996)

A Hungarian mathematician (his name is pronounced "AIR-dosh"), one of the greatest mathematicians of the twentieth century and, in terms of the number of papers published (more than 1,500), the most prolific in history–beating out even Leonhard **Euler** and inspiring the term "Erdös number." A mathematician has an Erdös number of 1 if he or she has published a paper with Erdös, of 2 if he or she has published with someone who published a paper with Erdös, and so on. Erdös worked almost nonstop, 19 hours a day, 7 days a week. "A mathematician," he quipped, "is a machine for turning coffee into theorems." At age 20, Erdös discovered an elegant proof of a famous theorem in number theory, known as *Chebyshev's theorem*, which says that for each number greater than one, there is always at least one **prime number** between it and its double. **Number theory** remained one of his chief interests, though his work spread across many fields, and he became renowned for posing and solving problems that were often simple to state but notoriously difficult to solve. He did groundbreaking work in a branch of mathematics known as **Ramsey theory** long before it became fashionable in the late 1950s. Bent and slight, often wearing sandals, Erdös had no time for the material side of life. "Property is nuisance," he said. Focused totally on mathematics, Erdös traveled from meeting to meeting, carrying a half-empty suitcase and staying with mathematicians wherever he went. His colleagues took care of him, lent him money, fed him, bought him clothes, and even did his taxes. In return, he showered them with ideas and challenges–with problems to be solved and brilliant ways of attacking them. Ernst Straus, who worked with both Albert Einstein and Erdös, wrote a tribute to Erdös shortly before his own death in 1983. He said of Erdös: "In our century, in which mathematics is so strongly dominated by 'theory doctors,' he has remained the prince of problem solvers and the absolute monarch of problem posers."[170]

ergodic

The property of a **dynamical system** such that all regions of a **phase space** are visited with similar frequency and that all regions will be revisited (within a small proximity) if given enough time.

Escher, Maurits Cornelius (1898–1972)

My work is a game, a very serious game.

A Dutch artist whose graphic explorations of **tiling**, figure-ground ambiguities, **impossible figure**s, and regression has attracted the interest of mathematicians and scientists. His experiences of Moorish art (see **Alhambra**) and his contact with mathematicians, most notably Harold **Coxeter**, led him to explore the way repetitive shapes can be used to tile the plane, and from this to ideas about duality and transformation. Escher's preoccupation with dualities is a constant presence in his work in the form of foreground/background, light and dark, flatness and dimensionality, representation and decoration, frame and scene, large and small, viewpoint and vanishing point, form and negative space, positive and negative, observer and observed, as well as the metaphysical aspects of good and evil. Self-referential images (see **self-referential sentence**) resonate throughout Escher's

works–reflections of the artist, hands that draw themselves, the visitor in a picture gallery who looks at a print that contains him. It was for this reason that Douglas **Hofstadter** wove Escher, along with Kurt Gödel and Bach, into the "eternal golden braid" at the heart of his Pulitzer Prize–winning book.[172] Having seen some of Escher's art, Roger **Penrose** was inspired to devise impossible figures, including the **Penrose triangle**, which Escher then incorporated into several of his later works. After the artist's death Penrose regretted that Escher had not lived long enough to take advantage of the discovery of **Penrose tiling**.

escribed circle

A circle that is **tangent** to one side of a triangle and to the extensions of the other sides.

Eternity Puzzle

An enormously difficult jigsaw consisting of 209 pieces, each one different and each made from a unique configuration of equilateral triangles and half-triangles with the same total area as six triangles. The puzzle was to fit them together into an almost-regular 12-sided figure aligned to a triangular grid. The puzzle's inventor, Christopher Monckton, announced a prize of $1 million when the puzzle was released commercially in June 1999, for the first correct solution submitted, assuming there was one, when all the solutions were opened in September 2000. Monckton had run computer searches on much smaller versions of the puzzle, which had convinced him that the sheer size of Eternity would make it intractable. However, the prize was won by two British mathematicians, Alex Selby and Oliver Riordan, with the help of a couple of computers, who sent in a correct tiling on May 15, six weeks ahead of the only other puzzler known to have found a correct solution. Early on, Selby and Riordan made a surprising discovery. As the number of pieces in an Eternity-like puzzle increased, so did the difficulty–but only up to a point. The critical size is about 70 pieces, which would be almost impossible to solve. For larger puzzles, however, the number of possible correct solutions increases. In the case of Eternity itself, with its 209 pieces, there are thought to be at least 10^{95} solutions–far more than the number of subatomic particles in the universe but far, far less than the number of nonsolutions. The puzzle itself is much too large to solve by an exhaustive search but not, as it turns out, by more savvy methods that take into account what shaped regions are easiest to tile and what shaped pieces are easiest to fit. By steadily refining their search algorithm, Selby and Riordan were able to prune out the vast majority of nonsolutions and, with a bit of

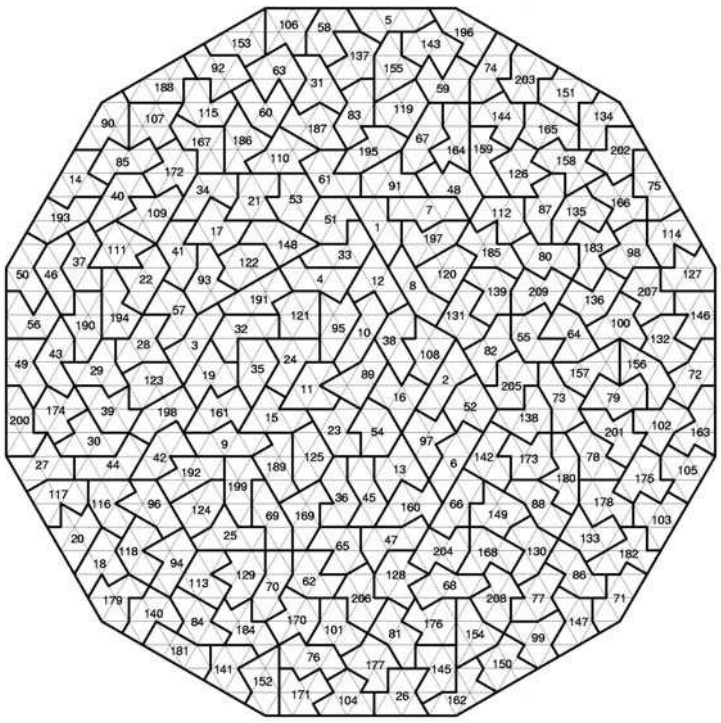

Eternity Puzzle The solution to the Eternity Puzzle that was awarded a $1 million prize. *Eternity pieces are copyright © 1999 by Christopher Monckton*

good fortune, to hit upon a correct solution and claim the prize.

Euclid of Alexandria (c. 330–270 B.C.)

A Greek mathematician who compiled and systematically arranged the geometry and number theory of his day into the famous text *Elements*. This text, used in schools for about 2,000 years, earned him the name "the father of geometry." Even today, the geometries that don't satisfy the fifth of Euclid's "common notions" (now called axioms or postulates) are called non-Euclidean geometries. When, according to the Greek philosopher Proclus, the Egyptian ruler Ptolemy asked if there was a shorter way to the study of geometry than the *Elements*, Euclid told the pharaoh that "there is no royal road to geometry." Little is known of Euclid's life. Proclus wrote (c. A.D. 350) that Euclid lived during the reign of Ptolemy and founded the first school of mathematics in Alexandria–the site of the most impressive library of ancient times with perhaps as many as 700,000 volumes. He wrote books on other subjects such as optics and conic sections, but most of them are now lost. See also **Euclidean geometry**.

Euclidean geometry

Geometry of the type described originally by **Euclid** in his book *Elements* and based on five axioms (see **Euclid's postulates**), one of which is the controversial **parallel postulate**. Various forms of **non-Euclidean geometry** began to emerge in the nineteenth century, with enormous implications for science and philosophy. See also **Euclidean space**.

Euclidean space

Any n-dimensional mathematical space that is a generalization of the familiar two- and three-dimensional spaces described by the axioms of **Euclidean geometry**. The term "n-dimensional Euclidean space" (where n is any positive whole number) is usually abbreviated to "Euclidean n-space", or even just "n-space". Formally, Euclidean n-space is the set $\mathbf{R}^n$ (where **R** is the set of **real numbers**) together with the *distance function*, which is obtained by defining the distance between two points $(x_1, \ldots, x_n)$ and $(y_1, \ldots, y_n)$ to be the square root of $\Sigma(x_i - y_i)^2$, where the sum is over $i = 1, \ldots, n$. This distance function is based on **Pythagoras's theorem** and is called the *Euclidean metric*.

Euclid's postulates

The five postulates, which together with 23 definitions and five "common notions," form the basis of **Euclid**'s great work on geometry, *Elements*. The postulates are:

1. A straight line may be drawn from any one point to any other point.
2. A finite straight line may be produced to any length in a straight line.
3. A circle may be described with any center at any distance from that center.
4. All right angles are equal.
5. If a straight line meets two other lines, so as to make the two interior angles on one side of it together less than two right angles, the other straight lines will meet if produced on that side on which the angles are less than two right angles.

The last postulate is not as obvious as the other four, and Euclid himself was reluctant to use it. Later mathematicians, finding the fifth postulate to be complicated, thought it might be possible to derive it from the other four. However, they only succeeded in replacing it with equivalent statements. The most common of these is the **parallel postulate**.

Eudoxus of Cnidus (c. 408–c. 355 B.C.)

A Greek astronomer, mathematician, and physician whose work on ratios formed the basis for Book V of **Euclid**'s *Elements* and anticipated some aspects of algebra, such as cross multiplying, which is otherwise absent from ancient Greek mathematics. Eudoxus constructed many geometric proofs, found formulas for measuring pyramids, cones, and cylinders, and developed the **method of exhaustion**, a forerunner of integration, later extended by Archimedes. He also studied the kampyle curve, often known as the **kampyle of Eudoxus**, in connection with the classical problem of **duplicating the cube**.

Euler, Leonhard (1707–1783)

A great Swiss mathematician; the second most prolific mathematician in history, after Paul **Erdös**. His greatest contributions were to **number theory**, but Euler also did important work in **calculus**, geometry, algebra, probability, acoustics, optics, mechanics, astronomy, artillery, navigation, and finance. He had a knack for coming up with important results by intuition, he cast calculus and trigonometry in their modern forms, and he showed the importance of the number e. Even the amusing puzzles he invented and, in some cases, solved have opened up new mathematical fields. The **bridges of Königsberg** problem, for example, heralded the beginning of **graph** theory and **topology**, while his **thirty-six officers problem** stimulated important work in **combinatorics**. Euler also worked on **magic squares** and the problem of the **knight's tour**. Having learned some math from his father, a Calvinist preacher, Euler studied at the University of

Basle where he became close friends with members of the **Bernoulli family**. In 1727, he moved to St. Petersburg, to the court of Catherine the Great, becoming professor of physics (1730) and of mathematics (1733). While in Russia, Euler, a devout Christian, met the encyclopedist and philosopher René Diderot, a notorious atheist. When Diderot heard that Euler had a mathematical proof of the existence of **God**, he asked for it and was quoted the equation now often referred to as **Euler's formula**.

Upon losing the use of his right eye, Euler said "Now I will have less distraction." Indeed, the quantity of his output seemed to be inversely proportional to the quality of his sight, because his rate of publication increased after he became almost totally blind in 1766. Euler died moments after calculating the orbit of Uranus on September 18, 1783.

Euler characteristic

An important kind of number, known as a *topological invariant,* that describes a closed surface. In the case of polyhedra, the Euler characteristic is the number of vertices and faces minus the number of edges (see **Euler's formula for polyhedra**).

Euler circuit

A **connected graph** such that starting at a **vertex** *a,* one can traverse every **edge** of the graph once to each of the other vertices and return to vertex *a.* In other words a Euler circuit is a **Euler path** that is a circuit. Thus, using the properties of odd and even degree vertices given in the definition of a Euler path, a Euler circuit exists if and only if every vertex of the graph has an even degree. See also **maze**s.

Euler line

A line that connects the **centroid** and the **circumcenter** of a triangle.

Euler path

A path along a **connected graph** that connects all the vertices (see **vertex**) and that traverses every **edge** of the graph only once. Note that a vertex with an odd degree allows one to travel through it and return by another path at least once, while a vertex with an even degree only allows a number of traversals through, but one cannot end a Euler path at a vertex with even degree. Thus, a connected graph has a Euler path which is a circuit (a **Euler circuit**) if all of its vertices have even degree. A connected graph has a Euler path which is non-circuitous if it has exactly two vertices with odd degree. See also **Hamilton path**.

Euler square

A square array made by combining n objects of two types such that the first and second elements form a **Latin square**. Euler squares are also known as *Graeco-Latin squares, Graeco-Roman squares,* or *Latin-Graeco squares.* For many years, Euler squares were known to exist for n = 3, 4, and for every odd n except $n = 3k$. *Euler's Graeco-Roman squares conjecture* maintained that there are no Euler squares of order $n = 4k + 2$ for $k = 1, 2, \ldots$. However, such squares were found to exist in 1959 by Bose and Shrikande, refuting the conjecture.

Euler-Mascheroni constant (γ)

Also known as *Euler's constant* or *Mascheroni's constant,* the limit (as n goes to infinity) of

$$1 + \tfrac{1}{2} + \tfrac{1}{3} + \tfrac{1}{4} + \tfrac{1}{5} + \ldots + 1/n - \log n$$

It is often denoted by a lowercase gamma, γ, and is approximately 0.5772156649 . . . . Even though over one million digits of this number have been calculated, it isn't yet known if it is a rational number (the ratio of two integers a/b). If it is rational, the denominator (b) must have more than 244,663 digits. The constant γ crops up in many places in **number theory**. For example, in 1898, the French mathematician Charles de la Vallée Poussin (who proved the **prime number** theorem) proved the following: Take any positive integer n and divide it by each positive integer m less than n. Calculate the average (mean) fraction by which the quotient n/m falls short of the next integer. The larger n gets, the closer the average gets to gamma.

Euler's conjecture

It always takes n terms to sum to an nth power: two squares, three cubes, four fourth powers, and so on. This hypothesis is now known to be wrong. In 1966, L. J. Lander and T. R. Parkin found the first counterexample: four fifth powers that sum to a fifth power. They showed that $27^5 + 84^5 + 110^5 + 133^5 = 144^5$. In 1988, Noam Elkies of Harvard University found a counterexample for fourth powers: $2{,}682{,}440^4 + 15{,}365{,}639^4 + 187{,}960^4 = 20{,}615{,}673^4$. Subsequently, Roger Frye of Thinking Machines Corporation did a computer search to find the smallest example: $95{,}800^4 + 217{,}519^4 + 414{,}560^4 = 422{,}481^4$.

Euler's constant

See **Euler-Mascheroni constant**.

Euler's formula

For any **real number** x, Euler's formula is

$$e^{ix} = \cos x + i \sin x$$

where e is a fundamental constant (the base of natural logarithms) and $i = \sqrt{-1}$. If we now put $x = \pi$, we get

$$e^{i\pi} = \cos \pi + i \sin \pi,$$

and since $\cos(\pi) = -1$ and $\sin(\pi) = 0$, this reduces to

$$e^{i\pi} = -1$$

so that

$$e^{i\pi} + 1 = 0.$$

This most extraordinary equation first emerged in Leonhard **Euler**'s *Introductio,* published in 1748. It is remarkable because it links the most important mathematical constants, e and π, the imaginary unit i, and the basic numbers used in counting, 0 and 1. In describing the equation to students, the Harvard mathematician Benjamin Peirce said: "Gentlemen, that is surely true, it is absolutely paradoxical; we cannot understand it, and we don't know what it means, but we have proved it, and therefore, we know it must be the truth."

Euler's formula for polyhedra

The earliest known equation in **topology**. If F is the number of faces of a **polygon**, E the number of edges, and V the number of vertices, Euler's formula can be written as

$$F - E + V = 2$$

where F − E + V is known as the **Euler characteristic**. For example, the surface of a cube has six (square) faces, twelve edges, and eight vertices and, sure enough, 6 − 12 + 8 = 2.

even function

A function $f(x)$ such that $f(x) = f(-x)$ for all x.

evolute

The **locus** of the centers of curvature (the envelope) of a plane curve's normals. The original curve is then said to be the **involute** of its evolute. For example, the evolute of an **ellipse** is a **Lamé curve** and the evolute of a **tractrix** is a **catenary**.

excluded middle law

A law in (two-valued) logic which states that there is no third alternative to truth or falsehood. In other words, for any statement *A,* either *A* or not-*A* must be true and the other must be false. This law no longer holds in three-valued logic, in which "undecided" is a valid state, nor does it hold in **fuzzy logic**.

existence

A term that has several different meanings within **mathematics**. In the broadest sense there is the question of what it means for certain concepts, such as **pi**, to exist. Was π, for example, invented or discovered? In other words, does π exist only as an intellectual construct or was it somehow already "out there" waiting for people to find it. If it does exist independently of the human mind, when did its existence start? Does π predate the physical universe? Such ontological questions become even more difficult when applied to more complex or abstract mathematical concepts such as the **Mandelbrot set**, **surreal number**s, or **infinity**. A narrower and more technical type of "existence" in math is implied by an *existence theorem.* Such a theorem is used to prove that a number or other object with particular properties definitely exists, but does not necessarily give a specific example. Finally, there is existence in the sense of particular solutions to problems. If at least one solution can be determined for a given problem, a solution to that problem is said to exist. Something of the flavor of all three types of mathematical existence mentioned here are captured in the following anecdote:

> An engineer, a chemist, and a mathematician are staying in three adjoining cabins at an old motel. First the engineer's coffee-maker catches fire. He smells the smoke, wakes up, unplugs the coffee maker, throws it out the window, and goes back to sleep. Later that night the chemist smells smoke, too. He wakes up and sees that a cigarette butt has set the trash can on fire. He thinks to himself, "How does one put out a fire? One can reduce the temperature of the fuel below the flash point, isolate the burning material from oxygen, or both. This could be accomplished by applying water." So he picks up the trash can, puts it in the shower stall, turns on the water, and, when the fire is out, goes back to sleep. The mathematician has been watching all this out the window. So later, when he finds that his pipe ashes have set the bed sheet on fire, he's not in the least taken aback. "Aha!" he says, "A solution exists!" and goes back to sleep.

exponent

A number that gives the **power** to which a **base** is raised. For example, in 3^2 the base is 3 and the exponent is 2.

exponential

> *Who has not been amazed to learn that the function* $y = e^x$, *like a phoenix rising again from its own ashes, is its own derivative?*
>
> –Francois le Lionnais

Anything that grows at a rate proportional to its size is said to grow exponentially. The simplest form of the exponential function is just $y = e^x$, where e is about 2.712 . . . The exponential function to **base** a can be written as $f(x) = a^x$.

extrapolate

See **interpolate**.

extravagant number

See **economical number**.

F

face
A **polygon** bounding a **polyhedron**. A **cube**, for example, has six square faces. The plane angle formed by adjacent edges of a polygonal angle in space is called a *face angle.*

factor
Also known as a *divisor,* a number or variable that divides evenly into another number or algebraic expression. For example, the factors of 28 are 1, 2, 4, 7, 14, and 28. Although it is true that 28 is also divisible by the negative of each of these, "factors" is usually taken to mean only the positive divisors. *Factorization,* or *factoring,* is the decomposition of an object into a product of factors. For example, the number 15 factorizes into **prime number**s as 3×5; and the **polynomial** $x^2 - 4$ factorizes as $(x - 2)(x + 2)$. The aim of factoring is usually to reduce something to basic building blocks, such as numbers to prime numbers, or polynomials to linear expressions. Factoring integers is covered by the **fundamental theorem of arithmetic** and factoring polynomials by the **fundamental theorem of algebra**. *Integer factorization* for large integers appears to be a difficult problem; there are no known methods for solving it quickly, and, for this reason, it has formed the basis of some public key cryptography algorithms.

factorial
The function, denoted *n!,* that is the product of the positive integers less than or equal to *n.* For example, $1! = 1$; $5! = 5 \times 4 \times 3 \times 2 \times 1 = 120$; $10! = 10 \times 9 \times 8 \times 7 \times 6 \times 5 \times 4 \times 3 \times 2 \times 1 = 3{,}628{,}800$. 0! is defined to be 1, by working the relationship $n! = n \times (n - 1)!$ backward. An interesting equality is 1! 10! 22! 1! = 11! 0! 2! 21! in which the same digits are broken up two different ways into factorials. This may be the smallest such example. Factorials are important in **combinatorics** because there are $n!$ different ways (permutations) of arranging n distinct objects in a sequence. They also turn up in formulas in calculus, for instance in *Taylor's theorem,* because the nth derivative of the function x^n is $n!$.

factorion
A natural number that equals of the sums of the **factorial**s of its digits in a given **base**. The only known **decimal** factorions are $1 = 1!$, $2 = 2!$, $145 = 1! + 4! + 5!$, and $40{,}585 = 4! + 0! + 5! + 8! + 5!$.

Fadiman, Clifton (1904–1999)
An American essayist, literary critic, and noted intellectual who, among many other works, edited *Fantasia Mathematica*[96] and *The Mathematical Magpie.*[97] He became well known for the encyclopedic knowledge he displayed on the *Information Please* radio programs in the 1930s and '40s.

Fagnano's problem
In a given acute triangle ABC, find the inscribed triangle whose perimeter is as small as possible. The answer is the *orthic triangle* of ABC, that is, the triangle whose vertices are endpoints of the altitudes from each of the vertices of ABC. The problem was proposed and solved using calculus by Giovanni Fagnano (1715–1797) in 1775. Once the answer became known, several purely geometric solutions were also discovered.

fair division
See **cake-cutting**.

Farey sequence
A sequence of numbers named after the English geologist John Farey (1766–1826) who wrote about such sequences in an article called "On a curious property of vulgar fractions" in the *Philosophical Magazine* in 1816. Farey says that he noted the "curious property" while examining the tables of *Complete decimal quotients* produced by Henry Goodwin. To obtain the Farey sequence for a fixed number n, consider all **rational number**s between 0 and 1 which, when expressed in their lowest terms, have a denominator (the number on the bottom of a fraction) not exceeding n. Write the sequence in ascending order of magnitude beginning with the smallest. The "curious property" is that each member of the sequence is equal to the rational number whose numerator (the number on top of a fraction) is the sum of the numerators of the fractions on either side, and whose denominator is the sum of the denominators of the fractions on either side. For example, the Farey sequence for $n = 5$ is ($0/1$, $1/5$, $1/4$, $1/3$, $2/5$, $1/2$, $3/5$, $2/3$, $3/4$, $4/5$, $1/1$), from which it can be seen that $2/5 = (1 + 1)/(3 + 2)$, $1/3 = (1 + 2)/(4 + 5)$, $1/2 = (2 + 3)/(5 + 5)$, $2/3 = (3 + 3)/(5 + 4)$, and so forth. Farey wrote: "I am not acquainted whether this curious property of vulgar fractions has been before pointed out?; or whether it may admit of some easy or general demonstration?; which are

points on which I should be glad to learn the sentiments of some of your mathematical readers."

One "mathematical reader" was Augustin **Cauchy**, who gave the necessary proof in his *Exercises de mathématique,* published in the same year as Farey's article. Farey was not the first to notice the property. C. Haros, in 1802, wrote a paper on the approximation of decimal fractions by common fractions. He explains how to construct what is in fact the Farey sequence for $n = 99$ and Farey's "curious property" is built into his construction.

Fechner, Gustav Theodor (1801–1887)

A German physicist and psychologist who studied aesthetic aspects of the **golden ratio** and published his findings in *Vorschule der Aesthetik* (Introduction to aesthetics) (1876), arguing that this ratio turns up commonly in human-made rectangular objects and is judged by people to be the most pleasing to the eye (though some later researchers have called his results into question).

Federov, E. S. (1853–1919)

A Russian geologist and crystallographer who helped lay the theoretical foundations for modern crystallography. In his famous two-part paper "Symmetry of Regular Systems of Figures" published in 1891, he proved that there are exactly 17 distinct symmetries in the **wallpaper group**.

feedback

The mutually **reciprocal** effect of one system or subsystem on another. *Negative feedback* is when two subsystems act to dampen the output of the other. For example, the relation of predators and prey can be described by a negative feedback loop since more predators lead to a decline in the population of prey, but when prey decrease too much so does the population of predators since they don't have enough food. *Positive feedback* means that two subsystems are amplifying each other's outputs, e.g., the screech heard in a public address system when the mike is too close to the speaker. The microphone amplifies the sound from the speaker which in turn amplifies the signal from the microphone, and so on. Feedback is a way of talking about the nonlinear interaction among the elements or components in a system and can be modeled by nonlinear differential or difference equations as well as by the activity of cells in a **cellular automaton** array.

Feigenbaum's constant

A universal constant, denoted δ, that governs the behavior of systems that are approaching **chaos**; it was discovered by the American mathematical physicist Mitchell Feigenbaum (1944–) in 1975 and has the value $\delta = 4.6692\ldots$. All one-dimensional chaotic systems have a behavior, as they approach instability, known as period doubling. The Feigenbaum constant gives the rate at which the period of the system doubles.

Fermat, Pierre de (1601–1665)

A French lawyer, magistrate, and gentleman scholar, often called the "Prince of Amateurs," who is best known for the **conjecture**, now proved, known as **Fermat's last theorem**. Although employed as a senior government official, Fermat somehow managed to find time to do an astonishing amount of math, for which he sought little acclaim or acknowledgment. In fact, he published only one important manuscript in his entire lifetime and even then used fake initials. When his fellow French mathematician Gilles Roberval offered to edit and publish some of his works, Fermat replied, "Whatever of my works is judged worthy of publication, I do not want my name to appear there." Most of his results are known through letters to friends, notes in book margins, and challenges to other mathematicians to find proofs for theorems he had devised.

Fermat was one of the founders, with René **Decartes**, of **analytical geometry** and, with Blaise **Pascal**, of **probability theory**. His work on the maxima and minima of curves and tangents to them was seen, by Isaac **Newton**, as a starting point for **calculus**. Yet his greatest love was for **number theory**. In 1640, while studying **perfect number**s, Fermat wrote to Mersenne that if p is prime, then $2p$ divides $2^p - 2$. Shortly after he expanded this into what is now called **Fermat's little theorem**. As usual, Fermat stated "I would send you a proof, if I did not fear its being too long." His most famous statement of this form accompanied his hasty notes on the "last theorem." See also **Fermat number**.

Fermat number

A number defined by the formula $F_n = 2^{2^n} + 1$ and named after Pierre **Fermat** who conjectured, wrongly, that all such numbers would be **prime**. The first five Fermat numbers, $F_0 = 3$, $F_1 = 5$, $F_2 = 17$, $F_3 = 257$, and $F_4 = 65{,}537$, are prime. However, in 1732, Leonhard **Euler** discovered that 641 divides F_5. It takes only two trial divisions to find this factor because Euler showed that every factor of a Fermat number F_n with n greater than 2 has the form $k \times 2^{n+2} + 1$. In the case of F_5 this is $128k + 1$, so we would try 257 and 641 (129, 385, and 513 are not prime). It is likely that there are only finitely many Fermat primes. Gauss proved that a **regular polygon** of n sides can be inscribed in a circle with Euclidean methods (e.g., by straightedge and compass) if and only if n is a power of two times a product of distinct Fermat primes.

Fermat, Pierre de

Fermat's last theorem

A challenge for many long ages
Had baffled the savants and sages.
Yet at last came the light:
Seems old Fermat was right–
To the margin add 200 pages.

–Paul Chernoff

A conjecture put forward by Pierre de **Fermat** in 1637 in the form of a note scribbled in the margin of his copy of the ancient Greek text *Arithmetica* by **Diophantus**. The note was found after his death, and the original is now lost. However, a copy was included in the appendix to a book published by Fermat's son. Fermat's note read: "It is impossible to write a cube as a sum of two cubes, a fourth power as a sum of fourth powers, and, in general, any power beyond the second as a sum of two similar powers. For this, I have found a truly wonderful proof, but the margin is too small to contain it."

Fermat claimed that the **Diophantine equation** $x^n + y^n = z^n$ has no integer solutions for $n > 2$. It turns out he was right. But the proof had to wait 350 years and involved such advanced techniques, virtually none of which existed in the seventeenth century, that is seems very unlikely that Fermat really had found an elementary proof. Fermat's last theorem–now truly a theorem–was finally proved correct by Andrew **Wiles** in 1994.[353] In order to reach that dizzy height, however, Wiles had to draw on and extend several ideas at the core of modern mathematics. In particular, he tackled the *Shimura-Taniyama-Weil conjecture,* which provides links between the branches of mathematics known as **algebraic geometry** and **complex analysis**. This conjecture dates back to 1955, when it was published in Japanese as a research problem by the late Yutaka Taniyama. Goro Shimura of Princeton and Andre Weil of the Institute for Advanced Study provided key insights in formulating the conjecture, which proposes a special kind of equivalence between the mathematics of objects called elliptic curves and the mathematics of certain motions in space. Interestingly, the Wiles proof of Fermat's last theorem was a byproduct of his deep inroads into proving the Shimura-Taniyama-Weil conjecture. Now, the Wiles effort could help point the way to a general theory of three variable Diophantine equations. Historically, mathematicians have always had to state and solve such problems on a case-by-case basis. An overarching theory would represent a tremendous advance. See also **ABC conjecture**.

Fermat's little theorem

If P is a **prime number** then for any number a, $(a^P - a)$ must be divisible by P. This theorem is useful for testing if a number is *not* prime, though it can't tell if a number is prime. As usual, Pierre de **Fermat** didn't provide a proof (this time saying "I would send you the demonstration, if I did not fear its being too long"). Leonhard **Euler** first published a proof in 1736, but Gottfried **Leibniz** left virtually the same proof in an unpublished manuscript from sometime before 1683.

Fermat's spiral

A parabolic **spiral**.

Fibonacci (c. 1175–1250)

The pen name of Leonardo of Pisa, one of the greatest mathematicians of the Middle Ages. The son of a Pisan merchant who also served as a customs officer in North Africa, he traveled widely in Barbary (Algeria) and was

later sent on business trips to Egypt, Syria, Greece, Sicily, and Provence. In 1200 he returned to Pisa and used the knowledge gained on his travels to write *Liber Abaci* (The book of the abacus), published in 1202, which introduced to western Europe the Hindu-Arabic numerals and **decimal** number system that remain in use today. The first chapter of Part 1 begins: "These are the nine figures of the Indians: 9 8 7 6 5 4 3 2 1. With these nine figures, and with this sign *0* which in Arabic is called zephirum, any number can be written, as will be demonstrated."

Fibonacci also showed he was capable of some amazing feats of calculation. For example, he found the positive solution of the **cubic** equation $x^3 + 2x^2 + 10x = 20$ using the Babylonian number system with base 60 (a strange choice, in view of his public advocacy of the decimal system!). He gave the result as 1, 22, 7, 42, 33, 4, 40 which is equivalent to

$$1 + \frac{22}{60} + \frac{7}{60^2} + \frac{42}{60^3} + \frac{33}{60^4} + \frac{4}{60^5} + \frac{40}{60^6}.$$

How on Earth he obtained this, nobody knows; it was 300 years before anyone else could obtain such accurate results. As well as serious mathematics, *Liber Abaci* contains many playful passages and it is for one of these, concerning a problem about counting the offspring of a pair of rabbits, that Fibonacci became best known after Edouard **Lucas** called the sequence of numbers discussed by the rabbit problem the **Fibonacci sequence**.

Fibonacci sequence

The sequence that arises in answer to this problem posed in **Fibonacci**'s great work *Liber Abaci:* "A certain man put a pair of rabbits in a place surrounded on all sides by a wall. How many pairs of rabbits can be produced from that pair in a year if it is supposed that every month each pair begins a new pair which from the second month on becomes productive?"

The number of pairs of rabbits in the nth month begins 1, 1, 2, 3, 5, 8, 13, 21, 34, 55, 89, . . . , where each term is the sum of the two terms preceding it. This sequence can be defined recursively as follows: $F(1) = F(2) = 1$, $F(n + 1) = F(n) + F(n - 1)$ for $n > 2$, where $F(n)$ is the nth Fibonacci number. Johannes **Kepler** was the first to point out that the growth rate of the Fibonacci numbers, that is, $F(n + 1) / F(n)$, converges to the **golden ratio**, ϕ (phi).

In the nineteenth century Fibonacci numbers were discovered in many natural forms. For example, many types of flower have a Fibonacci number of petals: certain types of daisies tend to have 34 or 55 petals, while sunflowers have 89 or, in some cases, 144. The seeds of sunflowers spiral outward both to the left and the right in a Fibonacci number of spirals. Similarly, the whorls on a pinecone, the numbers of rings on the trunks of palm trees, the patterns of snail shells, and the genealogy of the male bee all follow a sequence of Fibonacci numbers. The arrangement of plant leaves, or phyllotaxis, unfolds to the same pattern because this results in an optimal solution in terms of the spacing of the leaves or the amount of light that can reach them. A familiar spiral form, known as the **logarithmic spiral**, emerges when seeds on a plant grow and space themselves according the Fibonacci sequence. The logarithmic spiral is approximated by the rule: start at the origin of the Cartesian coordinate system, move $F(1)$ units to the right, move $F(2)$ units up, move $F(3)$ units to the left, move $F(4)$ units down, move $F(5)$ units to the right, and so on. By growing in this way, on structures such as sunflowers, pinecones, and pineapples, seeds are able to pack themselves together most efficiently.

Fibonacci numbers have so many interesting mathematical properties that an entire journal, *The Fibonacci Quarterly,* is devoted to them. The sequence of final digits in Fibonacci numbers repeats in cycles of 60. The last two digits repeat in 300, the last three in 1,500, the last four in 15,000, etc. The product of any four consecutive Fibonacci numbers is the area of a **Pythagorean triangle**. The shallow (least steep) diagonals of **Pascal's triangle** sum to Fibonacci numbers. Let m and n be positive integers, then

$F(n)$ divides $F(mn)$

$\gcd(F(n), F(m)) = F(\gcd(m, n))$, where "gcd" stands for "greatest common divisor."

$(F(n))^2 - F(n + 1)F(n - 1) = (-1)^{n-1}$.

$F(1) + F(3) + F(5) + \ldots + F(2n - 1) = F(2n)$.

For every n, there are n consecutive composite Fibonacci numbers.

An interesting use of the Fibonacci sequence is for converting miles to kilometers. For instance, if you want to know about how many kilometers 5 miles is, take the Fibonacci number (5) and look at the next one (8) (5 miles is about 8 kilometers). This works because it happens that the conversion factor between miles and kilometers is roughly equal to the Golden Ratio.

The first few Fibonacci numbers that are also **prime number**s are 3; 5; 13; 89; 233; 1,597; 28,657; 514,229; . . . . It seems likely that there are infinitely many Fibonacci primes, but this has yet to be proven. However, it is relatively easy to show that for $n \geq 4$, $u_n + 1$ is never prime. The Fibonacci sequence is a special case of the **Lucas sequence**.

The *tribonacci series* is made by adding the last two digits: 1, 1, 2, 4, 7, 13, 24, 44, 81, . . . and from this the quadbonacci series, the pentbonacci series, and the

Fibonacci sequence The number of spirals of seeds on a sunflower is always a Fibonacci number—an arrangement that keeps the seeds uniformly packed no matter how large the seed head. *Thomas Stromberg*

hexbonacci series, all the way up to the *n*-bonacci series. Each ratio of successive terms forms a special constant, analogous to ϕ.

field

A number system in which addition, subtraction, multiplication, and division (except by zero) are always defined, and the **associative** and **distributive** laws are valid. For example, the set of **rational number**s is a field, whereas the set of **integer**s is not a field, because the result of dividing one integer by another is not necessarily an integer. The **real number**s also constitute a field, as do the **complex number**s. Compare with **ring**.

Fields Medal

By convention, the most prestigious award for research in mathematics. It is awarded every four years to between two and four mathematicians under the age of 40.

Fifteen Puzzle

A sliding-tile puzzle invented by Sam **Loyd** in the 1870s that became a worldwide obsession, much as **Rubik's cube** did a century later. Fifteen little tiles, numbered 1 to 15, were placed in a four by four frame in serial order except for tiles 14 and 15, which were swapped around; the lower right-hand square was left empty. The object of the puzzle was to get all the tiles in the correct order; the only allowed moves were sliding counters into the empty square. Everyone it seemed was caught up with the craze–playing the game in horse-drawn trams, during their lunch breaks, or when they were supposed to be working. The game even made its way into the solemn halls of the German parliament. "I can still visualize quite clearly the gray-haired people in the Reichstag intent on a square small box in their hands," recalled the geographer and mathematician Sigmund Gunter who was a deputy during the puzzle epidemic. "In Paris the

Fifteen Puzzle A version of the Fifteen Puzzle produced in England by Fairylite. *Sue & Brian Young/Mr. Puzzle Australia, www.mrpuzzle.com.au*

puzzle flourished in the open air, in the boulevards, and proliferated speedily from the capital all over the provinces," wrote a contemporary French author. "There was hardly one country cottage where this spider hadn't made its nest lying in wait for a victim to flounder in its web." Loyd offered a $1,000 reward for the first correct solution. But, although many claimed it, none were able to reproduce a winning series of moves under close scrutiny. There is a simple reason for this, which is also the reason that Loyd was unable to obtain a U.S. patent for his invention. According to regulations, Loyd had to submit a working model so that a prototype batch could be manufactured from it. Having shown the game to a patent official, he was asked if it were solvable. "No," he replied. "It's mathematically impossible." Upon which the official reasoned there could be no working model and thus no patent!

The puzzle's theory reveals that the more than 20 billion possible starting arrangements of the tiles fall into just two groups: one in which all the tiles can be maneuvered into ascending numerical order (call this group I), and one in which tiles 14 and 15 will be inverted (group II). It's impossible to combine arrangements from these two groups and impossible to turn a group I arrangement into a group II, or vice versa, using the normal rules of the game. Given a random arrangement of tiles, can we know in advance if we have the unsolvable kind? Very easily. Simply count how many instances there are of a tile numbered n appearing after the tile numbered $n + 1$. If there are an even number of such inversions, the puzzle is solvable, otherwise you are wasting your time!

figurate number

A number sequence found by creating consecutive geometrical figures from arrangements of equally spaced points. Here is an example:

```
1   3   5   7
*   *   *   *
    **  *   *
        *** *
            ****
```

The points can be arranged in one, two, three, or more dimensions. There are many different kinds of figurate numbers, such as **polygonal number**s and **tetrahedral number**s.

films and plays involving mathematics

Mathematicians and mathematics rarely make an entrance on the silver screen or the stage, unless as parodies in the form of mad professors and meaningless scrawled equations. A notable exception is *A Beautiful Mind* (2001), directed by Ron Howard and starring Russell Crowe as the brilliant but mentally troubled mathematician John **Nash**. Although a fine love story and a well-crafted film, which won four Oscars, *A Beautiful Mind* is weak on math and inaccurate in many of its details of Nash's life and his battle with schizophrenia. *Rain Man* (1988), also based on a true story, costars Dustin Hoffman as an autistic savant with a photographic memory and a genius for mental arithmetic.

Good Will Hunting (1997), written by and starring Matt Damon and Ben Affleck, and also starring Robin Williams, is about a young man who has led a troubled life but has an amazing talent for mathematics. His abilities are discovered when he comes into conflict with the law, and he soon has to decide if he should pursue his mathematical future and leave his family and friends behind. In Darren Aronofsky's disturbing independent film *Pi* (1998), the main character is a mathematician obsessed with his search for patterns within **pi**'s infinite decimal places. He believes they can be used to predict chaotic behaviors, including that of the stock market. Throughout the film he is pursued by ruthless stock market players and by rabbis trying to find a mathematical way to communicate with God. In the science fiction film *Cube* (1997), six people awake to find themselves trapped in a deadly maze, and one of the characters uses mathematical skills to solve the puzzle and find a way to escape.

Lesser known films with strong mathematical themes include Mario Martone's *Death of a Neapolitan Mathematician;* Peter Greenaway's *Drowning by Numbers;* George Csicsery's *N Is a Number;* and *Moebius,* made by students and faculty at the Universidad del Cine of Buenos Aires. Mathematics has also found its way onto the stage. The musical *Fermat's Last Tango* (2000), a fictionalized account of Andrew **Wiles**'s struggle to prove **Fermat's last theorem**, was performed in New York by the York Theatre company. It followed the Pulitzer prize–winning play *Proof* by David Aubern, about the death of a brilliant mathematician and the repercussions for his daughters and his student.

finite

Limited in extent or scope. In mathematics, a *finite set* is such that the number of elements it contains can be described by a **natural number**. For instance, the set of integers between –18 and 5 is finite, because it has a natural number (17) of elements. The set of all **prime numbers**, on the other hand, is not finite. In physics, "finite" is used to mean both "not infinite" and "nonzero."

finite-state automaton (FSA)

The simplest computing device. Although it is not nearly powerful enough to perform universal computation, it can recognize **regular expression**s. FSAs are defined by a state transition table that specifies how the FSA moves from one state to another when presented with a particular input. FSAs can be drawn as **graph**s.

Fisher, Adrian

A British professional designer and constructor of **maze**s; his company, Adrian Fisher Maze Design, has built a huge variety of mazes in Britain, continental Europe, the United States, and elsewhere. These include the formal hedge maze at Leeds Castle and the largest brick pavement maze in the world at Kentwell Hall in Long Melford. The latter is based on a Tudor rose and has 15 sepals used as locations for a board game in which live players take part in Tudor costume.[101]

Fitchneal

An Irish version of the Viking game **Hnefa-Tafl**; played on a 7×7 board (as was the Scottish equivalent, known as *Ard-Ri,* "High King"), it is mentioned in the *Mabinogion* and *Cormac's Glossary* of the ninth century.

five

The length of the hypotenuse of the smallest **Pythagorean triangle** (a right triangle having integral sides). Five is the only **prime number** that is a member of two pairs of **twin primes.** Every integer is the sum of five positive or negative cubes in an infinite number of ways. Five is the smallest degree of a polynomial equation for which there is no general formula for the solutions (see **quintic**).

fixed-point attractor

An **attractor** that is represented by a particular point in **phase space**, sometimes called an *equilibrium point.* As a point it corresponds to a very limited range of possible behaviors of the system. For example, in the case of a

pendulum, the fixed-point attractor represents the pendulum when the bob is at rest. This state of rest attracts the system because of gravity and friction.

Flatland: A Romance of Many Dimensions

A satirical novel by Edwin A. **Abbott**,[1] first published in 1884, that portrays a **two-dimensional world**, like the surface of a map, over which its inhabitants move. Flatlanders have no concept of up and down, and appear to each other as mere points or lines. From our three-dimensional perspective we can look down on Flatland and see that its people are "really" a variety of shapes, including straight lines (females), narrow isosceles triangles (soldiers and workmen), equilateral triangles (lower middle-class men), squares and pentagons (professional men, including the pseudonymous author of the tale, A. Square), hexagons and other regular polygons with still more sides (the nobility), and circles (priests). Abbott uses these geometrical distinctions, especially the appearance of Flatland females and the working class, as a commentary on the discrimination against women, the rigid class stratification, and the lack of tolerance for "irregularity" that was prevalent in Victorian Britain.

In a dream, A. Square visits the one-dimensional world of Lineland where he tries, unsuccessfully, to persuade the king that there is such a thing as a second dimension. In turn, the narrator is told of three-dimensional space by a sphere who moves slowly through the plane of Flatland, growing and shrinking as his cross-section changes in size. (If a **hypersphere** were to move through our three-dimensional world, we would see a sphere appear, grow to a maximum size, and then shrink again before disappearing.) Abbott is aware that he cheats a little in his description of what the inhabitants of Flatland actually see. In his preface to the second edition, he gives a lengthy but not-too-convincing reply to the objection, raised by some readers, that a Flatlander, "seeing a Line, sees something that must be *thick* to the eye as well as *long* to the eye (otherwise it would not be visible . . .)." The curious and often-neglected fact is that we are just as unable to imagine what it would truly be like to see in two dimensions as we are to conceive of four dimensions! No matter how hard we try we cannot imagine being able to see a line of *zero* thickness.

flexagon

A flat model constructed from a folded strip of paper, which, when flexed, can be made to reveal a number of hidden faces. Flexagons are amusing toys but they have also caught the interest of mathematicians. They are usually square or rectangular (tetraflexagons) or hexagonal (hexaflexagons). A prefix can be added to the name to indicate the number of faces that the model can display, including the two faces (back and front) that are visible before flexing. For example, a hexaflexagon with a total of six faces is called a hexahexaflexagon. The discovery of the first flexagon, a trihexaflexagon, is credited to the British student Arthur H. Stone who was studying at

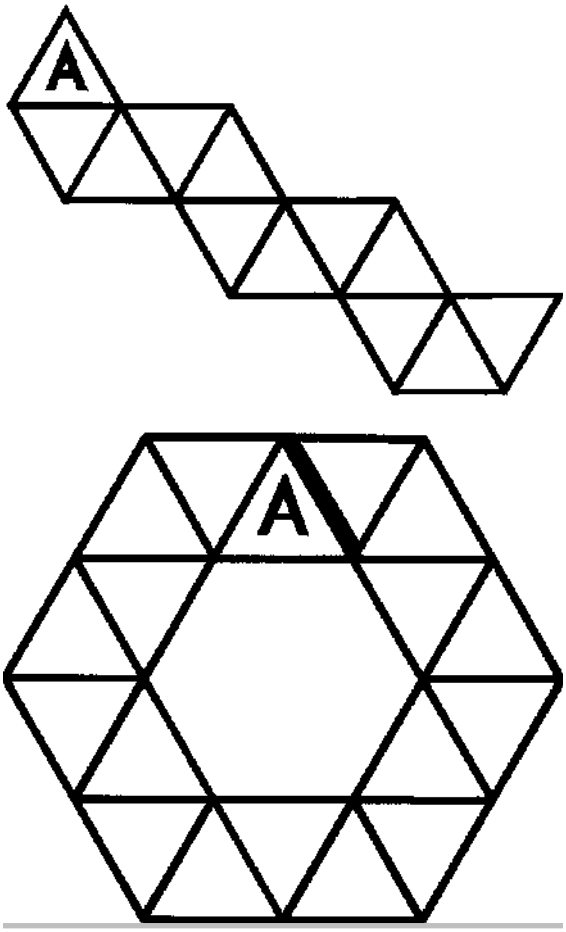

flexagon Two nets for folding into hexaflexagons: the 4-flexagon (top) and the 6-flexagon (bottom). To use the nets, photocopy and enlarge them, and label each side with these numbers:

4-flexagon $\begin{pmatrix} 2231 & 2231 & 2231 \\ 3144 & 3144 & 3144 \end{pmatrix}$,

6-flexagon $\begin{pmatrix} 662554 & 662554 & 662554 \\ 231431 & 231431 & 231431 \end{pmatrix}$.

Start at A using the top row of numbers. Number the other side of the net with the bottom row of numbers so that the top and bottom numbers appear on either side of the first triangle, and so on. *Jill Russell*

Princeton University in 1939. Stone's colleagues Bryant Tuckermann, Richard P. Feynman, and John W. Tukey became interested in the idea. Tuckerman worked out a topological method, called the *Tuckerman traverse,* for revealing all the faces of a flexagon. Tukey and Feynman developed a complete mathematical theory that has not been published. Flexagons were introduced to the general public by Martin **Gardner** writing in *Scientific American.*[110]

floor function
The greatest integer in x, that is, the largest integer less than or equal to x.

Flower of Life
One of the beautiful arrangements of circles found at the Temple of Osiris at Abydos, Egypt. The pattern also appears in Phoenician art from the ninth century B.C. The circles are placed with six-fold symmetry, forming a mesmerizing pattern of circles and lenses. A related design from the same temple, which recurs in Italian art from the thirteen century, is called the *Seed of Life.*

fly between trains problem
Two trains are approaching each another and a fly is buzzing back and forth between the two trains. Given the (constant) speed of the trains and their initial separation distance, and the (constant) speed of the fly, calculate how far the fly will travel before the trains collide. This problem appears to have been first posed by Charles Ange Laisant (1840–1921) in his *Initiation Mathématique.* There is a long-winded method of getting the answer and a much shorter way. Suppose the trains start out 200 miles apart and are each traveling at 50 miles per hour, and the fly–a speedster of its kind–is moving at 75 miles per hour. The long method involves considering the length of the back-and-forth path that the fly takes and evaluating this as the sum of an infinite series. The quick solution is to notice that the trains will collide in 2 hours and that in this time the fly will travel $2 \times 75 = 150$ miles! When this problem was put to John **von Neumann**, he immediately gave the correct answer. The poser, assuming he had spotted the shortcut, said: "It is very strange, but nearly everyone tries to sum the infinite series." Von Neumann replied: "What do you mean, strange? That's how I did it!"

focal chord
A **chord** of a **conic section** that passes through a **focus**.

focal radius
A line segment from the **focus** of an **ellipse** to a point on the **perimeter** of the ellipse.

focus
A defining point in the construction of a **conic section**. The word comes from the Latin for hearth or fireplace and appears to have been first used in mathematics, in describing an **ellipse**, by Johannes **Kepler**.

foliation
A decoration of a **manifold** in which the manifold is partitioned into sheets of some lower dimension, and the sheets are locally parallel. More technically, the foliated manifold is locally **homeomorphic** to a **vector space** decorated by cosets of a subspace.

folium
A curve, first described by Johannes **Kepler** in 1609, that corresponds to the general equation

$$(x^2 + y^2)(y^2 + x(x + b)) = 4axy^2, \text{ in Cartesian form, or}$$
$$r = -b\cos\theta + 4a\cos\theta\sin^2\theta, \text{ in polar coordinates.}$$

The Latin *folium* means "leaf-shaped." Three types, known as the simple folium, the bifolium (or double folium), and the trifolium, correspond to the cases when $b = 4a$, $b = 0$, and $b = a$, respectively. The *folium of Descartes* is given by the Cartesian equation $x^3 + y^3 = 3axy$ and was first discussed by René **Descartes** in 1638. Although he found the correct shape of the curve in the positive quadrant, he wrongly thought that this leaf shape was repeated in each quadrant like the four petals of a flower. The problem to determine the tangent to the curve was proposed to Gilles de Roberval who, having made the same incorrect assumption, called the curve *fleur de jasmin* after the four-petal jasmine bloom, a name that was later dropped. The folium of Descartes has an asymptote $x + y + a = 0$.

formal system
A mathematical formalism in which statements can be constructed and manipulated with logical rules. Some formal systems, such as **Euclidean geometry**, are built around a few basic **axiom**s and can be expanded with theorems that can be deduced through proofs.

formalism
A mathematical school of thought that was headed by the German mathematician David **Hilbert**. Formalists argue that mathematics must be developed through **axiom**atic systems. Formalists agree with Platonism on the principles of mathematical proof, but Hilbert's followers don't recognize an external world of mathematics. Formalists argue that mathematical objects don't exist until we define them. Humans create the **real number** system, for example, by establishing axioms to describe it. All that mathematics needs are inference rules to

progress from one step to the next. Formalists tried to prove that within the framework of established axioms, theorems, and definitions, a mathematical system is consistent and, in the mid-twentieth century, formalism became the predominant philosophical attitude in math textbooks. However, it was undermined by **Gödel's incompleteness theorem** and also the general recognition that results can be usefully applied without having to be proved or derived axiomatically.

Fortune's conjecture

A conjecture about **prime number**s made by the New Zealander social anthropologist Reo Fortune (1903–1979), who had a reputation for unstable behavior bordering on the psychotic. He once attempted to settle an academic dispute with a colleague, Thomas McIlwraith, at the University of Ontario, by challenging him to a duel with any weapon of his choice from the collections of the Royal Ontario Museum. Fortune proposed that if q is the smallest prime greater than $P + 1$, where P is the product of the first n primes, then $q - P$ is prime. For example, if n is 3, then P is $2 \times 3 \times 5 = 30$, $q = 37$, and $q - P$ is the prime 7. These numbers, $q - P$, are now known as *Fortunate numbers.* The conjecture remains unproven but is generally thought to be true. The sequence of Fortunate numbers begins

3, 5, 7, 13, 23, 17, 19, 23, 37, 61, 67, . . .

four

The smallest **composite number**, the second smallest **square number**, the first non-Fibonacci number (see **Fibonacci sequence**), the smallest **Smith number**, and the smallest number that can be written as the sum of two **prime number**s. Four is the number of dimensions that make up **space-time** (three of space and one of time). It is the most number of colors needed to color any map so that no two neighboring areas are the same color (see **four-color map problem**). There are four cardinal points on the compass, four Riders of the Apocalypse, and four Gospels.

four-color map problem

A long-standing problem that dates back to 1852 when Francis Guthrie, while trying to color a map of the counties of England noticed that four colors were enough to ensure that no adjacent counties were colored the same. He asked his brother Frederick if it was true that *any* map could be colored using four colors in such a way that adjacent regions (i.e., those sharing a common boundary segment, not just a point) receive different colors. Frederick Guthrie then passed on the conjecture to Augustus **de Morgan**. The first printed reference is due to Arthur **Cayley** in 1878. A year later the false "proof," by the English barrister Alfred Kempe, appeared; *its* incorrectness was pointed out by Percy Heawood 11 years later. Another failed proof is due to Peter **Tait** in 1880, a gap in *his* argument being pointed out by Julius Petersen in 1891. Both false proofs did have some value, though. Kempe discovered what became known as *Kempe chains,* and Tait found an equivalent formulation of the four-color theorem in terms of three-edge coloring.

The next major contribution came from George Birkhoff whose work allowed Philip Franklin in 1922 to prove that the four-color conjecture is true for maps with at most 25 regions. It was also used by other mathematicians to make various forms of progress on the four-color problem. In the 1970s, the German mathematician Heinrich Heesch developed the two main ingredients needed for the ultimate proof–reducibility and discharging. While the concept of reducibility was studied by other researchers as well, it seems that the idea of discharging, crucial for the unavoidability part of the proof, is due to Heesch, and that it was he who conjectured that a suitable development of this method would solve the four-color problem. This was confirmed by Kenneth Appel and Wolfgang Haken of the University of Illinois in 1977, when they published their proof of the four-color theorem.[12] Their controversial proof challenges the basic assumptions of what mathematical proof is. They used more than 1,200 hours of supercomputer time to analyze 1,478 different configurations that in turn can produce every possible map on a plane. Not everyone was happy with the method of the breakthrough, as Appel himself pointed out:

> For almost a century and a half, a Holy Grail of graph theory has been a simple incisive proof of the Four Color Theorem. It has troubled our profession that a problem that can be understood by a school child has yet to be solved in a way that better illuminates the reason that only four colors are needed for planar maps. The feelings of many mathematicians were summed up for me by Herb Wilf's response to being told that it appeared that one could prove the theorem by a long reducibility argument which used computers to test the reducibility of a large number of configurations. He simply said, "God would not allow such a beautiful theorem to have such an ugly proof."

Martin **Gardner** commented, "Whether a simple, elegant proof not requiring a computer will ever be found, is still an open question." It's interesting that such a simple, intuitive puzzle can be so difficult to settle! The four-color theorem is true for maps on a plane or on a sphere. The answer is different for geographic maps on a **torus**: in this case, seven colors are necessary and sufficient.[277]

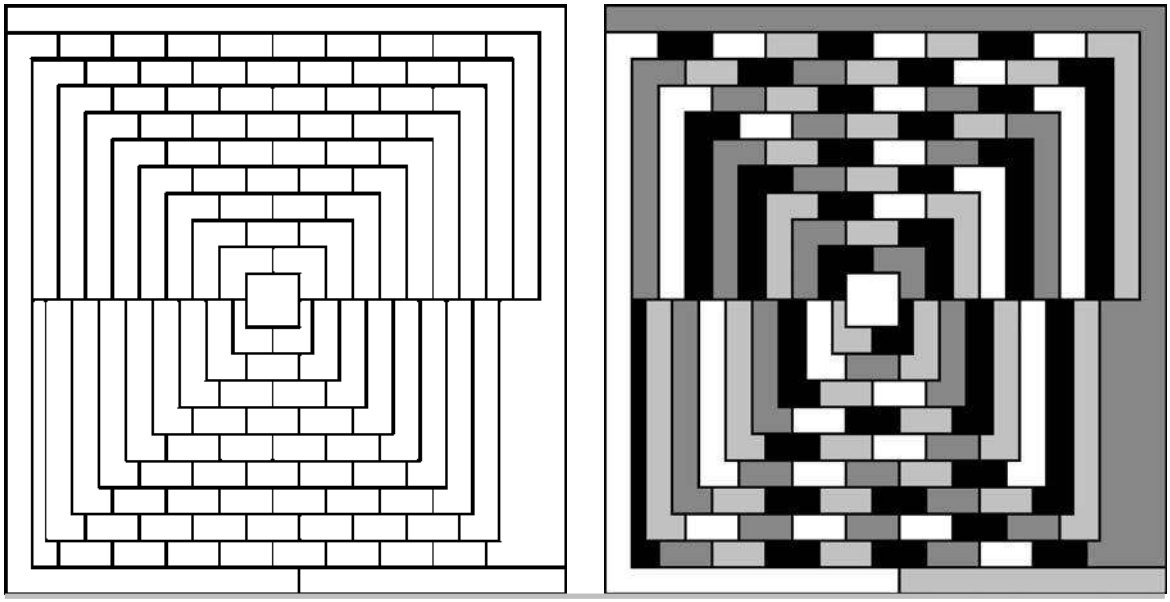

four-color map problem Martin Gardner's spoof counterexample to the four-color theorem (left) and a solution using four colors (right). The different colors are represented here in black, white, and gray.

four coins problem

Given three coins of possibly different sizes, which are arranged so that each is tangent to the other two, find the coin that is tangent to the other three coins. The solution is the inner **Soddy circle**.

four fours problem

Using arithmetic combinations of four 4's, express all the numbers from 1 to 100. For example, 1 = 44/44 and 2 = (4 × 4)/(4 + 4). The problem was first presented in *The Schoolmaster's Assistant: Being a Compendium of Arithmetic Both Practical and Theoretical* (first edition c. 1744), a popular textbook by the English schoolteacher and cleric Thomas Dilworth (d. 1780). Operations and symbols that are allowed include the four arithmetic operations (+, ×, −, /), concatenation (e.g., the use of 44), decimal points (e.g., 4.4), powers (e.g., 4^4), square roots, factorials (e.g., 4!), and overbars for repeating digits (e.g., .4 with an overbar to express $^4/_9$). Ordinary use of parentheses are allowed. One of the trickiest numbers to represent in this way is 73, which calls for something as contorted as

$$\sqrt{(\sqrt{(\sqrt{(4^4)})} + 4 \,/\, .4'}$$

(where .4′ is shorthand for .444 . . .). Of course, the problem can be extended to represent integers greater than 100. The highest value achievable in the four four's puzzle is $10^{8.0723047260281 \times 10153} = 4^{4^4}$.

four knights puzzle

On a 3 × 3 chessboard are two white knights at the top left-hand and top right-hand squares and two black knights at the bottom left-hand and bottom right-hand squares. The problem is to exchange the black knights with the white knights in the minimum possible number of moves. One move is a normal knight's move on any vacant cell of the board, which renders the center square inaccessible.

Fourier, (Jean Baptiste) Joseph, Baron (1768–1830)

A French mathematician known chiefly for his contribution to the mathematical analysis of heat flow. Although he trained for the priesthood, Fourier didn't take his vows but instead turned toward mathematics. He first studied and later taught mathematics at the newly created Ecole Normale. In 1798 he joined Napoleon's army in its invasion of Egypt as scientific advisor, to help establish educational facilities there and to carry out archaeological explorations. After his return to France in 1801 he was appointed prefect of the department of Isere. Fourier became famous for his *Theorie analytique de la Chaleur* (1822), a mathematical treatment of how heat conducts in solid bodies. He established the **partial differential equation** governing heat flow and solved it by using an

infinite series of trigonometric functions, now known as **Fourier series**. Though these series had been used before, Fourier investigated them in much greater detail and prepared the way for later work on trigonometric series and the theory of functions of a real variable. Fourier's belief that his health would be improved by wrapping himself up in blankets proved fatal: thus encumbered he tripped down the stairs of his house and died.

Fourier series

Named after Joseph **Fourier**, the expansion of a **periodic** function as an infinite sum of sines and cosines of various frequencies and amplitudes. This is similar to the approximation of an irrational number by a sum of a series of rational numbers (or a decimal expansion). Human ears effectively produce Fourier series automatically from complex sounds. Tiny hairs, known as *cilia,* vibrate at different specific frequencies. When a wave enters the ear, the cilia vibrate if the wave function contains any component of the corresponding frequency. This enables the hearer to distinguish sounds of various pitches. Fourier series are used a great deal in science and engineering to find solutions to **partial differential equations**, such as those in problems involving heat flow. They can also be used to construct some pathological functions such as ones that are continuous but nowhere differentiable. The study and computation of Fourier series is known as **harmonic analysis**.

fourth dimension

"Do you think that there are things which you cannot understand, and yet which are; that some people see things that others cannot?" said Dr. Van Helsing in Bram Stoker's *Dracula.* Instead of vampires, he may just as easily have been talking about the fourth dimension–an extension at right-angles to the three familiar directions of up-down, forward-backward, and side-to-side. In physics, especially **relativity theory**, **time** is often regarded as the fourth dimension of the **space-time** continuum in which we live. But what meaning can be attached to a fourth *spatial* dimension? The mathematics of the fourth dimension (4-d) can be approached through a simple extension of either the algebra or the geometry of one, two, and three dimensions.

Algebraically, each point in a multidimensional space can be represented by a unique sequence of **real number**s. One-dimensional space is just the **number line** of real numbers. Two-dimensional space, the plane, corresponds to the set of all **ordered pair**s (x, y) of real numbers, and three-dimensional space to the set of all ordered triplets (x, y, z). By extrapolation, four-dimensional space corresponds to the set of all ordered quadruplets (x, y, z, w). Linked to this concept is that of **quaternion**s, which can also be viewed as points in the fourth dimension.

Geometric facts about the fourth dimension are just as easy to state. The fourth dimension can be thought of as a direction perpendicular to every direction in three-dimensional space; in other words, it stretches out along an axis, say the *w*-axis, that is mutually perpendicular to the familiar *x*-, *y*-, and *z*-axes. Analogous to the cube is a hypercube or **tesseract**, and to the sphere is a 4-d **hypersphere**. Just as there are five regular polygons, known as the **Platonic solid**s, so there are six four-dimensional regular **polytope**s. They are: the 4-simplex (constructed from five tetrahedra, with three tetrahedra meeting at an edge); the tesseract (made from eight cubes, meeting three per edge); the 16-cell (made from 16 tetrahedra, meeting four per edge); the 24-cell (made from 24 octahedra, meeting three per edge); the 120-cell (made from 120 dodecahedra, meeting three per edge); and the monstrous 600-cell (made from 600 tetrahedra, meeting five per edge).

Geometers have no difficulty in analyzing, describing, and cataloging the properties of all sorts of 4-d figures. The problem starts when we try to *visualize* the fourth dimension. This is a bit like trying to form a mental picture of a color different from any of those in the known rainbow from red to violet, or a "lost chord," different from any that has ever been played. The best that most of us can hope for is to understand by analogy. For example, just as a sketch of a cube is a 2-d perspective of a real cube, so a real cube can be thought of as a perspective of a tesseract. At a movie, a 2-d picture represents a 3-d world, whereas if you were to watch the action live, in three-dimensions, this would be like a screen projection in four dimensions.

Many books have been written and schemes devised to nudge our imaginations into thinking four-dimensionally. One of the oldest and best is Edwin **Abbott**'s ***Flatland*** [1] written more than a century ago, around the time that mathematical discussion of **higher dimensions** was becoming popular. H. G. Wells also dabbled in the fourth dimension, most notably in *The Time Machine* (1895), but also in *The Invisible Man* (1897), in which the central character drinks a potion "involving four dimensions," and in "The Plattner Story" (1896), in which the hero of the tale, Gottfried Plattner, is hurled into a four-spatial dimension by a school chemistry experiment that goes wrong and comes back with all his internal organs switched around from right to left.[285] The most extraordinary and protracted attack on the problem, however, came from Charles **Hinton**, who believed that, through appropriate mental practice involving a complicated set of colored blocks, a higher reality would reveal itself, "bring[ing] forward a complete

system of four-dimensional thought [in] mechanics, science, and art."

Victorian-age spiritualists and mystics also latched on to the idea of the fourth dimension as a home for the spirits of the departed. This would explain, they argued, how ghosts could pass through walls, disappear and reappear at will, and see what was invisible to mere three-dimensional mortals. Some distinguished scientists lent their weight to these spiritualist claims, often after being duped by clever conjuring tricks. One such unfortunate was the astronomer Karl Friedrich Zöllner who wrote about the four-dimensional spirit world in his *Transcendental Physics* (1881) after attending séances by Henry Slade, the fraudulent American medium.

Art, too, became enraptured with the fourth dimension in the early twentieth century. When the Cubist painter and theorist Albert Gleizes said, "Beyond the three dimensions of Euclid we have added another, the fourth dimension, which is to say, the figuration of space, the measure of the infinite," he united math and art and brought together two major characteristics of the fourth dimension in early Modern Art theory–the geometric orientation as a higher spatial dimension and the metaphorical association with infinity.[159] See also **Klein bottle**.[25, 156, 163, 212, 213, 231, 254, 267, 271, 273, 340]

Fox and Geese

An English board game that dates back to the Middle Ages and is unusual in that the two sides are unequal, thus making this an example of a **Tafl game**. The lone fox attempts to capture 13 (or, in later versions, 17) geese, while the geese try to hem the fox in so that it can't move. The geese start out by filling up all the points on one side of the cross-shaped grid on the board. The fox–the one counter of a different color–begins on any vacant point remaining. The fox moves first. Each side, in its turn, may move one counter. Both fox and geese can move along a line, forwards, backwards, or sideways, to the next contiguous point. The fox may move along a line or jump over a goose to an empty point, capturing the goose and removing it from the board. Two or more geese may be captured by the fox in one turn, provided that he is able to jump to an empty point after each one. The fox wins if he depletes the gaggle of geese to a number that makes it impossible for them to trap him. The geese can't jump over the fox or capture the fox but instead must try to mob him and trap him in a corner. The geese win if they make it impossible for the fox to move. A modification of this game spread with the British to India, where during the Great Mutiny the game became known as "Officers and Sepoys." In this variant, two officers in a fort attempt to hold off 24 sepoys, who must storm the fort.

fractal

A geometric shape that can be subdivided at any scale into parts that are, at least approximately, reduced-size copies of the whole. The name "fractal," from the Latin *fractus* meaning a broken surface, was coined by Benoit **Mandelbrot** in 1975. The key property of fractals is **self-similarity**, which means that zooming in or zooming out of a fractal produces no overall change in appearance.

One of several technical definitions of a fractal is "a set of points whose topological dimension is less than its **Hausdorff dimension**." The topological dimension is an object's ordinary dimensionality–one in the case of a curve, two in the case of a surface, and so forth–and is always a whole number. The Hausdorff dimension, on the other hand, measures how much space an object fills, and can take non-integer values if the object is very complex and twisty.

Some fractals show a strong regularity and rigid self-similarity and are produced by the repeated application of a set of rules that may be quite simple. Among the best known of these "iterated function" systems are the **Koch snowflake**, the **Peano curve**s, the **Sierpinski carpet**, and the **Sierpinski gasket**. Other fractals, defined by a recurrence relation at each point in space, are among the most complex, beautiful, and beguiling mathematical structures known. They include the well-known **Mandelbrot set** and **Lyapunov fractal**s. Finally, there are random fractals generated by stochastic rather than deterministic processes, for example fractal landscapes. Random fractals have the greatest practical use, and can be used to describe many highly irregular real-world objects, including clouds, mountains, coastlines, and trees. See also **fractal dimension**.

fractal dimension

A non-integer measure of the irregularity or **complexity** of a system; it is an extension of the notion of dimension found in **Euclidean geometry**. Knowing the fractal dimension helps one determine the degree of irregularity and pinpoint the number of variables that are key to determining the dynamics of the system.

fraction

A number that represents a part, or several equal parts, of a whole; examples include one-half, two-thirds, and three-fifths. The word comes from the Latin *frangere,* meaning "to break." A *simple, common,* or *vulgar fraction* is of the form a/b, where a may be any integer and b may be any integer greater than 0. If $a < b$, the fraction is said to be *proper* ("bottom heavy"); otherwise it is *improper* ("top heavy"). A **decimal fraction** has a denominator (number on the bottom) of 10, 100, 1000, and so forth. See also **continued fraction**.

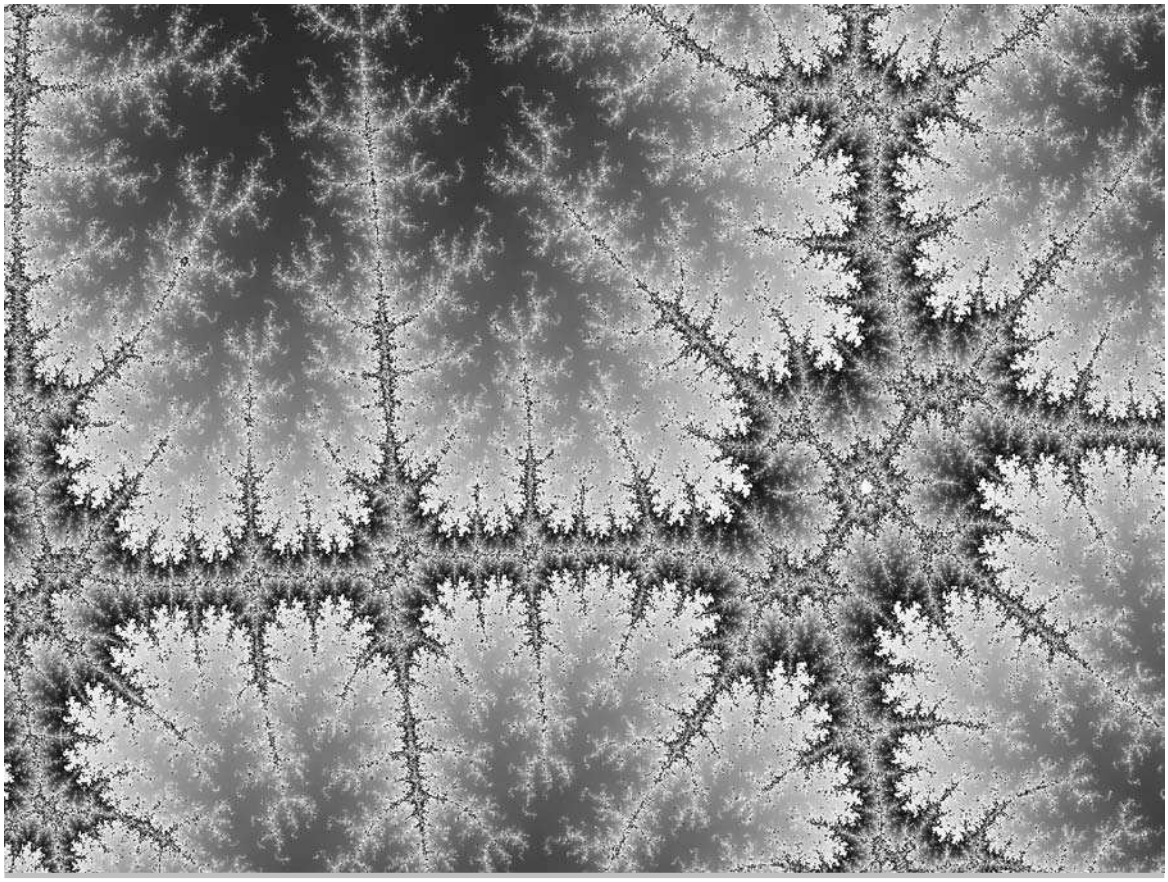

fractal A deep zoom of part of the Mandelbrot set. *Christopher Rowley*

Fraser spiral
A **distortion illusion** in which overlapping black arc segments appear to form a spiral but are in reality a series of overlapping concentric circles. This is easily demonstrated by following one of the curves with your finger. The illusion is named after the British psychologist James Fraser (1863–1936) who first published it in 1908.[104]

Fredholm, Erik Ivar (1866–1927)
A Swedish mathematician who founded the modern theory of **integral equation**s. This became a major research topic in the first quarter of the twentieth century and underpinned important theoretical developments in physics; David **Hilbert**, in particular, extended Fredholm's work to arrive at the concept of **Hilbert space**. Fredholm also devoted time to actuarial science and made a particularly important contribution by proposing an elegant formula to determine the surrender value of a life insurance policy. He earned his Ph.D. from the University of Uppsala but then spent the rest of his academic career at the University of Stockholm.

Freemish crate
See **impossible figure**.

Freeth's nephroid
See **nephroid**.

Frege, Friedrich Ludwig Gottlob (1848–1925)
A German mathematician and philosopher who virtually founded the modern discipline of mathematical logic. In *Die Grundlagen der Arithmetik* (The foundations of arithmetic, 1884), he used **set theory** to define the **cardinal number** of a given class as the class of all classes that are

similar (i.e. can be placed in a **one-to-one** correspondence) to the given class. In *Grundgesetze der Arithmetik* (The basic laws of arithmetic, 2 vols., 1893 and 1903), Frege began attempting to build up mathematics from arithmetic and symbolic logic on a rigorous and contradiction-free basis. When the second volume was in the process of being printed, Bernard **Russell** pointed out a paradox in Frege's work. The paradox, which became known as **Russell's paradox**, stems from the question: "Is the class of all classes that are not members of itself a member of itself or not?" The question leads to a contradiction and cannot be resolved. Frege was thus forced to admit that the foundation of his reasoning was worthless. As he stated at the end of his work, "A scientist can hardly encounter anything more undesirable than to have the foundation collapse just as the work is finished. I was put in this position by a letter from Mr. Bertrand Russell when the work was almost through the press."

Frénicle de Bessy, Bernard (1602–1675)

An eminent French amateur mathematician who extensively researched **magic square**s; his *Des quassez ou tables magiques,* published posthumously in 1693, first identified all 880 magic squares of the fourth order. Frénicle also corresponded with **Descartes**, **Fermat**, **Huygens**, and **Mersenne**, mostly on **number theory**, the work for which he is best known.

frequency

The number of times a value occurs in some time interval.

friendly number

See **amicable numbers**.

Frogs and Toads

A puzzle in which three counters or pegs representing frogs are placed on three successive positions on the left of a string of seven squares, and three different tokens representing toads are placed on the three rightmost squares. Frogs only move to the right, toads only to the left. Every move is either a slide to the adjacent square or a jump over one position, which is allowed only if the latter is occupied by a member of the other species. No two animals are ever allowed on the same square. The goal is to move the toads into the three leftmost positions and the frogs into three rightmost positions in the fewest possible moves. Many different versions of this puzzle have appeared over the centuries and it may be Arabic in origin. The number of pieces on each side may vary, as may the number of empty starting places in the middle; other names for the puzzle have included *Sheep and Goats* and *Sphinxes and Pyramids.*

frugal number

See **economical number**.

frustum

Part of a solid cut off between two parallel planes; in particular, for a **cone** or a **pyramid**, a frustum is determined by the plane of the base and a plane parallel to the base. *Frustum* is Latin for "a piece broken off."

function

> *Old mathematicians never die; they just lose some of their functions.*
>
> –Anonymous

A way of expressing the dependence of one quantity on another quantity or quantities. Traditionally, functions were specified as explicit rules or formulas that converted some input value (or values) into an output value. If f is the name of the function and x is a name for an input value, then $f(x)$ denotes the output value corresponding to x under the rule f. An input value is also called an *argument* of the function, and an output value is called a *value* of the function. The **graph** of the function f is the collection of all pairs $(x, f(x))$, where x is an argument of f. For example, the circumference C of a circle depends on its diameter d according to the formula $C = \pi d$; therefore, one can say that the circumference is a function of the diameter, and the functional relationship is given by $C(d) = \pi d$. Equally well, the diameter can be considered a function of the circumference, with the relationship given by $d(C) = d/\pi$. In modern mathematics, the insistence on specifying an explicit effective rule has been abandoned; all that is required is that a function f associate with every element of some **set** X a unique element of some set Y. This makes it possible to prove the existence of a function without necessarily being able to calculate its values explicitly. Also, it enables general properties of functions to be proved independently of their form. The set X of all admissible arguments is called the *domain* of f; the set Y of all admissible values is called the *codomain* of f. We write $f: X \to Y$.

fundamental group

A group of a **topological space** X that is constructed by looking at how closed paths in X can be combined to get new paths. Under a suitable way of identifying paths (known as **homotopy**) one can get a group structure on the set which gives an algebraic invariant of the space X.

fundamental theorem of algebra

The result that any **polynomial** with real or complex coefficients has a root in the complex plane.

fundamental theorem of arithmetic

Every positive **integer** greater than 1 is a **prime number** or can be expressed as a unique product of primes and powers of primes.

fuzzy logic

A departure from classical two-valued logic in which something is either true or false, to allow a continuous range of truth values. Fuzzy logic was introduced by Lotfi Zadeh of the University of California at Berkeley in the 1960s as a means to model the uncertainty of natural language.

G

Gabriel's horn

The **surface of revolution** of

$$y = 1/x$$

for x greater than 1. Surprisingly this has a finite volume of **pi** cubic units but an *infinitely large* surface area! Gabriel's horn is also known as *Torricelli's trumpet* because it was investigated by the Italian Evangelista Torricelli (1608–1647). As a young man Torricelli studied in Galileo's home at Arcetri, near Florence, and then, upon Galileo's death, succeeded his teacher as mathematician and philosopher for their good friend and patron, the grand duke of Tuscany. Torricelli was amazed by the strange property of his mathematical trumpet and tried various ways to avoid the conclusion that a finite volume could be enclosed by a vessel with an infinite surface area. Unfortunately, he lived before **calculus** came along to explain the apparent paradox in terms of **infinitesimal**s.

Galois, Évariste (1811–1832)

A French mathematician who led a short, dramatic life and is often credited with founding modern **group** theory, though the Italian Paolo Ruffini (1765–1822) came up with many of the ideas first. Galois's work wasn't widely acknowledged by his contemporaries, partly because he didn't present his material very well and partly because he held unpopular political views. In fact, he was a republican revolutionary who was twice imprisoned because of his activities. During his second incarceration he fell in love with the daughter of the prison physician, Stephanie-Felice du Motel, and after being released, was killed in a duel over her with Perscheux d'Herbinville. His death started republican riots and rallies which lasted for several days. See also **Galois theory**.

Galois theory

The study of certain **group**s, known as *Galois groups,* that can be associated with **polynomial** equations. Whether

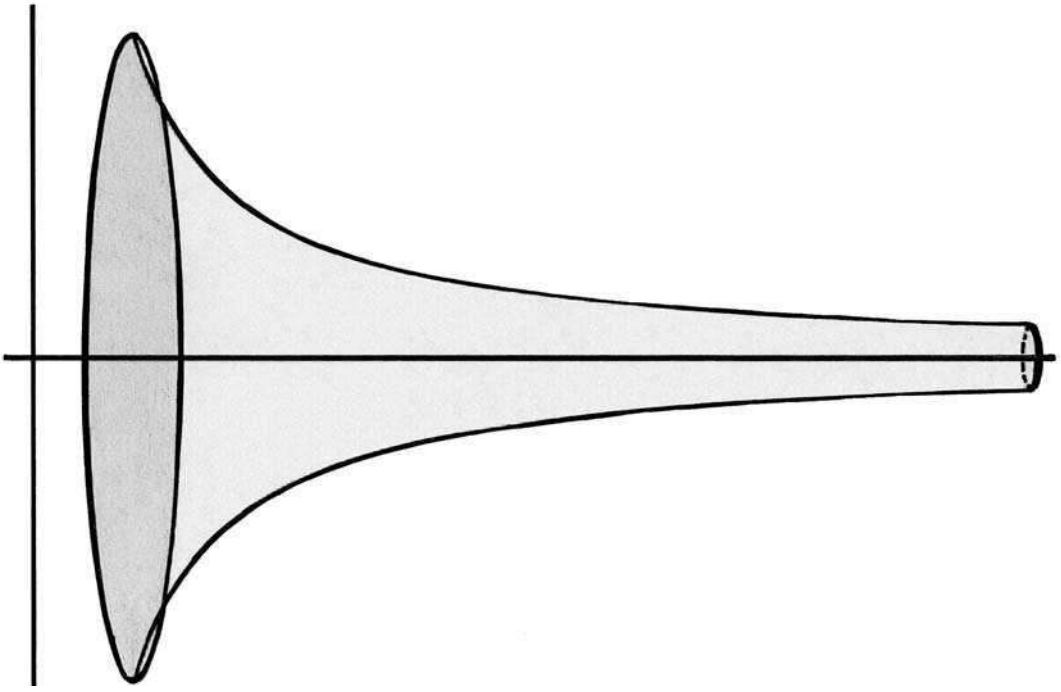

Gabriel's horn The horn for x values between 1 and 10.

or not the solutions to an equation can be written down using rational functions and square roots, cube roots, and so forth depends on certain group-theoretic properties of *Galois groups*.

game

A conflict, with formal rules and a finite number of choices of what to do at each stage, between two or more players. The study of games belongs to a branch of mathematics and logic known as **game theory**. If a game is simple enough, it can be solved for all possible outcomes. This is the case, for example, with **tic-tac-toe** and **Nim**. By harnessing the power of computers to check through vast numbers of moves, even more complicated games are succumbing to a complete analysis. In the 1990s, **nine men's morris** was shown, by searching through billions of possible endgames, to be a certain draw if both players work to an optimal strategy. Checkers may be the next to be fully determined: its roughly 500 million trillion possible positions may soon be within reach of the most powerful supercomputers. See also **blackjack**, **chess**, **Frogs and Toads**, **Ovid's game**, **TacTix**, and **Wythoff's game**.

game theory

A mathematical formalism used to study human **game**s, economics, military conflicts, and biology. The goal of game theory is to find the optimal **strategy** for one player to use when his opponent also plays optimally. A strategy may incorporate randomness, in which case it is referred to as a **mixed strategy**.

Early ideas of game theory can be found in writings throughout history as diverse as the Bible and works by René **Descartes**, Sun Tzu (author of the 2,400-year-old *The Art of War*), and Charles Darwin. The basis of modern game theory is an outgrowth of several books that deal with related subjects such as economics and probability. These include Augustin Cournot's *Researches into the Mathematical Principles of the Theory of Wealth* (1838), which gives an intuitive explanation of what would eventually be formalized by John **Nash** as *Nash equilibrium;* Francis Edgeworth's *Mathematical Psychics,* which explored the notion of competitive equilibria in a two-type (or two-person) economy; and Emile **Borel**'s *Algebre et calcul des probabilites* (1927), which gave the first insight into so-called mixed strategies.[49] Game theory finally came of age through the efforts of two European immigrants to the United States working at the Institute of Advanced Studies in Princeton. Around 1940, the idea of the **utility function** was taken up by John **von Neumann**, who had been forced to flee his native Hungary when the Nazis invaded, and the economist Oskar Morgenstern (1902–1976), who had left Austria because he loathed the National Socialists. In Princeton the two immigrants worked together on what they initially thought would be a short paper on the theory of games, but that kept growing until it finally appeared in 1944 as an opus of 600 pages with the title *Theory of Games and Economic Behavior.*[230]

GLOSSARY OF GAME THEORY

categorical game	A game in which a tie is impossible.
finite game	A game in which each player has a finite number of moves and a finite number of choices at each move.
futile game	A game that allows a tie when played properly by both players.
impartial game	A game in which the possible moves are the same for each player in any position.
mixed strategy	A collection of moves together with a corresponding set of weights which are followed probabilistically in the playing of a game.
partisan game	A game for which each player has a different set of moves in any position.
payoff matrix	An $m \times n$ matrix that gives the possible outcome of a two-person zero-sum game when player *A* has m possible moves and player *B* has n moves.
strategy	A set of moves that a player plans to follow while playing a game.
zero-sum game	A game in which players make payments only to each other. One player's loss is the other player's gain, so the total amount of "money" available is constant.

gamma

See **Euler-Mascheroni constant**.

gamma function

A generalization of the **factorial** function to the real line and to the complex plane. It is defined by:

$$\Gamma(n+1) = \int_0^\infty x^n e^{-x}\, dx$$

If n is an integer, then $\Gamma(n+1) = n!$ See also **beta function**.

Gardner, Martin (1914–)

An American recreational mathematician best known for his "Mathematical Games" column, which ran in *Scien-*

tific American for 25 years. Through this column he introduced many subjects, including **flexagon**s, **polyomino**s, Piet Hein's **Soma Cube**, and John Conway's Game of **Life**, to a wider audience. He is also an accomplished amateur magician and an active member of the skeptical movement associated with James Randi. Gardner is the author of more than 60 books, including various collections of his *Scientific American* columns, *The Ambidextrous Universe,* and *The Annotated Alice*.[108–131]

gauge theory
A force field in nature, or an analogous **vector** field in mathematics with an enormous amount of **symmetry** that expresses the redundancy or ambiguity of many parameters. The simplest example is the *electromagnetic field.*

Gauss, Carl Friedrich (1777–1855)
A German mathematician, often called the "Prince of Mathematics," whose stature and range of interests rivaled those of **Aristotle** and Isaac **Newton**. Some inkling of what was in store came when, as a 3-year-old, he corrected a mistake in one of his father's lengthy payroll calculations. In school, at age 10, when his teacher gave the class the task of adding all the integers from 1 to 100, Gauss immediately wrote down the correct answer, 5050, on his slate. He had spotted that the numbers can be paired off as (100 + 1), (99 + 2), (98 + 3), . . . , (51 + 50) so that the problem reduces to multiplying 101 by 50. At age 19, Gauss found a way to construct a heptadecagon (a **regular polygon** with 17 sides) using only a straightedge and compass–a feat that had eluded the Greeks. Then Gauss entered the mathematical stratosphere of his time by proving what is now called the *fundamental theorem of algebra,* namely, that every **polynomial** has at last one root that is a **complex number**; in fact, he gave four different proofs, the first of which appeared in his dissertation. In 1801, he proved the *fundamental theorem of arithmetic* (that every natural number can be represented as the product of **prime number**s in only one way); published a brilliant tour de force on the properties of integers in his *Disquisitiones Arithmeticae,* which systematized the study of **number theory**; and showed that every number is the sum of at most three **triangular number**s. In the same year, he also developed the method of least squares fitting and, though he didn't publish it, used it to calculate the orbit of the asteroid Ceres, that had recently been discovered by Piazzi, from only three observations. Gauss published his monumental treatise on celestial mechanics *Theoria Motus* in 1806. He became interested in the compass through surveying, and developed the magnetometer, an instrument with which, together with Wilhelm Weber, he measured the intensity of magnetic forces. With Weber, he also built the first successful telegraph.

Unfortunately for mathematics, Gauss reworked and improved papers incessantly, and, in keeping with his motto "*pauca sed matura*" (few but ripe), he published only a fraction of his work. Many of his results were subsequently repeated by and attributed to others, since his terse diary remained unpublished for years after his death. Only 19 pages long, this diary later confirmed his priority on many breakthroughs, including work on an alternative to the **parallel postulate**, which really makes him the earliest pioneer of **non-Euclidean geometry** despite the fact that János **Bólyai** and Nikolai **Lobachevsky** are normally given this accolade. Gauss did, however, publish his seminal treatment on **differential geometry** in *Disquisitiones circa superticies curvas,* and Gaussian **curvature** is named for him. Gauss wanted a heptadecagon placed on his gravestone, but the carver refused, saying it would be indistinguishable from a circle. The heptadecagon appears in the shape of a pedestal with a statue erected in his honor in his hometown of Braunschweig.

Gaussian
Normally distributed (with a bell-shaped curve) and having a **mean** at the center of the curve with tail widths proportional to the **standard deviation** of the data about the mean.

Gelfond's theorem
Also known as the *Gelfond-Schneider theorem:* a^b is a **transcendental number** if (1) a is an **algebraic number** and not equal to either 0 or 1, and (2) b is algebraic and also an **irrational number**. Gelfond's theorem enables the seventh of David **Hilbert**'s famous problems to be solved.

general relativity
See **relativity theory**.

general topology
See **point-set topology**.

genetic algorithm
A type of evolving computer program, developed by the computer scientist John Holland, whose strategy of arriving at solutions is based on principles taken from genetics. Basically, the genetic **algorithm** utilizes the mixing of genetic information in sexual reproduction, random mutations, and natural selection at arriving at solutions.

genus
In **topology**, roughly speaking, the number of **hole**s in a surface. Spheres, bowling balls (the finger holes aren't

true holes because they don't go all the way through), and wine glasses have a genus of 0 and can be represented by **quadratic** equations. Bagels, inner tubes, and teacups have a genus of 1 and can be described by **cubic** equations. Humans are more difficult to specify. However, you will certainly increase your genus by one if you have your ear pierced! Different definitions of genus apply to other types of mathematical objects such as a **curve**, a **knot**, or a **set**.

geoboard

A device commonly used in elementary schools to aid in the teaching of basic geometric concepts. A simple geoboard can be made from a square piece of wood and 25 nails arranged in an evenly spaced grid of 5 vertical lines and 5 horizontal lines. These nails represent the **lattice** points in the plane. Figures are made on the geoboard by stretching rubber bands from one nail to another until the desired shape is formed.

geodesic

A path on a given **surface** that is as straight as possible; in other words, a path that doesn't deviate either to the left or to the right, and only bends when forced to do so by the **curvature** (if any) of the surface. If the surface is an ordinary **plane**, the geodesics are straight lines; on a sphere the geodesics are **great circle**s.

geometric magic square

A square array of $n \times n$ cells each occupied by a distinct geometrical figure (or piece or tile), such that the n pieces contained in every row, column, and diagonal can be fitted together to produce (i.e., tile or pack) a constant shape known as the target. The figures may be of any dimension, but are normally planar (topological disks). In tessellating the target, which may be of any shape, planar pieces are allowed to be flipped. Pieces of three or more dimensions are considered distinct from their mirror images. Geometric **magic squares** using one-dimensional entries have been known for centuries; they are the traditional magic squares in which straight lines pave a constant length, as usually represented by numbers adding to a constant total. The properties of generalized geometric magic squares were first investigated by Lee **Sallows**.

geometric mean

The geometric mean of n numbers is the nth root of the product of the numbers.

geometric sequence

Also known as a *geometric progression,* a finite **sequence** of at least three numbers, or an infinite sequence, whose terms differ by a constant multiple, known as the *common ratio.* For example, starting with 3 and using a common ratio of 2 leads to the finite geometric sequence: 3, 6, 12, 24, 48, and also to the infinite sequence 3, 6, 12, 24, 48, . . . , (3×2^n). . . . In general, the terms of a geometric sequence have the form $a_n = ar^n$ $(n = 0, 1, 2, \ldots)$ for fixed numbers a and r. If the terms of a geometric sequence are added together the result is a *geometric series.* If it is a finite series, then we add its terms to get the series sum, $S_n = a + ar + ar^2 + \ldots + ar^n = (a - ar^{n+1})/(1 - r)$. In the case of an **infinite series**, if $|r| < 1$, the sum is $a/(1 - r)$. If $|r| \geq 1$, however, the series diverges and thus has no sum. See also **arithmetic sequence**.

geometry

The study of the properties of shapes and of spaces. See also **Euclidean geometry** and **non-Euclidean geometry**.

geometry puzzles

One of the attractions of puzzles involving shapes, especially **dissection** problems, is that they appeal to the eye and very often don't call for much ability in solving equations and the like. Anyone can try to assemble the pieces of a jigsaw, whether it be of a picture or of a geometric shape, so a mathematical game such as **tangrams** or the **Soma cube** is within everyone's reach. On the other hand, some geometric puzzles call for a basic knowledge of more abstract fields such as algebra and calculus. They may also exploit our sometimes faulty intuition about how different quantities vary in one, two, and three dimensions and about how much information is needed to solve a problem.

As an example of faulty intuition, imagine that Earth, taken to be a perfect sphere with a radius r of 6,378 km, is completely covered by a thin membrane. Now suppose that 1 square meter is added to the area of this membrane to form a larger sphere. By how much does the radius and the volume of this membrane increase? This can be worked out from the formulae for the volume of a sphere $(V = (4/3)\pi r^3)$ and the area of a sphere $(A = 4\pi r^2)$, respectively. It turns out that if the area of the cover is increased by 1 square meter, then the volume it contains is increased by about 3.25 million cubic meters. This seems like a huge amount. However, the new cover wouldn't be very high above the surface of the planet–only about 6 nanometers! As an example of a problem that is both counterintuitive *and* seems to lack sufficient data for its solution see **hole-through-a-sphere problem**.

Gergonne point

In a triangle, the point at which the lines from the vertices (see **vertex**) to the points of contact of the opposite sides with the **inscribed circle** meet.

Germain, Sophie (1776–1831)

A French mathematician who made notable contributions to **number theory** and to mathematical physics despite a lack of formal training and the social prejudices of her day. She taught herself, against her parents' wishes, often at night, during the Reign of Terror following the French Revolution, with books from her father's library. When deprived of heat and light, she would wrap herself in quilts and use candles. Finally her parents acquiesced to her "incurable" passion for mathematics and let her study. Through Joseph **Lagrange**, to whom she had originally submitted work under a pseudonym, she gained access to a circle of distinguished mathematicians, including Carl **Gauss**. Among her most important work was an analysis of Ernst **Chladni**'s studies of vibrating surfaces, and her proof that if $x, y,$ and z are integers and if $x^5 + y^5 = z^5$ then at least one of $x, y,$ or z must be divisible by 5 (a result now known as *Germain's theorem*); this was an important early step towards proving **Fermat's last theorem**.

Get Off the Earth

A famous **vanishment puzzle** by Sam **Loyd**. The picture is made from a rectangular background topped with a circular card, representing the world, that can be rotated. Parts of a number of Chinese men are on each piece. With the world orientated so that the large arrow on it points to the N.E. point on the background, 13 Chinamen can be counted. But when the earth is turned slightly, so that the arrow points N.W., there are only 12 characters. Where did the thirteenth Chinaman go? The cleverness of the puzzle is that there are many bits of Chinamen–arms, legs, bodies, heads, and swords–and each has tiny slivers missing. When the earth is turned, these pieces get slightly rearranged. In particular, each of the 12 Chinamen gains a sliver of a Chinaman from his neighbor.

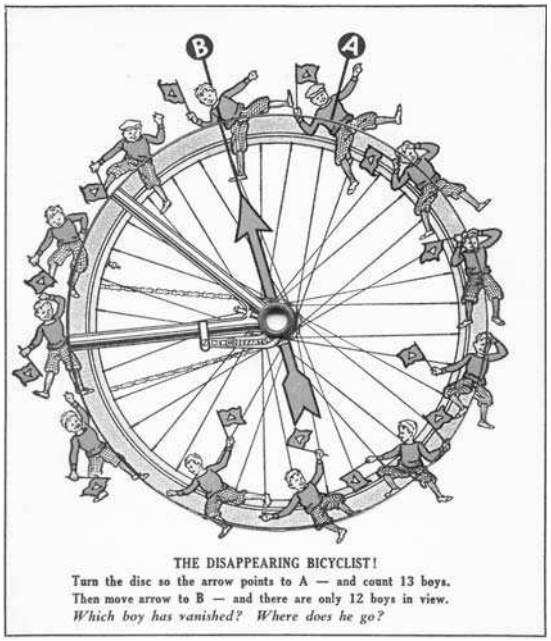

Get Off the Earth An unusual variant of Loyd's Get Off the Earth puzzle called "The Disappearing Bicyclist." *From the collection of William Waite*

Gettier problem

A thought experiment in philosophy that throws into question the long-held supposition that to know something is equivalent to holding a belief about something that is both true and for which there is justification. Consider a case in which a lecturer has two students in her class called Mr. Havenot and Mr. Havegot. Mr. Havenot claims to own a Ferrari, drives one around, and has papers that state that the car is his. But in fact he does not actually own the car. Mr. Havegot, on the other hand, who shows no sign of Ferrari ownership, secretly has one of these rare cars. On the basis of the evidence, the teacher concludes that one of her students owns a Ferrari–and is correct in this belief. However, there is something wrong. Despite the combination of truth, justification, and belief, it seems that there is no real knowledge. The first examples of such problems were published in 1963 by the American philosopher Edmund Gettier (1927–).

Giant's Causeway

A natural structure that occurs on the coast in County Antrim, Ireland; it is one of the few places in the world where volcanic basalt has cooled in a columnar formation. The columns approximately form a **hexagon**al tessellation (see **tiling**) and tend to break off to produce a pavement with this pattern. The full length of the columns can't be seen, but it is estimated that they may be 20 feet (about 6 meters) high before merging into the underlying irregular basaltic mass. About 99% of the columns are believed to be hexagonal and only one triangular column is known. Though many of the hexagons are fairly regular, some have a side twice as long as their smallest side. Side lengths vary from 8 to 18 inches (20 to 46 cm) and the pillars break up into sections 6 to 36 inches (15 to 90 cm) long, with a concavo-convex junction rather than a plane junction. Other examples of such formations occur at Kirkjubaejarklaustri, in Iceland, and the Devil's Postpile, in California.

Gilbreath's conjecture

A strange hypothesis concerning **prime number**s that was first suggested in 1958 by the American mathematician and amateur magician Norman L. Gilbreath following

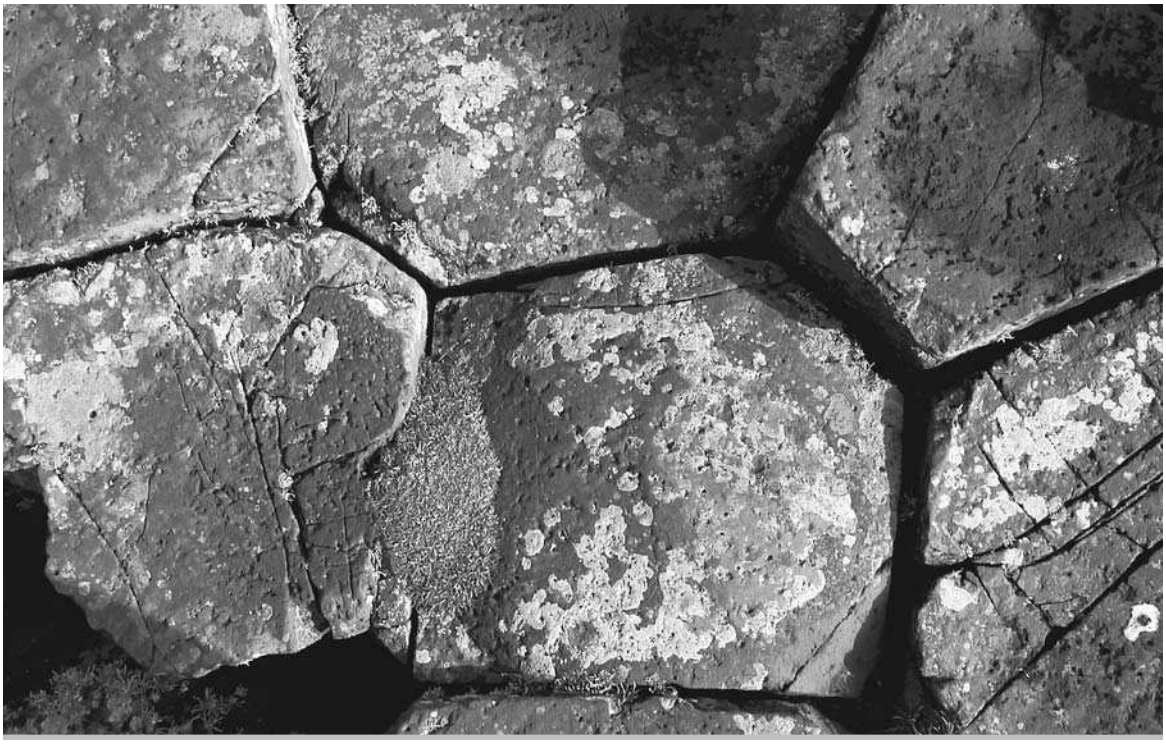

Giant's causeway Hexagonal paving on the Giant's Causeway. *Martin Melaugh, University of Ulster*

some doodlings on a napkin. Gilbreath started by writing down the first few primes:

2, 3, 5, 7, 11, 13, 17, 19, 23, 29, 31, . . .

Under these he put their differences:

1, 2, 2, 4, 2, 4, 2, 4, 6, 2, . . .

Under these he put the unsigned difference of the differences:

1, 0, 2, 2, 2, 2, 2, 2, 4, . . .

And he continued this process of finding iterated differences:

1, 2, 0, 0, 0, 0, 0, 2, . . .
1, 2, 0, 0, 0, 0, 2, . . .
1, 2, 0, 0, 0, 2, . . .
1, 2, 0, 0, 2, . . .
1, 2, 0, 2, . . .
1, 2, 2, . . .
1, 0, . . .
1, . . .

Gilbreath's conjecture is that, after the initial two rows, the numbers in the first column are all one. No exception has been found to date, despite searches out to several hundred billion rows, and the conjecture is generally assumed to be true. However, it may have nothing to do with primes as such. The English mathematician Hallard Croft has suggested the conjecture may apply to *any* sequence that begins with 2 and is followed by odd numbers that increase at a "reasonable" rate and with gaps of "reasonable" size. If this is the case, Gilbreath's conjecture may not be as mysterious as it first seems, though it may be very difficult to prove.

glissette

If there are two fixed curves, and a curve S of fixed shape and length that slides with its ends on the fixed curves, then the **locus** of a point moving with S is called a glissette. An example is the locus of the midpoint of a line segment sliding with its ends on two perpendicular lines; this locus is a circle.

gnomon magic square

A 3×3 array in which the elements in each 2×2 corner have the same sum. See also **magic square**.

Go

A two-player board game that originated in China in about 2000 B.C. It is often compared and contrasted with **chess**. Go is played on a board marked with 19×19 lines. Round, lens-shaped pieces called stones are placed, one per move, on the intersections of this grid, of which there are 361. As in chess, the pieces are colored black and white, but in Go black plays first. The board starts blank and pieces once played are not thereafter moved except to be taken off as prisoners. Pieces are captured singly or en masse by being surrounded so that they are not connected to any adjacent open intersection. The player with highest score at the end of the game, or following resignation or time expiry, wins. Go is considered to be a deeply strategic game, unlike chess, which is largely tactical. There are 32,940 opening moves, after symmetry is taken into account, 992 of which are deemed strong. Estimates of the number of possible board configurations vary but are typically on the order of 10^{174}.

God

I'm still an atheist, thank God.
–Luis Buñuel (Spanish film director, 1900–1983)

Mathematicians, logicians, and scientists have long debated the nature, existence, and dice-playing ability of a Higher Power. The pre-Renaissance French philosopher Jean Buridan (c. 1295–1358) used a version of the *liar paradox* to "prove" the existence of God. He wrote these two sentences:

God exists.

None of the sentences in this pair is true.

The only consistent way to have these two sentences be either true or false is for "God exists" to be true. (However, there is nothing to say that such consistency is necessary.) Blaise **Pascal** gave a more persuasive argument, not for the existence of God but for why we should believe in that existence: "If I believe in God and life after death and you do not, and if there is no God, we both lose when we die. However, if there is a God, you still lose and I gain everything." Pierre **Laplace**, on the other hand, replying to **Napoleon Bonaparte**, who had asked why his celestial mechanics made no mention of God, said: "Sir, I have no need of this hypothesis." The German mathematician Leopold **Kronecker** thought that "God made the Integers, all the rest is the work of man." In *The City of God,* however, Saint Augustine seems to imply that the integers were independent of God. He wrote: "**Six** is a number perfect in itself, and not because God created the world in six days; rather the contrary is true. God created the world in six days because this number is perfect, and it would remain perfect, even if the work of the six days did not exist." Augustine's statement can be taken to suggest that six would be a perfect number not only if the universe didn't exist, but even if God didn't exist. As to God's mathematical specialty, Plato said, "God ever geometrizes" while Charles Jacobi insisted that "God ever arithmetizes." James Jeans thought, "The Great Architect of the Universe now begins to appear as a pure mathematician," and Einstein ("God does not play dice") was sure He wasn't a probabilist.

Gödel, Kurt (1906–1978)

An Austrian-American mathematician and logician who, in 1931, proved that within a **formal system** questions exist that are neither provable nor disprovable on the basis of the **axiom**s that define the system. This is known as Gödel's undecidability theorem. He also showed that in a sufficiently rich formal system in which decidability of all questions is required, there will be contradictory statements. This is called **Gödel's incompleteness theorem**. In establishing these theorems Gödel showed that

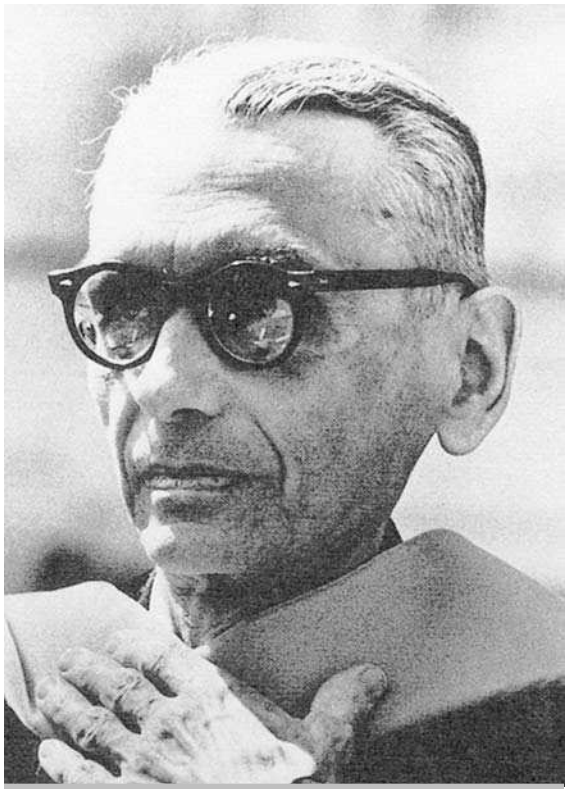

Gödel, Kurt

there are problems that can't be solved by any set of rules or procedures; instead, for these problems one must always extend the set of axioms. This disproved a common belief at the time that the different branches of mathematics could be integrated and placed on a single logical foundation. Gödel was a close friend of Albert Einstein at Princeton and contributed to his general **relativity theory** and cosmology. The so-called *Gödel universe* is a rotating model of the universe in which it is theoretically possible to travel into the past (see **time travel**).

Gödel's incompleteness theorem

In a nutshell: All consistent axiomatic systems contain undecidable propositions. What does this mean? An axiomatic system consists of some undefined terms, a number of **axiom**s that refer to those terms and partially describe their properties, and a rule or rules for deriving new propositions from already existing propositions. Axiomatic systems are powerful because they reduce large bodies of math to a simple description. Also, because they're very abstract, they allow all, and only, the results that follow from things having the formal properties specified by the axioms to be derived. An axiomatic system is *consistent* if, given the axioms and the derivation rules, it doesn't lead to any contradictions. One of the first modern axiomatic systems was a formalization of simple arithmetic (adding and multiplying whole numbers) by Giuseppe **Peano** and now known as *Peano arithmetic.* Kurt **Gödel** showed that every syntactically correct proposition in Peano arithmetic can be represented by a unique integer, called its *Gödel number.* The trick is to replace each symbol in the proposition, *including numerals,* by a different string of digits. If we represent "1" by 01, "2" by 02, "+" by 10, and "=" by 11, then the Gödel number of "1 + 1 = 2" is 0110011102. This allowed Gödel to write down, unambiguously, propositions about propositions. In particular, he was able to write down self-referential (see **self-referential sentence**) propositions–ones that include their own Gödel number. Gödel was then able to prove that, *either* the system of Peano arithmetic is inconsistent, *or* there are true propositions that can't be reached from the axioms by applying the derivation rules. The system is thus *incomplete,* and the truth of those propositions is *undecidable* (within that system). Such undecidable propositions are known as *Gödel propositions* or *Gödel sentences.* Nobody knows what the Gödel sentences for Peano arithmetic are, though people have their suspicions about the **Goldbach conjecture** (every even number is the sum of two prime numbers).

The results of an axiomatic system pertain to more than just Peano arithmetic, they apply to all kinds of things that satisfy the axioms. There are an immense number of other axiomatic systems, which either include Peano numbers among their basic entities or can be constructed from them. It follows that these systems, too, contain undecidable propositions, and are incomplete.

A common misconception is that Gödel's theorem imposes some profound limitation on knowledge, science, and mathematics. In the case of science, this ignores that Gödel's theorem applies to *deduction from axioms,* which is only one source of knowledge and not even a very common mode of reasoning in science. More generally, Gödel's incompleteness result doesn't touch directly on the most important sense of completeness and incompleteness, namely, descriptive completeness and incompleteness–the sense in which an axiom system describes a given field. In particular, the result represents no threat to the notion of truth.

Goldbach conjecture

One of the oldest and easiest-to-understand hypotheses in mathematics that remains unproven. In its original form, now known as the *weak Goldbach conjecture,* it was put forward by the Prussian amateur mathematician and historian Christian Goldbach (1690–1764) in a letter dated June 7, 1742, to Leonhard **Euler**. In this guise it says that every whole number greater than five is the sum of three **prime number**s. Euler restated this, in an equivalent form, as what is now called the *strong Goldbach conjecture* or, simply, the Goldbach conjecture: every even number greater than two is the sum of two primes. Thus, $4 = 2 + 2$, $6 = 3 + 3$, $8 = 3 + 5$, $10 = 3 + 7, \ldots,$ $100 = 53 + 47, \ldots$. In fact René **Descartes** knew about the two-prime version of Goldbach's conjecture before either Goldbach or Euler did. So, is it misnamed? Paul **Erdös** said, "It is better that the conjecture be named after Goldbach because, mathematically speaking, Descartes was infinitely rich and Goldbach was very poor." In any event, there is a much more important question, namely, is the conjecture true? The general assumption is that it is, but no one knows for sure. The most significant step toward a proof came in 1966 when the Chinese mathematician Chen Jing-Run showed that every sufficiently large even integer is the sum of a prime and a number that has at most two prime factors. Using powerful computers, the Goldbach conjecture has been checked out to about 400 trillion. But there is no great optimism among mathematicians that a final breakthrough is on the horizon. Even a reward of $1 million dollars for a proof offered by the publishing house Faber & Faber in 2000, to help publicize the novel *Uncle Petros and Goldbach's Conjecture* by the Greek mathematician and author Apostolos Doxiadis, went unclaimed.[85]

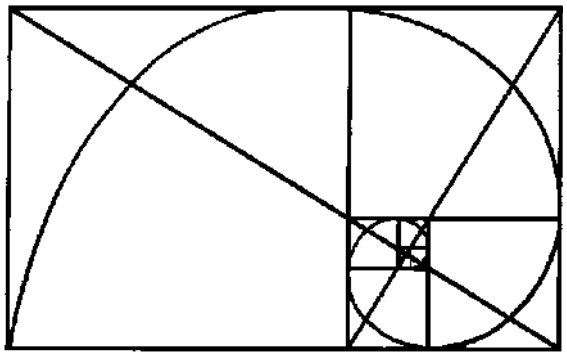

golden ratio A golden rectangle and a logarithmic spiral emerge from a whirling pattern of squares built up from two small squares of equal size at the spiral's center.

golden ratio (phi, ϕ)

A remarkable number that, like **pi** and ***e,*** pops up all over the place in mathematics but, in some ways, has a more "human" connection, in that it seems to be linked to aesthetics. Its name, which is also given as the *golden mean,* the *golden section,* the *golden number,* and the *divine proportion,* reflects this sense of a harmonious or pleasing ideal. The golden ratio is an **irrational number** of the type known as an **algebraic number** (in contrast with π and *e,* which are transcendental) and is represented by the Greek letter ϕ (phi). It can be defined in various ways. For example, it is the only number equal to its own reciprocal plus 1, that is, $\phi = (1/\phi) + 1$, so that $\phi^2 = \phi + 1$. From this comes the quadratic equation $\phi^2 - \phi - 1 = 0$ of which the golden ratio is the positive solution, $(1 + \sqrt{5}) / 2 \approx 1.6180339887 \ldots$. The golden ratio is also approximated by the ratio of successive terms in the **Fibonacci sequence**; in fact, $F(n + 1) / F(n)$ gets closer and closer to ϕ as n tends to infinity. Because $1/(1 - \phi) = \phi$, the **continued fraction** representation of ϕ is

$$\phi = 1 + 1/(1 + 1/(1 + 1/(1 + 1/(1 + 1/ \ldots$$
$$= [1;1,1,1,1, \ldots].$$

Two quantities are said to be in the golden ratio, if the ratio of the larger one, *a,* to the smaller one, *b,* is the same as the ratio of the smaller one to their difference, that is, $a/b = b/(a - b)$. The so-called *golden rectangle* is one whose sides *a* and *b* stand in the golden ratio. It is famously said to have great aesthetic appeal and is closely approximated by the dimensions of the front of the Parthenon in Rome. Leonardo da Vinci's masterpiece the *Mona Lisa* is said to have a face that is framed by a golden rectangle; what is certain is that Leonardo was a close personal friend of Luca **Pacioli**, who published a three-volume treatise on the golden ratio, *Divina Proportione,* in 1509. The Swiss-French architect and painter Le Corbusier designed an entire proportional system called the "Modulor," that was based on the golden ratio. The Modulor was supposed to provide a standardized system that would automatically confer harmonious proportions to everything, from door handles to high-rise buildings. Another artist who deliberately used the golden ratio is the surrealist Salvador Dali. The ratio of the dimensions of Dali's *Sacrament of the Last Supper* is equal to the golden ratio. Dali also incorporated in the painting a huge dodecahedron (a twelve-faced Platonic solid in which each side is a pentagon) engulfing the supper table. The dodecahedron, which according to Plato is the solid "which the god used for embroidering the constellations on the whole heaven," is intimately related to the golden ratio–both the surface area and the volume of a dodecahedron of unit edge length are simple functions of the golden ratio. In fact, ϕ turns up frequently in figures that have pentagonal symmetry. For instance the ratio of a regular pentagon's side and diagonal is equal to ϕ, and the vertices of a regular **icosahedron** are located on three orthogonal golden rectangles. The golden ratio is also related to **Penrose tiling** and to the **plastic number**.[205]

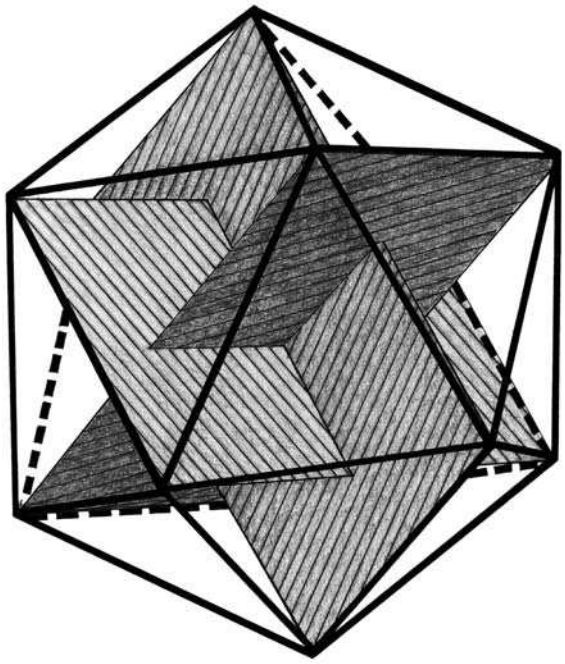

golden ratio The corners of an icosahedron meet the corners of three orthogonal golden rectangles.

Golomb, Solomon W. (1932–)

A mathematician and electrical engineer at the University of Southern California who is best known for his seminal studies of **polyomino**s. His article "Checker Boards and Polyominos," published in the *American Mathematical Monthly* in 1954 when Golomb was a 22-year-old graduate student at Harvard, defined a polyomino as a simply connected set of squares (i.e., a set of squares joined along their edges). Golomb also originated the idea of **graceful graph**s.[137]

golygon

A series of straight-line segments that have lengths of one, two, three, and so on, up to some finite number of units, with the property that every segment connects at a right angle to the segment that is one unit larger, except the longest segment, which meets the shortest segment at a right angle. The name "golygon" was invented by Lee **Sallows**. Golygons have inspired some interesting puzzles as well as some intriguing research problems.

googol

A named coined in 1938 by Milton Sirotta, the 9-year-old nephew of the mathematician Edward **Kasner**, when the child was asked by his uncle to come up with a name for a very **large number**; at the same time, *googolplex* was suggested for a still larger number. Kasner defined these numbers as follows:

1 googol = 10^{100} (i.e., 1 followed by 100 zeros);
1 googolplex = $10^{\text{googol}} = 10^{10^{100}}$ (i.e., 1 followed by a googol number of zeros)

A googol is very roughly the number of years thought to be needed for all the black holes in the universe to evaporate by a process known as Hawking radiation. It is much larger than the number of protons and neutrons in the known universe (about 10^{80}), but much smaller than the number of protons and neutrons needed to pack every cubic centimeter of the known universe (about 10^{128}). The googolplex is the largest number with a proper name of which many people have heard. It is dwarfed, however, by such esoterica as **Graham's number**.

Gordian knot

The earliest reference to a **string puzzle**. In Greek mythology, a Phrygian peasant called Gordius, the father of Minos (see **maze**), became king because he was first to arrive in town after an oracle commanded the Phrygians to select as ruler the first person to drive into the public square in a wagon. In gratitude, Gordius dedicated his wagon to Zeus and placed it in the temple grove, tying the wagon pole to the yoke with a rope of bark. The knot was so intricately entwined that no one could undo it. A saying developed that whoever succeeded in untying the knot would become ruler of all Asia. Many tried, but all failed. According to legend, even Alexander the Great was unable to untie the Gordian knot, so he drew his sword and cut it through with a stroke. The expression "to cut the Gordian knot" is used to refer to a situation in which a difficult problem is solved by a quick and decisive action.

graceful graph

A **graph** of points and connecting lines that can be numbered in a certain way. Say the graph has p points and e lines ("e" for edges) connecting them. Each of the points is assigned an integer; the lowest integer (by convention) is taken to be 0, and no two integers may be alike. Each of the lines is labeled with the difference between the two integers of the points that it connects. Then, if the numbers corresponding with the lines run from 0 through e, the graph is said to be graceful. Graceful graphs were originally defined and developed by Solomon **Golomb**.

gradient

A **vector** of partial **derivative**s of a **function** that operates on vectors. Intuitively, the gradient represents the slope of a high-dimensional surface.

Graham, Ronald L. (1936–)

An American mathematician and leading combinatorialist after whom **Graham's number** is named. Graham is also one of the country's best jugglers and former president of the International Juggler's Association. In his youth, he and two friends were professional trampolinists who performed with a circus as the Bouncing Baers. His office ceiling is covered with a large net that he can lower and attach to his waist so that when he practices juggling with six or seven balls, any that are dropped will roll back to him. Graham is a professor in the department of computer science and engineering at the University of California at San Diego.

Graham's number

A stupendously **large number** that found its way in to the *Guinness Book of Records* as the biggest number ever obtained as part of a mathematical proof; it is named after its discoverer, Ronald **Graham**. Graham's number is the upper bound solution to a very exotic problem in **Ramsey theory**, namely: What is the smallest dimension n of a **hypercube** such that if the lines joining all pairs of corners are two-colored, a planar complete graph K_4 of one color will be forced? This is exactly equivalent to a problem that can be stated in plain language: Take any number of people, list every possible committee that can be formed from them, and consider every possible pair of committees. How many people must be in the original group so that no

matter how the assignments are made, there will be four committees in which all the pairs fall in the same group, and all the people belong to an even number of committees. Graham's number is the *greatest* value that the answer could take. It is so large that it can only be written using special big-number notation, such as **Knuth's up-arrow notation**. Even then, it must be built up in stages. First, construct the number $G_1 = 3\uparrow\uparrow \ldots \uparrow\uparrow 3$, where there are $3\uparrow\uparrow\uparrow\uparrow 3$ up-arrows. This, in itself, is a number far, far beyond anyone's ability to even remotely comprehend. Next, construct $G_2 = 3\uparrow\uparrow \ldots \uparrow\uparrow 3$, where there are G_1 up-arrows; then construct $G_3 = 3\uparrow\uparrow \ldots \uparrow\uparrow 3$, where there are G_2 up-arrows; then continue this pattern until the number G_{62} has been made. Graham's number $G = 3\uparrow\uparrow \ldots \uparrow\uparrow 3$, where there are G_{62} up-arrows. While the unthinkably large upper boundary to the problem described earlier is given by Graham's number, nobody, including Graham himself, believes the solution is nearly so large. In fact, it is thought that the actual answer is probably 6![115]

grandfather paradox

One of the most powerful and commonly used arguments against **time travel**. It points out that if you were able to travel into the past you could (if you were so inclined) kill your grandfather when he was very young and thus render your own birth impossible. A simpler version is that you could kill a younger version of yourself so that you would not be alive in the future to travel back in time. The grandfather paradox shows how one form of time travel could violate **causality** by eliminating the cause of a phenomenon that has already taken place in the present.

The most bizarre adaptation of the grandfather paradox is found in Robert Heinlein's classic short story "All You Zombies." A baby girl is mysteriously left at an orphanage in Cleveland in 1945. "Jane" grows up lonely and dejected, not knowing who her parents are, until one day in 1963 she is strangely attracted to a drifter. She falls in love with him. But just when things are finally looking up for Jane, a series of disasters strike. First, she becomes pregnant by the drifter, who then disappears. Second, during the complicated delivery, doctors find that Jane has both sets of sex organs, and to save her life, they are forced to surgically convert "her" to a "him." Finally, a mysterious stranger kidnaps her baby from the delivery room. Reeling from these disasters, rejected by society, scorned by fate, "he" becomes a drunkard and drifter. Not only has Jane lost her parents and her lover, but he has lost his only child as well. Years later, in 1970, he stumbles into a lonely bar, called Pop's Place, and spills out his pathetic story to an elderly bartender. The bartender offers the drifter the chance to avenge the stranger who left her pregnant and abandoned, on the condition that he (Jane) join the "time travelers corps." Both of them enter a time machine, and the bartender drops off the drifter in 1963. The drifter is strangely attracted to a young orphan woman, who subsequently becomes pregnant. The bartender then goes forward nine months, kidnaps the baby girl from the hospital, and drops off the baby in an orphanage back in 1945. Then the bartender drops off the thoroughly confused drifter in 1985, to enlist in the time travelers corps. The drifter eventually gets his life together, becomes a respected and elderly member of the time travelers corps, and then disguises himself as a bartender and has his most difficult mission: a date with destiny, meeting a certain drifter at Pop's Place in 1970. The question is: who is Jane's mother, father, grandfather, grandmother, son, daughter, granddaughter, and grandson? The girl, the drifter, and the bartender, of course, are all the same person. As an exercise (on the road to insanity) try drawing Jane's family tree. You will find that not only is she her own mother and father, she is an entire family tree unto herself!

graph

> *I'll do algebra, I'll do trig, and I'll even do statistics, but graphing is where I draw the line!*
>
> –Anonymous

(1) In common usage, a plot of x values (the domain) against y values (the codomain) for a given **function**, $y = f(x)$. Such a graph is also known as a *function graph* or the *graph of a function.* (2) In strict mathematical usage, any set of dots, known as *nodes* or *vertices,* in which at least some pairs are joined by lines known as *edges* or *arcs.* What follows applies only to this second definition.

Often the lines on a graph are used to represent relationships between objects (represented by dots). Depending on the application, edges may or may not have a direction, as indicated by an arrow (see **directed graph**); edges joining a node to itself may or may not be allowed, and nodes and/or edges may be assigned weights. A *path* is a series of nodes such that each node is adjacent to both the preceding and succeeding node. A path is considered *simple* if none of the nodes in the path is repeated. The *length* of a path is the number of edges that the path uses, counting multiple edges multiple times. If it's possible to establish a path from any node to any other node of a graph, the graph is said to be a **connected graph**. A *circuit* or *cycle* is a path that begins and ends with the same node and has a length of at least two. A *tree* is a connected acyclic graph, that is, a graph without any circuits. A **complete graph** is one in which every node is adjacent to every other node. An **Euler path** in a graph is a path that uses each edge precisely once. If such a path exists, the graph is said to be *traversable.* An **Euler circuit** is a path that traverses each edge precisely once. A **Hamilton path**

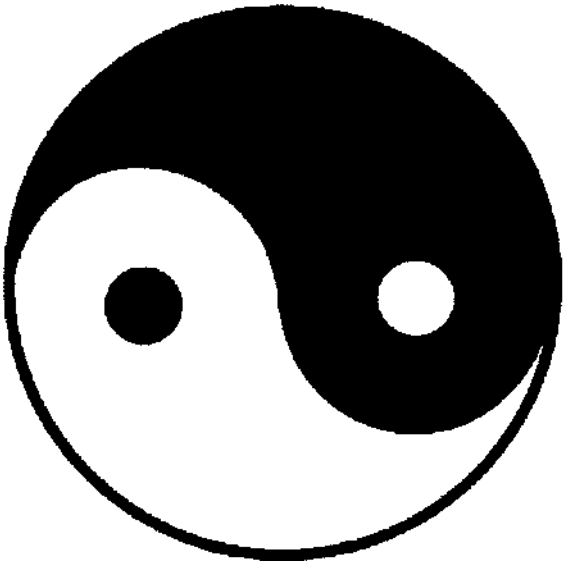

Great Monad

in a graph is a path that visits each node once and only once; a **Hamilton circuit** is a **circuit** that visits each node once and only once. Well known problems whose solution involves graphs and graph theory include the **four-color problem** and the **traveling salesman problem**.

graph theory

The study of **graph**s, either for their own sake, or as models of such diverse things as **group**s (in pure mathematics) or computer networks.

great circle

A circle that goes all the way around a **sphere** and is centered at the center of the sphere. The shortest route between two points on a sphere, such as Earth, is along the great circle that connects these points. A great circle is a **geodesic**.

Great Monad

Also known as *T'ai-Chi,* an important and ubiquitous symbol in traditional Chinese philosophy and cosmology. It represents the underlying harmony of the universe when its opposites or dualities–male and female (*yang* and *yin*), hard and soft, sun and moon, and so forth–are in balance. It occurs everywhere in Chinese art: in books, on walls, porcelain, tablets, and stitched into brocade.

greatest common divisor

The largest integer that divides each of a sequence of integers exactly. Also called the *greatest common factor.*

greatest lower bound

The largest **real number** that is smaller than each of the numbers in a **set** of real numbers.

Green, George (1793–1841)

An English mathematician who published work in the fields of hydrodynamics, electricity, and magnetism, but is best known for his theorem (see **Green's theorem**), which is the basis of **potential theory**. Green took over a bakery and adjoining windmill after the death of his father, but studied mathematics in his spare time. In 1828, he wrote his most important paper, "An Essay on the Application of Mathematical Analysis to the Theories of Electricity and Magnetism," which, though generally overlooked at the time, is now regarded as the beginning of mathematical physics in England.

Green's theorem

A connection between path integrals over a well-connected region in the plane and the area of the region bounded in the plane. Green's theorem is a form of the *fundamental theorem of calculus,* and is used today in almost all computer codes that solve **partial differential equation**s.

Grelling's paradox

An equivalent, from the world of words and grammar, of **Russell's paradox**. Grelling's paradox involves dividing all adjectives into two sets: self-applicable and not self-applicable. Words like "English," "written," and "short" are self-applicable, while "Russian," "spoken," and "long" are not self-applicable. Now, define the adjective *heterological* to mean "not self-applicable." To which set of adjectives does "heterological" belong? This strange quandry was devised by the logician and philosopher Kurt Grelling (1886–1941/2), who was persecuted by the Nazis; it is not certain whether he died with his wife in the Auschwitz concentration camp in 1942, or whether he was killed in 1941 in the Pyrenees while trying to escape into Spain.

gross

A group of 144 items. The word comes from the Latin *grossus,* for "thick" or "large," via the Old French *gross douzaine* or "large dozen" (12 dozen), though this grouping may have started out in Germany. "Grocer" has the same origins as "gross" because a grocer is someone who deals in large quantities of food. A *great gross,* or a dozen gross, is 1728. See also **twelve**.

group

> *Wherever groups disclosed themselves, or could be introduced, simplicity crystallized out of comparative chaos.*
>
> –Eric Temple Bell

An abstract and crucially important way of representing **symmetry** and one of the most fundamental concepts in modern **algebra**. Groups were brought into mathematics in the early nineteenth century by the radical young French student Evariste **Galois** as a tool to help solve one of the outstanding problems of his day: to find a formula for solving **polynomial** equations of order five–**quintic**s–and higher. Galois showed, in notes scribbled down the night before he died in a duel, that no such formula exists. The reason for this is that the possible symmetries, or permutations, of the **root**s of fifth-degree polynomial equations are more complex than are the symmetries that can be represented by arithmetical formulas. This fact emerged from the development of the idea of a *permutation group* by Galois and, independently at about the same time, by Niels **Abel**. Half a century later, another Norwegian, Sophus **Lie**, showed how important groups are to the whole of mathematics. The theory of what became known as **Lie group**s links the discrete structure of permutations with the continuous variation of **differential equation**s. Not surprisingly, because group theory forms a common underpinning to algebra and to geometric features such as rotation, reflection, and symmetry, it crops up routinely in modern physics, from the classification of elementary particles to crystallography.

A group is a **set** whose elements are defined by a single operation. The group is called *additive* if the symbol for the operation is "+" and is called *multiplicative* if the symbol is "·" for multiplication. But any other symbol can be substituted for these. There is always a unique element (1, for multiplicative, and 0, for additive, groups) that leaves elements unchanged under the defined operation, like $a + 0 = a$. Also, for every element a there exists a unique inverse b such that, for example, in the case of the additive symbol, $a + b = 0$ and $b + a = 0$. Most often, however, the inverse is denoted as a^{-1}. Lastly, the group operation must be **associative** as in $a \cdot (b \cdot c) = (a \cdot b) \cdot c$. A group is *commutative* or *Abelian* if its operation is symmetric, as in $a + b = b + a$.

Groups come in two types: finite and infinite. The symmetry group of the roots of a polynomial equation is a finite group, because there is only a limited number of permutations possible among the roots of a given polynomial. In contrast, the Lie groups that represent symmetries of solutions of differential equations are infinite because they represent continuous transformations, and continuity carries the potential of an infinite number of changes. Finite groups can be built up from combinations of smaller groups by a process analogous to multiplication. In the same way that a whole number can be written as a product of **prime number**s, a finite group can be expressed as a combination of certain factors known as *simple groups.* Most simple groups belong to one of three families: the *cyclic groups,* the *alternating groups,* or the *groups of Lie type.* Cyclic groups consist of cyclic permutations of a prime number of objects. Alternating groups consist of even permutations–those formed by interchanging the positions of two objects an even number of times. Sixteen subfamilies make up the simple groups of Lie type, each associated with a family of infinite Lie groups. (Confusingly, a Lie group is not a group of Lie type, since the former is infinite and the latter is finite!) Altogether, there are 18 specific families of finite simple groups. There are also 26 simple groups, known as *sporadic groups,* that are highly irregular and fall outside these families. Five sporadic groups were found in the nineteenth century by Emile Mathieu. Then came a hiatus until the 1960s, when suddenly a rush of new sporadics came to light. The most remarkable of these is the so-called **monster group**, which appears to be intimately related to the structure of the universe at the subatomic level.

Grundy's game

See **Nim**.

Guy, Richard Kenneth (1916–)

A British-born mathematician who is professor emeritus of mathematics at the University of Calgary, Canada, and an expert in **combinatorics** and in **number theory**. Guy is the author of more than 250 papers and 10 books, including (as a coauthor) the game theory classic *Winning Ways.* He has been an editor of the "Problems" section of the *American Mathematical Monthly* since 1971.

H

Haberdasher's puzzle

The greatest mathematical discovery of Henry **Dudeney**, it was first published in the *Weekly Dispatch in* 1902 and then as problem no. 26 in his *The Canterbury Puzzles* (1907).[87] One must decide how to cut an equilateral triangle into four pieces that can be rearranged to make a square. The accompanying diagram shows the solution, which Dudeney describes as follows:

> Bisect AB in D and BC in E; produce the line AE to F making EF equal to EB; bisect AF in G and describe arc AHF; produce EB to H, and EH is the length of the side of the required square; from E with distance EH, describe the arc HJ, and make JK equal to BE; now from the points D and K drop perpendiculars on EJ at L and M.

A remarkable feature of the solution is that each of the pieces can be hinged at one vertex, forming a chain that can be folded into the square or the original triangle. Two of the hinges bisect sides of the triangle, while the third hinge and the corner of the large piece on the base cut the base in the approximate ratio 0.982:2:1.018. Dudeney showed just such a model of the solution, made of polished mahogany with brass hinges, at a meeting of the Royal Society on May 17, 1905.

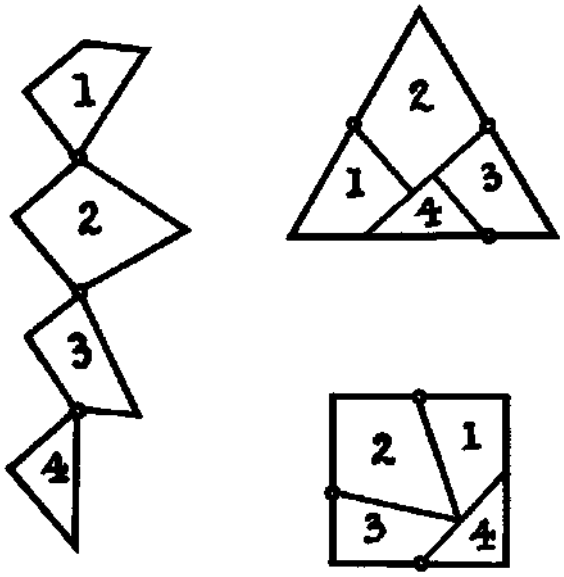

Haberdasher's puzzle The puzzle and its solution as illustrated by Henry Dudeney.

Hadwiger problem

In d dimensions, define $L(d)$ to be the largest integer n for which a cube cannot be cut into n cubes (not necessarily different). The Hadwiger problem is to find $L(d)$. Definite solutions are only known in two and three dimensions: $L(2) = 5$ and $L(3) = 47$. However, it is known that $L(4) \leq 853$ and $L(5) \leq 1{,}890$, and it is considered likely that $L(d)$ is odd for all values of d. See also **dissection**.

hailstone sequence

A sequence of numbers produced by the rules of the **Collatz problem**; in other words, a sequence formed in the following way: Start with any positive integer n. (1) If n is even, divide it by 2; if n is odd, multiply it by 3 and add 1. (2) If the result is not 1, repeat step (1) with the new number. For $n = 5$, this produces the sequence 5, 16, 8, 4, 2, 1, 4, 2, 1, ... For $n = 11$, the resulting sequence is 11, 34, 17, 52, 26, 13, 40, 20, 10, 5, 16, 8, 4, 2, 1, 4, 2, 1, ... The name "hailstone" comes from the fact that the numbers in these sequences rise and fall like hailstones in a cloud before finally falling to Earth. It seems from experiment that such a sequence will always eventually end in the repeating cycle 4, 2, 1, 4, 2, 1, . . . , but some values for n generate many values before the repeating cycle begins. An unsolved mystery is whether all such sequences eventually hit 1 (and then 4, 2, 1, 4, 2, 1, . . .) or whether there are some sequences that never settle down to a repeating cycle.

hairy ball theorem

If a sphere is covered with hair or fur, like a tennis ball, the hair cannot be brushed so that it lies flat at every point. In mathematical terms: any continuous tangent vector field on the sphere must have a point where the vector is zero. This theorem also means that somewhere on Earth's surface there has to be a point where the horizontal wind speed is zero, even if it's windy everywhere else. Does the same apply to a **torus**? Is there a hairy donut theorem? No! The number of "problem points," where the hair would stick up on a surface, is related to a quantity called the **Euler characteristic** of that surface. Basically, every

point on a surface has an index that describes how many times the vector field rotates in a neighborhood of the problem point. The sum of the indices of all the vector fields is the Euler characteristic. Since the torus has Euler number 0, it is possible to have a covering of hair–a vector field–on it that lies flat at every point.

half-line
A **ray**.

half-plane
The part of a **plane** that lies on one side of a given line.

halting problem
Given a program and inputs for it, decide whether it will run forever or will eventually stop. This is not the same thing as actually running a given program and seeing what happens. The halting problem asks whether there is any *general prescription* for deciding how long to run an arbitrary program so that its halting or non-halting will be revealed. In a celebrated 1936 paper,[337] Alan **Turing** proved that the halting problem is undecidable: there's no way to construct an **algorithm** that is *always* able to determine whether another algorithm halts or not. From this it follows that there can't be an algorithm that decides whether a given statement about **natural number**s is true or not. The undecidability of the halting problem provides an alternative proof of **Gödel's incompleteness theorem**. This is because if there were a complete and consistent axiomatization of all true statements about natural numbers, then we would be able to create a set of rules that decides whether such a statement is true or not. Another amazing consequence of the undecidability of the halting problem is *Rice's theorem,* which states that the truth of *any* nontrivial statement about the **function** that is defined by an algorithm is undecidable. So, for example, the decision problem "will this algorithm halt for the empty string" is already undecidable. Note that this theorem holds for the *function defined by the algorithm* and not the algorithm itself. It is, for example, quite possible to decide if an algorithm will halt within 100 steps, but this isn't a statement about the function that is defined by the algorithm. Many problems can be shown to be undecidable by reducing them to the halting problem. However, Gregory **Chaitin** has given an undecidable problem in algorithmic information theory that doesn't depend on the halting problem.

While Turing's proof shows that there can be no general method or algorithm to determine whether algorithms halt, individual instances of that problem may very well be susceptible to attack. Given a specific algorithm, one can often show that it must halt, and in fact computer scientists often do just that as part of a correctness proof. But every such proof requires new arguments: there is no *mechanical, general way* to determine whether algorithms halt. And there's another caveat. The undecidability of the halting problem relies on the fact that computers are assumed to have a memory of potentially infinite size. If the memory and external storage of a machine is limited, as it is for any real computer, then the halting problem for programs running on that machine can be solved with a general algorithm (albeit an extremely inefficient one).

ham sandwich theorem
Given a sandwich in which bread, ham, and cheese (three finite volumes) are mixed up, in any way at all, there is always a flat slice of a knife (a plane) that bisects each of the ham, bread, and cheese. In other words, however messed up the sandwich–even if it's been in a blender–you can always slice through it in such a way that the two halves have exactly equal amounts, by volume, of the three ingredients. This theorem generalizes to higher-dimensional ham sandwiches, when it essentially becomes the **Borsuk-Ulam theorem**: in n-dimensional space in which there are n globs of positive volume, there is always a hyperplane that cuts all the globs exactly in half.

Hamilton, William Rowan (1805–1865)
An Irish mathematician who, among other things, invented **quaternions** and a new theory of dynamics. Having excelled in Greek and mathematical physics at Trinity College, Cambridge, Hamilton was appointed Astronomer Royal of Ireland; in this position he served from 1827 to his death and, during all that time, lived in Dunsink Observatory, Dunsink Lane, to the northwest of Dublin. However, he quickly lost interest in staying up at nights to make observations–he hired three of his sisters to help run the place–and preferred instead to write poetry (badly). He was friends with Samuel Coleridge, who introduced him to the philosophy of Kant, which had a great influence on him, and with William Wordsworth, who advised him against writing any more poems.

Hamilton did early work on **caustic** curves and was led from this to his discovery of the *law of least action,* which enabled many physical problems to be expressed more elegantly. One of his greatest triumphs was his treatment of **complex number**s as pairs of real numbers, an approach that finally exorcised long-standing suspicions about the reality of **imaginary number**s, and helped clear the way for other algebras. From this he was led to consider ordered quartets of numbers, which he called quaternions. The idea for quaternions came to Hamilton suddenly on October 16, 1843, while he was standing on Brougham ("Broom") Bridge, where Broombridge Street crosses the Royal Canal, Dublin. A commemorative plaque under the bridge, on the towpath, was unveiled by the Taoiseach

(head of the Irish parliament), Eamon De Valera, on November 13, 1958. Of his invention, Hamilton wrote:

> The quaternion was born, as a curious offspring of a quaternion of parents, say of geometry, algebra, metaphysics, and poetry. . . . I have never been able to give a clearer statement of their nature and their aim than I have done in two lines of a sonnet addressed to Sir John Herschel:
>
> "And how the One of Time, of Space the Three
> Might in the Chain of Symbols girdled be."

Hamilton's interest in complex numbers was stimulated by his friend and compatriot John Graves, who pointed Hamilton in the direction of John Warren's *A Treatise on the Geometrical Representation of the Square Root of Negative Quantities.* This book explained the concept of the complex plane, which Hamilton turned from geometry into algebra. One of Hamilton's last inventions was a curiosity called the *icosian calculus,* which was another outcome of his friendship with Graves. After a visit to the latter's house, Hamilton wrote: "Conceive me shut up and revelling for a fortnight in John Graves' Paradise of Books! of which he has really an astonishingly extensive collection, especially in the curious and mathematical kinds. Such new works from the Continent he has picked up! and such rare old ones too!" Graves posed some puzzles to Hamilton, and either Graves or his books got Hamilton to thinking about regular polyhedra. When Hamilton returned to Dublin he thought about the symmetry group of the **icosahedron**, and used it to invent an algebra he called the "icosians" and also a game called the **Icosian game**. The only complete example of this game, inscribed to Graves, is now in the keeping of the Royal Irish Academy, of which Hamilton was the president from 1837 to 1847. (In early 1996, a second example of the Icosian game came to light but only included the board.)

In some ways, Hamilton was too far ahead of his time. The operator now referred to as the *Hamiltonian* and the so-called *Hamilton-Jacobi equation* that relates waves and particles only became important when **quantum mechanics** came along, and Felix **Klein** introduced Wernher Schrödinger, the father of wave mechanics, to Hamilton's work.

Hamilton's personal life was not always happy. He fell deeply in love with a woman named Catherine Disney, who was forced by her parents to marry a wealthy man 15 years older than her. Hamilton remained hopelessly in love with her the rest of his life, though he eventually married someone else. He became an alcoholic, then foreswore drink, then relapsed. Many years after their early romance, Catherine began a secret correspondence with Hamilton. Her husband became suspicious, and she attempted suicide by taking laudanum. Five years later, she became seriously ill. Hamilton visited her and gave her a copy of his *Lectures on Quaternions.* They kissed at last, and she died two weeks later. He carried her picture with him ever afterward and talked about her to anyone who would listen.[149]

Hamilton circuit

A **Hamilton path** that starts and ends at the same vertex. See also **traveling salesman problem**.

Hamilton path

Named after William **Hamilton**, a path that traverses every vertex of a **connected graph** once and only once. The problem of the **knight's tour** is equivalent to finding a Hamilton path (or, in the case of a reentrant tour, a **Hamilton circuit**) that corresponds to the legal moves of the knight. Compare with **Euler path**.

Hankel matrix

A **matrix** in which all the elements are the same along any **diagonal** that slopes from northeast to southwest.

happy number

If you iterate the process of summing the squares of the decimal digits of a number and if this process terminates in 1, then the original number is called a happy number. For example $7 \rightarrow (7^2)\ 49 \rightarrow (4^2 + 9^2)\ 97 \rightarrow (9^2 + 7^2)\ 130 \rightarrow (1^2 + 3^2)\ 10 \rightarrow 1$. See also **amicable number**.

Hardy, Godfrey Harold (1877–1947)

One of the most prominent English mathematicians of the twentieth century; his legendary collaboration with John Littlewood lasted 35 years and produced nearly 100 papers. Hardy was a precocious child, whose tricks included factorizing hymn numbers during sermons. In 1919, he became Savilian Professor of Geometry at Oxford but returned to Cambridge in 1931 as professor of pure mathematics. His work was mainly in **analysis** and **number theory**.

Hardy had only one other passion in his life–the game of cricket. His daily routine would begin with reading *The Times* and studying the cricket scores over breakfast. Then he would do mathematical research from 9 o'clock till 1 o'clock. After a light lunch, he would walk down to the university cricket ground to watch a game. In the late afternoon he would walk slowly back to his rooms at the college, and take dinner followed by a glass of wine. Hardy was known for his eccentricities. He couldn't stand having his photo taken and only five snapshots of him are known to exist. He also hated mirrors and his first action on entering any hotel room was to cover any mirror with a towel.

Hardy's book *A Mathematician's Apology* (1940)[151] is one of the most vivid descriptions of how a mathematician thinks and the pleasure of mathematics. But the book is more, as C. P. Snow writes:

> *A Mathematician's Apology* is . . . a book of haunting sadness. Yes, it is witty and sharp with intellectual high spirits: yes, the crystalline clarity and candor are still there: yes, it is the testament of a creative artist. But it is also, in an understated stoical fashion, a passionate lament for creative powers that used to be and that will never come again. I know nothing like it in the language: partly because most people with the literary gift to express such a lament don't come to feel it: it is very rare for a writer to realise, with the finality of truth, that he is absolutely finished.

See also **Ramanujan**.

harmonic analysis

The method of expressing **periodic** functions as sums of sines and cosines.

harmonic division

The division of a line segment by two points such that it is divided externally and internally in the same ratio.

harmonic mean

The harmonic mean of two numbers a and b is $2ab/(a+b)$.

harmonic sequence

The sequence: 1, $\frac{1}{2}$, $\frac{1}{3}$, $\frac{1}{4}$, $\frac{1}{5}$ . . . . Added together, these become the terms of the *harmonic series:* $1 + \frac{1}{2} + \frac{1}{3} + \frac{1}{4} + \frac{1}{5} + \ldots$. This series diverges (has no finite sum), though very slowly–a result first proved by the French philosopher and theologian, Nichole d' Oresme (c. 1325–1382). In fact, it still diverges if you take away every other term, and even if you take away nine out of every ten terms. However, if you take the sum of reciprocals of all natural numbers that do not contain the number nine (when written in decimal expansion) the series converges! To show this, group the terms based on the number of digits in their denominator. There are eight terms in $(\frac{1}{1} + \ldots + \frac{1}{8})$, each of which is no larger than 1. Consider the next group $(\frac{1}{10} + \ldots + \frac{1}{88})$. The number of terms is *at most* the number of ways to choose two ordered digits out of the digits 0 . . . 8, and each such term is clearly no larger than $\frac{1}{10}$. So this group's sum is no larger than $9^2/10$. Similarly, the sum of the terms in $(\frac{1}{100} + \ldots + \frac{1}{999})$ is at most $9^3/10^2$, etc. So the entire sum is no larger than

$$9 \times 1 + 9 \times (\tfrac{9}{10}) + 9 \times (9^2/10^2) + \ldots + 9 \times (9^n/10^n) + \ldots$$

This is a geometric series that converges. Thus by the comparison test, the original sum (which is smaller term-by-term) must converge.

Harshad number

A number that is divisible by the sum of its own digits; also known as a Niven number. For example, 1,729 is a Harshad number because $1 + 7 + 2 + 9 = 19$ and $1{,}729 = 19 \times 91$. A *Harshad amicable pair* is an amicable pair (m, n) such that both m and n are Harshad numbers (see **amicable numbers**). For example, 2,620 and 2,924 are a Harshad amicable pair because 2,620 is divisible by $2 + 6 + 2 + 0 = 10$ and 2,924 is divisible by $2 + 9 + 2 + 4 = 17$ ($2{,}924/17 = 172$). There are 192 Harshad amicable pairs in the first 5,000 amicable pairs.

hat problem

A team of three contestants, Alice, Bob, and Cedric, enter a room and a hat is placed on each one's head so that he or she can't see it. The color of each hat is based on a coin toss–blue (B) for heads, red (R) for tails. After all the contestants enter the room, they look at the colors of one anothers' hats and, based on this information, they guess the color of their own hat. Each can guess red or blue, or, if she can't make up her mind, she can pass. No communication is allowed during the competition, but the players are allowed to agree on a strategy before play begins. The team wins if at least one of them guesses correctly, and none of them guesses incorrectly. What is the team's best strategy? At first sight, it may seem as if no effective strategy is possible beyond each contestant guessing his or her own hat color. In fact, this is the very worst approach since, to succeed, it requires that everyone guess correctly and the probability of this is only $\frac{1}{2} \times \frac{1}{2} \times \frac{1}{2} = \frac{1}{8}$. A far better plan is for the contestants to agree that two of them will pass while the third takes a stab at the color of his own hat. Then the odds improve to one in two. Beyond this it's hard to see any way that the probability of success could be increased. Yet there is an even better strategy. The key is to realize that there are only two cases (RRR and BBB) where everyone's hat is the same color but *six* cases where two hats are the same color and the other hat is a different color (RRB, RBR, BRR, BBR, BRB, and RBB). This suggests the following strategy for members of the team: *if you see two hats of opposite colors, pass. If you see two hats of one color, guess that your hat is the other color.* If everyone's hat is the same color, all players on the team will guess wrong and the team will lose. But the chance of this happening is only $\frac{2}{8}$ ($= \frac{1}{4}$). In every other possible case, the odd person out will guess correctly and their teammates will pass, so the team will win. This strategy wins $\frac{6}{8}$ ($= \frac{3}{4}$) of the time, and can't be improved upon. Since half of each player's guesses will be wrong, it's impossible to do better than a strategy in which each player in turn guesses correctly alone three times out of four, and the fourth time all guess wrong.

What if there are more players in the team? Say the number of players is n. By the reasoning described previously, it's clear that the team can't hope to win more than $n/(n + 1)$ of the time. Yet it isn't obvious that it can do this well. Having more people, it seems, might make it harder for them to synchronize their wrong guesses. However, it turns out that, if the number of people in the team is *one less than a power of 2,* this best-possible value can be achieved. For example, with a team of 7, the team can win $^7/_8$ of the time, and with a team of 15, they can win $^{15}/_{16}$ of the time. The strategy involved is complicated but is closely linked to *Hamming codes* (see **coding theory**), which are a method of encoding and transmitting information so that even if a small number of errors occur during transmission, the original information can be entirely recovered. For teams of other sizes, such as 9, 10, or 13, mathematicians have yet to find an optimal strategy or establish what proportion of the time the team can be expected to win.

Hausdorff, Felix (1868–1942)

A German mathematician who is considered to be one of the founders of modern **topology** and who also did significant work in **set theory** and functional analysis. Among several concepts named after him is the **Hausdorff dimension**, which gives a way of assigning a fractional dimension to a curve or shape. Hausdorff also published philosophical and literary works under the pseudonym "Paul Mongré." He studied at Leipzig and taught mathematics there until 1910, when he became professor of mathematics at Bonn. When the Nazis came to power, Hausdorff, a Jew, felt that as a respected university professor he would be safe from persecution. However, his abstract mathematics was denounced as useless and "un-German" and he lost his position in 1935. He sent his daughter to Britain but stayed with his wife in Germany. In 1942, when he could no longer avoid being sent to a concentration camp, he committed suicide together with his wife and sister-in-law.

Hausdorff dimension

A way to accurately measure the **dimension** of complicated **set**s such as **fractal**s. The Hausdorff dimension, named after Felix **Hausdorff**, coincides with the more familiar notion of dimension in the case of well-behaved sets. For example, a straight line or an ordinary curve, such as a circle, has a Hausdorff dimension of 1; any **countable set** has a Hausdorff dimension of 0; and an n-dimensional **Euclidean space** has a Hausdorff dimension of n. But a Hausdorff dimension is not always a natural number. Think about a line that twists in such a complicated way that it starts to fill up the plane. Its Hausdorff dimension increases beyond 1 and takes on values that get closer and closer to 2. The same idea of ascribing a fractional dimension applies to a plane that contorts more and more in the third dimension: its Hausdorff dimension gets closer and closer to 3. As a specific example, the fractal known as the **Sierpinski carpet** has a Hausdorff dimension of just over 1.89.

Heesch number

The maximum number of times that a closed plane figure—a tile—can be completely surrounded by copies of itself. The Heesch number of a triangle, quadrilateral, regular hexagon, or any other single shape that can completely tile the plane (see **tiling**), is infinity. *Heesch's problem* is to find the largest possible *finite* Heesch number, or, more generally, what values other than zero and infinity can Heesch numbers take. In considering this problem, it's helpful to define the Heesch number more precisely. In a tiling, the *first corona* of a tile is the set of all tiles that have a common boundary point with the tile, including the original tile itself. The *second corona* is the set of tiles that share a point with anything in the first corona; and so on. The Heesch number is the maximum value of coronas (k) that can surround a shape. For a long time the record holder for the largest finite value of k was a shape found by the American computer scientist

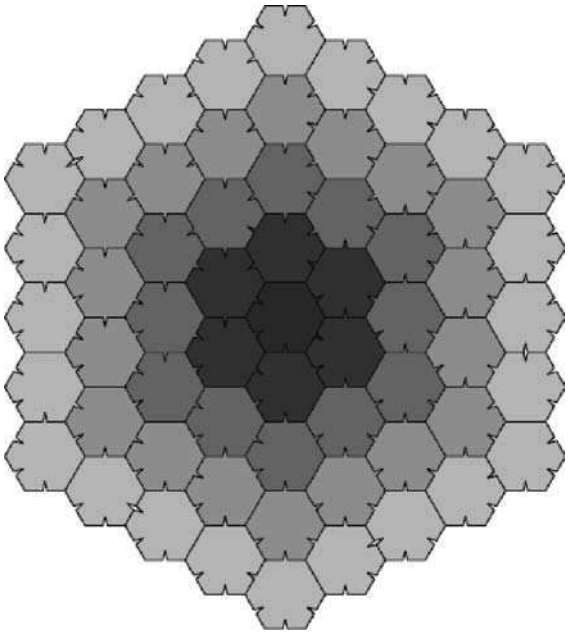

Heesch number A tiling in which copies of the same shape are used out to the fourth surrounding layer, or corona. *David Eppstein*

Robert Ammann, which consists of a regular hexagon with small bumps on two sides and matching notches on three sides. This was thought to have a Heesch number of three; however, in 2000, Alex Day argued that the Ammann hexagon actually has a Heesch number of four, though it isn't clear whether the difference has to do with a definition of tiling. In any event, it has since been shown by Casey Mann, of the University of Arkansas that there exists an infinite family of tiles (consisting of indented and outdented pentahex) with Heesch number five (or six by Day's reckoning)–the largest finite value currently known. Are there any polygons that have higher Heesch numbers? The answer is unknown but Mann thinks that more rounded **polyomino**s than the long skinny ones he's been using may have a better chance of giving unbounded Heesch numbers.

The Heesch number question is connected to two other famous unsolved tiling problems: the **domino problem** and the **Einstein problem**. Aperiodic tiling seems to act as a barrier to the existence of tiling algorithms, so it isn't expected that both of these problems have the same answer. On the other hand, if there's a maximum finite Heesch number *k,* then it seems that this could be used as the basis of an algorithm to test whether a shape tiles: simply attempt to fill out a tiling to the $(k + 1)$st corona; if successful, the shape must tile the plane, and if not, the shape will not tile. Similar questions can be asked about Heesch numbers for tilings in higher dimensions.

Hein, Piet (1905-1996)

An extraordinarily creative Danish mathematician, scientist, inventor, and poet who often wrote under the Old Norse pseudonym Kumbel, meaning "tombstone." A direct descendant of the Dutch naval hero of the sixteenth century who had the same name, Piet Hein was born in Copenhagen and studied at the Institute for Theoretical Physics of the University of Copenhagen (later the Niels Bohr Institute), the Technical University of Denmark, and the Royal Swedish Academy of Fine Art. He was later awarded an honorary doctorate by Yale University. A good friend of Albert Einstein, he is famed for his many mathematical games, including **Hex**, **Tangloids**, Polytaire, **TacTix**, and the **Soma cube**. These games were featured in numerous columns of Martin **Gardner**'s "Mathematical Recreations" column in *Scientific American* and often achieved worldwide attention in this way. As an artist and constructor, Hein gave form, in the 1950s and 1960s, to elegant pieces of furniture that helped "Scandinavian design" attract international recognition. These pieces, including a dining-room table created in cooperation with the Swedish designer Bruno Mathsson, were based on the **superellipse** curve–a shape that Hein also brought to bear in applications as varied as city planning (it's the basis for Sergel's Square in the center of Stockholm) and toy making (see **superegg**). Hein was a prolific and excellent writer of light verse, producing thousands of short, aphoristic poems known as Grooks. For him there was no unbridgeable gap between the subjectivity of fine art and the objective world of science. "Art," he said, "is a solution to problems which cannot be formulated clearly before they have been solved." His philosophy of life was summed up by his aphorism "co-existence or no existence."

helicoid

The second oldest known **minimal surface**; it was discovered by Jean-Baptiste Meusnier in 1776, thirty years after the **catenoid**. It is the only minimal surface, apart from the simple plane, that is also a **ruled surface**. The helicoid is the surface swept out by a line that always intersects a fixed axis at right angles and that rotates uniformly as its point of intersection moves uniformly along the axis. This line intersects any cylinder concentric with the axis in a **helix**. The helicoid has a wide variety of shapes and is a familiar sight in everyday life, taking the form of many things from spiraling parking ramps to screw threads.

helix

A curve in three dimensions, the tangent to which makes a constant angle with a fixed line. A *circular helix* is formed by winding a line around a **cylinder** so the radius is always the same. A *conical helix* is formed by winding a line around a **cone**, so that, consequently, its radius constantly changes. Springs often take the form of various kinds of helices. In nature, the DNA molecule is in the shape of a double helix.

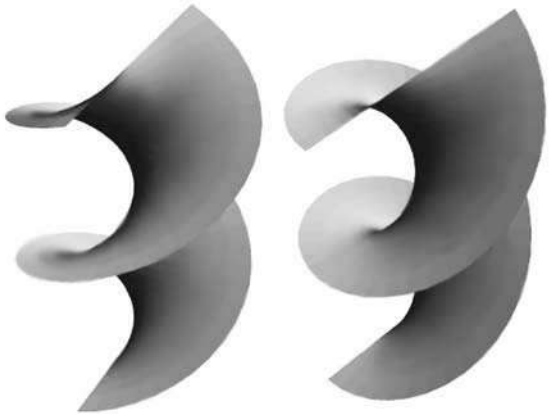

helicoid *Richard Palais*

Henon, Michele

An astronomer at the Nice Observatory in southern France. For a number of years, particularly during the 1960s, he studied the dynamics of stars moving within galaxies, using computers as a way to understand the stability of their motions. His work was very much in the spirit of Henri **Poincaré**'s approach to the classical **three-body problem**: What important geometric structures govern their behavior? The main property of these systems is that the energy of their motion is constant to a very good approximation. Consequently, their chaotic dynamics are not described by **simple attractor**s, but by objects that are markedly more difficult to analyze and visualize, existing on energy "surfaces" in three and higher dimensions. During the 1970s, Henon discovered a very simple iterated mapping that showed a **chaotic attractor**, now called *Henon's attractor,* that allowed him to make a direct connection between deterministic data and **fractal**s. The Henon attractor is self-similar (see **self-similarity**): if you zoom in on the attractor in its state space you find more and more layers, much like filo dough or a croissant.

Henstock integration

See **integration**.

heptagon

A **polygon** with 7 sides.

Hermann grid illusion

An illusion first described by the German physiologist Ludimar Hermann (1838–1914) in 1870. While reading a book on sound by the Irish physicist John Tyndall, Hermann saw gray spots in the intersections of spaces among the figures that Tyndall had arranged in a matrix. Despite the fact that the same intensity of light is reflected all the way along the white spaces in the Hermann Grid, the intersections appear gray. To explain this, consider two regions of the retina. One region views an intersection of a white horizontal and vertical band, while the other views a white band between two intersections (the region going away from the intersection). Although the two regions themselves receive the same amount of light, the situation in their neighboring regions is different. At the intersection, light comes in from all four sides, but the white band that lies between the two intersections is surrounded by two dark sides. This leads to an effect called *lateral inhibition,* which causes a bright surround to an area appear darker and, conversely, a dark surround to an area appear lighter. A similar but more powerful illusion, known as the *Lingelbach illusion* or the *Scintillating grid illusion,* was discovered in 1994 by Elke Lingelbach, the wife of a German mathematics professor, and has not

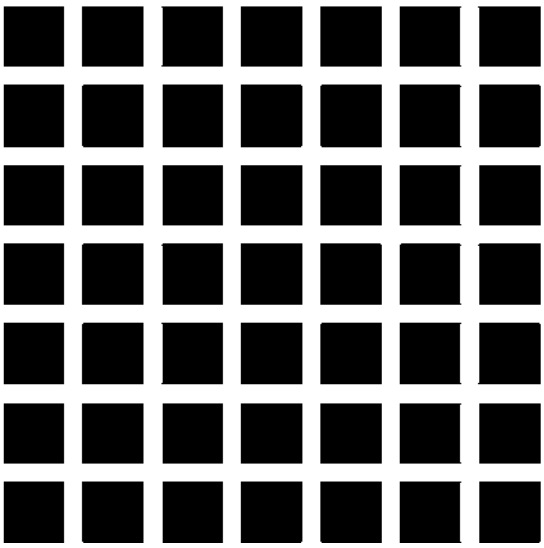

Hermann grid illusion The original illusion, in which the viewer sees gray spots at the intersections.

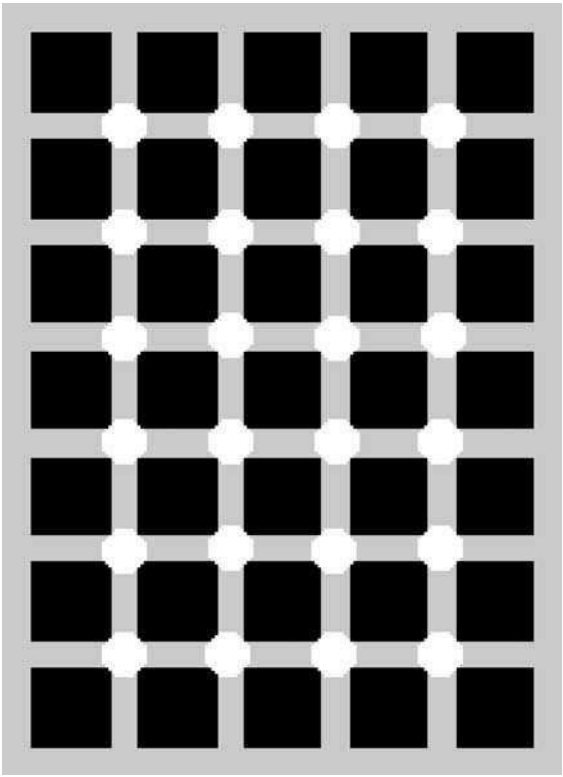

Hermann grid illusion The more striking and recently discovered "scintillating" version of the illusion.

yet been fully explained.[286] Curiously, the effect of the scintillation is lessened by tilting the head through 45°!

Hermite, Charles (1822–1901)

A French mathematician whose work in the theory of functions includes the application of **elliptic function**s to provide the first solution to the general equation of the fifth degree, the **quintic** equation. He also showed that e is a **transcendental number**, studied a class of **differential equation**s now known as *Hermite polynomials,* which later proved to be of importance in some applications of quantum mechanics, and discovered the properties of *Hermitian matrices.*

Heron of Alexandria (c. A.D. 60)

Also called *Hero,* a Greek geometer and inventor whose writings have helped preserve a knowledge of the mathematics and engineering of Babylonia, ancient Egypt, and the Greco-Roman world. His most important geometric work, *Metrica,* was lost until a fragment was discovered in 1894, followed by a complete copy in 1896. It is a compendium, in three books, of geometric rules and formulas, the best known of which is Proposition 1.8, now known as **Heron's formula**. He invented many devices operated by water, steam, or compressed air, including a fountain, a fire engine, siphons, and an engine in which the recoil of steam revolves a ball or a wheel.

Heron's formula

An important formula in plane geometry that allows the area of any triangle to be calculated without knowing the altitude (perpendicular height) of any of its sides. Let a, b, and c be the side lengths of a triangle and A its area. Heron's formula states that

$$A^2 = s(s-a)(s-b)(s-c),$$

where $s = (a+b+c)/2$. The origin of this formula is historically obscure. A medieval Arab source, for example, ascribes it to **Archimedes**. However, the first definite reference we have to it is by **Heron of Alexandria**. His proof is extremely convoluted, and it seems clear that it must have been determined by an entirely different thought process, and then dressed up in the usual synthetic form that the classical Greeks preferred for their presentations. Heron's formula contains **Pythagoras's theorem** as a degenerate case. A *Heronian triangle* is one with integer sides and integer area.

Herring illusion

A **distortion illusion** first published in 1861 by the German psychologist Ewald Herring (1834–1918), and now named after him. As in the case of the **Zöllner illusion** and others, it shows how geometrical relationships can

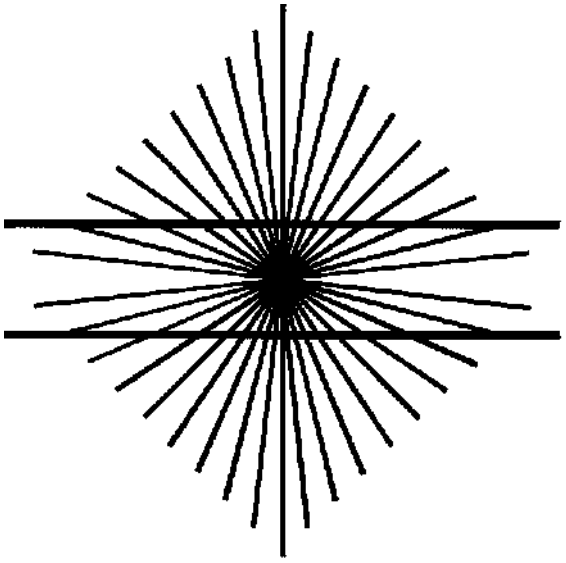

Herring illusion

seem to be distorted by their background (a lined background can make circles, squares, and triangles seem distorted, too). The straight horizontal lines in the illusion appear to bow out in the center. This can be explained if the brain interprets the radiating lines in terms of depth, making the central spot in the Herring diagram, and thus also the heavy black lines near the center of the diagram, appear to be farther away than the edges. Because the heavy black lines are the same thickness at the center as at the edges but are assumed to be farther away, the brain thinks they must be more widely spaced at the center.

heuristic argument

An educated guess: something that helps in finding the solution to a problem but is otherwise unjustified or incapable of justification.

Hex

A board game played by two players on a hexagonal grid, usually in the shape of an 11×11 rhombus. It was invented by Piet **Hein** in 1942 and independently by John **Nash** in 1948. Hein said that the game occurred to him while contemplating the **four-color problem** and it soon became popular in Denmark under the name *Polygon.* Nash's version was played by math students at Princeton and a number of other American campuses. Players use differently colored pieces–say, red and blue. They take alternate turns placing a piece of their color inside a hexagon, filling in that hexagon with their color. Red's goal is

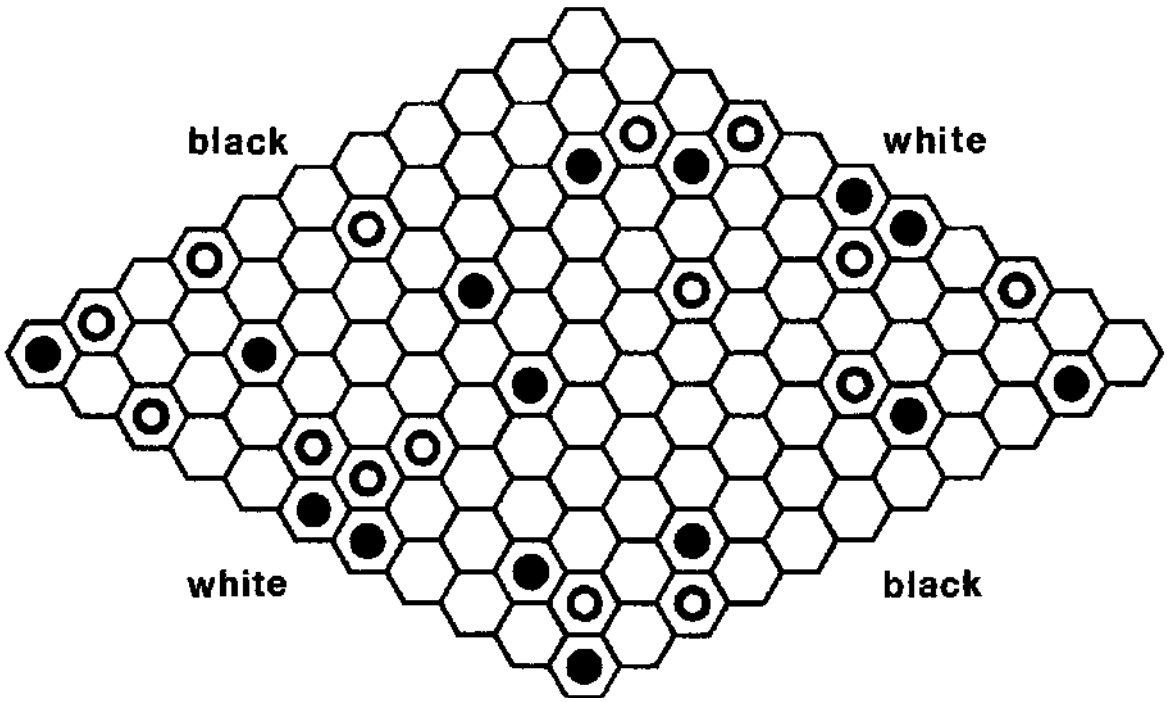

Hex A position in a game of Hex.

to form a red path connecting the top and bottom sides of the parallelogram; Blue's goal is to form a path connecting the left and right sides. The game can never end in a tie, a fact found by Nash. The only way to prevent your opponent from forming a connecting path is to form a path yourself. When the sides of the grid are equal, the game favors the first player and the first player has a winning strategy. There are two ways to make the game fairer. One is to make the second player's sides closer together, playing on a parallelogram rather than a rhombus; however, this has been proven to result in a win for the second player, so it theoretically doesn't improve matters. A better way is to allow the second player to choose his color after the first player makes the first move or to make the first three moves, which encourages the first player to intentionally even out the game.

hexa-

The Greek prefix meaning "six." A *hexagon* is a **six**-sided **polygon**. A *hexahedron* is a six-sided **polyhedron**, otherwise known as a **cube** if it is regular. *Hexadecimal* is the number system with **base** 16 (i.e., six more than the decimal system) and is used mostly in computing (because four binary digits can represent 16 different numbers). *Hexagonal numbers* are **figurate number**s (numbers that can be represented by a regular geometric arrangement of equally spaced points) of the form $n(2n - 1)$; the first few are 1, 6, 15, 28, 45, ... For *hexaflexagon* see **flexagon**. For *hexomino* see **polyomino**. See also **Giant's Causeway**.

higher dimensions

Dimensions beyond the familiar three spatial dimensions (up-down, left-right, back-forth) of which we are aware in every-day life. Intense speculation, both scientific and fictional, has naturally been directed toward the possibility of a **fourth dimension**. One way to think of points in four-dimensional space is as ordered sets of four numbers. Clearly, this algebraic representation can be extended to many arbitrary dimensions: n-dimensional space is defined as the set of the set of points $(a_1, a_2, \ldots, a_n)$ where a_1 to a_n can take any **real number** value. There has been much conjecture that the universe in which we live contains many more than three spatial dimensions. This speculation began with the **Kaluza-Klein theory** but is now firmly embedded in modern **string theory**.[25, 55, 81]

Hilbert, David (1862–1943)

> *One can measure the importance of a scientific work by the number of earlier publications rendered superfluous by it.*

A great German mathematician who was one of the colossi in the field in the twentieth century. His most important discovery was of what is now called **Hilbert space**. He was also a master of mathematical organization. During the early phase of his career, Hilbert reorganized **number theory**, crystallizing his conclusions in the classic book *Der Zahlbericht* (The theory of algebraic number fields, 1897). He then moved into geometry and performed a similar service by setting forth the first rigorous set of geometrical axioms in his *Grundlagen der Geometrie* (Foundations of geometry, 1899). He invented a simple **space-filling curve** now known as the *Hilbert curve* and also proved **Waring's conjecture**. At the Paris International Congress of 1900, Hilbert proposed 23 outstanding problems in mathematics to whose solutions he believed twentieth-century mathematicians should devote themselves. These problems have come to be known as *Hilbert's problems,* and a number still remain unsolved today. Hilbert's mathematical philosophy is partly re-vealed by a couple of remarks, one of which he made after learning that a student in his class had dropped the subject in order to become a poet. "Good," he said. "He did not have enough imagination to become a mathematician." Whether he really believed the second is open to question: "Mathematics is a game played according to certain simple rules with meaningless marks on paper."

Hilbert space

A space of infinite dimensions, named after David **Hilbert**, in which distance is preserved by making the sum of squares of coordinates a convergent sequence; it is of crucial importance in the mathematical formulation of **quantum mechanics**. See also **Fredholm, Erik Ivar**.

Hinton, Charles Howard (1853–1907)

An English-born mathematician best known for his writings and inventions aimed at helping to visualize the **fourth dimension**; he may also have coined the name ***tesseract*** for the four-dimensional analogue of a cube. Hinton matriculated at Oxford and continued to study there, earning a B.A. (1877) and an M.A. (1886), while he also taught, first at Cheltenham Ladies' School and then, from 1880 to 1886, at Uppingham School. At this time, another teacher at Uppingham was Howard Candler, who was a friend of Edwin **Abbott** and thus provides a possible link between these two explorers of other dimensions. In the early 1880s, Hinton published a series of pamphlets starting with "What Is the Fourth Dimension?" and "A Plane World" (a contemporary of Abbott's ***Flatland: A Romance of Many Dimensions***), which were reprinted in the two-volume *Scientific Romances* (1884). Hinton's descriptions owed much to the mathematical models of William **Clifford**, whose theories about four-dimensional spaces were then in vogue. But Hinton went much further in his attempts to break free of three-dimensional thought. He devised an elaborate set of small colored cubes to represent the various cross sections of a tesseract and then memorized the cubes and their many possible orientations in order to gain a window on the fourth dimension.

At the time he was teaching in England, Hinton married Mary Everest Boole, the eldest daughter of George **Boole**, the founder of mathematical logic. Regrettably, he also married a Maud Wheldon and was tried at the Old Bailey in London for bigamy. After serving a day in prison for the offence, he fled with his (first) family to Japan, where he taught for some years, before taking up a post at Princeton University. There, in 1897, he designed a species of baseball gun which, with the help of gunpowder charges, would shoot out balls at speeds of 40 to 70 miles per hour. It was used by the Princeton team for several seasons before being abandoned by the players in fear of their lives.

After a brief spell at the University of Minnesota, Hinton joined the Naval Observatory in Washington, D.C. At the same time, he more rigorously developed his ideas on the fourth dimension and presented his results before the Washington Philosophical Society in 1902. Hinton asked: What would prove the existence of a real fourth spatial dimension? He offered three possibilities, two of which involved a specific molecular structure and a particular case of electrical induction, and have since been explained by science in more mundane ways. However, Hinton's other case, pertaining to right- and left-handedness remains open because there are instances of right- and left-handedness in nature, such as the spin of elementary particles, to which his example could be applied. In any event, Hinton's final assessment that we can only regard a four-dimensional space as possible if three-dimensional mechanics fails to explain known physical phenomena still rings true today.[166, 167, 272] See also **Boole (Stott), Alicia**.

Hippias of Elis (c. 5th century B.C.)

An itinerant Greek philosopher who contributed significantly to mathematics by discovering the quadratrix, a special curve he may have used to trisect an angle (see **quadratrix of Hippias**). Hippias is one of the first mathematicians about whom a good deal is known. He came from a state in the northwest corner of Peloponnesia that

was the home of the Olympic games. According to Plato, Hippias boasted, during one of his visits to the Olympics, that everything he wore–his clothing, sandals, ring, and oil flask–he'd made himself. Later, in Athens, Hippias became one of the first to teach for money, a practice forbidden by the Pythagoreans and scorned by Plato. He and other paid teachers became known as "sophists," which was a derogatory term at the time but has since come to mean "wise man."

hippopede

A **quartic** curve described by the equation

$$(x^2 + y^2)^2 + 4b(b - a)(x^2 + y^2) - 4b^2x^2 = 0,$$

where a and b are positive constants. Hippopede means "foot of a horse." It is often known as the *hippopede of Proclus,* after **Proclus** who was the first to study it (together with **Eudoxus**, who used it in his theory of how the planets move), and also the *horse fetter* and the *curve of Booth* because of work done on it by J. Booth (1810–1878). Any hippopede is the intersection of a **torus** (donut) with one of its **tangent** planes–that is, a plane parallel to its axis of rotational symmetry. The curve takes any of a variety of forms depending on where the donut is sliced. It may be a simple oval; an indented oval or *elliptical lemniscate of Booth* ($0 < b < a$); two isolated circles; a figure-eight curve or **lemniscate of Bernoulli** (the only hippopede that is also a **Cassinian oval**); or a *hyperbolic lemniscate of Booth* ($0 < a < b$).

Hi-Q

See **peg solitaire**.

Hnefa-Tafl

The Viking equivalent of chess and a particular form of a **Tafl game**. It effectively models the kind of internal conflict familiar to the Vikings and recounted in *Njal's Saga,* the best known of the Icelandic sagas. The king or chieftain sits in his hall, surrounded by his thanes. His enemies gather in secret, and in numbers sufficient to overwhelm the king's standing forces in a lightning raid. They gather around the king's hall and set it alight, forcing the defenders to fight in the open or burn in the hall. If the king can, by some desperate stratagem, break free and escape the trap, he can rally his people and strike back at his enemies. If not, he dies. Hnefa-Tafl reflects this mode of contest. The board has 19×19 grid lines (though sometimes has as few as 7×7 grid lines), and the pieces are placed at the points of the intersections (curiously analogous to the oriental game of **Go**, which also uses 19×19 lines and where play occurs at the intersections). The opposing forces are unequal in size, and have different objectives: the attackers attempt to trap the king in his hall, while the defenders try to open an escape route for him.

Hoffmann, Louis "Professor" (1839–1919)

The pseudonym of Angelo John Lewis, an English barrister who was the leading writer on magic, cards, and "parlor amusements" at the turn of the twentieth century. His *Puzzles Old and New*[171] (1893) is a major source of information about mathematical recreations.

Hofstadter, Douglas R. (1945–)

A physicist and philosopher best known for his 1980 Pulitzer Prize–winning book *Gödel, Escher, Bach: An Eternal Golden Braid*.[172] He is currently a professor of cognitive science and computer science at Indiana University, Bloomington, and has particular interests in themes of the mind, consciousness, self-reference, translation, and mathematical games. He is the son of the Nobel Prize–winning physicist Robert Hofstadter.

Hofstadter's law

It always takes longer than you think, even when you take Hofstadter's law into account.

Hogben, Lancelot Thomas (1895–1975)

An English zoologist and geneticist famed for his best-selling *Mathematics for the Million* (1933)[173] of which Albert Einstein said, "It makes alive the contents of the elements of mathematics" and H. G. Wells said, "A great book, a book of first class importance." Hogben was born in Southsea, Hampshire, and studied at Cambridge and London. Imprisoned in 1916 as a conscientious objector during World War I, he was released only when his health went into serious decline. He held various academic posts in Britain, Canada, and South Africa, becoming professor of social biology at London University in 1930. During World War II he was put in charge of the medical statistics records for the British Army. After the war he became professor of medical statistics at the University of Birmingham, where he remained until his retirement in 1961. Hogben first began to apply mathematical principles to the study of genetics in the 1930s, focusing on the study of generations of the fruit fly *Drosophila* and how it related to research on heredity in humans. In addition to *Mathematics for the Million,* he authored half a dozen other books, including the popular *Science for the Citizen.* Though trained as a scientist, Hogben was passionately interested in linguistics. In *The Loom of Language,* which he edited, he set out the principles of his own invented language, "Interglossa," based on Greek and Latin roots but with a syntax resembling that of Chinese.

hole

A topological structure (see **topology**) that prevents any object in which it occurs from being continuously shrunk to a point. A **sphere** has no holes; a **torus** and a teacup each have one hole. See also **genus**.

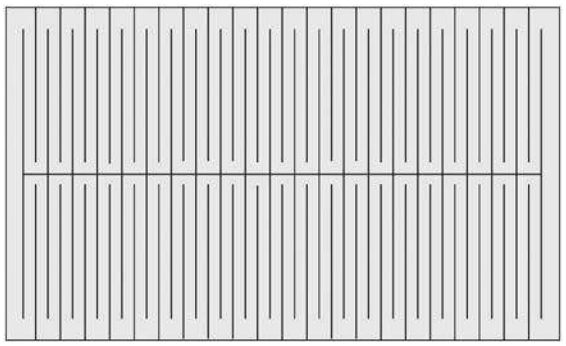

hole-in-a-postcard problem Photocopy the diagram, cut along the lines, and step through the postcard!

hole-in-a-postcard problem

With a pair of scissors, make cuts in a regular-sized postcard to create a hole large enough for a person to step through it. The solution is shown in the diagram. The number of lines determines the size of the resulting aperture. With enough cuts you could literally drive a horse and cart through the card!

hole-through-a-sphere problem

A number of **geometry puzzles** hinge on a surprising fact about spheres that have had holes bored through them. Imagine you have a round bead that is 1 inch (about 2.5 cm) in diameter and that you drill a hole exactly through the middle of this so that the remaining part of the sphere is only half an inch thick. Now imagine that an enormously large drill has been used to bore a hole though Earth so large that the part of Earth that is left behind is only half an inch thick. Amazingly, the residual volumes of these two holey spheres, the drilled bead and the drilled Earth, are exactly the same! It just happens that even though Earth is vastly larger than the bead, the drill has to take out proportionately more in order to make the thickness of the hole the same, so that the volume left doesn't depend separately on the initial size of the sphere or of the hole, but only on their *relation*, which is forced by requiring the hole to be half an inch long. This fact enables the following poem-problem to have a solution even though its seems as if not enough information has been provided:

Old Boniface he took his cheer,
Then he bored a hole through a solid sphere,
Clear through the center, straight and strong,
And the hole was just six inches long.
Now tell me, when the end was gained,
What volume in the sphere remained?
Sounds like I haven't told enough,
But I have, and the answer isn't tough.

Having already learned the secret that the volume that remains of a drilled sphere doesn't depend on the initial size of the sphere, we can cheat and give a kind of meta-argument that is much shorter than the geometric proof. The volume left behind of any sphere with a 6-inch-long hole through it must be the same as the volume left behind of a 6-inch-diameter sphere with a hole of 0 diameter drilled through it. This is equal to $\frac{4}{3}(\pi 6^3)$, or approximately 905 cubic inches.

hole-through-the-earth problem

I wonder if I shall fall right through *the earth!*
–Alice in *Alice in Wonderland*

Imagine there is a hole going from one point on Earth's surface, all the way through the center of Earth, to the exact opposite (antipodal) point on the other side. What would happen if you dropped something into this hole? The Greek historian Plutarch considered the problem some 2,000 years ago. In 1624, van Etten argued that a millstone dropped down such a hole at 1 mile per minute would take more than $2\frac{1}{2}$ days to reach the center, where "it would hang in the air." The first correct answer was given by Galileo is his *Dialogue Concerning the Two Chief World Systems* (1632). Galileo realized a dropped object would accelerate until it reached the center of Earth, travel through to the other side, then oscillate back and forth.

holism

The idea that the whole is greater than the sum of the parts. Holism is credible on the basis of **emergence** alone, since **reductionism** and bottom-up descriptions of nature often fail to predict complex higher-level patterns.

homeomorphic

In **topology**, two objects are said to be homeomorphic if they can be smoothly deformed into each other. See also **homeomorphism**.

homeomorphism

A **one-to-one** continuous transformation that preserves **open** and **closed** sets.

homology

A way of attaching **Abelian group**s, or more elaborate algebraic objects, to a **topological space** so as to obtain algebraic invariants. In a sense, it detects the presence of "holes" of various dimensions in the space. The methods developed to handle this led to what is now called *homological algebra,* a subject in which homological invariants are calculated for many purely algebraic structures.

homomorphism
A **function** that preserves the operators associated with the specified structure.

homotopy
A continuous transformation from one path in a **topological space** to another, or more generally, of one **function** to another (see **continuity**). Paths connected by a homotopy are called *homotopic* and are said to be in the same *homotopy class.* Properties left unchanged by such homotopies are known as *homotopy invariants.* Homotopy classes of paths can be composed to form the **fundamental group**, or *first homotopy group.* Other maps can be used to form *higher homotopy groups.*

Hordern, L. Edward (d. 2000)
An English puzzlist and leading authority and writer on **sliding-piece puzzles**.[175]

hundred
The smallest three-digit number in the decimal system and the smallest square of a two-digit number (10). A hundred today means 100 but, over the years and in different places, it has stood for different values including 112, 120, 124, and 132. The remnants of these old measures still persist in the *hundredweight* of some countries representing 112 or 120 pounds. A hundred is also a measure of land area, frequently used in colonial America and in England to signify a division of a county or a shire having its own court. A strange custom is invoked if a member of the English Parliament's lower house, the House of Commons, wishes to resign his seat (something that is technically illegal). That member accepts stewardship of the "Chiltern Hundreds," an area of chalk hills near Oxford and Buckingham, which effects his release from Parliament. The "Hundred Years' War" between the English and the French actually lasted 116 years.

hundred fowls problem
A Chinese puzzle found in the sixth-century work of the mathematician Zhang Qiujian. Similar problems involving two constraints and three unknowns are found in early European and Arabic mathematics from about the eighth century A.D. on.

PUZZLE

If a rooster is worth five coins, a hen three coins, and three chicks together are worth one coin, how many roosters, hens, and chicks totaling 100 can be bought for 100 coins? It turns out that there are three different solutions. These can be found the long way, by trial and error, or by using algebra. Call the number of roosters R, the number of hens H, and the number of chicks C. The problem gives two constraints. First, the total number of fowl must be 100, so $R + H + C = 100$. Second, the total cost of the fowl must be 100. The cost of roosters is $5R$, the cost of hens is $3H$, and the cost of chicks is $(\frac{1}{3})C$, so $5R + 3H + (\frac{1}{3})C = 100$. These two equations can be used to get rid of one of the unknowns; then it's a question of guess and check.

Solutions begin on page 369.

Hunter, James Alston Hope
An American mathematician and puzzlist who has written numerous articles and several books on recreational mathematics (two in partnership with Joseph **Madachy**), and was the author of a syndicated puzzle column read throughout the United States and Canada. In 1955, he coined the name "**alphametic**" and is probably the most prolific producer of **cryptarithm**s.

Huygens, Christiaan (1629–1695)
A Dutch scientist and mathematician who solved the **tautochrone problem**, proposed a new wave theory of light, designed a new pendulum clock, discovered Saturn's largest moon (Titan), and sketched the first feature on the surface of another planet (Syrtis Major on Mars). In his final years Huygens composed one of the earliest discussions of extraterrestrial life, published after his death as the *Cosmotheoros* (1698).

Hypatia of Alexandria (c. A.D. 370–417)
The first woman known to have made a significant contribution to mathematics. Although there is no evidence that Hypatia did any original research, she assisted her father, Theon of Alexandria, in writing his 11-part commentary on Ptolemy's great work on astronomy and mathematics, the *Almagest.* It's thought that she also helped in producing a new version of **Euclid**'s *Elements,* which formed the basis for all later editions of Euclid. Hypatia became head of the Platonist school at Alexandria in about A.D. 400 and, as a pagan, represented a menace to some Christian sects who felt threatened by her learning and depth of scientific knowledge. In the end, although the exact circumstances are unclear, she was murdered by a mob. The event served as a trigger for the departure of many scholars and the beginning of the decline of Alexandria as a major academic center.

hyperbola
One of the **conic section** family of curves, which also includes the **circle**, the **ellipse**, and the **parabola**; it is obtained if a double cone is cut by a plane inclined to the axis of the cone such that it meets both branches of the cone. Of the four conic curves, the hyperbola is the one least encountered in everyday life. A rare chance to see

the complete shape is when a lamp with a cylindrical or conical shade throws shadows on a nearby wall. Part of a hyperbola is produced by the liquid that climbs by capillary action between two microscope slides held vertically and almost touching.

A hyperbola is the path followed by a smaller object that is traveling fast enough to escape completely from the gravitational pull of a larger object. Some comets, for example, have hyperbolic or "open" orbits so that, after one swing around the Sun, they head off into interstellar space never to return. It can be difficult to tell, in some cases, whether a comet's orbit is hyperbolic or is highly elliptical and, therefore, closed. In fact, one way to think of a hyperbola is as a kind of ellipse that is split in half by infinity. Not surprisingly, the hyperbola and the ellipse share many inverse relationships. For example, whereas the eclipse is the **locus** of all points whose distances from two fixed points, called *foci,* have a constant sum, the hyperbola is the locus of all points whose distances, r_1 and r_2, from two fixed points, F_1 and F_2, is a constant difference, $r_2 - r_1 = k$. If a is the distance from the origin to either of the x intercepts of the hyperbola, then $k = 2a$. Also, let the distance between the foci, $F_2 - F_1 = 2c$. Then the *eccentricity,* a measure of the flatness of the hyperbola, is given by $e = c/a$. For all hyperbolas, $e > 1$; the larger the value of e, the more the hyperbola resembles two parallel lines. Just as the circle (for which $e = 0$) is the limiting case of the ellipse (for which $0 < e < 1$), so the parabola ($e = 1$) is the limiting case of both the ellipse and the hyperbola.

A hyperbola has two **asymptote**s: the never-quite-attainable limits of the curve's branches as they run away to infinity. The *transverse axis* of the hyperbola is the line on which both foci lie and that also intersects both vertices (turning points); the *conjugate axis* goes through the center and is perpendicular to the transverse axis.

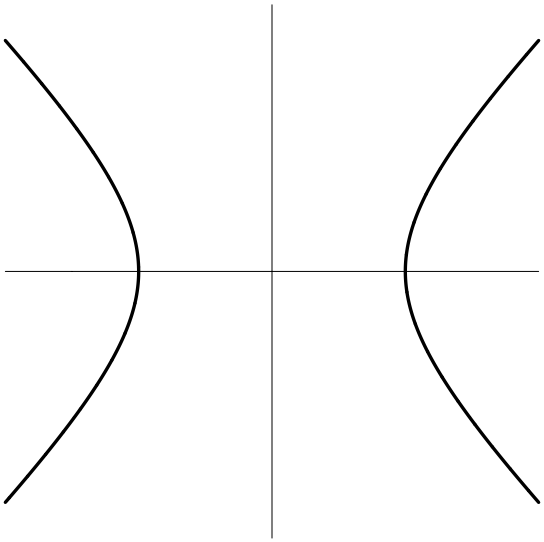

hyperbola © *Jan Wassenaar, www.2dcurves.com*

A *rectangular hyperbola* has an eccentricity of $\sqrt{2}$, asymptotes that are mutually perpendicular, and the property that when stretched along one or both of its asymptotes remains unchanged. This special case of the hyperbola was first studied by **Menaechmus**. **Euclid** and Aristaeus wrote about the general hyperbola but only studied one branch of it, while **Apollonius** was the first to study the two branches of the curve of the hyperbola and is generally thought to have given it its present name.

The **pedal curve** of a hyperbola with one focus as the pedal point is a circle. The pedal of a rectangular hyperbola with its center as pedal point is a **lemniscate of Bernoulli**. The **evolute** of a hyperbola is a **Lamé curve**. If the center of a rectangular hyperbola is taken as the center of inversion, the rectangular hyperbola inverts to a lemniscate. If the vertex is used as the center of inversion, the rectangular hyperbola inverts to a right **strophoid**. If the focus of a hyperbola is taken as the center of inversion, the hyperbola inverts to a limaçon (see **limaçon of Pascal**). In this last case if the asymptotes of the hyperbola make an angle of $\pi/3$ with the axis that cuts the hyperbola, then it inverts to the Maclaurin **trisectrix**. See also **hyperboloid**.

hyperbolic geometry

One of the two main types of **non-Euclidean geometry** and the first to be discovered. It is concerned with saddle-surfaces, which have negative **curvature** and on which the **geodesic**s are **hyperbolas**. In hyperbolic geometry, contrary to the **parallel postulate**, there exists a line m and a point p not on m such that at least two distinct lines parallel to m pass through p. As a result, the sum of the angles of a triangle is less than 180° and, for a right triangle, the square of the hypotenuse is greater than the sum of the squares of the other two sides. See also **elliptical geometry**.

hyperbolic spiral

The curve whose equation in **polar coordinates** is $r\theta = a$.

hyperboloid

A **quadratic** surface of which there are two basic forms: a *hyperboloid of one sheet,* generated by spinning a **hyperbola** around its conjugate axis, and a *hyperboloid of two sheets* produced by rotating a hyperbola about its transverse axis. The hyperboloid of one sheet, first described by **Archimedes**, has some particularly remarkable properties. In 1669 Christopher Wren, the architect who de-

hyperboloid The McDonnell Planetarium in St. Louis is an example of a hyperboloid. *Courtesy of the St. Louis Science Center*

signed St. Paul's Cathedral in London, showed that this kind if hyperboloid is what mathematicians now call a **ruled surface**–a surface composed of infinitely many straight lines. This fact enables a close approximation to a hyperboloid to be made in the form of a string model. Two circular disks, of the same size, are held parallel, one exactly above the other, by a framework. Strings are then run through holes near the circumference of one circle to corresponding holes in the other circle that are a fixed distance farther around the circumference. Each string is perfectly straight but the surface that emerges takes the curved form of a hyperboloid. For the same reason, a cube spun rapidly on one of its corners will appear to describe a hyperbolic curve when viewed side-on.

Prominent examples of hyperboloids can be seen in the form of cooling towers at power stations and, most strikingly, in the shape of the McDonnell Planetarium in St. Louis, Missouri. The designer of this building, Gyo Obata, chose the design because the hyperbolic paths of some comets suggest "the drama and excitement of space exploration."

hypercube

A higher dimensional analog of a cube. A four-dimensional hypercube is known as a **tesseract**.

hyperellipse

See **superellipse**.

hyperfactorial

A number such as 108, which is equal to $3^3 \times 2^2 \times 1^1$. In general, the nth hyperfactorial $H(n)$ is given by

$$H(n) = n^n \, (n-1)^{n-1} \ldots 3^3 \, 2^2 \, 1^1.$$

The first eight hyperfactorials are 1, 4, 108, 27,648, 86,400,000, 4,031,078,400,000, 3,319,766,398,771,200,000, and 55,696,437,941,726,556,979,200,000. See also **large numbers** and **superfactorials**.

hypergeometric function

The sum of the *hypergeometric series:*

$$F(a; b; c; x) = 1 + \frac{ab}{1.c}\, x + \frac{a(a+1)b(b+1)}{1.2.c(c+1)}\, x^2 + \ldots$$

Many common functions can be written as hypergeometric functions.

hyperreal number

Any of a colossal set of numbers, also known as *nonstandard reals,* that includes not only all the **real number**s but also certain classes of infinitely large (see **infinity**) and **infinitesimal** numbers as well. Hyperreals emerged in the 1960s from the work of Abraham **Robinson** who showed how infinitely large and infinitesimal numbers can be rigorously defined and developed in what is called **nonstandard analysis**. Because hyperreals represent an extension of the real numbers, R, they are usually denoted by *R.

Hyperreals include all the reals (in the technical sense that they form an ordered field containing the reals as a subfield) and they also contain infinitely many other numbers that are either infinitely large (numbers whose absolute value is greater than any positive real number) or infinitely small (numbers whose absolute value is less than any positive real number). No infinitely large number exists in the real number system and the only real infinitesimal is zero. But in the hyperreal system, it turns out that each real number is surrounded by a cloud of hyperreals that are infinitely close to it; the cloud around zero consists of the infinitesimals themselves. Conversely, every (finite) hyperreal number x is infinitely close to exactly one real number, which is called its *standard part,* $\mathrm{st}(x)$. In other words, there exists one and only one real number $\mathrm{st}(x)$ such that $x - \mathrm{st}(x)$ is infinitesimal.

hypersphere

A four-dimensional analog of a **sphere**; also known as a *4-sphere.* Just as the shadow cast by a sphere is a circle, the shadow cast by a hypersphere is a sphere, and just as the intersection of a sphere with a plane is a circle, the intersection of a hypersphere with a hyperplane is a sphere. These analogies are reflected in the underlying mathematics.

- $x^2 + y^2 = r^2$ is the Cartesian equation of a circle of radius *r;*
- $x^2 + y^2 + z^2 = r^2$ is the corresponding equation of a sphere;

hyperboloid A hyperboloidal sculpture at the Fermi National Accelerator Laboratory. *FNAL*

$x^2 + y^2 + z^2 + w^2 = r^2$ is the equation of a hypersphere, where w is measured along a **fourth dimension** at right angles to the x-, y-, and z-axes.

The hypersphere has a *hypervolume* (analogous to the volume of a sphere) of $\pi^2 r^4/2$, and a *surface volume* (analogous to the sphere's surface area) of $2\pi^2 r^3$. A solid angle of a hypersphere is measured in *hypersteradians,* of which the hypersphere contains a total of $2\pi^2$. The apparent pattern of 2π radians in a circle and 4π steradians in a sphere does not continue with 8π hypersteradians because the *n-volume, n-area,* and number of *n-radians* of an *n-sphere* are all related to the **gamma function** and the way it can cancel out powers of π halfway between integers. In general, the term "hypersphere" may be used to refer to any *n*-sphere.

hypocycloid

A curve formed by the path of a point attached to a circle of radius b that rolls around the inside of a larger circle of radius a. The parametric equations for a hypocycloid can be written as:

$$x = (a - b)\cos(t) + b\cos((a/b - 1)t)$$
$$y = (a - b)\sin(t) - b\sin((a/b - 1)t)$$

The type of hypocloid depends on where the point whose path is being traced is located on the rolling circle. If it lies on the circumference of the circle, the curve generated is an ordinary hypocycloid. If it lies elsewhere the result is a **hypotrochoid**. A hypocycloid has a closed form—that is, the moving point eventually retraces its steps—when the ratio of the rolling circle and the larger circle, fixed, is equal to a rational number. When this ratio is in its simplest form, the numerator is the number of revolutions covered inside the fixed circle before the curve closes. In the same family of curves as the hypocycloid (and hypotrochoid) are the **epicycloid** and **epitrochoid**.

hypoellipse

See **superellipse**.

hypotenuse

The longest side of a **right triangle**—the one opposite the right angle. The word comes from the Greek roots *hypo* meaning "under" (which also appears, for example, in hypodermic, "under the skin") and *tein* or *ten,* for stretch. Thus hypotenuse is the line segment "stretched under" the right angle.

hypothesis

See **conjecture**.

hypotrochoid

A curve formed by the path of a point attached to a point c, which is not on the circumference, of a circle of radius b that rolls around the inside of a larger circle of radius a. The parametric equations for a hypotrochoid can be written as:

$$x = (a - b)\cos(t) + c\cos((a/b - 1)t)$$
$$y = (a - b)\sin(t) - c\sin((a/b - 1)t)$$

The hypotrochoid is a generalized **hypocycloid** and comes in two varieties: a *prolate hypocycloid* if the starting point is outside the circumference of the rolling circle and a *curtate hypocycloid* if the starting point is inside the rolling circle. In the same family of curves as the hypotrochoid (and hypocycloid) are the **epicycloid** and **epitrochoid**.

i

The square root of minus one; *i* is also known as the *imaginary unit number,* $\sqrt{-1}$. The product of *i* and a real number is known as an *imaginary number.* For details, see **complex number**.

I-Ching

A system of Chinese divination based on 64 hexagrams, each consisting of six horizontal lines each of which may be solid (representing the male principle, or yang) or have a break in the middle (representing the female principle, or yin). The first three lines of the hexagram, from the bottom up, constitute the lower trigram and symbolize the inner world. The fourth, fifth, and sixth lines constitute the upper trigram and symbolize the outer world. One of the first Europeans to see the hexagram structure when it was brought out of China in the early 1700s was Gottfried **Leibniz**, the first mathematician to work with base two, or **binary**, arithmetic.

icosahedron

A **polyhedron** with 20 faces. A *regular icosahedron* has faces that are all equilateral **triangle**s, and is one of the five **Platonic solid**s. The length from **vertex** to opposing vertex of a regular icosahedron is $5^{1/4} \times \phi^{1/2} \times d$ where ϕ is the **golden ratio** and *d* is the length of the side of one of the triangular faces. Chopping off each vertex (corner) of a regular icosahedron reveals the 12 pentagonal and 20 hexagonal faces of the *truncated icosahedron,* which is one of the 13 **Archimedean solid**s (shapes made from truncating Platonic solids in certain ways). See also **buckyball**.

Icosian game

A game devised by William **Hamilton** and first described by him in 1857 at a meeting of the British Association for the Advancement of Science in Dublin. The object of the game is to find a way around the edges of a **dodecahedron** so that every vertex (corner) is visited once and only once. A path such as this became known as a **Hamilton circuit**, though the task of finding a circuit that passes just once through every vertex of a shape seems to have arisen first in connection with Leonhard **Euler**'s study of the **knight's tour**. Two years before Hamilton introduced his game, Thomas **Kirkman** posed the problem explicitly in a paper that he submitted to the Royal Society: Given a graph of a **polyhedron**, does there exist a cycle passing through every vertex?

The Icosian game stemmed from Hamilton's invention of a curious kind of algebra that he called *icosians,* based on the symmetry properties of the **icosahedron**. Hamilton connected the mathematics of his icosians with the problem of traveling along the edges of a dodecahedron, hitting each vertex just once, and coming back to the starting point. His friend and fellow Irishman John Graves (1806–1870) suggested turning the problem into a commercial game and put Hamilton in contact with the London company of John Jacques and Sons, toy-makers and manufacturer of high quality chess sets. Jacques bought the rights to the game for £25 and marketed two versions of it, under the name Around the World. One version, for the parlor, was played on a flat board; another, for the "traveler," consisted of an actual dodecahedron. In both cases, nails at each vertex stood for a major city of the world and the player wrapped a piece of string around these nails as they went. The game was a

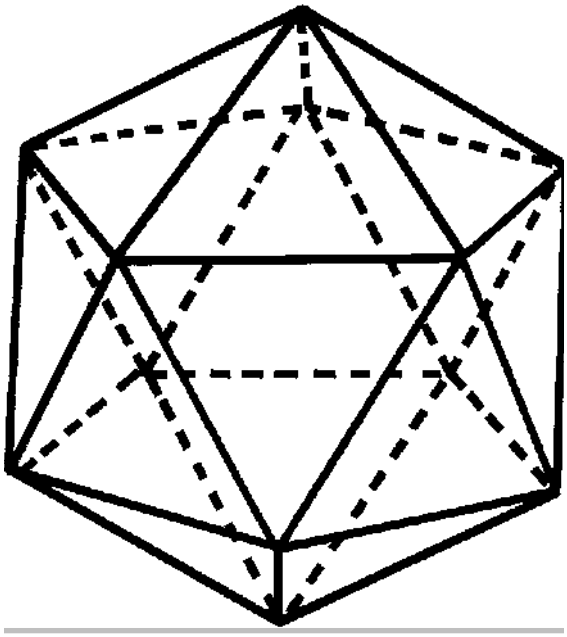

icosahedron The most multifaceted of the Platonic solids.

complete sales flop, mainly because it was too easy, even for children–but not for Hamilton himself who always used the icosian calculus to figure out his moves, instead of just trying different paths like everyone else! See also **traveling salesman problem**.

idempotent

The element x in some algebraic structures is called idempotent if $x \times x = x$.

identity

A statement that two expressions are always equal, for any values of their variables.

imaginary number

A number whose square is negative. Every imaginary number can be written in the form ib where b is a **real number** and $\boldsymbol{i}$ the *imaginary unit* with the property that $i^2 = -1$. Imaginary numbers are **complex number**s in which the real part is zero. The term "imaginary" is unfortunate because it suggests something that has less reality than a "real" number, which isn't the case.

impossibilities in mathematics

> *Alice laughed: "There's no use trying," she said; "one can't believe impossible things." "I daresay you haven't had much practice," said the Queen. "When I was younger, I always did it for half an hour a day. Why, sometimes I've believed as many as six impossible things before breakfast."*
>
> –Lewis Carroll, *Alice in Wonderland*

Mathematicians are used to believing things that most people would consider impossible or, at least, too outrageous to contemplate, such as the **Banach-Tarski paradox**. However, there are some genuine impossibilities, even in mathematics, including **trisecting an angle**, **duplicating the cube**, and **squaring the circle** using only a straightedge and compass; finding the center of a given circle with a straightedge alone; deriving Euclid's **parallel postulate** from the other four; and representing the **square root of 2** as a rational fraction a/b. Less well known is this little gem from Gustave Flaubert (1821–1880), who sounds as if he had seen too much of this type of problem in school:

> Since you are now studying geometry and trigonometry, I will give you a problem. A ship sails the ocean. It left Boston with a cargo of wool. It grosses 200 tons. It is bound for Le Havre. The mainmast is broken, the cabin boy is on deck, there are 12 passengers aboard, the wind is blowing East-North-East, the clock points to a quarter past three in the afternoon. It is the month of May. How old is the captain?

impossible figure

An image in two dimensions of an object that, because of spatial inconsistencies, is impossible to realize fully in three dimensions. Among the best known impossible figures are the **Penrose triangle**, the **Penrose stairway**, the **Impossible trident**, and the Freemish crate. Notable pioneers of this peculiar form of representation have been Ocar **Reutersvärd**, Roger **Penrose** (and his father), and M. C. **Escher**. See also **optical illusion**.

impossible tribar

See **Penrose triangle**.

impossible trident

One of the most notorious **impossible figure**s. It was first seen by many when it appeared on the cover of the March 1965 issue of *Mad* magazine. The two halves of the figure seem perfectly reasonable in themselves. When the top part is covered, the bottom part is taken to be three separate cylinders or tubes. With the bottom part hidden, the foreground figure is interpreted as being built of flat faces making two rectangular prongs. The trouble is that these two aspects of the figure are totally incompatible. Somewhere in the middle, the foreground and background swap places and give rise to an irreconcilable paradox. Over the years, countless adaptations of the trident have appeared with names such as the devil's fork, the three-stick clevis, the blivit, the impossible colonnade, the trichotometric indicator support, and, most extravagantly, the triple encabulator tuned manifold. Swedish artist Oscar **Reutersvärd**'s mastery of such figures has led him to draw thousands of variations on the theme. When the figure is drawn long, it is easy to perceive locally as a three-dimensional object and to overlook its inherent inconsistency, because the contradictory clues are too well separated. When the figure is of medium length, the figure is easily interpreted as a three-dimensional object, and its impossibility is quickly perceived. If the prongs are very short, the two different interpretations vie for acceptance within the same local area; thus there is no consistent interpretation and the illusion breaks down. Some early writers commented that the impossible trident couldn't be built in any form in three dimensions. However, this has been shown to be false. In 1985, the Japanese artist Shigeo Fukuda made a three-dimensional model of the trident in the form of classical columns in which the illusion works–from one critical angle.

The origins of the figure are uncertain. It turns out that *Mad* magazine bought the illustration rights from a con-

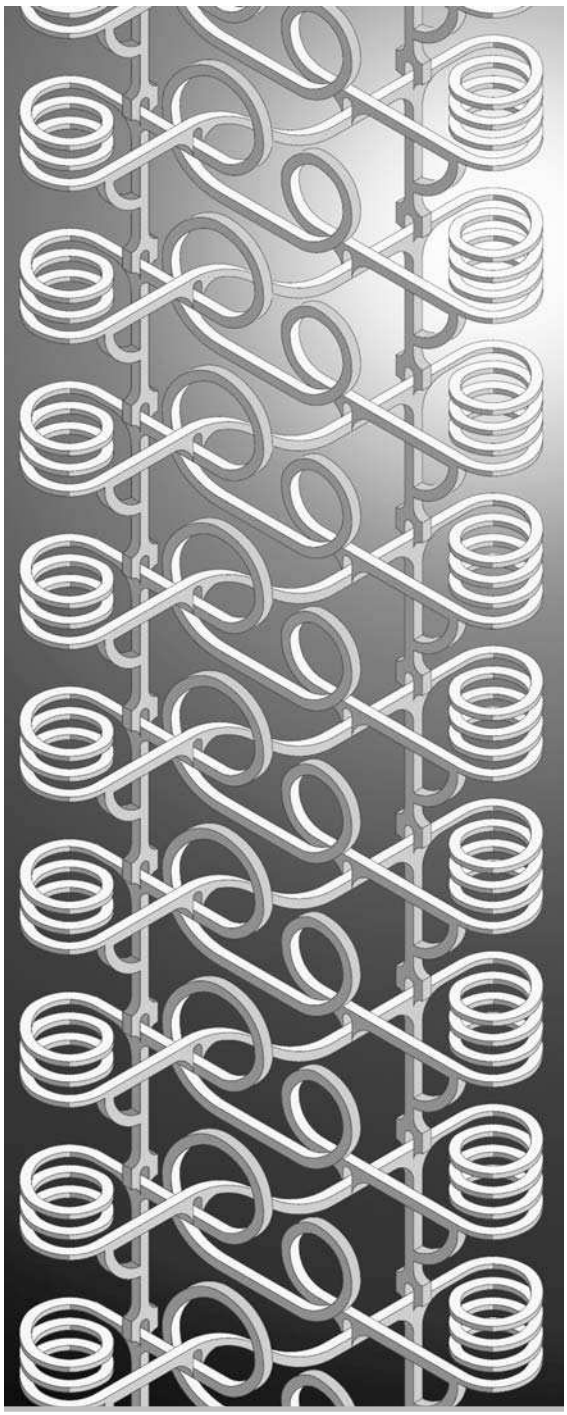

impossible figure "The Rollercoaster," a rendering in two dimensions of a structure impossible to build in three dimensions. *Jos Leys, www.josleys.com*

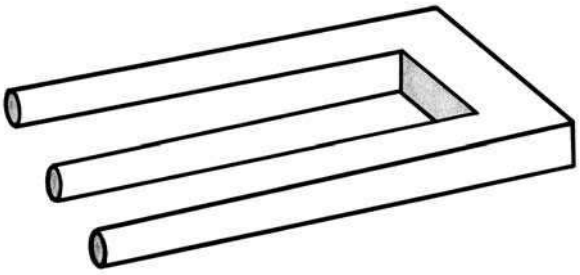

impossible trident

tributor who claimed that it was original; however, the magazine's management soon found out to their embarrassment that the figure had been previously published. It began to surface in several popular engineering, aviation, and science-fiction periodicals in May and June of 1964. D. H. Schuster published an article that same year in the *American Journal of Psychology,* which first brought the figure to the attention of the psychological community.

incircle

The **inscribed circle** of a triangle.

incomputable number

A **real number** with an infinite decimal (or binary) expansion that cannot be enumerated by any **universal computer**.

induction

A method of reasoning by which one infers a generalization from a series of instances. Say there is a hypothesis H that contains the variable n, which is a whole number. To prove by induction that H is true for every value of n is a two-step process: (1) prove that H is true for $n = 1$; (2) prove that H being true for $n = k$ implies that H is true for $n = k + 1$. This is sufficient because (1) and (2) together imply that H is true for $n = 2$, which, from (2), then implies H is true for $n = 3$, which implies H is true for $n = 4$, and so on. H is called an *inductive hypothesis.* Some philosophers don't accept this kind of proof, because it may take infinitely many steps to prove something; however, most mathematicians are happy to use it.

inequality

The statement that one quantity is less than or greater than another.

infinite dimensions

In mathematics, the concept of an infinite-dimensional space considered literally. It is a **vector space** with an infinite basis or a space with infinitely many coordinates.

infinite series

An infinite sum of the form

$$a_1 + a_2 + a_3 + \ldots = \sum_{k=1}^{\infty} a_k.$$

Such series crop up in many areas of modern mathematics. Their development began in the seventeenth century and was continued by Leonhard **Euler,** who, in the process, solved many important problems.

infinitesimal

A number that is greater than zero yet smaller than any positive **real number**. In a sense, infinitesimals are to small what **infinity** is to large. They were first introduced by Isaac **Newton** and Gottfried **Leibniz** in their early versions of **calculus**; however, the lack of a rigorous definition for them stood in the way of calculus being fully accepted. As Bertrand **Russell** later put it: "Calculus required continuity, and continuity was supposed to require the infinitely little; but nobody could discover what the infinitely little might be." In the 1800s, calculus was put on a firmer footing by Augustin **Cauchy**, Karl **Weierstrass**, and others, who clarified and redefined the notion of a **limit** without reference to infinitesimals. When a function $f(x)$ can be made as close as desired to L by taking x close enough to a, then L is the limit of $f(x)$ as x approaches a. This is the classical or *epsilon-delta* formulation of calculus, named for the common use of δ for $|x - a|$ and ε for $|f(x) - L|$. For a long time, this was the only rigorous foundation for calculus, and it is still the one taught in most calculus classes. But in 1960, Abraham **Robinson** discovered **nonstandard analysis**, which provides a rigorous formulation of infinitesimals, confers on them a new significance, and brings them closer to the vision of Newton and Leibniz.

infinity

> *Mystery has its own mysteries, and there are gods above gods. We have ours, they have theirs. That is what's known as infinity.*
>
> –Jean Cocteau (1889–1963), French author and filmmaker

A concept that has always fascinated philosophers and theologians, linked as it is to the notions of unending distance or space, eternity, and God, but that was avoided or met with open hostility throughout most of the history of mathematics. Only within the past century or so have mathematicians dealt with it head on and accepted infinity as a number–albeit the strangest one we know.

An early glimpse of the perils of the infinite came to Zeno of Elae through his paradoxes, the best known of which pits Achilles in a race against a tortoise (see **Zeno's paradoxes**). Confident of victory, Achilles gives the tortoise a head start. But then how can he ever overtake the sluggish reptile? First he must catch up to the point where it began, by which time the tortoise will have moved on. When he makes up the new distance that separated them, he finds his adversary has advanced again. And so it goes on, indefinitely. No matter how many times Achilles reaches the point where his competitor was, the tortoise has progressed a bit farther. So perplexed was Zeno by this problem that he decided not only was it best to avoid thinking about the infinite but also that motion was impossible!

A similar shock lay in store for **Pythagoras** and his followers who were convinced that everything in the universe could ultimately be understood in terms of whole numbers (even common fractions being just one whole number divided by another). The **square root of 2**–the length of the diagonal of a right-angled triangle whose shorter sides are both one unit long–refused to fit into this neat cosmic scheme. It was an **irrational number**, inexpressible as the ratio of two integers. Put another way, its decimal expansion goes on forever without ever settling into a recurring pattern.

These two examples highlight the basic problem in coming to grips with infinity. Our imaginations can cope with something that hasn't yet reached an end: we can always picture taking another step, adding one more to a total, or visualizing another term in a long series. But infinity, taken as a whole, boggles the mind. For mathematicians this was a particularly serious problem because mathematics deals with precise quantities and meticulously well-defined concepts. How could they work with things that clearly existed and went on indefinitely–a number like $\sqrt{2}$ or a curve that approached a line ever more closely–while avoiding a confrontation with infinity itself? **Aristotle** provided the key by arguing that there were two kinds of infinity. *Actual infinity,* or *completed infinity,* which he believed could not exist, is endlessness fully realized at some point in time. *Potential infinity,* which Aristotle insisted was manifest in nature–for example, in the unending cycle of the seasons or the indefinite divisibility of a piece of gold–is infinitude spread over unlimited time. This fundamental distinction persisted in mathematics for more than 2,000 years. In 1831, no less a figure than Karl **Gauss** expressed his "horror of the actual infinitude," saying: "I protest against the use of infinite magnitude as something completed, which is never permissible in mathematics. Infinity is merely a way of speaking, the true meaning being a limit which certain ratios approach indefinitely close, while others are permitted to increase without restriction."

By confining their attention to potential infinity, mathematicians were able to address and develop crucial

concepts such as those of **infinite series**, **limit**, and **infinitesimal**s, and so arrive at **calculus**, without having to grant that infinity itself was a mathematical object. Yet as early as the Middle Ages certain paradoxes and puzzles arose, which suggested that actual infinity was not an issue to be easily dismissed. These puzzles stem from the principle that it is possible to pair off, or put in *one-to-one correspondence,* all the members of one collection of objects with all those of another of equal size. Applied to indefinitely large collections, however, this principle seemed to flout a commonsense idea first expressed by **Euclid**: the whole is always greater than any of its parts. For instance, it appeared possible to pair off *all* the positive integers with *only those that are even:* 1 with 2, 2 with 4, 3 with 6, and so on, despite the fact that positive integers also include odd numbers. Galileo, in considering such a problem, was the first to show a more enlightened attitude toward the infinite when he proposed that "infinity should obey a different arithmetic than finite numbers." Much later, David **Hilbert** offered a striking illustration of how weird the arithmetic of the endless can get.

Imagine, said Hilbert, a hotel with an infinite number of rooms. In the usual kind of hotel, with finite accommodation, no more guests can be squeezed in once all the rooms are full. But "Hilbert's Grand Hotel" is dramatically different. If the guest occupying room 1 moves to room 2, the occupant of room 2 moves to room 3, and so on, all the way down the line, a newcomer can be placed in room 1. In fact, space can be made for an infinite number of new clients by moving the occupants of rooms 1, 2, 3, etc, to rooms 2, 4, 6, etc, thus freeing up all the odd-numbered rooms. Even if an infinite number of coaches were to arrive each carrying an infinite number of passengers, no one would have to be turned away: first the odd-numbered rooms would be emptied as above, then the first coach's load would be put in rooms $3n$ for $n = 1, 2, 3, \ldots$, the second coach's load in rooms $5n$ for $n = 1, 2, \ldots$, and so on; in general, the people aboard coach number i would empty into rooms p_n where p is the $(i + 1)$th prime number.

Such is the looking-glass world that opens up once the reality of **set**s of numbers with infinitely many elements is accepted. That was a crucial issue facing mathematicians in the late nineteenth century: Were they prepared to embrace actual infinity as a number? Most were still aligned with Aristotle and Gauss in opposing the idea. But a few, including Richard **Dedekind** and, above all, Georg **Cantor**, realized that the time had come to put the concept of infinite sets on a firm logical foundation.

Cantor accepted that the well-known pairing-off principle, used to determine if two finite sets are equal, is just as applicable to infinite sets. It followed that there really are just as many even positive integers as there are positive integers altogether. This was no paradox, he realized, but the *defining property* of infinite sets: the whole is no bigger than some of its parts. He went on to show that the set of all positive integers, 1, 2, 3, . . . , contains precisely as many members–that is, has the same **cardinal number** or cardinality–as the set of all rational numbers (numbers that can be written in the form p/q, where p and q are integers). He called this infinite cardinal number **aleph-**null, $\aleph_0$ ("aleph" being the first letter of the Hebrew alphabet). He then demonstrated, using what has become known as *Cantor's theorem,* that there is a hierarchy of infinities of which $\aleph_0$ is the smallest. Essentially, he proved that the cardinal number of all the subsets–the different ways of arranging the elements–of a set of size $\aleph_0$ is a bigger form of infinity, which he called $\aleph_1$. Similarly, the cardinality of the set of subsets of $\aleph_1$ is a still bigger infinity, known as $\aleph_2$. And so on, indefinitely, leading to an infinite number of different infinities.

Cantor believed that $\aleph_1$ was identical with the total number of mathematical points on a line, which, astonishingly, he found was the same as the number of points on a plane or in any higher n-dimensional space. This infinity of spatial points, known as the *power of the continuum, c,* is the set of all **real number**s (all rational numbers plus all irrational numbers). Cantor's **continuum hypothesis** asserts that $c = \aleph_1$, which is equivalent to saying that there is no infinite set with a cardinality between that of the integers and the reals. Yet, despite much effort, Cantor was never able to prove or disprove his continuum hypothesis. We now know why–and it strikes to the very foundations of mathematics.

In the 1930s, Kurt **Gödel** showed that it is impossible to *disprove* the continuum hypothesis from the standard **axiom**s of set theory. Three decades later, Paul Cohen showed that it *cannot be proven* from those same axioms either. Such a situation had been in the cards ever since the emergence of **Gödel's incompleteness theorem**. But the independence of the continuum hypothesis was still unsettling because it was the first concrete example of an important question that could not be proven either way from the universally accepted system of axioms on which most of mathematics is built.

Currently, the preference among mathematicians is to regard the continuum hypothesis as being false, simply because of the usefulness of the results that can be derived this way. As for the nature of the various types of infinities and the very existence of infinite sets, these depend crucially on what number theory is being used. Different axioms and rules lead to different answers to the question *what lies beyond all the integers?* This can make it difficult or even meaningless to compare the various types of infinities that arise and to determine their

relative size, although within any given number system the infinities can usually be put into a clear order. Certain extended number systems, such as the **surreal number**s, incorporate both the ordinary (finite) numbers and a diversity of infinite numbers. However, whatever number system is chosen, there will inevitably be inaccessible infinities–infinities that are larger than any of those the system is capable of producing.[198, 214, 275]

inflection
A point of inflection of a plane curve is a point where the curve has a stationary **tangent**, at which the tangent is changing from rotating in one direction to rotating in the opposite direction.

information theory
A mathematical theory of information born in 1948 with the publication of Claude **Shannon**'s landmark paper, "A Mathematical Theory of Communication." Its main goal is to discover the laws governing systems designed to communicate or manipulate information, and to set up quantitative measures of information and of the capacity of various systems to transmit, store, and otherwise process information. Among the problems it treats are finding the best methods of using various communication systems and the best methods for separating the wanted information, or signal, from the noise. Another of its concerns is setting upper bounds on what it is possible to achieve with a given information-carrying medium (often called an information channel). The theory overlaps heavily with communication theory but is more oriented toward the fundamental limitations on the processing and communication of information and less oriented toward the detailed operation of the devices used.

injection
A **one-to-one** mapping.

inscribed angle
The angle formed by two **chord**s of a curve that meet at the same point on the curve.

inscribed circle
A circle inside a triangle or other **polygon** whose edges are **tangent**s to the circle. Such a polygon is said to be *circumscribed* to the circle. The (unique) circle inscribed to a triangle is called the *incircle.*

instability
The condition of a system when it is easily disturbed by internal or external forces or events, in contrast to a *stable system,* which will return to its previous condition when disturbed. A pencil resting vertically on its eraser or a coin standing on edge are examples of systems that have the property of instability since they easily fall over at the slightest breeze or movement of the surface they are resting on. An unstable system is one whose **attractor**s can change; thus, instability is a characteristic of a system that is far from equilibrium or at **bifurcation**.

integer
Any positive or negative whole number or zero: . . ., –3, –2, –1, 0, 1, 2, 3, ... *Integer* is Latin for "whole" or "intact." The **set** of all integers is denoted by **Z**, which stands for *zahlen* (German for "numbers"). The integers are an extension of the **natural number**s to include **negative number**s and so make possible the solution of all equations of the form $a + x = b$, where a and b are natural numbers. Integers can be added and subtracted, multiplied, and compared. Like the natural numbers, the integers form a countably infinite set. However, the integers don't form a **field** since, for instance, there is no integer x such that $2x = 1$; the smallest field containing the integers is that of the **rational number**s. An important property of the integers is *division with remainder:* given two integers a and b with $b \neq 0$, it is always possible to find integers q and r such that $a = bq + r$, and such that $0 \leq r < |b|$. q is called the *quotient* and r is called the *remainder* resulting from division of a by b. The numbers q and r are uniquely determined by a and b. From this follows the *fundamental theorem of arithmetic,* which states that integers can be written as products of prime numbers in an essentially unique way.

integral
The area, or a generalization of area, under any section of a graph that is described by a **function**; in other words, the continuous cumulative sum of a function (see **continuity**). Not all functions have an exact formula that allows an integral to be found. In such cases, *numerical integration* has to be used, in which the area is found using approximate numerical techniques. Integrals, together with **derivative**s, are the fundamental objects of **calculus**.

integral equation
An equation that involves an **integral** of the **function** which is to be solved for.

integration
An operation that corresponds to the informal idea of finding the area under the graph of a **function**. The first theory of integration was developed by **Archimedes** with

his method of *quadratures,* but this could be applied only in circumstances where there was a high degree of geometric symmetry. In the seventeenth century, Isaac **Newton** and Gottfried **Leibniz** independently discovered the idea that integration was a sort of opposite of **differentiation** (which they had just invented); this allowed mathematicians to calculate a broad class of integrals for the first time. However, unlike Archimedes's method, which was based on **Euclidean geometry**, Newton's and Leibniz's integral calculus lacked a secure foundation.

In the nineteenth century, Augustin **Cauchy** finally developed a rigorous theory of **limit**s, and Bernhard **Riemann** followed this up by formalizing what is now called the **Riemann integral**. To define this integral, one fills the area under the graph with smaller and smaller rectangles and takes the limit of the sums of the areas of the rectangles at each stage. Unfortunately, some functions don't have well-defined limits to these sums, so they have no Riemann integral. Henri **Lesbesgue** invented another method of integration to solve this problem. He first presented his ideas in *Intégrale, Longueur, Aire* (Integral, length, area) in 1902. Instead of using the areas of rectangles, a method that puts the focus on the **domain** of the function, Lebesgue turned to the **codomain** of the function for his fundamental unit of area. Lesbesgue's idea was to build first the integral for what he called simple functions–functions that take only finitely many values. Then he defined it for more complicated functions as the upper bound of all the integrals of simple functions smaller than the function in question. *Lesbesgue integration* has the beautiful property that every function with a Riemann integral also has a Lebesgue integral, and the two integrals agree. But there are many functions with a Lebesgue integral that don't have a Riemann integral. As part of the development of Lebesgue integration, Lebesgue introduced the concept of *Lebesgue measure,* which measures lengths rather than areas. Lebesgue's technique for turning a measure into an integral generalizes easily to many other situations, leading to the modern field of **measure theory**.

The Lebesgue integral was deficient in one respect. The Riemann integral had been generalized to the *improper Riemann integral* to measure functions whose domain of definition was not a **closed** interval. The Lebesgue integral integrated many of these functions (always reproducing the same answer when it did), but not all of them. The *Henstock integral* is an even more general notion of integral (based on Riemann's theory rather than Lebesgue's) that subsumes both Lebesgue integration and improper Riemann integration. However, the Henstock integral depends on specific features of the real number line and so doesn't generalize as well as the Lebesgue integral does.

interesting numbers

Clearly some numbers are of greater interest (at least to mathematicians) than are others. The number **pi**, for instance, is far more interesting than 1.283–or virtually any other number for that matter. Confining our attention to integers, can there be such a thing as an uninteresting number? It is easy to show that the answer must be "no." Suppose there were a set U of uninteresting integers. Then it must contain a least member, u. But the property of being the smallest uninteresting integer makes u interesting! As soon as u is removed from U, there is a new smallest uninteresting integer, which must then also be excluded. And so the argument could be continued until U was empty. Given that all integers are interesting, can they be ranked from least to most interesting? Again, no. To be ranked as "least interesting" is an extremely interesting property, and thus leads to another logical contradiction!

When Srinivasa **Ramanujan**, the great Indian mathematician, was ill with tuberculosis in a London hospital, his colleague G. H. **Hardy** went to visit him. Hardy opened the conversation with: "I came here in taxicab number 1729. That number seems dull to me which I hope isn't a bad omen." Ramanujan replied, without hesitation: "Nonsense, the number isn't dull at all. It's quite interesting. It's the smallest number that can be expressed as the sum of two cubes in two different ways." ($1729 = 1^3 + 12^3$ and $9^3 + 10^3$.)

International Date Line

Is it possible to assign a time to every longitude on Earth, so that each longitude has a *different* time but the times at nearby longitudes are always close? The answer is no, which is mathematically equivalent to saying that there's no way to continuously map points on a **real number** line onto a circle. This explains why an International Date Line is needed. It allows most regions on Earth to have times similar to their neighbors, though, by convention, time changes are (usually) made in chunks of one hour between adjacent time zones. Then it takes care of the inevitable discontinuity by having it happen all at once, as a jump by one whole day, on a longitude that passes mostly through open water in the Pacific. The fact that there doesn't exist any continuous **one-to-one** function from the circle onto the line follows from the **Borsuk-Ulam theorem** in one dimension.

interpolate

To estimate the value of a point that lies between two known values of a **function**. This is often done by approximating a line or a smooth curve between the values, which is the literal meaning of the word. *Inter* is the

Latin prefix for "between," *polire* translates as "to adorn or polish," so together they mean "to smooth between." *Extrapolate* was created as an extension of interpolate to suggest the smoothing of a line *outside* the known points. This operation is often done in statistics when patterns are studied over time to predict future events.

intersection

A place where two or more things meet or overlap. Two lines intersect at a point, two planes can intersect in a line, and so forth. The intersection of two or more **set**s, represented by the symbol ∩, is the set of elements that all the sets have in common; in other words, all the elements contained in every one of the sets.

invariant

(1) Something that stays the same when a particular **transformation** is carried out. (2) A value that is unchanged when a particular **function** is applied. (3) In **topology**, a number, **polynomial**, or other quantity associated with a topological object such as a **knot** or 3-**manifold**, which depends only on the underlying object and not on its specific description or presentation.

invariant theory

The study of quantities that are associated with **polynomial** equations and that are left **invariant** under transformations of the variables. For example, the discriminant $b^2 - 4ac$ is an invariant of the **quadratic** form $ax^2 + bxy + cy^2$.

inverse

(1) The inverse of a number, or a **reciprocal**, is 1 divided by the number; for example, the inverse of 8 is $\frac{1}{8}$ and the inverse of $\frac{3}{5}$ is $\frac{5}{3}$. (2) The inverse of a **function** or a **transformation** is the function or transformation that reverses the effect of the function or transformation. For example, the inverse of addition is subtraction, and of clockwise rotation is anticlockwise rotation. (3) The inverse of an element of a **set**, or a number, with respect to a particular operation, is what has to be combined with the element or number in order to obtain that operation's *identity element*.

involute

Attach a string to a point on a curve. Extend the string so that it is **tangent** to the curve at the point of attachment. Then wind the string up, always keeping it taut. The **locus** of points traced out by the end of the string is called the involute of the original curve, and the original curve is called the **evolute** of its involute. Although a curve has a unique evolute, it has infinitely many involutes corresponding to different choices of initial point. An involute can also be thought of as any curve **orthogonal** to all the tangents to a given curve. See also **circle involute**.

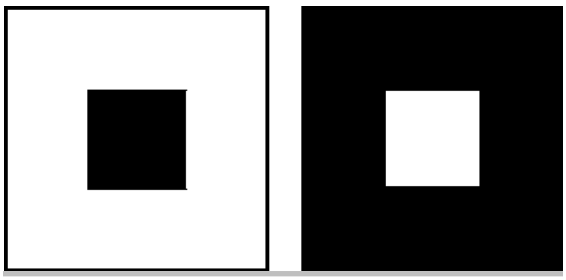

irradiation illusion Despite appearances, the inner squares are the same size.

irradiation illusion

A **distortion illusion** discovered by Hermann von Helmholtz in the nineteenth century. Despite the fact that the two figures are identical in size, the white hole looks bigger than the black one.

irrational number

A **real number** that can't be written as one whole number divided by another; in other words, a real number that isn't a **rational number**. The decimal expansion of an irrational number doesn't come to an end or repeat itself (in equal length blocks), though it may have a pattern such as 0.101001000100001000001 . . . . The vast majority of real numbers are irrational, so that if you were to pick a single point on the real **number line** at random the chances are overwhelmingly high that it would be irrational. Put another way, whereas the set of all rationals is countable, the irrationals form an **uncountable set** and therefore represent a larger kind of **infinity**. Indeed, as the Harvard logician Willard Van Orman Quine pointed out: "The irrationals exist in such variety . . . that no notation whatever is capable of providing a separate name for each of them."

There are two types of irrational number: **algebraic number**s, such as the **square root of 2**, which are the roots of algebraic equations, and the **transcendental number**s, such as **pi** and **e**, which aren't. In some cases it isn't known if a number is irrational or not; undecided cases include 2^e, π^e, π^2, and the **Euler-Mascheroni constant**, γ. An irrational number raised to a rational power can be rational; for instance, $\sqrt{2}$ to the power 2 is 2. Also, an irrational number to an irrational power can be rational. What kind of number is $\sqrt{2}^{\sqrt{2}}$? The answer is irrational. This follows from Gelfond's theorem, which

says that if a and b are roots of **polynomial**s, and a is not 0 or 1 and b is irrational, then a^b must be irrational (in fact, transcendental).

irreptile
See **rep-tile**.

Ishango bone
A bone tool handle discovered around 1960 in the African area of Ishango, near Lake Edward. It has been dated to about 9000 B.C. and was at first thought to have been a **tally** stick. At one end of the bone is a piece of quartz for writing, and the bone has a series of notches carved in groups on three rows running the length of the bone. The markings on two of these rows each add to 60. The first row is consistent with a number system based on 10, since the notches are grouped as 20 + 1, 20 − 1, 10 + 1, and 10 − 1, while the second row contains the **prime number**s between 10 and 20! A third seems to show a method for multiplying by 2 that was used in later times by the Egyptians. Additional markings suggest that the bone was also used as a lunar phase counter. The Ishango Bone is kept at the Royal Institute for Natural Sciences of Belgium in Brussels. See also **Lebombo bone**.[45, 157]

isochrone
A set of points with the property that a given process or trajectory will take the same length of time to complete starting from any of the points. The curve formed by such a set of points is called an *isochronous curve*. See also **tautochrone problem**.

isogonal conjugate
Isogonal lines of a triangle are cevians (see **Ceva, Giovanni**) that are symmetric with respect to the angle bisector. Two points are isogonal conjugates if the corresponding lines to the vertices are isogonal (see **vertex**).

isometry
A symmetry operation, which may involve **translation**, **rotation**, and **reflection**, that preserves the distance of any two points. Each isometry of a **wallpaper group**, for example, can be represented by a 3×3 matrix.

Ishango bone The marks on this 11,000-year-old bone speak of a surprisingly sophisticated mathematical knowledge. *Museum of Natural Sciences (Brussels)*

isomorphism

In geometry, a **transformation** that doesn't alter the side lengths and the angle sizes of the figure involved. Examples of such transformations include reflections, rotations, translations, or transformations by a glide. In **set theory**, an isomorphism is a **one-to-one** correspondence between the elements of two sets such that the result of an operation on elements of one set corresponds to the result of the analogous operation on their images in the other set.

isoperimetric inequality

For any closed, three-dimensional body with volume V and surface area A, the following inequality always holds:

$$36\pi V^2 \leq A^3$$

isoperimetric problem

Among all shapes of a given perimeter, which encloses the greatest area? This ancient conundrum is alluded to in the tale of Queen Dido in Virgil's *Aeneid*. Threatened by her brother, who had already murdered her father, the queen was obliged to hastily gather her valuables and flee her native city of Tyria in ancient Phoenicia. In due course, her ship landed in North Africa, where she made the following offer to a local chieftain: in return for her fortune he would give as much land as she could isolate with the skin of an ox. This was readily agreed to, whereupon the crafty queen sliced the skin into very fine threads, which she tied together and made into a giant semicircle. Combined with the natural boundary provided by the sea, this enclosed such a large area that a city—Carthage—was eventually built upon it. Two millennia later, Karl **Weierstrass** was the first to prove rigorously, using analysis and calculus, that the solution to the isoperimetric problem is a circle (something the Greeks suspected but were not able to prove geometrically). When the same question is asked in one dimension higher it becomes the **isovolume problem**.

isosceles

Having two sides of the same length, as in the case of an isosceles **triangle**. An isosceles **trapezoid** in the United States is the equivalent of a trapezium in Britain. *Isosceles* comes from the Greek *iso* ("same or equal") and *skelos* ("legs").

isotomic conjugate

Two points on the side of a triangle are *isotomic* if they are equidistant from the midpoint of that side. Two points inside a triangle are isotomic conjugates if the corresponding cevians (see **Ceva, Giovanni**) through these points meet the opposite sides in isotomic points.

isovolume problem

What surface encloses the maximum volume per unit surface? The answer is a **sphere**, for which

$$\text{volume/surface area} = (\tfrac{4}{3}\pi r^3)/(4\pi r^2) = \tfrac{1}{3}r,$$

where r is the sphere's radius. Proof of the solution to the isovolume problem came as recently as 1882 from Hermann Schwarz. See also **bubbles** and **isoperimetric problem**.

iterate

Do something repeatedly. Do something repeatedly. . . .

iteration

> *If at first you don't succeed, try, try, again. Then quit. There's no use being a damn fool about it.*
>
> —W. C. Fields

A **feedback** process that repeats n number of times. Iteration refers to the act of performing the calculation of a certain **function** and then picking the result, or output, as the starting value, or input, for the next calculation of the same function. The operation repeats on and on—even infinitely, despite Fields's comment!

J

Jacobi, Karl Gustav Jacob (1804–1851)

A German mathematician who did important work on **elliptic functions**, **partial differential equations**, and mechanics. Although he was preceded in many of his discoveries about elliptic functions by Carl **Gauss** (who didn't publish) and Niels **Abel**, Jacobi is nevertheless considered one of the founders of the subject. His name is probably best known from the *Jacobian,* an $n \quad n$ **determinant** formed from a set of n functions in n unknowns. He wasn't the first to use it–the "Jacobian" appears in an 1815 paper of Agustin **Cauchy**–but Jacobi did write a long memoir about it in 1841, and proved that the Jacobian of n functions vanishes if and only if the functions are related (Cauchy had proved the "if" part). He also did important work on partial differential equations and their application to physics. Along with William **Hamilton**, he developed an approach to mechanics based on generalized coordinates. In this method, the total energy of a mechanical system is represented as a function of generalized coordinates and corresponding generalized momenta; for example, in a double pendulum the two generalized coordinates could be two angles. *Hamilton-Jacobi theory* is the technique of solving the system by transforming coordinates so that the transformed coordinates and momenta are constants.

Jacobi was appointed to a position at the University of Königsberg in 1826. He gained a reputation as a gifted teacher and is credited with introducing the seminar method (giving lectures on his own ongoing research) into the university. After a collapse from overwork in 1843, Jacobi was allowed to stay in Berlin with a generous allowance from the king of Prussia. Five years later, revolution swept Europe and Jacobi was persuaded to run for parliament. This proved a disaster; not only did he loose the election, but his foray into politics annoyed his royal patron, who cut off his pension. Jacobi, with a large family to support, was faced with destitution. Only his reputation as the greatest German mathematician besides Gauss saved him; faced with the prospect of losing Jacobi to the University of Vienna, the king was prevailed upon to restore the pension. Jacobi was a notoriously hard worker (indeed, he had several breakdowns due to overwork), but his death in 1851 was the result of smallpox.

Johnson solid

Any convex **polyhedron** with regular faces that is not a **Platonic solid**, an **Archimedean solid**, or a **prism** (or an antiprism). There are 92 Johnson solids, which are named after Norman W. Johnson who was the first to catalog them in 1966. They include equilateral **deltahedra** and dipyramids (two pyramids placed symmetrically base to base) and any irregular convex solid that can be made by sticking together triangles, squares, pentagons, and so on, in a way that happens to close. Some of the simpler Johnson solids are assemblages of pyramids, prisms, and antiprisms; for example, a gyrobifastigium is two triangular prisms glued together with a twist. Others are fragments of Archimedean solids; for example, a pentagonal rotunda is half an icosidodecahedron. When stretched out with a prism this makes the marvelously named elongated pentagonal orthocupolarotunda.

Johnson's theorem

If three congruent circles all intersect in a single point, then the other three points of intersection will lie on another circle of the same radius. This simple little theorem was discovered by Roger Johnson in 1916.

Jordan, (Marie-Ennemond) Camille (1838–1922)

A French mathematician who made important contributions to **group** theory. He was the first to draw attention to the work of Evariste **Galois**, which had until then been almost entirely ignored. He built on Galois's study by grasping the intimate connection between groups of permutations and the solvability of **polynomial** equations. Jordan also introduced the idea of an infinite group. He passed on his interest in group theory to two of his most outstanding pupils, Felix **Klein** and Sophus **Lie**, both of whom went on to develop the subject in new and important ways.

Jordan curve

A simple, **closed curve**.

Jordan matrix

A **matrix** whose **diagonal** elements are all equal (and nonzero) and whose elements above the principal diagonal are equal to 1, but all other elements are 0.

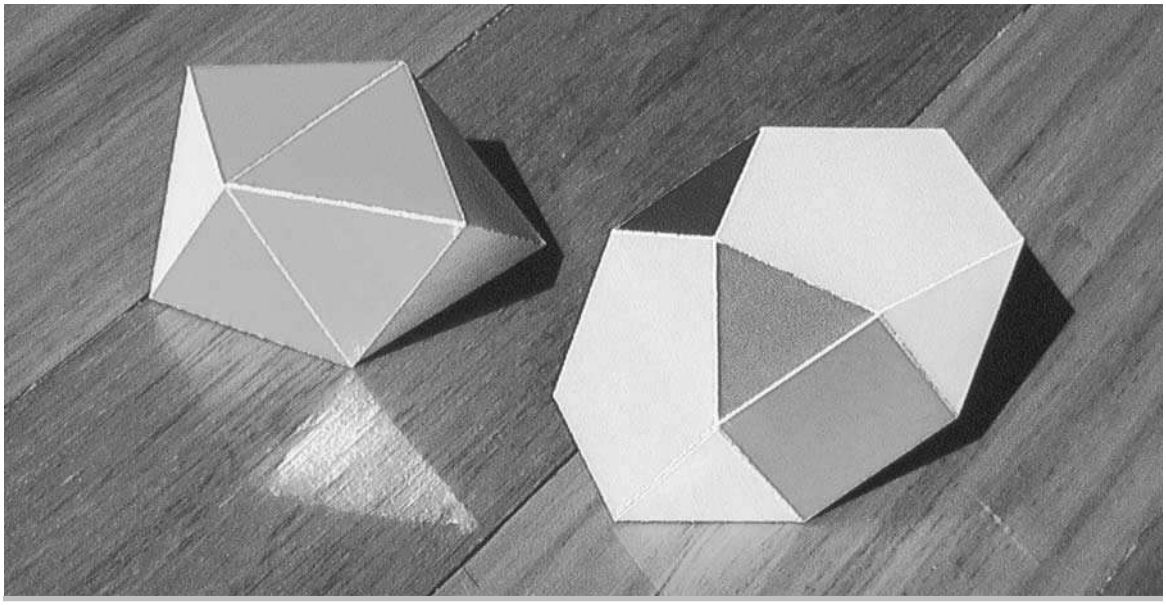

Johnson solid Two of the 92 Johnson solids: the bilunabirotunda (J91, right) and the snub disphenoid (J84, left). *Robert Webb, www.software3d.com; created using Webb's Stella program*

Journal of Recreational Mathematics

The only international journal devoted to the lighter side of mathematics. It was started in 1968 and is currently edited by Charles Ashbacher.

Julia set

Any of any infinite number of **fractal** sets of points on an **Argand diagram** (the complex plane) defined by a simple rule. Given two **complex number**s z and c, and the **recursion** $z_{n+1} = z_n^2 + c$, the Julia set for any given value of c, consists of all values of z for which z, when iterated in the equation above, does not "blow up" or tend to infinity. Julia sets are closely related to the **Mandelbrot set**, which is, in a way, an index of all Julia sets. For any point on the complex plane (which represents a value of c) a corresponding Julia set can be drawn. We can imagine a movie of a point moving about the complex plane with its corresponding Julia set. When the point lies inside the Mandelbrot set the corresponding Julia set is topologically unified or connected. As the point crosses the boundary of the Mandelbrot set, the Julia set explodes into a cloud of disconnected points called *Fatou dust.* If c is on the boundary of the Mandelbrot set, but not a waist point (where two large regions of the Mandelbrot set are connected by a narrow bridge), the Julia set of c looks like the Mandelbrot set in sufficiently small neighborhoods of c.

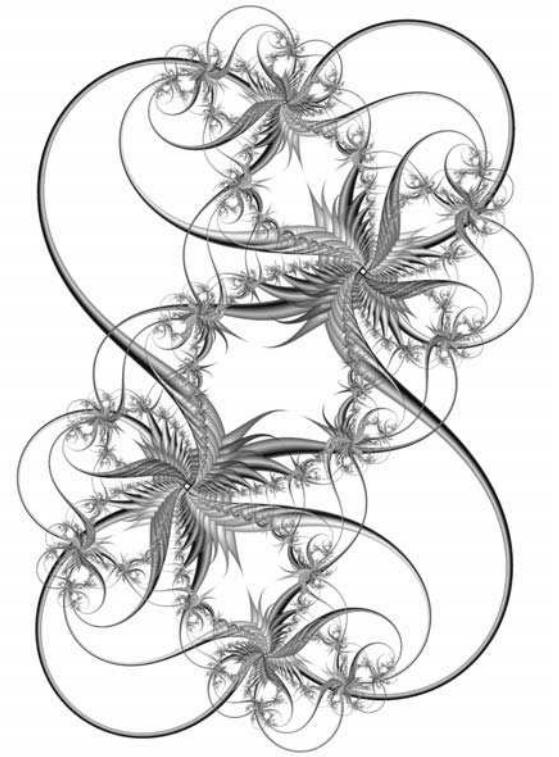

Julia set A fractal image based on a Julia set. *Jos Leys, www.josleys.com*

Julia sets are named after the French mathematician Gaston Julia (1893–1978), whose most famous work, *Memoire sur l'iteration des fonctions rationnelles,* provides the theory for Julia sets before computers were available. In 1918, at the age of 25 Julia was severely wounded in World War I and lost his nose. He wrote his greatest treatise in a hospital between the painful operations necessitated by his wounds.

jump discontinuity

A discontinuity in a **function** where the left- and right-hand limits exist but are not equal to each other.

K

Kaczynski, Theodore John (1942–)

Known as the Unabomber before his true identity was discovered, a Harvard graduate with a genius IQ who abandoned a promising career as a mathematician for a life of social isolation and intermittent terrorist attacks. Kaczynski eluded the FBI for 17 years, during which time he orchestrated 16 explosions that killed 3 people and injured 23 others. He avoided execution following his arrest in 1996 through a plea bargain and was given instead 4 life sentences plus 30 years in prison. During his mathematical career in the late 1960s, Kaczynski published a doctoral dissertation and several papers in academic journals and served as an assistant math professor at the University of California, Berkeley (1967–1969).

Kakeya needle problem

A famous problem named after the Japanese mathematician Sôichi Kakeya, who first posed it in 1917. It asks: What is the smallest-area plane figure inside which a unit straight-line segment can be rotated through 180°? For some years, the answer was thought to be a **deltoid**. However, in 1928, the Russian mathematician Abram Besicovitch shocked the mathematical world by showing that the problem *had no answer* or, to be more precise, that there was no minimum area.[39] In 1917 Besicovitch had been working on a problem in **Riemann integration**, and had reduced it to the question of existence of planar **set**s of **measure** 0, which contain a line segment in each direction. He then constructed such a set, and published his construction in a Russian journal in 1920. Due to the civil war and the blockade, there was hardly any communication between Russia and the rest of the world at the time, so Besicovitch hadn't heard about the challenge posed by Kakeya. Several years later, after he left Russia and learned about the needle problem, Besicovitch modified his original construction and was able to give the startling answer that the area in question may be made arbitrarily small.

Kaluza-Klein theory

A model that seeks to unite classical gravity and electromagnetism by resorting to **higher dimensions**. In 1919 the German mathematician Theodor Kaluza (1885–1954) pointed out that if general **relativity theory** is extended to a five-dimensional **space-time**, the equations can be separated out into ordinary four-dimensional gravitation plus an extra set (which is equivalent to Maxwell's equations for the electromagnetic field) plus an extra field known as the dilaton). Thus, electromagnetism is explained as a manifestation of curvature in a **fourth dimension** of physical space, in the same way that gravitation is explained in Einstein's theory as a manifestation of curvature in the first three. In 1926 the Swedish physicist Oskar Klein (1894–1977) proposed that the reason the extra spatial dimension goes unseen is that it is compact–curled up like a ball with a fantastically small radius. In the 1980s and 1990s, Kaluza-Klein theory experienced a big revival and can now be seen as a precursor of **string theory**.

Kampyle of Eudoxus

An hourglass-shaped curve that was first studied by **Eudoxus** in an attempt to solve the classical problem of **duplicating the cube**. It is described by the Cartesian equation

$$a^2x^4 = b^4(x^2 + y^2).$$

It is also the **radial curve** of the **catenary**.

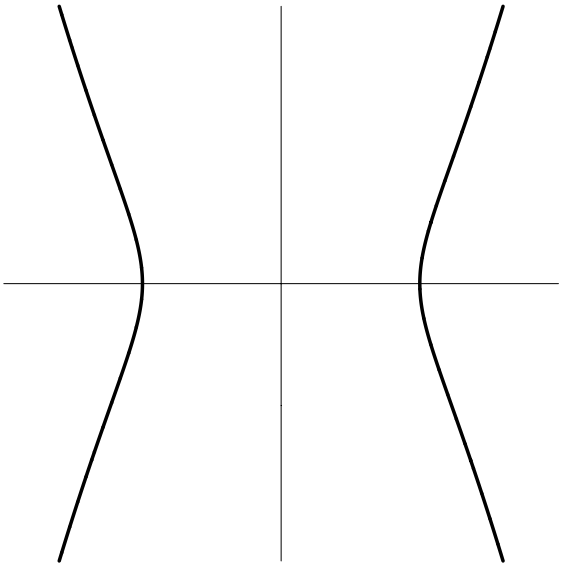

Kampyle of Eudoxus *© Jan Wassenaar, www.2dcurves.com*

kappa curve

Also known as *Gutschoven's curve,* named after Gérard van Gutschoven (1615–1668), who first studied it around 1662. The kappa curve, which resembles the Greek letter κ, was also investigated by Isaac **Newton** and, some years later, by Johann Bernoulli (see **Bernoulli family**). It is given by the Cartesian equation

$$y^2(x^2 + y^2) = a^2x^2.$$

Kaprekar constant

Take any four-digit number whose digits are not all identical. Rearrange the digits to make the largest and smallest 4-digit numbers possible. Subtract the smaller number from the larger. Use the resulting number and repeat the process. For example, starting with 4,731: 7,431 − 1,347 = 6,084; 8,640 − 468 = 8,172; 8,721 − 1,278 = 7,443; 7,443 − 3,447 = 3,996; 9,963 − 3,699 = 6,264; 6,642 − 2,466 = 4,176; 7,641 − 1,467 = 6,174. After this, the result is always 6174. Remarkably, *every* four-digit number whose digits are not all the same will eventually reach 6,174, in at most seven steps, and then stay there. This is called the Kaprekar constant for four-digit numbers, after the Indian mathematician Dattathreya Ramachandra Kaprekar who made the discovery in 1949. The Kaprekar constant for three-digit numbers is 495, which is arrived at for any three-digit number in no more than six iterations. The same process, or algorithm, can be applied to numbers of n-digits, where n is any whole number. Depending on the value of n, the algorithm will result in a nonzero constant, zero (the degenerate case), or a cycle.

Kaprekar number

Take a positive whole number n that has d number of digits. Take the square of n and separate the result into two pieces: a right-hand piece that has d digits and a left-hand piece that has either d or $d - 1$ digits. Add these two pieces together. If the result is n, then n is a Kaprekar number. Examples are 9 ($9^2 = 81$, $8 + 1 = 9$), 45 ($45^2 = 2{,}025$; $20 + 25 = 45$), and 297 ($297^2 = 88{,}209$; $88 + 209 = 297$). The first 10 Kaprekar numbers according to this definition are 1; 9; 45; 55; 99; 297; 703; 999; 2,223; and 2,728. Kaprekar numbers can also be defined by higher powers. For example, $45^3 = 91{,}125$; and $9 + 11 + 25 = 45$. The first 10 numbers with this property are: 1; 8; 10; 45; 297; 2,322; 2,728; 4,445; 4,544; and 4,949. For fourth powers, the sequence begins 1; 7; 45; 55; 67; 100; 433; 4,950; 5,050; 38,212. Notice that 45 is a Kaprekar number for second, third, and fourth powers ($45^4 = 4{,}100{,}625$; and $4 + 10 + 06 + 25 = 45$)–the only number in all three Kaprekar sequences, up to at least 400,000. See also **unique number**.

Kasner, Edward (1876–1955)

An American mathematician at Columbia University best remembered for introducing the words ***googol*** and *googolplex* into the popular mathematical lexicon. He is also well known as the coauthor, with James **Newman**, of *Mathematics and the Imagination,* first published in 1940.[186] In a later edition (1967), he spoke about the term *mathescope,* which was coined by the science reporter Wilson Davis after listening to one of Kasner's public lectures. In Kasner's words: "It is not a physical instrument; it is a purely intellectual instrument, the ever-increasing insight which mathematics gives into the fairyland which lies beyond intuition and beyond imagination." His main field of research was **differential geometry**, which he studied in its applications to mechanics, cartography, and stereographic projections, though he also wrote papers on circle packing and on the horn angle and studied an extension of right triangles to the complex plane.

Kepler, Johannes (1571–1630)

A German astronomer and mathematician best remembered for his three laws of planetary motion. He also did important work in optics, discovered two new regular polyhedra (1619), gave the first mathematical treatment of close **packing** of equal spheres (in 1611, leading to an explanation of the shape of the cells of a honeycomb), gave the first proof of how **logarithm**s work (1624), and devised a method of finding the volumes of **solids of revolution** that (with hindsight) can be seen as contributing to the development of **calculus** (1615–1616). Although his work eventually led to our modern view of the solar system, he himself held beliefs about the arrangement of the planets that smack of Pythagorean mysticism, though ultimately they stemmed from his belief that mathematical harmony was a reflection of God's perfection. In his first cosmological model (*Mysterium cosmographicum,* 1596) he suggested that if a sphere were drawn to touch the inside of the path of Saturn, and a cube were inscribed in the sphere, then the sphere inscribed in that cube would be the sphere circumscribing the path of Jupiter. Then if a regular tetrahedron were drawn in the sphere inscribing the path of Jupiter, the insphere of the tetrahedron would be the sphere circumscribing the path of Mars, and so inward, putting the regular dodecahedron between Mars and Earth, the regular icosahedron between Earth and Venus, and the regular octahedron between Venus and Mercury. Thus the number of (then-known) planets is explained perfectly in terms of the five convex regular solids–the **Platonic solid**s.

Kepler's second work on cosmology (*Harmonices mundi* [Harmony of the world], book V, 1619) offers a more elaborate mathematical model but still with the polyhedra in place. The mathematics in this work includes the first

systematic treatment of **tessellation**s, a proof that there are only 13 convex uniform polyhedra (the **Archimedean solid**s) and the first account of two non-convex regular polyhedra (see **Kepler-Poinsot solid**s).

Kepler's mathematical work was full time and continued even during the wedding to his second wife in 1613. The dedicatory letter to a book he wrote shortly after explains that at the wedding celebration he noticed that the volumes of wine barrels were estimated by means of a rod slipped in diagonally through the bunghole, which prompted him to wonder how that could work. The result was a study of the volumes of solids of revolution, *Nova Stereometria Doliorum* (New stereometry of wine barrels, 1615).

Kepler-Poinsot solids

The four regular nonconvex polyhedra that exist in addition to the five regular convex polyhedra known as the **Platonic solid**s. As with the Platonic solids, the Kepler-Poinsot solids have identical regular **polygon**s for all their faces, and the same number of faces meet at each vertex. What is new is that we allow for a notion of "going around twice," which results in faces that intersect each other. In the *great stellated dodecahedron* and the *small stellated dodecahedron,* the faces are pentagrams (five-pointed stars). The center of each pentagram is hidden inside the polyhedron. These two polyhedra were described by Johannes **Kepler** in 1619, and he deserves credit for first understanding them mathematically, though a sixteenth-century drawing by the Nuremberg goldsmith Wentzel Jamnitzer (1508–1585) is very similar to the former and a fifteenth-century mosaic attributed to the Florentine artist Paolo Uccello (1397–1475) illustrates the latter. The *great icosahedron* and *great dodecahedron* were described by Louis **Poinsot** in 1809, though Jamnitzer made a picture of the great dodecahedron in 1568. In these two, the faces (20 triangles and 12 pentagons, respectively) that meet at each vertex "go around twice" and intersect each other, in a manner that is

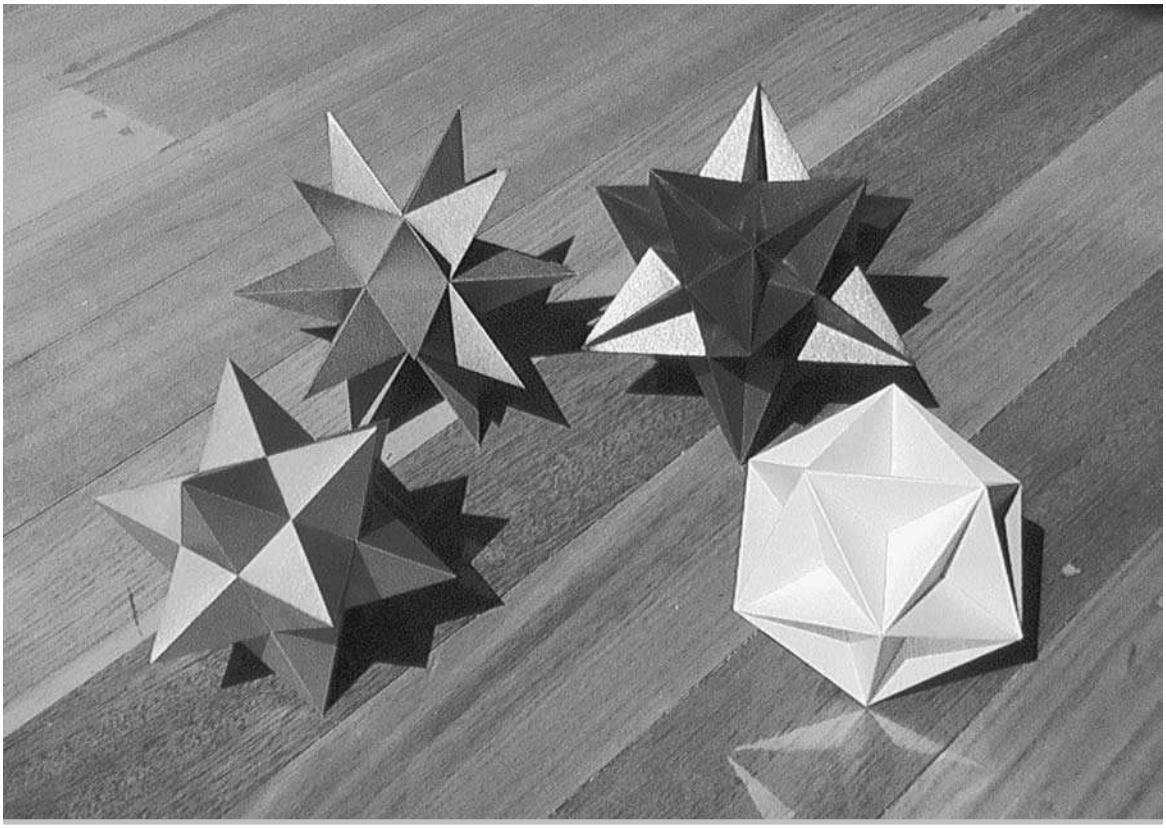

Kepler-Poinsot solids From left to right: the small stellated dodecahedron, great stellated dodecahedron, great icosahedron, and great dodecahedron. *Robert Webb, www.software3d.com; created using Webb's Stella program*

the three-dimensional analog to what happens in two dimensions with a **pentagram**. Together, the Platonic solids and the Kepler-Poinsot polyhedra form the set of nine *regular* polyhedra. Augustin **Cauchy** first proved that no other polyhedra can exist with identical regular faces and identical regular vertices.

Kepler's conjecture

No **packing** of spheres of the same radius in three dimensions has a density greater than the face-centered (hexagonal) cubic packing. This claim was first published by Johannes **Kepler** in his monograph *The Six-Cornered Snowflake* (1611), a treatise inspired by his correspondence with Thomas Harriot (see **cannonball problem**). In his slender essay, Kepler asserted that face-centered cubic packing–the kind greengrocers use to stack oranges–is "the tightest possible, so that in no other arrangement could more pellets be stuffed into the same container." The question of whether Kepler's conjecture is right or not has became known, not surprisingly, as *Kepler's problem*. In the nineteenth century, Carl **Gauss** proved that face-centered cubic packing is the densest arrangement in which the centers of the spheres form a regular lattice, but he left open the question of whether an irregular stacking of spheres might be still denser. In 1953, László Tóth reduced the Kepler conjecture to an enormous calculation that involved specific cases, and later suggested that computers might be helpful for solving the problem. This was the approach taken by Thomas Hales, a mathematician at the University of Michigan at Ann Arbor, and which led him, in 1998, to claim that he had proved Kepler was right all along. Hales's proof of Kepler's conjecture remains controversial simply because of the length of the computer calculations involved and the difficulty of verifying them. The casebook on this mystery remains open. See also **monster group**.

Khayyam, Omar (1044–1123)

An outstanding Persian mathematician and astronomer, whose full name was Abu al-Fath Omar ben Ibrahim al-Khayyam, or "tent-maker"–possibly his father's profession. His work on algebra was known throughout Europe in the Middle Ages. He made several important contributions: he discovered a geometrical method to solve **cubic** equations by intersecting a **parabola** with a circle, discussed what would become known as **Pascal's triangle**, and asked if a ratio could be regarded as a number. He is best known, however, as a poet. In 1859, Edward Fitzgerald (1809–1883) translated Khayyam's *Rubaiyat*–a popular collection 600 short four-line poems. Rosehips from Khayyam's tomb were germinated at Kew Gardens, London, and planted on Fitzgerald's tomb in St. Michael's Churchyard, Boulge, Suffolk, in 1893; the original plant has died, but its descendents continue to bloom.

Khintchine's constant

One of the most remarkable, yet poorly understood, constants in mathematics, which captures, in a fascinating way, the behavior of *almost all* **real number**s. Pick a real number at random and write it down as a **continued fraction**. Almost certainly, the **geometric mean** of the terms in this continued fraction will be Khintchine's constant, which has the value 2.685452 . . . . It is important to say "almost certainly" because there are some real numbers including all **rational number**s, roots of third-order **polynomial**s, and certain other classes of number, whose continued fractions would give a different result. These exceptions, however, form a tiny minority of all real numbers.

kings problem

The problem of determining how many nonattacking kings, $K(n)$, can be placed on an $n \times n$ chessboard. For $n = 8$, the solution is 16. The general solution is $K(n) = \frac{1}{4}n^2$ if n is even and $K(n) = \frac{1}{4}(n + 1)^2$ if n is odd. The minimum number of kings needed to attack or occupy all squares on an 8×8 chessboard is nine.

kinship puzzles

Like **age puzzles and tricks**, problems to do with how family members are related go back many centuries. Some of these can be fiendishly convoluted, especially if incestual pairings are allowed (in the puzzle!). Sketching a genealogical tree is sometimes helpful. The following all involve legitimate ties.

PUZZLES

1. Brothers and sisters have I none, but that man's father is my father's son. Who is that man? (This is one of the oldest problems of the kinship variety.)
2. What is the simplest way in which two people can be an uncle to each other? (From Dudeney's *A Puzzle-Mine*.)
3. A certain family party consisted of 1 grandfather, 1 grandmother, 2 fathers, 2 mothers, 4 children, 3 grandchildren, 1 brother, 2 sisters, 2 sons, 2 daughters, 1 father-in-law, 1 mother-in-law, and 1 daughter-in-law. Twenty-three people, you will say. No; there were only seven people present. Can you show how this might be? (From *Amusements in Mathematics*.)

Solutions begin on page 369.

Kirkman, Thomas Penyngton (1806–1895)

An English rector and mathematician who did important work in **combinatorics**. His **schoolgirls problem**, which he posed in 1850, led to a more general study of certain ways of combining objects. He also explored the possibility of finding a route around the edges of a given **polyhedron** that passes through each vertex (corner) of the shape once and only once. His rather complex and ultimately unprovable ideas were later picked up and refined successfully by William **Hamilton**, but not be-fore Kirkman had managed to supply a general proof of the fact that "if a polyhedron has an odd number of vertices and each face has an even number of edges, then there is no circuit which passes through all the vertices." This result introduces the concept of a *bipartite graph*—a **graph** that can be divided into two separate sets of vertices such that every edge in one set joins a vertex.

kite

A **quadrilateral**, with two pairs of congruent adjacent sides, that is named after one of the traditional forms of toy kite. The toy itself probably draws its name from the bird commonly called a kite, or kyte, in England. The old English form of the word, cyte, may in turn derive from an early German name for an owl. A nonconvex kite is often called a *dart,* a term used by Roger **Penrose** in his proof on a nonperiodic tiling of the plane (see also **Penrose tiling**). **Proclus** referred to this shape as a "four-sided triangle" and spoke of it as a geometric paradox. John **Conway** pointed out that there is no special name for a quadrilateral that has two pairs of equal sides that, unlike in the case of a kite, are not parallel sides. He proposed the name *strombus* for such a figure, from the Greek for a spinning top.

Klein, Christian Felix (1849–1925)

A German mathematician noted for his work on **non-Euclidean geometry**, the connections between geometry and **group** theory, and the theory of functions. His Erlangen Programm (1872) for unifying the diverse forms of geometry through the study of equivalence in transformation groups was profoundly influential, especially in the United States, for over 50 years. In his *Lectures on the Icosahedron and the Solution of Equations of the Fifth Degree* (1884, tr. 1888) he showed how the rotation groups of regular solids could be applied to the solution of difficult algebraic problems. Klein was a professor of mathematics successively at the University of Erlangen, the Technical Institute in Munich, and the universities of Leipzig and Göttingen, and was a prolific writer and lecturer on the theory, history, and teaching of mathematics. See also **Klein bottle**.

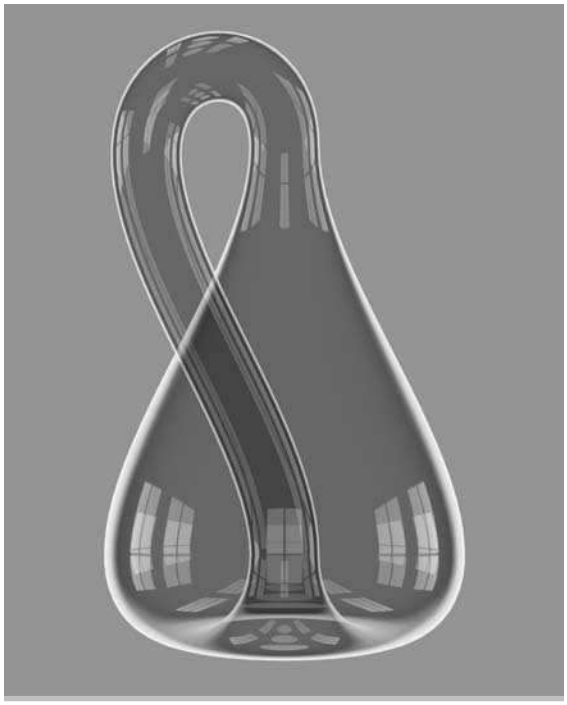

Klein bottle The famous container, with zero volume, rendered in the improbable form of a soap bubble. © *John M. Sullivan, University of Illinois and TU Berlin*

Klein bottle

A mathematician named Klein,
Thought the Möbius band was divine,
He said, "If you glue,
The edges of two,
You'll get a weird bottle like mine."

–Leo Moser

Take a rectangle and join one pair of opposite sides to make a cylinder. Now join the other pair with a half-twist. The result is a Klein bottle. Sound easy? It is if you have access to a **fourth dimension** because that's what is needed to carry out the second step and to allow the surface to pass through itself without a hole. A true Klein bottle is a four-dimensional object. It was discovered in 1882 by Felix **Klein** when he imagined, as in the limerick, joining two **Möbius band**s together to create a single-sided bottle with no boundary.

An ordinary (three-dimensional) bottle has a crease or fold around the opening where the inside and outside of the bottle meet. A sphere doesn't have this crease or fold, but it has no opening. A Klein bottle has an opening but no crease: like a Möbius band, it is a continuous one-sided structure. Because it has no crease or fold, there's

no verifiable definition of where its inside and outside begin. Therefore, the volume of a Klein bottle is considered to be zero, and the bottle has no real contents—except itself! As the joke goes: "In topological hell the beer is packed in Klein bottles." Take a coin, slide it across the surface of a Klein bottle until it returns to its starting point, and the coin, as if by magic, will be flipped over. This is because, unlike a sphere or a regular bottle, a Klein bottle is nonorientable.

Although a Klein bottle can't be "embedded" (that is, fully realized) in three dimensions, it can be "immersed" in three dimensions. Immersion is what happens when a higher dimensional object cuts through a lower dimensional one, producing a cross section. When a sphere is immersed in a plane, for example, it produces a circle. The computer-generated soap bubble structure shown here could be created by stretching the neck of a bottle through its side and joining its end to a hole in the base. Except at the side-connection (the nexus), this properly shows the shape of a four-dimensional Klein bottle. Just as the picture here is of a three-dimensional Klein bottle immersion, so an immersion in real life is like a drawing of the true four-dimensional bottle.

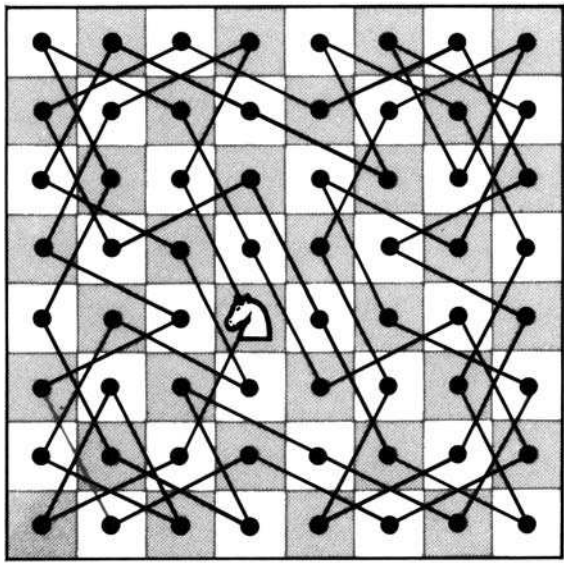

knight's tour After visiting every square of the chessboard exactly once, the knight returns to its starting point.

knights problem

To find the maximum number of knights that can be placed on an $n \times n$ chessboard in such a way that no two pieces are attacking each other. For a standard 8×8 chessboard, the answer is 32 (all on white squares or all on black). In the general, the solution is $\frac{1}{2} n^2$ if n is even and $\frac{1}{2} (n^2 + 1)$ if n is odd, giving the sequence 1, 4, 5, 8, 13, 18, ...

knight's tour

A classic **chess** puzzle: to find a sequence of moves by which a knight can visit each square of a chessboard exactly once. If the final position is a knight's move away from the first position, the tour is said to be *closed* or *reentrant.* The earliest recorded solution for a standard 8×8 chessboard was given by Abraham **de Moivre**; the earliest known reentrant solution came from the French mathematician Adrien-Marie Legendre (1752–1833). Not to be outdone Leonhard **Euler** found a reentrant tour that visits two halves of the board in turn. The problem can be generalized to an $n \times n$ board, with some surprising results; for example, a reentrant tour is not possible on a 4×4 board.

A knight's tour is called a **magic tour** if the resulting arrangement of numbers forms a **magic square**, and a *semimagic tour* if the resulting arrangement of numbers is a **semi-magic square**. It has long been known that magic knight's tours aren't possible on $n \times n$ boards if n is odd. It was also known that such tours are possible for all boards of size $4k \times 4k$ for $k > 2$. However, while a number of semi-magic knight's tours were known on the usual 8×8 chessboard, it was *not* known if any fully magic tours existed on the 8×8 board. This longstanding open problem was finally settled in the negative by an exhaustive computer enumeration of all possibilities. The software for the computation was written by J. C. Meyrignac, and a Web site was established by Guenter Stertenbrink to distribute and collect results for all possible tours. After 61.40 CPU-days, corresponding to 138.25 days of computation at 1 GHz, the project was completed on August 5, 2003. As well as netting a total of 140 distinct semi-magic knight's tours, the computation showed for the first time that no 8×8 magic knight's tour is possible.

More magical and mysterious tours can be conducted on boards on the surfaces of cubes, cylinders, toruses, and multidimensional shapes, such as hypercubes. See also **Hamilton path**.

knot

Never cut what you can untie.

–Joseph Joubert

A **closed** curve in three dimensions. The two simplest nontrivial knots are the trefoil knot, whose picture has three crossings, and the figure-eight knot, whose picture has four. To date, more than 1.7 million nonequivalent knots with

pictures of 16 or fewer crossings have been identified. The mathematical theory of knots was born out of attempts to model the atom. Near the end of the nineteenth century, William Thomson (Lord Kelvin) suggested that different atoms were actually different knots tied in the ether that was believed to permeate all of space. Physicists and mathematicians set to work making a table of distinct knots, believing they were making a table of the elements. A pioneer in this effort, alongside Thomson, was Peter **Tait**. By the time the theory of the ether vanished into thin air, *knot theory* was firmly tied into mainstream mathematics. It blossomed with the development of **topology** and eventually led to important applications in DNA research and molecular biology. Today it is one of the most active areas of mathematical research. See also **tie knot**, **loop**, and **braid**.

Knuth's up-arrow notation

A notation for **large number**s developed by the American mathematician Donald Knuth in 1976. A single up-arrow (↑) is the same as exponentiation:

$$m \uparrow n = m \times m \times \ldots \times m \ (n \text{ terms}) = m^n.$$

Two up-arrows together represent a **power tower**:

$$m \uparrow\uparrow n = m^{m^{\cdot^{\cdot^{\cdot^{m}}}}} \Big\} n.$$

(a tower of height n), which is the same as the operation known as *hyper4* or *tetration*. This can very rapidly generate huge numbers. For example:

$2 \uparrow\uparrow 2 = 2 \uparrow 2 = 4$
$2 \uparrow\uparrow 3 = 2 \uparrow 2 \uparrow 2 = 2 \uparrow 4 = 16$
$2 \uparrow\uparrow 4 = 2 \uparrow 2 \uparrow 2 \uparrow 2 = 2 \uparrow 16 = 65{,}536$
$3 \uparrow\uparrow 2 = 3 \uparrow 3 = 27$
$3 \uparrow\uparrow 3 = 3 \uparrow 3 \uparrow 3 = 3 \uparrow 27 = 7{,}625{,}597{,}484{,}987$
$3 \uparrow\uparrow 4 = 3 \uparrow 3 \uparrow 3 \uparrow 3 = 3 \uparrow 3 \uparrow 27 = 3^{7625597484987}$

Three up-arrows together represent a still more vastly powerful operator, equivalent to *hyper5* or *pentation*, or a power tower of power towers:

$$m \uparrow\uparrow\uparrow n = m \uparrow\uparrow m \uparrow\uparrow \ldots \uparrow\uparrow m \ (n \text{ terms})$$

For example:

$2 \uparrow\uparrow\uparrow 2 = 2 \uparrow\uparrow 2 = 4$
$2 \uparrow\uparrow\uparrow 3 = 2 \uparrow\uparrow 2 \uparrow\uparrow 2 = 2 \uparrow\uparrow 4 = 65{,}536$
$2 \uparrow\uparrow\uparrow 4 = 2 \uparrow\uparrow 2 \uparrow\uparrow 2 \uparrow\uparrow 2 = 2 \uparrow\uparrow 65{,}536 = 2 \uparrow 2 \uparrow \ldots \uparrow 2$ (65,536 terms)
$3 \uparrow\uparrow\uparrow 2 = 3 \uparrow\uparrow 3 = 7{,}625{,}597{,}484{,}987$
$3 \uparrow\uparrow\uparrow 3 = 3 \uparrow\uparrow 3 \uparrow\uparrow 3 = 3 \uparrow\uparrow 7{,}625{,}597{,}484{,}987 = 3 \uparrow 3 \uparrow \ldots \uparrow 3$ (a power tower 7,625,597,484,987 layers high)
$3 \uparrow\uparrow\uparrow 4 = 3 \uparrow\uparrow 3 \uparrow\uparrow 3 \uparrow\uparrow 3 = 3 \uparrow\uparrow 3 \uparrow\uparrow 7{,}625{,}597{,}484{,}987 = 3 \uparrow\uparrow 3 \uparrow \ldots \uparrow 3$ (a tower $3 \uparrow\uparrow$ 7,625,597,484,987 layers high)

Similarly,

$$m \uparrow\uparrow\uparrow\uparrow n = m \uparrow\uparrow\uparrow m \uparrow\uparrow\uparrow \ldots \uparrow\uparrow\uparrow m \ (n \text{ terms})$$

so that, for example:

$2 \uparrow\uparrow\uparrow\uparrow 2 = 2 \uparrow\uparrow\uparrow 2 = 4$
$2 \uparrow\uparrow\uparrow\uparrow 3 = 2 \uparrow\uparrow\uparrow 2 \uparrow\uparrow\uparrow 2 = 2 \uparrow\uparrow\uparrow 4 = 2 \uparrow 2 \uparrow \ldots \uparrow 2$ (65,536 terms)
$2 \uparrow\uparrow\uparrow\uparrow 4 = 2 \uparrow\uparrow\uparrow 2 \uparrow\uparrow\uparrow 2 \uparrow\uparrow\uparrow 2 = 2 \uparrow\uparrow\uparrow 2 \uparrow 2 \uparrow \ldots \uparrow 2$ (65,536 terms)
$3 \uparrow\uparrow\uparrow\uparrow 2 = 3 \uparrow\uparrow\uparrow 3 = 3 \uparrow 3 \uparrow \ldots \uparrow 3$ (7,625,597,484,987 terms)
$3 \uparrow\uparrow\uparrow\uparrow 3 = 3 \uparrow\uparrow\uparrow 3 \uparrow\uparrow\uparrow 3 = 3 \uparrow\uparrow\uparrow 3 \uparrow 3 \uparrow \ldots \uparrow 3$ (7,625,597,484,987 terms)
$= 3 \uparrow\uparrow 3 \uparrow 3 \uparrow \ldots \uparrow 3$ ($3 \uparrow 3 \uparrow \ldots \uparrow 3$ (7,625,597,484,987 terms)

Even up-arrow notation becomes cumbersome, however, when one is faced with staggeringly large numbers such as **Graham's number**. For such cases, more extensive systems such as **Conway's chained arrow notation** or *Steinhaus-Moser notation* are better suited. See also the **Ackermann function**, to which up-arrow notation is closely related.

Koch snowflake

One of the most symmetric and easy to understand **fractal**s; it is named after the Swedish mathematician Helge von Koch (1870–1924), who first described it in 1906. To make the snowflake, start with a straight line and split it into three equal parts. Replace the middle part with two lines, both of the same length as the first three, creating an

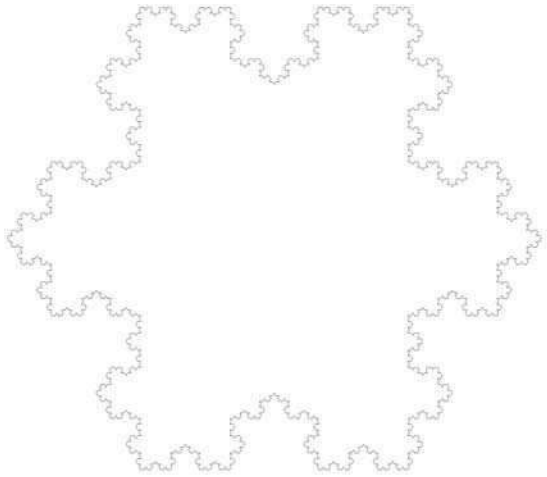

Koch snowflake This fractal shape emerges from continually sprouting equilateral triangles. *Xah Lee, www.xahlee.org*

equilateral triangle missing the bottom line. The shape now consists of four straight lines with the same length. For each of these lines, repeat this process, then continue the transformation indefinitely. The Koch snowflake has infinite length because each iteration increases the length of a line segment one-third, and the iterations go on forever.

The same kind of process can be applied to a tetrahedron. Take a regular tetrahedron (all side lengths the same) and glue to each of its faces a smaller regular tetrahedron. (Each smaller tetrahedron is scaled down by a factor of ½ from the larger one, and placed on each face in an inverted fashion, so that it divides the face into four equilateral triangles and covers the center one.) Then iterate this process. Intuition suggests that the end product might be a very strange-looking jagged object. But in fact, in the limit, as the number of iterations tends to infinity, the result is a perfect cube! The cube has side length $t/\sqrt{2}$, where t is the length of one of the edges of the regular tetrahedron you started with. Variations on the flat Koch snowflake include the *exterior snowflake,* the *Koch antisnowflake,* and the *flowsnake* curves.

Kolmogorov, Andrei Nikolaievich (1903–1987)

A Russian mathematician and physicist who advanced the foundations of **probability theory**, the **algorithm**ic theory of **random**ness, and made crucial contributions to the foundations of statistical mechanics, **stochastic** processes, **information theory**, fluid mechanics, and nonlinear dynamics. All of these areas, and their interrelationships, underlie **complex system**s as they are studied today. His work on reformulating probability started with a 1933 paper in which he built up probability theory in a rigorous way from fundamental axioms, similar to Euclid's treatment of geometry. Kolmogorov went on to study the motion of the planets and turbulent fluid flows, publishing two papers in 1941 on turbulence that even today are of fundamental importance.

In 1954 he developed his work on dynamical systems in relation to planetary motion, thus demonstrating the vital role of probability theory in physics and reopening the study of apparent randomness in deterministic systems, along the lines originally conceived by Henri **Poincaré**. In 1965 he introduced the algorithmic theory of randomness via a measure of complexity, now referred to as *Kolmogorov complexity.* According to Kolmogorov, the complexity of an object is the length of the shortest computer program that can reproduce the object. Random objects, in his view, were their own shortest description, whereas periodic sequences have low Kolmogorov complexity, given by the length of the smallest repeating "template" sequence they contain. Kolmogorov's notion of complexity is a measure of randomness, one that is closely related to Claude **Shannon**'s entropy rate of an information source.

Königsberg bridge problem

See **bridges of Königsberg**.

Kronecker, Leopold (1823–1891)

A German mathematician and pioneer in the field of **algebraic number**s who formulated the relationship between the theory of numbers, the theory of equations, and **elliptic function**s. He acquired a passion for **number theory** from Ernst Kummer, his instructor at the Liegnitz Gymnasium. Kronecker, who made a fortune in business before returning to his academic studies, claimed that mathematical argumentation should be based only on integers and finite procedures. He was one of Georg **Cantor**'s sternest critics and refused to accept the validity of **Weierstrass's nondifferentiable function.**

L

labyrinth
See **maze**.

Lagrange, Joseph Louis (1736–1813)
An Italian-born French mathematician who made important contributions to **number theory** and to classical and celestial mechanics. By his mid-twenties he was recognized as one of the greatest living mathematicians because of his papers on wave propagation and the maxima and minima of curves. His prodigious output included his textbook *Mécanique Analytique* (Analytical mechanics, 1788), the basis for all later work in this field. His remarkable discoveries include the *Lagrangian,* a differential operator characterizing a system's physical state, and the *Lagrangian points,* points in space where a small body in the gravitational fields of two large ones remains relatively stable. Under Napoleon, Lagrange was made both a senator and a count; he is buried in the Panthéon.

lambda calculus
A model of computation that is capable of **universal computation**. The Lisp programming language was inspired by lambda calculus.

Lamé curve
Any of a family of curves related to the **ellipse** and that was first recognized and studied in 1818 by the French physicist and mathematician Gabriel Lamé (1795–1870). The formula for the Lamé curve family is a generalization of the equation for an ellipse ($|x/a|^2 + |y/b|^2 = 1$), namely:

$$|x/a|^n + |y/b|^n = 1,$$

where n is any real number. When $n = 0$, the curve reduces to a pair of crossed lines. As n increases, the curve changes from a curved star shape to a rectangle, with diagonals a and b, when $n = 1$. The special case when $n = 2/3$ corresponds to the **astroid**. Between $n = 1$ and $n = 2$ the curve turns from a curved rectangle to an ellipse (or a circle when both a and b are 1). For values of n greater than 2, Lamé curves are known as **superellipse**s.

lamination
A decoration of a **manifold** in which some subset is partitioned into sheets of some lower dimension, and the sheets are locally parallel. It may or may not be possible to fill the gaps in a lamination to make a **foliation**.

Langley's adventitious angles
A seemingly simple problem first posed in 1922 by E. M. Langley[195] in connection with an isosceles triangle. In its original form, it is stated as follows: ABC is an isosceles triangle. B = C = 80°. CF at 30° to AC cuts AB in F. BE at 20° to AB cuts AC in E. Prove angle BEF = 30°. (No mention is made of D. Perhaps it is at the intersection of BE and CF.) A number of solutions appeared shortly after, including this one given by J. W. Mercer: Draw BG at 20° to BC, cutting CA in G. Then angle GBF = 60° and angles BGC and BCG are 80°. So BC = BG. Also angle BCF = angle BFC = 50°, so BF = BG and triangle BFG is equilateral. But angle GBE = 40° = angle BEG, so BG = GE = GF. And angle FGE = 40°, hence GEF = 70° and BEF = 30°.

Langton's ant
A type of **cellular automaton**, or a simple form of **artificial life**, named after its designer, Christopher Langton. The ant lives on an infinitely large chessboard, each square of which can be either black or white. Two pieces of information are associated with this digital insect: the

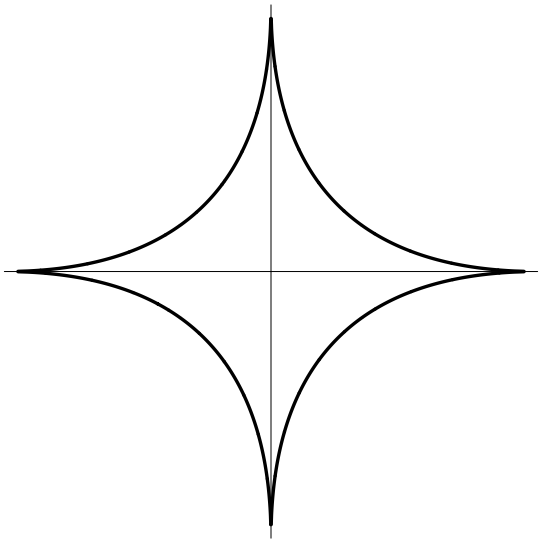

Lamé curve One example from the family of Lamé curves. © *Jan Wassenaar, www.2dcurves.com*

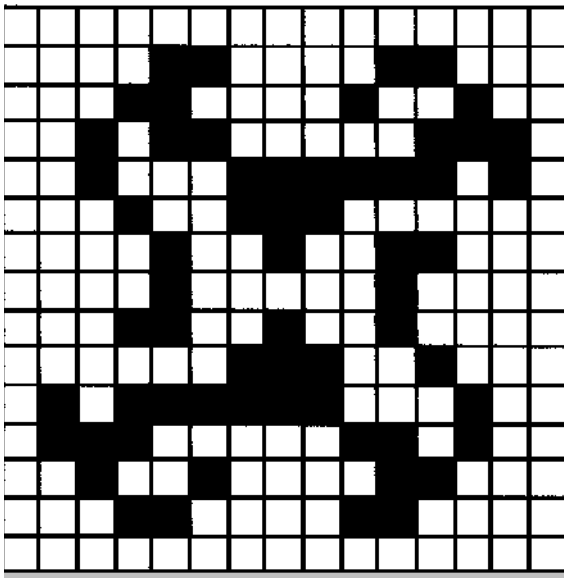

Langton's ant After 368 steps, a symmetrical pattern emerges.

direction that it's facing, and the state of the square that it currently occupies. Three simple rules govern the ant's behavior: (1) If it's on a black square, it turns left. (2) If it's on a white square, it turns right. (3) As it moves to the next square, the one it was on reverses color. Interest in Langton's ant stems from the fact that despite being a completely determined system governed by extremely simple rules, the patterns it produces are fantastically rich and complex. For the first 10,000 moves or so, the ant meanders around, building and then unbuilding structures with little pattern to them. Then, near the end of this chaotic phase, the ant begins to construct a diagonal highway off toward one edge of the board. In fact, this pattern stems from a sequence of 104 moves that, once started, will go on forever. In the language of **chaos** theory, the pattern is a *stable attractor* for the system. Remarkably, no matter what the initial arrangement of squares–even if the white and black squares are set up randomly–the ant will end up building a highway. The ant can be allowed to wrap around the edges of a finite board, thus allowing it to intersect its own path, and it will *still* end up building the highway. Are there any initial states that don't lead to the diagonal-road-building loop? No exceptions have been found from experiments–but proving it is another matter. Most mathematicians believe there is no general analytical method of predicting the position of the ant, or of any such chaotic system, after any given number of moves. Its behavior can't be reduced to the rules that govern it. In this sense, Langton's ant is a simple demonstration of the undecidability of the **halting problem**. The British mathematician Ian **Stewart** and biologist Jack Cohen, in their book *Figments of Reality*,[321] go a step further and use Langton's ant as an analog of an essential stage in the evolution of complex systems such as life: a stage in which the existence of chaotic behavior contains the potential for the spontaneous emergence of unpredictable forms of order.

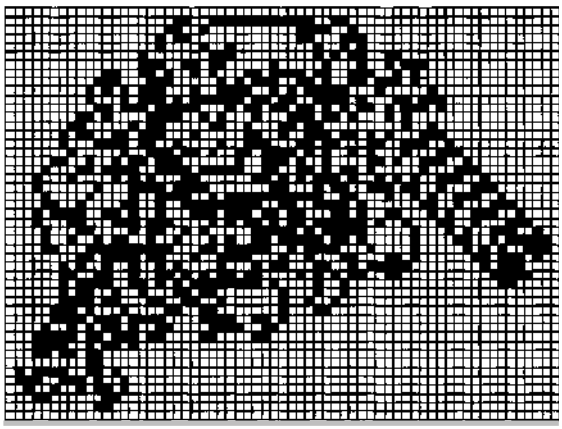

Langton's ant After 10,647 steps the "highway" is under construction.

Laplace, Pierre Simon (1749–1827)

A French mathematician and astronomer who was heavily involved with the development of celestial mechanics. He made an early impact by solving a complex problem of mutual gravitation that had eluded both Leonhard **Euler** and Joseph **Lagrange**. Laplace was among the most influential scientists of his time and was called the Newton of France for his study of and contributions to the understanding of the stability of the solar system. Laplace generalized the laws of mechanics for their application to the motion and properties of the heavenly bodies. He is also famous for his great treatises *Mécanique céleste* (Celestial mechanics, 1799–1825) and *Théorie analytique des probabilités* (Analytical theory of probabilities, 1812) which were advanced in large part by the mathematical techniques that Laplace developed early in his life.

large number

> *Bigger than the biggest thing ever and then some. Much bigger than that in fact, really amazingly immense, a totally stunning size, real "wow, that's big!" time. . . . Gigantic multiplied by colossal multiplied by staggeringly huge is the sort of concept we're trying to get across here.*
>
> –Douglas Adams, *The Restaurant at the End of the Universe*

Making, naming, and representing very large numbers is itself a big problem. A simple way to start is by adding zeros: 10; 100; 1,000; 10,000; . . . , 1,000,000; . . . . But this quickly gets tedious and exponentiation becomes a more attractive option: 10^1, 10^2, 10^3, . . . , 10^6, ... Naming the various powers of 10 follows a regular pattern of prefixes. In the United States, 10^3 is one thousand, 10^6 is one million, 10^9 is one billion, 10^{12} is one trillion, 10^{15} is one quadrillion, and so on. The "-illion" root kicks in at the sixth power of 10 prefixed by "m" for "mono"; then, every jump of three powers (factor of a thousand) comes the next prefix. Put another way, the U.S. name for 10^{3n} uses the Latinized prefix for $n - 1$. One centillion, which is the largest number with a single-word name in English, is 10^{303}. Elsewhere in the world, "billion," "trillion," and so on, can mean things other than they do in the U.S. system. A British billion, for example, is one million million, or 10^{12}, while the now largely obsolete term *milliard* was used for a thousand million. However, the American forms have become fairly standard internationally and are used without qualification in this book. It's also worth noting that, while "quadrillion," "quintillion," and so forth, are perfectly valid terms, "one thousand trillion," "one million trillion," and so forth, are generally preferred.

Exponentiating quite small numbers seems at first to be a pretty economical way of making and writing large numbers: 10^{30}, for example, is a highly effective shorthand for 1,000,000,000,000,000,000,000,000,000,000. But this method runs out of steam as the numbers get bigger and bigger. Take, for instance, the **googol** and the googolplex. One googol is the unofficial name for 10^{100}, or 1 followed by 100 zeros. This innocuous-looking number is larger than the number of atoms in the universe. What happens, therefore, if we want to represent the number that is 1 followed by *a googol number of zeros?* One way would be to write "1 followed by a googol number of zeroes"! But this is cheating because it couldn't be generalized without first giving a proper name to a fantastically large number of numbers. A better solution is to exponentiate using large numbers. Thus, 1 googolplex = $10^{\text{googol}} = 10^{10^{100}}$. This is the beginning of a **power tower**.

Are numbers as large as the googol, not to mention the googolplex, of any practical importance? Science has given us such colossi as the **Avogadro constant** (the number of molecules in a sample whose weight in grams equals its molecular weight) = 6.023×10^{23}, the **Eddington number** (astrophysicist Arthur Eddington's best estimate of the number of protons in the universe) = 1.575×10^{79}, and the Supermassive Black Hole Evaporation Time = 10^{100} years (or thereabouts)–which brings us to the level of the googol. But there's nothing known or that can be reasonably conjectured in the "real" world of physics that goes much beyond this.

Science fiction can carry us a bit further. In *The Hitchhiker's Guide to the Galaxy*[5] by Douglas Adams appears one of the largest numbers ever used in a work of fiction: 2^{260199}. These are the odds quoted against the characters Arthur Dent and Ford Prefect being rescued by a passing spaceship just after having been thrown out of an airlock. As it happens, they *are* rescued by a spaceship powered by the "infinite improbability drive." By contrast, some special numbers in mathematics make even the googolplex look tiny. **Skewes' number**, $10^{10^{10^{34}}}$, was long held up as an example of a googolplex-dwarfing number that nevertheless served a bonafide purpose in mathematics. However, even this seemingly immense integer is made to look ridiculously small by the likes of more recently described numbers, such as **Graham's number**, the *Mega,* and the *Moser,* which are so utterly vast that it takes a page or two simply to describe the various special notations used to represent them.

Just as writing out a number in full, or in place-value notation, becomes unwieldy with numbers as big as a googol, so exponentiation, in turn, endangers the world's forests if it tries to take on seriously large numbers. A more effective shorthand is *tetration–tetra* (from the Greek meaning "four") because it is the fourth dyadic operation in the series: addition, multiplication, exponentiation, tetration. Dyadic means that two numbers, or arguments, are involved in the operation. Multiplication is repeated addition (e.g., $2 \times 3 = 2 + 2 + 2$), exponentiation is repeated multiplication (e.g., $2^3 = 2 \times 2 \times 2$), and tetration is repeated exponentiation. For example, 2 tetrated to 3, represented as ${}^3 2$, is $2^{2^2} = 2^4 = 16$; 2 tetrated to 4, or ${}^4 2$, is $2^{2^{2^2}} = 2^{16} = 65{,}536$; and 2 tetrated to 5, or ${}^5 2$, is $2^{2^{2^{2^2}}} = 2^{65{,}536}$ = something too big to write out in full. Tetration goes by various other names including *superpower, superdegree,* and, the one used most commonly in mathematical circles and also here, *hyper4.*

Just as the exponentiation of two numbers, a and b, is represented as a^b and defined as $a \times a \times \ldots \times a$ (b terms), the hyper4 of a and b is represented as $a^{(4)}b$ and defined as $a^{a^{a^{\cdot^{\cdot^{\cdot}}}}}$ (a power tower with b levels). Alternatively, the hyper4 operator can be represented in **Knuth's up-arrow notation** as $a \uparrow\uparrow b$. Continuing this pattern:

hyper5 of a and $b = a^{(5)}b = a^{(4)}a^{(4)} \ldots a^{(4)} = a \uparrow\uparrow\uparrow b$
hyper6 of a and $b = a^{(6)}b = a^{(5)}a^{(5)} \ldots a^{(5)} = a \uparrow\uparrow\uparrow\uparrow b$
hyper7 of a and $b = a^{(7)}b = a^{(6)}a^{(6)} \ldots a^{(6)} = a \uparrow\uparrow\uparrow\uparrow\uparrow b$

To get some idea of the potency of this kind of representation, consider the sequence

1

10

10,000,000,000

10,000,000,000

least common multiple
The smallest **integer** that is an exact multiple of every number in a set of integers.

least upper bound
The smallest number that is larger than every member of a set of numbers.

Lebesgue, Henri Leon (1875–1941)
A French mathematician who introduced the modern definition of an **integral**. Lebesgue graduated from the École Normale Supériere and, from 1921, taught at the College de France. He and Emile **Borel** founded the modern theory of **function**s of a real variable, Lebesgue's great contribution being his new general definition of an integral (1902), which became known as the *Lebesgue integral* (see **integration**). This led to important advances in calculus, curve rectification, and trigonometric series, and, in Borel's hands, marked the start of **measure theory**. Although the Lebesgue integral was an example of the power of generalization, Lebesgue himself wasn't a fan of generalization and spent the rest of his life working on very specific problems, mostly in **analysis**.

Lebombo bone
One of the oldest mathematical artifacts known, a small piece of the fibula of a baboon, found near Border Cave in the Lebombo Mountains between South Africa and Swaziland. Discovered in the 1970s during excavations of Border Cave and dated about 35,000 B.C., the Lebombo bone is marked with 29 clearly defined notches. This suggests it may have been used as a lunar phase counter, in which case African women may have been the first mathematicians, because keeping track of menstrual cycles requires a lunar calendar. Certainly, the Lebombo bone resembles calendar sticks still used by Bushmen in Namibia. See also **Ishango bone**.

left-right reversal
See **mirror reversal problem**.

Leibniz, Gottfried Wilhelm (1646–1716)
A German philosopher, mathematician, and statesman who developed differential and integral **calculus** independently of Isaac **Newton**. He also invented a calculating machine, is considered a pioneer in mathematical logic, and proposed the metaphysical theory that we live in "the best of all possible worlds." In Leibniz's philosophical view, the universe is composed of countless conscious centers of spiritual force or energy known as *monads*. Leibniz talks about the "compossible" elements of any possible world–elements that allow a logically consistent structure. Though one of the finest minds of his age, Leibniz was not immune to blunders: he thought it just as easy to throw 12 with a pair of dice as to throw 11.

Leibniz harmonic triangle
A triangle of fractions that is related to the more famous **Pascal triangle** in a very simple way. Each row of the Leibniz harmonic triangle starts with the **reciprocal** of the row number (or the row number plus one depending on whether one starts counting from 1 or 0). Every entry is the sum of the two numbers just below it. The entries can thus be computed sequentially left to right and top to bottom using subtraction instead of addition.

$$\begin{array}{ccccccccc} & & & & 1/1 & & & & \\ & & & 1/2 & & 1/2 & & & \\ & & 1/3 & & 1/6 & & 1/3 & & \\ & 1/4 & & 1/12 & & 1/12 & & 1/4 & \\ 1/5 & & 1/20 & & 1/30 & & 1/20 & & 1/5 \end{array}$$

lemma
A short auxiliary proposition used in the proof of a larger **theorem**.

lemniscate of Bernoulli
A curve "shaped like a figure 8, or a knot, or the bow of a ribbon" in the words of Jacob Bernoulli (see **Bernoulli family**) in an article published in 1694. Bernoulli named the curve "lemniscate" after the Greek *lemniskus* for a pendant ribbon (the type fastened to a victor's garland). It has the Cartesian equation

$$(x^2 + y^2)^2 = a^2(x^2 - y^2).$$

At the time he wrote his article, Bernoulli wasn't aware that the curve he was talking about was a special case of a **Cassinian oval**, which had been described by Cassini in 1680. The general properties of the lemniscate were established by Giovanni Fagnano (1715–1797) in 1750; Leonhard **Euler**'s investigations of the length of arc of the curve (1751) led to later work on **elliptic function**s. There is a relationship between the lemniscate and the rectangular **hyperbola**. If a **tangent** is drawn to the hyperbola and the perpendicular to the tangent is drawn through the origin, the point where the perpendicular meets the tangent is on the lemniscate. See also **hippopede.**

Leurechon, Jean (c. 1591–1670)
A French Jesuit priest and mathematician who wrote *Recreations mathématiques* (1624) under the pseudonym Henrik van Etten. Much of the mathematical content centers around Claude **Bachet**'s problems and may have

been copied from it or some common source. The book also gives the earliest known description of the operation of an ear trumpet.

liar paradox

"This statement is false." What do we make of this statement (call it *S*)? If *S* is true, then *S* is false. On the other hand, if *S* is false, then it is true to say *S* is false; but, because the liar sentence is saying precisely that (namely that it is false), *S* is true. So *S* is true if and only if it is false. Since *S* is one or the other, it is both! Debate about sentences like *S* has been going on among philosophers and logicians for more than 2,000 years without any clear resolution.

The roots of the liar paradox stretch back to the philosopher Epimenides in the sixth century B.C. He said: "All Cretans are liars. . . . One of their own poets has said so." Another version of this can be found in the Bible, Titus 1:12–13, "Even one of their own prophets has said, 'Cretans are always liars, evil brutes, lazy gluttons.' This testimony is true." The poet's (or prophet's) statement is sometimes wrongly considered to be paradoxical because he himself is a Cretan. But actually there's no paradox here. A "liar," in everyday language, is someone who *on occasion* knowingly gives false answers. This isn't problematic: the poet, while lying occasionally, this time spoke the truth. However, most formulations of logic define a "liar" as an entity that always produces the negation of the true answer, that is, someone who does nothing but lie. Thus, the poet's statement can't be true: if it were, then he himself would be a liar who just spoke the truth, but liars don't do that. However, no contradiction arises if the poet's statement is taken to be false: the negation of "All Cretans are liars" is "Some Cretans aren't liars," in other words: some Cretans sometimes speak the truth. This doesn't contradict the fact that our Cretan poet just lied. Therefore, the statement "All Cretans are liars," if uttered by a Cretan, is necessarily false, but not paradoxical. Even the statement "I am a liar" is not paradoxical; depending on the definition of "liar" it may be true or false. However, the statement "I am lying now," first attributed to Eubulides of Miletus in the fourth century B.C., definitely is paradoxical. It is exactly equivalent to the sentence, we started with: "This statement is false."

Various elaborations of the basic Eubulides liar paradox have appeared over the ages. In the fourteenth century, the French philosopher Jean Buridan applied it in his argument for the existence of **God**. In 1913, the English mathematician Philip Jourdain (1879–1921) offered a version that is sometimes referred to as "Jourdain's card paradox." On one side of a card is written:

> The sentence on the other side of this card is true.

On the other side is written:

> The sentence on the other side of this card is false.

Yet another popular version of the liar paradox, guaranteed to perplex, is given by the following three sentences written on a card:

1. This sentence contains five words.
2. This sentence contains eight words.
3. Exactly one sentence on this card is true.

Lie, Marius Sophus (1842–1899)

A Norwegian mathematician who, along with his close friend Felix **Klein**, introduced **group** theory into geometry and used it to classify geometries. Lie discovered the *contact transformation,* which maps curves into surfaces (1870), and **Lie group**s, which use continuous or infinitesimal transformations. He used these groups to classify **partial differential equation**s, making the traditional methods of solution all reduce to a single principle. Lie groups also provided a basis for the growth of modern **topology**. See also **Lie algebra**.

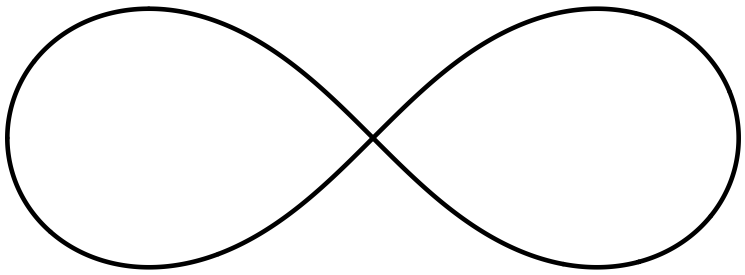

lemniscate of Bernoulli *© Jan Wassenaar, www.2dcurves.com*

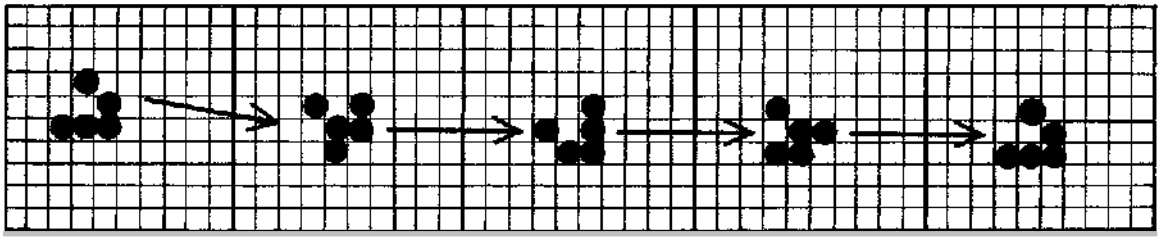

Life, Conway's game of A "glider" advances one cell down and one cell to the right.

Lie algebra

An **algebra**, named after M. Sophus **Lie**, in which multiplication satisfies properties similar to the *bracket operation* on matrices given by $[A, B] = AB - BA$, where the operation on the right-hand side involves ordinary multiplication and subtraction of matrices. The operation is not **associative**.

Lie group

A **group**, named after M. Sophus **Lie**, that is also a **manifold**. Groups of a real **matrix**, such as occur in quantum field theory, give naturally occurring examples of Lie groups. The tangent space at the identity element of a Lie group forms a **Lie algebra** in a natural way.

Life, Conway's game of

The best known example of a **cellular automaton**; it was invented by John **Conway** and first brought to public attention in Martin Gardner's *Scientific American* column in October 1970.[120] Conway's goal in creating Life was to devise a universal **Turing machine**–a sort of infinitely programmable computer. John **von Neumann** had described such a system in the 1950s, but it had very complex rules; Conway wanted to find one that was much simpler to describe and to operate. Life is played on a grid of squares on which each cell is either alive (occupied) or dead (empty). The game starts from an arbitrary initial configuration of live cells, and then progresses through generations as the life and death rules are applied. These rules are very simple: (1) A live cell survives to the next generation if it has two or three neighbors. (2) A live cell dies if it has four or more neighbors (overcrowding) or if it has only one neighbor or none (isolation). (3) A dead cell becomes a live cell in the next generation if it has exactly three neighbors (birth). The rules of Life were developed over a two-year-period during tea and coffee breaks by Conway and a group of graduate students and colleagues. Because **Go** boards and counters were used at this stage, instead of computers, it was important to have a death rule so that populations didn't tend to explode and quickly race off the board. On the other hand, to enable sufficiently interesting behavior so the game had a chance of being a universal system, it was equally important to have a birth rule that prevented populations from dying out. The rules eventually chosen provided a balance between birth and death so that the system tended to be fairly stable yet interesting enough to study. An early sign of success was the discovery of patterns, known as "gliders," that kept their shape while drifting across the plane. This was a hopeful step toward proving universality because it showed that the system had a way to transmit information from one place to another. Conway and his group went on to build nearly all the necessary configurations for arbitrary computations: AND gates, OR gates, and so on, just like the components of an ordinary computer. What they needed next was a way of producing gliders at will–a "glider gun." At this point, Conway sent a letter describing Life and the early findings to Martin Gardner, offering a prize of $50 for a configuration whose population tended toward infinity. The resulting *Scientific American* column sparked the public's imagination and very quickly a glider gun was discovered by a group at the Massachusetts Institute of Technology led by R. W. Gosper. Within two weeks of the discovery of the glider gun, both Conway's group and the group at MIT had shown that the system was indeed universal.

limaçon of Pascal

A snail-shaped curve (*limaçon* is French for "snail") named by the French mathematician Gilles Roberval after Etienne Pascal, the father of Blaise **Pascal**. It had been discovered earlier, however; Albrecht **Dürer** gave a method for drawing it as early as 1525 in his *Underweysung der Messung.* The limaçon of Pascal is a special case of an **epitrochoid** in which the rolling circle and the rolled circle have the same radius, and is also the cata**caustic** and the **pedal curve** of the **circle**. It has the **quartic** Cartesian equation

$$(x^2 + y^2 - 2rx)^2 = k^2(x^2 + y^2),$$

where r is the radius of the rolling circle or the rolled circle and k is a constant.

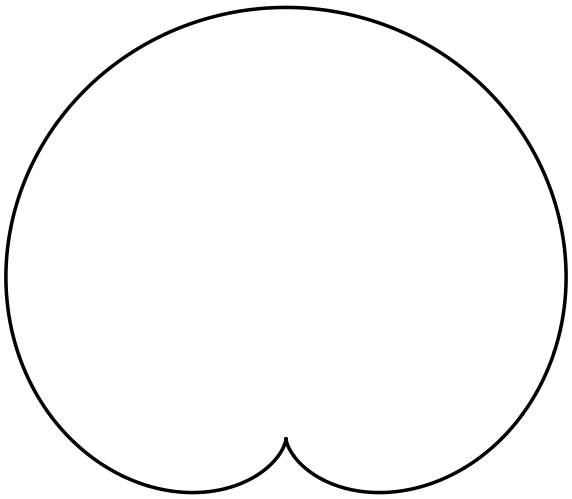

limaçon of Pascal © Jan Wassenaar, www.2dcurves.com

Sometimes the term *ordinary limaçon* is used to describe the curve when the value of k is greater than 0 and less than 1. When $k = 0$ the curve is a circle and when $k = 1$ the curve is a **cardioid**, so the ordinary limaçon is a transitional form between these two. The ordinary limaçon is also the **inverse** of the **ellipse**. For values of $k > 1$, a loop or noose appears in the curve. The inverse of a limaçon with a noose is a **hyperbola**. In fact, the constant k is the same as the eccentricity for a **conic section**. When $k = 2$, the limaçon is also called a **trisectrix**.

limerick

Why is this a limerick?:

$$((12 + 144 + 20) + 3\sqrt{4}/7) + 5 \times 11 = 9^2 + 0$$

Because, as its inventor, Jon Saxton, has pointed out:

A dozen, a gross, and a score,
Plus three times the square root of four,
Divided by seven,
Plus five times eleven,
Is nine squared and not a bit more.

limit

The target value that terms in a **sequence** of numbers get closer and closer to. This limit is not necessarily ever reached but can be approached arbitrarily close if the sequence is taken far enough.

limping triangle

A right **triangle** with two shorter sides (i.e., those other than the hypotenuse) that differ in length by one unit. An example is the 20-21-29 triangle ($20^2 + 21^2 = 29^2$).

line

The shortest distance between any two points in **Euclidean space**. A line is implicitly a *straight line;* the alternative is a **curve**. Mathematically, a line may be determined by the presence of any two points in an n-dimensional space (where n is two or more). A *line segment* is a piece of a line with definite endpoints.

linear

Having only a multiplicative factor. If $f(x)$ is a *linear **function***, then $f(a + b) = f(a) + f(b)$ and $cf(x) = f(cx)$ must both be true for all values of a, b, c, and x.

linear algebra

The study of **vector**s and **vector space**s. Linear algebra has a central place in modern mathematics, is used widely in both **abstract algebra** and functional **analysis**, and finds a concrete representation in the form of **analytical geometry**. Linear algebra began as the study of vectors in two- and three-dimensions but has now been extended to a generalized n-space.

linear group

A **group** of matrices under **matrix** multiplication.

linear programming

The problem, and associated area of mathematics, of maximizing or minimizing a linear **function** on a **convex** set, especially a **polytope**. Equivalently, maximizing a linear expression in some number of variables subject to linear equalities and inequalities.

linear system

Any system whose change of values of its variables can be represented as a series of points suggesting a straight **line** on a coordinate; hence, *linear* for "line." More generally, a linear system is one in which small changes result in small effects, and large changes in large effects. In a linear system, the components are isolated and noninteractive. Real linear systems are rare in nature since living organisms and their components are not isolated and do interact. Compare with **nonlinear system**.

Liouville number

A **transcendental number** that can be approximated very closely by a **rational number**. Normally, proving that any given number is transcendental is difficult. However, the French mathematician Joseph Liouville (1809–1882) showed the existence of a large (in fact, infinitely large) class of transcendentals whose nature is easy to ascertain. An example of a Liouville number is 0.1010010000001000000000000000000000001 . . . in which the successive groups of zeros are of length 1!, 2!, 3!, 4!, and so on.

Lissajous figure
A figure or graph of the type most often seen on an oscilloscope. The simplest Lissajous figures are circles or ellipses, but they can also take the form of **lemniscate**s and other, more complex shapes. They are named for the French scientist Jules Antoine Lissajous (1822–1880), who experimented with them in the 1850s, and are also known as *Bowditch curves,* because they had been written about earlier by the American astronomer and mathematician Nathanial Bowditch (1773–1838).

lituus
A **spiral** curve that was discovered by the English mathematician Roger Cotes (1682–1716) and named by the Scottish mathematician Colin Maclaurin (1698–1746) in 1722. The Latin *lituus* refers to a staff shaped like a bishop's crosier. The lituus is the locus of a point that moves in such a manner that the area of a circular sector remains constant; it has the polar equation

$$r^2 = a^2/\theta.$$

See **polar coordinates**.

Lobachevsky, Nikolai Ivanovich (1793–1856)
A Russian mathematician who was one of the pioneers of **non-Euclidean geometry**. He developed, independently of János **Bólyai**, the self-consistent system of **hyperbolic geometry** in which Euclid's **parallel postulate** is replaced by one allowing more than one parallel through the fixed point. Lobachevsky first announced his system in 1826 and subsequently wrote several expositions of it, including *Geometrical Researches on the Theory of Parallels* (originally published in 1840 in German). Lobachevsky studied and taught at the University of Kazan and eventually became rector of this institution in 1826. However, for some reason, despite serving his country and university well, he fell from favor and in 1846 was relieved by the government of his posts as professor and rector.

localized solution
A solution of a **differential equation**, or a similar mathematical object, that is confined to a small region even though it has the freedom to spread out.

loculus of Archimedes
A **dissection** game, similar to **tangrams**, which consists of 14 polygonal shapes that fit together to make a square. These pieces can be rearranged to make pictures of people, animals, and objects, or reassembled into their original form. There are many references to the game in ancient literature, including a description by the Roman poet and statesman Magnus Ausonius (A.D. 310–395). Only two fragmentary manuscripts, one an Arabic translation and the other a Greek manuscript dating from the tenth century discovered in Constantinople in 1899, connect the puzzle to **Archimedes** by calling it *loculus Archimedius* ("Archimedes's box"). More generally, but for unclear reasons, it is known as the *ostomachion* (Greek for "stomach"), or, in Latin texts, as the *syntemachion.* In 2003, William **Cutler** used a computer program to enumerate all 536 distinct ways (barring rotations and reflections) in which the pieces can be arranged into a square.

locus
The set of all points (usually forming a curve or surface) that satisfy some condition. For example, the locus of points in the plane equidistant from a given point is a circle. The Latin word *locus* simply means "place." (The Greek equivalent is *topos,* which crops up in "topology".)

logarithm
The logarithm of a number or variable x to base b, $\log_b x$, is the **exponent** of b needed to give x. The bases most commonly used in mathematics are e and 10. A logarithm to base e, written as $\log x$ or $\ln x$, is known as a *natural logarithm.* A logarithm to base 10 is written as $\log_{10} x$ and is known as a *common logarithm.*

logarithmic spiral
A type of **spiral**, also known as an *equiangular spiral,* that is very common in the natural world. Wonderful examples are found in the shells of some mollusks, such as that of the nautilus, and in spider webs. The angle any **tangent** to the curve makes with a tangent to a circle at the same radius, known as the *pitch angle,* is constant and results in a logarithmic spiral being *self-similar:* in other words, any part of it looks like any other part (though possibly rotated). Hawks approach their prey in the form of a logarithmic spiral and their sharpest view is at an angle to their flight direction that is the same as the spiral's pitch. On an altogether different scale, the arms of spiral galaxies are roughly logarithmic spirals. Our own galaxy, the Milky Way, is believed to have four major arms, each of which is a logarithmic spiral with pitch of about 12°. Approximate logarithmic spirals with a pitch of about 17° can be generated using the **Fibonacci sequence** or the **golden ratio**.

In **polar coordinates** (r, θ) the equation of the logarithmic spiral is

$$r = a\, b^{\theta},$$

with positive real numbers a and b. Changing a rotates the spiral while b controls how tightly and in which direction it is wrapped. It can be distinguished from the

Archimedean spiral by the fact that the distance between the arms of a logarithmic spiral increase in a **geometric sequence** while in an Archimedean spiral this distance is constant. Starting at a point P and moving inward along the spiral, one has to circle the origin infinitely often before reaching it; yet, the total distance covered is finite. This was first realized by the Italian physicist Evangelista Torricelli (1608–1647) even before calculus had been invented. The total distance covered is $r/\sin\theta$ where θ is the pitch angle and r is the straight-line distance from P to the origin.

The logarithmic spiral was first described by René **Descartes** and later studied in depth by Jakob Bernoulli (see **Bernoulli family**), who called it *Spiralis mirabilis* (the wonderful spiral) and wanted one engraved on his tombstone. He did get a spiral, but unfortunately it was a rather crudely cut Archimedean type.

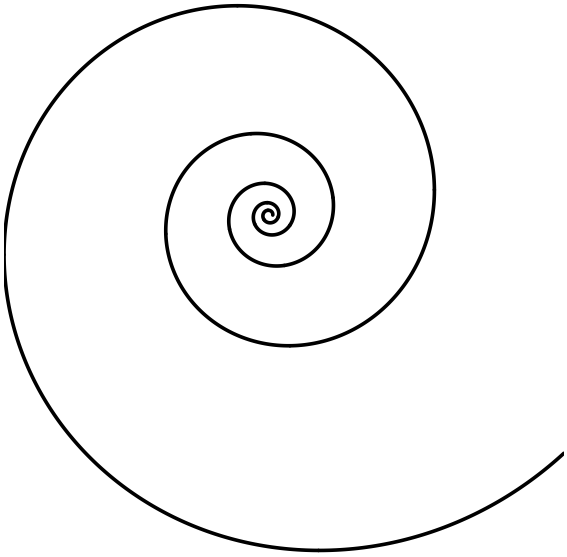

logarithmic spiral *© Jan Wassenaar, www.2dcurves.com*

logic

The branch of **mathematics** concerned with how one statement can imply others, or how sets of statements can

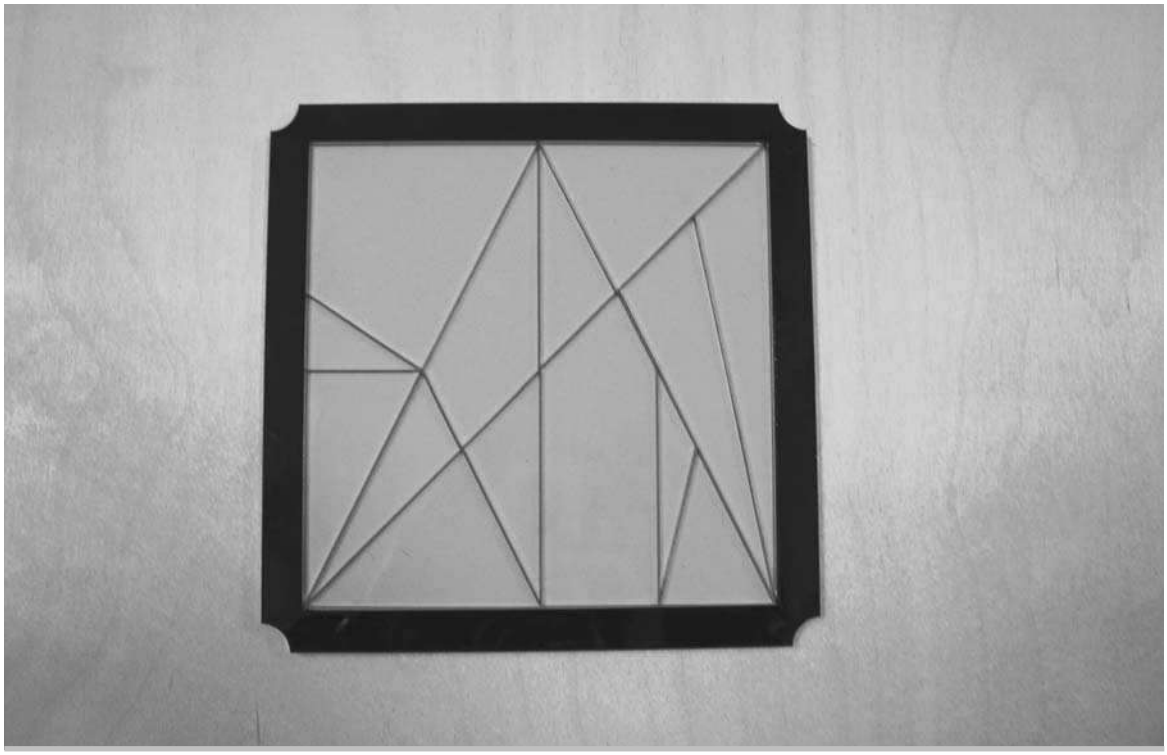

loculus of Archimedes The loculus of Archimedes is one of the most ancient dissection puzzles. *Kadon Enterprises, Inc., www.gamepuzzles.com*

be connected by chains of implication. Such relationships can be written down using special symbols, and different sets of rules can be studied to see how they give rise to different sorts of structures.

logical depth
A measure of the **complexity** of a system, developed in 1988 by the American computer scientist and mathematician Charles Bennett. It contrasts with another such measure, **algorithmic complexity**, but, like it, is a measure of the algorithms needed to generate the data from a system.

loop
(1) A **knot** or hitch that holds its form. (2) A degenerate edge of a **graph** that joins a vertex to itself. (3) A sequence of instructions that is repeated either a specified number of times or until a particular condition prevails. Loops lie at the heart of most computer programs. The most common type is the *iterative loop,* signified by keywords such as *for, while, do,* and *repeat,* or their equivalent, in which a given set of instructions is repeated a specified number of times. The *recursive loop* is a more powerful construct that carries out a given set of instructions, typically including **recursive** calls with modified parameters back to the instruction set itself, until a terminating condition is met. Recursive algorithms solve problems by reducing them to smaller and smaller subproblems until a solution is found, reusing the same set of instructions as often as needed.

Lorenz, Edward Norton (1917–)
A research meteorologist at the Massachusetts Institute of Technology who, in the early 1960s, using a simple system of equations to model convection in the atmosphere, ran headlong into the phenomenon of "sensitivity to initial conditions." In the process he sketched the outlines of one of the first recognized **chaotic attractor**s. In Lorenz's meteorological computer modeling, he discovered the underlying mechanism of deterministic chaos: simply formulated systems with only a few variables can display highly complicated behavior that is unpredictable. Using his digital computer, culling through reams of printed numbers and simple strip chart plots of the variables, he saw that slight differences in one variable had profound effects on the outcome of the whole system. This was one of the first clear demonstrations of sensitive dependence on initial conditions. Equally important, Lorenz showed that this occurred in a simple, but physically relevant model. He also appreciated that in real weather situations, this sensitivity could mean the development of a front or pressure-system where there never would have been one in previous models. In his famous 1963 paper, Lorenz picturesquely explained that a butterfly flapping its wings in Beijing could affect the weather thousands of miles away some days later. This sensitivity is now called the **butterfly effect**.

Lorenz system
A system of three **differential equation**s, named after its discoverer Edward **Lorenz**, that was the first concrete example of **chaos** and a **chaotic attractor**.

Lovelace, Lady
See **Byron, Ada**.

loxodrome
A path on Earth's surface that is followed when a compass is kept pointing in the same direction. It is a straight line on a Mercator projection of the globe precisely because such a projection is designed to have the property that all paths along Earth's surface that preserve the same directional bearing appear as straight lines. The loxodrome isn't the shortest distance between two points on a sphere. The shortest distance is an arc of a **great circle**. But, in the past, it was hard for a ship's navigator to follow a great circle because this required constant changes of compass heading. The solution was to follow a loxodrome (from

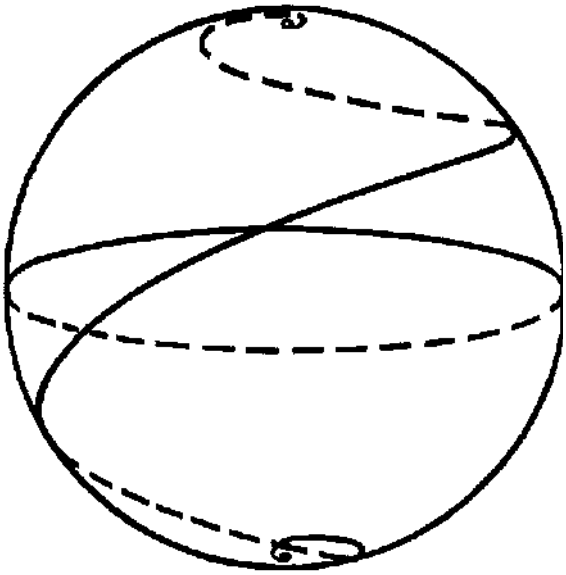

loxodrome Following a constant-compass heading between Earth's poles produces the winding path shown.

the Greek *loxos* for "slanted" and *drome* for "course"), also known as a *rhumb line,* by navigating along a constant direction. In middle latitudes, at least, this didn't lengthen the journey unduly. If a loxodrome is continued indefinitely around a sphere it will produce a spherical **spiral**, or a logarithmic spiral on a polar projection.

Loyd, Sam (1841–1911)

A great American inventor of puzzles among whose best-known creations are the Hoop-Snake Puzzle, **Get Off the Earth**, the **Pony Puzzle**, and, most famous of all, the **Fifteen Puzzle**. By age 17 he was already hailed as one of the world's leading writers of chess problems and had also just invented his deceptively simple-looking trick mules puzzle. The object of this is to cut apart three pieces that show two mules and two jockeys and then reassemble the pieces so that the jockeys are riding the mules. Loyd sold the puzzle to the showman Phineas T. Barnum (of Barnum & Bailey Circus fame) for some $10,000. This was to become his forte: devising puzzles that looked so simple to solve that people felt compelled to try them, only to find, hours later, that they were still trying to figure them out. Loyd became a full-time professional puzzlemaker only in the 1890s. He corresponded with his English counterpart Henry **Dudeney** and worked alongside his son Sam Loyd Jr. After the death of his father, Sam Loyd Jr. continued publishing puzzles that were mainly compilations of his father's work and in 1914 issued a now out-of-print and much sought-after mammoth collection of his father's puzzles called *Cyclopedia of 5,000 Puzzles, Tricks, and Conundrums*.[111, 207, 208]

lozenge

A **rhombus** with a 60° angle.

L-system

A method of constructing a **fractal** that is also a model for plant growth. L-systems use an **axiom** as a starting string and iteratively apply a set of parallel string substitution rules to yield one long string that can be used as instructions for drawing the fractal. Many fractals, including **Cantor dust**, the **Koch snowflake**, and the **Peano curve**, can be expressed as an L-system.

Lucas, (François) Edouard (Anatole) (1842–1891)

A French mathematician well known for his study of the **Fibonacci sequence** and the related **Lucas sequences** named after him. He devised methods of testing for **prime number**s–work that was later refined by D. H. Lehmer to yield the Lucas-Lehmer test for checking **Mersenne number**s to see if they are prime. Lucas was also interested in recreational mathematics, the **Tower of Hanoi** being his best known puzzle game. He worked at the Paris Observatory and later became a professor of mathematics in Paris.

Lucas sequences

Generalizations of the **Fibonacci sequence** first investigated by Edouard **Lucas**. One kind can be defined as follows: $L(0) = 0$, $L(1) = 1$, $L(n + 2) = PL(n + 1) + \underline{Q}L(n)$, where the normal Fibonacci sequence is the special case of $P = \underline{Q} = 1$. Another kind of Lucas sequence begins with $L(0) = 2$, $L(1) = P$. Such sequences are used in **number theory** and in testing for **prime number**s.

lucky number

A number in a sequence, first identified and named around 1955 by Stanislaw **Ulam**, that evades a particular type of number "sieve" (similar to the famous **sieve of Eratosthenes**), which works as follows. Start with a list of integers, including 1, and cross out every second number: 2, 4, 6, 8, ... The second surviving integer is 3. Cross out every third number not yet eliminated. This removes 5, 11, 17, 23, ... The third surviving number from the left is 7; cross out every seventh integer not yet eliminated: 19, 39, ... Repeat this process indefinitely and the numbers that survive are the "lucky" ones: 1, 3, 7, 9, 13, 15, 21, 25, 31, 33, 37, 43, 49, 51, 63, 67 . . . .

Amazingly, though produced by a sieve based solely on a number's position in an ordered list, the luckies have many properties in common with **prime number**s. For example, there are 25 primes less than 100 and 23 luckies less than 100. In fact, primes and luckies crop up about equally often between any two given integers. Also, the gaps between successive primes and the gaps between successive luckies widen at roughly the same rate as the numbers increase, and the number of twin primes (primes that differ by 2) is close to the number of twin luckies. The luckies even have their own equivalent of the famous (still unsolved) **Goldbach conjecture**, which states that every even number greater than 2 is the sum of two primes. In the case of luckies, it's conjectured that every even number is the sum of two luckies; no exception has yet been found. Another unresolved problem is whether there are an infinite number of lucky primes. See also **Ulam spiral**.

Ludolph's number

Also known as *Ludolphine,* a name by which the number **pi** was known in Germany for many years following its evaluation to 35 digits by Ludolph von Ceulen (1540–1610).

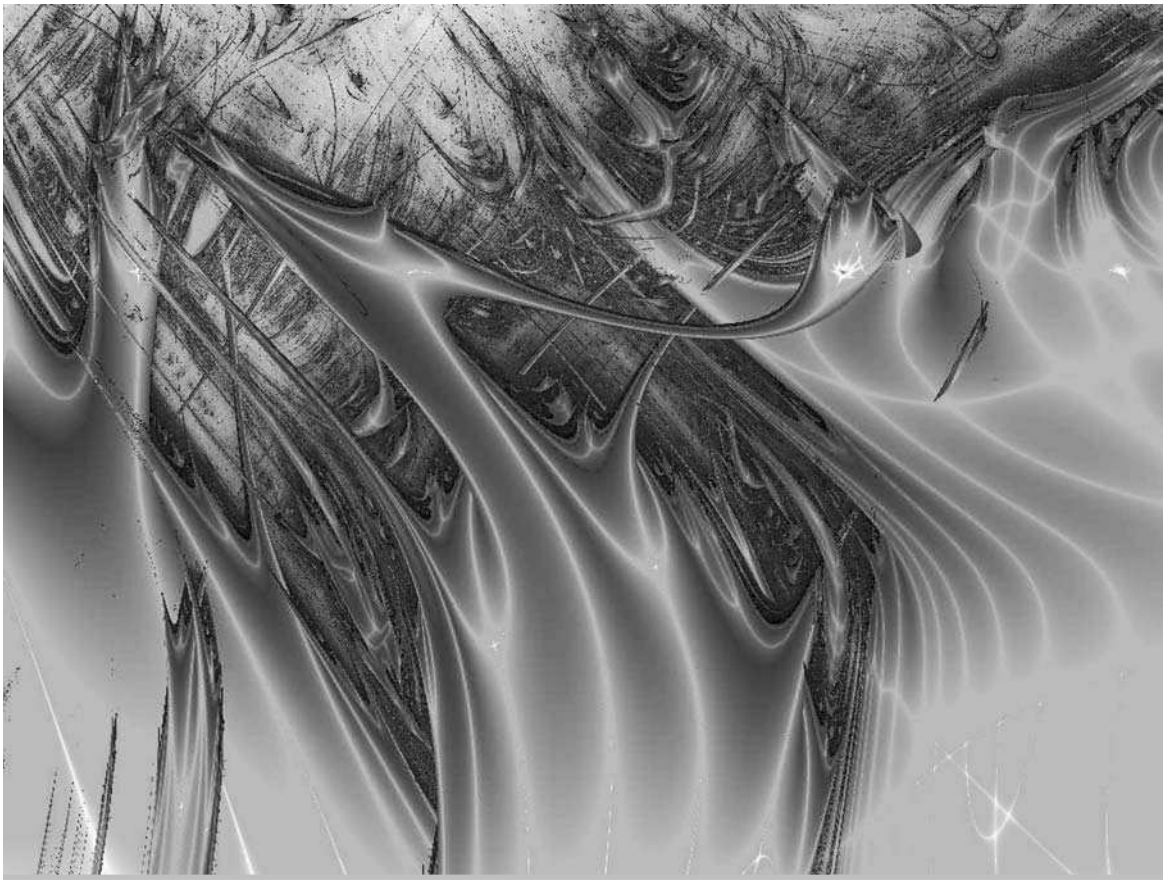

Lyapunov fractal A computer-generated image using Lyapunov exponents. *Radek Novak/Infojet*

lune

The portion of a **sphere** between two great semicircles (see **great circle**) having common endpoints (including the semicircles).

Lyapunov fractal

A particularly photogenic type of **fractal** that is popular with computer artists. It also represents a simple biological model of population growth in which the degree of the growth of the population can periodically alter between two values *a* and *b*.

M

Maclaurin, Colin (1698–1746)

A Scottish mathematician who developed and extended Isaac **Newton**'s work on **calculus** and gravitation, and did notable work on higher plane curves (see **Maclaurin trisectrix**). In his *Treatise of Fluxions* (1742), he gave the first systematic formulation of Newton's methods and set out a method for expanding functions about the origin in terms of series now known as *Maclaurin series*. Maclaurin also invented several devices, made astronomical observations, wrote on the structure of bees' honeycombs, and improved maps of the Scottish isles.

Maclaurin trisectrix

A curve first studied by Colin **Maclaurin** in 1742 with a view to solving one of the great geometric problems of antiquity: **trisecting an angle**. The Maclaurin trisectrix results from the Cartesian equation

$$y^2(a + x) = x^2(3a - x).$$

It is an **anallagmatic curve** that intersects itself at the origin.

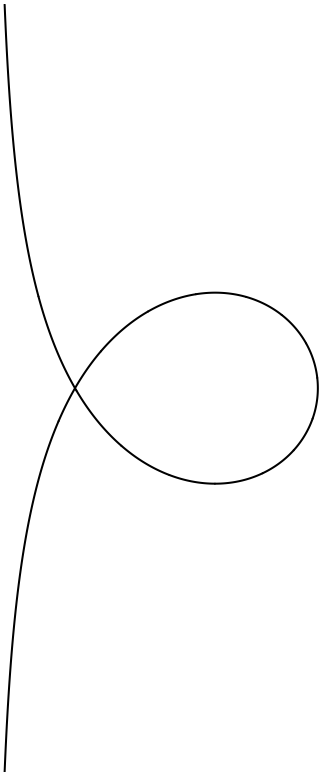

Maclaurin trisectrix *Jan Wassenaar, www.2dcurves.com*

MacMahon, Percy Alexander (1854–1929)

A British mathematician, physicist, and naval officer, born into a military family, whose leanings were evident early on when as a young child he showed a fascination with the way artillery was stacked. MacMahon later did work on missile trajectories, taking resistance into account, and on symmetric functions in the field of **combinatorics**, building on the results of James **Sylvester** and Arthur **Cayley**. His studies in symmetry led him to investigate partitions and to become a world authority on **Latin squares**. He wrote a two-volume treatise *Combinatory Analysis* (1915–1916), which became a classic, and a book on mathematical recreations called *New Mathematical Pastimes* (1921).[210] The latter shows another of the topics that intrigued MacMahon: the construction of patterns that can be repeated to fill the plane. However, much to his regret, as he wrote in the preface, "It has not been found possible to produce the book in colour." See also **MacMahon squares** and **thirty colored cubes puzzle**.

MacMahon squares

The concept of color-matching tiles based on all the permutations of colors on their edges dates from 1926, when Percy **MacMahon** invented and introduced three-color squares and four-color triangles as mathematical pastimes. MacMahon divided squares and triangles into triangles to give each edge of a piece its own color, in all possible combinations. Each set contains 24 different tiles, and MacMahon discovered that they could form a single figure with all adjacent edges matching and just one color all around the outside border. The most extensive research into these sets, over three decades, was done by the American engineer Wade Philpott (1918–1985), of Lima, Ohio, who identified all the possible symmetrical shapes that MacMahon squares and triangles could solve with both matching edge colors and uniform border color, and who calculated all the numbers of solutions for the MacMahon squares' 4×6 rectangle. See also **thirty colored cubes puzzle**.

Madachy, Joseph S.

An American mathematician, founder of *Recreational Mathematics Magazine,* editor of the ***Journal of Recreational Mathematics*** for nearly 30 years (now editor emeritus), the author of articles and books on the subject, and a well-known puzzlist.

magic cube

Similar to a **magic square** but having three dimensions instead of two. It contains the integers from 1 to n^3 and has $3n^2 + 4$ lines that sum correctly. All rows, columns, pillars, and the four triagonals (three-dimensional diagonals) must sum to the constant $\frac{1}{2}n(n^3 + 1)$. A cross section through a magic cube is a magic square.

magic square

An $n \times n$ square of the distinct whole numbers $1, 2, \ldots, n^2$, such that the sum of the numbers along any row, column, or main diagonal is the same. This sum is known as the *magic constant* and is equal to $\frac{1}{2}\, n(n^2 + 1)$. There is only one 3×3 magic square (not counting reflections and rotations), which was known to the Chinese as long ago as 650 B.C. as *lo-shu* and is bound up with a variety of myths. Associations between magic squares and the supernatural are also evident in early Indian and Arabian mathematics. The 3×3 square can be written as:

8 1 6
3 5 7
4 9 2

Each row, column, and main diagonal sums to 15. If the rows are read as three-digit numbers, forward and backward, and then squared, we find the interesting relation

$$816^2 + 357^2 + 492^2 = 618^2 + 753^2 + 294^2.$$

The reader may wish to see if the same rule holds for the columns and main diagonals.

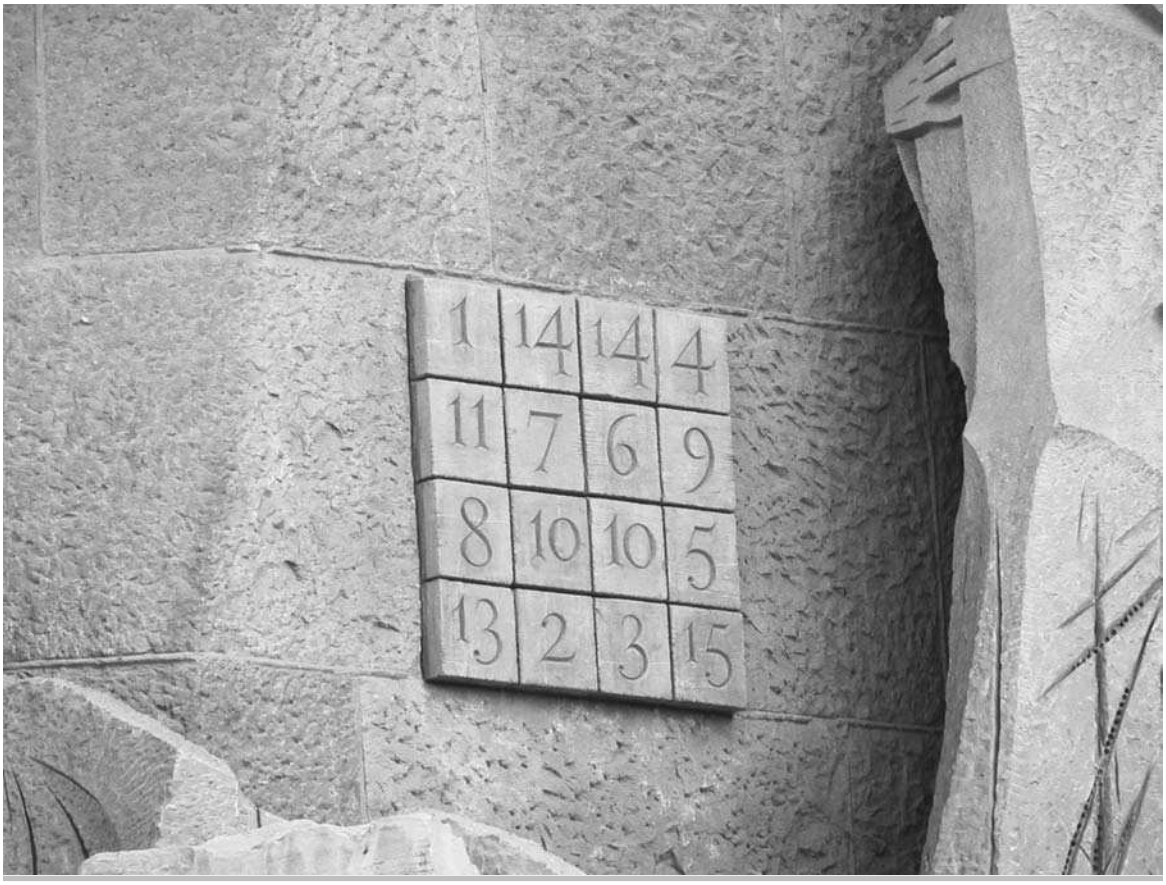

magic square A 4×4 magic square carved on the side of the Sagrada Familia cathedral in Barcelona.

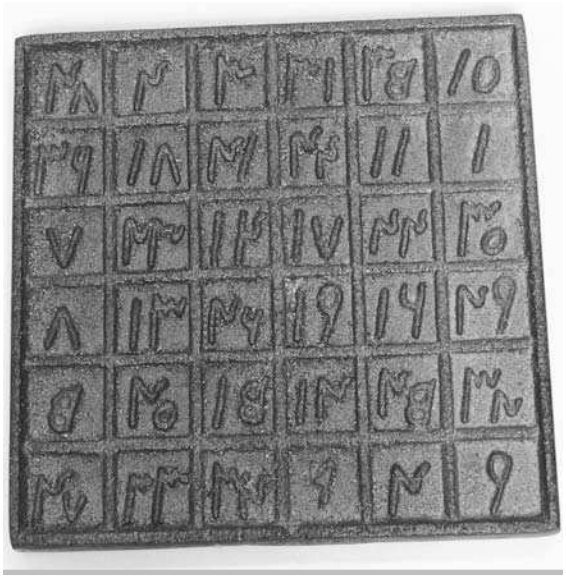

magic square A replica of a cast iron 6 × 6 magic square (vertical, horizontal, and main diagonal lines add to 111) from the Chinese Yuan dynasty (1271–1368), used as a sacred object to ward off evil spirits. *Sue & Brian Young/Mr. Puzzle Australia, www.mrpuzzle.com.au*

In the early sixteenth century Cornelius Agrippa constructed squares for $n = 3, 4, 5, 6, 7, 8$, and 9, which he associated with the seven "planets" then known (including the Sun and the Moon). Albrecht **Dürer**'s famous engraving of *Melancholia* (1514) includes a picture of an order-4 (4 × 4) magic square. There are 880 distinct squares of order-4 and 275,305,224 squares of order-5, but the number of larger squares is unknown. A square that fails to be magic only because one or both of the main diagonal sums don't equal the magic constant is called a *semi-magic square*. If *all* diagonals (including those obtained by wrapping around) of a magic square sum to the magic constant, the square is said to be a *pandiagonal square* (also known as a *panmagic* or *diabolical square*). Pandiagonal squares exist for all orders except 6, 10, 14, . . . , $2(2i + 1)$. There are 48 pandiagonal 4 × 4 squares. If replacing each number n_i by its square n_i^2 produces another magic square, the square is said to be a *bimagic* or *doubly magic square*. If a square is magic for n_i, n_i^2, and n_i^3, it is known as a *trebly magic square*.

A little trial and improvement is all it takes to construct the 3 × 3 magic square, but for building 4 × 4 squares and larger, a systematic method, or **algorithm**, is important. Interestingly, different algorithms are needed depending on whether the square is of an even order or an odd order. Odd order squares are the easier variety to make and there are several standard techniques, including the Siamese (sometimes called de la Loubere's or the Staircase), the Lozenge, and de Meziriac's methods. Here is yet another approach, known as the Pyramid or extended diagonals method: (1) Draw a pyramid of same size squares as the magic square's squares, on each side of the magic square; the number of squares on the pyramid's base should be two less than the number of squares on the side of the magic square. (2) Sequentially place the numbers 1 to n^2 of the $n \times n$ magic square in the diagonals. (3) Relocate any number not in the $n \times n$ square to the opposite hole inside the square.

An *antimagic square* is an $n \times n$ array of integers from 1 to n^2 in which each row, column, and main diagonal gives a different sum such that these sums form a sequence of consecutive integers. A 4 × 4 antimagic square is a square arrangement of the numbers 1 to 16 so that the totals of the four rows, four columns, and two main diagonals form a sequence of 10 consecutive integers, for example:

1	12	3	12
15	9	4	10
7	2	16	8
14	6	11	5

The principle of magic squares can be extrapolated from two dimensions to any number of **higher dimensions**, including **magic cube**s and *magic **tesseract**s,* whose cross sections consist of magic cubes, and so forth.[10, 160, 162] See also **Latin square**s and **magic tour**.

magic tour

A **tour** by a **chess** piece on an $n \times n$ chessboard, whose squares are numbered from 1 to n^2 along the path of the piece, such that the resulting arrangement of numbers is a **magic square**. The tour is a *semi-magic tour* if the resulting arrangement of numbers is a **semi-magic square**. Magic **knight's tour**s aren't possible on $n \times n$ boards if n is odd. They are possible for all boards of size $4k \times 4k$ for $k > 3$, but are believed to be impossible for $n = 8$.

main diagonal

In the $n \times n$ **matrix** $[a_{ij}]$, the elements $a_{11}, a_{22}, \ldots, a_{nn}$. See also **diagonal**.

major axis

The longest **chord** of an **ellipse**.

Malfatti circles

In 1803 the Italian mathematician Giovanni Malfatti (1731–1807) posed the following problem: Given a triangle, find three nonoverlapping circles inside it such that the sum of their areas is maximal. Malfatti and many other mathematicians thought that the solution is given by the three circles, each of which is **tangent** to the other

two and also to two sides of the triangle. Malfatti computed the radii of these circles, and they are now known as Malfatti's circles. Later it became clear that Malfatti's conjecture isn't true. In particular, Goldberg proved, in 1969, that the Malfatti circles *never* give a solution of the Malfatti problem! In other words, for any triangle there are three nonintersecting circles inside it, whose areas are bigger than the area of the Malfatti circles. So far as is known, the Malfatti problem hasn't been solved yet in the general case although it seems reasonable to suppose that the solution is given by what is called the *greedy algorithm:* First inscribe a circle in the given triangle; then inscribe a circle in the smallest angle of the triangle that is tangent to the first circle. The third circle is inscribed either in the same angle or in the middle angle of the triangle, depending on which of them has the bigger area.

Mancala

What is today almost universally called Mancala is, correctly speaking, the game of *Wari.* Mancala refers to a type of counting game of which Wari is a specific example, dating back to ancient times, known in Egypt and throughout Africa and Asia, and probably brought to Europe by sailors returning from those lands. Wari is played with a board and 48 markers or playing pieces, which are usually small colored stones or shells. The board consists of a piece of wood with two rows of six hollowed-out circular spaces, called *cups,* on each side, and one larger oval space at each end called a *reservoir.* The game is set up by placing four markers in each of the twelve cups. The first player picks up the markers in one of the cups on his side, then distributes the markers by placing one (and only one) in the other cups, going counterclockwise around the board. Markers are not placed in the reservoirs, which are for holding captured pieces only. Should there be enough markers that a complete circle of the board is made, the cup just emptied is skipped over. If the last marker put down goes into a cup on the opponent's side, and ends there with a total of two or three markers in that cup, then the markers in that cup are captured, and go into the reservoir at the player's right. Also, if the next cup clockwise from the captured cup has only two or three markers in it, that cup is likewise captured and the markers taken. This continues so long as the cup is clockwise to the last captured cup, has only two or three markers in it, and is an opponent's cup. However, a player can't capture all of an opponent's remaining pieces in a move, leaving him nothing to play. In capturing cups, if there's only one opponent cup left with markers in it, it can't be captured. Also, you cannot leave your opponent with all empty cups if you have a move that would put some pieces in one or more of his cups. When one side of the board is empty, play is ended. This happens when a player has to move his last markers onto his opponent's side. At the end of play each player takes any markers left on his side of the board and adds them to his reservoir. The winner is the person with the most markers in his reservoir.

Mandelbrot, Benoît B. (1924–)

A Polish-born French mathematician, largely responsible for the present interest in **fractal** geometry. A native of Warsaw, he spent most of his early life in France. Mandelbrot was born into a family with a strong academic tradition: his mother was a doctor and his uncle Szolem Mandelbrot was a famous Parisian mathematician. His family left Poland for Paris in the 1930s to escape Hitler's regime. There, Mandelbrot was introduced to mathematics by his two uncles. Educated in France, he developed the mathematics of Gaston **Julia**, and began the (now common) graphing of equations on a computer. Mandelbrot originated what became known as fractal geometry and the object known as the **Mandelbrot set** is named after him. His work on fractals as a mathematician at IBM earned him an emeritus fellowship at the Thomas J. Watson Research Laboratories. In addition to his study of fractals in mathematics, he showed that fractals can be found in many places in nature, leading to entire new fields of exploration in **chaos theory**. He joined the faculty of Yale in 1987.

Mandelbrot set

The best known **fractal** and one of the most complex and beautiful mathematical objects known. It was discovered by Benoît **Mandelbrot** in 1980 and named after him by Adrien Douady and J. Hubbard in 1982. The set is produced by the incredibly simple **iteration** formula

$$z_{n+1} = z_n^2 + c,$$

where z and c are complex numbers and $z_0 = 0$. This can be written without complex numbers as

$$x_{n+1} = x_n^2 - y_n^2 + a, \text{ and}$$
$$y_{n+1} = 2x_n y_n + b,$$

where $z = (x, y)$ and $c = (a, b)$. The Mandelbrot set consists of all the points on the **Argand diagram** for which the function $z^2 + c$ doesn't diverge under iteration. A computer is essential for carrying out the necessary calculations and for producing pictures of this remarkable structure. For the purposes of computation, the Argand diagram is broken down into pixels (picture elements), and the coordinates of each supply the constant c in $z^2 + c$. For each pixel (value of c) the function is iterated. If the function either rapidly diverges (blows up) or rapidly

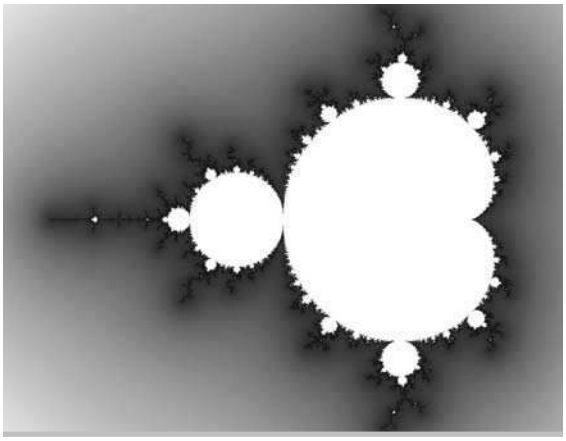

Mandelbrot set A general view of the Mandelbrot set.

converges (collapses), the pixel is left black. If the function is more indecisive about which way it is heading, it is allowed to iterate longer. In some cases the iterations could go on for a very long time before it became clear that the function would ultimately diverge, so a limit is established, known as the *depth,* beyond which iterations are stopped. If the depth is reached without divergence, the corresponding pixel is left black as though it were in the set. At locations where divergence becomes clear prior to hitting the limit, the pixel is displayed according to a scale that represents how many iterations are needed to show divergence. The whole Mandelbrot set lies within a circle of radius 2.5 centered at the origin of the Argand diagram. Although finite in area, the set has a boundary that is infinitely long and has a **Hausdorff dimension** of 2.

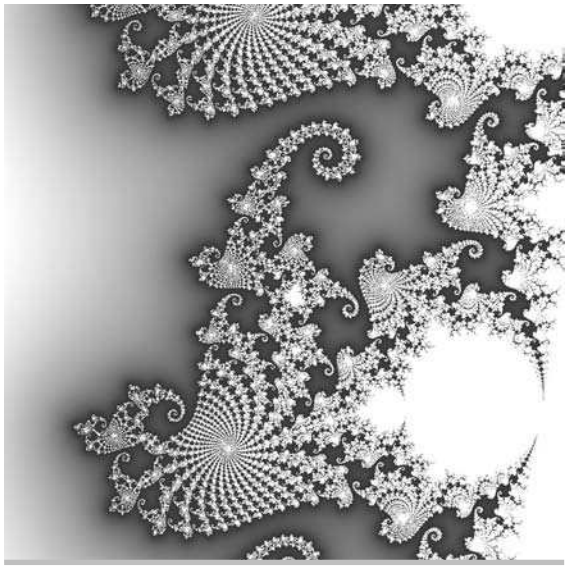

Mandelbrot set A zoom view of the Mandelbrot set reveals some of the infinite variety of remarkable patterns that inhabit it.

The overall appearance of the Mandelbrot set is that of a series of disks. These disks have irregular borders and decrease in size heading out along the negative real axis; moreover, the ratio of the diameter of one disk to the next approaches a constant. More complex shapes branch out from the disks. One region of the Mandelbrot set containing spiral shapes is known as *Seahorse Valley* because it resembles a seahorse's tail. A computer can be used, like a microscope, to zoom in on different parts of the set. This reveals that, although the shape is infinitely complex, it also displays **self-similarity** with regions that look like the outline of the entire set. The Mandelbrot set also reveals symmetry on different levels. It is identically symmetrical about the real axis, and almost symmetrical at smaller scales. This kind of "near-but-not-quite" symmetry is one of the most unexpected properties to find in an object generated from such a simple formula and process. The Mandelbrot set was created by Mandelbrot as an index to the **Julia set**s. Each point in the Argand diagram corresponds to a different Julia set, and those points within the Mandelbrot set correspond precisely to the connected Julia sets.

manifold

A mathematical object that, in geometrical terms, is nearly "flat" on a small scale (though on a larger scale it may bend and twist into exotic and intricate forms). More precisely, a manifold is a **topological space** that looks locally like ordinary **Euclidean space**. Every manifold has a *dimension,* which is the number of coordinates needed to specify it in the local coordinate system. A circle, although curved through two dimensions, is an example of a one-dimensional manifold, or one-manifold. A close-up view reveals that any small segment of the circle is practically indistinguishable from a straight line. Similarly, a sphere's two-dimensional surface, even though it curves through three dimensions, is an example of a two-manifold. Seen locally, the surface, like that of a small portion of Earth, appears flat. A manifold that is smooth enough to have locally well-defined directions is said to be *differentiable.* If it has enough structure to enable lengths and angles to be measured, then it is called a *Riemannian manifold.* Differentiable manifolds are used in mathematics to describe geometrical objects, and are also

the most natural and general settings in which to study differentiability. In physics, differentiable manifolds serve as the **phase space** in classical mechanics, while four-dimensional pseudo-Riemannian manifolds are used to model **space-time** in general relativity.

mantissa

The positive fractional part of the representation of a **logarithm**. For example, in the expression log 3,300 = 3.5185 . . . , 0.5185 is the mantissa.

many worlds hypothesis

> *Do you not think it a matter worthy of lamentation that when there is such a vast multitude of them [worlds], we have not yet conquered one?*
>
> –Alexander the Great

An interpretation of **quantum mechanics**, first proposed by the American physicist Hugh Everett III in 1957, according to which, whenever numerous viable possibilities exist, the world splits into many worlds, one world for each different possibility (in this context, the term *worlds* refers to what most people call "universes"). In each of these worlds, everything starts out identical, except for the one initial difference; but from this point on, they develop independently. No communication is possible between the separate universes, so the people living in them (and splitting along with them) would have no idea what was really going on. Thus, according to this view, the world branches endlessly. What is "the present" to us, lies in the pasts of an uncountably huge number of different futures. Everything that *can* happen does happen, somewhere. Until the many worlds interpretation, the generally accepted interpretation of quantum mechanics was (and perhaps still is) the *Copenhagen interpretation*. The Copenhagen interpretation makes a distinction between the observer and the observed; when no one is watching, a system evolves deterministically according to a wave equation, but when someone *is* watching, the wave function of the system "collapses" to the observed state, which is why the act of observing changes the system. The Copenhagen interpretation gives the observer special status, not accorded to any other object in quantum theory, and cannot explain the observer itself, while the many worlds hypothesis models the entire observer-observee system.

map

(1) A synonym for **function**, in which context it is also known as a *mapping*. More generally, the correspondence of elements in one **set** to elements in the same set or another set. (2) A representation, usually on a plane surface, of geographical regions. See **four-color map problem**.

Markov chain

A sequence of **random** variables in which the future variable is determined by the present variable but is independent of the way in which the present state arose from its predecessors. In other words, a Markov chain describes a chance process in which the future state can be predicted from its present state as accurately as if its entire earlier history was known. Markov chains are named after the Russian mathematician Andrei Andrevich Markov (1856–1922) who first studied them in a literary context, applying the idea to an analysis of vowels and consonants in a text by Pushkin. But his work launched the theory of **stochastic** processes and has since been applied in quantum theory, particle physics, and genetics.

Martingale system

A simple, popular, and ultimately disastrous gambling system that, on the face of it, seems like a dream come true. In the short run the player has a good chance of making a few dollars using this method. But, in the long run, two things conspire to defeat him–the table betting limits and the player's available funds. The Martingale system calls for an initial bet of, say, $2. If the player loses, he doubles his bet to $4. Another loss puts the net loss at $6 and requires a doubling of the bet to $8 to recoup the losses and show a profit. Assume the player loses five hands in a row. The sixth bet requires $64. Let's say this wins–the gambler has now won $128 but has lost $124–a net win of $4. Of course, any win, however small, if repeated over and over, could produce a fortune. The trouble is that many losing streaks run longer than 6 or 8 or 10 in a row. The Martingale quickly runs into the table limits. For example, if the player is at a $2 **blackjack** table with a $500 upper limit, he has to retire after 9 losses in a row and is down over $1,000. It would take another 500 winning hands to make up this loss! Basically, one losing streak will put the Martingale gambler in a hole he is unlikely ever to climb back out of.

Mascheroni construction

A construction done using a moveable compass alone, named after the Italian geometer Lorenzo Mascheroni (1750–1800), who, in his *Geometria del compasso* (1797), astonished the mathematical world by showing how every compass-and-straightedge construction can be done in this minimalist way. (Since straight lines can't be drawn with just a compass, it's assumed that two points, obtained by arc intersections, define a straight line.) It is now known that Georg Mohr (1640–1697) proved the same results earlier in his obscure *Euclides danicus* (1672). Mascheroni, or Mohr-Mascheroni, constructions are today primarily of

interest to puzzle enthusiasts who try to improve on the older solutions by finding ones with fewer steps.

matchstick puzzle

A form of **mechanical puzzle** that involves rearranging a pattern of ordinary matches, according to a given instruction, to make a new shape or solve some other mathematical problem.

mathematical lifespan

"The mathematical life of a mathematician is short. Work rarely improves after the age of twenty-five or thirty. If little has been accomplished by then, little will ever be accomplished." Thus wrote Alfred Adler in an article titled "Mathematics and Creativity" in the *New Yorker* magazine (1972), echoing a common belief that mathematicians tend to do their best work before the age of 30, physicists before the age of 40, and biologists before the age of 50 (though there are exceptions!). The mathematical physicist Freeman Dyson put it more succinctly: "Young men should prove theorems, old men should write books." On the other hand, there are compensations for early burnout, as G. H. **Hardy** pointed out (in *A Mathematician's Apology*): "Archimedes will be remembered when Aeschylus is forgotten, because languages die and mathematical ideas do not. 'Immortality' may be a silly word, but probably a mathematician has the best chance of whatever it may mean."

mathematics

> *Pure mathematics consists entirely of assertions to the effect that if such and such a proposition is true of anything, then such and such another proposition is true of that thing. It is essential not to discuss whether the first proposition is really true, and not to mention what the anything is of which it is supposed to be true. . . . Thus mathematics may be defined as the subject in which we never know what we are talking about, nor whether what we are saying is true.*
>
> –Bertrand Russell

The science of patterns, real or imagined; *mathematics* comes from the Greek *mathema* for "knowledge" or "that which is learned." Its roots lie in the practical need to carry out commercial calculations, to measure land, and to forecast astronomical events. These activities correspond roughly to the mathematics of structure, space, and change. The investigation of structure begins with numbers–initially the **natural number**s and **integer**s. The rules governing arithmetical operations are dealt with in elementary **algebra**, while the deeper properties of whole numbers are the province of **number theory**. The study of methods to solve equations leads to **abstract algebra**, which deals with structures that generalize the properties of familiar numbers. The physically important concept of **vector**, generalized to **vector space**s and studied in **linear algebra**, embraces both structure and space. The mathematics of space stems from **geometry**, first the **Euclidean geometry** and **trigonometry** of the everyday world, and later the various forms of **non-Euclidean geometry**. The modern fields of **differential geometry** and algebraic geometry generalize geometry in different ways. Differential geometry builds upon the concepts of coordinate system, smoothness, and direction, while algebraic geometry treats geometrical objects as sets of solutions to **polynomial** equations. **Group** theory places the concept of symmetry on an abstract footing and provides a bridge between space and structure. **Topology** links space and change through its emphasis on **continuity**. Analyzing and describing change in the physical world is a perennial theme of the natural sciences, and **calculus** was developed as a tool for doing this. The central concept used to describe a changing variable is that of a **function**. Many problems lead to relations between a quantity and its rate of change, and the methods to solve these are studied in the field of differential equations. The numbers used to represent continuous quantities are **real number**s, and the study of their properties and the properties of real-valued functions is known as real **analysis**. For various reasons, it's convenient to generalize to **complex number**s, which are dealt with in **complex analysis**. Functional analysis focuses attention on (typically infinite-dimensional) spaces of functions, laying the groundwork for **quantum mechanics** among many other things. In order to probe the foundations of mathematics, the fields of **set** theory, mathematical **logic**, and model theory were developed.

Since the time of the ancient Greeks, thought has been given to the ultimate nature of mathematics. What is its role and status in reality? Most crucially, is it invented or discovered? Leopold **Kronecker** was on the side of invention: "God made the integers; all the rest is the work of Man." Charles **Hermite**, by contrast, was clearly a Platonist: "There exists . . . an entire world, which is the totality of mathematical truths, to which we have access only with our mind, just as a world of physical reality exists, the one like the other independent of ourselves, both of divine creation." The German physicist Heinrich Hertz went even further: "One cannot escape the feeling that these mathematical formulas have an independent existence and an intelligence of their own, that they are wiser than we are, wiser even than their discoverers, that we get more

out of them than was originally put into them." G. H. **Hardy** summed up what many mathematicians today have a tendency to believe:[151] "that mathematical reality lies outside us, that our function is to discover or observe it, and that the theorems which we prove, and which we describe grandiloquently as our 'creations,' are simply the notes of our observations." In another passage, he made this point more precisely: "317 is a prime, not because we think so, or because our minds are shaped in one way rather than another, but because it is so, because mathematical reality is built that way." We are struck by how well mathematics describes the behavior of the world in which we live. The universe, in fact, appears to have a deep mathematical infrastructure. Martin **Gardner** makes the bold claim that: "Mathematics is not only real, but it is the only reality. [The] . . . entire universe is made of matter. . . . And matter is made of particles. . . . Now what are the particles made out of? They're not made out of anything. The only thing you can say about the reality of an electron is to cite its mathematical properties. So there's a sense in which matter has completely dissolved and what is left is just a mathematical structure."

matrix

A square or rectangular array of numbers, usually written enclosed in a large pair of parentheses. Matrices, which are added and multiplied using a special set of rules, are extremely useful for representing quantities, particularly in some branches of physics. A matrix can be thought of as a **linear** operator on **vector**s. Matrix-vector multiplication can be used to carry out geometric **transformation**s such as scaling, rotation, reflection, and translation.

Matrix comes from the same Latin root that gives us *mother,* and was used to refer to the womb and to pregnant animals. It became generalized to mean any situation or substance that contributes to the origin of something. The first mathematical use of the word *matrix* was around 1850 by James **Sylvester** who saw a matrix as a way of obtaining **determinant**s, but didn't fully appreciate its potential. Within a year of his first mention of the term, he introduced the idea to Arthur **Cayley** who was the first to publish the **inverse** of a matrix and to treat matrices as purely abstract mathematical forms. The use of mathematical arrays to solve problems predates the application of the name by about 2,000 years. Around 200 B.C. in the Chinese text *Juizhang Suanshu* (Nine Chapters on the Mathematical Arts) the author solves a system of three equations in three unknowns by placing the **coefficient**s on a counting board and solving by a process that today would be called *Gaussian elimination.*

maximum

The largest of a set of values.

maze

A network of winding and interconnected passageways that a traveler must negotiate in order to reach some goal. The terms *maze* and *labyrinth* are often used interchangeably, though sometimes a distinction is made based on the layout. A labyrinth is then defined as a construction that leads from a starting point to a goal by a *single* path, with no branches or dead ends. No matter how long and twisting the route, it is predetermined by the builder: a labyrinth, according to this definition, is *unicursal.* A maze, by contrast, is *multicursal* and calls for the traveler to make a series of decisions that affect how quickly the goal is reached. In this book, *maze* and *labyrinth* mean the same thing, and refer to unicursal and multicursal mazes.

The most famous of legendary mazes was the lair (or prison) of the Minotaur at Knossos on Crete. According to Greek mythology, King Minos of Crete had his chief engineer, Daedalus, build the labyrinth in order to keep the half-human half-bovine offspring of his wife Pasiphae and a bull out of the public eye. King Aegeus of Athens was forced to pay a periodic tribute to Minos (the Athenians having earlier murdered Minos's son) in the form of seven young men and seven maidens. These unfortunates were forced to enter the maze below Minos's palace where they would get hopelessly lost and eventually be eaten by the monster. King Aegeus' son, Theseus, decided to put a stop to this and offered to take the place

maze Possibly the world's oldest surviving labyrinth: a seven-ring labyrinth rock carving inside the Tomba del Labirinto, a Neolithic tomb at Luzzanas, Sardinia, dating somewhere between 2500 and 2000 B.C. *National University of Singapore*

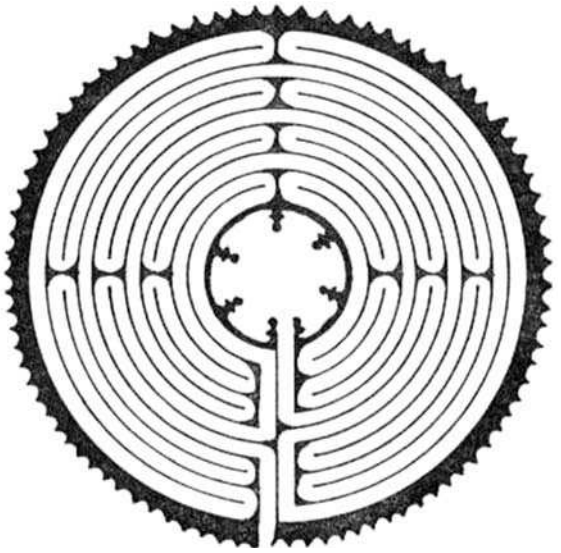

maze A plan of the maze in Chartres Cathedral as drawn by Henry Dudeney.

of one of the sacrificial virgins. He fell in love with Ariadne, one of Minos's daughters, who gave him a *clew,* or ball of yarn, to unravel as he entered the labyrinth so that he would be able to find his way back out. (Originally, *clue* and *clew* were alternative spellings of the same word. The modern sense of *clue* as a guide to solving a problem comes from the legend of the Minotaur, while *clew* retains its ancient meaning.) In true heroic style, Theseus slew the Minotaur but then spoiled the fairytale ending by abandoning Ariadne on the voyage home. Did this labyrinth really exist? In Roman times some writers suggested that a set of winding caves at Gortyan, in southern Crete, might have formed the basis for the tale. Although this complex of natural passages sounds similar to the maze in the myth, the story definitely places the labyrinth at the ancient Cretan capital. Archaeologists have found no evidence of a labyrinth structure at Knossos, but it has been suggested that the palace was so complicated, with its many levels, stairs, and rooms, that it may itself have inspired the story.

Minoan coins from about 300 B.C. bear a round, winding design, thought to be a representation of the labyrinth. A very similar geometric pattern recurs across many different cultures and times–scratched into caves in Cornwall (possibly by visiting Phoenician seafarers), on Roman coins, and in pictures drawn by native American Indians. Almost all these designs, including the one on the Minoan coins, are unicursal. Quite why Theseus would have needed a clew to navigate a maze that had only one way in and out is anybody's guess. But the underlying reason for the early unicursal design isn't hard to find. These mazes were intended not as intellectual puzzles but as symbolic representations of destiny as a matter of fate, beyond personal control. The world's oldest known maze-like designs, dating back about 3,500 years, have been found carved on rocks in northwest Spain and around the shores of the Mediterranean, and according to legend, were walked by fishermen before setting sail to ensure favorable winds and a good catch. In medieval times, mazes started to appear in churches, as art painted on walls or inlaid as "pavement mazes" on the floor. Some of the larger floor versions were traversed by people on their knees as a form of repentance or traversed as a substitute for an actual pilgrimage to the holy city, earning them the name "*Chemin de Jerusalem,*" or Road of Jerusalem. The oldest-known church labyrinth, at the Basilica of Reparatus at Orleansville, Algeria, dates from the fourth century A.D. and measures about 8 feet in diameter. One of the largest, built in 1288, formed part of the floor in the nave of Amiens Cathedral in France and spanned about 42 feet, but was destroyed in 1825. A splendid surviving example, however, is in Chartres Cathedral near Paris. Laid down in about 1200, this is an 11-circuit design (11 concentric windings) divided into quadrants, of the type often found in Gothic cathedrals. The only cathedral maze in Britain is at Ely, 16 miles north of Cambridge; when the Cathedral was restored around 1870, the architect, Gilbert Scott, installed a pavement maze of his own design under the west tower.

Mazes built primarily as puzzles or for recreation represent a different type of structure. For one thing, they are multicursal, offering those who enter a series of choices about which way to proceed. In his *Natural History,* the Roman historian Pliny comments that the classical type of labyrinth is quite distinct from "the mazes formed in the fields for the entertainment of children," suggesting that these diversions may have a long history. But it was in England that they really came of age. Church mazes never caught on in England, but turf mazes became tremendously popular. Ranging from 25 feet to over 80 feet across, they were constructed in or just outside villages across the countryside and were given names such as "Mizmaze," "Troy Town," "Shepherd's Race," and "Julian's Bower." A Welsh history book *Drych y Prif Oesoedd* (Mirror of the first age) published in 1740 notes the curious custom shepherds had of cutting the turf in the form of a labyrinth, which would seem to account for the origin of "Shepherd's Race." "Troy Town" probably refers to a legend that the city of Troy had seven exterior walls arranged as a maze to frustrate an attacking force.

From the turf maze it was no great leap to perhaps the most famous form of full-size maze–the topiary or hedge

maze. While the use of hedges in gardens dates back to Roman times, the earliest references to a topiary maze appears in thirteenth-century Belgium. By the sixteenth century the hedge maze had spread to England, as a landscape painting by Tintoretto attests. In the later part of the seventeenth century, Louis XIV had a labyrinth built as a part of the gardens at Versailles, which included 39 groups of hydraulic statuary representing the fables of Aesop. The most famous surviving historic hedge maze is that on the grounds of Hampton Court Palace in England, designed by George London and Henry Wise for William of Orange, planted between 1689 and 1694, and occupying about a third of an acre. The finest turf maze in England may be that at Bridge End Gardens in Saffron Walden, Essex, which was replanted with yew in 1838–1840, abandoned and lost by 1949, then restored in 1983. A second maze, an imitation of that at Hampton Court, is on the Common.

In August 1997, Adrian **Fisher** opened the "World's Largest Maze" at Millets Farm Centre, Frilford, Oxfordshire, England, cut from about six acres of grain. However, his 1995 effort in Shippensburg, Pennsylvania, was in a 30-acre field and the 1997 maze in Reignac sur Indre covers 37 acres.[101]

When faced with a maze, what is the best way of reaching the goal, whether this is a point in the middle of the maze or an exit that forms a second opening to the structure? A unicursal maze calls for no brainwork, only footwork, since it consists of a single winding passage with no offshoots. Multicursal mazes are a different story. The easiest solution is to place a hand on one wall at the outset and follow that wall, come what may. Each blind alley will be traversed one time in and out until the whole maze is completed, or the goal is found. This simple method isn't the most efficient and it will fail altogether if the goal lies within an island in the maze–that is, a section detached from any of the exterior walls. A classic general method of "threading a maze" is: (1) never traverse a path more than twice; (2) when arriving at a new branch point or node, select either path; (3) when arriving at an old node or at a dead end by a new path, return by the same path; and (4) when arriving at an old node by an old path, select a new path, if possible; otherwise, an old path. An

maze A handheld maze, the object of which is to get the silver ball from the starting rectangle on the left to the finishing rectangle on the right. Crafted from Tasmanian blackheart sassafrass by Kym Anderson. *Mr. Puzzle Australia, www.mrpuzzle.com.au*

explorer who follows these rules, using marks on the ground, as a record, can be assured of visiting every part of the maze.[48, 219, 240, 294]

See also **Rosamund's bower**.

mean

> *When she told me I was average, she was just being mean.*
>
> –Anonymous

A precisely calculated "typical" value of a group of numbers. There are several kinds of means. The *arithmetic mean,* which is usually what is meant when people talk about an **average**, is the sum of a set of values divided by the number of values. For example, the arithmetic mean of 3, 4, 7, and 10 is $(3 + 4 + 7 + 10)/4 = 6$. The *geometric mean* of n values is the nth root of the product of the values. For example, the geometric mean of 3, 8, and 10 is $(3 \times 8 \times 10)^{1/3}$ or the cube root of 240. The *harmonic mean* is the reciprocal of, or one over, the mean of the reciprocals of the values. For example, the harmonic mean of 3, 8, and 10 is $1/[(\frac{1}{3} + \frac{1}{8} + \frac{1}{10})/3]$. A different kind of average is *median,* which is generally the center term when a group of numbers are ordered by size. If there are an even number of values then the arithmetic mean of the center two is the median. The words *mean* and *median* both come from the Indo-European root *medhyo* meaning "middle."

measure

A way of gauging how big something is in terms of length, volume, or some other quality. One of the strangest facts in mathematics is that some objects exist that can't be measured. In the language of **set**s, the basic rules (somewhat simplified) of mathematical measures are as follows: (1) the measure of any set is a **real number**; (2) the **empty set** has measure zero; (3) if A and B are two sets with no elements in common then the measure of $A \cup B$ (the union of A and B) is equal to the measure of A plus the measure of B. The second of these rules can be very useful, for example, when integrating a **function**, since it allows us to ignore any points where the function jumps around, provided that such points are isolated. A slightly jittery function is one thing; a nonmeasurable set is a very different animal. Imagine a three-dimensional shape so fantastically intricate, so jagged and crinkled, that it is impossible to measure its volume and this gives some idea of the concept of nonmeasurability. From it flow such bizarre conclusions as the **Banach-Tarski paradox**.

measure theory

The part of **mathematics** that investigates the conditions under which **integration** can be carried out. It focuses mainly on the various ways in which the size, or **measure**, of a **set** can be estimated.

measuring and weighing puzzles

Problems that involve measuring a given quantity of liquid by pouring from one vessel into others of known capacity go back to medieval times. One of the earliest to appear in print was given by Niccoló **Tartaglia** and asks for 24 ounces of balsam to be divided into three equal portions using vessels that hold 5, 11, and 13 ounces, respectively. A similar problem was posed by a fellow traveler to the young Siméon **Poisson** while on a journey. Poisson's family had tried to steer him into careers ranging from a surgeon to a lawyer, the last on the theory that he was fit for nothing better. He seemed inept at everything he did. However, he saw the solution to the measuring problem immediately and realized his true calling. Thereafter, he threw himself into mathematics and became one of the greatest mathematicians of the nineteenth century.

The classic weighing problem was proposed by Claude-Gaspar **Bachet** and entails finding the least number of weights needed to weigh any integral number of pounds from 1 to 40 pounds inclusive, when no weights are allowed in either of the two pans. The answer is 1, 3, 9, and 27 pounds. Tartaglia had previously stated the same puzzle with the condition that the weights may only be placed in one pan, in which case the solution is 1, 2, 4, 8, 16, and 32 pounds.

PUZZLE

The following is a measuring problem from Henry **Dudeney**'s *Canterbury Puzzles,* which Dudeney claimed was the most popular of the whole collection and which the reader may like to try:

> Here be a cask of fine London ale, and in my hands do I hold two measures—one of five pints, and the other of three pints. Pray show how it is possible for me to put a true pint into each of the measures.

Solutions begin on page 369.

mechanical puzzle

A puzzle, involving several objects or a single object composed of one or more movable parts, whose solution requires moving from an initial state to a predefined final state. Mechanical puzzles were first classified by Louis **Hoffmann** in *Puzzles Old and New*[171] (1893). A modified form of his scheme is shown in the table "Mechanical Puzzles" on the following page.

medial triangle

The **triangle** whose vertices are the midpoints of the sides of a given triangle (see **vertex**).

Mechanical Puzzles

Type	Subtype	Examples
Assembly	2-dimensional assembly	**Tangrams**, **T-puzzle**, jigsaw
	3-dimensional assembly (noninterlocking)	**Soma cube**
	Matchstick puzzles	
	Miscellaneous	**Puzzle rings**
Disassembly	Trick or secret opening	**Puzzle jug**
	Miscellaneous	Trick locks, keys, etc.
Interlocking solid	**Burr puzzle**	
	3-dimensional jigsaws	
	Miscellaneous	Cubes, other objects
Disentanglement and entanglement	Wire puzzles	**Chinese rings**
	String puzzles	Cat's cradle
	Miscellaneous	
Sequential movement	**Peg solitaire** (peg removal)	
	Other counter (peg rearrangement)	
	Sliding-piece puzzles	**Fifteen Puzzle**
	Miscellaneous	**Tower of Hanoi**
Puzzle vessels	**Puzzle jug**	
	Miscellaneous	Bottom-fill teapots, pitchers
Vanishment puzzle		**Get Off the Earth**
Folding	**Origami**	
	Flexagon	
Impossible figure		**Penrose stairway**
		Penrose triangle
		Impossible trident

median
1. The line from a **vertex** of a **triangle** to the midpoint of the opposite side. 2. See **mean**.

Menaechmus (c. 380–c. 320 B.C.)
A Greek mathematician, thought to have been a pupil of **Eudoxus**, who is famed for his discovery of the **conic sections** and for being the first to show that **ellipse**s, **parabola**s, and **hyperbola**s are formed by cutting a cone in a plane that is not parallel to the base. Menaechmus made his discoveries on conic sections while attempting, unsuccessfully, to solve the problem of **duplicating the cube**. It has also been suggested that he served as a tutor to Alexander the Great.

Menger sponge
A famous **fractal** solid that is the three-dimensional equivalent of the **Sierpinski carpet** (which, in turn, is the

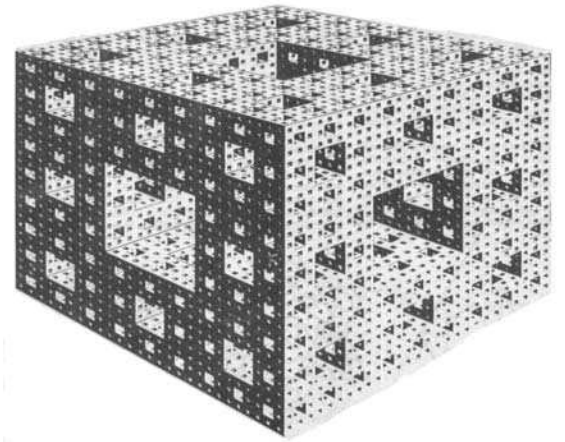

Menger sponge

two-dimensional equivalent of **Cantor dust**). To make a Menger sponge, take a cube, divide it into 27 (= 3 × 3 × 3) smaller cubes of the same size and remove the cube in the center and the six cubes that share faces with it. What's left are the eight small corner cubes and twelve small edge cubes holding them together. Now, imagine repeating this process on each of the remaining 20 cubes. Repeat it again. And again . . . ad infinitum. The Menger sponge was invented in 1926 by the Austrian mathematician Karl Menger (1902–1985).

Mersenne, Marin (1588–1648)

A French monk, philosopher, and mathematician best remembered for his work to find a formula to generate **prime number**s based on what are now known as **Mersenne number**s. However, in addition to being a mathematician, he wrote about music theory and other subjects; edited works of Euclid, Archimedes, and other Greek mathematicians; but most importantly, corresponded extensively with mathematicians and other scientists in many countries. At a time before scientific journals existed, Mersenne was at the heart of a network for information exchange.

Mersenne number

A number of the form $2^n - 1$ (one less than a power of 2), where n is a positive integer. Mersenne numbers are named after Marin **Mersenne** who wrote about them in his *Cogita Physico-Mathematica* (Physical Mathematics Knowledge 1644) and wrongly conjectured that they were prime for $n = 2, 3, 5, 7, 13, 17, 19, 31, 67$, and 257, and composite for $n < 257$. See also **Mersenne prime**.

Mersenne prime

A **prime number** of the form $2^p - 1$, where p is prime. A prime exponent is necessary for a **Mersenne number** to be prime but is not sufficient; for example, $2^{11} - 1 = 2{,}047 = 23 \times 89$. In fact, after an early clustering of Mersenne primes for fairly small values of p, further occurrences become increasingly rare. At the time of writing there are 40 known Mersenne primes, corresponding to values for p of 2; 3; 5; 7; 13; 17; 19; 31; 61; 89; 107; 127; 521; 607; 1,279; 2,203; 2,281; 3,217; 4,253; 4,423; 9,689; 9,941; 11,213; 19,937; 21,701; 23,209; 44,497; 86,243; 110,503; 132,049; 216,091; 756,839; 859,433; 1,257,787; 1,398,269; 2,976,221; 3,021,377; 6,972,593; 13,466,917; and 20,996,011. However, it isn't known if the current largest Mersenne prime is the fortieth in order of size because not all lower exponents have been checked. Mersenne primes rank among the largest of all known primes because they have a particularly simple test for primality, called the *Lucas-Lehmer test.*

The search for Mersenne primes has been going on for centuries. They are named after Marin **Mersenne** who, in 1644, helped the search gain wide recognition by writing to many mathematicians of his conjecture about which small exponents yield primes. Around the time that Mersenne's conjecture was finally settled, in 1947, digital computers gave a new impetus to the hunt for Mersenne primes. As time went on, larger and larger computers found many more Mersennes and, for a while the search belonged exclusively to those with the fastest computers. This changed in 1995 when the American computer scientist George Woltman began the *Great Internet Mersenne Prime Search* (*GIMPS*) by providing a database of what exponents had been checked, an efficient program based on the *Lucas-Lehmer test* that could check these numbers, and a way of reserving exponents to minimize the duplication of effort. Today GIMPS pools the combined efforts of dozens of experts and thousands of amateurs. This coordination has yielded several important results, including the discovery of the Mersennes $M_{3021377}$, $M_{2976221}$, and $M_{20996011}$ and the proof that M_{756839}, M_{859433}, and $M_{3021377}$ are the thirty-second, thirty-third, and thirty-fourth Mersennes.

meter

The basic unit of length adopted under the System International d'Unites (SI units). Over the years the definition of the meter has changed several times. Throughout all these definition changes the length of the meter hasn't changed, but the precision by which it is measured was improved. In 1793, the meter was defined to be 1/10,000,000 of the distance from the pole to the equator. During the nineteenth century, the definition was in terms of the length of standard bars of platinum kept under controlled conditions. In 1983, the current definition was adopted of the distance traveled by light in a vacuum in 1/299,792,458 of a second.

method of exhaustion

Finding an **area** by approximating it by the areas of a sequence of **polygon**s; for example, filling up the interior of a circle by inscribing polygons with more and more sides.

metric

Any **function** $d(x, y)$ that describes the *distance* between two points. Distance is formally defined as a single number with the following properties: (1) $d(x, y) = 0$ if and only if $x = y$; (2) $d(x, y) = d(y, x)$; (3) $d(x, y) + d(y, z) \geq d(x, z)$ (the triangle inequality).

metric space
A **set** that has a **metric**; in other words, a kind of space in which the concept of distance has meaning. Compare with **topological space**.

metrizable
For a **topological space**, the property that there exists a **metric** compatible with the topology. To say that a topological space is metrizable is to treat it as a **metric space**, but without distinguishing any specific or preferred distance function.

Michell, John (1724–1793)
An English natural philosopher and clergyman, educated at Queen's College, Cambridge, who discovered that the force between magnetic poles varies as $1/r^2$. In 1767, Michell became rector of Thornhill, now a suburb of Dewsbury, Yorkshire. Sometime in the early 1770s, he played music with the great astronomer William Herschel and gave Herschel his first telescope. In 1784, Michell deduced the existence of what are now called black holes from Newton's corpuscular theory of light, and suggested that some stars might have dark companions. He also devised and built the torsion balance for determining the universal gravitational constant *G,* but died before having the chance to use it. The balance was passed to the Cambridge physicist F. J. H. Wollaston, and from him to Henry Cavendish, who used it at his house in London and is often, mistakenly, identified as its inventor.

midpoint
The point M is the midpoint of line segment AB if $AM = MB$. That is, M is halfway between A and B.

mile
A measure of distance, the name of which is an abbreviation of the Latin *mille passes* or "one thousand paces." Since the paces (one step with each foot) of the Roman Army were supposed to be two steps, each 2.5 feet long, 1,000 paces is very close to the length now called a statute mile (5,280 feet). A *nautical mile* was developed to be a distance equal to 1 minute of arc ($\frac{1}{60}$ of a degree) distance along a great circle and is equal to 6,076 feet.

million
A thousand thousand, 1,000,000, or 10^6. The word comes from the Latin *mille* for "thousand" (which is also the root for ***mile*** and *millennium*) and the suffix *ion* that implies "large" or "great;" thus a million is literally a "great thousand." Although *million* seems to have come into use as early as the middle of the fourteenth century, most mathematicians would use the phrase "thousand thousands" to avoid confusion and it was not until the 1700s that "million" caught on. It appears in the King James Version of the Bible (Genesis 24:60) and in Shakespeare (*Hamlet* act II scene II)– "for the play, I remember, pleased not the million."

minimal prime
A **prime number** that is a substring of another prime when written in **base** 10. A string a is a substring of another string b, if a can be obtained from b by deleting zero or more of the characters in b. For example, 392 is a substring of 639,802. The minimal primes are:

2; 3; 5; 7; 11; 19; 41; 61; 89; 409; 449; 499; 881; 991; 6,469; 6,949; 9,001; 9,049; 9,649; 9,949; 60,649; 666,649; 946,669; 60,000,049; 66,000,049; 66,600,049

minimal surface
A surface that, bounded by a given closed curve or curves, has the smallest possible area. A minimal surface has a mean **curvature** of zero. Finding and classifying minimal surfaces and proving that certain surfaces are minimal have been major mathematical problems for over 200 years. If the closed curve is planar then the solution is trivial; for example, the minimal surface bounded by a circle is just a disk. But the problem becomes much more difficult if the bounding curve is nonplanar–in other words, is allowed to move up and down in the third dimension. The first nontrivial examples of minimal surfaces, the **catenoid** and the **helicoid**, were discovered by the French geometer and engineer Jean Meusnier (1754–1793) in 1776, but there was then a gap of almost 60 years before the German Heinrich Scherk found some more. In 1873 the Belgian physicist Joseph **Plateau** carried out experiments that led him to conjecture that soap **bubble**s and soap films always form minimal surfaces. Proving mathematically this was true became known as the **Plateau problem**. Most minimal surfaces are extremely hard to construct and visualize, in part because the majority of them are self-intersecting. However, the development of high-performance computer graphics has provided mathematicians with a powerful tool and the last couple of decades have seen a huge increase in the number of such surfaces that have been defined and investigated.

minimax theorem
A theorem that says there is always a rational solution to a precisely defined conflict between two people whose interests are completely opposite. It is rational in that both parties can convince themselves that they can't expect to do any better, given the nature of the conflict.

minimum
The smallest of a set of values.

minimal surface A Scherk Surface—a type of minimal surface—portrayed as a membrane. *Anders Sandberg*

Minkowski, Hermann (1864–1909)

A German mathematician, born in Lithuania, who played an important part in the early development of **relativity theory**. Minkowski was the first to realize that the work of Hendrik Lorentz and Albert **Einstein** could be best understood if space and time, formerly thought to be separate entities, were treated as part of a four-dimensional **space-time** with a **non-Euclidean geometry**. The concept of the space-time continuum, which provided a framework for all later mathematical work in relativity, appeared in Minkowski's book *Raum und Zeit* (Space and Time 1907). From 1896 to 1902, Minkowski taught at the Zurich Federal Institute of Technology when Einstein was a student. In fact, Einstein attended several of the courses he gave but didn't create a good impression at the time. Minkowski described him as a "lazy dog" who "never bothered about mathematics at all." In 1902, Minkowski accepted a chair at the University of Göttingen, where he stayed for the rest of his life. His main interest was in pure mathematics, including number theory and geometry, and it was through his understanding of the more abstract side of mathematics and geometry in more than three dimensions that he developed the idea of four-dimensional space-time.

Minkowski space

A finite-dimensional **vector space**, especially a four-dimensional one, together with an indefinite inner product with one positive or timelike direction and many negative or spacelike directions. In particular, Minkowski space is ordinary **space-time** in the special **relativity theory**.

minor axis

The smallest **chord** of an **ellipse**.

minute

(1) One sixtieth of an hour or of a **degree** of arc or angle. (2) One sixtieth of an hour. As a measure of both time and angle, it equals 60 **seconds**.

mirror reversal problem

Why does a mirror reverse right and left, but not up and down? This question crops up perennially in the letter and query columns of magazines and newspapers. It was the inspiration for Lewis **Carroll**'s *Alice through the Looking Glass*. Alice Raikes (not to be confused with Alice Liddell, after whom the fictional Alice was modeled) was another of Carroll's young friends. On one occasion, in 1868, Carroll put an orange in her right hand and then asked her to stand in front of a mirror and say which hand showed the reflection of the orange. She said the left hand and Carroll asked her to explain. She finally replied "If I was on the other side of the glass, wouldn't the orange still be in my right hand?" Carroll said this was the best answer he'd had and later said it gave him the idea for his book.

Others have struggled harder but not always convincingly to explain the phenomenon, appealing variously to gravity, the psychology of perception, and philosophy. Why *does* a mirror reverse right and left, but not up and down? A frequently given answer is that a mirror doesn't reverse right and left. It reverses *front and back.* This is certainly true: the looking glass you is facing in the opposite

mirror reversal problem A looking-glass world beckons the curious Alice in Lewis Carroll's book *Alice through the Looking Glass.*

direction to the "real" you. But this short, crisp explanation doesn't completely dispel the mystery. If you imagine that the mirror is not there and that instead you are looking at a flesh-and-blood twin of yourself, that twin is differently handed. If you have a watch on your left wrist, the person you are facing has his/her watch on the right wrist. The mirror *has* done a left-right swap, surely! At any rate, something has happened to left and right that hasn't happened to up and down. To be more convinced of this, hold this book up to the mirror and try to read it. If no left-right swap has happened, why is the reflected writing so hard to read? First, remember that you are only looking at an image! The mirror hasn't (Carrollian fantasies aside) created some*thing* of opposite handedness. Secondly, appreciate how the writing appears in the mirror's frame of reference. This is easy to do by looking at the writing from the other side of the page (i.e., back to front, thus undoing the back to front reversal caused by the reflection). From the mirror's point of view the writing looks perfectly normal.

missing dollar problem

A version of this problem first appeared in R. M. Abraham's *Diversions and Pastimes* in 1933.[2] See also **nine nooms paradox**.

PUZZLE

Three people dine at a restaurant and receive a total bill for $30. They agree to split the amount equally and pay $10 each. The waiter hands the bill and the $30 to the manager, who realizes there has been a mistake and the correct charge should be only $25. He gives the waiter five $1 bills to return to the customers, with the restaurant's apologies. However, the waiter is dishonest. He pockets $2, and gives back only $3 to the customers. So, each of the three customers has paid $9 and the waiter has stolen $2 making a total of $29. But the original bill was for $30. Where has the missing dollar gone?

Solutions begin on page 369.

Mittag-Leffler, (Magnus) Gösta (1846–1927)

A Swedish mathematician who, in 1882, founded the international journal *Acta Mathematica*, and was its chief editor for 45 years. He studied in Paris under Charles **Hermite** and in Berlin under Karl **Weierstrass**, and made significant contributions to **analysis**. His best known work concerned the analytic representation of a one-valued **function**s and culminated in the *Mittag-Leffler theorem.* Since he took a special interest in Georg **Cantor**'s discoveries, much of Cantor's work was published in *Acta Mathematica.* Inscribed on the mantlepiece of Mittag-Leffler's home–now a research institute–in Djursholm is the epitaph: "Number is the beginning and end of thought. Thought gave birth to number but reaches not beyond. ML 1903"

mixed strategy

In **game theory**, a **strategy** that uses **random**ness by employing different actions in identical circumstances with different probabilities.

Möbius band

A simple and wonderfully entertaining two-dimensional object, also known as the Möbius strip, that has only one surface and one edge. It is named after the German mathematician and theoretical astronomer August Ferdinand Möbius (1790–1868), who discovered it in September 1858, although his compatriot and fellow mathematician Johann Benedict Listing (1808–1882) independently devised the same object in July 1858. Making a Möbius band is simple: take an ordinary sheet of typing paper, cut an $11'' \times 1''$ rectangle, bring the two long ends together, twist one of the ends 180°, and tape the two ends together. To prove that the band is single-sided, take a pen and start drawing a line around the band's circumference. When drawing the line, never take the pen off the paper; just

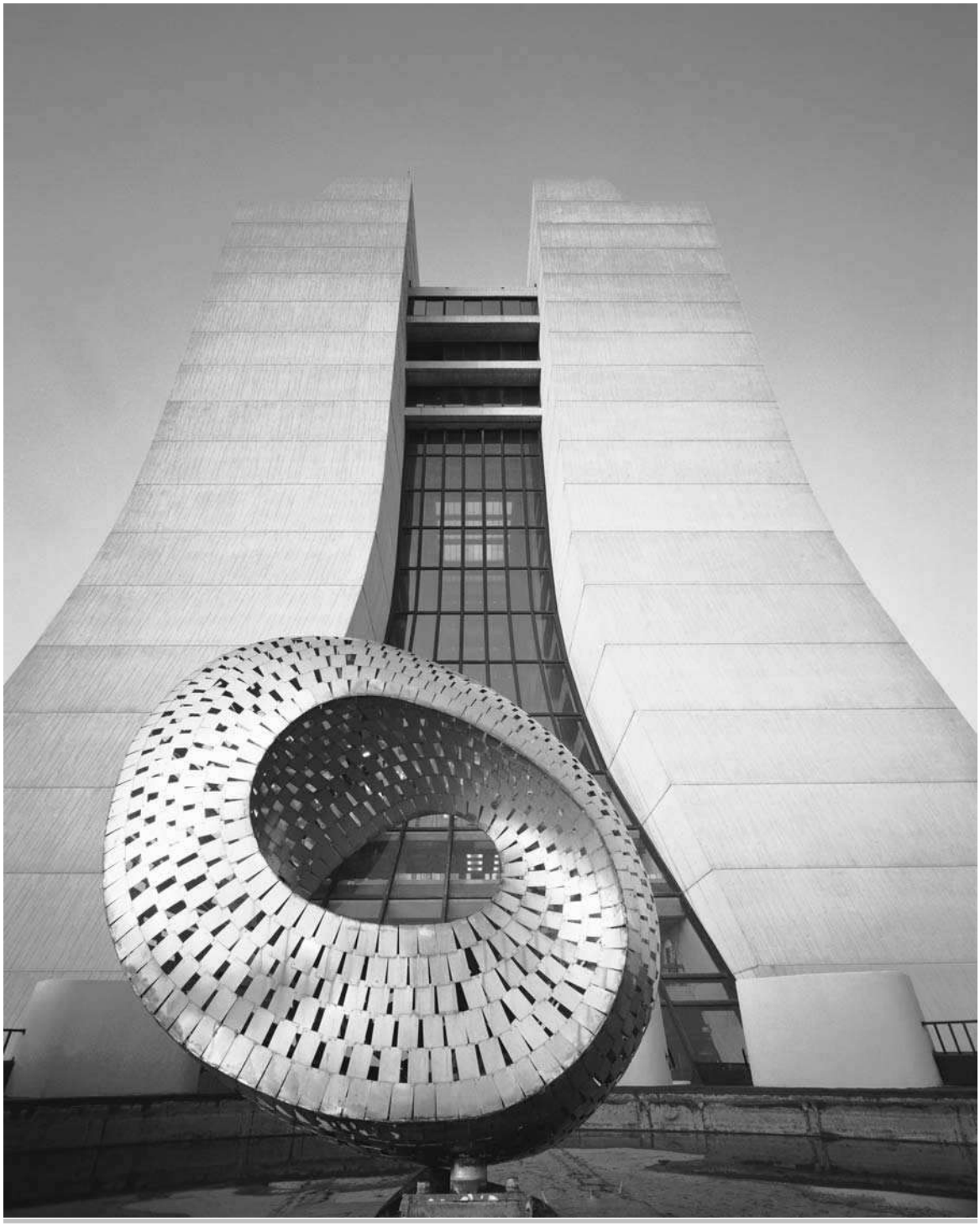

Möbius band A sculpture of a Möbius band outside the Fermi National Accelerator Laboratory. *FNAL*

keep drawing the line until the starting point is reached. Once you are finished, look at both sides: there should be a line on both sides, thus proving that it is all the same side because you never took the pen off the paper.

The Möbius band has a lot of curious properties. If you cut down the middle of the band, instead of getting two separate strips, it becomes one long strip with two half-twists in it. If you cut this one down the middle, you get two strips wound around each other. Alternatively, if you cut along the band, about a third of the way in from the edge, you will get two strips; one is a thinner Möbius band, the other is a long strip with two half-twists in it. Other interesting combinations of strips can be obtained by making Möbius bands with two or more flips in them instead of one. Cutting a Möbius band, giving it extra twists, and reconnecting the ends produces unexpected figures called *paradromic rings*.

The Möbius band has provided inspiration both for sculptures and for graphical art. M. C. **Escher** was especially fond of it and based many of his lithographs on it. It is also a recurrent feature in science fiction stories, such as Arthur C. Clarke's *The Wall of Darkness*. A common fictional theme is that our universe might be some kind of generalized Möbius band. There have been technical applications; giant Möbius bands have been used as conveyor belts (to make them last longer, since "each side" gets the same amount of wear) and as continuous-loop recording tapes (to double the playing time).

A closely related strange geometrical object is the **Klein bottle**, which can be produced by gluing two Möbius bands together along their edges; however, this can't be done in ordinary three-dimensional Euclidean space without creating self-intersections.[116]

mode
The most frequently occurring value in a sequence of numbers.

model of computation
An idealized version of a computing device that usually has some simplifications such as infinite memory. A **Turing machine** and the **lambda calculus** are models of computation.

model theory
The study of mathematical structures that satisfy a particular set of **axiom**s, especially in the field of **logic**.

modulo
The integers a and b are said to be congruent modulo m if $a - b$ is divisible by m.

Moiré pattern
A radiating curved pattern created when two repetitive patterns overlap and interfere with one another. A Moiré pattern is seen, for example, when someone on TV wears a herringbone jacket. *Moiré* is the French word for "silk", and *silk moiré,* introduced from China to France in 1754, is the fabric that shows the familiar shifting patterns.

Moivre, Abraham de
See **de Moivre, Abraham**.

monad
A central concept in the Pythagorean worldview (see **Pythagoras of Samos**), in which it is regarded as the first thing that came into existence. Following the monad came, in order: the *dyad,* numbers, lines, two-dimensional entities, three-dimensional entities, bodies, the four elements (earth, air, fire, and water), and the rest of the world. The monad plays a similarly fundamental role in the metaphysics of Leibnitz as an indivisible, impenetrable unit of mental experience. It also has several different technical meanings in modern mathematics. For example, in **nonstandard analysis**, a monad consists of all those numbers infinitesimally closer to a given number. The word comes from the Latin *monas* (single) and Greek *monos* (unit).

Monge, Gaspard (1746–1818)
A French mathematician and physicist who put descriptive geometry, introduced by Albrecht **Dürer**, on a firm mathematical footing. He became professor of mathematics at Mézières (1768) and of hydraulics at the Lycée in Paris (1780), and published his groundbreaking treatise on the application of geometry to the arts of construction in 1795.

monkeys and typewriters
Six monkeys pounding away on typewriters would, by pure chance, if given enough time, be bound to write out all the works held in the British Library (or in all other libraries, for that matter). This idea was first suggested by the biologist Julian Huxley (1887–1975); it was discussed by the physicist James Jeans (1877–1946) in his *Mysterious Universe* (1930); and it has been restated in various forms over the years, in terms of chimpanzees, Shakespeare's sonnets, and the like. It was also the subject of Russell Maloney's short story "Inflexible Logic," first published in the *New Yorker* magazine (1940) and reprinted in Clifton **Fadiman**'s *Fantasia Mathematica*,[96] which tells the tragic tale of what happens when the fantastically improbable comes true. See also **Universal Library**.

monochromatic triangle
A triangle whose vertices are all colored the same (see **vertex**).

monomial
An algebraic expression that consists of just one term.

monotonic
The property of a **function** that is always strictly increasing or strictly decreasing, but never both.

Monster curve
See **Peano curve**.

Monster group
The largest, most fascinating, and most mysterious of the so-called sporadic **group**s; it was constructed by Robert Griess at Princeton in 1982, having been predicted to exist by him and Bernd Fischer in 1973, and was named the Monster by John **Conway**. Think of the Monster group as a preposterous snowflake with more than 1,050 symmetries that exists in a space of 196,883 dimensions. It contains the following number of elements:

$$2^{46} \times 3^{20} \times 5^{9} \times 7^{6} \times 11^{2} \times 13^{3} \times 17 \times 19 \times 23 \times 29 \times 31 \times 41 \times 47 \times 59 \times 71$$
$$= 808{,}017{,}424{,}794{,}512{,}875{,}886{,}459{,}904{,}961{,}710{,}757{,}005{,}754{,}368{,}000{,}000{,}000$$
$$\approx 8 \times 10^{53}$$ (more than the number of quarks in the Sun).

Despite these impressive credentials, however, it is still classified as a *simple group,* meaning that it doesn't have any normal subgroups other than the identity element and itself. All 26 simple groups have now been classified and the Monster is far and away the biggest. At first, it seemed that the Monster was just a curiosity–a Guinness Book record of pure math. Its only "useful" application seemed to be to give the best way for packing spheres in 24 dimensions! In ordinary three-dimensional space (and also four and five dimensions), the grocer's way of stacking oranges in a hexagonal lattice is thought to be the tightest possible (see **Kepler's conjecture**). But as the number of dimensions increases, the optimal packing method changes. A 24-dimensional grocer would get the most efficient arrangement of his 24-dimensional oranges by using the same symmetry as that of the Monster. This is unlikely to be immediately useful. Much more interesting, however, is the connection that has been found between the symmetry of the Monster and one of the most promising unifying theories in physics–**string theory**–which has been revealed by the **Monstrous Moonshine conjecture**.[70]

Monstrous Moonshine conjecture
An outrageous idea that stemmed from an observation made by John McKay of Concordia University in 1978. McKay was leafing through a table of abstruse mathematical data, giving possible values for coefficients of the *j*-function of certain elliptic curves, when he noticed the number 196,884 in the expression $j(q) = q - 1 + 196884q + 21493760q^2 + \ldots$. In a moment of inspiration, he recognized this number as being one more than the number of dimensions in which the **Monster group** can be most simply represented. Looking into this "coincidence" more closely, he found that it was no coincidence at all. In fact, *all* the coefficients of the *j*-function were simple combinations of the degrees of possible representations of the Monster. This pointed to some deep connection between two seemingly unrelated areas of mathematics. On the one hand were the coefficients of what is called an elliptic modular function–exactly the kind of function that would play a key role in the proof of **Fermat's last theorem**. On the other was the number of dimensions, and combinations of degrees, of a crystal lattice whose symmetry rotations and reflections formed the Monster. Subsequently, McKay and a few other mathematicians, including John **Conway** and Simon Norton, drew out the link between elliptic modular functions and the Monster in a proposition christened, because of its fantastic nature, the Monstrous Moonshine. In 1998, this conjecture was proved by Richard Borcherds (a former student of Conway's) at the University of California at Berkeley. Astonishingly, Borcherds's proof reveals a deep relationship between elliptic curves, the Monster Group, and **string theory**–the most promising theory on offer to unify our understanding of nature at the subatomic level. Borcherds showed that the Monster is the group of symmetries of 26-dimensional strings expressed in a form known as *vertex algebra.* Some people believe the connection may run even deeper and that Monstrous Moonshine may hold clues to the very existence of the reality in which we live.[69]

Monte Carlo method
A method of estimating the true value of a quantity by carrying out a lot of **random** samples. For example, suppose we want to know the probability of getting a double six when we roll two dice. We could roll a pair of dice a thousand times, and count how many times, *n,* a double six came up; the estimated probability would then be *n*/1,000. A famous example of using the Monte Carlo method is to calculate **pi**. Get a computer to generate two random numbers *x* and *y,* each in the range –1 to 1, so that the point (*x, y*) lies somewhere randomly inside a square of side 2 units. Do this thousands of times, and count up what proportion of the points also lie inside the circle that inscribes

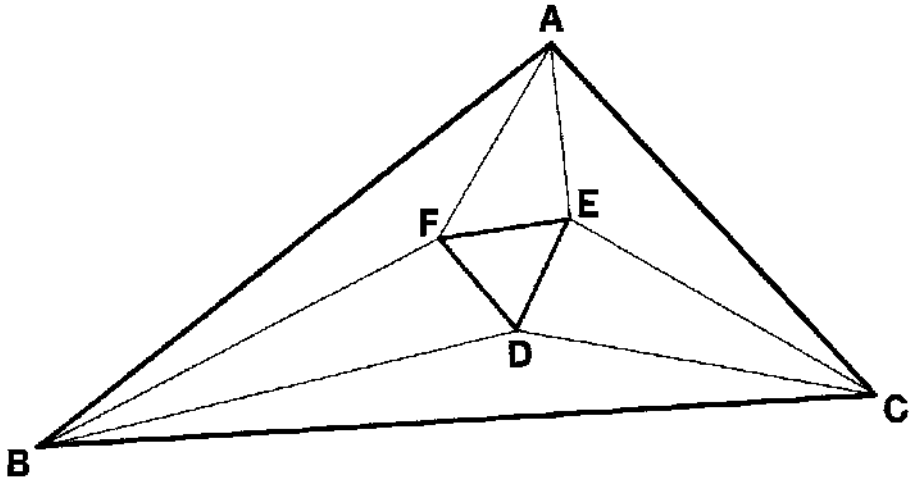

Morley's miracle The trisectors of the angles of triangle *ABC* meet the corners of a inner equilateral triangle *FED* known as Morley's triangle.

the square (you can tell whether a point does or not by working out whether $x^2 + y^2 < 1$). The proportion inside the circle is an approximation to $\pi/4$ (because the circle has area π but the square has area 4); millions of points are needed to obtain a good estimate.

This method was developed by researchers working on the Manhattan Project during World War II. To answer some of their scientific questions, they would repeatedly sample from their best estimates of the partial results, then apply the math they knew to the interactions and study the range of results. This process, which they named after the famous Monaco casino town of Monte Carlo, was created by John **von Neumann** and Stanislaw **Ulam**. The term and a description of the method seems not to have been published until some time after the war.

Montucla, Jean Etienne (1725–1799)

A French writer, mathematician, and scientist, who wrote several important early works on the history of mathematics. His *Histoire des mathématiques* (1758) was published in two volumes, the first of which covers the subject from ancient times to 1700, while the second is entirely devoted to seventeenth-century mathematics. It is considered the first attempt at a history of mathematical ideas and problems, in contrast to earlier works that were mostly lists of names, titles, and dates. Montucla had intended to produce a third volume covering the first half of the eighteenth century but the amount of new developments that had appeared during this time, and the difficulties of putting recent work into its historical context, led him to abandon this aim. A few years later he published another text for which he is famed–a new, greatly expanded and improved edition of Jacques **Ozanam**'s *Récréations mathématiques et physiques* (1778). Montucla's edition was particularly influential in popularizing geometric **dissection** problems. Charles Hutton translated it into English in 1803 and Riddle's edition was published in 1844, called *Recreations in science and natural philosophy.*

Monty Hall problem

A puzzle in probability that was inspired by the American game show *Let's Make a Deal,* hosted by Monty Hall. In its original form it goes like this: at the end of the show, you, the player, are shown three doors. Behind one of them is a new car, behind the other two are goats. Monty knows where the car is, but you don't. You choose a door. Before that door is opened however, Monty opens one of the two other doors with a goat behind it. He then gives you the option of switching to the other closed door. Should you switch or stick? At first glance, it seems as if it shouldn't make any difference. But the answer is surprising.

Suppose you stick. Your original choice made when all three doors were equally likely gives you a probability of winning the car of $\frac{1}{3}$. Now suppose you switch. In other words, you choose a door, wait for Monty to expose a goat, then switch to the other remaining door. This means that you win if the door you chose to begin with

had a goat behind it. The odds that your initial choice had a goat is two thirds, so you are twice as likely to win the car if you switch! This can be hard to grasp. To make it easier, suppose there are 100 doors to choose from, but still only one car. You pick a door, Monty opens 98 that have goats behind them, then he gives you the option of switching to the other remaining closed door. Should you? Of course–it's almost certain that the car is behind the other door, and very unlikely that it's behind your original choice.

In a generalization of the original problem there are n doors. In the first step, you choose a door. Monty then opens some other door that's a loser. If you want, you may then switch your choice to another door. Monty will then open an as yet unopened losing door, different from your current preference. Then you may switch again, and so on. This carries on until there are only two unopened doors left: your current choice and another one. How many times should you switch, and when, if at all? The answer is: stick all the way through with your first choice but then switch at the very end.

In another variation of the problem, consider that in the actual game show there were two contestants. Both of them were allowed to pick a door but not the same one. Monty then eliminated a player with a goat behind his door (if both players had a goat, one was eliminated randomly, without letting either player know about it), opened the loser's door, and then offered the remaining player a chance to switch. Should the remaining player switch? The answer is *no*. The reason: a switcher in this game will lose if and only if either of two initial choices of the two contestants was correct. How likely is that? Two-thirds. A sticker will win in those $\frac{2}{3}$ of the cases. So stickers will win twice as often as switchers.

Morley's miracle

A remarkable theorem, discovered in 1899, by Frank Morley, then professor of Mathematics at Haverford College. Take any triangle. Mark the three points that are the intersections of adjacent angle trisectors. Then, no matter what triangle you start with, these three points will form an equilateral triangle. That such a simple and elegant result was not known to the ancient Greeks may be because it is quite hard to prove.

One of the interesting auxiliary results of some of the proofs is that the side of the equilateral triangle is equal to $8r \sin(A/3) \sin(B/3) \sin(C/3)$, where A, B, and C are the angles of the larger triangle, and r is the radius of the circumcircle. A surprise awaits anyone who takes the intersections of the exterior, as well as the interior, angle trisectors. In addition to the interior equilateral triangle, four exterior equilateral triangles appear, three of which have sides that are extensions of a central triangle.

Moscow papyrus

See **Rhind papyrus**.

mousetrap

See **Cayley's mousetrap**.

moving sofa problem

In Douglas Adams's book *Dirk Gently's Holistic Detective Agency,* the character Richard MacDuff says at one point, "It would be really useful to know before you buy a piece of furniture whether it's actually going to fit up the stairs or around the corner." Mathematicians call this the moving sofa problem and it has been tackled in various forms over the past few decades. One version of it, formulated by Leo Moser in 1966, asks: What is the largest sofa (in terms of area) that can be moved around a right-angled corner in a hallway of unit width? The sofa can be any shape and doesn't even have to resemble a piece of furniture! The question simply asks for the biggest, unbendable area that can be maneuvered around the corner. Several different approaches suggest that the answer is about 2.21 square units. Variations on the problem involve negotiating pianos and other items around different types of bends and passageways.[133]

Mrs. Perkins's quilt

A square **dissection** problem first posed by Henry **Dudeney** in his *Amusements in Mathematics* (1917):[88]

PUZZLE

It will be seen that in this case the square patchwork quilt is built up of 169 pieces. The puzzle is to find the smallest possible number of square portions of which the quilt could be composed and show how they might be joined together. Or, to put it the reverse way, divide the quilt into as few square portions as possible by merely cutting the stitches.

Solutions begin on page 369.

Dudeney's problem can be generalized to the dissection of a square of side n into a number S_n of smaller squares. Unlike a perfect **squaring the square** problem, the smaller squares needn't be all different sizes. In addition, only prime dissections are considered so that patterns that can be dissected on lower order squares aren't allowed. The smallest number of relatively prime dissections of an $n \times n$ quilt for $n = 1, 2, \ldots$, are 1, 4, 6, 7, 8, 9, 9, 10, 10, 11, 11, 11, 11, 12, ...[66]

Müller-Lyer illusion

A **distortion illusion** in which the orientation of arrowheads makes one line segment look longer than another.

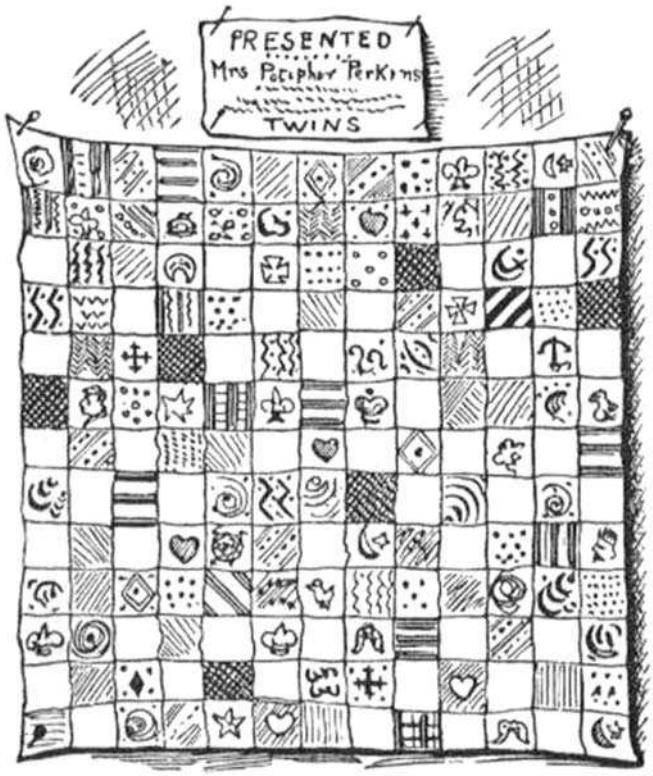

Mrs. Perkins's quilt Dudeney's drawing of one of his most famous puzzles.

multigrade

A set of equations in which the sums of powers of two different sets of numbers are the same for several different exponents. The simplest example is:

$1 + 6 + 8 = 2 + 4 + 9$
$1^2 + 6^2 + 8^2 = 2^2 + 4^2 + 9^2$

Another multigrade is:

$1 + 8 + 10 + 17 = 36 = 2 + 5 + 13 + 16$
$1^2 + 8^2 + 10^2 + 17^2 = 454 = 2^2 + 5^2 + 13^2 + 16^2$
$1^3 + 8^3 + 10^3 + 17^3 = 6426 = 2^3 + 5^3 + 13^3 + 16^3$

Remarkably, if any integer is added to all the terms of a multigrade it will still hold. Adding 1 to the example above, gives the multigrade (2, 9, 11, 18); (3, 6, 14, 17) (n = 1, 2, 3). Some high-order multigrades include: (1, 50, 57, 15, 22, 71); (2, 45, 61, 11, 27, 70); (5, 37, 66, 6, 35, 67) (n = 1, 2, 3, 4, 5), and (1, 9, 25, 51, 75, 79, 107, 129, 131, 157, 159, 173); (3, 15, 19, 43, 89, 93, 97, 137, 139, 141, 167, 171) (n = 1, 3, 5, 7, 9, 11, 13).

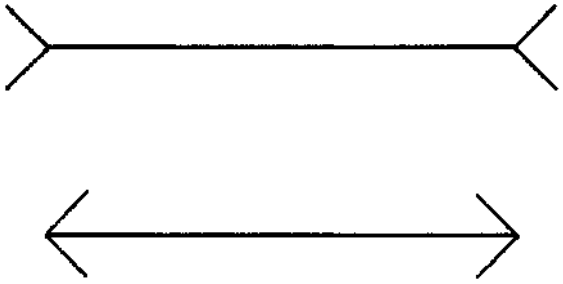

Müller–Lyer illusion Which of the horizontal lines is longer?

multiple

The integer b is a multiple of the integer a if there is an integer d such that $b = da$.

multiplication

A **binary operation** that is the equivalent of repeated addition and the **inverse** of **division**.

Mydorge, Claude (1585–1647)

A French mathematician who trained as a lawyer but was wealthy enough that he didn't have to work for a living. He was interested in mathematical puzzles and his book *Examen du livre des récréations mathématiques* (Study of the book of recreational mathematics, 1630) formed the basis for later works such as that by Denis Henrion (1659). Mydorge edited *Récréations mathématique* and left an unpublished manuscript of over 1,000 geometric problems and their solutions. He was also interested in optics and made a large number of instruments for his close friend René **Descartes**; the two shared a strong interest in explaining vision and the instruments and lenses were designed to help test their theories.

myriad

A term which today is normally synonymous with "very large number." Its origins go back to the Greek word *murious,* meaning "uncountable". The plural of this, *murioi,* evolved into the Latin *myriad,* which the Romans used to represent ten thousand. *Myriapod* is a general name for any many-legged anthropod, such as a millipede or a centipede

N

Nagel point
A point in a triangle where the lines from the vertices (see **vertex**) to the points of contact of the opposite sides with the excircles to those sides meet. (An excircle touches one side of a triangle and also touches the lines extended from the other two sides.)

nano-
Prefix for billionth (10^{-9}), from the Greek *nanos,* meaning "dwarf."

Napier, John (1550–1617)
A Scottish mathematician and theological writer who invented **logarithms** and wrote *Mirifici logarithmorum canonis descriptio* (The description of the wonderful canon of logarithms, 1614), which contains the first logarithmic table and the first use of the word *logarithm*. He also introduced the decimal point in writing numbers. His *Rabdologiae* (1617) describes various shortcuts for carrying out arithmetical calculations. One method of multiplication uses a system of numbered rods called *Napier's rods,* or *Napier's bones*–a major improvement on the ancient system of counters then in use. In 1619, after Napier's death, his *Mirifici logarithmorum canonis constructio,* which gave the method of construction of his logarithms, was published by his son Robert and edited by Henry **Briggs**.

Napoleon Bonaparte (1769–1821)

> *The advancement and perfection of mathematics are intimately connected with the prosperity of the state.*

Emperor of France and a very good amateur mathematician, having excelled in this subject as a student at school and at military college. Even after becoming first consul he was proud of his membership in the Institute de France (the nation's leading scientific society), and was close friends with several mathematicians and scientists, including Joseph **Fourier**, Gaspard **Monge**, Pierre Simon **Laplace**, Chaptal, and Berthollet. Indeed, in his grand expedition to Egypt in 1798 Napoleon brought along (in addition to 35,000 troops) over 150 experts in various fields, among them Monge, Fourier, and Berthollet, not to mention a complete *encyclopedie vivante* with libraries and instruments. One result of the expedition was that Fourier served for a time as the governor of lower Egypt. Likewise Laplace (who interviewed the young Napoleon for admission to the artillery) received titles and high office as a result of his friendship with Bonaparte. However, Laplace was relieved of his duties as the minister of the interior after only six weeks, and Napoleon later commented that Laplace had "sought subtleties everywhere, had only doubtful ideas, and carried the spirit of the infinitely small into administration." The most famous exchange between these two men occurred after Laplace had given Napoleon a copy of his great work, *Mecanique Celeste.* Napoleon looked it over, and remarked that in this massive volume about the universe there was not a single mention of **God**. Laplace replied "Sire, I had no need of that hypothesis." Regarding the idea that Napoleon might have discovered what is now called *Napoleon's theorem* (if equilateral triangles are constructed on the sides of any triangle (all outward or all inward), the centers of these equilateral triangles themselves form an equilateral triangle), Harold **Coxeter** and Samuel Greitzer have said that "The possibility of [Napoleon] knowing enough geometry for this feat is as questionable as the possibility of his knowing enough English to compose the famous palindrome, ABLE WAS I ERE I SAW ELBA."

nappe
Either of the two parts into which a **cone** is divided by the **vertex**. "Nappe" is the French for "tablecloth," which in turn comes from the Latin *mappa* (napkin).

narcissistic number
Also known as an *Armstrong number* or a *plus perfect number,* an *n*-digit number equal to the sum of its digits raised to the *n*th power. For instance, 371 is narcissistic because $3^3 + 7^3 + 1^3 = 371$, and 9474 is narcissistic because $9^4 + 4^4 + 7^4 + 4^4 = 9474$. The smallest narcissistic number of more than one digit is $153 = 1^3 + 5^3 + 3^3$. The largest narcissistic number (in base 10) is 115,132,219,018,763,992,565,095,597,973,971,522,401, which is the sum of the thirty-ninth powers of its digits. The reason there are no larger numbers is related to the fact that, as the number of digits increases, more and more nines are required to get a sum that has *n* digits. For example, $10^{70} - 1$ is a number consisting of 70 nines in a row, and the sum of the seventieth powers of its

digits is $70 \times 9^{70} \cong 4.386051 \times 10^{68}$, which is only 69 digits long. So there is no way any 70-digit number can be equal to the sum of the seventieth powers of its digits. The reason we see the last number occur at 39 digits is because, as the limit is approached, the number of big digits like eights and nines has to increase to make sure the sum will be big enough, but this means that there are a lot fewer combinations of digits to choose from.

Nash, John Forbes Jr. (1928–)

An American mathematician not very accurately portrayed in the Oscar-winning film *A Beautiful Mind* (2001), loosely based on the biography of the same name by Sylvia Nasar (1998).[229] Nash, who worked in **game theory** and **differential geometry**, shared the 1994 Nobel prize for economics with two other game theorists, Reinhard Selten and John Harsanyi. After a promising start to his mathematical career, Nash began to suffer from schizophrenia around the age of 30 and battled with the illness for the next quarter of a century. His Ph.D. dissertation, entitled "Non-cooperative Games," contained the definition and properties of what would later be called **Nash equilibrium** and the basis of the work that, 44 years later, would make him a Nobelist. Between 1966 and 1996, Nash published nothing. However, as his mental health slowly began to improve in the mid-1990s, his ability to tackle mathematical problems returned, and he also became interested in computer programming.

Nash equilibrium

In **game theory**, a pair of strategies (see **strategy**) for a game such that neither player can improve his outcome by changing his strategy. A Nash equilibrium sometimes takes the form of a **saddle** structure. In other cases, when a strategy is at a Nash equilibrium with itself, the strategy resembles an evolutionary stable strategy.

natural logarithm

Also called a *Naperian logarith,* a **logarithm** to base **e**. For example, $\log_e 10$ (also written as $1n\ 10$) is approximately 2.30258.

natural number

A number used for counting: 1, 2, 3, ... The debate about whether zero should also be included as a natural number has been going on for hundreds of years, and there's no general agreement even today. To avoid confusion, 0, 1, 2, 3, . . . , are often referred to as *nonnegative* ***integers*** or *whole numbers,* while 1, 2, 3, . . . , are called *positive integers*. Adding or multiplying natural numbers always produces other natural numbers. However, subtracting them can produce zero or negative integers, while dividing them produces **rational number**s. An important property of the natural numbers is that they are *well-ordered,* in other words, every set of natural numbers has a smallest element. The deeper properties of the natural numbers, such as the distribution of **prime number**s, are studied in **number theory**. Natural numbers can be used for two purposes: to describe the position of an element in an ordered sequence, which is generalized by the concept of **ordinal number**, and to specify the size of a finite set, which is generalized by the concept of **cardinal number**. In the finite world, these two concepts coincide; however, they differ when it comes to infinite sets (see **infinity**).

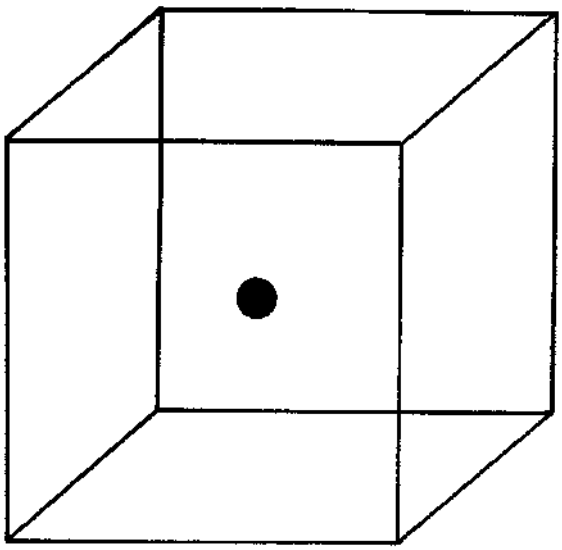

Necker cube Is the circle on the front face of the cube or the back?

Necker cube

A classic example of an **ambiguous figure**. In 1832, the Swiss crystallographer Louis Necker noticed, while examining crystals, that three-dimensional objects can fluctuate in appearance. He published pictures of an unusual **cube** that appeared to assume different orientations as one looked at it. The effect works because the drawing of the cube (an orthographic projection) carefully eliminates all depth cues. In attempting to fit the expected model of a cube to the picture, our brain must resolve the ambiguity as to which corner of the cube is closer.

negative base

The use of a negative **base** to represent numbers gives rise to some intriguing possibilities. Consider "negadecimal,"

for example, in which the base is *minus* 10 instead of the familiar positive 10. In this system, the number 365 is equivalent to the decimal number $5 + (6 \times -10) + (3 \times -10 \times -10)$, = 245, while 35 in negadecimal is equivalent to $5 + (3 \times -10)$, = –25, in ordinary decimal. This points to an interesting fact: the negadecimal equivalent of any positive or negative decimal number is always positive and therefore doesn't need to be accompanied by a sign. The Polish UMC-1, of which a few dozen were built in the late 1950s and earlier 1960s, is the only computer ever to use "nega**binary**" (base 2 arithmetic).

negative number

Long denied legitimacy in mathematics, negative numbers are nowhere to be found in the writings of the Babylonians, Greeks, or other ancient cultures. On the contrary, because Greek mathematics was grounded in geometry, and the concept of a negative distance is meaningless, negative numbers seemed to make no sense. They surface for the first time in bookkeeping records in seventh-century India and in a chapter of a work by the Hindu astronomer **Brahmagupta**. Their earliest documented use in Europe is in 1545 in the *Ars magna* of Girolamo **Cardano**. By the early seventeenth century, Renaissance mathematicians were explicitly using negative numbers but also meeting with heavy opposition. René **Descartes** called negative roots "false roots," and Blaise **Pascal** was convinced that numbers "less than zero" couldn't exist. Gottfried **Leibniz** admitted that they could lead to some absurd conclusions, but defended them as useful aids in calculation. By the eighteenth century, negative numbers had become an indispensable part of algebra.

Neile's parabola

Also known as the semi-cubical **parabola**, a curve discovered by the English mathematician William Neile (1637–1670) in 1657; it is the first **algebraic curve** to have its arc length calculated. (Before this, only the arc lengths of transcendental curves such as the **cycloid** and the **logarithmic spiral** had been calculated.) Neile's parabola is described in **Cartesian coordinate**s by the formula

$$y^3 = ax^2.$$

Christiaan **Huygens** showed that this curve satisfies the requirement requested by Gottfried **Leibniz** in 1687, namely, the curve along which a particle may descend under gravity so that it moves equal vertical distances in equal times. Neile's parabola is the **evolute** of a parabola.

nephroid

A type of curve often seen on the surface of a cup of coffee in the sunshine–a crescent of light formed by sunlight reflecting off the inside of the cup onto the surface of the drink. More generally, it is the shape made by parallel rays of light reflecting from the inside of any semicircle. In mathematical terms, this means that the nephroid is the cata**caustic** of a **circle** when the light source is at infinity, a fact first demonstrated by Christiaan **Huygens** in 1678 and published by him in his *Traité de la Lumière* (Treatise on light, 1690). A physical explanation wasn't forthcoming, however, until 1838 when George Airy gave a proof in terms of the wave theory of light. The name *nephroid* (from the Latin for "kidney-shaped") was introduced in 1878 by the English mathematician Richard Proctor in his book *The Geometry of Cycloids*. Prior to that it was known as a two-cusped **epicycloid**. Specifically, the nephroid is the epicycloid formed by a circle of radius a rolling around the outside on a fixed circle of radius $2a$. It has a length of $24a$, an area of $12\pi^2$, and is given by the parametric equations:

$$x = a(3\cos(t) - 3\cos(3t))$$
$$y = a(3\sin(t) - \sin(3t)).$$

The nephroid is the **involute** of **Cayley's sextic** and is also the **envelope** of circles with their centers on a given circle, touching a given diameter of that circle. The nephroid has been described as the perfect shape for a multiseat dining table. *Freeth's nephroid*, not to be mistaken for the ordinary nephroid just described, is named after the English mathematician T. J. Freeth (1819–1904) who first wrote about it in a paper published by the London Mathematical Society in 1879. Freeth's nephroid is

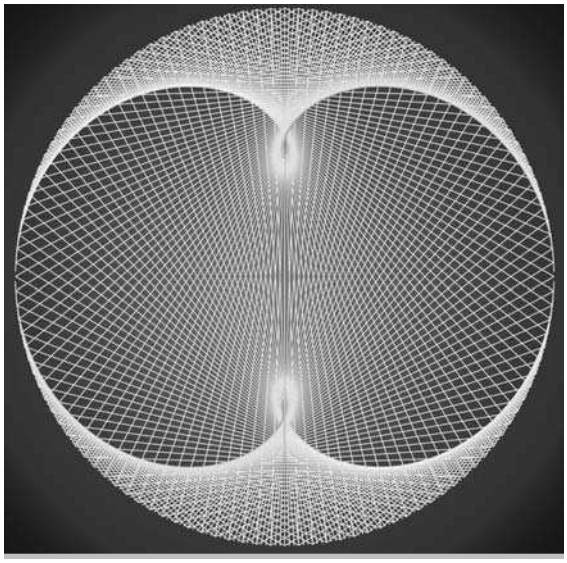

nephroid A nephroid curve spun by thread on a computer loom. *Jos Leys, www.josleys.com*

the **strophoid** of a circle and has the polar equation $r = a(1 + 2\sin(\theta/2))$. Freeth's nephroid is also the name of a group of mathematicians, mostly from Royal Holloway College, London, who gather weekly in a pub called the Beehive and compete in games of trivial pursuit.

net
A drawing of a **polyhedron** unfolded along its **edge**s, so as to lie flat in a plane. The earliest known examples of nets to represent polyhedra are by Albrecht **Dürer**.

neural network
An electronic automaton, similar in some ways to a **cellular automaton**, that offers a highly simplified model of a brain. As such, a neural network is a device for machine learning that is based on associative theories of human cognition. Using various algorithms and weightings of different connections between "neurons," neural networks are set up to learn how to recognize a pattern in applications such as voice recognition, visual pattern recognition, robotic control, symbol manipulation, and decision making. Generally, they consist of three layers: input neurons, output neurons, and a layer in between where information from input to output is processed. Initially the network is loaded with a random program, then the output is measured against a desired output which prompts an adjustment in the weights assigned to the connections in response to the discrepancy between the actual and desired output. This is repeated many times so that the network effectively learns as a child does: in a sense, the net discovers its own rules. Changing the rules of interaction between the "neurons" in the net can lead to interesting emergent behavior, so that neural networks have become another tool for investigating **emergence** and **self-organization**.

Neusis construction
A geometric construction that breaks the strict rules of classical Greek straightedge-and-compass construction (see **constructible**) by allowing a marked ruler to be slid into different positions. Neusis construction makes possible **duplicating the cube** and **trisecting an angle**. John **Conway** and Richard **Guy** have also shown how Neusis constructions, based on angle trisection, can be used to draw regular polygons with 7, 9, and 13 sides.

Newcomb's paradox
One of the most simply stated but astonishing of the so-called prediction paradoxes that bear on the problem of free will. It was devised in 1960 by William Newcomb, a theoretical physicist at the Lawrence Livermore Laboratory, while contemplating the **prisoner's dilemma**. A superior being, with super-predictive powers that have never been known to fail, has put $1,000 in box *A* and either nothing or $1 million in box *B*. The being presents you with a choice: (1) open box *B* only, or (2) open both box *A* and *B*. The being has put money in box *B* only if it predicted you will choose option (1). The being put nothing in box *B* if it predicted you will do anything other than choose option (1) (including choosing option (2), flipping a coin, etc.). The question is, what should you do to maximize your winnings? You might argue that since your choice now can't alter the contents of the boxes you may as well open them both and take whatever's there. This seems reasonable until you bear in mind that the being has never been known to have made an incorrect prediction. In other words, in some peculiar way, your mental state is highly correlated with the contents of the box: your choice is linked to the probability that there's money in box B. These arguments and many others have been put forward in favor of either choice. The fact is there is no known "right" answer, despite the concerted attentions of many philosophers and mathematicians over several decades.[123]

Newton, Isaac (1642–1727)
One of the great intellectual giants in human history; an English mathematician, physicist, and sometime head of the Royal Mint, Newton was one of the chief architects of **calculus** (though not in its modern form), discovered the **binomial theorem**, established the principles of universal gravitation, and saw through numerous other developments, any one of which would have brought a lesser person fame. Interestingly, his most productive period was 1665–1666, his so-called "miraculous year," when Cambridge University was closed because of the plague and Newton had to work at home. He was born in the same year that Galileo died. After publishing his *Principia* (1687), the most important and influential scientific book ever written, his interests drifted toward theology, politics, and, for a while, alchemy. His last two decades were largely spent in acrimonious debate with Gottfried **Leibniz**, over priority in the discovery of calculus, and with the astronomer John Flamsteed.

Newton's method
An iterative method for finding the zeros of a **function**.

n-gon
A **polygon** with *n* sides.

Nim
A **game**, of which there are many different versions, that involves two players alternately removing at least one item from one of two or more piles or rows. The person who picks up the last item wins. In one form of the game,

five rows of matches are laid out in such a way that there is one match in the first row, two matches in the second, and so on, down to five matches in the bottom row. Players take turns to remove any nonzero number of matches from any one row. The game may have originated in China. The name "Nim" was coined by Charles Bouton, an associate professor of mathematics at Harvard at the turn of the twentieth century, who took it from an archaic English word meaning to steal or to take away. In 1901 he published a full analysis of Nim and proof of a winning strategy.[50] The first Nim-playing computer, the Nimatron, a 1-ton behemoth, was built in 1940 by the Westinghouse Electrical Corporation and was exhibited at the New York World's Fair. It played 100,000 games against spectators and attendants, and won an impressive 90% of the time; most of its losses came at the hands of attendants who were instructed to reassure incredulous onlookers that the machine could be beaten! In 1951 a Nim-playing robot, the Nimrod, was shown at the Festival of Britain, and later at the Berlin trade fair. It was so popular that spectators entirely ignored a bar at the other end of the room where free drinks were being offered. Eventually the local police had to be called in to control the crowds.[110]

nine

A number long considered to have strange, mystic properties. A phrase in a book written during the Dark Ages gave rise to the superstition that cats have nine lives. English author and satirist William Baldwin wrote in his *Beware the Cat,* "It is permitted for a witch to take her cat's body nine times." There were nine Muses, nine rivers of Hades, and nine heads on the Hydra. It took nine days for Vulcan to fall from the heavens. The phrase "nine days' wonder" comes from the proverb "a wonder lasts nine days and then the puppy's eyes are open." A cat-o'-nine-tails is a whip, usually made of nine knotted lines or cords fastened to a handle that produces scars like the scratches of a cat. Being on "cloud nine" may have its origin in Dante's ninth heaven of Paradise, whose inhabitants are blissful because they are closest to God.

The term "the whole 9 yards" came from World War II fighter pilots in the Pacific. When arming their planes on the ground, the .50-caliber machine gun ammo belts measured exactly 27 feet, before being loaded into the fuselage. If the pilots fired all their ammo at a target, it got "the whole 9 yards." Less certain–though there is no shortage of theories–is the source of the expression "dressed to the nines."

Nine is the largest single-digit number and the one that occurs least frequently in most situations; an exception is the tendency of businesses to set prices that end with one or more nines. Because nine is one less than the base of our number system, it is easy to see if a number is divisible by 9 by adding the digits (and repeating on the result if necessary: the result should be nine). This process is sometimes called **casting out nines**. Similar processes can be developed for divisibility by 99, 999, etc. or any number that divides one of these numbers. Nine has many other interesting properties. For example, write down a number containing as many digits as you like, add these digits together, and deduct the sum from the first number. The sum of the digits of this new number will always be a multiple of nine.

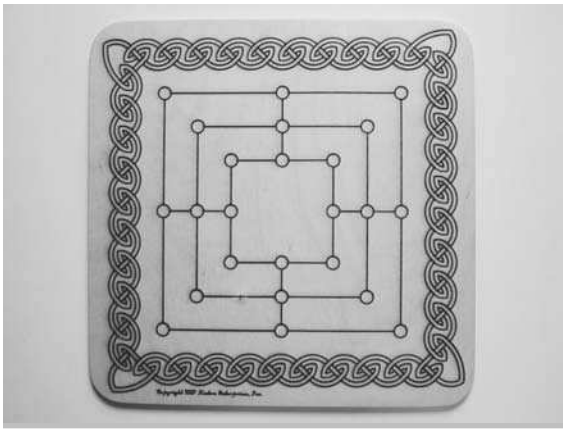

nine men's morris A modern version of the playing board.
Kadon Enterprises, Inc., www.puzzlegames.com

nine holes

See **three men's morris**.

nine men's morris

> *The nine-men's morris is filled up with mud;*
> *And the quaint mazes in the wanton green,*
> *For lack of tread, are indistinguishable.*
> –*Midsummer Night's Dream* (Act 2, scene 1), Shakespeare

One of the oldest of board games, known by different names and played with variations of rules in different places and periods. In France it is Marelle, in Austria it is Muhle, and in England it was known as Peg Meryll, Meg Marrylegs, and other names, all referring to a "mill" because that is the name of a run of three counters in the game. Versions of it have been found etched into the roof of the Temple of Kurna in Egypt (dated to about 1400 B.C.), cut into the oak planks that form the deck of the great Viking ship discovered at Gokstad in 1880, and carved in the choir stalls of several English cathedrals. A typical board layout is shown in the

accompanying figure; diagonal lines may or may not be included. Joseph Strutt in *The Sports and Pastimes of the People of England* (1801) described the rules in this way:

> Two persons, having each of them nine pieces, or men, lay them down alternately, one by one upon the spots; and the business of either party is to prevent his antagonist from placing three of his pieces so as to form a row of three, without the intervention of an opponent piece. If a row be formed, he that made it is at liberty to take up one of his competitor's pieces from any part he thinks most to his advantage; excepting he has made a row, which must not be touched if he have another piece upon the board that is not a component part of that row. When all the pieces are laid down, they are played backwards and forwards, in any direction that the lines run, but only can move from one spot to another (next to it) at one time. He that takes off all his antagonist's pieces is the conqueror.

In 1996, the German mathematician Ralph Gasser used a computer to prove that nine men's morris is a guaranteed draw if both players make optimal moves from the outset. He programmed the computer to figure out and tabulate 10 billion positions that were known to be a win for one side or the other, then worked forward 18 moves from the beginning of the game until his opening analysis met his endgame analysis. As a result he showed that every potentially winning position could be countered by the opponent in the early stages of the game. See also **three men's morris**.[132]

nine rooms paradox

A puzzle that was first published in *Current Literature* vol. 2, April 1889. It takes the form of a poem and is similar to that of the **missing dollar**.

PUZZLE

Ten weary, footsore travellers,
All in a woeful plight,
Sought shelter at a wayside inn
One dark and stormy night.

'Nine rooms, no more,' the landlord said
'Have I to offer you.
To each of eight a single bed,
But the ninth must serve for two.'

A din arose. The troubled host
Could only scratch his head,
For of those tired men not two
Would occupy one bed.

The puzzled host was soon at ease—
He was a clever man—
And so to please his guests devised
This most ingenious plan.

In a room marked A two men were placed,
The third was lodged in B,
The fourth to C was then assigned,
The fifth retired to D.

In E the sixth he tucked away,
In F the seventh man.
The eighth and ninth in G and H,
And then to A he ran,

Wherein the host, as I have said,
Had laid two travellers by;
Then taking one—the tenth and last—
He logged him safe in I.

Nine single rooms—a room for each—
Were made to serve for ten;
And this it is that puzzles me
And many wiser men.

How has the host managed to bamboozle his patrons?

Solutions begin on page 369.

nine-point circle

Draw a triangle, any triangle (although it may be best to start with an acute triangle). Mark the midpoints of each side. Drop an altitude from each vertex to the opposite side, and mark the points where the altitudes intersect the opposite side. (If the triangle is obtuse, an altitude will be outside the triangle, so extend the opposite side until it intersects.) Notice that the altitudes intersect at a common point. Mark the midpoint between each vertex and this common point. No matter what triangle you start

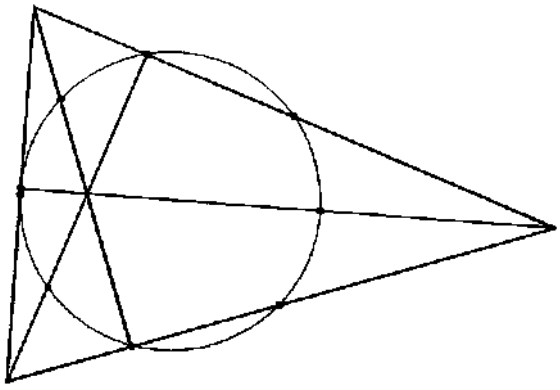

nine-point circle

with, these nine points all lie on a perfect circle! This result was known to Leonhard **Euler** in 1765, but was rediscovered by the German mathematician Karl Feuerbach (1800–1834) in 1822.

node
See **crunode**.

Noether, Emmy (Amalie) (1882–1935)
A German mathematician, one of the most talented of the early twentieth century. The crucial result now known as *Noether's theorem,* which is important in other symmetries in natural systems, is of great importance in physics. She received her doctorate in 1907 and rapidly built an international reputation, but the University of Göttingen refused to let her teach, and her colleague David **Hilbert** had to advertise her courses in the university's catalog under his own name. A long controversy ensued, with her opponents asking what the country's soldiers would think when they returned home and were expected to learn at the feet of a woman. Allowing her on the faculty would also mean letting her vote in the academic senate. Said Hilbert, "I do not see that the sex of the candidate is against her admission as a privatdozent. After all, the university senate is not a bathhouse." She was finally admitted to the faculty in 1919. A Jew, Noether was forced to flee Nazi Germany in 1933 and joined the faculty at Bryn Mawr in the United States.

non-Abelian
Non**commutative** or order-dependent. For example, the group of manipulations of **Rubik's cube** is non-Abelian because the state of the cube depends greatly on the order of the moves performed on it. See also **Abelian group**.

nonagon
A **polygon** with nine sides. A *nonagonal number* is a number of the form $n(7n - 5)/2$.

nonconvex uniform polyhedron
A **uniform polyhedron** of a type obtained by relaxing the conditions used to produce the **Archimedean solid**s (which have regular convex faces and identical convex vertices) to allow both nonconvex faces and vertex types, as in the case of the **Kepler-Poinsot solid**s. The condition that every vertex must be identical, but the faces need not be, gives rise to 53 nonconvex uniform polyhedra. An example is the *great truncated dodecahedron,* obtained by truncating the corners of the great dodecahedron at a depth which gives regular decagons.

non-Euclidean geometry
Any **geometry** in which Euclid's **parallel postulate** doesn't hold. (One way to state the parallel postulate is: given a straight line and a point A not on that line, there is only one exactly straight line through A that never intersects the original line.) The two most important types of non-Euclidean geometry are **hyperbolic geometry** and **elliptical geometry**. The different models of non-Euclidean geometry can have positive or negative **curvature**. The sign of curvature of a surface is indicated by drawing a straight line on the surface and then drawing another straight line perpendicular to it: both these lines are **geodesic**s. If the two lines curve in the same direction, the surface has a positive curvature; if they curve in opposite directions, the surface has negative curvature. Elliptical (and spherical) geometry has positive curvature whereas hyperbolic geometry has negative curvature.

The discovery of non-Euclidean geometry had immense consequences. For more than 2,000 years, people had thought that **Euclidean geometry** was the only geometric system possible. Non-Euclidean geometry showed that there are other conceivable descriptions of space–a realization that transforms mathematics into an altogether more abstract science. Thereafter, it was clear that in mathematics, one could start out with *any* set of self-consistent

Types of Geometry

	Euclidean	Elliptical	Hyperbolic
Curvature	Zero	Positive	Negative
Given a line m and a point P not on m, the number of lines passing through P and parallel to m	1	0	Many
Sum of interior angles of a triangle	180°	> 180°	< 180°
Square of hypotenuse of a right triangle with sides a and b	$a^2 + b^2$	$< a^2 + b^2$	$> a^2 + b^2$
Circumference of a circle with diameter 1	π	$< \pi$	$> \pi$

postulates and follow through their ramifications. The discovery of non-Euclidean geometry has been compared with Copernicus's theory and Einstein's **relativity theory**, the analogy being that each freed people from long-held models of thought. In fact, Einstein said about non-Euclidean geometry: "To this interpretation of geometry, I attach great importance, for should I have not been acquainted with it, I never would have been able to develop the theory of relativity."

It's important to realize that both Euclidean and non-Euclidean geometry are consistent in that the assumptions on which they rest don't involve any contradictions. In response to a question as to which geometry is true, Henri **Poincaré** said: "One geometry cannot be more true than the other; it can only be more convenient." Which geometry is valid in the physical space in which we live? On a small scale, and for all practical purposes on Earth, Euclidean geometry works just fine. But on larger scales this is no longer true. Einstein's general theory of relativity uses non-Euclidean geometry as a description of **space-time**. According to this idea, space-time has a positive curvature near gravitating matter and the geometry is non-Euclidean. When a body revolves around another body, it appears to move in a curved path due to some force exerted by the central body, but it is actually moving along a **geodesic**, without any force acting on it. Whether all of space-time contains enough matter to give itself an overall positive curvature is one of the many unanswered question in physics today, but it is generally accepted that the geometry of space-time is more non-Euclidean than Euclidean. It is proposed that if space-time does happen to have an overall positive curvature, then the universe will stop expanding after a fixed amount of time and start to shrink resulting in a "big crunch," as opposed to the "big bang" that resulted in its creation. At the moment, astronomical observations seem to favor a universe that is "open" and has a hyperbolic geometry. Another consequence of non-Euclidean geometry is the possibility of the existence of a **fourth dimension**. Just as the surface of the sphere curves in the direction of the third dimension, i.e., perpendicular to its surface, it is believed that space-time curves in the direction of the fourth dimension. Non-Euclidean geometry has applications in other areas of mathematics, including the theory of elliptic curves, which was important in the proof of **Fermat's last theorem**.[72, 140] (See table, "Types of Geometry.")

nonlinear system

Any system in which the data points coming from the measurement of the values of its variables can be represented as a curvilinear pattern on a coordinate plane; hence, "nonlinear" for "not-a-line." More generally, a system in which small changes can result in large effects, and large changes in small effects. Thus, sensitive dependence on initial conditions (see **butterfly effect**) in chaotic systems illustrates the extreme nonlinearity of these systems. In a nonlinear system the components are interactive, interdependent, and exhibit feedback effects.

nonstandard analysis

In a broad sense, the study of the infinitely small; more specifically, the study of **hyperreal number**s, their functions and properties. Nonstandard analysis, which was pioneered by Abraham **Robinson** in the 1960s, puts the concept of **infinitesimal**s on a firm mathematical footing and is, for many mathematicians, more intuitive than real **analysis**.

normal

A line that is perpendicular to a given line or plane.

normal number

A number in which digit sequences of the same length occur with the same frequency. A constant is considered normal to base 10 if any single digit in its decimal expansion appears one-tenth of the time, any two-digit combination one-hundredth of the time, any three-digit combination one-thousandth of the time, and so on. In the case of **pi**, the digit 7 is expected to appear 1 million times among the first 10 million digits of its decimal expansion. It actually occurs 1,000,207 times—very close to the expected value. Each of the other digits also turns up with approximately the same frequency, showing no significant departure from predictions. A number is said to be *absolutely normal* if its digits are normal not only to base 10 but also to every integer base greater than or equal to 2. In base 2, for example, the digits 1 and 0 would appear equally often. Émile **Borel** introduced the concept of normal numbers in 1909 as a way to characterize the resemblance between the digits of a mathematical constant such as π and a sequence of **random number**s. He quickly established that there are lots of normal numbers, though finding a specific example of one proved to be a major challenge. The first to be found was **Champernowne's number**, which is normal to base 10. Analogous normal numbers can be created for other bases. To date, no specific "naturally occurring" **real number** has been proved to be absolutely normal, even though it is known that almost all real numbers are absolutely normal! However, in 2001, Greg Martin of the University of Toronto found some examples of the opposite extreme—real numbers that are normal to no base whatsoever. To start with, he noted that every

rational number is absolutely abnormal. For example, the fraction $1/7$ can be written in decimal form as 0.1428571428571 . . . . The digits 142857 just repeat themselves. Indeed, an expansion of a rational number to any base b or b^k eventually repeats. Martin then focused on constructing a specific *irrational* absolutely abnormal number. He nominated the following candidate, expressed in decimal form, for the honor:

$\alpha = 0.656249999995699\underline{1999999 \ldots 9999998}528404201690728 \ldots$

The middle portion (underlined) of the given fragment of α consists of 23,747,291,559 nines. Martin's formulation of this number and proof of its absolute abnormality involved so-called **Liouville number**s.[216]

nothing

The absence of anything; nonexistence. Nothing is not the same as the **empty set**, which exists as the set that mathematically denotes nothing, nor is it the same as **zero**, which exists as the number that denotes how many members the empty set contains. In physics, nothing is not a **vacuum**, because a vacuum not only contains energy but exists in space and time; nor is it a singularity, which contains a great deal of concentrated matter and energy. So, can there be nothing? No. "To be" implies existence of some sort: the one thing we can be absolutely sure has never existed, or will exist, is nothing.

noughts and crosses

See **tic-tac-toe**.

NP-hard problem

A mathematical problem for which, even in theory, no shortcut or smart **algorithm** is possible that would lead to a simple or rapid solution. Instead, the only way to find an optimal solution is a computationally intensive, exhaustive analysis in which all possible outcomes are tested. Examples of NP-hard problems include the **traveling salesman problem** and the popular game **Tetris**. NP stands for "non-deterministic polynomial-time."

nucleation

A process in a physical system, or a mathematical model such as a **cellular automaton** or a statistical model, whereby a bubble or other structure appears spontaneously at a random or unpredictable spot.

null hypothesis

The **hypothesis** that is being tested in a hypothesis-testing situation.

null set

See **empty set**.

number

An abstract measure of quantity. The most familiar numbers are the **natural number**s, 0, 1, 2, . . . , used for counting. If negative numbers are included, the result is the **integer**s. Ratios of integers are called **rational number**s, which can be expressed as terminating or repeating decimals. If all infinite and nonrepeating decimal expansions are thrown in as well, the scope of numbers extends to all **real numbers**, which can be extended to the **complex numbers** in order to include all possible solutions to algebraic equations. More recent developments are the **hyperreal number**s and the **surreal number**s, which extend the real numbers by adding infinitesimal and infinitely large numbers. For measuring the size of infinite **set**s, the natural numbers have been generalized to the **ordinal number**s and to the **cardinal number**s. See also **numeral** and **number system**.

number line

A way of representing numbers by thinking of them as the positions of points on a line.

number system

A way of counting using a particular **base**. The familiar **decimal** number system is a base 10 system, because it uses 10 different digits, 0, 1, 2, 3, 4, 5, 6, 7, 8, 9, and combinations of these. Other number systems, used for special purposes or by certain cultures, are the **binary** (base 2), trinary (base 3), hexadecimal (base 16), **vigesimal** (base 20), and **sexagesimal** (base 60). In a *positional number system* of base b, b basic symbols (or digits) corresponding to the first b **natural number**s, including zero, are used. To generate the rest of the numbers, the position of the symbol in the figure is used. The symbol in the last position has its own value, and as it moves to the left its value is multiplied by b. In this way, with only finitely many different symbols, every number can be expressed. This is unlike systems, such as that of **Roman numeral**s, which use different symbols for different orders of magnitude.

number theory

The study of the whole numbers and their properties and relationships. Often, a problem in number theory can be restated in terms of finding the solution, or showing that there is no solution, to a **Diophantine equation**. A Diophantine equation is one where the coefficients are whole numbers and where the solution is also con-

strained to be a whole number. Sometimes, what appears to be a simple Diophantine equation can lead to an **elliptic curve**.[30]

numeral
A symbol, or combination of symbols, that describes a number. See **Arabic numeral** and **Roman numeral**.

numerator
The number above the fraction bar that indicates the number of parts of the whole there are in a **rational number**.

numerical analysis
The study of methods for approximating the solutions of various classes of mathematical problems including *error analysis*.

obelus
The name of the symbol "÷", used as a sign for division. It comes from the Greek *obelos* meaning a pointed stick (a spit) used for cooking. This root word also gave rise to *obelisk* for a pointed stone pillar. The "÷" symbol was originally used as an editing mark in early manuscripts, sometimes only as a line without the two dots, to point out material that the editor thought needed cutting. It was also used occasionally as a symbol for subtraction. As a division symbol it was first employed by the Swiss mathematician Johann Rahn (1622–1676) in his *Teutsche Algebra* in 1659. By a misunderstanding of a credit to John Pell about other material in the book, many English writers started using the symbol and calling it "Pell's notation." Although it appears regularly in literature produced in Britain and the United States, it is virtually unknown in the rest of the world.

oblate spheroid
An **ellipsoid** produced by rotating an **ellipse** through 360° about its **minor axis**.

oblique
Slanted or not perpendicular. *Oblique coordinates* are measured on a plane coordinate system whose axes are not perpendicular. An *oblique angle* is any angle except a **right angle** and an *oblique triangle* is any triangle that doesn't contain a right angle. The first reference to "oblique angled triangles" may have been by Thomas Blundevil in his *Exercises* in 1594.

oblong
An alternate name for any **rectangle** that is not a square. The word comes from the Latin *ob* ("excessive") and *longus* ("long").

oblong number
Any positive integer that is not a **perfect square**.

obtuse
An *obtuse angle* is an **angle** greater than 90° but less than 180°. An *obtuse triangle* is a **triangle** that contains an obtuse angle. The word comes from the Latin *ob* ("against") and *tundere* ("to beat") and thus refers to things that are blunt, dull, or rounded.

octa-
The Greek prefix meaning "eight."

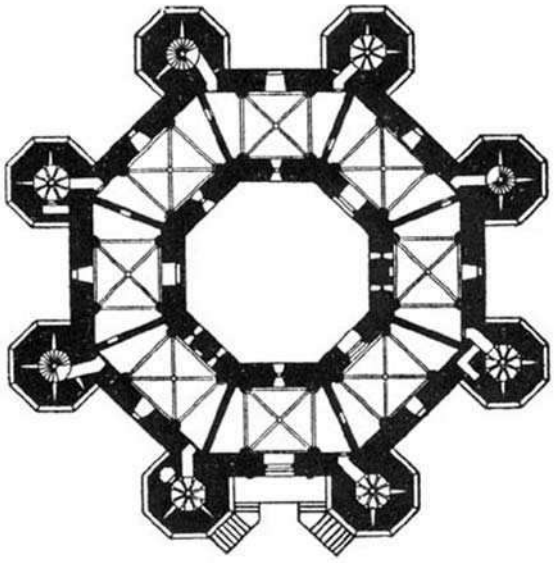

octa- An aerial view of Castel del Monte in Italy's Apulien region.

octagon
An eight-sided **polygon**. One of the most remarkable examples of octagonal design in architecture is the Castel del Monte, in southern Italy, which consists of a central octagonal core containing an inner octagonal courtyard that is surrounded by eight tall, perfectly octagonal towers. Another famous octagon is Oxford University's Radcliffe Observatory tower, built from 1772 to 1794, vaguely based on the Tower of the Winds in Athens, and considered architecturally the finest observatory in Europe.[139]

octahedron
A **polyhedron** with eight faces, each of which is an equilateral triangle. A regular octahedron, whose sides are all equilateral triangles, is one of the **Platonic solid**s; it looks like two square pyramids with their square bases stuck together. See also **octa-**.

octant
Any one of the eight portions of space determined by the three coordinate planes.

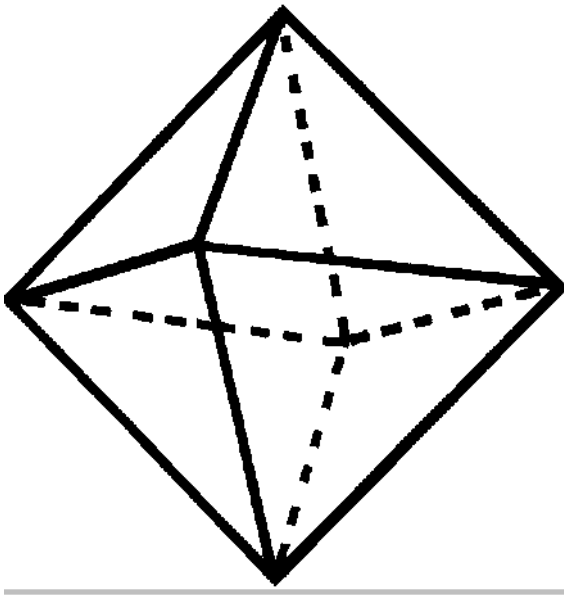

octahedron One of the Platonic solids.

octonion
Also known as a *Cayley number.* Octonions are a non**associative** generalization of the **quaternion**s and the **complex number**s involving numbers with one real **coefficient** and seven imaginary coefficients.

odd
Not divisible by two. An *odd function* is a **function** $f(x)$ with the property that $f(-x) = -f(x)$ for any value of x; an example is $\sin(x)$.

officer problem
See **thirty-six officers problem**.

omega
See **Chaitin's constant**.

one
The first positive **integer** and the first odd number; it is also known as *unity.* From the time of Euclid to the late 1500s, one wasn't generally considered to be a number but instead was thought of as the unit of which bonafide numbers were composed. The Old English (c. 550–c. 1100) *ane* served both for counting and as the indefinite article. Toward the end of the Old English period and the beginning of Middle English (c. 1100–c. 1500), *ane* developed two pronunciations, the first being used for 1 and the other for the indefinite article *an, a.* The existence of different words for the number one and the indefinite article seems to be unique to the English language. "One" can be traced back to the Latin *unus* and the Greek *oine* but probably came into English from the German *eine.*

153
A number with some very curious properties. It is the smallest number that can be expressed as the sum of the cubes of its digits: $153 = 1^3 + 5^3 + 3^3$. It is equal to the sum of the factorials of 1 to 5: $153 = 1! + 2! + 3! + 4! + 5!$ The sum of the digits of 153 is a perfect square: $1 + 5 + 3 = 9 = 3^2$. The sum of the **aliquot part**s of 153 is also a perfect square: $1 + 3 + 9 + 17 + 51 = 81 = 9^2$. On adding the number 153 to its reverse (351), the result is 504 whose square is the smallest square that can be expressed as the product of two different numbers that are the reverse of one another: $153 + 351 = 504$; $504^2 = 288 \times 882$. It can be expressed as the sum of all integers from 1 to 17. In other words, 153 is the seventeenth triangular number; its reverse is also a triangular number. In addition, 153 and its reverse are **Harshad number**s. It can be expressed as the product of two numbers formed from its own digits: $153 = 3 \times 51$. A reference to 153 occurs in the New Testament: the net that Simon Peter drew from the Sea of Tiberias held 153 fishes.

one-to-one
A **function** or map that for every possible output has only one input that yields that particular output; if $f(a) = f(b)$, then $a = b$.

open
An *open interval* is a piece of a straight line that doesn't contain its endpoints; a *half-open interval* contains one endpoint. An *open set* is one in which every point in the set has a neighborhood lying in the set.

operator
Something that acts on a **function** to give another function.

optical illusion
A picture or figure that deceives or confuses the eye and/or brain. Categorization of optical illusions is difficult because several underlying mechanisms may contribute to an effect, or the cause of the illusions may not be completely understood. For the purposes of this book illusions are grouped as shown in the table "Some Types and Examples of Optical Illusions." See individual entries for details. See also **anamorphosis**.

Some Types and Examples of Optical Illusions

Type	Examples
Distortion illusion	Fraser spiral Müller-Lyer illusion Orbison's illusion Poggendorff illusion Titchener illusion Zöllner illusion
Impossible figures and objects	Freemish crate Penrose triangle Penrose stairway Tribar illusion
Ambiguous figure	Ames room Necker cube Schröder's reversible staircase Thiery figure
Lateral inhibition illusion	Hermann grid illusion
Antigravity houses and hills	

Orbison's illusion

A **distortion illusion** in which a background of radiating lines appears to distort the shape of a superimposed figure, such as a square or circle.

orbit

(1) The path, in the form of a **conic section**, that an object takes when under the gravitational influence of another body. (2) More generally, the trajectory of a **differential equation**.

order

A word with many different meanings in mathematics. Among these are: (1) the sequence in which a set of objects or numbers is placed; (2) the number of elements in a set; (3) the number of times a shape can be fitted back onto its own outline during a complete turn (*order of symmetry*); (4) the highest order **power** in a one-variable **polynomial** (*order of a polynomial*, also known as its *degree*); (5) the type of curve described by such a polynomial (*order of a curve*).

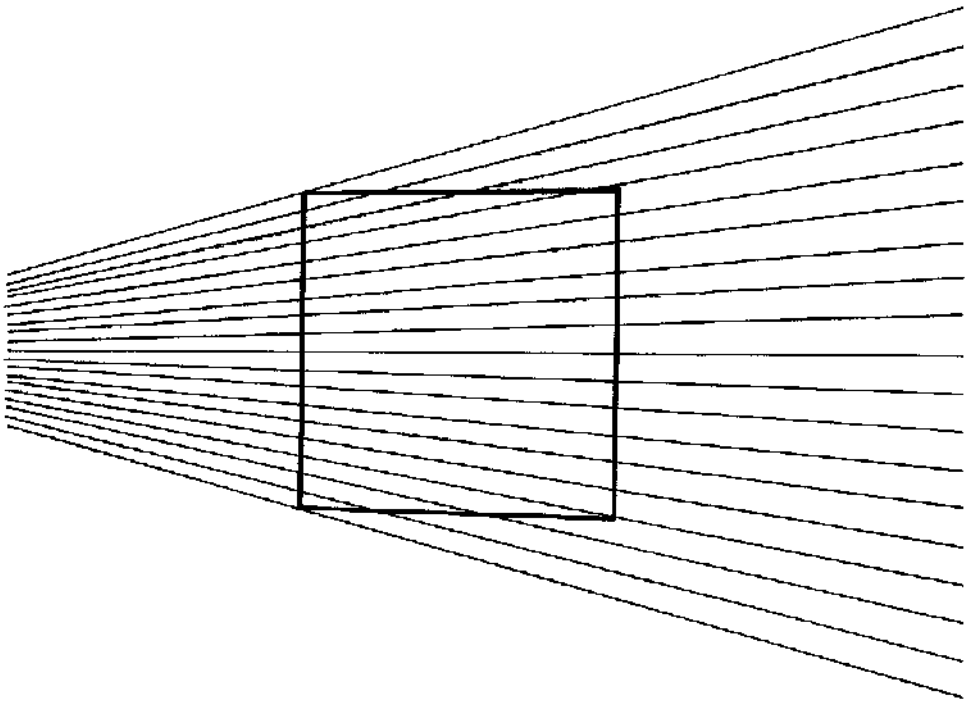

Orbison's illusion Is the square really a square?

ordered pair
A collection of two objects such that one can be distinguished as the *first element* and the other as the *second element.* An ordered pair with first element a and second element b is usually written as (a, b). Two such ordered pairs (a_1, b_1) and (a_2, b_2) are equal if and only if $a_1 = a_2$ and $b_1 = b_2$. *Ordered triples* and *ordered n-tuples* (ordered lists of n terms) are defined in the same way. An ordered triple (a, b, c) can be defined as $(a, (b, c))$, that is, as two nested pairs.

ordinal number
A number used to give the position in an ordered sequence: first, second, third, fourth, ...Ordinal numbers are distinct from **cardinal number**s (one, two, three, four, . . .), which describe the *size* of a collection. The mathematician Georg **Cantor** showed in 1897 how to extend the concept of ordinals beyond the **natural number**s to the infinite and how to do arithmetic with the resulting *transfinite ordinals* (see **infinity**).

ordinary differential equation
Any equation relating a **function** of one variable to its **derivative**s. Compare with **partial differential equation**.

ordinate
The y-coordinate, or vertical distance from the x-axis, in a system of **Cartesian coordinates**. Compare with **abscissa**.

origami
The Japanese art of the paper-folding, without cutting and joining, to form definite objects.

origin
The point (0, 0) on the coordinate axes.

orthic triangle
The triangle whose vertices (see **vertex**) are the feet of the **altitude**s of a given triangle.

orthocenter
The point of intersection of the **altitude**s of a **triangle.**

orthogonal
At right angles to; independent of. *Orthogonal curves* are two families of curves with the property that each member of one family meets members of the other family at right angles.

osculating
To share the same **tangent** and **curvature** and at a given point, as in the case of two *osculating curves*. For example the curve $y = x^3$ and the x-axis osculate at the origin.

Oughtred, William (1574–1660)
An English clergyman and mathematician who invented the **slide rule** and who, in the first English edition of his *Clavis Mathematicae* in 1647, first used the name "**pi**" for the number 3.141 . . . . He wrote it $\pi.\delta$, where π stood for the English word *periphery* (what we would call circumference), the dot was his symbol for division, and δ stood for the English word *diameter.* The use of π to represent words starting with the letter *p,* like *periphery,* was not uncommon. Before $\pi = 3.14 \ldots$ caught on, π was variously used to indicate a point, a polygon, a positive number, a power, a proportion, the number of primes in a series, and a factorial (which is a product). Oughtred used the same notation in all later English and Latin editions of his book, but not in the earlier first Latin edition. He was a prodigious inventor of mathematical symbols, though most of them have not survived. He did, however, introduce a couple of other symbols we still use: $\times$ for multiplication (as distinct from the letter x, which he also used for this purpose) and $\pm$ for "plus or minus." Oughtred served as rector of Albury from 1608 or 1610 until his death. There he tutored many young mathematicians of the time, including John **Wallis**, Seth Ward, Charles Scarburgh, and Christopher Wren. Moreover, all English mathematicians for the next century, including Isaac **Newton**, learned algebra from *Clavis Mathematicae* (first published in 1631).

oval
A curve that looks like a squashed **circle** but, in contrast with the **ellipse**, doesn't have a precise mathematical definition. The word *oval* comes from the Latin *ovus* for "egg." Unlike ellipses, ovals sometimes have only a single axis of reflection symmetry (instead of two).

Ovid's game
A board game, described by the Roman poet Ovid in Book III of his *Art of Love,* that was popular in ancient Greece, Rome, and China. Each player has three counters, which they place alternately on to nine points laid out in a 3×3 grid, with the object of getting three in a line and so winning. This may sound like **tic-tac-toe**, and there is no doubt that both Ovid's game and **nine men's morris** are antecedents of the familiar noughts and crosses. But in Ovid's game play continues after the six counters are down, if no one has yet won, by moving a single counter on each turn, though not diagonally, to any adjacent square. As in the case of tic-tac-toe, two experts (i.e., "rational" players) will always draw. Because the first player is ensured a win by covering the center square, this move is usually not allowed. Ovid advised women to master the game in order to gain the attention of men!

Ozanam, Jacques (1640–1717)

A French mathematician, scientist, and writer best remembered for his book on mathematical and scientific puzzles *Récréations Mathématiques et Physiques* (four volumes, 1694), which later went through 10 editions. Based on earlier works by Claude **Bachet**, Claude **Mydorge**, Jean **Leurechon**, and Daniel Schwenter (1585–1636), it was later revised and enlarged by Jean **Montucla**, then translated into English by Charles Hutton (1803, 1814). Edward Riddle edited a new edition, which was published in 1844, removing some old material and adding new material so that "[T]he work might continue to be to the present generation a useful manual of scientific recreation, as its predecessors have been to the generation which has passed." Ozanam's original edition contained an early example of a problem about orthogonal **Latin square**s: "Arrange the 16 court cards so that each row and each column contains one of each suit and one of each value."

P

Pacioli, Luca (1445–1517)

An Italian mathematician and Franciscan monk who wrote several influential books. His encyclopedic *Summa de Arithmetica, Geometria, Proportioni et Proportionalita* (Summary of arithmetic, geometry, proportion and proportionality, 1494) summarized what was known about contemporary arithmetic, algebra, geometry, and trigonometry and gave a basis for the major progress in mathematics which subsequently took place in Europe. *Divina proportione* (1509), with drawings by none other than Leonardo da Vinci (surely no mathematical text was more impressively illustrated!), deals with the **golden ratio**, a subject that Pacioli treats from an architectural standpoint in a second volume. At his death, he left a major book unpublished, *De Viribus Amanuensis,* on recreational problems, geometrical problems, and proverbs. It makes frequent reference to Leonardo, who assisted him with the project: many of the problems in this treatise are also in Leonardo's notebooks. Again it is a work for which Pacioli claimed no originality, describing it as a compendium.

packing

A way to place objects of the same kind so that they touch in some specified way, often inside a container with specified properties. The objects to be packed may be polyhedra, polygons, spheres, ellipsoids, hyperspheres, or any other type of shape, and the number of dimensions involved may range upward from two. The fraction of a space filled by a given collection of objects is called the *packing density.* The densest packing of circles in the plane is the hexagonal lattice of the bee's honeycomb, which has a packing density of 0.9069 . . . . In 1611, Johannes **Kepler** proposed that hexagonal, or face-centered cubic, packing is also the densest possible way to arrange spheres in three dimensions–an assertion known as **Kepler's conjecture**. Currently, the worst known **convex** packer in two-dimensions is the smoothed octagon, with a packing density of about 0.902. Stanislaw **Ulam** conjectured that the sphere was the worst packing object in three-dimensional space.

Padovan sequence

See **plastic number**.

palindrome

A word, verse, sentence, or passage that reads the same forward or backward; the term comes from the Greek *palindromos* for "running back again." Well-known examples include: "Madam, I'm Adam;" "A man, a plan, a canal–Panama!;" and "Able was I ere I saw Elba." A slightly longer one, devised by Peter Hilton, a code-breaker on the British team that cracked the German Enigma, is "Doc, note. I dissent. A fast never prevents a fatness. I diet on cod." Credit for inventing the palindrome is often given to Sotades the Obscene of Maronea (third century B.C.). Though only eleven lines of his work have survived, he is thought to have recast the entire Iliad in palindromic verse. Sotades also wrote lines (now sometimes called Sotadic verses) that, when read backward, had the opposite meaning. His acid tongue eventually landed him in jail by order of Ptolemy II, though worse was to follow. Sotades escaped but was captured by Ptolemy's admiral Patroclus, who sealed him in a leaden chest and tossed him into the sea. A musical palindrome is formed by Haydn's Symphony No. 47 in G, sometimes referred to as *The Palindrome,* because in both the minuet and the trio the orchestra plays the music twice forward and then twice backward to arrive at the beginning. See also **palindromic number**.

palindromic number

A number such as 1,234,321 that reads the same forward and backward; more generally, a symmetrical number written in some **base** a as $a_1\ a_2\ a_3 \ldots | \ldots a_3\ a_2\ a_1$. In the familiar base 10 system, there are nine two-digit palindromic numbers: 11, 22, 33, 44, 55, 66, 77, 88, 99; there are 90 palindromics with three digits: 101, 111, 121, 131, 141, . . . , 959, 969, 979, 989, 999; and there are 90 palindromics with four digits: 1,001; 1,111; 1,221; 1,331; 1,441; . . . , 9,559; 9,669; 9,779; 9,889; 9,999, giving a total of 199 palindromic numbers below 10^4. Below 10^5 there are 1,099 palindromics and for other exponents of 10^n there are 1,999; 10,999; 19,999; 109,999; 199,999; 1,099,999; . . . . It is conjectured, but has not been proven, that there are an infinite number of palindromic **prime number**s. With the exception of 11, palindromic primes must have an odd number of digits. A normally quick way to produce a palindromic number is to pick a positive integer of two or more

digits, reverse the digits, and add to the original, then repeat this process with the new number, and so on. For example, 3,462 gives the sequence 3,462; 6,105; 11,121; 23,232. Does the series formed by adding a number to its reverse always end in a palindrome? It used to be thought so. However, this conjecture has been proven false for bases 2, 4, 8, and other powers of 2, and seems to be false for base 10 as well. Among the first 100,000 numbers, 5,996 numbers are known that have not produced palindromic numbers by the add-and-reverse method in calculations carried out to date. The first few of these are 196; 887; 1,675; 7,436; 13,783; 52,514; . . . . A proof that these numbers never produce palindromes, however, has yet to be found. The largest known palindromic prime, containing 30,913 digits, was found by David Broadhurst in 2003.

pandiagonal magic square

A **magic square** in which all the broken diagonals as well as the main diagonals add up to the magic constant.

pandigital number

An integer that contains each of the digits from zero to nine exactly once and whose leading digit is nonzero. The smallest pandigital numbers are 1,023,456,789; 1,023,456,798; 1,023,456,879; 1,023,456,897; and 1,023,456,978. Like all pandigitals these are divisible by nine. The first few "zeroless" pandigitals are 123,456,789; 123,456,798; 123,456,879; 123,456,897; 123,456,978; and 123,456,987; and the first few zeroless pandigital primes are 1,123,465,789; 1,123,465,879; 1,123,468,597; 1,123,469,587; and 1,123,478,659. The sum of the first 32,423 (a **palindromic number**) consecutive primes is 5,897,230,146, which is pandigital. No other palindromic number shares this property. Examples of palindromic numbers that are the product of pandigital numbers are 2,970,408,257,528,040,792 (= 1,023,687,954 × 2,901,673,548) and 5,550,518,471,748,150,555 (= 1,023,746,895 × 5,421,768,309), both found in 2001. See also **pandigital product**.

pandigital product

A product in which the digits of the multiplicand, multiplier, and product, taken together, form a **pandigital number**.

pangram

A phrase or sentence that contains every letter of the alphabet at least once. The best known example in English and a familiar typing test is "The quick brown fox jumps over the lazy dog." One of the shortest known that still makes some kind of sense is "The five boxing wizards jump quickly."

Pappus of Alexandria (c. A.D. 300)

The last of the great Greek geometers whose eight-volume *Mathematical Collection* summarized the bulk of mathematics known at that time. In this compendium, Pappus added a considerable number of his own explanations and amplifications of the earlier work of **Euclid**, **Archimedes**, **Apollonius**, and others.

parabola

One of the **conic section**s and one of the most studied curves in the history of mathematics. A parabola is the outline of the figure obtained if a right circular **cone** is cut by a plane that is exactly parallel to the cone's side. Just as the circle is a limiting case of the **ellipse** when the two foci coincide, the parabola is a limiting case of the ellipse when one of the foci is moved to infinity. As the French mathematician Henri Fabre eloquently put it, the parabola is an ellipse that "seeks in vain for its second, lost center." Johannes **Kepler** drew this further connection between the parabola and other conic sections: "Because of its intermediate nature the parabola occupies a middle position [between the ellipse and the **hyperbola**]. As it is produced it does not spread out its arms like the hyperbola but contracts them and brings them nearer to parallel, always encompassing more, yet always striving for less–whereas the hyperbola, the more it encompasses, the more it tries to obtain."

A parabola is the **locus** of all points in a plane that are equidistant from a given line, known as the *directric*, and

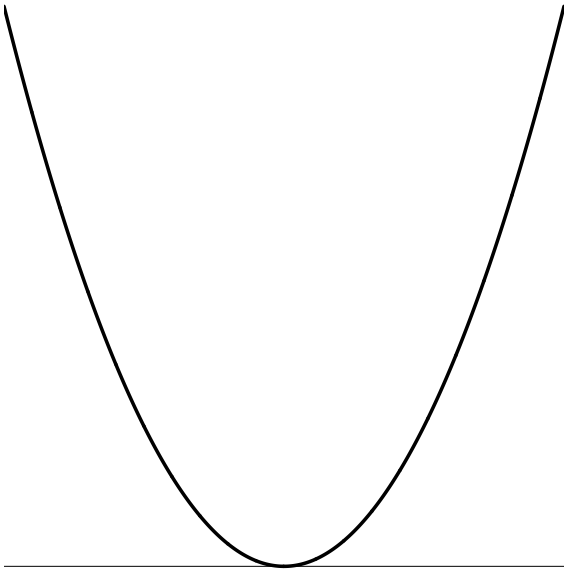

parabola *Jan Wassenaar, www.2dcurves.com*

a given point not on the line, known as the focus. The Cartesian equation of a parabola that opens upward and has its vertex (turning point) at the origin is $y = 4ax^2$, where a is the distance from the vertex to the focus, and the quantity $4a$ is known as the *latus rectum*. More generally, any **quadratic** equation of the form $y = ax^2 + bx + c$, where a is not zero, graphs a parabola. The simplest form of this, when $a = 1$, and both b and c are zero, is $y = x^2$. Like the circle, but unlike the ellipse and the hyperbola, the parabola has only one distinct shape. In other words, any parabola can be superimposed exactly on any other parabola simply by rotating, translating (sliding), and/or enlarging or shrinking it.

Euclid dealt with the parabola in his *Conic Sections,* and, although this treatise was lost, it provided a foundation for the first four books by **Apollonius** of the same name. Galileo (1564–1642) discovered that a cannonball, or any other projectile launched at an angle to ground, follows a parabolic path: a result that immediately grabbed the attention of not only scientists but of monarchs and military leaders. René **Descartes**, in writing *La Géométrie* (1637), chose the parabola to illustrate his innovative **analytical geometry**. In 1992, Rudolph Marcus of the California Institute of Technology won the Nobel Prize in Chemistry for his work showing that parabolic reaction surfaces can be used to calculate how fast electrons travel in molecules. His most famous theoretical result, an inverted rate-energy parabola, predicts electron transfer will slow down at very high-reaction free energies.

paraboloid

The surface of revolution of the **parabola**. It is a **quadratic** surface described by the equation $z = a(x^2 + y^2)$.

paradox

> *Please accept my resignation. I don't want to belong to any club that will accept me as a member.*
>
> –Groucho Marx (1895–1977)

A statement that seems to lead to a logical self-contradiction, or to a situation that contradicts common intuition. The word *paradox* comes from the Greek *para* ("beyond") and *doxa* ("opinion" or "belief"). The identification of a paradox based on seemingly simple and reasonable concepts has often led to significant advances in science, philosophy, and mathematics. See **Allais paradox**, **Arrow paradox**, **Banach-Tarski paradox**, **Berry's Paradox**, **birthday paradox**, **Burali-Forti paradox**, **coin paradox**, **grandfather paradox**, **Grelling's paradox**, **liar paradox**, **Newcomb's paradox**, **nine rooms paradox**, **Parrondo's paradox**, **raven paradox**, **Russell's paradox**, **St. Petersburg paradox**, **Siegel's paradox**, **unexpected hanging**, and **Zeno's paradoxes**.

parallel

Said of two or more things, such as lines or planes, that are equally distant from one another at all points.

parallel postulate

The fifth and most controversial of **Euclid's postulates** set forth in the Greek geometer's great work, *Elements.* To later mathematicians, the parallel postulate seemed less obvious than the other four and many attempts were made to derive it from them, but without success. In 1823, János **Bólyai** and Nikolai **Lobachevsky** independently realized that entirely self-consistent types of **non-Euclidean geometry** could be created in which the parallel postulate doesn't hold. Carl **Gauss** had made the same discovery earlier but kept the fact secret.

parallelepiped

A **polyhedron** with six faces bounded by three pairs of parallel planes, so that all its faces are **parallelogram**s. It is also a **prism** with a parallelogram for a base. A *rectangular parallelepiped* has the shape of a shoebox. The word comes from the Greek *parallelepipedon* for the same shape, which in turn comes from the roots *para* ("beside"), *allel* ("other"), *epi* ("on"), and *pedon* ("ground"). *Parallelepipedon* may have been first used in English by Billingsley in his 1570 translation of Euclid. It seems to have then given way to *parallelepiped* in the last quarter of the nineteenth century.

parallelogram

A **quadrilateral** (four-sided figure) whose opposite sides are parallel, and whose opposite angles, therefore, are equal. The diagonals of a parallelogram bisect each other. A parallelogram of base b and height h has an area

$$bh = ab\sin A = ab\sin B.$$

The height of a parallelogram is $h = a\sin A = a\sin B$. The sides a, b, c, and d and diagonals p and q of a parallelogram satisfy the equality

$$p^2 + q^2 = a^2 + b^2 + c^2 + d^2.$$

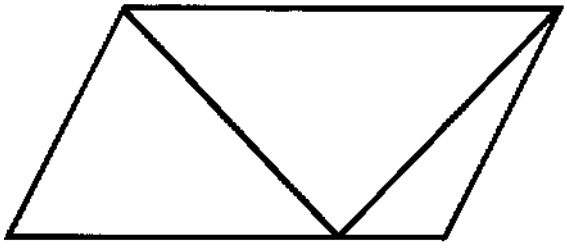

parallelogram The two lines drawn inside this parallelogram have the same length.

Special cases of a parallelogram are a **rhombus**, which has sides of equal length; a **rectangle**, which has two sets of parallel sides that are perpendicular to each other; and a **square**, which meets the conditions of both a rectangle and a rhombus.

In the *parallelogram illusion* shown, despite appearances to the contrary, the interior diagonal lines are of equal length.

parameter

An independent variable; one of the inputs for a **function**. *Parametric equations* are equations in which the variables of interest are given in terms of another variable.

parity

(1) The sum of the digits in a **binary** representation of a number. (2) An indication of whether two numbers are both even or both odd (same parity), or are such that one is even and one is odd (opposite parity). This concept, of same or opposite parity, can be applied to any things that can have two different states–the sense in which a knot is tied, the color of a chessboard square, and so on.

Parrondo's paradox

Two losing gambling games can be set up so that when they are played one after the other, they become winning. This paradox is named after the Spanish physicist Juan Parrondo who, in the late 1990s, discovered how to construct such a scenario. The simplest way is to use three biased coins. Imagine you are standing on stair zero, in the middle of a long staircase with 1001 stairs numbered from –500 to 500. You win if you can get to the top of the staircase, and the way you move depends on the outcome of flipping one of two coins. Heads you move up a stair, tails you move down a stair. In game 1, you use coin *A,* which is slightly biased and comes up heads 49.5% of the time and tails 50.5%. Obviously, these are losing odds. In game 2, you use two coins, *B* and *C.* Coin *B* comes up heads only 9.5% of the time, tails 90.5%. Coin *C* comes up heads 74.5% of the time, tails 25.5%. In game 2 if the number of the stair you are on at the time is a multiple of 3 (that is, . . . , –9, –6, –3, 0, 3, 6, 9, 12, . . .), then you flip coin *B;* otherwise you flip coin *C.* Game 2, it turns out, is also a losing game and would eventually take you to the bottom of the stairs. What Parrondo found, however, is that if you play these two games in succession in random order, keeping your place on the staircase as you switch between games, you will steadily rise to the top of the staircase! This kind of process has been called a *Brownian motion*.[153]

partial differential equation

An equation that involves **derivative**s with respect to more than one variable. Many of the equations used to model the physics of the real world are partial differential equations.

partition number

A number that gives the number of ways of placing n indistinguishable balls into n indistinguishable urns. For example:

1: (*)

2: (**) (*)(*)

3: (***) (**)(*) (*)(*)(*)

5: (****) (***)(*) (**)(**) (**)(*)(*) (*)(*)(*)(*)

7: (*****) (****)(*) (***)(**) (***)(*)(*) (**)(**)(*) (**)(*)(*)(*)(*)(*)(*)(*)

11: (******) (*****)(*) (****)(**) (****)(*)(*) (***)(***) (***)(**)(*)(***)(*)(*)(*) (**)(**)(**) (**)(**)(*)(*) (**)(*)(*)(*)(*) (*)(*)(*)(*)(*)(*)

The sequence runs: 1, 2, 3, 5, 7, 11, 15, 22, 30, 42, 56, 77, 101, 135, 176, 231, 297, 385, ... If the urns are distinguishable, the number of ways is 2^n. If the balls are distinguishable, the number of ways is given by the nth **Bell number**.

Pascal, Blaise (1623–1662)

A French mathematician, philosopher, and pioneer of **probability theory** whose short life was rich with mathematical invention but whose name, ironically, is most familiar from its association with an array of numbers known as **Pascal's triangle** (which he didn't discover, though he did important work on it). Educated by his father (after whom the **limaçon of Pascal** is named), Pascal showed his intellectual prowess early on by proving one of the most important theorems in **projective geometry** at the age of 16. Three years later he devised the world's second mechanical calculating machine (the first was made by Wilhelm Schickard in 1623) to help with his father's business; he sold about 50 of these "Pascalines," several of which survive. In 1654, he and Pierre de **Fermat**, in an exchange of correspondence, laid the foundation for **probability theory**. They considered the dice problem, already studied by Girolamo **Cardano**, and the problem of points also considered by Cardano and, around the same time, by Luca **Pacioli** and Niccoló **Tartaglia**. The dice problem asks how many times one can expect to throw a pair of dice before getting a double six; the problem of points asks how to divide the stakes if

a game of dice is incomplete. Pascal and Fermat solved the problem of points for a two-player game but didn't develop powerful enough methods to solve it for three or more players. In the same year, Pascal was almost killed in an incident in which the horses pulling his carriage bolted and the carriage was left hanging over a bridge above the river Seine. Though rescued unharmed, he shortly after converted to the rigorous Jansenist sect of the Catholic Church. His philosophical work *Pensées,* written between 1656 and 1658 contains his famous argument, often called Pascal's wager, for belief in **God**. Having suffered poor health for most of his adult life, he died in great pain of cancer at the age of 39.

Pascal's mystic hexagon

If a **hexagon** *ADBFCE* (not necessarily convex) is inscribed in a **conic section** (in particular a circle), then the points of intersections of opposite sides (*AD* with *FC*, *DB* with *CE* and *BF* with *EA*) are collinear. This line is called the *Pascal line* of the hexagon. A special case is when the conic degenerates into two lines; the theorem still holds but is then usually called *Pappus's theorem.*

Pascal's triangle

A triangular pattern of numbers in which each number is equal to the sum of the two numbers immediately above it:

$$
\begin{array}{ccccccccccc}
 & & & & & 1 & & & & & \\
 & & & & 1 & & 1 & & & & \\
 & & & 1 & & 2 & & 1 & & & \\
 & & 1 & & 3 & & 3 & & 1 & & \\
 & 1 & & 4 & & 6 & & 4 & & 1 & \\
1 & & 5 & & 10 & & 10 & & 5 & & 1 \\
 & \vdots & & & & & & & & \vdots &
\end{array}
$$

Although named after Blaise **Pascal**, who studied it, this arithmetic triangle has been recognized since the twelfth century and has a variety of other names. In Italy it is called *Tartaglia's triangle* and in many parts of Asia it is referred to as *Yang Hui's triangle.* Yang Hui was a minor Chinese official who wrote two books, dated 1261 and 1275, that use decimal fractions (long before they appeared in the West) and contain one of the earliest accounts of the triangle. At about the same time, Omar **Khayyam** also wrote about it. The Chinese triangle appears again in 1303 on the front of Chu Shi-Chieh's *Ssu Yuan Yü Chien* (Precious mirror of the four elements), a book in which Chu says the triangle was known in China more than two centuries before his time.

The numbers in Pascal's triangle give the number of ways of picking r unordered outcomes from n possibilities. This is equivalent to saying that the numbers in each row are the **binomial coefficient**s in the expansion of $(x+y)^n$:

$$
\begin{aligned}
(x+y)^0 &= 1 \\
(x+y)^1 &= 1x + 1y \\
(x+y)^2 &= 1x^2 + 2xy + 1y^2 \\
(x+y)^3 &= 1x^3 + 3x^2y + 3xy^2 + 1y^3 \\
(x+y)^4 &= 1x^4 + 4x^3y + 6x^2y^2 + 4xy^3 + 1y^4
\end{aligned}
$$

and so on. In addition, the shallow diagonals of the triangle sum to give the **Fibonacci sequence**.

path

See **trajectory**.

pathological curve

A curve often specifically devised to show the falseness of certain intuitive concepts. In particular, the image of **continuity** as a smooth curve in our mind's eye severely misrepresents the situation and is the result of a bias stemming from an overexposure to the much smaller class of differentiable functions (see **differentiation**). A chief lesson of pathological curves is that continuity is a weaker notion than differentiability. Many pathological curves are **fractal**s, such as **Cantor dust**, including **space-filling curve**s, such as the **Peano curve**. The earliest known example is the graph of **Weierstrass' nondifferentiable function**.

payoff

In **game theory**, the amount that a player wins, given the player's and his opponent's actions.

Peano, Guiseppe (1858–1932)

An Italian pioneer of mathematical **logic** and the axiomatization of mathematics. In 1889, he published his first version of a system of mathematical logic in *Arithmetics Principia,* which included his famous **axiom**s of natural numbers, now known as *Peano's axioms.* Two years later, he established a journal, the *Rivista,* in which he proposed the symbolizing of all mathematical propositions into his system. The project, which became known as the *Formulario,* was his chief focus for the next fifteen years.

Peano curve

The first known example of a **space-filling curve**. Discovered by Guiseppe **Peano** in 1890, its effect was like that of an earthquake on the traditional structure of mathematics. Commenting in 1965 on the impact of the curve in Peano's day, N. Ya Vilenkin said: "Everything has come unstrung! It's difficult to put into words the effect that

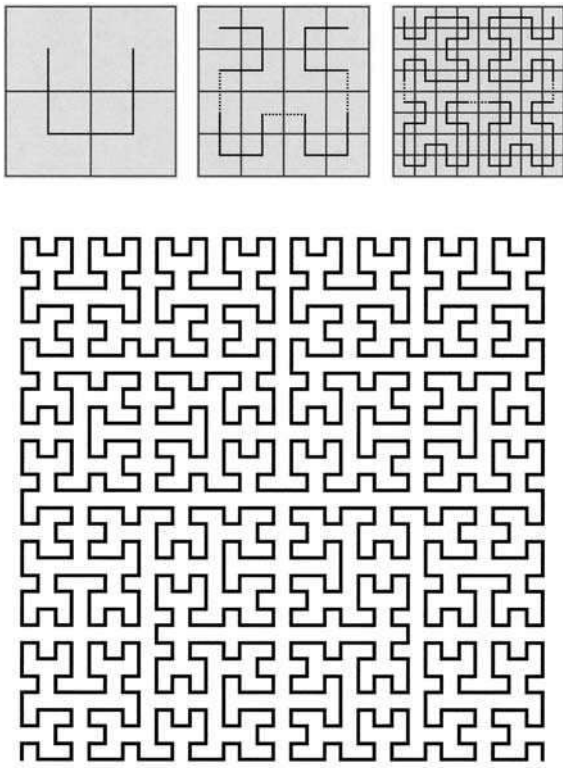

Peano curve A simple iterative process produces a remarkable space-filling shape.

Peano's result had on the mathematical world. It seemed that everything was in ruins, that all the basic mathematical concepts had lost their meaning." Today, the Peano curve is recognized as just one of an infinite class of familiar objects known as **fractal**s. But at the end of the nineteenth century it was an extravagant, completely counterintuitive thing; indeed, it was something that had been believed impossible. Writing of Peano's result in *Grundzüge der Mengenlehre* (Basic features of set theory) in 1914, Felix **Hausdorff** said: "This is one of the most remarkable facts of set theory." Originally, the Peano curve was derived purely analytically, without any kind of drawing or attempt at visualization. But the first few steps in drawing it, as shown in the diagrams, are easy enough, even though the finished product is unattainable in this way–and totally unimaginable. To fill the unit square, as the Peano curve does, without leaving any holes, the curve has to be both continuous and self-intersecting.

pearls of Sluze

Curves that are generated by the Cartesian equation

$$y^n = k(a - x)^p x^m,$$

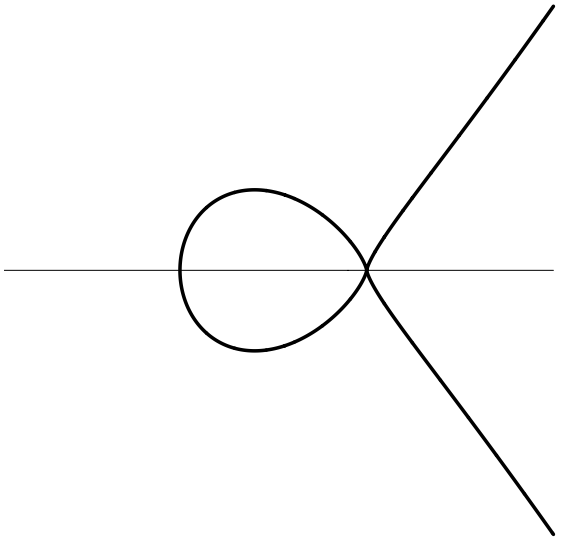

pearls of Sluze *Jan Wassenaar, www.2dcurves.com*

where n, m, and p are integers. They were first studied by the French mathematician René de Sluze (1622–1685) and named the pearls of Sluze by Blaise **Pascal**.

pedal curve

The locus of the feet of the perpendiculars from a given point to the **tangent**s to the given figure. The "given point" is known as the *pedal point*.

pedal triangle

The pedal triangle of a point P with respect to a triangle ABC is the triangle whose vertices (see **vertex**) are the feet of the perpendiculars dropped from P to the sides of triangle ABC.

peg solitaire

Also known as Hi-Q, a game that, in its commonest form, is played with 32 pegs or marbles on a rectangular grid, the middle position of which starts out empty. A peg may jump horizontally or vertically, but not diagonally, over a peg in an adjacent hole into a vacant hole immediately beyond. The peg that was jumped over is then removed. The object is to be left with a single peg in the center position.

The quickest solution of peg solitaire was found by Ernest Bergholt in 1912 and was proved to be minimal by John Beasley in 1964. Suppose the rows and columns of the board are each labeled 1 to 7 so that, for example, a peg on the fourth row and the third column is in position 43. The quickest solution is: (1) 46→44. (2) 65→45.

peg solitaire A version of peg solitaire made of tin with marbles by the British firm MAR Toys in the 1950s. *Sue & Brian Young/Mr. Puzzle Australia, www.mrpuzzle.com.au*

(3) 57→55. (4) 54→56. (5) 52→54. (6) 73→53. (7) 43→63. (8) 75→73→53. (9) 35→55. (10) 15→35. (11) 23→43→63→65→45→25. (12) 37→57→55→53. (13) 31→33. (14) 34→32. (15) 51→31→33. (16) 13→15→35. (17) 36→34→32→52→54→34. (18) 24→44.[28]

Pell equation

An equation of the form $y^2 = ax^2 + 1$, where a is any positive whole number except a square number. The name comes from the English mathematician John Pell (1611–1685); however, he was wrongly credited. In writing about some of the work done on this type of equation, Leonhard **Euler** gave priority to Pell whereas, in fact, Pell had done no more than copy it in his papers from some of Pierre de **Fermat**'s letters. Fermat had been the first to state that an equation of this form always has an unlimited number of integer solutions. For example, the equation $y^2 = 92x^2 + 1$, has the solutions $x = 0$, $y = 1$; $x = 120$, $y = 1{,}151$; $x = 276{,}240$, $y = 2{,}649{,}601$; and so on. Each successive solution is about 2,300 times the previous solution. In fact, the solutions are every eighth partial fraction (where x is the numerator and y is the denominator) of the **continued fraction** for $\sqrt{92}$. A Pell equation was used in finding the solution to **Archimedes's cattle problem**.

Pell numbers

Numbers, named after John Pell (1611–1685), that are similar to the **Fibonacci sequence** and are generated by the formula $A_n = 2A_{n-1} + A_{n-2}$. The sequence runs: 1; 2; 5; 12; 29; 70; 169; 408; 985; 2,378; 5,741; 13,860; 33,461; 80,782; 195,025; . . . . The ratio of successive terms approaches 1 plus the **square root of 2**.

Penrose, Roger (1931–)

An English mathematical physicist famous for his important contributions to cosmology and the physics of black holes, for his controversial views on the nature of human consciousness and its relationship to **quantum mechanics**, and for his work in the field of recreational mathematics. The **Penrose tiling** and the **Penrose triangle** are named after him (but not the **Penrose stairway**, which is named after his father). In his book *The Emperor's New Mind* he argues that there must be errors in the known laws of physics, notably in quantum mechanics, and that true **artificial intelligence** is impossible.[242] The latter claim is based on his assertion that humans can do things outside the power of formal logic systems, such as knowing the truth of unprovable statements, or solving the **halting problem** (claims that were originally made by the philosopher John Lucas of Merton College, Oxford). These are controversial views, with which most of the mathematical and computer science communities disagree.

Penrose stairway

An **impossible figure** named after the British geneticist Lionel Penrose (1898–1972), father of Roger **Penrose**. It served as an inspiration for the staircase in M. C. **Escher**'s famous print "Ascending and Descending." Although the Penrose stairway cannot be realized in

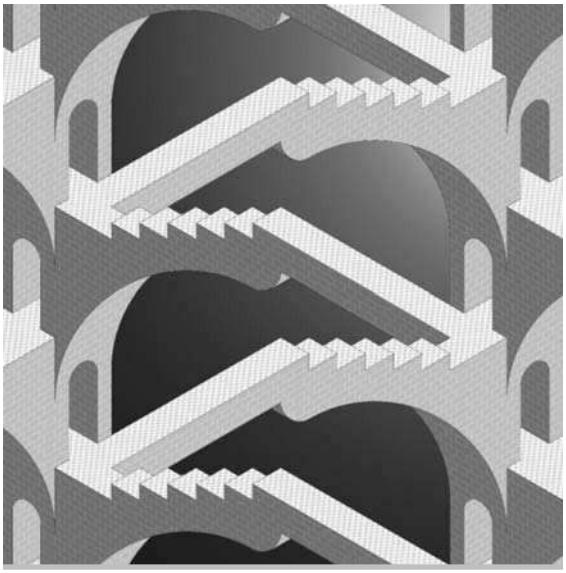

Penrose stairway Steps that ascend and descend simultaneously. *Jos Leys, www.josleys.com*

three dimensions, this impossibility is not immediately perceived and, in fact, the paradox is not even apparent to many people at a quick glance. Although Escher and the Penroses made the Stairway famous, it was, unbeknownst to them, independently discovered and refined years before by the Swedish artist Oscar **Reutersvärd**. In the 1960s the Stanford psychologist Roger Shepard created an auditory analogue of the Stairway. See also **Penrose triangle**.

Penrose tiling

A kind of **aperiodic tiling** discovered by Roger **Penrose**. In 1973 he announced a tiling made from a set of six tiles and then, by slicing and re-gluing, was able to reduce the number of tiles to just two. The most elegant of Penrose tilings use two rhombi (see **rhombus**), a thick one called a "kite" and a thin one called a "dart," which are fitted together so that no two tiles are aligned to form a single parallelogram (otherwise, a single rhombus could be used to make a periodic tiling). All angles are multiples of $\pi/5$ radians (36°, or one-tenth of a circle). Each tile has four sides with a length of one unit. One tile has four corners with the angles 72°, 72°, 108°, and 108° (2, 2, 3, and 3 multiples of 36°); the other has angles of 36°, 36°, 144°, and 144° (1, 1, 4, and 4 multiples of 36°). On each tile one of the vertices (corners) is colored black and two of the sides are marked with arrows. The only rules for assembling the tiles to ensure an aperiodic tiling are that two adjacent vertices must be of the same color, and two adjacent edges must have arrows pointing in the same direction or have no arrows at all. These rules ensure that, taken over a large enough area of the plane, the pattern of tiles doesn't repeat. In a correct Penrose tiling, the ratio of kites to darts is always the same and is equal to the **golden ratio**. Although Penrose tilings started out as nothing more than an interesting mathematical diver-

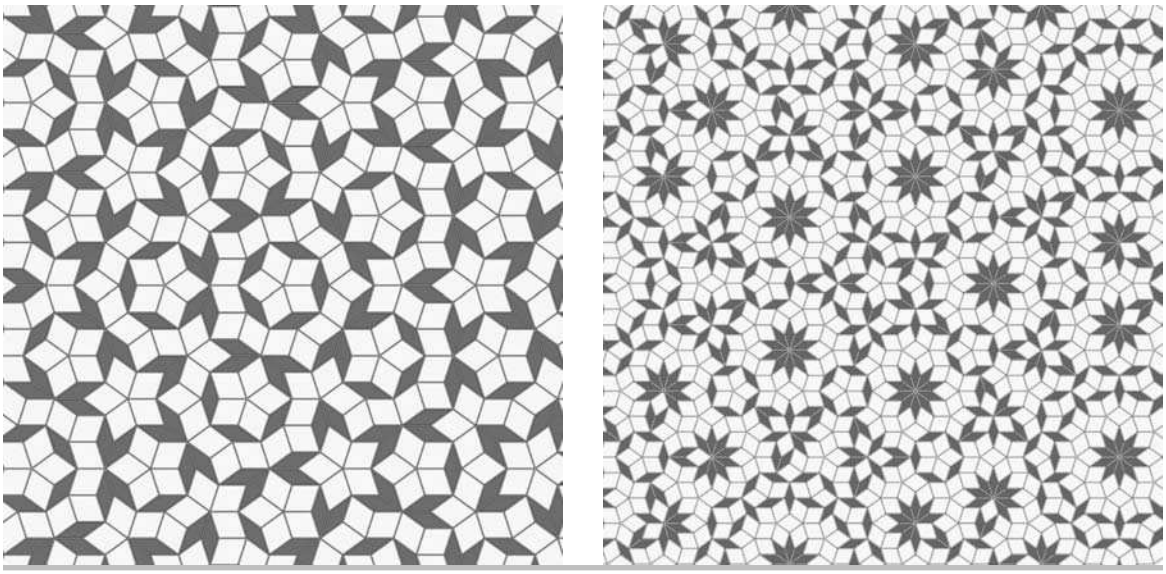

Penrose tiling Two of an infinite variety of nonperiodic patterns possible using Penrose tiles. *Jos Leys, www.josleys.com*

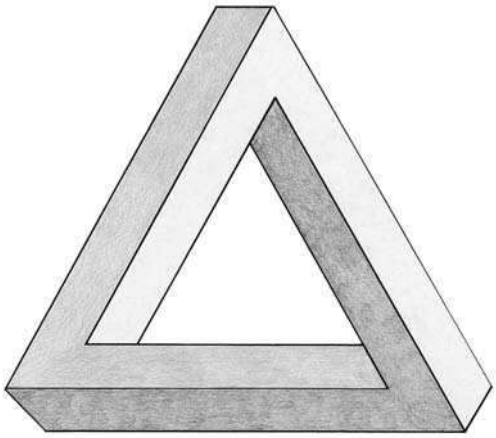

Penrose triangle

sion, they have turned out to mimic the arrangements of atoms in some newly discovered materials, known as **quasicrystals**.[127]

Penrose triangle

The most famous and one of the simplest **impossible figures**. Its roots go back to 1934 when Oscar **Reutersvärd** made the first recognizable impossible triangle out of a strange two-dimensional representation of cubes; this artwork appeared on a Swedish postage stamp issued in 1982. In 1954, Roger **Penrose**, after attending a lecture by the artist M. C. **Escher**, rediscovered the impossible triangle and drew it in its most familiar form, which he published in a 1958 article in the *British Journal of Psychology,* coauthored with his father Lionel.[241] Penrose was unfamiliar with the work of Reutersvärd, Giovanni Piranesi, and others who had previously created impossible figures. Penrose's impossible triangle, unlike Reutersvärd's earlier version, was drawn in perspective, which added an additional size paradox to the object. In 1961, Escher, inspired by Penrose's version of the impossible triangle (he was sent a copy of the article by the Penroses), incorporated it into his famous lithograph *Waterfall.*

penta-

The Greek prefix meaning "five." A *pentagon* is a five-sided **polygon** and a *pentahedron,* such as the Great Pyramid of Gisa, is a five-sided **polyhedron**. A *pentagram,* or *pentacle,* is a five-pointed star formed by the pairwise extension of the sides of a regular polygon so that each side meets not with the next side but with the one after that. The Pythagoreans (see **Pythagoras of Samos**) used the pentagram as a secret identification emblem; later it became a trademark of alchemists and, perhaps because of its repeating properties, a sign of the occult. According to legend, a pentagram was used by Doctor Faustus to exorcise Mephistopheles. *Pentagonal numbers* are **figurate numbers** (numbers that can be represented by a regular geometric arrangement of equally spaced points) of the form $n(3n - 1)/2$; the first few are 1, 5, 12, 22, ...

pentomino

A five-square **polyomino**.

Perelman, Yakov Isidorovitch (1882–1942)

A Russian scientist and exponent of recreational mathematics whose stature in his own country was, and remains, similar to that of Martin **Gardner** in the United States. Between 1913 and his death, Perelman authored a dozen books and scores of articles covering many different aspects of popular mathematics, physics, and astronomy. His books have been republished so often in Russia that Perelman is universally known among both amateur and professional mathematicians across several generations. He was also a leading proponent of the ideas of the spaceflight visionary Konstantin Tsiolkovsky.

perfect cube

An integer of the form n^3 where n is an integer.

perfect cuboid problem

See **cuboid**.

perfect number

A whole number that is equal to the sum of all its factors except itself. For example, 6 is a perfect number because its factors, 1, 2, and 3 add to give 6. The next smallest is 28 (the sum of 1 + 2 + 4 + 7 + 14). Augustine (354–430) argued that God could have created the world in an instant but chose to do it in a perfect number of days, 6. Early Jewish commentators saw the perfection of the universe in the Moon's period of 28 days. The next in line are 496, 8,128, and 33,550,336. As René **Descartes** pointed out: "Perfect numbers like perfect men are very rare." All end in six or eight, though what seems to be an alternating pattern of sixes and eights for the first few perfect numbers doesn't continue. All are of the form $2^{n-1}(2^n - 1)$, where $2^n - 1$ is a **Mersenne prime**, so that the search for perfect numbers is the search for Mersenne primes. The largest one found is $2^{3021376}(2^{3021377} - 1)$. It isn't known if there are infinitely many perfect numbers or if there are any odd perfect numbers. A *pseudoperfect number* or *semi-perfect number* is a number equal to the sum of some of its divisors, for example, 12 = 2 + 4 + 6, 20 = 1 + 4 + 5 + 10. An *irreducible semi-perfect number* is a semi-perfect number, none of whose factors is semi-perfect, for example, 104. A *quasi-perfect number*

would be a number n whose divisors (excluding itself) sum to $n + 1$, but it isn't known if such a number exists. A *multiply perfect number* is a number n whose divisors sum to a multiple of n. An example is 120, whose divisors (including itself) sum to $360 = 3 \times 120$. If the divisors sum to $3n$, n is called multiply perfect of order 3, or *tri-perfect*. Ordinary perfect numbers are multiply perfect of order 2. Multiply perfect numbers are known of order up to 8. See also **abundant number**.

perfect power
An integer of the form m^n where m and n are integers and $n > 1$.

perfect square
A number that is the product of two equal whole numbers; for example, $1 = 1 \times 1$, $4 = 2 \times 2$, $9 = 3 \times 3$, $16 = 4 \times 4$.

Perigal, Henry (1801–1898)
An English amateur mathematician best known for his elegant **dissection** proof of **Pythagoras's theorem**, a diagram of which is carved on his gravestone. Perigal also discovered a number of other interesting geometrical dissections and, though employed modestly for much of his life as a stockbroker's clerk, was well known in British scientific society.

perimeter
The distance around a two-dimensional shape.

period, of a decimal expansion
The length of the smallest block of repeating digits in the decimal expansion of a **rational number** that does not terminate. For example:

$1/3 = 0.333333333333\ldots$
repeating block = 3, period = 1
$5/7 = 0.71428571428571\ldots$
repeating block = 714285, period = 6
$89/26 = 3.4230769230769\ldots$
repeating block = 230769, period = 6

periodic
Refers to motion or to an entity that goes through a finite number of regions, returns to a previous state, and repeats the same fixed pattern forever.

periodic attractor
Also called a *limit cycle attractor,* an **attractor** that consists of a periodic movement back and forth between two or more values. The periodic attractor represents more possibilities for system behavior than does the **fixed-point attractor**. An example of a period two attractor is the oscillating movement of a metronome or, in psychiatry, a bipolar disorder that causes a person's mood to shift back and forth from elation to depression.

periodic tiling
A **tiling** in which a region can be outlined that tiles the plane by translation, that is, by shifting the position of the region without rotating or reflecting it. M. C. **Escher** is famous for his many pictures of periodic tilings with shapes that resemble living things. An infinity of shapes–for instance, the regular hexagon–tile only periodically, though all these fall into 17 distinct **wallpaper group**s. An infinity of other shapes tile both periodically and aperiodically. But it was only quite recently that the first **aperiodic tiling**s were discovered.

periphery
A curved **perimeter**.

permutable prime
Also known as an *absolute prime,* a **prime number** with at least two distinct digits, which remains prime on every rearrangement (permutation) of the digits. For example, 337 is a permutable prime because 337, 373, and 733 are all prime. Most likely, in base 10, the only permutable primes are 13, 17, 37, 79, 113, 199, 337, and their permutations. Permutable primes can't have any of the digits 2, 4, 6, 8 or 5, nor can they have all four of the digits 1, 3, 7, and 9 simultaneously.

permutation
A particular ordering of a collection of objects. For example, if an athlete has won three medals, a bronze one (B), a silver one (S), and a gold one (G), there are six ways they can be permuted or lined up: BSG, BGS, SBG, SGB, GBS, and GSB. If six people want to sit on the same park bench, there are 720 ways in which they can organize themselves. In general, n things can be permuted in $n \times (n - 1) \times (n - 2) \times \ldots \times 2 \times 1 = n!$ ways (where "!" is the symbol for **factorial**). How about if there are n distinct objects but we want to permute them in groups of k (where $k \leq n$): how many ways can that be done? The first member of the group can be picked in n ways because there are n objects to pick from. The second member can be filled in $(n - 1)$ ways since one of the n elements has already been taken. The third member can be filled in $(n - 2)$ ways since 2 elements have already been used, and so on. This pattern continues until k things have been chosen. This means that the last member can be filled in $(n - k + 1)$ ways. Therefore a total of $n(n - 1)(n - 2)\ldots(n - k + 1)$ different permutations of k

objects, taken from a pool of n objects, exist. If we denote this number by $P(n, k)$, we can write $P(n, k) = n! / (n - k)!$

perpendicular
At right angles. Two lines, planes, etc., are said to be perpendicular if they are 90° apart.

Perrin sequence
The sequence of integers defined by the recurrence relation $P(n) = P(n - 2) + P(n - 3)$, with the initial conditions $P(0) = 3$, $P(1) = 0$, $P(2) = 2$. Although the sequence is named after R. Perrin who studied it in 1899, it had been explored earlier, in 1876, by Édouard **Lucas**. As in the case of the similar *Padovan sequence,* the ratio of consecutive Perrin numbers tends toward the **plastic number**. More importantly, it appears that n divides $P(n)$ exactly if and only if n is a **prime number**. For example, 19 is prime, $P(19) = 209$ and $^{209}/_{19} = 11$; on the other hand, 18 is composite, $P(18) = 158$ and $^{158}/_{18} = 8.777$, which is not a whole number. Lucas conjectured that this is true for all values of n so that the Perrin sequence can be used as a test for non-primality: any number n that does not divide $P(n)$ is composite. Whether this conjecture is correct remains an open question. No one has ever found a composite n that divides $A(n)$, nor has anyone been able to prove that such numbers, known as *Perrin pseudoprimes,* don't exist. In 1991 Steven Arno of the Supercomputing Research Center in Bowie, Maryland, proved that Perrin pseudoprimes must have at least 15 digits.[15] The conjecture that no Perrin pseudoprimes exist is important, because the remainder on dividing $P(n)$ by n can be calculated very rapidly.

perturbation
A slight nudge that, temporarily or permanently, displaces an object or system out of **equilibrium**.

peta-
Prefix for 10^{15}, from the Greek *pentakis,* meaning "five times."

phase space
The mathematical space of all possibilities in a given situation. A motion is then described by a *path, trajectory,* or *orbit* in this space. This is not the usual kind of path laid out on the ground, but a series of locations in phase space, describing motion or change over a period of time. The terms do, however, recall the origins of qualitative dynamics in Henri **Poincaré**'s study of planetary motion. The *dimension* of the phase space is the number of initial conditions needed to uniquely specify a path and is equal to the number of variables in the dynamical system. The temporal behavior of the system is viewed as the succession of states in the system's state space. In the case of a simple pendulum, for example, the instantaneous configuration is given by just two numbers–the position of the pendulum bob and its velocity–which completely describe the system's state. For more complex systems, such as a chain of n pendulums coupled together, the state of the system is much larger. It requires, in this case, $2n$ numbers to specify the state of the entire system. This collection of all possible configurations is the phase space.

phase transition
In physics, a change from one state of matter to another. In **dynamical system**s theory, a change from one mode of behavior to another.

phi
See **golden ratio**.

Phillips, Hubert (1891–1964)
An English compiler of crosswords and word puzzles who wrote under the pseudonyms "Dogberry" in the *News Chronicle* magazine and "Caliban" in the *New Statesman.* He was also a prolific writer of epigrams, parodies, and satirical verse, and appeared on many radio quizzes. Phillips earned a first class degree in history at Oxford, served in the army throughout World War I, taught economics at Bristol University, and was active in the British Liberal Party. He was an accomplished player of contract bridge, captaining England in 1937 and 1938. Among his many publications are *Caliban's Problem Book, The Complete Book of Card Games, Brush Up Your Wits, My Best Puzzles in Mathematics,* over a hundred crime-problem stories, and a novel, *Charteris Royal.*[249, 250, 251]

Phutball
Also known as *philosopher's football,* a two-player board **game** first described by Elwyn Berlekamp, John **Conway**, and Richard **Guy**, in their book *Winning Ways for your Mathematical Plays.* Phutball is played on the intersections of a 19×15 grid using one white piece and as many black pieces as necessary. The objective is to score goals by using the men (black pieces) to move the football (white piece) onto or over the opponent's goal line, that is, either rows 1 or 0 or rows 19 and 20 (rows 0 and 20 being off the board). At the start of the game the football is placed on the central point, although a handicapping scheme exists where the ball can start nearer to the stronger player's goal line. Players alternate making moves, which consist either of adding a man to any vacant point on the board or of moving the ball. There is no difference between men played by the two opponents. The football is moved by a series of jumps over adjacent men. One jump is from the football's current

point to the first vacant point in a straight line orthogonally or diagonally over one or more men. The jumped men are then removed from the board (before any subsequent jump occurs). Jumping is optional and can be repeated for as long as there are men available to be jumped and the player desires to do so. In contrast to checkers, multiple men in a row are jumped and removed as a group. If the football ends the move on or over the opponent's goal line then a goal has been scored. If the football passes through a goal line, but ends up elsewhere due to further jumps, the game continues. The game is sufficiently complex that, although theoretically one of the players has a winning strategy, this strategy is not known.

pi (π)

The ratio of the circumference to the diameter of a **circle**. Pi, sometimes known as *Archimedes' constant,* is one of the most important and ubiquitous numbers in mathematics, popping up in all kinds of seemingly unrelated areas. Its approximate value is 3.1419 but, being an **irrational number**, it can't be written as a terminating or recurring decimal. The fact that π can't be expressed as the ratio of two integers was proved by Johann Lambert in 1761. Then, in 1881, Ferdinand Lindemann showed that it is a **transcendental number**, meaning that there is no polynomial with integer or rational coefficients of which π is a root. Because of this, it's impossible to write π in terms of *any* finite number of integers or fractions or their roots. From the outset, this dooms any attempt at **squaring the circle**, that is, constructing a square whose area is equal to the area of a given circle, using straightedge and compass alone.

The association of the Greek letter π with the number 3.141 . . . started with William **Oughtred** in 1647 who used π.δ as a stand-in for "periphery-diameter" in his *Clavis mathematicae.* The Welsh mathematician William Jones was the first to use π as a symbol on its own in his 1706 *Synopsis palmariorum matheseos.* But it fell to the great Leonhard **Euler** to popularize the notation 30 years later.

Calculating π with greater and greater precision became a popular pursuit. Around 1600, Ludolph van Ceulen computed the first 35 decimals and was so proud of his accomplishment that he had the number inscribed on his tombstone. In 1789, the Slovene mathematician Jurij Vega extended known π to 140 places (of which only 137 were correct), while, in 1873, William Shanks pushed back the frontier to 707 places–a record that stood until 1949 when the first electronic computers appeared on the scene. In September 2002, Yasumasa Kanada and his colleagues at Tokyo University used 400 hours of supercomputer time to calculate π to 1.24 trillion places, beating their previous best, set in 1999, of 206 billion places. Although such an exercise may seem pointless, it serves as a benchmark for new high-speed computers and algorithms, and also to test the long-standing, but still unproven assertion that the distribution of digits in π is completely random.

For the record, the first 100 digits of π are: 3.1415926535 8979323846 2643383279 5028841971 6939937510 5820974944 5923078164 0628620899 8628034825 3421170679. The wonderfully pointless pastime of "piphilology" is concerned with devising mnemonics for remembering some of these: the number of letters in each word of the mnemonic gives the corresponding digit. A famous example is Isaac Asimov's "How I want a drink, alcoholic of course, after the heavy lectures involving quantum mechanics!" For the more ambitious, there is Michael Keith's 1995 poem that supplies the first 42 digits:

Poe, E. Near A Raven
Midnights so dreary, tired and weary,
Silently pondering volumes extolling all by-now obsolete lore.
During my rather long nap, the weirdest tap!
An ominous vibrating sound disturbing my chamber's antedoor.
"This," I whispered quietly, "I ignore."

There are some reasonably good approximations to π in the form of ordinary (rational) fractions. The best known is $^{22}/_{7}$, but this is only accurate to two decimal places. A fraction with a larger denominator offers a better chance of getting a more refined estimate. There is also $^{333}/_{106}$, which is good to 5 places. But an outstanding approximation is $^{355}/_{113}$ which is accurate to 6 places; in fact, there is no better approximation among all fractions with denominators less than 30,000. See also **continued fraction**.

In 1897 the General Assembly of the state of Indiana tried to pass legislation to the effect that the exact value of π is 3.2. The bill was referred, for some bizarre reason, to the House Committee on Canals. But then the true motive for the attempted change to the law became clear. By chance a professor of mathematics happened to be present during a debate and heard an ex-teacher saying "The case is perfectly simple. If we pass this bill, which establishes a new and correct value for π, the author offers to our state without cost the use of his discovery and its free publication in our school textbooks, while everyone else must pay him a royalty." Fortunately, the professor was able to teach the senators a little math and the bill was stopped in its tracks.

Any formulas to do with circles or spheres, not surprisingly, have π in them. For example, the circumference

of a circle of radius r is $2\pi r$, the area of a circle is πr^2, the volume of a sphere is $(4/3)\pi r^3$, and the surface area of a sphere is $4\pi r^2$. But π also has a strange habit of appearing in the most unexpected places. In the eighteenth century, the French naturalist Comte de Buffon showed that you could estimate π by experiment using the unlikely apparatus of a repeatedly dropped needle and a shove-halfpenny board (see **Buffon's needle**). Two of the most important, but (as far as is known) unrelated, equations in modern physics, Heisenberg's uncertainty principle ($\Delta x\ \Delta p = h/4\pi$) in **quantum mechanics** and Einstein's field equation ($R_{ik} - \frac{1}{2}\ g_{ik}\ R + \Lambda\ g_{ik} = 8\pi G/c^4\ T_{ik}$) in general **relativity theory** include π. The ever-present constant also emerges as a result of various remarkable **infinite series**. These include:

$1/1^2 + 1/2^2 + 1/3^2 + 1/4^2 + \ldots = \pi^2/6$
(found by Leonhard **Euler**)

$1/1 - 1/3 + 1/5 - 1/7 + 1/9 - \ldots = \pi/4$
(found by Gottfried **Leibniz**)

$2/1 \times 2/3 \times 4/3 \times 4/5 \times 6/5 \times 6/7 \times 8/7 \times 8/9 \times \ldots = \pi/2$
(found by John **Wallis**)

Among many other formulas that give rise to or contain π are

the integral

$$\int_{-\infty}^{\infty} e^{-x^2}\,dx = \sqrt{\pi},$$

Stirling's formula, $n! \sim \sqrt{2\ \pi\ n}\ (n/e)^n$ and, the most intriguing equation in mathematics, $e^{i\pi} + 1 = 0$.

In **number theory**, the probability that two randomly chosen integers have no common divisors (in other words, that they're *relatively prime*) is $6/\pi^2$ or 1 in 1.644934 . . . , and the average number of ways to write a positive integer as the sum of two **perfect square**s is $\pi/4$. Both of these facts are astonishing because it is hard to see how a basically geometric constant to do with circles has any bearing at all on how various types of numbers are distributed. Deep truths are buried here!

In 1995, David Bailey, Peter Borwein, and Simon Plouffe of the University of Quebec at Montreal discovered a new formula for π as an infinite series:[21]

$$\pi = \sum_{k=0}^{8} \frac{1}{16^k}\left[\frac{4}{8k+1} - \frac{2}{8k+4} - \frac{1}{8k+5} - \frac{1}{8k+6}\right]$$

What is so remarkable about this is that it enables the calculation of *isolated digits* of π—say, the trillionth digit—without computing and keeping track of all the preceding digits. How such a formula could possibly arise constitutes a mystery in itself. The only catch is that the formula works for base 2 (**binary**) and 16 (**hexadecimal**) but not base 10. So, it's possible to use the formula to determine, for example, that the five-trillionth binary digit of π is 0, but there's no way to convert the result into its decimal equivalent without knowing all the binary digits that come before the one of interest. The new formula allows the calculation of the nth base 2 or base 16 digit of π in a time that is essentially linear in n, with memory requirements that grow logarithmically (very slowly) in n. One possible use of the Bailey-Borwein-Plouffe formula is to help shed light on whether the distribution of π's digits are truly random, as most mathematicians suppose.[29, 42, 68, 114] See also **pyramid**.

Pick's theorem

First published in 1899, a theorem that was brought to broad attention as recently as 1969 through Hugo **Steinhaus**'s popular book *Mathematical Snapshots*.[316] Pick's theorem gives an elegant formula for the area of *lattice polygons*—**polygon**s that have vertices located at the integral nodes of a square grid or lattice that are spaced a unit distance from their immediate neighbors. Pick's theorem says that the area of such a polygon can be found simply by counting the lattice points on the interior and boundary of the polygon. The area is given by

$$i + (b/2) - 1,$$

where i is the number of interior lattice points and b is the number of boundary lattice points. The Austrian mathematician Georg Pick (1859–1942) after whom the result is named, was born in Vienna and perished during World War II in the Theresienstadt concentration camp. Over the past few decades, beginning with a paper by J. E. Reeve in 1957, various generalizations of Pick's theorem have been made to more general polygons, to higher-dimensional polyhedra, and to lattices other than square lattices. Most recently, mathematicians have become interested in the theorem because it provides a link between traditional Euclidean geometry and the modern subject of digital (discrete) geometry.

pico-

Prefix meaning a trillionth (10^{-12}), from the Italian *piccolo*, meaning "small."

pitch drop experiment

The world's longest running experiment. It started in 1927 when Thomas Parnell, the first professor of physics at the University of Queensland in Brisbane, Australia, heated a sample of pitch (a derivative of tar) and poured it into a glass funnel with a sealed stem. Three years were allowed for the pitch to settle, then, in 1930, the sealed stem was cut. From that date on the pitch has slowly dripped out of the funnel—so slowly that, up to the present time, only eight drops have fallen! The experiment

pitch drop experiment Professor John Mainstone alongside the world's longest-running experiment. *John Mainstone, University of Queensland*

stands in a display cabinet in the foyer of the Department of Physics at the University of Queensland demonstrating for all to see the fact that pitch, though it feels like a solid and is brittle enough to smash with a hammer, is really a fluid of very high viscosity (about 100 billion times as viscous as water).[91]

pizza

Order a pizza, pick an arbitrary point in it, and cut the pizza into eight slices by slicing at 45° angles through the chosen point. Color the alternate pieces red, with ketchup, and yellow, with mustard. Measure the area of the red slices and the yellow slices. Surprisingly, it will be found that these areas are the same! This fact holds true for any multiple of four slices cut by using equal angles through a fixed arbitrary point in the pizza. See also **tautology**.

place-value system

A **number system** in which the value of a number symbol depends not only on the symbol itself but also on the position where it occurs.

Planck time

In **quantum mechanics**, the shortest meaningful period of **time**; any two events that are separated by less than this amount of time can be considered simultaneous. It has the value 5.390×10^{-44} second. Related to this is the *Planck length* of 6.160×10^{-35} meters, which is the distance that light can travel in the Planck time.

plane

A flat surface such that a straight **line** joining any two points on it will also lie entirely on the surface.

plane partition

A stack of unit cubes in a rectangular box or in the positive **octant** in space such that to the left, behind, and below every cube lies either another cube or a wall. A plane partition in a box is equivalent to a **lozenge** tiling of a hexagon in the plane.

plastic number

A little-known number that has much in common with the **golden ratio** in that it is closely linked to architecture and to aesthetics. The concept of the plastic number was first described by the Dutchman Hans van der Laan (1904–1991) in 1928, shortly after he had abandoned his

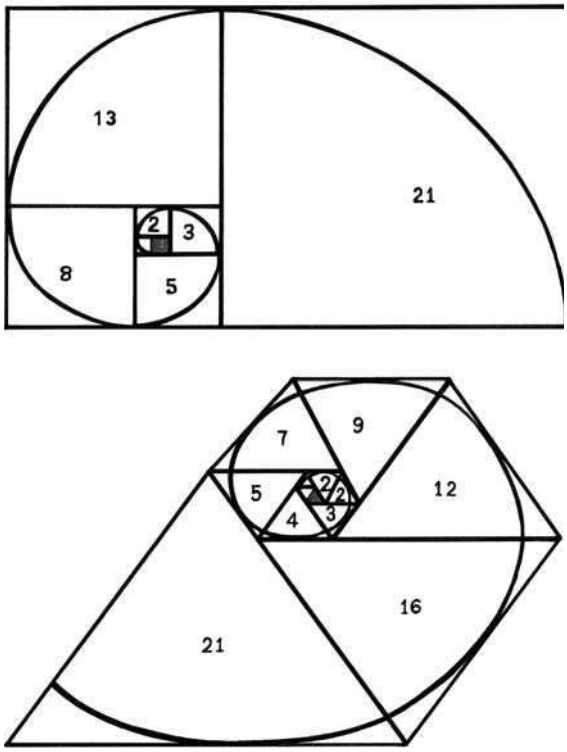

plastic number Spiraling systems illustrate the Fibonacci numbers (top) and the Padovan sequence.

architectural studies and become a novice monk, and has subsequently been explored by the English architect Richard Padovan (1935–). It is derived from a **cubic** equation, rather than a **quadratic** in the case of the golden ratio, and is intimately linked to two ratios, approximately 3:4 and 1:7, which van der Laan considered fundamental in the relationship between human perception and shape and form. These ratios, he believed, express the lower and upper limits of our normal ability to perceive differences of size among three-dimensional objects. The lower limit is that at which things differ just enough to be of distinct types of size. The upper limit is that beyond which they differ too much to relate to each other; they then belong to different orders of size. According to van der Laan, these limits are precisely definable. The mutual proportion of three-dimensional things first becomes perceptible when the largest dimension of one thing equals the sum of the two smaller dimensions of the other. This initial proportion determines, in turn, the limit beyond which things cease to have any perceptible mutual relation.

In mathematical terms, the plastic number is the unique **real number** solution to the equation $x^3 - x - 1 = 0$ and has the approximate value 1.324718 . . . . Just as the golden ratio is approximated better and better by successive terms of the **Fibonacci sequence**, $F(n + 1) = F(n) + F(n - 1)$, where $F(0) = F(1) = 1$, so the plastic number arises as the limit of the ratio of successive numbers in the sequence $P(n + 1) = P(n - 1) + P(n - 2)$ where $P(0) = P(1) = P(2) = 1$. This sequence has been called the *Padovan sequence,* and its members the *Padovan numbers.* The Padovan sequence increases much more slowly than does the Fibonacci sequence. Some numbers, such as 3, 5, and 21, are common to both sequences; however, it is not known if there are finitely many or infinitely many such pairs. Some Padovan numbers, such as 9, 16, and 49, are perfect squares; the square roots of these (3, 4, and 7) are also Padovan numbers, but it is not known if this is a coincidence or a general rule. Another way to generate the Padovan numbers is to mimic the use of squares for Fibonacci numbers, but with cuboid structures–boxes with rectangular faces. A kind of three-dimensional spiral of boxes emerges. Start with a cube of side 1 and place another adjacent to it: the result is a $1 \times 1 \times 2$ cuboid. On the 1×2 face, add another $1 \times 1 \times 2$ box to produce a $1 \times 2 \times 2$ cuboid. Then on a 2×2 face, add a $2 \times 2 \times 2$ cube to form a $2 \times 2 \times 3$ cuboid overall. To a 2×3 face, add a $2 \times 2 \times 3$ to get a $2 \times 3 \times 4$ box overall, and so on. Continue this process, always adding cuboids in the sequence east, south, down, west, north, and up. At each stage the new cuboid formed will have three consecutive Padovan numbers as its sides. Moreover, if successive square faces of the added cuboids are connected by straight lines, the result is a spiral that lies in a plane. The Padovan sequence is very similar to the **Perrin sequence**.[319]

Plateau, Joseph Antoine Ferdinand (1801–1883)

A Belgian physicist who did pioneering experimental work on soap bubbles and soap films, which stimulated the mathematical study of bubbles as **minimal surface**s. In 1829 Plateau carried out an optical experiment that involved looking at the Sun for 25 seconds: this damaged his eyes, and he eventually became blind.

Plateau curves

A set of curves, named after Joseph **Plateau**, that are described by the parametric equations:

$$x = a \sin(m + n)t \,/\, \sin(m - n)t$$
$$y = 2a \sin(mt) \sin(nt) \,/\, \sin(m - n)t$$

If $m = 2n$ the Plateau curves become a circle with a center at (1, 0) and a radius of 2.

Plateau problem

The general problem of determining the shape of the **minimal surface** constrained by a given boundary. It is named after Joseph **Plateau** who noticed that a handful of simple patterns seemed to completely describe the geometry of how soap **bubble**s fit together. Plateau claimed that soap bubble surfaces always make contact in one of two ways: either three surfaces meet at 120° angles along a curve; or six surfaces meet at a vertex, forming angles of about 109°. For instance, in a cluster of bubbles, two intersecting bubbles (of possibly different sizes) will have a common dividing wall (the third surface) that meets the outer surfaces of the bubbles in 120° angles. On the other hand, the edges of the six soap-film faces that emerge within a tetrahedral wire frame, when dipped in a soapy solution, form angles of roughly 109° at a central vertex. Until the American mathematician Jean Taylor came along in the mid-1970s, Plateau's patterns were just a set of empirical rules. However, as a follow-up to her doctoral thesis, Taylor was able to prove that Plateau's rules were a necessary consequence of the energy-minimizing principle–no other yet unobserved configurations were possible–thus settling a question that had been open for more than a century. The forces acting along the surface of a soap bubble all have the same magnitude in all directions. In crystals this is not the case (magnitudes of surface forces differ in different directions, though they may exhibit a grain, analogous to that in a piece of wood), but they still require the least energy to enclose a given volume. Minimal surfaces that model these conditions, like a cube with its corners chopped off or the bottom half of a cone

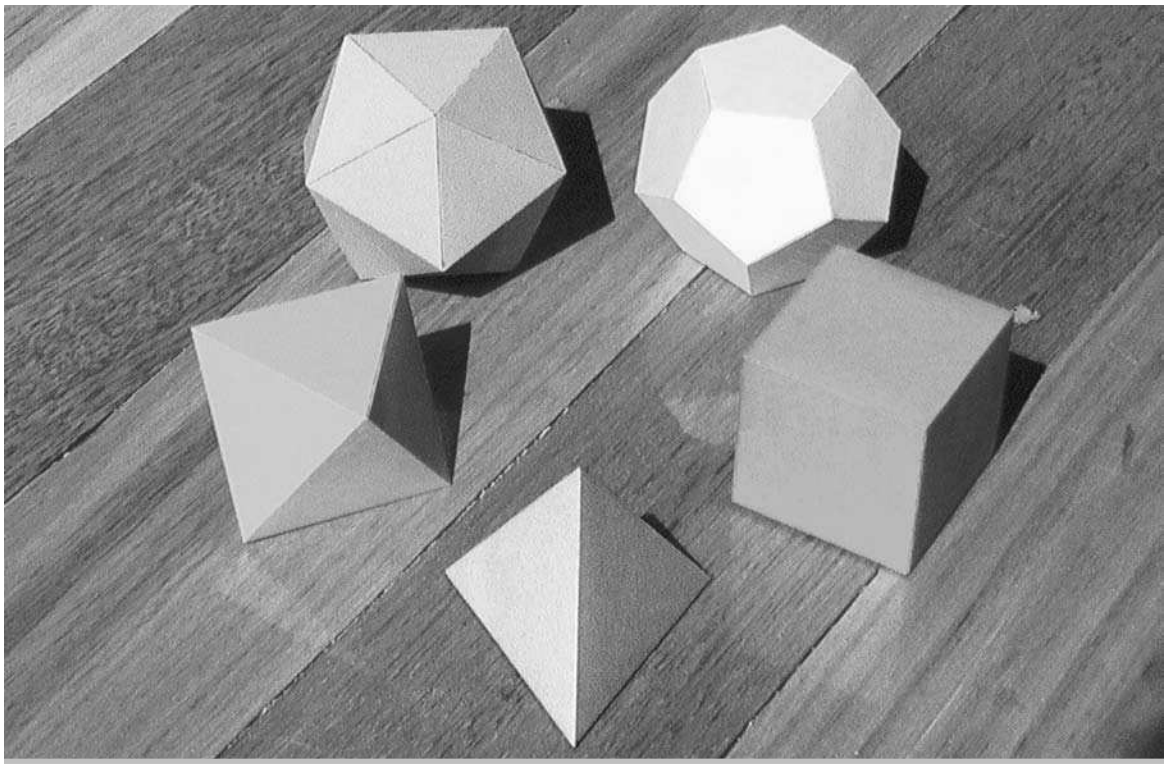

Platonic solid Clockwise from the extreme right: the cube, tetrahedron, octahedron, icosahedron, and dodecahedron. *Robert Webb, www.software3d.com; created using Webb's Stella program*

mounted on a cylinder, are known as *Wullf Shapes*, and provide fertile ground for mathematical study today.[328]

Platonic solid

Any of the five regular **polyhedron**s–solids with regular **polygon** faces and the same number of faces meeting at each corner–that are possible in three dimensions. They are the **tetrahedron** (a pyramid with triangular faces), the **octahedron** (an eight-sided figure with triangular faces), the **dodecahedron** (a 12-sided figure with pentagonal faces), the **icosahedron** (a 20-sided figure with triangular faces), and the **cube** (see table, "The Platonic Solids"). They are named after **Plato** who described them in one of his books, though it was **Euclid** who proved that there are only five regular polyhedra. A regular solid with hexagonal faces cannot exist because if it did, the sum of the angles of any three hexagonal corners that meet would already equal 360°, so such an object would be

The Platonic Solids

	Number of			
Name	**Faces**	**Edges**	**Vertices**	**Schläfi Symbol**
Tetrahedron	4	6	4	{3,3}
Cube	6	12	8	{4,3}
Octagon	8	12	6	{3,4}
Dodecahedron	12	30	20	{5,3}
Icosahedron	20	30	12	{3,5}

planar. See also **Archimedean solid**, **Catalan solid**, and **Johnson solid**.

Platonism
The belief that mathematical objects exist independent of physical models. It is, at the very least, a useful pretense in mathematics, especially in **geometry**.

pleated surface
A surface in **Euclidean space** or hyperbolic space (see **hyperbolic geometry**) that resembles a **polyhedron** in the sense that it has flat faces that meet along edges. Unlike a polyhedron, a pleated surface has no corners, but it may have infinitely many edges that form a **lamination**.

Poggendorff illusion
A **distortion illusion** in which the two ends of a straight line passing behind a rectangle appear offset when, in fact, they are aligned. It was discovered in 1860 by the physicist J. C. Poggendorff, editor of *Annalen der Physik und Chemie* (Annals of physics and chemistry), after receiving a letter from the astronomer Friedrich Zöllner. In this letter, Zöllner described an illusion (see **Zöllner illusion**) he had noticed on a fabric design in which parallel lines intersected by a pattern of short diagonal lines appear to diverge.[134]

Poincaré, (Jules) Henri (1854–1912)
A French theoretical physicist and mathematician who almost discovered **relativity theory** before Einstein and who is most famous in mathematics because of his hypothesis known as the **Poincaré conjecture**. Poincaré, who taught for most of his life at the University of Paris, was sometimes referred to as "the last universalist," because of his huge published output on a wide variety of mathematics and mathematical physics. Strangely, he was also clumsy, absent-minded, and inept at simple

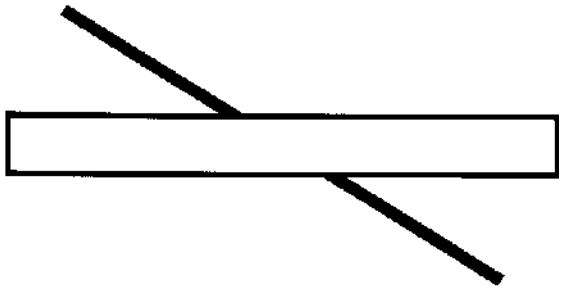

Poggendorff illusion

arithmetic. In order to translate problems in **topology** into questions in **algebra**, he devised (or discovered) ***homotopy*** *groups*–quantities that capture the essence of multidimensional spaces in algebraic terms, and have the power to reveal similarities between them.

Poincaré conjecture
A proposition in **topology** put forward by Henri **Poincaré** in 1904. Poincaré was led to make his conjecture during his pioneering work in topology, the mathematical study of the properties of objects that stay unchanged when the objects are stretched or bent. In loose terms, the conjecture is that every three-dimensional object that has a set of spherelike properties (i.e., is topologically equivalent to a sphere) can be stretched or squeezed until it is a three-dimensional sphere (a 3-sphere) without tearing (i.e., making a hole in) it. Strictly speaking, the conjecture says that every **closed**, **simply connected** three-**manifold** is **homeomorphic** to the 3-sphere.

Poincaré proved the two-dimensional case and he guessed that the principle would hold in three dimensions. Determining if the Poincaré conjecture is correct has been widely judged the most important outstanding problem in topology–so important that, in 2000, the Clay Mathematics Institute in Boston named it as one of seven Millennium Prize Problems and offered a $1 million prize for its solution. Since the 1960s, mathematicians have shown by various means that the generalized conjecture is true for all dimensions higher than three–the four-dimensional case finally falling in 1982. But none of these strategies work in three dimensions. On April 7, 2002, came reports that the Poincaré conjecture might have been proved by Martin Dunwoody of Southampton University, but within a few days a fatal flaw was found in his proof. Then, in April 2003, what appears to be a genuine breakthrough emerged during a series of lectures delivered at the Massachusetts Institute of Technology by the Russian mathematician Grigori Perelman of the Steklov Institute of Mathematics (part of the Russian Academy of Sciences in St. Petersburg). His lectures, entitled "Ricci Flow and Geometrization of Three-Manifolds," constituted Perelman's first public discussion of important results contained in two earlier preprints. Mathematicians will now scrutinize the validity of Perelman's work (which does not actually mention the Poincaré conjecture by name). In any event, the Clay Institute requires a two-year cooling-off period before the prize can be awarded.

Poincaré disk
The region inside (but not including) a bounding circle, where straight lines are defined to be either diameters of the bounding circle, or arcs of circles that are perpendicular to the bounding circle. The Poincaré disk is a model

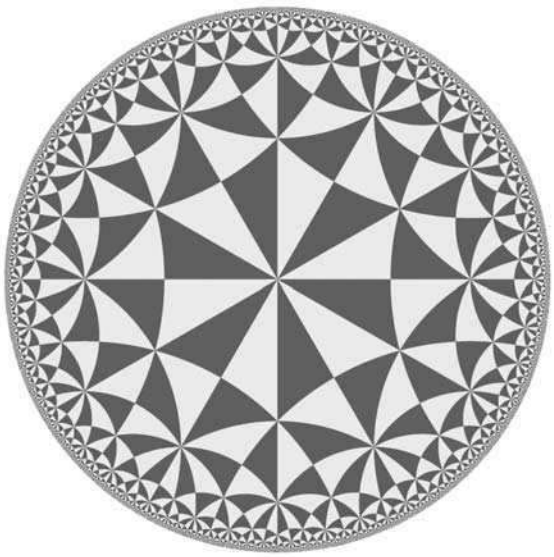

Poincaré disk A pattern on a hyperbolic surface. *Jos Leys, www.josleys.com*

of **hyperbolic geometry**. The great flexibility it allows in specifying the angles of a triangle leads to an infinite variety of ways in which the disk can be tiled.

Poinsot, Louis (1777–1859)

A French mathematician who invented *geometrical mechanics* while investigating how a system of forces acting on a rigid body can be resolved into a single force and a couple (a pair of equal and oppositely directed forces, as when you try to unscrew a bottle cap). Together with Gaspard **Monge**, he helped geometry regain its leading role in mathematical research in France in the eighteenth century. He wrote an important work on polyhedra in 1809, discovering four new regular polyhedra, which are now known as the **Kepler-Poinsot solids**. Two of these had been found by Johannes **Kepler** in 1619 but Poinsot was unaware of this; the two additional ones that Poinsot discovered were the *great dodecahedron* and the *great icosahedron*. In 1810 Augustin **Cauchy** proved that, with this definition of regular, the enumeration of regular polyhedra is complete (although a mistake was discovered in Poinsot's, and hence Cauchy's, definition in 1990 when an internal inconsistency became apparent). Poinsot also worked in number theory, studying **Diophantine equation**s with a view to expressing numbers as the difference of two squares and primitive roots.

point

A dimensionless geometric object having no properties other than location or place. More generally, an element in a geometrically described **set**.

point-set topology

Also known as *general topology,* a branch of **topology** concerned with how to put a structure on a **set** in such a way as to generalize the idea of **continuity** for maps from the real numbers to itself. A topology on a set X is a certain set of *open subsets* of the set X which satisfy various axioms. The set X together with this topology is called a **topological space**.

Poisson, Siméon Denis (1781–1840)

A French mathematician whose main interest lay in the application of mathematics to physics, especially in electrostatics and magnetism. He developed a two-fluid theory of electricity and provided theoretical support for the experimental results of others, notably Charles de Coulomb. Poisson also made important contributions to mechanics, especially the theory of elasticity; optics; calculus, especially definite integrals; differential geometry; and probability theory. In all, he wrote more than 300 papers on mathematics, physics, and astronomy, and his *Traité de Mécanique* (1811) was long a standard work.

polar coordinates

A **coordinate** system in which distances are measured from a fixed reference point (the pole) and angles from a fixed reference line. A *polar equation* is one that uses polar coordinates.

pole

(1) The **origin** of a system of **polar coordinates**. (2) In **complex analysis**, a function of a certain simple type of **singularity**. (3) One of the two points, where the axis of rotation of a rotating body, such as Earth, passes through the surface. (4) An old unit of length, also called a *rod*, equal to 5.5 yards.

Pólya's conjecture

A hypothesis put forward by the Hungarian mathematician George Pólya (1887–1985) in 1919. A positive integer is said to be of *even type* if it factorizes into an even number of **prime number**s; otherwise it is said to be of *odd type*. For example, $4, = 2 \times 2$, is of even type, whereas $18, = 2 \times 3 \times 3$, is of odd type. Let $O(n)$ be the number of odd type and $E(n)$ be the number of even type integers in the first n integers. Pólya's conjecture says that $O(n) \geq E(n)$ for all $n \geq 2$. After the conjecture had been checked for all values of n up to 1 million, many mathematicians assumed it was

probably true. However, in 1942 A. E. Ingham came up with an ingenious method to show how a counterexample could be constructed, even though there wasn't enough computing power around at the time to do the necessary calculations.[177] Twenty years later, R. S. Lehman ran Ingham's method on a computer to find a counterexample to Pólya's conjecture at $n = 906180359$.[199]

polychoron

An unofficial name (from the Greek *poly* meaning "many" and *choros* meaning "room" or "space") for a four-dimensional **polytope**; it was first advocated by George Olshevsky.

polycube

A **polyhedron** formed by joining unit cubes by their faces. Examples of puzzles that involve polycubes are the **Soma cube** and **Rubik's cube**.

polygon

A plane closed figure whose sides are straight lines. The term *polygon* (from the Greek *poly* for "many" and *gwnos* for "angle") sometimes also refers to the *interior* of the polygon (the open area that this path encloses) or to the **union** of both. A polygon is *simple* if it is described by a single, nonintersecting boundary; otherwise it is said to be *complex*. A simple polygon is called *convex* if it has no internal angles greater than 180°; otherwise it is called *concave*. A polygon is called *regular* if all its sides are of equal length and all its angles are equal (see table, "Regular Polygons"). Any polygon, regular or irregular, has as many angles as it has sides. See **constructible** (for constructible polygons).

Regular Polygons

Name	Sides	Angle (= 180°–360°/sides)
Equilateral **triangle**	3	60°
Square	4	90°
Regular **penta**gon	5	108°
Regular **hexa**gon	6	120°
Regular heptagon	7	128.57° (approx.)
Regular **octa**gon	8	135°
Regular nonagon	9	140°
Regular **decagon**	10	144°
Regular hectagon	100	176.4°
Regular megagon	10^6	179.99964°
Regular **googol**gon	10^{100}	180° (approx.)

polygonal number

The number of equally spaced dots needed to draw a **polygon**. Polygonal numbers, which are a type of **figurate number**, include square numbers, triangular numbers, and hexagonal numbers.

polyhedron

A three-dimensional object whose faces are all **polygon**s and whose edges are shared by exactly two polygons. *Polyhedron* comes from the Greek *poly* for "many" and *-hedron* meaning "base," "seat," or "face." Every polyhedron in three-dimensional space consists of (two-dimensional) faces, (one-dimensional) edges, and (zero-dimensional) vertices. Sometimes the term *polyhedron* is used to apply to figures in more than three dimensions; however, analogs of polyhedra in the **fourth dimension** or higher are also referred to as **polytope**s. Polyhedrons, like polygons, may be *convex* or *nonconvex*. If a line that connects any two points on the surface of a polyhedron is completely inside or on the polyhedron, the figure is convex. Otherwise, it is nonconvex or *concave*. A polygon is *regular* if all of its faces are exactly the same size and shape and if the same number of faces meet at each vertex. There are only five regular convex polyhedra–the **Platonic solid**s. Another four regular nonconvex polyhedra are called **Kepler-Poinsot solid**s. However, the term *regular polyhedra* is sometimes used to describe only the Platonic solids. A convex polyhedron is said to be *semi-regular* if its faces have a similar arrangement of nonintersecting regular plane convex polygons of two or more different types about each vertex. These solids, of which there are 13 different kinds, are commonly called the **Archimedean solids**. A *dual* of a polyhedron is another polyhedron in which faces and vertices occupy complementary locations. The duals of the Archimedean solids are known as the **Catalan solid**s. A **quasi-regular polyhedron** is the solid region interior to two dual regular polyhedra; only two exist: the cuboctahedron and the icoidodecahedron. There are also infinite families of **prism**s and **antiprism**s. In total there are 92 convex polyhedra with regular polygonal faces (and not necessarily equivalent vertices); these are the **Johnson solids**.

The oldest known examples of man-made polyhedra were found on the islands of northeastern Scotland and date back to Neolithic times, between 2000 and 3000 B.C. These stone figures are about 2 inches in diameter and many are carved into rounded forms of regular polyhedra. Examples including cubical, tetrahedral, octahedral, and dodecahedral forms, one which is the dual of the pentagonal prism, are on display in the Museum of Scotland and in Oxford's Ashmolean Museum.

polyiamond

A shape made from identical equilateral **triangle**s that have been joined at their edges.

polynomial

An expression in which whole-numbered powers of a variable multiplied by numerical coefficients are added together. The powers of the variable must be positive integers, or zero. An example of a polynomial is $3x^3 + 7x - 2$. A polynomial *equation* has a polynomial expression, or zero, on each side of the equal sign: for example, $4a^2 - 5.6a + 1.7 = 0$ or $5x^2 - 1 = 8x + 2x^4$. The type of polynomial expression or equation is determined by the highest power present of the variable. A **quadratic**, for example, has nothing higher than a squared term. **Cubic**s, **quartic**s, and **quintic**s have maximum powers of three, four, and five, respectively. Mathematicians who have done pioneering work on each of these higher types of polynomial equations tended, for some reason, to have had colorful and star-crossed lives. Niccolo **Tartaglia**, who first solved the cubic, failed miserably as a mathematician for the rest of his life, largely because he spent it trying to discredit Girolamo **Cardano**. Tartaglia told Cardano his method of solution and swore him to secrecy but Cardano went ahead and published the solution anyway. Cardono himself lived a long unhappy life and his only son was executed for murder. Lodovico Ferrara, Cardano's student, who solved the general quartic, was poisoned, probably by his sister, over an inheritance dispute. Finally, Evariste **Galois**, who showed that the general quintic was unsolvable, died in a duel at the age of 20.

polyomino

A two-dimensional shape made by connecting n squares of the same size along their edges. The polyomino is a generalization of the **domino**, which can be thought of as a polyomino with $n = 2$. Several puzzles involving polyominoes made from three or more squares stuck together became popular around the beginning of the twentieth century. The best-known of these is the Broken Chessboard, presented as problem no. 74 in Henry **Dudeney**'s book *The Canterbury Puzzles* (1907).[87] Dudeney gives an amusing introduction to the problem, first quoting from Hayward's *Life of William the Conqueror* (1613) about an incident in which Prince Henry,

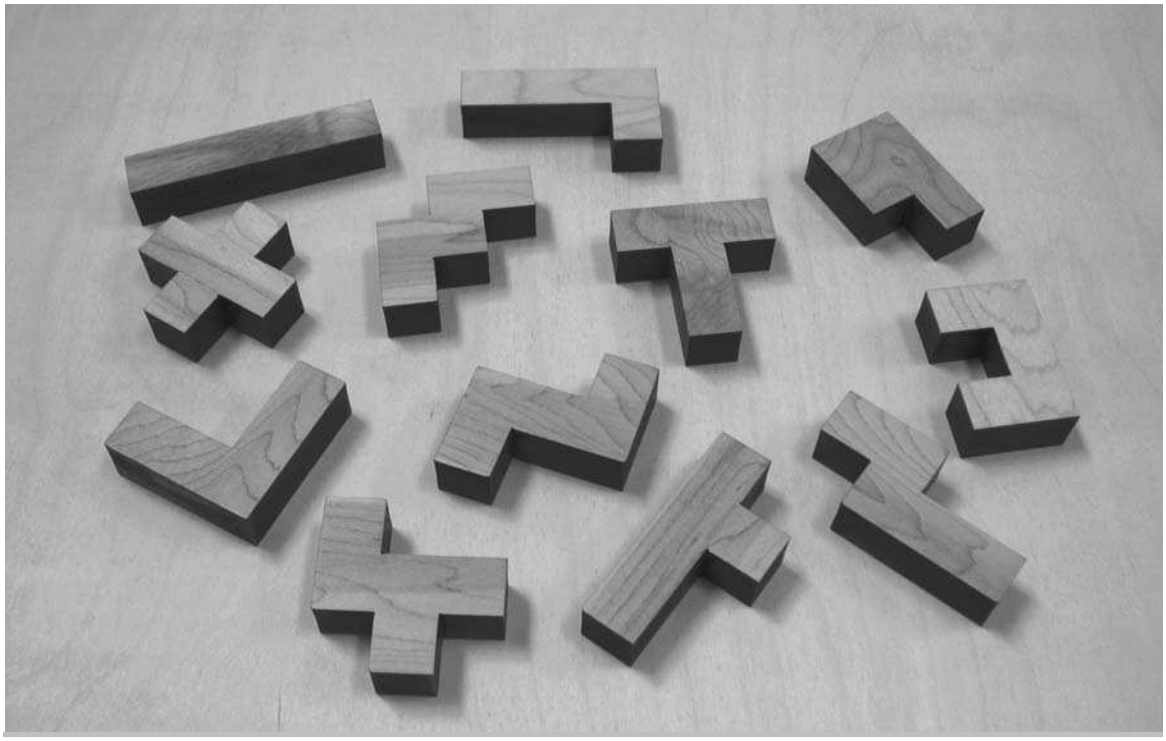

polyomino A complete set of 12 solid pentominos, also known as planar pentacubes. *Kadon Enterprises, Inc., www.gamepuzzles.com*

one of William's sons, smashes a chessboard over the head of his brother, Prince Robert, and then adding his own mathematical appendix. By a curious quirk, Dudeney reveals, the board breaks into 13 pieces, 12 of which are the different possible ways in which five squares can be arranged and one square 2×2 piece. The puzzle is to reconstitute the board from these fragments. This is the earliest example of a mathematical recreation that involves pentominoes, a name that wasn't coined until 1953 when Solomon **Golomb** first used it in a talk to the Harvard Math Club. Golomb not only invented the nomenclature for polyominoes but did much of the pioneering research on them; his work was brought to a wide audience and popularized by Martin **Gardner** in his *Scientific American* column, beginning in 1957.[114, 136, 137]

Golomb was particularly interested in the pentomino, for a reason that becomes clear (see table, "Types of Polyomino"). The familiar domino comes in just one configuration as, obviously, does the trivial monomino. A triomino can have two different shapes–three squares in a line or in an L shape. The tetromino (or tetramino) has five distinct arrangements and is used in the popular video game **Tetris**. Thus for $n \leq 4$ the number of distinct pieces is ≤ 5, which restricts the variety of combinations possible. On the other hand, for $n > 5$, the number of different pieces is large, making analysis of problems difficult and games based on such polyominoes difficult and unwieldy. However, pentominoes, for which $n = 5$, come in 12 unique configurations, which is just about an ideal balance between tractability and combinatorial richness, hence the high level of interest in this particular type of polyomino. The problem of tiling an 8×8 chessboard with a square hole in the center using pentominoes was first solved in 1935 and found, by computer in 1958, to have exactly 65 solutions. Another standard pentomino puzzle is to arrange the set of 12 possible shapes into rectangles without holes: 3×20, 4×15, 5×12, and 6×10. Pentominoes are prominently featured in a subplot of the novel *Imperial Earth* by Arthur C. Clarke.

Hexominoes and heptominoes come in 35 and 108 unique arrangements, respectively. One of the 108 heptomino configurations, however, has a hole–a region that is not tiled with squares but that is unconnected to the exterior of the polyomino–and may or may not be counted as a valid piece depending on the rules of a particular game. All polyominoes made of seven or more squares may contain holes. There is no known algorithm or formula for calculating how many distinct polyominoes of each order there are.

Related to polyominoes are **polyiamond**s (formed from equilateral triangles) and polyhexes (formed from regular hexagons). The three-dimensional analog of polyominoes uses cubes instead of squares; an example is the **Soma cube**.

Types of Polyomino

Name	Number of Unit Squares	Number of Distinct Configurations
Monomino	1	1
Domino	2	1
Triomino	3	2
Tetromino	4	5
Pentomino	5	12
Hexomino	6	35
Heptomino	7	108

polytope

A higher-dimensional analogue of a **polygon** or **polyhedron**. The number of possible regular polytopes depends on the number of dimensions. In two dimensions there

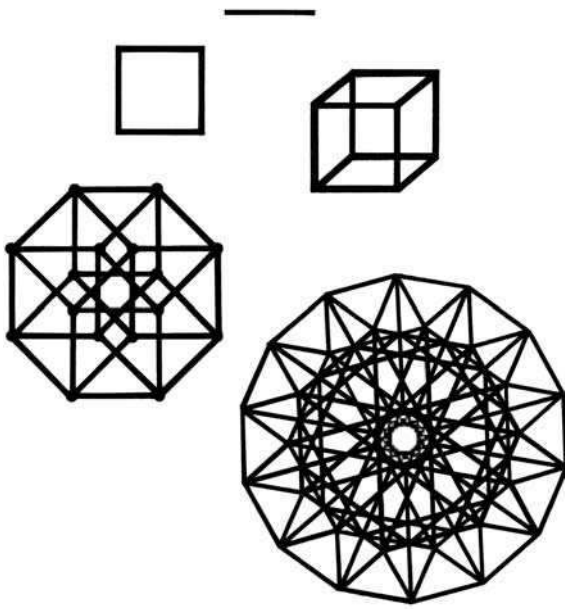

polytope In descending order: a straight line, a square, a cube, a tesseract (four-dimensional cube), and a regular, multidimensional polytope.

are infinitely many possible regular polygons; in three dimensions there are five possible regular polyhedra; in four dimensions there are six possible regular polytopes; and in each number of dimensions higher than four, there are just three possible regular polytopes, analogous to the three-dimensional tetrahedron, cube, and octahedron. A four-dimensional polytope is also sometimes called a *polyhedroid* or a *polychoron*. Just as a polygon has vertices and edges, and a polyhedron has vertices, edges, and faces, a four-dimensional polytope has vertices, edges, faces, and cells, where a cell is a three-dimensional figure.[75] See also **Boole (Stott), Alicia**.

Poncelet, Jean Victor (1788–1867)

A French mathematician who substantially advanced **projective geometry**. With Brianchon, he proved *Feuerbach's theorem* on the **nine-point circle** in 1820–1821, and also suggested the theorem proved by Jakob **Steiner** and now called the *Poncelot-Steiner theorem* that Euclidean constructions (see **constructible**) can be done with a straightedge alone. As a soldier in Napoleon's army, he was captured and imprisoned in Russia. While in prison from 1813–1814, he organized and wrote down his discoveries, and the result was published as *Traité des Propriétés Projectives des Figures* (Treatise on the properties of the projections of shapes, 1822). To serve as an introduction to this work, he also wrote *Applications D'analyse et de Géométrie* (Applications of analysis and geometry, 2 vols., 1862–1864).

Poncelet's theorem

Given an **ellipse**, and a smaller ellipse entirely inside it, start at a point on the outer ellipse, and, moving clockwise, follow a line that is **tangent** to the inner ellipse until you hit the outer ellipse again. Repeat this over and over again. It may be that this path will never hit the same points on the outer ellipse twice. However, if it *does* close up in a certain number of steps, then something amazing is true: *all* such paths, starting at *any point* on the outer ellipse, close up in the same number of steps. This fact is Poncelet's theorem, also known as *Poncelet's closure theorem,* and is named after the Jean **Poncelet**.

Pony Puzzle

One of Sam **Loyd**'s best known and commercially successful puzzles. It consists of just six pieces of the silhouette of a horse that have to be assembled in the most sensible way. Loyd got the idea for the puzzle from the governor of Philadelphia, Andrew Curtin, when the two were on a steamer returning from Europe and talking about the White Horse of Uffington–a famous chalk figure carved on a hillside in Berkshire, England.

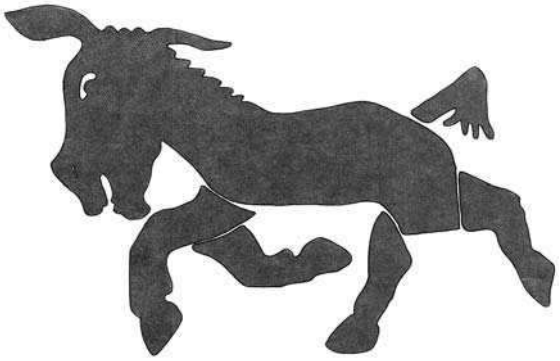

Pony Puzzle One of Sam Loyd's best known brain-teasers.

postage stamp problems

Mathematical puzzles that involve postage stamps have been around almost as long as postage stamps themselves, the first of which, the Penny Black, was issued by Great Britain on May 6, 1840. Some such puzzles ask what postage amounts can or can't be made with stamps of certain values. Others are based on the ways that a block of stamps can be folded or torn along the perforations.

PUZZLE

One of this type appears as problem no. 285 in Henry **Dudeney**'s *Amusements in Mathematics* (1917).[88] It starts by saying you have just bought 12 stamps in a rectangular block of three rows with four stamps in each. (In Dudeney's diagram, they are labeled 1, 2, 3, 4 across the top row, and so on.) He goes on: "[A] friend asks you to oblige him with four stamps, all joined together—no stamp hanging on by a mere corner. In how many different ways is it possible for you to tear off those four stamps? You see, you can give him 1, 2, 3, 4, or 2, 3, 6, 7, . . . , and so on. Can you count the number of different ways in which those four stamps might be delivered?" This can be thought of as a problem involving tetrominoes, which are a type of **polyomino**.

Solutions begin on page 369.

The postage stamp problem, also known as the *Frobenius problem,* is a long-standing challenge in **number theory** and in **computer science**. Suppose a country issues n different denominations of stamps but allows no more than m stamps to be put on a single letter. The postage stamp problem is to write and implement an algorithm (a stepwise set of rules) that, for any given values of m and

n, computes the greatest consecutive range of postage values, from one on up, and all possible sets of denominations that realize that range. For example, for $n = 4$ and $m = 5$, the stamps with values (1, 4, 12, 21) allow the postage values 1 through 71. If the values of the stamps are constant and not part of the input, algorithms can be, and have been, devised that give a short-cut solution. However, in the general case where the number of stamp values *is* part of the input, the postage stamp problem has been shown to be an **NP-hard problem**, and thus not susceptible to an efficient algorithmic approach.

potato paradox

Fred brings home 100 pounds of potatoes, which (being purely mathematical potatoes) consist of 99 percent water. He then leaves them outside overnight so that they consist of 98 percent water. What is their new weight? The surprising answer is 50 pounds!

potential theory

The study of *harmonic functions.* These functions satisfy **Laplace**'s equation, a certain type of **partial differential equation** that commonly arises in physics in problems to do with gravity and electromagnetism.

power

A word that is almost never used in its correct, original sense any more. Strictly speaking, if we write $8 = 2^3$, then 2 is the **base**, 3 is the **exponent**, and 8 is the power. But almost everyone, including most mathematicians, would say that 3 is the power, and that "power" and "exponent" mean the same thing. The misuse has probably come about from a misunderstanding of statements such "eight is the third power of two."

power law

A type of mathematical pattern in which the frequency of an occurrence of a given size is inversely **proportional** to some **power** (or exponent) of its size. For example, in the case of avalanches or earthquakes, large ones are fairly rare, smaller ones are much more frequent, and in between are cascades of different sizes and frequencies. Power laws define the distribution of catastrophic events in self-organized critical systems (see **self-organization**).

power series

An infinite sum of the form

$$a_0 + a_1x + a_2x^2 + a_3x^3 + \ldots,$$

where a is a number of any type and x is the variable. Power series are commonly used to define **function**s. For example, the **sine** function can be written

$$\sin x = x - x^3/3! + x^5/5! - x^7/7! + \ldots,$$

where "!" stands for **factorial**. Although the series has infinitely many terms, these get small so quickly that only the first few terms make much of a contribution.

power set

The **set** of all **subsets** of a given set, including the **empty set** and the original set. For example, if the original set is {*a, b,* c} then the power set is {{∅, {*a*}, {*b*}, {*c*}, {*a, b*}, {*a, c*}, {*b, c*}, {*a, b,* c}}.

power tower

A way of representing very large numbers in terms of stacks of **exponent**s. For example:

$$10^{3^{3^3}} = 10^{3^{27}} = 10^{3^{2541865828329}} = \text{enormous}$$

In general, and especially if the number at the top of the tower is fairly large, adding another exponent to the bottom of a tower will make the value of the tower much larger than will increasing the size of the bottom exponent. This leads to the (somewhat counterintuitive) result that to know which of two towers is the larger, you can look at how many exponents are in the tower and know right away which is larger. For example:

$$1.1^{1.1^{1.1^{1,000}}} \text{ is much larger than } 1{,}000^{1{,}000^{1{,}000}}$$

In the case of an infinite power tower of the form

$$x^{x^{x^{\cdots}}},$$

the maximum value that x can take and still cause the tower to converge to a finite value is $e^{(1/e)} = 1.444667\ldots$. The minimum value of x that will produce convergence is $1/e^e = 0.065988\ldots$.

powerful number

Also known as a *squarefull number,* a positive whole number n such that for every **prime number** p dividing n, p^2 also divides n. Every powerful number can be written as a^2b^3, where a and b are positive integers. The first few powerful numbers are 1, 4, 8, 9, 16, 25, 27, 32, 36, 49, 64, 72, 81, 100, and 108. Pairs of consecutive powerful numbers exist, such as (8,9), (288,289), and (675,676). However, no three consecutive powerful numbers are known and, in 1978, Paul **Erdös** conjectured that none exist.

practical number

A number n such that every positive integer less than n is either a divisor or a sum of distinct divisors of n. The first few practical numbers are 1, 2, 4, 6, 8, 12, 16, 18, 20, and 24. All **perfect number**s are practical.

prime number

> *[U]pon looking at prime numbers one has the feeling of being in the presence of one of the inexplicable secrets of creation.*
>
> –Don Zagier

An **integer** greater than 1 that is divisible only by 1 and itself. Prime numbers have fascinated mathematicians for centuries, in large part because of how they are distributed. At first sight, their occurrence looks random; yet, on closer inspection, they reveal a subtle order or pattern, that seems to hold deep truths about the nature of mathematics and of the world in which we live. The German-born American mathematician Don Zagier (1951–), in his inaugural lecture at Bonn University, put it this way:

> There are two facts about the distribution of prime numbers which I hope to convince you. . . . The first is that despite their simple definition and role as the building blocks of the natural numbers, the prime numbers . . . grow like weeds among the natural numbers, seeming to obey no other law than that of chance, and nobody can predict where the next one will sprout. The second fact is even more astonishing, for it states just the opposite: that the prime numbers exhibit stunning regularity, that there are laws governing their behavior, and that they obey these laws with almost military precision.

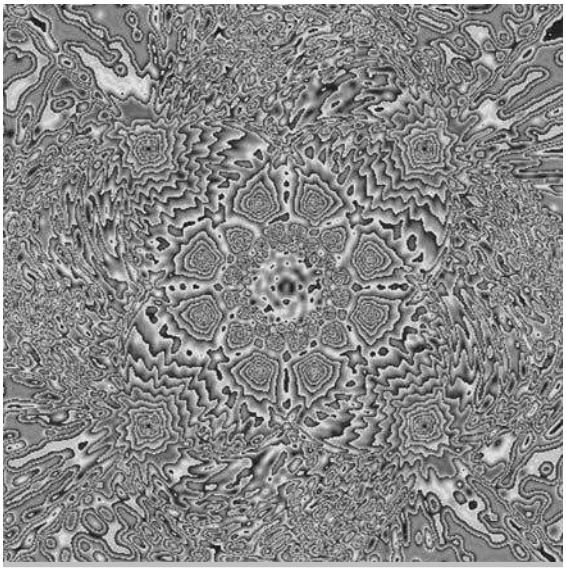

prime number A remarkable pattern generated by the distribution of the first few billion primes. *Jean-Francois Colonna/Ecole Polytechnique*

The prime numbers are 2, 3, 5, 7, 11, 13, 17, 19, 23, 29, 31, 37, 41, 43, 47, 53, 59, ... The *fundamental theorem of arithmetic* declares that the primes are the building blocks of the positive integers: every positive integer is a product of prime numbers in one and only one way, except for the order of the factors. This is the key to their importance: the prime factors of an integer determine its properties. The ancient Greeks proved (c. 300 B.C.) that there are infinitely many primes and that they are irregularly spaced; in fact, there can be arbitrarily large gaps between successive primes. On the other hand, in the nineteenth century it was shown that the number of primes less than or equal to n approaches $n/\log n$, as n gets very large (a result known as the *prime number theorem*), so that a rough estimate for the nth prime is $n \log n$. In his *Disquisitiones Arithmeticae* (1801), Carl **Gauss** wrote: "The problem of distinguishing prime numbers from composite numbers and of resolving the latter into their prime factors is known to be one of the most important and useful in arithmetic. It has engaged the industry and wisdom of ancient and modern geometers to such an extent that it would be superfluous to discuss the problem at length. . . . Further, the dignity of the science itself seems to require that every possible means be explored for the solution of a problem so elegant and so celebrated." The earliest known primality test is the **sieve of Eratosthenes**, which dates from around 240 B.C. However, high-speed computers and fast algorithms are needed to identify large primes. New record-breaking primes tend to be of the variety known as **Mersenne primes**, since these are the easiest to find. About 6,000 prime numbers are known of which the largest is $2^{20996011} - 1$.

Much remains unknown about the primes. As Martin **Gardner** said:[113] "No branch of **number theory** is more saturated with mystery. . . . Some problems concerning primes are so simple that a child can understand them and yet so deep and far from solved that many mathematicians now suspect they have no solution. Perhaps they are 'undecideable.' Perhaps number theory, like quantum mechanics, has its own uncertainty principle that makes it necessary, in certain areas, to abandon exactness for probabilistic formulations." One of the greatest unsolved problems in mathematics is the **Riemann hypothesis** concerning the distribution of prime numbers. See also **Goldbach's conjecture**, **twin primes**, **Ulam spiral**, and **Ishango bone**.

primitive root

A primitive root for a **prime number** p is one whose powers generate all the nonzero integers **modulo** (or mod) p. For example, 3 is a primitive root modulo 7 since $3 = 3^1$, $2 = 3^2 \bmod 7$, $6 = 3^3 \bmod 7$, $4 = 3^4 \bmod 7$, $5 = 3^5 \bmod 7$, $1 = 3^6 \bmod 7$.

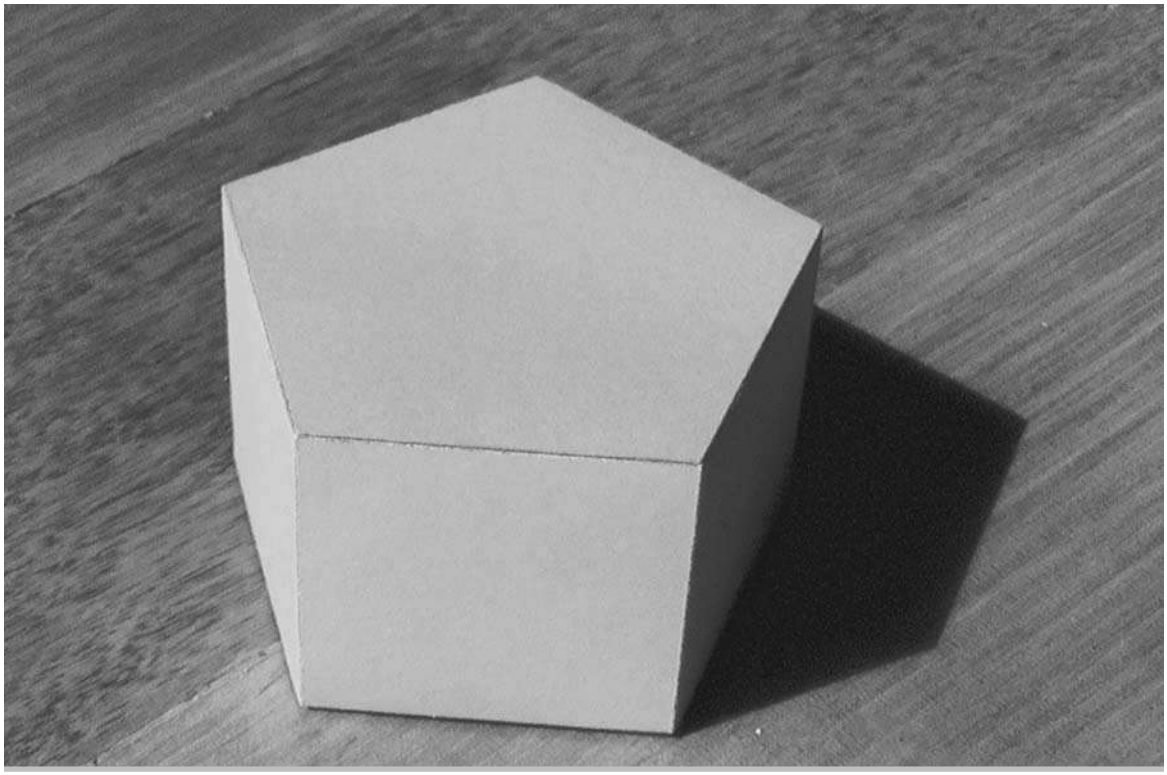

prism A pentagonal prism. *Robert Webb, www.software3d.com; created using Webb's Stella program*

primitive root of unity
The **complex number** z such that $z^n = 1$ but z^k is not equal to 1 for any positive integer k less than n.

primorial
Also known as a *prime factorial*, the product of all **prime number**s that are less than or equal to a given prime p; it is denoted $p\#$. For example $3\# = 2 \times 3 = 6$, $5\# = 2 \times 3 \times 5 = 30$, and $13\# = 2 \times 3 \times 5 \times 7 \times 11 \times 13 = 30{,}030$.

Prince Rupert's problem
The problem of pushing a **cube** through a hole in another cube of equal or less size; it is named after Prince Rupert (1619–1682), a nephew of England's King Charles I, who won a wager that a hole could be made in one of two equal cubes large enough for the other cube to slide through. The mathematics of cubes passing through cubes was considered by John **Wallis**. Later, in 1816, a solution was published posthumously by the Dutch mathematician Pieter Nieuwland (1764–1794) to the question: What is the largest cube that can be passed through a unit cube (a cube of which each side is one unit long)? Nieuwland answered this by finding the largest square that fits inside a unit cube. When viewed from directly above one apex, a unit cube has the outline of a regular hexagon of side $\sqrt{3}/\sqrt{2}$. The largest square that will go into a cube has a face that can be inscribed within this hexagon; the length of its edge is $\sqrt{6} - \sqrt{2} = 1.03527618$.

prism
A **semi-regular polyhedron** constructed from two **congruent** *n-sided* **polygons** and n **parallelogram**s. The word comes from the Greek *prizma*, which relates to cutting or sawing. A *prismoid* resembles a prism but has bases that are **similar** rather than congruent, and sides that are **trapezoids** rather than parallelograms. An example of a prismoid is the **frustum** of a **pyramid**. A *prismatoid* is a polyhedron with all its vertices lying in two parallel planes.

prisoner's dilemma
A problem in **game theory** first described by the Canadian-born Princeton mathematician Albert Tucker (1905–1995) in 1950, while addressing an audience of psychologists at Stanford University, where he was a visiting professor. It runs along these lines: Al and Bob have been arrested for holding up the Anyapolis State Bank

and have been put in separate cells. Each cares a lot more about his personal freedom than he does about his accomplice's welfare. A clever prosecutor makes the following offer to each. "You may choose to confess or remain silent. If you confess and your accomplice remains silent, I'll drop all charges against you and use your testimony to ensure that your accomplice does serious time. Likewise, if your accomplice confesses while you remain silent, he'll go free while you do the time. If you both confess I get two convictions, but I'll see to it that you both get early parole. If you both remain silent, I'll have to settle for token sentences on firearms possession charges. If you wish to confess, you must leave a note with the jailer before I come back tomorrow morning." The dilemma faced by the prisoners is that, whatever the other does, each is better off confessing than remaining silent. But the outcome when both confess is worse for each than the outcome if both stay silent!

Tucker's paradox was based on puzzles with a similar structure that had been devised in 1950 by Merrill Flood and Melvin Dresher as part of the Rand Corporation's investigations into game theory (which Rand pursued because of possible applications to global nuclear strategy). Flood and Dresher hadn't published much about their work, but the prisoner's dilemma attracted an enormous amount of attention in subjects as diverse philosophy, biology, sociology, political science, and economics, as well as game theory itself. A common view is that the puzzle illustrates a conflict between individual and group rationality. A group whose members pursue rational self-interest may all end up worse off than a group whose members act contrary to rational self-interest. More generally, if the payoffs aren't assumed to represent self-interest, a group whose members rationally pursue any goals may all meet less success than if they hadn't rationally pursued their goals individually.

probability

A measure of how likely it is that some event will occur, given as a number between 0 (impossible) and 1 (certain). Usually, probability is expressed as a ratio: the number of experimental results that would produce the event divided by the number of experimental results considered possible. For example, the probability of drawing the five of hearts from an ordinary deck of cards is one in fifty-two (1:52).

probability theory

The branch of **mathematics** that deals with the possible outcomes of events and their relative likelihoods. While mathematicians agree on how to calculate the probability of certain events and how to use those calculations in certain ways, there's plenty of disagreement as to what the numbers actually mean. Probability divides into two main concepts: *aleatory probability,* which represents the likelihood of future events whose occurrence is governed by some random physical phenomenon like tossing dice or spinning a wheel; and *epistemic probability,* which represents our uncertainty of belief about past events that either did or didn't occur, or uncertainty about the causes of future events. An example of the latter is when we say that it's "probable" that a certain suspect committed a crime based on the available evidence. It is an open question whether aleatory probability is reducible to epistemic probability based on our inability to precisely predict every force that might affect the roll of a die, or whether such uncertainties exist in the nature of reality itself, particularly at the level of **quantum mechanics**. One of the earliest mathematical studies on probability was written by Girolamo **Cardano**. Among other important contributions to the development of the subject were those by Blaise **Pascal**, Pierre de **Fermat**, Jakob Bernouilli (see **Bernouilli family**), Joseph **Lagrange**, Pierre **Laplace**, Carl **Gauss**, Siméon **Poisson**, Abraham **de Moivre**, Pafnuty Chebyshev, Andrei Markov (see **Markov chain**), and Andrei **Kolmogorov**.

PUZZLES

The following are two problems in probability. Both are easier to solve if the various possible outcomes are written down in the form of a table.

1. You meet a stranger on the street, and ask how many children he has. He truthfully says two. You ask "Is the older one a girl?" He truthfully says yes. What is the probability that both children are girls? What would the probability be if your second question had been "Is at least one of them a girl?", with the other conditions unchanged?
2. You are in a game of Russian roulette, but this time the gun (a six-shooter revolver) has three bullets in a row in three of the chambers. The barrel is spun only once. Each player then points the gun at his head and pulls the trigger. If he is still alive, the gun is passed to the other player who then points it at his own head and pulls the trigger. The game stops when one player dies. Would you stand a better chance of surviving if you shoot first or second, or does it make any difference?

Solutions begin on page 369.

See also **Buffon's needle**, **birthday problem**, **Monty Hall problem**, and **St. Petersburg paradox**.

Proclus Diadochus (c. A.D. 410–485)

The last major Greek philosopher; his *Commentary on Euclid* is the main original source we have on the early history of Greek geometry. He also wrote *Hypotyposis,* which gives a detailed account of the Earth-centered astronomical theories of Hipparchus and Ptolemy.

product

The result of one or more multiplications.

projectile

An object, such as a baseball, spear, or cannonball, that is thrown, fired, or otherwise propelled but that can't propel itself. For centuries, philosophers and mathematicians debated what path a projectile follows under gravity. Galilei Galileo was the first to establish that (in the absence of air resistance) this path is a **parabola**.

projective geometry

The branch of **geometry** that deals with properties of geometric figures that remain unchanged under projection. A mathematical theory of perspective grew out of the studies of Renaissance architects and painters who asked themselves how to best represent a three-dimensional object on a two-dimensional surface. The Greeks had done some early work on perspective, and the great geometer **Pappus of Alexandria** is credited with the first theorem in projective geometry. However, the subject reached mathematical maturity through the efforts first of Girard **Desargues**, and then, much later through the work of Jean **Poncelet** and by Karl von Staudt (1798–1867).

The basic elements of projective geometry are points, lines, and planes. These elements retain their characteristics under projection; for example, the projection of a line is another line, and the point of intersection of two lines is projected into another point that is the intersection of the projections of the two original lines. However, lengths and ratios of lengths are not invariant under projection, nor are angles or the shapes of figures. The concept of parallelism doesn't appear at all in projective geometry; any pair of distinct lines intersects in a point, and if these lines are parallel in the sense of **Euclidean geometry**, then their point of intersection is at infinity. The plane that includes the ideal line, or line at infinity, consisting of all such ideal points, is called the **projective plane**. Two properties that are invariant under projection are the order of three or more points on a line and the harmonic relationship, or cross-ratio, among four points, *A, B, C, D,* that is, $AC/BC : AD/BD$. The most remarkable concept in projective geometry is that of duality. In the plane, the terms *point* and *line* are dual and can be interchanged in any valid statement to yield another valid statement; in space, the terms *plane, line,* and *point* are interchanged with *point, line,* and *plane,* respectively, to yield dual statements. Entire theorems also occur in dual pairs, so that one can be instantly transformed into the other. For example, *Pascal's theorem* (given a hexagon inscribed in a **conic section**, the three pairs of the continuations of opposite sides meet on a straight line) is the dual of *Brianchon's theorem* (given a hexagon circumscribed on a conic section, the lines joining opposite diagonals meet in a single point). In fact, *all* the propositions in projective geometry occur in dual pairs.

projective plane

The surface you would get if you glued the edge of a disk to the edge of a **Möbius band**. This sounds easy to do, since a disk and a Möbius band each have one edge. But the process becomes hopelessly tangled and is, in fact, impossible. The projective plane needs a **fourth dimension**, in addition to the three we live in (up-down, left-right, and back-forth), to be fully realized. The idea of the projective plane arose from the study of perspective by mathematicians and painters in the Renaissance. In trying to represent parallel lines in space on the two-dimensional surface of a painting, it was found useful to introduce the notion of a *line at infinity* on which parallel lines met. The study of the geometry that adds this extra line of ideal points to the ordinary familiar plane came to be known as **projective geometry**, because of its use in studying projections of figures onto different lines. This idea was even more important in three dimensions, since projections are used for representing three-dimensional figures on planes. An interesting property of the projective plane is that any "straight" line on it, followed far enough, comes back to the starting point. (The old arcade version of the game of Asteroids was played on a virtual projective plane: the screen was a disk, and when an asteroid went off one edge of the screen it emerged on the opposite side.) The projective plane is also *nonorientable,* as a result of which any two-dimensional object pushed along a path back to its starting point would be reversed.

prolate

(1) Rounded like an **egg**. (2) Having a polar diameter greater than the equatorial diameter. See also **spheroid**.

pronic number

Also known as a *rectangular* or *oblong number,* a number that is the product of two consecutive integers: 2 (1×2), 6 (2×3), 12 (3×4), 20 (4×5), ... The pronic numbers are twice the **triangular number**s, and represent the lengths that produce the musical intervals: octave (1:2),

fifth (2:3), fourth (3:4), major third (4:5) . . . . Pronic seems to be a misspelling of *promic,* from the Greek *promekes,* for "rectangular" or "oblong"; however, the "n" form goes back at least as far as Leonhard **Euler** who used it in series one, volume fifteen of his *Opera.*

proof
A sequence of statements in which each subsequent statement is derivable from one of the previous statements or from an **axiom** of a **formal system**. The final statement of a proof is usually the **theorem** that one has set out to prove.

proper divisor
See **aliquot part**.

proportional
A variable a is said to be *directly proportional* to b if a/b is a constant. The relationship is written $a \propto b$, which implies that $a = kb$, where k is a constant. If a is *inversely proportional* to b, this is written $a \propto 1/b$.

pseudoprime
A number that passes the test of **Fermat's little theorem** (FLT) for **prime number**s but actually isn't a prime. FLT says that if p is prime and a is **coprime** to p, then $a^{p-1} - 1$ is divisible by p. If a number x is not prime, a is coprime to x, and x divides $a^{x-1} - 1$, then x is called a *pseudoprime to base a.* A number x that is a pseudoprime for all values of a that are coprime to x is called a **Carmichael number**. The smallest pseudoprime in base 2 is 341. This isn't prime because $341 = 11 \times 31$; however, it satisfies FLT: $2^{340} - 1$ is divisible by 341.

pseudosphere
A saddle-shaped surface that is produced by rotating a **tractrix** about its **asymptote**. The name *pseudosphere,* which means "false sphere," is misleading because it suggests something that is spherelike; however, a pseudosphere is almost exactly the opposite of a sphere. Whereas a sphere has a constant positive **curvature** (equal to $+1/r$, where r is the radius) at every point on its surface, a pseudosphere has a constant negative curvature (equal to $-1/r$) everywhere. As a result, a sphere has a closed surface and a finite area, while a pseudosphere has an open surface and an infinite area. In fact, although both the two-dimensional plane and a pseudosphere are infinite, the pseudosphere manages to have more room! One way to think of this is that a pseudosphere is more intensely infinite than the plane. Another result of the pseudosphere's negative curvature is that the angles of a triangle drawn on its surface add up to less than 180°. The geometry on the surfaces of both the sphere and the pseudosphere is a two-

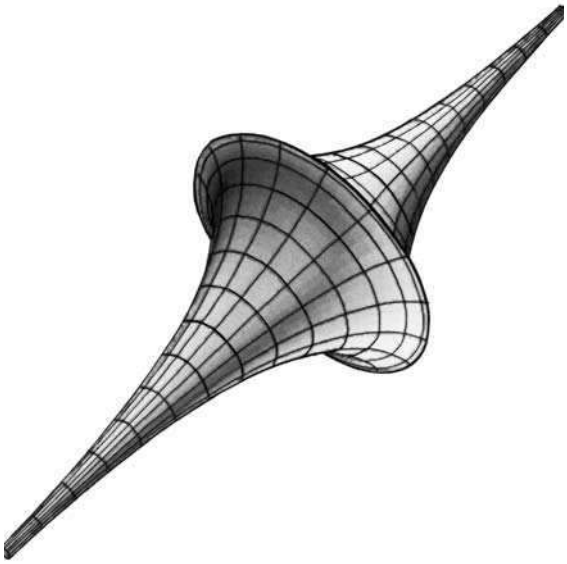

pseudosphere

dimensional **non-Euclidean geometry**–spherical (or elliptical) geometry in the case of the sphere and **hyperbolic geometry** in the case of the pseudosphere. Astronomers currently suspect that the universe we live in may have a hyperbolic geometry and thus have properties analogous to those of a pseudosphere.

Ptolemy's theorem
The sum of the products of the two pairs of opposite sides of a convex cyclic **quadrilateral** (see **cyclic polygon**) is equal to the product of the lengths of the diagonals. The theorem is named after the mathematician, astronomer, and geographer Ptolemy of Alexandria.

pure mathematics
Mathematics for the sake of its internal beauty or logical strength. Compare with **applied mathematics**.

pursuit curve
The path an object takes when chasing after another object in the most effective way. Pursuit curves can arise in a variety of situations, for example when a lion is chasing after a gazelle or a heat-seeking missile is homing in on a moving target. Suppose that four ants are at the corners of a square. They start to crawl clockwise at a constant rate, each moving toward its neighbor. At any instant, they mark the corners of a square. As the ants get closer to

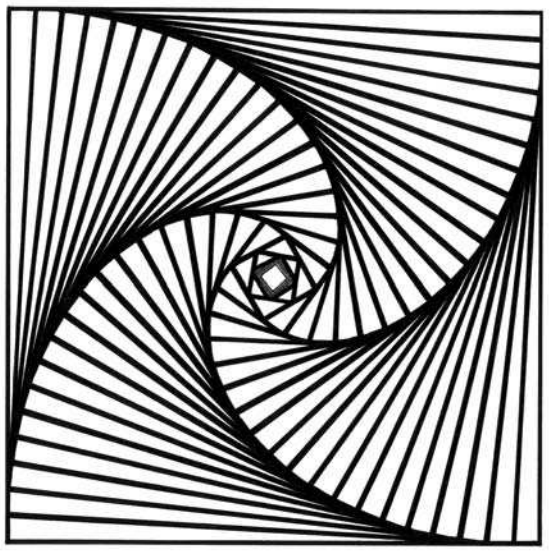

pursuit curve A set of superimposed snapshots shows the lines of sight at regular intervals of four bugs chasing one another, all moving at the same speed after starting at the corners of a square. *John Sharp*

the original square's center, the new square they define rotates and diminishes in size. In reaching the center, each ant travels on a **logarithmic spiral** with a length equal to the side of the original square. Superimposed snapshots of the ants' progress give rise to an intriguing pattern.

puzzle jug

A practical joke in the form of a drinking vessel that, unless the trick is known, spills all over the user when he tries to take a sip. As the jug is tilted, liquid pours out from the pierced decoration surrounding the pot. The puzzle is to learn the secret of how to successfully drink without getting wet. Puzzle jugs are the oldest known **mechanical puzzle**s. Several Phoenician examples are in New York's Metropolitan Museum of Art, and in ninth-century Turkey they were especially popular. Puzzle jugs have been manufactured in Germany, Holland, France, and several other European countries since the end of the thirteenth century. The Exeter puzzle jug, on display in the Royal Albert Museum in Exeter, Devon, was probably made in the Saintonge region of western France, around 1300, and is one of the finest examples of medieval pottery imported to England. Puzzle jugs came back into vogue in the eighteenth and nineteenth centuries and are still manufactured by ceramicists in France, Germany, and Britain. And the secret? That is really quite open, and can be handled by anyone prepared to get to the bottom of it.

puzzle rings

A **mechanical puzzle** consisting of a group of interlocking rings that fit together to form an intricate design; when apart, the rings remain interconnected and pose a challenging puzzle. The puzzle itself has ancient origins in Egypt, though many stories have been told of its use throughout the Middle East. According to one, a person would give the ring to their lover telling them of the magical qualities of the ring. If the ring was ever worn while being amorous to another, it would tell the giver of the ring about the unfaithfulness of the ring wearer. The wearer, wishing to avoid the watchfulness of the ring, might remove it from their finger so that it wouldn't witness an unfaithful act. But once removed, the ring would fall into its separate pieces and so the giver would know their lover had been cheating.

pyramid

A **polyhedron** whose base is a **polygon** and whose other faces are triangles that meet at a common **vertex**, sometimes called the *apex*. A right pyramid has its apex directly above the center of its base. A square-based pyramid, like the pyramids in Egypt, has a square base and four triangular sides. A triangular pyramid, or **tetrahedron**, is made from four triangular sides; if regular, it is one of the **Platonic solid**s. The volume of a pyramid is $\frac{1}{3}A_b h$, where A_b is the area of the base and h is the perpendicular height of the apex above the base; the surface area is ps, where p is the base perimeter and s is the slant height.

Pyramidology, which (in its original form) claims links between biblical prophesy and the construction of the Egyptian pyramids, stemmed from the publication in 1859 of *The Great Pyramid: Why Was It Built? And Who Built It?* by

pyramid The Great Pyramid of Cheops at Giza.

John Taylor, a British amateur mathematician and astronomer who was editor of the *London Observer.* Taylor became convinced that the Great Pyramid of Cheops, in its architectural proportions, embodied various remarkable and deeply meaningful geometric and mathematical properties. Chief among these, Taylor noted, was that the ratio of the perimeter of the pyramid's base to twice its height closely approximates the universal constant **pi**. The said ratio of the Great Pyramid gives a better value for pi than any found in written Egyptian records. The **Rhind papyrus** contains several problems that involve a multistep method for finding the area of a circle from its diameter. This method implies a value of π equal to $^{256}/_{81}$, or 3.1605, which is less than 1% larger than the true value of 3.14159 . . . . The values Taylor used for the Great Pyramid's base and height gave him a value of π correct to two decimal places. Further analysis of the pyramid's dimensions and various manipulations of numbers led him to conclude that the builders of the edifice had used a unit that he called "pyramid inch" (equal to about 1.01 times a standard inch). Twenty-five pyramid inches made a "pyramid cubit," and 10 million pyramid cubits, Taylor pointed out, approximate the length of Earth's polar radius. These and a series of similar calculations provided what Taylor considered to be adequate evidence that the Great Pyramid had been built as a model of Earth. Taylor's fantastic claims may never have become popular had not Charles Piazzi Smyth, the Astronomer Royal of Scotland taken up the cause of pyramidology. He popularized it in Britain, the rest of Europe, and the United States, through a number of books including *Our Inheritance in the Great Pyramid* (1864) and *Life and Work at the Great Pyramid* (1867). (In the churchyard in Sharow, North Yorkshire, Smyth has a pyramidal grave marker.) Others who espoused pyramid numerology have included Helena Blavatsky, the theosophist; Charles Taze Russell, founder of the Watchtower Bible and Tract Society; and Edgar Cayce, the American psychic; not to mention a variety of more recent pseudohistorians who have linked the Great Pyramid to everything from lost civilizations to UFOs. Yet Taylor himself was well aware of other, less dramatic explanations for the pyramid's dimensions, including the possibility that the pyramid had been constructed so that the area of one of its faces would equal the square of its height. The mathematical sophistication required to achieve this is not great and would have resulted in a ratio of the perimeter of the base to twice the height of 3.145–about as close as the approximation of pi used by Smyth in his studies. So, the ratio could have occurred as a completely coincidental byproduct of a design that had nothing to do with the ratio of the circumference of a circle to its diameter. The pyramid is a rich source of the kind of data that Taylor and Smyth worked with, and it would be surprising if they'd been unable to come up with some interesting number combinations given the extent of their efforts.

pyramidal number

The number of dots that may be arranged in a **pyramid** with a regular **polygon** as a base.

Pythagoras of Samos (c. 580–500 B.C.)

A Greek philosopher and mathematician, a native of the Aegean island of Samos, and the founder of a secretive pseudoreligious community in Croton, southern Italy. Pythagoras left no writings and virtually nothing is known about him as an individual, so it is almost impossible to disentangle the beliefs and discoveries of the "Pythagoreans" from those of their leader. To the Pythagoreans, "everything is number" and every number was supposed to be a quantity that could be expressed as the ratio of two integers. We now call such a number a **rational number**. The Pythagoreans used music as an example of the perfection and harmony of numbers that can be expressed as ratios. They showed that pitch could be represented as a simple ratio that came from the length of equally tight strings that could be plucked. Perhaps the most famous of the Pythagoreans' mathematical results is **Pythagoras's theorem**. Then the sky fell in on the Pythagoreans' worldview. Using their very own theorems they showed that not all numbers are rational. Their discovery that the **square root of 2** (the length of the hypotenuse of a triangle with sides 1 and 1) can't be expressed as ratio of two whole numbers was to have been kept a closely guarded a secret, but was later revealed by one of the cult's members.

Pythagoras's lute

The **kite**-shaped figure that forms the enclosing shape for a progression of diminishing **penta**gons and pentagrams, linking the vertices together. The resulting diagram is replete with lines in the **golden ratio**.

Pythagoras's theorem

The square of the length of the **hypotenuse** of a right **triangle** is the sum of the squares of the lengths of the two sides. This is usually expressed as $a^2 + b^2 = c^2$. See also **Pythagorean triplet**.

Pythagorean square puzzle

A deceptively hard assembly puzzle in which a small square piece must be combined with four pieces forming a larger square to make an even larger square.

PUZZLE

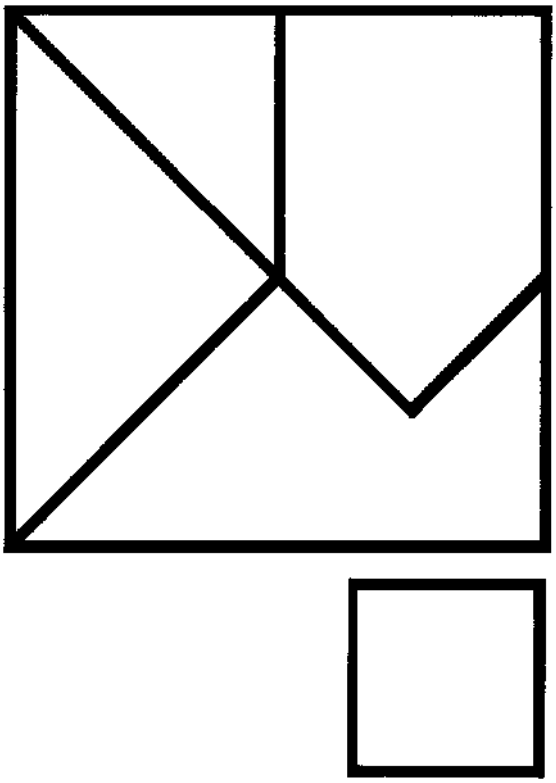

Rearrange the pieces in the Pythagorean square puzzle, including the small square, to make a single larger square.

Solutions begin on page 369.

Pythagorean triangle

A right triangle whose sides are integers. A *primitive Pythagorean triangle* is one whose sides are **coprime**.

Pythagorean triplet

Also called a *Pythagorean triple,* a set of three whole numbers that satisfies **Pythagoras's theorem**, that is, the squares of two of the numbers add up to the square of the third number. Examples include (3, 4, 5), (5, 12, 13), and (7, 24, 25). These are called *primitive triplets* because they have no common divisors. If the members of a primitive triplet are multiplied by the same integer, the result is a new (but not primitive) triplet. In any primitive Pythagorean triplet, one, and only one, of the three numbers must be even (but can't equal 2); the other two numbers are **coprime**. There are infinitely many such triplets, and they are easy to generate using a classic formula, known since ancient times. If the numbers in the triplet are *a, b,* and *c,* then: $a = n^2 - m^2$, $b = 2mn$, $c = m^2 + n^2$, where m and n are two integers and m is less than n. Because the **square root of 2** is irrational, there can't be any Pythagorean triplets (*a, a, c*). However, there are an infinite number of triplets (*a, a* + 1, *c*), the first three of which (apart from the trivial (0, 1, 1)) are (3, 4, 5), (20, 21, 29), and (119, 120, 169).

There are also an infinite number of Pythagorean quartets (*a, b, c, d*) such that $a^2 + b^2 + c^2 = d^2$. This is simply the three-dimensional form of Pythagoras's theorem and can be interpreted as the fact that the point in three-dimensions with Cartesian coordinates (*a, b, c*) lies an integer distance *d* from the origin. A formula that generates Pythagorean quartets is: $a = m^2$, $b = 2mn$, $c = 2n^2$, $d = (m^2 + 2n^2) = a + c$. Also note that $b^2 = 2ac$. When $m = 1$ and $n = 1$, we get the quartet (1, 2, 2, 3)–the simplest example.

Although there are an infinite number of Pythagorean triplets, **Fermat's last theorem**, which is now know to be true, ensures that there are no triplets for higher powers. See also **Euler's conjecture** and **multigrade**.

Q

QED
Abbreviation for *quod erat demonstrandum* ("that which was to be shown"), used to denote the end of a proof.

quadrangle
A plane figure consisting of four points, each of which is joined to two other points by a line segment. A quadrangle may be **concave** or **convex** depending on whether the line segments do or don't intersect. A convex quadrangle is a **quadrilateral**. The word is from the Latin *quadrangulum* for "four-cornered" and is also used to describe a rectangular area surrounded on all four sides by buildings, or to such buildings themselves.

quadrant
Any one of the four portions of the plane into which the plane is divided by the Cartesian coordinate axes.

quadratic
An expression or an equation that contains the variable squared, but not raised to any higher power. For instance a *quadratic equation* in x contains x^2 but not x^3. Similarly a *quadratic expression,* or a *quadratic form,* contains its variable(s) squared but not raised to any higher power. If there is more than one variable (say, x and y), quadratic can mean that they are multiplied together in pairs (xy) but not in threes (such as x^2y). The graph of a quadratic equation is known as a *quadratic curve;* the curve of the general quadratic equation $y = ax^2 + bx + c$ is a **parabola**.

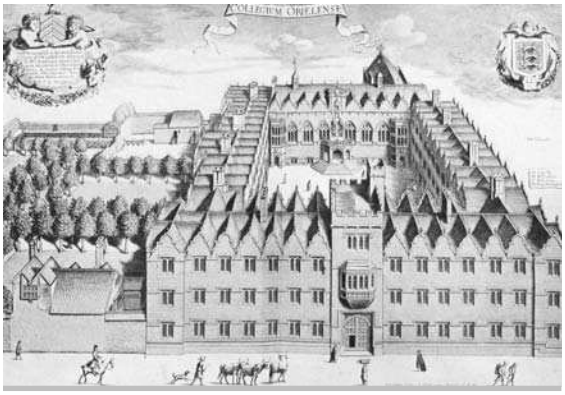

quadrangle The sixteenth-century quadrangle of Oxford University's Oriel College. *Oriel College, Oxford*

quadratrix of Hippias
The first curve in recorded history that was not part of a line or a circle, and the first curve known that is not **constructible** in the classical sense; in other words, it can't be drawn using a straightedge and a compass alone, but instead has to be plotted point by point. The quadratrix can be thought of as the intersection of two lines moving with constant velocity: the first line rotates (e.g., counterclockwise) while the second line moves along (say, in the direction of the positive y-axis). It has the Cartesian equation $y = x\ cot(\pi x/2a)$. The quadratrix was discovered by **Hippias of Elis** in about 430 B.C. and was used by him in his work on **trisecting an angle** and **squaring the circle**. In fact, its name refers to its use in turning curvilinear space into a rectangular area.

quadrature
The determination of the area of a geometric figure.

quadric
A surface in three dimensions that is described by equations containing the squares of x, y, and z, but no higher powers of them. Examples of such surfaces include the **sphere**, **ellipsoid**, **cone**, and **cylinder**.

quadrifolium
See **rose curve**.

quadrilateral
A **polygon** that has four sides and four vertices (corners). Quadrilaterals, and polygons in general, may be **convex** or **concave**. A convex quadrilateral may be further classified as a **trapezoid** or a British **trapezium** (one pair of opposite sides are parallel), a trapezium (no sides parallel); an isosceles trapezoid (United States) or an isosceles trapezium (United Kingdom) (two of the opposite sides parallel, the two other sides equal, and the two ends of each parallel side of equal angles); a **parallelogram** (opposite sides are parallel); a **kite** (two

adjacent sides of equal length, the other two sides of equal length); a **rhombus** (four sides of equal length); a **rectangle** (each angle is a right angle); or a **square** (four sides of equal length, each angle a right angle). *Quadrangular prisms* and *quadrangular pyramids* are ones whose bases are quadrilateral.

quantifier

In symbolic logic, the *universal quantifier* ∀ indicates "for every" or "for all." For example, ∀ *x A, p*(*x*) means for all *x* belonging to *A,* the **proposition** *p*(*x*) is valid. The *existential quantifier* ∃ indicates "there exists." So, for instance, ∃ *x A, p*(*x*) means there exists at least one *x,* belonging in *A,* for which the proposition *p*(*x*) is valid.

quantum field theory

The study of force fields such as the electromagnetic field in the context of **quantum mechanics**, and often special **relativity theory**. The mainstay of modern high-energy physics.

quantum mechanics

The science and mathematics that describe the behavior of nature at the atomic and subatomic level. At the heart of quantum mechanics are two basic concepts: (1) that every small bit of matter or energy can behave as if it were either a particle or a wave; and (2) that certain combinations of properties such as position and velocity, and energy and time, can't be known with arbitrary precision. The latter idea is encapsulated in *Heisenberg's uncertainty principle.* See also **many worlds hypothesis**.

quartic

A **polynomial** or polynomial equation that contains the fourth power of the variable, but no higher power. Many famous curves are described by such equations, including the **bicorn**, **Cartesian oval**, **conchoid**, **deltoid**, **devil's curve**, **folium**, **kampyle of Eudoxus**, and **limacon of Pascal**.

quartile

The first quartile of a **sequence** of numbers is the number such that one quarter of the numbers in the sequence are less than this number.

quasicrystal

A strange type of solid whose atomic structure is very regular but never quite repeats. Quasicrystalline structures don't have a simple unit cell that can be repeated periodically in all directions to fill space, although they do have local patterns that repeat almost periodically. They also have local rotational symmetries, such as those of a **pentagon**, that can't exist in ordinary crystals. Prior to the discovery of quasicrystals, it was thought that five-fold crystal symmetry was impossible, because there are no space-filling periodic tilings of this kind. The best known examples of quasicrystals resemble **Penrose tilings**, which use repeated copies of two different rhombi to cover an infinite plane in intricate, interlocking patterns. In fact, some quasicrystals can be sliced in such a way that the atoms on the surface follow the exact pattern of the Penrose tiling.[293]

quasiperiodic

Refers to a form of motion that is regular but never exactly repeating. Quasiperiodic motion is always composed of multiple but simpler **periodic** motions. In the general case for motion that is the sum of simpler periodic motions, if there exists a length of time that evenly divides the frequencies of the underlying motions, then the composite motion will also be periodic; however, if no such length of time exists, then the motion will be quasiperiodic.

quasiregular polyhedron

A **polyhedron** that consists of two sets of regular **polygons**, *m*-sided and *n*-sided respectively, and is constructed so that each polygon in one set is surrounded by members of the other set. There are three convex quasiregular solids: the *cuboctahedron* ($m = 3$, $n = 4$), the *icosidodecahedron* ($m = 3$, $n = 5$), and the **octahedron** ($m = n = 3$). In each case four faces meet at each vertex in the cyclic order (*m, n, m, n*). Because of this, these polyhedra have some special properties, one of which is that their edges form a system of **great circle**s. The edges of the octahedron form three squares; the edges of the cuboctahedron form four hexagons, and the edges of the icosidodecahedron form six decagons. Among the nonconvex polyhedra are two examples of type (*m, n, m, n*): the *dodecadodecahedron* ($m = 5$, $n = 5/2$) and the *great icosidodecahedron* ($m = 3$, $n = 5/2$), which can be made by truncating the **Kepler-Poinsot polyhedra** at their edge midpoints. There are also three nonconvex examples of type (*m, n, m, n, m, n*): the *small triambic icosidodecahedron* ($m = 3$, $n = 5/2$), the *triambic dodecadodecahedron* ($m = 5/3$, $n = 5$), and the *great triambic icosidodecahedron* ($m = 3$, $n = 5$). Finally, there is a group of nine *hemihedra,* in which some faces pass through the polyhedron's center. These hemifaces each cut a sphere into two hemispheres.

quaternion

An ordered **set** of four numbers. Quaternions, first introduced by William **Hamilton**, can also be written in the

quaternion An Irish stamp showing the quaternion equations in Hamilton's own hand.

form $a + bi + cj + dk$, where a, b, c, and d are real numbers and i, j, and k are imaginary numbers, which is similar to that of **complex number**s. Whereas complex numbers can be represented by points of a two-dimensional plane, quaternions can be viewed as points in the **fourth dimension**. For a while, quaternions were very influential: they were taught in many mathematics departments in the United States in the late 1800s, and were a mandatory topic of study at Dublin, where Hamilton ran the observatory. But then they were driven out by the **vector** notation of William Gibbs and Oliver Heaviside. Had quaternions come along later, when theoretical physicists were trying to understand patterns among subatomic particles, they may have found a place in modern science; after all, the unit quaternions form the group SU(2), which is perfect for studying spin-½ particles. But the way things turned out, quaternions had fallen from favor by the twentieth century and Wolfgang Pauli used 2×2 complex matrices instead to describe the generators of SU(2).

queens puzzle

A famous **chess** problem that asks in how many ways eight queens can be placed on a chessboard so that no two attack each other. The generalized problem, to find how many ways n queens can be placed on an $n \times n$ board so that no two attack each other, was first posed by Franz Nauck in 1850. In 1874 Günther and Glaisher described methods for solving this problem based on **determinant**s. The number of distinct solutions, not counting rotations and reflections, for board sizes ranging from 1×1 to 10×10 is 1, 0, 0, 1, 2, 1, 6, 12, 46, and 92, respectively. The 6×6 puzzle, for which there is a solitary unique solution, was sold for one penny in Victorian London in the form of a wooden board with 36 holes into which pins were placed.

quine

> *Before we put the motion "that the motion be now put," should we not first put the motion "that the motion 'that the motion be now put' be now put?"*
> –Chairman of the meeting of the Society of Logicians

A term named by Douglas **Hofstadter** after the Harvard logician Willard van Orman Quine. It can be used either as a noun or a verb. (1) Quine (noun). A computer program that produces an exact copy of itself (or, alternatively, that prints its own listing.) This means that when the program is run, it must duplicate (or print out) precisely those instructions that the programmer wrote as part of the program, including the instructions that do the copying (or printing) and the data used in the copying (or printing.) A respectable quine–one that doesn't cheat–is not allowed to do anything as underhand or trivial as seeking the source file on the disk, opening it, and copying (or printing) its contents. Although writing a quine is not always easy, and in fact may seem impossible, it can always be done in any programming language that is Turing complete (see **Turing machine**), which includes every programming language actually in use. (2) Quine (verb). To write a sentence fragment a first time, and then to write it a second time, but with quotation marks around it. For example, if we quine "say," we get "say 'say' "). Thus, if we quine "quine", we get "quine 'quine,' " so that the sentence "quine 'quine' " is a quine. In this linguistic analogy, the verb "to quine," plays the role of the code, and "quine" in quotation marks plays the role of the data.

quintic

A **polynomial** or polynomial equation that contains the fifth power of the variable, but no higher power. Niels **Abel** and Evariste **Galois** independently proved that although there exist formulas for the general solution of **quadratic**, **cubic**, and **quartic** equations, no such formula exists for quintic equations.

quipu

A recording device generally associated with the Incas, who ruled Peru before the Spanish conquest. Quipu consisted of a number of color-coded cords; knots of various kinds were tied on these cords to represent a variety of information. An important use of quipu was to record numbers for use in trade, keeping accounts, and calendars, but the knotted strings might also have served

as mnemonics for important historical events, astronomical data, and mythology (the Incas had no written language). Some evidence supports the idea that the knots and cords followed in a decimal system. Similar devices were used by several other Indian tribes and also described in Chinese and Persian documents from the fifth and sixth centuries B.C., and are still used by shepherds in the Andes for keeping accounts of their herds.

quotient

The number of times that one number can be divided exactly into another.

R

radian
A unit of angular measurement such that there are 2π radians in a complete circle. One radian = $180/\pi$ degrees. One radian is approximately 57.3°.

radical
The symbol that indicates a **root**, $\sqrt[n]{}$. It seems to have been first used in 1525 by Christoff Rudolff (1499–1545) in his *Die Coss*.

radical axis
The **locus** of points of equal power with respect to two **circle**s. The *radical center* of three circles is the common point of intersection of the radical axes of each pair of circles.

radius
The distance from the center of a **circle** to its circumference, or from the center of a regular **polygon** to any one of its vertices. The *radius of curvature, r,* at any point of a curve is $r = 1/\kappa$, where κ is the **curvature**.

radix
See **base**.

railroad problems
See **shunting puzzles**.

Ramanujan, Srinivasa Aaiyangar (1887–1920)
An extraordinary, largely self-taught, Indian mathematician who, in the most unorthodox way, made significant contributions to **number theory**, including the subject of **elliptic function**s, **continued fraction**s, and **infinite series**. During much of his early work, he was unaware that he was rediscovering results that had taken other mathematicians centuries to achieve. But even in cases where he arrived at conclusions already known, he'd often travel an original route, and, in many cases, almost purely by intuition. Ramanujan was employed in a lowly clerk's position in Madras, when, in 1913, he wrote letters to three eminent mathematicians in England describing some of his results. Two of the three letters were returned unopened. However, G. H. **Hardy** recognized Ramanujan's abilities and arranged for him to come to Cambridge. Because of his lack of formal training, Ramanujan sometimes failed to distinguish between formal proof and apparent truth based on intuition or numerical evidence. His extraordinary innate familiarity with numbers was revealed by an incident recalled by Hardy:[150] "I remember once going to see him when he was lying ill at Putney. I had ridden in taxi cab number 1729 and remarked that the number seemed to me rather a dull one, and that I hoped it was not an unfavorable omen. 'No,' he replied, 'it is a very interesting number; it is the smallest number expressible as the sum of two cubes in two different ways [$1729 = 1^3 + 12^3 = 9^3 + 10^3$].' "

Unfortunately, Ramanujan's health deteriorated rapidly in England, perhaps due to the unfamiliar climate and food, and to the isolation which Ramanujan felt as the sole Indian and a devout Hindu in a culture which was alien to him. Ramanujan was sent home to recuperate in 1919, but tragically died the following year at the age of only 32. Although he published some of his results in journals, much of his work and conclusions have only

Ramanujan, Srinivasa Aaiyangar The enigmatic mathematician on an Indian commemorative stamp.

come to light more recently, from a scrutiny of his disorganized but fascinating notebooks.[184]

Ramsey theory

A branch of mathematics that asks questions such as: Can order always be found in what appears to be disorder? If so, how much can be found and how big a chunk of disorder is needed to find a particular amount of order in it? Ramsey theory is named after the English mathematician Frank P. Ramsey (1904–1930) who started the field in 1928 while wrestling with a problem in logic. (Frank's one-year-younger brother, Arthur, served as Archbishop of Canterbury from 1961 to 1974.) His life was cut short at the age of 26, following a bout of jaundice. Ramsey suspected that if a system was big enough, even if it seemed to be disorderly to an arbitrary degree, it was bound to contain pockets of order from which information about the system could be gleaned.

random

Without cause; not **compressible**; obeying the statistics of a fair coin toss.

random number

A number generated by a process that is fundamentally nondeterministic and unpredictable. Computer-generated "random numbers," which are calculated through a deterministic process, cannot, by definition, be **random**. Given knowledge of the **algorithm** used to create the numbers and its internal state, it's possible to predict all of the numbers returned by subsequent calls to the algorithm. For this reason the numbers produced by computer-based "random number generators" are often referred to as *pseudo-random numbers*. In the case of genuinely random numbers, knowledge of one number or an arbitrarily long sequence of numbers offers no clue of the next number to be generated. Humans are among the worst random number gen-

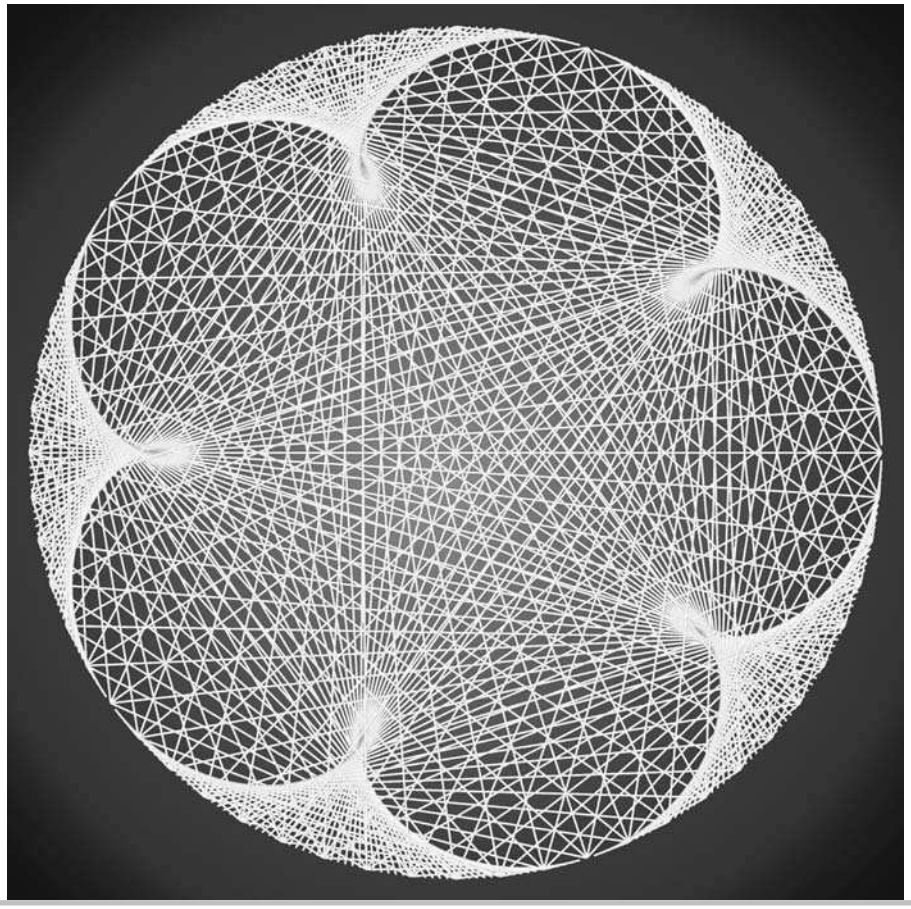

ranunculoid A ranunculoid curve spun by thread on a computer loom. *Jos Leys, www.josleys.com*

erators. Ask someone to pick a number "at random" between 1 and 20, and the number they're most likely to choose is 17. *Psychologically random numbers,* such as 17, are usually odd and don't end in 5, so that they frequently tend to be **prime number**s. See also **Chaitin's constant**.

random walk

A process in which the position of a particle changes by discrete steps of fixed length, and the direction of each step is chosen randomly. Random walks have interesting mathematical properties that vary greatly depending on the number of dimensions in which the walk takes place and whether it is confined to a **lattice**. For a random walk in one dimension there are only two directions to choose from. Imagine a drunken person wandering on the **number line** who starts at 0, and then moves left or right (+/−1) with probability ½. The probability that the walker will eventually return to his starting point is 1; in other words, it is certain to happen. The same is true for a random walk in the plane, moving on the integer lattice points, with probability ¼ in each of the coordinate directions: the probability of ending up back at the starting point is 1. However, the situation changes in three dimensions. Suppose a drunken fly moves randomly from one point to another in a three-dimensional lattice with a probability of 1 in 6 of arriving at any of the six adjacent lattice points on each move. No matter how long the fly roams, it has only a 0.34054 . . . probability of ever getting back to where it started. Probabilists say that random walks on the line and plane are *recurrent,* whereas random walks in three dimensions or more are *transient.* Effectively, this is because there is so much more "space" in three or more dimensions. The numbers giving the probability of eventually returning to the starting point are known as *random walk constants.* The random thermal perturbations in a liquid are responsible for a random walk phenomenon known as *Brownian motion,* and the collisions of molecules in a gas are a random walk responsible for *diffusion.*

range

(1) The set of possible values in which a **function**'s output can be. See also **codomain**. (2) The set of all points on a **line segment**.

rank

(1) Any of the rows of squares running crosswise to the files on a playing board in **chess** or checkers. (2) The rank of a **matrix** is equal to the dimension of the largest submatrix that can be obtained by deleting rows and columns of the parent matrix and that has a nonzero determinant. See also **tensor**.

ranunculoid

An **epicycloid** with five cusps ($n = 5$), named after the buttercup genus *Ranunculus.*

ratio

A **rational number** of the form a/b where a is called the *numerator* and b is called the *denominator.* It may be written with a colon (:), as a fraction, or with the word *to.*

rational number

A number that can be written as an ordinary **fraction**—a ratio, a/b, of two integers, a and b, where b isn't zero—or as a decimal expansion that either stops (like 4.58) or is periodic (like 1.315315 . . .). Other examples include 1, 1.2, 385.66, and ⅓. Rational numbers are countable, which means that, although there are infinitely many of them, they can always be put in a definite order, from smallest to largest, and can thus be counted. They also form what's called a *densely ordered set;* in other words, between any two rationals there always sits another one—in fact infinitely many others. The rational numbers are a subset of the **real number**s; real numbers that aren't rational are called, rationally enough, **irrational number**s. Although rationals are dense on the real **number line**, in the sense that any **open** set contains a rational, they're pretty sparse in comparison with the irrationals. One way to think of this is that the **infinity** of rationals (which, strangely enough, is exactly the same size as the infinity of whole numbers) is smaller than the infinity of irrational numbers. Another way to grasp the scarcity versus density issue, is to realize that the rationals can be covered by a set whose "length" is arbitrarily small. In other words, given a string of any positive length, no matter how short, it will still be long enough to cover all the rationals. In mathematical parlance, the rationals are a **measure** *zero* set. The irrationals, by contrast, are a measure one set. This difference in measure means that the rationals and irrationals are quite different even though a rational can always be found between any two irrationals, and an irrational exists between any two rationals.

raven paradox

A **paradox** put forward by the German logician Carl Hempel (1905–1997) in the 1940s to highlight a situation where the logic of **induction** seems to fly in the face of intuition. According to the *principle of induction,* the more that a theory is supported by observation, the greater the probability that the theory is true. Consider, said Hempel, the theory that all ravens are black. After each observation of a black raven, our belief in the theory "all ravens are black" increases. But here's the rub. The state-

ment "all ravens are black" is logically equivalent to the statement "all nonblack things are nonravens." The observation of a white swan is consistent with this statement. A white swan is a nonblack thing, and when we examine it, we observe that it is a nonraven. So by the principle of induction, observing a white swan should increase our belief that all ravens are black!

Many solutions have been offered to this enigma. The American logician Nelson Goodman (1906–1998) suggested imposing restrictions to our reasoning, such as never considering an instance as support for "All P are Q" if it would also support "No P are Q." Others have questioned the *principle of equivalence.* Perhaps seeing a white swan should strengthen our belief in the theory "all nonblack things are nonravens," without increasing our conviction that "all ravens are black." Yet others have argued that our intuition is flawed. Observing a white swan really does increase the probability that all ravens are black! After all, if you were shown all the nonblack things in existence, and you noticed that none was a raven, then you could properly conclude that all ravens were black. The example only seems counterintuitive because the set of nonblack things is vastly larger than the set of ravens. Thus observing one more nonblack thing that is not a raven should make a tiny difference to our degree of belief in the proposition compared to the difference made by observing one more raven that is black.

A way to sidestep the paradox is by using **Bayes's theorem**. According to this the probability of a hypothesis H must be multiplied by the ratio:

$$\frac{\text{probability of observing } X \text{ if } H \text{ is true}}{\text{probability of observing } X}$$

If a swan is picked at random, the probability of it being white is independent of the colors of ravens. The numerator in the above ratio will equal the denominator, the ratio will equal one, and the probability will remain unchanged. Seeing a white swan doesn't affect our belief about whether all ravens are black. If a nonblack thing is chosen at random, and a white swan is shown, then the numerator will be bigger than the denominator by a tiny amount. Seeing the white swan will only slightly increase our belief that all ravens are black. We'd have to see almost every nonblack thing in the universe (and see that they're all nonravens) before our belief in "all ravens are black" would increase appreciably. In both cases, these results are in line with intuition.

ray
A straight path of points that begins at one point and continues in one direction.

real number
Any number that can be represented as a decimal, possibly infinitely long and nonrepeating. Real numbers stand in one-to-one correspondence with the points on a continuous line, known as the *real number line,* that stretches from zero to infinity in both directions. The set of real numbers contains the set of all **rational number**s and the set of all **irrational number**s. The name "real number" is a retronym, coined by René **Descartes** in response to the concept of **imaginary number**s. Number systems that are even more general than the real numbers include the **complex numbers** and, of much more recent discovery, **hyperreal number**s and **surreal number**s.

realm
A term advocated for a three-dimensional version of the two-dimensional **plane**.

reciprocal
One over a given number; for example, the reciprocal of 4 is ¼.

Recorde, Robert (c. 1510–1558)
A Welsh physician and mathematician, born in Tenby, Pembrokeshire, and trained at Oxford and Cambridge, who held various positions, including master of the mint in Bristol and later in Ireland, and wrote a number of influential math textbooks. These books formed a complete course and were written in English, rather than the usual Latin or Greek, so that they could be read by anyone. In one of them Recorde introduces the "=" sign for "equals."

rectangle
A **quadrilateral** whose interior angles are all 90°. If all of its sides are the same length, it is a **square**. The smallest square that can be cut into $m \times n$ rectangles, such that all m and n are different integers, is the 11×11 square, and the **tiling** uses five rectangles. The smallest rectangle that can be cut into $m \times n$ rectangles, such that all m and n are different integers, is the 9×13 rectangle; this tiling also uses five rectangles.

rectangular coordinates
See **Cartesian coordinates**.

rectangular hyperbola
See **hyperbola**.

recursion
See **recursion**.
No, seriously. Recursion is a process that wraps back on itself and feeds the output of a process or function back

in as the input. Using some sort of *recurrence relation,* an entire class of objects can be built up from a few initial values and a small number of rules. The **Fibonacci sequence**, for example, is defined recursively, as are many **fractal** figures. *Self-recursion,* of which the first two lines of this entry are an example, leads to an endless feedback loop. One, somewhat disturbing, notion of reality is that we live in a *recursive universe* in which nature resembles an infinite nest of Russian dolls. One day, we will simulate the big bang in one of our supercomputers. Inside this artificial universe (rather like an immense *Star Trek* "holodeck" simulation) will evolve new star systems and new life forms. They too will evolve intelligence one day and invent computers. And they too may one day simulate the big bang inside one of their supercomputers. This chain of existence will continue as long as we continue to run our simulation. Our universe will continue to exist as long as our parent universes' continue to run their simulations. And therein lies madness.

recursive function
Strictly speaking, a **function** that is *computable;* however, in the usual sense of the word, a function is said to be recursive if its definition makes reference to itself (see **recursion**). For example, **factorial** can be defined as $x! = x(x - 1)!$ with the base case of 1! equal to 1. See also **self-referential sentence**.

recursively enumerable set
A potentially infinite **set** whose members can be enumerated by a **universal computer**; however, a universal computer may not be able to determine that something is not a member of a recursively enumerable set. The *halting set,* a concept related to the **halting problem**, is recursively enumerable but not recursive.

reductio ad absurdum
"Reduction to the absurd"; the process of demonstrating that an idea is probably false by first assuming its truth, and then showing how that truth leads to conclusions that can't possibly be true. In *A Mathematician's Apology* (1941),[151] G. H. **Hardy** said: "Reductio ad absurdum, which Euclid loved so much, is one of a mathematician's finest weapons. It is a far finer gambit than any chess play: a chess player may offer the sacrifice of a pawn or even a piece, but a mathematician offers the game."

reductionism
The idea that nature can be understood by taking it apart. In other words, knowing the lowest-level details of how things work (at, say, the level of subatomic physics) reveals how higher-level phenomena come about. This is a bottom-up way of looking at the universe, and is the exact opposite of **holism**.

redundancy
The existence of repetitive patterns or structures. In an important sense, redundancy refers to *order* in a **complex system** since order is defined as the existence of structures that maintain themselves over time. In **information theory**, redundancy refers to repetition in patterns of messages in a communication channel. If the message contains these redundancies, they can be compressed further; for example, a message containing a series of 250 ones, could be compressed into a command that effectively says "and then repeat one 250 times," instead of writing out all 250 ones.

reentrant angle
An inward-pointing angle of a **concave** polygon.

reflection
A way of transforming a shape in the same way that a mirror does. The reflection of a shape in a mirror line is an identical shape that has been flipped over. When an object is placed a certain distance in front of a mirror, its image in the mirror appears the same distance away from the edge of the mirror. Likewise, all the points on a shape and all the points on its image are the same distance away from the mirror line.

reflex angle
An angle between 180° and 360°.

reflexible
Having a plane of mirror symmetry. Compare with **chiral**.

regular polygon
A **polygon** in which all the sides are equal and all the angles are equal.

regular polyhedron
A polyhedron in which every face and vertex figure is regular. There are nine regular polyhedra: the five **Platonic solid**s and the four **Kepler-Poinsot solid**s. However, others are sometimes allowed, depending on the definition of polyhedron.

relativity theory
The physical and mathematical theory due to Albert Einstein (1879–1955) that revolutionized our understanding of **space**, **time**, and gravity. In it, space and time are seen as a unified and inseparable whole–the

four-dimensional continuum of **space-time**. The curvature of space-time due to the presence of matter becomes the extraordinary new explanation and interpretation of gravity. Einstein's theory of relativity was published by him in two great parts. Special relativity, published in 1905, deals exclusively with *inertial* frames of reference, that is, reference frames that don't accelerate with respect to one another. Its two central premises are that the laws of physics are the same in all reference frames and that the speed of light (in a vacuum) is constant in all reference frames. General relativity, published in 1915, centers on the *equivalence principle,* the idea that acceleration and gravity are equivalent. See also **non-Euclidean space**.

renormalization

A mathematical technique for looking at a physical system at different levels of magnification.

repdigit

A number composed of repetition of a single digit in a given base, generally taken as base 10 unless otherwise specified. For example, the **beast number** 666 is a (base-10) repdigit.

representation theory

A theory that seeks to understand an abstract algebraic system such as a **group** by obtaining it in a more concrete way as a *permutation group* or as a group of matrixes (see **matrix**).

rep-tile

A repetitive **tiling**: a shape with the property that it tiles a larger version of itself, using identical copies of itself. A simple example is a square because four copies of any square tile a larger square. Any triangle also is a rep-tile, because four copies of it tile a larger version of this triangle. Rep-tiles that require n tiles to build a larger version of themselves are said to be rep-n; thus a square is rep-4. Since any of these larger replicas can be combined to give an even larger, second-generation copy, a rep-n tile is also rep-n^2, rep-n^3, and so on. Often tiles have several rep-numbers. If a tile is rep-n and rep-m, it is also rep-mn, since replicas can be built with n tiles, then combined, m at a time, to give a yet larger version.

The set of rep-tiles is a subset of the set of *irreptiles.* An irreptile is any shape that tiles a larger version of itself using either differently sized or identical copies of itself. The problem to find all irreptiles in the Euclidean plane has been studied but not yet completely solved. A

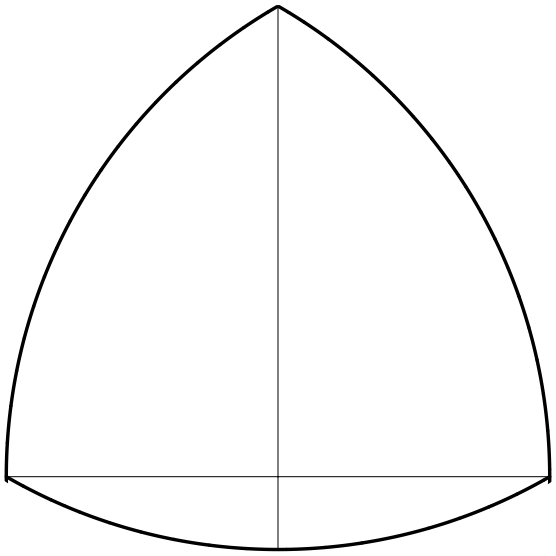

Reuleaux triangle *© Jan Wassenaar, www.2dcurves.com*

Reutersvärd, Oscar A Swedish stamp depicting one of Reutersvärd's impossible figures.

re-lated set of problems is to find for each irreptile the minimum number of smaller copies needed to tile the original shape; in many cases it is difficult to prove such a minimality. The name "rep-tile" was coined by Simon **Golomb**.

rep-unit

A number whose digits are all units; the rep-unit (repeated unit) with n digits is denoted R_n. For example, $R_1 = 1$, $R_2 = 11$, $R_3 = 111$, and $R_n = (10^n - 1)/9$. R_n divides R_m whenever n divides m. No rep-unit can be a square, but it is not known if one can be a cube. *Rep-unit primes* are rep-units that are **prime number**s. The only known rep-unit primes are R_2 (11), R_{19}, R_{23}, R_{317}, and R_{1031}, though R_{49081} and R_{86453} are suspected primes.

resultant

A **vector** that is the sum of a given set of vectors.

Reuleaux polytope

A **convex** body in the plane or in higher dimensions that, like the **Reuleaux triangle**, consists of pieces of round spheres, each centered at one of the corners of the convex body.

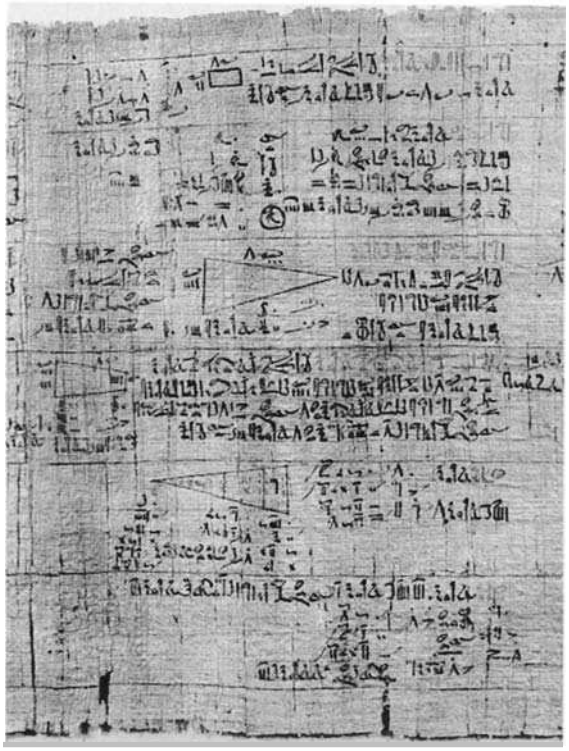

Rhind papyrus *British Museum*

Reuleaux triangle

The simplest noncircular **curve of constant width**; also known as the *Reuleaux wheel,* it is named after the German engineer and mathematician Franz Reuleaux (1829–1905). Although it was known to earlier mathematicians, Reuleaux was the first to show its constant-width properties. To form a Reuleaux triangle, take the three points at the corners of an equilateral triangle and connect each pair of points by a circular arc centered at the remaining point. The ratio of the circumference to the width of the triangle is, remarkably, **pi**. By rotating the centroid of a Reuleaux triangle appropriately, the figure can be made to trace out a square, perfect except for slightly rounded corners. This idea has formed the basis of a drill that will carve out squares, first patented by Harry Watts in 1914. Bits for square, pentagonal, hexagonal, and octagonal holes are still sold by the Watts Brothers Tool Works in Wilmerding, Pennsylvania. The actual drill bit for the square is a Reuleaux triangle made concave in three spots to allow for unobstructed corner-cutting and the discharge of shavings. The Reuleaux triangle may also form the shape of the piston in a rotary, or Wankel, engine, in which gasoline burns in crescent-shaped chambers, turning a rotating piston that drives an axle through its center.

Reutersvärd, Oscar (1915–)

A Swedish artist who pioneered the creation and design of **impossible figure**s. His work in this area goes back to one day in 1934 when, as a young student in Stockholm, he started doodling in the margins of a textbook during a long lecture. Reutersvärd's doodle began with an outline of a perfect six-pointed star. Once the star was complete he added cubes around the star, nestled into the spaces between the points. He soon realized that what he'd drawn was paradoxical: something that couldn't be built in the real world. A different version of this figure, independently created by Roger **Penrose**, would later be called the **Penrose triangle**. Thus began a lifelong fascination with such objects, which later included work on the impossible staircase (a design he sketched in 1950 while on a cross-country train ride), which is known as the **Penrose stairway**, and the discovery of the **tribar illusion**. In the early 1980s the Swedish government honored Reutersvärd's achievements by issuing a set of three stamps depicting impossible figures, including a version of his 1934 weird cubes design.

Rhind papyrus

A papyrus scroll, 33 cm high and 565 cm wide, found in a tomb in Thebes, that is the most valuable source of information we have about Egyptian mathematics. The

scroll was bought at a market in Luxor in 1858 by a 25-year-old Scotsman, Henry Rhind, who went to Egypt for health reasons and became interested in archeology. After his early death at the age of 30, the scroll found its way to the British Museum in London in 1864 and has remained there ever since. It is often referred to as the *Rhind mathematical papyrus,* or RMP for short. The hieroglyphs on the papyrus were deciphered in 1842, while the Babylonian clay-tablet cuneiform writing was deciphered later in the nineteenth century. The text begins by stating that the scribe "Ahmes" is writing it (in about 1600 B.C., and he is thus the earliest named individual in the history of mathematics) but that he has copied it from "ancient writings," which probably go back to at least 2000 B.C. Although there is some strictly practical mathematics on the papyrus, including calculations needed for surveying, building, and accounting, some of which involve **Egyptian fraction**s, many of the problems in the RMP take the form of arithmetic puzzles. One of these is: Seven houses contain seven cats. Each cat kills seven mice. Each mouse had eaten seven ears of grain. Each ear of grain would have produced seven hekats of wheat. What is the total of all of these? This is very similar to the **St. Ives problem**.

There are also four lesser documents preserving Egyptian arithmetic: the Moscow papyrus and the Berlin papyrus (named for the places they are kept), the Kahun papyrus (named for where it was found), and the Leather Roll (named for its composition). The Moscow papyrus is sometimes called the Golenischev papyrus after the Russian V. S. Golenischev, who purchased it in 1893 from two Egyptian brothers who found it in a tomb at Deir el-Bahri. It measures 8 cm high and 540 cm wide and contains 25 problems and their solutions. The most unusual are the tenth, which seems to give the area of the surface of a hemisphere or perhaps a cylinder, and the fourteenth, which gives the formula for the volume of the frustum of a **pyramid**.

rhombus

A **quadrilateral** in which both pairs of opposite sides are parallel and all sides are the same length, that is, an equilateral **parallelogram**. A rhombus is also sometimes called a *rhomb* or a diamond. A rhombus whose acute angles are 45° is called a *lozenge.* The diagonals p and q of a rhombus are perpendicular and satisfy the relationship $p^2 + q^2 = 4a^2$. The area of a rhombus is given by $A = \frac{1}{2}\, pq$.

Richard's paradox

See **Berry's paradox**.

Riemann, (Georg Friedrich) Bernhard (1826–1866)

A German mathematician who was the first person to provide a thorough treatment of **non-Euclidean geometry** and to see how it might be applied in physics; he thus helped pave the way for the general **relativity theory**. Among several profound aspects of mathematics now named after him are the **Riemann hypothesis** and the related **Riemann zeta function**. His father, a Lutheran pastor, encouraged him to study theology at Göttingen. But even as a child Riemann had shown a tremendous aptitude for mathematics and, in 1847, he persuaded his father to let him go to Berlin to learn mathematics from the likes of Karl **Jacobi**, Peter **Dirichlet**, and Jakob **Steiner**. Two years later, he returned to Göttingen to study for his Ph.D. and begin his climb up the professorial ladder. In 1854, his inaugural lecture, "Concerning the hypotheses which underlie geometry," covered a breathtaking array of topics, including a workable definition of the curvature of space and how it could be measured, the first description of **elliptical geometry**, and, most important of all, the extension of geometry into more than three dimensions with the aid of algebra.

Riemann hypothesis

> *If I were to awaken after having slept for a thousand years, my first question would be: Has the Riemann Hypothesis been proven?*
>
> –David Hilbert

The most important open question in **number theory** and, possibly, in the whole of mathematics. A $1 million prize has been offered by the Clay Mathematics Institute for a proof. The hypothesis was first formulated by Bernhard **Riemann** in 1859, was included in David **Hilbert**'s list of challenging problems for twentieth-century mathematicians, and is widely believed to be true. Yet a proof remains tantalizingly out of reach. What the Riemann hypothesis says is that the nontrivial zeros of the **Riemann zeta function** all have real parts equal to $\frac{1}{2}$. In plain language, the hypothesis asserts that there is an underlying order, akin to musical harmonics, in the way **prime number**s are distributed. It's known that for any given number n there are approximately $n/\log n$ prime numbers that are less than n. The formula is not exact: sometimes it is a little high and sometimes it is a little low. Riemann looked at these deviations and found that they contain periodicities. His hypothesis quantifies and formalizes this discovery, positing that the zeros of the zeta function can be regarded as the harmonic frequencies in the distribution of primes. If the Riemann hypothesis turns out to be true, what do these harmonics in the "music" of the primes mean? Remarkably, it is been found by the English physicist Michael Berry and his colleagues that there is a deep connection between the harmonics–the Riemann zeros–and the allowable energy states of physical systems that are on the border between the quantum world (see **quantum**

mechanics) and the everyday world of classical physics. The Riemann harmonics, or "magic numbers," behave exactly like the energy levels in quantum systems that classically would be chaotic. This deep connection between number theory and the physics of the real universe, if upheld, is utterly astonishing. If the Riemann hypothesis is proved true, it could open an entirely new window on the nature of reality and the relationship between the abstract world of mathematics and the behavior of matter and energy. On the other hand, if it is disproven, there will be an even deeper mystery to explore: How can the Riemann zeta function so convincingly mimic a quantum system without actually being one?[40]

Riemann integral

The kind of **integral** familiar from **calculus** texts and normally used by scientists and engineers, in which the process of **integration** of function on an interval amounts to finding the area under the curve.

Riemann sphere

A topological sphere consisting of the **complex plane** and the point at infinity; an example of a **Riemann surface**.

Riemann surface

Also known as a *complex curve,* a complex **manifold** with one complex dimension. The Riemann surface is a conformal structure (see **conformal mapping**).

Riemann zeta function ζ(*s*)

> *We may—paraphrasing the famous sentence of George Orwell—say that "all mathematics is beautiful, yet some is more beautiful than the other." But the most beautiful in all mathematics is the zeta function. There is no doubt about it.*
>
> —Krzysztof Maslanka, Polish cosmologist

One of the most profound and mysterious objects in modern mathematics; from it has sprung the **Riemann hypothesis** and all that this conjecture seems to imply. The Riemann zeta function is closely tied to the distribution of **prime number**s. It is an extension of the *Euler zeta function,* first studied by Leonhard **Euler**, which is the sum

$$\zeta(s) = 1 + 1/2^s + 1/3^s + 1/4^s + \ldots = \sum_{n=1}^{\infty} 1/n^s.$$

Euler found that this function is linked to the occurrence of prime numbers by the following fundamental relationship:

$$\zeta(s) = 1 + 1/2^s + 1/3^s + 1/4^s + \ldots = 2^n/(2^n - 1) \times 3^n/(3^n - 1) \times 5^n/(5^n - 1) \times 7^n/(7^n - 1) \times \ldots = \prod_p 1/(1 - p^{-s})$$

The Riemann zeta function extends the definition of Euler's zeta function to all **complex number**s.

Riemannian geometry

See **elliptical geometry**.

right

A *right angle* is an angle of 90°. A *right triangle* is a triangle that contains a right angle.

ring

(1) Another name for an **annulus**. (2) A number system in which addition, subtraction, and multiplication are always defined and the **associative** and **distributive** laws are valid. Compare with **field**.

Rithmomachia

A medieval, chesslike board game for two players that is based on the number theories of Pythagoras and Boethius. Rithmomachia or "battle of numbers" (*rithmo,* "arithmetic, numbers"; *machia* "battle") dates back to about A.D. 1150 although the earliest publication of the rules was by Jean de Boissiere in the sixteenth century. Used as an educational tool (the only game allowed in medieval schools and universities) and as an intellectual exercise, it enjoyed a last wave of popularity during the Renaissance before the early Scientific Revolution led to its disappearance.

The game is played on an 8 × 16 board. Each player starts with either 24 black or white pieces: 8 circles, 8 triangles, 7 squares, and 1 pyramid. Each of these has a *number,* which is how many places it can move. A square can move 4 spaces, a triangle 3, a circle 1, and the pyramid as many spaces as the player chooses. Opponent pieces can be captured in a variety of ways: *siege capture* (surrounding the opponent piece on all four sides; *meeting capture* (attacking a piece with the same type of piece); *assault capture* (achieved if the piece's number times the number of spaces it moved lands it next to an opposing piece that equals the product); *ambuscade* (achieved if two pieces of a player that are on either sides of a piece sum to equal the opponent's piece). There are also a number of different ways to win, including: *de corpore* (players agree on a number of pieces to be captured); *de bonis* (players agree on a number value target); *de lite* (the winner is determined by the sum of the pieces as well as the number of digits on all those pieces); *victoria magna* (if there is a common difference between the pieces a player has captured, or the squares of three consecutive integers are captured; or there is a difference of 2, 4, and 6 in even pieces, or 3, 5, and 7 in odd pieces).

river-crossing problem

A puzzle in which a variety of objects and living things, some of them mutually incompatible, must be conveyed in small groups from one side of a river to another without any loss along the way. The earliest known examples are in *Propositiones ad Acuendos Juvenes* (Propositions for sharpening youths), which is generally attributed to Abbott **Alcuin**. They are: the problem of three jealous husbands (each of whom won't let another man be alone with his wife), the problem of the two adults and two children where the children weigh half as much as the adults (and the boat has a limited weight capacity), and the problem of the wolf, the goat, and the cabbage. In the last case, the difficulty is that only one item can be ferried across at once but, if left unattended, the sheep will eat the cabbage and the wolf will eat the sheep. The solution, which involves a stratagem common to all these types of problems, is to bring back to the starting bank of the river an item that has already been taken across. In this case, the sheep must be taken across first, followed by either the cabbage or the wolf, but then the sheep must be brought back before the next item is taken across to avoid the sheep becoming either a diner or a dinner.

These medieval puzzles were considered and elaborated on by Niccoló **Tartaglia**, Luca **Pacioli**, and Claude-Gaspar **Bachet**, and even more so by later mathematicians such as Edouard **Lucas** and Gaston **Tarry**. Ways of complicating river-crossing problems include adding more people and objects, using a bigger boat, and inserting an island in the river. The reader may care to try the problem of the missionaries and the cannibals.

PUZZLE

Three missionaries and three cannibals must cross a river in a boat that holds a maximum of two people. If the cannibals outnumber the missionaries, on either side of the river, the missionaries are in trouble. Each missionary and each cannibal is capable of rowing the boat. How can all six get across the river safely?

Solutions begin on page 369.

Robinson, Abraham (1918–1974)

A German-born mathematician who founded **nonstandard analysis** and did important work in a wide diversity of fields from aerodynamics to mathematical logic. A modern counterpart to Gottfried **Leibniz** in his range of interests and the significance of his research on **infinitesimal**s, Robinson (he changed his name from Robinsohn) taught at various universities in Israel, England, Canada, and the United States.

Rolle's theorem

Suppose a continuous function (see **continuity**) crosses the *x*-axis at two points *a* and *b* and is differentiable at all points between *a* and *b;* that is, it has a **tangent** at all points on the curve between *a* and *b*. Then there's at least one point between *a* and *b* where the **derivative** is 0, and the tangent is parallel to the *x*-axis.

Roman numerals

A **number system** in which each symbol represents a fixed value regardless of its position; this differs from the place-value system of **Arabic numeral**s. The earliest form of the Roman system was, however, decimal. In this primitive version a series of I's represented any number from 1 to 9, and a new symbol was introduced for each higher power of 10: X for 10, C for 100, and M for 1,000. The symbols V, L, and D, which stand for 5, 50, and 500, are thought to have been introduced by the Etruscans. A common remark is that multiplication and division using Roman numerals is so awkward that it is totally impractical. However, an article by James G. Kennedy in *The American Mathematical Monthly* in 1980 gives algorithms for these operations that are actually more straightforward in the Roman system than in the Arabic. In multiplication the first step is to rewrite the numbers in a simple place-value notation. Seven columns are set up, headed by the symbols M, D, C, L, X, V, and I, and tallies are marked in each column corresponding to the number of times that symbol appears in the multiplicand. For example, if the multiplicand is XIII (13), one tally is marked in the X column and three tallies are marked in the I column. The multiplier is written in the same way. The multiplication itself is done by forming partial products according to two simple rules. In most cases the partial product given by any one tally in the multiplier is simply the set of tallies that represents the multiplicand, shifted to the left an appropriate number of columns. If the multiplier digit is I, the multiplicand is not shifted at all; the multiplicand is shifted one place to the left for V, two places for X, three places for L, and so on. The second rule is applied only when one Etruscan character is multiplied by another. In such cases the tallies representing the multiplicand digit are written twice in the appropriately shifted column and an additional tally is written one column to the right. Once a partial product has been formed for every tally in the multiplier, the tallies in each column are accumulated and replaced by the Roman symbol at the head of the column, giving the final answer. Only a slight change in the method is needed for Roman numerals in "subtractive notation," where 10 is written as IX, and so on. If all this sounds not quite so simple, the method for multiplying Arabic numbers is just as

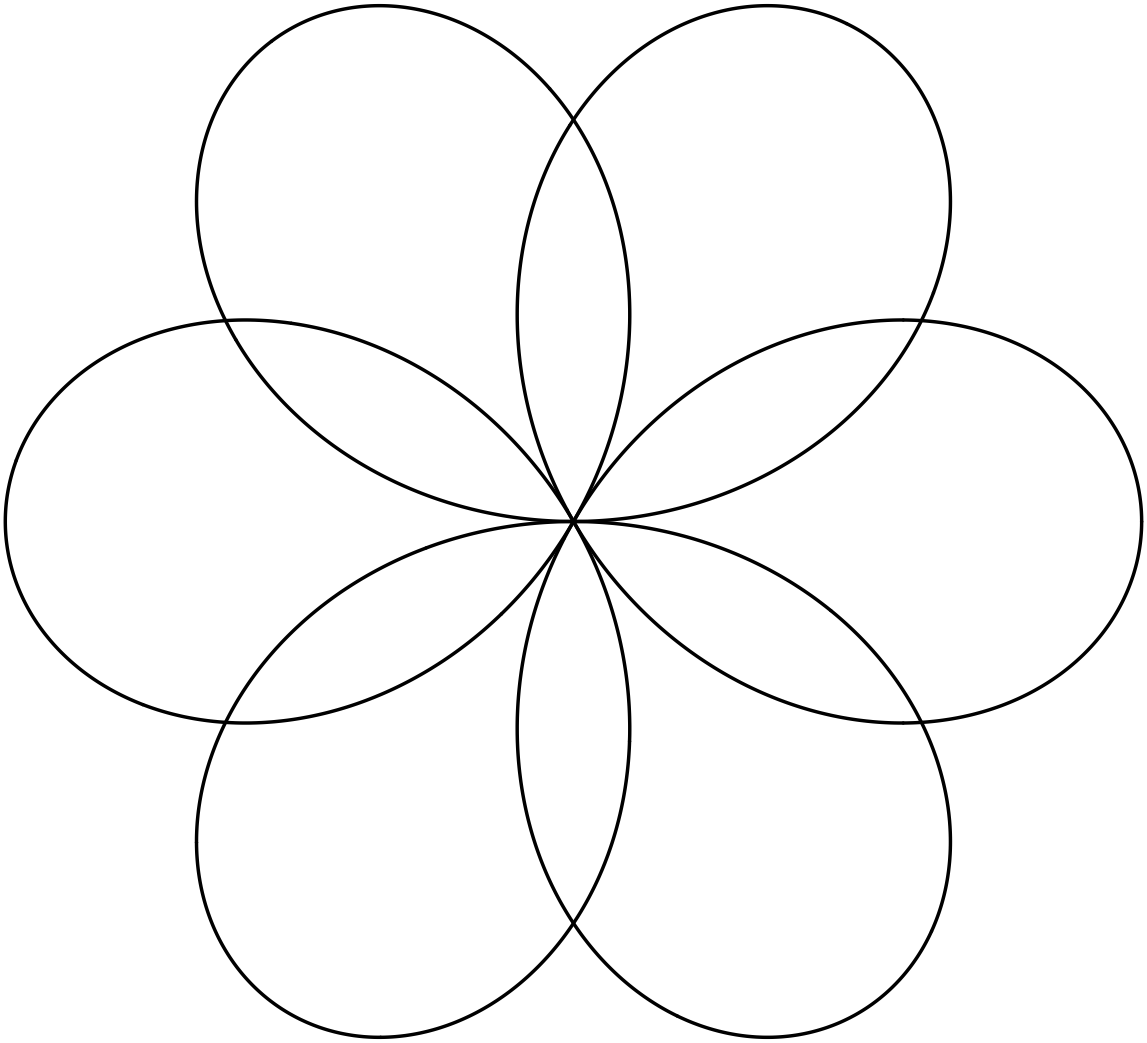

rose curve *© Jan Wassenaar, www.2dcurves.com*

involved if they are written in explicit form. Furthermore, Arabic operations require a multiplication table giving the 100 products of all the possible pairs of Arabic digits. No comparable table is needed with Roman numerals, where all arithmetical operations can be defined in terms of shifting rules, addition, and subtraction.

rooks problem

To find the maximum number of rooks that can be placed on an $n \times n$ **chess**board such that no rook attacks another. Since each rook attacks all squares in the rank and file upon which it rests, this number is *n:* the rooks may be placed along the main diagonal. The total number of ways of placing n nonattacking rooks is n factorial ($n!$).

root

(1) A number used to build up another number by repeated multiplication. For example, since $2 \times 2 \times 2 = 8$, two is said to be the third root or cube root of eight. (2) A solution of an equation. For example, 3 is a root of the

Rubik's cube *Peter Knoppers, www.buttonius.com*

equation $x^2 = 9$. A root is also called a *zero of a function* because it is a value that will make the function zero ($x = 3$ will make the function $f(x) = x^2 - 9$ zero. The word comes from the Indo-European *werad*, which originally meant the roots of a plant but was later generalized to mean the origins or beginnings of something, whether it was physical or mental.

root of unity

A solution of the equation $x^n = 1$, where n is a positive integer.

rope around the earth puzzle

Imagine a rope that fits snugly all the way around Earth like a ring on a person's finger. Now imagine the rope is made just 1 meter longer and lifted uniformly off the surface until it is once again taught. What will its height be above the surface? This puzzle, or one very like it, appeared in a students' book on Euclid written in 1702 by the English clergyman, mathematician, and natural philosopher William Whiston (1667–1752). The answer in the form just given is remarkable: about 16 cm. It comes simply from the formula for the circumference of a circle. If the extra radius of the rope is r and Earth's radius is R, then

$$2\pi(R + r) = 2\pi R + 100$$
so that $r = 100/2\pi \cong 15.9$.

Rosamund's bower

A legendary **maze**, located in Woodstock Park, Oxfordshire, whose purported site is marked today by a well and fountain. It was supposedly intended to conceal Rosamund Clifford, the mistress of King Henry II (1133–1189), from the queen, Eleanor of Aquitaine. Legend has it that about 1176, Eleanor managed to solve the maze and confronted Rosamund with the choice of a dagger or poison; she drank the poison and Henry

never smiled again. Historically, Henry had imprisoned Eleanor for fomenting rebellion by her sons, and Rosamund was his acknowledged mistress. Rosamund probably spent her last days at a nunnery in Godstow, near Oxford. The legend of the bower dates from the fourteenth century and her murder is a later addition. In the nineteenth century, many puzzle collections had a maze called Rosamund's bower.

rose curve

A curve that has the shape of a flower with petals; it was named *rhodonea* ("rose") by the Italian mathematician Guido Grandi in the 1720s. It is given by the polar equation

$$r = a \sin (n\theta).$$

If n is odd the rose has n petals, if n is even the rose has $2n$ petals, and if $n = 2$ the rose becomes the **quadrifolium**. If n is an *irrational* **number**, then there are an infinite number of petals.

rotation

A **transformation** in which a figure turns through a specific angle about a fixed point, called the center of rotation. The center of rotation may be inside or outside the figure that is being transformed. If the figure is turned anticlockwise, the rotation is considered positive, while a negative rotation turns the figure clockwise.

rotor

A **convex** figure that can be rotated inside a **polygon** (or **polyhedron**) while always touching every side (or face). The least area rotor in a square is the **Reuleaux triangle**. The least area rotor in an equilateral triangle is a lens with two 60° arcs of circles and a radius equal to the triangle's altitude. There exist nonspherical rotors for the tetrahedron, octahedron, and cube, but not for the dodecahedron and icosahedron. See also **curve of constant width**.

roulette

(1) The curve traced by a fixed point on a closed **convex** curve as that curve rolls without slipping along a second curve. (2) A gambling game in which players bet on which slot of a rotating disk a small ball will come to rest in. On August 18, 1913, on an unbiased roulette wheel at Monte Carlo, evens came up 26 times in a row. The probability of this occurring is 1 in 136,823,184.

round

In **topology**, the terms ***circle*** and ***sphere*** refer to topological objects and not geometric ones, so that the surface of an egg shape is a sphere. A *round sphere* is, topologically speaking, not a tautology, but a sphere with constant **curvature**; that is, a sphere in the sense of geometry.

rounding

Replacing a number by another number having fewer **significant digits** or, for integer numbers, fewer value-carrying (nonzero digits). For example, 386.804 may be rounded successively to 386.80, 386.8, 387, 390, and 400. Rounding may be carried out in two ways: by *rounding down,* which is equivalent to truncation, and by *rounding up* the last digit to be retained by one unit. See also **banker's rounding**.

round-off error

The error accumulated during a calculation due to rounding intermediate results. See also **banker's rounding**.

Rubik's cube

A $3 \times 3 \times 3$ cube in which the 26 subcubes on the outside are internally hinged in such a way that rotation (by a quarter turn in either direction or a half turn) is possible in any plane of cubes. Each of the six sides is painted a distinct color, and the goal of the puzzle is to return the cube to a state in which each side has a single color after it has been randomized by repeated rotations. Invented in 1974 by the Hungarian Ernö Rubik, patented in 1975, and put on the market in Hungary in 1977, it went on to sell some 100 million copies worldwide over the next decade. Since there are over 43 million trillion different arrangements of the small cubes, only one of which corresponds to the desired goal, to solve Rubik's cube in a time significantly less than the current age of the universe (let alone the world record, which stands at around 20 seconds) calls for some kind of methodical approach. Algorithms exist for solving a cube from an arbitrary initial position, but they are not necessarily optimal (i.e., requiring a minimum number of turns).[270, 297]

Rucker, Rudy (Rudolf von Bitter) (1946–)

An American mathematician best known for his entertaining popular mathematics, science, and science fiction books, including *Infinity and the Mind,*[275] *The Fourth Dimension,*[273] and *Mind Tools.*[274] Rucker has a doctorate in mathematical logic from Rutgers and teaches at San José State University. His great-great-great-grandfather was the famous German philosopher Georg Hegel.

ruled surface

A surface that is built up from an infinite number of perfectly straight lines. A **cylinder**, for example, is a ruled

surface of parallel straight lines. A **cone** is a ruled surface of straight lines that meet at the apex of the cone. Also known as *scrolls,* ruled surfaces have been studied for centuries by geometers such as the Jesuits Roger Boscovich and Andre Tacquet as well as by their famous students, including Gaspar **Monge** and Phillippe de Lahire. Examples that stand out because of both their striking shape and their relative ease of construction include **hyperboloid**s, **helicoid**s and **Möbius band**s. Most ruled surfaces, however, are so complicated that, before the computer age, they were almost impossible to construct.

ruler-and-compass construction

See **Mascheroni construction**.

Russell, Bertrand Arthur William (1872–1970)

A British philosopher, mathematician, and logician who rose to prominence with his first major work, *The Principles of Mathematics* (1902), in which he attempted to remove mathematics from the realm of abstract philosophical notions and to give it a precise scientific framework. Russell then collaborated for eight years with the British philosopher and mathematician Alfred North Whitehead (1861–1947) to produce the monumental work *Principia Mathematica* (3 volumes, 1910–1913). This work showed that mathematics can be stated in terms of the concepts of general **logic**, such as class and membership in a class. It became a masterpiece of rational thought. Russell and Whitehead proved that numbers can be defined as classes of a certain type, and in the process they developed logic concepts and a logic notation that established symbolic logic as an important specialization within the field of philosophy. In his next major work, *The Problems of Philosophy* (1912), Russell borrowed from the fields of sociology, psychology, physics, and mathematics to refute the tenets of idealism, the dominant philosophical school of the period, which held that all objects and experiences are the product of the intellect. Russell, a realist, believed that objects perceived by the senses have an inherent reality independent of the mind.

Russell condemned both sides in World War I, and for his uncompromising stand he was fined, imprisoned, and deprived of his teaching post at Cambridge. In prison he wrote *Introduction to Mathematical Philosophy* (1919). After the war he visited the Soviet Union, and in his book *Practice and Theory of Bolshevism* (1920) he expressed his disappointment with the form of socialism practiced there. He felt that the methods used to achieve a Communist system were intolerable and that the results obtained were not worth the price paid. Russell taught at Beijing University during 1921 and 1922, and in the United States from 1938 to 1944, though he was barred from teaching at the College of the City of New York (now City College of the City University of New York) by the state supreme court because of his attacks on religion and his advocacy of sexual freedom. Russell returned to England in 1944 and was reinstated as a fellow of Trinity College. Although he abandoned pacifism to support the Allied cause in World War II, he became an ardent opponent of nuclear weapons. Russell received the 1950 Nobel Prize for Literature and was cited as "the champion of humanity and freedom of thought." He led a movement in the late 1950s advocating unilateral nuclear disarmament by Britain, and at the age of 89 he was imprisoned after an antinuclear demonstration.[276]

Russell's paradox

A **paradox** uncovered by Bertrand **Russell** in 1901 that forced a reformulation of **set theory**. One version of Russell's paradox, known as the barber paradox, considers a town with a male barber who, every day, shaves every man who doesn't shave himself, and no one else. Does the barber shave himself? The scenario as described requires that the barber shave himself if and only if he does not! Russell's paradox, in its original form considers the set of all sets that aren't members of themselves. Most sets, it would seem, aren't members of themselves–for example, the set of elephants is not an elephant–and so could be said to be "run-of-the-mill." However, some "self-swallowing" sets *do* contain themselves as members, such as the set of all sets, or the set of all things except Julius Caesar, and so on. Clearly, every set is either run-of-the-mill or self-swallowing, and no set can be both. But then, asked Russell, what about the set *S* of all sets that aren't members of themselves? Somehow, *S* is neither a member of itself nor not a member of itself. Russell discovered this strange situation while studying a foundational work in symbolic logic by Gottlob **Frege**. After he described it, set theory had to be reformulated axiomatically in a way that avoided such problems. Russell himself, together with Alfred North Whitehead (1861–1947), developed a comprehensive system of types in *Principia Mathematica.* Although this system does avoid troublesome paradoxes and allows for the construction of all of mathematics, it never became widely accepted. Instead, the most common version of axiomatic set theory in use today is the *Zermelo-Fraenkel set theory,* which avoids the notion of types and restricts the universe of sets to those that can be built up from given sets using certain axioms. Russell's paradox underlies the proof of **Gödel's incompleteness theorem** as well as Alan **Turing**'s proof of the undecidability of the **halting problem**.

Russian multiplication

Multiplication by repeated doubling, also known as *peasant multiplication*. For example to multiply 17 by 13, double the 17 and halve the 13 rounding down to the next whole number where necessary; then add the doubles that correspond to an odd number in the other column.

So	17×13
doubled and halved	34×6
doubled and halved	68×3
doubled and halved	136×1

adding up the numbers in the first column that correspond to an odd number in the second
$(17 + 68 + 136) = 221 = 17 \times 13$.

S

Saccheri, Giovanni Girolamo (1667–1733)

A Jesuit priest, philosopher, and mathematician who did early work on **non-Euclidean geometry**, although he didn't see it as such. His *Euclides ab Omni Naevo Vindicatus* (1733) was actually an attempt to prove Euclid's **parallel postulate** but ended up laying the groundwork for both **hyperbolic geometry** and **elliptical geometry**.

saddle

A type of surface that is neither a peak nor a valley but still has a zero gradient. Saddle points are situated such that moving in one direction takes one uphill, while moving in another direction would be downhill. A *saddle function* is a **function** $f(x, y)$ of two vectors x and y (which typically lie in different **vector spaces**) that is **concave** up in x and concave down in y. See also **pseudosphere**.

St. Ives problem

A well-known and simple puzzle in arithmetic set by Mother Goose in the rhyme "As I Was Going to St. Ives":

> As I was going to St. Ives, I met a man with seven wives. Every wife had seven sacks, and every sack had seven cats, every cat had seven kittens. Kittens, cats, sacks, and wives, how many were going to St. Ives?

The various individuals and items make up a **geometric sequence**: 7 wives + 7^2 sacks + 7^3 cats + 7^4 kittens = 7 + 49 + 343 + 2,401. This gives a total of 2,800 (or 2,801 if the narrator also happens to be a wife). It's been said that the real answer to this rhyme is 1, since "I *met* a man with seven wives" means the 2,800 were going in the *opposite* direction!

A similar problem, and solution, is contained in the **Rhind papyrus** by Ahmose, written about 1650 B.C. (some of which is copied from an older document of about 1800 B.C.). Here the geometric series has one more power of 7: 7 houses + 49 cats + 343 mice + 2,401 ears of grain + 16,807 hekats (a measure) of grains, giving a total of 19,607.

St. Petersburg paradox

A strange state of affairs that arises from a game proposed by Nikolaus (I) Bernoulli (see **Bernoulli family**) in 1713. It is named after the fact that a treatise on the paradox was written by Nikolaus' cousin, Daniel, and published (1738) in the *Commentaries of the Imperial Academy of Science of St. Petersburg.* The game goes as follows. You toss a coin. If it shows heads, you win whatever is in the pot and the game is over. If it shows tails, the pot is doubled and you get to toss the coin again. If the coin shows heads on the first toss you win \$2; if it shows tails, you toss again. If the coin now shows heads you win \$4, and so on. After n tosses you get $\$2^n$ if heads appear for the first time. The only catch is you have to pay to play the game. How much should you be willing to pay? Classical decision theory says that you should be willing to pay any amount up to the expected prize, the value of which is obtained by multiplying all the possible prizes by the probability that they are obtained and adding the resulting numbers. The chance of winning \$2 is ½ (heads on the first toss); the chance of winning \$4 is ¼ (tails followed by heads); the chance of winning \$8 is ⅛ (tails followed by tails followed by heads); and so on. Since the expected payoff of each possible consequence is \$1 (\$2 × ½, \$4 × ¼, etc.) and there are an infinite number of them, the total expected payoff is an infinite sum of money. A rational gambler would enter a game if and only if the price of entry was less than the expected value. In the St. Petersburg game, any finite price of entry is smaller than the expected value of the game. Thus, the rational gambler would play no matter how large the entry price was! But there's clearly something wrong with this. Most people would offer between \$5 and \$20 on the grounds that the chance of winning more than \$4 is only 25% and the odds of winning a fortune are very small. And therein lies the paradox: If the expected payoff is infinite, why is no one willing to pay a huge amount to play?

The classical solution to this mystery, provided by Daniel Bernoulli and another Swiss mathematician, Gabriel Cremer, goes beyond probability theory to touch areas of psychology and economics. Bernoulli and Cremer pointed out that a given amount of money isn't always of the same use to its owner. For example, to a millionaire \$1 is nothing, whereas to a beggar it can mean not going hungry. In a similar way, the utility of \$2 million is not twice the utility of \$1 million. Thus, the important quantity in the St. Petersburg game is the *expected utility* of the game (the utility of the prize multiplied by its probability) which is far less than the *expected prize.* This explanation forms the theoretical basis of the insurance business. The existence of a **utility function**

means that most people prefer, for example, having \$98 in cash to gambling in a lottery where they could win \$70 or \$130 each with a chance of 50%, even though the lottery has the higher expected prize of \$100. The difference of \$2 is the premium most of us would be willing to pay for insurance. That many people pay for insurance to avoid any risk, yet at the same time spend money on lottery tickets in order to take a risk of a different kind, is another paradox, which is still waiting to be explained.

salient

At a *salient point,* two branches of a curve meet and stop, and have different **tangent**s. A *salient angle* is an outward-pointing angle of a **polygon**; compare with **reentrant angle**.

salinon

A figure formed from four connected semicircles. The word *salinon* is Greek for "salt cellar," which the figure resembles. In his *Book of Lemmas,* **Archimedes** proved that the salinon has an area equal to the circle having the line segment joining the top and bottom points as its diameter. See also **arbelos**.

Sallows, Lee C. F. (1944–)

A British electronics engineer and puzzle enthusiast at the University of Nijmegen in the Netherlands. Among his many accomplishments in recreational mathematics, he devised the first **self-enumerating sentence** (published in 1982), introduced **alphamagic square**s in 1986, coined the word ***golygon*** in 1990, invented reflexicons (minimal self-enumerating phrases) in 1992, demonstrated the parallelogram theorem for 3×3 **magic square**s in 1997, and discovered **geometric magic squares** in 2001.

scalar

A quantity specified by a single number or value (as opposed to a vector, matrix, or array) that contains multiple values. Examples of scalars include mass, volume, and temperature. A *scalar field* is an arrangement of scalar values distributed in a space.

scalene triangle

A **triangle** whose sides are all unequal.

schizophrenic number

An informal name for an **irrational number** that displays such persistent patterns in its decimal expansion, that it

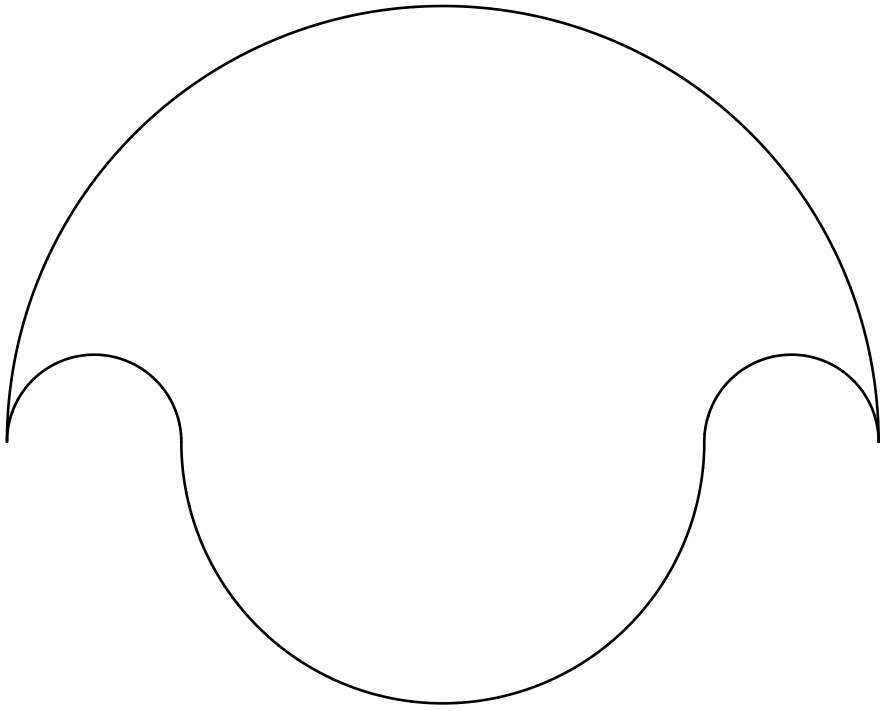

salinon *© Jan Wassenaar, www.2dcurves.com*

has the appearance of a **rational number**. A schizophrenic number can be obtained as follows. For any positive integer n let $f(n)$ denote the integer given by the recurrence $f(n) = 10f(n-1) + n$ with the initial value $f(0) = 0$. Thus, $f(1) = 1, f(2) = 12, f(3) = 123$, and so on. The square roots of $f(n)$ for odd integers n give rise to a curious mixture appearing to be rational for periods, and then disintegrating into irrationality. This is illustrated by the first 500 digits of $\sqrt{f(49)}$:

```
11111111111111111111111.11111111111111111111          0860
55555555555555555555555555555555555555555555          2730541
66666666666666666666666666666666666666666666          0296260347
22222222222222222222222222222222222222                0426563940928819
44444444444444444444444444444444                      38775551250401171874
99999999999999999999999999                            80824968771148630533854l
66666666666666666666                                  59871857386214406386555989 58
33333333333333333333                                  08434604076276082069402770996093 74
99999999999999                                        06422275875559830666394303215874565 97
222222222                                             18634920167911808330818 44 . . . .
```

The repeating strings become progressively shorter and the scrabbled strings become larger until eventually the repeating strings disappear. However, by increasing n we can forestall the disappearance of the repeating strings as long as we like. The repeating digits are always 1, 5, 6, 2, 4, 9, 6, 3, 9, 2, ...

Schläfli, Ludwig (1814–1895)

A German mathematician whose work centered on geometry, arithmetic, and the theory of functions. He made an important contribution to **non-Euclidean geometry** when he proposed that spherical three-dimensional space could be thought of as the surface of a **hypersphere** in Euclidean four-dimensional space. Schläfli started out as a schoolteacher and amateur mathematician. He was also an expert linguist and spoke many languages, including Sanskrit. In 1843 he served as a translator for the great mathematicians Jakob **Steiner**, Karl **Jacobi**, and Peter **Dirichlet** during their visit to Rome and learned a great deal from them. Ten years later he became professor of mathematics at Bern. However, his true importance was only appreciated following the publication of his magnum opus *Theory of Continuous Manifolds* in 1901, several years after his death.

Schläfli symbol

A notation, devised by Ludwig **Schläfli**, which describes the number of edges of each **polygon** meeting at a **vertex** of a regular or semi-regular **tessellation** or solid. For a **Platonic solid**, it is written $\{p, q\}$, where p is the number of sides each face has, and q is the number of faces that touch at each vertex.

schoolgirls problem

A problem in **combinatorics** posed by the Rev. Thomas **Kirkman** in a letter in 1850 following a paper he wrote on the same subject in 1847:[188] A school mistress has fifteen girl pupils and she wishes to take them on a daily walk. The girls are to walk in five rows of three girls each. It is required that no two girls should walk in the same row more than once per week. Can this be done?

In fact, provided n is divisible by 3, we can ask the more general question about n schoolgirls walking for $(n-1)/2$ days so that no girl walks with any other girl in the same triplet more than once. Solutions for $n = 9$, 15, and 27 were given in 1850 and much work was done on the problem thereafter. The general problem of how many triads can be made out of **n** symbols, so that no pair of symbols is comprised more than once among them gave rise to the study of Steiner triple systems. However, Jakob **Steiner** had little to do with them and they should rightfully be named after Kirkman. They are important in the modern theory of **combinatorics**.

Schröder's reversible staircase

A classic example of an **ambiguous figure**, first drawn by Schröder in 1858. Not to be confused with the **Penrose stairway**.

Schubert, Hermann Cäsar Hannibal (1848–1911)

A German mathematician who worked mainly in enumerative geometry–the parts of algebraic geometry that

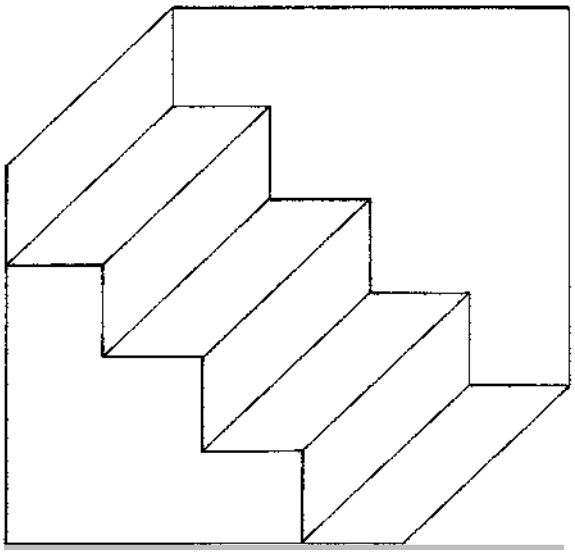

Schröder's reversible staircase

involve a finite number of solutions. He also wrote extensively on recreational math.

Schuh, Frederick (1875–1966)
A Dutch mathematician who wrote many textbooks and a number of books on recreational mathematics, including *The Master Book of Mathematical Recreations* (1943), the English edition of which appeared in 1968 (Dover Publications).[291] Schuh was professor of mathematics at the Technische Hoogeschool at Delft (1907–1909 and 1916–1945) and professor of mathematics at Groningen (1909–1916).

scientific notation
A number of the form $a \times 10^n$, where n is an integer, positive or negative, and a is a **real number** larger than or equal to 1, but less than 10. Scientific notation provides a compact way of writing **large number**s.

scintillating grid illusion
See **Hermann grid illusion**.

score
A group of 20 items. The word comes from the Old Norse *skor* for a heavy mark used to indicate a string of 20 smaller marks; *skor,* in turn, is descended from the Indo-European *sker,* for "cutting" or "slicing." From about 1400, *score* was also the word for a record or an amount due–the total of the score marks on a tally. It became a common word for the total of a tradesman's or innkeeper's account. So, *to settle the score* originally meant just to pay one's bill. But it acquired the figurative sense of taking revenge on somebody, and that's usually what is meant by the expression now. The more general meaning of score, as a tally, is used daily when the results of sports competitions are reported.

search space
A characterization of every possible solution to a problem instance.

secant
A straight line that meets a curve in two or more points.

second
One-sixtieth of a **minute** in both time and angle. Literally, the second division of the hour or the circle, the minute being the first; from the Latin *secundus.* In the System International d'Unites (SI units) one second is defined as the duration of 9,192,631,770 periods of radiation corresponding to the transition between two hyperfine levels of cesium-133 in a ground state at a temperature of 0°K (Kelvin).

secretary problem
See **sultan's dowry**.

sector
Part of a **circle** bounded by two radii and the included **arc**.

segment
Part of a **circle** bounded by a **chord** and the **arc** subtending the chord.

self-enumerating sentence
Also known as an *autogram,* a **self-referential sentence** whose text consists solely of the enumeration of its letter content. The answer to the question whether such a sentence exists in English was given by Lee **Sallows**, and was first published in *Scientific American* in January 1982:

> Only the fool would take trouble to verify that his sentence was composed of ten a's, three b's, four c's, four d's, forty-six e's, sixteen f's, four g's, thirteen h's, fifteen i's, two k's, nine l's, four m's, twenty-five n's, twenty-four o's, five p's, sixteen r's, forty-one s's, thirty-seven t's, ten u's, eight v's, eight w's, four x's, eleven y's, twenty-seven commas, twenty-three apostrophes, seven hyphens and, last but not least, a single !

This remarkable sentence counts not only its own letters, but also its punctuation marks, although it fails to enumerate three letters of the alphabet (j, q, and z). Sallows went on to devise a "pangram machine"–a computer purposely built to search for sentences of this type. Among its many successes is:

> This pangram lists four a's, one b, one c, two d's, twenty-nine e's, eight f's, three g's, five h's, eleven i's, one j, one k, three l's, two m's, twenty-two n's, fifteen o's, two p's, one q, seven r's, twenty-six s's, nineteen t's, four u's, five v's, nine w's, two x's, four y's, and one z.

self-intersecting
A *self-intersecting polygon* is a **polygon** with edges that cross other edges. A *self-intersecting polyhedron* is a **polyhedron** with faces that cross other faces.

self-organization
A process in a **complex system** whereby new emergent structures, patterns, and properties arise without being externally imposed on the system. Not controlled by a centralized, hierarchical "command and control" center, self-organization is usually distributed throughout a system. It requires a complex, **nonlinear system** under

appropriate conditions, variously described as "far-from-equilibrium," critical values of control parameters leading to "bifurcation," or the "edge of chaos." First investigated in the 1960s in physical systems by Ilya Prigogine and his followers, as well as the Synergetics School founded by Hermann Haken, self-organization is now studied mainly through computer simulations (see **cellular automaton**), Boolean networks, and other phenomena of **artificial life**. However, self-organization is now recognized as a crucial way of understanding emergent, collective behavior in a large variety of systems including the economy, the brain and nervous system, the immune system, and ecosystems. The buildup of system order via self-organization is now conceived as a primary tendency of complex systems in contrast to the past emphasis on the degrading of order in association with the principle of entropy (Second Law of Thermodynamics). However, rather than denying entropy, self-organization can be understood as a way that entropy increases in complex, nonlinear systems.

self-organized criticality

A mathematical theory that describes how systems composed of many interacting parts can tune themselves toward dynamical behavior that is critical in the sense that it is neither stable nor unstable but at a region near a **phase transition**. See also **edge of chaos** and **self-organization**.

self-referential sentence

A sentence that refers to itself and nothing else. Here are some examples:

> This statement is short.
>
> This sentence has five words.
>
> The last word of this sentence is "wrong."
>
> "Pentasyllabic" is pentasyllabic.
>
> How long is the answer to this question? Ten letters.

Some self-referential statements take the form of jokes. For example:

> The two rules for success are: Never tell them everything you know.
>
> There are three kinds of people in the world: those who can count and those who can't.

Finally, some take the form of maxims, as in this case by Thomas Macaulay (1800–1859):

> Nothing is so useless as a general maxim.

See also **Hofstadter's law**.

self-similarity

The property an object has when a part of itself looks the same or similar to the whole. Many objects in the real world, such as coastlines, are statistically self-similar: parts of them show the same statistical properties at many scales. Self-similarity is a defining characteristic of **fractal**s.

semigroup

A **set** together with a method of combining elements, such as addition or multiplication, to get new ones, which satisfies only some of the properties required to get a **group**. In particular, a semigroup need not have an **identity** element and elements need not have **inverse**s.

semi-magic square

A square array of n numbers such that sum of the n numbers in any row or column is a constant (known as the magic sum). See also **magic square**.

semi-regular polyhedron

A **polyhedron** that consists of two or more types of **regular polygon**s, all of whose vertices are identical. This category includes the **Archimedean solid**s, **prism**s and **antiprism**s, and the nonconvex uniform polyhedra (see **nonconvex uniform polyhedron**).

Senet

A popular two-player board game in ancient Egypt, enjoyed by both commoners and nobility, that may be an ancestor of modern **backgammon**. The rules are not known, though about 40 sets have been found in tombs, some in very good condition, together with paintings of games on tomb walls, dating back to the reign of Hesy (c. 2686–2613 B.C.). Senet, or the "game of passing," was played on a rectangular board consisting of three rows of 10 squares called "houses" that represented good or bad fortune. The board could be a grid drawn on a smooth surface or an elaborate box of wood and other precious materials. A perfectly preserved traveling version of Senet was found in Tutankhamen's tomb. The pieces, called *ibau* ("dancers" in Egyptian), varied in number from five to ten per player–five and seven being commonest. Cone-shaped pieces were pitted against reel-shaped pieces. The object was to get one's pieces on the board, then around the board in an S-shaped pattern, and finally off again at the far end. Strategy was mixed with chance (as it is in backgammon), introduced by the throw of four, two-sided sticks (as depicted in the Hesy painting) or, in later times, of knucklebones. Later depictions of the game, in the New Kingdom period, often showed just one player in competition–the opponent being a spirit from the afterlife. This has been interpreted as a change

Senet A modern version of the ancient Egyptian board game. *Fundex Games Ltd.*

in the significance of Senet, from a simple amusement to a symbolic representation of the deceased's journey through the underworld. See also **nine men's morris**.

sensitivity
The tendency of a system, which may be chaotic (see **chaos**) to change dramatically with only small **perturbation**s.

sequence
An ordered list of values that may be finite or infinite in length. Among the different types of sequence are **arithmetic sequence**s, **geometric sequence**s, and the **harmonic sequence**.

series
A sum of all or some of the terms of a **sequence**. A series may or may not *converge* to a particular value as more and more terms are included. A series is said to be *absolutely convergent* if the sum of the absolute values of the terms converges; in this case the series converges no matter how the terms of the sum are arranged. Series that are *conditionally convergent* only converge for some arrangements of the terms and, even then, converge to different values for different arrangements.

serpentine
A curve named and studied by Isaac **Newton** in 1701 and contained in his classification of **cubic curve**s. It had been studied earlier by **de L'Hôpital** and Christiaan **Huygens** in 1692. The curve is given by the Cartesian equation

$$y(x) = abx/(x^2 - a^2).$$

set
A finite or infinite collection of objects known as *elements*. Sets are one of the most basic and important concepts in mathematics. An example of a finite set is the set of whole numbers from 1 to 58; an example of an infinite set is the set of all the **rational number**s. Two sets are equal if, and only if, they contain the same objects. Standard notation uses braces around the list of elements, as in: {red, green, blue}. If A and B are two sets and every x in A is also contained in B, then A is said to be a *subset* of B. Every set has as subsets itself, known as the *improper subset*, and the **empty set**. The *union* of a collection of sets $S = \{S_1, S_2, S_3, \ldots\}$ is the set of all elements contained in at least one of the sets $S_1, S_2, S_3, \ldots$. The *intersection* of a collection of sets $T = \{T_1, T_2, T_3, \ldots\}$ is the set of all elements contained in all of the sets. The union and intersection of sets, say A_1 and A_2, is denoted $A_1 \cup A_2$ and $A_1 \cap A_2$, respectively. The set of all subsets of X is called its *power set* and is denoted 2^X or $\mathrm{P}(X)$. See also **set theory**, **Venn diagram**, and **Russell's paradox**.

set of all sets
See **Russell's paradox**.

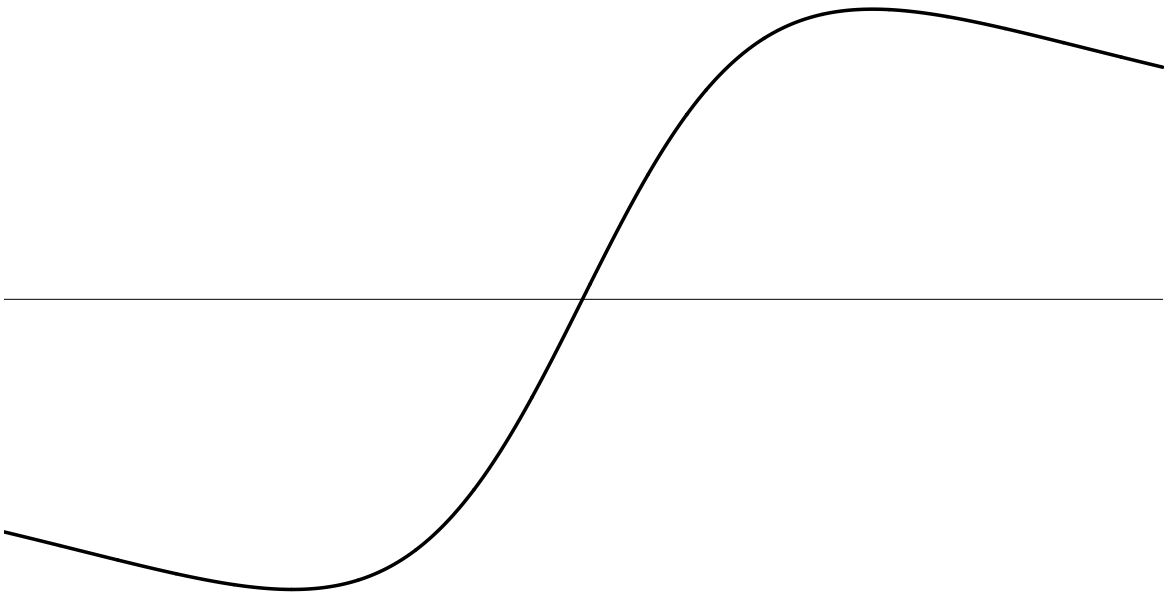

serpentine The serpentine curve. © *Jan Wassenaar, www.2dcurves.com*

set theory

A branch of **mathematics** created by Georg **Cantor** at the end of the nineteenth century. Initially controversial, set theory has come to play a foundational role in modern mathematics, in that it is used to justify assumptions made concerning the existence of mathematical objects (such as numbers or functions) and their properties. Formal versions of set theory also figure centrally in specifying a theoretical ideal of mathematical rigor in proofs. Cantor's basic discovery was that if we define two sets A and B to have the same number of members (the same *cardinality*), then there is a way of pairing off members of A exhaustively with members of B. The appearance around the turn of the century of set-theoretical paradoxes, such as **Russell's paradox**, prompted the formulation in 1908 by Ernst Zermelo of an axiomatic theory of sets. The axioms for set theory now most often studied and used are those called the *Zermelo-Fraenkel axioms,* usually together with the **axiom of choice**. The Zermelo-Fraenkel axioms are commonly abbreviated to ZF, or ZFC if the axiom of choice is included. An important feature of ZFC is that every object that it deals with is a set. In particular, every element of a set is itself a set. Other familiar mathematical objects, such as numbers, must be subsequently defined in terms of sets.

seven

A lucky number in the eyes of many people and one that has been given much spiritual significance. The early religious and cultural use of the seven-day week almost certainly stems from the fact that the Moon goes through its four phases in a bit over 28 days, which divides nicely into seven days per phase. There are seven moving objects in the sky visible to the naked eye (the Sun, Moon, Mercury, Venus, Mars, Jupiter, and Saturn), seven seas, seven orders of architecture, seven deadly sins, seven liberal arts and sciences, and seven dwarfs. The seventh son of a seventh son is supposed to be born gifted (Donny Osmond was such a person). In the Bible, there were seven years of famine and seven years of plenty, and seven years were taken to construct King Solomon's Temple. The Pythagoreans were especially intrigued by the number as it is the sum of three and four, which are the number of sides of a triangle and a square–shapes of enormous importance to the sect. These links with Solomon's Temple and the Pythagoreans help explain the importance of seven in freemasonry. Seven is the smallest positive integer whose reciprocal has a pattern of more than one repeating digit: $1/7 = 0.142857142857\ldots$ and is the smallest number for which the digit sequence of $1/n$ is of length $n - 1$ (the longest such a sequence can be). The next such numbers are 17, 19, 23, 29, 47, 59, 61, 97,

109, 113, ... Other curios: the citrus soda 7-UP, created in 1929, was so called because the original containers were 7 ounces and "up" was the direction of the bubbles, and seven is the maximum number of times you can fold any sheet of paper (try it!).

seventeen

The number most often picked in response to the request "Pick a random number from 1 to 20." Seventeen is a *Fermat prime* (a **prime number** of the form $2^{2^n} + 1$, where n is a positive integer), the exponent of a *Mersenne prime* (a prime p for which $2^p - 1$ is prime), and the only prime that is the sum of four consecutive primes ($2 + 3 + 5 + 7$). Seventeen is also the smallest number for which the sum of the digits of its cube is equal to the number: $17^3 = 4913$, $4 + 9 + 1 + 3 = 17$, and the smallest number that can be written as $a^2 + b^3$ in two different ways: $17 = 3^2 + 2^3 = 4^2 + 1^3$. The pair (8, 9), whose sum is 17, is the only pair of consecutive numbers where one is a square and the other is a cube (a result proved by Leonhard **Euler**.) There are 17 planar crystallographic groups, called **wallpaper groups**. The minimum number of faces on a convex **polyhedron** that has only one stable face is 17. (A stable face is one that the figure can rest on without falling over; most polygons have more than one such face.) Seventeen is also the answer to the following problem: At a party where any two people have previously met each other in one of three other places, what is the least number of people who must be at the party to guarantee that there is at least one group of three people who have met each other before in the same place?

sexagesimal

Of, relating to, or based on the number 60. Sexagesimal refers especially to the **number system** with base 60. The Babylonians began using such a scheme around the beginning of the second millennium B.C. in what was the first example of a **place-value system**. Our degree of 60 minutes, minute of 60 seconds (in both time and angle measure), and hour of 60 minutes hark back to this ancient method of numeration. Why the Babylonians counted using sexagesimal isn't known, but 60 certainly has more factors than any other number of comparable size.

Shannon, Claude Elwood (1916–2001)

An American mathematician and a pioneer of **information theory**. Shannon was the first to realize that any sort of message can be transmitted as a series of 0's and 1's, regardless of whether it consists of words, numbers, pictures, or sound. In his master's thesis, he explained how electrical switches could represent **binary** digits–a 1 when the switch is on and 0 when it is off. He also used **Boolean algebra** to show that complex operations could be carried out automatically on these electrical circuits, thus manipulating the data they were storing. It was in one of his papers, "A Mathematical Theory of Communication" published in 1948, that the word "bit" (short for binary digit) was used for the first time. In fact the framework and terminology for information theory he developed remains standard today. Shannon was driven by curiosity, and in his own words he "just wondered how things were put together." Among his inventions were rocket-powered Frisbees, motorized Pogo sticks, a device that could solve the **Rubik's cube** puzzle, and a juggling machine. (He could ride a unicycle while juggling three balls.) He was involved in pioneering **artificial intelligence** research, which included building the electromechanical mouse called "Theseus" that could navigate a metal **maze** using magnetic signals. Shannon also built a **chess**-playing computer, many years before IBM's Deep Blue, that played well against the world champion of the time, Mikhail Botvinnik (the computer lost only after 42 moves).

shell curve

See **Dürer's shell curve**.

shuffle

How many shuffles does it take to **randomize** a deck of cards–in other words, to mix up the cards about as thoroughly as dropping them all on the table and stirring them around for several minutes (the author's usual method). The answer depends on the kind of shuffle used. The beginner's *overhand shuffle,* for example, is a really bad way to mix cards: about 2,500 such shuffles are need to randomize a deck of 52 cards. A magician's *perfect shuffle,* on the other hand, in which the cards are cut exactly in half and then perfectly interlaced, *never* produces randomization (see below). One of the most effective ways to get a random deck is the *riffle shuffle* in which the deck is cut in half and imperfectly interlaced by dropping cards one by one from either half of the deck with a probability proportional to the current sizes of the deck splits. In 1992 Persi Diaconis (then at Harvard) and David Bayer demonstrated that, starting with a completely ordered deck, it takes *seven* riffle shuffles to produce randomization.[27] Any more than this and there's no significant increase in the randomness; any less and the shuffle is far from random. In fact, not only are five or six riffles not enough to randomize, there are some configurations of cards that are impossible to reach in this number of shuffles! To understand this, suppose the starting order of the cards is marked 1 to 52, top to bottom. After one shuffle, only configurations with two or fewer rising sequences are possible. A rising sequence is a maximal increasing

sequential ordering of cards that appear in the deck (with other cards possibly interspersed) as it is run through from top to bottom. For instance, in an eight-card deck, 12345678 is the ordered deck and it has one rising sequence. After one shuffle, 16237845 is a possible configuration, and there are two rising sequences (the underlined numerals form one, the nonunderlined numerals form the other). Clearly the rising sequences are formed when the deck is cut before the cards are interleaved in the shuffle. After two shuffles, there can be at most four rising sequences, since each of the two rising sequences from the first shuffle has a chance of being cut in the second. This pattern continues: the number of rising sequences can at most double during each shuffle. After five shuffles, there are at most 32 rising sequences. But the *reversed* deck, numbered 52 down to 1, has 52 rising sequences. Thus, this is one (of many) arrangements that are unattainable in five riffle shuffles. Interestingly, Diaconis and other researchers have also found that decks can undergo sudden changes in their degree of randomness; after six riffle shuffles, a deck is still visibly ordered, but this order vanishes one shuffle later.

Perfect shuffles do the exact opposite of randomizing: they preserve order at every stage. There are two kinds of perfect shuffles. The *out-shuffle* is one in which the top card stays on top; the *in-shuffle* is one in which the top card moves to the second position of the deck. Amazingly, eight perfect out-shuffles restore the deck to its original order! Magicians use combinations of out and in shuffles to perform a variety of baffling tricks and to control the position of any given card in a deck. How could you make the top card (call it position 0) go to position *n*? Easy: write *n* in **binary** (base 2), read the 0's and 1's from left to right, perform an out-shuffle for a 0 and an in-shuffle for a 1, and, as if by magic, the top card will have materialized at position *n*.

shunting puzzles

Railroad modelers, especially those with limited space available for their layouts, often enjoy setting up track that allows interesting shunting problems to be tried out and solved. The most famous mathematical puzzle of this type, called the *railroad shunting puzzle,* comes in a number of variations, but basically the problem is that there are two trains (*A* and *B* in the diagram) facing each other on a single line with just one short siding, which will only hold one item of rolling stock at a time. In order to enable the two trains to pass each other and to continue their journey, a series of movements using the siding is required. First time around it's quite a brain-teaser, which probably explains why railroad companies all over the world took the more costly but easier way out and built passing sidings!

Siegel's paradox

If a fixed fraction x of a given amount of money P is lost, and then the same fraction x of the remaining amount is gained, the result is less than the original and equal to the final amount if a fraction x is first gained, then lost.

Sierpinski, Waclaw Franciszek (1882–1969)

A Polish mathematician who made outstanding contributions to **set theory**, which included research on the **axiom of choice** and the **continuum hypothesis**, **number theory**, and **topology**. Two well-known fractals, the **Sierpinski carpet** and the **Sierpinski gasket**, are named after him.

Sierpinski carpet

A fractal, named after Waclaw **Sierpinski**, that is derived from a square by cutting it into nine equal squares with a 3×3 grid, removing the central piece, and then applying the same procedure ad infinitum to the remaining eight squares. It is one of two generalizations of the Cantor set to two dimensions; the other is the **Cantor dust**. The carpet's **Hausdorff dimension** is log 8/log 3 = 1.8928. . . .

Sierpinski gasket

A fractal, also known as the *Sierpinski triangle* or *Sierpinski sieve* after its inventor Waclaw **Sierpinski**. It is produced by the following set of rules: (1) start with any triangle in a plane; (2) shrink the triangle by ½, make three copies, and translate them so that each triangle touches the two other triangles at a corner; (3) repeat step 2 ad infinitum. The gasket can also be made by starting with **Pascal's**

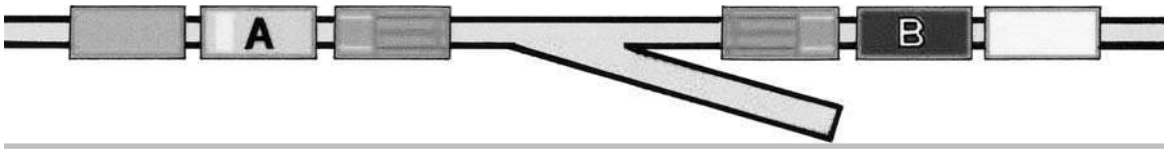

shunting puzzles How can two trains, traveling in opposite directions on a single track, get past each other by using a siding that can only accommodate a single item of rolling stock at a time?

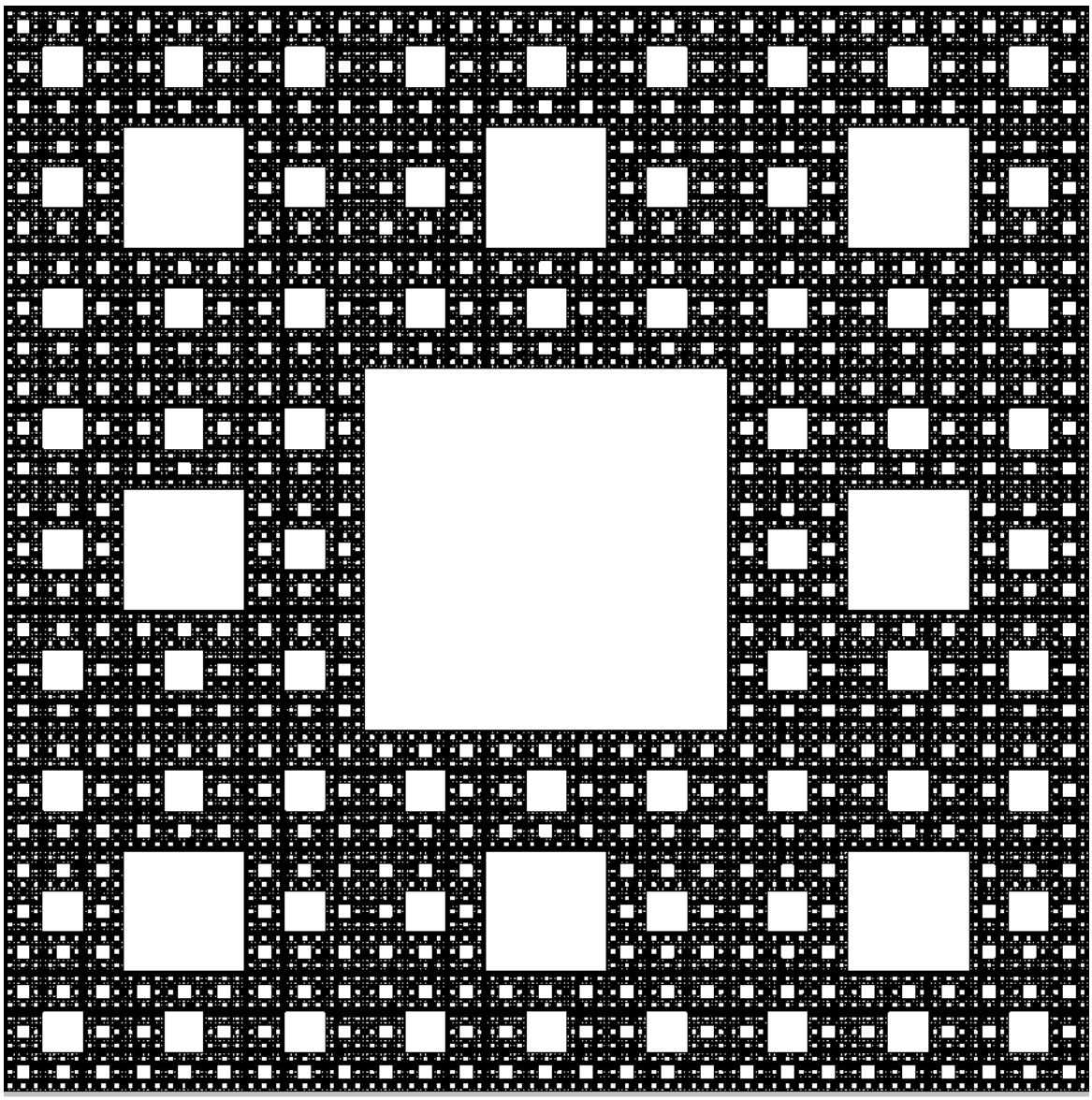

Sierpinski carpet

triangle, then coloring the even numbers white and the odd numbers black. Most curiously, it can be generated by a game of chance. Begin with three points, labeled 1, 2, and 3, and any starting point, *S*. Then select randomly 1, 2, or 3, using a die or some other method. Each random number defines a new point halfway between the latest point and the labeled point that the random number indicates. When the game has gone on long enough the pattern produced is the Sierpinski gasket. The gasket has a **Hausdorff dimension** of $\log 3/\log 2 = 1.585\ldots$, which follows from the fact that it is a union of three copies of itself, each scaled by a factor of $\frac{1}{2}$. Adding rounded corners to the defining curve gives a nonintersecting curve that traverses the gasket from one corner to another and which Benoit **Mandelbrot** called the *Sierpinski arrowhead*.

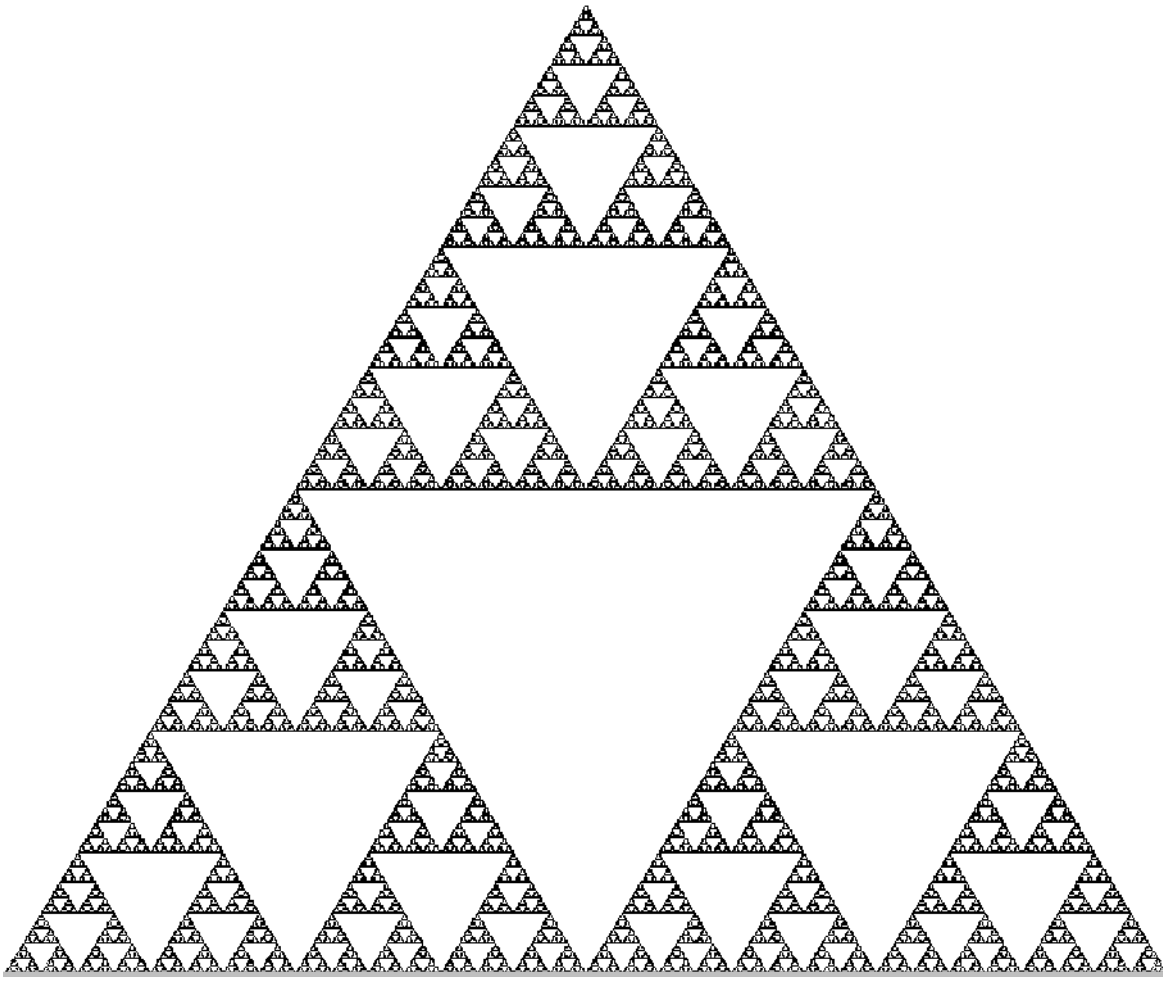

Sierpinski gasket

Sierpinski number

A positive, odd integer k such that k times $2^n + 1$ is *never* a **prime number** for any value of n. In 1960 Waclaw **Sierpinski** showed that there were infinitely many such numbers (though he didn't give a specific example). This is a strange result. Why should it be that while the vast majority of expressions of the form m times $2^n + 1$ eventually produce a prime, some don't? For now, mathematicians are focused on a more manageable problem posed by Sierpinski: What is the smallest Sierpinski number? In 1962, John Selfridge discovered the smallest known Sierpinski number, $k = 78{,}557$. The next largest is 271,129. Is there a smaller Sierpinski number? No one yet knows. However, to establish that 78,557 is really the smallest, it would be sufficient to find a prime of the form $k(2^n + 1)$ for every value of k less than 78,557. In early 2001, there were only 17 candidate values of k left to check: 4,847; 5,359; 10,223; 19,249; 21,181; 22,699; 24,737; 27,653; 28,433; 33,661; 44,131; 46,157; 54,767; 55,459; 65,567; 67,607; and 69,109. In March 2002, Louis Helm of the University of Michigan and David Norris of the University of Illinois started a project called "Seventeen or Bust," the goal of which is to harness the computing power of a worldwide network of hundreds of personal computers to check for primes among the remaining candidates. The team's effort have so far eliminated six candidates–5,359; 44,131; 46,157; 54,767; 65,567; and 69,109. Despite this encouraging start, it may take as long as a decade, with many additional participants, to check the eleven remaining candidates.

sieve of Eratosthenes

The most efficient way to find all of the smallest **prime numbers**. First described by **Eratosthenes of Cyrene**, it involves making a list of all the integers less than or equal to n (and greater than one), then striking out the multiples of all primes less than or equal to the square root of n. The numbers that are left are the primes. For example, to find all the primes less than or equal to 30, we list the numbers from 2 to 30:

2, 3, 4, 5, 6, 7, 8, 9, 10, 11, 12, 13, 14, 15, 16, 17, 18, 19, 20, 21, 22, 23, 24, 25, 26, 27, 28, 29, 30

The first number, 2, is prime, so we keep it and strike out all of its multiples, leaving

2, 3, 5, 7, 9, 11, 13, 15, 17, 19, 21, 23, 25, 27, 29

The next number left, 3, is prime, so again we retain it and delete all of its multiples, leaving

2, 3, 5, 7, 11, 13, 17, 19, 23, 25, 29

Now we do the same thing for 5, another prime, to give

2, 3, 5, 7, 11, 13, 17, 19, 23, 29

The next number, 7, is larger than the square root of 30, so all of the numbers left are primes.

significant digits

The digits that define a numerical value. The significant digits of a given number begin with the first nonzero integer digit or, if this number is less than unity, with the first (zero or nonzero) decimal digit. They end with the final (zero or nonzero) decimal digit; the final zero or zeros of an integer may or may not be significant.

similar

Having the same shape but not necessarily the same size. Two triangles are similar if they have equal angles and their corresponding sides, say, a_1, b_1, c_1 and a_2, b_2, c_2, have a common ratio, r: $a_1/a_2 = b_1/b_2 = c_1/c_2$. In general, a *similarity* is a transformation under which the distance between any corresponding pair of points changes by the same factor.

simple group

A **group** that has no nontrivial proper normal **subgroup**s. Simple groups are important because they can be thought of as the blocks out of which other groups can be built. Much activity has been expended in the classification of all finite simple groups.

simplex

The n-dimensional generalization of the **triangle** and the **tetrahedron**; in other words, a **polytope** in n dimensions with $n + 1$ vertices.

simply connected

The condition of a geometrical object if it consists of one piece and doesn't have any holes or "handles." For example, a line, disk, and sphere are simply connected, but a torus (doughnut) and teapot are not. See also **connected**.

simulation

Experimentation in the space of theories, or a combination of experimentation and theorization. Some numerical simulations are programs that represent a model for how nature works. Usually, the outcome of a simulation is as much a surprise as the outcome of a natural event, due to the richness and uncertainty of computation.

sine

The **trigonometric function** of an angle of a right-angled triangle other than the right angle that is equal to the length of the side adjacent to the angle divided by the length of the hypotenuse. The curve of $y = \sin x$ is called the sine curve, or *sinusoid*.

Singmaster, David

A professor at the school of computing, information systems, and mathematics at South Bank University, London, who is one of the world's leading compilers and historians of mathematical puzzles.

singularity

(1) A point at which the **derivative** does not exist for a given **function** but every neighborhood of which contains points for which the derivative exists. (2) A point in **space-time** at which gravitational forces cause matter to have infinite density and infinitesimal volume, and space and time to become infinitely distorted.

six

The smallest **perfect number**, the number of faces of a **cube**, and the number of sides of a **hexagon**. There are six players on a volleyball team, six kinds of chessmen, and six types of quark (not including antiquarks). A touchdown in American football earns six points and a hit across the boundary rope of a cricket field without bouncing scores six runs. Long ago people indicated a number by pointing to a part of their body; this is echoed in the New Guinea word for six, which is the same as that for "wrist."

six circles theorem

Given a triangle and a circle inside it that touches two of the triangle's sides, draw a second circle touching another two sides and touching the first circle. Draw a third circle

touching two sides and the second circle, and so on. This chain ends with the sixth circle, which will touch the first.

sixty
See **sexagesimal**.

skeletal division
A long division in which most or all of the digits are replaced by symbols (usually asterisks) to form a **cryptarithm**.

skew lines
Also known as *crossing lines,* lines that lie in different planes and do not intersect one another.

Skewes' number
A famous **large number**, commonly given as $10^{10^{10^{34}}}$, that was first derived in 1933 by the South African mathematician Samuel Skewes in a proof involving **prime number**s.[299] G. H. **Hardy** once described Skewes' number as "the largest number which has ever served any definite purpose in mathematics," though it has long since lost that distinction. Skewes' numbers—there are actually two of them—came about from a study of the frequency with which **prime number**s occur. Gauss's well-known estimate of the number of prime numbers less than or equal to n, $\mathrm{pi}(n)$, is the integral from $u = 0$ to $u = n$ of $1/(\log u)$; this integral is called $\mathrm{Li}(n)$. In 1914 the English mathematician John Littlewood proved that $\mathrm{pi}(x) - \mathrm{Li}(x)$ assumes both positive and negative values infinitely often. For all values of n up to 10^{22}, which is as far as computations have gone so far, $\mathrm{Li}(n)$ has turned out to be an overestimate. But Littlewood's result showed that above some value of n it becomes an underestimate, then at an even higher value of n it becomes an overestimate again, and so on. This is where Skewes' number comes in. Skewes showed that, if the **Riemann hypothesis** is true, the first crossing can't be greater than $e^{e^{e^{79}}}$. This is called the first or *Riemann true Skewes' number.* Converted to base 10, the value can be approximated as $10^{10^{10^{34}}}$, or more accurately as $10^{10^{8.852142\times10^{33}}}$ or $10^{10^{8852142197543270606106100452735038.55}}$. In 1987, the Dutch mathematician Herman te Riele[330] reduced dramatically the upper bound of the first crossing to $e^{e^{27/4}}$, or approximately 8.185×10^{370}, while John **Conway** and Richard Guy[68] have made the contradictory claim that the lower bound is 10^{1167}. In any event, Skewes' number is now only of historical interest. Skewes also defined the limit if the Riemann hypothesis is false: $10^{10^{10^{1000}}}$. This is known as the second Skewes' number.

slide rule
A calculating device consisting of two sliding logarithmic scales.

sliding-piece puzzle
A type of *sequential-movement puzzle,* within the larger category of **mechanical puzzle**s, that involves sliding one piece at a time into a single vacant opening in order to advance toward the solution—a certain orderly arrangement of the pieces. The best known is Loyd's **Fifteen Puzzle**.

Slocum, Jerry
An American historian of and writer on **mechanical puzzles**.

slope
"Rise over run." For a straight line in the plane, the *slope* is the **tangent** of the angle it forms with the positive x-axis. For a curve, the slope is, by definition, the slope of the *tangent* line. Therefore, if the slope is constant, a line is straight.

Slothouber-Graatsma puzzle
A **packing** puzzle in which six $1 \times 2 \times 2$ blocks and three $1 \times 1 \times 1$ blocks must be fitted together to make a $3 \times 3 \times 3$ cube. There is only one solution. A similar but much more difficult puzzle, named after its inventor, John **Conway**, calls for packing three $1 \times 1 \times 3$ blocks, one $1 \times 2 \times 2$ block, one $2 \times 2 \times 2$ block, and thirteen $1 \times 2 \times 4$ blocks into a $5 \times 5 \times 5$ box.

Smith number
A **composite number**, the sum of whose digits equals the sum of the digits of its prime factors (its **factor**s that are **prime number**s). The name stems from a phone call in 1984 by the mathematician Albert Wilansky to his brother-in-law Smith, during which Wilansky noticed that the phone number, 493-7775, obeyed the condition just mentioned. Specifically:

$$4{,}937{,}775 = 3 \times 5 \times 5 \times 65{,}837$$
$$4 + 9 + 3 + 7 + 7 + 7 + 5 = 3 + 5 + 5 + 6 + 5 + 8 + 3 + 7$$

Trivially, all **prime numbers** have this property, so they are excluded. The first few Smith numbers are: 4, 22, 27, 58, 85, 94, 121, 166, 202, 265, 274, 319, 346, ... In 1987, Wayne McDaniel proved that there are infinitely many Smiths.

smooth
(1) Infinitely differentiable; possessing infinitely many **derivative**s. For example, $\sin(x)$ is a smooth function, while $|x|^3$ is not. More complicated mathematical objects such as **manifold**s are called smooth if they are defined or described by smooth functions. (2) Continuously differentiable (see **continuity**); possessing a continuous **tangent** or derivative.

Smullyan, Raymond (1919–)

An American mathematical logician, puzzle-maker, and magician, who has taught in various colleges but is best known for his books on recreational mathematics. Among these are *What Is the Name of This Book?, The Lady or the Tiger, The Tao is Silent,* and *This Book Needs No Title: A Budget of Living Paradoxes.*[304–311] Smullyan is an inventive maker of logic paradoxes and a pioneer of chess problems that involve "retrograde analysis," in which the object is to deduce the past history of a game from some given present position.

snow

It is often said that no two snowflakes are alike. While this is hard to prove, individual samples can be captured on a chilled glass microscope slide and preserved with artist's spray fixative. All are six-sided and the more ornate kind, called *dendritic snowflakes,* form when the air temperature is between –12°C and –16°C (10°F and 3°F). Typical snowflakes fall at a rate of a meter or two per second; assuming 1.5 m/s and a cloud base of 3,000 m (roughly the height of nimbostratus clouds) gives a descent time of 20 minutes. One of the great urban legends is that the Inuit have *n* words for "snow," where *n* is a large number. This story may have started in 1911 when anthropologist Franz Boaz casually mentioned that the Inuit–he called them "Eskimos," using the derogatory term of a tribe to the south of them for eaters of raw meat–had four different words for snow. With each succeeding reference in textbooks and the popular press the number grew to as many as 400 words. A problem with trying to pin down exactly how many Inuit words there are for snow and/or ice, or for anything else, is that the various dialects of Inuit are polysynthetic, which means that words can effectively be made up on the spot by concatenating various particles to the root word. For example, the suffix *-tluk,* for "bad," might be added to *kaniktshaq,* for "snow," to give *kaniktshartluk,* "bad snow." This can give rise to any number of snow terms, from *akelrorak* ("newly drifting snow") to *mitailak* ("soft snow over an opening in an ice floe").

snowball prime

Also known as a *right-truncatable prime,* a **prime number** whose digits can be chopped off, one by one, from the right-hand side, yet still leave a prime number. This means that even if you stop writing before you finish the number, you will still have written a prime. The largest snowball prime is 73,939,133 (7, 73, 739, . . . , 73,939,133 are all prime).

snowflake curve

See **Koch snowflake**.

soap film

See **bubbles**.

Soddy circle

A solution to the three-circle form of the **Apollonius problem** in which each of the given circles is tangent to (just touches) the other two.[312] There are two Soddy circles: the *outer Soddy circle,* which surrounds the three given circles, and the *inner Soddy circle,* which is interior to them. The inner Soddy circle is the solution to the **four coins problem**.

Soddy's formula

If four circles *A, B, C,* and *D,* of radii r_1, r_2, r_3, and r_4, are drawn so that they do not overlap but each touches the other three, and if we let $b_1 = 1/r_1$, etc., then

$$(b_1 + b_2 + b_3 + b_4)^2 = 2(b_1^2 + b_2^2 + b_3^2 + b_4^2).$$

solid

Of or relating to three-dimensional geometric figures or bodies.

solid angle

An angle formed by three or more planes intersecting at a common point. Solid angles are measured in **steradian**s.

solid geometry

The geometry of three-dimensional space.

solidus

The slanted line in a fraction such as *a/b* dividing the **numerator** from the **denominator**.

solitaire

See **peg solitaire**.

solitary number

A number that is not one of a pair of **amicable numbers**. Examples include all **prime number**s, all integer powers or primes, and other numbers such as 9, 16, 18, 52, and 160.

soliton

A solitary wave that can travel for long distances without changing its shape or losing energy. Mathematically, a soliton is a solution to a **partial differential equation** that is localized in some directions but not localized in time, and which does not change its shape. The first soliton to be described was a water wave seen by the engineer and shipbuilder John Scott Russell (1808–1882) in 1834 when he was riding by the Grand Union Canal at Hermiston, Glasgow. He observed that when a canal boat stopped, its bow wave continued onward as a well-

defined elevation of the water at constant speed. (Another account says Scott Russell observed it on the Glasgow and Ardrossan Canal when a horse bolted with a light canal boat in tow.) The phenomenon was largely forgotten until the 1960s, when the American physicist Martin Kruskal rediscovered it and called it a soliton wave. On July 12, 1995, a viaduct at Hermiston was renamed the John Scott Russell viaduct, with Kruskal unveiling plaques and attempting to re-create a soliton wave. A classic soliton occurs on the River Severn in England, which starts at the head of the triangular Bristol Channel and narrows rapidly upstream. When the tide comes in, it is greatly compressed and produces the Severn Bore, a tidal wave up to 6 feet (2 m) high which rushes about 20 miles (32 km) up the river to Gloucester at a speed of up to 10 mph (16 km/hr). It is strongest at the spring tides, i.e. at full and new moons, and is now popular with surfers and canoeists.

solution

A value that satisfies the requirements of an equation. See also **lost solutions**.

Soma cube

A mathematical puzzle devised by Piet **Hein** in 1936 during a lecture on quantum mechanics by Werner Heisenberg in which the great German physicist was describing a space sliced into cubes. In a moment of genius, Hein grasped that the result of combining all seven of the irregular shapes that can be made from no more than four unit cubes joined at their faces is a single larger ($3 \times 3 \times 3$) cube. The Soma cube was first brought to popular attention by Martin **Gardner** in his "Mathematical Games" column in *Scientific American* in 1958. All 240 possible solutions were first identified by John **Conway** and Mickael Guy in 1961. The pieces can also be used to make a variety of other interesting three-dimensional

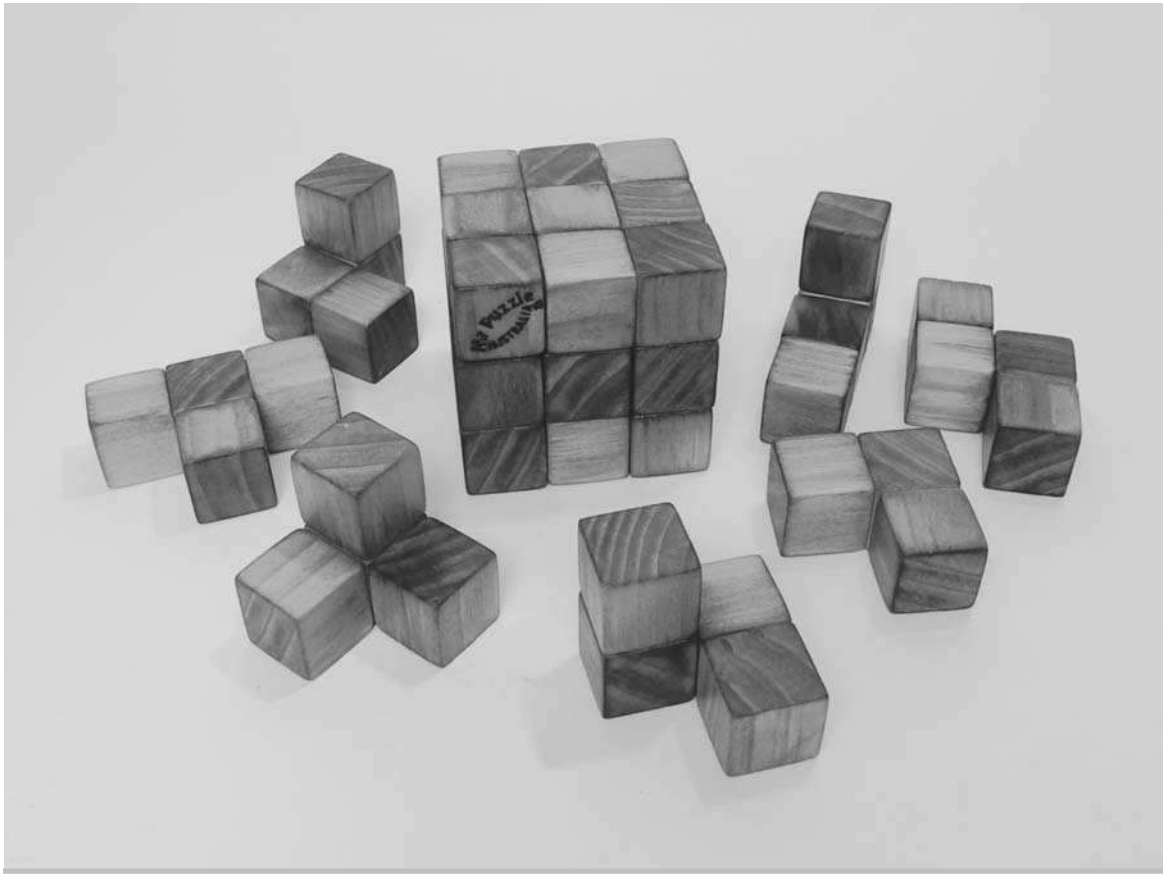

Soma cube How the pieces of the cube fit together. *Mr. Puzzle Australia, www.mrpuzzle.com.au*

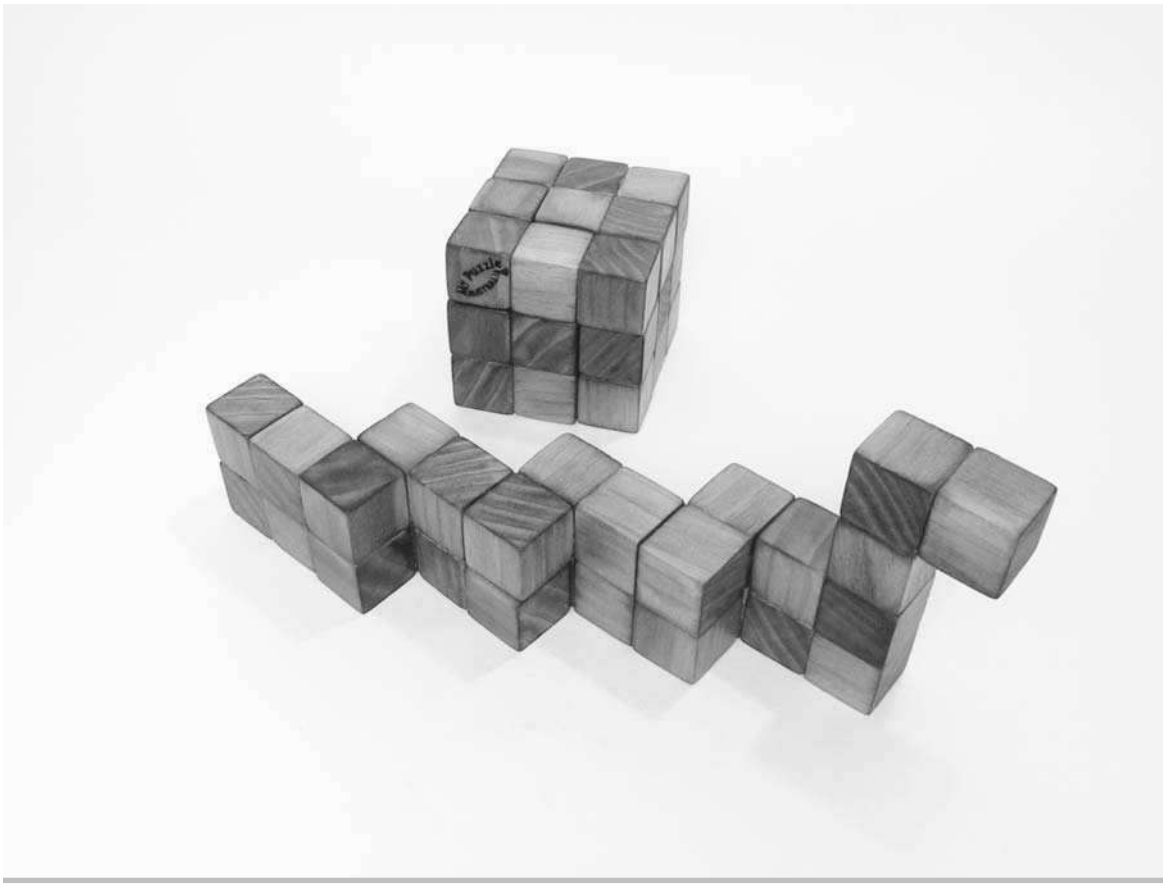

Soma cube One of many animals into which the cube pieces can be arranged. *Mr. Puzzle Australia, www.mrpuzzle.com.au*

shapes so that the Soma cube is often regarded as a three-dimensional analog of **tangrams**. It is possible that the puzzle is named after the fictitious drug "soma" in Aldous Huxley's novel *Brave New World*. See also **polyomino**.[112]

Sophie Germain prime

Any **prime number** p such that $2p + 1$ is also prime; the smallest examples are 2, 3, 5, 11, 23, 29, 41, 53, 83, 89, 113, and 131. Around 1825 Sophie **Germain** proved that the first case of **Fermat's last theorem** (FLT) is true for such primes. Soon after, Adrien-Marie Legendre began to generalize this by showing the first case of FLT also holds for odd primes p such that $kp + 1$ is prime, $k = 4$, 8, 10, 14, and 16. In 1991 Fee and Granville extended this to $k < 100$, where k is not a multiple of three. Many similar results were also shown, but now that FLT has been proven correct, they are of less interest.

soroban

See **abacus**.

space

(1) The three-dimensional theater in which things as we know them can exist or in which events can take place. In the Einsteinian worldview, space and **time** are united inextricably in a **space-time** continuum and there is also the possibility of **higher dimensions**. (See also **fourth dimension**.) (2) In mathematics, there are additionally many other types of space, most of them too abstract to imagine or to describe accurately in a few sentences. Generally, a mathematical space is a **set** of points with additional features. In a *topological space* (see **topology**) every point has a collection of neighborhoods to which it belongs. In an *affine space,* which is a generalization of the familiar concepts of a straight line, a plane, and ordinary three-dimensional space, a defining feature is the ability

to fix a point and a set of coordinate axes through it so that every point in the space can be represented as a "tuple," or ordered set, of coordinates. Other examples of mathematical spaces include *vector spaces, measure spaces,* and *metric spaces.*

space-filling curve

A curve that passes through every point of a finite region (such as a unit square or unit cube) of an *n*-dimensional space, where $n \geq 2$. A well-known example is the **Peano curve**.

space-time

The inseparable four-dimensional **manifold**, or combination, which **space** and **time** are considered to form in the special and general theories of relativity (see **relativity theory**). A point in space-time is known as an *event.* Each event has four coordinates (x, y, z, t). Just as the x, y, z coordinates of a point depend on the axes being used, so distances and time intervals, (which are invariant in Newtonian physics) may depend (in relativistic physics) on the reference frame of an observer; this can lead to bizarre effects such as *length contraction* and *time dilation.* A *space-time interval* between two events is the invariant quantity analogous to distance in **Euclidean space**. The space-time interval s along a curve is defined by the quantity

$$ds^2 = dx^2 + dy^2 + dz^2 - c^2dt^2,$$

where c is the speed of light. A basic assumption of relativity theory is that coordinate transformations leave intervals invariant. However, note that whereas distances are always positive, intervals may be positive, zero, or negative. Events with a space-time interval of zero are separated by the propagation of a light signal. Events with a positive space-time interval are in each other's future or past, and the value of the interval defines the proper time measured by an observer traveling between them.

special function

A **function**, often named after the person who introduced it, that has a particular use in physics or some branch of mathematics. Examples include *Bessel functions, Lagrange polynomials,* **beta function**s, **gamma function**s, and **hypergeometric function**s.

special relativity

See **relativity theory**.

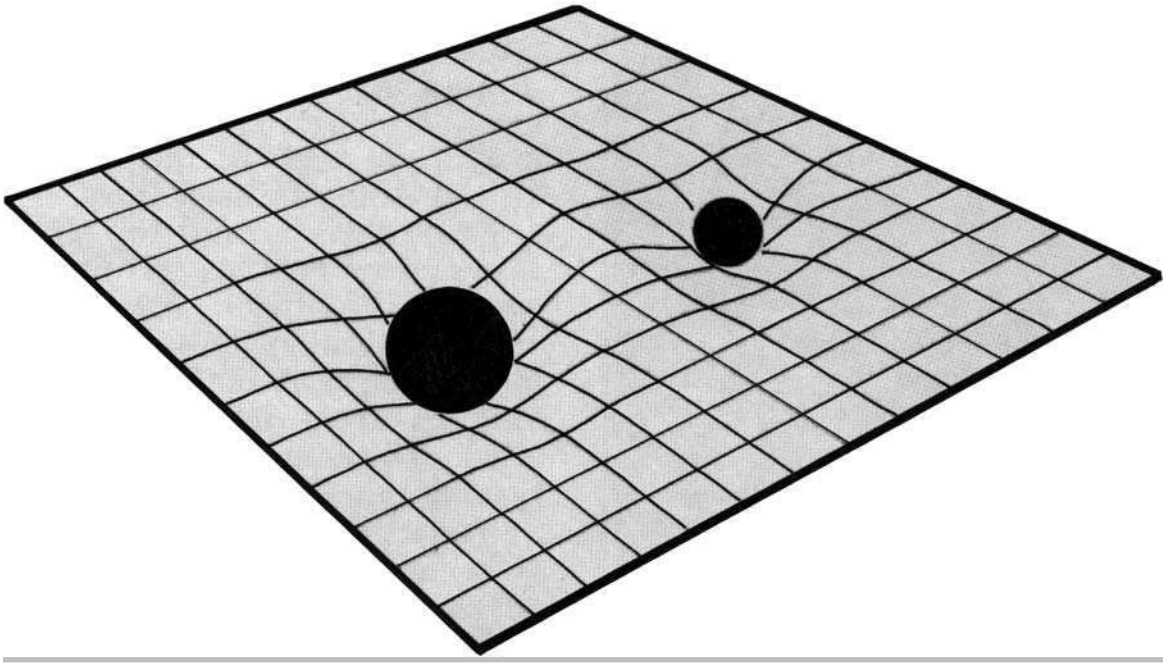

space-time Gravity seen as a curvature of the fabric of space and time.

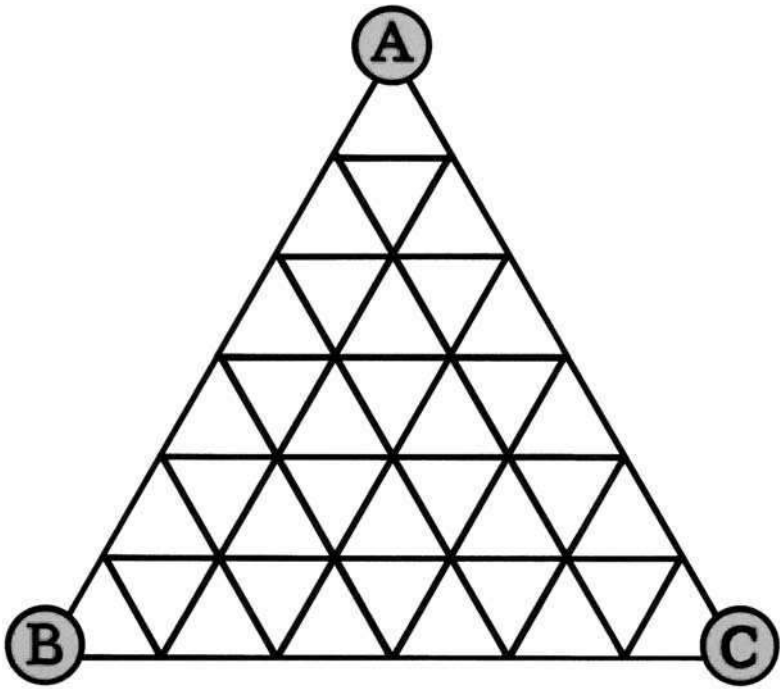

Sperner's lemma A triangular lattice that can be used for demonstrating Sperner's lemma. To understand how, see the accompanying entry.

spectrum

(1) In **quantum mechanics**, the set of allowable energy levels of a particle or system. It is directly related to bright or dark lines in a spectrum of light produced by a prism. (2) In mathematics, the set of **eigenvalue**s of a linear transformation. By historical coincidence, it is equivalent to the notion of a spectrum in quantum mechanics.

Sperner's lemma

Take a triangle ABC, labeled counterclockwise, and subdivide it into lots of smaller triangles in any arbitrary way. Then label all the new vertices as follows: (1) vertices along AB may be labeled either A or B, but not C; (2) vertices along BC may be labeled either B or C, but not A; (3) vertices along CA may be labeled either C or A, but not B; (4) vertices inside triangle ABC may be labeled A or B or C. Now shade in every small triangle that has three different labels. Use two different shadings to distinguish the triangles that have been labeled counterclockwise (i.e., in the same sense as triangle ABC) from the triangles that have been labeled clockwise (i.e., in the sense opposite to that of triangle ABC). Then there will be exactly one more counterclockwise triangle than clockwise triangles. In particular, the number of shaded triangles will be odd. This is Sperner's lemma, named after its discoverer, the German mathematician Emanuel Sperner (1905–1980). Sperner's lemma is equivalent to the **Brouwer fixed-point theorem**; a version of it holds in all dimensions.

sphere

Roughly speaking, a ball-shaped object. In everyday usage a sphere is often considered to be solid; mathematicians call this the *interior* of the sphere. In mathematics, a sphere is a **quadric** consisting only of a surface and is therefore hollow. More precisely, a sphere is the set of all points in three-dimensional **Euclidean space** that lie at distance r, the radius, from a fixed point. In **analytical geometry** a sphere with center (x_0, y_0, z_0) and radius r is the set of all points (x, y, z) such that

$$(x - x_0)^2 + (y - y_0)^2 + (z - z_0)^2 = r^2.$$

A sphere can also be defined as the **surface of revolution** formed by rotating a circle about its diameter. If the cir-

cle is replaced by an **ellipse**, the shape becomes a **spheroid**. The surface area of a sphere is $4\pi r^2$ and its volume is $4\pi r^3/3$. The sphere has the smallest surface area among all surfaces enclosing a given volume and it encloses the largest volume among all closed surfaces with a given surface area. In nature, **bubbles** and water drops tend to form spheres because surface tension always tries to minimize surface area. The circumscribed cylinder for a given sphere has a volume which is 3/2 times the volume of the sphere. If a spherical egg were cut up by an egg-slicer with evenly spaced wires, the bands between the cuts (on the surface of the sphere) would have exactly the same area. Spheres can be generalized to other dimensions. For any natural number n, an n-sphere is the set of points in $(n + 1)$-dimensional **Euclidean space** that lie at distance r from a fixed point of that space. A 2-sphere is therefore an ordinary sphere, while a 1-sphere is a **circle** and a 0-sphere is a pair of points. An n-sphere for which $n = 3$ or more is often called a **hypersphere**.

sphere packing

See **packing**, **Kepler's conjecture**, and **cannonball problem**.

spherical geometry

See **elliptical geometry**.

sphericon

A curious and mathematically delightful three-dimensional object made from a right double-**cone**–two identical, 90° cones joined base to base–and an added twist. To create a sphericon, a right double-cone is sliced along a plane that includes both vertices. The resulting cross section is a square, which enables one of the halves to be rotated through a right angle and the two halves to be glued back together without any overlap. This final twist enables the sphericon to roll in an unusual way. An ordinary cone placed on a flat surface rolls around in circles. A double-cone can roll in a clockwise circle or a counterclockwise one. A sphericon, in contrast, performs a controlled wiggle, with first one conical sector in contact with the flat surface, then the other. Two sphericons placed next to each other can roll on each other's surfaces. Four sphericons arranged in a square block can all roll around one another simultaneously. And eight sphericons can fit on the surface of one sphericon so that any one of the outer solids can roll on the surface of the central one. The sphericon was first found by the En-glishman Colin Roberts in 1969, while he was still in school. In 1999 he brought his discovery to the attention of Ian **Stewart** who subsequently wrote about the new object in his "Mathematical Recreations" column in *Scientific American*.[322]

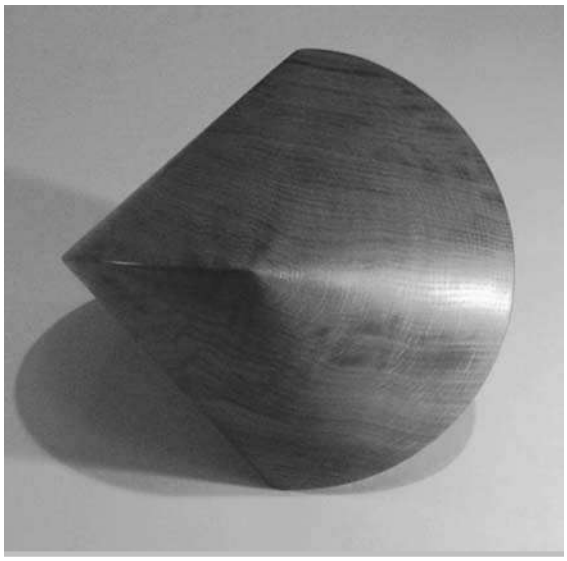

sphericon A model in oak of this remarkable shape. *Paul and Colin Roberts*

spheroid

A surface in three dimensions obtained by rotating an **ellipse** about one of its principal axes. If the ellipse is rotated about its major axis, the surface is called a *prolate spheroid* (similar to the shape of a rugby ball). If the minor axis is chosen, the surface is called an *oblate spheroid* (similar to the shape of Earth). The **sphere** is a special case of the spheroid in which the generating ellipse is a **circle**. A spheroid is a special case of an **ellipsoid** where two of the three major axes are equal.

Sphinx riddle

In Greek mythology, the Sphinx sat outside Thebes and asked this riddle of all travelers who passed by. If the traveler failed to solve the riddle, then the Sphinx killed him/her. And if the traveler answered the riddle correctly, then the Sphinx would destroy herself. The riddle: what goes on four legs in the morning, on two legs at noon, and on three legs in the evening? Oedipus solved the riddle, and the Sphinx destroyed herself. The solution: a man, who crawls on all fours as a baby, walks on two legs as an adult, and walks with a cane in old age. Of course morning, noon, and night are metaphors for the times in a person's life. Such metaphors are common in riddles. There were two Thebes; apparently the Thebes in this myth was the one in Greece, and the Sphinx was different from the one that stands at Giza, in Egypt.

spider-and-fly problem

A puzzle that was originally posed in the *Weekly Dispatch,* an English newspaper, on June 14, 1903, by Henry **Dudeney**, and that appears as one of the problems in *The Canterbury Puzzles* (1907).[87] A simple but elegant exercise in **geodesic**s, it is Dudeney's best-known brain-teaser. In a cuboidal (shoebox-shaped) room measuring 30′ × 12′ × 12′, a spider is in the middle of one 12′ × 12′ wall, 1 foot away from the ceiling. A fly is in the middle of the opposite wall 1 foot away from the floor. If the fly remains stationary, what is the shortest total distance (the geodesic) the spider must crawl along the walls, ceiling, and floor in order to get to the fly? The answer, 40′, can be obtained by flattening out the walls. Note that this distance is shorter than the 42′ the spider would have to travel if it first crawled along the wall to the floor, then across the floor, then up 1′ to get to the fly. A twist to the problem can be obtained by a spider that suspends himself from a strand of cobweb and thus takes a shortcut by not being forced to remain glued to a surface of the room. If the spider attaches a strand of cobweb to the wall at his starting position and lowers himself down to the floor (thus not crawling a single inch), he can then walk across the length of the room (30′) and ascend a single foot, thus reaching his prey after a total crawl of 31′ (although the total distance traveled is of course 42′). If the spider is not proficient with fastening strands to vertical walls, he must first ascend 1′ to the ceiling, from where it can lower himself to the floor, traverse the length of the room, and climb one foot to get to the fly, for a total distance crawled of 32′.

Dudeney and Sam **Loyd** offered several versions of the problem in a rectangular room. In 1926 Dudeney gave a version on a cylindrical glass with the source and the target on opposite sides.

spinor

A mathematical object similar to a **vector**, but which changes sign when rotated through 360°. Spinors were invented by Wolfgang Pauli and Paul **Dirac** (they were named by Paul Ehrenfest) to represent the spin of a subatomic particle. In the early 1930s, Dirac, Piet **Hein**, and others at the Niels Bohr Institute created games such as **Tangloids** to teach and model the calculus of spinors.

spiral

A curve that turns around some central point, getting progressively closer to it or progressively farther from it, depending on which way the curve is followed. Among the best known types are the **Archimedean spiral**, the **logarithmic spiral**, the **circle involute**, and the **lituus**. Like their space-curve cousin the **helix**, all spirals are asymmetric and each come in two forms that are mirror reflections of one another.

spirograph curve

See **roulette**.

Sprague-Grundy theory

A theory of certain classes of games called *impartial games,* discovered independently by Roland Percival Sprague (in 1936) and Patrick Michael Grundy (in 1939)

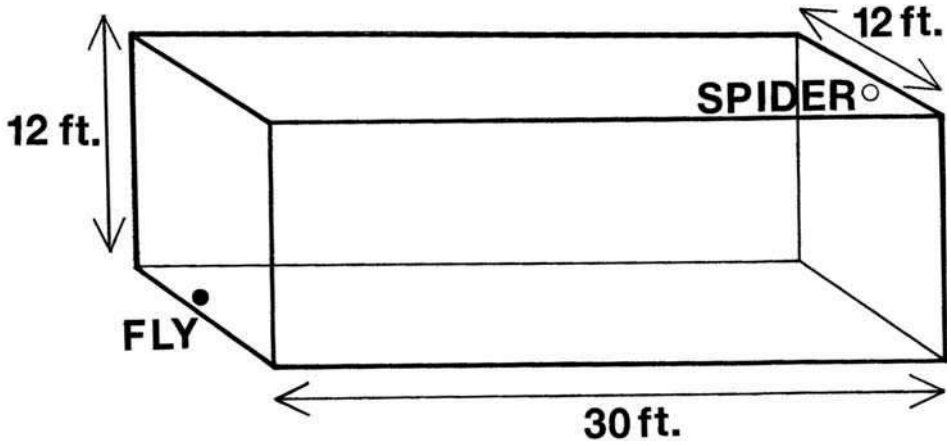

Spider-and-fly problem What is the shortest route for the spider to catch its prey?

and originally applied to **Nim**. In simple terms, they showed that one could take any impartial game and analyze it in terms of Nim heaps that could grow or decrease in size. The theory was developed further by E. R. Berlekamp, John **Conway**, and others, and presented comprehensively in the books *Winning Ways for Your Mathematical Plays* and *On Numbers.* Sprague-Grundy theory has been applied to other combinatorial games, including kayles.

Sprouts

A pencil-and-paper game invented by John **Conway** and Michael S. Paterson at Cambridge University in 1967. Sprouts is played by two players, starting with a few dots (called *spots*) drawn on a sheet of paper. To make a move, a player draws a curve between two spots or a loop from a spot to itself; the curve may not cross any other curve. The player marks a new spot on the curve, dividing it in two. Each spot can have at most three curves connected to it. The player who makes the last move wins. Sprouts has been studied from the perspectives of **graph** theory and of **topology**. It can be proven that a game started with n spots will last at least $2n$ moves and at most $3n - 1$ moves. By enumerating all possible moves, one can show that the first player is guaranteed a win in games involving three, four, or five spots, while the second player can always win a game that starts with one, two, or six spots. Following a 1990 computer analysis of the game at Bell Labs out to 11 spots, David Applegate, Guy Jacobsen, and Daniel Sleator conjectured that the first player has a winning strategy when the number of spots divided by six leaves a remainder of three, four, or five. Sprouts was featured in the plot of the first part of the science fiction novel *Macroscope* by Piers Anthony.

square

(1) A **quadrilateral** with four equal sides that meet at right angles. (2) To square something is to multiply it by itself. To take the *square root* is the reverse process. A *square number* is the square of a whole number (see also **figurate number**). A well-known formula for the *difference of squares* is $a^2 - b^2 = (a + b)(a - b)$. This formula enables some otherwise difficult calculations to be done easily in the head. For example, $43 \times 37 = (40 + 3)(40 - 3) = 40^2 - 3^2 = 1600 - 9 = 1591$.

square free

An integer that is not divisible by a perfect square, n^2, for $n > 1$.

square pyramid problem

See **cannonball problem**.

square root of 2 ($\sqrt{2}$)

The first number shown to be what is now known as an **irrational number** (a number that can't be written in the form a/b, where both a and b are integers). This discovery was made by **Pythagoras** or, at any rate, by the Pythagorean group that he founded. The square root of 2 is the length of the hypotenuse (longest side) of a right **triangle** whose other two sides are each one unit long. A ***reductio ad absurdum*** proof that $\sqrt{2}$ is irrational is straightforward. Suppose that $\sqrt{2}$ is rational, in other words that $\sqrt{2} = a/b$, where a and b are coprime integers (that is, they have no common factors other than 1) and $b > 0$. It follows that $a^2/b^2 = 2$, so that $a^2 = 2b^2$. Since a^2 is even (because it has a factor of 2), a must be even, so that $a = 2c$, say. Therefore, $(2c)^2 = 2b^2$, or $2c^2 = b^2$, so b must also be even. Thus, in a/b, both a and b are even. But we started out by assuming that we'd reduced the fraction to its lowest terms. So there is a contradiction and therefore $\sqrt{2}$ must not be irrational. This type of proof can be generalized to show that any root of any natural number is either a natural number or irrational.

As a **continued fraction**, $\sqrt{2}$ can be written $1 + 1/(2 + 1/(2 + 1/(2 + \ldots)))$, which yields the series of rational approximations: 1/1, 3/2, 7/5, 17/12, 41/29, 99/70, 239/169, ... Multiplying each numerator (number on the top) by its denominator (number on the bottom) gives the series 1; 6; 35; 204; 1,189; 6,930; 40,391; 235,416; . . . which follows the pattern: $A_n = 6A_{n-1} - A_{n-2}$. Squaring each of these numbers gives 1; 36; 1,225; 41,616; 1,413,721; 48,024,900; 1,631,432,881; . . . each of which is also a **triangular number**. The numbers in this sequence are the only numbers that are both square and triangular.

squarefull number

See **powerful number**.

squaring the circle

The problem to find a construction (see **constructible**), using only a straightedge and compass, that would give a square of the same area as a given circle. It is now known that this is impossible because, as the German mathematician Ferdinand von Lindemann showed in 1882, it would amount to finding a **polynomial** expression for **pi**, which can't be done as π is a **transcendental number**. (All the coordinates of all points that can be constructed with ruler and compass are algebraic numbers.) This minor inconvenience, however, hasn't prevented some amateur mathematicians from continuing to claim they have found proofs that the circle can be squared. Some of the most bizarre attempts have involved proposing a different and rational value for π. In 1897, the Indiana

State Legislature came within a hair's breadth of introducing a bill to set the value of π equal to 3.2! In fact, long before π was finally proved to be transcendental, most learned societies had conjectured that a proof was impossible and had stopped considering circle-squaring arguments sent to them.

squaring the square

The problem of how to tile a square with *integral squares* (squares of integral side-length). Of course squaring the square is a trivial task unless additional conditions are set. The most studied restriction is the *perfect squared square:* a square such that each of the smaller squares has a different size. The name was coined in humorous analogy with **squaring the circle** and is first recorded as being studied by R. L. Brooks, C. A. B. Smith, A. H. Stone, and W. T. Tutte at Cambridge University. The first perfect squared square was found by Roland Sprague in 1939. If such a **tiling** is enlarged so that the formerly smallest tile becomes as big as the original square, it becomes clear that the whole plane can be tiled with integral squares, each having a different size. It is still an unsolved problem, however, whether the plane can be tiled with a set of integral square tiles such that each natural number is used exactly once as the size of a tile. A *simple squared square* is one where no subset of the squares forms a rectangle. The smallest simple perfect squared square was discovered by A. J. W. Duijvestin using a computer search. His tiling uses 21 squares, and has been proved to be minimal. Other possible conditions that lead to interesting results are nowhere-neat squared squares and no-touch squared squares. Developments leading to squaring the square can be traced back to 1902 and the first appearance of Henry **Dudeney**'s Lady Isabel's casket, later published as problem #40 in *The Canterbury Puzzles*.[87]

standard deviation

A measure of the spread of a **set** of data. For a **Gaussian** distribution, the standard deviation hints at the width of the tails of the distribution **function**.

Stanhope, Earl

A line of English earls, several of whom were notable mathematicians and polymaths. The third earl, Charles Stanhope (1753–1816), invented the process of stereotyping and, in 1777, devised the first mechanical logical calculator. The fourth earl, Philip Henry Stanhope (1781–1855) was a mathematician who applied his knowledge to mapmaking and **maze** design. From 1818 to 1830 he planted a maze according to a basic plan laid down by the second earl (1714–1786) that was probably the first to incorporate islands that defeat the familiar "hand-on-wall" method. (There are islands in the famous Hampton Court maze, yet the hand-on-wall method solves it.) His designs often had a number of islands, or just isolated lengths of hedge.

Star of David

Also known as a *hexagram,* the six-pointed star obtained by extending the sides of a regular **hexa**gon to the points of intersection.

star of Lakshmi

An eight-pointed star design often used in architecture, particularly as a tiling or other decoration on the floor of a room that has four- or eight-fold symmetry. A notable example is in the **octagonal** central lobby in the Houses of Parliament in London. It was used by Hindus to symbolize *Ashtalakshmi,* the eight forms of wealth.

state space

See **phase space**.

stationary point

A point on the graph of a **function** where the **tangent** to the graph is parallel to the *x*-axis or, equivalently, where the **derivative** of the function is 0. There are four kinds of stationary points: (1) a *local minimum,* where the derivative of the function changes from negative to positive; (2) a *local maximum,* where the derivative changes from positive to negative; (3) a *rising point of inflection,* where the derivative is positive on both sides of the stationary point; and (4) a *falling point of inflection,* where the derivative is negative on both sides of the stationary point.

statistical mechanics

The study of statistical and thermal properties of physical materials and their idealized mathematical models.

statistics

The study of ways that lots of data can be represented using a few numbers and the study of how such numbers can be chosen and used to draw reasonable conclusions about the data. The word *statistics* comes from the Latin *statis* for "political state"; one of the main tasks of the subject involves analyzing facts and figures about governments, resources, and populations. Although a powerful tool, statistics is open to abuse, both intentional and unintentional. Benjamin Disraeli (1804–1881) may have gone a little over the top when he said, "There are lies, damned lies, and statistics," but Scottish author Andrew Lang (1844–1912) could have been describing many a politician when he remarked, "He uses statistics as a drunken man uses lamp posts–for support rather than

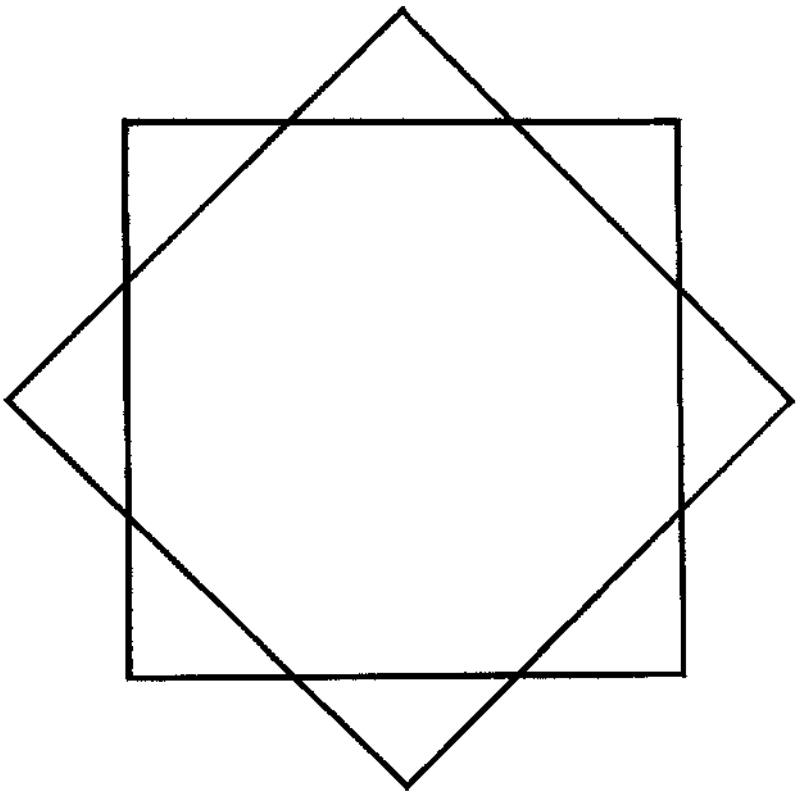

star of Lakshmi

illumination." The branch of statistics most commonly used in recreational mathematics is **probability theory.**

Steiner, Jakob (1796–1863)

A Swiss mathematician, considered by many to be the greatest geometer since **Apollonius** of Perga. Largely self-taught, he became a professor at the University of Berlin, and was a pioneer in the field of **projective geometry**. He had an important influence on his students, including Bernhard **Riemann**.

Steiner-Lehmus theorem

Any triangle that has two equal angle bisectors (each measured from a vertex to the opposite sides) is an **isosceles** triangle. In 1840, a Berlin professor Ludolph Lehmus wondered if this statement is true, given that it is the inverse of the already proven rule: If a triangle is isosceles then two of its internal bisectors are equal. He put the problem to Jakob **Steiner** who was quickly able to show its validity. Shortly after, Lehmus himself found a neater proof and it is has since become a favorite pastime of geometry hobbyists to search for still simpler proofs of the theorem.

Steinhaus, Hugo Dyonizy (1887–1972)

A Polish mathematician who was an influential member of the *Lvov school,* based at the Jan Kazimierz University in Lvov, which also included Stefan **Banach** and which focused on problems in functional **analysis**, real functions, and probability in the 1920s and '30s. Early on, Steinhaus's work revolved around applications of the **Lebesque** measure and integral. In 1923 he published the first rigorous account of the theory of tossing coins based on **measure theory**, and in 1925 was the first to define and discuss the concept of strategy in **game theory**. During World War II, as a Jew he was compelled to hide from persecution by the Nazis, yet continued his mathematical work despite great hardship. In 1944, Steinhaus proposed the problem of dividing a cake into *n* pieces so that it is proportional and envy free (see **cake-cutting**). He is also well known as the author of the widely read *Mathematical Snapshots.*[316]

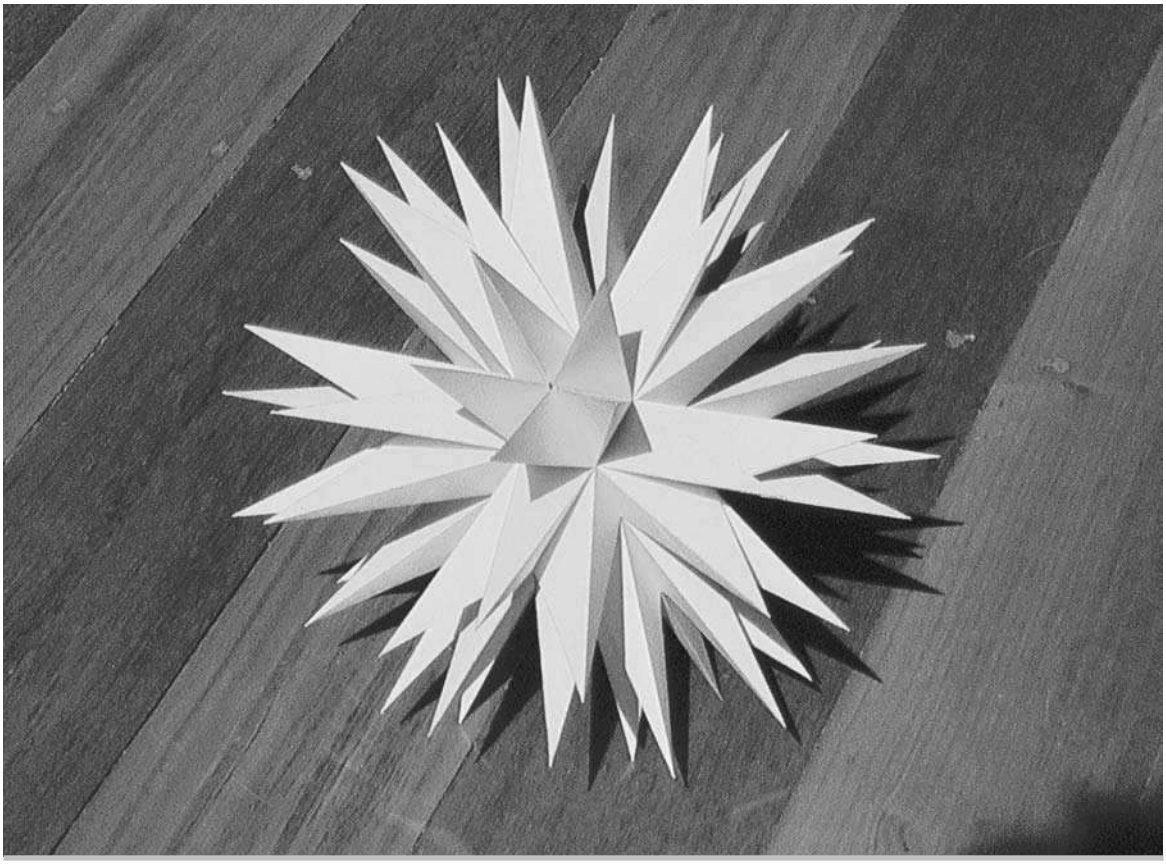

stellation The final stellation of the icosahedron. *Robert Webb, www.software3d.com; created using Webb's Stella program*

stellation

(1) The process of constructing a new **polyhedron** by extending the face planes of a given polyhedron past their edges. (2) The new polyhedron thus obtained. Starting with the **icosahedron**, for example, there are 59 possible stellations, including the *great icosahedron*, which is one of the **Kepler-Poinsot solids**.

steradian

The international (SI) unit in which **solid angle**s are measured. The steradian (sr) is a solid angle with its **vertex** in the center of a **sphere** and which cuts off from the spherical surface an area equal to the square of the radius of the sphere. The full sphere represents a spherical angle of 4π steradians.

Stewart, Ian (1945–)

A British mathematician at Warwick University who has written many books and articles on recreational math and popular science. From 1990 to 2001 he wrote the "Mathematical Recreations" column in *Scientific American*. His books include *Flatterland: Like Flatland Only More So* (a modern version of Edwin Abbott's classic ***Flatland: A Romance of Many Dimensions***); *Does God Play Dice: The New Mathematics of Chaos*, and *Evolving the Alien* (with Jack Cohen).[317, 318, 321, 323]

Stewart toroid

A **polygon** with a hole through it that meets some or all of the criteria specified by Bonnie Madison Stewart in his 1980 book *Adventures among the Toroids*. These criteria are as follows: all faces must be regular; faces that meet mustn't lie in the same plane; the polygon must be quasi-convex; the hole through the polygon must change its **genus**; and, the faces aren't allowed to intersect with themselves or each other. Stewart toroids, pierced relatives of the familiar Platonic solids, combine dazzling complexity with attractive symmetry.

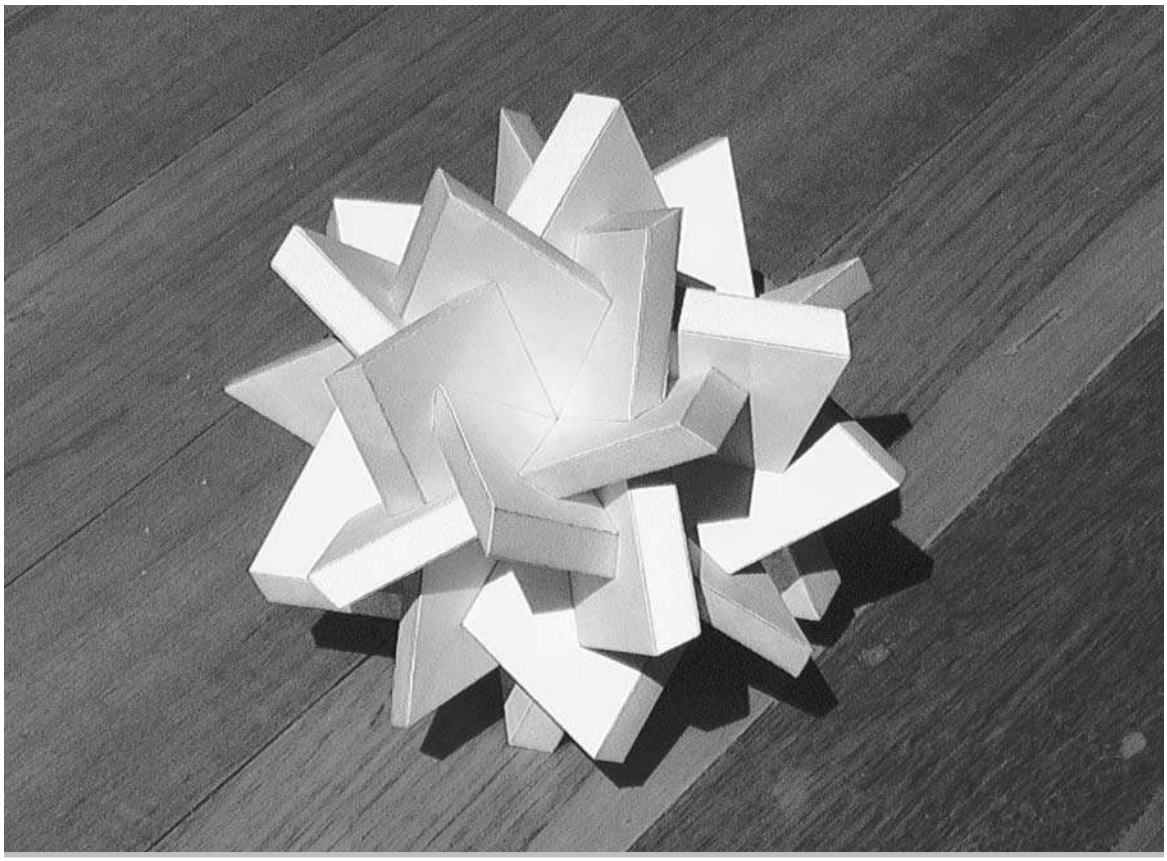

stellation A stellation of the small stellated truncated dodecahedron, a uniform polyhedron. *Robert Webb, www.software3d.com; created using Webb's Stella program*

stochastic
Something that is **random**.

stochastic process
A **dynamical system** with **random** fluctuations at each iteration or that is influenced by random noise. A random variable that, at each stage in time, depends on its previous values and on further random choices. For example, the price of a stock is often modeled as a stochastic process.

Stomachion
See **Loculus of Archimedes**.

straight
Having no deviations. A *straight line* is usually simply called a **line**. A *straight angle,* or *flat angle,* is exactly 180°.

strange attractor
See **chaotic attractor**.

strange loop
A phenomenon in which, whenever movement is made upward or downward through the levels of some hierarchical system, the system unexpectedly arrives back where it started. Douglas **Hofstadter** has used the strange loop as a paradigm in which to interpret paradoxes in logic, such as **Grelling's paradox** and **Russell's paradox**, and has called a system in which a strange loop appears a *tangled hierarchy.*

strategy
In **game theory**, a policy for playing a game. A strategy is a complete recipe for how a player should act in a game under all circumstances. A policy may employ **randomness**, in which case it is referred to as a **mixed strategy**.

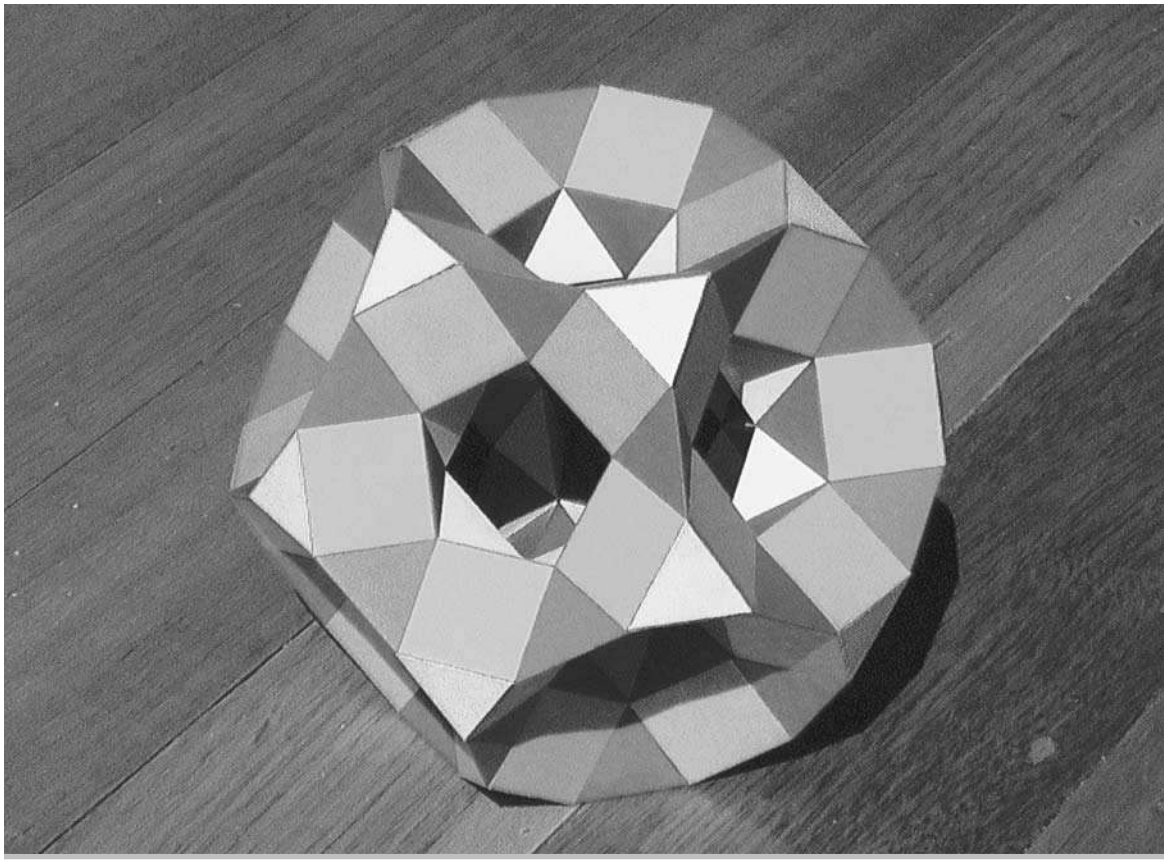

Stewart toroid A drilled truncated dodecahedron. *Robert Webb, www.software3d.com; created using Webb's Stella program*

string

Any sequence of letters, numbers, digits, **bit**s, or symbols.

string puzzle

The origins of puzzles using string, a form of *disentanglement puzzle,* are lost in antiquity but one of the earliest stories involving this type of problem is that of the **Gordian knot**. Today many kinds of string puzzles are available, most of which involve removing a ring from loops of string that are threaded through a solid (typically wooden) body. See also **mechanical puzzle**s and **knot**.

string theory

An important theory in modern physics in which the fundamental particles in nature are thought of as the "musical notes" or excitation modes of vibrating elementary strings. These strings have the shortest meaningful physical length, the so-called *Planck length* (equal to about 10^{-33} cm), and no thickness. Even more bizarre, for the theory to make sense, the universe must have nine space dimensions and one time dimension, for a total of 10 dimensions. This idea of a 10-dimensional universe first appeared in the **Kaluza-Klein theory**. We're familiar with time and three of the space dimensions: the other six together are known as **Calabi-Yau space**s. In string theory, as in the case of a stringed instrument, the string must be stretched under tension in order to vibrate. This tension is fantastically high—equivalent to a weight of about 10^{39} tons. String theories are classified according to whether or not the strings are required to be closed loops, and whether or not the particle spectrum includes *fermions.* In order to include fermions in string theory, there must be a special kind of symmetry called *supersymmetry,* which means that for every *boson* (a particle, of integral spin, that transmits a

force) there is a corresponding fermion (a particle, of half-integral spin, that makes up matter). So supersymmetry relates the particles that transmit forces to the particles that make up matter. Supersymmetric partners to currently known particles have not been observed in particle experiments, but theorists believe this is because supersymmetric particles are too massive to be produced by present-day high-energy accelerators. Particle accelerators could be on the verge of finding evidence for high energy supersymmetry in the next decade. Evidence for supersymmetry at high energy would be compelling evidence that string theory was a good mathematical model for nature at the smallest distance scales. In string theory, all of the properties of elementary particles–charge, mass, spin, and so forth–come from the vibration of the string. The easiest of these to understand is mass. The more frantic the vibration, the more energy; and since mass and energy are the same thing, higher mass comes from faster vibration.

strobogrammatic prime

A **prime number** that remains unchanged when rotated through 180°. An example is 619, which looks the same when read upside-down. To be strobogrammatic, a prime cannot contain digits other than 0, 1, and 8, which have a horizontal line of symmetry (ignoring font variations), and 6 and 9, which are vertical reflections of each other. An *invertible prime* is one that yields a different prime when the digits are inverted. Of course, these definitions are not taken seriously by mathematicians!

strophoid

A looping curve, first studied in 1670 by Isaac Barrow (1630–1677), the first Lucasian Professor of Mathematics at Cambridge and the immediate predecessor of Isaac **Newton** in this job. The strophoid, which is a special case of the general **cissoid**, was named by Enrico Montucci in 1846 from the Latin for "twisted belt shape." The elaborate rules for drawing a strophoid are as follows. Let C be a curve, let O be a fixed point called the pole, and let O' be a second fixed point. Let P and P' be points on a line through O meeting C at Q such that $P'Q = QP = QO'$. The locus of P and P' is the strophoid of C with respect to the pole O and fixed point O'. If the curve C is a straight line, the pole P is not on C, and the second point O' is on C, the resulting strophoid is called an *oblique strophoid.* If these same conditions apply except that O' is the point where the perpendicular from O to C cuts C, then the strophoid produced is called a *right strophoid.* On the other hand if C is a circle, O is the center of the circle, and O' a point on its circumference, then the strophoid that results is known as *Freeth's nephroid.* The French mathematician Gilles Roberval (1602–1675) found the strophoid in a different way–as the result of planes cutting a **cone**. When the plane rotates (about the tangent at its vertex) the collection of foci of the obtained conics gives the strophoid.

subgroup

A subset of a **group** that is a group under the same operation.

sublime number

A number such that both the *sum* of its divisors and the *number* of its divisors are **perfect number**s. The smallest sublime number is 12. There are 6 divisors of 12–1, 2, 3, 4, 6, and 12–the sum of which is 28. Both 6 and 28 are perfect. The second sublime number begins 60,865 . . . , ends . . . 91,264, and has a total of 76 digits! It is not known if there are larger even sublime numbers, nor if there are any odd sublime numbers.

subset

A **set** whose members are members of another set; a set contained within another set.

substitution cipher

A **cipher** that replaces each plaintext (original message) symbol with a ciphertext (coded text) symbol. The receiver decodes using the inverse substitution. A simple example is the **Caesar cipher**.

subtraction

The **binary operation** of finding the difference between two quantities or numbers.

sultan's dowry

A sticky problem in **probability** that first came to light in Martin **Gardner**'s "Mathematical Recreations" column in the February 1960 issue of *Scientific American.* Gardner's original version has become known as the secretary problem. In the exactly equivalent form called the sultan's dowry problem, a sultan has granted a commoner the chance to marry one of his hundred daughters. The commoner will be shown the daughters one at a time and will be told each daughter's dowry. The commoner has only one chance to accept or reject each daughter; he can't go back and choose one that he has previously rejected. The sultan's catch is that the commoner may only marry the daughter with the highest dowry. What is the commoner's best strategy, assuming that he knows nothing in advance about the way the dowries are distributed?

Many mathematicians have tackled this question and numerous papers have been written on the subject. It has even spawned its own area of study within the field of

management science. The consensus among those who have worked on the problem is that the commoner's best strategy is to let a certain fraction of the daughters pass and then choose the next one who has a dowry higher than any of the ones seen up to that point. The exact number to skip is determined by the condition that the odds that the highest dowry has already been seen is just greater than the odds that it remains to be seen *and that if it is seen it will be picked*. This amounts to finding the smallest x such that:

$$x/n > x/n \times [1/(x+1) + \ldots + 1/(n-1)]$$

Substituting $n = 100$ leads to the conclusion that the commoner should wait until he has seen 37 of the daughters, then pick the first daughter with a dowry that is bigger than any that have already been revealed. With this strategy, his odds of choosing the daughter with the highest dowry are surprisingly high: about 37%.[224]

supercomputer

A computer that, in its day, is faster than any contemporary conventional computer. Supercomputers are typically used for enormous number-crunching tasks such as weather-forecasting, simulations of fusion experiments or galaxy evolution, design of cars and planes, and code-cracking. At the start of 2004, the world's most powerful computer, by a long way, is the Earth Simulator in Japan, which is capable of a maximum of 40,960 gigaflops, that is, 40.96 trillion "floating point operations" per second. The top 500 supercomputers are listed at the following Web site: http://www.top500.org.

superegg

The **surface of revolution** of a **superellipse** given by the formula $|x/a|^{2.5} + |y/b|^{2.5} = 1$, where $a/b = 4/3$. The superegg was named by Piet **Hein** and singled out by him because of an unusual property: stood on either end it has a peculiar and surprising stability. Supereggs, made of metal, wood, and other materials, were sold as novelties in the 1960s; small, solid-steel ones were marketed as an "executive toy." The world's largest superegg, made of steel and aluminum and weighing 1 ton, was placed outside Kelvin Hall in Glasgow in 1971 to honor Hein's appearance there as a speaker.

superellipse

A **Lamé curve**, described by the formula $|x/a|^n + |y/b|^n = 1$, for which $n > 2$. Superellipses have a form partway between an **ellipse** and a rounded rectangle (or, if $a = b$, partway between a circle and a rounded square). The Danish poet and architect Piet **Hein** decided that the superellipse with $n = 5/2$ and $a/b = 6/5$ is the most pleasing to the eye. This so-called *Piet Hein ellipse* was quickly adopted as the basic motif for planning an open space at the center of Stockholm and was also incorporated into Scandinavian designs for office tables, desks, beds, and even roundabouts in roads. The **surface of revolution** of a superellipse is a *superellipsoid*, one special form of which has been nicknamed the **superegg**.

superegg

superfactorial

A **function** based on the **factorial** that produces **large number**s very quickly. It is a recent creation that has not yet entered the mathematical mainstream, and has been defined in a couple of different ways. In 1995, in his book *Keys to Infinity*, Clifford Pickover gave the superfactorial as

$$n\$ = \underbrace{n!^{n!^{\cdot^{\cdot^{\cdot^{n!}}}}}}_{n!\text{ terms}}$$

In the same year, Sloane and Plouffe offered an alternative definition:

$$n\$ = \prod_{i}^{n} i!$$

Pickover's superfactorial grows with extraordinary speed. The first two terms are 1 and 4, but the third term 3$, already has more digits than could be written down on this page. Sloan and Plouffe's factorial grows sedately by comparison–the first few values are 1, 1, 2, 12, 288, and 345,690–and is related to **Bell number**s.

supersymmetry
A theory in physics that postulates a counterintuitive symmetric relationship between fermions, which are particles such as electrons that obey the Pauli exclusion principle and thus cannot occupy the same quantum state, and bosons, which are particles such as photons that can coexist in the same state.

supertetrahedral number
A type of **figurate number** in four dimensions (see **fourth dimension**). Supertetrahedral numbers are obtained by piling up the **tetrahedral number**s 1, 4, 10, 20, 35, etc., as in:

$$\begin{aligned} 1 &= 1 \\ 1 + 4 &= 5 \\ 1 + 4 + 10 &= 15 \\ 1 + 4 + 10 + 20 &= 35 \\ 1 + 4 + 10 + 20 + 35 &= 70 \end{aligned}$$

etc.

supplementary angles
Two angles that add up to 180°.

surd
A **radical** that expresses an **irrational number**. Surds may be *quadratic* (e.g., $\sqrt{2}$), *cubic* (e.g., $\sqrt[3]{2}$), *quartic* (e.g., $\sqrt[4]{2}$), and so on. (The term is sometimes used as a synonym for irrational number.) A *pure surd,* or entire surd, contains no **rational number**; that, is, all its factors or terms are surds (e.g., $\sqrt{2} + \sqrt{3}$). A *mixed surd* contains at least one rational number (e.g., $2 + \sqrt{3}$ or $3\sqrt{2}$).

surface
In mathematics, any object that locally (if you zoom in close enough to it) looks like a piece of a flat **plane**. A **sphere**, a **torus**, a **pseudosphere**, and a **Klein bottle** are examples of different types of surfaces.

surface of revolution
A surface produced by rotating a line or a curve about some axis. For example, a **sphere** is the surface of revolution generated when a circle spins about its diameter.

surreal number
A member of a mind-boggling vast class of numbers that includes all of the **real number**s, all of Georg Cantor's infinite **ordinal number**s (different kinds of infinity), a set of **infinitesimal**s (infinitely small numbers) produced from these ordinals, and strange numbers that previously lived outside the known realm of mathematics. Each real number, it turns out, is surrounded by a "cloud" of surreals that lie closer to it than do any other real numbers. One of these surreal clouds occupies the curious space between zero and the smallest real number greater than zero and is made up of the infinitesimals.

Surreal numbers were invented or discovered (depending on your philosophy) by John **Conway** to help with his analysis of certain kinds of games. The idea came to him after watching the British **Go** champion playing in the mathematics department at Cambridge. Conway noticed that endgames in Go tend to break up into a sum of games, and that some positions behave like numbers. He then found that, in the case of infinite games, some positions behaved like a new kind of number–the surreals. The name "surreal" was introduced by Donald **Knuth** in his 1974 book *Surreal Numbers: How Two Ex-Students Turned on to Pure Mathematics and Found Total Happiness.*[191] This novelette is notable as being the only instance where a major mathematical idea has been first presented in a work of fiction. Conway went on to describe the surreal numbers and their use in analyzing games in his 1976 book *On Numbers and Games.*[67] The surreals are similar to the **hyperreal number**s, but they are constructed in a very different way and the class of surreals is larger and contains the hyperreals as a subset.

swastika
An ancient ideogram, signs of which have been found in the Euphrates-Tigris Valley, and in some areas of the Indus Valley, dating back 3,000 years; it became commonly used

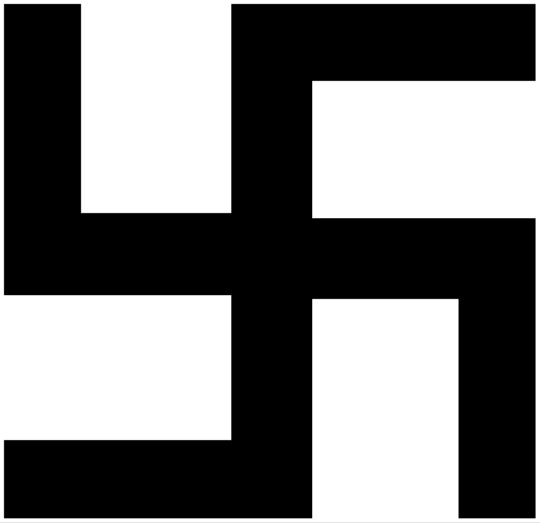

swastika

around 1000 B.C., possibly first in ancient Troy, in the northwest of modern Turkey. The swastika is an irregular icosagon (a 20-sided **polygon**), which in Arabic and Indian culture originally represented good luck. Of course, in more recent times, it was adopted as the symbol of the Nazi Party in Hitler's Germany and thus came to stand for anti-Semitism.

syllogism
An argument composed of three parts–a major premise, a minor premise, and a conclusion. For example: All men are mortal (major premise). Socrates is a man (minor premise). Therefore, Socrates is mortal (conclusion). The syllogism forms the basis of Aristotle's system of logic, which went unchallenged for over 2,000 years. Aristotle believed that by setting out any argument in syllogistic form, it should be possible to avoid fallacies. However, Bertrand **Russell** discovered several formal errors in the doctrine of syllogism.

Sylvester, James Joseph (1814–1897)
An English mathematician and lawyer who, in 1850, first used the term ***matrix*** in mathematics and gave it its present meaning of a rectangular array of numbers from which **determinant**s may be formed. Together with Arthur **Cayley**, he founded the *theory of invariants.* Hotheaded and vociferous in opposition of anti-Semitism, he was thrown out of the University of London for threatening another student with a table knife. Later he studied at Cambridge, emerging as Second Wrangler but without a degree (though in 1871 he earned an MA) because, as a Jew, he refused to accept the articles of the Church of England. After a spell working as an actuary and a barrister, and also taking private pupils (one of whom was Flor-ence Nightingale), he met Cayley, with whom he forged a lifelong friendship and collaboration, and returned to mathematics. He became professor of mathematics at the Royal Military Academy at Woolwich (1855–1870) and at the newly established Johns Hopkins University at Baltimore (1877–1883), founding the *American Journal of Mathematics,* before accepting the Savilian chair at Oxford (1883–1894). Remarkably, especially in the field of mathematics, he produced an extraordinary flood of ideas well into his old age. At 82, he worked out the theory of compound partitions. He also published on the roots of **quintic** equations and on **number theory**. His partnership with Cayley worked perfectly, since Cayley supplied the rigor which the brilliantly creative Sylvester lacked.

Sylvester's problem of collinear points
A problem posed in 1893 by James **Sylvester** who wrote: "Prove that it is not possible to arrange any finite number of real points so that a right line through every two of them shall pass through a third, unless they all lie in the same right line." No correct proof was forthcoming at the time, but the problem was revived by Paul **Erdös** in 1943 and correctly solved by T. Grünwald in 1944.

symmedian
Reflection of a **median** of a triangle about the corresponding angle **bisector**.

symmetric group
The **group** of all **permutation**s of a finite set. The symmetric group of a **set** of size n is denoted S_n and has $n!$ elements.

symmetry
An intrinsic property of a mathematical object that allows it to remain unchanged under certain types of **transformation**, such as rotation, reflection, or more abstract operations. The mathematical study of symmetry is systematized and formalized in the extremely powerful subject known as **group** theory. Symmetries and apparent symmetries in the laws of nature have played a part in the construction of physical theories since the time of Galileo and Newton. The most familiar symmetries are spatial or geometric ones. In a **snow**flake, for example, the presence of a symmetrical pattern can be detected at a glance. One of the most remarkable developments of the past half century has been the emergence of symmetry as a central theme of subatomic physics. This came about through a series of subtle evolutions in the concept of symmetry itself. Many researchers believe that this evolutionary process has not come to an end, and that further meaning of the concept of symmetry, with perhaps new mathematical structures, will develop in the coming years.

symmetry group
The **group** formed by the set of all rigid motions (translations, rotations, reflections, etc.) of Euclidean space that map all points of a subset F into F.

system
Something that can be studied as a whole. Systems may consist of subsystems that are interesting in their own right. Or they may exist in an environment that consists of other similar systems. Systems are generally understood to have an internal state, inputs from an environment, and methods for manipulating the environment or themselves. Since cause and effect can flow in both directions of a system and environment, interesting systems often possess **feedback**, which is self-referential in the strongest case.

Szilassi polyhedron

A **toroid**al heptahedron (seven-sided **polyhedron**) first described in 1977 by the Hungarian mathematician Lajos Szilassi. It has 7 faces, 14 vertices, 21 edges, and 1 hole. The Szilassi polyhedron is the **dual** of the **Császár polyhedron** and, like it, shares with the **tetrahedron** the property that each of its faces touches all the other faces. Whereas a tetrahedron demonstrates that four colors are necessary for a map on a surface topologically equivalent to a sphere, the Szilassi and Császár polyhedra show that seven colors are necessary for a map on a surface topologically equivalent to a **torus**.

T

tachyon

A hypothetical particle that travels faster than the speed of light. Tachyons were first proposed in prerelativistic times by the physicist Arnold Sommerfeld and named in the 1960s by Gerald Feinberg from the Greek *tachys* meaning "swift." By extension of this terminology, particles that travel slower than light are called *tardyons* (or *bradyons* in more modern usage) and particles, such as photons, that travel exactly at the speed of light are called *luxons.* The existence of tachyons is allowed by the mathematics of special **relativity theory**, one of the basic equations of which is

$$E = m/\sqrt{(1 - v^2/c^2)}$$

where E is the mass-energy of a particle, m its rest mass, v its velocity, and c the speed of light. This shows that for tardyons (particles of ordinary matter), E increases as v increases and becomes infinite when $v = c$, thus preventing an initially slower-than-light particle from being accelerated up to the speed of light and beyond. What about a particle for which v is always greater than c? In this case, $v^2/c^2 > 1$, so that the denominator in the equation above is an **imaginary number**—the square root of a negative real number. If m has a real value, E is imaginary, which is hard for physicists to swallow because E is a measurable quantity. If m takes an imaginary value, however (because one imaginary number divided by another is real), then E is real. Tachyons are allowed, therefore, providing (a) they never cross from one side of the light-barrier to the other, and (b) they have an imaginary rest mass (which is physically more acceptable, since the rest mass of an object that never stops isn't directly measurable). Tachyons would slow down if they lost energy, and accelerate if they gained energy. This leads to a problem in the case of charged tachyons because charged particles that move faster than the speed of light in the surrounding medium give off energy in the form of Cherenkov radiation. Charged tachyons would continuously lose energy, even in a vacuum, through Cherenkov emission. This would cause them to gain speed, thus lose energy at an even greater rate, thus accelerate even more, and so on, leading to a runaway reaction and the release of an arbitrarily large amount of energy.

More worrisome, as the physicist Gregory Benford and his colleagues first pointed out in their 1970 paper "The Tachyonic Antitelephone," tachyons seem to lead to a **time travel** paradox because of their ability to send messages into the past. Suppose Alice on Earth and Boole on a planet circling around Sirius can communicate using what has been called a tachyon "antitelephone." They agree in advance that when Boole receives a message from Alice, he will reply immediately. Alice promises to send a message to Boole at noon her time, if and only if she has not received a message from Boole by 10 A.M. The snag is that both messages, being superluminal, travel back in time. If Alice sends her message at noon, Boole's reply could reach her before 10 A.M. "Then," as Benford and colleagues wrote, "the exchange of messages will take place if and only if it does not take place. . . ." Perhaps not surprisingly, despite numerous searches, no tachyon detection has so far been confirmed. The same is true of another hypothetical faster-than-light particle called a dybbuk (Hebrew for a "roving spirit"), which would have imaginary mass, energy, and momentum. Dybbuks, proposed by Raymond Fox of the Israel Institute of Technology, have properties even stranger than those of tachyons yet, interestingly, they avoid the **causality** problem that affects their superluminal cousins.

TacTix

A two-player game of strategy, devised by Piet **Hein**, that is essentially a two-dimensional version of **Nim**. Though the game is nontrivial, the first player can always win, at least in the 5×5 matrix version by choosing the center piece and symmetrically mirroring the second player's moves. On a 5×5 grid, players alternate taking away as many contiguous pieces as desired from a single row or column.

Tafl game

A type of board game in which the contest is between two forces of unequal number or strength. The earliest form of Tafl (old Norse for "table"), known as **Hnefa-Tafl** ("king's table"), originated in Scandinavia before A.D. 400 and was then exported by the Vikings to Greenland, Iceland (where it is mentioned in the *Grettis Saga* dating back to A.D. 1300), Ireland, England, Wales, and as far east as the Ukraine. Several boards unearthed in both Viking and Anglo-Saxon contexts, including the board found at the Gokstad ship burial, have had

Hnefa-Tafl on one side and **nine men's morris** on the other. Later variants of Tafl include Tabula (the medieval ancestor of **backgammon**, introduced from the French as *Quatre* and thus *Kvatru-Tafl*), **fox and geese** (*Ref-Skak,* "fox chess", *Hala-Tafl* or *Freys-Tafl*), **three men's morris** (*Hræ-Tafl,* "Quick-Tafl"), and **nine men's morris.**

Tait, Peter Guthrie (1831–1901)

A Scottish scientist and mathematician who carried out the world's first systematic investigation of **knot** theory. Early in his career he formed a friendship with William **Hamilton** and became fascinated in the application of Hamilton's **quaternion**s to problems in physics. In 1857, he also took an interest in Hermann Helmholtz's theories on the behavior of vortex rings, and began experimenting with smoke rings and their interactions. These experiments greatly impressed William Thomson (Lord Kelvin) who saw in them a possible way (wrong, as we now know) to explain atomic structure and the buildup of different elements. This idea, in turn, led Tait, Thomson, and James Maxwell to do seminal work on knot theory, since the basic building blocks in Thomson's vortex atom model were rings knotted in three dimensions. Without any rigorous theory, which would have been well beyond nineteenth-century mathematics, Tait began to classify knots using his geometric intuition. By 1877 he had classified all knots with seven crossings. He then went on to consider the coloring of **graph**s and put forward a hypothesis (see **Tait's conjecture**) that, if true (which it wasn't), would have proved the **four-color map problem**. Among his many other accomplishments, Tait wrote a classic paper on the trajectory of golf balls (1896). This was a subject close to his heart because the third of his four sons was Frederick Gutherie Tait, the leading amateur golfer in 1893 and winner of the Open Golf Championship in 1896 and 1898.

Tait's conjecture

A hypothesis put forward by Peter **Tait** in 1884, which says that every **polyhedron** has a **Hamilton circuit** through its vertices. In other words, it is possible to travel around all the edges of a polyhedron, passing through each vertex (corner) exactly once and arriving back at the starting point. If true, Tait's conjecture would have provided an immediate proof of the **four color map problem**. However, in 1946, the British mathematician William Tutte (1917–2002), whose work at Bletchley Park on cracking the German FISH cipher played an important role in World War II, found a counterexample to the conjecture in the form of a polygon with 25 faces, 69 edges, and 46 vertices.

tally

To count or keep score. In the past this was often done by making marks on a stick; the word comes from the Latin *talea* meaning "one who cuts," which is also the root of *tailor.* The oldest known tally stick is thought to be the **Lebombo bone** dating back about 37,000 years. Until around 1828 British tax records were kept on wooden tally sticks. When the system was finally abandoned, the government was left with a mountain of wood which, in 1834, it decided to dispose of by having a giant bonfire. So successful was that blaze that it also burned down the parliament buildings. What Guy Fawkes had failed to do with dynamite, the Exchequer did with tally sticks!

tangent

(1) A straight line that touches a given curve exactly once, at a given point. (2) In a right triangle, if one of the angles is θ, then the tangent of θ is the ratio of lengths of the side opposite θ to the side next to θ. See also **trigonometric function**.

tangle

A system in which a **strange loop** appears.

tangled graph

A **graph** in 3-dimensional space; equivalently, a graph drawn in the plane so that when edges cross, one edge goes over the other.

Tangloids

A mathematical game for two players devised by Piet **Hein** to model the calculus of **spinor**s. Two flat blocks of wood each pierced with three tiny holes are joined with three parallel strings. Each player holds one of the blocks of wood. The first player holds one block of wood still, while the other player rotates the other block of wood around any axis for 4π radians (two full revolutions). Then the first player tries to untangle the strings without rotating either piece of wood. Only translations (sliding the pieces) are allowed. Afterward, the players reverse roles; whoever can untangle the strings fastest is the winner.

tangrams

A puzzle of Chinese origin, the objective of which is to form given shapes using a set of seven pieces (five triangles of various sizes, one square, and one parallelogram) that come from slicing up a square. The produced shape has to contain all the pieces, which mustn't overlap. Tangrams became popular in England around the middle of the nineteenth century, having been brought back by sailors from Hong Kong. It received a further boost when Lewis **Carroll** used the pieces to create illustrations of the characters in the Alice books. The origin of the name

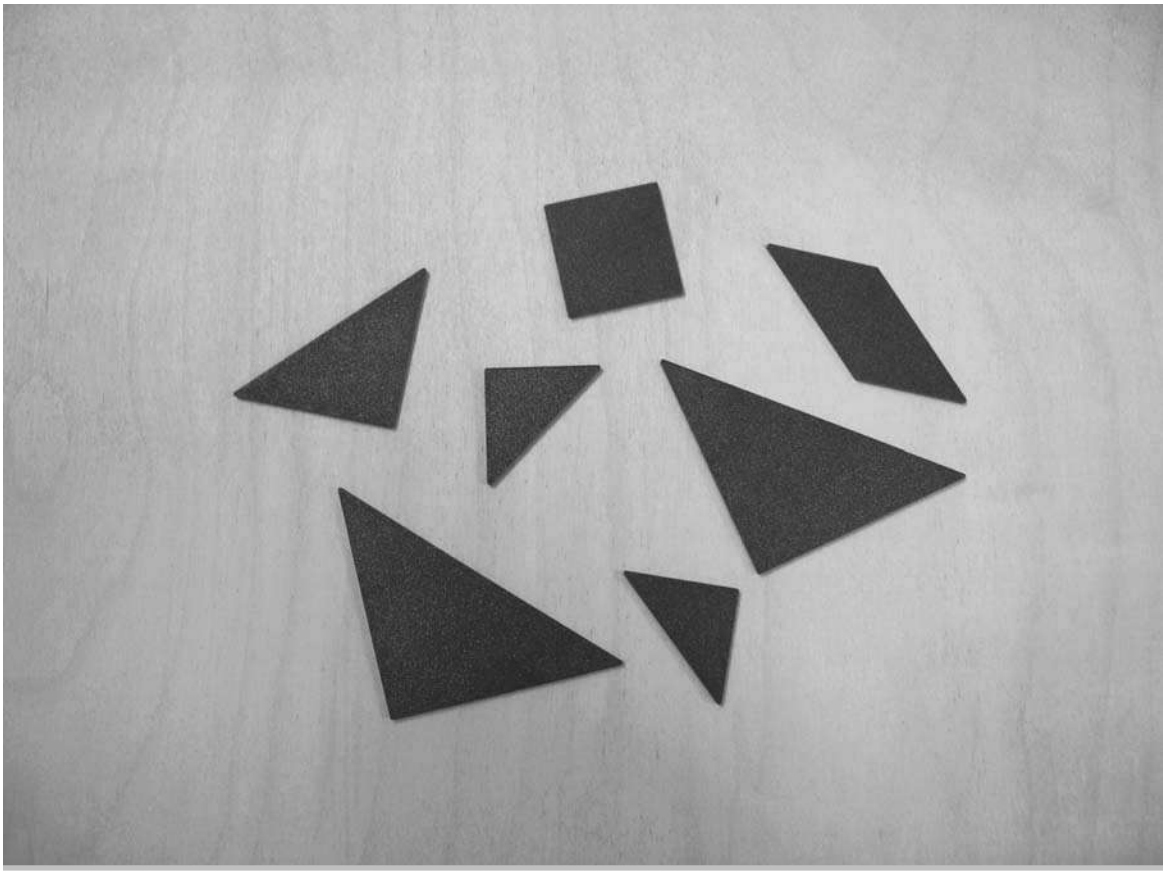

tangrams The seven tangrams. *Kadon Enterprises, Inc., www.gamepuzzles.com*

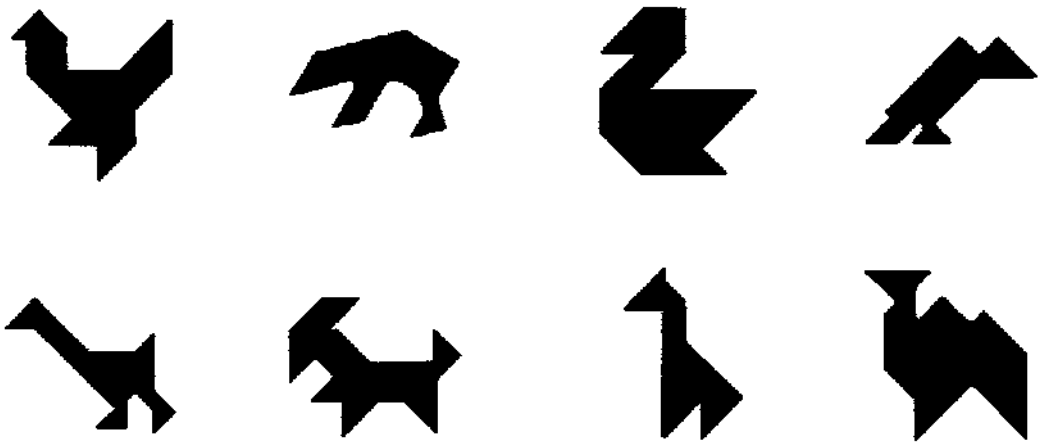

tangrams A tangram menagerie built up from the seven simple shapes.

isn't certain. One theory is that it comes from the Cantonese word for chin. A second is that it stems from a mispronunciation of a Chinese term that the sailors used for the ladies of the night from whom they learned the game! A third suggestion is that it is from the archaic Chinese root for seven, which still persists in the Tanabata festival held on July 7 in Japan. The first definitive appearance of tangrams in the Far East seems to be in Japan in the early eighteenth century; by around 1805 it had become a fad in both China and Europe. The **loculus of Archimedes** is a similar game and it has been suggested, though without evidence, that this was a direct precursor of tangrams, having been transmitted to the East via Arab sources.[93, 265]

Tarry, Gaston (1843–1913)

A French civil servant and amateur mathematician who spent the whole of his working career in Algeria. He published numerous articles on geometry, **number theory**, and **magic square**s from 1882 until his death, and is best known for his contribution to Euler's **thirty-six officers problem**. He also published an algorithm for exploring **maze**s that is named after him.

Tarski, Alfred (1902–1983)

A Polish-American mathematician who, along with Aristotle, Friedrich **Frege**, and Kurt **Gödel** is considered one of the greatest logicians of all time and certainly the most prolific: his collected works, excluding books, runs to 2,500 pages. Tarski made important contributions in many areas of mathematics, including **set theory**, **topology**, algebraic **logic**, and metamathematics. His most important contribution to logic is the *semantic method*–a technique that allows a more exacting study of formal scientific languages.

Tartaglia, Niccoló Fontana (1499–1557)

An Italian mathematician who, along with Girolamo **Cardano**, discovered the algebraic solution of the **cubic**. He was also a well-known inventor of mathematical recreations. He devised many arithmetical problems, and contributed especially to **measuring and weighing puzzles** and to **river-crossing problem**s. Although his real name was Niccoló Fontana, he is always referred to as Tartaglia, "the stammerer."

tautochrone problem

Find the curve down which an object can slide from any point to the bottom (accelerated by gravity and ignoring friction), always in the same length of time. *Tautochrone* comes from the Greek *tauto* for "the same" (which also gives us ***tautology***) and *chronos* for "time." The solution, first found by Christiaan **Huygens** and published in his *Horologium oscillatorium* (1673), is a **cycloid**. Thus, if you were to upturn a cycloid, in the manner of an inverted arch, and then release a marble from any point on it, it would take exactly the same time to reach the bottom, no matter where on the curve you started. Huygens used his discovery to design a more accurate pendulum–one with curved jaws from the point of support that forced the string to follow the right curve no matter how large or small the swing. The cycloid's unique property is mentioned in the following passage from Herman Melville's *Moby Dick:* "[The try-pot] is also a place for profound mathematical meditation. It was in the left-hand try-pot of the *Pequod*, with the soapstone diligently circling round me, that I was first indirectly struck by the remarkable fact, that in geometry all bodies gliding along a cycloid, my soapstone, for example, will descend from any point in precisely the same time." The cycloid is also the curve that answers the **brachistochrone problem**.

tautology

In mathematics, a logical statement in which the conclusion is equivalent to the premise. According to the school of thought known as *logicism,* all of mathematics is derived from **logic** and is thus inherently tautological. Tautology is also the needless, pointless, meaningless, and unwarranted repetition of words and phrases that mean the same thing. Examples are to be found in the previous sentence and the next one. Have a slice of pizza (*pizza* is Italian for "slice") and spin the **roulette** wheel (*roulette* is French for "little wheel").

ten

The **base** of our familiar **number system**, which stems directly from the fact that we have 10 fingers on which to count. Ten is the only **triangular number** that is a sum of consecutive odd squares ($10 = 1^2 + 3^2$) and the only composite integer such that all of its positive integer divisors other than 1 are of the form $x^2 + 1$ ($2 = 1^2 + 1$, $5 = 2^2 + 1$, $10 = 3^2 + 1$). Strange but true: the life span of a taste bud is 10 days.

tensor

A generalization of the concept of a **vector**. A *scalar* is a tensor of rank zero and a vector is a tensor of rank one. There are tensors of rank two, three, and so on, used mainly in manipulating and transforming sets of equations within and between different coordinate systems. A tensor of order n has n^2 components and is often best thought of as an array of values that can be manipulated like a **matrix**. To illustrate a tensor of rank two, imagine a plane surface area with a force acting on it. The total effect depends on two things: the magnitude and direction of the force, and the size of the area and its orientation. In

fact this latter property can be represented uniquely by a vector of magnitude proportional to the size of the area, and in a direction normal to the area. So the effect of the force upon the surface depends on two vectors and is equivalent to a tensor of rank two. Tensors were used by Einstein in deriving his law of gravitation in general **relativity theory**.

tera-
Prefix for 10^{15}, from the Greek *pentakis* for "five times."

terminating decimal
A decimal fraction that comes to an end, as in 0.3 or 0.7194. All terminating decimals are **rational number**s, but not all rational numbers have terminating decimal expansions. For example, $\frac{1}{3}$ is rational, but its decimal expansion goes on forever.

ternary
(1) Having the **base** three. (2) Involving three **variable**s. From the Latin *ternarius* ("three each").

tessellation
See **tiling**.

tesseract
The four-dimensional analogue of a cube, also known as a 4-space **hypercube** or an 8-cell. The name, possibly coined by Charles **Hinton**, comes from *tesser,* meaning "four," and *aktis,* meaning "ray," thus "four rays." Just as a cube is obtained by "thickening" a square in the third dimension, which can be imagined as stacking infinitely many infinitely thin sheets of paper, a tesseract is a cube thickened in the **fourth dimension**. We can't imagine this because we can't think four dimensionally but it is possible to appreciate that just as perspectives of cubes can be drawn on a 2-d surface, so real cubes can serve as perspectives of tesseracts. A square drawn inside a larger square with the vertices connected by lines is one way to provide a perspective of a cube. Similarly, a hypercube is sometimes portrayed as a small cube within a larger cube with lines drawn from the vertices of the smaller cube to the vertices of the larger cube. This kind of representation is a bit misleading, however, and reveals very little of the nature of a tesseract. It doesn't show, for instance, how a tesseract can be subdivided into smaller 4-d blocks in the same way that a cube can be divided into smaller cubes, or a square into smaller squares. A more useful way to think of a tesseract is as a folding, in the fourth dimension, of a 3-d net of eight cubes, just as a cube is a folding in the third dimension of a 2-d net of six squares. Start with a stack of four cubes, with four more cubes arranged in a cross around the second cube from the top. A tesseract is made by folding (in the fourth dimension) so that the top face of the cube at the top of the stack merges with the bottom face of the bottom cube, and so that the adjacent edges of the cubes in the cross join. (See table, "A Comparison of the Square, Cube, and Tesseract.")

A Comparison of the Square, Cube, and Tesseract

	Vertices	Edges	Squares	Cubes
Square	4	4	1	–
Cube	8	12	6	1
Tesseract	16	32	24	8

A tesseract is bounded by eight hyperplanes, each of which intersects it to form a cube. Two cubes, and so three squares, intersect at each edge. There are three cubes meeting at every vertex, the vertex polyhedron of which is a regular tetrahedron, leading to the **Schläfli symbol** {4,3,3}. The distance between opposite corners of a hypercube is twice the length of a side–much tidier than the corresponding values of $\sqrt{2}$ for a square and $\sqrt{3}$ for a cube.

If a cube is hung from one of its vertices and sliced horizontally through its center, the result is a hexagon. What if the same is done to a tesseract? The slice will yield a 3-dimensional object–but what kind? The answer is an octahedron. By analogy with the slice of the 3-cube, the slice of the 4-cube must cut every "face." The number of faces of a 4-cube is eight and the only regular eight-sided solid is an octahedron.

Tesseracts turn up in both art and literature. Salvador Dali's *Christus Hypercubus* shows Christ being crucified on a tesseract. In Robert Heinlein's short story "And He Built a Crooked House" (1940), a house built as a three-dimensional projection of a tesseract collapses, or folds up, to become a real tesseract–with unusual consequences for the person trapped inside. The tesseract is also mentioned in Madeleine l'Engles children's fantasy *A Wrinkle in Time* as a way of introducing the concept of higher dimensions.[161, 338]

tetragon
The less familiar name for what's normally called a **quadrilateral**.

tetrahedral number
A number that can be made by considering a tetrahedral pattern of beads in three dimensions. For example, if a tri-

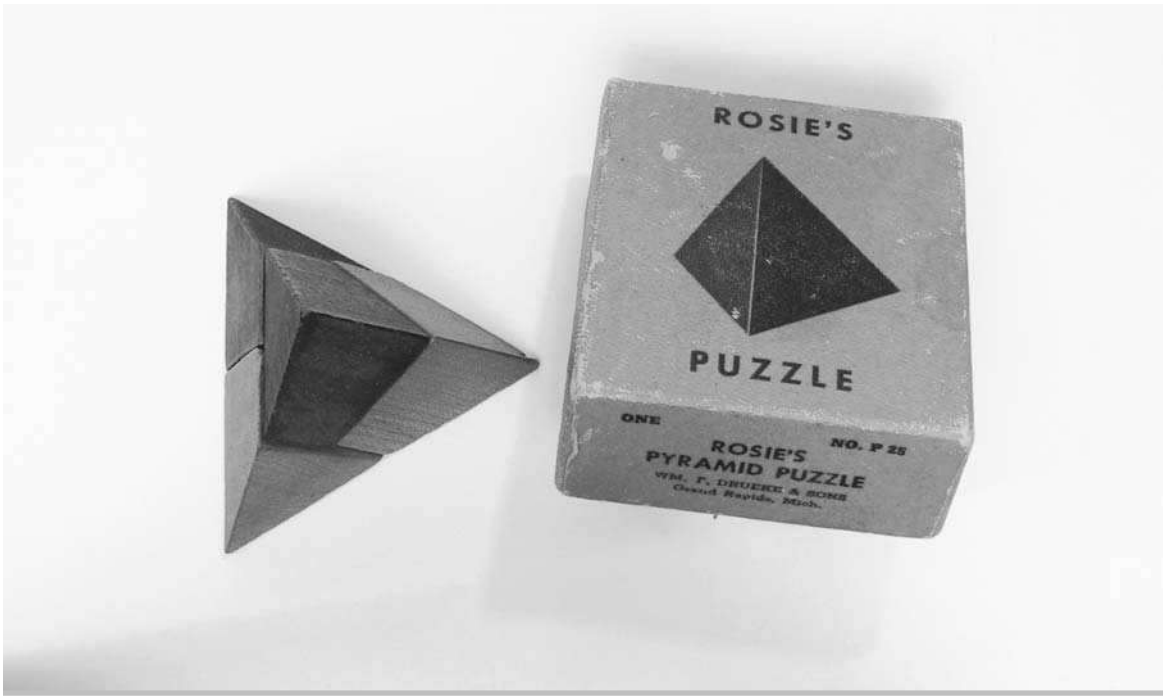

tetrahedron Rosie's pyramid puzzle, a vintage game that calls for four pieces to be assembled into a tetrahedron. *Sue & Brian Young/Mr. Puzzle Australia, www.mrpuzzle.com.au*

angle of beads is made with three beads to a side, and on top of this is placed a triangle with two beads to a side, and on top of that a triangle with one bead to a side, the result is a tetrahedron of beads. In this case the total number of beads is (third triangular number) + (second triangular number) + (first triangular number) = 6 + 3 + 1 = 10. In general the nth tetrahedral number is equal to the sum of the first n triangular numbers. This is the same as the fourth number from the left in the $(n + 3)$th row of **Pascal's triangle**. We can use the **binomial** formula for numbers in Pascal's triangle to show that the nth tetrahedral number is ${}^{n+2}C_3$, or $(n + 2)(n + 1)n/6$. The only numbers that are both tetrahedral and square are 4 $(= 2^2 = T_2)$ and 19,600 $(= 140^2 = T_{48})$.

tetrahedron

A four-sided **polyhedron**. A regular tetrahedron, one of the **Platonic solid**s, is a regular three-sided pyramid in which the base-edges and side-edges are of equal length. The projection of a regular tetrahedron can be an equilateral triangle or a square. The centers of the faces of a tetrahedron form another tetrahedron.

tetraktys

The sum 1 + 2 + 3 + 4 = 10 (the fourth **triangular number**), held in reverence by the Pythagoreans (see **Pythagoras of Samos**). The tetraktus, or "holy fourfoldness," was taken to represent the four elements: fire, water, air, and earth.

Tetris

A video and computer game, invented in 1985 by the Russian Alexey Pajitnov, that has become one of the most widely played games of all time. In 2002, computer scientists Erik Demaine, Susan Hohenberger, and David Liben-Nowell of the Massachusetts Institute of Technology (MIT) analyzed the game to determine its computational complexity and found it to be an **NP-hard problem** (one that is immune to simple solution and instead demands exhaustive analysis to work out the best way to be completed). Many people first played Tetris on the Nintendo Gameboy handheld console but it has since become available for virtually every personal computer–based device. The game gives the player the task of creating complete lines from a series of regularly shaped blocks–tetrominos, which are a type of **polyomino**–that advance steadily

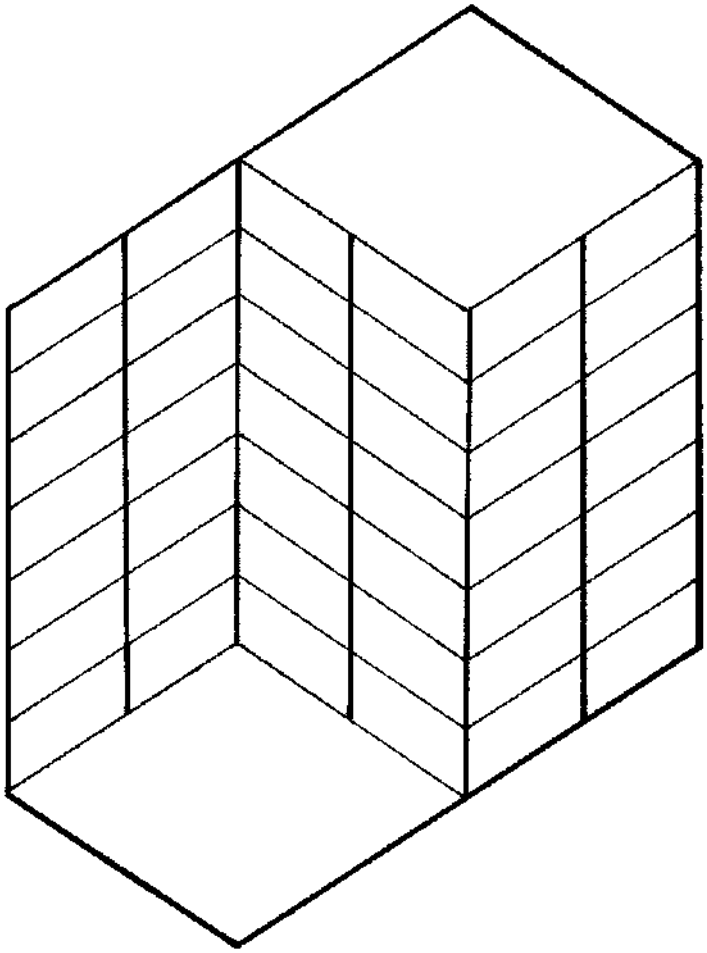

Thiery figure

down a narrow grid. The blocks can be spun to make them fit together better and complete lines. The game gets faster as levels are completed, making it harder to spin and fit blocks together fast enough to form lines. The MIT team found that, subject to certain conditions, Tetris has much in common with some of the knottiest mathematical conundrums, including the **traveling salesman problem**. Because Tetris is NP-hard, there is no easy way to maximize a score for the game, even when the sequence of blocks is known in advance.

tetromino
A four-square **polyomino**.

theorem
A major mathematical proposition that has been proved correct. More precisely, a statement in a **formal system** for which there exists a **proof**. See also **conjecture** and **lemma**.

theory of everything
A unified theory of all fundamental forces and interactions in nature; a grand unified theory that also includes gravity or general relativity (see **relativity theory**).

Thiery figure
A classic **ambiguous figure** devised by the psychologist A. Thiery in the late nineteenth century.

thirteen
The unluckiest of numbers if you happen to be superstitious. This belief has a couple of historical roots. According to biblical tradition, there were 13 people at Christ's Last Supper, and Christ was crucified on a Friday the thirteenth. Further back in time, Alexander the Great decided he wanted to be the thirteenth god alongside the 12 that already stood for each month of the year, so he had a thirteenth statue built on the place of his capital. His death

shortly after gave the number a bad name. Many buildings don't have a floor labeled 13 and many hotels will have a room numbered 12A instead of 13. There is even a name for a morbid fear of 13: triskaidekaphobia.

Fresh disasters involving the number hardly help triskaidekaphobics overcome their affliction. The most notorious of these involved the Apollo 13 Moon mission, which was launched on April 11, 1970 (the sum of 4, 11, and 70 equals 85, the digital sum of which is 13), from Pad 39 (3×13) at 13:13 local time, and suffered an explosion on April 13. (The astronauts did, however, make it home safely, which could be considered good luck.) There is always at least one Friday the thirteenth in each year; in some years there are two, and rarely three (e.g., 1998 and 2009). There were 13 original U.S. colonies (hence the 13 stripes on the American flag) and 13 signers of the Declaration of Independence. In Japan, the numbers 4 and 9 are considered unlucky, not because 13 can be represented as sum of these two perfect squares but because of their pronunciation. In Japanese, four is *shi,* which is pronounced the same as the word for death; nine is *ku,* which sounds like the word for torture. And speaking of torture, it was not unusual in times past for bakers to come in for stiff punishment if they short-changed their customers. In ancient Egypt, someone found selling light loaves might end up with his ear nailed to a doorpost, while in medieval Britain the punishment was likely to be a spell in the pillory. This led to the custom of adding a thirteenth loaf to every batch of 12 to be on the safe side, and hence the expression "a baker's dozen."

Mathematically, the reverse of the square of 13 is the same as the square of the reverse of 13: $13^2 = 169$; the reverse of 169 is 961 and the reverse of 13 is 31; $31^2 = 961$. Thirteen is the smallest **prime number** that can be expressed as the sum of the squares of two prime numbers: $13 = 2^2 + 3^2$. Also the sum of all prime numbers up to 13 ($2 + 3 + 5 + 7 + 11 + 13$) is equal to the thirteenth prime number (41), and this is the largest such number. On the anagrammatical front is this nice equation:

$$\text{ELEVEN} + \text{TWO} = \text{TWELVE} + \text{ONE}$$

See also **dollar**.

thirty colored cubes puzzle

A game devised in 1921 by Percy **MacMahon**, which was marketed under the name "Mayblox." It is played with 30 cubes that have all possible permutations of six different colors on their faces. A number of different games can be played with the blocks. One is to choose a cube at random and then choose seven other cubes to make a $2 \times 2 \times 2$ cube with the same arrangement of colors for its faces as the first chosen cube. Each face of the $2 \times 2 \times 2$ cube has to be a single color and the interior faces have to match in color. After building one such cube, only one other with the same properties can by made from the remaining 22 cubes—the mirror image of the first.

thirty-six officers problem

Arrange 36 officers in a 6×6 square so that one officer from each of six regiments appears in each row and one from each of six ranks appears in each column. This problem, first posed by Leonhard **Euler** in 1779, is equivalent to finding two mutually orthogonal **Latin square**s of order six. Euler correctly conjectured that there was no solution; the search for a proof led to important developments in **combinatorics**.

Thompson, D'Arcy Wentworth (1860–1948)

A Scottish naturalist and polymath. Thompson held a professorial chair at St. Andrews and Dundee, Scotland, for the amazing period of 64 years, a record for tenure unlikely ever to be broken. Although he wrote more than 300 scientific articles and books, his reputation is based primarily on his efforts to reduce biological phenomena to mathematics in his magnum opus *On Growth and Form* (1917).[332] In this book, full of marvelous sketches of such things as nautilus shells and honeycombs, Thompson claimed that much about animals and plants could be understood by the laws of physics, as mirrored in the

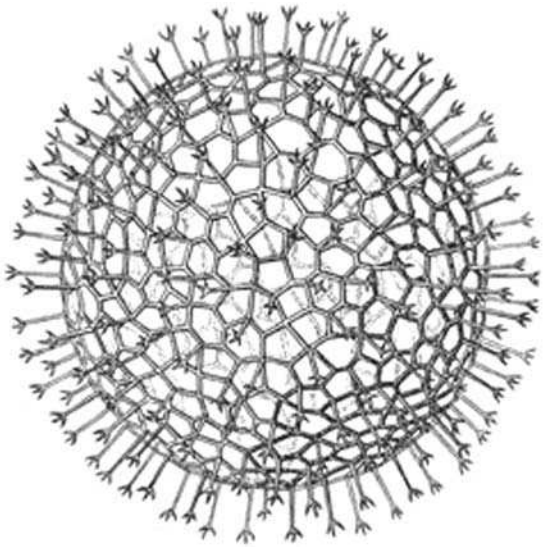

Thompson, D'Arcy Wentworth An illustration from Thompson's *On Growth and Form:* the shell of the radiolarian Aulastrum triceros.

structures and patterns of mathematics. His most novel idea was to show how mathematical functions could be applied to the shape of one organism to continuously transform it into other, physically similar organisms. One memorable example is the squeezing and stretching of a rectangular Cartesian grid that transforms the fish species *Scarus sp.* to the species *Pomacanthus.* Thompson used the same principle to transform skulls of baboons into those of other primates, and to show how corresponding bones like the shoulder blade are related in different species. Doubtless, if he were alive today, he would be heavily into "morphing"–the digital technique that allows a computer to do exactly the same kind of transformation of one object to another, but vastly more efficiently. Thompson acquired a local reputation as a mild eccentric; indeed, older inhabitants of St. Andrews still recall seeing him strolling about town with a parrot on his shoulder.

thousand

A number that, linguistically, comes from an extension of "hundred" and has roots in the Germanic *teue* and *hundt. Teue* refers to a thickening or swelling, and *hundt* is the source of our present-day hundred. A thousand, then, literally means a swollen or large hundred. The root *teue* is the basis of such common words today as thigh, thumb, tumor, and tuber. One thousand is the answer to the question: If you were to spell out numbers, how far would you have to go until you would find the letter "A"? While Americans may say "Thanks a million" to express gratitude, Norwegians offer "Thanks a thousand" ("*tusen takk*").

three

> *1 + 1 = 3, for large values of 1.*
>
> –Anonymous

The number of dimensions of space in which we live; three is also the smallest odd **prime number**, the second **triangular number**, and member of the **Fibonacci sequence**. Three is often the number of repetitions in jokes and children's stories (for example, the tale of the *Three Little Pigs* and of the number of chairs, beds, and porridge-eating bears in *Goldilocks*), because it is the minimum number needed to establish a pattern (such as a regular tempo) or to convey the impression of an ongoing sequence or succession. In the Christian tradition, three plays a crucial role: Christ represents one third of the Trinity (the Father, Son, and Holy Spirit), was visited by the three wise men and, 33 years later, when Peter disowned him three times, rose on the third day after the crucifixion, having died at 3 P.M. Other things that come in threes: musketeers, primary colors, wishes, blind mice, bad luck, and London buses. See also **Triangular Lodge** and **tinner's rabbits**.

three-hat problem

See **hat problem**.

three men's morris

An old game played on a 3×3 board that is thought to be a direct ancestor of **tic-tac-toe**; it is known by many other names, including nine holes, and is related to six men's morris and **nine men's morris**. The game involves two differently colored sets of four pieces (one set for each player). Players take turns placing pieces on intersection points, and the first person to place three along a line wins the game. The earliest known board for three men's morris was found on the roof of the temple in Kurna, Egypt, dating back almost three and a half thousand years. Its earliest known appearance in literature is in Ovid's *Ars Amatoria.* The Chinese are believed to have played it under the name *Luk tsut K'i* during the time of Confucius (c. 500 B.C.). Boards for three men's morris dating back to the thirteenth century can be found carved into the cloister seats at the cathedrals at Canterbury, Gloucester, Norwich, and Salisbury, and at Westminster Abbey.

three-body problem

The problem of determining the future positions and velocities of three gravitational bodies. The problem was proved unsolvable in the general case by Henri **Poincaré**, which foreshadowed the importance of **chaos**. Although no analytical solutions are possible in the worst case, a numerical solution is sometimes sufficient for many tasks.

Thue-Morse constant

Also known as the *parity constant,* the number defined as follows: Take a string of 1's and 0's and follow it by its complement (the same string with 1's switched to 0's and vice versa) to give a string twice as long. Repeat this process forever (starting with 0 as the initial string) to get the sequence 0110100110010110100101100 . . . . Make this a binary fraction, $0.0110100110010110\ldots_2$, and rewrite it in base 10. The resulting **transcendental number**, 0.41245403364 . . . , is the Thue-Morse constant.

tic-tac-toe

Also known as noughts and crosses, and spelled in a variety of ways (such as ticktacktoe), this well-known pastime is not as ancient as popularly believed, though it certainly has roots in older games. The earliest clear description of the rules, but without a name, comes

from Charles **Babbage** around 1820. Later on, Babbage started to call the game tit tat to and by slight variants on this, gave the first detailed analysis of it, and designed the first robot to play it! He speculated that "[T]he machine might consist of the figures of two children playing against each other, accompanied by a lamb and a cock. That the child who won the game might clap his hands whilst the cock was crowing, after which, that the child who was beaten might cry and wring his hands whilst the lamb was bleating."

His plan was to exhibit the machine in London to raise money for his more serious projects, including the fabulous Analytical Engine. However, on hearing that similar devices, such as a mechanical composer of Latin verse, had flopped financially he abandoned the scheme.

Two expert players of tic-tac-toe will always draw. In other words, there is no winning strategy against an opponent who knows the game well. Nor is it difficult to become unbeatable. Despite the fact that there are $9 \times 8 \times 7 \times 6 \times 5$ (= 15,120) possible layouts of noughts and crosses for the first five moves alone, these reduce to just a few basic patterns of play and counterplay that ensure the canny contestant never loses. The game is only interesting when at least one novice is involved. The strongest opening play is in a corner because an unwary opponent will be trapped unless her countermove is in the center. By the same token, a center opening must be countered by a corner response or the first player has an easy win. Of course, a master player will not only never lose but will learn his opponent's weaknesses and exploit them in the most devastating way.

The game also becomes more interesting when played on a larger board and/or in more dimensions. An exception to this is the $3 \times 3 \times 3$ cube which gives an easy win to the first player; in fact, it cannot end in a draw because the first player has 14 plays and it is impossible to make all of these without scoring. The $4 \times 4 \times 4$ cube is much more interesting and is sold commercially as the well-known Score Four game. For the ambitious, tic-tac-toe can be played in four dimensions on a **tesseract** by sectioning it into two-dimensional squares. Older, similar, and mathematically more interesting relatives of tic-tac-toe include **nine men's morris** and **Ovid's game**.

tie knots

How many ways can you tie a tie? For many years there were just three styles of **knot**: the Four-in-Hand, the Windsor, and the Half-Windsor. Then the Pratt was introduced to the world on the cover of the *New York Times* in 1989. Intrigued that only one new knot had been added to the tie-tying repertoire in more than half a century, two researchers from the University of Cambridge's physics department, Thomas Fink and Yong Mao, decided to see how many tie knots were actually possible. To this end, they applied **random walk** theory–a technique useful for describing movement which, although unpredictable in detail, reveals large-scale patterns. Such patterns, the researchers realized, were essential to a successfully accomplished tie-knot. For example, if the end of the tie is moved to the right, its next move can't be to the right again–it has to be either to the left or to the center. This means that each move made in tying a tie can only be followed by one of two alternatives. Fink and Mao found that the simplest possible knot involves just three moves. They went on to discover 85 possible tie-knots, including the four popular knots, six new knots that they consider aesthetically pleasing, and two complicated nine-move knots.[100]

tiling

Also called a *tesselation,* a collection of smaller shapes that precisely covers a larger shape, without any gaps or overlaps. Usually, the shape to be tiled is a flat plane but other shapes and three-dimensional objects can be tiled, too. In a game that involves tiling, certain conditions are applied; for example, all the tiles may have to be identical, or they may all have to be squares but every one of a different size. It's been known for some time that all simple regular tilings in the plane belong to one of the 17 plane symmetry groups known as **wallpaper group**s. All 17 of these patterns are known to exist in the **Alhambra** palace. This doesn't exhaust the apparently simple problem of tiling the plane: adding extra constraints or removing the requirement for regularity leads to a large number of interesting problems. These include *alternating tilings,* for examples of squares or dominoes, such that two tiles have a side or a part of a side in common, or *colored tilings,* in which no two adjacent tiles have the same color. Colored tilings are also called *colored maps.* The most famous problem relating to colored tilings is the **four-color map problem**, which has been solved. Other problems involve *n*-tesselations, in which each tile has an integral area and for each natural number *n* there is exactly one tile with area *n.* See also **Penrose tiling**, **rep-tile**, **rectangle**, **squaring the square**, **dissection**, and **packing**.

time

> *Time is a great teacher. Unfortunately, it kills all its pupils.*
>
> –Hector Berlioz (1803–1869)

One of the most familiar and yet mysterious properties of the universe. The "flow" of time is one of the strongest impressions we have, yet it may simply be

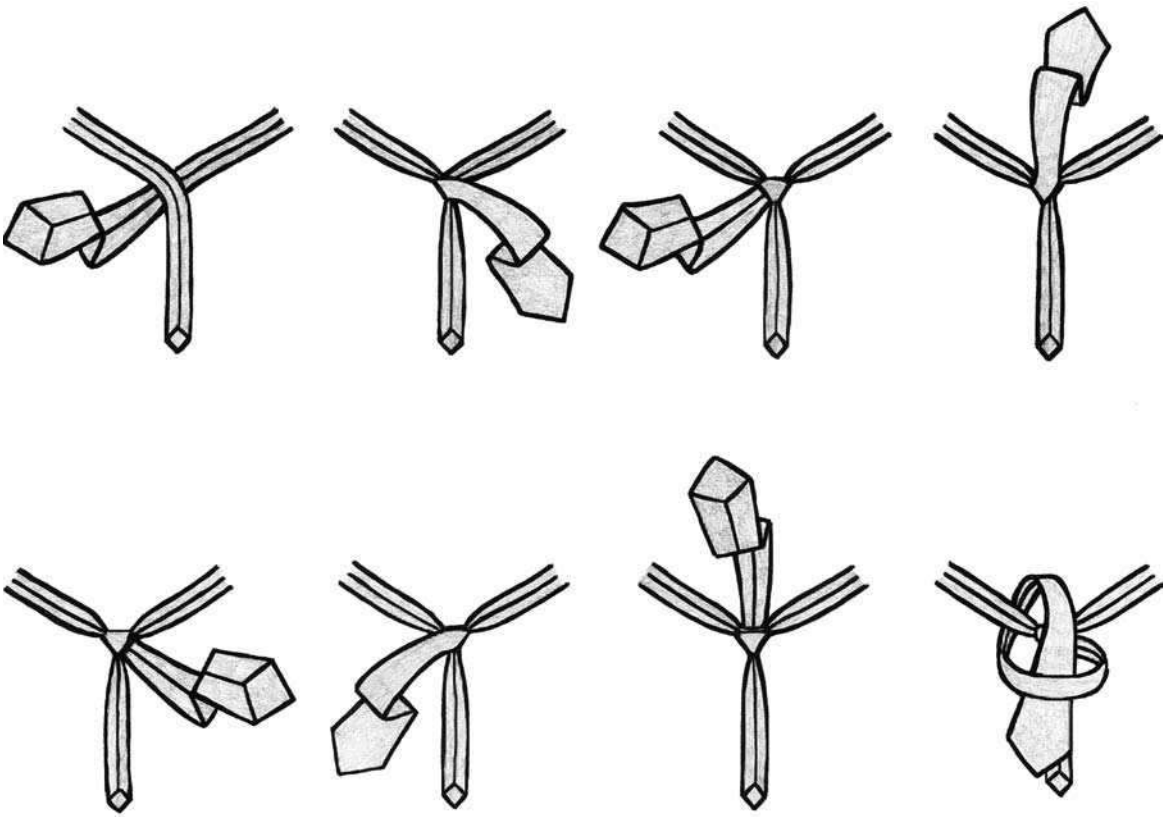

tie knots The "St. Andrew": one of several new tie knots recently discovered. *Thomas Fink*

an illusion or a product of the conscious mind. The very notion that time somehow moves leads to a logical paradox because, as the Australian philosopher J. J. C. Smart asked: "In what units is the rate of time flow to be measured? Seconds per ____?" John Dunne in his classic book *An Experiment with Time,* argued that the human mind has the ability to rove back and forth along the time line so that precognition is a physical possibility. However his theory involves an infinite regress of time and of the observer that is philosophically hard to swallow. All the same, it may be that the apparent movement from past to present to future has less to do with the universe at large than it has to do with our individual subjective experience. In some way, still to be fathomed, time, consciousness, free will, and the individual are intimately entwined. In physics, by contrast, time is treated no differently (with one important exception, noted below) than space. It is simply another **dimension**–another axis, or extension, of physical reality. Just as the various spatial dimensions prevent everything from happening at a single point, so time prevents everything from happening all at once. As one wag put it, "Time is just one damned thing after another!" In Einstein's **relativity theory**, time is effectively "spatialized" so that, instead of speaking of an absolute three-dimensional space and a separate one-dimensional time, there is a four-dimensional **space-time** continuum. So closely related are time and space in relativity theory that time can be converted into space and vice versa. In particular, different observers may not agree on the distance or the duration between any two events in space-time, but they will always agree on the *space-time interval.* If the two points events occur at (t, x, y, z) and $(t + dt, x + dx, y + dy, z + dz)$, then the (constant) space-time interval between them is given by

$$s^2 = c^2(t_2^2 - t_1^2) - (x_2^2 - x_1^2) - (y_2^2 - y_1^2) - (z_2^2 - z_1^2).$$

But the time of relativity, like that of classical physics, remains reversible.

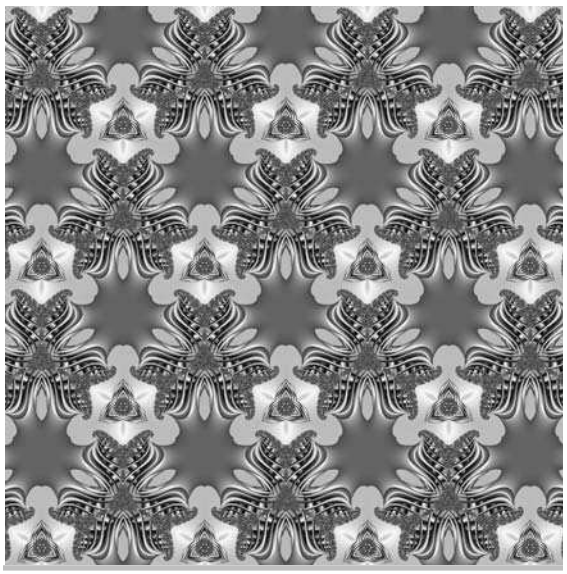

tiling A computer-generated periodic tiling. *Jos Leys, www.josleys.com*

time travel The game of Chrononauts, in which players must resolve a series of paradoxes that threaten the time line. *Looney Labs, www.LooneyLabs.com*

time complexity

A **function** that describes the amount of time required for a program to run on a computer to perform a particular task. The function is parameterized by the length of the program's input.

time dilation

See **relativity theory**.

time-reversible

A property of **dynamical system**s that can be run unambiguously both forward and backward in time. The **Lorenz system**, for example, is time-reversible.

time travel

Can we travel through **time**? Of course, we do it all the time! But can we do it at a different rate than normal? Again, the answer is "yes" because of the phenomenon known as *time dilation* in Einstein's **relativity theory**. However, time dilation enables, even in principle, only a limited kind of leap into the future–one from which we cannot return to the present. Genuine time travel is the ability to jump forward or backward through time at a rate other than that of the ordinary progression of events or that enabled by the relativistic time dilation effect.

The possibility of traveling through time poses such a threat to **causality** and opens the door to so many disturbing paradoxes that many scientists feel inclined to dismiss it out of hand. However, it has been a favorite theme of science fiction since the 1880s. In *The Time Machine* (1895), H. G. Wells gives a pleasant preamble about the nature of the **fourth dimension** before whisking his hero 802,000 years into the future. Says the Time Traveller (we never learn his real name), "[A]ny real body must have extension in four directions: it must have Length, Breadth, Thickness, and–Duration. There are really four dimensions, three of which we call the three planes of Space, and a fourth, Time. There is, however, a tendency to draw an unreal distinction between the former three dimensions and the latter, because it happens that our consciousness moves intermittently in one direction along the latter from the beginning to the end of our lives."

Unfortunately for would-be chrononauts (an early version of *The Time Machine* was called *The Chronic Astronauts*), Wells is not specific about how his time traveling

device works, though we know that "Parts were of nickel, parts of ivory, parts had certainly been filed or sawn out of rock crystal." In more recent times, physicists, speculating on some of the more esoteric byways of relativity and **quantum mechanics**, have been a little more forthcoming about how time travel might be achieved in practice. These speculations have variously involved wormholes (shortcuts outside of normal space and time), faster-than-light particles known as **tachyon**s, and unusual cosmological models, such as the ***Gödel** universe,* which allow movement to any point in the future or the past. Let us leave aside the practical aspects, however, and focus on the logic of breaking the time barrier.

The various time travel possibilities dealt with in science fiction fall into two broad categories. In the first the timeline, from deepest past to darkest future, is frozen and immutable, like a filmstrip. Any time traveling that takes place is constrained by this preordained structure–effectively, already written into the narrative of the world (the "block universe" of Einsteinian physics)–and is thus prevented from leading to paradoxes. In one variant of this scenario, the *Novikov self-consistency principle* applies. Named after Igor Novikov, an astrophysicist at Copenhagen University, this asserts that any attempt at time travel that would lead to a paradox, such as the **grandfather paradox**, is bound to fail even if the cause of failure is an extremely improbable event. In other words, try as you might to introduce a contradiction into the timeline, like killing yourself or one of your ancestors in the past, circumstances will always conspire to prevent you. An excellent example of this type of universe is found in Robert L. Forward's novel *Timemaster.* Another variant on the fixed timeline concept is that any event that appears to have caused a paradox has, in fact, created a new timeline. The old timeline remains unaltered, and the time traveler becomes part of a new temporal branch line. One difficulty with this arrangement is that it might violate the principle of conservation of mass-energy, unless the mechanics of time travel demand that mass-energy be exchanged in precise balance between past and future at the moment of travel. However, the concept of branching universes and alternative histories is not outrageous in physics where the **many worlds hypothesis** and of Feynmann's sum-over-histories are routinely debated.

The second main type of time travel entertained in science fiction assumes that the timeline is flexible and changeable. This can lead to all sorts of mind-boggling difficulties and contradictions. A way to offset some of these problems is to stipulate that the timeline is very resistant to change. In the extreme case, as writer Larry Niven has argued, it may be a fundamental rule that in any universe where time travel is allowed, no actual time machine is ever invented. The English physicist and mathematician Stephen Hawking put this idea on a more formal footing with his *chronology protection conjecture.* On the other hand if the timeline is presumed to be easily changed, paradoxes threaten to spring up at every turn. One of the most remarkable of these is the *closed causal curve paradox* in which, it seems, something can be gotten for nothing. Samuel Mines summarized the plot of his 1946 short story as follows:

> A scientist builds a time machine, goes 500 years into the future. He finds a statue of himself commemorating the first time traveler. He brings it back to his own time and it is subsequently set up in his honor. You see the catch here? It had to be set up in his own time so that it would be there waiting for him when he went into the future to find it. He had to go into the future to bring it back so it could be set up in his own time. Somewhere a piece of the cycle is missing. When was the statue made?

Closed loops in time can also conjure knowledge out of thin air. A man builds a time machine and travels into the past to give the plans for the device to his younger self who then builds the machine, travels into the past, and so on. Where did the plans originate? A curious thing about time loops is that they have no easily discernible future or past because all the events taking place in them affect one another in a circular way. Time loops also put a question mark over free will. What happens if the younger man, given the time machine plans by his older self, decides not to build the device? *Can* he make that choice given that, in some sense, he has already built it? Perhaps the apparent absence of time travelers and time machines in the real world is a sign that we do not have to worry about such issues–at least, for the present.

tinner's rabbits

A name that has emerged recently to describe a pattern of three rabbits or hares that has been found in many parts of the world, including England and Wales, mainland Europe, China, and Russia. It occurs, for example, on the medieval roof bosses of some churches in Devon and Cornwall and is thought to be connected with the local tin-mining industry. One theory suggests the following link: Tin is alloyed with copper to make bronze, copper came from Cyprus (the words *Cyprus* and *copper* have the same root), Cyprus is the island of the goddess Venus or Aphrodite (she was born there), rabbits are symbols of Venus. Three intertwined fishes are a common Christian symbol, so the three rabbits may also have stood for the Trinity.

Tippee Top

Also known as a *Tippy Top,* a type of top, patented in Britain in 1953, that consists of a peg with a ball-shaped body. If the top is spun quickly on the rounded body, with the peg pointing upward, it flips itself over and spins on its peg. Crucial to this counterintuitive behavior is the shape of the body, which is smooth and spheroidal with no sharp point. After release, the top, like tops of every description, begins to show precession, that is, its axis of rotation moves in a small circle. After a while, the contact point of the top with the table no longer coincides with the rotation axis but instead moves to other points of the top's head. Due to frictional forces and precession, the top seeks a more stable position, which it finds by flipping on to its stalk. See also **celt**.

Titchener illusion

Also known as the *Ebbinghaus size illusion,* a well-known **distortion illusion**. Two circles are surrounded by either six big circles or six small circles. Despite appearances, the two center circles are exactly the same size.

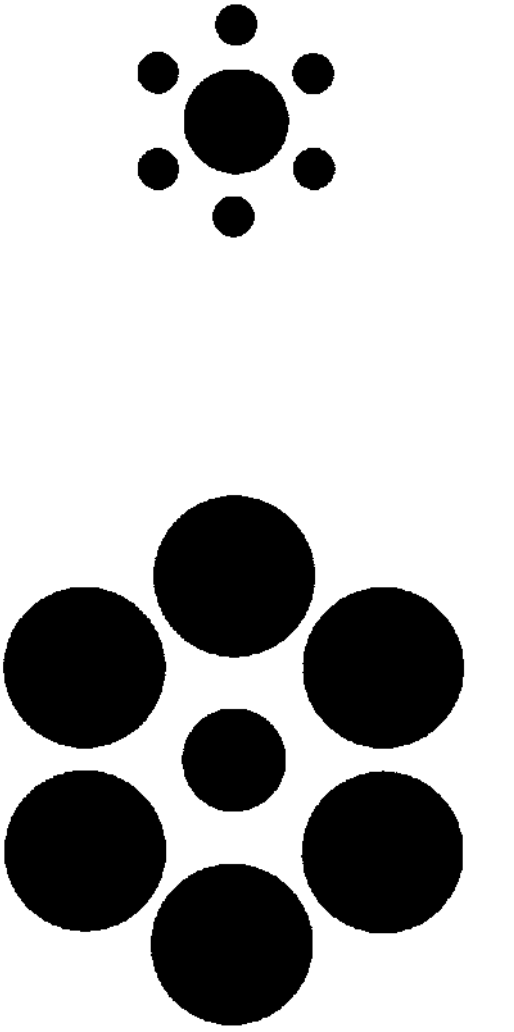

Titchener illusion The center circles are the same size.

Toeplitz matrix

A **matrix** in which all the elements are the same along any **diagonal** that slopes from northwest to southeast.

topological group

Also called a *continuous group,* a **set** that has both the structure of a **group** and of a **topological space** in such a way that the operations defining the group structure give continuous maps in the topological structure. Many groups of matrices (see **matrix**) give topological groups.

topological dimension

An integer that defines the number of coordinates needed to specify a given point of an object of set *X*. A single point, therefore, has a topological dimension equal to zero; a curve has dimension one, a surface has dimension two, and so on.

topological space

A type of generalized mathematical space in which the idea of closeness, or limits, is described in terms of relationships between **set**s rather than in terms of distance. Every topological space consists of: (1) a set of points; (2) a class of subsets defined axiomatically as open sets; and (3) the set operations of union and intersection.

topology

The study of those properties of mathematical objects that remain unaffected by smooth deformations, such as stretching and squeezing, but that don't involve tearing. The word comes from the Greek *topos* for "place," and was introduced into English by Solomon Lefschetz in the late 1920s. A topologist has been described as someone who doesn't know the difference between a doughnut and a coffee cup. Substitute "care about" for "know" and this becomes more accurate. Imagine a donut made of soft clay. A potter can easily shape this into a cup with a handle without removing or creating any new holes. Both shapes, in topology, are said to be genus 1—objects with a single hole. A sphere, by contrast, is genus 0 (no holes), while an eyeglass frame, with the lenses removed, is genus 2. For more on topologically intriguing structures, see **Möbius band** and **Klein bottle**.

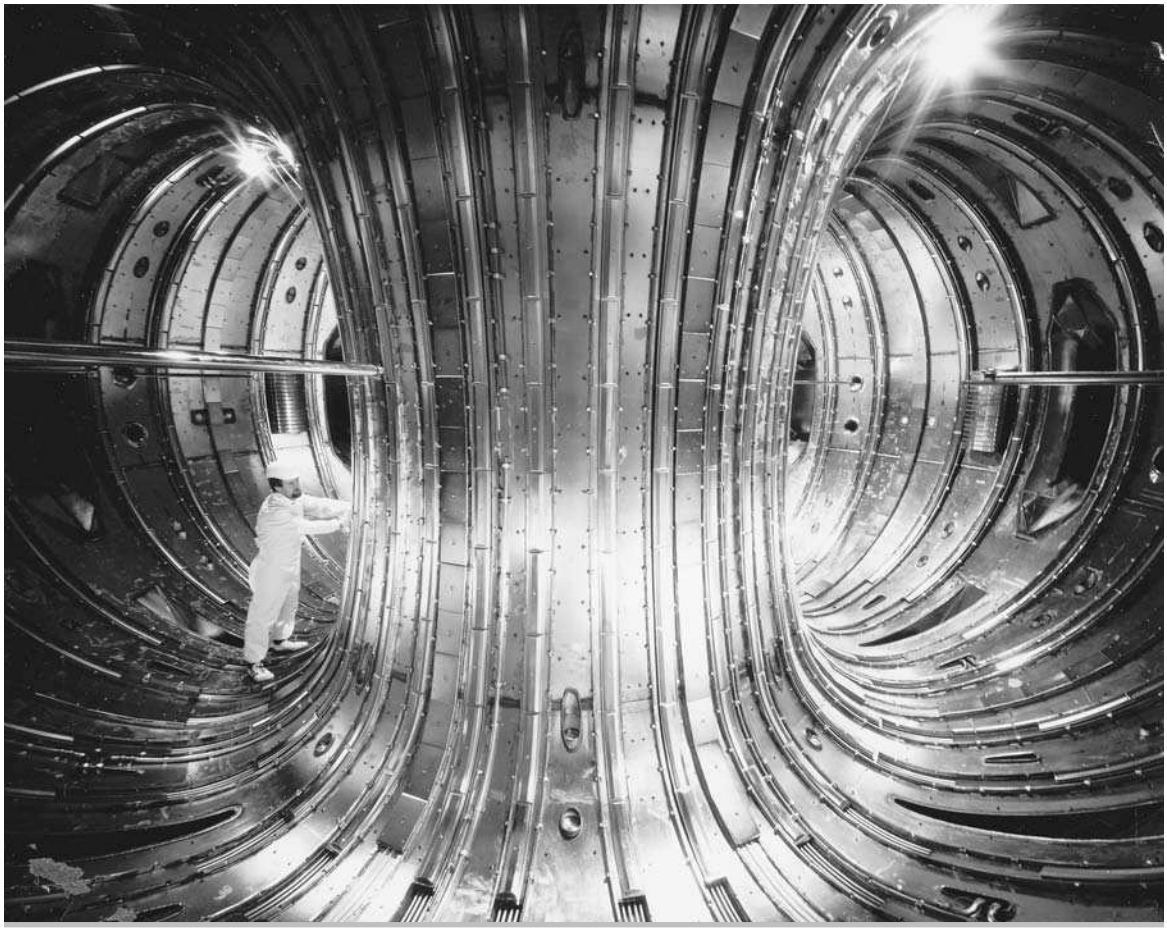

torus Inside the torus of an experimental nuclear fusion reactor. *Joint European Torus*

torus

A doughnut, bagel, or inner-tube shape; the word comes from the Latin for "bulge" and was first used to describe the molding around the base of a column. One way to think of a torus is as a **surface of revolution** obtained by rotating a circle around an axis that lies in the plane of the circle but doesn't intersect the circle. In the general case, where the shape being so rotated is any closed plane curve, the resulting surface is called a *toroid*. Although the usual torus in three-dimensional space is shaped like a doughnut, the concept of the torus is extremely useful in higher dimensional space as well.

tour

A sequence of moves by a **chess** piece on a chessboard in which each square of the board is visited exactly once. See also **knight's tour** and **magic tour**.

Tower of Brahma

A romantic legend manufactured by Edouard **Lucas** as an accompaniment to the popular game he invented, the **Tower of Hanoi**. According to the tale of the Tower of Brahma, in the Indian city of Benares, beneath a dome that marked the center of the world, is to be found a brass plate in which are set three diamond needles, "each a cubit high and as thick as the body of a bee." Brahma placed 64 disks of pure gold on one of these needles at the time of Creation. Each disk is a different size, and each is placed so that it rests on top of another disk of greater size, with the largest resting on the brass plate at the bottom and the smallest at the top. Within the temple are priests whose job it is to transfer all the gold disks from their original needle to one of the others, without ever moving more than one disk at a time. No priest can ever place any disk on top of a smaller one, or anywhere

Tower of Hanoi A vintage version of the game called Pyramids, manufactured by Knapp Electric, Inc., of New York. *Sue & Brian Young/Mr. Puzzle Australia, www.mrpuzzle.com.au*

else except on one of the needles. When the task is done, and all 64 disks have been successfully transferred to another needle, "tower, temple, and Brahmins alike will crumble into dust, and with a thunder-clap the world will vanish." The prediction (thunder-clap aside) seems fairly safe given that the number of steps required to transfer all the disks is $2^{64} - 1$, which is approximately 1.8447×10^{19}. Assuming one second per move, this would take about five times longer than the current age of the universe! Interestingly, $2^{64} - 1$ is also the answer to the **wheat and chessboard problem**.

Tower of Hanoi

A game invented by Edouard **Lucas** and sold as a toy in 1883. Early versions of it carried the name "Prof. Claus" of the College of "Li-Sou-Stain," but these were quickly discovered to be anagrams for "Prof. Lucas" of the College of "Saint Louis." The game, in its usual form, consists of three pegs on one of which are eight disks, stacked from largest to smallest. The problem is to transfer the tower to either of the vacant pegs in the fewest possible moves, by moving one disk at a time and never placing any disk on top of a smaller one. The minimum number of moves turns out to be $2^n - 1$, where n is the number of disks; this equals 255 in the case of eight disks. The original toy came with a description saying that it was a small version of the great **Tower of Brahma**.[257]

T-puzzle

A surprisingly difficult puzzle, given that there are only four pieces; it dates back to the start of the twentieth century. Photocopy and cut out the four pieces shown in the figure on the following page, and then try to arrange them to make the symmetric capital T. You are allowed to rotate the pieces as you wish and even turn them over, but they mustn't overlap in the final letter. In fact *two* different symmetric capital T letters can be made from the pieces. Also, two other symmetric shapes can be formed from the set, including an isosceles trapezoid. Can you find all of these?

trace

The sum of the terms along the **main diagonal** of a **matrix**.

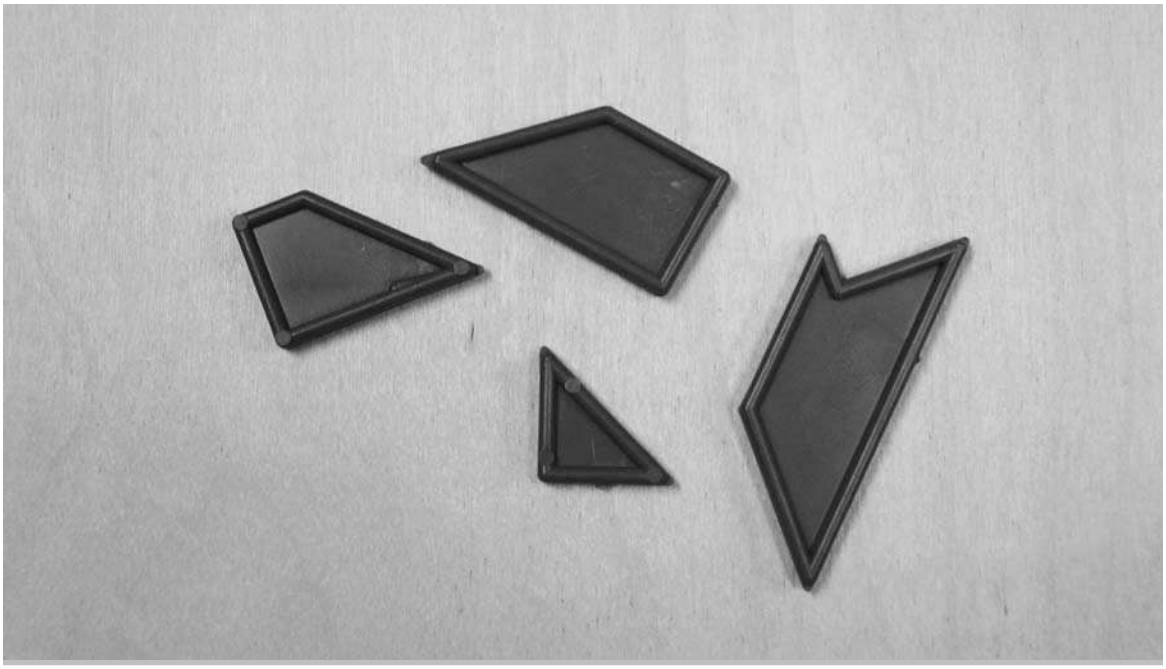

T-puzzle The pieces of the T-puzzle. *Kadon Enterprises, Inc., www.puzzlegames.com*

tractrix

A curve, sometimes called the *trajectory curve* or *equitangential curve,* that is the answer to a question asked by the Frenchman Claude Perrault (1613–1688). Perrault is not a giant in the annals of mathematics; in fact, he trained as a doctor and gained a minor reputation as an architect and an anatomist before dying in unusual style as a result of an infection he caught while dissecting a camel. His greatest claim to fame, aside from his connection with the tractrix, is that he was the brother of the author of "Cinderella" and "Puss-in-Boots."

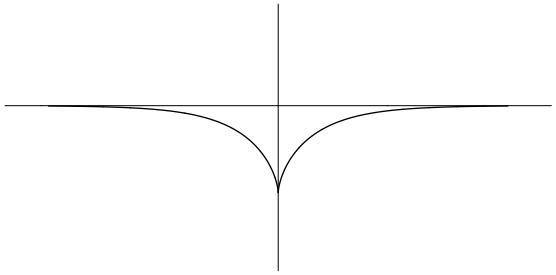

tractrix © *Jan Wassenaar, www.2dcurves.com*

In 1676, at about the time Gottfried **Leibniz** was doing groundbreaking work on the calculus, Perrault placed his pocket watch on the middle of a table, pulled the end of its chain along the edge of the table, and asked: What is the shape of the curve traced by the watch? The first known solution was given in a letter to a friend in 1693 by Christiaan **Huygens**, who also coined the name "tractrix" from the Latin *tractus* for something that is pulled along. (The corresponding German name is *hundkurve*, or "hound curve," which makes sense if you imagine the path a dog might follow on its leash as its master walks away.) The tractrix can also be found by taking the **involute** of a **catenary**. (Imagine a horizontal bar held at the vertex of the catenary and the point of contact marked as *P*. When the bar is rolled against the catenary without slipping, the path of *P* is a tractrix.) It is described by the parametric equations: $x = 1/\cosh(t)$, $y = t - \tanh(t)$. The **surface of revolution** of the tractrix is the **pseudosphere**, which is the classic model for **hyperbolic geometry** and one possible three-dimensional analog for the shape of the four-dimensional space-time in which we live.

trajectory
(1) The path of a **projectile** or other moving body through space. (2) A curve that intersects all curves of a given family at the same angles; if the intersection is at a right angle, this is an *orthogonal trajectory.* (3) The path through **phase space** taken by a system.

transcendental number
A number that can't be expressed as the root of a **polynomial** equation with integer coefficients. Transcendental numbers are one of the two types of **irrational number**, the other being **algebraic number**s. Their existence was proved in 1844 by the French mathematician Joseph Liouville (1809–1882). Although transcendentals make up the vast majority of real numbers, it is often surprisingly hard, and may even be impossible, to tell whether a certain number is transcendental or algebraic. For example it is known that both **pi** (π) and ***e*** are transcendental and also that at least one of $\pi + e$ and $\pi \times e$ must be transcendental, but it is not known which. It is also known that e^{π} is transcendental. This follows from the *Gelfond-Schneider theorem,* which says that if a and b are algebraic, a is not 0 or 1, and b is not rational, then a^b is transcendental. Using Euler's formula, $e^{i\pi} = -1$, and taking both sides to the power $-i$ gives $(-1)^{-i} = (e^{i\pi})^{-i} = e^{\pi}$. Since the theorem tells us that the left-hand side is transcendental, it follows that the right-hand side is too. (It also follows that $e \times \pi$ and $e + \pi$ are not both algebraic, because if they were, then the equation $x^2 + x(e + \pi) + e\pi = 0$ would have roots e and π, making both numbers algebraic.) But although it is known that e^{π} is transcendental, the status of e^e, π^e, and π^{π} remains uncertain.

transfinite number
Any of the infinite **ordinal number**s first described by Georg **Cantor**.

transformation
In geometry, a change to an object due to a process such as **rotation**, **reflection**, enlargement, or **translation**. In algebra, a transformation is the action of a **function**; in other words, what happens when there is a **one-to-one** mapping between sets of objects.

translation
Any **transformation** that takes the form of a constant offset with no rotation or distortion.

transpose
An operation that flips a **matrix** about the **main diagonal**.

transposition cipher
A **cipher** that encodes a message by reordering the plaintext. The receiver decodes the message using the inverse transposition. A simple kind of transposition cipher writes the message in a rectangle by rows, for example:

Asimplekin
doftranspo
sitionciph
erwritesth
emessagein
toarectang
lebyrowsan
dreadsitou
tbycolumns

and reads it by columns:

Adsee tldts oirmo erbif tweab eymti rsrya cproi serdo lanta cosle ncegt wiuks iseas tmipp tinao nnohh ngnus.

This type of cipher can be made more difficult to crack by permuting the rows and columns. See also **substitution cipher**.

transversal
A line that cuts across parallel lines, intersecting each of them.

trapezoid
A **quadrilateral** with one pair of parallel sides; in Britain this shape is known as a **trapezium**. If the parallel sides are of length a and b, and h is the perpendicular distance between them, then the area of the trapezoid is given by $A = \frac{1}{2}(a + b)h$.

trapezium
The American definition of a trapezium is a **quadrilateral** with no parallel sides. The British definition is equivalent to that of a **trapezoid**.

traveling salesman problem
Given a number n of cities, along with the cost of travel between each pair of them, find the cheapest way of visiting all the cities and returning to the starting point. This is equivalent to finding the **Hamilton circuit** of minimum weight in a weighted **complete graph**. Mathematical problems related to the traveling salesman problem (TSP) were treated in the nineteenth century by William **Hamil-**

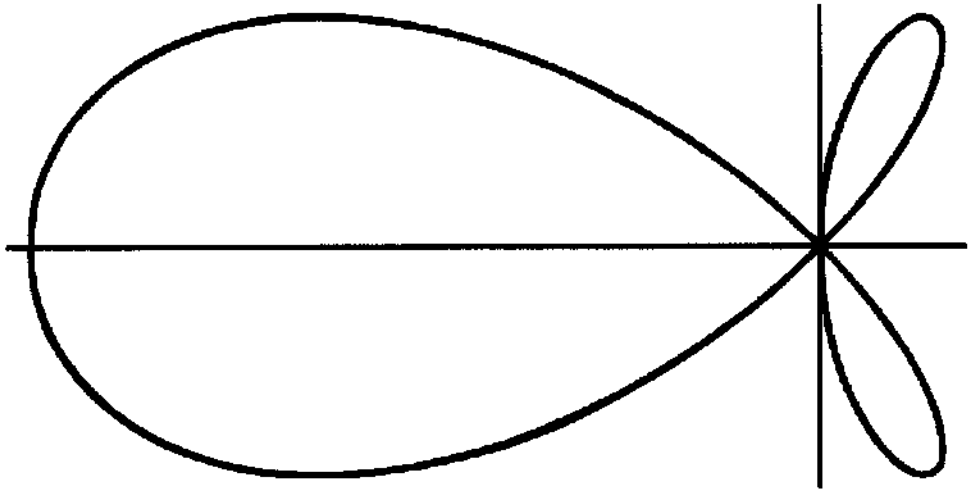

trefoil curve

ton, for example in his **Icosian game**, and by Thomas **Kirkman**. The general form of the TSP appears to be have been first studied by mathematicians in the 1930s, notably by Karl Menger in Vienna and Harvard, and later promoted by Hassler Whitney and Merrill Flood at Princeton. It has become a classic challenge to computer scientists seeking fast **algorithm**s to complex problems. An approximate solution to the TSP for 15,112 cities, towns, and villages in Germany was found in 2001 by Princeton researchers using 110 computer processors and the equivalent of more than five years computer time on a 2 GHz machine.

tree

A **graph** with the property that there is a unique path from any **vertex** to any other vertex traveling along the **edge**s.

trefoil curve

The plane curve given by the equation

$$x^4 + x^2y^2 + y^4 = x(x^2 - y^2).$$

triangle

A three-sided **polygon**. The sum of the interior angles of a triangle is always 180°, unless the triangle is drawn in a **non-Euclidean geometry**. Triangles can be classified either by their angles, as **acute**, **obtuse**, or **right**; or by their sides, as scalene (all different), **isosceles** (two the same), or **equilateral** (all equal).

Triangular Lodge

One of the few triangular buildings in England; it was built by Sir Thomas Tresham in about 1595 at Rushton, Northamptonshire. Tresham was a Catholic (spending some 15 years in prison because of this) and also a mystic numerologist. The whole design of the Lodge is based on the number **three**, which Tresham saw connected with his own surname and as an expression of his faith in the Christian Trinity. The Lodge's ground plan is a perfect **equilateral** triangle, each side 33 feet long–by tradition, the age of Christ at his death. The building has three floors, each floor has three windows, and each window is a three-fold **trefoil**. There are three gables and three gargoyles on each side. Even the central chimney is three-sided. The inscriptions all have 33 letters. Other buildings with a three-sided equilateral theme in Europe include a triangular castle at Gripsholm in Sweden and part of the Chateau de Chantilly in France, which is based on an equilateral plan of gigantic scale.

triangular number

Any number that can be represented by a triangular array of dots: 1, 3, 6, 10, ... The nth triangular number is $n(n + 1)/2$. Every integer is the sum of at most three triangular numbers. Every triangular number is a **perfect number**. If T is a triangular number, $8T + 1$ is a perfect square and $9T + 1$ is another triangular number. The square of the nth triangular number is equal to the sum of the first n cubes. Certain triangular numbers

are also squares, but no triangular number can be a third, fourth, or fifth power, nor can one end in 2, 4, 7, or 9.

triangulation
A **tiling** of some object such as a **manifold** by simplices (see **simplex**).

tribar illusion
See **Penrose triangle**.

tricuspoid
See **deltoid**.

trident of Newton
A curve investigated and named "trident" by Isaac **Newton** as part of his systematic study of **cubic** equations. René **Descartes** also studied it and it is sometimes called the parabola of Descartes, although it isn't a parabola. It has the Cartesian equation

$$xy = cx^3 + dx^2 + ex + f.$$

trifolium
See **rose curve**.

trigonometric curve
Any of the curves produced when a **trigonometric function** is graphed.

trigonometric function
Any of the **function**s *sine* (sin), *cosine* (cos), *tangent* (tan), *secant* (sec), *cosecant* (cosec), or *cotangent* (cot), or their inverses, sin^{-1}, etc, which deal with certain proportions in right **triangle**s. For example, the sine of an angle θ, sin θ, in a right triangle, is equal to the side opposite the angle divided by the hypotenuse (the longest side). Similarly cos is adjacent over hypotenuse and tan is opposite over adjacent. Sec, cosec, and cot are the multiplicative inverses of cos, sin, and tan, respectively: $\sec \theta = 1/\cos \theta$, and so forth. These are not the same as the inverse functions $\cos^{-1}$, $\sin^{-1}$, and $\tan^{-1}$, which are also known as arccos, arcsin, and arctan. Graphs of trigonometric functions produce **trigonometric curve**s.

trigonometry
The branch of **mathematics** that deals with the relationships between the sides and the angles of **triangle**s and the calculations based on them, particularly the **trigonometric function**s. Sherlock Holmes relies on a little trigonometry to solve a 250-year-old mystery known as the Musgrave Ritual (in a short story of the same name)—an enigmatic series of clues that refers to the shadow of an elm tree when the sun is just visible at the top of a nearby oak to point toward buried treasure. The great detective recalls to Watson his conversation with Reginald Musgrave:

> "Have you any old elms?" . . .
>
> "There used to be a very old one over yonder, but it was struck by lightening ten years ago, and we cut down the stump."
>
> "You can see where it used to be?"
>
> "Oh, yes." . . .
>
> "I suppose it is impossible to find out how high the elm was?"
>
> "I can give it to you at once. It was sixty-four feet. . . . When my old tutor used to give me an exercise in trigonometry, it always took the shape of measuring heights." . . .
>
> I went with Musgrave to his study and whittled myself this peg, to which I tied this long string with a knot at each yard. Then I took two lengths of a fishing-rod, which came to just six feet. . . . The sun was just grazing the top of the oak. I fastened the rod on end, marked out the direction of the shadow. . . . It was nine feet in length. Of course, the calculation was now a simple one. If a rod of six feet threw a shadow of nine, a tree of sixty-four feet would throw one of ninety-six. . . . I measured out the distance . . . and I thrust a peg into the spot.

trillion
In American and general usage, a million million—1,000,000,000,000 or 10^{12}. A European trillion is a million times larger than this, or 10^{18}. Counting one number every second, 24 hours a day, it would take 31,688 years to reach one (American) trillion. The first trillion-dollar lawsuit ($116 trillion) was filed in August 2002 by 600 family members against a company run by Osama bin Laden's family, Saudi Arabian princes, and Sudan. See also **large number**.

trimorphic number
See **automorphic number**.

trinomial
An algebraic expression consisting of three terms.

triomino
Also called a *tromino,* a three-square **polyomino**.

triple
A multiple of **three**. A *triple integral* is one in which the integrand is integrated three times. See also **Pythagorean triplet**.

trisecting an angle

Whereas **bisecting an angle** could hardly be simpler, splitting an angle in three equal parts with compass and straightedge alone is impossible, except in a few special cases such as when the angle happens to be 90°. Trisecting an arbitrary angle can be done if you cheat by using a measuring ruler instead of a plain straightedge, or even if you draw just two marks on the straightedge, but not if you play by the rules and the straightedge is completely blank. The Greeks put a huge effort into the problem but couldn't crack it. In fact, the question of whether trisection could ever be done in the general case remained open until 1837, when it was finally shown to be impossible by Pierre Wantzel, a 23-year-old French mathematician. Why is it impossible? Wantzel showed that the two problems of trisecting an angle and of solving a cubic equation are equivalent. Moreover, he showed that only a very few cubic equations can be solved using the straightedge-and-compass method. He thus deduced that most angles cannot be trisected.

trisector theorem

See **Morley's miracle**.

trisectrix

A general name for curves that can be used in **trisecting an angle**. The name "trisectrix," on its own, is often applied specifically to the **limaçon of Pascal**. Other famous trisectrix curves include the **Maclaurin trisectrix** and the **conchoid** of Nicomedes.

triskaidekaphobia

See **thirteen**.

trochoid

The curve formed by the path of a point on the extension of a radius of a circle as it rolls along a curve or line. It is also the curve formed by the path of a point on a perpendicular to a straight line as the straight line rolls along the convex side of a base curve. By the first definition, the trochoid is derived from the **cycloid**; by the second definition it is derived from the **involute**. See also **roulette**.

truel

A three-cornered gunfight or its logical equivalent. Imagine a truel between Arnie, Bullseye, and Clint, who are standing at the corners of an equilateral triangle. All know that Arnie's chance of hitting a target is 0.3 and Clint's is 0.5, while Bullseye never misses. They have to fire at their choice of target in the order Arnie then Bullseye then Clint until only one man is left. A man who's been hit is out of the fight and can no longer be shot at. What should Arnie's strategy be?

Truels, like this one, have become a significant topic in **game theory** because they're analogs of various real-life situations, from rivalry among animals to competition between television networks. Small changes in the rules can lead to strikingly different, sometimes counterintuitive outcomes. Different firing rules are possible: sequential in fixed order (players fire one at a time in a predetermined, repeating sequence), sequential in random order (the first player to fire and each subsequent player is chosen at random from among the survivors), or simultaneous (all surviving players fire at the same time in every round). In certain truels, a participant is allowed to shoot at the ground rather than try to eliminate an opponent (an optimal strategy if the firing order is fixed and each player has only one bullet and is a perfect shot). If the first shooter misses on purpose, he eliminates himself as a threat, and the other two fight it out, leaving two survivors in the end. Any other course of action would lead to the first shooter's own demise, with only one survivor. Even if the players have an unlimited supply of bullets, the truel may still end with more than one survivor because no player wants to be the first to shoot. Indeed, under the fixed firing order rule, no player has an incentive to eliminate another player. Only in the case of simultaneous firing is there a chance that nobody will survive.

Most of the mathematical research on truels concerns the relationship between a player's marksmanship (probability of hitting a target) and his or her survival probability. It's possible to show, for example, that better marksmanship can hurt in many situations. In a sequential truel in which contendors aren't allowed to shoot in the air, a player maximizes his probability of survival by firing at the opponent against whom he'd less prefer to fight in a duel–regardless of what the other players do. If his shot misses, it makes no difference who the target was. If the shot hits the target, the shooter is better off because his opponent in the next duel is weaker. Thus, the first shooter fires at the opponent who's the better marksman. In general, depending on the marksmanship values, the survival probabilities of the truelists could end up in any order, including one that is the reverse order of shooting skill. Optimal play can be very sensitive to slight changes in the rules, such as the number of rounds of play allowed. On the other hand, some factors are fairly constant: the disadvantage of being the best marksman, the weakness of pacts, the possibility that an endless supply of ammunition may stabilize rather than undermine cooperation, and the

deterrent effect of an indefinite number of rounds of play (which can prevent players from trying to get the last shot). Some of these findings are counterintuitive, even paradoxical. An understanding of them might well dampen the desire of aggressive players to score quick but temporary wins, rendering them more cautious. In particular, contemplating the consequences of a long, drawn-out conflict, truelists may come to realize that their own actions, while immediately beneficial, may trigger forces that ultimately lead to their own destruction.

truncate
To slice off a corner of a **polyhedron** around a **vertex**.

truncatable prime
A **prime number** *n* that remains a prime when digits are deleted from it one at a time. For example 410,256,793 is a truncatable prime because each number created by the removal of the digit underlined produces a new prime: 41<u>0</u>,256,793; 41,256,7<u>9</u>3; 4,1<u>2</u>5,673; 4<u>1</u>5,673; 45,67<u>3</u>; 4,<u>5</u>67; <u>4</u>67; <u>6</u>7; 7. It is conjectured that there are infinitely many of these primes. If the digits from a prime can be deleted only from the right, to leave a prime, then *n* is called a *right truncatable prime.* If they can be deleted only from the left, to leave a prime, then *n* is a *left truncatable prime.* The list of primes from which *any* digit can be deleted at each step to leave a prime is very short indeed, because it demands that each digit be a prime and also that no digit occurs twice. Only these numbers satisfy this requirement: 2, 3, 5, 7, 23, 37, 53, and 73.

Tschirnhaus's cubic
A curve with the Cartesian equation $3ay^2 = x(x - a)^2$.

Turing, Alan Mathison (1912–1954)
An English mathematician considered to be one of the fathers of modern digital computing. At an early age, Turing showed signs of the genius and eccentricity that became hallmarks of his adult personality. He taught himself to read in three weeks and made a habit of stopping at street corners to read the serial numbers of traffic lights. Later, he became a near-Olympic-class runner and ran long distances with an alarm clock tied to his waist to time himself.

At Cambridge, Turing studied under G. H. **Hardy** and got involved with problems that David **Hilbert** and Kurt **Gödel** had proposed to do with completeness and decidability in mathematics. In 1936, he introduced the idea of what became known as **Turing machine**s–formal devices capable of solving any conceivable mathematical problem that could be represented by an **algorithm**. However, the Turing machine was only a theoretical possibility at that time and not a working implementation. It would remain for later researchers to solve the various practical difficulties required to make the computer a reality. Turing also showed that there were mathematical problems that a Turing machine could never solve. One of these is the **halting problem**. While his proof was published after that of Alonzo **Church**, Turing's work is more accessible and intuitive. During World War II, Turing was a major player at Bletchley Park, near present-day Milton-Keynes (a town built after the war), in the successful efforts to crack the Nazi Enigma ciphers. While serving at Bletchley Park (1939–1944), he stayed at the Crown Inn, Shenley Brook End, and somewhere near here he buried two silver bars, carefully recording the site with respect to local landmarks. When he returned to recover them, the area had been rebuilt and all his landmarks were gone. Despite several attempts with metal detectors, he never recovered them and no one else is known to have found them. The Crown is now a private house and the area where he buried the bars is a housing estate.

Turing, Alan Mathison

Turing's interest in computing continued after the war, when he worked at the National Physical Laboratory on the development of a stored-program computer (the ACE or Automatic Computing Engine). In 1948 he moved to the University of Manchester, where the first stored-program digital computer ran later that year (see

Babbage, Charles for a photo of this machine). In 1950, in the article "Computing Machinery and Intelligence," Turing tackled the problem of **artificial intelligence**, and proposed an experiment now known as the **Turing test**.

In 1952 his lover helped a compatriot to break into Turing's house and commit larceny. Turing went to the police to report the crime. As a result of the police investigation, he was charged with homosexuality (formerly a crime), offered no defense, and was convicted. Following the well-publicized trial, he was given a choice between incarceration and libido-reducing hormone injections. He chose the latter, which lasted for a year and had side effects including the development of breasts during that period. In 1954 he died of poisoning after eating a cyanide-laced apple. Most (though not his mother) believed that his death was intentional, and the death was ruled a suicide. According to one urban legend the Apple company's logo is symbolic of this event: an apple with two bites (or possibly bytes) out of it and rainbow colors that code for homosexuality. See also **Church-Turing thesis**.[168]

Turing machine

An abstract model of computer execution and storage introduced in 1936 by Alan **Turing** to give a mathematically precise definition of **algorithm**. A Turing machine can be thought of as a black box that carries out a calculation of some kind on an input number. If the calculation reaches a conclusion, or halts, then an output number is returned. Otherwise, the machine theoretically carries on forever (see **halting problem**). There are an infinite number of Turing machines, as there are an infinite number of calculations that can be done with a finite list of rules. A Turing machine that can simulate any other Turing machine is called a *universal Turing machine* or a **universal computer**. The concept of Turing machines is still widely used in theoretical computer science, especially in **complexity theory** and the theory of computation.

Turing test

A proposed way of deciding if a machine has human-level intelligence. First described by Alan **Turing** in 1950, it goes like this: A human judge engages in a natural language conversation with other parties; if the judge can't reliably tell whether the other party is human or machine, then the machine is said to pass the test. It is assumed that both the human and the machine try to appear human. The origin of the test is a party game in which guests try to guess the gender of a person in another room by writing a series of questions on notes and reading the answers sent back. In Turing's original proposal, the human participants had to pretend to be the other gender, and the test was limited to a 5-minute conversation. These features are nowadays not considered to be essential and are generally not included in the specification of the Turing test. Turing proposed the test in order to replace the emotionally charged and, for him, meaningless question "Can machines think?" with a more well-defined one. Turing predicted that machines would eventually be able to pass the test. In fact, he estimated that by the year 2000, machines with 10^9 bits (about 119MB) of memory would be able to fool 30% of human judges during a 5-minute test. He also predicted that people would then no longer consider the phrase "thinking machine" contradictory.

It has been argued that the Turing test can't serve as a valid definition of **artificial intelligence** for at least two reasons: (1) A machine passing the Turing test might be able to simulate human conversational behavior, but this could be much weaker than true intelligence. The machine might just follow some cleverly devised rules. (2) A machine might well be intelligent without being able to chat like a human. Simple conversational programs, such as ELIZA, have fooled people into believing they are talking to another human being; however, such limited successes don't amount to passing the Turing test. Most obviously, the human party in the conversation has no reason to suspect he is talking to anything other than a human, whereas in a real Turing test the questioner is actively trying to determine the nature of the entity he is chatting with. The Loebner Prize is an annual competition to determine the best Turing test competitors. See also **Chinese room**.

twelve

A number heavily used for grouping things (inches, hours, 12-packs), partly because it can be divided evenly in several different ways (by 2, 3, 4, and 6) and partly because there are roughly 12 cycles of the Moon for every one of the Sun. The Latin *duodecim* (two + ten) for 12 forms the root of dodecagon (originally duodecagon), meaning a 12-sided shape, and duodenum, the first part of the intestine that is about 12 inches long. Contracted and modified over the years, *duodecim* became "dozen." Multiples of 12 have also been used by many cultures for various units and measures. A "shock" was 60 or five dozen (a dozen for each finger on one hand), and many cultures had a "great hundred" of 120 or 10 dozen (a dozen for each finger on both hands). The Romans used a fraction system based on 12 and the smallest part, an *uncil*, became our word for "ounce." The French emperor Charlemagne established a monetary system that had a base of 12 and 20, the remnants of which persist. Until 1970, the En-

glish pound sterling consisted of 20 shillings, and each shilling contained 12 pence. In 1944, The Duodecimal Society was formed in New York with the purpose of proposing a switch to base 12 for all scientific work. There are 12 signs of the zodiac and there were 12 apostles of Christ. Twelve is the smallest **abundant number**, a **Harshad number**, and a semiperfect number (because 12 = 1 + 2 + 3 + 6; see **perfect number**). See also **gross**.

twelve-color map problem

If on a plane or sphere each country has at the most one colony, requiring the same color as its parent country, at most 12 different colors are needed to distinguish the political regions on a map. The problem of determining if this is true or not remains open. See also **four-color map problem**.

twenty

Many early cultures, including some in Europe; the Mayans of Central America; and the Ainu, the indigenous people of the Japanese islands, used a **base** of 20 for counting. The base 20 system was retained until about 1970 in the British monetary system, in which there were 20 shillings to the pound. A group of 20 is often called a **score**. Two of the five Platonic solids involve 20: the **icosahedron** has 20 triangular faces and the **dodecahedron** has 20 vertices. Twenty is a **Harshad number**, a semiperfect number (see **perfect number**), and a **practical number**. It is also a tetratrahedral number–the sum of consecutive triangular numbers (1 + 3 + 6 + 10).

twin primes

Pairs of **prime numbers** that differ by two, the first of which are 3 and 5, 5 and 7, 11 and 13, and 17 and 19. The largest example known, as of February 2003, is a pair of 51,090-digit primes discovered by Yves Gallot and Daniel Papp, with the value $33{,}218{,}925 \times 2^{169690} \pm 1$. Other than the first, all twin primes have the form $\{6n - 1, 6n + 1\}$; also, the integers n and $n + 2$ form twin primes if and only if $4[(n - 1)! + 1] = -n \pmod{n(n + 2)}$. In 1919 the Norwegian mathematician Viggo Brun (1885–1978) showed that the sum of the reciprocals of the twin primes converges to a sum now known as *Brun's constant:*

$$(1/3 + 1/5) + (1/5 + 1/7) + (1/11 + 1/13) + (1/17 + 1/19) + \ldots$$

In 1994, by calculating the twin primes up to 10^{14} (and discovering the infamous Pentium bug in the process), Thomas Nicely of Lynchburg College estimated Brun's constant to be 1.902160578. According to the (unsolved) *twin-prime conjecture* there are infinitely many twin primes. The twin-prime conjecture generalizes to prime pairs that differ by any even number n, and generalizes even further to certain finite patterns of numbers separated by specified even differences. For example, the following triplets of primes all fit the pattern k, $k + 2$, and $k + 6$: 5, 7, and 11; 11, 13, and 17; 17, 19, and 23; 41, 43, and 47. It is believed that for any such pattern not outlawed by divisibility considerations there are infinitely many examples. (The pattern k, $k + 2$, and $k + 4$ has only one solution in primes, 3, 5, and 7, because any larger such triplet would contain a number divisible by 3.) Quartets of the form k, $k + 2$, $k + 6$, and $k + 8$ (the smallest example is 5, 7, 11, and 13) are thought to be infinite. For some patterns no example is known, or only one.

twins paradox

See **relativity theory**.

twisted cubic

A curve in three-dimensional space or projective space whose points are given by $(x(t), y(t), z(t))$ for a parameter t and where x, y, z are **polynomials** of at most degree 3.

two

The first even number and the only even **prime number**. The word comes from the Greek *dyo* and the Latin *duo* through the Old English *twa.* Early languages often had both feminine and masculine forms for two and so there are a lot of diverse roots related to "two-ness." Many "two" words use the Greek root *bi* such as biannual, binary, biscuit, and biceps. Others come from the Old English *twa,* such as between, twilight, twist, and twin. From *duo* we get dual, duet, dubious (of two minds), duplex (two layers), and double. The Latin *di* gives us diploma (two papers) and dihedral. The earlier Greek *dyo* produces dyad, composed of two parts. Two is the only positive real number that gives the same result when added to itself as when multiplied by itself. It is conjectured that 2 is the only even integer that cannot be written as the sum of two primes (see **Goldbach conjecture**) and it has recently been proven that 2 is the largest value of n for which the equation $x^n + y^n = z^n$ has nonzero integer solutions (see **Fermat's last theorem**). Two is the base of the **binary** number system.

two-dimensional world

Life in three dimensions is familiar and there is a huge body of literature on the **fourth dimension**. But what would a universe of just two dimensions be like? The first and the most charming book on the subject is Edwin Abbott's ***Flatland: A Romance of Many Dimensions***

(1884).[1] This was followed by Charles **Hinton**'s lengthier *An Episode of Flatland* (1907)[272] in which the 2-d world is not a plane, as in Abbott's yarn, but the rim of a large circular world called Astria. Hinton was the first to explore in some depth what science and technology might be like in two dimensions; in fact, an earlier pamphlet of his called "A Plane World," (reprinted in *Scientific Romances* in 1884) may have helped inspire Abbott's novel. Hinton's speculations were taken much further by Alexander **Dewdney** in *Planiverse* (1984).[81]

U

Ulam, Stanislaw Marcin (1909–1984)

A Polish-born American mathematician and physicist who solved the problem of how to initiate fusion in the hydrogen bomb and also devised the **Monte Carlo method** of solving mathematical problems using statistical sampling. He first came to the United States in 1935 following an invitation from John **von Neumann**. One morning in 1946 an event happened that changed Ulam's life, as colleague Gian-Carlo Rota recalled:

> Ulam, a newly appointed professor at the University of Southern California, awoke to find himself unable to speak. A few hours later, he underwent a dangerous surgical operation after the diagnosis of encephalitis. . . . In time, however, some changes in his personality became obvious to those who knew him . . . [H]is ideas, which he spouted out at odd intervals, were fascinating beyond anything I have witnessed before or since. However, he seemed to studiously avoid going into details . . . . [H]e came to lean on his unimpaired imagination for his ideas, and on . . . others for technical support . . . . A crippling technical weakness coupled with an extraordinarily creative imagination is the drama of Stan Ulam.

Ulam spiral

A remarkable geometric pattern accidentally found among the **prime number**s by Stanislaw **Ulam**;[314] it is also known as the *Prime Spiral*. During a boring meeting one day in 1963, Ulam drew a square, marked the number 1 at the center, and then wrote the increasing whole numbers as a spiral that wound its way out to the edge of the paper. He then circled all the prime numbers and was immediately struck by how they tended to fall on diagonal lines radiating from the central 1. In Ulam's words the arrangement of primes "appears to exhibit a strongly nonrandom appearance." Ulam rushed home and

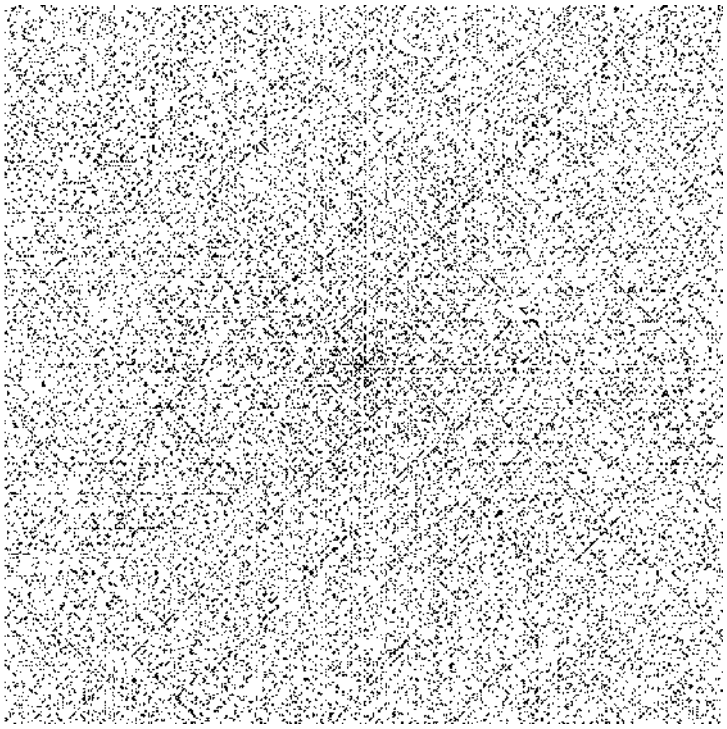

Ulam spiral Patterns amid the primes.

expanded the spiral to cover a much larger portion of the number sequence. The strange pattern persisted. Primes had a tendency to occur in clusters and all clusters tended to make a beautiful image that couldn't be predicted. With the help of computers this pattern can now be explored almost indefinitely and it reveals a wonderfully rich combination of symmetry and surprise–very reminiscent of some **fractal**s.

The Ulam spiral should perhaps be known as the "Clarke spiral" in view of the fact that Arthur C. Clarke described the phenomenon in his novel *The City and the Stars* (1956, ch. 6, p. 54),[63] predating Ulam's discovery by several years. Clarke wrote:

> Jeserac sat motionless within a whirlpool of numbers. The first thousand primes. . . . Jeserac was no mathematician, though sometimes he liked to believe he was. All he could do was to search among the infinite array of primes for special relationships and rules which more talented men might incorporate in general laws. He could find how numbers behaved, but he could not explain why. It was his pleasure to hack his way through the arithmetical jungle, and sometimes he discovered wonders that more skillful explorers had missed. He set up the matrix of all possible integers, and started his computer stringing the primes across its surface as beads might be arranged at the intersections of a mesh.

Ulam's conjecture

See **Collatz problem**.

uncountable set

A **set** of numbers that can't be put in a definite order from smallest to largest and so can't be counted. All uncountable sets are infinite, but not all infinite sets are uncountable. The best known uncountable set is the set of all **real number**s. By contrast the set of all **natural number**s, which represents the "smallest" type of **infinity**, is countable.

undulating number

An integer whose digits, in a given **base**, alternate–that is, one written in the form *ababab* . . . , where *a* and *b* are digits. For example, 434,343 and 101,010,101 are undulating numbers.

unduloid

A member of a family curves that is formed by films or liquid drops suspended between certain boundaries. Examples of unduloids are seen on a spider web when viewed through a microscope. They consist of blobs of viscous liquid that make up the sticky part of the web and are mostly gathered into a lemon shape. The family of unduloids includes shapes ranging from very thin to almost spherical, depending on the diameter of the thread and the volume of liquid in the blob. The shape of the curve is a result of the equality of pressure throughout the blob, which means that the total **curvature** at all points on the surface must be the same. The total curvature is the sum as the curvatures in two planes at right angles, and so varies from one blob to the next. A common property of all unduloids, however, is that they have a constant nonzero main curvature.

unexpected hanging

A remarkable logical **paradox** that appears to have begun circulating by word of mouth in the 1940s, often in the form of a puzzle about a man condemned to be hanged. A judge, with a reputation for reliability, tells a prisoner on Saturday that he will be hung on one of the next seven days but that he will not know which day until he is informed on the morning of the execution. Back in his cell, the prisoner reasons that the judge must be wrong. The hanging cannot be left until Saturday, because the prisoner would certainly know, if this day dawned, that it was his last. But if Saturday is eliminated, the hanging cannot take place on Friday either, because if the prisoner survived Thursday he would know that the hanging was scheduled for the next day. By the same argument, Thursday can be crossed off, then Wednesday, and so forth, all the way back to Sunday. But with every other day ruled out for a possible unexpected hanging, the hangman cannot arrive on Sunday without the prisoner knowing in advance. Thus, the condemned man reasons, the sentence can't be carried out as the judged decreed. But then Wednesday morning comes around and, with it, the hangman–unexpectedly! The judge was right after all and something was awry with the prisoner's seemingly impeccable logic. But what? More than half a century of attack by numerous logicians and mathematicians has failed to produce a resolution that is universally accepted. The paradox seems to stem from the fact that whereas the judge knows beyond doubt that his words are true (the hanging will occur on a day unknown in advance to the prisoner), the prisoner does not have this same degree of certainty. Even if the prisoner is alive on Saturday morning, can he be certain that the hangman will arrive?[61, 260]

uniform polyhedron

A **polyhedron** in which each face is regular and each **vertex** is equivalently arranged. Uniform polyhedra include the **Platonic solid**s, the **Archimedean solid**s, the **prism**s and **antiprism**s, and the nonconvex uniform polyhedra (see **nonconvex uniform polyhedron**).

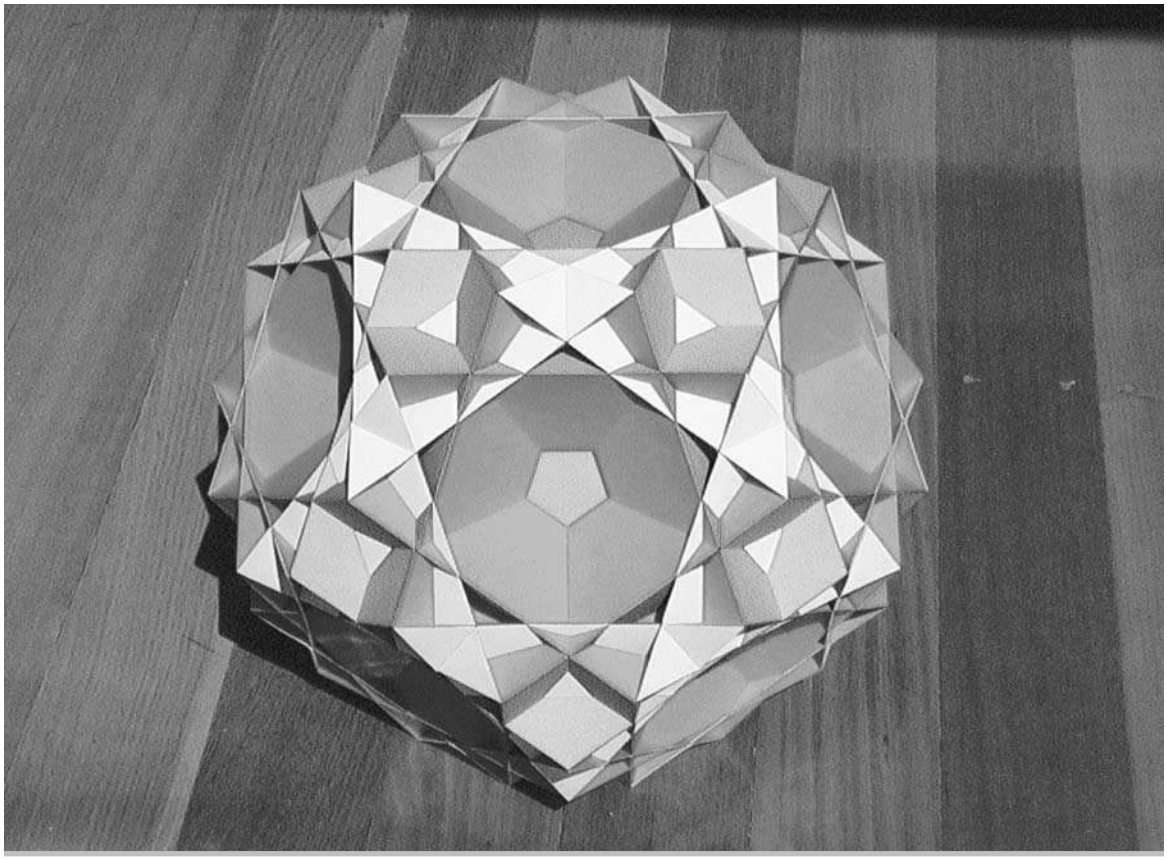

uniform polyhedron The great icosicosidodecahedron, a uniform polyhedron. *Robert Webb, www.software3d.com; created using Webb's Stella program*

unilluminable room problem

Imagine an L-shaped room in which Amy is standing near one corner holding a match. If Bob stands round the corner, he can see light from the match because a light ray can bounce off the two opposite walls. This is true wherever Bob stands in the room: the whole room is illuminated by the one match. Would this be true for a room of *any* shape, or is there at least one room that is *so* complicated that there's somewhere inside it that light from the match never reaches. This problem was first asked by Ernst Strauss in the 1950s. Nobody knew the answer until 1995, when George Tokarsky of the University of Alberta showed that the answer is "yes," there *is* a room that is not completely illuminable. His published floor plan showed a room with 26 sides–the smallest such room currently known. But a mystery remains. The room Tokarsky found contains one particular place where the match can be held which leaves part of the room dark. But if the match is moved slightly, the whole room is lit up again. Is there a room so fiendishly complicated that *wherever* the match is held there are some places that its light can never reach? For the moment we remain in the dark.[320, 334]

unique number

The constant U_n that results if a number A_n consisting of n consecutive digits, in ascending order, is subtracted from the number A_n' obtained by reversing the digits of A_n. For example, a three-digit number 345, if subtracted from its reverse 543, yields a difference of 198. Any other three-digit number subtracted from its reverse gives the same difference. Thus $U_3 = 198$. Similarly for a number with four consecutive digits, the unique number $U_4 = 3{,}087$. The first ten unique numbers are: $U_1 = 0$, $U_2 = 9$, $U_3 = 198$, $U_4 = 3{,}087$, $U_5 = 41{,}976$, $U_6 = 530{,}865$, $U_7 = 6{,}419{,}754$, $U_8 = 75{,}308{,}643$, $U_9 = 864{,}197{,}532$, and $U_{10} = 9{,}753{,}086{,}421$. Unique numbers are related to **Kaprekar numbers**, K_n, by the formula

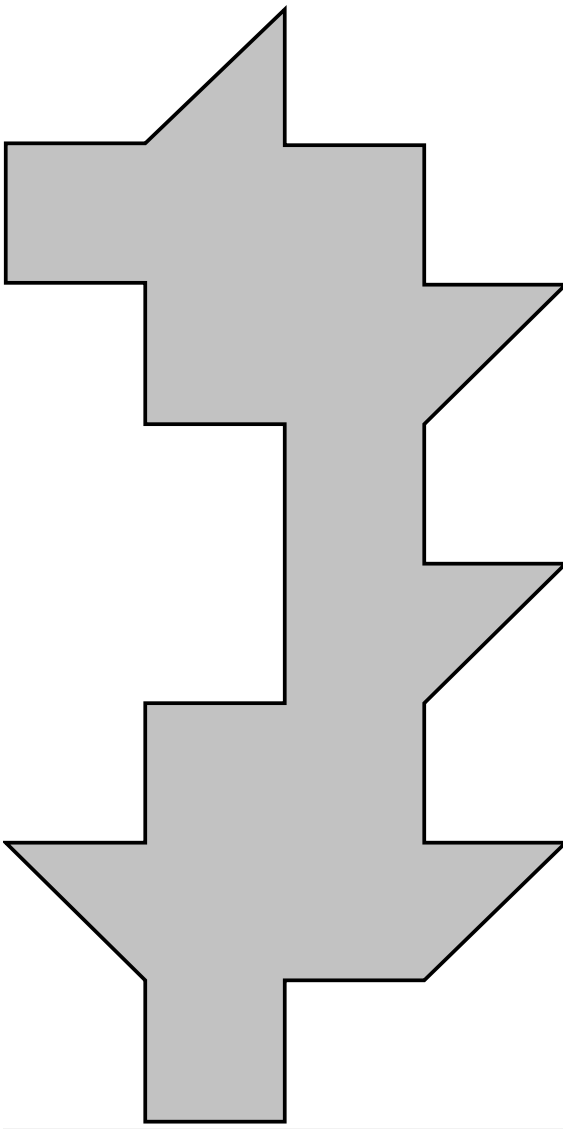

unilluminable room problem No single light source can light up every corner of a room with this shape.

$$U_n + U'_n = K_n + K'_n.$$

For example, when $n = 4$, $K_4 = 6{,}174$, $K_4' = 4{,}716$, $U_4 = 3{,}087$, $U_4' = 7{,}803$, and

$$3{,}087 + 7{,}803 = 10{,}890 = 6{,}174 + 4{,}716.$$

unimodal sequence
A **sequence** that first increases and then decreases.

unimodular matrix
A square **matrix** whose **determinant** is 1.

union
The **set** of all elements that belong to at least one of two or more given sets. It is denoted by the symbol ∪.

unit circle
A circle with radius 1.

unit cube
A cube with edge length 1. A *unit square* has a side length of 1.

unit fraction
A fraction whose **numerator** (number on top) is 1.

universal approximation
Having the ability to approximate any **function** to an arbitrary degree of accuracy. **Neural network**s are universal approximators.

universal computation
Capable of computing anything that can in principle be computed; being equivalent in computing power to a **Turing machine** or the **lambda calculus**.

universal computer
A computer that is capable of **universal computation**, which means that given a description of any other computer or program and some data, it can perfectly emulate this second computer or program. Strictly speaking, home PCs are not universal computers because they have only a finite amount of memory. However, in practice, this is usually ignored.

Universal Library
A library that contains not just one copy of every book that has ever been printed but one copy of every book that it is possible to print. A version of such a fantastic place is described by Jorge Luis **Borges** in his melancholic short story "Library of Babel" from *The Garden of Forking Paths* (1941). It begins: "The universe (which others call the Library) is composed of an indefinite, perhaps infinite number of hexagonal galleries." Each gallery is identical to all the others and contains 800 books identical in format. "[E]ach book contains four hundred ten pages; each page, forty lines, each line, approximately eighty black letters. . . ." There are 25 symbols–22 letters, the comma, the period, and the space. Because the library contains every possible combination of these

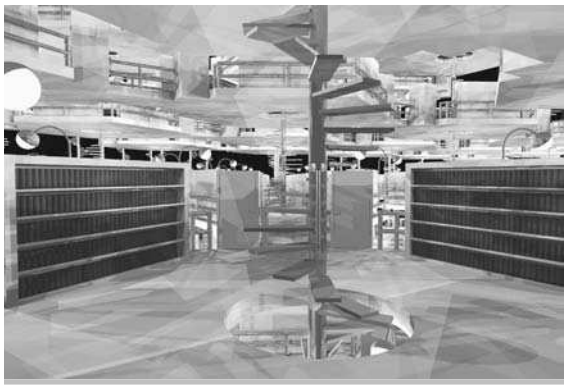

Universal Library Inside the library that goes on forever.
Joseph Formoso

symbols it contains, in addition to vast tracts of gibberish, every truth, falsehood, idea, novel, thought, and description of events, past and future, that are possible. It contains, writes Borges,

> *All*–the detailed history of the future, the autobiographies of the archangels, the faithful catalog of the Library, thousands and thousands of false catalogs, the proof of the falsity of those catalogs, a proof of the falsity of the *true* catalog, the gnostic gospel of Basilides, the commentary upon that gospel, the commentary on the commentary of that gospel, the true story of your death, the translation of every book into every language, the interpolations of every book into all books, the treatise Bede could have written (but did not) on the mythology of the Saxon people, the lost books of Tacitus.

The name "Universal Library" was first used by the German philosopher and science fiction writer Kurt Lasswitz (1848–1910) as the title of a short story published in 1901. He, in turn, borrowed the concept from the German psychologist **Theodor Fechner**. But to get to the root of speculation about listing all possible combinations of words and meanings, we have to go back much further, to Ramon Lully (1235–1315), a Spaniard who was a missionary and a mystic philosopher and who had an idea that later became known as Lully's Great Art. His idea was simply this: if one property of a thing is chosen, say the color of blood, and all the possibilities for that property are listed–blood is green, blood is yellow, etc.–then one of them must be true. One list alone might not be enough to point out the truth. However, other lists could be made that would eliminate some of the possible colors. Done in the right way, the one and only true answer should emerge. Lully even tried to build a device that used a series of concentric rings to bring different combinations of words into alignment. Eventually, the idea came down to Fechner who ruminated on the idea of permuting all combinations of letters to express all possible statements and concepts. There are, however, two barriers to this dream of ultimate truth. The first is that there isn't enough matter or space in the universe to represent all the different ways that book-length sequences of letters can expressed. Second, even if there were, it would take an all-seeing, all-knowing intelligence to sort the rare grain of meaningful wheat from the vast quantities of vapid chaff. See also **monkeys and typewriters**.

universal set

The **set** that contains all elements capable of being accepted to the problem. Also known as the *universe*, as in the **universe of discourse**, it is usually denoted *U*.

universe of discourse

The part of the world under discussion; more precisely, the **set** of all objects presumed or hypothesized to exist for some specific purpose. Objects may be concrete (e.g., a specific carbon atom, Confucius, the Sun) or abstract (e.g., the number 2, the set of all integers, the concept of justice). Objects may be primitive or composite (e.g., a circuit that consists of many subcircuits). Objects may even be fictional (e.g., a unicorn, Sherlock Holmes). The universe of discourse is a familiar concept in **logic**, linguistics, and mathematics.

unknown

A quantity, denoted by a letter, that is to be found by solving one or more equations.

untouchable number

A number that is not the sum of the **aliquot part**s of any other number. The first few untouchable numbers are 2, 5, 52, 88.

up-arrow notation

See **Knuth's up-arrow notation**.

upside-down picture

A picture (or figure) that, when inverted, looks the same or changes into the picture of a different subject. Possibly the most remarkable examples of upside-down art were the cartoons drawn by Gustave Verbeek for the *Sunday New York Herald* in the early 1900s. The first part of the cartoon is read normally; then the newspaper is turned

upside-down picture An upside-down figure from China.
Sue & Brian Young/Mr. Puzzle Australia, www.mrpuzzle.com.au

through 180° and the second part read from the same boxes in reverse order. As if by magic, Little Lady Lovekins transforms into Old Man Muffaroo, a giant fish becomes a giant bird, and a pouncing tiger turns into a tiger buried under a pile of stones.

Ussher, James (1581–1656)

An Irish clergyman, born in Fishamble Street, Dublin, who studied at Trinity College, Dublin, and later became a fellow there. He entered the Church and eventually became Archbishop of Armagh. In 1650 he published his famous assertion that the Creation had taken place "upon the entrance of the night preceding" Sunday, October 23, 4004 B.C.

utility function

The lesson of the **St. Petersburg paradox** is that people do not play games as if they are maximizing the expected monetary value they receive. However, certain rationality assumptions about the way people behave, known as the *von Neumann and Morganstern axioms,* imply that people *do* act as though they are maximizing *something.* This "something" is often referred to as a utility function.

V

vampire number
A natural number x that can be factorized as $y \times z$ in such a way that the number of occurrences of a particular digit in the representation of x in a given **base** (say 10) appears the same number of times in the representations in that same base of y and z together. For example, 2,187 is a vampire number since $2{,}187 = 21 \times 87$; similarly 136,948 is a vampire because $136{,}948 = 146 \times 938$. Vampire numbers are a whimsical idea that was introduced by Clifford Pickover in 1995.[253]

van der Pol, Balthazar (1889–1959)
A Dutch electrical engineer who began the modern experimental study of **dynamical system**s in the 1920s and '30s. Van der Pol discovered that electrical circuits employing vacuum tubes display stable oscillations, now called limit cycles, but that when these circuits are driven with a signal whose frequency is near that of the limit cycle, the periodic response shifts its frequency to that of the driving signal. The resulting waveform, however, can be quite complicated and contain a rich structure of harmonics and subharmonics. In 1927, van der Pol and his colleague van der Mark reported that an "irregular noise" was heard at certain driving frequencies between the natural entrainment frequencies. It's now clear that, without realizing it, they had described one of the first experimental instances of **chaos**.

vanishment puzzle
A **mechanical puzzle** in which the total area of a collection of pieces, or the number of items in a picture, appear to change following some manipulation. A well-known puzzle, first seen in 1868, involves an 8×8 square that is divided up into two triangles and two trapezoids. The pieces are reassembled into an oblong shape that measures 5×13. Where did the extra bit of area come from? The answer is that final shape is not perfectly rectangular but instead has a narrow gap that runs the length of one of the diagonals. Most famous of all vanishment puzzles is **Get off the Earth**.

variable
An **unknown** that has no fixed quantitative value.

vector
A quantity that is specified by a number, indicating size or "magnitude," and a direction; for example, "80 kilometers per hour, heading due south." More generally, a vector is any element of a **vector space** and is also a type of **tensor**. A vector is usually shown in a graph or other diagram as an arrow whose length and direction represent the vector's magnitude and direction, respectively. In n-dimensional space, it is easy to deal with vectors algebraically in the form of n-tuples, which are ordered lists (one-dimensional arrays) of n components.

vector space
Also known as a *linear space,* the most fundamental concept in **linear algebra**. It is a generalization of the set of all geometric **vector**s and is used throughout modern mathematics. Like the concepts of **group**, **ring**, and **field**, that of a vector space is entirely abstract.

Venn diagram
A simple way of representing **set**s and subsets, which makes use of overlapping circles. Venn diagrams are named after the Englishman John Venn (1834–1923), a fellow of Cambridge University. Venn was a cleric in the Anglican Church, an authority on what was then called "moral science," the compiler of a massive index of all Cambridge alumni, and a rather mundane mathematician who worked in logic and probability theory. The diagrams he used for representing **syllogism**s appear to have been first called "Venn diagrams" by Clarence Irving in his book *A Survey of Symbolic Logic* in 1918. However, Venn was lucky to be so immortalized. Both Gottfried **Leibniz** and Leonhard **Euler** used very similar forms of representation many years earlier.

vertex
The point where two sides of a closed figure, or two sides of an angle, meet; otherwise known as a *corner.* A cube, for example, has eight vertices.

vertex figure
The **polygon** that appears if a **polyhedron** is **truncate**d at a **vertex**. The vertex figure of a cube, for example, is an equilateral triangle. To ensure consistency, the truncation may be done at the midpoints of the edges.

vertical-horizontal illusion
Vertical lines looks considerably longer than horizontal ones of the same length. For centuries, it has been known

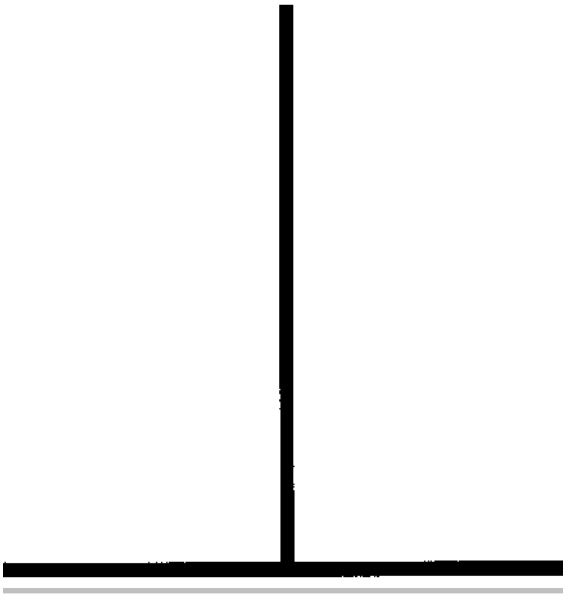

vertical-horizontal illusion

that the height of trees and buildings is perceived to be greater than the horizontal distance between them. This may be because we live in gravity. Rotate the book and you will see that the vertical line in the diagram appears to shrink in relation to what was originally the horizontal line. See also **distortion illusion**.

Vesica Piscis

Literally "fish's bladder," the almond shape formed when two identical circles overlap so that the outside edge of each just touches the center of the other. The Vesica Piscis appears as the Christian fish symbol and also frequently in medieval art and architecture. Most significantly, it provides the template for the pointed Gothic **arch**.

Vickrey auction

A silent auction in which the object being sold goes to the *second-highest bidder.* In a normal silent auction prospective buyers place their bids in sealed envelopes and the highest bid wins. This makes it risky for the seller because if the object is highly valuable and all buyers think they are the only ones who recognize this fact, they may offer much less than they think the object is actually worth. However, a Vickrey auction induces people to bid truthfully. Why? Because when all other bids are fixed and unknown to a given bidder, that bidder's optimal strategy is to bid what she thinks the object is worth. Suppose Alice places a bid for an antique vase. Let V be the amount that Alice thinks the vase is actually worth, and B the bid that she actually makes. Let M be the maximum of all other bids. If M is more than V, then Alice should set her bid B less than or equal to V, so that she does not get the vase for more than she thinks it is worth. If M is less than V, then Alice should set $B = V$, because if she bids any less, she will not get the vase any cheaper, and she may lose it altogether.

vigesimal

Of, relating to, or based on the number 20; the term comes from the Latin *vigesimus* for "twentieth." Mayan arithmetic, which took account of all the toes as well as the fingers, used a vigesimal system. In place of the multiples of 10 used in the decimal system: 1; 10; 100; 1,000; 10,000, . . . , the Mayans dealt in multiples of 20: 1; 20; 400; 8,000; 160,000; . . . .

vinculum

The bar that is placed over repeating decimal fractions to indicate the portion of the pattern that repeats. In the original Latin, *vinculum* referred to a small cord for binding the hands or feet. The symbol was once used in the same way that parentheses and brackets are now used to bind together a group of numbers or symbols. Originally the line was placed under the items to be grouped. What today might be written $7(3x + 4)$ the early users of the vinculum would write $\underline{3x + 4}\ 7$. Sometimes the horizontal fraction bar is called a vinculum as it binds the numerator and denominator into a single value.

Vinogradov's theorem

Every sufficiently large odd number can be expressed as the sum of three **prime number**s. The theorem was named after the Russian mathematician Ivan Vinogradov (1891–1983) who proved it in 1937. This is a partial solution of the **Goldbach conjecture** and is related to **Waring's conjecture**.

Viviani's curve

The space curve that marks the intersection of the cylinder $(x - a)^2 + y^2 = a^2$ and the sphere $x^2 + y^2 + z^2 = a^2$. It is given by the parametric equations:

$$x = a(1 + \cos t)$$
$$y = a \sin t$$
$$z = 2a \sin(\tfrac{1}{2} t)$$

Viviani's theorem

For a given point inside an equilateral **triangle**, the sum of the perpendicular distances from the point to the sides is equal to the height of the triangle. If the point is outside the triangle, the relationship still holds if one or more of the perpendiculars is treated as a negative value.

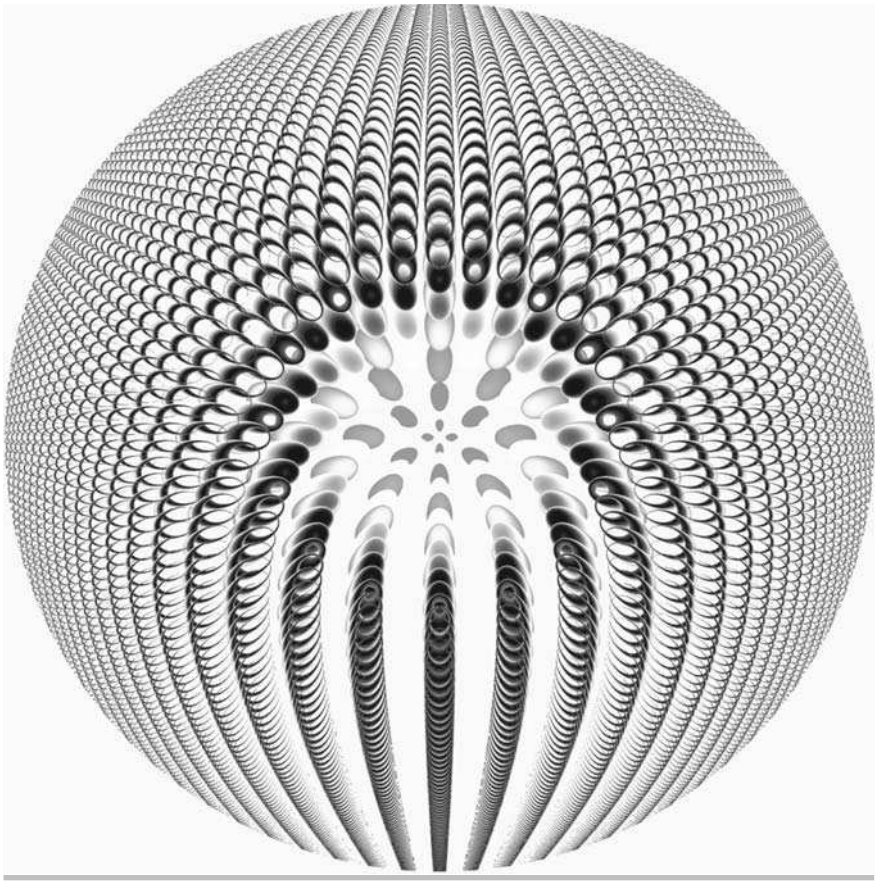

Volvox fractal *Jos Leys, www.josleys.com*

Viviani's theorem generalizes to a regular *n*-sided **polygon**: the sum of the perpendicular distances from an interior point to the *n* sides being *n* times the **apothem** of the figure. The theorem is named for Vincenzo Viviani (1622–1703), a pupil of Galileo and Torricelli, who is also remembered for a reconstruction of a book on the **conic section**s of **Apollonius** and for finding a way of **trisecting an angle** through the use of an equilateral hyperbola.

volume

The measure of space occupied by a solid body.

Volvox fractal

A **fractal** that is similar in appearance to *Volvox*–a unicellular life form that lives in spherical colonies with thousands of members.

von Neumann, John (1903–1957)

> *Young man, in mathematics you don't understand things, you just get used to them.*

A Hungarian-American mathematician who made important contributions to **set theory**, computer science, economics, and **quantum mechanics**. He received a Ph.D. in mathematics from the University of Budapest and later he worked at the Institute for Advanced Study in Princeton. *Theory of Games and Economic Behavior,*[230] which he coauthored with Oskar Morgenstern in 1944, is considered a seminal work in the field of **game theory**. Von Neumann devised the von Neumann architecture used in all modern computers and studied cellular automata (see **cellular automaton**) in order to construct the first examples of self-replicating automata, now known as **von Neumann machine**s. Von Neumann had a mind of great

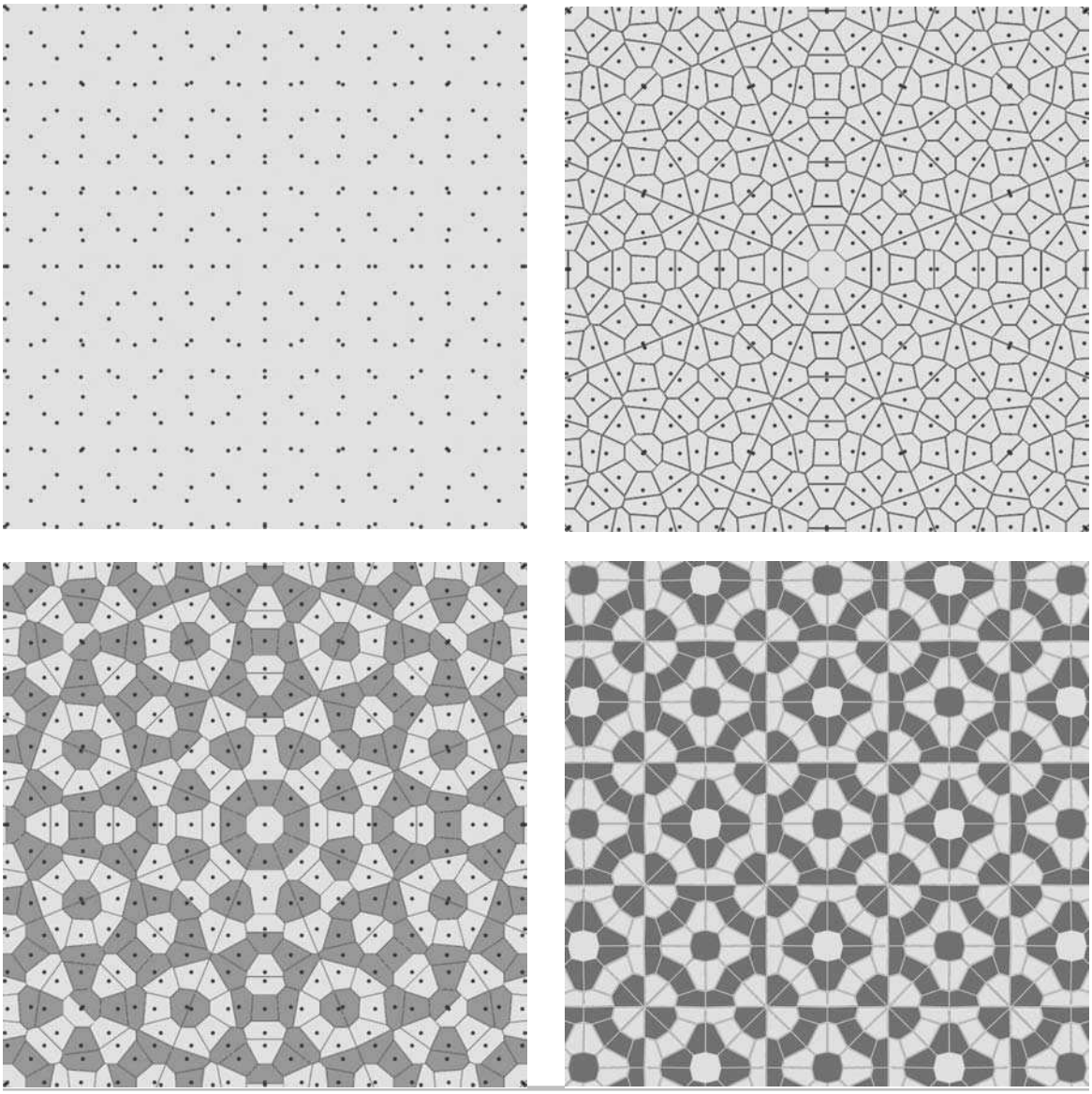

Voronoi diagram Top (left to right): Start from a grid of points. Draw lines that limit areas closest to the points of the grid. Bottom (left to right): Color the areas in some fashion. An infinite variety of patterns is possible. *Jos Leys, www.josleys.com*

ingenuity, nearly total recall of what he'd learned, immense arrogance, and a great love of jokes and humor.[259]

von Neumann machine

(1) A model for a computing machine that uses a single storage structure to hold both the set of instructions on how to perform the computation and the data required or generated by the computation. John **von Neumann** helped to create the model as an example of a general-purpose computing machine. By treating the instructions in the same way as the data, the machine could easily change the instructions. In other words the machine was reprogrammable. (2) A self-replicating machine. In principle, if a machine (e.g., an industrial

robot) could be given enough capability, raw material, and instructions, then that robot could make an exact physical copy of itself. The copy would need to be programmed in order to do anything. If both robots were reprogrammable, then the original robot could be instructed to copy its program to the new robot. Both robots would now have the capability of building copies of themselves. Since such a machine is capable of reproduction, it could arguably qualify as a simple form of life.

Voronoi diagram

Also known as a *Dirichlet tesselation,* a partitioning of space into cells, each of which consists of the points closer to one particular object than to any others. More specifically, in two dimensions a Voronoi diagram consists of breaking up a plane containing *n* points into *n* convex **polygon**s in such a way that each polygon contains exactly one point and every point in a given polygon is closer to its central point than to any other. Voronoi diagrams, their boundaries (known as *medial axes*), and their **dual**s (called *Delaunay triangulations*) have been reinvented, given different names, generalized, studied, and applied many times over in many different fields. Voronoi diagrams tend to be involved in situations where a space should be partitioned into "spheres of influence"; examples include models of crystal and cell growth and protein molecule volume analysis.

vulgar fraction

See **common fraction**.

W

walking in the rain problem
The question is whether you get wetter by walking or running a given distance through rain that is falling at a constant rate. An early appearance of this problem was in Bagley's *Paradox Pie* (1944). A simple answer is that moving faster is better. If the rain falls vertically and the density of water in the air is assumed constant, then, no matter what your speed, you'll sweep out the same volume and will always get the same amount of water hitting your front. However, running rather than walking will reduce the amount of water landing on your head.

Wallis, John (1616–1703)
The most influential English mathematician before Isaac **Newton** and an important contributor to the origins of **calculus**. He was a skilled linguist, was one of the first to proclaim in public Harvey's discovery of the circulation of the blood, and had an extraordinary memory for figures. His *Arithmetica Infinitorum* was described as "the most stimulating mathematical work so far published in England" and introduced the symbol ∞ for infinity (see also **aleph**). It contained the germs of the differential calculus, and it suggested to Newton, who was delighted by it, the **binomial theorem**.

Wallis formula
See **pi**.

wallpaper group
Also known as a *crystallographic group,* a distinct way to tile the plane that repeats indefinitely in two dimensions; that is, a collection of two-dimensional symmetric patterns on a plane surface, containing two nonparallel **translation**s (see **periodic tiling**). There are only 17 kinds of these patterns, known as isometries (see **isometry**), each uniquely identified by its translation and rotation symmetries, as discovered in the late nineteenth century by E. S. **Fedorov** and, independently, by the German A. M. Schoenflies and the Englishman William Barlow. Thirteen of the isometries include some kind of rotational symmetry, while four do not; twelve show rectangular symmetries, while five involve hexagonal symmetries. Every two-dimensional repetitive pattern in wallpaper, textiles, brickwork, or the arrangement of atoms in a plane of a crystal is just a minor variation on one of these 17 patterns.

Wari
See **Mancala**.

Waring's conjecture
A hypothesis given, without proof, by the English mathematician Edward Waring (1734–1798) in his *Meditationes algebraicae* (1770). It states that for every number k, there is another number s such that every natural number can be represented as the sum of s kth powers. For example, every natural number can be written as a sum of 4 squares, 9 cubes and so on. Waring's conjecture was first proven in full by David **Hilbert** in 1909.

weak inequality
An **inequality** that permits the equality case. For example, a is less than or equal to ($\leq$) b.

Weierstrass, Karl Wilhelm Theodor (1815–1897)
A German mathematician who is considered the father of modern **analysis**. Compelled by his father to study law, he instead spent four years at the University of Bonn, fencing, drinking, and reading math. He left under a cloud and

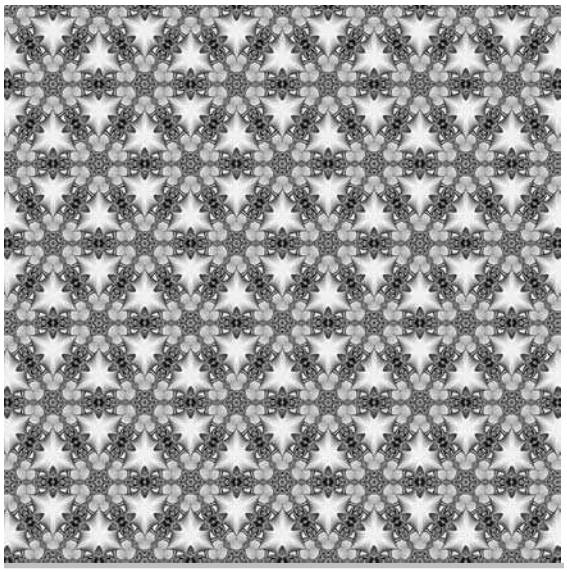

wallpaper group A pattern made from one of the wallpaper groups. *Jos Leys, www.josleys.com*

ended up teaching in secondary schools for many years. In 1854 he published a paper, written 14 years earlier when he was fresh out of college, in *Crelle's Journal*, on *Abelian functions* which completed work that Niels **Abel** and Karl **Jacobi** had begun. Its importance was immediately recognized and Weierstrass was appointed a professor at the Royal Polytechnic School and a lecturer at the University of Berlin. He went on to give the first rigorous definitions of **limit**, **derivative**, differentiability, and **convergence**, and investigated under what conditions a power series will converge.

Weierstrass's nondifferentiable function

The earliest known example of a *pathological function*–a **function** that gives rise to a **pathological curve**. It was investigated by Karl **Weierstrass**, but had been first discovered by Bernhard **Riemann**, and is defined as:

$$f(x) = \sum_{k=1}^{\infty} \frac{\sin(\pi k^2 x)}{\pi k^2}$$

The Weierstrass function is everywhere continuous (see **continuity**) but nowhere differentiable; in other words, no **tangent** exists to its curve at any point. Constructed from an infinite sum of trigonometric functions, it is the densely nested oscillating structure that makes the definition of a tangent line impossible.

weighing puzzles

See **measuring and weighing puzzles**.

weird number

See **abundant number**.

Wessel, Caspar (1745–1818)

A Norwegian surveyor whose mathematical fame rests on a single paper, published in 1799, that gave the first geometrical interpretation of **complex number**s. His priority in this discovery, however, went unrecognized for many years. Thus what should really be called a *Wessel diagram* is known instead as an **Argand diagram** after the man whose work on the same subject, published in 1806, first came to the attention of the mathematical world. Wessel's paper, by contrast, wasn't noticed by the mathematical community until 1895 when the Danish mathematician Sophus Juel drew attention to it and, in the same year, Sophus **Lie** republished Wessel's paper. Astonishingly, Wessel's remarkable work was not translated into English until 1999–its bicentenary!

Weyl, Hermann Klaus Hugo (1885–1955)

A German mathematician (known as "Peter" to his close friends) whose work involved symmetry theory, **topology**, and **non-Euclidean geometry**. Weyl studied under David **Hilbert** at Göttingen. Then, as a colleague of Albert Einstein at Zurich 1913, he got involved with **relativity theory** and came to believe (erroneously) that he had found a way to unite gravity and electromagnetism. From 1923 to 1938 he concentrated on **group** theory and made some important contributions to **quantum mechanics**. As the Nazi tide swept over Europe, Weyl came to the United States and spent the rest of his career at the Institute for Advanced Studies at Princeton. He said: "My work always tried to unite the truth with the beautiful, but when I had to choose one or the other, I usually chose the beautiful." See also **beauty and mathematics**.

wff

A well-formed formula.

what color was the bear?

A hunter walks one mile due south, then one mile due east, then one mile north and arrives back at his starting point. He shoots a bear. What color was it? Such a trip is possible if the hunter starts from one of the geographical poles, then circumnavigates the sides of a spherical triangle (see **elliptical geometry**). Since there are no bears in Antarctica, the trip is assumed to have taken place in the Arctic where there are polar bears and thus the answer is "white." Versions of this problem began to appear in the 1940s. A closer examination reveals that there are many more points on the globe, other than an exact pole, from which the hunter could have begun his trek. One example is any point (of which there are an infinite number) on a circle drawn at a distance of slightly more than $1 + \frac{1}{2}\pi$ mile (about 1.16 miles) from a pole–"slightly more" because of Earth's curvature. But this is not all. The hunter could also satisfy the conditions by starting at points closer to the pole, so that the walk east would carry him exactly twice around the pole, or three times, and so on. Of course, the bear would still be white (except that polar bears don't live that far north!).

wheat and chessboard problem

According to one myth, **chess** was invented by Grand Vizier Sissa Ben Dahir and then given to King Shirham of India. The king was so pleased that he offered his subject a great reward in gold, but the wily vizier said that he would be happy merely to have some wheat: one grain for the first square of the chessboard, two grains for the second square, four for the third, and so on, doubling each time. The king thought this was a very modest request, granted it, and asked for a bag of wheat to be brought in. However the bag was emptied by the twentieth square. The king asked for another bag, but then realized that this entire bag was needed for the next square. In 20 more squares, as many bags would have been exhausted as there

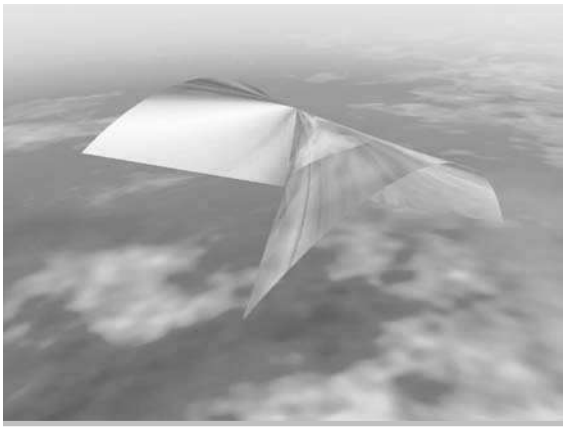

Whitney's umbrella *Takashi Nishimura*

were grains in the first bag! The number of grains on the sixty-fourth square would have been 2^{63}, and the total for the whole board $2^{64} - 1 = 18{,}446{,}744{,}073{,}709{,}551{,}615$. This is more wheat than in the entire whole world; in fact, it would fill a building 40 km long, 40 km wide, and 300 meters tall. See also **Tower of Brahma**.

Whitney's umbrella

A strange-looking, whimsically named geometrical object first studied by Hassler Whitney in the 1940s. It can be pictured as a self-intersecting rectangle in three dimensions. A *pinch point,* also known as a *Whitney singularity* or a *branch point* occurs at the top endpoint of the segment of self-intersection: every neighborhood of the pinch point intersects itself.

Wiener, Norbert (1894–1964)

An American mathematician who established the subject of **cybernetics.** As a precocious youngster, Wiener hopped from subject to subject at college, finally earning a Ph.D. in mathematics from Harvard at 19, before embarking on an even more erratic early career that took him into a variety of activities, including journalism. Having settled upon mathematical research, obtaining a post at the Massachusetts Institute of Technology in 1919, he nevertheless continued to range across fields, from random processes, including ergodic theory (concerned with the onset of chaos in a system), to integral equations, quantum mechanics, and potential theory. Wartime work that involved applying statistical methods to control and communication engineering, led to him extending these studies into control and communication in complex electronic systems and in animals, especially humans–the science of cybernetics.

Wiles, Andrew (1953–)

The English mathematician who, in 1994, finally proved **Fermat's last theorem**. Wiles studied at Oxford (B.A. 1974) and Cambridge (Ph.D. 1977) and has held posts at Cambridge, Oxford, and Princeton. From the mid-1980s his work was focused on proving a proposition known as the *Shimura-Taniyama conjecture,* since from this, it had been shown, Fermat's last theorem would follow. In 1993 he gave a series of lectures at Cambridge University ending on June 23, 1993. At the end of the final lecture he announced he had a proof of Fermat's last theorem. However, when the results were written up for publication, a subtle error was found. Wiles worked hard for about a year, helped in particular by a colleague, R. Taylor, and by September 19, 1994, having almost given up, he decided to have one last try. As he recalled, "suddenly, totally unexpectedly, I had this incredible revelation. It was the most important moment of my working life. . . . [I]t was so indescribably beautiful, it was so simple and so elegant . . . [that] I just stared in disbelief for twenty minutes, then during the day I walked round the department. I'd keep coming back to my desk to see it was still there–it was still there."

In 1994 Wiles was appointed Eugene Higgins Professor of Mathematics at Princeton. His paper that proves Fermat's last theorem is called "Modular elliptic curves and Fermat's Last Theorem" and appeared in the *Annals of Mathematics* in 1995.[296]

Wilson's theorem

Any number p is a **prime number** if, and only if, $(p-1)! + 1$ is divisible by p. We can easily check this for some small numbers: $(2-1)! + 1 = 2$, which is divisible by 2; $(5-1)! + 1 = 25$, which is divisible by 5; $(9-1)! + 1 = 40{,}321$, which is not divisible by 9. The theorem is named for Sir John Wilson (1741–1793), who came across it (but left no formal proof) while he was a student at Peterhouse College, Cambridge. Wilson went on to become a judge and seems to have done little else in mathematics. The theorem was first published and named after Wilson by Edward Waring (1734–1798) around 1770. However, it is now clear that the result was known to Gottfried **Leibniz** and perhaps, much earlier to Ibn al-Haytham (965–1040). The first known proof was provided by Joseph **Lagrange**.

winding number

The number of times a **closed** curve in the plane passes around a given point in the counterclockwise direction.

wine

The creation of a fine wine may be a complex business, but it is not mathematically intractable according to a Cali-

fornian winemaker and businessman, Leo McCloskey, who runs a consulting firm. McCloskey's formula takes into account color, fragrance, and flavor and attempts to predict wine quality two to three years in advance. The formula stems from a comparison of key chemical characteristics for a range of wines with what experts made of the final product. Putting this information into a database, McCloskey has claimed, enables the math of wine flavor to be derived. More than 50,000 wines were analyzed for the database but, in each case, only a handful of the 400 to 500 constituent chemicals were considered crucial flags to future color, taste, and bouquet. The proportion of tannins and phenols is particularly crucial in determining a wine's future, thus reducing the number of essential flags for an accurate mathematical model to just 10 or 20. With this system, McCloskey believes, he can predict what a wine will be like before it is bottled, giving winemakers the opportunity to modify the flavor if necessary. However, whether any wine formula can effectively take into account the subjective impressions of the end user remains to be seen. See also **bottle sizes**.

Witch of Agnesi curve

See **Agnesi**.

word puzzles

1. What positive integer, when spelled out, has a Scrabble score equal to that integer?
2. What is the only English word that ends in "mt?"
3. Only four words in the English language end in "-dous." What are they?
4. What is the shortest complete sentence in the English language?
5. Name the only word (not including proper names) in the English language that has two "i" 's together.
6. Name a one-syllable word that becomes a three-syllable word by adding one letter to the end of it.
7. What word begins and ends with "und?"

Solutions begin on page 369.

word trivia

- The hardest word to define briefly is thought to be the word *mamihlapinatopai* from the Fuegian language spoken by the natives of the Andaman Islands. Its simplest definition is "two people looking at each other without speaking hoping that the other will offer to do something which both parties desire but neither are willing to do."
- No word in the English language rhymes with orange, silver, purple, or month.
- The only 15-letter word that can be written without repeating a letter is *uncopyrightable.*
- The combination "ough" can be pronounced in nine different ways. The following sentence contains them all: "A rough-coated, dough-faced, thoughtful ploughman strode through the streets of Scarborough; after falling into a slough, he coughed and hiccoughed."
- *Facetious* and *abstemious* contain all the vowels in the correct order, as does *arsenious,* meaning "containing arsenic."
- The longest word in the English language, according to the Oxford English Dictionary, is *pneumonoultramicroscopicsilicovolcanoconiosis.* The only other word with the same amount of letters is its plural: *pneumonoultramicroscopicsilicovolcanoconioses.* It means an infection of the lungs.
- The longest English word with one vowel is *strengths.*
- The "sixth sick sheik's sixth sheep's sick" is said to be the toughest tongue twister in the English language.
- Richard Millhouse Nixon was the first U.S. president whose name contains all the letters from the word *criminal.*
- In Scotland, a new game was invented. It was called Gentlemen Only Ladies Forbidden and thus the word GOLF entered the vocabulary.
- The longest English words that don't use any of vowels a, e, i, o, or u are "rhythm" and "syzygy."
- The verb *cleave* is one of many English words with two synonyms which are antonyms of each other: adhere and separate.
- There is a seven letter word in the English language that contains ten words without rearranging any of its letters, *therein:* the, there, he, in, rein, her, here, ere, therein, herein.
- The longest English word that consists entirely of consonants is *crwth,* which is from the fourteenth century and means crowd.
- The word *trivia* comes from the Latin *tri-* + *via,* and means "three streets." This is because in ancient times, at an intersection of three streets in Rome, they would have a type of kiosk where ancillary information was listed. You might be interested in it, you might not, hence they were bits of "trivia."

worldline

The path of an object through **space-time**. On a *Minkowski diagram,* in which the three dimensions of space are represented by the horizontal axis and time is represented by the vertical axis, worldlines appear as wiggly curves extending from the past into the future. *My*

Worldline is the title of the autobiography of George Gamow, the Ukrainian-American physicist.

Wundt illusion

A **distortion illusion** devised by the German "father of experimental psychology," and one-time assistant to the physicist Hermann von Helmholtz at Heidelberg, Wilhelm Wundt (1832–1920). In the figure, two horizontal lines are both straight, although they look as if they bow in at the middle. The distortion is induced by crooked lines on the background, as in **Orbison's illusion**. The simplest of all distortion illusions–the **vertical-horizontal illusion**–was also discovered by Wundt.

Wythoff's game

A variation on the game of **Nim** suggested by W. A. Wythoff in 1907. It is played with two heaps of counters in which a player may take any number from either heap or the same number from both. The player who takes the last counter wins.

x

The most frequently used symbol for an unknown in an expression or equation.

x-axis

The horizontal axis of a two-dimensional plot in **Cartesian coordinates**.

X-pentomino

A pentomino, a five-square **polyomino**, in the shape of the letter X.

Y

yard
A unit of distance equal to 3 feet (36 inches) or 0.9144 meters. The name originates with the old German word *gazdaz* for a staff or stick, which could be used for measurement. This changed to *gierd* in Old English and eventually to *yard*. The yard-arm of a sailing ship—a tapered spar used to support a square sail—harkens back to the earlier meaning. In France, the equivalent of the yard measure is called a "verge," from the Latin *virga* for a stick or rod.

y-axis
The vertical axis of a two-dimensional plot in **Cartesian coordinates**.

yin-yang symbol
See **Great Monad**.

yocto-/yotta-
The prefix yocto-, for 10^{-24}, derives from the Greek *oktakis* ("eight times"). The prefix yotta-, for 10^{24}, comes from the same source.

Z

Zeller's formula

A formula invented by the German clergyman Christian Zeller (1824–1899) for figuring out the day of the week of a given date, without the need of tables. Let

J be the century-number,

K the last two digits in the year,

e the residue, which remains when J is divided by 4,

m the number of the month,

q the day of the month,

h the number of the day of the week.

Then h is the remainder that results when

$$h = q + 26(m + 1)/10 + K + K/4 - 2e$$

is divided by 7. For the formula to work, January and February have to be taken as months 13 and 14 of the preceding year. For example, Frederick the Great was born on 24 January 1712, so $J = 17$, $e = 1$, $K = 11$ (not 12 because of the special way of numbering the months), $m = 13$, and $q = 24$. Plugging these values into the formula, we get

$$\begin{aligned} &24 + 26(13 + 1)/10 + 11 + 11/4 - 2 \times 1 \\ &\quad = 71 = 70 \times 1 + 1. \end{aligned}$$

The remainder h is 1, so Frederick the Great was born on the first day of the week, Sunday.

Zenodorus (c. 180 B.C.)

The Greek mathematician and philosopher who proposed in *On Isometric Figures* that the circle has the maximum area of all isoperimetric figures in a plane, and that the sphere has the maximum volume of all bodies with equal surface.

Zeno's paradoxes

A series of **paradox**es posed by the philosopher Zeno of Elea (c. 490–c. 425 B.C.). Little is known about Zeno's life. He was born in Elea (now Lucania) in southern Italy and was a friend and student of Parmenides. None of his writings survive but he is known to have written a book, which **Proclus** says contained 40 paradoxes. Four of these, which all concern motion, have had a profound influence on the development of mathematics. They are described in Aristotle's great work *Physics* and are called the Dichotomy, Achilles (and the Tortoise), the Arrow, and the Stadium.

The Dichotomy argues that "there is no motion because that which is moved must arrive at the middle of its course before it arrives at the end." In order to traverse a line segment it's necessary to reach the halfway point, but this requires first reaching the quarter-way point, which first requires reaching the eighth-way point, and so on without end. Hence motion can never begin. This problem isn't alleviated by the well-known infinite sum $\frac{1}{2} + \frac{1}{4} + \frac{1}{8} + \ldots = 1$ because Zeno is effectively insisting that the sum be tackled in the reverse direction. What is the first term in such a series?

Zeno's paradox of Achilles is told by Aristotle in this way: "The slower when running will never be overtaken by the quicker; for that which is pursuing must first reach the point from which that which is fleeing started, so that the slower must necessarily always be some distance ahead." Thus, Achilles, however fast he runs, will never catch the plodding Tortoise who started first. And yet, of course, in the real world, faster things do overtake slower ones. So how is the paradox to be solved? The German set theorist Adolf Frankel (1891–1965) is one of many modern mathematicians (Bertrand Russell is another) who have pointed out that 2,000 years of attempted explanations have not cleared away the mysteries of Zeno's paradoxes: "Although they have often been dismissed as logical nonsense, many attempts have also been made to dispose of them by means of mathematical theorems, such as the theory of convergent series or the theory of sets. In the end, however, the difficulties inherent in his arguments have always come back with a vengeance, for the human mind is so constructed that it can look at a continuum in two ways that are not quite reconcilable."

zepto-/zetta-

The prefix zepto-, for 10^{-21}, derives from the Greek *heptakis* ("seven times"). The prefix zetta-, for 10^{21}, comes from the same source.

zero

The **integer**, denoted 0, which, when used as a counting number, indicates that no objects are present. It is the only integer that is neither negative nor positive. Zero is both a **number** and a **numeral**. The number zero is the

size of the **empty set** but it is not the empty set itself, nor is it the same thing as **nothing**. The numeral or digit zero is used in positional **number system**s, where the position of a digit signifies its value, with successive positions having higher values, and the digit zero is used to skip a position. The earliest roots of the numeral zero stretch back 5,000 years to the Sumerians in Mesopotamia, who inserted a slanted double wedge between cuneiform characters for numbers, written positionally, to indicate a number's absence. The symbol changed over time as positional notation made its way to India, via the Greeks (in whose own culture zero made a late and only occasional appearance). Our word *zero* derives from the Hindi *sunya* for "void" or "emptiness," through the Arabic *sifr* (which also gives us *cipher*), and the Italian *zevero*. As a number in its own right, aside from its use as a position marker, zero took a much longer time to become established, and even now is not equal in status to other numbers: division by zero is not allowed.

zero divisors

Nonzero elements of a **ring** whose product is 0.

zero of a function

See **root**.

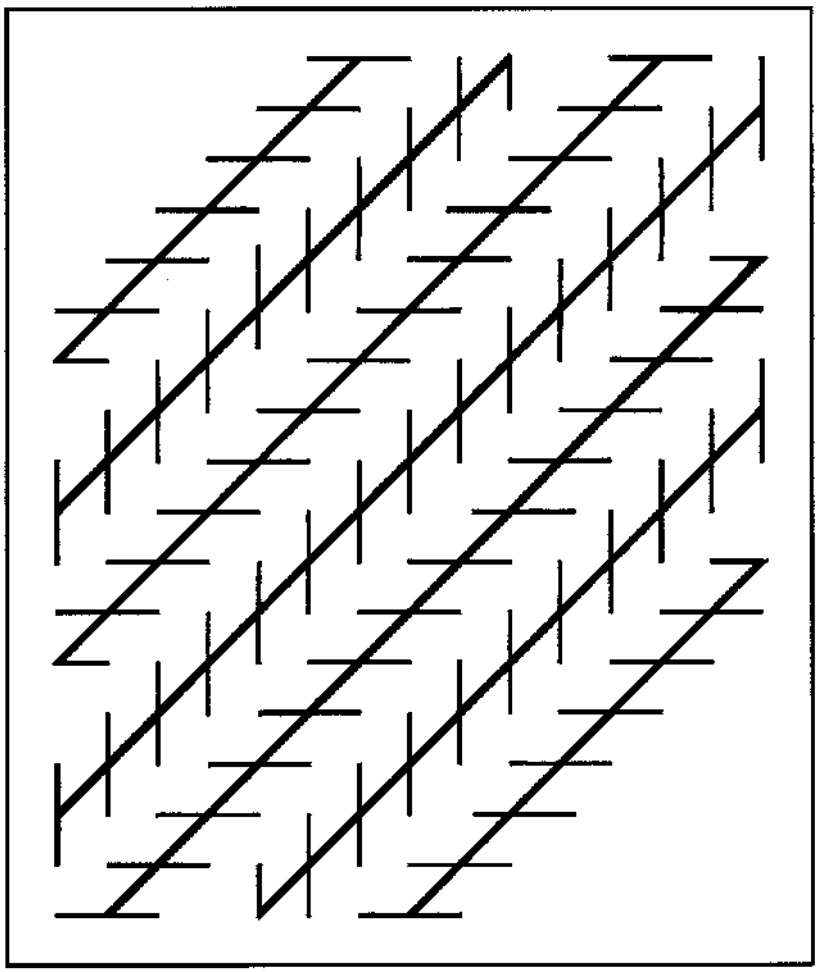

Zöllner illusion

zero-sum game
In **game theory**, a game in which a win for one player results in an equal but opposite loss for the other players.

zeta function
A **function** that has certain properties and is calculated as an infinite sum of negative powers. The most commonly encountered zeta function is the **Riemann zeta function**.

zigzag
A general word for a type of curve that consists of several straight lines joined at points. A zigzag usually goes alternately from side to side.

Zöllner illusion
A line **distortion illusion** first published by the astronomer Johann Zöllner in 1860. The diagonal lines, although parallel, appear not to be. The illusion was one of a series specifically designed to cause errors in optical equipment of that time. They did cause errors, and also great concern among scientists over the validity of all human observations. See also **Poggendorff illusion**.

zombie
A hypothetical being that behaves like us and may share our functional organization and even, perhaps, our neurophysiological makeup, but lacks consciousness or any form of subjective awareness. The concept is used in discussions of **artificial intelligence**.

zone
The portion of a **sphere** between two parallel planes.

zonohedron
A **polyhedron** in which the faces are all **parallelogram**s or parallel-sided. The faces of a zonohedron can be grouped into *zones*–encircling bands of faces which share a common edge direction (and length).

References

1. Abbott, Edwin A. *Flatland: A Romance of Many Dimensions.* London: Seely and Co., 1884. Reprint, Mineola, N.Y.: Dover, 1992.

2. Abraham, R. M. *Diversions and Pastimes.* London: Constable & Co., 1933. Reprinted, 1964.

3. Ackermann, A. S. E. *Scientific Paradoxes and Problems.* London, 1925.

4. Adams, Douglas. *Life, the Universe and Everything.* New York: Harmony Books, 1982.

5. Adams, Douglas. *The Hitchhiker's Guide to the Galaxy.* New York: Ballantine, 1995.

6. Ahrens, W. *Mathematische Unterhaltungen und Spiele.* Leipzig, Germany: Teubner, 1910.

7. Ainley, Stephen. *Mathematical Puzzles.* London: Bell, 1977.

8. Allais, M. "Le comportement de l'homme rationnel devant le risque: Critique des postulats et axiomes de l'école américaine." *Econometrica,* 21: 503–546 (1953).

9. Amthor, A., and B. Krumbiegel. "Das Problema bovinum des Archimedes." *Zeitschrift für Mathematik und Physik,* 25: 121–171 (1880).

10. Andrews, William S. *Magic Squares and Cubes,* 2nd ed. Mineola, N.Y.: Dover, 1960.

11. Apéry, R. "Irrationalité de ζ(2) et ζ(3)." *Astérisque,* 61: 11–13 (1979).

12. Appel, K., and W. Haken. "The Solution of the Four-Color Map Problem." *Scientific American,* 237: 108–121 (1977).

13. ApSimon, Hugh. *Mathematical Byways in Ayling, Beeling, and Ceiling.* New York: Oxford University Press, 1984.

14. Argand, R. *Essai sur une manière de représenter les quantités imaginaires dans les constructions géométriques.* Paris: Albert Blanchard, 1971. Reprint of the 2nd ed., published by G. J. Hoel in 1874. First published in 1806 in Paris.

15. Arno, Steven. "A Note on Perrin Pseudoprimes." *Mathematics of Computation,* 56(193): 371–376 (1991).

16. Arrow, Kenneth. *Social Choice and Individual Values.* New York: John Wiley & Sons, 1951.

17. Ascher, Marcia. *Ethnomathematics: A Multicultural View of Mathematical Ideas.* Pacific Grove, Calif.: Brooks/Cole Publishing Co., 1991.

18. Avedon, Elliot M., and Brian Sutton-Smith. *The Study of Games.* New York: John Wiley & Sons, 1971.

19. Averbach, Bonnie, and Orin Chein. *Mathematics: Problem Solving through Recreational Mathematics.* New York: W. H. Freeman, 1980.

20. Bagley, William A. *Puzzle Pie: A Unique Collection of Scientific Paradoxes, Posers and Oddities.* London: Vawser and Wiles, 1944.

21. Bailey, D. H., P. B. Borwein, and S. Plouffe. "On the Rapid Computation of Various Polylogarithmic Constants." *Mathematics of Computation,* 66(218): 903–913 (1997).

22. Bakst, Aaron. *Mathematical Puzzles and Pastimes.* New York: Van Nostrand, 1954.

23. Bakst, Aaron. *Mathematics: Its Magic and Mystery,* 3rd ed. Princeton, N.J.: Van Nostrand, 1967.

24. Ball, Walter William Rouse. *Mathematical Recreations and Problems.* London: Macmillan, 1892. (Ball, W. W. Rouse and H. S. M. Coxeter. *Mathematical Recreations and Essays,* 13th ed. Mineola, N.Y.: Dover, 1987.)

25. Banchoff, Thomas F. *Beyond the Third Dimension: Geometry, Computer Graphics, and Higher Dimensions.* New York: W. H. Freeman, 1990.

26. Barnsley, Michael. *Fractals Everywhere,* 2nd edition. San Francisco: Morgan Kaufmann, 1993.

27. Bayer, D., and P. Diaconis. "Trailing the Dovetail Shuffle to Its Lair." *Annals of Applied Probability,* 2(2): 294–313 (1992).

28. Beasley, John D. *The Ins and Outs of Peg Solitaire.* New York: Oxford University Press, 1985.

29. Beckmann, P. *A History of Pi,* 3rd ed. New York: Dorset Press, 1989.

30. Beiler, Albert H. *Recreations in the Theory of Numbers.* Mineola, N.Y.: Dover, 1964.

31. Bell, A. H. " 'Cattle Problem.' By Archimedes 251 B.C." *American Mathematical Monthly,* 2: 140 (1895).

32. Bell, E. T. *Men of Mathematics.* New York: Simon & Schuster, 1937.

33. Bell, Robbie, and Michael Cornelius. *Board Games Round the World: A Resource Book for Mathematical Investigations.* New York: Cambridge University Press, 1990.

34. Benford, F. "The Law of Anomalous Numbers."

Proceedings of the American Philosophical Society, 78: 551–572 (1938).

35. Bergholt, E. *Complete Handbook to the Game of Solitaire on the English Board of Thirty-Three Holes.* Routledge: London, 1920.

36. Berlekamp, Elwyn R., John Horton Conway, and Richard K. Guy. *Winning Ways for Your Mathematical Plays,* 2 vols. New York: Academic Press, 1982.

37. Berloquin, Pierre. *Le Jardin du Sphinx.* Paris: Dunod, 1981.

38. Berrondo, Marie. *Mathematical Games.* Englewood Cliffs, N.J.: Prentice Hall, 1983.

39. Besicovitch, A. S. "On Kakeya's Problem and a Similar One." *Mathematische Zeitschrift,* 27: 312–320, (1928).

40. Berry, Michael. "Quantum Physics on the Edge of Chaos." *New Scientist,* 116: 44–47 (1987).

41. Birtwistle, Claude. *The Calculator Puzzle Book.* New York: Bell Publishing Co., 1978.

42. Blatner, David. *The Joy of Pi.* New York: Walker, 1997.

43. Blocksma, Mary. *Reading the Numbers: A Survival Guide to the Measurements, Numbers, and Sizes Encountered in Everyday Life.* New York: Viking Penguin, 1989.

44. Blyth, Will. *Match-Stick Magic, Puzzles, Games and Conjuring Tricks.* London: C. A. Pearson Ltd., 1921.

45. Bogoshi, J., Naidoo, K., and Webb, J. "The Oldest Mathematical Artifact." *Mathematical Gazette,* 71: 458 (1987).

46. Bond, Raymond T. *Famous Stories of Code and Cipher.* New York: Rinehart & Co., 1947.

47. Bondi, Hermann. "The Rigid Body Dynamics of Unidirectional Spin." *Proceedings of the Royal Society,* A405: 265–274, 1986.

48. Bord, Janet. *Mazes and Labyrinths of the World.* London: Latimer, 1976.

49. Borel, Emile. *Algebre et Calcul des Probabilites,* vol. 184. Paris: Comptes Rendus Academie des Sciences, 1927.

50. Bouton, Charles L. "Nim, a Game with a Complete Mathematical Theory." *Annals of Mathematics,* Series 2. 3: 35–39, (1901–1902).

51. Brams, S. J., and A. D. Taylor. "An Envy-Free Cake Division Protocol." *American Mathematical Monthly,* 102: 9–19 (1995).

52. Brams, S. J., and A. D. Taylor. *Fair Division: From Cake-Cutting to Dispute Resolution.* New York: Cambridge University Press, 1996.

53. Brandreth, Gyles. *Numberplay.* New York: Rawson, 1984.

54. Branges, L., de, "A Proof of the Bieberbach Conjecture." *Acta Mathematica,* 154: 137–152 (1985).

55. Burger, Dionys. *Sphereland: A Fantasy about Curved Spaces and an Expanding Universe.* New York: Barnes & Noble, 1983.

56. Cadwell, J. H. *Topics in Recreational Mathematics.* New York: Cambridge University Press, 1966.

57. Carroll, Lewis. *Mathematical Recreations of Lewis Carroll.* 2 vols. Mineola, N.Y.: Dover, 1958.

58. Carroll, Lewis. *Symbolic Logic and the Game of Logic.* 2 vols. Mineola, N.Y.: Dover, 1958.

59. Carroll, Lewis. *Pillow Problems and A Tangles Tale.* New York: Dover, 1958.

60. Chaitin, G. J. "The Berry Paradox." *Complexity,* 1: 26–30 (1995).

61. Chow, T. Y. "The Surprise Examination or Unexpected Hanging Paradox." *American Mathematical Monthly,* 105: 41–51 (1998).

62. Church, Alonzo. *Introduction to Mathematical Logic.* Princeton, N.J.: Princeton University Press, 1956.

63. Clarke, Arthur C. *The City and the Stars.* New York: Harcourt, Brace, 1956.

64. Coffin, Stewart T. *The Puzzling World of Polyhedral Dissections.* New York: Oxford University Press, 1990.

65. Collins, A. Frederick. *Fun with Figures.* New York: D. Appleton & Co., 1928.

66. Conway, J. H. "Mrs. Perkins's Quilt." *Proceedings of the Cambridge Philosophical Society,* 60: 363–368, 1964.

67. Conway, John Horton. *On Numbers and Games.* New York: Academic Press, 1976.

68. Conway, John Horton, and Richard K. Guy. *The Book of Numbers.* New York: Springer-Verlag, 1996.

69. Conway, J. H., and S. P. Norton. "Monstrous Moonshine." *Bulletin London Mathematical Society,* 11: 308–339 (1979).

70. Conway, J. H., and N. J. A. Sloane. "The Monster Group and its 196884-Dimensional Space" and "A Monster Lie Algebra?" Chs. 29–30 in *Sphere Packings Lattices, and Groups,* 2nd ed. New York: Springer-Verlag, pp. 554–571, 1993.

71. Cooper, Necia Grant (ed.). *From Cardinals to Chaos: Reflections on the Life and Legacy of Stanislaw Ulam.* Cambridge: Cambridge University Press, 1989.

72. Coxeter, H. S. M. *Non-Euclidean Geometry.* Toronto: The University of Toronto Press, 1942.

73. Coxeter, H. S. M., M. S. Longuet-Higgins, and J. C. P. Miller. "Uniform Polyhedra." *Philosophical Transactions of the Royal Society of London,* Series, *A* 246: 401–450, 1954.

74. Coxeter, H. S. M. *Introduction to Geometry,* 2nd ed. New York: John Wiley & Sons, 1969.

75. Coxeter, H. S. M. *Regular Polytopes,* 3rd ed. New York: Dover, 1973.

76. Coxeter, H. S. M., P. DuVal, H. T. Flather, and J. F. Petrie. *The Fifty-Nine Icosahedra.* Toronto: University of

Toronto Press, 1938. Reprint, New York: Springer-Verlag, 1982.

77. Coxeter, H. S. M., M. Emmer, R. Penrose, and M. L. Teuber, (eds). *M. C. Escher: Art and Science.* New York: North-Holland, 1986.

78. Cromwell, Peter R. *Polyhedra.* Cambridge: Cambridge University Press, 1997.

79. Császár, Ákos. "A polyhedron without diagonals." *Acta Univ Szegendiensis, Acta Scientia Math,* 13: 140–142, 1949.

80. Cundy, H. Martyn, and A. P. Rollett. *Mathematical Models,* 3rd ed. Oxford: Clarendon Press, 1961; Diss, England: Tarquin Publications, 1981.

81. Dewdney, A. K. *The Planiverse: Computer Contact with a Two-dimensional World.* New York: Simon & Schuster, 1984.

82. Dickson, Leonard E. *History of the Theory of Numbers.* 3 vol. London: Chelsea Pub. Co., 1919–23. Reprint, Providence, R.I.: American Mathematical Society, 1999.

83. Domoryad, A. P. *Mathematical Games and Pastimes.* Elmsford, N.Y.: Pergamon Press, 1963.

84. Dötzel, Gunter. "A Function to End All Functions." *Algorithm: Recreational Programming 2.4,* 16–17 (1991).

85. Doxiadis, Apostolos K. *Uncle Petros and Goldbach's Conjecture.* New York: Bloomsbury, 2000.

86. Dresner, Simon (ed.). *Science World Book of Brain Teasers.* New York: Scholastic Book Services, 1962.

87. Dudeney, H. E. *The Canterbury Puzzles.* London: Nelson, 1907. Reprinted Mineola, N.Y.: Dover, 1958.

88. Dudeney, H. E. *Amusements in Mathematics.* New York: Dover, 1917. Reprinted Mineola, N.Y.: Dover, 1958.

89. Dudeney, Henry E. *The World's Best Word Puzzles.* London: Daily News, 1925.

90. Dudeney, H. E. *536 Puzzles and Curious Problems,* ed. by Martin Gardner. New York: Charles Scribner, 1967.

91. Edgeworth, R., Dalton, B. J., and Parnell, T. "The Pitch Drop Experiment." *European Journal of Physics,* 5: 198–200 (1984).

92. Eiss, Harry Edwin. *Dictionary of Mathematical Games, Puzzles, and Amusements.* Westport, Conn.: Greenwood Press, 1988.

93. Elffers, J. *Tangram—The Ancient Chinese Puzzle.* New York: Harry N. Abrams, 1979.

94. Escher, M. C. *The Graphic Work of M. C. Escher,* New York: Ballantine, 1971.

95. Ewing, John, and Kosniowski, Czes. *Puzzle It Out: Cubes, Groups and Puzzles.* New York: Cambridge University Press, 1982.

96. Fadiman, Clifton. *Fantasia Mathematica: Being a set of stories, together with a group of oddments and diversions, all drawn from the universe of mathematics.* New York: Simon and Schuster, 1958.

97. Fadiman, Clifton. *The Mathematical Magpie: Being more stories, mainly transcendental, plus subsets of essays, rhymes, music, anecdotes, epigrams and other prime oddments and diversions, rational or irrational, all derived from the infinite domain of mathematics.* New York: Simon and Schuster, 1962.

Federico, P. J. "The Melancholy Octahedron." *Mathematics Magazine,* 45: 30–36, 1972.

98. Filipiak, Anthony S. *100 Puzzles: How to Make and Solve Them.* New York: A. S. Barnes, 1942.

99. Filipiak, Anthony S. *Mathematical Puzzles and Other Brain Twisters.* New York: A. S. Barnes, 1964.

100. Fink, Thomas M., and Yong Mao Mao. "Designing Tie Knots Using Random Walks." *Nature,* 398: 31 (1999).

101. Fisher, Adrian. Arian Fisher Maze Design Web site: http://www.mazemaker.com.

102. Fisher, John (ed.). *The Magic of Lewis Carroll.* New York: Simon and Schuster, 1973.

103. Foster, James E. *Mathematics as Diversion.* Astoria, IL: Fulton County Press, 1978.

104. Fraser, James. "A new visual illusion of direction." *British Journal of Psychology,* 2: 307–337 (1908).

105. Frederickson, Greg N. *Dissections: Plane and Fancy.* Cambridge: Cambridge University Press, 1997.

106. Frey, Alexander H., Jr., and David Singmaster. *Handbook of Cubik Math.* Hillside, N.J.: Enslow, 1982.

107. Gamow, G., and M. Stern. *Puzzle-Math.* New York: Viking, 1958.

108. Gardiner, M. *Mathematical Puzzling.* New York: Oxford University Press, 1987.

109. Gardner, Martin. *Mathematics, Magic and Mystery.* Mineola, N.Y.: Dover, 1956.

110. Gardner, M. *Mathematical Puzzles and Diversions.* New York: Simon and Schuster, 1959.

111. Gardner, Martin, ed. *The Mathematical Puzzles of Sam Loyd,* 2 vols. Mineola, N.Y.: Dover, 1959.

112. Gardner, M. *The Second Scientific American Book of Mathematical Puzzles & Diversions.* New York: Simon and Schuster, 1961.

113. Gardner, Martin. "The Remarkable Lore of the Prime Numbers," *Scientific American,* March 1964.

114. Gardner, M. *New Mathematical Diversions from Scientific American.* New York: Simon and Schuster, 1966.

115. Gardner, M. "Mathematical Games." *Scientific American,* 237, 18–28, Nov. 1977.

116. Gardner, Martin. *Mathematical Magic Show: More Puzzles, Games, Diversions, Illusions and Other Mathematical Sleights-of-Mind from Scientific American.* New York: Vintage, 1978.

117. Gardner, Martin. *The Ambidextrous Universe.* New York: Charles Scribner's Sons, 1978.

118. Gardner, Martin. *Mathematical Circus: More Games, Puzzles, Paradoxes, and Other Mathematical*

Entertainments from Scientific American. New York: Alfred A. Knopf, 1979.

119. Gardner, Martin. *Science Fiction Puzzle Tales.* New York: Clarkson N. Potter, 1981.

120. Gardner, Martin. *Wheels, Life, and other Mathematical Amusements.* New York: W. H. Freeman, 1983.

121. Gardner, Martin. *Martin Gardner's Sixth Book of Mathematical Diversions from Scientific American.* Chicago: University of Chicago Press, 1983.

122. Gardner, Martin. *The Magic Numbers of Dr. Matrix.* Buffalo, N.Y.: Prometheus Books, 1985.

123. Gardner, M. *Knotted Doughnuts and Other Mathematical Entertainments.* New York: W. H. Freeman, 1986.

124. Gardner, Martin. *Riddles of the Sphinx And Other Mathematical Puzzle Tales.* Washington, DC: Mathematical Association of America, 1987.

125. Gardner, Martin. *Time Travel and Other Mathematical Bewilderments.* New York: W. H. Freeman, 1987.

126. Gardner, Martin. *Hexaflexagons and Other Mathematical Diversions.* Chicago: University of Chicago Press, 1988.

127. Gardner, Martin. *Penrose Tiles and Trapdoor Ciphers . . . and the Return of Dr. Matrix.* New York: W. H. Freeman, 1989.

128. Gardner, Martin. *Mathematical Carnival.* Washington, D.C.: Mathematical Association of America, 1989.

129. Gardner, Martin. *Mathematical Magic Show.* Washington, D.C.: Mathematical Association of America, 1990.

130. Gardner, M. *Fractal Music, Hypercards, and More Mathematical Recreations from Scientific American Magazine.* New York: W. H. Freeman, 1992.

131. Gardner, Martin (introduction and notes). *The Annotated Alice: Alice's Adventures in Wonderland and Through the Looking Glass.* New York: Random House, 1998.

132. Gasser, Ralph. "Solving Nine Men's Morris." *Computational Intelligence,* 12: 24–41 (1996).

133. Gerver, J. L. "On Moving a Sofa Around a Corner." *Geometriae Dedicata,* 42: 267–283 (1992).

134. Gillam, B. "Geometrical Illusions." *Scientific American,* 242: 102–111 (Jan. 1980).

135. Gleick, James. *Chaos: Making a New Science.* New York: Penguin, 1988.

136. Golomb, S. W. "Checker Boards and Polyominoes." *American Mathematical Monthly,* 61: 675–682 (1954).

137. Golomb, Solomon W. *Polyominoes: Puzzles, Patterns, Problems, and Packings.* New York: Charles Scribner's, 1965. Reprint, Princeton, N.J.: Princeton University Press, 1995.

138. Gomme, Alice Bertha. *Traditional Games of England, Scotland and Ireland.* 2 vols. London: Thames and Hudson, 1894–1898.

139. Gotze, Heinz. *Castel del Monte, Geometric Marvel of the Middle Ages.* New York: Prestel, 1998.

140. Greenberg, Marvin J. *Euclidean and non-Euclidean Geometries: Development and History.* San Francisco: W. H. Freeman, 1974.

141. Greenblatt, M. H. *Mathematical Entertainments.* London: George Allen and Unwin, 1968.

142. Gregory, R. L. "Analogue Transactions with Adelbert Ames." *Perception,* 16: 277–282 (1987).

143. Grunbaum, B., and G. C. Shephard. *Tilings and Patterns.* New York: W. H. Freeman, 1987.

144. Guy, Richard K. *Unsolved Problems in Number Theory,* 2nd ed. New York: Springer-Verlag, 1994.

145. Guy, Richard K., and Robert E. Woodrow (eds). *The Lighter Side of Mathematics: Proceedings of the Eugène Strens Memorial Conference on Recreational Mathematics and its History.* Washington, D.C.: Mathematical Association of America, 1994.

146. Haeckel, Ernst. Kunstformen der Natur (Art Forms in Nature). Leipzig, Wien: Bibliographisches Institut 1899–1904. Reprinted Mineola, N.Y.: Dover, 1974.

147. Haldeman-Julius, E. *Problems, Puzzles and Brain-Teasers.* Girard, KS: Appeal to Reason, 1937.

148. Hall, Trevor H. *Old Conjuring Books.* London: Duckworth, 1972.

149. Hankins, Thomas L. *Sir William Rowan Hamilton.* Baltimore: Johns Hopkins University Press, 1980.

150. Hardy, G. H. *Ramanujan: Twelve Lectures on Subjects Suggested by His Life and Work.* London: Cambridge University Press, 1940.

151. Hardy, G. H. *A Mathematician's Apology.* London: Cambridge University Press, 1940.

152. Hargrave, Catherine Perry. *A History of Playing Cards and a Bibliography of Cards and Gaming.* New York: Houghton Mifflin, 1930. Reprint, New York: Dover, 1966.

153. Harmer, G. P., and D. Abbott. "Losing Strategies Can Win by Parrondo's Paradox." *Nature,* 402: 864 (1999).

154. Hartley, Miles C. *Patterns of Polyhedra.* Ann Arbor, MI: Edwards Brothers, 1957.

155. Heafford, Philip. *The Math Entertainer.* New York: Vintage Press, 1983.

156. Heinlein, Robert. "And He Built a Crooked House," in Isaac Asimov (ed.) *Where Do We Go From Here?* New York: Doubleday, 1971.

157. Heinzelin, J., de, "Ishango." *Scientific American,* 206(6): 105–116 (Jun. 1962).

158. Held, Richard (ed.). *Image, Object and Illusion.* San Francisco: W. H. Freeman, 1974.

159. Henderson, Linda Dalrymple. *The Fourth Dimension and Non-Euclidean Geometry in Modern Art.* Princeton, N.J.: Princeton University Press, 1983.

160. Hendricks, John R. "Magic Tesseracts and N-Dimensional Magic Hypercubes." *Journal of Recreational Mathematics.* 6(3) (Summer 1973).

161. Hendricks, John R. "Black and White Vertices of a Hypercube." *Journal of Recreational Mathematics,* 11(4), 1978–1979.

162. Hendricks, John R. "Magic Hypercubes." Winnipeg, Canada: self-published pamphlet, 1988.

163. Hendricks, John R. "Images from the Fourth Dimension." Winnipeg, Canada: self-published pamphlet, 1993.

164. Hill, T. P. "The First Digit Phenomenon." *American Scientist,* 86: 358–363 (1998).

165. Hilton, Peter, and Jean Pedersen. *Build Your Own Polyhedra.* New York: Addison Wesley, 1988.

166. Hinton, Charles Howard. *A New Era of Thought.* London: Swan Sonnenschein, 1888.

167. Hinton, Charles Howard. *The Fourth Dimension.* London: Allen & Unwin, 1904.

168. Hodges, Andrew, and Douglas Hofstadter. *Alan Turing: The Enigma.* New York: Walker & Co., 2000.

169. Hoffman, Paul. *Archimedes' Revenge: The Joys and Perils of Mathematics.* New York: W. W. Norton, 1988.

170. Hoffman, Paul. *The Man Who Loved Only Numbers: The Story of Paul Erdos and the Search for Mathematical Truth.* New York: Hyperion, 1998.

171. Hoffmann, Professor (Angelo Louis). *Puzzles Old and New.* London: Frederick Warne, 1893. Reprint, L. Edward Hordern, 1993.

172. Hofstadter, Douglas R. *Gödel. Escher, Bach: An Eternal Golden Braid.* New York: Basic Books, 1999.

173. Hogben, Lancelot. *Mathematics for the Million.* New York: W. W. Norton, 1933.

174. Holden, Alan. *Shapes, Spaces and Symmetry.* New York: Columbia University Press, 1971. Reprint, Mineola, N.Y.: Dover, 1991.

175. Hordern, Edward. *Sliding Piece Puzzles.* New York: Oxford University Press, 1986.

176. Hovis, R. Corby, and Helge Kragh. "P. A. M. Dirac and the Beauty of Physics." *Scientific American,* 268(5): 104–109, May 1993.

177. Ingham, A. E. "On Two Conjectures in the Theory of Numbers." *American Journal of Mathematics,* 64: 313–319 (1942).

178. Ittelson, W. H., and F. P. Kilpatrick. "Experiments in Perception." *Scientific American,* 185(2), 50–55, August 1951.

179. Jackson, John. *Rational Amusement for Winter Evenings.* London: Longmans & Co., 1821.

180. Jayne, Caroline Furness. *String Figures and How to Make Them: A Study of Cat's-Cradle in Many Lands.* New York: Dover, 1975.

181. Jones, John Winter. *Riddles, Charades, and Conundrums.* London, 1821.

182. Jones, Samuel Isaac. *Mathematical Nuts for Lovers of Mathematics.* Nashville, 1932.

183. Kadesch, Robert R. *Math Menagerie.* New York: Harper & Row, 1970.

184. Kanigal, Robert. *The Man Who Knew Infinity: A Life of the Genius Ramanujan.* New York: Scribner, 1991.

185. Kapur, J. N. *The Fascinating World of Mathematics.* 3 vols. New Delhi, India: Mathematical Sciences Trust Society, 1989.

186. Kasner, Edward, and James R. Newman, *Mathematics and the Imagination.* New York: Simon and Schuster, 1940.

187. King, T. *The Best 100 Puzzles Solved and Answered.* Slough, England: W. Foulsham & Co., 1927.

188. Kirkman, T. P. "On a Problem in Combinatorics." *Cambridge and Dublin Math. J.,* 2: 191–204 (1847).

189. Klarner, David A., ed. *The Mathematical Gardner.* Boston: Prindle, Weber and Schmidt, 1981.

190. Klarner, David A., ed. *Mathematical Recreations: A Collection in Honor of Martin Gardner.* New York: Dover, 1998.

191. Knuth, Donald. *Surreal Numbers: How Two Ex-Students Turned On to Pure Mathematics and Found Total Happiness.* Reading, Mass.: Addison-Wesley, 1974.

192. Körner, T. W. *The Pleasures of Counting.* Cambridge: Cambridge University Press, 1997.

193. Kraitchik, Maurice. *Mathematical Recreations.* New York: Norton, 1942.

194. Krasnikov, S. V. "Causality Violations and Paradoxes." *Physical Review D,* 55(6): 3427–30 (1997).

195. Langley, E. M. "Problem 644." *Mathematical Gazette,* 11: 173, 1922.

196. Langman, H. *Play Mathematics.* New York: Hafner, 1962.

197. Lausmann, Raymond F. *Fun With Figures.* New York: McGraw-Hill, 1965.

198. Lavine, S. *Understanding the Infinite.* Cambridge, Mass.: Harvard University Press, 1994.

199. Lehman, R. S. "On Liouville's Function." *Mathematics of Computation,* 14: 311–320, 1960.

200. Licks, H. E. *Recreations in Mathematics.* New York: D. Van Nostrand, 1921.

201. Lindgren, Harry. *Geometric Dissections.* New York: Van Nostrand Reinhold, 1964.

202. Lindgren, Harry. *Recreational Problems in Geometrical Dissections and How to Solve Them.* New York: Dover Publications, 1972.

203. Lines, Malcolm. *Think of a Number.* New York: Adam Hilger, 1990.

204. Littlewood, J. E. *A Mathematician's Miscellany.* London: Methuen and Co., 1953.

205. Livio, Mario. *The Golden Ratio: The Story of Phi, the World's Most Astonishing Number.* New York: Broadway Books, 2002.

206. Locher J. L., ed. *M. C. Esher: His Life and Complete Graphic Work.* New York: Abradale Press, 1982.

207. Loyd, Sam. *Sam Loyd's Cyclopedia of 5000 Puzzles, Tricks, and Conundrums.* 1914. Reprint, New York: Pinnacle, 1976.

208. Loyd, Sam. *Sam Loyd's Picture Puzzles with Answers.* Brooklyn: S. Loyd, 1924. Reprint, Ontario, Canada: Algrove, 2000.

209. Lucas, Edouard. *Récréations Mathématiques,* 4 vols. Paris: Gauthier-Villars et fils, 1881–1894. Reprinted by Paris: A. Blanchard, 1960–1974.

210. MacMahon, Alexander: *New Mathematical Pastimes.* Cambridge: Cambridge University Press, 1921.

211. Madachy, Joseph S. *Mathematics on Vacation.* New York: Charles Scribner's, 1966. Republished as *Madachy's Mathematical Recreations.* New York: Dover, 1979.

212. Manning, H. P. *Geometry of Four Dimensions.* New York: Dover, 1956.

213. Manning, H. P. *The Fourth Dimension Simply Explained.* New York: Dover, 1960.

214. Maor, E. *To Infinity and Beyond: A Cultural History of the Infinite.* Boston, Mass.: Birkhäuser, 1987.

215. Maor, E. *e: The Story of a Number.* Princeton, N.J.: Princeton University Press, 1994.

216. Martin, G. "Absolutely abnormal numbers." *American Mathematical Monthly,* 108: 746–754, 2001.

217. Matijasevic, Yu. V. "Solution of the Tenth Problem of Hilbert." *Matematikai Lapok,* 21: 83–87 (1970).

218. Matijasevic, Yu. V. *Hilbert's Tenth Problem.* Cambridge, Mass.: MIT Press, 1993.

219. Matthews, W. H. *Mazes & Labyrinths: A General Account of Their History and Development.* London: Longmans, Green and Co., 1922. Reprint, New York: Dover, 1970.

220. Maxwell, E. A. *Fallacies in Mathematics.* New York: Cambridge University Press, 1959.

221. Meeus, J., and P. J. Torbijn. *Polycubes.* Paris: Cedic, 1977.

222. Melzak, Z. A. *Companion to Concrete Mathematics.* 2 vols. New York: John Wiley, 1973, 1976.

223. Mercer, J. W., et al. "Solutions to Langley's Adventitious Angles Problem." *Mathematical Gazette,* 11: 321–323, 1923.

224. Mosteller, F. *Fifty Challenging Problems in Probability with Solutions,* Reading, Mass.: Addison-Wesley, 1965, #47; "Mathematical Plums," edited by Ross Honsberger, pp. 104–110.

225. Mott-Smith, Geoffrey. *Mathematical Puzzles for Beginners and Enthusiasts,* 2nd rev. ed. New York: Dover, 1954.

226. Moyer, Ann E. *The Philosophers' Game: Rithmomachia in Medieval and Renaissance Europe.* Ann Arbor, Mich.: University of Michigan Press, 2001.

227. Murray, H. J. R. *History of Chess.* Oxford: Clarendon Press, 1913.

228. Murray, H. J. R. *A History of Board-Games Other than Chess.* Oxford: Clarendon Press, 1952.

229. Nasar, Sylvia. *A Beautiful Mind: A Biography of John Forbes Nash, Jr.* New York: Simon & Schuster, 1998.

230. Neumann, J. von, and Morgenstern, O. *Theory of Games and Economic Behavior.* New York: Wiley, 1964.

231. Neville, E. H. *The Fourth Dimension.* Cambridge: Cambridge University Press, 1921.

232. Newcomb, S. "Note on the Frequency of the Use of Digits in Natural Numbers." *American Journal of Mathematics,* 4: 39–40, 1881.

233. Newing, Angela. "The Life and Work of H. E. Dudeney." *Mathematical Spectrum,* 21: 37–44 (1988–1989).

234. Northrop, Eugene P. *Riddles in Mathematics. A Book of Paradoxes.* Princeton, N.J.: Van Nostrand, 1944.

235. O'Beirne, T. H. *Puzzles and Paradoxes: Fascinating Excursions in Recreational Mathematics.* Mineola, N.Y.: Dover, 1984.

236. Ogilvy, C. Stanley. *Tomorrow's Math: Unsolved Problems for the Amateur,* 2nd ed. New York: Oxford University Press, 1972.

237. Olivastro, Dominic. *Ancient Puzzles.* New York: Bantam, 1993.

238. Panofsky, Erwin. *The Life and Art of Albrecht Durer,* Princeton, N.J.: Princeton University Press, 1955.

239. Pardon, G. F. *Parlour Pastimes: A Repertoire of Acting Charades, Fire-Side Games, Enigmas, Riddles, Etc.* London, 1868.

240. Pennick, Nigel. *Mazes and Labyrinths.* London: Robert Hale, 1990.

241. Penrose, L. S., and R. Penrose. "Impossible Objects: A Special Type of Illusion," *British Journal of Psychology,* 49: 31, 1958.

242. Penrose Roger. *The Emperor's New Mind.* New York: Oxford University Press, 1989.

243. Péter, Rózsa. *Playing with Infinity: Mathematical Explorations and Excursions.* Mineola, N.Y.: Dover, 1976.

244. Peterson, Ivars. *The Mathematical Tourist: Snapshots of Modern Mathematics.* New York: W. H. Freeman, 1988.

245. Peterson, Ivars. *Islands of Truth: A Mathematical Mystery Cruise.* New York: W. H. Freeman, 1990.

246. Peterson, Ivars. *The Jungles of Randomness: A Mathematical Safari.* New York: Wiley, 1997.

247. Peterson, Ivars. *The Mathematical Tourist: New and Updated Snapshots of Modern Mathematics.* New York: W. H. Freeman, 1998.

248. Peterson, Ivars. *Mathematical Treks: From Surreal Numbers to Magic Circles.* Washington, D.C.: Mathematical Association of America, 2001.

249. Phillips, Hubert. *Journey to Nowhere: A Discursive Autobiography.* London: Macgibbon & Kee, 1960.

250. Phillips, Hubert. *My Best Puzzles in Mathematics.* Mineola, N.Y.: Dover, 1961.

251. Phillips, Hubert. *My Best Puzzles in Logic and Reasoning.* Mineola, N.Y.: Dover, 1961.

252. Picciotto, Henri. *Pentomino Activities.* Mountain View, Calif.: Creative Publications, 1986.

253. Pickover, Clifford. *Keys to Infinity.* New York: W. H. Freeman, 1995.

254. Pickover, Clifford. *Surfing Through Hyperspace.* New York: Oxford University Press, 1999.

255. Pickover, Clifford A. *Wonders of Numbers: Adventures in Mathematics, Mind, and Meaning.* Oxford: Oxford University Press, 2001.

256. Pickover, C. A. *The Zen of Magic Squares, Circles, and Stars: An Exhibition of Surprising Structures across Dimensions.* Princeton, N.J.: Princeton University Press, 2002.

257. Poole, D. G. "The Towers and Triangles of Professor Claus (or, Pascal Knows Hanoi)." *Mathematics Magazine,* 67: 323–344 (1994).

258. Poundstone, William. *The Recursive Universe.* New York: William Morrow, 1984.

259. Poundstone, William. *Prisoner's Dilemma: John Von Neumann, Game Theory and the Puzzle of the Bomb.* New York: Doubleday, 1992.

260. Quine, W. V. O. "On a So-Called Paradox." *Mind,* 62: 65–67 (1953).

261. Rabinowitz, Stanley. *Index to Mathematical Problems 1980–1984.* Westford, Mass.: Mathpro Press, 1992.

262. Rademacher, Hans, and Otto Toeplitz. *The Enjoyment of Mathematics: Selections from Mathematics for the Amateur.* Princeton, N.J.: Princeton University Press, 1957.

263. Raimi, R. A. "The Peculiar Distribution of First Digits." *Scientific American,* 221: 109–119 (Dec. 1969).

264. Ransom, William R. *One Hundred Mathematical Curiosities.* Portland, Maine: Weston Walch, 1955.

265. Read, Ronald C. *Tangrams: 330 Puzzles.* Mineola, N.Y.: Dover, 1965.

266. Ribenboim, P. *Catalan's Conjecture.* Boston, Mass.: Academic Press, 1994.

267. Robbin, Tony. *Fourfield: Computers, Art, and the Fourth Dimension.* Boston: Little, Brown, 1992.

268. Robertson, J., and Webb, W. *Cake-cutting Algorithms.* Natick, Mass.: A. K. Peters, 1998.

269. Rossi, Hugo. "Mathematics Is an Edifice, Not a Toolbox." *Notices of the AMS,* 43(10) (Oct. 1996).

270. Rubik, Erno, et al. *Rubik's Cubic Compendium.* New York: Oxford University Press, 1987.

271. Rucker, Rudolf v.B. *Geometry, Relativity, and the Fourth Dimension.* New York: Dover, 1977.

272. Rucker, R. (ed). *Speculations on the Fourth Dimension: Selected Writings of C. H. Hinton.* New York: Dover, 1980.

273. Rucker, Rudy. *The Fourth Dimension.* Boston: Houghton Mifflin, 1984.

274. Rucker, Rudy. *Mind Tools.* Boston: Houghton Mifflin, 1987.

275. Rucker, Rudy. *Infinity and the Mind.* Princeton, N.J.: Princeton University Press, 1995.

276. Russell, Bertrand. *Bertrand Russell Autobiography.* New York: Routledge, 1992.

277. Saaty, T. L., and P. C. Kainen. *The Four-Color Problem: Assaults and Conquest.* New York: Dover, 1986.

278. Sallows, L. C. F. "Alphamagic squares." *Abacus* 4 (No. 1): 28–45, 1986.

279. Sallows, L. C. F. "Alphamagic squares, part II". *Abacus* 4 (No. 2): 20–29, 43, 1987.

280. Sallows, L. C. F. "Alphamagic squares." In *The Lighter Side of Mathematics: Proceedings of the Eugène Strens Memorial Conference on Recreational Mathematics and Its History,* R. K. Guy and R. E. Woodrow, eds. Washington, D.C.: Mathematical Association of America, 1994.

281. Sanford, Vera. *A Short History of Mathematics.* Boston, Mass.: Houghton Mifflin, 1930.

282. Scarne, John. *Scarne's New Complete Guide to Gambling.* New York: Simon and Schuster, 1986.

283. Schaaf, William Leonard. *A Bibliography of Recreational Mathematics.* 4 vols. Washington, D.C.: National Council of Teachers of Mathematics, 1955–78.

284. Schattschneider, Doris. *M. C. Escher: Visions of Symmetry.* New York: W. H. Freeman, 1990.

285. Scheick, William J. "The Fourth Dimension in Wells's Novels of the 1920s." *Criticism,* 20: 167–190, 1978.

286. Schrauf, M., B. Lingelbach, E. Lingelbach, and E. R. Wist. "The Hermann Grid and the Scintillation Effect." *Perception,* 24, suppl. A: 88–89, 1995.

287. Schreiber, P. "A New Hypothesis on Durer's Enigmatic Polyhedron in His Copper Engraving 'Melencholia I'," *Historia Mathematica,* 26: 369–377, 1999.

288. Schubert, Hermann. *Mathematical Essays and Recreations.* Thomas J. McCormack, trans. Chicago: Open Court, 1899.

289. Schubert, Hermann. *Mathematische Mussestunden.* Walter de Gruyter, 1940. First published 1900? (German).

290. Schubert, Hermann. *Mathematische Mussestunden II.* Berlin: G. J. Goshen'sche, 1909.

291. Schuh, Fred. *The Master Book of Mathematical Recreations.* Mineola, N.Y.: Dover, 1968.

292. Searle, John R. "Minds, Brains and Programs" in *The Brain and Behavioral Sciences,* vol. 3. Cambridge: Cambridge University Press, 1980.

293. Senechal, M. *Quasicrystals and Geometry.* New York: Cambridge University Press, 1995.

294. Shepherd, Walter. *For Amazement Only.* New York: Penguin, 1942. Reprinted as *Mazes and Labyrinths: A Book of Puzzles.* New York: Dover, 1961.

295. Simon, William. *Mathematical Magic.* New York: Charles Scribner's, 1964.

296. Singh, Simon. *Fermat's Enigma: The Epic Quest to Solve the World's Greatest Mathematical Problem.* New York: Walker & Co., 1997.

297. Singmaster, David. *Notes on Rubik's 'Magic Cube.* Hillside, N.J.: Enslow, 1981.

298. Singmaster, David. *Sources in Recreational Mathematics: An Annotated Bibliography,* 7th prelim, ed. Unpublished.

299. Skewes, S. "On the difference $\pi(x) - \mathrm{li}(x)$." *Journal of the London Mathematical Society,* 8: 277–283 (1933).

300. Slocum, Jerry. *Compendium of Mechanical Puzzles.* 3rd ed. Slocum and Haubrich, 1977.

301. Slocum, Jerry. *The Tangram Book: The Story of the Chinese Puzzle with Over 2000 Puzzles to Solve.* New York: Sterling, 2003.

302. Smith, David Eugene. *Number Stories of Long Ago.* Washington, D.C.: National Council of Teachers of Mathematics, 1919.

303. Smith, David Eugene. *A Source Book in Mathematics.* 2 vols. New York: McGraw-Hill, 1929.

304. Smullyan, Raymond M. *What Is the Name of This Book? The Riddle of Dracula and Other Logical Puzzles.* Englewood Cliffs, N.J.: Prentice Hall, 1978.

305. Smullyan, Raymond M. *The Chess Mysteries of Sherlock Holmes.* New York: Alfred A. Knopf, 1979.

306. Smullyan, Raymond. *This Book Needs No Title: A Budget of Living Paradoxes.* Englewood Cliffs, N.J.: Prentice-Hall, 1980.

307. Smullyan, Raymond M. *The Lady or the Tiger? And Other Logic Puzzles.* New York: Alfred A. Knopf, 1982.

308. Smullyan, Raymond M. *Alice in Puzzleland.* New York: William Morrow, 1982.

309. Smullyan, Raymond M. *To Mock a Mockingbird.* New York: Alfred A. Knopf, 1985.

310. Smullyan, Raymond M. *Forever Undecided: A Puzzle Guide to Godel.* New York: Alfred A. Knopf, 1987.

311. Smullyan, Raymond. *The Tao is Silent.* New York: HarperCollins, 1992.

312. Soddy, F. "The Kiss Precise." *Nature,* 137: 1021, 1936.

313. Sprague, Roland. *Recreation in Mathematics.* Mineola, N.Y.: Dover, 1963.

314. Stein, M. L., S. M. Ulam, and M. B. Wells. "A Visual Display of Some Properties of the Distribution of Primes." *American Mathematical Monthly,* 71: 516–520, 1964.

315. Steinhaus, H. "Sur la division pragmatique." *Ekonometrika* (*Supp.*), 17: 315–319, 1949.

316. Steinhaus, Hugo. *Mathematical Snapshots.* 3rd rev. ed. New York: Dover, 1983.

317. Stewart, Ian. *Does God Play Dice: The New Mathematics of Chaos.* Cambridge, Mass.: Basil Blackwell, 1989.

318. Stewart, Ian. *Game, Set, and Math: Enigmas and Conundrums.* Cambridge, Mass.: Basil Blackwell, 1989.

319. Stewart, Ian. "Tales of a Neglected Number." *Scientific American,* 274: 102–103 (Jun. 1996).

320. Stewart, Ian. "Unilluminable Rooms." *Scientific American,* 275(2), 100–103 (Aug. 1996).

321. Stewart, Ian and Cohen, Jack Cohen. *Figments of Reality.* Cambridge: Cambridge University Press, 1997.

322. Stewart, Ian. "Cone with a Twist." *Scientific American,* 281: 116–117 (Oct. 1999).

323. Stewart, Ian. *Flatterland: Like Flatland Only More So.* New York: Perseus, 2001.

324. Stromberg, K. "The Banach-Tarski Paradox." *American Mathematical Monthly,* 86: 3, 1979.

325. Stubbs, A. Duncan. *Miscellaneous Puzzles.* London: Frederick Warne, 1931.

326. Struik, Dirk Jan, ed. *A Source Book in Mathematics 1200–1800.* Princeton, N.J.: Princeton University Press, 1969.

327. Strutt, Joseph. *The Sports and Pastimes of the People of England.* London: J. White, 1801.

328. Stuwe, M. *Plateau's Problem and the Calculus of Variations.* Princeton, N.J.: Princeton University Press, 1989.

329. Swade, Doron. *The Difference Engine: Charles Babbage and the Quest to Build the First Computer.* New York: Viking, 2000.

330. te Riele, H. J. J. "On the Sign of the Difference $\pi(x) - \mathrm{Li}(x)$." *Mathematics of Computation,* 48: 323–328 (1987).

331. Thom, R. *Structural Stability and Morphogenesis: An Outline of a General Theory of Models.* Reading, Mass.: Addison-Wesley, 1972.

332. Thompson, d'Arcy W. *On Growth and Form.* Cambridge: Cambridge University Press, 1917. (Reprint, New York: Dover, 1992.)

333. Thorpe, Edward O. *Beat the Dealer,* rev. ed. New York: Random House, 1966.

334. Tokarsky, George W. "Polygonal Rooms Not Illuminable from Every Point." *American Mathematical Monthly,* 102(10): 867–879, 1995.

335. Toole, Betty A. (ed.). *Ada, the Enchantress of Numbers: A Selection from the Letters of Lord Byron's Daughter and Her Description of the First Computer.* Mill Valley, Calif.: Strawberry Press, 1998.

336. Tormey, Alan and Tormey, Judith Farr. "Renaissance Intarsia: The Art of Geometry." *Scientific American,* 247: 136–143, July 1982.

337. Turing, A. M. "On Computable Numbers, with an Application to the Entscheidungsproblem." *Proceedings*

of the London Mathematical Society, Series 2, 42: 230–265, 1937.

338. Turney, P, "Unfolding the Tesseract." *Journal of Recreational Mathematics,* 17(1): 1–16, 1984–1985.

339. Underwood, Dudley. "The First Recreational Mathematics Book." *Journal of Recreational Mathematics,* 3, 164–169, 1970.

340. Van Cleve, James. "Right, Left, and the Fourth Dimension." *The Philosophical Review,* 96: 33–68 (1987).

341. Vardi, I. "Archimedes' Cattle Problem." *American Mathematical Monthly,* 105: 305–319 (1998).

342. Vardi, Ilan. *Computational Recreations in Mathematica.* Redwood City, Calif.: Addison-Wesley, 1991.

343. Wagon, S. *The Banach-Tarski Paradox.* New York: Cambridge University Press, 1993.

344. Waller, Mary D. *Chladni Figures: A Study in Symmetry.* London: G. Bell & Sons, 1961.

345. Watson, G. N. "The Problem of the Square Pyramid." *Messenger of Mathematics,* 48: 1–22 (1918–1919).

346. Weisstein, Eric W. *The CRC Concise Encyclopedia of Mathematics.* Boca Raton, Fla.: CRC Press, 1998.

347. Wells, David Graham. *Hidden Connections, Double Meanings: A Mathematical Exploration.* Cambridge: Cambridge University Press, 1988.

348. Wells, David. *The Penguin Dictionary of Curious and Interesting Geometry.* London: Penguin Books, 1991.

349. Wells, David. *The Penguin Book of Curious and Interesting Mathematics.* New York: Penguin, 1997.

350. Wells, Kenneth. *Wooden Puzzles and Games.* New York: Sterling Publications, 1983.

351. Weyl, Hermann. *Symmetry.* Princeton, N.J.: Princeton University Press, 1952.

352. White, Alain C. *Sam Loyd and His Chess Problems.* Leeds, England: Whitehead & Miller, 1913.

353. Wiles, A. "Modular Elliptic-Curves and Fermat's Last Theorem." *Annals of Mathematics,* 141: 443–551, 1995.

354. Williams, W. T., and Savage, G. H. *The First Penguin Problems Book.* New York: Penguin Books, 1940.

355. Wyatt, Edwin Mather. *Puzzles in Wood.* Milwaukee, Wis.: Bruce Publishing Company, 1928.

356. Yan, Li, and Du, Shiran. *Chinese Mathematics: A Concise History.* Oxford: Oxford University Press, 1988.

357. Zaslavsky, Claudia. *Africa Counts.* Brooklyn, N.Y.: Lawrence Hill Books, 1973.

Solutions to Puzzles

abracadabra

To solve this problem, redraw the diamond and replace every letter on the outside top half of the diamond with a 1 and every other point in the diamond with a dot. This gives

```
          1
        1   1
      1   .   1
    1   .   .   1
  1   .   .   .   1
1   .   .   .   .   1
  .   .   .   .   .
    .   .   .   .
      .   .   .
        .   .
          .
```

Next, replace each of the dots, starting at the top, with the sum of the two numbers in the northwest and northeast positions, so that the pyramid now starts

```
          1
        1   1
      1   2   1
    1   3   3   1
```

After you have worked your way down to the very bottom, the bottom number in the diamond is the answer to Polya's problem: 252.

age puzzles and tricks

1. 18.
2. 16½ (Mary is 27½).

alphametic

1.
```
   67432 (EARTH)
     704 (AIR)
    8046 (FIRE)
+  97364 (WATER)
---------------
  173546 (NATURE)
```

A = 7, E = 6, F = 8, H = 2, I = 0, R = 4, T = 3, W = 9

2.
```
   127503 (SATURN)
   502351 (URANUS)
  3947539 (NEPTUNE)
+  46578 (PLUTO)
-----------------
  4623971 (PLANETS)
```

A = 2, E = 9, L = 6, N = 3, O = 8, P = 4, R = 0, S = 1, T = 7, U = 5

3.
```
   862903 (MARTIN)
+ 1627342 (GARDNER)
-------------------
  2490245 (RETIRES)
```

A = 6, D = 7, E = 4, G = 1, I = 0, M = 8, N = 3, R = 2, S = 5, T = 9

anagram

1. Wolfgang Amadeus Mozart.
2. Thomas Alva Edison.
3. William Shakespeare.

Carroll, Lewis

1. There is as much water in the milk/water mixture as milk in the water/milk mixture.
2. There are 30 ways of painting the cube. If the restriction that each face be painted a different color is dropped, there are 2,226 ways of painting the cube.
3. FOUR → FOUL → FOOL → FOOT → FORT → FORE → FIRE → FIVE

Alternatively:

FOUR → POUR → POUT → ROUT → ROUE → ROVE → DOVE → DIVE → FIVE

(Thanks to my editor, Stephen Power, for this one.)

4. Carroll didn't have an answer in mind when he wrote the riddle, though he later came up with: "Because it can produce a few notes, though they are *very* flat; and it is nevar put wrong end in front!" (Note the variant spelling of "never.") Other authors have come up with: "Because Poe wrote on both"

(Sam Loyd); "Because it slopes with a flap" (Cyril Pearson); and "Because both have quills dipped in ink" (David Jodrey).

clock puzzles

1. Approximately 27 minutes and 42 seconds (exactly 360/13 minutes) after 6.
2. The stopped clock, because it will give the right time twice a day, whereas the other is only correct approximately every two years.
3. The positions of the hands shown in the illustration could only indicate that the clock stopped at 44 min. 51 1,143/1,427 sec. after eleven o'clock. The second hand would next be "exactly midway between the other two hands" at 45 min. 52 496/1,427 sec. after eleven o'clock. If we had been dealing with the points on the circle to which the three hands are directed, the answer would be 45 min. 22 106/1,427 sec. after eleven; but the question applied to the hands, and the second hand would not be between the others at that time, but outside them.

cone

The simple rule is that the cone must be cut at one-third of its height.

de Morgan, Augustus

43 (the only number that, when squared, gives a number between the years of de Morgan's birth and death).

domino

No! Suppose it *were* possible to totally cover the modified chessboard with nonoverlapping dominos. In any complete tiling, every domino must cover exactly one white square and one black square. Thus the modified board must have exactly the same number of black and white squares. But the two removed squares, from diagonally opposite corners of a chessboard, must be same color. Since there can't be the same number of white squares and black squares on the modified board it must be impossible to tile the modified board with nonoverlapping dominos.

hundred fowls problem

Using the two equations to eliminate C, gives the equation $7R + 4H = 100$. R must be less than 15 (since $7 \times 15 = 105$). Trial-and-error shows that values of R that allow whole number values of H are 4, 8, and 12, from which it follows that the three possible solutions to the problem are 4 roosters, 18 hens, and 78 chicks; 8 roosters, 11 hens, and 81 chicks; and 12 roosters, 4 hens, and 84 chicks.

kinship puzzles

1. Your son.
2. Sons of two men who married each other's mothers.
3. The party consisted of two girls and a boy, their father and mother, and their father's father and mother.

measuring and weighing puzzles

The innkeeper first filled the 5-pint and 3-pint measures, then turned the tap on the barrel and allowed the rest of its contents to run to waste. He closed the tap and emptied the 3-pint into the barrel; filled the 3-pint from the 5-pint; emptied the 3-pint into the barrel; transferred the 2 pints from the 5-pint to the 3-pint; filled the 5-pint from the barrel, leaving 1 pint now in the barrel; filled the 3-pint from the 5-pint; allowed the company to drink the contents of the 3-pint; filled the 3-pint from the 5-pint, leaving 1 pint now in the 5-pint; drank the contents of the 3-pint; and finally drew off 1 pint from the barrel into the 3-pint. He now had 1 pint of ale in each measure!

missing dollar problem

There is no missing dollar (of course!). Adding $27 and $2 (to get $29) is a bogus operation. They paid $27, $2 went to the dishonest waiter, and $25 went to the restaurant. You have to subtract $27 minus $2 to get $25. There never was a $29; it has nothing to do with anything.

Mrs. Perkins's quilt

The following diagram shows how the quilt should be made.

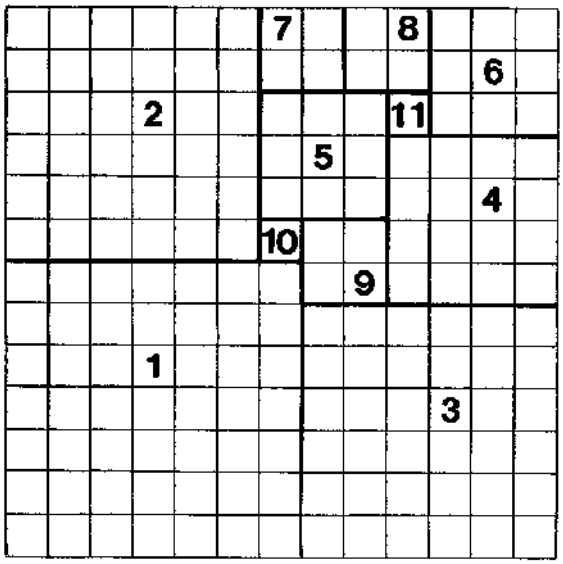

The solution of Mrs. Perkins's quilt.

In *Amusements in Mathematics,* Dudeney writes: "There is, I believe, only one solution to this puzzle. The fewest separate squares must be eleven. The portions must be of the sizes given, the three largest pieces must be arranged as shown, and the remaining group of eight squares may be 'reflected,' but cannot be differently arranged."

nine rooms paradox

One of the two customers who is initially placed in room A, whom we refer to as the "first" customer, is later transferred to room I and treated as if he were also the tenth customer!

postage stamp problems

Dudeney gives the solution to his "The Four Postage Stamps" problem as follows: "[T]he four stamps may be given in the shape 1, 2, 3, 4, in three ways; in the shape 1, 2, 5, 6, in six ways; in the shape 1, 2, 3, 5, or 1, 2, 3, 7, or 1, 5, 6, 7, or 3, 5, 6, 7, in twenty-eight ways; in shape 1, 2, 3, 6, or 2, 5, 6, 7, in fourteen ways; in shape 1, 2, 6, 7, or 2, 3, 5, 6, or 1, 5, 6, 10, or 2, 5, 6, 9, in fourteen ways. Thus there are sixty-five ways in all."

probability theory

1. There are four possibilities:

Oldest Child	Youngest Child
1. Girl	Girl
2. Girl	Boy
3. Boy	Girl
4. Boy	Boy

If your friend says "My oldest child is a girl," he has eliminated cases 3 and 4, and in the remaining cases both are girls ½ of the time. If your friend says "At least one of my children is a girl," he has eliminated case 4 only, and in the remaining cases both are girls ⅓ of the time.

2. There are six possible bullet configurations (B = bullet, E = empty):

B B B E E E → player 1 dies
E B B B E E → player 2 dies
E E B B B E → player 1 dies
E E E B B B → player 2 dies
B E E E B B → player 1 dies
B B E E E B → player 1 dies

One therefore has a ⅔ probability of winning (and a ⅓ probability of dying) by shooting second.

Pythagorean square puzzle

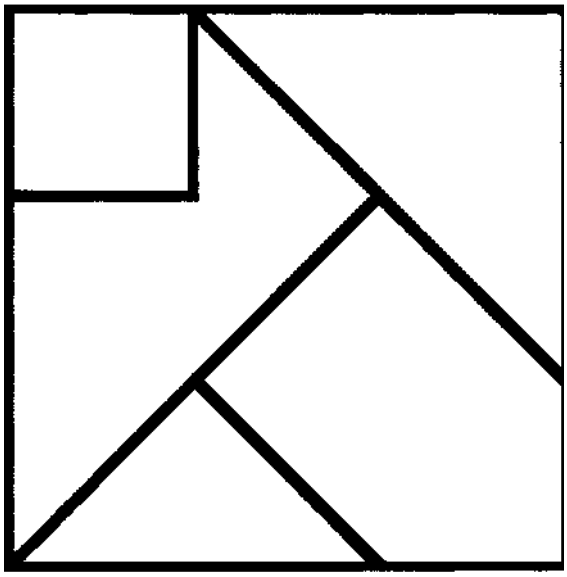

Pythagorean puzzle solution.

river-crossing problem

The missionaries (M) can avoid being eaten by the cannibals (C) if the crossings of the river and the returns are arranged as follows. Crossing #1: 1M + 1C; return #1: 1M; crossing #2: 2C; return #2: 1C; crossing #3: 2M; return #3: 1M + 1C; crossing #4: 2M; return #4: 1C; crossing #5: 2C; return #5: 1C; crossing #6: 2C.

word puzzles

(1) $T_1W_4E_1L_1V_4E_1$.

(2) Dreamt.

(3) Tremendous, horrendous, stupendous, and hazardous.

(4) I am.

(5) skiing

(6) "Are" by an adding an "a" becomes "area."

(7) underground.

9:1 Magnetic Longwire Balun / Unun

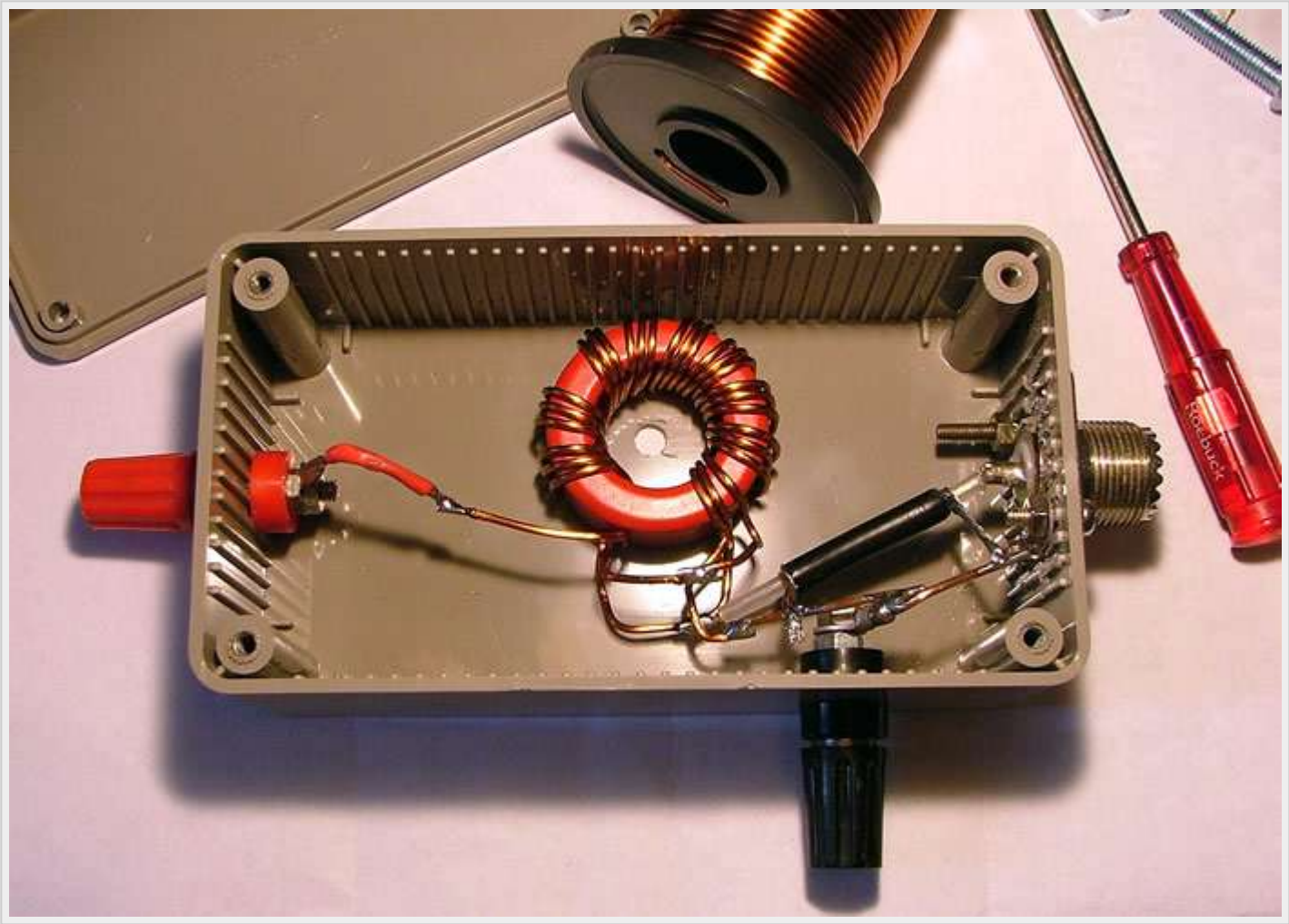

Completed 9:1 UnUn

These are sometimes known as a *Magnetic Longwire Balun*. Its really an impedance transformer (9:1) to feed a high impedance, end fed (unbalanced) random wire which is likely to be a few hundred ohms, and transform it into something closer to a 50Ω (unbalanced) coaxial input, hence UnUn. It can however also be used as a balun by not grounding the other half of the balanced output. The toroid is a T130-2 Iron Powder core, with 3 x 9 turns of 18SWG enammeled copper wire, and the connections can be seen below.

This website uses cookies to improve your experience. We'll assume you're ok with this, but you can opt-out if you wish.

Read More

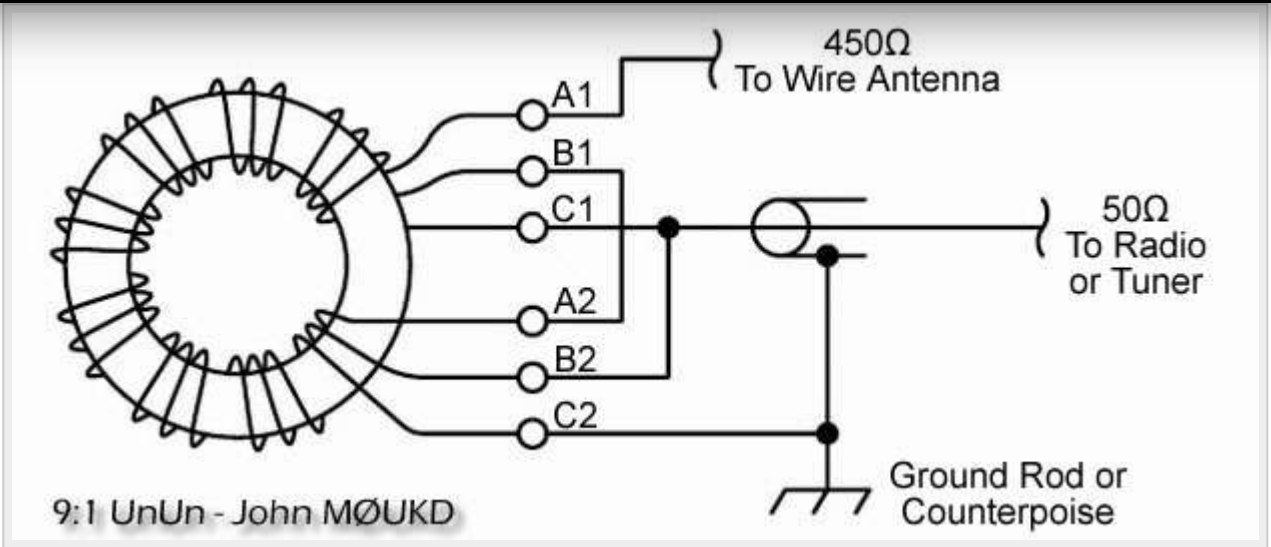

The triple winding connections. 8 turns is shown here, but more turns is preferred. 10 would be ideal.

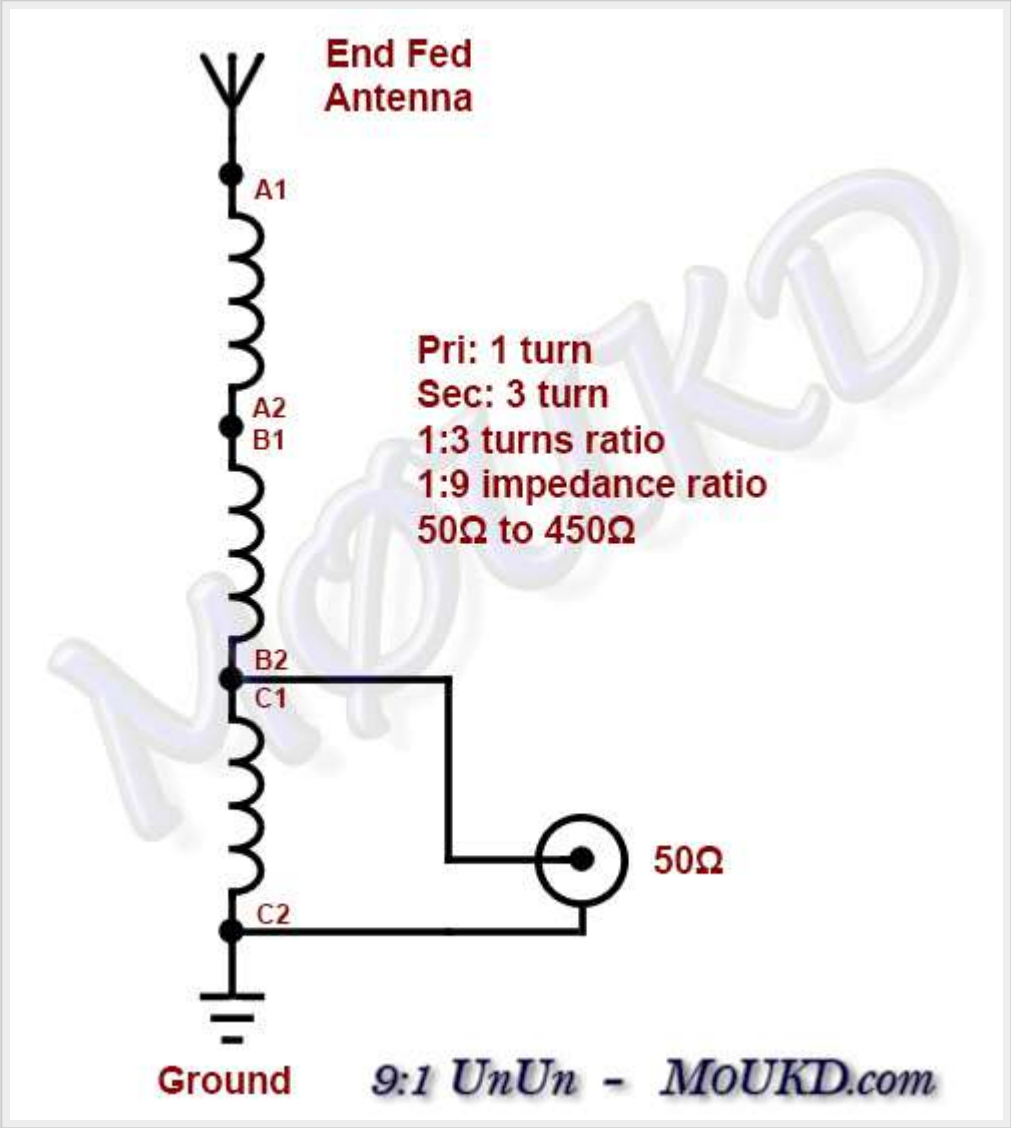

9:1 UnUn Schematic

This website uses cookies to improve your experience. We'll assume you're ok with this, but you can opt-out if you wish.

Read More

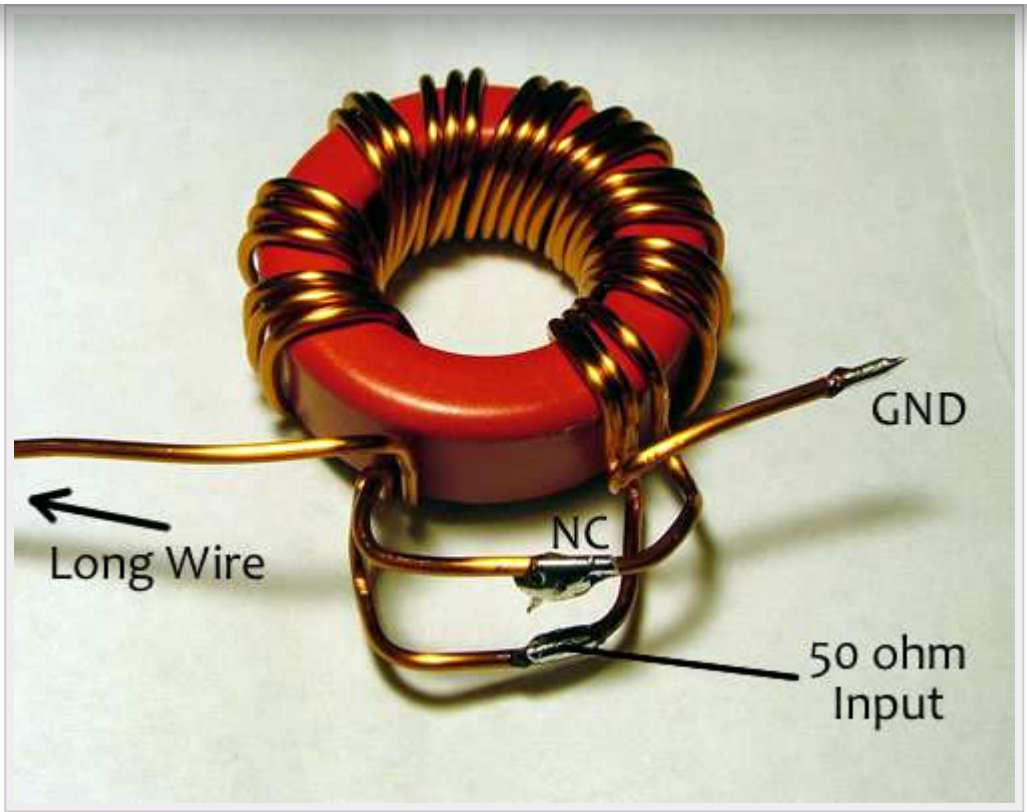

Completed windings

The completed unit.

This website uses cookies to improve your experience. We'll assume you're ok with this, but you can opt-out if you wish.

Read More

1:1 Voltage Balun for HF wire dipoles

Heres a neat 1:1 50 ohm balun for use on HF horizontal wire dipoles. It uses an AM radio ferrite rod, with 3×14 turns of wire. 10-14 turns should be good for 2-30MHz. I used 18SWG enammeled copper wire. It all fits in a small project box. Great for setting up portable. For 20 metres, I started with 6 metres of wire per element, and trimmed each down until it has minimum S.W.R. I managed to get a 1:1.1 S.W.R. on my desired frequency. Bandwidth from the resonant frequency is about 200KHz either way, any more needs an ATU. The wire and ferrite core I had already, the box, terminal plugs and SO-239 came to about £6. The balun can also be built on a ferrite toroid such as an FT140-43 or FT240-43.

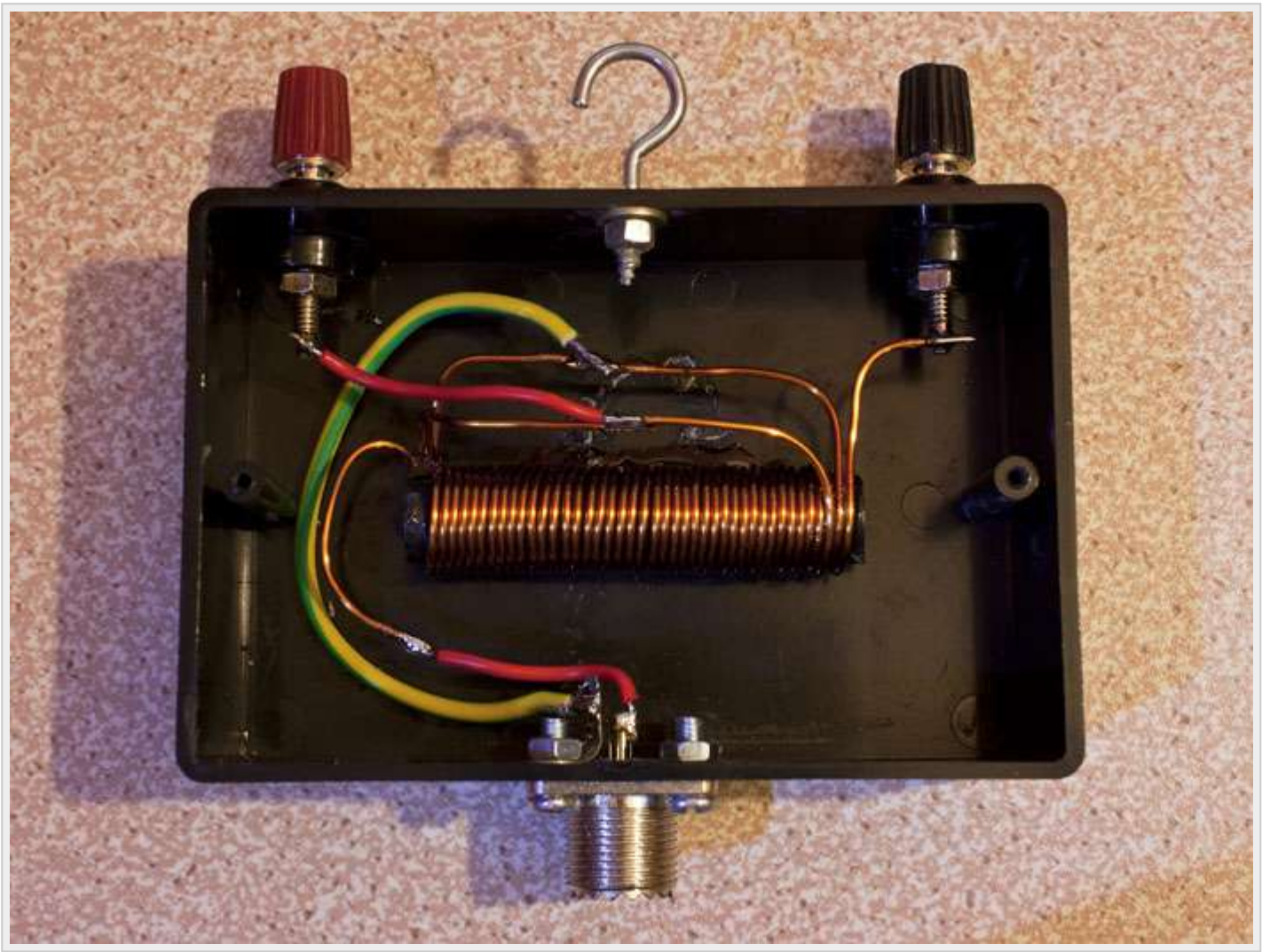

1:1 ferrite rod voltage balun

This website uses cookies to improve your experience. We'll assume you're ok with this, but you can opt-out if you wish.

Accept Read More

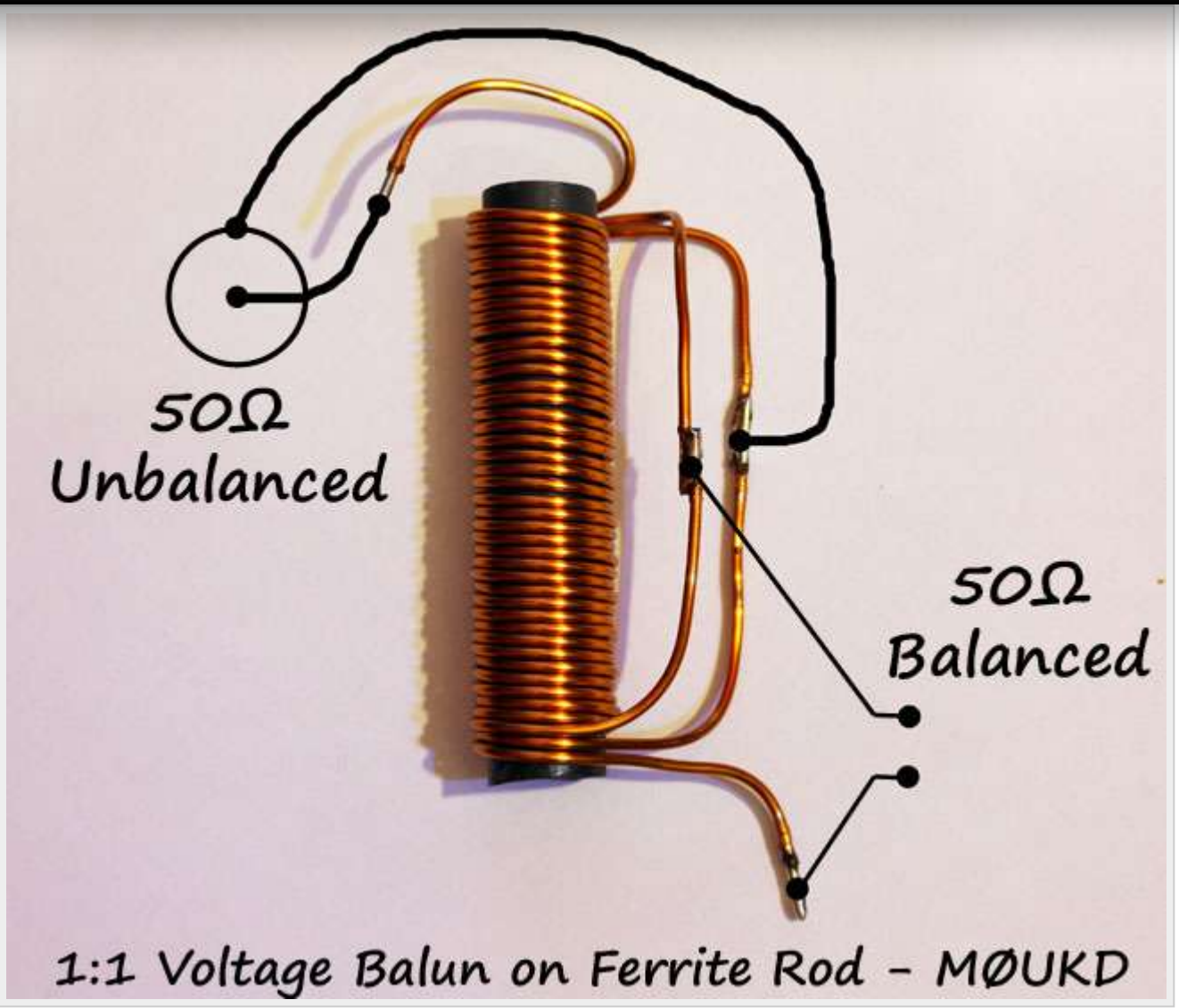

Bandwidth may be increased by more spacing between each trifilar turn. I didn't have room on this tiny ferrite rod, but it performs OK.

This website uses cookies to improve your experience. We'll assume you're ok with this, but you can opt-out if you wish.

Read More

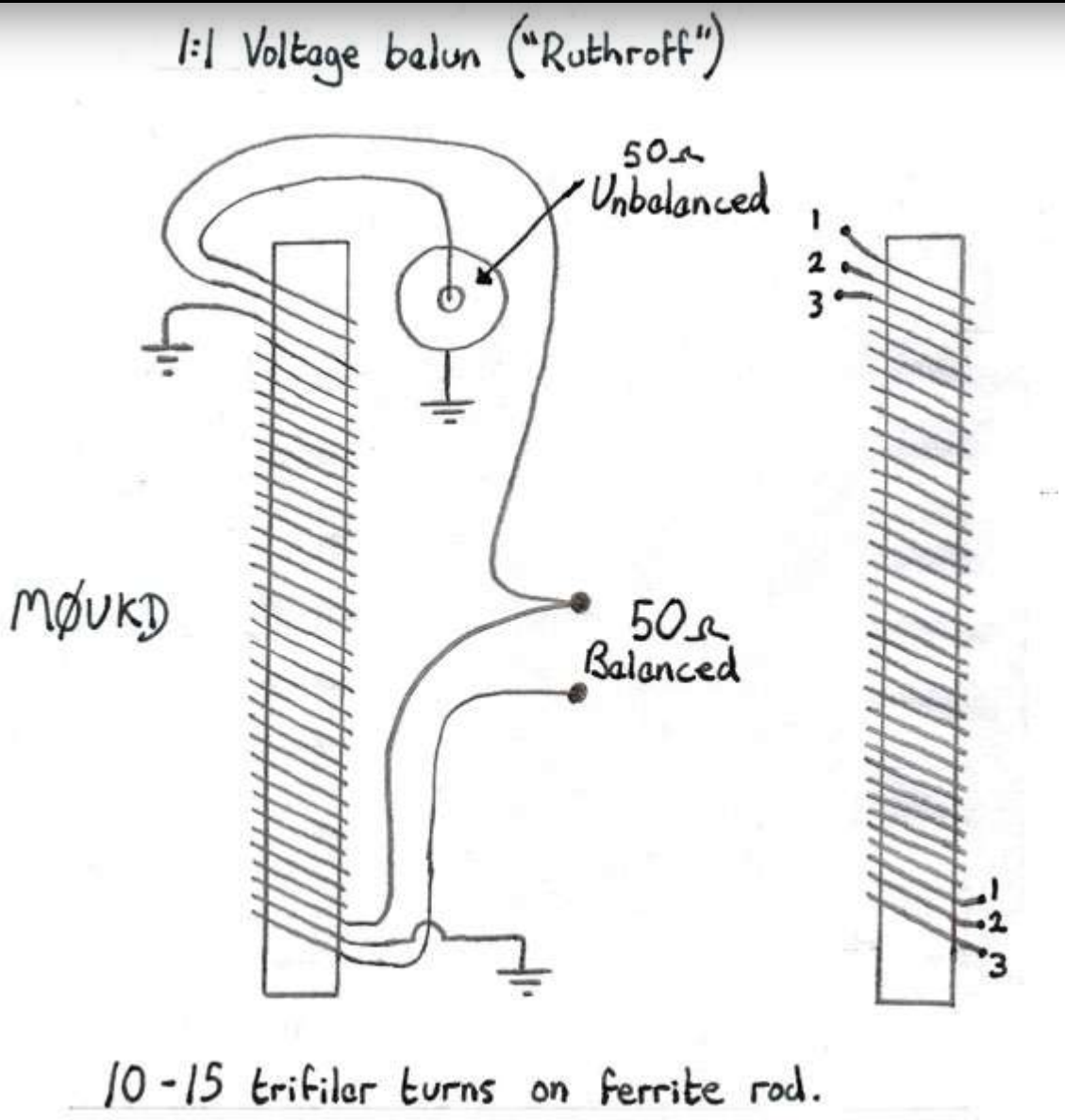

This website uses cookies to improve your experience. We'll assume you're ok with this, but you can opt-out if you wish.

Read More

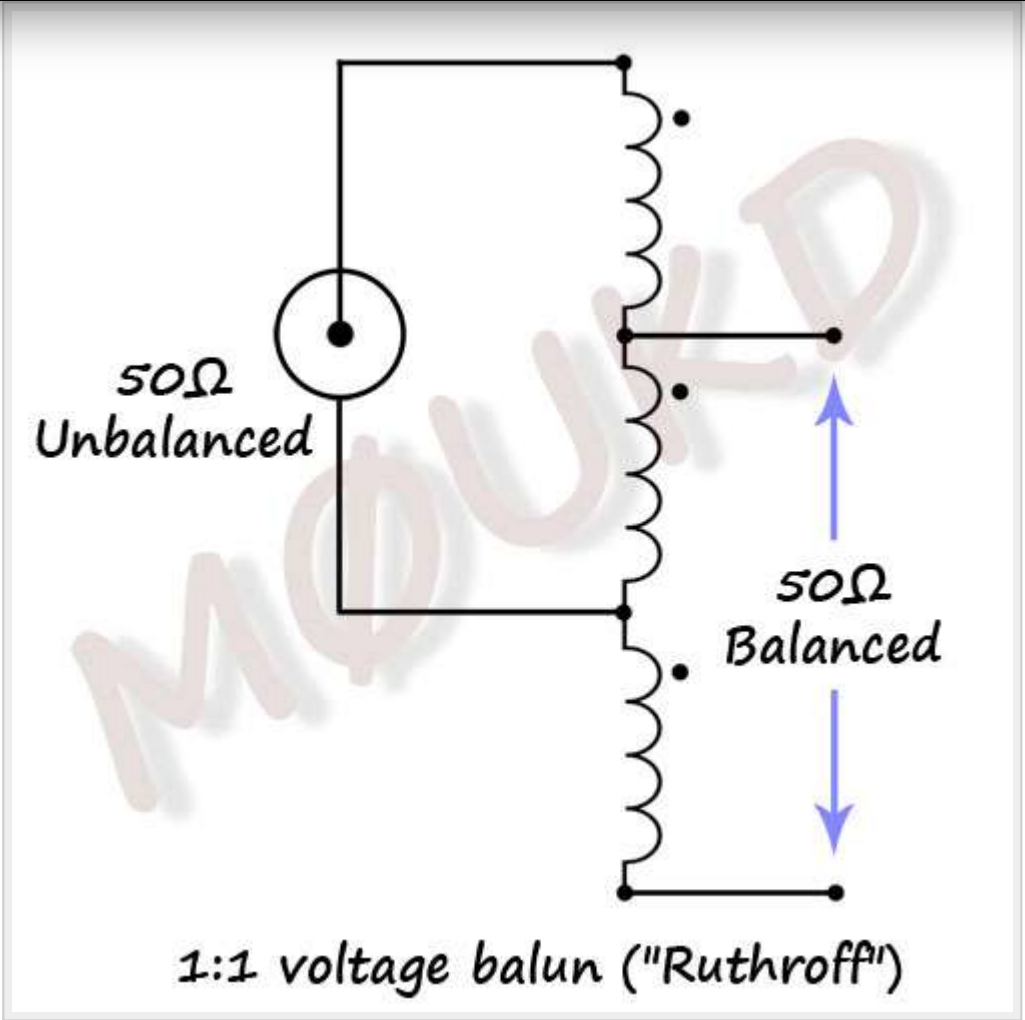

Schematic Diagram

This website uses cookies to improve your experience. We'll assume you're ok with this, but you can opt-out if you wish.

Read More

End Fed Half Wave Antenna Coupler (EFHW)

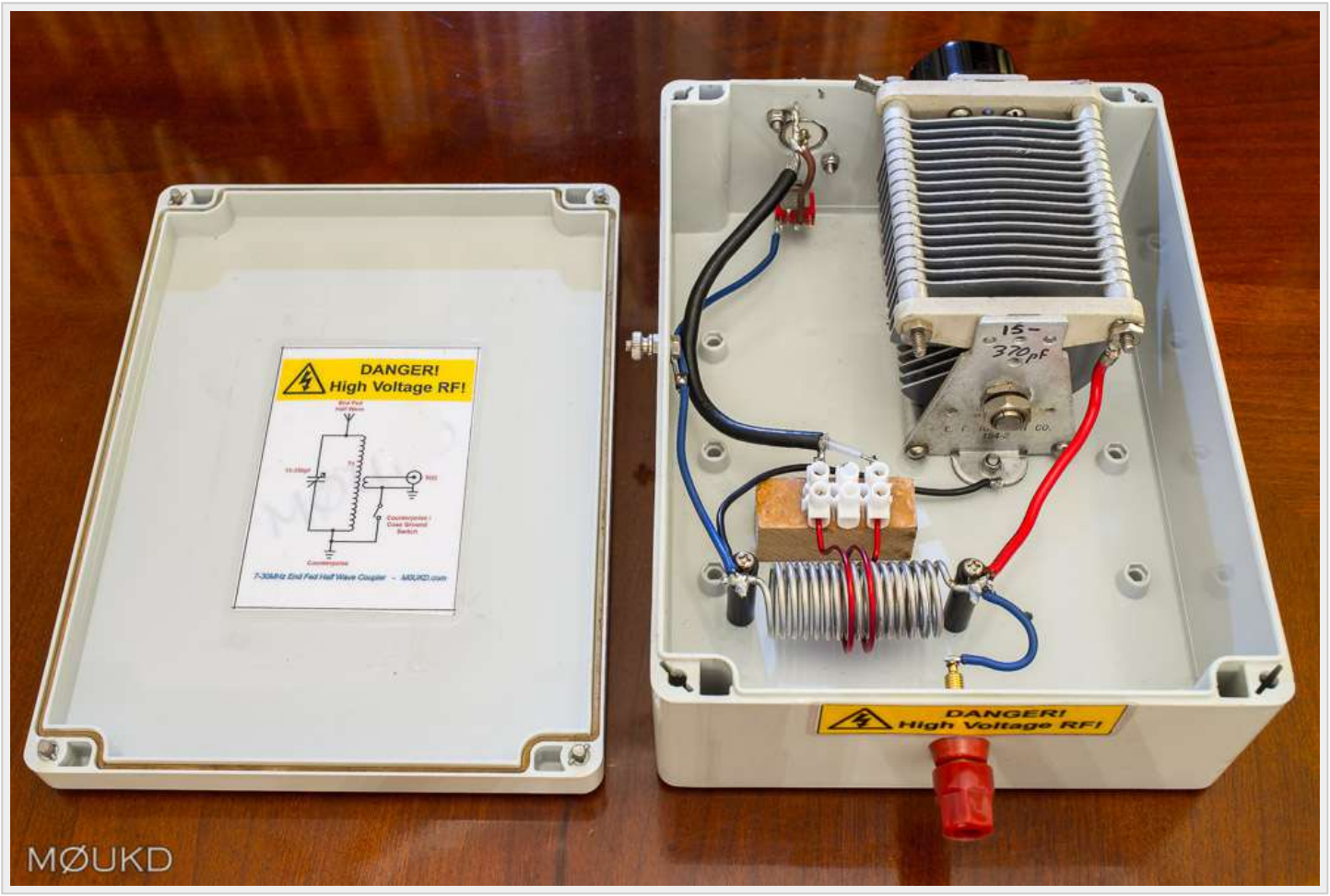

The finished End Fed Half Wave antenna coupler.

Centre fed half wave dipoles make great, simple and effective antennas for the HF bands. Sometimes however, the centre feed is not ideal, for example when you want to use it as a vertical. Being able to feed the dipole from one end gives you more options on how to erect an antenna and makes portable operation easier. A vertical, a sloper, a piece of wire hung in a hedge are all good examples. A ground mounted half wave vertical has a peak radiation angle of 20°, so it makes a good choice for DX.

I have been experimenting with feeding end fed half wave antennas matched by a parallel tuned circuit coupler. This article will explain my findings and reasons for constructing it the way I did.

A dipole can be fed anywhere along its length. A centre feed gives around 70Ω. A 'Windom' type off centre fed dipole (fed 38% along its length) provides around a 200Ω feed. The feed impedance at the very end of a half wave is thousands of ohms, usually somewhere between 2000Ω to 5000Ω, which we need to match to our 50Ω transceiver. The problem with end feeding a half wave is also its advantage. The high impedance means that the feedpoint has a very high voltage but low current, therefore very little ground is required. A very small counterpoise should be adequate from 7 to 30MHz, or you can even use the coax and transceiver

This website uses cookies to improve your experience. We'll assume you're ok with this, but you can opt-out if you wish.

Accept Read More

Below is the schematic of the final build.

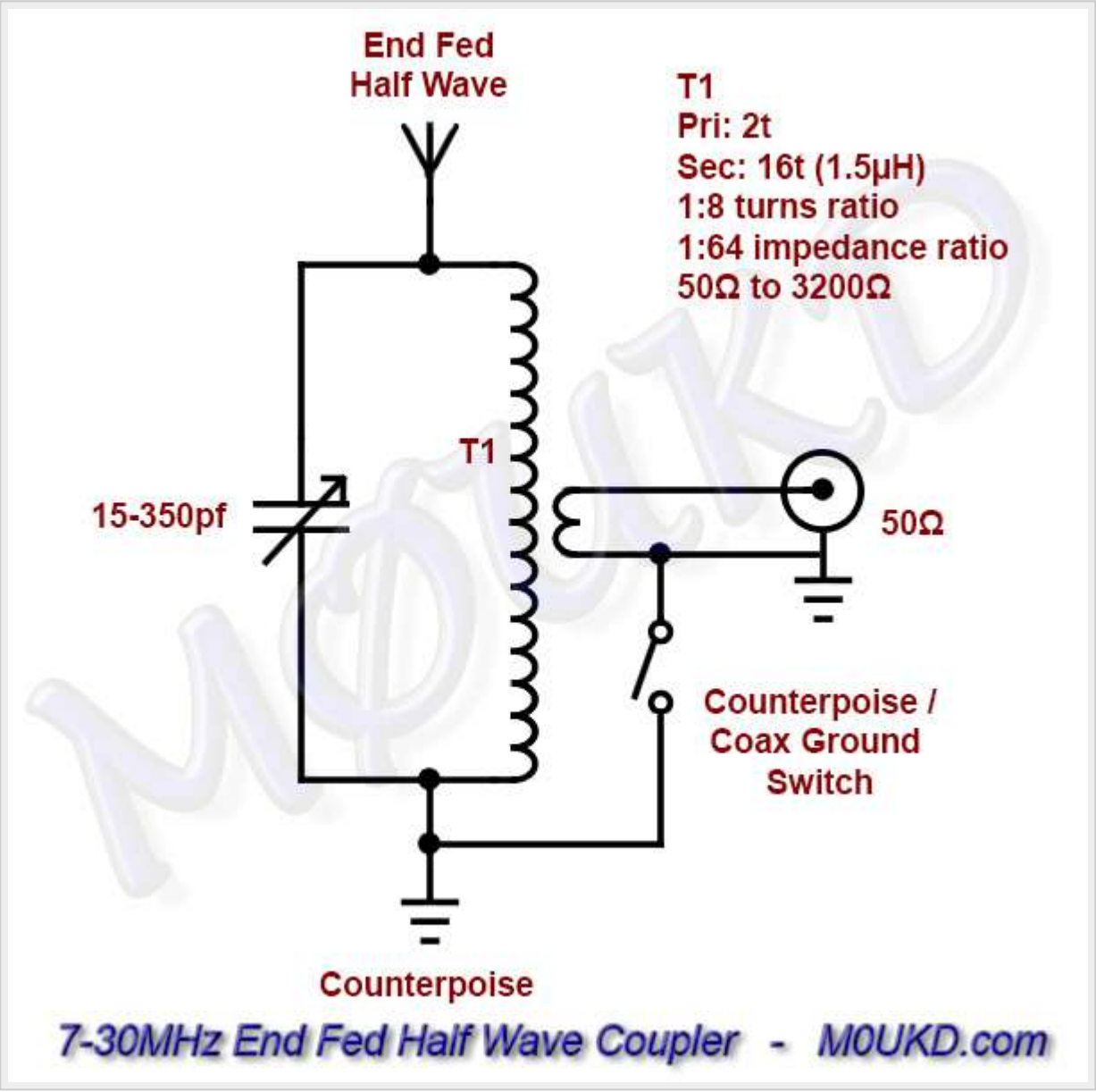

End Fed Half Wave Antenna Coupler Schematic – 7-30MHz

For calculating the length of a half wave in metres, I use $141 \div f$(MHz) for wire elements. These dimensions were derived from modelling the antenna in EZNEC. I have found this calculation to work well, however it depends on many factors such as wire used, location etc. I have made a javascript calculator below for simplicity with a 15m half wave ready to go!

Enter the frequency: 21.25 MHz

Calculate

Half Wave antenna is: Metres

This website uses cookies to improve your experience. We'll assume you're ok with this, but you can opt-out if you wish.

Read More

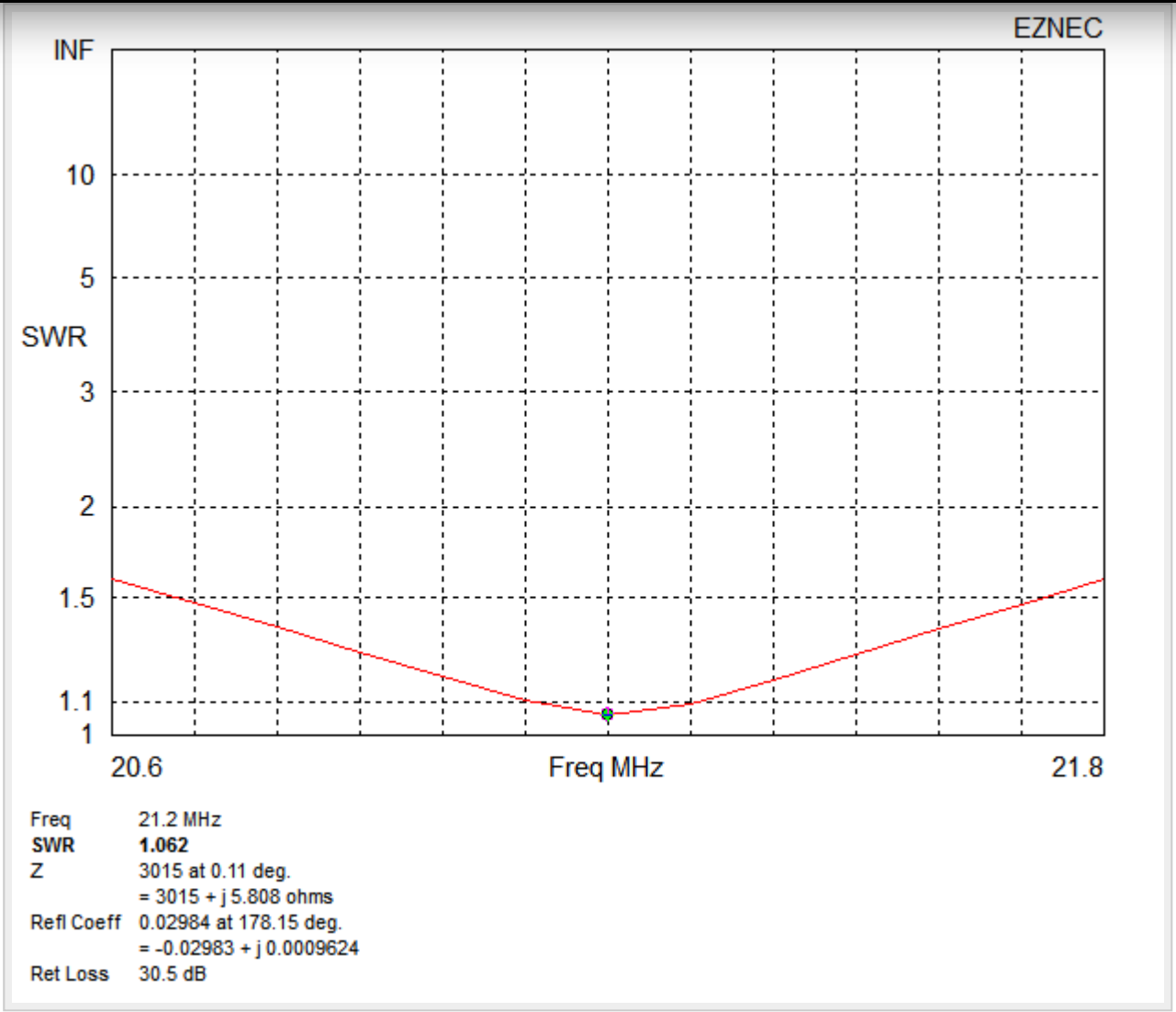

End Fed Half Wave (6.65m @ 21.2MHz, ground mounted) SWR – Actual bandwidth on the 50Ω side of the coupler will be much narrower, due to the tuned circuit we are using. This is showing the feed point SWR at 3200Ω

This website uses cookies to improve your experience. We'll assume you're ok with this, but you can opt-out if you wish.

Read More

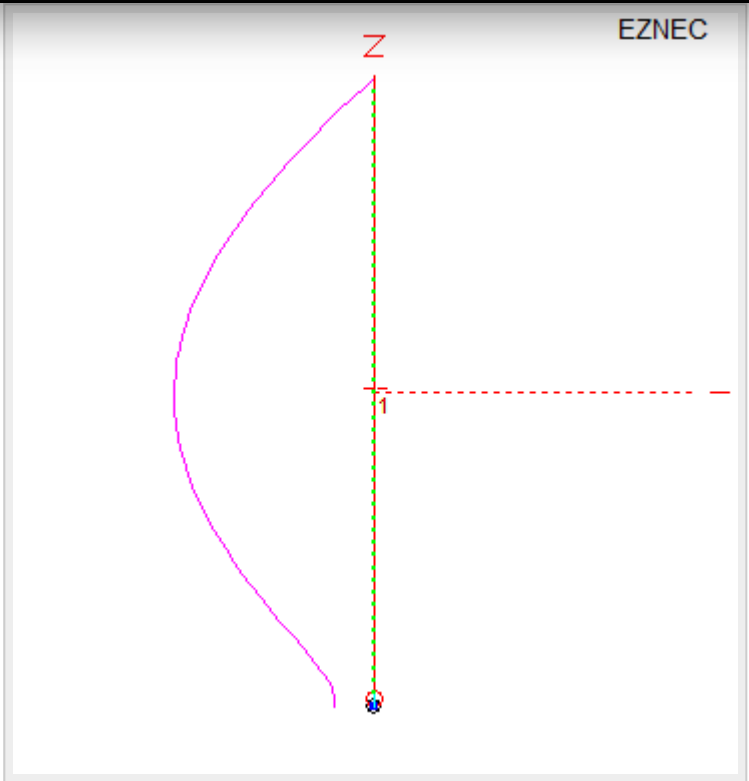

Current along the half wave. Notice how the feedpoint is not quite as high impedance as the top of the antenna.

First off, construction will be a juggle between available components and the desired band coverage. I had a capacitor that I wanted to use, which is a Johnson 154-2 air variable capacitor, with a range of 15-353pf. I would like to cover 7 to 30MHz with my coupler if possibe, so the next thing I needed to design was an inductor that would resonate in a parallel LC circuit at just above 30MHz when the capacitor is at minimum. Using this **Resonant LC Calculator**, I worked out that an inductance of 1.5µH will resonate at about 33MHz when the capacitor is at 15pf and 6.9MHz when the capacitor is at its maximum of 353pf. Sounds perfect to me! If you have a smaller value capacitor, for example 200pf maximum, it should still cover 10MHZ to 30MHz. A switch could be added to add a further capacitance of 150-200pf to include 7MHz operation.

So, lets build the secondary transformer inductor first. I wanted to transform 50Ω to around 3000Ω. This would require a 1:8 turns ratio. Impedance transformation is calculated by squaring the secondary turns ratio (note ratio, not actual turns) 8^2 is 64. 50×64=3200Ω (our input impedance x 8^2). I looked at using a **T200-6** iron powder toroid, but the problem was 1.5µH required *only* 12 turns. As I wanted a 1:8 turns ratio (for a 1:64 impedance ratio), I needed a primary of 1.33 turns, which was going to be impossible. I could have made it 16 turns and a 2 turn primary, but then the inductance would be too large for 30MHz.

So, I decided to use an air wound transformer. This way, I can build it with a 16 turn secondary, *and* at the inductance I wanted by altering the diameter and/or length of the coil. Using this **Air Inductance Calculator**, I worked out that a 19mm diameter, 52mm long, 16 turn inductor should give an inductance of 1.5uH, so this is what I built.

This website uses cookies to improve your experience. We'll assume you're ok with this, but you can opt-out if you wish.

Read More

Winding the secondary inductor

Once it was wound, I tested it on an LC meter, which confirmed it was around 1.5µH. You can expand or contract the inductor to fine tune the impedance to suit. The importance is that it remains 16 turns to match with the 2 turn primary. I then wound the primary coil, which had to be a slightly larger diameter so that it could fit over the secondary coil and provide inductive coupling. You can see the finished 2 turn primary and 16 turn secondary below.

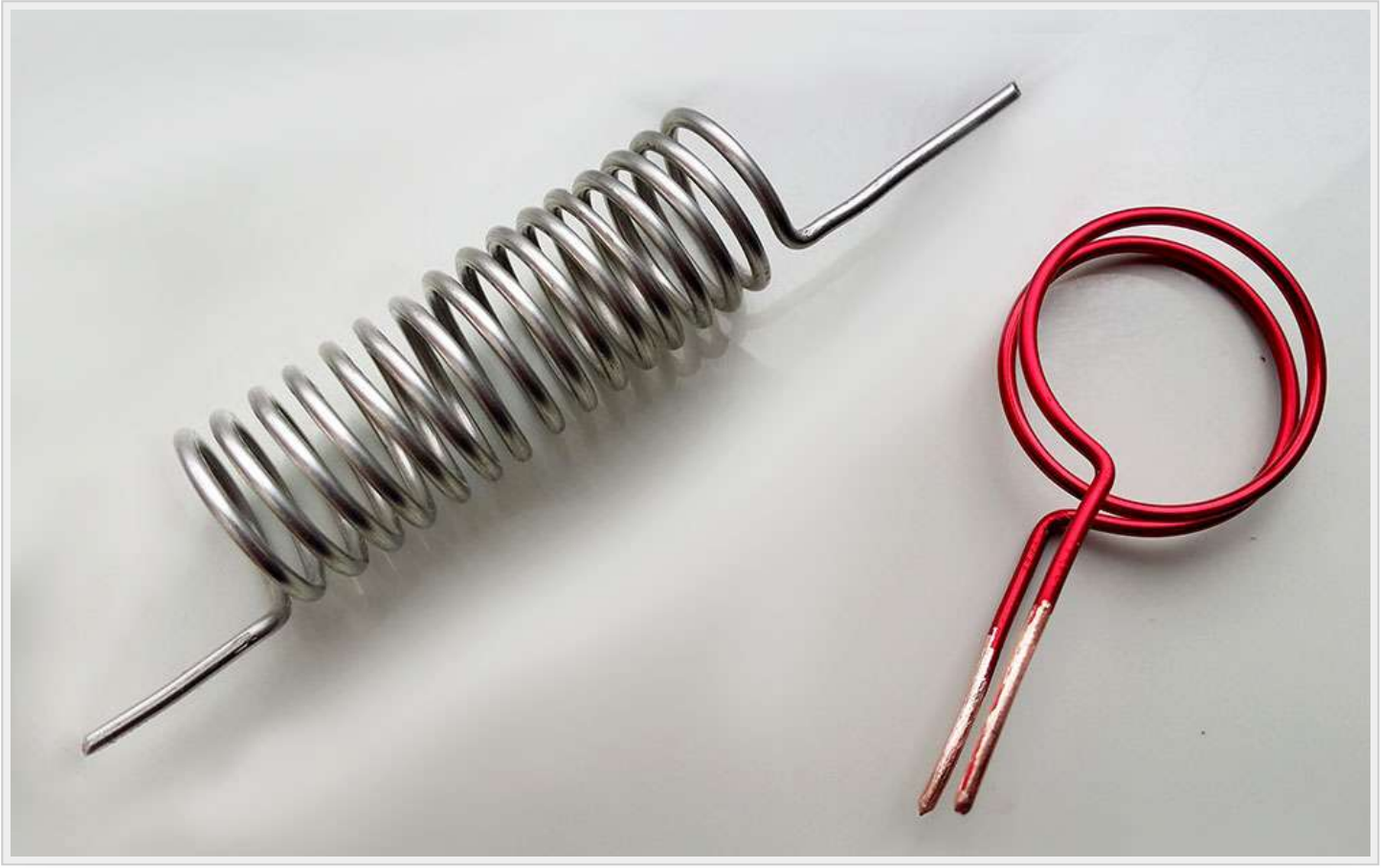

The completed inductors. They have their differences, but I will make them a happy ‘couple’!

This website uses cookies to improve your experience. We'll assume you're ok with this, but you can opt-out if you wish.

Read More

secondary and a terminal block glued to a small block of MDF for the primary. The coax is soldered to the primary, the terminal block is just to hold it in place. There is a counterpoise connection on the side, the antenna connection on the front and the capacitor, SO239 and counterpoise/coax ground switch on the rear. Some photos of the completed unit are below.

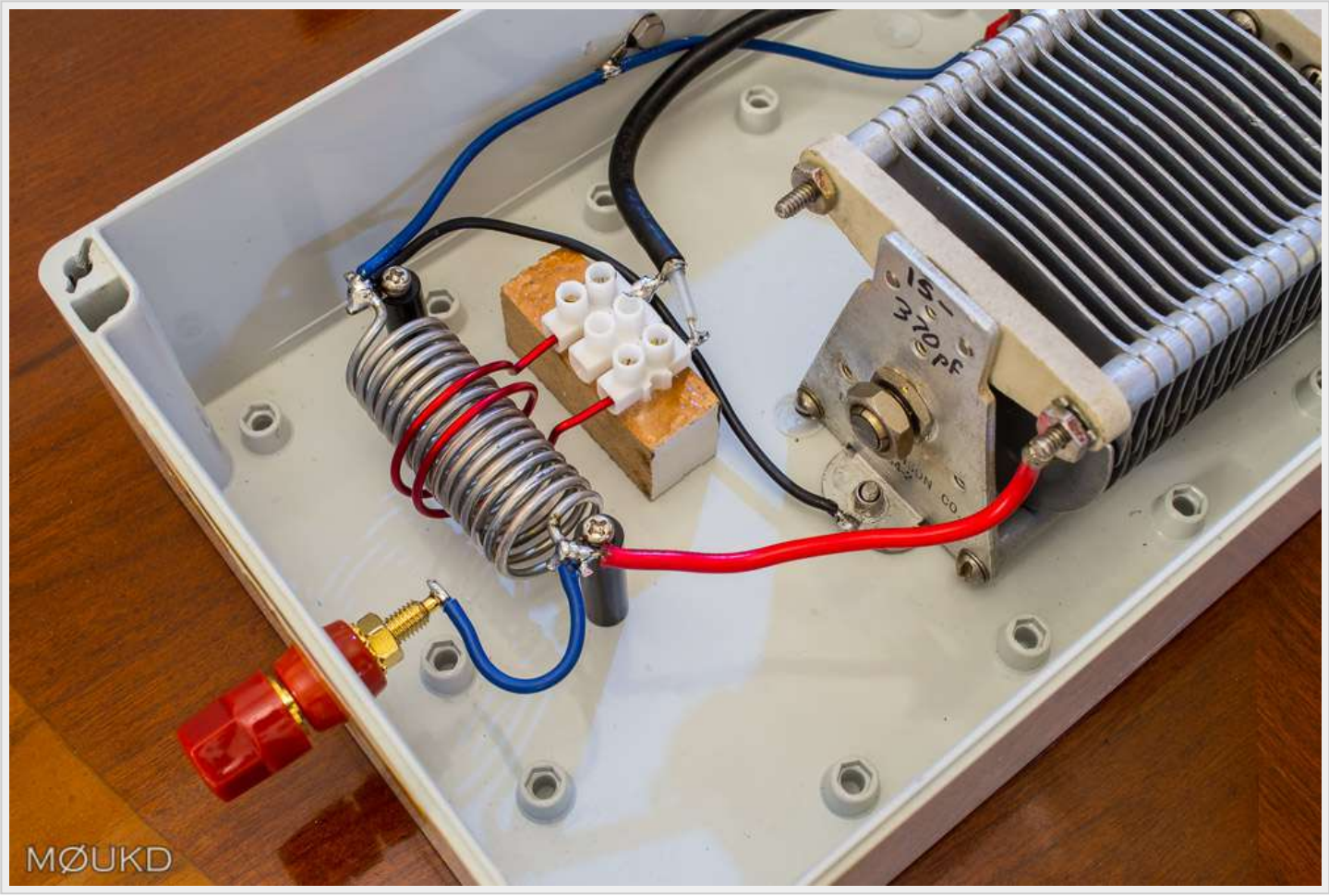

The completed End Fed Half Wave Coupler

This website uses cookies to improve your experience. We'll assume you're ok with this, but you can opt-out if you wish.

Read More

The tuning control, SO239, ground switch and on the right, the counterpoise connection.

The antenna connection. The second hand box had a few holes in it, so I made this sticker to cover them up!

This website uses cookies to improve your experience. We'll assume you're ok with this, but you can opt-out if you wish.

Read More

this is due to extra stray capacitance. I tuned the coupler to resonance into a resistor (in my case 3.2kΩ) so a 1:1 SWR was obtained on my chosen frequency of 21.25MHz, then I removed the resistor and attached the half wave antenna (6.65m) and counterpoise (66cm) from the above calculator. Without adjusting the variable capacitor, I had a 1:1 SWR. This confirmed that I had a resonant half wave and that I was feeding it at or very close to the peak voltage point and the feed impedance was around 3200Ω. I found that a small counterpoise was required. Sometimes, the stray capacitance to ground was good enough on its own, especially on the higher bands and if the coupler was laying on the ground. If its all away from ground, I get consistent results using the above setup. I have had good success also by using the coax as the return, by connecting the 'bottom' of the primary and secondary together via a switch to use the coax shield and transceiver as a counterpoise.

You may be able to adjust the capacitor to match the antenna if its not a perfect half wave, but then it will be a higher current feed and the simple ground system will be inadequate. The coupler will also not be working as it was designed and will be inefficient, generating heat. The coupler is a tuned impedance transformer, not an antenna 'tuning' unit. Stick to the above, and it should be a sure thing!

This website uses cookies to improve your experience. We'll assume you're ok with this, but you can opt-out if you wish.

Read More

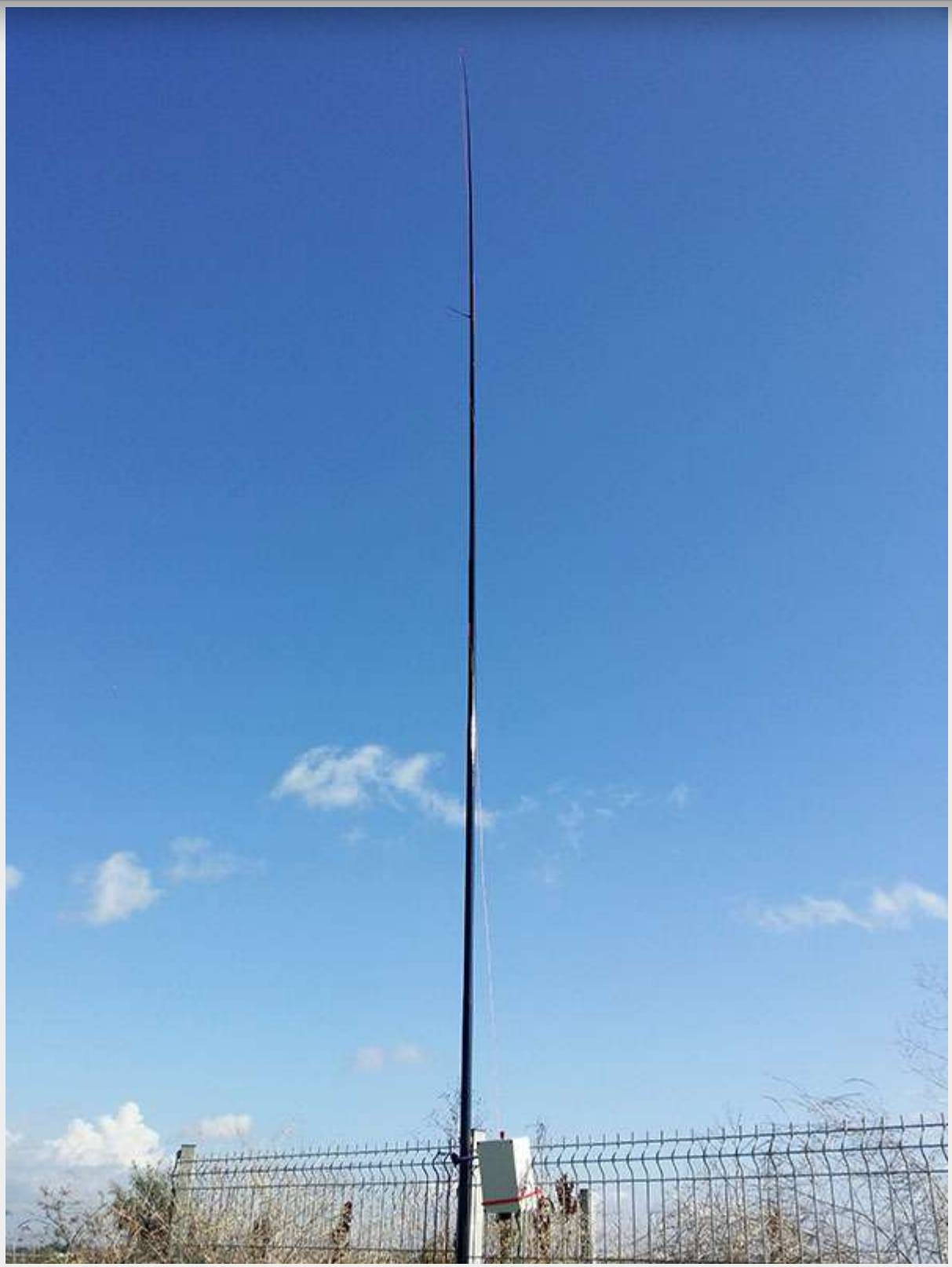

A half wave vertical for 21MHz. 6.65 metres of wire on a 9 metre fibreglass pole. The coupler is mounted 2 metres up and attached to the top of the fence. The 67cm counterpoise just hangs down in free air.

Below is a short video from my second test with the coupler, here on 17m.

This website uses cookies to improve your experience. We'll assume you're ok with this, but you can opt-out if you wish.

Read More

END FED 6–40 Meter Multiband HF Antenna

Introduction

This EARC project produces an inexpensive, multiband, end fed HF antenna matchbox that is quick and easy to setup and use. The end fed feature adds portable convenience, but does present another issue. The problem with an end fed half wave antenna is that the antenna presents high impedance, creating a significant miss match with the usual transceiver impedance of 50 ohms. This miss match is significantly greater than typical tuners can accommodate without a matching transformer.

This project creates a trifilar wound, 9:1 UNUN (unbalance to unbalance) toroid matching transformer that will match the high input impedance of an end fed antenna into the range where most antenna tuners can produce good performance. The matchbox handles 100 watts of power. ***This project requires an antenna tuner to achieve satisfactory SWR***. If you need an auto tuner, we recommend the LDG line of auto tuners, shown to work well with these matchbox antennas, and highly rated by users. They are reasonably priced and available at most ham stores.

The matchbox project uses readily available common hardware and materials listed below.

Matchbox Parts List

1	small plastic enclosure (shown right)
1	powdered iron toroid T130-2
3	20” pieces of 18 AWG solid insulated copper wire in red, green, and black
2	# 8-32 x 3/4” hex head machine screws
2	# 8 lock washers
2	# 8 ring wire lugs
2	# 8 flat washers
2	# 8 lock washer/nut combination
2	# 8 wing nut
1	SO-239 panel mount connector to fit keyed enclosure opening

30’ # 18 AWG insulated stranded wire antenna with ring lug attached Small amount of clear silicone caulk to secure toroid in place

Preparing the MATCHBOX Plastic Enclosure

The enclosure needs one 5/8” hole for the SO-239 connector, and one 11/64” hole for the counterpoise wing nut on the lower side of the enclosure. An 11/64” hole on the upper right side of the box facilitates antenna connector mounting.

TOROID WINDING

First, wind the three 20” pieces of insulated solid wire onto the toroid. Place the wires as shown green-black-red, and wrap the toroid 9 turns so that it looks like the photo on the right. Notice there are three wires extending from the left winding and three wires extending from the right winding. As the connections are completed, the steps refer to the specific wires by left or right and color.

NOTE: Count turns by counting the number of times the wire goes thru the toroid center.

Crimp together and solder ***the left black wire*** with the ***right red wire*** When the step is completed, it will look like the right photo.

The next three steps should appear as shown in the first photo on page 3. Crimp and solder a # 8 lug to the ***left red*** wire about 2” from the toroid. The completed lug will later connect to the antenna connection bolt on the upper inside of the enclosure.

Twist the **left green** wire with the ***right black*** wire. Strip the ends of the two wires and twist together at about 2”. This twisted pair will solder to the center connection of the SO-239 connector in a later step.

Trim and strip the remaining ***right green*** wire at about 2”. Cut an additional 2” piece of green wire, and crimp and solder both wires to a # 8 lug. The 2” green wire will connect to the ground

connector on the SO-239 already installed in the enclosure. Strip remaining green wire end 3/8” and bend into a hook for connection to the SO-239 ground connector.

The SO-239 connector and ground lug should be installed through the keyed hole in the lower right with the mounting nut securely tightened.

Solder the green and black twisted pair to the SO-239 center connector. Solder the green wire hook to the ground lug on the SO-239 connector.

From inside the box, place an 8-32 machine screw through a lock washer, the # 8 lug on the green wire, then through the lower 11/64’” mounting hole. Place a flat washer on the outside protruding machine screw followed by # 8 lock washer/nut and tighten securely. Place a # 8 wing nut on the machine screw to finish the **counterpoise connector**.

Position the toroid inside the box to allow connection of the red antenna wire lug to an 832 machine screw and lock- washer on the upper box side. Place a flat washer on the outside of the box followed with a # 8 lock washer/nut. Tighten the nut securely. Next, place the wing nut on the **antenna connector** and your project appears as shown above.

A small spot of clear silicone compound is used to secure the toroid from movement in the enclosure. The final assembly step is to secure the box cover in place with four screws.

Preparing the Antenna Wire

Matchbox performance will be determined by two factors: The length of the antenna wire, and the capability of the tuner. The length of the antenna wire should be between 24 and 60 feet for best performance. Additional counterpoise is not normally required, as the coax shield provides the counterpoise function. Wires longer than 60 feet may have excessive impedance for some tuners to properly match. Wires shorter than 24 feet may not radiate as effectively. A 30 foot insulated 18 gauge stranded wire antenna and connecting lug is included with the project and should meet most requirements without need for any counterpoise.

Experience has shown that most external tuners and some internal tuners will tune 80–6 meters with an antenna length of 24’ to 30’. If a longer antenna is desired, the provided antenna can be lengthened.

Some tuners, in particular internal tuners, may not tune the full 80-6 meter range. You may need to try different wire lengths to optimize your antenna configuration. If you are having difficulty getting your rig to tune, start with a 26’ wire. This should produce good results on at least 40-6 meters using the narrowest performance range of internal tuners.

Best performance is achieved with a coax of 16’ or longer, with the coax shield providing the counterpoise function. Additional counterpoise is usually not required in this design, although the lower wing nut provides a convenient counterpoise connector if needed. The end fed antenna system works well in horizontal, sloper, and vertical configurations.

Observe established safety practices when working with antennas, and avoid proximity to power or utility wires. Permanent installations should be equipped with appropriate static and lighting protection.

Keep amateur radio safe and fun!

Toroid Wiring Schematic

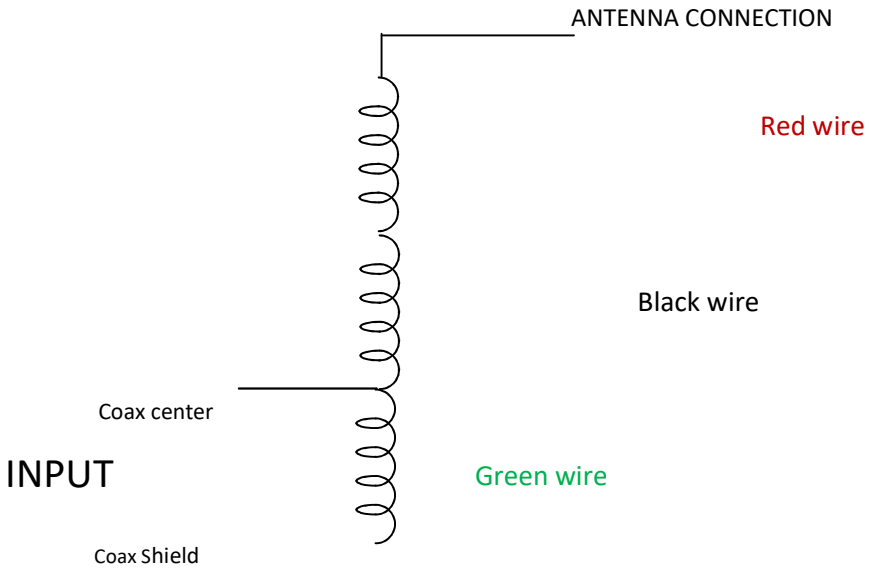

Feedback on 6-40 End Fed Matchbox Antennas

The antenna is amazing. I receive fantastic signal report from DX stations as well as hams around the country. I previously used a short version GR5V that was in an inverted V configuration on the roof of our house. This antenna was noisy but worked. Your antenna out performs the prior antenna and is much quieter. Thanks again for the fine product that your club offers. ***May 2012***

It took me 10 minutes to install and WOW - within 10 minutes I made my first HF contact (from CT to GA). And in the span of 4 hours made 3 more !! I was transmitting just 5 Watts from Yaesu 857ND using this antenna. This antenna rocks ! Thanks a ton ! 73 ***May 2012***

The 6 - 40 Matchbox antenna works great! Easily tunes with the Z100 tuner - very low SWR's on 20m thru 10m. Antenna was up about 45 feet on tree branch - wire length was about 52.5 feet, slight slope, 55 feet of coax, line isolator at radio. ***Work Hawaii for the very first time. Guess the antenna wanted to call home :-) 57 report, 100 watts, 15 Meter band, Icom 718.*** A great portable antenna that I will use often at Montrose Harbor along the lakefront in Chicago. Thank you for a fine, well made product. ***April 2012***

It arrived today in fine shape. I got is up in the air this afternoon using a 31 foot radiator. Top is at 45 feet. Loads on all bands 80-10M with my LDG auto-tuner absolutely no problem, My first QSO was KH7X in the ARRL SS contest with 100W. Amazing. This thing rocks! It's a great antenna! Nice job and a great buy. ***November 2011***

I set-up my jackite pole today and tried a 68' wire with the 9:1 unun matchbox. I set it up as an inverted L with about 26 feet vertical and 42 feet horizontal. With my IC-703 it tuned 80 through 6 all well below 1.5:1. I am going to leave the antenna up a few days and make a few contacts. I think the matchbox is terrific. ***October 2011***

My 6 – 40 meter end fed arrived through the UK holiday mail and I departed from my norm of a sloper and mounted it vertically on a 10m fishing pole. It is surprisingly effective and rewarded me with a surprise contact on 17m into the Falkland Islands at 20:30UT last night. ***January 2012***
When I attached it to a 10m fiberglass fishing pole and went vertical - wow! Easy 5/9 contacts out to 6,000+ miles when propagation was anything better than the worst. My simple ATU easily matches the antenna with SWR never greater than about 1.4 on any band it is built for. ***December 2012***

You can dither and procrastinate, but with this antenna, you'll be talking to the world in no time on any band that happens to be hot - and with your hard-earned cash hardly touched! ***January 2012***

Just wanted to report back that I have tossed the antenna into a tree about 20' up in an inverted vee shape and I am pleased to report that I can tune anywhere I need on 40-10M using the TS-590 internal tuner!! My first contact was on 40M within 10 minutes of erecting the antenna and was all the way to TX from my condo here in MI using just 10 watts. This is by far the best HAM related investment I have made in a long time. Living in a condo with strict association rules, I am able to conceal this wire in a tree out my bedroom window and talk all over. I'm very happy and would recommend this antenna to anyone in a similar situation. ***March 2013***

I have had your multiband end fed antenna installed here in Singapore for a few weeks now and am very pleased. I used the wire from my previous antenna which is 66 feet long. It works beautifully! I have it hanging vertically outside my 15th story apartment window on a 5 foot horizontal pole (to get it away from the reinforced concrete building). A couple of fish weights on the end keep it from blowing around too much. I would recommend this antenna to anyone who is facing a challenging QTH. ***April 2013*** I received my antenna yesterday, a quick 4 days since I ordered it. I attached it to a 31 foot pole and my IC-706MK2. Within minutes, I made my first contact with 9A4KW in Zagreb, Croatia on 20 meters. Being able to reach out over 4,000 miles gives me real confidence that I have found my portable antenna. Thanks for your rapid response and fine product. ***May 2013***

In only 2 weeks of casual on-air time. If you could see how I had to zig-zag it through a big tree above the roof of my RV, you'd be saying like I am, "how the heck can that work? I worked 90% of the stations I called, and just added Mexico City on 15m that gave me a 5x9. ***September 2013***

Just wanted to let you know how pleased I am with my ERAC matchbox antenna. I put the EARC antenna in the backyard with the feed point at 4 feet and the wire sloping up to 35 feet. I have 125 feet of coax feed line. My transceiver's built-in antenna tuner will adjust the SWR to below 1.2 to 1 on all bands 80-6 meters. Last weekend I worked 65 countries on 5 continents. I live in an antenna restricted community and this antenna has allowed me to enjoy ham radio again. ***February 2014***

I used the EARC Matchbox today. It works GREAT on 20m with a 30 ft radiator in vertical positioning, fed with 25ft of RG175/u coax. I've been talking up and down the east coast with 3W on SSB all afternoon! People ask me to repeat my power output again and again. I can't wait until I get the chance to use it at night, where I think it'll really shine! This has a permanent place in my portable kit. Thanks for the great product! ***April 2014***

I performed a simple install in Virginia making it vertical by using a 28 foot fiber glass kite pole. Within 30 minutes (NO KIDDING) I was receiving Lebanon on 17 meters! I also worked Russia and Eastern Europe that night on 20 meters. I love this antenna and I give it a 100% (5 STAR) rating. ***May 2014***

This little box is magic. NY, IA and NM from GA with ease on 100w ***June 2014***

Just wanted to let you guys know, this matchbox is wonderful. I built the matchbox, connected it to 55 feet of solid #14 about 20 feet in the air. My rig is a Yaesu FT-817ND connected to a MFJ-971 tuner with coax running between the tuner and the matchbox. So far I have worked Slovenia twice, Morocco, St. Helena Island, Cuba, Cost Rica, Vermont, Wyoming, Florida, North Dakota, Brazil, and Colombia. This setup works really well on the higher bands. Thank you for putting this design on the internet. I like it so much its become permanent here. ***September 2014***

This antenna continues to amaze me. It worked well U-shaped "indoors" with 50 watts, and now outdoors as a sloper. It easily loads 10-40m with my TS-570s internal tuner. I'm sold on it and own two of them now. I'm working at least 90% of the DX I chase. I have no RFI in the shack either. ***November 2014***

EARC Antennas are operating in virtually every state, these countries and more!

Argentina Australia Belgium Brazil Canada Chile Denmark Greece

Hong Kong India Ireland Israel Italy Mexico Mozambique New Zealand Russia Singapore Sweden Tasmania United Kingdom

ORDERING A MATCHBOX ANTENNA FROM EARC

Volunteers of the Honolulu Emergency Amateur Radio Club (EARC) carefully assemble the 6-40 End Fed matchbox antennas for those who prefer not to build one. For a donation of **$56** (Including USPS priority mail shipping) club volunteers will build and deliver a 6-40 matchbox with a 30 foot antenna wire anywhere in the U.S., we do not ship internationally. Note that coax cable is not included.

Payment by PayPal

To pay via **PayPal**, make your payment to paypal@earchi.org using any major credit card. Include your name, mailing address, and email address with the order.

We will ship promptly and you will likely receive the order in the US in 7 days or less. If you have any questions about your order, please email webmaster@earchi.org

Thank you for your interest in the activities of Honolulu Emergency Amateur Radio Club and amateur radio.

GPS coordinates for 20 of the Top HAARP facilities

GPS coordinates for 20 of the Top HAARP facilities:

1- High Frequency Active Auroral Research Programn (HAARP)
Gakona Alaska
+62° 23’ 30.00″, -145° 8’ 48.00″

2- High Power Auroral Stimulation Observatory (HIPAS)
Fairbanks Alaska
64° 52’ 19″ N 146° 50’ 33″ W

3- Poker Flat Research Range
Near Chatanika, Alaska
+65° 7’ 23.90″, -147° 28’ 7.05″

4- Platteville Atmospheric Observatory
Platteville, Colorado
+40° 10’ 54″, -104° 43’ 30″

5- Millstone Hill Radio Observatory
Westford, Massachusetts
+42° 37’ 09.25″, -71° 29’ 28.49″

6- The Arecibo Observatory radio telescope
Arecibo Puerto Rico.
18° 20’38.97″N 66° 45’9.77″W

7- Jicamarca Radio Observatory
Lima, Peru
11° 57’ 08.25″ S 76° 52’ 30.67″ W

8- São Luiz Space Observatory
Cruzeiro Santa Bárbara, Sao Luis-MA, Brasil
-2° 35’ 40.47″, -44° 12’ 35.90″

9- Nerc MST Radar Facility
Capel Dewi, Carmarthenshire, Wales, United Kingdom
+52° 25’ 28.26″, -4° 00’ 19.59″

10- European Incoherent Scatter Scientific Association EISCAT
Ramfjordmoen, Near Tromsø, Norway

+69° 35’ 10.94″, +19° 13’ 20.89″

11- Sura Facility
Nizhniy Novgorod, Russia
+56° 7’ 9.70″, +46° 2’ 3.66″

12- The Russian Woodpecker
Duga Radar Array, Chenobyl, Ukraine
51° 18’20.17″N, 30° 04’02.60″E

13- National MST Radar Facility NMRF
Gadanki, India
+13° 27’ 26.68″, +79° 10’ 30.74″

14- China Research Institute of Radiowave Propagation (CRIRP)
Xinjiang (Sinkiang) Region
40° 24’15.91″N, 93° 38’09.74″E

15- Sheshan, Shanghai,
China
31° 5′ 41.98″ N, 121° 11′ 29.72″ E

16- Mu Radar
in Japan
34° 51’14.80″N 136° 6’19.45″E

17- Jindalee Operational Radar Network (JORN)
Laverton, West Australia
-28° 19’ 36.29″, +122° 0’ 18.84″

18- Jindalee Operational Radar Network (JORN)
Longreach, Queensland, Australia
-23° 39’ 29.53″, +144° 8’ 49.58″

19- Australia Naval Communications Station Harold E Holt (NCS HEH)
Exmouth, Western Australia. 21° 48’ 59.47″s, 114° 09’ 55.60″

20- Zhong Shan Antarctic Polar Station (China)
69º 22’ 43.69″ S 76º 23’ 15.07″ E

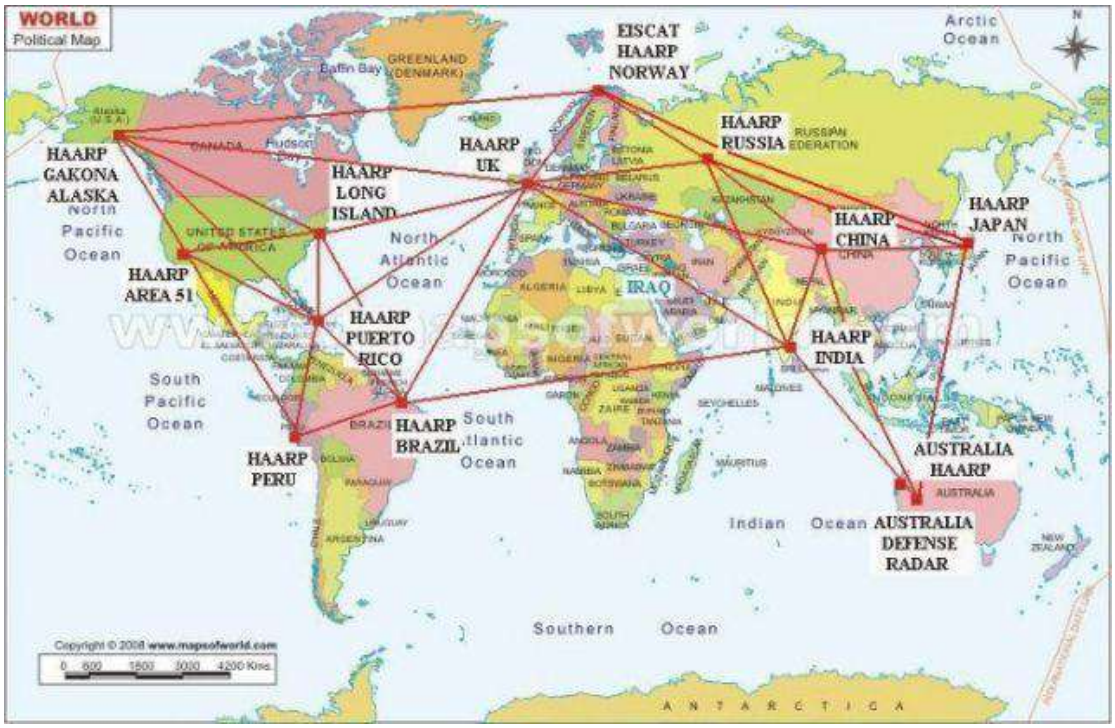
WORLD
Political Map
EISCAT
HAARP
NORWAY
HAARP
RUSSIA
HAARP
UK
HAARP
LONG
ISLAND
HAARP
GAKONA
ALASKA
HAARP
AREA 51
HAARP
PUERTO
RICO
HAARP
BRAZIL
HAARP
PERU
HAARP
CHINA
HAARP
JAPAN
HAARP
INDIA
AUSTRALIA
HAARP
AUSTRALIA
DEFENSE
RADAR
IRAQ
Arctic
Ocean
North
Pacific
Ocean
North
Atlantic
Ocean
South
Pacific
Ocean
South
Atlantic
Ocean
Indian
Ocean
Southern
Ocean
ANTARCTICA
Baffin Bay
GREENLAND
(DENMARK)
CANADA
Hudson
Bay
UNITED STATES
OF AMERICA
RUSSIAN
FEDERATION
CHINA
AUSTRALIA
NEW
ZEALAND
Copyright © 2008 www.mapsofworld.com
0 600 1800 3000 4200 Kms

The Future of the High frequency Active Auroral Research Program (HAARP)

Robert P. McCoy
Geophysical Institute, University of Alaska Fairbanks
903 Koyukuk Drive, P. O. Box 757320
Fairbanks, Alaska 99775

ABSTRACT

The HAARP facility, located in Gakona Alaska, is the world's premier laboratory for active experimentation in the ionosphere and upper atmosphere. Understanding the ionosphere is particularly important because it affects long-distance communication, navigation, and radar applications relying upon radio propagation through this ionized atmospheric region. The primary component of HAARP, the Ionospheric Research Instrument (IRI), is a phased array of 180 HF tower antennas spread across 33 acres and capable of radiating 3.6 MW into the upper atmosphere and ionosphere. The array is fed by five 2500 kW generators, each driven by a 3600 hp diesel engine (4 + 1 spare). Transmit frequencies are selectable in the range 2.8 to 10 MHz. HAARP is owned by the Space Vehicles Directorate of the Air Force Research Laboratory (AFRL/RV) in Albuquerque, NM. In 2013 AFRL/RV decided that they no longer needed the facility, and by prior arrangement, were prepared to remediate the site. In response to a letter writing campaign and petition by the scientific community, the Secretary of the Air Force directed that the demolition be postponed until May, 2015 to allow time for another federal agency, a consortium of academic or research institutions, or the University of Alaska, to build a plan to sustain the facility and preserve its capability to enable fundamental ionospheric research. For the past year the Geophysical Institute of the University of Alaska Fairbanks has been in active negotiations with the Air Force and a sustainment plan for HAARP, using a pay per use model may soon be approved and implemented preserving HAARP for future upper atmospheric investigations.

OVERVIEW

The HAARP facility, located in Gakona Alaska, is the world's premier laboratory for active experimentation in the ionosphere and upper atmosphere. Scientists at HAARP use high frequency (HF) radio transmitters to heat selected regions of the ionosphere and observe the effects. With a facility like HAARP, the ionosphere becomes a laboratory to study a range of physics phenomena. For traditional space research using ground-based observations or experiments on sounding rockets, it can take an extremely long time (days, weeks, years) to get the desired natural overhead conditions. Satellites can amass much larger databases but it is difficult to coordinate the satellite with the desired phenomena. With a facility like HAARP, it is possible to perform an experiment at

Figure 1 Overhead Photo of HAARP Courtesy of M. McCarrick

will to create plasma structures and irregularities; use the ionosphere like an antenna to excite low frequency waves; create weak luminous aurora-like glows; and a variety of other experiments. Ground-based instruments or satellite overflights are used to collect the necessary data for the investigation.

The primary component of HAARP is the Ionospheric Research Instrument (IRI), a phased array of 180 HF tower antennas spread across 33 acres and capable of radiating 3.6 MW into the upper atmosphere and ionosphere. The array is fed by five 2500 kW generators, each driven by a 3600 hp diesel engine (4 + 1 spare). Transmit frequencies can be chosen anywhere in the range 2.8 to 10 MHz and since the antennas are part of an array, the transmitted beam can take many shapes, can be scanned over a wide angular range (down to 30° deg. elevation angle) and multiple beams can be formed and steered. The facility employs 30 transmitter shelters each with six pairs of 10 KW transmitters (6 x 2 x 30 x 10) to achieve the 3.6 MW transmit power.

The facility is located at 62.39° N, 145.15° W in the subarctic which is an ideal location for a wide range of scientific experiments. The location is just south of the auroral region which allows active experiments outside of the aurora. During substorms HAARP's location is under the aurora or inside the auroral oval. The high latitude location is also ideal for experiments generating low frequency waves which propagate along magnetic field lines high into the magnetosphere.

Figure 2 HAARP Antennas Courtesy USRA

Figure 3 HAARP Antennas and Transmitter Shelters Courtesy USRA

Initiated in 1989 with congressional earmarks (~$180M), HAARP was completed around 2009 with additional investments of $110M from the Air Force Research Laboratory (AFRL), the Office of Naval Research (ONR) and Defense Advanced Research Program Agency (DARPA) and represents a total investment of ~$290M. HAARP is currently owned by the AFRL Space Vehicles Directorate (AFRL/RV) in Albuquerque NM.

There are two other ionospheric heaters in the world, EISCAT in Norway and Sura in Russia. The National Science Foundation is currently building a fourth hearter in Arecibo Puerto Rico. HAARP is by far the most powerful and capable heater in the world.

HAARP SCIENCE

A full discussion of the science capabilities, accomplishments and future science potential of HAARP is not practical here but the 2013 National Research Council Workshop Report: ***Opportunities for High-Power, High-Frequency Transmitters to Advance Ionospheric/Thermospheric Research*** (see below) is an excellent resource. As a scientific tool for active experimentation in the ionosphere HAARP has a number of characteristics that make it unsurpassed in the world including:

- Effective radiated power (ERP) = power x antenna gain;
- Steerability of the beam and ability to create multiple beams;
- Frequency range and ability to select frequency;
- Polarization control;
- Modulation control;
- Location – relative to the aurora and on high latitude magnetic field lines;
- Accessibility of the site from either Anchorage or Fairbanks Alaska.

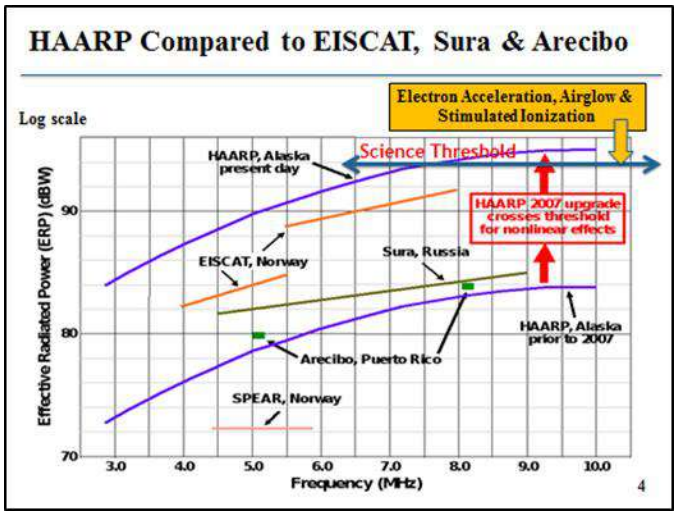

Figure 1 Comparison of Existing Ionospheric Heaters (Kennedy, 1998)

A short summary of HAARP science highlights in a few topic areas includes:

RADIO SCIENCE: Production of artificial plasma layers to study radio frequency propagation at a range of frequencies from a few Hz to a few GHz (including GPS frequencies). Studies include guidance, redirection, enhancement and degradation and loss of signals.

MESOSPHERE-THERMOSPHERE DIAGNOSTICS: Production of artificial periodic irregularities; neutral density and temperature measurements and generation of optical emissions. Upper atmospheric heating has been used to change density, composition, neutral diffusion, thermospheric winds and potentially – drag on orbiting debris or satellites. HAARP can be used in studies of polar mesospheric clouds.

SPACE WEATHER: The use of HAARP to make comparisons quiet ionospheric conditions to substorms and mapping up into the plasmasphere. Use of the facility to study a variety of transient phenomena including subauroral polarization stream (SAPS); subauroral ion drift (SAID), high electron temperature regions and troughs, and ion-outflow-created atmospheric gravity waves.

MAGNETOSPHERE-RADIATION BELTS: This line of investigation primarily involves using the ionosphere in a variety of modes as a "virtual antenna" to inject a variety of waves including whistler waves, shear Alfvén, and magnetosonic waves and waves at frequencies down to a few Hz and study resonance and amplification effects. There are a wide range investigations of wave/particle interactions in the magnetosphere enabled by HAARP (Rietveld et al., 1989; Barr, 1998; Papadopoulos et al., 1990, 2005).

FUTURE SCIENCE POSSIBILITIES

Recent experiments at HAARP (Fallen et al., 2011) demonstrated experimental techniques to continuously generate artificial plasma ducts that extend from the upper ionosphere into the earth's magnetosphere. These plasma structures facilitate the ducting of VLF waves generated artificially either by, HAARP signals interacting with the ionosphere, from other ground based sources, or generated in space. This new discovery is relevant to the efforts to reduce high energy electrons in the radiation belts (see below).

Continued basic science efforts on this topic should reveal how this technique may be optimized for a variety of geophysical conditions. Measurements of duct geometry may then be used in conjunction with numerical models and simulation to estimate levels of VLF power density that may be deposited in the equatorial region of the earth's magnetosphere within the radiation belts. This efficient injection of artificially created VLF waves into the radiation belts acts to scatter and remove high levels of energetic electrons injected from high-altitude nuclear burst.

DOD APPLICATIONS

Interest by the DoD (AFRL, ONR and DARPA) in HAARP is obvious by the $105M they invested to complete and upgrade the facility. Historically, most of the applications of interest stem from the ability of HAARP to generate low frequency waves that propagate both within the Earth – atmosphere waveguide around the globe and which propagate upward along magnetic field lines into the magnetosphere. More recently the focus has been on using HAARP to stimulate artificial glows in the upper atmosphere and creating artificial plasma clouds.

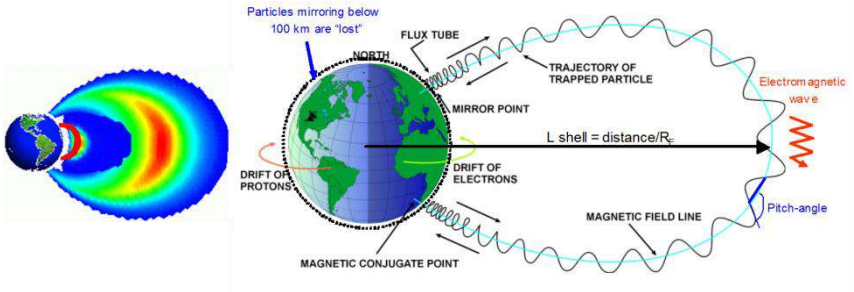

Figure 2 Radiation Belts and Trapped Electrons in Magnetic Flux Tubes

REDUCTION OF ELECTRONS IN THE SPACE RADIATION BELTS: The highest priority application for HAARP and the one stimulating most of the investment involves using low frequency waves to cause high energy million-electron-volt "killer" electrons in the magnetosphere to precipitate out. The Earth's natural radiation belts contain high energy electrons trapped in magnetic bottles (flux tubes) and propagating for extended periods from pole to pole spiraling along magnetic field lines. The density of these trapped particles can go up dramatically from a solar coronal mass ejection (SME) or from a manmade event like a high altitude nuclear burst. A 1000 fold electron density increase can easily be obtained from the latter and these electrons can persist for months or years in the radiation belts. These killer electrons can damage and destroy electronics in low Earth orbiting satellites and there is an estimated $100B of non-DoD satellites at risk.

Experiments with HAARP and other radio frequency transmitters have shown that a variety of low frequency waves can be generated in the ionosphere which propagate along magnetic field lines to interact with these trapped electrons. Wave-particle interaction occur which modify the angle between the trapped electron and the magnetic field line, the pitch angle. On subsequent reflections near either pole these electrons penetrate deeper into the upper atmosphere colliding

with neutral atoms and molecules and are lost. This process reduces the density of electrons trapped in the radiation belts.

There have been a number of HAARP investigations on this topic sponsored by several agencies. Based on results observations and models, AFRL/RV built the DSX satellite to investigate the effect of emitting low frequency waves directly in space and will soon launch this vehicle soon to test the effect. Neither HAARP nor DSX provide a comprehensive solution for this problem but both provide valuable insights into the science of wave-particle interactions on the radiation belts.

SUBMARINE COMMUNICATION: The Navy's interest in HAARP was frequently related to using the ionosphere as a large antenna to excite extremely long wavelength (ELF) waves to propagate long distances and penetrate the oceans to communicate with submarines.

DETECTION OF CAVITIES IN THE EARTH: The same ELF waves that penetrate the oceans can also penetrate into the Earth's lithosphere and experiments with HAARP have been used to detect cavities; mines and caves underground.

OVER THE HORIZON RADAR: The current HAARP site was originally an over the horizon (OTH) radar site. OTH radar depends on reflecting HF waves off the ionosphere. Solar and geomagnetic activity produce problems for HF radar propagation in the Arctic. Auroral activity creates irregularities and bubbles in the ionosphere causing scintillation and loss of HF signals. Recent HAARP experiments (Pedersen et al., 2010) demonstrate the ability to create sustainable artificial plasma clouds or plasma balls at altitudes below the natural ionosphere which may be useable as an artificial mirror to reflect HF radar and other RF communication signals.

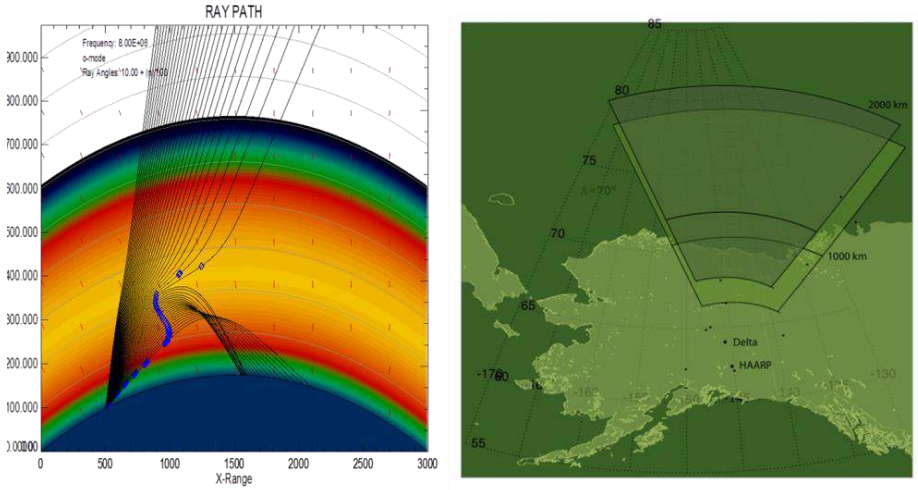

Figure 3 Ionospheric propagation of 8MHz rays and potential OTH footprint from HAARP
Courtesy of Bill Bristow

As the sea ice in the Arctic continues to melt opening up polar navigation routes, there is increasing interest by the US Northern Command and NORAD in the possibility of deploying a system of OTH radars across North America for increased Arctic maritime domain awareness. HAARP may play an important role as an OTH test bed and demonstration platform for this new capability.

TRANSIONOSPHERIC RF PROPAGATION: As HAARP heats the ionosphere it can create bubbles and irregularities. These irregularities can then interfere with a wide range of space to ground RF propagation at frequencies up to 10 GHz. A facility like HAARP could be used to cause interference with communication signals, GPS navigation or blur space-based synthetic aperture radar.

LASER FUSION APPLICATIONS: Another application of an ionospheric heater is to use the natural ionosphere to perform nonlinear plasma experiments in unbounded plasma. The power levels of HAARP are small compared to those in fusion experiments but the lack of walls in the ionosphere, combined with HAARP's tunability and phase array transmissions allow a wide range of experimentation in parametric instabilities and nonlinear plasma physics.

THERMOSPHERIC HEATING EXPERIMENTS: Through coupling between the ionosphere and thermosphere it is possible to heat the neutral atmosphere above HAARP. This heating can be used to create density plumes and drive neutral waves over HAARP to test applications to increase drag on selected orbiting satellites or orbital debris.

HAARP GROUND-BASED DIAGNOSTICS

The IRI at HAARP creates the effects in the ionosphere but it is the diagnostic ground-based instruments which allow scientific investigations. The state of the diagnostic instruments at HAARP is in flux and many of the sensors have been temporarily removed. Most of the sensors are slated to be returned and restored to service during the spring/summer 2015. The discussion that follows lists the instruments that were traditionally resident at HAARP and used to support science and may represent the set of diagnostics later in 2015.

The primary diagnostic tool at HAARP is the digisonde. This instrument, basically a swept frequency HF radar, measures the bottom side of the electron layer in the ionosphere. Additional sensors at the facility include:

- All-sky Riometer
- Imaging Riometer (8 X 8 Array)
- Fluxgate Magnetometer
- Induction Magnetometer
- Optics
  - All-sky imager
  - Telescopic imager
  - Photometers
  - 14 ft Optical Dome
- Tomography Chain (Cordova -> Kaktovik)
- VHF Radar (139 MHz)
- MUIR (Modular UHF Ionospheric Radar
- Ionospheric Scintillation Receivers
  - SATSIN (offsite)
  - GPS-NOVATEL
  - Total Electron Content
- HF 2-30 MHz High Angle Receiving Antenna
- Scanning Doppler Interferometer (SDI)

Figure 4 HAARP Optics Facility

Figure 5 MUIR Radar

- Radio Background Receivers
  - Broadband ELF / VLF Receiver network.
  - SEE Receiver string.
  - HF to UHF Spectrum Monitor

Figure 6 HF High Angle Receive Array

NATIONAL ACADEMY OF SCIENCE INPUT

The National Research Council (NRC), the operating arm of the National Academy of Sciences has taken up the issue of HAARP twice over the past two years. In 2013 the NRC completed a Decadal Survey in Solar and Space Physics. One of the priority recommendations of that study included:

> **Priority** - ***Fully realize the potential of ionospheric modification techniques through collocation of modern heating facilities with a full complement of diagnostic instruments including incoherent scatter radars. This effort requires coordination between NSF and DOD agencies in planning and operation of existing and future ionospheric modification facilities.***

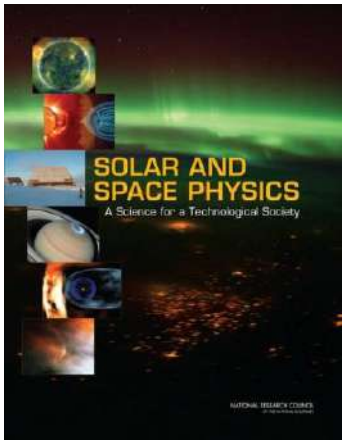

Figure 7 2013 Space Physics Decadal Study

In March 2013 in response to a request by AFRL and NSF the NRC conducted a workshop entitled: **Opportunities for High-Power, High-Frequency Transmitters to Advance Ionospheric/Thermospheric Research** focused primarily on HAARP. Topics addressed in that three day workshop included:

- Geospace and space weather;
- Stimulated emission and radiation belts;
- Radio science; and
- Communications.

NRC Workshops do not produce recommendations, but the NRC published a report containing 72 pages by 40+ scientists documenting past science results from HAARP and a wealth of prospects for future science from the facility.

The report reiterated the importance of co-locating an incoherent scatter radar to HAARP to maximize the science potential of the facility. The NRC report can be obtained at:

http://www.nap.edu/booksearch.php?booksearch=1&term=sale&record_id=18620

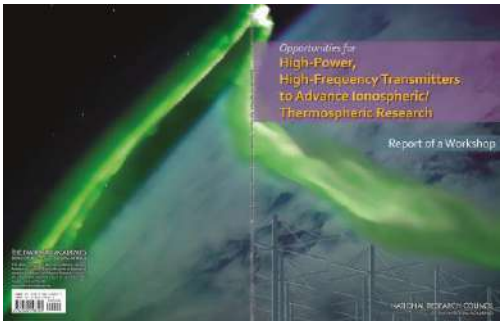

Figure 8 2013 NRC Workshop Report

NEED FOR AN INCOHERENT SCATTER RADAR

A diagnostic instrument noticeably missing from HAARP is an incoherent scatter radar (ISR). An ISR is one of the most powerful tools for studying the ionosphere from the ground. An ISR can routinely measure vertical profiles of electron density, electron and ion temperatures, bulk ion motion, ion masses, ion-neutral collision frequencies. Over the years there have been several plans to build an ISR at HAARP but because of funding variability for the facility it was never completed. There have been several studies, workshops and panels which made recommendations to install an ISR at HAARP, most notably the two NRC studies mentioned above but also a DoD sponsored panel in 2001 entitled HAARP "Future Directions" but usually called the "Tether Panel" after the chairman Dr. Tony Tether.

The NSF owns and operates a chain of ISRs from near the north magnetic pole to the magnetic equator at such sites as: Resolute Bay Canada; Sondrestrom Greenland; Millstone Hill Massachusetts; Arecibo Puerto Rico and Jicamarca Peru. Additionally, they own one more outside of that chain at Poker Flat Alaska about 300 miles north of HAARP. Older ISRs have a conventional radiating transmitter and dish reflector design, but two of the newer ISRs in Canada and Alaska are built with phased array transmitters and are far more flexible and capable. Both of these ISRs are called Advanced Modular Incoherent Scatter Radar (AMISR) and for distinction the Resolute Bay is commonly referred to as RISR and the Alaskan ISR is called the PFISR.

Figure 9 PFISR Incoherent Scatter Radar

The NSF PFISR is located on the property of the University of Alaska owned Poker Flat Research Range (PFRR) which is used by NASA to launch sounding rockets to study space physics in the arctic. The PFISR is employed for routine and campaign ionospheric science and frequently supports NASA sounding rocket launches. The radar consists of 128 identical panels which constitute the phased array. The MUIR radar at HAARP (Figure 9) is built with the same technology but with only 16 panels. That radar has some capability to sound the ionosphere but it does not have ISR capability. Expanding the MUIR to a total of 96 panels should give it ISR capability. There have been discussions of temporarily relocating PFISR to HAARP for a year, or two, to test out the heater/ISR combination to enable space research. Other options which have been discussed include reducing PFISR to 96 panels by transferring panels to HAARP and expanding the (adding panels) to the MURI array with a potential of ending up with two ISRs in Alaska.

EDUCATIONAL OPPORTUNITIES AT HAARP

With sponsorship from NSF and AFRL HAARP has provided numerous opportunities for graduate and undergraduate research projects and there are several ionospheric scientists working in the field who got degree in heater science with experiments at HAARP. For several years NSF and AFRL sponsored the Polar Aeronomy and Radio Science (PARS) summer school which gave undergraduates and graduate students opportunities to work with their advisors to perform science experiments at HAARP. This summer school also included tours and classes at the Geophysical Institute at the University of Alaska Fairbanks (UAF-GI) and tours of PFRR.

RECENT DEVELOPMENTS WITH HAARP

In 2012, anticipating budget cuts, AFRL/RV contacted the University Space Research Associates (USRA) and the UAF-GI to see if we could help them find a way to lower operating costs and/or divest themselves of management/operation of HAARP. USRA and UAF-GI formed a team and submitted a proposal to operate HAARP under an extended use lease arrangement which was not funded.

In 2013, after the release of the NRC workshop report and after a workshop sponsored by the Office of Science Technology Policy (OSTP), the UAF-GI proposed the creation of a Federal Facility Partnership for HAARP spreading the operating costs across five federal agencies (AFRL, ONR, DARPA, NSF and DOE), selling each a two-week campaign with an operating cost similar to what EISCAT charges customers. That proposal was not successful.

In July 2013, in response to a letter writing campaign by the scientific community; letters of support from leadership of the American Meteorological Society (AMS) and the Space Physics and Aeronomy Section of the American Geophysical Union (AGU/SPA); and a letter from U. S. Senator Lisa Murkowski; Air Force Secretary Deborah Lee James decided to postpone decommissioning plans for HAARP which had been scheduled for June 2014. She allowed time (May, 2015) for the "University of Alaska or a consortium of academic or research institutions" to develop a plan to take ownership of HAARP for the purpose of keeping the facility open covering operating costs from the user base.

In June 2014, DARPA completed a phase of the Basic Research on Ionospheric Characteristics and Effects (BRIOCHE) campaign and soon after the facility was placed in cold-storage. Transmitter tubes were removed from the transmitter shelters and moved into the heated main building to minimize heating costs for the winter. The diesel generators were winterized and many of the diagnostics were transported to AFRL at Kirtland AFB.

Since then negotiations have progressed well and the UAF-GI is working with AFRL/RV on a cooperative research and development agreement (CRADA) to transition ownership of the facility to the University of Alaska to allow the UAF-GI to bring it back on line for continued ionospheric, thermospheric and magnetospheric research. Current projections are that the UAF-GI will take ownership in the fall of 2015. Plans are being finalized to return the diagnostics to HAARP in the spring 2015. The UAF-GI is working to develop a plan to reduce the operating costs of the facility and is actively seeking customers, both domestically and internationally, to come to HAARP to do active experiments at the world's premier upper atmospheric active research facility.

REFERENCES

Barr, R. 1998. The generation of ELF and VLF radio waves in the ionosphere using powerful HF transmitters. Advances in Space Research 21:677-687, doi =10.1016/S0273-1177(97)01003-X.

Fallen, C. T., J. A. Secan, and B. J. Watkins. 2011. In-situ measurements of topside ionosphere electron density enhancements during an HF-modification experiment, Geophys. Res. Lett., VOL. 38, L08101, doi:10.1029/2011GL046887.

This is Google's cache of http://lucianarchy.proboards.com/index.cgi?board=zorgon&action=print&thread=8872. It is a snapshot of the page as it appeared on 18 Apr 2011 10:28:22 GMT. The current page could have changed in the meantime. Learn more

These search terms are highlighted: **vlf haarp** These terms only appear in links pointing to this page: **thompson manitoba**

'Special Guest' Boards » The Zorgon Zone, with Special Guest Ron Schmidt » **Every One Speaks about HAARP, but did you know...**
http://lucianarchy.proboards.com/index.cgi?board=zorgon&action=display&thread=8872

Every One Speaks about HAARP, but did you know...
Post by zorgon on Sept 21, 2010, 6:46pm

Every One Speaks about **HAARP**...

It gets blames for everything, it has magical abilities etc...

While it is true that it does indeed have some interesting abilities, there are many threads and documents on **HAARP**. I have been collecting material for years BUT, though its been hinted at from time to time that other countries also have a version of **HAARP** and that incoherent scatter sites have a similar function as **HAARP** and EISCAT has been mentioned...

Very few people have taken the time to follow the leads in the various documents and threads and put together the GLOBAL NETWORK

While **HAARP** itself may not have the power to create a planetary shield (for missile defense and solar radiation) the world wide network certainly does.

So for this thread I will leave the much discussed Alaskan **HAARP** in the side lines for now and lets do a tour of the other facilities around the world.

First a little bit on connections to other facilities. In reports like the NAVY Press Release of Dr Paul A. Bernhard... we see some terms already...

Dr. Bernhardt used the high-power HF facility near Arecibo, Puerto Rico, and Nizhny Novgorod, Russia, from 1985 to 1999...

Dr. Bernhardt has conducted over eight experiments from 1985 to the present, using the Space Shuttle Orbital Maneuver Subsystem (OMS) engines, to modify the ionosphere with high-speed exhaust injections into the upper atmosphere. The results of these dedicated engine burns have been recorded using the VHF and UHF radars at Arecibo, Puerto Rico; Kwajalein, Marshall Islands; Millstone Hill, Massachusetts; and Jicamarca, Peru. Currently, Dr. Bernhardt is the principal investigator for the Charged Aerosol Release Experiment (CARE) program, designed to study the scattering of radar from electrons in the vicinity of charged particulates that form artificial "dusty plasmas."

...Coherent Electromagnetic Radio Tomography (CERTO)
...Computerized Ionospheric Tomography Receiver in Space (CITRIS)

http://www.nrl.navy.mil/pao/pressRelease.php?Y=2006&R=17-06r

So from this single press release we have three search terms. Just ignore the facts about the chemical releases and the shuttle spewing fumes, we already have a thread on that)

...Incoherent Scatter Radar (ISR) (Like EISCAT for European Incoherent Scatter Radar)
...Coherent Electromagnetic Radio Tomography (CERTO)
...Computerized Ionospheric Tomography Receiver in Space (CITRIS)

and these locations mentioned directly

Arecibo, Puerto Rico
Nizhny Novgorod, Russia
Kwajalein, Marshall Islands
Millstone Hill, Massachusetts
Jicamarca, Peru

From our research collected at Pegasus we can add these...

HIPAS - High Power Auroral Stimulation Observatory
IRIS - Imaging Riometer for Ionospheric Studies

The problem is I have gathered so much material on these sites and still have more to do... that it may get lost in a single thread...

So lets start with the best **HAARP** like arrays and Incoherent Scatter facilities.

Now this will take me a while to pull up all my pages so I won't be answering any posts for a while

continued...

Re: Every One Speaks about HAARP, but did you know
Post by zorgon on Sept 21, 2010, 6:50pm

Sura Facility

HAARP Like Facility
Nizhniy Novgorod, Russia
+56° 7' 9.70", +46° 2' 3.66"

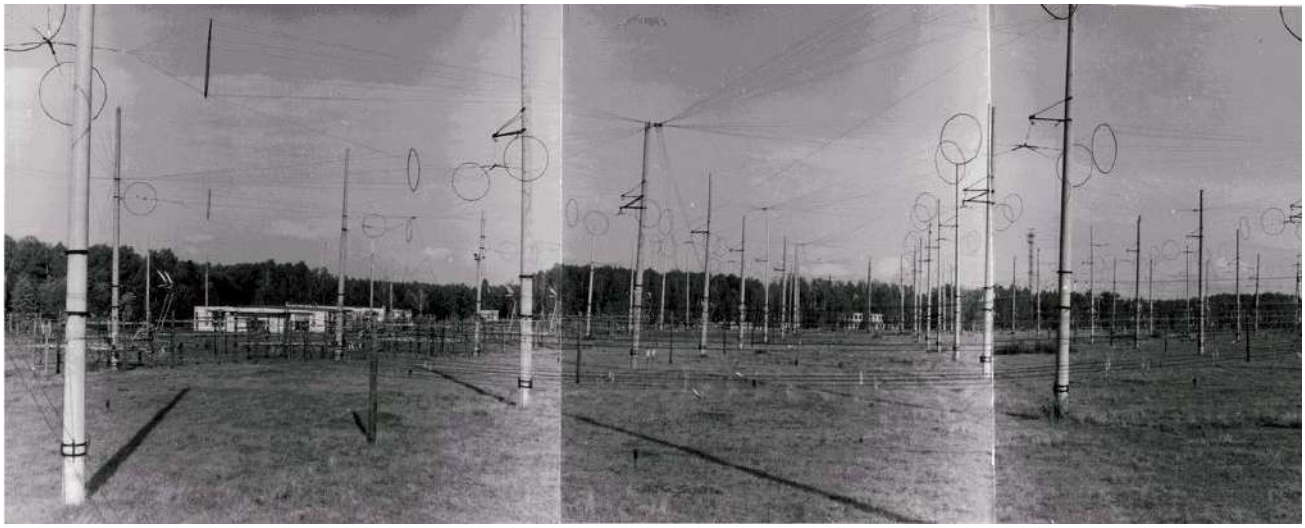

courtesy http://sura.nirfi.sci-nnov.ru/Photogalery/Photogalery.html

SURA Official Site Russian

The Sura Ionospheric Heating Facility, located near the small town of Vasilsursk about 100 km eastward from Nizhniy Novgorod in Russia, is a laboratory for ionosphere research. Sura is capable of radiating about 190 MW, effective radiated power (ERP) on short waves. This facility is operated by the radiophysical research institute NIRFI in Nizhny Novgorod. The Sura facility was commissioned in 1981. Using this facility, Russian researchers achieved extremely interesting results regarding the ionosphere behavior and discovered the effect of generation of low-frequency emission at the modulation of ionosphere current[1]. At the beginning, Soviet Defense Department mostly footed the bill. The American **HAARP** ionospheric heater is similar to the Sura facility. The **HAARP** project began in 1993.

Technical information

The frequency range of the heating facility is from 4.5 to 9.3 MHz. The facility consists of three 250 kW broadcasting transmitters and a 144 crossed dipole antenna-array with dimensions of 300 m x 300 m. At the middle of the operating frequency range (4.5 – 9.3 MHz) a maximum zenith gain of about 260 (~24 dB) is reached, the ERP of the facility is 190 MW (~83 dbW).

http://en.wikipedia.org/wiki/Sura_Ionospheric_Heating_Facility

http://www.thelivingmoon.com/45jack_files/03files/SURA_Radar_Facility.html

Artificial Ionospheric Turbulence and Radio Wave Propagation (Sura/**HAARP**)

PDF File

Russian US cooperation

In March and May 2006 two
sessions of measurements in the framework of the SURA–**HAARP** experiment were carried out.

Re: Every One Speaks about HAARP, but did you know
Post by zorgon on Sept 21, 2010, 6:52pm

São Luiz Space Observatory

HAARP Like Facility
Cruzeiro Santa Bárbara, Sao Luis-MA, Brasil
-2° 35' 40.47", -44° 12' 35.90"

Coherent Back-Scatter Radar 50 MHz (RESCO)

The Coherent Back-Scatter Radar of 50 MHz (RESCO) was installed at the Space Observatory of São Luís / INPE, whose operation begun in August of 1998, is capable to accomplish measures of dynamics of the plasma of the electrojet and of bubbles equatorial ionospheric. This radar was projected to map the turbulence and the electromagnetic drift of the irregularities of short length scale (3 meters) in a height range that extends from ~90 km to ~1000 km of the equatorial ionosphere. Such plasma irregularities have big influence in the propagation trans-ionosphere of waves in a great frequency range, VHF to UHF, and, therefore, it influence all of the activities of space communications of the Brazilian tropical area. The formation, the development and the space distribution of these irregularities are highly sensitive to the space climatic change (in other words, "Space Weather") besides the convection processes and of the storms of the troposphere.

This radar resulted of the development and construction begun in INPE there are several years. It transmits signs pulse of high potency through an network antenna with 768 dipoles which allow to concentrate all the energy transmitted in only narrow beam radiation. The same antenna also captures the echo signs spread by the irregularities ionosphere. The transmitted maximum power (120 kW) it is reached through the use of a modular system of 8 transmitters in phase to maximize the transmitted energy. The operational control of the radar is made by a computer, which also accomplishes the acquisition, the treatment and processing 'on line' of the received data of the ionosphere. The data recorded are available also for the processing and analyze subsequent. This radar was already operated in several campaigns since 1998 and now it is collecting in a routine way data of the dynamics of the equatorial electrojet.

This radar, with the FCI radar of 30 MHz together offers great opportunities to the researchers of studying the peculiar phenomenon of the equatorial area. These, beside the radars of Peru (Jicamarca), of the India (Thumba) and of the Indonesia, are some of the few radars of this type that exist in the world around of the magnetic equator. Due to the peculiar configuration of the geomagnetic field, the Brazilian equatorial area have characteristics very different from the other areas. It was for this reason that NASA of the USA, in collaboration of INPE, accomplished in Alcântara in 1994 the campaign GUARÁ when 26 rockets were thrown (in the period of September-October) to study the equatorial electrojet and the bubbles ionosphere. In this campaign were used another radar similar to the radar RESCO (which was brought of the USA), Digissonde (which provided the diagnoses of the ionosphere) and of the magnetometers operated by INPE in the Space Observatory of São Luís. The radar RESCO, that is now in a phase of technological improvement, offers great potential to promote researches of the environment of the Brazilian equatorial area.

Rua Horto Florestal, 100, Cruzeiro Santa Bárbara, Sao Luis-MA - Brasil

SOURCE: São Luiz Space Observatory
http://www.dae.inpe.br/slz/english/resco.html

http://www.thelivingmoon.com/45jack_file....bservatory.html

Re: Every One Speaks about HAARP, but did you know
Post by zorgon on Sept 21, 2010, 6:54pm

Millstone Hill Radio Observatory

EISCAT Like Facility
Westford, Massachusetts
+42° 37' 09.25", -71° 29' 28.49"

Millstone Hill

Millstone Hill, Westford, Massachusetts, USA (Longitude: W Latitude: N)

The Millstone Hill Steerable Antenna, or MISA, is a fully steerable dish antenna, 46 meters in diameter, designed by the Stanford Research Institute (SRI) in 1959. It is currently located at MIT Haystack Observatory in Westford, Massachusetts. It was originally installed at the Sagamore Hill Radio Observatory in Hamilton, Massachusetts in 1963. The antenna operated at that location until 1978, at which time it was relocated to Millstone Hill. Since that time it has been primarily used as a UHF radar antenna to provide measurements of the near space environment using the incoherent scatter radar technique. It is one of two surviving dish antennas of this type in the world with the other antenna being located at the Stanford University radio science field site in Stanford, California. MISA is used to provide wide radar coverage in latitude and longitude.

MISA is a broad-based observatory capable of addressing a wide range of atmospheric science investigations. The incoherent scatter radar facility at Millstone Hill has been supported by the National Science Foundation since 1974 for studies of the earth's upper atmosphere and ionosphere. During this time the facility has evolved from a part-time research operation sharing radar cooling and power supply elements with the M.I.T. Lincoln Laboratory Millstone satellite tracking radar, to a separately funded, operationally independent system dedicated to upper atmospheric research. The scientific capability of the Millstone Hill facility was greatly expanded in 1978 with the installation of a fully-steerable 46 meter antenna to complement the 67 meter fixed zenith pointing dish.

The favorable location of Millstone Hill at sub-auroral latitudes combined with the great operational range afforded by the steerable antenna permit observations over a latitude span encompassing the region between the polar cap and the near-equatorial ionosphere. Since 1982 the Haystack Observatory Atmospheric Sciences Group has been supported for operating the Millstone Hill research radar as a part of the incoherent scatter radar chain and for associated studies of the auroral and sub-auroral ionosphere and thermosphere. The meridional radar chain extends from Sondre Stromfjord, Greenland through Millstone Hill at mid-latitudes, beyond Arecibo at low latitudes, to the Jicamarca facility at the magnetic equator in Peru. The radar chain forms an integral part of the NSF-supported CEDAR (Coupling, Energetics, and Dynamics of Atmospheric Regions) observing network and Millstone Hill observations and analysis have contributed extensively to the successes of the CEDAR initiative.

The Millstone Hill Radar uses Thomson backscatter from ionospheric electrons to deduce height- and time-resolved plasma drift velocities, electron and ion temperatures, electron densities, ion composition, and ion-neutral collision frequencies. These parameters provide further information about the neutral gas, neutral temperatures and winds, and electric fields present in the medium. The incoherent scatter technique provides observations of many of these parameters over an altitude range extending from less than 100 km to a thousand kilometers or more. Methods have been developed that allow these measurements to be made with an altitude resolution of hundreds of meters. The complete steerability of the radar allows horizontal gradients and structure to be examined along with vertical variations.

The Observatory is the premier scientific facility in the world for studying the equatorial ionosphere. It has a 2-MW transmitter and a main antenna with 18,432 dipoles covering an area of nearly 85,000 square meters.

SOURCE: Wikipedia Millstone Hill
http://en.wikipedia.org/wiki/Millstone_Hill

Related Links:
MIT Haystack Observatory
http://www.haystack.mit.edu/

Credit: Haystack Observatory

http://www.thelivingmoon.com/45jack_file...bservatory.html

Re: Every One Speaks about HAARP, but did you know
Post by zorgon on Sept 21, 2010, 6:56pm

The first American '**HAARP**'

Platteville Atmospheric Observatory

HAARP Like Facility
+40° 10' 54", -104° 43' 30"

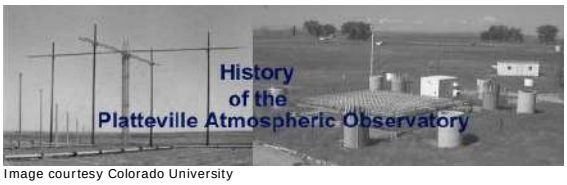

Image courtesy Colorado University

The Platteville Atmospheric Observatory was envisioned in 1962 by what is now the Institute of Telecommunication Sciences (ITS), a part of the National Telecommunications and Information Administration (NTIA), as a site for high-powered radio experiments. While the initial experiment, that took place in 1968, studied over-the-horizon radar, the majority of later experiments used high power radio waves to modify the ionosphere in a process that is sometimes called ionospheric heating because it raises the electron temperature in the ionosphere.

The ionospheric heater was still used until 1984, when the last ionospheric experiments were performed. In the same year, the transmitters were loaned to the Office of Naval Research and sent to HIPAS in Alaska where they are still used.

With the removal of the transmitters, the focus of the facility changed to smaller-powered observation of the atmosphere rather than modifying it. In 1988 the 404 MHz RASS was installed and the ownership of the facility was transferred from NTIA to NOAA-ERL.

SOURCE: Platteville Atmospheric Observatory
http://grison.colorado.edu/Radar_Stations/Platteville/Platteville.html

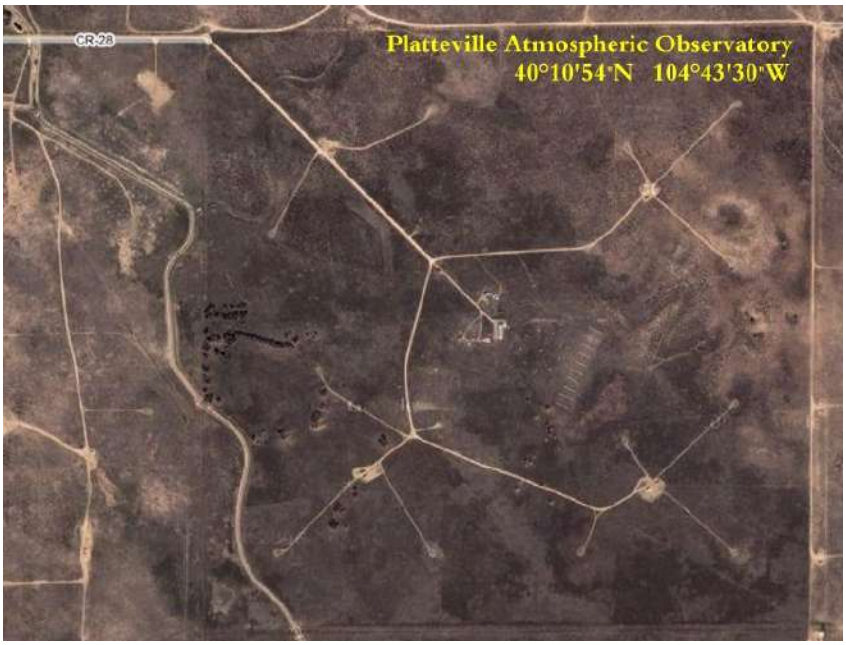

http://www.thelivingmoon.com/45jack_file....bservatory.html

Re: Every One Speaks about HAARP, but did you know
Post by zorgon on Sept 21, 2010, 6:58pm

High Power Auroral Stimulation Observatory

HIPAS
Fairbanks Alaska
64° 52' 19" N 146° 50' 33" W

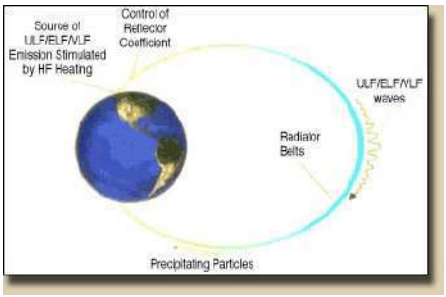

HIPAS is located 30 miles Northeast of Fairbanks Alaska; in the small community of Two Rivers. It occupies 120 acres of land and has six buildings. The facility is located at: latitude and longitude. The facility operates year-round.

The HIPAS facility is engaged in the study of the Ionosphere through the use of high power radio transmission as well as a state-of-the-art LIDAR (LIght Detection And Ranging) facility.

The Heater system consists of 8 transmitters capable of conducting amplitude modulation of 100 Hz - 20 kHz and phase modulation of 0 -20 kHz. Each transmitter can transmit up to 150kW at 2.85 or 4.53 MHz on CW mode.

The Heater antenna system consists of a circular array of 8 crossed dipoles, copper wire ground-planes and resonant triaxial baluns.

The LIDAR facility consists of a 2.7 meter LMT (Liquid Mirror Telescope) with a 4.5 meter focal length as well as 6 state-of-the-art lasers.

SOURCE: HIPAS Home Page
http://www.hipas.alaska.edu/hipasweb/hipas.htm
Link invalid... Internet Archive Page
http://web.archive.org/web/20080212193205/http://www.hipas.alaska.edu/hipasweb/hipas.htm

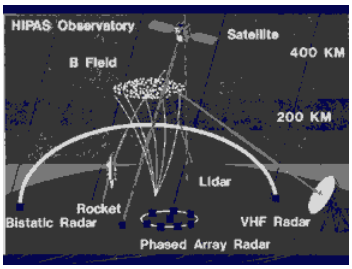

Courtesy HIPAS

http://www.thelivingmoon.com/45jack_file...bservatory.html

Re: Every One Speaks about HAARP, but did you know
Post by zorgon on Sept 21, 2010, 6:59pm

European Incoherent Scatter Scientific Association
EISCAT
Ramfjordmoen, Near Tromsø, Norway
+69° 35' 10.94", +19° 13' 20.89"

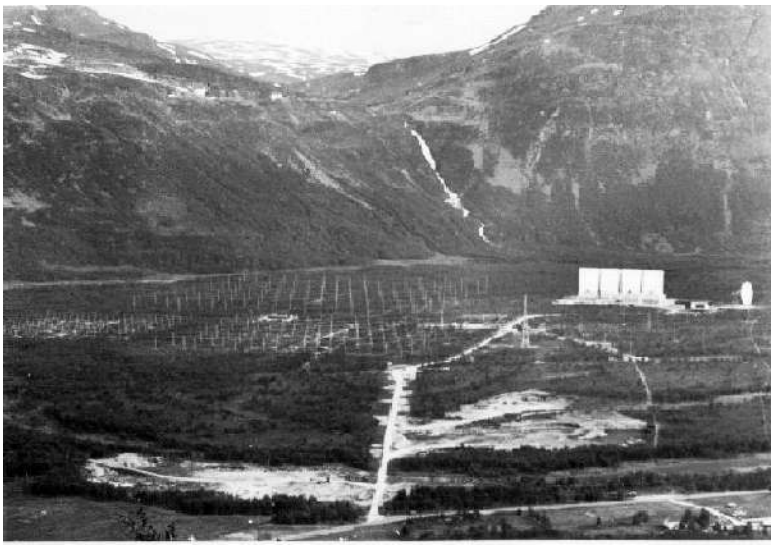

The EISCAT Scientific Association is an international research organisation operating three incoherent scatter radar systems, at 931 MHz, 224 MHz and 500 MHz, in Northern Scandinavia. It is funded and operated by the research councils of Norway, Sweden, Finland, Japan, France, the United Kingdom and Germany (collectively, the EISCAT Associates).

EISCAT (European Incoherent Scattter) studies the interaction between the Sun and the Earth as revealed by disturbances in the magnetosphere and the ionised parts of the atmosphere (these interactions also give rise to the spectacular aurora, or Northern Lights). The radars are operated in both Common and Special Programme modes, depending on the particular research objective, and Special Programme time is accounted and distributed between the Associates according to rules which are published from time to time.

One EISCAT transmitter site is located close to the city of Tromsø, in Norway, and additional receiver stations are located in Sodankylä, Finland, and Kiruna, Sweden. See an animation that shows the basic operation. The EISCAT Headquarters are also located in Kiruna. 1996 the EISCAT Scientific Association constructed a second incoherent scatter radar facility, the EISCAT Svalbard Radar, near Longyearbyen on the island of Spitsbergen, far to the North of the Norwegian mainland.

The Incoherent Scatter Radar technique requires sophisticated technology and EISCAT engineers are constantly involved in upgrading the systems.

In addition to the incoherent scatter radars, EISCAT also operates an Ionospheric Heater facility at Ramfjordmoen (including a Dynasonde) to support various active plasma physics experiments in the high latitude ionosphere.

SOURCE ARTICLE
http://www.eiscat.se:8080/about.html

Tromsø 931 MHz Ultra High Frequency Radar [facts]
These signals are also received at Kiruna and Sodankylä

Tromsø 224 MHz Very High Frequency Radar [facts]
We have also a heating facility and a Dynasonde

http://www.thelivingmoon.com/45jack_file....mso_Norway.html

Re: Every One Speaks about HAARP, but did you know
Post by zorgon on Sept 21, 2010, 7:01pm

Nerc MST Radar Facility

NMRF
HAARP Like Facility
+52° 25' 28.26", -4° 00' 19.59"
Capel Dewi, Carmarthenshire, Wales, United Kingdom
near Aberystwyth, Wales, UK

This one is different but included anyway

The Natural Environment Research Council (NERC) Mesosphere-Stratosphere-Troposphere (MST) Radar at Aberystwyth

SOURCE: NERC
http://mst.nerc.ac.uk/index.html

http://www.thelivingmoon.com/45jack_files/03files/NERC_MST_Radar_Facility.html

---

Re: Every One Speaks about HAARP, but did you know
Post by zorgon on Sept 21, 2010, 7:03pm

National MST Radar Facility

NMRF
HAARP Like Facility
+13° 27' 26.68", +79° 10' 30.74"
Gadanki, near Tirupati, in southern Andra Pradesh, India

I found this one on Google Earth so Pegasus has first find on that one

Visiting the National MST Radar Facility in Gadanki, near Tirupati, in southern Andra Pradesh, India

ABOUT NATIONAL MST RADAR FACILITY

Indian scientists have carried out pioneering research work in the fields of astronomy and astrophysics, solar/interplanetary medium, earth's upper atmosphere/ionosphere, aeronomy/middle atmosphere and weather/climate phenomena. The nationally coordinated Indian Middle Atmosphere Programme (IMAP) was implemented during the period 1982-89 with well focussed campaign experiments with ground based, balloon, rocket and satellite based techniques. The IMAP programme led to the decision to conduct in-depth studies of atmosphericdynamical phenomena by developing a versatile ground based radar technique...

...The MST Radar is a state of the art instrument capable of providing estimates of atmospheric parameters with very high resolution on a continuous basis which are essential in the study of different dynamical processes in the atmosphere. It is an important research tool in the investigation of prevailing winds, waves (including gravity waves) turbulence, and atmospheric stability & other mesoscale phenomena . A reliable three dimensional model of the atmosphere over the low latitudes improves our understanding of the climatic and weather variations...

Establishment of NMRF

Attaching great importance to the scientific utilisation of the Indian MST Radar, the Government of India decided to create an autonomous Scientific Society called the National MST Radar Facility (NMRF). This society is affliated to the Department Of Space. The NMRF was registered on January 11, 1993 under the Indian Societies Act 1860.
This society is administered by a Governing Council under the chairmanship of Dr. K. Kasturirangan, Secretary DOS with, Director , NMRF as the member secretary . The present Director of NMRF is Prof D. Narayan Rao .The Governing Council consists of other eminent scientists, representatives of the National Laboratories and some of the funding agencies.The Governing Council sets broad policy guidelines to ensure the effective scientific utilisation of the facility, supported by a Scientific Advisory Commitee & a Finance Commitee.

Location Of NMRF

The scientific requirements dictated that the Indian MST Radar should be located preferably below 15 degrees North latitude. Hence after careful consideration of the various constraints, a site at Gadanki Village, near the temple town of Tirupati in the Chitoor district of Andhra Pradesh was selected for locating the Indian MST Radar . NMRF is located off the Chitoor -Tirupati main road in a picturesque landscape spreading over an area of about 42 acres. Regular train and bus services are operated between Tirupati and Bangalore/Madras. On request NMRF may provide transport between Tirupati and Gadanki.

SOURCE: The National MST Radar Facility (NMRF)
http://www.isro.org/nmrf/default.htm

http://www.thelivingmoon.com/45jack_file...r_Facility.html

Cherenkov Radiation around Antennas

Image courtesy ISRO

Re: Every One Speaks about HAARP, but did you know
Post by zorgon on Sept 21, 2010, 7:05pm

Jicamarca Radio Observatory

HAARP Like Facility
Lima, Peru
11° 57' 04.82" S 78° 52' 27.43" W

Image courtesy Colorado University

Introduction

The Jicamarca Radio Observatory is the equatorial anchor of the Western Hemisphere chain of incoherent scatter radar (ISR) observatories extending from Lima, Perú, to Søndre Strømfjord, Greenland. It is part of the Geophysical Institute of Peru (Instituto Geofísico del Perú, or IGP) and receives the majority of its financial support from the National Science Foundation of the U.S. through a Cooperative Agreement with Cornell University.

The Observatory is the premier scientific facility in the world for studying the equatorial ionosphere. It has a 2-MW transmitter and a main antenna with 18,432 dipoles covering an area of nearly 85,000 square meters.

SOURCE: Jicamarca Radio Observatory
http://jicamarca.ece.cornell.edu/overview.html

Piura facility: Jicamarca Radio Observatory

The Observatory is about a half-hour drive inland (east) from Lima, Peru at a geographic latitude of 11.95° south and a longitude of 76.87° west. The altitude of the Observatory is about 500 m ASL.

It is about 10 km from the Carretera Central, the main highway east in Peru.

The Jicamarca Radio Observatory was built in 1960-61 by the Central Radio Propagation Laboratory (CRPL) of the National Bureau of Standards (NBS).

Station Database
http://jro.igp.gob.pe/english/database/database_en.htm

Image Courtesy Cornell University

The Jicamarca Radio Observatory - Cornell University
http://jicamarca.ece.cornell.edu/

The 49.92 MHz ISR is the principal facility of the Observatory. The radar antenna consists of a large square array of 18,432 half-wave dipoles arranged into 64 separate modules of 12 x 12 crossed dipoles. Each linear polarization of each module can be separately phased (by hand, changing cable lengths), and the modules can be fed separately or connected in almost any desired fashion. There is great flexibility, but changes cannot be made rapidly. The individual modules have a beam width of about 7 deg, and the array can be steered within this region by proper phasing. The one way half power beam width of the full array is about 1.1 deg; the two way (radar) half power width is about 0.8 deg. The frequency bandwidth is about 1 MHz. The isolation between the linear polarizations is very good, at least 50 dB, which is important for certain measurements. Since the array is on the ground and the Observatory is the only sign of man in a desert region completely surrounded by mountains, there is no RF interference. The transmitter consists of four completely independent modules which can be operated together or separately. Only two of these modules are currently in operation. Each can deliver ~1.5 MW peak power, with a maximum duty cycle of 6%, and pulses as short as 0.8-1.0 μs. Pulses as long as 2 ms show little power droop; considerably longer pulses are probably possible. Two additional modules with the same properties will eventually be available. The third is more than 90% complete; the fourth is well advanced but its completion will require additional funding. The drivers of the main transmitter can also be used as transmitters for applications requiring only 50- 100 KW of peak power...

SOURCE: Jicamarca Radio Observatoryhttp://www.kurasc.kyoto-u.ac.jp/radar-group/local/isr/jicamarca/overview.html

MUCH BIGGER THAN **HAARP**
Main Array

Visit the Jicamarca Radio Observatory homepage
http://jro.igp.gob.pe/

http://www.thelivingmoon.com/45jack_file....bservatory.html

Re: Every One Speaks about HAARP, but did you know
Post by zorgon on Sept 21, 2010, 7:07pm

Jindalee Operational Radar Network

JORN
JP 2025
Laverton, West Australia
-28° 19' 36.29", +122° 0' 18.84"

Two Part System

CAND98/0153-03
JORN PROJECT RECEIVER SITE, LAVERTON W.A.
PIC BY CPL DAVE BROOS, DEFENCE PUBLIC AFFAIRS.

Projects
JP 2025 - Jindalee Operational Radar Network (JORN)

The JORN project arose out of extensive research undertaken by the Defence Science and Technology Organisation (DSTO) into over-the horizon radar (OTHR) beginning in the early 1970s. As part of the 1987 Defence White Paper, the Government placed a high priority on wide area surveillance of the north and north western approaches to Australia and OTHR was seen to be the most cost effective solution. As a consequence, in December 1990, the Government approved the design and construction of JORN.

The Jindalee Operational Radar Network (JORN) consists of two OTHR, one near Longreach, Qld. and the other near Laverton, WA, jointly operated from the JORN Coordination Centre (JCC) at RAAF Base Edinburgh, SA by No 1 Radar Surveillance Unit. The radars are an advanced development of the Australian designed Jindalee radar at Alice Receiver Site, Laverton WA - click on image to enlargeSprings which is in operational use as well as being a research and development facility used by DSTO for ongoing OTHR improvement. JORN radars are capable of all weather detection of air and surface targets inside an arc of up to 3,000 km range extending from Geraldton in the west around to Cairns in the east. JORN makes a crucial contribution to broad area surveillance of Australia's strategically important northern approaches.

SOURCE:
Australian Department of Defence
Defence Materiel Organization
http://www.defence.gov.au/dmo/esd/jp2025/jp2025.cfm

Electronic Warfare & Radar Division - DSTO, Australia
http://www.dsto.defence.gov.au/page/3603/

CAND98-0153-25
JORN PROJECT RECEIVER SITE ANTENNA ARRAY, LAVERTON W.A.
PIC BY CPL DAVE BROOS, DEFENCE PUBLIC AFFAIRS.
Courtesy Australian Department of Defence

Courtesy Australian Department of Defence

http://www.thelivingmoon.com/45jack_file...k_Laverton.html

Re: Every One Speaks about HAARP, but did you know
Post by zorgon on Sept 21, 2010, 7:09pm

Jindalee Operational Radar Network

JORN
Longreach, Queensland, Australia
-23° 39' 29.53", +144° 8' 49.58"

JORN Part Two

Communications '92: Communications Technology, Services and Systems; Getting It All Together

The Jindalee Operational Radar Network Communications and the Operational Concept
Nicholson, P1; Cameron, A2

Abstract: The operational concept of the Jindalee over-the-horizon operational radar network (JORN) is the centralised control and co-ordination of remote sensors. The radar sites are in Laverton, WA and Longreach, Queensland, while the co-ordination centre is situated in Adelaide, South Australia. An extensive communications network is needed to control the radars and their associated frequency management systems, transfer partly processed data for final analysis at the co-ordination centre, and pass track information to the command support systems of the Australian Defence Force and other users. The principle of operation, configuration and concept of the Jindalee project are briefly outlined to provide the context of the communications requirement. The communications infrastructure to support this operational concept is then described together with the main factors which have influenced the design of JORN communications.

Papers Available Here
http://search.informit.com.au/documentSummary;dn=563982181256363;res=IELENG

Consultancy Projects

Jindalee Operational Radar Network

RayTec Consulting has since its inception offered sub-contract services on the JORN project across a broad spectrum of Systems Engineering disciplines from Requirements Analysis and Design, Verification and Validation to
Integration and Test.

SOURCE: http://www.raytec.com.au/wp/projects

Electronic Warfare & Radar Division

High frequency surface wave radar. Credit DSTO

Electronic Warfare & Radar Division

Electronic Warfare & Radar Division provides scientific leadership and support to the Australian Defence Organisation on the exploitation of the electromagnetic spectrum to enhance the performance of our own sensors, weapons, platforms and command systems, together with the ability to destroy the effectiveness of adversarial systems.

Weapons Systems Division

Weapons Systems Division provides scientific leadership and support covering all aspects of weapon systems - including sensors, guidance, propulsion and warheads, and their integration into combat platforms and command and control systems.

Command, Control, Communications & Intelligence Division

Command, Control, Communications & Intelligence Division provides scientific leadership and support for Defence command, intelligence, communications, and business processes, at both the operational and theatre levels of command. Support to the Australian Defence Organisation includes Information Operations with special capabilities in Information Security and Digital Forensics; Communications with special capabilities in Satellite Communications, Mobile Networks and Network Management; Intelligence Processing and Analysis with special capabilities in signals analysis, communications analysis, automated fact extraction, and speech processing. The Division has organised its work program to have a strong emphasis on support achieving the goals as outlined in the Network Centric Warfare roadmap.

Intelligence, Surveillance & Reconnaissance Division

Intelligence, Surveillance & Reconnaissance Division provides scientific leadership and support for strategic intelligence, surveillance and reconnaissance systems, with a focus on the needs of the intelligence community.

Land Operations Division

Land Operations Division provides scientific leadership and support to the Land Force through structured and analytical approaches to capability development.

SOURCE: DSTO
http://www.dsto.defence.gov.au/page/3603/

http://www.thelivingmoon.com/45jack_file.... Longreach.html

Re: Every One Speaks about HAARP, but did you know
Post by zorgon on Sept 21, 2010, 7:12pm

[quote]*Originally posted by zorgon*

Poker Flat Research Range

Near Chatanika, Alaska
+65° 7' 23.90", -147° 28' 7.05"

Still looking for the actual array in this area but Poker Flats covers a wide terrain and the array is most likely hidden in the trees

Gate sign says NASA is lurking about and they mention the Aurora studies...

HAARP likely not Primary Ionospheric array in Alaska by Guy Cramer
http://www.superforce.com/**haarp**/index.htm

How to hide a **HAARP** by Guy Cramer

This first photo shows **HAARP**

The second photo shows **HAARP** with a camouflaged Array

The third image shows a completely concealed array, road and power generation center, to show how easy it is to hide a large facility in a location like Alaska.

"The above illustrations demonstrate the capability to effectively conceal large land areas containing hardware and buildings. In a similar initiative comprising the the most comprehensive infrastructure concealment program since World War II, the design team of Dr. Resnick, Lt. Col. Timothy R. O'Neill, PhD (U.S. Army, Ret.) and Mr. Guy Cramer have produced remarkable results. Using specially designed "Fractal Based" camouflage patterns in projects related to concealment of critical infrastructure under the auspices of the US Department of the Interior's Bureau of Land Management, the team continues to achieve desired objectives such as those shown below."

SOURCE: Guy Cramer Hyperstealth Tech
http://www.superforce.com/**haarp**/index.htm

We have found this one...

Chatanika Incoherent Scatter Facility

EISCAT Like Facility
Poker Flats
+65° 7' 1.34", -147° 27' 37.23"

Also found one small Array...
+65° 7' 55.61", -147° 27' 14.98"

And several 'suspicious' areas like this one

But Poker Flats is still a work in progress

Re: Every One Speaks about HAARP, but did you know
Post by zorgon on Sept 21, 2010, 7:20pm

Baikal-1 and IGR sites
Semipalatinsk-21, Kazakhstan

This one is a direct tie in with Remote Viewing success and Tesla technology.

It is said Russia has several **HAARP** like facilities, bt so far I have only found SURA

Back in the scalar weapon and Tesla research days there are several objects left in Russia that are very impressive. As they deal with antennas and as they are cool I will add them here as well...

You will also have to visit my pages at the bottom of each post as I am only using a few of the images and a little of the text... the full collection is on each page as I get new data...

First one is...

URDF-3 (Unidentified Research and Development Facility-3)
Baikal-1, Semipalatinsk, Kazakhstan
50°10'12.69"N, 78°22'36.84"W

This first appeared as a CIA satellite image

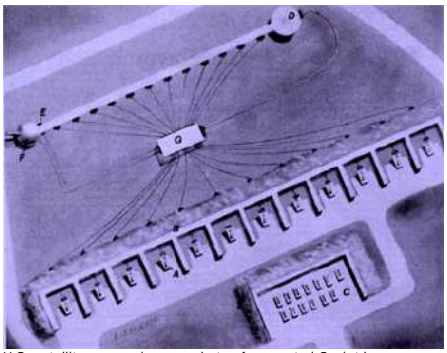

U.S. satellite reconnaissance photo of suspected Soviet beam weapon installation near Semipalatinsk.
Published July 28, 1980. (Courtesy Aviation Week & Space Technology)

Much has been written about the CIA search for Russia's Tesla Beam Weapon facility and it is even one of the biggest cases for the Remote Viewing Project Stargate that the CIA ran. One of the things that was a positive hit from the RV Team was the huge crane at the site...

Well that crane is STILL THERE...

Space Nuclear Facility test capability at the Baikal-1 and IGR sites
Semipalatinsk-21, Kazakhstan

Hill, T. J.; Stanley, M. L.; Martinell, J. S.
Presented at the Nuclear Power Engineering in Space Nuclear Rocket Engines, Kazakhstan, Russia, 22-26 Sep. 1992

The International Space Technology Assessment Program was established 1/19/92 to take advantage of the availability of Russian space technology and hardware. DOE had two delegations visit CIS and assess its space nuclear power and propulsion technologies. The visit coincided with the Conference on Nuclear Power Engineering in Space Nuclear Rocket Engines at Semipalatinsk-21 (Kurchatov, Kazakhstan) on Sept. 22-25, 1992. Reactor facilities assessed in Semipalatinski-21 included the IVG-1 reactor (a nuclear furnace, which has been modified and now called IVG-1M), the RA reactor, and the Impulse Graphite Reactor (IGR), the CIS version of TREAT. Although the reactor facilities are being maintained satisfactorily, the support infrastructure appears to be degrading. The group assessment is based on two half-day tours of the Baikals-1 test facility and a brief (2 hr) tour of IGR; because of limited time and the large size of the tour group, it was impossible to obtain answers to all prepared questions. Potential benefit is that CIS fuels and facilities may permit USA to conduct a lower priced space nuclear propulsion program while achieving higher performance capability faster, and immediate access to test facilities that cannot be available in this country for 5 years. Information needs to be obtained about available data acquisition capability, accuracy, frequency response, and number of channels. Potential areas of interest with broad application in the U.S. nuclear industry are listed.

SOURCE: Harvard Abstracts
http://adsabs.harvard.edu/abs/1993STIN...9416773H

Here is the crane sketch from the CIA RV Team members

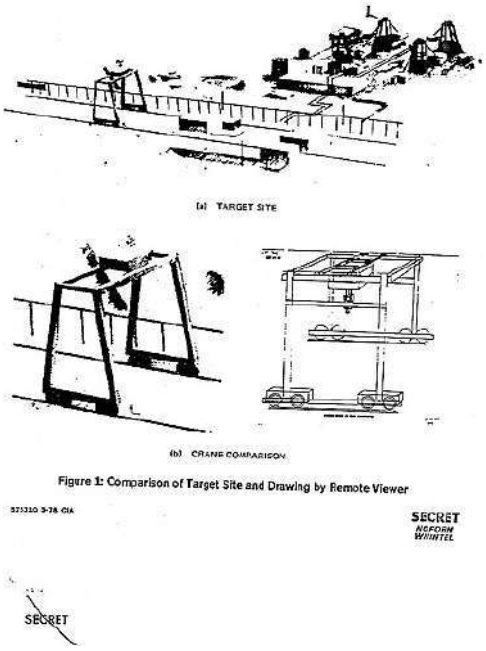

Here is the large crane on Google Earth

Credit for the find and info gathering goes to
admiraltogo
Fort Smith, AR
Google Earth poster

This base was also the spot where the Russians tested their version of a Nuclear Rocket

http://www.thelivingmoon.com/45jack_file....Kazakhstan.html [/quote]

Re: Every One Speaks about HAARP, but did you know
Post by zorgon on Sept 21, 2010, 7:26pm

Strange Towers in a Russian Forest
Tesla Generators

Sychëvka, Moskovskaya Oblast' (Russia)
+55°55'26.15"N,36°49'10.97"

Yet another old Russian project tied into Tesla research... I have included these because they are related, and just plain cool

Update 2007-12-02 09:59:49

"These were part of the experiments do by the SU with Teslas work towards power transmission and communication. Pictures all over the place on the internet. Nothing mysterious or new about it. Or perhaps its a secret installation for taking over the world. Take you pick."

Below is the entry gate from Google Earth images... the caption translates to...
"Isled. the center of the high energies"

Test benches VNITS - ALL-UNION SCIENTIFIC RESEARCH INSTITUTE OF CEMENT VEI
(high-voltage scientific research center of All-Russian electrotechnical institute).

Satellite View of the Installation near Sychëvka, Moskovskaya Oblast' (Russia)

http://www.thelivingmoon.com/47john_lear....ian_Forest.html

Re: Every One Speaks about HAARP, but did you know
Post by zorgon on Sept 21, 2010, 7:29pm

The Russian Woodpecker

Duga Radar Array, Chenobyl, Ukraine
51°18'20.17"N, 30°04'02.60"E

"Woodpecker" Duga radar array, Chenobyl, Ukraine by Necator

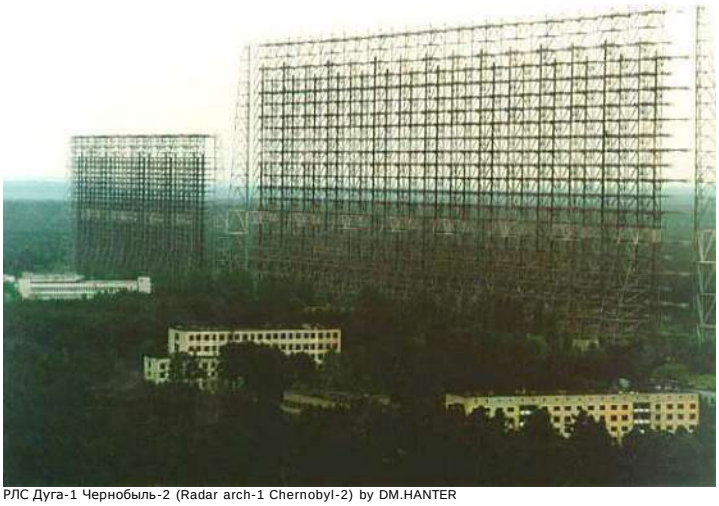

РЛС Дуга-1 Чернобыль-2 (Radar arch-1 Chernobyl-2) by DM.HANTER

History

The Soviets had been working on early warning radars for their anti-ballistic missile systems through the 1960s, but most of these had been line-of-sight systems that were useful for raid analysis and interception only. None of these systems had the capability to provide early-warning of a launch, which would give the defenses time to study the attack and plan a response. At the time the Soviet early-warning satellite network was not well developed, so work started on over-the-horizon radar systems for this associated role in the late 1960s.

The first experimental system, Duga-1, was built outside Mykolaiv in the Ukraine, successfully detecting rocket launches from Baikonur Cosmodrome at 2,500 kilometers. This was followed by the prototype Duga-2, built on the same site, which was able to track launches from the far east and submarines in the Pacific Ocean as the missiles flew towards Novaya Zemlya. Both of these radars were aimed east and were fairly low power, but with the concept proven work began on an operational system. The new Duga-3 systems used a transmitter and receiver separated by about 60 km.[2]

http://en.wikipedia.org/wiki/Russian_Woodpecker

Чорнобиль-2. Приймальні антени (Chernobyl-2. Receiving Antenna) by djcrok

MANY more pictures

http://www.thelivingmoon.com/45jack_file....ar_Ukraine.html

Main Stream Media coverage..

The Missing Secrets Of Nikola Tesla - Woodpecker Signal
Russia makes Aurora's with Woodpecker Array

Re: Every One Speaks about HAARP, but did you know
Post by zorgon on Sept 21, 2010, 7:33pm

China Research Institute of Radiowave Propagation (CRIRP)
HAARP Like Facility
Ionospheric Laboratory

Ionospheric Laboratory, Xinjiang (Sinkiang) Region
40°24'15.91"N, 93°38'09.74"E

So far I have only found ONE of China's Arrays and one EISCAT type dish.

Not much data to go on either but the name...
CRIRP
China Research Institute of Radiowave Propagation

This facility is closest to Urumchi (Urumqi), Xinjiang Region, China. Actually the whole region is filled with odd markings and will be a whole thread on its own but not related to radio waves...

Ionospheric sounding network and data in China

Wu Jian Jiao Peinan Xiao Zuo Wan Weixing Liu Ruiyuan Zhao Zhengyu
LEME, China Res. inst. of Radiowave Propagation, Beijing;

This paper appears in: Antennas, Propagation and EM Theory, 2000. Proceedings. ISAPE 2000. 5th International Symposium on
Publication Date: 2000
On page(s): 688-691
Meeting Date: 08/15/2000 - 08/18/2000
Location: Beijing, China
ISBN: 0-7803-6377-9
References Cited: 10
INSPEC Accession Number: 6963766
Digital Object Identifier: 10.1109/ISAPE.2000.894880
Current Version Published: 2002-08-06

Abstract
Ionospheric sounding has been conducted routinely for more than 60 years in China. A complete network of ground-based sounding sites covers the Chinese subcontinent, including vertical and oblique sounding, GPS measurement of ionospheric TEC and scintillation, **VLF** receivers measuring the lower ionosphere etc. In this paper, we give a picture of the sounding network, equipment situation and data acquired with emphasis on vertical ionosonde network

SOURCE: IEEE
http://ieeexplore.ieee.org/xpl/freeabs_a...&isnumber=19345

The Ionospheric Sounding in China

The ionospheric sounding in China has a long history and has a well spread network, which is still keeping routine operation, providing a good background to do the ionospheric long-term prediction and short-term forecasting. The ionospheric sounding in China started in early 1940s (Wu et al., 2002). Fig.1 shows the ionospheric sounding network in China. The sounding equipments and operation periods are listed in Table 1. Among them 11 ionosonde stations are still in operation in China mainland. The data at integer UT hours are sent to forecasting center in Beijing twice a day through Internet.

There is also a daily exchange of ionospheric data with Russian (for 4 stations) and with Australia (for 4 stations) respectively. A method of predicting the ionospheric F2 layer in the Asia and Oceania Region (AOR Method [Sun X.R., 1987]) was adopted as a regional ionospheric long-term prediction method in China and its surrounding area. Then this was cooperated with the International Reference Ionosphere and became the Reference Ionosphere in China (CRI) [Liu et al., 1994].

http://www.irf.se/~christer/China_IONO.doc

Preliminary studies on ionospheric forecasting in China and its surrounding area

R. Liua, Corresponding Author Contact Information
E-mail The Corresponding Author, Z. Xua, J. Wub, S. Liua, B. Zhanga and G. Wangb

Polar Research Institute of China, 451 Jinqiao Road., Shanghai 200136,
China bChina Research Institute of Radiowave Propagation, Xinxiang 453003, China

Abstract

The ionospheric sounding in China has a long history and has a well spread network, which is still keeping routine operation. The autocorrelation method is adopted for the short-term forecasting of ionospheric characteristics. The performances of the forecasts at Chongqing have been examined for different combination of parameters and algorithms by estimating the prediction errors. Preliminary results show that for predictions of more than 10 h ahead the “at once” method with f0F2 is preferable. For predictions of less than 10 h ahead the “iterations” method with View the MathML source is the best. A corrected method of the International Reference Ionosphere used in China region (the CRI model) is described in this paper. By introducing an effective ionospheric index Ic into the CRI model the regional forecasting could be realized.

SOURCE: Science Direst

Home Address:
National Key Lab of Electromagnetic Environment, China Research Institute of Radiowave Propagation (CRIRP), P.O. Box 6301, Beijing 102206, China,

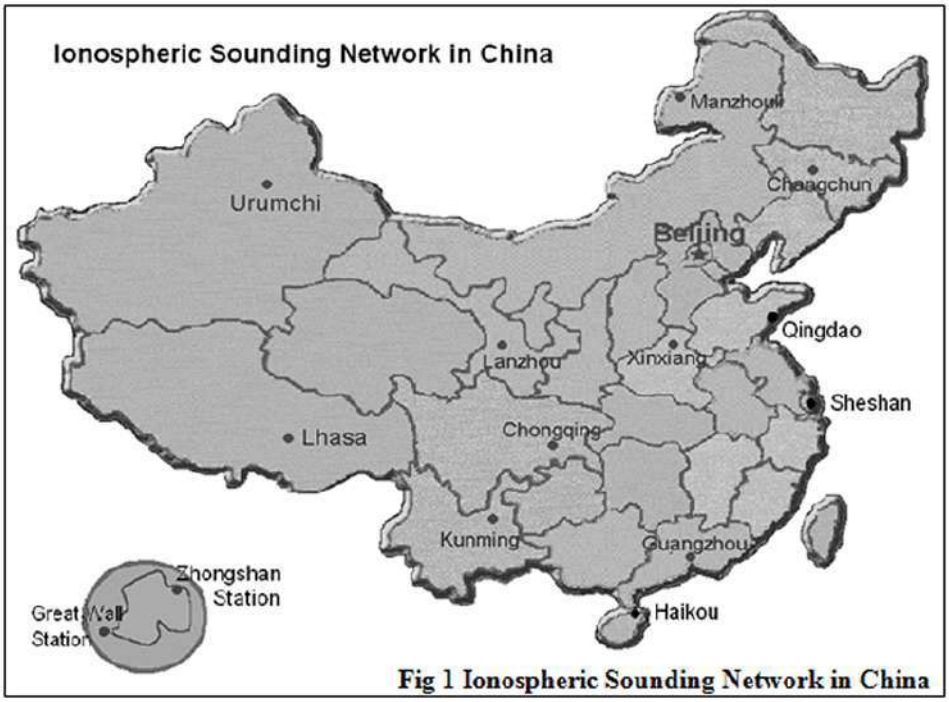

Fig 1 Ionospheric Sounding Network in China

Table 1 Ionospheric sounding equipments and operating periods in China

Site	Ionosonde	GPS TEC receiver	GPS scintillation receiver	VLF signal receiver	Dif. Doppler receiver	Polarimeter TEC and scintillation
Manzhouli	1954—now				1982—1991	
Changchun	1956—now					
Urumchi	1957—now				1982—1992	
Beijing	1953—now	1998—now			1994—1996	1980—1992
Lanzhou	1956—now					
Qingdao	1999—now	1994—now		1997—now	1994—1996	
Xinxiang	1988—now	1994—now		1978—now	1982—1992	1981—1992
Sheshan	1957—1966					
Wuhan	1957—now	1994—now		1988—now		1980—1990
Lhasa	1970—now					
Chongqing	1944—now				1981—1992	
Guangzhou	1955—now				1985—1989	
Haikou	1956—now	1994—now	1998—now	1999—now	1982—1987	1986—1989
Great wall	1986—now		1998—now	1998—now	1989—1996	
Zhongshan	1990—now		1998—now	1998—now		

http://www.thelivingmoon.com/45jack_file....ropagation.html

Zhong Shan Antarctic Polar Station (China)

69° 22' 23.63" S 76° 22' 19.11" E

Introduction

Of the two Chinese scientific stations in Antarctic, the one in Zhong Shan is closely conjugated with the Svalbard area in the northern hemisphere. This makes it a valuable place for coordinated measurements both with the EISCAT Svalbard Radar (ESR) and the Polar satellite. In 1991 a cooperation agreement was signed between the Ionospheric Laboratory of the China Research Institute of Radiowave Propagation (CRIRP) in Xinxiang, China, and the Department of Physical Sciences, University of Oulu, Finland, to build an auroral photometer system for the Zhong Shan station (Kaila et al, 1997). The multichannel scanning photometer agreed upon was constructed in Oulu by April 1995, and delivered to China in May. Measurements were supposed to start in March 1997, to be continued during the local winter time until October (the same schedule of measurements is planned for every year). However, due to problems mentioned above, the current status of the system is unknown!

The Zhong Shan Station, Antarctica
http://www.thelivingmoon.com/45jack_file....Zhong_Shan.html

Re: Every One Speaks about HAARP, but did you know
Post by zorgon on Sept 21, 2010, 7:36pm

Sheshan, Shanghai, China

EISCAT Like Facility
31°5′41.98″N, 121°11′29.72″E

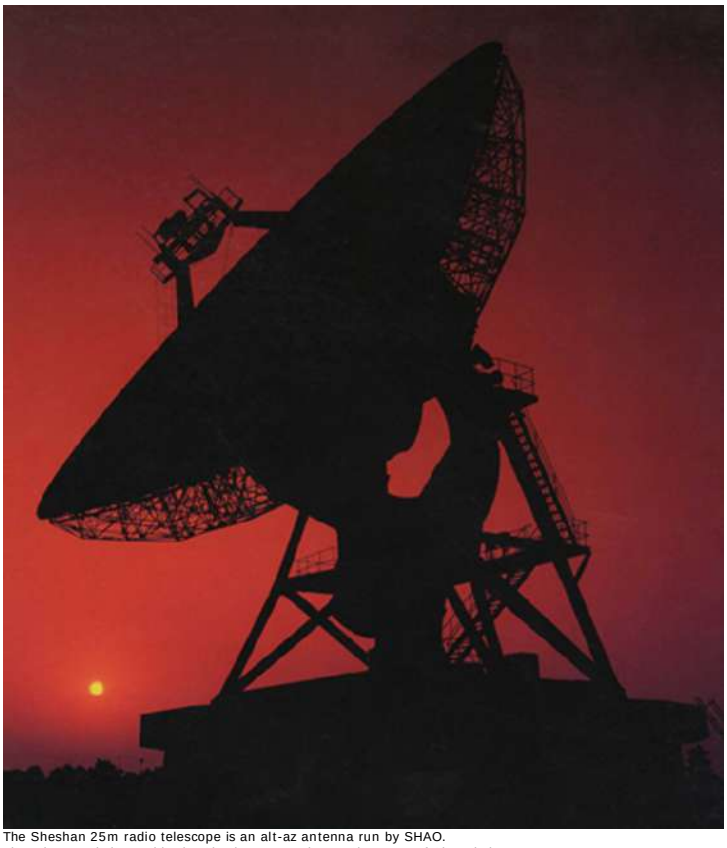

The Sheshan 25m radio telescope is an alt-az antenna run by SHAO.
The telescope is located in the Sheshan area, about 40km west of Shanghai.

This one is in the middle of the Old Jesuit Cathedral lot. They have an observatory there as well

Observatory and Church

http://www.thelivingmoon.com/45jack_files/03files/China_Sheshan.html

Been a lot of rumors around that the Jesuits still have a lot of control in the world...

Look up Wheeling Jesuit University... search for NASA grants and ask why is NASA giving money to a Church organization?
http://www.wju.edu/

Look up the National Technology Transfer Center (NTTC) These guys are in charge of who gets new technology

The National Technology Transfer Center (NTTC) has entered its 20th year of providing technology transfer services for federal facilities of our nation. Our work has provided clients with technical and market research expertise dedicated to meeting the complex needs of technology transfer organizations, while providing close support focusing on customer service. NTTC is inspired by the technologies developed at our federal R&D institutions, and is proud of our work commercializing and disseminating federal innovation for the betterment of our nation's economy.

Ask why do the Jesuits control technology transfer?

©2009 National Technology Transfer Center, Wheeling Jesuit University
http://www.nttc.edu/

But that is a whole new story

Back to **HAARP**/EISCAT like stuff...

Re: Every One Speaks about HAARP, but did you know
Post by zorgon on Sept 21, 2010, 7:51pm

HAARP High Frequency Active Auroral Research Program
Gacona, Alaska

There are more but that is all I have cataloged so far

But each one of those sites links to documents that link to other cogs in the wheel...

I am sure I have missed a few

I will add more as I have time to create the webpages. Feel free to add anything that you find from those links...

I will finish with some of the original **HAARP** images. You can also go to Jack Arnesons page and look under **HAARP** and Similar Facilities

HAARP cam image...

http://www.thelivingmoon.com/45jack_file...ona_Alaska.html

This is the **HAARP** 'home page'
http://www.**haarp**.alaska.edu/

But remember that the real **HAARP** project is run by the US NAVY NRL (Naval Research Laboratory

High Frequency Active Auroral Research Program
http://www.nrl.navy.mil/content.php?P=04REVIEW106

HAARP Photo Gallery and web cam access links

http://www.thelivingmoon.com/45jack_file...Gallery_01.html

Re: Every One Speaks about HAARP, but did you know
Post by zorgon on Sept 21, 2010, 8:00pm

Going through my old thread for relevant posts... here is one...

Quote:
Originally posted by TheWretched
Many of the ones you have listed are nothing but observatories for looking into the stars. Some are nothing but radar stations.

If you believe THAT then you haven't read anything about them. So much for your 'expertise' Most of the ones listed came from EISCAT and **HAARP** OFFICIAL websites

I haven't even listed all yet..but the antennas at
Kiruna, Sweden
Longyearbyen, Svalbard (Spitsbergen), Norway
Sodankylä, Finland
Søndre Strømfjord, Greenland
Ramfjordmoen, near Tromsø, Norway

Are most certainly used for Ionosphere manipulation and research which is after all THE POINT of these facilities and hence the thread

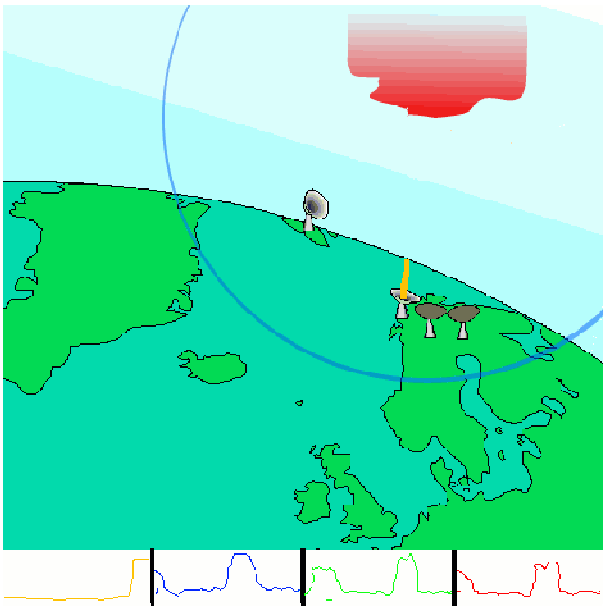

Why do these skeptics always have nasty names?

Re: Every One Speaks about HAARP, but did you know
Post by zorgon on Sept 21, 2010, 8:10pm

Lot of weird stuff happening lately... Ocker has noticed it too, he said so in an ATS thread...

Stuff I have been looking for for years is suddenly posted on Wikipedia, Buzz Aldrin now posts the confirming data on his site about Aquila and the very day I made that **HAARP** thread at ATS...

Quote:

Originally posted by autowrench
Great post, starred and flagged. Did anyone happen to watch the History Channel last night? They had as show called "That's Impossible," and the show as all about **HAARP**, and the different facilities around the world, and how they use it as a weather weapon. I too have researched this thing, but the show had all of the tech, plus computer animation, and was fabulously presented.

Now how is that for coincidence? Same dang thing happened with PBS NOVA... A week before I was going to post all the original Secret Astronaut material we had collected, NOVA does :Astrospies"

{{{insert score to 'Twilight Zone' here}}}

Re: Every One Speaks about HAARP, but did you know
Post by dragar on Sept 21, 2010, 10:09pm

Zorgon im going to add this in please feel free to delete this post.
Take alook at it see if this is a bit strange.
HAARP= High Frequency Active Auroral Research Program
The Prince Albert Radar Laboratory (PARL):The original study that led to PARL came about as the side effect of questions about the effects of the aurora on radar systems.
Work on the **HAARP** Station began in 1993
Prince Albert Radar Laboratory limited operations started in 1959.
Could this be what sparked **HAARP**?

The Prince Albert Radar Laboratory

A satellite is any smaller object traveling around a larger one. This means that the moon is a satellite to the Earth. However, the term satellite often refers to a human-made spacecraft placed in space to orbit another body.

The first "communicatons satellite" was the moon. The USA started using the moon for communications trials in the early 1950's. Signals beamed towards the moon were reflected and received back on Earth. It was a very inefficient means of communication requiring high power and large antennas to produce a detectable system. In addition, communication was only possible while the moon was above the horizon.

DRTE staff participated in the trials starting in 1959 using a large radar station at the newly-built Prince Albert Radar Laboratory (PARL) in Saskatchewan. The first demonstration was given when Prime Minister John Diefenbaker inaugurated the station on June 6, 1959. Here are some photos of the inauguration. A pre-taped greeting* from President Eisenhower was transmitted from a station at Millstone Hill near Boston and received by the PARL station. Each station was equipped with a 26-m dish antenna. Diefenbaker used the occasion to announce that Canada would initiate its own satellite program. Here* is part of Mr. Diefenbaker's speech.

http://www.friendsofcrc.ca/Projects/PARL/PARL.html

As a side note :MY family and I have been there twice. It is very active many upgrades including a new security fence around it.
You may have to dig around in the link I gave for further info . ty

At the beginning, the work of the laboratory was focused on high frequency radio and the problem of forecasting the ionospheric conditions which determined the availability of any given frequency and transmission path. To this end, a new ionospheric sounder was designed by a team led by Bill McLeish. These sounders were constructed at RPL and were installed in a number of stations established across Canada. Most of the components were those which had been removed from surplus military equipment. The stations were manned by DOT personnel who were trained in their operation by Bob Stevens in a small building below the main laboratory by the shore of the Rideau Canal.

A second project arose from some of the HFDF work during the war. It had been noted that transmissions passing through the auroral zone had been deflected by as much as 20 degrees. To investigate this phenomenon further. Jack Meek proposed what became known as the "Mobile" experiment. A railroad car was equipped with a laboratory, diesel generators, accommodation, and cooking and eating facilities. Ionospheric sounders were installed, a crew was chosen and the car was hauled up to The Pas in Manitoba. From there, it was attached to the train which ran to Churchill and was shunted onto sidings at various points along the route. Antennas would be erected, and a series of ionospheric soundings taken. The car would then be hauled to the next siding and the process repeated. A line of soundings was thus obtained crossing the auroral zone. Jack Meek was in charge of the operation for the first period from the autumn of 1947 to January 1948 when Claire McKerrow took over. With Claire were Harold Serson, Cam Baker, and Sgt. Len Hagg on loan from the Canadian Army. The cook, provided by CNR, had an unfortunate habit of disappearing whenever the expedition arrived in The Pas. He was usually found in one of the local bars shortly before the train left. On one occasion, the town was searched from end to end to no avail. He was finally located in the local hospital, and they had to carry on without him. Claire called for volunteers to do the cooking with no success until Harold Serson finally admitted that he could cook a little. (In fact, Harold could have competed with most professional chefs.) Claire and Harold then shared the task until the cook's return. Food was supplied by the CNR from Winnipeg. Both Claire and Harold were inordinately fond of Winnipeg goldeye, and they ordered several cases of this delicacy.. The rest of the crew ate smoked goldeye, like it or not.

Re: Every One Speaks about HAARP, but did you know
Post by zorgon on Sept 22, 2010, 6:14am

Nice addition Did not have that one yet

Location, Location, Location

The requirements for the radar's site were twofold.

1. The site should permit the radar beam to illuminate the ionosphere over the Churchill, Manitoba region at the height at which the Aurora Borealis (Northern Lights) normally occurs. This would enable the comparison of auroral radar returns with simultaneous geophysical measurements made from Churchill.
2. The site should be accessible to scientists from the Physics department of the University of Saskatchewan, Saskatoon, where considerable expertise in auroral studies existed.

So it seems the location was specifically chosen to mess with the Aurora's.. so yeah... not only the predecessor for HAARP but proof that all big EISCAT and other huge radar dishes can effect the ionosphere

Nice catch

Re: Every One Speaks about HAARP, but did you know
Post by dragar on Sept 22, 2010, 3:58pm

University of Saskatchewan
Auroral Radar - Saskatchewan

Early 1948
Peter Forsyth was preparing for medical school when Balfour Currie, returning from meeting in Ottawa, asked if he would help modify a radar to be borrowed from the Navy to seek radar echoes from aurora.
This turned out to be a 3000 MHz surveillance radar. It was modified and operated, but no auroral echoes were detected.

Auroral Radar - Saskatchewan

1948-49
With the aid of Nate Gerson, the USAF provided two huge 106 MHz early-warning radars. One went to Saskatoon, the other to NRC (McKinley), where it was to be modified to 56 MHz
First Canadian auroral echoes were detected with this radar in 1949 (paper in Nature, April, 1950).
As a result, Peter Forsyth decided to do his PhD on auroral echoes, rather than go into medicine.

Auroral Radar - Saskatchewan

1948-49 - Postscript
Around 1990 a phone call came to the Department of Physics at the University of Saskatchewan asking if they had an SCR-270 radar with a particular serial number
They did! It was the original radar which detected the incoming Japanese planes arriving to bomb Pearl Harbor (that information was ignored).
For over 40 years that radar had been sitting "buried" in Saskatoon. It is now at the Historical Electronics Museum near Baltimore.

Auroral Radar - Saskatchewan

1951-52
The modified radar came to Saskatoon from Ottawa, and a combined dual-frequency antenna was constructed.
Simultaneous observations of auroral echoes were observed at 56 and 106 MHz (1953 paper)
In 1951, Peter Forsyth finished his PhD and was hired to work at the Defence Research Telecommunications Establishment(DRTE) at Shirley Bay, near Ottawa, but since the facility didn't exist yet, he continued at Saskatoon for another year. It was a year later when he moved to DRTE, where he remained until 1958, rising to the position of Superintendent of the Radio Physics Lab.

Pre-History

1931 - NRC Radio Section established
1932 - Dr. John Henderson (PhD with Appleton)
1935 - Maj.-Gen. A.G.L. McNaughton new NRC President helped invent a cathode-ray tube direction-finder in the 1920s
1936-38 - Henderson developed direction-finder for marine and air use, installed in Nova Scotia in 1938
1938 - McNaughton was consulting with DND re detection of aircraft by electrical means
1939 - Henderson sent to UK to be briefed on radar developments

World War II

McNaughton contacted by Sir Charles Wright
you have expertise, get into this radar development
send physics graduates to UK Navy - badly needed
Peter Forsyth developed air-borne radar in UK, 1942-45
NRC became centre of radar development in Canada
McGill, Queens, Toronto, Western also involved in radar research
REL (Crown corporation) established to manufacture optical equipment, radar
During course of war, NRC designed more than a dozen different radars at many frequencies: 75, 95, 150, 200, 215, 2,800, 3,000, 10,000 and 24,000 MHz.
REL manufactured over 2000 radar sets, mostly for Navy, Army

Post-war

NRC
microwave experience --> Covington's 10.7cm solar radio-telescope (1946)
McKinley --> meteor radar program (1947)
DRB
established 1947 to take over defence research role which NRC refused to continue with after the war.
took over labs from services (e.g. Naval Research Establishment, CARDE), and started new ones (DRTE, DRNL, Ft. Churchill)
Weather radar
started in 1943 as a Canadian Army project in Ottawa, led by Stewart Marshall.
Post-war, at DRB & McGill, until 1950, then McGill alone. (Stormy Weather)

Re: Every One Speaks about HAARP, but did you know
Post by dragar on Sept 22, 2010, 4:09pm

EISCAT

In addition to the incoherent scatter radars, EISCAT also operates an Ionospheric Heater facility at Ramfjordmoen (including a Dynasonde) to support various active plasma physics experiments in the high latitude ionosphere.

Description of the EISCAT heating facility:

The Heating facility is situated next to the UHF and VHF incoherent scatter radars.
The Heater is used for ionospheric modification experiments applying high-power transmissions of high-frequency electro-magnetic waves to study plasma parameters in the ionosphere. The name Heating stems from the fact that these high power electromagnetic waves, which are transmitted into the ionosphre with high-gain antennas, heat the electrons and thus modify the plasma state. To create plasma turbulence, the transmitted frequencies have to be close to the plasma resonances, which are 4 to 8 MHz.

Re: Every One Speaks about HAARP, but did you know
Post by gigas on Sept 23, 2010, 9:32am

Here in wisconsin up north of me, we have clam lake and they run an ELF facility there to communicate with subs deep under the sea. This ELF transmitter is connected by another facility 128 miles east in michigan. I would guess this also holds true for the underground communications of other secret facilities regular radio communications cannot be linked up with.

This facility was said to be shut down some years ago but according to the dot mil link below, it still operates.

http://enterprise.spawar.navy.mil/UploadedFiles/fs_clam_lake_elf2003.pdf

---

Re: Every One Speaks about HAARP, but did you know
Post by pman35 on Sept 27, 2010, 11:46am

Hi guys have'nt read any of this but i have to say i'm pretty impressed zorgon with what u've posted to me it looks like if all these were connected they would indeed create a shield around the globe and because there are so many if one was to fail it might not affect the rest.

I will read this post as i have an interest in haarp.

Respect And May Disclosure Keep Moving Forwards

Re: Every One Speaks about HAARP, but did you know
Post by magooollo on Oct 5, 2010, 11:25am

buzz aldrin and edgar mitchell (apollo astronauts) are involved in the UFO community, perhaps as information conduits tho that isnt offically acknolwedged , would make good intermediatries in the disclosure race

---

Re: Every One Speaks about HAARP, but did you know
Post by somamech on Oct 5, 2010, 4:14pm

Interesting pdf Gigas!

EDIT

For anyone curious as to when Zorgon mentioned that sometimes documents coming from us mil sites cannot be accessed by folk abroad, this is what you may see showing in your browser. *Obviously I'm in Australia... and this is how our allie treats us?*

You are not authorized to view this page

You do not have permission to view this directory or page using the credentials that you supplied.

Please try the following:

- Contact the Web site administrator if you believe you should be able to view this directory or page.
- Click the Refresh button to try again with different credentials.

HTTP Error 401.1 - Unauthorized: Access is denied due to invalid credentials.
Internet Information Services (IIS)

Technical Information (for support personnel)

- Go to Microsoft Product Support Services and perform a title search for the words **HTTP** and **401**.
- Open **IIS Help**, which is accessible in IIS Manager (inetmgr), and search for topics titled **Authentication**, **Access Control**, and **About Custom Error Messages**.

EDIT: PDF in question which Gigas posted is this link below:

http://enterprise.spawar.navy.mil/UploadedFiles/fs_clam_lake_elf2003.pdf

---

Re: Every One Speaks about HAARP, but did you know
Post by winniethepooh4102 on Oct 5, 2010, 4:47pm

I found a torrent for it, but the downloading is very slow:

http://extratorrent.com/torrent_download....s+HAARP.torrent

But there is something more to HAARP if one
could believe in some claims.

Re: Every One Speaks about HAARP, but did you know
Post by gigas on Oct 5, 2010, 5:37pm

Oct 5, 2010, 4:14pm, somamech wrote:

Interesting pdf Gigas!

EDIT

For anyone curious as to when Zorgon mentioned that sometimes documents coming from us mil sites cannot be accessed by folk abroad, this is what you may see showing in your browser. *Obviously I'm in Australia... and this is how our allie treats us?*

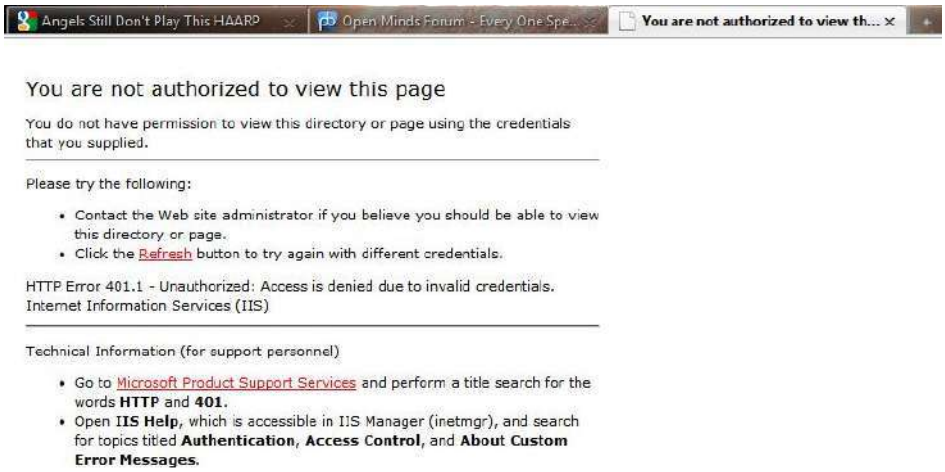

EDIT: PDF in question which Gigas posted is this link below:

http://enterprise.spawar.navy.mil/UploadedFiles/fs_clam_lake_elf2003.pdf

I can no longer access that pdf as well with I am not authorized to access that page. It appears they locked it from web access. I tried to navigate to the pdf with a proxy web service and it says I am not authorized to see the pdf.

Looks like they don't like this information being out there for all to see.

Re: Every One Speaks about HAARP, but did you know
Post by somamech on Oct 5, 2010, 5:41pm

I saved a copy

EDIT

Re-reading that PDF I can clearly see why they don't like that info in the public domain

[image]

Re: Every One Speaks about HAARP, but did you know
Post by zorgon on Oct 5, 2010, 5:56pm

Oct 5, 2010, 4:14pm, somamech wrote:

For anyone curious as to when Zorgon mentioned that sometimes documents coming from us mil sites cannot be accessed by folk abroad, this is what you may see showing in your browser.

FAS.org has a copy

http://www.fas.org/nuke/guide/usa/c3i/fs_clam_lake_elf2003.pdf

---

Re: Every One Speaks about HAARP, but did you know
Post by winniethepooh4102 on Oct 5, 2010, 6:02pm

The ELF cannot conquer the Elves.

Re: Every One Speaks about HAARP, but did you know
Post by gigas on Oct 5, 2010, 6:04pm

Oct 5, 2010, 5:41pm, somamech wrote:

I saved a copy

EDIT

Re-reading that PDF I can clearly see why they don't like that info in the public domain

[image]

Reading that pdf, it looks like the facility is still operating when it was supposed to be closed sept 30 2004.

Read the following link to see whats happening in the wisc land of dot mil.

http://www.zcommunications.org/project-elf-rip-by-site-administrator

---

Re: Every One Speaks about HAARP, but did you know
Post by gigas on Oct 5, 2010, 6:13pm

Thanks zorgon and somamech.

I thought I had saved it when found but maybe not since I looked and could not find it on this pc. Maybe on my other machine. I did save it from zorgons link though. really I did.

I tried to use the cache way back machines and it is scrubbed from the web as is the link to http://enterprise.spawar.navy.mil. I can't access that link as well.

Re: Every One Speaks about HAARP, but did you know
Post by winniethepooh4102 on Oct 5, 2010, 6:13pm

My favourite movie was "The Mad Max", the day after tomorrow.

Re: Every One Speaks about HAARP, but did you know
Post by somamech on Oct 5, 2010, 6:31pm

Oct 5, 2010, 6:13pm, gigas wrote:

Thanks zorgon and somamech.

I thought I had saved it when found but maybe not since I looked and could not find it on this pc. Maybe on my other machine. I did save it from zorgons link though. really I did.

I tried to use the cache way back machines and it is scrubbed from the web as is the link to http://enterprise.spawar.navy.mil. I can't access that link as well.

Me neither

I was always able to view that previously

Re: Every One Speaks about HAARP, but did you know
Post by zorgon on Oct 5, 2010, 6:34pm

One thing I need to mention....

Normally I will NEVER post a direct link to a file at a .mil site...

Why?

1) Many cannot get access from overseas
2) Many .mil sites that I visit require a certificate acceptance, which means you give them permission to monitor you. Some are several levels deep. This scares off the looky loos
3) Some ,mil sites like Maxwell AFB Archives will 'ping' back on the IP... happened once at ATS... everyone simply opening the page on that thread with the direct link got a warning pop up... I believe that contributed to ATS getting the rep of being government owned
4) This is the most important FILES GET MOVED because of the sudden traffic

Look at it this way An obscure document from 2003 has been idle for years... then suddenly I post a link say at ATS where several thousand viewers suddenly look at that file... well that sends up a red flag real fast

I have over 16,000 files I have saved... haven't even read them all yet but a friendly spook at ATS once told me that my posts generate unique hits on sites that they would rather remain quiet

So best bet is download the file and save it then post it somewhere else to share

One time I found a link to NASA Apollo photos... the FULL RS TIFF copies... I d/led a few posted something on a thread and while ArMaP was in the middle of a d/l the directory vanished. I never got all of them and I never found them again yet...

Another case I had a link to all the Rover images in full true color... that directory also moved... but fortunately I found that one again...

Because there are 40,000 pics on each Rover, I cannot d/l them all so I keep that link to myself now

Keith Laney has some of them on his site
http://www.keithlaney.net

Re: Every One Speaks about HAARP, but did you know
Post by somamech on Oct 5, 2010, 6:48pm

Good advice!

But in my case I don't mind clicking on those sites that require accepting a security certificate. In this case the whole site is offline...

Code:
```
http://enterprise.spawar.navy.mil/
```

Re: Every One Speaks about HAARP, but did you know
Post by somamech on Oct 5, 2010, 6:50pm

BTW..the moon boggy better not look like that POS LOL

Re: Every One Speaks about HAARP, but did you know
Post by zorgon on Oct 5, 2010, 6:51pm

Oct 5, 2010, 6:31pm, somamech wrote:

Me neither
I was always able to view that previously

Well see? You have just witnessed the system in action... I posted that link mainly because the word 'enterprise' was in that url. A similar one before was 'hyperspace.nrl.navy.mil/TiPS/' That was the info on the other tether satellite that flew at the same time the NASA one did (STS75)

It is still available on wayback machine

LINK

But this is what happens and that is why I have stopped posting direct links to sites like that because it means that I lose my sources when they plug the 'leaks'

Grab this one quick... it offers a 'public' access portal to the enterprise link, though I doubt the really cool stuff will be found there... but you never know

http://nesipublic.spawar.navy.mil/docs/misc/PEO_C4I_NESI_Memo.pdf

---

Re: Every One Speaks about HAARP, but did you know
Post by somamech on Oct 5, 2010, 7:13pm

Thanks Zorg!

That pesky system... Arrgh. When I get time after the weeks break i will show you my own instance of posting a link in an email that had way too many coincindes to be called so.

I don't mind posting DSTO links though... USA gets way too much attention... and lets face it, a good idea is as simple as placing some magnets and concrete together ala Ed. It does not need wads of cash thrown at it. Heck any country can come up with THE right idea

---

Re: Every One Speaks about HAARP, but did you know
Post by gigas on Oct 5, 2010, 8:30pm

Oct 5, 2010, 6:34pm, zorgon wrote:

One thing I need to mention....

Normally I will NEVER post a direct link to a file at a .mil site...

Why?

1) Many cannot get access from overseas
2) Many .mil sites that I visit require a certificate acceptance, which means you give them permission to monitor you. Some are several levels deep. This scares off the looky loos
3) Some ,mil sites like Maxwell AFB Archives will 'ping' back on the IP... happened once at ATS... everyone simply opening the page on that thread with the direct link got a warning pop up... I believe that contributed to ATS getting the rep of being government owned
4) This is the most important FILES GET MOVED because of the sudden traffic

Who knew, cept master zorgon. Ok my friend, the lesson has surely been learned and in the future, I will follow your proven advice and keep dot mil links on the low.

Thanks again exalted one for sharing that important bit of information on dot mil. We have seen it in action and know it to be true .

Now, all hail zorgon .

Re: Every One Speaks about HAARP, but did you know
Post by zorgon on Oct 5, 2010, 8:38pm

Oct 5, 2010, 6:02pm, winniethepooh4102 wrote:

The ELF cannot conquer the Elves.

I hope not I like Elves... have a few myself

Re: Every One Speaks about HAARP, but did you know
Post by winniethepooh4102 on Oct 6, 2010, 7:38am

Observing those very strange clouds and chemtrails
in the sky above me I'm inclined to believe, as though
the atmosphere is growing wiser and overripe. Do you
admit the claims about the HAARP and the elves?

P.S. I meant exactly this and some claims surrounding it:

http://www.educate-yourself.org/cn/sylphandchemtrailindex.shtml

http://educate-yourself.org/zsl/sylphessayindex.shtml

If the elves and the sylphs really exist they have to be in one category. Considering the UFO problem every possible information has to be processed.

Re: Every One Speaks about HAARP, but did you know
Post by zorgon on Oct 7, 2010, 9:00am

Elves and Sprites Play above huge thunderstorms

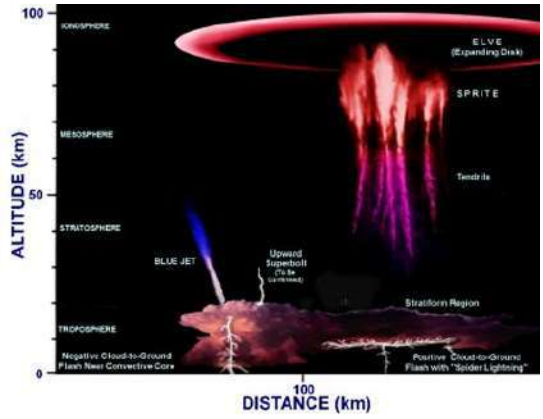

The Sylphs on the other hand only reveal themselves to those who can see them. I have a magnificent collections of Dragons... perhaps I may do a thread

They have little to do with HAARP as the Sylphs play in the atmosphere while HAARP messes several miles higher in the ionosphere, home of the Aurora...

The Dragons will come though... all you need to do is ask them to appear

---

Re: Every One Speaks about HAARP, but did you know
Post by winniethepooh4102 on Oct 7, 2010, 11:21am

I would leave the theme in this ouroboros style
not knowing how exactly the matrix is structured.
Anyway those creatures from under the ground
and under the water flying also everywhere in
the air and into the space cannot be unknown
for The Big Brother. The question is why they are
so big secret and what is their relation to us
indepedently of those massive space ships
and the ETs.

Re: Every One Speaks about HAARP, but did you know
Post by dragar on Nov 4, 2010, 5:51pm

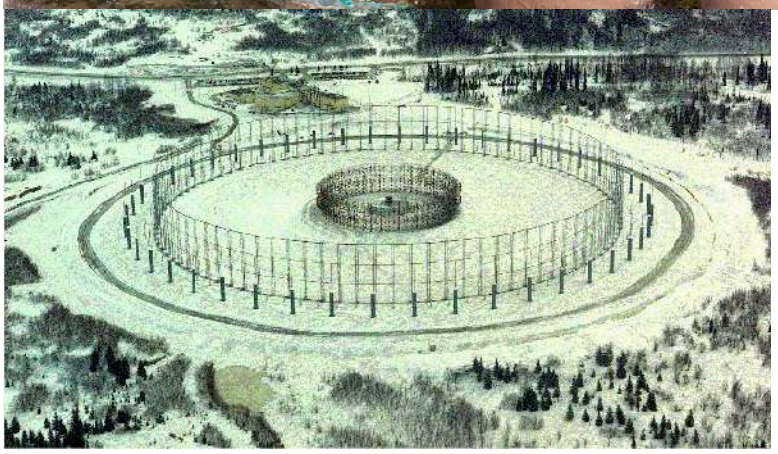

The AN/FLR-9, operated by the Air Intelligence Agency, is part of the DOD World Wide High Frequency Direction Finding System. High-frequency radio communication signals travel to receivers over the horizon by bouncing off the ionosphere. The shell of ionised particles which surrounds the earth refracts the signals so that they return to earth rather than disappear out into space. The clarity of the signal received depends on atmospheric and topographical conditions. HF-DF stations detect radio signals from aircraft or ships, and calculate the direction, or line of bearing, of the radio transmitter from the direction finding antenna. When the same signal is received by two or more antennae, the intersection of the lines of bearing mark the transmitter's location, using either precision single station location (SSL) capability, or in a network of DF stations using both multi-station azimuth triangulation and SSL. High Frequency Acquisition (AQ) and Direction Finding (DF) operations are performed with the Narrowband System (NBS) and Wideband Direction Finding (WBDF) Subsystem in support of normal and degraded communications modes, using both adaptive reception and super-resolution direction finding techniques.

Re: Every One Speaks about HAARP, but did you know
Post by ivalen on Nov 9, 2010, 7:50pm

Sept 21, 2010, 7:03pm, zorgon wrote:

http://www.thelivingmoon.com/45jack_file...r_Facility.html

Cherenkov Radiation around Antennas

Image courtesy ISRO

http://en.wikipedia.org/wiki/Cherenkov_radiation

> Cherenkov radiation (also spelled Cerenkov or Čerenkov) is electromagnetic radiation emitted when a charged particle (such as an electron) passes through an insulator at a constant speed greater than the speed of light in that medium. The charged particles polarize the molecules of that medium, which then turn back rapidly to their ground state, emitting radiation in the process.

For this to be the case in the above photograph - what is the insulating medium?

Re: Every One Speaks about HAARP, but did you know
Post by sarentack on Nov 11, 2010, 4:10am

one would think some of these facilities was like ginormous computer chip.

or signals or landmarks for ET like that Triangle look from above.

Wonder if their any relation to what we see in Peru?

Re: Every One Speaks about HAARP, but did you know
Post by somamech on Dec 5, 2010, 5:26pm

Hey HAARP is old news to the mountain people

The uncanny resemblance to a mil array

^compare that...

To this:

Re: Every One Speaks about HAARP, but did you know
Post by zorgon on Dec 7, 2010, 8:55am

Nov 9, 2010, 7:50pm, ivalen wrote:

For this to be the case in the above photograph - what is the insulating medium?

Good question... I might have said 'plasma' but that would require even more explanation. I do need to pinpoint exactly what these glows are... related to another glowing object on the Moon

St. Elmo's fire (also St. Elmo's light) is an electrical weather phenomenon in which luminous plasma is created by a coronal discharge originating from a grounded object in an atmospheric electric field Physically, St. Elmo's fire is a bright blue or violet glow, appearing like fire in some circumstances, from tall, sharply pointed structures

Working on it

Re: Every One Speaks about HAARP, but did you know
Post by zorgon on Dec 7, 2010, 9:12am

Nov 4, 2010, 5:51pm, dragar wrote:

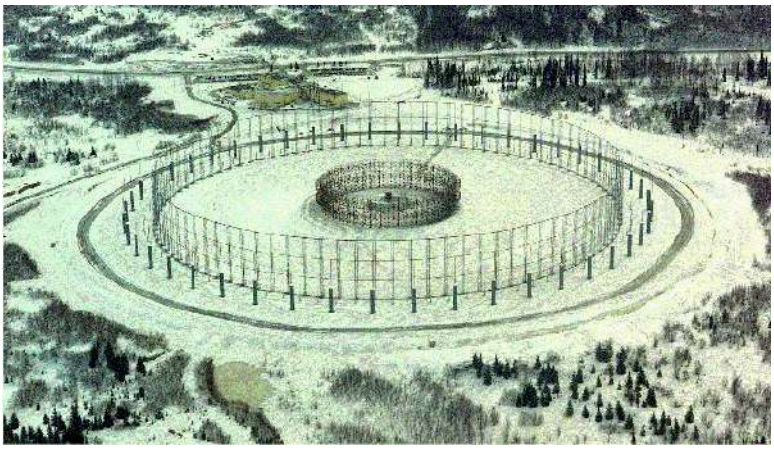

We have one of those in Japan too

Misawa, Japan
Misawa NSA Echelon Station
Code Name: Ladylove
+40° 43' 22.91", +141° 19' 43.57"

Quite a NAVY and AF presence there as well as an ECHELON station. We have nukes in storage in that area as well

http://www.thelivingmoon.com/45jack_files/03files/ECHELON_Misawa.html

---

Re: Every One Speaks about HAARP, but did you know
Post by zaggan on Dec 7, 2010, 3:31pm

I'm late in the game on this discussion, but it surfaced in June of last year in one of Dan's threads (think Reality 101). Someone had brought up one of the antenna arrays, along with a picture, and I commented back in late June. Dan got snippy and deleted all references to it, but want to add it back in here:

Received a reply to an inquiry to POA Elmendorf AFB, listed as follows:

Good Afternoon Sir,

My name is SrA Xxxxxx Xxxxxxxxx from the 3rd Wing Public Affairs on Elmendorf and I contacting you in regards to the question about the structure you saw on Google Earth.

It is a HF Antenna. If you would like more information you can go to the following link. http://www.fas.org/irp/program/collect/an-flr-9.htm

If you have any other questions, comments or concerns please do not hesitate to contact me at 552-8915 or by email.

Hope this helps!

Thank You and have a nice day!

XXXXXX XXXXXXXXX, SRA, USAF
COMMUNITY RELATIONS

3WG PUBLIC AFFAIRS
DSN: 552-8915 COMM: 552-8915

The link is pretty interesting.

Re: Every One Speaks about HAARP, but did you know
Post by gigas on Dec 7, 2010, 8:22pm

Dec 7, 2010, 9:12am, zorgon wrote:

Nov 4, 2010, 5:51pm, dragar wrote:

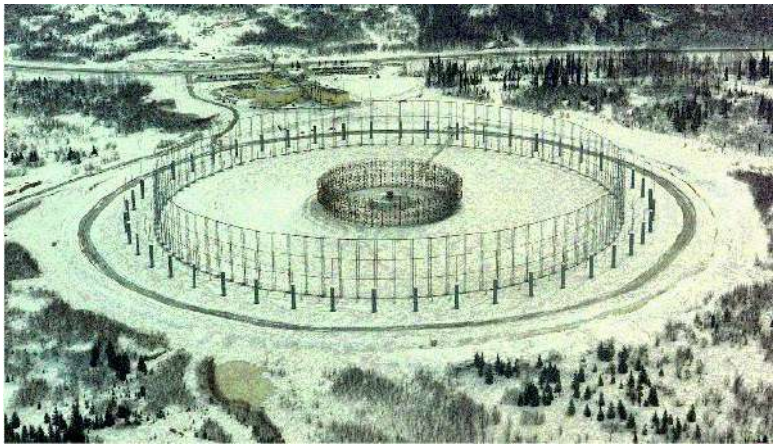

We have one of those in Japan too

Misawa, Japan
Misawa NSA Echelon Station
Code Name: Ladylove
+40° 43' 22.91", +141° 19' 43.57"

Looks like they had one back 5,000 years ago in the UK around salisbury called stonehenge as well.

THE CHEMTRAIL DIARY (/)

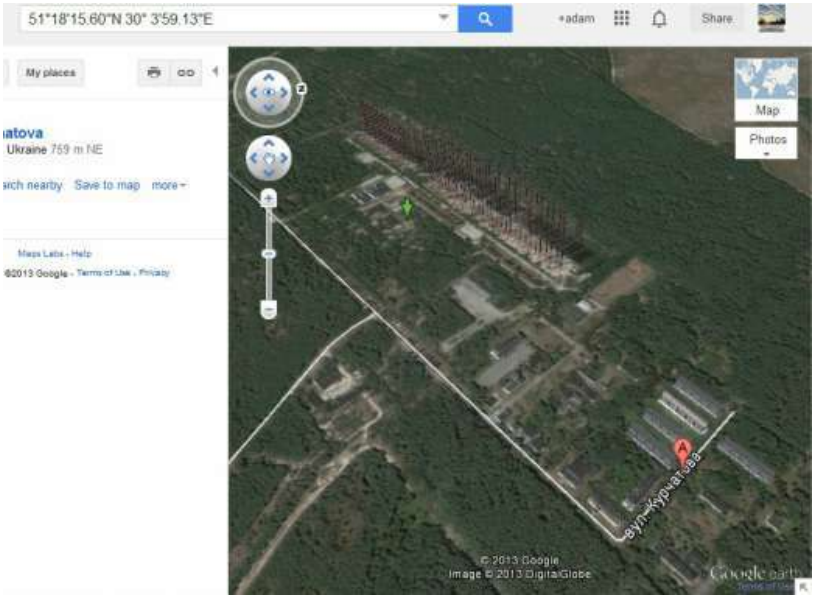

HAARP LOCATIES

- GPS Locaties -

(/haarp.html)

- GEBRUIK / USE GOOGLE MAPS -

1. High Frequency Active Auroral Research Programn (HAARP)
Gakona Alaska
+62° 23’ 30.00”, -145° 8’ 48.00”

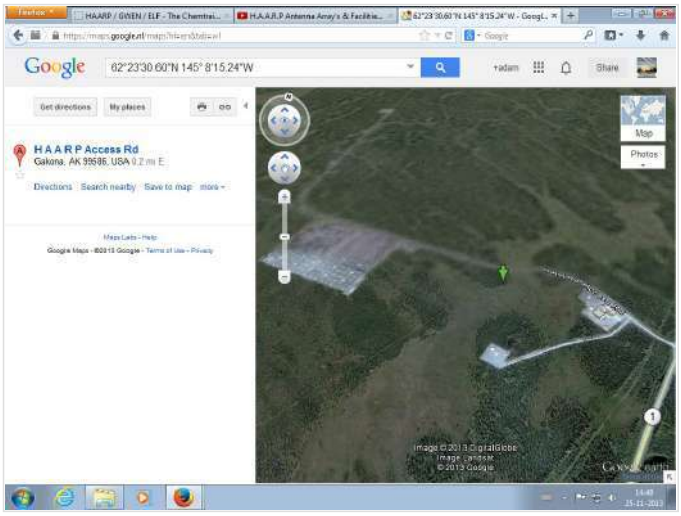

(/uploads/2/3/1/7/23175228/4799260_orig.jpg)

2. High Power Auroral Stimulation Observatory (HIPAS)
Fairbanks Alaska
64° 52’ 19” N 146° 50’ 33” W

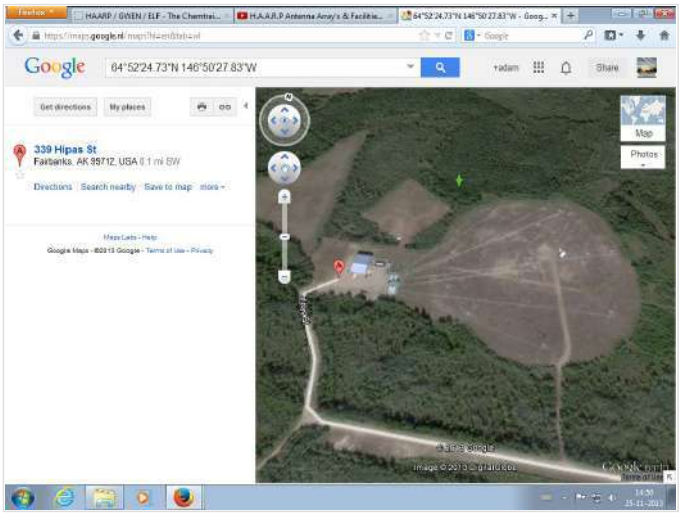

(/uploads/2/3/1/7/23175228/7260176_orig.jpg)

3. Poker Flat Research Range
Near Chatanika, Alaska
+65° 7’ 23.90”, -147° 28’ 7.05”

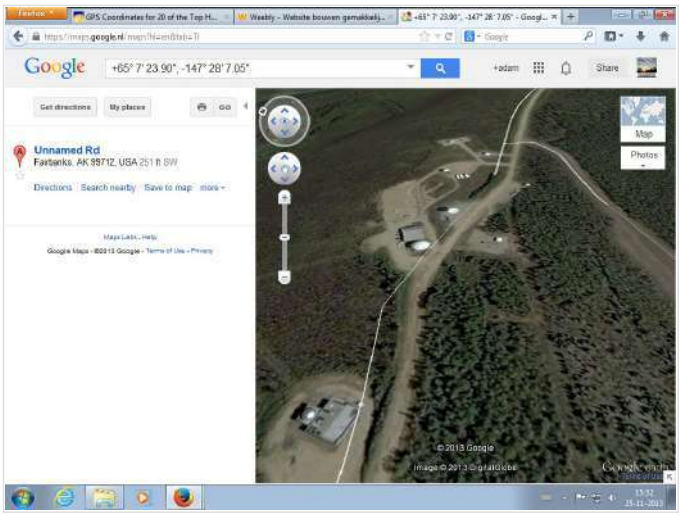

(/uploads/2/3/1/7/23175228/7191263_orig.jpg)

4. Platteville Atmospheric Observatory
Platteville, Colorado
+40° 10’ 54”, -104° 43’ 30”

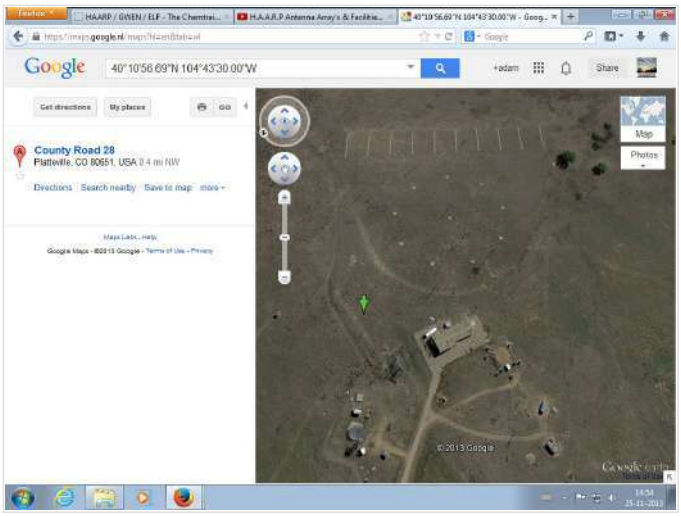

(/uploads/2/3/1/7/23175228/2019020_orig.jpg)

5. Haarp - Westford, Massachusetts, USA (EISCAT-like)
42°37'6.89"N 71°29'25.72"W

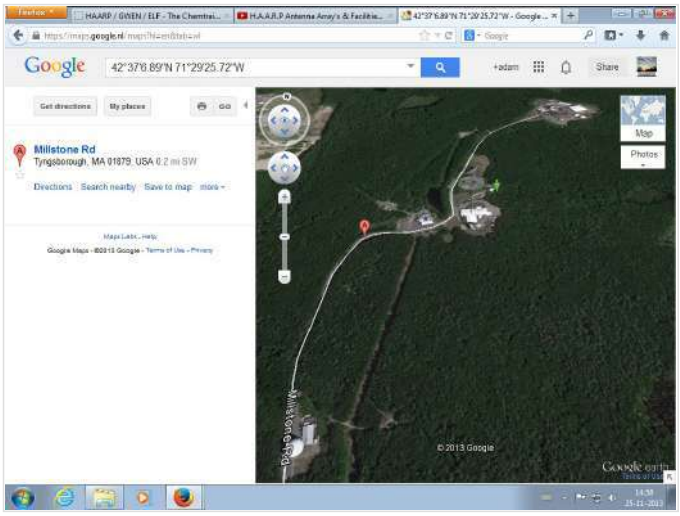

(/uploads/2/3/1/7/23175228/7575768_orig.jpg)

6. Haarp - Westford, Massachusetts, USA (EISCAT-like) Construction
42°37'26.36"N 71°29'16.10"W

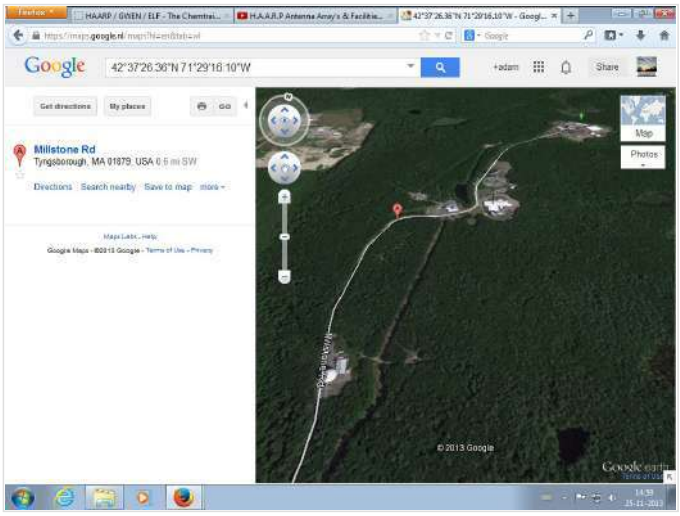

(/uploads/2/3/1/7/23175228/1981341_orig.jpg)

7. Nerc MST Radar Facility
Capel Dewi, Carmarthenshire, Wales, United Kingdom
52°25'25.95"N 4° 0'19.48"W

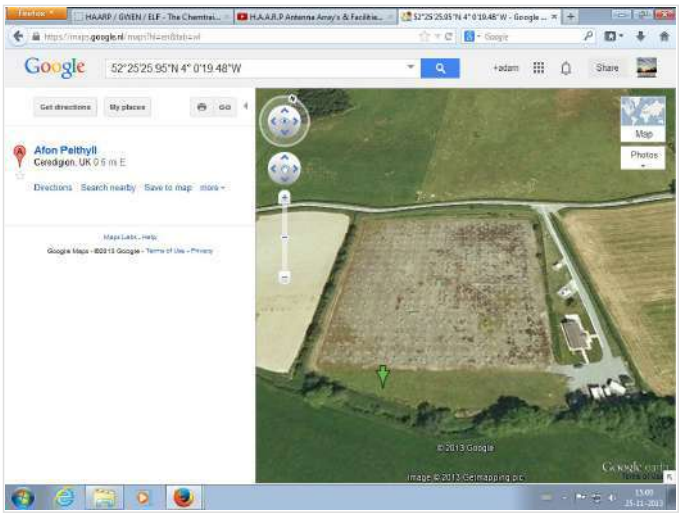

(/uploads/2/3/1/7/23175228/5483133_orig.jpg)

8. The Russian Woodpecker
Duga Radar Array, Chenobyl, Ukraine
51°18'20.17"N, 30°04'02.60"E

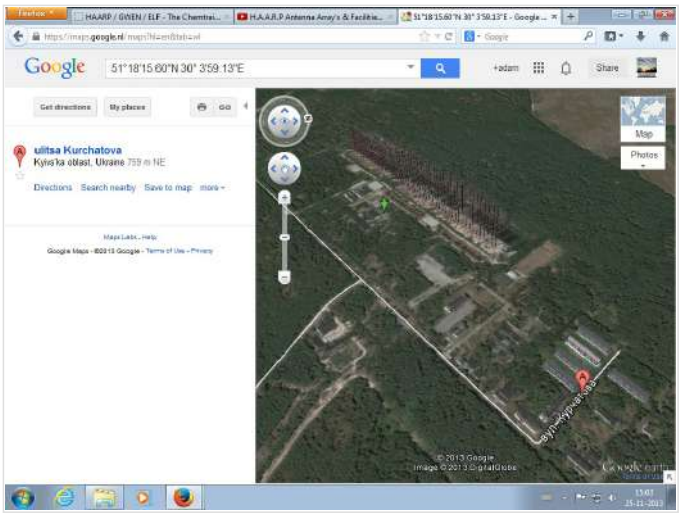

(/uploads/2/3/1/7/23175228/4301759_orig.jpg)

9. The Arecibo Observatory radio telescope
Arecibo Puerto Rico.
18°20'38.97"N 66°45'9.77"W

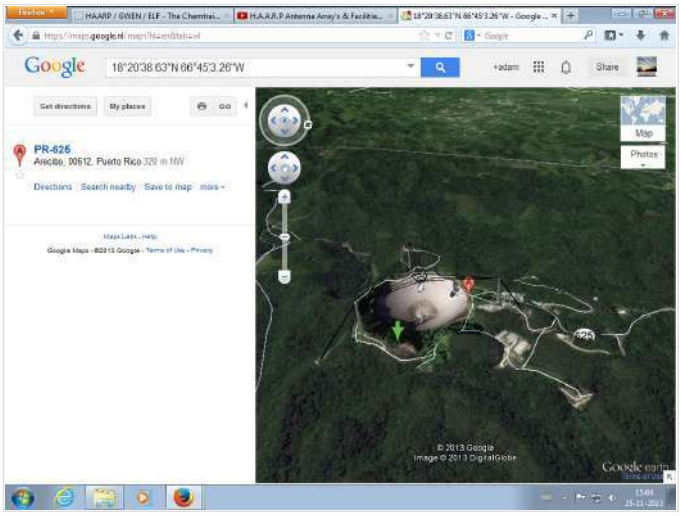

(/uploads/2/3/1/7/23175228/7398577_orig.jpg)

10. National MST Radar Facility NMRF
Gadanki, India
+13° 27' 26.68", +79° 10' 30.74"

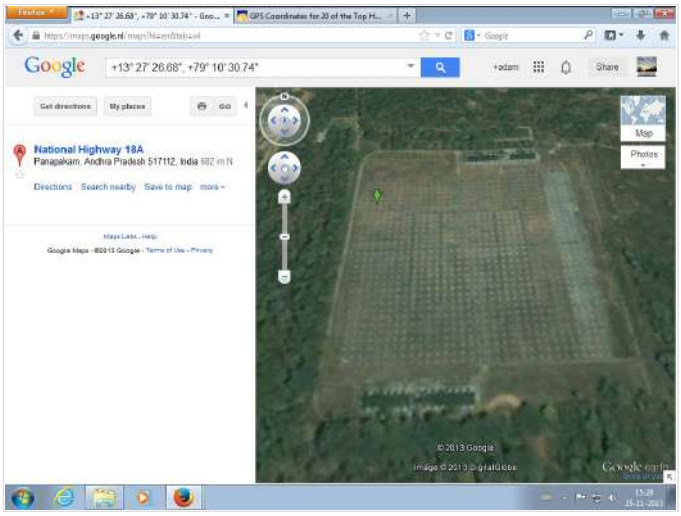

(/uploads/2/3/1/7/23175228/6048676_orig.jpg)

11. Jicamarca Radio Observatory
Lima, Peru
11° 57' 08.25" S 76° 52' 30.67" W

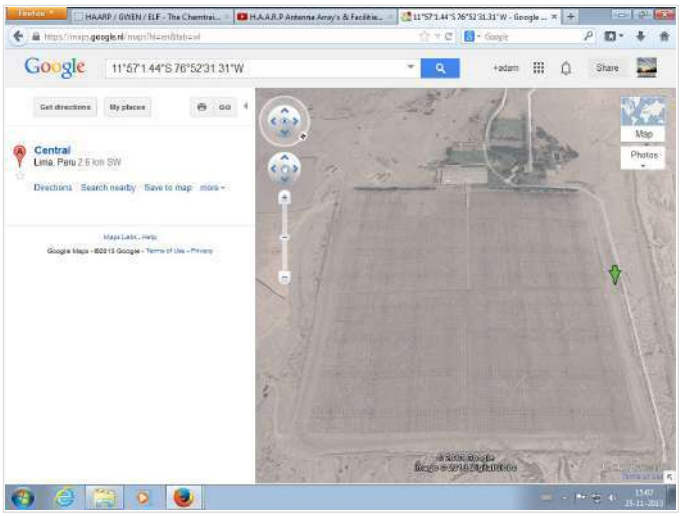

(/uploads/2/3/1/7/23175228/6266894_orig.jpg)

12. São Luiz Space Observatory
Cruzeiro Santa Bárbara, Sao Luis-MA, Brasil
-2° 35' 40.47", -44° 12' 35.90"

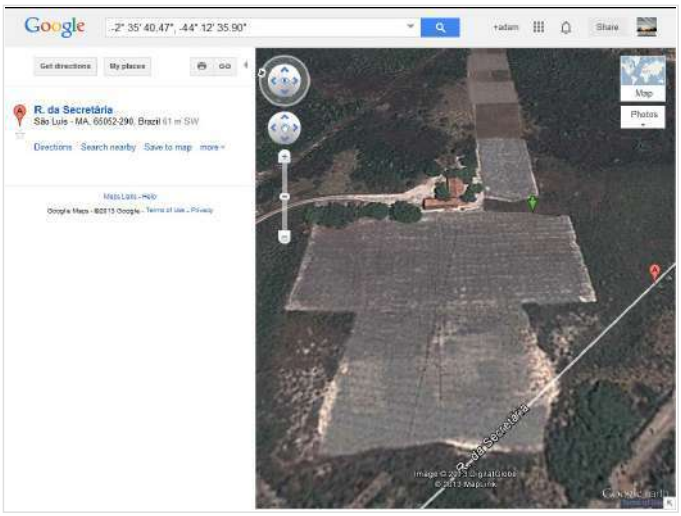

(/uploads/2/3/1/7/23175228/7926199_orig.jpg)

13. European Incoherent Scatter Scientific Association EISCAT
Ramfjordmoen, Near Tromsø, Norway
+69° 35' 10.94", +19° 13' 20.89"

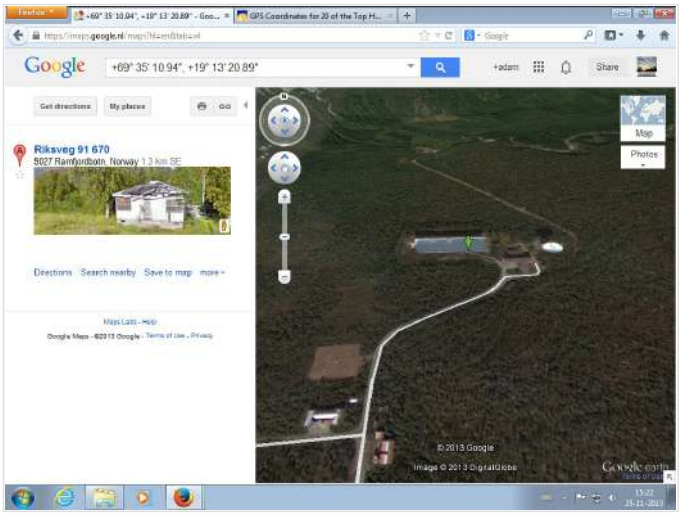

(/uploads/2/3/1/7/23175228/3199053_orig.jpg)

14. Sura Facility
Nizhniy Novgorod, Russia
+56° 7' 9.70", +46° 2' 3.66"

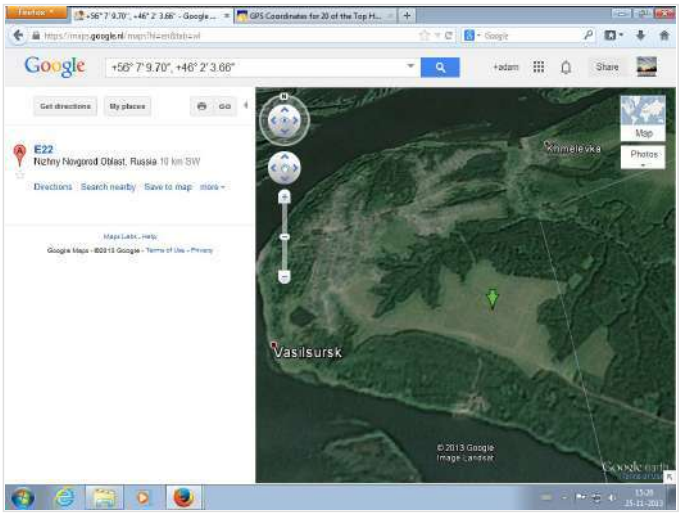

(/uploads/2/3/1/7/23175228/5474744_orig.jpg)

15. China Research Institute of Radiowave Propagation (CRIRP)
Xinjiang (Sinkiang) Region
40°24'15.91"N, 93°38'09.74"E

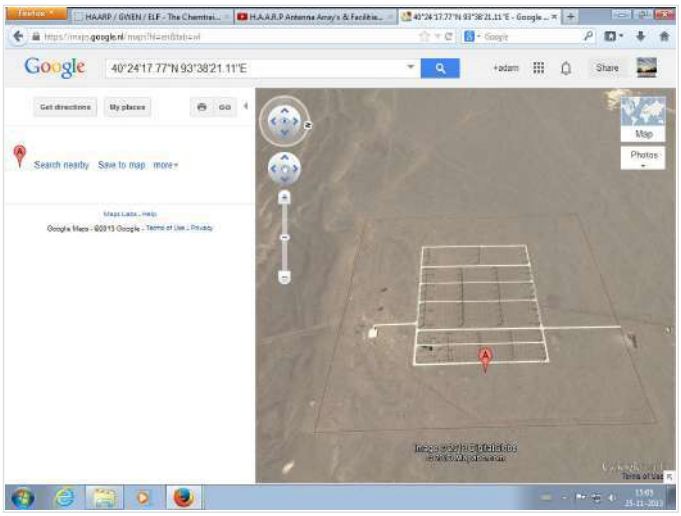

(/uploads/2/3/1/7/23175228/7563411_orig.jpg)

16. Sheshan, Shanghai,
China
31°5'41.98"N, 121°11'29.72"E

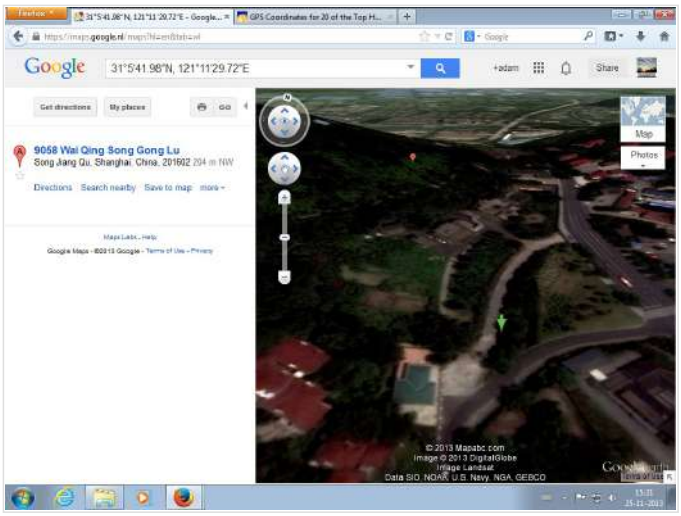

(/uploads/2/3/1/7/23175228/6051246_orig.jpg)

17. Mu Radar
in Japan
34°51’14.80”N 136° 6’19.45”E

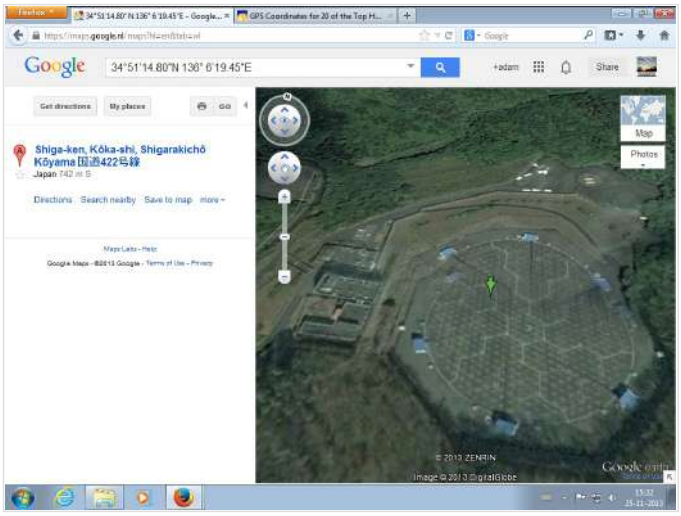

(/uploads/2/3/1/7/23175228/4904711_orig.jpg)

18. Jindalee Operational Radar Network (JORN)
Laverton, West Australia
-28° 19’ 36.29”, +122° 0’ 18.84”

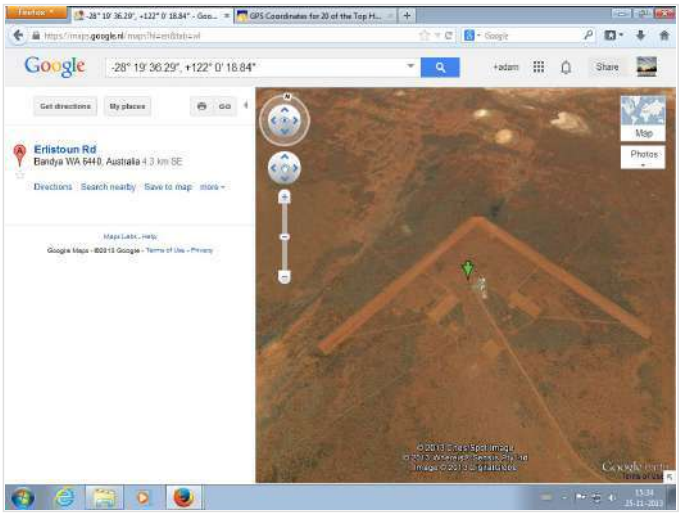

(/uploads/2/3/1/7/23175228/97514_orig.jpg)

19. Jindalee Operational Radar Network (JORN)
Longreach, Queensland, Australia
-23° 39’ 29.53”, +144° 8’ 49.58”

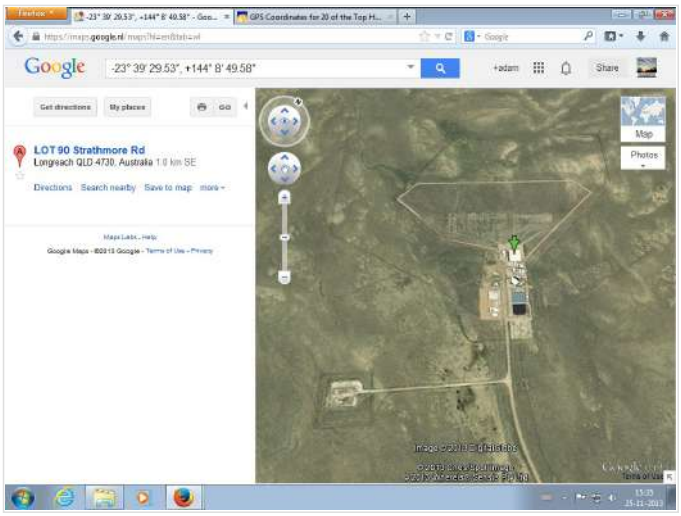

(/uploads/2/3/1/7/23175228/908329_orig.jpg)

20. Australia Naval Communications Station Harold E Holt (NCS HEH)
Exmouth, Western Australia.

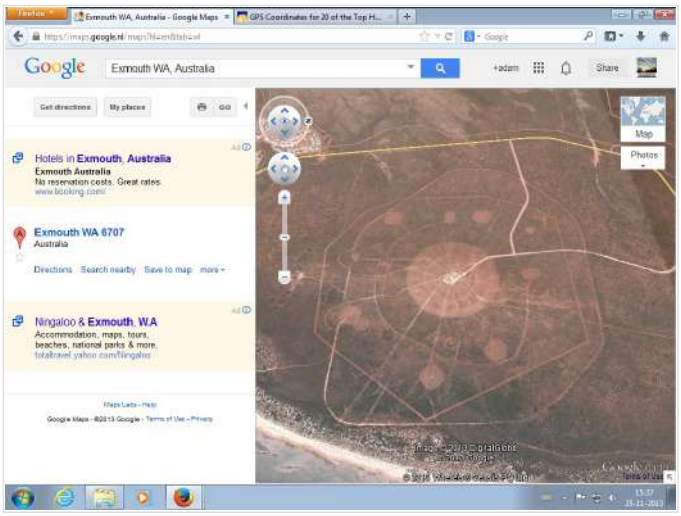

(/uploads/2/3/1/7/23175228/3863477_orig.jpg)

(/uploads/2/3/1/7/23175228/8315126_orig.jpg)

21. Zhong Shan Antarctic Polar Station (China)
69º 22’ 43.69” S 76º 23’ 15.07” E

(/uploads/2/3/1/7/23175228/4903180_orig.jpg)

22. 43°04'51.75"N/92°48'26.85"E

(/microwaves.html)

(/)

- Chemtrails in Nederland en meer -

CREATE A FREE WEBSITE

POWERED BY

MFJ-971 Portable Antenna Tuner Modifications

Ads by Google Mods Guitar Tuner Tuner Tuner Antenna

The MFJ-971 has the potential to be a great portable tuner. It is a small, compact tuner that has a sensitive SWR circuit allowing precise tuning with low power thanks to its 6w FSD setting and it has outputs for coax, wire and balanced feeder (although I won't talk about the MFJ 'heavy duty' 1:4 voltage baluns here!). To make it the almost perfect portable / QRP tuner, there were a couple of things that needed to be solved...

Full SiC Modules ROHM
Constructed by Original SiC-MOS/SBD
Suited for replacemet of IGBT
www.rohm.com

Coil Bobbins
Inch and Metric coil bobbins 5000+ standard range available
www.milesplatts.co.uk

Isolators and Circulators
300MHz to 20GHz: Coax, Drop-in & WG
Fast Delivery, Manufactured in UK.
www.mcsmicrowave.co.uk

The problems I had with this tuner are:

1) No bypass switch

2) Not enough inductance to tune on 1.8MHz

The first thing that I would want in any tuner, is a bypass switch. Its nice to flick a switch and be able to receive on all bands and the lack of a bypass switch is frustrating. This was easily added by mounting a DPDT switch to the front panel, and connecting it appropriately, as seen in the pictures below.

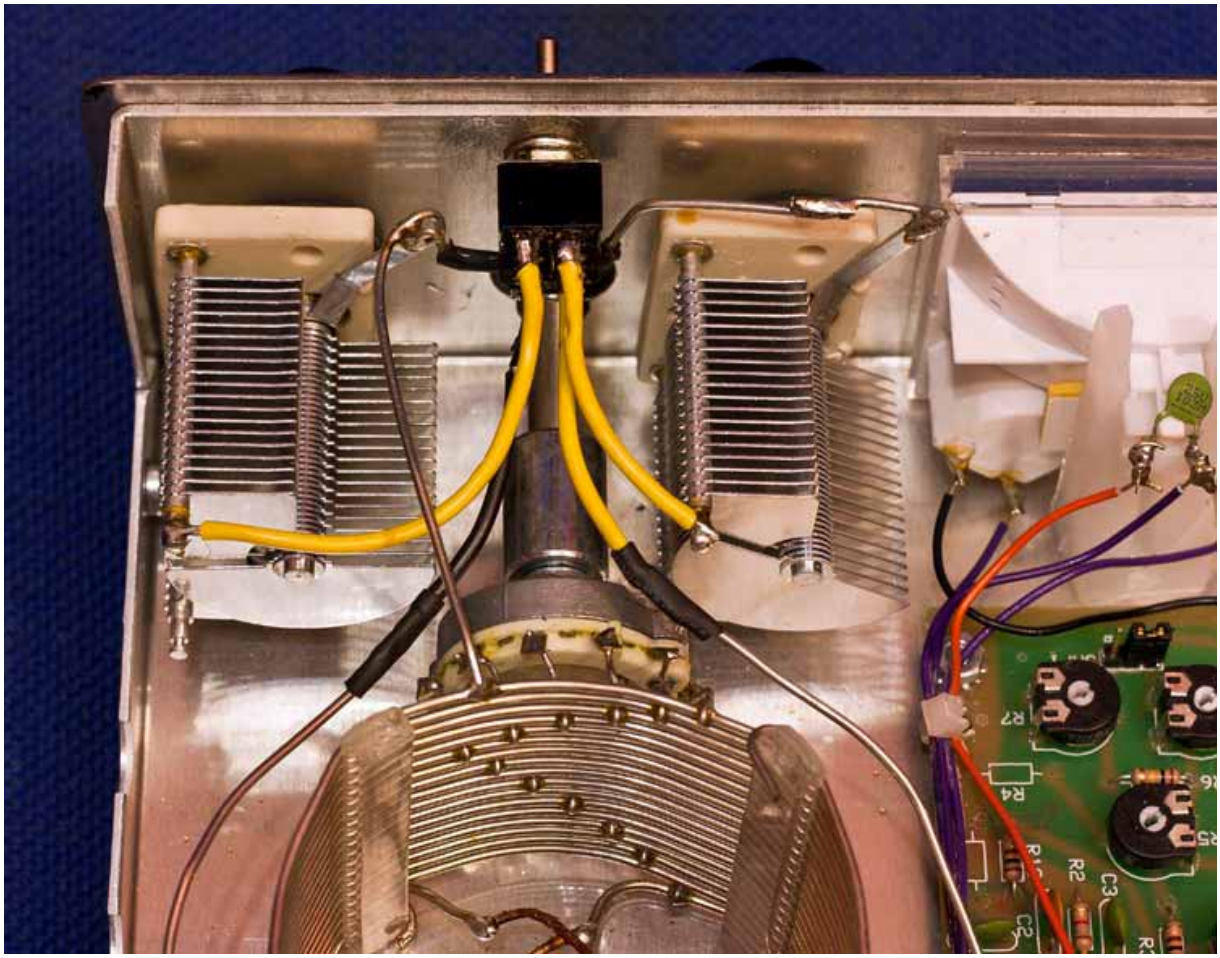

Usually, the signal comes off the PCB and straight into the 'transmitter' capacitor and the output of the 'antenna' capacitor goes to the coax/wire connection on the rear. The switch has been added to provide a way to bypass the tuner section. A drawing of the DPDT switch wiring is below.

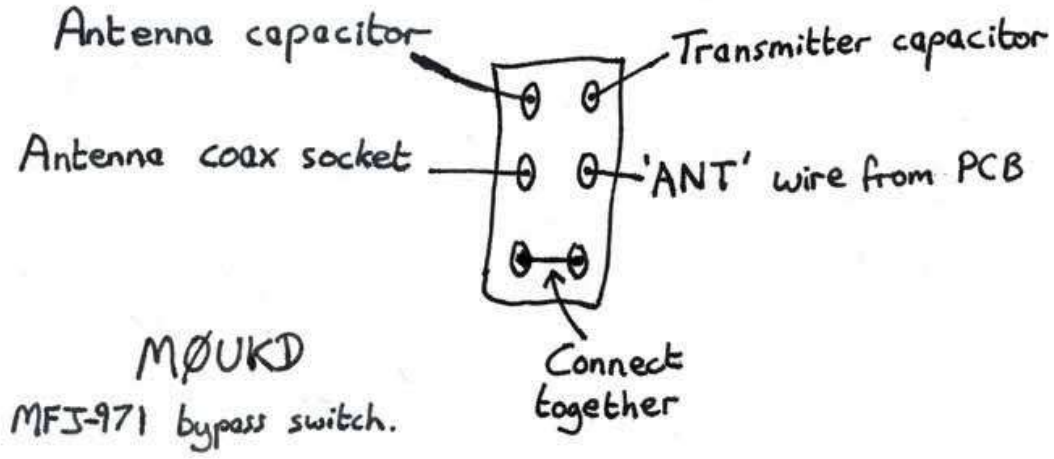

OK, now that annoyance is out of the way, lets fix the top band issue. MFJ say *'The [MFJ-971] T-match tuner covers*

1.8-30 MHz'. It may well do, if you want to match a perfect 50Ω load on 1.8MHz! The inductor inside this tuner, although adequate for 80-10m, does not have enough inductance to be useful on 160m.

To overcome this problem, I included extra inductance by winding 29 turns of enamelled copper wire (any suitable insulated wire will do) on a T130-2 iron powder toroid, so when the tuner is on the 'L' inductance setting, the whole original inductor is used *plus* the extra inductance provided by the toroid. This does not affect any of the other settings from A-K.

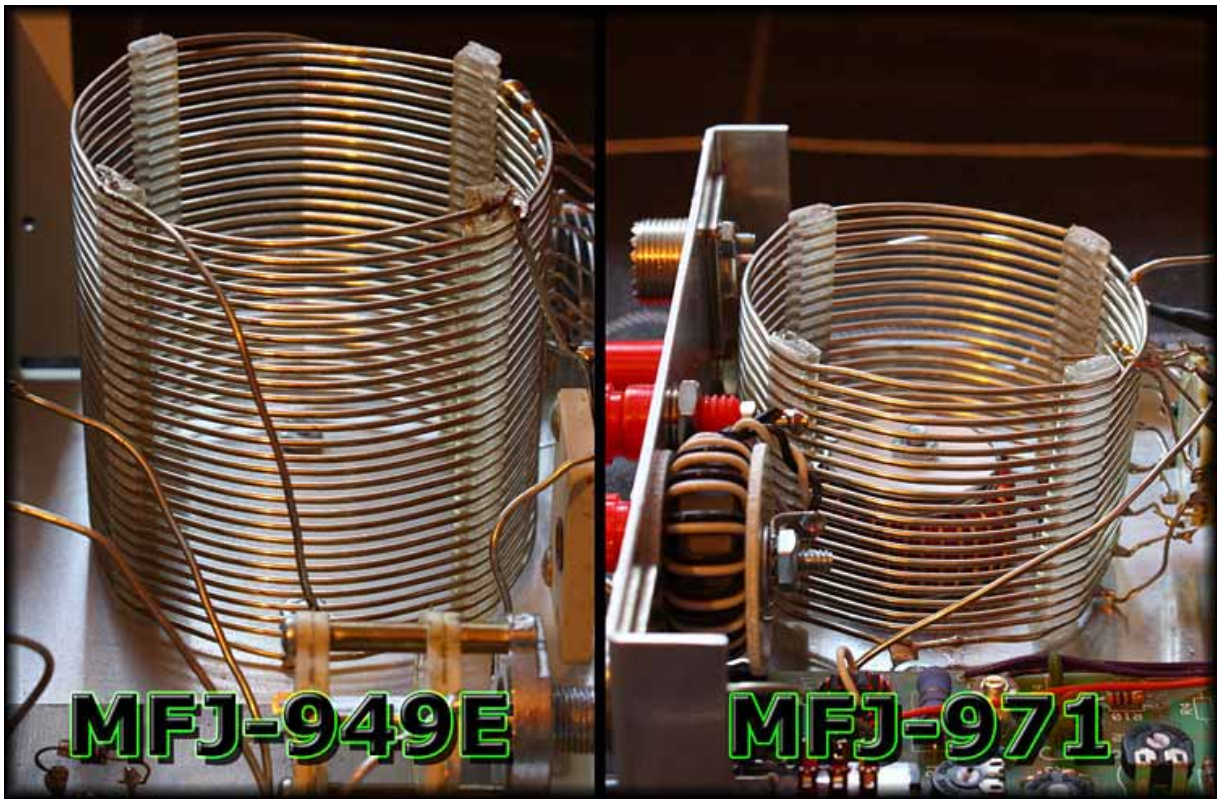

The MFJ-949E inductor has 27 turns, 75mm long and 75mm diameter which is about 37µH.
The MFJ-971 inductor has 17 turns, 43mm long and 66mm diameter which is about 17µH.
Adding on the extra inductance means we have a max inductance of around 27µH which allows matching on 1.8MHz.
Air inductance coils can be calculated **here** and the T130-2 toroid **here**.

High Power Fiber Laser 15W single frequency with low noise 1064 and 1550 nm ranges www.nktphotonics.com/high_power

1553 Box/Flange Couplers Mfr of flight worthy, 1 to 8 stub, 4-hole mount bus couplers. www.databusproducts.com

Coil Winding Specialist Design and Manufacturing of Chokes, Inductors, Transformers, Coils, CTs www.coilws.c

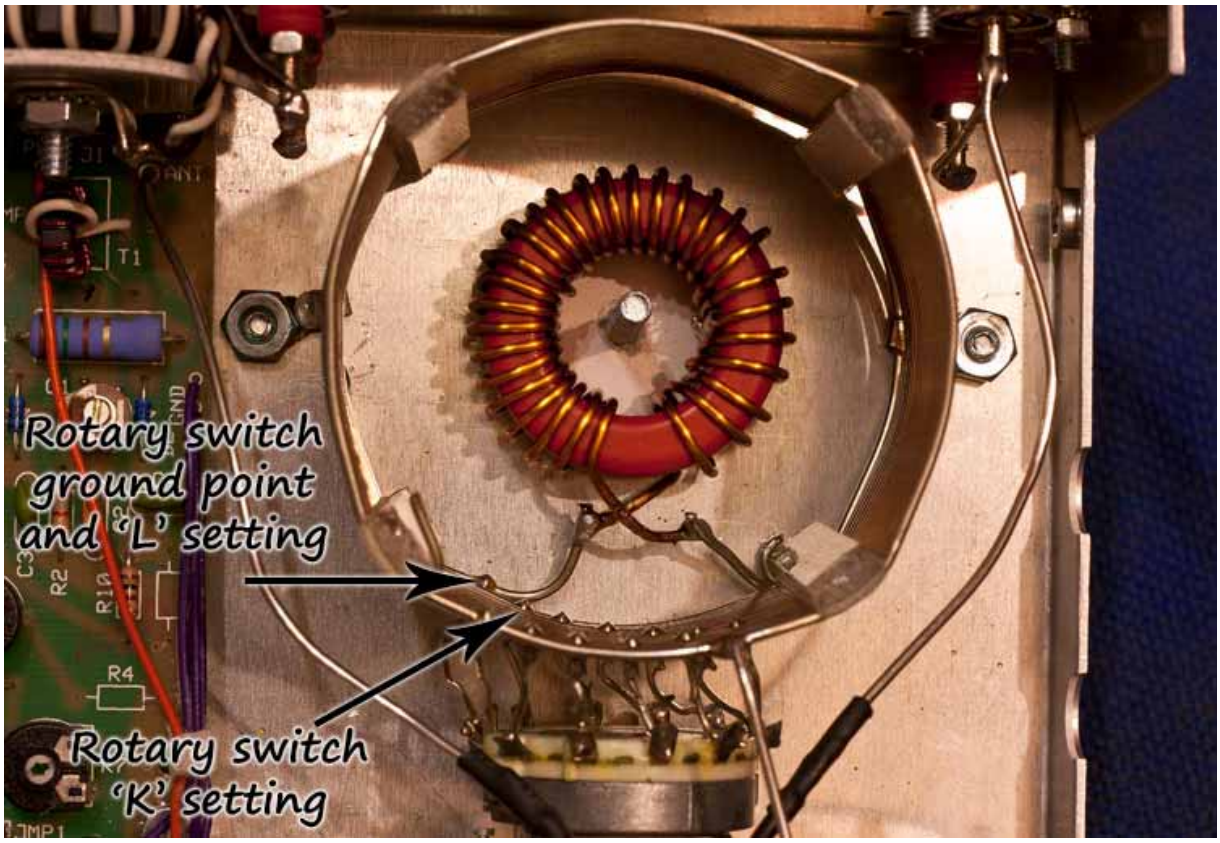

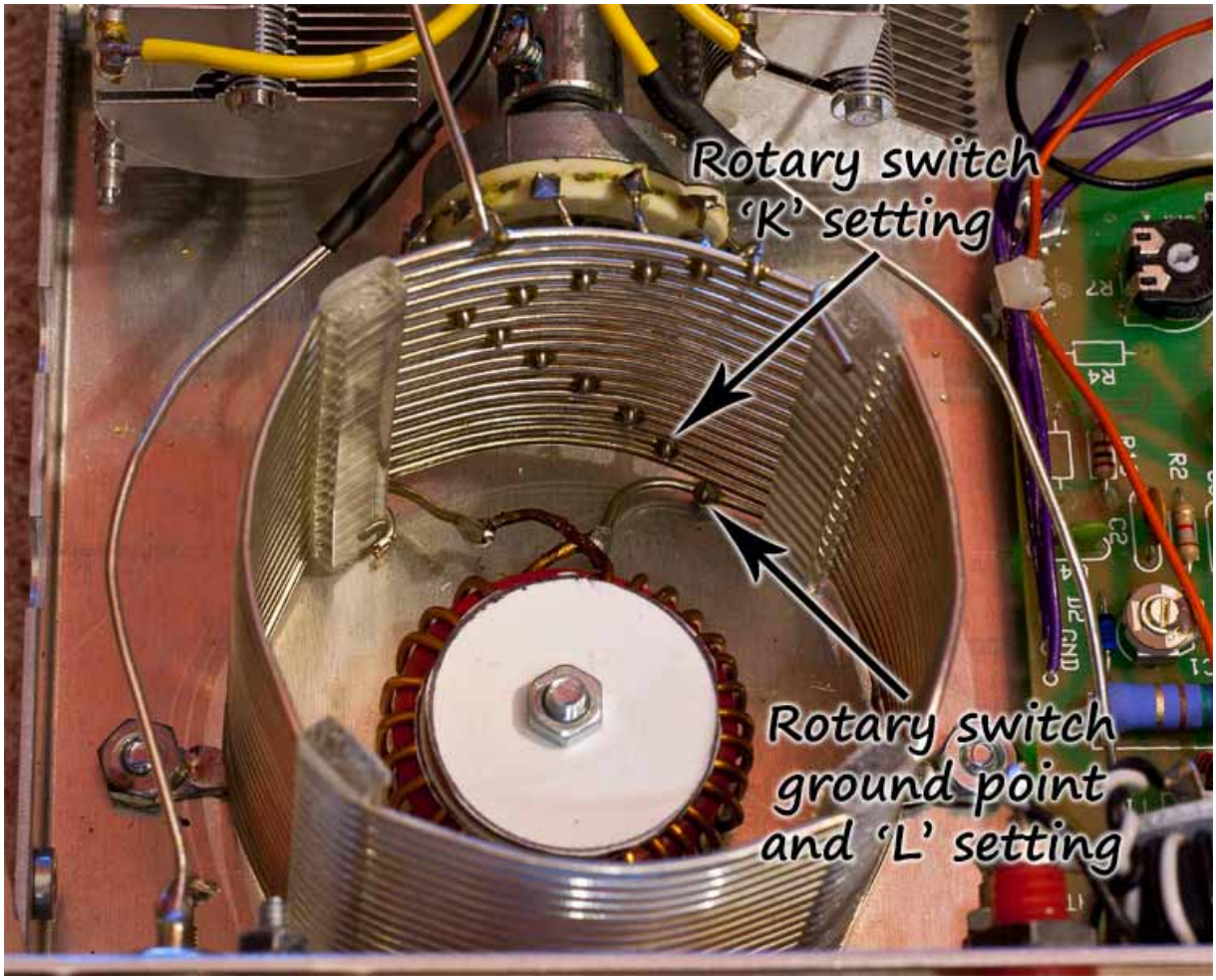

The inductor switch picks up its ground from the bottom of the inductor and this is also the 'L' setting, meaning the whole coil is in use when 'L' is selected. The 'K' inductance setting is 2 turns up from this point. I cut the wire just after the 'L' tap and inserted the extra inductance. Now, when 'L' is selected, the whole original inductor is in use, plus the extra inductance of the toroid, making it suitable for use on 160m! Of course, the 'K' setting still uses the whole original coil (less 2 turns) so nothing is really lost. The wires cross to keep any magnetic fields circulating the same way between the 2 inductors. The toroid is then fixed with a nut & bolt and suitable insulation washers either side of the toroid.

The completed, modified, much improved MFJ-971 is seen below. Please let me know if you perform any of these modifications, I'd be interested to know what you think.

There is one small problem remaining and that is RF BURNS! The nuts that hold the variable capacitors in place on many MFJ tuners are at RF potential. Most of the time they are hard to come into contact with being tucked away behind the control knobs, however, on the MFJ-971 the knobs must be pulled forward a little otherwise the metal inside the knob comes into contact with the metal shaft causing the grub screws that hold the two control knobs on to be at a high RF voltage. This can give you RF burns whilst you are tuning, even at 5 watts. I hate to imagine what the result would be if you put the 'rated' 200w into this thing and touched a control! One problem with pulling the knobs forward a little is that then the nuts themselves are more visible, although anything is better than an RF burn! 73 de M0UKD.

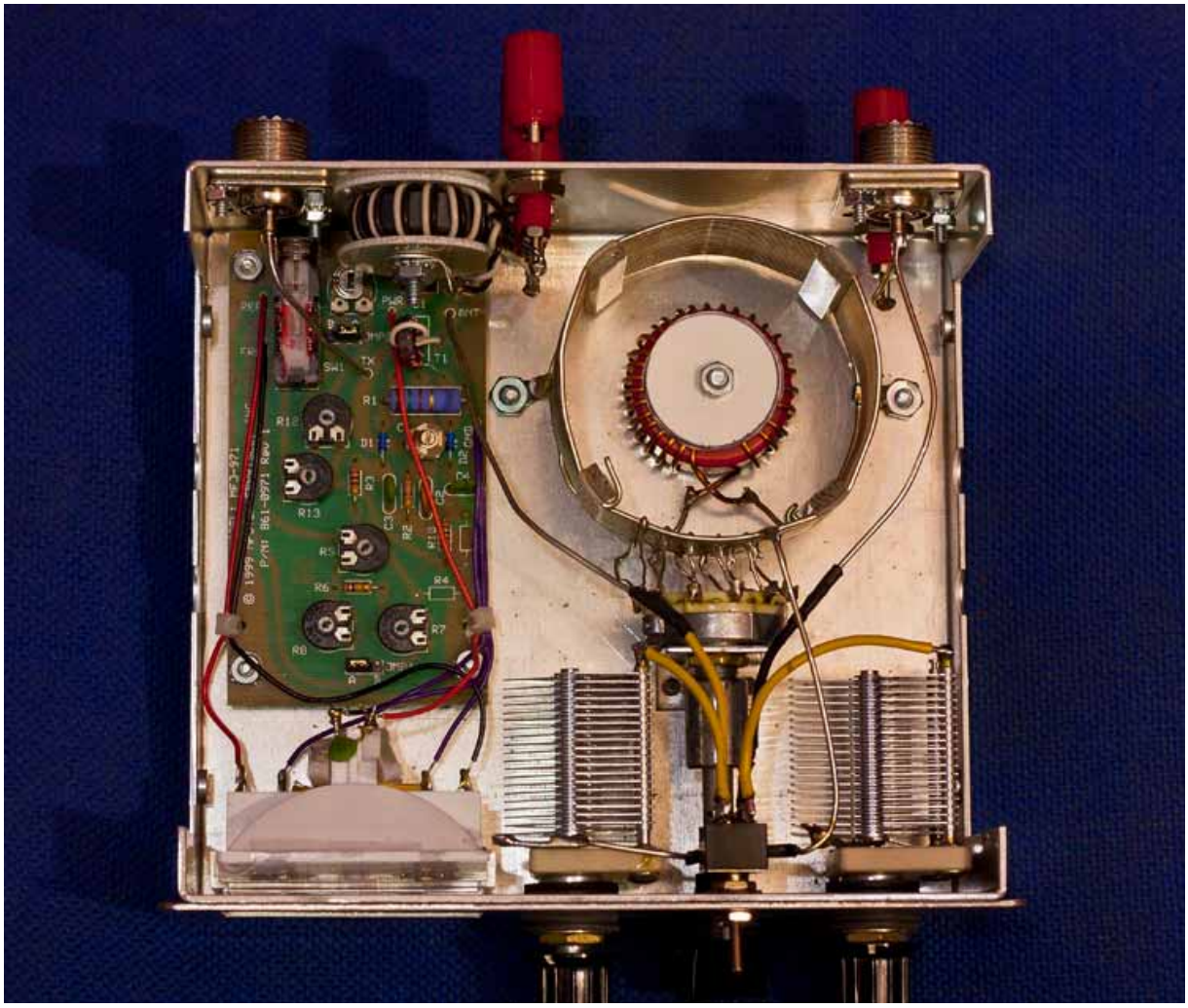

Ads by Google Mods Guitar Tuner Tuner Tuner Antenna

Ugly/Ground Plane Construction

The Method I Use in Building My Simple Receivers

Oct. 7, 2006 by Rick Andersen, KE3IJ

Occasionally I get emails from readers who want to know how I build these simple radio receiver circuits on an "L-shaped chassis" without cutting and scoring the copper, what I mean by "L-shaped chassis," or "what's all this about 10 megohm resistors?", etc. I tend to forget that not everybody has done this before, and I usually take it for granted that the reader is an accomplished "basement-tinkerer" and should therefore be able to just look at a schematic diagram and then come up with his own layout and method of construction. Sorry if I have annoyed anyone -- that wasn't my intention.

When I first design a circuit, I make what a friend of mine used to refer to as a "spider" (or, "spider-web")-- basically just construct the circuit by soldering the components together, lead by lead, into a reasonable facsimile of the schematic (no chassis or pc board necessary-- the stiffness of the soldered leads themselves hold the "spider" circuit together). This method is quick, and allows me to modify things fairly easily. It also grows rather quickly into a "haywire monstrosity" if I allow it.

Sometimes I do use a piece of copper-clad pc board as a ground plane, even during the "spider" stage, as the photo below illustrates:

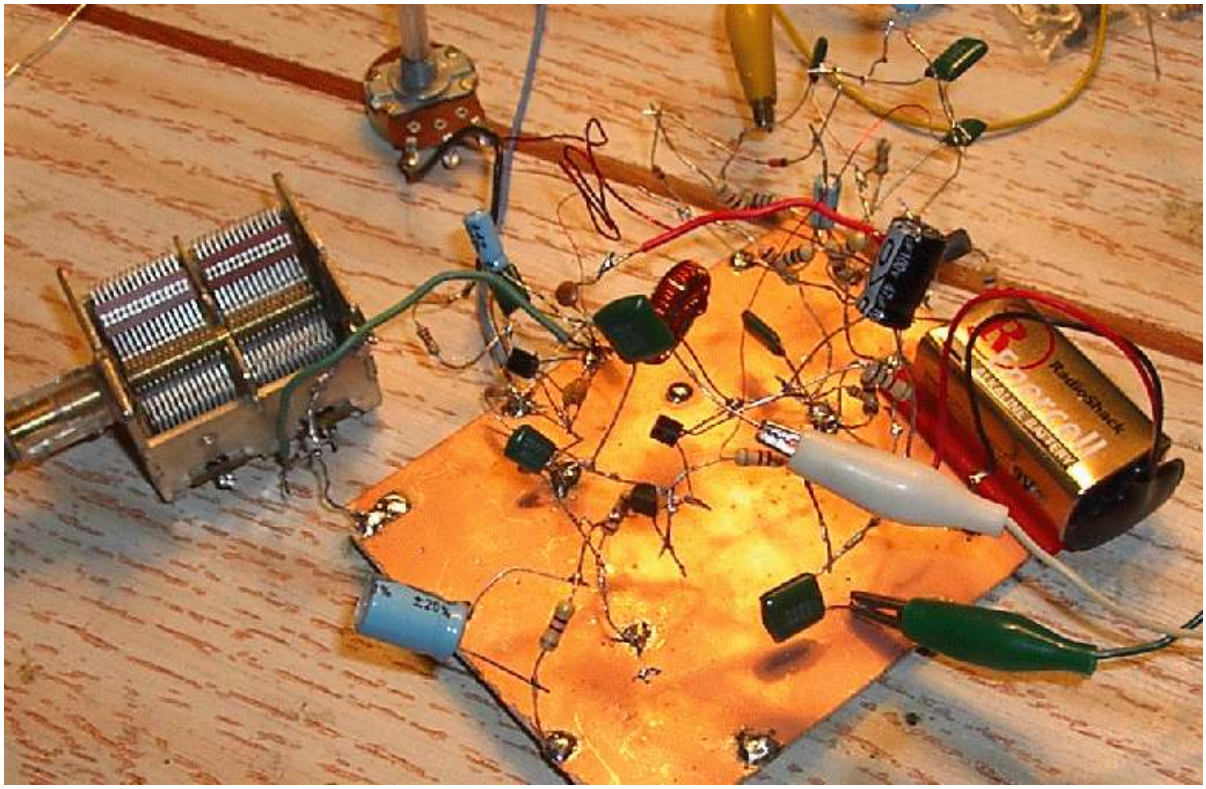

A "haywire" mess of my "AGC-80" Regen receiver in its early, experimental stage

To make things a bit clearer to you who have never built projects in this way before, I have attempted a free-hand diagram using Microsoft "Paint", which I converted to a .gif file and which you see below.

In the top-center of the diagram is the schematic for a simple common-emitter audio amplifier stage. The left side of the diagram illustrates how one might translate that schematic into an actual circuit on the copper-clad pc board. At right is a diagram of the "L-shaped Chassis." This is the style in which I build most of my circuits.

Basically, I use 2 pieces of 5x7 inch copper-clad pc board, available in the USA at **Radio Shack** [free plug]. One piece lies flat (the bottom piece), which is what I have shown in the diagram. I build my circuit on this bottom piece, using the copper floor as my ground connections ("ground plane"). Any resistors, caps, etc., that go to ground in the schematic, are literally soldered to this bottom ground plane and stood upright. At their top ends, the rest of the circuit is soldered, suspended up above the ground plane. Anywhere that I think I need some mechanical stability, I use a vertical 10 Megohm resistor, which acts to prop up and support the rest of the wiring above the ground plane. For most of the circuits I build, 10 Megohms is much higher a resistance value than any of the resistors in the circuit itself; therefore, the circuit pretty much ignores the 10M "posts", electrically, and they remain simply a mechanical "standoff insulator". The 2nd piece of copper clad board is drilled for switches, potentiometers, tuning caps, and earphone jacks, etc., and then is soldered at right

angles to the flat bottom piece, making an "L-shaped chassis". It also helps to solder triangular pieces of copper-clad board as mechanical braces, at the corners where the front panel is soldered to the bottom ground plane.

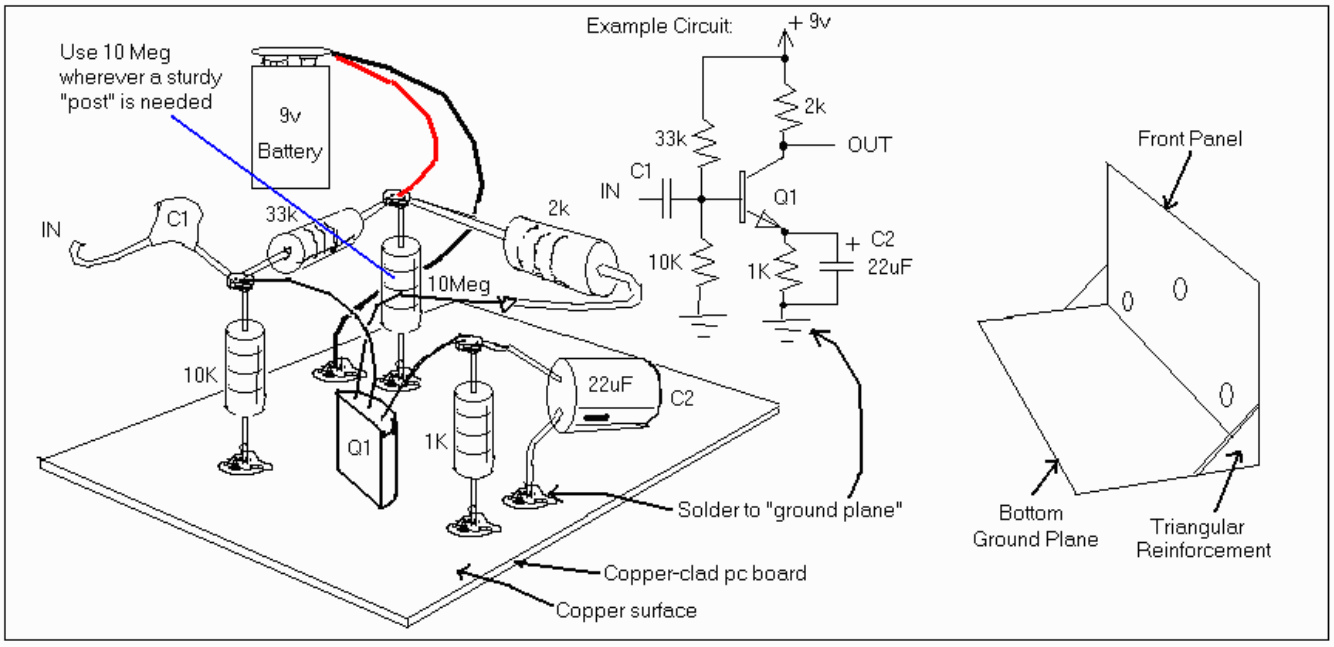

Below is a photo of my 2006 creation, the "AGC-80", a Regen receiver for the 80 Meter ham band with audio-derived AGC. There's an article on this receiver elsewhere on this website; meanwhile, notice that it is built in the same way outlined above-- an "L-shaped" chassis made of a bottom piece of copper-clad board, soldered to a vertical piece of the same kind of board which is the front panel. [I also added a back wall to hold the antenna jack, and a right wall to hold the audio output jack, as well as a triangular reinforcement piece of copper-clad, at bottom-left between the front panel and bottom piece, although you can't see it in this photo.]

To the right of the AGC-80 is the infamous Radio Shack/Archer little beige Amplified Speaker that I'm always mentioning. I may knock Radio Shack for other reasons [for example, that they have pretty much left us hobbyists behind, and have become just another consumer electronics store] but I will always say good things about their little $12.95 beige-colored Amplified Speaker. It works like a charm for the kind of projects I build. I also run an audio cable out of the Radio Shack amp to a bigger speaker, for better-quality sound-- in the photo you can see a white "Optimus" computer speaker pressed into this service. While the Radio Shack's speaker does a fine job, the Optimus sounds quite a bit louder and way nicer. Of course, you may argue that a *real* Electronics Geek rolls his *own* audio amp rather than rely on a commercially-made, external one. Well, I'm often too impatient to build the audio power amp myself, after having spent hours or days getting the RF part of the radio to work the way I want. Also, homemade audio amps tend to oscillate (squeal, motorboat, howl) in mysterious ways once lovingly installed on the same circuit board as the RF circuitry.... After a while one grows tired of trying 50 ways to make it happy, and would rather just hook up an Amplified Speaker and be done with it.

To each his own.

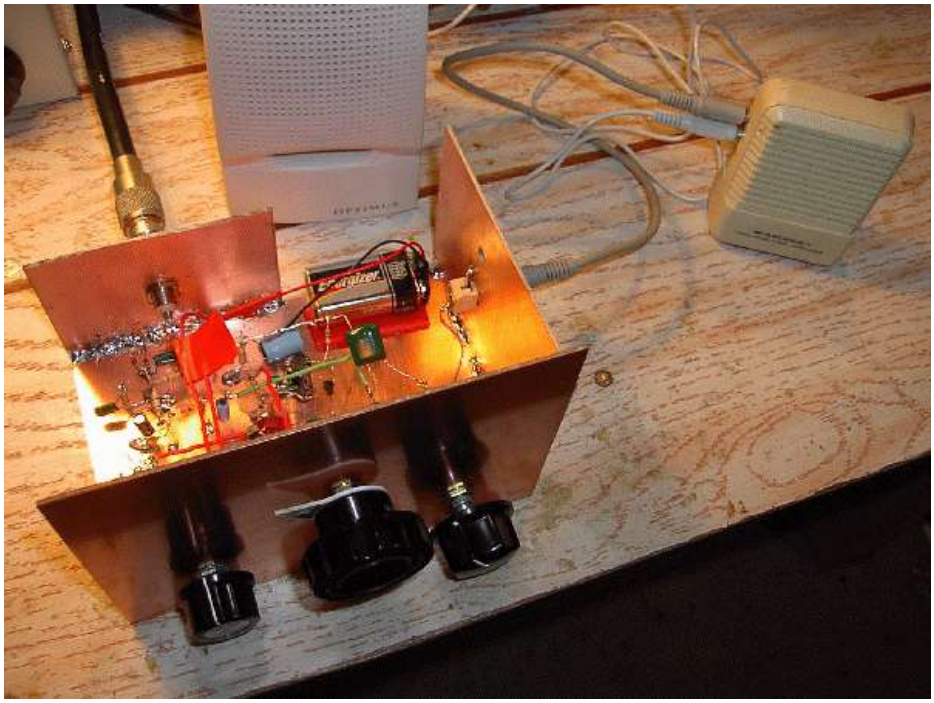

Please realize that you don't have to follow this method of construction (usually called "Ugly Construction" by hams), but I would advise you to make sure there is some equivalent of a copper ground plane in most of your radio projects... it helps to shield the circuit from outside influence (particularly when connected to earth ground) and contributes to stability.

I hope this has helped to give you a little better idea of the methods I use!
73 de Rick, KE3IJ

Back

ON6MU's "Vipormutant" Antenna RE-AHFV14P

Versatile Inexpensive Portable Multi-band Tunable Antenna

de ON6MU
revision 2

AdChoices RF Antenna Design Antenna 2M 70CM Antenna

Features

- Only 3 meters high fully extended (effective radiating element height)
- Less then one meter inserted (no element is larger then one meter including the tunable section)
- Tunable without the use of an extra tuner (just switch till you get the best SWR)
- Covers all frequencies from UHF to 7 MHz without a tuner
- UHF (tuned by de- or increasing the length of the antenna) 3/4 2*5/8 4*5/8
- VHF (tuned by de- or increasing the length of the antenna) 1/4 5/8 2*5/8
- HF (tuned by switching)
  6 meters (1/4 1/2)
  10 meters (1/4)
  12 meters
  15 meters

17 meters
20 meters
30 meters
40 meters: with large counterpoise and/or with longer radiating element, or extra tuner
80 meters: if radiating element is > 5 meters, or with large counterpoise and/or with extra tuner

- Works with or without cointerpoise
- Ideal as portable or balcony antenna
- Compact and extremly portable
- Not too critical on the material or sizes of the elements
- +- 50 watt input
- SWL's Note: tunable on all frequencies between the bands mentioned above

What you need to build the "Vipormutant"

- 5 (or more depending on how high you want your boom) alu tubes
- piece of hard insulating tube (+- 7 cm), examples: plastic, nylon, bamboo...
- some low loss RG174 50 Ohm coax
- carbon/ferrite bead or toroid (to act as a choke)
- a few meters of 0,75mm enamelled copper wire to make the coil
- SO239 (PL259 female)
- Paint, silicon, glue etc. to seal things up
- Plastic box to mount over the coil and where we'll put the switch and SO239 connector
- 12 position rotary switch
- a few innox hose clamps

About the "Vipormutant" antenna:

Well yes, one must have a name HI...It is nothing more then a base coil loaded antenna, but with a selector direct on the base to tune the antenna.
Most of us don't have the luxury of building a 1/4, 1/2 or even a 5/8 wavelength vertical antenna for HF. We have to settle for something a little shorter. (A lot shorter, in the case of people following the FCC's Part 15 rules, which limit them to 3 meters in size.) Shorter vertical antennas can give acceptable (but not spectacular) performance.
I needed a highly (HF) portable antenna to use with my FT-817 which should have the highest possible frequency range (also VHF) and still compact enough to take along almost anywhere! The antenna should be versatile enough to allow further experimenting, to allow being mounted on a balcony, caravan, outdoors etc... So I came up with a compact vertical (dismounted no higher then 1 meter) with a "tuner" directly connected to the antenna radiating element (the best possible place a tuner can be).
The "Vipormutant" tuning principle gets energy into the antenna on a wide range of frequencies, but the design of an antenna is what controls what happens to the RF energy from there. For some antennas, the antenna is simply not complete without a radial system, or at least a counterpoise. Other types of antennas need no RF ground system at all. Most reference books on antennas provide solid guidance on radials and counterpoises, but only for antennas cut to a specific frequency. When using the "Vipormutant" it will also act like tuner and at the best place a tuner should be: directly beneeth the antenna! So the rules have to change somewhat because the "Vipormutant" almost operates across the full range of HF frequencies unto UHF. It doesn't need a counterpoise to work, but the efficiency will increase when you do use it.

Considerations:

- If the length of the conductor is very short compared to a wavelength (< wave/4), the electric and magnetic fields will decrease dramatically within a distance of one or two wavelengths.
- It is impossible to make a small antenna to radiate as efficient like a big antenna.
- Ground losses affect radiation patterns and cause high signal losses for some frequencies. Such losses can be greatly reduced if a good conducting ground is provided in the vicinity of the antenna.

The coil/tuner

Wind 0,8mm enamelled copper wire around the isolator (+- 16mm diamter) and make a tap every xx turns (see fig. 2 and 3)

Fig.1

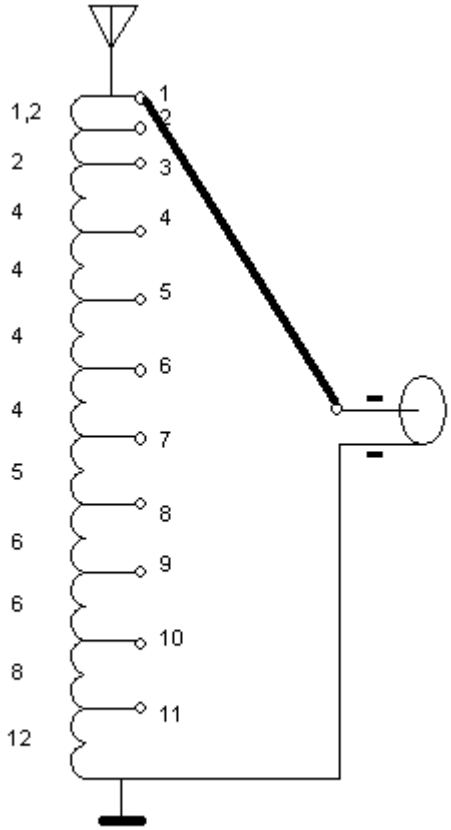

Fig.2 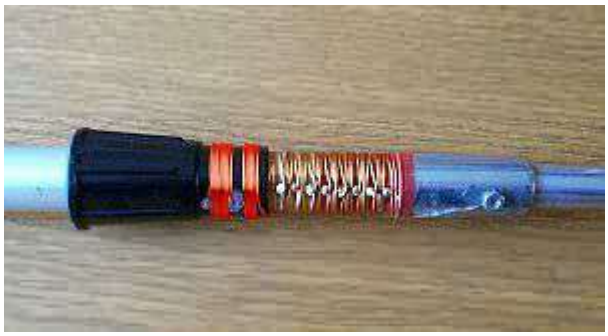 The coil dimensions isn't too critical.

Relatively short antennas behave like lossy capacitors and present a high impedance load to the transmitter due to the large amount of capacitive reactance that is present. The loading coil helps to tune out that reactance. Tuning out the reactance is important because a tuned antenna will accept and radiate much more power than a mismatched antenna.

When the loading coil is installed at the bottom of the vertical radiator, we call it a "base loaded" antenna. Base loading requires the smallest amount of inductance to achieve resonance.

The shoke

Is made out of miniature 50 Ohm coax (rg174) that goes a few turns through the carbon/ferrite bead or toroid. You can also use a Snap-Together Ferrite Choke Core.
If a ferrite is put over a cable which includes both signal and return lines, it will have no effect on the signal (differential-mode) current but it will increase the impedance to common-mode currents. This is because the differential currents, by definition, sum to zero in each wire pair and therefore there is no net magnetic field. If there is no field, the ferrite is invisible. But the common mode currents do produce a net magnetic flux and this flux is concentrated in the bulk of the ferrite, leading to an increased impedance for these currents only. The choke should prevent any mantle currents flowing and should decrease RFI.

The effectiveness can be increased by looping the cable several times through the core, but the benefit is limited at higher frequencies by the stray capacitance between the turns of the cable.

Fig 3.

4 turns

Highlighted

Start Download - View PDF
Convert From Doc to PDF, PDF to Doc Simply With The Free Online App! download.fromdoctopdf.com

The base insulator

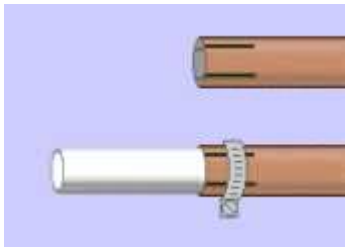

The vertical radiator "driver" element and tuning box
I used a plastic box of 130x70x40mm. On top and bottom I drilled a hole to fit the driver element (radiator of +/- 40cm length)and boom (also +/- 40cm length).
On the side I drilled a hole for the rotary switch and the SO239 connector, whilest on the opposite side I drilled a hole to fit a "ground" bolt where I can easily connect the counterpoise and/or ground to if needed.

Fig 4

Fig 5

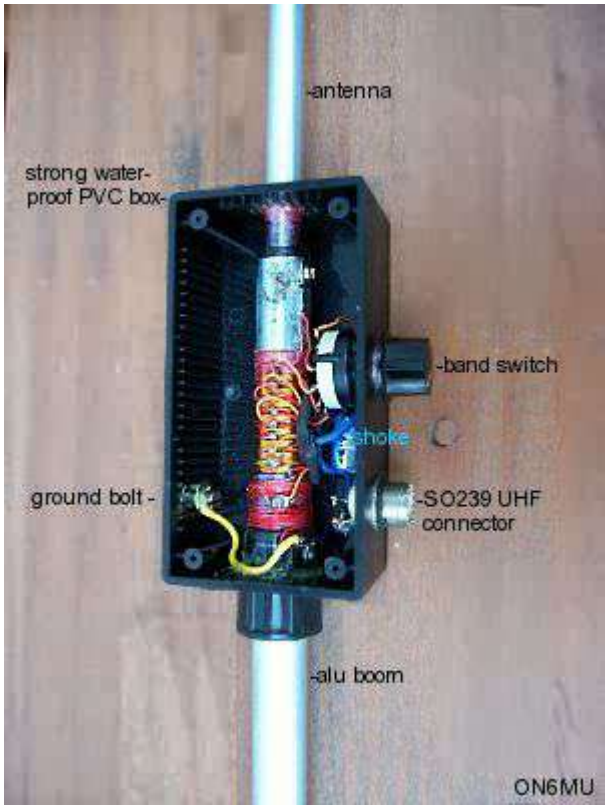

This is how things are connected inside the box:

Fig. 6

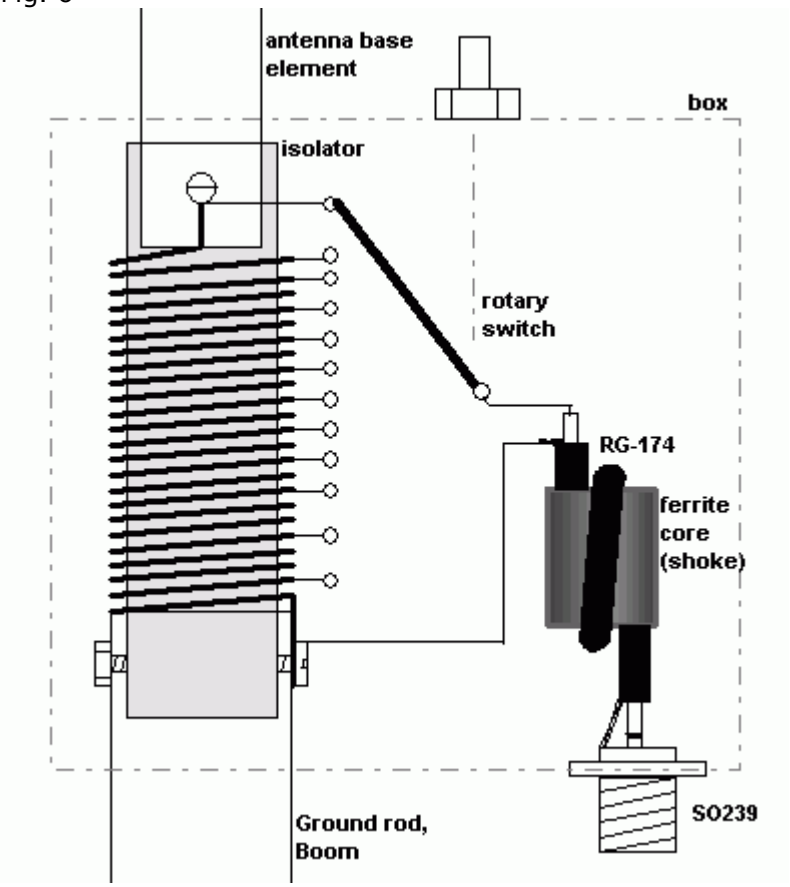

Example

The rotary switch is used for tuning the antenna on each band. The first position allows UHF/VHF ranges.
Tuning is done by sliding in/out of the elements.
The "lower" the switch (higher inductance) the lower the resonance frequency of the antenna.

Remember, and this is important too, to seal everything up so no moisture can penetrate the antenna! Because the radiating vertical antenna elements are made out of separate pieces that fits inside each other and are tightened by hose clamps, the construction isn't waterproof.
If you use a hollow isolating piece you need to to prevent moisture from getting inside the box (via the places where the elements are hold together). I've used a rubber "stopper" that fits snugly on the bottom of the driver element and glued tight.

Black paint finishes the job:

fig. 7

using a round box
In my first design I used a plastic box of 50mm diameter and 9 cm heigh. On top I drilled two holes: one for the driver element (radiator of 40cm) and a hole for the rotary switch (as was used in the first prototype).

fig.8: The main driver element and tuning unit finished

This allows it to be used on almost any boom or can be extended to use with or without vertical elements! Ideal for experimenting!

Featuring Today

The antenna construction specs

All elements are made out of aluminum.
Fig. 9

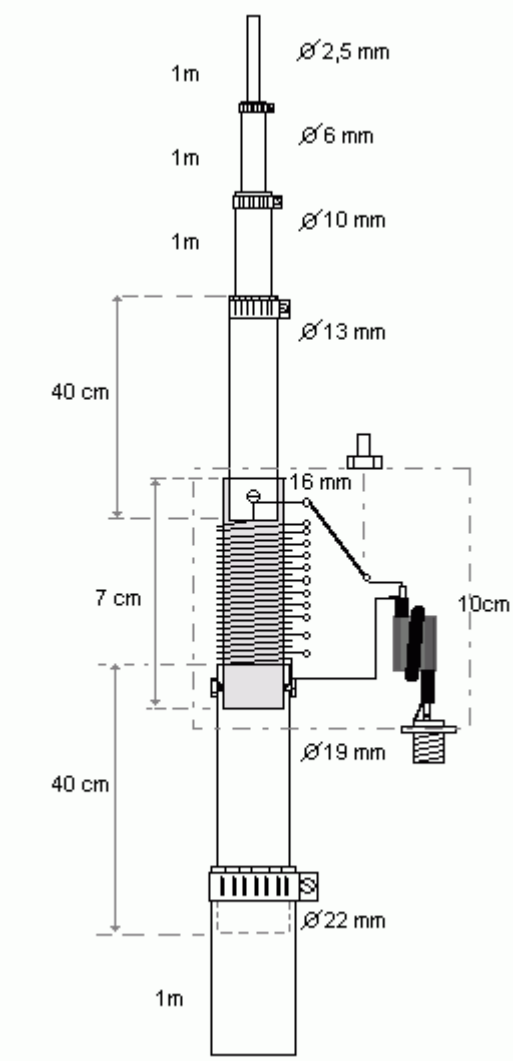

This makes the antenna effective radiating elements a total length of 3 meters. The boom elements can be chosen freely and on your needs. A short one (one element of a meter), a medium sized one of several 1 meter tubes or none at all! The bottom piece where the boom is "connected" too is 40 cm and can/could be put directly in the ground (if made pointed for sure). Or you could fix it in a umbrella stand. Use your imagination HI.

Examples of "Vipormutant's" utilization

Used it on a balcony:

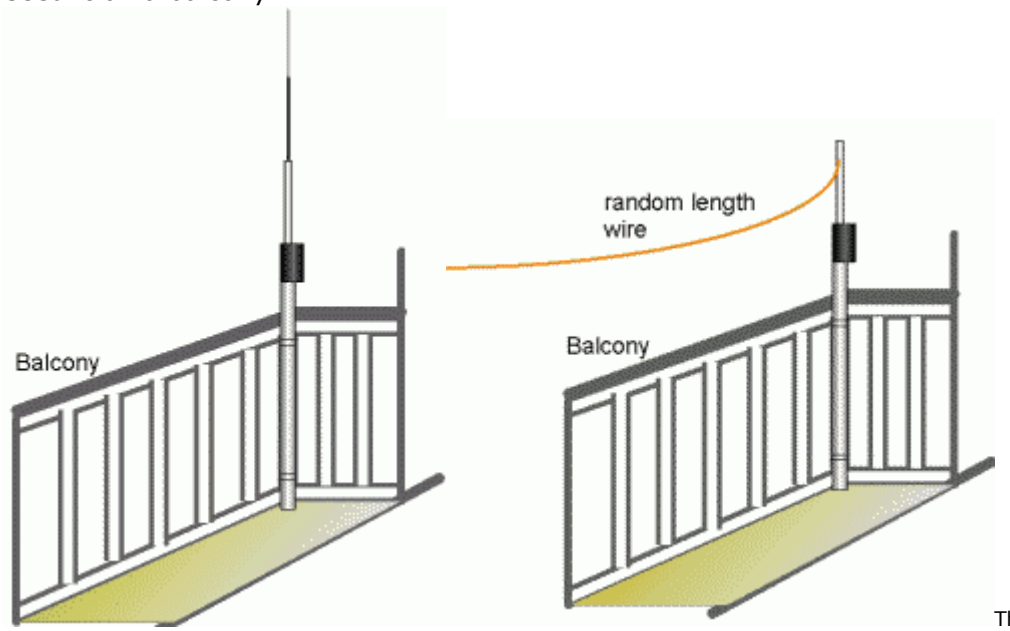

This could cover even the lowest HF-bands!

Use it outdoors without grounding:

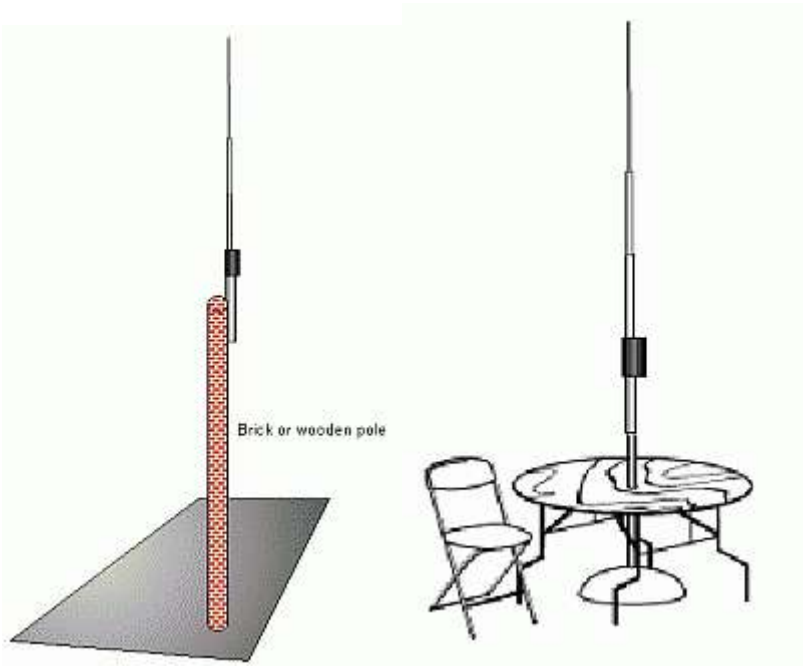

Use it outdoors as a shortened "dipole" balanced antenna (rotary switch set approx. in the middle):

Frequencies below 7 MHz could easily be match 1:1 SWR if total length of the "dipole" > 4 meters
Further tuning can be done with selecting a different impedance using the rotary switch.
Different lengths of wire can be used (an example: one part 3 meter, the other 5 meter or more)

Use it outdoors with ground or counterpoise:

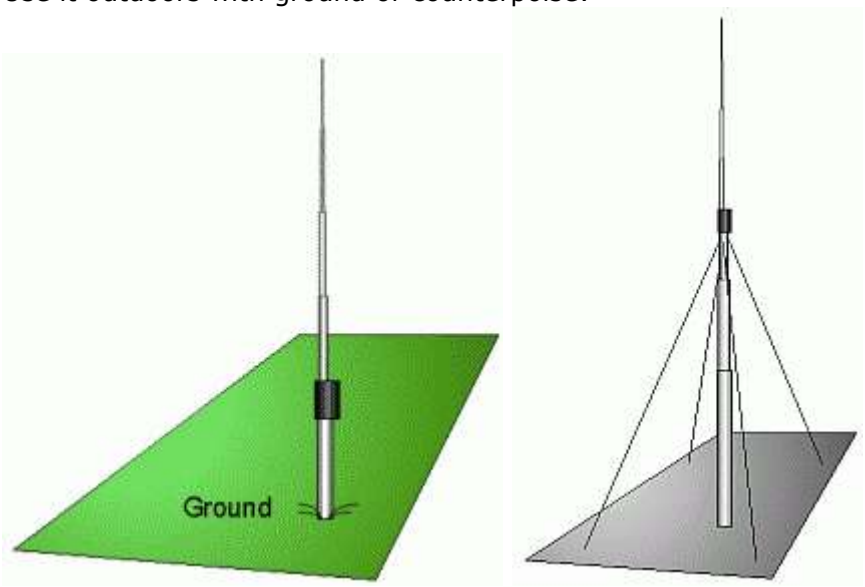

Radials and Counterpoises basic purposes:

1. To improve the RF ground conductivity for the ground current return path. Unless you live in a salt-water swamp, your ground conductivity makes a very poor path for the return of ground currents. This increases the ground losses and reduces the efficiency of an antenna that needs a good RF ground.

2. To provide a counterbalance for the feed point of the antenna to reduce RF radiation back to the radio room. The "Vipormutant" changes the rules because there is no single frequency that you will be operating on, so all of the thumb rules for 1/4 and 1/2 wavelength radials don't apply. It is possible to be either a purist or a pragmatist in deciding what radials to put in place.

3. Number of radials: More is better, up to a point. In carefully controlled experiments, it has been proved that increasing the number of radials from 2 to 15, or from 4 to 16, produces significant increases in signal strength. Further increasing the number of radials to 60 only produces 1 to 2 dB of increase in field strength. Follow this link to see some of the empirical data.

4. Where to put the radials: For a semi-permanent installation, it is customary to bury the radials a few inches down in the soil. This makes it much easier to mow and walk in the area around the antenna. However, some experimenters have gotten an improvement in performance by raising the radials and the antenna base a few inches above the soil. Raising the antenna and ground system several meters above the earth, for example by installing the base of the antenna on a roof-top, can improve the antenna's performance by reducing capacitive earth losses.

While the "Vipormutant" will provide a good match with a poor RF ground system which will will able you to transmit, your antenna efficiency will be low. Nevertheless, by using a tuning circuit directly at the antenna

radiating element losses are kept to a miminum. Getting the greatest efficiency out of your antenna system needs a proper RF ground unless you're using a balanced antenna system

The efficiency of the antenna increases by using a counterpoise. However, the antenna can be tuned perfectly without!

Don't forget to check these out:

ON6MU Homebrew projects
Radioamateur related projects

ON6MU Ham mods
Modifications of transceivers

73"

Have fun and my best 73"

Guy, ON6MU
http://www.qsl.net/on6mu

Comments, pictures or experiences with my antenna are always welcome!

ON6MU

New Journal of Physics
The open access journal at the forefront of physics

Deutsche Physikalische Gesellschaft DPG IOP Institute of Physics

The Large Hadron Collider

To cite this article: Lyndon Evans 2007 *New J. Phys.* **9** 335

View the article online for updates and enhancements.

Related content

- Protection of the CERN Large Hadron Collider
  R Schmidt, R Assmann, E Carlier et al.
- Accelerator physics at LEP
  D Brandt, H Burkhardt, M Lamont et al.
- LHC as nucleus--nucleus collider
  John M Jowett

Recent citations

- Alexandru Iosup *et al*
- Design of distributed JT (Joule-Thomson) effect heat exchanger for superfluid 2 K cooling device
  S Jeong *et al*
- LHC optics measurement with proton tracks detected by the Roman pots of the TOTEM experiment
  The TOTEM Collaboration *et al*

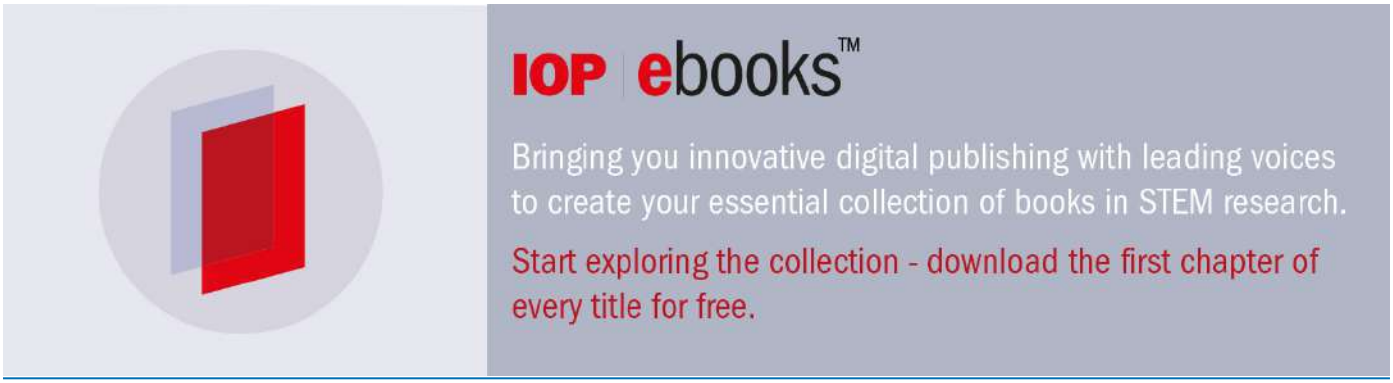

This content was downloaded from IP address 172.0.74.23 on 15/01/2019 at 06:21

New Journal of Physics
The open-access journal for physics

The Large Hadron Collider

Lyndon Evans
CERN – European Organization for Nuclear Research, Geneva, Switzerland

New Journal of Physics **9** (2007) 335
Received 8 May 2007
Published 19 September 2007
Online at http://www.njp.org/
doi:10.1088/1367-2630/9/9/335

Abstract. The Large Hadron Collider (LHC), now close to completion at CERN will provide proton–proton collisions with unprecedented luminosity and energy. It will allow the Standard Model of physics to be explored in an energy range where new phenomena can be studied. This includes the validity of the Higgs mechanism, supersymmetry and CP violation. The machine presents a number of novel features discussed in detail below.

Contents

1. Introduction **2**
2. Machine design **2**
2.1. Machine layout 4
2.2. Main hardware systems 6
2.3. Magnets 6
2.4. Cryogenics 8
2.5. The radiofrequency acceleration system 11
2.6. The vacuum system 14
3. Accelerator physics issues **15**
3.1. Dynamic aperture 15
3.2. The beam–beam interaction 16
3.3. Intrabeam scattering 16
3.4. Coherent instabilities 19
3.5. Electron cloud effects 20
4. Conclusions **21**
References **22**

PII: S1367-2630(07)50015-7
© IOP Publishing Ltd and Deutsche Physikalische Gesellschaft

1. Introduction

The Large Hadron Collider (LHC) at CERN is now in its final installation and commissioning phase. It is a two-ring superconducting proton–proton collider housed in the 27 km tunnel previously constructed for the large electron positron collider (LEP). It is designed to provide proton–proton collisions with unprecedented luminosity ($10^{34}\,\mathrm{cm}^{-2}\,\mathrm{s}^{-1}$) and a centre-of-mass energy of 14 TeV for the study of rare events such as the production of the Higgs particle if it exists. In order to reach the required energy in the existing tunnel, the dipoles must operate at 1.9 K in superfluid helium. In addition to p–p operation, the LHC will be able to collide heavy nuclei (Pb–Pb) with a centre-of-mass energy of 1150 TeV (2.76 TeV $\mathrm{u}^{-1}$and 7 TeV per charge). By modifying the existing obsolete antiproton ring (LEAR) into an ion accumulator (LEIR) in which electron cooling is applied, the luminosity can reach $10^{27}\,\mathrm{cm}^{-2}\,\mathrm{s}^{-1}$.

The LHC presents many innovative features and a number of challenges which push the art of safely manipulating intense proton beams to extreme limits. The beams are injected into the LHC from the existing super proton synchrotron (SPS) at an energy of 450 GeV. After the two rings are filled, the machine is ramped to its nominal energy of 7 TeV over about 28 min. In order to reach this energy, the dipole field must reach the unprecedented level for accelerator magnets of 8.3 T. This high field can only be achieved using 'conventional' and affordable superconducting material (NbTi), by cooling the magnets in superfluid helium at 1.9 K. The cryogenic equipment needed to produce the 100 tons or so of superfluid helium is unprecedented in scale and complexity.

The tunnel diameter in the regular arc is only 3.8 m, insufficient for the installation of two separate rings. The two rings are therefore incorporated into a single magnetic structure with two sets of coils in a common yoke and cryostat.

2. Machine design

At nominal luminosity, the energy stored in each beam is more than 350 MJ (equivalent to 80 kg of TNT). This is more than two orders of magnitude in stored energy, and three orders of magnitude in energy density (due to the very small beam emittance) than in any other previous machine (figure 1). It imposes unprecedented conditions on the reliability of the safety systems which must abort the beams cleanly if necessary as well as on the collimation systems which protect the machine and detectors from halo particles.

The number of events per second generated by beam–beam collisions for a given process is given by:

$$N = L\sigma,$$

where σ is the cross-section for the process in question and L is the luminosity. For the study of very rare events the luminosity must be as high as possible. The luminosity depends only on beam parameters and can be written for a Gaussian beam profile as:

$$L = \frac{N_\mathrm{b}^2\, n\, f_\mathrm{r}\, \gamma}{4\pi\, \varepsilon_\mathrm{n}\, \beta^*},$$

where N_b is the number of particles per bunch, n the number of bunches per beam, f_r the revolution frequency (11.245 kHz), γ the relativistic γ factor, ε_n the normalized transverse emittance and β^* the β function at the collision point. As well as the rare hard collisions between

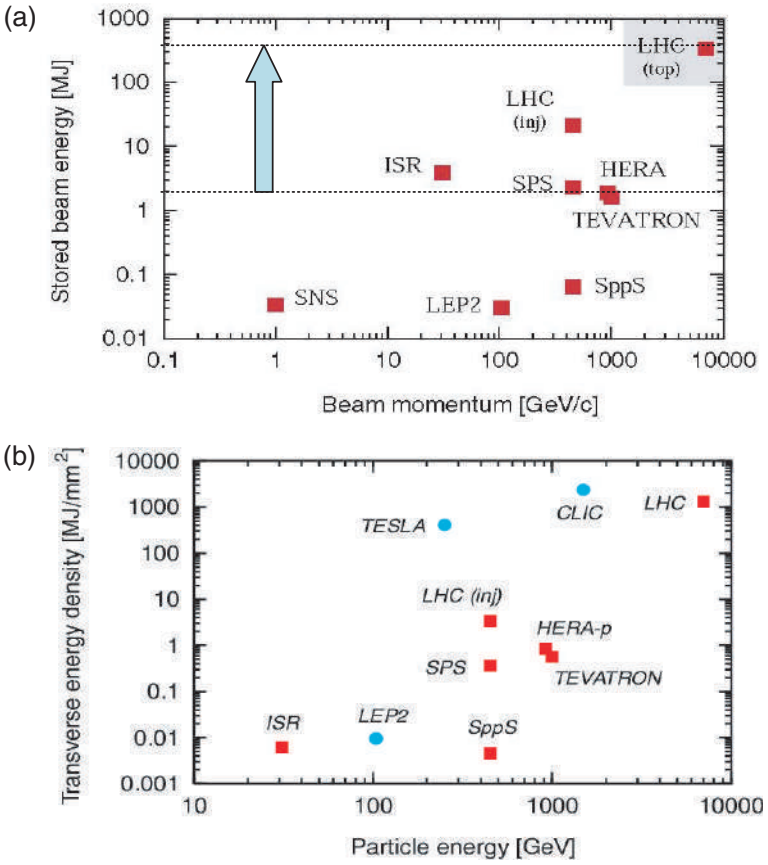

Figure 1. (a) Energy stored in the accelerator beam, as a function of beam momentum. At less than 1% of nominal intensity LHC enters new territory. (b) Stored energy density as a function of beam momentum. Transverse energy density is a measure of damage potential and is proportional to luminosity.

particles, the particles in one beam experience the global electromagnetic field of the other beam (the beam–beam interaction). This force is very nonlinear and gives rise to unwanted effects if not limited to as small a value as possible. Therefore, the bunches must have a crossing angle in order to limit the beam–beam force to the colliding bunches. This produces a geometrical luminosity reduction factor F given by:

$$F = 1/\sqrt{1 + \left(\frac{\theta_c \sigma_z}{2\sigma^*}\right)},$$

where θ_c is the full crossing angle at the interaction point (IP), σ_z the rms bunch length and σ^* the transverse rms beam size at the crossing point.

Table 1 shows the main parameters required to reach a peak luminosity of $10^{34}\,\mathrm{cm}^{-2}\,\mathrm{s}^{-1}$ for proton–proton collisions at 14 TeV centre-of-mass. It can be seen from the table that for the first time in a hadron machine, the synchrotron radiation at top energy is not negligible. At 3.6 kW per beam it is still very small compared with lepton storage rings and has no influence on the design of the radio frequency system, but this power is radiated into a cryogenic environment and strongly influences the design of the vacuum and cryogenic systems.

Table 1. Performance parameters.

Circumference	26.7 km
Beam energy at collision	7 TeV
Beam energy at injection	0.45 TeV
Dipole field at 7 TeV	8.33 T
Luminosity	10^{34} cm^{-2} s^{-1}
Beam current	0.56 A
Protons per bunch	1.1×10^{11}
Number of bunches	2808
Nominal bunch spacing	24.95 ns
Normalized emittance	3.75 μm
Total crossing angle	300 μrad
Energy loss per turn	6.7 keV
Critical synchrotron energy	44.1 eV
Radiated power per beam	3.8 kW
Stored energy per beam	350 MJ
Stored energy in magnets	11 GJ
Operating temperature	1.9 K

2.1. Machine layout

The basic layout of the LHC follows the LEP tunnel geometry and is shown in figure 2. The machine has eight arcs and straight sections. Each straight section is approximately 528 m long. Four of the straight sections house the LHC detectors whilst the other four are used for machine utilities, radio frequency, collimation and beam abort. The two high luminosity detectors are located at diametrically opposite straight sections. The ATLAS detector is located at point 1 and CMS at point 5, which also incorporates the small angle scattering experiment TOTEM. Two more detectors are located at point 2 (ALICE) and at point 8 (LHCb), which also contain the injection systems for the two rings. The beams only cross from one ring to the other at these four locations.

In order to leave enough space for the LHCb spectrometer magnet in the already existing experimental cavern at point 8, the IP at this location is shifted by 11.25 m towards point 7. Bunches with the nominal 25 ns separation collide at all four crossing points simultaneously. However, because of this displacement, the only other bunch separation with simultaneous collisions in all four detectors is 75 ns. For early commissioning, this bunch separation is interesting because there is no possibility of electron cloud buildup (see below) and the number of long-range beam–beam interactions is reduced, simplifying early machine operation. The 25 GeV proton synchrotron (the first circular machine in the injector chain), where the LHC bunch structure is generated, has therefore been equipped with the means to provide either of these two bunch separations.

Straight sections at points 3 and 7 contain two collimation systems for capturing stray particles. Point 3 is designed to capture off-momentum particles (momentum collimation) and point 7 for removing the beam halo (betatron collimation). Point 4 contains the two radio frequency systems, one independent system for each beam operating at 400 MHz, twice the

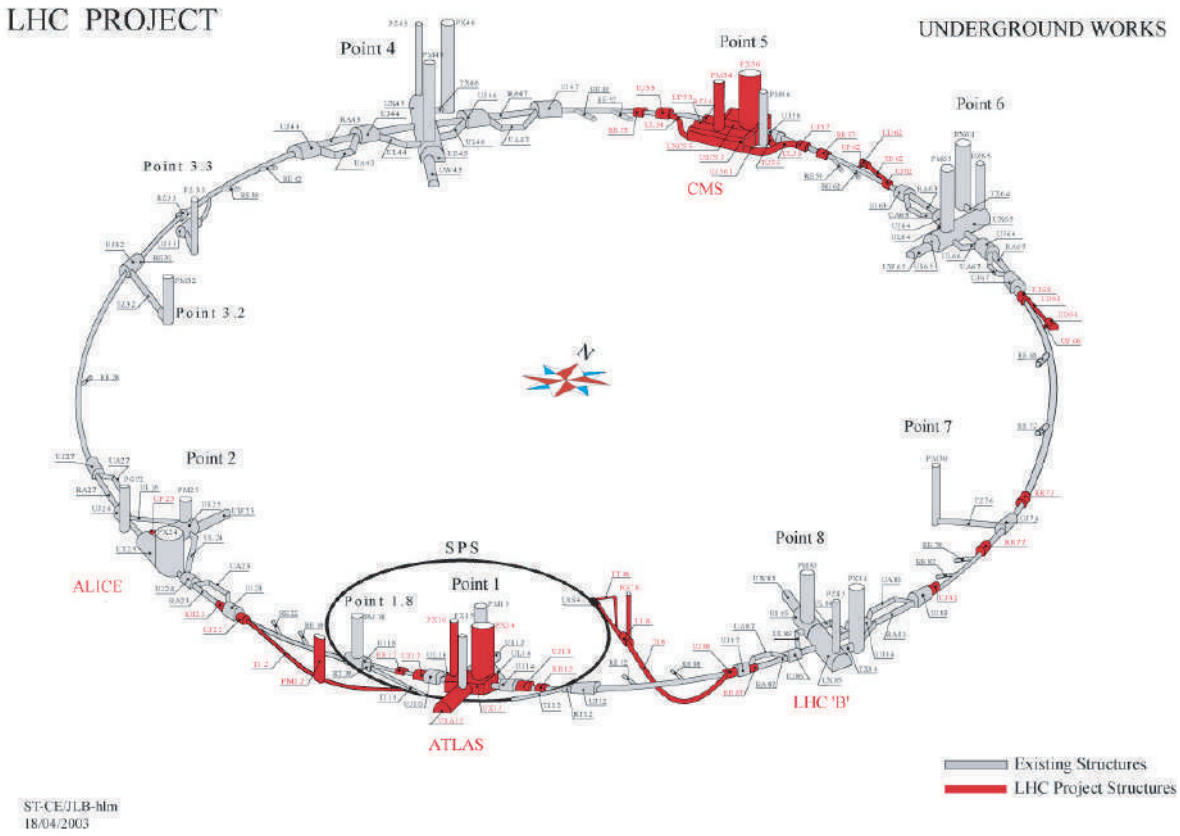

Figure 2. LHC layout.

frequency of the LHC injector. Finally, point 6 contains the two beam abort systems which will allow the beams to be extracted safely and dumped onto external absorbers.

The regular LHC lattice was designed to maximize the amount of bending power in the arc by making the dipoles as long as reasonably possible. This minimizes the amount of dead space between interconnects as well as the number of dipoles to be manufactured, tested and interconnected. After careful optimization, the dipole length was chosen to be 14.2 m (magnetic), 15 m overall with 23 regular lattice periods per arc. Each period is 106.9 m long and is made up of six dipoles and two short straight sections (SSSs) each of 6.6 m length containing the main quadrupoles and lattice correctors. The two apertures of rings 1 and 2 are separated by 194 mm. Both dipole apertures are connected in series whereas the quadrupoles are powered in two families, all focusing quadrupoles of rings one and two in series and likewise for the defocusing quadrupoles.

The transition from the regular arc contains a dispersion suppressor consisting of two perturbed lattice periods. The purpose of the dispersion suppressor is threefold:

1. adapt the LHC reference orbit to the geometry of the tunnel,
2. cancel the horizontal dispersion generated in the arc and by the separation and recombination dipoles,
3. help with the matching of the beams between the arcs and straight sections.

A generic design of a dispersion suppressor can be made using standard arc cells with missing dipoles and dipoles of different length to those in the arc. However, due to the constraints imposed by the geometry of the existing tunnel and the economy of having only one standard dipole length, the dispersion can only be fully cancelled by individual powering of the quadrupoles in the dispersion suppressor cells. These quadrupoles also provide additional parameters for matching the insertion optics.

The SSSs in the arcs contain the main quadrupoles and also the correction sextupoles for chromaticity control and the orbit correction dipoles. Depending on their location, they can also contain trim normal or skew quadrupoles or Landau damping octupoles.

The optics of the long straight sections differ according to their functionality. At points 1 and 5 in the high luminosity insertions the small β (0.5 m) at the collision point is generated with the help of a quadrupole triplet assembly. At points 2 and 8, the optics at the 450 GeV injection level must allow beam injection whereas at top field the beams must be focused to a moderate β. At the utility insertions the optics is tailored to their functionality. Details of the optics in the various insertions can be found elsewhere [1].

2.2. Main hardware systems

The main hardware systems include magnets, vacuum, cryogenics, radio frequency, power converters, injection and extraction equipment, beam instrumentation, collimation and controls, far too numerous for an article of this size. Details can be found in the LHC design report [1]. Only a few selected systems of general interest will be treated here.

2.3. Magnets

The LHC contains more than 7000 superconducting magnets ranging from the 15 m long main dipoles to the 10 cm long octupole/decapole correctors inside the dipole cold masses as well as more than 100 conventional warm magnets not counting the 500 or so conventional magnets in the two 2.6 km long transfer lines between the SPS and the LHC. The most challenging are the superconducting dipoles and the quadrupoles in the arcs, dispersion suppressor and matching regions.

The three large superconducting accelerators operating today, the Tevatron (FNAL), HERA (DESY) and RHIC (BNL) all use magnets made with classical Nb–Ti superconductor cooled with supercritical helium at a temperature slightly above 4.2 K. In each case, the nominal field is below or around 5 T. In order to increase the field to above 8 T, two possibilities exist today.

Figure 3 shows the critical current density of two superconductors available commercially today. The Nb–Ti conductor at 4.5 K has a critical current density that is too low to reach the LHC objective. The other commercially available conductor made from Nb_3Sn gives a shift of about 3 T upwards at 4.5 K and could be used for such high field magnets. However, Nb_3Sn superconductor is a very brittle material and cannot be used to wind magnet coils. Instead, the coils have to be wound before the heat treatment needed to produce the superconducting state, which requires them to be heated to over 600° for many tens of hours. Whilst this may be reasonable for a small number of specialized magnets, it is clearly not feasible for a large series.

The other way to high fields is to cool conventional superconductor to lower temperature. It can be seen from figure 3 that Nb–Ti cooled to 1.8 K gives the same 3 T shift as Nb_3Sn. This is a much more economical way to getting the high fields needed. However, it does not come without difficulties. First of all, there is a phase transition in helium at 2.17 K when the liquid

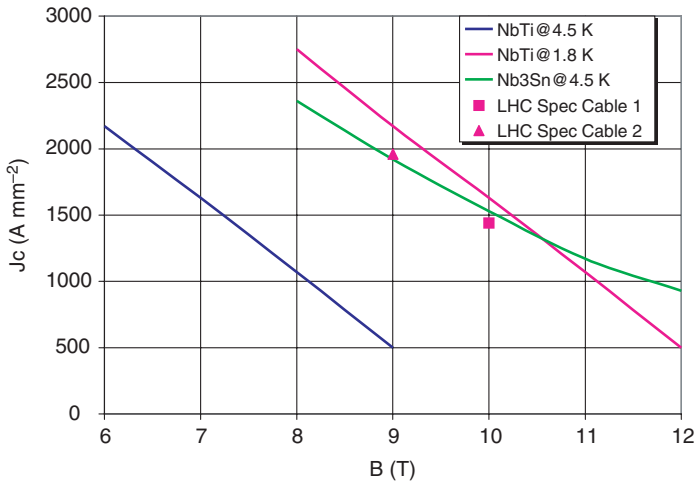

Figure 3. Critical current density of superconductors.

becomes superfluid. The advantages and disadvantages of this are discussed below. In addition, the heat capacity of the superconductor decreases by an order of magnitude between 4.5 and 1.8 K, so for a given heat inleak into the cable, for example due to small movement under the very high electromagnetic force or heating due to beam loss, the temperature rise is much higher, making the magnets much more sensitive to quenches. However, the superfluid helium can help if the coils are properly engineered.

A twin aperture dipole consists of two dipoles in a common iron yoke (figure 4). The two coils are clamped with austenitic steel collars with very low permeability surrounded by a yoke of low carbon steel which carries the magnetic flux. Figure 5 shows the flux plot as computed for the whole structure of the main dipole.

The requirement that the field must be in the opposite directions in the two apertures (for a proton–proton collider) ensures that there is no saturation of the central part of the yoke. The stored energy of 500 kJ m^{-1} in the magnet at nominal field requires active quench protection. If a quench is detected, the whole coil is made resistive by firing a capacitor bank into resistive strips (quench heaters) built into the coil. The current is then diverted through a diode until the power supply can be switched off.

The cross-section of a coil is shown in figure 6. The coil is wound in two layers in six blocks separated with copper wedges. The geometry of the conductor distribution has been carefully optimized to achieve as pure a dipole field as possible. The optimum geometry, which minimizes the higher harmonics of the field distribution, has been computed using a genetic algorithm [2]. Once the coil geometry has been fixed, then it is very important to keep it constant during the whole series production.

Equipment has been provided to the magnet manufacturers to allow the measurement of the field harmonics in the collared coil before assembly into the yoke. In this way, a tight quality control can be kept throughout the manufacturing run. Figure 7 shows the sextupole component of the field in about 1000 produced magnets. At the beginning of production it was necessary to make two small iterations on the geometry of the copper wedges in order to bring the harmonics inside the required control limits.

Apart from the field quality, it is also important to keep the integrated transfer function (effectively the bending angle for a given current) inside tight limits and identical for all three

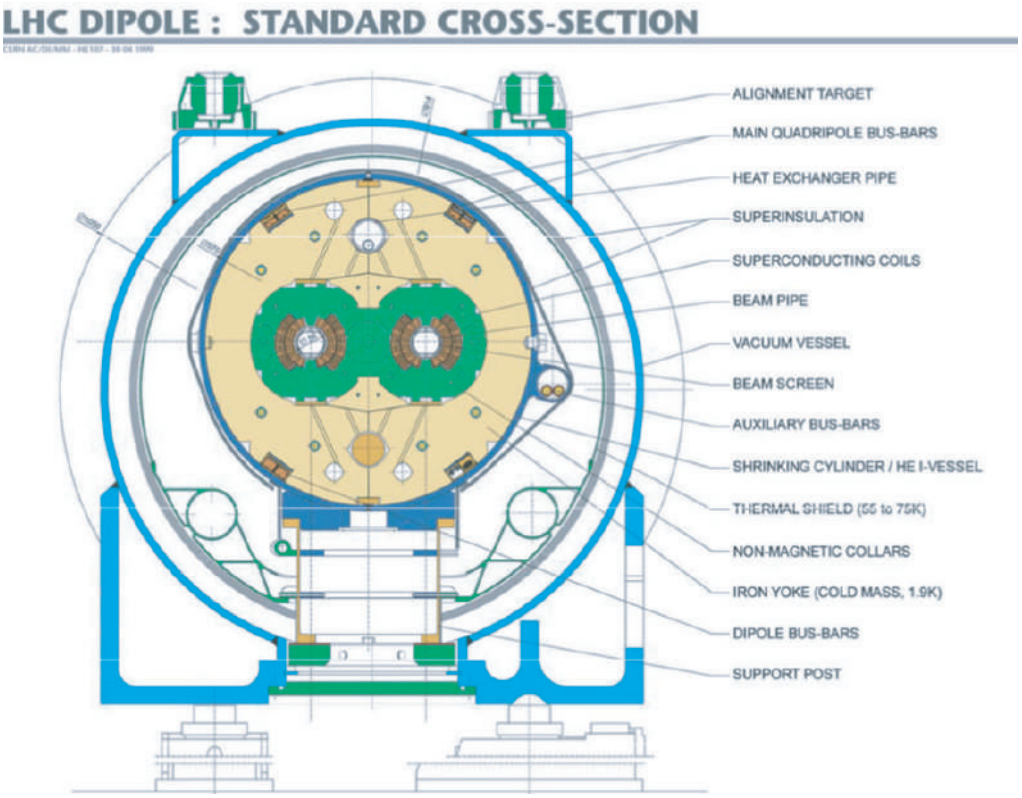

Figure 4. Dipole cross-section.

manufacturers. Too large dispersion in bending angle would result in very large orbit distortion which would be difficult to correct and variation in the mean for the three manufacturers would require that they are sorted into different octants depending on the manufacturer. Figure 8 shows what has been achieved for 1000 dipoles produced. The dispersion is much smaller than specified and the variation in the mean is so small that magnets from the three manufacturers can freely be mixed, simplifying enormously the logistics.

The main arc quadrupoles, 3.25 m long, are made with the same superconducting cable as the outer layer of the dipoles. Since the electromagnetic forces are much less and the geometry is more suited, the coils have separate austenitic steel collars instead of the combined collar structure of the dipoles. Each quadrupole is integrated into a SSS, each containing a sextupole for chromaticity correction and a closed orbit correction dipole. Depending on its position in the arc, a SSS can also contain a trim quadrupole or a Landau octupole.

In addition to the main arc magnets, the LHC contains many more elements for correction of dipole imperfections, matching of the optics and in the final focus. Table 2 gives a full list of all superconducting magnets, their number and function.

2.4. Cryogenics

The LHC magnets are cooled with pressurized superfluid helium, which has some interesting properties that make it a unique engineering material. Best known is its very low bulk viscosity which allows it to permeate the smallest cracks. This is used to advantage in the magnet

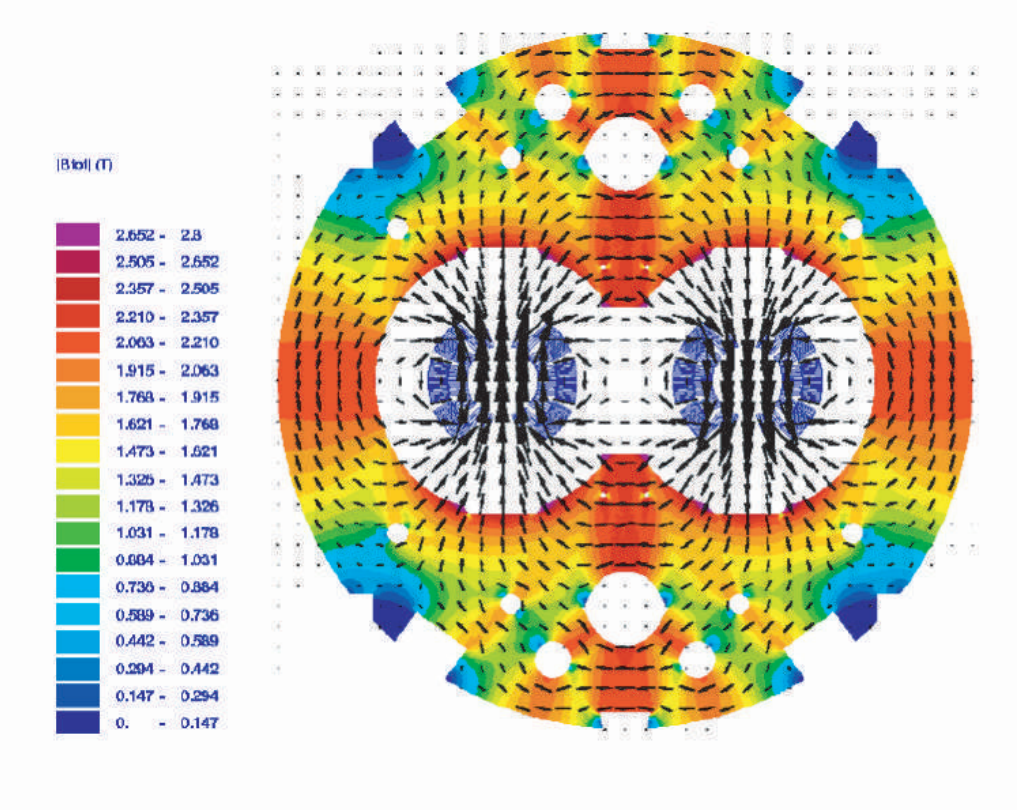

Figure 5. Flux plot in dipole.

design by making the coil insulation porous and enabling the fluid to be in contact with the strands of the superconductor. It also has a very large specific heat, 100 000 times that of the superconductor per unit mass and 2000 times per unit volume. Finally the thermal conductivity peaks at 1.9 K (figure 9) and is approximately 1000 times higher than that of cryogenic grade OFHC copper. The helium in the coil can therefore make up for the very low specific heat of the conductor at this temperature by helping to absorb unwanted thermal loads and transporting them efficiently outside the coil.

The most usual method of making superfluid helium in the laboratory is by pumping on the helium bath. Figure 10 shows the phase diagram of helium in the region of the point of the phase transition (the lambda point). Pumping on the bath reduces the pressure and at around 50 mbar and at a temperature of 2.17 K it crosses the lambda point. Further reduction of the pressure to 15 mbar lowers the temperature to 1.9 K.

The magnets themselves are cooled in a bath of superfluid at atmospheric pressure. This is achieved through a linear heat exchanger traversing each 107 m period of magnets (figure 11) containing superfluid at 15 mbar pressure, cooling the helium in the magnets at 1 bar to the same temperature as the saturated superfluid inside the heat exchanger. One big advantage of this system is that there is no problem with the bad dielectric strength of gaseous helium since the coil is permanently in liquid.

The machine is cooled using 8 cryogenic plants, each of 18 kW capacity at 4.5 K, located in pairs at the even points except for one singularity at point 2. Figure 12 shows the cryogenic

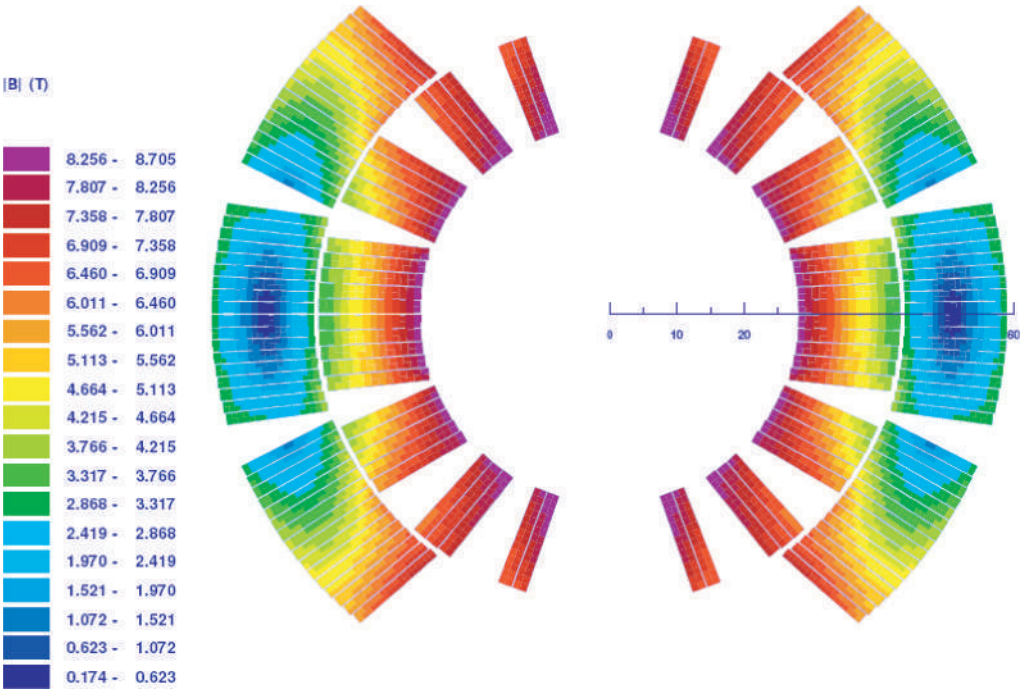

Figure 6. Distribution of conductors in dipole coil. The coil blocks are separated by copper wedges.

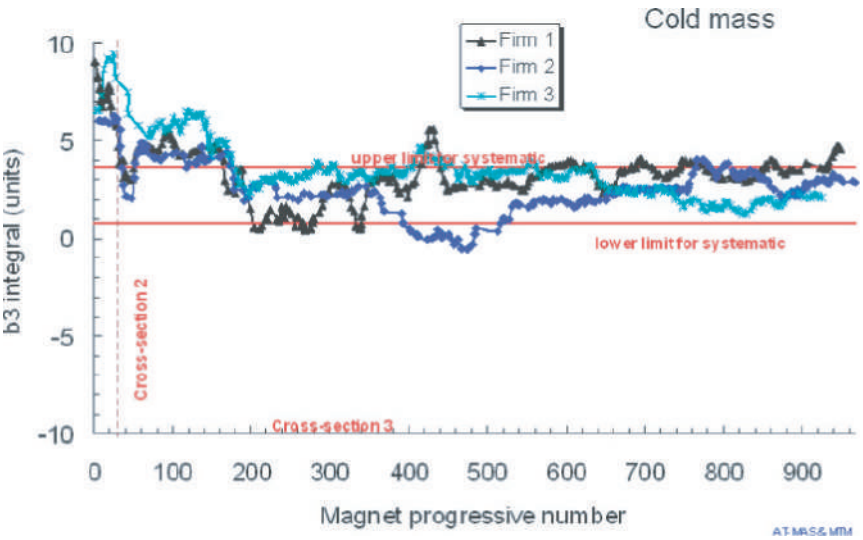

Figure 7. Sextupole component (b_3) of magnetic field in 1000 of the 1232 dipoles.

architecture at an even point. Four of the refrigerators are recuperated and upgraded from LEP, the other four are new.

The LEP refrigerators have their cold box split between surface and tunnel level whereas the new plants are located on the surface. At the tunnel level, the conventional refrigerators are supplemented by cold compressors. These multi-stage axial centrifugal compressors (figure 13)

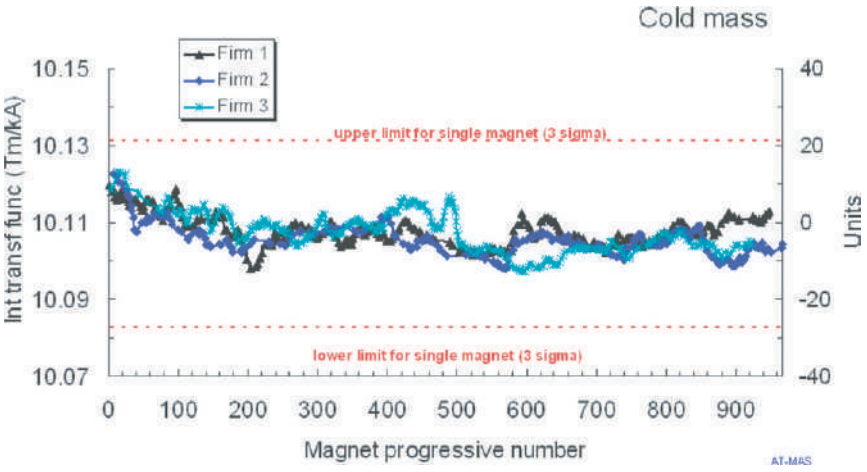

Figure 8. Integrated bending strength measured over 1000 dipoles from three manufacturers.

Table 2. List of superconducting magnets and their function.

Type	Number	Function
MB	1232	Main dipoles
MQ	392	Arc quadrupoles
MBX/MBR	16	Separation and recombination dipoles
MSCB	376	Combined chromaticity and closed orbit correctors
MCS	2464	Sextupole correctors for persistent currents at injection
MCDO	1232	Octupole/decapole correctors for persistent currents at injection
MO	336	Landau damping octupoles
MQT/MQTL	248	Tuning quadrupoles
MCB	190	Orbit correction dipoles
MQM	86	Dispersion suppressor and matching section quadrupoles
MQY	24	Enlarged-aperture quadrupoles in insertions
MQX	32	Low-β insertion quadrupoles

pump the cold helium gas, producing the 15 mbar pressure in the linear heat exchangers inside the magnets in order to produce the primary superfluid. The connection to the magnets is made through a cryogenic distribution line running in the tunnel parallel to the machine. An interconnect box allows the plants to be used in the arc either side of the even point or if needed, for the full power of both plants to be used in one arc.

Using a single cryogenic plant boosted with a liquid nitrogen precooler, a sector can be cooled down in less than 15 days. By coupling two plants to the same octant, this time can be reduced by a factor of two. Warming of a sector takes about the same time.

2.5. The radiofrequency acceleration system

The RF system is located at point 4. Two independent sets of cavities operating at 400 MHz (twice the frequency of the SPS injector) allow independent control of the two beams. The

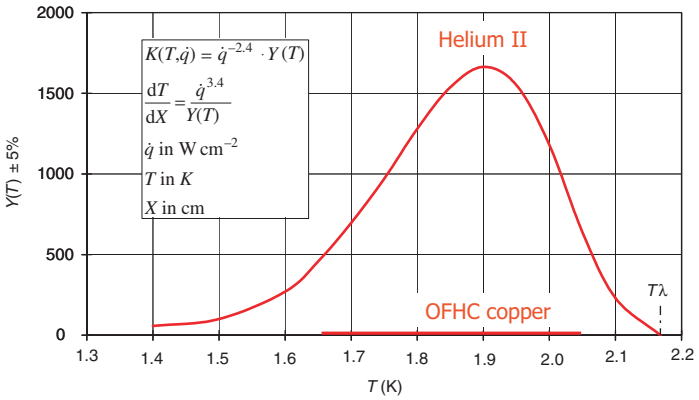

Figure 9. Thermal conductivity of He II.

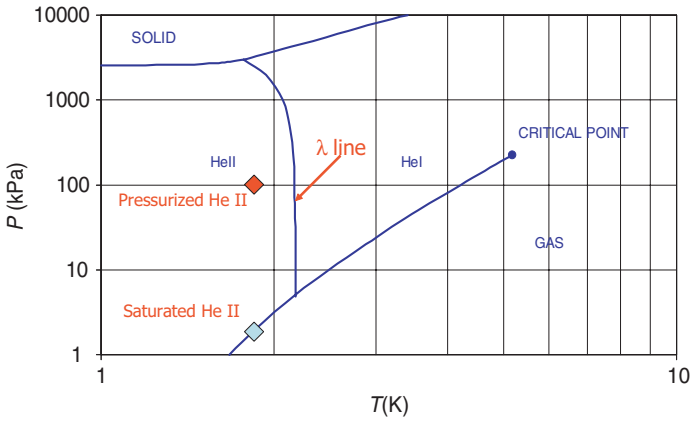

Figure 10. Phase diagram of helium.

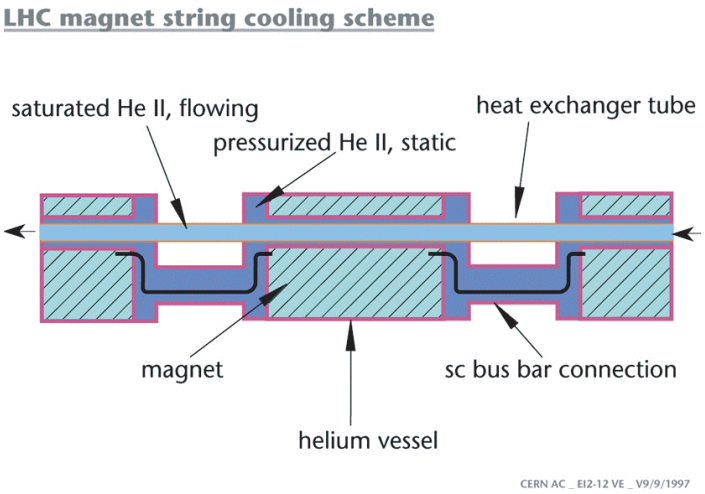

Figure 11. Linear heat exchanger.

IOP Institute of Physics DEUTSCHE PHYSIKALISCHE GESELLSCHAFT

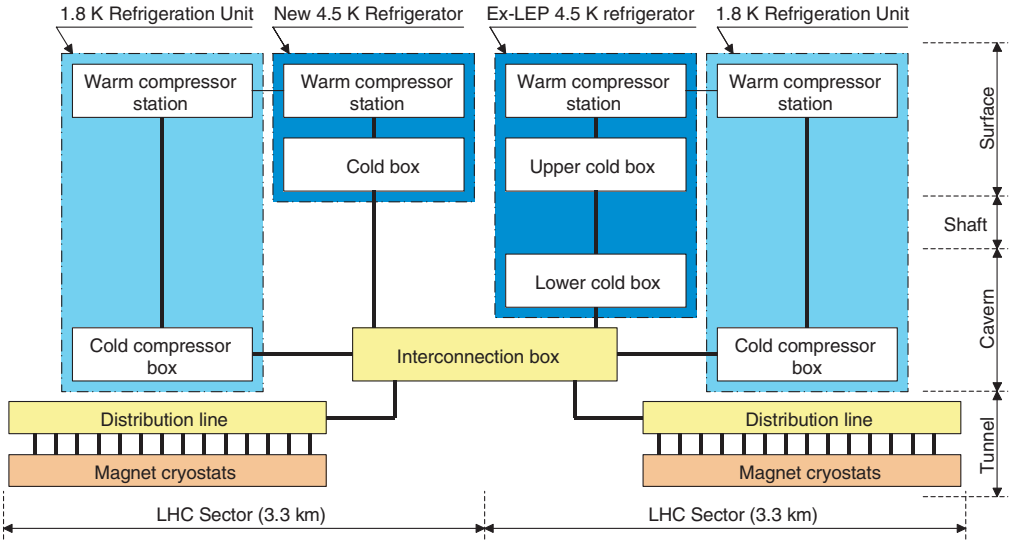

Figure 12. Cryoplant architecture at an even point.

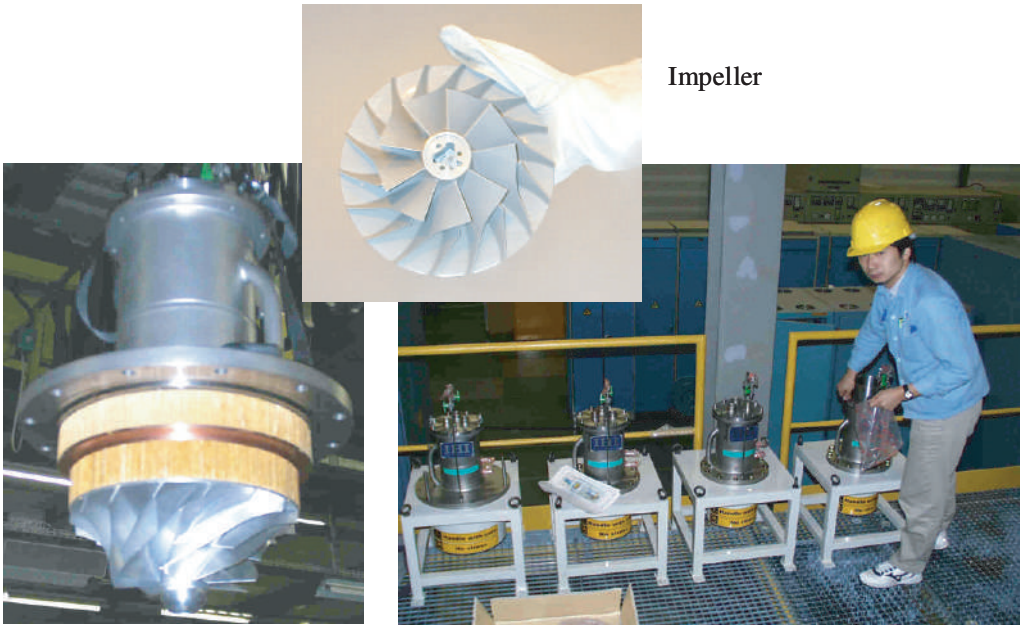

Figure 13. Cold compressor impeller stages.

superconducting cavities are made from copper on which a thin film of a few microns of niobium is sputtered on to the internal surface. In order to allow for the lateral space, the beam separation must be increased from 194 mm in the arcs to 420 mm. In order to combat intrabeam scattering (see below), each RF system must provide 16 MV during coast while at injection 8 MV is needed. For each beam there are 8 single cell cavities, each providing 2 MV, with a conservative gradient of 5.5 MV m^{-1}. The cavities are grouped into two modules per beam, each containing four cells (figure 14). Each cavity is driven by an independent RF system, with

Figure 14. Four-cavity module during assembly.

independent klystron, circulator and load. Although the RF hardware required is much smaller than LEP due to the very small synchrotron radiation power loss, the real challenges are in controlling beam loading and RF noise.

2.6. The vacuum system

The LHC presents several original requirements compared with classical vacuum systems. It has to ensure adequate beam lifetime in a cryogenic system where heat input to the 1.9 K helium circuit must be minimized and where significant quantities of gas can be condensed on the vacuum chamber. The main heat sources are:

1. synchrotron light radiated by the beam at high energy (0.2 W m^{-1}per beam), with a critical energy of about 44 eV;
2. image currents (0.2 W m^{-1} per beam);
3. energy dissipated by the development of electron clouds (see below);
4. energy loss by nuclear scattering (30 mW m^{-1}per beam).

In order to remove the heat from all these processes but the last with high thermodynamic efficiency, the 1.9 K cold bore of the magnets is shielded with a beam screen cooled to between 5 and 20 K (figure 15). This beam screen is perforated with about 4% of the surface area to allow the cold bore of the magnets at 1.9 K to act as a distributed cryopump, allowing gas to be condensed on the cold bore surface protected against desorption by bombardment with synchrotron radiation photons.

For roughly 3 km of the 27 km circumference, mainly in the long straight sections, the vacuum chambers are at room temperature, requiring a low residual pressure without the benefit

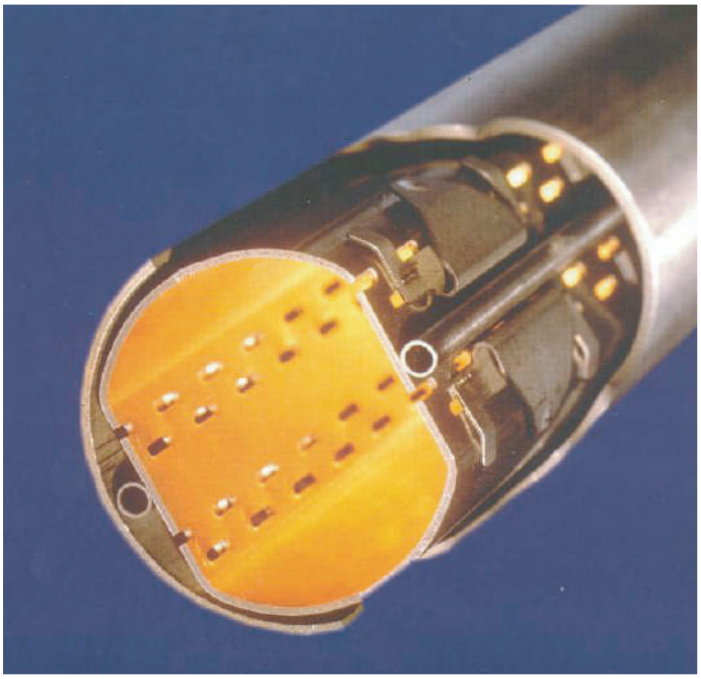

Figure 15. LHC beam screen.

of the distributed cryopumping. As a spin-off of the development of sputtering technology for superconducting cavities a new getter material (TiZrV) has been developed which can be sputtered on the internal surface of the copper vacuum chambers and can be activated at the very low temperature of 200° (conventional getters require activation at 600°). When activated, the chamber wall itself becomes a distributed pump, producing very low residual pressure and at the same time a very low secondary emission yield (SEY), preventing the buildup of an electron cloud. All warm chambers, including those inside the detectors, are treated in this way.

3. Accelerator physics issues

More than 30 years of accumulated experience from the first hadron collider, the intersecting storage rings as well as the proton–antiproton colliders at CERN and FNAL and the superconducting storage rings at BNL and DESY has gone into the LHC design. In the following chapters, the different effects that could limit machine performance and the remedies adopted are described.

3.1. Dynamic aperture

In superconducting magnets of the type used in the LHC, the field quality is determined by the precision of the positioning of the superconductor and not by the geometry of the iron yoke, so it can never be as good as in conventional magnets. It has been shown by experience in the different superconducting machines and by particle tracking that the aperture inside which particle orbits are stable is much smaller than the physical aperture of the beam pipe. This is called the dynamic aperture and is limited by a complex interplay between the

unwanted higher field harmonics due to magnet imperfections. Sophisticated computer codes have been developed to track particle orbits around virtual machines with distributed random and systematic imperfections [3]. And these results are used to define maximum systematic and random deviations of each field multipole. It was from this work that the control limits for the sextupole component of the dipole field shown in figure 7 were derived. Even with present day computers it is not possible to perform full scale simulation over a large number of virtual machines over 4×10^7 turns, which corresponds to 1 h of storage time. The dynamic aperture obtained from tracking of existing machines is always too optimistic when compared to experiment by 20% or more. For the LHC, in order to insure a dynamic aperture of 6 sigmas it has been decided that the tracked dynamic aperture over 10^6 turns should be a factor of 2 larger. These results have been used to supply the tables of allowed multipole errors to the magnet builders.

Since the dynamic aperture depends strongly on the horizontal and vertical tunes, the tracking studies are also used to find the best working points.

3.2. The beam–beam interaction

When the beams are brought into collision, a much stronger nonlinearity than the magnet imperfections comes into play. It is called the beam–beam interaction and is caused by the force due to the electromagnetic field of one beam on the particles in the other beam. It produces two main effects.

The first is to cause a variation of the tune with amplitude. This means that the beam does not occupy a point on the Qh, Qv tune diagram but produces an extended 'footprint'. The second effect is that because of the periodic nature of the force (particles experience a delta function kick on each revolution) it excites nonlinear resonances which can strongly limit the beam lifetime. Figure 16 is an example of a tune scan made many years ago on the SPS proton–antiproton collider [4]. The lower figure shows the tune diagram with nests of 10th, 7th and 11th order resonances. The beams are scanned across these resonances in steps, the lines corresponding to each scan position being intended to indicate approximately the size of the footprint. The upper diagram shows a chart recorder output of the intensity decay of the beams for each position in tune space. In this experiment, the antiproton intensity was very low so that the effect of the beam–beam interaction of the antiprotons on the protons is very small. Consequently, as observed, the decay rate of the protons is completely insensitive to the tune. On the other hand, the strong proton beam affects the antiprotons much more, producing a clear effect as the beams are scanned across the resonances. Experiments like this indicate that the total tune spread due to the sum of the tune spreads from each IP should not exceed 0.015. With three proton detectors requiring almost head-on collisions this implies that the tune shift per experiment should not exceed 0.005, a value routinely achieved in previous and existing colliders.

The long-range beam–beam interaction between successive bunches must also be avoided by colliding the beams with a small crossing angle of about 400 μrad.

3.3. Intrabeam scattering

As particles perform their betatron and synchrotron oscillations, they exchange energy due to multiple Coulomb scattering. The correct frame of reference to understand the phenomenon

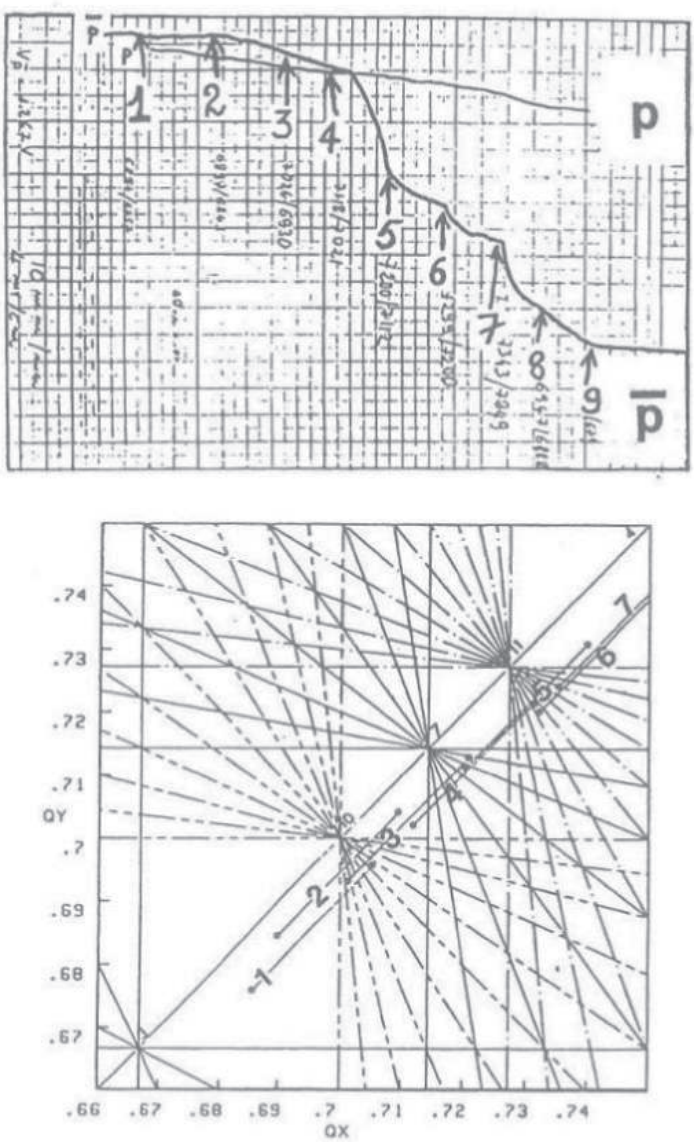

Figure 16. A beam–beam resonance scan at the SPS collider.

is the rest frame of the beam [5]. The transverse rms momenta $\sigma'_{x,y}$ are unchanged by this transformation whereas the longitudinal momentum σ_p is transformed into σ_p/γ. In a highly relativistic beam like the LHC, the longitudinal plane is therefore very 'cold' compared with the transverse planes and one would expect a damping of the transverse dimensions and an increase in the energy spread, which would be good for luminosity preservation. This indeed does occur in the vertical plane although the damping time is very long. Unfortunately, in the regions where the dispersion is not zero (most of the machine), a particle changes its energy by Coulomb scattering but does not change its position and therefore finds itself on the wrong orbit for its momentum. It can only make a betatron oscillation around its new equilibrium orbit, adding a heating term that completely swamps the slow damping in the radial plane.

Intrabeam scattering has been clearly observed in the SPS proton–antiproton collider (figure 17) [6] and the growth rate is in quite good agreement with the theory. In the LHC,

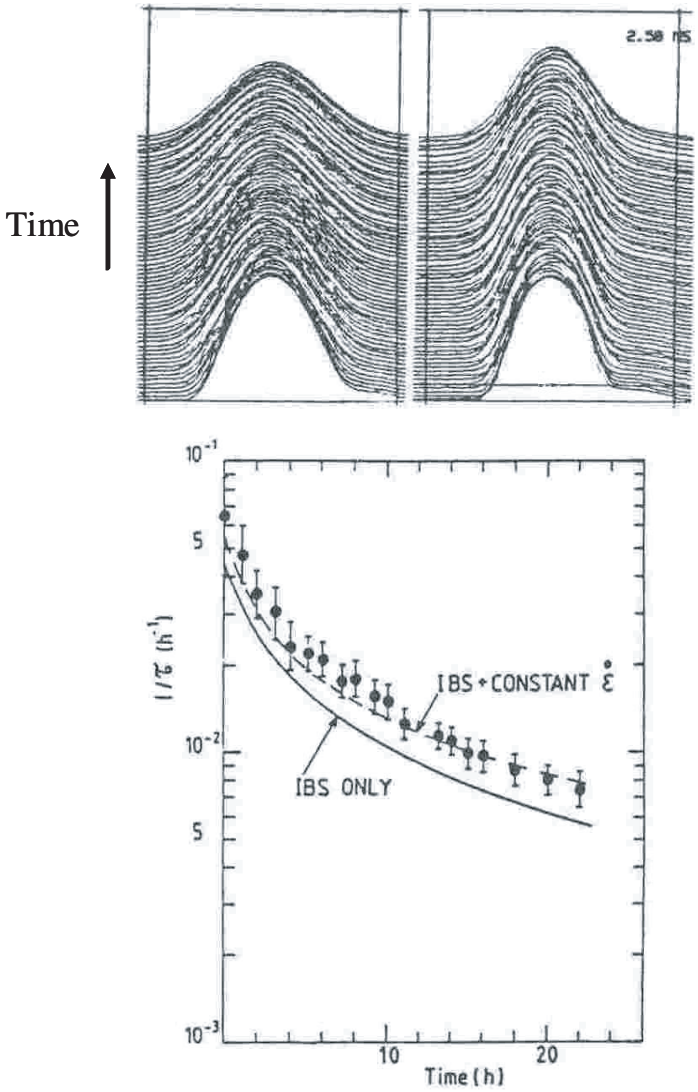

Figure 17. Intrabeam scattering in the SPS. Top bunch lengthening with time for a strong proton bunch (left) and a weak antiproton bunch (right) bottom. IBS growth rate compared with theory.

if no action is taken, the beam would blow up so fast that the luminosity lifetime would be reduced to a few hours.

The growth rate depends strongly on the six-dimensional phase space density. The longitudinal emittance of the beam arriving from the SPS is about 1 eV s. During the acceleration, the emittance is increased to 2.5 eV s using RF noise to blow up the energy spread and bunch length. This reduction in phase space density is sufficient to increase the transverse emittance growth time to about 80 h, making its effect on luminosity lifetime negligible compared to other processes. A consequence of this is that the RF voltage during coast must be increased to 16 MV to provide a big enough bucket for the large emittance beam.

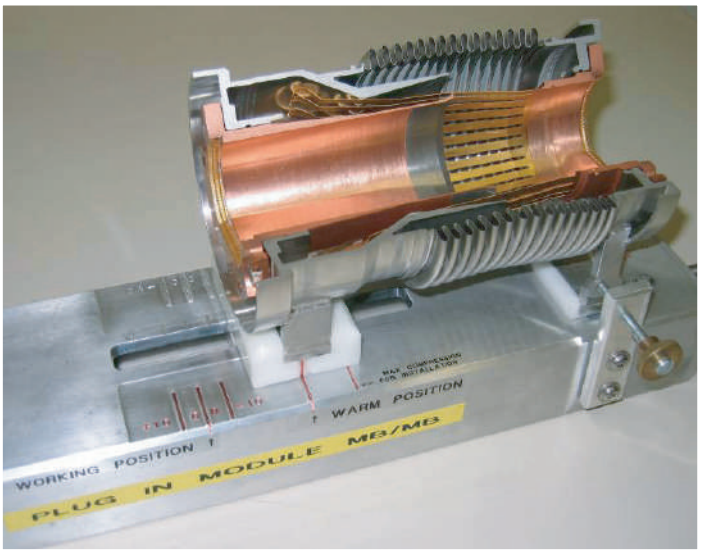

Figure 18. A vacuum interconnect.

3.4. Coherent instabilities

The interaction of the beam with its environment generates electromagnetic fields which can react back on it and drive it unstable. The first remedial action is to design the vacuum chamber to reduce this coupling as much as possible. The chamber should be as smooth as possible without discontinuities. As an example, figure 18 shows an interconnect module between two dipoles. When the magnets are cold, the bellows is stretched and the RF 'fingers' ensure a smooth transition from one beam screen to the other. The material of the beam screen is stainless steel to give it structural strength in case of quench co-laminated with a 75 μm layer of copper on its inner surface. The resistivity of the copper layer is reduced by cooling it to between 5 and 20 K. In the room temperature regions the vacuum chamber is made of 2 mm thick high conductivity copper.

Reducing the impedance of the environment can reduce the growth rate of the instabilities but cannot eliminate them all together. In the LHC, the two instabilities that must be controlled are the transverse coupled bunch instability (resistive wall) and the single bunch head-tail instability.

The resistive wall instability is driven mainly by the long-range wake fields due to image currents in the beam screen. The instability can occur at the frequencies of the so-called slow waves:

$$f_n = (n - Q)\, f_r,$$

where f_r is the revolution frequency (11.245 kHz), Q is the tune and n is the mode number. Only modes with $n > Q$ are unstable. The other modes drive backward waves which are stable.

The lowest and fastest growing mode is around 8 kHz ($Q = 59.3$) with a rise time of around 300 turns (26 ms). It must be damped with active feedback. A signal from a transverse pickup is delayed by one turn, amplified and fed back into a pair of electrostatic deflectors placed at a betatron phase of 90° with respect to the pickup. The bandwidth of the system is around 20 MHz, allowing many modes to be damped simultaneously. Very high frequency modes have such slow

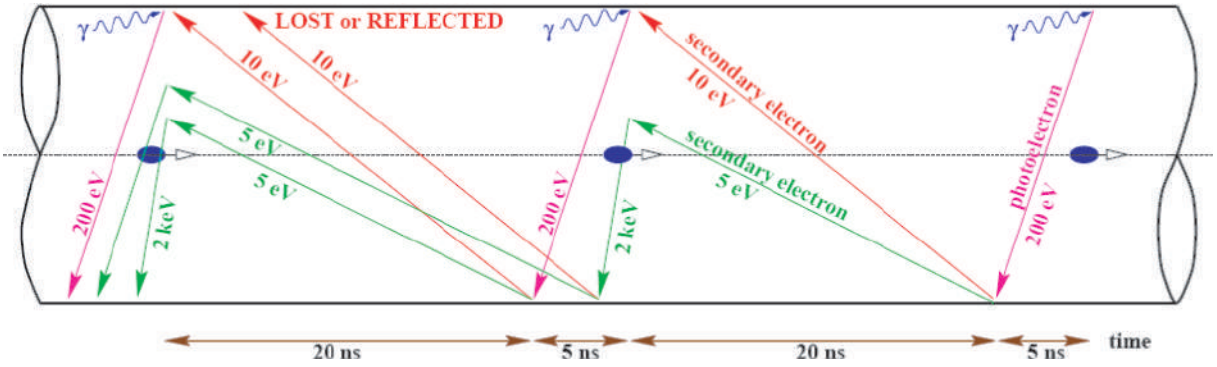

Figure 19. The electron cloud effect.

growth rates that they will be damped by Landau damping (see below). The transverse feedback system is also useful for damping injection errors to avoid filamentation and emittance growth.

The head–tail instability is a well-known single bunch effect driven by short-range wakefields where the tail of the bunch is driven by the head and half a synchrotron period later the roles are reversed, driving the bunch unstable. For the lowest head-tail mode this can only happen if the chromaticity is negative. The chromatic aberrations must anyway be corrected by the sextupoles integrated into the short straight sections. To control the head–tail instability it is sufficient to keep the chromaticity slightly positive at all times. This will be particularly critical at the start of acceleration where persistent currents in the superconducting magnets can produce a large and rapid change in the chromaticity.

The ultimate panacea for beam instabilities is Landau damping where the tune spread in the beam is large enough to stop it from oscillating coherently. To provide Landau damping, two families of strong octupoles are integrated into the lattice in selected short straight sections. Octupoles give a variation of tune with betatron amplitude and will allow instability control at high energy without active feedback. This will be particularly important if the transverse feedback system has noise problems. During collisions, the tune spread due to the beam–beam footprint should be enough to keep the beams stable.

3.5. Electron cloud effects

A significant number of electrons can accumulate in the LHC vacuum chamber through ionization of residual gas molecules or by the impact of synchrotron radiation on the beam screen. When a proton bunch passes, these electrons will be given an impulse and can hit the beam screen with energies of several hundred electron volts. The primary electrons produce secondaries (figure 19) and if the transit time of the electrons across the chamber is resonant with the 25 ns bunch separation, the electron cloud can grow exponentially. This process is called beam-induced multipacting and is known to limit the performance of storage rings with small bunch separation, notably the two B factories, PEP-II and KEKB.

The threshold for the buildup of the electron cloud depends on the bunch current, the geometry of the beam screen and the SEY of the surface of the beam screen. It has been shown that it can occur in the LHC under some conditions with the nominal bunch separation and has already been observed in the SPS with LHC-like beams. The main effect is an additional heat load in the cryogenic system and can also lead to instabilities.

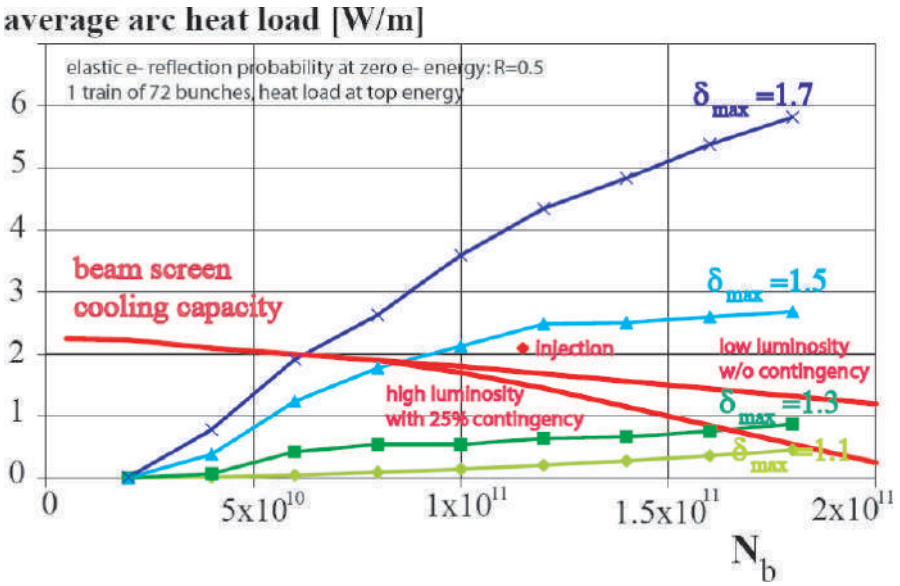

Figure 20. Heat load on the beam screen for different values of SEY.

A considerable amount of work has been done in order to understand the phenomenon, both experimentally and through the development of simulation codes which have been calibrated on experimental data from the SPS [7]. Figure 20 shows the predicted heat load on the beam screen as a function of bunch intensity for the nominal 25 ns bunch separation with different values of the SEY of the beam screen surface. The available cooling capacity of the cryogenic system is also shown. At zero intensity, all of the capacity is available for the electron cloud but as the intensity increases, part of the capacity is used for image currents and synchrotron radiation. The main conclusions are the following.

For the raw surface of the beam screen with a SEY of around 1.7, the electron cloud will limit the intensity to about half nominal. It has been shown experimentally that the presence of the cloud 'scrubs' the surface and the SEY reduces quickly to below 1.3, where this effect should no longer be a problem up to and beyond nominal intensity. Simulations also show that for larger bunch separations, above 50 ns, the threshold is well above nominal intensity. For this reason, the LHC injector chain has been equipped to provide beam a beam of 75 ns as well as the nominal one, so that early commissioning can be done without the need for a scrubbing run.

4. Conclusions

The LHC is now in its final stage of installation and commissioning. A beam has already been extracted from the SPS with the parameters needed to achieve design luminosity and has been transported along the 2.6 km tunnel TI8 to the LHC injection point. The stored energy in this beam at 7 TeV is two orders of magnitude higher than in any previous machine and one of the biggest challenges will be to ensure that the machine protection systems work with an extremely high degree of reliability in order to protect both machine and detectors.

The accelerator physics is well understood and the appropriate means to combat the various effects have been integrated into the machine design. The one new effect not seen in hadron

machines before is the electron cloud. Simulations and experiments on the SPS have shown that a moderate scrubbing of the surface of the beam screen by electron bombardment will quickly reduce the SEY to a low enough value to allow design luminosity to be reached.

References

[1] 2004 *LHC Design Report* CERN-2004-03
[2] Ramberger S and Nussenschuck S 1998 *IEEE Trans. Magn.* **34** 2944
[3] Koutchouk J P 1999 *Proc. 1999 Particle Accelerator Conference, LHC Project Report 296*
[4] Evans L *AIP Conf. Proc.* **153** 1722
[5] Piwinski A 1974 *Proc. 9th Int. Conf. on High Energy Accelerators* (*Stanford*)
[6] Evans L 1984 *Proc. 12th Int. Conf. on High Energy Accelerators* (*Batavia*)
[7] Jimenez J M *et al* 2004 *AIP Conf. Proc.* **773** 211

My Home Page

Amateur Radio
Operating Conditions
Antennas
Accessories
Projects & Kits
Data Modes
Information
Portable
QSL
RSGB Ltd
Links
QRM
Bits 'n' Bobs
Contact

WSPR
Weak Signal Propagation Reporter

Site Map

MDS975 Home

Feedback

Site Search
Find
powered by FreeFind

Get on the air with TOP QUALITY BRITISH

M0MTJ | Operating Conditions | Antennas / Aerials | /P Portable Operating | Accessories | Projects & Kits | Useful Information
Contact MØMTJ | Contact M6ORS | Links to Amateur Radio Sites | RSGB | QSL | The Amateur Radio Mini Site Map
News, Developments, Events, Photographs and other 'Bits 'n' Bobs' | WSPR Weak Signal Propagation Reporter

AERIALS (ANTENNAS) 2

Antennas 1 | Antennas 3 | Antennas 4 | Antennas 5 | Antennas 6 | Antennas 7

Index To Other Antenna Pages:
Antennas 1 : Aerials used at M0MTJ
Antennas 2 : Including ideas for compact aerkals for Top Band /160 metres
Antennas 3 : Felix Scerri VK4FUQ discusses Loop Antennas, baluns, masts & other antenna related topics
Antennas 4 : Many antenna ideas from various sources particularly for multi-band operation & also gives information about
antenna trimming, knots for wire antennas and useful antenna rigging accessory ideas.
Antennas 5 : Half Wave End Fed aerials for 144 MHz VHF / 430 MHz UHF and 50 MHz 6 Metre band & J-Pole Aerials
Antennas 6 : Simple and effective H.F. Antenna ideas - Ground Plane and All Band Doublet
Antennas 7 : Omni-Directional - Circularly (Mixed) Polarized Aerial for VHF / 2 Meters.

Compact Top Band Antenna - An Inverted L for stealth with low(ish) visual impact

With a small back garden there is no way that I could accommodate an aerial for the 160m band that would be anything approaching full size. A full size dipole would be about 65 metres long and would need to be mounted at a very good height to be at its most effective. A full size vertical 1/4 wave would be about 37.5 meters tall. Impossible! Bending a 1/4 wave wire into an inverted L would still result in a very long wire - say 10 metres vertically and 27.5 metres horizontally. Still too large.

Full size top band antennas are big, far too big for my small plot, so I have tried a few different shortened 160m aerials. I really would prefer to use a balanced dipole not only for the radiation efficiency, but just as importantly for the lower noise on receive - like a ground mounted vertical aerial an inverted L can be rather noisy on RX. However I have to settle for a compromise, so shown in the drawings and photographs below is my current top band aerial, along with some previous experiments and ideas further down the page.

This incarnation of my Top Band aerial takes two forms. A compact Inverted L and, in its lower position, a less conspicuous sloping wire, shown below:

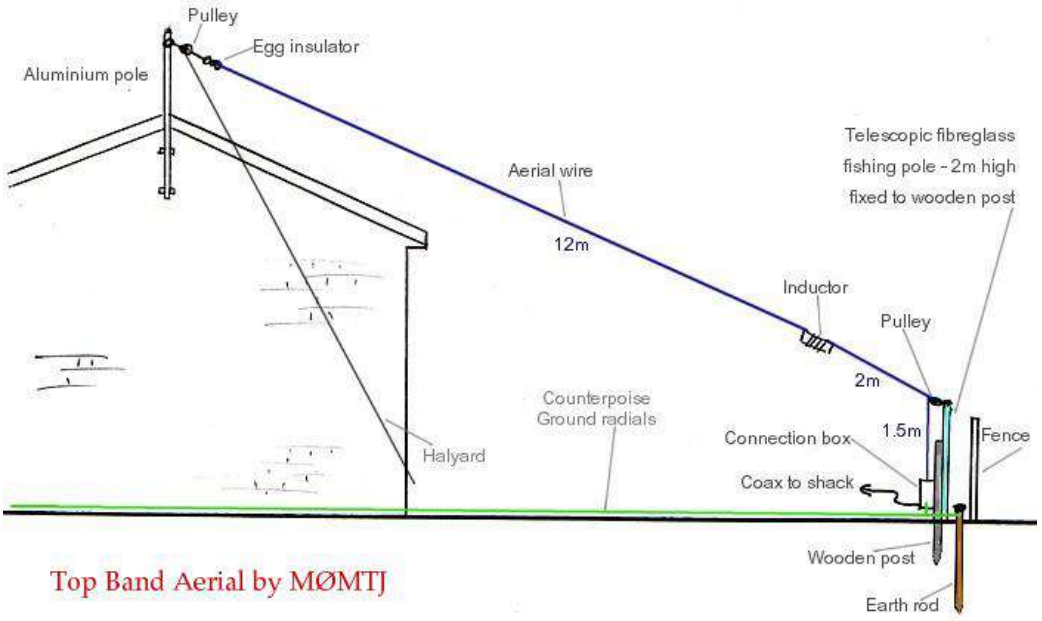

General layout of Top Band Aerial with fibreglass pole retracted to a height of 2 metres
Wire lengths are approximate: Inductor 5cm dia with approx 40 turns of 0.9mm e.c.w.

G-WHIP ANTENNAS

My first experiments were with a base loaded sloper which worked ok-ish for local ground wave, but could have been better. The first weak link that I wanted to change was moving the base loading coil further up the aerial wire so that it would be positioned on the more horizontal section.

It was also very low, so could surely benefit from some additional vertical height. However I could not realistically erect another permanent pole in the garden for fear of upsetting the XYL!

Therefore I decided that I needed a design that could be semi-permanent and offer two slightly different configurations: The idea is that, as a sloping wire, the aerial can be left in place at all times for RX and still be operable on TX. Since it is essentially just a wire sloping from fence height (2m) up to the roof apex it has fairly minimal visual impact. Alternatively, when required - at night - the telescopic pole can be extended to transform the aerial into the larger Inverted L.

The Earth and Radials: The aerial is fed against ground, so the ground needs to be as good as possible. At the base of the aerial a copper earth rod is driven into the ground. Additional ground radial wires are also added to provide a counterpoise and help reduce earth loss. The more the merrier.

The Support: A 10 metre long telescopic fibreglass fishing pole is used as part of the support. A wooden post was driven into the ground, adjacent to the earth rod. The connector box is screwed on to the post and the fishing pole was fixed to the post using nylon straps.

Since the top sections of a fishing pole are too thin to support the aerial wire, the last four sections were removed, leaving the pole 6 metres in length, which is a respectable height in a small back garden, though being even taller would be better.

A small lightweight pulley is fixed to the top of the fibreglass pole using two nylon ties - as seen in the photograph. As a sloping wire, the fishing pole is collapsed to 2m in height while being extended to 6 metres when being used as the 'full' Inverted L. The pole is quite flexible and so will tend to bend quite noticeably when 6 metres long with the wire attached to the top. This could be remedied by adding a back guy rope of required.

The far end of the aerial wire is tied to a egg type insulator and nylon halyard which is suspended through a pulley on a pole attached near the apex of the roof. The nylon halyard is tied off on a cleat hook near ground level to enable easy raising and lowering of the aerial wire.

The Wire: Aerial wire is PVC covered stranded wire of about 16/18 swg http://www.whwestlake.co.uk. The wires were cut for the maximum length that could be fitted into the available space - so as much wire was in the air as possible. This was about 3.5 metres from the feed point to inductor and around 12 to 13 metres from the inductor to the far end.

(If you make one of these get the vertical portion as high as possible and the horizontal section as long as possible and reduce the coil's inductance accordingly).

The Inductor and Resonance:

The resonance of the aerial system was adjusted not by altering the length of the wires, but by changing the inductance of the loading coil.

I had some 0.9mm (20 s.w.g.) enamelled copper wire on a reel, so I used that to wind the coil. The coil former is 5cm in diameter and about 15 cm long, cut from an empty tube of silicone bath sealant (the 'gun' type). Two holes are drilled in the former for the fixing bolts and wing nuts that secure the aerial and coil wires.

I used an MFJ antenna analyzer to check resonance and adjust the number of turns. Initially the coil was wound with 60 turns, but the resonance was well below 1800 kHz. Turns were gradually removed until resonance was around 1940 kHz, leaving 39 turns on the coil. (Thicker e.c.wire might have been better, I would have preferred to use something like 18.swg 1.2mm diameter and this may possibly get changed in the future)

Enamelled copper wire:
http://www.esr.co.uk/electronics/cable-copper.htm

When the adjustments were finished the aerial wires and coil wires are terminated with lugs and fixed in place with the bolts and wing nuts. The winding was also covered in duck tape. All exposed connections should be suitably protected against the weather for a permanent installation.

When setting up any aerial an antenna analyzer is extremely useful - allowing all the measurements to be done in the garden or back yard thereby simplifying and speeding up the process considerably. These simple

measurements can be made using the transceiver and VSWR meter, though that is obviously less convenient and will involve transmitting regular short burst of carrier, so it's very important to ensure that the power used is the absolute minimum and that the frequency being used is clear.

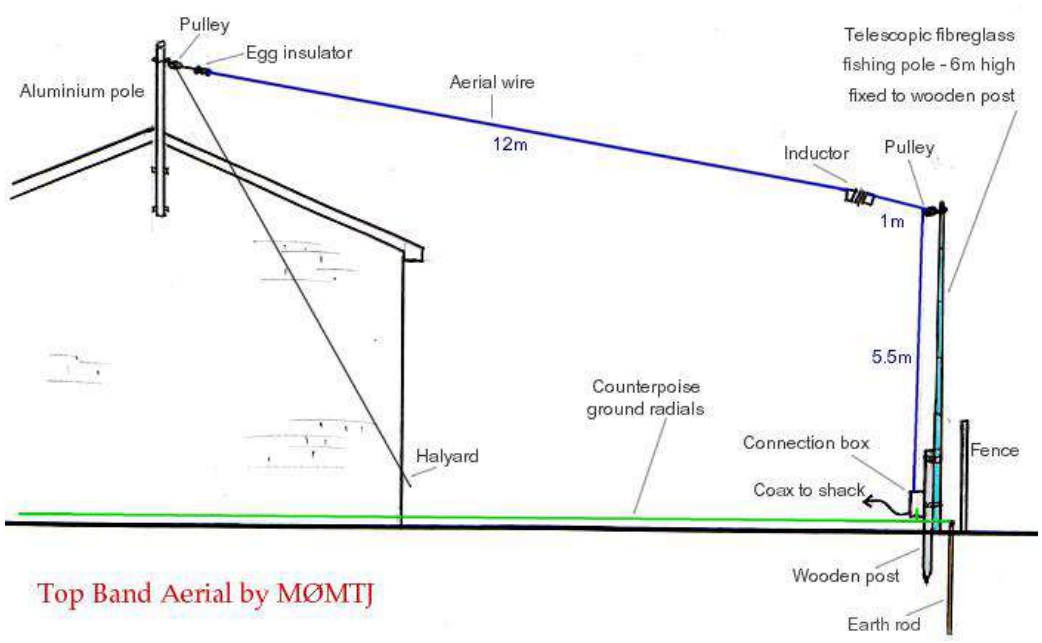

General layout of Top Band Aerial with a fibreglass pole extended to a height of 6 metres
Wire lengths are approximate: Inductor 5cm dia with approx 39 turns of 0.9mm e.c.w.

To transform the aerial to the Inverted L format (shown in the above diagram) I envisaged that changing the first length of wire, from a 3.5 metre length to 6.5 metre length, and the inductor would be necessary. I had assumed that a coil with less inductance (fewer turns) would be required due to the longer length of aerial wire used in the Inverted L arrangement.

I was, however, proved wrong. On first attempt I left the original coil in place, just adding the longer wire section (from connection box to coil) and raising the pole to its full 6 metres. The point of resonance was only about 20 kHz away from where it was as a sloper.

This, I think, can be explained by the fact that in the sloper configuration, the wire is close to the ground, other objects and vegetation which will in effect add loading to the aerial, Consequently a loading coil with less inductance than might otherwise be expected is required. So, by happy coincidence, the same coil is also suitable for the longer wire that is at a greater height (and therefore is influenced less by ground loading).

This, quite by chance, made the swap from Sloper to Inverted L a little easier since there was no need to wind a second coil - the change being made by merely adding the longer first wire section and pushing up the pole to its full 6 metre height.

If there are no concerns or objections to installing a tall pole at the bottom of the garden, then the Inverted L arrangement could be left as a permanent installation. In that case the pole need not be a fibreglass fishing pole, although it is still an attractive lightweight method, instead a couple of 3 metre long sections of treated timber could be joined together to form a 6 metre high post - the higher and longer the better though!

These links may be useful in helping to calculate loading coils:

Antenna Loading Coil Calculator : http://eweb.chemeng.ed.ac.uk/jack/radio/software/loading.html

Coil winding design program : http://ecosse.org/jack/radio/software/newcoil3.html

Loaded dipole calculator by K7MEM : http://www.k7mem.com/Electronic_Notebook/antennas/shortant.html

Ring Core Calculato r: http://www.dl5swb.de/html/mini_ring_core_calculator.htm

Top Band Inverted L - photograph showing the wooden support post with telescopic pole attached with connection box, cables and earth rod. The cable entering from the left is the earthing strap which is connected to ground rods and radial wires. The coaxial feeder cable exits from the bottom right of the box and is wound around a length of white plastic pipe to form a simple RF Choke.

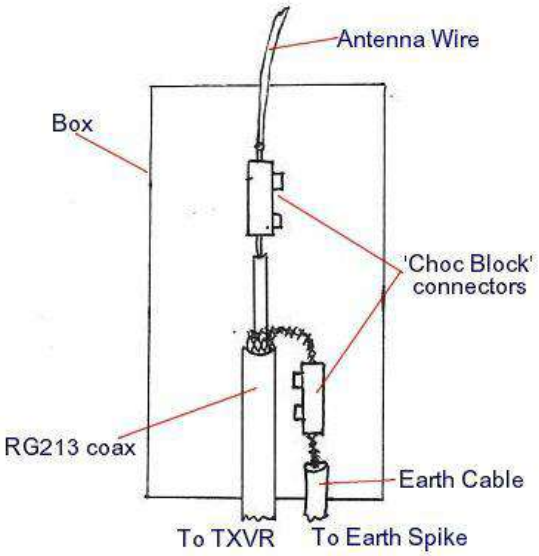

My original implementation which used 'choc block' connectors. The final design has all soldered joints with a stainless steel bolt and wing not at the top of the connecting box.

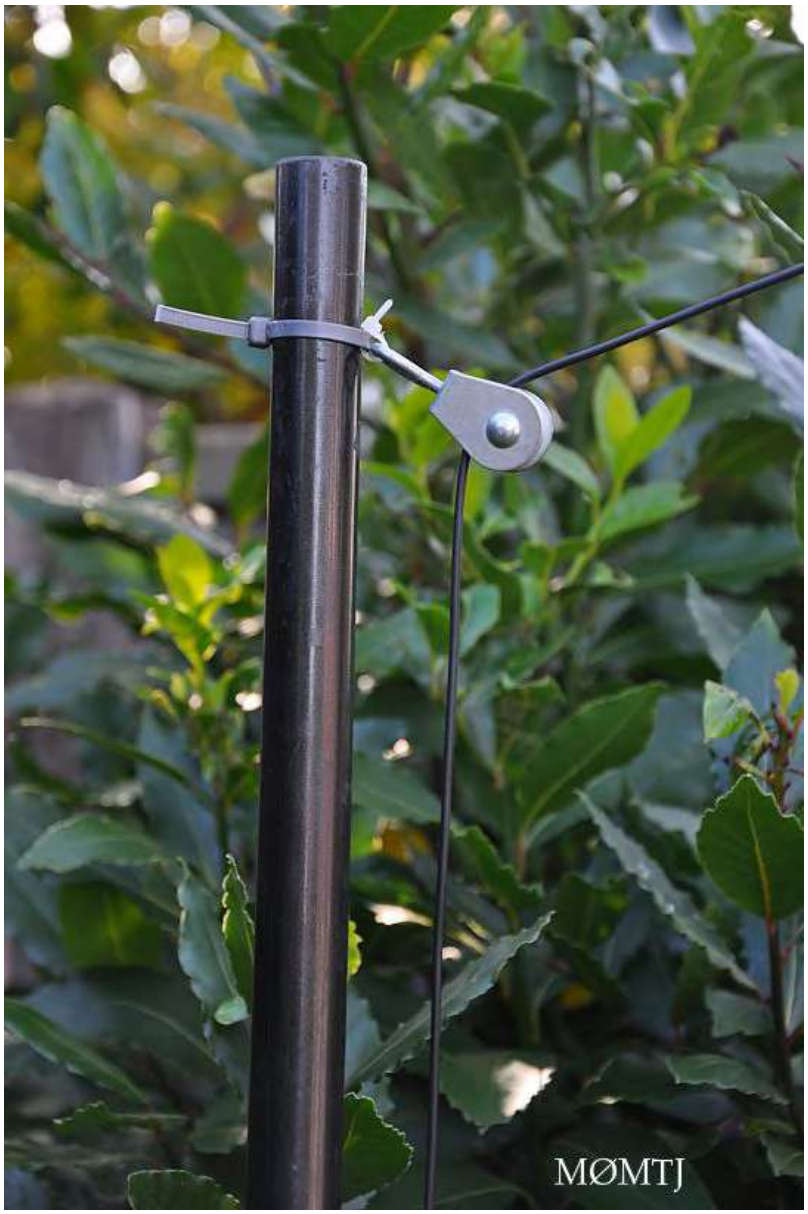

Top Band Inverted L - pulley on top of the 6m telescopic pole

Top Band Inverted L - loading inductor.

This is the unfinished coil, the connections on the left are properly finished off using lugs, but the connections on the right are unfinished to allow adjustment of the number of turns. When that is settled the final lug is soldered to the end of the enamelled copper wire and held in place with the bolt and wing nut. The coil is 39 turns of 0.9mm e.c.w., wound on a 5cm diameter former made out of an empty silicone bathroom sealant tube. (I would have preferred to use slightly thicker e.c.w. of about 18 swg 1.2mm diameter, so that may get changed in the future)

Enamelled copper wire:
http://www.sycomcomp.co.uk
http://www.esr.co.uk/electronics/cable-copper.htm

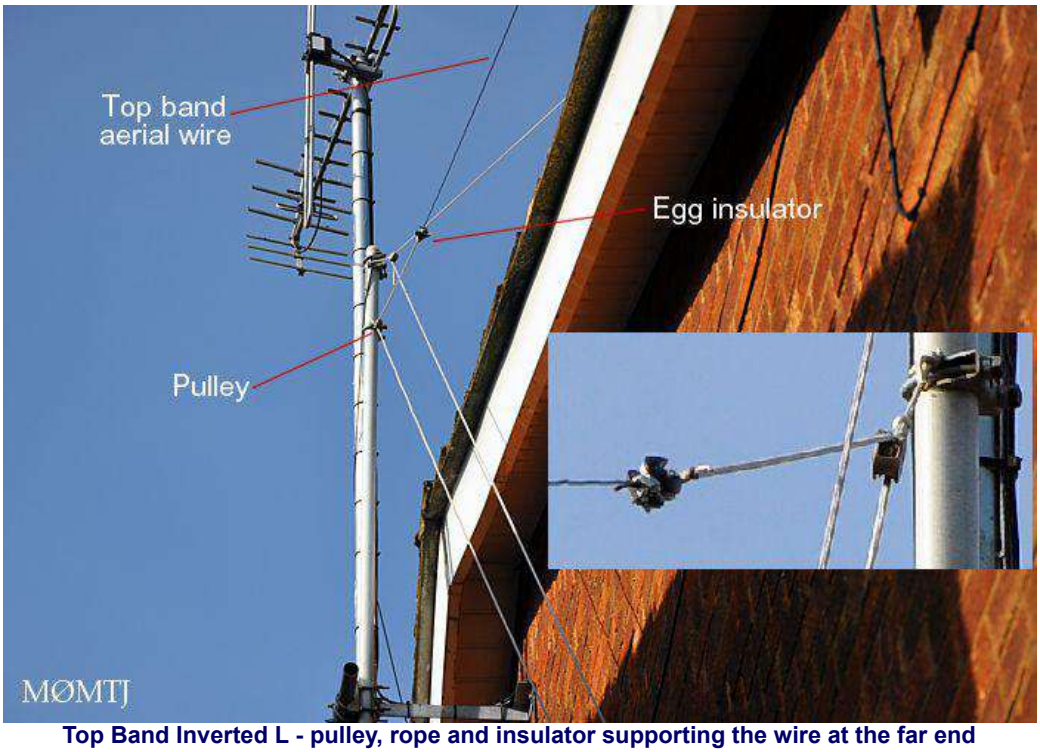

Top Band Inverted L - pulley, rope and insulator supporting the wire at the far end

Top Band Inverted L - supported by a 6m long fibrelass (roach) pole

Top Band Inverted L - looking up!

The photo exaggerates the bend a little, but it's not enough to worry about. The bend could easily be corrected by adding a back guy to pull the pole back towards the vertical position, but for this job it's fine as it is.

DOES IT WORK?

Yes! This aerial does work, I am glad to say!

It works better than my initial short sloping wire shown further down this page, which is what one would expect!

Rather than merely settling for a local ground wave signal I was very pleased to contact Top Band enthusiast Steve G7KLJ on my first attempt. Steve is 170 miles distant from me and the night time sky wave provided a pretty good result. G7KLJ gave me a 5 / 8 with my 100 watts on 1843kcs using my small aerial. I gave G7KLJ 5 / 9+10 with Steve's large doublet and 400 watts (lovely audio too Steve!).

Admittedly that's potentially a 16dB difference, which is pretty huge, but G7KLJ had the benefit of 300 more watts - that's a 6dB advantage. It also depends on how the individual S meters compare. Steve seemed to indicate that his S meter was a bit on the lazy side - 1 S Point pessimistic? But maybe my S meter similarly pessimistic?

Compared to a full size inverted L my loaded aerial is less than half the size and is obviously going to lose out, but by how much? Half the size, half the effective power - 3dB down? Probably a lot more - 6dB? There's one S point lost already (Who wants to bet that it's a lot more than that?). Since I have a ground system that is far from ideal there's another few dB's lost - another 6dB? That would be 2 S Points lost before taking into account anything else. This is all pure guesswork and speculation admittedly and probably quite groundless (almost literally in my case), and might best be described as pointless ramblings! (Where did the delete key go?) The pessimist? The realist?

The only thing proved by this single event is that my aerial radiates at least something useful - and that G7KLJ has a great station! www.g7klj.com

Droitwich

OK so it's not Droitwich, but it does work and gets me on Top Band when otherwise there would be no chance.

I am happy - but as with anything improvements can always be made. The aerial could be taller perhaps, though I cannot make it any longer. The earth system could be far far better, though I would struggle to accommodate any improvements at the present QTH. I could use better coaxial cable and also (importantly) attempt to lower the received noise by experimenting with chokes or burying the feeder to reduce common mode currents.

Plenty to think about and plenty to play with!

Important notes on effective Grounding by Jim K8OZ

Mike - I was reading about your work on the 160 meter Inverted L, and it makes me want to go out and build some more antennas! Congratulations. Your story is fascinating, and very well documented.

The only thing I can offer as a suggestion is to get as much radial wire along the edge of your property as possible (assuming your XYL will not allow you to bury radial wire all over your yard). Even if you can only run multiple wires 1/8th of a meter apart from each other, and parallel to each other, your losses will be reduced. The ground losses have quite an impact on your transmitted signal, so any wire you can "hide" along the edge of your property will help improve your signal strength - little, by little...! { It may also affect your resonant frequency slightly, but that's easy to deal with by adjusting with an antenna tuner or slightly changing the loading coil. }

Good luck OM, and keep up the refinements on your antenna system. You're doing great! 73,

Jim, K8OZ
Albuquerque, NM

Top Band Antenna by Mark, G0MGX and Vince G0ORC

Mike, I've been reading with interest your musings on top band antennas and have tried to build a replica of yours today with a fellow ham G0ORC. Thanks very much for the information and the link. You can see the results of my attempts here:

Construction: http://g0mgx.blogspot.co.uk/2012/08/top-band-what-happens-there-then.html

It Works!: http://g0mgx.blogspot.co.uk/2012/08/well-this-top-band-twig-does-it-work.html

Mark. G0MGX

Mike,

I know you have been in contact with my good friend Mark G0MGX but I felt I needed to say thanks and acknowledge your work on a 160m sloper.

It works very well here and, thanks to Mark who built several inductors until one gave us an SWR of 1.1 on the CW end of the band and also braised several copper rods together for form a reasonable earth under a large pine tree. He has passed on to me details of the website of K7MEM which may well inspire me to try a sloper for 80m as well.

I've always wanted a top band antenna but felt that I didn't have the room - but thanks to your idea and Mark's enthusiasm for the project I now have what I wanted - I'm being heard (and can hear) into European Russia with it so it certainly works!

Thanks again - I enjoyed your website very much. (Just heard A65BP as well!)

73, Vince G0ORC http://www.qrz.com/db/G0ORC

Further Developments of this antenna...

Another Top Band Aerial by MØMTJ

After reading the article "Top Band in a Small Garden" in the August 2012 edition of Practical Wireless Magazine ('PW'), I investigated further development of my Top Band Sloper / Inverted L Antenna (shown above).

The article by Stuart Craigen G4GTX described a compact wire antenna for top band that could be accommodated in small gardens. The antenna is shunt fed at the base, the coax being connected across a 7 turn coil (wound on an off-cut of an empty silicone sealant cartridge), with the braid connected to the earth stake and radial ground wires. The centre conductor is connected to the aerial wire.

I could not quite accommodate the shape that Stuart suggested for the aerial wire, but it is very similar: For my version the feed point is at the bottom of the garden near the fence immediately adjacent the earth stake. The first section of aerial is about 9.14 metres long - the wire rises 3.5 metres vertically up the 6.5 metre tall telescopic pole, at the 3.5 metre point the wire is held in place on the mast by a small bungee and then folds over almost horizontally

and runs for a further 5.64 metres where it connects to the loading inductor.

The inductor consists of 36 turns of 18 swg (1.2mm diameter) enamelled copper wire on a 50mm diameter, lightweight plastic former (again made from an off-cut of an empty silicone sealant cartridge). After the inductor there is a further 6 metres (approx) of wire rising to a dog-bone insulator, fixed to the end of a length of para cord that runs up to the pulley shown in a previous photograph. From the dog-bone insulator the aerial wire runs back, in the opposite direction, for about 12 metres, returning to the top of the 6.5 metre tall mast at the bottom of the garden, tied off to an egg insulator which is itself fixed to the top of the mast by a very short length of para-cord fixed to the mast by a thick nylon cable tie.

If the wire dimensions are changed, the number of turns on the inductor will have to be changed accordingly. Similarly my antenna is located quite near the 80m/40m Inverted L and the interaction of the antenna affects the tuning and hence the number of turns required on the loading coil.

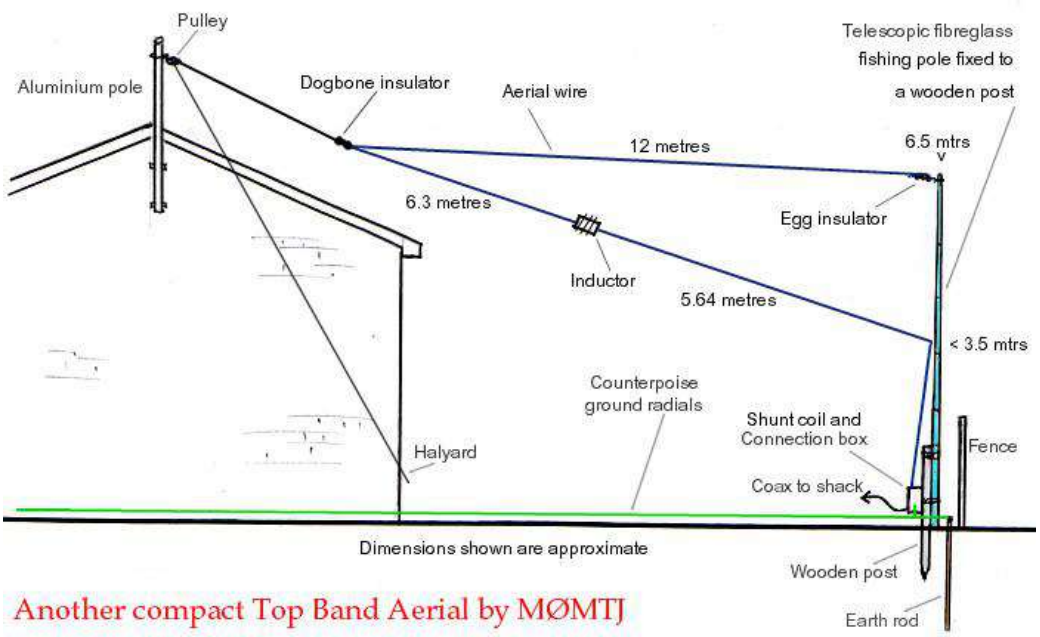

Another Top Band Aerial (drawing not to scale)
The inductor is 36 turns of 1.2mm diameter (18 swg) enamelled copper wire on a 2 inch former

With that arrangement there is about 27 metres of wire in the air. The point of resonance is 1900 kHz, but this can be adjusted by altering the number of turns on the inductor. As expected bandwidth is quite narrow. As with any antenna fed against ground the earthing needs to as extensive as possible - as noted previously, above. I suspect that it may be better that the top wire should be horizontal, or sloping slightly upwards, however with the available space and materials available the best that I could achieve had the top wire sloping slightly downwards to the post. Lowering the position of the dog-bone insulator or using a taller post could overcome this.

Photograph of the feed-point of the compact, folded, Top Band antenna showing the 7 turn shunt fed coil in the weatherproof housing. Nuts and bolts are stainless steel.

First Test: A brief on air test on 8th September 2012 between 2100 and 2130 UTC on 1.933 MHz brought in two prizes: Peter EI7JM near Malin Head and Tony M3LTD in Naseby, Leicestershire. EI7JM was a true 5/9 to me and he gave me a report of a true 5/9. M3LTD was 5/7. Many thanks to both stations for the useful contacts.

For different sized gardens the best idea might be to get as much aerial wire into the air and then make adjustments to the point of resonance by simply adjusting the number of turns on the inductor.

Practical Wireless Magazine
Obtain the article "Top Band in a Small Garden" by Stuart Craigen G4GTX from Practical Wireless Back Issues department

Stuart Craigen G4GTX comments:

Hi Mike, I have just been looking at your fascinating antenna page on top band antennas! Glad to see that you had a

go at building my shunt fed wire vertical that I did for Practical Wireless! I found it tremendous. A few weeks ago I was talking to G3YFN in Newcastle at about 4pm when I was called by G4BIM in the Isle of Wight! I also got a QSL 5/9 from Luxembourg!. Have fun.with it!

Thanks for the nice comments about my shunt fed 160m aerial. I enclose some QSL cards which you might find interesting to look at! Note the times of the QSO's and the reports! At night I have been told that I sound like the BBC from some European stations!!

Note G4BIM Isle of Wight 5/7 from Sunderland at 4.30 pm and Aberdeen at night. It certainly works for me. I think that the shunt feeding is the answer as it taps into the aerial at the 50 ohm point. Putting the loading coil away from the base should increase efficiency hence approx midway. A chap near Newcastle built one of these a few years ago and his groundwave signal was 5/9+20 here in Sunderland 12 miles away!!!
73
Stuart G4GTX

More ideas....

Adding Top Band to the 40m / 80m Inverted L antenna using a switchable loading coil:

Due to an aborted house move in 2010 I had removed all the antennas. While re-establishing the aerials in 2011, and considering space limitations, I decided to experiment with adding a loading coil to the 40m / 80m Inverted L aerial. The loading coil has a link wire to short it out of circuit when using the aerial for 80 metres and 40 metres. The link wire is removed when Top Band is required. The coil consists of approximately 37 turns wound on a piece of 68mm (2.8 inch approx) diameter PVC pipe:

Work In Progress! - Adding 160 metre loading coil to the 80m / 40m Inverted L Aerial.
The loading coil has a link wire to short it out of circuit when using the aerial for 80 metres and 40 metres.
The link wire is removed when Top Band is required.
The coil consists of approximately 37 turns wound on a piece of 68mm (2.7 inch approx) diameter PVC pipe.

More about the 80 / 40 metre Inverted L Aerial on Antennas Page 1 >

Simple Vertical Top Band Aerial Using A Fibreglass Telescopic Fishing Pole (Roach Pole)?

If there really is no space to accommodate a top band dipole, inverted V or even the inverted L above, then another option could be a simple vertical. Again based on a 10 metre long fibreglass roach pole, this could be installed as a

permanent aerial, or only deployed as and when required on a temporary and stealthy basis.

The 10 metre long fishing pole would be erected by standing it on the ground, using three or four nylon guy ropes as support, or tying it to a wooden ground stake driven into the ground. The vertical radiator would consist of about 9.5 metres of PVC covered wire fixed at the top of the pole and with a loading coil at the centre. As with the design above, the loading coil could be wound on a 5 cm diameter using 1.2 mm diameter enamelled copper wire. To make the former as light weight as possible, once again, the tube from an empty bathroom sealant (or silicone sealer etc) gun could be used. They are, conveniently, 50mm in diameter.

I have not experimented with the number of turns required for the centre loading coil, but from experience with the above aerial, the figure may lie somewhere between 50 and 100 turns.

The aerial would be fed with coaxial cable and would need a good earth rod at its base and a good number of ground radials, as along as possible.

Previous Top Band Aerial Experiments:

Top Band Inverted V

This is a considerably shortened dipole for 160 metres, using loading coils to reduce the length of each leg to about 7.5 metres length. Each coil is wound on a 5 cm diameter former and consists of approximately 120 turns of 1.2mm diameter enamelled copper wire. The dipole was arranged in an inverted V configuration.

Being as a dipole is a balanced aerial, it was fed at its centre using balanced twin feeder for lowest loss and, being balanced, lowest noise.

In this configuration it was very quiet, but did also appear to receive very well. At my QTH the noise on top band generally ranges from S7 to S9, on this inverted V the noise was S4 to S6. However it did not transmit well at all - I believe this to be not only because the dipole is very short (only 15m) but because the angle at which the wires at the top of the V was far too acute - only about 45 degrees. The angle at the top of the V really should be over well 90 degrees - maybe something like 110 degrees would be best. Clearly this seems to be a problem.

I had not got the space to separate the wires any further, but it was an interesting experiment that appeared to demonstrate that a balanced dipole fed with balanced twin feeder could help reduce noise. If more space was available this is an antenna that I would wish to pursue further.

Top Band Shortened (loaded) Inverted V

Short Base Loaded Sloper - a first attempt at a top band antenna

160m metres is probably the noisiest band, but I wanted to give it a go anyway even though space at my QTH is at a premium and fitting in a suitable antenna is quite challenging. The most promising candidate that I initially found, apart from small commercially available antennas, was the "Practical Antenna For 160 metres" described by Frank G3YCC and featured on the website of IW5EDI and linked to on the pages of www.dxzone.com

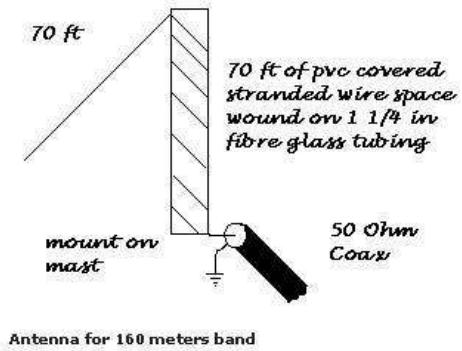

G3YCC Top Band Antenna

This Top Band antenna consists of 140 feet of wire, 70 feet space wound around a non-conductive (fibreglass) pole or tube about 6 feet long, with remainder forming a sloping wire falling back to near ground level. The antenna is UN-Balanced and is therefore fed with unbalanced coaxial cable, with the braid connected to a ground stake at the base of the aerial.

The above design is intended to have the coil section mounted on top of a mast or pole with the wire running downwards. I could not accommodate that arrangement, so I adapted the design to produce the antenna shown below:

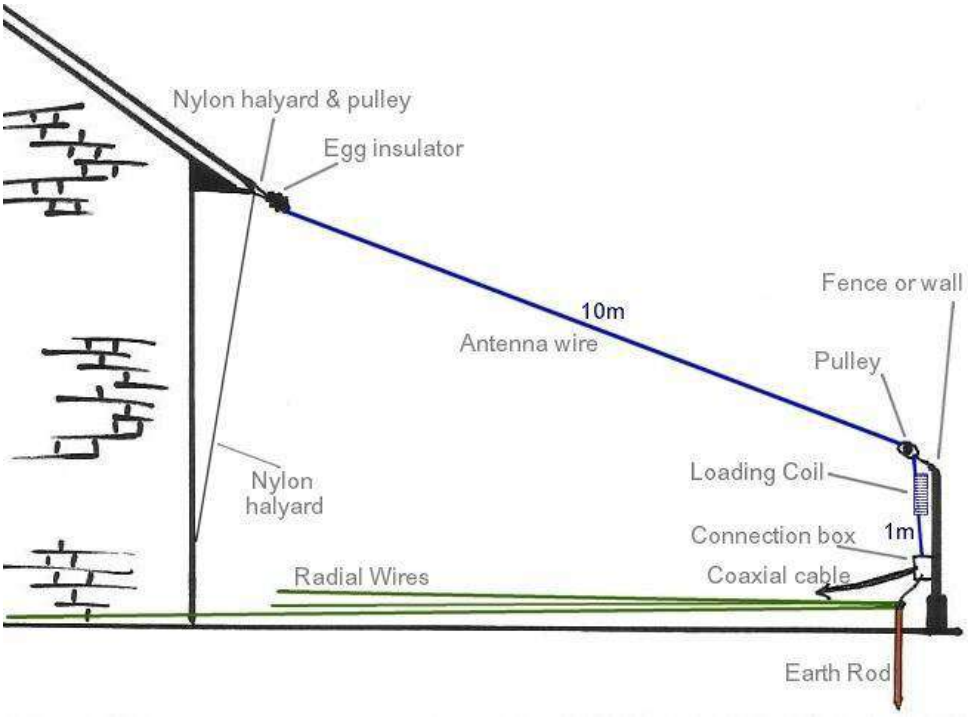

The drawing above shows the loaded Top-Band Antenna - a first attempt at an aerial for 160m - consisting of the radiating top wire, a base loading coil, earth stake and additional earth radials that act as a counterpoise: The top wire is about 10 metres long and slopes down to the loading coil which consists of 64 turns of the aerial cable wound around a 4" diameter PVC pipe and then falls vertically for about 1 metre where it enters the connection box. The halyard arrangement allows the antenna wire to be quickly dropped for adjustment and then raised back into position. There is an earth rod at the base of the antenna connected to several ground radials and a second earth rod a few metres away.After performing some tests I find that it does work reasonably well for local contacts ground wave contacts around the town, but it could be better and is certainly very disappointing for longer distance work.

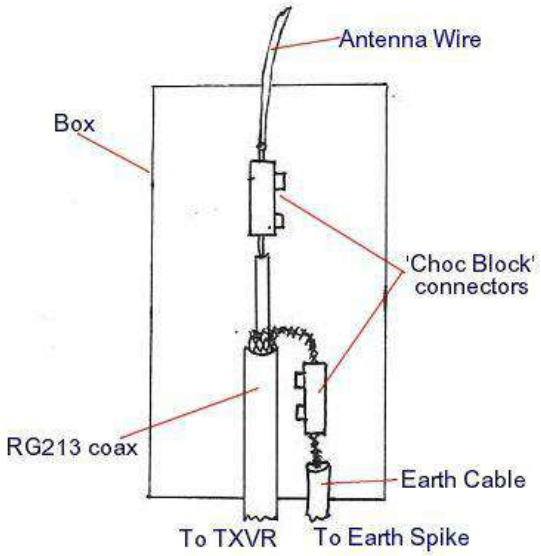

Above: The Connection Box

Read more developments here>

Efficiency

The aerial shown above is obviously very much shortened and therefore is very inefficient when compared to a full size resonant quater wave aerial. A shortened aerial still needs to make best use of the space - so the antenna wire

needs to be as long as possible. Resonance is adjusted by varying the inductance of the loading coil. Also it is necessary to use the largest earth system as is practicable to obtain the best possible efficiency.

Performance

In my configuration described above it is admittedly a very low efficiency antenna - but at least it gets one on Top Band! It's ok for local working around a town or a city, but it's certainly not a DX aerial by any stretch of the imagination. I could hear many stations 100 to 200 miles away, but they could not read my signals. For local ground wave work it was adequate.

I suspect that if the original design by G3YCC was employed, i.e. the coil mounted at the top of a pole and the loading wire running down, that it may work rather better than my implementation. The problem that my implementation has is that the loading coil is at the bottom of the aerial, near the ground. Better efficiency may be acheived with centre loading. The longer the radiating wire the better too.

More Details

The antenna was fed by coaxial cable from the shack in the bedroom at the front of the house to the feed point at the base of the fence at the bottom of the back garden. The coaxial cable enters a small plastic box, screwed to the fence post, where it is terminated: The outer conductor of the coax is connected to the earth cable with a 'chock block' connecter, the earth cable going to a four foot long earth rod hammered into the ground near by. The centre conductor of the coax is connected to the antenna cable also using a 'choc block' connector.

The antenna wire runs vertically up the fence for about 1 metre to the loading coil which consists of 64 turns of the antenna wire wound around a piece of 4 inch diameter PVC pipe. About 32 turns a close wound and the other 32 turns space wound; The inductance, and therefore the point of resonance could be easily adjusted by altering the spacing of the windings. Once set at the required point of resonance the windings can be held in place with duck tape.

The antenna wire exits the coil at the top and passes through a pully secured to the top of the fence and then slopes upwards for about 10 metres to the fixing point at a convenient point on the house, in this case the eaves. The end of the wire is tied off to a plastic 'egg insulator'. The egg insulator is tied to a nylon halyard wich passes through a second pully at the fixing point. This allows the antenna wire to be quickly dropped for adjustment and then raised back into position.

The earth system should be as extensive as possible for better efficiency; e.g. earth stake and a number earth radials, as long as possible around the garden to provide a counterpoise.

Link:

Visit www.g7klj.com - the website of 160 metre entusiast Steve G7KLJ

OTHER THINGS

Antennas for HF

There are dozens, if not hundreds, of antenna designs from which to choose. All have their own proponents. Some are genuinely good while others might be considered as nothing more than glorified dummy loads! The key thing for me was to choose the most effective an antenna that could fit within the constrains of my small back garden and also one that would not be too ugly.

I decided that wire antennas, made from PVC covered stranded wire, would be least objectionable on visual grounds. After all they look like glorified washing lines and almost everyone has a washing line**!**

Knots to use when fixing Wire Antennas

It's important to use the correct knot for the job. I find that the Bowline is very useful for fixing end, egg and dog-bone insulators to the ends of the wire and/or ropes. The Round Turn & Two Hitches, Anchor Bend and Buntline Hitch knots are very good for tying a rope to a pole or a mast. A Double Sheet Bend can join two pieces of rope together - even if they are of unequal size. 'Animated Knots' will show you how to do them: http://www.animatedknots.com

The antenna or antennas really are the key to an effective amateur radio station. The most expensive radio will be of little value unless it is used with the best possible and most effective antenna; so I had to set about finding the best antennas that I could accommodate for HF and VHF work.

The dilemma facing most radio amateurs is that antennas for HF are often large and difficult to accommodate in modern small back gardens. Additionally there may be objections on the grounds of visual impact. Some people do

not regard antennas as the beautiful creations that radio enthusiasts do!

Cables and Feeders

As I have learned by experience and from the tutorials I have studied as part of the licensing exam process, a very important consideration concerning the antenna system is the loss incurred in the cable that connects the radio to the antenna. A loss of 3dB sounds like a small amount when you say it quickly, but that equates to only HALF of your transmitter power reaching the aerial! We'd soon complain if our new 100 watt transceiver only produced 50 watts - so why stand the chance of losing this much power in the feed line?

Starting off as an M3 licensee I could only use 10dBw (10 watts) power at the antenna termination, so if I had a feeder with a loss of 3dB I would have to run the transmitter at 20 Watts to get 10 watts to the aerial!

Coaxial Cables

For HF using a single band resonant antenna, a dipole for example, Mini 8 or even RG58 is probably fine since the SWR should be between 1:1 and 2:1. However if one was to consider using the antenna on non resonant frequencies the VSWR will be higher, maybe very much higher, and the consequential losses in coaxial cable will be greatly magnified and power losses very significant. I did not want to run such an inefficient station.

For this reason I chose to use low loss RG213 coaxial cable for my Inverted L since I may need to use it on bands other than the 40 metre and 80 metres that it is intended for and where the SWR may be 4:1 or 5:1. RG213 will help keep feedline losses to a minimum. No lossy RG58 on Mini8 for me! Westflex 103 would be even better, of course.

For VHF and UHF I now consider Westflex103 as the minimum standard of cable to use, it's half the loss of even RG213. Losses at VHF are much higher than HF and at UHF they are even higher, so Westflex 103 helps preserve as much of that precious transmitter power as possible.

See more about Coaxial Cable Losses here >

Balanced Feeders = Low Noise

It's difficult to feed a centre fed wire dipole with RG213 or Westflex 103, both cables are really too thick and heavy. RG58 or Mini 8 are lighter and therefore more suitable for suspended wire dipoles, but to match the unbalanced coaxial cable to the balanced dipole would need a 1:1 'choke balun' at its centre, as I have learned. However, as mentioned above, when attempting to use the dipole at non-resonant frequencies the VSWR will be higher and the losses in the coaxial cable will be very much larger too, and hence much less of the precious transmitter power will be actually radiated by the antenna. Not an ideal situation

I have learned that the only really sensible way to feed dipole type antennas, which are 'balanced', is to use a balanced feeder such as 300 ohm ribbon cable, 450 ohm ladder line or the best option, it seems, might be 75 ohm Twin Feeder. All such twin feeders are extremely low loss, much much lower than any coaxial cable, so low that it could almost be considered lossless by comparison. Of course nothing is lossless, but twin feeder is as near as you'll get, so that's how I will feed my dipoles from now on! See the note on Doublet antennas below.

Tony Nailer of Spectrum Communications notes that: "75 ohm twin feeder is lower loss than coax. It allows the aerial to be properly balanced and the very close spacing of the wires prevents pickup or radiation from the feeder. It does not need to be spaced off, unlike ribbon feeder. Use of twin feeder makes this aerial much lower noise than one fed with coax. Also importantly it generates less TVI !! Note that the [trapped dipole] aerial is generally 72 ohms, and will need to be used with an ATU with transistorised rigs which are unforgiving about SWR mismatches."

Spectrum Communications are now supplying a new design of top quality, very low loss, twin feeder. It is rated at 2kW at 100 ohms. It can be supplied by 100 metre reel or by the meter, or in various lengths with the ends expertly terminated and made off. I can confirm the superior quality of this product and its low noise properties.

Spectrum Communications also supply a very high quality, well made 1:1 Balun that is perfect for connecting the twin feeder to the unbalanced input of an A.T.U. of transceiver.

Doublet or Dipole (Horizontal or Sloper)

I have also experimented with a second HF antenna - the 'doublet' style antenna. I fed this with low loss twin feeder and cut it for the lowest frequency of operation, in my case 20 metres (14 MHz).

Some initial experiments have shown that it is very effective on 20 metres, better than my Inverted L - which is designed essentially for 80m and 40m.

In theory a doublet antenna, when fed by twin feeder (NOT coaxial cable) and matched at the transmitter end via a

1:1 balun and an ATU (or to use a more correct term, Antenna Matching Unit) at the transceiver should be able to work on all bands with a higher frequency than the band that it is cut for.

On other bands such as 17m (18 MHz), 15m (21 MHz), 12m (24 MHz) and 10m 28 MHz) the doublet showed generally lower VSWR than the Inverted L ..... however (and here is a nice lesson) it is actually not quite as effective as the Inverted L! I think that size may matter here - the overall length of the Inverted L is much longer.

This short 14 MHz doublet is only about 10 metres in total length and was suspended at about 25 feet high at one end from the same fibreglass pole fixed at the apex of the roof and taken down to another 16 foot high wooden pole installed on the other side of the back garden in somewhat of a 'sloper' style.

Trapped Horizontal Dipole or Vertical Antenna for 20m / 10m

I also experimented with a trapped wire dipole cut to be resonant for 20 metres and 10 metres, again fed with twin feeder and matched at the radio end via a 1:1 balun and the ATU (AMU !).

I may also try an antenna for 20m / 15m and 10m in a Vertical 'ground plane' arrangement which should give a lower angle of radiation than a horizontal dipole - therefore better for longer distance DX.

At the moment I am using the 20m / 10m trapped dipole in a rather unorthodox arrangement. I have installed a fibreglass fishing pole, mounted vertically on a stake on one side of the garden. Most of the wire dipole is fixed to the vertical pole, but being as the dipole is somewhat longer than 7 metres, a portion of the wire runs away from the pole horizontally along a fence panel about 1.5 meters above ground level. It's vaguely L shaped, but mostly vertical which should help with the angle of radiation. It seems to work very well indeed - I like the mostly vertical idea.
The antenna can be seen on this page >

Other Dipoles:

Spectrum Communications can supply a full size W3DZZ style antenna with a 7MHz trap for use on 40m and 80m and usable on 20m, 15m and 10m. A half size version with a 14 MHz trap for use on 40m and 20 metres, plus 15m and 10m is also available. As a special order an even shorter version using a 28 MHz trap is available for 20 metres and 10 metres. http://www.spectrumcomms.co.uk/G2DYM.htm Al versions designed to be used with balanced line feeder - lince they are balanced aerials - for low noise and lowest loss.

PDF Document - The W3DZZ Antenna -
http://www.users.icscotland.net/~len.paget/GM0ONX%20trap%20dipole.pdf (But rather than using coaxial cable with a 'choke balun' at the centre of the dipole, try using twin feeder with the Choke Balun at the radio end for less power loss!)

Links

Enamelled copper wire supply: http://www.esr.co.uk/electronics/cable-copper.htm

Loading coil calculators: http://www.k7mem.com/Electronic_Notebook/antennas/shortant.html

Ring Core Calculator: http://www.dl5swb.de/html/mini_ring_core_calculator.htm

Vertical Antenna For 50 MHz, 144 MHz and 430 MHz

Watson W-2000 on Telescopic Mast at the lowest position
more on this page

OTHER ANTENNAS

Our good friend in Australia Felix Scerri, VK4FUQ, uses Inverted V antennas but also highly recommends the Quad Loop style antenna for HF work. These are well worth investigating, and you can read more here: Antennas 3 see the antennas at the MØMTJ QTH here with many more antenna ideas on Antennas 4 and the Links Page here and here

Antennas 1 | Antennas 3 | Antennas 4 | Antennas 5 | Antennas 6 | Antennas 7

G-Whip Antenna Products
Geoff G4ICD offers a multitude of high quality solutions for portable, mobile and permenant base installations

M0MTJ | Operating Conditions | Antennas / Aerials | /P Portable Operating | Accessories | Projects & Kits | Useful Information

Contact MØMTJ | Contact M6ORS | Links to Amateur Radio Sites | RSGB | QSL | The Amateur Radio Mini Site Map

WSPR Weak Signal Propagation Reporter

News, Developments, Events, Photographs and other 'Bits 'n' Bobs'

MDS975 Home

Feedback

Mike Smith - MDS975.co.uk © 2003 - 2016

M0MTJ

Amateur Radio; Ham Radio; Radio; Transceivers; HF; VHF; UHF; Data Modes; Morse Code; RTTY; PSK31; SSTV; FSTV; Amtor; Sitor Antennas; Aerials; Cable; Coaxial Cable; Twin Lead; Masts; Poles; Propagation; Computer; PC; USB Computer Interface; Microphone Loudspeaker; Filters; Noise Reduction; DSP; Digital Signal Processing; Morse Key; SWR ; Inverted L; Inverted V; Dipole; Doublet.

Amateur Radio M0MTJ

MDS975.co.uk HOME PAGE

My Home Page

Amateur Radio
Operating Conditions
Antennas
Accessories
Projects & Kits
Data Modes
Information
Portable
QSL
RSGB Ltd
Links
QRM
Bits 'n' Bobs
Contact

WSPR Weak Signal Propagation Reporter

PORTABLE

Site Map

MDS975 Home

Feedback

QRM from PLT

Site Search
Find
powered by FreeFind

M0MTJ | Operating Conditions | Antennas / Aerials | /P Portable Operating | Accessories | Projects & Kits | Useful Information
Contact MØMTJ | Contact M6ORS | Links to Amateur Radio Sites | RSGB | QSL | The Amateur Radio Mini Site Map
News, Developments, Events, Photographs and other 'Bits 'n' Bobs' | WSPR Weak Signal Propagation Reporter

"Everything should be made as simple as possible, but not simpler." - *Albert Einstein*

AERIALS (ANTENNAS) 4 - Notes and Queries

Antennas 1 | **Antennas 2** | **Antennas 3** | **Antennas 5** | **Antennas 6** | **Antennas 7**

Index To Other Antenna Pages:
Antennas 1 : Aerials used by M0MTJ
Antennas 2 : Including ideas for compact aerials for Top Band /160 metres
Antennas 3 : Felix Scerri VK4FUQ discusses Loop Antennas, baluns, masts & other antenna related topics
Antennas 4 : Many antenna ideas from various sources particularly for Multi-Band operation & also gives information about...
antenna trimming, knots for wire antennas and useful antenna rigging accessory ideas.
Antennas 5 : Half Wave End Fed antennas for 144 MHz VHF / 430 MHz UHF and 50 MHz 6 Metre band & J-Pole Aerials
Antennas 6 : Simple and effective H.F. Antenna ideas - Ground Plane and All Band Doublet
Antennas 7 : Omni-Directional - Circularly (Mixed) Polarized Antenna for VHF / 2 Meters.

Multi Band Aerial Options | Useful Aerial Rigging Accessories | Aerial Trimming Chart | Useful Knots | A few antenna related Links

As G4ILO notes: An antenna may have two of the attributes: Small; Efficient or Broadband (works over a wide frequency range without retuning) but never all three.

Marconi spins in his grave every time a ham buys an aerial instead of building it ! *(W1GFH)*

THE QUEST FOR MULTI - BAND OPERATION - In A Limited Space

The aerial is arguably the most important part of any station. No matter what transceiver is being used it is the aerial that is the last and most vital link in the chain and needs to be efficient and effective to radiate the signal to best best effect. Some amateurs are quite content to operate on one or two bands while others might want to be able to operate on many or even all of the amateur HF bands. When I gained my licence I definitely fell into the latter camp!

It seems, then, that the holy grail of many amateurs is the perfect multi-band aerial!

Luckily N4UJW has designed a new limited space 160m through to 70cm marvel antenna the plans of which can be found here:
http://www.hamuniverse.com/antwish.html

Having experimented with various types of antenna I am of the opinion that, perhaps along with many other amateurs, for simplicity a resonant dipole is the most efficient and effective of aerial. A resonant dipole it is only a single band aerial of course, but it is extremely cheap and very simple to make - and it's a very efficient radiator. So one could make a dipole for every band of interest and simply swap aerials to work different individual bands. Unfortunately the aerial described by N4UJW does not exist and compromises, such as lack of bandwidth or poor radiation efficiency, have to be made.

The principal of lowering a dipole cut for one band, removing it and hoisting another dipole cut for a different band in to place sounds pretty straightforward, but would the process become frustrating after a while. I think it could, so what about an antenna that will allow operation on several bands?

The Quest For A Multi - Band Aerial

Here is a collection of commercial and 'home brew' (DIY) antenna ideas that will allow multi-band operation, many of which could also be used in a location that offers limited space. Perhaps this only scratches the surface, but hopefully will provide a good starting point and fuel the mind in a quest for a good multi-band HF aerial. Do check out the manufacturer and supplier websites given on this page for lots more options and details.

Home Brew! It has been said that no radio amateur should ever buy an aerial - especially a wire aerial! Joe Tyburczy WB1GFH also comments about suitable antenna installing weather on his web pages:

"When you put up your antenna is also crucial. I must mention here the importance of what many early hams called "antenna weather". That is, snow, sleet, freezing rain, or combination of all the above. It has been proven time and time again that any antenna installed in conditions better than abysmal will not function worth a darn. Or, put another way, it takes bad weather to put up a decent antenna. Dark and cold New England winter days are ideal for this activity. Any antenna erected on such a day will inevitably produce miracles." Joe Tyburczy WB1GFH

G-WHIP
Antenna Products
Top Quality
British Manufacture

Most of what is available commercially could be 'home-brewed' if one has the time and a few suitable mechanical skills.

It's worth bearing in mind that Joe Tyburczy's $4.00 Special may well be more effective than a commercial antenna costing $400.00. Perhaps the equally inexpensive Zepp Antenna could produce far greater Value For Money than shelling out £$hundreds on a commercial antenna?

I give no particular recommendation here, but a good rule of thumb is not to believe the marketing hype of any commercial company supplying antennas.

A good place to start is, I think, the classic All Band Doublet Antenna, which is mentioned several times below. Plenty of links are also provide further down this page.

As important as not believing any of the marketing hype is remembering the words of the Star Ship Enterprise's Chief Engineer Mongomery Scott; (paraphrasing) *You cannae change the laws of physics!* - Size matters. A coil loaded 5 foot long aerial probably won't be that much good on the H.F. bands. Indeed, a a 5 meter long antenna may be perfect for the 10 metre band but it won't be a great antenna on 20m, and certainly even less effective on 40m and 80m

So, before falling for all the marketing hyperbole its wise to read up on a little antenna theory and do some lengthy research into the antennas being considered before making an expensive decision.

Below are a few clues and ideas listed in no particular order - some of the antennas will be great while some of the commercial designs shown below may promise great things but fail to meet high expectations.

There is no "miracle antenna". If one understands the theory and the compromises made with shortened, under-sized, multi-band (and often very expensive) antennas there may not be so much disappointment. However most will be compromised in one way or another, so if one is happy to live with those compromises, understand what they mean, and are happy to have a lighter bank balance then that's fine!

Low SWR across all the bands does not indicate a good antenna. My dummy load has very low SWR across all the bands but it is most certainly not a good antenna!

Someone telling you that the antenna that they're using is great and that they've worked the world doesn't mean it really is a good antenna - it's just 'hearsay'. One could quite possibly work around the globe on a coat hanger in the right conditions - it doesn't suddenly make a coat hanger the great antenna that should be widely heralded!

The best way to learn about antennas is to go out and make some - well actually go out and make many antennas.

Here are a few ideas. Some that are easily 'home brewed' and some commercial ideas that could be adapted to 'home brewing'. I don't have any particular recommendation, but I hope that this list will provide some good food for thought. (Some of the commercial antennas may be okay, some may be awful).

Remember; ***Marconi spins in his grave every time a radio amateur buys an aerial instead of building it !***

The Doublet Antenna - the classic all band / multi-band Aerial

The Doublet Antenna is my favourite Multi-Band aerial. The main benefits of a Doublet Antenna are that it can be

used on whatever frequency it is cut for, and higher frequencies. Usefully, there can be some useful gain on higher frequencies, although there will be some petal shaped lobes on the higher frequency bands.

In fact my 20 meter long Doublet for the 40meter band to the 6 metre band also works quite well on 80 meters! Not only a very good starter antenna for those looking to work as many bands as possible, but also an aerial that would be useful and efficient for years and years to come.

Ladder line or open wire feeder must be used (NOT coaxial cable). Ladder Line or open wire ensures low loss at High Frequencies so that as much of your precious transmitter power as possible will be radiated. Likewise receive efficiency should be maximized. Assuming that the aerial is successfully balanced, the feeder should not radiate, even when there is (inevitably) high SWR

High SWR is not an especially bad thing and will not reduce the aerial's performance, but note that high SWR on the balanced feeder does increase feeder loss compared to a when matched - but the losses will be a lot less significant then if coaxial cable were to be used. This ensures that efficiency should be better so that all the power that reaches the antenna wires will be radiated - save for any losses in the antenna tuning unit (AMU) or the balanced feeder cable.

Remember: Ladder Line = Lower Loss - Read more about my M0MTJ Doublet Antenna HERE >> and more notes on this page here >>

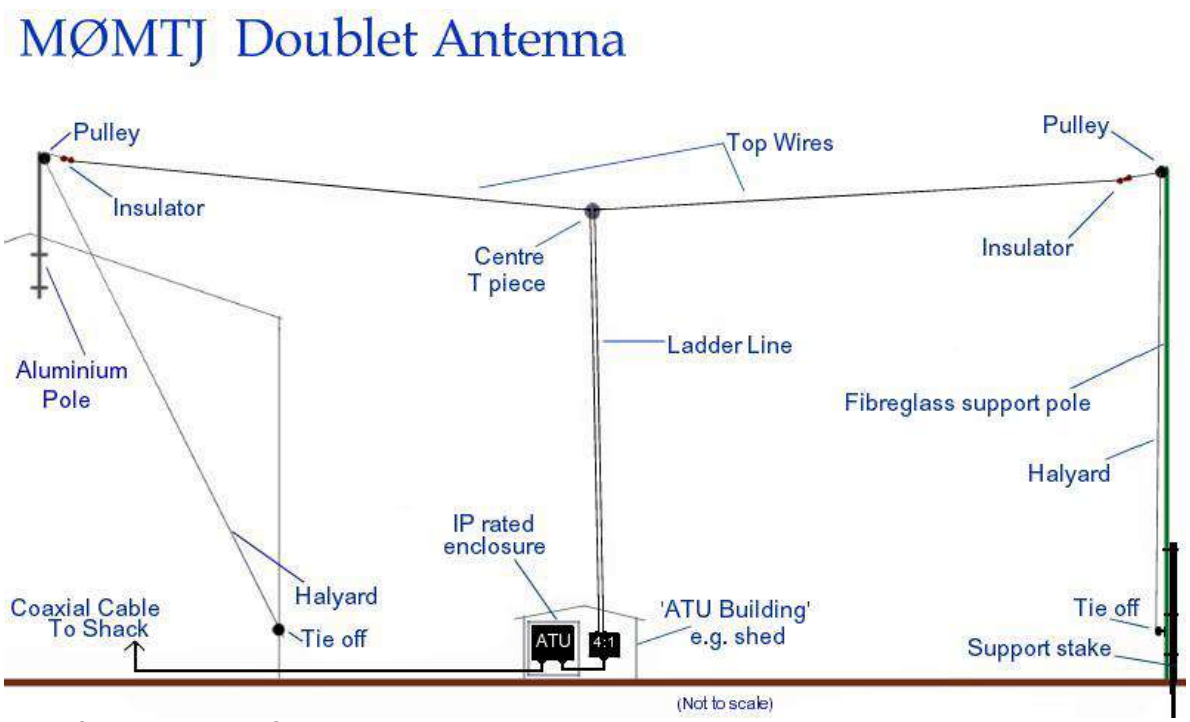

The Classic All Band DOUBLET ANTENNA - Read More about my M0MTJ All Band Doublet Aerial Here >>>

The G5RV and more about Doublets & Dipoles

The G5RV - (Even Louis Varney himself said that a Doublet would be better!)

Why the G5RV continues to remain popular is a mystery. The 'legendary' name, perhaps? That it can be 'thrown up' without too much thought? The fact that it' cheap and cheerful? Well, cheap anyway. There has been much written about the G5RV and the overall conclusion is that it's not a very good multi-band antenna. Certainly it will work quite well on, perhaps, a couple of bands, but there are better alternatives, especially when one considers the wide availability of remote automatic antenna matching units (remote auto 'a.t.u.'s) that will greatly assist in minimizing antenna feeder losses.

Perhaps the best thing that can be done with a G5RV is cut off the coax, re-size the top wires and turn it into a true Doublet Antenna - or, better than that, don't buy a G5RV in the first place and simply make (home brew) a true All Band HF Balanced Doublet Antenna.

The G5RV and its derivatives such as the Western HF-10 and the ZS6BKW are a bodge. In fact, Louis Varney G5VA himseld stated that a much better alternative to any of these 'G5RV' designs is to run the open-wire line from the center of a dipole all the way to a balanced antenna tuner!! This aerial arrangement will work on ANY band from 80 metres through to 10 meters.

The G5RV is, therefore, not the most efficient aerial and, as users report, may not always be the easiest to use, but because it is coax fed, it remains an ever popular choice because it's easy to feed the coax cable from the antenna's location back to the shack. Unfortunately this easy (lazy?) approach means lots of loss due to high SWR on the coaxial cable.

One may say, Oh well, there's perhaps only 2 or 3 S points in it. (Cough!). A difference of 3 S points is the difference between radiating 100 watts or only radiating 1.6 watts. Um, - I'm sure we'd soon complain if our shiny, new 100 watt transceiver only produced 1.6 watts!!

QRP and lower power portable operators should be especially keen to minimize antenna system losses so that as much power as possible is radiated. Losing 3 S points from a 5 watt FT-817 results in only 0.08 watts. QRP operators may likely favour resonant, single band antennas for greatest efficiency.

Coaxial Cable is only 'low loss' when the antenna impedance is similar to the cable's designed impedance of 50 Ohms, or near 1:1 SWR (or at least less than 2:1). Coax cable is therefore fine for a Dipole antenna that is designed to be resonant on one band of choice, which will have a reasonably low SWR across that band, but coax' is entirely unsuitable when one wants to use the aerial on several bands. The G5RV will be used an multiple bands and will therefore present widely varying impedance values (and SWR) depending on the band of operation and so the power losses will be significant.

Note: The antenna's true impedance (SWR) must be measured at the antenna's feed point (i.e outside and up in the air) not at the radio end of the cable, in the shack, where the coaxial cable's losses will mask the true SWR reading. Unfortunately 50 Ohms, or a near 1:1 match, will not be encountered on any band on a G5RV. The best band will be 20 metres at typically 2:1 (100 Ohms), but on any other band the impedance will be very much higher. One might expect rersults like these: 80 metres 3:1 to 5:1, 40 meters 5:1, 30 metres 20:1 or more, 17 metres 15:1 or more, 15 metres 6:1 to 12:1, 12 meters 3:1, 10 meters 10:1 to 20:1.

1000 Ohms into 50 Ohm coaxial cable will result in a massive dumping of your power - lost as heat in the coaxial cable instead of being radiated as a useful signal. However, high SWR is not in itself a bad thing - it's just that the correct type of feeder and impedance transformation method needs to be used. The *incorrect* feeder is coaxial cable - the correct type of feeder is balanced Line or Ladder Line feeder. This can be the typical slotted 300 Ohm type or the 450 Ohm 'window line' which are commercially available. Even better, make your own open wire, balanced line feeder. Spacers can be bought commercially or 'home brewed'. The spacing for this parallel line should be about 2 to 3 inches (50 to 80 mm) - the width of the spacing is not particularly critical, but whatever width is chosen should be maintained as accurately as possible along the length of the feeder - i.e. it should be parallel.

The Doublet can take more time and effort to tune, prune and adjust. It will also need a good antenna matching unit (so-called "ATU") and low loss balun, but the reward will be more effective performance due to the much reduced loss in the balanced line feeder system.

Doublet Aerials - a better alternative to a G5RV

Check out the The classic All Band Doublet and the NorCal Doublet for very simple, effective and versatile antennas for multi band operation:

The ALL BAND Doublet Antenna

This could very well be the first antenna that one should try in order to get on at least one band very efficiently but also several other bands with the use of a good ATU.

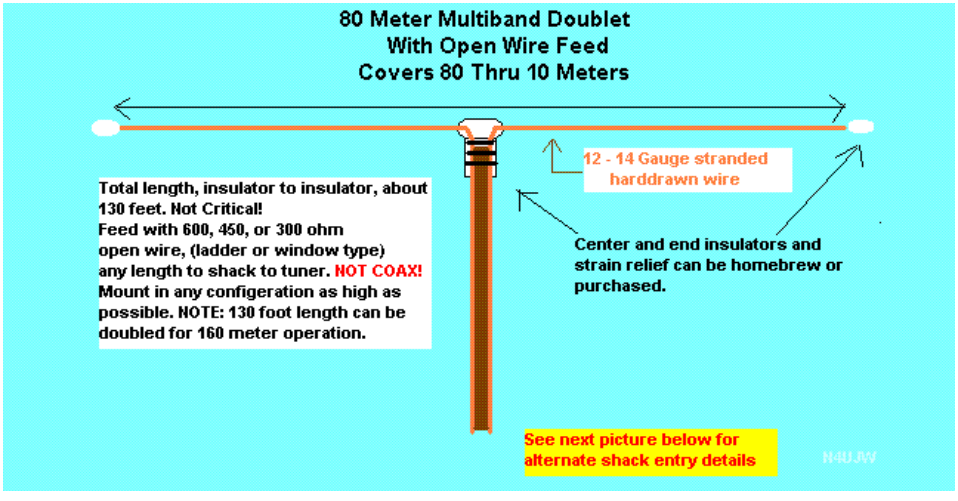

All Band Doublet - http://www.hamuniverse.com
See My All Band Doublet Antenna here

The all band Doublet antenna is nothing more than a 1/2 wave dipole cut for your lowest operating frequency and fed with twin lead, ladder line, open wire, etc to a tuner that will accept a balanced line connection. IT MUST NOT BE FED WITH COAXIAL CABLE !

It can be designed for use from 160 through to 10 meters very easily using the standard 1/2 wave dipole formula:

468/freq MHz = total length (ft)
The exact length is not critical!

If there is insufficient room for a lower frequency version (160m or 80m), then the Doublet can be designed to the shorter wavelength of the 40 metre band and used up to the 10 metre band. (Do not attempt to operate on a lower frequency than 7 MHz in that case since this could damage the a.t.u.) It may be possible to connect the ends together and tune it against earth - if you have a good enough earth - and use lower frequency bands. For best results a doublet should be mounted as high as possible (as with many aerials) and can be erected as a flat top or inverted V.

A Doublet Antenna needs a good antenna matching unit with a wide impedance matching range (obviously not the one in the radio!). Preferably this should be a balanced antenna matching unit, but an unbalanced matching unit can also be used together with a good low loss current / Guanella balun, such as the extremely high quality items available from G-Whip Antennas. I use a 4:1 G-Whip guanella current balun with my Doublet, but many users recommend using a 1:1 ratio current balun - again, this is a case for individual experimentation.

A more detailed description of the Doublet Antenna can be found here >>

External Links

The All Band HF Doublet can also be found on Ham Universe: http://www.hamuniverse.com/hfdoublet.html

Introducing The All Band Doublet by the late L.B. Cebik W4RNL: http://www.cebik.com/content/edu/edu6.html
N.B. Create a free account at http://www.cebik.com

The Norcal Doublet

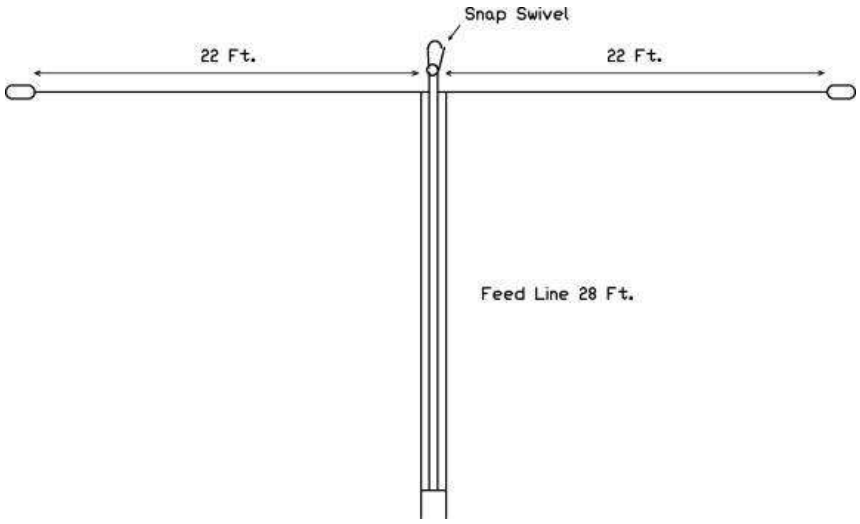

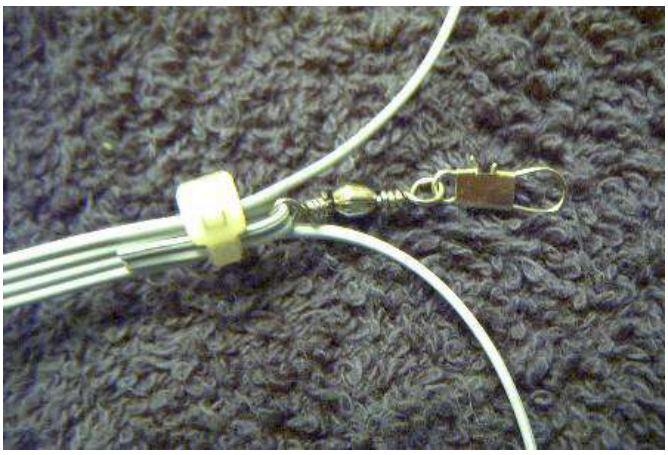

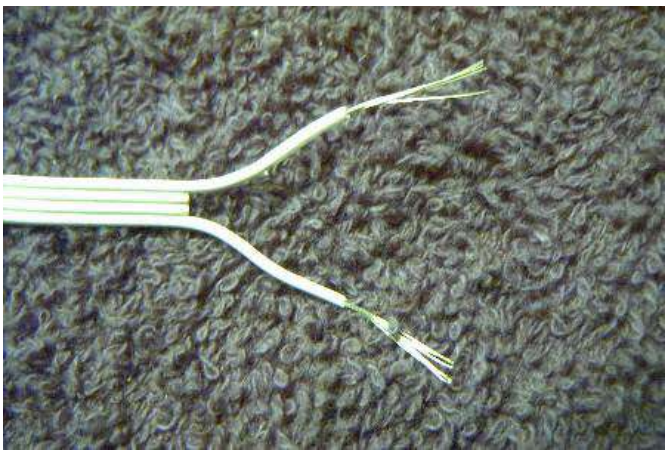

The Norcal Doublet Antenna: http://www.norcalqrp.org/norcaldoublet.htm

The Norcal Doublet is a simple antenna that is 44 feet (13.4 metres) long, 22 feet (6.7 metres) per side. The Norcal pages report "...that the antenna would have basically the same radiation patterns on all bands from 40 - 10 meters. This would be very handy to have for field operation..... You will need the following materials: 50 feet of 4 core stranded computer cable; 1 #0 Fishing Swivel; 1 Cable tie; 2 pieces of fishing cord."

The antenna can be hung from trees or cheap telescopic 'roach' / Sota poles. Doubling the size would allow operation on 80 metres and even 160 metres by shorting the twin feed together at the transmitter end and feeding it against a good earth as a 'Marconi' type antenna.

An effective multi-band "4 Dollar Special" by Joe Tyburcy - W1GFH (An Inverted Vee Doublet Antenna - super cheap - super effective - multi-band)

Joe Tyburczy, W1GFH provides some sensible insight and advice, he writes: *"I am a big fan of "balanced line" (twin lead, open wire line, etc.) vs. coax. By using balanced line and a tuner you can have one, single-element antenna that works well on all bands. You can't do that as easily with coax. The basic "W1GFH $4 SPECIAL" shown below is a variation on the type of versatile skyhook I've been using for years.....Now at this point, some of you may be looking at the diagram and muttering, "Jeez Joe, that's just a dipole fed with twin lead and used with a tuner". Well of course it is. Virtually all antennas are "di-poles" (i.e. "two sides") in some form or another. This one just happens to be made from low-cost materials.....I won't go into the theory here, but trust me: balanced feed line, properly used, does not "leak" RF and is less lossy than coax. I've tried the commercial 450-ohm ladder line, but prefer 300-ohm TV twin lead, and the cheaper the better. Radio Shack TV twin lead is ideal. Home Depot has some good stuff, too. Forget all the obsessive junk about standing waves, impedance and velocity factor. What you really need to concentrate on is getting an interesting set of antenna insulators."*

Read Joe's excellent article in its entirety here: http://www.qsl.net/wb1gfh/antenna.html

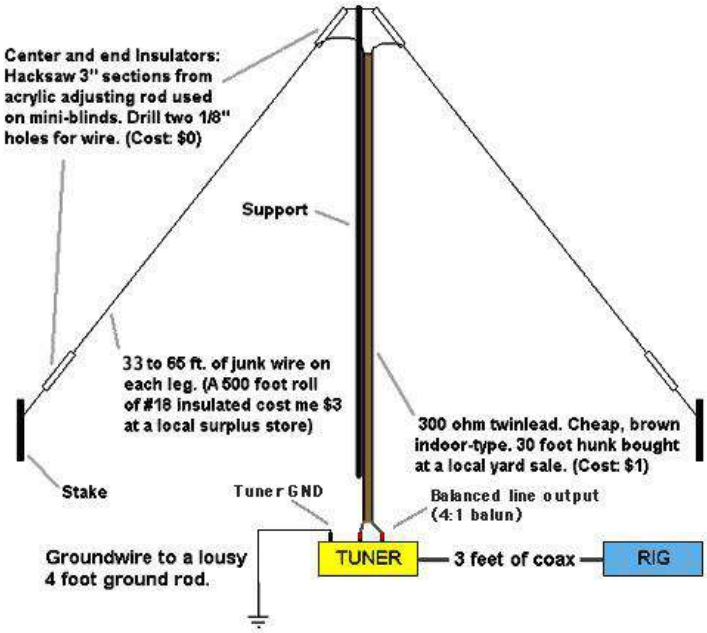

4 Dollar Special by W1GFH
http://www.qsl.net/wb1gfh/antenna.html

Inverted L - 80 metres to 10 metres

A typical Inverted L antenna will be trapped for 40m/80m using a 7.1 MHz trap. It is essentially one half of a W3DZZ dipole so can be accommodated very much more easily into a small plot or garden - especially as part of the antenna is running vertically up a wooden or fibreglass (non conductive) pole. This should allow it to be fitted into quite a small garden such as mine. It's a very useful antenna in this respect, and because there is a good length of wire in the air, it radiates quite well.

The Inverted L is also a very effective aerial because it has the benefit of both vertical and horizontal radiation. While Inverted L's might make good TX aerials, like ground mounted vertical aerials they do have the potential to be a little noisy on RX. This will depend upon local circumstances and noise sources. However the fact that the feed point will generally at the bottom of the garden, well away from the house may help to keep QRM to a minimum.

The Inverted L is extremely easy to 'home brew'. Spectrum Communications can also supply the complete aerial as shown below. It should give excellent performance on 80m and 40 metres, with 20 metres also being good but also allowing use on 15m and 10m and possibly one or two of the WARC bands.

If you fancy home-brewing the complete antenna, except for the 7 MHz trap, traps are available to buy commercially from suppliers such as Spectrum Communications and Sotabeams who supply very neat and lightweight devices,

Use a Remote Automatic Antenna Coupler : The use of a good Automatic Antenna Coupler, such as the CG Antennas CG-3000, at the feed-point with a simple inverted L wire will provide a very good Multi-Band aerial that could be used on all bands between 160m and 10m and should be very simple to deploy.

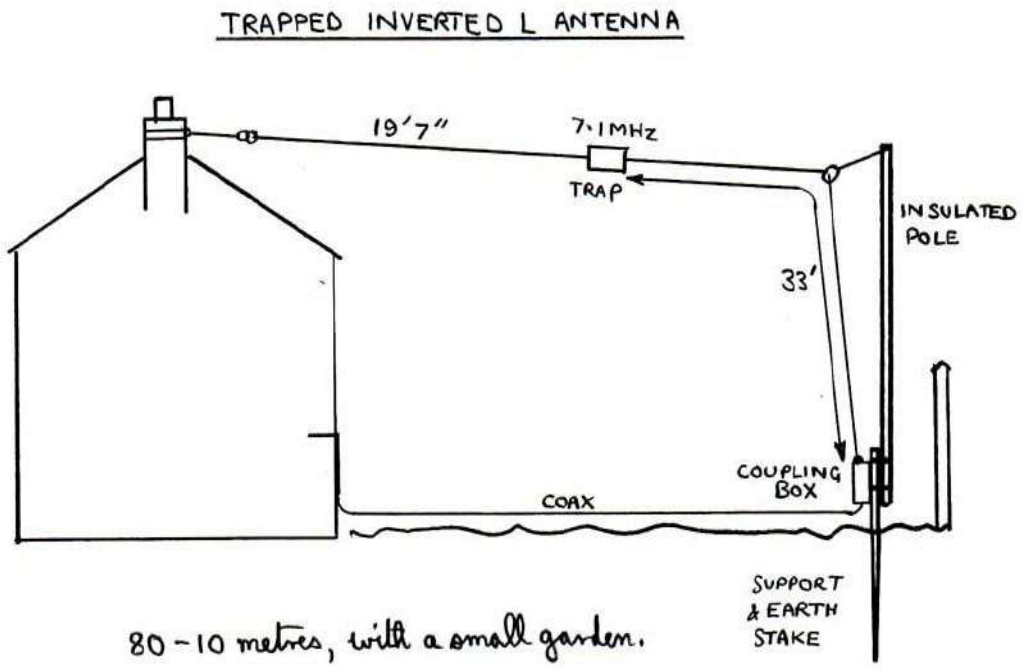

Spectrum Communications Inverted L - benefits from both vertical and horizontal radiation
http://www.spectrumcomms.co.uk

More about Inverted L Aerials:

The Inverted L for 40m/80m is shown below is essentially one half of a W3DZZ dipole fed against ground using one 7.1 MHz trap. It's a very compact antenna and is simple to construct. It is most efficient, of course, on 80 metres and 40 metres, but can also be used, with an a.t.u., on 20m, 15m and 10m.

Find out how to make one here: http://www.users.icscotland.net/~len.paget/5%20band%20Inverted%20L.pdf

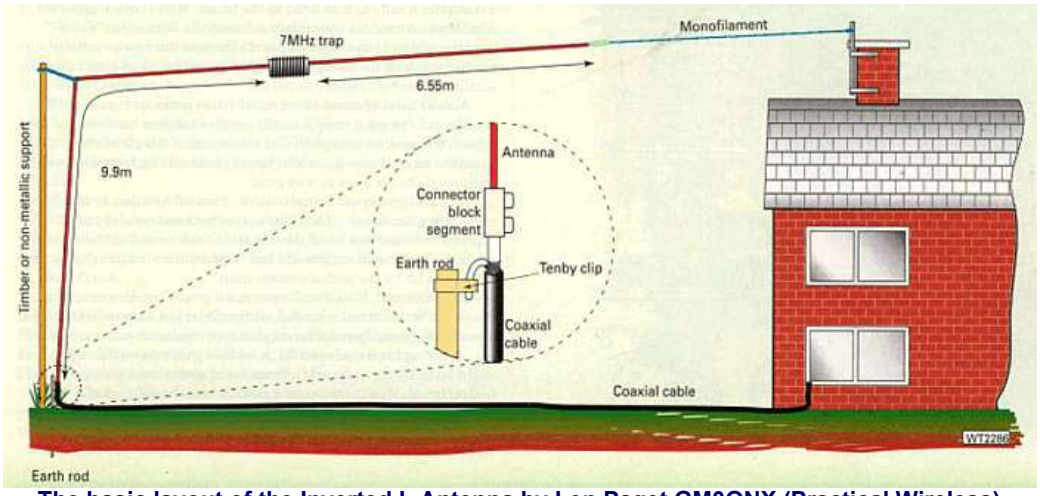

The basic layout of the Inverted L Antenna by Len Paget GM0ONX (Practical Wireless)

Adding 160m / Top Band to an Inverted L

The 160 metre Top Band can be added to this aerial by connecting a 3.5 MHz trap at the end of the 80 metre wire (where to monofilament joins the 6.55m section of wire below) with another length of wire on the other side, increasing the overall length of the antenna.

Find out how to do it here: http://www.users.icscotland.net/~len.paget/Inverted%20L%20adding%20top%20band.pdf

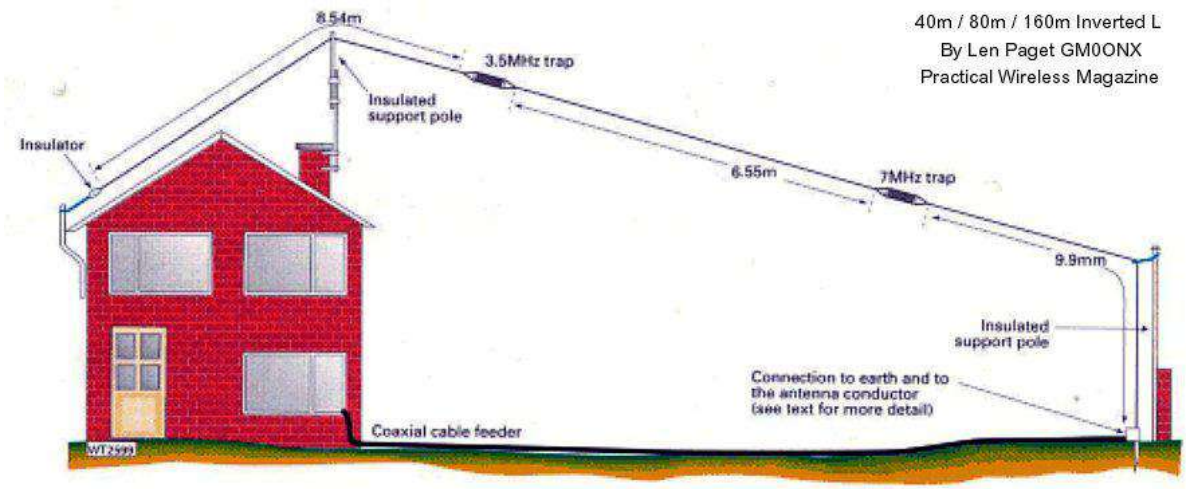

Adding Top Band to an Inverted L by Len Paget GM0ONX (Practical Wireless magazine)

160m Top Band 'Inverted L' Wire Antenna

At the time of writing I am using a 40m/80m Inverted L aerial and in an attempt to get on Top Band I have also been experimenting with a shortened 160m antenna in an inverted L configuration that uses a wire about 19 metres long - about half the size of a full size inverted L for 160 Metres.

A Top Band aerial of this type also needs a very good ground / counterpoise and can suffer the disadvantage, like ground mounted vertical aerials, of being rather noisy on RX . The drawing below shows the general idea. Read more here >

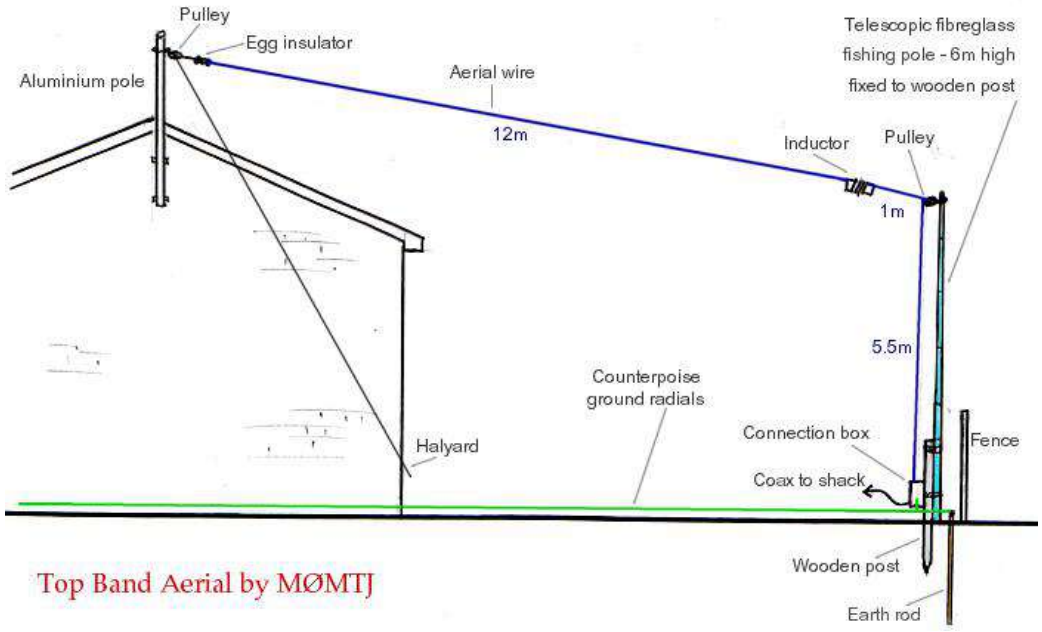

General layout of Top Band Aerial with fibreglass pole retracted to a height of 2 metres
Wire lengths are approximate: Inductor 5cm dia with approx 40 turns of enamelled copper wire

Full Wave Loops and Delta Loops - An easy to install and effective antenna for multi band operation

Easy and low visual impact - a full wave loop: With a larger garden a full wave loop could be easily accommodated horizontally without the neighbours even noticing. A garden with a perimeter of 40 metres would

easily accommodate a full wave loop for the 40 metre band and would work up to 10 metres or even 6 metres with an 'ATU'. A garden with a perimeter of 80 meters would accommodate a full wave loop for the 80 metre band and would work up to 10 metres.

Small Loop for 20 metres to 10 metres: A loop for 20 metres or 17 meters is relatively compact and could easily be installed in small 'postage stamp' sized gardens. A loop antenna could be triangular, square (Quad) or circular, but a square loop (and indeed a circular loop) would need more supporting points than a delta (triangular) loop, so a Delta loop is likely to be the easier option.

The loop is really a single band antenna cut for one wavelength on the band of interest, however it can also work quite well as a cheap and easy to install multi-band H.F. aerial. A loop consisting of a 17 metre length of thin antenna wire, for example, will work well on 17 metres but may also give 15m, 12m and 10m with an ATU. My own loop is made from an 16 metre length of wire, tuned for the 17m band, but can work on higher bands. A 40 metre loop will be considerably larger, but it might still possible to accommodate in many fairly compact gardens. Performance will depend on height and orientation.

Feeding the loop at the top or bottom will give horizontal polarisation, while placing the feed point on the side will give vertical polarisation. The apex can be at the top or the bottom, but performance should be better with the apex at the bottom with the flat wire across the top - however for ease it may be more convenient to support a Delta Loop on a single pole, meaning that the apex would be at the top.

Ideally a loop should be fed with balanced line back to the shack, connected to a balanced line ATU or other ATU via a 4:1 balun. Alternatively use a 4:1 balun at the antenna end and run 50 ohm coax back to the ATU / txvr - though losses will be greater doing it by this method if the coaxial cable is quite long.

If one can install a separate antenna for the lower frequency bands of say 160m, 80m and 40m, then a Loop Antenna could be a good partner to allow operation on the higher bands of 20 metres to 10 meters or even 6 metres.

A loop should be really very easy to install using a single support pole and very cheap too! All that's needed is the supporting pole, some cheap wire, a 4:1 balun which can be 'home brewed' and some thin cord and insulators which should not be an eyesore either.

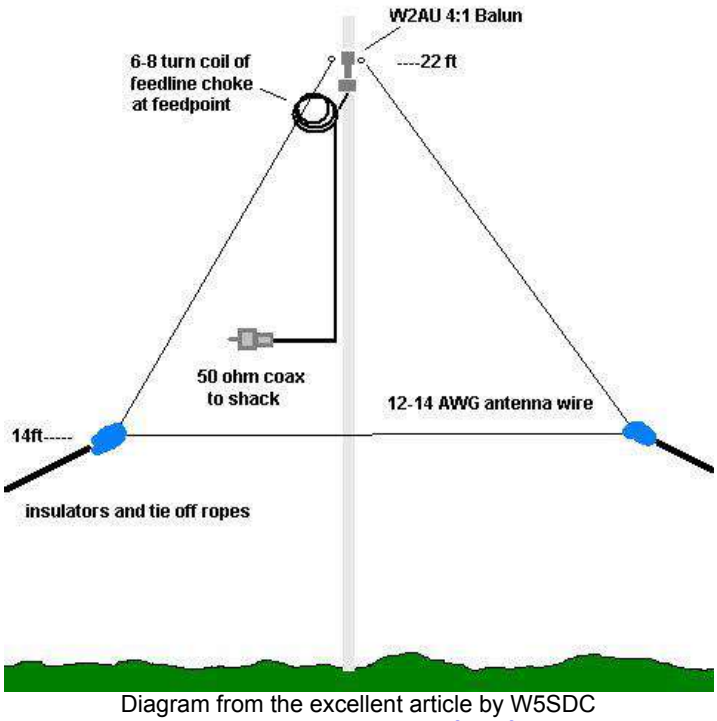

Diagram from the excellent article by W5SDC
http://w5sdc.net/delta_loop_for_hf.htm

Band	Length of antenna wire at mid band in metres
10	10.617
12	12.282
15	14.432
17	16.90

20	21.502
30	29.622
40	42.842
80	82.234
160	161.223

Delta or Quad Loop Antenna - An ideal multi band antenna solution?

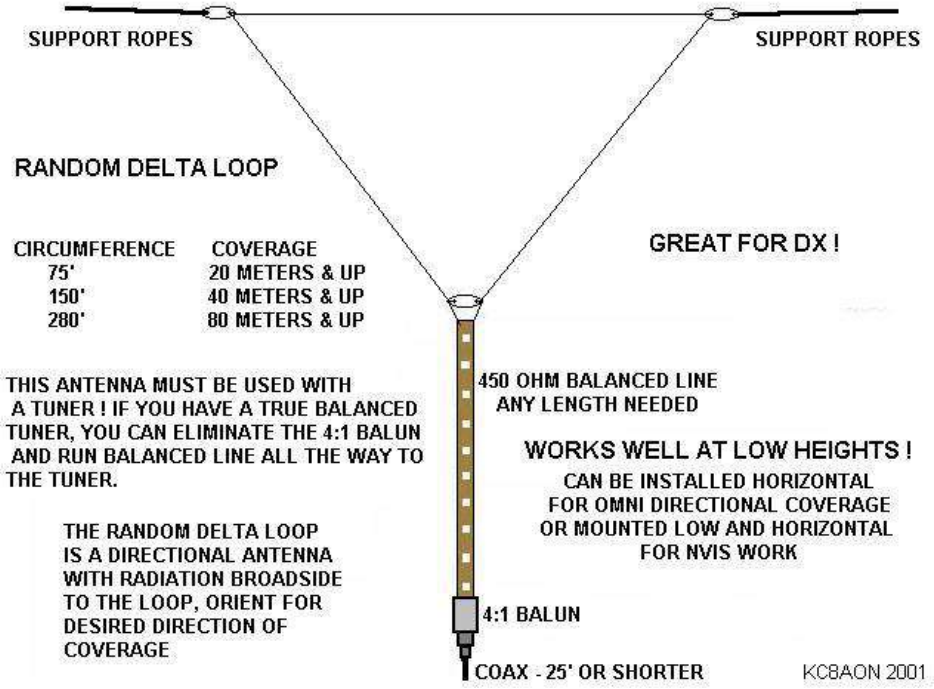

A Multi Band Wire DX Loop Antenna by KC8AON
http://www.i1wqrlinkradio.com/antype/ch10/chiave1827.htm

Delta Loop by Arthur M0PLK (SQ2PLK)
Details at http://pdxa.one.pl/articles.php?article_id=17
Available at http://ham-radio.urbasket.eu and http://www.vpa-systems.pl/

Using fibreglass fishing poles (Sota Poles) two 7 metre long poles can be erected in an inverted V shape and used to support a 20 metre delta loop which will be usable on 20m to 10m and also adaptable for use on the 40 metre band.

The two aerial wires used are connected directly to a 4:1 balun which is, in turn, connected to an ATU such as the Z-11 Pro or Z-100 via coaxial cable. See this page which shows the W6ZO delta loop to get for the general idea of what will be achieved. The finished aerial will be very much like the commercially available ProAntennas DMV-Pro.

W6ZO Delta Loop - fed with 4:1 Balun - 40m to 10m
http://www.fros.com/KI0GU/w6zodelta.htm

The Loop Antenna. Ideal - cheap, easy, multi-band, simples! -
Lots of links to other Loop Antenna information on the links page here

Omni Directional Multi-Band Horizontally Polarized Delta Loop

If all that can be erected is a single pole, masts or telescopic pole, here is an option that will provide a horizontally polarized signal on 20 / 17 / 15 / 12 / 10 metres - the Sandpiper Aerial Technology GM3 (designed by GM3VLB). A similar idea, providing omni-directional horizontally polarized signals, is the G3TPW Cobwebb Antenna from Steve Webb.

These look like good ideas, though I have yet to make one to test.

G-WHIP
Antenna Products
Top Quality
British Manufacture

Site Search
Find
powered by FreeFind

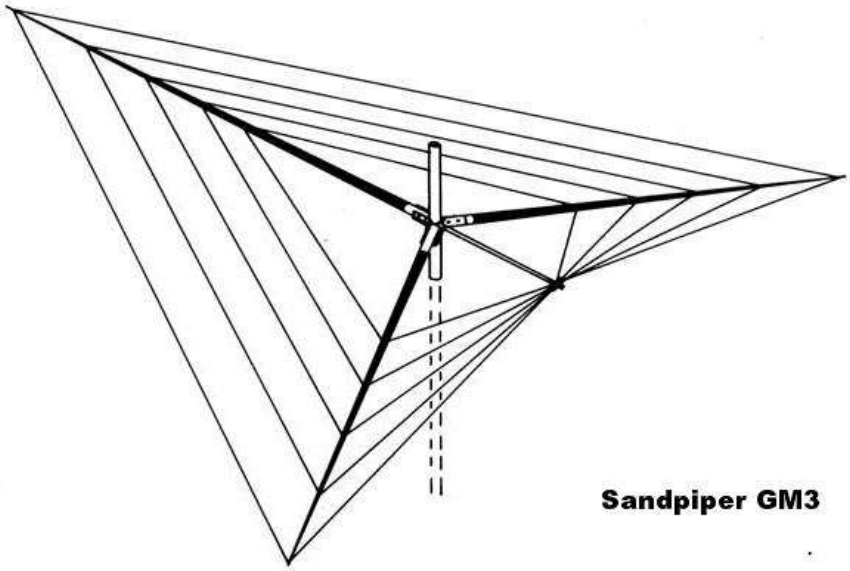

Sandpiper GM3VLB Antenna
http://www.sandpiperaerials.co.uk/

G3TPW Cobwebb Antenna from Steve Webb - photo by G3TXQ
http://www.g3tpw.co.uk http://www.karinya.net/g3txq

Resonant Vertical Antennas

Low SWR: Having a low v.s.w.r. across the whole of HF may seem, at first glance, to be a good thing - but my dummy load has a very low v.s.w.r. from HF to UHF, it does not make it a good antenna! As far as aerial systems are concerned, having a low v.s.w.r. across the whole of HF is probably not the best way to judge an antenna - a wide band low v.s.w.r. could indicate a fault with the aerial or feeder system - or just that lossy matching transformer that is gently heated up by the power applied from the transmitter!

A low v.s.w.r. is a good thing in a resonant antenna. It will help demonstrate the antenna's point of resonance - but the v.s.w.r. will rise either side of resonance. So:

The next commercial option is an antenna that is truly resonant on a number, but perhaps not all, bands. The Hustler and Butternut varieties are very well known and offer well reported good performance.

Some vertical antennas use traps to achieve multi-band performance and as such are essentially one half of a trap dipole, fed against ground. A consideration is that the traps themselves, particularly if multiple traps are used, will introduce losses to the antenna system. It should also be noted as an additional consequence of using traps on a ground mounted vertical antenna, is that the highest frequency element will inevitably be positioned at the lowest position on the aerial - not a good position to be, especially for local ground wave radiation where signals will more easily be screened by local structures. Ground conductivity also needs to be good for verticals to operate efficiently.

The Hustler 4-BTV, 5-BTV & 6-BTV aerials are examples of multi-band verticals that use traps; many amateurs report great success with Hustler aerials - and it is very low profile too, indeed an amateur friend of mine uses a Hustler with great success and has even modified an additional top resonator so that the aerial can be used on 160 metres..

Other manufacturers of resonant vertical antennas, using varying design methods, include GAP, Cushcraft, Diamond, HyGain, and the well known British names Moonraker and Sandpiper.

Advisory: These are perhaps a good idea for limited space situations, but the shorter versions will not work well on the lower HF bands. A 6 metre tall antenna cannot possibly work terribly well on 40m or 80m, but may work well on the 20 metre band and above. However one could easily 'home brew' an equally effective antenna for a fraction of the cost of a commercial antenna.

Sandpiper Aerials

Sandpiper Aerial Technology offer an enormous range of amateur radio antennas from HF to UHF. For HF working Sandpiper offer numerous options including simple multi band resonant antennas supported on fibreglass telescopic poles using either changeable or plug-in coils for different bands to the famous V range and shorter and more compact MV range and the Portable MV antenna on its own tripod base. The V and MV ranges use a rather innovative design, seen above right. The V and MV antennas are available in versions that cover all the HF bands - or as cheaper versions that just cover the particular bands of interest. http://www.sandpiperaerials.co.uk/

Vertical antennas will be quite short when compared to the wavelengths of some of the longer wavelength bands (particularly 40m, 80m and 160m) and so will not radiate as efficiently as a full size resonant aerial. The bandwidth will also be quite narrow. Setting up a multi band antenna to be resonant at the required portion of each band can sometimes be a little time consuming, but for the convenience it might be a price worth paying. A vertical antenna will generally have a low angle of radiation which is a good thing for long distance DX but verticals can be very noisy on RX compared to a balanced dipole and as previously alluded to, radiation efficiency will be very low when compared to a full size single band resonant antenna. Attractive options?

Alternatives: My favourite way of experimenting with aerials is using a 10 metre long fibreglass telescopic fishing pole as the support. These fibreglass poles are lightweight and easy to carry, put up and take down, ideal for supporting lightweight v.h.f. and u.h.f. yagis, wire dipoles and doublets and also for supporting vertical wire aerials.

The telescopic pole must be made from fibreglass, not carbon fibre which is electrically conductive.

One great design is by Dave G4AON who writes on his web page: "There seems to be a myth among many newly licensed radio amateurs that an antenna works better if it costs a lot of money..... The antenna shown here costs around one tenth the price of a commercial vertical, yet it will perform as well as (and in many cases better than) a trapped vertical antenna. This antenna is based on a 10 Metre long fibreglass fishing pole.....the poles will collapse inside the sections unless each joint is secured with PVC tape, for more permanent installations glue could be used.

...The wire lengths are calculated from the formula L = 234/F, where F is the frequency in MHz and L is the wire length in feet. These lengths work out to around 33' 3", 23' 2" and 16' 7" for the 7, 10 and 14 MHz bands. The lengths for 7 and 10 MHz were more or less correct, however probably due to interaction between the wires the 14 MHz wire needed lengthening by around 4" for minimum SWR. Wire size is not critical, but it is probably better to avoid the thinnest "hookup" wire. Note, ground conductivity/loss and elevated/buried radials make a significant impact on both the performance and tuning of a ground mounted vertical. In the case of buried radials the vertical may resonate significantly lower in frequency than expected."

The antenna shown on the right is made for triple band operation on 7 MHz, 10 MHz and 14 MHz by the use of parallel wires, but an aerial based on a fibreglass pole could be single, dual, triple or even - at a push - quadruple band.

The more bands included the more difficult it will be able to trim to tune for resonance (as with a fan dipole) so to keep interaction to a minimum the wires should be quite well spaced. Like all quarter wave verticals aerials a good ground plane will be needed.

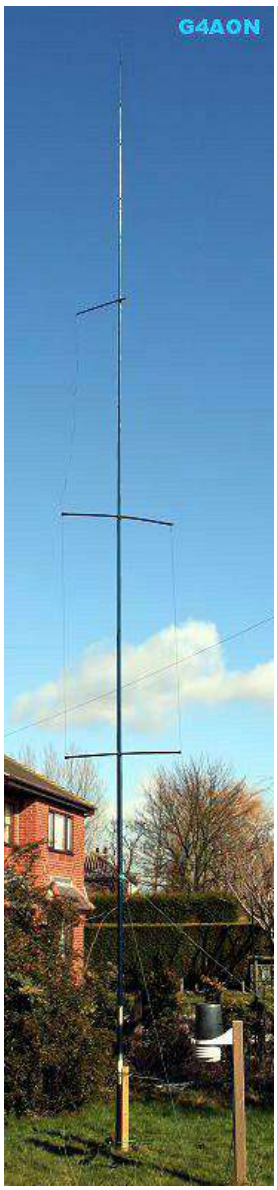

See G4AON's excellent full article here: http://www.qsl.net/g4aon/vertical/

Horizontal Resonant Wire Aerials

The great advantage of a vertical antenna is that they have a very small footprint, i.e. they can be installed in the corner of many small plots and gardens. True resonant verticals can properly cover many, if not all, the HF bands. However to be reasonably effective a vertical needs a very good ground and also must be quite tall, in the order of 6 to 9 meters in many cases (about 19 to 30 feet). This may cause objections from the XYL. Another disadvantage might be that a vertical has little near vertical incidence skywave radiation (NVIS), a consideration for the lower HF bands, so after the local ground wave coverage there will be little or no signal until after about 500 miles, not good for inter G working. (ref. G8JNJ) - So try some Dipole Antennas:

Dipole Antennas

The dipole antenna is possibly the simplest and cheapest antenna to make. It it cut for single band operation where it should make a very efficient radiator. The simple wire dipole should be quite discrete, though not entirely invisible, but should not raise too many objections from the XYL or neighbours.

For some dipole ideas see this page:
http://www.qsl.net/ta1dx/amator/practical_dipole_antenna.htm

How to make a basic dipole by Marshall N1FN : http://www.morsex.com/dipole/index.htm

Also see this detailed and useful page: http://www.dxzone.com/cgi-bin/dir/jump2.cgi?ID=7499

Calculator:
http://www.sean1226.pwp.blueyonder.co.uk/design_your_own_antennas%201.htm

TRAP Dipoles:

The next type of antenna to consider might, then, be a horizontal or sloping wire antenna. Perhaps the most familiar multi band wire aerial is the trap dipole. The traps, in simplest terms, divide a wire dipole into two or more resonant sections so that two or more bands can be covered.

As far as commercial options go then there are quite a number. Tony Nailer of Spectrum Communications produces a great deal of useful equipment and accessories including some well designed and well made trapped dipole aerials based on the very effective W3DZZ design. In particular the Full Size G4CFY resonant on 80m and 40m and also allowing operation on 20m, 15m and 10m, also the Half Size G4CFY resonant on 40m and 20m and additionally allowing operation on 15m and 10m.

Visit http://www.spectrumcomms.co.uk/G2DYM.htm for more information.

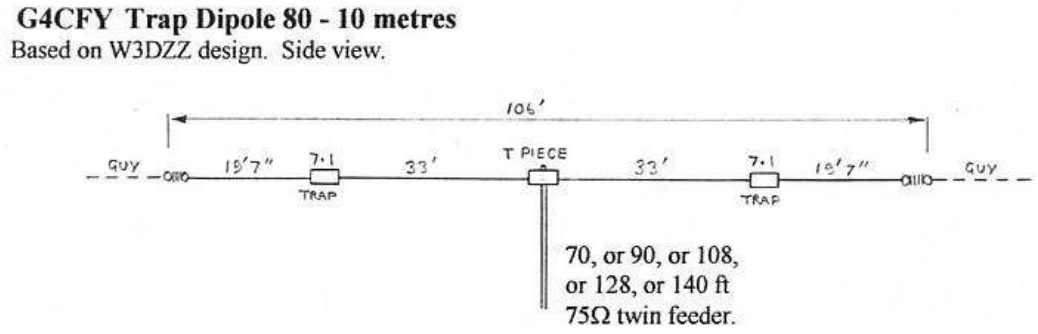

Spectrum Communications G4CFY Trapped Dipole
http://www.spectrumcomms.co.uk

Spectrum Communications G4CFY Trapped Dipole
http://www.spectrumcomms.co.uk

More about Coaxial Trapped Dipoles

A trapped dipole for 40m and 80m offers the advantage of being somewhat shorter than a full size single band 80m resonant dipole plus it offers 40m as a resonant band plus the possibility of working on 20m, 15m and 10m. There are several designs available on the web for this type of aerial so Google W3DZZ. One of the most comprehensive sets of instructions is by Len Paget G0ONX. Fine out more here:
http://www.users.icscotland.net/~len.paget/GM0ONX%20trap%20dipole.pdf

This would be my choice if I had the space, though since a dipole is a balanced aerial it would make more sense to use balanced twin feeder (as in the Spectrum Communications implementation of this design) rather than coaxial cable which is an un-balanced and more lossy feeder.

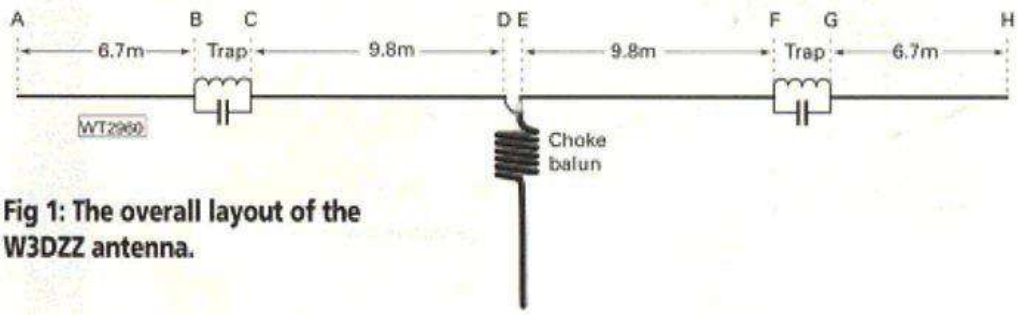

The W3DZZ Trapped Dipole - a balanced aerial, so use balanced twin feeder!

Here is a variation on the W3DZZ antenna by the Maidstone Amateur Radio Society that adds a dedicated 10 meter (28MHz) resonant element as a 'fan'.

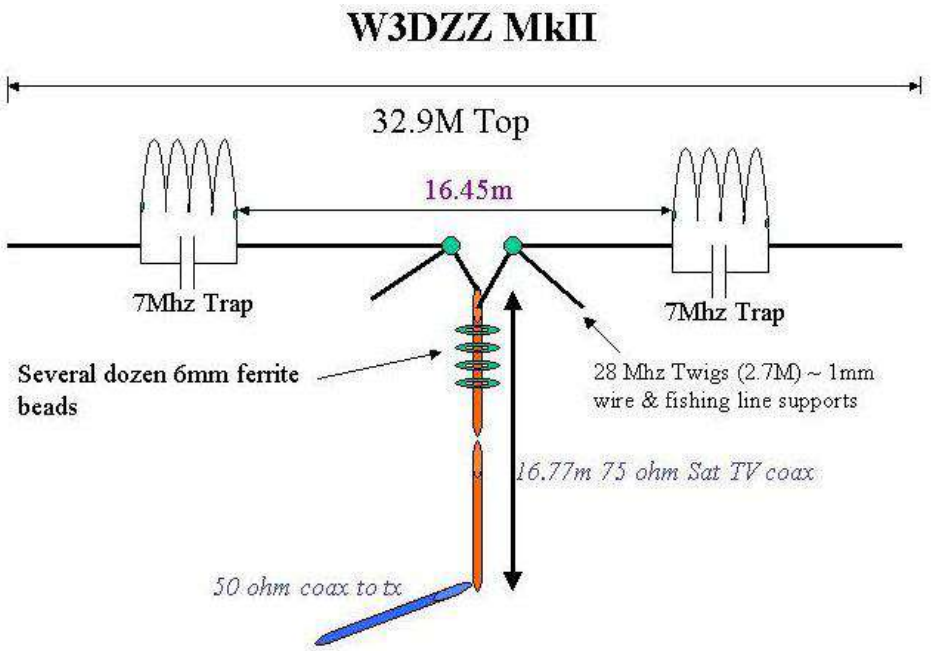

W3DZZ Dipole Aerial design by the Maidstone Amateur Radio Society
http://www.btinternet.com/~shaun.scannell/club/w3dzz.htm

Moonraker supply a whole range of wire trap dipoles covering from 2 to 5 HF bands (MTD1; MTD2; MTD3; MTD4; MTD5; MTD6). Diamond also produce trapped wire antennas, the W-721, W-728 and W735. Comet and Diamond each produce similar interesting 5 band wire dipoles that utilize both traps and a fan arrangement - the Diamond W8010 and the Comet CWA-1000. If space really is limited then look out for KZJ Communications (dongo1950 on ebay) - he produces 'Limited Space Inductive Dipoles'. These are inductively loaded and shortened dipoles so they will have reduced efficiency, of course, but are very nicely made, so might be very useful in a tight spot.

Alpha Delta Communications produce a couple of substantial parallel dipole models: http://www.alphadeltacom.com

To obtain good efficiency and achieve a low angle of radiation, desirable for longer distance DX, a horizontal dipole needs to be installed at a good height - over 20 feet would be desirable and it is quite common to install horizontal dipoles at around 30 to 40 feet above ground level. This might be a problem at some QTH's, it certainly is at mine!

Allan Copland, GM1SXX comments: "The dipole will operate well on the band it has been sized for , if placed at a suitable height, but will also operate as a' three-half-wave' aerial at three times the frequency and so on, so it's not strictly a single band aerial. An 80M dipole (132 feet typical) will work nicely on 30 metres (three half waves) but not on 40m (two half waves)… because on 40M the feed-point is at a voltage node and not at a current node, for easy feeding. Most aerials are current fed.

The radiation pattern changes when a dipole is not used on its design frequency. The pattern will break up into multiple 'petals'. This can be either a disadvantage or an advantage depending on what you expect from it. Since most of us use co-ax, an UN-BAL should really be used to connect the unbalanced feeder to the balanced aerial, but how many people actually bother? Not many I suspect. It's possible of course to use a balanced feed-line system instead with a dipole and just have a delta match (no centre insulator… none needed). There are many choices and permutations, but in general, dipoles are centre fed at a point of current maximum (and minimum voltage).

A normal dipole is current fed but of course can be voltage fed instead. This is what's done in the EFHWA or Fuchs aerial where a resonant half wave wire is fed at one end (max voltage / min current) from an L/C tank, against a very short counterpoise wire.

Fan Dipoles (a.k.a. Parallel) Dipoles:

Another design of multi band wire dipole is the fan dipole, or parallel dipole. A fan (or parallel) dipole will have, perhaps, two, three or four individual resonant dipoles with the arms arranged in a fan shape.

A fan dipole is a very handy way of using a dipole that will be resonant on several bands - typically three or four. The fan dipole (a.k.a. Parallel Dipole)

See M0WYM's page for a QRP Fan Dipole design: http://www.radiowymsey.org/FanDipole/fandiploe.htm

See this page for construction details: http://www.hamuniverse.com/multidipole.html

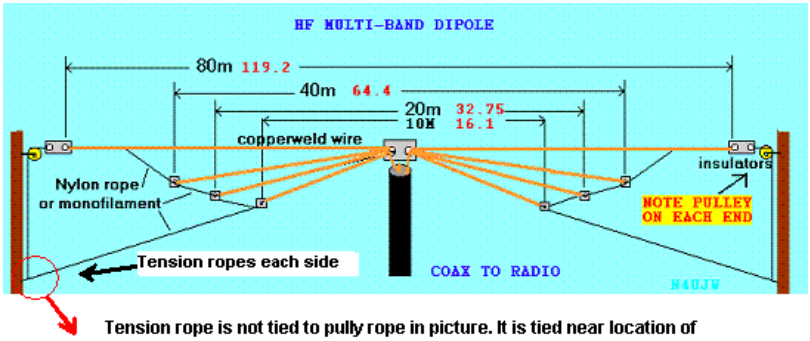

Tension rope is not tied to pully rope in picture. It is tied near location of pully rope down on supports within easy reach. It is tied last after final SWR adjustment and the antenna is in it's final position.

Suggested total lengths:
80 meters - 120 feet
40 meters - 65 to 66 feet
20 meters - 34 feet
10 meters - 17 feet
These lengths are not exact. Some tuning may be required. Use the standard formula 468 / freqmhz for total feet for each band (freq) of interest. Adjust each length longer or shorter as needed.

Fan Dipole shown on Ham Universe

KI4NRH built a really neat fan dipole shown in the photograph below:

Fan Dipole by ki4nrh

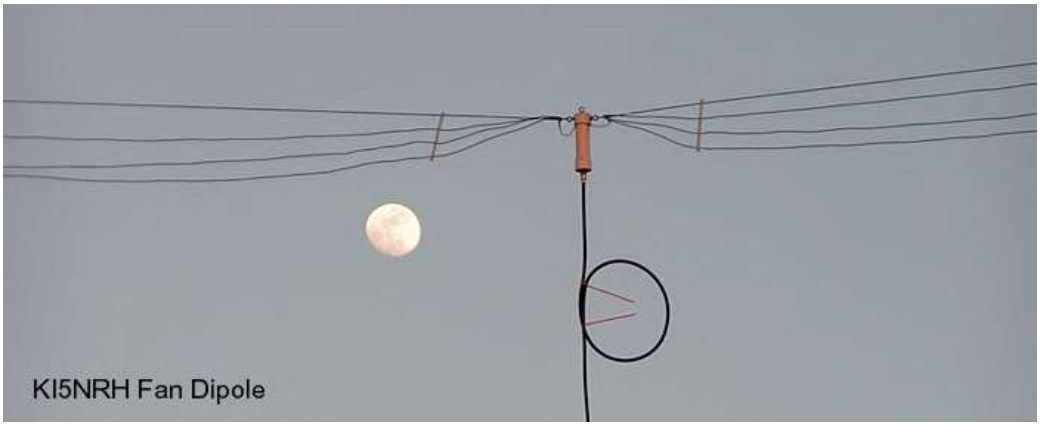

Fan Dipole by ki4nrh
http://forums.qrz.com/showthread.php?t=159953

Link Dipoles

Link Dipoles (a.k.a Jumpered Dipoles) facilitate multi band operation by simply connecting the jumpers (one on each side of the aerial) to achieve the desired resonant band. Perhaps a bit bothersome for frequent band changes, but a very simple and effective aerial and very handy for portable operation, not to mention efficient for QRP.

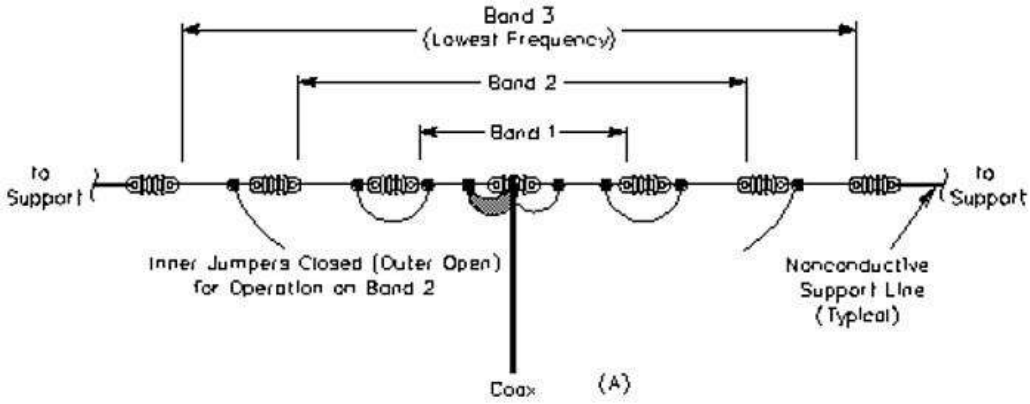

Link Dipole - ref ARRL

Sloper Aerials

Alternatively a dipole can be installed as a sloper; one end fixed to a high point on the house or building, or a tall post maybe 8 to 10 metres high, with the other end attached to a lower point such as a post maybe 3 or 4 metres high. This will give the aerial some directivity.

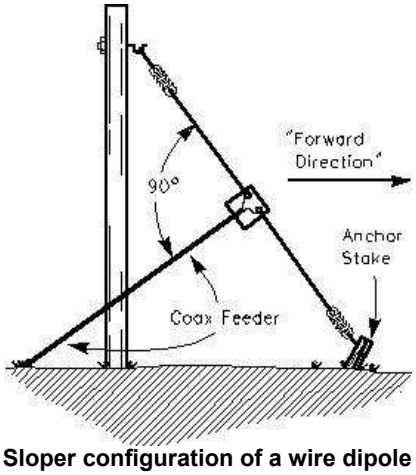

Sloper configuration of a wire dipole

Inverted V Aerials

Another option maybe to support the dipole at its centre on a tall pole, or roof apex, with each end sloping downwards to lower fixing points. This will give the aerial an upside down V shape. As with a sloper, the Inverted V arrangement will give the aerial some directivity - a different radiation pattern compared to a straight horizontal dipole.

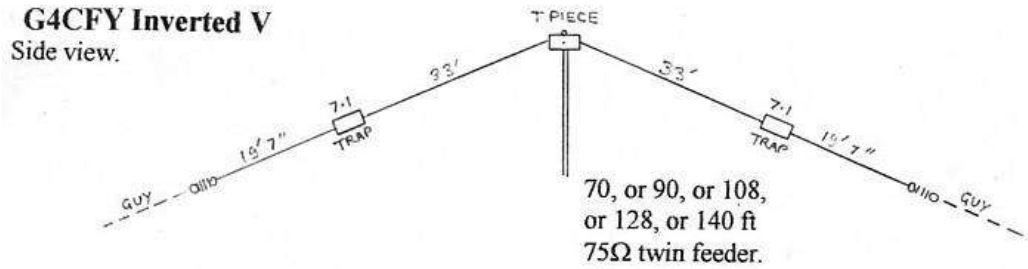

Spectrum Communications G4CFY Trapped Dipole in "Inverted V" configuration
http://www.spectrumcomms.co.uk

The Classic Doublet Antenna Again. This time in an Inverted V formation:

Using an Inverted V can help fit a dipole into a slightly restricted space. The Inverted V arrangement can be used for single band resonant dipoles, trapped dipoles and fan dipoles. The Doublet must be fed with Ladder Line or Open Wire balanced feeder for efficient Multi-Band operation.

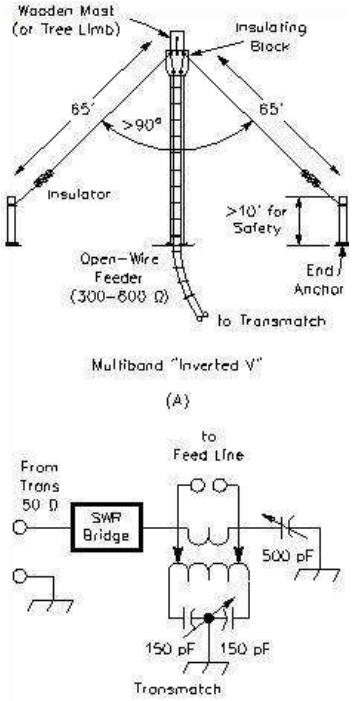

At A, details for an inverted V fed with open-wire line for multi-band HF operation. A Transmatch is shown at B, suitable for matching the antenna to the transmitter over a wide frequency range. The included angle between the two legs should be greater than 90° for best performance. [ref: QSL.net]

Vee Configuration

Comet and Diamond produce Vee antennas that can be mounted on the side of a building at roof height, or on a pole, telescopic pole or other suitable support. These are trapped dipoles in an upright V configuration, not made of wire but of aluminium tubing for solid construction. Typically covering 40m, 20m, 15m and 10m. The Comet model is H-422V. The Diamond Model is HFV5 which also covers 6m.

These are shortened antennas so cannot be expected to have high performance on the lower HF bands, but if space is restricted the RF compromise may one that has to be taken.

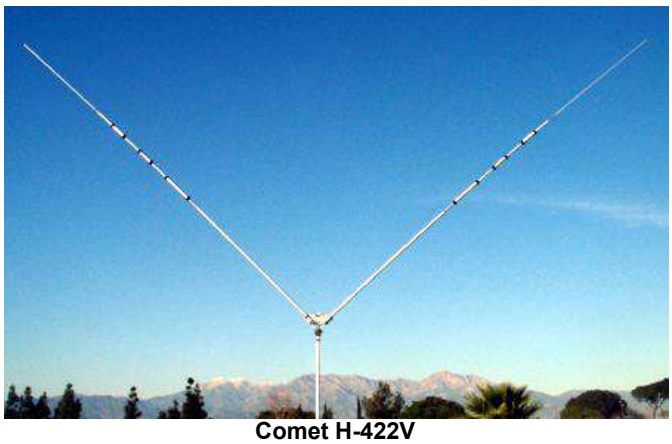

Comet H-422V
http://www.cometantenna.com

Diamond HFV5 Antenna
http://www.diamond-ant.co.jp/english/amateur/antenna/ante_2base/ante_base7.html

Thoughts from Martin G8JNJ on multi-band wire antennas:

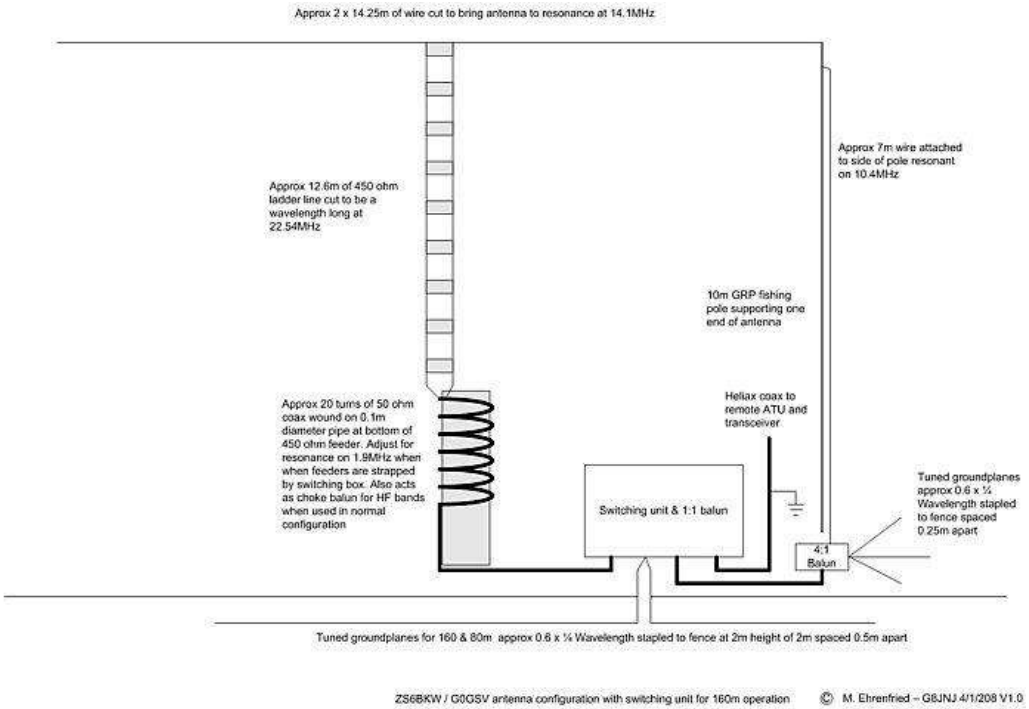

Multiband Wire Antenna by Martin G8JNJ
http://g8jnj.webs.com/

Linear Loading

Linear loading a dipole can reduce the length to help fit a ling dipole into a shorted space by essentially folding back some of the dipole elements. Here is a design by K4VX for a 7MHz Linear Loaded Dipole:
http://www.arrl.org/files/file/Technology/tis/info/pdf/0207040.pdf

End Loaded Dipole

End loading can also help reduce the size of antennas, particularly useful for dipoles used on the 80m and 160m bands.

An end loaded dipole will produce an antenna that is H shaped. There are several commercial designs available produced in designs that cover a single band and others that cover multiple bands. The version shown below is only 3 metres tall so will be suitable for very unobtrusive, low profile use. It is the ProAntennas Multi-band I-PRO: 20m 17m 15m 12m 11m & 10m which uses a capacity hat with some loading at the centre.
http://www.proantennas.co.uk/

Other similar antennas were available from Force12 Antennas in the form of, amongst others, the Sigma 5 and Sigma GT5. The Sigma design used T-bars at each end of the vertical dipole for loading technique and off-center loading coils. http://www.force12inc.com This was supplied supplied in the UK by Vine Antennas at one time http://www.vinecom.co.uk . Transworld Antennas also have produce antennaa using a similar concept - the TW2010 Adventurer and Backpacker http://transworldantennas.com

K9AY Notes that: "I have come to the conclusion from my experiments, readings and observations, that a capacity hatted vertical dipole, a few feet over ground, is less compromised than a 1/4 w/l vertical of the same height fed against a less than perfect ground. Let's face it, most amateur's ground systems are mediocre at best. Also, the dipole is easier and cheaper to rig, and is two dimensional..Very important in my situation, as I cannot run out radials on my neighbours property. Or, to quote W4RNL.."Since only a handful of hams can ever have 160-meter antennas high enough to yield a low angle DX signal, more practical are vertical arrays such as yours. Vertical dipoles with hats (or Tees) save a plethora of wire needed by monopoles." http://www.dxzone.com/cgi-bin/dir/jump2.cgi?ID=7466

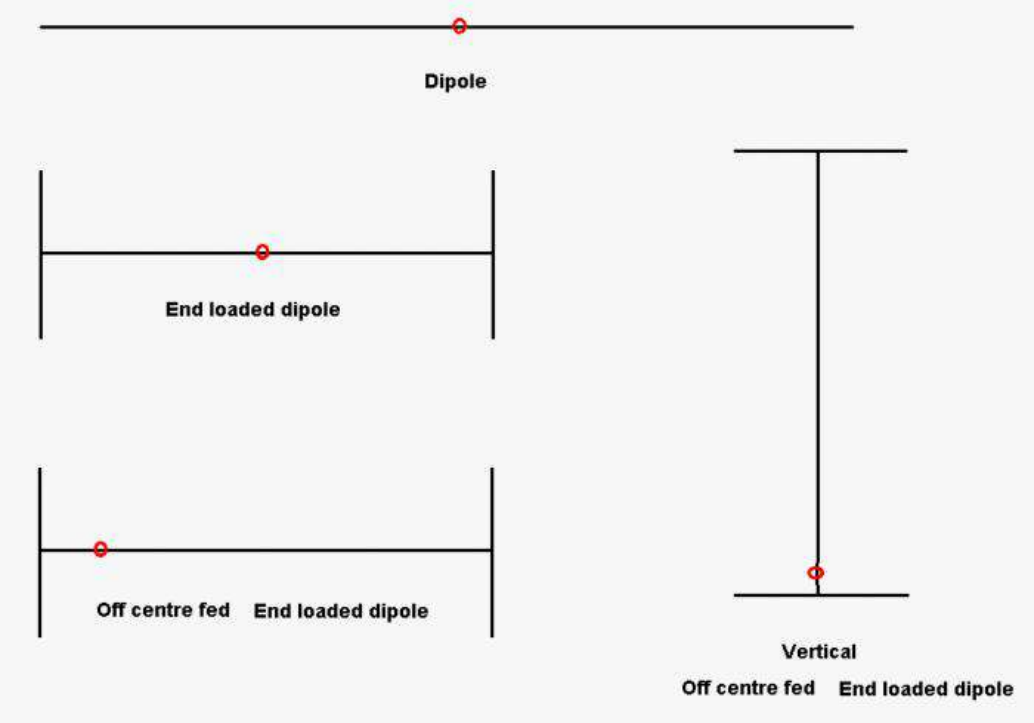

Information by K9AY

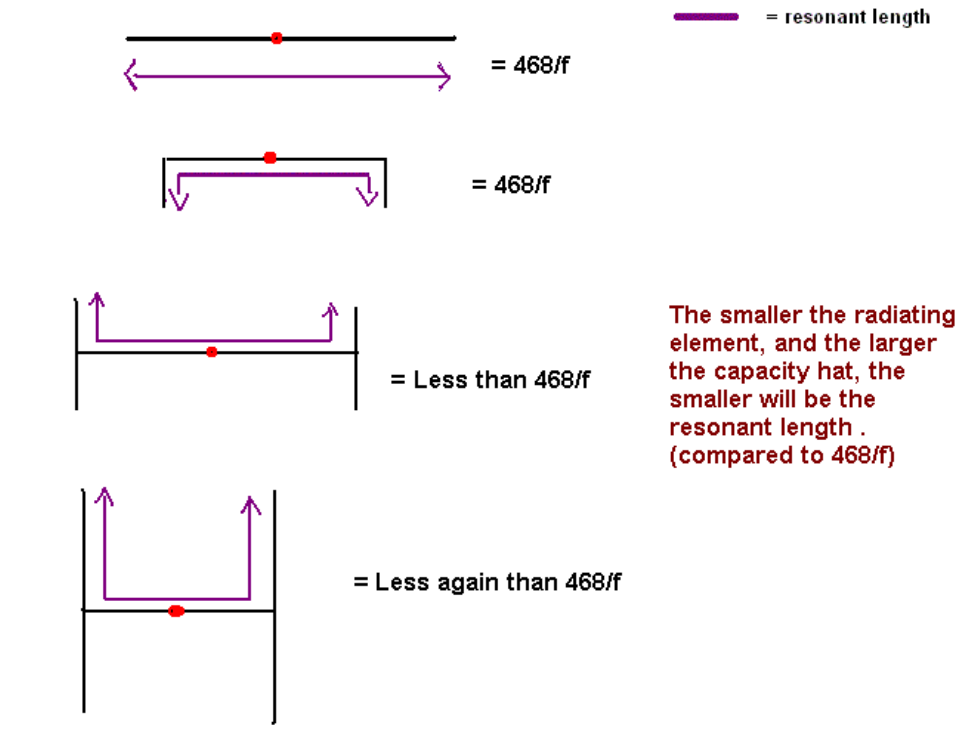

Information by K9AY

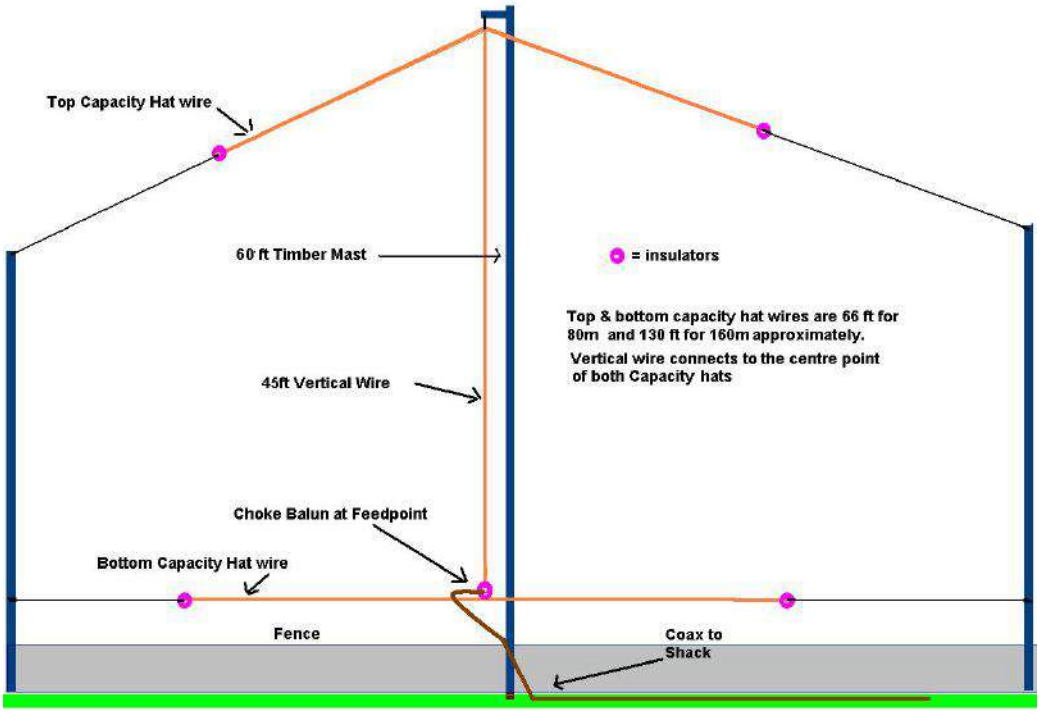

Interesting concepts from K9AY

End Fed Half Wave Antenna

The End Fed Half Wave Antenna (EFHWA) is fed at a voltage node via a parallel resonant circuit against a 'short counterpoise', it is a favourite of backpackers and outdoor types. It can be considered as a half wave dipole that's end-fed at a voltage node rather than the current node, as is more usual. This is a very handy arrangement for portable QRP work.

EFHWA Link: http://www.aa5tb.com/efha.html

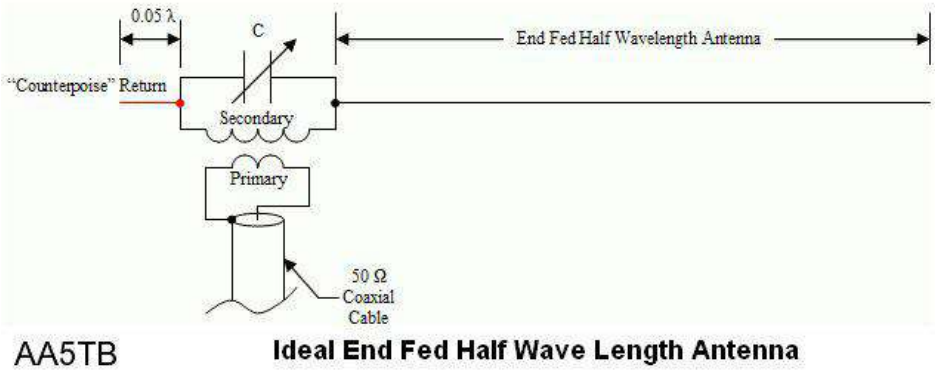

End Fed Half Wave Antenna by AA5TB
http://www.aa5tb.com/efha.html

"I suspect that nothing new or radical has happened in the field of radio aerials in a VERY long time, like at least many tens of decades. Most of the new wonder aerials are really a con. Choke off the feed-line and then see how good they really are. Prime among the baddies is the CFA. It doesn't really work, at least if you place a choke in the feed-line. With any real aerial, there should be minimal radiation from the feed system… so a choke should really make no difference at all, but for the CFA it does! The CFA is not alone, there are others. The popular G5RV is another design with a radiating feed, deliberately so, but of course G5RV planned it that way. He wasn't cheating… merely being a bit devious, to make it multi-band".

"Lots of stuff to pass on to my fellow radio club members, most of whom are of the 'if it's not expensive, it can't be any good' school of thought when it comes to aerials. Nothing of course could be further from the truth! Aerials are one area where it makes a lot of sense to build our own." : Website of GM1SXX - www.observations.biz

Thanks for your email Allan. It's a good idea to point out that an antenna could be pressed into use on odd multiples of its resonant frequency, hence a 3.6MHz antenna for 80m could be useful near the 30 metre, 10.1MHz, band - near to the third harmonic of 3.5 MHz although, as you observe, the radiation pattern may be quite distorted from the traditionally expected dipole pattern and be more petal shaped. The same goes for a 7.1 MHz antenna for 40m being usable on its third harmonic of 21.3 MHz for the 15m band - a 40m dipole being three half waves an the 21 MHz band.

I have not experimented with a full size 80m dipole, but I would guess that it might be useful at 5 times 3.6Mhz in the 18 MHz / 17m band?

The point made about feeding a familiar dipole at the current node rather than the voltage node is obviously very important and, I imagine, sometimes overlooked.

PLANS: Download the pdf plans produced by G0KYA here > http://g0kya.blogspot.com More from G0KYA here:

W3EDP Antenna

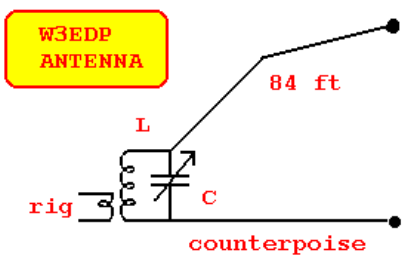

Frank, G3YCC comments on his website: The W3EDP needs a simple matching unit is needed to couple the wire to the rig and a counterpoise is required for some bands, however there is room for experimentation. It has been shown that different lengths or removal of the counterpoise altogether, can improve performance, as described in RadCom, August 1996 by G3LCK.

The Tuning capacitor in the AMU can be a 365 - 500pF broadcast type or a miniature version is OK for QRP use.

Counterpoise lengths: 3.5 & 7.0Mhz - 17ft ; 14Mhz - 6.5ft ; 28Mhz - none

Tuning Unit: Values for coils in the unit, based on a 2 inch former and 16 swg wire:
3.5Mhz 21 turns ; 7.0Mhz 7 turns ; 14.0Mhz - 5 turns.

K3HRN Notes: "Some folks have told me the modifications below make the antenna something other than a W3EDP. I can tell you that it works very well with 5 watts. Create a "bundle" of counterpoise wires, 1/4 wave length for each band you will use. Attach the bundle to the tuner in place of the counterpoise pictured above. Be cautious, 1/4 wave length elements can have high RF voltages present, even at QRP power levels. I've been able to work 160-10, including WARC bands with this type of antenna".

W3EDP or Zepp ?

It's the antenna favoured by VA3QV for all band Portable QRP operating!

VA3QV uses this home-brewed antenna with a small LDG Z100 antenna tuner for portable QRP work.

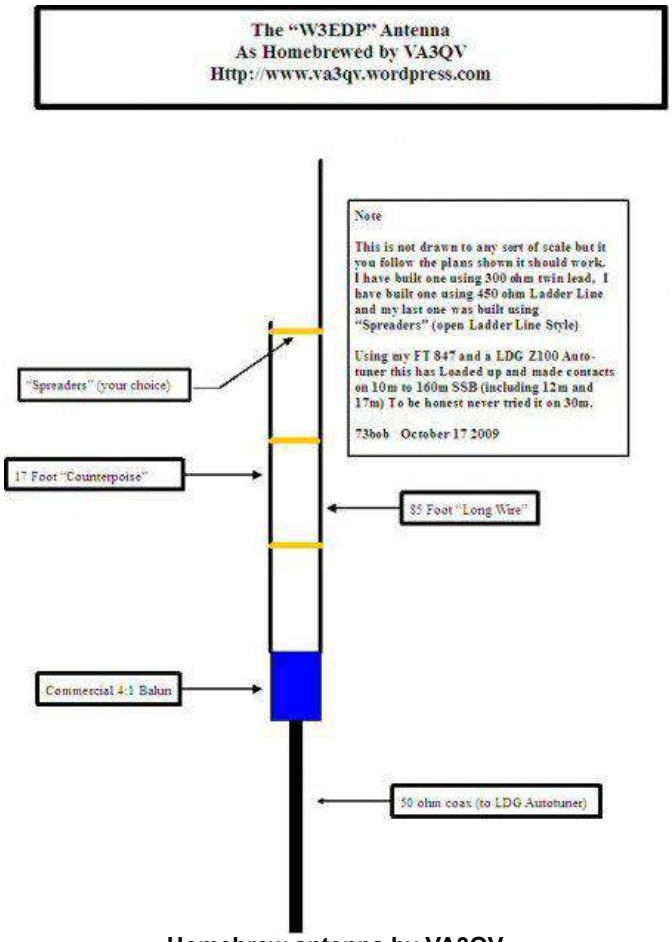

Homebrew antenna by VA3QV
http://va3qv.wordpress.com

Ye Olde Zepp

Marconi spins in his grave every time a ham buys an aerial instead of building it ! (W1GFH)

Here is a wonderful olde worlde style cartoon from WB1GFH that certainly inspires antenna experimentation with

antenna designs:

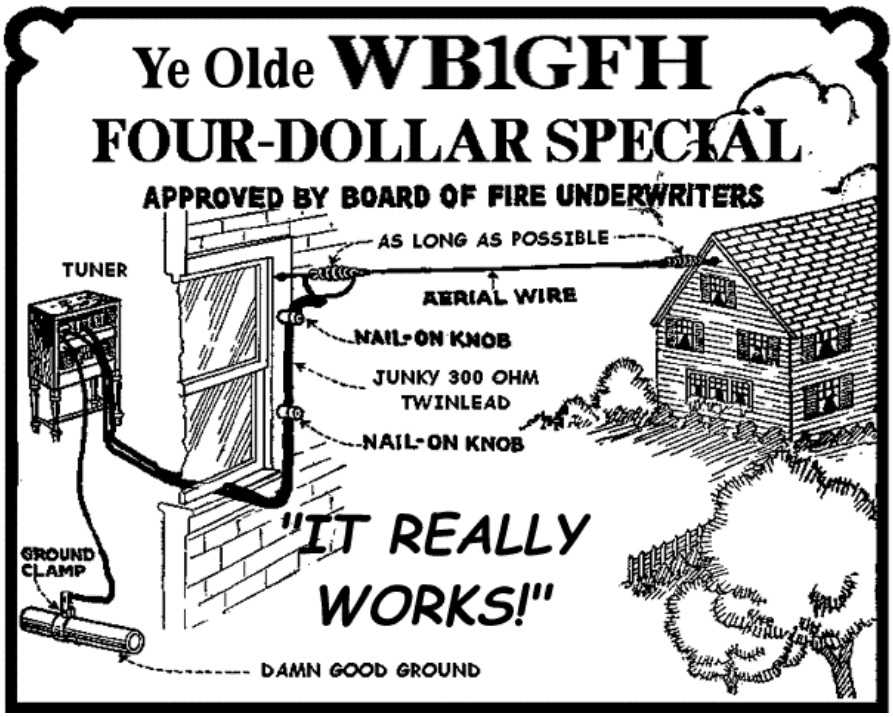

Superb. I love it!

See more inspiration from Joe Tyburczy, W1GFH, here: http://www.hamuniverse.com/fourdollarspecialw1gfh.html

End Fed Zepp "Zepp"

The End Fed Zepp consists of a 1/2 wavelength horizontal radiator wire connected to one conductor of a length of parallel open wire feeder, 300 ohm or 450 ohm twin feeder. The feeder is often quoted as being 1/4 wavelength long.

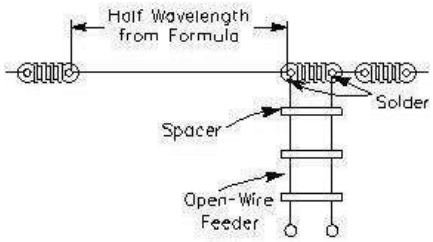

Basic design of an end fed Zepp

G Whip Antenna Products manufacture and supply a version of the Zepp antenna. Geoff G4ICD explains: "The end fed Zepp shown below has no counterpoise, just a tuned circuit in the feedpoint plus a half wave radiator. This is a most interesting antenna and can be used on other bands with the use of an Antenna Matching Unit."

A high quality End Fed Zepp style antenna: This variation uses a tuned circuit rather than a tuned twin feeder.
Supplied by G Whip Antenna Products of the UK
www.gwhip.co.uk

The end fed zepp is a popular antenna often used to save space and gets its name from the fact that it was used as an end fed wire trailing out from the rear of Zeppelin airships. It consists of a 1/2 wavelength horizontal radiator wire connected to one conductor of a length of parallel 300 ohm or 450 ohm twin feeder, often quoted as being 1/4 wavelength long.

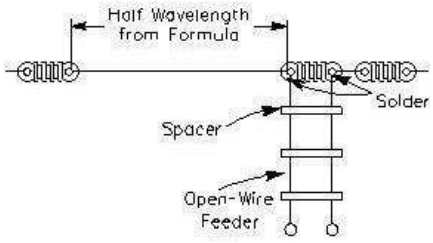

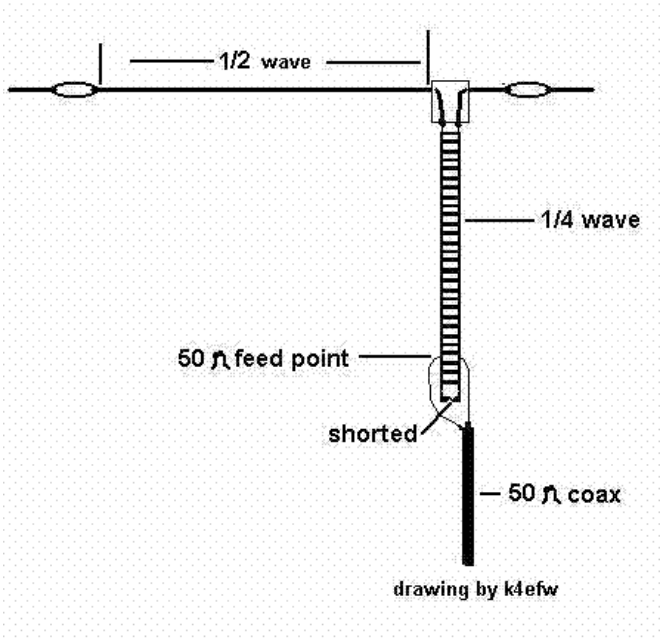

Zepp Antenna by K4EFW
http://www.hamuniverse.com/n4jaantennabook.html

K4EFW notes: "...A half-wave resonant antenna can be fed from its end. When fed this way, it is also known as an end-fed zepp. An end-fed zepp will work on its fundamental frequency and on odd and even harmonic frequencies. The end of a half-wave antenna has very high impedance, and an antenna fed this way is said to be voltage fed. Feeding a half-wave resonant dipole in the center means it is current fed. The normal way of feeding the end-fed antenna is with ladder-line. One side of the ladder-line is connected to one end of the antenna and the other side of the ladder-line is connected to nothing. To secure the unconnected side of the ladder-line, it is connected to a short wire running between two insulators. Since the antenna is connected at its high impedance point, no current flows into an antenna, but there will be a large current in the center of this antenna. No current flows from the open side of the feed-line because it is at a zero current point. The end-fed zepp can be matched by cutting the ladder-line to a quarter wavelength with the bottom end of the ladder-line shorted. A certain distance above the short is a 50-ohm feet-point and it can be fed directly with coax. You will have to find the 50-ohm point by trial and error. This method of feed makes it a single band antenna". Quoted from K4EFW.

Here is a commercial product made by G-Whip Antennas of the UK offering their version of a Zepp antenna design: http://www.gwhip.co.uk/

Martin G8JNJ highlights a very interesting antenna designed by Mike G7FEK here:-

The G7FEK antenna goes several stages further than the simple single band End Fed Zepp. G7FEK has produced a design for Multi-Band operation claimed to offer much improved performance over a half sized G5RV or 'Windom' antenna while additionally providing access to the 80 Metre Band.

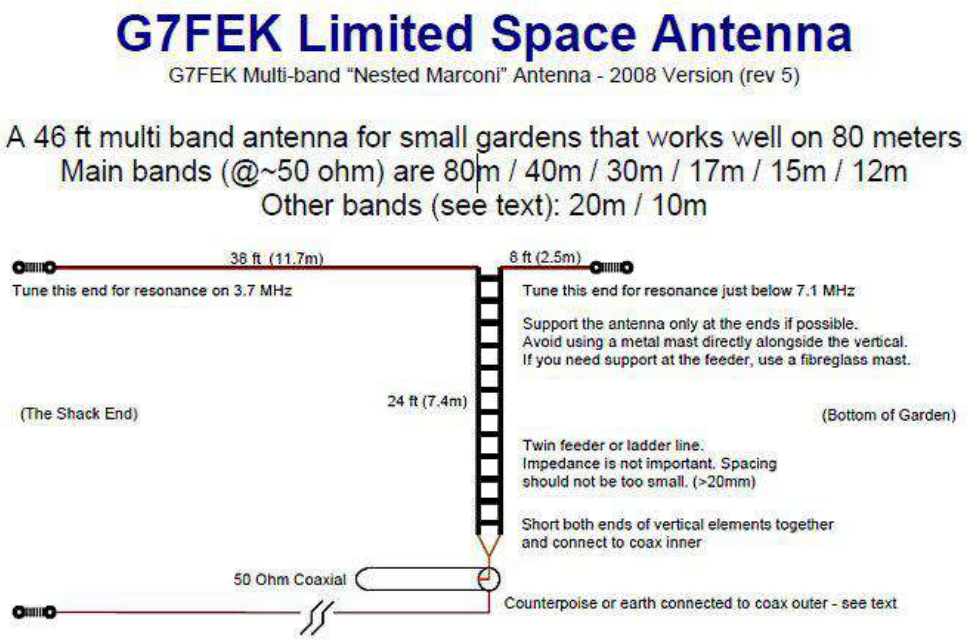

G7FEK Limited Space Multi-Band Antenna

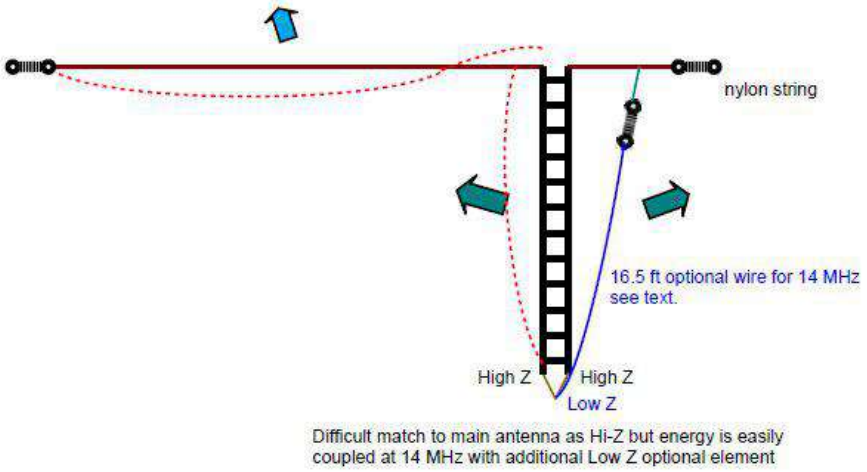

Adding 14MHz to the G7FEK Limited Space Multi-Band Antenna

The G7FEK design will allow operation on 80m / 40m / 30m / 17m / 15m / 12m with the possibility to add the 20m band.

G7FEK Plans: Download the plans for the G7FEK antenna from G7FEK's website here or from this website here

Tuner Design For Half Wave Vertical and Similar Length End Fed Antennas by G4FGQ

http://www.radioaficion.com/HamNews/articles/8218-tuner-design-for-half-wave-vertical-a-similar-length-end-fed-antennas.html

Off Centre Fed Dipole (OCFD) - so called 'Windom' Antenna

The "Windom Antenna" was described by Loren G. Windom W8GZ. It could be an ideal wire aerial for use in restricted spaces for multi-band operation. It may also be an good candidate for portable work.

It is a wire antenna, similar to a dipole, but unlike a dipole or doublet which is fed at the exact centre, a Windom or Off Centre Fed Dipole, as the name suggests, has the feed point off center.

Current versions of the Windom are not actually Windom antennas at all - instead they are fed with coaxial cable and have a balun placed at the feed point. These are Off Centre Fed Dipole antennas - OCFD. They are similar in

appearance to a true wire Windom, but they are different.

As with all aerials the aerial should be as high as possible. With the feed point at between 20 and 40 feet above ground the typical claimed impedance will be somewhere in the region of 200 Ohms so a 4:1 balun will typically be required. At greater heights, and depending upon the exact position of the feed point, the impedance may be higher and a 5:1 or 6:1 balun might be a better choice although balun losses will be greater.

The point at which a Windom is fed in the original design, which used an open wire to feed the aerial, was 15 percent off-centre. The current designs, which are fed with coaxial cable, are typically fed about 33 percent off centre, so one leg is 67 percent of the total length and the other leg is 33 percent of the overall length of the aerial.

The bands that are covered depends upon the overall length of the aerial:

11 metres long (approx) should cover 20m, 15m and 10m and the WARC bands with a tuner.

21 metres long (approx) should cover 40m, 20m, 15m and the 10m bands and WARC with a tuner.

41 metres long (approx) should cover 80m, 40m, 20m, 15m and 10m and WARC with a tuner.

80 metres long (approx) should cover 160m, 80m, 40m, 20m, 15m and 10m and WARC with a tuner.

Cut the aerial for the lowest band to be used. In imperial measurements using a familiar formula:
The longer leg will be 468 divided by the frequency and multiplied by .67 = length in feet
The shorter leg will be 468 divided by the frequency and multiplied by .33 = length in feet

OCFD Formulas:

The offset proportions differ according to which sources one refers. Some sources suggest 33% / 67% but other dimensions are also to be found:

62.2% for one side and 37.8% for the other leg. So:
The longer leg will be 468 divided by the frequency and multiplied by .622 = length in feet
The shorter leg will be 468 divided by the frequency and multiplied by .378 = length in feet
[Source: New Caroline Windom - http://www.hamuniverse.com/k4iwlnewwindom.html]

Other ideas:

The proportions of 69% / 37% are used by Buxcomm who say that "One third plus two thirds will not work. Use the formula below, as is: Do not be concerned with the off-set of the feed point, as this formula takes into consideration, the correct off-set for feeding the (BUXCOMM) Windom.for the other leg." **So:**
The longer leg will be 468 divided by the frequency and multiplied by .69 = length in feet
The shorter leg will be 468 divided by the frequency and multiplied by .37 = length in feet
[Source Buxcom: http://www.buxcomm.com/windom_files/WINDOM.htm]

Given the fairly simple formula it should be quite easy to make an OCFD Windom - however a Windom can be purchased at very reasonable cost commercially, for example from M0CVO at http://m0cvoantennas.webs.com alternatively G-Whip Antennas of the UK supply extremely high quality, high efficiency 4:1 baluns (and other baluns) that could be used at the centre of any Off Centre Fed Dipole - just add the correct wire lengths to each side.

Geoff G4ICD / GJ4ICD of GWhip highlighted his website which has an interesting page with comments concerning the quality and construction of balun products. This feature on the G-Whip site can be seen here:
http://www.g4icd.co.uk/baluns.htm

Here is a photograph of the very high quality G-Whip OCFD antenna product www.gwhip.co.uk :

An 'Off Set Centre Dipole' - OSCD - Fed made by G Whip Antennas
G-Whip Antennas - www.gwhip.co.uk

HW-20HP Off Centre Fed Dipole - produced by M0CVO
6.76 metres long one side and 3.38 metres on the other side.
http://m0cvoantennas.webs.com

M0CVO produces a couple of off centre fed dipoles, the HW-40HP and the HW-20HP. Both antennas handle 400 watts - the HP designation refers to high power.

The M0CVO HW-20HP is 10.14m in length and covers 6 bands - 20, 17, 15, 12, 10 & 6m, no ATU, and is said to also work on 30m & 40m with an ATU. Can be mounted as a horizontal, inverted vee or a sloper. VSWR is said to be 1.4 on 20m, 2.8 on 17m, 1.1 on 15m, 1.0 on 12m, 1.0 on 10m and 1.5 on 6m. The antenna is6.76 metres long on one side and 3.38 metres long on the other side. This uses a 66.6% / 33.3% formula.

The HW-20P was reviewed by Steve Nichols, G0KYA, in the January 2012 edition of RadCom.

The HW-40HP is 20.28m in length and will operate on 40, 20 and 10m without an ATU and 80, 60, 15, 6 and WARC Bands with an ATU. (Presuably one leg is 13.52 metres long and the other 6.76 metres if it follows the same 66.6% / 33.3% formula as the HW-20HP).

Here is a graphic of an Off Centre Fed Dipole typical of those available in the USA:

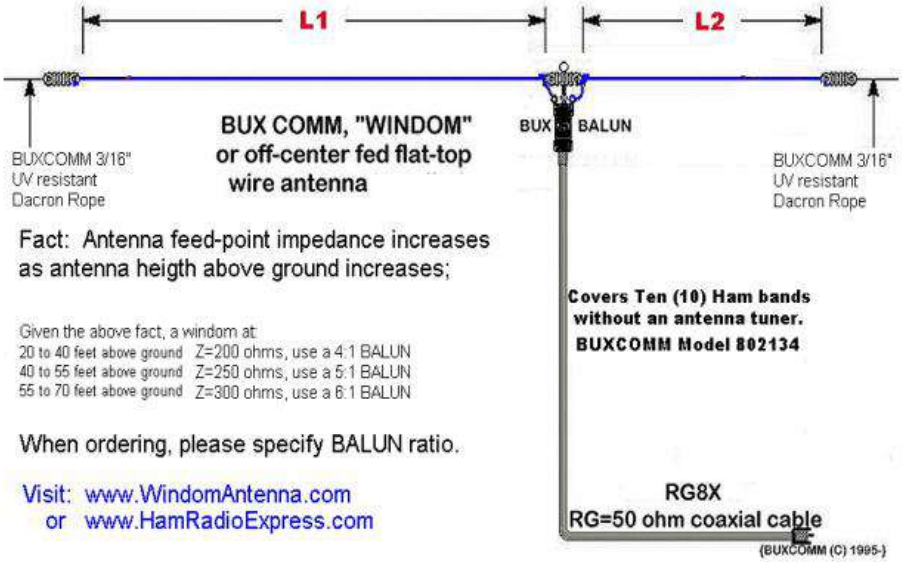

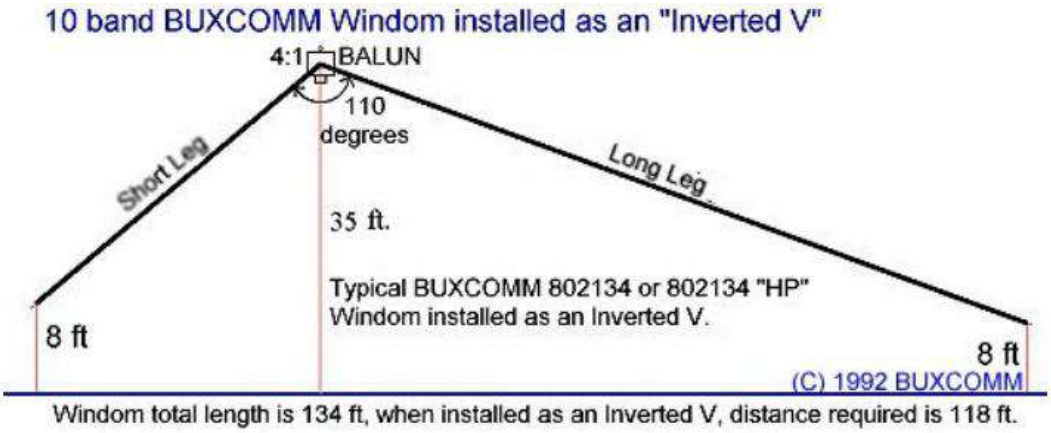

http://www.buxcomm.com

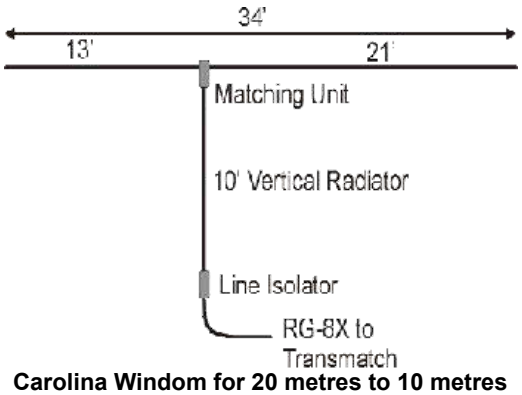

Carolina Windom for 20 metres to 10 metres
http://www.radioworks.com/ccwcover.html

M0UKD - 4:1 balun. It is 17 bifilar turns on a half inch ferrite rod. 50Ω - 200Ω, 1-30MHz
http://www.m0ukd.com/Carolina_Windom/index.php

M0UKD Line isolator - 10 turns RG8 on a half inch ferrite rod
http://www.m0ukd.com/Carolina_Windom/index.php

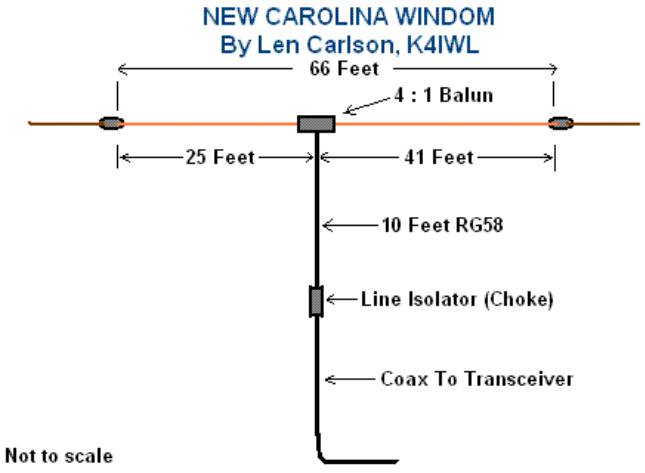

Windom design for 40m 20m 15m and 10m by K4IWL
http://www.hamuniverse.com/k4iwlnewwindom.html

More information on this general subject at BucksCom: http://www.packetradio.com/windom.htm **or** http://www.buckscom.com/pdfzips/windom.pdf

Commercial Suppliers:

G-WHIP Antennas (UK) : http://www.gwhip.co.uk
M0CVO OCFD Antennas (UK) : http://m0cvoantennas.webs.com

In the U.S.A:
Bux Comm Windom Antennas : http://www.buxcomm.com
Buck Master OFC Dipole Antennas : http://hamcall.net/
Alpha Delta : http://www.alphadeltacom.com
Carolina Windom : http://www.radioworks.com/ccwcover.html

See some Windom - Off Centre Fed Dipole - designs at these links:
http://users.erols.com/k3mt/windom/windom.htm
http://www.dxzone.com/cgi-bin/dir/jump2.cgi?ID=7478
http://www.radioelectronicschool.net/files/downloads/ocfdipole.pdf
http://www.hamuniverse.com/k4iwlnewwindom.html
http://www.g4nsj.co.uk/windom.shtml
http://www.m0ukd.com/Carolina_Windom/index.php

Semi-Permanent Antenna Installations

If it impossible to install a permanent aerial, then another option is to use an antenna designed for portable or mobile work deploying it only as and when necessary in the back yard or garden - perhaps supported with a portable tripod and/or guy ropes.

From the ideas above it should be possible to rig up a semi-permanent or removable antenna for low visual impact.

There are also very many portable antennas produced commercially that might be very useful to utilize on a semi-permanent basis. Commercially bought antennas can be very expensive indeed, especially when compared to 'home brew' aerials, but examples that immediately spring to mind for consideration include: The DMV-Pro, I-Pro, G Whip or G Whip Backpacker, the TW2010 from Transworld Antennas, the Sigma5 from Force 12 and aerials from SuperAntennas. Sandpiper Aerial Technology offer a very good choice of aerials such as the MV and MV-Portable, Buttie or Walkabout mk11 at very attractive prices. http://www.sandpiperaerials.co.uk There are very many other compact and portable antenna systems that are widely available. Check out all the amateur radio dealers for more ideas.

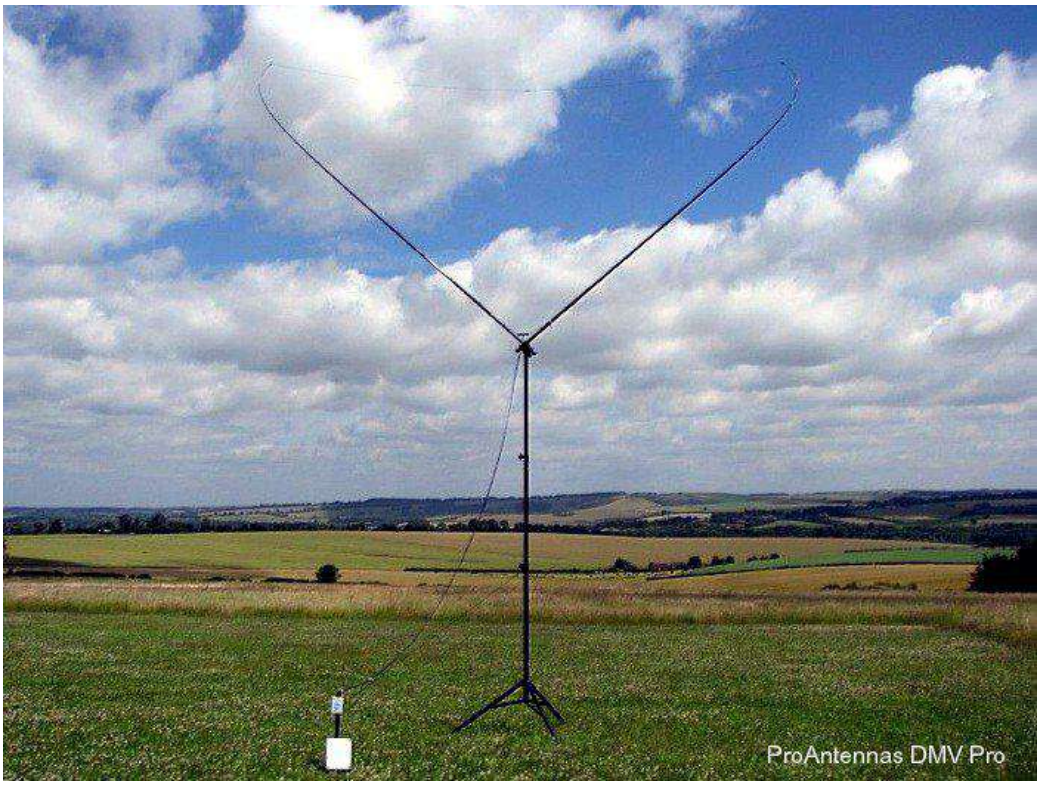

The DMV-Pro Antenna from ProAntennas (shown above) could be used in a back garden whenever required as could the company's I-Pro antenna. The DMV-Pro uses two fibreglass arms that allow the wire aerial to be supported in a number of different configurations such a "V" shaped, "L" shaped, "M" shaped and Delta. The aerial elements are fed to a 4:1 balun using low loss twin feeder, the balun is then connected to an auto ATU, such as the LDG Z-11 Pro, which is connected to the transceiver using coaxial cable. A versatile idea that could also be implemented on a DIY basis with a little experimentation! http://www.proantennas.co.uk

Geoff G4ICD / GJ4ICD mentions the original design, the JJ1VKL published in CQ ham radio Sep' 2000 in Japan. "This one goes back to 2000 and is now copied by several antenna manufacturers in the UK" It is an HF multi-band Delta loop antenna for 3.5-50MHz
http://www.geocities.jp/yoshiki_ja/deltae.htm

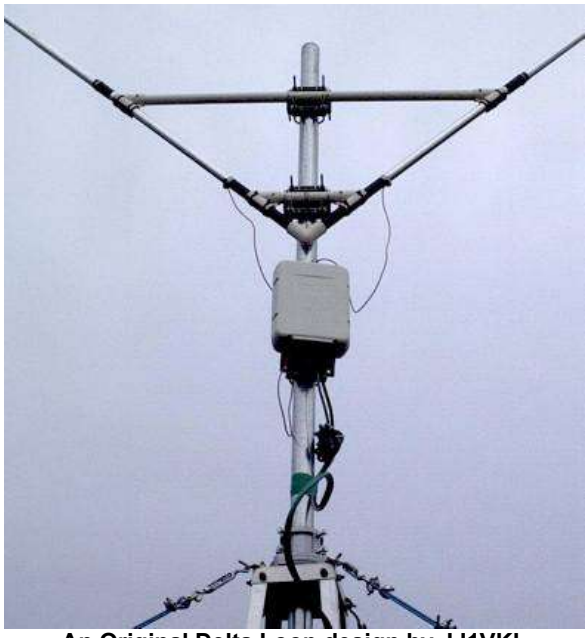

An Original Delta Loop design by JJ1VKL
Read more here: http://www.geocities.jp/yoshiki_ja/deltae.htm

Delta Loop by Arthur M0PLK (SQ2PLK)
Details at http://pdxa.one.pl/articles.php?article_id=17
Available at http://ham-radio.urbasket.eu and http://www.vpa-systems.pl/

STEALTH / COVERT / HIDDEN or DISGUISED ANTENNAS:

Ideas from **G4ILO** - Stealth Antennas: http://www.g4ilo.com/stealth.html

VK2ZOI - "Flowerpot" Antennas

Some ideas by VK2ZOI about producing inconspicuous antennas - perhaps disguised as a plant in a flower pot! There are ideas for 6 metre, 2metre and 70cm antennas including a dual band 2,/70cm design.

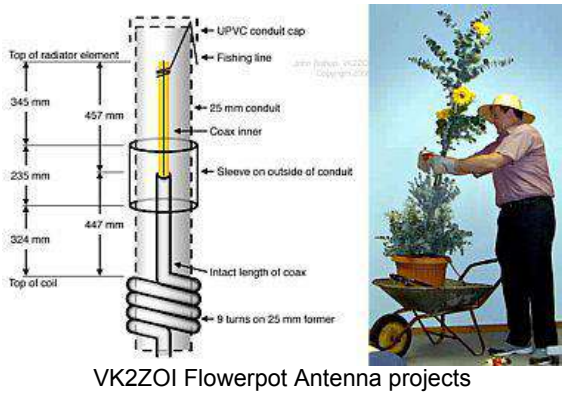

VK2ZOI Flowerpot Antenna projects
http://vk2zoi.com

All Band HF Vertical Antennas (non resonant) - 'Untennas'

So this is where the search for a multi-band antenna begins. It's a difficult task especially if space is limited. First considerations might lie with the commercially available options that are available. Commercially manufactured aerials are available at widely varying price points - perhaps from under £100 to many many £100's

One of the first commercial multi-band antennas that many keen new amateurs come across is something like the Comet CHA250B, or the Diamond BB7V or Moonraker GP2500 (pictured right). These are broad-band antennas and look like large CB antennas with a matching network at the base. Such antennas claim to allow operation of all bands between 80 metres and 6 metres with acceptably low v.s.w.r. Sounds like the perfect multi-band solution, especially as Comet and Moonraker are well known names that make excellent products.

These multi-band antennas have their critics though: Sure enough, they exhibit a seemingly acceptably low v.s.w.r. across the whole of HF, but low v.s.w.r. isn't everything. Ctitics do, in fact, call these types of broadband antennas glorified dummy loads - a bit unfair possibly, but maybe they have a point when most of your transmitter's precious power is wasted as heat rather than radiated as a useful RF signal!

The only way a simple, single vertical radiator can be made to work on across such a wide range of frequencies is by having a broad band matching transformer at the base of the radiator. This will inevitably result in the absorption of some - or much of the transmitter's power - the power loss represented by the heating up of the coils/transformer rather than actually being radiated as a useful signal by the antenna's vertical element.

Such antennas could present a loss of around 6 - 12 dB compared to a resonant antenna - how do do fancy putting all 100 of your precious watts in to the antenna and only getting 6.31 watts of effective power radiated?

Maybe that's a bit simplistic, so Martin G8JNJ has many superb articles analyzing the CHA250B and similar antenna designs here: http://g8jnj.webs.com/cometcha250b.htm

The article Anatomy Of The Comet CHA250B by VK5ZBD can be found here:
http://www.radiomanual.info/schemi/ACC_antenna/Comet_CHA-250BX2_anatomy.pdf
(Formerly found at this site http://www.vk5zdb.com/CHA250BXII.htm)

G8JNJ is also developing a better version of this type of antenna here:
http://g8jnj.webs.com/broadbandhfvertical.htm

I admit that, due to limited space, I considered this type of antenna when first starting out - but in the end dismissed them due to the extreme inefficiency and power loss problems. They should not be entirely discounted however, because if this really is all that can be accommodated at one's QTH then at least such an aerial will at get you on the air - and on all bands - at least in some sort of fashion. Many amateurs use these aerials with success, so they do have a place. Have a look and decide for yourself.

Other similar types of broad-band antenna:

There are a number of very similar designs (i.e. longish vertical radiator, with a transformer / unun at the base) available from some other British suppliers:

The G Pro-Whip 'Widebander' antenna (see http://www.gwhip.co.uk/);
The ProWhip Portable Antenna (see http://www.prowhipantennas.co.uk/);
Snowdonia Radio Company (SRC) - various types of wideband antennas (see http://www.snowdonia-radio-company.co.uk)

All these antennas appear to be based around an UNUN (typically 9:1) matching transformer at the base of the aerial. These aerials cost considerably less than those previously mentioned. The G Pro Whip and Pro Whip Portable offer particularly convenient portable operating opportunities as they are based on one of my favourite methods of antenna support - a long telescopic fibreglass (fishing) pole. Really neat!

For the 'fishing pole' types, essentially there is a vertical radiating wire of about 7 to 10 meters long, a 10m long horizontal counterpoise wire and the 9:1 unun at the base. This makes for a simple and attractive installation proposition (but remember the penalty of power losses) - all these aerials will be easy to install for permanent, semi-permanent use and easily removable or portable operating.

Considering the 10 meter vertical type, the performance on 40 meters (1/4 wave) should be quite reasonable, with reduced performance on other bands.

G-WHIP G Pro Whip antennas (now discontinued)
by Geoff Brown G4ICD
2011/2 - See G-WHIP'S WideBander Antenna as an alternative
http://www.gwhip.co.uk/

Buy (or build) a 9:1 UNUN and Make Your Own:

If you already have a 10m telescopic fibreglass fishing pole and some wire, then you could easily wind a 9:1 unun, or even buy one from suppliers such as G WHip Antenna products for a reasonable cost. So, you could make your own aerial with 10m vertical radiator working against the 10m counterpoise and fed to the ATU via the 9:1 unun at the aerial's base - just for fun, for experimentation, analysis or for permanent installation or portable work. (The telescopic pole must be fibreglass not carbon fibre)

Martin G8JNJ, suggests that a slightly better way to home-brew a broadband HF aerial might be to cut a vertical aerial for about 8.5 MHz, i.e. not a resonant 1/4 wave on any amateur band, but optimised to present a moderate impedance on as many bands as possible. In which case the vertical wire would be about 8.8 metres long, working against the counterpoise, and fed to the a.t.u. via an unun - perhaps 6:1 or 9:1 - this is all open to further research and experimentation! See http://g8jnj.webs.com/currentprojects.htm

G0KYA has also written lots of interesting articles about antennas and several pieces about using a 9:1 unun and a length of wire. He found that a wire length of 19.8 metres offered a good compromise for a multi band aerial. Read G0KYA's blog here: http://g0kya.blogspot.com/search/label/antennas

More : http://g0kya.blogspot.co.uk/search/label/antennas

Interestingly 2W0SAK of Snowdonia Radio Company recommended an antenna wire length of 7.13 metres with their 9:1 unun - or for better efficiency a wire that is 19.8 metres long which would be run out horizontally. Both the 7.13 m and 19.8 metre lengths should cover the 80m to 10m bands.

Freq Coverage	Wire Length	or try
7 - 29 (50) MHz	2.74 m	6 m
3.5 - 29 (50) Mhz	7.13 m	9.8 m or 16.1 m
3.5 - 29 (50) MHz	19.8 m	21.9 m or 26.8 m
1.8 - 29 MHz	29.0 m	29.9 m
1.8 - 29 (50) MHz	39.6 m	36.6 m

High Quality Baluns and UnUns Available From www.gwhip.co.uk - either boxed and ready to use or just the core and quality windings suitable to put into own box or project.

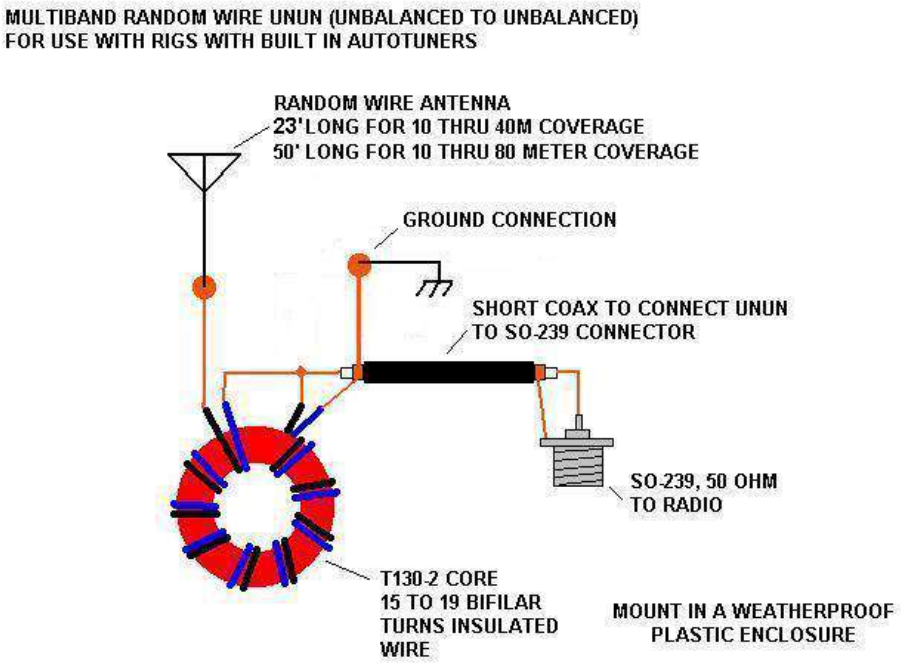

Above is a neat design for an "Untenna" KC8AON - Link: http://www.angelfire.com/electronic2/qrp/ununn.html

For a jack of all trades try a high quality GWhip "Widebander Antenna"

G0KYA writes a very useful piece in his blog:

http://g0kya.blogspot.com/search/label/antennas

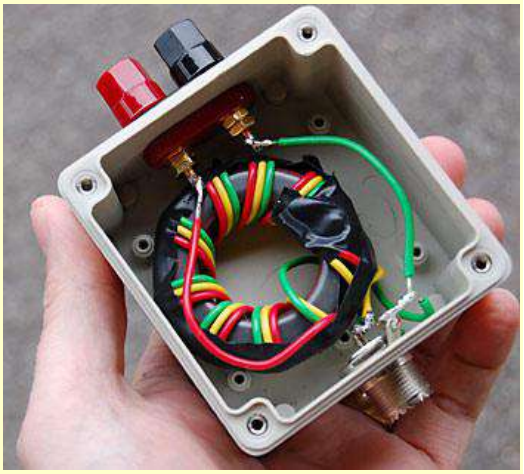

In the next round of tests I used the same 9:1 Un-Un wound using PVC covered cable and a T200-2 toroid. Note in the photograph that the PVC tape is only used to keep the turns neatly arranged.

If you want to build your own follow these instructions:

Building a 9:1 unun
To understand how to construct an unun lets build a 9:1 version. You will need a T-200 (red) toroid and three pieces of wire, each 24 inches (60cm) long . It will also help if you a small plastic box with an SO239 socket mounted at one end and with two wing nuts or mounting posts at the other. In the UK you can buy a small plastic box from Maplin which is watertight with a rubber seal, yet inexpensive.
It will help if the wires are different colours, although that isn't critical if you have a multimeter available. It just makes it a lot easier to follow these instructions.
For the sake of this explanation I'll assume that you are using green, red and black pieces of wire.
Put the three pieces of wire together and wind them carefully onto the T130-2 toroid. Place the wires (left to right) green-black-red, and wrap nine turns on to the toroid.
Try not to let the wires overlap.
You should end up with a toroid with three wires extending from the left winding and three wires extending from the right.
Now twist and solder the left black wire with the right red wire. This can be covered with PVC tape once complete.
Now twist the left green wire with the right black wire. Strip the ends of the two wires, twist and solder them together leaving the length about 2” long from the toroid.
Finally trim and strip the remaining right green wire and solder another 5” piece of green solid wire to it.
Now take the left green wire and right black wires that you twisted together and connect them to the centre pin of the SO239 socket – this is the input side and will connect to your radio via a length of coax.
One of the green wires is now soldered to the ground connection of the SO239 socket. The other end of the wire you soldered on (which is connected to it) becomes the earth connection for the unun and typically goes to a ground stake and ground radials.
This leaves the remaining red wire which connects to the other wingnut and will become the connection for the antenna.
If you are worried about the wires unravelling you can either use PVC tape to hold them in place or plastic cable ties.
So how do we use an unun? Lets look at a typical example.

This time I erected a 10m high fishing pole and attached a 65ft quarter wave antenna for 80m in an inverted L fashion. That is, 10m up and then 9.8m out to the nearby summerhouse.

This was arranged away from the house and fed with 12m of RG8 coax, a single earth stake and two 20ft radials at the feed point..

Here are the SWR readings at the end of the coax:
3.5MHz – SWR 3:1
3.65MHz – SWR 4.2
3.8MHz – SWR 5.9
7.10MHz - SWR 13.6:1
10.1MHz – SWR 2.5:1
14.2MHz – SWR 3.3:1

18.14MHz – SWR 1.8:1
21.2MHz – SWR 2.4:1
24.9MHz – SWR 1.9:1
28.5MHz – SWR 1.2:1

From this you can see that by shortening the wire to 65ft from the original 85ft you gain 80m, but lose 40m. The rig (FT2000) would quite happily tune seven bands with its internal ATU. Here are the quick comparison results against my 80m Windom and parallel-fed dipoles in the loft for 40m, 20m, 17, and 10m.

80m
Not as good around the UK as the Windom - probably due to the maximum current being in the vertical section. Modelling shows the antenna to be down about 10dB on a low dipole.
30m
Lithuania similar. Other EU and Italy similar. Bulgaria down 2 S points
17m
Similar – inverted L has slight edge at times. Slightly noisier
15m
Better than Windom by about 1 S point.
10m
Much better than Windom, dipole and mag loop around Europe via Es, by about 2 S points. Slightly more noise (+ 1 S point).

From this I can see that I need to do more tests, especially on 20m, but for an all-in cost for the antenna of about £15-£20 it shows promise. If you have a tree then the up and out idea with a 65ft wire looks quite good. A way to get 40m back would be to put a 40m trap in the wire at the 10m mark. If you don't fancy making your own UnUn you can buy the whole antenna from the Snowdonia Radio Company for £35 inc P&P – see http://www.snowdonia-radio-company.co.uk/srcproducts.html [From a collection of excellent articles from G0KYA] Link to SRC: http://www.snowdonia-radio-company.co.uk

GWhip Antennas, and ProWhip Antennas all supply this type of antenna as a commercial item.

CONCLUSIONS?

Arguably the most effective, simplest and, indeed, cheapest way to attain multi-band operation is by using a full size resonant dipole for each band of interest - perhaps having a couple suspended at any one time and swapping aerials when other bands are needed.

As mentioned in the introduction this is a little inconvenient which is why the holy grail of so many amateurs is one antenna that that will do everything - perfectly. As we have seen such an aerial does not exist, and never will due to those pesky laws of physics. Compromises will always have to be made; compromises of efficiency, size, number of bands and bandwidth per band etc - nevertheless there are enough options available to be able to choose a configuration of antenna or antennas that should be able to make the best use of precious transmitter power for a particular circumstance.

My two key criteria are that the antenna should be truly resonant on the band(s) of interest and that the radiating elements should be as near to full size as possible, relative to the wavelength(s) being used, to ensure the best possible efficiency (i.e. lowest loss of power). This means full size quarter wave vertical or full size half wavelength long trapped dipole.

I don't especially like aerials that are shortened by using a loading coil, but accept that such an arrangement is sometimes necessary for the longer wavelength bands. Top Band is a real problem in average size gardens. Where the is a coil, a trap, or transformer there will be some loss or reduced efficiency introduced into the antenna system. I do find that using a trap is an excellent compromise - the 80m / 40m Inverted L and the 20m / 10m trapped dipole work especially well. If I could not use the Inverted L, my next favourite option is the Loop or a fan (Parallel) dipole.

All the pros and cons have to be weighed up to find the best compromise for particular operating circumstances. I hope that this page has given new operators some ideas to take away and mull over, but remember those words from Joe Tyburczy WB1GFH that this page started with:

"When you put up your antenna is also crucial. I must mention here the importance of what many early hams called "antenna weather". That is, snow, sleet, freezing rain, or combination of all the above. It has been proven time and time again that any antenna installed in conditions better than abysmal will not function worth a darn. Or, put another way, it takes bad weather to put up a decent antenna. Dark and cold New England winter days are ideal for this activity. Any antenna erected on such a day will inevitably produce miracles."

Some Further Reading:

Understanding Antennas For The Non-Technical Ham
A Book By Jim Abercrombie, N4JA
basicantennas.pdf

More Antenna Ideas by other amateurs (.doc)

ARRL document Multi Band Dipoles Compared (.pdf)

High Quality Baluns and UnUns Available From www.gwhip.co.uk

Useful Aerial Rigging Accessories

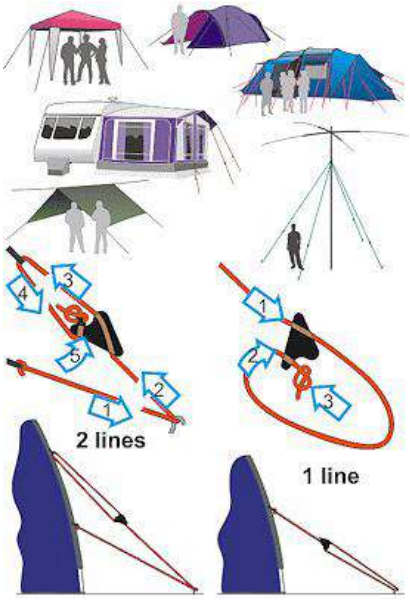

Line-Lok guy runners from ClamCleats - fantastic for guying antenna masts quickly and successfully
http://www.cleats.co.uk http://www.clamcleat.com

Reusable Nylon Hose Clip / Reusable Circular Clamps
Useful for securing telescopic fibreglass poles - e.g. holding each section in place in windy weather or to use as a guying ring (spider)
(Herbie Clips) (Kaf-flex Nylon Clamps)
http://www.malpasonline.co.uk
http://news.thomasnet.com
http://www.hclfasteners.co.uk/acatalog/Herbie-Clip.html
http://www.cheapham.com/products/S9V31-Replacement-Clamps.html
http://rotocon.homestead.com/shoponline2.html

OTHER THINGS THAT MAY BE NEEDED:

POLE(S) Aluminium, fibreglass or wood ; POLE TO POLE CLAMPS ; MET POST(S) ; NYLON CORD or PARA CORD ; SPIDERS / 3 or 4 WAY GUY RINGS ; PULLEYS ; SNAP HOOKS ; DEE SHACKELS ; GROUND STAKES for anchoring guy ropes ; DOG BONE or EGG INSULATORS ; DIPOLE CENTRES ; EARTHING STAKE ; V BOLTS ; ROPE GRIPS ; THIMBLES ; SLEEVE JOINER(S) ; T&K BRACKETS ; TRIPOD or other GROUND MOUNTING HARDWARE ; STAINLESS STEEL M6 Nuts Bolts and Washers ; SPADE and / LUG TERMINALS ; SELF AMALGAMATING TAPE ; HEATSHRINK ; WEATHERPROOFING SEALANT ; STAINLESS STEEL JUBILEE CLIPS.

TRIMMING AERIALS

Antenna Trimming Chart

This following information below could be very useful indeed when constructing aerials and is compiled by DX Zone / Radio Works from the web page at: http://www.dxzone.com/cgi-bin/dir/jump2.cgi?ID=13444

Use this chart as an aid in trimming the length of your antenna. It gives you an idea of the change in wire length needed to move antenna resonance a specific number of KHz.

* Dimensions are for each leg of a half-wave dipole
* For quarter-wave antennas (i.e. verticals) use the dimensions directly from this chart
* Full-wavelength antennas (loops) - multiply the chart dimensions by four (4) and change the overall length of the antenna by that amount.

Lengths are estimates. Many factors will affect their exact value.

To move	80/75 m	40 m	20 m	15 m	10 m
-500 kHz	+8' 4"	+2'	+8"	+3"	+1.5"
-400 kHz	+6' 8"	+1' 9"	+6.5"	+2.5"	+1.25'
-300 kHz	+5'	+1' 4"	+5"	+1.75"	+1"
-200 kHz	+3' 4"	+10"	+3.25"	+1.25	+5/8"
-100 kHz	+1' 7"	+5"	+1.5"	+1/2"	+3/8
00 kHz	0	0	0	0	0
+100 kHz	-1' 7"	-5"	-1.5"	-1/2"	-3/8"
+200 kHz	-3' 4"	-10"	-3.25"	-1.25	-5/8"
+300 kHz	-5'	-1' 4"	-5"	-1.75"	-1"
+400 kHz	-6' 8"	-1' 9"	-6.5"	-2.5"	-1.25'
+500 kHz	-8' 4"	-2'	-8"	-3"	-1.5"

Example:

You have measured the SWR of your 40 meter dipole at various frequencies across the band. You have determined that the SWR is lowest at 7.00 MHz. You actually want the lowest SWR to occur up in the sideband portion of the band, so you need to move resonance up in frequency about 200 KHz.

According to the chart, to move +200 KHz on 40 meters, you will have to shorten each leg of the dipole 10" (-10"). The overall length of the antenna is shortened a total of 20 inches.

Lengthening or shortening the antenna is done at the end insulators. To shorten the antenna, unwind the antenna wire as it wraps around itself at the end insulator. Move the insulator several inches toward the center of the antenna. Re wrap the antenna wire to secure the end insulator. Do not cut the wire. Wrap it back around the antenna wire. You may need to increase the antenna later. [From Radio Works / DXZone]

KNOTS FOR SECURING WIRE ANTENNAS

I have found the Bowline to be one of the most useful, it is strong and easy to tie. A Bowline will not slip in any circumstances and, usefully, the more load that is put on it, the tighter it gets.

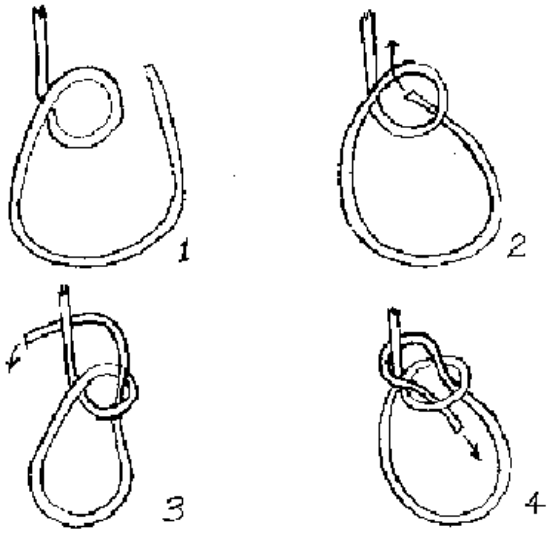

The Bowline Knot

A Bowline can be used to tie two ropes together and should be used to tie a support rope to a pulley, dipole centre and other antenna items.

It's important to use the correct knot for the job when fixing up wire antennas. I find the Bowline is a very useful for fixing end, egg and dog-bone insulators to the ends of the wire and/or ropes.

The Buntline Hitch is an excellent knot as is the Round Turn & Two Hitches, Anchor Bend (Anchor Hitch) knots which are very good for tying a rope to a pole or a mast.

The Bowline is most useful for fixing end, egg and dog-bone insulators to the ends of the wire and/or ropes.

A Double Sheet Bend can join two pieces of rope together - even if they are of unequal size.

'Animated Knots' will show you how to do them. Visit http://www.animatedknots.com

More websites with knot information : http://www.netknots.com/ http://www.southee.com/Knots/Index.htm

The correct knot will ensure that the antenna will be as strong as possible.

LINKS

Understanding Antennas For The Non-Technical Ham - A Book By Jim Abercrombie, N4JA :
PDF Book: http://www.hamuniverse.com/basicantennas.pdf
HTML page: http://www.hamuniverse.com/n4jaantennabook.html

G4ILO - Stealth Antennas: http://www.g4ilo.com/stealth.html

All Band Doublet Antenna by M0MTJ :
http://www.mds975.co.uk/Content/amateur_radio_antennas_06.html#All_Band_Doublet_Antenna

All Band Doublet Antenna : http://www.hamuniverse.com/hfdoublet.html

All Band Doublet Antenna by AI4JI : http://www.ai4ji.com/Projects/antennas/doublet.htm

Amateur Radio MØMTJ

MDS975.co.uk HOME PAGE

My Home Page

Amateur Radio
Operating Conditions
Antennas
Accessories
Projects & Kits
Data Modes
Information
Portable
QSL
RSGB Ltd
Links
QRM
Bits 'n' Bobs
Contact

WSPR
Weak Signal Propagation Reporting

PORTABLE

Site Map

MDS975 Home

Feedback

Site Search
Find
powered by FreeFind

QRM from PLT

M0MTJ | Operating Conditions | Antennas / Aerials | /P Portable Operating | Accessories | Projects & Kits | Useful Information
Contact MØMTJ | Contact M6ORS | Links to Amateur Radio Sites | RSGB | QSL | The Amateur Radio Mini Site Map
News, Developments, Events, Photographs and other 'Bits 'n' Bobs' | WSPR Weak Signal Propagation Reporter

AERIALS (ANTENNAS) 1

Antennas 2 | Antennas 3 | Antennas 4 | Antennas 5 | Antennas 6 | Antennas 7

"Success is 90% antenna and 10% rig. Hobby is 90% listening 10% transmitting" *- MM0HDW.*

AERIALS used by MØMTJ

This page shows some the antennas that I have used over the course of time.

Index To Other Antenna Pages:
Antennas 1 : Aerials used by M0MTJ
Antennas 2 : Including ideas for compact aerials for Top Band /160 metres
Antennas 3 : Felix Scerri VK4FUQ discusses Loop Aerials, baluns, masts & other antenna related topics
Antennas 4 : Many antenna ideas from various sources particularly for multi-band operation & also gives information about
antenna trimming, knots for wire antennas and useful aerial rigging accessory ideas.
Antennas 5 : Half Wave (physically end fed) aerials for 144 MHz VHF / 430 MHz UHF and 50 MHz 6 Metre band & J-Pole Aerials
Antennas 6 : Simple and effective H.F. Aerial ideas: The All Band Doublet, an All Band Sloper & a Ground Plane Aerial
Antennas 7 : Omni-Directional - Circularly (Mixed) Polarized Aerial for VHF / 2 Meters.

2014 : Current Set Up - as at September 2014:

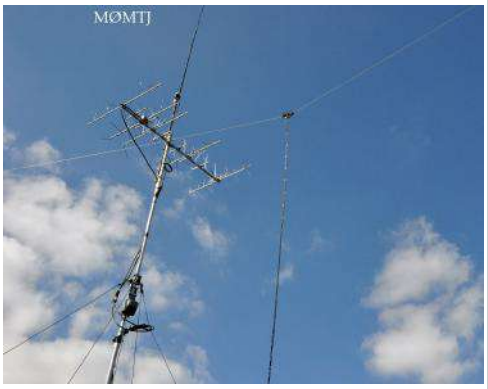

The Summer of 2014 has seen a few changes of aerials. The 80m/40m Inverted L was removed and replaced with a newly constructed Doublet Antenna fed with ladder line via a 4:1 G-Whip current balun and an LDG "ATU". The Tecadi support pole originally used for the Inverted L is now used to support one end of the Doublet. You have probably read this elsewhere, but I can confirm that the All Band Doublet (fed with ladder line *not coax*) is a superb all round HF aerial. Highly recommended.

The SGC-230 Automatic Antenna Coupler was moved from the original feedpoint of the Inverted L antenna to the second feed-point on the other side of the garden. This now feeds a sloping wire of approximately 20 meters length to ensure that the 80 Meter Band and Top Band (160 meters) remain available. This antenna will also 'tune' on most other bands, so remains a very useful second antenna, though the All Band Doublet is often considerably better, particularly on the higher frequencies. The old SGC-230 was also faulty and I replaced it with a new CG-3000 auto coupler from Martin Lynch and Sons.

The J-Pole for 4 Meters (70 MHz) was removed since it wasn't used much, being only connected to a 4m hand-held radio - it seemed to be a waste of precious antenna space. This was replaced with a newly constructed Half Wave "CFR" Antenna (Coaxial Dipole) for 6 Meters (50 MHz) connected to the main HF radio via Westflex 103 coax. The DK7ZB dual band Yagi antenna remains, as does the 10m / 6m Fan Dipole in the loft space. Also remaining in place at the apex of the house is the home-brew 2m / 70cm "CFR" Antenna (Coaxial Dipole) for VHF/UHF FM operation - this has been a particularly effective antenna.

To sumarise:

1) A 20 meter long doublet antenna fed with balanced ladder line for 40 meters to 6 meters. The 'old timers' really knew their stuff, this an excellent all round antenna that is easy and cheap to make and should be quite easy to accommodate and install. See photograph below and read more here

2) A Sloper Antenna consisting of two parallel wires - one wire being 20 meters long with a second parallel wire

Get on the air with TOP QUALITY BRITISH G-WHIP ANTENNAS

that is 10 meters in length. The first 2.5 meters (approx) of wire runs vertically up a non metallic post, then the remainder slopes back towards the house being finished off with an insulator which is attached to a Para-Cord lanyard that runs through a pulley on a pole at the apex of the roof. The antenna wire can therefore easily be let down for maintenance or adjustment whenever required. For lowest possible loss, the antenna is fed via a GC3000 automatic antenna coupler located at the bottom of the garden. The antenna is primarily for lower HF bands including 160 meters, 80 meters and and 40 meters, but it also works very well on some higher bands. The GC3000 itself is mounted in a waterproof IP56 rated enclosure near ground level at the bottom of the garden. Grounding is achieved from two 4 foot long copper ground stakes and several radial grounding wires.

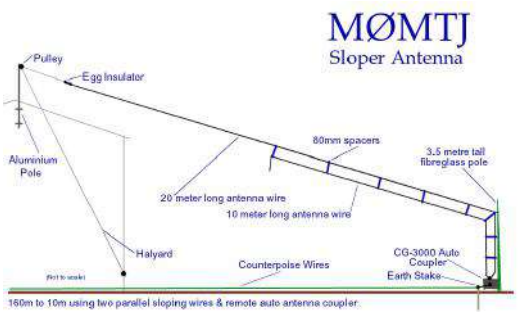

Read more about the Sloper Antenna and the CG3000 here.

3) A 'home-brew' omnidirectional, vertical dual band, end fed antenna for 2 metres and 70cm. This is of the Controlled Feeder Radiation design (CFR) by VK2ZOI; effectively an end fed half wave dipole on 2m with an aluminium sleeve dipole section to achieve 70cms with a few extra dB's of gain. It is mounted on an aluminium mast. It's feed-point is about 11 metres a.g.l. read more here

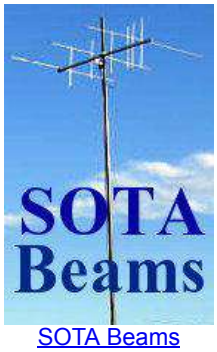

SOTA Beams Lightweight 2 metre & 70cms Yagis, Dipole, Accessories & Poles www.sotabeams.co.uk

4) A DK7ZB design dual band Yagi antenna, with 5 elements for 2 metres and 8 elements for 70cms, mounted horizontally for SSB. A lightweight antenna rotator is employed and uses a push-up telescopic mast. Height above ground level is again approximately 7 metres. The DK7ZB is an excellent twin band Yagi antenna. read more here

5) A Half Wave End Fed / Controlled Feeder Radiation (CFR) antenna for 6 meters / 50 MHz. Supported by a 3 meter long telescopic fibreglass fishing pole attached to the top of the aluminium push up mast that supports the DK7ZB dual band yagi and rotator.

6) Dual Band Fan Dipole, made from thick loudspeaker wire, mounted horizontally in the loft space for 10 meters an 6 metres. Cheap & quite effective.

Other Options that can be deployed on an 'as required basis' :

7) A half wave Wire J-Pole fixed to a telescopic fibreglass fishing pole for 10m. Cheap and effective. more about J-Poles here and also here on Antenna page 5

8) Compact Loaded Top Band Antenna, based on a design idea by Stuart Craigen G4GTX more

9 & 10) G Whip End Fed Zepps (EFZ's) for either 20m, 15m or 17m or the G-Whip "WideBander" which is an 'UnTenna' style antenna that can be used for 20m through to 10m using good quality G Whip 9:1 UnUn; useful additions for antenna flexibility. more

11) N9TAX Dual Band Slim Jim (J-Pole) antenna mounted in the loft as a back-up antenna for 2m and 70cms. Very good. more

12) Delta Loop Antenna - 16 metre loop of wire in triangular Delta shape, hung from the top of the pole supporting the inverted L antenna and fed via RG213 coaxial cable via a 4:1 balun. The loop is really a single band antenna cut for one wavelength on the band of interest, however it also can be pressed into service for some higher bands - a good, cheap and easy to install aerial; Often works better than the inverted L on the higher bands, but on 10 metres the tuned 10 metre dipole in the loft is sometimes better. more

Knots: Knots for securing wire aerials and other things more here

H.F. ANTENNAS used by M0MTJ

All Band Doublet Antenna

The Doublet Antenna consists of two 10 meter long top wires to form the 20 meter long 'dipole' section. The centre is fed with Ladder Line rather than coaxial cable. A dipole fed with coaxial cable is essentially a single band (mono band) antenna. Feeding such an aerial with ladder line, or open wire twin feeder makes a much more effective multi-band antenna.

The ladder line runs down to a high efficiency 4:1 Current Balun (G-Whip) which is connected to an LDG AT-200 automatic antenna matching unit via a very short RG213 patch lead to ensure lowest losses. The Antenna tuner and balun are housed in a box which is itself contained in a small garden shed to protect it from the weather. The LDG antenna matching unit is then connected back to the 'shack' via a run of RG-213 coaxial cable. Read more

about the All Band Doublet Antenna here.

A view of part of the MØMTJ All Band Doublet Antenna
Read more here

ANTENNAS FOR VHF and UHF - 2 m & 70 cms

The main antennas are as follows:

Home-Brew dual band end (physically end fed) half wave "Coaxial Dipole" for 2m & 70cm

For 2m and 70cm FM I use a mounted on a lightweight aluminium telescopic pole on the apex of the hose. The base of the antenna (the bottom of the radiating element) is approximately 11 metres above ground level. This antenna is based on the Controlled Feeder Radiation principle (CFR) and is described by VK2ZOI. Read more about its construction here. Also seen in the photograph below are the ropes that support the H.F. wire aerials.

Home brew dual band vertical antenna for 2 metres and 70 cms
Read more about its construction here

Dual Band Yagi for 2m & 70cm

For 2 metres and 70cms SSB there is a horizontal DK7ZB design dual band Yagi antenna. This has 5 elements for 2 metres and 8 elements for 70 cms. A lightweight antenna rotator is employed and uses the same push-up telescopic mast that the Home-Brew 70MHz J-Pole is mounted on. Height above ground level is again approximately 7 metres. The DK7ZB is an excellent twin band Yagi antenna**.**

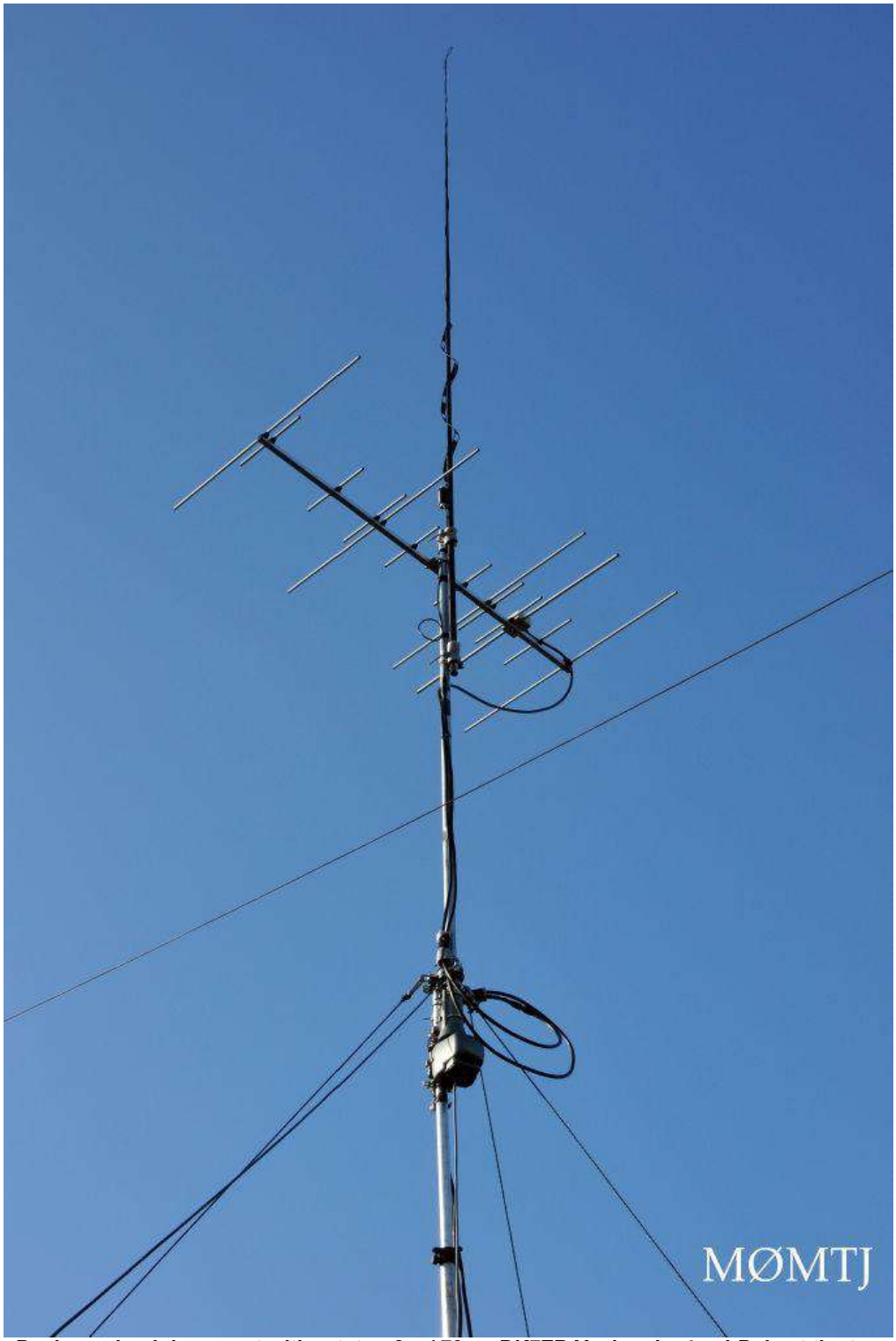

Push up aluminium mast with rotator, 2m / 70cm DK7ZB Yagi and a 4m J-Pole at the top

The DK7ZB 5 + 8 element dual band yagi for 2m and 70 cm - designed by Martin Steyer DK7ZB
Available from Arthur M0PLK (SQ2PLK) at Ham Radio Shop:
http://stores.ebay.co.uk/urbasket-eu
http://ham-radio.urbasket.eu
Also available from VPA SYSTEMS by SQ9VPA http://www.vpa-systems.pl
Kits available from NUXCOM.de : http://shop.nuxcom.de

2 Meter J-Pole Antenna for the garden shed - and other J-Pole antennas for 6 metres and 10 metres :

While experimenting with antennas in the garden in the summer of 2012 I thought that it would be good to have a hand-held radio in the shed to do some monitoring and make a few contacts. To improve upon the performance of the 'rubber duck' antenna I quickly made a J-Pole antenna for the 2 metre band.

It is made from a 47cm length of 450 ohm Wireman ladder line as the 1/4 wave matching section, plus a 97cm length of stranded wire as the 1/2 wave radiator. It is fed with 3 metres of Mil spec RG58 c/u coaxial cable that is soldered to the 1/4 wave matching section's impedance matching point at 3.5 cm from the bottom. The coax feeder is wound around some PVC tube to form a choke. The completed antenna is taped to a 2.2 metre long fibreglass fishing pole that I purchased from Poundland (for £1.00). It took about 20 minutes to make followed by some testing and adjustment with the antenna analyser. The fishing pole is lashed to the shed with some cable ties.

This simple antenna works pretty well, but being so low down signal strengths are not huge, but it's pleasing to get on the air with something so simple and cheap!

Find out how easy it is to construct J-Pole Antennas here

Now, if it was at the top of my 10 metre long fishing pole. . . . . (!)

The Shed Antenna - a 2m J-Pole by M0MTJ
Note the simple choke balun at its base made by winding 8 turns
of the coaxial cable around a small off cut of white PVC water pipe.
Find out how easy it is to construct J-Pole Antennas here

The feed point of a J-Pole antenna made from Wireman 450 ohm ladder line.
More here

More Antennas . . .

Inverted L Antenna for 80m and 40m (and some other HF Bands from 80m to 10m)

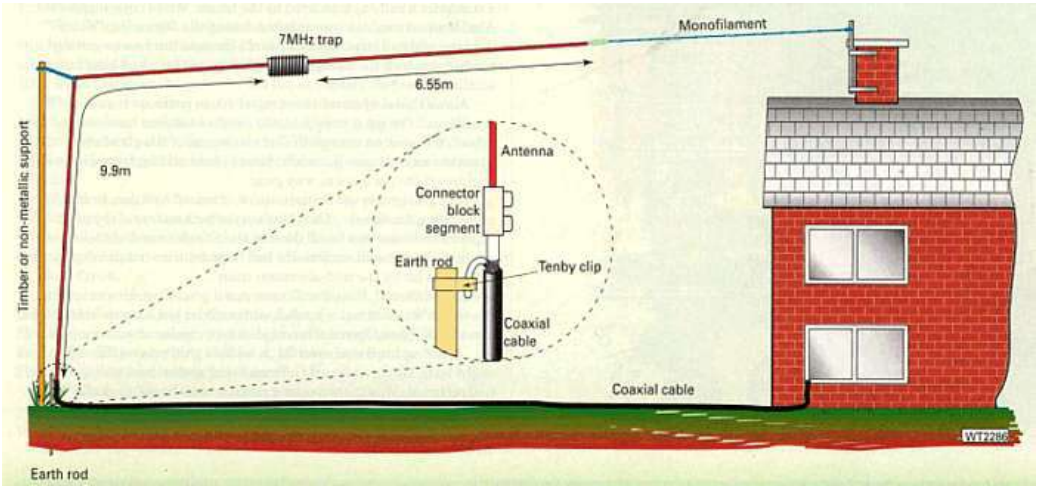

The basic layout of the Inverted L Antenna (Practical Wireless)

The first antenna that I installed was for HF. I decided on an Inverted L that incorporates a 7MHz trap so that it can be used on both 7MHz (40 metres) and 3.5 MHz (80 metres).

The design of this Inverted L is well known and a good design has been published previously in Practical Wireless by Len Paget GM0ONX. It is based on one half of the famous W3DZZ trapped dipole antenna.

It can be made entirely from scratch as a DIY project, or the 7MHz trap could be purchased commercially as a ready made item, or whole antenna can bought as a complete kit from Tony Nailer, G4CFY, at Spectrum Communications. I opted to buy the 7MHz trap from Spectrum Communications, as I already had most of the other materials required - rope, egg insulator, plastic box, and some good aerial wire. The Spectrum Communications trap is solid and well made and 'potted' to protect against the elements.

This antenna is tuned for 40 metres and 80 metres, but the VSWR is acceptable on several other bands being in the region of 2:1 to 5:1. The designer anticipated that this antenna would be usable on five of the H.F. bands between 80m and 10m.

I have found that with the use of the Antenna Tuning Unit it can be used on all of the H.F. bands. However the polar radiation pattern may very well be less predictable on bands other than the intended 40 and 80 metres, and it may well be less effective than might be desirable - but it does work!

The antenna is in the back garden, while the shack (radio room) is in a bedroom at the front of the house. It is fed by a 30 metre length of RG213 coaxial cable (it is not possible to use twin feeder for this type of antenna as the Inverted L is an UN-Balanced aerial, whereas twin feeder is balanced). With this length of cable I estimate the loss in the feeder alone to be about 1dB at 7MHz. The feed point of the aerial is located at the base of a 16 foot high wooden pole near the bottom of the garden. The horizontal top wire returns to a fibreglass pole installed at the apex of the roof.

+ 17 + 160: I have since added a separate sloping wire element for the 17 Metre Band and a switchable loading coil for Top Band - see notes below...

Photograph showing the wooden support post and termination point of the Inverted L antenna The post is coloured green with green fence treatment to mast it somewhat. I have also placed it near the bush to provide further camouflage.

The low loss RG213 coaxial cable runs from the shack at the front of the house up into the loft and exits into the back garden down the rear wall, through some garden hose to offer some protection along the flower bed to the bottom of the garden where it is connected to the base of the Inverted L antenna.

The suspended Inverted L aerial with 7 MHz trap.

The Inverted L antenna - lower section now nicely camouflaged. The wooden support post is some 6 metres long.

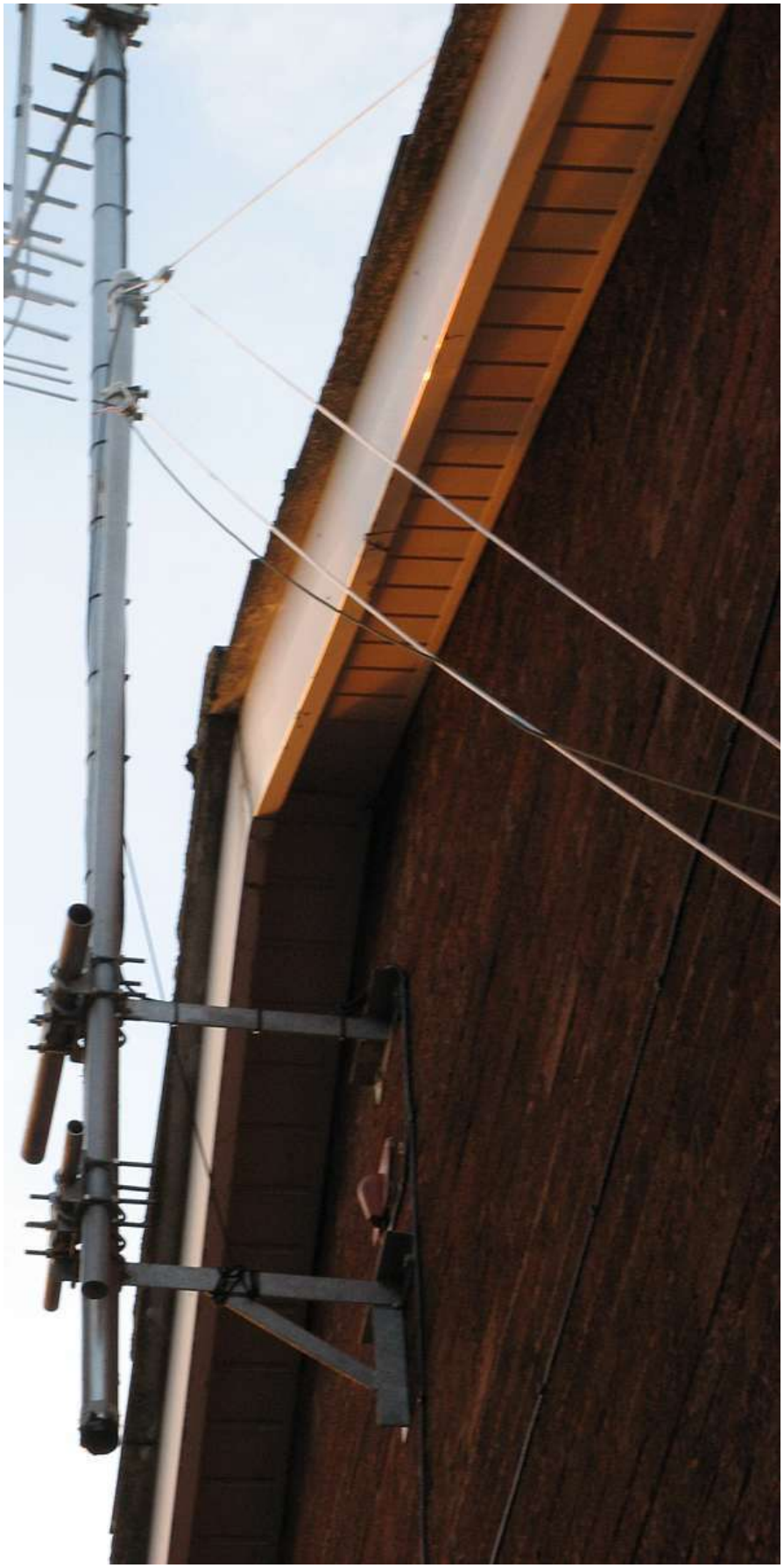

The photograph above shows the Dacron ropes supporting the ends of the Inverted L and Dipole antennas are held in place at the top of the fibreglass support mast by a pulley - one pulley for each support rope. This facilitates rapid lowering of either antenna for adjustment or replacement. This photograph also shows a second rope and pulley system that was originally used to support the 20m dipole and is now used for the top band inverted L wire

aerial.

I needed a good reliable knot for securing ropes when installing wire antennas and have found the Bowline to be one of the most useful, it is strong and easy to tie. A Bowline will not slip in any circumstances and, usefully, the more load that is put on it, the tighter it gets.

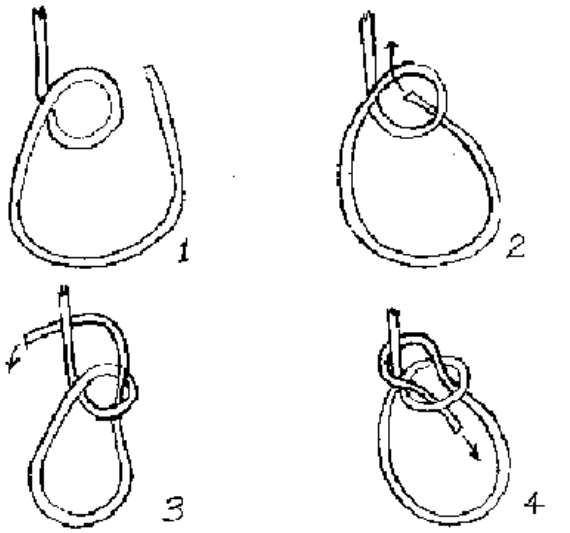

The Bowline Knot

A Bowline can be used to tie two ropes together and should be used to tie a support rope to a pulley, dipole centre and other antenna items.

It's important to use the correct knot for the job when fixing up wire antennas. I find the Bowline is a very useful for fixing end, egg and dog-bone insulators to the ends of the wire and/or ropes. The Round Turn & Two Hitches, Anchor Bend (Anchor Hitch) and Buntline Hitch knots are very good for tying a rope to a pole or a mast. A Double Sheet Bend can join two pieces of rope together - even if they are of unequal size. 'Animated Knots' will show you how to do them: http://www.animatedknots.com

Photo showing pulley fixed to the top of the wooden support post and the aerial support rope that it holds in place.

The Spectrum Communications Trap

View of trap showing that the joints have been thoroughly sealed against the weather with self amalgamating tape and silicone sealant.

Just for good measure I sealed the internal side of the machine screw that forms the connection terminal against the weather with Watson sealant putty.

Adding Top Band to the 80 / 40 metre Inverted L Antenna:

Due to an aborted house move in 2010 I had removed all the antennas. While re-establishing the aerials in 2011, and considering space limitations, I decided to experiment with adding a loading coil to the 40m / 80m Inverted L aerial. The loading coil has a link wire to short it out of circuit when using the aerial for 80 metres and 40 metres. The link wire is removed when Top Band is required.

I also took the opportunity to replace the original wooden post with a strong 6 metre tall fibreglass pole.

The coil consists of approximately 37 turns of PVC covered antenna wire wound on a short piece of PVC pipe. Once the required points of resonance were set for 40 metres and 80 metres, the link wire was removed and number of turns on the coil were adjusted until the required point of resonance was found on the 160 metre band. I set it to around 1900 kHz - the bandwidth is quite narrow.

Once the work was done, the joints and connections were sealed with either Liquid Electrical Tape or self amalgamating tape, then the connecting box, V bolts and white PVC pipe were sprayed with green paint to help it all blend in with the surroundings a little better.

Adding the 17 Metre (18 MHz) Band to the 80 / 40 metre Inverted L Antenna:

The Inverted L is not too good for the 'WARC' bands so to obtain better performance on the 17 Metre band I added a single slightly sloping wire element cut for that band. The lower end of the wire is permanently connected to the feed terminal on the junction box, the other end is tied to a small dog bone insulator. This dog bone is then supported by a length of thin para-cord which is tied to the horizontal wire of the main Inverted L element. (N.B. The 17 metre modification is not currently shown in the photographs below.)

Work In Progress! - September 2011
Reconfiguring Inverted L with additional Top Band Loading Coil for 160 metres.
A strong 6 metre tall fibreglass pole replaces the original heavy wooden post.

Adding 160 metre loading coil to the 80m / 40m Inverted L Aerial.
The loading coil has a link wire to short it out of circuit when using the aerial for 80 metres and 40 metres.
The link wire is removed when Top Band is required.
The coil consists of approximately 37 turns wound on a piece of PVC pipe.

Adding 160 metre loading coil to the 80m / 40m Inverted L Aerial.
The loading coil has a link wire to short it out of circuit when using the aerial for 80 metres and 40 metres.
The link wire is removed when Top Band is required.
The coil consists of approximately 37 turns wound on a piece of PVC pipe.

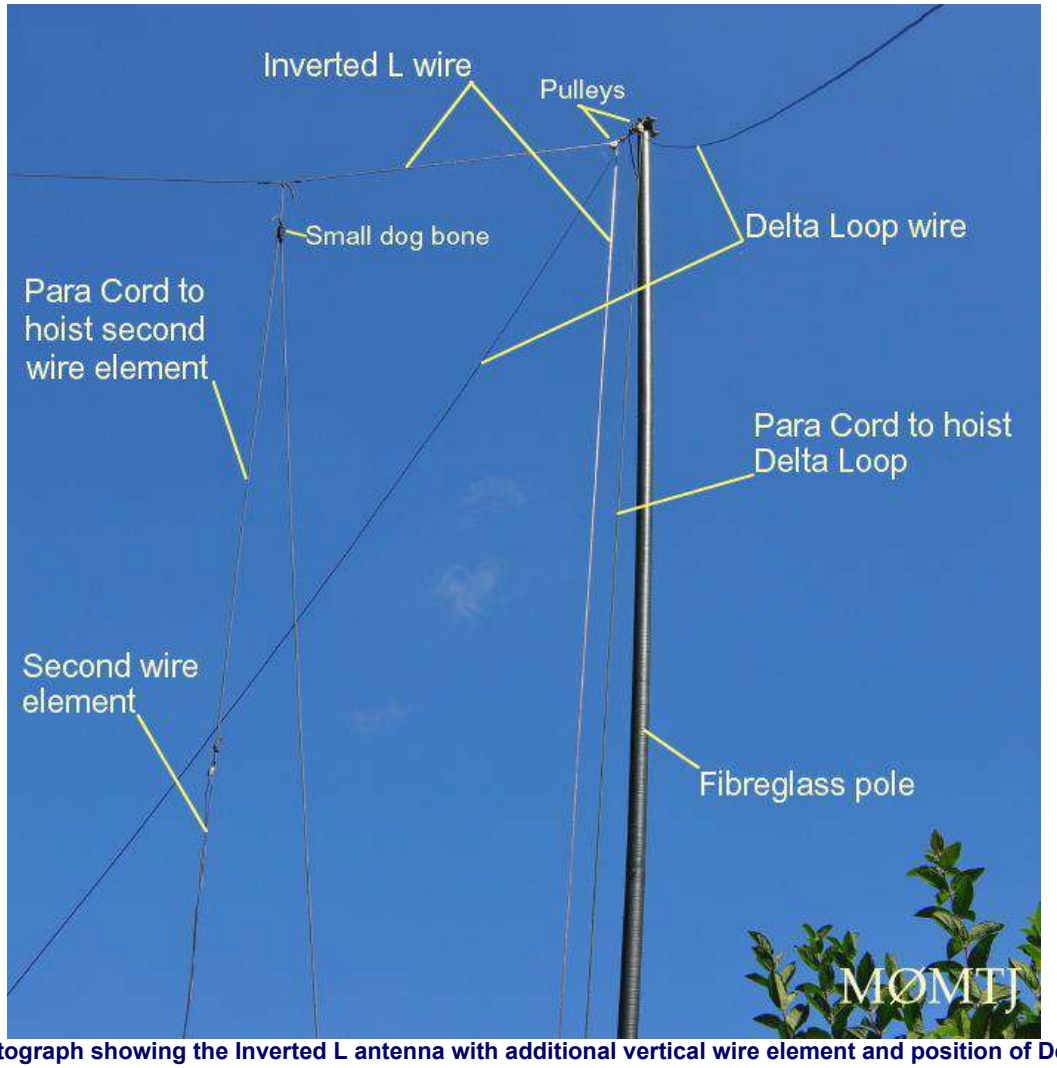

Photograph showing the Inverted L antenna with additional vertical wire element and position of Delta Loop

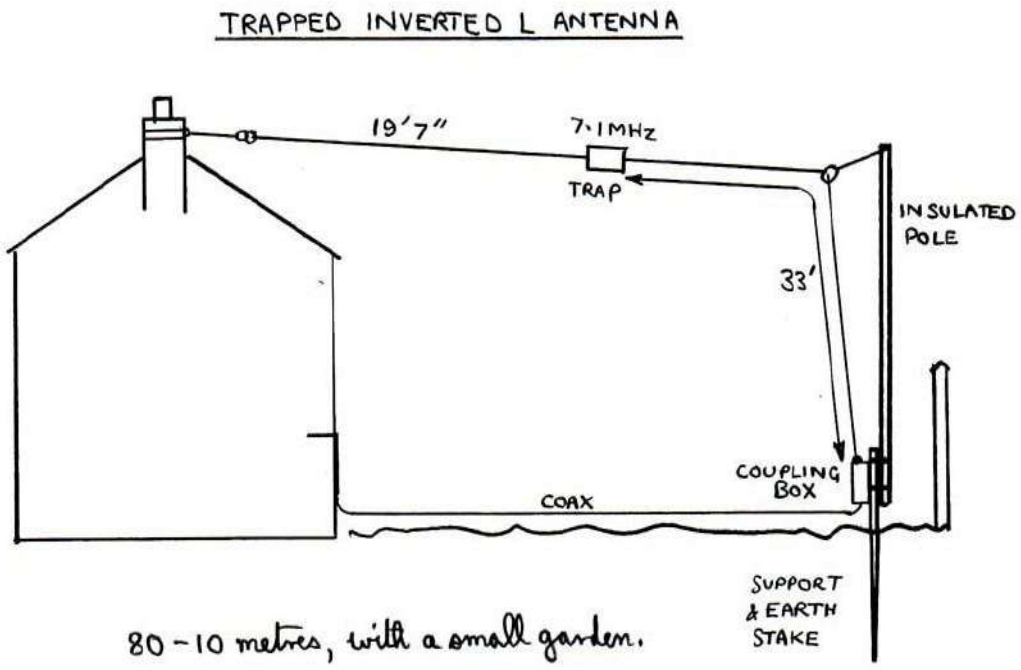

The commercial version of the basic 80m - 10m Inverted L is available from Tony Nailer at Spectrum Communications

Important notes on effective Grounding by Jim K8OZ

Mike - I was reading about your work on the 160 meter Inverted L, and it makes me want to go out and build some more antennas! Congratulations. Your story is fascinating, and very well documented.

The only thing I can offer as a suggestion is to get as much radial wire along the edge of your property as possible (assuming your XYL will not allow you to bury radial wire all over your yard). Even if you can only run multiple wires 1/8th of a meter apart from each other, and parallel to each other, your losses will be reduced. The ground lossses have quite an impact on your transmitted signal, so any wire you can "hide" along the edge of your property will help improve your signal strentgh - little, by little...! { It may also affect your resonant frequency slightly, but that's easy to deal with by adjusting with an antenna tuner or slightly changing the loading coil. }

Good luck OM, and keep up the refinements on your antenna system. You're doing great! 73,

Jim, K8OZ
Albuquerque, NM

Delta Loop Antenna - Tuned for the 17 metre band but also usable as a multi-band operation

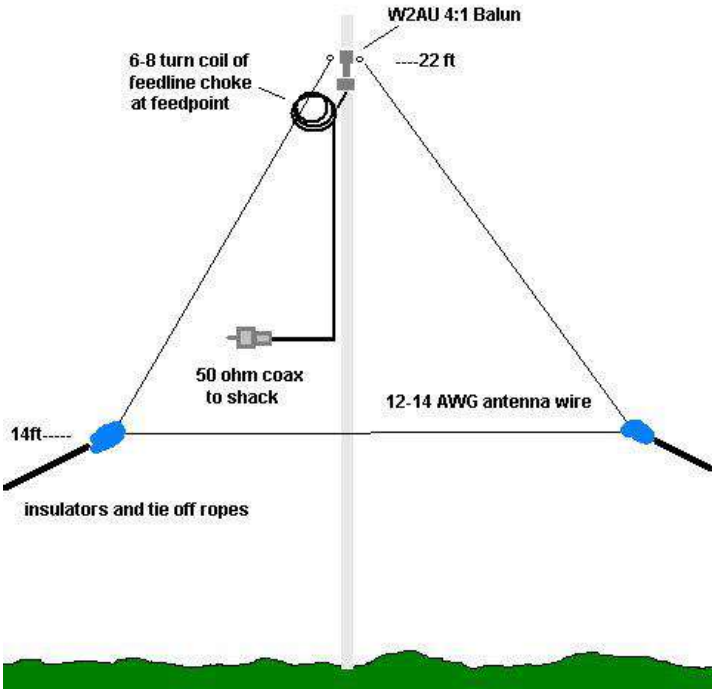

A typical Delta Loop antenna - diagram by W5SDC - gives multi-band operation with minimal cost.
My Delta Loop is fed near the bottom corner - it cannot be fed at the top, as in the diagram above, due to unwanted interaction with the antenna wire of the Inverted L antenna which is supported on the same pole.

My Delta Loop is fed near the bottom at one corner - it cannot be fed at the top, as in the diagram above, due to unwanted interaction with the antenna wire of the Inverted L antenna which is supported on the same pole.

It consists of a 16 metre long loop of wire in triangular Delta shape, hung from the top of the pole supporting the inverted L antenna and fed via RG213 coaxial cable via a home-brew 4:1 balun. A loop is really a single band antenna cut for one wavelength on the band of interest, however it can also work on higher bands with an ATU - as a good, cheap and easy to install multi-band H.F. aerial. Performance is a little better than the inverted L on the higher bands, but on 10 metres the tuned 10 / 6 metre wire 'fan' dipole in the loft can still be better.

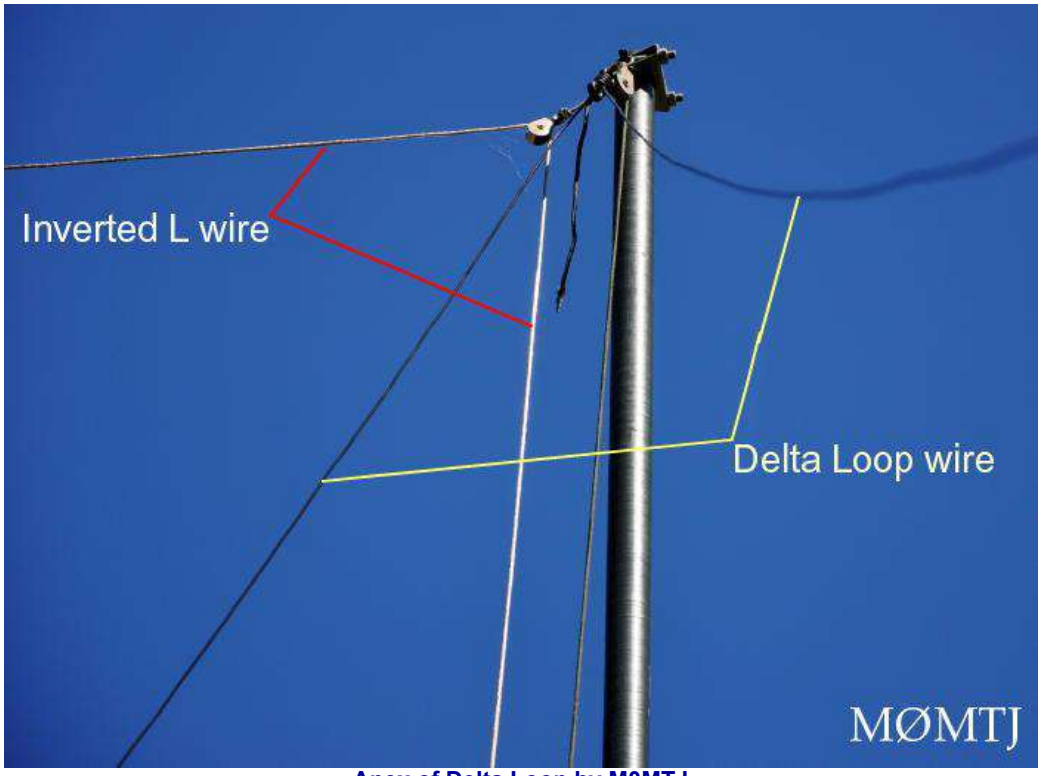

Apex of Delta Loop by M0MTJ

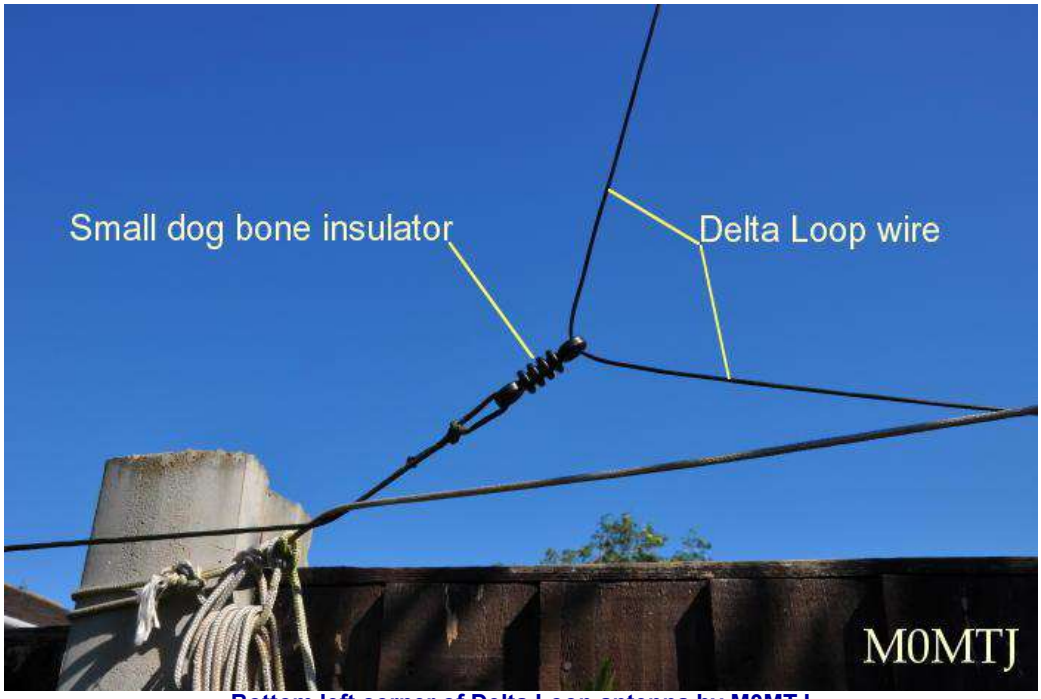

Bottom left corner of Delta Loop antenna by M0MTJ

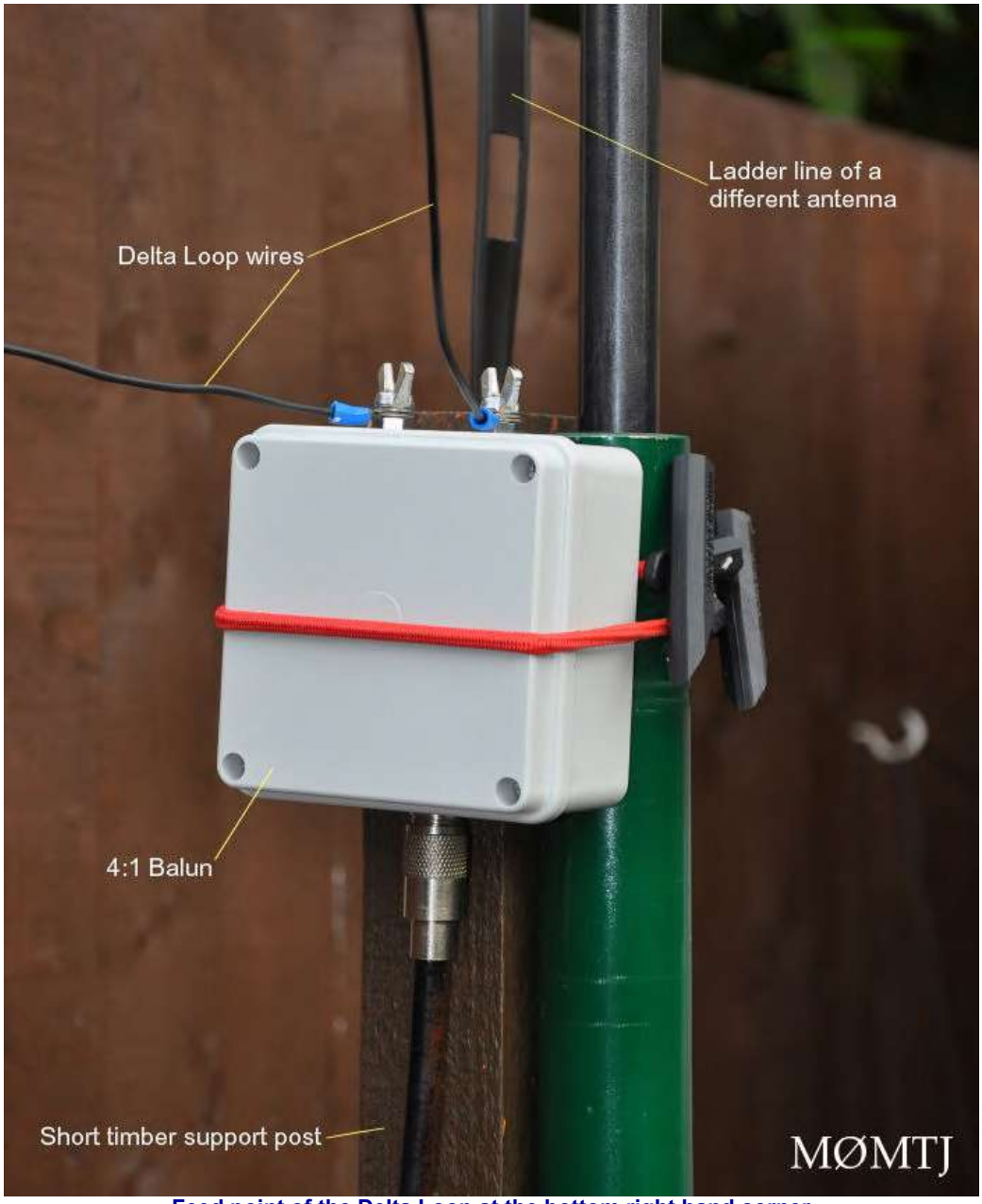

Feed point of the Delta Loop at the bottom right hand corner

The Feed Point of the Delta Loop Antenna is at the bottom right hand corner
The Antenna is fed via a 'home brew' 4:1 balun by M0MTJ

Below are the VSWR measurements for the 16 metre long loop which has been measured an cut for resonance in the 17 metre band. For comparison are the measurements for the 12 metre long loop (which has not been optimised) and an 18 metre long loop which is of arbitrary length:

16 metre long loop of wire for the 17 Metre Band (optimised for 17m band)		
BAND	VSWR	VSWR
20m	14.0 MHz = 6.5	14.35 MHz = 4.9
17m	18.07 MHz = 1.2	18.16 MHz = 1.2
15m	21.0 MHz = 3.1	21.45 MHz = 3.7
12m	24.8 MHz = 5.9	25.9 MHz = 6.1
10m	28.0 MHz = 4.1	29.5 MHz = 4.4

12 metre long loop of wire for the 12 Metre Band (NOT optimised)		
BAND	VSWR	VSWR
20m	14.0 MHz = 22.1	14.35 MHz = 21.1
17m	18.07 MHz = 8.4	18.16 MHz = 8.1
15m	21.0 MHz = 5.0	21.45 MHz = 4.6
12m	24.8 MHz = 1.9	25.9 MHz = 2.0
10m	28.0 MHz = 5.0	29.5 MHz = 6.1

18 metre long loop of wire (An arbitary length between 20m & 17m)		
BAND	VSWR	VSWR
20m	14.0 MHz = 2.1	14.35 MHz = 1.4

17m	18.07 MHz = 2.6	18.16 MHz = 2.5
15m	21.0 MHz = 6.8	21.45 MHz = 8.4
12m	24.8 MHz = 6.3	25.9 MHz = 6.5
10m	28.0 MHz = 2.9	29.5 MHz = 2.5

Many users claim that loop aerials are quieter than typical vertical antennas. There are many plans available in the internet and given a suitable support or pole and a 4:1 balun it can take only a few minutes to install a loop antenna.

Arthur M0PLK (SQ2PLK) at Ham Radio Shop supplies an interesting lightweight self supporting Delta Loop antenna: http://ham-radio.urbasket.eu - see the review on the Polonia DX Award here: http://pdxa.one.pl/articles.php?article_id=17

LOOP ANTENNA LINKS: See lots more links to Loop Antennas on my links page here

Dipole or Doublet Antenna for 20m and 10m

This is an antenna trapped dipole for 20m and 10m. Currently it is fed by 75 ohm twin feeder to a 1:1 balun in the loft, then on to the ATU (AMU) via a short RG213 coaxial cable. Although it was initially installed horizontally, it is now installed with one leg supported vertically on a 7 metre fibreglass 'Sota' pole with the other leg supported horizontally about 2 metres above the ground. This is a rather unorthodox arrangement for a balanced dipole, but it seems to work ok and was inspired by another radio amateur's idea - although I don't recommend balanced feeder for this arrangement!

It looks much neater than the horizontally strung dipole and offers a more omnidirectional radiation pattern too.

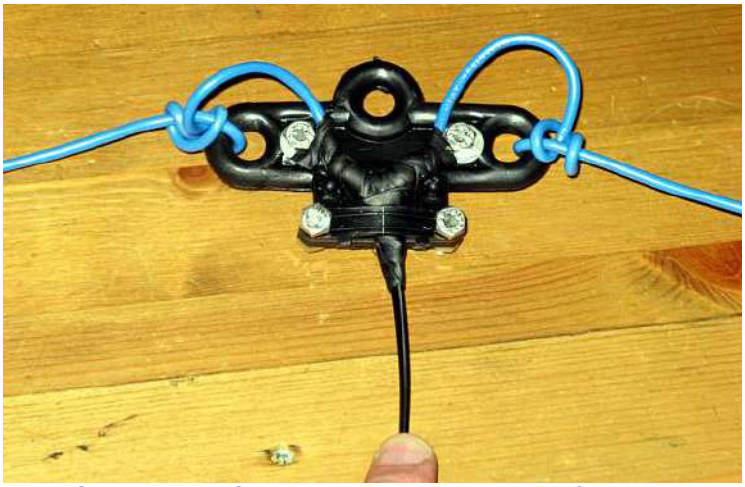

Dipole Centre with PVC covered wire and 75 ohm twin feeder attached.

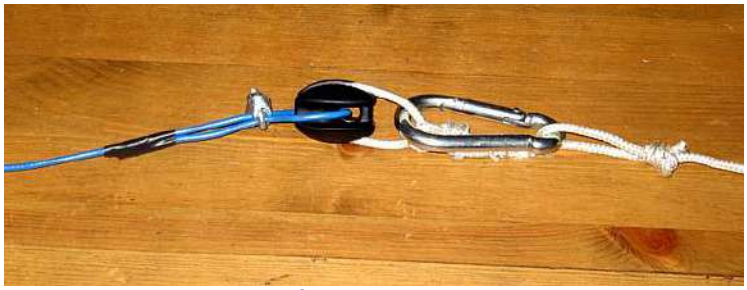

Removable end support method for wire dipole using a plastic antenna insulator, snap-hook and Dacron rope.

Photo showing how the wooden support posts are held in the ground by the steel Met Post.
This Met Post and wooden pole now supports the 7 metre high fibreglass Sota Pole (fishing pole).

The 'deformed dipole'.

A Dipole for 20m and 10m.

One leg is vertical, giving a more omnidirectional pattern and supported by the 7 metre long fibreglass fishing pole, while the other leg runs off horizontally at about 2 metres above the ground.

This antenna is fed by 75 ohm twin feeder.

The Deformed Dipole

Compact Antenna for Top Band

A Shortened Inverted L for 160 Metres

Despite the dreadful noise on top band caused by modern electronic gadgets and the difficulty in accommodating a necessarily large aerial in a small garden, I was keen to try to get on to top band. I experimented with some different ideas during 2009, some of which are shown on this page.

Eventually I settled on the design shown below. It is an Inverted L type aerial, shortened by the use of a loading coil. It uses a fibreglass telescopic fishing pole to allow it to be easily lowered out of sight when not in use. Read more on Antennas page 2 here>

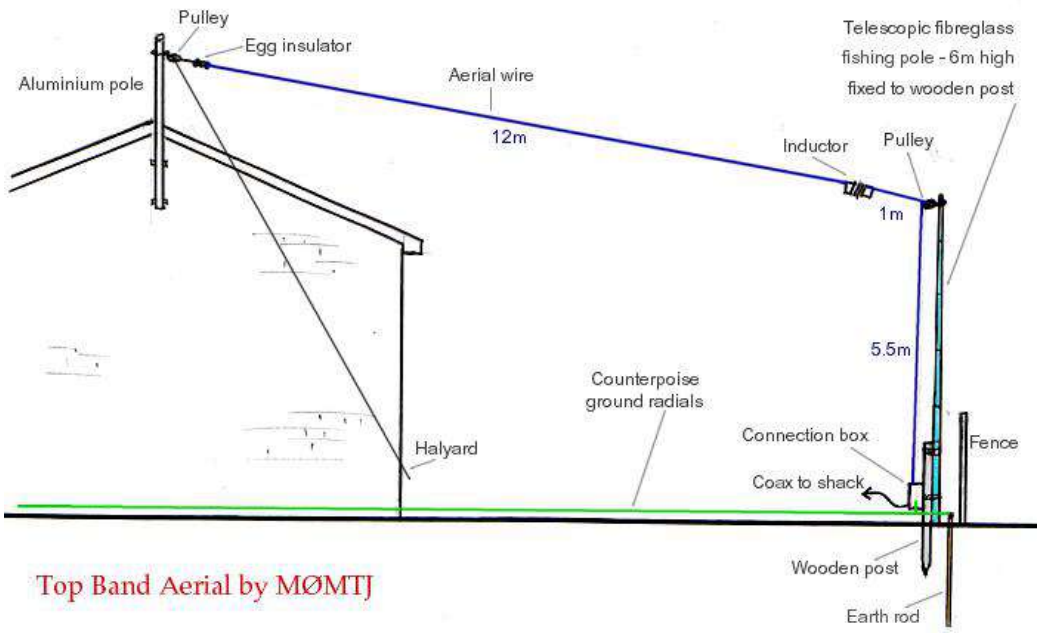

Shortened Base Loaded Top Band Antenna For Small Gardens
uses a fibreglass telescopic fishing pole to allow it to be easily lowered out of sight when not in use.

Read more about Top Band Antennas on Antennas page 2 >

Other Antennas:

End Fed Zepp Antennas for 20m / 17m and 15m :

High quality commercially built Zepp antenna from G Whip Antenna Products.
http://www.gwhip.co.uk/

Above is a high efficiency, high quality commercially built Zepp style antenna using a half wave radiator. However there is a difference - unlike the traditional Zepp antennas, G4ICD's design dispenses with the long trailing 1/4 wave twin feeder matching section and counterpoise and, instead, uses a G-Whip's helical tuned unit.

The end fed Zepp is extremely versatile - it can simply be hung from the fascia board or guttering just outside one's window: The 1/2 wave wire radiator made of high strength Kevlar is easily sloped down the garden and is a camouflage green in colour so as to be almost invisible. The G-Whip Zepp is supplied with a fascia board insulator, a throwing line with plus cable strain relief and fittings, the IP65 waterproof resin potted box fitted with UHF connectors (SO239) for coax feeder. The Zepp can be mounted vertically (e.g. using a telescopic fibreglass pole), horizontally or sloping and can be ready in a matter of minutes.

I then decided to try an excellent new design developed by Geoff G4ICD - an End Fed Zepp antenna with a difference. The G-Whip End Fed Zepps are high efficiency, resonant mono band antennas utilising a half wave radiator, however this new G-Whip design by G4ICD dispenses with the long trailing 1/4 wave twin feeder matching section and counterpoise and, instead, uses a helical tuned unit. Using versions for 20m, 17m and 15m will enable me to get on the air with the minimum of fuss since the G-Whip end fed Zepp can simply be hung from the facia board or guttering just outside one's window. The high-strength Kevlar, camouflage green 1/2 wave wire radiator is easily sloped down the garden to be almost invisible.

G-Whip Widebander :

GWhip Widebander antenna.

Using the popular idea of feeding a large but non resonant antenna with an impedance converting 9:1 unun.

The G Whip wideband antenna consists of a 9:1 unun of GWhip's customary high quality for best efficiency, two 20metre lengths of kevlar wire for the radiator and counterpoise which provide operation from 3.6MHz to 50MHz. Feed with good quality low loss coax and use an ATU to match. The 20 metre radiator wire can be used as a sloper, or supported by convenient supports such as poles or trees in a straight line or 'dog legged'. I use a shorter radiator wire run up a telescopic fibreglass pole for operation on 20 metres an above.

Dual Band J-Pole :

There is a dual band vertical J-Pole antenna in the loft as a back up for the 2m and 70cm bands.

The excellent Dual Band N9TAX Slim Jim antenna that I use in the loft as a reserve antenna.
More information from Joe N9TAX at: www.n9tax.com
www.ebay.co.uk/itm/VHF-UHF-Slim-Jim-J-Pole-Dual-Band-2m-70cm-Antenna-jpole

Previous Antenna installations:

(2011 - 2013)

1) A trapped Inverted L for 80m and 40m with an SGC-230 auto antenna coupler at its feed-point at the bottom of the garden. RG213 coaxial cable is used to feed the output of the auto-coupler back to the shack. This can be used on all bands from 160 through to 10 metres. The support post is installed at the bottom of the garden with the end of the antenna wire being supported by Dacron rope that is attached to a pulley on a pole at the apex of the roof. A simple, single sloping wire element provides use on the 17 metre band. Although too short to be really effective on 160 metres, Top Band can be tuned by the SGC coupler. A pretty good all-round antenna. more

2) A half wave Wire J-Pole fixed to a telescopic fibreglass fishing pole for 10m. Cheap and effective. more about J-Poles

3) A 'home-brew' omnidirectional, vertical dual band, end fed antenna for 2 metres and 70cm. This is of the Controlled Feeder Radiation design (CFR) by VK2ZOI; effectively an end fed half wave dipole on 2m with an aluminium sleeve to achieve 70cms with a few extra dB's of gain. It is mounted on an aluminium mast 10 metres a.g.l. more

4) A DK7ZB design dual band Yagi antenna, with 5 elements for 2 metres and 8 elements for 70cms, mounted horizontally for SSB. A lightweight antenna rotator is employed and uses a push-up telescopic mast. Height above ground level is again approximately 7 metres. The DK7ZB is an excellent twin band Yagi antenna. more

5) Dual Band Fan Dipole, made from thick loudspeaker wire, mounted horizontally in the loft space for 10 meters an 6 metres. Cheap & effective.

6) (Installed late September 2013) Wire J-Pole antenna for 4 Metres (70 MHz) supported on a 3 metre long telescopic fibreglass pole to be attached to the top of the aluminium push up mast that supports the DK7ZB dual band yagi and rotator,

Other Options that can be deployed on an 'as required basis':

7) Compact Loaded Top Band Antenna, based on a design idea by Stuart Craigen G4GTX more

8 & 9) G Whip End Fed Zepps (EFZ's) for either 20m, 15m or 17m or the G-Whip "WideBander" which is an 'UnTenna' style antenna that can be used for 20m through to 10m using good quality G Whip 9:1 UnUn; useful additions for antenna flexibility. more

10) N9TAX Dual Band Slim Jim (J-Pole) antenna mounted in the loft as a back-up antenna for 2m and 70cms. Very good. more

11) Delta Loop Antenna - 16 metre loop of wire in triangular Delta shape, hung from the top of the pole supporting the inverted L antenna and fed via RG213 coaxial cable via a 4:1 balun. The loop is really a single band antenna cut for one wavelength on the band of interest, however it also can be pressed into service for some higher bands - a good, cheap and easy to install aerial; Often works better than the inverted L on the higher bands, but on 10 metres the tuned 10 metre dipole in the loft is sometimes better. more

(2011)

In mid 2011 I experimented with an excellent N9TAX designed dual band Slim-Jim (J-Pole) antenna for 2m and 70cms. This is made from lightweight 450 Ohm ladder line which can be fixed to the top of a 10m tall fibreglass, telescopic, fishing pole. The N9TAX works extremely well indeed. More information from Joe N9TAX at: www.n9tax.com and buy at: www.ebay.co.uk/itm/VHF-UHF-Slim-Jim-J-Pole-Dual-Band-2m-70cm-Antenna-jpole

N.B. I tried to home-brew the DJB-1 dual band J-Pole antenna using plans published by the ARRL in QST magazine. I wanted a neat antenna that could be enclosed in a protective tube to minimise weathering effects. However trying to tune this antenna at UHF frequencies proved to be frustratingly difficult to do and after two full days work I could not get the thing resonate accurately at the correct frequency. Sadly, for this reason, I cannot recommend the Dual Band J-Pole as a home-brew project.

The N9TAX antenna on the other hand works very well. However it cannot be enclosed in a tube due to the velocity factor effect de-tuning the antenna's resonant frequencies.

(Late 2011)

Due to difficulties with the stability of a lightweight fishing pole as a support I moved back to using the lightweight aluminium telescopic mast, with stays, to support a Watson W-50 vertical dual band collinear for 2 metres and 70 cms FM.

The excellent N9TAX dual band Slim Jim is now installed in the loft.

(Antennas used up until 2010)

1) A trapped Inverted L for 80m and 40m fed by RG213 coaxial cable to the LDG Z-11 Pro antenna matching unit in the shack. This can be used on all bands from 80 through to 10 metres. The support post is installed at the bottom of the garden with the end of the antenna wire being supported by Dacron rope that is attached to a pulley on a pole at the apex of the roof. This excellent antenna is still use. *more*

2) A trapped dipole for 20m and 10m. This was fed by 75 ohm twin feeder to a 1:1 balun then on to the AMU via RG213 coaxial cable. It was initially installed horizontally, but more latterly installed with one leg supported vertically on a 7 metre fibreglass 'Sota' pole with the other leg supported horizontally about 2 metres above the ground. A rather unorthodox arrangement for a balanced dipole, but it seemed to work ok, it looked much neater than a horizontally slung dipole and also offered a more omnidirectional radiation pattern. *more*

4) A compact Inverted L for the 160 metre band - Top Band - shortened with a loading coil. *more*

5) As N9TAX Dual Band Slim Jim (J-Pole) antenna for 2m and 70cms. This was fixed near the top of a 10m telescopic fibreglass fishing pole that I pushed up whenever it was required. *more*

(2008)

W-2000 - Vertical Collinear mounted on a temporary 10m telescopic pole:

I no longer have the Watson W-2000 but this is how it was used previously:

The Watson W-2000 covered VHF (2 metres / 144 MHz) and UHF (70 cms / 430 MHz) and also, rather usefully, 6 metres (50 MHz) too. The W-2000 is 2.5 metres long and enclosed in white fibreglass with three radial elements at the base.

Unfortunately I had nowhere practical to install a separate mast for the VHF / UHF antenna, so this was mounted on top of a 30 foot (10 metre) high telescopic aluminium mast in the back garden. The base of the mast was placed in a handy metal sleeved hole that was already present in a small wall in the garden. Very fortunate indeed!

The antenna is connected to the radio via the very low loss Westflex 103 coaxial cable. The cable was left in place permanently, running from the shack in the front bedroom, up into the loft and out of a small hole in the back of the house, down a drain pipe into the back garden. From there the aerial can be connected as an when required:

When VHF or UHF operation is required I have to connect the coaxial cable to the Watson W-2000, fix it to the top of the telescopic mast, which is very quick using two V bolts and 4 wing nuts, put the mast in the hole and raise it to a good height. I tend to extend it so that the bottom of the antenna is at about 24 feet in the air, the height of the apex of the house, so it is in fairly clear space.

A VHF and UHF aerial needs to be as high as possible since at these frequencies communication is essentially local and 'line of sight' - unless heightened propagation conditions, such as Sporadic E or a Temperature Inversion is prevailing at the time.

Even at 24 feet the mast is rather wobbly, so it was tied down using three nylon guy ropes.

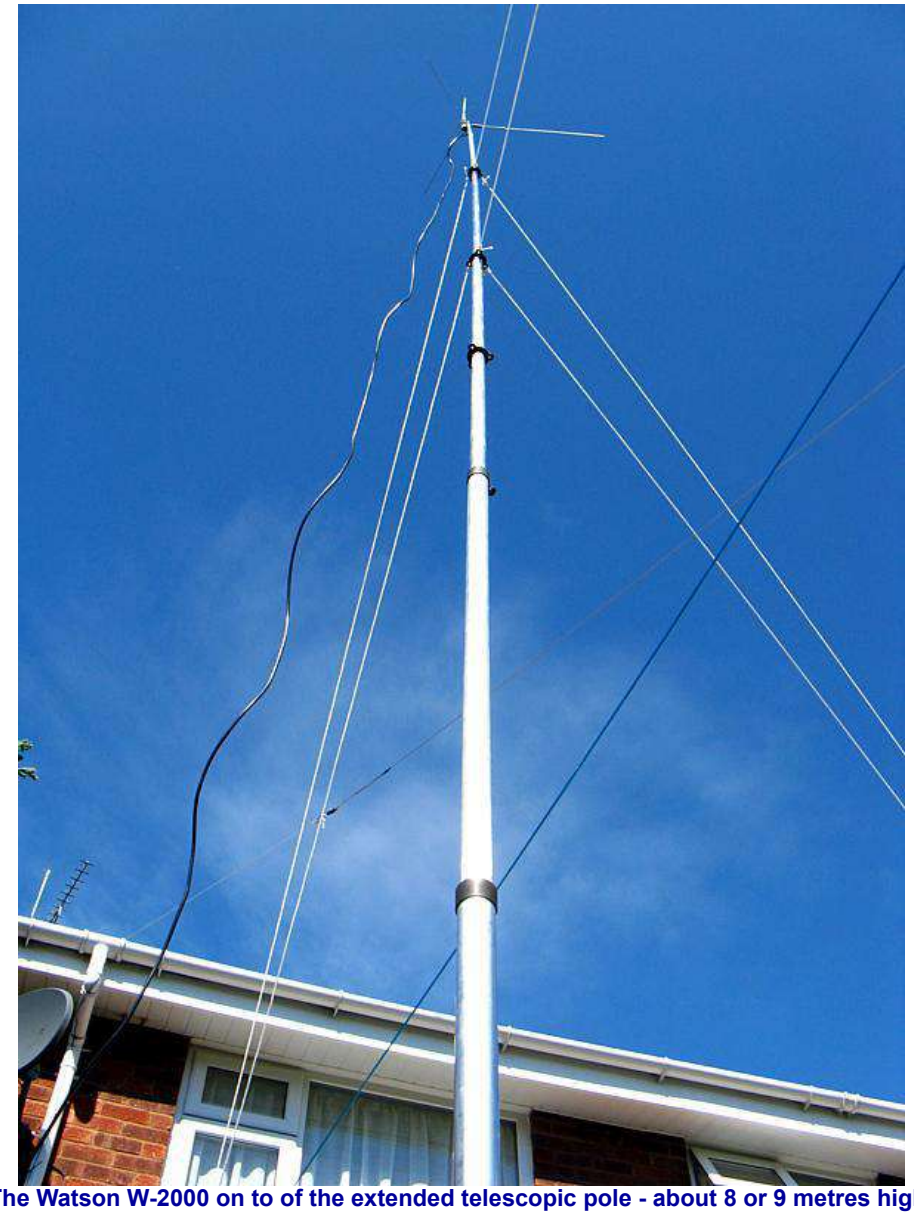

The Watson W-2000 on to of the extended telescopic pole - about 8 or 9 metres high.

Photograph of a Watson W-2000 on Telescopic Mast at the lowest position.

MORE ANTENNAS

Our good friend in Australia Felix Scerri, VK4FUQ, uses Inverted V antennas but also highly recommends the Quad Loop style antenna for HF work. These are well worth investigating, and you can read more here: Antennas 3 with more antenna ideas on Antennas 2 and Antennas 4 and the Links Page here and here

KNOTS FOR SECURING WIRE ANTENNAS

I have found the Bowline to be one of the most useful, it is strong and easy to tie. A Bowline will not slip in any circumstances and, usefully, the more load that is put on it, the tighter it gets. Read more about good knots for amateur radio aerials here...

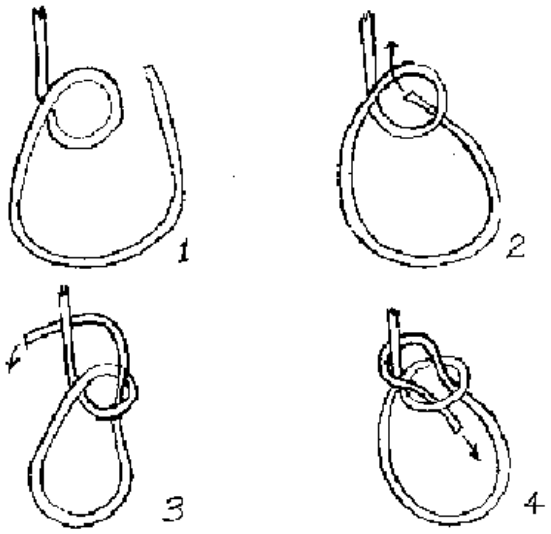

The Bowline Knot - Read more about knots here ...

Antenna Trimming Chart and useful Antenna Rigging Accessory ideas

On Antennas 4 I have included a helpful Antenna Trimming Chart and some useful ideas for Antenna Rigging Accessories

More project ideas here>

73

Mike, M0MTJ 2011 / 2012

Antennas 2 | **Antennas 3** | **Antennas 4** | **Antennas 5** | **Antennas 6**

Links to further reading:

Introducing The All Band Doublet: http://www.cebik.com/content/edu/edu6.html ***N.B. Create a free account at*** http://www.cebik.com

The All Band Doublet - http://www.cebik.com/wire/abd.html

The ALL Band HF Doublet on Ham Universe - http://www.hamuniverse.com/hfdoublet.html

Multi Band Dipoles Compared - by ARRL on QST and DX Zone:
http://www.arrl.org/tis/info/pdf/9611073.pdf http://www.dxzone.com/cgi-bin/dir/jump2.cgi?ID=7499

PDF Document - The W3DZZ Antenna -
http://www.users.icscotland.net/~len.paget/GM0ONX%20trap%20dipole.pdf (**!!! But don't use coaxial cable with a 'choke balun' at the centre of the dipole! Use twin feeder with the Choke Balun at the other end. Less power loss.!!!***)

See Practical Dipole Antennas Compared: http://www.qsl.net/ta1dx/amator/practical_dipole_antenna.htm

Practical Antenna For 160 Metres - http://www.iw5edi.com/ham-radio/?a-practical-antenna-for-160-metres.32
http://www.ik1mnj.net/id202.htm

More:

The website of GM0ONX http://www.gm0onx.co.uk/

The Inverted L - PDF document: http://www.users.icscotland.net/~len.paget/5%20band%20Inverted%20L.pdf

Adding Top Band To The Inverted L - PDF Document:
http://www.users.icscotland.net/~len.paget/Inverted%20L%20adding%20top%20band.pdf

The All Band Inverted L - http://www.antennex.com/preview/archive3/ltv.htm

Q.T.H. Move in 2010 !%*?"*!?!

We decided that we'd like to move house in 2009, we found a new property in early 2010. My amateur radio aerials were duly taken down and the ham shack packed away. However after months of delays we still had not moved by August 2010, but we were still hoping to move. However after months of messing about and stringing us along our buyer pulled out the very day before we were to exchange contracts later in August 2010.

This cost us a lot of time and a great deal of wasted money. Thank you Mrs xxxxxx :-(

After a wasted year we decided to stay where we were and take the house of the market. Instead we spent the next eight months remodelling and redecorating. No time for playing radio of course and besides everything was still all packed away in boxes!

In mid 2011 I was getting frustrated that I had no radio. So I suppose it's time to think about re-establishing the station and to start planning the installation of some antennas. Of course Jules, my XYL, understandably questions my antennas and experiments!

Due to time constraints I will probably start again with a somewhat temporary antenna. I was thinking along the lines of an "Untenna" - so I installed a 7.2 ish long wire supported on a vertical fibreglass pole with a horizontal 'counterpoise' connected via a 9:1 balun to the coax back to the shack. Of course it is a fairly low efficiency multi-band (wideband) antenna, but easy to get going quickly. The GWhip Widebander antenna by Geoff Brown G4ICD is possibly the highest quality antenna of this type available, using a very high efficiency, top quality 9:1 UnUn with a 17 meter wire radiator and 10 metre long counterpoise - a very useful, versatile 'all situations' antenna.

As time progressed I re-established my full size trapped Inverted L antenna for 80metres and 40 metres and added a switchable loading coil at its base for use on 160 meters, as described above.

Then I gradually re-established the 2 metres and 70 cms antennas with the vertical W-50 and horizontal dual band DK7ZB Yagi - as detailed above.

Antennas 2 | Antennas 3 | Antennas 4 | Antennas 5 | Antennas 6

Index To Other Antenna Pages:
Antennas 1 : Aerials used at M0MTJ
Antennas 2 : Including ..... Ideas for compact aerials for Top Band /160 metres
Antennas 3 : Felix Scerri VK4FUQ discusses Loop Antennas, baluns, masts & other antenna related topics
Antennas 4 : Including ..... Many antenna ideas from various sources particularly for multi-band operation & also gives information about
antenna trimming, knots for wire antennas and useful antenna rigging accessory ideas.
Antennas 5 : Including ..... Half Wave End Fed aerials for 144 MHz VHF / 430 MHz UHF and 50 MHz 6 Metre band & J-Pole Aerials
Antennas 6 : Including .... Simple and effective H.F. Antenna ideas - Ground Plane and All Band Doublet

G-Whip Antenna Products
Geoff Brown G4ICD offers a multitude of high quality solutions for portable, mobile and permanent base installations

G-WHIP G Pro Whip antennas
http://www.gwhip.co.uk/

http://www.gwhip.co.uk/

Just For Fun:

A tower that we may like to have to attach our antennas to - but I don't think that Health And Safety was taken into account here:

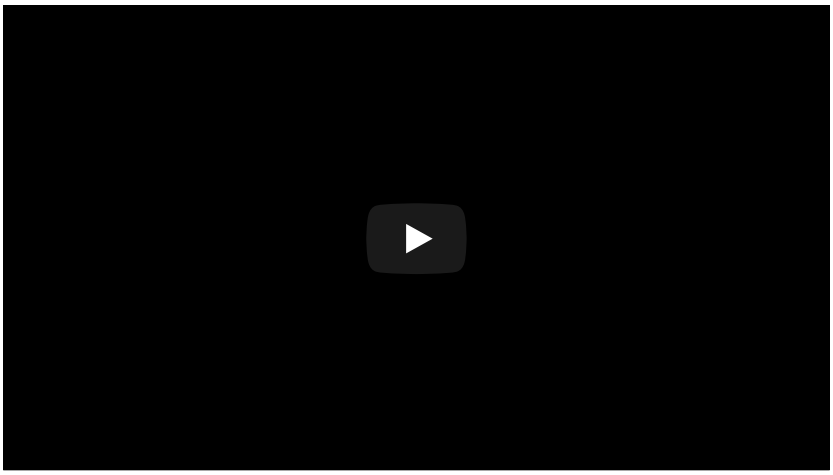

M0MTJ | Operating Conditions | Antennas / Aerials | /P Portable Operating | Accessories | Projects & Kits

Useful Information | Contact MØMTJ | Contact M6ORS | Links to Amateur Radio Sites

RSGB | QSL | The Amateur Radio Mini Site Map

WSPR Weak Signal Propagation Reporter

News, Developments, Events, Photographs and other 'Bits 'n' Bobs'

MDS975 Home

Feedback

Mike Smith - MDS975.co.uk © 2003 - 2016

M0MTJ

Amateur Radio; Ham Radio; Radio; Transceivers; HF; VHF; UHF; Data Modes; Morse Code; RTTY; PSK31; SSTV; FSTV; Amtor; Sitor Antennas; Aerials; Cable; Coaxial Cable; Twin Lead; Masts; Poles; Propagation; Computer; PC; USB Computer Interface; Microphone Loudspeaker; Filters; Noise Reduction; DSP; Digital Signal Processing; Morse Key; SWR ; Inverted L; Inverted V; Dipole; Doublet.

http://www.freeradio.co.uk/

Amateur Radio MØMTJ

MDS975.co.uk HOME PAGE

My Home Page

Amateur Radio
Operating Conditions
Antennas
Accessories
Projects & Kits
Data Modes
Information
Portable
QSL
RSGB Ltd
Links
QRM
Bits 'n' Bobs
Contact

WSPR
Weak Signal Propagation Reporter

PORTABLE

Site Map

MDS975 Home

Feedback

PLT QRM

Site Search
Find
powered by FreeFind

M0MTJ | Operating Conditions | Antennas / Aerials | /P Portable Operating | Accessories | Projects & Kits | Useful Information
Contact MØMTJ | Contact M6ORS | Links to Amateur Radio Sites | RSGB | QSL | The Amateur Radio Mini Site Map
News, Developments, Events, Photographs and other 'Bits 'n' Bobs' | WSPR Weak Signal Propagation Reporter

AERIALS (ANTENNAS) 5

Antennas 1 | Antennas 2 | Antennas 3 | Antennas 4 | Antennas 6 | Antennas 7

Index To Other Antenna Pages:
Antennas 1 : Aerials used by M0MTJ
Antennas 2 : Including ideas for compact antennas for Top Band /160 metres
Antennas 3 : Felix Scerri VK4FUQ discusses Loop Antennas, baluns, masts & other antenna related topics
Antennas 4 : Many antenna ideas from various sources particularly for multi-band operation & also gives information about
antenna trimming, knots for wire antennas and useful antenna rigging accessory ideas.
Antennas 5 : Half Wave End Fed antennas for 144 MHz VHF / 430 MHz UHF and 50 MHz 6 Metre band & J-Pole Aerials
Antennas 6 : Simple and effective H.F. Antenna ideas - Ground Plane and All Band Doublet
Antennas 7 : Omni-Directional - Circularly (Mixed) Polarized Antenna for VHF / 2 Meters.

The VK2ZOI "Flowerpot Antenna" - A physically end fed Half Wave "Coaxial Dipole" for 2 metres and 70 centimetres

For 2m and 70cm FM I use a mounted on a lightweight aluminium telescopic pole on the apex of the hose. The base of the antenna (the bottom of its radiating element) is approximately 11 metres above ground level. This antenna is based on the Controlled Feeder Radiation principle (CFR) and is described by VK2ZOI on his website. Also known as a "Coaxial Dipole". My version is described below.

Also seen in the photograph are the ropes that support the H.F. wire aerials.

G-Whip Antenna Products
Get on the air with
TOP QUALITY
BRITISH
G-WHIP
ANTENNAS

Home brew dual band vertical antenna for 2 metres and 70 cms
(Coaxial Dipole / Controlled Feeder Radiation Antenna / 'Flowerpot Antenna')

VK2ZOI has produced some extremely interesting and potentially very useful dipole antenna designs. The designs could form the basis for a great home-brew antenna project since it is physically end fed and can also be made into a dual band aerial for 2 metres and 70 centimetres, so forming the basis of a viable alternative to buying an expensive commercially manufactured 'white stick' antenna.

The final dual band version works very well and can form the basis of a viable alternative to commercially made 'white stick' antennas, because there's nothing better than using your own home-brew antenna!

Physically, the feeder cable enters the antenna at the bottom end, so it looks like an end fed aerial. VK3TWO / VK6TWO describes it as a "Coaxial Dipole". 'Electrically' it is a simple dipole. The RF is travelling 'inside' the bottom 'element' and doesn't 'feed' the antenna until where the coax is cut - in the centre of the antenna, as shown in the diagram below. Where the outer braid is cut (electrically the centre feed point), the RF then radiates like a simple dipole, via the top radiator (coax core), and via the outside of the coax - the bottom half of the dipole. The top radiator is thinner than the lower radiator (hence why the lower radiator is slightly shorter than the upper radiator).

The coiling of the coax is simply forming an RF choke (high impedance point), to stop the RF continuing down the outside of the braid, thus electrically it 'appears' to be the end of the radiating element.

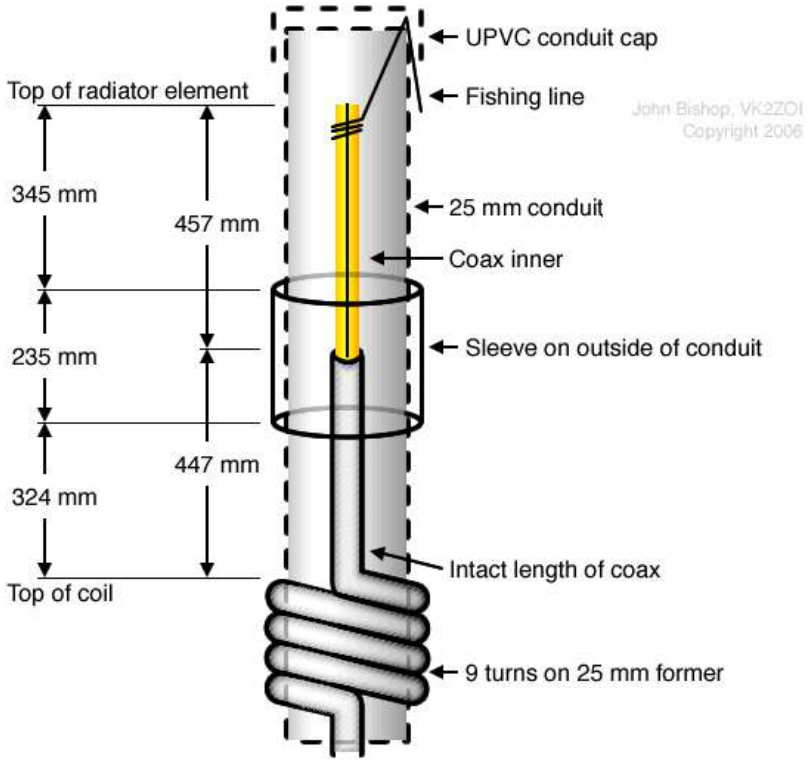

http://vk2zoi.com/articles/half-wave-flower-pot/

I purchased a 3 metre length of 25mm diameter conduit from B&Q, our local DIY centre and ordered some 25mm end caps and heatshrink from ebay. I already had some good quality RG58 for the feeder and main 2 metre radiating element and some aluminium foil for the 70cm sleeve dipole.

First of all I cut the RG58 cable to form the 2m radiating section and choke coil. Because the UK's 2m allocation of 144 to 146 MHz is narrower than the 144 to 148 MHz available in Australia, I varied slightly from the design shown. The centre of the UK's 2m band is about 1% longer in wavelength, so I decided to make both the top and bottom measurements 1% longer.

I therefore stripped 460 mm of the outer sheath and braid from the cable to form the top 1/4 wave element of the dipole. I then measured down 450 mm and marked the point where the lower 1/4 wave element would finish and the choke coil would start.

Next I attached a thin nylon cord to the top of the top radiator, the coax inner.

I then cut the 3 meter length of 25 mm conduit down to about 2.3 metres and drilled a hole where the coil would start, wound 9 turns of RG58 cable from that hole and marked the position of the lower hole. I then removed the coaxial cable and drilled the second, lower, hole.

I then pushed the radiating section of RG58 into the top hole and fed it up towards the top of the tube, stopping when the marker tape reached the hole. I then wound the coil and pushed the remainder of the RG58 through to lower hole and fitted a PL259 plug on the end.

I pulled the top of the radiator wire tight using the nylon cord and pushed the end cap on. The antenna was then ready to be tested on the 2 metre band. I found that the resonant frequency was rather too high, just above 146 MHz, so I pushed an additional 10 mm of coaxial cable into the upper section of the tube - therefore making the lower 1/4 wave section of the dipole 460 mm long - the same as the top section. I tightened up the choke coil winding again and performed another test.

This time the resonant point was just over 145.000 MHz - near enough the centre if the UK's 2 metre band. That was perfect, so the 70 cm sleeve element was then added - this is a 235 mm long tube of kitchen foil positioned exactly at the centre (feed) point of the 2 meter dipole within the tube.

The SWR was tested and found to be acceptable across both the 2m and 70cm bands.

I then fitted the end cap, applied the heatshrink to the coil and to the aluminium foil sleeve. I noticed that when the antenna tube was moved around the cable inside rattled around making a noise that may be rather annoying to anyone near its final location.

To help hold prevent the cable from rattling I pushed up 4 or 5 small pieces of foam material up the tube from the bottom to rest at various positions along its length. With these pieces in place the cable was certainly silenced, however it may have had a deleterious effect on the SWR.

With the antenna now in its finished physical state I naturally checked the SWR again to compare against the performance in its semi-complete state. I was pleased to find that the SWR was still fine across the 2m band, in fact the SWR was a little lower. However the SWR at the edges of the 70cm band was considerably higher - 1.8 at 440 MHz and about 2.2 at 430 MHz.

I conjectured that the heatshrink covering the foil sleeve dipole may have caused the change in response so I removed it, but the SWR was little different and the bandwidth on 70cm was now disappointingly narrower than expected and hoped for.

Although I cannot say for certain, because they cannot now be easily removed, but it may be possible that the pieces of foam may be the culprits for the difference.

While the bandwidth could not be improved, I decided to move the centre point of resonance down a little by increasing the length of the sleeve element from 235 mm to 245 mm. With that adjustment the SWR was now approximately 1.6 at 430 MHz but rising to 2.0 at 440 MHz. (Unfortunately I forgot to note the exact figures down in all cases).

When the antenna was connected to the 20 meter length of Westflex-103 back to the shack, the SWR reading were as follows:

2 Metres - SWR		70cms - SWR	
144.00	1.3	430.00	1.2
144.50	1.2	431.00	1.4
145.00	1.2	432.00	1.4
145.50	1.2	433.40	1.0
146.00	1.2	434.00	1.3
		435.00	1.8
		436.00	1.6
		437.00	1.0
		438.00	1.5
		439.00	2.0
		440.00	2.1

The SWR readings in the shack for 2 meters are lower than at the feed point, which is presumably due the losses in the feeder. The SWR readings for 70 cms look rather erratic, with a strange peak at 435 MHz, while the 430 MHz figure is lower than at the feed point of the antenna, and the 439 and 440 MHz figures are disappointingly higher than hoped for. The peculiar readings are likely due to feeder effects.

However the SWR at 433.4, in the FM simplex portion of the band, is very low.

The completed antenna was mounted to the aluminium mast by utilising brackets of the Watson W50 antenna. The brackets had to be reversed so that the narrower diameter of the 25mm tube could be held in place by the V Bolt, while the circular section that previously fitted over the base of the W50 now slid over the mast, which was coincidentally a similar diameter.

I made a small addition to the design in the form of a second small 150mm length of of the 25 mm conduit glued to a coupler section. This is slid into place at the bottom of the antenna to provide additional weather protection to the joint between the W-103 feeder and the RG58 of the antenna - which itself is covered in self amalgamating tape.

Shown in the table below are some signal comparisons with the Watson W-50 antenna; both were mounted on the same mast in the same position and at a height of approximately 7 metres above ground level. Becuase the S-Meter of the transceiver is not calibrated in absolute values, the figres are for relative comparison only - also bear in mind that a typical S Point represents 6dB - therefore the accuracy of these readings will be coarse and might be considered to be +/- 3dB - that's a rather wide variation.

Despite the relative crudeness of these comparisons, the results do seem to indiacte that the VK2ZOI antenna is marginally or slightly better than the W-50 on 2 metres and marginally worse on 70cms. I am quite pleased with this result and beleive that this antenna really could replace the need to buy an expensive commercially manufactured antenna.

My only concern with this type of antenna is that there is no path to ground from the top element, as there would be with a folded dipole or a J-Pole type antenna. This may be a cause for concern as far as static build up is concerned.

Signal comparisons		
	Watson W-50	**"Flowerpot Antenna"**
2 Metres		
Station A	S7	S9
Station B	S5	S6
Station C	S4	S4
Station D	S9	S9
Station E	S6	S6
Station F	S0	S1
Station G	S2	S2
Station H	S2	S3
Station I	S6	S6
70 cms		
Station J	S0	S1
Station K	S5	S5
Station L	S5	S4
Station M	S0	S0
Station N	S9	S9
Station O	S6	S6
Station P	S7	S6

Please see the photographs below for a visual explanation of this project. Mike, MØMTJ. 05/03/2013

First stage of construction of the 2m / 70cm dual band antenna
Cutting the 25mm diameter conduit to the desired length and drilling
the two holes allowing the coil to be wound. MØMTJ

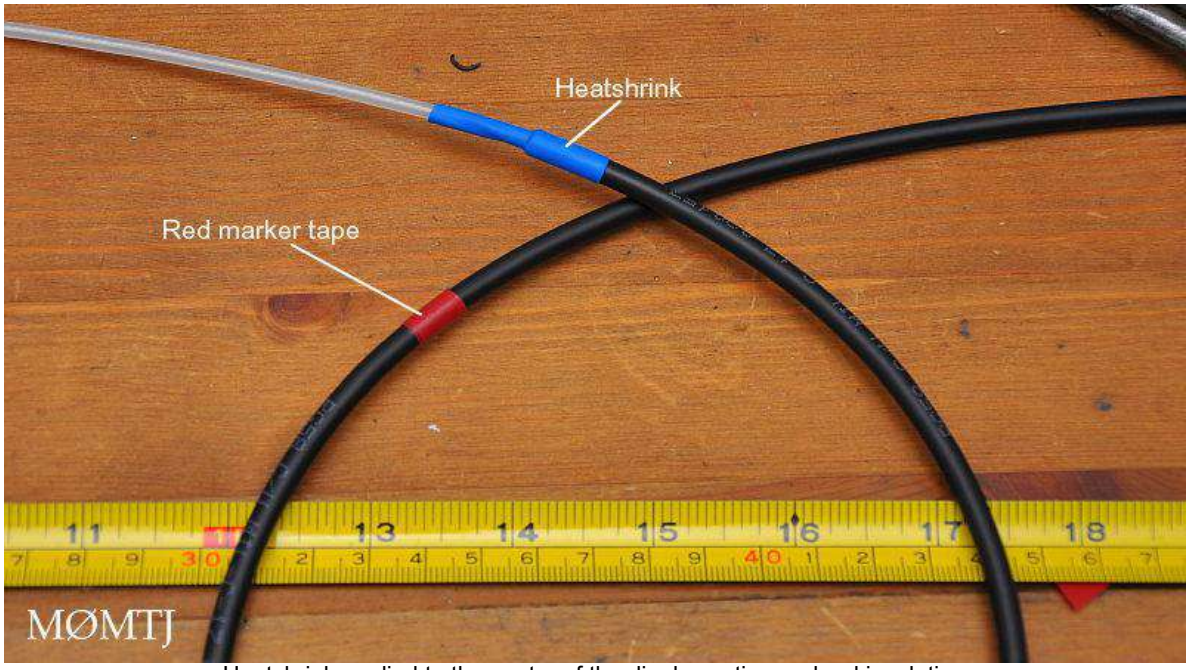

Heatshrink applied to the centre of the dipole section and red insulation tape added to mark the bottom of the dipole where the coil starts. MØMTJ

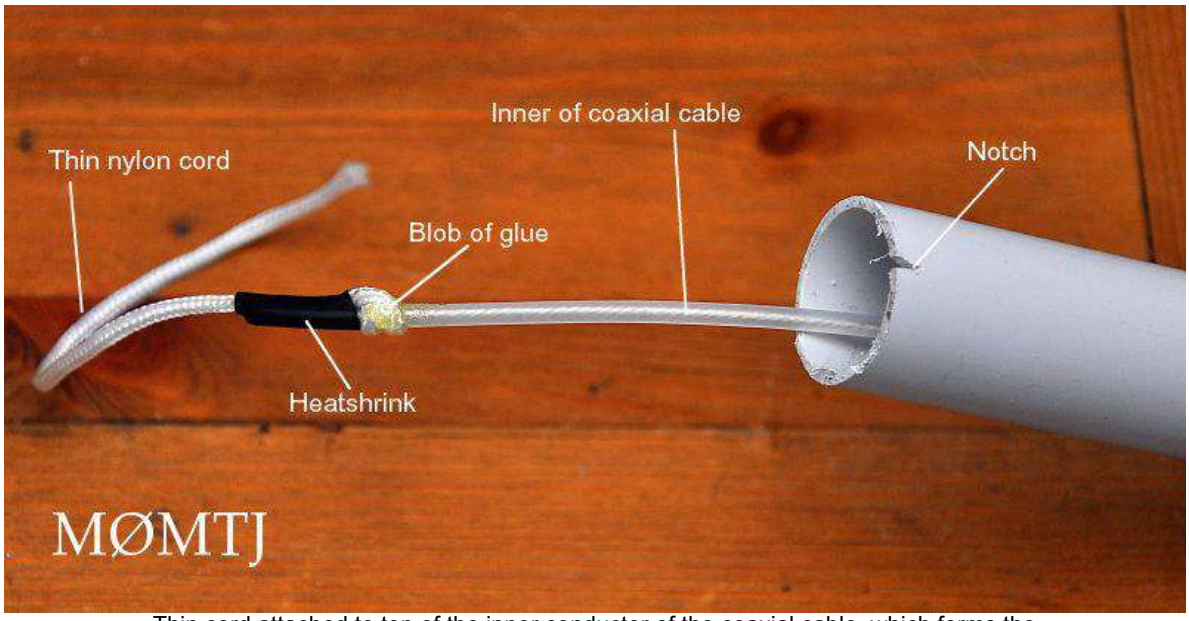

Thin cord attached to top of the inner conductor of the coaxial cable, which forms the top 1/4 wave section of the dipole with a piece of heatshrink and a blob of glue. MØMTJ

The line isolator choke is formed by winding 9 turns of the RG58 coaxial cable around the 25mm diameter conduit tubing. MØMTJ

The thin cord that holds the 1/4 wave radiator in place is located in the notch and will be trapped in place when the end cap is fitted. MØMTJ

After testing, the coil was covered in heatshrink to prevent water entering the plastic tube.

The foil sleeve dipole for 70cms is covered in heatshrink.

Oops. Lesson learned. When applying heat to the heatshrink I held the tube above the ground and the plastic of the tube started to go soft and bend out of shape. The buckle in the tube can be seen in this photograph.
Lesson: When applying heat, keep the tube flat on the ground or work bench and roll the tube along as the heatshrink shrinks into place ensuring that the tube does not distort or bend.

25 mm end cap sealed in place by heatshrink.

The completed antenna in place, mounted at the top of my aluminium push-up mast. The fixings used are the brackets from the Watson W-50 antenna which have been reversed so that the smaller diameter PVC tube is held in place by the V Bolts.

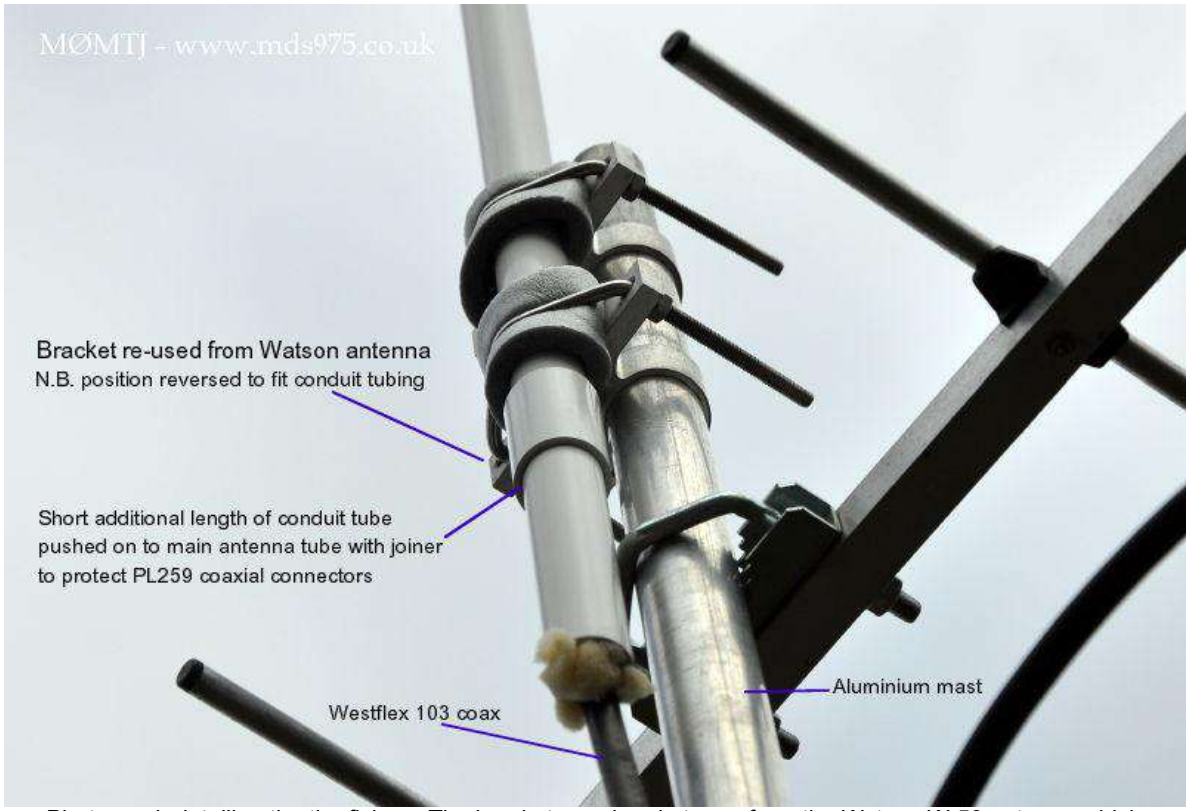

Photograph detailing the the fixings. The brackets are brackets are from the Watson W-50 antenna which have been reversed so that the smaller diameter PVC tube is held in place by the V Bolts.

For further detailed information and reading, please visit the excellent website of John Bishop VK2ZOI here:
http://vk2zoi.com/articles/half-wave-flower-pot/

6 Metre Half Wave Coaxial Dipole - An end fed CFR Dipole antenna supported by a 3 metre long fibreglass fishing pole for 50 MHz

In 2014 I decided to remove the 4 Metre J-Pole antenna from my push-up mast due to the fact that the band is relatively quiet and that I only have the 5 watt Wouxon handheld transceiver for 70 MHz.

I decided that having a good, full size antenna, for the 6 Metre band would be more useful and potentially more rewarding since it can be used with a 100watt HF radio that covers 50 MHz.

The choice of antenna was an easy one. With the great success of the "flowerpot antenna", I decided to build a version for 6 Metres.

Similar designs of Coaxial Dipole antennas had also been featured in recent editions of the RSGB publication RadCom during 2012 and 2013. The antennas in RadCom are described as Controlled Feeder Radiation (C.F.R.) Dipole antennas - the tuned choke at the feed-point controlling, or choking off, the common mode current that would otherwise flow down the outside of the coaxial feeder cable causing E.M.C. issues on transmit, high S.W.R. reduced efficiency and noise on receive. See references below

The advantage of this design is that it can be physically end fed, so there is no feeder cable to route away from the centre of the dipole. Electrically, however, the feed point is at the centre of this dipole aerial, as explained earlier.

Rather than fit the antenna inside a PVC pipe, as with the previous dual band 2m / 70cm antenna described above, I decided to use a lighter weight and less conspicuous 3 metre long fibreglass fishing pole as the support. The completed radiating element simply being taped to the fishing pole.

I cut a length of MIL spec RG58 cable, about 4.5 metres long, to form the bottom half of the radiating section and the choke coil, leaving enough to form a short length (about 30 cm) of cable below the choke coil on to which is soldered a PL259 plug.

The choke consists of 15 turns of the RG58 coaxial cable wound on a 50mm diameter plastic former cut from the empty tube of a cartridge gun that previously contained silicone sealant - allowing a 30cm tail on to which the PL259 plug is fixed on one side and and about 1.31 metre length on the other side that will form part of the radiating element.

The half wave radiator therefore consists of a quarter wave bottom section of the RG58 cable and a quarter wave top section consisting of a length of multi-strand (single conductor) P.V.C. covered antenna wire.

A quarter wavelength at the mid point of the 6 Metre band is: 300 ÷ 51 MHz = 5.88 metres ÷ 4 = 1.47 metres

Due to velocity factor the actual length of the quarter wave sections will be shorter. With the materials that I used, I found that a factor of about 87% was about right, the 1/4 wave length being 1.29 metres.

The top tip of the bottom 1/4 wave section of the coaxial cable is stripped of about 2 cm of outer sheath and braid leaving the length of braided section, measured from where it exits the coil, 129 cm long. The inner conductor is then stripped of 1cm of insulation. This is effectively the centre point of the dipole. To this point is soldered the 129 cm length of the P.V.C. covered aerial wire to form the top half of the antenna. In practice, use a slightly longer length of wire, and then fold over the excess to for the 129 cm length - this can then be used to adjust for lowest SWR at 51 MHz.

The length of the radiating section was therefore about 260 centimetres, plus about 13 centimeters for the coil former giving a total length of 273 cm. This allows about 27 cm of the bottom section of a 3 metre fishing pole to be used to fix to a supporting pole or mount - e.g. to the top of an aluminium mast.

Drill four small holes in the choke former so that when the fishing pole is placed through the centre of the former it can be fixed to the pole using two cable ties.

The radiating section (coax and PVC covered wire) is fixed to the top section of the fishing pole with good quality insulating tape.

The aerial can now be temporarily fixed to the mounting pole using suitable brackets - taking care not to crush the delicate fibreglass! Connect the PL259 plug to the antenna feeder cable using an SO239 back-to-back coupler and test the SWR with an antenna analyzer or SWR bridge. The lowest SWR should be centred on 51MHz and be low - less than 1.5. My reading was 1.2.

If the point of lowest SWR is significantly away from 51 MHz and/or the SWR at the band edges is too high (i.e. over 2) then length of the radiator will need to be adjusted. If the point is too low in frequency, the antenna is too long and will need to be shortened. If the point is too high in frequency, the antenna is too short and will need to be lengthened.

Adjustment can be achieved by pulling the coax through the coil to make it longer, or pushing the coaxial cable back

into the coil to make it shorter. Also ensure that the coil winding are adjusted to that they remain tight and neat. The top PVC covered wire section will also need to be lengthened or shortened accordingly by adjusting the folded over section.

Note that in practice, to obtain the very lowest SWR, the top PVC covered wire section may need to be slightly longer by perhaps 1 or 2 centimetres. This is probably due to the fact that the velocity factor of the PVC covered antenna wire is a little greater than the coaxial cable.

Once the antenna is adjusted correctly, ensure that the wires are securely taped to the fishing pole. Connect the permanent antenna feeder to the aerial using the SO239 coupler and weatherproof the joint thoroughly using self amalgamating tape. Use the very best quality coaxial cable possible to ensure lowest loss. I use Westflex 103, but consider MIL Spec RG8 or RG213 as the minimum standard.

50 MHz Coaxial Dipole / Controlled Feeder Radiation Antenna / 'Flowerpot Antenna'
A physically end fed fed half wave dipole antenna for 6 Metres

Choke Coil - 15 turns of the RG58 coaxial cable on a 50mm diameter former

VHF Band II Broadcast Band antenna for 88 to 108MHz -
Physically end fed, Coaxial Dipole / Controlled Feeder Radiation Antenna (CFR Dipole) for VHF broadcasts

I used a 2 metre long length of 25mm white plastic pipe, strengthened with with a 2 metre length of 21.5mm overflow pipe pushed up the inside.

The radiating element is made from good quality 75 Ohm coaxial cable. Since VHF/FM broadcast tuners are designed to be fed with 75 Ohm coaxial cable, use high quality, low loss double shielded satellite grade coaxial cable for the feed between the aerial and the radio tuner. Use satellite F type connectors and joiners for lowest loss.

The top half of the radiating section is 670mm of the centre conductor (or a length of multi-strand PVC covered wire). The bottom half of the dipole is 650mm of the complete coaxial cable - choked off at the bottom by the coil section. The top part is held in place by a a short length of thin nylon cord, trapped in place by the top PVC cap. The cap itself is sealed on the outside by some self amalgamating tape.

The choke coil is 22 turns of the 75 Ohm coax wound around the 25mm pipe. Tightly spacing the windings of the coil will minimize the bandwidth covered but provide the lowest SWR at the centre point. A looser winding of the coil will widen the bandwidth covered, but lowest SWR achived will be a little higher.

Once the tuning of the radiating elements, coil winding and band coverage has been checked with an Antenna Analyzer, the coil section should be covered with heat shrink, taking great care not to overheat and deform the plastic pipe.

The actual final dimensions (as shown below) may well need some adjustment in length due to differences in cable and type of pipe used. However, with the dimensions shown, I achieved a minimum SWR of 1.3 at 97.4 MHz. The band edges at 88MHz and 108MHz were at an SWR of around 3.8 to 4.0 - which is probably OK for broadcast band reception. The frequency of lowest SWR can can be changed, if desired, by changing the lengths of the radiating sections - slightly longer for a lower frequency and slightly shorter for a higher frequency.

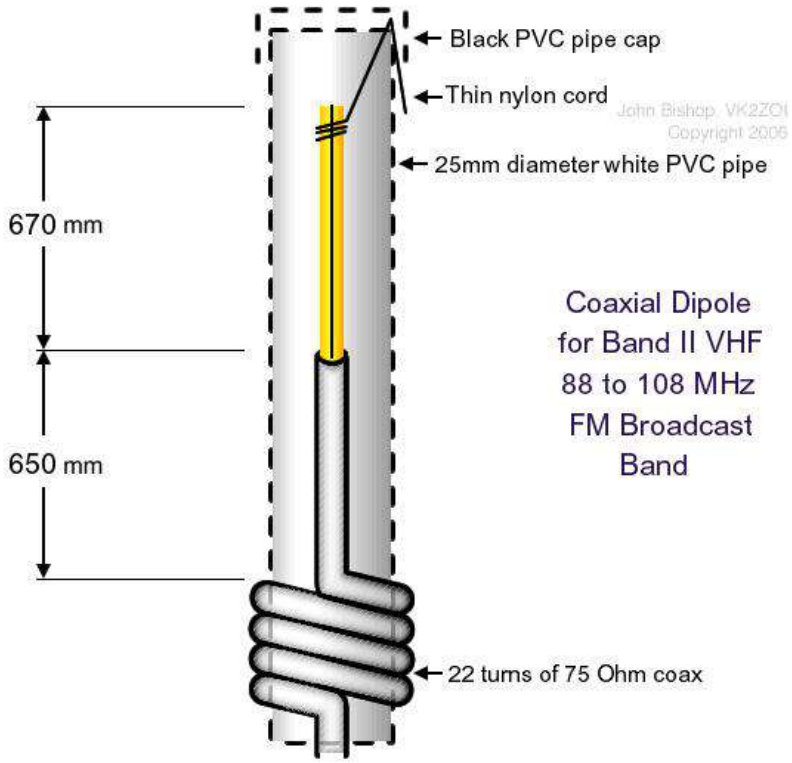

Coaxial Dipole for the 88 to 108 MHz Band II Broadcast Band
An effective, cheap and simple vertical antenna that is fed at its base

RSGB RadCom Articles:

The Controlled Feeder Radiation Dipole. Peter Dodd. RadCom, September 2012, page 22.

More On The CFR Dipole and Coax Chokes. Peter Dodd. RadCom, October 2012, page 54.

VHF CFR Dipoles and More on Common Modes Chokes. Peter Dodd. RadCom, January 2013, page 24.

The HAK Chokes Coaxial Dipole. Encouraging results from 2m to 20m. Peter Grant. RadCom, April 2013, page 22.

Join the RSGB to receive your monthly RadCom magazine: http://rsgb.org/main/publications-archives/radcom/

VK3TWO / VK6TWO Comments:

Many years ago when I was working for a Service Centre, by accident we broke a commercial white stick antenna whilst using it for a task it wasn't intended for. I found that inside the fairly expensive commercial antenna the basis for the design was very similar to the coaxial dipole (as I call them).

Our local repeater club calls them "pogo sticks", which I can only assume is due to the coax coil resembling the spring of a pogo stick. This design had RG213 being fed inside an aluminium tube (the bottom radiator), and the outer braid was then terminated to this. The inner of the coax, then terminated to an identical aluminium tube which was of course the top radiator. Where this design largely differs, is that there was also a 1/4 wave stub of coax running parrallel with the bottom radiator (note that this was for single band operation, not dual band). The whole lot then slid inside the typical white tapered fibreglass housing. I didn't cut open the bottom mounting section to see how it was choking the RF, but I assume it had a handful of ferrites inside the metal base (an alternative way of making the RF choke).

The repeater group has built probably hundreds of these and sells them for $40 at local hamfests. We had a 'Jig' made so that all of the measurements were 'pre-marked' etc, and allowed us to mass manufacture them. Last year, we had planned the typical 'working bee' to make about 30 of them, but this time we had a very expensive Anritsu Sitemaster at our disposal. We discovered that the whilst the design we'd used for decades had a good SWR, it actually was far from optimal. With a heap of 'trial and error' (and with excellent visibility of what was really going on via the Anritsu - not just SWR) we were able to fine tune the design.

From memory, we actually needed more turns of the coax than we had been using (10.5 turns from memory), and our cutting measurements altered slightly. As to be expected, the number of turns was largely dependent on the size of the conduit being used, even changing from 25mm to 30mm etc.

We took several screenshots of the final SWR plots etc. These showed that the bandwidth of this antenna as VERY wide from an SWR point of view. I'll see if I can dig some of them up for you if you'd like.

73, Heath, VK3TWO / VK6TWO
MEngSc, GDipCompSc, DipEE
www.spooktech.net

http://www.warg.org.au - The West Australian Repeater Group Inc (WARG) is the largest amateur radio club in Western Australia (VK6).

D.I.Y. J-Pole Antennas - A really simple, quick and very cheap 'home brew' project J-Pole Antennas

J-Pole antennas for 2 meters, 4 metres, 6 metres and 10 metres :

While experimenting with antennas in the garden in the summer of 2012 I thought that it would be good to have a hand-held radio in the shed to do some monitoring and make a few contacts. To improve upon the performance of the 'rubber duck' antenna I quickly made a J-Pole antenna for the 2 metre band.

It is made from a 47cm length of 450 ohm Wireman ladder line as the 1/4 wave matching section, plus a 97cm length of stranded wire as the 1/2 wave radiator. It is fed with 3 metres of Mil spec RG58 c/u coaxial cable that is soldered to the 1/4 wave matching section's impedance matching point at 3.5 cm from the bottom. The coax feeder is wound around some PVC tube to form a choke. The completed antenna is taped to a 2.2 metre long fibreglass fishing pole that I purchased from Poundland (for £1.00). It took about 20 minutes to make followed by some testing and adjustment with the antenna analyser. The fishing pole is lashed to the shed with some cable ties.

This simple antenna works pretty well, but being so low down signal strengths are not huge, but it's pleasing to get on the air with something so simple and cheap!

The Shed Antenna - a 2m J-Pole by M0MTJ
Note the simple choke balun at its base made by winding 8 turns
of the coaxial cable around a small off cut of white PVC water pipe.

The feed point of a J-Pole antenna made from Wireman 450 ohm ladder line.
For the 145 MHz antenna this feed point is 3.5 cm from the bottom of the ladder line section which is on the right hand side in this photograph. The coaxial cable used in this case was Mil spec RG58 c/u. But any good quality, low loss 50 ohm coaxial cable could be used. The wire radiator section is connected to the same conductor of the ladder line as the coaxial cable's centre conductor. For my antenna, fixed to a fibreglass fishing pole, the radiator wire was 97cm in length.

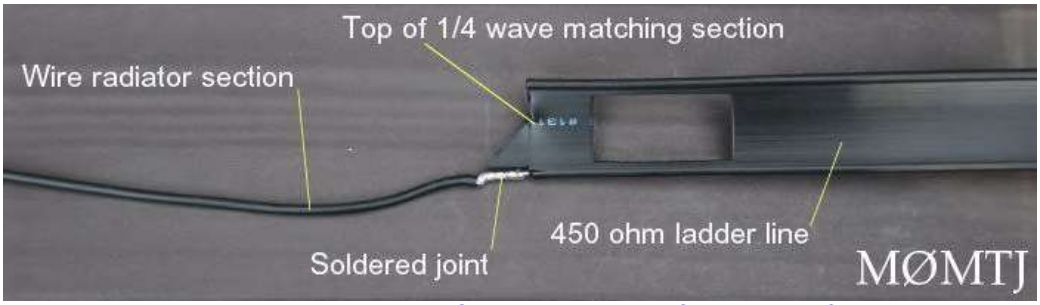

Photograph showing the point where the PVC covered wire that forms the half wave radiator section is soldered onto the top of the 450 ohm ladder line that forms the quarter wave matching section.

Inspired by DK7ZB. The J-Pole is a very effective antenna and being made of wire it is very light weight making it quite easy to fix in different positions. If you have problems installing a permanent antenna then making a wire antenna that can be easily supported on a lightweight push up telescopic fishing pole can make an ideal alternative.

The formulas to make a J-Pole antenna from 450 Ohm Wireman ladder line in this way are:

Length of 1/4 wave impedance matching section (450 ohm ladder line) Wavelength x 0.223
Length of 1/2 wave radiator (any reasonably strong PVC covered stranded wire) Wavelength x 0.471
The point at which the coax is connected to the 450 ohm ladder line will be about 5 to 10% of the length of the ladder line section up from the bottom.

The wavelength at mid point of the 2 metre band (145.00 MHz) is found by the quick calculation 300 ÷ 145 = 2.068 metres

So, to make a practical antenna:

The 1/4 wave section of 450 ladder line will be 2.07 x 0.223 = 0.47 metres long
The 1/2 wave wire radiator will be worked out as 2.07 x .471 = 0.975 metres long
The connecting point of the coax will be about 3.5 cm from the bottom of the 1/4 wave section. The optimal point may have to be found by some experimentation - as will the best length for the wire radiator.

The length of the wire radiator will be affected by surroundings. For example I fixed the wire to a fishing pole. The proximity of the fishing pole has the effect of electrically lengthening the wire; so using a 97.5cm length of wire fixed to a pole I found that it resonated (as expected) at a lower frequency, it therefore had to be shortened until the point of resonance (indicated by lowest SWR) was around 145.00 MHz. This should be done in the antenna's expected final position since the J-Pole is quite sensitive to its surroundings, so if these checks are done near the ground, once it is raised into its final position the SWR will have changed and the adjustments will have to be done again.

I found that 3.5 cm was good for the 2 metre band antenna, but for the 10 metre band version of the antenna a little more experimentation was required:

The VSWR reading may not be especially low, even though the point of resonance for the wire radiator may have been found. For the 10 metre band antenna at this this stage was about 1.7 indicating that the connection point of the coaxial cable to the 450 ladder line needs to be adjusted. The ladder line is used as an impedance transformer, transforming the very high impedance (hundreds of ohms) of the half wave wire radiator down to the 50 ohms required by the transceiver and the coaxial feeder cable. This connection point therefore affects the impedance of the antenna, the higher up the matching section it is the higher the impedance will be, and visa versa.

Once the length of the wire radiator has been set, the connection point can be moved up and down the ladder line until lowest SWR is achieved. A few centimetres of the PVC insulation has to be carefully scraped away from the copper conductor on each side of the ladder line using a craft knife. The inner conductor of the coaxial cable is quickly tack soldered on the side that is connected to the 1/2 wave wire radiator. The coaxial cable's braid is quickly tack soldered to the opposite side of the ladder line at this point, ensuring that both points are equal distance from the bottom. At this point temporary croc clips could be used, but I preferred a quick solder joint.

With radiator trimmed for resonance, the connection point of the coaxial cable can then be moved up or down the ladder line little by little; un-soldering and re-soldering the coax to the ladder line until a lowest possible SWR is achieved, indicating that the antenna is near the ideal 50 ohm impedance.

Once the ideal point is found the coaxial cable can be properly and permanently soldered to the ladder line.

6 Metre Band J Pole on the antenna analyser - it's getting close!

Each J-Pole took about 20 minutes to physically make out of the wire components. However the testing and adjusting took a bit more time. I used an antenna analyser which saved having to key the mike every time when using a basic VSWR bridge and causing unnecessary QRM, but even so, hoisting the fishing pole up and down numerous times took a little more time:

10 Meter J-Pole. For the 10 metre band J-Pole antenna this took perhaps another 20 or 30 minutes until I was satisfied with the adjustments. It may take a little longer if using an SWR meter.

6 Meter J-Pole. For the 6 metre band antenna the radiator wire had to be trimmed a little and the feed point adjusted to 6 cm, taking about 10 additional minutes to complete.

4 Metre J-Pole. For the 4 metre band, centred on 70.37 MHz

2 Meter J-Pole. For the 2 metre band antenna the wire radiator took a couple of attempts to get it to the correct length when attached to a fishing pole, but the feed point was spot on first time at 3.0 cm, again taking about 10 additional minutes to complete.

Here are some suggested dimensions for the 2 metre, 6 metre and 10 metre band versions, when supported by a fibreglass fishing pole:

Wire J-Pole Antennas	1/2 Wave Radiator	1/4 Wave Section	Feed Point
2 Metre Band Antenna	0.975 m	0.47 m	3.0 cm

4 Metre Band Antenna	**1.90 m**	**0.95 m**	**6.1 cm**
6 Metre Band Antenna	**2.815 m**	**1.33 m**	**6 cm**
10 Metre Band Antenna	**4.96 m**	**2.45 m**	**15 cm**

N.B. The 1/2 wave wire radiator section will be shorter than calculated when fixed to a fibreglass pole or other object.

To re-cap, the 1/2 wave section should be adjusted for resonance and the feed point position adjusted for minimum VSWR.

Sealing and waterproofing. Once the antenna is complete and has been checked and tested all the bare joints should be sealed against the weather with liquid electrical tape and self amalgamating tape. The coax should also be secured against the ladder line with a nylon cable tie as a strain relief to prevent the soldered feed point joints from breaking.

These J-Pole Antennas were inspired by DK7ZB - http://www.qsl.net/dk7zb/J_Pole/wiremanjpole.htm

---

Antennas 1 | Antennas 2 | Antennas 3 | Antennas 4 | Antennas 5 | Antennas 6 | Antennas 7

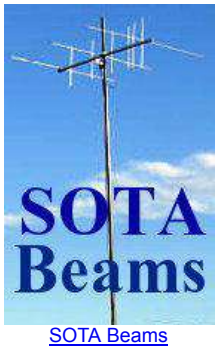

SOTA Beams
Lightweight 2 metre & 70cms Yagis, Dipole, Accessories & Poles
www.sotabeams.co.uk

G-Whip Antenna Products
Get on the air with TOP QUALITY BRITISH G-WHIP ANTENNAS
End Fed Zepps and many more designs and products

Radio Interference?:
PLT & PLA: Radio Interference
British Telecom, BT Home Plug
P C World, Powerline Adapters
YouView, Belkin Linksys
Netgear Devolo, BT Vision - BPL
Radio Interference
PLT Page 1

Antennas 1 | Antennas 2 | Antennas 3 | Antennas 4 | Antennas 5 | Antennas 6 | Antennas 7

Top of page ^

M0MTJ | Operating Conditions | Antennas / Aerials | /P Portable Operating | Accessories | Projects & Kits | Useful Information

Contact MØMTJ | Contact M6ORS | Links to Amateur Radio Sites | RSGB | QSL | The Amateur Radio Mini Site Map

WSPR Weak Signal Propagation Reporter

News, Developments, Events, Photographs and other 'Bits 'n' Bobs'

MDS975 Home

Feedback

Mike Smith - MDS975.co.uk © 2003 - 2016

M0MTJ

Amateur Radio; Ham Radio; Radio; Transceivers; HF; VHF; UHF; Data Modes; Morse Code; RTTY; PSK31; SSTV; FSTV; Amtor; Sitor Antennas; Aerials; Cable; Coaxial Cable; Twin Lead; Masts; Poles; Propagation; Computer; PC; USB Computer Interface; Microphone Loudspeaker; Filters; Noise Reduction; DSP; Digital Signal Processing; Morse Key; SWR ; Inverted L; Inverted V; Dipole; Doublet.

Amateur Radio MØMTJ

MDS975.co.uk HOME PAGE

My Home Page

Amateur Radio
Operating Conditions
Antennas
Accessories
Projects & Kits
Data Modes
Information
Portable
QSL
RSGB Ltd
Links
QRM
Bits 'n' Bobs
Contact

WSPR Weak Signal Propagation Reporter

PORTABLE

Site Map

MDS975 Home

Feedback

PLT QRM

Site Search
Find
powered by FreeFind

M0MTJ | Operating Conditions | Antennas / Aerials | /P Portable Operating | Accessories | Projects & Kits
Useful Information | Contact MØMTJ | Contact M6ORS | Links to Amateur Radio Sites
RSGB | QSL | The Amateur Radio Mini Site Map
News, Developments, Events, Photographs and other 'Bits 'n' Bobs' | WSPR Weak Signal Propagation Reporter

AERIALS (ANTENNAS) 7

Antennas 1 | Antennas 2 | Antennas 3 | Antennas 4 | Antennas 5 | Antennas 6 | Antennas 7

Index To Other Antenna Pages:
Antennas 1 : Aerials used by M0MTJ
Antennas 2 : Including ideas for compact antennas for Top Band /160 metres
Antennas 3 : Felix Scerri VK4FUQ discusses Loop Antennas, baluns, masts & other antenna related topics
Antennas 4 : Many antenna ideas from various sources particularly for multi-band operation & also gives information about
antenna trimming, knots for wire antennas and useful antenna rigging accessory ideas.
Antennas 5 : Half Wave End Fed antennas for 144 MHz VHF / 430 MHz UHF and 50 MHz 6 Metre band & J-Pole Aerials
Antennas 6 : Simple and effective H.F. Antenna ideas - Ground Plane and the All Band Doublet Aerial
Antennas 7 : Experimental Omni-Directional - Circularly (Mixed) Polarized Antenna for VHF / 2 Meters.

"Everything should be made as simple as possible, but not simpler." - *Albert Einstein*

MØMTJ - Experimental (Almost) Omni-Directional - Circularly (Mixed) Polarized Antenna for 144 MHz / VHF / 2 Meters.

Introduction and Background

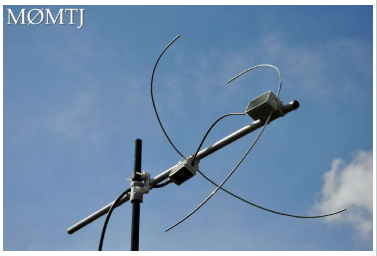

This is an experimental project that may lead to further development in the future, but even as presented below, it does work and may prove very useful.

I have therefore included this page of information so that you may can construct the aerial and develop these ideas further - either just out of interest and for the sake good old traditional Amateur Radio experimentation or for more permanent and practical uses!

The idea was sparked by the fact that I had been toying with the idea of removing the rotator and dual-band horizontal Yagi from my lightweight push-up aluminium mast to reduce mass and visual impact. I certainly did not want to lose access to the horizontally polarized portions of the 2 Metre (144 MHz) or 70cms (432 MHz) bands, so decided upon trying an Omni-Directional, horizontally polarized aerial.

The question was which antenna would I use to replace the rotatable dual-band Yagi?

Due to the weight of the rotator, the lightweight aluminium mast could not safely be pushed up higher than about 6 meters. Therefore, the Yagi on the stub mast was never much higher than 6 or 7 metres above the ground. A lighter weight omnidirectional aerial, without the heavy rotator, would allow the past to be pushed up to, perhaps, 8 or 9 meters. Maybe even to its full 10 meters on a fine day!

My thinking is that this additional height may compensate slightly for the loss of gain from the Yagi. The additional height would also benefit my vertical Coaxial Dipole for 6 Meters (50 MHz) which sits at the top of this mast. A small bonus.

I decided that I would try simple Halo antennas (HAlf wave LOop) and Big Wheel antennas for 2 Meters and 70cms.

Circularly Polarized, Omnidirectional Antenna for VHF 2 Meters / 144 MHz

.
However, before embarking on those particular experiments and possible future changes, I wanted to experiment with mixed polarization, or more correctly in this case, Circular Polarization - the subject of this project and article.

Why? - Well, when the IBA (Independent Broadcasting Authority) began building transmitters for their Independent Local Radio (ILR) in 1973, they specified that mixed polarized aerials should be used used at each of their VHF/FM

G Whip Antenna Products
Get on the air with TOP QUALITY BRITISH G-WHIP ANTENNAS

transmitter sites, starting with Croydon for LBC and Capital Radio in London, then Black Hill for Radio Clyde in Glasgow and Lichfield for BRMB in Birmingham and the many other sites that followed. The aerial systems were either described as "Mixed", "Slant" or "Circular".

The reason that mixed polarization was chosen was to improve reception on car radios and portable radios that generally used a vertical or slanted telescopic rod aerial. The BBC, at the time, used horizontal polarization for VHF/FM radio which was good for permanently installed roof-top receiving aerials, but provided poorer reception for listeners with portable sets and car radios. Some years later the BBC followed the IBA and began converting that majority of their transmitter sites to mixed polarization to improve reception and reduce mobile 'flutter' effects.

I thought that I would like to experiment with mixed polarisation and took some inspiration from some of the more recent, and simpler, antennas that have been installed at commercial radio ("ILR") transmitter sites. Two examples are shown below, both from the Radio Wave transmitter site at Blackpool Tower. The original aerial and its more recent replacement.

Original SBS transmitting aerial for
Radio Wave Blackpool 96.5 MHz
Photo from MB21.co.uk

The newer antenna viewed from below
Photo from MB21.co.uk

What's Needed

4 x 500mm lengths of 4mm diameter aluminium rod
2 x Dipole Centres

6 x Solder Tags with 3mm diameter hole
2 x Dipole Mounting Boxes - e.g. IP54 85 x 45 x 40mm
2 x Stainless Steel Nuts, Bolts and Washers M4 x 20mm
2 x Stainless Steel Nuts, Bolts and Washers M4 x 14mm
4 x Stainless Steel Self Tapping Screws No. 4 (2.9mm) diameter by 9.5mm long
1 meter of 20mm or 25mm Diameter PVC Pipe
8 x Pipe Clamps to suit diameter of boom and diameter of supporting mast
4 x Stainless Steel Nuts, Bolts and Washers
2 x End Caps to suit diameter of PVC boom (i.e. either 20mm or 25mm)
1 x SO239 Chassis Mount Socket
500mm length of small diameter coaxial cable, e.g. RG188 A / U - 50 Ohms PTFE coaxial cable
1 x piece of PVC tube for choke balun - 16mm diameter x 30mm long
1 x length of coaxial cable for phasing section
Some small self tapping screws to fix the pipe clamps to the boom

These items will be available from many and various sources, but Nuxcom is a good supplier - http://shop.nuxcom.de/

The antennas essentially comprise of two Crossed Dipoles, set a 90 degrees from each other. In the first photo, the antenna can be seen to have one dipole positioned vertically and the other horizontally. The second photograph shows that the to dipoles are again set at right angles, but one slopes 45 / 225 degrees and the other at 315 / 135 degrees.

The two dipoles are connected to each other, but have to be fed with the current to each dipole 90 degrees out of phase. This is called phase quadrature. It is a very common method used for other types of antenna, such as the Turnstile which is often used for communication with satellites where circular polarization must be used.

One dipole is connected directly to the coaxial cable. (I used Westflex 103 coaxial cable, for lowest loss, to feed the antenna). The second dipole has to be fed via a 1/4 wave (90 degrees) matching section. I had an off-cut of RG58, so used this for my initial experiment.

A quarter wave at 145.00 MHz is 300 / 145 = 2.068m / 4 = 51.7 cm. However the Velocity Factor (VF) of the cable has to be taken into account because radio waves travel more slowly through transmission lines than the do through free space.

Ideally I should have measured the VF with my antenna analyzer, however I took the typical VF of RG58 as being 0.66. So 51.7cm x 0.66 = 34.1cm. I cut the cable to 34.1 cm and used this to connect the two dipoles together.

Initially I cut the 4mm diameter aluminium rod into four 50cm long pieces and mounted them into the two dipole mounting boxes using the Nuxcom Dipole Centres. A small hole has to be very carefully drilled into the end of each rod to align with the fixing hole of the dipole centre. Then very carefully screw the 2.9mm stainless steel self tapping screws into each hole being sure not break off the head of the screws. When tapping these holes it is best to ease back and forth until the hole is successfully tapped.

The dipole centres and pipe clamps are fixed to the box with the 20mm diameter M4 hex bolts, washers and nuts.

The second pipe clamp is fixed to the box with the 14mm long M4 stainless steel hex bolt, washer and nut.

Each mounting box is fixed to the boom by clipping on the pipe clamp. The two dipoles are mounted at right angles (90 degrees) to each other, approximately 335mm apart. Once the final adjustments have been made and the positions along the boom are decided, the clamps are held firmly in place by screwing them to the boom, as can be seen in the photographs below.

Each dipole is then carefully bent into a semi-circle.

The SO239 socket is then fitted to the box and the choke balun is wound and one end of the coaxial cable soldered to the socket and the other end fitted with the solder tags. The small 2.9mm x 9.5mm stainless steel self tapping screws are then used to fix the tags to the dipole centre.

Now connect this dipole to an antenna analyzer (or SWR meter) and check the point of resonance. I decided to centre the aerial on 144.3 MHz. Almost certainly the dipole will be too long. I had to cut off 1mm of rod from each end.

Once complete, do the same for the other dipole so that they are exactly the same size.

Next, the phasing cable is prepared, as mentioned above. A suitable diameter hole is drilled in the end of the box opposite the SO239 socket and the phasing cable passed through this and soldered on to the two tags, as can be seen in the photograph below.

A similar small hole is then drilled into the other dipole mounting box and the other end of the phasing coaxial cable is passed through this, two solder tags are soldered on to the end and then fixed into place on the dipole centre using the small self tapping screws.

Now connect the antenna analyzer again, using a few metres of low loss coaxial cable, and mount the antenna in some free space, preferably outside on a pole about two or three metres above the ground a. It will almost certainly be found that the point of resonance is now two low, so each dipole will now need to be carefully trimmed, cutting small and equal amounts off each of the four ends until the point of resonance is around 144.3 MHz.

It should be possible to obtain an SWR of 1.5:1 or less across the 2 Meter band - to achieve this it may be necessary to move one of the dipole mounting boxes further away, or closer together to the other. Also, it may be necessary to bend the dipole rod of each dipole element inwards, or outwards slightly. I was able to achieve an SWR of 1:1 with an impedance of 50 Ohms according to the antenna analyzer.

Once the adjustment were complete, I used 20 meters of Westflex 103 to connect the antenna to the Icom IC-706 mk2g. A similar length of the same cable is used to connect the 5 element horizontal Yagi to the radio. A low loss coaxial switch was used to make instand comparisons between each antenna.

I raised the experimental antenna to 8 meters above ground level on the telescopic pole and began to make some comparisons.

My guess was that the experimental omni-directional circular polarized antenna would be noticeably inferior to the much higher gain, horizontal, directional Yagi.

The Yagi has a quoted gain of 8.4dDBd (i.e. gain with reference to a standard dipole - not dBi).

A standard straight dipole has a gain of 0 dBd. However if it used horizontally and is bent into a circle to produce a roughly omni-directional radiation pattern, then the gain must be reduced, so I assumed that the 'gain' must now be negative, perhaps -1 or -2 dBd.

Additionally, being as this is a circularly (mixed) polarised antenna, the power is essentially divided in half across the horizontal plane and the vertical plane. i.e. another 'loss' of 3dBd.

Therefore the gain of the antenna may be assumed to be -5dBd (minus 5 dBd), i.e. about 1 S point down on a simple straight linearly polarized aerial and about 13 dBd down compared to the Yagi - i.e. about 2 or 3 S points worse.

Here, at my QTH in Staffordshire, the Kent beacon on 144.430MHz on my 5 element Yagi is just audible, although there is no S Meter reading. I therefore did not expect to be able to hear it on the experimental antenna as it is so weak, but to my surprise, the beacon was still there - obviously a bit weaker, but still audible. That was an encouraging start!

I therefore went ahead and made some QSO's with other stations who were using both vertical and horizontal polarization and also made some comparisons purely on receive.

I therefore went ahead and made some QSO's with other stations who were using both vertical and horizontal polarization and also made some comparisons purely on receive.

I haven't recorded enough data to draw truly meaningful conclusions. It's not scientific either. However, my impression from what I have recorded and from other general use is that the performance is broadly in line with my expectations - i.e. about 2 or 3 S points, or around 12dB, down on the Yagi.

Station	Location	QSO or RX	Mode	Other station's Aerial	Rprt Sent (Yagi)	Rprt Rec'd (Yagi)	Rprt Sent (Omni)	Rprt Rec'd (Omni)
G3XEV	Sedgley	QSO	SSB	V2000 Vertical	S2-3	S7	S6-7	S7
2W0JYN	Rhos	QSO	SSB	3 Ele Horiz Yagi	S6	S9	S5	S7
2W0JYN	Rhos	QSO	SSB	Vertical Colinear	S1	S1	S0	S0
G8WEG	SW B'Ham	RX	FM	Unknown (Vert?)	N/A	N/A	S9+20	N/A
MW0WML/p	GWNW012	QSO	FM	Vertical Dipole	N/A	N/A	S9+10	S8
G7HEM	Stourbridge	QSO	SSB	6 Ele Horiz Yagi	S7	S9	S2	S3
N/K	Burton	RX	SSB	Unknown (Horiz?)	S9	N/A	S5	N/A

With particular thanks for John G3XEV and Steven 2W0JYN for their assistance with these initial tests!

I hope this information is useful and may encourage you to experiment further and make some much better scientific comparisons!

If you have any comments, please do email them to me via the contact page here.

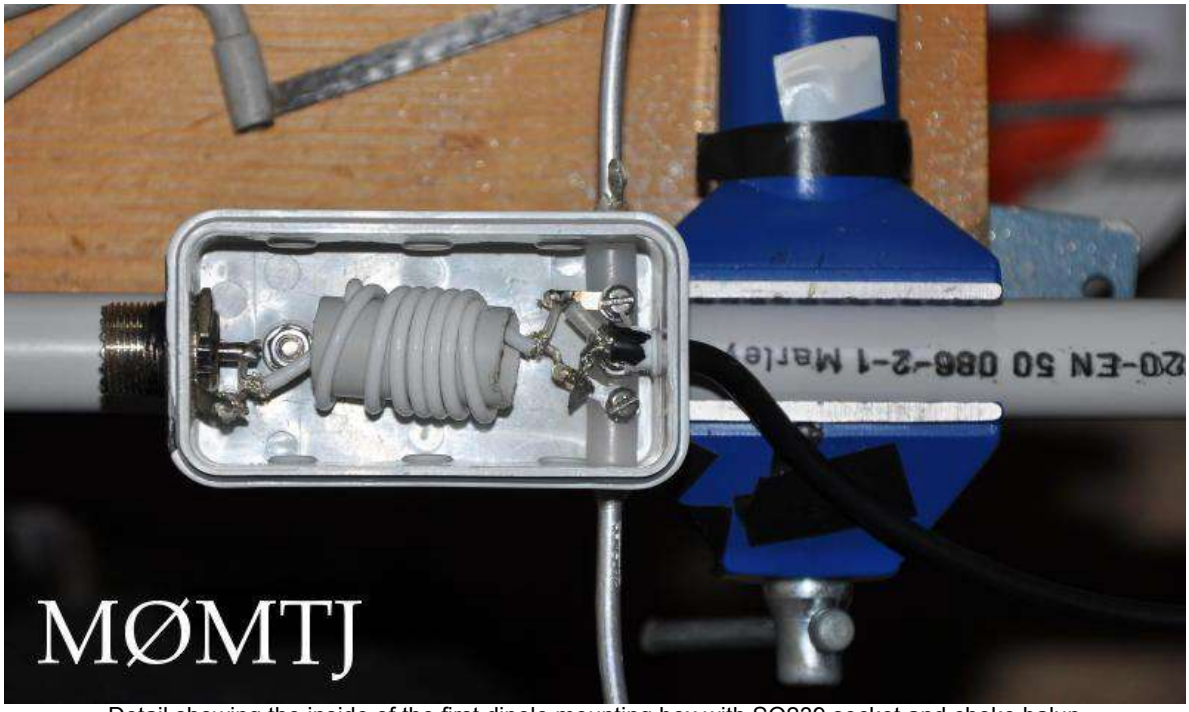

Detail showing the inside of the first dipole mounting box with SO239 socket and choke balun

Nuxcom Dipole Centre for 4 mm dipole rods
10 mm space between dipole rods
Three holes: One in the middle for fixing the box on the boom. The other two for connecting the cable to the dipole rods.
Length: 36 mm
Space in the between rods: 10 mm
Outer diameter: 8.4 mm
Inner diameter: 4,1 mm
Material: Polyamid
http://shop.nuxcom.de/

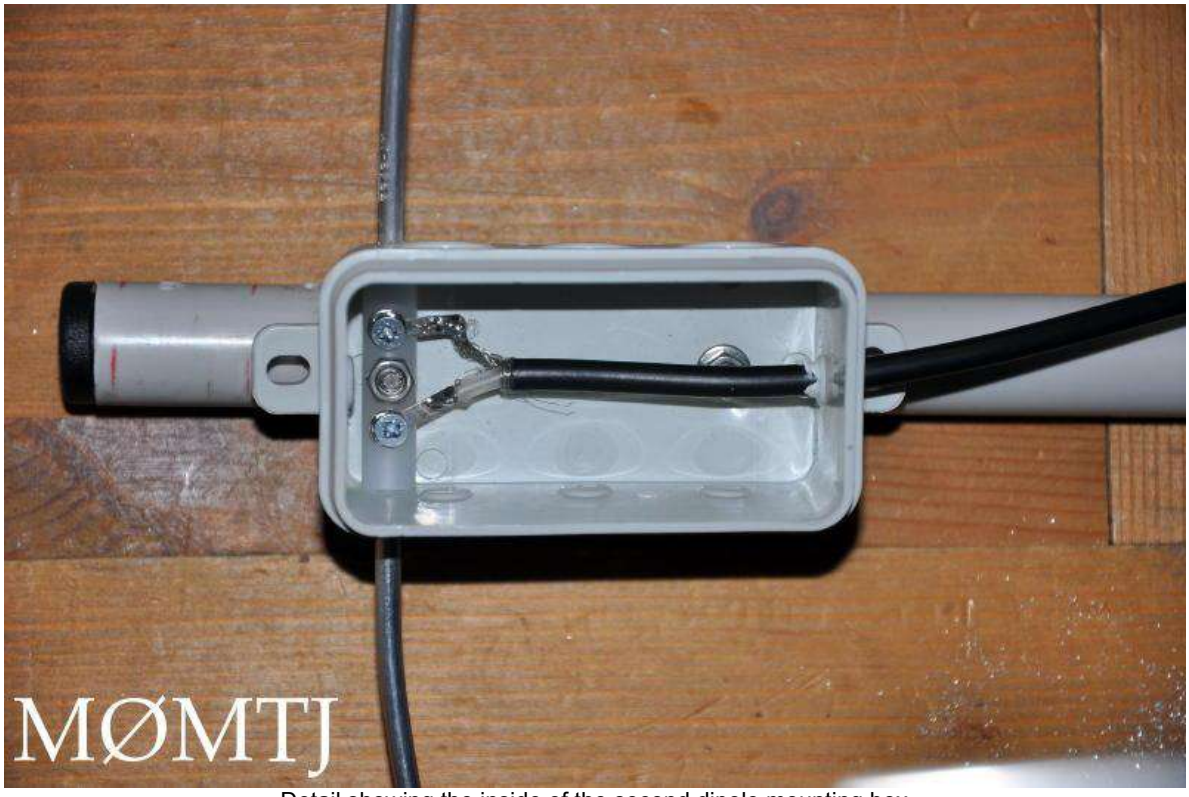

Detail showing the inside of the second dipole mounting box

Detail showing how the dipole mounting box is fixed to the plastic pipe with pipe clamps and firmly secured in place with small self tapping screws.

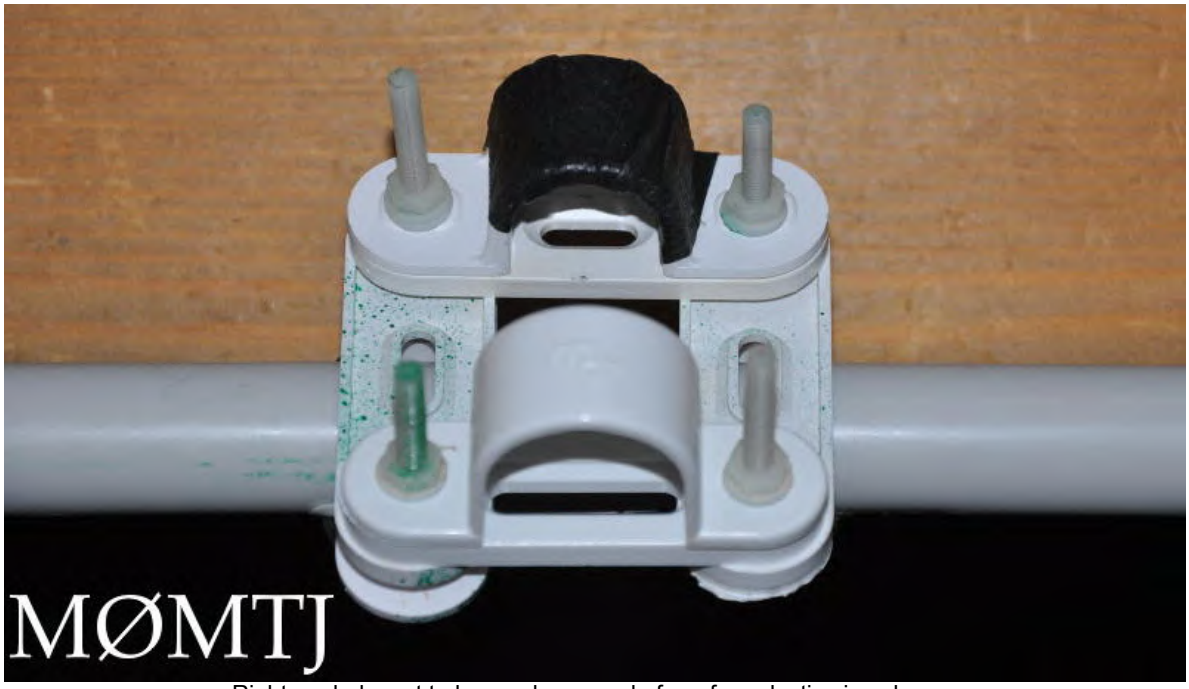

Right angled mast to boom clamp made from four plastic pipe clamps

Right angled mast to boom clamp made from four plastic pipe clamps

Antenna under initial test and adjustment at approximately 2 metres a.g.l.
The coaxial cable is low loss Westflex 103
(My HF Doublet antenna, fed with open wire balanced line can be seen in the background on the left)

After adjustment to element lengths and dipole positions along the boom arm, the antenna shows a good match.

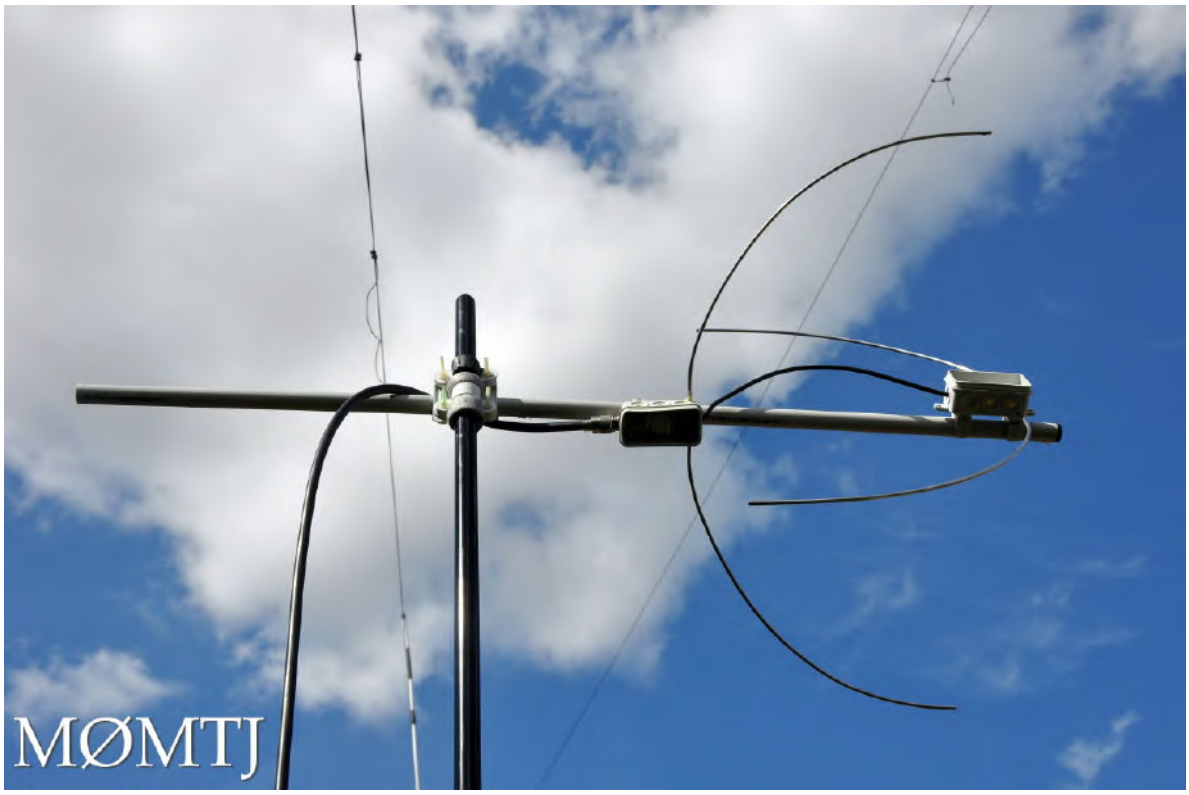

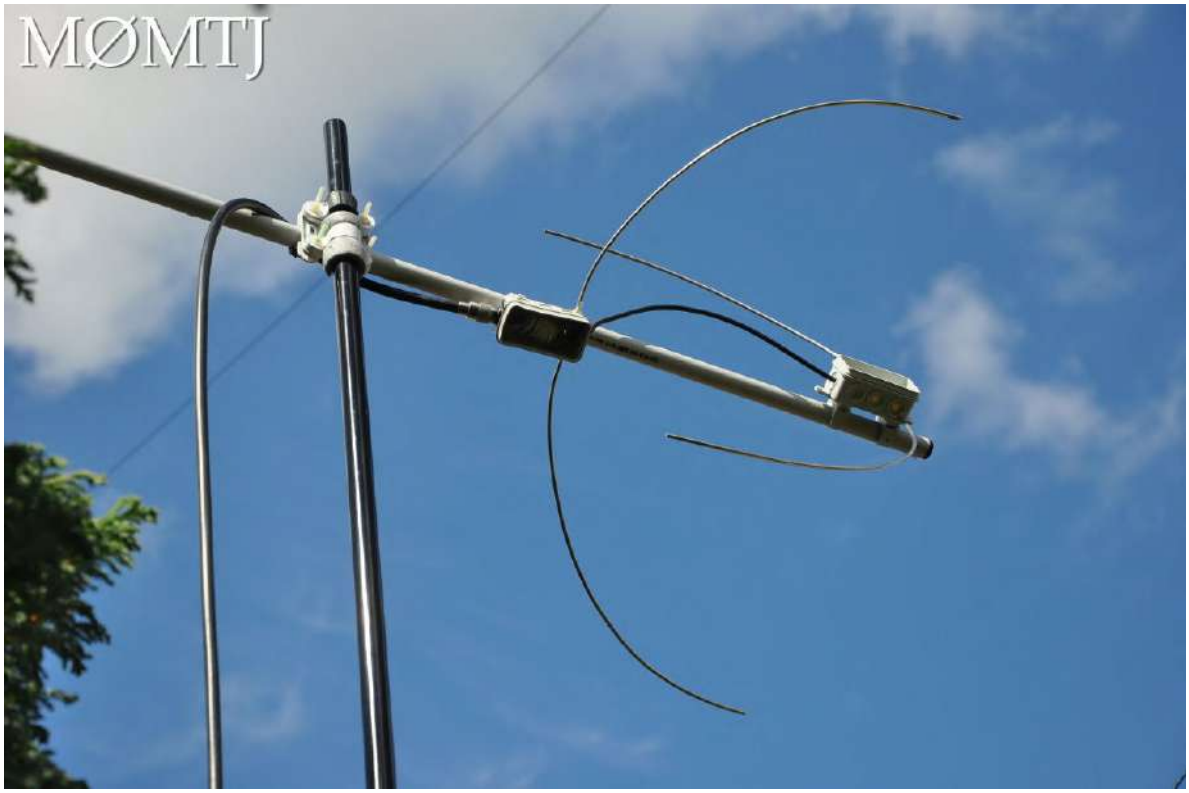
MØMTJ

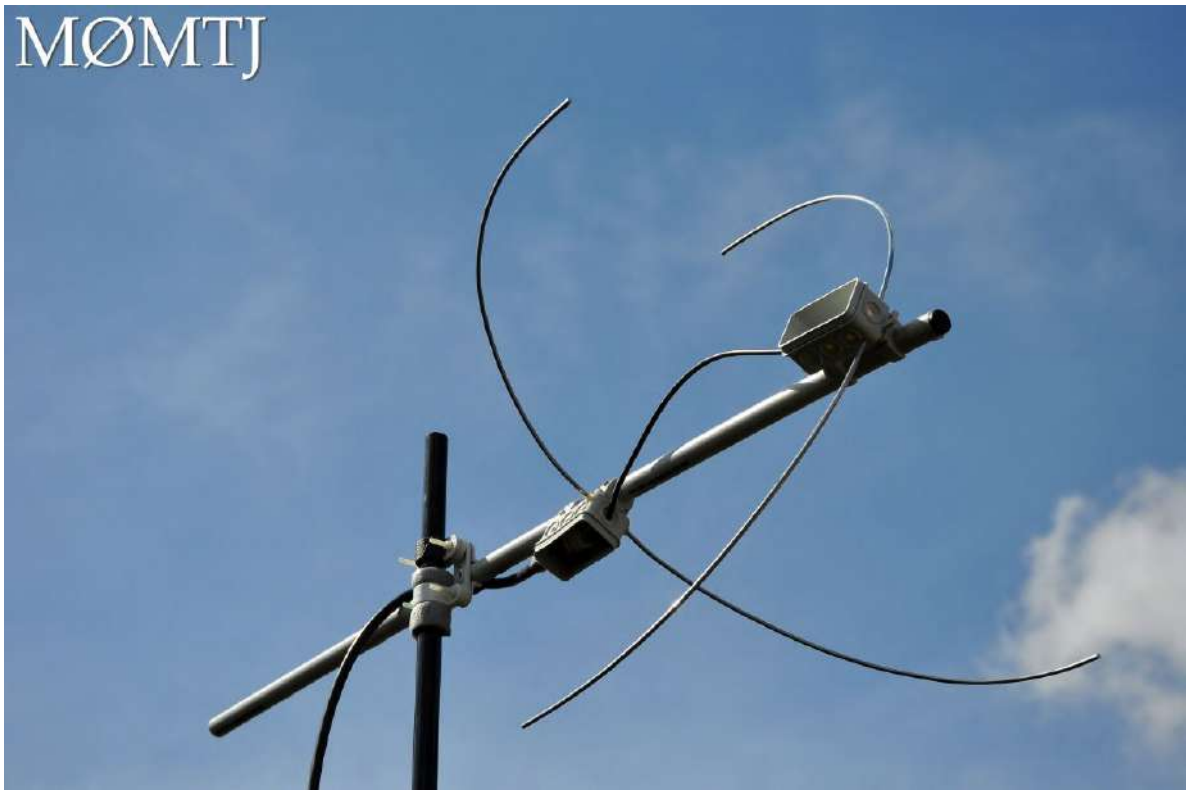
MØMTJ

MØMTJ

MØMTJ

The Test 'Rig' comprised of a heavy duty Spiderbeam 12m fibreglass telescopic pole with the antenna mounted approximately 8 meters a.g.l.

If you have any comments, please do email them to me via the contact page here.

Antennas 1 | Antennas 2 | Antennas 3 | Antennas 4 | Antennas 5 | Antennas 6 | Antennas 7

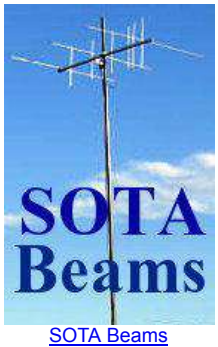

SOTA Beams
Lightweight 2 metre &
70cms Yagis, Dipole.

G-Whip Antenna Products
Get on the air with
TOP QUALITY
BRITISH
G-WHIP
ANTENNAS
End Fed Zepps and
many more designs
and products

Accessories & Poles
www.sotabeams.co.uk

Radio Interference?:
PLT & PLA: Radio Interference
British Telecom, BT Home Plug
P C World, Powerline Adapters
YouView, Belkin Linksys
Netgear Devolo, BT Vision - BPL
Radio Interference
PLT Page 1

Antennas 1 | Antennas 2 | Antennas 3 | Antennas 4 | Antennas 5 | Antennas 6

Top of page ^

M0MTJ | Operating Conditions | Antennas / Aerials | /P Portable Operating | Accessories | Projects & Kits | Useful Information

Contact MØMTJ | Contact M6ORS | Links to Amateur Radio Sites | RSGB | QSL | The Amateur Radio Mini Site Map

WSPR Weak Signal Propagation Reporter

News, Developments, Events, Photographs and other 'Bits 'n' Bobs'

MDS975 Home

Feedback

MAIL

Mike Smith - MDS975.co.uk © 2003 - 2016

M0MTJ

Amateur Radio; Ham Radio; Radio; Ground Plane Vertical; Sloper; HF Antenna; Dipole;
Doublet; Antenna - The Best Multi-Band Antenna for Easiest Construction, Quickest Deployment and Lowest Cost

Wire Antennas for Ham Radio

Iulian Rosu YO3DAC / VA3IUL,

http://www.qsl.net/va3iul

***Note:** Dimensions of the antennas presented below are either in: feet ('), inch ("), meters (m), or centimeters (cm)*

01 - Tee Antenna
02 - Half-Lamda Tee Antenna
03 - Twin-Led Marconi Antenna
04 - Swallow-Tail Antenna
05 - Random Length Radiator Wire Antenna
06 - Windom Antenna
07 - Windom Antenna - Feed with coax cable
08 - Quarter Wavelength Vertical Antenna
09 - Folded Marconi Tee Antenna
10 - Zeppelin Antenna
11 - EWE Antenna
12 - Dipole Antenna - Balun
13 - Multiband Dipole Antenna
14 - Inverted-Vee Antenna
15 - Sloping Dipole Antenna
16 - Vertical Dipole
17 - Delta Fed Dipole Antenna
18 - Bow-Tie Dipole Antenna
19 - Bow-Tie Folded Dipole Antenna for RX
20 - Multiband Tuned Doublet Antenna
21 - G5RV Antenna
22 - Wideband Dipole Antenna
23 - Wideband Dipole for Receiving
24 - Tilted Folded Dipole Antenna
25 - Right Angle Marconi Antenna
26 - Linearly Loaded Tee Antenna
27 - Reduced Size Dipole Antenna
28 - Doublet Dipole Antenna
29 - Delta Loop Antenna
30 - Half Delta Loop Antenna
31 - Collinear Franklin Antenna
32 - Four Element Broadside Antenna
33 - The Lazy-H Array Antenna
34 - Sterba Curtain Array Antenna
35 - T-L DX Antenna
36 - 1.9 MHz Full-wave Loop Antenna
37 - Multi-Band Portable Antenna
38 - Off-center-fed Full-wave Doublet Antenna
39 - Terminated Sloper Antenna
40 - Double Extended Zepp Antenna
41 - TCFTFD Dipole Antenna
42 - Vee-Sloper Antenna
43 - Rhombic Inverted-Vee Antenna
44 - Counterpoise Longwire
45 - Bisquare Loop Antenna
46 - Piggyback Antenna for 10m
47 - Vertical Sleeve Antenna for 10m
48 - Double Windom Antenna
49 - Double Windom for 9 Bands
50 - Collinear Trap Antenna
51 - Short Dipole Antenna for 40m - 80m - 160m
52 - Center Fed-Zepp Antenna for 80m - 40m
53 - All Bands Antenna
54 - All-Bands Dipole Antenna
147 - KE4PT OCEF All-Band Dipole
148 - Wire Quad Antenna for 40m
149 - Inclined Dipole Antenna for 80m, 40m
150 - Pyramidal Wire Antenna for 80m
151 - Random Wire Antenna All Bands
152 - Multiband Dipole Antenna for 80m, 40m,15m, 10m
153 - Slim Jim Wire Antenna for 4m
154 - Delta Loop for 6m
155 - Re-Configurable Antenna for 160m and 80m
156 - Very Low Frequency Inverted-L Antenna
157 - Reduced Size Half Sloper Antenna for 160m
158 - Tree-Mounted HF Antenna
159 - Multiband Vertical Antenna for 80m, 40m, 20m
160 - Marconi Antenna for 136 kHz
161 - Simple Killer Antenna for 40m
162 - Stub-Directed V Antenna for 80m
163 - KT0NY Over-and-Under DX Antenna for 20m
164 - Horizontal Loop Antennas
165 - Ribbon J-Pole for 2m
166 - Dual Band Ribbon J-Pole for 2m, 70cm
167 - Square Vertical Loop Antenna for 40m
168 - Tri-Band Quad Antenna for 20m, 15m, 10m
169 - 3D Quad Antenna for 80m, 40m, 20m, 15m, 10m
170 - Sloping Wire Antenna for 30m, 20m, 17m, 15m, 12m, 10m
171 - Broadband Dipole Antenna with Coaxial Resonator for 80m
172 - Resonant Feedline Dipole Antenna for 80m
173 - Dual-Band Loading Wire Antenna for 80m, 30m
174 - Stub Matching Antennas
175 - J-Style Vertical Wire Antenna for 10m
176 - Dual Band Vertical with Zepp Feeders for 40m, 20m
177 - RCA Double Doublet for 40m to 12m
178 - RCA Spiderweb Antenna for 40m to 6m
179 - Folded Dipole with Shorted Straps
180 - Twin-Lead Marconi Antenna for 160m, 80m
181 - Broadband Antenna Quarter-Wave Balun for 80m
182 - Three-Quarter-Wave Folded Doublet for Dual-Band
183 - Three-Quarter-Wave Folded Doublet No-Switch for Dual-Band
184 - Wideband Omni-Directional Discone Antenna
185 - Wideband Rhombic Antenna for 40m to 10m
186 - Pre-Cut Linear Array Antenna 3dB-Gain for 40m
187 - X-Array Antenna 6dB-Gain for 20m, 15m, 10m
188 - Double-Bruce Array Antenna 5dB-Gain for 20m, 10m
189 - Bi-Square Broadside Array 4dB-Gain for 20m, 15m, 10m
190 - Six-Shooter Broadside Array 7.5dB-Gain for 20m, 15m, 10m
191 - Triplex Flat-Top Beam 4.5dB-Gain for 20m, 15m, 10m
192 - Dual-Band Tilt Antenna for 20m, 10m
193 - Super Space Multiband Dipole Antenna for 80m to 10m
194 - Bi-Square Beam Antenna Gain=5.5dB for 10m
195 - Cousin of G5RV Multiband Antenna for 40m to 10m
196 - Cayman Quad Antenna for 20m
197 - Hentenna Gain=3dB with Bazooka Match for 6m
198 - X-Beam Antenna Gain=3dB for 20m

55 - Multiband Z Antenna
56 - Multiband Dipole Antenna
57 - Five-Bands No-Tuner Antenna
58 - Dualband Full-wave Loop Antenna for 80m-40m
59 - Loop Antenna for 10m
60 - Lazy Quad Antenna for 10m
61 - Tri-band Delta Loop Antenna for 80m - 40m - 30m
62 - Dual-band Loop Antenna for 30m - 40m
63 - Wire-Beam Antenna for 80m
64 - Dual-Band Sloper Antenna
65 - Inverted-V Beam Antenna for 30m
66 - ZL-Special Beam Antenna for 15m
67 - Half-Sloper Antenna for 160m
68 - Two-Bands Half Sloper for 80m - 40m
69 - Linear Loaded Sloper Antenna for 160m
70 - Super-Sloper Antenna
71 - Tower Pole as a Vertical Antenna for 80m
72 - Clothesline Antenna
73 - Curtain Zepp Antenna for 160m, 80m, 40m
74 - Collinear Array Antenna for 40m, 30m, 20m
75 - 160m Inverted Delta Loop
76 - Half Rhombic Unidirectional Vertical for 20m to 6m
77 - Capacitance Loaded Vertical Antenna for 160m
78 - Fan Dipole Antenna for 80m to 6m
79 - Wire Ground Plane Antenna
80 - Inverted Delta Loop Antenna for 160m
81 - Inverted-L for 160m
82 - 300ohm-Ribbon Dual Band Dipole
83 - Tri-Band Beam for 20m, 15m, 10m
84 - Mini-Horse Yagi Antenna
85 - Backpack J-Pole Antenna for 10m, 6m, 2m
86 - Fan-Dipole Antenna for 80m, 40m, 20m
87 - Capacity Tuned Folded Loop Antenna for 20m
88 - Indoor Loop Antenna for 80m to 30m
89 - Indoor Loop Antenna for 80m
90 - Double-Delta Antenna 80m and 40m
91 - Inductance-Loaded Shortened Dipole for 160m
92 - V-Beam Antenna for 15m
93 - Picnic Vertical Wire Antenna
94 - Laid-Back Quad Antenna for 80m
95 - Phased Loop Antenna
96 - Loop Antenna for TX for 160m
97 - Morgain-Dipole Antenna for 160m and 80m
98 - ZL-Special for 20m, 15m, 10m
99 - Biconical Antenna
100 - Directive Delta-Birdcage Antenna for 20m to 10m
101 - Dual Polarization Antenna for 80m and 40m
102 - Directive 300-ohm-Ribbon Folded Dipole for 15m
103 - Miniature Directive Antenna for 10m
104 - Biquad Antenna 12dBi-Gain for 2.4GHz
105 - Dual-Rhomboid Antenna for 435MHz to 870MHz
106 - Double-Bazooka Antenna for 80m
107 - J-Style Antenna
108 - Vertical / Horizontal / Circular Polarization Antenna
109 - Coax Inverted-L Antenna for 80m
110 - Indoor Compact Loop Antenna for 80m
111 - Helix Antenna
112 - Novice Vertical Antenna for 80m, 40m, 15m, 10m
113 - Stub-Loaded Shortened Dipole for 80m
114 - Six-Band Wire-Stub Trap Antenna for 40m-10m
115 - Multiband Half-Wave Delta-Loop Antenna
199 - Twin Delta Loop Antenna Gain=6dB for 160m, 80m, 40m
200 - Inverted-V Beam Antenna for 30m
201 - FD4 Windom Antenna for 80m, 40m, 20m, 10m
202 - Two Elements Phased Delta Loop for 40m
203 - Three Elements Wire Yagi for 10m
204 - Low Radiation Angle Full-Wave Loop Antenna for 80m
205 - Collinear Antenna Gain=3dB for 2m
206 - X-Ray Monoband Antenna Gain=6.5dBd
207 - Broadside Collinear Curtain Array for 20m
208 - Shrunk Loop Antenna for 80m, 40m
209 - λ/3 Multiband Dipole for 40m, 20m, 17m, 15m, 13m, 10m
210 - K3LR Sloper Antenna Gain=3dB for 160m
211 - Mini Folded Vertical Monopole Antenna for 160m, 80m, 40m
212 - Three Band Dipole for 80m, 40m, 20m
213 - Stub Matched Dipole Antenna
214 - Inverted-Vee Antenna with Bazooka Match
215 - Multiband Long Wire Antenna for 40m, 20m, 15m, 10m
216 - Converted Vee Antenna for 80m, 40m
217 - Swiss Quad Antenna for 20m, 15m, 10m
218 - Japanese Quad Antenna for 20m, 15m, 10m
219 - Seven-Elements Triangle Beam Antenna for 20m
220 - Log Periodic Wire Antenna for 40m
221 - Three-Elements 90-degrees Wire Beam for 20m
222 - Two-Elements Wire Beam for 20m
223 - Suitcase-Fit Dipole Antenna for 80m, 40m, 20m
224 - Multiband Coaxial Dipole for 80m, 40m
225 - Vertical Log Periodic Antenna for 80m, 40m
226 - Inverted Vertical Log Periodic Antenna for 40m
227 - Double Extended Zepp Antenna Gain=7dB for 15m
228 - Double Lazy-H Antenna G=10dB for 70cm
229 - Wire Log Periodic Antenna G=12dB for 15m, 20m
230 - Five-Elements Vertical Log Periodic for 80m, 40m, 20m
231 - Sloping Delta Loop Antenna for 40m
232 - Doublet Antenna for 160m
233 - Log Periodic Wire Beam for 40m
234 - G3LDO Wire Beam Antenna for 20m, 15m, 10m
235 - Phased Delta Loop Array for 20m
236 - Dual Band V-dipole for 80m, 40m
237 - Collinear Array 5dB-Gain for 15m
238 - Two-Band Quad Loop Antenna 80m, 40m
239 - K7CW Quad Antenna
240 - Broadband Short Dipole for 80m
241 - Off-Center Fed Dipole for 40m, 20m, 10m
242 - Broadband Sloper Antenna for 80m
243 - Two-Frequency Dipole Antenna for 80m
244 - Top Loaded Vertical Antenna for 160m
245 - Two Loop Beam Antenna for 20m, 15m
246 - Corner-Fed Delta Loop Antenna for 80m, 40m, 20m
247 - Loaded Delta Loop Antenna for 40m, 20m
248 - Compact Size Dipole for 80m
249 - JAWS 3dB Gain Antenna for 40m
250 - Inverted-V Antenna for 160m
251 - Lazy-U Antenna for 160m
252 - AF3V Compact Antenna for 160m
253 - Hot Beam Wire Antenna for 40m
254 - Sloping Delta Loop for 40m
255 - K6FD Multiband Antenna with T-tuner
256 - Dual Band Dipole Antenna for 17m, 10m
257 - Compact Travel Dipole Antenna for 10m, 15m, 20m
258 - End-Fire Antenna for 160m, 80m, 40m, 20m
259 - Four Band Loop for 40m, 20m, 15m, 10m

116 - Hybrid Vee for 20m, 17m
117 - Six-Shooter Array Antenna, Gain=7.5dB
118 - Multiband Ground-Plane Antenna for 10m, 15m, 20m
119 - Wire Superbeam Antenna for 10m, 15m, 20m
120 - Two Elements Delta-Loop Antenna
121 - Sterba Curtain Antenna
122 - Half-Wave Vertical Zepp Antenna
123 - Lazy-Loop Antenna for 40m
124 - Terminated Folded Dipole for 80m, 40m
125 - Short-Fat Antenna for 15m
126 - Cobra Antenna for 80m
127 - Log-Periodic Wire Antenna for 20m, 15m, 10m
128 - 5-Element Log-Periodic Vertical Antenna for 80m, 40m, 20m
129 - 2m Vertical Wire Antennas
130 - Earth-Mover Inverted-V Antenna for 40m
131 - Coax-Cable Collinear Antennas
132 - Double Bobtail Antenna for 20m
133 - Collinear Zepp Antenna
134 - Taylor Vee Antenna for 20m
135 - Collinear Vertical Antenna 6dB-Gain for 2m, 1.3m, 73cm
136 - Bi-Loop Antenna for 20m
137 - Wire Beam 6dBd-Gain for 10m
138 - Sloping Diamond Antenna 4dB-Gain for 40m
139 - Twisted Loop Antenna for 160m
140 - DX RX Loop Antenna for 160m
141 - Hentenna 3dB-Gain for 10m, 6m, 2m
142 - VK2AAR Wire Antenna for 20m
143 - 2-Elements Quad Antenna for 6m
144 - Hula-Loop Bidirectional 6dB-Gain Antenna for 17m
145 - Moxon Rectangle Beam for 15m-10m
146 - Double-D Beam 4dB-Gain
260 - Carolina Windom Antenna for 80 to 10m
261 - Shortened Loaded Dipole for 40m
262 - Shortened Loaded Dipole for 80m
263 - Low Radiation Angle Inverted Delta Loop for 80m
264 - Compact Dipole Antenna for 40m, 15m
265 - Vertical Delta Loop for 40m to 10m
266 - Delta Loop Antenna for 17m
267 - Bi-Square Beam Gain=3dBd for 17m
268 -Trap Dipole Antenna for 17m,13m
269 - Hanging Unipole Antenna for 160m, 80m
270 - Wideband Sloping Vee Antenna - 30m to 6m
271 - 5/8 Wavelength Antenna
272 - C-Pole Vertical Antenna
273 - Bobtail Antenna for 30m
274 - Bobtail Antenna for 40m
275 - Two Elements Vertical Loop Antenna for 40m
276 - Double Extended Zepp Antenna for 40m
277 - Reversible Moxon Flip Beam for 40m
278 - Spitwire Antenna for 40m
279 - Fork Antenna for 40m
280 - Veebeam Antenna 3dB-Gain for All Bands
281 - Vertical Moxon Antenna for 10m
282 - Half-Square Antenna for 30m
283 - Rotatable Vertical Delta Loop for 20m
284 - Mini-Horse Antenna 10dB-Gain for 40m-to-2m
285 - Compact Moxon Antenna 5dB-Gain for 40m
286 - Two Elements Sloping Delta Loop 8dB-Gain for 10m
287 - Two Elements Phased Vertical Antenna 3dB-Gain for 40m

---

01 - Tee Antenna

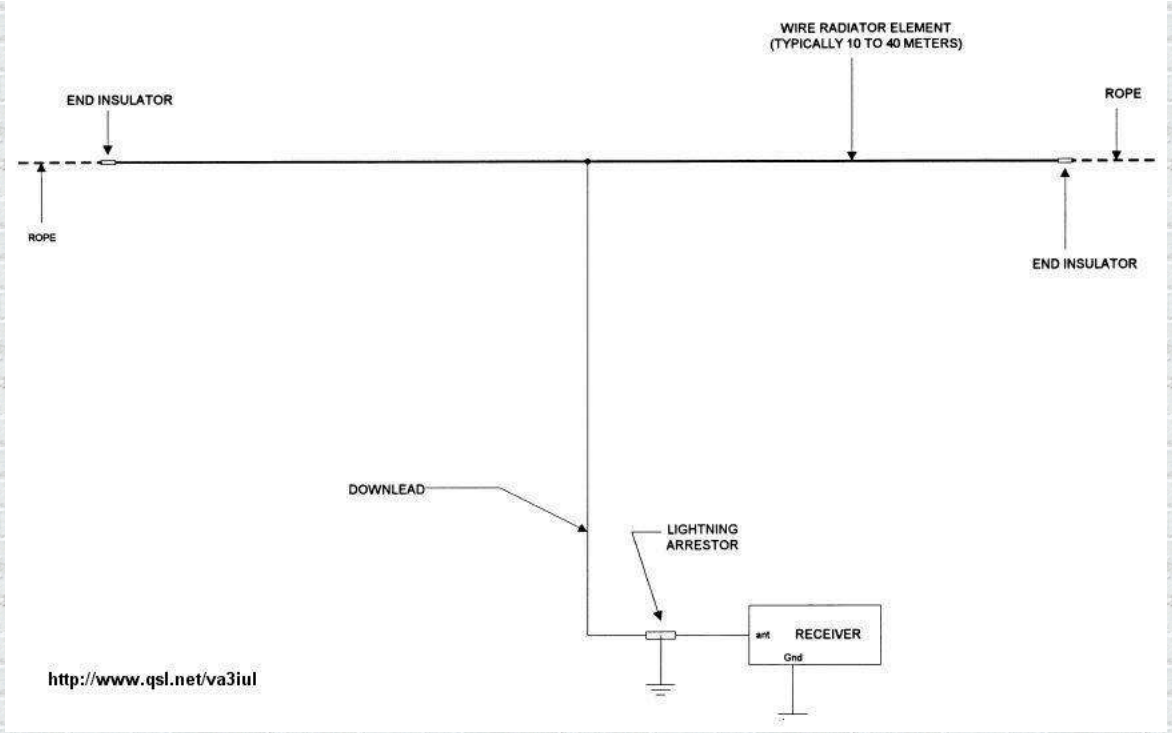

02 - Half-Lamda Tee Antenna

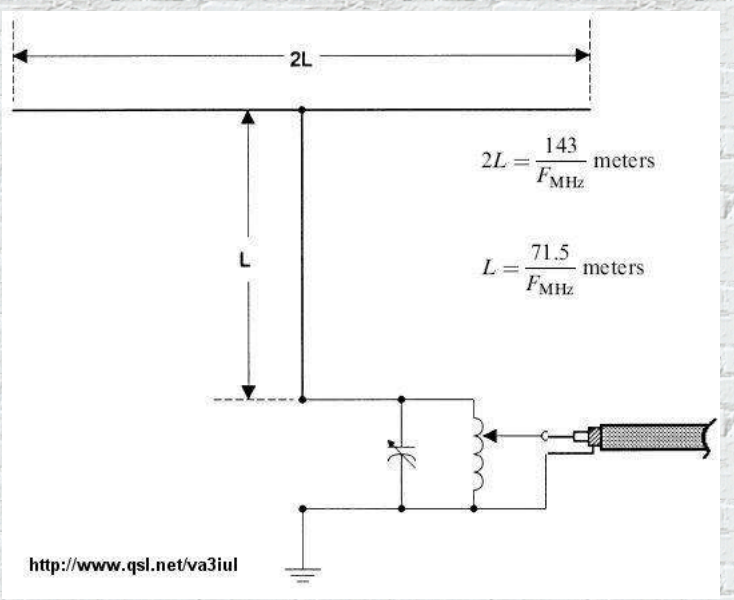

03 - Twin-Led Marconi Antenna

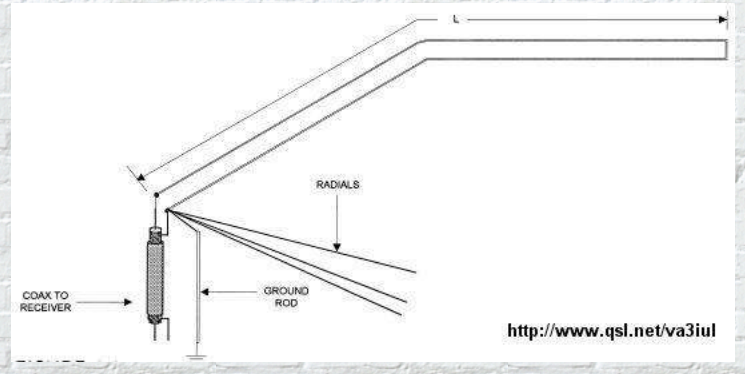

04 - Swallow-Tail Antenna

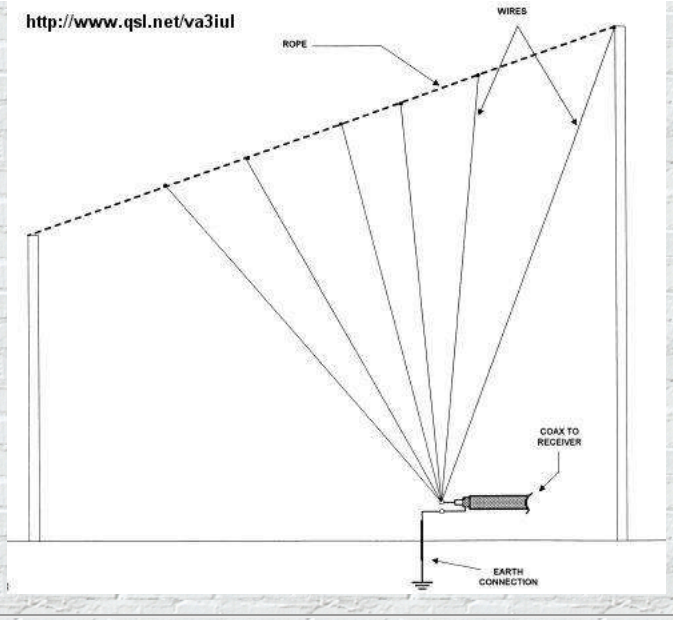

05 - Random Length Radiator Wire Antenna

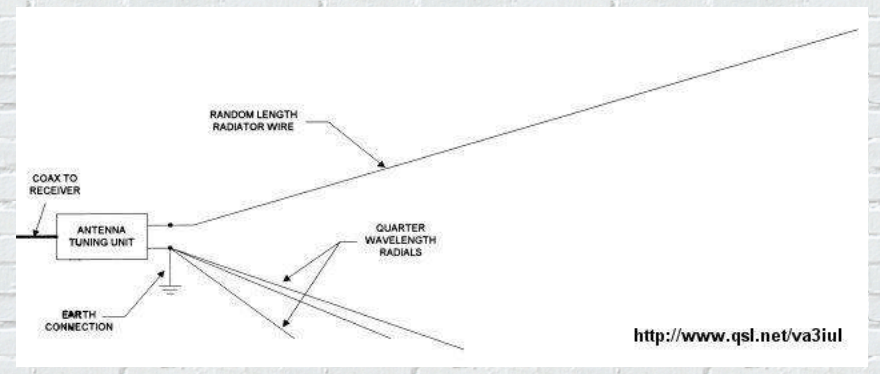

06 - Windom Antenna

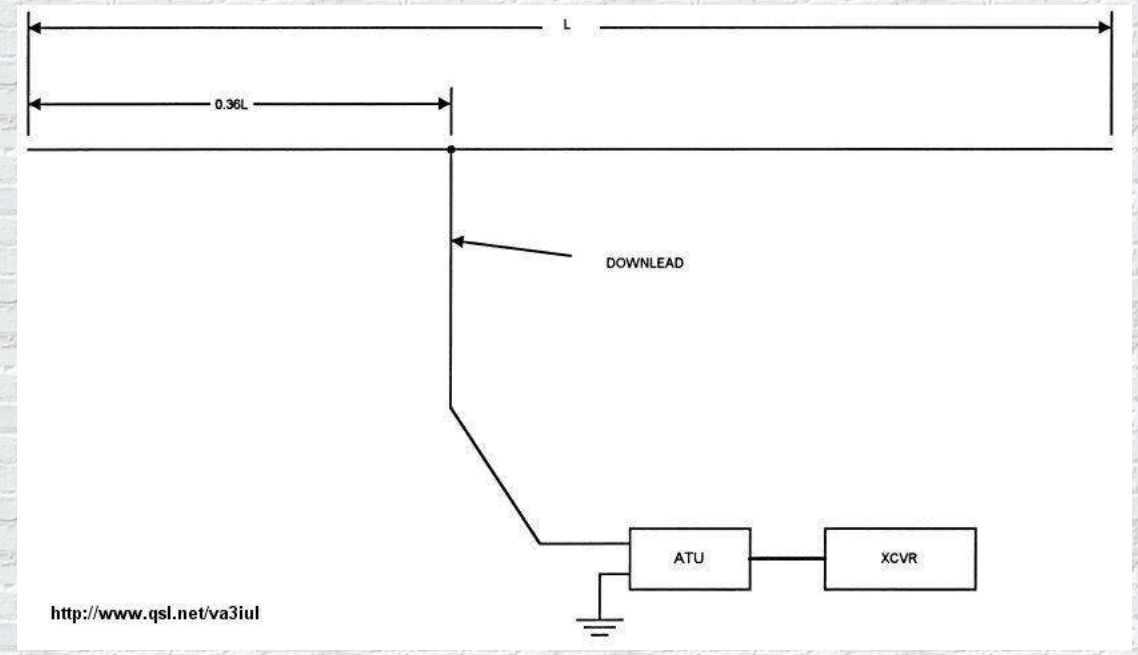

07 - Windom Antenna - Feed with coax cable

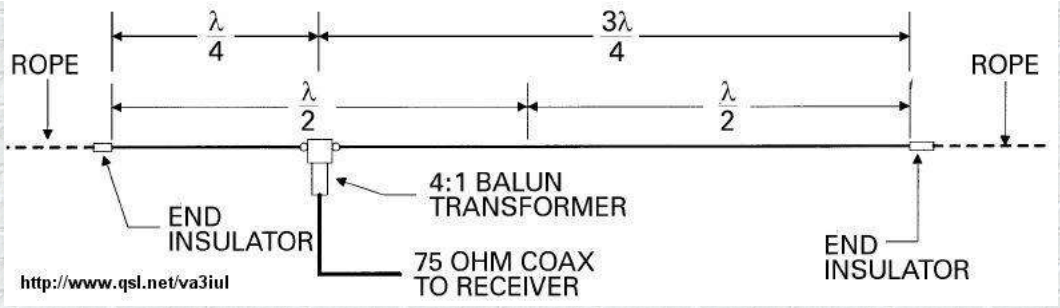

08 - Quarter Wavelength Vertical Antenna

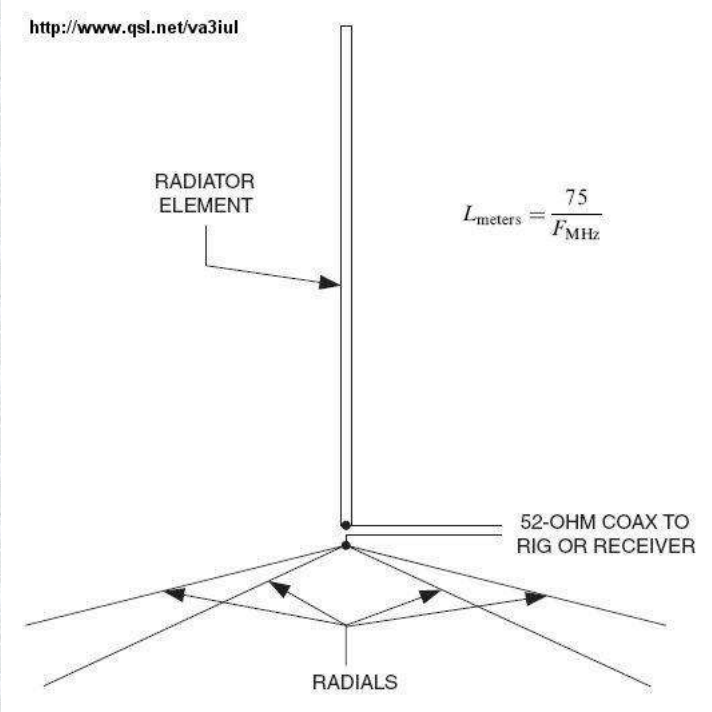

09 - Folded Marconi Tee Antenna

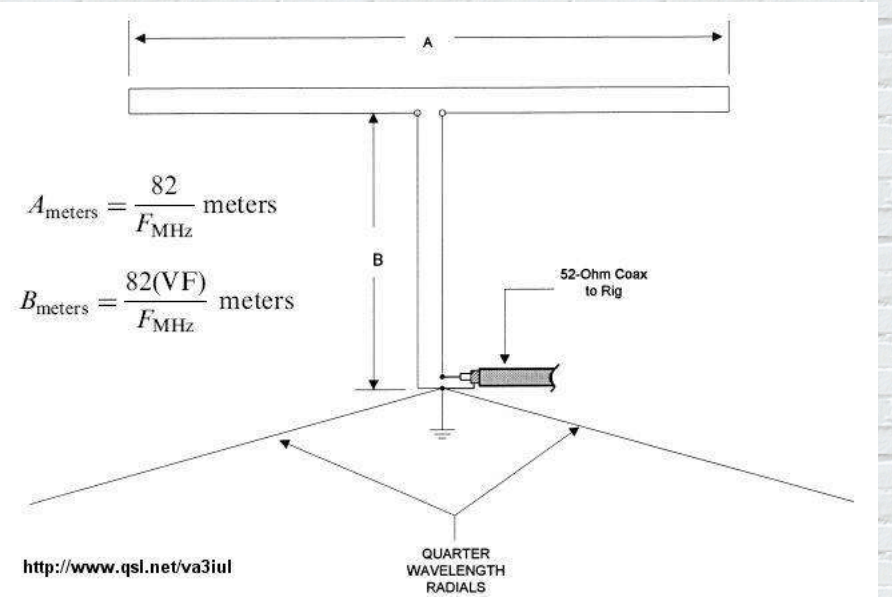

10 - Zeppelin Antenna

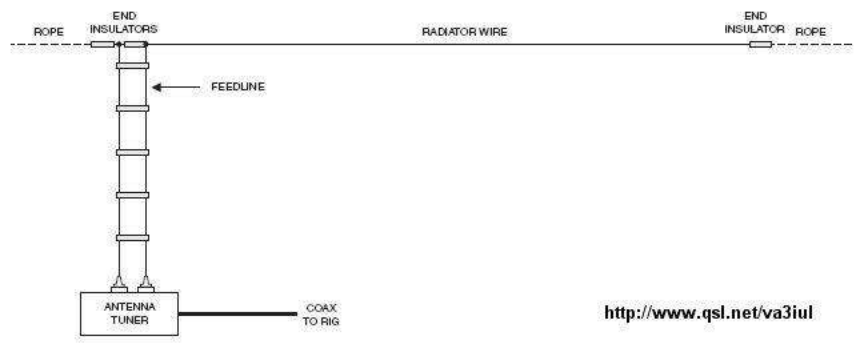

11 - EWE Antenna

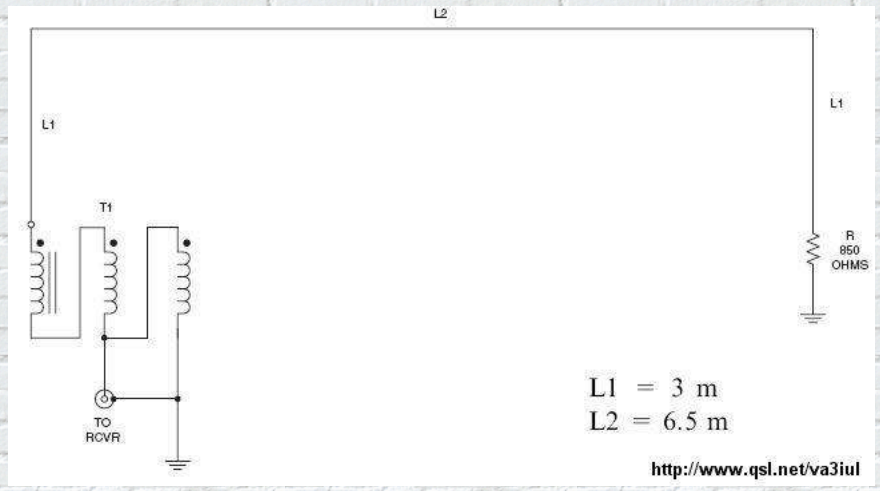

12 - Dipole Antenna - Balun

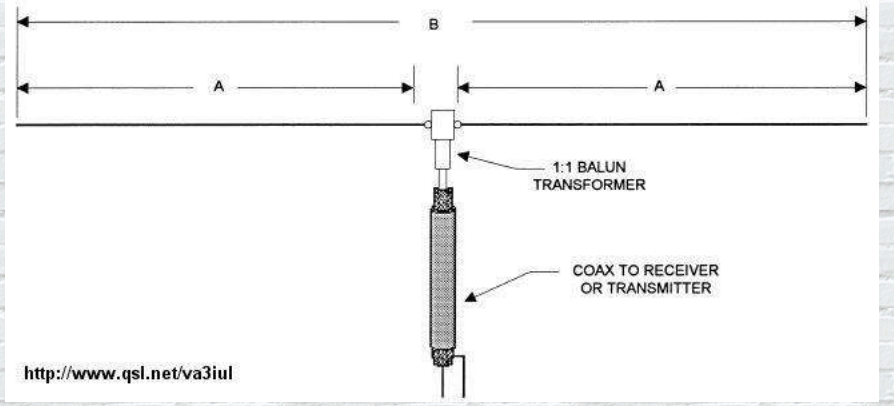

13 - Multiband Dipole Antenna

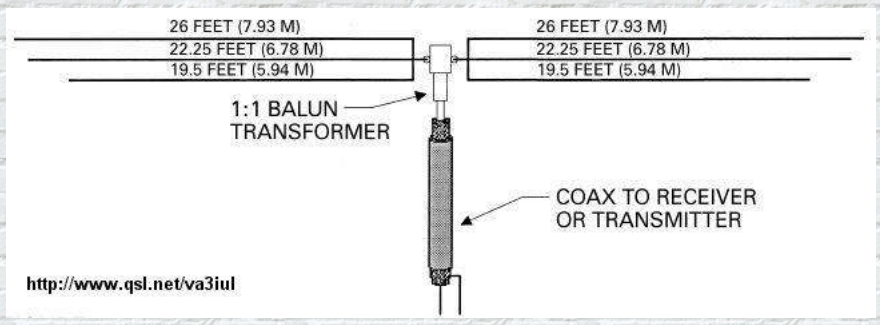

14 - Inverted-Vee Antenna

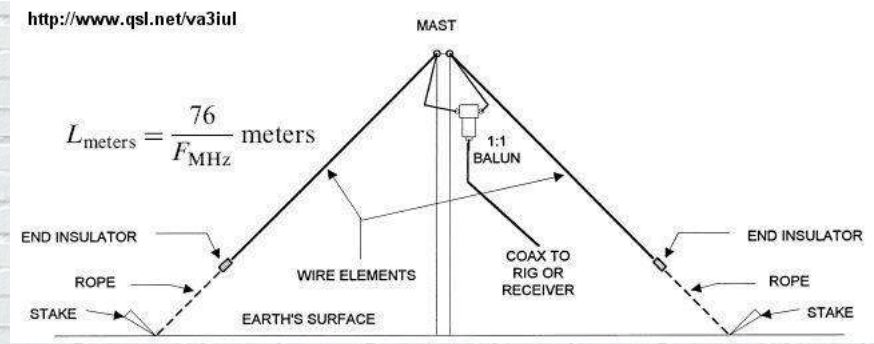

15 - Sloping Dipole Antenna

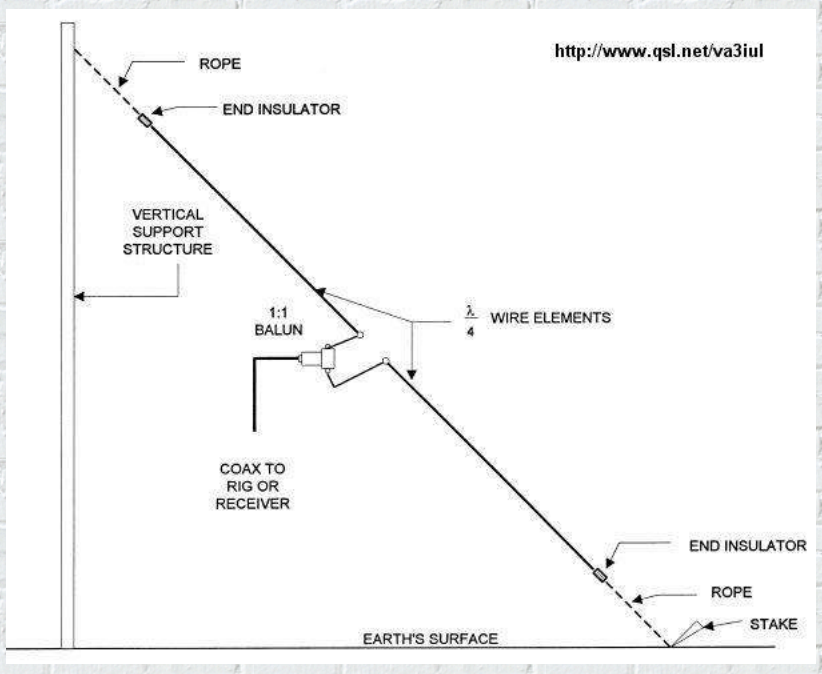

16 - Vertical Dipole

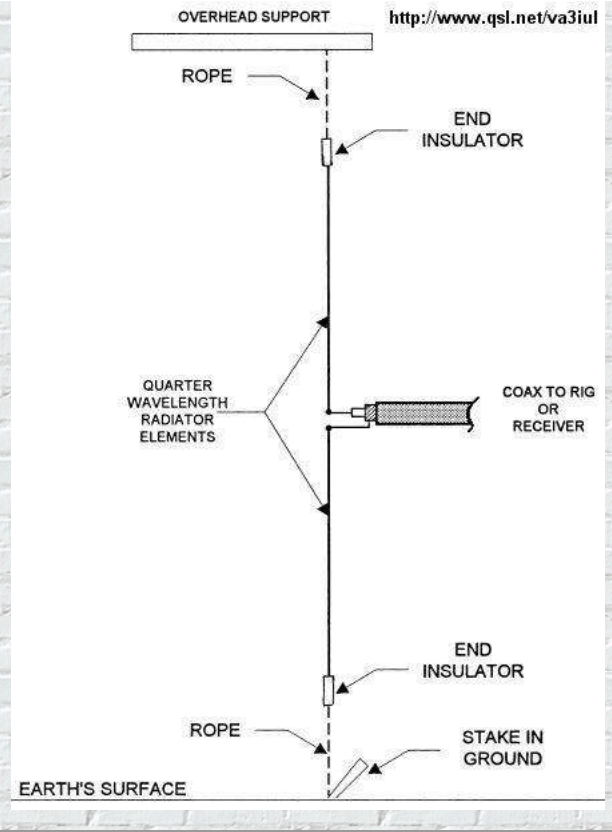

17 - Delta Fed Dipole Antenna

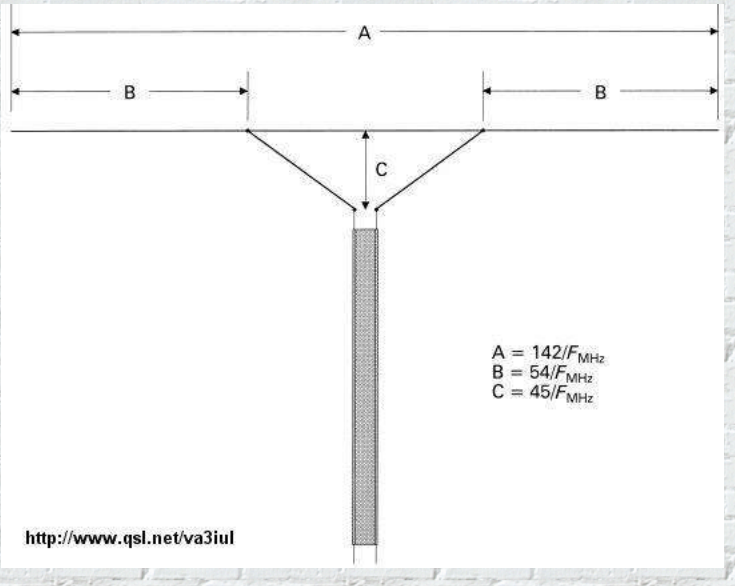

18 - Bow-Tie Dipole Antenna

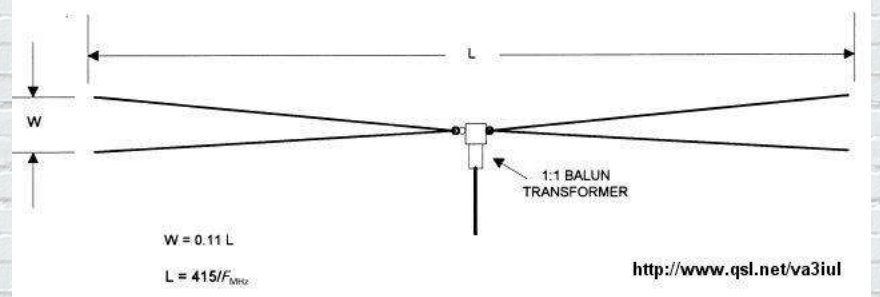

19 - Bow-Tie Folded Dipole Antenna for RX

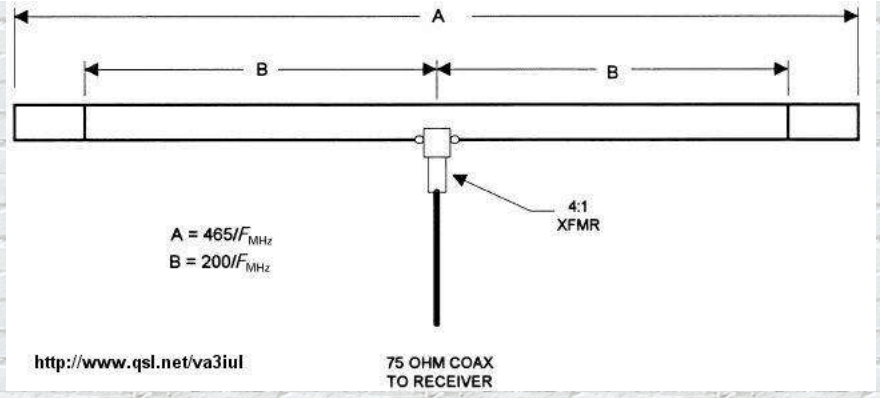

20 - Multiband Tuned Doublet Antenna

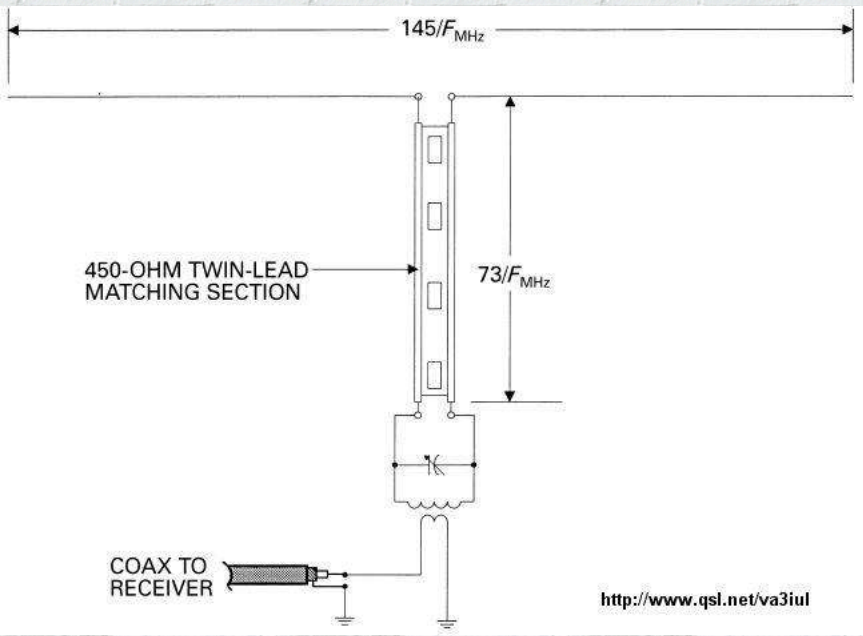

21 - G5RV Antenna

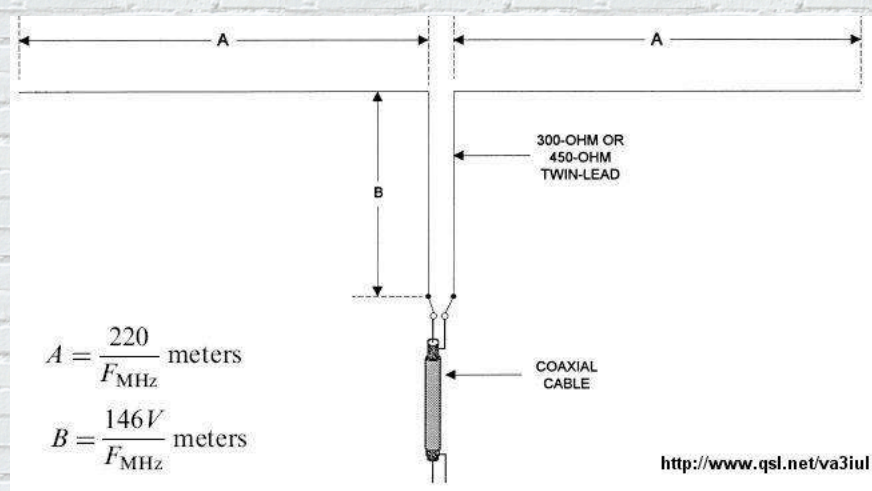

22 - Wideband Dipole Antenna

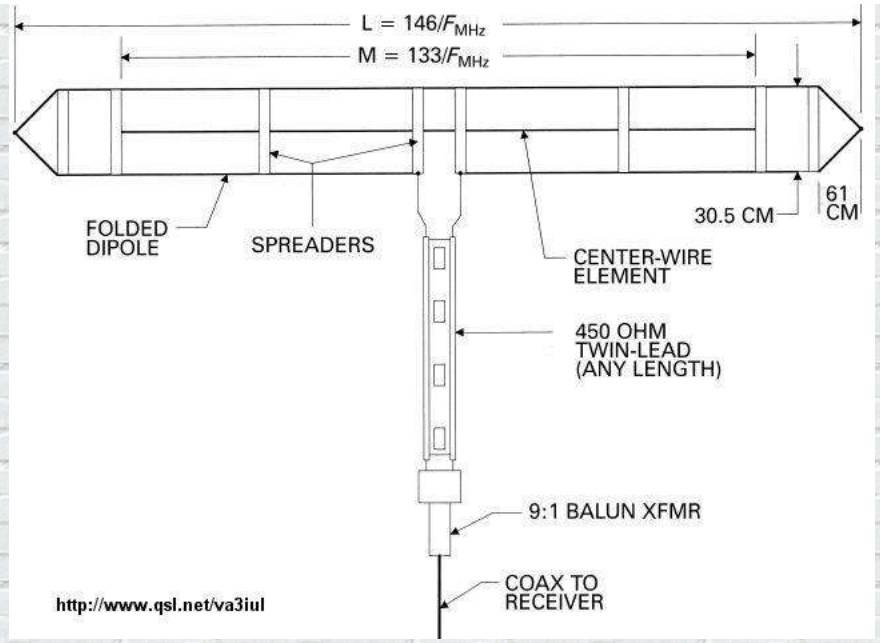

23 - Wideband Dipole for Receiving

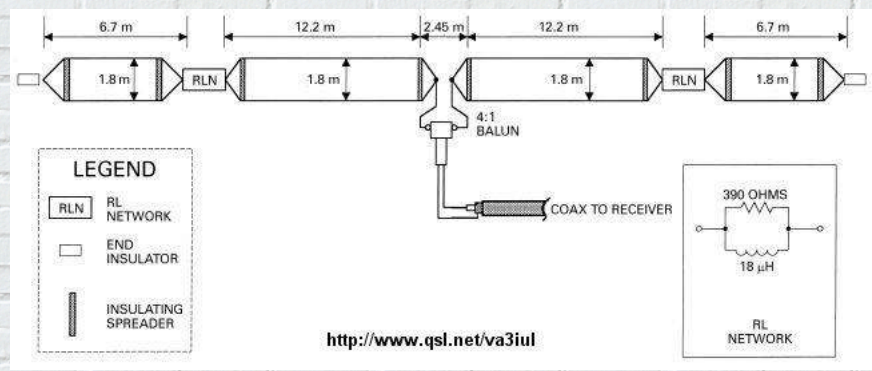

24 - Tilted Folded Dipole Antenna

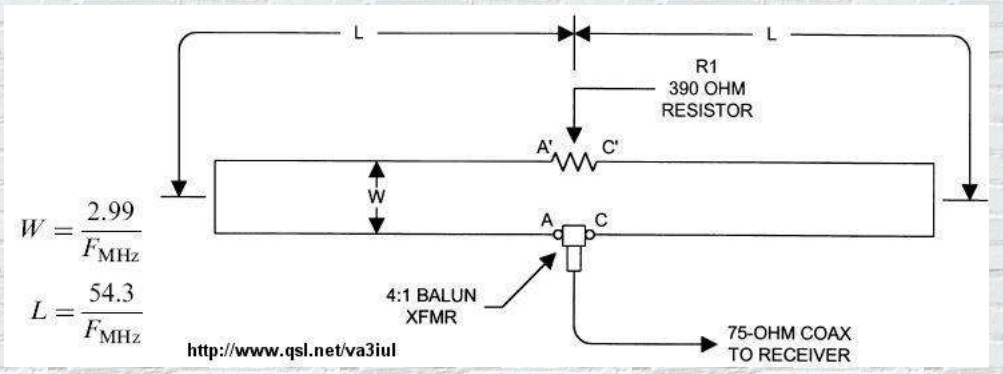

25 - Right Angle Marconi Antenna

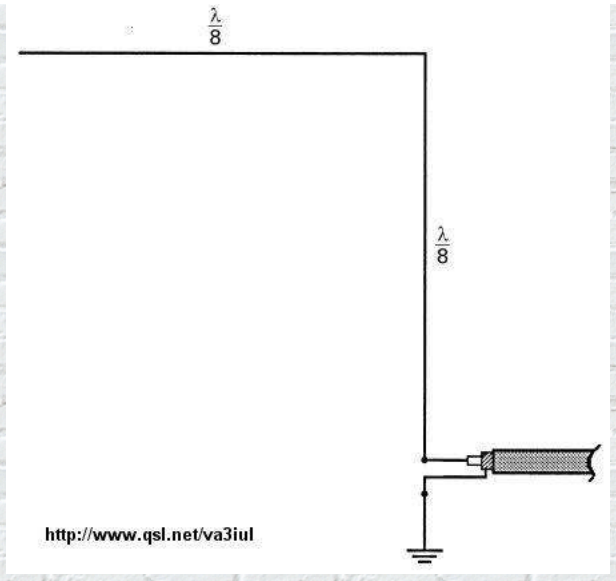

26 - Linearly Loaded Tee Antenna

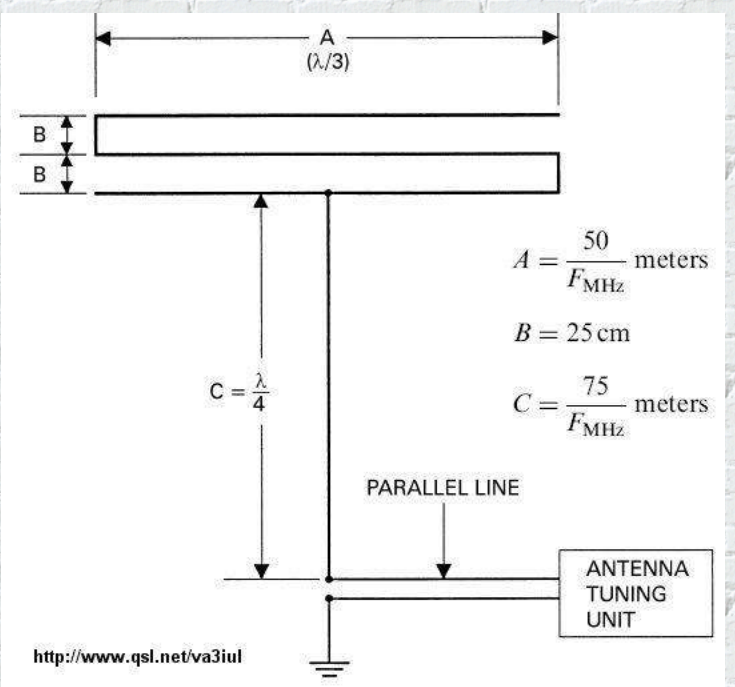

27 - Reduced Size Dipole Antenna

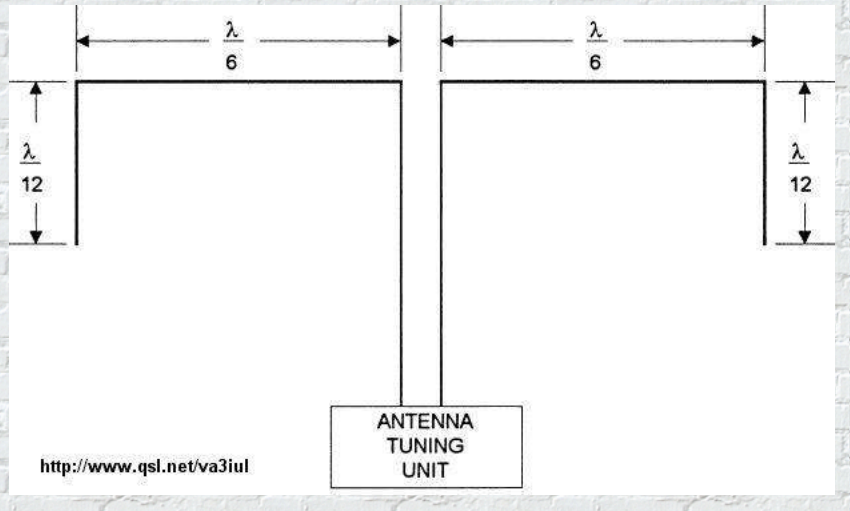

28 - Doublet Dipole Antenna

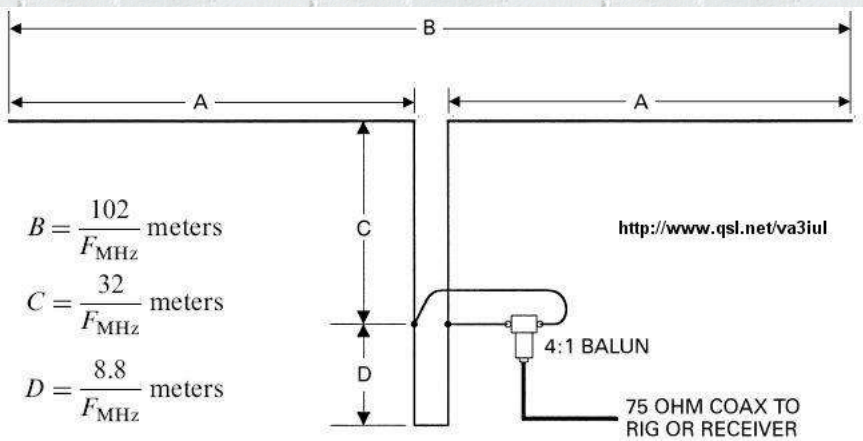

29 - Delta Loop Antenna

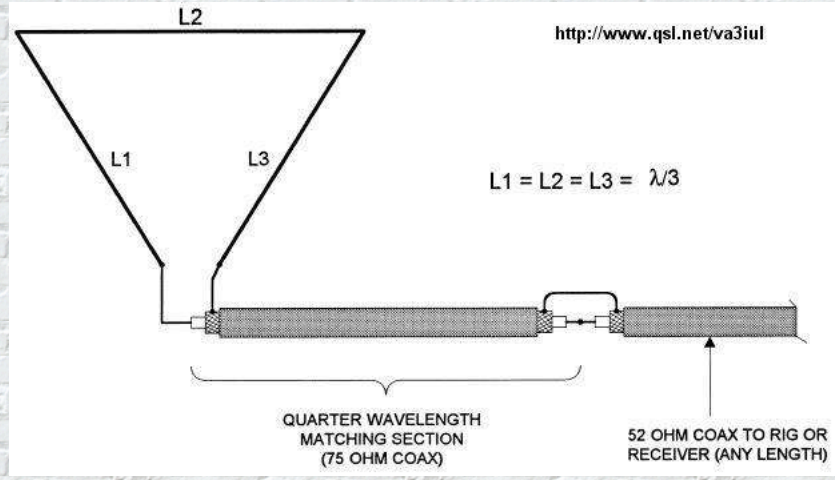

30 - Half Delta Loop Antenna

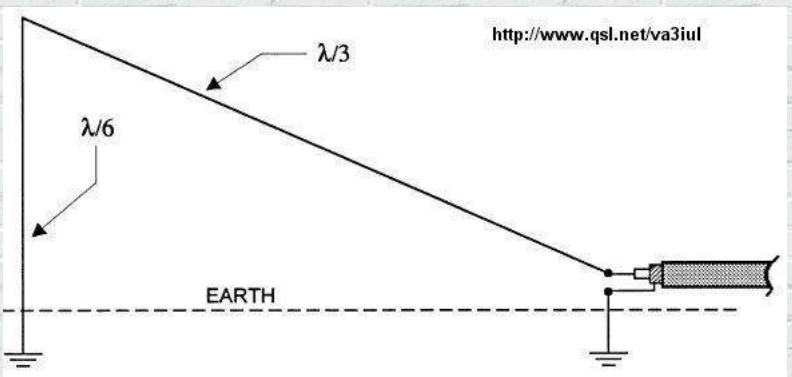

31 - Collinear Franklin Antenna

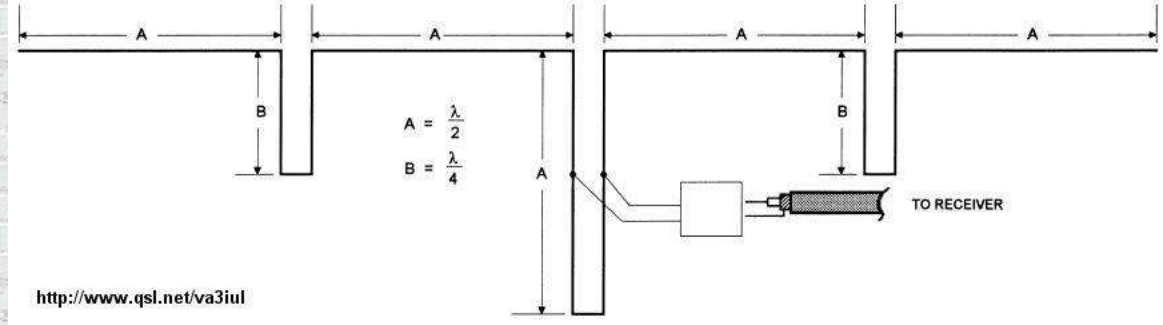

32 - Four Element Broadside Antenna

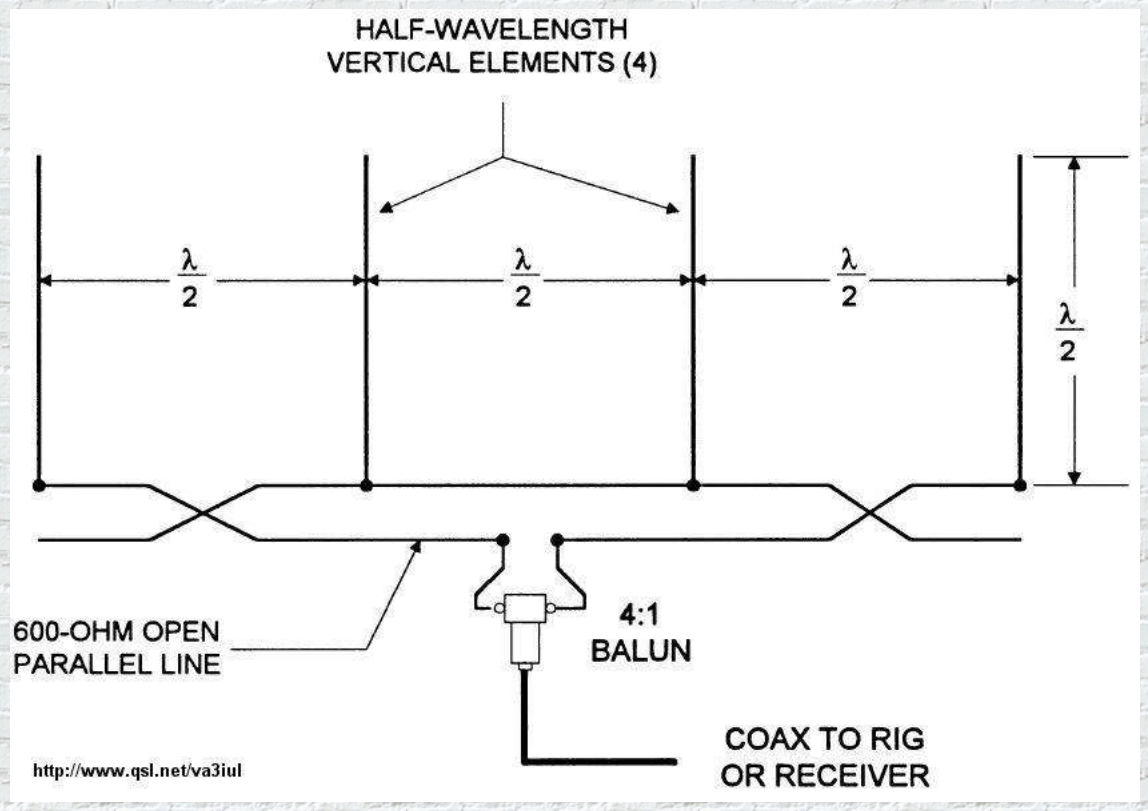

33 - The Lazy-H Array Antenna

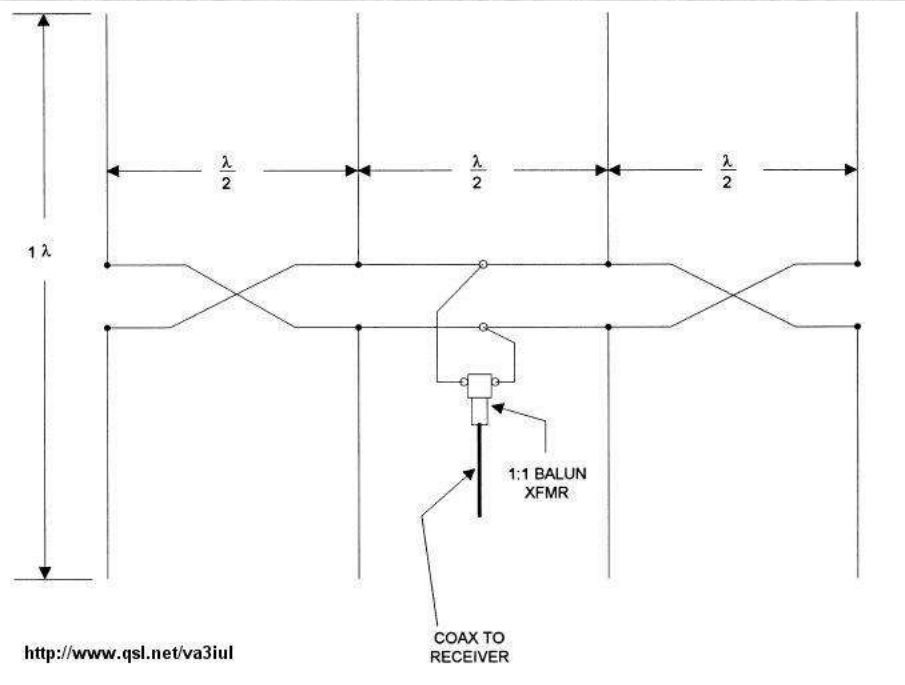

34 - Sterba Curtain Array Antenna

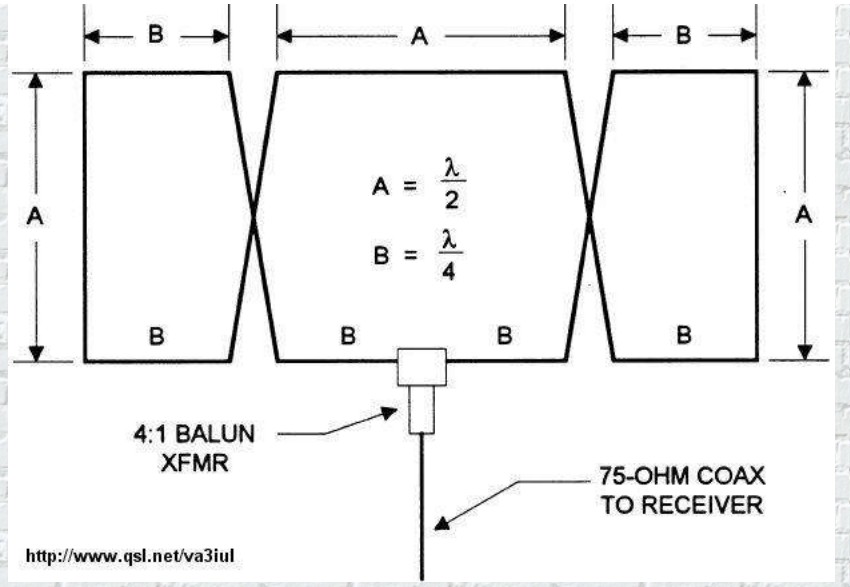

35 - T-L DX Antenna

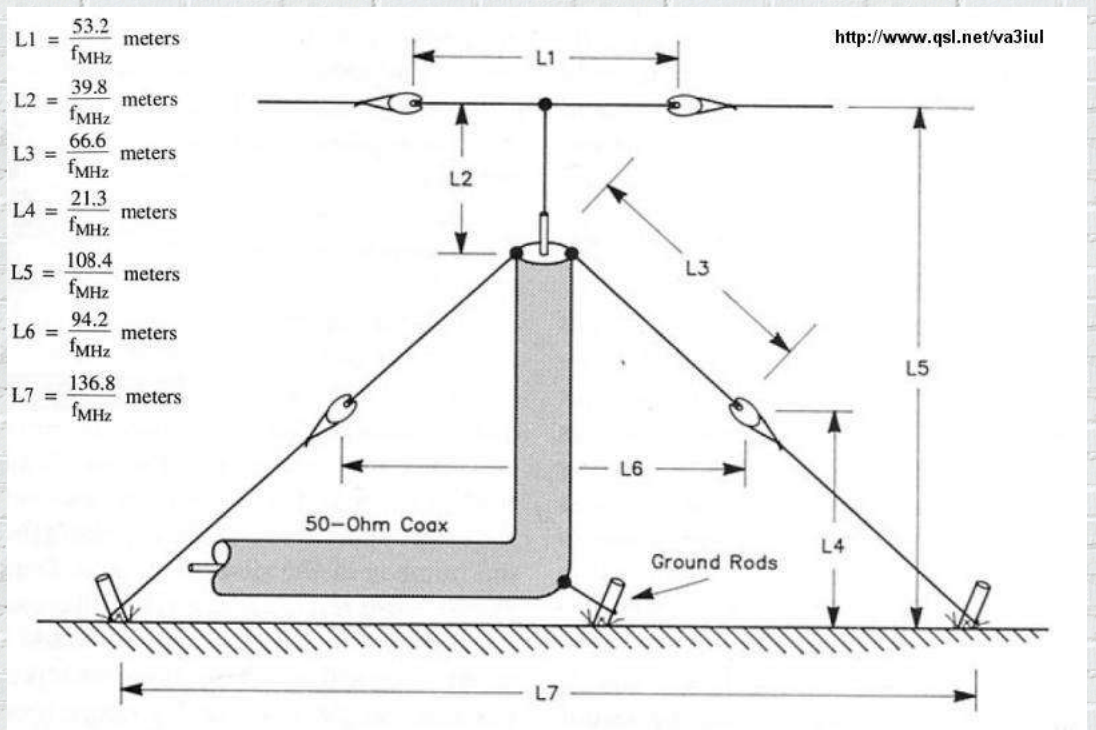

36 - 1.9 MHz Full-wave Loop Antenna

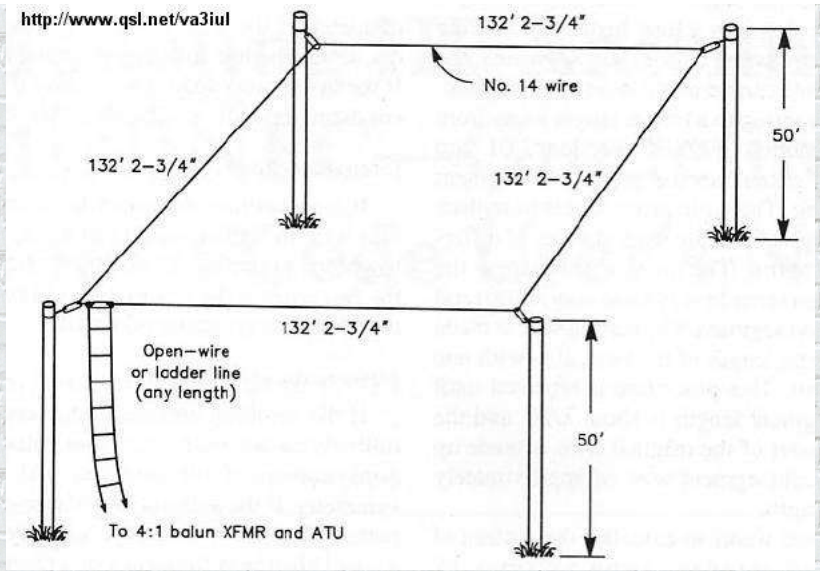

37 - Multi-Band Portable Antenna

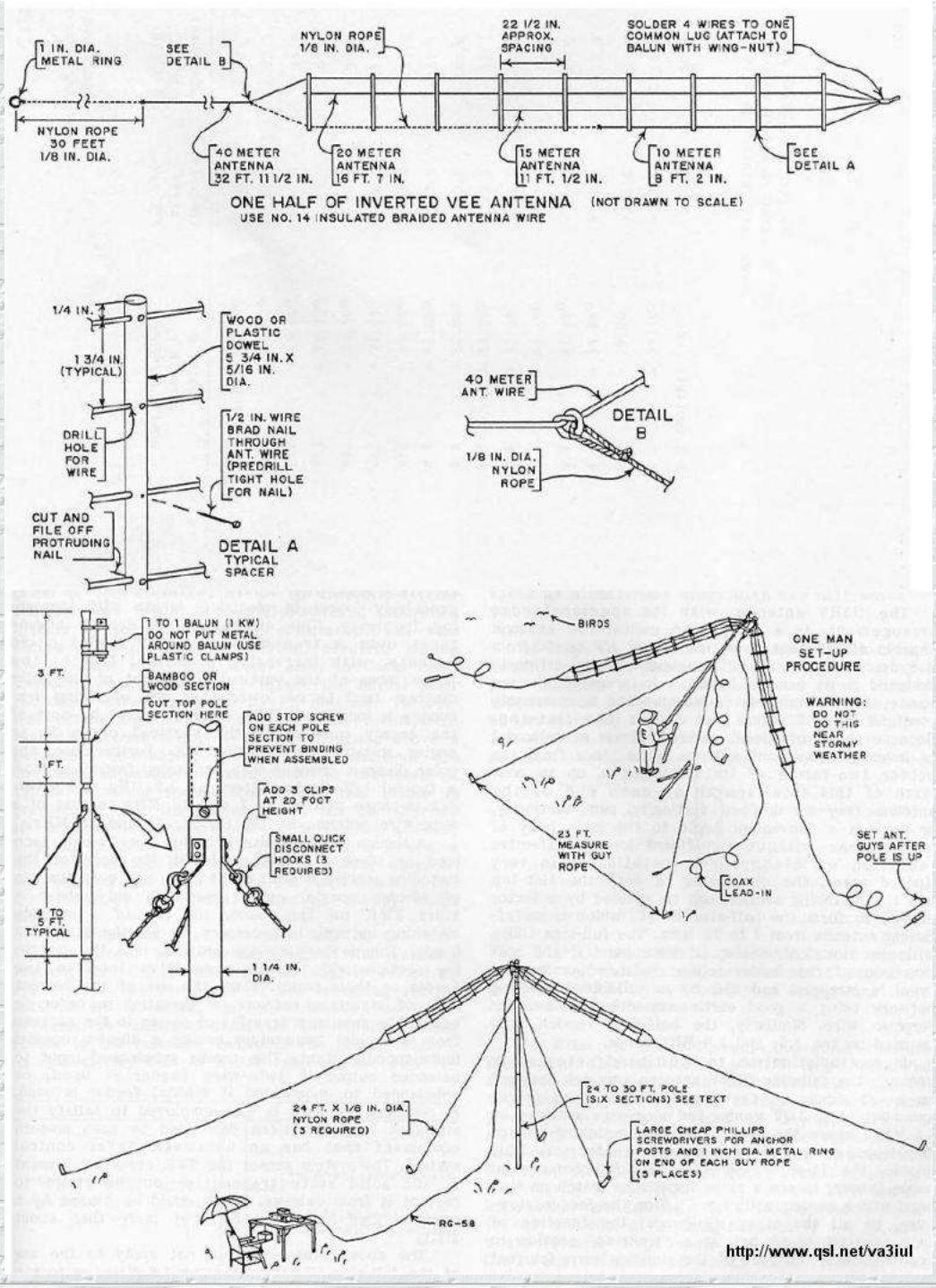

38 - Off-center-fed Full-wave Doublet Antenna

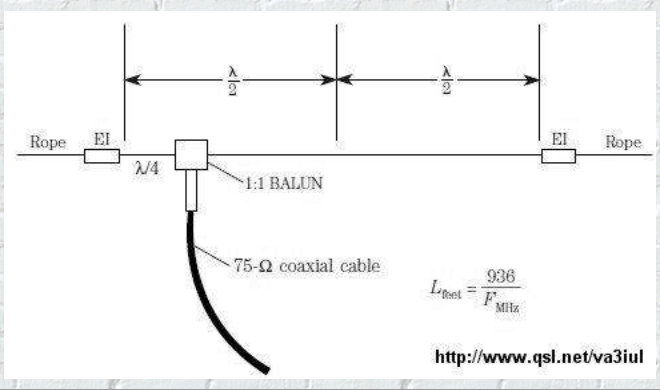

39 - Terminated Sloper Antenna

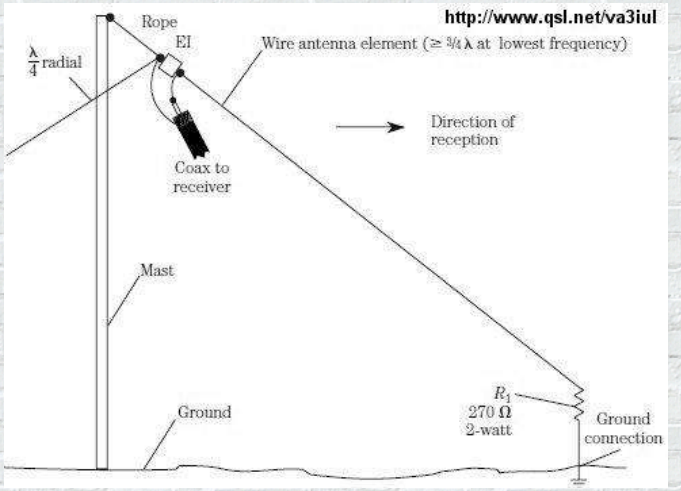

40 - Double Extended Zepp Antenna

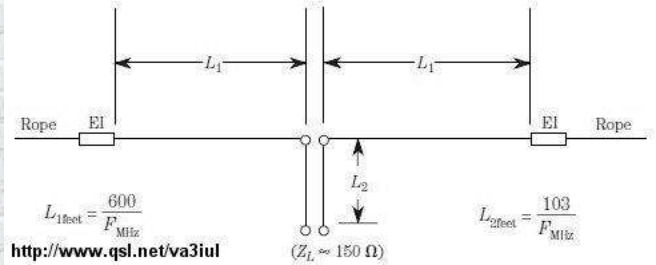

41 - TCFTFD Dipole Antenna

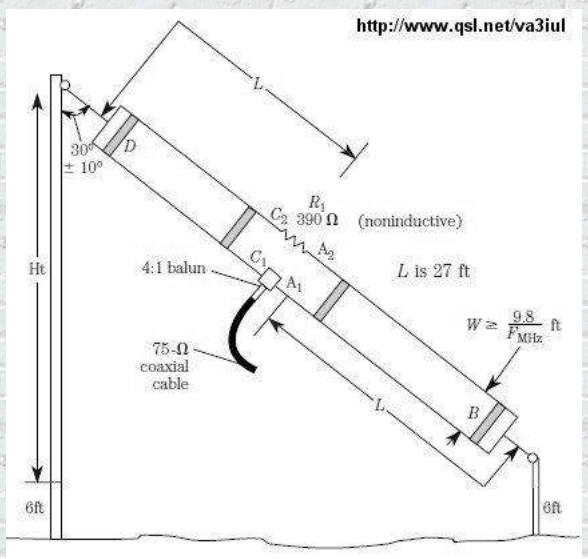

42 - Vee-Sloper Antenna

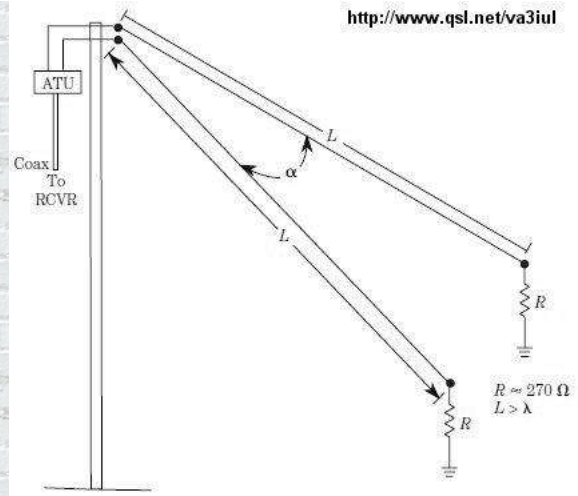

43 - Rhombic Inverted-Vee Antenna

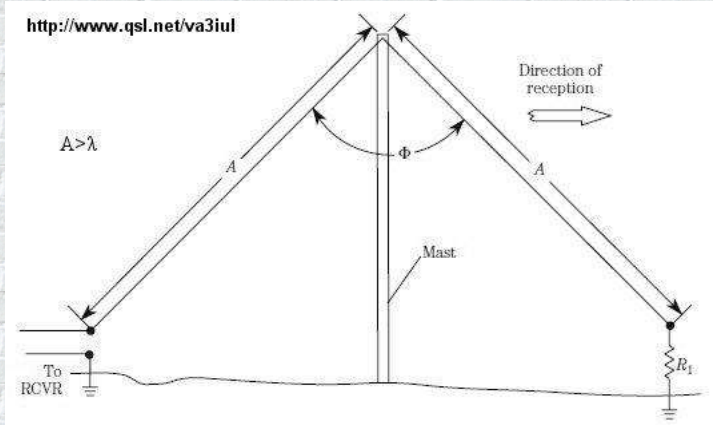

44 - Counterpoise Longwire

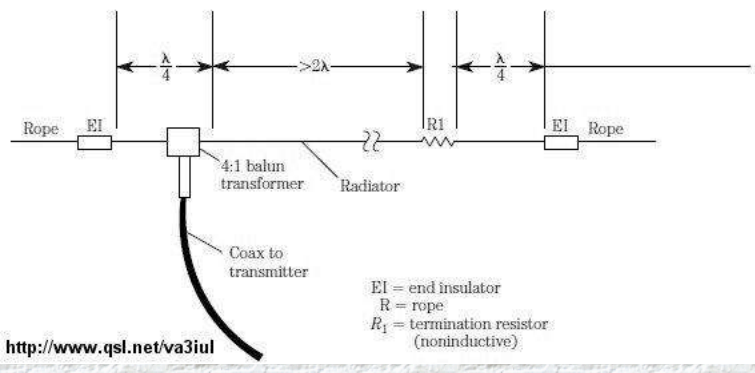

45 - Bisquare Loop Antenna

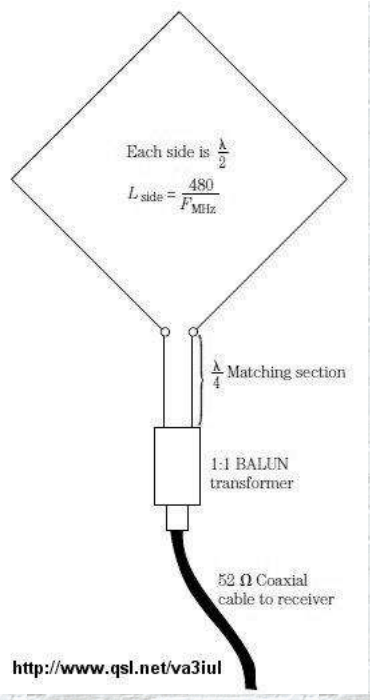

46 - Piggyback Antenna for 10m

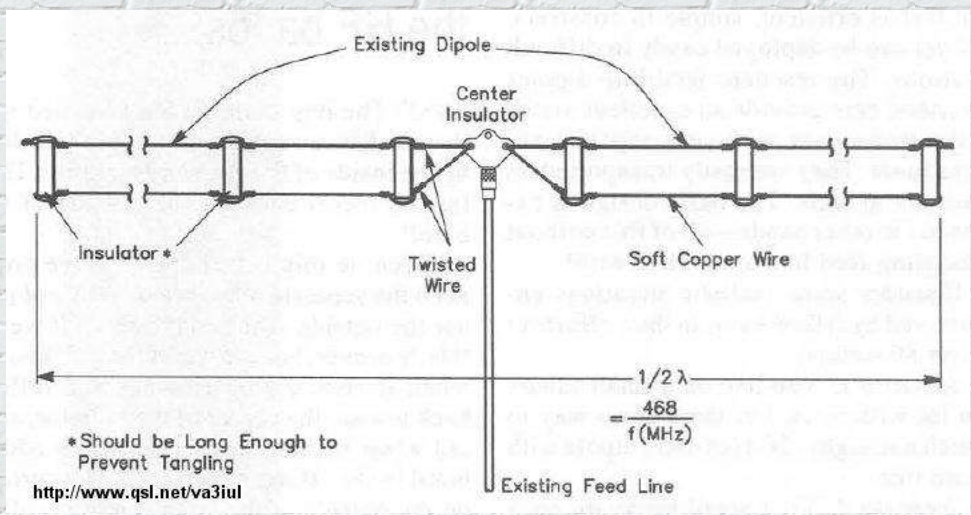

47 - Vertical Sleeve Antenna for 10m

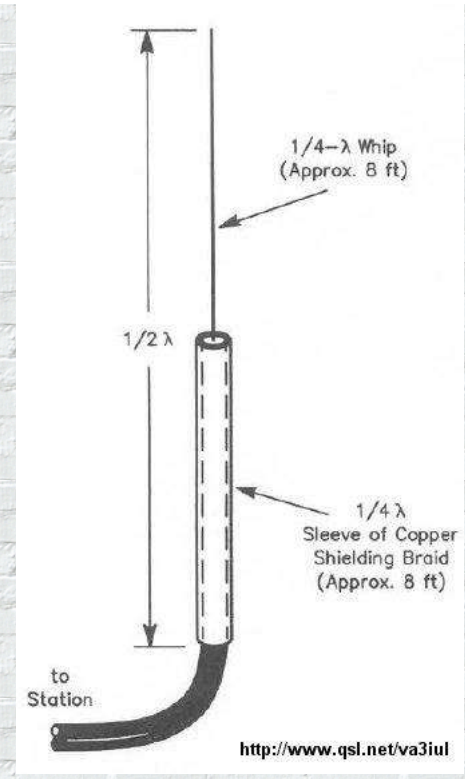

48 - Double Windom Antenna

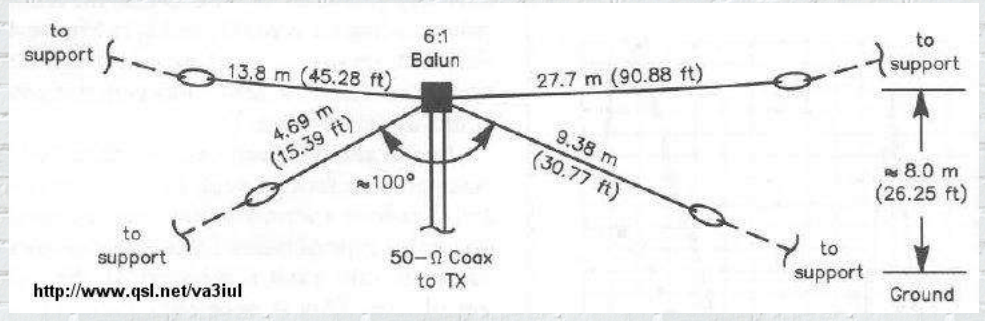

49 - Double Windom for 9 Bands

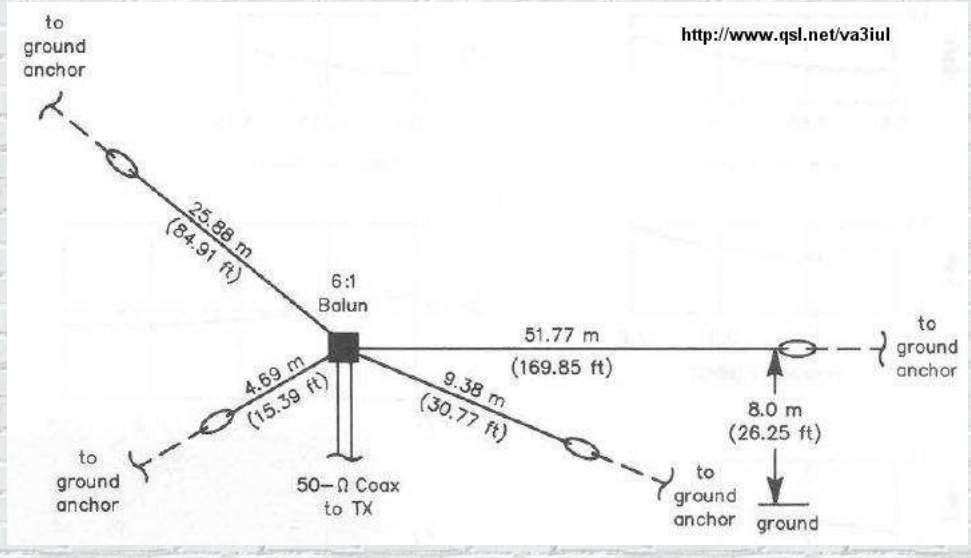

50 - Collinear Trap Antenna

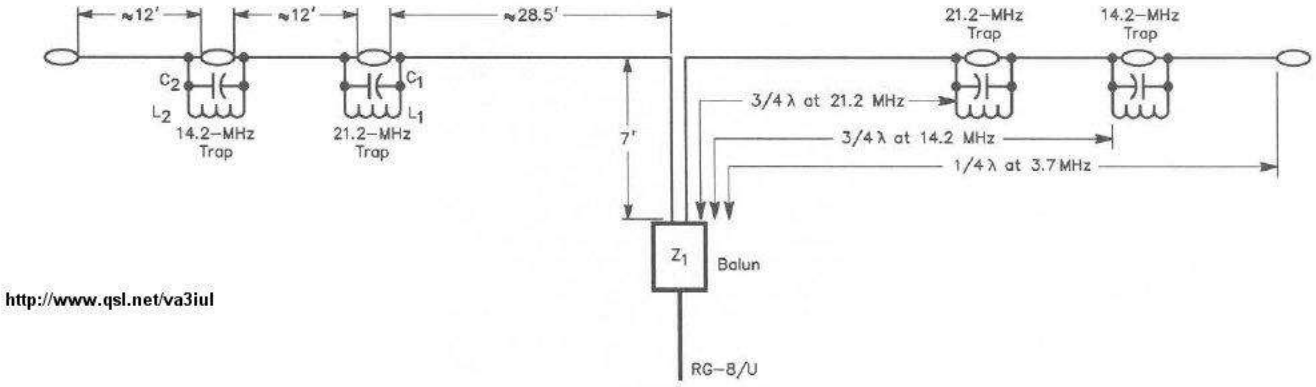

C1, C2—25-pf. 6000-volt disk ceramic. See text.
L_1—Approx. 2 µH–4¾ turns No. 18, 2¼-inches diam., ⅜ inch long, or 5 turns No. 18, 2-inch diam., 16 tpi. See text.
L_2—Approx. 5 µH.—8 turns No. 18, 2¼-inch dia., ⅝ inch long, or 9 turns No. 18, 2-inch diam. 16 tpi. See text.
Z_1—1 to 1 balun.

51 - Short Dipole Antenna for 40m - 80m - 160m

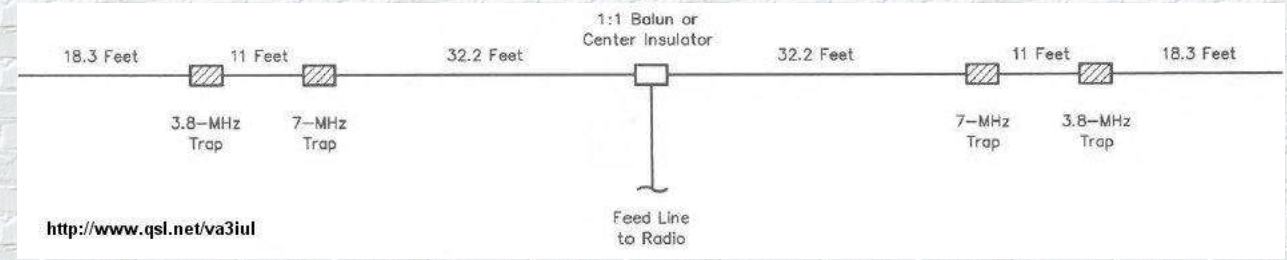

52 - Center Fed-Zepp Antenna for 80m - 40m

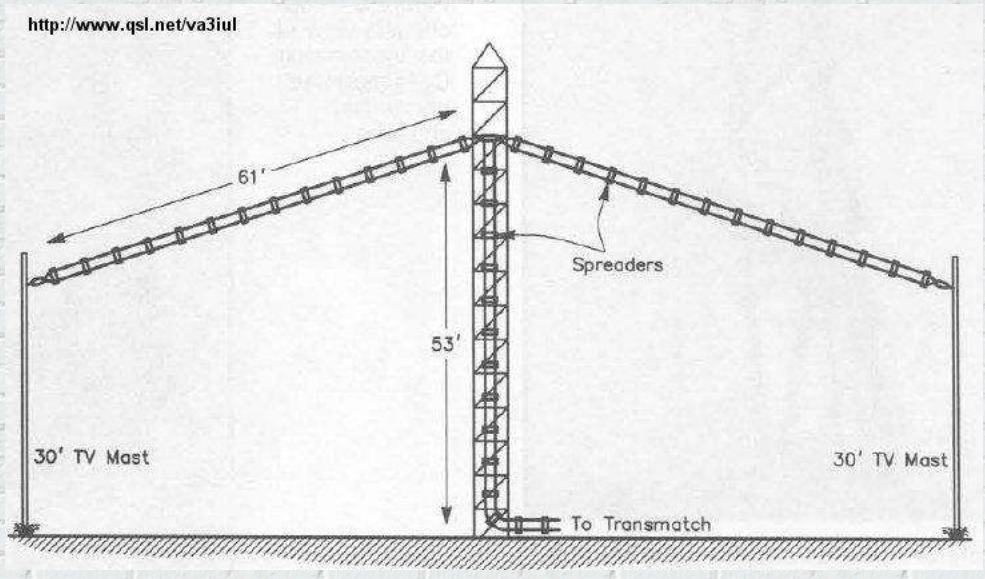

53 - All-Bands Antenna

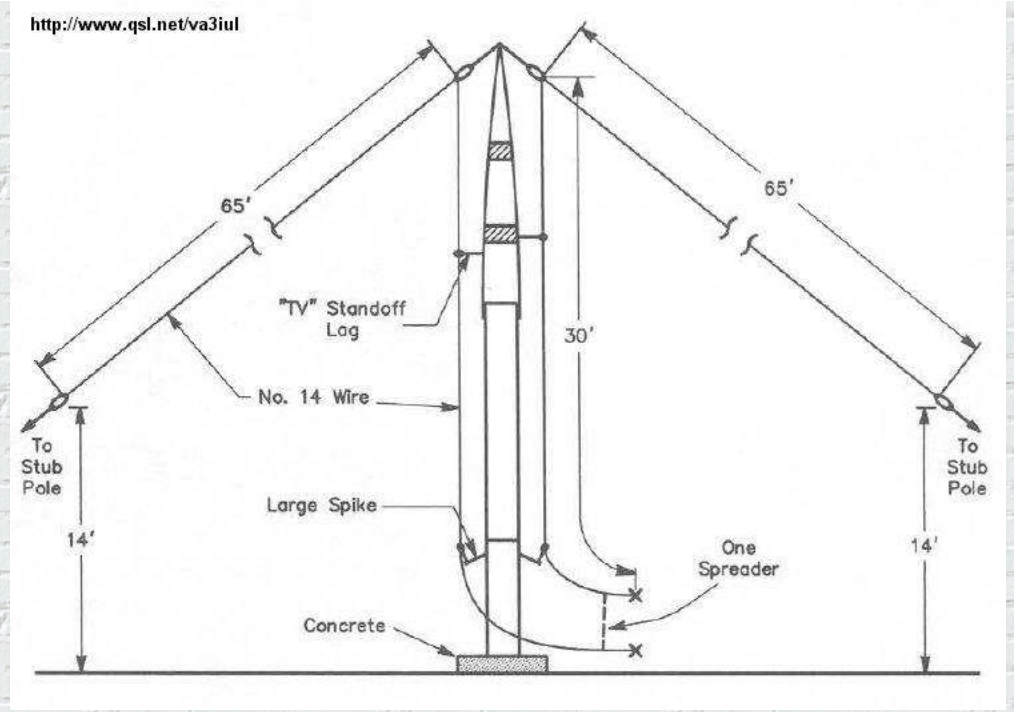

54 - All-Bands Dipole Antenna

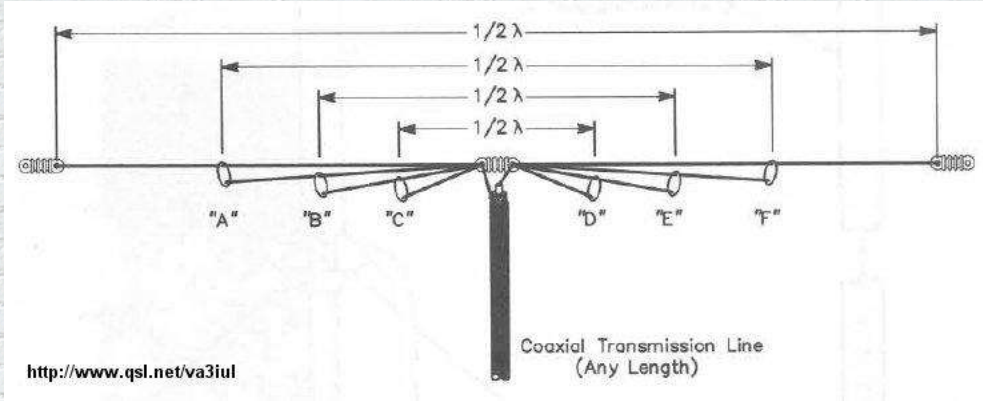

55 - Multiband Z Antenna

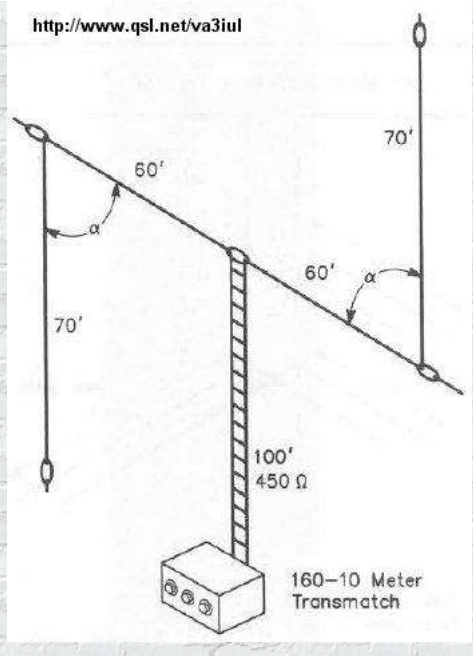

56 - Multiband Dipole Antenna

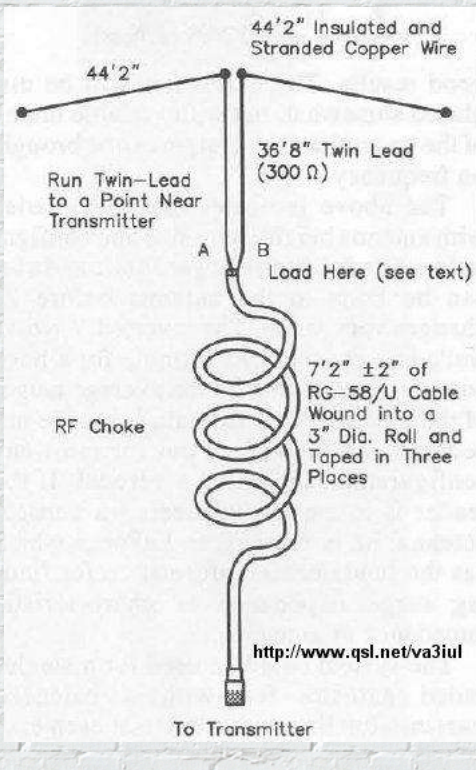

57 - Five-Bands No-Tuner Antenna

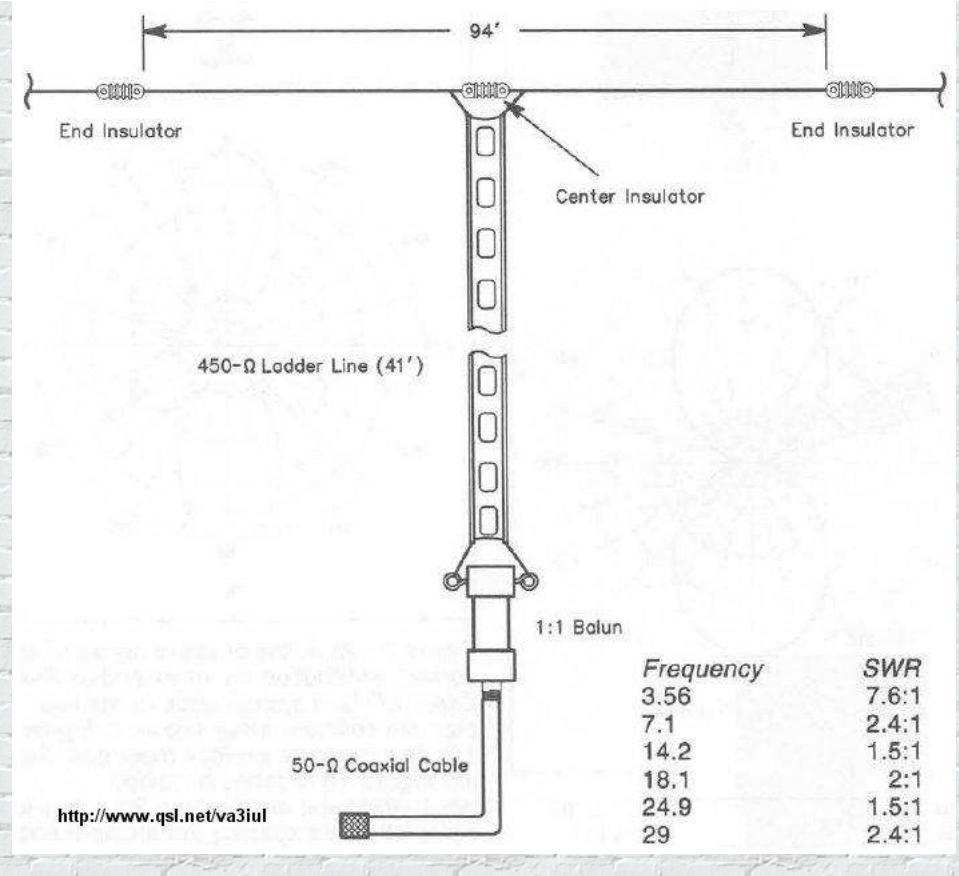

58 - Dualband Full-wave Loop Antenna for 80m-40m

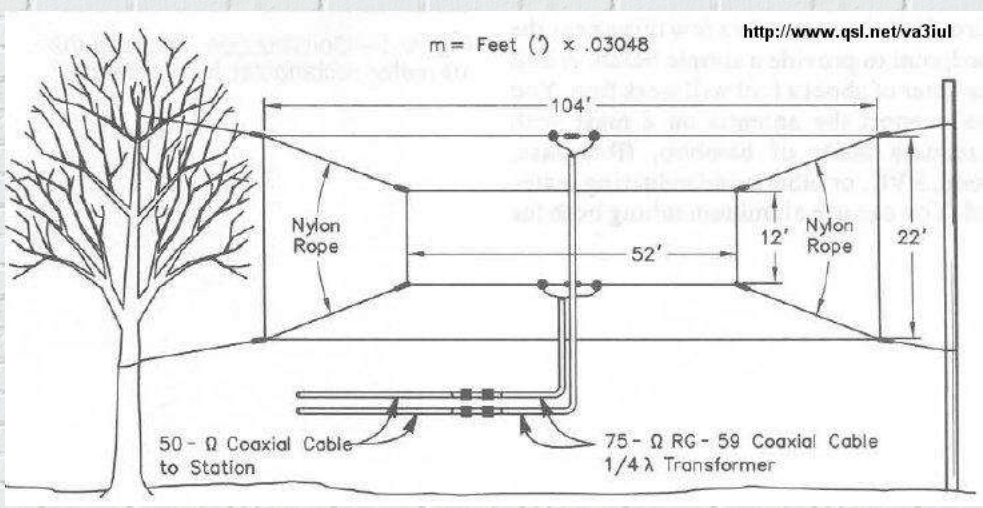

59 - Loop Antenna for 10m

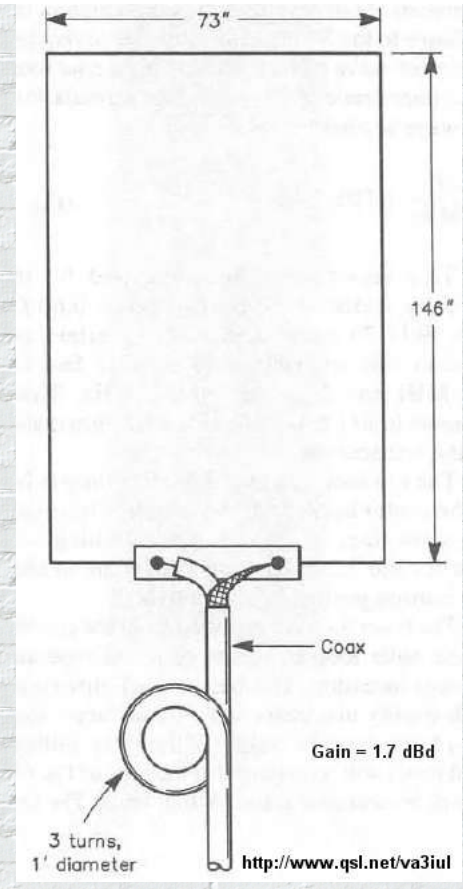

60 - Lazy Quad Antenna for 10m

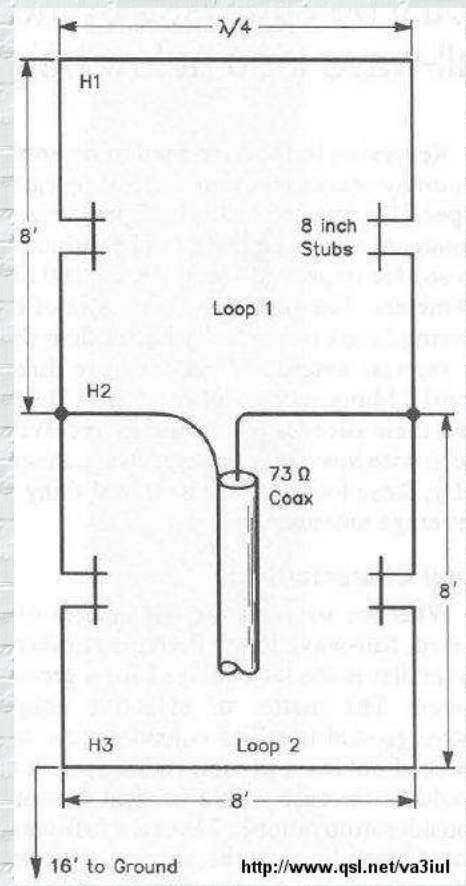

61 - Tri-band Delta Loop Antenna for 80m - 40m - 30m

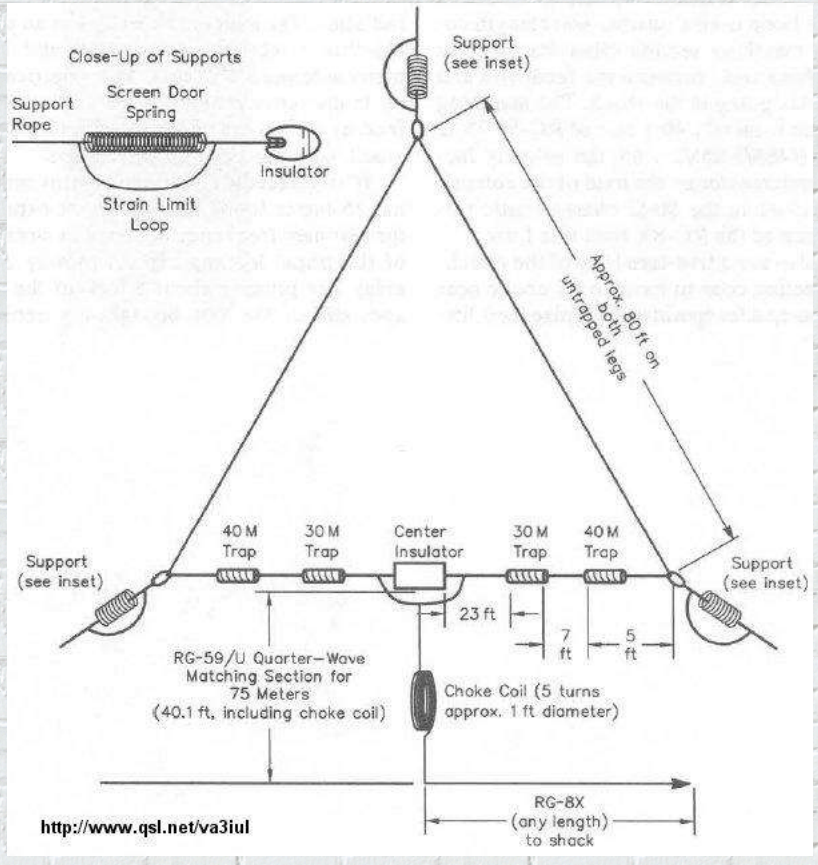

62 - Dual-band Loop Antenna for 30m - 40m

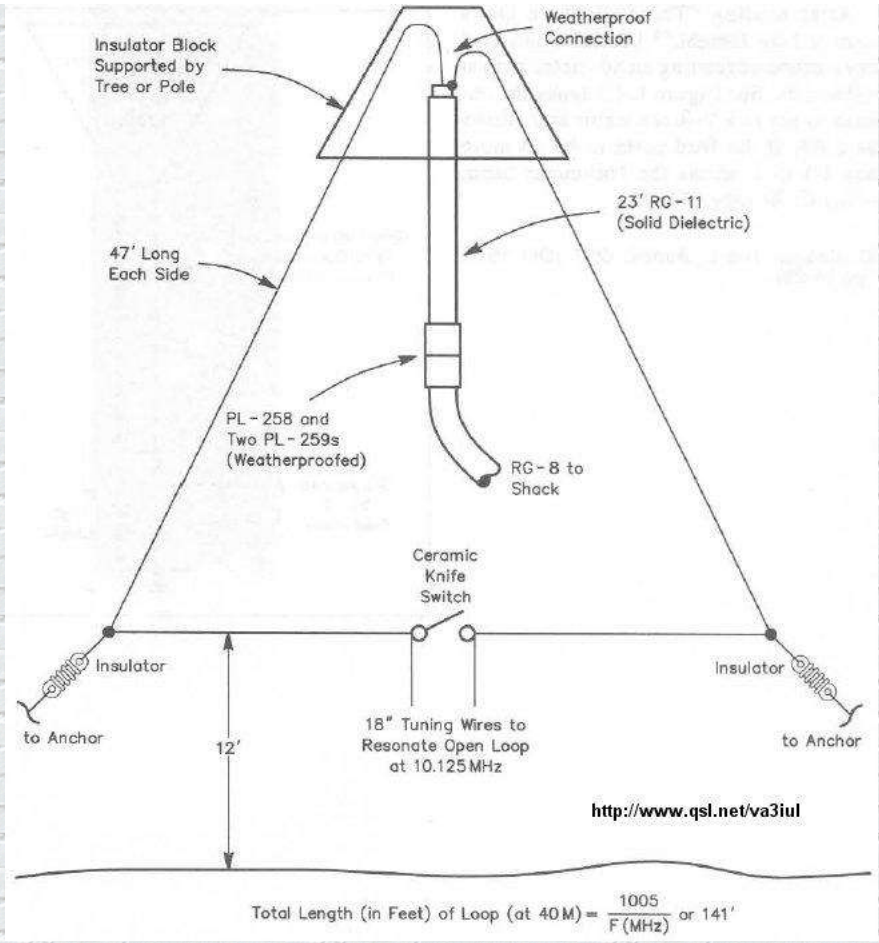

63 - Wire-Beam Antenna for 80m

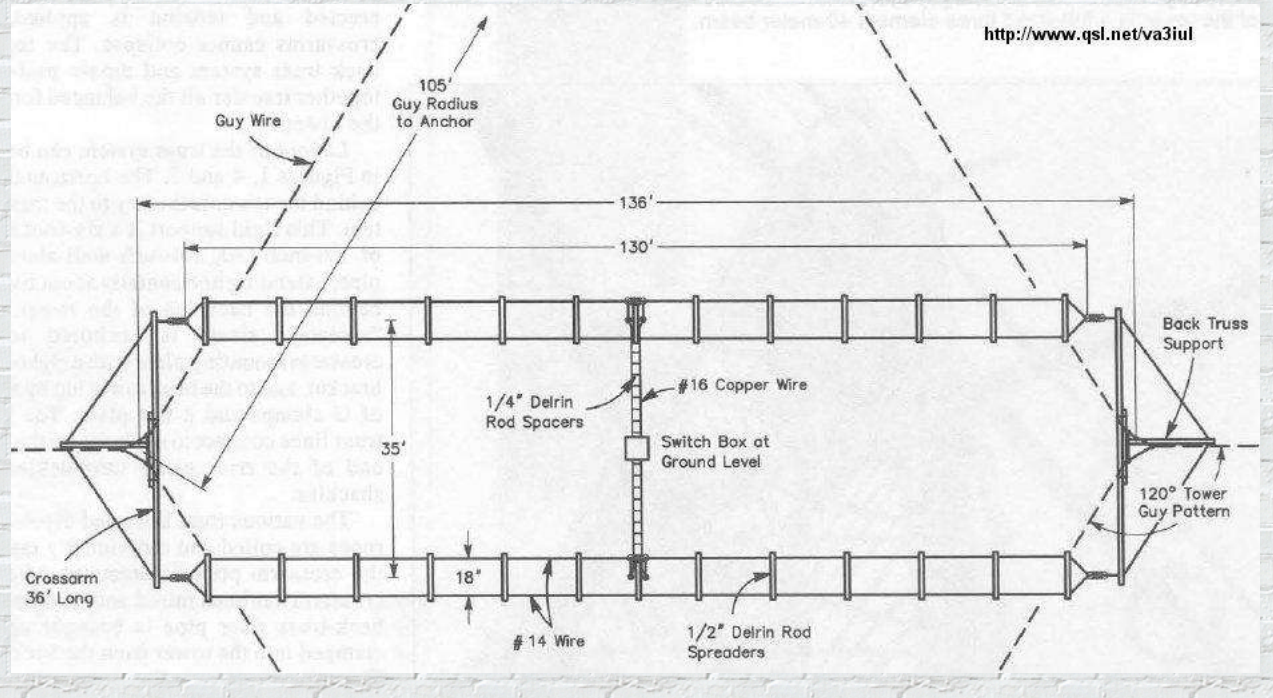

64 - Dual-Band Sloper Antenna

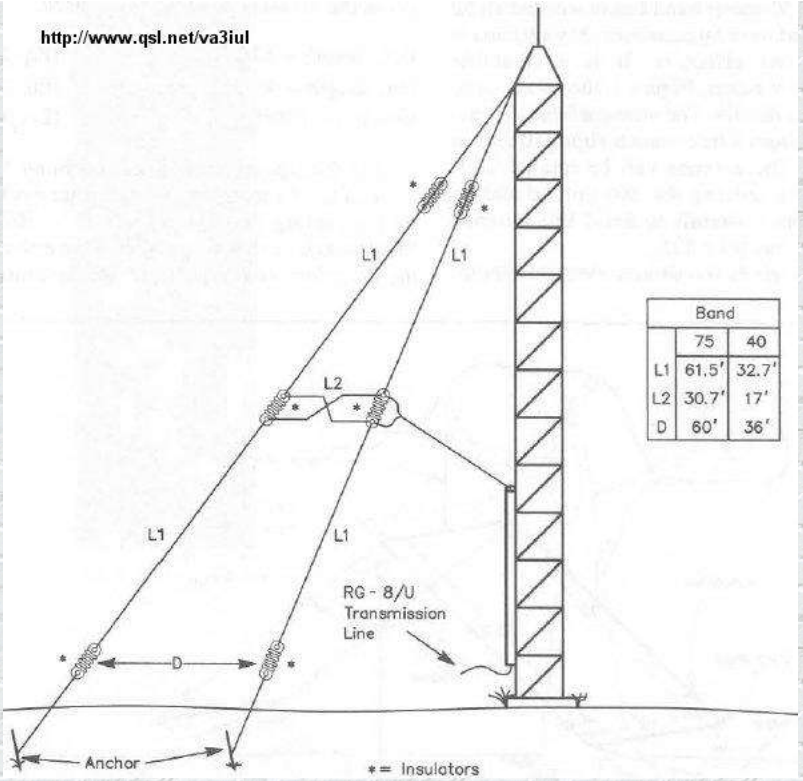

65 - Inverted-V Beam Antenna for 30m

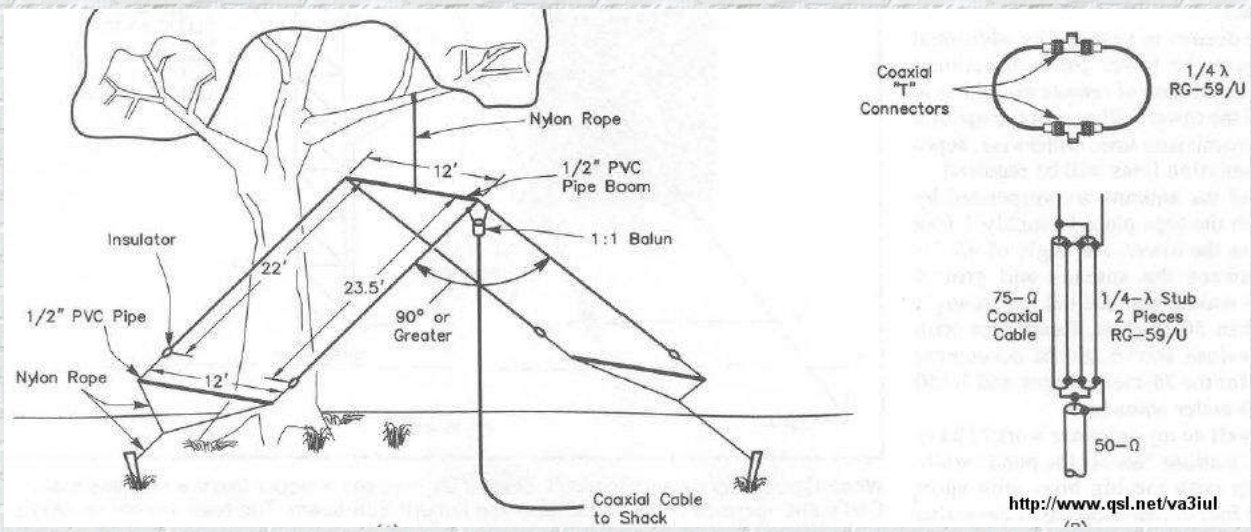

66 - ZL-Special Beam Antenna for 15m

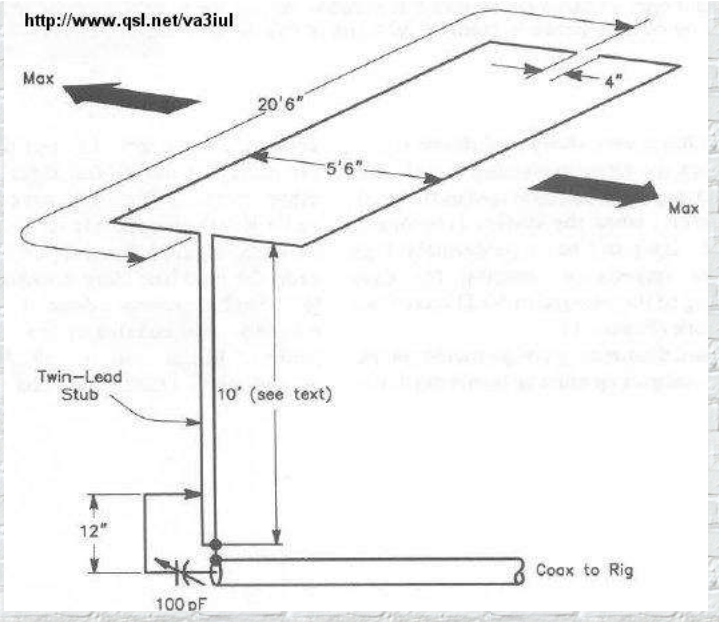

67 - Half-Sloper Antenna for 160m

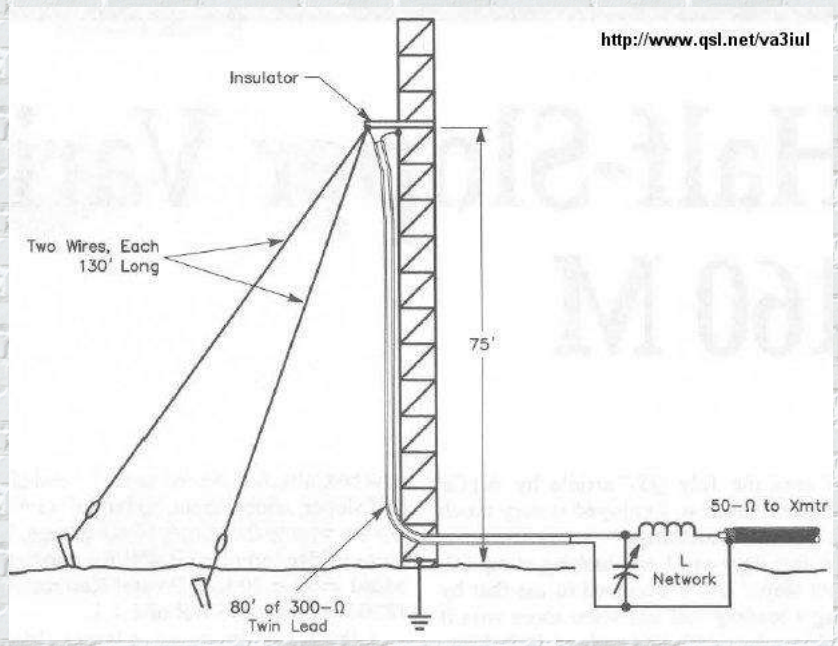

68 - Two-Bands Half Sloper for 80m - 40m

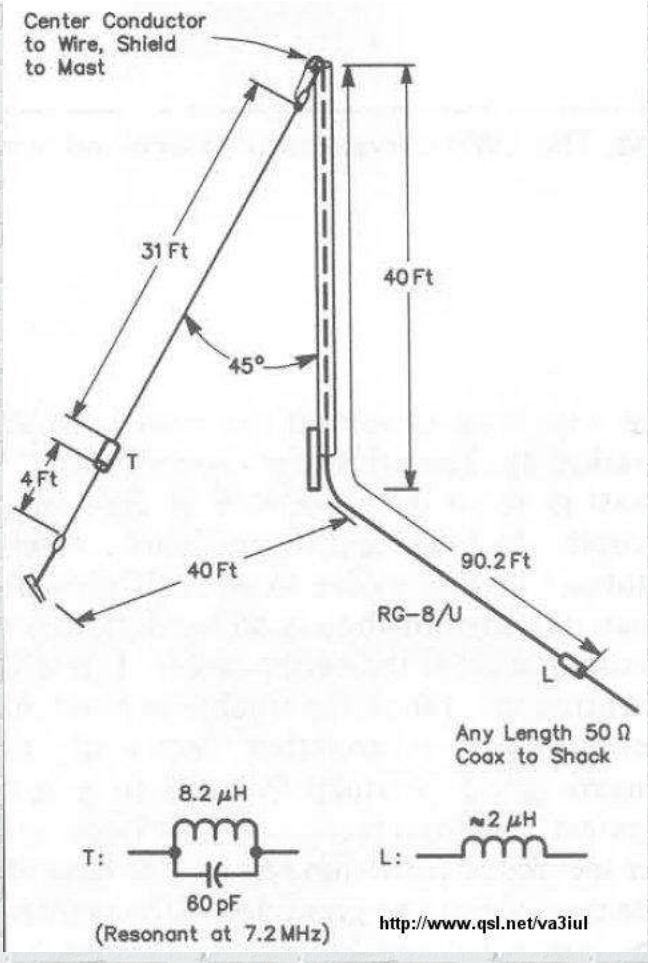

69 - Linear Loaded Sloper Antenna for 160m

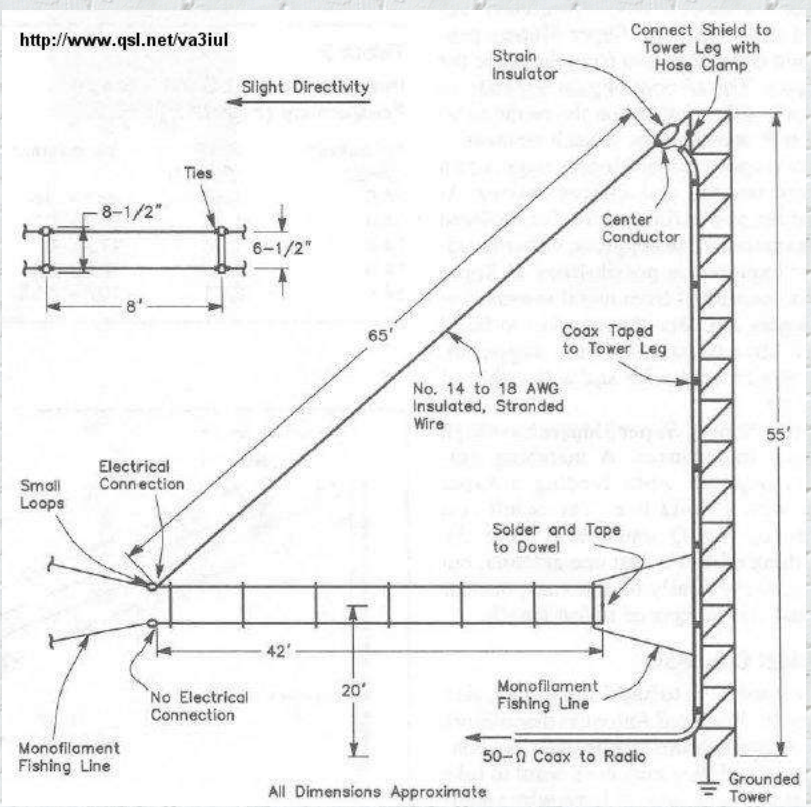

70 - Super-Sloper Antenna

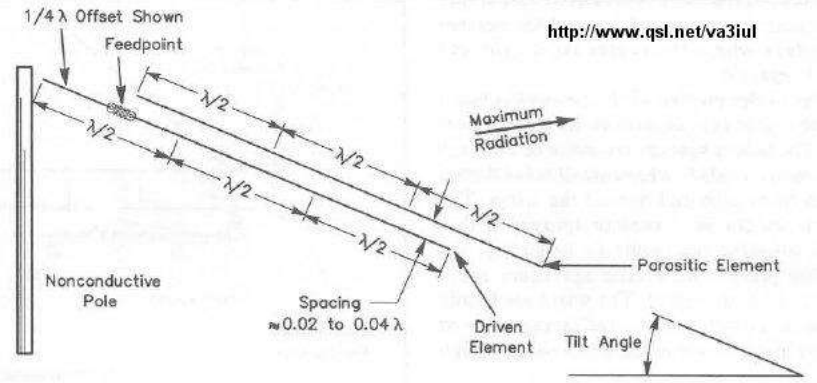

71 - Tower Pole as a Vertical Antenna for 80m

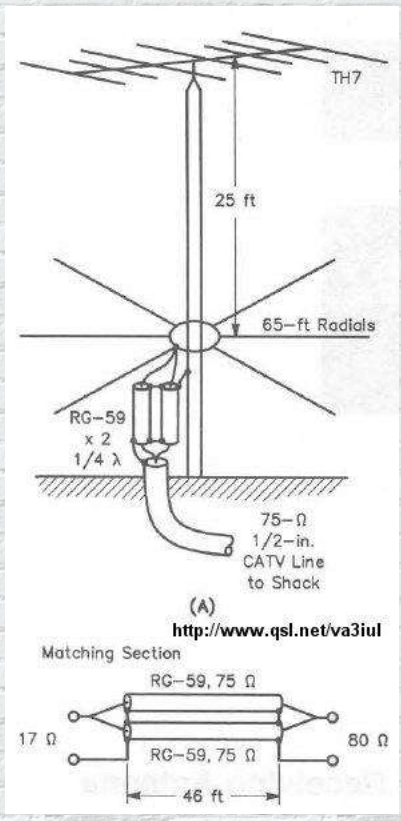

72 - Clothesline Antenna

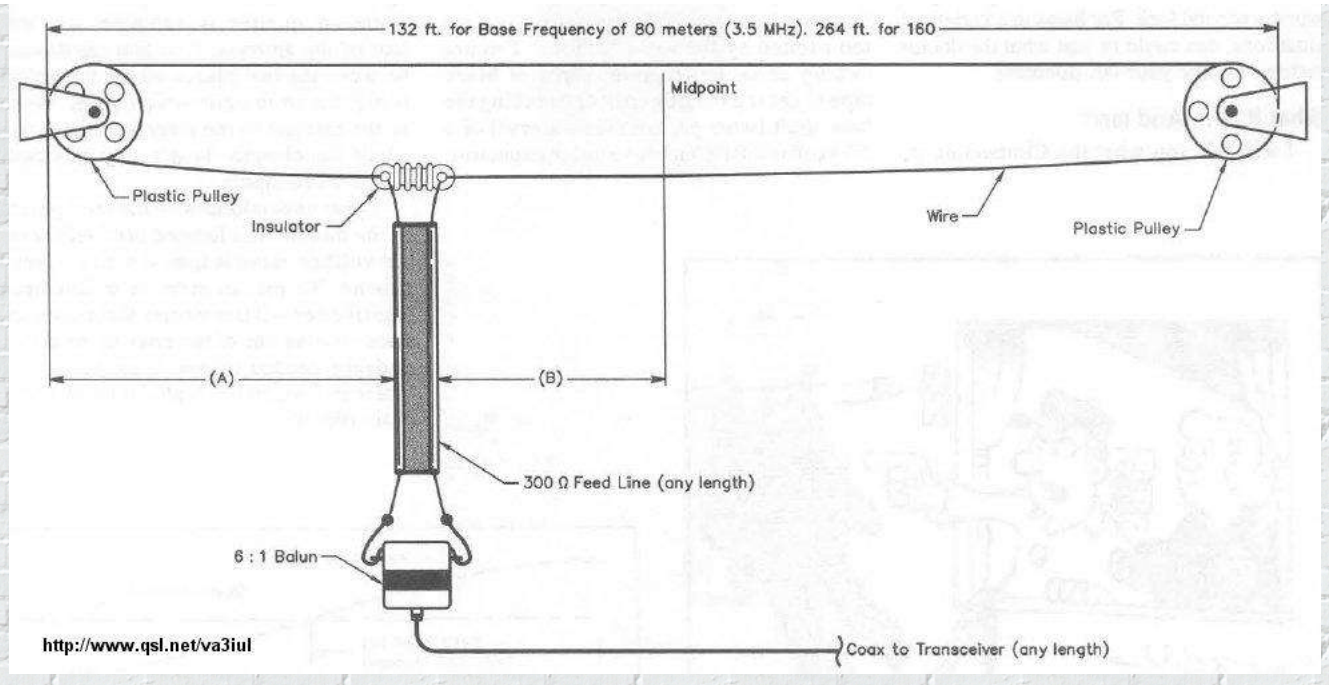

73 - Curtain Zepp Antenna for 160m, 80m, 40m

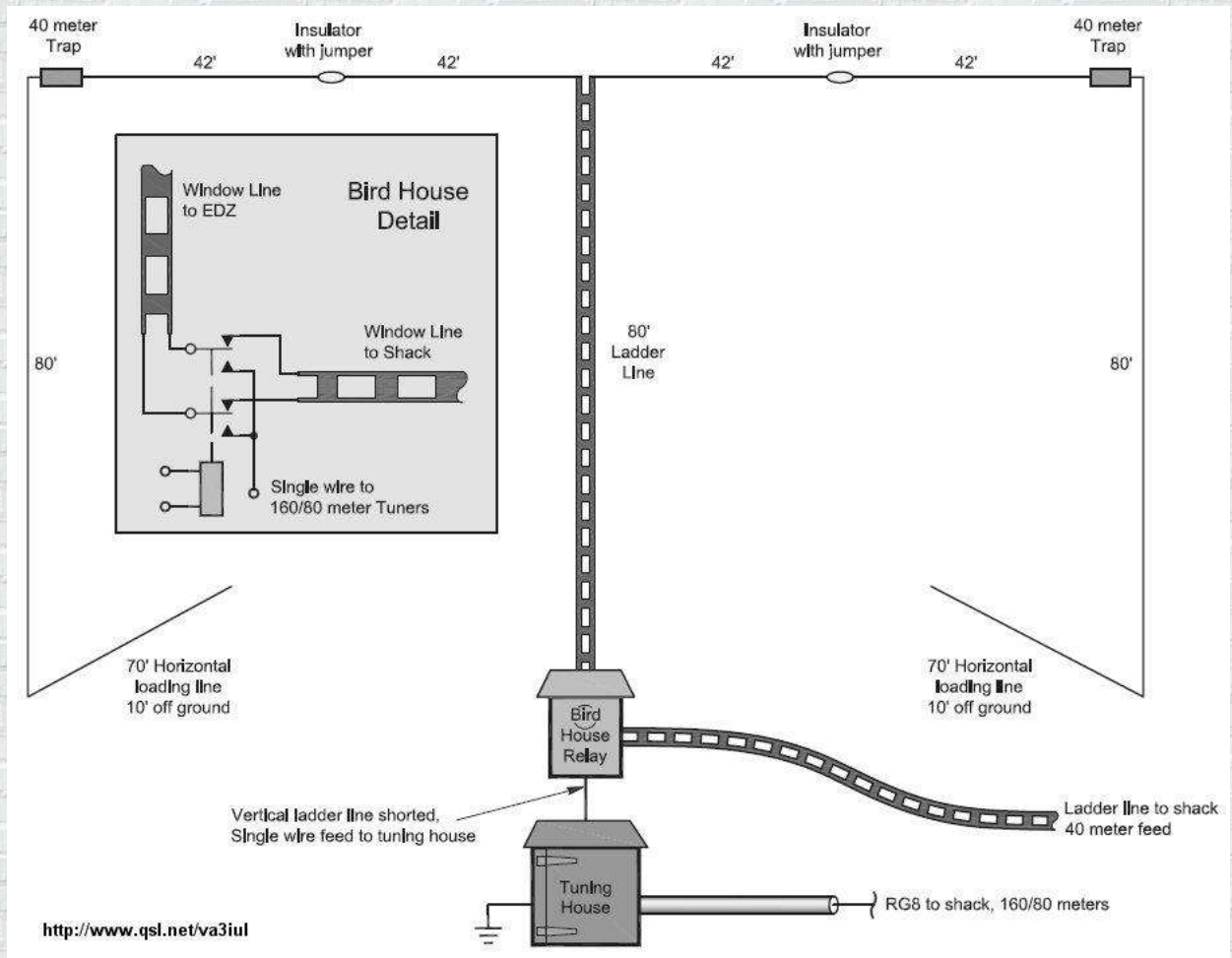

74 - Collinear Array Antenna for 40m, 30m, 20m

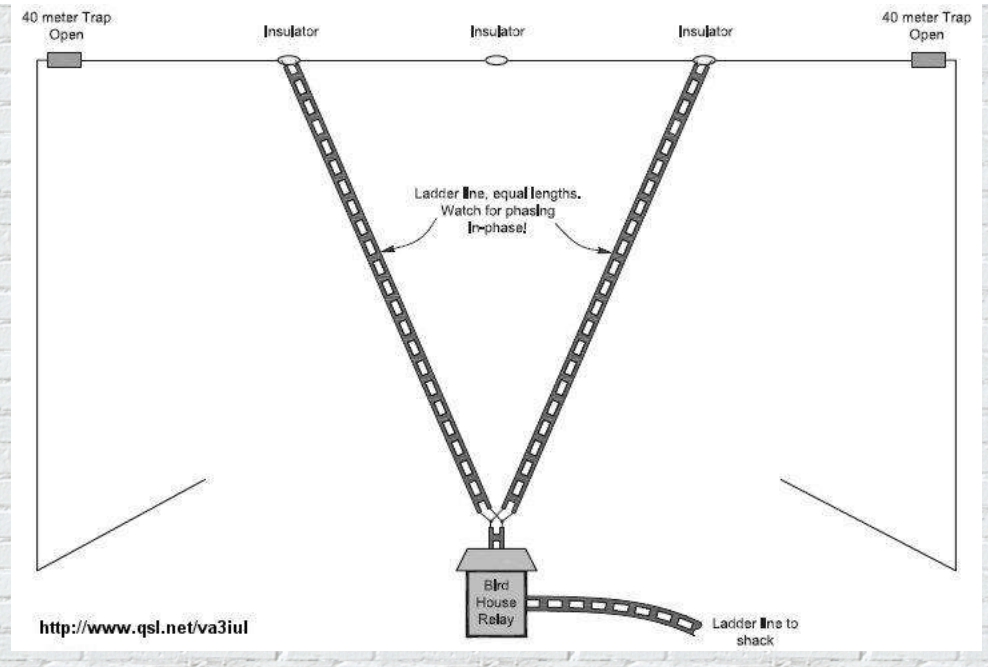

75 - 160m Inverted Delta Loop

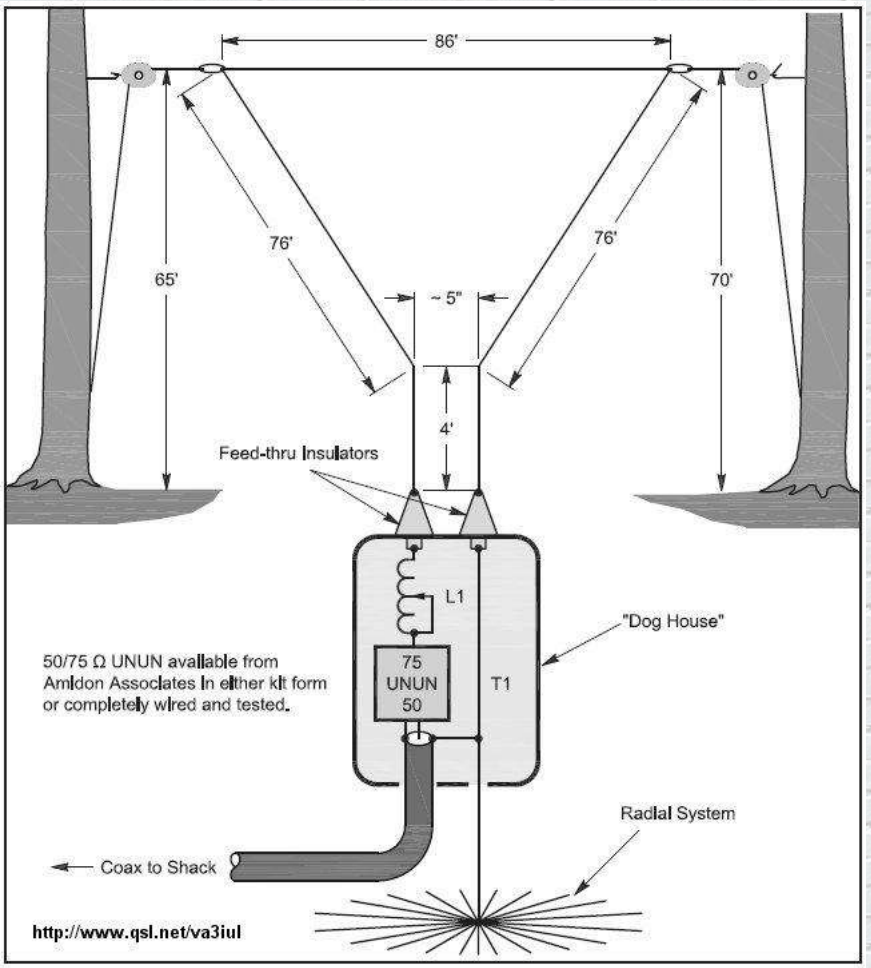

76 - Half Rhombic Unidirectional Vertical for 20m to 6m

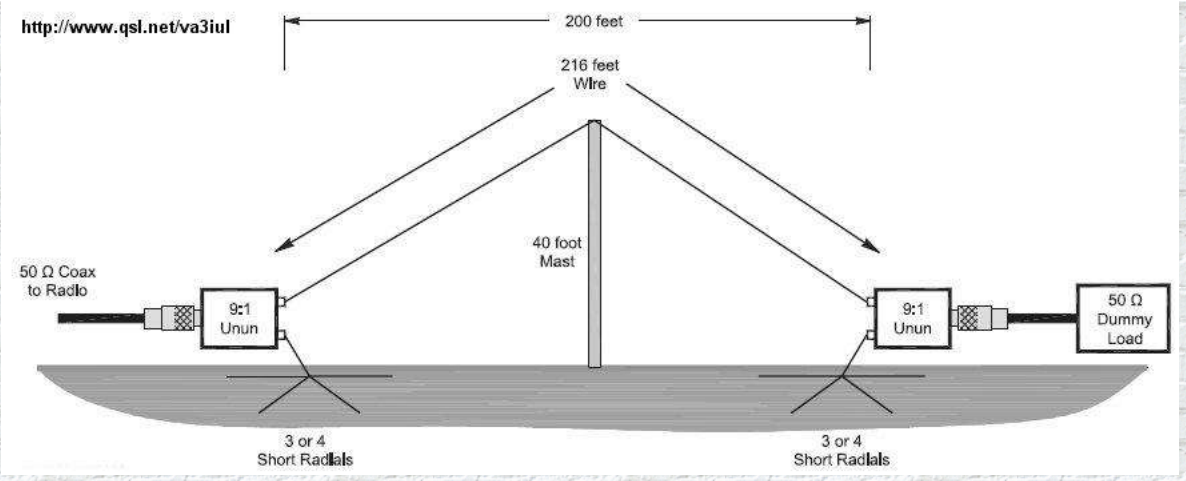

77 - Capacitance Loaded Vertical Antenna for 160m

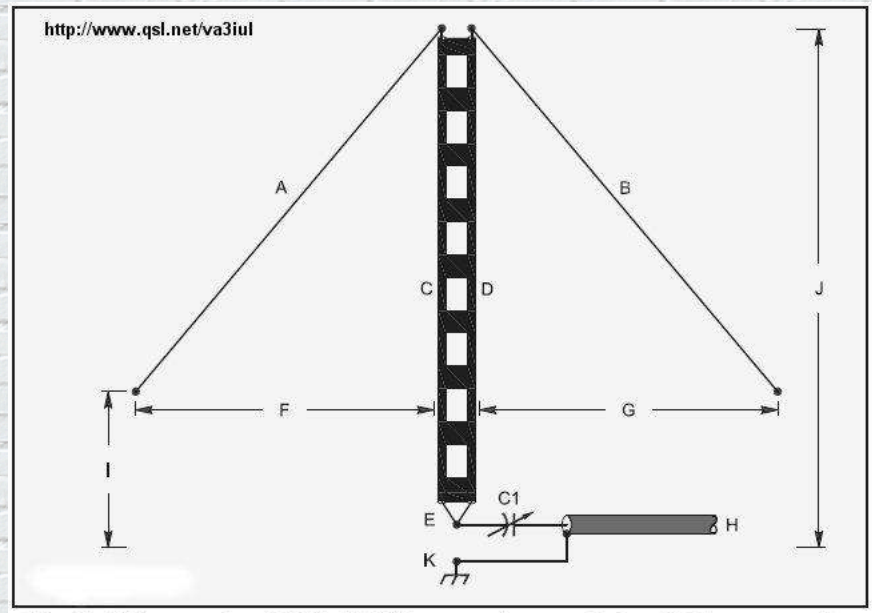

C1 — Variable capacitor, 0-1500 pF, 7 kV.
A, B — Sloping segments of 66 foot, 4 inch pieces of #16 AWG enameled copper wire soldered to the top of segments C and D and forming a 45° angle.
C, D — 59 feet of 450 Ω open wire or window line or, alternatively, two parallel lengths of #16 AWG enameled copper wire with a 1 inch separation.
E — 1 inch triangle formed by the bottom ends of the open wire line. Solder them tightly at the vertex and connect to C1.
F, G — Distance between the lower ends of segments A and B from segments C and D, 51 feet.
H — Any length of 50 Ω coaxial cable (RG-213 in this case). The central conductor must be soldered to C1, and the braid to the ground radials.
I — Approximately 16 feet from ground to lower ends of sloping segments A and B.
J — 60 feet from antenna top to bottom.
K — Ground radials, 60 ¼ λ (the more the better — 32 will form a reasonable ground).

78 - Fan Dipole Antenna for 80m to 6m

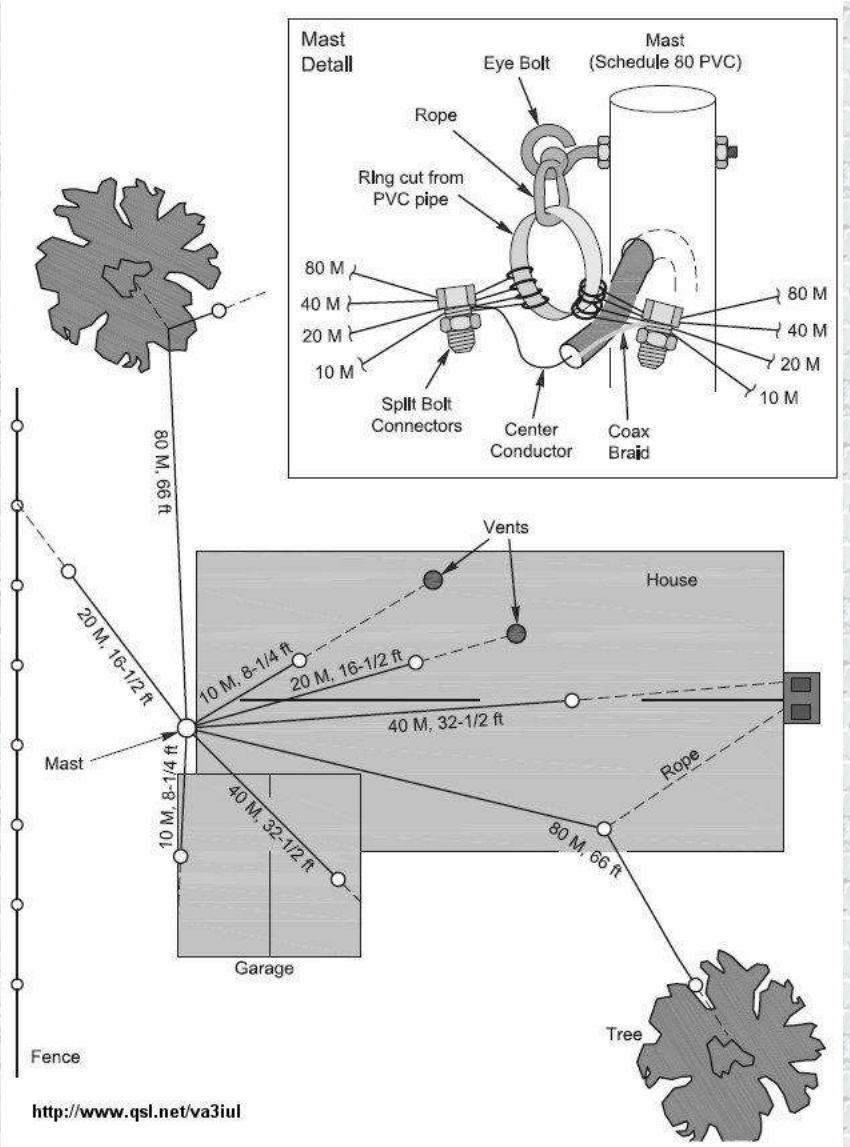

79 - Wire Ground Plane Antenna

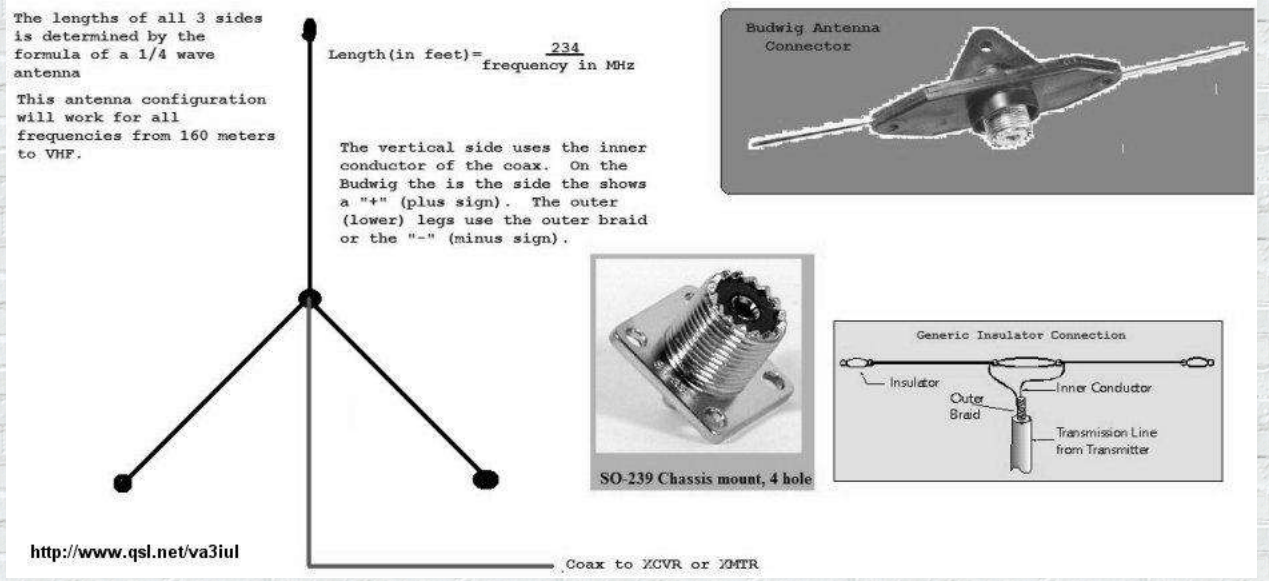

80 - Inverted Delta Loop Antenna for 160m

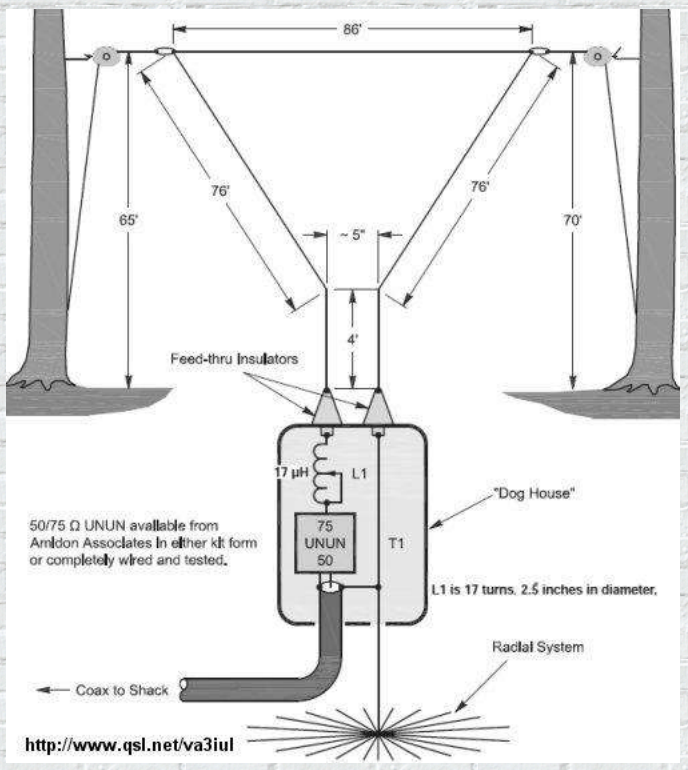

81 - Inverted-L for 160m

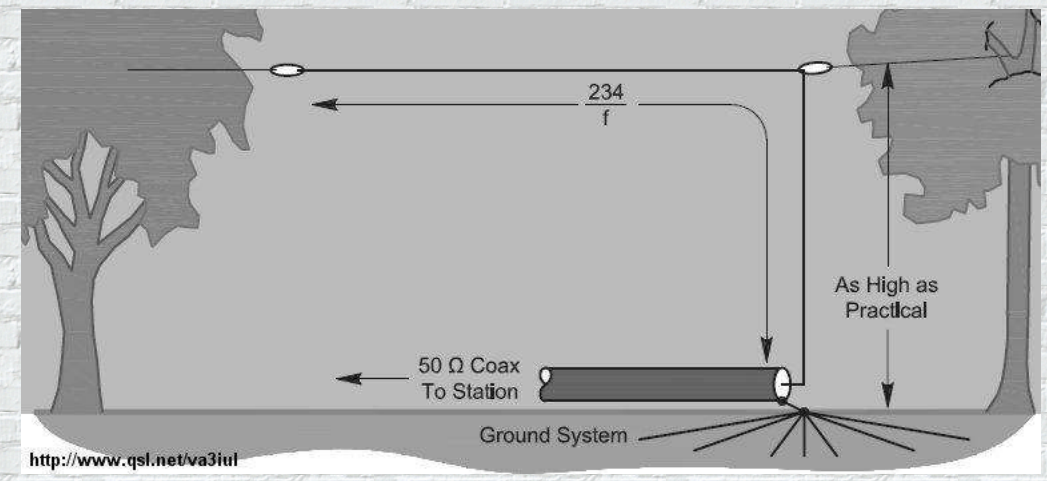

82 - 300ohm-Ribbon Dual Band Dipole

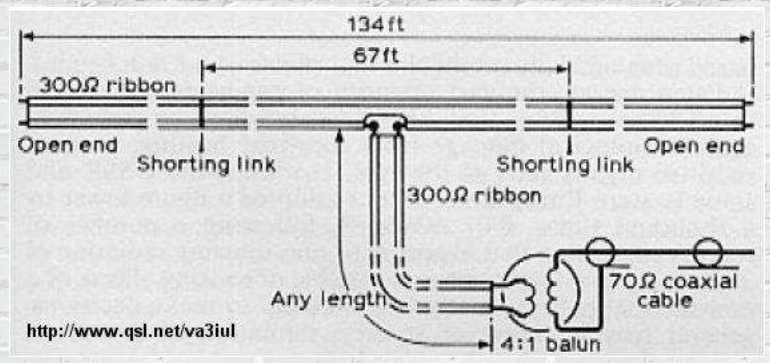

83 - Tri-Band Beam for 20m, 15m, 10m

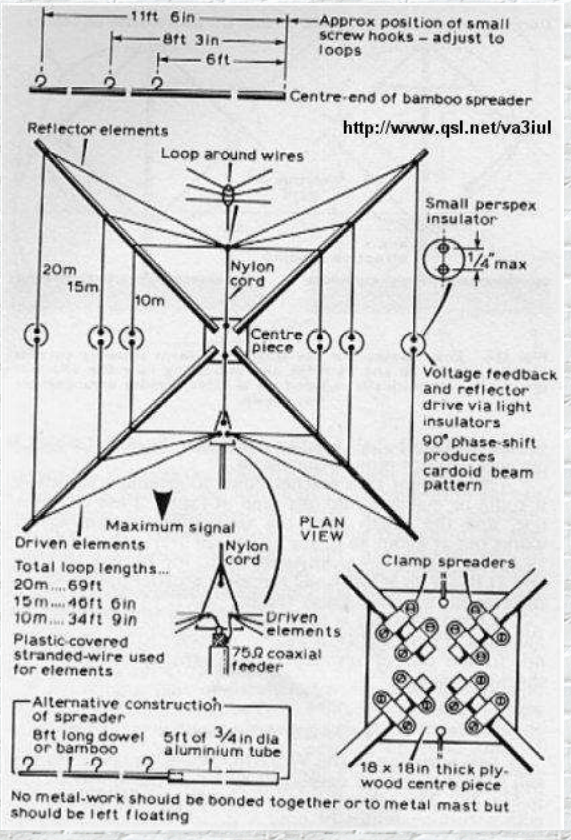

84 - Mini-Horse Yagi Antenna

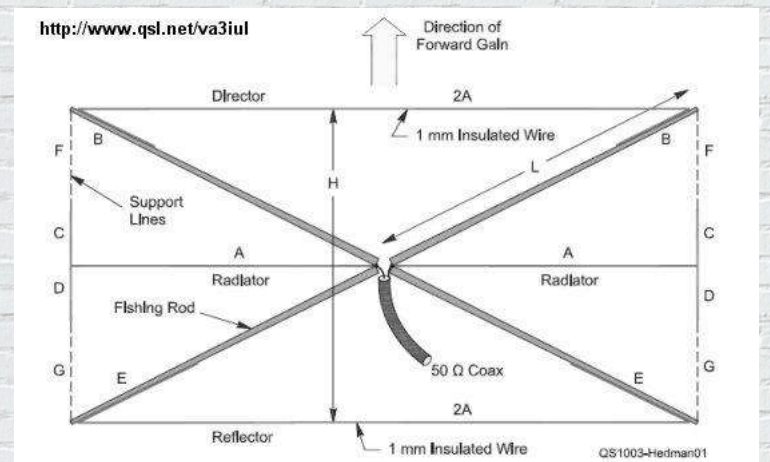

MHz	A	B	C	D	E	F	G	H	L
144	1' 2.2"	0' 4.7"	0' 3.5"	0' 1.8"	0' 7.1"	0' 4.7"	0' 6.5"	1' 4.5"	1' 4.3"
28	5' 11.6"	1' 10.8"	1' 6.9"	0' 9.4"	2' 11.8"	1' 10.8"	2' 8.3"	6' 11.4"	6' 11.0"
21	7' 11.6"	2' 6.3"	2' 1.2"	1' 0.6"	3' 11.6"	2' 6.3"	3' 6.9"	9' 3.0"	9' 2.6"
14	11' 11.3"	3' 9.7"	3' 1.8"	1' 6.9"	5' 11.2"	3' 9.7"	5' 4.6"	13' 10.9"	13' 9.7"
7.1	23' 10.5"	7' 7.3"	6' 3.6"	3' 1.8"	11' 10.5"	7' 7.3"	10' 9.1"	27' 9.8"	27' 7.4"

85 - Half-Rhombic Directive Antenna for 20m to 6m

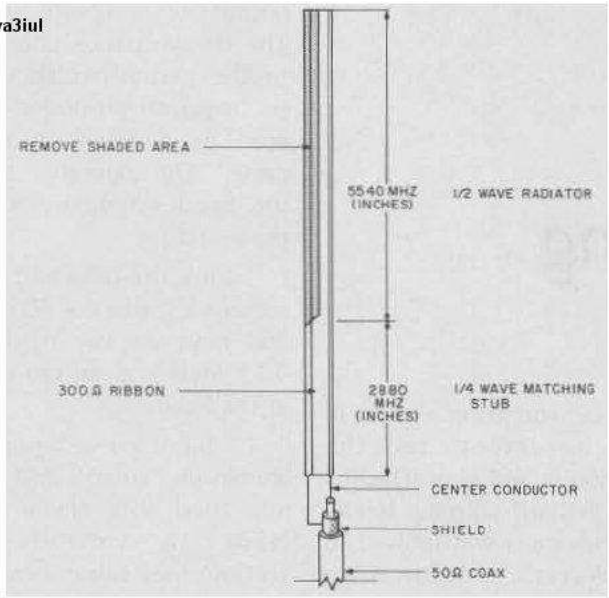

Frequency (MHz)	28.0	28.5	29.0	50.0	51.0	52.0	144	145	146	147
Radiator (inches)										
½ wave	197.8	194.3	191.0	110.8	108.6	106.5	38.4	38.2	37.9	37.7
Stub (inches)										
¼ wave	102.8	101.0	99.3	57.6	56.4	55.3	20.0	19.8	19.7	19.6

86 - Fan-Dipole Antenna for 80m, 40m, 20m

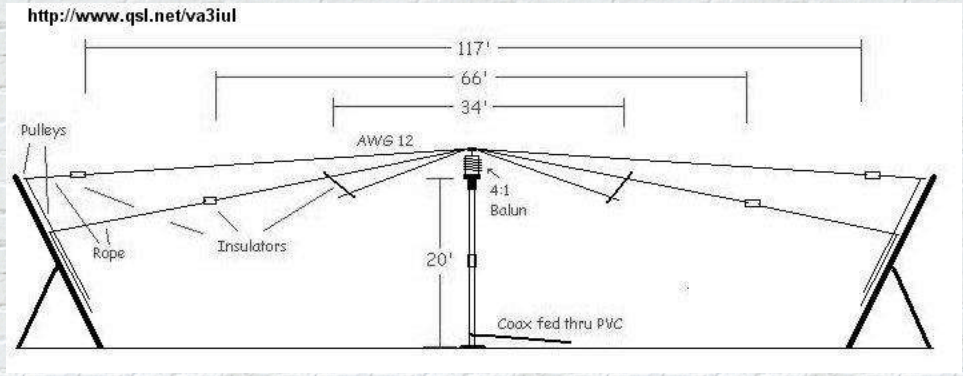

87 - Capacity Tuned Folded Loop Antenna for 20m

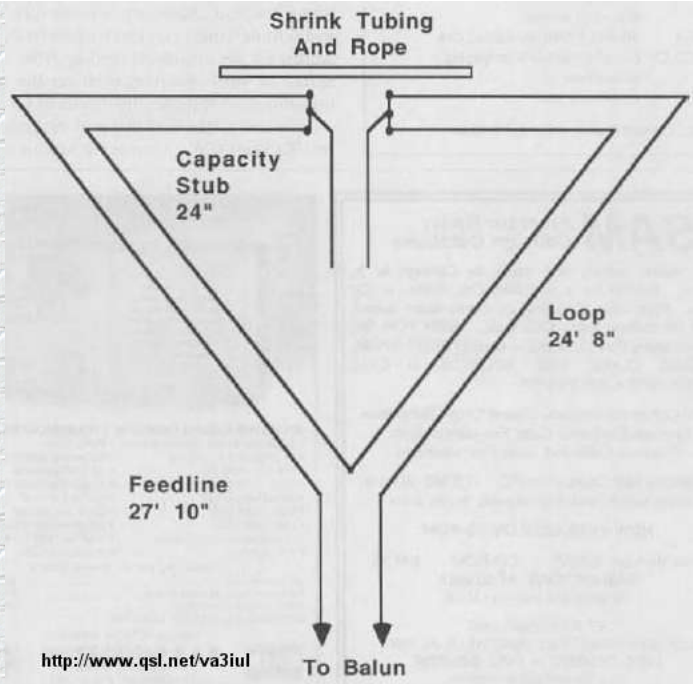

88 - Indoor Loop Antenna for 80m to 30m

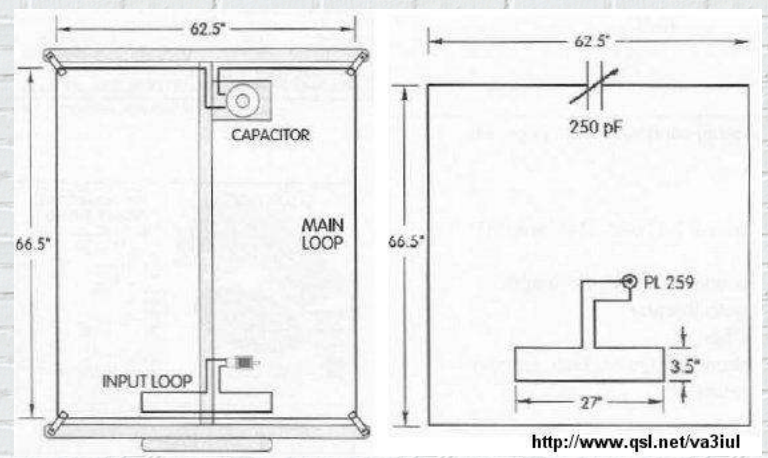

89 - Indoor Loop Antenna for 80m

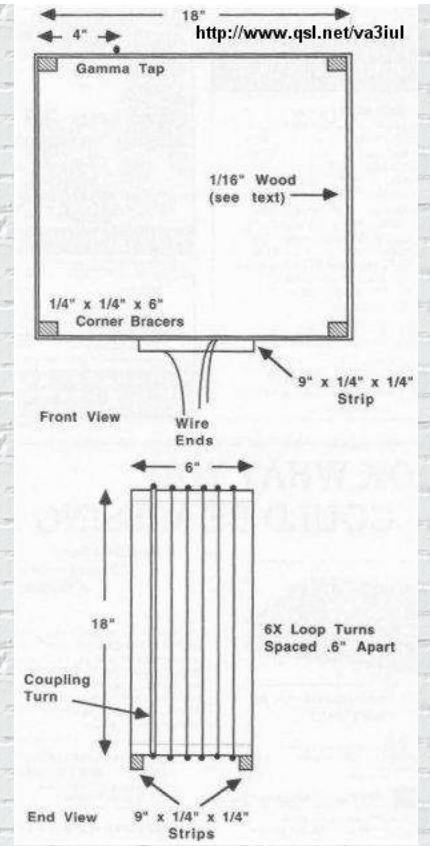

90 - Double-Delta Antenna 80m and 40m

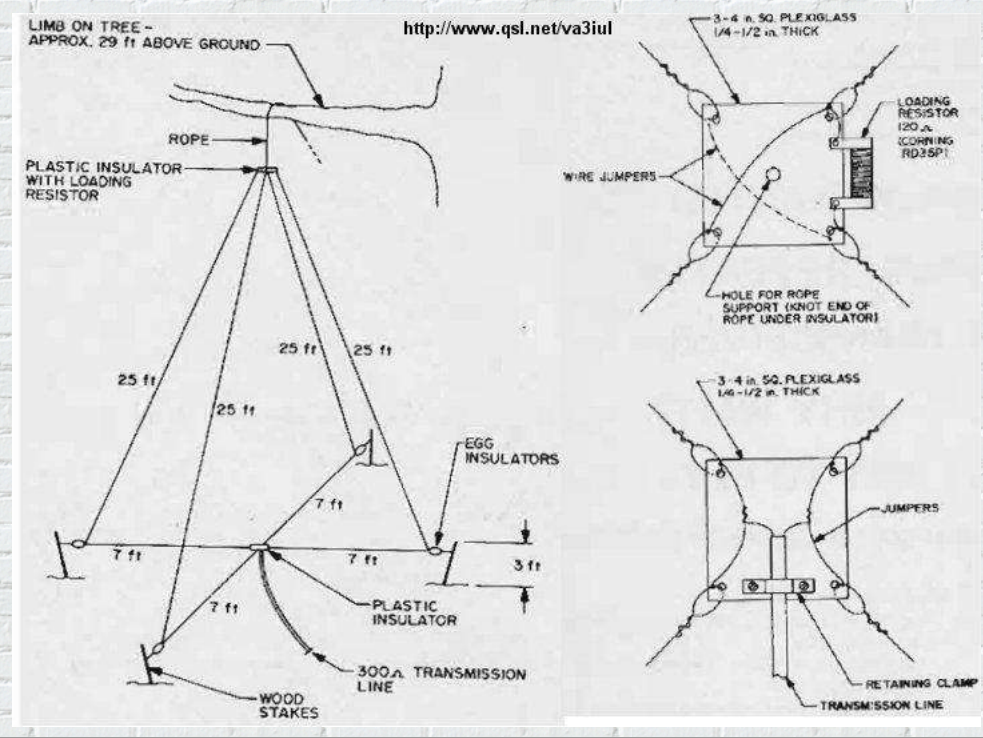

91 - Inductance-Loaded Shortened Dipole for 160m

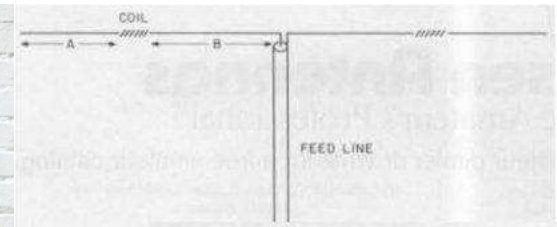

Overall Length (ft.)	Element A Length	Number Of Coil Turns	Element B Length
246.3	full-size antenna		
221.3	66.5	10	44.3
197.1	59.1	20	39.4
172.4	51.7	33	34.5
147.8	44.3	48	29.6
123.2	36.9	65	24.6
98.5	29.6	86	19.7

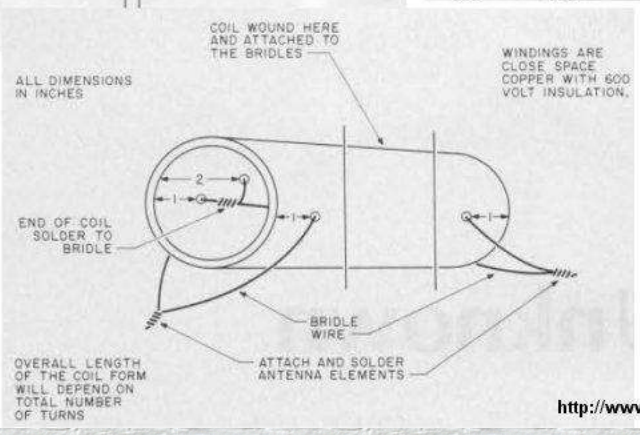

92 - V-Beam Antenna for 15m

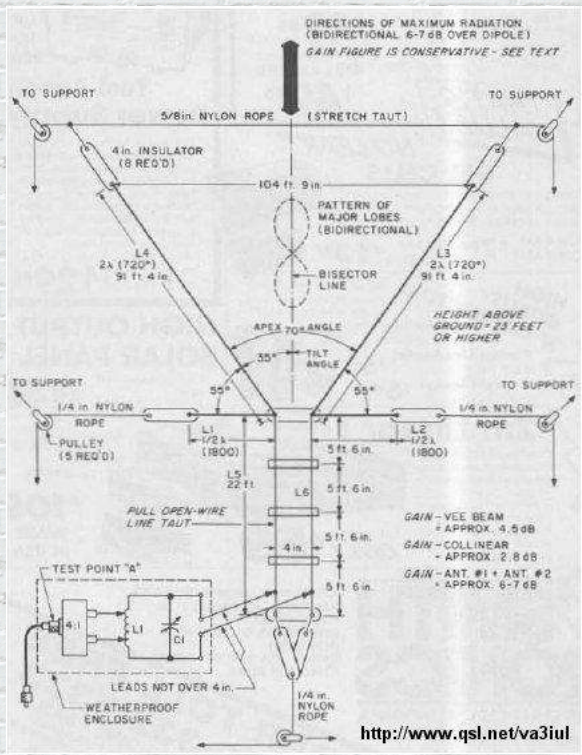

93 - Picnic Vertical Wire Antenna

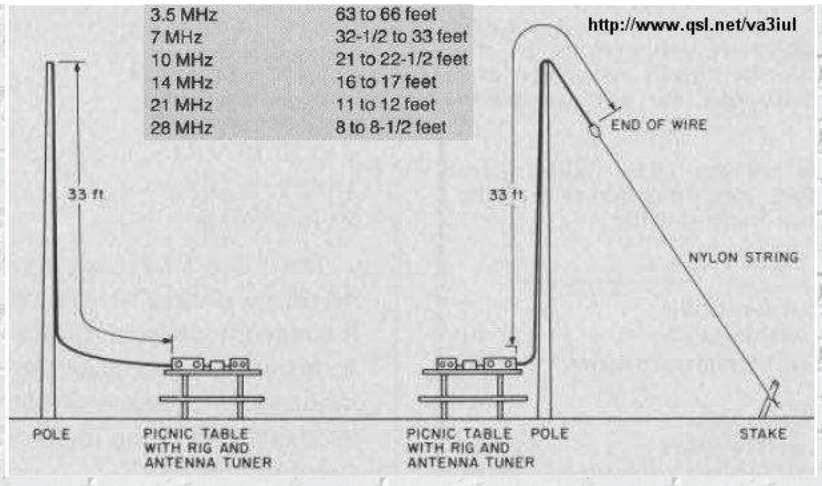

94 - Laid-Back Quad Antenna for 80m

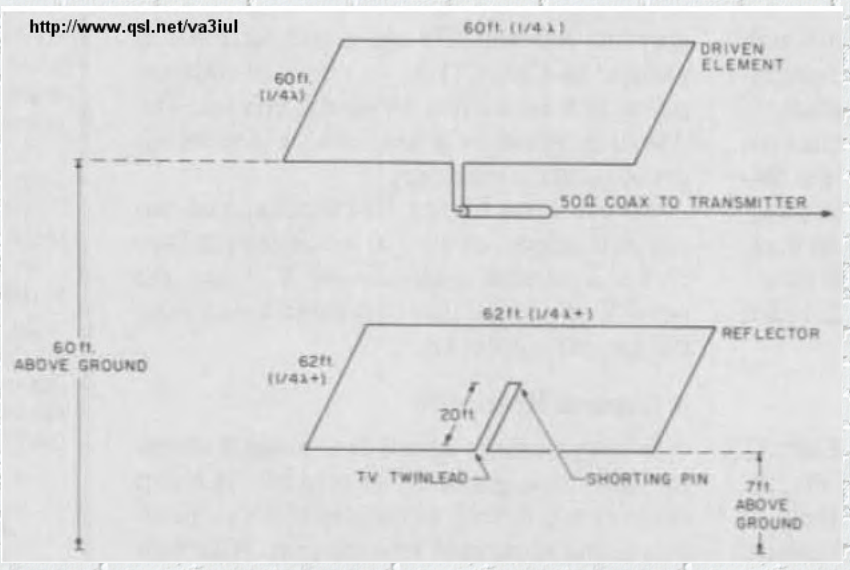

95 - Phased Loop Antenna

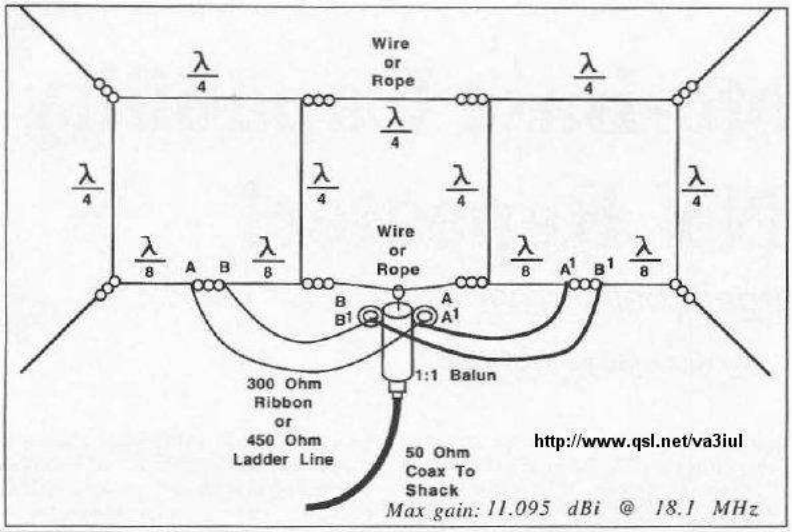

	λ/4	λ/8	300Ω Ribbon	450Ω Ladderline
40m	34.9 ft.	17.5 ft.	53.3 ft.	62.2 ft.
20m	17.6 ft.	8.8 ft.	27.0 ft.	31.2 ft.
17m	13.9 ft.	6.9 ft.	21.2 ft.	25.2 ft
15m	11.8 ft.	5.9 ft.	18.1 ft.	21.97 ft.
10m	8.67 ft.	4.33 ft.	13.2 ft.	15.33 ft.

96 - Loop Antenna for TX for 160m

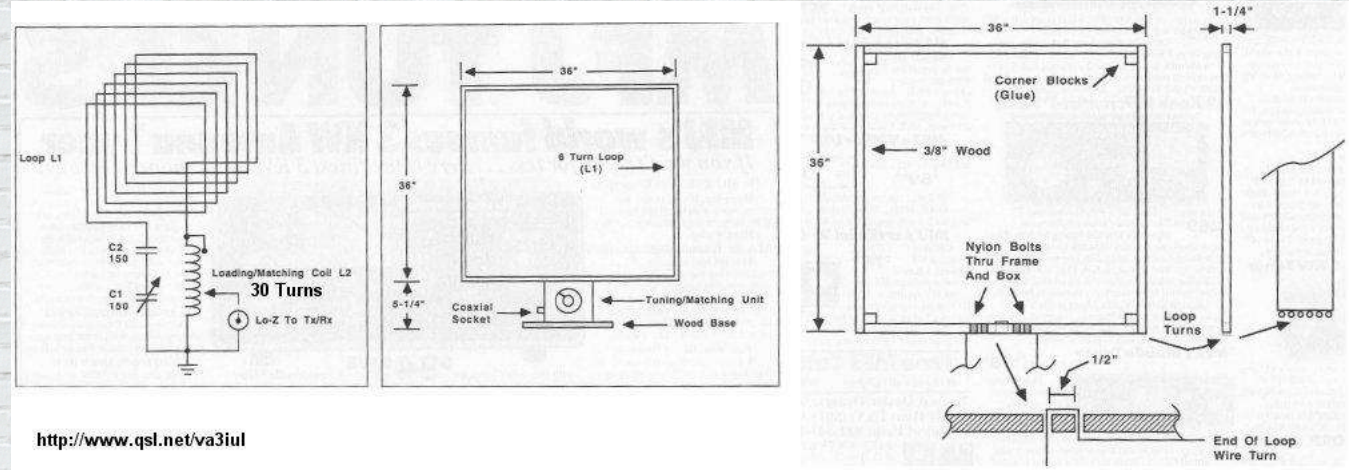

97 - Morgain-Dipole Antenna for 160m and 80m

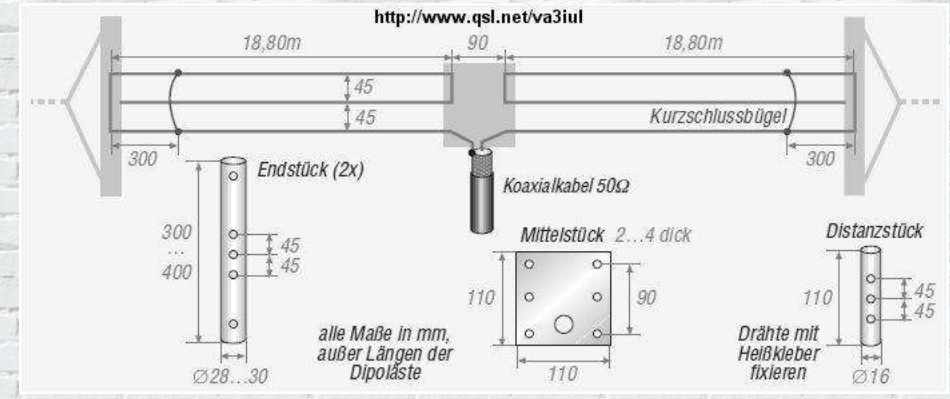

98 - ZL-Special for 20m, 15m, 10m

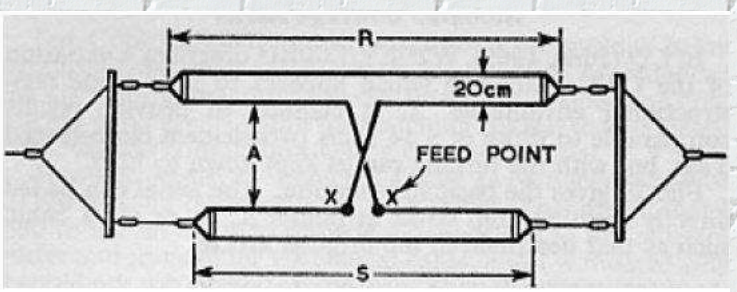

	S	R	A	A
28 Mc/s	5·09m	5·39m	1·29m	½λ
	4·17m	4·42m	1·06m	$\frac{1}{10}\lambda$
21 Mc/s	6·85m	7·24m	1·72m	½λ
	5·62m	5·94m	1·41m	$\frac{1}{10}\lambda$
14 Mc/s	10·30m	10·85m	2·58m	½λ
	8·45m	8·90m	2·12m	$\frac{1}{10}\lambda$

http://www.qsl.net/va3iul

99 - Biconical Antenna

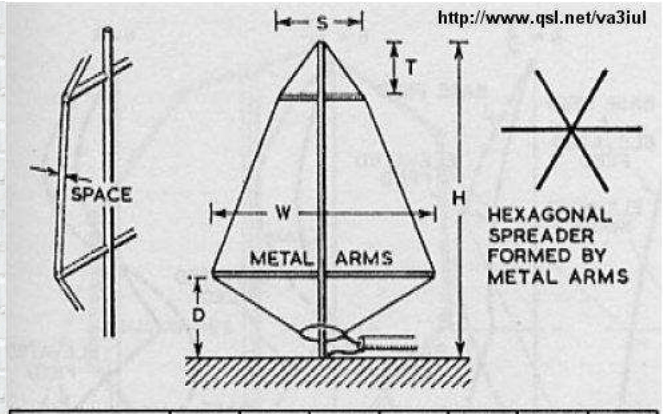

	H	W	D	T	S	SPACE	WIRE
3·5 - 15 Mc/s	43'	17'-8"	16'-10"	2'-2"	5'-10"	3"	NR 8
7 - 28 Mc/s	23'	9'-6"	9'	12"	3'-2"	2"	NR10
14 - 56 Mc/s	12'	5'	4'-9"	8"	1'-8"	1"	NR12

100 - Directive Delta-Birdcage Antenna for 20m to 10m

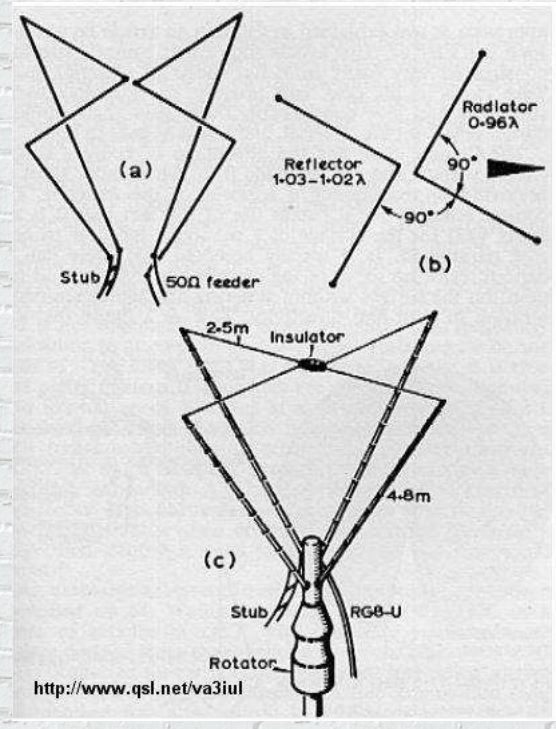

101 - Dual Polarization Antenna for 80m and 40m

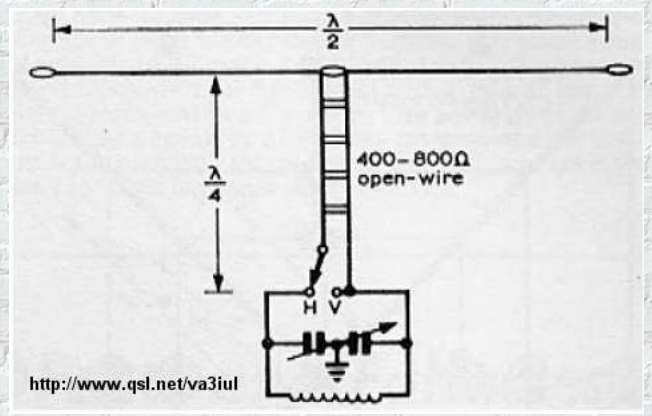

102 - Directive 300-ohm-Ribbon Folded Dipole for 15m

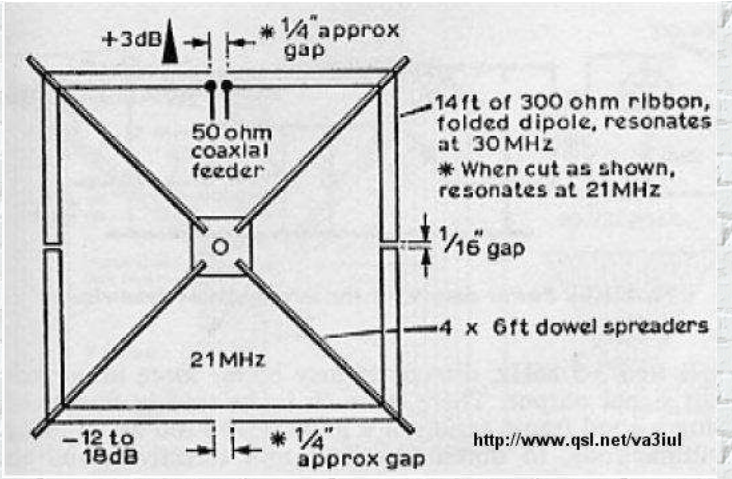

103 - Miniature Directive Antenna for 10m

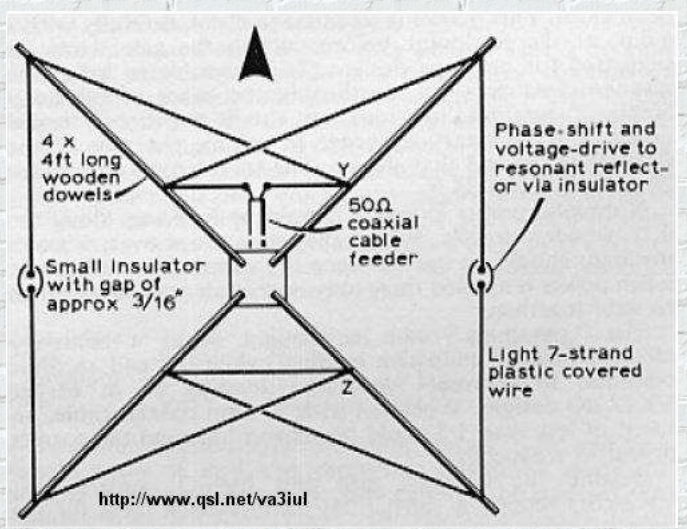

104 - Biquad Antenna 12dBi-Gain for 2.4GHz

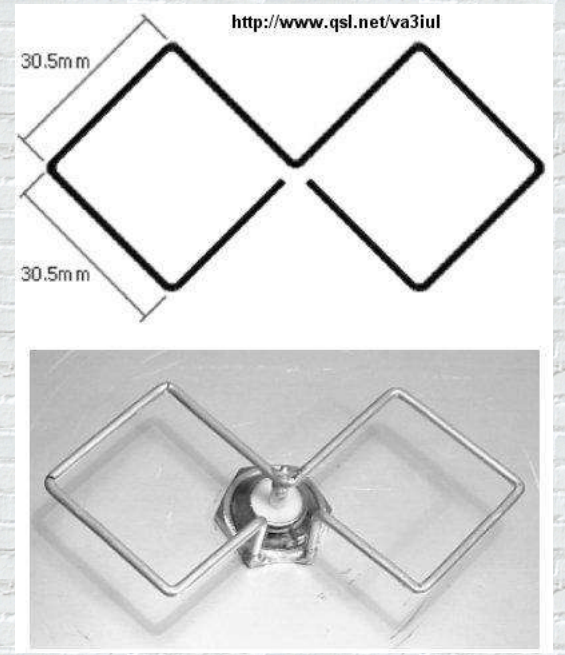

105 - Dual-Rhomboid Antenna for 435MHz to 870MHz

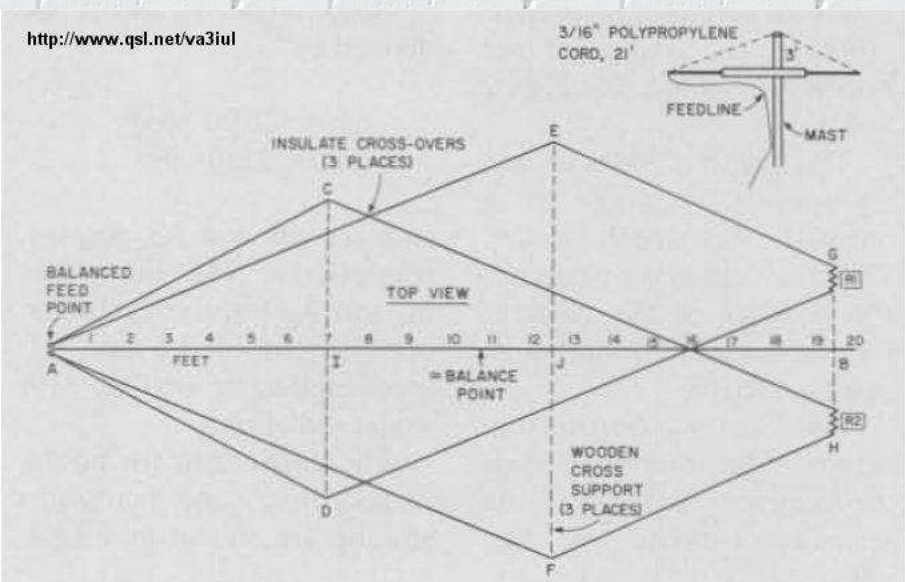

Dual rhomboid antenna for 435-870 MHz. Beamwidth ≈ 10° H x 6° V. Gain over DP ≈ 26 dB. Boom length: AB = 19'6". Support spacing : AI = 7'; IJ = 5'6"; JB = 7'. Support length: CD = 7'3"; EF = 10'3"; GH = 3'0". Rhomboid sides: AC, AD, EG, FH = 7'9.5"; AE, AF, CH, DG = 13'5.5". Feedline: Wire needed: 14 AWG formvar, ≈ 86'0". Boom material: AI, JB = wood; IJ = metal. Cross support: CD, EF, GH = wood. Terminators: R1, R2 = 600 Ohms; Watts

106 - Double-Bazooka Antenna for 80m

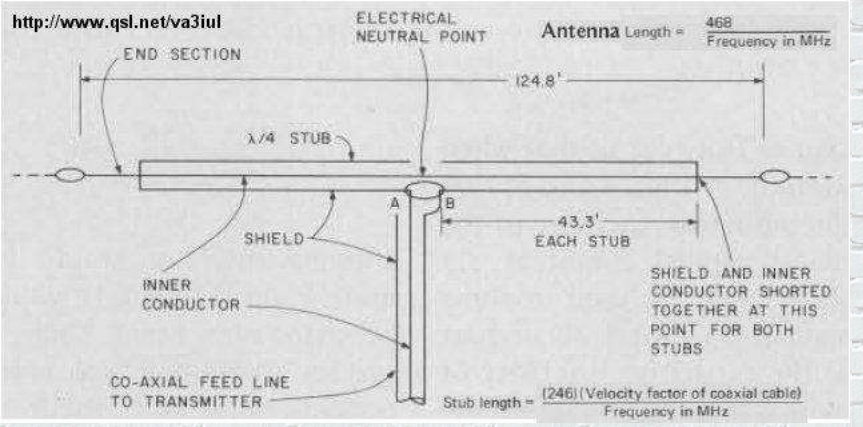

107 - J-Style Antenna

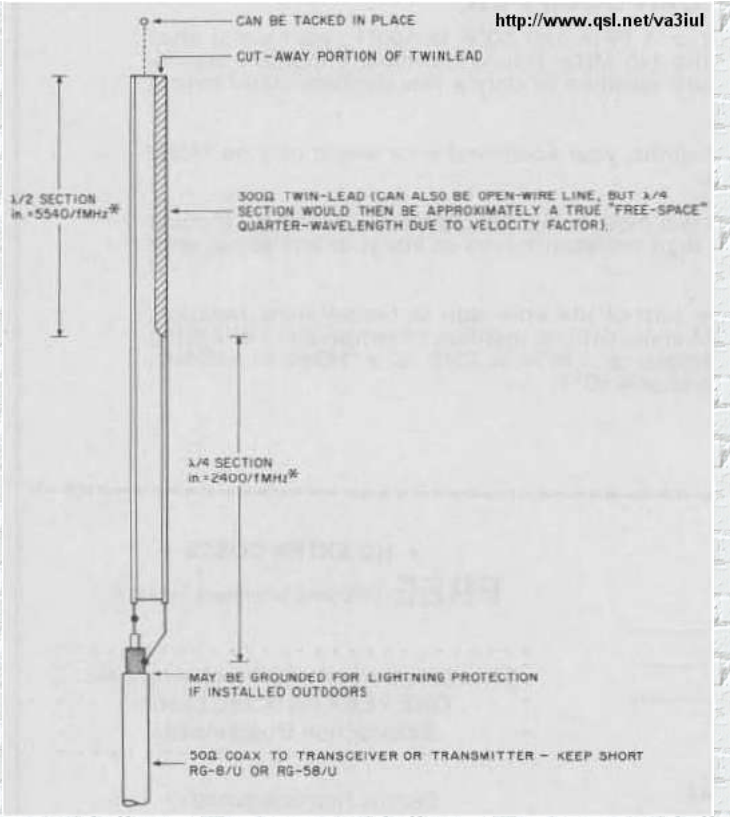

108 - Vertical / Horizontal / Circular Polarization Antenna

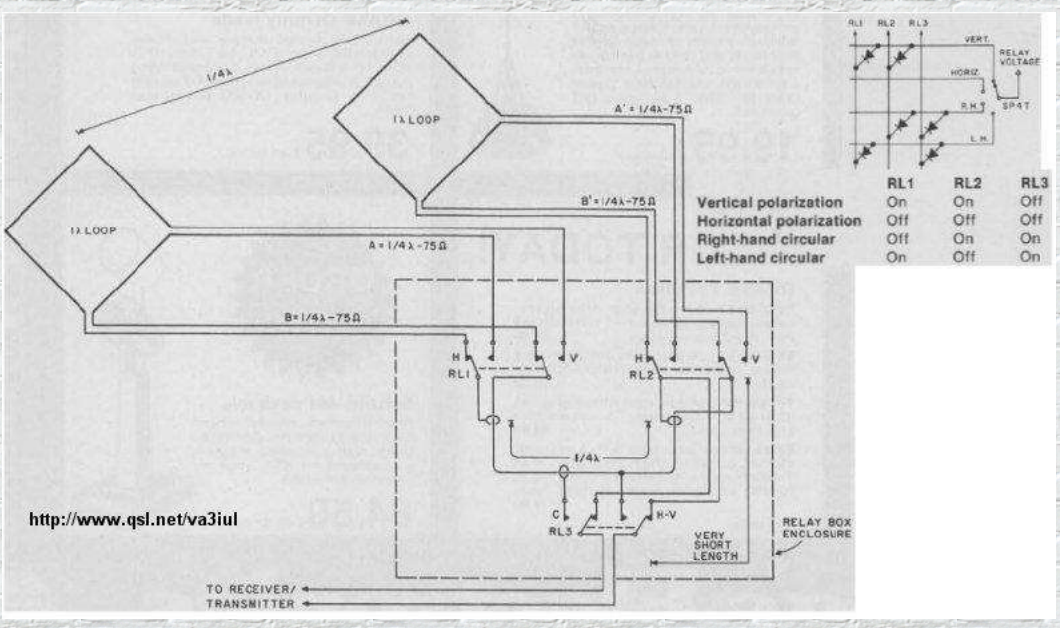

	RL1	RL2	RL3
Vertical polarization	On	On	Off
Horizontal polarization	Off	Off	Off
Right-hand circular	Off	On	On
Left-hand circular	On	Off	On

109 - Coax Inverted-L Antenna for 80m

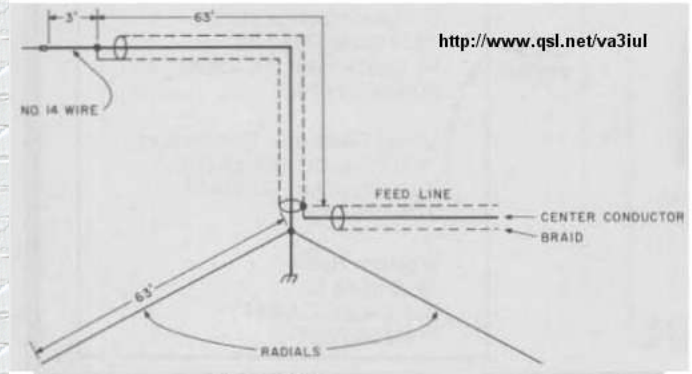

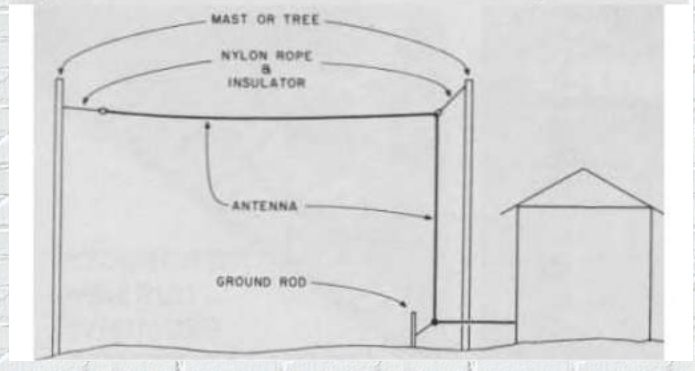

110 - Indoor Compact Loop Antenna for 80m

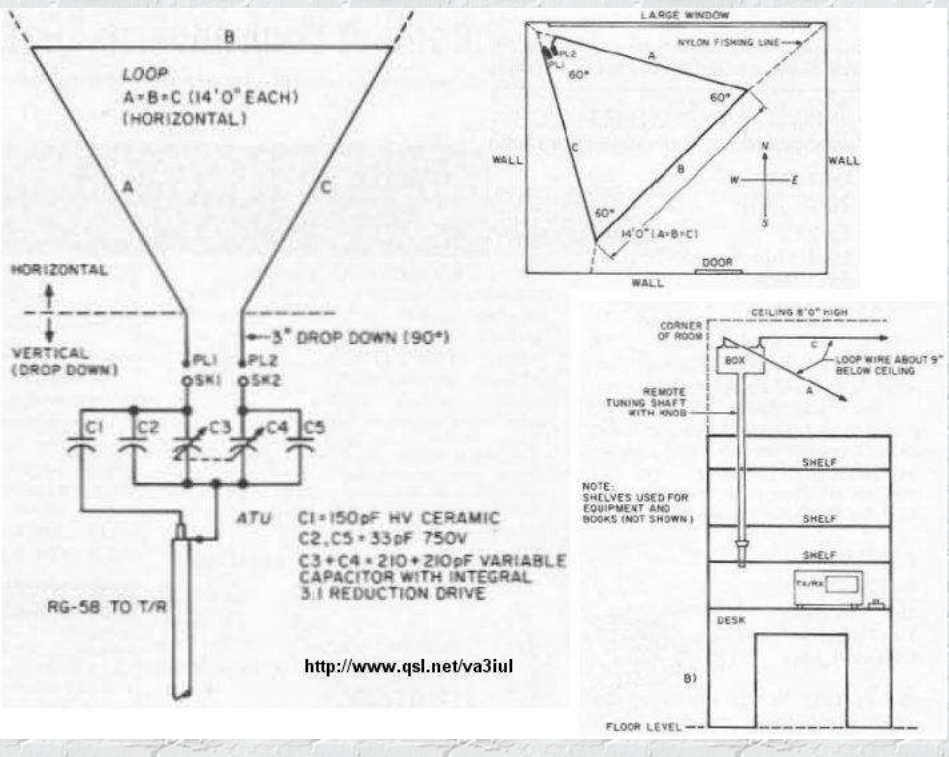

111 - Helix Antenna

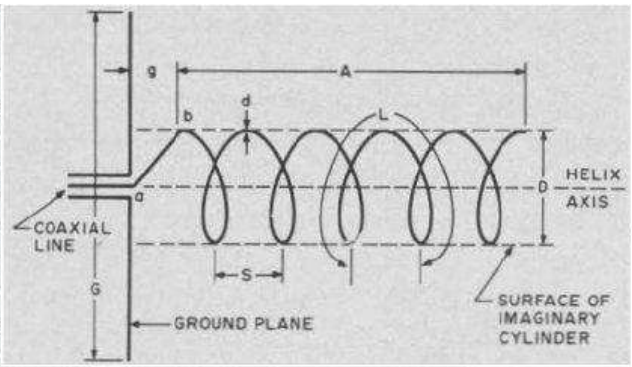

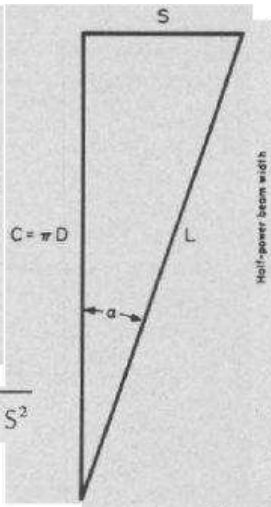

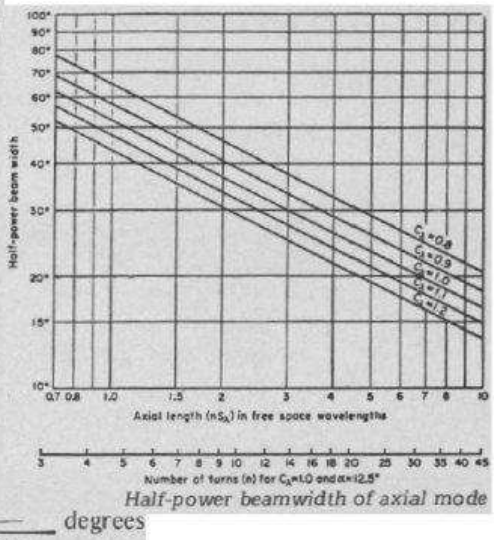

Half-power beamwidth of axial mode

D = Diameter of the helix
S = Spacing between turns
α = Pitch angle = Arctan $\left(\frac{S}{\pi D}\right)$
L = Length of 1 turn
n = Number of turns
A = Axial length = nS
d = Diameter of conductor
g = Distance of ground plane to first turn
G = Ground plane diameter

$L = \sqrt{(\pi D)^2 + S^2}$

$D = 0.32\lambda$
$S = 0.22\lambda$
$G \geq 0.80\lambda$
$g = \frac{S}{2} = 0.12\lambda$

$\beta = \frac{52}{C_\lambda \sqrt{nS_\lambda}}$ degrees

http://www.qsl.net/va3iul

112 - Novice Vertical Antenna for 80m, 40m, 15m, 10m

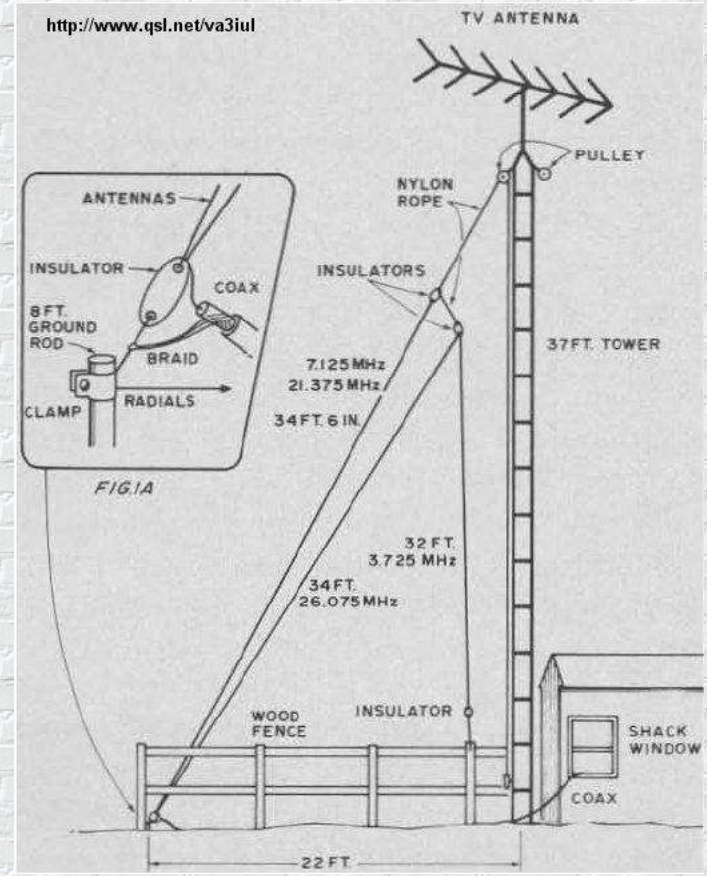

113 - Stub-Loaded Shortened Dipole for 80m

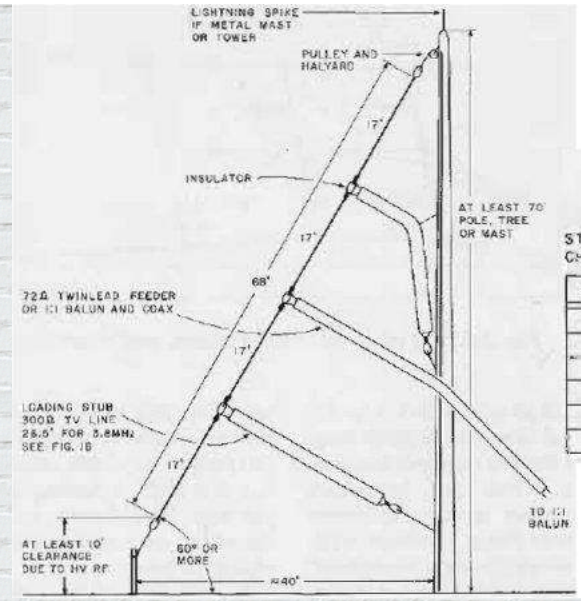

http://www.qsl.net/va3iul

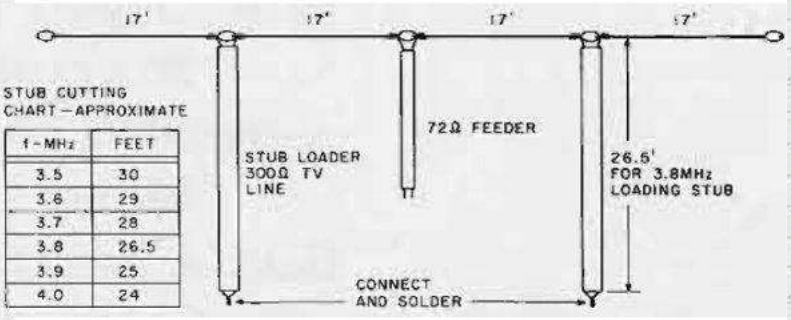

f-MHz	FEET
3.5	30
3.6	29
3.7	28
3.8	26.5
3.9	25
4.0	24

114 - Six-Band Wire-Stub Trap Antenna for 40m-10m

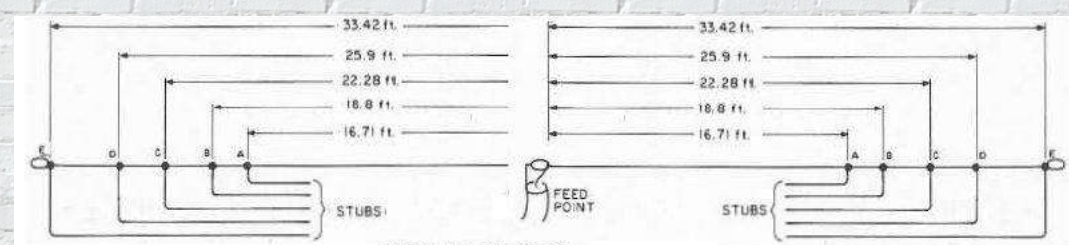

Point	Length (feet)
A	8.37
B	9.40
C	11.14
D	12.95
E	16.72

http://www.qsl.net/va3iul

40m
20m
17m
15m
12m
10m

115 - Multiband Half-Wave Delta-Loop Antenna

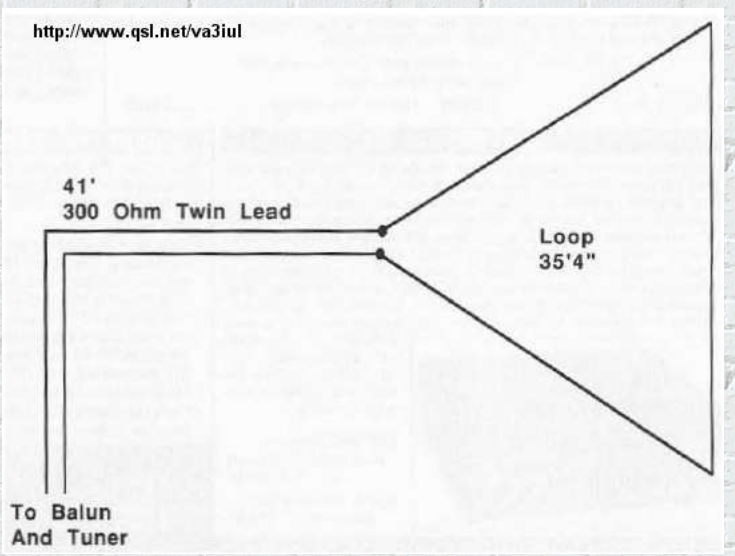

116 - Hybrid Vee for 20m, 17m

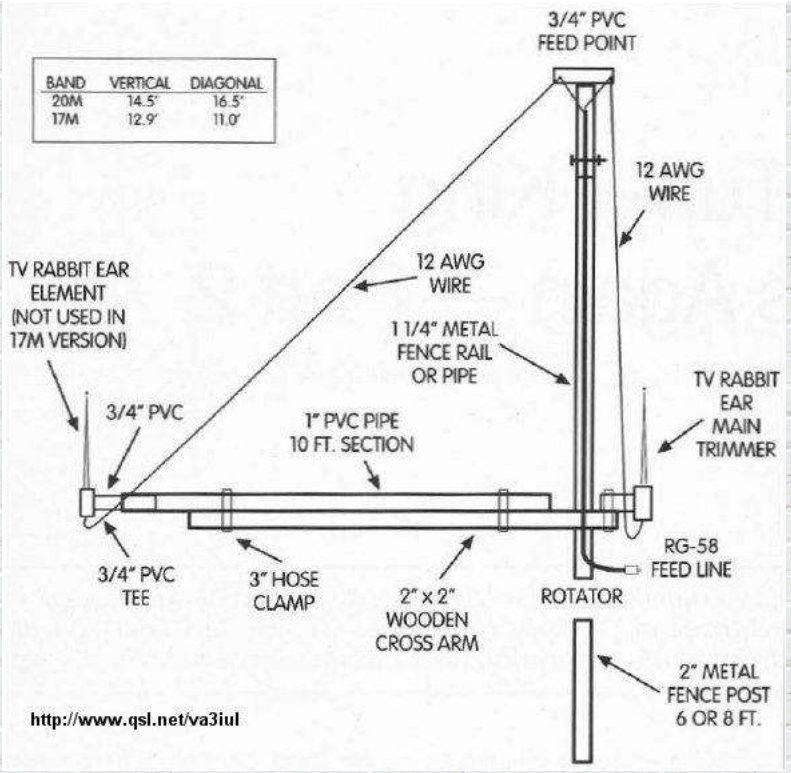

117 - Six-Shooter Array Antenna, Gain=7.5dB

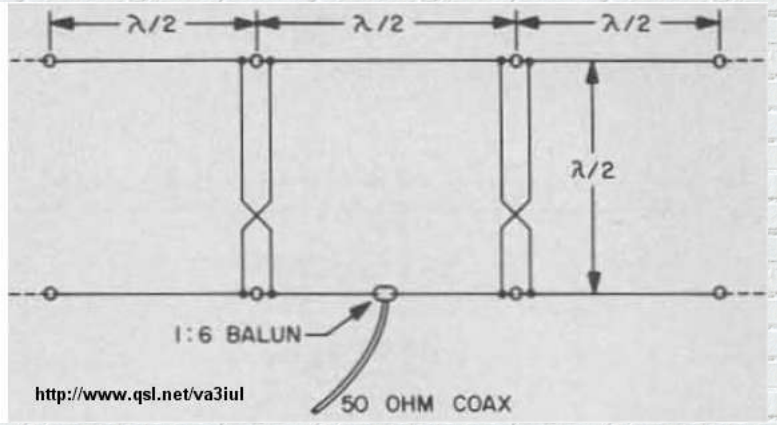

118 - Multiband Ground-Plane Antenna for 10m, 15m, 20m

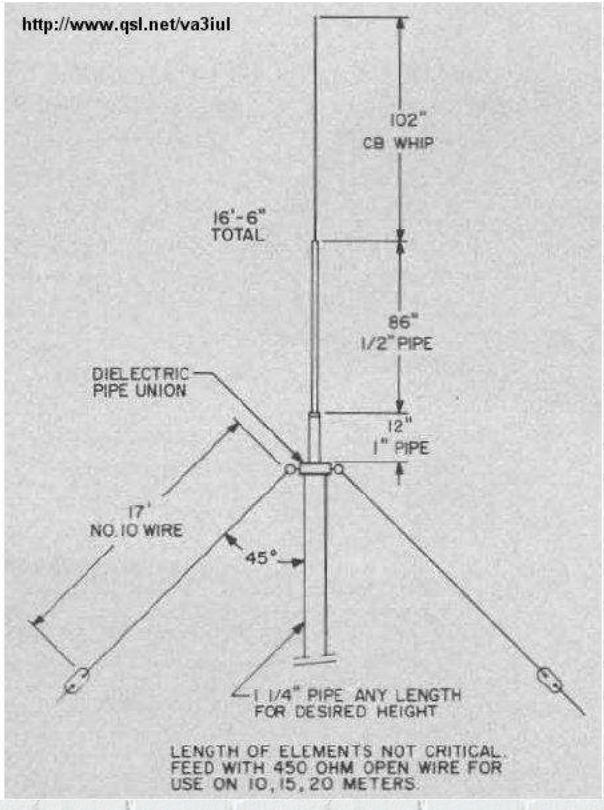

119 - Wire Superbeam Antenna for 10m, 15m, 20m

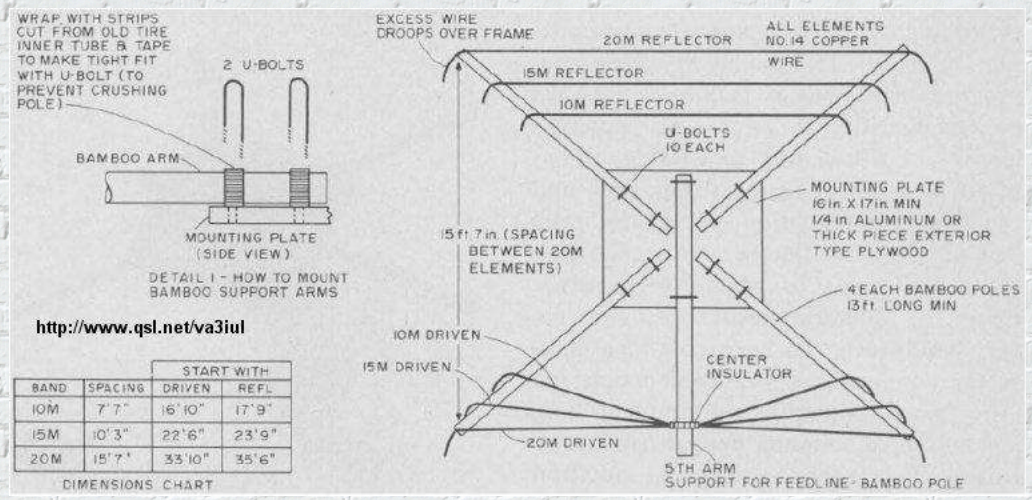

BAND	SPACING	START WITH DRIVEN	START WITH REFL
10M	7'7"	16'10"	17'9"
15M	10'3"	22'6"	23'9"
20M	15'7"	33'10"	35'6"

DIMENSIONS CHART

120 - Two Elements Delta-Loop Antenna

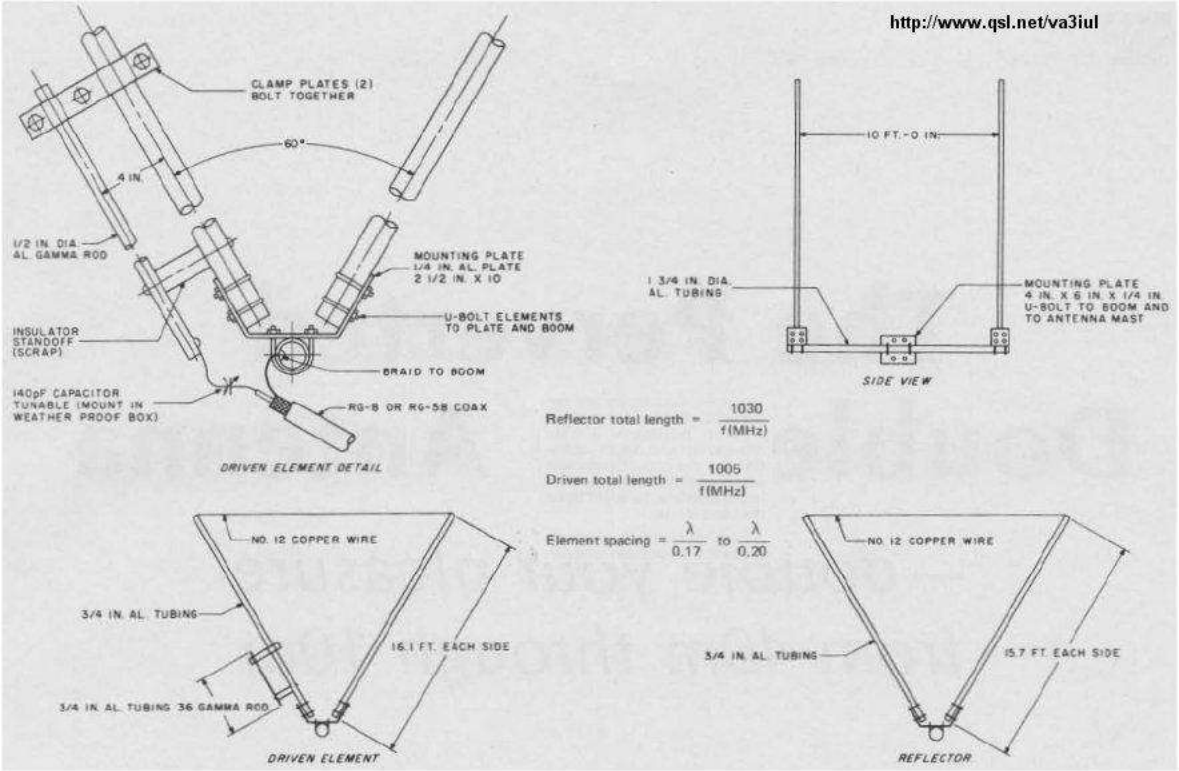

121 - Sterba Curtain Antenna

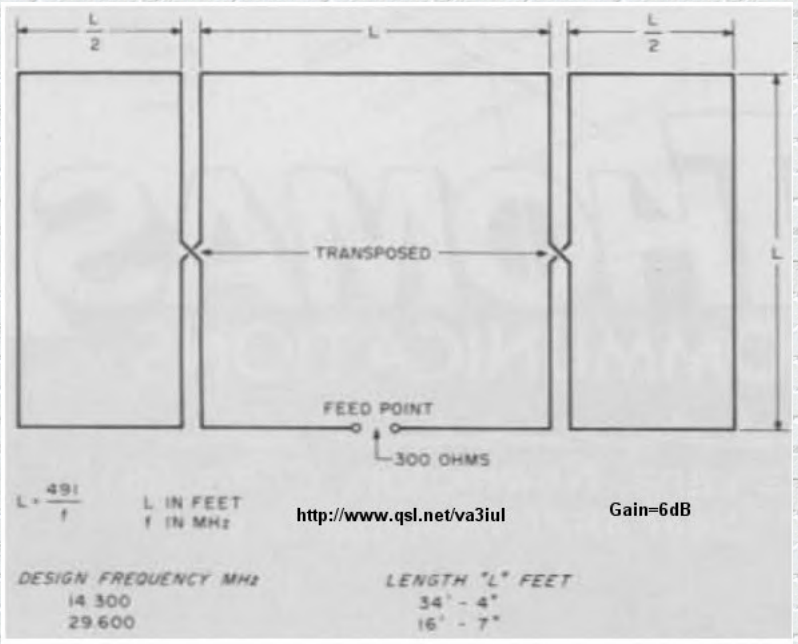

122 - Half-Wave Vertical Zepp Antenna

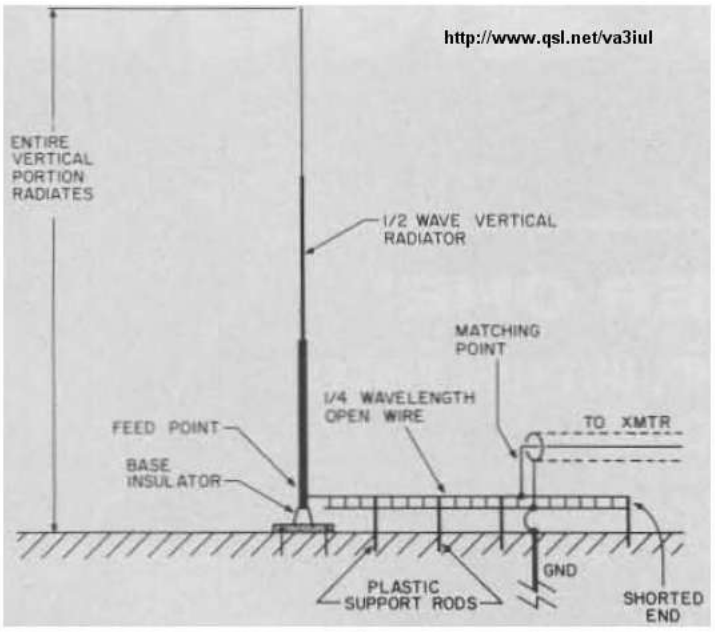

123 - Lazy-Loop Antenna for 40m

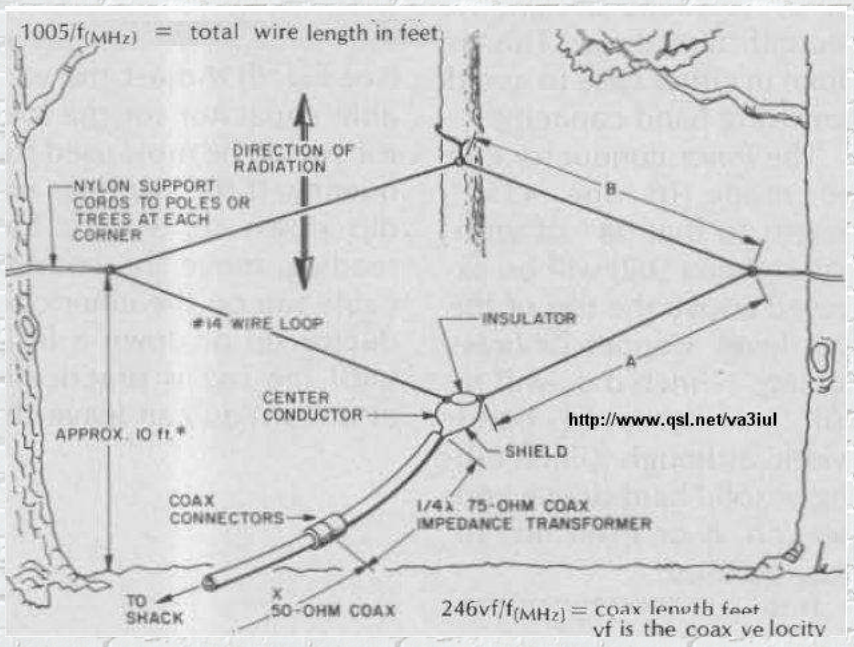

124 - Terminated Folded Dipole for 80m, 40m

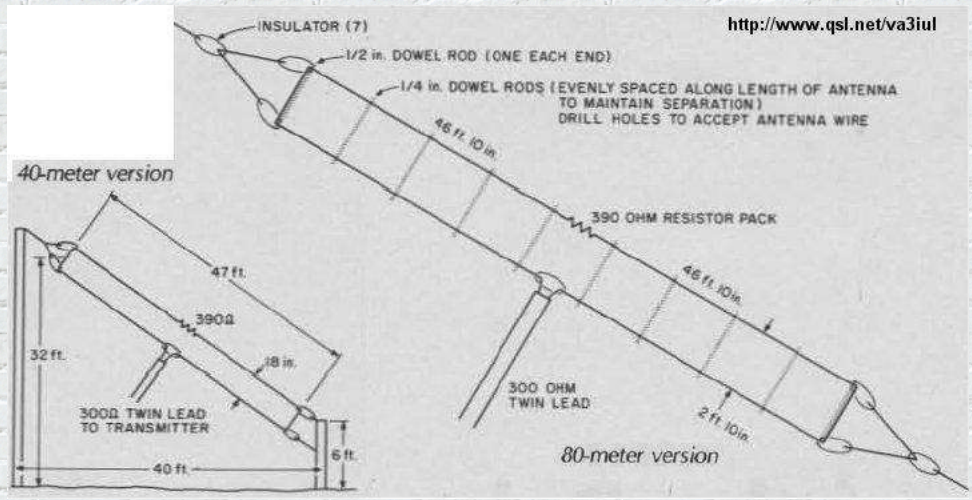

125 - Short-Fat Antenna for 15m

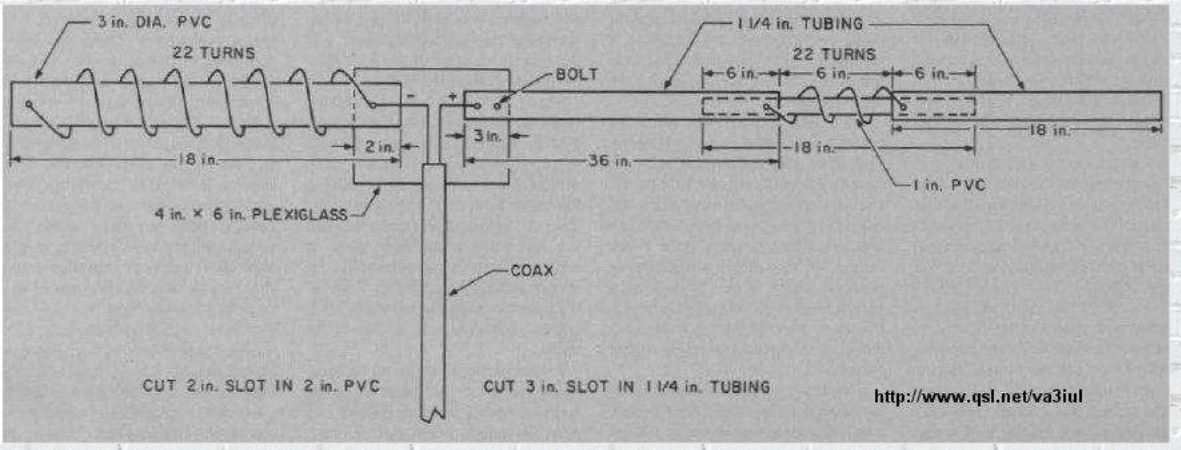

126 - Cobra Antenna for 80m

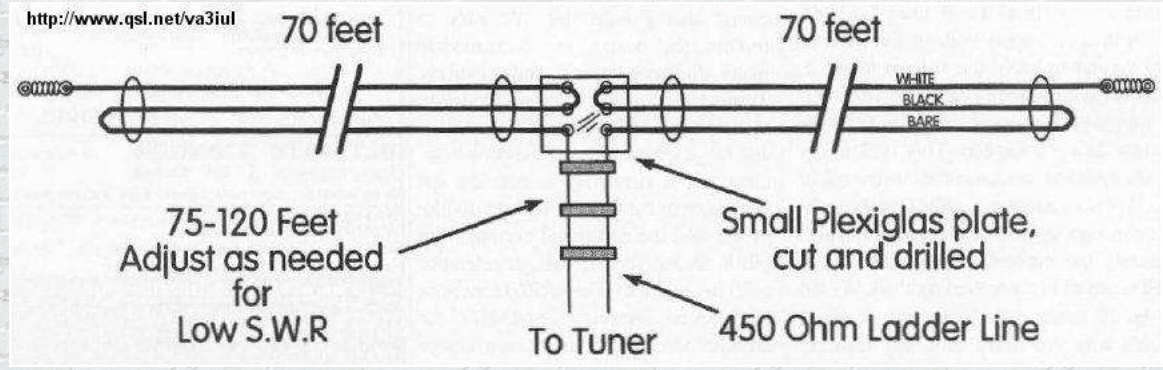

127 - Log-Periodic Wire Antenna for 20m, 15m, 10m

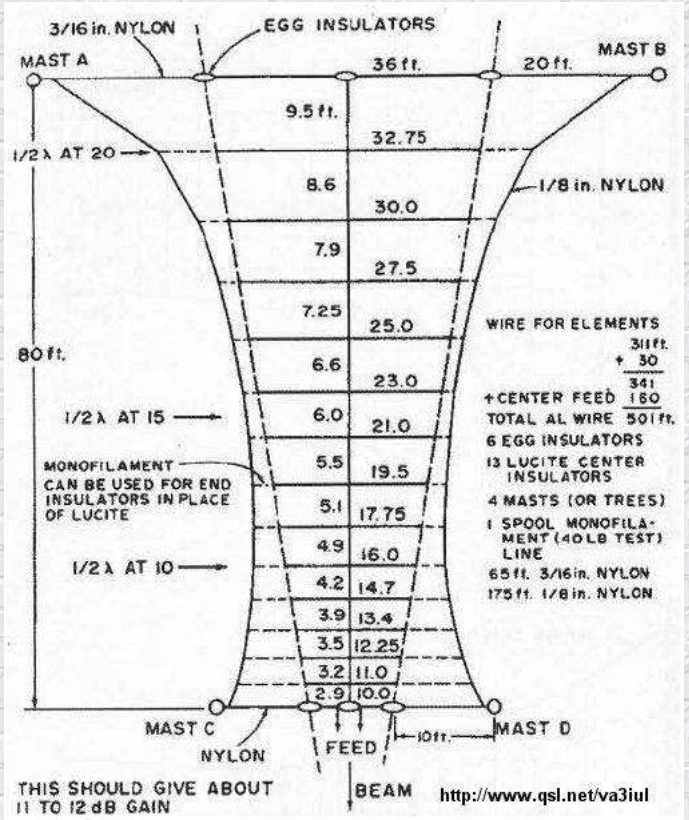

128 - 5-Element Log-Periodic Vertical Antenna for 80m, 40m, 20m

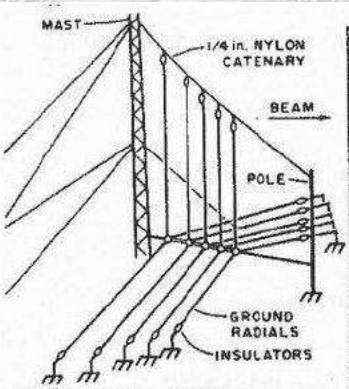

MHz BAND →	NOTE 1 3.5-4.0	NOTE 2 3.8-4.0	NOTE 2 7.0-7.3	NOTE 1 14.0-14.
L-1 •	70'	65'	35'	17.5'
L-2 •	67	62	33	16.5
L-3 •	59	55	28	14.0
L-4 •	50	45	24.5	12.25
L-5 •	43	40	20	10.0
S-1 •	30'	26'	14'	7.0'
S-2 •	27	24	13	6.5
S-3 •	24	23	12	6.0
S-4 •	19	18	9	4.5
TOTAL LENGTH	100'	91'	48'	24'
MAST HEIGHT	80	75	50	30
POLE HEIGHT	45	40	25	20

NOTE 1 - ESTIMATED (NOT TESTED)

NOTE 2 - CONSTRUCTED & TESTED. SWR LESS THAN 1.5 : 1 OVER FREQUENCY SPECIFIED

http://www.qsl.net/va3iul

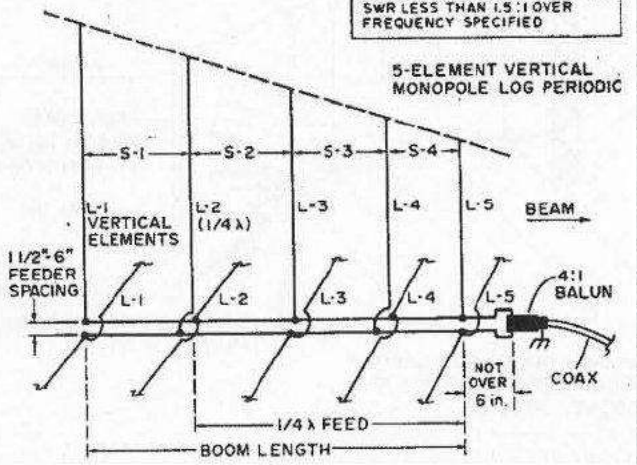

129 - 2m Vertical Wire Antennas

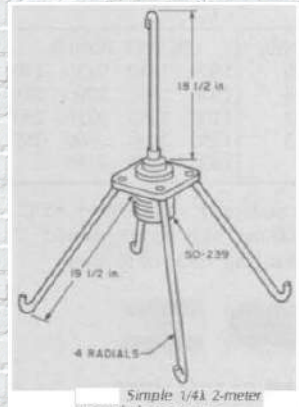

Simple 1/4λ 2-meter ground-plane antenna.

http://www.qsl.net/va3iul

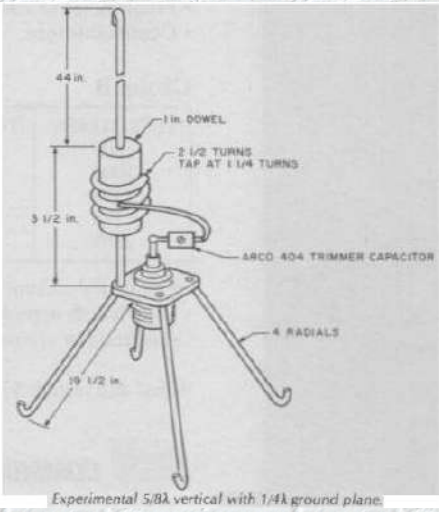

Experimental 5/8λ vertical with 1/4λ ground plane.

130 - Earth-Mover Inverted-V Antenna for 40m

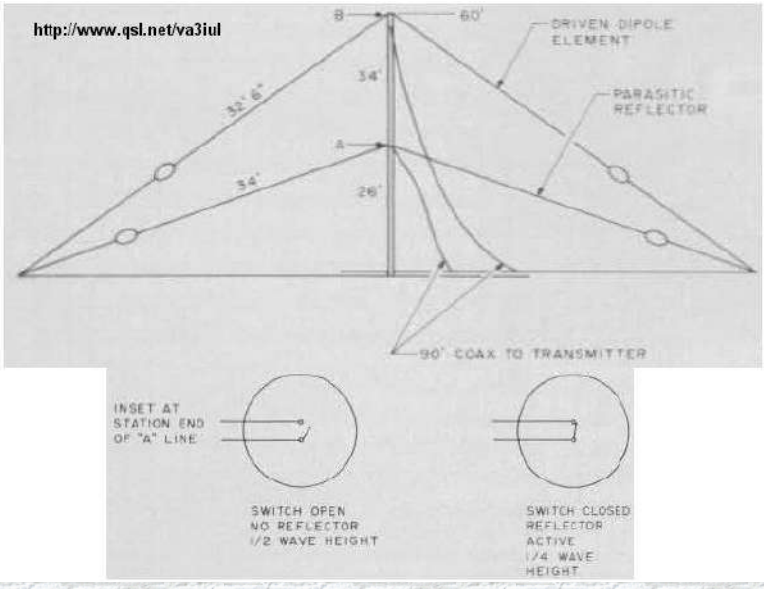

131 - Coax-Cable Collinear Antennas

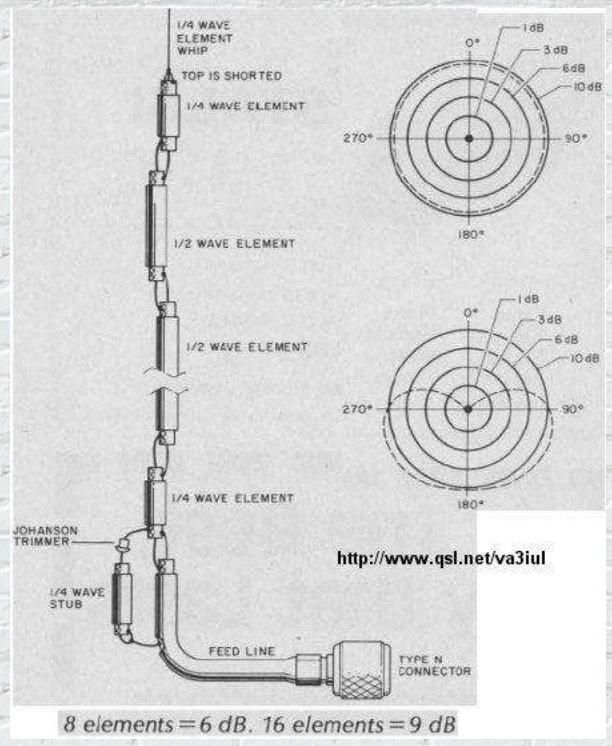

8 elements = 6 dB. 16 elements = 9 dB

132 - Double Bobtail Antenna for 20m

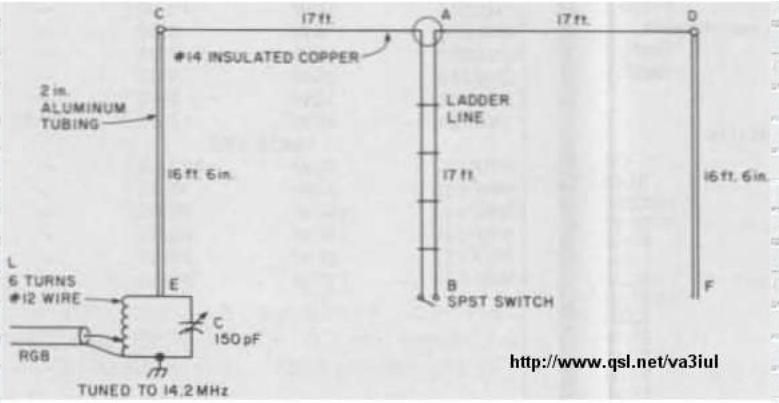

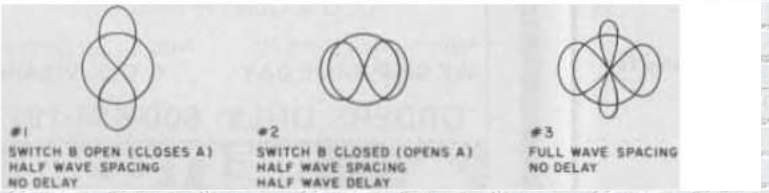

133 - Collinear Zepp Antenna

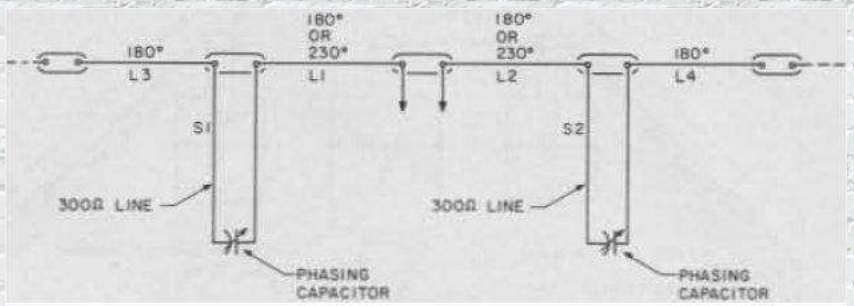

L1 - L2 = 180° - 468/f WHERE f = MHz
L1 - L2 = 230° - 600/f WHERE f = MHz

S1 - S2 = 246 × 0.82/f WHERE f = MHz
S1 - S2 MADE FROM 300Ω TV RIBBON.
MAKE ABOUT 6 inches LONGER THAN
CALCULATED VALUES. TRIM IF NECESSARY.

http://www.qsl.net/va3iul

134 - Taylor Vee Antenna for 20m

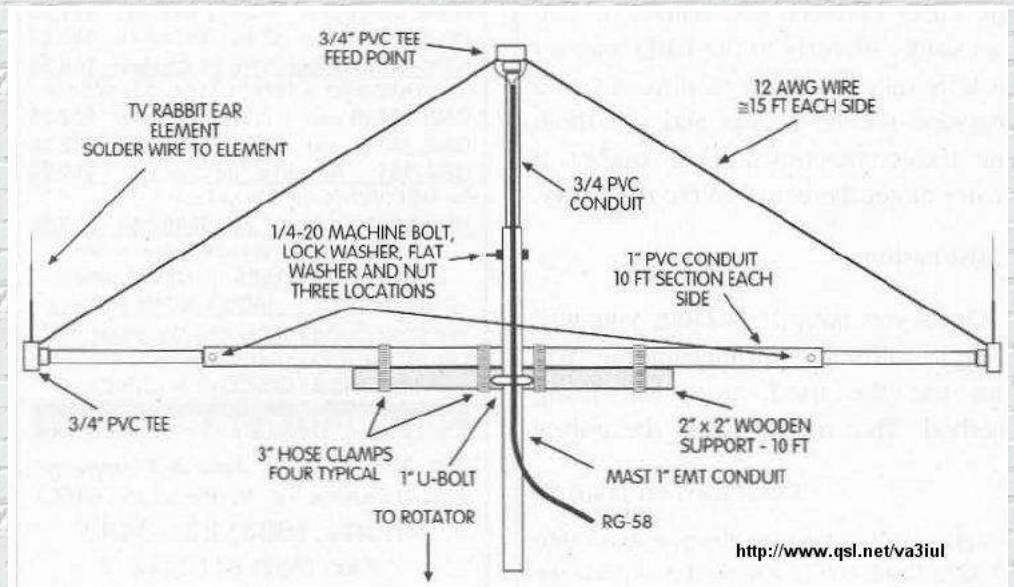

135 - Collinear Vertical Antenna 6dB-Gain for 2m, 1.3m, 73cm

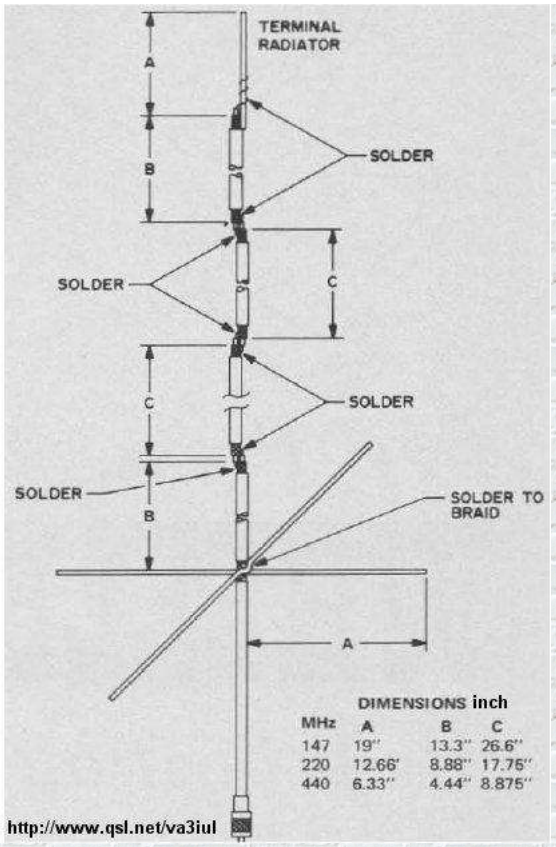

136 - Bi-Loop Antenna for 20m

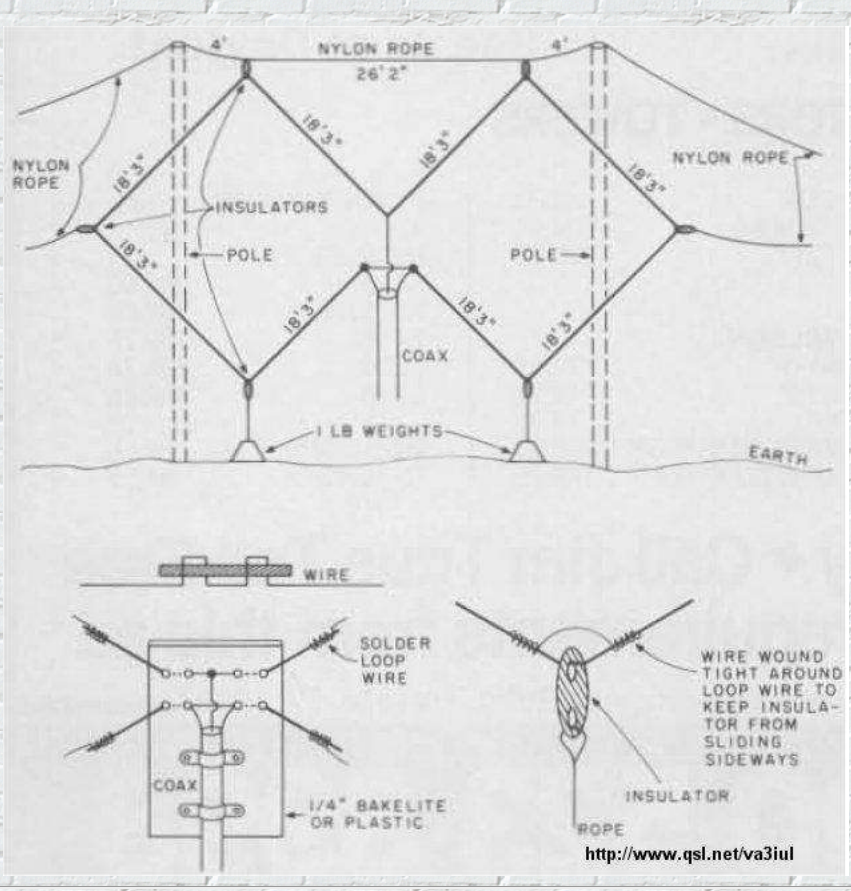

137 - Wire Beam 6dBd-Gain for 10m

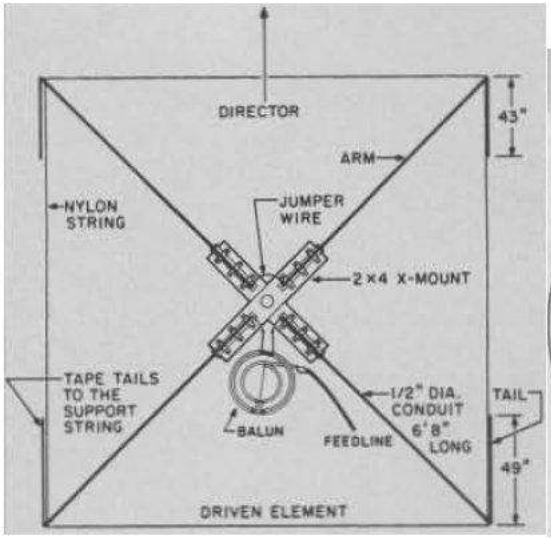

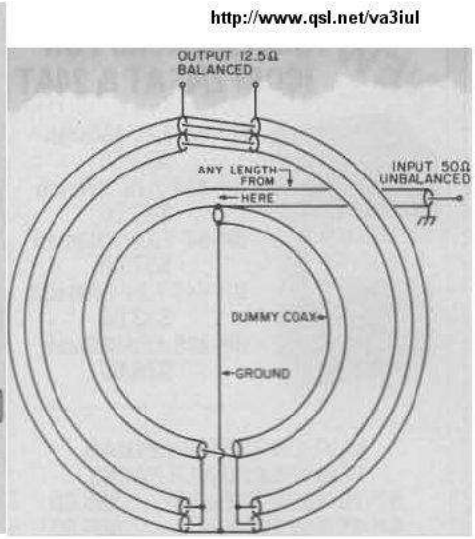

138 - Sloping Diamond Antenna 4dB-Gain for 40m

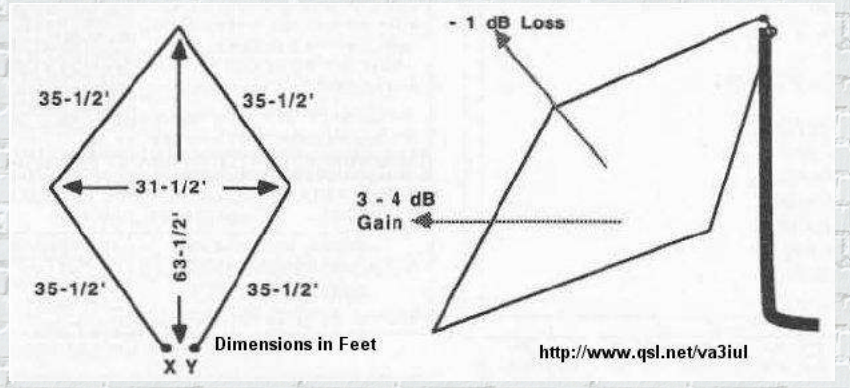

139 - Twisted Loop Antenna for 160m

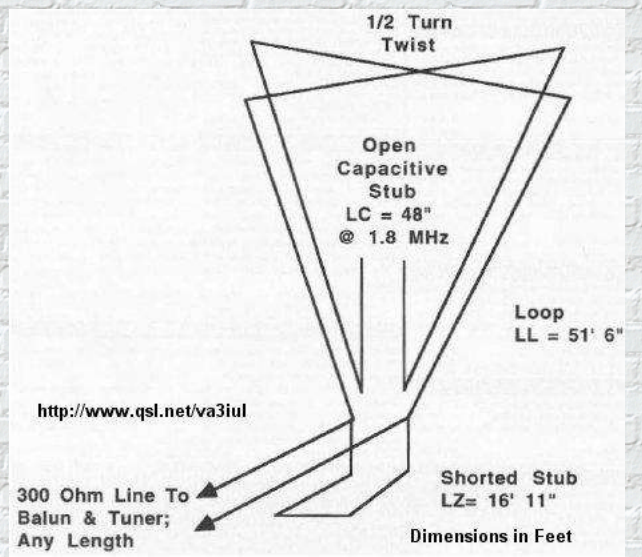

140 - DX RX Loop Antenna for 160m

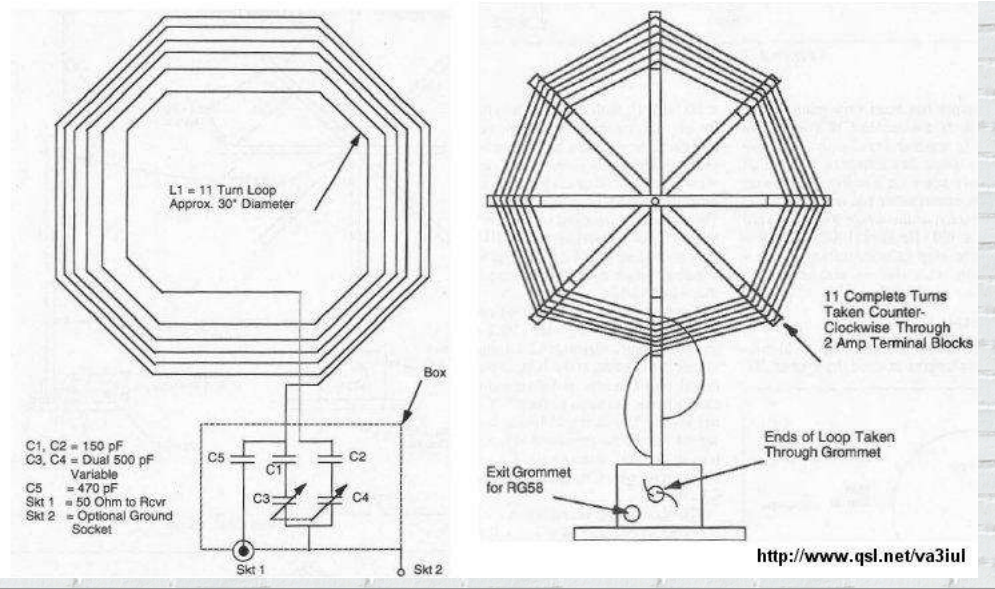

141 - Hentenna 3dB-Gain for 10m, 6m, 2m

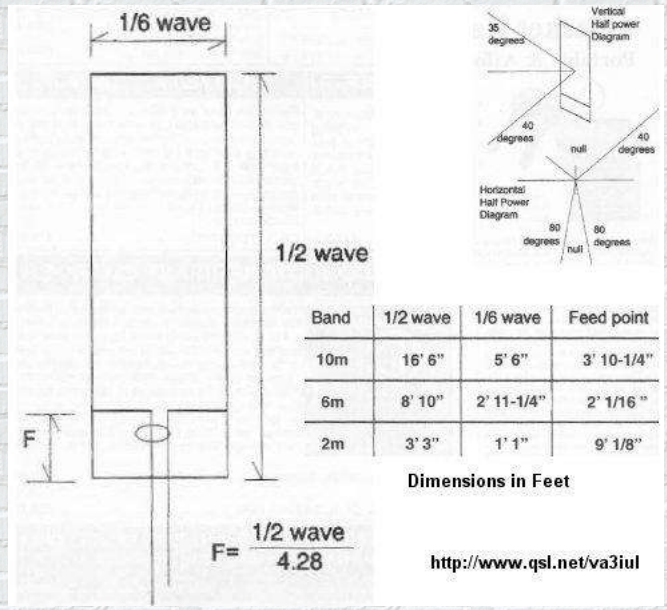

142 - VK2AAR Wire Antenna for 20m

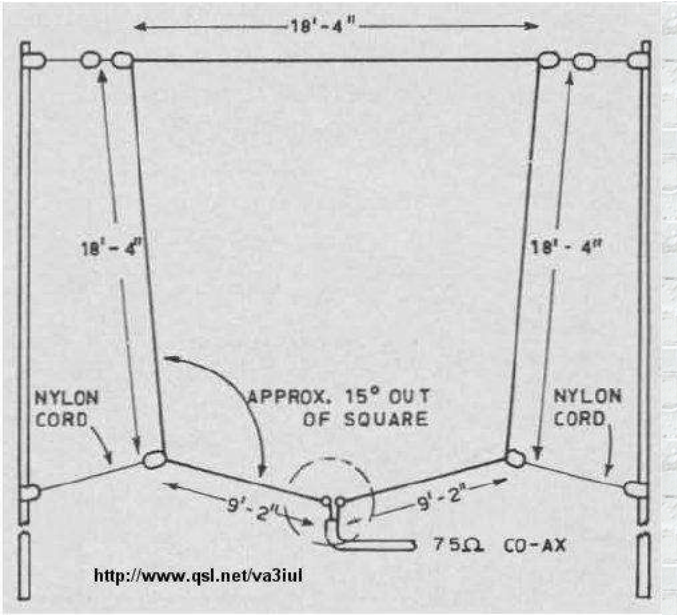

143 - 2-Elements Quad Antenna for 6m

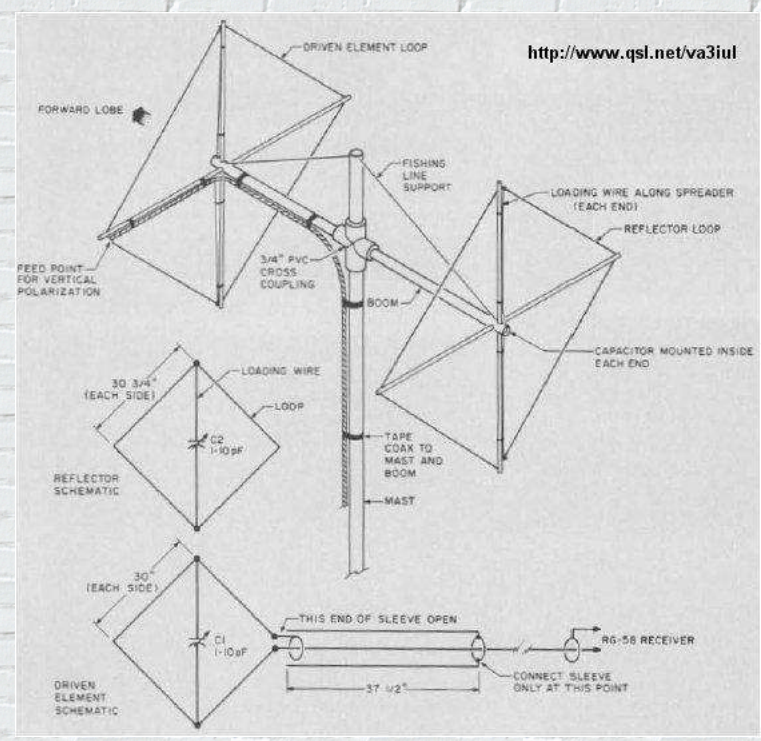

144 - Hula-Loop Bidirectional 6dB-Gain Antenna for 17m

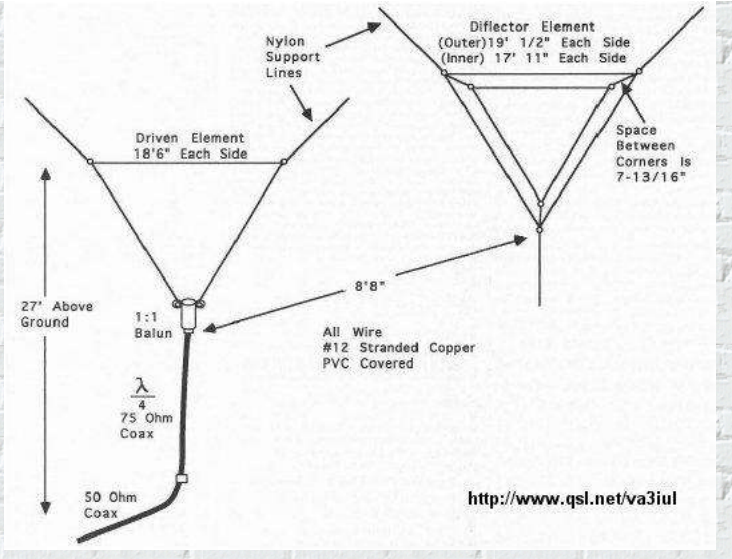

145 - Moxon Rectangle Beam for 15m-10m

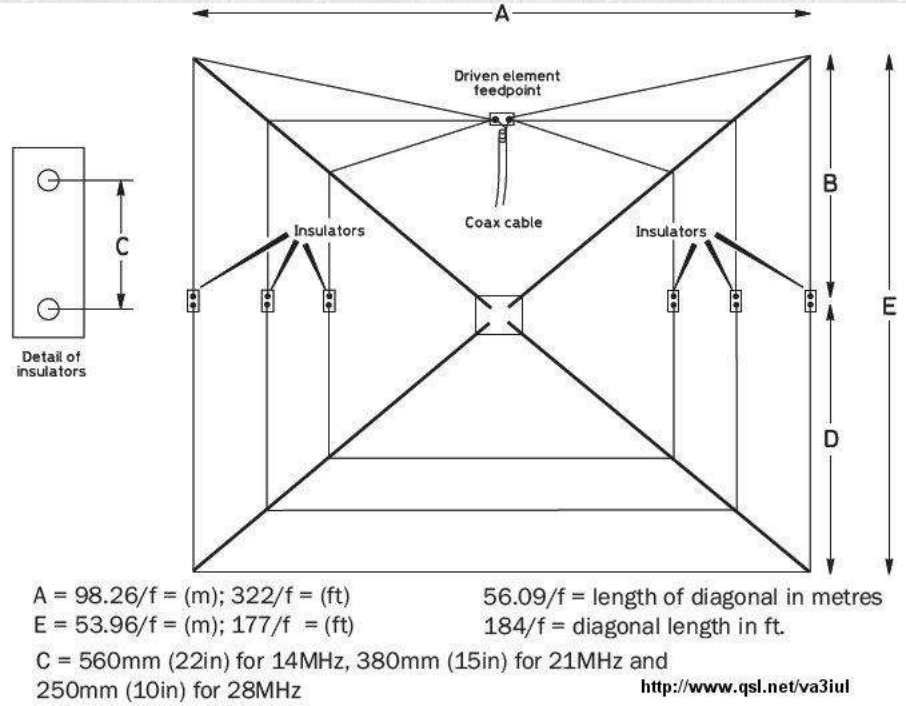

146 - Double-D Beam 4dB-Gain

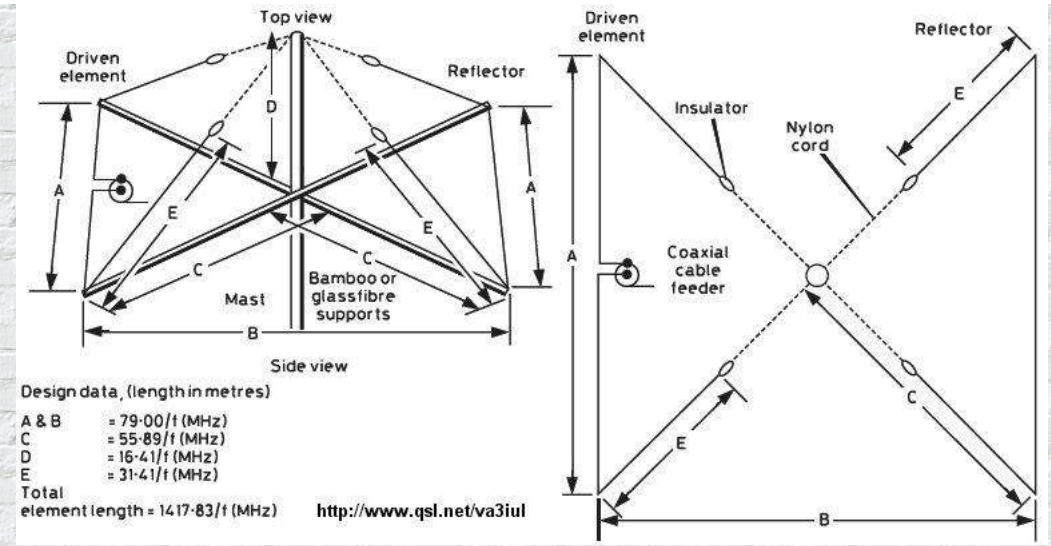

147 - KE4PT OCEF All-Band Dipole

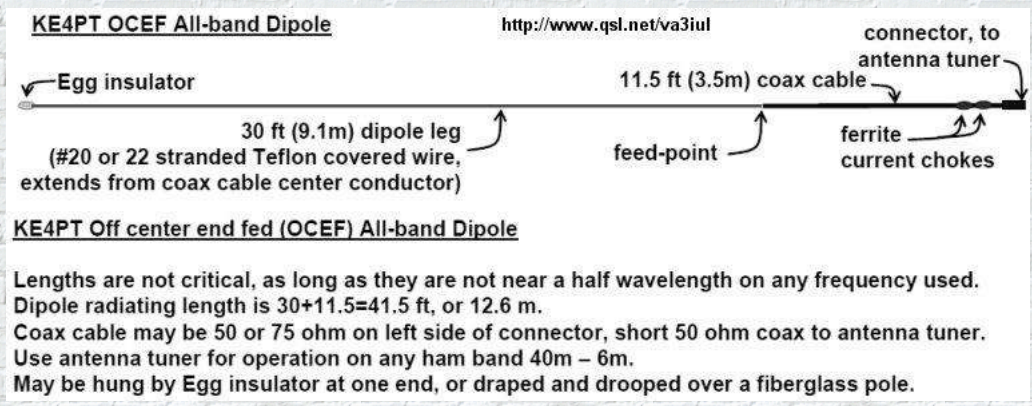

148 - Wire Quad Antenna for 40m

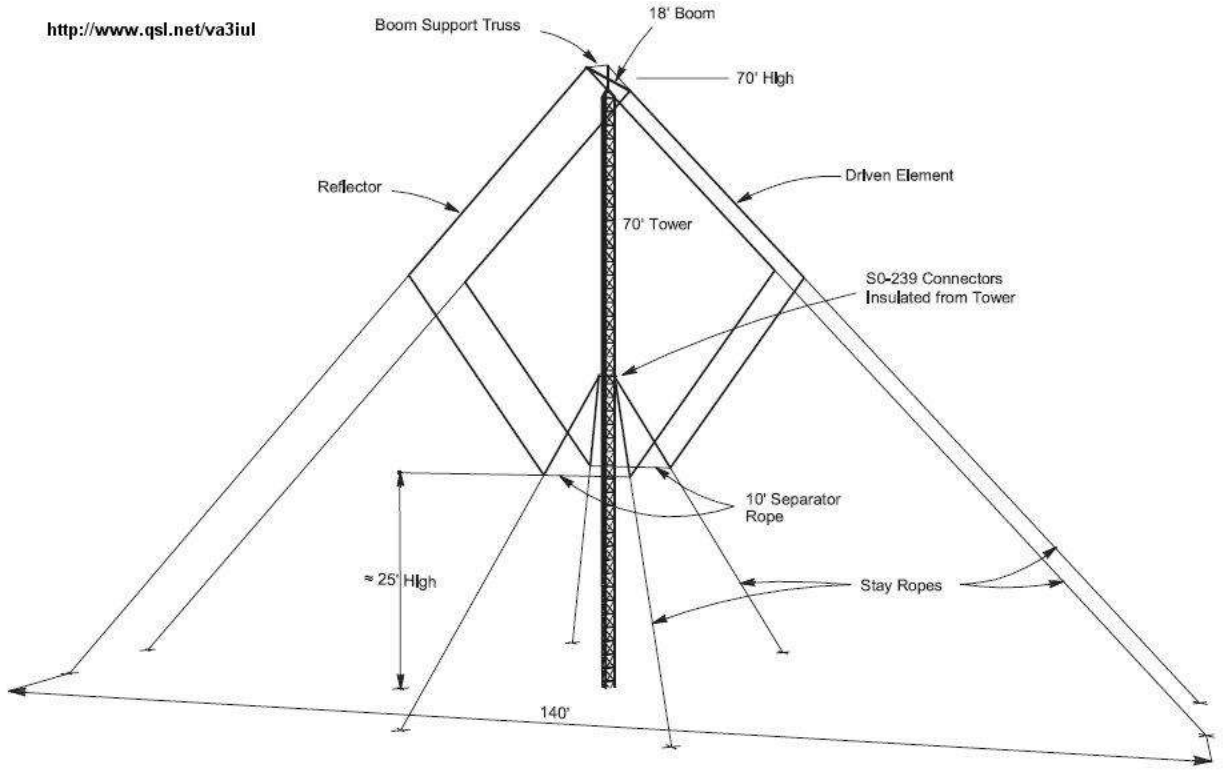

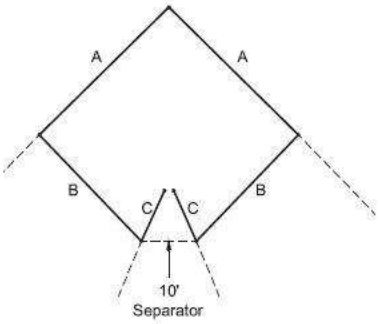

	7050 kHz, CW	7200 kHz, SSB
Length A, Reflector	31'6"	30'10-¾"
Length B, Reflector	28'2-¼"	27'7"
Length C, Reflector	15'7-¼"	15"
Total, Half Reflector	75'3-½"	73'5-¾"
Resonant Frequency	7030 kHz	7205 kHz
Length A, Driven	30'7-¼"	30"
Length B, Driven	27'3-½"	26'8-½"
Length C, Driven	14'7-½"	14"
Length, Half Driven	72'6-¼"	70'8-½"
Self-Resonant Frequency	7295 kHz	7480 kHz

149 - Inclined Dipole Antenna for 80m, 40m

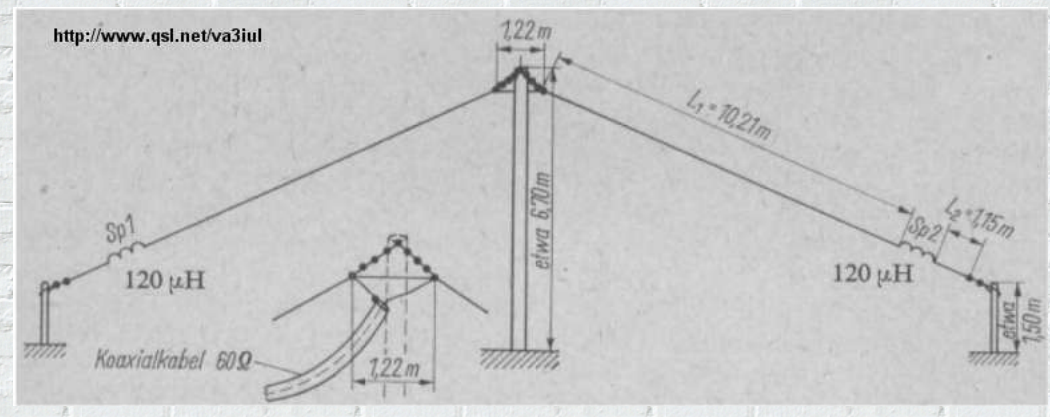

150 - Pyramidal Wire Antenna for 80m

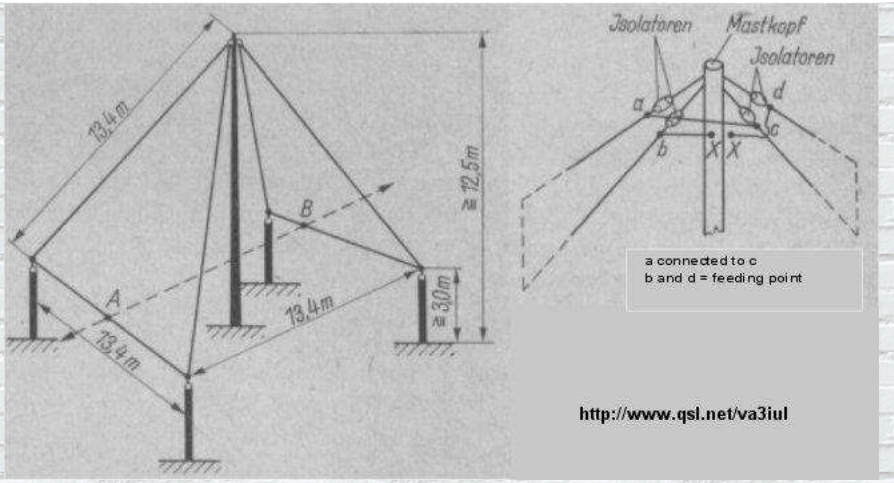

151 - Random Wire Antenna All Bands

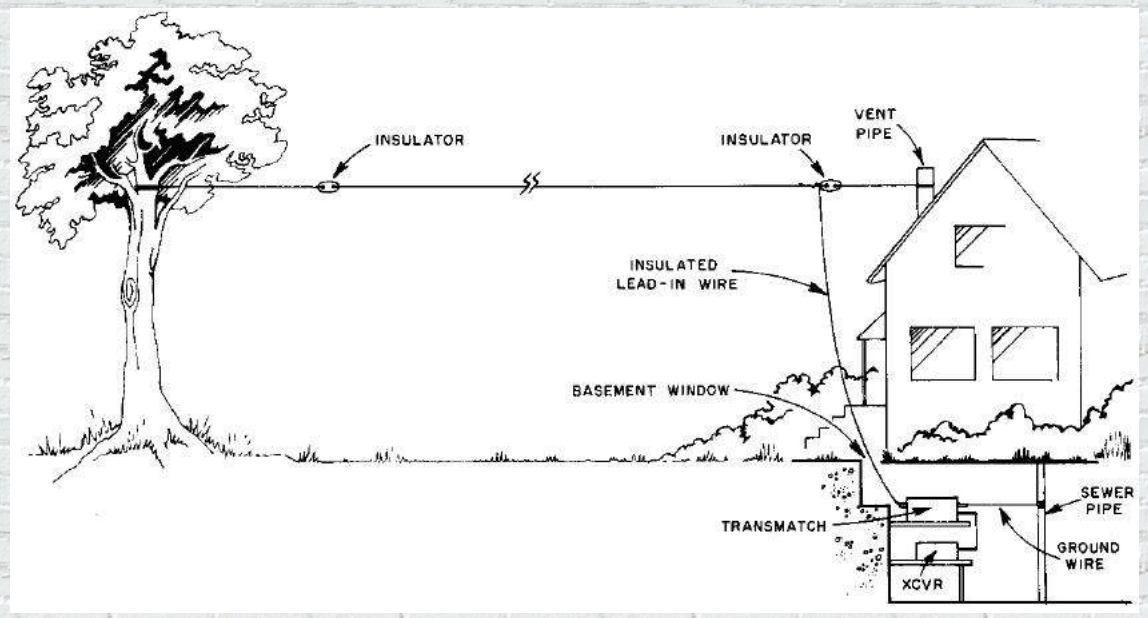

152 - Multiband Dipole Antenna for 80m, 40m,15m, 10m

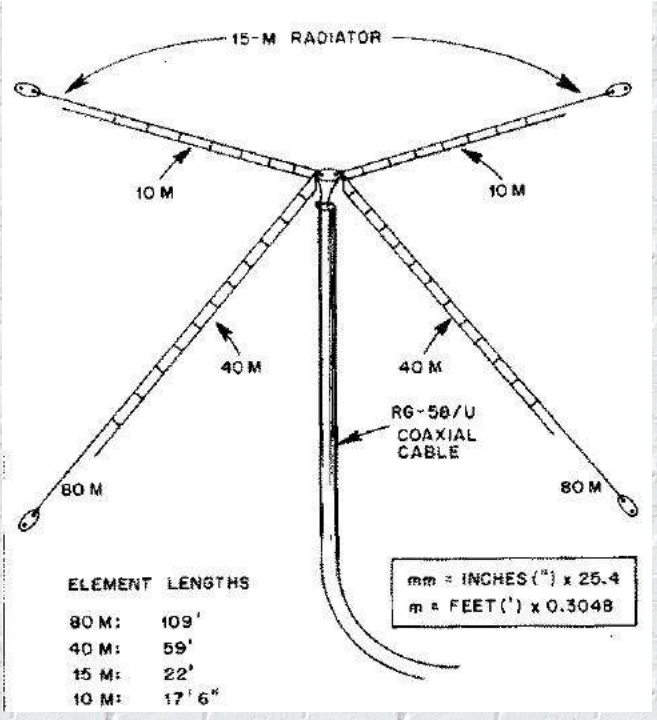

153 - Slim Jim Wire Antenna for 4m

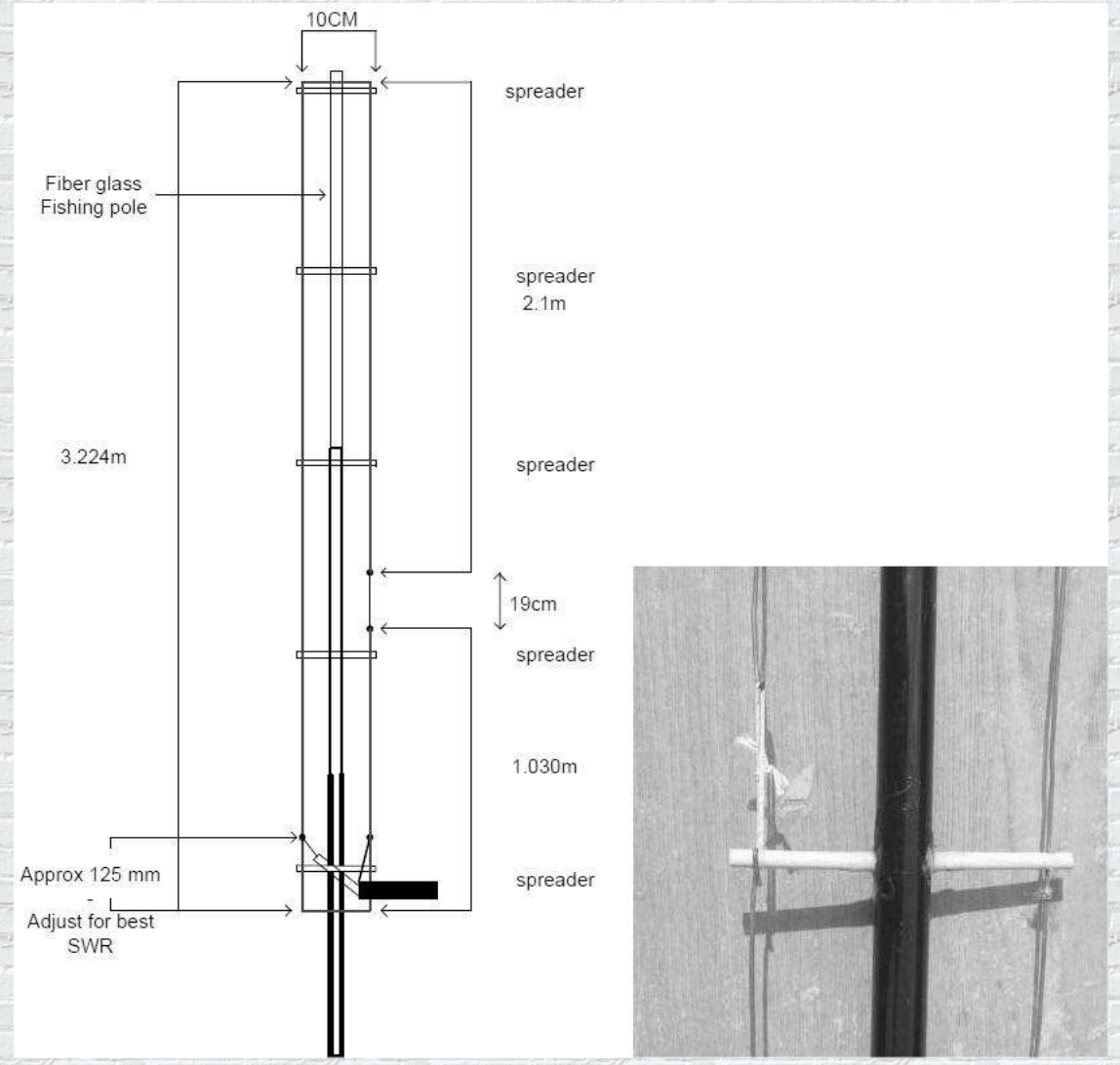

154 - Delta Loop for 6m

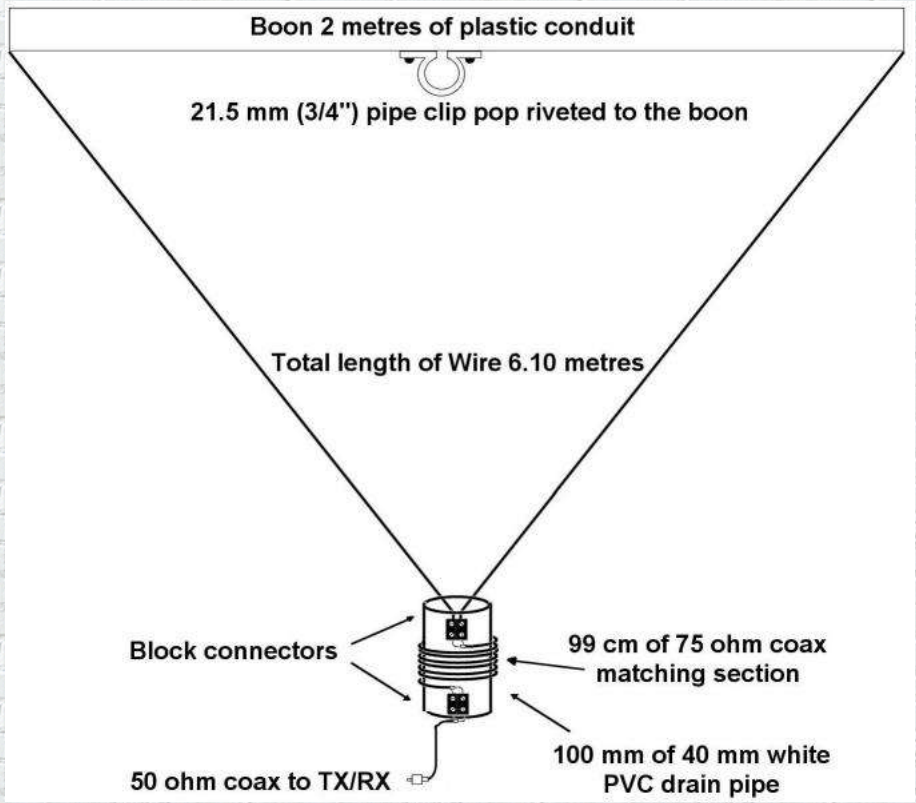

155 - Re-Configurable Antenna for 160m and 80m

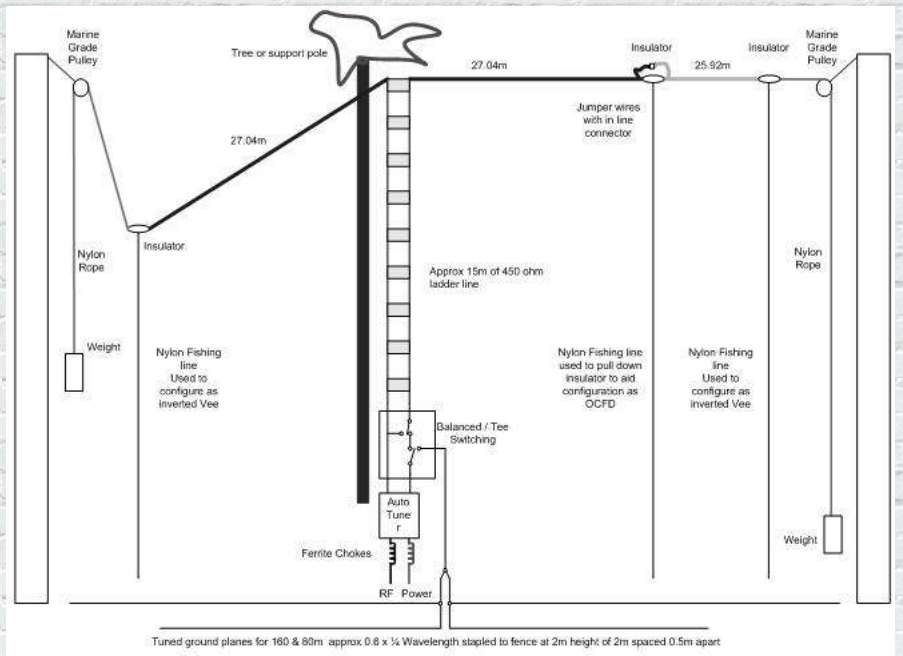

156 - Very Low Frequency Inverted-L Antenna

f(kc)	X (ohms)	CALCULATED Rrad (ohms)
45	-j 785	0.49
50	690	0.60
60	555	0.85
70	450	1.20
80	375	1.55
90	320	2.00
100	268	2.40
120	188	3.6
140	125	5.2
160	75	7.2
180	30	9.9
195	0	12.8

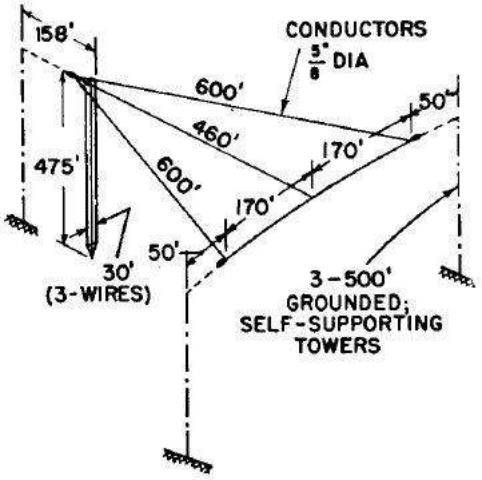

157 - Reduced Size Half Sloper Antenna for 160m

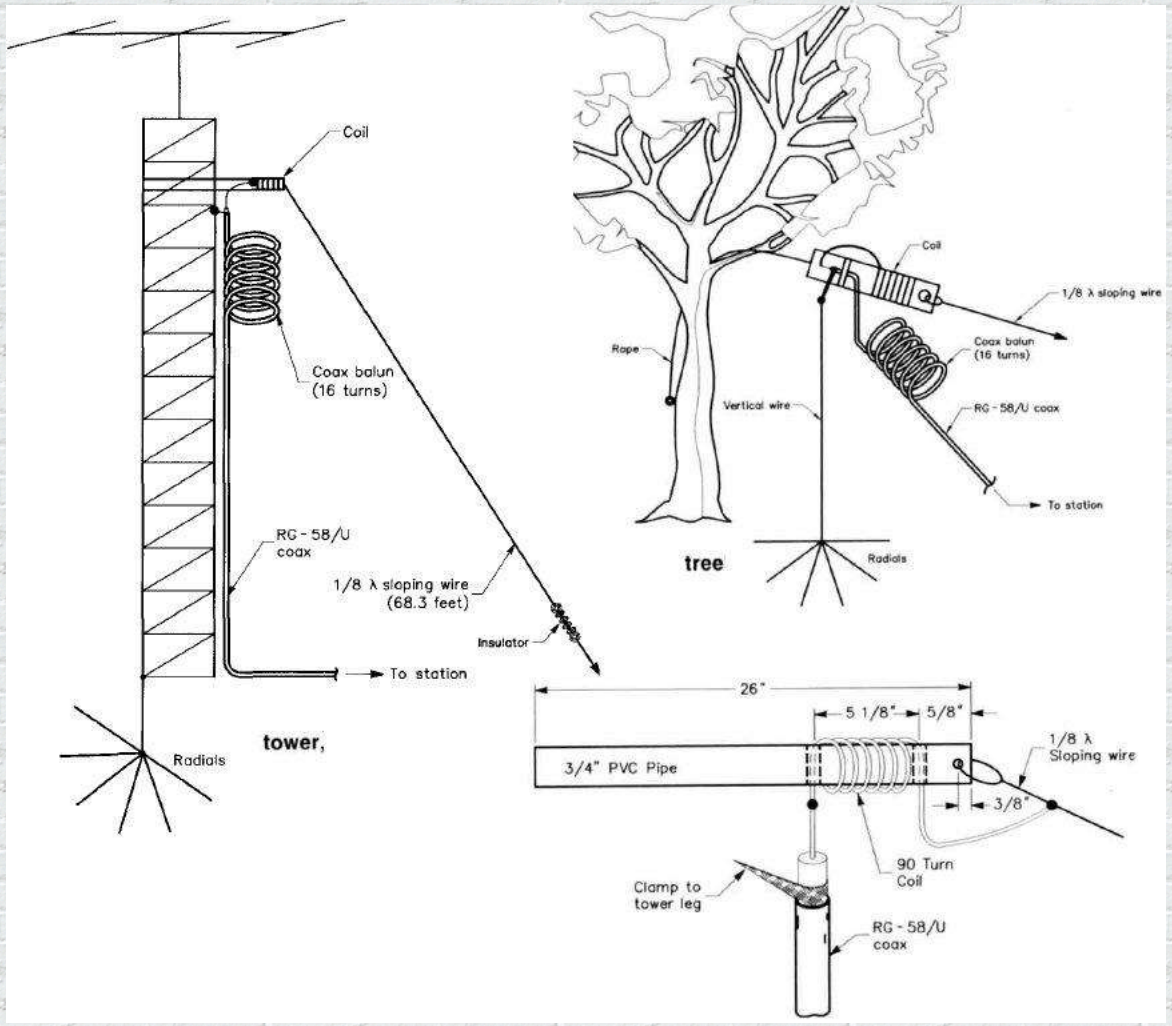

158 - Tree-Mounted HF Antenna

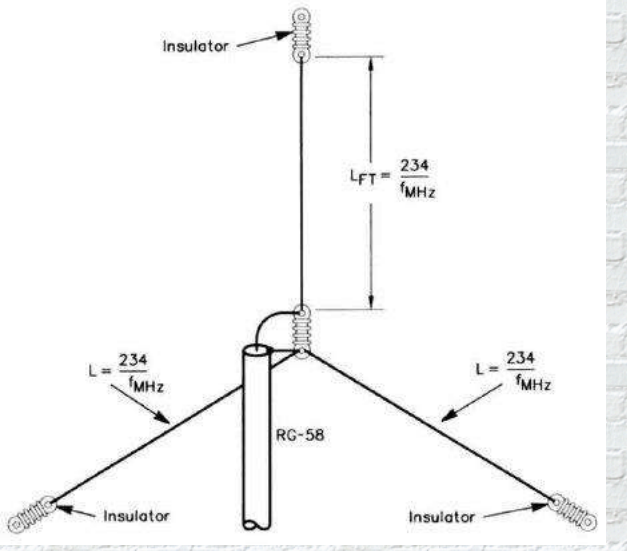

159 - Multiband Vertical Antenna for 80m, 40m, 20m

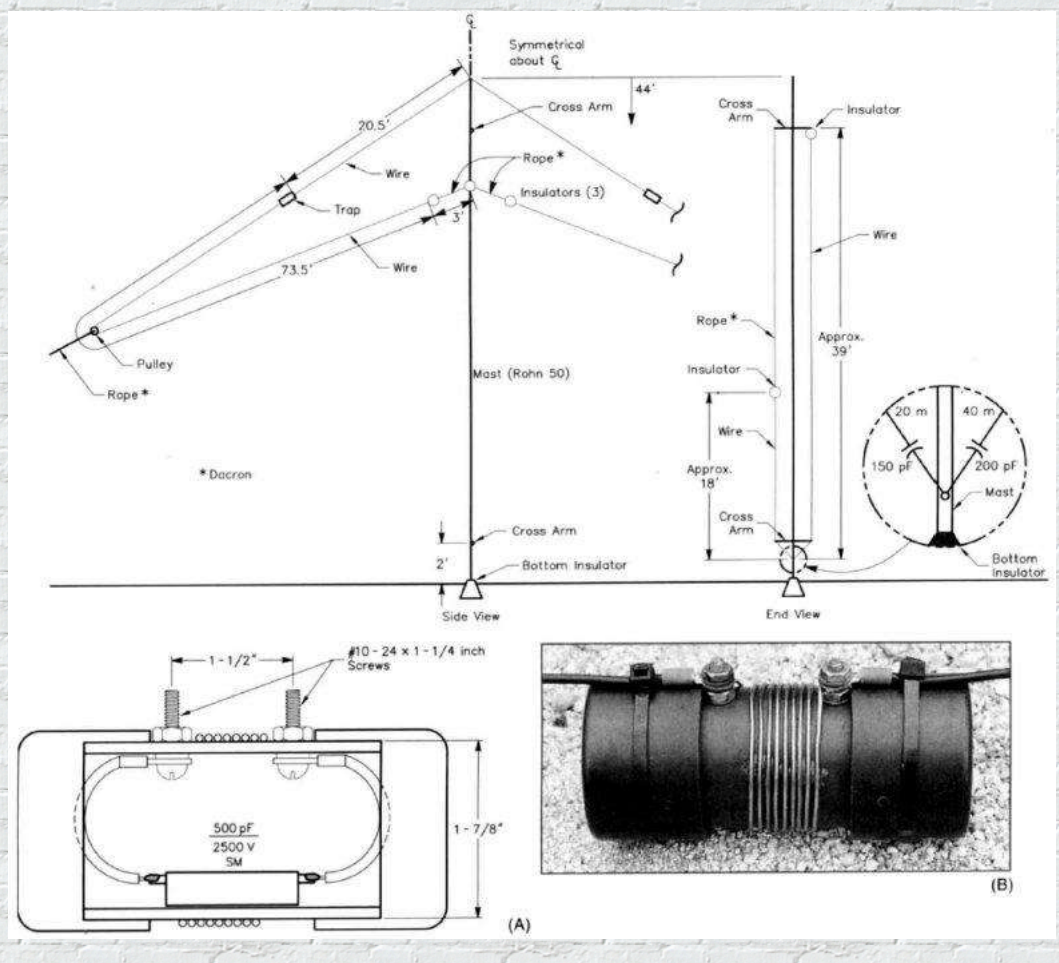

160 - Marconi Antenna for 136 kHz

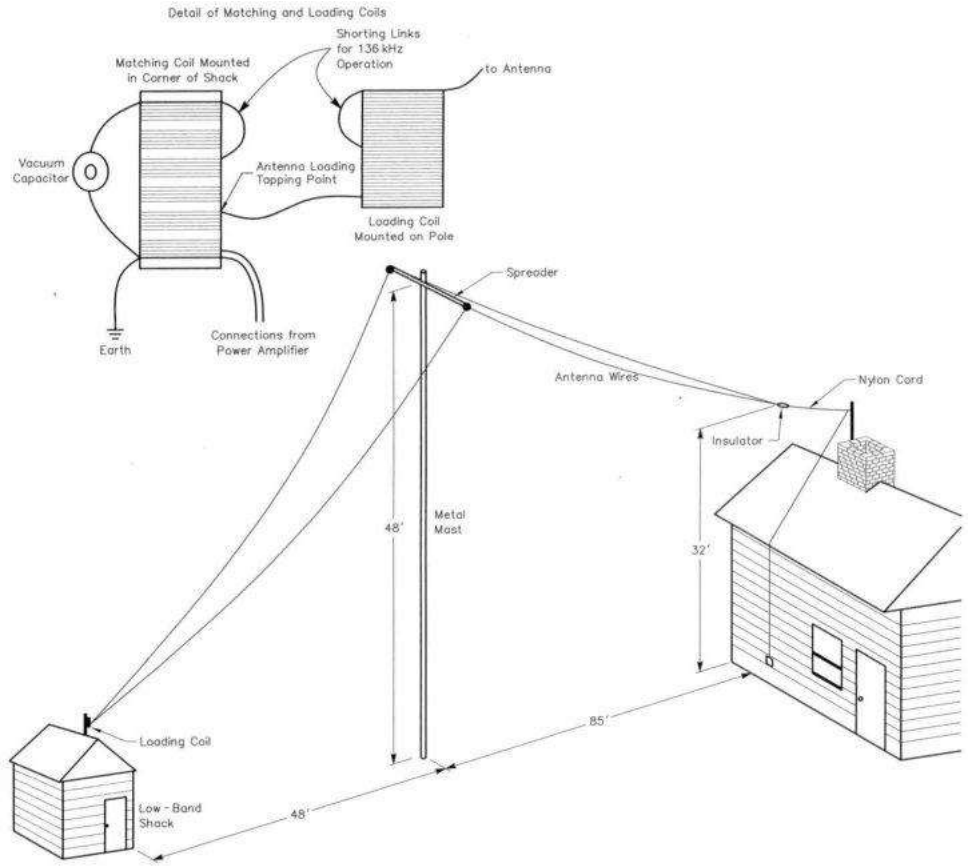

161 - Simple Killer Antenna for 40m

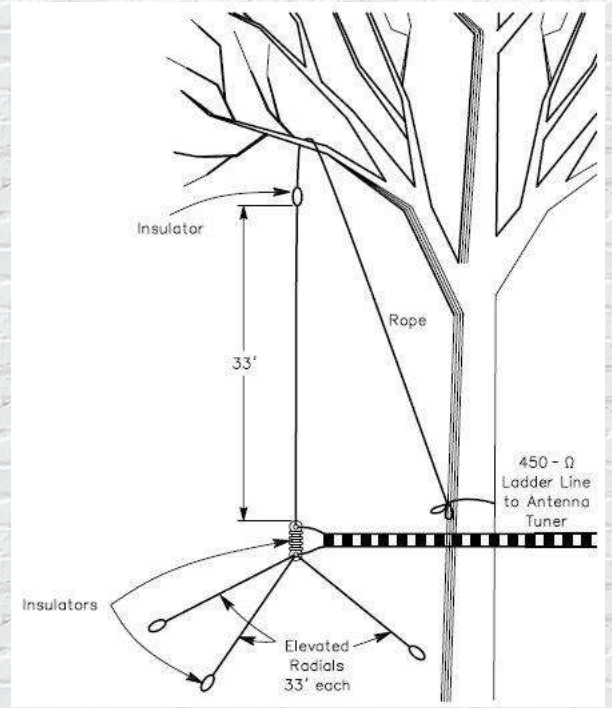

162 - Stub-Directed V Antenna for 80m

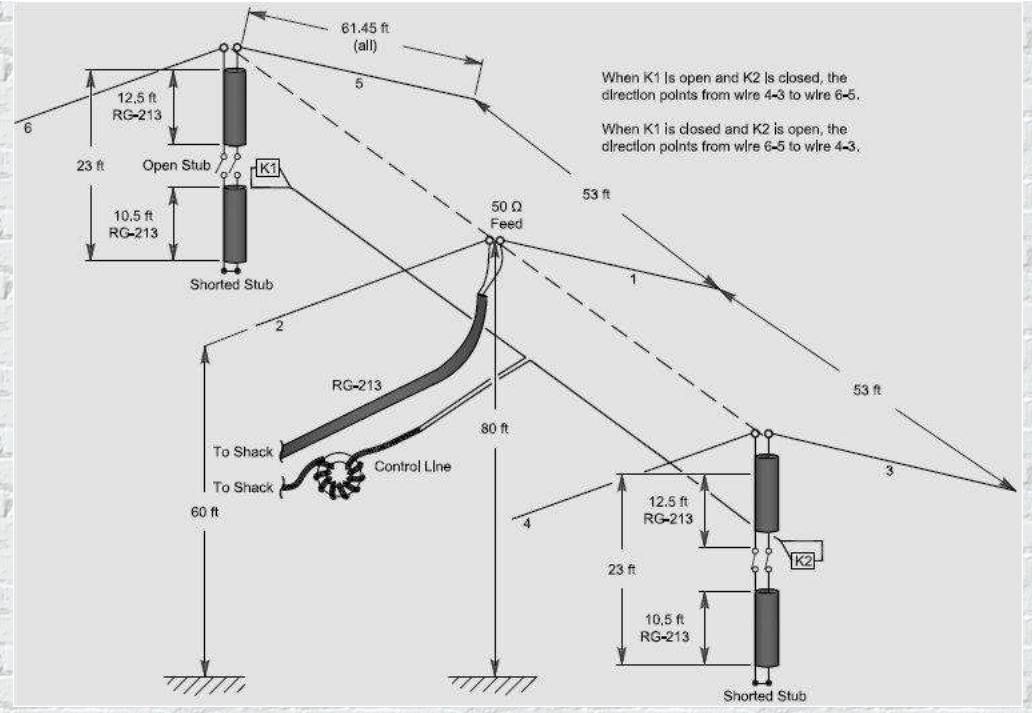

163 - KT0NY Over-and-Under DX Antenna for 20m

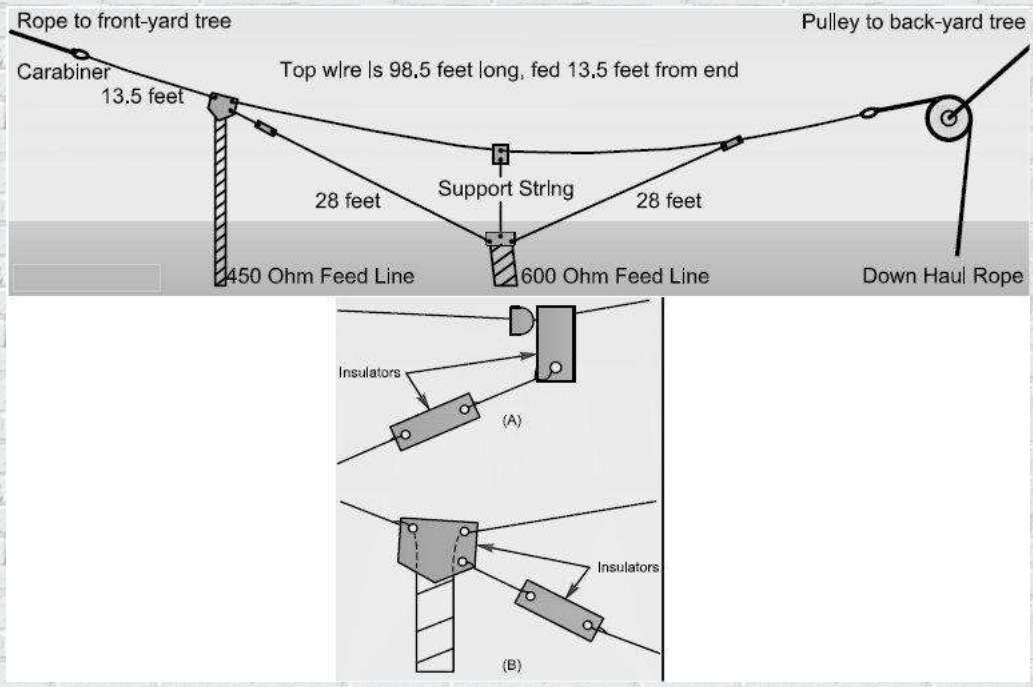

164 - Horizontal Loop Antennas

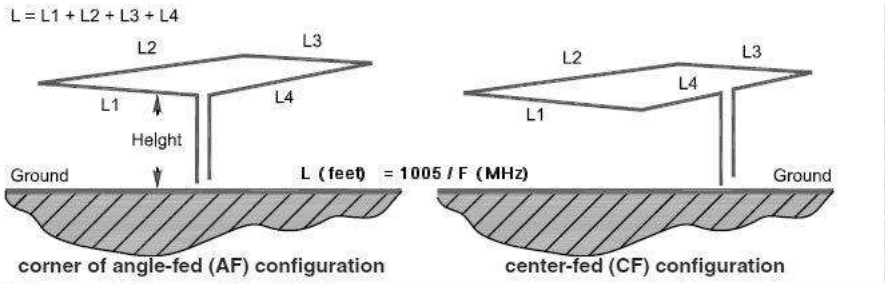

Loop Performance by Shape and Feed Point

	Circular Loop		*Square Loop AF*		*Triangle Loop AF*		*Square Loop CF*		*Triangle Loop CF*	
	Gain (dBi)	*Elev*	*Gain (dBi)*	*Elev*	*Gain (dBi)*	*Elev*	*Gain (dBi)*	*Elev*	*Gain (dBi)*	*Elev*
1.9 MHz	3.93	90°	3.46	90°	2.88	90°	3.70	90°	2.67	90°
3.9 MHz	8.47	90°	8.13	90°	7.76	90°	8.23	90°	8.04	90°
7.2 MHz	7.76	50°	7.35	50°	7.98	45°	7.64	45°	7.30	45°
10.1 MHz	8.34	35°	10.68	35°	7.35	30°	8.17	35°	7.24	30°
14.2 MHz	10.44	25°	12.50	25°	11.27	25°	10.25	25°	8.50	25°
18.1 MHz	11.18	20°	14.03	20°	12.32	20°	11.40	20°	8.84	20°
21.2 MHz	10.16	15°	14.55	15°	12.42	15°	11.28	15°	8.29	15°
24.9 MHz	10.77	15°	13.69	15°	14.09	15°	10.58	15°	10.10	15°
28.5 MHz	11.39	15°	12.85	10°	13.84	10°	11.19	10°	12.66	10°

165 - Ribbon J-Pole for 2m

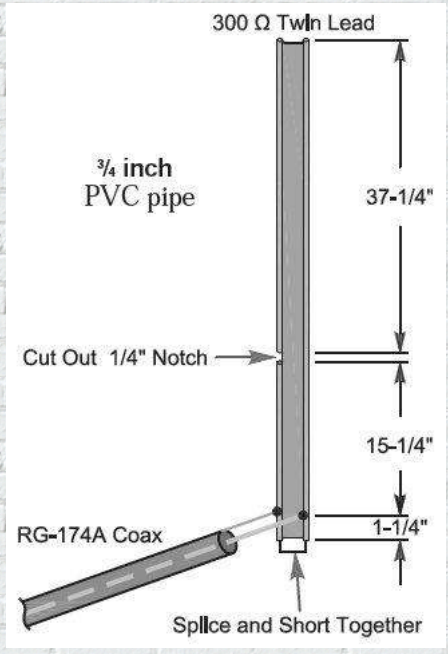

166 - Dual Band Ribbon J-Pole for 2m, 70cm

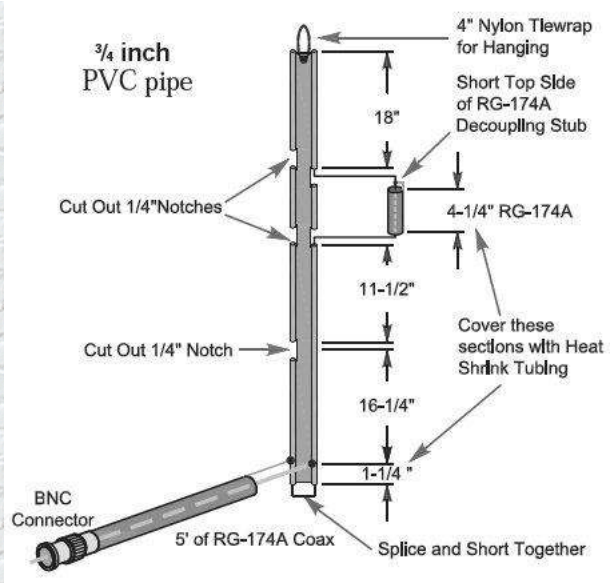

167 - Square Vertical Loop Antenna for 40m

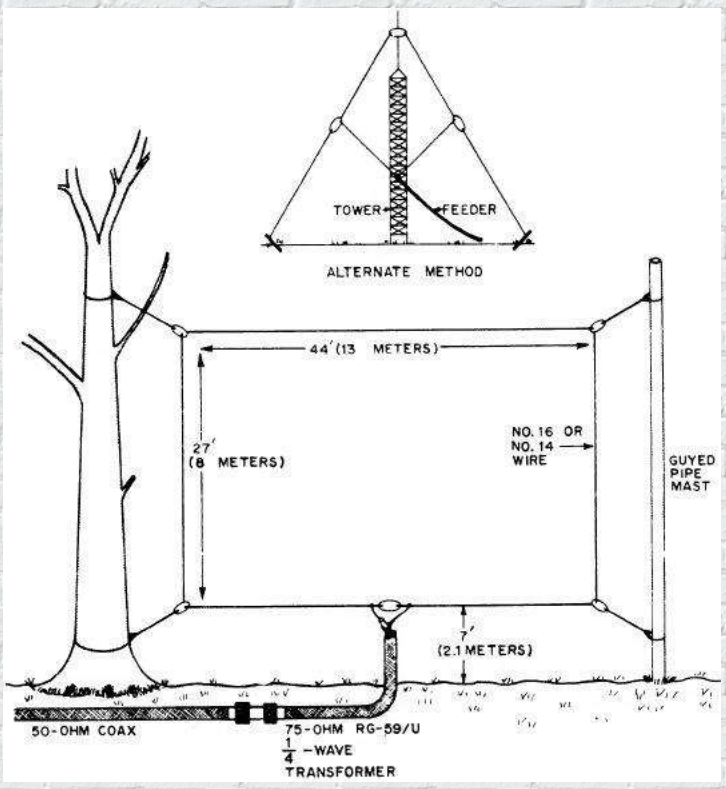

168 - Tri-Band Quad Antenna for 20m, 15m, 10m

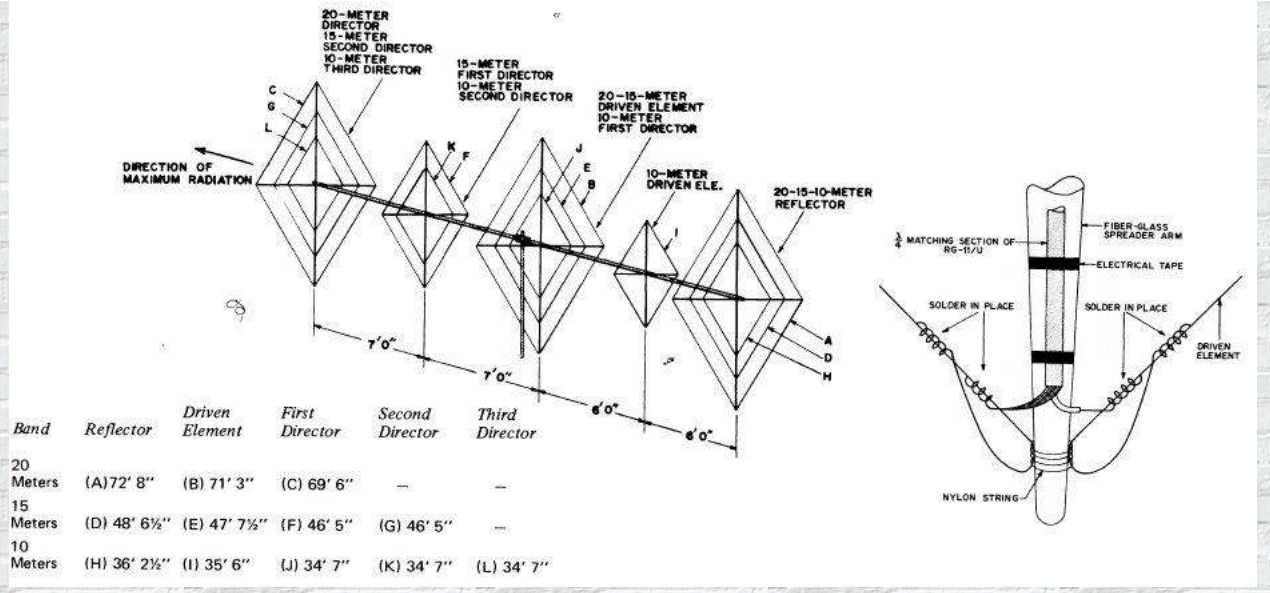

Band	Reflector	Driven Element	First Director	Second Director	Third Director
20 Meters	(A) 72' 8"	(B) 71' 3"	(C) 69' 6"	–	–
15 Meters	(D) 48' 6½"	(E) 47' 7½"	(F) 46' 5"	(G) 46' 5"	–
10 Meters	(H) 36' 2½"	(I) 35' 6"	(J) 34' 7"	(K) 34' 7"	(L) 34' 7"

169 - 3D Quad Antenna for 80m, 40m, 20m, 15m, 10m

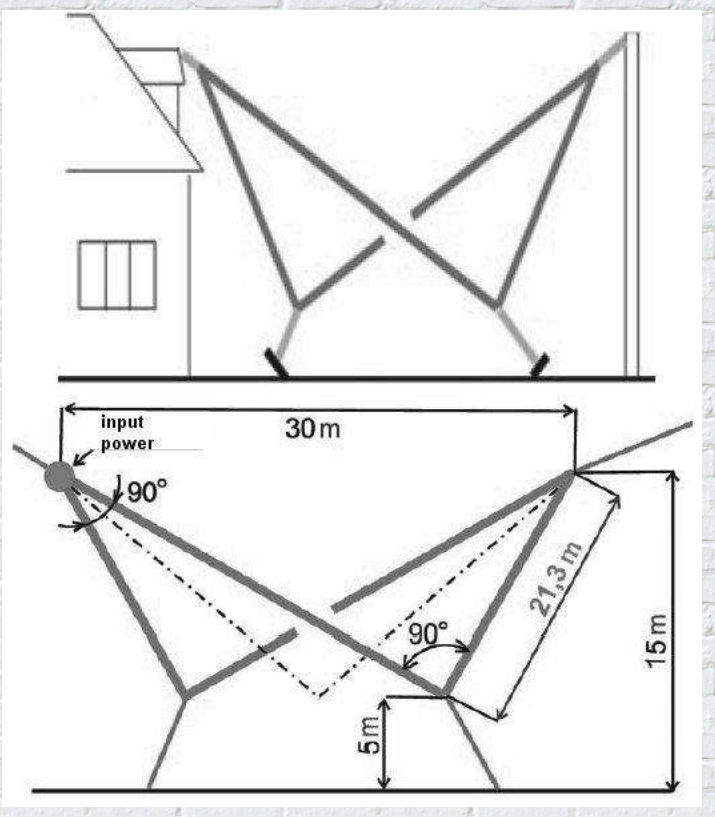

170 - Sloping Wire Antenna for 30m, 20m, 17m, 15m, 12m, 10m

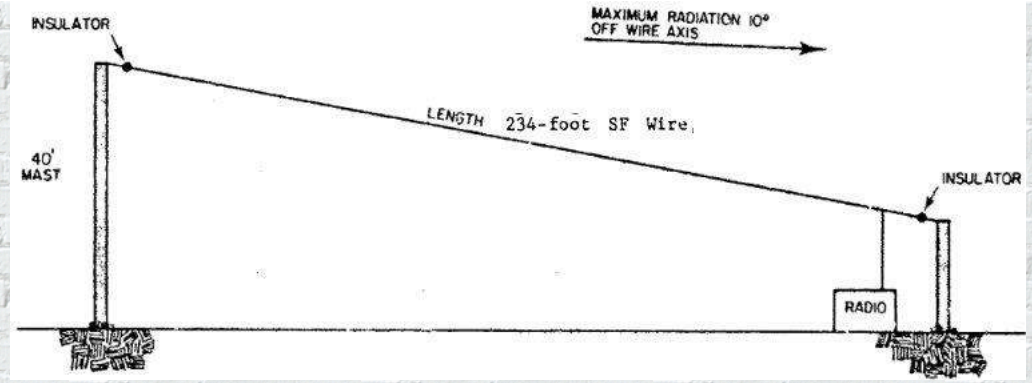

171 - Broadband Dipole Antenna with Coaxial Resonator for 80m

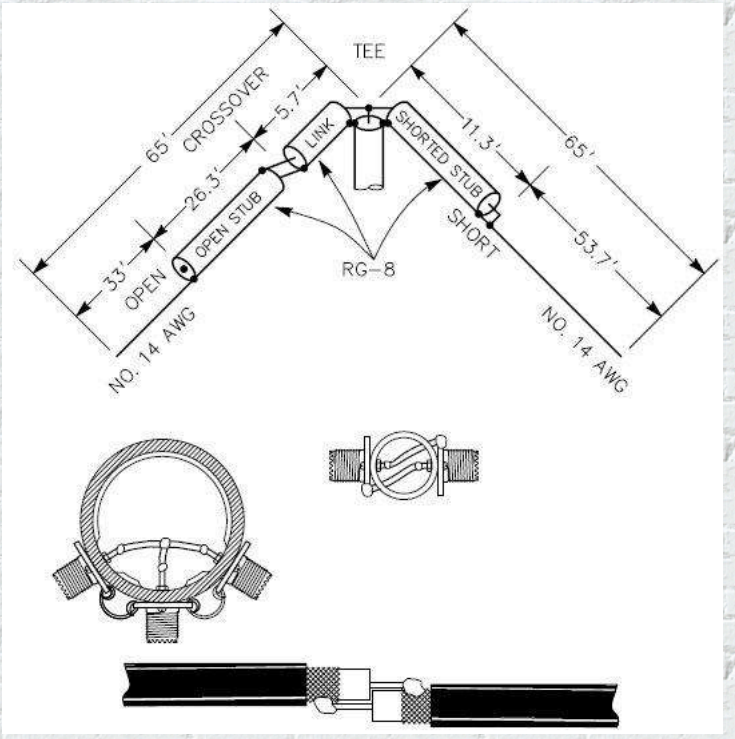

172 - Resonant Feedline Dipole Antenna for 80m

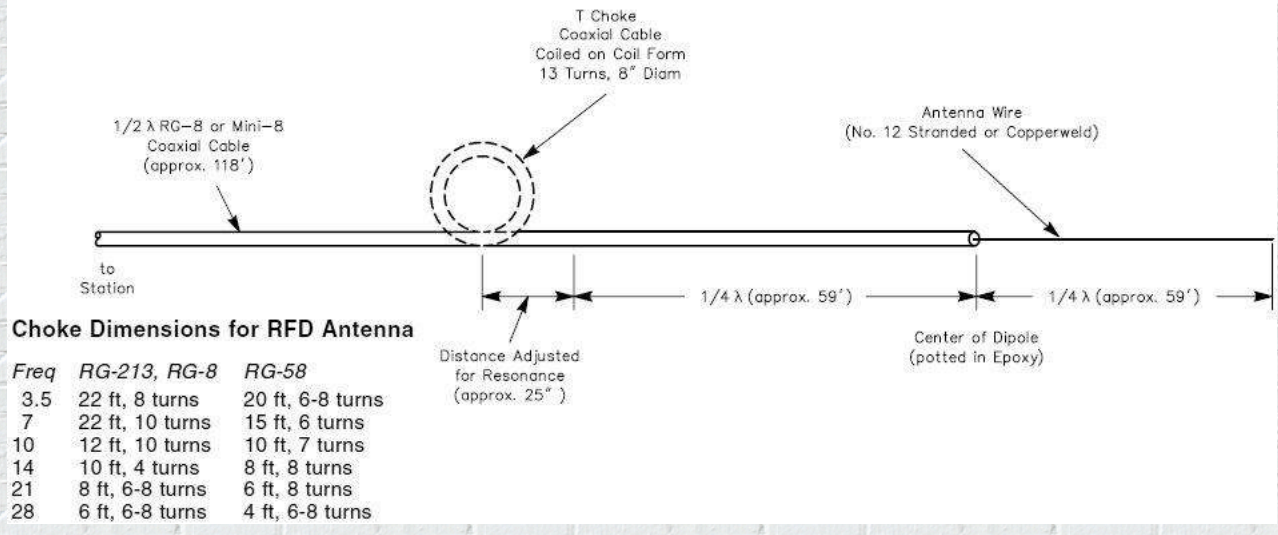

Choke Dimensions for RFD Antenna

Freq	*RG-213, RG-8*	*RG-58*
3.5	22 ft, 8 turns	20 ft, 6-8 turns
7	22 ft, 10 turns	15 ft, 6 turns
10	12 ft, 10 turns	10 ft, 7 turns
14	10 ft, 4 turns	8 ft, 8 turns
21	8 ft, 6-8 turns	6 ft, 8 turns
28	6 ft, 6-8 turns	4 ft, 6-8 turns

173 - Dual-Band Loading Wire Antenna for 80m, 30m

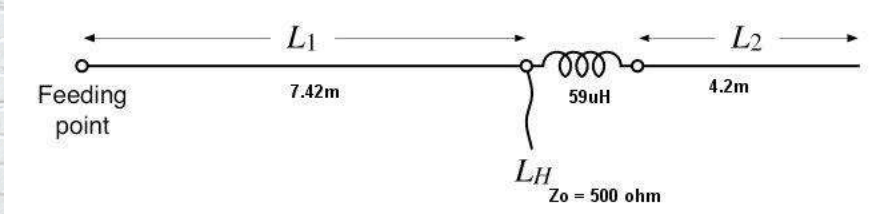

174 - Stub Matching Antennas

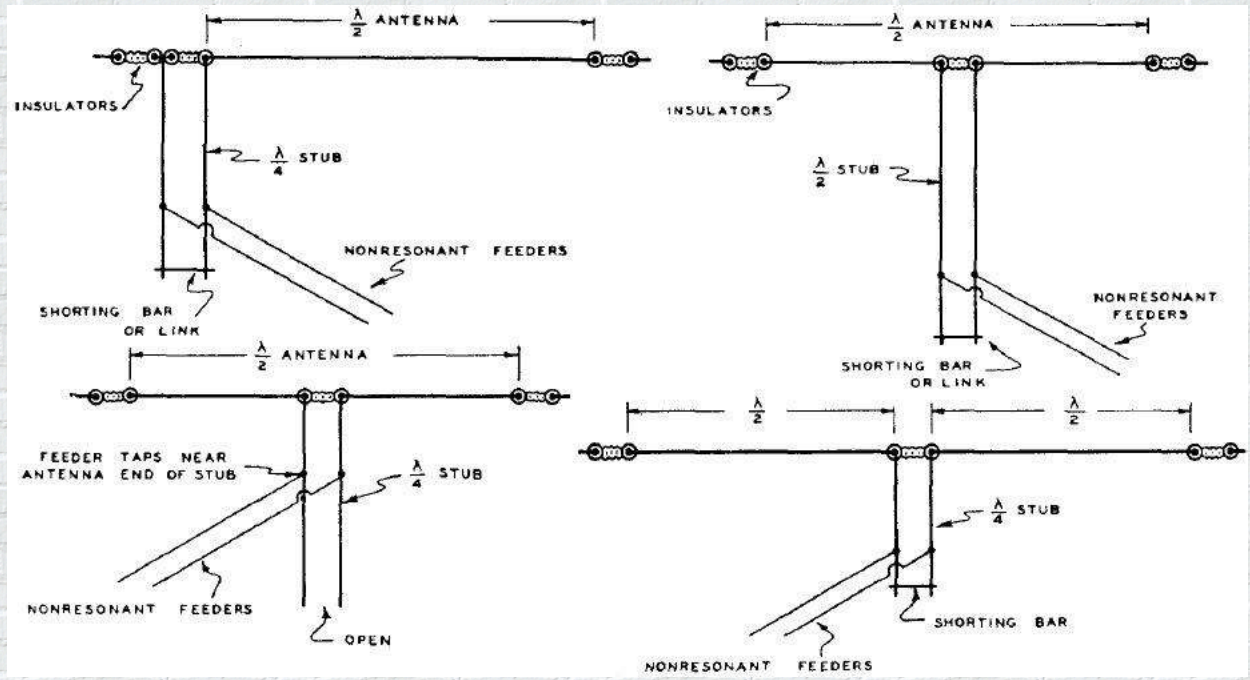

175 - J-Style Vertical Wire Antenna for 10m

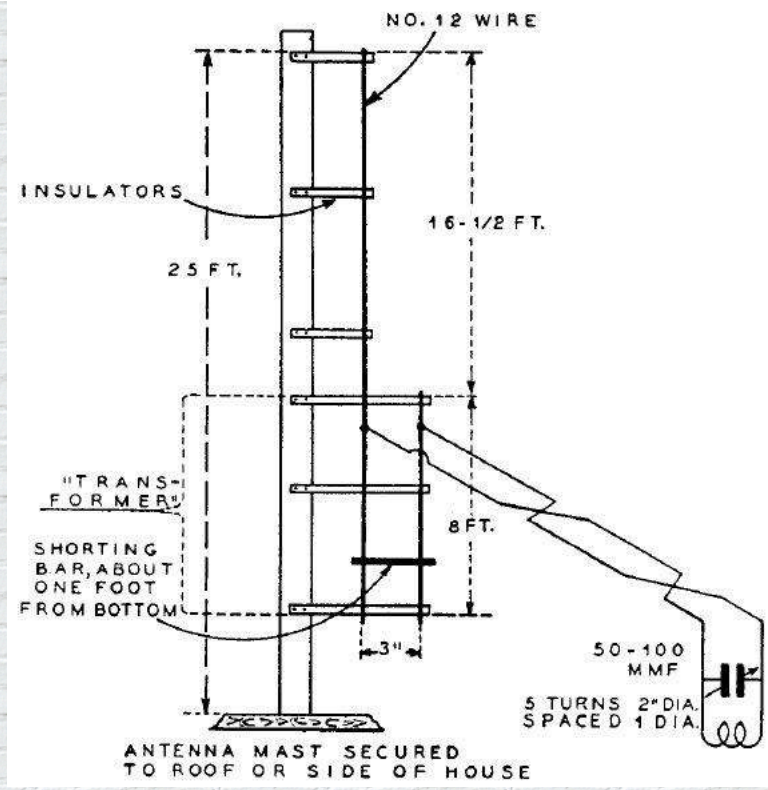

176 - Dual Band Vertical with Zepp Feeders for 40m, 20m

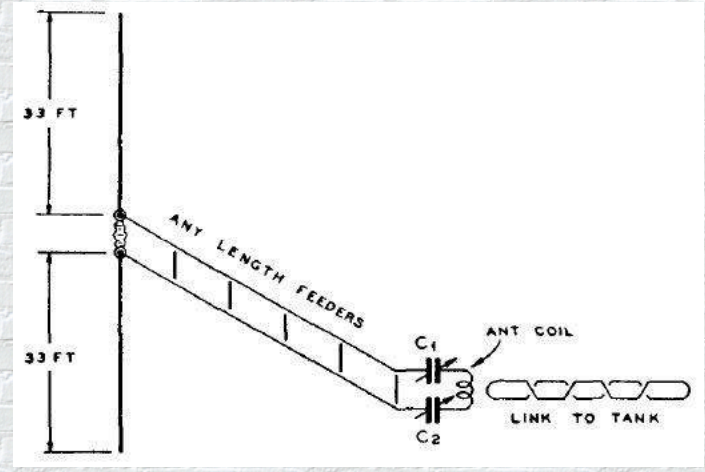

177 - RCA Double Doublet for 40m to 12m

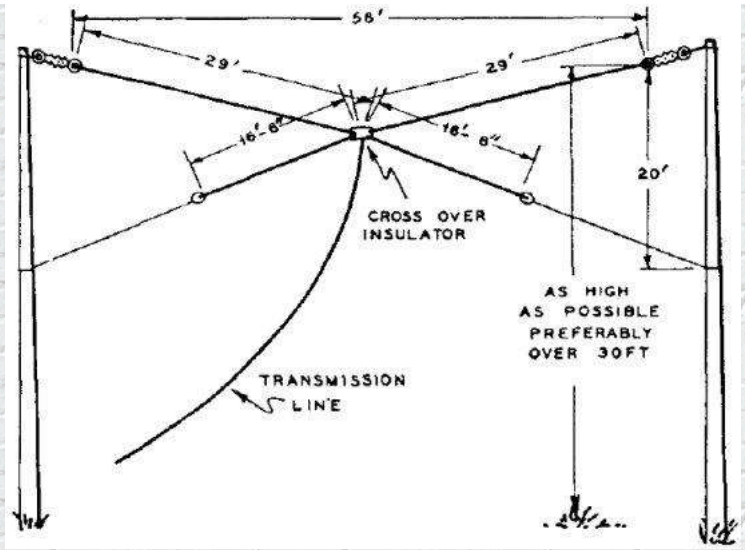

178 - RCA Spiderweb Antenna for 40m to 6m

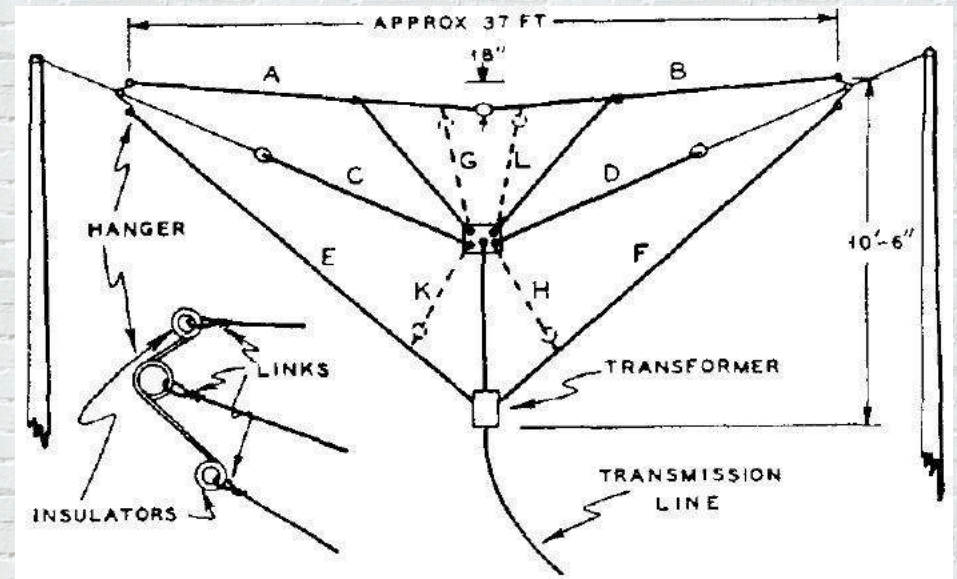

179 - Folded Dipole with Shorted Straps

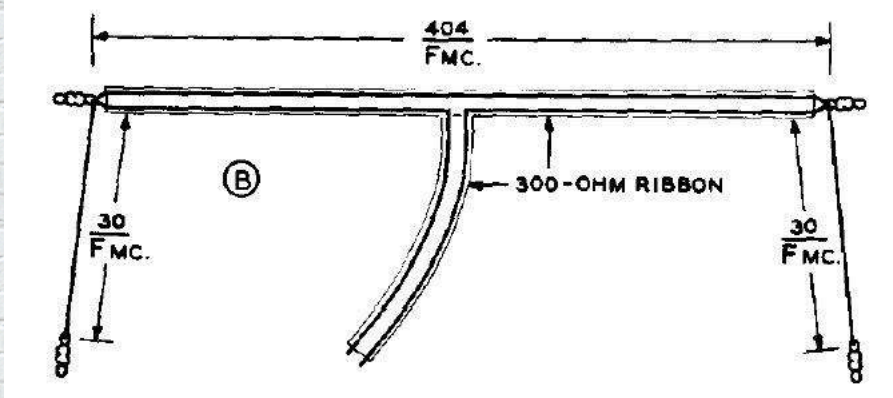

180 - Twin-Lead Marconi Antenna for 160m, 80m

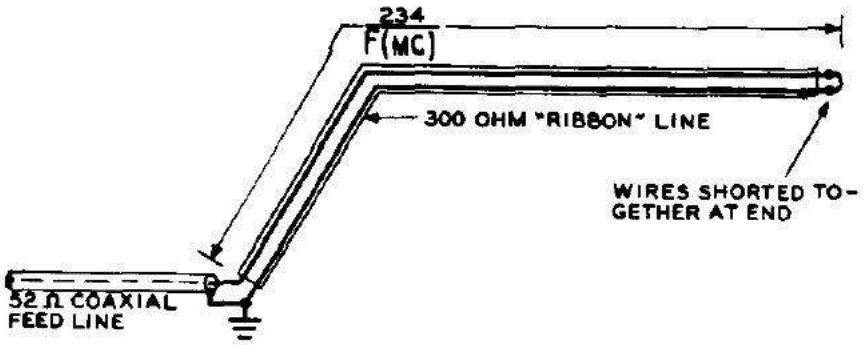

181 - Broadband Antenna Quarter-Wave Balun for 80m

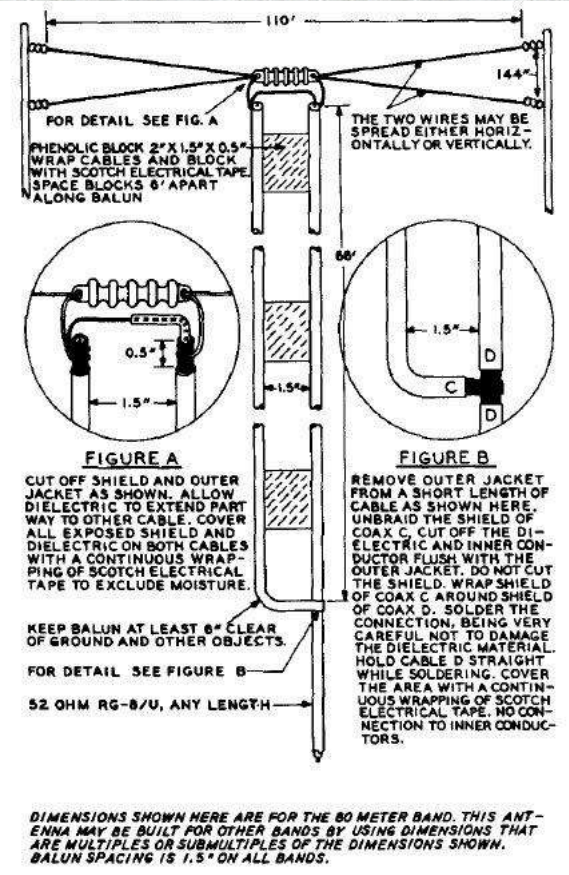

182 - Three-Quarter-Wave Folded Doublet for Dual-Band

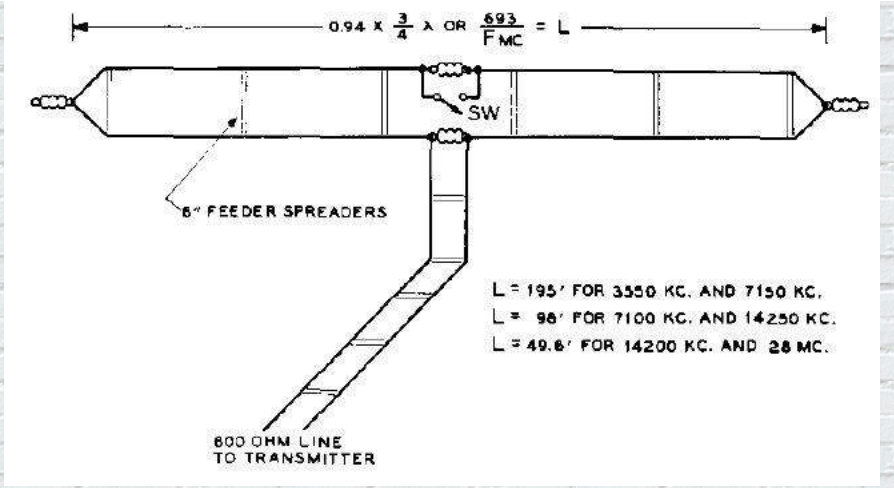

183 - Three-Quarter-Wave Folded Doublet No-Switch for Dual-Band

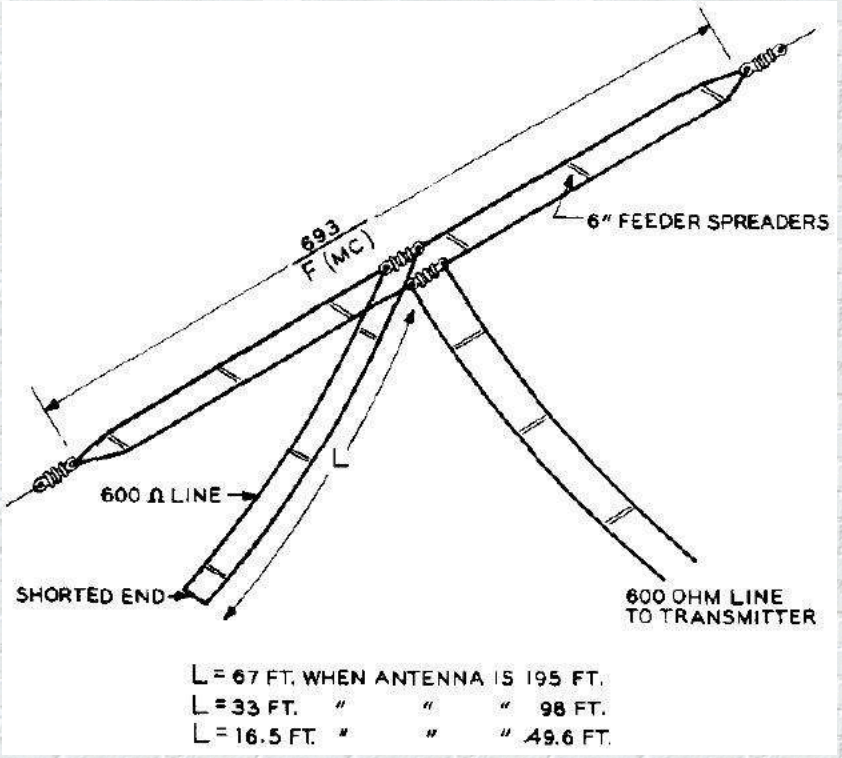

184 - Wideband Omni-Directional Discone Antenna

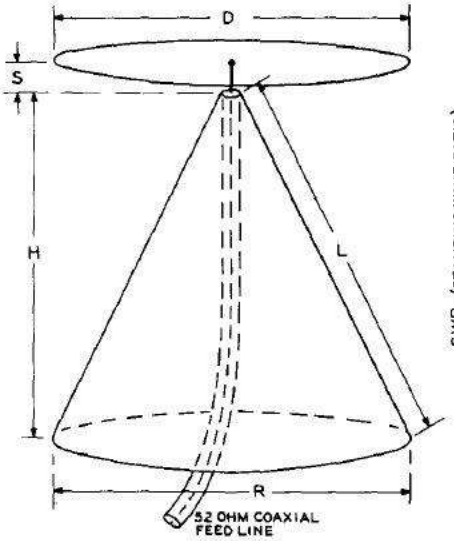

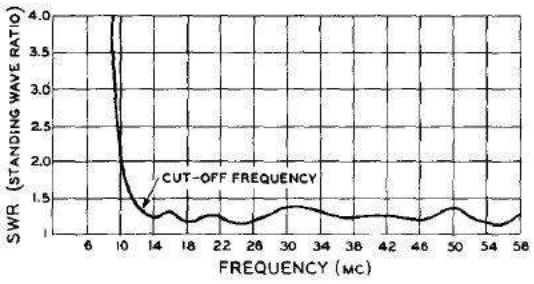

DIMENSIONS

20, 15, 11, 10, 6 METERS	15, 11, 10, 6 METERS	11, 10, 6, 2 METERS
D= 12′ L= 18′	D= 8′ L= 12′	D= 6′ L= 9′6″
S= 10″ R= 18′	S= 6″ R= 12′	S= 4″ R= 9′6″
H= 15′7″	H= 10′5″	H= 8′3″

185 - Wideband Rhombic Antenna for 40m to 10m

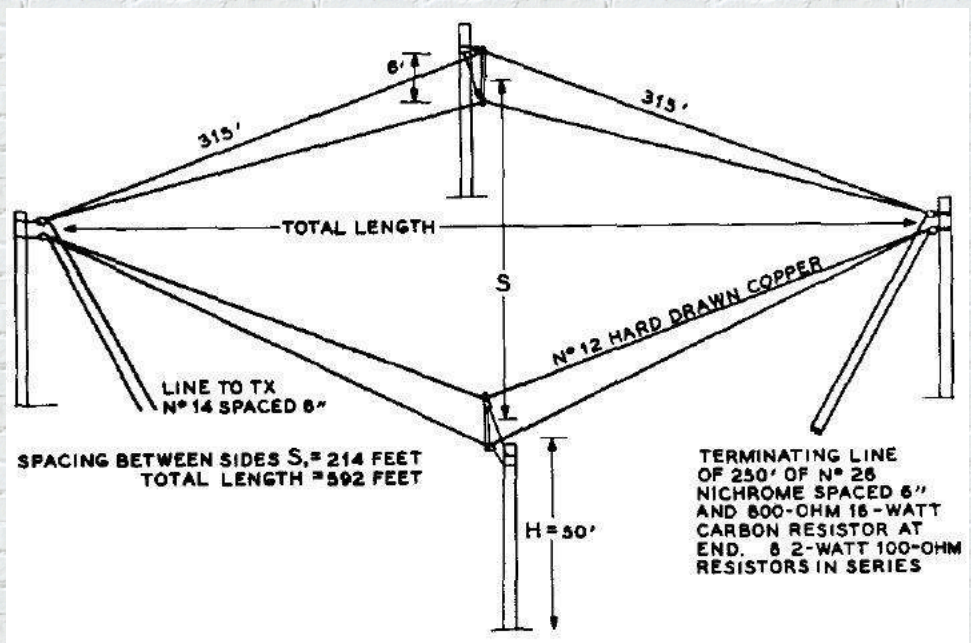

186 - Pre-Cut Linear Array Antenna 3dB-Gain for 40m

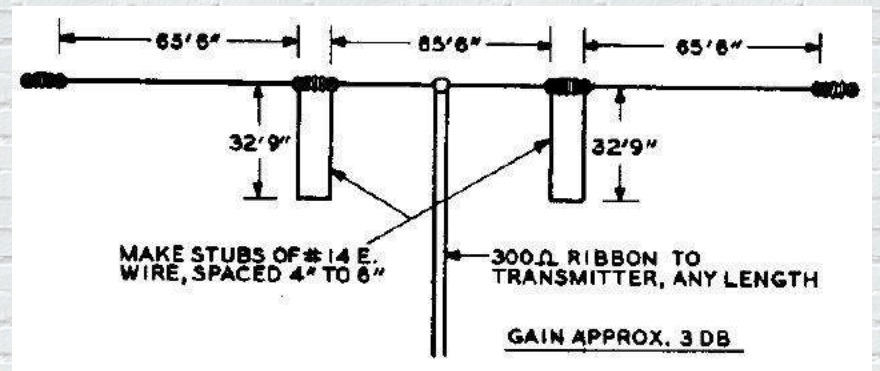

187 - X-Array Antenna 6dB-Gain for 20m, 15m, 10m

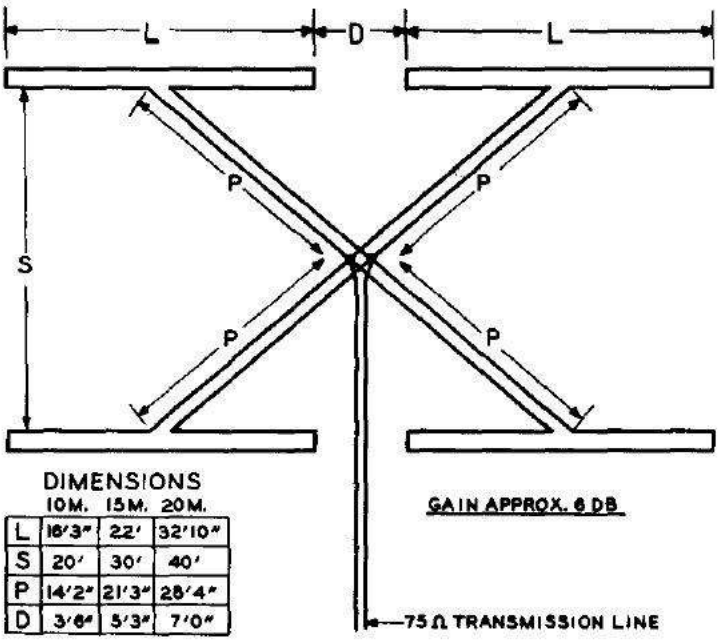

	10M.	15M.	20M.
L	16'3"	22'	32'10"
S	20'	30'	40'
P	14'2"	21'3"	28'4"
D	3'6"	5'3"	7'0"

The entire array (with the exception of the 75-ohm feed line) is constructed of 300-ohm ribbon line. Be sure phasing lines (P) are poled correctly, as shown.

188 - Double-Bruce Array Antenna 5dB-Gain for 20m, 10m

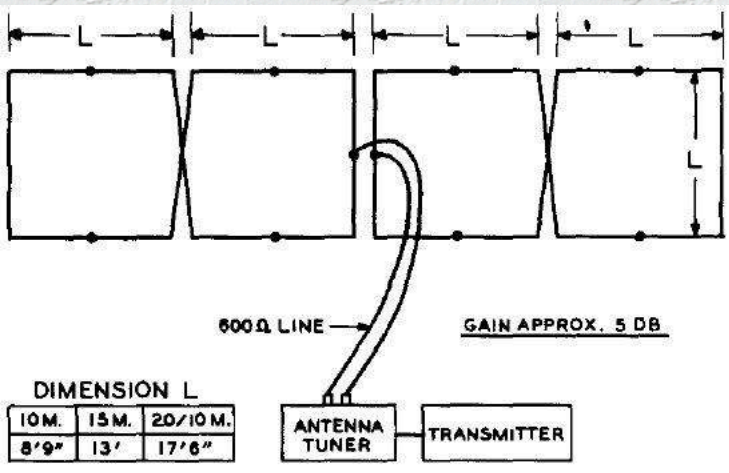

10M.	15M.	20/10M.
8'9"	13'	17'6"

189 - Bi-Square Broadside Array 4dB-Gain for 20m, 15m, 10m

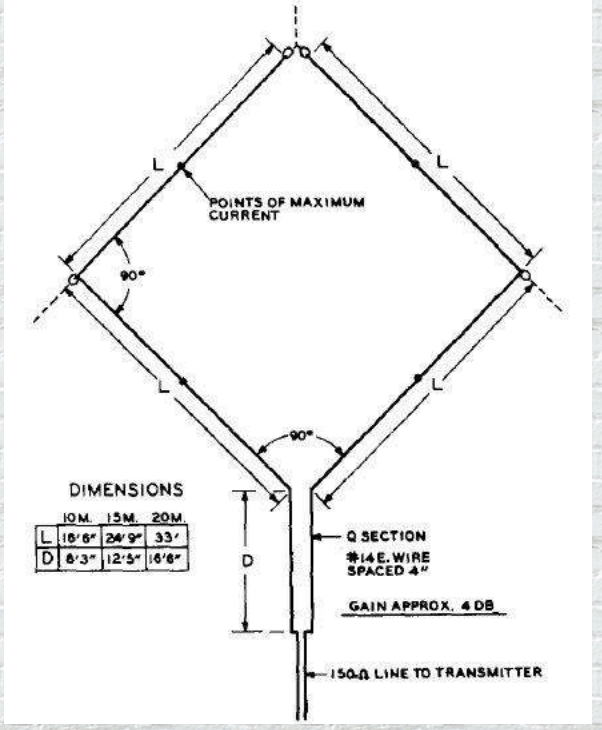

190 - Six-Shooter Broadside Array 7.5dB-Gain for 20m, 15m, 10m

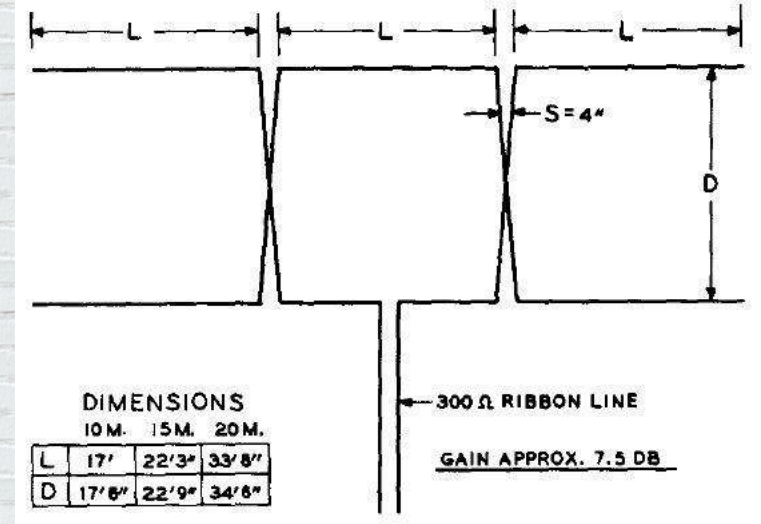

191 - Triplex Flat-Top Beam 4.5dB-Gain for 20m, 15m, 10m

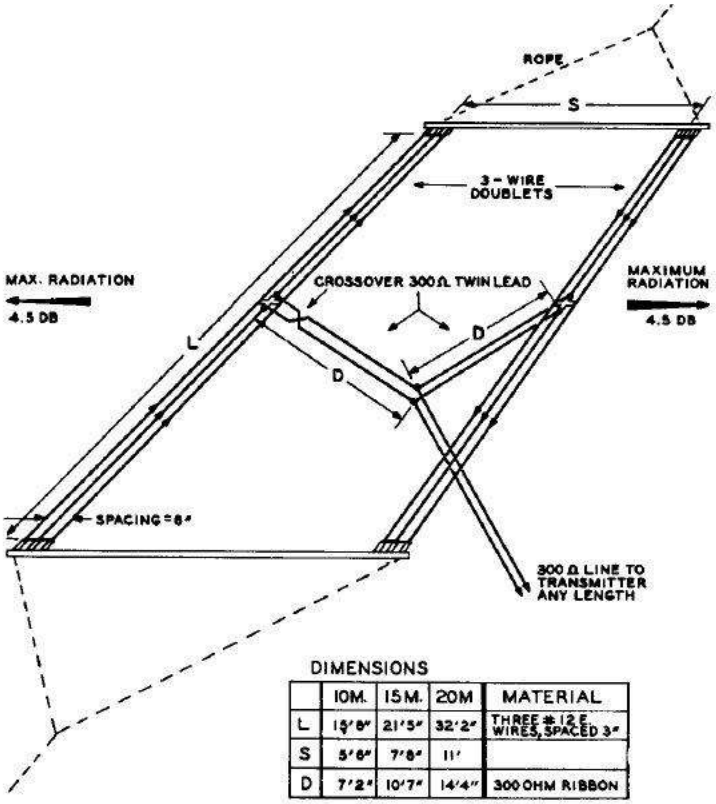

DIMENSIONS

	10M.	15M.	20M	MATERIAL
L	15'8"	21'5"	32'2"	THREE # 12 E. WIRES, SPACED 3"
S	5'6"	7'8"	11'	
D	7'2"	10'7"	14'4"	300 OHM RIBBON

192 - Dual-Band Tilt Antenna for 20m, 10m

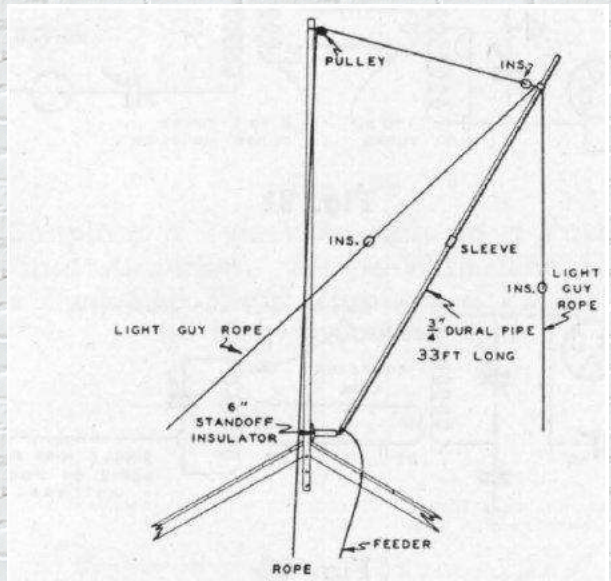

TWO BAND (10-20 METER) TILT ANTENNA — VERTICAL FOR 20 METERS - TILT 54° FROM HORIZON FOR 10 METERS

193 - Super Space Multiband Dipole Antenna for 80m to 10m

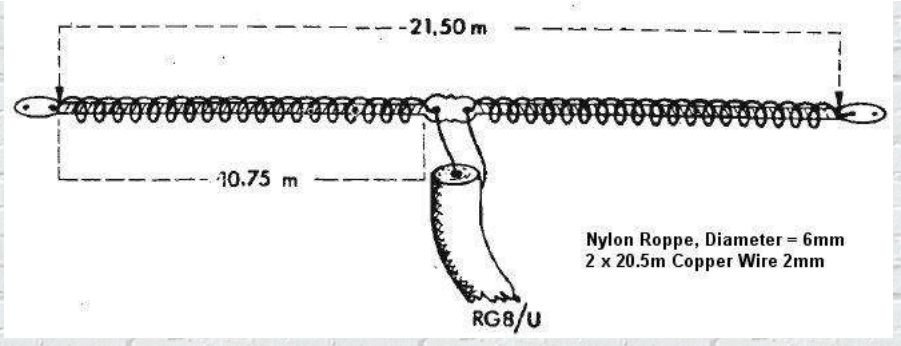

194 - Bi-Square Beam Antenna Gain=5.5dB for 10m

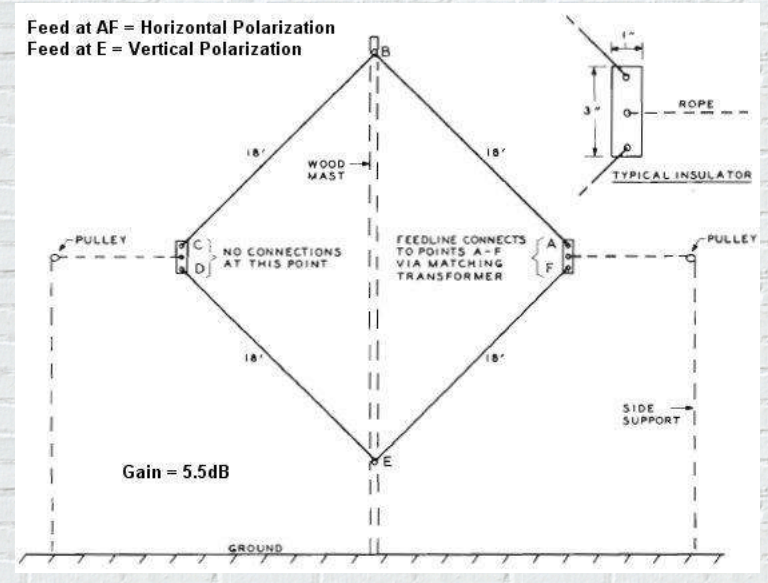

195 - Cousin of G5RV Multiband Antenna for 40m to 10m

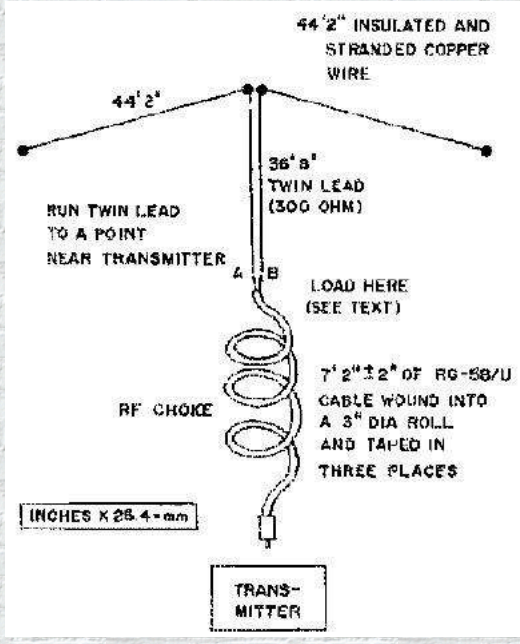

196 - Cayman Quad Antenna for 20m

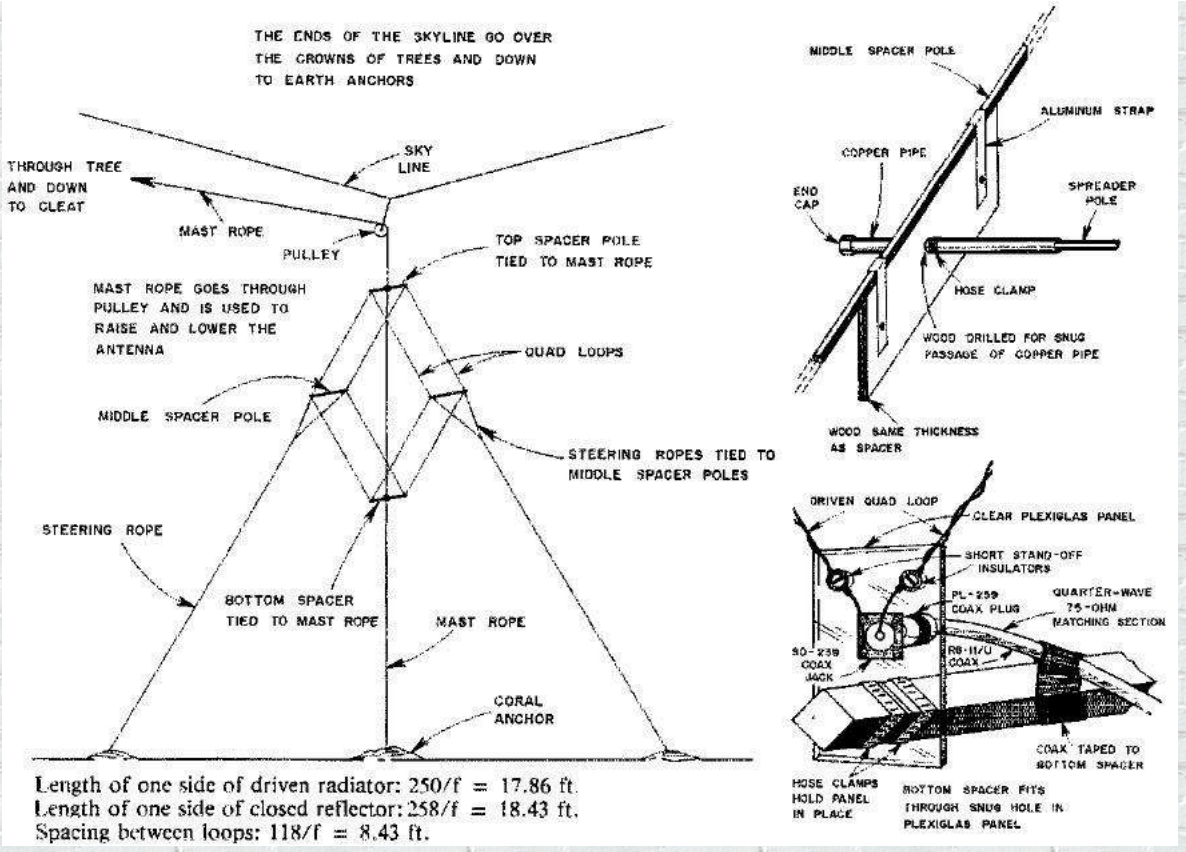

197 - Hentenna Gain=3dB with Bazooka Match for 6m

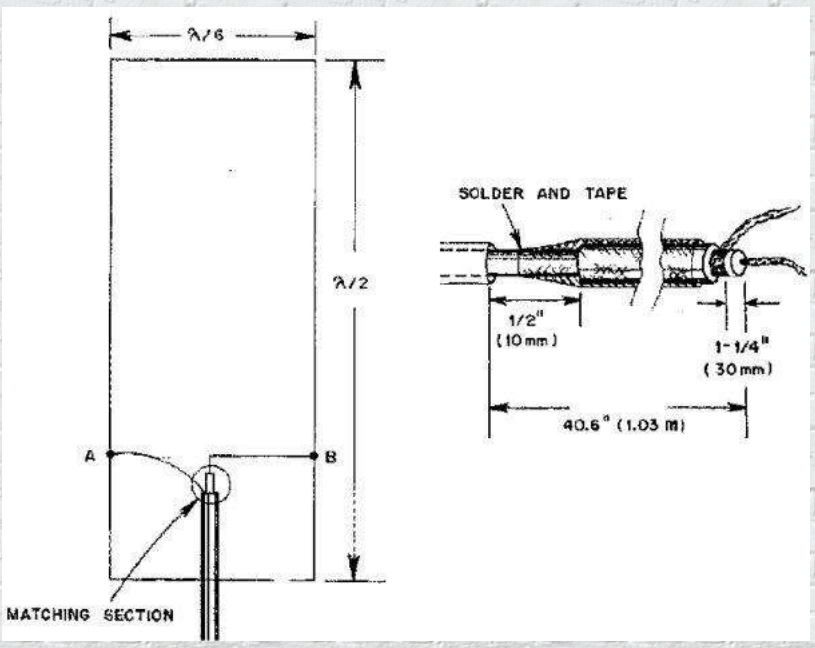

198 - X-Beam Antenna Gain=3dB for 20m

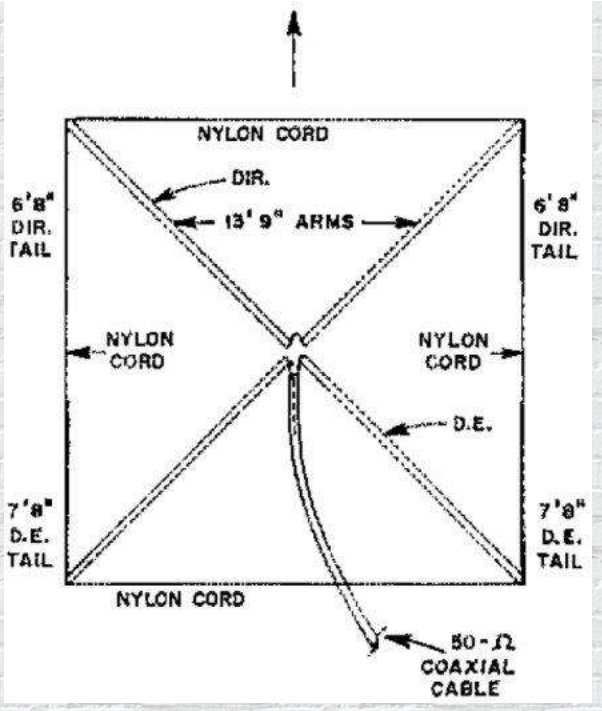

199 - Twin Delta Loop Antenna Gain=6dB for 160m, 80m, 40m

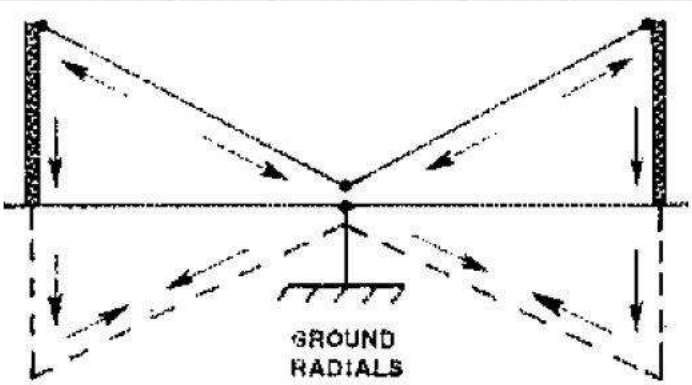

Twin- Delta Loop, with the Image in the ground plane.

Band	*Tower Height (ft)*	*Length of Sloping Wires (ft)*
160 m†	102.03	204.06
80 m	49.86	99.72
40 m	25.92	51.84

200 - Inverted-V Beam Antenna for 30m

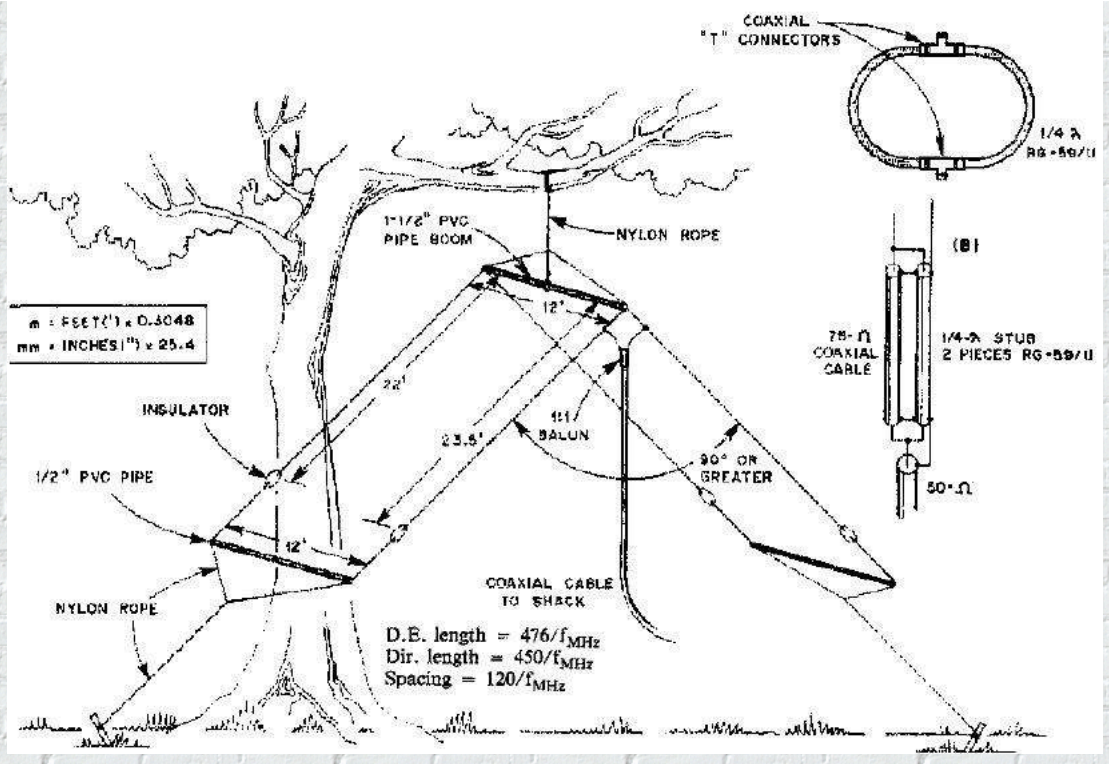

201 - FD4 Windom Antenna for 80m, 40m, 20m, 10m

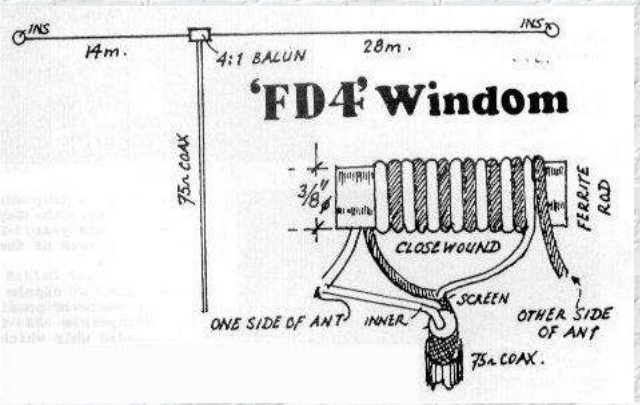

202 - Two Elements Phased Delta Loop for 40m

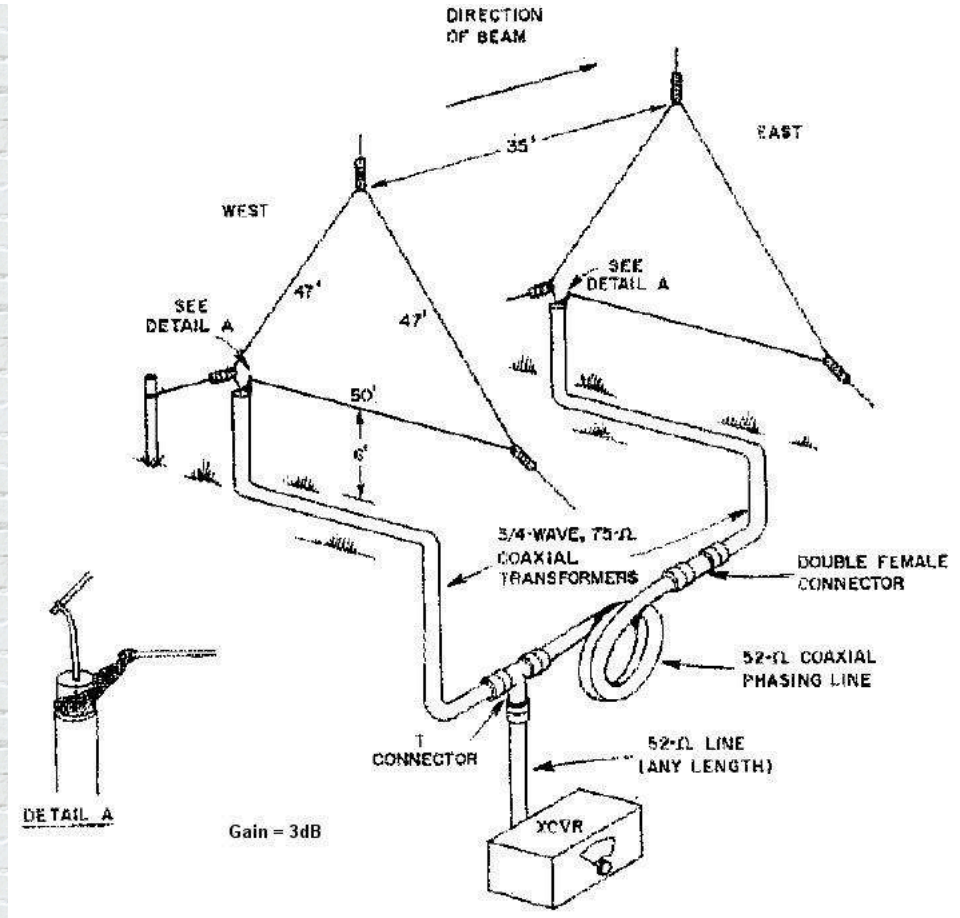

203 - Three Elements Wire Yagi for 10m

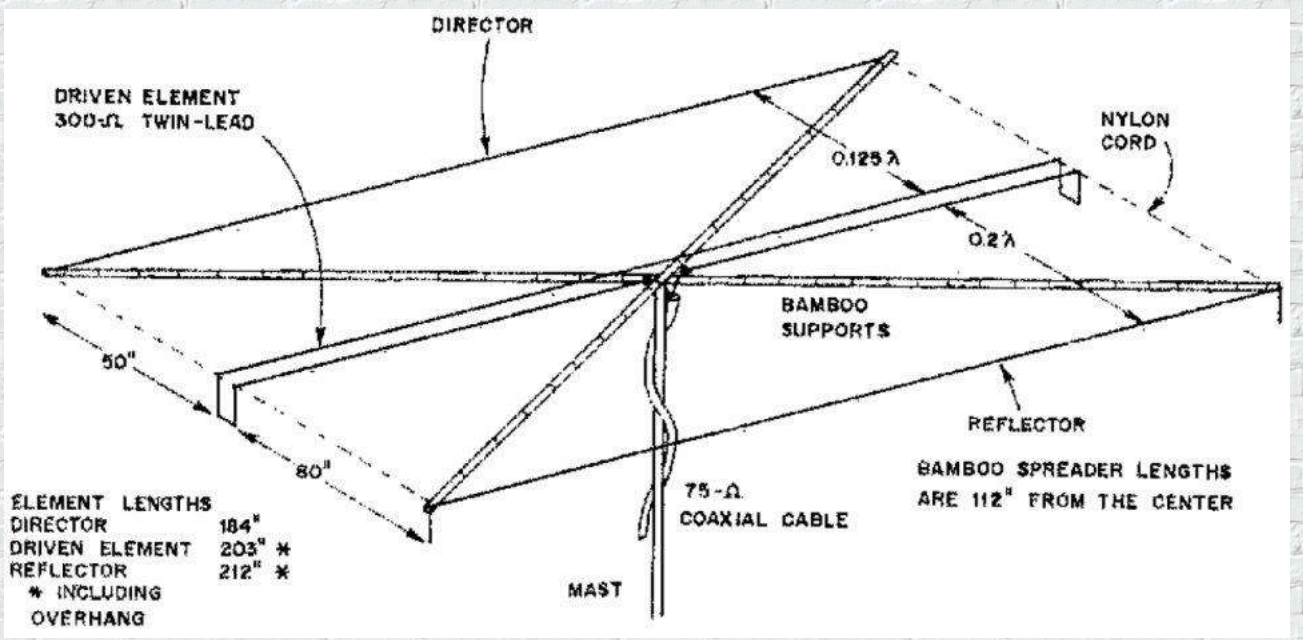

204 - Low Radiation Angle Full-Wave Loop Antenna for 80m

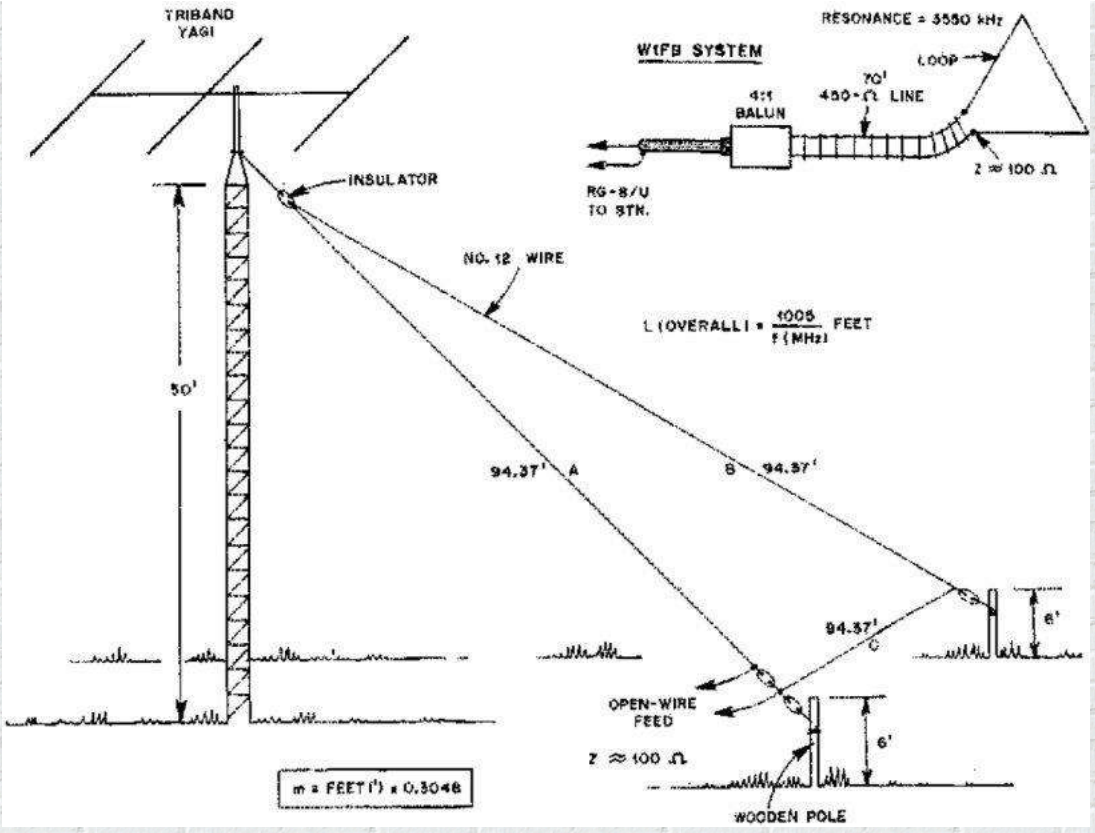

205 - Collinear Antenna Gain=3dB for 2m

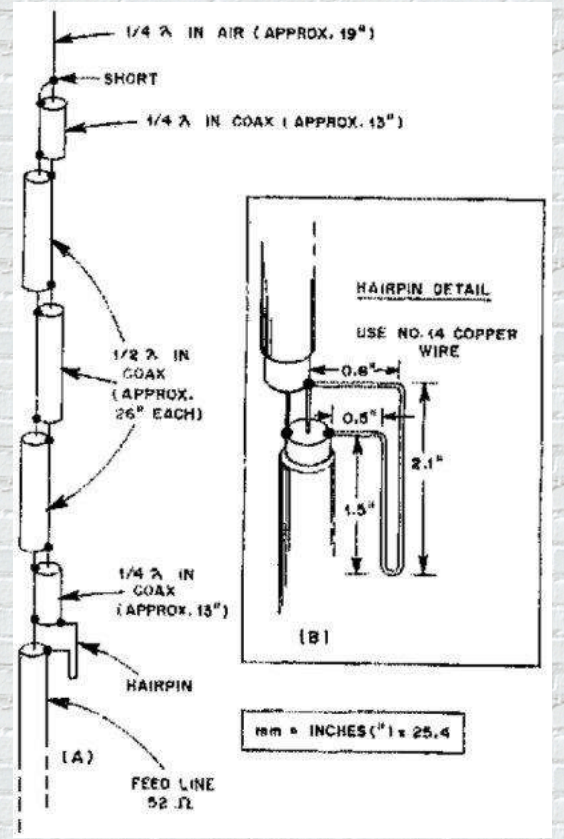

206 - X-Ray Monoband Antenna Gain=6.5dBd

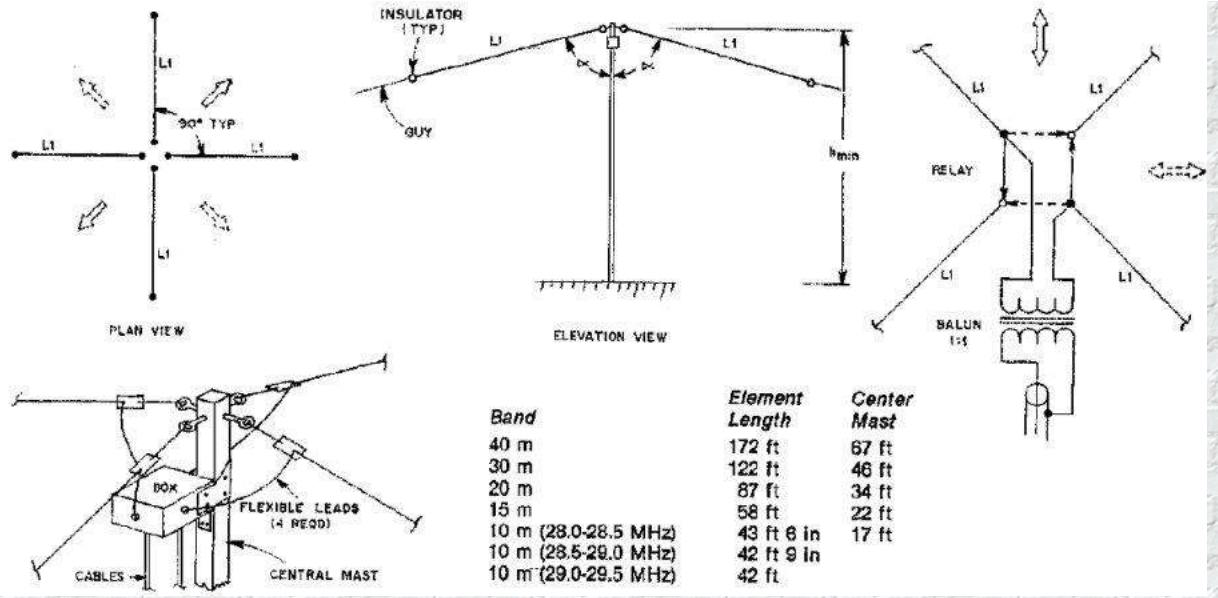

Band	Element Length	Center Mast
40 m	172 ft	67 ft
30 m	122 ft	46 ft
20 m	87 ft	34 ft
15 m	58 ft	22 ft
10 m (28.0-28.5 MHz)	43 ft 6 in	17 ft
10 m (28.5-29.0 MHz)	42 ft 9 in	
10 m (29.0-29.5 MHz)	42 ft	

207 - Broadside Collinear Curtain Array for 20m

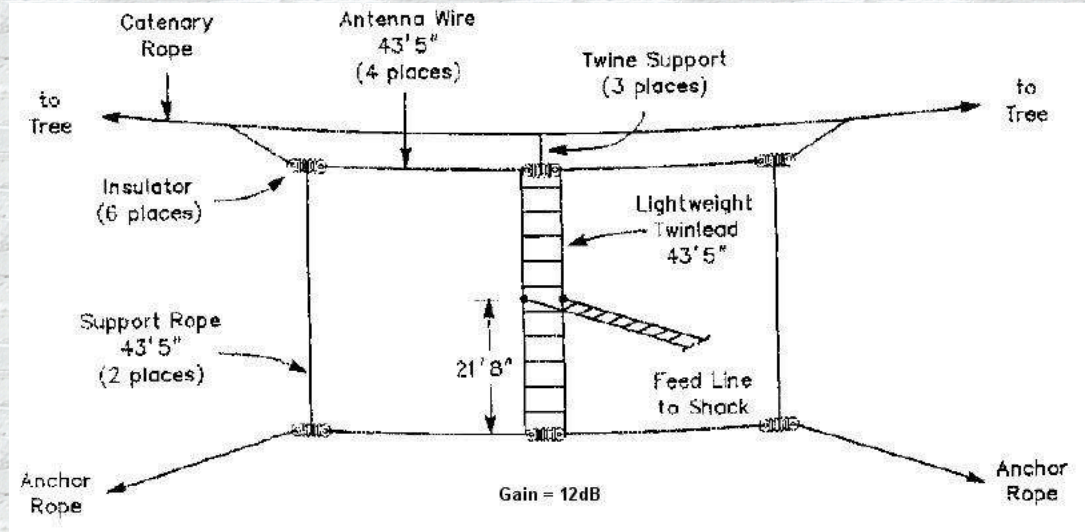

208 - Shrunk Loop Antenna for 80m, 40m

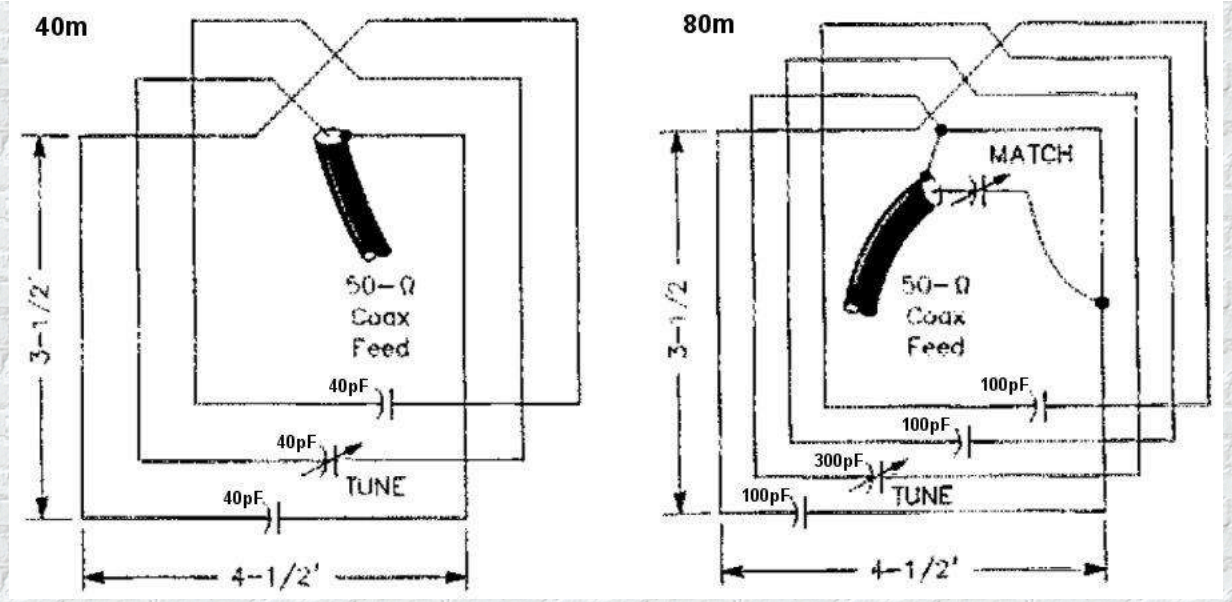

209 - λ/3 Multiband Dipole for 40m, 20m, 17m, 15m, 13m, 10m

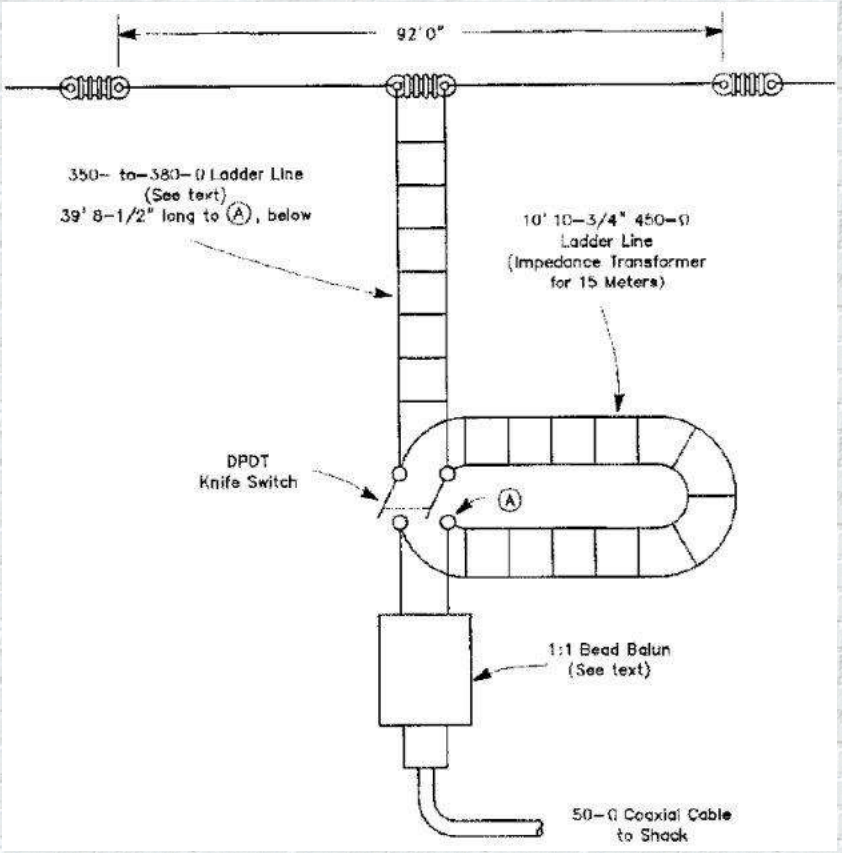

210 - K3LR Sloper Antenna Gain=3dB for 160m

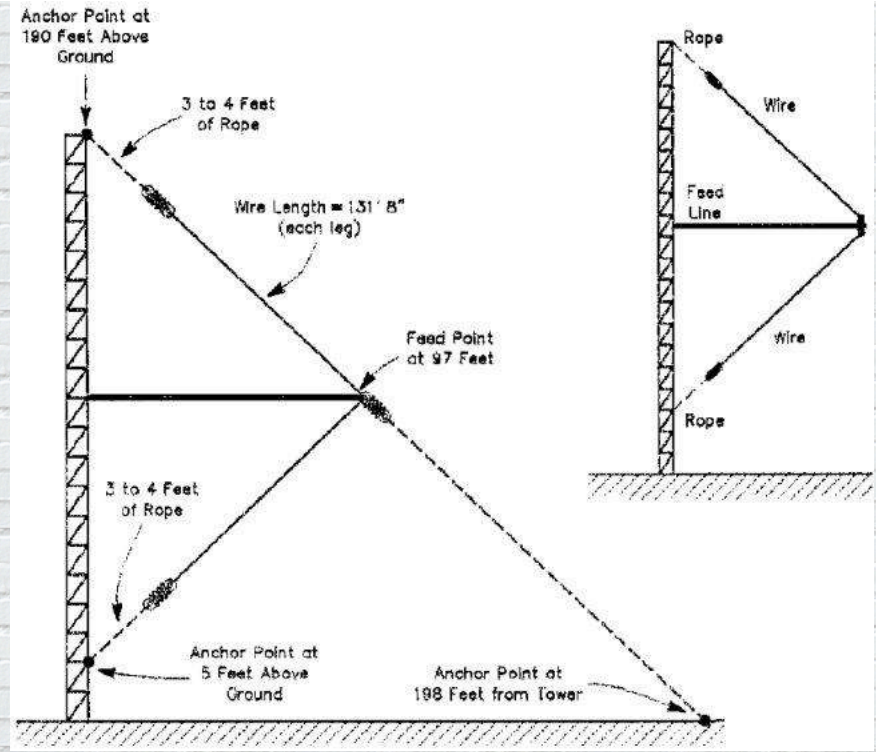

211 - Mini Folded Vertical Monopole Antenna for 160m, 80m, 40m

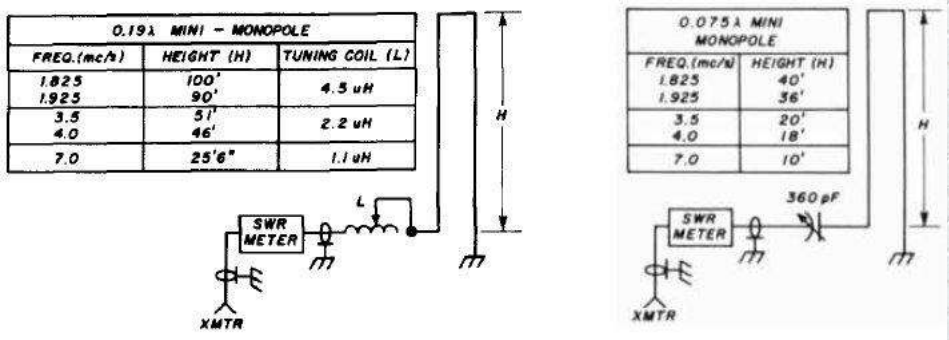

0.19λ MINI – MONOPOLE		
FREQ.(mc/s)	HEIGHT (H)	TUNING COIL (L)
1.825 1.925	100' 90'	4.5 uH
3.5 4.0	51' 46'	2.2 uH
7.0	25'6"	1.1 uH

0.075λ MINI MONOPOLE	
FREQ.(mc/s)	HEIGHT (H)
1.825 1.925	40' 36'
3.5 4.0	20' 18'
7.0	10'

212 - Three Band Dipole for 80m, 40m, 20m

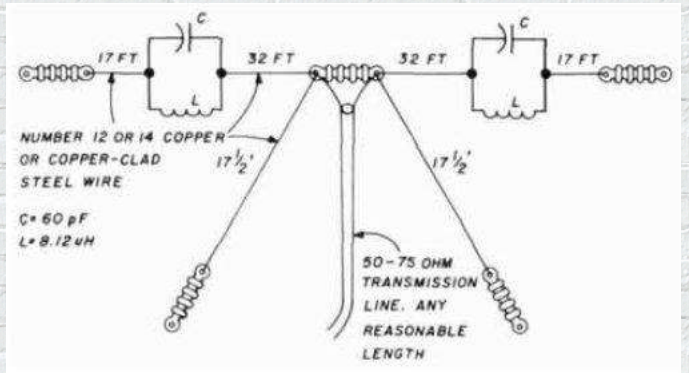

213 - Stub Matched Dipole Antenna

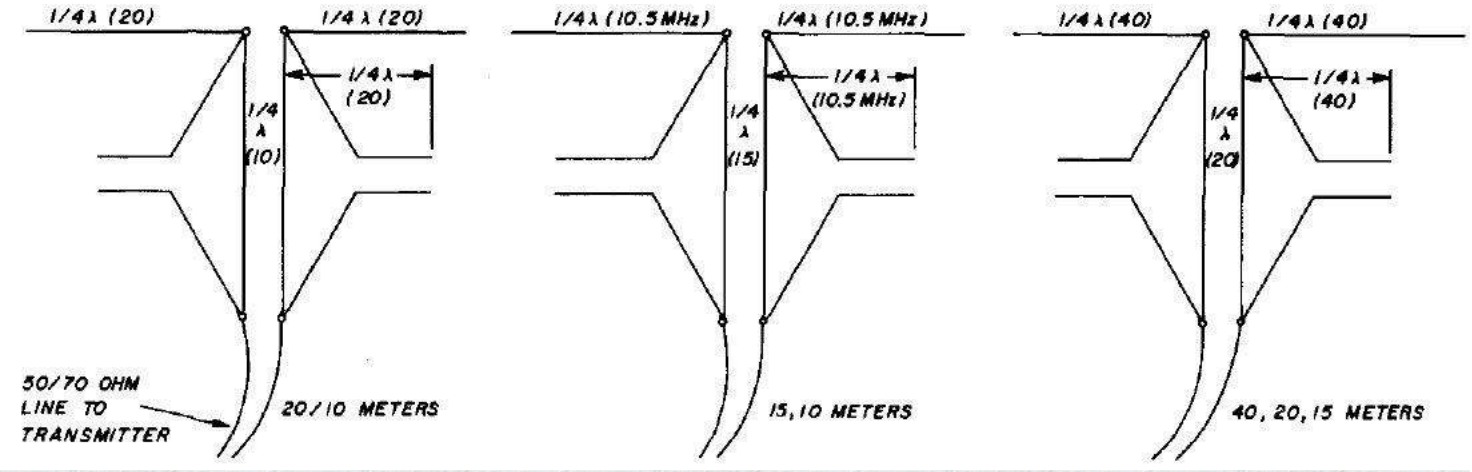

214 - Inverted-Vee Antenna with Bazooka Match

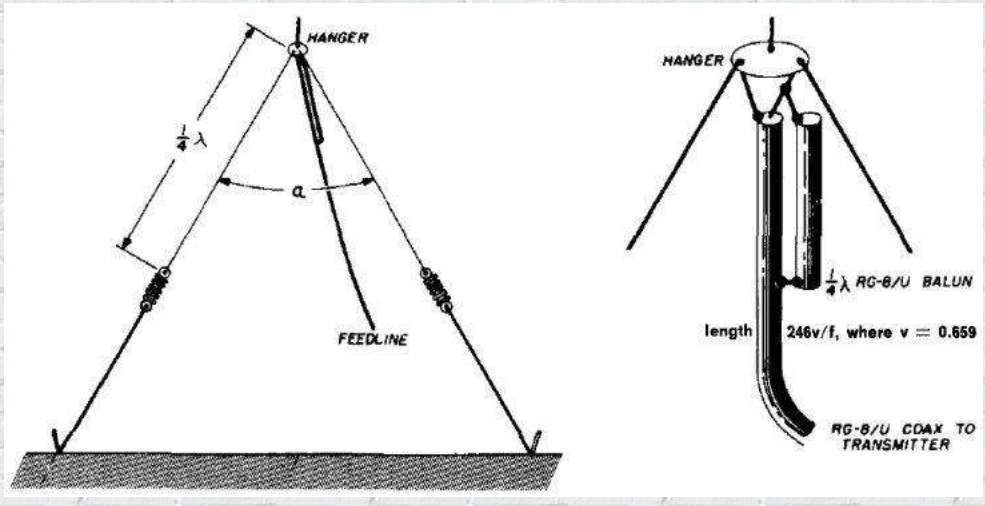

215 - Multiband Long Wire Antenna for 40m, 20m, 15m, 10m

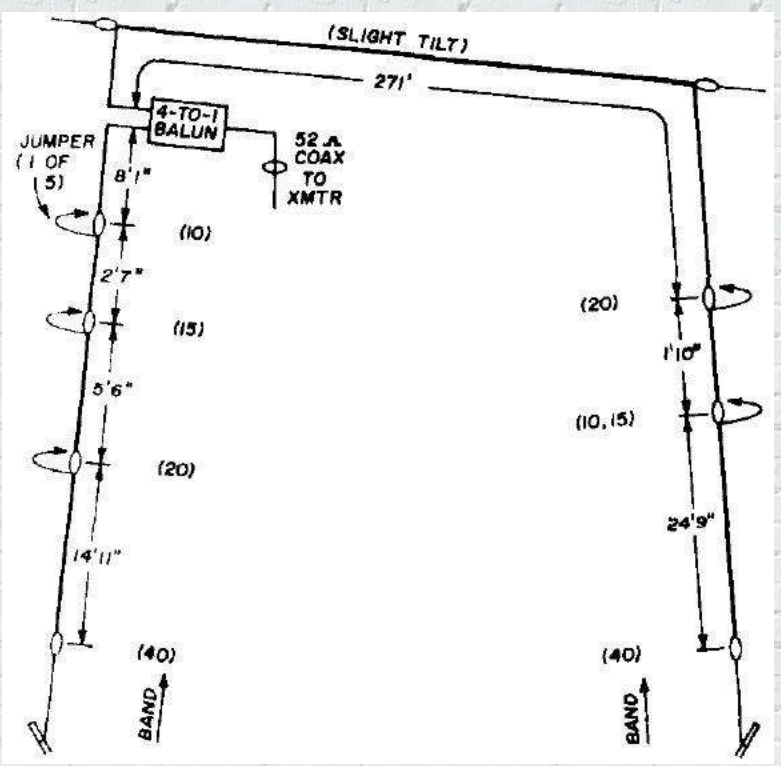

216 - Converted Vee Antenna for 80m, 40m

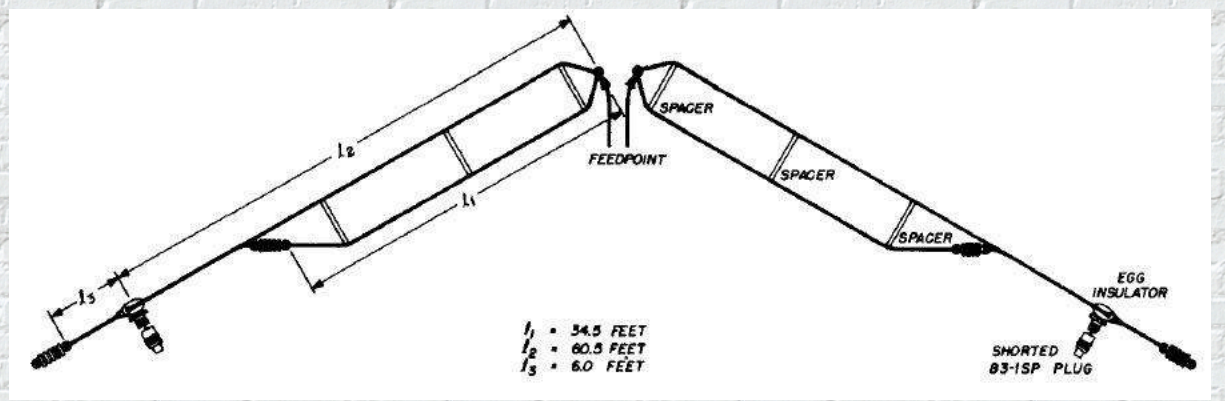

217 - Swiss Quad Antenna for 20m, 15m, 10m

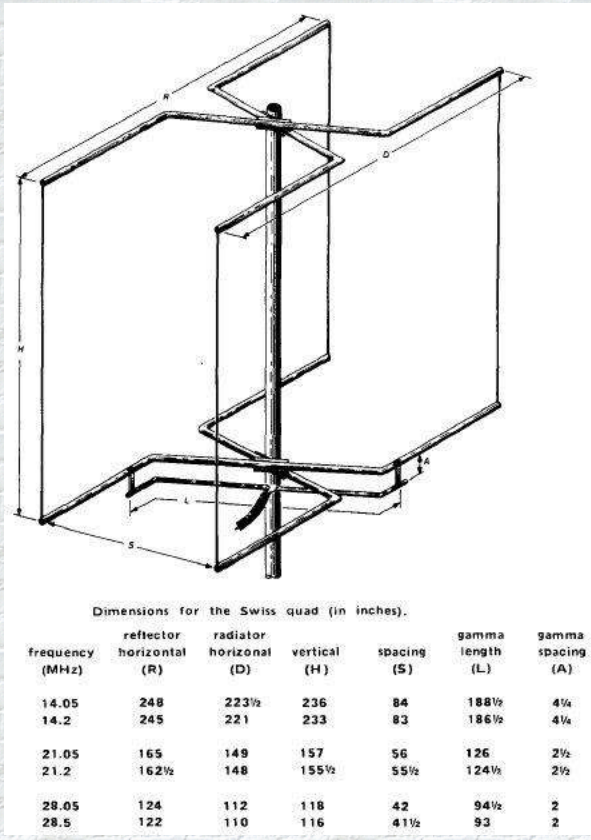

Dimensions for the Swiss quad (in inches).

frequency (MHz)	reflector horizontal (R)	radiator horizonal (D)	vertical (H)	spacing (S)	gamma length (L)	gamma spacing (A)
14.05	248	223½	236	84	188½	4¼
14.2	245	221	233	83	186½	4¼
21.05	165	149	157	56	126	2½
21.2	162½	148	155½	55½	124½	2½
28.05	124	112	118	42	94½	2
28.5	122	110	116	41½	93	2

218 - Japanese Quad Antenna for 20m, 15m, 10m

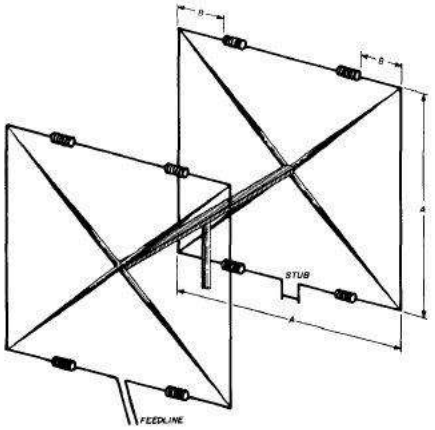

Construction details of the Japanese quad (in inches).

frequency (MHz)	quad side (A)	spacing	coil location (B)	coil (μH)	winding info
14	152	101	38	3.0	17½ turns no. 14, 1½" diameter, 5" long
21	98	67	24½	2.0	11 turns no. 14, 1½" diameter, 3½" long
28	77	50	19¼	1.5	9½ turns no. 14, 1½" diameter, 3½" long

219 - Seven-Elements Triangle Beam Antenna for 20m

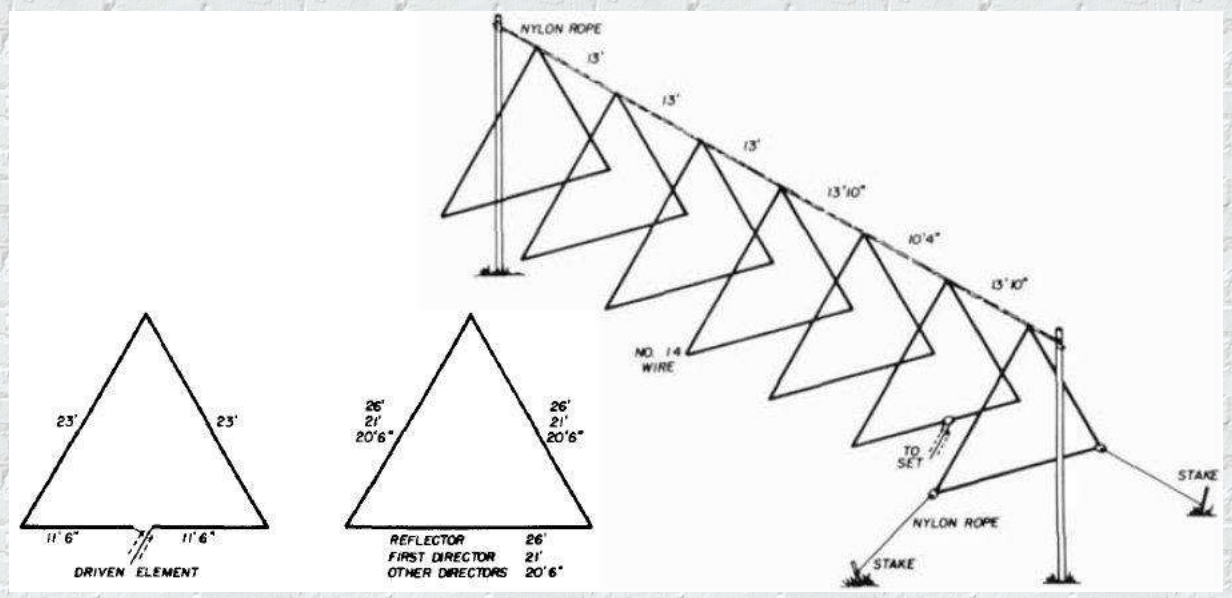

220 - Log Periodic Wire Antenna for 40m

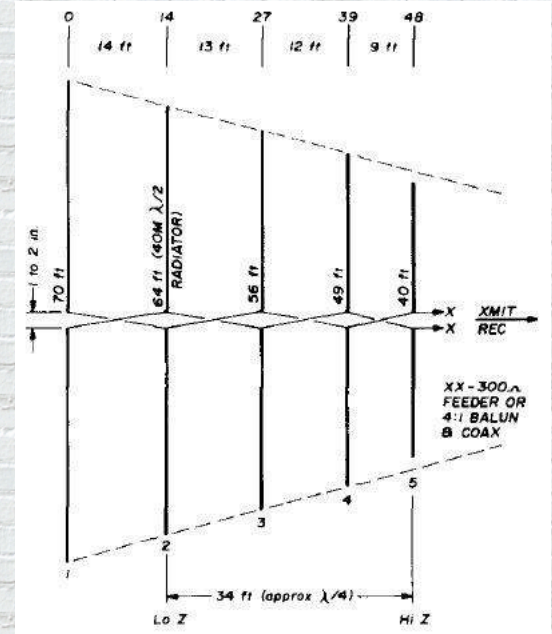

221 - Three-Elements 90-degrees Wire Beam for 20m

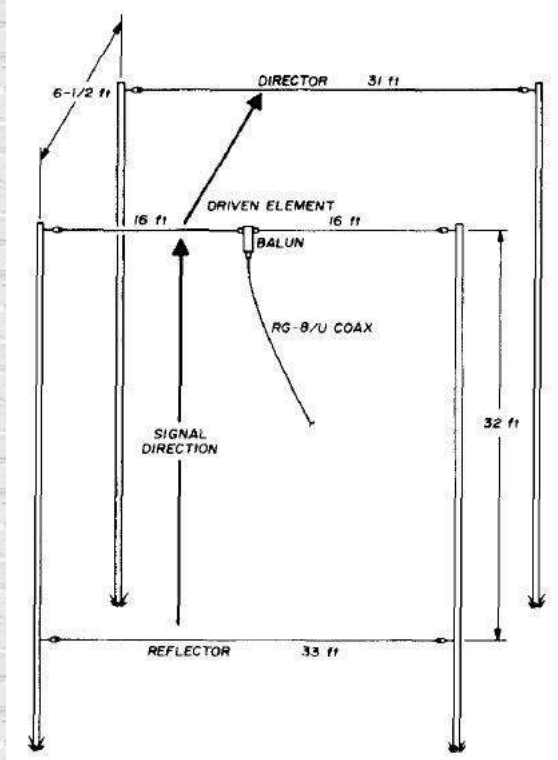

---

222 - Two-Elements Wire Beam for 20m

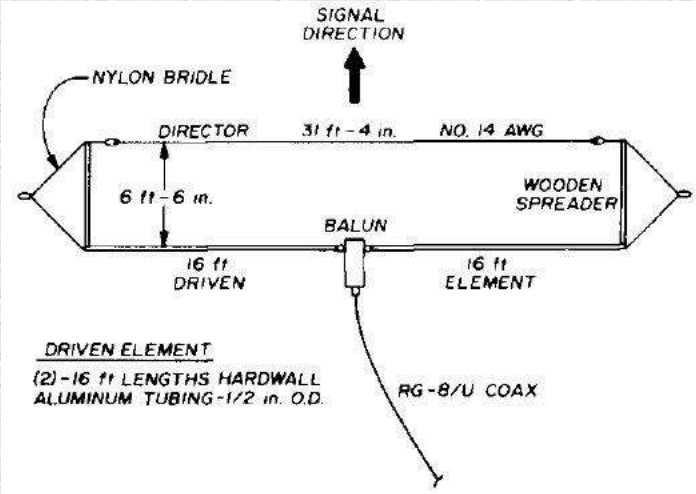

---

223 - Suitcase-Fit Dipole Antenna for 80m, 40m, 20m

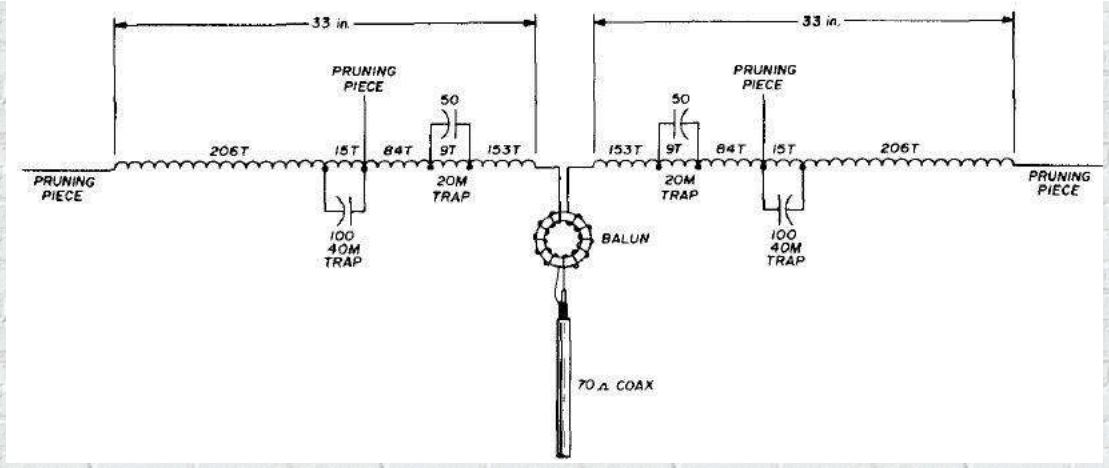

224 - Multiband Coaxial Dipole for 80m, 40m

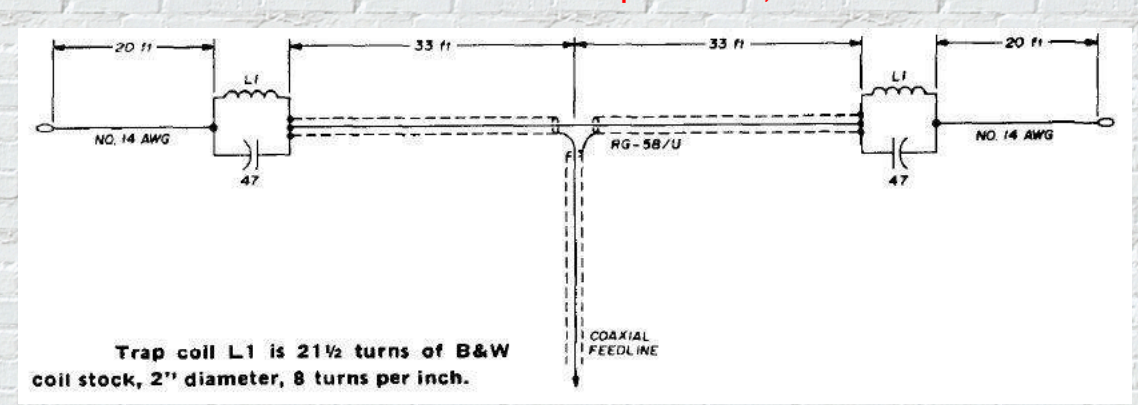

225 - Vertical Log Periodic Antenna for 80m, 40m

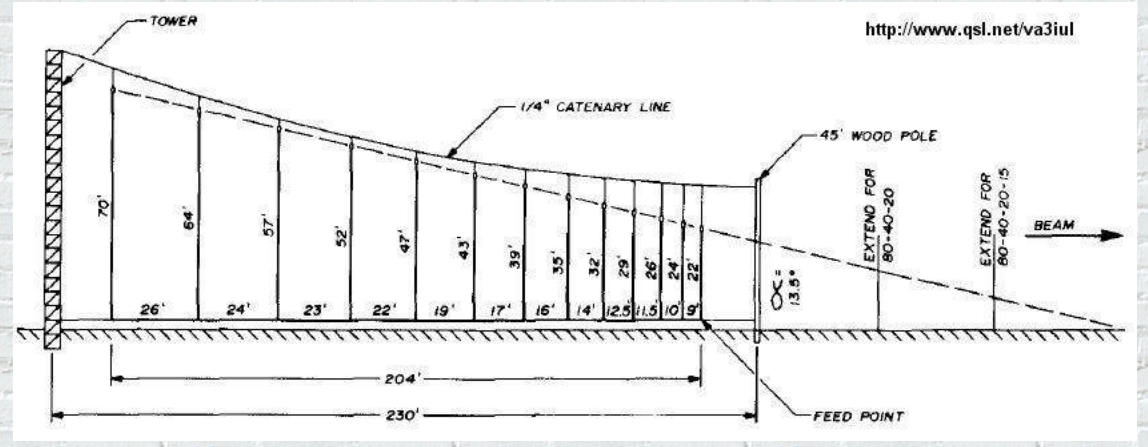

226 - Inverted Vertical Log Periodic Antenna for 40m

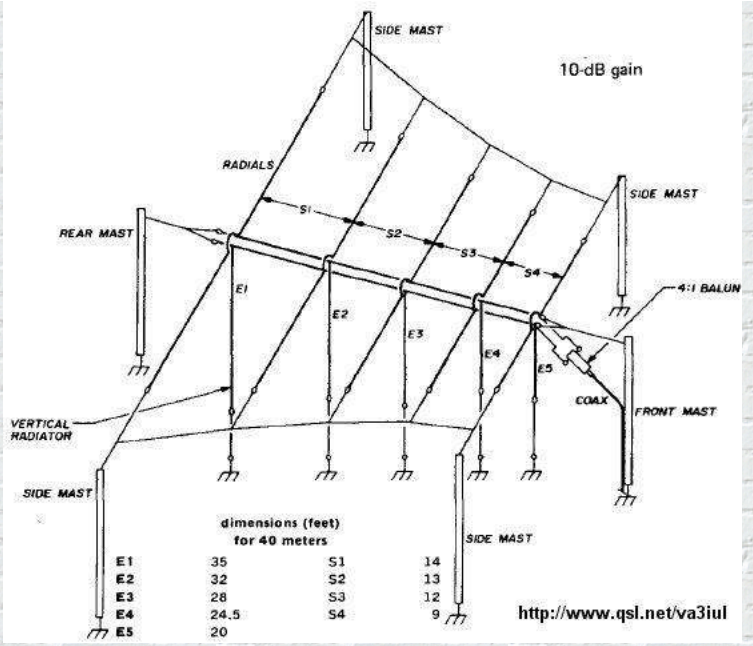

227 - Double Extended Zepp Antenna Gain=7dB for 15m

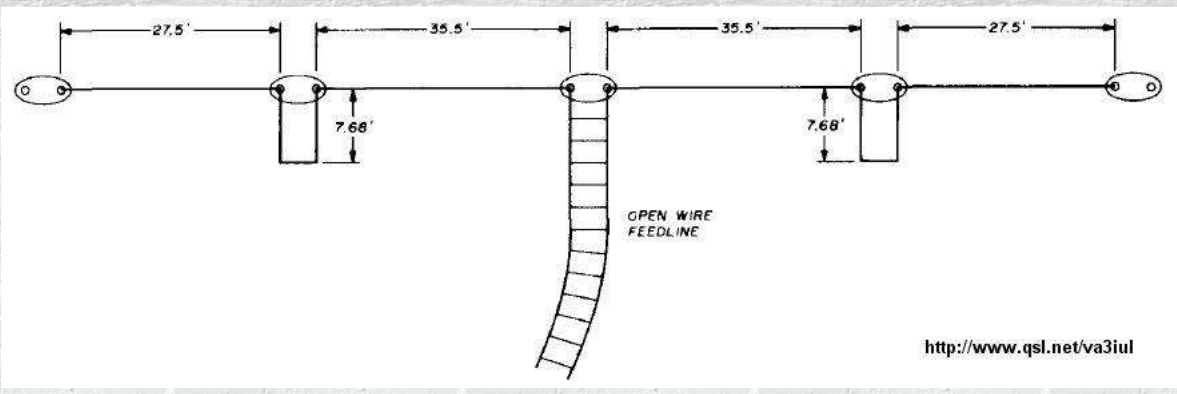

228 - Double Lazy-H Antenna G=10dB for 70cm

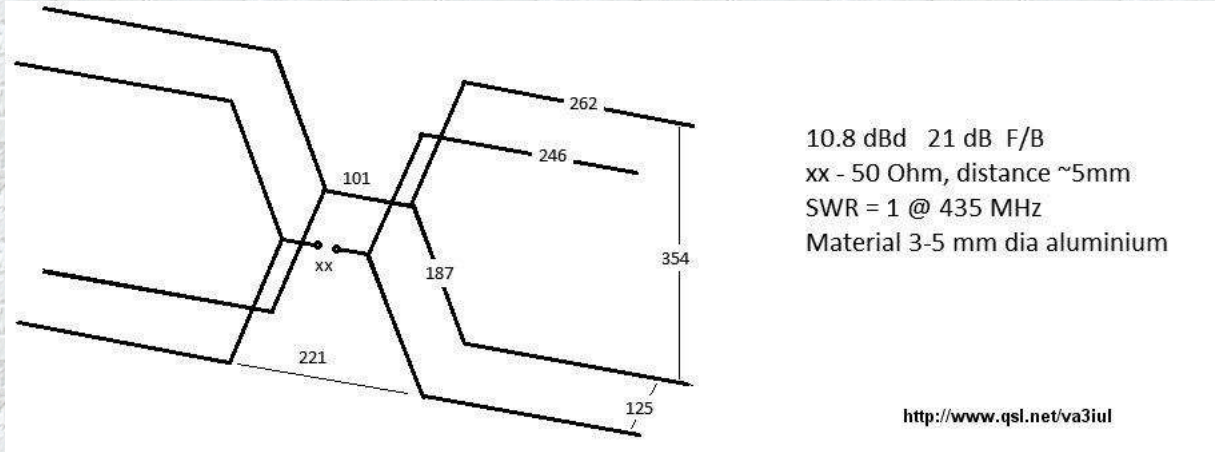

229 - Wire Log Periodic Antenna G=12dB for 15m, 20m

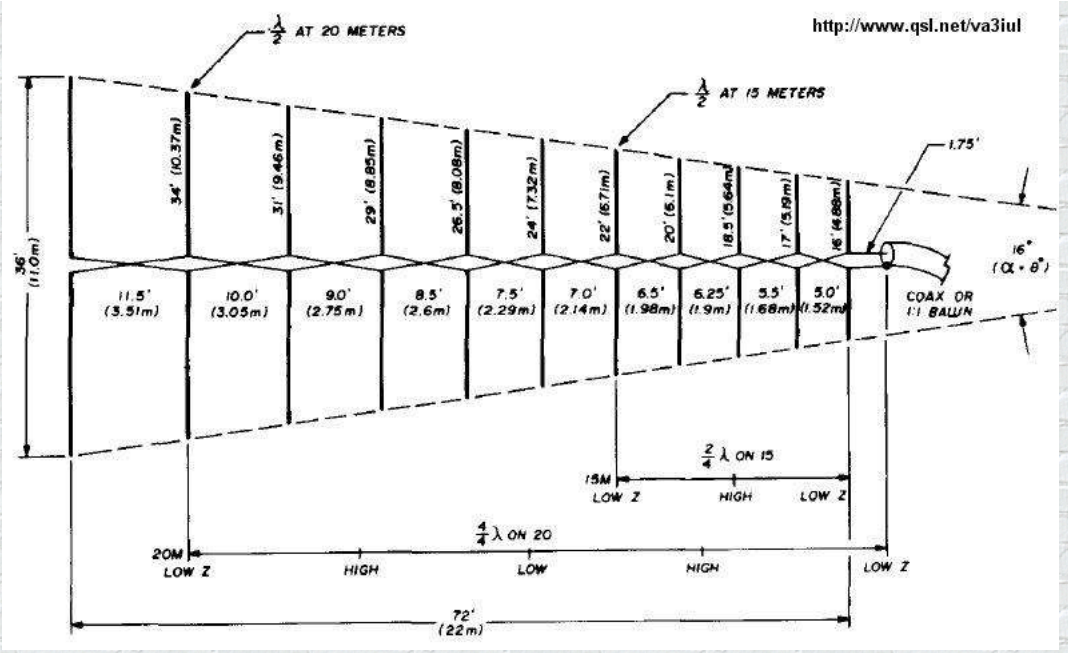

230 - Five-Elements Vertical Log Periodic for 80m, 40m, 20m

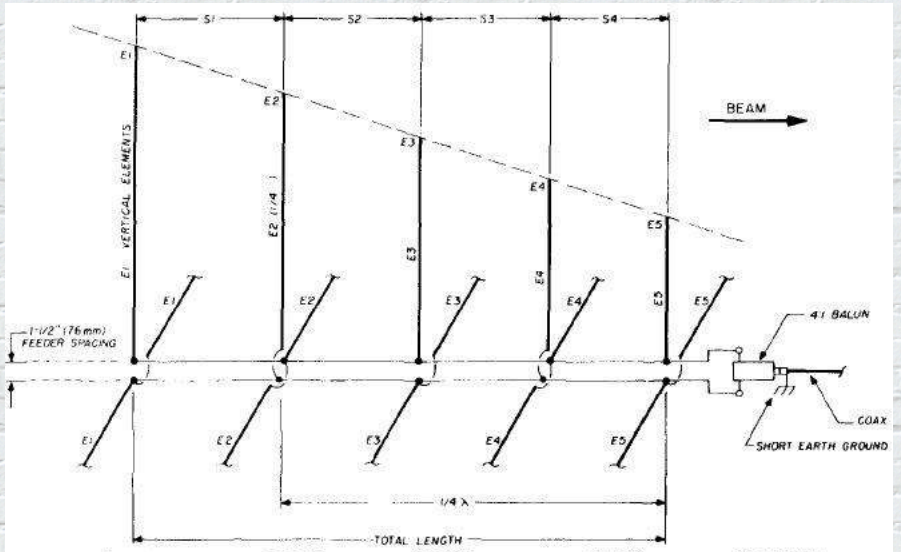

element	3.5-4.0[1]	3.8-4.0[2]	7.0-7.3[2]	14.0-14.35[1]
E1	70' (21.4 m)	65' (19.8 m)	35' (10.7 m)	17.5' (5.3 m)
E2	67' (20.4 m)	62' (18.9 m)	33' (10.0 m)	16.5' (5.0 m)
E3	58' (17.7 m)	55' (16.8 m)	28' (8.5 m)	14.0' (4.3 m)
E4	50' (15.3 m)	45' (13.7 m)	24.5' (7.5 m)	12.2' (3.7 m)
E5	43' (13.1 m)	40' (12.2 m)	20' (6.1 m)	10.0' (3.0 m)
S1	30' (9.2 m)	26' (7.9 m)	14' (4.3 m)	7.0' (2.1 m)
S2	27' (8.2 m)	24' (7.3 m)	13' (4.0 m)	6.5' (2.0 m)
S3	24' (7.3 m)	23' (7.0 m)	12' (3.7 m)	6.0' (1.8 m)
S4	19' (5.8 m)	18' (5.5 m)	9' (2.7 m)	4.5' (1.4 m)
total length	100' (30.5 m)	91' (27.8 m)	48' (14.6 m)	24' (7.3 m)
mast height	80' (24.4 m)	75' (22.9 m)	50' (15.3 m)	30' (9.2 m)
pole height	45' (13.7 m)	40' (12.2 m)	25' (7.6 m)	20' (6.1 m)

http://www.qsl.net/va3iul

231 - Sloping Delta Loop Antenna for 40m

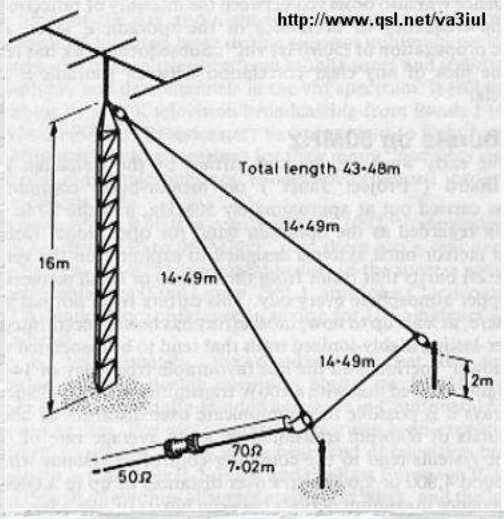

232 - Doublet Antenna for 160m

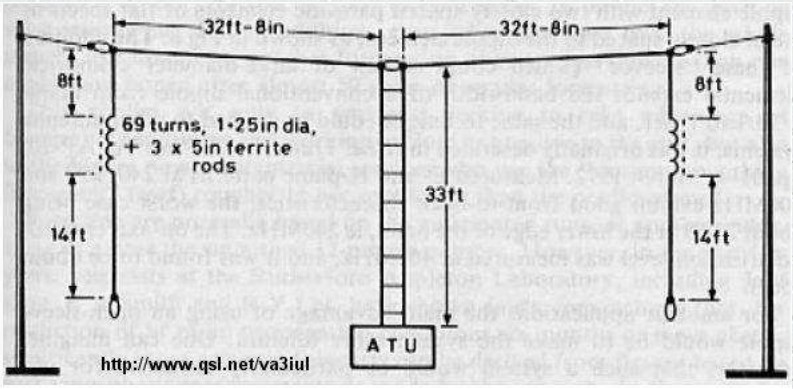

233 - Log Periodic Wire Beam for 40m

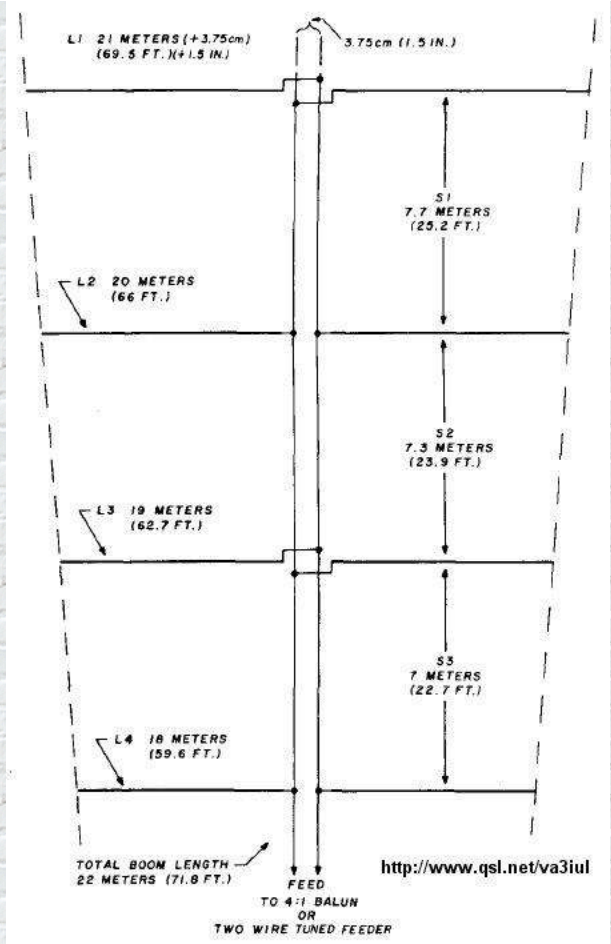

234 - G3LDO Wire Beam Antenna for 20m, 15m, 10m

http://www.qsl.net/va3iul

Data for the G3LDO wire-beam antenna. All dimensions are in inches and are for insulated wire; multiply by 1.04 for uninsulated wire. Dimension C is approximate.

band	reflector	driven element	A	B	C	D
20	452	417	245	263	180	33
15	302	279	154	166	113	22
10	225	208	114	122	85	15

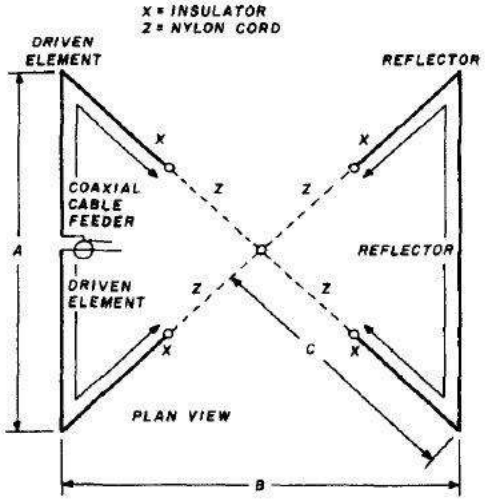

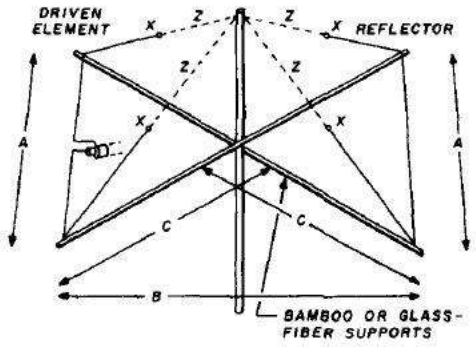

GENERAL CONSTRUCTION DETAILS WITH DIMENSION REFERENCES

235 - Phased Delta Loop Array for 20m

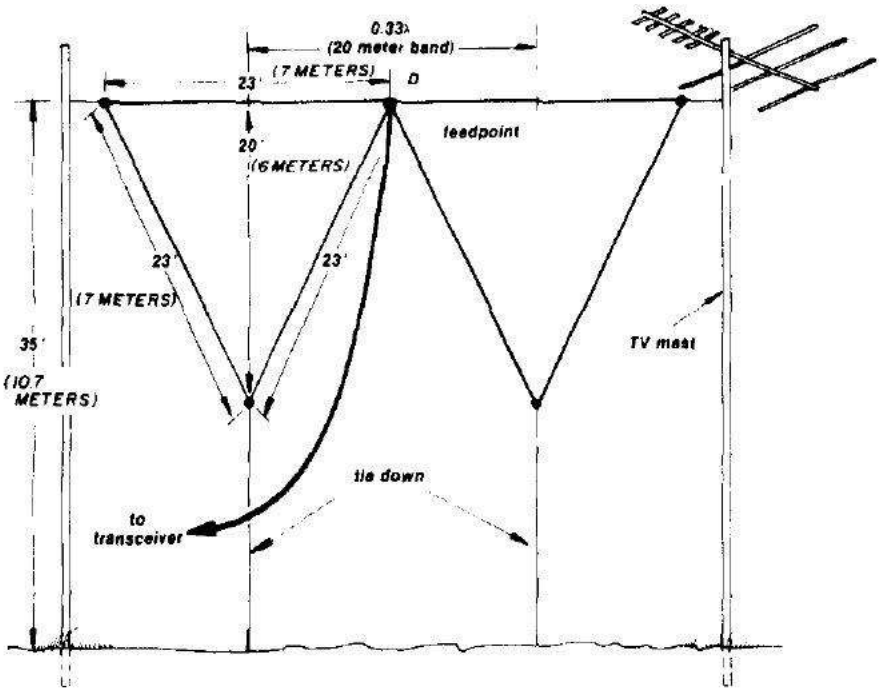

spacing wavelength	feet	(meters)	gain (dB)
0.33	23	(7)	2.0
0.40	27	(8)	2.8
0.50	34	(10)	4.0
0.65	44	(13)	4.8

http://www.qsl.net/va3iul

236 - Dual Band V-dipole for 80m, 40m

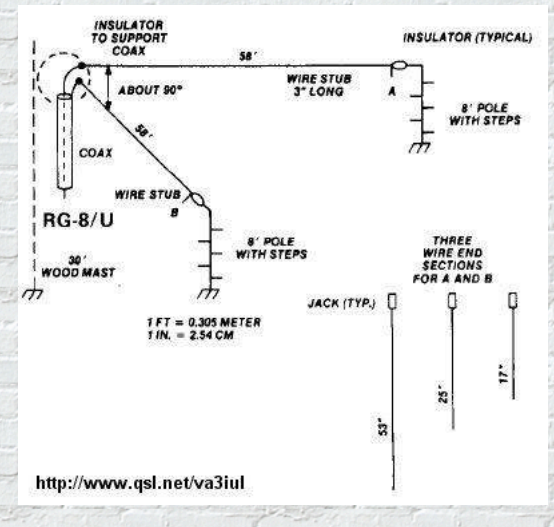

http://www.qsl.net/va3iul

237 - Collinear Array 5dB-Gain for 15m

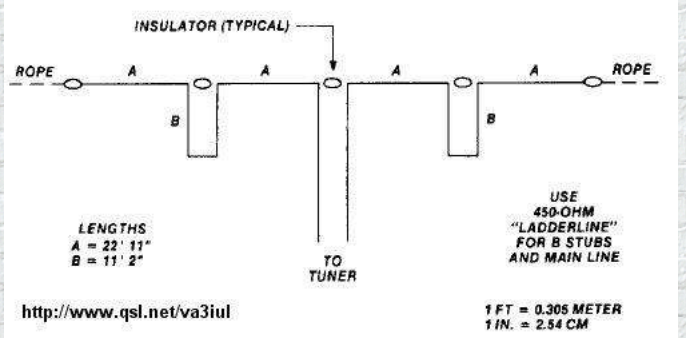

http://www.qsl.net/va3iul

238 - Two-Band Quad Loop Antenna 80m, 40m

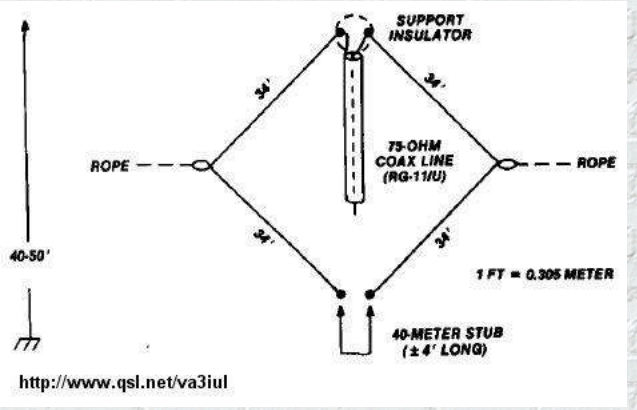

http://www.qsl.net/va3iul

239 - K7CW Quad Antenna

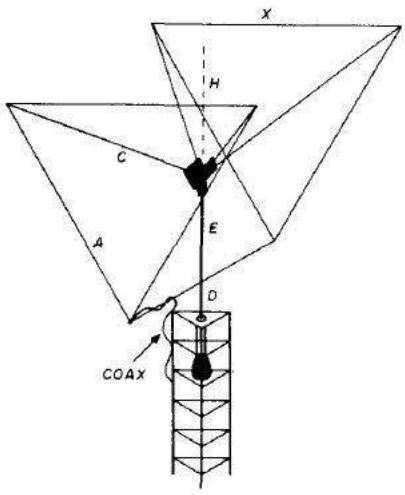

http://www.qsl.net/va3iul

$X = \frac{1030}{9.84F}$

$A = \frac{1005}{9.84F}$

$H = \frac{X}{2}$

$D = .2\lambda$

$E = \sqrt{X_2 - H^2} - H$

$C = \sqrt{2H^2 + \left(\frac{D}{2}\right)^2}$

Where F = design frequency of antenna (3X = total distance around reflector loop).

3A = total distance around driven element loop.

= distance from main hub to top of antenna (the imaginary plane which contains the tips of all four spreaders).

where λ = wavelength at design frequency.
D = element spacing
= length of bottom spreader.

= distance from bottom spreader to main hub.

= distance from hub to where loop is attached to main spreader.

antenna design frequencies (in mete

	3.575 MHz	3.8 MHz	7.05 MHz	7.2 MHz	14.
X	29.2722	27.5389	14.8437	14.5344	
Y	87.8165	82.6168	44.5311	43.6033	2
A	28.5617	26.8705	14.4834	14.1817	
B	85.685	80.6116	43.4502	42.5450	2
H	14.6361	13.7695	7.42184	7.26722	
D	16.7832	15.7895	8.51064	8.33333	
E	10.7144	10.0800	5.43317	5.31998	
C	22.3349	21.0124	11.3258	11.0899	

	21.3 MHz	28.15 MHz	28.6 MHz	29 MHz	50
X	4.91305	3.71751	3.63902	3.60855	
Y	14.7392	11.1525	10.9771	10.8257	
A	4.79380	3.62728	3.57021	3.52097	
B	14.3814	10.8818	10.7106	10.5629	
H	2.45653	1.85876	1.82951	1.80428	
D	2.81690	2.13144	2.09790	2.06897	
E	1.79830	1.36070	1.33929	1.32082	
C	3.74870	2.83649	2.79186	2.75335	

Note: X = length of reflector loop side
Y = distance around reflector loop
A = length of driven element loop side
B = total distance around driven element loop
H = distance from hub to top of antenna
D = bottom spreader length – element spacing
E = distance from bottom spreader to main hub
C = distance from hub to where loop is attached to main spreader, that is, spreader length

240 - Broadband Short Dipole for 80m

http://www.qsl.net/va3iul

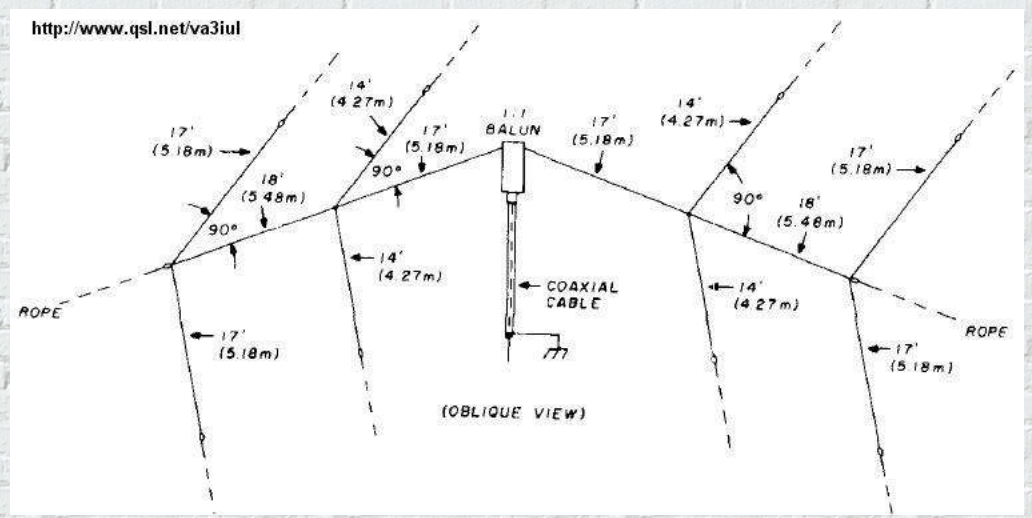

241 - Off-Center Fed Dipole for 40m, 20m, 10m

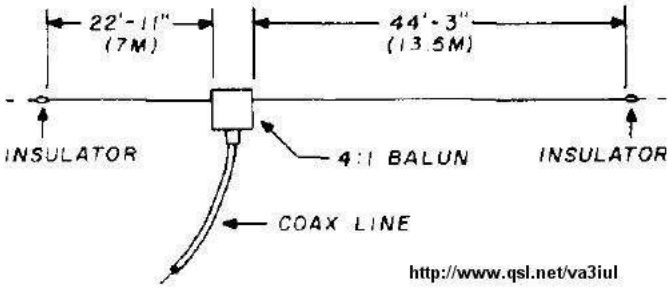

242 - Broadband Sloper Antenna for 80m

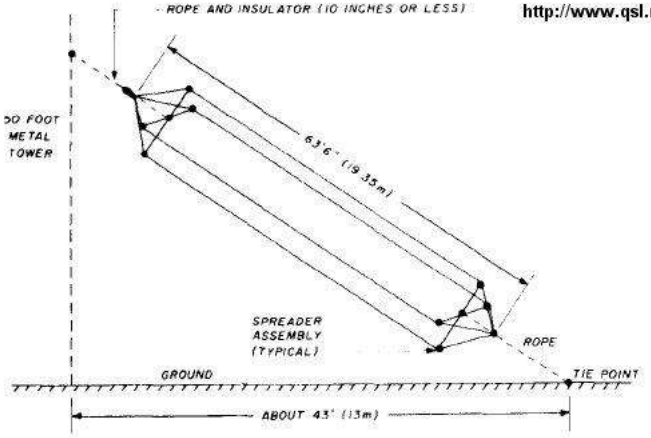

80-meter WD4FAB broadband sloper. Spreader assemblies are made of 36-inch long fiberglass tubes. The four antenna wires are tied together about 24 inches past each spreader assembly. A nylon line may be required from the crossover point of the spreader to the outer insulator to prevent bowing. The SWR plot of the antenna falls below 1.4-to-1 at 3.5 MHz; 1.25-to-1 at 3.8 MHz and 1.4-to-1 at 4.0 MHz. Feedpoint resistance of the antenna may be changed by altering the slope angle. The resonant frequency is adjusted by changing length — no climbing necessary!

243 - Two-Frequency Dipole Antenna for 80m

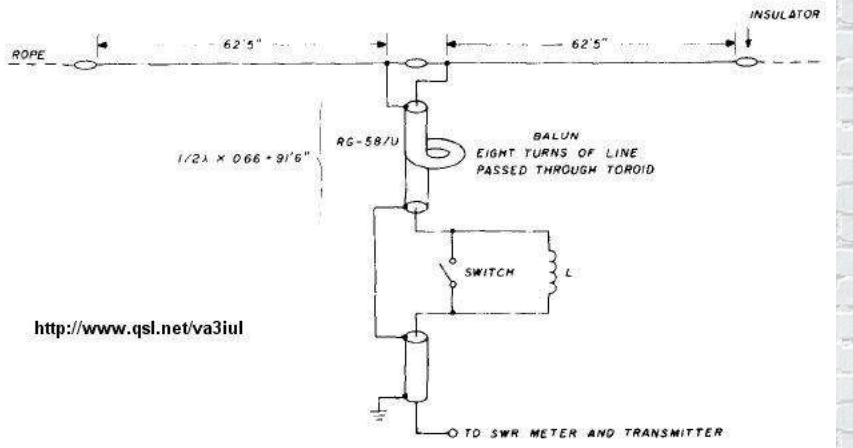

The W6TC two-frequency dipole for 80 meters. Antenna is cut for resonance at high frequency end of band. A single loading coil for operation at the low frequency end of the band is placed an electrical half-wavelength down the transmission line. The line is decoupled from the antenna by a simple balun placed directly at the antenna insulator. Toroid is powdered iron material T-200 (2″ OD) (1.25″ ID), 2-mix (red, μ = 10 (Amidon T-200-2), or equivalent.

244 - Top Loaded Vertical Antenna for 160m

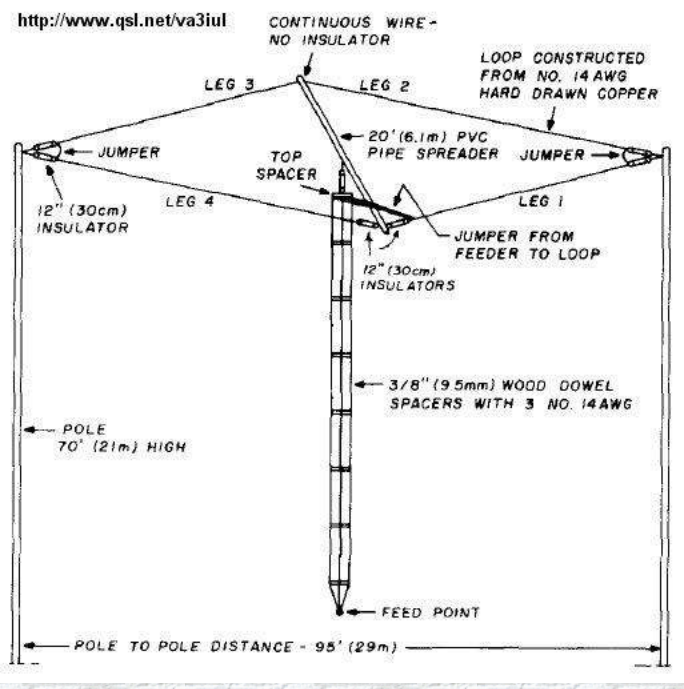

245 - Two Loop Beam Antenna for 20m, 15m

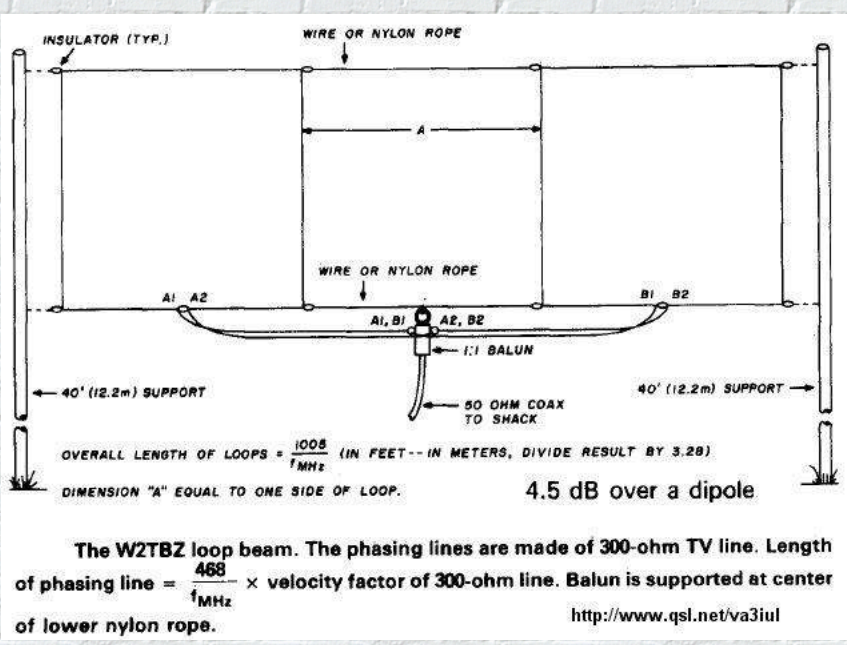

The W2TBZ loop beam. The phasing lines are made of 300-ohm TV line. Length of phasing line = $\frac{468}{f_{MHz}}$ × velocity factor of 300-ohm line. Balun is supported at center of lower nylon rope.

http://www.qsl.net/va3iul

246 - Corner-Fed Delta Loop Antenna for 80m, 40m, 20m

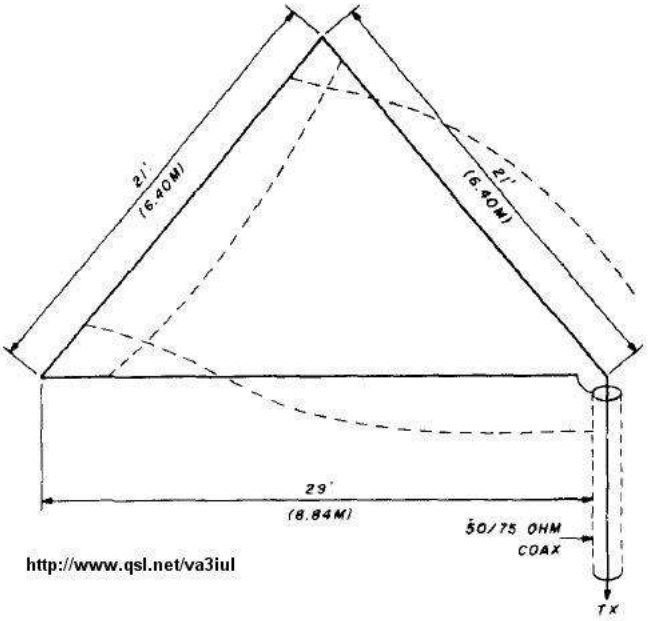

DIMENSIONS FOR FULL-SIZE CORNER-FED DELTA LOOPS

frequency (MHz)	total loop circumference (feet)	(meters)	length of each side (feet)	(meters)	length of base (feet)	(meters)
3.800	279 ft. 2 in.	(85.09)	82 ft.	(24.99)	115 ft. 2 in.	(35.10)
7.075	142 ft. 0 in.	(43.28)	42 ft.	(12.80)	58 ft. 0 in.	(17.68)
14.150	71 ft. 0 in.	(21.64)	21 ft.	(6.40)	29 ft. 0 in.	(8.84)

247 - Loaded Delta Loop Antenna for 40m, 20m

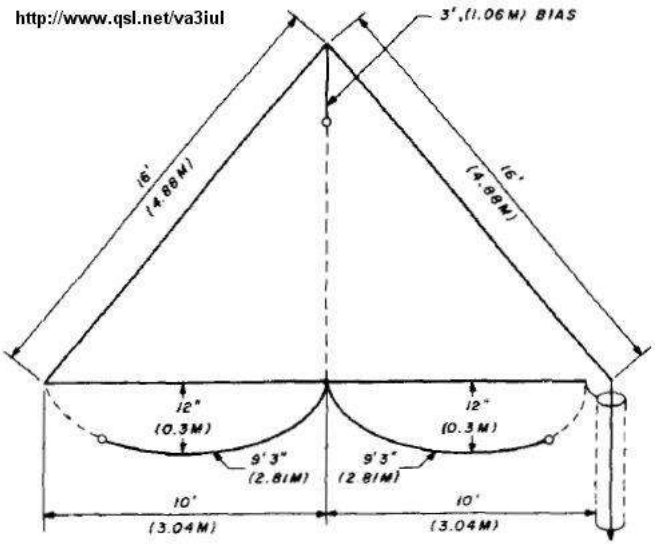

The final loaded loop for 14 MHz. All dimensions are doubled for operation on 7 MHz. Base loading wires are each 18 feet 4 inches (5.59 meters). The top loading wire is made taut by securing to base with thin light nylon cord.

248 - Compact Size Dipole for 80m

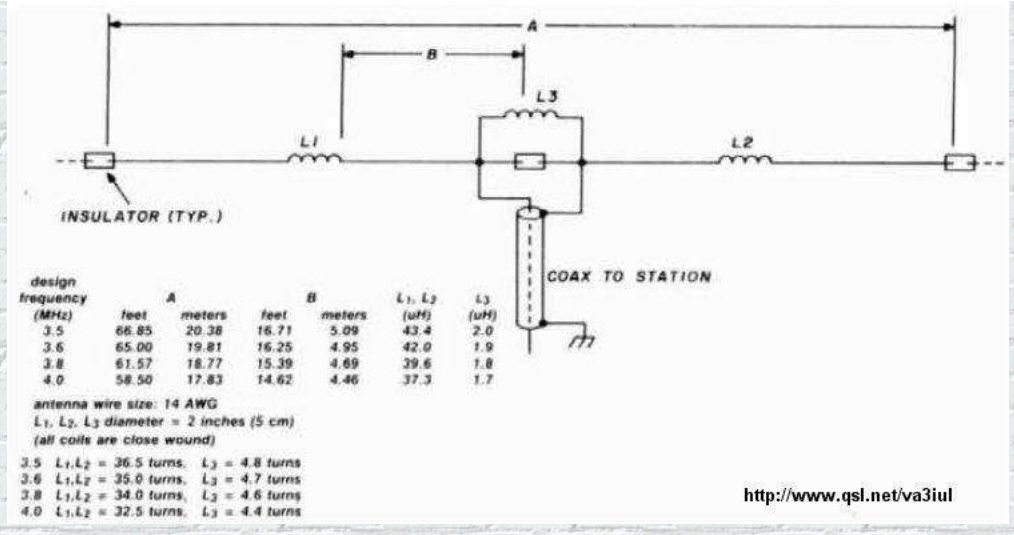

design frequency (MHz)	A feet	A meters	B feet	B meters	L_1, L_2 (uH)	L_3 (uH)
3.5	66.85	20.38	16.71	5.09	43.4	2.0
3.6	65.00	19.81	16.25	4.95	42.0	1.9
3.8	61.57	18.77	15.39	4.69	39.6	1.8
4.0	58.50	17.83	14.62	4.46	37.3	1.7

antenna wire size: 14 AWG
L_1, L_2, L_3 diameter = 2 inches (5 cm)
(all coils are close wound)

3.5 L_1,L_2 = 36.5 turns, L_3 = 4.8 turns
3.6 L_1,L_2 = 35.0 turns, L_3 = 4.7 turns
3.8 L_1,L_2 = 34.0 turns, L_3 = 4.6 turns
4.0 L_1,L_2 = 32.5 turns, L_3 = 4.4 turns

http://www.qsl.net/va3iul

249 - JAWS 3dB Gain Antenna for 40m

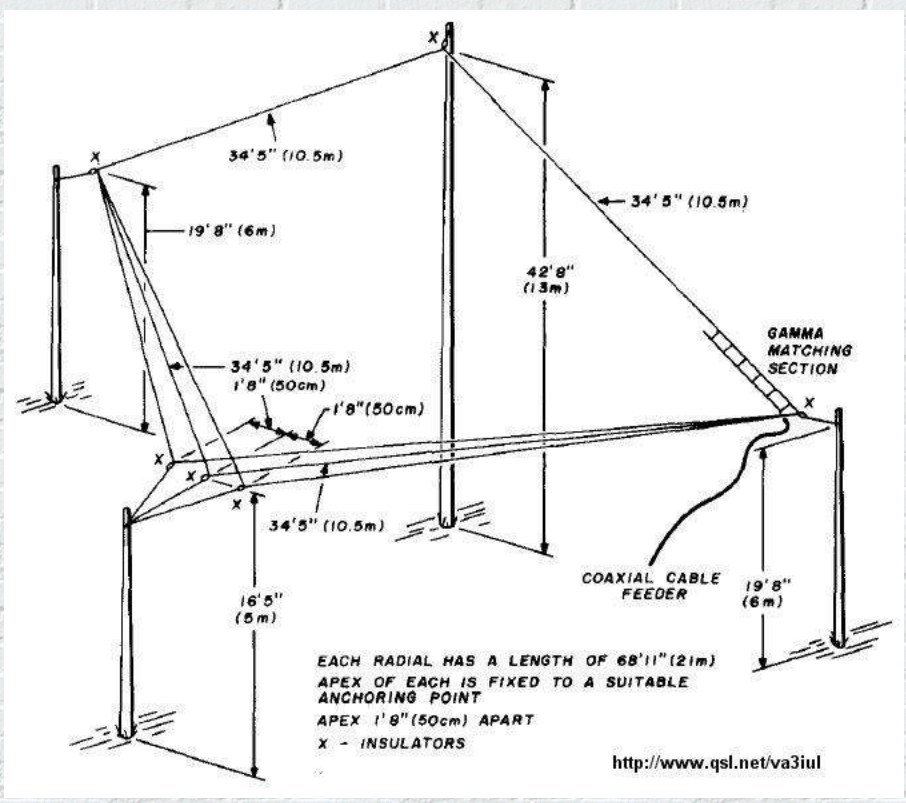

250 - Inverted-V Antenna for 160m

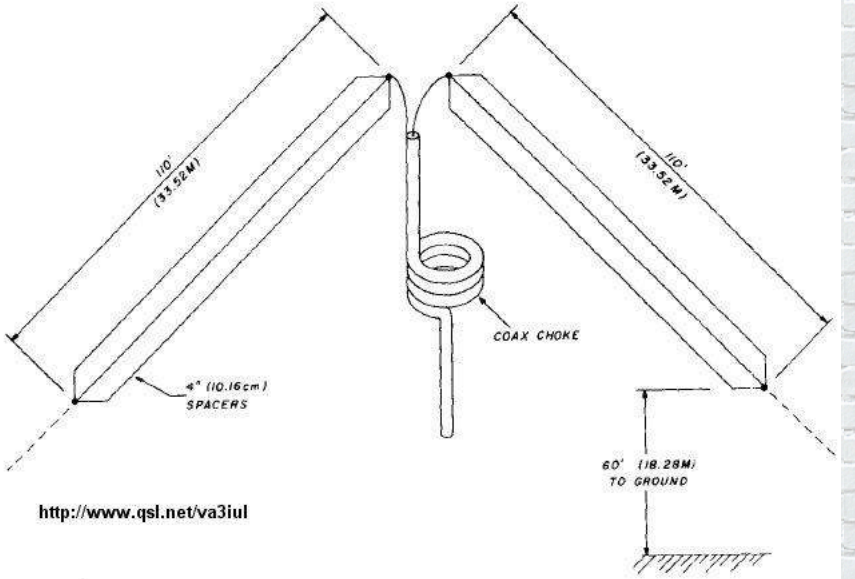

The inverted-V antenna for 160 meters at VE7BS. Wires all lie in the same plane. Apex is at 105 feet (32 meters).

251 - Lazy-U Antenna for 160m

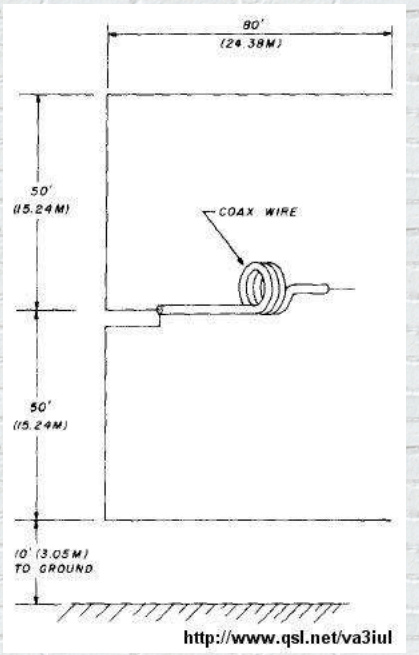

252 - AF3V Compact Antenna for 160m

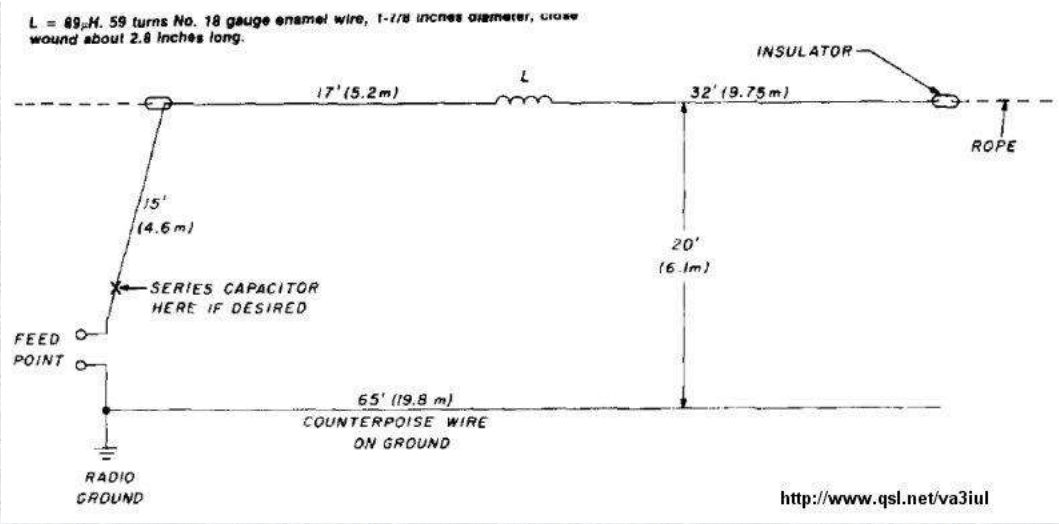

253 - Hot Beam Wire Antenna for 40m

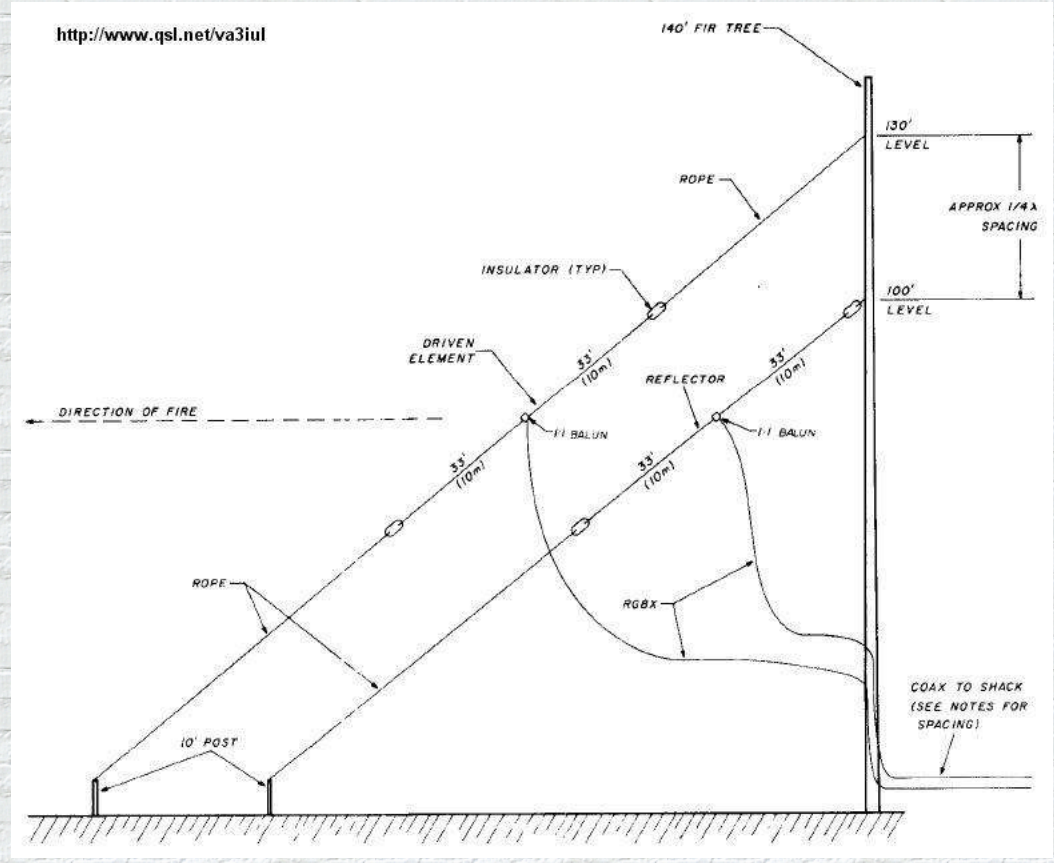

254 - Sloping Delta Loop for 40m

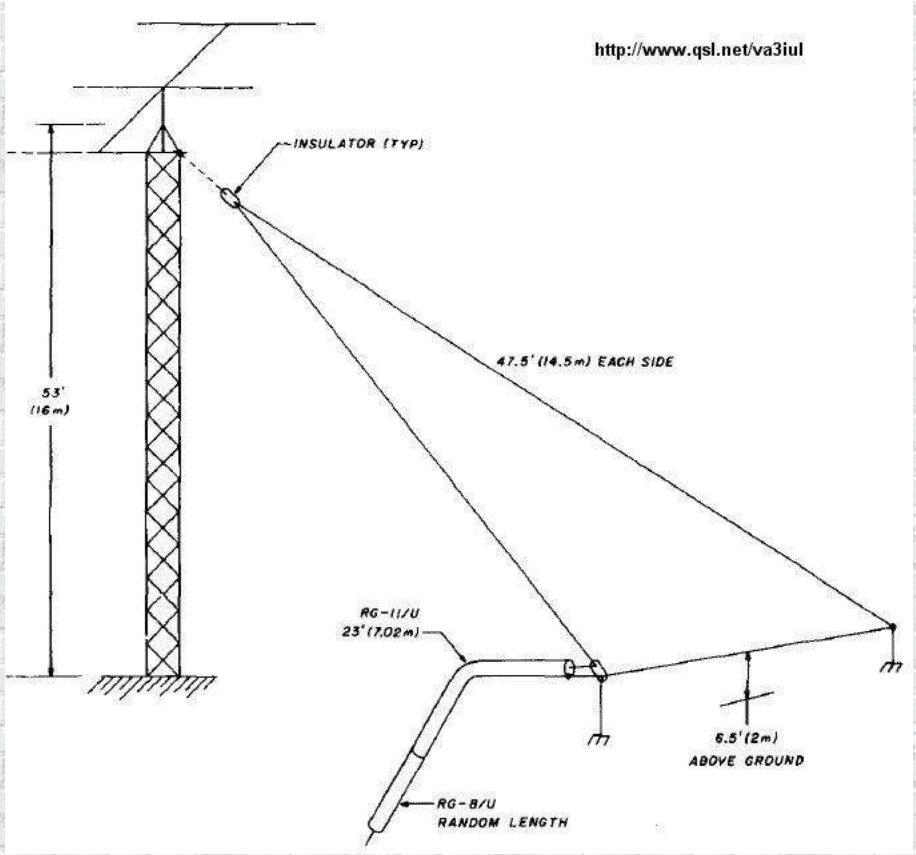

255 - K6FD Multiband Antenna with T-tuner

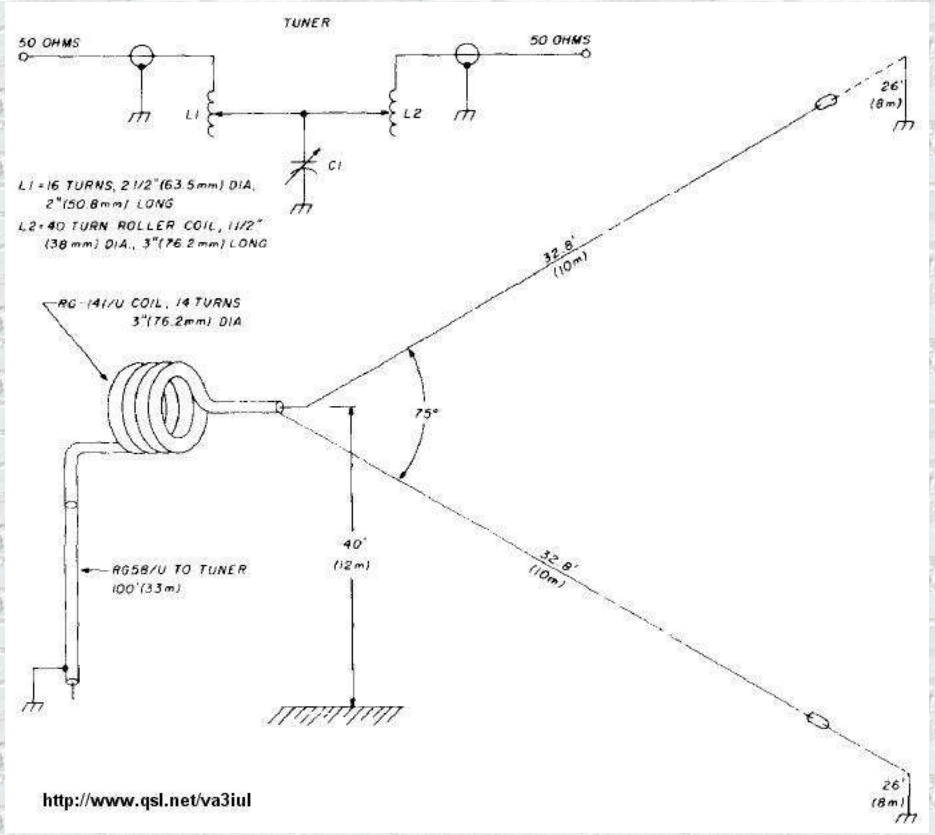

256 - Dual Band Dipole Antenna for 17m, 10m

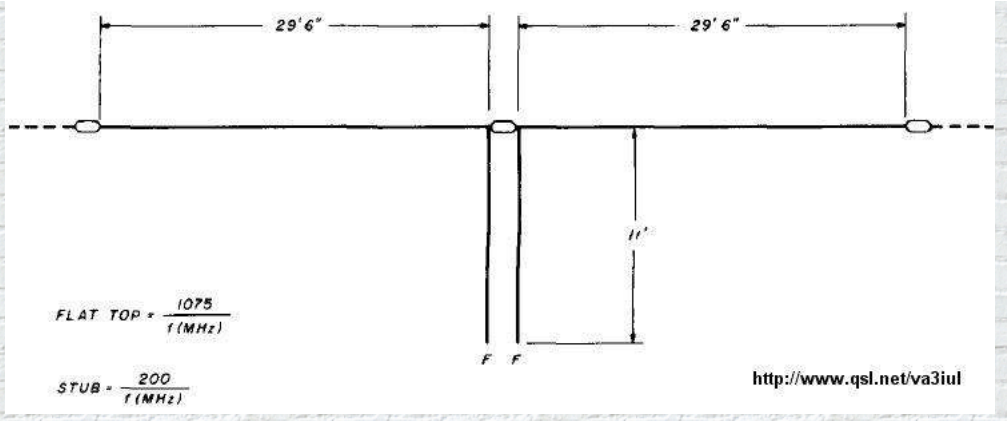

257 - Compact Travel Dipole Antenna for 10m, 15m, 20m

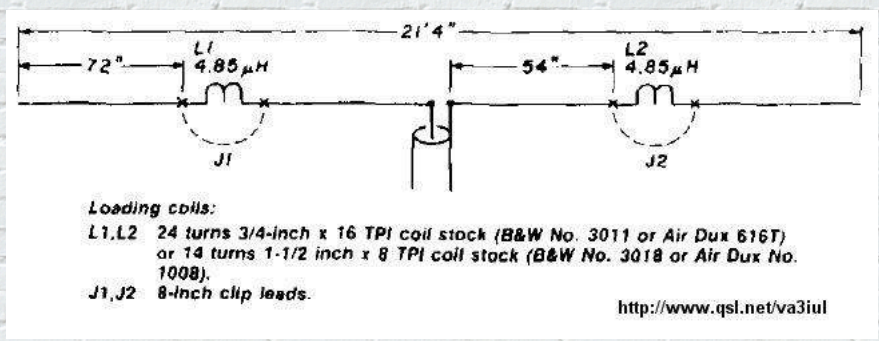

258 - End-Fire Antenna for 160m, 80m, 40m, 20m

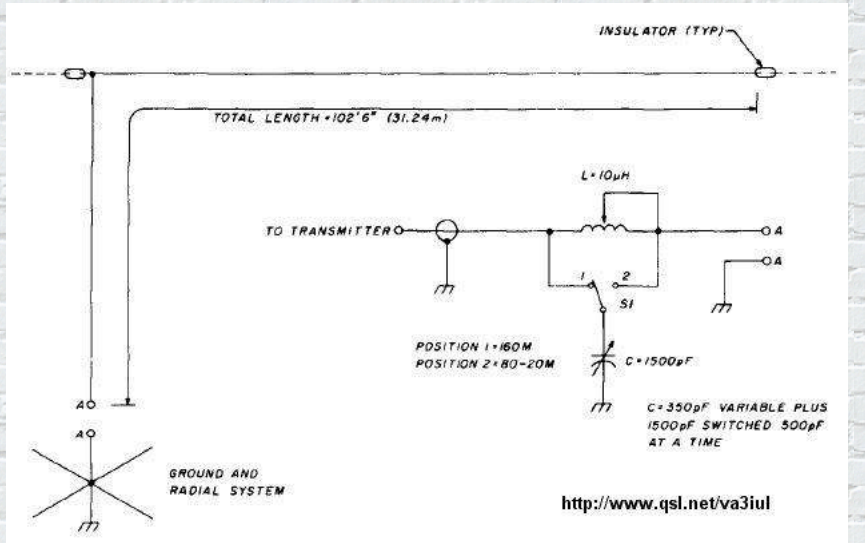

259 - Four Band Loop for 40m, 20m, 15m, 10m

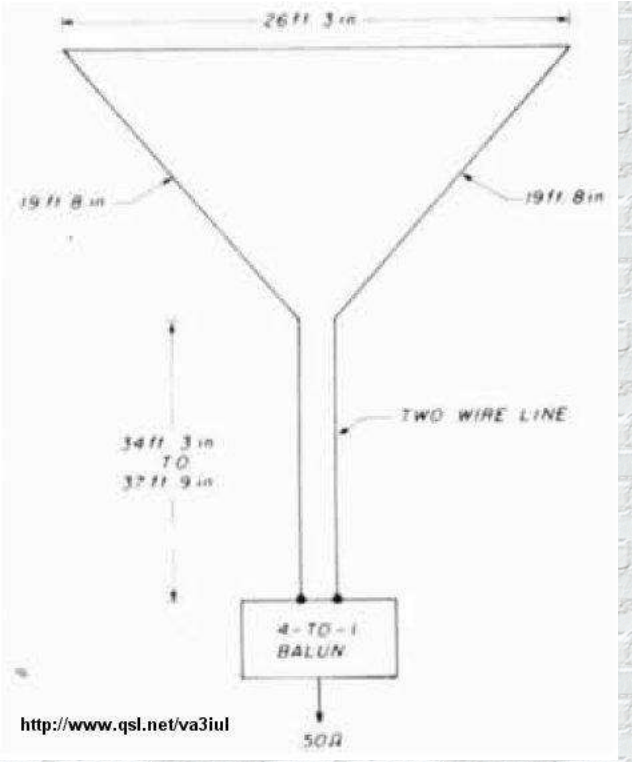

260 - Carolina Windom Antenna for 80 to 10m

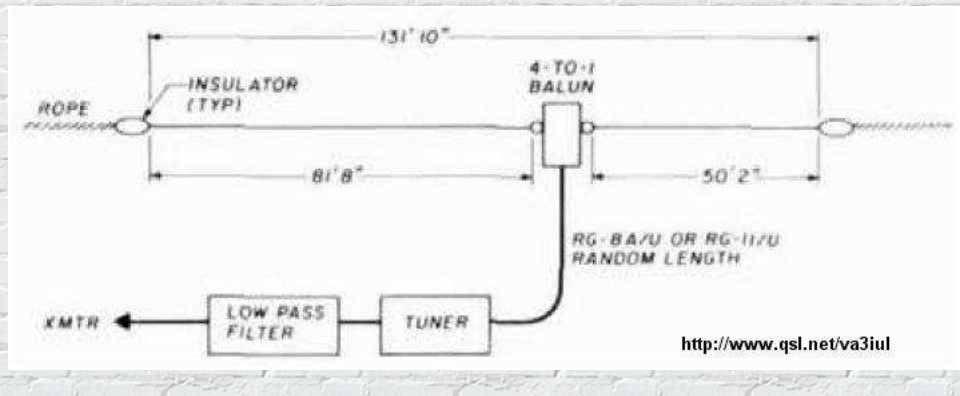

261 - Shortened Loaded Dipole for 40m

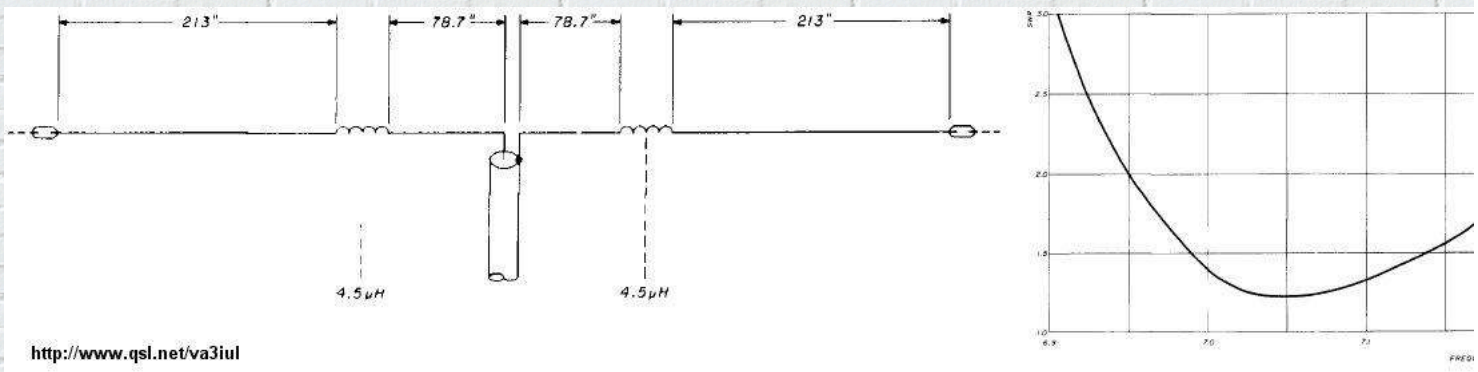

262 - Shortened Loaded Dipole for 80m

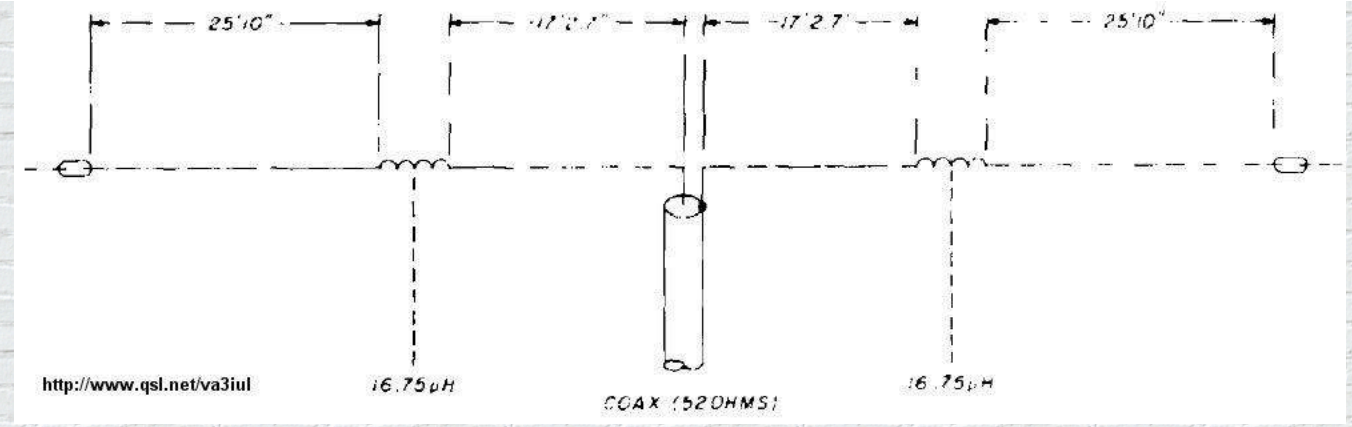

263 - Low Radiation Angle Inverted Delta Loop for 80m

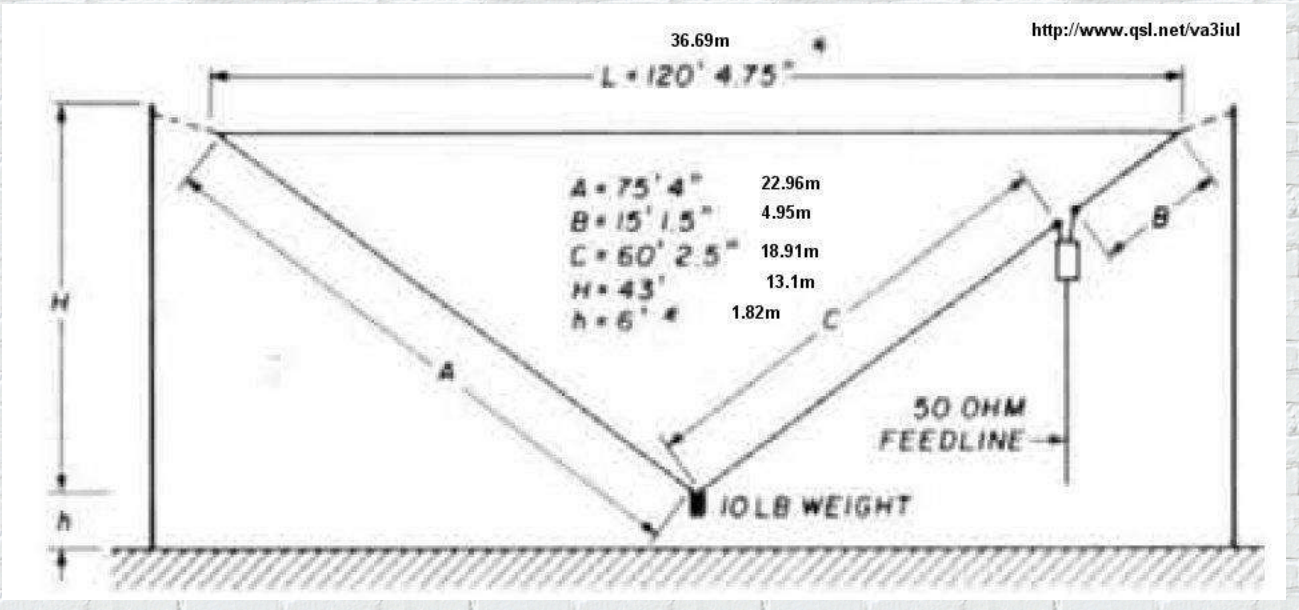

264 - Compact Dipole Antenna for 40m, 15m

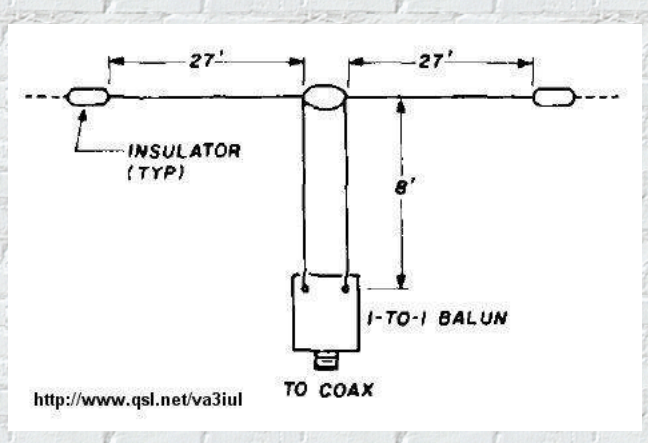

265 - Vertical Delta Loop for 40m to 10m

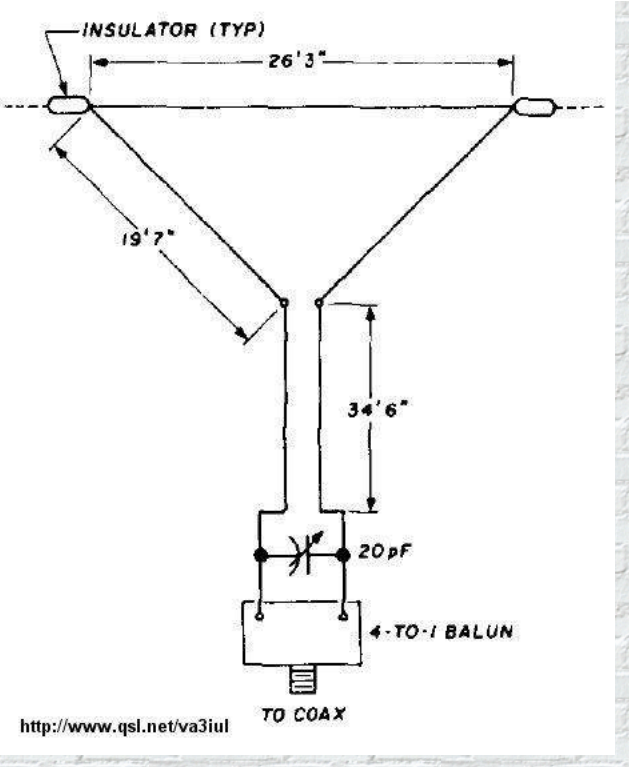

266 - Delta Loop Antenna for 17m

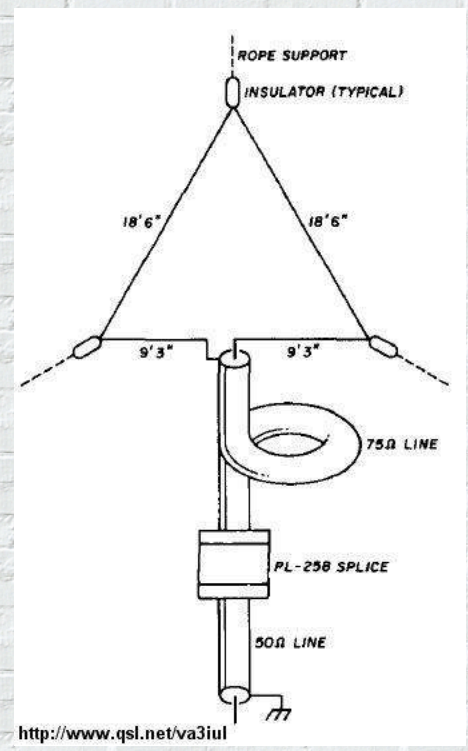

267 - Bi-Square Beam Gain=3dBd for 17m

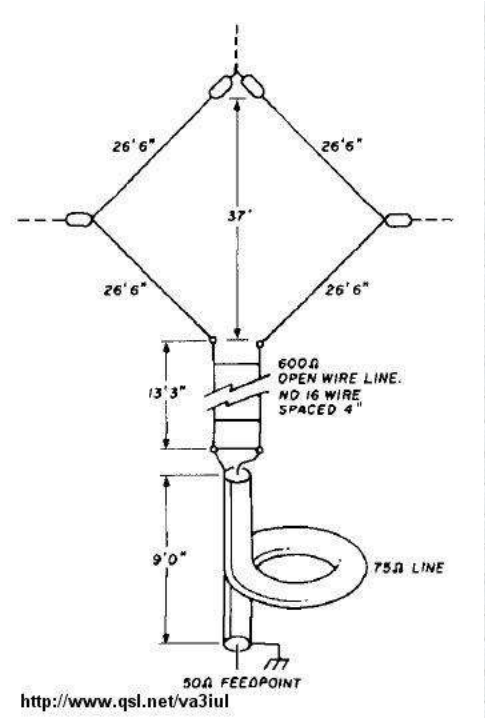

268 -Trap Dipole Antenna for 17m,13m

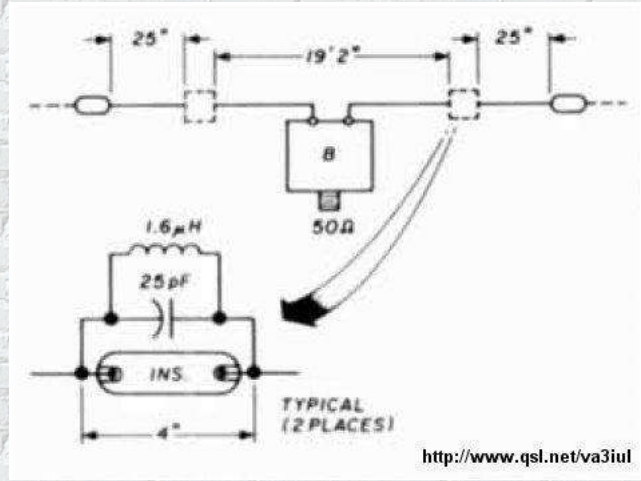

269 - Hanging Unipole Antenna for 160m, 80m

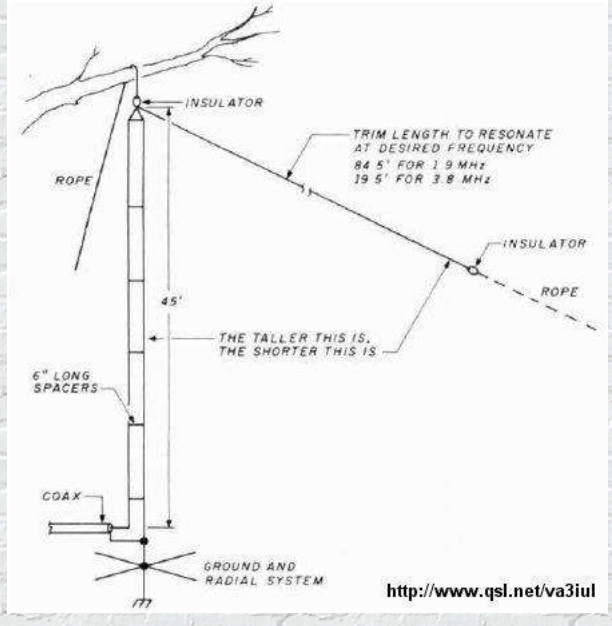

270 - Wideband Sloping Vee Antenna - 30m to 6m

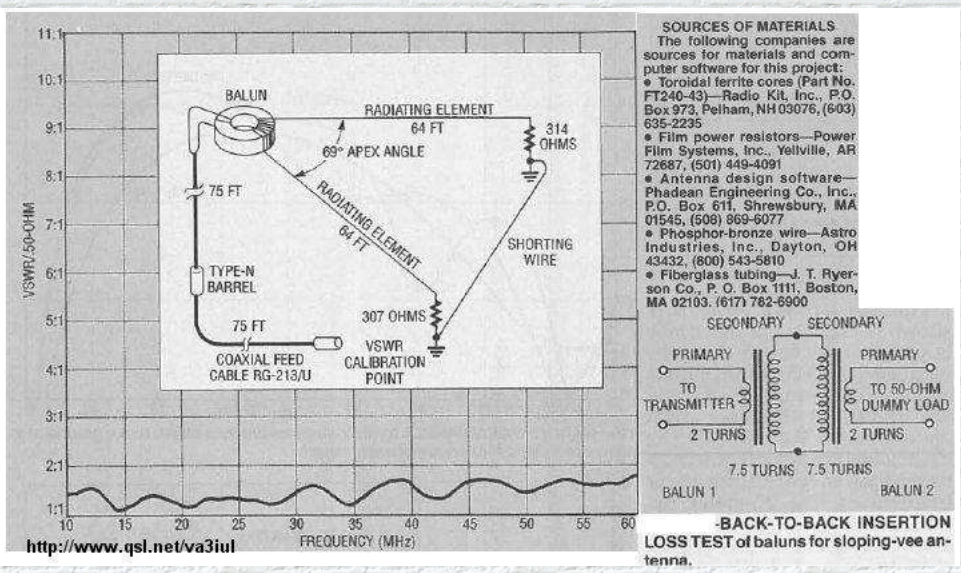

271 - 5/8 Wavelength Antenna

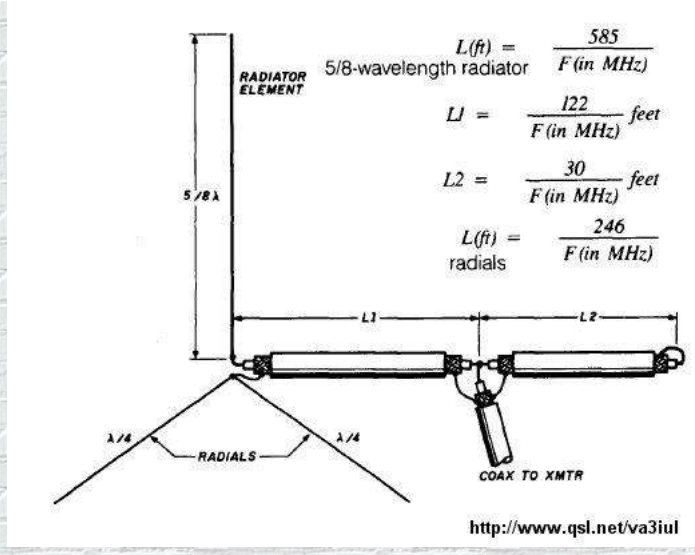

272 - C-Pole Vertical Antenna

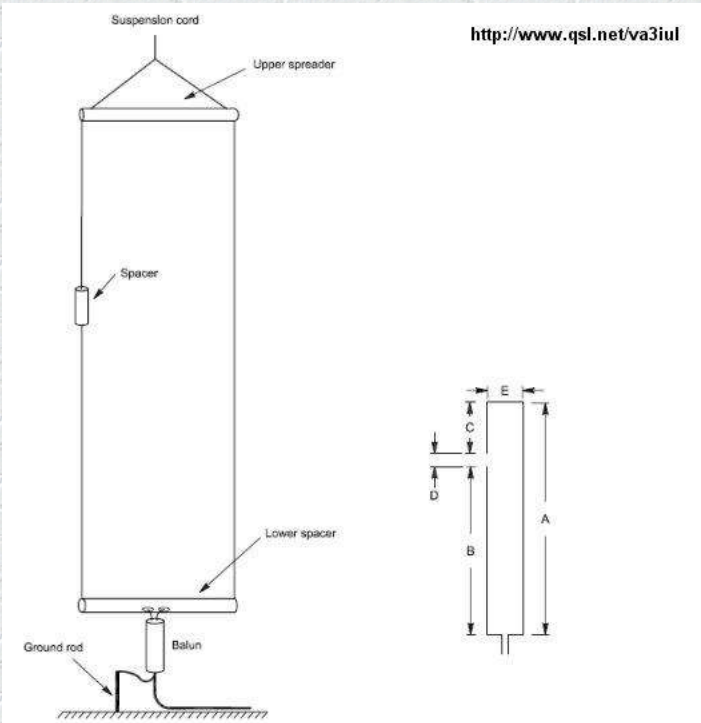

Band (meters)	A (inches)	B (inches)	C (inches)	D (inches)	E (inches)	2:1 SWR bandwidth (kHz)
160	1666	924	994	60	80	58
80	840	460	360	30	40	120
60	591	322	249	20	26	250
40	450	240	190	20	20	260
30	320	167	139	14	14	360
20	177	85	84	8	40	400
15	124	60	60	4	20	600
10	87	46	37	4	20	800

Wire diameter is 1/16-inch. Height of the lower horizontal wire is 12 inches to 24 inches and is non-critical.

273 - Bobtail Antenna for 30m

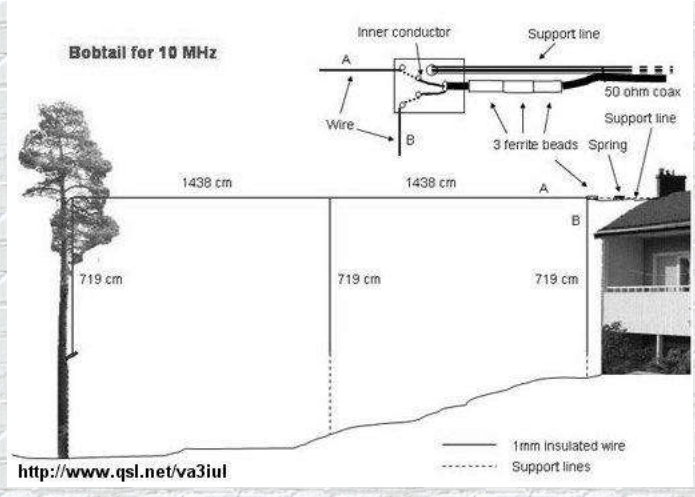

274 - Bobtail Antenna for 40m

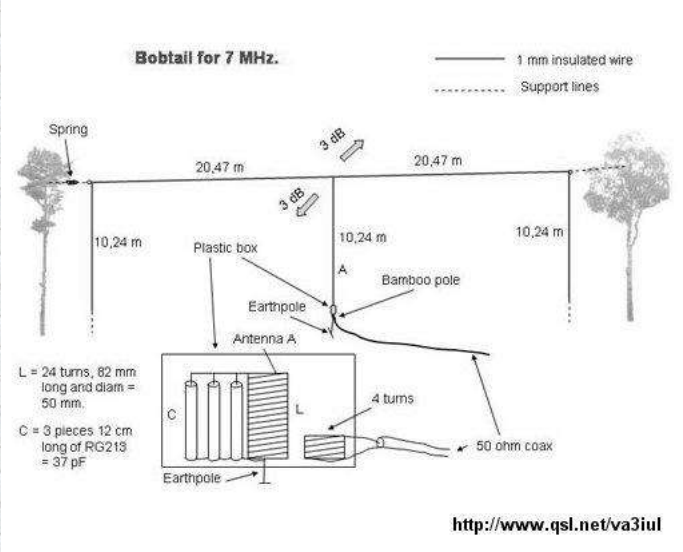

275 - Two Elements Vertical Loop Antenna for 40m

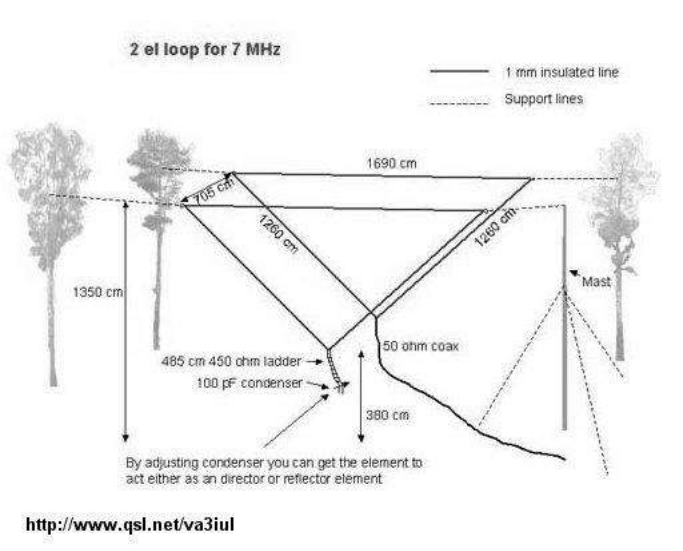

276 - Double Extended Zepp Antenna for 40m

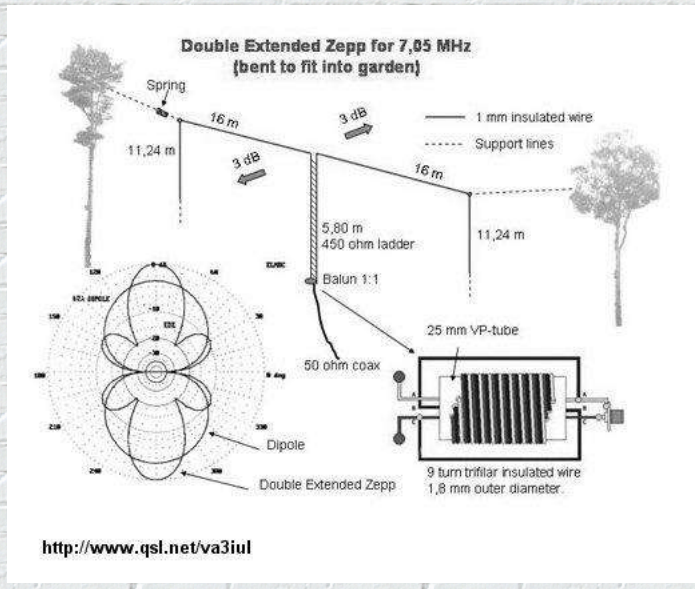

277 - Reversible Moxon Flip Beam for 40m

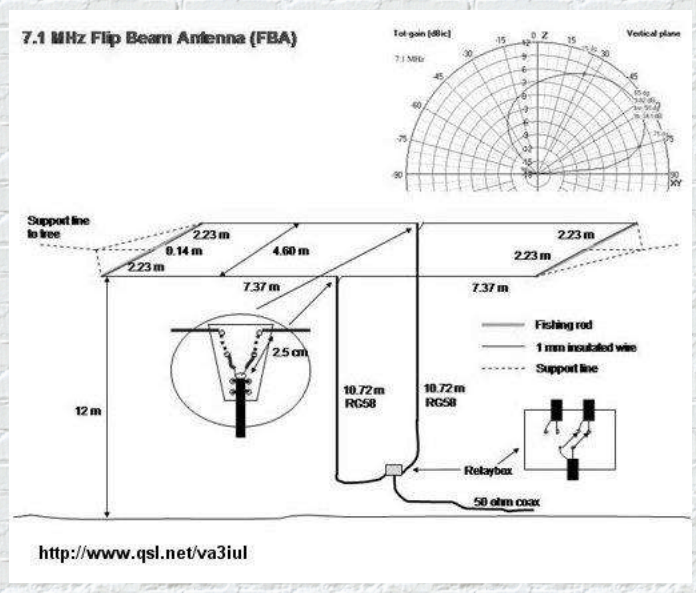

278 - Spitwire Antenna for 40m

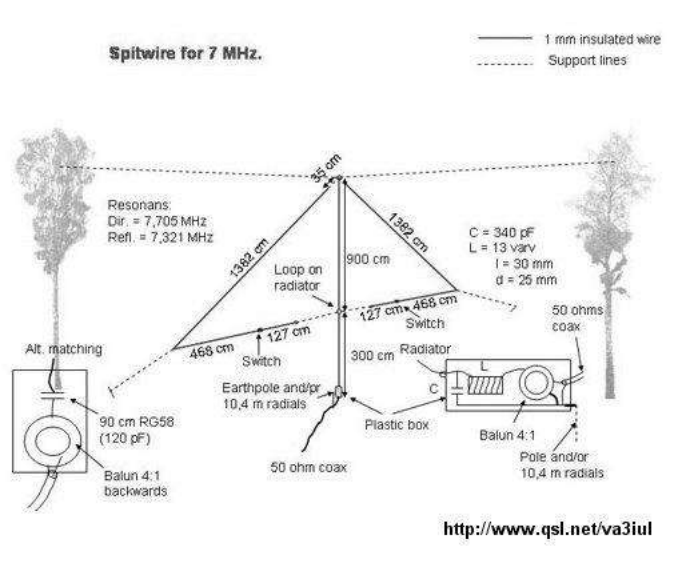

279 - Fork Antenna for 40m

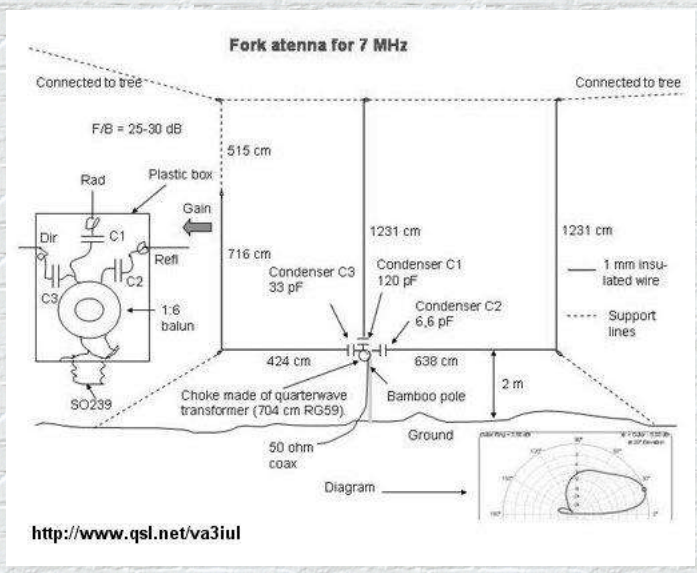

280 - Veebeam Antenna 3dB-Gain for All Bands

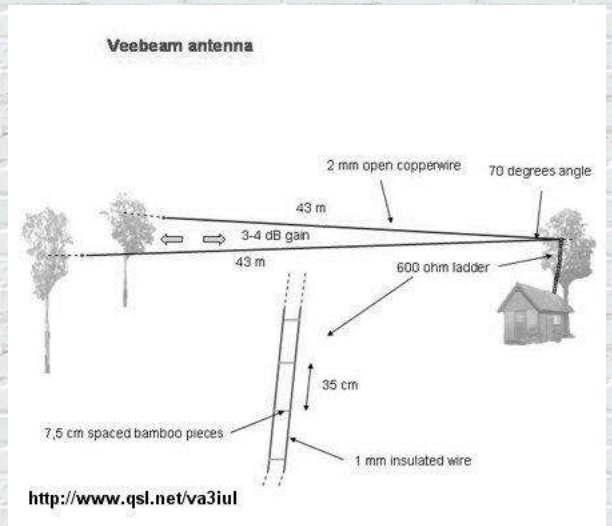

281 - Vertical Moxon Antenna for 10m

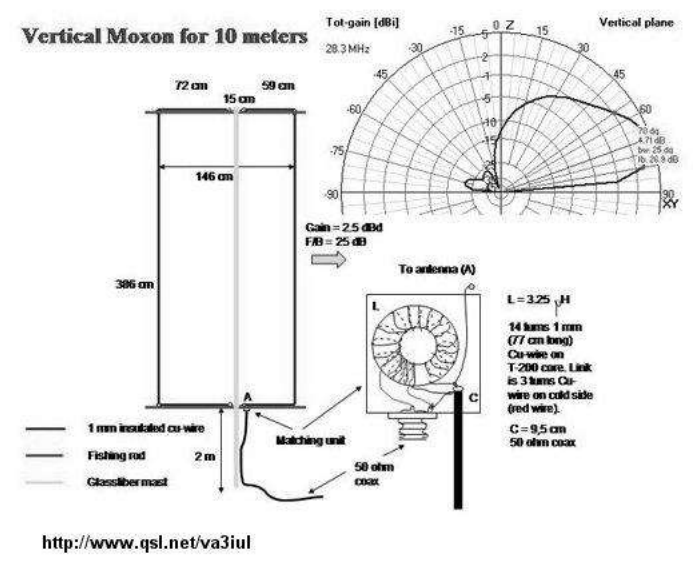

---

282 - Half-Square Antenna for 30m

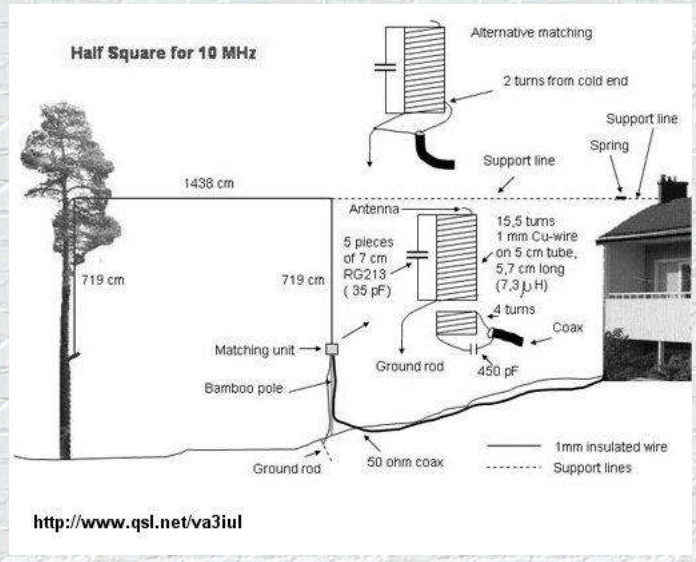

---

283 - Rotatable Vertical Delta Loop for 20m

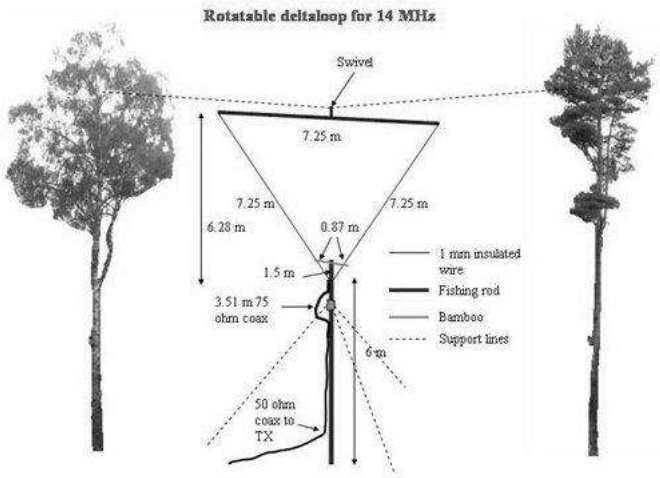

284 - Mini-Horse Antenna 10dB-Gain for 40m-to-2m

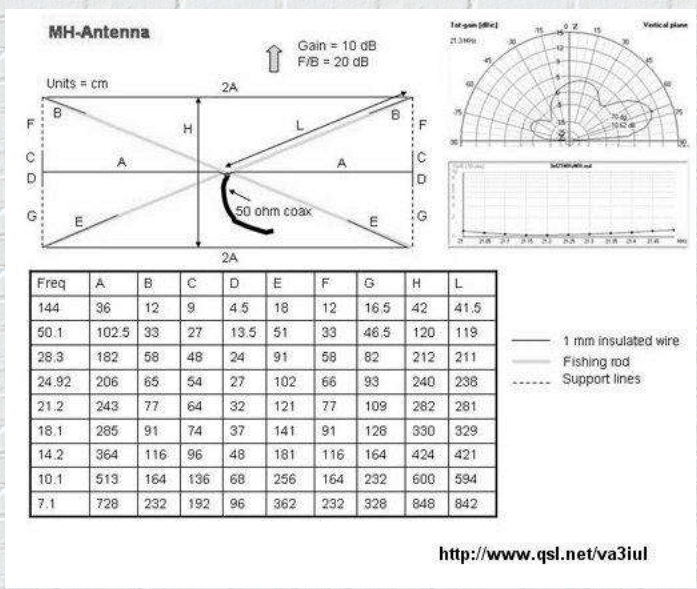

Freq	A	B	C	D	E	F	G	H	L
144	36	12	9	4.5	18	12	16.5	42	41.5
50.1	102.5	33	27	13.5	51	33	46.5	120	119
28.3	182	58	48	24	91	58	82	212	211
24.92	206	65	54	27	102	66	93	240	238
21.2	243	77	64	32	121	77	109	282	281
18.1	285	91	74	37	141	91	128	330	329
14.2	364	116	96	48	181	116	164	424	421
10.1	513	164	136	68	256	164	232	600	594
7.1	728	232	192	96	362	232	328	848	842

285 - Compact Moxon Antenna 5dB-Gain for 40m

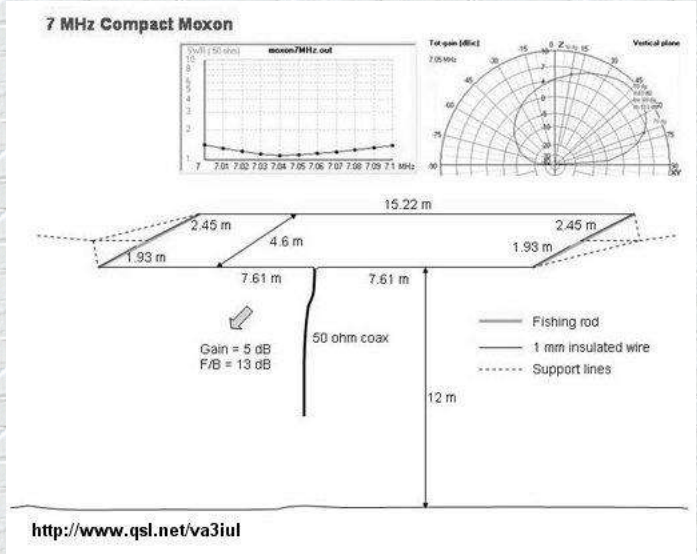

286 - Two Elements Sloping Delta Loop 8dB-Gain for 10m

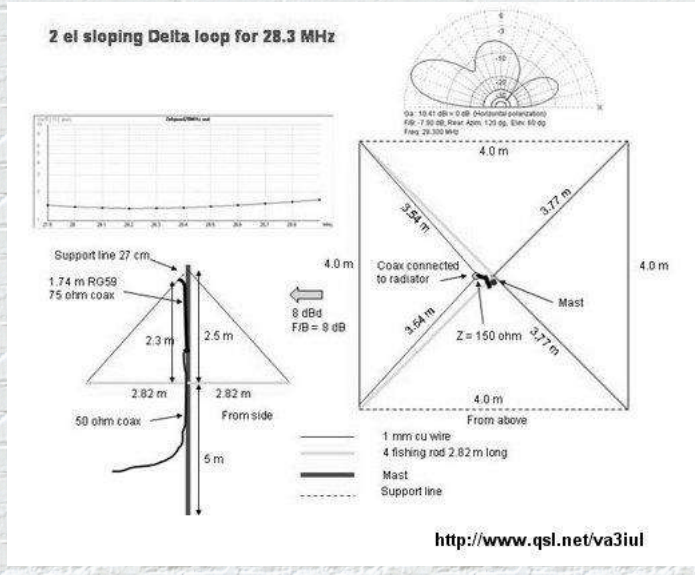

287 - Two Elements Phased Vertical Antenna 3dB-Gain for 40m

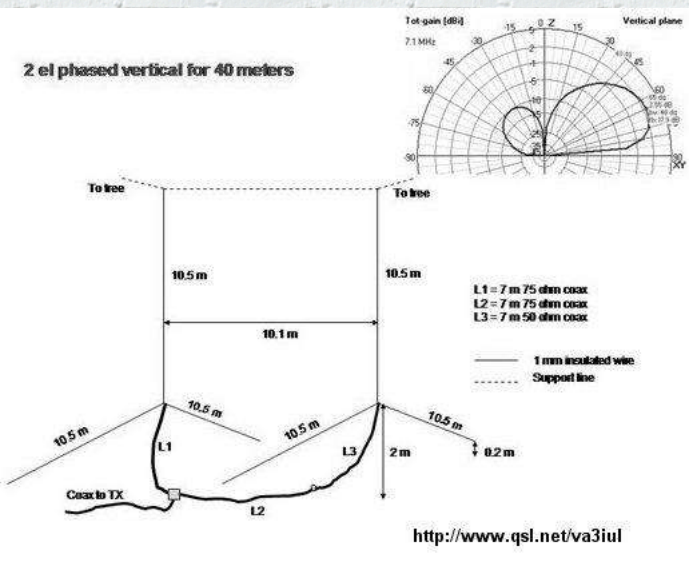

References:

Antenna Toolkit - J. Carr
Practical Antenna Handbook - J. Carr
More Antenna Classics - C. Hutchinson
Amateur Radio Techniques - P. Hawker
The Radio Handbook - W. Orr (editor), 15th edition
The Radio Antenna Handbook - Engineering Staff of "Radio"
Jones Antenna Handbook - Frank C. Jones
SM0DTK - http://www.sm0dtk.se/antennas.htm
ARRL Antenna Handbook 1990-2007
ARRL Handbook 1937-2009
ARRL Antenna Compendium
73 Magazine 1970-2002
Funkamateur Magazine 1990-2011
RSGB Handbook - 2007 - 2010
QST Magazine - 1980 - 2010
Ham Radio Magazine - 1969 - 1990
Radio-Electronics Magazine - 1986 - 1990

home: ***http://www.qsl.net/va3iul***

Live Traffic Feed

Watch Live | Get FEEDJIT

Richmond, California, United States arrived 0 secs ago.
United Kingdom arrived 2 mins ago.
Kundan, Kashmir, India arrived 3 mins ago.
San Francisco, California, United States arrived 9 mins ago.
Rostock, Mecklenburg-Vorpommern, Germany arrived 13 mins ago.
Russia arrived 16 mins ago.
Abu Dhabi, United Arab Emirates arrived 32 mins ago.
United States arrived 35 mins ago.
Menlo Park, California, United States arrived 58 mins ago.
Québec, Canada arrived 59 mins ago.

$44.95

The ARRL

ANTENNA BOOK

21st Edition

The *ultimate* reference for Amateur Radio antennas, transmission lines and propagation

INSIDE: Includes the fully searchable book on CD-ROM

The ARRL Antenna Book

All the information you need to design your own complete antenna system.

Since the first edition in September 1939, radio amateurs and professional engineers have turned to **The ARRL Antenna Book** as THE source of current antenna theory and a wealth of practical how-to construction projects. Use this book to discover even the most basic antenna designs— wire and loop antennas, verticals, and Yagis—and for advanced antenna theory and applications. Many of the antennas in this edition benefit directly from advances in sophisticated computer modeling.

This 21st edition has been extensively revised to include information you can use to build highly optimized or specialized antennas. The book includes new content on Near Vertical Incidence Skywave (NVIS) techniques, phased arrays, S-parameters as used in modern vector network analyzers (VNA), Beverage receiving antennas, mobile "screwdriver" antennas, ionospheric area-coverage maps, *and much…much more*.

Fully searchable CD-ROM included!
Bundled with this book is a CD-ROM containing **The ARRL Antenna Book** in its entirety, using the popular Adobe® Reader® software for Microsoft® Windows® and Macintosh® systems. View, search and print from the entire text, including images, photographs, drawings…**everything!**

The CD-ROM contains additional utility programs, including:

- **YW**—Yagi for Windows
- **TLW**—Transmission Line for Windows
- **HFTA**—HF Terrain Assessment for Windows
- **Range-Bearing**— compute range/bearing or latitude/longitude
- **Arrayfeed1**— designing phased-array feed systems
- **EZNEC-ARRL**— antenna modeling for Windows

PLUS propagation forecast tables for more than 170 locations around the world for all portions of the solar cycle!

CONTENTS

Safety First
Antenna Fundamentals
The Effects of Ground
Antenna Modeling and System Planning
Loop Antennas
Low-Frequency Antennas
Multiband Antennas
Multielement Arrays
Broadband Antenna Matching
Log Periodic Arrays
HF Yagi Arrays
Quad Arrays
Long-Wire and Traveling-Wave Antennas
Direction Finding Antennas
Portable Antennas
Mobile and Maritime Antennas
Repeater Antenna Systems
VHF and UHF Antenna Systems
Antenna Systems for Space Communications
Antenna Materials and Accessories
Antenna Products Suppliers
Antenna Supports
Radio Wave Propagation
Transmission Lines
Coupling the Transmitter to the Line
Coupling the Line to the Antenna
Antenna and Transmission-Line Measurements
Smith Chart Calculations

Includes a comprehensive glossary and index

Published by:
ARRL The national association for AMATEUR RADIO
225 Main Street, Newington, CT 06111-1494 USA
www.arrl.org

ISBN-13: 978-0-87259-987-1
ISBN-10: 0-87259-987-6
54495
EAN
9 780872 599871
ISBN 0-87259-987-6 Order No. 9876

The ARRL

Antenna Book

21st Edition

Editor
R. Dean Straw, N6BV

Contributing Editors
L. B. Cebik, W4RNL
Dave Hallidy, K2DH
Dick Jansson, WD4FAB
Roy Lewallen, W7EL
Rudy Severns, N6LF
Frank Witt, AI1H

Production
Michelle Bloom, WB1ENT
Sue Fagan, KB1OKW—Cover Art
Jodi Morin, KA1JPA
David Pingree, N1NAS
Kathy Ford

Software Beta Testers
Ahti Aintila, OH2RZ
Alan Bloom, N1AL
L. B. Cebik, W4RNL
Loney Duncan, WØGZV
Chuck Hutchinson, K8CH
Steve London, N2IC
Dan Maguire, AC6LA
Steve Miller, N8SM (SK)
Bob Neece, KØKR,
Danny Richardson, K6MHE
Rudy Severns, N6LF
Jim Tabor, KU5S
Bill Tippett, W4ZV
Don Toman, K2KQ
Pete Smith, N4ZR
Scott Tuthill, K7ZO
Frank Witt, AI1H.

The Covers:

Tower photo at sunset (front and back): Tower and beam at the station of Francisco R.F. Aragao, PT2TD, in Brasilia, Brazil.

Center image: Kurt Andress, K7NV, working on 40-meter Yagi at N6RO in Oakley, CA. Photo by Dean Straw, N6BV.

Upper right image: UHF antenna. Photo credit: ShutterStock.com.

Lower right image: Some of the members of the C5Z contest DXpedition near Banjul, The Gambia. Photo by Henryk Kotowski, SMØJHF.

ARRL The national association for AMATEUR RADIO
225 Main Street, Newington, CT 06111-1494 USA
www.arrl.org/

Contents

1 Safety First
2 Antenna Fundamentals
3 The Effects of Ground
4 Antenna Modeling & System Planning
5 Loop Antennas
6 Low-Frequency Antennas
7 Multiband Antennas
8 Multielement Arrays
9 Broadband Antenna Matching
10 Log Periodic Arrays
11 HF Yagi Arrays
12 Quad Arrays
13 Long-Wire and Traveling-Wave Antennas
14 Direction Finding Antennas
15 Portable Antennas
16 Mobile and Maritime Antennas

upfront.pmd 4 3/20/2007, 2:58 PM

17 Repeater Antenna Systems
18 VHF and UHF Antenna Systems
19 Antenna Systems for Space Communications
20 Antenna Materials and Accessories
21 Antenna Products Suppliers
22 Antenna Supports
23 Radio Wave Propagation
24 Transmission Lines
25 Coupling the Transmitter to the Line
26 Coupling the Line to the Antenna
27 Antenna and Transmission-Line Measurements
28 Smith Chart Calculations
A-1 Appendix
AB-1 Index of Advertisers
931 Index

upfront.pmd 5 3/20/2007, 2:58 PM

Schematic Symbols Used in Circuit Diagrams

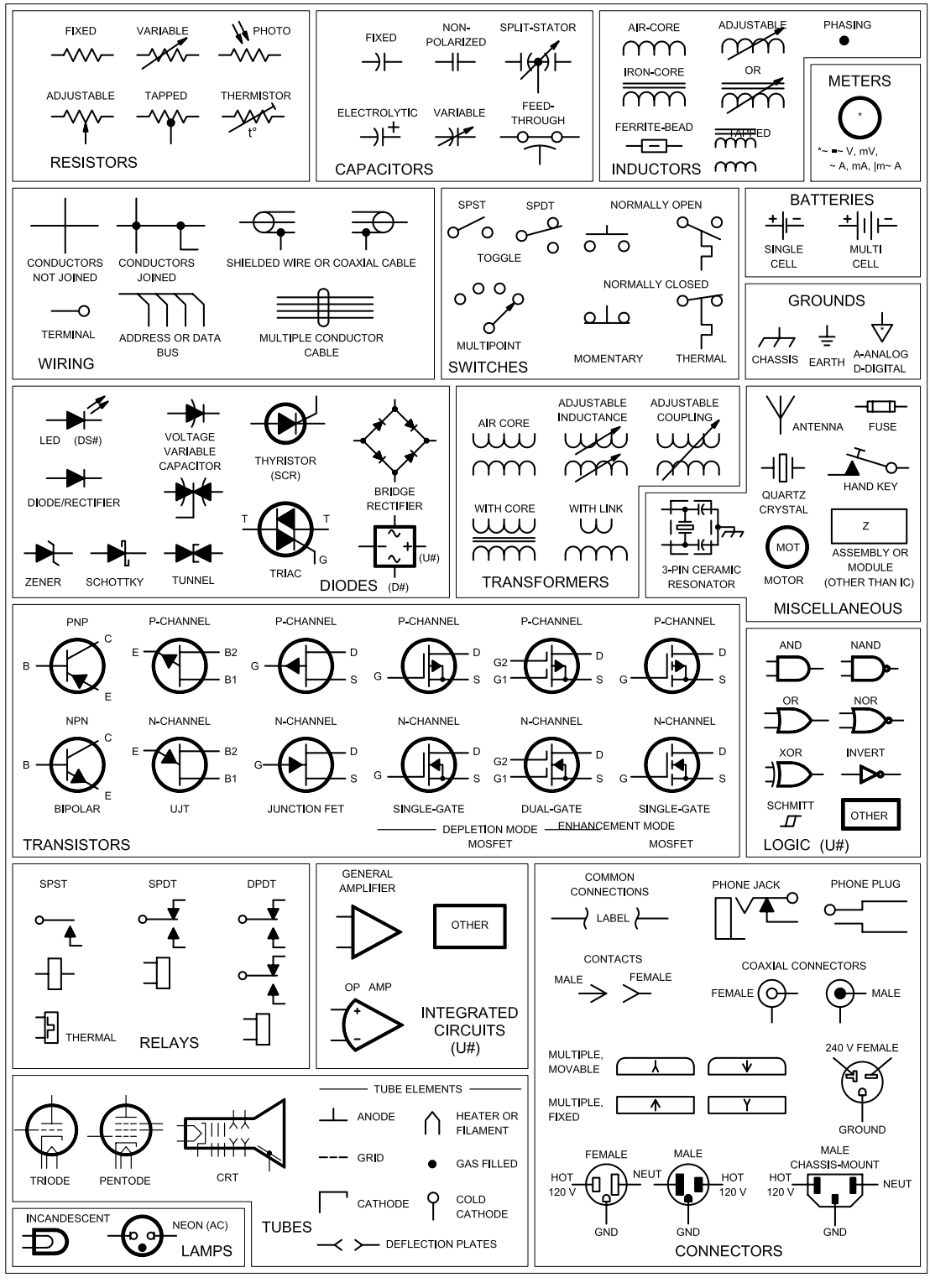

About the ARRL

The seed for Amateur Radio was planted in the 1890s, when Guglielmo Marconi began his experiments in wireless telegraphy. Soon he was joined by dozens, then hundreds, of others who were enthusiastic about sending and receiving messages through the air—some with a commercial interest, but others solely out of a love for this new communications medium. The United States government began licensing Amateur Radio operators in 1912.

By 1914, there were thousands of Amateur Radio operators—hams—in the United States. Hiram Percy Maxim, a leading Hartford, Connecticut inventor and industrialist, saw the need for an organization to band together this fledgling group of radio experimenters. In May 1914 he founded the American Radio Relay League (ARRL) to meet that need.

Today ARRL, with approximately 150,000 members, is the largest organization of radio amateurs in the United States. The ARRL is a not-for-profit organization that:

- promotes interest in Amateur Radio communications and experimentation
- represents US radio amateurs in legislative matters, and
- maintains fraternalism and a high standard of conduct among Amateur Radio operators.

At ARRL headquarters in the Hartford suburb of Newington, the staff helps serve the needs of members. ARRL is also International Secretariat for the International Amateur Radio Union, which is made up of similar societies in 150 countries around the world.

ARRL publishes the monthly journal *QST*, as well as newsletters and many publications covering all aspects of Amateur Radio. Its headquarters station, W1AW, transmits bulletins of interest to radio amateurs and Morse code practice sessions. The ARRL also coordinates an extensive field organization, which includes volunteers who provide technical information and other support services for radio amateurs as well as communications for public-service activities. In addition, ARRL represents US amateurs with the Federal Communications Commission and other government agencies in the US and abroad.

Membership in ARRL means much more than receiving *QST* each month. In addition to the services already described, ARRL offers membership services on a personal level, such as the ARRL Volunteer Examiner Coordinator Program and a QSL bureau.

Full ARRL membership (available only to licensed radio amateurs) gives you a voice in how the affairs of the organization are governed. ARRL policy is set by a Board of Directors (one from each of 15 Divisions). Each year, one-third of the ARRL Board of Directors stands for election by the full members they represent. The day-to-day operation of ARRL HQ is managed by a Chief Executive Officer.

No matter what aspect of Amateur Radio attracts you, ARRL membership is relevant and important. There would be no Amateur Radio as we know it today were it not for the ARRL. We would be happy to welcome you as a member! (An Amateur Radio license is not required for Associate Membership.) For more information about ARRL and answers to any questions you may have about Amateur Radio, write or call:

ARRL—The national association for Amateur Radio
225 Main Street
Newington CT 06111-1494
Voice: 860-594-0200
Fax: 860-594-0259
E-mail: **hq@arrl.org**
Internet: **www.arrl.org/**

Prospective new amateurs call (toll-free):
800-32-NEW HAM (800-326-3942)
You can also contact us via e-mail at **newham@arrl.org**
or check out *ARRLWeb* at **http://www.arrl.org/**

upfront.pmd 7 3/20/2007, 2:58 PM

Chapter 1

Safety First

Safety begins with your attitude. If you make it a habit to plan your work carefully and to consider the safety aspects of a project before you begin the work, you will be much safer than "Careless Carl," who just jumps in, proceeding in a haphazard manner. Learn to have a positive attitude about safety. Think about the dangers involved with a job before you begin the work. Don't be the one to say, "I didn't think it could happen to me."

Having a good attitude about safety isn't enough, however. You must be knowledgeable about common safety guidelines and follow them faithfully. Safety guidelines can't possibly cover all the situations you might face, but if you approach a task with a measure of "common sense," you should be able to work safely.

This chapter offers some safety guidelines and protective measures for you and your Amateur Radio station. You should not consider it to be an all-inclusive discussion of safety practices, though. Safety considerations will affect your choice of materials and assembly procedures when building an antenna. Other chapters of this book will offer further suggestions on safe construction practices. For example, Chapter 22 includes some very important advice on a tower installation.

PUTTING UP SIMPLE WIRE ANTENNAS

No matter what type of antenna you choose to erect, you should remember a few key points about safety. If you are using a slingshot or bow and arrow to get a line over a tree, make sure you keep everyone away from the "downrange" area. Hitting one of your helpers with a rock or fishing sinker is considered not nice, and could end up causing a serious injury.

Make sure the ends of the antenna are high enough to be out of reach of passers-by. Even when you are transmitting with low power there may be enough voltage at the ends of your antenna to give someone nasty "RF burns." If you have a vertical antenna with its base at ground level, build a wooden safety fence around it at least 4 feet away from it. Do not use metal fence, as this will interfere with the proper operation of the antenna. Be especially certain that your antenna is not close to any power wires. That is the only way you can be sure it won't come in contact with them!

Antenna work often requires that one person climb up on a tower, into a tree or onto the roof of a house. Never work alone! Work slowly, thinking out each move before you make it. The person on the ladder, tower, tree or rooftop should wear a safety belt, and keep it securely anchored. It is helpful (and safe!) to tie strings or lightweight ropes to all tools. If your tools are tied on, you'll save time getting them back if you drop them, and you'll greatly reduce the risk of injuring a helper on the ground. (There are more safety tips for climbing and working on towers later in this chapter. Those tips apply to any work that you must do above the ground to install even the simplest antenna.)

Tower Safety

Working on towers and antennas is dangerous, and possibly fatal, if you do not know what you are doing. Your tower and antenna can cause serious property damage and personal injury if any part of the installation should fail. Always use the highest quality materials in your system. Follow the manufacturer's specifications, paying close attention to base pier and guying details. Do not overload the tower. If you have any doubts about your ability to work on your tower and antennas safely, contact another amateur with experience in this area or seek professional assistance.

Chapter 22, Antenna Supports, provides more detailed guidelines for constructing a tower base and putting up a tower. It also explains how to properly attach guy wires and install guy anchors in the ground. These are extremely important parts of a tower installation, and

you should not take shortcuts or use second-rate materials. Otherwise the strength and safety of your entire antenna system may be compromised.

Any mechanical job is easier if you have the right tools. Tower work is no exception. In addition to a good assortment of wrenches, screwdrivers and pliers, you will need some specialized tools to work safely and efficiently on a tower. You may already own some of these tools. Others may be purchased or borrowed. Don't start a job until you have assembled all of the necessary tools. Shortcuts or improvised tools can be fatal if you gamble and lose at 70 feet in the air. The following sections describe in detail the tools you will need to work safely on a tower.

CLOTHING

The clothing you wear when working on towers and antennas should be selected for maximum comfort and safety. Wear clothing that will keep you warm, yet allow complete freedom of movement. Long denim pants and a long-sleeve shirt will protect you from scrapes and cuts. (A pull-on shirt, like a sweat shirt with no openings or buttons to snag on tower parts, is best.) Wear work shoes with heavy soles, or better yet, with steel shanks (steel inserts in the soles), to give your feet the support they need to stand on a narrow tower rung.

Gloves are necessary for both the tower climber and all ground-crew members. Good quality leather gloves will protect hands from injury and keep them warm. They also offer protection and a better grip when you are handling rope. In cooler weather, a pair of gloves with light insulation will help keep your hands warm. The insulation should not be so bulky as to inhibit movement, however.

Ground-crew members should have hard hats for protection in case something falls from the tower. It is not uncommon for the tower climber to drop tools and hardware. A wrench dropped from 100 feet will bury itself several inches in soft ground; imagine what it might do to an unprotected skull.

SAFETY BELT AND CLIMBING ACCESSORIES

Any amateur with a tower must own a high-quality safety belt, such as the one shown in **Fig 1**. *Do not attempt* to climb a tower, even a short distance, without a belt. The climbing belt is more than just a safety device for the experienced climber. It is a tool to free up both hands for work. The belt allows the climber to lean back away from the tower to reach bolts or connections. It also provides a solid surface to lean against to exert greater force when hoisting antennas into place.

A climber must trust his life to his safety belt. For this reason, nothing less than a professional quality, commercially made, tested and approved safety belt is acceptable. Check the suppliers' list in Chapter 21, Antenna Product Suppliers, and ads in *QST* for suppliers of climbing belts and accessories. Examine your belt for defects

Fig 1—Bill Lowry, W1VV, uses a good quality safety belt, a requirement for working on a tower. The belt should contain large steel loops for the strap snaps. Leather loops at the rear of the belt are handy for holding tools. (*Photo by K1WA*)

before each use. If the belt or lanyard (tower strap) are cracked, frayed or worn in any way, destroy the damaged piece and replace it with a new one. You should never have to wonder if your belt will hold.

Along with your climbing belt, you should seriously consider purchasing some climbing accessories. A canvas bucket is a great help for carrying tools and hardware up the tower. Two buckets, a large one for carrying tools and a smaller one for hardware, make it easier to find things when needed. A few extra snap hooks like those on the ends of your belt lanyard are useful for attaching tool bags and equipment to the tower at convenient spots. These hooks are better than using rope and tying knots because in many cases they can be hooked and unhooked with one hand.

Many hams use climbing belts such as shown in Fig 1. But fully integrated fall-arrest and positioning safety harnesses are preferable. The model ASL-301 in **Fig 2** has a D-ring on the back of the harness to which a safety lanyard is attached. These harnesses are available through Champion Radio Products, Box 572, Woodinville, WA 98072, **www.championradio.com**.

Rope and Pulley

Every amateur who owns a tower should also own a

Fig 2—Fall-arrest safety harness integrated with positioning safety belt for tower climbing. *(Courtesy of Champion Radio Products)*

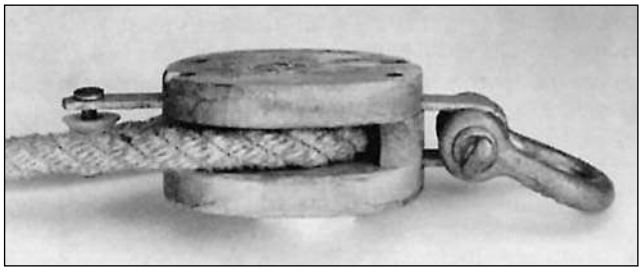

Fig 3—A good quality rope and pulley are essential for anyone working on towers and antennas. This pulley is encased in wood so the rope cannot jump out of the pulley wheel and jam.

good quality rope at least twice as long as the tower height. The rope is essential for safely erecting towers and installing antennas and cables. For most installations, a good quality 1/2-inch diameter manila hemp rope will do the job, although a thicker rope is stronger and may be easier to handle. Some types of polypropylene rope are acceptable also; check the manufacturer's strength ratings. Nylon rope is not recommended because it tends to stretch and cannot be securely knotted without difficulty.

Check your rope before each use for tearing or chafing. Do not attempt to use damaged rope; if it breaks with a tower section or antenna in mid-air, property damage and personal injury are likely results. If your rope should get wet, let it air dry thoroughly before putting it away.

Another very worthwhile purchase is a pulley like the one shown in **Fig 3**. Use the right size pulley for your rope. Be sure that the pulley you purchase will not jam or bind as the rope passes through it.

THE GIN POLE

A gin pole, like the one shown in **Fig 4**, is a handy device for working with tower sections and masts. This gin pole is designed to clamp onto one leg of Rohn No. 25 or 45 tower. The tubing, which is about 12 feet long,

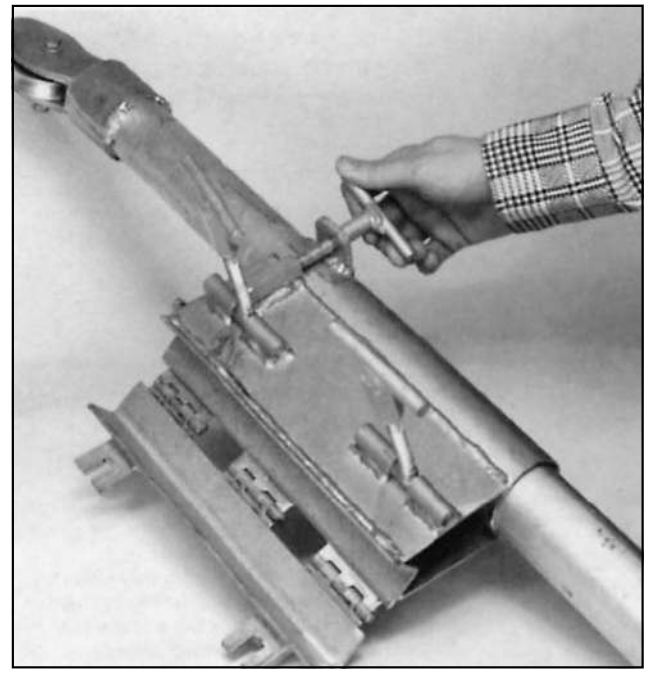

Fig 4—A gin pole is a mechanical device that can be clamped to a tower leg to aid in the assembly of sections as well as the installation of the mast. The aluminum tubing extends through the clamp and may be slipped into position before the tubing clamp is tightened. A rope should be routed through the tubing and over the pulley mounted at the top.

Fig 5—The assembly of tower sections is made simple when a gin pole is used to lift each one into position. Note that the safety belts of both climbers are fastened below the pole, thereby preventing the strap from slipping over the top section. (*Photo by K1WA*)

has a pulley on one end. The rope is routed through the tubing and over the pulley. When the gin pole is attached to the tower and the tubing extended into place, the rope may be used to haul tower sections or the mast into place. **Fig 5** shows the basic process. A gin pole can be expensive for an individual to buy, especially for a one-time tower installation. Some radio clubs own a gin pole for use by their members. Stores that sell tower sections to amateurs and commercial customers frequently will rent a gin pole to erect the tower. If you attempt to make your own gin pole, use materials heavy enough for the job. Provide a means for securely clamping the pole to the tower. There are many cases on record where homemade gin poles have failed, sending tower sections crashing down amidst the ground crew.

When you use a gin pole, make every effort to keep the load as vertical as possible. Although gin poles are strong, you are asking for trouble if you apply too much lateral force.

INSTALLING ANTENNAS ON THE TOWER

All antenna installations are different in some respects. Therefore, thorough planning is the most important first step in installing any antenna. At the beginning, before anyone climbs the tower, the whole process should be thought through. The procedure should be discussed to be sure each crew member understands what is to be done. Plan how to work out all bugs. Consider what tools and parts must be assembled and what items must be taken up the tower. Extra trips up and down the tower can be avoided by using forethought.

Getting ready to raise a beam requires planning. Done properly, the actual work of getting the antenna into position can be accomplished quite easily with only one person at the top of the tower. The trick is to let the ground crew do all the work and leave the person on the tower free to guide the antenna into position.

Before the antenna can be hoisted into position, the tower and the area around it must be prepared. The ground crew should clear the area around the base while someone climbs the tower to remove any wire antennas or other objects that might get in the way. The first person to climb the tower should also rig the rope and pulley that will be used to raise the antenna. The time to prepare the tower is before the antenna leaves the ground, not after it becomes hopelessly entwined with your 3.5-MHz dipole.

SOME TOWER CLIMBING TIPS

The following tower climbing safety tips were compiled by Tom Willeford, N8ETU. The most important safety factor in any kind of hazardous endeavor is the right attitude. Safety is important and worthy of careful consideration and implementation. The right attitude toward safety is a requirement for tower climbers. Lip service won't do, however; safety must be practiced.

The safe ham's safety attitude is simple: *Don't take any unnecessary chances*. There are no exceptions to this plain and simple rule. It is the first rule of safety and, of course, of climbing. The second rule is equally simple: *Don't be afraid to terminate an activity* (climbing, in this case) at any time if things don't seem to be going well.

Take time to plan your climb; this time is never wasted, and it's the first building block of safety. Talk the climb over with friends who will be helping you. Select the date and alternative dates to do the work. Choose someone to be responsible for all activities on the ground and for all communication with the climbers. Study the structure to be climbed and choose the best route to your objective. Plan emergency ascent and descent paths and methods.

Make a list of emergency phone numbers to keep by your phone, even though they may never be used. Develop a plan for rescuing climbers from the structure, should that become necessary.

Give careful thought to how much time you will need to complete the project. Allow enough time to go up, do the work, and then climb down during daylight hours. Include time for resting during the climb and for completing the work in a quality fashion. Remember that the

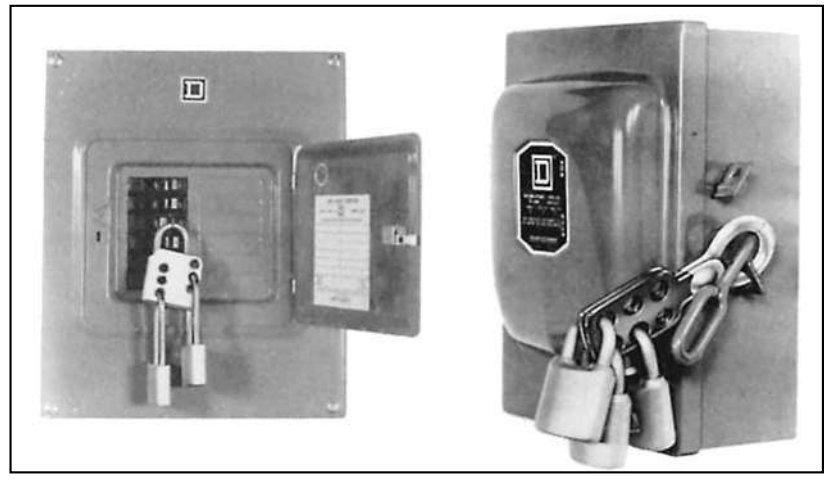

Fig 6—If the switch box feeding power to equipment on your tower is equipped with a lock-out hole, use it. With a lock through the hole on the box, the power cannot be accidentally turned back on. (*Photos courtesy of American ED CO®, at left, and Osborn Mfg Corp, at right.*)

temperature changes fast as the sun goes down. Climbing up or down a tower with cold hands and feet is very difficult—and dangerous.

Give careful consideration to the weather, and climb only in good weather. Investigate wind conditions, the temperature, and the weather forecast. The weather can change quickly, so if you're climbing a really tall tower, it may be a good idea to have a weather alert radio handy during the climb. *Never* climb a wet tower.

The person who is going to do the climbing should be the one to disconnect and tag all sources of power to the structure. All switches or circuit breakers should be labeled clearly with DO NOT TOUCH instructions. Use locks on any switches designed to accept them. (See **Fig 6**.) Only the climber should reconnect power sources.

An important part of the climbing plan is to review notes on the present installation and any previous work. It's a good idea to keep a notebook, listing every bolt and nut size on your tower/antenna installation. Then, when you have to go up to make repairs, you'll be able to take the minimum number of tools with you to do the job. If you take too many tools up the tower, there is a much greater chance of dropping something, risking injury to the ground crew and possibly damaging the tool.

It is also a good idea to review the instruction sheets and take them with you. In other words, plan carefully what you are going to do, and what you'll need to do it efficiently and safely.

It's better to use a rope and pulley to hoist tools. Climbing is hard work and there's no sense making it more difficult by carrying a big load of tools. Always rig the pulley and rope so the ground crew raises and lowers tools and equipment.

Climbing Equipment

Equipment is another important safety consideration. By equipment, we don't just mean tools. We mean safety equipment. Safety equipment should be selected and cared for as if your life depends on it—because it does!

The list of safety equipment essential to a safe climb and safe work on the tower should include:

1) A first class safety belt,
2) Safety glasses,
3) Hard hat,
4) Long-sleeved, pull-over shirt with no buttons or openings to snag (long sleeves are especially important for climbing wooden poles),
5) Long pants without cuffs,
6) Firm, comfortable, steel-shank shoes with no-slip soles and well-defined heels, and
7) Gloves that won't restrict finger movement (insulated gloves if you MUST work in cold weather).

Your safety belt should be approved for use on the structure you are climbing. Different structures may require different types of safety hooks or straps. The belt should be light weight, but strength should not be sacrificed to save weight. It should fit you comfortably. All moving parts, such as snap hooks, should work freely. You should inspect safety belts and harnesses carefully and thoroughly before each climb, paying particular attention to stitching, rivets and weight-bearing mechanical parts.

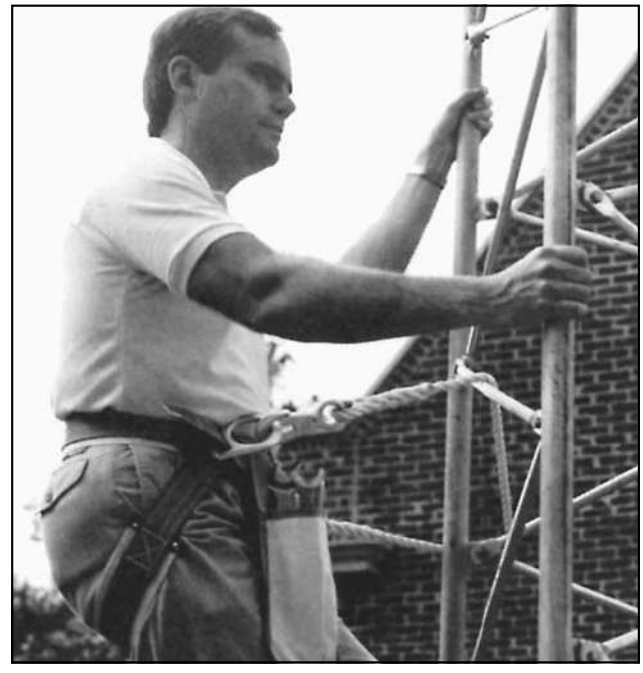

Fig 7—Mark Wilson, K1RO, shows the proper way to attach a safety hook, with the hook opening facing away from the tower. That way the hook can't be accidentally released by pressing it against a tower leg.

Support belt hooks should always be hooked to the D rings in an outward configuration. That is, the opening part of the hook should face away from the tower when engaged in the D rings (see **Fig 7**). Hooks engaged this way are easier to unhook deliberately but won't get squeezed open by a part of the tower or engage and snag a part of the tower while you are climbing. The engagement of these hooks should always be checked visually. A snapping hook makes the same sound whether it's engaged or not. Never check by sound—look to be sure the hook is engaged properly before trusting it.

Remember that the D rings on the safety belt are for support hooks *only*. No tools or lines should be attached to these hooks. Such tools or lines may prevent the proper engagement of support belt hooks, or they may foul the hooks. At best, they could prevent the release of the hooks in an emergency. No one should have to disconnect a support hook to get a tool and then have to reconnect the support hook before beginning to work again. That's foolish.

Equipment you purchase new is best. Homemade belts or home-spliced lines are dangerous. Used belts may have worn or defective stitching, or other faulty components. Be careful of so-called "bargains" that could cost you your life.

Straps, lanyards and lines should be as short as possible. Remember, in general knots reduce the load strength of a line by approximately 50%.

Before actually climbing, check the structure visually. Review the route. Check for obstacles, both natural (like wasp's nests) and man-made. Check the structure supports and add more if necessary. Guy wires can be obstacles to the climb, but it's better to have too many supports than not enough. Check your safety belt, support belts and hooks at the base of the tower. Really test them before you need them. Never leave the ground without a safety belt—even 5 or 10 feet. After all of this, the climb will be a "cake walk" if you are careful.

Climb slowly and surely. Don't overreach or overstep. Patience and watchfulness is rewarded with good hand and foot holds. Take a lesson from rock climbers. Hook on to the tower and rest periodically during the climb. Don't try to rest by wedging an arm or leg in some joint; to rest, hook on. Rests provide an opportunity to review the remainder of the route and to make sure that your safety equipment feels good and is working properly. Rest periods also help you conserve a margin of energy in case of difficulty.

Finally, keep in mind that the most dangerous part of working on a tower occurs when you are actually climbing. Your safety equipment is not hooked up at this time, so be extra careful during the ascent or descent.

You must climb the tower to install or work on an antenna. Nevertheless, any work that can be done on the ground should be done there. If you can do any assembly or make any adjustments on the ground, that's where you should do the work! The less time you have to spend on the tower, the better off you'll be.

When you arrive at the work area, hook on to the tower and review what you have to do. Determine the best position to do the work from, disconnect your safety strap and move to that position. Then reconnect your safety strap at a safe spot, away from joints and other obstacles. If you must move around an obstacle, try to do it while hooked on to the tower. Find a comfortable position and go to work. Don't overreach—move to the work.

Use the right tool for the task. If you don't have it, have the ground crew haul it up. Be patient. Lower tools, don't drop them, when you are finished with them. Dropped tools can bounce and cause injury or damage, or can be broken or lost. It's a good idea to tie a piece of string or light rope to the tools, and to tie the other end to the tower or some other point so if you do drop a tool, it won't fall all the way to the ground. Don't tie tools to the D ring or your safely belt, however!

Beware of situations where an antenna may be off balance. It's hard to obtain the extra leverage needed to handle even a small beam when you are holding it far from the balance point. Leverage can apply to the climber as well as the device being levered. Many slips and skinned knuckles result from such situations. A severely injured hand or finger can be a real problem to a climber.

Before descending, be sure to check all connections and the tightness of all the bolts and nuts that you have worked with. Have the ground crew use the rope and pulley to lower your tools. Lighten your load as much as possible. Remember, you're more tired coming down than going up. While still hooked on, wiggle your toes and move a little to get your senses working again. Check your downward route and begin to descend slowly and even more surely than you went up. Rest is even more important during the descent.

The ground captain is the director of all activities on the ground, and should be the only one to communicate with a person on a tower. Hand-held transceivers can be very helpful for this communication, but no one else should transmit to the workers on the tower. Even minor confusion or misunderstanding about a move to be made could be very dangerous.

"Antenna parties" can be lots of fun, but the joking and fooling around should wait until the job is done and everyone is down safely. Save the celebrating until after the work is completed, even for the ground crew.

These are just a few ideas on tower climbing safety; no list can include everything that you might run into. Check Chapter 22 for additional ideas. *Just remember—you can't be too careful when climbing*. Keep safety in mind while doing antenna work, and help ensure that after you have fallen *for* ham radio, you don't fall *from* ham radio.

THE TOWER SHIELD

A tower can be legally classified as an "attractive nuisance" that could cause injuries. You should take some precautions to ensure that "unauthorized climbers" can't get hurt on your tower. This tower shield was originally described by Baker Springfield, W4HYY, and Richard Ely, WA4VHM, in September 1976 *QST*, and should eliminate the worry.

Generally, the attractive-nuisance doctrine applies to your responsibility to trespassers on your property. (The law is much stricter with regard to your responsibility to an invited guest.) You should expect your tower to attract children, whether they are already technically trespassing

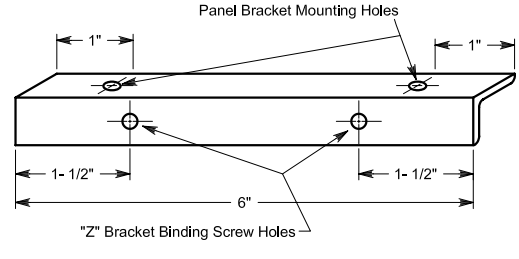

Fig 8—Z-bracket component pieces.

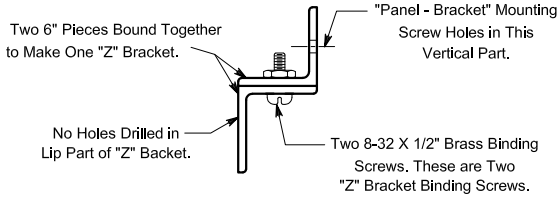

Fig 9—Assembly of the Z bracket.

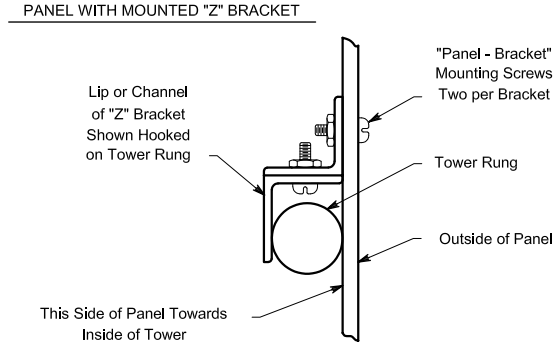

Fig 10—Installation of the shield on a tower rung.

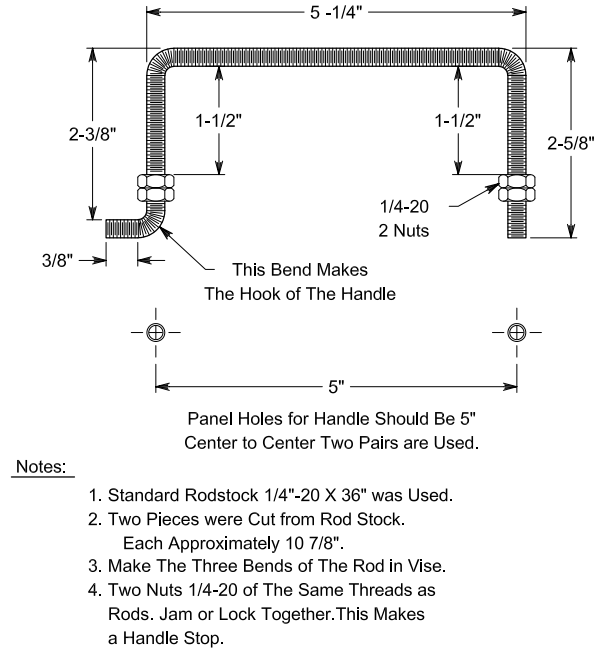

Fig 11—Removable handle construction.

or whether the tower itself lures them onto your property. A tower is dangerous to children, especially because of their inability to appreciate danger. (What child could resist trying to climb a tower once they see one?) Because of this danger, you have a legal duty to exercise reasonable care to eliminate the danger or otherwise protect children against the perils of the attraction.

The tower shield is composed simply of panels that enclose the tower and make climbing practically impossible. These panels are 5 feet in height and are wide enough to fit snugly between the tower legs and flat against the rungs. A height of 5 feet is sufficient in almost every case. The panels are constructed from 18-gauge galvanized sheet metal obtained and cut to proper dimensions from a local sheet-metal shop. A lighter gauge could probably be used, but the extra physical weight of the heavier gauge is an advantage if no additional means of securing the panels to the tower rungs are used. The three types of metals used for the components of the shield are supposedly rust proof and nonreactive. The panels are galvanized sheet steel, the brackets aluminum, and the screws and nuts are brass. For a triangular tower, the shield consists of three panels, one for each of the three sides, supported by two brackets. Construct these brackets from 6-inch pieces of thin aluminum angle stock. Bolt two of the pieces together to form a Z bracket (see **Figs 8**, **9** and **10**). The Z brackets are bolted together with binding head brass machine screws.

Lay the panels flat for measuring, marking and drilling. First measure from the top of the upper mounting rung on the tower to the top of the bottom rung. (Mounting rungs are selected to position the panel on the tower.) Then mark this distance on the panels. Use the same size brass screws and nuts throughout the shield. Bolt the top vertical portion of each Z bracket to the panel. Drill the mounting-screw holes about 1 inch from the end of the Z

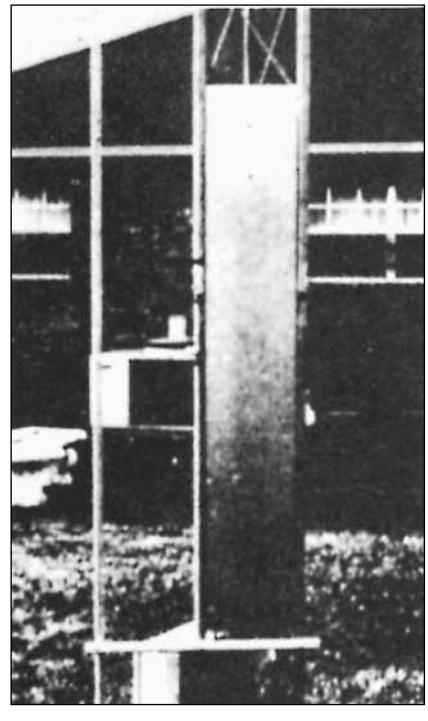

Fig 12—Installed tower shield. Note the holes for using the handles.

brackets so there is an offset clearance between the Z-bracket binding-screw holes and the panel-bracket mounting-screw holes. Drill holes in each panel to match the Z-bracket holes.

The panels are held on the tower by their own weight. They are not easy to grasp because they fit snugly between the tower legs. If you feel a need for added safety against deliberate removal of the panels, this can be accomplished by means of tie wires. Drill a small hole in the panel just above, just below, and in the center of each Z bracket. Run a piece of heavy galvanized wire through the top hole, around the Z bracket, and then back through the hole just below the Z bracket. Twist together the two ends of the wire. One tie wire should be sufficient for each panel, but use two if desired.

The completed panels are rather bulky and difficult to handle. A feature that is useful if the panels have to be removed often for tower climbing or accessibility is a pair of removable handles. The removable handles can be constructed from one threaded rod and eight nuts (see **Fig 11**). Drill two pair of handle holes in the panels a few inches below the top Z bracket and several inches above the bottom Z bracket. For panel placement or removal, you can hook the handles in these panel holes. The hook, on the top of the handle, fits into the top hole of each pair of the handle holes. The handle is optional, but for the effort required it certainly makes removal and replacement much safer and easier.

Fig 12 shows the shield installed on a tower. This relatively simple device could prevent an accident.

Electrical Safety

Although the RF, ac and dc voltages in most amateur stations pose a potentially grave threat to life and limb, common sense and knowledge of safety practices will help you avoid accidents. Building and operating an Amateur Radio station can be, and is for almost all amateurs, a perfectly safe pastime. However, carelessness can lead to severe injury, or even death. The ideas presented here are only guidelines; it would be impossible to cover all safety precautions. Remember, there is no substitute for common sense.

A fire extinguisher is a requirement for the well-equipped amateur station. The fire extinguisher should be of the carbon-dioxide type to be effective in electrical fires. Store it in an easy-to-reach spot and check it at recommended intervals.

Family members should know how to turn the power off in your station. They should also know how to apply artificial respiration. Many community groups offer courses on cardiopulmonary resuscitation (CPR).

AC AND DC SAFETY

The primary wiring for your station should be controlled by one master switch, and other members of your household should know how to kill the power in an emergency. All equipment should be connected to a good ground. All wires carrying power around the station should be of the proper size for the current to be drawn and should be insulated for the voltage level involved. Bare wire, open-chassis construction and exposed connections are an invitation to accidents. Remember that high-current, low-voltage power sources are just as dangerous as high-voltage, low-current sources. Possibly the most-dangerous voltage source in your station is the 120-V primary supply; it is a hazard often overlooked because it is a part of everyday life. Respect even the lowliest power supply in your station.

Whenever possible, kill the power and unplug equipment before working on it. Discharge capacitors with an insulated screwdriver; don't assume the bleeder resistors are 100% reliable. In a power amplifier, always short the tube plate cap to ground just to be sure the supply is discharged. If you must work on live equipment, keep one hand in your pocket. Avoid bodily contact with any grounded object to prevent your body from becoming the return path from a voltage source to ground. Use insulated tools for adjusting or moving any circuitry. Never work alone. Have someone else present; it could save your life in an emergency.

National Electrical Code

The National Electrical Code® is a comprehensive document that details safety requirements for all types of electrical installations. In addition to setting safety standards for house wiring and grounding, the Code also contains a section on Radio and Television Equipment — Article 810. Sections C and D specifically cover Amateur Transmitting and Receiving Stations. Highlights of the section concerning Amateur Radio stations follow. If you are interested in learning more about electrical safety, you may purchase a copy of *The National Electrical Code* or *The National Electrical Code Handbook*, edited by Peter Schram, from the National Fire Protection Association, Batterymarch Park, Quincy, MA 02269.

Antenna installations are covered in some detail in the Code. It specifies minimum conductor sizes for different length wire antennas. For hard-drawn copper wire, the Code specifies #14 wire for open (unsupported) spans less than 150 feet, and #10 for longer spans. Copper-clad

steel, bronze or other high-strength conductors may be #14 for spans less than 150 feet and #12 wire for longer runs. Lead-in conductors (for open-wire transmission line) should be at least as large as those specified for antennas.

The Code also says that antenna and lead-in conductors attached to buildings must be firmly mounted at least 3 inches clear of the surface of the building on nonabsorbent insulators. The only exception to this minimum distance is when the lead-in conductors are enclosed in a "permanently and effectively grounded" metallic shield. The exception covers coaxial cable.

According to the Code, lead-in conductors (except those covered by the exception) must enter a building through a rigid, noncombustible, nonabsorbent insulating tube or bushing, through an opening provided for the purpose that provides a clearance of at least 2 inches or through a drilled window pane. All lead-in conductors to transmitting equipment must be arranged so that accidental contact is difficult.

Transmitting stations are required to have a means of draining static charges from the antenna system. An antenna discharge unit (lightning arrester) must be installed on each lead-in conductor (except where the lead-in is protected by a continuous metallic shield that is permanently and effectively grounded, or the antenna is permanently and effectively grounded). An acceptable alternative to lightning arrester installation is a switch that connects the lead-in to ground when the transmitter is not in use.

Grounding conductors are described in detail in the Code. Grounding conductors may be made from copper, aluminum, copper-clad steel, bronze or similar erosion-resistant material. Insulation is not required. The "protective grounding conductor" (main conductor running to the ground rod) must be as large as the antenna lead-in, but not smaller than #10. The "operating grounding conductor" (to bond equipment chassis together) must be at least #14. Grounding conductors must be adequately supported and arranged so they are not easily damaged. They must run in as straight a line as practical between the mast or discharge unit and the ground rod.

The Code also includes some information on safety inside the station. All conductors inside the building must be at least 4 inches away from conductors of any lighting or signaling circuit except when they are separated from other conductors by conduit or a nonconducting material. Transmitters must be enclosed in metal cabinets, and the cabinets must be grounded. All metal handles and controls accessible by the operator must be grounded. Access doors must be fitted with interlocks that will disconnect all potentials above 350 V when the door is opened.

Ground

An effective ground system is necessary for every amateur station. The mission of the ground system is twofold. First, it reduces the possibility of electrical shock if something in a piece of equipment should fail and the chassis or cabinet becomes "hot." If connected properly, three-wire electrical systems ground the chassis, but older amateur equipment may use the ungrounded two-wire system. A ground system to prevent shock hazards is generally referred to as "dc ground."

The second job the ground system must perform is to provide a low-impedance path to ground for any stray RF current inside the station. Stray RF can cause equipment to malfunction and contributes to RFI problems. This low-impedance path is usually called "RF ground." In most stations, dc ground and RF ground are provided by the same system.

The first step in building a ground system is to bond together the chassis of all equipment in your station. Ordinary hookup wire will do for a dc ground, but for a good RF ground you need a low-impedance conductor. Copper strap, sold as "flashing copper," is excellent for this application, but it may be hard to find. Braid from coaxial cable is a popular choice; it is readily available, makes a low-impedance conductor, and is flexible.

Grounding straps can be run from equipment chassis to equipment chassis, but a more convenient approach is illustrated in **Fig 13**. In this installation, a $^1/_2$-inch diameter copper water pipe runs the entire length of the operating bench. A thick braid (from discarded RG-8 cable) runs from each piece of equipment to a clamp on the pipe. Copper water pipe is available at most hardware stores and home centers. Alternatively, a strip of flashing copper may be run along the rear of the operating bench.

After the equipment is bonded to a common ground bus, the ground bus must be wired to a good earth ground. This run should be made with a heavy conductor (braid is a popular choice, again) and should be as short and direct as possible. The earth ground usually takes one of two forms.

In most cases, the best approach is to drive one or more ground rods into the earth at the point where the conductor from the station ground bus leaves the house. The best ground rods to use are those available from an electrical supply house. These rods are 8 to 10 feet long and are made from steel with a heavy copper plating. Do not depend on shorter, thinly plated rods sold by some home electronics suppliers. These rods begin to rust almost immediately after they are driven into the soil, and they become worthless within a short time. Good ground rods, while more expensive initially, offer long-term protection.

If your soil is soft and contains few rocks, an acceptable alternative to "genuine" ground rods is $^1/_2$-inch diameter copper water pipe. A 6- to 8-foot length of this material offers a good ground, but it may bend while being driven into the earth. Some people have recommended that you make a connection to a water line and run water down through the copper pipe so that it forces its own

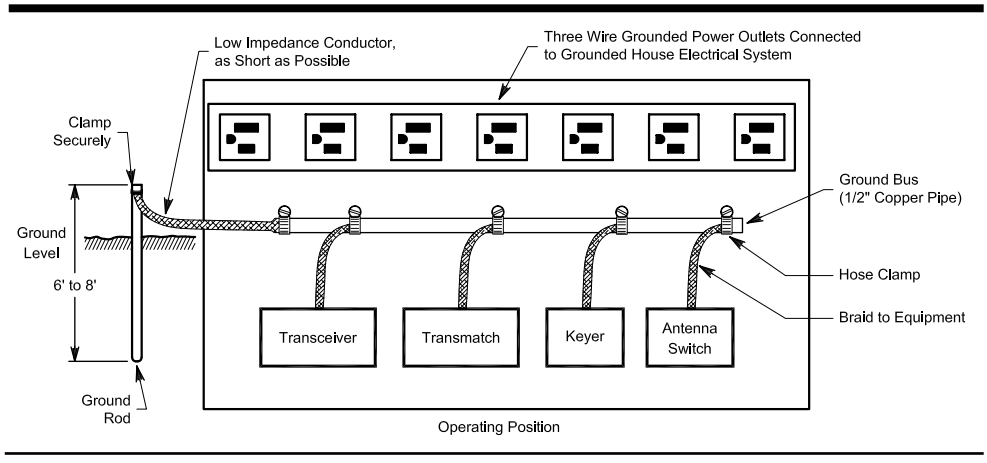

Fig 13—An effective station ground bonds the chassis of all equipment together with low-impedance conductors and ties into a good earth ground.

hole in the ground. There may be a problem with this method, however. When the ground dries, it may shrink away from the pipe and not make proper contact with the ground rod. This would provide a rather poor ground.

Once the ground rod is installed, clamp the conductor from the station ground bus to it with a clamp that can be tightened securely and will not rust. Copper-plated clamps made especially for this purpose are available from electrical supply houses, but a stainless-steel hose clamp will work too. Alternatively, drill several holes through the pipe and bolt the conductor in place.

Another popular station ground is the cold water pipe system in the building. To take advantage of this ready-made ground system, run a low-impedance conductor from the station ground bus to a convenient cold water pipe, preferably somewhere near the point where the main water supply enters the house. Avoid hot water pipes; they do not run directly into the earth. The advent of PVC (plastic) plumbing makes it mandatory to inspect the cold water system from your intended ground connection to the main inlet. PVC is an excellent insulator, so any PVC pipe or fittings rule out your cold water system for use as a station ground.

For some installations, especially those located above the first floor, a conventional ground system such as that just described will make a fine dc ground but will not provide the necessary low-impedance path to ground for RF. The length of the conductor between the ground bus and the ultimate ground point becomes a problem. For example, the ground wire may be about $^1/_4$ λ (or an odd multiple of $^1/_4$ λ) long on some amateur band. A $^1/_4$-λ wire acts as an impedance inverter from one end to the other. Since the grounded end is at a very low impedance, the equipment end will be at a high impedance. The likely result is RF hot spots around the station while the transmitter is operating. A ground system like this may be worse than having no ground at all.

An alternative RF ground system is shown in **Fig 14**. Connect a system of $^1/_4$-λ radials to the station ground bus. Install at least one radial for each band used. You

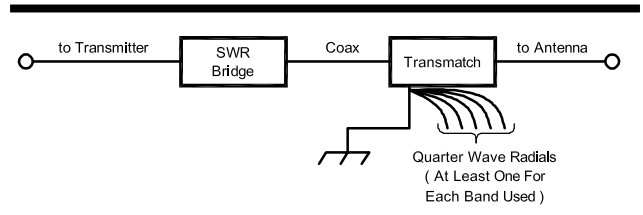

Fig 14—Here is an alternative to earth ground if the station is located far from the ground point and RF in the station is a problem. Install at least one $^1/_4$-λ radial for each band used.

should still be sure to make a connection to earth ground for the ac power wiring. Try this system if you have problems with RF in the shack. It may just solve a number of problems for you. Be careful, however, to prevent contact with the ends of the radials, where there is high-voltage RF for powers greater than QRP level.

Ground Noise

Noise in ground systems can affect sensitive radio equipment. It is usually related to one of three problems:

1) Insufficient ground conductor size,
2) Loose ground connections, or
3) Ground loops.

These matters are treated in precise scientific research equipment and some industrial instruments by paying attention to certain rules. The ground conductor should be at least as large as the largest conductor in the primary power circuit. Ground conductors should provide a solid connection to both ground and to the equipment being grounded. Liberal use of lock washers and star washers is highly recommended. A loose ground connection is a tremendous source of noise, particularly in a sensitive receiving system.

Ground loops should be avoided at all costs. A short discussion of what a ground loop is and how to avoid them may lead you down the proper path. A ground loop

is formed when more than one ground current is flowing in a single conductor. This commonly occurs when grounds are "daisy-chained" (series linked). The correct way to ground equipment is to bring all ground conductors out radially from a common point to either a good driven earth ground or to a cold water system.

Ground noise can affect transmitted as well as received signals. With the low audio levels required to drive amateur transmitters, and with the ever-increasing sensitivity of our receivers, correct grounding is critical.

Lightning and EMP Protection

The National Fire Protection Association (NFPA) publishes a booklet called *Lightning Protection Code* (NFPA no. 78-1983) that should be of interest to radio amateurs. For information about obtaining a copy of this booklet, write to the National Fire Protection Association, Batterymarch Park, Quincy, MA 02269. Two paragraphs of particular interest to amateurs are presented below:

"3-26 Antennas. Radio and television masts of metal, located on a protected building, shall be bonded to the lightning protection system with a main size conductor and fittings.

"3-27 Lightning arresters, protectors or antenna discharge units shall be installed on electric and telephone service entrances and on radio and television antenna lead-ins."

The best protection from lightning is to disconnect all antennas from equipment and disconnect the equipment from the power lines. Ground antenna feed lines to safely bleed off static buildup. Eliminate the possible paths for lightning strokes. Rotator cables and other control cables from the antenna location should also be disconnected during severe electrical storms.

In some areas, the probability of lightning surges entering homes via the 120/240-V line may be high. Lightning produces both electrical and magnetic fields that vary with distance. These fields can be coupled into power lines and destroy electronic components in equipment that is miles from where the lightning occurred. Radio equipment can be protected from these surges to some extent by using transient-protective devices.

ELECTROMAGMETIC PULSE AND THE RADIO AMATEUR

The following material is based on a 4-part *QST* article by Dennis Bodson, W4PWF, that appeared in the August through November 1986 issues of *QST*. The series was condensed from the National Communications System report NCS TIB 85-10.

An equipment test program demonstrated that most Amateur Radio installations can be protected from lightning and electromagnetic pulse (EMP) transients with a basic protection scheme. Most of the equipment is not susceptible to damage when all external cabling is removed. You can duplicate this stand-alone configuration simply by unplugging the ac power cord from the outlet, disconnecting the antenna feed line at the rear of the radio, and isolating the radio gear from any other long metal conductors. Often it is not practical to completely disconnect the equipment whenever it is not being used. Also, there is the danger that a lightning strike several miles away could induce a large voltage transient on the power lines or antenna while the radio is in use. You can add two transient-protection devices to the interconnected system, however, that will also closely duplicate the safety of the stand-alone configuration.

The ac power line and antenna feed line are the two important points that should be outfitted with transient protection. This is the minimum basic protection scheme recommended for all Amateur Radio installations. (For fixed installations, consideration should also be given to the rotator connections—see **Fig 15**.) Hand-held radios equipped with a "rubber duck" require no protection at the antenna jack. If a larger antenna is used with the hand-held, however, a protection device should be installed.

General Considerations

Because of the unpredictable energy content of a nearby lightning strike or other large transient, it is possible for a metal-oxide varistor (MOV) to be subjected to an energy surge in excess of its rated capabilities. This may result in the destruction of the MOV and explosive rupture of the package. These fragments can cause damage to nearby components or operators and possibly ignite flammable material. Therefore, the MOV should be physically shielded.

A proper ground system is a key factor in achieving protection from lightning and EMP transients. A low-impedance ground system should be installed to eliminate transient paths through radio equipment and to provide a good physical ground for the transient-suppression devices. A single-point ground system is recommended (**Fig 16**) to help prevent lightning from getting into the shack on the shields of antenna feed-line coaxes. Many hams use a well-grounded radio-entrance panel mounted *outside* the shack to ground their coaxes before they enter the house. **Fig 17** shows an entrance panel at K8CH's home in Michigan. All external conductors going to the radio equipment should enter and exit the station through this panel. Install all transient-suppression devices directly on the panel. Use

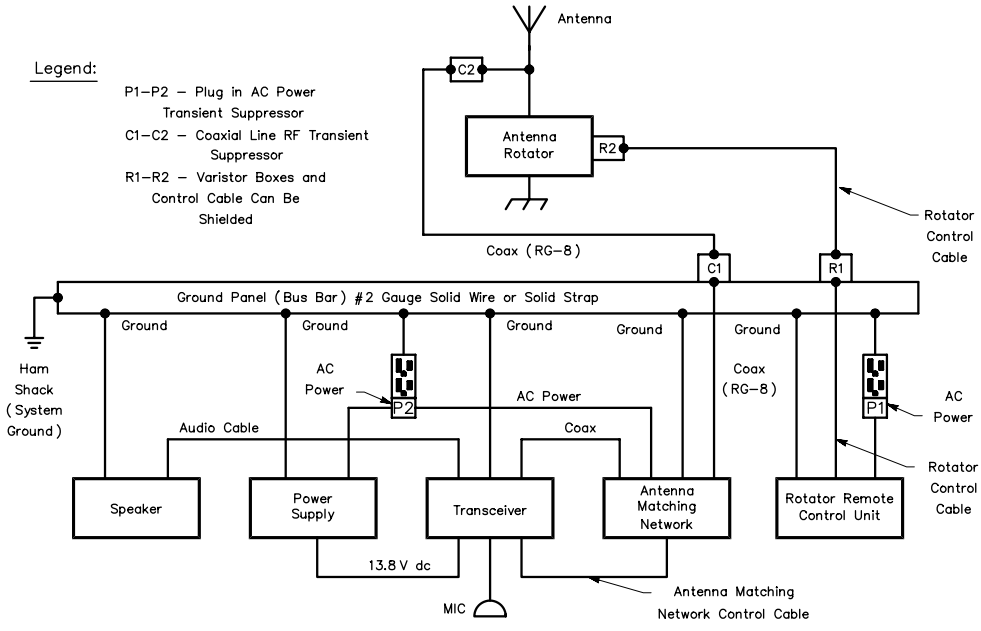

Fig 15—Transient suppression techniques applied to an Amateur Radio station.

the shortest length(s) possible of #6 solid wire to connect the radio equipment case(s) to the ground bus.

Ac Power-Line Protection

Tests have indicated that household electrical wiring inherently limits the maximum transient current that it will pass to approximately 120 A. Therefore, if possible, the amateur station should be installed away from the house ac entrance panel and breaker box to take advantage of these limiting effects.

Ac power-line protection can be provided with easy-to-install, plug-in transient protectors. Ten such devices were tested for the article series in 1986. The plug-in-strip units are the best overall choice for a typical amateur installation. They provide the protection needed, they're simple to install and can be easily moved to other operating locations with the equipment.

In their tests, NCS found that the model that provided transient paths to ground from the hot and neutral lines (common mode) as well as the transient path between the hot and neutral lines (normal mode) performed best. The best model used three MOVs and a 3-electrode gas-discharge-tube arrester to provide fast operation and large power dissipation capabilities. This unit was tested repeatedly and operated without failure.

The flood of low-cost computers in the 1990s spawned a host of surge protection devices designed to limit transient voltage spikes coming from the ac line and also through the telephone line into a modem connected to a computer. Many of these devices are well-designed and can be relied upon to provide the protection they claim.

You can, however, easily find a variety of really low-cost bargain strips at flea markets and discount hardware stores. A bargain-brand $6 unit may prove to be a poor bargain indeed if it allows a spike to get through to damage your $2000 computer or $4000 transceiver.

You should be careful to find one that carries a sticker indicating that it meets Underwriters Laboratories safety standard UL 1449. This defines the minimum level of clamping voltage beyond which a surge protector will "fire" to protect the device connected to its output. The UL 1149 limit is 330 V ac. Prices for brand-name units from Tripp Lite, APC or Curtis vary from about $30 to $80, depending on how many ac sockets they have and the number of indicator lights and switched/unswitched sockets. A brand-name device is well worth the small additional cost over the bargain-basement units.

A transient suppressor requires a 3-wire outlet; the outlet should be tested to ensure all wires are properly connected. In older houses, an ac ground may have to be installed by a qualified electrician. The ac ground must be available for the plug-in transient suppressor to function properly. The ac ground of the receptacle should be attached to the station ground bus, and the plug-in receptacle should be installed on the ground panel behind the radio equipment.

Emergency Power Generators

Emergency power generators provide two major transient-protection advantages. First, the station is disconnected from the commercial ac power system. This isolates the radio equipment from a major source of damaging transients. Second, tests have shown that the emergency power generator may not be susceptible to EMP transients.

When the radio equipment is plugged directly into the generator outlets, transient protection may not be

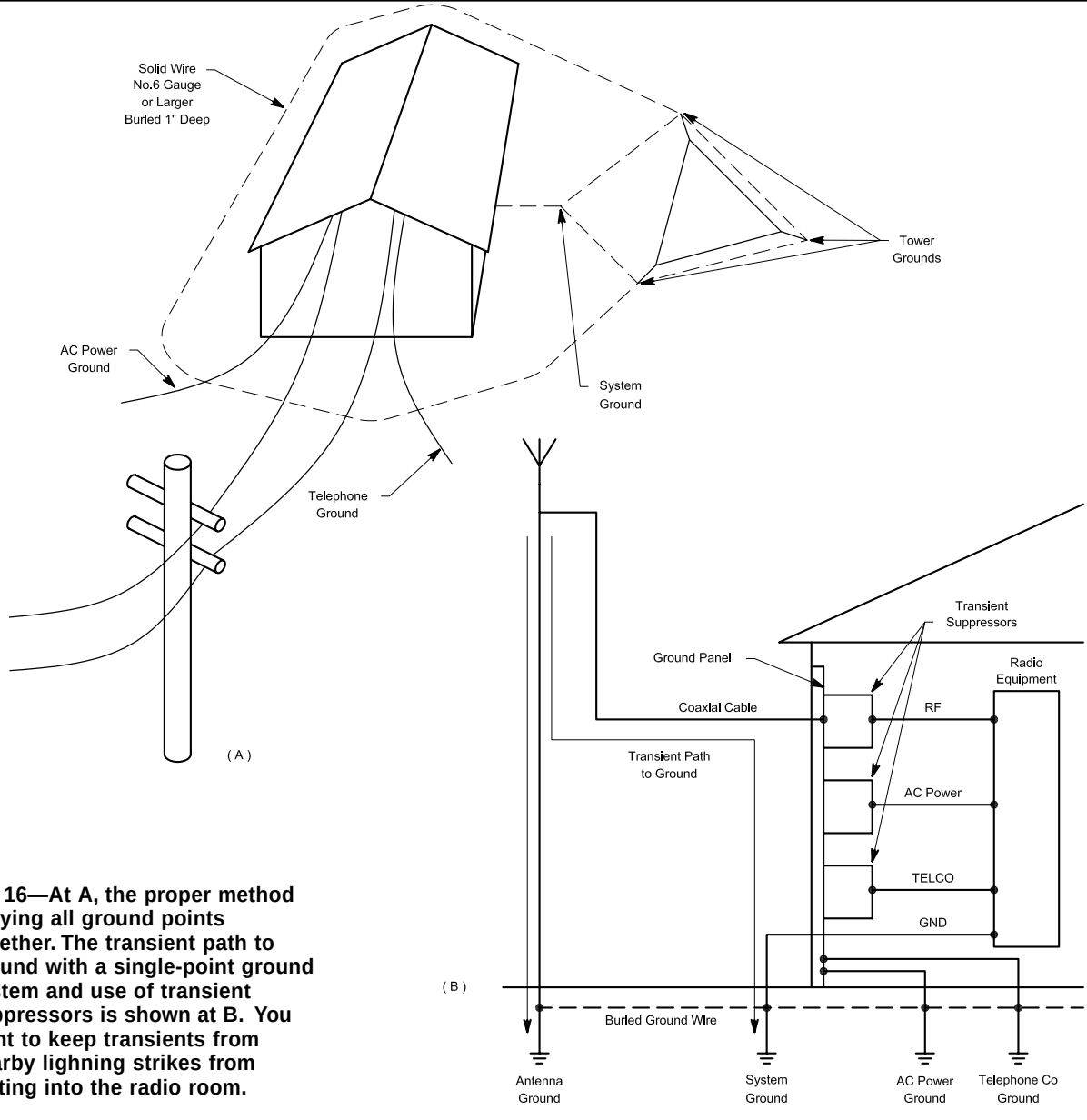

Fig 16—At A, the proper method of tying all ground points together. The transient path to ground with a single-point ground system and use of transient suppressors is shown at B. You want to keep transients from nearby lighning strikes from getting into the radio room.

needed. If an extension cord or household wiring is used, transient protection should be employed.

An emergency power generator should be wired into the household circuit only by a qualified electrician. When properly connected, a switch is used to disconnect the commercial ac power source from the house lines before the generator is connected to them. This keeps the generator output from feeding back into the commercial power system. If this is not done, death or injury to unsuspecting linemen can result.

Feed-Line Protection

Coaxial cable is recommended for use as the transmission line because it provides a certain amount of transient surge protection for the equipment to which it is attached. The outer conductor shields the center conductor from the transient field. Also, the cable limits the maximum conducted transient voltage on the center by arcing the differential voltage from the center conductor to the grounded cable shield.

By providing a path to ground ahead of the radio equipment, the gear can be protected from the large currents impressed upon the antenna system by lightning and EMP. A single protection device installed at the radio antenna jack will protect the radio, but not the transmission line. To protect the transmission line, another tran-

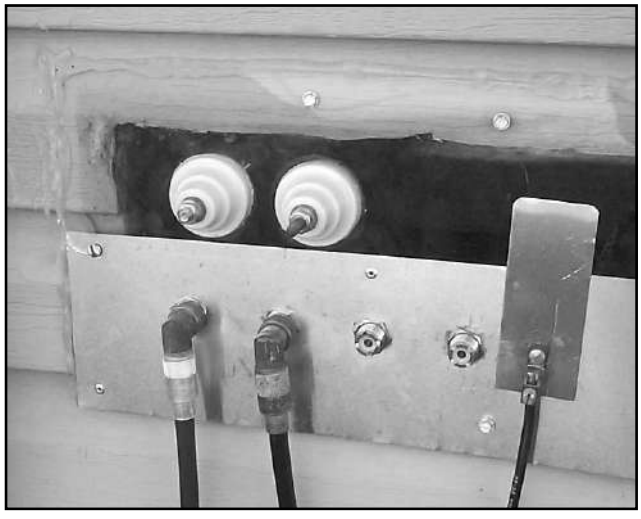

Fig 17—Radio-entrance panel at K8CH. A flat aluminum plate serves as a common grounding point for all coax cables to prevent transients from nearby lightning strikes from getting into the shack on the feed lines. "Spark-gap" protectors to kill transients on the coax inner conductors are located behind the panel. A spark-gap protector is also used on the two open-wire feeder insulators mounted on the Plexiglas sheet behind the aluminum panel.

Table 1
RF Coaxial-Line Protectors

Manufacturer	*Device*	*Approximate Cost (US Dollars)*	*Measured High-Z Clamping Voltage (Volts)*
Fischer	FCC-250-300-UHF	55	393
Fischer	FCC-250-350-UHF	55	260
Fischer	FCC-250-150-UHF	55	220
Fischer	FCC-250-120-UHF	55	240
Fischer	FCC-450-120-UHF	55	120
Polyphaser	IS-NEMP	83	140
Polyphaser	IS-NEMP-1	83	150
Polyphaser	IS-NEMP-2	83	160

Note: The transmitter output power, frequency of operation, and transmission line SWR must be considered when selecting any of these devices.

sient protector must be installed between the antenna and the transmission line. (See Fig 15).

RF transient protection devices from several manufacturers were tested (see **Table 1**) using RG-8 cable equipped with UHF connectors. All of the devices shown can be installed in a coaxial transmission line. Recall that during the tests the RG-8 cable acted like a suppressor; damaging EMP energy arced from the center conductor to the cable shield when the voltage level approached 5.5 kV.

Low price and a low clamping-voltage rating must be considered in the selection of an RF transient-protection device. The lower cost devices have the higher clamping voltages, however, and the higher-cost devices have the lower clamping voltages. Because of this, medium-priced devices manufactured by Fischer Custom Communications were selected for testing. The Fischer Spikeguard Suppressors ($55 price class) for coaxial lines can be made to order to operate at a specific clamping voltage. The Fischer devices satisfactorily suppressed the damaging transient pulses, passed the transmitter RF output power without interfering with the signal, and operated effectively over a wide frequency range.

Polyphaser Corporation devices are also effective in providing the necessary transient protection. The devices available limited the transmitter RF output power to 100 W or less, however. These units cost approximately $83 each.

RF coaxial protectors should be mounted on the station ground bus bar. If the Fischer device is used, it should be attached to a grounded UHF receptacle that will serve as a hold-down bracket. This creates a conductive path between the outer shield of the protector and the bus bar. The Polyphaser device can be mounted directly to the bus bar with the bracket provided.

Attach the transceiver or antenna matching network to the grounded protector with a short (6 foot or less) piece of coaxial cable. Although the cable provides a ground path to the bus bar from the radio equipment, it is not a satisfactory transient-protection ground path for the transceiver. Another ground should be installed between the transceiver case and the ground bus using solid #6 wire. The coaxial cable shield should be grounded to the antenna tower leg at the tower base. Each tower leg should have an earth ground connection and be connected to the single-point ground system as shown in Fig 16.

Antenna Rotators

Antenna rotators can be protected by plugging the control box into a protected ac power source and adding protection to the control lines to the antenna rotator. When the control lines are in a shielded cable, the shield must be grounded at both ends. MOVs of the proper size should be installed at both ends of the control cable. At the station end, terminate the control cable in a small metal box that is connected to the station ground bus. Attach MOVs from each conductor to ground inside the box. At the antenna end of the control cable, place the MOVs inside the rotator case or in a small metal box that is properly grounded.

For example, the Alliance HD73 antenna rotator uses a 6-conductor unshielded control cable with a maximum control voltage of 24.7 V dc. Select an MOV with a clamping voltage level 10% higher (27 V or more) so the MOV won't clamp the control signal to ground. If the control voltage is ac, be sure to convert the RMS voltage value to peak voltage when considering the clamping voltage level.

Mobile Power Supply Protection

The mobile amateur station environment exposes radio equipment to other transient hazards in addition to those of lightning and EMP. Currents as high as 300 A are switched when starting the engine, and this can produce voltage spikes of over 200 V on the vehicle's electrical system. Lightning and EMP are not likely to impact the vehicle's electrical system as much as they would that of a fixed installation because the automobile chassis is not normally grounded. This would not be the case if the vehicle is inadvertently grounded; for example, when the vehicle is parked against a grounded metal conductor. The mobile radio system has two advantages over a fixed installation: Lightning is almost never a problem, and the vehicle battery is a natural surge suppressor.

Mobile radio equipment should be installed in a way that takes advantage of the protection provided by the battery. See **Fig 18**. To do this, connect the positive power lead of the radio directly to the positive battery post, not to intermediate points in the electrical system such as the fuse box or the auxiliary contacts on the ignition switch. To prevent equipment damage or fire, in-line fuses should be installed in the positive lead where they are attached to the battery post.

An MOV should be installed between the two leads of the equipment power cord. A GE MOV (V36ZA80) is recommended for this application. This MOV provides the lowest measured clamping voltage (170 V) and is low in cost.

Mobile Antenna Installation

Although tests indicate that mobile radios can survive an EMP transient without protection for the antenna system, protection from lightning transients is still required. A coaxial-line transient suppressor should be installed on the vehicle chassis between the antenna and the radio's antenna connector.

A Fischer suppressor can be attached to a UHF receptacle that is mounted on, and grounded to, the vehicle chassis. The Polyphaser protector can be mounted on, and grounded to, the vehicle chassis with its flange. Use a short length of coaxial cable between the radio and the transient suppressor.

Clamping Voltage Calculation

When selecting any EMP-protection device to be used at the antenna port of a radio, several items must be considered. These include transmitter RF power output, the SWR, and the operating frequency. The protection device must allow the outgoing RF signal to pass without clamping. A clamping voltage calculation must be made for each amateur installation.

The RF-power input to a transmission line develops a corresponding voltage that becomes important when a voltage-surge arrester is in the line. SWR is important because of its influence on the voltage level. The maximum voltage developed for a given power input is determined by:

$$V = \sqrt{2 \times P \times Z \times SWR} \qquad \text{(Eq 1)}$$

where

P = peak power in W
Z = impedance of the coaxial cable (Ω)
V = peak voltage across the cable

Eq 1 should be used to determine the peak voltage present across the transmission line. Because the RF transient-protection devices use gas-discharge tubes, the voltage level at which they clamp is not fixed; a safety margin must be added to the calculated peak voltage. This is done

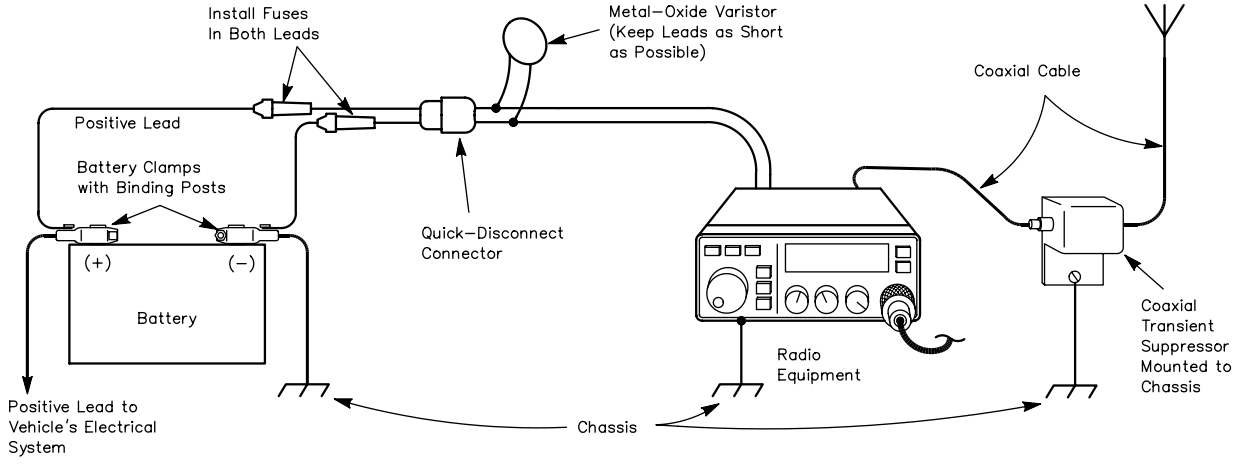

Fig 18—Recommended method of connecting mobile radio equipment to the vehicle battery and antenna.

by multiplying the calculated value by a factor of three. This added safety margin is required to ensure that the transmitter's RF output power will pass through the transient suppressor without causing the device to clamp the RF signal to ground. The final clamping voltage obtained is then high enough to allow normal operation of the transmitter while providing the lowest practical clamping voltage for the suppression device. This ensures the maximum possible protection for the radio system.

Here's how to determine the clamping voltage required. Let's assume the SWR is 1.5:1. The power output of the transceiver is 100 W PEP. RG/8 coaxial cable has an impedance of 52 Ω. Therefore:

P = 100 W
Z = 52 Ω
SWR = 1.5

Substituting these values into Eq 1:

$$V = \sqrt{2 \times 100 \times 52 \times 1.5} = 124.89 \text{ V peak}$$

Note that the voltage, V, is the peak value at the peak of the RF envelope. The final clamping voltage (FCV) is three times this value, or 374.7 V. Therefore, a coaxial-line transient suppressor that clamps at or above 375 V should be used.

The cost of a two-point basic protection scheme is estimated to be $100 for each fixed amateur station. This includes the cost of a good quality plug-in power-line protector ($45) and one Fischer coaxial-line protector ($55).

Inexpensive Transient-Protection Devices

Here are two low-cost protection devices you can assemble. They performed flawlessly in the tests.

The radio antenna connection can be protected by means of another simple device. As shown in **Fig 19**, two spark gaps (Siemens BI-A350) are installed in series at one end of a coaxial-cable T connector. Use the shortest practical lead length (about 1/4 inch) between the two spark gaps. One lead is bent forward and forced between the split sections of the inner coaxial connector until the spark gaps approach the body of the connector. A short length of insulating material (such as Mylar) is placed between the spark gaps and the connector shell. The other spark-gap lead is folded over the insulator, then conductive (metallic) tape is wrapped around the assembly. This construction method proved durable enough to allow many insertions and removals of the device during testing. Estimated cost of this assembly is $9. Similar devices can be built using components from Joslyn, General Electric, General Semiconductor or Siemens.

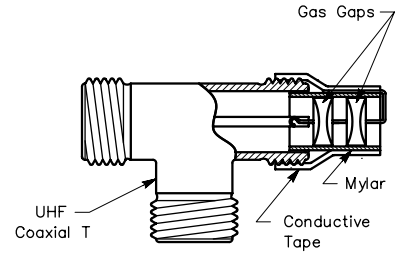

Fig 19—Pictorial diagram of an inexpensive, homemade RF coax transient protector.

Summary

Amateurs should be aware of which components in their radio system are most likely to be damaged by EMP. They should also know how to repair the damaged equipment. Amateurs should know how to reestablish communications after an EMP event, taking into consideration its adverse effects on the earth's atmosphere and radio equipment. One of the first things that would be noticed, providing the radio equipment is operative, is a sudden silence in radio transmissions across all frequencies below approximately 100 MHz. This silence would be caused in part by damage to unprotected radio gear from the EMP transient. Transmissions from one direction, the direction of the nuclear blast, would be completely out. RF signal loss by absorption and attenuation by the nuclear fireball are the reasons for this.

After an EMP event, the amateur should be prepared to operate CW. CW gives the most signal power under adverse conditions. It also provides a degree of message security from the general public.

Amateurs should develop the capability and flexibility to operate in more than one frequency band. The lower ground-wave frequencies should be useful for long-distance communications immediately after an EMP event. Line-of-sight VHF would be of value for local communications.

What can be done to increase the survivability of an Amateur Radio station? Here are some suggestions:

1) If you have spare equipment, keep it disconnected; use only the primary station gear. The spare equipment would then be available after an EMP event.
2) Keep equipment turned off and antenna and power lines disconnected when the equipment is not in use.
3) Connect only those external conductors necessary for the current mode of operation.
4) Tie all fixed equipment to a single-point earth ground to prevent closed loops through the ground.
5) Obtain schematic diagrams of your equipment and tools for repair of the equipment.
6) Have spare parts on hand for sensitive components of the radio equipment and antenna system.
7) Learn how to repair or replace the sensitive components of the radio equipment.
8) Use nonmetallic guy lines and antenna structural parts where possible.
9) Obtain an emergency power source and operate from

it during periods of increased world political tension. The power source should be completely isolated from the commercial power lines.

10) Equipment power cords should be disconnected when the gear is idle. Or the circuit breaker for the line feeding the equipment should be kept in the OFF position when the station is off the air.
11) Disconnect the antenna lead-in when the station is off the air. Or use a grounding antenna switch and keep it in the GROUND position when the equipment is not in use.
12) Have a spare antenna and transmission line on hand to replace a damaged antenna system.
13) Install EMP surge arresters and filters on all primary conductors attached to the equipment and antenna.
14) Retain tube type equipment and spare components; keep them in good working order.
15) Do not rely on a microprocessor to control the station after an EMP event. Be able to operate without microprocessor control.

The recommendations contained in this section were developed with low cost in mind; they are not intended to cover all possible combinations of equipment and installation methods found in the amateur community. Amateurs should examine their own requirements and use this report as a guideline in providing protection for the equipment.

RF Radiation and Electromagnetic Field Safety

Amateur Radio is basically a safe activity. In recent years, however, there has been considerable discussion and concern about the possible hazards of electromagnetic radiation (EMR), including both RF energy and power-frequency (50-60 Hz) electromagnetic (EM) fields. FCC regulations set limits on the maximum permissible exposure (MPE) allowed from the operation of radio transmitters. These regulations do not take the place of RF-safety practices, however. This section deals with the topic of RF safety.

This section was prepared by members of the ARRL RF Safety Committee and coordinated by Dr Robert E. Gold, WBØKIZ. It summarizes what is now known and offers safety precautions based on the research to date.

All life on Earth has adapted to survive in an environment of weak, natural, low-frequency electromagnetic fields (in addition to the Earth's static geomagnetic field). Natural low-frequency EM fields come from two main sources: the sun, and thunderstorm activity. But in the last 100 years, man-made fields at much higher intensities and with a very different spectral distribution have altered this natural EM background in ways that are not yet fully understood. Researchers continue to look at the effects of RF exposure over a wide range of frequencies and levels.

Both RF and 60-Hz fields are classified as *nonionizing radiation*, because the frequency is too low for there to be enough photon energy to ionize atoms. (*Ionizing radiation*, such as X-rays, gamma rays and even some ultraviolet radiation has enough energy to knock electrons loose from their atoms. When this happens, positive and negative ions are formed.) Still, at sufficiently high power densities, EMR poses certain health hazards. It has been known since the early days of radio that RF energy can cause injuries by heating body tissue. (Anyone who has ever touched an improperly grounded radio chassis or energized antenna and received an *RF burn* will agree that this type of injury can be quite painful.) In extreme cases, RF-induced heating in the eye can result in cataract formation, and can even cause blindness. Excessive RF heating of the reproductive organs can cause sterility. Other health problems also can result from RF heating. These heat-related health hazards are called *thermal effects*. A microwave oven is a positive application of this thermal effect.

There also have been observations of changes in physiological function in the presence of RF energy levels that are too low to cause heating. These functions return to normal when the field is removed. Although research is ongoing, no harmful health consequences have been linked to these changes.

In addition to the ongoing research, much else has been done to address this issue. For example, FCC regulations set limits on exposure from radio transmitters. The Institute of Electrical and Electronics Engineers, the American National Standards Institute and the National Council for Radiation Protection and Measurement, among others, have recommended voluntary guidelines to limit human exposure to RF energy. The ARRL has established the RF Safety Committee, consisting of concerned medical doctors and scientists, serving voluntarily to monitor scientific research in the fields and to recommend safe practices for radio amateurs.

THERMAL EFFECTS OF RF ENERGY

Body tissues that are subjected to *very high* levels of RF energy may suffer serious heat damage. These effects depend on the frequency of the energy, the power density of the RF field that strikes the body and factors such as the polarization of the wave.

At frequencies near the body's natural resonant frequency, RF energy is absorbed more efficiently, and an increase in heating occurs. In adults, this frequency usually is about 35 MHz if the person is grounded, and about 70 MHz if insulated from the ground. Individual body parts may be resonant at different frequencies. The adult head, for example, is resonant around 400 MHz, while a baby's smaller head resonates near 700 MHz. Body size thus determines the frequency at which most RF energy is absorbed. As the frequency is moved farther from resonance, less RF heating generally occurs. *Specific absorption rate (SAR)* is a term that describes the rate at which RF energy is absorbed in tissue.

Maximum permissible exposure (MPE) limits are based on whole-body SAR values, with additional safety factors included as part of the standards and regulations. This helps explain why these safe exposure limits vary with frequency. The MPE limits define the maximum electric and magnetic field strengths or the plane-wave equivalent power densities associated with these fields, that a person may be exposed to without harmful effect—and with an acceptable safety factor. The regulations assume that a person exposed to a specified (safe) MPE level also will experience a safe SAR.

Nevertheless, thermal effects of RF energy should not be a major concern for most radio amateurs, because of the power levels we normally use and the intermittent nature of most amateur transmissions. Amateurs spend more time listening than transmitting, and many amateur transmissions such as CW and SSB use low-duty-cycle modes. (With FM or RTTY, though, the RF is present continuously at its maximum level during each transmission.) In any event, it is rare for radio amateurs to be subjected to RF fields strong enough to produce thermal effects, unless they are close to an energized antenna or un- shielded power amplifier. Specific suggestions for avoiding excessive exposure are offered later in this chapter.

ATHERMAL EFFECTS OF EMR

Research about possible health effects resulting from exposure to the lower level energy fields, the athermal effects, has been of two basic types: epidemiological research and laboratory research.

Scientists conduct laboratory research into biological mechanisms by which EMR may affect animals including humans. Epidemiologists look at the health patterns of large groups of people using statistical methods. These epidemiological studies have been inconclusive. By their basic design, these studies do not demonstrate cause and effect, nor do they postulate mechanisms of disease. Instead, epidemiologists look for associations between an environmental factor and an observed pattern of illness. For example, in the earliest research on malaria, epidemiologists observed the association between populations with high prevalence of the disease and the proximity of mosquito infested swamplands. It was left to the biological and medical scientists to isolate the organism causing malaria in the blood of those with the disease, and identify the same organisms in the mosquito population.

In the case of athermal effects, some studies have identified a weak association between exposure to EMF at home or at work and various malignant conditions including leukemia and brain cancer. A larger number of equally well designed and performed studies, however, have found no association. A risk ratio of between 1.5 and 2.0 has been observed in positive studies (the number of observed cases of malignancy being 1.5 to 2.0 times the "expected" number in the population). Epidemiologists generally regard a risk ratio of 4.0 or greater to be indicative of a strong association between the cause and effect under study. For example, men who smoke one pack of cigarettes per day increase their risk for lung cancer tenfold compared to nonsmokers, and two packs per day increases the risk to more than 25 times the nonsmokers' risk.

Epidemiological research by itself is rarely conclusive, however. Epidemiology only identifies health patterns in groups—it does not ordinarily determine their cause. And there are often confounding factors: Most of us are exposed to many different environmental hazards that may affect our health in various ways. Moreover, not all studies of persons likely to be exposed to high levels of EMR have yielded the same results.

There also has been considerable laboratory research about the biological effects of EMR in recent years. For example, some separate studies have indicated that even fairly low levels of EMR might alter the human body's circadian rhythms, affect the manner in which T lymphocytes function in the immune system and alter the nature of the electrical and chemical signals communicated through the cell membrane and between cells, among other things. Although these studies are intriguing, they do not demonstrate any effect of these low-level fields on the overall organism.

Much of this research has focused on low-frequency magnetic fields, or on RF fields that are keyed, pulsed or modulated at a low audio frequency (often below 100 Hz). Several studies suggested that humans and animals can adapt to the presence of a steady RF carrier more readily than to an intermittent, keyed or modulated energy source.

The results of studies in this area, plus speculations concerning the effect of various types of modulation, were and have remained somewhat controversial. None of the research to date has demonstrated that low-level EMR causes adverse health effects.

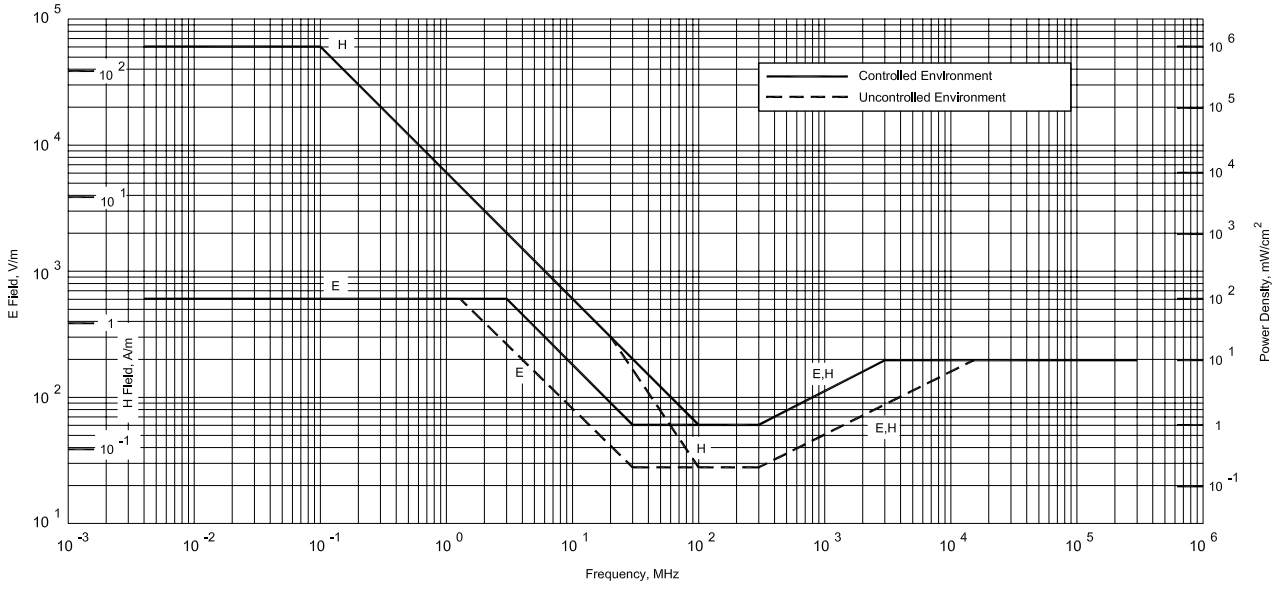

Fig 20—1991 RF protection guidelines for body exposure of humans. It is known officially as the "IEEE Standard for Safety Levels with Respect to Human Exposure to Radio Frequency Electromagnetic Fields, 3 kHz to 300 GHz."

Given the fact that there is a great deal of ongoing research to examine the health consequences of exposure to EMF, the American Physical Society (a national group of highly respected scientists) issued a statement in May 1995 based on its review of available data pertaining to the possible connections of cancer to 60-Hz EMF exposure. This report is exhaustive and should be reviewed by anyone with a serious interest in the field. Among its general conclusions were the following:

1. The scientific literature and the reports of reviews by other panels show no consistent, significant link between cancer and power line fields.
2. No plausible biophysical mechanisms for the systematic initiation or promotion of cancer by these extremely weak 60-Hz fields has been identified.
3. While it is impossible to prove that no deleterious health effects occur from exposure to any environmental factor, it is necessary to demonstrate a consistent, significant, and causal relationship before one can conclude that such effects do occur.

In a report dated October 31, 1996, a committee of the National Research Council of the National Academy of Sciences has concluded that no clear, convincing evidence exists to show that residential exposures to electric and magnetic fields (EMFs) are a threat to human health.

A National Cancer Institute epidemiological study of residential exposure to magnetic fields and acute lymphoblastic leukemia in children was published in the *New England Journal of Medicine* in July 1997. The exhaustive, seven-year study concludes that if there is any link at all, it is far too weak to be concerned about.

Readers may want to follow this topic as further studies are reported. Amateurs should be aware that exposure to RF and ELF (60 Hz) electromagnetic fields at all power levels and frequencies has not been fully studied under all circumstances. "Prudent avoidance" of any avoidable EMR is always a good idea. Prudent avoidance doesn't mean that amateurs should be fearful of using their equipment. Most amateur operations are well within the MPE limits. If any risk does exist, it will almost surely fall well down on the list of causes that may be harmful to your health (on the other end of the list from your automobile). It does mean, however, that hams should be aware of the potential for exposure from their stations, and take whatever reasonable steps they can take to minimize their own exposure and the exposure of those around them.

Safe Exposure Levels

How much EM energy is safe? Scientists and regulators have devoted a great deal of effort to deciding upon safe RF-exposure limits. This is a very complex problem, involving difficult public health and economic considerations. The recommended safe levels have been revised downward several times over the years —and not all scientific bodies agree on this question even today. An Institute of Electrical and Electronics Engineers (IEEE) standard for recommended EM exposure limits was published in 1991 (see Bibliography). It replaced a 1982 American National Standards Institute (ANSI) standard. In the new standard, most of the permitted exposure levels were revised downward (made more stringent), to better reflect the current research. The new IEEE stan-

FCC RF-Exposure Regulations

FCC regulations control the amount of RF exposure that can result from your station's operation (§§97.13, 97.503, 1.1307 (b)(c)(d), 1.1310 and 2.1093). The regulations set limits on the maximum permissible exposure (MPE) allowed from operation of transmitters in all radio services. They also require that certain types of stations be evaluated to determine if they are in compliance with the MPEs specified in the rules. The FCC has also required that five questions on RF environmental safety practices be added to Novice, Technician and General license examinations.

These rules went into effect on January 1, 1998 for new stations or stations that file a Form 605 application with the FCC. Other existing stations have until September 1, 2000 to be in compliance with the rules.

The Rules

Maximum Permissible Exposure (MPE)

All radio stations regulated by the FCC must comply with the requirements for MPEs, even QRP stations running only a few watts or less. The MPEs vary with frequency, as shown in **Table A**. MPE limits are specified in maximum electric and magnetic fields for frequencies below 30 MHz, in power density for frequencies above 300 MHz and all three ways for frequencies from 30 to 300 MHz. For compliance purposes, all of these limits must be considered *separately*. If any one is exceeded, the station is not in compliance.

The regulations control human exposure to RF fields, not the strength of RF fields. There is no limit to how strong a field can be as long as no one is being exposed to it, although FCC regulations require that amateurs use the minimum necessary power at all times (§97.311 [a]).

Environments

The FCC has defined two exposure environments — *controlled* and *uncontrolled*. A controlled environment is one in which the people who are being exposed are aware of that exposure and can take steps to minimize that exposure, if appropriate. In an uncontrolled environment, the people being exposed are not normally aware of the exposure. The uncontrolled environment limits are more stringent than the controlled environment limits.

Although the controlled environment is usually intended as an occupational environment, the FCC has determined that it generally applies to amateur operators and members of their immediate households. In most cases, controlled-environment limits can be applied to your home and property to which you can control physical access. The uncontrolled environment is intended for areas that are accessible by the general public, such as your neighbors' properties.

The MPE levels are based on average exposure. An averaging time of 6 minutes is used for controlled exposure; an averaging period of 30 minutes is used for uncontrolled exposure.

Table A—(From §1.1310) Limits for Maximum Permissible Exposure (MPE)

(A) Limits for Occupational/Controlled Exposure

Frequency Range (MHz)	*Electric Field Strength (V/m)*	*Magnetic Field Strength (A/m)*	*Power Density (mW/cm^2)*	*Averaging Time (minutes)*
0.3-3.0	614	1.63	(100)*	6
3.0-30	1842/f	4.89/f	($900/f^2$)*	6
30-300	61.4	0.163	1.0	6
300-1500	—	—	f/300	6
1500-100,000	—	—	5	6

f = frequency in MHz

* = Plane-wave equivalent power density (see Note 1).

(B) Limits for General Population/Uncontrolled Exposure

Frequency Range (MHz)	*Electric Field Strength (V/m)*	*Magnetic Field Strength (A/m)*	*Power Density (mW/cm^2)*	*Averaging Time (minutes)*
0.3-1.34	614	1.63	(100)*	30
1.34-30	824/f	2.19/f	($180/f^2$)*	30
30-300	27.5	0.073	0.2	30
300-1500	—	—	f/1500	30
1500-100,000	—	—	1.0	30

f = frequency in MHz

* = Plane-wave equivalent power density (see Note 1).

Note 1: This means the equivalent far-field strength that would have the E or H-field component calculated or measured. It does not apply well in the near field of an antenna. The equivalent far-field power density can be found in the near or far field regions from the relationships: $P_d = |E_{total}|^2 / 3770$ mW/cm^2 or from $P_d = \left|H_{total}\right|^2 \times 37.7$ mW/cm.^{2}

Station Evaluations

The FCC requires that certain amateur stations be evaluated for compliance with the MPEs. Although an amateur can have someone else do the evaluation, it is not difficult for hams to evaluate their own stations. The ARRL book *RF Exposure and You* contains extensive information about the regulations and a large chapter of tables that show compliance distances for specific antennas and power levels. Generally, hams will use these tables to evaluate their stations. Some of these tables have been included in the FCC's information — *OET Bulletin 65* and its *Supplement B*. If hams choose, however, they can do more extensive calculations, use a computer to model their antenna and exposure, or make actual measurements.

Table B—Power Thresholds for Routine Evaluation of Amateur Radio Stations

Wavelength Band	*Evaluation Required if Power* (watts) Exceeds:*
MF	
160 m	500
HF	
80 m	500
75 m	500
40 m	500
30 m	425
20 m	225
17 m	125
15 m	100
12 m	75
10 m	50
VHF (all bands)	50
UHF	
70 cm	70
33 cm	150
23 cm	200
13 cm	250
SHF (all bands)	250
EHF (all bands)	250
Repeater stations (all bands)	*non-building-mounted antennas*: height above ground level to lowest point of antenna < 10 m *and* power > 500 W ERP *building-mounted antennas*: power > 500 W ERP

*Transmitter power = Peak-envelope power input to antenna. For repeater stations ***only,*** power exclusion based on ERP (effective radiated power).

Categorical Exemptions

Some types of amateur stations do not need to be evaluated, but these stations must still comply with the MPE limits. The station licensee remains responsible for ensuring that the station meets these requirements.

The FCC has exempted these stations from the evaluation requirement because their output power, operating mode and frequency are such that they are presumed to be in compliance with the rules.

Stations using power equal to or less than the levels in **Table B** do not have to be evaluated. For the 100-W HF ham station, for example, an evaluation would be required *only* on 12 and 10 meters.

Hand-held radios and vehicle-mounted mobile radios that operate using a push-to-talk (PTT) button are also categorically exempt from performing the routine evaluation. Repeater stations that use less than 500 W ERP or those with antennas not mounted on buildings, if the antenna is at least 10 meters off the ground, also do not need to be evaluated.

Correcting Problems

Most hams are already in compliance with the MPE requirements. Some amateurs, especially those using indoor antennas or high-power, high-duty-cycle modes such as a RTTY bulletin station and specialized stations for moonbounce operations and the like may need to make adjustments to their station or operation to be in compliance.

The FCC permits amateurs considerable flexibility in complying with these regulations. As an example, hams can adjust their operating frequency, mode or power to comply with the MPE limits. They can also adjust their operating habits or control the direction their antenna is pointing.

More Information

This discussion offers only an overview of this topic; additional information can be found in *RF Exposure and You* and on *ARRLWeb* at **www.arrl.org/news/rfsafety/**. *ARRLWeb* has links to the FCC Web site, with *OET Bulletin 65* and *Supplement B* and links to software that hams can use to evaluate their stations.

dard was adopted by ANSI in 1992.

The IEEE standard recommends frequency-dependent and time-dependent maximum permissible exposure levels. Unlike earlier versions of the standard, the 1991 standard recommends different RF exposure limits in controlled environments (that is, where energy levels can be accurately determined and everyone on the premises is aware of the presence of EM fields) and in uncontrolled environments (where energy levels are not known or where people may not be aware of the presence of EM fields). FCC regulations also include controlled/occupational and uncontrolled/general population exposure environments.

The graph in **Fig 20** depicts the 1991 IEEE standard. It is necessarily a complex graph, because the standards differ not only for controlled and uncontrolled environments but also for electric (E) fields and magnetic (H) fields. Basically, the lowest E-field exposure limits occur at frequencies between 30 and 300 MHz. The lowest H-field exposure levels occur at 100-300 MHz. The ANSI standard sets the maximum E-field limits between 30 and 300 MHz at a power density of 1 mW/cm^2 (61.4 V/m) in controlled environments—but at one-fifth that level (0.2 mW/cm^2 or 27.5 V/m) in uncontrolled environments. The H-field limit drops to 1 mW/cm^2 (0.163 A/m) at 100-300 MHz in controlled environments and 0.2 mW/cm^2 (0.0728 A/m) in uncontrolled environments. Higher power densities are permitted at frequencies below 30 MHz (below 100 MHz for H fields) and above 300 MHz, based on the concept that the body will not be resonant at those frequencies and will therefore absorb less energy.

In general, the 1991 IEEE standard requires averaging the power level over time periods ranging from 6 to

30 minutes for power-density calculations, depending on the frequency and other variables. The ANSI exposure limits for uncontrolled environments are lower than those for controlled environments, but to compensate for that the standard allows exposure levels in those environments to be averaged over much longer time periods (generally 30 minutes). This long averaging time means that an intermittently operating RF source (such as an Amateur Radio transmitter) will show a much lower power density than a continuous-duty station—for a given power level and antenna configuration.

Time averaging is based on the concept that the human body can withstand a greater rate of body heating (and thus, a higher level of RF energy) for a short time than for a longer period. Time averaging may not be appropriate, however, when considering nonthermal effects of RF energy.

The IEEE standard excludes any transmitter with an output below 7 W because such low-power transmitters would not be able to produce significant whole-body heating. (Recent studies show that hand-held transceivers often produce power densities in excess of the IEEE standard within the head.)

There is disagreement within the scientific community about these RF exposure guidelines. The IEEE standard is still intended primarily to deal with thermal effects, not exposure to energy at lower levels. A small but significant number of researchers now believe athermal effects also should be taken into consideration. Several European countries and localities in the United States have adopted stricter standards than the recently updated IEEE standard.

Another national body in the United States, the National Council for Radiation Protection and Measurement (NCRP), also has adopted recommended exposure guidelines. NCRP urges a limit of 0.2 mW/cm^2 for nonoccupational exposure in the 30-300 MHz range. The NCRP guideline differs from IEEE in two notable ways: It takes into account the effects of modulation on an RF carrier, and it does not exempt transmitters with outputs below 7 W.

The FCC MPE regulations are based on parts of the 1992 IEEE/ANSI standard and recommendations of the National Council for Radiation Protection and Measurement (NCRP). The MPE limits under the regulations are slightly different than the IEEE/ANSI limits. Note that the MPE levels apply to the FCC rules put into effect for radio amateurs on January 1, 1998. These MPE requirements do not reflect and include all the assumptions and exclusions of the IEEE/ANSI standard.

Cardiac Pacemakers and RF Safety

It is a widely held belief that cardiac pacemakers may be adversely affected in their function by exposure to electromagnetic fields. Amateurs with pacemakers may ask whether their operating might endanger themselves or visitors to their shacks who have a pacemaker. Because of this, and similar concerns regarding other sources of electromagnetic fields, pacemaker manufacturers apply design methods that for the most part shield the pacemaker circuitry from even relatively high EM field strengths.

It is recommended that any amateur who has a pacemaker, or is being considered for one, discuss this matter with his or her physician. The physician will probably put the amateur into contact with the technical representative of the pacemaker manufacturer. These representatives are generally excellent resources, and may have data from laboratory or "in the field" studies with specific model pacemakers.

One study examined the function of a modern (dual chamber) pacemaker in and around an Amateur Radio station. The pacemaker generator has circuits that receive and process electrical signals produced by the heart, and also generate electrical signals that stimulate (pace) the heart. In one series of experiments, the pacemaker was connected to a heart simulator. The system was placed on top of the cabinet of a 1-kW HF linear amplifier during SSB and CW operation. In another test, the system was placed in close proximity to several 1 to 5-W 2-meter hand-held transceivers. The test pacemaker was connected to the heart simulator in a third test, and then placed on the ground 9 meters below and 5 meters in front of a three-element Yagi HF antenna. No interference with pacemaker function was observed in these experiments.

Although the possibility of interference cannot be entirely ruled out by these few observations, these tests represent more severe exposure to EM fields than would ordinarily be encountered by an amateur—with an average amount of common sense. Of course, prudence dictates that amateurs with pacemakers, who use hand-held VHF transceivers, keep the antenna as far as possible from the site of the implanted pacemaker generator. They also should use the lowest transmitter output required for adequate communication. For high power HF transmission, the antenna should be as far as possible from the operating position, and all equipment should be properly grounded.

Low-Frequency Fields

Although the FCC doesn't regulate 60-Hz fields, some recent concern about EMR has focused on low-frequency energy rather than RF. Amateur Radio equipment can be a significant source of low-frequency magnetic fields, although there are many other sources of this kind of energy in the typical home. Magnetic fields can be measured relatively accurately with inexpensive 60-Hz meters that are made by several manufacturers.

Table 2 shows typical magnetic field intensities of Amateur Radio equipment and various household items. Because these fields dissipate rapidly with distance, "prudent avoidance" would mean staying perhaps 12 to 18 inches away from most Amateur Radio equipment (and

24 inches from power supplies with 1-kW RF amplifiers).

Determining RF Power Density

Unfortunately, determining the power density of the RF fields generated by an amateur station is not as simple as measuring low-frequency magnetic fields. Although sophisticated instruments can be used to measure RF power densities quite accurately, they are costly and require frequent recalibration. Most amateurs don't have access to such equipment, and the inexpensive field-

Table 2

Typical 60-Hz Magnetic Fields Near Amateur Radio Equipment and AC-Powered Household Appliances

Values are in milligauss.

Item	*Field*	*Distance*
Electric blanket	30-90	Surface
Microwave oven	10-100	Surface
	1-10	12″
IBM personal computer	5-10	Atop monitor
	0-1	15″ from screen
Electric drill	500-2000	At handle
Hair dryer	200-2000	At handle
HF transceiver	10-100	Atop cabinet
	1-5	15″ from front
1-kW RF amplifier	80-1000	Atop cabinet
	1-25	15″ from front

(Source: measurements made by members of the ARRL RF Safety Committee)

Table 3

Typical RF Field Strengths Near Amateur Radio Antennas

A sampling of values as measured by the Federal Communications Commission and Environmental Protection Agency, 1990

Antenna Type	*Freq (MHz)*	*Power (W)*	*E Field (V/m)*	*Location*
Dipole in attic	14.15	100	7-100	In home
Discone in attic	146.5	250	10-27	In home
Half sloper	21.5	1000	50	1 m from base
Dipole at 7-13 ft	7.14	120	8-150	1-2 m from earth
Vertical	3.8	800	180	0.5 m from base
5-element Yagi at 60 ft	21.2	1000	10-20	In shack
			14	12 m from base
3-element Yagi at 25 ft	28.5	425	8-12	12 m from base
Inverted V at 22-46 ft	7.23	1400	5-27	Below antenna
Vertical on roof	14.11	140	6-9	In house
			35-100	At antenna tuner
Whip on auto roof	146.5	100	22-75	2 m antenna
			15-30	In vehicle
			90	Rear seat
5-element Yagi at 20 ft	50.1	500	37-50	10 m antenna

Table 4

RF Awareness Guidelines

These guidelines were developed by the ARRL RF Safety Committee, based on the FCC/EPA measurements of Table 3 and other data.

- Although antennas on towers (well away from people) pose no exposure problem, make certain that the RF radiation is confined to the antennas' radiating elements themselves. Provide a single, good station ground (earth), and eliminate radiation from transmission lines. Use good coaxial cable or other feed line properly. Avoid serious imbalance in your antenna system and feed line. For high-powered installations, avoid end-fed antennas that come directly into the transmitter area near the operator.
- No person should ever be near any transmitting antenna while it is in use. This is especially true for mobile or ground-mounted vertical antennas. Avoid transmitting with more than 25 W in a VHF mobile installation unless it is possible to first measure the RF fields inside the vehicle. At the 1-kW level, both HF and VHF directional antennas should be at least 35 ft above inhabited areas. Avoid using indoor and attic-mounted antennas if at all possible. If open-wire feeders are used, ensure that it is not possible for people (or animals) to come into accidental contact with the feed line.
- Don't operate high-power amplifiers with the covers removed, especially at VHF/UHF.
- In the UHF/SHF region, never look into the open end of an activated length of waveguide or microwave feed-horn antenna or point it toward anyone. (If you do, you may be exposing your eyes to more than the maximum permissible exposure level of RF radiation.) Never point a high-gain, narrow-bandwidth antenna (a paraboloid, for instance) toward people. Use caution in aiming an EME (moonbounce) array toward the horizon; EME arrays may deliver an effective radiated power of 250,000 W or more.
- With hand-held transceivers, keep the antenna away from your head and use the lowest power possible to maintain communications. Use a separate microphone and hold the rig as far away from you as possible. This will reduce your exposure to the RF energy.
- Don't work on antennas that have RF power applied.
- Don't stand or sit close to a power supply or linear amplifier when the ac power is turned on. Stay at least 24 inches away from power transformers, electrical fans and other sources of high-level 60-Hz magnetic fields.

strength meters that we do have are not suitable for measuring RF power density.

Table 3 shows a sampling of measurements made at Amateur Radio stations by the Federal Communications Commission and the Environmental Protection Agency in 1990. As this table indicates, a good antenna well removed from inhabited areas poses no hazard under any of the IEEE/ANSI guidelines. However, the FCC/EPA survey also indicates that amateurs must be careful about using indoor or attic-mounted antennas, mobile antennas, low directional arrays or any other antenna that is close to inhabited areas, especially when moderate to high power is used.

Ideally, before using any antenna that is in close proximity to an inhabited area, you should measure the RF power density. If that is not feasible, the next best option is make the installation as safe as possible by observing the safety suggestions listed in **Table 4**.

It also is possible, of course, to calculate the probable power density near an antenna using simple equations. Such calculations have many pitfalls. For one, most of the situations where the power density would be high enough to be of concern are in the near field. In the near field, ground interactions and other variables produce power densities that cannot be determined by simple arithmetic. In the far field, conditions become easier to predict with simple calculations.

The boundary between the near field and the far field depends on the wavelength of the transmitted signal and the physical size and configuration of the antenna. The boundary between the near field and the far field of an antenna can be as much as several wavelengths from the antenna.

Computer antenna-modeling programs are another approach you can use. *MININEC* or other codes derived from *NEC* (Numerical Electromagnetics Code) are suitable for estimating RF magnetic and electric fields around amateur antenna systems.

These models have limitations. Ground interactions must be considered in estimating near-field power densities, and the "correct ground" must be modeled. Computer modeling is generally not sophisticated enough to predict "hot spots" in the near field—places where the field intensity may be far higher than would be expected, due to reflections from nearby objects. In addition, "nearby objects" often change or vary with weather or the season, so the model so laboriously crafted may not be representative of the actual situation, by the time it is running on the computer.

Intensely elevated but localized fields often can be detected by professional measuring instruments. These "hot spots" are often found near wiring in the shack, and metal objects such as antenna masts or equipment cabinets. But even with the best instrumentation, these measurements also may be misleading in the near field.

One need not make precise measurements or model the exact antenna system, however, to develop some idea of the relative fields around an antenna. Computer modeling using close approximations of the geometry and power input of the antenna will generally suffice. Those who are familiar with *MININEC* can estimate their power densities by computer modeling, and those who have access to professional power-density meters can make useful measurements.

While our primary concern is ordinarily the intensity of the signal radiated by an antenna, we also should remember that there are other potential energy sources to be considered. You also can be exposed to RF radiation directly from a power amplifier if it is operated without proper shielding. Transmission lines also may radiate a significant amount of energy under some conditions. Poor microwave waveguide joints or improperly assembled connectors are another source of incidental radiation.

Further RF Exposure Suggestions

Potential exposure situations should be taken seriously. Based on the FCC/EPA measurements and other data, the "RF awareness" guidelines of Table 4 were developed by the ARRL RF Safety Committee. A longer version of these guidelines, along with a complete list of references, appeared in a *QST* article by Ivan Shulman, MD, WC2S ("Is Amateur Radio Hazardous to Our Health?" *QST* , Oct 1989, pp 31-34). For more information or background, see the list of RF Safety References in the next section.

In addition, the ARRL has published a book, *RF Exposure and You*, that is helping hams comply with the FCC's RF-exposure regulations. The ARRL also maintains an RF-exposure news page on its Web site. See **www.arrl.org/news/rfsafety**. This site contains reprints of selected *QST* articles on RF exposure and links to the FCC and other useful sites.

Chapter 2

Antenna Fundamentals

Antennas belong to a class of devices called *transducers*. This term is derived from two Latin words, meaning literally "to lead across" or "to transfer." Thus, a transducer is a device that transfers, or converts, energy from one form to another. The purpose of an antenna is to convert radio-frequency electric current to *electromagnetic waves*, which are then *radiated* into space. [For more details on the properties of electromagnetic waves themselves, see Chapter 23, Radio Wave Propagation.]

We cannot directly see or hear, taste or touch electromagnetic waves, so it's not surprising that the process by which they are launched into space from our antennas can be a little mystifying, especially to a newcomer. In everyday life we come across many types of transducers, although we don't always recognize them as such. A comparison with a type of transducer that you can actually see and touch may be useful. You are no doubt familiar with a *loudspeaker*. It converts audio-frequency electric current from the output of your radio or stereo into acoustic pressure waves, also known as *sound waves*. The sound waves are propagated through the air to your ears, where they are converted into what you perceive as sound.

We normally think of a loudspeaker as something that converts electrical energy into sound energy, but we could just as well turn things around and apply sound energy to a loudspeaker, which will then convert it into electrical energy. When used in this manner, the loudspeaker has become a microphone. The loudspeaker/microphone thus exhibits the principle of *reciprocity*, derived from the Latin word meaning to move back and forth.

Now, let's look more closely at that special transducer we call an *antenna*. When fed by a transmitter with RF current (usually through a transmission line), the antenna launches electromagnetic waves, which are propagated through space. This is similar to the way sound waves are propagated through the air by a loudspeaker. In the next town, or perhaps on a distant continent, a similar transducer (that is, a receiving antenna) intercepts some of these electromagnetic waves and converts them into electrical current for a receiver to amplify and detect.

In the same fashion that a loudspeaker can act as a microphone, a radio antenna also follows the principle of reciprocity. In other words, an antenna can transmit as well as receive signals. However, unlike the loudspeaker, an antenna does not require a *medium*, such as air, through which it radiates electromagnetic waves. Electromagnetic waves can be propagated through air, the vacuum of outer space or the near vacuum of the upper ionosphere. This is the miracle of radio—electromagnetic waves can propagate without a physical medium.

Essential Characteristics of Antennas

What other things make an antenna different from an ordinary electronic circuit? In ordinary circuits, the dimensions of coils, capacitors and connections usually are small compared with the wavelength of the frequency in use. Here, we define wavelength as the distance in free space traveled during one complete cycle of a wave. The velocity of a wave in free space is the speed of light, and the wavelength is thus:

$$\lambda_{\text{meters}} = \frac{299.7925\times10^{6}\ \text{meters/sec}}{\text{f hertz}} = \frac{299.7925}{\text{f MHz}} \qquad \text{(Eq 1)}$$

where λ_{meters}, the Greek letter lambda, is the free-space wavelength in meters.

Expressed in feet, Eq 1 becomes:

$$\lambda_{feet} = \frac{983.5712}{f\ MHz} \approx \frac{983.6}{f\ MHz} \qquad \text{(Eq 2)}$$

When circuit dimensions are small compared to λ, most of the electromagnetic energy is confined to the circuit itself, and is used up either performing useful work or is converted into heat. However, when the dimensions of wiring or components become significant compared with the wavelength, some of the energy escapes by radiation in the form of electromagnetic waves.

Antennas come in an enormous, even bewildering, assortment of shapes and sizes. This chapter on fundamentals will deal with the theory of simple forms of antennas, usually in *free space*, away from the influence of ground. Subsequent chapters will concentrate on more exotic or specialized antenna types. Chapter 3 deals with the complicated subject of the effect of ground, including the effect of uneven local terrain. Ground has a profound influence on how an antenna performs in the real world.

No matter what form an antenna takes, simple or complex, its electrical performance can be characterized according to the following important properties:

1. Feed-point Impedance
2. Directivity, Gain and Efficiency
3. Polarization

FEED-POINT IMPEDANCE

The first major characteristic defining an antenna is its *feed-point impedance*. Since we amateurs are free to choose our operating frequencies within assigned bands, we need to consider how the feed-point impedance of a particular antenna varies with frequency, within a particular band, or even in several different bands if we intend to use one antenna on multiple bands.

There are two forms of impedance associated with any antenna: *self impedance* and *mutual impedance*. As you might expect, self impedance is what you measure at the feed-point terminals of an antenna located completely away from the influence of any other conductors.

Mutual, or coupled, impedance is due to the parasitic effect of nearby conductors; that is, conductors located within the antenna's reactive near field. (The subject of fields around an antenna will be discussed in detail later.) This includes the effect of ground, which is a lossy conductor, but a conductor nonetheless. Mutual impedance is defined using Ohm's Law, just like self impedance. However, mutual impedance is the ratio of voltage in one conductor, divided by the current in another (coupled) conductor. Mutually coupled conductors can distort the pattern of a highly directive antenna, as well as change the impedance seen at the feed point.

In this chapter on fundamentals, we won't directly deal with mutual impedance, considering it as a side effect of nearby conductors. Instead, here we'll concentrate on simple antennas in free space, away from ground and any other conductors. Mutual impedance will be considered in detail in Chapter 11, HF Yagi Arrays, where it is essential for proper operation of these beam antennas.

Self Impedance

The current that flows into an antenna's feed point must be supplied at a finite voltage. The self impedance of the antenna is simply equal to the voltage applied to its feed point divided by the current flowing into the feed point. Where the current and voltage are exactly in phase, the impedance is purely resistive, with zero reactive component. For this case the antenna is termed *resonant*. (Amateurs often use the term "resonant" rather loosely, usually meaning "nearly resonant" or "close-to resonant.")

Please recognize that an antenna *need not be resonant* in order to be an effective radiator. There is in fact nothing magic about having a resonant antenna, provided of course that you can devise some efficient means to feed the antenna. Many amateurs use non-resonant (even random-length) antennas fed with open-wire transmission lines and antenna tuners. They radiate signals just as well as those using coaxial cable and resonant antennas, and as a bonus they usually can use these antenna systems on multiple frequency bands. It is important to consider an antenna and its feed line as a *system*, in which all losses should be kept to a minimum. See Chapter 24, Transmission Lines, for details on transmission-line loss as a function of impedance mismatch.

Except at the one frequency where it is truly resonant, the current in an antenna is at a different phase compared to the applied voltage. In other words, the antenna exhibits a feed-point *impedance*, not just a pure resistance. The feed-point impedance is composed of either capacitive or inductive reactance in series with a resistance.

Radiation Resistance

The power supplied to an antenna is dissipated in two ways: radiation of electromagnetic waves, and heat losses in the wire and nearby dielectrics. The radiated power is what we want, the useful part, but it represents a form of "loss" just as much as the power used in heating the wire or nearby dielectrics is a loss. In either case, the dissipated power is equal to I^2R. In the case of heat losses, R is a real resistance. In the case of radiation, however, R is a "virtual" resistance, which, if replaced with an actual resistor of the same value, would dissipate the power actually radiated from the antenna. This resistance is called the *radiation resistance*. The total power in the antenna is therefore equal to $I^2(R_0+R)$, where R_0 is the radiation resistance and R represents the total of all the loss resistances.

In ordinary antennas operated at amateur frequencies, the power lost as heat in the conductor does not exceed a few percent of the total power supplied to the antenna. Expressed in decibels, the loss is less than 0.1 dB. The RF loss resistance of copper wire even as small as #14 is very low compared with the radiation resistance of an antenna that is reasonably clear of surrounding objects and is not too close to the ground. You can therefore assume that the ohmic loss in a reasonably well-located antenna is negligible, and that the total resistance shown by the antenna (the feed-point resistance) is radiation resistance. As a radiator of electromagnetic waves, such an antenna is a highly efficient device.

Impedance of a Center-Fed Dipole

A fundamental type of antenna is the *center-fed half-wave dipole*. Historically, the λ/2 dipole has been the most popular antenna used by amateurs worldwide, largely because it is very simple to construct and because it is an effective performer. It is also a basic building block for many other antenna systems, including beam antennas, such as Yagis.

A center-fed half-wave *dipole* consists of a straight wire, one-half wavelength long as defined in Eq 1, and fed in the center. The term "dipole" derives from Greek words meaning "two poles." See **Fig 1**. A λ/2-long dipole is just one form a dipole can take. Actually, a center-fed dipole can be any length electrically, as long as it is configured in a symmetrical fashion with two equal-length legs. There are also versions of dipoles that are not fed in the center. These are called *off-center-fed dipoles*, sometimes abbreviated as "OCF dipoles."

In free space—with the antenna remote from everything else—the theoretical impedance of a physically half-wave long antenna made of an infinitely thin conductor is 73 + *j* 42.5 Ω. This antenna exhibits both resistance and reactance. The positive sign in the + *j* 42.5-Ω reactive term indicates that the antenna exhibits an inductive reactance at its feed point. The antenna is slightly long electrically, compared to the length necessary for exact resonance, where the reactance is zero.

The feed-point impedance of any antenna is affected by the wavelength-to-diameter ratio (λ/dia) of the conductors used. Theoreticians like to specify an "infinitely thin" antenna because it is easier to handle mathematically.

What happens if we keep the physical length of an antenna constant, but change the thickness of the wire used in its construction? Further, what happens if we vary the frequency from well below to well above the half-wave resonance and measure the feed-point impedance? **Fig 2** graphs the impedance of a 100-foot long, center-fed dipole in free space, made with extremely thin wire—in this case, wire that is only 0.001 inches in diameter. There is nothing particularly significant about the choice here of 100 feet. This is simply a numerical example.

We could never actually build such a thin antenna (and neither could we install it in free space), but we can model how this antenna works using a very powerful piece of computer software called *NEC-4.1*. See Chapter 4, Antenna Modeling and System Planning, for details on antenna modeling.

The frequency applied to the antenna in Fig 2 is varied from 1 to 30 MHz. The x-axis has a logarithmic scale because of the wide range of feed-point resistance seen over the frequency range. The y-axis has a linear scale representing the reactive portion of the impedance. Inductive reactance is positive and capacitive reactance is negative on the y-axis. The bold figures centered on the spiraling line show the frequency in MHz.

At 1 MHz, the antenna is very short electrically, with a resistive component of about 2 Ω and a series capaci-

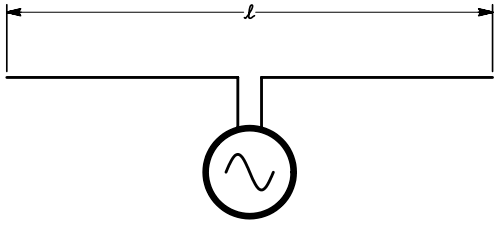

Fig 1—The center-fed dipole antenna. It is assumed that the source of power is directly at the antenna feed point, with no intervening transmission line. Most commonly in amateur applications, the overall length of the dipole is λ/2, but the antenna can in actuality be any length.

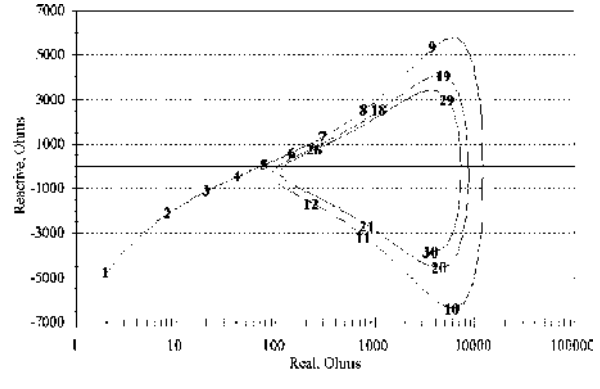

Fig 2—Feed-point impedance versus frequency for a theoretical 100-foot long dipole in free space, fed in the center and made of extremely thin 0.001-inch diameter wire. The y-axis is calibrated in positive (inductive) series reactance up from the zero line, and negative (capacitive) series reactance in the downward direction. The range of reactance goes from –6500 Ω to +6000 Ω. Note that the x-axis is logarithmic because of the wide range of the real, resistive component of the feed-point impedance, from roughly 2 Ω to 10,000 Ω. The numbers placed along the curve show the frequency in MHz.

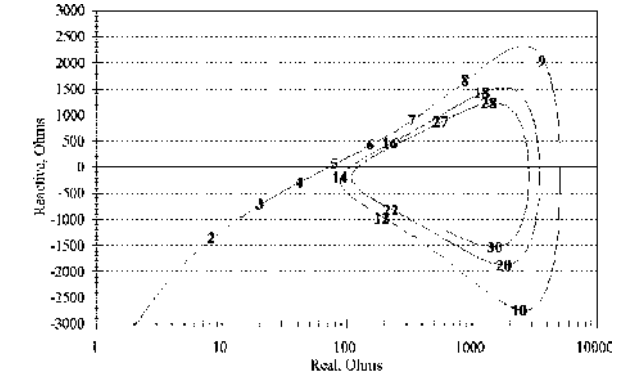

Fig 3—Feed-point impedance versus frequency for a theoretical 100-foot long dipole in free space, fed in the center and made of thin 0.1-inch (#10) diameter wire. Note that the range of change in reactance is less than that shown in Fig 2, ranging from –2700 Ω to +2300 Ω. At about 5,000 Ω, the maximum resistance is also less than that in Fig 2 for the thinner wire, where it is about 10,000 Ω.

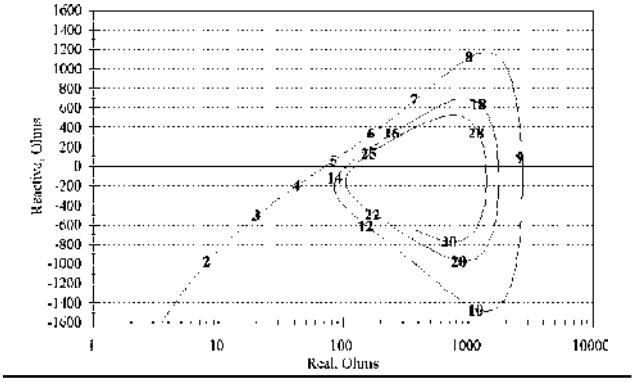

Fig 4—Feed-point impedance versus frequency for a theoretical 100-foot long dipole in free space, fed in the center and made of thick 1.0-inch diameter wire. Once again, the excursion in both reactance and resistance over the frequency range is less with this thick wire dipole than with thinner ones.

tive reactance about –5000 Ω. Close to 5 MHz, the line crosses the zero-reactance line, meaning that the antenna goes through half-wave resonance there. Between 9 and 10 MHz the antenna exhibits a peak inductive reactance of about 6000 Ω. It goes through full-wave resonance (again crossing the zero-reactance line) between 9.5 and 9.6 MHz. At about 10 MHz, the reactance peaks at about –6500 Ω. Around 14 MHz, the line again crosses the zero-reactance line, meaning that the antenna has now gone through 3/2-wave resonance.

Between 19 and 20 MHz, the antenna goes through 4/2-wave resonance, which is twice the full-wave resonance or four times the half-wave frequency. If you allow your mind's eye to trace out the curve for frequencies beyond 30 MHz, it eventually spirals down to a resistive component somewhere between 200 and 3000 Ω. Thus, we have another way of looking at an antenna—as a sort of *transformer*, one that transforms the free-space impedance into the impedance seen at its feed point.

Now look at **Fig 3**, which shows the same kind of spiral curve, but for a thicker-diameter wire, one that is 0.1 inches in diameter. This diameter is close to #10 wire, a practical size we might actually use to build a real dipole. Note that the y-axis scale in Fig 3 is different from that in Fig 2. The range is from ±3000 Ω in Fig 3, while it was ±7000 Ω in Fig 2. The reactance for the thicker antenna ranges from +2300 to –2700 Ω over the whole frequency range from 1 to 30 MHz. Compare this with the range of +5800 to –6400 Ω for the very thin wire in Fig 2.

Fig 4 shows the impedance for a 100-foot long dipole using really thick, 1.0-inch diameter wire. The reactance varies from +1000 to –1500 Ω, indicating once again that a larger diameter antenna exhibits less of an excursion in the reactive component with frequency. Note that at the

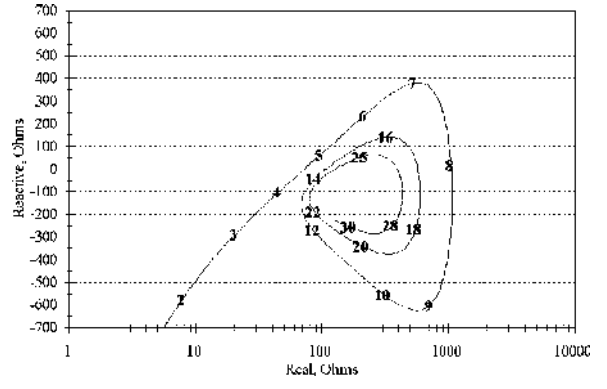

Fig 5—Feed-point impedance versus frequency for a theoretical 100-foot long dipole in free space, fed in the center and made of very thick 10.0-inch diameter wire. This ratio of length to diameter is about the same as a typical rod type of dipole element commonly used at 432 MHz. The maximum resistance is now about 1,000 Ω and the peak reactance range is from about –625 Ω to +380 Ω. This performance is also found in "cage" dipoles, where a number of paralleled wires are used to simulate a fat conductor.

half-wave resonance just below 5 MHz, the resistive component of the impedance is still about 70 Ω, just about what it is for a much thinner antenna. Unlike the reactance, the half-wave radiation resistance of an antenna doesn't radically change with wire diameter, although the maximum level of resistance at full-wave resonance is lower for thicker antennas.

Fig 5 shows the results for a very thick, 10-inch diameter wire. Here, the excursion in the reactive component is even less: about +400 to –600 Ω. Note that the full-wave resonant frequency is about 8 MHz for this

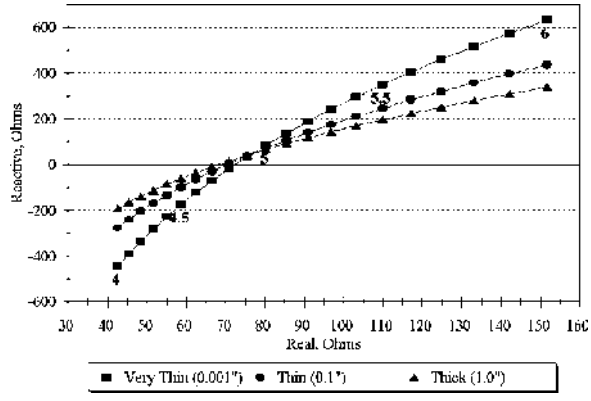

Fig 6—Expansion of frequency range around half-wave resonant point of three center-fed dipoles of three different thicknesses. The frequency is shown along the curves in MHz. The slope of change in series reactance versus series resistance is steeper for the thinner antennas than for the thick 1.0-inch antenna, indicating that the Q of the thinner antennas is higher.

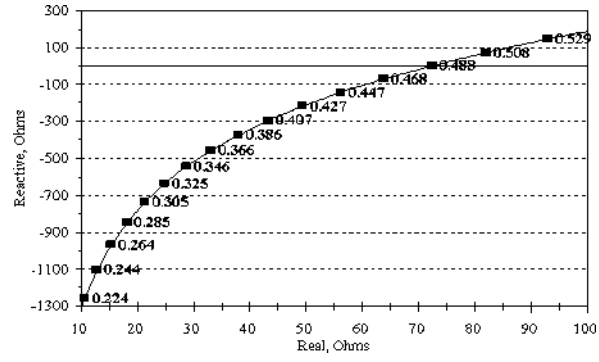

Fig 7—Another way of looking at the data for a 100-foot, center-fed dipole made of #14 wire in free space. The numbers along the curve represent the fractional wavelength, rather than frequency as shown in Fig 6. Note that this antenna goes through its half-wave resonance about 0.488 λ, rather than exactly at a half-wave physical length.

extremely thick antenna, while thinner antennas have full-wave resonances closer to 9 MHz. Note also that the full-wave resistance for this extremely thick antenna is only about 1,000 Ω, compared to the 10,000 Ω shown in Fig 2. All half-wave resonances shown in Figs 2 through 5 remain close to 5 MHz, regardless of the diameter of the antenna wire. Once again, the extremely thick, 10-inch diameter antenna has a resistive component at half-wave resonance close to 70 Ω. And once again, the change in reactance near this frequency is very much less for the extremely thick antenna than for thinner ones.

Now, we grant you that a 100-foot long antenna made with 10-inch diameter wire sounds a little odd! A length of 100 feet and a diameter of 10 inches represent a ratio of 120:1 in length to diameter. However, this is about the same length-to-diameter ratio as a 432-MHz half-wave dipole using 0.25-inch diameter elements, where the ratio is 109:1. In other words, the ratio of length-to-diameter for the 10-inch diameter, 100-foot long dipole is not that far removed from what might actually be used at UHF.

Another way of highlighting the changes in reactance and resistance is shown in **Fig 6**. This shows an expanded portion of the frequency range around the half-wave resonant frequency, from 4 to 6 MHz. In this region, the shape of each spiral curve is almost a straight line. The slope of the curve for the very thin antenna (0.001-inch diameter) is steeper than that for the thicker antennas (0.1 and 1.0-inch diameters). **Fig 7** illustrates another way of looking at the impedance data above and below the half-wave resonance. This is for a 100-foot dipole made of #14 wire. Instead of showing the frequency for each impedance point, the wavelength is

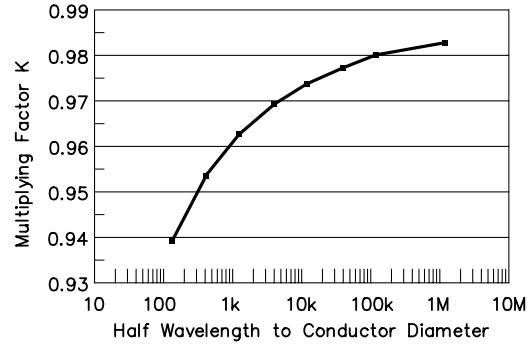

Fig 8—Effect of antenna diameter on length for half-wavelength resonance, shown as a multiplying factor, K, to be applied to the free-space, half-wavelength.

shown, making the graph more universal in application.

Just to show that there are lots of ways of looking at the same data, **Fig 8** graphs the constant "K" used to multiply the free-space half-wavelength as a function of the ratio between the half-wavelength and the conductor diameter. The curve approaches the value of 1.00 for an infinitely thin conductor, in other words an infinitely large ratio of half-wavelength to diameter.

The behavior of antennas with different λ/diameter ratios corresponds to the behavior of ordinary series-resonant circuits having different values of Q. When the Q of a circuit is low, the reactance is small and changes rather slowly as the applied frequency is varied on either side of resonance. If the Q is high, the converse is true. The

response curve of the low-Q circuit is *broad*; that of the high-Q circuit *sharp*. So it is with antennas—the impedance of a thick antenna changes slowly over a comparatively wide band of frequencies, while a thin antenna has a faster change in impedance. Antenna Q is defined

$$Q = \frac{f_0 \Delta X}{2 R_0 \Delta f} \qquad \text{(Eq 3)}$$

where f_0 is the center frequency, ΔX is the change in the reactance for a Δf change in frequency, and R_0 is the resistance the f_0. For the "Very Thin," 0.001-inch diameter dipole in Fig 2, a change of frequency from 5.0 to 5.5 MHz yields a reactance change from 86 to 351 Ω, with an R_0 of 95 Ω. The Q is thus 14.6. For the 1.0-inch-diameter "Thick" dipole in Fig 4, ΔX = 131 Ω and R_0 is still 95 Ω, making Q = 7.2 for the thicker antenna, roughly half that of the thinner antenna.

Let's recap. We have described an antenna first as a transducer, then as a sort of transformer to a range of free-space impedances. Now, we just compared the antenna to a series-tuned circuit. Near its half-wave resonant frequency, a center-fed λ/2 dipole exhibits much the same characteristics as a conventional series-resonant circuit. Exactly at resonance, the current at the input terminals is in phase with the applied voltage and the feed-point impedance is purely resistive. If the frequency is below resonance, the phase of the current leads the voltage; that is, the reactance of the antenna is capacitive. When the frequency is above resonance, the opposite occurs; the current lags the applied voltage and the antenna exhibits inductive reactance. Just like a conventional series-tuned circuit, the antenna's reactance and resistance determines its Q.

ANTENNA DIRECTIVITY AND GAIN

The Isotropic Radiator

Before we can fully describe practical antennas, we must first introduce a completely theoretical antenna, the *isotropic radiator*. Envision, if you will, an infinitely small antenna, a point located in outer space, completely removed from anything else around it. Then consider an infinitely small transmitter feeding this infinitely small, point antenna. You now have an isotropic radiator.

The uniquely useful property of this theoretical *point-source* antenna is that it radiates equally well in all directions. That is to say, an isotropic antenna favors no direction at the expense of any other—in other words, it has absolutely no *directivity*. The isotropic radiator is useful as a *measuring stick* for comparison with actual antenna systems.

You will find later that real, practical antennas all exhibit some degree of directivity, which is the property of radiating more strongly in some directions than in others. The radiation from a practical antenna never has the same intensity in all directions and may even have zero radiation in some directions. The fact that a practical antenna displays directivity (while an isotropic radiator does not) is not necessarily a bad thing. The directivity of a real antenna is often carefully tailored to emphasize radiation in particular directions. For example, a receiving antenna that favors certain directions can discriminate against interference or noise coming from other directions, thereby increasing the signal-to-noise ratio for desired signals coming from the favored direction.

Directivity and the Radiation Pattern—a Flashlight Analogy

The directivity of an antenna is directly related to the *pattern* of its radiated field intensity in free space. A graph showing the actual or relative field intensity at a fixed distance, as a function of the direction from the antenna system, is called a *radiation pattern*. Since we can't actually see electromagnetic waves making up the radiation pattern of an antenna, we can consider an analogous situation.

Fig 9 represents a flashlight shining in a totally darkened room. To quantify what our eyes are seeing, we might use a sensitive light meter like those used by photographers, with a scale graduated in units from 0 to 10. We place the meter directly in front of the flashlight and adjust the distance so the meter reads 10, exactly full scale. We also carefully note the distance. Then, always keeping the meter the same distance from the flashlight and keeping it at the same height above the floor, we move the light meter around the flashlight, as indicated by the

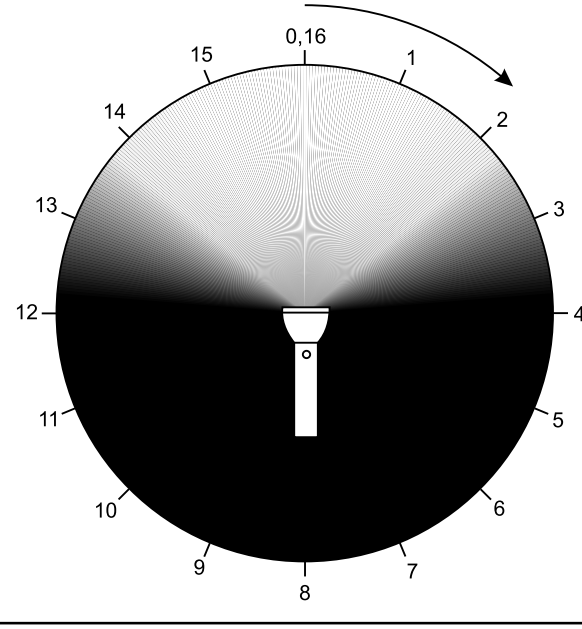

Fig 9—The beam from a flashlight illuminates a totally darkened area as shown here. Readings taken with a photographic light meter at the 16 points around the circle may be used to plot the radiation pattern of the flashlight.

arrow, and take light readings at a number of different positions.

After all the readings have been taken and recorded, we plot those values on a sheet of polar graph paper, like that shown in **Fig 10**. The values read on the meter are plotted at an angular position corresponding to that for which each meter reading was taken. Following this, we connect the plotted points with a smooth curve, also shown in Fig 10. When this is finished, we have completed a radiation pattern for the flashlight.

Antenna Pattern Measurements

Antenna radiation patterns can be constructed in a similar manner. Power is fed to the antenna under test, and a field-strength meter indicates the amount of signal. We might wish to rotate the antenna under test, rather than moving the measuring equipment to numerous positions about the antenna. Or we might make use of antenna reciprocity, since the pattern while receiving is the same as that while transmitting. A source antenna fed by a low-power transmitter illuminates the antenna under test, and the signal intercepted by the antenna under test is fed to a receiver and measuring equipment. Additional information on the mechanics of measuring antenna patterns is contained in Chapter 27, Antennas and Transmission-Line Measurements.

Some precautions must be taken to assure that the measurements are accurate and repeatable. In the case of the flashlight, let's assume that the separation between the light source and the light meter is 2 meters, about 6.5 feet. The wavelength of visible light is about one-half micron, where a micron is one-millionth of a meter.

For the flashlight, a separation of 2 meters between source and detector is $2.0/(0.5\times10^{-6}) = 4$ million λ, a very large number of wavelengths. Measurements of practical HF or even VHF antennas are made at much closer distances, in terms of wavelength. For example, at 3.5 MHz a full wavelength is 85.7 meters, or 281.0 feet. To duplicate the flashlight-to-light-meter spacing in wavelengths at 3.5 MHz, we would have to place the field-strength measuring instrument almost on the surface of the Moon, about a quarter-million miles away!

The Fields Around an Antenna

Why should we be concerned with the separation between the source antenna and the field-strength meter, which has its own receiving antenna? One important reason is that if you place a receiving antenna very close to an antenna whose pattern you wish to measure, mutual coupling between the two antennas may actually alter the pattern you are trying to measure.

This sort of mutual coupling can occur in the region very close to the antenna under test. This region is called the *reactive near-field* region. The term "reactive" refers to the fact that the mutual impedance between the transmitting and receiving antennas can be either capacitive

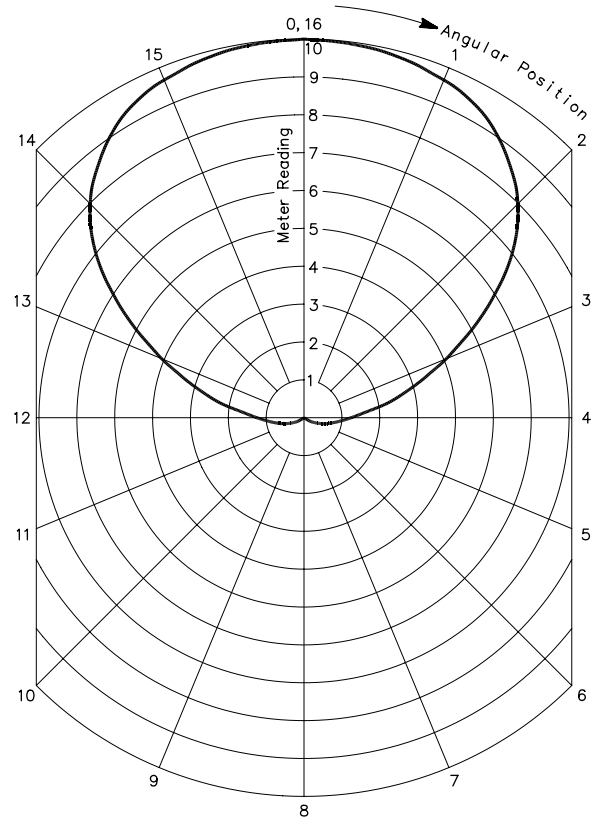

Fig 10—The radiation pattern of the flashlight in Fig 9. The measured values are plotted and connected with a smooth curve.

or inductive in nature. The reactive near field is sometimes called the "induction field," meaning that the magnetic field usually is predominant over the electric field in this region. The antenna acts as though it were a rather large, lumped-constant inductor or capacitor, storing energy in the reactive near field rather than propagating it into space.

For simple wire antennas, the reactive near field is considered to be within about a half wavelength from an antenna's radiating center. Later on, in the chapters dealing with Yagi and quad antennas, you will find that mutual coupling between elements can be put to good use to purposely shape the radiated pattern. For making pattern measurements, however, we do not want to be too close to the antenna being measured.

The strength of the reactive near field decreases in a complicated fashion as you increase the distance from the antenna. Beyond the reactive near field, the antenna's radiated field is divided into two other regions: the *radiating near field* and the *radiating far field.* Historically, the terms *Fresnel* and *Fraunhöfer* fields have been used for the radiating near and far fields, but these terms have been largely supplanted by the more descriptive terminology used here. Even inside the reactive near-field

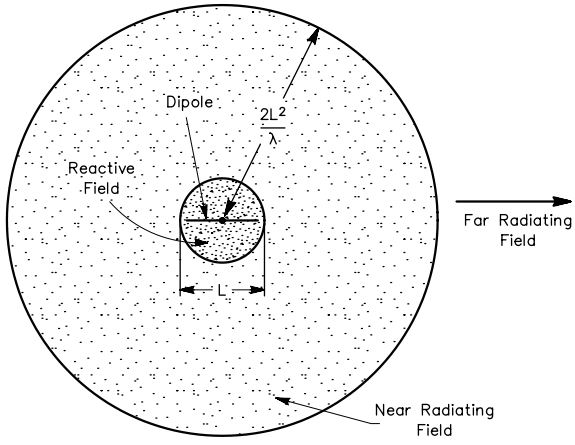

Fig 11—The fields around a radiating antenna. Very close to the antenna, the reactive field dominates. Within this area mutual impedances are observed between antenna and any other antennas used to measure response. Outside of the reactive field, the near radiating field dominates, up to a distance approximately equal to $2L^2/\lambda$, where L is the length of the largest dimension of the antenna. Beyond the near/far field boundary lies the far radiating field, where power density varies as the inverse square of radial distance.

region, both radiating and reactive fields coexist, although the reactive field predominates very close to the antenna.

Because the boundary between the fields is rather fuzzy, experts debate where one field begins and another leaves off, but the boundary between the radiating near and far fields is generally accepted as:

$$D \approx \frac{2L^2}{\lambda} \qquad \text{(Eq 4)}$$

where L is the largest dimension of the physical antenna, expressed in the same units of measurement as the wavelength λ. Remember, many specialized antennas do not follow the rule of thumb in Eq 4 exactly. **Fig 11** depicts the three fields in front of a simple wire antenna.

Throughout the rest of this book we will discuss mainly the radiating far-fields, those forming the traveling electromagnetic waves. Far-field radiation is distinguished by the fact that the intensity is inversely proportional to the distance, and that the electric and magnetic components, although perpendicular to each other in the wave front, are in time phase. The total energy is equally divided between the electric and magnetic fields. Beyond several wavelengths from the antenna, these are the only fields we need to consider. For accurate measurement of radiation patterns, we must place our measuring instrumentation at least several wavelengths away from the antenna under test.

Pattern Planes

Patterns obtained above represent the antenna radiation in just one plane. In the example of the flashlight, the plane of measurement was at one height above the floor. Actually, the pattern for any antenna is three dimensional, and therefore cannot be represented in a single-plane drawing. The *solid* radiation pattern of an antenna in free space would be found by measuring the field strength at every point on the surface of an imaginary sphere having the antenna at its center. The information so obtained would then be used to construct a solid figure, where the distance from a fixed point (representing the antenna) to the surface of the figure is proportional to the field strength from the antenna in any given direction. **Fig 12B** shows a three-dimensional wire-grid representation of the radiation pattern of a half-wave dipole.

For amateur work, *relative* values of field strength (rather than absolute) are quite adequate in pattern plotting. In other words, it is not necessary to know how many microvolts per meter a particular antenna will produce at a distance of 1 mile when excited with a specified power level. (This is the kind of specifications that AM broadcast stations must meet to certify their antenna systems to the FCC.)

For whatever data is collected (or calculated from theoretical equations), it is common to normalize the plotted values so the field strength in the direction of maximum radiation coincides with the outer edge of the chart. On a given system of polar coordinate scales, the *shape* of the pattern is not altered by proper normalization, only its size.

E and H-Plane Patterns

The solid 3-D pattern of an antenna in free space cannot adequately be shown with field-strength data on a flat sheet of paper. Cartographers making maps of a round Earth on flat pieces of paper face much the same kind of problem. As we discussed above, cross-sectional or plane diagrams are very useful for this purpose. Two such diagrams, one in the plane containing the straight wire of a dipole and one in the plane perpendicular to the wire, can convey a great deal of information. The pattern in the plane containing the axis of the antenna is called the *E-plane pattern*, and the one in the plane perpendicular to the axis is called the *H-plane pattern*. These designations are used because they represent the planes in which the electric (symbol E), and the magnetic (symbol H) lines of force lie, respectively.

The E lines represent the *polarization* of the antenna. Polarization will be covered in more detail later in this chapter. As an example, the electromagnetic field pictured in Fig 1 of Chapter 23, Radio Wave Propagation, is the field that would be radiated from a vertically polarized antenna; that is, an antenna in which the conductor is mounted perpendicular to the earth.

When a radiation pattern is shown for an antenna mounted over ground rather than in free space, we automatically gain two frames of reference—an *azimuth angle* and an *elevation angle*. The azimuth angle is usually ref-

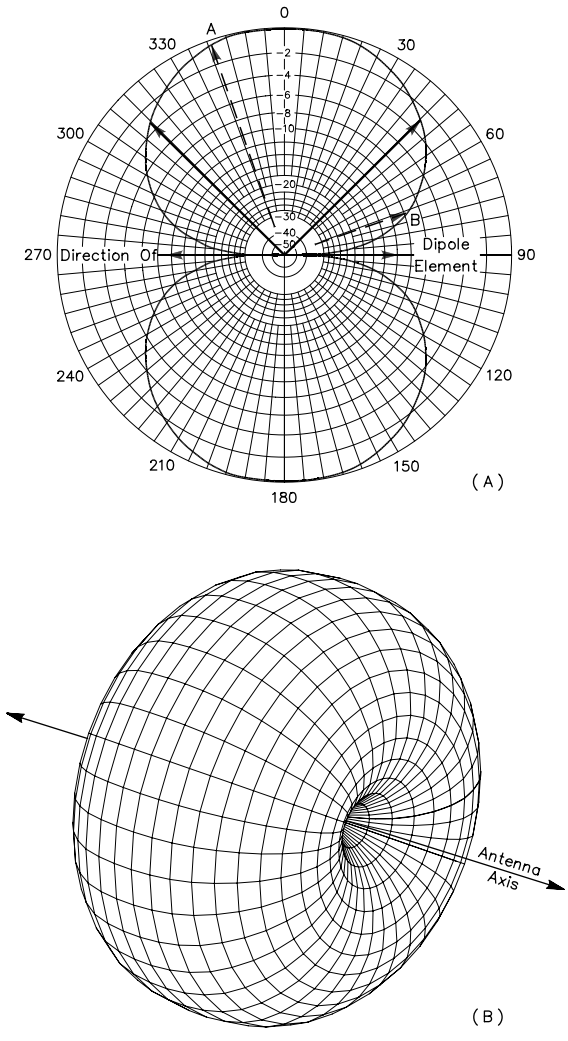

Fig 12—Directive diagram of a free-space dipole. At A, the pattern in the plane containing the wire axis. The length of each dashed-line arrow represents the relative field strength in that direction, referenced to the direction of maximum radiation, which is at right angles to the wire's axis. The arrows at approximately 45° and 315° are the half-power or –3 dB points. At B, a wire grid representation of the solid pattern for the same antenna. These same patterns apply to any center-fed dipole antenna less than a half wavelength long.

Introduction to the Decibel

The power gain of an antenna system is usually expressed in *decibels*. The decibel is a practical unit for measuring power ratios because it is more closely related to the actual effect produced at a distant receiver than the power ratio itself. One decibel represents a just-detectable change in signal strength, regardless of the actual value of the signal voltage. A 20-decibel (20-dB) increase in signal, for example, represents 20 observable steps in increased signal. The power ratio (100 to 1) corresponding to 20 dB gives an entirely exaggerated idea of the improvement in communication to be expected. The number of decibels corresponding to any power ratio is equal to 10 times the common logarithm of the power ratio, or

$$dB = 10 \log_{10} \frac{P_1}{P_2}$$

If the voltage ratio is given, the number of decibels is equal to 20 times the common logarithm of the ratio. That is,

$$dB = 20 \log_{10} \frac{V_1}{V_2}$$

When a *voltage* ratio is used, both voltages must be measured across the same value of impedance. Unless this is done the decibel figure is meaningless, because it is fundamentally a measure of a *power* ratio.

The main reason a decibel is used is that successive power gains expressed in decibels may simply be added together. Thus a gain of 3 dB followed by a gain of 6 dB gives a total gain of 9 dB. In ordinary power ratios, the ratios must be multiplied together to find the total gain.

A *reduction* in power is handled simply by subtracting the requisite number of decibels. Thus, reducing the power to ½ is the same as *subtracting* 3 decibels. For example, a power gain of 4 in one part of a system and a reduction to ½ in another part gives a total power gain of 4 × ½ = 2. In decibels, this is 6 – 3 = 3 dB. A power reduction or *loss* is simply indicated by including a negative sign in front of the appropriate number of decibels.

erenced to the maximum radiation lobe of the antenna, where the azimuth angle is defined at 0°, or it could be referenced to the Earth's True North direction for an antenna oriented in a particular compass direction. The E-plane pattern for an antenna over ground is now called the *azimuth pattern*.

The elevation angle is referenced to the horizon at the Earth's surface, where the elevation angle is 0°. Of course, the Earth is round but because its radius is so large, it can in this context be considered to be flat in the area directly under the antenna. An elevation angle of 90° is straight over the antenna, and a 180° elevation is toward the horizon directly behind the antenna.

Professional antenna engineers often describe an antenna's orientation with respect to the point directly overhead—using the *zenith angle*, rather than the elevation angle. The elevation angle is computed by subtracting the zenith angle from 90°.

Referenced to the horizon of the Earth, the H-plane pattern is now called the *elevation pattern*. Unlike the free-space H-plane pattern, the over-ground elevation pattern is drawn as a half-circle, representing only positive elevations above the Earth's surface. The ground reflects or blocks radiation at negative elevation angles, making below-surface radiation plots unnecessary.

After a little practice, and with the exercise of some imagination, the complete solid pattern can be visualized with fair accuracy from inspection of the two planar diagrams, provided of course that the solid pattern of the antenna is *smooth*, a condition that is true for simple antennas like λ/2 dipoles.

Plane diagrams are plotted on polar coordinate paper, as described earlier. The points on the pattern where the radiation is zero are called *nulls*. The curved section from one null to the next on the plane diagram, or the corresponding section on the solid pattern, is called a *lobe*. The strongest lobe is commonly called the *main lobe*. Fig 12A shows the E-plane pattern for a half-wave dipole. In Fig 12, the dipole is placed in free space. In addition to the labels showing the main lobe and nulls in the pattern, the so-called *half-power* points on the main lobe are shown. These are the points where the power is 3 dB down from the peak value in the main lobe.

Directivity and Gain

Let us now examine directivity more closely. As mentioned previously, all practical antennas, even the simplest types such as dipoles, exhibit directivity. Here's another picture that may help explain the concept of directivity. **Fig 13A** shows a balloon blown into its usual spherical shape. This represents a "reference" isotropic source. Squeezing the balloon in the middle in Fig 13B produces a dipole-like figure-8 pattern whose peak levels at top and bottom are larger than the reference sphere. Compare this with Fig 13C. Next, squeezing the bottom end of the balloon produces a pattern that gives even more "gain" compared to the reference.

Free-space directivity can be expressed quantitatively by comparing the three-dimensional pattern of the antenna under consideration with the perfectly spherical three-dimensional pattern of an isotropic antenna. The field strength (and thus power per unit area, or *power density*) is the same everywhere on the surface of an imaginary sphere having a radius of many wavelengths and having an isotropic antenna at its center. At the surface of the same imaginary sphere around an antenna radiating the same total power, the directive pattern results in greater power density at some points on this sphere and less at others. The ratio of the maximum power density to the average power density taken over the entire sphere (which is the same as from the isotropic antenna under the specified conditions) is the numerical measure of the directivity of the antenna. That is,

$$D = \frac{P}{P_{av}} \qquad \text{(Eq 5)}$$

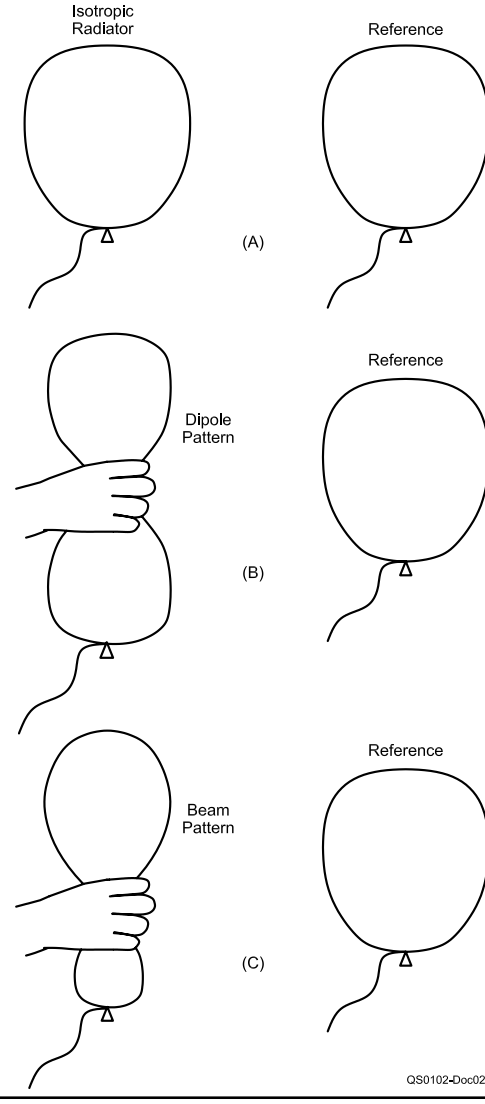

Fig 13—Demonstrating antenna pattern gain with balloons. Take a balloon, blow it up so that it is roughly circular in shape and then declare that this is a radiation pattern from an isotropic radiator. Next, blow up another balloon to the same size and shape and tell the audience that this will be the "reference" antenna (A). Then, squeeze the first balloon in the middle to form a sort of figure-8 shape and declare that this is a dipole and compare the maximum size to that of the reference "antenna" (B). The dipole can be seen to have some "gain" over the reference isotropic. Next, squeeze the end of the first balloon to come up with a sausage-like shape to demonstrate the sort of pattern a beam antenna creates (C).

where

D = directivity
P = power density at its maximum point on the surface of the sphere
P_{av} = average power density

The *gain* of an antenna is closely related to its direc-

tivity. Because directivity is based solely on the *shape* of the directive pattern, it does not take into account any power losses that may occur in an actual antenna system. To determine gain, these losses must be subtracted from the power supplied to the antenna. The loss is normally a constant percentage of the power input, so the antenna gain is

$$G = k\frac{P}{P_{av}} = kD \qquad \text{(Eq 6)}$$

where

G = gain (expressed as a power ratio)
D = directivity
k = efficiency (power radiated divided by power input) of the antenna
P and P_{av} are as above

For many of the antenna systems used by amateurs, the efficiency is quite high (the loss amounts to only a few percent of the total). In such cases the gain is essentially equal to the directivity. The more the directive diagram is compressed—or, in common terminology, the *sharper* the lobes—the greater the power gain of the antenna. This is a natural consequence of the fact that as power is taken away from a larger and larger portion of the sphere surrounding the radiator, it is added to the volume represented by the narrow lobes. Power is therefore concentrated in some directions, at the expense of others. In a general way, the smaller the volume of the solid radiation pattern, compared with the volume of a sphere having the same radius as the length of the largest lobe in the actual pattern, the greater the power gain.

As stated above, the gain of an antenna is related to its directivity, and directivity is related to the shape of the directive pattern. A commonly used index of directivity, and therefore the gain of an antenna, is a measure of the width of the major lobe (or lobes) of the plotted pattern. The width is expressed in degrees at the half-power or –3 dB points, and is often called the *beamwidth*.

This information provides only a general idea of relative gain, rather than an exact measure. This is because an absolute measure involves knowing the power density at every point on the surface of a sphere, while a single diagram shows the pattern shape in only one plane of that sphere. It is customary to examine at least the E-plane and the H-plane patterns before making any comparisons between antennas.

A simple approximation for gain over an isotropic radiator can be used, but only if the sidelobes in the antenna's pattern are small compared to the main lobe and if the resistive losses in the antenna are small. When the radiation pattern is complex, numerical integration is employed to give the actual gain.

$$G \approx \frac{41253}{H_{3dB} \times E_{3dB}} \qquad \text{(Eq 7)}$$

where H_{3dB} and E_{3dB} are the half-power points, in degrees, for the H and E-plane patterns.

Radiation Patterns for Center-Fed Dipoles at Different Frequencies

Earlier, we saw how the feed-point impedance of a fixed-length center-fed dipole in free space varies as the frequency is changed. What happens to the radiation pattern of such an antenna as the frequency is changed?

In general, the greater the length of a center-fed antenna, in terms of wavelength, the larger the number of lobes into which the pattern splits. A feature of all such patterns is the fact that the main lobe—the one that gives the largest field strength at a given distance—always is the one that makes the smallest angle with the antenna wire. Furthermore, this angle becomes smaller as the length of the antenna is increased.

Let's examine how the free-space radiation pattern changes for a 100-foot long wire made of #14 wire as the frequency is varied. (Varying the frequency effectively changes the wavelength for a fixed-length wire.) **Fig 14** shows the E-plane pattern at the λ/2 resonant frequency of 4.8 MHz. This is a classical dipole pattern, with a gain in free space of 2.14 dBi referenced to an isotropic radiator.

Fig 15 shows the free-space E-plane pattern for the same antenna, but now at the full-wave (2λ/2) resonant frequency of 9.55 MHz. Note how the pattern has been pinched in at the top and bottom of the figure. In other words, the two main lobes have become sharper at this frequency, making the gain 3.73 dBi, higher than at the λ/2 frequency.

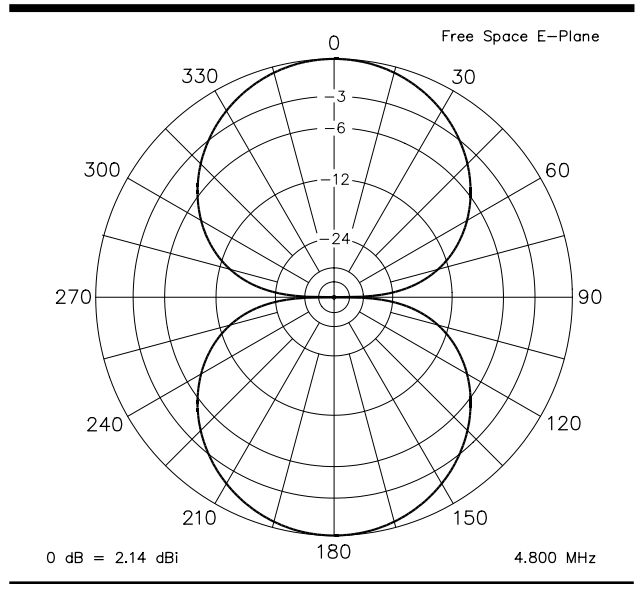

Fig 14—Free-space E-Plane radiation pattern for a 100-foot dipole at its half-wave resonant frequency of 4.80 MHz. This antenna has 2.14 dBi of gain. The dipole is located on the line from 90° to 270°.

Coordinate Scales for Radiation Patterns

A number of different systems of coordinate scales or *grids* are in use for plotting antenna patterns. Antenna patterns published for amateur audiences are sometimes placed on rectangular grids, but more often they are shown using polar coordinate systems. Polar coordinate systems may be divided generally into three classes: linear, logarithmic and modified logarithmic.

A very important point to remember is that the shape of a pattern (its general appearance) is highly dependent on the grid system used for the plotting. This is exemplified in **Fig A**, where the radiation pattern for a beam antenna is presented using three coordinate systems discussed in the paragraphs that follow.

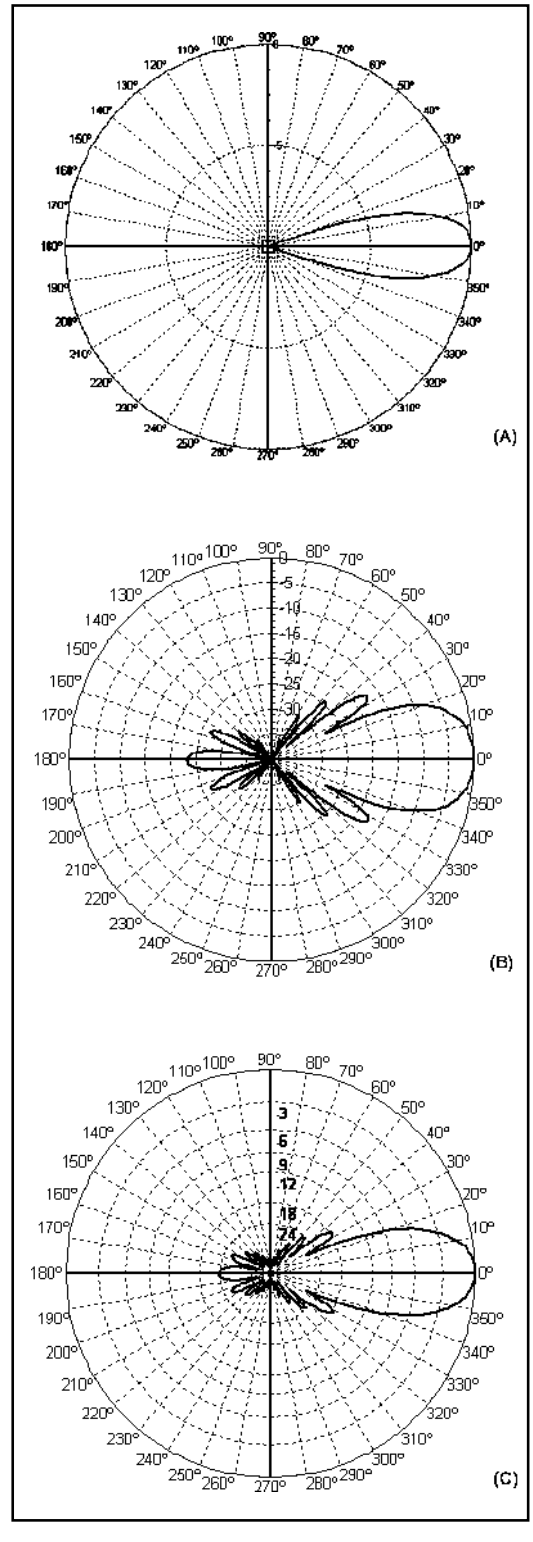

Linear Coordinate Systems

The polar coordinate system for the flashlight radiation pattern, Fig 10, uses linear coordinates. The concentric circles are equally spaced, and are graduated from 0 to 10. Such a grid may be used to prepare a linear plot of the power contained in the signal. For ease of comparison, the equally spaced concentric circles have been replaced with appropriately placed circles representing the decibel response, referenced to 0 dB at the outer edge of the plot. In these plots the minor lobes are suppressed. Lobes with peaks more than 15 dB or so below the main lobe disappear completely because of their small size. This is a good way to show the pattern of an array having high directivity and small minor lobes.

Logarithmic Coordinate System

Another coordinate system used by antenna manufacturers is the logarithmic grid, where the concentric grid lines are spaced according to the logarithm of the voltage in the signal. If the logarithmically spaced concentric circles are replaced with appropriately placed circles representing the decibel response, the decibel circles are graduated linearly. In that sense, the logarithmic grid might be termed a linear-log grid, one having linear divisions calibrated in decibels.

This grid enhances the appearance of the minor lobes. If the intent is to show the radiation pattern of an array supposedly having an omnidirectional response, this grid enhances that appearance. An antenna having a difference of 8 or 10 dB in pattern response around the compass appears to be closer to omnidirectional on this grid than on any of the others. See Fig A-(B).

ARRL Log Coordinate System

The modified logarithmic grid used by the ARRL has a system of concentric grid lines spaced according to the logarithm of 0.89 times the value of the signal voltage. In this grid, minor lobes that are 30 and 40 dB down from the main lobe are distinguishable. Such lobes are of concern in VHF and UHF work. The spacing between plotted points at 0 dB and –3 dB is significantly greater than the spacing between –20 and –23 dB, which in turn is significantly greater than the spacing between –50 and –53 dB.

For example, the scale distance covered by 0 to –3 dB is about $^{1}/_{10}$ of the radius of the chart. The scale distance for the next 3-dB increment (to –6 dB) is slightly less, 89% of the first, to be exact. The scale distance for the next 3-dB increment (to –9 dB) is again 89% of the second. The scale is constructed so that the progression ends with –100 dB at chart center.

The periodicity of spacing thus corresponds generally to the relative significance of such changes in antenna performance. Antenna pattern plots in this publication are made on the modified-log grid similar to that shown in Fig A-(C).

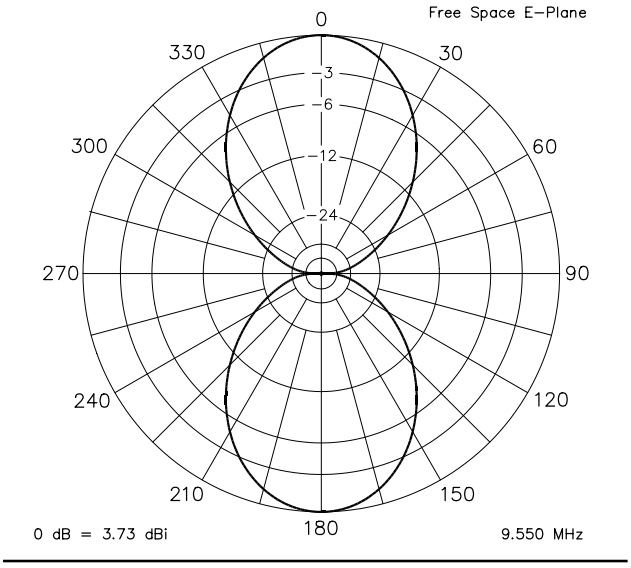

Fig 15—Free-space E-Plane radiation pattern for a 100-foot dipole at its full-wave resonant frequency of 9.55 MHz. The gain has increased to 3.73 dBi, because the main lobes have been focused and sharpened compared to Fig 13.

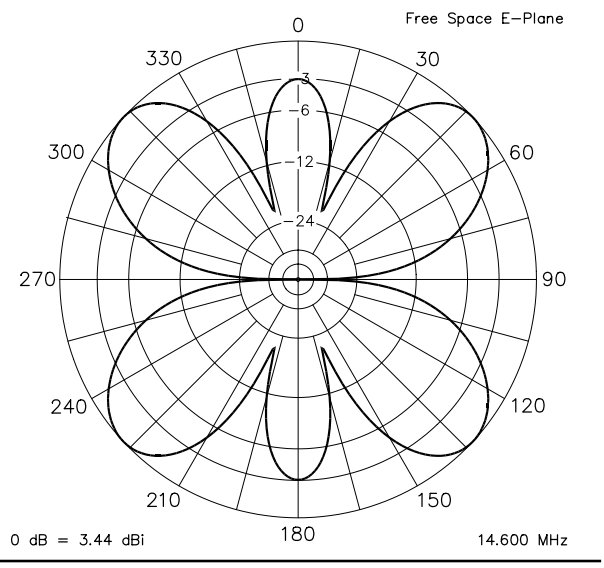

Fig 16—Free-space E-Plane radiation pattern for a 100-foot dipole at its 3/2λ resonant frequency of 14.60 MHz. The pattern has broken up into six lobes, and thus the peak gain has dropped to 3.44 dBi.

Fig 16 shows the pattern at the 3λ/2 frequency of 14.6 MHz. More lobes have developed compared to Fig 14. This means that the power has split up into more lobes and consequently the gain decreases a small amount, down to 3.44 dBi. This is still higher than the dipole at its λ/2 frequency, but lower than at its full-wave frequency. **Fig 17** shows the E-plane response at 19.45 MHz, the 4λ/2, or 2λ, resonant frequency. Now the pattern has reformed itself into only four lobes, and the gain has as a consequence risen to 3.96 dBi.

In **Fig 18** the response has become quite complex at the 5λ/2 resonance point of 24.45 MHz, with ten lobes showing. Despite the presence all these lobes, the main lobes now show a gain of 4.78 dBi. Finally, **Fig 19** shows the pattern at the 3λ (6λ/2) resonance at 29.45 MHz. Despite the fact that there are fewer lobes taking up power than at 24.45 MHz, the peak gain is slightly less at 29.45 MHz, at 4.70 dBi.

The pattern—and hence the gain—of a fixed-length antenna varies considerably as the frequency is changed. Of course, the pattern and gain change in the same fashion if the frequency is kept constant and the length of the wire is varied. In either case, the wavelength is changing. It is also evident that certain lengths reinforce the pattern to provide more peak gain. If an antenna is not rotated in azimuth when the frequency is changed, the peak gain may occur in a different direction than you might like. In other words, the main lobes change direction as the frequency is varied.

Fig A—Radiation pattern plots for a high-gain Yagi antenna on three different grid coordinate systems. At A, the pattern on a linear-power dB grid. Notice how details of sidelobe structure are lost with this grid. At B, the same pattern on a grid with constant 5 dB circles. The sidelobe level is exaggerated when this scale is employed. At B, the same pattern on the modified log grid used by ARRL. The side and rearward lobes are clearly visible on this grid. The concentric circles in all three grids are graduated in decibels referenced to 0 dB at the outer edge of the chart. The patterns look quite different, yet they all represent the same antenna response!

POLARIZATION

We've now examined the first two of the three major properties used to characterize antennas: the radiation pattern and the feed-point impedance. The third general property is *polarization*. An antenna's polarization is defined to be that of its electric field, in the direction where the field strength is maximum.

For example, if a λ/2 dipole is mounted horizontally over the Earth, the electric field is strongest perpendicular to its axis (that is, at right angle to the wire) and parallel to the earth. Thus, since the maximum electric field is horizontal, the polarization in this case is also considered to be *horizontal* with respect to the earth. If the dipole is mounted vertically, its polarization will be *vertical*. See **Fig 20**. Note that if an antenna is mounted in free space, there is no frame of reference and hence its

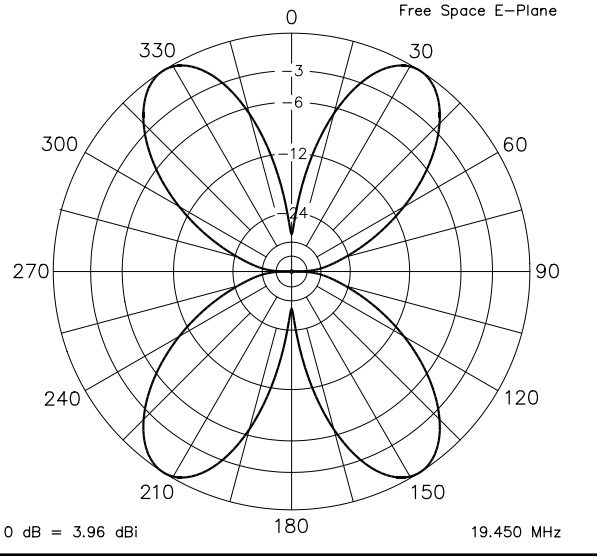

Fig 17—Free-space E-Plane radiation pattern for a 100-foot dipole at twice its full-wave resonant frequency of 19.45 MHz. The pattern has been refocused into four lobes, with a peak gain of 3.96 dBi.

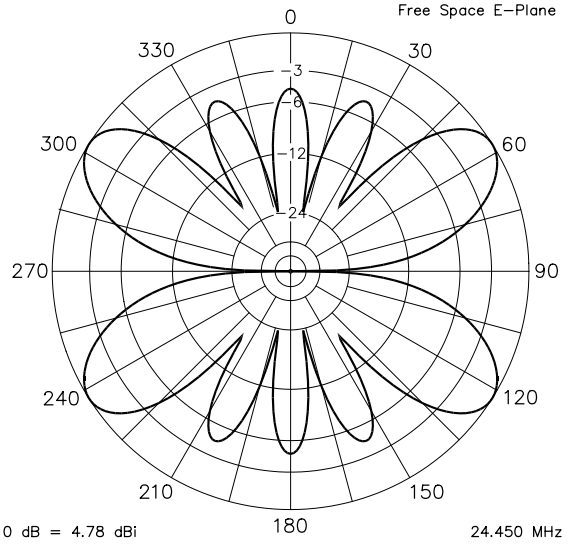

Fig 18—Free-space E-Plane radiation pattern for a 100-foot dipole at its 5/2λ resonant frequency of 24.45 MHz. The pattern has broken down into ten lobes, with a peak gain of 4.78 dBi.

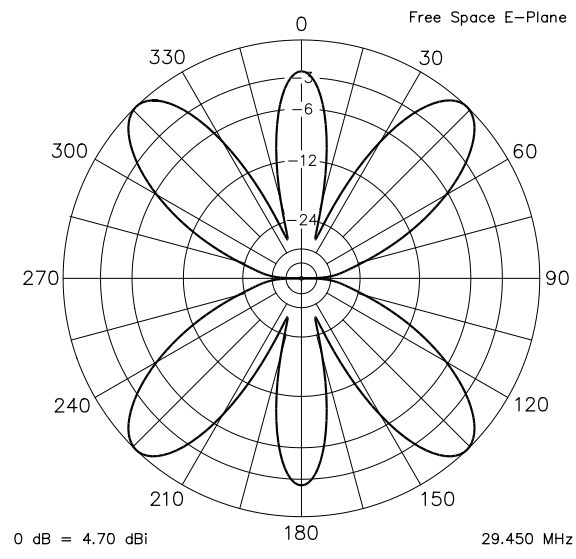

Fig 19—Free-space E-Plane radiation pattern for a 100-foot dipole at three times its full-wave resonant frequency of 29.45 MHz. The pattern has returned to six lobes, with a peak gain of 4.70 dBi.

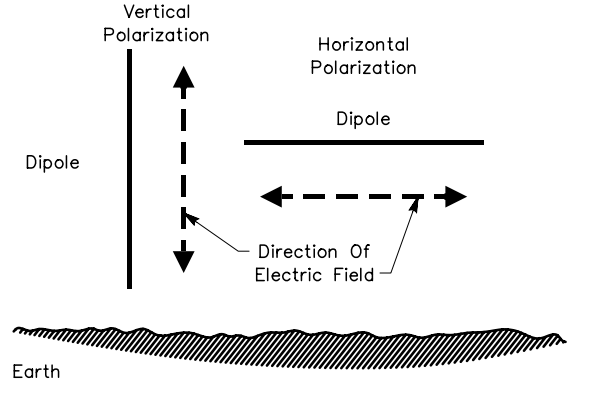

Fig 20—Vertical and horizontal polarization of a dipole above ground. The direction of polarization is the direction of the maximum electric field with respect to the earth.

polarization is indeterminate.

Antennas composed of a number of λ/2 elements arranged so that their axes lie in the same or parallel directions have the same polarization as that of any one of the elements. For example, a system composed of a group of horizontal dipoles is horizontally polarized. If both horizontal and vertical elements are used in the same plane and radiate in phase, however, the polarization is the *resultant* of the contributions made by each set of elements to the total electromagnetic field at a given point some distance from the antenna. In such a case the resultant polarization is still *linear*, but is tilted between horizontal and vertical.

In directions other than those where the radiation is maximum, the resultant wave even for a simple dipole is a combination of horizontally and vertically polarized components. The radiation off the ends of a horizontal dipole is actually vertically polarized, albeit at a greatly reduced amplitude compared to the broadside horizontally polarized radiation—the sense of polarization

changes with compass direction.

Thus it is often helpful to consider the radiation pattern from an antenna in terms of polar coordinates, rather than trying to think in purely linear horizontal or vertical coordinates. See **Fig 21**. The reference axis in a polar system is vertical to the earth under the antenna. The zenith angle is usually referred to as θ (Greek letter theta), and the azimuth angle is referred to as ϕ (Greek letter phi). Instead of zenith angles, most amateurs are more familiar with *elevation angles*, where a zenith angle of 0° is the same as an elevation angle of 90°, straight overhead. Native *NEC* or *MININEC* computer programs use zenith angles rather than elevation angles, although most commercial versions automatically reduce these to elevation angles.

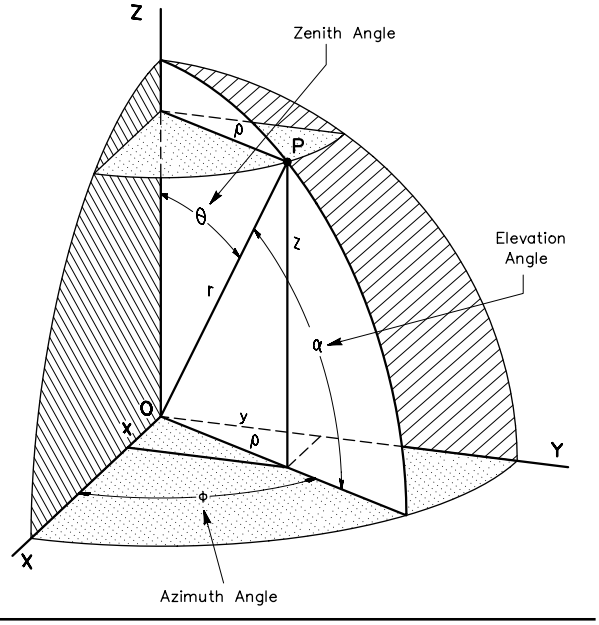

Fig 21—Diagram showing polar representation of a point P lying on an imaginary sphere surround a point-source antenna. The various angles associated with this coordinate system are shown referenced to the x, y and z-axes.

If vertical and horizontal elements in the same plane are fed out of phase (where the beginning of the RF period applied to the feed point of the vertical element is not in time phase with that applied to the horizontal), the resultant polarization is *elliptical*. Circular polarization is a special case of elliptical polarization. The wave front of a circularly polarized signal appears (in passing a fixed observer) to rotate every 90° between vertical and horizontal, making a complete 360° rotation once every period. Field intensities are *equal* at all instantaneous polarizations. Circular polarization is frequently used for space communications, and is discussed further in Chapter 19, Antenna Systems for Space Communications.

Sky-wave transmission usually changes the polarization of traveling waves. (This is discussed in Chapter 23, Radio Wave Propagation.) The polarization of receiving and transmitting antennas in the 3 to 30-MHz range, where almost all communication is by means of sky wave, need not be the same at both ends of a communication circuit (except for distances of a few miles). In this range the choice of polarization for the antenna is usually determined by factors such as the height of available antenna supports, polarization of man-made RF noise from nearby sources, probable energy losses in nearby objects, the likelihood of interfering with neighborhood broadcast or TV reception and general convenience.

Other Antenna Characteristics

Besides the three main characteristics of impedance, pattern (gain) and polarization, there are some other useful properties of antennas.

RECIPROCITY IN RECEIVING AND TRANSMITTING

Many of the properties of a resonant antenna used for reception are the same as its properties in transmission. It has the same directive pattern in both cases, and delivers maximum signal to the receiver when the signal comes from a direction in which the antenna has its best response. The impedance of the antenna is the same, at the same point of measurement, in receiving as in transmitting.

In the receiving case, the antenna is the source of power delivered to the receiver, rather than the load for a source of power (as in transmitting). Maximum possible output from the receiving antenna is obtained when the load to which the antenna is connected is the same as the impedance of the antenna. We say that the antenna is *matched* to its load.

The power gain in receiving is the same as the gain in transmitting, when certain conditions are met. One such condition is that both antennas (usually λ/2-long antennas) must work into load impedances matched to their own impedances, so that maximum power is transferred in both cases. In addition, the comparison antenna should be oriented so it gives maximum response to the signal used in the test. That is, it should have the same polarization as the incoming signal and should be placed so its direction of maximum gain is toward the signal source.

In long-distance transmission and reception via the ionosphere, the relationship between receiving and transmitting, however, may not be exactly reciprocal. This is because the waves do not always follow exactly the same

paths at all times and so may show considerable variation in the time between alternations between transmitting and receiving. Also, when more than one ionospheric layer is involved in the wave travel (see Chapter 23, Radio Wave Propagation), it is sometimes possible for reception to be good in one direction and poor in the other, over the same path.

Wave polarization usually shifts in the ionosphere. The tendency is for the arriving wave to be elliptically polarized, regardless of the polarization of the transmitting antenna. Vertically polarized antennas can be expected to show no more difference between transmission and reception than horizontally polarized antennas. On the average, however, an antenna that transmits well in a certain direction also gives favorable reception from the same direction, despite ionospheric variations.

FREQUENCY SCALING

Any antenna design can be scaled in size for use on another frequency or on another amateur band. The dimensions of the antenna may be scaled with Eq 8 below.

$$D = \frac{f1}{f2} \times d \qquad \text{(Eq 8)}$$

where

D = scaled dimension
d = original design dimension
f1 = original design frequency
f2 = scaled frequency (frequency of intended operation)

From this equation, a published antenna design for, say, 14 MHz can be scaled in size and constructed for operation on 18 MHz, or any other desired band. Similarly, an antenna design could be developed experimentally at VHF or UHF and then scaled for operation in one of the HF bands. For example, from Eq 8, an element of 39.0 inches length at 144 MHz would be scaled to 14 MHz as follows: D = 144/14 × 39 = 401.1 inches, or 33.43 feet.

To scale an antenna properly, *all* physical dimensions must be scaled, including element lengths, element spacings, boom diameters and element diameters. Lengths and spacings may be scaled in a straightforward manner as in the above example, but element diameters are often not as conveniently scaled. For example, assume a 14-MHz antenna is modeled at 144 MHz and perfected with $^3/_8$-inch cylindrical elements. For proper scaling to 14 MHz, the elements should be cylindrical, of 144/14 × $^3/_8$ or 3.86 inches diameter. From a realistic standpoint, a 4-inch diameter might be acceptable, but cylindrical elements of 4-inch diameter in lengths of 33 feet or so would be quite unwieldy (and quite expensive, not to mention heavy). Choosing another, more suitable diameter is the only practical answer.

Diameter Scaling

Simply changing the diameter of dipole type elements during the scaling process is not satisfactory without making a corresponding element-length correction. This is because changing the diameter results in a change in the λ/dia ratio from the original design, and this alters the corresponding resonant frequency of the element. The element length must be corrected to compensate for the effect of the different diameter actually used.

To be more precise, however, the purpose of diameter scaling is not to maintain the same resonant frequency for the element, but to maintain the same ratio of self-resistance to self-reactance at the operating frequency—that is, the Q of the scaled element should be the same as that of the original element. This is not always possible to achieve exactly for elements that use several telescoping sections of tubing.

Tapered Elements

Rotatable beam antennas are usually constructed with elements made of metal tubing. The general practice at HF is to taper the elements with lengths of telescoping tubing. The center section has a large diameter, but the ends are relatively small. This reduces not only the weight, but also the cost of materials for the elements. Tapering of HF Yagi elements is discussed in detail in Chapter 11, HF Yagi Arrays.

Length Correction for Tapered Elements

The effect of tapering an element is to alter its electrical length. That is to say, two elements of the same length, one cylindrical and one tapered but with the same average diameter as the cylindrical element, will not be resonant at the same frequency. The tapered element must be made longer than the cylindrical element for the same resonant frequency.

A procedure for calculating the length for tapered elements has been worked out by Dave Leeson, W6NL (ex-W6QHS), from work done by Schelkunoff at Bell Labs and is presented in Leeson's book, *Physical Design of Yagi Antennas*. In the software accompanying this book is a subroutine called EFFLEN.FOR. It is written in Fortran and is used in the *SCALE* program to compute the effective length of a tapered element. The algorithm uses the W6NL-Schelkunoff algorithm and is commented step-by-step to show what is happening. Calculations are made for only one half of an element, assuming the element is symmetrical about the point of boom attachment.

Also, read the documentation SCALE.PDF for the *SCALE* program, which will automatically do the complex mathematics to scale a Yagi design from one frequency to another, or from one taper schedule to another.

The Vertical Monopole

So far in this discussion on Antenna Fundamentals, we have been using the free-space, center-fed dipole as our main example. Another simple form of antenna derived from a dipole is called a *monopole*. The name suggests that this is one half of a dipole, and so it is. The monopole is always used in conjunction with a *ground plane*, which acts as a sort of electrical mirror. See **Fig 22**, where a λ/2 dipole and a λ/4 monopole are compared. The *image antenna* for the monopole is the dotted line beneath the ground plane. The image forms the missing second half of the antenna, transforming a monopole into the functional equivalent of a dipole. From this explanation you can see where the term *image plane* is sometimes used instead of ground plane.

Although we have been focusing throughout this chapter on antennas in free space, practical monopoles are usually mounted vertically with respect to the surface of the ground. As such, they are called *vertical monopoles*, or simply *verticals*. A practical vertical is supplied power by feeding the radiator against a ground system, usually made up of a series of paralleled wires radiating from and laid out in a circular pattern around the base of the antenna. These wires are termed *radials*.

The term *ground plane* is also used to describe a vertical antenna employing a λ/4-long vertical radiator working against a *counterpoise* system, another name for the ground plane that supplies the missing half of the antenna. The counterpoise for a ground-plane antenna usually consists of four λ/4-long radials elevated well above the earth. See **Fig 23**.

Chapter 3, The Effects of Ground, devotes much attention to the requirements for an efficient grounding system for vertical monopole antennas, and Chapter 6, Low-Frequency Antennas, gives more information on ground-plane verticals.

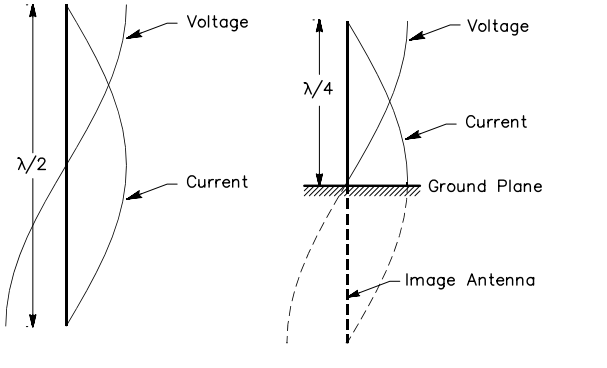

Fig 22—The λ/2 dipole antenna and its λ/4 ground-plane counterpart. The "missing" quarter wavelength is supplied as an image in "perfect" (that is, high-conductivity) ground.

Characteristics of a λ/4 Monopole

The free-space directional characteristics of a λ/4 monopole with its ground plane are very similar to that of a λ/2 antenna in free space. The gain for the λ/4 monopole is slightly less because the H-plane for the λ/2 antenna is compressed compared to the monopole. Like a λ/2 antenna, the λ/4 monopole has an *omnidirectional* radiation pattern in the plane perpendicular to the monopole.

The current in a λ/4 monopole varies practically sinusoidally (as is the case with a λ/2 wire), and is highest at the ground-plane connection. The RF voltage is highest at the open (top) end and minimum at the ground plane. The feed-point resistance close to λ/4 resonance of a vertical monopole over a perfect ground plane is one-half that for a λ/2 dipole at its λ/2 resonance. In this case, a "perfect ground plane" is an infinitely large, lossless conductor.

See **Fig 24**, which shows the feed-point impedance of a vertical antenna made of #14 wire, 50 feet long, located over perfect ground. This is over the whole HF range from 1 to 30 MHz. Again, there is nothing special about the choice of 50 feet for the length of the vertical radiator; it is simply a convenient length for evaluation. **Fig 25** shows an expanded portion of the frequency range above and below the λ/4 resonant point, but now calibrated in terms of wavelength. Note that this particular antenna goes through λ/4 resonance at a length of 0.244 λ, not at exactly 0.25 λ. The exact length for resonance varies with the diameter of the wire used, just as it does for the λ/2 dipole at its λ/2 resonance.

The word *height* is usually used for a vertical monopole antenna whose base is on or near the ground, and in this context, height has the same meaning as *length* when applied to λ/2 dipole antennas. Older texts often refer to heights in electrical degrees, referenced to a free-space wavelength of 360°, but here height is expressed in terms of the free-space wavelength. The range shown in Fig 24 is from 0.132 λ to 0.300 λ, corresponding to a frequency range of 2.0 to 5.9 MHz.

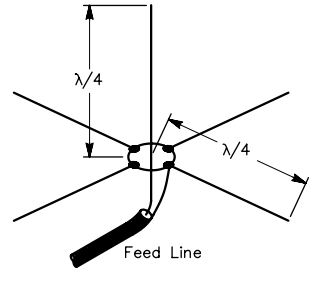

Fig 23—The ground-plane antenna. Power is applied between the base of the vertical radiator and the center of the four ground plane wires.

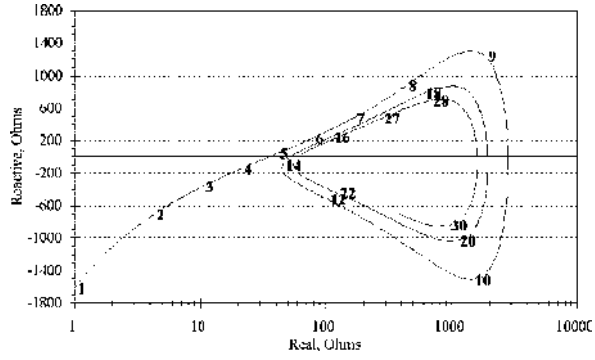

Fig 24—Feed-point impedance versus frequency for a theoretical 50-foot-high grounded vertical monopole made of #14 wire. The numbers along the curve show the frequency in MHz. This was computed using "perfect" ground. Real ground losses will add to the feed-point impedance shown in an actual antenna system.

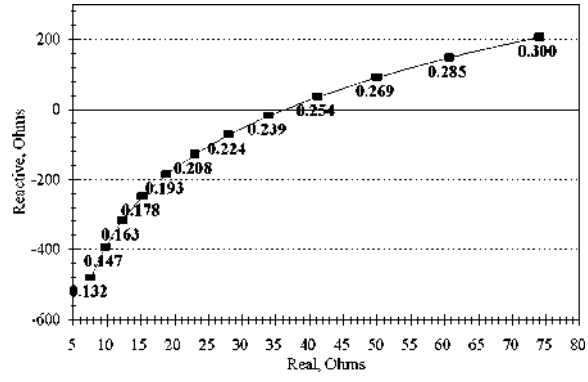

Fig 25—Feed-point impedance for the same antennas as in Fig 21, but calibrated in wavelength rather than frequency, over the range from 0.132 to 0.300λ, above and below the quarter-wave resonance.

The reactive portion of the feed-point impedance depends highly on the length/dia ratio of the conductor, as was discussed previously for a horizontal center-fed dipole. The impedance curve in Figs 24 and 25 is based on a #14 conductor having a length/dia ratio of about 800 to 1. As usual, thicker antennas can be expected to show less reactance at a given height, and thinner antennas will show more.

Efficiency of Vertical Monopoles

This topic of the efficiency of vertical monopole systems will be covered in detail in Chapter 3, The Effects of Ground, but it is worth noting at this point that the efficiency of a real vertical antenna over real earth often suffers dramatically compared with that of a λ/2 antenna. Without a fairly elaborate grounding system, the efficiency is not likely to exceed 50%, and it may be much less, particularly at monopole heights below λ/4.

BIBLIOGRAPHY

J. S. Belrose, "Short Antennas for Mobile Operation," *QST*, Sep 1953.

G. H. Brown, "The Phase and Magnitude of Earth Currents Near Radio Transmitting Antennas," *Proc IRE*, Feb 1935.

G. H. Brown, R. F. Lewis and J. Epstein, "Ground Systems as a Factor in Antenna Efficiency," *Proc IRE*, Jun 1937, pp 753-787.

G. H. Brown and O. M. Woodward, Jr., "Experimentally Determined Impedance Characteristics of Cylindrical Antennas," *Proc IRE*, April 1945.

A. Christman, "Elevated Vertical Antenna Systems," *QST*, Aug 1988, pp 35-42.

R. B. Dome, "Increased Radiating Efficiency for Short Antennas," *QST*, Sep 1934, pp 9-12.

A. C. Doty, Jr., J. A. Frey and H. J. Mills, "Characteristics of the Counterpoise and Elevated Ground Screen," Professional Program, Session 9, Southcon '83 (IEEE), Atlanta, GA, Jan 1983.

A. C. Doty, Jr., J. A. Frey and H. J. Mills, "Efficient Ground Systems for Vertical Antennas," *QST*, Feb 1983, pp 20-25.

A. C. Doty, Jr., technical paper presentation, "Capacitive Bottom Loading and Other Aspects of Vertical Antennas," Technical Symposium, Radio Club of America, New York City, Nov 20, 1987.

A. C. Doty, Jr., J. A. Frey and H. J. Mills, "Vertical Antennas: New Design and Construction Data," *The ARRL Antenna Compendium, Volume 2* (Newington: ARRL, 1989), pp 2-9.

R. Fosberg, "Some Notes on Ground Systems for 160 Meters," *QST*, Apr 1965, pp 65-67.

G. Grammer, "More on the Directivity of Horizontal Antennas; Harmonic Operation—Effects of Tilting," *QST*, Mar 1937, pp 38-40, 92, 94, 98.

H. E. Green, "Design Data for Short and Medium Length Yagi-Uda Arrays," *Trans IE Australia*, Vol EE-2, No. 1, Mar 1966.

H. J. Mills, technical paper presentation, "Impedance Transformation Provided by Folded Monopole Antennas," Technical Symposium, Radio Club of America, New York City, Nov 20, 1987.

B. Myers, "The W2PV Four-Element Yagi," *QST*, Oct 1986, pp 15-19.

L. Richard, "Parallel Dipoles of 300-Ohm Ribbon," *QST*, Mar 1957.

J. H. Richmond, "Monopole Antenna on Circular Disc," *IEEE Trans on Antennas and Propagation*, Vol. AP-32, No. 12, Dec 1984.

W. Schulz, "Designing a Vertical Antenna," *QST*, Sep 1978, pp 19- 21.

J. Sevick, "The Ground-Image Vertical Antenna," *QST*, Jul 1971, pp 16-17, 22.
J. Sevick, "The W2FMI 20-Meter Vertical Beam," *QST*, Jun 1972, pp 14-18.
J. Sevick, "The W2FMI Ground-Mounted Short Vertical," *QST*, Mar 1973, pp. 13-18, 41.
J. Sevick, "A High Performance 20-, 40- and 80-Meter Vertical System," *QST*, Dec 1973.
J. Sevick, "Short Ground-Radial Systems for Short Verticals," *QST*, Apr 1978, pp 30-33.
J. Sevick, *Transmission Line Transformers*, 3rd ed. (Tucker, GA: Noble Publishing, 1996).
C. E. Smith and E. M. Johnson, "Performance of Short Antennas," *Proc IRE*, Oct 1947.
J. Stanley, "Optimum Ground Systems for Vertical Antennas," *QST*, Dec 1976, pp 13-15.
R. E. Stephens, "Admittance Matching the Ground-Plane Antenna to Coaxial Transmission Line," Technical Correspondence, *QST*, Apr 1973, pp 55-57.
D. Sumner, "Cushcraft 32-19 'Boomer' and 324-QK Stacking Kit," Product Review, *QST*, Nov 1980, pp 48-49.
W. van B. Roberts, "Input Impedance of a Folded Dipole," *RCA Review*, Jun 1947.
E. M. Williams, "Radiating Characteristics of Short-Wave Loop Aerials," *Proc IRE*, Oct 1940.

TEXTBOOKS ON ANTENNAS

C. A. Balanis, *Antenna Theory, Analysis and Design* (New York: Harper & Row, 1982).
D. S. Bond, *Radio Direction Finders*, 1st ed. (New York: McGraw-Hill Book Co).
W. N. Caron, *Antenna Impedance Matching* (Newington: ARRL, 1989).
K. Davies, *Ionospheric Radio Propagation*—National Bureau of Standards Monograph 80 (Washington, DC: U.S. Government Printing Office, Apr 1, 1965).
R. S. Elliott, *Antenna Theory and Design* (Englewood Cliffs, NJ: Prentice Hall, 1981).
A. E. Harper, *Rhombic Antenna Design* (New York: D. Van Nostrand Co, Inc, 1941).
K. Henney, *Principles of Radio* (New York: John Wiley and Sons, 1938), p 462.
H. Jasik, *Antenna Engineering Handbook*, 1st ed. (New York: McGraw-Hill, 1961).
W. C. Johnson, *Transmission Lines and Networks*, 1st ed. (New York: McGraw-Hill Book Co, 1950).
R. C. Johnson and H. Jasik, *Antenna Engineering Handbook*, 2nd ed. (New York: McGraw-Hill, 1984).
R. C. Johnson, *Antenna Engineering Handbook*, 3rd ed. (New York: McGraw-Hill, 1993).
E. C. Jordan and K. G. Balmain, *Electromagnetic Waves and Radiating Systems*, 2nd ed. (Englewood Cliffs, NJ: Prentice-Hall, Inc, 1968).
R. Keen, *Wireless Direction Finding*, 3rd ed. (London: Wireless World).
R. W. P. King, *Theory of Linear Antennas* (Cambridge, MA: Harvard Univ. Press, 1956).
R. W. P. King, H. R. Mimno and A. H. Wing, *Transmission Lines, Antennas and Waveguides* (New York: Dover Publications, Inc, 1965).
King, Mack and Sandler, *Arrays of Cylindrical Dipoles* (London: Cambridge Univ Press, 1968).
M. G. Knitter, Ed., *Loop Antennas—Design and Theory* (Cambridge, WI: National Radio Club, 1983).
M. G. Knitter, Ed., *Beverage and Long Wire Antennas*—Design and Theory (Cambridge, WI: National Radio Club, 1983).
J. D. Kraus, *Electromagnetics* (New York: McGraw-Hill Book Co).
J. D. Kraus, *Antennas*, 2nd ed. (New York: McGraw-Hill Book Co, 1988).
E. A. Laport, *Radio Antenna Engineering* (New York: McGraw-Hill Book Co, 1952).
J. L. Lawson, *Yagi-Antenna Design*, 1st ed. (Newington: ARRL, 1986).
P. H. Lee, *The Amateur Radio Vertical Antenna Handbook*, 2nd ed. (Port Washington, NY: Cowen Publishing Co., 1984).
A. W. Lowe, *Reflector Antennas* (New York: IEEE Press, 1978).
M. W. Maxwell, *Reflections—Transmission Lines and Antennas* (Newington: ARRL, 1990). Out of print.
M. W. Maxwell, *Reflections II—Transmission Lines and Antennas* (Sacramento: Worldradio Books, 2001).
G. M. Miller, *Modern Electronic Communication* (Englewood Cliffs, NJ: Prentice Hall, 1983).
V. A. Misek, *The Beverage Antenna Handbook* (Hudson, NH: V. A. Misek, 1977).
T. Moreno, *Microwave Transmission Design Data* (New York: McGraw-Hill, 1948).
L. A. Moxon, *HF Antennas for All Locations* (Potters Bar, Herts: Radio Society of Great Britain, 1982), pp 109-111.
Ramo and Whinnery, *Fields and Waves in Modern Radio* (New York: John Wiley & Sons).
V. H. Rumsey, *Frequency Independent Antennas* (New York: Academic Press, 1966).
P. N. Saveskie, *Radio Propagation Handbook* (Blue Ridge Summit, PA: Tab Books, Inc, 1980).
S. A. Schelkunoff, *Advanced Antenna Theory* (New York: John Wiley & Sons, Inc, 1952).
S. A. Schelkunoff and H. T. Friis, *Antennas Theory and Practice* (New York: John Wiley & Sons, Inc, 1952).
J. Sevick, *Transmission Line Transformers* (Atlanta: Noble Publishing, 1996).
H. H. Skilling, *Electric Transmission Lines* (New York: McGraw-Hill Book Co, Inc, 1951).
M. Slurzburg and W. Osterheld, *Electrical Essentials of Radio* (New York: McGraw-Hill Book Co, Inc, 1944).
G. Southworth, *Principles and Applications of Waveguide*

Transmission (New York: D. Van Nostrand Co, 1950).
F. E. Terman, *Radio Engineers' Handbook*, 1st ed. (New York, London: McGraw-Hill Book Co, 1943).
F. E. Terman, *Radio Engineering*, 3rd ed. (New York: McGraw-Hill, 1947).
S. Uda and Y. Mushiake, *Yagi-Uda Antenna* (Sendai, Japan: Sasaki Publishing Co, 1954). [Published in English—Ed.]
P. P. Viezbicke, "*Yagi Antenna Design*," NBS Technical Note 688 (U. S. Dept of Commerce/National Bureau of Standards, Boulder, CO), Dec 1976.
G. B. Welch, *Wave Propagation and Antennas* (New York: D. Van Nostrand Co, 1958), pp 180-182.
The GIANT Book of Amateur Radio Antennas (Blue Ridge Summit, PA: Tab Books, 1979), pp 55-85.
IEEE Standard Dictionary of Electrical and Electronics Terms, 3rd ed. (New York: IEEE, 1984).
Radio Broadcast Ground Systems, available from Smith Electronics, Inc, 8200 Snowville Rd, Cleveland, OH 44141.
Radio Communication Handbook, 5th ed. (London: RSGB, 1976).
Radio Direction Finding, published by the Happy Flyer, 1811 Hillman Ave, Belmont, CA 94002

Chapter 3

The Effects of Ground

The ground around and under an antenna is part of the environment in which any actual antenna must operate. Chapter 2, Antenna Fundamentals, dealt mainly with theoretical antennas in free space, completely removed from the influence of the ground. This chapter is devoted to exploring the interactions between antennas and the ground.

The interactions can be analyzed depending on where they occur relative to two areas surrounding the antenna: the *reactive near field* and the *radiating far field*. You will recall that the reactive near field only exists very close to the antenna itself. In this region the antenna acts as though it were a large lumped-constant inductor or capacitor, where energy is stored but very little is actually radiated. The interaction with the ground in this area creates mutual impedances between the antenna and its environment and these interactions not only modify the feed-point impedance of an antenna, but also often increase losses.

In the radiating far field, the presence of ground profoundly influences the radiation pattern of a real antenna. The interaction is different, depending on the antenna's polarization with respect to the ground. For horizontally polarized antennas, the *shape* of the radiated pattern in the elevation plane depends primarily on the antenna's height above ground. For vertically polarized antennas, both the *shape* and the *strength* of the radiated pattern in the elevation plane strongly depend on the nature of the ground itself (its dielectric constant and conductivity at the frequency of operation), as well as on the height of the antenna above ground.

The Effects of Ground in the Reactive Near Field

FEED-POINT IMPEDANCE VERSUS HEIGHT ABOVE GROUND

Waves radiated from the antenna directly downward reflect vertically from the ground and, in passing the antenna on their upward journey, induce a voltage in it. The magnitude and phase of the current resulting from this induced voltage depends on the height of the antenna above the reflecting surface.

The total current in the antenna consists of two components. The amplitude of the first is determined by the power supplied by the transmitter and the free-space feed-point resistance of the antenna. The second component is induced in the antenna by the wave reflected from the ground. This second component of current, while considerably smaller than the first at most useful antenna heights, is by no means insignificant. At some heights, the two components will be in phase, so the total current is larger than is indicated by the free-space feed-point resistance. At other heights, the two components are out of phase, and the total current is the difference between the two components.

Changing the height of the antenna above ground will change the amount of current flow, assuming that the power input to the antenna is constant. A higher current at the same power input means that the effective resistance of the

antenna is lower, and vice versa. In other words, the feed-point resistance of the antenna is affected by the height of the antenna above ground because of mutual coupling between the antenna and the ground beneath it.

The electrical characteristics of the ground affect both the amplitude and the phase of reflected signals. For this reason, the electrical characteristics of the ground under the antenna will have some effect on the impedance of that antenna, the reflected wave having been influenced by the ground. Different impedance values may be encountered when an antenna is erected at identical heights but over different types of earth.

Fig 1 shows the way in which the radiation resistance of horizontal and vertical half-wave antennas varies with height above ground (in λ, wavelengths). The height of the vertical half-wave is the distance from the bottom of the antenna to ground. For horizontally polarized half-wave antennas, the differences between the effects of perfect ground and real earth are negligible if the antenna height is greater than 0.2 λ. At lower heights, the feed-point resistance over perfect ground decreases rapidly as the antenna is brought closer to a theoretically perfect ground, but this does not occur so rapidly for actual ground. Over real earth, the resistance actually begins increasing at heights below about 0.08 λ. The reason for the increasing resistance at very low heights is that more and more of the reactive (induction) field of the antenna is absorbed by the lossy ground in close proximity. This results in increased loss that is reflected in the increased value of the feedpoint resistance.

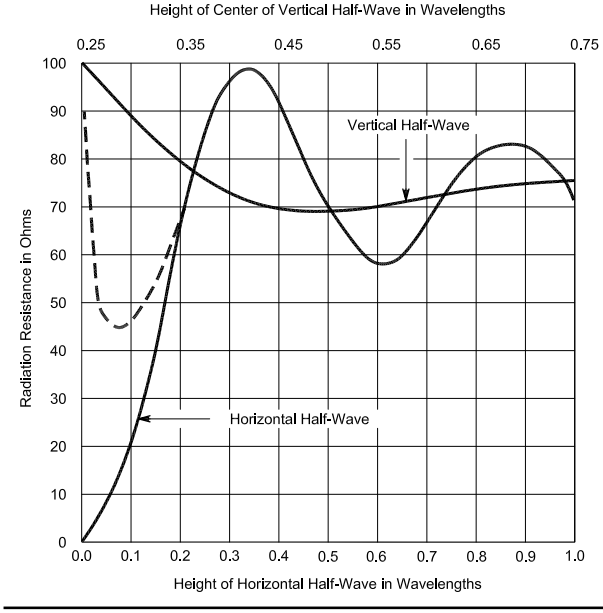

Fig 1—Variation in radiation resistance of vertical and horizontal half-wave antennas at various heights above flat ground. Solid lines are for perfectly conducting ground; the broken line is the radiation resistance of horizontal half-wave antennas at low height over real ground.

For a vertically polarized λ/2-long dipole, differences between the effects of perfect ground and real earth on the feed-point impedance is negligible, as seen in **Fig 1**. The theoretical half-wave antennas on which this chart is based are assumed to have infinitely thin conductors.

GROUND SYSTEMS FOR VERTICAL MONOPOLES

In this section, we'll look at vertical monopoles, which require some sort of ground system in order to make up for the "missing" second half of the antenna and reduce the power lost in the near field. Rudy Severns, N6LF, contributed much of the new material in this chapter.

In Chapter 2, Antenna Fundamentals, and up to this point in this chapter, the discussion about vertical monopoles has mainly been for antennas where *perfect ground* is available. We have also briefly looked at the ground-plane vertical in free space, where the four ground-plane radials form a built-in ground system.

Perfect ground makes a vertical monopole into the functional equivalent of a center-fed dipole, although the feed-point resistance at resonance is half that of the center-fed dipole. But how can we manage to create that elusive perfect ground, or at least a reasonable approximation, for our real vertical antennas?

Simulating a Perfect Ground in the Reactive Near Field

The effect of a perfectly conducting ground (so far as feed-point resistance and losses are concerned) can be simulated under a real antenna by installing a very large metal screen or mesh, such as poultry netting (chicken wire) or hardware cloth, on or near the surface of the ground. The screen (also called a *counterpoise system*, especially if it is elevated off the ground) should extend at least a half wavelength in every direction from the antenna. The feed-point resistance of a quarter-wave long, thin vertical radiator over such a ground screen will approach the theoretical value of 36.6 Ω. Of course on the lower HF bands such a screen is not practical for most amateurs.

Based on the results of a study published in 1937 by Brown, Lewis and Epstein (see Bibliography), a grounding system consisting of 120 wires, each at least λ/2 long, extending radially from the base of the antenna and spaced equally around a circle, is also the practical equivalent of perfectly conducting ground for reactive-field currents. The wires can either be laid directly on the surface of the ground or buried a few inches below.

Another approach to simulating a perfect ground system is to utilize the ground-plane antenna, with its four ground-plane radials elevated well above lossy earth. Heights (between the bottom of the ground-plane and the surface of the ground) greater than λ/8 have proven to yield excellent

results. See Chapter 6, Low-Frequency Antennas, for more details on practical ground-plane verticals.

For a vertical antenna, a large ground screen, either made of wire mesh or a multitude of radials, or an elevated system of ground-plane radials will reduce ground losses near the antenna. This is because the screen conductors are solidly bonded to each other and the resistance is much lower than that of the lossy, low-conductivity earth itself. If the ground screen or elevated ground plane were not present, RF currents would be forced to flow through the lossy, low-conductivity earth to return to the base of the radiator. The ground screen or elevated ground plane in effect shield ground-return currents from the lossy earth.

Less-Than-Ideal Ground Systems

Now, what happens when something less than an ideal ground screen is used as the ground plane for a vertical monopole? Typically this will take the form of an on-ground wire radial system. A great deal of mystery and lack of information seems to surround the vertical antenna ground system. In the case of ground-mounted vertical antennas, many general statements such as "the more radials the better" and "lots of short radials are better than a few long ones" have served as rules of thumb, but many questions as to relative performance differences and optimum number for a given length remain unanswered, as is the justification for the rules of thumb. Most of these questions boil down to one: namely, how many radials, and how long, should be used in a given vertical antenna installation?

A ground system with 120 $\lambda/2$ radials is not very practical for many amateur installations, which often must contend with limited space and funding. Unfortunately the ground resistance, R_g, increases rapidly when the number of radials is reduced. To minimize ground loss where a large, optimum ground system is not possible requires that we understand how ground losses occur and how to optimize the design of a ground system that can fit within the space and budget available.

E and H Fields

E and H fields were introduced in Chapter 2, Antenna Fundamentals, to explain some basic concepts concerning antennas. To understand the reasons for ground loss we need to look at the E and H fields in the near field, but we need to have some feeling for what E and H fields are. The following is a brief description of these fields. It is certainly not a rigorous description but should give at least an intuitive feeling for what is happening.

In 1820 Hans Oerstad discovered that a current flowing in a wire would deflect the needle of a nearby compass. We attribute this effect to a *magnetic* or *H-field*, which at any given location is denoted by the bold-faced letter **H**. **H** is a vector, with an amplitude expressed in A/m (Amperes/meter) and a direction. **Fig 2** shows a typical experimental arrangement. The shape of the magnetic field is roughly shown by the distribution of the iron filings. This field distribution is very similar to that for a vertical antenna.

A compass needle (a small magnet itself) will try to align itself parallel to **H.** As the compass is moved around the conductor, the orientation of the needle changes accordingly. The orientation of the needle gives the direction of **H**. If you attempt to turn the needle away from alignment you will discover a torque trying to restore the needle to its original position. The torque is proportional to the strength of the magnetic field at that point. This is called the *field intensity* or amplitude of **H** at that point. If a larger current flows in the conductor going through the piece of paper holding the iron filings, the amplitude of **H** will be larger. Currents flowing in the conductors of an antenna also generate a magnetic field, one component of the near field.

An antenna will also have an *electric* or *E-field*, which can be visualized using a parallel-plate capacitor, as shown in **Fig 3**. If we connect a battery with a potential V_{dc} across the capacitor plates there will be an electric field **E** established between the plates, as indicated by the lines and directional arrows between the plates. The magnitude of vector **E** is expressed in V/m (volts per meter), so for a potential of V volts and a spacing of d meters, E = V/d V/m. The amplitude of **E** will increase with greater voltage and/or a smaller distance (d). In an antenna, there will be ac potential differences between different parts of the antenna and from the antenna to ground. These ac potential differences establish the electric field associated with the antenna.

Conduction And Displacement Currents

If we replace the dc voltage source in Fig 3 with an ac source, a steady ac current will flow in the circuit. In the

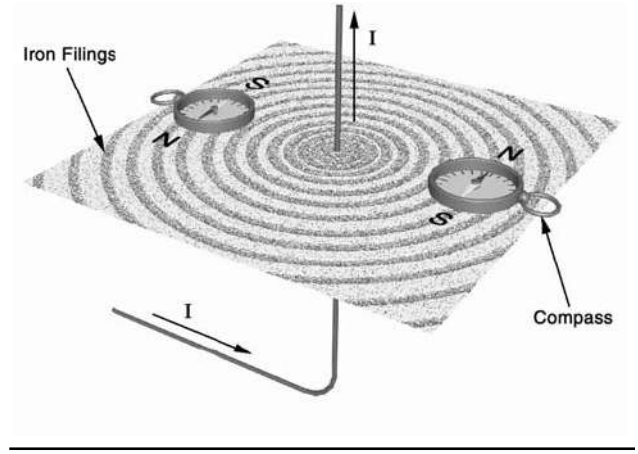

Fig 2—The magnetic lines of force that surround a conductor with an electric current flowing in it are shown by iron filings and small compass needles. The needles point in the direction of the magnetic or H-field. The filings give a general view of the field distribution in the plane perpendicular to the conductor.

conductors between the ac source and the capacitor plates, current (I_c) flows, because of the movement of charge, usually electrons. But in the space between the capacitor plates—particularly in a vacuum—there are no charge carriers available to carry a conduction current. Nonetheless, current still flows in the complete circuit, and we attribute this to a *displacement current* (I_d) flowing between the capacitor plates to account for the continuity of current in the circuit. Displacement and conduction currents are two different phenomena but they both represent current, just two different kinds. Some observers prefer to call conduction currents "currents" and displacement currents "imaginary currents." That terminology is OK, but to account for the current flow in a closed circuit with capacitance you have to keep track of both kinds of current, whatever you call them.

In an antenna over ground, the displacement current represents the current flow from the antenna surface through the air into the ground. The currents flowing in the ground are predominantly conduction currents, but there may also be displacement currents.

Where the dielectric material between the capacitor plates is not a perfect insulator, both conduction and displacement currents can flow between the capacitor plates. A good example of this would be a soil dielectric, which has both resistive and capacitive characteristics. Soil can be represented in the circuit of **Fig 4**, where there is a resistor with a conduction current I_c in parallel with a capacitor with a displacement current I_d. The two currents add up (vectorially) as the total current I_T.

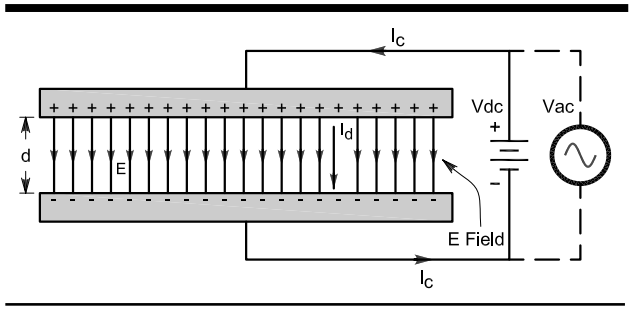

Fig 3—Example of an electric field, $E=V_{dc}/d$. When the dc source is replaced with an ac source there will be a displacement current (I_d) flowing between the capacitor plates.

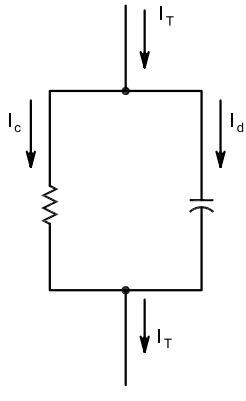

Fig 4—When the capacitor dielectric is less than perfect there will be a conduction current (I_c) in addition to the displacement current (I_d). Soil will typically have both resistive and capacitive components. Power loss in the soil is due to the current flowing through the resistive component.

A Closer Look at Verticals

A vertical antenna has two field components that induce currents in the ground around the antenna. **Fig 5** shows in a general way the electric-field component (E_z, in V/m) and magnetic-field component (H_ϕ, in A/m) in the region near a vertical. Because the soil near the antenna usually has relatively high resistance, both of these field components will induce currents (I_V and I_H) in the ground, resulting in losses. While the worms may enjoy the heated ground, power dissipated in the ground is subtracted from the radiated power, weakening your signal.

As shown in Fig 5, the tangential component of the H-field (H_ϕ) induces horizontal currents (I_H) flowing radially. The normal component (perpendicular to the ground surface) of the E-field (E_z) induces vertically flowing currents (I_v). Actually, things are more complex than this but we don't need to thrash through that to understand conceptually what's going on.

When modeling an antenna we account for the radiated power (P_r) by assuming there is a resistor we call the *radiation resistance* (R_r) through which the antenna base current (I_o) flows. The radiated power is then $P_r = I_o^2 R_r$. Similarly, we can account for the power dissipated in the ground (P_g) by adding a loss resistance (R_g) in series with R_r. The ground loss is then $P_g = I_o^2 R_g$. Additional losses due to conductors, loading coils, etc can also be simulated

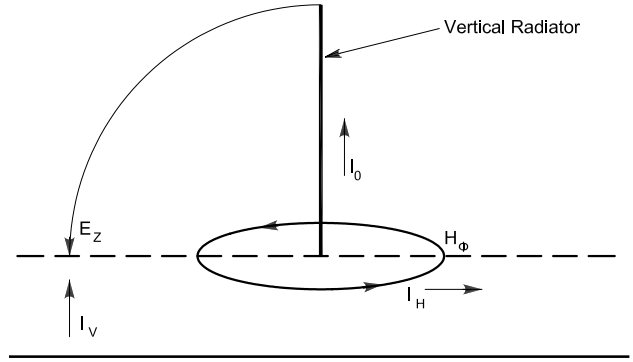

Fig 5—A general view of the fields and ground currents near the base of a vertical antenna. Note that the H-field distribution is equivalent to that shown in Fig 3.

by adding more series loss resistances. Putting aside for the moment these additional losses, the efficiency (η) of a vertical can be expressed as:

$$\eta = \frac{P_r}{P_r + P_g} \qquad \text{(Eq 1)}$$

This can be restated in terms of resistances as:

$$\eta = \frac{R_r}{R_r + R_g} = \frac{1}{1 + \frac{R_g}{R_r}} \qquad \text{(Eq 2)}$$

In essence, efficiency is the ratio of the radiated power to the total input power ($P_T = P_r + P_g$). Another way of saying this is that efficiency depends on the ratio of ground loss resistance (R_g) to radiation resistance (R_r), as Eq 2 shows. The smaller we make R_g the more power will be radiated for a given input power. Reducing R_g is the purpose of the ground system.

A sketch of current flow in the antenna and the surrounding ground (due to H-field), near the base of a vertical, is shown in **Fig 6**. I_z represents the total *zone current* flowing radially through a cylindrical zone at a given radius (r) due to the H field, while I_o is the current at the feed point at the base of the antenna. Technically speaking, the cylinder is infinitely deep, with I_z being the total current integrated over the surface of the cylinder at a given radius.

Fig 7 is a graph of the amplitude of I_z for several antenna heights in wavelengths (h) as we move away from the base of the antenna. Fig 7 shows the zone current that would flow in the ground returning to the base of the antenna, assuming a single ground rod is placed at the feed point for the vertical radiator. The heights indicated are the effective electrical heights. For example, if you use some top loading on the vertical, the effective electrical height will be greater than the physical height.

It is important to recognize that simply adding a top hat to a vertical of a given physical height may reduce ground losses. We can see this from the effect of h on ground current amplitude in Fig 7. Increasing h reduces the ground current. Even something as simple as moving a loading coil from the base up to the center of the antenna may reduce ground losses because it reduces ground current amplitude. But we do have to be careful that the loss introduced by the loading coil does not overcome the reduction in ground loss! Both loading-coil and top-hat schemes also increase the radiation resistance R_r, which further improves efficiency.

The currents in Fig 7 have been adjusted for constant radiated power at the base of the antenna by varying I_o to compensate for the change in R_r as we vary h. To maintain constant radiated power as R_r is falling, you must increase I_o. The base feed-point impedance is a strong function of h. For example, for h = 0.25 λ, R_r will be in the neighborhood of 36 Ω. However, for h = 0.1 λ, R_r will be less than 4 Ω. More information on short antennas can be found in Chapter 16, Mobile and Maritime Antennas.

Fig 7 clearly shows the high currents that flow in the ground near the base of a short antenna due to the antenna's H field. Compared to a 0.25-λ vertical, the 0.1-λ vertical has about three times the base current. As you shorten the antenna further, the zone current increases even more quickly. The ground loss is proportional to the square of the ground current ($P_g = I_g^2 R_g$), so the power loss in the immediate

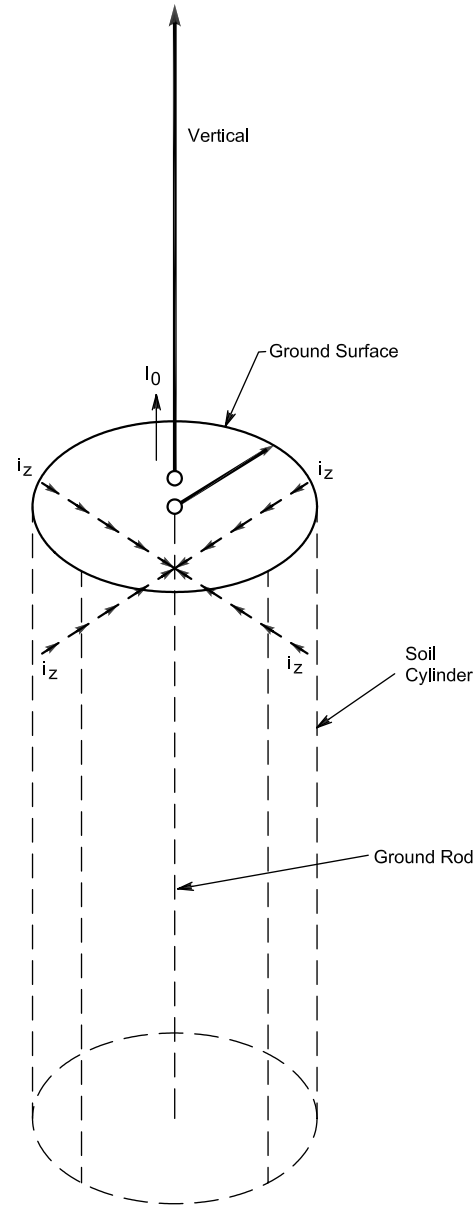

Fig 6—Representation of the zone current near the base of a vertical antenna. Individual i_z components of current flow into a cylinder of soil, with a radius r centered on the base of the vertical. The total current, I_z, thus represents the net current induced in the soil by the H-field for a given radius. (I_z was labeled I_H in Fig 5.)

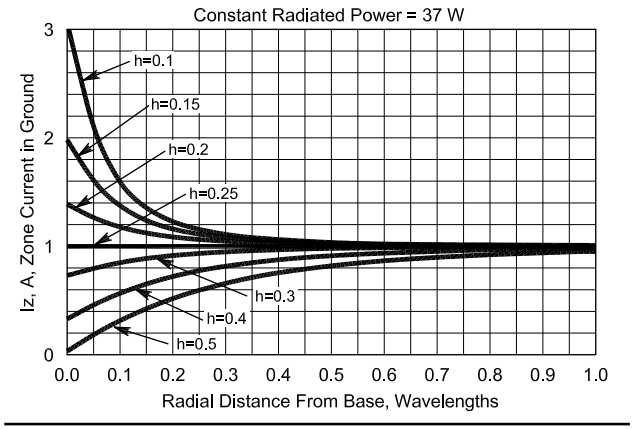

Fig 7—Plot of zone current (I_z) in amperes near the base of a vertical as a function of height (h) and radius (r) in wavelengths. The current in the base of the 0.25-λ antenna is assumed to be 1 A and the current for other values of h is adjusted to maintain the same radiated power ($P_r = I_0^2 R_r = 37$ W) as the radiation resistance (R_r) changes with h.

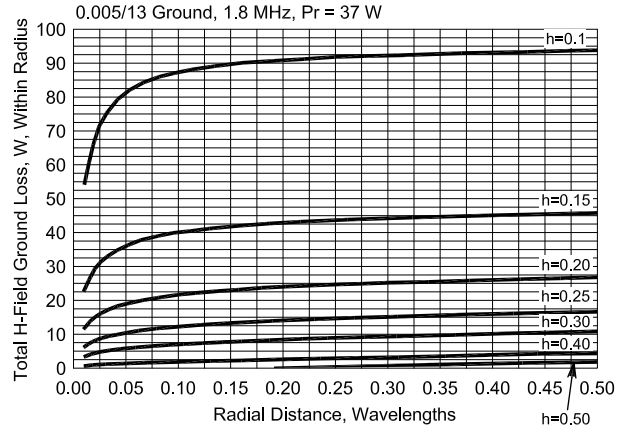

Fig 8—Total H-field induced ground loss within a circle of radius r around the base of a vertical for different values of h and constant P_r = 37 W. Note how the total loss increases rapidly near the base of the antenna indicating high loss. Beyond r = 0.15 λ, however, the additional loss is much lower and the curves flatten out. Note also how much higher the loss is for shorter antennas.

region of the base is much higher for a short antenna operating with the same input power as for a quarter-wave vertical.

We can calculate the losses induced in the soil by either the E- or H-field intensity. **Fig 8** shows an example of the H-field losses for several different antenna heights, given a constant radiated power of 37 W. Note that the total loss within 0.5 λ of the base for h = 0.25 λ is about 16 W (right side of the graph). This gives η = 37/(37 + 16) = 70%. However, for h = 0.1 λ, the total loss is about 94 W. Taking into consideration only the H-field losses, η = 37/(37 + 94) = 28%. Note that in both cases the majority of the loss is near (< 0.1 λ) the antenna, with the rate of increase of total loss decreasing rapidly as we move farther away from the base, where the lines are almost flat.

Fig 9 is a graph of the E-field intensity around a vertical with 1500 W radiated power, for three values of h. The E-field intensity doesn't depend on the exact type of ground system. (You can see this when you consider that the voltage across a capacitor doesn't depend on the size of the capacitor's plates.) Notice that close to the base, the E-field intensity for the 0.1-λ vertical is almost 100 times that for the 0.25-λ vertical. Because loss is proportional to the square of the voltage, the E-field losses close to the base will be ten thousand times larger in the 0.1-λ vertical! At a 1500-W power level the field intensity near the base of a short vertical is high enough to pose some risk of igniting grass and bushes that grow above any radial system close to the vertical's base. The grass should be kept mowed within 0.1 λ of the base.

Fig 10 shows a computation for the E-field losses, again for a constant radiated power of 37 W and several values of h. For the 0.25-λ vertical, the electric field intensity is quite low and so are the losses associated with it, at only 1.5 W.

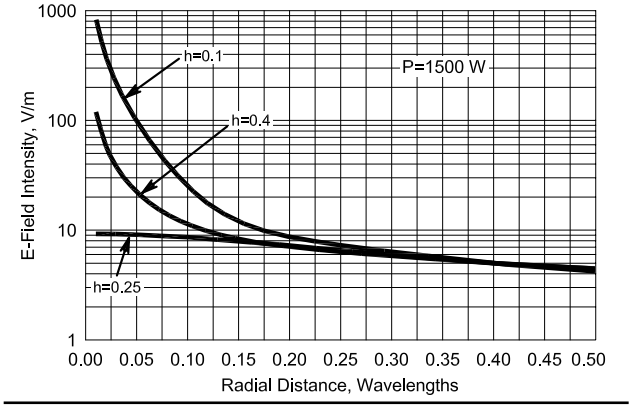

Fig 9—Electric field intensity near the base of a vertical for different values of h. P_r is held constant at 1500 W.

With any reasonable ground system, the E-field losses for a 0.25-λ vertical will be insignificant.

For shorter or longer verticals, however, the picture is different. This is why we see the very high losses (> 100 W) in Fig 10 for h = 0.1 λ. This loss, when added to the H-field loss, reduces the efficiency of the 0.1-λ vertical to 16% or less without a good ground system. In short antennas the E-field losses cannot be ignored, since they get worse exponentially as the antenna is shortened further.

The presence of a top-loading hat will also increase the E-field intensity in the area below the hat. However, most practical amateur hats will be quite small and the associated E-field loss small. The benefit, however, of reducing I_o because of the addition of the hat—which reduces the field

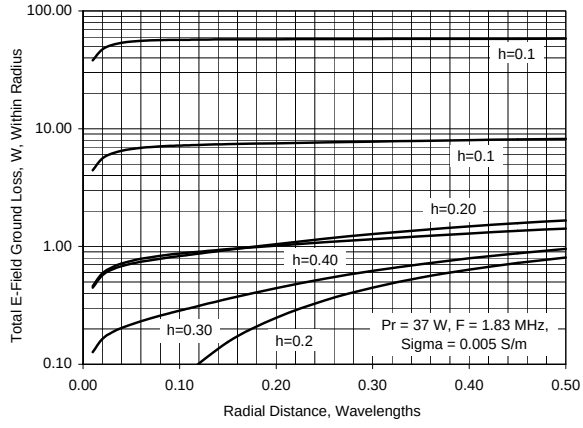

Fig 10—Total E-field induced ground loss within a circle of radius r around the base of a vertical for different values of h and constant P_r = 37 W. Note how the total loss increases rapidly near the base of the antenna, indicating high loss. Beyond r = 0.05 λ, however, the additional loss is much lower and the curves flatten out. Note again how much higher the loss is for shorter antennas. For h = 0.1 λ the E-field loss is greater than the H-field loss.

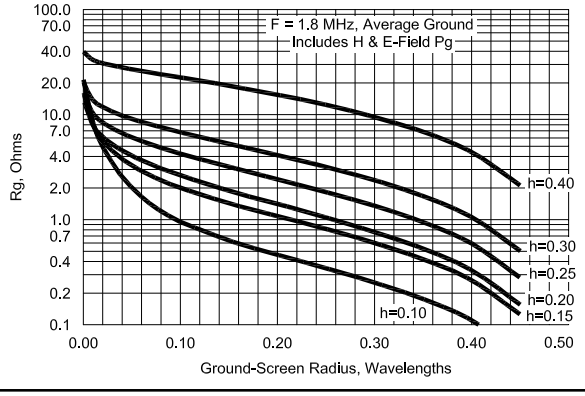

Fig 11—Effective ground resistance (R_g) at the base of the vertical as a function of the radius of a ground screen for several different antenna heights. Note how R_g falls as power dissipation in the soil is eliminated by the highly conducting ground screen.

from the vertical part of the antenna—more than compensates for the small additional E-field loss due to the hat.

Verticals taller than 0.25 λ also display increased E-field intensity, but not nearly so severe as short verticals. In verticals both shorter and longer than a 0.25 λ, the critical loss region is within a radius of about 0.05 λ. We can see this in Fig 10, where the power-loss curves for the shorter antennas flatten out by the time we reach a radius of 0.05 λ.

It's not widely known, but while radial wire systems reduce the H-field losses very effectively, Larsen (see Bibliography) has shown that the E-field losses with the same radial system do not fall in the same fashion as H-field losses. For h > 0.15 λ this doesn't matter much because the E-field loss is so low anyway. However, for short antennas it is very helpful to install either a ground screen or a dense radial system within 0.05 λ of the base.

We can take the data in Figs 8 and 10 and calculate the effective value of the ground resistance R_g. **Fig 11** shows the results of such a computation. Fig 11 assumes a perfect ground screen that varies in radius from 0.001 λ to 0.5 λ. As we would expect, when the ground screen is very small the ground losses are high, meaning R_g is high and the efficiency is low. As we increase the radius of the ground screen, forcing current out of the lossy soil and into the very low-loss screen, R_g drops rapidly and the efficiency increases.

Fig 11 demonstrates why it is desirable to have a good ground system out to at least 0.125 λ, and better yet, even farther. The shorter the antenna, the more important the ground system becomes, especially close to the base. In this example the ground system consists of a highly conductive, bonded ground screen, not always practical for amateur installations. A more typical ground system would consist of a number of individual radial wires. This kind of ground will be inferior to a screen but represents a practical compromise. We'll examine this in more detail shortly.

Note that as we reduce h in Fig 11, R_g actually goes down—even though the ground losses are higher. When h is made smaller the radiation resistance declines rapidly (see Chapter 16, Mobile and Maritime Antennas), so that for a given radiated power I_o must increase. If we measure R_g as we reduce h over a given ground system, we would see that the value for R_g goes down as shown in Fig 11. But because I_o^2 is rising more rapidly than R_g is falling, the power lost in the ground increases and efficiency decreases. The point here is that the value of R_g depends on the ground system, soil characteristics *and* the antenna configuration. You cannot assign an arbitrary value to R_g independent of the antenna system.

Wire Radial Systems

Fig 11 shows R_g for a dense, perfectly conducting ground screen, but what we really need to know is the effect of length and number of individual radials on R_g in a wire radial system. We can calculate the current division between a radial system and the soil and use this to determine R_g. A typical graph of the proportion of the zone current flowing in the radial system, as a function of radius and various numbers of radials (N), is shown in **Fig 12**.

The radial currents decrease as we move away from the base, and the lower the number of radials, the more rapidly the radial current decreases. This means that close to the base of the antenna most of the current is in the radial system, but as we move away from the base the current increasingly flows in the lossy ground. When only a few radials are used, the outer ends of the radials contribute little to reducing ground loss.

Why is this? The problem is that I_z does not go immediately to the nearest radial but may flow for some distance in the soil. This is illustrated in a general way in **Fig 13**. As

we move away from the base of the antenna, adjacent radials are further apart from each other and the current must flow further in the soil before it reaches one of the radials. When we use more radials, the distance between radials is less and more of the total current will be in the radials and less in the soil. This reduces ground loss.

When we know the current distribution in the ground we can calculate the power loss and R_g. A typical example for h = 0.25 λ is given in **Fig 14**. We can learn a lot about radial system design from Fig 14 and similar graphs. If we use only a few radials, the radial current drops off very rapidly. Most of the current is flowing in the soil.

Such a ground system is by nature inefficient—that is, R_g is large. We can also see that if we have only 16 radials, R_g falls an ohm or two as we lengthen the radials, but is essentially flat by 0.1 λ. There is no point in making them longer because there is little current in the outer portions and R_g is essentially constant beyond 0.1 λ. As we increase the number of radials, we gather more current further out, making longer radials more useful. The result is cumulative—more radials allow longer radials to be effective and both together reduce ground loss. We can see this in Fig 14, where the initial value of R_g drops as N increases and flattens out at longer radial lengths. For 128 radials, for example, lengths of 0.25 λ or more are useful.

The example in Fig 14 uses #12 wire for the radials. Compared to soil, the resistance of the radial wires is very small, especially if many radials are used, and does not greatly affect overall losses no matter how small the wire. The effect of changing wire size is to slowly change the current division between ground and the radial system. Larger wire results in only a small decrease in R_g. In principle, very small wire could be used for radials but from a mechanical point of view, #18 or #20 wire is about as small as is practical. Any smaller wire breaks too easily to be buried, and also breaks easily when left on the ground surface and is walked on or driven over.

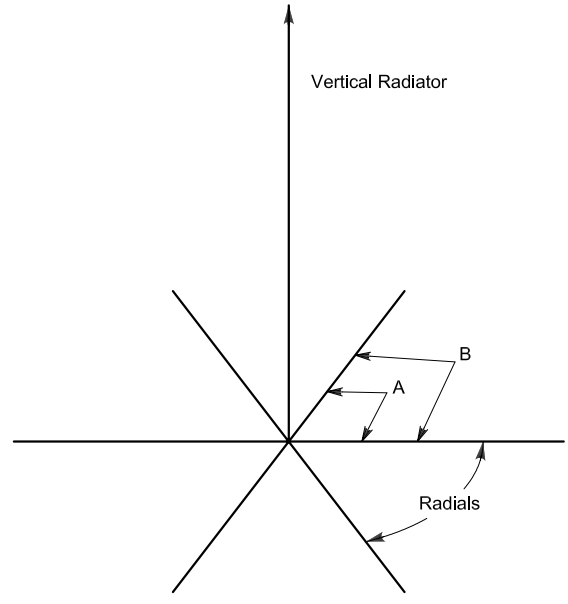

Fig 13—An example of current entering the ground between the radials and flowing for some distance before being picked up by a radial.

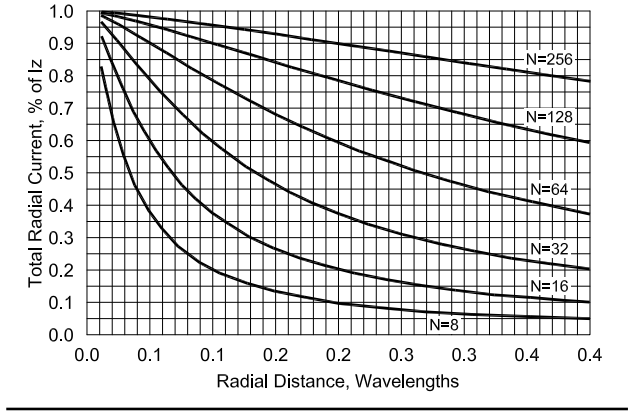

Fig 12—An example of the portion of the zone current flowing in the radial system as you move away from the base of a 0.25 λ vertical for different numbers of radials (N). Note that when more radials are used, more of the zone current flows in the radials and not in the ground, reducing ground loss. The proportion of current in the radial system falls rapidly when only a few radials are used. This leads to high ground loss because most of the zone current is flowing in the ground rather than in the radials.

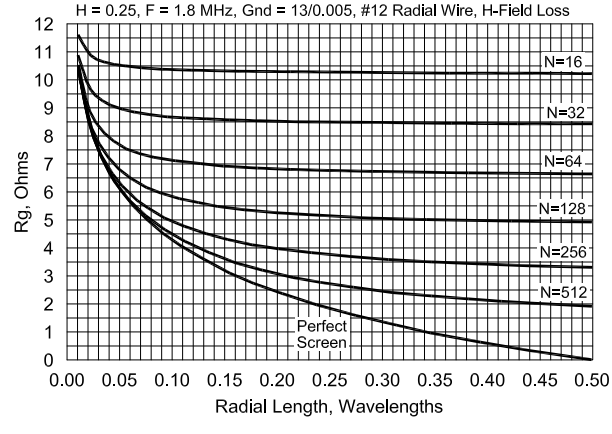

Fig 14—An example of the variation of R_g with radial length and number of radials (N) for h = 0.25 λ. When only a few radials are used there is little point in making them longer than 0.1 λ. Increasing N reduces R_g at a given radius and also makes longer radials useful, further reducing R_g. R_g for other values of h behave similarly.

On the other hand, wire larger than #12 is expensive. Thousands of feet of #8 wire may be affordable for broadcast stations but not for most hams. Increasing the wire size from #20 to #10 would result in only a small reduction in R_g. Of course, if you happen to have a few thousand feet of old RG-8 cable lying around (the diameter is comparable to #0000 wire) then that might indeed help to reduce R_g, as W9QQ has shown (see Bibliography). You are still better off, however, using many radials with small wire than a few radials with large wire. Radial wire size is usually a mechanical and financial issue, not an electrical one.

If the example in Fig 14 were changed for different ground characteristics, then the curves would have a similar shape but would be shifted either up or down. For example, poorer ground will result in higher R_g but the usable length for the radials for a given N would increase somewhat. For better-quality ground, with higher conductivity, R_g will be lower but the usable length of the radials for a given N will be shorter.

For short antennas, the initial drop in R_g will be more rapid and the curves flatten out sooner. This implies that somewhat shorter radials are useful with short antennas. However, given the high losses, it is still a very good idea to use lots of radials with short antennas. As in the above example, increasing N also increases the usable length.

As you go up in frequency from 160 meters, R_g generally rises slowly and then stabilizes around 7 MHz, depending on the ground characteristics. This effect is related to the change in skin depth with frequency, which is discussed in a later section of this chapter. There is also a small shift in current division between the radials and ground as the frequency increases.

A Word Of Caution

In the preceding discussion we presented a number of graphs and the CD-ROM accompanying this book contains some spreadsheets containing the equations from which these graphs were derived. From these graphs we extracted a number of observations on how to design radial systems. Basic to each graph is the assumption that we know the ground characteristics: conductivity and permitivity. In the real world, we amateurs very rarely have more than a rough idea of the ground characteristics under our antennas. Even when careful measurements are made, the characteristics will vary through the year with rainfall or the lack thereof.

Soils are always stratified vertically and can vary by factors or two or more horizontally over distances comparable to radial length, so that even good ground measurements are at best an average. In addition, there will frequently be constraints on the size and shape of the ground system. As a result, we use the calculated information and the previous graphs for general guidance and preliminary design, but when actually installing a ground system we try to measure—or at least estimate—R_g as we go along.

When R_g stops falling, or our patience and/or money run out, we stop adding ground radials. We can measure the feed-point resistance with an impedance bridge to estimate of R_g. The impedance seen at the feed point of the antenna is the sum of the loss and the radiation resistance. To determine R_g you have to estimate R_r (from the antenna height) and other losses due to loading or conductors, and then subtract that from the total measured input resistance. The remainder is R_g, and R_g should fall as we add radials. When R_g stops falling we probably have as many radials of a given length as will be useful. Further reduction in R_g would require more, longer radials.

Practical Suggestions For Vertical Ground Systems

At least 16 radials should be used if at all possible. Experimental measurements and calculations show that with this number, the loss resistance decreases the antenna efficiency by 30% to 50% for a 0.25 λ vertical, depending on soil characteristics. In general, a large number of radials (even though some or all of them must be short) is preferable to a few long radials for a vertical antenna mounted on the ground. The conductor size is relatively unimportant as mentioned before: #12 to #22 copper wire is suitable.

Table 1 summarizes these conclusions. John Stanley, K4ERO, first presented this material in December 1976 *QST*. Another source of information on ground-system design is *Radio Broadcast Ground Systems* (see the Bibliography at the end of this chapter). Most of the data presented in Table 1 is taken from that source, or derived from the interpolation of data contained therein.

Table 1 is based on the number of radials. For each configuration, there is a corresponding optimum radial length. Each configuration also includes the amount of wire used, expressed in wavelengths. Using radials considerably longer than suggested for a given N or using a lot more radials than suggested for a given length, while not adverse to performance, does not yield significant improvement either. That would represent a non-optimum use of wire and construction time. Each suggested configuration represents an optimum relationship between length and number for the given amount of total wire used. Table 1 leads to these conclusions:

- If you install only 16 radials (in configuration A), they need not be very long—0.1 λ is sufficient. The total length of wire will be 1.6 λ, which is about 875 feet at 1.8 MHz.
- If you have the wire, the space and the patience to lay down 120 radials (optimal configuration F), they should be 0.4 λ long. This radial system will gain about 3 dB over the 16-radial case and you'll use 48 λ of wire, or about 26,000 feet at 1.8 MHz.
- If you install 36 radials that are 0.15 λ long, you will lose 1.5 dB compared to optimal configuration F. You will use 5.4 λ of wire, or almost 3,000 feet at 1.8 MHz.

The loss figures in Table 1 assume h = 0.25 λ. A very rough approximation of loss when using shorter antennas can be obtained by doubling the loss in dB each

Table 1
Optimum Ground-System Configurations

	Configuration Designation					
	A	*B*	*C*	*D*	*E*	*F*
Number of radials	16	24	36	60	90	120
Length of each radial in wavelengths	0.1	0.125	0.15	0.2	0.25	0.4
Spacing of radials in degrees	22.5	15	10	6	4	3
Total length of radial wire installed, in wavelengths	1.6	3	5.4	12	22.5	48
Power loss in dB at low angles with a quarter-wave radiating element	3	2	1.5	1	0.5	0*
Feed-point impedance in ohms with a quarter-wave radiating element	52	46	43	40	37	35

Note: Configuration designations are indicated only for text reference.
*Reference: The loss of this configuration is negligible compared to a perfectly conducting ground.

time the antenna height is halved. For taller antennas the losses decrease, approaching 2 dB for configuration A of Table 1 for a half-wave radiator. Even longer antennas yield correspondingly better performance.

Table 1 is based on average ground conductivity. Variation of the loss values shown can be considerable, especially for configurations using fewer radials. Those building antennas over dry, sandy or rocky ground should expect more loss. On the other hand, higher than average soil conductivity and wet soils would make the compromise configurations (those with the fewest radials) even more attractive.

When antennas are combined into arrays, either parasitic or all-driven types, mutual impedances lower the radiation resistance of the elements. This drastically increases the effects of ground loss because I_o will be higher for the same power level. For instance, an antenna with a 50-Ω feed-point impedance, of which 10 Ω is ground-loss resistance, will have an efficiency of approximately 83%. An array of two similar antennas in a driven array with similar ground losses may have an efficiency of 70% or less.

Special precautions must be taken in such cases to achieve satisfactory operation. Generally speaking, a wide-spaced broadside array presents little problem because R_r is high, but a close-spaced end-fire array should be avoided because R_r is much lower, unless low-loss radial system configurations are used or other precautions taken. Chapter 8, Multielement Arrays, covers the subject of vertical arrays in great detail.

In cases where directivity is desirable or real-estate limitations dictate, longer, more closely spaced radials can be installed in one direction, and shorter, more widely spaced radials in another. Multiband ground systems can be designed using different optimum configurations for different bands. Usually it is most convenient to start at the lowest frequency with fewer radials and add more short radials for better performance on the higher bands.

There is nothing sacred about the exact details of the configurations in Table 1, and small changes in the number of radials and lengths will not cause serious problems. Thus, a configuration with 32 or 40 radials of 0.14 λ or 0.16 λ will work as well as configuration C shown in the table.

If less than 90 radials are contemplated, there is no need to make them a quarter wavelength long. This differs rather dramatically from the case of a ground-plane antenna, where resonant radials are installed above ground. For a ground-mounted antenna, quarter-wave long radials may not be optimum. Because the radials of a ground-mounted vertical are actually on, if not slightly below the surface, they are coupled by capacitance or conduction to the ground, and thus resonance effects are not important. The basic function of radials is to provide a low-loss return path for ground currents.

Radio Broadcast Ground Systems states, "Experiments show that the ground system consisting of only 15 radial wires need not be more than 0.1 wavelength long, while the system consisting of 113 radials is still effective out to 0.5 wavelength." Many graphs in that publication confirm this statement. This is not to say that these two systems will perform equally well; they most certainly will not. However, if 0.1 λ is as long as the radials can be, there is little point in using more than 15 of them unless the vertical radiator's height is also small.

The antenna designer should:

1. Study the cost of various radial configurations versus the gain of each.
2. Compare alternative means of improving transmitted signal and their cost (more power, etc).
3. Consider increasing the physical antenna height (the electrical length) of the vertical radiator, instead of improving the ground system.
4. Use multi-element arrays for directivity and gain, observing the necessary precautions related to mutual impedances discussed in Chapter 8, Multielement Arrays.

The Effect of Ground in the Far Field

The properties of the ground in the far field of an antenna are very important, especially for a vertically polarized antenna, as discussed above. Even if the ground-radial system for a vertical has been optimized to reduce ground-return losses in the reactive near field to an insignificant level, the electrical properties of the ground may still diminish far-field performance to lower levels than "perfect-ground" analyses might lead you to expect. The key is that *ground reflections* from horizontally and vertically polarized waves behave very differently.

Reflections in General

First, let us consider the case of flat ground. Over flat ground, either horizontally or vertically polarized downgoing waves launched from an antenna into the far field strike the surface and are reflected by a process very similar to that by which light waves are reflected from a mirror. As is the case with light waves, the angle of reflection is the same as the angle of incidence, so a wave striking the surface at an angle of, say, 15° is reflected upward from the surface at 15°.

The reflected waves combine with direct waves (those radiated at angles above the horizon) in various ways. Some of the factors that influence this combining process are the height of the antenna, its length, the electrical characteristics of the ground, and as mentioned above, the polarization of the wave. At some elevation angles above the horizon the direct and reflected waves are exactly in phase—that is, the maximum field strengths of both waves are reached at the same time at the same point in space, and the directions of the fields are the same. In such a case, the resultant field strength for that angle is simply the sum of the direct and reflected fields. (This represents a theoretical increase in field strength of 6 dB over the free-space pattern at these angles.)

At other elevation angles the two waves are completely out of phase—that is, the field intensities are equal at the same instant and the directions are opposite. At such angles, the fields cancel each other. At still other angles, the resultant field will have intermediate values. Thus, the effect of the ground is to increase radiation intensity at some elevation angles and to decrease it at others. When you plot the results as an elevation pattern, you will see *lobes* and *nulls*, as described in Chapter 2, Antenna Fundamentals.

The concept of an *image antenna* is often useful to show the effect of reflection. As **Fig 15** shows, the reflected ray has the same path length (AD equals BD) that it would if it originated at a virtual second antenna with the same characteristics as the real antenna, but situated below the ground just as far as the actual antenna is above it.

Now, if we look at the antenna and its image over perfect ground from a remote point on the surface of the ground, we will see that the currents in a horizontally polarized antenna and its image are flowing in opposite directions, or in other words, are 180° out of phase. But the currents in a vertically polarized antenna and its image are flowing in the *same* direction—they are *in* phase. This 180° phase difference between the vertically and horizontally polarized reflections off ground is what makes the combinations with direct waves behave so very differently.

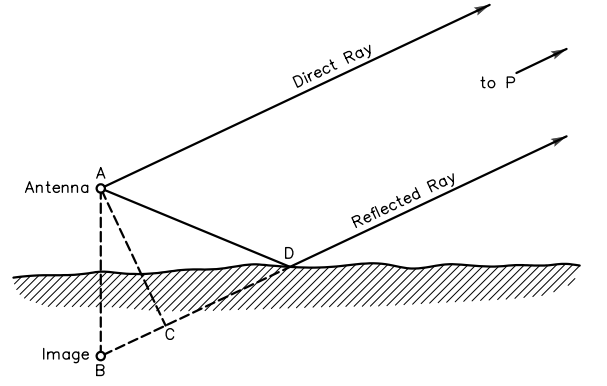

Fig 15—At any distant point, P, the field strength will be the vector sum of the direct ray and the reflected ray. The reflected ray travels farther than the direct ray by the distance BC, where the reflected ray is considered to originate at the *image* antenna.

FAR-FIELD GROUND REFLECTIONS AND THE VERTICAL ANTENNA

A vertical's azimuthal directivity is omnidirectional. A λ/2 vertical over ideal, perfectly conducting earth has the elevation-plane radiation pattern shown by the solid line in **Fig 16**. Over real earth, however, the pattern looks more like the shaded one in the same diagram. In this case, the low-angle radiation that might be hoped for because of perfect-ground performance is not realized in the real world.

Now look at **Fig 17A**, which compares the computed elevation-angle response for two half-wave dipoles at 14 MHz. One is oriented horizontally over ground at a height of λ/2 and the other is oriented vertically, with its center just over λ/2 high (so that the bottom end of the wire doesn't actually touch the ground). The ground is "average" in dielectric constant (13) and conductivity (0.005 S/m). At a 15° elevation angle, the horizontally polarized dipole has almost 7 dB more gain than its vertical brother. Contrast Fig 17A to the comparison in Fig 17B, where the peak gain of a vertically polarized half-wave dipole over seawater, which is virtually perfect for RF reflections, is quite comparable with the horizontal dipole's response at 15°, and exceeds the horizontally polarized antenna dramatically below 15° elevation.

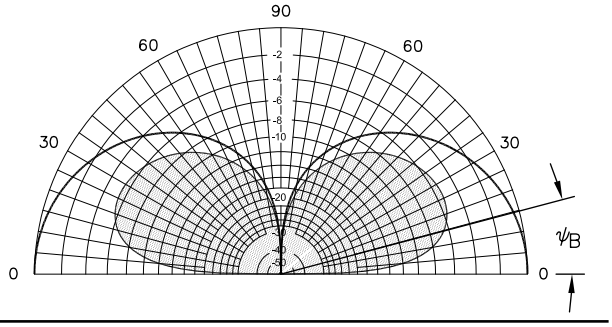

Fig 16—Vertical-plane radiation pattern for a ground-mounted quarter-wave vertical. The solid line is the pattern for perfect earth. The shaded pattern shows how the response is modified over average earth (k = 13, G = 0.005 S/m) at 14 MHz. ψ is the pseudo-Brewster angle (PBA), in this case 14.8°.

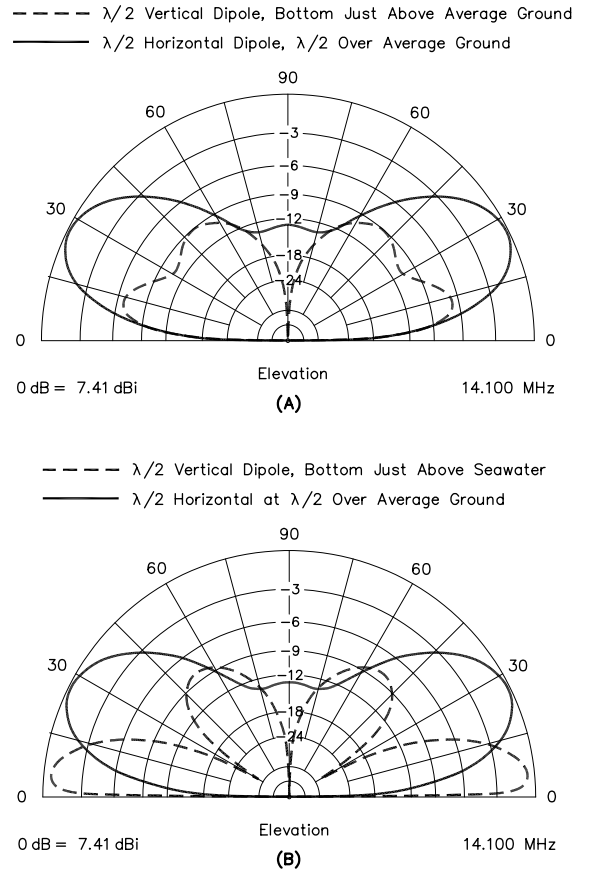

Fig 17—At A, comparison of horizontal and vertical λ/2 dipoles over average ground. Average ground has conductivity of 5 mS/m and dielectric constant of 13. Horizontal dipole is λ/2 high; vertical dipole's bottom wire is just above ground. Horizontal antenna is much less affected by far-field ground losses compared with its vertical counterpart. At B, comparison of 20-meter λ/2 vertical dipole whose bottom wire is just above seawater with λ/2-high horizontal dipole over average ground. Seawater is great for verticals!

To understand in a qualitative fashion why the desired low-angle radiation from a vertical is not delivered when the ground isn't "perfect," examine **Fig 18A**. Radiation from each antenna segment reaches a point P in space by two paths; one directly from the antenna, path AP, and the other by reflection from the earth, path AGP. (Note that P is so far away that the slight difference in angles is insignificant—for practical purposes the waves are parallel to each other at point P.)

If the earth were a perfectly conducting surface, there would be no phase shift of the vertically polarized wave upon reflection at point G. The two waves would add together with some phase difference because of the different path lengths. This difference in path lengths of the two waves is why the free-space radiation pattern differs from the pattern of the same antenna over ground.

Now consider a point P that is close to the horizon, as in Fig 18B. The path lengths AP and AGP are almost the same, so the magnitudes of the two waves add together, producing a maximum at zero angle of radiation. The arrows on the waves point both ways since the process works similarly for transmitting and receiving.

With real earth, however, the reflected wave from a vertically polarized antenna undergoes a change in both *amplitude* and *phase* in the reflection process. Indeed, at a low-enough elevation angle, the phase of the reflected wave will actually change by 180° and its magnitude will then subtract from that of the direct wave. At a zero takeoff angle, it will be almost equal in amplitude, but 180° out of phase with the direct wave.

Note that this is very similar to what happens with horizontally polarized reflected and direct waves at low elevation angles. Virtually complete cancellation will result in a deep null, inhibiting any radiation or reception at 0°. For real-world soils, the vertical loses the theoretical advantage it has at low elevation angles over a horizontal antenna, as Fig 17A so clearly shows.

The degree that a vertical works better than a horizontal antenna at low elevation angles is largely dependent on the characteristics of the ground around the vertical, as we'll next examine.

THE PSEUDO-BREWSTER ANGLE AND THE VERTICAL ANTENNA

Much of the material presented here regarding pseudo-Brewster angle was prepared by Charles J. Michaels, W7XC, and first appeared in July 1987 *QST*, with additional information in *The ARRL Antenna Compendium, Vol 3*. (See the Bibliography at the end of this chapter.)

Most fishermen have noticed that when the sun is low, its light is reflected from the water's surface as glare, obscuring the underwater view. When the sun is high, however, the sunlight penetrates the water and it is possible to see objects below the surface of the water. The angle at which this transition takes place is known as the *Brewster angle*,

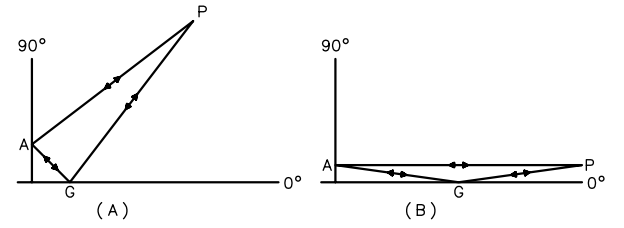

Fig 18—The direct wave and the reflected wave combine at point P to form the pattern (P is very far from the antenna). At A the two paths AP and AGP differ appreciably in length, while at B these two path lengths are nearly equal.

named for the Scottish physicist, Sir David Brewster (1781-1868).

A similar situation exists in the case of vertically polarized antennas; the RF energy behaves as the sunlight in the optical system, and the earth under the antenna acts as the water. The *pseudo-Brewster angle* (PBA) is the angle at which the reflected wave is 90° out of phase with respect to the direct wave. "Pseudo" is used here because the RF effect is similar to the optical effect from which the term gets its name. Below this angle, the reflected wave is between 90° and 180° out of phase with the direct wave, so some degree of cancellation takes place. The largest amount of cancellation occurs near 0°, and steadily less cancellation occurs as the PBA is approached from below.

The factors that determine the PBA for a particular location *are not related to the antenna itself, but to the ground around it*. The first of these factors is earth conductivity, G, which is a measure of the ability of the soil to conduct electricity. Conductivity is the inverse of resistance. The second factor is the dielectric constant, k, which is a unitless quantity that corresponds to the capacitive effect of the earth. For both of these quantities, the higher the number, the better is the ground (for vertical antenna purposes). The third factor determining the PBA for a given location is the frequency of operation. The PBA increases with increasing frequency, all other conditions being equal. **Table 2** gives typical values of conductivity and dielectric constant for different types of soil. The map of **Fig 19** shows the approximate conductivity values for different areas in the continental United States.

As the frequency is increased, the role of the dielectric constant in determining the PBA becomes more significant. **Table 3** shows how the PBA varies with changes in ground conductivity, dielectric constant and frequency. The table shows trends in PBA dependency on ground constants and frequency. The constants chosen are not necessarily typical of any geographical area; they are just examples.

At angles below the PBA, the reflected vertically polarized wave subtracts from the direct wave, causing the radiation intensity to fall off rapidly. Similarly, above the PBA, the reflected wave adds to the direct wave, and the radiated pattern approaches the perfect-earth pattern. Fig 16 shows the PBA, usually labeled ψ_B.

When plotting vertical-antenna radiation patterns over real earth, the reflected wave from an antenna segment is multiplied by a factor called the *vertical reflection coefficient*, and the product is then added vectorially to the direct wave to get the resultant. The reflection coefficient consists of an attenuation factor, A, and a phase angle, ϕ, and is usually expressed as $A\angle\phi$. (ϕ is always a negative angle, because the earth acts as a lossy capacitor in this situation.) The following equation can be used to calculate the reflection coefficient for vertically polarized waves, for earth of given conductivity and dielectric constant at any frequency and elevation angle (also called the wave angle in many texts).

Table 2
Conductivities and Dielectric Constants for Common Types of Earth

Surface Type	*Dielectric Constant*	*Conductivity (S/m)*	*Relative Quality*
Fresh water	80	0.001	
Salt water	81	5.0	
Pastoral, low hills, rich soil, typ Dallas, TX, to Lincoln, NE areas	20	0.0303	Very good
Pastoral, low hills, rich soil typ OH and IL	14	0.01	
Flat country, marshy, densely wooded, typ LA near Mississippi River	12	0.0075	
Pastoral, medium hills and forestation, typ MD, PA, NY, (exclusive of mountains and coastline)	13	0.006	
Pastoral, medium hills and forestation, heavy clay soil, typ central VA	13	0.005	Average
Rocky soil, steep hills, typ mountainous	12-14	0.002	Poor
Sandy, dry, flat, coastal	10	0.002	
Cities, industrial areas	5	0.001	Very Poor
Cities, heavy industrial areas, high buildings	3	0.001	Extremely poor

Table 3
Pseudo-Brewster Angle Variation with Frequency, Dielectric Constant, and Conductivity

Frequency (MHz)	*Dielectric Constant*	*Conductivity (S/m)*	*PBA (degrees)*
7	20	0.0303	6.4
	13	0.005	13.3
	13	0.002	15.0
	5	0.001	23.2
	3	0.001	27.8
14	20	0.0303	8.6
	13	0.005	14.8
	13	0.002	15.4
	5	0.001	23.8
	3	0.001	29.5
21	20	0.0303	10.0
	13	0.005	15.2
	13	0.002	15.4
	5	0.001	24.0
	3	0.001	29.8

$$A_{Vert} \angle \phi = \frac{k' \sin\psi - \sqrt{k' - \cos^2 \psi}}{k' \sin\psi + \sqrt{k' - \cos^2 \psi}} \qquad \text{(Eq 3)}$$

where

$A_{Vert} \angle \phi$ = vertical reflection coefficient

ψ = elevation angle

$$k' = k - j\left|\frac{1.8 \times 10^4 \times G}{f}\right|$$

k = dielectric constant of earth (k for air = 1)

G = conductivity of earth in S/m

f = frequency in MHz

j = complex operator ($\sqrt{-1}$)

Solving this equation for several points indicates what effect the earth has on vertically polarized signals at a particular location for a given frequency range. **Fig 20** shows the reflection coefficient as a function of elevation angle at 21 MHz over average earth (G = 0.005 S/m, and k = 13).

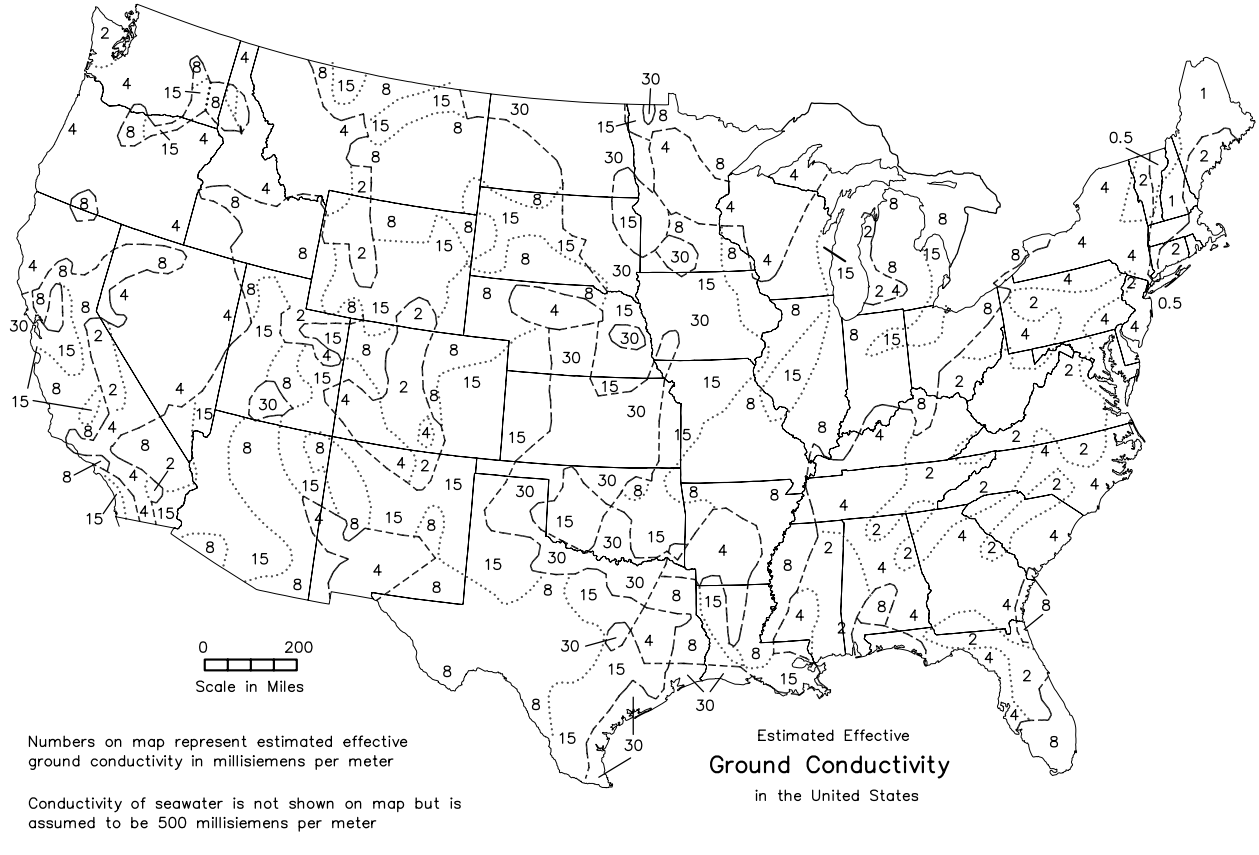

Fig 19—Typical average soil conductivities for the continental United States. Numeric values indicate conductivities in millisiemens per meter (mS/m), where 1.0 mS/m = 0.001 S/m.

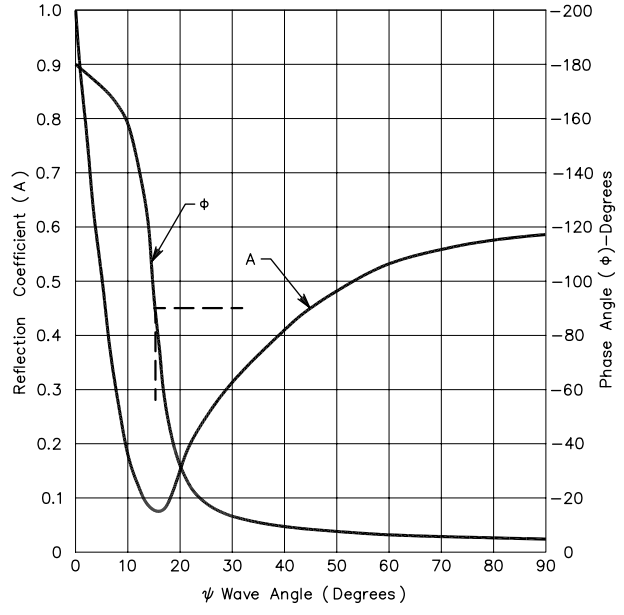

Fig 20—Reflection coefficient for vertically polarized waves. A and ϕ are magnitude and angle for wave angles ψ. This case is for average earth, (k = 13, G = 0.005 S/m), at 21 MHz.

Note that as the phase curve, ψ, passes through 90°, the attenuation curve (A) passes through a minimum at the same wave angle ψ. This is the PBA. At this angle, the reflected wave is not only at a phase angle of 90° with respect to the direct wave, but is so low in amplitude that it does not aid the direct wave by a significant amount. In the case illustrated in Fig 20 this elevation angle is about 15°.

Variations in PBA with Earth Quality

From Eq 3, it is quite a task to search for either the 90° phase point or the attenuation curve minimum for a wide variety of earth conditions. Instead, the PBA can be calculated directly from the following equation.

$$\psi_B = \arcsin\sqrt{\frac{k-1+\sqrt{(x^2+k^2)^2(k-1)^2+x^2[(x^2+k^2)^2-1]}}{(x^2+k^2)^2-1}} \qquad \text{(Eq 4)}$$

where k, G and f are as defined for Eq 3, and

$$x = \frac{1.8\times10^4\times G}{f}$$

Fig 21 shows curves calculated using Eq 4 for several different earth conditions, at frequencies between 1.8 and 30 MHz. As expected, poorer earths yield higher PBAs. Unfortunately, at the higher frequencies (where low-angle radiation is most important for DX work), the PBAs are highest. The PBA is the same for both transmitting and receiving.

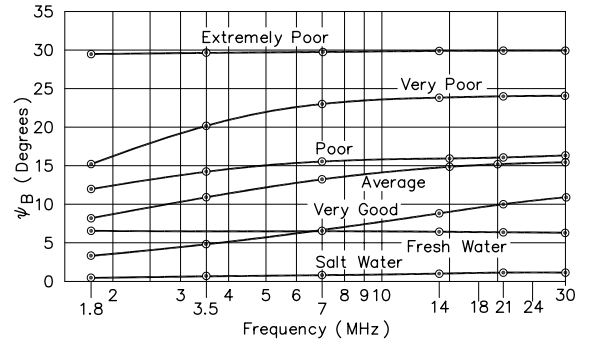

Fig 21—Pseudo-Brewster angle (ψ) for various qualities of earth over the 1.8 to 30-MHz frequency range. Note that the frequency scale is logarithmic. The constants used for each curve are given in Table 2.

Relating PBA to Location and Frequency

Table 2 lists the physical descriptions of various kinds of earth with their respective conductivities and dielectric constants, as mentioned earlier. Note that in general, the dielectric constants and conductivities are higher for better earths. This enables the labeling of the earth characteristics as extremely poor, very poor, poor, average, very good, and so on, without the complications that would result from treating the two parameters independently.

Fresh water and salt water are special cases; in spite of high resistivity, the fresh-water PBA is 6.4°, and is nearly independent of frequency below 30 MHz. Salt water, because of its extremely high conductivity, has a PBA that never exceeds 1° in this frequency range. The extremely low conductivity listed for cities (the last case) in Table 2 results more from the clutter of surrounding buildings and other obstructions than any actual earth characteristic. The PBA at any location can be found for a given frequency from the curves in Fig 21.

FLAT-GROUND REFLECTIONS AND HORIZONTALLY POLARIZED WAVES

The situation for horizontal antennas is different from that of verticals. **Fig 22** shows the reflection coefficient for horizontally polarized waves over average earth at 21 MHz. Note that in this case, the phase-angle departure from 0° never gets very large, and the attenuation factor that causes the most loss for high-angle signals approaches unity for low angles. Attenuation increases with progressively poorer earth types.

In calculating the broadside radiation pattern of a horizontal λ/2 dipole, the perfect-earth image current, equal to the true antenna current but 180° out of phase with it) is multiplied by the horizontal reflection coefficient given by Eq 5 below. The product is then added vectorially to the direct wave to get the resultant at that elevation angle. The

reflection coefficient for horizontally polarized waves can be calculated using the following equation.

$$A_{Horiz} \angle \phi = \frac{\sqrt{k' - \cos^2 \psi} - \sin \psi}{\sqrt{k' - \cos^2 \psi} + \sin \psi} \qquad \text{(Eq 5)}$$

where

$A_{Horiz} \angle \phi$ = horizontal reflection coefficient

ψ = elevation angle

$$k' = k - j\left(\frac{1.8 \times 10^4 \times G}{f}\right)$$

k = dielectric constant of earth

G = conductivity of earth in S/m

f = frequency in MHz

j = complex operator ($\sqrt{-1}$)

For a horizontal antenna near the earth, the resultant pattern is a modification of the free-space pattern of the antenna. **Fig 23** shows how this modification takes place for a horizontal λ/2 antenna over a perfectly conducting flat surface. The patterns at the left show the relative radiation when one views the antenna from the side; those at the right show the radiation pattern looking at the end of the antenna. Changing the height above ground from λ/4 to λ/2 makes a significant difference in the high-angle radiation, moving the main lobe down lower.

Note that for an antenna height of λ/2 (Fig 23, bottom), the out-of-phase reflection from a perfectly conducting surface creates a null in the pattern at the zenith (90° elevation angle). Over real earth, however, a *filling in* of this null occurs because of ground losses that prevent perfect reflection of high-angle radiation.

At a 0° elevation angle, horizontally polarized antennas also demonstrate a null, because out-of-phase reflection cancels the direct wave. As the elevation angle departs from 0°, however, there is a slight filling-in effect so that over other-than-perfect earth, radiation at lower angles is enhanced compared to a vertical. A horizontal antenna will often outperform a vertical for low-angle DX work, particularly over lossy types of earth at the higher frequencies.

Reflection coefficients for vertically and horizontally polarized radiation differ considerably at most angles above ground, as can be seen by comparison of Figs 20 and 22. (Both sets of curves were plotted for the same ground constants and at the same frequency, so they may be compared directly.) This is because, as mentioned earlier, the image of a horizontally polarized antenna is out-of-phase with the antenna itself, and the image of a vertical antenna is in-phase with the actual radiator.

The result is that the phase shifts and reflection magnitudes vary greatly at different angles for horizontal and vertical polarization. The magnitude of the reflection coefficient for vertically polarized waves is greatest (near unity) at very low angles, and the phase angle is close to 180°. As mentioned earlier, this cancels nearly all radiation at very low angles. For the same range of angles, the magnitude of the reflection coefficient for horizontally polarized waves is also near unity, but the phase angle is near 0° for the specific conditions shown in Figs 20 and 22. This causes reinforcement of low-angle horizontally polarized waves. At some relatively high angle, the reflection coefficients for

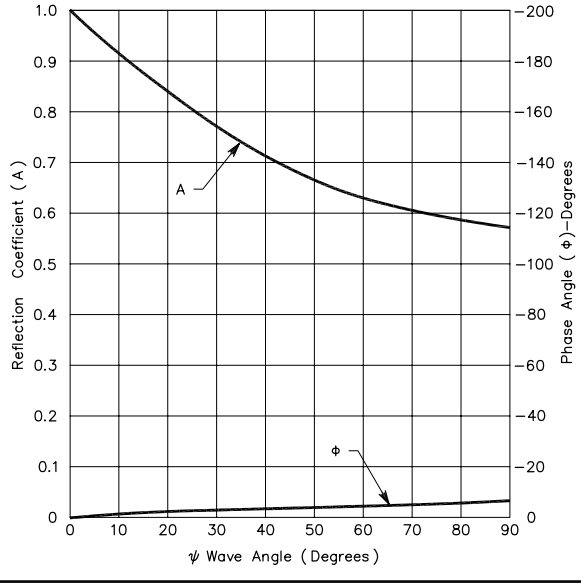

Fig 22—Reflection coefficient for horizontally polarized waves (magnitude A at angle ϕ), at 21 MHz over average earth (k = 13, G = 0.005 S/m).

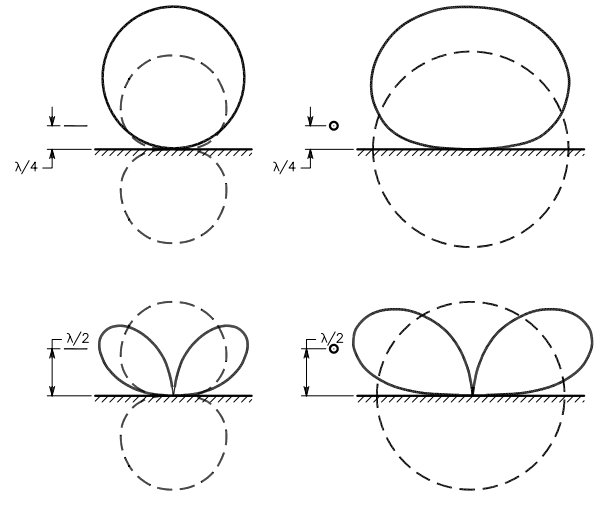

Fig 23—Effect of the ground on the radiation from a horizontal half-wave dipole antenna, for heights of one-fourth and one-half wavelength. Broken lines show what the pattern would be if there were no reflection from the ground (free space).

horizontally and vertically polarized waves are equal in magnitude and phase. At this angle (approximately 81° for the example case), the effect of ground reflection on vertically and horizontally polarized signals will be the same.

DEPTH OF RF CURRENT PENETRATION

When considering earth characteristics, questions about depth of RF current penetration often arise. For instance, if a given location consists of a 6-foot layer of soil overlying a highly resistive rock strata, which material dominates? The answer depends on the frequency, the soil and rock dielectric constants, and their respective conductivities. The following equation can be used to calculate the current density at any depth.

$$e^{-pd} = \frac{\text{Current Density at Depth d}}{\text{Current Density at Surface}} \qquad \text{(Eq 6)}$$

where

d = depth of penetration in cm

e = natural logarithm base (2.718)

$$p = \left(\frac{X \times B}{2} \times \left(\sqrt{1 + \frac{G^2 \times 10^{-4}}{B^2}} - 1 \right) \right)^{1/2}$$

$X = 0.008 \times \pi^2 \times f$

$B = 5.56 \times 10^{-7} \times k \times f$

k = dielectric constant of earth

f = frequency in MHz

G = conductivity of earth in S/m

After some manipulation of this equation, it can be used to calculate the depth at which the current density is some fraction of that at the surface. The depth at which the current density is 37% (1/*e*) of that at the surface (often referred to as *skin depth*) is the depth at which the current density would be zero if it were distributed uniformly instead of exponentially. (This 1/*e* factor appears in many physical situations. For instance, a capacitor charges to within 1/*e* of full charge within one RC time constant.) At this depth, since the power loss is proportional to the square of the current, approximately 91% of the total power loss has occurred, as has most of the phase shift, and current flow below this level is negligible.

Fig 24 shows the solutions to Eq 6 over the 1.8 to 30-MHz frequency range for various types of earth. For example, in very good earth, substantial RF currents flow down to about 3.3 feet at 14 MHz. This depth goes to 13 feet in average earth and as far as 40 feet in very poor earth. Thus, if the overlying soil is rich, moist loam, the underlying rock stratum is of little concern. However, if the soil is only average, the underlying rock may constitute a major consideration in determining the PBA and the depth to which the RF current will penetrate.

The depth in fresh water is about 156 feet and is nearly independent of frequency in the amateur bands below 30 MHz. In salt water, the depth is about seven inches at 1.8 MHz and decreases rather steadily to about two inches at 30 MHz. Dissolved minerals in moist earth increase its conductivity.

The depth-of-penetration curves in Fig 24 illustrate a noteworthy phenomenon. While skin effect confines RF current flow close to the surface of a conductor, the earth is so lossy that RF current penetrates to much greater depths than in most other media. The depth of RF current penetration is a function of frequency as well as earth type. Thus, the only cases in which most of the current flows near the surface are with very highly conductive media (such as salt water), and at frequencies above 30 MHz.

DIRECTIVE PATTERNS OVER REAL GROUND

As explained in Chapter 2, Antenna Fundamentals, because antenna radiation patterns are three-dimensional, it is helpful in understanding their operation to use a form of representation showing the elevation-plane directional characteristic for different heights. It is possible to show selected elevation-plane patterns oriented in various directions with respect to the antenna axis. In the case of the horizontal half-wave dipole, a plane running in a direction along the axis and another broadside to the antenna will give a good deal of information.

The effect of reflection from the ground can be expressed as a separate *pattern factor*, given in decibels. For any given elevation angle, adding this factor algebraically to the value for that angle from the free-space pattern for that antenna gives the resultant radiation value at that

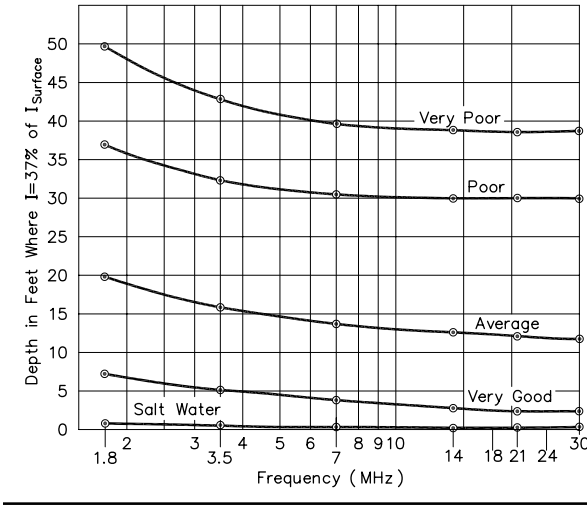

Fig 24—Depths at which the current density is 37% (1/*e*) of that at the surface for different qualities of earth over the 1.8- to 30-MHz frequency range. The depth for fresh water, not plotted, is 156 feet and almost independent of frequency below 30 MHz. See text and Table 2 for ground constants.

angle. The limiting conditions are those represented by the direct ray and the reflected ray being exactly in-phase and exactly out-of-phase, when both (assuming there are no ground losses) have equal amplitudes. Thus, the resultant field strength at a distant point may be either 6 dB greater than the free-space pattern (twice the field strength), or zero, in the limiting cases.

Horizontally Polarized Antennas

The way in which pattern factors vary with height for horizontal antennas over flat earth is shown graphically in the plots of **Fig 25**. The solid-line plots are based on perfectly conducting ground, while the shaded plots are based on typical real-earth conditions. These patterns apply to horizontal antennas of any length. While these graphs are, in fact, radiation patterns of horizontal single-wire antennas (dipoles) as viewed from the axis of the wire, it must be remembered that the plots merely represent pattern factors.

Fig 26 shows vertical-plane radiation patterns in the directions off the ends of a horizontal half-wave dipole for various antenna heights. These patterns are scaled so they may be compared directly to those for the appropriate heights in Fig 25. Note that the perfect-earth patterns in Figs 26A and 25B are the same as those in the upper part of Fig 23. Note also that the perfect-earth patterns of Figs 26B and 25D are the same as those in the lower section of Fig 23. The reduction in field strength off the ends of the wire at the lower angles, as compared with the broadside field strength, is quite apparent. It is also clear from Fig 26 that, at some heights, the high-angle radiation off the ends is nearly as great as the broadside radiation, making the antenna essentially an omnidirectional radiator.

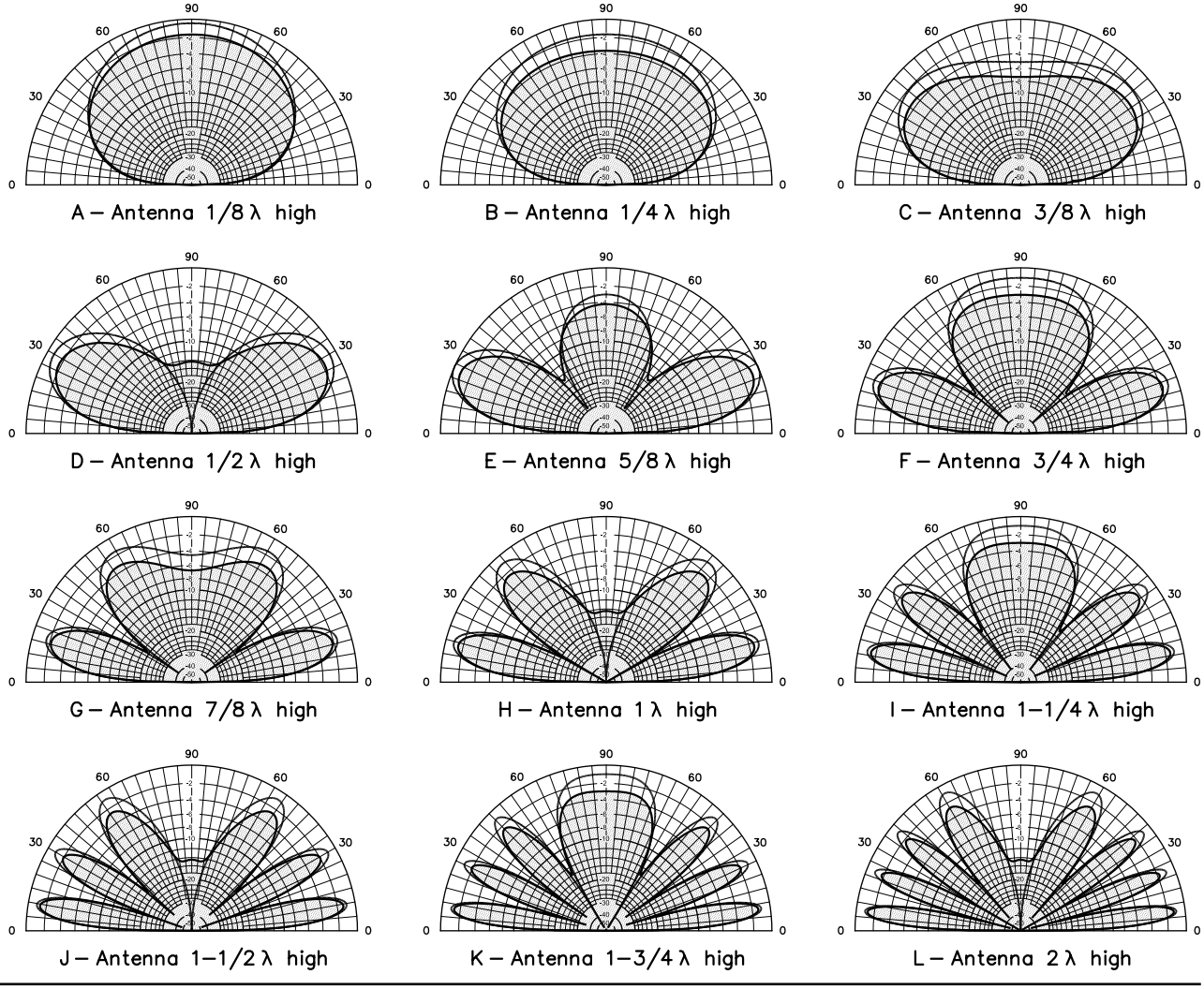

Fig 25—Reflection factors for horizontal dipole antennas at various heights above flat ground. The solid-line curves are the perfect-earth patterns (broadside to the antenna wire); the shaded curves represent the effects of average earth (k = 13, G = 0.005 S/m) at 14 MHz. Add 7 dB to values shown for absolute gain in dBd referenced to dipole in free space, or 9.15 dB for gain in dBi. For example, peak gain over perfect earth at $^{5}/_{8}$ λ height is 7 dBd (or 9.15 dBi) at 25° elevation.

In vertical planes making some intermediate angle between 0° and 90° with the wire axis, the pattern will have a shape intermediate between the broadside and end-on patterns. By visualizing a smooth transition from the end-on pattern to the broadside pattern as the horizontal angle is varied from 0° to 90°, a fairly good mental picture of the actual solid pattern may be formed. An example is shown in **Fig 27**. At A, the elevation-plane pattern of a half-wave dipole at a height of λ/2 is shown through a plane 45° away from the favored direction of the antenna. At B and C, the pattern of the same antenna is shown at heights of 3λ/4 and 1λ (through the same 45° off-axis plane). These patterns are scaled so they may be compared directly with the broadside and end-on patterns for the same antenna (at the appropriate heights) in Figs 25 and 26.

The curves presented in **Fig 28** are useful for determining heights of horizontal antennas that give either maximum or minimum reinforcement at any desired wave angle. For instance, if you want to place an antenna at a height so that it will have a null at 30°, the antenna should be placed where a broken line crosses the 30° line on the horizontal scale. There are two heights (up to 2 λ) that will yield this null angle: 1 λ and 2 λ.

As a second example, you may want to have the ground reflection give maximum reinforcement of the direct ray from a horizontal antenna at a 20° elevation angle. The antenna height should be 0.75 λ. The same height will give a null at 42° and a second lobe at 90°.

Fig 28 is also useful for visualizing the vertical pattern of a horizontal antenna. For example, if an antenna is erected at 1.25 λ, it will have major lobes (solid-line crossings) at 12° and 37°, as well as at 90° (the zenith). The nulls in this pattern (dashed-line crossings) will appear at 24° and 53°.

The Y-axis in Fig 28 plots the wave angle versus the height in wavelength above flat ground on the X-axis. Fig 28 doesn't show the elevation angles required for actual

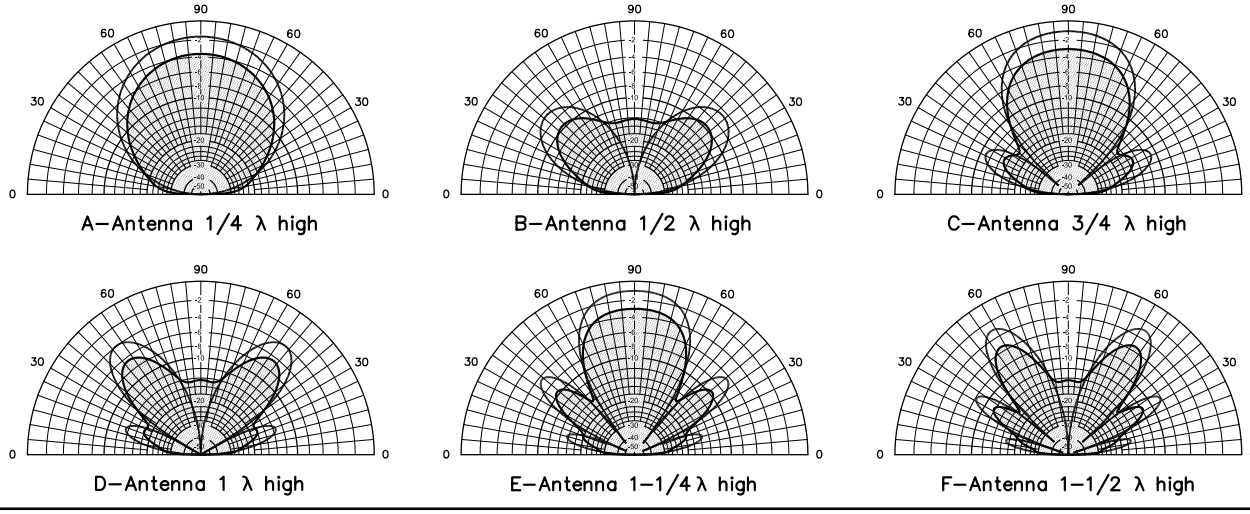

Fig 26—Vertical-plane radiation patterns of horizontal half-wave dipole antennas off the ends of the antenna wire. The solid-line curves are the flat, perfect-earth patterns, and the shaded curves represent the effects of average flat earth (k = 13, G = 0.005 S/m) at 14 MHz. The 0-dB reference in each plot corresponds to the peak of the main lobe in the favored direction of the antenna (the maximum gain). Add 7 dB to values shown for absolute gain in dBd referenced to dipole in free space, or 9.15 dB for gain in dBi.

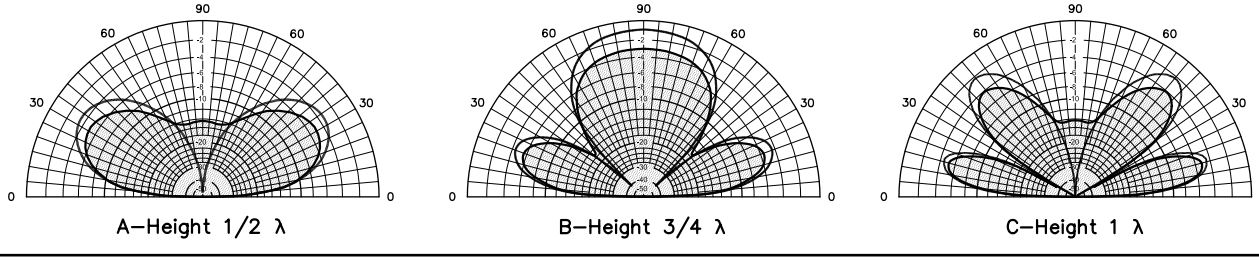

Fig 27—Vertical-plane radiation patterns of half-wave horizontal dipole antennas at 45° from the antenna wire over flat ground. The solid-line and shaded curves represent the same conditions as in Figs 25 and 26. These patterns are scaled so they may be compared directly with those of Figs 25 and 26.

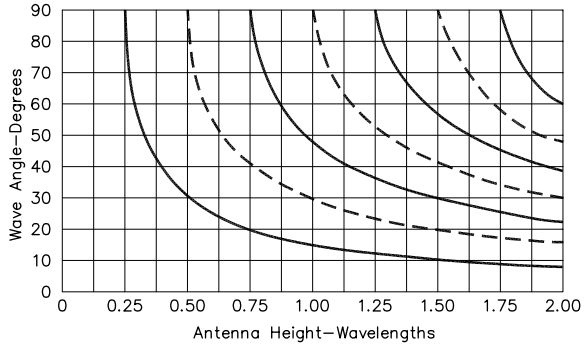

Fig 28—Angles at which nulls and maxima (factor = 6 dB) in the ground-reflection factor appear for antenna heights up to two wavelengths over flat ground. The solid lines are maxima, dashed lines nulls, for all horizontal antennas. See text for examples. Values may also be determined from the trigonometric relationship θ = arc sin (A/4h), where θ is the wave angle and h is the antenna height in wavelengths. For the first maximum, A has a value of 1; for the first null A has a value of 2, for the second maximum 3, for the second null 4, and so on.

communications to various target geographic locations of interest. Chapter 23, Radio Wave Propagation, and the CD-ROM in the back of this book give details about the range of angles required for target locations around the world. It is very useful to overlay plots of these angles together with the elevation pattern for horizontally polarized antennas at various heights above flat ground. This will be demonstrated in detail later in this chapter.

Vertically Polarized Antennas

In the case of a vertical λ/2 dipole or a ground-plane antenna, the horizontal directional pattern is simply a circle at any elevation angle (although the actual field strength will vary, at the different elevation angles, with the height above ground). Hence, one vertical pattern is sufficient to give complete information (for a given antenna height) about the antenna in any direction with respect to the wire. A series of such patterns for various heights is given in **Fig 29**. Rotating the plane pattern about the zenith axis of the graph forms the three-dimensional radiation pattern in each case.

The solid-line curves represent the radiation patterns of the λ/2 vertical dipole at different feed-point heights over perfectly conducting ground. The shaded curves in Fig 29 show the patterns produced by the same antennas at the same heights over average ground (G = 0.005 S/m, k = 13) at 14 MHz. The PBA in this case is 14.8°.

In short, far-field losses for vertically polarized antennas are highly dependent on the conductivity and dielectric constant of the earth around the antenna, extending far beyond the ends of any radials used to complete the ground return for the near field. Putting more radials out around the antenna may well decrease ground-return losses in the reactive near field for a vertical monopole, but will not increase radiation at low elevation launch angles in the far field, unless the radials can extend perhaps 100 wavelengths in all directions! Aside from moving to the fabled "salt water swamp on a high hill," there is very little that someone can do to change the character of the ground that affects the far-field pattern of a real vertical. Classical texts

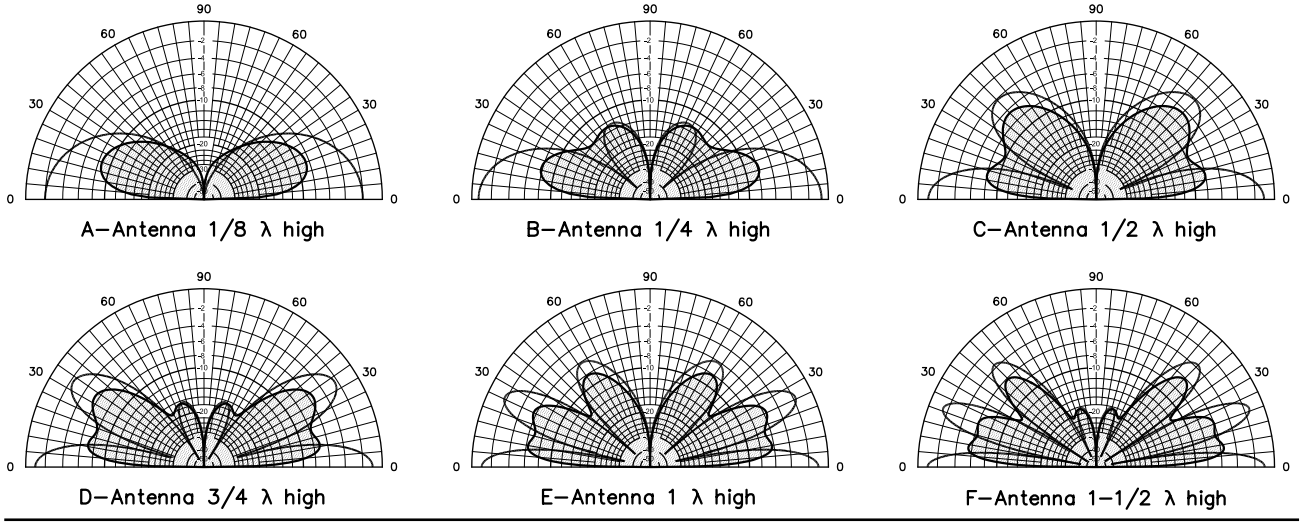

Fig 29—Vertical-plane radiation patterns of a ground-plane antenna above flat ground. The height is that of the ground plane, which consists of four radials in a horizontal plane. Solid lines are perfect-earth patterns; shaded curves show the effects of real earth. The patterns are scaled—that is, they may be directly compared to the solid-line ones for comparison of losses at any wave angle. These patterns were calculated for average ground (k = 13, G = 0.005 S/m) at 14 MHz. The PBA for these conditions is 14.8°. Add 6 dB to values shown for absolute gain in dBd over dipole in free space.

on verticals often show elevation patterns computed over an "infinitely wide, infinitely conducting ground plane." Real ground, with finite conductivity and less than perfect dielectric constant, can severely curtail the low-angle radiation at which verticals are supposed to excel.

While real verticals over real ground are not a surefire method to achieve low-angle radiation, cost versus performance and ease of installation are still attributes that can highly recommend verticals to knowledgeable builders. Practical installations for 160 and 80 meters rarely allow amateurs to put up horizontal antenna high enough to radiate effectively at low elevation angles. After all, a half-wave on 1.8 MHz is 273 feet high, and even at such a lofty height the peak radiation would be at a 30° elevation angle.

The Effects of Irregular Local Terrain in the Far Field

The following material is condensed and updated from an article by R. Dean Straw, N6BV, in July 1995 *QEX* magazine. *HFTA* (HF Terrain Assessment) and supporting data files are included on the CD-ROM at the back of this book. *HFTA* is the latest version of the *YT* program included with earlier editions of *The ARRL Antenna Book*.

Choosing a QTH for DXing

The subject of how to choose a QTH for working DX has fascinated hams since the beginning of amateur operations. No doubt, Marconi probably spent a lot of time wandering around Newfoundland looking for a great radio QTH before making the first transAtlantic transmission. Putting together a high-performance HF station for contesting or DXing has always followed some pretty simple rules. First, you need the perfect QTH, preferably on a rural mountaintop or at least on top of a hill. Even better yet, you need a mountaintop surrounded by seawater! Then, after you have found your dream QTH, you put up the biggest antennas you possibly can, on the highest towers you can afford. Then you work all sorts of DX—sunspots willing, of course.

The only trouble with this straightforward formula for success is that it doesn't always work. Hams fortunate enough to be located on mountain tops with really spectacular drop-offs often find that their highest antennas don't do very well, especially on 15 or 10 meters, but often even on 20 meters. When they compare their signals with nearby locals in the flatlands, they sometimes (but not always) come out on the losing end, especially when sunspot activity is high.

On the other hand, when the sunspots drop into the cellar, the high antennas on the mountaintop are usually the ones crunching the pileups—but again, not always. So, the really ambitious contest aficionados, the guys with lots of resources and infinite enthusiasm, have resorted to putting up antennas at all possible heights, on a multitude of towers.

There is a more scientific way to figure out where and how high to put your antennas to optimize your signal during all parts of the 11-year solar cycle. We advocate a *system approach* to HF station design, in which you need to know the following:

1. The range of elevation angles necessary to get from point A to point B
2. The elevation patterns for various types and configurations of antennas
3. The effect of local terrain on elevation patterns for horizontally polarized antennas.

WHAT IS THE RANGE OF ELEVATION ANGLES NEEDED?

Up until 1994, *The ARRL Antenna Book* contained only a limited amount of information about the elevation angles needed for communication throughout the world. In the 1974 edition, Table 1-1 in the Wave Propagation chapter was captioned: "Measured vertical angles of arrival of signals from England at receiving location in New Jersey."

What the caption didn't say was that Table 1-1 was derived from measurements made during 1934 by Bell Labs. The highest frequency data seemed pretty shaky, considering that 1934 was the low point of Cycle 17. Neither was this data applicable to any other path, other than the one from New Jersey to England. Nonetheless, many amateurs located throughout the US tried to use the sparse information in Table 1-1 as the only rational data they had for determining how high to mount their antennas. (If they lived on hills, they made estimates of the effect of the terrain, assuming that the hill was adequately represented by a long, unbroken slope. More on this later.)

In 1993 ARRL HQ embarked on a major project to tabulate the range of elevation angles from all regions of the US to important DX QTHs around the world. This was accomplished by running many thousands of computations using the *IONCAP* computer program. *IONCAP* has been under development for more than 25 years by various agencies of the US government and is considered the standard of comparison for propagation programs by many agencies, including the Voice of America, Radio Free Europe, and more than 100 foreign governments throughout the world. *IONCAP* is a real pain in the neck to use, but it is the standard of comparison.

The calculations were done for all levels of solar activity, for all months of the year, and for all 24 hours of the

day. The results were gathered into some very large databases, from which special custom-written software extracted detailed statistics. The results appeared in summary form in Tables 4 through 13 printed in Chapter 23, Radio Wave Propagation, of the 17th Edition and in more detail on the diskette included with that book. (This book, the 20th Edition, contains even more statistical data, for more areas of the world, on the accompanying CD-ROM.)

Fig 30 shows the full range of elevation angles (represented as vertical bars) for the 20-meter path from New England (centered on Newington, Connecticut) to all of Europe. This is for all openings, in all months, over the entire 11-year solar cycle. The most likely elevation angle occurs at 5° for about 13% of the times when the 20-meter band is open to Europe from New England. From 4° to 6° the band is open a total of about 34% of the times the band is open. There is a secondary peak between 10° to 12°, occurring for a total of about 25% of the times the band is open.

Overlaid on Fig 30 along with the elevation-angle statistics are the elevation-plane responses for three different horizontally polarized Yagi beams, all over flat ground. The first is mounted 140 feet high, 2 λ in terms of wavelength. The second Yagi is mounted 70 feet high (at 1 λ) and the third is 35 feet (0.5 λ). The 140-foot high antenna has a deep null at 15°, but it also has the highest response (13.4 dBi) of the three at the statistical peak elevation angle of 5°. However, at 12°—where the band is open some 9% of the time—the 140-foot high Yagi is down 4 dB compared to the 70-foot antenna.

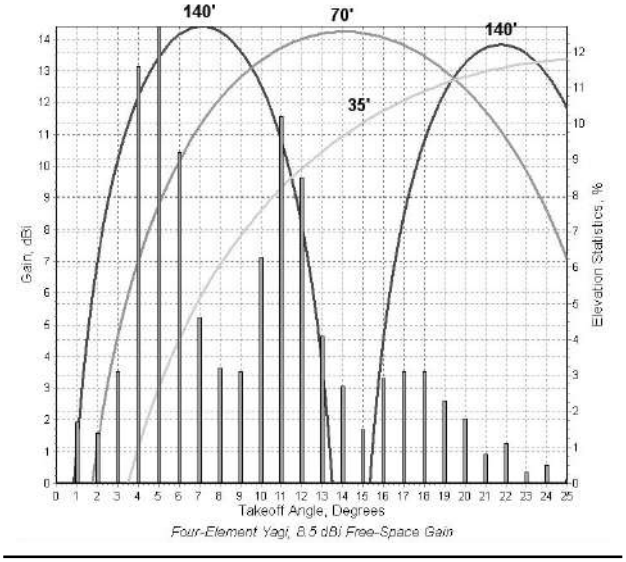

Fig 30—Graph showing 20-meter percentage of all openings from New England to Europe versus elevation angles, together with overlay of elevation patterns over flat ground for three 20-meter antenna systems. The most statistically likely angle at which the band will be open is 5°, although at any particular hour, day, month and year, the actual angle will likely be different. Note the deep null exhibited by the 140-foot high antenna centered at 14°.

The 70-foot high Yagi arguably covers the overall range best, since it has no disastrous nulls in the 1° to 25° range, where most of the action is occurring on 20 meters. At 5°, however, its response is only 8.8 dBi, 4.6 dB down from the 140-foot high antenna at that angle. The 35-foot antenna peaks above 26° in elevation angle, and is down some 10.4 dB compared to the 140-foot antenna at 5°. Obviously, no single antenna covers the complete range of elevation angles needed.

Note that the highest Yagi has a strong *second lobe* peaking at 22°. Let's say that you could select between two antennas, one at 140 and one at 70 feet, and that the incoming angle for a particular distant station is 22°. You might be fooled into thinking that the incoming angle is around 6°, favoring the first peak of the higher antenna, when in truth the angle is relatively high. The 70-foot antenna's response would be lower at 22° than the higher one, but only because the 140-foot antenna is operating on its second lobe. (What would clinch a determination of the correct incoming angle—6° or 22°—would be the response of the 35-foot high Yagi, which would be close to its peak at 22°, while it would be very far down at 6°.)

Now, we must emphasize that these elevation angles are *statistical entities*— in other words, just because 5° is the "statistically most likely angle" for the 20-meter path from New England to Europe doesn't mean that the band will be open at 11° at any particular hour, on a particular day, in a particular month, in any particular year. In fact, however, experience agrees with the *IONCAP* computations: the 20-meter path to Europe usually opens at a low angle in the New England morning hours, rising to about 11° during the afternoon, when the signals remain strongest throughout the afternoon until the evening in New England.

What would happen if we were to feed all three Yagi at 140, 70 and 35 feet in-phase as a stack? **Fig 31** shows this situation, along with a more highly optimized stack at 120, 80 and 40 feet that better covers the overall range of elevation angles from Connecticut to Europe.

Now see **Fig 32**, which uses the same 120/80/40-foot stack of 20-meter antennas as in Fig 31, but this time from Seattle, Washington, to Europe. For comparison, the response of a single 4-element Yagi at 100 feet over flat ground is also shown in Fig 32. Just because 5º is the statistically most prevalent angle (occurring some 13% of the time) from Seattle to Europe on 20 meters, this doesn't mean that the actual angle *at any particular moment in time* might not be 10º, or even 2º. The statistics for W7 to Europe say that 5º is the most likely angle, but 20-meter signals from Europe arrive at angles ranging from 1º to 18º. Note that this range of angles is quite a bit less than from W1 to Europe, which is much closer geographically to Europe than is the Pacific Northwest coast of the US. If you design an antenna system to cover all possible angles needed to talk to Europe from Seattle (or from Seattle to Europe) on 20 meters, you would need to cover the full range from 1º to 18º equally well.

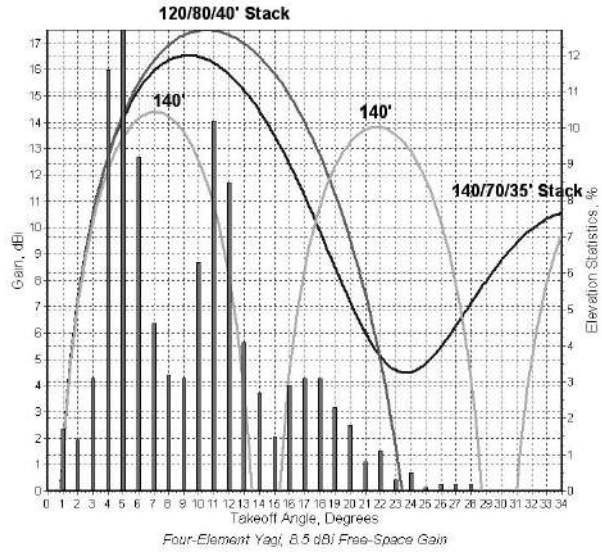

Fig 31—Graph showing results of stacking antennas at different heights on the same tower to cover a wider range of elevation angles, in this case for the path from Connecticut (W1) to all of Europe on 20 meters. The optimized stack at 120/80/40 feet covers the needed range of elevation angles better than the stack at 140/70/35 feet or the single Yagi at 140 feet.

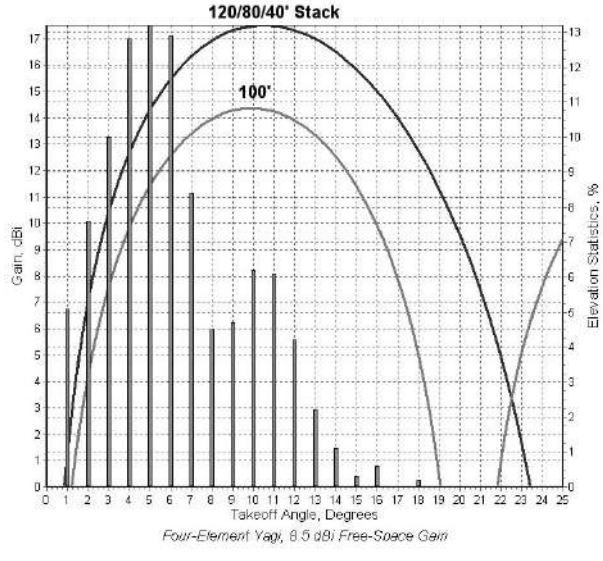

Fig 32—Graph showing 20-meter percentage of all openings, this time from Seattle, WA, to Europe, together with an overlay of elevation patterns over flat ground for two 20-meter antenna systems. The statistically most likely angle on this path is 5°, occurring about 13% of the time when the band is actually open. Higher antennas predominate on this low-angle path.

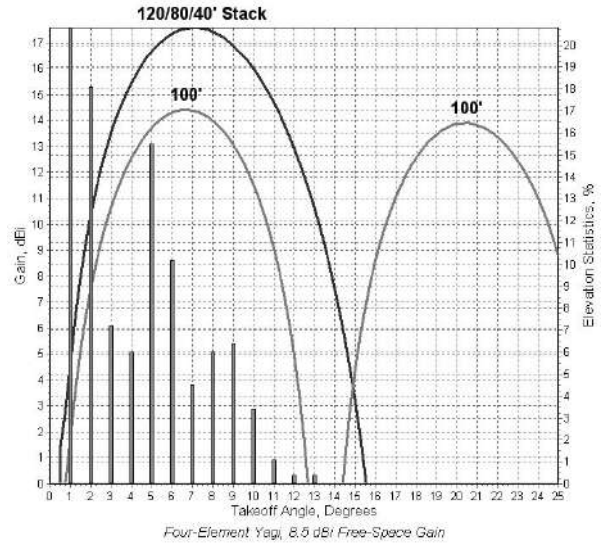

Fig 33—Graph showing 15-meter percentage of all openings from Chicago to Southern Africa, together with overlay of elevation patterns over flat ground for two 15-meter antenna systems. On this long-distance, low-angle path, higher antennas are again most effective.

Similarly, if you wish to cover the full range of elevation angles from Chicago to Southern Africa on 15 meters, you would need to cover 1º to 13º, even though the most statistically likely signals arrive at 1º, for 21% of the time when that the band is open for that path. See **Fig 33**.

It is important to recognize that Figs 30 through 33 are for flat ground. When the antennas are mounted over irregular local terrain, things get much more complicated. First, however, we'll discuss general-purpose antenna modeling programs as they try to model real terrain.

DRAWBACKS OF COMPUTER MODELS FOR ANTENNAS OVER REAL TERRAIN

Modern general-purpose antenna modeling programs such as *NEC* or *MININEC* (or their commercially upgraded equivalents, such as *NEC-Win Plus*, *EZNEC* and *EZNEC ARRL*) can accurately model almost any type of antenna commonly used by radio amateurs. In addition, there are specialized programs specifically designed to model Yagis efficiently, such as *YO* or *YW* (Yagi for Windows, bundled on the CD-ROM with this book) or *YagiMax*. These programs however are all unable to model antennas accurately over anything other than *purely flat ground*.

While both *NEC* and *MININEC* can simulate irregular ground terrain, they do so in a decidedly crude manner, employing step-like concentric rings of height around an antenna. The documentation for *NEC* and *MININEC* both clearly state that diffraction off these steps is not modeled.

Common experience among serious modelers is that the warnings in the manuals are worth heeding.

Although you can analyze and even optimize antenna designs using free-space or flat-earth ground models, it is *diffraction* that makes the real world a very, very complicated place. This should be clarified—diffraction is hard, even tortuous, to analyze properly, but it makes analysis of real world results far more believable than a flat-world reflection model does.

RAY-TRACING OVER UNEVEN LOCAL TERRAIN

The Raytracing Technique

First, let's look at a simple raytracing procedure involving only horizontally polarized reflections, with no diffractions. From a specified height on the tower, an antenna shoots "rays" (just as though they were bullets) in 0.25° increments from +35° above the horizon to –35° below the horizon. Each ray is traced over the foreground terrain to see if it hits the ground at any point on its travels in the direction of interest. If it does hit the ground, the ray is reflected following the classical *law of reflection*. That is, the outgoing angle equals the incoming angle, reflected through the normal to the slope of the surface. Once the rays exit into the ionosphere, the individual contributions are vector-summed to create the overall far-field elevation pattern.

The next step in terrain modeling involves adding *diffractions* as well as reflections. At the Dayton antenna forum in 1994, Jim Breakall, WA3FET, gave a fascinating and tantalizing lecture on the effect of foreground terrain. Later Breakall, Dick Adler, K3CXZ, Joel Young and a group of other researchers published an extremely interesting paper entitled "The Modeling and Measurement of HF Antenna Skywave Radiation Patterns in Irregular Terrain" in July 1994 *IEEE Transactions on Antennas and Propagation*. They described in rather general terms the modifications they made to the *NEC-BSC* program. They showed how the addition of a ray-tracing reflection and diffraction model to the simplistic stair-stepped reflection model in regular *NEC* gave far more realistic results. For validation, they compared actual pattern measurements made on a site in Utah (with an overflying helicopter) to computed patterns made using the modified *NEC* software. However, because the US Navy funded this work the software remained for a long time a military secret.

Thumbnail History of the Uniform Theory of Diffraction

It is instructive to look briefly at the history of how *Geometric Optics* (GO) evolved (and still continues to evolve) into the *Uniform Theory of Diffraction* (UTD). The following is summarized from the historical overview in one book found to be particularly useful and comprehensive on the subject of UTD: *Introduction to the Uniform Geometrical Theory of Diffraction*, by McNamara, Pistorius, and Malherbe.

Many years before the time of Christ, the ancient Greeks studied optics. Euclid is credited with deriving the law of reflection about 300 BC. Other Greeks, such as Ptolemy, were also fascinated with optical phenomena. In the 1600s, a Dutchman named Snell finally figured out the law of refraction, resulting in *Snell's law*. By the early 1800s, the basic world of classical optics was pretty well described from a mathematic point of view, based on the work of a number of individuals.

As its name implies, classical geometric optical theory deals strictly with geometric shapes. Of course, the importance of geometry in optics shouldn't be minimized—after all, we wouldn't have eyeglasses without geometric optics. Mathematical analysis of shapes utilizes a methodology that traces the paths of straight-line *rays* of light. (Note that the paths of rays can also be likened to the straight-line paths of particles.) In classical geometric optics, however, there is no mention of three important quantities: phase, intensity and polarization. Indeed, without phase, intensity or polarization, there is no way to deal properly with the phenomenon of *interference*, or its cousin, *diffraction*. These phenomena require theories that deal with *waves* rather than rays.

Wave theory has also been around for a long time, although not as long as geometry. Workers like Hooke and Grimaldi had recorded their observations of interference and diffraction in the mid 1600s. Huygens had used elements of wave theory in the late 1600s to help explain refraction. By the late 1800s, the work of Lord Rayleigh, Sommerfeld, Fresnel, Maxwell and many others led to the full mathematic characterization of all electromagnetic phenomena, light included.

Unfortunately, ray theory doesn't work for many problems, at least ray theory in the classical optical form. The real world is a lot more jagged, pointy and fuzzy in shape than can be described in a totally rigorous mathematic fashion. Some properties of the real world are most easily explained on the micro level using electrons and protons as conceptual objects, while other macro phenomena (like resonance, for example) are more easily explained in terms of waves. To get a handle on a typical real-world physical situation, a combination of classical ray theory and wave theory was needed.

The breakthrough in the combination of classical geometric optics and wave concepts came from J. B. Keller of Bell Labs in 1953, although he published his work in the early 1960s. In the very simplest of terms, Keller introduced the notion that shooting a ray at a diffraction *wedge* causes wave interference at the tip, with an infinite number of diffracted waves emanating from the diffraction point. Each diffracted wave can be considered to be a point source radiator at the place of generation, the diffraction point. Thereafter, the paths of individual waves can be traced as

though they were individual classical optic rays again. What Keller came up with was a reasonable mathematical description of what happens at the tip of the diffraction wedge.

Fig 34 is a picture of a simple diffraction wedge, with an incoming ray launched at an angle of α_r, referenced to the horizon, impinging on it. The diffraction wedge here is considered to be perfectly conducting, and hence impenetrable by the ray. The wedge generates an infinite number of diffracted waves, going in all directions not blocked by the wedge itself. The amplitudes and phases of the diffracted waves are determined by the interaction at the wedge tip, and this in turn is governed by the various angles associated with the wedge. Shown in Fig 34 are the included angle a of the wedge, the angle ϕ' of the incoming ray (referenced to the incoming surface of the wedge), and the observed angle ϕ of one of the outgoing diffracted waves, also referenced to the wedge surface.

The so-called *shadow boundaries* are also shown in Fig 34. The Reflection-Shadow Boundary (RSB) is the angle beyond which no further reflections can take place for a given incoming angle. The Incident-Shadow Boundary (ISB) is that angle beyond which the wedge's face blocks any incident rays from illuminating the observation point.

Keller derived the amplitude and phase terms by comparing the classical Geometric Optics (GO) solution with the exact mathematical solution calculated by Sommerfeld for a particular case where the boundary conditions were well known—an infinitely long, perfectly conducting wedge illuminated by a plane wave. Simply speaking, whatever was left over had to be diffraction terms. Keller combined these diffraction terms with GO terms to yield the total field everywhere.

Keller's new theory became known as the *Geometric Theory of Diffraction* (abbreviated henceforth as GTD). The beauty of GTD was that in the regions where classical GO predicted zero fields, the GTD "filled in the blanks," so to speak. For example, see **Fig 35**, showing the terrain for a hypothetical case, where a 60-foot high 4-element 15-meter Yagi illuminates a wide, perfectly flat piece of ground. A 10-foot high rock has been placed 400 feet away from the tower base in the direction of outgoing rays. **Fig 36** shows the elevation pattern predicted using reflection-only GO techniques. Due to blockage of the direct wave (A) trying to shoot past the 10-foot high rock, and due to blockage of (B) reflections from the flat ground in front of the rock by the rock, there is a *hole* in the smooth elevation pattern.

Now, doesn't it defy common sense to imagine that a single 10-foot high rock will really have such an effect on a 15-meter signal? Keller's GTD took diffraction effects into account to show that waves do indeed sneak past and over the rock to fill in the pattern. The whole GTD scheme is very clever indeed.

However, GTD wasn't perfect. Keller's GTD predicts some big spikes in the pattern, even though the overall shape of the elevation pattern is much closer to reality than a simple GO reflection analysis would indicate. The region right at the RSB and ISB shadow boundaries is where problems are found. The GO terms go to zero at these points because of blockage by the wedge, while Keller's diffraction terms tend to go to infinity at these very spots. In mathematical terms this is referred to as a *caustic problem*. Nevertheless, despite these nasty problems at the ISB and RSB, the GTD provided a remarkably better solution to diffraction problems than did classical GO.

In the early 1970s, a group at Ohio State University under R. G. Kouyoumjian and P. H. Pathak did some pivotal work to resolve this caustic problem, introducing what amounts to a clever *fudge factor* to compensate for the tendency of the diffraction terms at the shadow boundaries to go to infinity. They introduced what is known as a *transition function*, using a form of Fresnel integral. Most importantly, the Ohio State researchers also created several FORTRAN computer programs to compute the amplitude and phase of diffraction components. Now computer hackers could get to work!

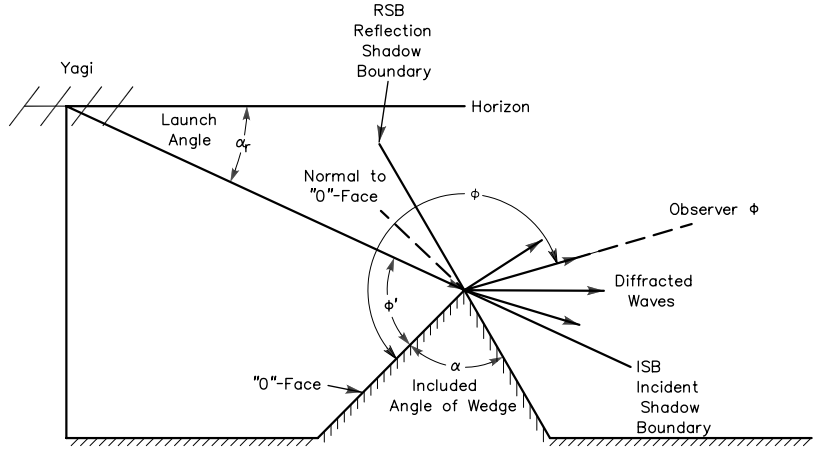

Fig 34—Diagram showing diffraction mechanism of ray launched at angle α_r below the horizon at a diffraction wedge, whose included angle is α. Referenced to the incident face (the *o-face* as it is called in UTD terminology), the incoming angle is ϕ' (phi prime). The wedge creates an infinite number of diffracted waves. Shown is one whose angle referenced to the o-face is ϕ, the so-called *observation angle* in UTD terminology.

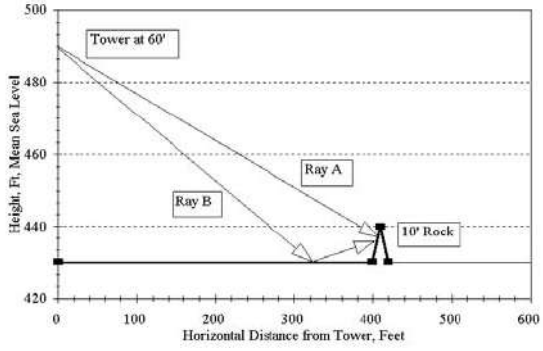

Fig 35—Hypothetical terrain exhibiting so-called "10-foot rock effect." The terrain is flat from the tower base out to 400 feet, where a 10-foot high rock is placed. Note that this forms a diffraction wedge, but that it also blocks direct waves trying to shoot through it to the flat surface beyond, as shown by Ray A. Ray B reflects off the flat surface before it reaches the 10-foot rock, but it is blocked by the rock from proceeding further. A simple Geometric Optics (GO) analysis of this terrain without taking diffraction into account will result in the elevation response shown in Fig 36.

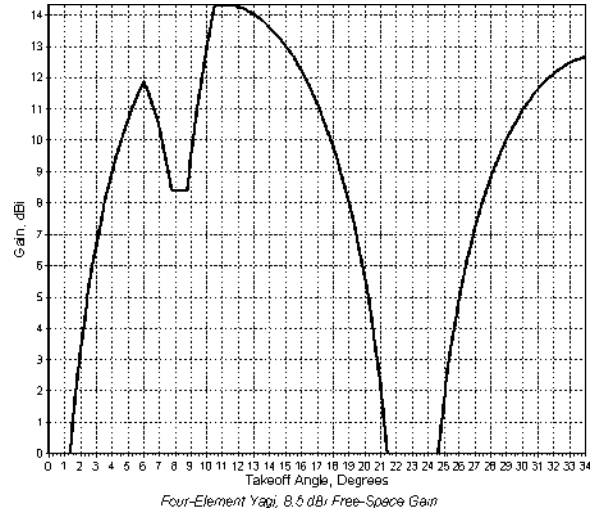

Fig 36—Elevation response for rays launched at terrain in Fig 35 from a height of 60 feet using a 4-element Yagi. This was computed using a simple Geometrical Optics (GO) reflection-only analysis. Note the *hole* in the response between 6° to 10° in elevation. It is not reasonable for a 10-foot high rock to create such a disturbance at 21 MHz!

The program that finally resulted is called *HFTA*, standing for "HF Terrain Assessment." (The DOS version of *HFTA* was known as *YT*, standing for "Yagi Terrain.") As the name suggests, *HFTA* analyzes the effect of local terrain on HF propagation through the ionosphere. It is designed for horizontally polarized Yagis, although it will model the effects of a simple flattop dipole also. The accurate appraisal of the effect of terrain on vertically polarized signals is a far more complex problem than for horizontally polarized waves, and *HFTA* doesn't do verticals.

SIMULATION OF REALITY—SOME SIMPLE EXAMPLES FIRST

We want to focus first on some simple results, to show that the computations do make some sense by presenting some simulations over simple terrains. We've already described the "10-foot rock at 400 feet" situation, and showed where a simple GO reflection analysis is inadequate to the task without taking diffraction effects into account.

Now look at the simple case shown in **Fig 37**, where a very long, continuous downslope from the tower base is shown. Note that the scales used for the X and Y axes are different: the Y-axis changes 300 feet in height (from 800 to 1100 feet), while the X-axis goes from 0 to 3000 feet. This exaggerates the apparent steepness of the downwards slope, which is actually a rather gentle slope, at $\tan^{-1}(1000 - 850) / (3000 - 0) = -2.86°$. In other words, the terrain falls 150 feet in height over a range of 3000 feet from the base of the tower.

Fig 38 shows the computed elevation response for this terrain profile, for a 4-element horizontally polarized Yagi on a 60-foot tower. The response is compared to that of an identical Yagi placed 60 feet above flat ground. Compared to the "flatland" antenna, the hilltop antenna has an elevation response shifted over by almost 3° towards the lower elevation angles. In fact, this shift is directly due to the –2.86° slope of the hill. Reflections off the slope are tilted by the slope. In this situation there is a single diffraction at the bottom of the gentle slope at 3000 feet, where the program assumes that the terrain becomes flat.

Look at **Fig 39**, which shows another simple terrain profile, called a "Hill-Valley" scenario. Here, the 60-foot high tower stands on the edge of a gentle hill overlooking a long valley. Once again the slope of the hill is exaggerated by the different X and Y-axes. **Fig 40** shows the computed elevation response at 21.2 MHz for a 4-element Yagi on a 60-foot high tower at the edge of the slope.

Once again, the pattern is overlaid with that of an identical 60-foot-high Yagi over flat ground. Compared to the flatland antenna, the hilltop antenna's response above 9° in elevation is shifted by almost 3° towards the lower elevation angles. Again, this is due to reflections off the downward slope. From 1° to 9°, the hilltop pattern is enhanced even more compared to the flatland antenna, this time by diffraction occurring at the bottom of the hill.

Now let's see what happens when there is a hill ahead in the direction of interest. **Fig 41** depicts such a situation, labeled "Hill-Ahead." Here, at a height of 400 feet above mean sea level, the land is flat in front of the tower, out to a distance 500 feet, where the hill begins. The hill then rises 100 feet over the range 500 to 1000 feet away

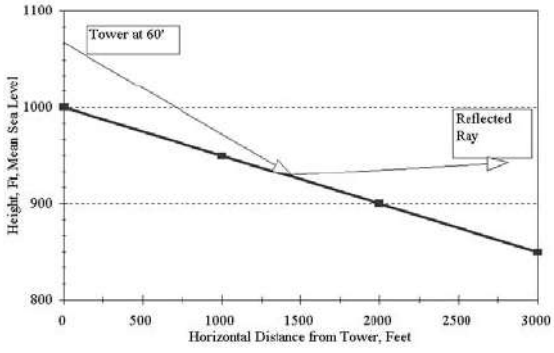

Fig 37—A long, gentle downwards-sloping terrain. This terrain has no explicit diffraction points and can be analyzed using simple GO reflection techniques.

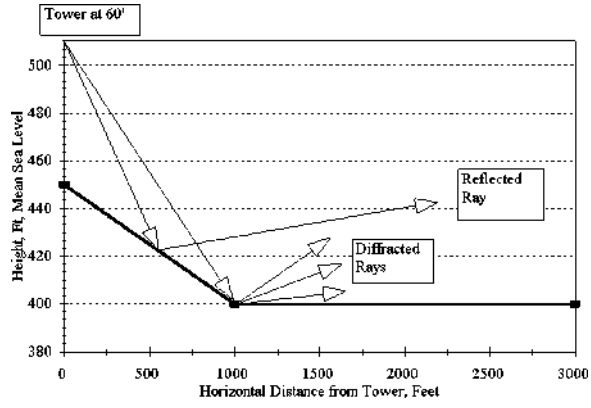

Fig 39—"Hill-Valley" terrain, with reflected and diffracted rays.

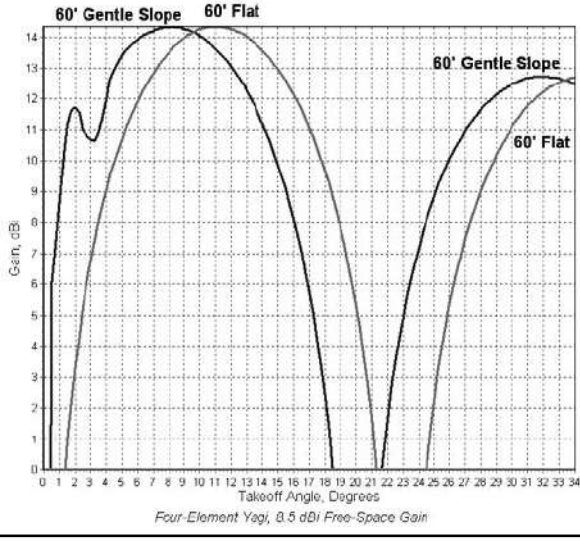

Fig 38—Elevation response for terrain shown in Fig 37, using a 4-element 15-meter Yagi, 60-foot high. Note that the shape of the response is essentially shifted towards the left, towards lower elevation angles, by the angle of the sloping ground. For reference, the response for an identical Yagi placed over flat ground is also shown.

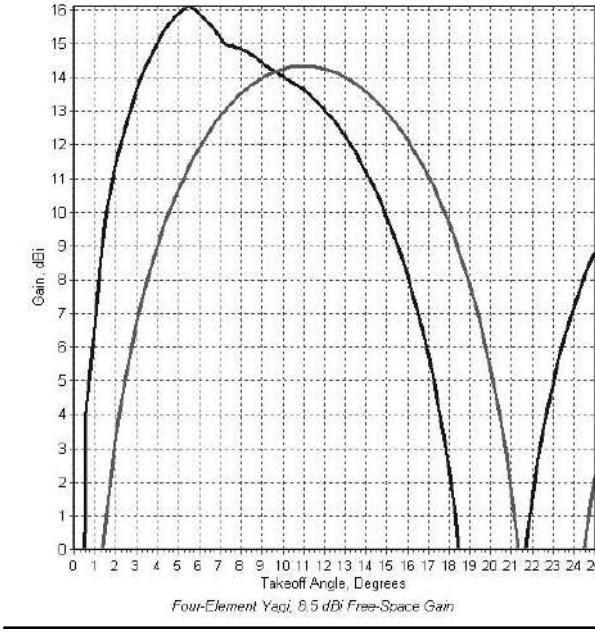

Fig 40—Elevation response computed by *HFTA* program for single 4-element 15-meter Yagi at 60 feet above "Hill-Valley" terrain shown in Fig 39. Note that the slope has caused the response in general to be shifted towards lower elevation angles. At 5° elevation, the diffraction components add up to increase the gain slightly above the amount a GO-only analysis would indicate.

from the tower base. After that, the terrain is a plateau, at a constant 500 feet elevation.

Fig 42 shows the computed elevation pattern for a 4-element 21-MHz Yagi 60-feet high on the tower, compared again with an overlay for an identical 60-foot high antenna over flat ground. The hill blocks low-angle waves directly radiated from the antenna from 0° to 2.3°. In addition, waves that would normally be reflected from the ground, and that would normally add in phase from about 2.3° to 12°, are blocked by the hill also. Thus the signal at 8° is down almost 5 dB from the signal over flat ground, all due to the effect of the hill. Diffracted waves start kicking in once the direct wave rises enough above the horizon to illuminate the top edge of the hill. These diffracted waves tend to augment elevation angles above about 12°, which reflected waves can't reach.

Is there is any hope for someone in such a lousy QTH for DXing? **Fig 43** shows the elevation response for a truly heroic solution. This involves a stack of four 4element Yagis, mounted at 120, 90, 60 and 30 feet on the tower. Now, the total gain at low angles is just about comparable to that from a single 4-element Yagi mounted over flat ground. Where there's a ham, there is a way!

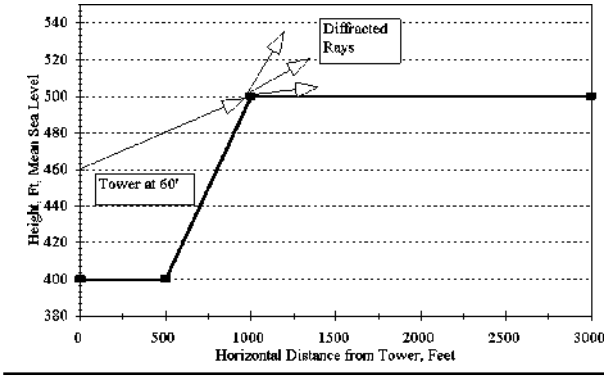

Fig 41—"Hill-Ahead" terrain, shown with diffracted rays created by illumination of the edge of the plateau at the top of the hill.

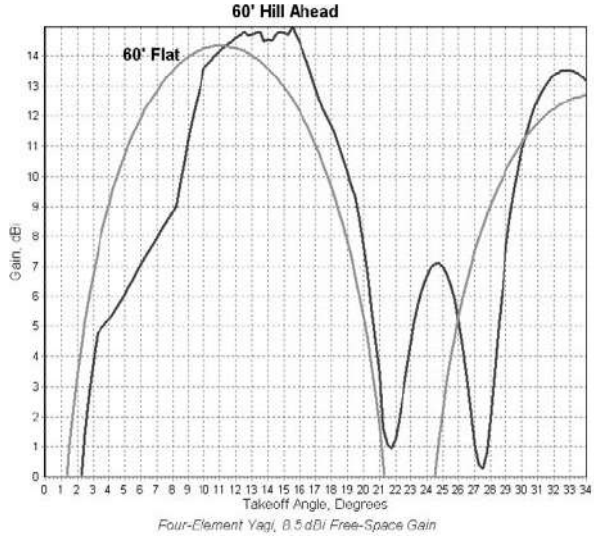

Fig 42—Elevation response computed by *HFTA* for "Hill-Ahead" terrain shown in Fig 41. Now the hill blocks direct rays and also precludes possibility of any constructive reflections. Above 10°, diffraction components add up together with direct rays to create the response shown.

At 5° elevation, four diffraction components add up (there are zero reflection components) to achieve the far-field pattern. This seems reasonable, because each of the four antennas is illuminating the diffraction point separately and we know that none of the four antennas can *see over* the hill directly to produce a reflection at a low launch angle.

At an elevation angle of 5°, 15-meter signals arrive from Europe from New England about 13% of the total time when the band is actually open. We can look at this another way. For about two-thirds of the times when the band is open on this path, the incoming angle is between 3° to 12°. For about one-third of the time, signals arrive above 10°, where the "heroic" four-stack is really beginning to come into its own.

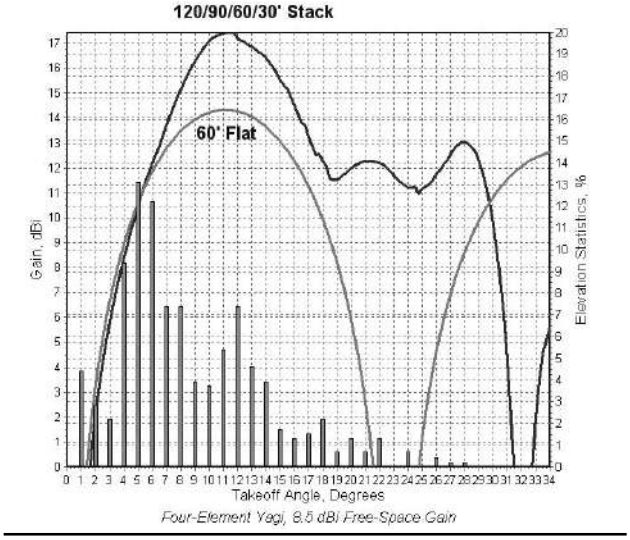

Fig 43—Elevation response of "heroic effort" to surmount the difficulties imposed by hill in Fig 41. This effort involves a stack of four 4-element Yagis in a stack starting at 120 feet and spaced at 30-foot increments on the tower. The response is roughly equivalent to a single 4-element Yagi at 60 feet above flat ground, hence the characterization as being a "heroic effort." The elevation-angle statistics from New England to Europe are overlaid on the graph for reference.

A More Complex Terrain

The results for simple terrains look reasonable; let's try a more complicated real-world situation. **Fig 44** shows the terrain from the New Hampshire N6BV/1 QTH towards Japan. The terrain was complex, with 52 different points *HFTA* identifies as diffraction points. **Fig 45** shows a labeled *HFTA* output for three different types of antennas on 20 meters: a stack at 120 and 60 feet, the 120-foot antenna by itself, and then a 120/60-foot stack over flat ground, for reference. The elevation-angle statistics for New England to Japan are overlaid on the graph also, making for a very complicated looking picture—it is a *lot* easier to decipher the lines on the color CRT, by the way than on a black-and-white printer.

Comparison of the same 120/60-foot stacks over irregular terrain and flat ground is useful to show where the terrain itself is affecting the elevation response. The flatland stack has more gain in the region of 3° to 7° than the same stack over the N6BV/1 local terrain towards Japan. On the other hand, the N6BV/1 local terrain boosts signals in the range of 8° to about 12°. This demonstrates the conservation of energy—you may gain a stronger signal at certain elevation angles, but you will lose gain at others. In this case, the N6BV/1 station always felt "weak" towards Japan on 20 meters, because the dominant angles are low.

Examination of the detailed data output from *HFTA* shows that at an elevation angle of 5°, there are 6159

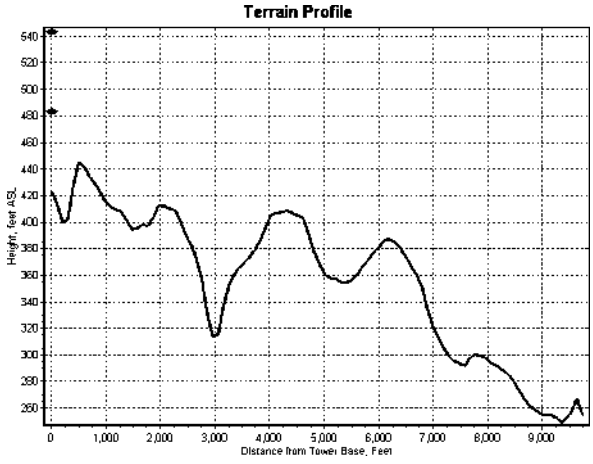

Fig 44—Terrain of N6BV in Windham, NH, towards Japan. *HFTA* identifies 52 different points where diffraction can occur.

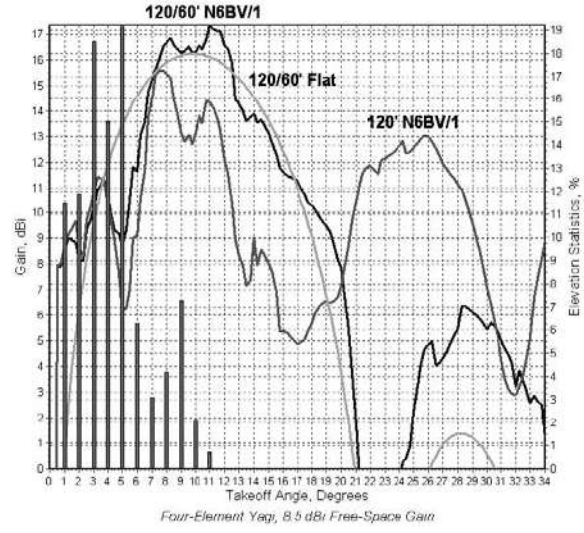

Fig 45—Elevation responses computed by *HFTA* for N6BV/1 terrain shown in Fig 44, for a stack of two 4-element 20-meter Yagis at 120 and 60 feet, together with the response for a single Yagi at 120 feet and a 120/60-foot stack over flat ground for reference. The response due to many diffraction and reflection components is quite complicated!

diffraction components. There are many, many signals bouncing around off the terrain on their trip to Japan! Note that because of blockage of some parts of the terrain, the 60-foot high Yagi cannot illuminate all the diffraction points, while the higher 120-foot Yagi is able to see these diffraction points.

It is fascinating to reflect on the thought that received signals coming down from the ionosphere to the receiver are having encounters with the terrain, but from the opposite direction. It's not surprising, given these kinds of interactions, that transmitting and receiving might not be totally reciprocal.

The 120/60-foot stack in Fig 45 achieves its peak gain of 17.3 dBi at 11° elevation, where it is about 3 dB stronger than the single Yagi at 120 feet. It maintains this 3-dB advantage over most of the range of incoming signals from Japan. This difference in performance between the stack and each antenna by itself was observed many times on the air. Much of the time when comparisons are being made, however, the small differences in signal are difficult to measure meaningfully, especially when the QSB varies signals by 20 dB or so during a typical QSO. It should be noted that the stack usually exhibited less fading compared to each antenna by itself.

USING *HFTA*

Manually Generating a Terrain Profile

The *HFTA* program uses two distinct algorithms to generate the far-field elevation pattern. The first is a simple reflection-only Geometric Optics (GO) algorithm. The second is the diffraction algorithm using the Uniform Theory of Diffraction (UTD). These algorithms work with a digitized representation of the terrain profile for a single azimuthal direction—for example, towards Japan or towards Europe.

You can generate a terrain file manually using a topographic map and a ruler or a pair of dividers. The HFTA.PDF file (accessed by clicking on the **Help** button) and on the accompanying CD-ROM gives complete instructions on how to create a terrain file manually (or automatically). The manual process is simple enough in concept. Mark on your US Geological Survey 7.5-minute map the exact location of your tower. You will find 7.5-minute maps available from some local sources, such as large hardware stores, but the main contact point is the U.S. Geological Survey, Denver, CO 80225 or Reston, VA 22092. Call 1-800-MAPS-USA. Ask for the folder describing the topographic maps available for your geographic area. Many countries outside the USA have topographic charts also. Most are calibrated in meters. To use these with *HFTA*, you will have to convert meters to feet by multiplying meters by 3.28 or else inserting a single line at the very beginning of the disk file, saying "meters" for *HFTA* to recognize meters automatically.

Mark off a pencil line from the tower base, in the azimuthal direction of interest, perhaps 45° from New England to Europe, or 335° to Japan. Then measure the distance from the tower base to each height contour crossed by the pencil line. Enter the data at each distance/height into an ASCII computer file, whose filename extension is "PRO," standing for *profile*.

Fig 46 shows a portion of the USGS paper map for the N6BV QTH in Windham, NH, along with lines scribed in several directions towards various parts of Europe and the Far East. Note that the elevation heights of the intermediate

contour lines are labeled manually in pencil in order to make sense of things. It is very easy to get confused unless you do this!

The terrain model used by *HFTA* assumes that the terrain is represented by flat *plates* connecting the elevation points in the *.PRO file with straight lines. The model is two dimensional, meaning that range and elevation are the only data for a particular azimuth. In effect, *HFTA* assumes that the width of a terrain plate is wide relative to its length. Obviously, the world is three-dimensional. If your shot in a particular direction involves aiming your Yagi down a canyon with steep walls, then it's pretty likely that your actual elevation pattern will be different than what *HFTA* tells you. The signals must careen horizontally from wall to wall, in addition to being affected by the height changes of the terrain. *HFTA* isn't designed to do canyons.

To get a true 3-D picture of the full effects of terrain, a terrain model would have to show azimuth, along with range and elevation, point-by-point for about two miles in every direction around the base of the tower. After you go through the pain of creating a profile for a single azimuth, you'll appreciate the immensity of the process if you were you try to create a full 360° 3D profile manually.

Terrain Data from the Internet

At one time digitized terrain data commonly available from the Internet didn't have sufficient resolution to be accurate enough for *HFTA*. Nowadays, the complete, accurate set of USGS topographic 7.5-minute maps are available at no cost on the Internet. You can use a program called *MicroDEM*, written by Professor Peter Guth at the US Naval Academy, to quickly and easily produce terrain data files suitable for *HFTA* from topographic data files. Dr Guth and the US Naval Academy have graciously allowed ARRL to include the *MicroDEM* program on the CD-ROM accompanying this book. It should be noted that besides automatically creating terrain profiles for *HFTA*, *MicroDEM* is a full-featured mapping program on its own.

Instructions for using *MicroDEM* are in the Help file for *HFTA* (HFTA.PDF), which you can access from the *HFTA* main window by clicking on the **Help** button. **Fig 47** shows a screen capture of the *MicroDEM* program for the N6BV/1 location in New Hampshire for an azimuth of 45° into Europe. The black/white rendering of the screen capture doesn't do justice to the same information in color. The computed terrain profile is plotted in the window at the right of Fig 47 and the data file is shown in the inset window at the top right.

Using *MicroDEM* and on-line USGS topographic map data, you can also automatically create up to 360 terrain profiles with 1° spacing of azimuths in a few seconds. (Specifying a 1° spacing is really overkill; most operator choose to create 72 profiles with 5° spacing.) On a topographic DEM (digital elevation model) map that covers the geographic

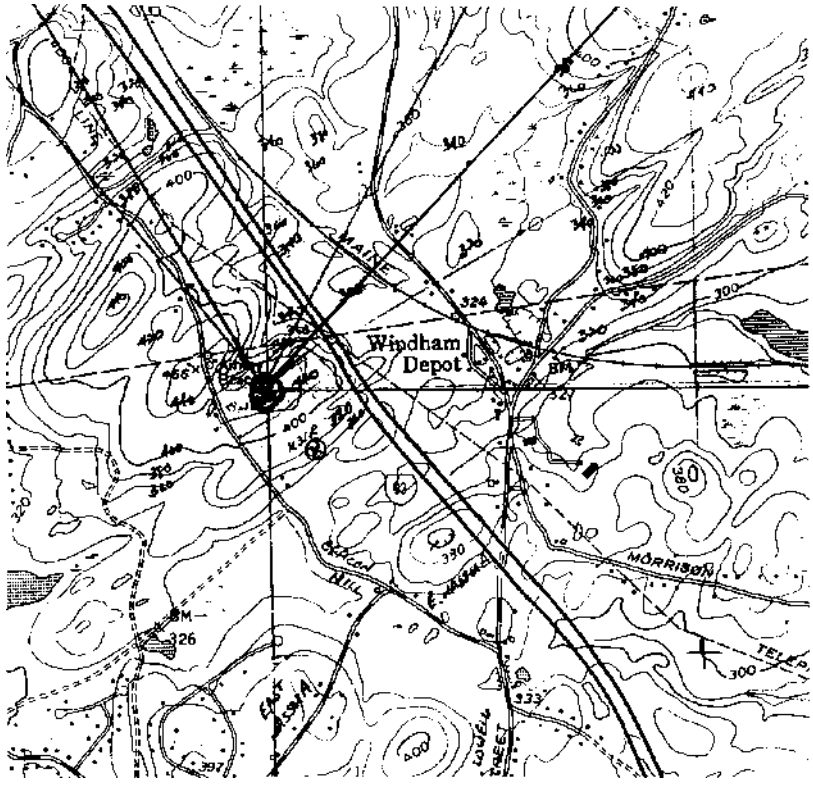

Fig 46—A portion of USGS 7.5 minute topographic map, showing N6BV/1 QTH, together with marks in direction of Europe and Japan from tower base. Note that the elevations contours were marked by hand to help eliminate confusion. This required a magnifying glass and a steady hand!

area of interest, you simply specify the latitude and longitude of a tower's location—found using a GPS receiver—and then ask *MicroDEM* for a **Viewshed**. See the *HFTA* **Help** file for the details.

Compare this automated several-second *MicroDEM* process to creating manual profiles on a paper topographic map—It can take up to an hour of meticulous measurements to manually create a single terrain profile!

Algorithm for Ray-Tracing the Terrain

Once a terrain profile is created, there are a number of mechanisms that *HFTA* takes into account as a ray travels over that terrain:

1. Classical ray reflection, with Fresnel ground coefficients.
2. Direct diffraction, where a diffraction point is illuminated directly by an antenna, with no intervening terrain features blocking the direct illumination.
3. When a diffracted ray is subsequently reflected off the terrain.
4. When a reflected ray encounters a diffraction point and causes another series of diffracted rays to be generated.
5. When a diffracted ray hits another diffraction point, generating another whole series of diffractions.

Certain unusual, bowl-shaped terrain profiles, with sheer vertical faces, can conceivably cause signals to reflect or diffract in a backwards direction, only to be reflected back again in the forward direction by the sheer-walled terrain to the rear. *HFTA* does not accommodate these interactions, mainly because to do so would increase the computation time too much. It only evaluates terrain in the forward direction along one azimuth of interest.

Fig 48 shows a portion of an *HFTA* screen capture in the direction towards Europe from the N6BV/1 location in New Hampshire on 21.2 MHz. It compares the results for a 90/60/30-foot stack of TH7DX tribanders to the same stack over flat land, and to a single antenna at 70 feet over flat ground. The 70-foot single antenna represents a pretty typical station on 15 meters. The terrain produces excellent gain at lower elevation angles compared to the same stack over flat ground. The stack is very close to or superior to the single 70-foot high Yagi at all useful elevation angles. Terrain can indeed exhibit a profound effect on the launch of signals into the ionosphere—for good or for bad.

HFTA's Internal Antenna Model

The operator selects the antenna used inside *HFTA* to be anything from a dipole to an 8-element Yagi. The default assumes a simple cosine-squared mathematic response, equivalent to a 4-element Yagi in free space. *HFTA* traces rays only in the forward direction from the tower along the azimuth of interest. This keeps the algorithms reasonably simple and saves computing time.

HFTA considers each antenna in a stack as a separate *point source*. The simulation begins to fall apart if a traveling wave type of antenna like a rhombic is used, particularly if the terrain changes under the antenna—that is, the ground is not flat under the entire antenna. For a typical Yagi, even a long-boom one, the point-source assumption is reasonable. The internal antenna model also assumes that the Yagi is horizontally polarized. *HFTA* does not do vertically polarized antennas, as discussed previously. The documentation for *HFTA* also cautions the user to work with practical spacings between stacked Yagis—0.5 λ or more

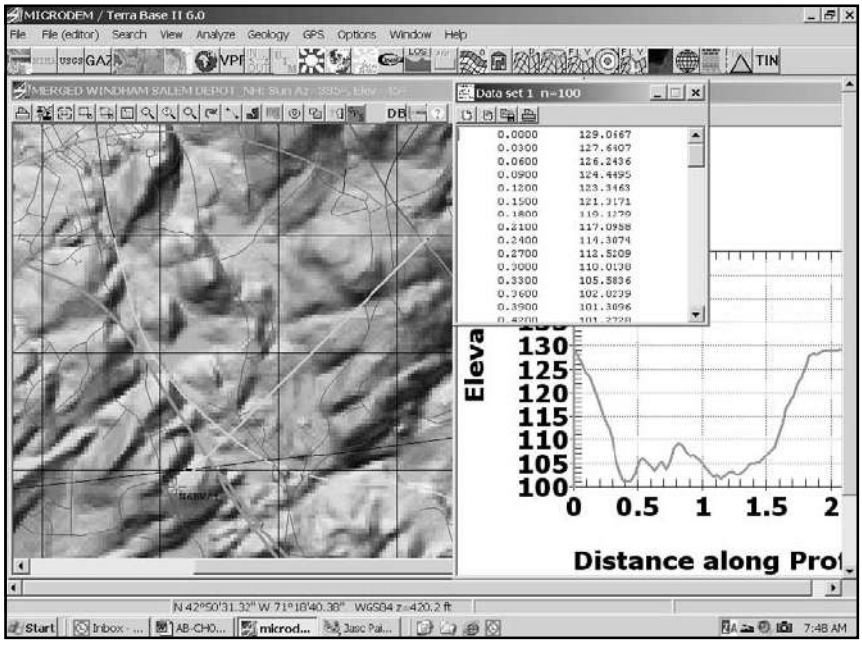

Fig 47—A screen-capture of the *MicroDEM* program, showing the topographic map for the same terrain shown in Fig 46, together with the computed terrain profile along an azimuth of 45° on the path towards Europe from the N6BV/1 location in Windham, NH.

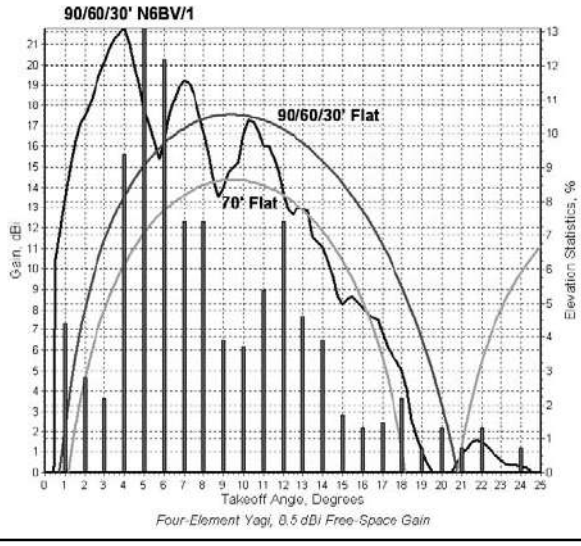

Fig 48—The 21-MHz elevation response for a stack of three TH7DX Yagis mounted on a single tower at 90/60/30 feet, at the N6BV/1 QTH for a 45° azimuth towards Europe. The terrain focuses the energy at low elevation angles compared to the same stack over flat ground. This illustrates once again the conservation of energy—Energy squeezed down into low elevation angles is stolen from other, higher, angles.

because *HFTA* doesn't explicitly model mutual coupling between Yagis in a stack.

HFTA compares well with the measurements for the horizontal antennas described earlier by Jim Breakall, WA3FET, using a helicopter in Utah. Breakall's measurements were done with a 15-foot high horizontal dipole.

More Details About *HFTA*

Frequency Coverage

HFTA can be used on frequencies higher than the HF bands, although the graphical resolution is only 0.25°. The patterns above about 100 MHz thus look rather grainy. The UTD is a *high-frequency-asymptotic* solution, so in theory the results become more realistic as the frequency is raised. Keep in mind too that *HFTA* is designed to model launch angles for skywave propagation modes, including E- and F-layer, and even Sporadic-E. Since by definition the ionospheric launch angles include only those above the horizon, direct line-of-sight UHF modes involving negative launch angles are not considered in *HFTA*.

See the HFTA.PDF documentation file for further details on the operation of *HFTA*. This file, as well as sample terrain profiles for some *big-gun* stations, is located on the CD-ROM accompanying this book.

BIBLIOGRAPHY

Source material and more extended discussion of the topics covered in this chapter can be found in the references listed below and in the textbooks listed at the end of Chapter 2, Antenna Fundamentals.

B. Boothe, "The Minooka Special," *QST*, Dec 1974.

Brown, Lewis and Epstein, "Ground Systems as a Factor in Antenna Efficiency," *Proc. IRE* , Jun 1937.

G. Brown, "The Phase And Magnitude Of Earth Currents Near Radio Transmitting Antennas," *Proc. IRE*, Feb 1935, pp 168-182.

R. Collin and F. Zucker, *Antenna Theory*, Chap 23 by J. Wait, Inter-University Electronics Series (New York: McGraw-Hill, 1969), Vol 7, pp 414-424.

T. Hullick, W9QQ, "A Two-Element Vertical Parasitic Array For 75 Meters," *QST*, Dec 1995, pp 38-41.

R. Jones, "A 7-MHz Vertical Parasitic Array," *QST*, Nov 1973.

T. Larsen, "The E-Field and H-Field Losses Around Antennas With a Radial Ground Wire System," *Journal of Research of the National Bureau of Standards*, D. Radio Propagation, Vol 66D, No. 2, Mar-Apr 1962, pp 189-204.

D. A. McNamara, C. W. I. Pistorius, J. A. G. Malherbe, *Introduction to the Geometrical Theory of Diffraction* (Norwood, MA: Artech House, 1994).

C. J. Michaels, "Some Reflections on Vertical Antennas," *QST*, Jul 1987.

C. J. Michaels, "Horizontal Antennas and the Compound Reflection Coefficient," *The ARRL Antenna Compendium, Vol 3* (Newington: ARRL, 1992).

R. Severns, N6LF, "Verticals, Ground Systems and Some History," *QST*, Jul 2000, pp 38-44.

J. Sevick, "The Ground-Image Vertical Antenna," *QST*, Jul 1971.

J. Sevick, "The W2FMI 20-Meter Vertical Beam," *QST*, Jun 1972.

J. Sevick, "The W2FMI Ground-Mounted Short Vertical," *QST*, Mar 1973.

J. Sevick, "A High Performance 20-, 40- and 80-Meter Vertical System," *QST*, Dec 1973.

J. Sevick, "The Constant-Impedance Trap Vertical," *QST*, Mar 1974.

J. Stanley, "Optimum Ground Systems for Vertical Antennas," *QST*, Dec 1976.

F. E. Terman, *Radio Engineers' Handbook*, 1st ed. (New York, London: McGraw-Hill Book Co, 1943).

Radio Broadcast Ground Systems, available from Smith Electronics, Inc, 8200 Snowville Rd, Cleveland, OH 44141.

The last major study that appeared in the Amateur literature on the subject of local terrain as it affects DX appeared in four *QST* "How's DX" columns, by Clarke Greene, K1JX, from October 1980 to January 1981. Greene's work was an update of a landmark Sep 1966 *QST* article entitled "Station Design for DX," by Paul Rockwell, W3AFM. The long-range profiles of several prominent, indeed legendary, stations in Rockwell's article are fascinating: W3CRA, W4KFC and W6AM.

Chapter 4

Antenna Modeling & System Planning

OVERVIEW: ANTENNA ANALYSIS BY COMPUTER

As pointed out in Chapter 3, The Effects of Ground, irregular local terrain can have a profound effect on the launch of HF signals into the ionosphere. A *system approach* is needed to create a scientifically planned station. We pointed out in Chapter 3 that antenna modeling programs do not generally take into account the effects of irregular terrain, and by "irregular" we mean any sort of ground that is not flat. Most modeling programs based on *NEC-2* or *MININEC* do model reflections, but they do not model diffractions.

On the other hand, while a ray-tracing program like *HFTA* (HF Terrain Assessment) does take into account diffraction, it doesn't explicitly factor in the mutual impedance between an antenna and the ground. Instead, *HFTA* makes the basic assumption that the antenna is mounted sufficiently high above ground so that the mutual impedance between an antenna and the ground is minimal.

In this chapter we'll look at modeling the antennas themselves on the PC. We'll evaluate some typical antennas over flat ground and also in free space. Once characterized—or even optimized for certain characteristics—these antennas can then be analyzed over real terrain using *HFTA* and the other tools discussed in Chapter 3.

A Short History of Antenna Modeling

With the proliferation of personal computers since the early 1980s, amateurs and professionals alike have made significant strides in computerized antenna system analysis. It is now possible for the amateur with a relatively inexpensive computer to evaluate even complicated antenna systems. Amateurs can obtain a keener grasp of the operation of antenna systems—a subject that has been a great mystery to many in the past. We might add that modern computing tools allow hams to debunk overblown claims made about certain antennas.

The most commonly encountered programs for antenna analysis are those derived from a program developed at US government laboratories called *NEC*, short for "Numerical Electromagnetics Code." *NEC* uses a so-called *Method of Moments* algorithm. This intriguing name derives from a mathematical convention dealing with how "momentous" the accumulated error becomes when certain simplifying assumptions are made about the current distribution along an antenna wire. If you want to delve into details about the method of moments, John Kraus, W8JK, has an excellent chapter in his book *Antennas*, 2nd edition. See also the article "Programs for Antenna Analysis by the Method of Moments," by Bob Haviland, W4MB, in *The ARRL Antenna Compendium, Vol 4*.

The mathematics behind the method-of-moments algorithm are pretty formidable, but the basic principle is simple. An antenna is broken down into a number of straight-line wire *segments*, and the field resulting from the RF current in each segment is evaluated by itself and also with respect to other mutually coupled segments. Finally, the field from each contributing segment is vector-summed to yield the total field, which can be computed for any elevation or azimuth angle desired. The effects of flat-earth ground reflections, including the effect of ground conductivity and dielectric constant, may be evaluated as well.

In the early 1980s, *MININEC* was written in BASIC for use on personal computers. Because of limitations in

memory and speed typical of personal computers of the time, several simplifying assumptions were necessary in *MININEC* and these limited potential accuracy. Perhaps the most significant limitation was that perfect ground was assumed to be directly under the antenna, even though the radiation pattern in the far field did take into account real ground parameters. This meant that antennas modeled closer than approximately 0.2 λ over ground sometimes gave erroneous impedances and inflated gains, especially for horizontal polarization. Despite some limitations, *MININEC* represented a remarkable leap forward in analytical capability. See Roy Lewallen's (W7EL) "*MININEC*—the Other Edge of the Sword" in Feb 1991 *QST* for an excellent treatment on pitfalls when using *MININEC*.

Because source code was made available when *MININEC* was released to the public, a number of programmers produced some very capable commercial versions for the amateur market, many incorporating exciting graphics showing antenna patterns in 2D or 3D. These programs also simplify the creation of models for popular antenna types, and several come with libraries of sample antennas.

By the end of the 1980s, the speed and capabilities

Commercial Implementations of *MININEC* and *NEC-2* Programs

Ever since the source code for *NEC-2* and *MININEC* came into in the public domain, enterprising programmers have been upgrading, extending and improving these programs. There are a number of "freeware" versions available nowadays, and there are also a variety of commercial implementations.

This sidebar deals only with the most popular commercial versions, programs that many hams use. You should keep in mind that whatever program you choose will require an investment in learning time, if not in dollars. Your time is valuable, of course, and so is the ability to swap modeling files you create with other modelers. Other peoples' modeling files, particularly when you are just starting out, are a great way to learn how the "experts" do their modeling. For example, there are archives of *EZNEC/ELNEC* files available on the Internet, since this popular modeling program has been around for a number of years. (*ELNEC* is the DOS-only, *MININEC*-core predecessor of EZNEC.)

The following table summarizes the main features and the pricing as of 2006 for some popular commercial antenna modeling programs. The programs that use the *NEC-4* core require separate licenses from Lawrence Livermore National Laboratories.

Commercial Implementations of *MININEC* and *NEC 2* programs

Name	*EZNEC 4.0 (+ ver.)*	*EZNEC-M Pro*	*EZNEC/4*	*NEC-Win Plus +*	*NEC-Win Pro*	*GNEC*	*Antenna Model*
Manufacturer	Roy Lewallen	Roy Lewallen	Roy Lewallen	Nittany Scientific	Nittany Scientific	Nittany Scientific	Teri Software
Core	*NEC-2*	*NEC-2*	*NEC-4*	*NEC-2*	*NEC-2*	*NEC-2/NEC-4*	*MININEC*
Operating System	Windows 32-bit	Windows 32-bit	Windows 32-bit	Windows 32-bit	Windows 32-bit	Windows 32-bit	Windows 32-bit
Number Segments	500 (1500, + ver.)	20,000	20,000	10,000	10,000	80,000	Limited by memory
NEC-Card Inputs	No	Yes	Yes	Yes	Yes	Yes	No
Other Input	ASCII (NEC, + ver.)	ASCII, NEC	ASCII, NEC	CAD *.DXF	CAD *.DXF	CAD *.DXF	No
Wires by Equation	No	No	No	Yes	Yes	Yes	Yes
Source Setting	By %	By %	By %	By %	By %	By %	By %
Source Type	Current/ Voltage/Split	Current/ Voltage/Split	Current /Voltage/Split	Current/ Voltage/Split	All types	All types	Current/Voltage
R + *j* X Loads	Yes	Yes	Yes	Yes	Yes	Yes	Yes
RLC Loads	Series, Parallel, Trap	Series, Parallel, Trap	Series, Parallel, Trap	Series, Parallel	Series, Parallel	Series, Parallel	Series, Parallel
True Trap Loads	Yes	Yes	Yes	No	No	No	No
Laplace Loads	Yes	Yes	Yes	Yes	Yes	Yes	No
Conductivity Table	Yes *	Yes *	Yes *	Yes	Yes	Yes	Yes
Average Gain Test	Yes	Yes	Yes	Yes	Yes	Yes	Yes
Transmission Lines	Yes	Yes	Yes	Yes	Yes	Yes	No
View Geometry	Excellent	Excellent	Excellent	Good	Good	Good	Very Good
Geometry Checking	Yes	Yes	Yes	Yes	Yes	Yes	Yes
Easy Height Change	Yes	Yes	Yes	No	No	No	No
Polar Plots	ARRL, linear-dB Az/El, Circ. (+ ver.)	ARRL, linear-dB Az/El, Circ.	ARRL, linear-dB Az/El, Circ.	ARRL, linear-dB Az/El Patterns	ARRL, linear-dB Az/El Patterns	ARRL, linear-dB Az/El Patterns	ARRL, Linear -dB Az/El Patterns
Rectangular Plots	SWR	SWR	SWR	SWR, Zin	SWR, Zin, Az/El, Near/Far Plots, Currents	SWR, Zin, Az/El, Near/Far Plots, Currents	Gain, SWR, F/B, F/R, Rin, Xin
Operating Speed	Fast	Fast	Fast	Very Fast	Very Fast	Very Fast	Slow
Smith Chart	Data for Ext. Smith program	Data for Ext. Smith program	Data for Ext. Smithprogram	No	Yes	Yes	Yes
Near/Far Field Tables	Both	Both	Both	Far	Both	Both	Both
Ground Wave Analysis	No	Yes	Yes	No	Yes	Yes	No
Pricing	$89 Web; $99 CD-ROM, $139 (+ ver.)	$450	$600; must have *NEC-4* license	$150	$425	$795	$85

* Wire conductivity is the same for all wires.

Excellent, Very Good, Good ratings done by *Antenna Book* editor.

of personal computers had advanced to the point where PC versions of *NEC* became practical, and several versions are now available to amateurs. The most recent public-domain version is *NEC-2* and this is the computational core that we'll use as an example throughout this chapter.

Like *MININEC*, *NEC-2* is a general-purpose modeling package and it can be difficult to use and relatively slow in operation for certain specialized antenna forms. Thus, custom commercial software has been created for more user-friendly and speedier analysis of specific antenna varieties, mainly Yagi arrays. See Chapter 11, HF Yagi Arrays. Also see the sidebar, "Commercial Implementations of *MININEC* and *NEC-2* Programs."

For this edition of *The ARRL Antenna Book*, Roy Lewallen, W7EL, has graciously provided a special version of his *EZNEC 3.0* program, called *EZNEC-ARRL*. This version works with the specific antenna models also bundled on the CD-ROM. Please note that this ARRL-specific version of *EZNEC* is limited to a maximum of 20 segments (we'll explain segments later) for all models except for the special ones included on this CD-ROM. You can find information on how to purchase the full-fledged version of *EZNEC* in the **Help** section of the *EZNEC-ARRL* program.

The following material on antenna modeling is by necessity a summary, since entire books have been written on this subject. Serious modelers would be well-advised to enroll in the online Antenna Modeling course, part of the ARRL Certification and Continuing Education series. L. B. Cebik, W4RNL created the ARRL Antenna Modeling course and it contains a great deal of information, tips and techniques concerning modeling by computer. See: **http://www.arrl.org/news/stories/2002/02/06/2/** for more information. We also strongly recommend that you read the Help files in *EZNEC-ARRL*. There is a wealth of practical information on the finer points of antenna modeling there.

THE BASICS OF ANTENNA MODELING

This chapter will discuss the following antenna-modeling topics for an *NEC-2*-based modeling software, using *EZNEC-ARRL* as an example:

- Program outputs
- Wire geometry
- Segmentation, warnings and limitations
- Source (feed point) placement
- Environment, including ground types and frequency
- Loads and transmission lines
- Testing the adequacy of a model

PROGRAM OUTPUTS

Instruction manuals for software programs traditionally start out describing in detail the input data needed by the program. They then demonstrate the output data the program can generate. We feel it is instructive, however, to turn things around and start out with a brief overview of the output from a typical antenna-modeling program.

We'll look at the output from public-domain *NEC-2*. Next, we'll look at the output information available from commercial adaptations of *NEC-2*, using *EZNEC-ARRL* provided by W7EL. After this brief overview of the output data, we'll look in detail at the input data needed to make a modeling program work. In the following discussions it will be very instructive if you to bring up *EZNEC-ARRL* on your computer and open the specific modeling files used in each example. [From now on in this chapter we'll refer merely to *EZNEC* rather than *EZNEC 3.0*, the official name or *EZNEC-ARRL*, a specialized subset of *EZNEC 3.0*. Where there are specific differences between *EZNEC 3.0* and the limited-edition *EZNEC-ARRL* we'll identify them.]

Native *NEC-2*

The native *NEC-2* program produces pages and pages of output formatted for a mainframe "line printer." You may be old enough to remember the stacks of green-and-white, tractor-feed, 132-column computer paper that such a line printer produced. Corporate MIS departments stored untold number of boxes of that paper.

Native *NEC-2* was written in the Fortran language, which stands for *Formula Translation*. Programmers used punched cards to enter the program itself and its accompanying input data into huge mainframe computers. To say that the paper output from *NEC-2* is massive, even intimidating, is putting it mildly. There is a strong distinction between "useful information" and "raw data" and the raw output from native *NEC-2* bombards the user with raw data.

Commercial versions that use the *NEC-2* computational core shield the user from the ugliness of raw line-printer output, as well as punched-card input (or disk surrogates for punched cards). Commercial versions like *EZNEC* do produce output numerical tables where this is useful. These tables show parameters such as the source impedance and SWR at a single frequency, or the characteristics of a load or a transmission line. But as the old saying goes, "One picture is worth a thousand words." This is as true for modeling programs as it is for other endeavors dealing with reams of numbers. Thus, most commercial modeling software packages create *graphs* for the user. *EZNEC* produces the following types of graphs:

- Polar (linear-dB or ARRL-style) graphs of the far-field elevation and azimuth responses.
- 3-D wire-frame graph of the total far-field response.
- Graph of the SWR across a frequency band.
- Graphical display of the RF currents on various conductors in a model.
- Rotatable, zoomable 3-D views of the wires used to make a model.
- Output to programs capable of generating Smith charts.

Fig 1A and 1B shows the computed far-field 2-D elevation and azimuth patterns for a 135-foot long horizontal dipole, mounted in a flattop configuration 50 feet above flat ground. These figures were generated using *EZNEC* at 3.75 MHz. Fig 1C shows a 3-D wire-frame picture of the far-field response, but this time at 14.2 MHz. For comparison, **Table 1** shows a short portion of the line-printer output for the azimuth pattern at 3.75 MHz. The actual printout is many pages long. One picture can indeed replace thousands of numbers!

Fig 2 shows the computed SWR curve over the frequency range 3.0 to 4.0 MHz for this dipole, fed with lossless 50-Ω transmission line. *EZNEC* generated this plot using the "SWR" button. Figs 1 and 2 are typical of the kind of graphical outputs that commercial implementations of the *NEC-2* computing core can produce.

Now, let's get into the details of what kind of input data is required to run a typical method-of-moments antenna-modeling program.

PROGRAM INPUTS: WIRE GEOMETRY

Coordinates in an X, Y and Z World

The most difficult part of using a *NEC*-type of modeling program is setting up the antenna's geometry—you must condition yourself to think in three-dimensional, Cartesian coordinates. Each end point of a wire is represented by three numbers: an x, y and z coordinate. These coordinates represent the distance from the origin (x-axis), the width of an antenna (y-axis), and the height (z-axis).

An example should help sort things out. **Fig 3** shows a simple model of a 135-foot center-fed dipole, made of #14 copper wire placed 50 feet above flat ground. The common term for this antenna is *flattop dipole*. For convenience, the ground is located at the *origin* of the coordinate system, at (0, 0, 0) feet, directly under the center of the dipole. **Fig 4** shows the *EZNEC* spreadsheet-like input data for this antenna. (Use model file: **Ch4-Flattop Dipole.EZ**.) *EZNEC* allows you to specify the type of conductor material from its main window, using the **Wire Loss** button to open a new window. We will click on the **Copper** button for this dipole.

Above the origin, at a height of 50 feet on the z-axis, is the dipole's *feed point*, called a *source* in *NEC* terminology. The width of the dipole goes toward the left (that is, in the "negative-y" direction) one-half the overall length of 135 feet, or –67.5 feet. Toward the right, our dipole's other end is at +67.5 feet. The x-axis dimension of our dipole is zero, meaning that the dipole wire is parallel to and directly above the x-axis. The dipole's ends are thus represented by two points, whose coordinates are (0, –67.5, 50) and (0, 67.5, 50) feet. The use of parentheses with a sequential listing of (x, y, z) coordinates is a common practice among antenna modelers to describe a wire end point.

Fig 3B includes some other useful information about this antenna beyond the wire geometry. Fig 3B overlays the wire geometry, the current distribution along the wire and the far-field azimuth response, in this case at an elevation angle of 30°.

Although not shown specifically in Fig 3, the thickness of the antenna is the diameter of the wire, #14 gauge. Note that native *NEC* programs specify the *radius* of the

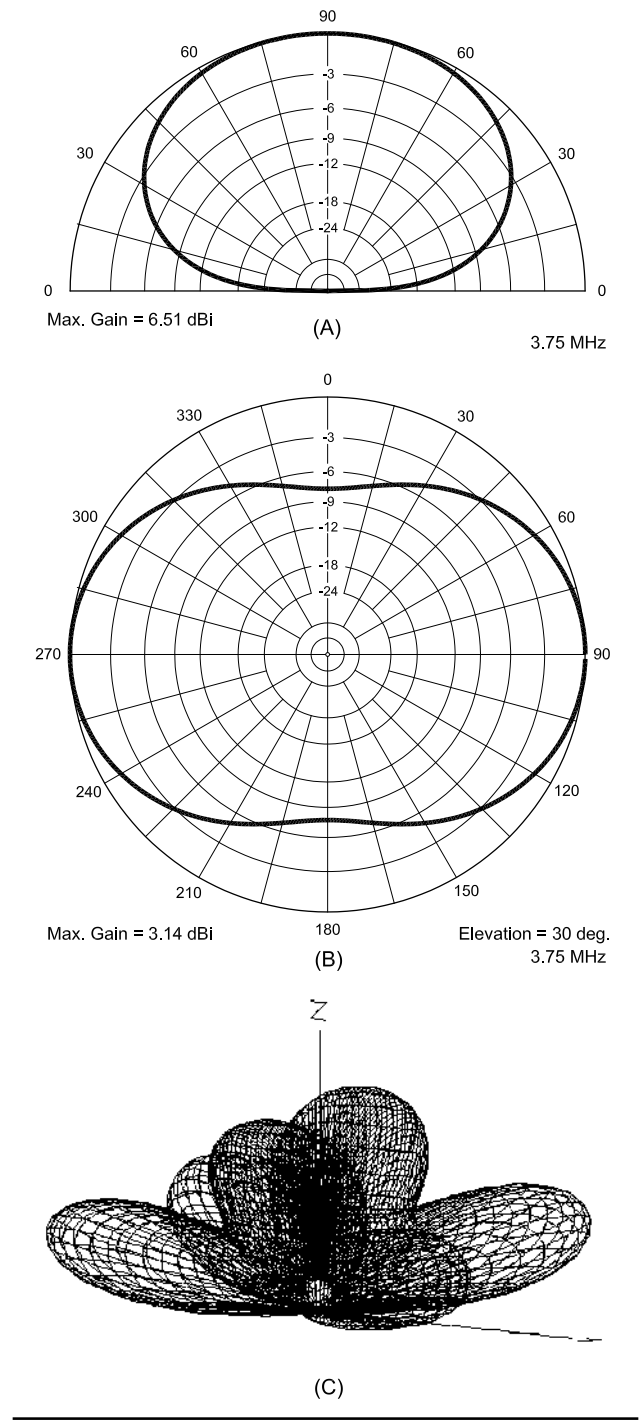

Fig 1—At A, far-field elevation-plane pattern for a 135-foot-long horizontal dipole, 50 feet above flat ground, at 3.5 MHz. At B, the far-field azimuth-plane pattern at an elevation angle of 30°.

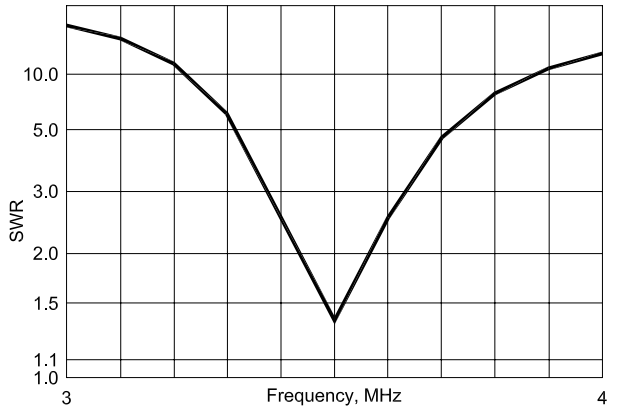

Fig 2—SWR curve for 135-foot flattop dipole over the frequency range 3.0 to 4.0 MHz for a 50-Ω feed line. This antenna is an example and is not optimized for the amateur band.

wire, rather than the diameter, but programs like *EZNEC* use the more intuitive diameter of a wire rather than the radius. *EZNEC* (and other commercial programs) also allows the user to specify the wire as an AWG gauge, such as #14 or #22, for example.

We've represented our simple dipole in Fig 3 using a single, straight wire. In fact, all antenna models created for method-of-moment programs are made of combinations of straight wires. This includes even complex antennas, such as helical antennas or round loops. (The mathematical basis for modeling complex antennas is that they can be simulated using straight-wire *polygons*. A circular loop, for example, can be modeled using an octagon.)

Segmentation and Specifying a Source Segment

We've specified the physical geometry of this simple one-wire dipole. Now several more modeling details surface—you must specify the number of *segments* into which the dipole is divided for the method-of-moment analysis and you must somehow feed the antenna. The *NEC-2* guideline for setting the number of segments is to use at least 10 segments per half-wavelength. This is a general rule of thumb, however, and in many models more dense segmentation is mandatory for good accuracy.

In Fig 3, we've specified that the dipole be divided into 11 segments for operation on the 80-meter band. This follows the rule of thumb above, since the 135-foot dipole is about a half-wavelength long at 3.5 MHz.

Setting the Source Segment

The use of 11 segments, an odd rather than an even number such as 10, places the dipole's feed point (the

Table 1
Portion of line-printer output from *NEC-2* for 135-foot dipole.

- - - RADIATION PATTERNS - - -

- - ANGLES - -		- POWER GAINS -			- - - POLARIZATION - - -			- - - E(THETA) - - -		- - - E(PHI) - - -	
Theta Degrees	Phi Degrees	Vert dB	Hor dB	Total dB	Axial Ratio	Tilt Degrees	Sense	Magnitude Volts	Phase Degrees	Magnitude Volts	Phase Degrees
60.00	0.00	–999.99	3.14	3.14	0.00000	90.00	LINEAR	0.00000E+00	0.00	6.62073E-01	–66.87
60.00	1.00	–37.87	3.13	3.14	0.00301	89.52	LEFT	5.89772E-03	–86.64	6.61933E-01	–66.87
60.00	2.00	–31.85	3.13	3.13	0.00603	89.04	LEFT	1.17915E-02	–86.64	6.61512E-01	–66.87
60.00	3.00	–28.33	3.12	3.12	0.00904	88.56	LEFT	1.76776E-02	–86.64	6.60812E-01	–66.87
60.00	4.00	–25.84	3.11	3.11	0.01206	88.08	LEFT	2.35520E-02	–86.64	6.59834E-01	–66.87
60.00	5.00	–23.91	3.09	3.10	0.01508	87.59	LEFT	2.94109E-02	–86.64	6.58577E-01	–66.87
60.00	6.00	–22.34	3.07	3.08	0.01810	87.11	LEFT	3.52504E-02	–86.64	6.57045E-01	–66.87
60.00	7.00	–21.01	3.05	3.06	0.02112	86.62	LEFT	4.10669E-02	–86.63	6.55237E-01	–66.87
60.00	8.00	–19.87	3.02	3.04	0.02415	86.14	LEFT	4.68565E-02	–86.63	6.53158E-01	–66.87
60.00	9.00	–18.86	2.99	3.02	0.02718	85.65	LEFT	5.26156E-02	–86.63	6.50808E-01	–66.87
60.00	10.00	–17.96	2.95	2.99	0.03022	85.15	LEFT	5.83405E-02	–86.63	6.48190E-01	–66.87
60.00	11.00	–17.15	2.91	2.96	0.03327	84.66	LEFT	6.40278E-02	–86.63	6.45308E-01	–66.86
60.00	12.00	–16.42	2.87	2.92	0.03631	84.16	LEFT	6.96739E-02	–86.63	6.42165E-01	–66.86
60.00	13.00	–15.75	2.83	2.89	0.03937	83.66	LEFT	7.52755E-02	–86.63	6.38764E-01	–66.86
60.00	14.00	–15.13	2.78	2.85	0.04243	83.16	LEFT	8.08291E-02	–86.63	6.35108E-01	–66.86
60.00	15.00	–14.56	2.72	2.80	0.04550	82.65	LEFT	8.63317E-02	–86.62	6.31203E-01	–66.86
60.00	16.00	–14.03	2.66	2.76	0.04858	82.14	LEFT	9.17800E-02	–86.62	6.27051E-01	–66.86
60.00	17.00	–13.53	2.60	2.71	0.05166	81.62	LEFT	9.71711E-02	–86.62	6.22657E-01	–66.85
60.00	18.00	–13.07	2.54	2.66	0.05475	81.10	LEFT	1.02502E-01	–86.62	6.18027E-01	–66.85

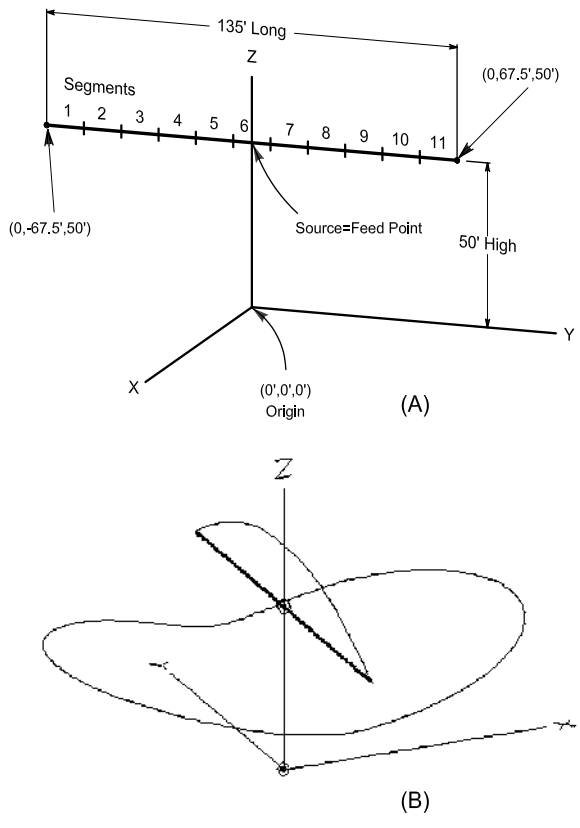

Fig 3—At A, simple model for a 135-foot long horizontal dipole, 50 feet above the ground. The dipole is over the y-axis. The wire has been segmented into 11 segments, with the center of segment number 6 as the feed point. The left-hand end of the antenna is -67.5 feet from the center feed point and that the right-hand end is at 67.5 feet from the center. At B, *EZNEC* "View Antenna" drawing, showing geometry of wire and the x, y and z axes. Overlaid on the wire geometry drawing are the current distribution along the wire and the far-field azimuthal response at an elevation angle of 30°.

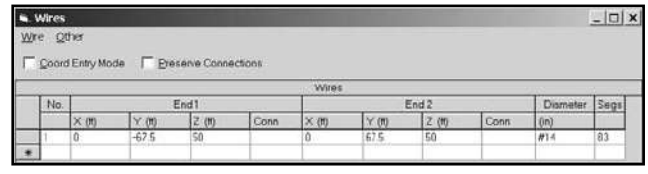

Fig 4—*EZNEC* "Wires" spreadsheet for simple flattop dipole in Fig 3. The numbers shown are in feet, except for the wire diameter, which *EZNEC* allows you to specify as an AWG gauge, in this case #14. Note that 83 segments have been specified for this antenna for analysis over the range from 3.5 to 29.7 MHz.

source in *NEC*-speak, a word choice that can befuddle beginners) right at the antenna's center, at the center of segment number six. In concert with the "EZ" in its name, *EZNEC* makes choosing the source segment easy by allowing the user to specify a percentage along the wire, in this case 50% for center feeding.

At this point you may very well be wondering why no center insulator is shown in the middle of our center-fed dipole. After all, a real dipole would have a center insulator. However, method-of-moment programs assume that a source generator is placed across an infinitely small gap in the antenna wire. While this is convenient from a mathematical point of view, the unstated use of such an infinitely small gap often confuses newcomers to the world of antenna modeling. We'll get into more details, caveats and limitations in source placement later in this chapter. For now, just trust us that the model we've just described with 11 segments, fed at segment 6, will work well over the full amateur band from 3.5 to 4.0 MHz.

Now, let's consider what would happen if we want to use our 135-foot long dipole on all HF amateur bands from 3.5 to 29.7 MHz, rather than just from 3.5 to 4.0 MHz. Instead of feeding such an antenna with coax cable, we would feed it with open-wire line and use an antenna tuner in the shack to create a 50-Ω load for the transmitter. To comply with the segmentation rule above, the number of segments used in the model should vary with frequency—or at least be segmented at or above the minimum recommended level at the highest frequency used. This is because a half wavelength at 29.7 MHz is 16.6 feet, while a half wavelength at 3.5 MHz is 140.6 feet. So the number of segments for proper operation on 29.7 MHz should be 10 × 135/16.6 = 81. We'll be a little more conservative than the minimum requirement and specify 83 segments. **Fig 4** shows the *EZNEC* input spreadsheet for this model. (Use model file: **Ch4-Multiband Dipole.EZ**.)

The penalty for using more segments in a program like *NEC* is that the program slows down roughly as the square of the segments—double the number of segments and the speed drops to a fourth. If we try to use too few segments, we'll introduce inaccuracies, particularly in computing the feed-point impedance. We'll delve into this area of segmentation density in more detail later when we discuss testing the adequacy of a model.

Segment Length-to-Wire-Diameter Ratio

Even if you're willing to live with the slowdown in computing speed for situations involving a large number of wire segments, you should make sure the ratio between the segment length and the diameter of any wire is greater than 1:1. This is to say that the length of each segment is longer than the diameter of the wire. Doing so stays away from internal limitations in the *NEC* program.

For the #14 wire specified in this simple 135-foot long dipole, it's pretty unlikely that you'll bump up against this limitation for any reasonable level of segmentation. After all, #14 wire has a diameter of 0.064 inches and 135 feet is 1620 inches. To keep above a segment length of 0.064 inches, the maximum number of segments is 1620/

0.064 = 25,312. This is a *very* large number of segments and it would take a very long time to compute, assuming that your program can handle that many segments.

Keeping above a 1:1 ratio in segment length to wire diameter can be more challenging at VHF/UHF frequencies, however. This is particularly true for fairly large "wires" made of aluminum tubing. Incidentally, this is another point where newcomers to antenna modeling can be led astray by the terminology. In a *NEC*-type program, all conductors in a model are considered to be *wires*, even if they consist of hollow aluminum or copper tubes. Surface effect keeps the RF current in any conductor confined to the outer surface of that conductor, and thus it doesn't matter whether the conductor is hollow or solid, or even made using a number of stranded wires twisted together.

Let's look at a half-wave dipole at 420 MHz. This would be about 14.1 inches long. If you use 1/4-inch diameter tubing for this dipole, the maximum segment length meeting the 1:1 diameter-to-length ratio requirement is also 1/4 inches long. The maximum number of segments then would be 14.1/0.25 = 56.4, rounded down to 56. From this discussion you should now understand why method-of-moment programs are known for using a "thin-wire approximation." Really fat conductors can get you into trouble, particularly at VHF/UHF.

Some Caveats and Limitations Concerning Geometry

Example: Inverted-V Dipole

Now, let's get a little more complicated and specify another 135-foot-long dipole, but this time configured as an *inverted V*. As shown in **Fig 5**, you must now specify two wires. The two wires join at the top, at (0, 0, 50) feet. (Again, the program doesn't use a center insulator in the model.)

If you are using a native version of *NEC*, you may have to go back to your high-school trigonometry book to figure out how to specify the end points of our "droopy" dipole, with its 120° included angle. Fig 5 shows the details, along with the trigonometric equations needed. *EZNEC* is indeed more "easy" here, since it allows you to tilt the ends of each wire downwards an appropriate number of degrees (in this case –30° at each end of the dipole) to automatically create an inverted-V configuration. **Fig 6A** shows the *EZNEC* spreadsheet describing this inverted-V dipole with a 120° included angle between the two wires.

See the *EZNEC* **Help** section under "Wire Coordinate Shortcuts" for specific instructions on how to use the "elevation rotate end" shortcut "RE–30" to create the sloping wires easily by rotating the end of the wire down 30°. Now the specification of the source becomes a bit more complicated. The easiest way is to specify two sources, one on each end segment at the junction of the two wires. *EZNEC* does this automatically if you specify a so-called *split-source* feed. Fig 6B shows the two sources as two open circles at the top ends of the two wires making up the inverted-V dipole. What *EZNEC* is doing is creating two sources, each on the closest segments on either side of the junction of the two wires. *EZNEC* sums up the two source impedances to provide a single readout.

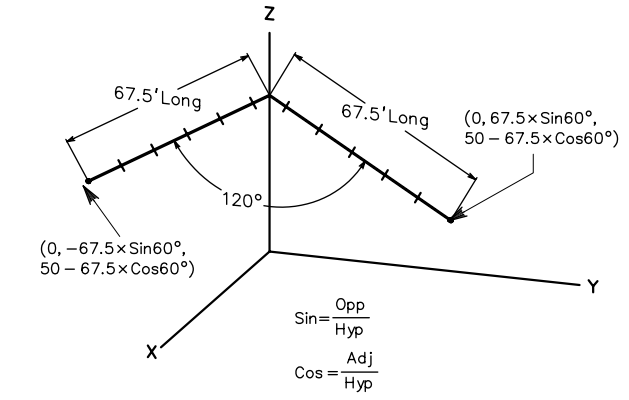

Fig 5—Model for an inverted-V dipole, with an included angle between the two legs of 120°. Sine and cosine functions are used to describe the heights of the end points for the sloping arms of the antenna.

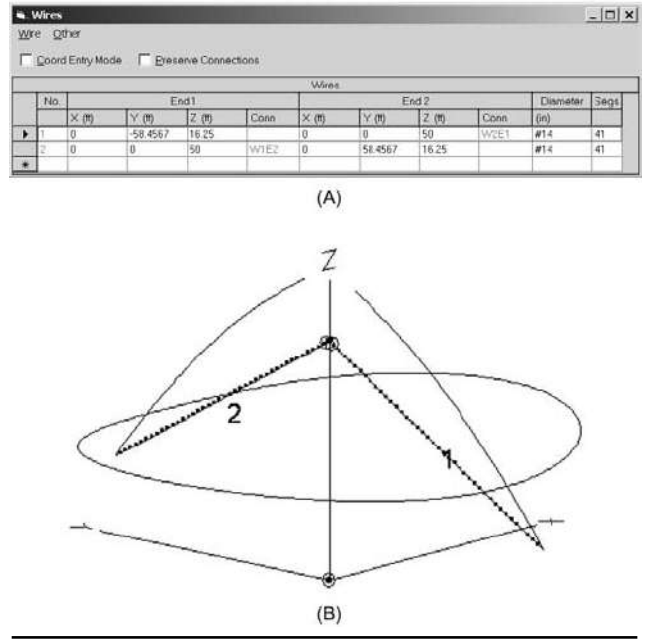

Fig 6—At A, *EZNEC* spreadsheet for inverted-V dipole in Fig 5. Now the ends of the inverted-V dipole are 16.25 feet above ground, instead of 50 feet for the flattop dipole. At B, *EZNEC* "View Antenna" drawing, with overlay of geometry, current distribution and azimuth plot.

Navigating in the View Antenna Window

At this point it's worthwhile to explore some of the ways you can see what the wire geometry looks like using the *EZNEC* **View Ant** button on the main window. Bring up the file **Ch4-Inverted V Dipole.EZ** in *EZNEC*, and click on the **View Ant** button. You will see a small inverted-V dipole raised over the (0, 0, 0) origin on the ground directly under the feed point of the inverted-V dipole. First, "rotate" the dipole by holding down the left-mouse button and moving the mouse. You can orient the picture any way you wish.

Let's take a closer look at the junction of the two wires at the feed point. Click the **Center Ant Image** checkbox toward the bottom of the window to anchor the center of the image at the center of the window, and then move the **Zoom** slider upwards to zoom in on the image. At some point the junction of the two slanted wires will move up off the edge of the window, so you will need to click on the left-hand side of the **Z Move Image** slider to bring the junction back into view. Now you should be able to see a zoomed view of the junction, along with the two open circles that represent the location of the split sources in the middle of the segments adjacent to the wire junction.

Now put the mouse cursor over one of the slanted wires and double click the left-mouse button. *EZNEC* will now identify that wire and show its length, as well as the length of each segment on that wire. Pretty slick, isn't it?

Short, Fat Wires and the Acute-Angle Junction

Another possible complication can arise for wires with short, fat segments, particularly ones that have only a small included angle between them. These wire segments can end up inter-penetrating within each other's volumes, leading to problems in a model. Once you think of each wire segment as a thick cylinder, you can appreciate the difficulty in connecting two wires together at their ends. The two wires always inter-penetrate each other's volume to some extent. **Fig 7** depicts this problem graphically for two short, fat wires joined at their ends at an acute angle. A rule of thumb is to avoid creating junctions where more than 1/3 of the wire volumes inter-penetrate. You can achieve this by using longer segment lengths or thinner wire diameters.

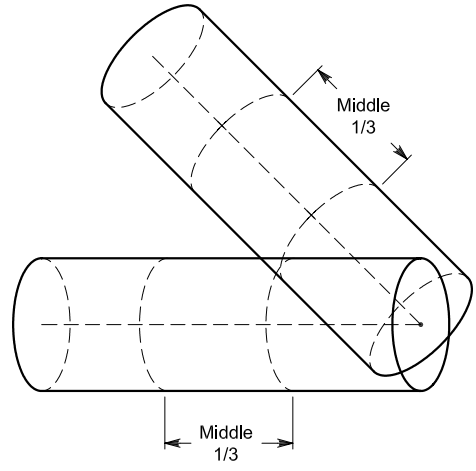

Fig 7—A junction of two short, fat wire segments at an acute angle. This results in inter-penetration of the two wire volumes beyond the middle-1/3 recommended limit.

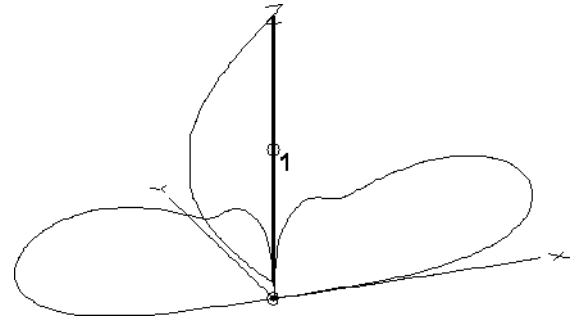

Fig 8—A vertical half-wave dipole, created by turning the dipole in Fig 3 on its end, with a minimum height at the lower end of 8 feet to keep the antenna away from people and animals. The current distribution and the elevation pattern for this antenna are also shown overlaid on the wire geometry.

Some Other Practical Antenna Geometries

A Vertical Half-Wave Dipole

If you turn the 135-foot-long horizontal dipole in Fig 1 on its end you will create a vertical half-wave dipole that is above the origin of the x, y and z axes. See **Fig 8**, where the bottom end of the dipole is placed 8 feet off the ground to keep it away from humans and animals for safety, at (0, 0, 8) feet. The top end is thus at 8 + 135 = 143 feet off the ground at (0, 0, 143). Fig 8 also shows the current distribution and the elevation pattern for this antenna. (Use *EZNEC* model file: **Ch4-Vertical Dipole.EZ**.)

A Ground-Plane Antenna

The ground-plane model is more complicated than previous ones because a total of five wires are now needed: one for the vertical radiator and four for the radials. **Fig 9** shows the *EZNEC* view for a 20-meter ground plane mounted 15 feet off the ground (perhaps on a garage roof), with the overlay of both the current distribution and the elevation-plane plot. (Use *EZNEC* model file: **Ch4-GP.EZ**.) Note that the source has been placed at the

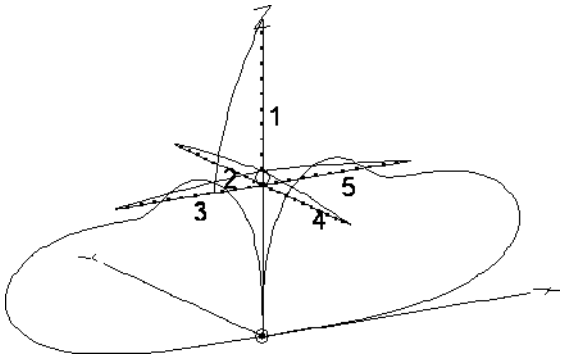

Fig 9—A vertical ground-plane antenna. The radials and the bottom of the vertical radiator are located 15 feet off the ground in this model. The current distribution along each wire and the far-field elevation-plane pattern are overlaid on the antenna geometry.

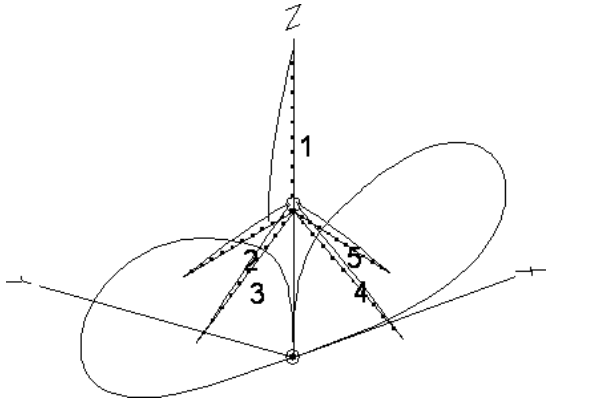

Fig 10—*EZNEC* View Antenna for the ground-plane antenna with its four radials tilted downwards by 40° to improve the SWR at the feed point.

bottom segment of the vertical radiator. Once again, the program needs no bottom insulator, since all five wires are connected together at a common point. *EZNEC* reports that this antenna has a resonant feed-point impedance of about 22 Ω, which would show an SWR of 2.3:1 for a 50-Ω coax feed line if no matching system is used, such as a gamma or hairpin match.

Fig 10 shows the same antenna, except that the radials have now been tilted downwards by 35° to facilitate an almost perfect 50-Ω match (SWR = 1.08:1). In addition, the length of the radiator in this model was shortened by 6 inches to re-resonate the antenna. (Use *EZNEC* model file: **Ch4-Modified GP.EZ**.) The trick of tilting the radials downwards for a ground-plane antenna is an old one, and the modeling programs validates what hams have been doing for years.

A 5-Element Horizontal Yagi

This is a little more challenging modeling exercise. Let's use a 5-element design on a 40-foot boom, but rather than using telescoping aluminum tubing for the elements, we'll use #14 wire. The *SCALE* program included with this book on the CD-ROM converted the aluminum-tubing 520-40.YW to a design using #14 copper wire. **Table 2** shows the element lineup for this antenna. (Later in this chapter we'll see what happens when telescoping aluminum tubing is used in a real-world Yagi design.)

Some explanations of what Table 3 means are in order. First, only one half of each element is shown. The *YW* program (Yagi for Windows), also included on the CD-ROM, computes the other half of the Yagi automatically, essentially mirroring the other half on the opposite side of the boom. Having to enter the dimensions for only half of a real-world Yagi element that uses telescoping aluminum tubing is much easier this way.

Second, the placement of the elements along the boom starts at 0.0 inches for the reflector. The distance between adjacent elements defined in this particular file is the spacing between the element itself and the element just before it. For example, the spacing between the driven element and the reflector is 72 inches, and the spacing between the first director and the driven element is also 72 inches. The spacing between the second director and the first director is 139 inches.

Fig 11A shows the wire geometry for this Yagi array when it is mounted 720 inches (60 feet) above flat ground and Fig 11B shows the *EZNEC* Wires spreadsheet that describes the coordinates. (Use *EZNEC* model file: **Ch4-520-40W.EZ**.) You can see that the x-axis coordinates for the elements have been automatically moved by the *SCALE* program so that the center of the boom is located directly above the origin. This makes it easier to evaluate the effects of stacking different monoband Yagis on a rotating mast in a "Christmas Tree" arrangement. A typical Christmas Tree stack might include 20, 15 and 10-meter monobanders on a single rotating mast sticking out of the top of the tower.

Fig 12 shows the computed azimuth pattern for this Yagi at 14.175 MHz, at an elevation angle of 15°, the angle where the peak of the forward lobe occurs at this

Table 2

520-40W.YW, using #14 wire from 520-40H.YW
14.000 14.174 14.350 MHz
5 elements, inches

Spacing	.064
0.000	210.923
72.000	200.941
72.000	199.600
139.000	197.502
191.000	190.536

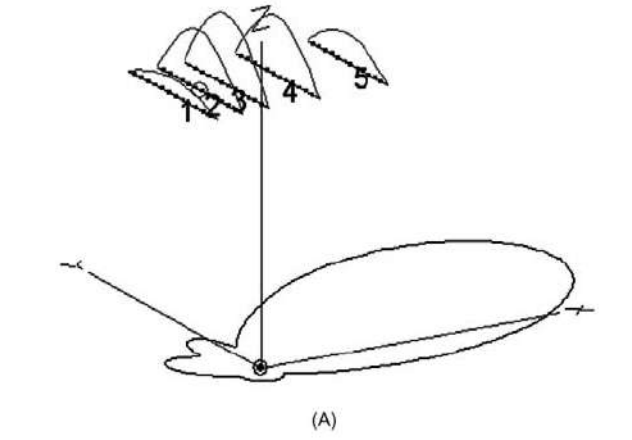

(A)

Wires

Wire Other

Coord Entry Mode Preserve Connections

Wires

No.	End1				End2				Diameter	Segs
	X (in)	Y (in)	Z (in)	Conn	X (in)	Y (in)	Z (in)	Conn	(in)	
1	-237.188	-210.923	720		-237.188	210.923	720		0.064	13
2	-165.188	-200.941	720		-165.188	200.941	720		0.064	13
3	-93.188	-199.6	720		-93.188	199.6	720		0.064	13
4	45.812	-197.502	720		45.812	197.502	720		0.064	13
5	236.812	-190.536	720		236.812	190.536	720		0.064	13

(B)

Fig 11—At A, geometry for 5-element Yagi on a 40-foot boom, mounted 720 inches (60 feet) above flat ground, with an overlay of current and the azimuth pattern. At B, *EZNEC* Wires spreadsheet for this antenna. This design uses #14 wire for simplicity.

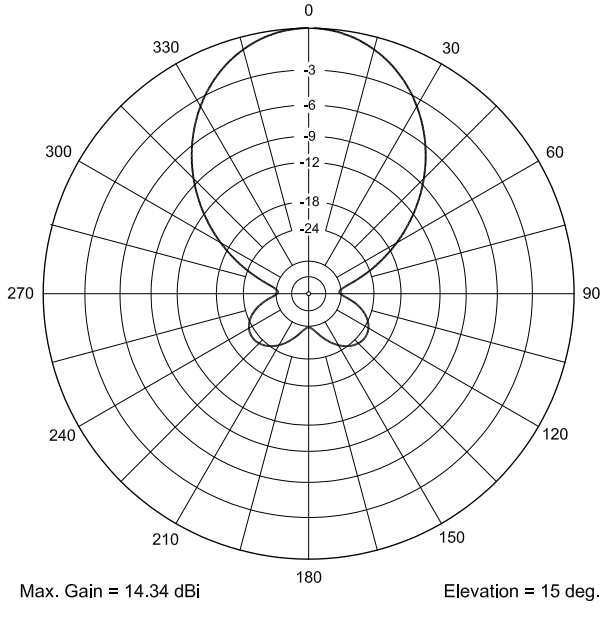

Fig 12—*EZNEC* azimuth-plane pattern at an elevation angle of 15° for #14 wire Yagi described in Fig 11.

height above flat ground. The antenna exhibits excellent gain at 13.1 dBi, as well as a clean pattern behind the main lobe. The worst-case front-to-rear ratio at any point from 90° to 270° in azimuth is better than 23 dB. *EZNEC* says the feed-point impedance is 25 – *j* 23 Ω, just the right impedance suited for a simple hairpin or gamma match.

A Monoband 2-Element Cubical Quad

Unlike a Yagi, with its elements existing only in the x-y plane, a quad type of beam is a three-dimensional sort of antenna. A quad loop has height in the z-axis, as well as width and length in the x-y plane. Each individual loop for a monoband quad consists of four wires, joined together at the corners. **Fig 13** shows the coordinates for a 2-element 15-meter quad, consisting of a reflector and a driven element on a 10-foot boom.

You can see that the axis of symmetry, the x-axis, runs down the center of this model, meaning that the origin of this particular x, y and z-coordinate scheme is in the center of the reflector. The (0, 0, 0) origin is placed this way for convenience in assigning corner coordinates for each element. For actual placement of the antenna at a particular height above real ground, the heights of all z-axis coordinates are changed accordingly. *EZNEC* has a convenient built-in function to change the height of all wires at a single stroke.

Fig 14 shows the input *EZNEC* spreadsheet for this quad in free space, clearly showing the symmetrical nature of the corner coordinates. (Use *EZNEC* model file: **Ch4-Quad.EZ**.) This is a good place to emphasize that you should enter the wire coordinates in a logical

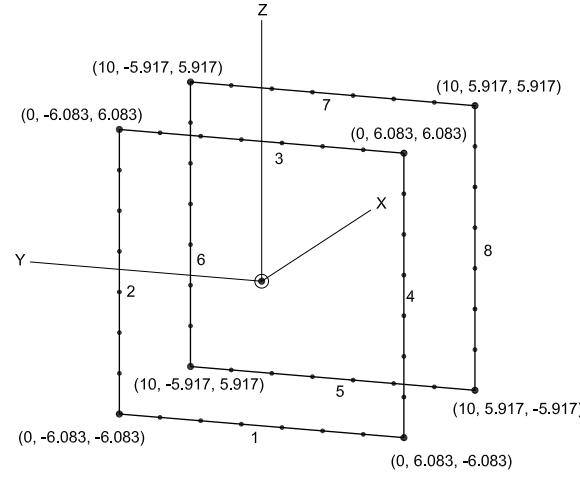

Fig 13—Wire geometry for a 2-element cubical quad, with a reflector and driven element. The x-axis is the axis of symmetry for this free-space model.

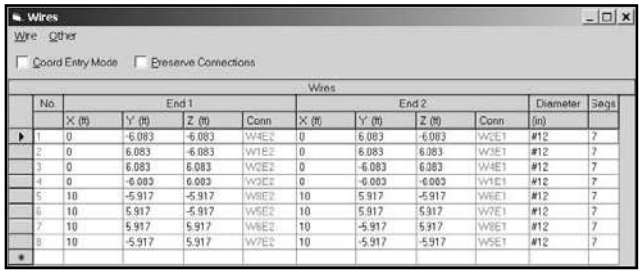

Fig 14—*EZNEC* Wires spreadsheet showing the coordinates used for the quad in Fig 13. Note how the x-axis describes the position of an element on the 10-foot boom and also is the axis of symmetry for each element. The values for the z-axis and y-axis vary above and below the axis of symmetry.

sequence. The most obvious example in this particular model is that you should group all the wires associated with a particular element together—for example, the four wires associated with the reflector should be in one place. In Fig 14 you can see that all four wires with an x-coordinate of zero represent the reflector.

It's best to follow a convention in entering wires in a loop structure in a logical fashion. The idea to connect the end point of one wire to the starting point of the next wire. For example, in Fig 13 you can see that the left-hand end of Wire 1 is connected to the bottom of Wire 2, and that the top of Wire 2 connects to the left-hand end of Wire 3. In turn, Wire 3 connects to the top of Wire 4, whose bottom end connects to the right-hand end of Wire 1. The pattern is known as "going around the horn" meaning that the connections proceed smoothly in one direction, in this case in a clockwise direction.

You can see that the entry for the wires making up the elements in the 5-element Yagi in Fig 11B also proceeded in an orderly fashion by starting with the reflector, then the driven element, then director 1, then director 2 and finally director 3. This doesn't mean that you couldn't mix things up, say by specifying the driven element first, followed by director 3, and then the reflector, or whatever. But it's a pretty good bet that doing so in this quasi-random fashion will result in some confusion later on when you revisit a model, or when you let another person see your model.

THE MODELING ENVIRONMENT

The Ground

Above, when considering the 135-foot dipole mounted 50 feet above flat earth, we briefly mentioned the most important environmental item in an antenna model—the ground beneath it. Let's examine some of the options available in the *NEC-2* environment in *EZNEC*:

- Free space
- Perfect ground
- *MININEC* type ground
- "Fast" type ground
- Sommerfeld-Norton ground.

The free space environment option is pretty self-explanatory—the antenna model is placed in free space away from the influence of any type of ground. This option is useful when you wish to optimize certain characteristics of a particular antenna design. For example, you might wish to optimize the front-to-rear ratio of a Yagi over an entire amateur band and this might entail many calculation runs. The free-space ground will run the fastest among all the ground options.

Perfect ground is useful as a reference case, especially for vertically polarized antennas over real ground. Antenna evaluations over perfect ground are shown in most classical antenna textbooks, so it is useful to compare models for simple antennas over perfect ground to those textbook cases.

MININEC type ground is useful when modeling vertical wires, or horizontal wires that are higher than 0.2 λ above ground. A *MININEC* type ground will compute faster than either a "Fast" ground or a Sommerfeld-Norton type of ground because it assumes that the ground under the antenna is perfect, while still taking into account the far-field reflections for ground using user-specified values of ground conductivity and dielectric constant. The fact that the ground under the antenna is perfect allows the *NEC-2* user of a *MININEC* type ground to specify wires that touch (but don't go below) the ground surface, something that only users of the advanced *NEC-4* program can do with the more accurate Sommerfeld-Norton type of ground described below. (*NEC-4* is presently not in the public domain and is strictly restricted and licensed by the US government.) The ability to model grounded wires is useful with vertical antennas. The modeler must be wary of the feed-point source impedances reported for either horizontally or vertically polarized wires because of the perfect-ground assumption inherent in a *MININEC*-type ground.

The "fast" type of ground is a hybrid type of ground that makes certain simplifying assumptions that allow it to be used provided that horizontal wires are higher than about 0.1 λ above ground. With today's fast computers the Sommerfeld-Norton model is preferred.

The Sommerfeld-Norton ground (referred to in *EZNEC* as the "high accuracy" ground) is preferable to the other ground types because it has essentially no practical limitations for wire height. It has the disadvantage that it can run about four times slower than a *MININEC* type of ground, but today's fast computers make that almost a non-issue. Again, *NEC-2*-based programs cannot model wires that penetrate into the ground (although there are work-arounds described below).

As mentioned above, for any type of ground other than perfect ground or free space, the user must specify the conductivity and dielectric constant of the soil. *EZNEC*

allows the entry by several user-friendly categories, where σ is conductivity in Siemens/meter and ε is dielectric constant:

- Extremely poor: cities, high buildings (σ = 0.001, ε = 3)
- Very Poor: cities, industrial (σ = 0.001, ε = 5)
- Sandy, dry (σ = 0.002, ε = 10)
- Poor: rocky, mountainous (σ = 0.002, ε = 13)
- Average: pastoral, heavy clay (σ = 0.005, ε = 13)
- Pastoral: medium hills and forestation (σ = 0.006, ε = 13)
- Flat, marshy, densely wooded (σ = 0.0075, ε = 12)
- Pastoral, rich soil, US Midwest (σ = 0.010, ε = 14)
- Very Good: pastoral, rich, central US (σ = 0.0303, ε = 20)
- Fresh water (σ = 0.001, ε = 80)
- Saltwater (σ = 5, ε = 80)

Let's use *EZNEC*'s ability to overlay one or more plots together on one graph to compare the response of the vertical ground plane antenna in Fig 9 for two different types of ground: Saltwater and Poor. Open the **Ch4-GP.EZ** file in *EZNEC*. Click the **Ground Descrip** button and then right-click anywhere in the Media window that opens up. Choose first the "Poor: rocky, mountainous" option button, click **OK** and then **FF Plot**. When the elevation plot appears, click the **File** menu at the top of the main window, and then **Save As**. Choose an appropriate name for the trace, perhaps "Poor Gnd.PF."

Go back and select saltwater as your **Ground Descrip** and follow the same procedure to compute the far-field plot for saltwater ground. Now, add the Poor Gnd.PF trace, by clicking menu selection **File**, **Add Trace**. **Fig 15** shows this comparison, which greatly favors the saltwater environment, particularly at low elevation angles. At 5° the ground plane mounted over saltwater has about a 10 dB advantage compared to its landlocked cousin.

You might be wondering what happens if we move the ground-plane antenna down closer to the ground. The lower limit to how far the radials can approach the lossy earth is 0.001 λ or twice the diameter of the radial wire. A distance of 0.001 λ at 1.8 MHz is about 6 inches, while it is 0.4 inches at 30 MHz. While *NEC-2*-based programs cannot model wires that penetrate the ground, radial systems just above the ground with more than about eight radial wires can provide a work-around to simulate a direct-ground connection.

Modeling Environment: Frequency

It's always a good idea to evaluate an antenna over a *range of frequencies*, rather than simply at a single spot frequency. Trends that become quite apparent on a frequency sweep are frequently lost when looking simply at a single frequency. Native *NEC-2* has built-in frequency sweep capabilities, but once again the commercial programs make the process easier to use and understand. You

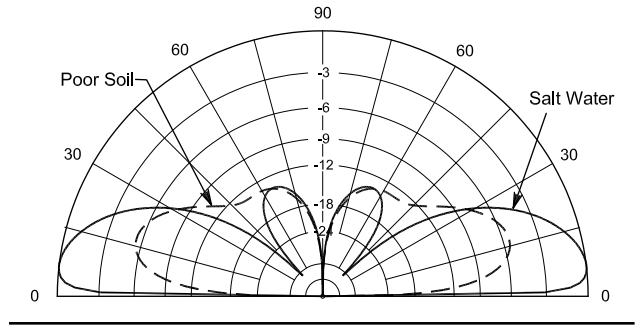

Fig 15—A comparison of the elevation response for the vertical ground plane in Fig 9 over saltwater and over "poor: rocky, mountainous" soil. Saltwater works wonders for verticals, providing excellent low-angle signals.

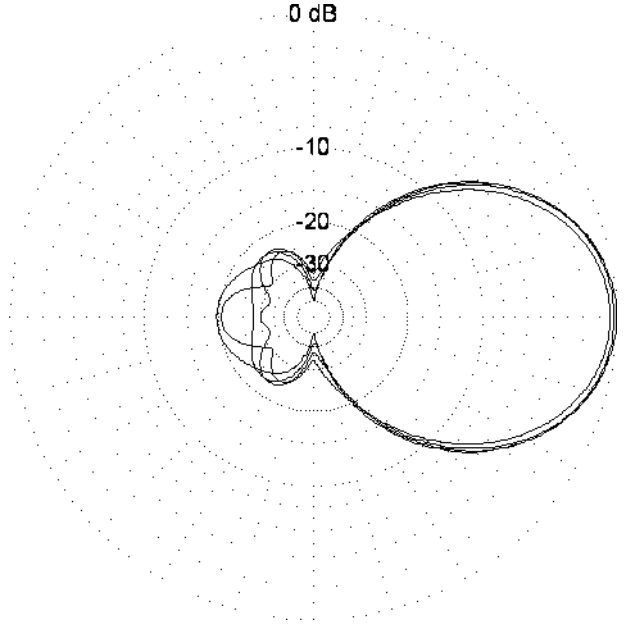

Fig 16—Frequency sweep of 5-element Yagi described in Fig 11, showing how the azimuth pattern changes with frequency.

saw in the SWR curve in Fig 2 the result of one such frequency sweep using *EZNEC*. **Fig 16** shows a frequency sweep of the azimuth response for the 5-element Yagi in Fig 11 across the 20-meter band, using steps of 117 kHz so there are four evaluation frequencies. At 14.0 MHz this Yagi's gain is down a small amount compared to the gain at 14.351 MHz but the rearward pattern is noticeably degraded, dropping to a front-to-back ratio of just under 20 dB.

EZNEC can save to a series of output plot files a frequency sweep of elevation (or azimuth) patterns. In essence, this automates the process described above for

saving a plot to disk and then overlaying it on another plot. *EZNEC* can save to a text file for later analysis (or perhaps importation into a spreadsheet) the following parameters, chosen by the user:

- Source data
- Load data
- Pattern data
- Current data
- MicroSmith numeric data
- Pattern analysis summary.

Frequency Scaling

EZNEC has a very useful feature that allows you to create new models *scaled* to a new frequency. You invoke the algorithm used to scale a model from one frequency to another by checking the **Rescale** box after you've clicked the **Frequency** button. *EZNEC* will scale all model dimensions (wire length, height and diameter) except for one specific situation—the wire diameter will stay the same at the new frequency if you originally specified wire size by AWG gauge. For example, #14 copper wire for a half-wave 80-meter dipole will stay #14 copper wire for a 20-meter half-wave dipole. If, however, you specified diameter as a floating point number originally, the diameter will be scaled by the ratio of new to old frequency, along with wire length and height.

Start up *EZNEC* and open up the file **Ch4-520-40W.EZ** for the 5-element 20-meter Yagi on a 40-foot boom. Click the **Frequency** box and then check the **Rescale** check box. Now, type in the frequency of 28.4 MHz and click **OK**. You have quickly and easily created a new 5-element 10-meter Yagi, that is mounted 29.9949 feet high, the exact ratio of 28.4 MHz to 14.1739 MHz, the original design frequency on 20 meters. Click the **FF Plot** button to plot the azimuth pattern for this new Yagi. You will see that it closely duplicates the performance of its 20-meter brother. Click **Src Dat** to see that the source impedance is 25.38 – *j* 22.19 Ω, again very close to the source data for the 20-meter version.

REVISITING SOURCE SPECIFICATION

Sensitivity to Source Placement

Earlier, we briefly described how to specify a source on a particular segment using *EZNEC*. The sources for the relatively simple dipole, Yagi and quad models investigated so far have been in the center of an easy-to-visualize wire. The placement for the source on the vertical ground plane was at the bottom of the vertical radiator, an eminently logical place. In the other cases we specified the position of the source at 50% of the distance along a wire, given that the wire being fed had an odd number of segments. Please note that in each case so far, the feed point (source) has been placed at a relatively low-impedance point, where the current changes relatively slowly from segment to segment.

Now we're going to examine some subtler source-placement problems. *NEC-2* is well-known as being very sensitive to source placement. Significant errors can result from a haphazard choice of the source segment and the segments surrounding it.

Let's return to the inverted-V dipole in Fig 5. The first time we evaluated this antenna (**Ch4-Inverted V Dipole.EZ**) we specified a split source in *EZNEC*. This function uses two sources, one on each of the segments immediately adjacent to the junction of the two downward slanting wires.

Another common method to create a source at the junction of two wires that meet at an angle is to separate these two slanted wires by a short distance and bridge that gap with a short straight wire, which is fed at its center. **Fig 17** shows a close-up of this scheme. In Fig 17 the length of the segments surrounding the short middle wire are purposely made equal to the length of the middle wire. The segmentation for the short middle wire is set to one. **Table 3** lists the source impedance and the maximum gain the *EZNEC* computes for three different models:

1. **Ch4-Inverted V Dipole.EZ** (the original model)
2. **Ch4-Inverted V Dipole Triple Segmentation.EZ**
3. **Ch4-Modified Inverted V Dipole.EZ** (as shown in Fig 17, for the middle wire set to be 2 feet long)
4. **Ch4-Mod Inverted V Poor Segmentation.EZ** (where the number of segments on the two slanted wires have been increased to 200)

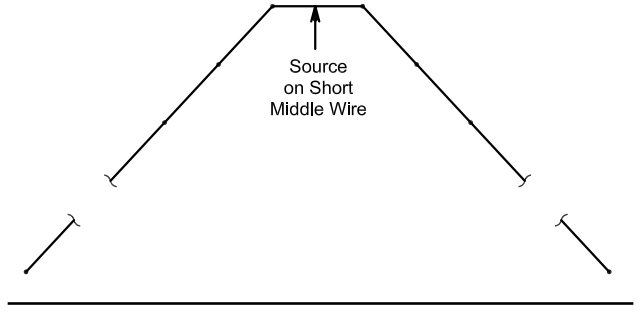

Fig 17—Model of inverted-V dipole using a short center wire on which the source is placed.

Table 3
135-Foot Inverted-V Dipole at 3.75 MHz

Case	*Segments*	*Source Impedance Ω*	*Max. Gain dBi*
1	82	72.64 + *j* 128.2	4.82
2	246	73.19 + *j* 128.9	4.82
3	67	73.06 + *j* 129.1	4.85
4	401	76.21 + *j* 135.2	4.67

Case 2 shows the effect of tripling the number of segments in Case 1. This is a check on the segmentation, to see that the results are stable at a lower level compared to a higher level of segmentation (which theoretically is better, although slower in computation). We purposely set up Case 4 so that the lengths of the segments on either side of the single-segment middle wire are significantly different (0.33 feet) compared to the 2-foot length of the middle wire.

The feed-point and gain figures for the first three models are close to each other. But you can see that the figures for the fourth model are beginning to diverge from the first three, with about a 5% overall change in the reactance and resistance compared to the average values, and about a 3% change in the maximum gain. This illustrates that it is best to keep the segments surrounding the source equal or at least close to equal in length. We'll soon examine a figure of merit called the *Average Gain* test, but it bears mentioning here that the average gain test is very close for the first three models and begins to diverge for the fourth model.

Things get more interesting if the source is placed at a high-impedance point on an antenna—for example, in the center of a full-wave dipole—the value computed for the source impedance will be high, and things will be quite sensitive to the segment lengths. We'll repeat the computations for the same inverted-V models, but this time at twice the operating frequency, at 7.5 MHz.

Table 4 summarizes the results. The impedance is high, as expected. Note that the resistance term varies quite a bit for all four models, a range of about 23% around the average value. Interestingly, the poorly segmented model's resistance falls in between the other three. The reactive terms are closer for all four models but still cover a range of 4% around the average value. The maximum gain shows the same tendancy to be somewhat lower in the fourth model compared to the first three and thus looks as potentially untrustworthy at 7.5 MHz as it does at 3.75 MHz.

This is, of course, but a small sampling of segmentation schemes, and caution dictates that you shouldn't take these results as being representative of all possibilities. Nevertheless, the lesson to be learned here is that the feed-point (source) impedance can vary significantly at a point where the current is changing rapidly, as it does where a high impedance feed is involved. Another general conclusion that can be drawn from Table 5 is that more segments, particularly if they surround the source segment improperly, is not necessarily better.

Table 4
135-Foot Inverted-V Dipole at 7.5 MHz

Case	*Segments*	*Source Impedance Ω*	*Max. Gain dBi*
1	82	2297 – *j* 2668	5.67
2	246	1822 – *j* 2553	5.66
3	67	1960 – *j* 2583	5.66
4	401	2031 – *j* 2688	5.48

Voltage and Current Sources

Before we leave the topic of sources, you should be aware that programs like *EZNEC* and others have the ability to simulate both voltage sources and current sources. Although native *NEC-2* has several source types, voltage sources are the most commonly used by hams. Native *NEC-2* doesn't have a current source, but a current source is nothing more than a voltage source delivering current through a high impedance. Basic network theory says that every Thevenin voltage source has a Norton current source equivalent. Various commercial implementations of *NEC-2* approach the creation of a current source in slightly different fashions. Some use a high value of inductive reactance as a series impedance, while others use a high value of series resistance.

Why would we want to use a current source instead of a voltage source in a model? The general-purpose answer is that models containing a single source at a single feed point can use a voltage source with no problems. Models that employ multiple sources, usually with different amplitudes and different phase shifts, do best with current sources.

For example, *phased arrays* feed RF currents at different amplitudes and phase shifts into two or more elements. The impedances seen at each element may be very different—some impedances might even have negative values of resistance, indicating that power is flowing out of that element into the feed system due to mutual coupling to other elements. Having the ability to specify the amplitude and phase of the current, rather than a feed voltage, at a feed point in a program like *EZNEC* is a valuable tool.

Next, we examine one more important aspect of building a model, setting up loads. After that, we'll look into two tests for the potential accuracy of a model. These tests can help identify source placement, as well as other problems.

LOADS

Many ham antennas, in particular electrically short ones, employ some sort of *loading* to resonate the system. Sometimes loading takes the form of *capacitance hats*, but these can and should be modeled as wires connected to the top of a vertical radiator. A capacitance hat is not the type of loading we'll explore in this section.

Here, the term *loads* refers to discrete inductances, capacitances and resistances that are placed at some point (or points) in an antenna system to achieve certain effects. One fairly common form of a load is a *loading coil* used to resonate an electrically short antenna. Another form of load often seen in ham antennas is a *trap*. *EZNEC* has

a special built-in function to evaluate parallel-resonant traps, even at different frequencies beyond their main parallel resonance.

Just for reference, a more subtle type of load is a *distributed* material load. We encountered just such a load in our first model antenna, the 135-foot long flattop dipole—although we didn't identify it specifically as a load at that time. Instead, it was identified as a "wire loss" associated with copper.

The *NEC-2* core program has the capability of simulating a number of built-in loads, including distributed material and discrete loads. *EZNEC* implements the following discrete loads:

- Series R ± *j* X loads.
- Series R-L-C loads, specified in Ω of resistance, µH of inductance and pF of capacitance.
- Parallel R-L-C loads, specified in Ω of resistance, µH of inductance and pF of capacitance.
- Trap loads, specified in Ω of resistance in series with µH of inductance, shunted by pF of capacitance, at a specific frequency.
- Laplace loads, specified as mathematical Laplace coefficients (sometimes used in older modeling programs and left in *EZNEC* for backwards compatibility).

It is important to recognize that the discrete loads in an antenna modeling program *do not radiate* and they have zero size. The *NEC-2* discrete loads are described by L. B. Cebik in his antenna modeling course as being *mathematical loads*. The fact that *NEC-2* loads do not radiate means that the popular mobile antennas that use helical loading coils wound over a length of fiberglass whip cannot be modeled with *NEC-2*, because such coils do radiate.

Let's say that we want to put a air-wound loading coil with an unloaded Q of 400 at the center of a 40-foot long, 50-foot high, flattop dipole so that it is resonant at 7.1 MHz. The schematic of this antenna is shown in **Fig 18**. Examine the modeling file **Ch4-Loaded Dipole.EZ** to see how a discrete series RL load is used to resonate this short dipole at 7.1 MHz, with a feed-point (source) impedance of 25.3 Ω. This requires a series resistance of 1.854 Ω and an inductive reactance of +741.5 Ω. Note that we again used a single wire to model this antenna, and that we placed the load at a point 50% along the length of the wire.

This load represents a 16.62 µH coil with an unloaded Q of 741.5/1.854 = 400, just what we wanted. Let's assume for now that we use a perfect transformer to transform the 25.3-Ω source impedance to 50 Ω. If we now attempt to run a frequency sweep over the whole 40-meter band from 7.0 to 7.3 MHz, the load reactance and resistance will not change, since we specified fixed values for reactance and resistance. Hence, the source impedance will be correct only at the frequency where the reactance and resistance are specified, since the reactance changes with frequency.

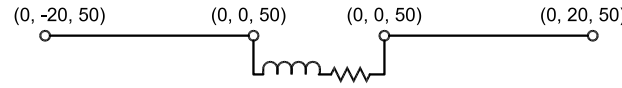

Fig 18—Schematic diagram of a 40-foot long flattop dipole with a loading coil placed at the center. This coil has an unloaded Q of 400 at 7.1 MHz.

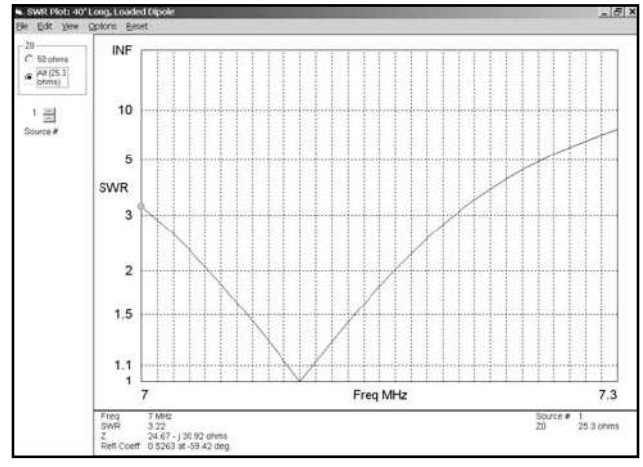

Fig 19—SWR graph of the loaded 40-foot long flattop dipole shown in Fig 18.

So let's use another load capability and substitute a 16.62 µH coil with a series 1.854-Ω resistance at 7.1 MHz. We'll let *EZNEC* take care of the details of computing both the reactance and the changing series resistance at various frequencies. The degree that both reactance and series loss resistance of the coil change with frequency may be viewed using the **Load Dat** button from the main *EZNEC* window.

Fig 19 shows the computed SWR curve for a 25.3-Ω **Alt SWR Z0** reference resistance. The 2:1 SWR bandwidth is about 120 kHz. As could be expected, the antenna has a rather narrow bandwidth because it is electrically short.

ACCURACY TESTS

There are two tests that can help identify accuracy problems in a model:

- The Convergence test.
- The Average Gain test.

Convergence Test

The idea behind the *Convergence* test is simple: If you increase the segmentation in a particular model and the results changes more than you'd like, then you increase the segmentation until the computations converge

to a level that is suitable to you. This process has the potential for being subjective, but simple antenna models do converge quickly. In this section, we'll review several more of the antennas discussed previously to see how they converge.

Let's go back to the simple dipole in Fig 3. The original segmentation was 11 segments, but we'll start with a very low value of segmentation of three, well below the minimum recommended level. **Table 5** shows how the source impedance and gain change with increase in segmentation at 3.75 MHz. For this simple antenna, the gain levels off at 6.50 dBi by the time the segmentation has reached 11 segments. Going to ten times the minimum-recommended level (to 111 segments) results in an increase of only 0.01 dBi in the gain.

Arguably, the impedance has also stabilized by the time we reach a segmentation level of 11 segments, although purists may opt for 23 segments. The tradeoff is a slowdown in computational speed.

Let's see how the 5-element Yagi model converges with changes in segmentation level. **Table 6** shows how the source impedance, gain, 180° front-to-back ratio and worst-case front-to-rear ratio change with segmentation density. By the time the segmentation has reached 11 segments per wire, the impedance and gain have stabilized quite nicely, as has the F/R. The 180° F/B is still increasing with segmentation level until about 25 segments, but a relatively small shift in frequency will change the maximum F/B level greatly. For example, with 11 segments per wire, shifting the frequency to 14.1 MHz—a shift of only 0.5%— will change the maximum 180° F/B from almost 50 dB down to 27 dB. For this reason the F/R is considered a more reliable indicator of the adequacy of the segmentation level than is F/B.

Table 5
135-Foot Flattop Dipole at 3.75 MHz

Segments	*Source Impedance Ω*	*Max. Gain dBi*
3	85.9 + *j* 128.0	6.34
5	86.3 + *j* 128.3	6.45
7	86.8 + *j* 128.8	6.48
11	87.9 + *j* 129.5	6.50
23	88.5 + *j* 130.3	6.51
45	89.0 + *j* 130.8	6.51
101	89.4 + *j* 131.1	6.51

Table 6
5-element Wire Yagi at 14.1739 MHz

Segments	*Source Impedance Ω*	*Max. Gain dBi*	*180° F/B dB*	*F/R dB*
3	28.5 – *j* 30.6	12.79	23.2	22.4
5	26.3 – *j* 25.6	13.02	30.5	23.1
7	25.6 – *j* 24.0	13.07	34.8	23.1
11	25.1 – *j* 22.9	13.09	39.9	23.1
25	24.9 – *j* 22.0	13.10	43.7	23.1
99	24.7 – *j* 21.5	13.10	44.2	23.1

Average Gain Test

The theory behind the *Average Gain* test is a little more involved. Basically, if you remove all intentional losses in a model, and if you place the antenna either in free space or over perfect ground, then all the power fed to the antenna should be radiated by it. Internally, the program runs a full 3-D analysis, adding up the power in all directions and then dividing that sum by the total power fed to the antenna. Since *NEC-2* is very sensitive about source placement, as mentioned before, the Average Gain test is a good indicator that something is wrong with the specification of the source.

Various commercial versions of *NEC-2* handle the Average Gain test in different ways. *EZNEC* requires the operator to turn off all distributed losses in wires or set to zero any discrete resistive losses in loads. Next you set the ground environment to free space (or perfect ground) and request a 3-D pattern plot. *EZNEC* will then report the average gain, which will be 1.000 if the model has no problems. The average gain can be lower or higher than 1.000, but if it falls within the range 0.95 to 1.05 it is usually considered adequate.

As L. B. Cebik, W4RNL, stated in his ARRL Certification and Continuing Education Course on antenna modeling: "Like the convergence test, the average gain test is a necessary but not a sufficient condition of model reliability." Pass both tests, however, and you can be pretty well sure that your model represents reality. Pass only one test, and you have reason to worry about how well your model represents reality.

Once again, open the model file **Ch4-Mod Inverted V Poor Segmentation.EZ** and set **Wire Loss** to zero, **Ground Type** to Free Space and **Plot Type** to 3-Dimensional. Click on the **FF Plot** button. *EZNEC* will report that the Average Gain is 0.955 = –0.2 dB. This is very close to the lower limit of 0.95 considered valid for excellent accuracy. This is a direct result of forcing the segment lengths adjacent to the source segment to be considerably shorter than the source segment's length. The gain reported using this test would be approximately –0.2 dB from what it should be—just what Table 4 alludes to also.

Now, let's revisit the basic model **Ch4-Inverted V Dipole.EZ** and look at Case 2 in Table 4. Case 2 amounts to a Convergence test for the basic inverted-V model. Since the impedance and gain changes were small comparing the basic model to the one using three times the number of segments, the model passed the Convergence test. The Average Gain test for the basic model yields a value of 0.991, well within the limits for good accuracy. This model has thus passed both tests and can be considered accurate.

Running the Average Gain test for the 5-element Yagi (using 11 segments per wire and whose convergence we examined in Table 6) yields a value of 0.996, again well within the bounds indicating a good model. And the simple flattop dipole with 11 segments at 3.75 MHz yields an Average Gain result of 0.997, again indicating a very accurate model.

OTHER POSSIBLE MODEL LIMITATIONS

Programs based on the *NEC-2* core computational code have several well-documented limitations that you should know about. Some limitations have been removed in the restricted-access *NEC-4* core (which is not generally available to users), but other limitations still exist, even in *NEC-4*.

Closely Spaced Wires

If wires are spaced too close to each other, the *NEC-2* core can run into problems. If the segments are not carefully aligned, there also can be problems with accuracy. The worst-case situation is where two wires are so close together that their volumes actually merge into each other. This can happen where wires are thick, parallel to each other and close together. You should keep parallel wires separated by at least several diameters.

For example, #14 wire is 0.064 inches in diameter. The rule then is to keep parallel #14 wires separated by more than $2 \times 0.064 = 0.128$ inches. And you should run the Convergence test to assure yourself that the solution is indeed converging when you have closely spaced wires, especially if the two wires have different diameters. To model antennas containing closely spaced wires, very often you will need many more segments than usual and you must also carefully ensure that the segments line up with each other.

Things can get a little more tricky when wires cross over or under each other, simply because such crossings are sometimes difficult to visualize. Again, the rule is to keep crossing wires separated by more than two diameters from each other. And if you intend to join two wires together, make sure you do so at the ends of the two wires, using identical end coordinates. When any or all of these rules are violated, the Convergence and Average Gain tests will usually warn you of potential inaccuracies.

Parallel-Wire Transmission Lines and LPDAs

A common example of problems with closely spaced wires is when someone attempts to model a parallel-wire transmission line. *NEC-2*-based programs usually do not work as well in such situations as do *MININEC*-based programs. The problems are compounded if the diameters are different for the two wires simulating a parallel-wire transmission line. In *NEC-2* programs, it is usually better to use the built-in "perfect transmission line" function than to try to model closely spaced parallel wires as a transmission line.

For example, a Log Periodic Dipole Array (LPDA) is composed of a series of elements fed using a transmission line that reverses the phase 180° at each element. In other words, the elements are connected to a transmission line that reverses connections left-to-right at each element. It is cumbersome to do so, but you could model such a transmission line using separate wires in *EZNEC*, but it is a potentially confusing and a definitely painstaking process. Further, the accuracy of the resulting model is usually suspect, as shown by the Average Gain test.

It is far easier to use the **Trans Lines** function from the *EZNEC* main window to accurately model an LPDA. See **Fig 20**, which shows the **Trans Lines** window for the **9302A.EZ** 16-element LPDA. There are 15 transmission lines connecting the 16 elements, placed at the 50% point on each element, with a 200-Ω characteristic impedance and with Reversed connections.

Fat Wires Connected to Skinny Wires

Another inherent limitation in the *NEC-2* computational core shows up when modeling several popular ham-radio antennas: many Yagis and some quads.

Tapered Elements

As mentioned before, many Yagis are built using telescoping aluminum tubing. This technique saves weight and makes for a more flexible and usually stronger element, one that can survive wind and ice loading better than a "monotaper" element design. Many vertical antennas are also constructed using telescoping aluminum tubing.

Unfortunately, native *NEC-2* doesn't model accurately such *tapered elements*, as they are commonly called. There is, however, a sophisticated and accurate work-around for such elements, called the *Leeson corrections*. The Leeson corrections, derived by Dave Leeson, W6NL, from pioneering work by Schelkunoff at Bell Labs, compute the diameter and length of an element that is electrically equivalent to a tapered element. This monotaper element is much easier to use in a pro-

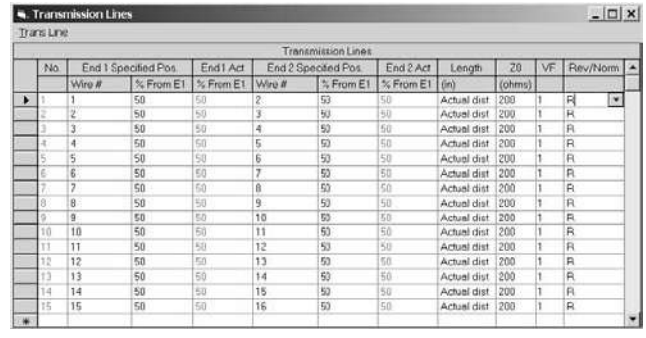
Transmission Lines

Trans Line

Transmission Lines

No.	End 1 Specified Pos.		End 1 Act	End 2 Specified Pos.		End 2 Act	Length	Z0	VF	Rev/Norm
	Wire #	% From E1	% From E1	Wire #	% From E1	% From E1	(in)	(ohms)		
1	1	50	50	2	50	50	Actual dist	200	1	R
2	2	50	50	3	50	50	Actual dist	200	1	R
3	3	50	50	4	50	50	Actual dist	200	1	R
4	4	50	50	5	50	50	Actual dist	200	1	R
5	5	50	50	6	50	50	Actual dist	200	1	R
6	6	50	50	7	50	50	Actual dist	200	1	R
7	7	50	50	8	50	50	Actual dist	200	1	R
8	8	50	50	9	50	50	Actual dist	200	1	R
9	9	50	50	10	50	50	Actual dist	200	1	R
10	10	50	50	11	50	50	Actual dist	200	1	R
11	11	50	50	12	50	50	Actual dist	200	1	R
12	12	50	50	13	50	50	Actual dist	200	1	R
13	13	50	50	14	50	50	Actual dist	200	1	R
14	14	50	50	15	50	50	Actual dist	200	1	R
15	15	50	50	16	50	50	Actual dist	200	1	R

Fig 20—Transmission-line window for the 9302A.EZ 16-element LPDA. Note that the transmission lines going between elements are "reversed," meaning that they are 180° out-of-phase at each element, a requirement for properly feeding an LPDA.

Table 7
5-element Yagi at 14.1739 MHz with Telescoping Aluminum Elements

	With Leeson Corrections			Without Leeson Corrections		
Freq. MHz	*Source Impedance Ω*	*Gain dBi*	*F/R dB*	*Source Impedance Ω*	*Gain dBi*	*F/R dB*
14.0	23.2 – *j* 26.5	14.82	23.3	22.4 – *j* 12.7	14.92	23.1
14.1	22.7 – *j* 20.5	14.87	22.8	18.6 – *j* 12.5	14.70	21.6
14.2	22.8 – *j* 14.8	14.87	22.7	6.6 – *j* 4.6	14.01	16.2
14.3	22.5 – *j* 11.9	14.76	21.5	1.9 + *j* 10.6	10.61	3.1
14.4	14.5 – *j* 10.5	14.45	19.9	1.6 + *j* 23.7	11.15	–11.4

gram like *NEC-2*. See Chapter 2, Antenna Fundamentals, for more information on the Leeson corrections.

EZNEC and other *NEC-2* programs can automatically invoke the Leeson corrections, providing that some basic conditions are met—and happily, these conditions are true for the telescoping aluminum-tubing elements commonly used as Yagi elements. *EZNEC* gives you the ability to disable or enable Leeson corrections, under the **Option** menu, under **Stepped Diameter Correction**, *EZNEC*'s name for the Leeson corrections. Open the modeling file **520-40H.EZ**, which contains tapered aluminum tubing elements and compare the results using and without using the Leeson corrections.

Table 7 lists the differences over the 20-meter band, with the 5-element Yagi at a height of 70 feet above flat ground. You can see that the non-Leeson corrected figures are very different from the corrected ones. At 14.3 MHz, the pattern for the non-corrected Yagi has degenerated to a F/R of 3.1 db, while at 14.4 MHz, just outside the top of the Amateur band, the pattern for the non-corrected antenna actually has reversed. Even at 14.2 MHz, the non-corrected antenna shows a low source impedance, while the corrected version exhibits smooth variations in gain, F/R and impedance across the whole band, just as the actual antenna exhibits.

Some Quads

Some types of cubical quads are made using a combination of aluminum tubing and wire elements, particularly in Europe where the "Swiss" quad has a wide following. Again, *NEC-2*-based programs don't handle such tubing/wire elements well. It is best to avoid modeling this type of antenna, although there are some ways to attempt to get around the limitations, ways that are beyond the scope of this chapter.

NEAR-FIELD OUTPUTS

FCC regulations set limits on the maximum permissible exposure (MPE) allowed from the operation of radio transmitters. These limits are expressed in terms of the electric (V/m) and magnetic fields (A/m) close to an antenna. *NEC-2*-based programs can compute the electric and magnetic *near fields* and the FCC accepts such computations to demonstrate that an installation meets their regulatory requirements. See Chapter 1, Safety, in this book.

Table 8
E- and H-Field Intensities for 1500 W into 5-Element Yagi at 70 Feet on 14.2 MHz

Height Feet	*H-Field (A/m)*	*E-Field (V/m)*
0	0.04	4.1
10	0.03	13.8
20	0.04	20.6
30	0.06	22.6
40	0.08	25.8
50	0.10	33.8
60	0.12	41.5
70	0.12	44.3

We'll continue to use the 5-element Yagi at 70 feet to demonstrate a near-field computation. Open **Ch4-520-40H.EZ** in *EZNEC* and choose **Setups** and then **Near Field** from the menu at the top of the main window. Let's calculate the E-field and H-field intensity for a power level of 1500 W (chosen using the **Options**, **Power Level** choices from the main menu) in the main beam at a fixed distance, say 50 feet, from the tower base. We'll do this at various heights, using 10-foot increments of height, in order to see the lobe structure of the Yagi at 70 feet height.

Table 8 summarizes the total H- and E-field intensities as a function of height. As you might expect, the fields are strongest directly in line with the antenna at a height of 70 feet. At ground level, the total fields are well within the FCC limits for rf exposure for both fields. In fact, the fields are within the FCC limits if someone were to stand at the tower base, directly under the antenna.

ANTENNA MODELING SUMMARY

This section on antenna modeling is by necessity only a brief introduction to the science of antenna modeling. The subject is partly art as well as science because there are usually several ways of creating a model for a particular antenna or antennas.

Indeed, the presence of other wires surrounding a particular antenna can affect the performance of that antenna. Finally, there are the practical aspects of putting a actual antenna up in the real world. We'll explore this next.

Practical Aspects, Designing Your Antenna System

The most important time spent in putting together an antenna system is the time spent in planning. In Chapter 3, The Effects of Ground, we outlined the steps needed to evaluate how your local terrain can affect HF communications. There we emphasized that you need to compare the patterns resulting from your own terrain to the statistically relevant elevation angles needed for coverage of various geographic areas. (The elevation-angle statistics were developed in Chapter 23, Radio Wave Propagation and are located on the CD-ROM included with this book, as is the terrain-assessment program *HFTA*.)

The implicit assumptions in Chapter 3 are (1) that you know where you want to talk to, and (2) that you'd like the most effective system possible. At the start of such a theoretical analysis, cost is no object. Practical matters, like cost or the desires of your spouse, can come later! After all, you're just checking out all the possibilities. If nothing else, you will use the methodology in Chapter 3 to evaluate any property you are considering buying so that you can build your "dream station."

Next, in the first part of this chapter we described modeling tools used to evaluate different types of antennas. These modeling tools can help you evaluate what type of antenna might be suitable to your own particular style of operating. Do you want a Yagi with a lot of rejection of received signals from the rear? Let's say that terrain analysis shows that you need an antenna at least 50 feet high. Do you really need a steel tower, or would a simple dipole in the trees serve your communication needs just fine? How about a vertical in your backyard? Would that be inconspicuous enough to suit your neighbors and your own family, yet still get you on the air?

In short, using the techniques and tools we've presented in Chapters 3, 23 and here in Chapter 4, you can scientifically plan an antenna *system* that will be best suited for your own particular conditions. Now, however, you have to get practical. Thinking through and planning the installation can save a lot of time, money and frustration. While no one can tell you the exact steps you should take in developing your own master plan, this section, prepared originally by Chuck Hutchinson, K8CH, should help you with some ideas.

WHAT DO YOU REALLY WANT?

Begin planning by spelling out your communications *desires*. What bands are you interested in? Who (or where) do you want to talk to? When do you operate? How much time and money are you willing to spend on an antenna system? What physical limitations affect your master plan?

From the answers to the above questions, begin to formulate *goals*—short, intermediate and long range. Be realistic about those goals. Remember that there are three station effectiveness factors that are under your control. These are: operator skill, equipment in the shack, and the antenna system. There is no substitute for developing operating skills. Some tradeoffs are possible between shack equipment and antennas. For example, a high-power amplifier can compensate for a less than optimum antenna. By contrast, a better antenna has advantages for receiving as well as for transmitting.

Consider your *limitations*. Are there regulatory restrictions on antennas in your community? Are there any deed restrictions or covenants that apply to your property? Do other factors (finances, family considerations, other interests, and so forth) limit the type or height of antennas that you can erect? All of these factors must be investigated because they play a major role determining the type of antennas you erect.

Chances are that you won't be able to immediately do all you desire. Think about how you can budget your resources over a period of time. Your resources are your money, your time available to work, materials you may have on hand, friends that are willing to help, etc. One way to budget is to concentrate your initial efforts on a given band or two. If your major interest is in chasing DX, you might want to start with a very good antenna for the 14-MHz band. A simple multiband antenna could initially serve for other frequencies. Later you can add better antennas for those other bands.

SITE PLANNING

A map of your property or proposed antenna site can be of great help as you begin to consider alternative antennas. You'll need to know the size and location of buildings, trees and other major objects in the area. Be sure to note compass directions on your map. Graph or quadrille paper (or a simple CAD program) can be very useful for this purpose. See **Fig 21** for an example. It's a good idea to make a few photocopies of your *site map* so you can mark on the copies as you work on your plans.

Use your map to plan antenna layouts and locations of any supporting towers or masts. If your plan calls for more than one tower or mast, think about using them as supports for wire antennas. As you work on a layout, be sure to think in three dimensions even though the map shows only two.

Be sensitive to your neighbors. A 70-foot guyed tower in the front yard of a house in a residential neighborhood is not a good idea (and probably won't comply with local ordinances!). You probably will want to locate that tower in the back yard.

ANALYSIS

Use the information earlier in this chapter and in Chapters 3 and 23 to analyze antenna patterns in both

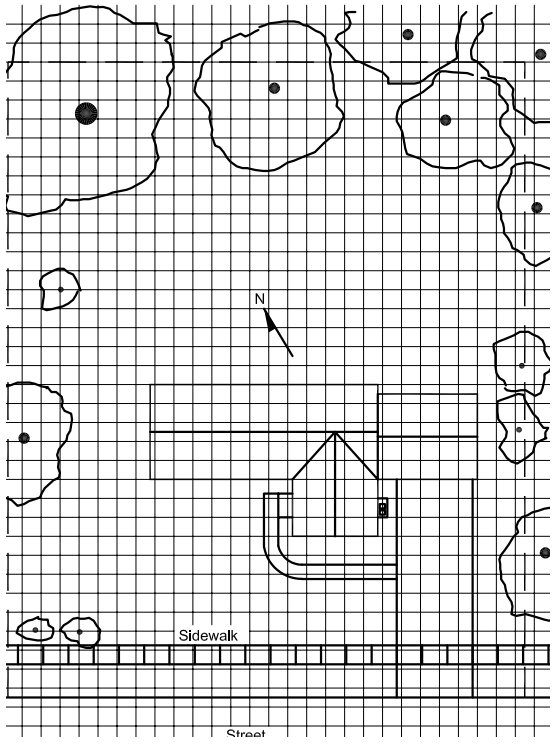

Fig 21—A site map such this one is a useful tool for planning your antenna installation.

horizontal and vertical planes towards geographic areas of interest. If you want to work DX, you'll want antennas that radiate energy at low as well as intermediate angles. An antenna pattern is greatly affected by the presence of ground and by the local topography of the ground. Therefore, be sure to consider what effect ground will have on the antenna pattern at the height you are considering. A 70-foot high antenna is approximately $^1/_2$, 1, $1^1/_2$ and 2 wavelengths (λ) high on 7, 14, 21 and 28 MHz respectively. Those heights are useful for long-distance communications. The same 70-foot height represents only $\lambda/4$ at 3.5 MHz, however. Most of the radiated energy from a dipole at that height would be concentrated straight up. This condition is not great for long-distance communication, but can still be useful for some DX work and excellent for short-range communications.

Lower heights can be useful for communications. However, it is generally true that "the higher, the better" as far as communications effectiveness is concerned. This general rule of thumb, of course, should be tempered by an exact analysis of your local terrain. Being located at the top of a steep hill can mean that you can use lower tower heights to achieve good coverage.

There may be cases where it is not possible to install low-frequency dipoles at $\lambda/4$ or more above the ground. A vertical antenna with many radials is a good choice for long-distance communications. You may want to install both a dipole and a vertical for the 3.5- or 7-MHz bands. On the 1.8-MHz band, unless extremely tall supports are available, a vertical antenna is likely to be the most useful for DXing. You can then choose the antenna that performs best for a given set of conditions. A low dipole will generally work better for shorter-range communications, while the vertical will generally be the better performer over longer distances.

Consider the azimuthal pattern of fixed antennas. You'll want to orient any fixed antennas to favor the directions of greatest interest to you.

BUILDING THE SYSTEM

When the planning is completed, it is time to begin construction of the antenna system. Chances are that you can divide that construction into a series of *phases* or steps. Say, for example, that you have lots of room and that your long-range plan calls for a pair of towers, one 100-feet high, and the other 70-feet high, to support monoband Yagi antennas. The towers will also support a horizontal 3.5-MHz dipole, for DX work. On your map you've located them so the 80-meter dipole will be broadside to Europe. You decide to build the 70-foot tower with a "triband" beam and 80- and 40-meter inverted-V dipoles to begin the project.

In your master plan you design the guys, anchors and all hardware for the 70-foot tower to support the load of stacked 4-element 10- and 15-meter monobanders Yagis. So you make sure you buy a heavy-duty rotator and the stout mast needed for the monoband antennas later. Thus you avoid having to buy, and then sell, a medium-duty rotator and lighter weight tower equipment later on when you upgrade the station. You could have saved money in the long run by putting up a monoband beam for your favorite band, but you decided that for now it is more important to have a beam on 14, 21 and 28 MHz, so you choose a commercial triband Yagi.

The second step of your plan calls for installing the second tower and stacking a 2-element 40-meter and a 4-element 20-meter monoband Yagi on it. You also plan to replace the tribander on the 70-foot tower with stacked 4-element 10- and 15-meter monoband Yagis. Although this is still a "dream system" you can now apply some of the modeling techniques discussed earlier in this chapter to determine the overall system performance.

Modeling Interactions at Your Dream Station

In this analysis we're going to assume that you have sufficient real estate to separate the 70- and 100-foot towers by 150 feet so that you can easily support an 80-meter dipole between them. We'll also assume that you want the 80-meter dipole to have its maximum response at a heading of 45° into Europe from your location in Newington, Connecticut. The dipole will also have a lobe

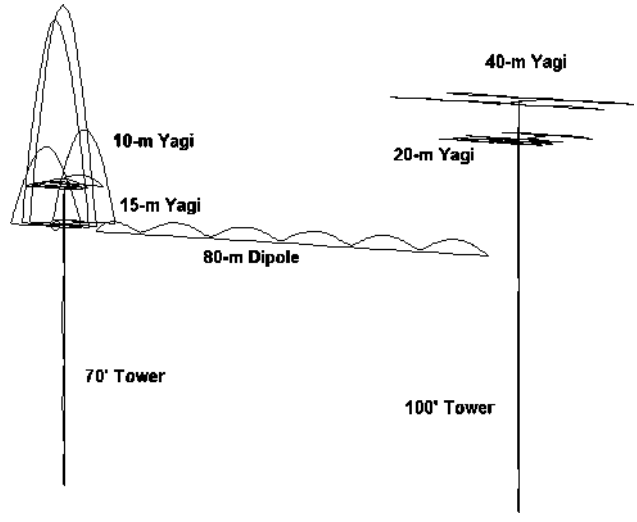

Fig 22—Layout for two-tower antenna system, at 70 and 100 feet high and 150 feet apart. The 70-foot tower has a 4-element 10-meter Yagi at 80 feet on a 10-foot rotating mast and a 4-element 15-meter Yagi at 70 feet. An 80-meter dipole goes from the 70-foot tower to the 100-foot tower, which holds a 2-element 40-meter Yagi at 110 feet and a 4-element 20-meter Yagi at 100 feet. In this figure all the rotatable Yagis are facing the direction of Europe and the currents on the 15-meter Yagi are shown. Note the significant amount of current re-radiated by the nearby 80-meter dipole.

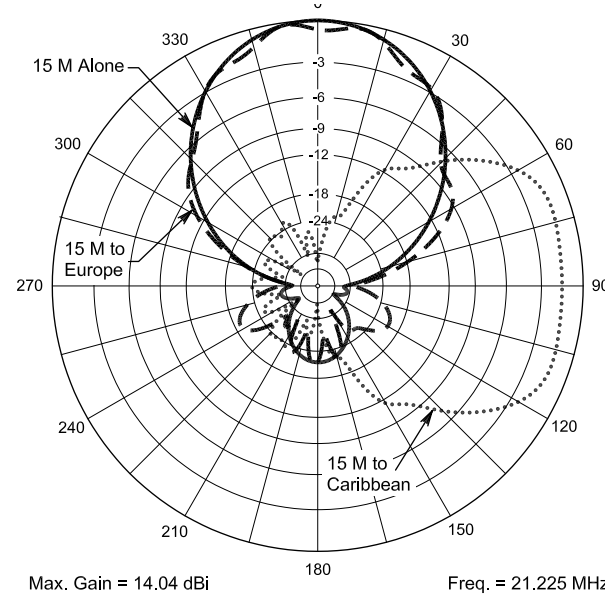

Fig 23—An overlay of azimuth patterns. The solid line is the radiation pattern for the 15-meter Yagi all by itself. The dashed line is the pattern for the 15-meter Yagi, as affected by all the other antennas. The dotted line is the pattern for the 15-meter Yagi when it is pointed toward the Caribbean, with the Yagis on the 100-foot tower pointed toward the 70-foot tower. The peak response of the 15-meter Yagi has dropped by about 1.5 dB.

facing 225° towards the USA and New Zealand, making it a good antenna for both domestic contacts and DX work.

Let's examine the interactions that occur between the rotatable Yagis for 10, 15, 20 and 40 meters. See **Fig 22**, which purposely exaggerates the magnitude of the currents on the 4-element 15-meter Yagi mounted at 70 feet. Here, both sets of Yagis have been rotated so that they are pointing into Europe. There is a small amount of current radiated onto the 10-meter antenna but virtually no current is radiated onto the 40- and 20-meter Yagis. This is good.

However, significant current is radiated onto, and then re-radiated, by the 80-meter dipole. This undesired current affects the radiation pattern of the 15-meter antenna, as shown in **Fig 23**, which overlays the pattern of the 4-element 15-meter Yagi by itself with that of the Yagi interacting with the other antennas. You can see "ripples" in the azimuthal response of the 15-meter Yagi due to the effects of the 80-meter dipole's re-radiation. The magnitude of the ripples is about 1 dB at worst, so they don't seriously affect the forward pattern (into Europe), but the rearward lobes are degraded somewhat, to just below 20 dB.

Fig 23 also shows the worst-case situation for the 15-meter Yagi. Here, the 15- and 10-meter stack has been turned clockwise 90°, facing the Caribbean, while the 40-

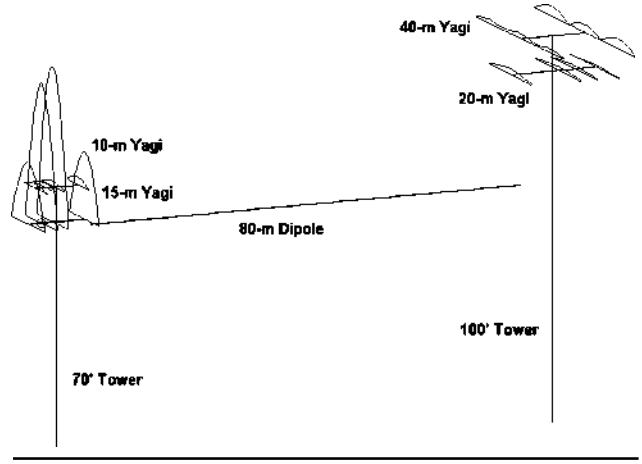

Fig 24—The layout and 15-meter currents when the Yagis on the 100-foot tower are pointed toward the 70-foot tower. The 15-meter Yagi has been rotated to face the direction of the 100-foot tower (toward the Caribbean).

and 20-meter Yagis on the 100-foot tower have been turned counter-clockwise 90° (in the direction of Japan) to face the 70-foot tower holding the 10/15-meter Yagis. You can see the layout and the currents in **Fig 24**. Now the 40- and 20-meter Yagis re-radiate some 15-meter

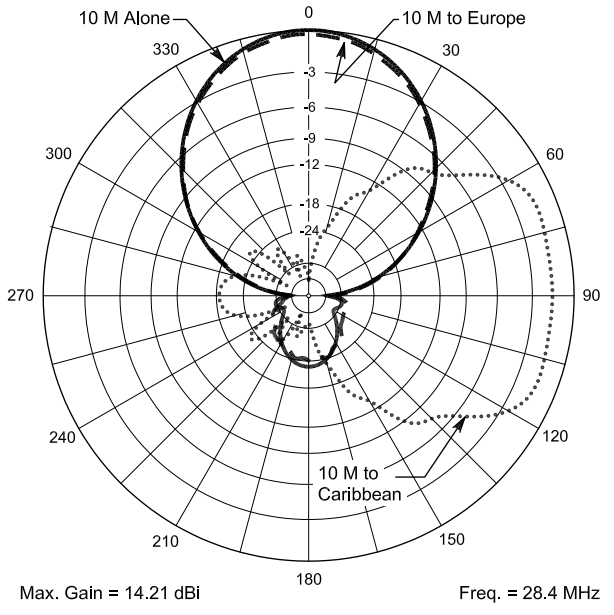

Fig 25—The radiation patterns for the 10-meter Yagi. The solid line is the 10-meter Yagi by itself. The dashed line is for the same Yagi, with all other antenna interactions. The dotted line shows the worst-case pattern, with the stacked Yagis on the 100-foot tower facing the 70-foot tower and the 10-meter Yagi pointed toward the Caribbean. Again, the peak response of the 10-meter Yagi has dropped about 1.5 dB in the worst-case situation.

energy and reduce the maximum gain by about 1.5 dB. Note that in this direction the 80-meter dipole no longer has 15-meter energy radiated onto it by the 15-meter Yagi.

The shape of the patterns will change depending on whether you specify "current" or "voltage" sources in the models for the other antennas, since this effectively opens up or shorts the feed points at the other antennas so far as 15-meter energy is concerned. In practice, this means that the interaction between antennas will vary somewhat depending on the length of the feed lines going to each antenna and whether each feed line is open-circuited or short-circuited when it is not in use.

You can now see that interactions between various antennas pointing in different directions can be significant in a real-world antenna system. In general, higher-frequency antennas are affected by re-radiation from lower-frequency antennas, rather than the other way around. Thus the presence of a 10- or 15-meter stack does not affect the 20-meter Yagi at all.

Modeling can also help determine the minimum stacking distance required between monoband Yagis on the same rotating mast. In this case, stacking the 10- and 15-meter monobanders 10 feet apart holds down interaction between them so that the pattern and gain of the 10-meter Yagi is not impacted adversely. **Fig 25** demonstrates this in the European direction, where the patterns for the 10-meter beam by itself looks very clean compared to the same Yagi separated by 10 feet from the 15-meter Yagi below it. The worst-case situation is pointing towards the Caribbean, when the 40- and 20-meter stack is facing the 70-foot tower. This drops the 10-meter gain down about 1.5 dB from maximum, indicating significant interaction is occurring.

In this situation you might find it best to place the 70-foot tower in the direction closest to the Caribbean if this direction is very important to you. Doing so will, however, cause the pattern in the direction of the Far East to be affected on 10 and 15 meters. You have the modeling tools necessary to evaluate various configurations to achieve whatever is most important to you.

COMPROMISES

Because of limitations, most amateurs are never able to build their dream antenna system. This means that some compromises must be made. Do not, under any circumstances, compromise the *safety* of an antenna installation. Follow the manufacturer's recommendations for tower assembly, installation and accessories. Make sure that all hardware is being used within its ratings.

Guyed towers are frequently used by radio amateurs because they cost less than more complicated unguyed or freestanding towers with similar ratings. Guyed towers are fine for those who can climb, or those with a friend who is willing to climb. But you may want to consider an antenna tower that folds over, or one that cranks up (and down). Some towers crank up (and down) and fold over too. See **Fig 26**. That makes for convenient access to antennas for adjustments and maintenance without climbing. Crank-up towers also offer another advantage. They allow antennas to be lowered during periods of no operation, such as for aesthetic reasons or during periods of high winds.

A well-designed monoband Yagi should outperform a multiband Yagi. In a monoband design the best adjustments can be made for gain, front-to-rear ratio (F/R) and matching, *but only for a single band*. In a multiband design, there are always tradeoffs in these properties for the ability to operate on more than one band. Nevertheless, a multiband antenna has many advantages over two or more single band antennas. A multiband antenna requires less heavy-duty hardware, requires only one feed line, takes up less space and it costs less.

Apartment dwellers face much greater limitations in their choice of antennas. For most, the possibility of a tower is only a dream. (One enterprising ham made arrangements to purchase a top-floor condominium from a developer. The arrangements were made before construction began, and the plans were altered to include a roof-top tower installation.) For apartment and condominium dwellers, the situation is still far from hopeless. A later section presents ideas for consideration.

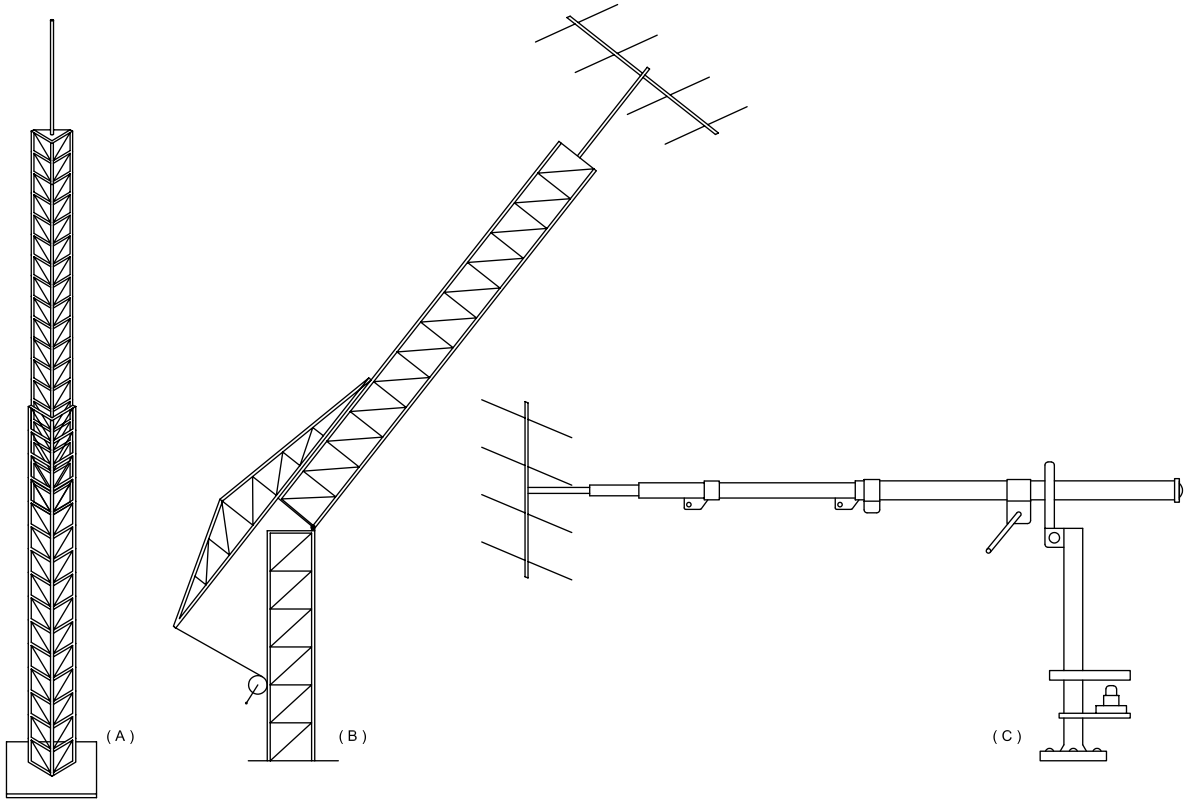

Fig 26—Alternatives to a guyed tower are shown here. At A, the crank-up tower permits working on antennas at reduced height. It also allows antennas to be lowered during periods of no operation. Motor-driven versions are available. The fold-over tower at B and the combination at C permit working on antennas at ground level.

EXAMPLES

You can follow the procedure previously outlined to put together modest or very large antenna systems. What might a ham put together for antennas when he or she wants to try a little of everything, and has a modest budget? Let's suppose that the goals are (1) low cost, (2) no tower, (3) coverage of all HF bands and the repeater portion of one VHF band, and (4) the possibility of working some DX.

After studying the pages of this book, the station owner decides to first put up a 135-foot center-fed antenna. High trees in the back yard will serve as supports to about 50 feet. This antenna will cover all the HF bands by using a balanced feeder and an antenna tuner. It should be good for DX contacts on 10 MHz and above, and will probably work okay for DX contacts on the lower bands. However, her plan calls for a vertical for 3.5 and 7 MHz to enhance the DX possibilities on those bands. For VHF, a chimney-mounted vertical is included.

ANOTHER EXAMPLE

A licensed couple has bigger ambitions. Goals for their station are (1) a good setup for DX on 14, 21 and 28 MHz, (2) moderate cost, (3) one tower, (4) ability to work some DX on 1.8, 3.5 and 7 MHz, and (5) no need to cover the CW portion of the bands.

After considering the options, the couple decides to install a 65-foot guyed tower. A large commercial triband Yagi will be mounted on top of the tower. The center of a trap dipole tuned for the phone portion of the 3.5- and 7-MHz bands will be supported by a wooden yardarm installed at the 60-foot level of the tower, with ends drooping down to form an inverted V. An inverted L for 1.8 MHz starts near ground level and goes up to a similar yardarm on the opposite side of the tower. The horizontal portion of the inverted L runs away from the tower at right angles to the trap dipole. Later, the husband will experiment with sloping antennas for 3.5 MHz. If those experiments are not successful, a $\lambda/4$ vertical will be used on that band.

Apartment Possibilities

A complete and accurate assessment of antenna types, antenna placement and feed-line placement is very important for the apartment dweller. Among the many possibilities for types are balcony antennas, *invisible* ones (made of fine wire), vertical antennas disguised as flag poles or as masts with a TV antenna on top, and indoor antennas.

A number of amateurs have been successful negotiating with the apartment owner or manager for permission to install a short mast on the roof of the building. Coaxial lines and rotator control cables might be routed through conduit troughs or through ductwork. If you live in one of the upper stories of the building, routing the cables over the edge of the roof and in through a window might be the way to go. There is a story about one amateur who owns a triband beam mounted on a 10-foot mast. But even with such a short mast, he is the envy of all his amateur friends because of his superb antenna height. His mast stands on top of a 22-story apartment building.

Usually the challenge is to find ways to install antennas that are unobtrusive. That means searching out antenna locations such as balconies, eaves, nearby trees, etc. For example, a simple but effective balcony antenna is a dangling vertical. Attach a thin wire to the tip of a mobile whip or a length of metal rod or tubing. Then mount the rigid part of the antenna horizontally on the balcony rail, dangling the wire over the edge. The antenna is operated against the balcony railing or other metallic framework. A matching network is usually required at the antenna feed point. Metal in the building will likely give a directivity effect, but this may be of little consequence and perhaps even an advantage. The antenna may be removed and stored when not in use.

Frequently, the task of finding an inconspicuous route for a feed line is more difficult than the antenna installation itself. When Al Francisco, K7NHV, lived in an apartment, he used a tree-mounted vertical antenna. The coax feeder exited his apartment through a window and ran down the wall to the ground. Al buried the section of line that went from under the window to a nearby tree. At the tree, a section of enameled wire was connected to the coax center conductor. He ran the wire up the side of the tree away from foot traffic. A few short radials completed the installation. The antenna worked fine, and was never noticed by the neighbors.

See Chapters 6, Low-Frequency Antennas, and Chapter 15, Portable Antennas, for ideas about low-frequency and portable antennas that might fit into your available space. Your options are limited as much by your imagination and ingenuity as by your pocketbook. Another option for apartment dwellers is to operate away from home. Some hams concentrate on mobile operation as an alternative to a fixed station. It is possible to make a lot of contacts on HF mobile. Some have worked DXCC that way.

Suppose that you like VHF contests. Because of other activities, you are not particularly interested in operating VHF outside the contests. Why not take your equipment and antennas to a hilltop for the contests? Many hams combine a love for camping or hiking with their interest in radio.

Antennas for Limited Space

It is not always practical to erect full-size antennas for the HF bands. Those who live in apartment buildings may be restricted to the use of minuscule radiators because of house rules, or simply because the required space for full-size antennas is unavailable. Other amateurs may desire small antennas for aesthetic reasons, perhaps to keep peace with neighbors who do not share their enthusiasm about high towers and big antennas. There are many reasons why some amateurs prefer to use physically-shortened antennas. This section discusses proven designs and various ways of building and using them effectively. You will find that modeling antennas by computer, even compromised "stealth antennas," can help you determine the most practical system possible for your particular circumstances—before you go through the effort of stringing up wires.

Few compromise antennas are capable of delivering the performance you can expect from the full-size variety. But the patient and skillful operator can often do as well as some who are equipped with high power and full-size antennas. Someone with a reduced-size antenna may not be able to "bore a hole" in the bands as often and with the commanding dispatch enjoyed by those who are better equipped, but DX can be worked successfully when band conditions are suitable.

INVISIBLE ANTENNAS

We amateurs don't regard our antennas as eyesores; in fact, we almost always regard them as works of art! But there are occasions when having an outdoor or visible antenna can present problems.

When we are confronted with restrictions—self-imposed or otherwise—we can take advantage of a number of options toward getting on the air and radiating at least a moderately effective signal. In this context, a poor antenna is certainly better than no antenna at all! This section describes a number of techniques that enable us to use indoor antennas or "invisible" antennas outdoors.

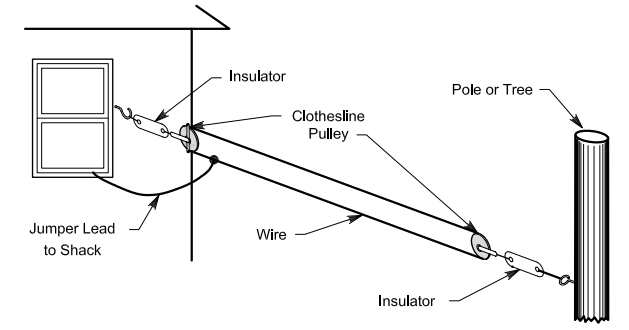

Fig 27—The clothesline antenna is more than it appears to be.

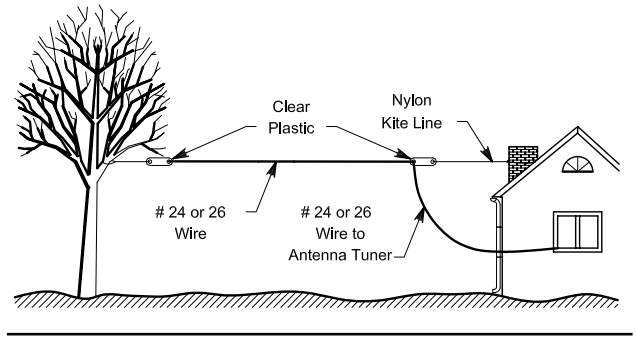

Fig 28—The "invisible" end-fed antenna.

Many of these systems will yield good-to-excellent results for local and DX contacts, depending on band conditions at any given time. *The most important consideration is that of not erecting any antenna that can present a hazard (physical or electrical) to humans, animals and buildings. Safety first!*

Clothesline Antenna

Clotheslines are sometimes attached to pulleys (**Fig 27**) so that the user can load the line and retrieve the laundry from a back porch. Laundry lines of this variety are accepted parts of the neighborhood "scenery," and can be used handily as amateur antennas by simply insulating the pulleys from their support points. This calls for the use of a conducting type of clothesline, such as heavy gauge stranded electrical wire with Teflon or vinyl insulation. A high quality, flexible steel cable (stranded) is suitable as a substitute if you don't mind cleaning it before clothing is hung on it.

A jumper wire can be brought from one end of the line to the ham shack when the station is being operated. If a good electrical connection exists between the wire clothesline and the pulley, a permanent connection can be made by connecting the lead-in wire between the pulley and its insulator. An antenna tuner can be used to match the "invisible" random-length wire to the transmitter and receiver.

Invisible Long Wire

A wire antenna is not actually a "long wire" unless it is one wavelength or greater in length. Yet many amateurs refer to (relatively) long physical spans of conductor as *long wires*. For the purpose of this discussion we will assume we have a fairly long span of wire, and refer to it as an *end-fed* wire antenna.

If we use small-diameter enameled wire for our end-fed antenna, chances are that it will be very difficult to see against the sky and neighborhood scenery. The smaller the wire, the more invisible the antenna will be. The limiting factor with small wire is fragility. A good compromise is #24 or #26 magnet wire for spans up to 130 feet; lighter-gauge wire can be used for shorter spans, such as 30 or 60 feet. The major threat to the longevity of fine wire is icing. Also, birds may fly into the wire and break it. Therefore, this style of antenna may require frequent service or replacement.

Fig 28 illustrates how you might install an invisible end-fed wire. It is important that the insulators also be lacking in prominence. Tiny Plexiglas blocks perform this function well. Small-diameter clear plastic medical vials are suitable also. Some amateurs simply use rubber bands for end insulators, but they will deteriorate rapidly from sun and air pollutants. They are entirely adequate for short-term operation with an invisible antenna, however.

Rain Gutter and TV Antennas

A great number of amateurs have taken advantage of standard house fixtures when contriving inconspicuous antennas. A very old technique is the use of the gutter and downspout system on the building. This is shown in **Fig 29**, where a lead wire is routed to the operating room

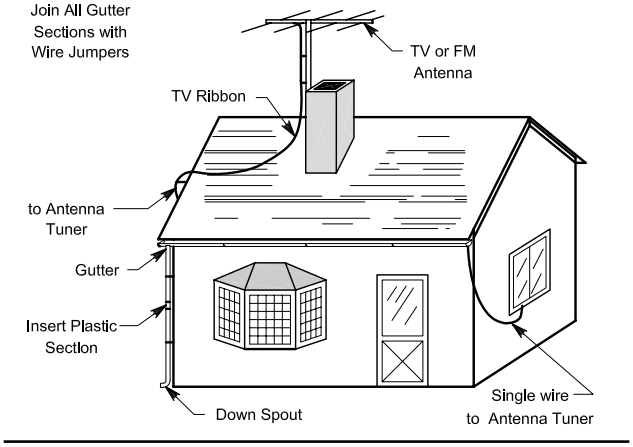

Fig 29—Rain gutters and TV antenna installations can be used as inconspicuous Amateur Radio antennas.

from one end of the gutter trough. We must assume that the wood to which the gutter is affixed is dry and of good quality to provide reasonable electrical insulation. The rain gutter antenna may perform quite poorly during wet weather or when there is ice and snow on it and the house roof.

All joints between gutter and downspout sections must be bonded electrically with straps of braid or flashing copper to provide good continuity in the system. Poor joints can permit rectification of RF and subsequently cause TVI and other harmonic interference. Also, it is prudent to insert a section of plastic downspout about 8 feet above ground to prevent RF shocks or burns to passersby while the antenna is being used. Improved performance may result if you join the front and back gutters of the house with a jumper wire to increase the area of the antenna.

Fig 29 also shows a TV or FM antenna that can be employed as an invisible amateur antenna. Many of these antennas can be modified easily to accommodate the 144- or 222-MHz bands, thereby permitting the use of the 300-Ω line as a feeder system. Some FM antennas can be used on 6 meters by adding #10 bus wire extensions to the ends of the elements, and adjusting the match for an SWR of 1:1. If 300-Ω line is used it will require a balun or antenna tuner to interface the line with the station equipment.

For operation in the HF bands, the TV or FM antenna feeders can be tied together at the transmitter end of the span and the system treated as a random length wire. If this is done, the 300-Ω line will have to be on TV standoff insulators and spaced well away from phone and power company service entrance lines. Naturally, the TV or FM radio must be disconnected from the system when it is used for amateur work! Similarly, masthead amplifiers and splitters must be removed from the line if the system is to be used for amateur operation. If the system is mostly vertical, a good RF ground system with many radials around the base of the house should be used to improve performance.

A very nice top-loaded vertical can be made from a length of TV mast with a large TV antenna on the top. Radials can be placed on the roof or at ground level with the TV "feed line" acting as part of the vertical. There is an extensive discussion of loaded verticals and radial systems in Chapter 6, Low-Frequency Antennas.

Flagpole Antennas

We can exhibit our patriotism and have an invisible amateur antenna at the same time by disguising our antenna as shown in **Fig 30**. The vertical antenna is a wire that has been placed inside a plastic or fiberglass pole.

The flagpole antenna shown is structured for a single amateur band, and it is assumed that the height of the pole corresponds to a quarter wavelength for the chosen band. The radials and feed line can be buried in the ground

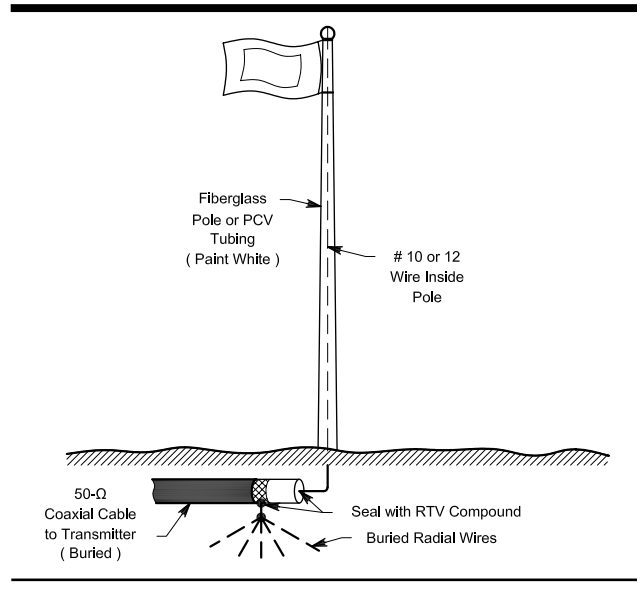

Fig 30—A flagpole antenna.

as shown. In a practical installation, the sealed end of the coax cable would protrude slightly into the lower end of the plastic pole.

If a large-diameter fiberglass pole were available, a multiband trap vertical may be concealed inside it. Or you might use a metal pole and bury a water-tight box at its base, containing fixed-tuned matching networks for the bands of interest. The networks could then be selected remotely by means of relays inside the box. A 30-foot flagpole would provide good results in this kind of system, provided it was used in conjunction with a buried radial system.

Still another technique is one that employs a wooden flagpole. A small diameter wire can be stapled to the pole and routed to the coax feeder or matching network. The halyard could by itself constitute the antenna wire if it were made from heavy-duty insulated hookup wire. There are countless variations for this type of antenna, and they are limited only by the imagination of the amateur.

Other Invisible Antennas

Some amateurs have used the metal fence on apartment verandas as antennas, and have had good results on the upper HF bands (14, 21 and 28 MHz). We must presume that the fences were not connected to the steel framework of the building, but rather were insulated by the concrete floor to which they were affixed. These verandah fences have also been used effectively as ground systems (counterpoises) for HF-band vertical antennas put in place temporarily after dark.

One amateur in New York City uses the fire escape on his apartment building as a 7-MHz antenna, and he reports good success working DX stations with it. Another

apartment dweller makes use of the aluminum frame on his living room picture window as an antenna for 21 and 28 MHz. He works it against the metal conductors of the baseboard heater in the same room.

Many jokes have been told over the years about *bedspring antennas*. The idea is by no means absurd. Bedsprings and metal end boards have been used to advantage as antennas by many apartment dwellers as 14, 21 and 28 MHz radiators. A counterpoise ground can be routed along the baseboard of the room and used in combination with the bedspring. It is important to remember that any independent (insulated) metal object of reasonable size can serve as an antenna if the transmitter can be matched to it. An amateur in Detroit once used his Shopsmith craft machine (about 5 feet tall) as a 28 MHz antenna. He worked a number of DX stations with it when band conditions were good.

A number of operators have used metal curtain rods and window screens for VHF work, and found them to be acceptable for local communications. Best results with any of these makeshift antennas will be had when the "antennas" are kept well away from house wiring and other conductive objects.

INDOOR ANTENNAS

Without question, the best place for your antenna is outdoors, and as high and in the clear as possible. Some of us, however, for legal, social, neighborhood, family or landlord reasons, are restricted to indoor antennas. Having to settle for an indoor antenna is certainly a handicap for the amateur seeking effective radio communication, but that is not enough reason to abandon all operation in despair.

First, we should be aware of the reasons why indoor antennas do not work well. Principal faults are:

- Low height above ground—the antenna cannot be placed higher than the highest peak of the roof, a point usually low in terms of wavelength at HF
- The antenna must function in a lossy RF environment involving close coupling to electrical wiring, guttering, plumbing and other parasitic conductors, besides dielectric losses in such nonconductors as wood, plaster and masonry
- Sometimes the antenna must be made small in terms of a wavelength
- Usually it cannot be rotated.

These are appreciable handicaps. Nevertheless, global communication with an indoor antenna is still possible, although you must be sure that you are not exposing anyone in your family or nearby neighbors to excessive radiation. See Chapter 1, Safety, in this book.

Some practical points in favor of the indoor antenna include:

- Freedom from weathering effects and damage caused by wind, ice, rain and sunlight (the SWR of an attic antenna, however, can be affected somewhat by a wet or snow-covered roof).
- Indoor antennas can be made from materials that would be altogether impractical outdoors, such as aluminum foil and thread (the antenna need support only its own weight).
- The supporting structure is already in place, eliminating the need for antenna masts.
- The antenna is readily accessible in all weather conditions, simplifying pruning or tuning, which can be accomplished without climbing or tilting over a tower.

Empiricism

A typical house or apartment presents such a complex electromagnetic environment that it is impossible to predict theoretically which location or orientation of the indoor antenna will work best. This is where good old fashioned cut-and-try, use-what-works-best *empiricism* pays off. But to properly determine what really is most suitable requires an understanding of some antenna measuring fundamentals.

Unfortunately, many amateurs do not know how to evaluate performance scientifically or compare one antenna with another. Typically, they will put up one antenna and try it out on the air to see how it "gets out" in comparison with a previous antenna. This is obviously a very poor evaluation method because there is no way to know if the better or worse reports are caused by changing band conditions, different S-meter characteristics or any of several other factors that could influence the reports received.

Many times the difference between two antennas or between two different locations for identical antennas amounts to only a few decibels, a difference that is hard to discern unless instantaneous switching between the two is possible. Those few decibels are not important under strong signal conditions, of course, but when the going gets rough, as is often the case with an indoor antenna, a few dB can make the difference between solid copy and no possibility of real communication.

Very little in the way of test equipment is needed for casual antenna evaluation, other than a communications receiver. You can even do a qualitative comparison by ear, if you can switch antennas instantaneously. Differences of less than 2 dB, however, are still hard to discern. The same is true of S-meters. Signal strength differences of less than a decibel are usually difficult to see. If you want to measure that last fraction of a decibel, you should use a good ac voltmeter at the receiver audio output (with the AGC turned off).

In order to compare two antennas, switching the coaxial transmission line from one to the other is necessary. No elaborate coaxial switch is needed; even a simple double-throw toggle or slide switch will provide more than 40 dB of isolation at HF. See **Fig 31**. Switching by means of manually connecting and disconnecting coaxial lines is not recommended because that takes too long.

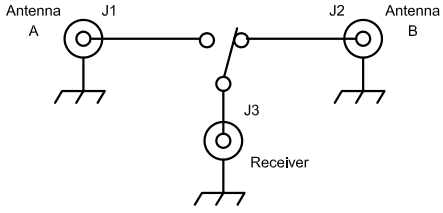

Fig 31—When antennas are compared on fading signals, the time delay involved in disconnecting and reconnecting coaxial cables is too long for accurate measurements. A simple slide switch will do well for switching coaxial lines at HF. The four components can be mounted in a tin can or any small metal box. Leads should be short and direct. J1 through J3 are coaxial connectors.

Fading can cause signal-strength changes during the changeover interval.

Whatever difference shows up in the strength of the received signal will be the difference in performance between the two antennas in the direction of that signal. For this test to be valid, both antennas must have nearly the same feed-point impedance, a condition that is reasonably well met if the SWR is below 2:1 on both antennas.

On ionospheric propagated signals (sky wave) there will be constant fading, and for a valid comparison it will be necessary to take an average of the difference between the two antennas. Occasionally, the inferior antenna will deliver a stronger signal to the receiver, but in the long run the law of averages will put the better antenna ahead.

Of course with a ground-wave signal, such as that from a station across town, there will be no fading problems. A ground-wave signal will enable the operator to properly evaluate the antenna under test in the direction of the source. The results will be valid for ionospheric-propagated signals at low elevation angles in that direction. On 28 MHz, all sky-wave signals arrive and leave at low angles. But on the lower bands, particularly 3.5 and 7 MHz, we often use signals propagated at high elevation angles, almost up to the zenith. For these angles a ground-wave test between local stations may not provide a proper evaluation of the antenna, and use of sky wave signals becomes necessary.

Dipoles

At HF the most practical indoor antenna is usually the dipole. Attempts to get more gain with parasitic elements will usually fail because of close proximity to the ground or coupling to house wiring. Beam antenna dimensions determined outdoors will not usually be valid for an attic antenna because the roof structure will cause dielectric loading of the parasitic elements. It is usually more worthwhile to spend time optimizing the location and performance of a dipole than to try to improve results with parasitic elements.

Most attics are not long enough to accommodate half-wave dipoles for 7 MHz and below. If this is the case, some folding of the dipole will be necessary. The final shape of the antenna will depend on the dimensions and configuration of the attic. Remember that the center of the dipole carries the most current and therefore does most of the radiating. This part should be as high and unfolded as possible. Because the dipole ends radiate less energy than the center, their orientation is not as important. They do carry the maximum voltage, nevertheless, so care should be taken to position the ends far enough from other conductors to avoid arcing.

The dipole may end up being L-shaped, Z-shaped, U-shaped or some indescribable corkscrew shape, depending on what space is available, but reasonable performance can often be had even with such a non-straight arrangement. **Fig 32** shows some possible configurations. Multiband operation is possible with the use of open-wire feeders and an antenna tuner.

One alternative not shown here is the aluminum-foil dipole, which was conceived by Rudy Stork, KA5FSB. He suggests mounting the dipole behind wallpaper or in the attic, with portability, ease of construction and adjustment, and economy in design among its desirable features. This antenna should also display reasonably good bandwidth resulting from the large area of its conductor material. If coaxial feed is used, some pruning of an attic antenna to establish minimum SWR at the band center will be required. Tuning the antenna outdoors and then installing it inside is usually not feasible since the behavior of the antenna will not be the same when placed in the attic. Resonance will be affected somewhat if the antenna is bent.

Even if the antenna is placed in a straight line, parasitic conductors and dielectric loading by nearby wood structures can affect the impedance. Trap and loaded dipoles are shorter than the full-sized versions, but are comparable performers. Trap dipoles are discussed in Chapter 7, Multiband Antennas, and loaded dipoles in Chapter 6, Low-Frequency Antennas.

Dipole Orientation

Theoretically a vertical dipole is most effective at low radiation angles, but practical experience shows that the horizontal dipole is usually a better indoor antenna. A high horizontal dipole does exhibit directional effects at low radiation angles, but you will not be likely to see much, if any, directivity with an attic-mounted dipole. Some operators place two dipoles at right angles to each other with provisions at the operating position for switching between the two. Their reasoning is the radiation patterns will inevitably be distorted in an unpredictable manner by nearby parasitic conductors. There will be little coupling between the dipoles if they are oriented a right

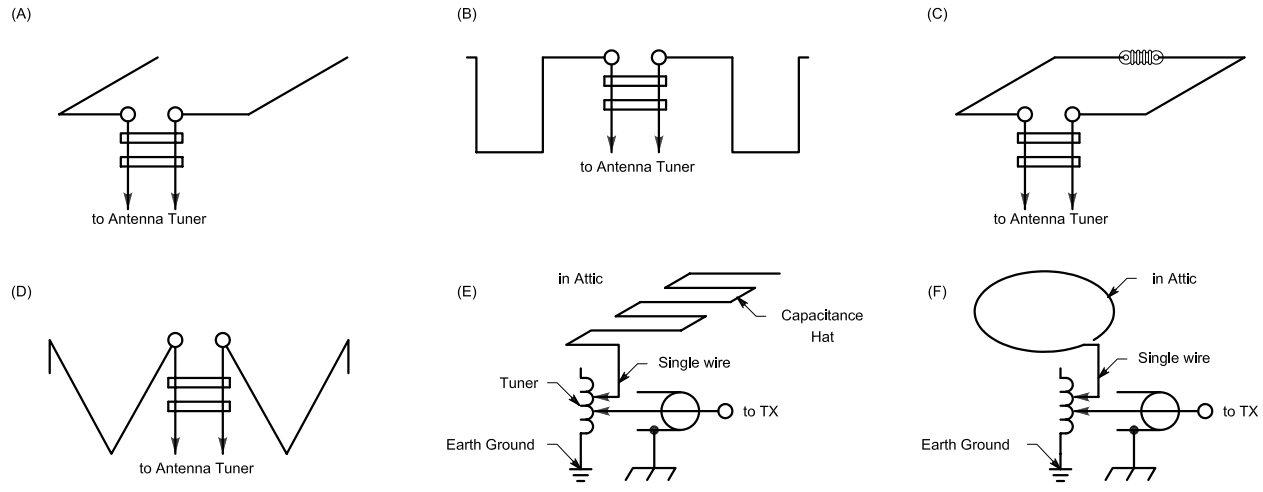

Fig 32—Various configurations for small indoor antennas. See text for discussion.

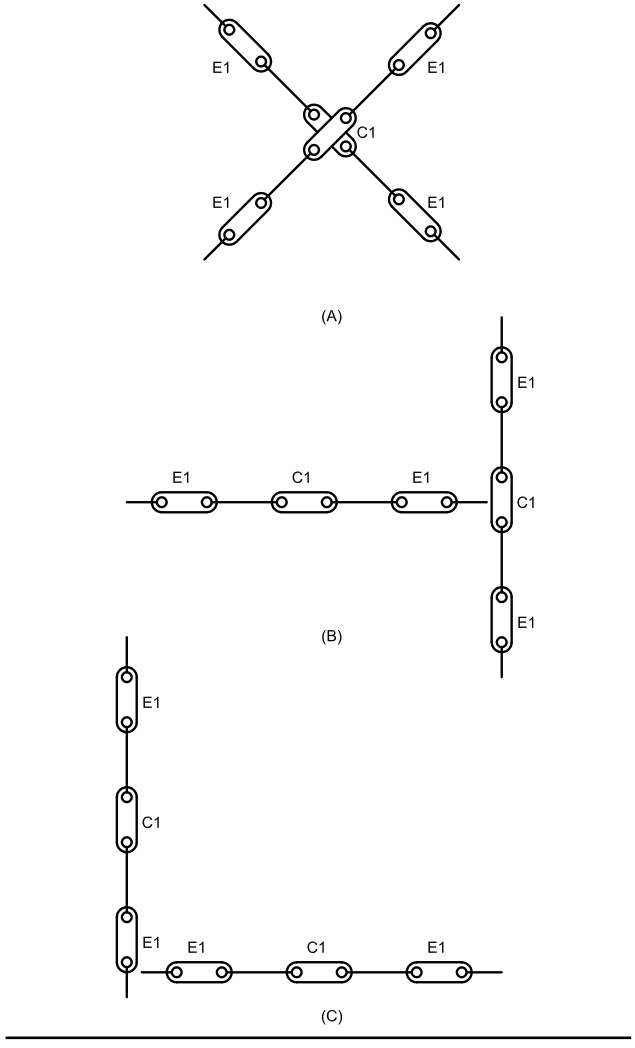

angles to each other as shown in **Figs 33A** and 33B. There will be some coupling with the arrangement shown in Fig 33C, but even this orientation is preferable to a single dipole.

With two antennas mounted 90° apart, you may find that one dipole is consistently better in nearly all directions, in which case you will want to remove the inferior dipole, perhaps placing it someplace else. In this manner the best spots in the house or attic can be determined experimentally.

Parasitic Conductors

Inevitably, any conductor in your house near a quarter wave in length or longer at the operating frequency will be parasitically coupled to your antenna. The word *parasitic* is particularly appropriate in this case because these conductors usually introduce losses and leave less energy for radiation into space. Unlike the parasitic elements in a beam antenna, conductors such as house wiring and plumbing are usually connected to lossy objects such as earth, electrical appliances, masonry or other objects that dissipate energy. Even where this energy is reradiated, it is not likely to be in the right phase in the desired direction; it is, in fact, likely to be a source of RFI.

Fig 33—Ways to orient a pair of perpendicular dipoles. The orientation at A and B will result in no mutual coupling between the two dipoles, but there will be some coupling in the configuration shown at C. End (EI) and center (CI) insulators are shown.

There are, however, some things that can be done about parasitic conductors. The most obvious is to reroute them at right angles to the antenna or close to the ground, or even underground—procedures that are usually not feasible in a finished home. Where these conductors cannot be rerouted, other measures can be taken. Electrical wiring can be broken up with RF chokes to prevent the flow of radio-frequency currents while permitting 60-Hz current (or audio, in the case of telephone wires) to flow unimpeded. A typical RF choke for a power line can be 100 turns of #10 insulated wire close wound on a length of 1-inch diameter plastic pipe. Of course one choke will be needed for each conductor. A three-wire line calls for three chokes. The chokes can be simplified by winding them bifilar or trifilar on a single coil form.

THE RESONANT BREAKER

Obviously, RF chokes cannot be used on conductors such as metal conduit or water pipes. But it is still possible, surprising as it may seem, to obstruct RF currents on such conductors without breaking the metal. The resonant breaker was first described by Fred Brown, W6HPH, in Oct 1979 *QST*.

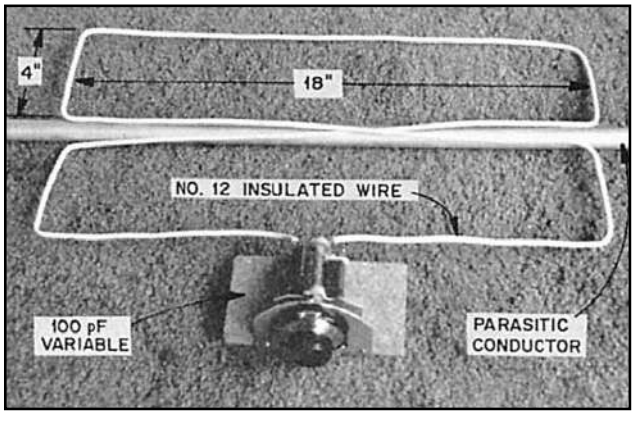

Fig 34—A "resonant breaker" such as shown here can be used to obstruct radio-frequency currents in a conductor without the need to break the conductor physically. A vernier dial is recommended for use with the variable capacitor because tuning is quite sharp. The 100-pF capacitor is in series with the loop. This resonant breaker tunes from 14 through 29.7 MHz. Larger models may be constructed for the lower frequency bands.

Fig 34 shows a method of accomplishing this. A figure-eight loop is inductively coupled to the parasitic conductor and is resonated to the desired frequency with a variable capacitor. The result is a very high impedance induced in series with the pipe, conduit or wire. This impedance will block the flow of radio-frequency currents. The figure-eight coil can be thought of as two turns of an air-core toroid and since the parasitic conductor threads through the hole of this core, there will be tight coupling between the two. Inasmuch as the figure-eight coil is parallel resonated, transformer action will reflect a high impedance in series with the linear conductor.

Before you bother with a *resonant breaker* of this type, be sure that there is a significant amount of RF current flowing in the parasitic conductor, and that you will therefore benefit from installing one. The relative magnitude of this current can be determined with an RF current probe of the type described in Chapter 27, Antenna and Transmission-Line Measurements. According to the rule of thumb regarding parasitic conductor current, if it measures less than $^1/_{10}$ of that measured near the center of the dipole, the parasitic current is generally not large enough to be of concern.

The current probe is also needed for resonating the breaker after it is installed. Normally, the resonant breaker will be placed on the parasitic conductor near the point of maximum current. When it is tuned through resonance, there will be a sharp dip in RF current, as indicated by the current probe. Of course, the resonant breaker will be effective only on one band. You will need one for each band where there is significant current indicated by the probe.

Power-Handling Capability

So far, our discussion have not considered the full power-handling capability of an indoor antenna. Any tendency to flash over must be determined by running full power or, preferably, somewhat more than the peak power you intend to use in regular operation. The antenna should be carefully checked for arcing or RF heating before you do any operating. Bear in mind that attics are indeed vulnerable to fire hazards. A potential of several hundred volts exists at the ends of a dipole fed by the typical Amateur Radio transmitter. If a power amplifier is used, there could be a few thousand volts at the ends of the dipole. Keep your antenna elements well away from other objects. *Safety first*!

Construction Details and Practical Considerations

Ultimately the success of an antenna project depends on the details of how the antenna is fabricated. A great deal of construction information is given in other chapters of this book. For example the construction of HF Yagis is discussed in Chapter 11, Quad arrays in Chapter 12, VHF antennas in Chapter 18, and in Chapter 20 there is an excellent discussion of antenna materials, particularly wire and tubing for elements. Here is still more helpful antenna construction information.

END EFFECT

If the standard expression $\lambda/2 \approx 491.8/f$ (MHz) is used for the length of a $\lambda/2$ wire antenna, the antenna will resonate at a somewhat lower frequency than is desired. The reason is that in addition to the effect of the conductor diameter and ground effects (Chapter 3, The Effects of Ground) an additional "loading" effect is caused by the insulators used at the ends of the wires to support the antenna. The insulators and the wire loops that tie the insulators to the antenna add a small amount of capacitance to the system. This capacitance helps to tune the antenna to a slightly lower frequency, in much the same way that additional capacitance in any tuned circuit lowers the resonant frequency. In an antenna this is called *end effect*. The current at the ends of the antenna does not quite reach zero because of the end effect, as there is some current flowing into the end capacitance. Note that the computations used to create Figs 2 through 7 in Chapter 2, Antenna Fundamentals, did not take into account any end effect.

End effect increases with frequency and varies slightly with different installations. However, at frequencies up to 30 MHz (the frequency range over which wire antennas are most commonly used), experience shows that the length of a practical $\lambda/2$ antenna, including the effect of diameter and end effect, is on the order of 5% less than the length of a half wave in space. As an average, then, the physical length of a resonant $\lambda/2$ wire antenna can be found from:

$$\lambda = \frac{491.8 \times 0.95}{\text{f (MHz)}} \approx \frac{468}{\text{f (MHz)}} \qquad \text{(Eq 1)}$$

Eq 1 is reasonably accurate for finding the physical length of a $\lambda/2$ antenna for a given frequency, but does not apply to antennas longer than a half wave in length. In the practical case, if the antenna length must be adjusted to exact frequency (not all antenna systems require it) the length should be "pruned" to resonance. Note that the use of plastic-insulated wire will typically lower the resonant frequency of a half-wave dipole about 3%.

INSULATORS

Wire antennas must be insulated at the ends. Commercially available insulators are made from ceramic, glass or plastic. Insulators are available from many Amateur Radio dealers. RadioShack and local hardware stores are other possible sources. Acceptable homemade insulators may be fashioned from a variety of material including (but not limited to) acrylic sheet or rod, PVC tubing, wood, fiberglass rod or even stiff plastic from a discarded container. **Fig 35** shows some homemade insulators. Ceramic or glass insulators will usually outlast the wire, so they are highly recommended for a safe, reliable, permanent installation. Other materials may tear under stress or break down in the presence of sunlight. Many types of plastic do not weather well.

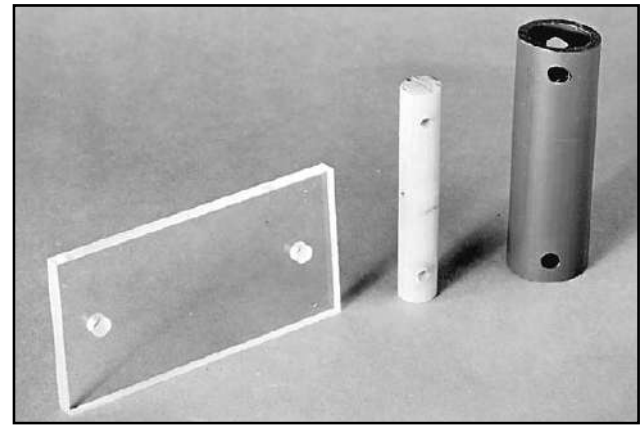

Fig 35—Some ideas for homemade antenna insulators.

INSTALLING TRANSMISSION LINES

Many wire antennas require an insulator at the feed point. Although there are many ways to connect the feed line, there are a few things to keep in mind. If you feed your antenna with coaxial cable, you have two choices. You can install an SO-239 connector on the center insu-

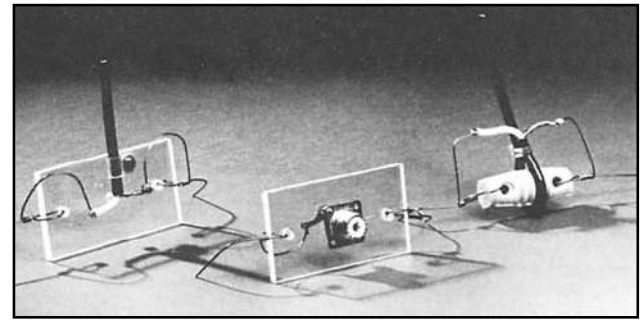

Fig 36—Some homemade dipole center insulators. The one in the center includes a built-in SO-239 connector. Others are designed for direct connection to the feed line.

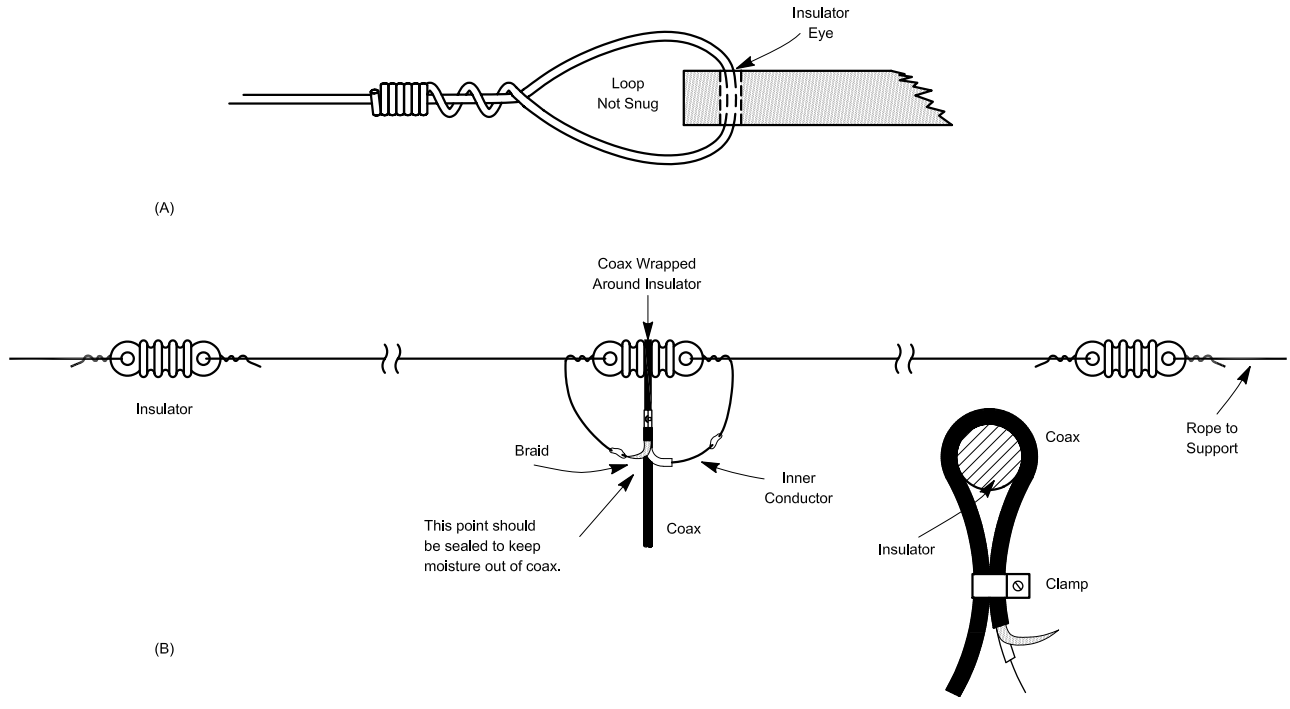

Fig 37—Details of dipole antenna construction. At A, the end insulator connection is shown. At B, the completed antenna is shown. A balun (not shown) is often used at the feed point, since this is a balanced antenna.

lator, as shown by the center example in **Fig 36,** and use a PL-259 on the end of your coax, or you can separate the center conductor from the braid and connect the feed line directly to the antenna wire as shown in the other two examples in Fig 36 and the example in **Fig 37**. Although it costs less to connect direct, the use of connectors offers several advantages. Coaxial cable braid soaks up water like a sponge unless it is very well waterproofed. If you do not adequately seal the antenna end of the feed line, water will find its way into the braid. Water in the feed line will lead to contamination, rendering the coax useless long before its normal lifetime is up. Many hams waterproof the coax, first with vinyl electrical tape, and then using a paint-on material called "PlastiDip," which is sold by RadioShack (part number 910-5166 for the white variety).

It is not uncommon for water to drip from the end of the coax inside the shack after a year or so of service if the antenna connection is not properly waterproofed. Use of a PL-259/SO-239 combination (or connector of your choice) makes the task of waterproofing connections much easier. Another advantage to using the PL-259/SO-239 combination is that feed-line replacement is much easier, should that become necessary.

Whether you use coaxial cable, ladder line, or twin lead to feed your antenna, an often overlooked consideration is the mechanical strength of the connection. Wire antennas and feed lines tend to move a lot in the breeze, and

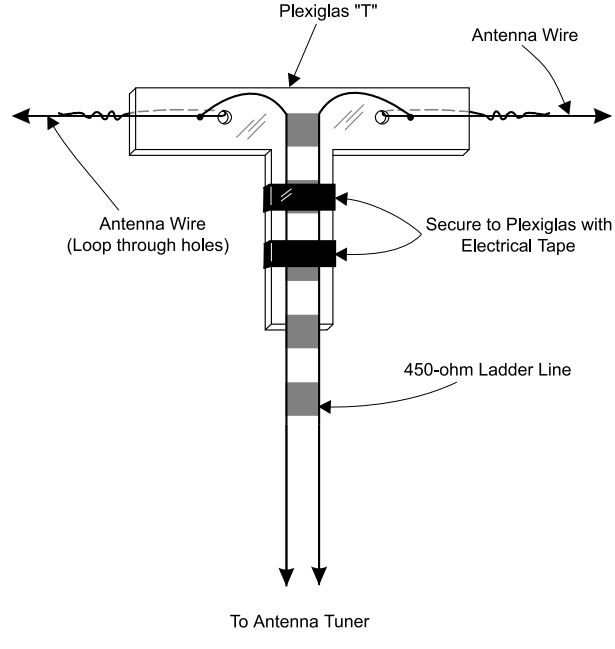

Fig 38—A piece of cut Plexiglas can be used as a center insulator and to support a ladder-line feeder. The Plexiglas acts to reduce the flexing of the wires where they connect to the antenna. Use thick Plexiglas in areas subject to high winds.

unless the feed line is attached securely, the connection will weaken with time. The resulting failure can range from a frustrating intermittent electrical connection to a complete separation of feed line and antenna. Fig 37 and **Fig 38** illustrate different ways of attaching either coax or ladder line to the antenna securely.

When open-wire feed line is used, the conductors of the line should be anchored to the insulator by threading them through the eyes of the insulator two or three times, and twisting the wire back on itself before soldering. A slack tie wire should then be used between the feeder conductor and the antenna, as shown in Fig 38. (The tie wires may be extensions of the line conductors themselves.) When window-type line is suspended from an antenna in a manner such as that shown in Fig 38, the line should be twisted—at several twists per foot—to prevent stress hardening of the wire because of constant flexing in the wind.

When using plastic-insulated open-wire line, the tendency of the line to twist and short out close to the antenna can be counteracted by making the center insulator of the antenna longer than the spacing of the line, as shown in Fig 38. In severe wind areas, it may be necessary to use ¼-inch thick Plexiglas for the center insulator rather than thinner material.

RUNNING THE FEED LINE FROM THE ANTENNA TO THE STATION

Chapter 24, Transmission Lines, contains some general guidelines for installing feed lines. More detailed information is contained in this section. Whenever possible, the transmission line should be lead away from the antenna at a 90° angle to minimize coupling from the antenna to the transmission line. This coupling can cause unequal currents on the transmission line, which will then radiate and it can detune the antenna.

Except for the portion of the line in close proximity to the antenna, coaxial cable requires no particular care in running from the antenna to the station entrance, other than protection from mechanical damage. If the antenna is not supported at the center, the line should be fastened to a post more than head high located under the center of the antenna, allowing enough slack between the post and the antenna to take care of any movement of the antenna in the wind. If the antenna feed point is supported by a tower or mast, the cable can be taped to the mast at intervals or to one leg of the tower.

Coaxial cable rated for direct burial can be buried a few inches in the ground to make the run from the antenna to the station. A deep slit can be cut by pushing a square-end spade full depth into the ground and moving the handle back and forth to widen the slit before removing the spade. After the cable has been pushed into the slit with a piece of 1-inch board 3 or 4 inches wide, the slit can be tamped closed. Many hams run coax cables through PVC pipe buried in the ground deeper than the frost line

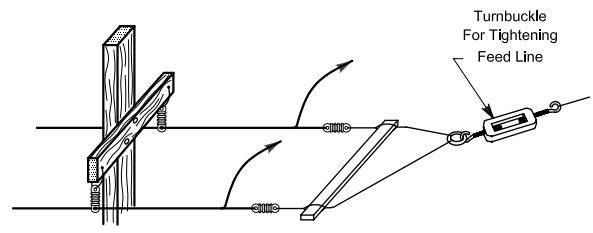

Fig 39—A support for open-wire line. The support at the antenna end of the line must be sufficiently rigid to stand the tension of the line.

and slanted downwards slightly so that water will drain, rather than pooling inside the length of the pipe.

Solid ribbon or the newer *window* types of line should be kept reasonably well spaced from other conductors running parallel to it for more than a few feet. TV-type standoff insulators with strap clamp mountings can be used for running this type of line down a mast or tower leg. Similar insulators of the screw-in type can be used in supporting the line on wooden poles for a long run.

Open-wire lines with bare conductors require frequent supports to keep the lines from twisting and shorting out, as well as to relieve the mechanical strain. One method of supporting a long horizontal run of heavy open-wire line is shown in **Fig 39**. The line must be anchored securely at a point under the feed point of the antenna. Window-type line can be supported similarly with wire links fastened to the insulators or with black cable ties (ones not affected by UV radiation from the sun).

To keep the line clear of pedestrians and vehicles, it is usually desirable to anchor the feed line at the eaves or rafter line of the station building (see **Fig 40**), and then drop it vertically to the point of entrance. The points of anchorage and entrance should be chosen to permit the vertical drop without crossing windows for aesthetic reasons.

If the station is located in a room on the ground floor, one way of bringing coax transmission line into the house is to go through the outside wall below floor level, feed it through the basement or crawl space and then up to the station through a hole in the floor. When making the entrance hole in the side of the building, suitable measurements should be made in advance to be sure the hole will go through the sill 2 or 3 inches above the foundation line (and between joists if the bore is parallel to the joists). The line should be allowed to sag below the entrance hole level outside the building to allow rain water to drip off.

Open-wire line can be fed in a similar manner, although it will require a separate hole for each conductor. Each hole should be insulated with a length of polystyrene or Lucite tubing. If available, ceramic tubes salvaged from old-fashioned *knob and tube* electrical

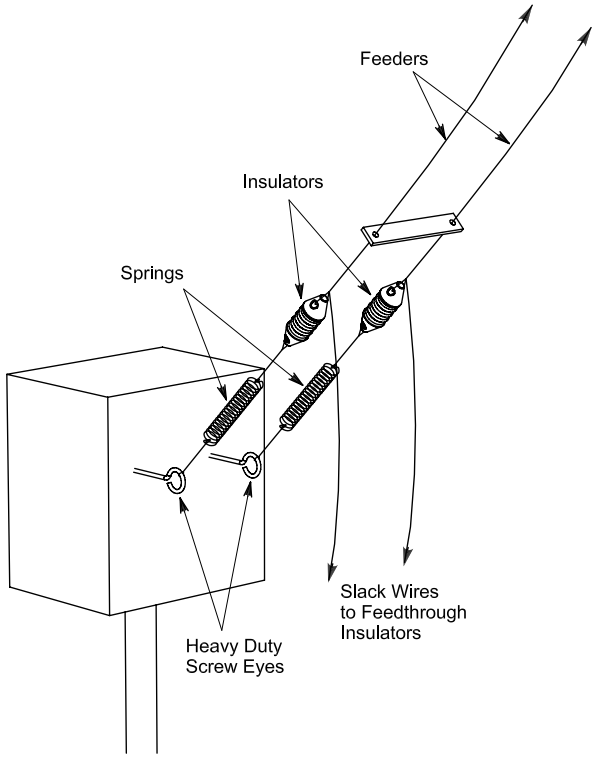

Fig 40—Anchoring open-wire line at the station end. The springs are especially desirable if the line is not supported between the antenna and the anchoring point.

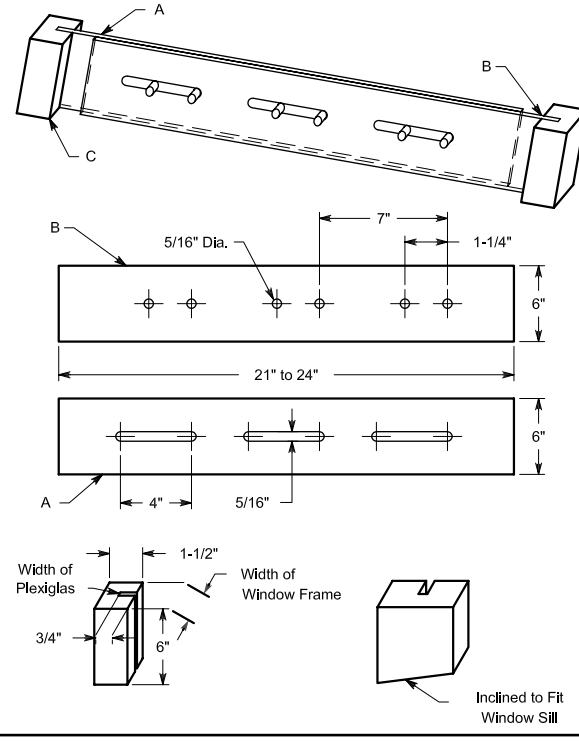

Fig 41—An adjustable window lead-in panel made up of two sheets of Lucite or Plexiglas. A feedthrough connector for coax line can be made as shown in Fig 28. Ceramic feedthrough insulators are suitable for open-wire line. (W1RVE)

installations, work very well for this purpose. Drill the holes with a slight downward slant toward the outside of the building to prevent rain seepage. With window ladder line, it will be necessary to remove a few of the spreader insulators, cut the line before passing through the holes (allowing enough length to reach the inside) and splice the remainder on the inside.

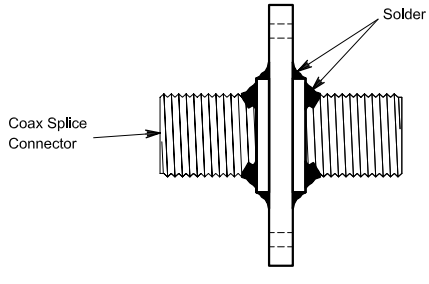

Fig 42—Feedthrough connector for coax line. An Amphenol 83-1J (PL-258) connector, the type used to splice sections of coax line together, is soldered into a hole cut in a brass mounting flange. An Amphenol bulkhead adapter 83-1F may be used instead.

If the station is located above ground level, or if there is other objection to the procedure described above, entrance can be made at a window, using the arrangement shown in **Fig 41**. An Amphenol type 83-1F (UG-363) connector can be used as shown in **Fig 42**; ceramic feedthrough insulators can be used for open-wire line. Ribbon line can be run through clearance holes in the panel, and secured by a winding of tape on either side of the panel, or by cutting the retaining rings and insulators from a pair of TV standoff insulators and clamping one on each side of the panel.

LIGHTNING PROTECTION

Two or three types of lightning arresters for coaxial cable are available on the market. If the antenna feed point is at the top of a well-grounded tower, the arrester can be fastened securely to the top of the tower for grounding purposes. A short length of cable, terminated in a coaxial plug, is then run from the antenna feed point to one receptacle of the arrester, while the transmission line is run from the other arrester receptacle to the station. Such arresters may also be placed at the entrance point to the station, if a suitable ground connection is available at that point (or arresters may be placed at both points for added insurance).

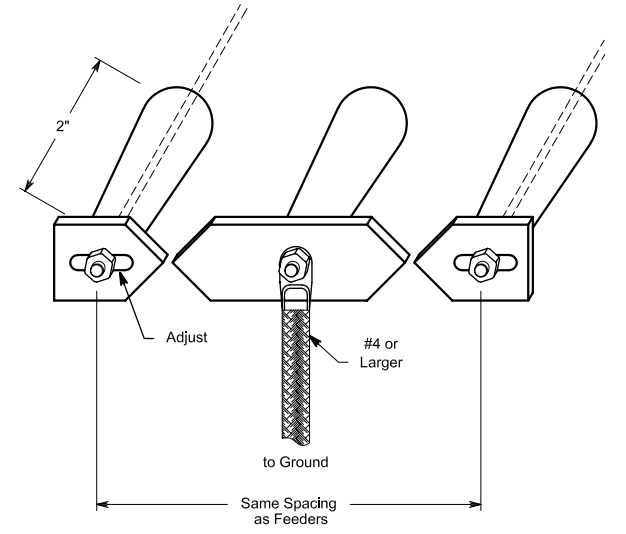

Fig 43—A simple lightning arrester for open-wire line made from three standoff or feedthrough insulators and sections of 1/8 × 1/2-inch brass or copper strap. It should be installed in the line at the point where the line enters the station. The heavy ground lead should be as short and as direct as possible. The gap setting should be adjusted to the minimum width that will prohibit arcing when the transmitter is operated.

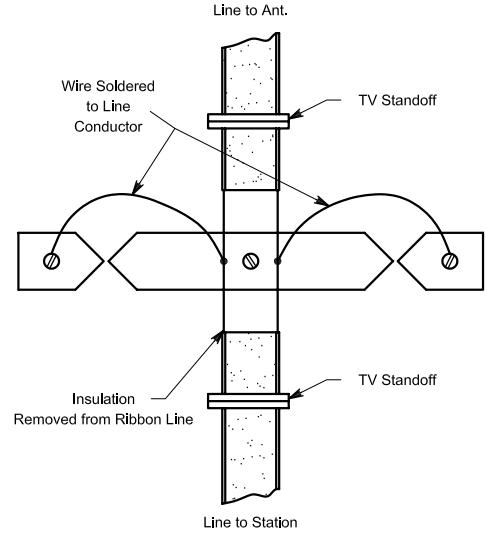

Fig 44—The lightning arrester of Fig 39 may be used with 300-Ω ribbon line in the manner shown here. The TV standoffs support the line an inch or so away from the grounded center member of the arrester

The construction of a homemade arrester for open-wire line is shown in **Fig 43**. This type of arrester can be adapted to ribbon line an inch or so away from the center member of the arrester, as shown in **Fig 44**. Sufficient insulation should be removed from the line where it crosses the arrester to permit soldering the arrester connecting leads.

Lightning Grounds

Lightning-ground connecting leads should be of conductor size equivalent to at least #10 wire. The #8 aluminum wire used for TV-antenna grounds is satisfactory. Copper braid 3/4-inch wide (Belden 8662-10) is also suitable. The conductor should run in a straight line to the grounding point. The ground connection may be made to a water pipe system (if the pipe is not plastic), the grounded metal frame of a building, or to one or more 5/8-inch ground rods driven to a depth of at least 8 feet. More detailed information on lightning protection is contained in Chapter 1, Safety.

A central grounding panel for coax cables coming into the house is highly recommended. See **Fig 45** for a photo of the homemade grounding panel installed by Chuck Hutchinson, K8CH, at his Michigan home. The coax cables screwed into dual-female feed-through UHF connectors. K8CH installed this aluminum panel under the outside grill for a duct that provided combustion air to an unused fireplace. He used ground strap to connect to ground rods located under the panel. See the ARRL book *Simple and Fun Antennas* for more information about ground panels.

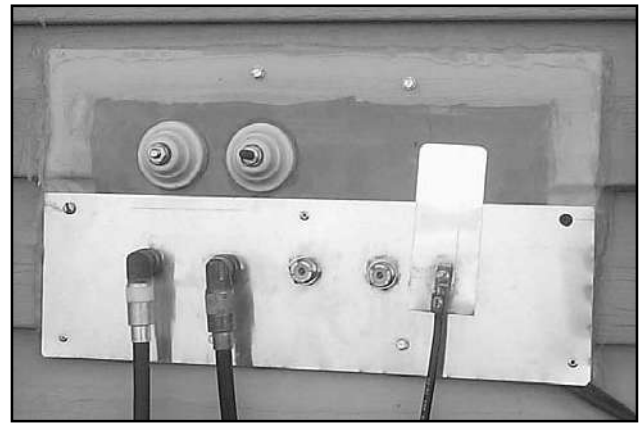

Fig 45—K8CH's coax entry panel mounted on exterior wall (later covered by grill that provides combustion to an unused fireplace). The ground braid goes to a ground rod located beneath the panel. (Photo courtesy: *Simple and Fun Antennas for Hams*)

Before a lightning storm approaches, a prudent ham will disconnect all feed lines, rotor lines and control lines inside the shack to prevent damage to sensitive electronics. When lightning is crashing about outside, you certainly don't want that lightning inside your shack!

Chapter 5

Loop Antennas

A loop antenna is a closed-circuit antenna—that is, one in which a conductor is formed into one or more turns so its two ends are close together. Loops can be divided into two general classes, those in which both the total conductor length and the maximum linear dimension of a turn are very small compared with the wavelength, and those in which both the conductor length and the loop dimensions begin to be comparable with the wavelength.

A "small" loop can be considered to be simply a rather large coil, and the current distribution in such a loop is the same as in a coil. That is, the current has the same phase and the same amplitude in every part of the loop. To meet this condition, the total length of conductor in the loop must not exceed about 0.1 λ. Small loops are discussed later in this chapter, and further in Chapter 14, Direction Finding Antennas.

A "large" loop is one in which the current is not the same either in amplitude or phase in every part of the loop. This change in current distribution gives rise to entirely different properties compared with a small loop.

Half-Wave Loops

The smallest size of "large" loop generally used is one having a conductor length of $^1/_2$ λ. The conductor is usually formed into a square, as shown in **Fig 1**, making each side $^1/_8$ λ long. When fed at the center of one side, the current flows in a closed loop as shown in Fig 1A. The current distribution is approximately the same as on a $^1/_2$ λ wire, and so is maximum at the center of the side opposite the terminals X-Y, and minimum at the terminals themselves. This current distribution causes the field strength to be maximum in the plane of the loop and in the direction looking from the low-current side to the high-current side. If the side opposite the terminals is opened at the center as shown in Fig 1B (strictly speaking, it is then no longer a loop because it is no longer a closed circuit), the direction of current flow remains unchanged but the maximum current flow occurs at the terminals. This reverses the direction of maximum radiation.

The radiation resistance at a current antinode (which is also the resistance at X-Y in Fig 1B) is on the order of 50 Ω. The impedance at the terminals in Fig 1A is a few thousand ohms. This can be reduced by using two identical loops side by side with a few inches spacing between them and applying power between terminal X on one loop and terminal Y on the other.

Unlike a $^1/_2$ λ dipole or a small loop, there is no direction in which the radiation from a loop of the type shown in Fig 1 is zero. There is appreciable radiation in the direction perpendicular to the plane of the loop, as well as to the "rear"—the opposite direction to the arrows shown. The front-to-back (F/B) ratio is approximately 4 to 6 dB. The small size and the shape of the directive pattern result in a loss of about 1 dB when the field strength in the optimum direction from such a

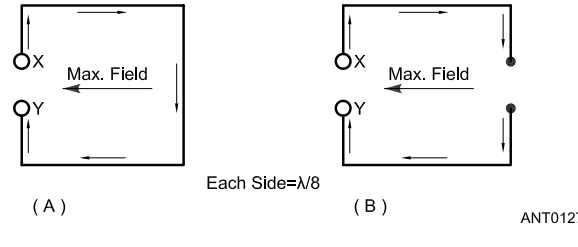

Fig 1—Half-wave loops, consisting of a single turn having a total length of $^1/_2$ λ.

loop is compared with the field from a $^1/_2$ λ dipole in its optimum direction.

The ratio of the forward radiation to the backward radiation can be increased, and the field strength likewise increased at the same time to give a gain of about 1 dB over a dipole, by using inductive reactances to "load" the sides joining the front and back of the loop. This is shown in **Fig 2**. The reactances, which should have a value of approximately 360 Ω, decrease the current in the sides in which they are inserted and increase it in the side having terminals. This increases the directivity and thus increases the efficiency of the loop as a radiator. Lossy coils can reduce this advantage greatly.

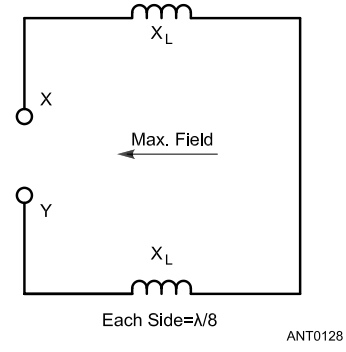

Fig 2—Inductive loading in the sides of a $^1/_2$-λ loop to increase the directivity and gain. Maximum radiation or response is in the plane of the loop, in the direction shown by the arrow.

One-Wavelength Loops

Loops in which the conductor length is 1 λ have different characteristics than $^1/_2$-λ loops. Three forms of 1 λ loops are shown in **Fig 3**. At A and B the sides of the squares are equal to $^1/_4$ λ, the difference being in the point at which the terminals are inserted. At C the sides of the triangle are equal to $^1/_3$ λ. The relative direction of current flow is as shown in the drawings. This direction reverses halfway around the perimeter of the loop, as such reversals always occur at the junction of each $^1/_2$-λ section of wire.

The directional characteristics of loops of this type are opposite in sense to those of a small loop. That is, the radiation is maximum perpendicular to the plane of the loop and is minimum in either direction in the plane containing the loop. If the three loops shown in Fig 3 are mounted in a vertical plane with the terminals at the bottom, the radiation is horizontally polarized. When the terminals are moved to the center of one vertical side in Fig 3A, or to a side corner in B, the radiation is vertically polarized. If the terminals are moved to a side corner in C, the polarization will be diagonal, containing both vertical and horizontal components.

In contrast to straight-wire antennas, the electrical length of the circumference of a 1-λ loop is shorter than the actual length. For a loop made of bare #18 wire and operating at a frequency of 14 MHz, where the ratio of conductor length to wire diameter is large, the loop will be close to resonance when

$$\text{Length}_{\text{feet}} = \frac{1032}{f_{\text{MHz}}}$$

The radiation resistance of a resonant 1 λ loop is approximately 120 Ω, under these conditions. Since the loop dimensions are larger than those of a $^1/_2$-λ dipole, the radiation efficiency is high.

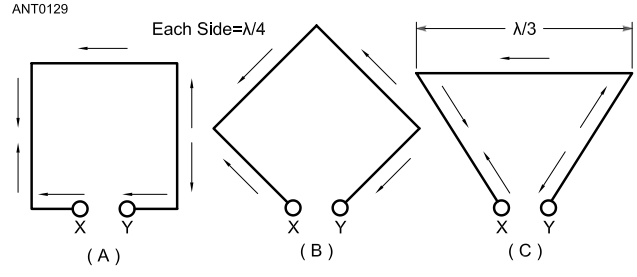

Fig 3—At A and B, loops having sides $^1/_4$ λ long, and at C having sides $^1/_3$ λ long (total conductor length 1 λ). The polarization depends on the orientation of the loop and on the position of the feed point (terminals X-Y) around the perimeter of the loop.

In the direction of maximum radiation (that is, broadside to the plane of the loop, regardless of the point at which it is fed) the 1-λ loop will show a small gain over a $^1/_2$-λ dipole. Theoretically, this gain is about 1 dB, and measurements have confirmed that it is of this order.

The 1-λ loop is more frequently used as an element of a directive antenna array (the quad and delta-loop antennas described in Chapter 12, Quad Arrays) than singly, although there is no reason why it cannot be used alone. In the quad and delta loop, it is nearly always driven so that the polarization is horizontal.

Small Loop Antennas

The electrically small loop antenna has existed in various forms for many years. Probably the most familiar form of this antenna is the ferrite *loopstick* found in portable AM broadcast-band receivers. Amateur applications of the small loop include direction finding, low-noise directional receiving antennas for 1.8 and 3.5 MHz, and small transmitting antennas. Because the design of transmitting and receiving loops requires some different considerations, the two situations are examined separately in this section. This information was written by Domenic M. Mallozzi, N1DM.

The Basic Loop

What is and what is not a small loop antenna? By definition, the loop is considered to be electrically small when its total conductor length is less than 0.1 λ—0.085 is the number used in this section. This size is based on the fact that the current around the perimeter of the loop must be in phase. When the winding conductor is more than about 0.085 λ long, this is no longer true. This constraint results in a very predictable figure-eight radiation pattern, shown in **Fig 4**.

The simplest loop is a 1-turn untuned loop with a load connected to a pair of terminals located in the center of one of the sides, as shown in **Fig 5**. How its pattern is developed is easily pictured if we look at some "snapshots" of the antenna relative to a signal source. **Fig 6** represents a loop from above, and shows the instantaneous radiated voltage wave. Note that points A and B of the loop are receiving the same instantaneous voltage. This means that no current will flow through the loop, because there is no current flow between points of equal potential. A similar analysis of **Fig 7**, with the loop turned 90° from the position represented in Fig 6, shows that this position of the loop provides maximum response. Of course, the voltage derived from the passing wave is small because of the small physical size of the loop. Fig 4 shows the ideal radiation pattern for a small loop.

The voltage across the loop terminals is given by

$$V = \frac{2\,\pi A\,N\,E\,\cos\theta}{\lambda} \qquad \text{(Eq 1)}$$

where

V = voltage across the loop terminals
A = area of loop in square meters
N = number of turns in the loop
E = RF field strength in volts per meter
θ = angle between the plane of the loop and the signal source (transmitting station)
λ = wavelength of operation in meters

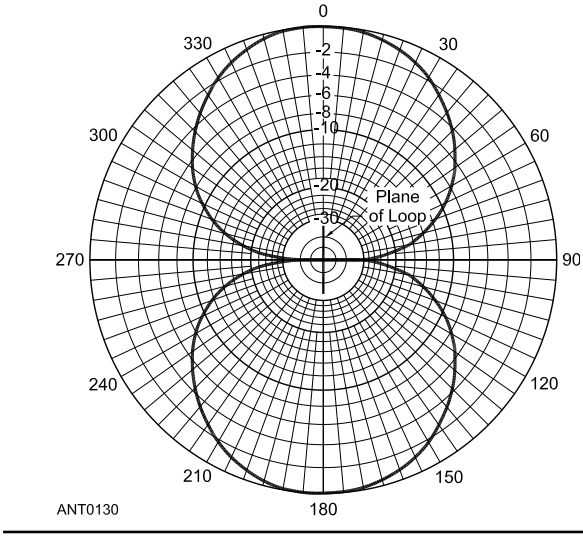

Fig 4—Calculated small loop antenna radiation pattern.

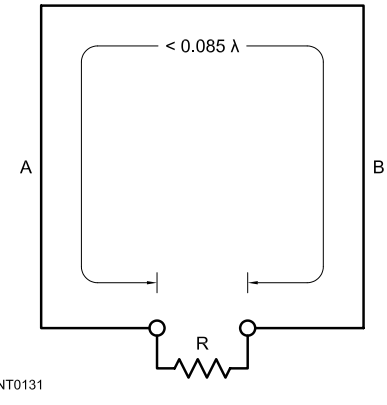

Fig 5—Simple untuned small loop antenna.

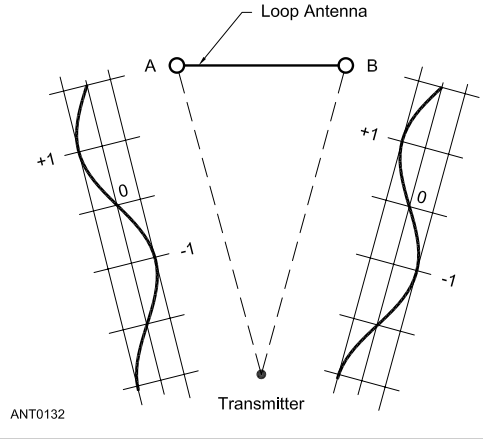

Fig 6—Example of orientation of loop antenna that does not respond to a signal source (null in pattern).

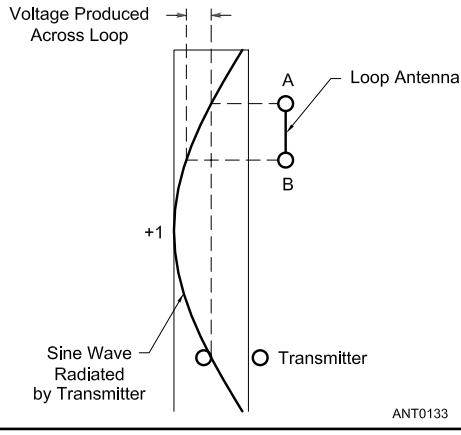

Fig 7—Example of orientation of loop antenna for maximum response.

This equation comes from a term called *effective height*. The effective height refers to the height (length) of a vertical piece of wire above ground that would deliver the same voltage to the receiver. The equation for effective height is

$$h = \frac{2\pi N A}{\lambda} \qquad \text{(Eq 2)}$$

where h is in meters and the other terms are as for Eq 1.

A few minutes with a calculator will show that, with the constraints previously stated, the loop antenna will have a very small effective height. This means it will deliver a relatively small voltage to the receiver, even with a large transmitted signal.

TUNED LOOPS

We can tune the loop by placing a capacitor across the antenna terminals. This causes a larger voltage to appear across the loop terminals because of the Q of the parallel resonant circuit that is formed.

The voltage across the loop terminals is now given by

$$V = \frac{2\pi A N E Q \cos\theta}{\lambda} \qquad \text{(Eq 3)}$$

where Q is the loaded Q of the tuned circuit, and the other terms are as defined above.

Most amateur loops are of the tuned variety. For this reason, all comments that follow are based on tuned-loop antennas, consisting of one or more turns. The tuned-loop antenna has some particular advantages. For example, it puts high selectivity up at the "front" of a receiving system, where it can significantly help factors such as dynamic range. Loaded Q values of 100 or greater are easy to obtain with careful loop construction.

Consider a situation where the inherent selectivity of the loop is helpful. Assume we have a loop with a Q of 100 at 1.805 MHz. We are working a DX station on 1.805 MHz and are suffering strong interference from a local station 10 kHz away. Switching from a dipole to a small loop will reduce the strength of the off-frequency signal by 6 dB (approximately one S unit). This, in effect, increases the dynamic range of the receiver. In fact, if the off-frequency station were further off frequency, the attenuation would be greater.

Another way the loop can help is by using the nulls in its pattern to null out on-frequency (or slightly off-frequency) interference. For example, say we are working a DX station to the north, and just 1 kHz away is another local station engaged in a contact. The local station is to our west. We can simply rotate our loop to put its null to the west, and now the DX station should be readable while the local will be knocked down by 60 or more dB. This obviously is quite a noticeable difference. Loop nulls are very sharp and are generally noticeable only on ground-wave signals (more on this later).

Of course, this method of nulling will be effective only if the interfering station and the station being worked are not in the same direction (or in exact opposite directions) from our location. If the two stations were on the same line from our location, both the station being worked and the undesired station would be nulled out. Luckily the nulls are very sharp, so as long as the stations are at least 10° off axis from each other, the loop null will be usable.

A similar use of the nulling capability is to eliminate local noise interference, such as that from a light dimmer in a neighbor's house. Just put the null on the offending light dimmer, and the noise should disappear.

Now that we have seen some possible uses of the small loop, let us look at a bit of detail about its design. First, the loop forms an inductor having a very small ratio of winding length to diameter. The equations for finding inductance given in most radio handbooks assume that the inductor coil is longer than its diameter. However, F. W. Grover of the US National Bureau of Standards has provided equations for inductors of common cross-sectional shapes and small length-to-diameter ratios. (See the Bibliography at the end of this chapter.) Grover's equations are shown in **Table 1**. Their use will yield relatively accurate numbers; results are easily worked out with a scientific calculator or home computer.

The value of a tuning capacitor for a loop is easy to calculate from the standard resonance equations. The only matter to consider before calculating this is the value of distributed capacitance of the loop winding. This capacitance shows up between adjacent turns of the coil because of their slight difference in potential. This causes each turn to appear as a charge plate. As with all other capacitances, the value of the distributed capacitance is based on the physical dimensions of the coil. An exact mathematical analysis of its value is a complex problem. A simple approximation is given by Medhurst (see Bibliography) as:

$$C = HD \qquad \text{(Eq 4)}$$

where

C = distributed capacitance in pF

H = a constant related to the length-to-diameter ratio of the coil (**Table 2** gives H values for length-to-diameter ratios used in loop antenna work.)

D = diameter of the winding in cm

Medhurst's work was with coils of round cross section. For loops of square cross section the distributed capacitance is given by Bramslev (see Bibliography) as

$$C = 60S \qquad \text{(Eq 5)}$$

where

C = the distributed capacitance in pF

S = the length of the side in meters

If you convert the length in this equation to centimeters, you will find Bramslev's equation gives results in the same order of magnitude as Medhurst's equation.

This distributed capacitance appears as if it were a capacitor across the loop terminals. Therefore, when determining the value of the tuning capacitor, the distributed capacitance must be subtracted from the total capacitance required to resonate the loop. The distributed capacitance also determines the highest frequency at which a particular loop can be used, because it is the minimum capacitance obtainable.

Electrostatically Shielded Loops

Over the years, many loop antennas have incorporated an electrostatic shield. This shield generally takes the form of a tube around the winding, made of a conductive but nonmagnetic material (such as copper or aluminum). Its purpose is to maintain loop balance with respect to ground, by forcing the capacitance between all portions of the loop and ground to be identical. This is illustrated in **Fig 8**. It is necessary to maintain electrical loop balance to eliminate what is referred to as the *antenna effect*. When the antenna becomes unbalanced it appears to act partially as a small vertical antenna. This vertical pattern gets superimposed on the ideal figure-eight pattern, distorting the pattern and filling in the nulls. The type of pattern that results is shown in **Fig 9**.

Adding the shield has the effect of somewhat reducing the pickup of the loop, but this loss is generally offset by the increase in null depth of the loops. Proper balance of the loop antenna requires that the load on the loop also be balanced. This is usually accomplished by use of a balun transformer or a balanced input preamplifier. One important point regarding the shield is that it cannot form a continuous electrical path around the loop perimeter, or it will appear as a shorted coil turn. Usually the insulated break is located opposite the feed point to maintain symmetry. Another point to be considered is that the shield should be of a much larger diameter than the loop winding, or it will lower the Q of the loop.

Various construction techniques have been used in

Table 1
Inductance Equations for Short Coils (Loop Antennas)

Triangle:

$$L\,(\mu H) = 0.006N^2\,s \left[\ln\left(\frac{1.1547\,sN}{(N+1)\,\ell}\right) + 0.65533 + \frac{0.1348\,(N+1)\,\ell}{sN}\right]$$

Square:

$$L\,(\mu H) = 0.008N^2\,s \left[\ln\left(\frac{1.4142sN}{(N+1)\,\ell}\right) + 0.37942 + \frac{0.3333\,(N+1)\,\ell}{sN}\right]$$

Hexagon:

$$L\,(\mu H) = 0.012N^2\,s \left[\ln\left(\frac{2sN}{(N+1)\,\ell}\right) + 0.65533 + \frac{0.1348\,(N+1)\,\ell}{sN}\right]$$

Octagon:

$$L\,(\mu H) = 0.016N^2 \left[\ln\left(\frac{2.613sN}{(N+1)\,\ell}\right) + 0.75143 + \frac{0.07153\,(N+1)\,\ell}{sN}\right]$$

where

N = number of turns

s = side length in cm

ℓ = coil length in cm

Note: In the case of single-turn coils, the diameter of the conductor should be used for ℓ.

Table 2
Values of the Constant H for Distributed Capacitance

Length to Diameter Ratio	*H*
0.10	0.96
0.15	0.79
0.20	0.78
0.25	0.64
0.30	0.60
0.35	0.57
0.40	0.54
0.50	0.50
1.00	0.46

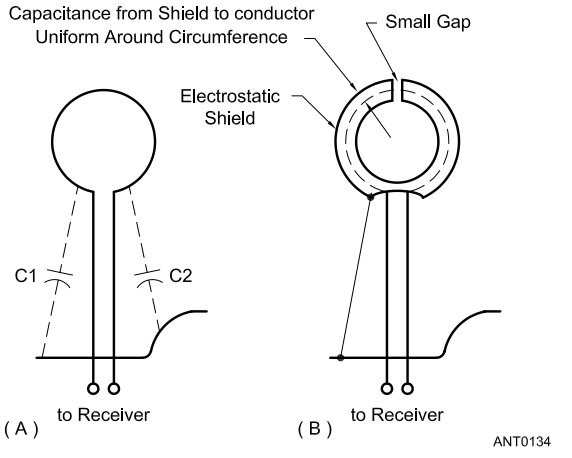

Fig 8—At A, the loop is unbalanced by capacitance to its surroundings. At B, the use of an electrostatic shield overcomes this effect.

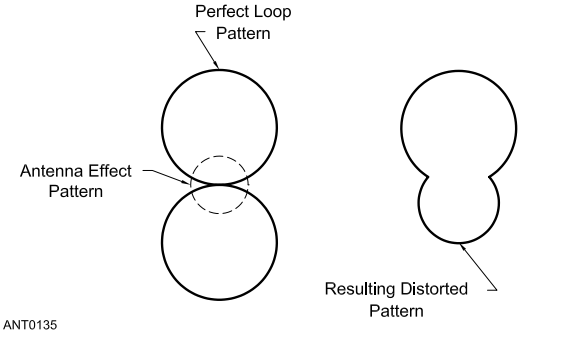

Fig 9—Distortion in loop pattern resulting from antenna effect.

making shielded loops. Genaille located his loop winding inside aluminum conduit, while True constructed an aluminum shield can around his winding. Others have used pieces of Hardline to form a loop, using the outer conductor as a shield. DeMaw used flexible coax with the shield broken at the center of the loop conductor in a multiturn loop for 1.8 MHz. Goldman uses another shielding method for broadcast receiver loops. His shield is in the form of a barrel made of hardware cloth, with the loop in its center. (See Bibliography for above references.) All these methods provide sufficient shielding to maintain the balance. It is possible, as Nelson shows, to construct an unshielded loop with good nulls (60 dB or better) by paying great care to symmetry.

LOOP Q

As previously mentioned, Q is an important consideration in loop performance because it determines both the loop bandwidth and its terminal voltage for a given field strength. The loaded Q of a loop is based on four major factors. These are (1) the intrinsic Q of the loop winding, (2) the effect of the load, (3) the effect of the electrostatic shield, and (4) the Q of the tuning capacitor.

The major factor is the Q of the winding of the loop itself. The ac resistance of the conductor caused by skin effect is the major consideration. The ac resistance for copper conductors may be determined from

$$R = \frac{0.996 \times 10^{-6} \sqrt{f}}{d} \qquad \text{(Eq 6)}$$

where

R = resistance in ohms per foot
f = frequency, Hz
d = conductor diameter, inches

The Q of the inductor is then easily determined by taking the reactance of the inductor and dividing it by the ac resistance. If you are using a multiturn loop and are a perfectionist, you might also want to include the loss from conductor proximity effect. This effect is described in detail later in this chapter, in the section on transmitting loops.

Improvement in Q can be obtained in some cases by the use of Litz wire (short for *Litzendraht*). Litz wire consists of strands of individual insulated wires that are woven into bundles in such a manner that each conductor occupies each location in the bundle with equal frequency. Litz wire results in improved Q over solid or stranded wire of equivalent size, up to about 3 MHz.

Also, the Q of the tuned circuit of the loop antenna is determined by the Q of the capacitors used to resonate it. In the case of air variables or dipped micas this is not usually a problem. But if variable-capacitance diodes are used to remotely tune the loop, pay particular attention to the manufacturer's specification for Q of the diode at the frequency of operation. The tuning diodes can have a significant effect on circuit Q.

Now we consider the effect of load impedance on loop Q. In the case of a directly coupled loop (as in Fig 5), the load is connected directly across the loop terminals, causing it to be treated as a parallel resistance in a parallel-tuned RLC circuit. Obviously, if the load is of a low value, the Q of the loop will be low. A simple way to correct this is to use a transformer to step up the load impedance that appears across the loop terminals. In fact, if we make this transformer a balun, it also allows us to use our unbalanced receivers with the loop and maintain loop symmetry. Another solution is to use what is referred to as an inductively coupled loop, such as DeMaw's four turn electrostatically shielded loop. A one-turn link is connected to the receiver. This turn is wound with the four-turn loop. In effect, this builds the transformer into the antenna.

Another solution to the problem of load impedance on loop Q is to use an active preamplifier with a high imped-

ance balanced input and unbalanced output. This method also has the advantage of amplifying the low-level output voltage of the loop to where it can be used with a receiver of even mediocre sensitivity. In fact, the Q of the loop when used with a balanced preamplifier having high input impedance may be so high as to be unusable in certain applications. An example of this situation would occur where a loop is being used to receive a 5 kHz wide AM signal at a frequency where the bandwidth of the loop is only 1.5 kHz. In this case the detected audio might be very distorted. The solution to this is to put a Q-degrading resistor across the loop terminals.

FERRITE-CORE LOOP ANTENNAS

The ferrite-core loop antenna is a special case of the air-core receiving loops considered up to now. Because of its use in every AM broadcast-band portable radio, the ferrite-core loop is, by quantity, the most popular form of the loop antenna. But broadcast-band reception is far from its only use; it is commonly found in radio-direction-finding equipment and low-frequency-receiving systems (below 500 kHz) for time and frequency standard systems. In recent years, design information on these types of antennas has been a bit sparse in the amateur literature, so the next few paragraphs are devoted to providing some details.

Ferrite-loop antennas are characteristically very small compared to the frequency of use. For example, a 3.5-MHz version may be in the range of 15 to 30 cm long and about 1.25 cm in diameter. Earlier in this chapter, effective height was introduced as a measure of loop sensitivity. The effective height of an air-core loop antenna is given by Eq 2.

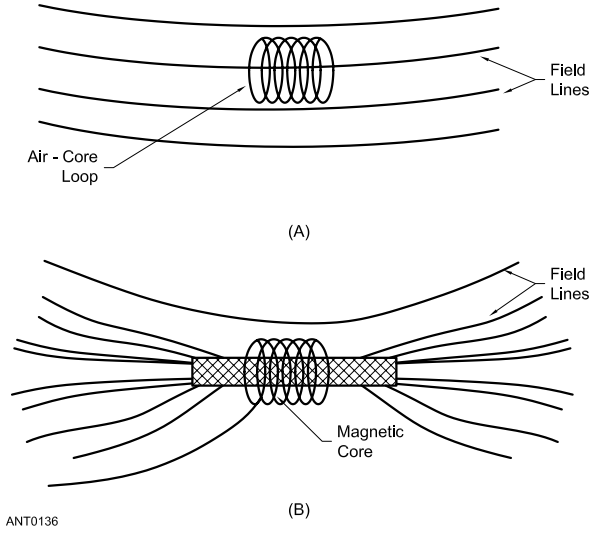

Fig 10—At A, an air-core loop has no effect on nearby field lines. B illustrates the effect of a ferrite core on nearby field lines. The field is altered by the reluctance of the ferrite material.

If an air-core loop is placed in a field, in essence it cuts the lines of flux without disturbing them (**Fig 10A**). On the other hand, when a ferrite (magnetic) core is placed in the field, the nearby field lines are redirected into the loop (Fig 10B). This is because the reluctance of the ferrite material is less than that of the surrounding air, so the nearby flux lines tend to flow through the loop rather than passing it by. (Reluctance is the magnetic analogy of resistance, while flux is analogous to current.) The reluctance is inversely proportional to the permeability of the rod core, μ_{rod}. (In some texts the rod permeability is referred to as effective permeability, μ_{eff}). This effect modifies the equation for effective height of a ferrite-core loop to

$$h = \frac{2\pi N A \mu_{rod}}{\lambda} \qquad \text{(Eq 7)}$$

where

h = effective height (length) in meters
N = number of turns in the loop
A = area of loop in square meters
μ_{rod} = permeability of the ferrite rod
λ = wavelength of operation in meters

This obviously is a large increase in "collected" signal. If the rod permeability were 90, this would be the same as making the loop area 90 times larger with the same number of turns. For example, a 1.25-cm diameter ferrite-core loop would have an effective height equal to an air-core loop 22.5 cm in diameter (with the same number of turns).

By now you might have noticed we have been very careful to refer to rod permeability. There is a very important reason for this. The permeability that a rod of ferrite exhibits is a combination of the material permeability or μ, the shape of the rod, and the dimensions of the rod. In ferrite rods, μ is sometimes referred to as initial permeability, μ_i, or toroidal permeability, μ_{tor}. Because most amateur ferrite loops are in the form of rods, we will discuss only this shape.

The reason that μ_{rod} is different from μ is a very complex physics problem that is well beyond the scope of this book. For those interested in the details, books by Polydoroff and by Snelling cover this subject in considerable detail. (See Bibliography.) For our purposes a simple explanation will suffice. The rod is in fact not a perfect director of flux, as is illustrated in **Fig 11**. Note that some lines impinge on the sides of the core and also exit from the sides. These lines therefore would not pass through all the turns of the coil if it were wound from one end of the core to the other. These flux lines are referred to as *leakage flux*, or sometimes as flux leakage.

Leakage flux causes the flux density in the core to be nonuniform along its length. From Fig 11 it can be seen that the flux has a maximum at the geometric center of the length of the core, and decreases as the ends of the core are approached. This causes some noticeable effects. As a short

coil is placed at different locations along a long core, its inductance will change. The maximum inductance exists when the coil is centered on the rod. The Q of a short coil on a long rod is greatest at the center. On the other hand, if you require a higher Q than this, it is recommended that you spread the coil turns along the whole length of the core, even though this will result in a lower value of inductance. (The inductance can be increased to the original value by adding turns.) **Fig 12** gives the relationship of rod permeability to material permeability for a variety of values.

The change in μ over the length of the rod results in an adjustment in the term μ_{rod} for its so called "free ends" (those not covered by the winding). This adjustment factor is given by

$$\mu' = \mu_{rod} \sqrt[3]{\frac{a}{b}} \qquad \text{(Eq 8)}$$

where

μ′ = the corrected permeability
a = the length of the core
b = the length of the coil

This value of μ′ should be used in place of μ_{rod} in Eq 7 to obtain the most accurate value of effective height.

All these variables make the calculation of ferrite loop antenna inductance somewhat less accurate than for the air-core version. The inductance of a ferrite loop is given by

$$L = \frac{4\pi N^2 A \mu_{rod} \times 10^{-4}}{\ell} \qquad \text{(Eq 9)}$$

where

L = inductance in μH
N = number of turns
A = cross-sectional area of the core in square mm
ℓ = magnetic length of core in mm

Experiments indicate that the winding diameter should be as close to that of the rod diameter as practical in order to maximize both inductance value and Q. By using all this information, we may determine the voltage at the loop terminals and its signal-to-noise ratio (SNR). The voltage may be determined from

$$V = \frac{2\pi A N \mu' Q E}{\lambda} \qquad \text{(Eq 10)}$$

where

V = output voltage across the loop terminals
A = loop area in square meters
N = number of turns in the loop winding
μ′ = corrected rod permeability
Q = loaded Q of the loop
E = RF field strength in volts per meter
λ = wavelength of operation in meters

Lankford's equation for the sensitivity of the loop for a 10 dB SNR is

$$E = \frac{1.09 \times 10^{-10} \lambda \sqrt{f L b}}{A N \mu' \sqrt{Q}} \qquad \text{(Eq 11)}$$

where

f = operating frequency in Hz
L = loop inductance in henrys
b = receiver bandwidth in Hz

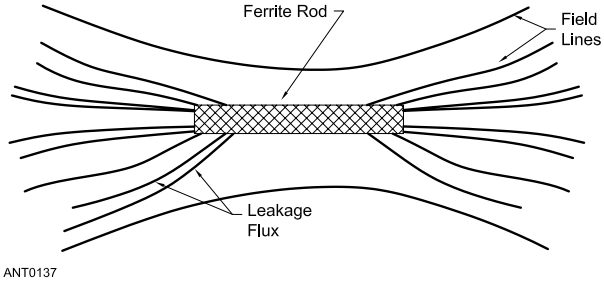

Fig 11—Example of magnetic field lines near a practical ferrite rod, showing leakage flux.

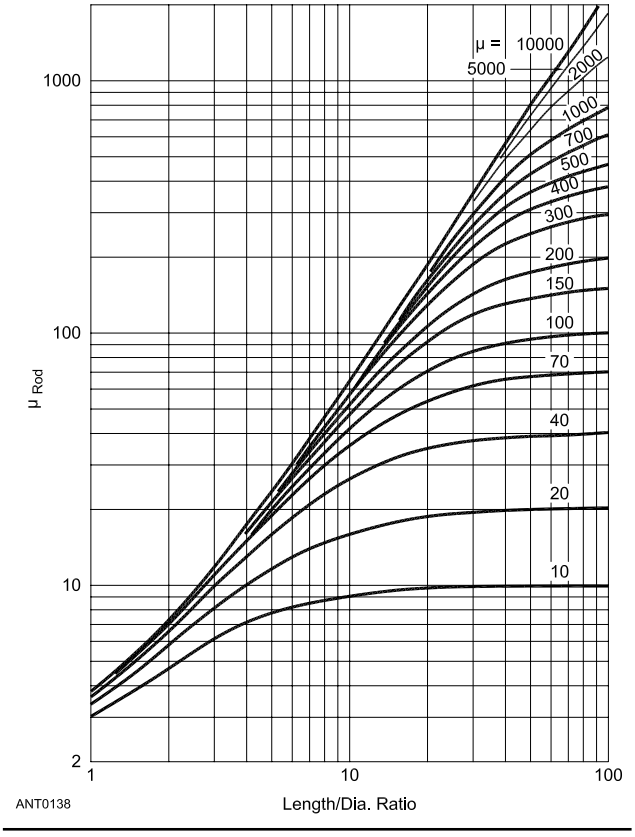

Fig 12—Rod permeability, μ_{rod}, versus material permeability, μ, for different rod length-to-diameter ratios.

Similarly, Belrose gives the SNR of a tuned loop antenna as

$$SNR = \frac{66.3\,N\,A\,\mu_{rod}\,E}{\sqrt{b}}\sqrt{\frac{Qf}{L}} \qquad \text{(Eq 12)}$$

From this, if the field strength E, μ_{rod}, b, and A are fixed, then Q or N must increase (or L decrease) to yield a better SNR. Higher sensitivity can also be obtained (especially at frequencies below 500 kHz) by bunching ferrite cores together to increase the loop area over that which would be possible with a single rod. High sensitivity is important because loop antennas are not the most efficient collectors of signals, but they do offer improvement over other receiving antennas in terms of SNR. For this reason, you should attempt to maximize the SNR when using a small loop receiving antenna. In some cases there may be physical constraints that limit how large you can make a ferrite-core loop.

After working through Eq 11 or 12, you might find you still require some increase in antenna system gain to effectively use your loop. In these cases the addition of a low noise preamplifier may be quite valuable even on the lower frequency bands where they are not commonly used. Chapter 14 contains information on such preamplifiers.

The electrostatic shield discussed earlier with reference to air-core loops can be used effectively with ferrite-core loops. (Construction examples are presented in Chapter 14.) As in the air-core loop, a shield will reduce electrical noise and improve loop balance.

PROPAGATION EFFECTS ON NULL DEPTH

After building a balanced loop you may find it does not approach the theoretical performance in the null depth. This problem may result from propagation effects. Tilting the loop away from a vertical plane may improve performance under some propagation conditions, to account for the vertical angle of arrival. Basically, the loop performs as described above only when the signal is arriving perpendicular to the axis of rotation of the loop. At incidence angles other than perpendicular, the position and depth of the nulls deteriorate.

The problem can be even further influenced by the fact that if the loop is situated over less than perfectly conductive ground, the wave front will appear to tilt or bend. (This bending is not always detrimental; in the case of Beverage antennas, sites are chosen to take advantage of this effect.)

Another cause of apparent poor performance in the null depth can be from polarization error. If the polarization of the signal is not completely linear, the nulls will not be sharp. In fact, for circularly polarized signals, the loop might appear to have almost no nulls. Propagation effects are discussed further in Chapter 14.

SITING EFFECTS ON THE LOOP

The location of the loop has an influence on its performance that at times may become quite noticeable. For ideal performance the loop should be located outdoors and clear of any large conductors, such as metallic downspouts and towers. A VLF loop, when mounted this way, will show good sharp nulls spaced 180° apart if the loop is well balanced. This is because the major propagation mode at VLF is by ground wave. At frequencies in the HF region, a significant portion of the signals is propagated by sky wave, and nulls are often only partial.

Most hams locate their loop antennas near their operating position. If you choose to locate a small loop indoors, its performance may show nulls of less than the expected depth, and some skewing of the pattern. For precision direction finding there may be some errors associated with wiring, plumbing, and other metallic construction members in the building. Also, a strong local signal may be reradiated from the surrounding conductors so that it cannot be nulled with any positioning of the loop. There appears to be no known method of curing this type of problem. All this should not discourage you from locating a loop indoors; this information is presented here only to give you an idea of some pitfalls. Many hams have reported excellent results with indoor mounted loops, in spite of some of the problems.

Locating a receiving loop in the field of a transmitting antenna may cause a large voltage to appear at the receiver antenna terminals. This may be sufficient to destroy sensitive RF amplifier transistors or front-end protection diodes. This can be solved by disconnecting your loop from the receiver during transmit periods. This can obviously be done automatically with a relay that opens when the transmitter is activated.

LOOP ANTENNA ARRAYS

Arrays of loop antennas, both in combination with each other and with other antenna types, have been used for many years. The arrays are generally used to cure some "deficiency" in the basic loop for a particular application, such as a 180° ambiguity in the null direction, low sensitivity, and so forth.

A Sensing Element

For direction-finding applications the single loop suffers the problem of having two nulls that are 180° apart. This leads to an ambiguity of 180° when trying to find the direction to a transmitting station from a given location. A sensing element (often called a *sense antenna*) may be added to the loop, causing the overall antenna to have a cardioid pattern and only one null. The sensing element is a small vertical antenna whose height is equal to or greater than the loop effective height. This vertical is physically close to the loop, and when its omnidirectional pattern is adjusted so that its amplitude and phase are equal to one of the loop

lobes, the patterns combine to form a cardioid. This antenna can be made quite compact by use of a ferrite loop to form a portable DF antenna for HF direction finding. Chapter 14 contains additional information and construction projects using sensing elements.

Arrays of Loops

A more advanced array that can develop more diverse patterns consists of two or more loops. Their outputs are combined through appropriate phasing lines and combiners to form a phased array. Two loops can also be formed into an array that can be rotated without physically turning the loops themselves. This method was developed by Bellini and Tosi in 1907 and performs this apparently contradictory feat by use of a special transformer called a *goniometer*. The goniometer is described in Chapter 14.

Aperiodic Arrays

The aperiodic loop array is a wide-band antenna. This type of array is useful over at least a decade of frequency, such as 2 to 20 MHz. Unlike most of the loops discussed up to now, the loop elements in an aperiodic array are untuned. Such arrays have been used commercially for many years. One loop used in such an array is shown in **Fig 13**. This loop is quite different from all the loops discussed so far in this chapter because its pattern is not the familiar figure eight. Rather, it is omnidirectional.

The antenna is omnidirectional because it is purposely unbalanced, and also because the isolating resistor causes the antenna to appear as two closely spaced short monopoles. The loop maintains the omnidirectional characteristics over a frequency range of at least four or five to one. These loops, when combined into end-fire or broadside phased arrays, can provide quite impressive performance. A commercially made end-fire array of this type consisting of four loops equally spaced along a 25-meter baseline can provide gains in excess of 5 dBi over a range of 2 to 30 MHz. Over a considerable portion of this frequency range, the array can maintain F/B ratios of 10 dB. Even though the commercial version is very expensive, an amateur version can be constructed using the information provided by Lambert. One interesting feature of this type of array is that, with the proper combination of hybrids and combiners, the antenna can simultaneously feed two receivers with signals from different directions, as shown in **Fig 14**. This antenna may be especially interesting to one wanting a directional receiving array for two or more adjacent amateur bands.

SMALL TRANSMITTING LOOP ANTENNAS

The electrically small transmitting-loop antenna involves some different design considerations compared to receiving loops. Unlike receiving loops, the size limitations of the antenna are not as clearly defined. For most purposes, any transmitting loop whose physical circumference is less than ¼ λ can be considered "small." In most cases, as a consequence of their relatively large size (when compared to a receiving loop), transmitting loops have a nonuniform current distribution along their circumference. This leads to some performance changes from a receiving loop.

The transmitting loop is a parallel-tuned circuit with a large inductor acting as the radiator. As with the receiving

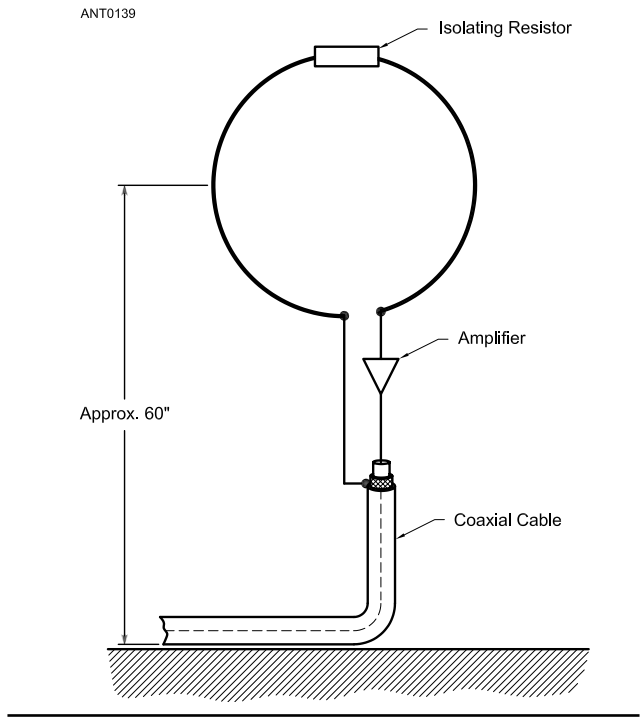

Fig 13—A single wide-band loop antenna used in an aperiodic array.

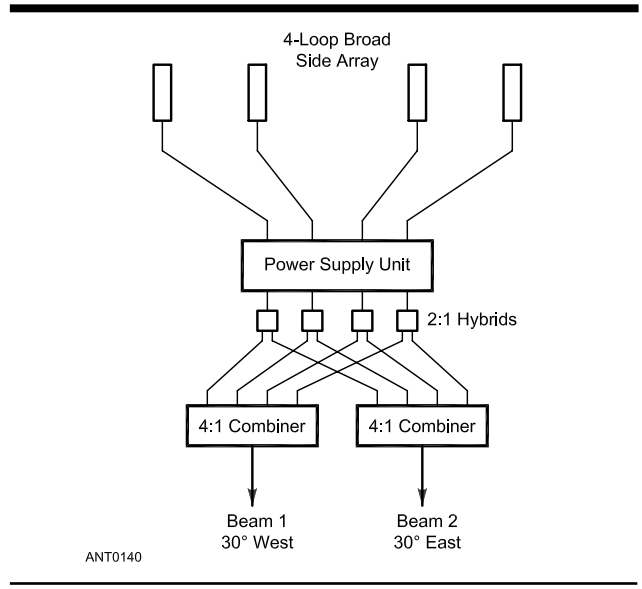

Fig 14—Block diagram of a four-loop broadside array with dual beams separated by 60° in azimuth.

Table 3
Transmitting Loop Equations

$$X_L = 2\pi fL \text{ ohms}$$

$$Q = \frac{f}{\Delta f} = \frac{X_L}{2(R_R + R_L)}$$

$$R_R = 3.12 \times 10^4 \left[\frac{NA}{\lambda^2}\right]^2 \text{ ohms}$$

$$V_C = \sqrt{P X_L Q}$$

$$I_L = \sqrt{\frac{PQ}{X_L}}$$

where

X_L = inductive reactance, ohms
f = frequency, Hz
Δf = bandwidth, Hz
R_R = radiation resistance, ohms
R_L = loss resistance, ohms (see text)
N = number of turns
A = area enclosed by loop, square meters
λ = wavelength at operating frequency, meters
V_C = voltage across capacitor
P = power, watts
I_L = resonant circulating current in loop

loop, the calculation of the transmitting-loop inductance may be carried out with the equations in Table 1. Avoid equations for long solenoids found in most texts. Other fundamental equations for transmitting loops are given in **Table 3**.

In the March 1968 *QST*, Lew McCoy, W1ICP, introduced the so-called "Army Loop" to radio amateurs. This was an amateur version of a loop designed for portable use in Southeast Asia by Patterson of the US Army and described in 1967. The Army Loop is diagrammed in **Fig 15A**, showing that this is a parallel tuned circuit fed by a tapped-capacitance impedance-matching network.

The Hart "high-efficiency" loop was introduced in the June 1986 *QST* by Ted Hart, W5QJR. It is shown schematically in Fig 15B and has the series-tuning capacitor separate from the matching network. The Hart matching network is basically a form of gamma match. Other designs have used a smaller loop connected to the transmission line to couple into the larger transmitting loop.

The approximate radiation resistance of a loop in ohms is given by

$$R_R = 3.12 \times 10^4 \left(\frac{NA}{\lambda^2}\right)^2 \qquad \text{(Eq 13)}$$

where

N = number of turns
A = area of loop in square meters
λ = wavelength of operation in meters

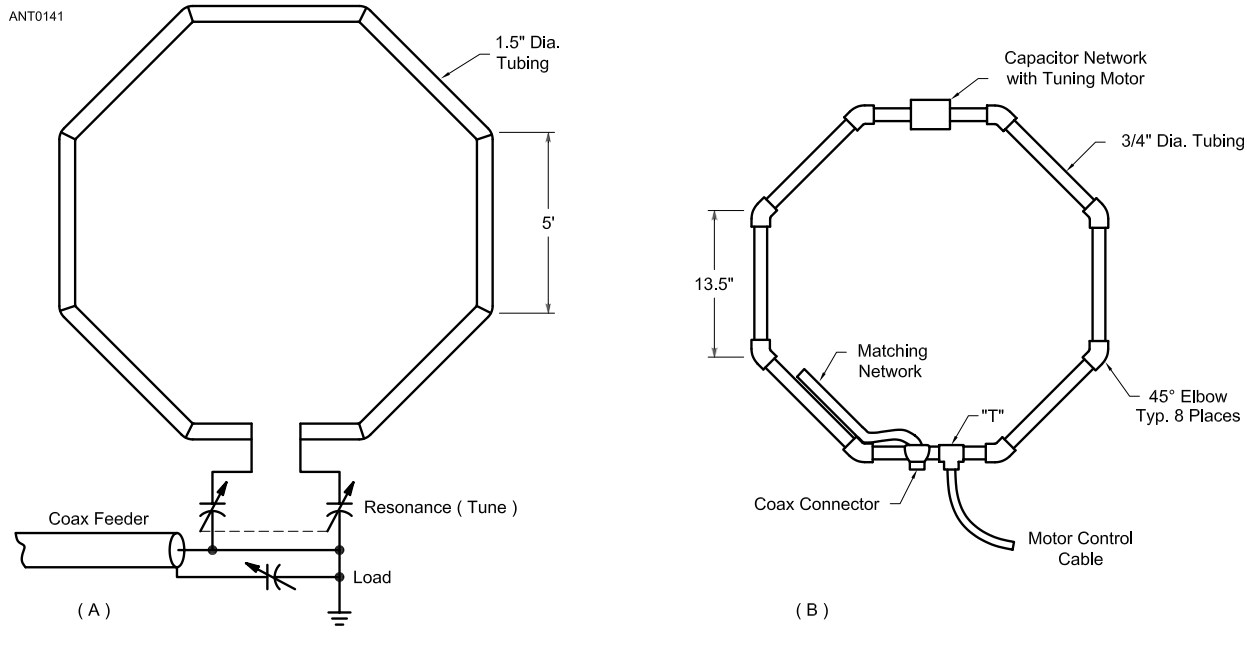

Fig 15—At A, a simplified diagram of the Army Loop. At B, the W5QJR loop, which is described in more detail later in this chapter.

The radiation resistance of a small transmitting loop is usually very small. For example, a 1-meter diameter, single-turn circular loop has a radius of 0.5 meters and an enclosed area of $\pi \times 0.5^2 = 0.785\ m^2$. Operated at 14.0 MHz, the free-space wavelength is 21.4 meters and this leads to a computed radiation resistance of only $3.12 \times 10^{-4}\ (0.785/21.4^2)^2 = 0.092\ \Omega$.

Unfortunately the loop also has losses, both ohmic and from skin effect. By using this information, the radiation efficiency of a loop can be calculated from

$$\eta = \frac{R_R}{R_R + R_L} \qquad \text{(Eq 14)}$$

where

η = antenna efficiency, %

R_R = radiation resistance, Ω

R_L = loss resistance, Ω, which includes the loop's conductor loss plus the loss in the series-tuning capacitor.

A simple ratio of R_R versus R_L shows the effects on the efficiency, as can be seen from **Fig 16**. The loss resistance is primarily the ac resistance of the conductor. This can be calculated from Eq 6. A transmitting loop generally requires the use of copper conductors of at least ¾ inch in diameter in order to obtain reasonable efficiency. Tubing is as useful as a solid conductor because high-frequency currents flow only along a very small depth of the surface of the conductor; the center of the conductor has almost no effect on current flow.

Note that the R_L term above also includes the effect of the tuning capacitor's loss. Normally, the unloaded Q of a capacitor can be considered to be so high that any loss in the tuning capacitor can be neglected. For example, a very high-quality tuning capacitor with no mechanical wiping contacts, such as a vacuum-variable or a transmitting butterfly capacitor, might have an unloaded Q of about 5000. This implies a series loss resistance of less than about 0.02 Ω for a capacitive reactance of 100 Ω. This relatively tiny loss resistance can become significant, however, when the radiation resistance of the loop is only on the order of 0.1 Ω! Practical details for curbing capacitor losses are covered later in this chapter.

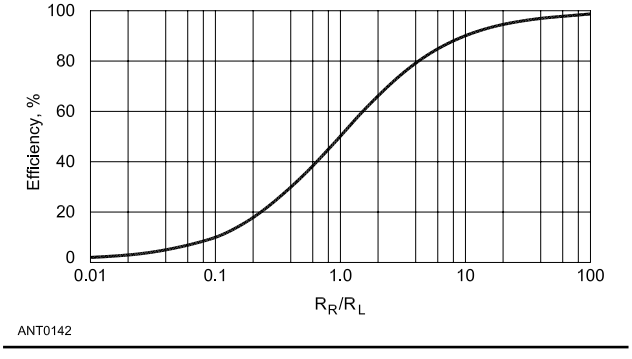

Fig 16—Effect of ratio of R_R/R_L on loop efficiency.

In the case of multiturn loops there is an additional loss related to a term called *proximity effect*. The proximity effect occurs in cases where the turns are closely spaced (such as being spaced one wire diameter apart). As these current-carrying conductors are brought close to each other, the current density around the circumference of each conductor gets redistributed. The result is that more current per square meter is flowing at the surfaces adjacent to other conductors. This means that the loss is higher than a simple skin-effect analysis would indicate, because the current is bunched so it flows through a smaller cross section of the conductor than if the other turns were not present.

As the efficiency of a loop approaches 90%, the proximity effect is less serious. But unfortunately, the less efficient the loop, the worse the effect. For example, an 8-turn transmitting loop with an efficiency of 10% (calculated by the skin-effect method) actually only has an efficiency of 3% because of the additional losses introduced by the proximity effect. If you are contemplating construction of a multiturn transmitting loop, you might want to consider spreading the conductors apart to reduce this effect. G. S. Smith includes graphs that detail this effect in his 1972 IEEE paper.

The components in a resonated transmitting loop are subject to both high currents and voltages as a result of the large circulating currents found in the high-Q tuned circuit formed by the antenna. This makes it important that any fixed capacitors have a high RF current rating, such as transmitting micas or the Centralab 850 series. Be aware that even a 100-W transmitter can develop currents in the tens of amperes, and voltages across the tuning capacitor in excess of 10,000 V. This consideration also applies to any conductors used to connect the loop to the capacitors. A piece of #14 wire may have more resistance than the rest of the loop conductor!

It is therefore best to use copper strips or the braid from a piece of large coax cable to make any connections. Make the best electrical connection possible, using soldered or welded joints. Using nuts and bolts should be avoided, because at RF these joints generally have high resistance, especially after being subjected to weathering.

An unfortunate consequence of having a small but high-efficiency transmitting loop is high loaded Q, and therefore limited bandwidth. This type of antenna may require retuning for frequency changes as little as 5 kHz. If you are using any wide-band mode such as AM or FM, this might cause fidelity problems and you might wish to sacrifice a little efficiency to obtain the required bandwidth.

A special case of the transmitting loop is that of the ferrite-loaded loop. This is a logical extension of the transmitting loop if we consider the improvement that a ferrite core makes in receiving loops. The use of ferrites in a transmitting loop is still under development. (See the Bibliography reference for DeVore and Bohley.)

PRACTICAL COMPACT TRANSMITTING LOOPS

The ideal small transmitting antenna would have performance equal to a large antenna. A small loop antenna can approach that performance except for a reduction in bandwidth, but that effect can be overcome by retuning. This section is adapted and updated from material written by Robert T. (Ted) Hart, W5QJR.

As pointed out above, small antennas are characterized by low radiation resistance. For a typical small antenna, such as a short dipole, loading coils are often added to achieve resonance. However, the loss inherent in the coils can result in an antenna with low efficiency. If instead of coils a large, low-loss capacitor is added to a low-loss conductor to achieve resonance, and if the antenna conductor is bent to connect the ends to the capacitor, a loop is formed.

Based on this concept, the small loop is capable of relatively high efficiency, compared to its coil-loaded cousin. In addition, the small loop, when mounted vertically, can radiate efficiently over the wide range of elevation angles required on the lower frequency bands. This is because it has both high-angle and low-angle response. See **Fig 17**, which shows the elevation response for a compact transmitting loop only 16.2 inches wide at 14.2 MHz. This loop is vertically polarized and its bottom is 8 feet above average ground, which has a conductivity of 5 mS/m and a dielectric constant of 13. For comparison, Fig 17 also shows the responses of three other reference antennas—the same small loop flipped sideways at a height of 30 feet to produce horizontal radiation, a full-sized ¼-λ ground plane antenna mounted 8 feet above average ground using two tuned radials, and finally a simple ½ λ flattop dipole mounted 30 feet above flat ground. The considerably smaller transmitting loop comes to within 3 dB of the larger ¼-λ vertical at a 10° elevation angle, and it is far stronger for high elevation angles because it does not have the null at high elevation angles that the ground plane has. Of course, this characteristic does make it more susceptible to strong signals received at high elevation angles. Incidentally, just in case you were wondering, adding more radials to the λ/4 ground plane doesn't materially improve its performance when mounted at an 8-foot height on 20 meters.

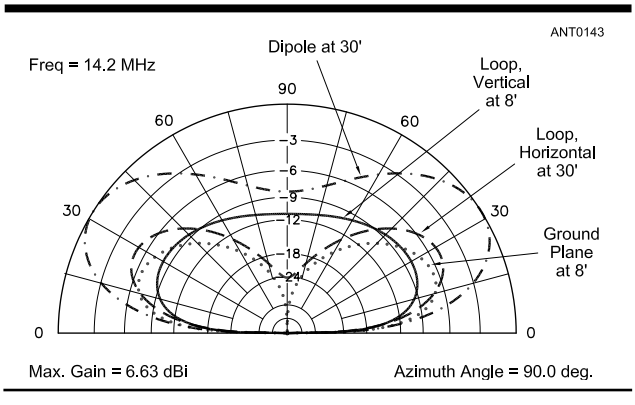

Fig 17—Elevation-plane plot at 14.2 MHz, showing response of an 8.5-foot circumference octagonal copper loop (width of 16.2 inches), compared to a full-sized λ/4 ground-plane vertical with two elevated λ/4 radials, the same small loop flipped horizontally at a height of 30 feet, and lastly, a λ/2 flattop dipole also at a height of 30 feet. Both the λ/4 ground-plane vertical and the vertically polarized loop are elevated 8 feet above typical ground, with σ = 5 mS/m and ε = 13. The low vertically polarized loop is surprisingly competitive, only down about 2.5 dB compared to the far larger ground plane at low elevation angles. Note that the vertical loop has both high-angle as well as low-angle radiation, and hence would be better at working close-in local stations than the ground-plane vertical, with its deep nulls at higher angles. The simple flattop dipole, however, is better than either vertical because of the poor ground reflection for a vertically polarized compared to a horizontally polarized signal.

The simple horizontal dipole in Fig 17 would be the clear winner in any shootout because its horizontally polarized radiation does not suffer as much attenuation at reflection from ground as does a vertically polarized wave. The case is not quite so clear-cut, however, for the small loop mounted horizontally at 30 feet. While it does have increased gain at medium elevation angles, it may not be worth the effort needed to mount it on a mast, considering the slight loss at low angles compared to its twin mounted vertically only 8 feet above ground.

A physically small antenna like the 16.2-inch-wide vertically polarized loop does put out an impressive signal compared to far larger competing antennas. Though somewhat ungainly, it is a substantially better performer than most mobile whips, for example. The main deficiency in a compact transmitting loop is its narrow bandwidth—it must be accurately tuned to the operating frequency. The use of a remote motor drive allows the loop to be tuned over a wide frequency range.

For example, for fixed-station use, two loops could be constructed to provide continuous frequency coverage from 3.5 to 30 MHz. A loop with an 8.5 foot circumference, 16 inches wide, could cover 10 through 30 MHz and a loop with a 20-foot circumference, 72 inches wide, could cover 3.5 to 10.1 MHz.

Table 4 presents summary data for various size loop antennas for the HF amateur bands. Through computer analysis, the optimum size conductor was determined to be ¾-inch rigid copper water pipe, considering both performance and cost. Performance will be compromised, but only slightly, if ⅝-inch flexible copper tubing is used. This tubing can easily be bent to any desired shape, even a circle. The rigid ¾-inch copper pipe is best used with 45° elbows to make an octagon.

The loop circumference should be between ¼ and ⅛ λ at the operating frequency. It will become self-resonant above ¼ λ, and efficiency drops rapidly below ⅛ λ. In the frequency ranges shown in Table 4, the high fre-

Table 4

Design Data for Loops

Loop Circumference = 8.5' (Width = 32.4"), Vertically Polarized

Frequency, MHz	10.1	14.2	21.2	29.0
Max Gain, dBi	–4.47	–1.42	+1.34	+2.97
Max Elevation Angle	40°	30°	22°	90°
Gain, dBi @10°	–8.40	–4.61	–0.87	+0.40
Total Capacitance, pF	145	70	29	13
Peak Capacitor kV	23	27	30	30

Loop Circumference = 8.5' (Width = 32.4"), Horizontally Polarized, @30'

Frequency, MHz	10.1	14.2	21.2	29.0
Max Gain, dBi	–3.06	+1.71	+5.43	+6.60
Max Elevation Angle	34°	28°	20°	16°
Gain, dBi @10°	–9.25	–3.11	+2.61	+5.34
Total Capacitance, pF	145	70	29	13
Peak Capacitor kV	23	27	30	30

Loop Circumference = 20' (Width = 6'), Vertically Polarized

Frequency, MHz	3.5	4.0	7.2	10.1
Max Gain, dBi	–7.40	–6.07	–1.69	–0.34
Max Elevation Angle	68°	60°	38°	30°
Gain, dBi @10°	–11.46	–10.12	–5.27	–3.33
Capacitance, pF	379	286	85	38
Peak Capacitor kV	22	24	26	30

Loop Circumference = 20' (Width = 6'), Horizontally Polarized, @30'

Frequency, MHz	3.5	4.0	7.2	10.1
Max Gain, dBi	–13.32	–10.60	–0.20	+3.20
Max Elevation Angle	42°	42°	38°	34°
Gain, dBi @10°	–21.62	–18.79	–7.51	–3.22
Capacitance, pF	379	286	85	38
Peak Capacitor kV	22	24	26	30

Loop Circumference = 38' (Width = 11.5'), Vertically Polarized

Frequency, MHz	3.5	4.0	7.2
Max Gain, dBi	–2.93	–2.20	–0.05
Max Elevation Angle	46°	42°	28°
Gain, dBi @10°	–6.48	–5.69	–2.80
Capacitance, pF	165	123	29
Peak Capacitor kV	26	27	33

Notes: These loops are octagonal in shape, constructed with ¾-inch copper water pipe and soldered 45° copper elbows. The gain figures assume a capacitor unloaded Q_C = 5000, typical for vacuum-variable type of tuning capacitor. The bottom of the loop is assumed to be 8 feet high for safety and the ground constants are "typical" at conductivity = 5 mS/m and dielectric constant = 13. Transmitter power is 1500 W. The voltage across the tuning capacitor for lower powers goes down with a multiplier of $\sqrt{\frac{P}{1500}}$. For example, at 100 W using the 38-foot-circumference loop at 7.2 MHz, the peak voltage would be $33\ \text{kV} \times \sqrt{\frac{100}{1500}} = 8.5\ \text{kV}$.

quency is tuned with a minimum capacitance of about 29 pF—including stray capacitance.

The low frequency listed in Table 4 is that where the loop response is down about 10 dB from that of a full-sized elevated ground plane at low elevation angles suitable for DX work. **Fig 18** shows an overlay at 3.5 MHz of the elevation responses for two loops: one with an 8.5-foot circumference and one with a 20-foot circumference, together with the response for a full-sized 80-meter ground plane elevated 8 feet off average ground with 2 tuned radials. The 20-foot circumference loop holds its own well compared to the full-sized ground plane.

Controlling Losses

Contrary to earlier reports, adding quarter-wave ground radials underneath a vertically polarized transmitting loop doesn't materially increase loop efficiency. The size of the conductor used for a transmitting loop, however, does directly affect several interrelated aspects of loop performance.

Data for Table 4 was computed for ¾-inch copper water pipe (nominal OD of 0.9 inch). Note that the efficiency is higher and the Q is lower for loops having a circumference near ¼ λ. Larger pipe size will reduce the loss resistance, but the Q increases. Therefore the bandwidth decreases, and the voltage across the tuning capacitor increases. The voltage across the tuning capacitor for high-power operation can become very impressive, as shown in Table 4. Rigid ¾-inch copper water pipe is a good electrical compromise and can also help make a small-diameter loop mechanically sturdy.

The equivalent electrical circuit for the loop is a parallel resonant circuit with a very high Q, and therefore a narrow bandwidth. The efficiency is a function of radiation resistance divided by the sum of the radiation plus loss resistances. The radiation resistance is much less than 1 Ω, so it is necessary to minimize the loss resistance, which is largely the skin-effect loss of the conductor, assuming that the tuning capacitor has very low loss. Poor construction techniques must be avoided. All joints in the

loop must be brazed or soldered.

However, if the system loss is too low, for example by using even larger diameter tubing, the Q may become excessive and the bandwidth may become too narrow for practical use. These reasons dictate the need for a complete analysis to be performed before proceeding with the construction of a loop.

There is another source of additional loss in a completed loop antenna besides the conductor and capacitor losses. If the loop is mounted near lossy metallic conductors, the large magnetic field produced will induce currents into those conductors and be reflected as losses in the loop. Therefore the loop should be as far from other conductors as possible. If you use the loop inside a building constructed with large amounts of iron or near ferrous materials, you will simply have to live with the loss if the loop cannot otherwise be relocated.

The Tuning Capacitor

Fig 19 demonstrates the selection of loop size versus tuning capacitance for any desired operating frequency range for the HF amateur bands. This is for octagonal-shaped loops using ¾-inch copper water pipe with 45° copper elbows. For example, a capacitor that varies from 5 to 50 pF, used with a loop 10 feet in circumference, tunes from 13 to 27 MHz (represented by the left dark vertical bar). A 25 to 150-pF capacitor with a 13.5-foot loop circumference covers the 7 to 14.4-MHz range, represented by the right vertical bar.

Fig 20 illustrates how the 29-MHz elevation pattern becomes distorted and rather bulbous-looking for the 10-foot circumference loop, although the response at low elevation angles is still better than that of a full-sized ground-plane antenna.

Air Variable Capacitors

Special care must be taken with the tuning capacitor if an air-variable type is used. The use of a split-stator capacitor eliminates the resistance of wiper contacts, resistance that is inherent in a single-section capacitor. The ends of the loop are connected to the stators, and the rotor forms the variable coupling path between the stators. With this arrangement the value of capacitance is divided by two, but the voltage rating is doubled.

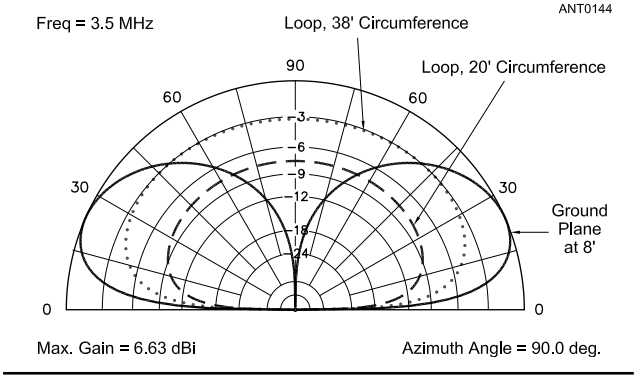

Fig 18—Elevation-plane response of three antennas at 3.5 MHz—a 20-foot circumference octagonal copper loop, a 38-foot circumference copper loop and a full-sized λ/4 ground plane with two elevated radials. The bottom of each antenna is mounted 8 feet above ground for safety. The 38-foot circumference loop (which has a "wingspan" of 11.5 feet) is fairly competitive with the much large ground-plane, being down only about 4 dB at low elevation angles. The 20-foot circumference loop is much more lossy, but with its top only about 14 feet off the ground is very much of a "stealth" antenna.

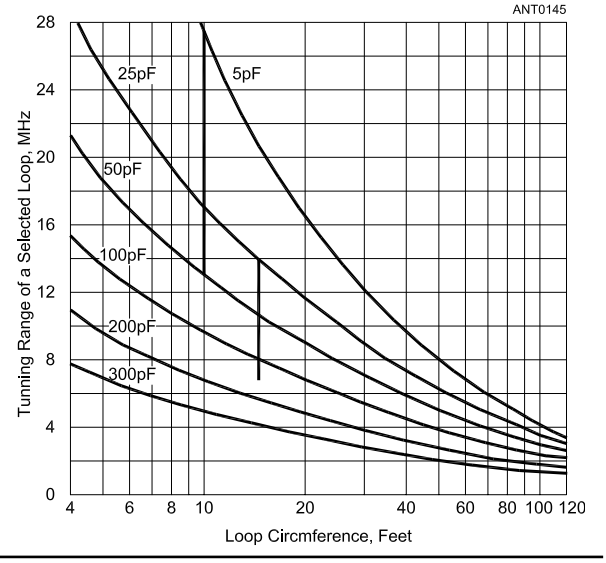

Fig 19—Frequency tuning range of an octagon-shaped loop using $^{3}/_{4}$-inch copper water pipe, for various values of tuning capacitance and loop circumference.

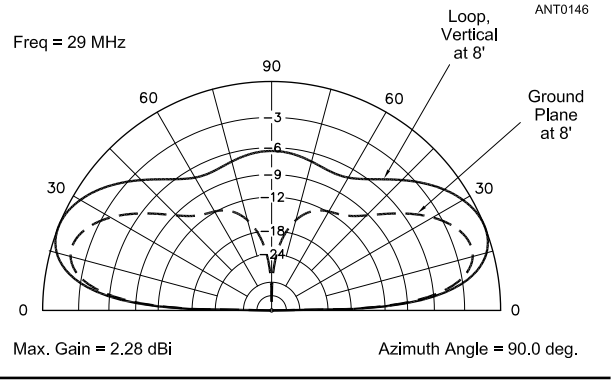

Fig 20—Elevation-plane plot for a 16.2-inch wingspan octagonal copper loop at 29 MHz, compared to a λ/4 ground-plane antenna with two resonant elevated radials. The gains at low angles are almost identical, but the loop exhibits more gain at medium and high elevation angles. Again, the bottom of each antenna is located 8 feet above ground for safety.

You must carefully select a variable capacitor for transmitting-loop application—that is, all contacts must be welded, and no mechanical wiping contacts are allowed. For example, if the spacers between plates are not welded to the plates, there will be loss at each joint, and thus degraded loop efficiency. (Earlier transmitting loops exhibited poor efficiency because capacitors with wiping contacts were used.)

There are several suitable types of capacitors for this application. A vacuum variable is an excellent choice, provided one is selected with an adequate voltage rating. Unfortunately, those capacitors are very expensive.

W5QJR used a specially modified air-variable capacitor in his designs. This had up to 340 pF maximum per section, with 1/4-inch spacing, resulting in 170 pF when both sections were in series as a butterfly capacitor. Another alternative is to obtain a large air variable, remove the aluminum plates, and replace them with copper or double-sided PC board material to reduce losses. Connect all plates together on the rotor and on the stators. Solder copper straps to the capacitor for soldering to the loop itself.

The spacing between plates in an air-variable capacitor determines the voltage-handling capability, rated at 75,000 V per inch. For other power ratings, multiply the spacing (and voltage) by the square root of the ratio of your power to 1000 W. For example, for 100 W, the ratio would be = 0.316.

Table 5
KD7S Loop-Tuning Capacitor Parts List for Nominal 50-pF Capacitor

Qty	*Description*
2	10-inch length of ¾-inch-ID type M copper water pipe
2	10-inch length of ½-inch-ID type M copper water pipe
1	3-inch length of ½-inch-ID type M copper water pipe
2	½-inch, 90° copper elbows
2	¾-inch, 90° copper elbows
2	10 × 22-inch piece of 0.005-inch-thick Teflon sheet plastic
1	12-inch length of #8-32 threaded brass rod
1	#8-32 brass shoulder nut
2	22 × 5½ × ¼-inch ABS plastic sheet (top and bottom covers)
3	1 × 5½ × ¼-inch ABS plastic sheet (end pieces and center) brace/guide
2	1 × 22 × ¼-inch ABS plastic sheet (side rails)
1	50 to 200-rpm gear-head dc motor
1	DPDT center-off toggle switch (up/down control)
2	SPDT microswitches (limit switches)
50 feet	3-conductor control cable
1	Enclosure for control switch

A Teflon-Insulated Trombone Variable Capacitor

Another type of variable capacitor discussed in the amateur literature for use with a compact transmitting loop is the so-called "trombone" type of capacitor. **Fig 21** shows a practical trombone capacitor created by Bill Jones, KD7S, for Nov 1994 *QST*. This capacitor uses downward pointing extensions of the two 3/4-inch OD main conductor copper pipes, with a Teflon-insulated trombone section made of 1/2-inch ID copper pipe. The trombone telescopes into the main pipes, driven by a lead screw and a 180-rpm gear-head motor. Like the butterfly air variable capacitor, the trombone works without lossy wiper contacts. Jones' capacitor varied from 12 pF (including strays) to almost 60 pF, making it suitable to tune his 3-foot circumference loop from 14 to 30 MHz at the 100-W level.

KD7S used 5-mil (0.005 inch) thick Teflon sheet as an insulator. Since Teflon is conservatively rated at more than 1 kV per mil of thickness, the voltage breakdown capability of this capacitor is well in excess of 5 kV. The parts list is given in **Table 5**.

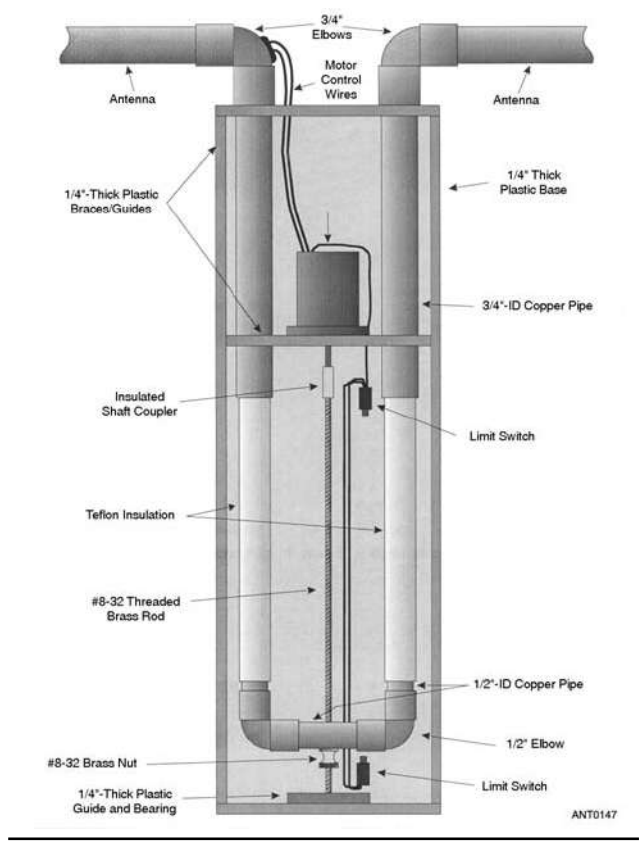

Fig 21—A practical trombone capacitor designed by Bill Jones, KD7S, for his compact transmitting loop. This capacitor has a tuning range from 12 to almost 60 pF, and can withstand at least 5 kV peak. The 10-inch ½-inch ID tubes are covered with Teflon-sheet insulation and slide into the ¾-inch ID copper pipes.

A short length of plastic tubing connects the threaded brass rod to the motor. The tubing acts as an insulator and a flexible coupling to smooth out minor shaft-alignment errors. The other end of the rod is threaded into a brass nut soldered to the crossbar holding the 1/2-inch pipes together. Jones used a 12-V motor rated at 180 rpm, but it has sufficient torque to work with as little as 4 V applied. Instead of a sophisticated variable duty-cycle speed control circuit, he used an LM327 adjustable voltage regulator to vary the motor-control voltage from 4 to 12 V. Tuning speeds ranged from 11 seconds per inch at 12 V to 40 seconds per inch at 4 V. The higher speed is necessary to jump from band to band in a reasonable length of time. The lower speed makes it easy to fine-tune the capacitor to any desired frequency within a band.

When building the capacitor, keep in mind that the smaller tubes must telescope in and out of the larger tubes with silky smoothness. Any binding will cause erratic tuning. For the same reason, the #8-32 brass threaded rod must be straight and properly aligned with the brass nut. *Take your time with this part of the project*.

Perhaps the easiest way to form the insulator is to precut a length of Teflon sheet to the proper size. Place a lengthwise strip of double-sided tape on the tube to secure one end of the Teflon sheet. Begin wrapping the Teflon around the tube while keeping it as tight as possible. *Don't allow wrinkles or ridges to form*. Secure the other end with another piece of tape. Once both tubes are covered, ensure they are just short of being a snug fit inside the larger tubes. Confirm that the insulation completely overlaps the open end of the small tubes. If not, the capacitor is certain to arc internally with more than a few watts of power applied to it.

Route the motor wiring inside the antenna pipes to minimize the amount of metal within the field of the antenna. Bring the wires out next to the coaxial connector. A three-wire system allows the use of limit switches to restrict the movement of the trombone section. Be sure to solder together all metal parts of the capacitor. Use a small propane torch, a good quality flux and 50/50 solid solder. Do not use acid-core solder! Clean all parts to be joined with steel wool prior to coating them with flux.

A Cookie-Sheet and Picture-Frame-Glass Variable Capacitor

In Vol 2 of *The ARRL Antenna Compendium* series, Richard Plasencia, WØRPV, described a clever high-voltage variable capacitor he constructed using readily available materials. See **Fig 22**, which shows Plasencia's homebrew high-voltage variable capacitor, along with the coil and other parts used in his homemade antenna coupler. This capacitor could be varied from 16 to 542 pF and tested at a breakdown of 12,000 V.

The capacitor sits on four PVC pillars and consists of two $4^1/_2 \times 4^1/_2$-inch aluminum plates separated by a piece of window glass that is $8^1/_2 \times 5^1/_2$ inches in size. The lower plate is epoxied to the glass. The upper plate is free to move in a wooden track epoxied to the upper surface of the glass. The motor is reversible and moves the upper capacitor plate by rotating a threaded rod in a wing nut pinned to a tab on the capacitor plate. The four pillars are cut from PVC pipe to insulate the capacitor from the chassis and to elevate it into alignment with the motor shaft.

WØRPV used a piece of 0.063-inch thick single-weight glass that exhibited a dielectric constant of 8. He removed the glass from a dime-store picture frame. In time-honored ham fashion, he improvised his wooden tracks for the upper capacitor plate from a single wooden paint stirrer, and for the capacitor plates, he used aluminum cookie sheets.

The wooden track for the upper plate is made by splitting the wooden paint stirrer with a knife into one narrow and one wide strip. The narrow strip is cemented on top and overhangs the movable plate, creating a slotted track. Since the wood is supported by the glass plate, its insulating qualities are of no importance.

The principle of operation is simple. The reversible motor turns a threaded 1/4-inch rod with a pitch of 20 threads to the inch. This rod engages a wing nut attached to the movable capacitor plate. Although WØRPV grounded his capacitor's movable plate with a braid, an insulator similar to that used in the trombone capacitor above should be used to isolate the lead-screw mechanism. Several pieces of braid made from RG-8 coax shield should be used to connect to the ends of the compact transmitting loop conductors to form low-loss connections.

WØRPV used a 90-rpm motor from a surplus vending machine. It moved his variable capacitor plate $4^1/_2$ inches, taking about a minute to travel from one end to the other. Since he wished to eliminate the complexity and dubious reliability of limit switches when used outdoors, he monitored the motor's dc current through two 3 Ω, 2W resistors

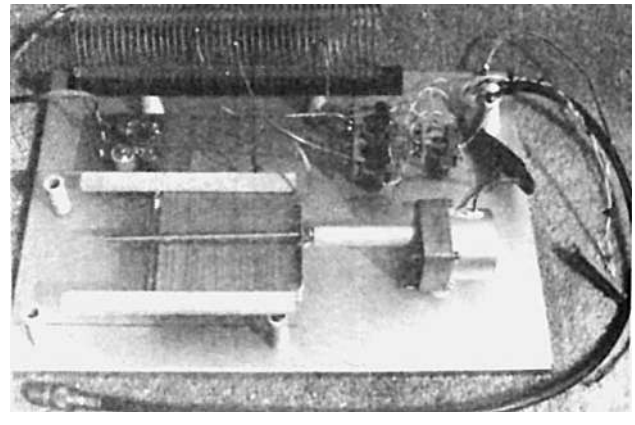

Fig 22—The picture-frame-glass variable capacitor design of Richard Plasencia, WØRPV. Two aluminum plates separated by a piece of glass scavenged from a picture frame create a variable capacitor that can withstand 12,000 V, with a variable range from 16 to 542 pF.

placed in series with each lead of the motor and shunted by red LEDs at the control box. When the motor stalled by jamming up against the PVC limit stop or against the inside of the plastic mounting box, the increased motor current caused one or the other of the LEDs to light up.

TYPICAL LOOP CONSTRUCTION

After you select the electrical design for your loop application, you must consider how to mount it and how to feed it. If you wish to cover only the upper HF bands of 20 through 10 meters, you will probably choose a loop that has a circumference of about 8.5 feet. You can make a reasonably sturdy loop using 1-inch diameter PVC pipe and $^5/_8$-inch flexible copper tubing bent into the shape of a circle. Robert Capon, WA3ULH, did this for a QRP-level transmitting loop described in May 1994 *QST*. **Fig 23** shows a picture of his loop, with PVC H-frame stand.

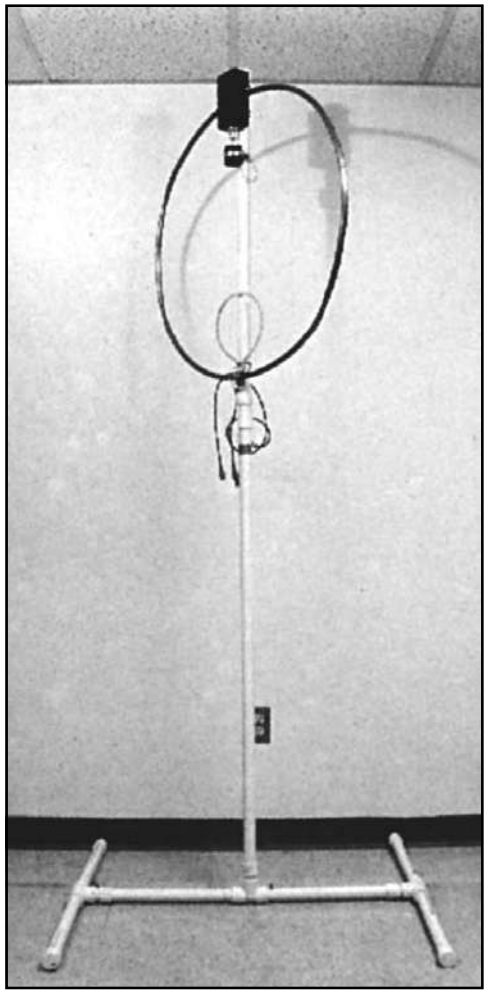

Fig 23—Photo of compact transmitting loop designed by Robert Capon, WA3ULH. This uses a 1-inch PVC H-frame to support the loop made of flexible $^5/_8$-inch copper tubing. The small coupling loop made of RG-8 coax braid couples the loop to the coax feed line. The tuning capacitor and drive motor are at the top of the loop, shown here in the ARRL Laboratory during testing.

This loop design used a 20-inch long coupling loop made of RG-8 coax to magnetically couple into the transmitting loop rather than the gamma-match arrangement used by W5QJR in his loop designs. The coupling loop was fastened to the PVC pipe frame using 2-inch long #8 bolts that also held the main loop to the mast.

A more rugged loop can be constructed using rigid $^3/_4$-inch copper water pipe, as shown in the W5QJR design in **Fig 24**. While a round loop is theoretically a bit more efficient, an octagonal shape is much easier to construct. The values presented in Table 4 are for octagons.

For a given loop circumference, divide the circumference by 8 and cut eight equal-length pieces of $^3/_4$ inch copper water pipe. Join the pieces with 45° elbows to form the octagon. With the loop lying on the ground on scraps of 2 × 4 lumber, braze or solder all joints.

W5QJR made a box from clear plastic to house his air-variable capacitor and drive motor at the top of the loop. The side of the box that mounts to the loop and the capacitor should be at least ¼-inch thick, preferably $^3/_8$-inch. The remainder of the box can be $^1/_8$-inch plastic sheet. He mounted the loop to the plastic using $^1/_4$-inch bolts (two on either side of center) after cutting out a section of pipe 2 inches wide in the center. On the motor side of the capacitor, he cut the pipe and installed a copper T for the motor wiring.

W5QJR's next step was to solder copper straps to the loop ends and to the capacitor stators, then he remounted the loop to the plastic. If you insert wood dowels, the pipe will remain round when you tighten the bolts. Next he installed the motor drive cable through the loop and connected it to the motor. Antenna rotator cable is a good choice for this cable. He completed the plastic box using short pieces of aluminum angle and small sheet-metal screws to join the pieces.

The loop was then ready to raise to the vertical position. Remember, no metal is allowed near the loop. W5QJR made a pole of 2 × 4-inch lumber with 1 × 4-inch boards on either side to form an I section. He held the boards together with $^1/_4$-inch bolts, 2 feet apart and tied rope guys to the top. This made an excellent mast up to 50 feet high. The pole height should be one foot greater than the loop diameter, to allow room for cutting grass or weeds at the bottom of the loop. W5QJR installed a pulley at the top so that his loop could be raised, supported by rope. He supported the bottom of the loop by tying it to the pole and tied guy ropes to the sides of the loop to keep it from rotating in the wind. By moving the anchor points, he could rotate his loop in the azimuth plane.

W5QJR used a gamma-matching arrangement made of flexible $^1/_4$-inch copper tubing to couple the loop to the transmission line. In the center of one leg, he cut the pipe and installed a copper T. Adjacent to the T, he installed a mount for the coax connector. He made the mount from copper strap, which can be obtained by splitting a short piece of pipe and hammering it flat.

While the loop was in the vertical position he cut a piece of $^1/_4$-inch flexible copper tubing the length of one

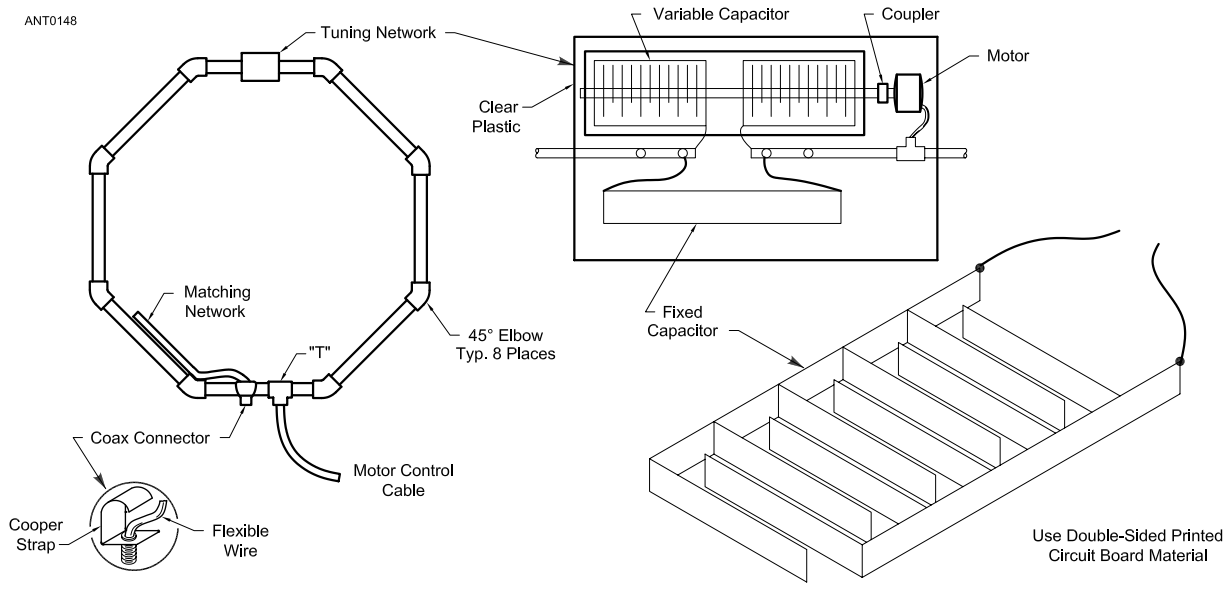

Fig 24—Octagonal loop construction details. Table 4 gives loop design data for various frequency ranges.

of the straight sides of the loop. He then flattened one end and soldered a piece of flexible wire to the other. He wrapped the tubing with electrical tape for insulation and connected the flexible wire to the coax connector. He then installed the tubing against the inside of the loop, held temporarily in place with tape. He soldered the flat part to the loop, ending up with a form of gamma match, but without reactive components. This simple feed provided better than 1.7:1 SWR over a 2:1 frequency range. For safety, he installed a good ground rod under the loop and connected it to the strap for the coax connector, using large flexible wire.

TUNE-UP PROCEDURE

The resonant frequency of the loop can be readily found by setting the receiver to a desired frequency and rotating the capacitor (by remote control) until signals peak. The peak will be very sharp because of the high Q of the loop.

Turn on the transmitter in the tune mode and adjust either the transmitter frequency or the loop capacitor for maximum signal on a field-strength meter, or for maximum forward signal on an SWR bridge. Adjust the matching network for minimum SWR by bending the matching line. Normally a small hump in the 1/4-inch tubing line, as shown in Fig 24, will give the desired results. For a loop that covers two or more bands, adjust the feed to give equally low SWR at each end of the tubing range. The SWR will be very low in the center of the tuning range but will rise at each end.

If there is metal near the loop, the additional loss will reduce the Q and therefore the impedance of the loop. In those cases it will be necessary to increase the length of the matching line and tap higher up on the loop to obtain a 50-Ω match.

PERFORMANCE COMPARISON

As previously indicated, a compact transmitting loop can provide performance approaching full-size dipoles and verticals. To illustrate one case, a loop 100 feet in circumference would be 30 feet high for 1.8 MHz. However, a good dipole would be 240 feet (1/2 λ) in length and at least 120 feet high (1/4 λ). A 1/4-λ vertical would be 120 feet tall with a large number of radials on the ground, each 120 feet in length. The smaller loop could replace both of those antennas with only a moderate degradation in performance and a requirement for a high-voltage variable capacitor.

On the higher frequencies, the same ratios apply, but full-size antennas are less dramatic. However, very few city dwellers can erect good verticals even on 7 MHz with a full-size counterpoise. Even on 14 MHz a loop about 3 feet high can work the world.

Other than trading small size for narrow bandwidth and a high-voltage capacitor, the compact transmitting loop is an excellent antenna and should find use where large antennas are not practical.

The Loop Skywire

Are you looking for a multiband HF antenna that is easy to construct, costs nearly nothing and yet works well? You might want to try this one. The *Loop Skywire* antenna is a full-sized horizontal loop. Early proponents suggested that the antenna could be fed with coaxial cable with little concern for losses, but later analysis proved that this was a bit of wishful thinking—the relatively low values for SWR across multiple bands indicate that cable losses were part and parcel of performance. The best way to feed this versatile antenna is with open-wire ladder line, with an antenna tuner in the shack to present the transmitter with a low value of SWR.

THE DESIGN

The Loop Skywire is shown in **Fig 25**. The antenna has one wavelength of wire in its perimeter at the design or fundamental frequency. If you choose to calculate L_{total} in feet, the following equation should be used:

$$L_{total} = \frac{1005}{f}$$

where f equals the frequency in MHz.

Given any length of wire, the maximum possible area the antenna can enclose is with the wire in the shape of a circle. Since it takes an infinite number of supports to hang a circular loop, the square loop (four supports) is the most practical. Further reducing the area enclosed by the wire loop (fewer supports) brings the antenna closer to the properties of the folded dipole, and both harmonic-impedance and feed-line voltage problems can result. Loop geometries other than a square are thus possible, but remember the two fundamental requirements for the Loop Skywire—its horizontal position and maximum enclosed area.

There is another great advantage to this antenna system. It can be operated as a vertical antenna with top-hat loading on other bands as well. This is accomplished by simply keeping the feed line run from the antenna to the shack as vertical as possible and clear of objects. Both feedline conductors are then tied together, and the antenna is fed against a good ground.

CONSTRUCTION

Antenna construction is simple. Although the loop can be made for any band or frequency of operation, the following two Loop Skywires are good performers. The 10-MHz band can also be operated on both.

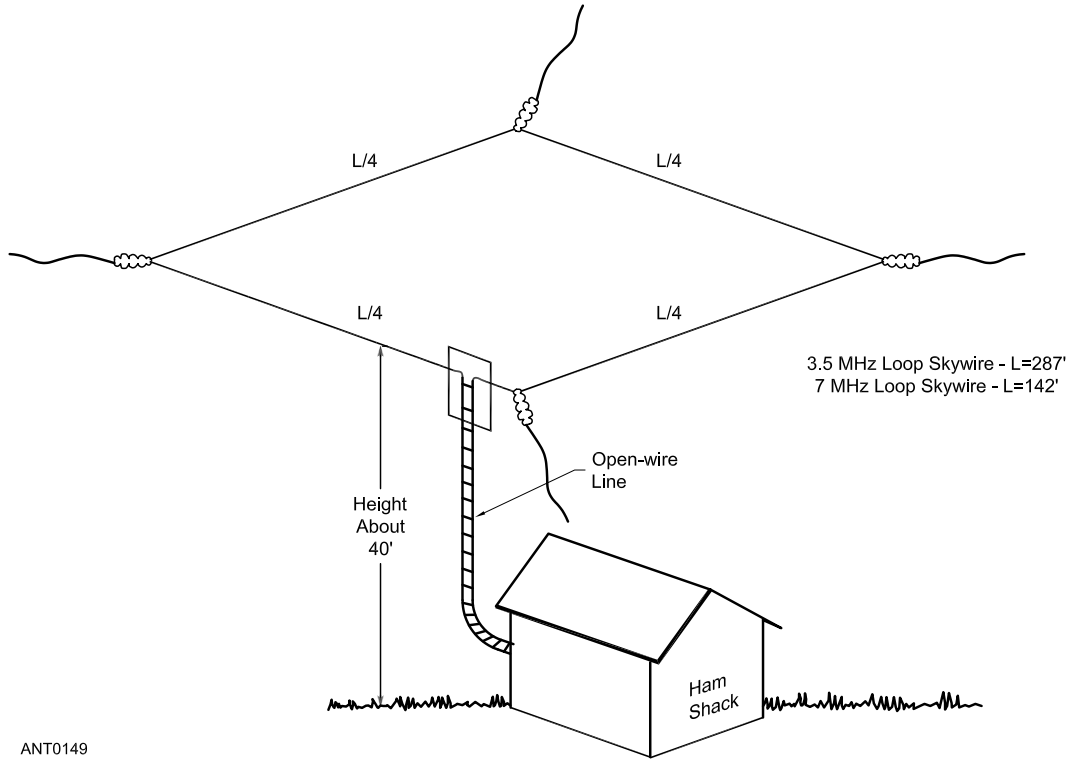

Fig 25—A complete view of the Loop Skywire. The square loop is erected horizontal to the earth.

3.5-MHz Loop Skywire
(3.5-28 MHz loop and 1.8-MHz vertical)
Total loop perimeter: 272 feet
Square side length: 68 feet

7-MHz Loop Skywire
(7-28 MHz loop and 3.5-MHz vertical)
Total loop perimeter: 142 feet
Square side length: 35.5 feet

The actual total length can vary from the above by a few feet, as the length is not at all critical. Do not worry about tuning and pruning the loop to resonance. No signal difference will be detected on the other end when that method is used.

Bare #14 copper wire is used in the loop. **Fig 26** shows the placement of the insulators at the loop corners. Two common methods are used to attach the insulators. Either lock or tie the insulator in place with a loop wire tie, as shown in Fig 26A, or leave the insulator free to "float" or slide along the wire, Fig 26B. Most loop users float at least two insulators. This allows pulling the slack out of the loop once it is in the air, and eliminates the need to have all the supports exactly placed for proper tension in each leg. Floating two opposite corners is recommended.

Fig 27A shows the azimuth-plane performance on 7.2 MHz of a 142-foot long, 7-MHz Loop Skywire, 40 feet high at an elevation angle of 10º, compared to a regular flattop $^1/_2$-λ dipole at a height of 30 feet. The loop comes into its own at higher frequencies. Fig 27B shows the response at 14.2 MHz, compared again to a $^1/_2$–λ 14.2-MHz

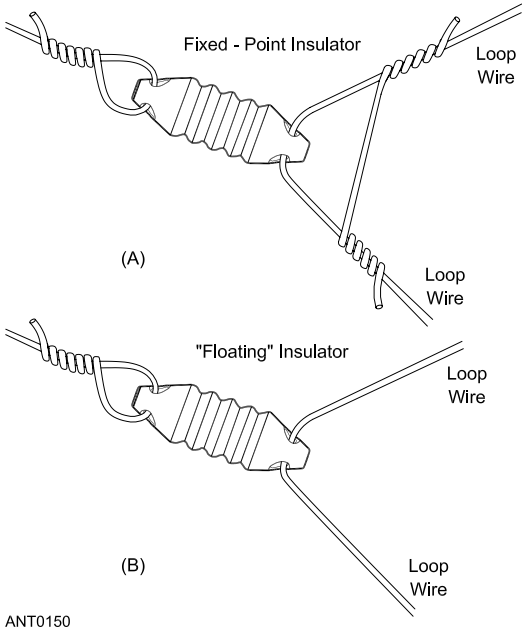

Fig 26—Two methods of installing the insulators at the loop corners.

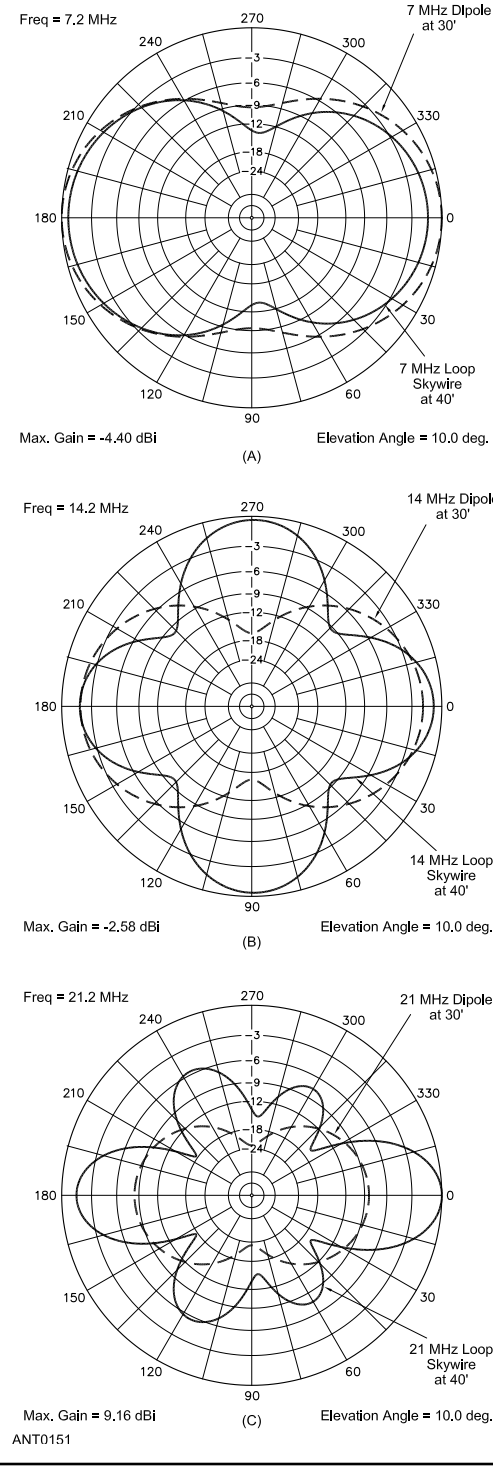

Fig 27—At A, azimuth-plane response of 142-foot long, 7-MHz Loop Skywire, 40 feet in the air at 7.2 MHz, compared with ½-λ dipole 30 feet in the air. At B, response of same Loop Skywire at 14.2 MHz, compared with ½-λ 14.2-MHz dipole 30 feet in the air. Now the loop has some advantage in certain directions. At C, response of the same Loop Skywire at 21.2 MHz compared to a 21.2-MHz dipole at 30 feet. Here, the Loop Skywire has more gain in almost all directions than the simple dipole. All azimuth-plane patterns were made at 10° elevation.

dipole at a height of 30 feet. Now the loop has several lobes that are stronger than the dipole. Fig 27C shows the response at 21.2 MHz, compared to a dipole. Now the loop has superior gain compared to the $^1/_2$-λ dipole at almost any azimuth. In its favored direction on 21.2 MHz, the loop is 8 dB stronger than the dipole.

The feed point can be positioned anywhere along the loop that you wish. However, most users feed the Skywire at a corner. **Fig 28** depicts a method of doing this, using a piece of plexiglass to provide insulation as well as strain relief for the open-wire ladder line. It is advantageous to keep the feed-point mechanicals away from the corner support. Feeding a foot or so from one corner allows the feed line to exit more freely. This method keeps the feed line free from the loop support.

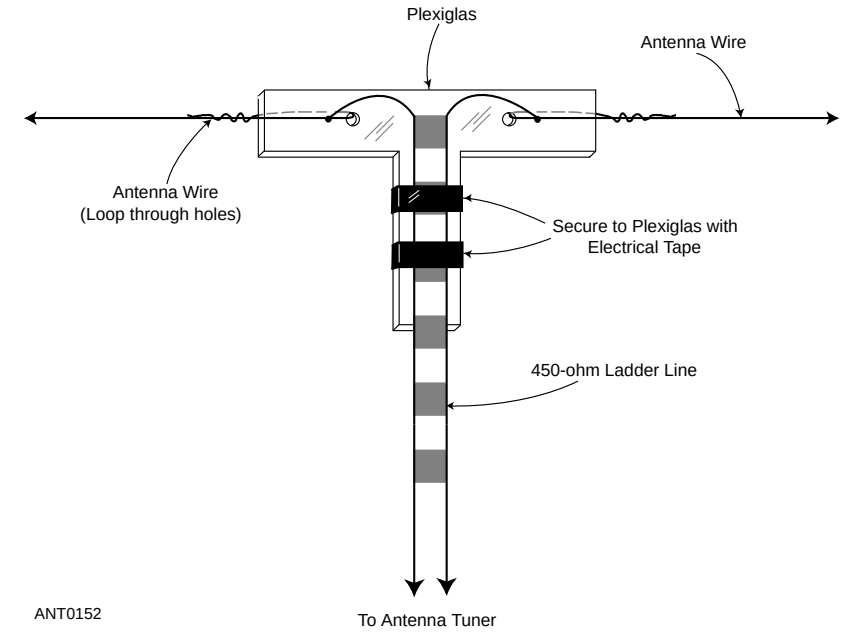

Fig 28—Most users feed the Skywire at a corner. A high-impedance weather-resistant insulator should be used for the feed-point insulator.

Generally a minimum of four supports is required. If trees are used for supports, then at least two of the ropes or guys used to support the insulators should be counterweighted and allowed to move freely. The feed-line corner is almost always tied down, however. Very little tension is needed to support the loop (far less than that for a dipole). Thus, counterweights are light. Several such loops have been constructed with bungie cords tied to three of the four insulators. This eliminates the need for counterweighting.

Recommended height for the antenna is 40 feet or more. The higher the better, especially if you wish to use the loop in the vertical mode. However, successful local and DX operation has been reported in several cases with the antenna at 20 feet. **Fig 29** shows the feed arrangement for using the Loop Skywire as a top-loaded vertical fed against ground on the lower bands.

Because the loop is high in the air and has considerable electrical exposure to the elements, proper methods should be employed to eliminate the chance of induced or direct lightning hazard to the shack and operator. Some users simply completely disconnect the antenna from the antenna tuner and rig and shack during periods of possible lightning activity.

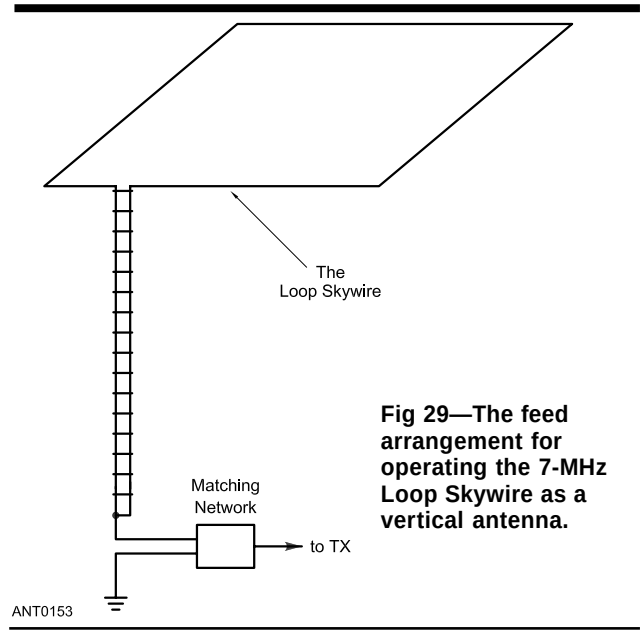

Fig 29—The feed arrangement for operating the 7-MHz Loop Skywire as a vertical antenna.

7-MHz Loop

An effective but simple 7MHz antenna that has a theoretical gain of approximately 1 dB over a dipole is a full-wave, closed vertical loop. Such a loop need not be square, as illustrated in **Fig 30A**. It can be trapezoidal, rectangular, circular, or some distorted configuration in between those shapes. For best results, however, you should attempt to make the loop as square as possible. The more rectangular the shape, the greater the cancellation of energy in the system, and the less effective it will be. In the limiting case, the antenna loses its identity as a loop and becomes a folded dipole.

You can feed the loop in the center of one of the vertical sides if you want vertical polarization. For horizontal polarization, you feed either of the horizontal sides at the center. Since optimum directivity occurs at right angles to the plane of the loop (or in more simple terms, broadside to the loop), you should hang the loop to radiate the maximum amount in some favored direction.

Fig 31A shows the azimuthal response at a takeoff angle of 15°, a typical angle for 40-meter DX, for vertical and horizontal feed systems over ground with "average" conductivity and dielectric constant. Fig 31A includes, for reference, the response of a flattop dipole 50 feet high. For DX work on 40 meters, the vertically polarized loop can perform as well as or substantially better than either a horizontally polarized loop or a flattop dipole, particularly in the azimuthal nulls of the dipole.

For the low elevation angles that favor DX work, the optimal feed point is at the center of one of the vertical wires. Feeding the loop at one of the corners at the bottom gives a

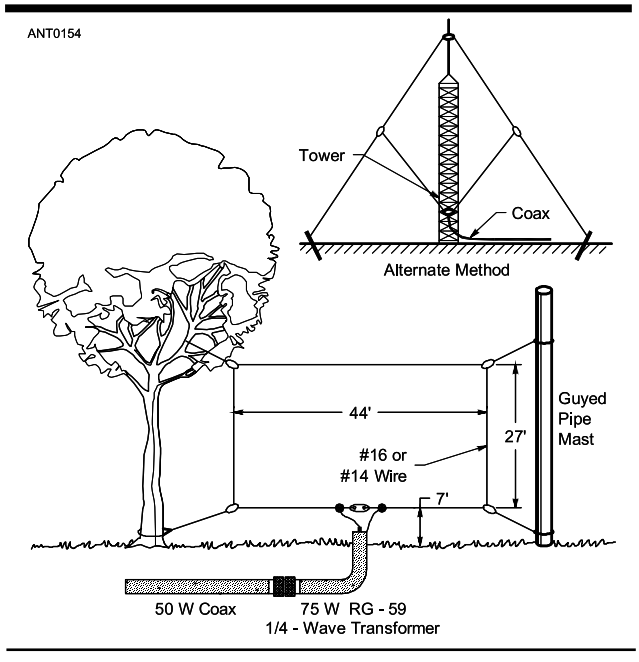

Fig 30—At A, details of the rectangular full-wave loop. The dimensions given are for operation at 7.05 MHz. The height above ground was 7 feet in this instance, although improved performance should result if the builder can install the loop higher above ground without sacrificing length on the vertical sides. At B, illustration how a single supporting structure can be used to hold the loop in a diamond-shaped configuration. Feeding the diamond at the lower tip provides radiation in the horizontal plane. Feeding the system at either side will result in vertical polarization of the radiated signal.

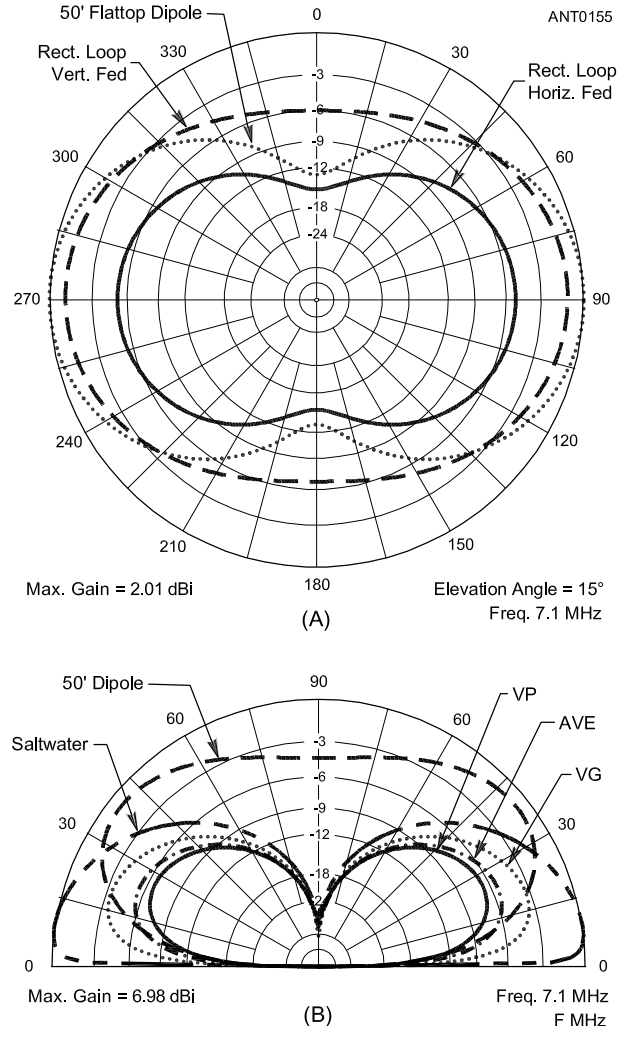

Fig 31—At A, azimuthal plane responses for the vertically and horizontally polarized 7-MHz loop, compared to a flattop 50-foot high dipole, all at a takeoff angle of 15° for DX work. The solid line is for feeding the loop horizontally at the bottom; the dashed line is for feeding the loop vertically at a side, and the dotted line is for a simple flattop horizontal dipole at 50 feet in height. For DX work, the vertically polarized loop is an excellent performer.

compromise result for both local and DX work. The actual impedance is roughly the same at each point: bottom horizontal center, corner or vertical side center.

Fig 31B demonstrates how the gain for vertical polarization changes over different type of grounds: saltwater, very poor ground (conductivity = 1 mS/m, dielectric constant = 5) very good (conductivity = 30 mS/m, dielectric constant = 20) and average ground (conductivity = 5 mS/m, dielectric constant = 13). Again, for reference a 50-foot high flattop dipole's elevation response is included. As has been mentioned previously in other chapters, a seaside location is a wonderful environment for verticals!

Just how you erect such a loop will depend on what is available in your backyard. Trees are always handy for supporting loop antennas. A disadvantage to the rectangular loop shown in Fig 30A is that two 34-foot high supports are needed, although in many instances your house may be high enough to serve as one of these supports. If you have a tower higher than about 50 feet, Fig 30B demonstrates how you can use it to support a diamond-shaped loop for 40 meters. The elevation and azimuthal responses are almost the same for either loop configuration, rectangular- or diamond-shaped.

The overall length of the wire used in a loop is determined in feet from the formula 1005/f (MHz). Hence, for operation at 7.125 MHz the overall wire length will be 141 feet. The matching transformer, an electrical $^1/_4$ λ of 75Ω coax cable, can be computed by dividing 246 by the operating frequency in MHz, then multiplying that number by the velocity factor of the cable being used. Thus, for operation at 7.125 MHz, 246/7.125 MHz = 34.53 feet. If coax with solid polyethylene insulation is used, a velocity factor of 0.66 must be employed. Foam-polyethylene coax has a velocity factor of 0.80. Assuming RG-59 is used, the length of the matching transformer becomes 34.53 (feet) × 0.66 = 22.79 feet, or 22 feet, $9^1/_2$ inches.

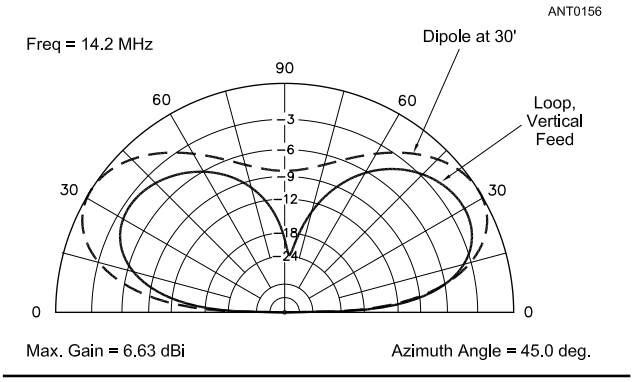

Fig 32—Elevation-plane response of 7-MHz loop used on 14.2 MHz. This is for a feed point at the center of one of the two vertical wires. The dashed line is the response of a flattop 20-meter dipole at 30 feet in height for comparison.

This same loop antenna in Fig 30A fed vertically may be used on the 14 and 21MHz bands, although its pattern will not be as good as that on its fundamental frequency and you will have to use an open-wire transmission line to feed the loop for multiband use. **Fig 32** shows the response at the peak lobe of the loop, at a 45° angle to the plane of the loop, compared to the peak response for a simple halfwave 20-meter dipole, 30 feet high. The gain from a simple flattop dipole, mounted at 30 feet, will be superior to the loop operated on a harmonic frequency.

A Receiving Loop for 1.8 MHz

You can use a small shielded-loop antenna to improve reception under certain conditions, especially at the lower amateur frequencies. This is particularly true when high levels of man-made noise are prevalent, when the second-harmonic energy from a nearby broadcast station falls in the 1.8MHz band, or when interference exists from some other amateur station in the immediate area. A properly constructed and tuned small loop will exhibit approximately 30 dB of front-to-side response, the minimum response being at right angles to the plane of the loop. Therefore, noise and interference can be reduced significantly or completely nulled out, by rotating the loop so that it is sideways to the interference-causing source.

Generally speaking, small shielded loops are far less responsive to man-made noise than are the larger antennas used for transmitting and receiving. But a trade-off in performance must be accepted when using the loop, for the strength of received signals will be 10 or 15 dB less than when using a full-size resonant antenna. This condition is not a handicap on 1.8 or 3.5 MHz, provided the station receiver has normal sensitivity and overall gain. Because a front-to-side ratio of 30 dB may be expected, a shielded loop can be used to eliminate a variety of receiving problems if made rotatable, as shown in **Fig 33**.

To obtain the sharp bidirectional pattern of a small loop, the overall length of the conductor must not exceed 0.1 λ. The loop of **Fig 34** has a conductor length of 20 feet. At 1.81 MHz, 20 feet is 0.037 λ. With this style of loop, 0.037 λ is about the maximum practical dimension if you want to tune the element to resonance. This limitation results from the distributed capacitance between the shield and inner conductor of the loop. RG-59 was used for the loop element in this example. The capacitance per foot for this cable is 21 pF, resulting in a total distributed

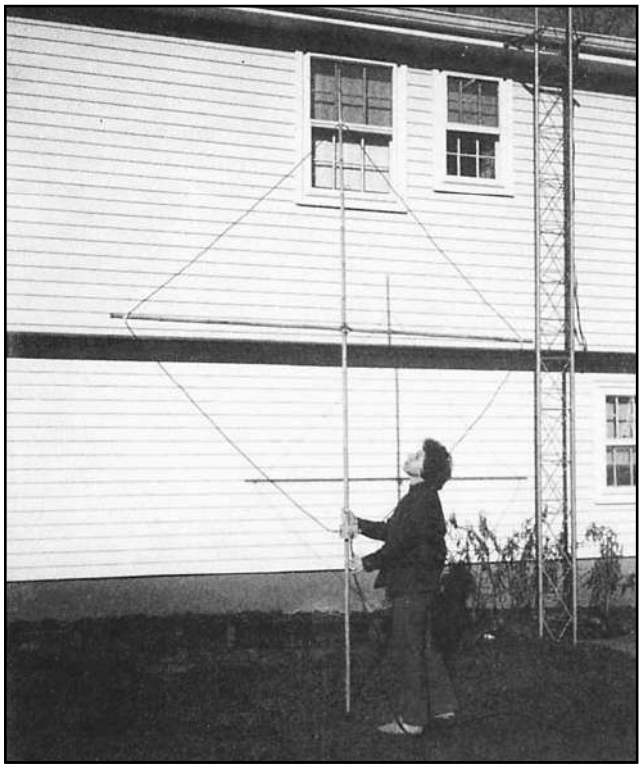

Fig 33—Jean DeMaw, W1CKK, tests the 1.8-MHz shielded loop. Bamboo cross arms are used to support the antenna.

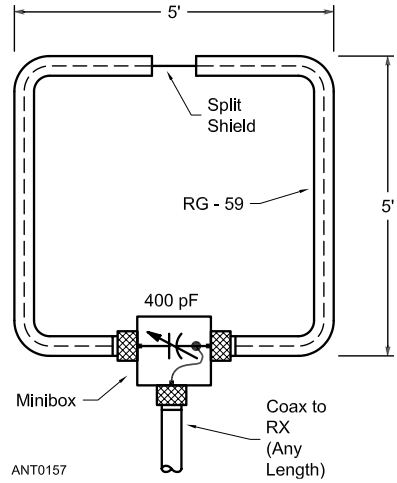

Fig 34—Schematic diagram of the loop antenna. The dimensions are not critical provided overall length of the loop element does not exceed approximately 0.1 λ. Small loops which are one half or less the size of this one will prove useful where limited space is a consideration.

capacitance of 420 pF. An additional 100 pF was needed to resonate the loop at 1.810 MHz.

Therefore, the approximate inductance of the loop is 15 μH. The effect of the capacitance becomes less pronounced at the higher end of the HF spectrum, provided the same percentage of a wavelength is used in computing the conductor length. The ratio between the distributed capacitance and the lumped capacitance used at the feed point becomes greater at resonance. These facts should be contemplated when scaling the loop to those bands above 1.8 MHz.

There will not be a major difference in the construction requirements of the loop if coaxial cables other than RG-59 are used. The line impedance is not significant with respect to the loop element. Various types of coaxial line exhibit different amounts of capacitance per foot, however, thereby requiring more or less capacitance across the feed point to establish resonance.

Shielded loops are not affected noticeably by nearby objects, and therefore they can be installed indoors or out after being tuned to resonance. Moving them from one place to another does not significantly affect the tuning.

You can see in the model shown in Fig 33 that a supporting structure was fashioned from bamboo poles. The X frame is held together at the center with two U bolts. The loop element is taped to the cross-arms to form a square. You could likely use metal cross arms without seriously degrading the antenna performance. Alternatively, wood can be used for the supporting frame.

A Minibox was used at the feed point of the loop to hold the resonating variable capacitor. In this model a 50 to 400-pF compression trimmer was used to establish resonance. You must weatherproof the box for outdoor installations.

Remove the shield braid of the loop coax for one inch directly opposite the feed point. You should treat the exposed areas with a sealing compound once this is done.

In operation this receiving loop has proven very effective for nulling out second-harmonic energy from local broadcast stations. During DX and contest operations on 1.8 MHz it helped prevent receiver overloading from nearby 1.8-MHz stations that share the band. The marked reduction in response to noise has made the loop a valuable station accessory when receiving weak signals. It is not used all of the time, but is available when needed by connecting it to the receiver through an antenna selector switch. Reception of European stations with the loop has been possible from New England at times when other antennas were totally ineffective because of noise.

It was also discovered that the effects of approaching storms (with attendant atmospheric noise) could be nullified considerably by rotating the loop away from the storm front. It should be said that the loop does not exhibit meaningful directivity when receiving sky-wave signals. The directivity characteristics relate primarily to ground-wave signals. This is a bonus feature in disguise, for when nulling out local noise or interference, one is still able to copy sky-wave signals from all compass points!

For receiving applications it is not necessary to match the feed line to the loop, though doing so may enhance the performance somewhat. If no attempt is made to obtain an SWR of 1, the builder can use 50 or 75-Ω coax for a feeder, and no difference in performance will be observed. The Q of this loop is sufficiently low to allow the operator to peak it for resonance at 1.9 MHz and use it across the entire 1.8MHz band. The degradation in performance at 1.8 and 2 MHz will be so slight that it will be difficult to discern.

An Indoor Stealth Loop

Ted Phelps, W8TP, wrote an article in *The ARRL Antenna Compendium, Vol 7* describing his attic-mounted wire loop antenna, fed with an automatic antenna tuner. Here is a shortened version of that article.

If you drive down my street in Whitechapel Village in Newark, DE, trying to find my ham location by looking for my antenna, you wouldn't find it. Even if you pulled up in front of my condo, you wouldn't notice any telltale signs, because my multiband antenna is completely hidden. It's in the attic of my two-bedroom condominium in a small retirement community completed in 1999.

Before the move, I had given considerable thought to what type of antenna I might use, if any. I already knew that permanent outdoor types were out of the question, due to restrictive real estate and condo association rules. So I planned a clause for any sales contract I might sign, specifically mentioning amateur radio and my desire to set up a station in my new living quarters. I decided I would not move where my lifelong hobby would be severely restricted or prohibited.

That meant that to be reasonably sure I could continue enjoying Amateur Radio as before, I would have to install an indoor antenna that could perform as well as a typical outdoor system. What kind? In Ohio, I had tried a horizontally polarized attic dipole made with #14 wire. It didn't work very well—it was just too low to the ground.

I learned about a high-tech method of remote antenna tuning using an antenna coupler which contains a microprocessor. I found this kind of automatic tuner available from two American manufacturers and within a reasonable price range. Although our move was still a few months ahead, I purchased a model SG-230 antenna coupler made by SGC Inc, Bellevue, WA, for use in Delaware.

Fig 35 shows the final dimensions of my hidden loop, which is a single-turn rectangular loop, erected in a north-south vertical plane and made from nearly 78 feet of #6 stranded, aircraft primary wire in a PVC jacket, held taut at the lower corners and supported by a pulley and guy rope at each upper corner. Because it's vertically polarized, it supports low-angle radiation reasonably well. By the way, if you're wondering why I used such a relatively large-gauge wire as #6 for the loop antenna, it was readily available from my son-in-law!

Fig 36 shows my completed condo unit. Note the dog-house dormer on the roof about 12 feet above ground at the attic floor. This is the level of my hidden loop's base leg.

In constructing my system I had to overcome RFI problems on my own premises. Each condo unit has its own electronic security panel on an upper shelf in a closet. As soon as I applied moderate power to my radio and loop, the Fire Alarm sounded and firefighters came to my door! The burglar/intrusion signal was triggered a couple of times, too. Working with a security installation technician, I found that *there was no ground wire connected to my security panel.* "We don't bother with that," said the tech, and then, reacting to my surprise, connected a #14 ground between the security panel and the house water-pipe ground. I then installed a ferrite bead on each lead entering the security panel. I also placed ferrite beads on keyer-paddle leads, GFCI electrical outlets, etc. Those

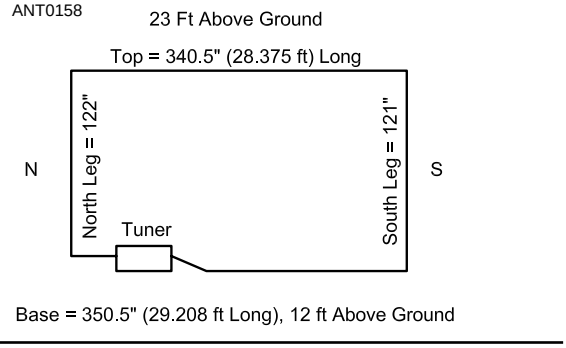

Fig 35—Diagram showing layout of W8TP's indoor hidden loop antenna.

Fig 36—Can you see W8TP's antenna in this photograph? Of course you can't—it's hidden from view inside his attic!

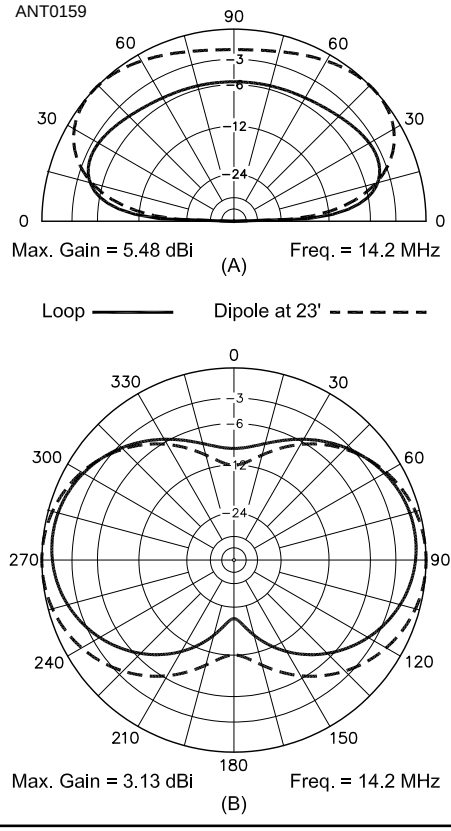

Fig 37—At A, computed elevation pattern at 14.2 MHz for W8TP's hidden loop (solid line), compared to a 20-meter dipole (dashed line) at a height of 23 feet. At B, a comparison of the azimuth patterns at a 20°-elevation angle for W8TP's loop (solid line) and the same 20-meter dipole (dashed line). The loop has a slightly asymmetrical response because it is fed at a corner, but its performance is competitive to an outdoor dipole. In fact, it has superior low-angle performance, typical of a vertically polarized antenna compared to a low horizontal antenna.

measures seem to have eliminated my RFI problems.

When we moved into our condo, I took the obvious precaution of not using a linear amplifier. I took extra care to establish a single-point ground for my station equipment by connecting all equipment grounds to the cover plate of the dedicated metallic outlet box behind the operating position, and thence to a separate ground rod in our front yard. I use a 1-kW RL Drake low-pass filter in the transceiver-antenna feed line.

Is this indoor antenna system safe? I believe so. In the attic it is not at all close to our living space. It is fixed firmly in place and unlike most amateur antennas it is *out of the weather*! I therefore do not use a quick-grounding system for times when a thunderstorm approaches.

Fig 37 shows the computed elevation and azimuth patterns on 20 meters. The tuner is able to hold the SWR down low enough so that my JRC-245 transceiver can operate through its internal antenna tuner.

BIBLIOGRAPHY

Source material and more extended discussion of topics covered in this chapter can be found in the references given below and in the textbooks listed at the end of Chapter 2.

C. F. W. Anderson, "A Crossed-Loop/Goniometer DF Antenna for 160 Meters," *The ARRL Antenna Compendium, Vol 1* (Newington: ARRL, 1985), pp 127-132.

J. S. Belrose, "Ferromagnetic Loop Aerials," *Wireless Engineer*, Feb 1955, pp 41-46.

J. S. Belrose, "An Update on Compact Transmitting Loops," *QST*, Nov 1993, pp 37-40.

D. S. Bond, *Radio Direction Finders*, 1st ed. (New York: McGraw-Hill Book Co, 1944).

G. Bramslev, "Loop Aerial Reception," *Wireless World*, Nov 1952, pp 469-472.

R. W. Burhans, "Experimental Loop Antennas for 60 kHz to 200 kHz," *Technical Memorandum (NASA) 71*, (Athens, OH: Ohio Univ, Dept of Electrical Engr), Dec 1979.

R. W. Burhans, "Loop Antennas for VLF-LF," *Radio-Electronics*, Jun 1983, pp 83-87.

D. DeMaw, "Beat the Noise with a Scoop Loop," *QST*, Jul 1977, pp 30-34.

M. F. DeMaw, *Ferromagnetic-Core Design and Application Handbook* (Englewood Cliffs, NJ: Prentice-Hall Inc, 1981).

D. DeMaw and L. Aurick, "The Full-Wave Delta Loop at Low Height," *QST*, Oct 1984, pp 24-26.

R. Devore and P. Bohley, "The Electrically Small Magnetically Loaded Multiturn Loop Antenna," *IEEE Trans on Ant and Prop*, Jul 1977, pp 496-505.

T. Dorbuck, "Radio Direction-Finding Techniques," *QST*, Aug 1975, pp 30-36.

R. G. Fenwick, "A Loop Array for 160 Meters," *CQ*, Apr 1986, pp 25-29.

D. Fischer, "The Loop Skywire," *QST*, Nov 1985, pp 20-22. Also "Feedback," *QST*, Dec 1985, p 53.

R. A. Genaille, "V.L.F. Loop Antenna," *Electronics World*, Jan 1963, pp 49-52.

G. Gercke, "Radio Direction/Range Finder," *73*, Dec 1971, pp 29-30.

R. S. Glasgow, *Principles of Radio Engineering* (New York: McGraw-Hill Book Co, Inc, 1936).

S. Goldman, "A Shielded Loop for Low Noise Broadcast Reception," *Electronics*, Oct 1938, pp 20-22.

F. W. Grover, *Inductance Calculation-Working Formulas and Tables* (New York: D. VanNostrand Co, Inc, 1946).

J. V. Hagan, "A Large Aperture Ferrite Core Loop Antenna for Long and Medium Wave Reception," *Loop Antennas Design and Theory*, M.G. Knitter, Ed. (Cambridge, WI: National Radio Club, 1983), pp 37-49.

T. Hart, "Small, High-Efficiency Loop Antennas," *QST*, Jun 1986, pp 33-36.

T. Hart, *Small High Efficiency Antennas Alias The Loop* (Melbourne, FL: W5QJR Antenna Products, 1985)

H. Hawkins, "A Low Budget, Rotatable 17 Meter Loop," *QST*, Nov 1997, p 35.

F. M. Howes and F. M. Wood, "Note on the Bearing Error and Sensitivity of a Loop Antenna in an Abnormally Polarized Field," *Proc IRE*, Apr 1944, pp 231-233.

B. Jones, KD7S, "You Can Build: A Compact Loop Antenna for 30 Through 12 Meters," Nov 1994 *QST*, pp 33-36.

J. A. Lambert, "A Directional Active Loop Receiving Antenna System," *Radio Communication*, Nov 1982, pp 944-949.

D. Lankford, "Loop Antennas, Theory and Practice," *Loop Antennas Design and Theory*, M. G. Knitter, Ed. (Cambridge, WI: National Radio Club, 1983), pp 10-22.

D. Lankford, "Multi-Rod Ferrite Loop Antennas," *Loop Antennas Design and Theory*, M. G. Knitter, Ed. (Cambridge, WI: National Radio Club, 1983), pp 53-56.

G. Levy, "Loop Antennas for Aircraft," *Proc IRE*, Feb 1943, pp 56-66. Also see correction, *Proc IRE*, Jul 1943, p 384.

J. Malone, "Can a 7 foot 40m Antenna Work?" *73*, Mar 1975, pp 33-38.

R. Q. Marris, "An In-Room 80-Meter Transmitting Multiturn Loop Antenna," *QST*, Feb 1996, pp 43-45. Feedback. *QST*, May 1996, p 48.

L. G. McCoy, "The Army Loop in Ham Communications," *QST*, Mar 1968, pp 17, 18, 150, 152. (See also Technical Correspondence, *QST*, May 1968, pp 49-51 and Nov 1968, pp 46-47.)

R. G. Medhurst, "HF Resistance and Self Capacitance of Single Layer Solenoids," *Wireless Engineer*, Feb 1947, pp 35-43, and Mar 1947, pp 80-92.

G. P. Nelson, "The NRC FET Altazimuth Loop Antenna," *N.R.C. Antenna Reference Manual Vol. 1*, 4th ed., R. J. Edmunds, Ed. (Cambridge, WI: National Radio Club, 1982), pp 2-18.

K. H. Patterson, "Down-To-Earth Army Antenna," *Electronics*, Aug 21, 1967, pp 111-114.

R. C. Pettengill, H. T. Garland and J. D. Meindl, "Receiving Antenna Design for Miniature Receivers," *IEEE Trans on Ant and Prop*, Jul 1977, pp 528-530.

T. Phelps, W8TP, "A Hidden Loop Antenna," *The ARRL Antenna Compendium, Vol 7* (Newington: ARRL, 2002), pp 160-162.

R. Z. Plasencia, WØRPV, "Remotely Controlled Antenna Coupler," *The ARRL Antenna Compendium, Vol 2* (Newington: ARRL, 1989), pp 182-186.

W. J. Polydoroff, *High Frequency Magnetic Materials—Their Characteristics and Principal Applications* (New York: John Wiley and Sons, Inc, 1960).

E. Robberson, "QRM? Get Looped," *Radio and Television News*, Aug 1955, pp 52-54, 126.

G. S. Smith, "Radiation Efficiency of Electrically Small Multiturn Loop Antennas," *IEEE Trans on Ant and Prop*, Sep 1972, pp 656-657.

E. C. Snelling, *Soft Ferrites—Properties and Applications* (Cleveland, OH: CRC Press, 1969).

G. Thomas, "The Hot Rod—An Inexpensive Ferrite Booster Antenna," *Loop Antennas Theory and Design*, M. G. Knitter, Ed. (Cambridge, WI: National Radio Club, 1983), pp 57-62.

J. R. True, "Low-Frequency Loop Antennas," *Ham Radio*, Dec 1976, pp 18-24.

E. G. VonWald, "Small-Loop Antennas," *Ham Radio*, May 1972, pp 36-41.

"An FET Loop Amplifier with Coaxial Output," *N.R.C. Antenna Reference Manual, Vol 2*, 1st ed., R. J. Edmunds, Ed. (Cambridge, WI: National Radio Club, Oct 1982), pp 17-20.

Aperiodic Loop Antenna Arrays (Hermes Electronics Ltd, Nov 1973).

Reference Data for Radio Engineers, 6th ed. (Indianapolis: Howard W. Sams & Co, subsidiary of ITT, 1977).

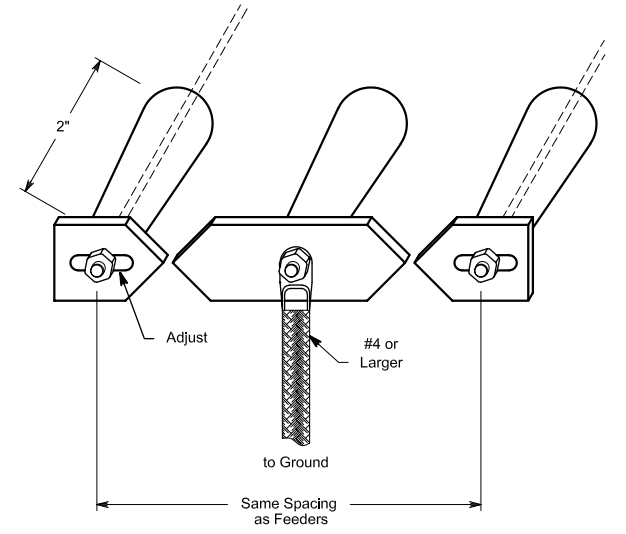

Fig 43—A simple lightning arrester for open-wire line made from three standoff or feedthrough insulators and sections of $^1/_8 \times {}^1/_2$-inch brass or copper strap. It should be installed in the line at the point where the line enters the station. The heavy ground lead should be as short and as direct as possible. The gap setting should be adjusted to the minimum width that will prohibit arcing when the transmitter is operated.

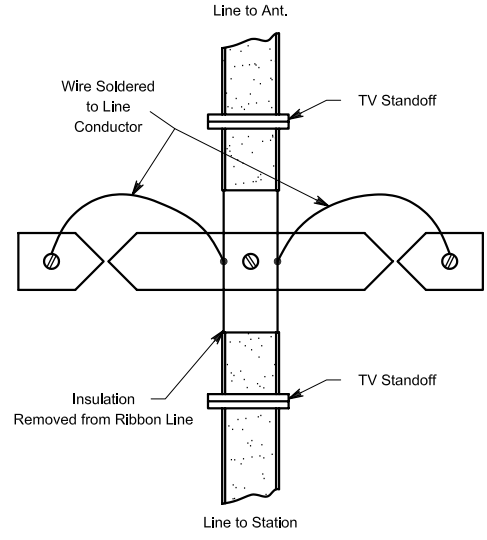

Fig 44—The lightning arrester of Fig 39 may be used with 300-Ω ribbon line in the manner shown here. The TV standoffs support the line an inch or so away from the grounded center member of the arrester

The construction of a homemade arrester for open-wire line is shown in **Fig 43**. This type of arrester can be adapted to ribbon line an inch or so away from the center member of the arrester, as shown in **Fig 44**. Sufficient insulation should be removed from the line where it crosses the arrester to permit soldering the arrester connecting leads.

Lightning Grounds

Lightning-ground connecting leads should be of conductor size equivalent to at least #10 wire. The #8 aluminum wire used for TV-antenna grounds is satisfactory. Copper braid $^3/_4$-inch wide (Belden 8662-10) is also suitable. The conductor should run in a straight line to the grounding point. The ground connection may be made to a water pipe system (if the pipe is not plastic), the grounded metal frame of a building, or to one or more $^5/_8$-inch ground rods driven to a depth of at least 8 feet. More detailed information on lightning protection is contained in Chapter 1, Safety.

A central grounding panel for coax cables coming into the house is highly recommended. See **Fig 45** for a photo of the homemade grounding panel installed by Chuck Hutchinson, K8CH, at his Michigan home. The coax cables screwed into dual-female feed-through UHF connectors. K8CH installed this aluminum panel under the outside grill for a duct that provided combustion air to an unused fireplace. He used ground strap to connect to ground rods located under the panel. See the ARRL book *Simple and Fun Antennas* for more information about ground panels.

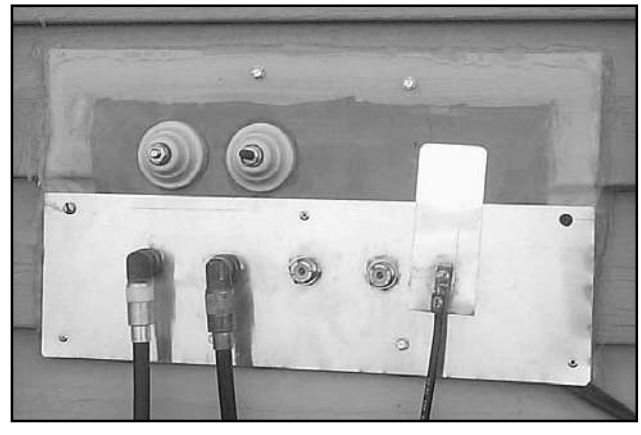

Fig 45—K8CH's coax entry panel mounted on exterior wall (later covered by grill that provides combustion to an unused fireplace). The ground braid goes to a ground rod located beneath the panel. (Photo courtesy: *Simple and Fun Antennas for Hams*)

Before a lightning storm approaches, a prudent ham will disconnect all feed lines, rotor lines and control lines inside the shack to prevent damage to sensitive electronics. When lightning is crashing about outside, you certainly don't want that lightning inside your shack!

Chapter 6

Low-Frequency Antennas

In theory there is no difference between antennas at 10 MHz and up and those for lower frequencies. In reality however, there are often important differences. It is the size of the antennas, which increases as frequency is decreased, that creates practical limits on what can be realized physically at reasonable cost.

At 7.3 MHz, 1λ = 133 feet and by the time we get to 1.8 MHz, 1 λ = 547 feet. Even a λ/2 dipole is very long on 160 meters. The result is that the average antenna for these bands is quite different from the higher bands, where Yagis and other relatively complex antennas dominate. In addition, vertical antennas can be more useful at low frequencies than they are on 20 meters and above because of the low heights (in wavelengths) usually available for horizontal antennas on the low bands. Much of the effort on the low bands is focused on how to build simple but effective antennas with limited resources. This section is devoted to antennas for use on amateur bands between 1.8 to 7 MHz.

The Importance of Low Angles for Low-Band DXing

In Chapter 3, The Effects of Ground, we emphasized the importance of matching the elevation response of your antennas as closely as possible to the range of elevation angles needed for communication with desired geographic areas. **Fig 1** shows the statistical 40-meter elevation angles needed over the entire 11-year solar cycle to cover the path from Boston, Massachusetts, to all of Europe. These angles range from 1° (at 9.6% of the time when the 40-meter band is open to Europe) to 28° (at 0.3% of the time).

Fig 1 also overlays the elevation pattern response of a 100-foot high flattop dipole on the elevation-angle statistics, illustrating that even at this height the coverage is hardly optimum to cover all the necessary elevation angles. While Fig 1 is dramatic in its own right, the data can be viewed in another way that emphasizes even more the importance of low elevation angles. **Fig 2** plots the the *cumulative distribution function*, the total percentage of time 40 meters is open from Boston to Europe, at or below each elevation angle. For example, Fig 2 says that 40 meters is open to Europe from Boston 50% of the time at an elevation angle of 9° or less. The band is open 90%

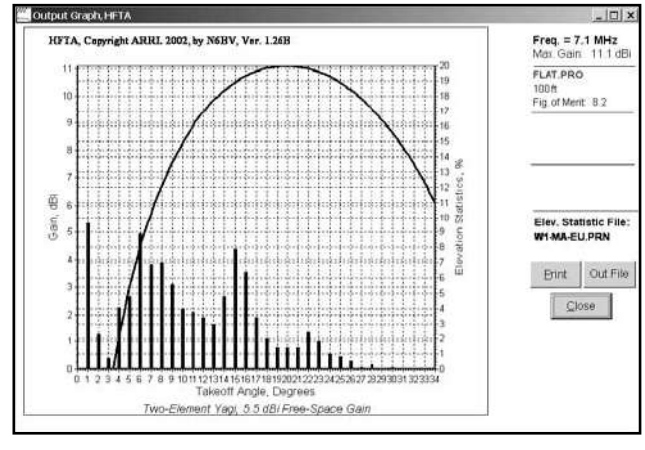

Fig 1—Screen capture from *HFTA* (HF Terrain Assessment) program showing elevation response for 100-foot high dipole over flat ground on 7.1 MHz, with bar-graph overlay of the statistical elevation angles needed over the whole 11-year solar cycle from New England (Boston) to all of Europe. Even a 100-foot high antenna cannot cover all the necessary angles.

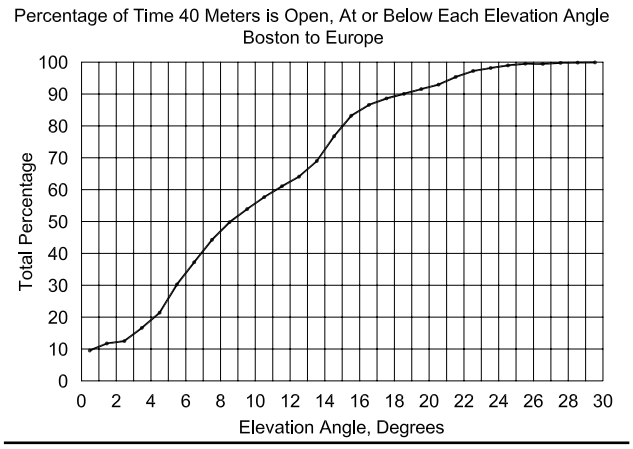

Fig 2—Another way of looking at the elevation statistics from Fig 1. This shows the percentage of time the 40-meter band is open, at or below each elevation angle, on the path from Boston to Europe. For example, the band is open 50% of the time at an angle of 9° or lower. It is open 90% of the time at an angle of 19° or lower.

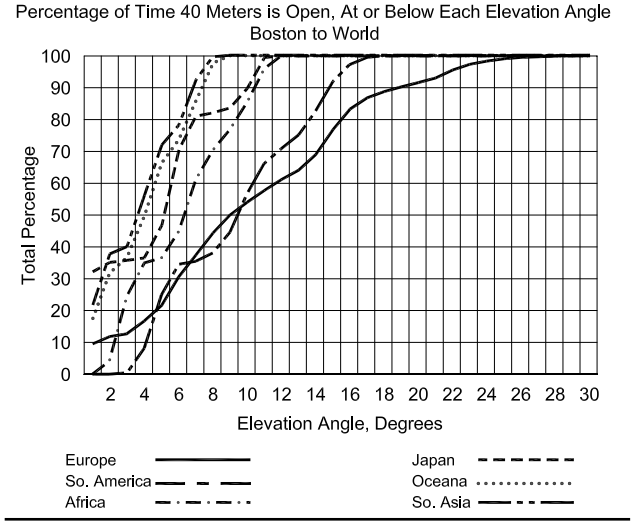

Fig 3—The percentage of time the 40-meter band is open, at or below each elevation angle, for various DX paths from Boston: to Europe, South America, southern Africa, Japan, Oceania and south Asias. The angles are predominantly quite low. For example, on the path from Boston to Japan, 90% of the time when the 40-meter band is open, it is open at elevation angles less than or equal to 10°. Achieving good performance at these low takeoff angles requires very high horizontally polarized antennas, or efficient vertically polarized antennas.

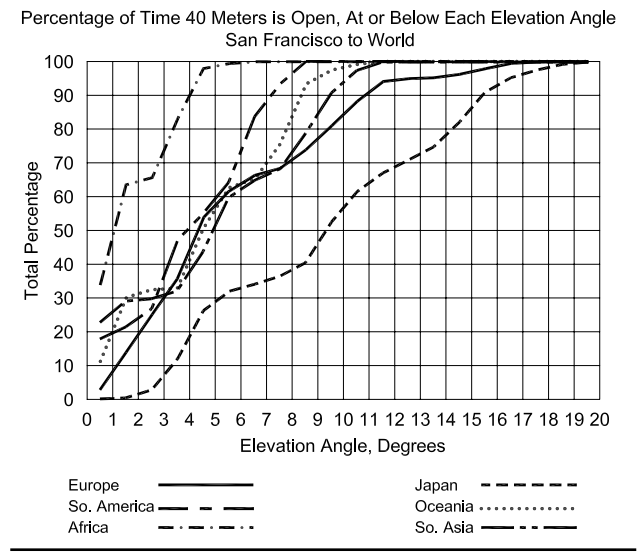

Fig 4—The 40-meter statistics from the West Coast: from San Francisco to the rest of the DX world. Here, 90% of the time the path to Europe is open, it is at takeoff angles less than or equal to 11°. No wonder the hams living on mountain tops do best into Europe from the West Coast.

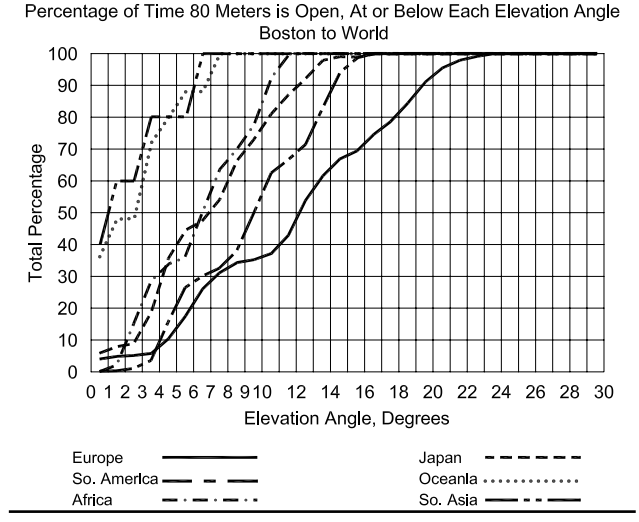

Fig 5—The situation on 80 meters from Boston to the rest of the DX world. Into Europe, 90% of the time the elevation angle is less than or equal to 20°. Into Japan from Boston, 90% of the time the angle is less than or equal to 12°.

of the time at an elevation angle of 19° or less.

Fig 3 plots the 40-meter elevation-angle data for six major geographic areas around the world from Boston. In general, the overall range of elevation angles for far-distant locations is smaller, and the angles are lower than for closer-in areas. For example, from Boston to southern Asia (India), 50% of the time the takeoff angles are 4° or less. On the path to Japan from Boston, the takeoff angles is less than or equal to 6° about 70% of the time. These are low angles indeed.

Fig 4 shows similar data for the 40-meter band from San Francisco, California, to the rest of the world. The path to southern Africa from the US West Coast is a very long-distance path, open some 65% of the time it is open at angles of 2° or less! The 40-meter path to Japan involves takeoff angles of 10° or less more than 50% of the time. If you are

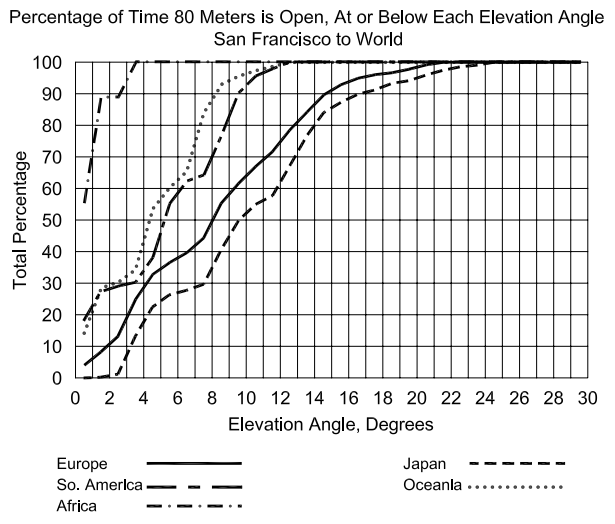

Fig 6—From San Francisco to the rest of the world on 80 meters: 90% of the time on the path to Japan, the takeoff angle is less than or equal to 17°; 50% of the time the angle is less than or equal to 10°; 25% of the time the angle is less than or equal to 6°. A horizontally polarized antenna would have to be 600 feet above flat ground to be optimum at 6°!

fortunate enough to have a 100-foot high flattop dipole for 40 meters, at a takeoff angle of 10° the response would be down about 3 dB from its peak level at 20°. At an elevation angle of 5° the response would be about 8 dB down from peak. You can see why the California stations located on mountain tops do best on 40 meters for DXing.

Fig 5 shows the same percentage-of-time data for the 80-meter band from Boston to the world. Into Europe from Boston, the 80-meter elevation angle is 13° or less more than 50% of the time. Into Japan from Boston, 90% of the time the band is open is at a takeoff angle of 13° or less. (Note that these elevation statistics are computed for "undisturbed" ionospheric conditions. There are times when the incoming angles are affected by geomagnetic storms, and generally speaking the elevation angles rise under these conditions.)

Fig 6 shows the 80-meter data from San Francisco to the world. Low elevation angles dominate in this graph and high horizontal antennas would be necessary to optimal coverage. In fact, 50% of the time for all paths, the elevation angle is less than 10°.

In the rest of this chapter, we'll often compare horizontally polarized antennas at practical heights with vertically polarized antennas, usually at takeoff angles of 5° or 10°, angles useful for DX work. But first, let us look at situations where *high* takeoff angles are most useful.

Short/Medium-Range Communications

Not all hams are interested in working stations thousands of miles from them. Traffic handlers and rag chewers may, in fact, only be interested in *nearby* communications—perhaps out to 600 miles from their location.

For example, a ham in Boston may want to talk with his brother-in-law in Cleveland, OH, a path that is just over 550 miles away. Or an operator in Buffalo, NY, may be the net control station (NCS) for a regional net involving the states of New York and New Jersey. She needs to cover distances up to about 300 miles away.

Depending on the time of day, the most appropriate ham frequencies needed for nearby communications are the 40 and 80/75-meter bands, with 160 meters also a possibility during the night hours, particularly during low portions of the sunspot cycle. The elevation angles involved in such nearby distances are usually high, even almost directly overhead for distances beyond ground-wave coverage (which may be as short as a few miles on 40 meters). For example, the distance between the Massachusetts cities of Boston and Worchester is about 40 miles. On 40 meters, 40 miles is beyond ground-wave coverage. So you will need sky-wave signals that use the ionosphere to communicate between these two cities, where the elevation angle is 83°—very nearly straight up.

Hams using vertical antennas for communications with nearby stations may well find that their signals will be below the noise level typical on the lower bands, especially if they aren't running maximum legal power. Such relatively short-range paths involve so-called *NVIS*, "Near Vertical Incidence Skywave," a fancy name for HF communication systems covering nearby geographic areas. The US military discusses NVIS out to about 500 miles, encompassing the territory a brigade might cover. Elevation angles needed to cover distances from 0 to 500 miles range from about 40º to 90º. This also covers the circumstances involved in amateur communications, particularly in emergency situations.

The following section is adopted from the article "What's the Deal About NVIS?" that appeared in December 2005 *QST*. This article used an example of a hypothetical earthquake in San Francisco to analyze HF emergency communication requirements.

HAM RADIO RESPONSE IN NATURAL DISASTERS

One of San Francisco's somewhat less endearing nicknames is "the city that waits to die." When the *Big Earthquake* does come, you can be assured that all the cell phones and the land-line telephones will be totally jammed, making calling in or out of the San Francisco Bay Area virtually impossible. The same thing occurred in Manhattan on September 11, 2001. The Internet will also be severely affected throughout northern California because of its trunking via the facilities of the telephone network. Commercial electricity will be out

in wide areas because power lines will be down. It's virtually certain that water mains will be out of commission too.

If the repeaters on the hills around the San Francisco Bay Area haven't been damaged by the shaking itself, there will be some ham VHF/UHF voice coverage in the intermediate area, at least until the backup batteries run down. But connecting to the dysfunctional telephone system will be difficult at best through amateur repeaters.

With little or no telephone coverage, an obvious need for ham radio communications to aid disaster relief would be from San Francisco to Sacramento, the state capital. Sacramento is 75 miles northeast of the Bay Area, well outside VHF/UHF coverage, so amateur HF will be required on this radio circuit. On-the-ground communications directly between emergency personnel (including the armed-forces personnel who will be brought into the rescue and rebuilding effort) will often be difficult on VHF/UHF since San Francisco is a hilly place. So HF will probably be needed even for short distance, operator-to-operator or operator-to-communications center work. Throughout the city, portable HF stations will have to be quickly set up and staffed to provide such communications.

Hams used to half jokingly call short range HF communications on 40 and 80 meters "cloud warming." This is an apt description, because the takeoff angles needed to launch HF signals up into the ionosphere and then down again to a nearby station are almost directly upwards. **Table 1** lists the distance and takeoff angles from San Francisco to various cities around the western part of the USA. The distance between San Francisco and Sacramento is about 75 miles, and the optimum takeoff angle is about 78°. Launching such a high-angle signal is best done using horizontally polarized antennas mounted relatively close to the ground.

GEOGRAPHIC COVERAGE FOR NVIS

Figure 7A shows the geographic area coverage around San Francisco for a 100-W, 7.2-MHz station using an inverted V dipole. The center of this antenna is 20 feet above flat

Table 1
Average Elevation Angles for Target Destinations from San Francisco

Location	*Distance Miles*	*Average Elevation Angle, Degrees*
San Jose, CA	43	80
Sacramento, CA	75	78
Fresno, CA	160	63
Reno, NV	185	60
Los Angeles	350	44
San Diego	450	42
Portland, OR	530	30
Denver, CO	950	18
Dallas, TX	1500	8

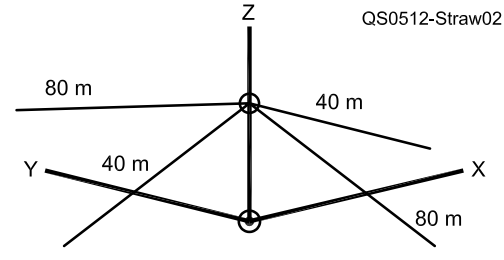

Fig 8—Layout for two band inverted V dipoles for 40 and 80 meters. The two dipoles are fed together at the center and are laid out at right angles to each other to minimize interaction between them. Each end of both dipoles is kept 8 feet above ground for personnel safety.

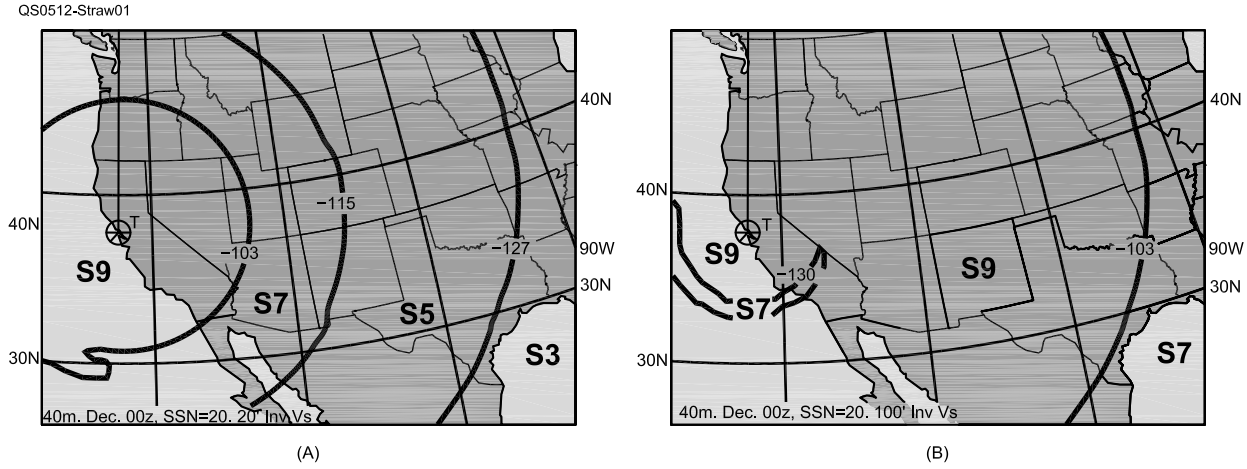

Fig 7—At A, Predicted 40 meter geographic coverage plot for a 100 W transmitter in December at 0000 UTC (near sunset), for a SSN (Smoothed Sunspot Number) of 20. The antennas used are 20 foot-high inverted V dipoles. At B, 40 meter coverage for same date and time, but for 100 foot-high flattop dipoles. Most of California is well covered with S9 signals in both cases, but there is more susceptibility in the higher dipole case to thunderstorm crashes coming from outside California, for example from Arizona or even Texas. Such noise can interfere with communications inside California.

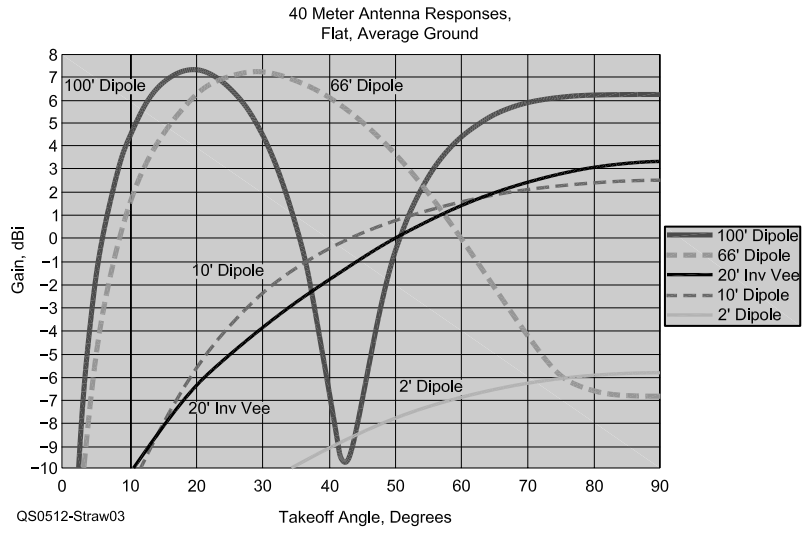

Fig 9—Elevation plots for different 40 meter antennas above flat ground with average ground characteristics (5 mS/m conductivity and dielectric constant of 13). The 10 foot-high flattop dipole and the 20 foot-high inverted V dipoles both have close to the same characteristics. Note that there is a null in the response of the 100 foot-high flattop dipole at a 42° elevation angle. The gain there is roughly that of a 2 foot-high dipole!

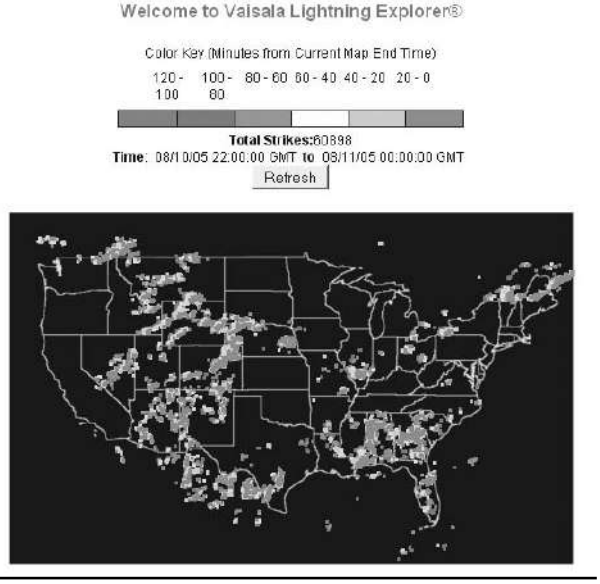

Fig 10—The distribution of lightning strikes across the USA for August 10, 2005 from 2200 to 0000 UTC, in the afternoon California time. There are lots of lightning strikes in the US during the summer—60,898 of them in this two-hour period! (*Courtesy Vaisala Lightning Explorer.*)

ground and the ends are 8 feet high. An actual implementation of such an antenna could be as an 80-meter inverted V, fed in parallel with a 40-meter inverted V dipole at a 90° angle. See **Fig 8**. The 8-foot height puts the ends high enough to prevent RF burns to humans (or most animals). The low height of the antenna above ground means that the azimuthal pattern is omnidirectional for high elevation angles.

Fig 7 was generated using the *VOAAREA* program, part of the *VOACAP* propagation-prediction suite, for the month of December. This was for 0000 UTC, close to sundown, for a low period of solar activity (Smoothed Sunspot Number, SSN of 20). The receiving stations were also assumed to be using identical inverted-V dipoles.

You can see that almost the whole state of California is covered with S9 signals, minus only a thin slice of land near the Mexican border in the southeast portion of the state, where the signal drops to S7. Signals from Texas are predicted to be only S5 or less in strength. Signals (or thunderstorm static) coming from, say, Louisiana would be several S units weaker than signals from central Texas.

Now take a look at Fig 7B. Here, the date, time and solar conditions remain the same, but now the antennas are 100-foot high flattop dipoles. California is still blanketed with S9 signals, save for an interesting crescent-shaped slice near Los Angeles, where the signal drops down to S7. Close investigation of this intriguing drop in signal strength reveals that the necessary elevation angle, 44°, from San Francisco to this part of southern California falls in the first null of the 100-foot high antenna's elevation pattern. See **Fig 9**, which shows the elevation patterns for five 40-meter antennas at different heights. In the null at a 44° takeoff angle, the 100-foot high dipole is just about equal to a 2-foot high dipole. We'll discuss 2-foot high dipoles in more detail later.

For most of California, the problem with 100-foot high 40-meter antennas is that interfering signals from Texas, Colorado or Washington State will *also* be S9 in San Francisco. So will static crashes coming from thunderstorms all over the West and much of the Gulf Coast. (Ed Farmer, AA6ZM, joked once that the Army doesn't have any problem with interfering signals—they just call in an airstrike. We hams don't generally have this ability, although we occasionally call in the FCC.) See **Fig 10**, which shows a typical distribution of thunderstorms across the US in the late afternoon, California time, in mid-August. There certainly are a lot of thunderstorms raging around the country in the summer.

The signal-to-noise and signal-to-interference ratios for a 20-foot high inverted V dipole will be superior for medium-

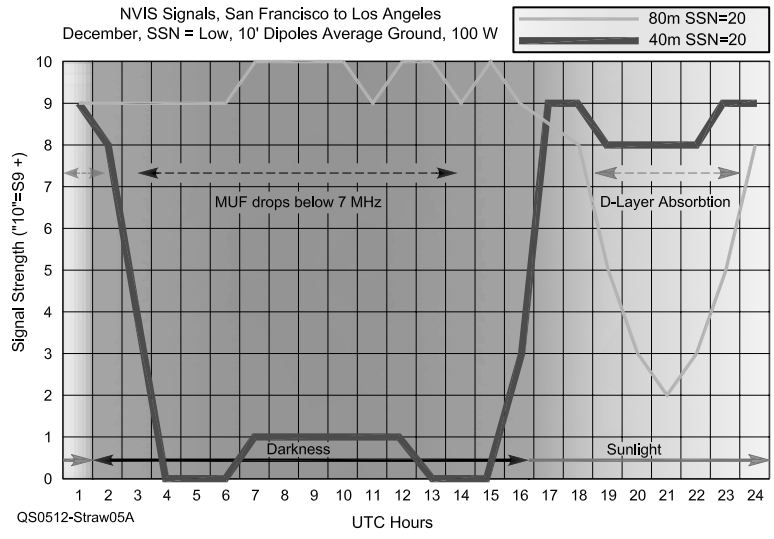

Fig 11—VOACAP calculations for a 350 mile path from San Francisco to Los Angeles, using 10 foot-high flattop dipoles. This plot shows the signal strength in S Units ("S10" = S9+10) for a worst-case month/SSN combination—winter solstice, in December, for a low level of solar activity (SSN = 20). The 40-meter signal drops to a very low level during the night because the MUF drops well below 7.2 MHz. The 80-meter signal drops in the afternoon because of D-layer absorption. For 24-hour communications on this path, the rule of thumb is to select 40 meters during the day and 80 meters during the night.

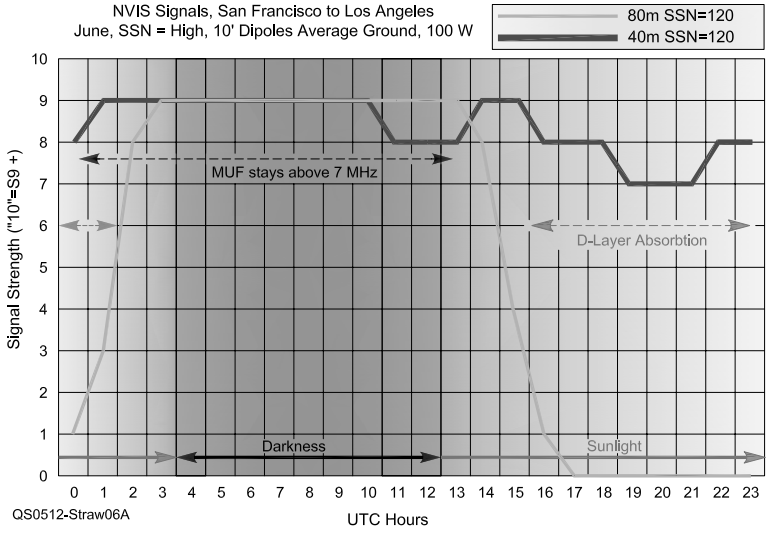

Fig 12—Signal strengths for the San Francisco to Los Angeles path for a worst-case month/SSN combination—summer solstice, in June, for a high level of solar activity (SSN = 120). Now 80 meters drops out more dramatically during the daylight hours, due to increased D-layer absorption. At this high level of solar activity, 40 meters remains open 24 hours with reasonable signal levels. However, the NVIS rule-of-thumb still holds: Use 40 meters during the day; 80 meters at night.

range distances, say out to 500 miles from the center, compared to a 100-foot high antenna. The 20-foot high antenna can discriminate against medium-angle thunderstorm noise in the late afternoon coming from the Arizona desert, although it wouldn't help much for thunderstorms in the Sierra Nevada in central Nevada, which are arriving in San Francisco at high angles, along with the desired NVIS signals.

This is the essence of what NVIS means. NVIS exploits the difference in elevation pattern responses of low horizontally polarized antennas compared to higher horizontal antennas, or even verticals. Over the years, many hams have been lead to believe that higher is always better. This is not quite so true for consistent coverage of medium or short distance signals!

If NVIS only involved putting up a low horizontally polarized antenna on 40 meters the story would end here. However, real cloud warming is more complicated. It also involves the intelligent choice of more than just one operating frequency to achieve reliable all day, all-night communications coverage.

Fig 11 shows the signal strength predicted using *VOACAP* for the 350-mile path from San Francisco to Los Angeles for the month of December for a period of low solar activity (SSN of 20). The antennas used in this case are 10-foot high dipoles, just for some variety. These act almost like 20-foot high Inverted V dipoles. December at a low SSN was chosen as a worst-case scenario because the *winter solstice* occurs on December 21. This is the day that has the fewest hours of daylight in the year. (Contrast this with the *summer solstice*, on June 21, which has the most hours of daylight in the year.) Note that the upper signal limit in Fig 11 is "S10"—a fictitious quantity that allows easier graphing.

S10 is equivalent to S9+, or at least S9+10 dB.

The 40-meter curve in Fig 11 shows that the MUF (maximum usable frequency) actually drops below the 7.2 MHz amateur band after sunset. The signal becomes quite weak for about 14 hours during the night, from about 0300 to 1700 UTC. In a period of low solar activity the 40-meter band thus becomes strictly a *daytime band* on this medium-distance path.

The 80-meter curve in Fig 11 shows strong signals after dusk, through the night and up until about an hour after sunrise. After sunrise, 80 meters starts to suffer absorption in the D layer of the ionosphere and hence the signal strength drops. Here, 80 meters is a true *nighttime band*.

Let's see what happens from San Francisco to Los Angeles during a period of high solar activity (SSN of 120) during the summer solstice in June. **Fig 12** shows that 40 meters now stays open all hours of the day due to the greater number of hours of sunlight in June and because the ionosphere becomes more highly ionized by higher solar activity. Meanwhile, 80 meters still remains a nighttime band during these conditions on this path.

Now, let's look at a shorter-distance path—our 75-mile emergency communications path from San Francisco to Sacramento. We'll again use June during the summer solstice, at a high level of solar activity (SSN of 120) because this represents another worst-case scenario. **Fig 13** shows that 40 meters remains open on this path all day, dropping to a lower signal level just before sunrise. At sunrise, the MUF drops close to 7.2 MHz. 80 meters is still mainly a nighttime band to Sacramento, even though it does yield workable signal levels even during the daylight hours. However, 40 meters is better from 1200 to 0400 UTC, so 40 would be still the right daytime band for this path during the day.

CHOOSING THE RIGHT NVIS FREQUENCY

You can see that a pattern is developing here for efficient NVIS short/medium-distance communications out to 500 miles:

- You should pick a frequency on 40 meters during the day.
- You should pick a frequency on 80 meters during the night.
- You should choose an antenna that emphasizes moderate to high elevation angles, from 40° to almost directly overhead at 90°.

"What about 60 meters?" you might ask. The characteristics on 60 meters fall in-between 40 and 80 meters, although it resembles 40 meters more closely. With characteristics close to that of 40, but with only five channels available and a 50-W power limit, the 60-meter band is of low utility for serious NVIS use.

What about 160 meters? For 100-W level radios, even at the worst-case month or during low solar activity, the critical frequency doesn't fall below 3.8 MHz often enough to destroy the ability to communicate, even for short distances. That is a relief, considering that installing a 160-meter half-wave dipole involves a 255-foot wingspan, and it would need to be elevated at least 30 feet in the center. A short loaded vertical such as a 160-meter mobile whip would have poor response at the high elevation angles needed for NVIS. You could probably put a monster 160-meter horizontal dipole up at a permanent location, but hauling such a thing around in the field would not be an easy task.

SOME OTHER OBSERVATIONS ABOUT NVIS—STRATEGY

You could pose the question about whether NVIS is an operating *mode* or whether it is actually an operating *strategy*. We maintain that NVIS is a strategy. It involves choosing both appropriate frequencies and then appropriate antennas for those frequencies. Fig 13 does show that on short-distance

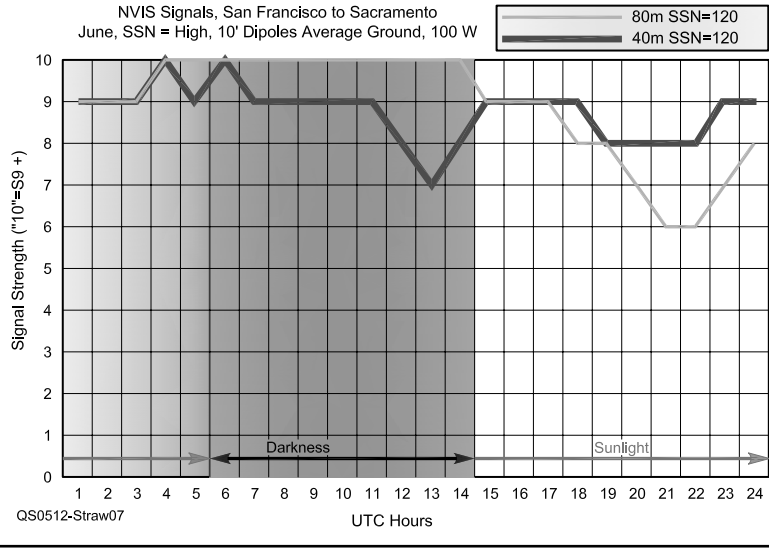

Fig 13—Signal strengths for a 75 mile path—San Francisco to Sacramento. This is for June and SSN = 120. Either band could be used successfully over the full 24-hour period because signal levels are always higher than S6. But the simple NVIS rule-of-thumb still holds: Use 40 meters during the day; 80 meters at night. This simplifies giving instructions to operators unaccustomed to the use of HF.

paths, such as between San Francisco and Sacramento, you could stay on 80 meters all day and night. But if you have to give a single rule-of-thumb to operators who are not very experienced at operating HF, we would tell them to operate on the higher frequency band during the day and on the lower frequency band at night.

SOME OTHER OBSERVATIONS ABOUT NVIS—ANTENNA HEIGHT

Some NVIS aficionados have advocated placing dipoles only a few feet over ground, something akin to saying, "If low is good for NVIS, then lower must be even better." Now we are not claiming that a very low antenna *won't* work in specific instances—for example, covering a small state such as Rhode Island or even just the San Francisco Bay Area.

It certainly is convenient to mount a 40-meter dipole on some 2-foot high red traffic cones! You should be very skeptical, however, about the ability of such antennas to cover all of a large state, such as California or Texas, especially on 80 meters. **Fig 14** shows the computed elevation responses for a number of 80-meter antennas, including a 2-foot-high dipole.

Fig 15B shows the 80 meter geographic coverage plot for 2-foot-high flattop dipoles, compared with the plot in Fig 15A for 20-foot-high inverted V dipoles on both ends of the path. The 2-foot-high dipoles produce about two S-units less signal across all of California than the 20-foot-high inverted V dipoles, at 0300 UTC in December, with an SSN of 20. The reason is that a low dipole will suffer more losses in the ground under it.

The differential between California signals and possible interfering signals from, say, New Mexico, is predicted to be four S-units, the same as it is for the higher inverted V dipole

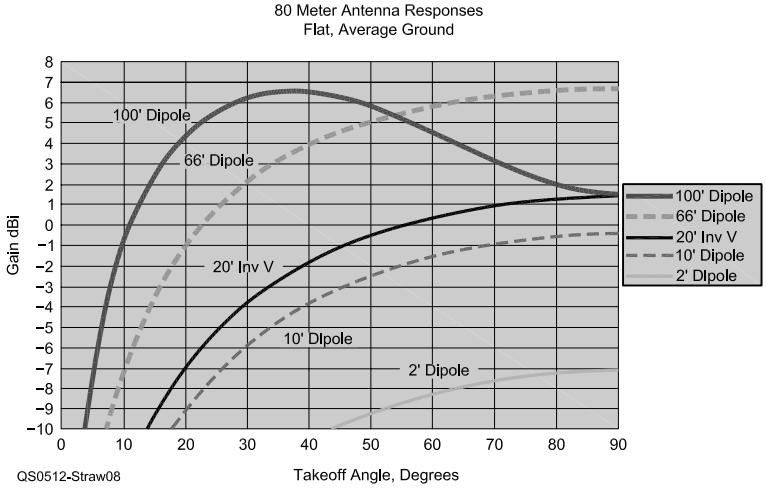

Fig 14—Elevation response patterns for 80 meter antennas over average soil. The shapes track each other rather well, remaining parallel for heights from 2 to 66 feet over flat ground. The 2 foot dipole is substantially down, about 9 dB, from the 20 foot inverted V dipole at all angles.

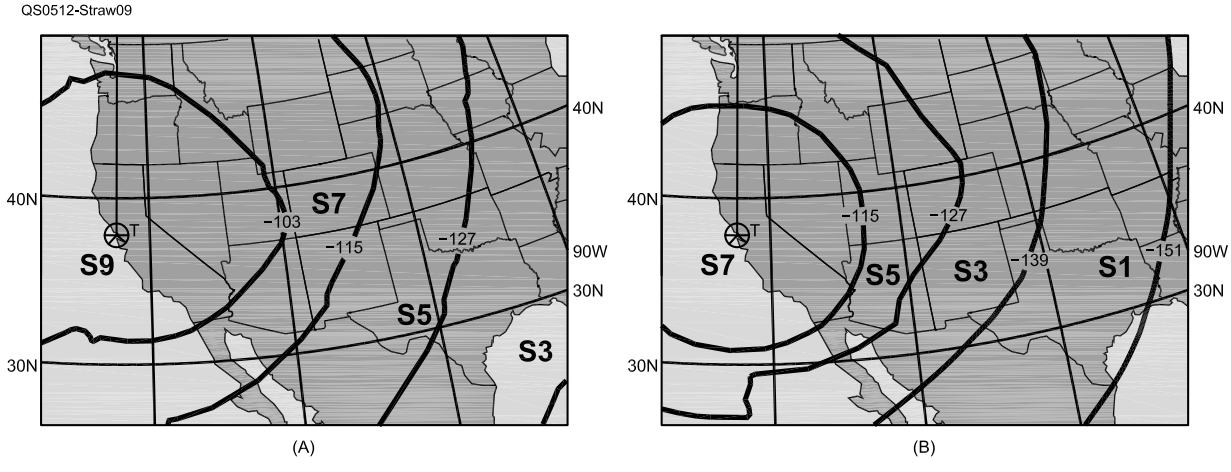

Fig 15—Geographic coverage plots for December, SSN = 20, 0300 UTC. At A, antennas are 20 foot-high inverted V dipoles over Average soil. At B, antennas are 2-foot-high flattop dipoles over Average soil. The response for the 2-foot-high antennas is down about 2 S Units, 8 to 12 dB for a typical communications receiver.

at 20 feet. Thus there is no real advantage in terms of signal-to-interference ratio or signal-to-noise ratio (for thunderstorm static crashes) for either height. This is because the shape of all the response curves in Fig 14 below 20 feet essentially track each other in parallel.

However, the lower the antenna, the lower the transmitted signal strength. Physics remain physics. And if you are in an emergency situation operating on batteries, you could reduce power from 100 W to 10 W with a 20-foot high inverted-V antenna and still maintain the same signal strength as a 2-foot high dipole at 100W.

LOW NVIS ANTENNAS AND LOCAL POWERLINE NOISE

Some advocates of really low antennas have stated that the received noise is much lower than that received from higher antennas, and this therefore leads to better signal-to-noise ratios (SNR). How much this is true depends on the source of the noise. If the noise comes from distant thunderstorms, then the SNR advantage going to a 2-foot antenna from a 20-foot-high one is insignificant, as Fig 15 indicates.

If noise is from an arcing insulator on a HV power line half a mile away, that noise will arrive at the antenna as a ground-wave signal. We calculate that the 2-foot antenna receives 4.4 dB less noise by groundwave than a 20-foot-high inverted V dipole. However, at an incoming elevation angle of 45º—suitable for a signal going from Los Angeles to San Francisco—the signal would be down 7.1 dB on the low dipole compared to the higher antenna. The net loss in SNR for the 2-foot-high dipole is thus 7.1– 4.4 or 2.7 dB. Close, but no cigar. Summarizing about really low NVIS antennas:

- A 2-foot-high dipole yields weaker signals, but without an SNR advantage compared to its more elevated brethren.
- A 2-foot-high dipole is a lot easier to trip over at night. We would call this a “knee biter” (or maybe an “ankle biter” if you’re really tall).
- You (and your dog) can easily get RF burns from an antenna that is only 2 feet off the ground.

This is not a winning strategy to make friends or QSOs, it seems. But still, a really low dipole may serve your short-range communication needs just fine. But remember, that just as “higher is better” isn’t universally true for NVIS (or even longer range) applications, “lower is better” isn’t a panacea either.

ELEVATION ANGLES FOR MODERATE DISTANCES ON 75/80 METERS

Fig 16 shows the elevation angles statistics for a 75-meter, 550-mile path from Boston to Cleveland, together with overlays of the elevation patterns for several different types of antennas. These elevation statistics cover all parts of the 11-year solar cycle for this path. The responses for the popular G5RV antenna (described later in this chapter) are shown for two different heights above flat ground: 50 and 100 feet. An 80-meter half-wave sloper (“full sloper”) and an 80-meter ground-plane antenna are also shown. All

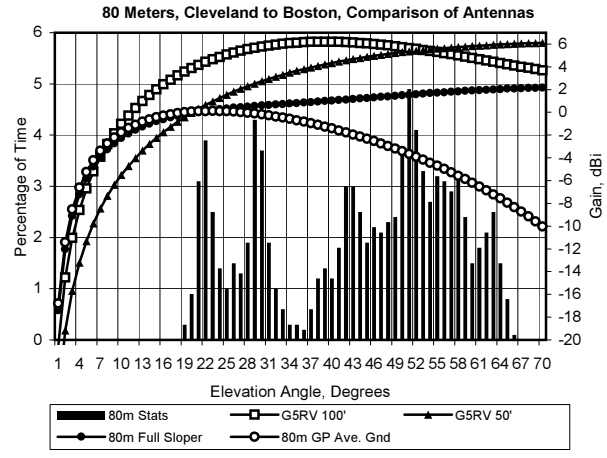

Fig 16—80/75-meter elevation statistics for all portions of the 11-year solar cycle for the path from Cleveland, Ohio, to Boston, Massachusetts, together with the elevation responses for four different multiband antennas. The 100-foot high horizontally polarized G5RV performs well over the entire range of necessary takeoff elevation angles.

antenna patterns are for “average ground” constants of 5 mS/m conductivity and a dielectric constant of 13.

At the statistically most significant takeoff angles around 50°, the two horizontally polarized G5RV antennas are about equal. At the second-highest elevation peak near 30°, the 100-foot G5RV has about a 4-dB advantage over its lower counterpart. The full sloper has comparable performance to the 100-foot high G5RV from 1° to about 20° and then gradually rises to its peak at angles higher than 70°. The full sloper is superior to the 50-foot horizontal G5RV at low takeoff elevation angles. The 80-meter ground plane has a deep null directly overhead. At an elevation angle of 70° it is down some 16 dB compared to the 50-foot high horizontal G5RV.

The advantage of antennas suitable for high-angle radiation was vividly demonstrated during a 75-meter QSO one fall evening between N6BV/1 in southern New Hampshire and W1WEF in central Connecticut. This involved a distance of about 100 miles and W1WEF was using his Four Square vertical array. Although W1WEF’s signal was S9 on the Four Square, N6BV/1 suggested an experiment. Instead of connecting the so-called “dump power” connector on his Comtek ACB-4 hybrid phasing coupler to a 50-Ω dummy load (the normal configuration), W1WEF switched the dump power to his 100-foot high 80-meter horizontal dipole. W1WEF’s signal came up more than 20 dB! The approximately 100-W of power that would otherwise be “wasted” in the dummy load was converted to useful signal.

ELEVATION ANGLES FOR MODERATE DISTANCES ON 40 METERS

Fig 17 shows the situation for the 40-meter band, from Boston to Cleveland, together with the same antennas used for 80 meters in Fig 16. Note that the 100-foot high horizontally

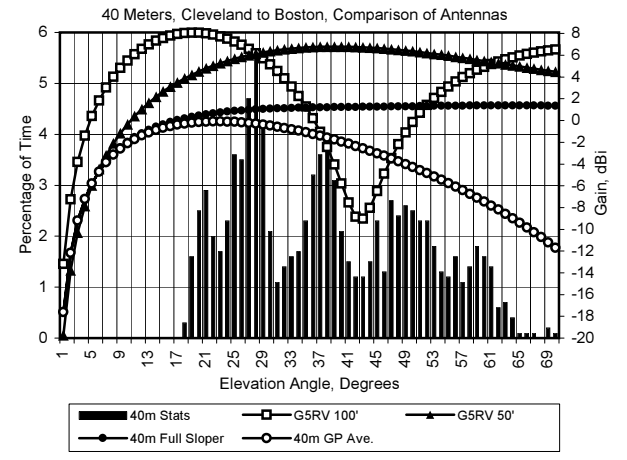

Fig 17—40-meter elevation statistics for the Cleveland to Boston path, together with elevation patterns for four antennas. Here, the 100-foot high horizontally polarized G5RV would have a null in the middle of the range of elevation angles needed for consistent performance on this path. For multiband use on this path to relatively nearby stations, the 50-foot high horizontal antenna would be a better choice than the 100-foot high antenna.

polarized G5RV has about a 16-dB null at an elevation angle of 43°. This doesn't affect things for low elevation angles, but it certainly has a profound effect on signals arriving between about 30° to 60°, especially when compared to the 50-foot high horizontal G5RV. The 40-meter full sloper beats out the high horizontal antenna from about 35° to 50°. And the ground plane is obviously not the antenna of choice for this moderate-range path from Boston to Cleveland, although it is still a good performer on longer-distance paths, with their low takeoff angles.

A 100-foot high multiband dipole is about ⅜-λ high on 75/80 meters. It is an excellent antenna for general-purpose local and DXing operation. But the same dipole used on 40 meters becomes ¾-λ high. At that height, the nulls in its elevation pattern give large holes in coverage for nearby 40-meter contacts. Many operators have found that a 40- to 50-foot high dipole on 40 meters gives them far superior performance for close-in QSOs, when compared to a high dipole, or even a high 2-element 40-meter Yagi.

NVIS SUMMARY

The use of NVIS strategies to cover close-in and intermediate distance communications within about 600 miles involves the intelligent choice of low HF frequencies. As a rule-of-thumb for ham band NVIS, 40 meters is recommended for use during the day; 80 meters during the night.

NVIS involves the choice of antennas suitable for this strategy. Horizontally polarized dual-band 80 and 40-meter flattop dipoles that are mounted higher than about 10 feet high will work adequately for portable operations. Dual-band 80 and 40-meter inverted V dipoles supported 20 feet above the ground at the center can also work well in portable operations.

Single-band 40-meter flattop antennas about 30 feet high and 80-meter flattop antennas about 60 feet high can do a good job for fixed locations.

Horizontal Antennas for the Low Bands

As shown in Chapter 3, The Effects of Ground, and here, radiation angles from horizontal antennas are a very strong function of the height above ground in wavelengths. Typically for DX work heights of λ/2 to 1 λ are considered to be a minimum. As we go down in frequency these heights become harder to realize. For example, a 160-meter dipole at 70 feet is only 0.14 λ high. This antenna will be very effective for local and short distance QSOs but not very good for DX work. Despite this limitation, horizontal antennas are very popular on the lower bands because the low frequencies are often used for short range communications, local nets and rag chewing. Also horizontal antennas do not require extensive ground systems to be efficient.

DIPOLE ANTENNAS

Half-wave dipoles and variations of these can be a very good choice for a low band antenna. A variety of possibilities are shown in **Fig 18**. An untuned or "flat" feed line is a logical choice on any band because the losses are low, but this generally limits the use of the antenna to one band. Where only single-band operation is wanted, the λ/2 antenna fed with open-wire line is one of the most popular systems on the 3.5 and 7-MHz bands.

If the antenna is a single-wire affair, its impedance is in the vicinity of 60 Ω, depending on the height and the ground characteristics. The most common way to feed the antenna is with 50- or 75-Ω coaxial line. Heavy coaxial lines present support problems because they are a concentrated weight at the center of the antenna, tending to pull the center of the antenna down. This can be overcome by using an auxiliary pole to take at least some of the weight of the line. The line should come away from the antenna at right angles, and it can be of any length.

Folded Dipoles

A folded dipole (Fig 18B and C) has an impedance of about 300 Ω, and can be fed directly with any length of 300-Ω line. The folded dipole can be made of ordinary wire spaced by lightweight wooden or plastic spacers, 4 or 6 inches long, or a piece of 300 or 450-Ω twin-lead or ladder line.

A folded dipole can be fed with a 600-Ω open wire line with only a 2:1 SWR, but a nearly perfect match can be ob-

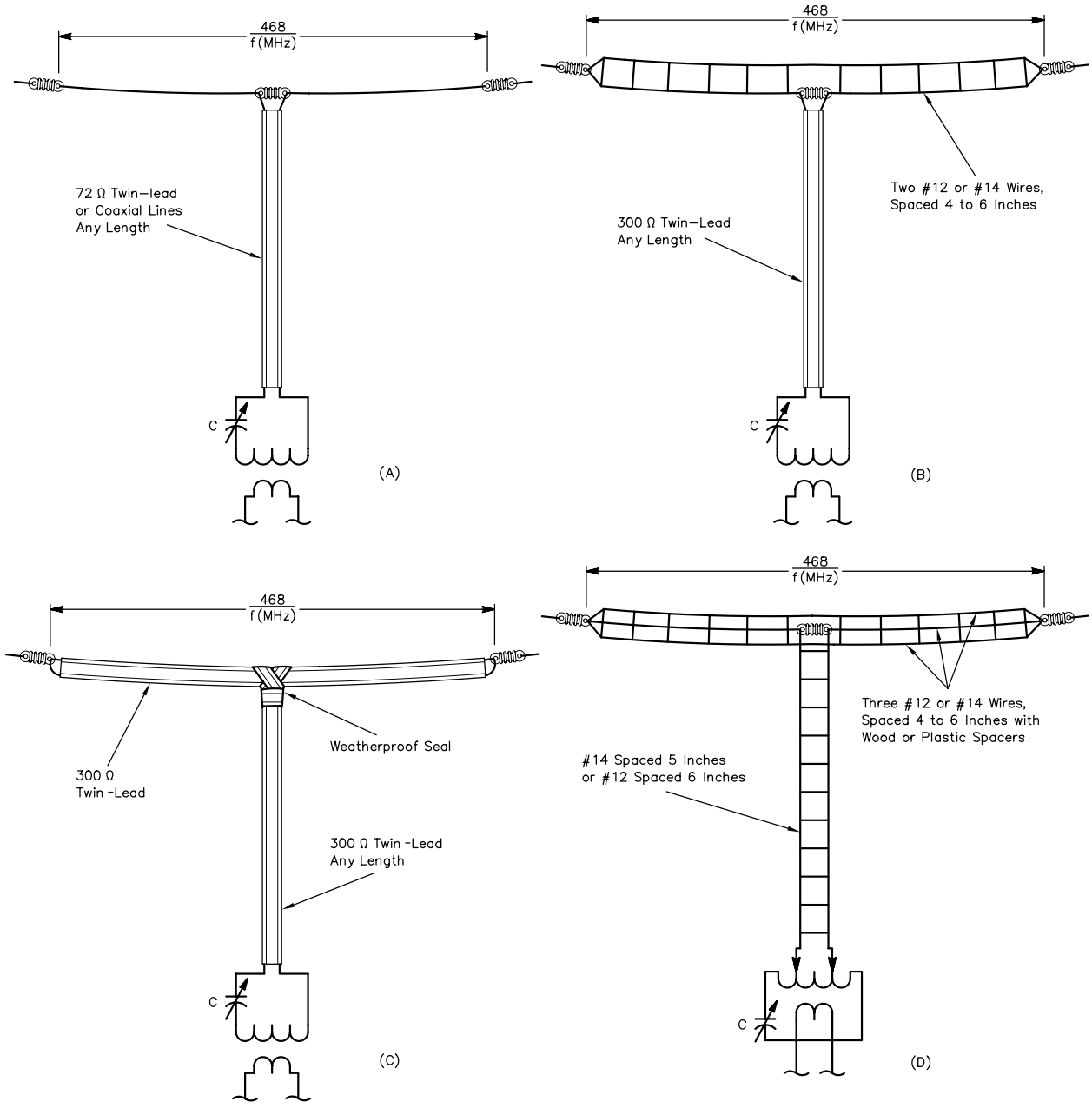

Fig 18—Half-wavelength antennas for single band operation. The multiwire types shown in B, C and D offer a better match to the feeder over a somewhat wider range of frequencies but otherwise the performances are identical. The feeder should run away from the antenna at a right angle for as great a distance as possible. In the coupling circuits shown, tuned circuits should resonate to the operating frequency. In the series-tuned circuits of A, B, and C, high L and low C are recommended, and in D the inductance and capacitance should be similar to the output-amplifier tank, with the feeders tapped across at least ½ the coil. The tapped-coil matching circuit shown in Chapter 25 can be substituted in each case.

tained with a three-wire dipole fed with either 450-Ω ladder line or 600-Ω open wire line. One advantage of the two- and three-wire antennas over the single wire is that they offer a better match over a wider band. This is particularly important if full coverage of the 3.5-MHz band is contemplated.

Inverted-V Dipole

The halves of a dipole may be sloped to form an inverted V, as shown in **Fig 19**. This has the advantages of requiring only a single high support and less horizontal space. There will be some difference in performance between a normal horizontal dipole and the inverted V as shown by the radiation patterns in **Fig 20**. There is small loss in peak gain and the pattern is less directional.

Sloping of the wires results in a raising of the resonant frequency and a decrease in feed-point impedance and

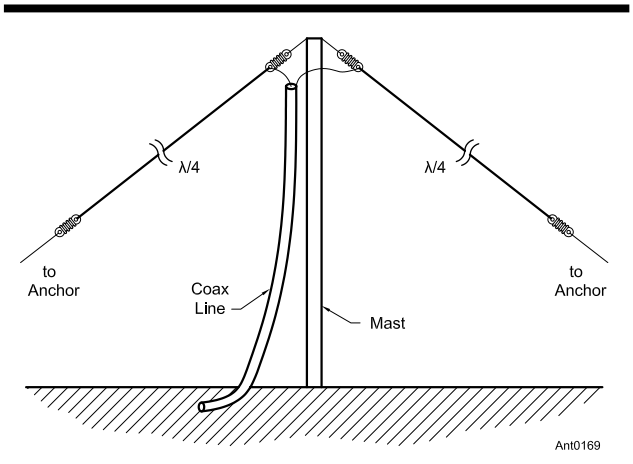

Fig 19—The inverted-V dipole. The length and apex angle should be adjusted as described in the text.

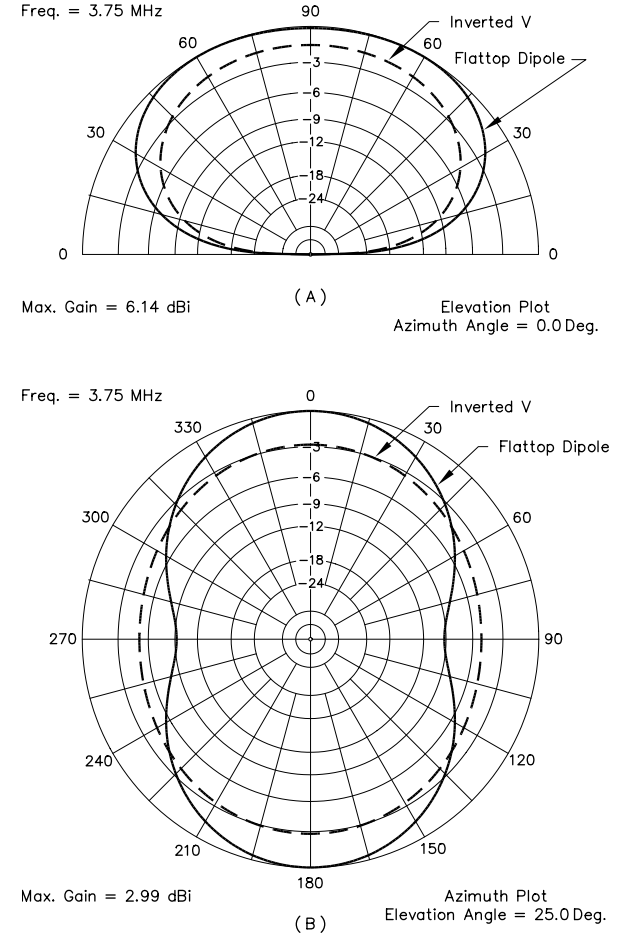

Fig 20—At A, elevation and at B, azimuthal radiation patterns comparing a normal 80-meter dipole and an inverted-V dipole. The center of both dipoles is at 65 feet and the ends of the inverted V are at 20 feet. The frequency is 3.750 MHz.

bandwidth. Thus, for the same frequency, the length of the dipole must be increased somewhat. The angle at the apex is not critical, although it should probably be made no smaller than 90°. Because of the lower impedance, a 50-Ω line should be used. For those who are dissatisfied with anything but a perfect match, the usual procedure is to adjust the angle for lowest SWR while keeping the dipole resonant by adjustment of length. Bandwidth may be increased by using multiconductor elements, such as a cage configuration.

PHASED HORIZONTAL ARRAYS

Phased arrays with horizontal elements, which provide some directional gain, can be used to advantage at 7 MHz, if they can be placed at least 40 feet above ground. At 3.5 MHz heights of 70 feet or more are needed for any real advantage.

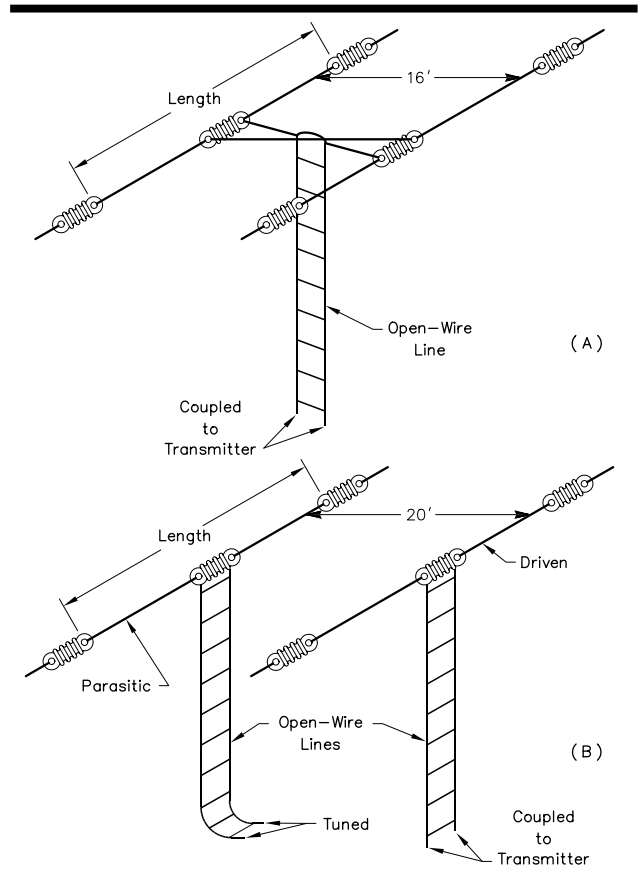

Fig 21—Directional antennas for 7 MHz. To realize any advantage from these antennas, they should be at least 40 feet high. At A, system is bidirectional. At B, system is unidirectional in a direction depending upon the tuning conditions of the parasitic element. The length of the elements in either antenna should be exactly the same, but any length from 60 to 150 feet can be used. If the length of the antenna at A is between 60 and 80 feet, the antenna will be bidirectional along the same line on both 7 and 14 MHz. The system at B can be made to work on 7 and 14 MHz in the same way, by keeping the length between 60 and 80 feet.

Many of the driven arrays discussed in Chapter 8 and even some of the Yagis discussed in Chapter 11 can be used as fixed directional antennas. If a bidirectional characteristic is desired, the W8JK array, shown in **Fig 21A**, is a good one. If a unidirectional characteristic is required, two elements can be mounted about 20 feet apart and provision included for tuning one of the elements as either a director or reflector, as shown in Fig 21B.

The parasitic element is tuned at the end of its feed line with a series or parallel-tuned circuit (whichever would normally be required to couple power into the line), and the proper tuning condition can be found by using the system for receiving and listening to distant stations along the line to the rear of the antenna. Tuning the feeder to the parasitic element can minimize the received signals from the back of the antenna. This is in effect adjusting the antenna for maximum front-to-back ratio. Maximum front-to-back does not occur at the same point as maximum forward gain but the loss in forward gain is very small. Adjusting the antenna for maximum forward gain (peaking received signals in the forward direction) may increase the forward gain slightly but will almost certainly result in relatively poor front-to-back ratio.

A MODIFIED EXTENDED DOUBLE ZEPP

If the distance between the available supports is greater than λ/2 then a very simple form of a single wire collinear array can be used to achieve significant gain. The *extended double Zepp* antenna has long been used by amateurs and is discussed in Chapter 8, Multielement Arrays. A simple variation of this antenna with substantially improved bandwidth can be very useful on 3.5 and 7.0 MHz. The following material has been taken from an article by Rudy Severns, N6LF, in *The ARRL Antenna Compendium Vol 4*.

The key to improving the characteristics of a standard double-extended Zepp is to modify the current distribution. One of the simplest ways to do this is to insert a reactance(s) in series with the wire. This could either be an inductor(s) or a capacitor(s). In general, a series capacitor will have a higher Q and therefore less loss. With either choice it is desirable to use as few components as possible.

As an initial trial at 7 MHz, only two capacitors, one on each side of the antenna, were used. The value and position of the capacitors was varied to see what would happen. It quickly became clear that the reactance at the feed point could be tuned out by adjusting the capacitor value, making the antenna look essentially like a resistor over the entire band. The value of the feed-point resistance could be varied from less than 150 Ω to over 1500 Ω by changing the location of the capacitors and adjusting their values to resonate the antenna.

A number of interesting combinations were created. The one ultimately selected is shown in **Fig 22**. The antenna is 170 feet in length. Two 9.1 pF capacitors are located 25 feet out each side of the center. The antenna is fed with 450-Ω transmission line and a 9:1 three-core Guanella balun used at the transmitter to convert to 50 Ω. The transmission line can be any convenient length and it operates with a very low SWR.

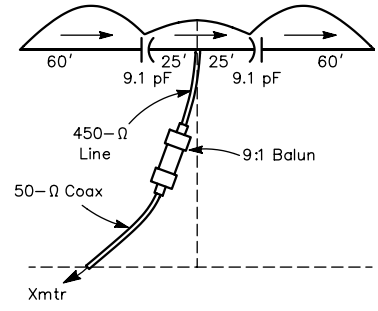

Fig 22—Schematic for modified N6LF Double Extended Zepp. Overall length is 170 feet, with 9.1 pF capacitors placed 25 feet each side of center.

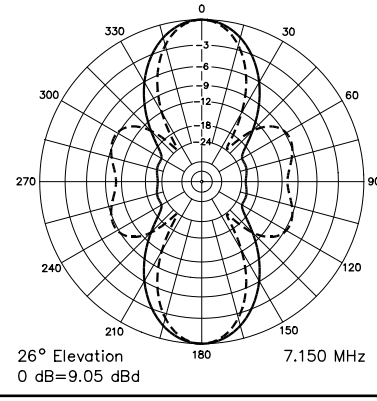

Fig 23—Azimuth pattern for N6LF Double Extended Zepp (solid line), compared to classic Double Extended Zepp (dashed line). The main lobe for the modified antenna is slightly broader than that of the classic model, and the sidelobes are suppressed better.

That's all there is to it. The radiation pattern, overlaid with that for a standard DEZepp for comparison, is shown in **Fig 23**. The sidelobes are now reduced to below 20 dB. The main lobe is now 43° wide at the 3-dB points, as opposed to 35° for the original DEZepp. The antenna has gain over a dipole for > 50° now and the gain of the main lobe has dropped only 0.2 dB below the original DEZepp.

Experimental Results

The antenna was made from #14 wire and the capacitors were made from 3.5-inch sections of RG-213, shown in **Fig 24A**. Note that great care should be taken to seal out moisture in these capacitors. The voltage across the capacitor for 1.5 kW will be about 2000 V so any corona will quickly destroy the capacitor.

A silicon sealant was used and then both ends covered

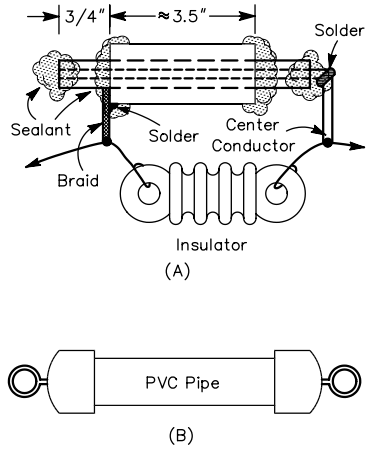

Fig 24—Construction details for series capacitor made from RG-213 coaxial cable. At A, the method used by N6LF is illustrated. At B, a suggested method to seal capacitor better against weather is shown, using a section of PVC pipe with end caps.

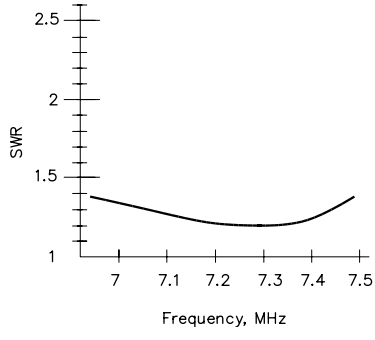

Fig 25—Measured SWR curve across 40-meter band for N6LF DEZepp.

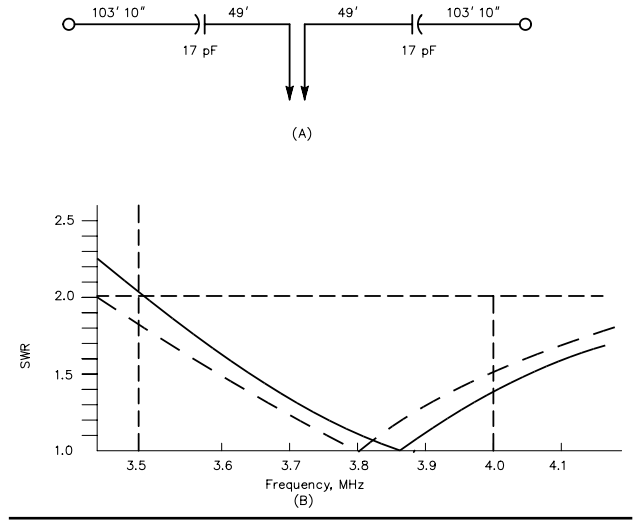

Fig 26—75/80-meter modified Double Extended Zepp, designed using *NEC Wires*. At A, a schematic is shown for antenna. At B, SWR curve is shown across 75/80-meter band. Solid line shows measured curve for W7ISV antenna, which was pruned to place SWR minimum higher in the band. The dashed curve shows the computed response when SWR minimum is set to 3.8 MHz.

with coax seal, finally wrapping it with plastic tape. The solder balls indicated on the drawing are to prevent wicking of moisture through the braid and the stranded center conductor. This is a small but important point if long service out in the weather is expected. An even better way to protect the capacitor would be to enclose it in a short piece of PVC pipe with end caps, as shown in Fig 24B.

Note that all RG-8 type cables do not have exactly the same capacitance per foot and there will also be some end effect adding to the capacitance. If possible the capacitor should be trimmed with a capacitance meter. It isn't necessary to be too exact—the effect of varying the capacitance ±10% was checked and the antenna still worked fine.

The results proved to be close to those predicted by the computer model. **Fig 25** shows the measured value for SWR across the band. These measurements were made with a Bird directional wattmeter. The worst SWR is 1.35:1 at the low end of the band.

Dick Ives, W7ISV, erected an 80-meter version of the antenna, shown in **Fig 26A**. The series capacitors are 17 pF. Since he isn't interested in CW, Dick adjusted the length for the lowest SWR at the high end of the band, as shown in the SWR curve (Fig 26B). The antenna could have been tuned somewhat lower in frequency and would then provide an SWR < 2:1 over the entire band, as indicated by the dashed line.

This antenna provides wide bandwidth and moderate gain over the entire 75/80-meter band. Not many antennas will give you that with a simple wire structure.

Vertical Antennas

On the low bands quarter-wave high vertical antennas become increasingly attractive, especially for DX work, because they provide a means for lowering the radiation angle. This is especially true where practical heights for horizontally polarized antennas are too low. In addition, verticals can be very simple and unobtrusive structures. For example, it is very easy to disguise a vertical as a flagpole. In fact an actual flagpole may be used as a vertical. Performance of a vertical is determined by several factors:

- Height of the vertical portion of the radiator
- The ground or counterpoise system efficiency, if one is used
- Ground characteristics in the near- and far-field regions
- The efficiency of loading elements and matching networks

THE HALF-WAVE VERTICAL DIPOLE (HVD)

The simplest form of vertical is that of a half-wave vertical dipole, an HVD. This is a horizontal dipole turned 90° so that it is perpendicular to the ground under it. Of course, the top end of such an antenna must be at least a half wave above the ground or else it would be touching the ground. This poses quite a construction challenge if the builder wants a free-standing low-frequency antenna. Hams fortunate enough to have tall trees on their property can suspend wire HVDs from these trees. Similarly, hams with two tall towers can run rope catenaries between them to hold up an HVD.

A vertical half-wave dipole has some operational advantages compared to a more-commonly used vertical configuration—the quarter-wave vertical used with some sort of above-ground counterpoise or an on-ground radial system. See **Fig 27** and 27B, which shows the two configurations discussed here. In each case, the lowest part of each antenna is 8 feet above ground, to prevent passersby from being able to touch any live wire. Each antenna is assumed to be made of #14 wire resonant on 80 meters.

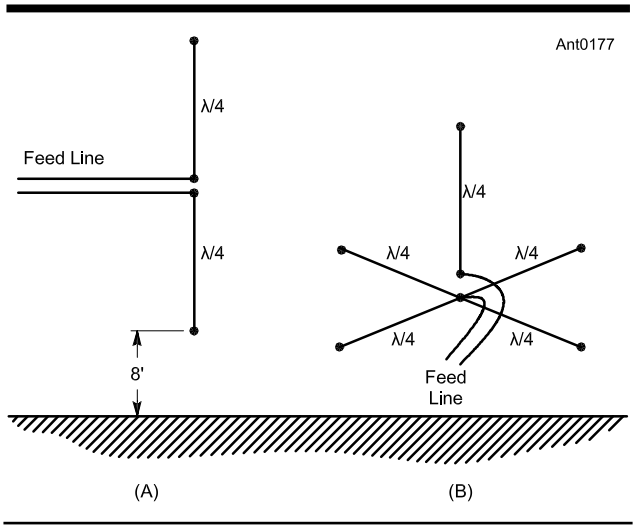

Fig 27—At A, a 80-meter half-wave vertical dipole elevated 8 feet above the ground. The feed line is run perpendicularly away from the dipole. At B, a "ground plane" type of quarter-wave vertical, with four elevated resonant radials. Both antennas are mounted 8 feet above the ground to keep them away from passersby.

Feeding a Half-Wave Vertical Dipole

Fig 28 compares elevation patterns for the two antennas for "average ground." You can see that the half-wave vertical dipole has about 1.5 dB higher peak gain, since it compresses the vertical elevation pattern down somewhat closer to the horizon than does the quarter-wave ground plane. Another advantage to using a half-wave radiator besides higher gain is that less horizontal "real estate" is needed compared to a quarter-wave vertical with its horizontal radials.

The obvious disadvantage to an HVD is that it is taller than a quarter-wave ground plane. This requires a higher support (such as a taller tree) if you make it from wire, or a longer element if you make it from telescoping aluminum tubing.

Another problem is that theory says you must dress the feed line so that it is perpendicular to the half-wave radiator. This means you must support the coax feed line above ground for some distance before bringing the coax down to ground level. A question immediately arises: How far must you go out horizontally with the feed line before going to ground level to eliminate common-mode currents that are radiated onto the coax shield? Such common-mode currents will affect the feed-point impedance as well as the radiation pattern for the antenna system. Quite a bit of distortion in the azimuthal pattern can be created if common-mode currents aren't suppressed, usually by using a common-mode choke, also known as a current balun.

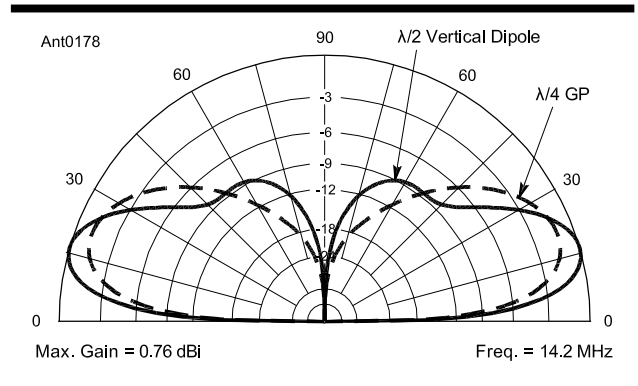

Fig 28—A comparison of the elevation patterns for the two antennas in Fig 27. The peak gain of the HVD is about 1.5 dB higher than that for the quarter-wave ground-plane radiator with radials.

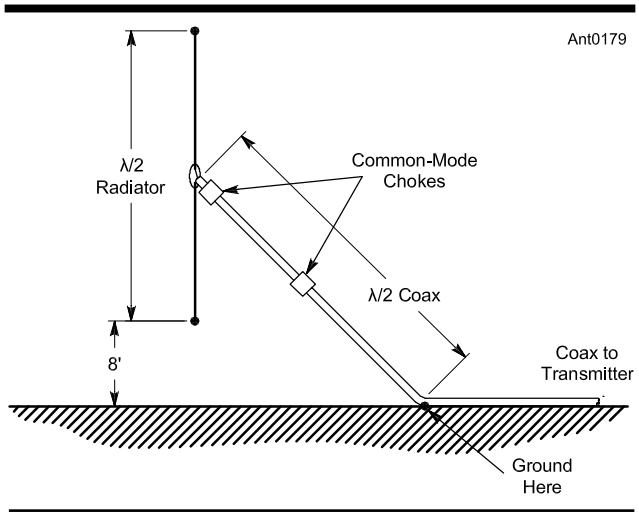

Fig 29—A 20-meter HVD whose bottom is 8 feet above ground. This is fed with a λ/2 of RG-213 coax. This system uses a common-mode choke at the feed point and another λ/4 down the line. The resulting azimuthal radiation pattern is within 0.4 dB of being perfectly circular. The "wingspan" of this antenna system is 27 feet from the radiator to the point where the coax comes to ground level.

Constructing such a common-mode choke is very simple: Three large ferrite beads are slipped over the coax (before the connectors are soldered on or else they won't fit!) and taped in place. The only problem with this scheme is that an additional support (some sort of "skyhook") is required to support the coax horizontally. Let's try to simplify the installation, by slanting the feed-line coax down to ground from the feed point at a fairly steep angle of about 30° from vertical. See **Fig 29**.

Note that the bottom end of the coax in Fig 29 is grounded to a ground rod. This serves several purposes—this serves as a mechanical connection to hold the coax in place and it provides some protection against lightning strikes. Now, as a purely practical matter, just how picky are we being here? What if we skip the second common-mode choke and just use one at the feed point? The computer models predicts that there will be some distortion in the azimuthal pattern—about 1.1 dB worth. Whether this is serious is up to you. However, you may find other problems with common-mode currents on the coax shield—problems such as RF in the shack or variable SWR readings depending on the way coax is routed in the shack. The addition of three extra ferrite beads to suppress the common-mode currents is cheap insurance.

Later in this chapter we'll discuss shortened vertical antennas, ones arranged both as vertical dipoles and as vertical monopoles with radial systems.

MONOPOLE VERTICALS WITH GROUND PLANE RADIALS

For best performance the vertical portion of a ground-plane type of antenna should be λ/4 or more, but this is not an absolute requirement. With proper design, antennas as short as 0.1 λ or even less can be efficient and effective. Antennas shorter than λ/4 will be reactive and some form of loading and perhaps a matching network will be required.

If the radiator is made of wire supported by nonconducting material, the approximate length for λ/4 resonance can be found from:

$$\ell_{\text{feet}} = \frac{234}{f_{\text{MHz}}} \qquad \text{(Eq 1)}$$

For tubing, the length for resonance must be shorter than given by the above equation, as the length-to-diameter ratio is lower than for wire (see Chapter 2, Antenna Fundamentals). For a tower, the resonant length will be shorter still. In any case, after installation the antenna length (height) can be adjusted for resonance at the desired frequency.

The effect of ground characteristics on losses and elevation pattern is discussed in detail in Chapter 3, The Effects of Ground. The most important points made in that discussion are the effect of ground characteristics on the radiation pattern and the means for achieving low ground-loss resistance in a buried ground system. As ground conductivity increases, low-angle radiation improves. This makes a vertical very attractive to those who live in areas with good ground conductivity. If your QTH is on a saltwater beach, then a vertical would be very effective, even when compared to horizontal antennas at great height.

When a buried-radial ground system is used, the efficiency of the antenna will be limited by the loss resistance of the ground system. The ground can be a number of radial wires extending out from the base of the antenna for about λ/4. Driven ground rods, while satisfactory for electrical safety and for lightning protection, are of little value as an RF ground for a vertical antenna, except perhaps in marshy or beach areas. As pointed out in Chapter 3, many long radials are desirable. In general, however, a large number of short radials are preferable to only a few long radials, although the best system would have 60 or more radials longer than λ/4. An elevated system of radials or a ground screen (*counterpoise*) may be used instead of buried radials, and can result in an efficient antenna.

ELEVATED RADIALS AND COUNTERPOISES

Elevated radials, isolated from ground, can be used in place of an extensive buried radial system. Work by Al Christman, K3LC (ex-KB8I), has shown that 4 to 8 elevated radials can provide performance comparable to a 120 λ/4-long buried wires. This is especially important for the low bands, where such a buried ground system is very large and impractical for most amateurs. An elevated ground system is sometimes referred to as a *ground plane* or *counterpoise*. **Fig 30** compares buried and elevated ground systems, showing the difference in current flow in the two systems.

An elevated ground can take several forms. A number of wires arranged with radial symmetry around the base of the antenna is shown in Fig 30B. Four radials are normally

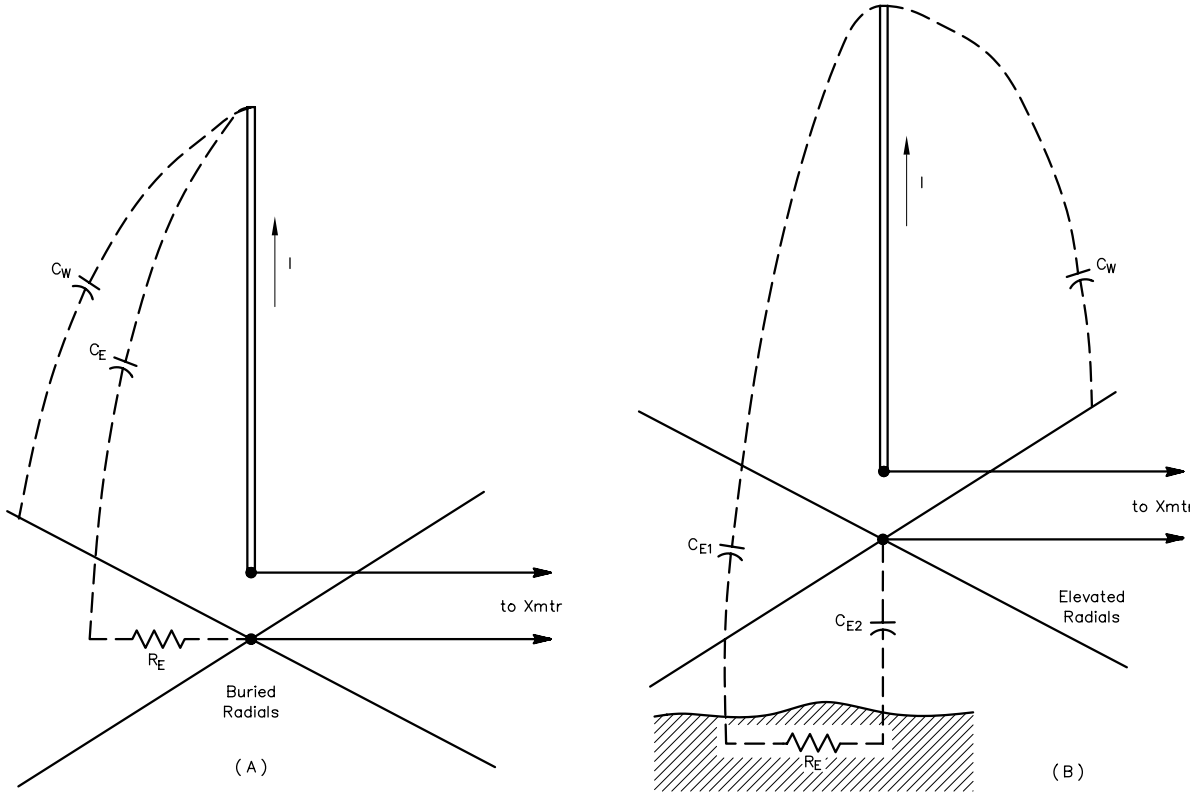

Fig 30—How earth currents affect the losses in a short vertical antenna system. At A, the current through the combination of C_E and R_E may be appreciable if C_E is much greater than C_W, the capacitance of the vertical to the ground wires. This ratio can be improved (up to a point) by using more radials. By raising the entire antenna system off the ground, C_E (which consists of the series combination of C_{E1} and C_{E2}) is decreased while C_W stays the same. The radial system shown at B is sometimes called a *counterpoise*.

used, but as few as two, or as many as eight, can be used. For a given height of vertical, the length of the radials can be adjusted to resonate the antenna. For a λ/4 vertical, the radials are normally λ/4 long.

In the case of a multiband vertical, two or more sets of radials, with different lengths, may be interleaved. The radials associated with each band are adjusted for resonance on their associated band.

A counterpoise is most commonly a system of elevated radials, where the radial wires are interconnected with jumpers, as shown in **Fig 31**. As illustrated in Fig 30, the purpose of the elevated-ground system is to provide a return path for the displacement currents flowing in the vicinity of the antenna. The idea is to minimize the current flowing through the ground itself, which is usually very lossy. By raising the radials above ground most of the current will flow in the radials, which are good conductors. This allows a simple radial system to provide a very efficient ground. However, there is a price to be paid for this.

The ground system now has a direct effect on the feedpoint impedance, introducing reactance as well as resistance, and is relatively narrow band. For a given vertical height, the

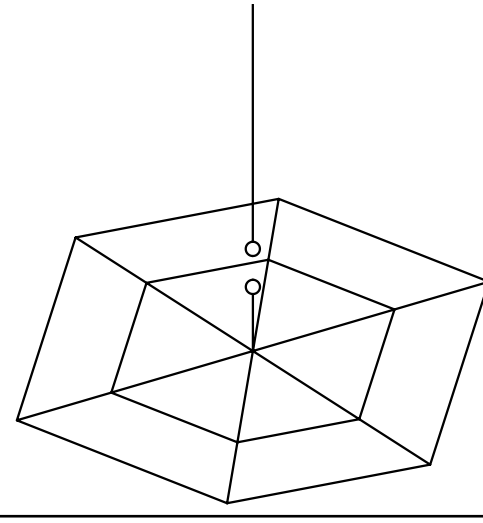

Fig 31—Counterpoise, showing the radial wires connected together by cross wires. The length of the perimeter of the individual meshes should be < λ/4 to prevent undesired resonances. Sometimes the center portion of the counterpoise is made from wire mesh.

Table 2

Illustration of the effect of variable vertical height (L_1) on elevated radial length (L2) and R_R. #12 wire, elevated 5 feet over average ground at 3.525 MHz.

L_1 (λ)	L_1 (feet)	L_2 (feet)	R_R (Ω)
0.225	62.8	94	28.8
0.25	69.8	67	38.4
0.27	75.0	45	51.0
0.3	83.7	24	75.9

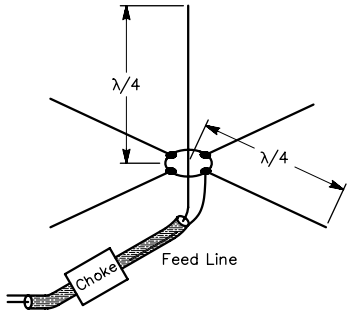

Fig 32—The ground-plane antenna. Power is applied between the base of the vertical radiator and the center of the ground plane, as indicated in the drawing. Decoupling from the transmission line and any conductive support structure is highly desirable.

radial length must be adjusted to resonate the antenna. The length of the radials must be readjusted for each band if a multiband vertical is used. As pointed out above, this usually means the installation of a set of radials for each band. To minimize current flowing in the ground, the antenna, ground plane and feed line must be isolated from ground for RF. More on this later.

The height of the vertical does not have to be exactly $\lambda/4$. Other lengths may be used and the antenna may be resonated by adjusting the length of the radials. **Table 2** gives a comparison between three different vertical lengths in an antenna using four elevated radials at 3.525 MHz.

An important feature of Table 2 is the dramatic reduction in radial length (L_2) with even a small increase in vertical height (L_1). For example, increasing the height by 5 feet reduces the radial length by 22 feet on 80 meters. On the other hand even a small decrease in L_1 can cause a substantial increase in L_2. This would be very undesirable, since the area required by the radials is already considerable. Notice also that the small increase in height raises R_R to 51 Ω. This trick of increasing the height slightly to reduce the size of the elevated ground system and to increase the input resistance can be very useful. In a following section the use of *top loading* for short antennas will be discussed. Top loading can also be used on a $\lambda/4$ vertical to achieve the same effect as increasing the height—the ability to use shorter radials and a better match.

GROUND-PLANE ANTENNAS

The ground-plane antenna is a $\lambda/4$ vertical with four radials, as shown in **Fig 32**. The entire antenna is elevated above ground. A practical example of a 7-MHz ground-plane antenna is given in **Fig 33**. As explained earlier, elevating the antenna reduces the ground loss and lowers the radiation angle somewhat. The radials are sloped downward to make the feed-point impedance closer to 50 Ω.

The feed-point impedance of the antenna varies with the height above ground, and to a lesser extent varies with the ground characteristics. **Fig 34** is a graph of feed-point resistance (R_R) for a ground-plane antenna with the radials parallel to the ground. R_R is plotted as a function of height above ground. Notice that the difference between perfect ground and average ground (ε=13 and σ = 0.005 S/m) is small, except when quite close to ground. Near ground R_R is between 36 and 40 Ω. This is a reasonable match for 50-Ω feed line but as the antenna is raised above ground R_R drops to approximately 22 Ω, which is not a very good match. The feed-point resistance can be increased by sloping the radials downward, away from the vertical section.

The effect of sloping the radials is shown in **Fig 35**. The

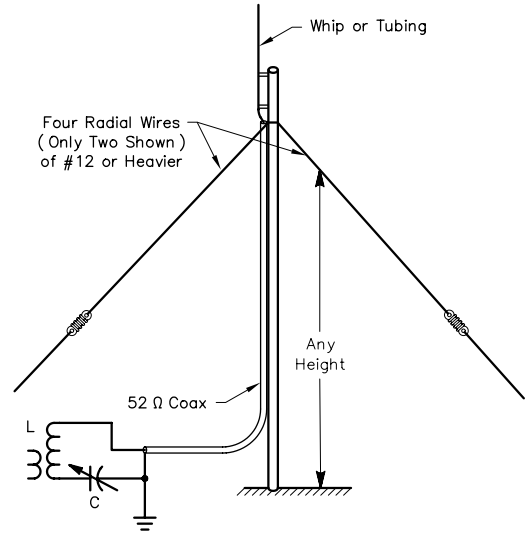

Fig 33—A ground-plane antenna is effective for DX work on 7 MHz. Although its base can be any height above ground, losses in the ground underneath will be reduced by keeping the bottom of the antenna and the ground plane as high above ground as possible. Feeding the antenna directly with 50-Ω coaxial cable will result in a low SWR. The vertical radiator and the radials are all $\lambda/4$ long electrically. Contrary to popular myth, the radials need not necessarily be 5% longer than the radiator. Their physical length will depend on their length-to-diameter ratios, the height over ground and the length of the vertical radiator, as discussed in text.

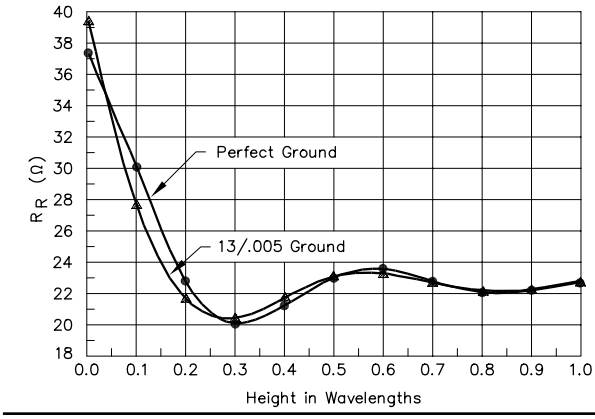

Fig 34—Radiation resistance of a 4-radial ground-plane antenna as a function of height over ground. Perfect and average ground are shown. Frequency is 3.525 MHz. Radial angle (θ) is 0°.

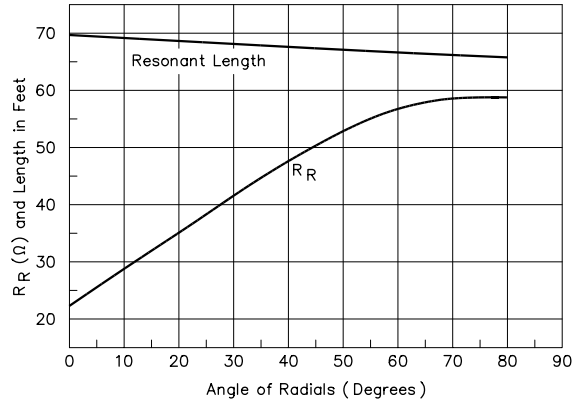

Fig 35—Radiation resistance and resonant length for a 4-radial ground-plane antenna > 0.3 λ above ground as a function of radial droop angle (θ).

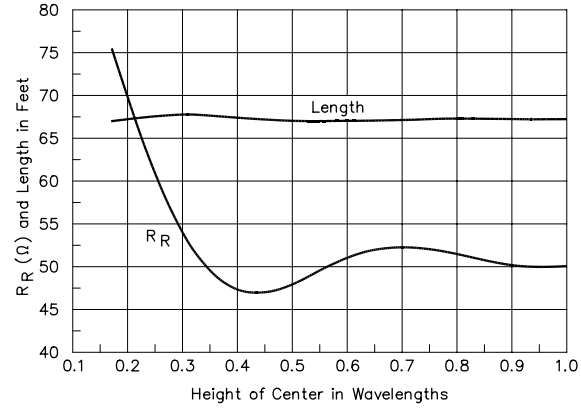

Fig 36—Radiation resistance and resonant length for a 4-radial ground-plane antenna for various heights above average ground for radial droop angle θ = 45°.

graph is for an antenna well above ground (> 0.3 λ). Notice that R_R = 50 Ω when the radials are sloped downward at an angle of 45°, a convenient value. The resonant length of the antenna will vary slightly with the angle. In addition, the resonant length will vary a small amount with height above the ground. It is for these reasons, as well as the effect of conductor diameter, that some adjustment of the radial lengths is usually required. When the ground-plane antenna is used on the higher HF bands and at VHF, the height above ground is usually such that a radial sloping angle of 45° will give a good match to 50-Ω feed line.

The effect of height on R_R with a radial angle of 45° is shown in **Fig 36**. At 7 MHz and lower, it is seldom possible to elevate the antenna a significant portion of a wavelength and the radial angle required to match to 50-Ω line is usually of the order of 10° to 20°. To make the vertical portion of the antenna

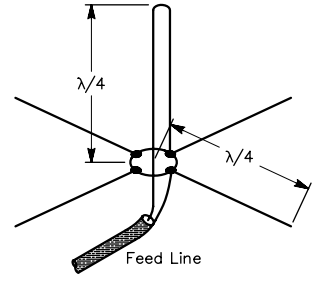

Fig 37—The folded monopole antenna. Shown here is a ground plane of four λ/4 radials. The folded element may be operated over an extensive counterpoise system or mounted on the ground and worked against buried radials and the earth. As with the folded dipole antenna, the feed-point impedance depends on the ratios of the radiator conductor sizes and their spacing.

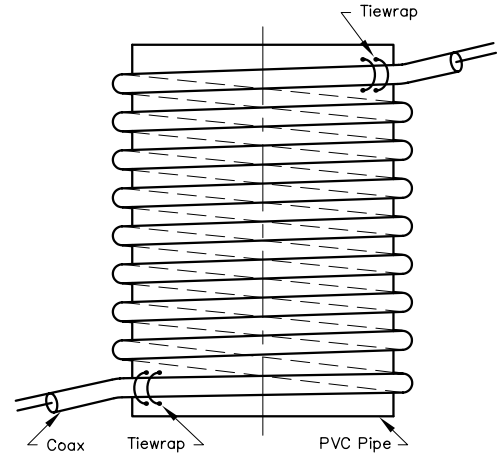

Fig 38—A choke balun with sufficient impedance to isolate the antenna properly can be made by winding coaxial cable around a section of plastic pipe. Suitable dimensions are given in the text.

as long as possible, it may be better to accept a slightly poorer match and keep the radials parallel to ground.

The principles of the folded dipole (Fig 18) can also be applied to the ground-plane antenna, as shown in **Fig 37**. This is the *folded monopole* antenna. The feed-point resistance can be controlled by the number of parallel vertical conductors and the ratios of their diameters.

As mentioned earlier, it is important in most installations to isolate the antenna from the feed line and any conductive supporting structure. This is done to minimize the return current conducted through the ground. A return current on the feed line itself or the support structure can drastically alter the radiation pattern, usually for the worse. For these reasons, a balun (see Chapter 26, Coupling the Line to the Antenna) or other isolation scheme must be used. 1:1 baluns are effective for the higher bands but at 3.5 and 1.8 MHz commercial baluns often have too low a shunt inductance to provide adequate isolation. It is very easy to recognize when the isolation is inadequate. When the antenna is being adjusted while watching an isolated impedance or SWR meter, adjustments may be sensitive to your touching the instrument. After adjustment and after the feed line is attached, the SWR may be drastically different. When the feed line is inadequately isolated, the apparent resonant frequency or the length of the radials required for resonance may also be significantly different from what you expect.

In general, an isolation choke inductance of 50 to 100 μH will be needed for 3.5 and 1.8-MHz ground-plane antennas. One of the easiest ways to make the required isolation choke is to wind a length of coaxial cable into a coil as shown in **Fig 38**. For 1.8 MHz, 30 turns of RG-213 wound on a 14-inch length of 8-inch diameter PVC pipe, will make a very good isolation choke that can handle full legal power continuously. A smaller choke could be wound on 4-inch diameter plastic drain pipe using RG-8X or a Teflon insulated cable. The important point here is to isolate or decouple the antenna from the feed line and support structure.

A full-size ground-plane antenna is often a little impractical for 3.5-MHz and quite impractical for 1.8 MHz, but it can be used at 7 MHz to good advantage, particularly for DX work. Smaller versions can be very useful on 3.5 and 1.8 MHz.

EXAMPLES OF VERTICALS

There are many possible ways to build a vertical antenna—the limits are set by your ingenuity. The primary problem is creating the vertical portion of the antenna with sufficient height. Some of the more common means are:

- A dedicated tower
- Using an existing tower with an HF Yagi on top
- A wire suspended from a tree limb or the side of a building
- A vertical wire supported by a line between two trees or other supports
- A tall pole supporting a conductor
- Flagpoles
- Light standards
- Irrigation pipe
- TV masts

If you have the space and the resources, the most straightforward means is to erect a dedicated tower for a vertical. While this is certainly an effective approach, many amateurs do not have the space or the funds to do this, especially if they already have a tower with an HF antenna on the top. The existing tower can be used as a top-loaded vertical, using shunt feed and a ground radial system. A system like this is shown in **Fig 39B**.

For those who live in an area with tall trees, it may be possible to install a support rope between two trees, or between a tree and an existing tower. (Under no circumstances should you use an active utility pole!) The vertical portion of the antenna can be a wire suspended from the support line to ground, as shown in Fig 39C. If top loading is needed, some or all of the support line can be made part of the antenna.

Your local utility company will periodically have older power poles that they no longer wish to keep in service. These are sometimes available at little or no expense. If you see a power line under reconstruction or repair in your area you might stop and speak with the crew foreman. Sometimes they will have removed older poles they will not use again and will have to haul them back to their shop for disposal. Your offer for local "disposal" may well be accepted. Such a pole can be used in conjunction with a tubing or whip extension such as that shown in Fig 39A. Power poles are not your only option. In some areas of the US, such as the southeast or northwest, tall poles made directly from small conifers are available.

Freestanding (unguyed) flagpoles and roadway illumination standards are available in heights exceeding 100 feet. These are made of fiberglass, aluminum or galvanized steel. All of these are candidates for verticals. Flagpole suppliers are listed under "Flags and Banners" in your Yellow Pages. For lighting standards (lamp posts), you can contact a local electrical hardware distributor. Like a wooden pole, a fiberglass flagpole does not require a base insulator, but metal poles do. Guy wires will be needed.

One option to avoid the use of guys and a base insulator is to mount the pole directly into the ground as originally intended and then use shunt feed. If you want to keep the pole grounded but would like to use elevated radials, you can attach a cage of wires (four to six) at the top as shown in Fig 39D. The cage surrounds the pole and allows the pole (or tower for that matter) to be grounded while allowing elevated radials to be used. The use of a cage of wires surrounding the pole or tower is a very good way to increase the effective diameter. This reduces the Q of the antenna, thereby increasing the bandwidth. It can also reduce the conductor loss, especially if the pole is galvanized steel, which is not a very good RF conductor.

Aluminum irrigation tubing, which comes in diameters of 3 and 4 inches and in lengths of 20 to 40 feet, is widely available in rural areas. One or two lengths of tubing con-

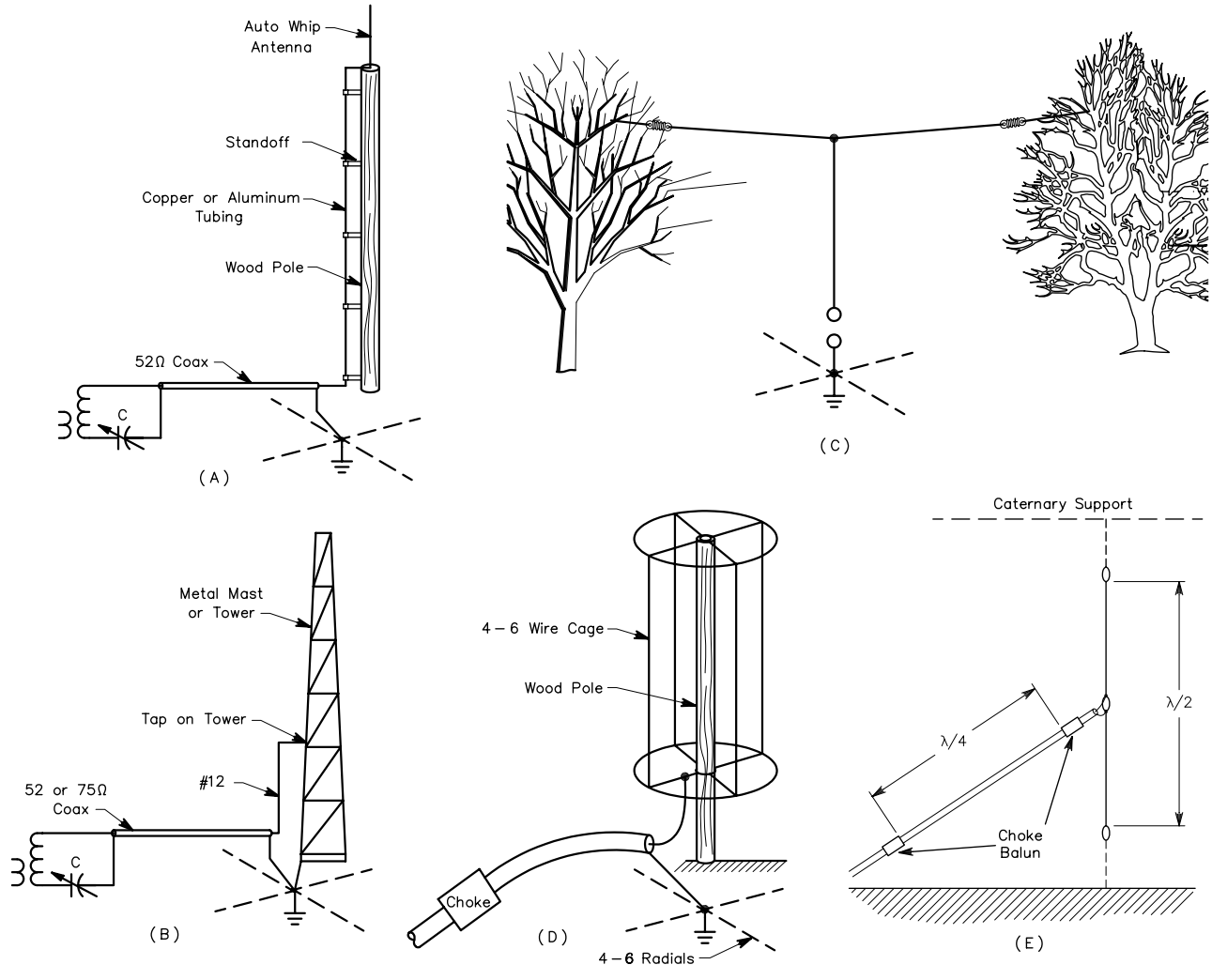

Fig 39—Vertical antennas are effective for 3.5- or 7-MHz work. The λ/4 antenna shown at A is fed directly with 50-Ω coaxial line, and the resulting SWR is usually less than 1.5 to 1, depending on the ground resistance. If a grounded antenna is used as at B, the antenna can be shunt fed with either 50- or 75-Ω coaxial line. The tap for best match and the value of C will have to be found by experiment. The line running up the side of the antenna should be spaced 6 to 12 inches from the antenna. If tall trees are available the antenna can be supported from a line suspended between the trees, as shown in C. If the vertical section is not long enough then the horizontal support section can be made of wire and act as top loading. A pole or even a grounded tower can be used with elevated radials if a cage of four to six wires is provided as shown in D. The cage surrounds the pole which may be wood or a grounded conductor.

nected together can make a very good vertical when guyed with non-conducting line. It is also very lightweight and relatively easy to erect. A variety of TV masts are available which can also be used for verticals.

1.8 TO 3.5-MHz VERTICAL USING AN EXISTING TOWER

A tower can be used as a vertical antenna, provided that a good ground system is available. The shunt-fed tower is at its best on 1.8 MHz, where a full λ/4 vertical antenna is rarely possible. Almost any tower height can be used. If the beam structure provides some top loading, so much the better, but anything can be made to radiate—if it is fed properly. W5RTQ (now K6SE) uses a self-supporting, aluminum, crank-up, tilt-over tower, with a TH6DXX tribander mounted at 70 feet. Measurements showed that the entire structure has about the same properties as a 125-foot vertical. It thus works quite well as an antenna on 1.8 and 3.5 MHz for DX work requiring low-angle radiation.

Preparing the Structure

Usually some work on the tower system must be done before shunt-feeding is tried. If present, metallic guys should be broken up with insulators. They can be made to simulate

top loading, if needed, by judicious placement of the first insulators. Don't overdo it; there is no need to "tune the radiator to resonance" in this way since a shunt feed is employed. If the tower is fastened to a house at a point more than about one-fourth of the height of the tower, it may be desirable to insulate the tower from the building. Plexiglas sheet, ¼-inch or more thick, can be bent to any desired shape for this purpose, if it is heated in an oven and bent while hot.

All cables should be taped tightly to the tower, on the inside, and run down to the ground level. It is not necessary to bond shielded cables to the tower electrically, but there should be no exceptions to the down-to-the-ground rule.

A good system of buried radials is very desirable. The ideal would be 120 radials, each 250 feet long, but fewer and shorter ones must often suffice. You can lay them around corners of houses, along fences or sidewalks, wherever they can be put a few inches under the surface, or even on the earth's surface. Aluminum clothesline wire may be used extensively in areas where it will not be subject to corrosion. Neoprene-covered aluminum wire will be better in highly acid soils. Contact with the soil is not important. Deep-driven ground rods and connection to underground copper water pipes may be helpful, if available, especially to provide some protection from lightning.

Installing the Shunt Feed

Principal details of the shunt-fed tower for 1.8 and 3.5 MHz are shown in **Fig 40**. Rigid rod or tubing can be used for the feed portion, but heavy gauge aluminum or copper wire is easier to work with. Flexible stranded #8 copper wire is used at W5RTQ (now K6SE) for the 1.8-MHz feed, because when the tower is cranked down, the feed wire must come down with it. Connection is made at the top, 68 feet, through a 4-foot length of aluminum tubing clamped to the top of the tower, horizontally. The wire is clamped to the tubing at the outer end, and runs down vertically through standoff insulators. These are made by fitting 12-inch lengths of PVC plastic water pipe over 3-foot lengths of aluminum tubing. These are clamped to the tower at 15- to 20-foot intervals, with the bottom clamp about 3 feet above ground. These lengths allow for adjustment of the tower-to-wire spacing over a range of about 12 to 36 inches, for impedance matching.

The gamma-match capacitor for 1.8 MHz is a 250-pF variable with about ⅛-inch plate spacing. This is adequate for power levels up to about 200 W. A large transmitting or a vacuum-variable capacitor should be used for high-power applications.

Tuning Procedure

The 1.8-MHz feed wire should be connected to the top of the structure if it is 75 feet tall or less. Mount the standoff insulators so as to have a spacing of about 24 inches between wire and tower. Pull the wire taut and clamp it in place at the bottom insulator. Leave a little slack below to permit adjustment of the wire spacing, if necessary.

Adjust the series capacitor in the 1.8-MHz line for minimum reflected power, as indicated on an SWR meter connected between the coax and the connector on the capacitor housing. Make this adjustment at a frequency near the middle of your expected operating range. If a high SWR is indicated, try moving the wire closer to the tower. Just the

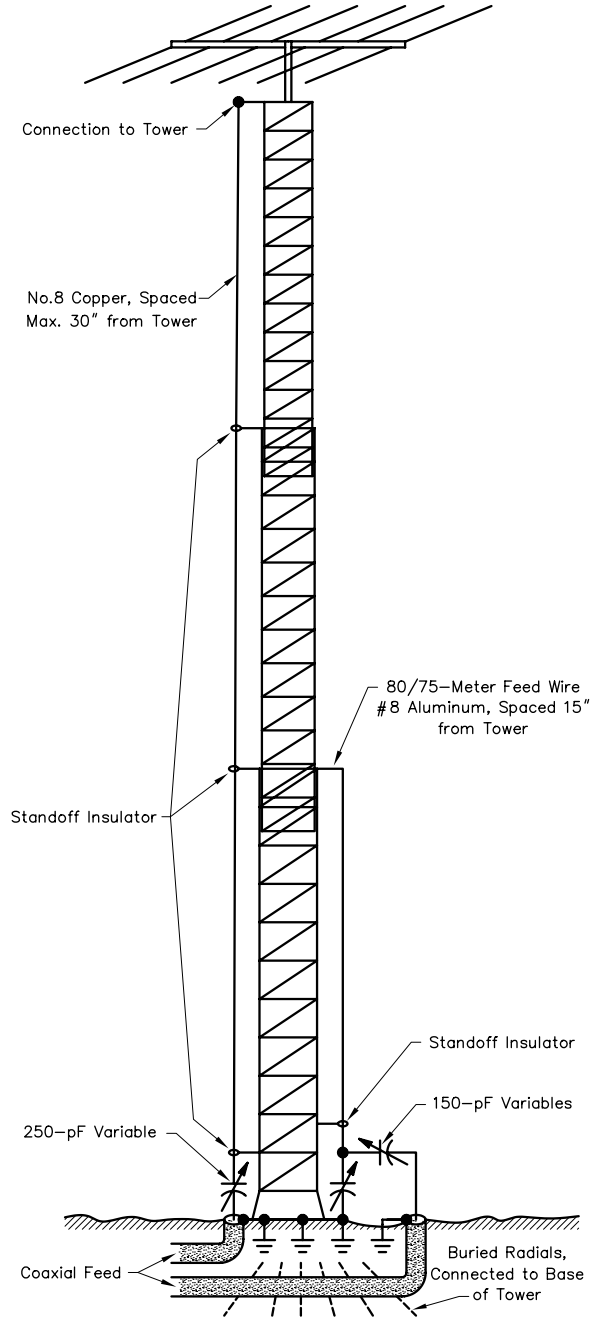

Fig 40—Principal details of the shunt-fed tower at W5RTQ (now K6SE). The 1.8-MHz feed, left side, connects to the top of the tower through a horizontal arm of 1-inch diameter aluminum tubing. The other arms have standoff insulators at their outer ends, made of 1-foot lengths of plastic water pipe. The connection for 3.5-4 MHz, right, is made similarly, at 28 feet, but two variable capacitors are used to permit adjustment of matching with large changes in frequency.

lower part of the wire need be moved for an indication as to whether reduced spacing is needed. If the SWR drops, move all insulators closer to the tower, and try again.

If the SWR goes up, increase the spacing. There will be a practical range of about 12 to 36 inches. If going down to 12 inches does not give a low SWR, try connecting the top a bit farther down the tower. If wide spacing does not make it, the omega match shown for 3.5-MHz work should be tried. No adjustment of spacing is needed with the latter arrangement, which may be necessary with short towers or installations having little or no top loading.

The two-capacitor arrangement in the omega match is also useful for working in more than one 25-kHz segment of the 1.8-MHz band. Tune up on the highest frequency, say 1990 kHz, using the single capacitor, making the settings of wire spacing and connection point permanent for this frequency. To move to the lower frequency, say 1810 kHz, connect the second capacitor into the circuit and adjust it for the new frequency. Switching the second capacitor in and out then allows changing from one segment to the other, with no more than a slight retuning of the first capacitor.

SIMPLE, EFFECTIVE, ELEVATED GROUND-PLANE ANTENNAS

This section describes a simple and effective means of using a grounded tower, with or without top-mounted antennas, as an elevated ground-plane antenna for 80 and 160 meters. It first appeared in a June 1994 *QST* article by Thomas Russell, N4KG.

From Sloper to Vertical

Recall the quarter-wavelength sloper, also known as the *half sloper*. [The half sloper is covered later in this chapter in more detail.—*Ed.*] It consists of an isolated quarter wavelength of wire, sloping from an elevated feed point on a grounded tower. Best results are usually obtained when the feed point is somewhere below a top-mounted Yagi antenna. You feed a sloper by attaching the center conductor of a coaxial cable to the wire and the braid of the cable to the tower leg. Now, imagine four (or more) slopers, but instead of feeding each individually, connect them together to the center conductor of a single feed line. Voilà! Instant elevated ground plane.

Now, all you need to do is determine how to tune the antenna to resonance. With no antennas on the top of the tower, the tower can be thought of as a fat conductor and should be approximately 4% shorter than a quarter wavelength in free space. Calculate this length and attach four insulated quarter-wavelength radials at this distance from the top of the tower. For 80 meters, a feed point 65 feet below the top of an unloaded tower is called for. The tower guys must be broken up with insulators for all such installations. For 160 meters, 130 feet of tower above the feed point is needed.

What can be done with a typical grounded-tower-and-Yagi installation? A top-mounted Yagi acts as a large capacitance hat, top loading the tower. Fortunately, top loading is the most efficient means of loading a vertical antenna.

The examples in **Table 3** should give us an idea of how much top loading might be expected from typical amateur antennas. The values listed in the *Equivalent Loading* column tell us the approximate vertical height replaced by the antennas listed in a top-loaded vertical antenna. To arrive at the remaining amount of tower needed for resonance, subtract these numbers from the non-loaded tower height needed for resonance. Note that for all but the 10-meter antennas, the equivalent loading equals or exceeds a quarter wavelength on 40 meters. For typical HF Yagis, this method is best used only on 80 and 160 meters.

Construction Examples

Consider this example: A TH7 triband Yagi mounted on a 40-foot tower. The TH7 has approximately the same overall dimensions as a full-sized 3-element 20-meter beam, but has more interlaced elements. Its equivalent loading is estimated to be 40 feet. At 3.6 MHz, 65 feet of tower is needed without loading. Subtracting 40 feet of equivalent loading, the feed point should be 25 feet below the TH7 antenna.

Ten quarter-wavelength (65-foot) radials were run from a nylon rope tied between tower legs at the 15-foot level, to various supports 10 feet high. Nylon cord was tied to the insulated, stranded, #18 wire, without using insulators. The radials are all connected together and to the center of an exact half wavelength (at 3.6 MHz) of RG-213 coax, which will repeat the antenna feed impedance at the other end. **Fig 41** is a drawing of the installation. The author used a Hewlett-Packard low-frequency impedance analyzer to measure the input impedance across the 80-meter band. An exact resonance (zero reactance) was seen at 3.6 MHz, just as predicted. The radiation resistance was found to be 17 Ω. The next question is, how to feed and match the antenna.

One good approach to 80-meter antennas is to tune them to the low end of the band, use a low-loss transmission line, and switch an antenna tuner in line for operation in the higher portions of the band. With a 50-Ω line, the 17-Ω radiation resistance represents a 3:1 SWR, meaning that an antenna tuner should be in-line for all frequencies. For short runs, it

Table 3
Effective Loading of Common Yagi Antennas

Antenna	*Boom Length (feet)*	*S (area, ft²)*	*Equivalent Loading (feet)*
3L 20	24	768	39
5L 15	26	624	35
4L 15	20	480	31
3L 15	16	384	28
5L 10	24	384	28
4L 10	18	288	24
3L 10	12	192	20
TH7	24	—	40 (estimated)
TH3	14	—	27 (estimated)

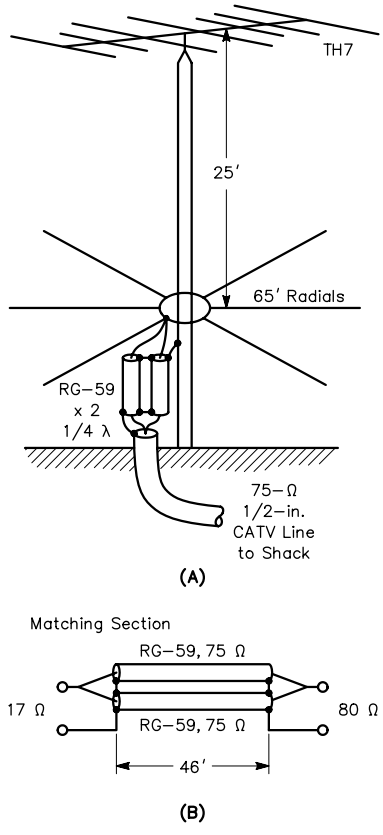

Fig 41—At A, an 80-meter top-loaded, reverse-fed elevated ground plane, using a 40-foot tower carrying a TH7 triband Yagi antenna. At B, dimensions of the 3.6-MHz matching network, made from RG-59.

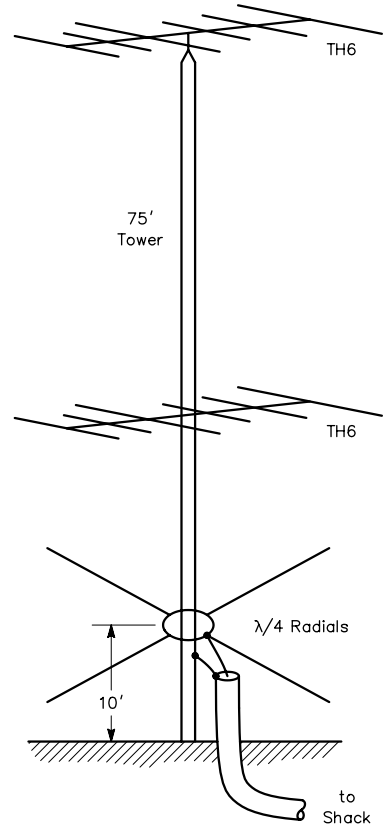

Fig 42—A 160-meter antenna using a 75-foot tower carrying stacked triband Yagis.

would be permissible to use RG-8 or RG-213 directly to the tuner. If you have a plentiful supply of low-loss 75-Ω CATV rigid coax, you can take another approach.

Make a quarter-wave (70 feet × 0.66 velocity factor = 46 feet) 37-Ω matching line by paralleling two pieces of RG-59 and connecting them between the feed point and a run of the rigid coax to the transmitter. The magic of quarter-wave matching transformers is that the input impedance (R_i) and output impedance (R_o) are related by:

$$Z_0^2 = R_i \times R_o \qquad \text{(Eq 2)}$$

For R_i = 17 Ω and Z_0 = 37 Ω, R_o = 80 Ω, an almost perfect match for the 75-Ω CATV coax. The resulting 1.6:1 SWR at the transmitter is good enough for CW operation without a tuner.

160-Meter Operation

On the 160-meter band, a resonant quarter-wavelength requires 130 feet of tower above the radials. That's a pretty tall order. Subtracting 40 feet of top loading for a 3-element 20-meter or TH7 antenna brings us to a more reasonable 90 feet above the radials. Additional top loading in the form of more antennas will reduce that even more.

Another installation, using stacked TH6s on a 75-foot tower, is shown in **Fig 42**. The radials are 10 feet off the ground.

PHASED VERTICALS

Two or more vertical antennas spaced apart can be operated as a single antenna system to obtain additional gain and a directional pattern. There is an extensive discussion of phased arrays in Chapter 8, Multielement Arrays. Much of the material in Chapter 8 is useful for low-band antennas.

The Half-Square Antenna

The *half-square* antenna is a very simple form of vertical two-element phased array that can be very effective on the low bands. The following section was originally presented in *The ARRL Antenna Compendium Vol 5*, by Rudy Severns, N6LF.

A simple modification to a standard dipole is to add two λ/4 vertical wires, one at each end, as shown in **Fig 43**. This makes a *half-square antenna*. The antenna can be fed at one corner (low-impedance, current fed) or at the lower end of one of the vertical wires (high-impedance, voltage fed).

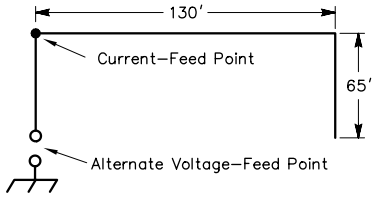

Fig 43—Typical 80-meter half-square, with λ/4-high vertical legs and a λ/2-long horizontal leg. The antenna may be fed at the bottom or at a corner. When fed at a corner, the feed point is a low-impedance, current-feed. When fed at the bottom of one of the wires against a small ground counterpoise, the feed point is a high-impedance, voltage-feed.

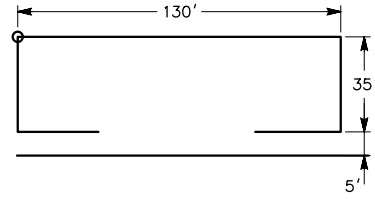

Fig 44—An 80-meter half-square configured for 40-foot high supports. The ends have been bent inward to reresonate the antenna. The performance is compromised surprisingly little.

Other feed arrangements are also possible.

The "classical" dimensions for this antenna are λ/2 (131 feet at 3.75 MHz) for the top wire and λ/4 (65.5 feet) for the vertical wires. However, there is nothing sacred about these dimensions! They can vary over a wide range and still obtain nearly the same performance.

This antenna is two λ/4 verticals, spaced λ/2, fed in-phase by the top wire. The current maximums are at the top corners. The theoretical gain over a single vertical is 3.8 dB. An important advantage of this antenna is that it does not require the extensive ground system and feed arrangements that a conventional pair of phased λ/4 verticals would.

Comparison to a Dipole

In the past, one of the things that has turned off potential users of the half-square on 80 and 160 meters is the perceived need for λ/4 vertical sections. This forces the height to be > 65 feet on 80 meters and > 130 feet on 160 meters. That's not really a problem. If you don't have the height there are several things you can do. For example, just fold the ends in, as shown in **Fig 44**. This compromises the performance surprisingly little.

It is helpful to compare the examples given in Figs 43 and 44 to dipoles at the same height. Two heights, 40 and 80 feet, and average, very good and sea water grounds, were used for this comparison. It is also assumed that the lower end of the vertical wires had to be a minimum of 5 feet above ground.

At 40 feet the half-square is really mangled, with only 35-foot long (≈ λ/8) vertical sections. The elevation-plane comparison between this antenna and a dipole of the same height is shown in **Fig 45**. Over average ground the half-square is superior below 32° and at 15° is almost 5 dB better. That is a worthwhile improvement. If you have very good soil conductivity, like parts of the lower Midwest and South, then the half-square will be superior below 38° and at 15° will be nearly 8 dB better. For those fortunate few with saltwater frontal property the advantage at 15° is 11 dB! Notice also that above 35°, the response drops off rapidly. This is great for DX but is not good for local work.

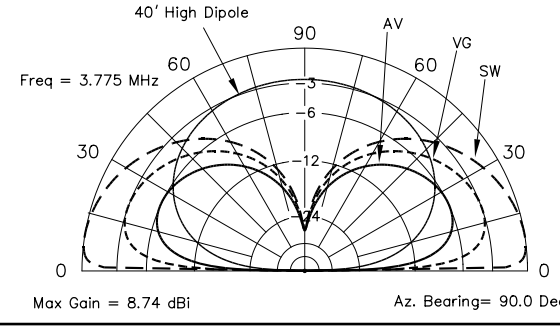

Fig 45—Comparison of 80-meter elevation response of 40-foot high, horizontally polarized dipole over average ground and a 40-foot high, vertically polarized half-square, over three types of ground: average (conductivity σ = 5 mS/m, dielectric constant ε = 13), very good (σ = 30 mS/m, ε = 20) and salt water (σ = 5000 mS/m, ε = 80). The quality of the ground clearly has a profound effect on the low-angle performance of the half-square. Even over average ground, the half-square outperforms the low dipole below about 32°.

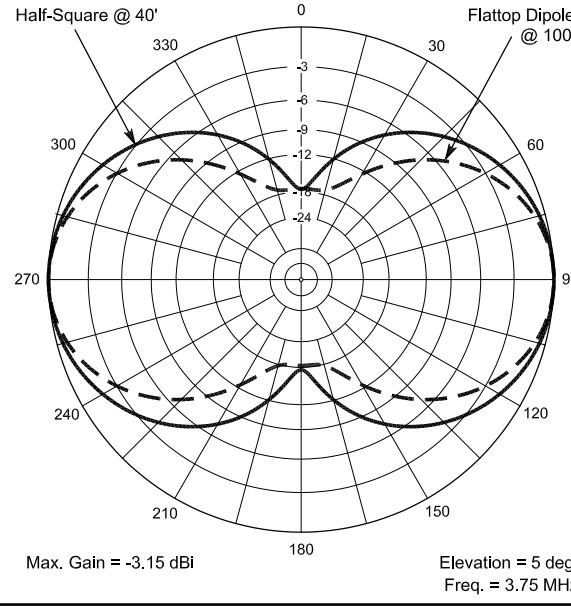

Fig 46—80-meter azimuth patterns for shortened half-square antenna (solid line) shown in Fig 44, compared with flattop dipole (dashed line) at 100 feet height. Average ground is assumed for these cases.

Fig 46 shows the azimuthal-plane pattern for the 80-meter half-square antenna in Fig 44, but this time compared with the response of a flattop horizontal dipole that is 100 feet high. These comparisons are for average ground and are for an elevation angle of 5°. The message here is that the lower your dipole and the better your ground, the more you have to gain by switching from a dipole to a half-square. The half-square antenna looks like a good bet for DXing.

Changing the Shape of the Half Square

Just how flexible is the shape? There are several common distortions of practical importance. Some have very little effect but a few are fatal to the gain. Suppose you have either more height and less width than called for in the standard version or more width and less height, as shown in **Fig 47A**.

The effect on gain from this type of dimensional variation is given in **Table 4**. For a top length (L_T) varying between 110 and 150 feet, where the vertical wire lengths (L_V) readjusted to resonate the antenna, the gain changes only by 0.6 dB. For a 1-dB change the range of L_T is 100 to 155 feet, a pretty wide range.

Another variation results if we vary the length of the horizontal top wire and readjust the vertical wires for resonance, while keeping the top at a constant height. See Fig 47B. **Table 5** shows the effect of this variation on the peak gain. For a range of L_T = 110 to 145 feet, the gain changes only 0.65 dB.

The effect of bending the ends into a V shape, as shown in Fig 47C, is given in **Table 6**. The bottom of the antenna is kept at a height of 5 feet and the top height (H) is either 40 or 60 feet. Even this gross deformation has only a relatively small effect on the gain. Sloping the ends outward as shown in Fig 47D and varying the top length also has only a small effect on the gain. While this is good news because it allows you dimension the antenna to fit different QTHs, not all distortions are so benign.

Table 4

Variation in Gain with Change in Horizontal Length, with Vertical Height Readjusted for Resonance (see Fig 47A)

L_T (feet)	*L_V (feet)*	*Gain (dBi)*
100	85.4	2.65
110	79.5	3.15
120	73.7	3.55
130	67.8	3.75
140	61.8	3.65
150	56	3.05
155	53	2.65

Table 5

Variation in Gain with Change in Horizontal Length, with Vertical Length Readjusted for Resonance, but Horizontal Wire Kept at Constant Height (see Fig 47B)

L_T (feet)	*L_V (feet)*	*Gain (dBi)*
110	78.7	3.15
120	73.9	3.55
130	68	3.75
140	63	3.35
145	60.7	3.05

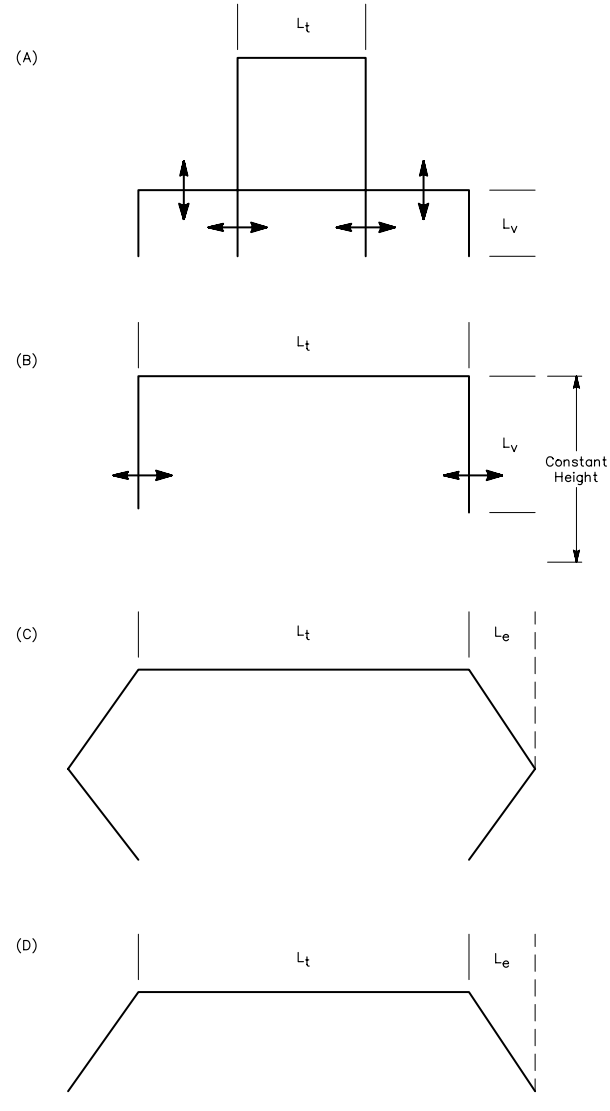

Fig 47—Varying the horizontal and vertical lengths of a half-square. At A, both the horizontal and vertical legs are varied, while keeping the antenna resonant. At B, the height of the horizontal wire is kept constant, while its length and that of the vertical legs is varied to keep the antenna resonant. At C, the length of the horizontal wire is varied and the legs are bent inwards in the shape of "vees." At D, the ends are sloped outward and the length of the flattop portion is varied. All these symmetrical forms of distortion of the basic half-square shape result in small performance losses. At E, a "halfwave vertical dipole" (HVD) with the feed coax isolated with common-mode choke baluns to keep RF current off the coax shield.

Table 6

Gain for Half-Square Antenna, Where Ends Are Bent Into V-Shape (see Fig 47 C)

Height ⇒	*H=40 feet*	*H=40 feet*	*H=60 feet*	*H=60 feet*
L_T (feet)	*L_e (feet)*	*Gain (dBi)*	*L_e (feet)*	*Gain (dBi)*
40	57.6	3.25	52.0	2.75
60	51.4	3.75	45.4	3.35
80	45.2	3.95	76.4	3.65
100	38.6	3.75	61.4	3.85
120	31.7	3.05	44.4	3.65
140	—	—	23	3.05

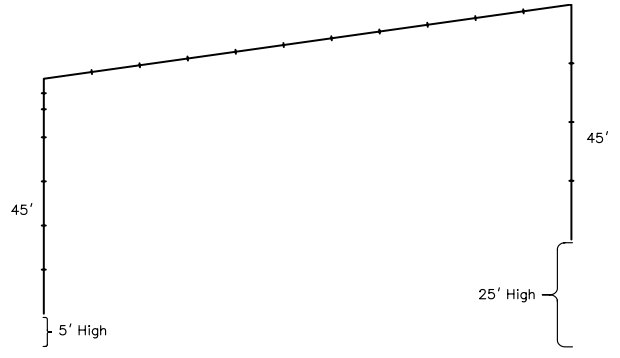

Fig 48—An asymmetrical distortion of the half-square antenna, where the bottom of one leg is purposely made 20 feet higher than the other. This type of distortion does affect the pattern!

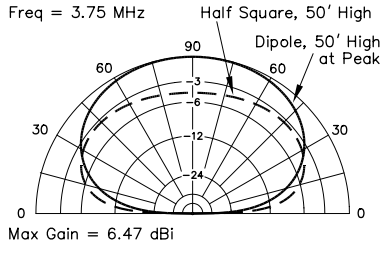

Fig 49—Elevation pattern for the asymmetrical half-square shown in Fig 48, compared with pattern for a 50-foot high dipole. This is over average ground, with a conductivity of 5 mS/m and a dielectric constant of 13. Note that the zenith-angle null has filled in and the peak gain is lower compared to conventional half-square shown in Fig 43 over the same kind of ground.

Suppose the two ends are not of the same height, as illustrated in **Fig 48**, where one end of the half-square is 20 feet higher than the other. The elevation-plane radiation pattern for this antenna is shown in **Fig 49** compared to a dipole at 50 feet. This type of distortion does affect the pattern. The gain drops somewhat and the zenith null goes away. The nulls off the end of the antenna also go away, so that there is some end-fire radiation. In this example the difference in height is fairly extreme at 20 feet. Small differences of 1 to 5 feet do not affect the pattern seriously.

If the top height is the same at both ends but the length of the vertical wires is not the same, then a similar pattern distortion can occur. The antenna is very tolerant of symmetrical distortions but it is much less accepting of asymmetrical distortion.

What if the length of the wires is such that the antenna is not resonant? Depending on the feed arrangement, that may or may not matter. We will look at that issue later on, in the section on patterns versus frequency. The half-square antenna, like the dipole, is very flexible in its proportions.

Half-Square Feed-Point Impedance

There are many different ways to feed the half-square. Traditionally the antenna has been fed either at the end of one of the vertical sections, against ground, or at one of the upper corners as shown in Fig 43.

For voltage feed at the bottom against ground, the impedance is very high, on the order of several thousand ohms. For current feed at a corner, the impedance is much lower and is usually close to 50 Ω. This is very convenient for direct feed with coax.

The half-square is a relatively high-Q antenna (Q ≈ 17). **Fig 50** shows the SWR variation with frequency for this feed arrangement. An 80-meter dipole is not particularly wideband either, but a dipole will have less extreme variation in SWR than the half-square.

Patterns Versus Frequency

Impedance is not the only issue when defining the bandwidth of an antenna. The effect on the radiation pattern of changing frequency is also a concern. For a voltage-fed half-square, the current distribution changes with frequency. For an antenna resonant near 3.75 MHz, the current distribution is nearly symmetrical. However, above and below resonance the current distribution increasingly becomes asymmetrical. In effect, the open end of the antenna is constrained to be a voltage maximum but the feed point can behave less as a voltage point and more like a current maxima. This allows the current distribution to become asymmetrical.

The effect is to reduce the gain by –0.4 dB at 3.5 MHz and by –0.6 dB at 4 MHz. The depth of the zenith null is reduced from –20 dB to –10 dB. The side nulls are also reduced. Note that this is exactly what happened when the antenna was made physically asymmetrical. Whether the asymmetry is due to current distribution or mechanical arrangements, the antenna pattern will suffer.

When current-feed at a corner is used, the asymmetry introduced by off-resonance operation is much less, since both ends of the antenna are open circuits and constrained to be voltage maximums. The resulting gain reduction is only –0.1 dB. It is interesting that the sensitivity of the pattern to changing frequency depends on the feed scheme used.

Of more concern for corner feed is the effect of the transmission line. The usual instruction is to simply feed

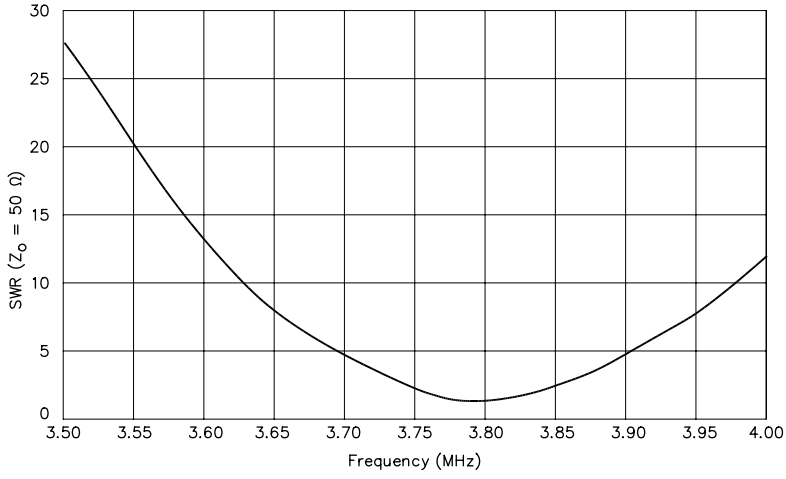

Fig 50—Variation of SWR with frequency for current-fed half-square antenna. The SWR bandwidth is quite narrow.

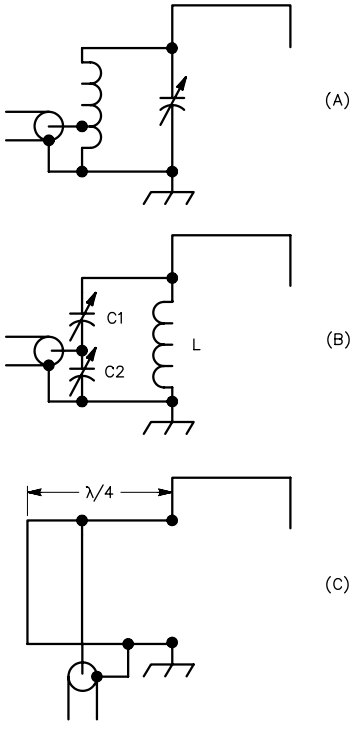

Fig 51—Typical matching networks used for voltage-feeding a half-square antenna.

the antenna using coax, with the shield connected to vertical wire and the center conductor to the top wire. Since the shield of the coax is a conductor, more or less parallel with the radiator, and is in the immediate field of the antenna, you might expect the pattern to be seriously distorted by this practice. This arrangement seems to have very little effect on the pattern. The greatest effect is when the feed line length was near a multiple of λ/2. Such lengths should be avoided.

Of course, you may use a choke balun at the feed point if you desire. This might reduce the coupling to the feed line even further but it doesn't appear to be worth the trouble. In fact, if you use an antenna tuner in the shack to operate away from resonance with a very high SWR on the transmission line, a balun at the feed point would take a beating.

Voltage-Feed at One End of Antenna: Matching Schemes

Several straightforward means are available for narrow-band matching. However, broadband matching over the full 80-meter band is much more challenging. Voltage feed with a parallel-resonant circuit and a modest local ground, as shown in **Fig 51**, is the traditional matching scheme for this antenna. Matching is achieved by resonating the circuit at the desired frequency and tapping down on the inductor in Fig 51A or using a capacitive divider (Fig 51B). It is also possible to use a λ/4 transmission-line matching scheme, as shown in Fig 51C.

If the matching network shown in Fig 51B is used, typical values for the components would be: L = 15 μH, C1 = 125 pF and C2 = 855 pF. At any single point the SWR can be made very close to 1:1 but the bandwidth for SWR < 2:1 will be very narrow at <100 kHz. Altering the L-C ratio doesn't make very much difference. The half-square antenna has a well-earned reputation for being narrow-band.

Short Vertical Antennas

On the lower frequencies it becomes increasingly difficult to accommodate a full λ/4 vertical height and full-sized λ/4 radials, or even worse, a full-sized half-wave vertical dipole (HVD). In fact, it is not absolutely necessary to make the antenna full size, whether it is an HVD, a grounded monopole antenna or a ground-plane type of monopole antenna. The size of the antenna can be reduced by half or even more and still retain high efficiency and the desired radiation pattern. This requires careful design, however. And if high efficiency is maintained, the operating bandwidth of the shortened antenna will be reduced because the shortened antenna will have a higher Q.

This translates into a more rapid increase of reactance away from resonance. The effect can be mitigated to some extent by using larger-diameter conductors. Even doing this however, bandwidth will be a problem, particularly on the 3.5 to 4-MHz band, which is very wide in proportion to the center frequency.

If we take a vertical monopole with a diameter of 2 inches and a frequency of 3.525 MHz and progressively shorten it from λ/4 in length, the feed-point impedance and efficiency (using an inductor at the base to tune out the capacitive reactance) will vary as shown in **Table 7**. In this example perfect ground and conductor are assumed. Real ground will not make a great difference in the impedance but will introduce ground loss, which will reduce the efficiency further. Conductor loss will also reduce efficiency. In general, higher R_R will result in better efficiency.

The important point of Table 7 is the drastic reduction in radiation resistance R_R as the antenna gets shorter. This combined with the increasing loss resistance of the inductor (R_L) used to tune out the increasing base reactance (X_C) reduces the efficiency.

BASE LOADING A SHORT VERTICAL ANTENNA

The base of the antenna is a convenient point at which to add a loading inductor, but it is usually not the lowest loss point at which an inductor, of a given Q, could be placed. There is an extensive discussion of the optimum location of the loading in a short vertical as a function of ground loss and inductor Q in Chapter 16 for mobile antennas, which by necessity are electrically and physically short. This information should be reviewed before using inductive loading.

On the accompanying CD-ROM is a copy of the program *MOBILE.EXE*. This is an excellent tool for designing short, inductively loaded antennas. In most cases, where top loading (discussed below) is not used, the optimum point is near or a little above the middle of the vertical section. Moving the loading coil from the base to the middle of the vertical antenna can make an important difference, increasing R_R and reducing the inductor loss. For example, in an antenna operating at 3.525 MHz, if we make L_1 = 34.9 feet (0.125 λ) the amount of loading inductor placed at the center is 25.2 μH. This resonates the antenna. In this configuration R_R will increase from 6.8 Ω (base loading) to 13.5 Ω (center loading). This substantially increases the efficiency of the antenna, depending on the ground loss and conductor resistances.

Instead of a lumped inductance being inserted at some point in the antenna, it is also possible to use "continuous loading," where the entire radiator is wound as a small diameter coil. The effect is to distribute the inductive loading all along the radiator. In this version of inductive loading the coil is the radiator. An example of a short vertical using this principle is given later in this chapter.

OTHER WAYS OF LOADING A SHORT ANTENNA FOR RESONANCE

Inductive loading is not the only, or even the best, way to compensate for reduced antenna height. *Capacitive top loading* can also be used as indicated in **Fig 52** to bring a vertical monopole to resonance. **Table 8** gives information on a shortened 3.525-MHz vertical using top loading. The vertical portion (L_1) is made from 2-inch tubing. The top loading is also 2-inch tubing extending across the top like a T. The length of the top loading T ($\pm L_2$) is adjusted to resonate the

Table 7

Effect of Shortening a Vertical Radiator Below λ/4 Using Inductive Base Loading.

Frequency is 3.525 MHz and for the Inductor Q_L = 200. Ground and conductor losses are omitted.

Length (feet)	Length (λ)	R_R (Ω)	X_C (Ω)	R_L (Ω)	Efficiency (%)	Loss (dB)
14	0.050	0.96	–761	3.8	20	–7.0
20.9	0.075	2.2	–533	2.7	45	–3.5
27.9	0.100	4.2	–395	2.0	68	–1.7
34.9	0.125	6.8	–298	1.5	82	–0.86
41.9	0.150	10.4	–220	1.1	90	–0.44
48.9	0.175	15.1	–153	0.77	95	–0.22
55.8	0.200	21.4	–92	0.46	98	–0.09
62.8	0.225	29.7	–34	0.17	99	–0.02

Table 8

Effect of Shortening a Vertical Using Top Loading

L_1 (feet)	L_2 (feet)	Length (λ)	R_R (Ω)
14.0	48.8	0.050	4.0
20.9	38.6	0.075	8.5
27.9	30.1	0.100	14.0
34.9	22.8	0.125	19.9
41.9	17.3	0.150	25.5
48.9	11.9	0.175	30.4
55.8	7.0	0.200	33.9
62.8	2.4	0.225	35.7

antenna. Again, the ground and the conductors are assumed to be perfect in Table 8.

For a given vertical height, resonating the antenna with top loading results in much higher radiation resistance R_R—2 to 4 times. In addition, the loss associated with the loading element will be smaller. The result is a more efficient antenna for low heights. A comparison of R_R for both capacitive top loading and inductive base loading is given in **Fig 53**. For heights below 0.15 λ the length of the top-loading elements becomes impractical but there are other, potentially more useful, top-loading schemes.

A multiwire system such as the one shown in **Fig 54** has more capacitance than the single-conductor arrangement, and thus does not need to be as long to resonate at a given frequency. This design does, however, require extra supports for the additional wires. Ideally, an arrangement of this sort should be in the form of a cross, but parallel wires separated by several feet give a considerable increase in capacitance

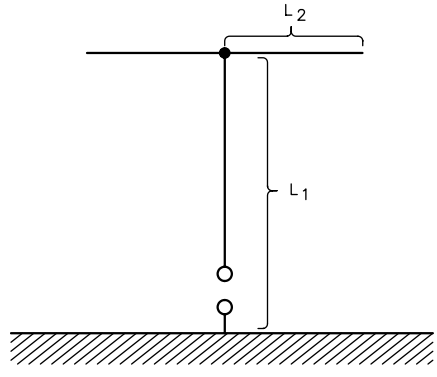

Fig 52—Horizontal wire used to top load a short vertical.

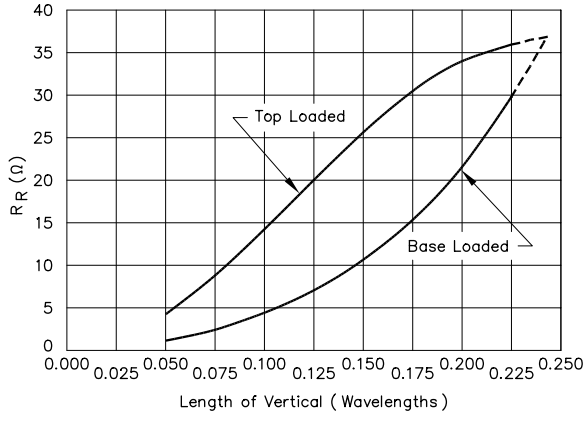

Fig 53—Comparison of top (capacitive) and base (inductive) loading for short verticals. Sufficient loading is used to resonate the antenna.

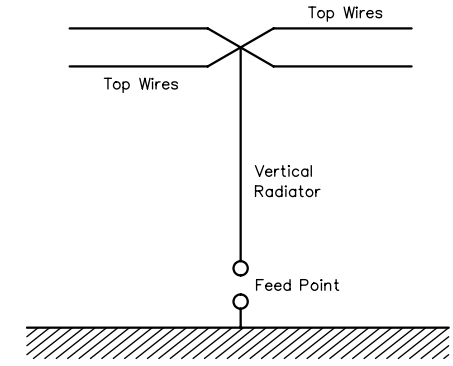

Fig 54—Multiple top wires can increase the effective capacitance substantially. This allows the use of shorter top wires to achieve resonance.

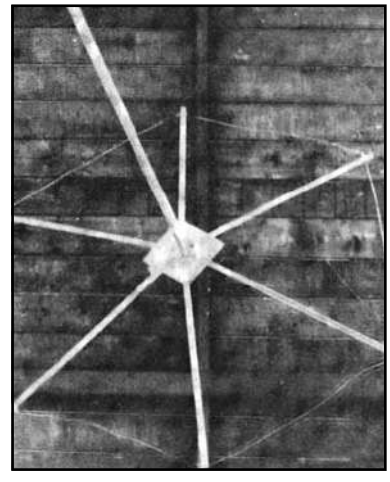

Fig 55—A close-up view of the capacitance hat for a 7-MHz vertical antenna. The ½-in. diameter radial arms terminate in a loop of copper wire.

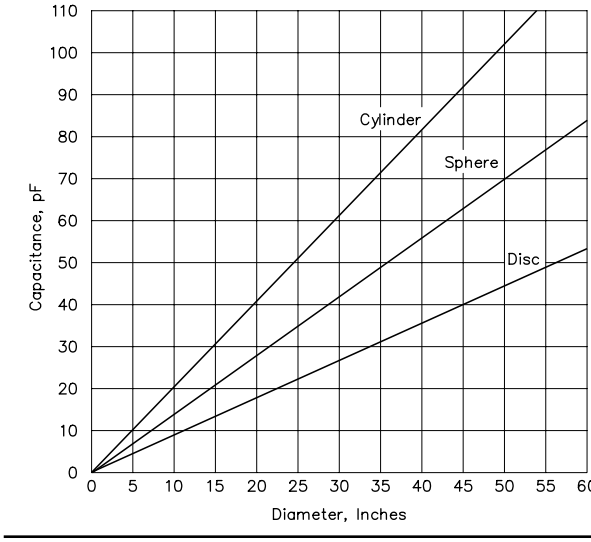

Fig 56—Capacitance of sphere, disc and cylinder as a function of their diameters. The cylinder length is assumed equal to its diameter.

over a single wire.

The top loading can be supplied by a variety of metallic structures large enough to have the necessary self-capacitance. For example, as shown in **Fig 55**, a multi-spoked structure with the ends connected together can be used. One simple way to make a capacitance hat is to take four to six 8-foot fiberglass CB mobile whips, arrange them like spokes in a wagon wheel and connect the ends with a peripheral wire. This arrangement will produce a 16-foot diameter hat that is economical and very durable, even when loaded with ice. Practically any sufficiently large metallic structure can be used for this purpose, but simple geometric forms such as the sphere, cylinder and disc are preferred because of the relative ease with which their capacitance can be calculated.

The capacitance of three geometric forms can be estimated from the curves of **Fig 56** as a function of their size. For the cylinder, the length is specified equal to the diameter. The sphere, disc and cylinder can be constructed from sheet metal, if such construction is feasible, but the capacitance will be practically the same in each if a "skeleton" type of construction with screening or networks of wire or tubing are used.

Finding Capacitance Hat Size

The required size of a capacitance hat may be determined from the following procedure. The information in this section is based on a September 1978 *QST* article by Walter Schulz, K3OQF. The physical length of a shortened antenna can be found from:

$$h_{inches} = \frac{11808}{F_{MHz}} \qquad \text{(Eq 3)}$$

where h = length in inches.

Thus, using an example of 7 MHz and a shortened length of 0.167 λ, h = 11808/7 × 0.167 = 282 inches, equivalent to 23.48 feet.

Consider the vertical radiator as an open-ended transmission line, so the impedance and top loading may be determined. The characteristic impedance of a vertical antenna can be found from

$$Z_0 = 60 \left(\ln\left(\frac{4h}{d}\right) - 1 \right) \qquad \text{(Eq 4)}$$

where

ln = natural logarithm

h = length (height) of vertical radiator in inches (as above)

d = diameter of radiator in inches

The vertical radiator for this example has a diameter of 1 inch. Thus, for this example,

$$Z_0 = 60 \left(\ln\left(\frac{4\times 281}{1}\right) - 1 \right) = 361\ \Omega$$

The capacitive reactance required for the amount of top loading can be found from

$$Z_0 = 60\ \ln\left(\frac{4\times 281}{1}\right) - 1 = 361\ \Omega \qquad \text{(Eq 5)}$$

where

X = capacitive reactance, ohms

Z_0 = characteristic impedance of antenna (from Eq 4)

θ = amount of electrical loading, degrees.

This value for a 30° hat is 361/tan 30° = 625 Ω. This capacitive reactance may be converted to capacitance with the following equation,

$$C = \frac{10^6}{2\pi f X_C} \qquad \text{(Eq 6)}$$

where

C = capacitance in pF

f = frequency, MHz

X_C = capacitive reactance, ohms (from above).

For this example, the required $C = 10^6/(2\ \pi \times 7 \times 625)$ = 36.4 pF, which may be rounded to 36 pF. A disc capacitor is used in this example. The appropriate diameter for 36 pF of hat capacitance can be found from Fig 56. The disc diameter that yields 36 pF of capacitance is 40 inches.

The skeleton disc shown in Fig 55 is fashioned into a wagonwheel configuration. Six 20-inch lengths of ½-inch OD aluminum tubing are used as spokes. Each is connected to the hub at equidistant intervals. The outer ends of the spokes terminate in a loop made of #14 copper wire. Note that the loop increases the hat capacitance slightly, making a better approximation of a solid disc. The addition of this hat at the top of a 23.4-foot radiator makes it quarter-wave resonant at 7 MHz.

After construction, some slight adjustment in the radiator length or the hat size may be required if resonance at a specific frequency is desired. From Fig 53, the radiation resistance of a 0.167-λ high radiator is seen to be about 13 Ω without top loading. With top loading Rr ≈ 25 Ω or almost double.

THE COMPACT VERTICAL DIPOLE

A variation on the HVD (half-wave vertical dipole) theme is the *compact vertical dipole*, or CVD. The CVD uses capacitance-hat loading on each end of a shortened vertical radiator, as shown in **Fig 57C**. Some call this "top hat" and "bottom hat" loading. Les Moxon, G6XN, called this method of loading a shortened antenna simply "end loading." The vertical wire for his 40-meter CVD is 25 feet high, with 15-foot long horizontal loading wires on each side, top and bottom.

K8CH Compact Vertical Dipole

The top loading wires needn't be perpendicular to the vertical radiator, although that is convenient if you construct the antenna from aluminum tubing. K8CH described a wire 30-meter CVD in the 2006 Edition of *The ARRL Handbook*. This used #14 wire throughout, with sloping top loading wires. It was designed to be suspended from a tree at least

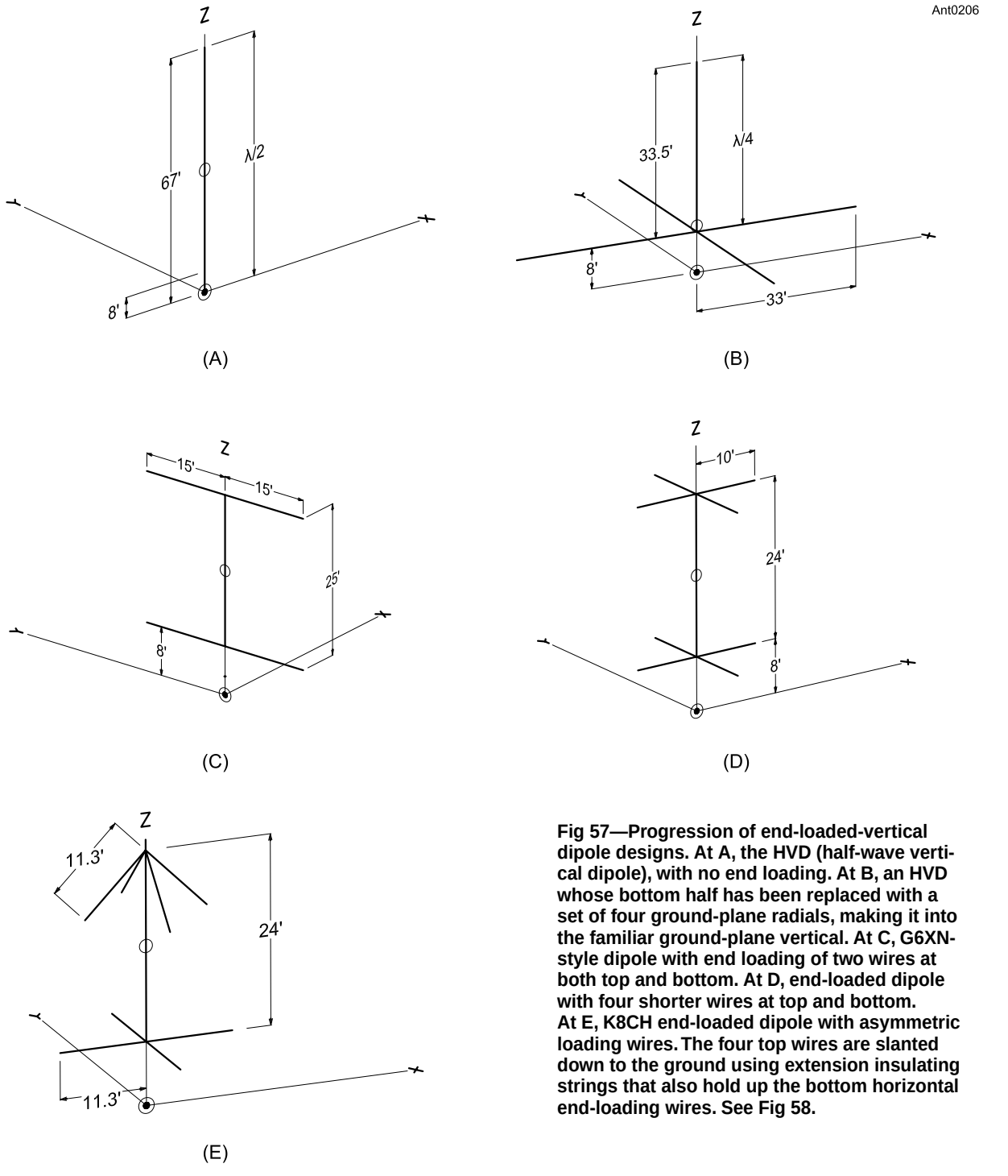

Fig 57—Progression of end-loaded-vertical dipole designs. At A, the HVD (half-wave vertical dipole), with no end loading. At B, an HVD whose bottom half has been replaced with a set of four ground-plane radials, making it into the familiar ground-plane vertical. At C, G6XN-style dipole with end loading of two wires at both top and bottom. At D, end-loaded dipole with four shorter wires at top and bottom. At E, K8CH end-loaded dipole with asymmetric loading wires. The four top wires are slanted down to the ground using extension insulating strings that also hold up the bottom horizontal end-loading wires. See Fig 58.

32 feet high to keep all wires 8 feet or more above humans and animals. The vertical radiating wire is 24 feet long, and the eight top and bottom end-loading wires are all 5 feet 9 inches long. See Fig 57E and **Table 9**, CVD 1.

The top loading wires slant at an angle of 45º down to the ground, using insulating strings that also support the ends of the bottom loading wires, holding them out so that they are horizontal. See **Fig 58**. There is a small loss of gain because of the "umbrella" shape of the top loading wires, and the 2:1 SWR bandwidth is diminished slightly from the horizontal case. This isn't a problem on a narrow band like 30 meters.

A 40-meter version of this antenna, CVD 6, also uses a 24-foot long vertical radiator, 8 feet high at its bottom. It uses 11.3-foot long radial wires made of #14 wire, again with the top four slanted down at 45º. This CVD has a 2:1

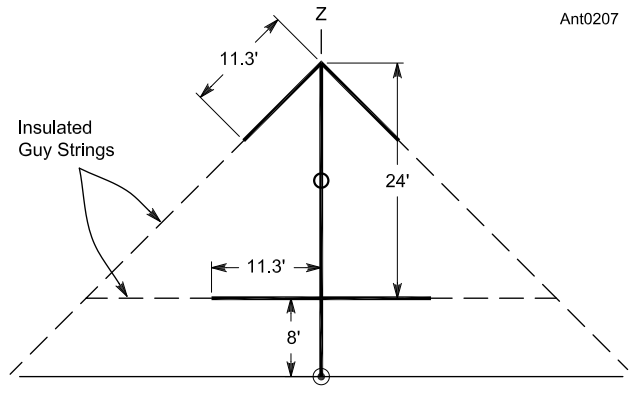

Fig 58—Layout of CVD made using #14 wire suspended from a tree branch.

SWR bandwidth of 250 kHz. It is directly fed with 50-Ω coax with ferrite-core common-mode choke baluns in the middle of the vertical radiator. An additional choke balun is used where the coax reaches ground level in order to knock down common-mode currents that might otherwise radiate onto the coax shield.

You should note the comparison of 40-meter ground-plane vertical antennas in Table 9. GP 1 is for horizontal radials that are 8 feet off the ground, while GP 2 has its radials only 2 feet high. There is some loss in gain because of the proximity of the lossy ground. The 40-meter CVD 1 and CVD 2 cases illustrate the same effect of being close to the lossy ground.

Some of the cases in Table 9 require Center Load coils to bring the antenna to resonance. Where the loading coil inductance is equal to the "Hairpin Coil" inductance, the loading coil also serves as a hairpin matching coil. Where the amount of Hairpin Coil inductance is less than the Load Coil inductance, a match is achieved by tapping the Center Load Coil symmetrically out from the center.

80-Meter CVD

The size of a CVD becomes a real challenge on 80 meters, requiring either very tall support structures or multiple loading methods to keep the vertical radiator to a reasonable length. The CVD 2 design in Table 9 shows a K8CH-style CVD wire antenna whose vertical radiator is 46.5 feet long. It requires a 54.5-foot high tree to keep the bottom end of the vertical radiator 8 feet above ground for safety. Compare this to an HVD that requires a 143-foot support of some sort to keep it 8 feet off the ground at the bottom. The CVD 2 sacrifices some 0.7 dB in gain for this difference in size, and about 75 kHz in 2:1 SWR bandwidth.

The CVD 2 would require retuning when going from

Table 9
Variations on a Vertical Center-Fed Dipole

Name	*Style Fig 57*	*Vertical Length feet*	*Spoke Length feet*	*Min. Ht feet*	*Max. Gain dBi*	*2:1 SWR kHz*	*Hairpin Coil μH*	*Center Load μH*
20 Meters								
GP	B	17.53	16.53	8	0.29	400	—	—
CVD 1	C	13	7.57	8	0.12	625	—	—
CVD 2	D	12	5.1	8	0.00	550	0.68	0.68
CVD 3	E	12.15	5.6	8	–0.01	450	0.5	0.5
30 Meters								
GP	B	24.54	23.14	8	0.04	400	—	—
CVD 1	E	24	5.33	8	–0.2	500	—	—
CVD 2	E	17	7.60	8	–0.36	400	0.82	0.82
40 Meters								
HVD	A	66	—	8	0.13	450	—	—
GP 1	B	35	33	8	–0.12	325	—	—
GP 2	B	34.5	33	2	–0.37	400	—	—
CVD 1	C	25	15	8	–0.42	450	—	—
CVD 2	C	24	15	2	–1.09	400	—	—
CVD 3	D	24	10	8	–0.55	425	—	0.25
CVD 4	D	24	5	8	–0.85	225	—	8.7
CVD 5	D	16	8	8	–1.18	175	0.94	6.8
CVD 6	E	24	11.3	8	–0.59	250	—	—
80 Meters								
HVD	A	135	—	8	0.19	225	—	—
GP	B	65.5	61	8	0.11	200	—	—
CVD 1	C	48.3	30	8	–0.27	200	—	—
CVD 2	E	46.5	21.9	8	–0.50	150	—	—

CW to phone, probably by changing the length of the four bottom horizontal wires equally.

LINEAR LOADING

Another alternative to inductive loading is *linear loading*. This little-understood method of shortening radiators can be applied to almost any antenna configuration—including parasitic arrays. Although commercial antenna manufacturers make use of linear loading in their HF antennas, relatively few hams have used it in their own designs. Linear loading can be used to advantage in many antennas because it introduces relatively little loss, does not degrade directivity patterns, and has low enough Q to allow reasonably good bandwidth. Some examples of linear-loaded antennas are shown in **Fig 59**.

Since the dimensions and spacing of linear-loading devices vary greatly from one antenna installation to another, the best way to employ this technique is to try a length of conductor 10% to 20% longer than the difference between the shortened antenna and the full-size dimension for the linear-loading device. Then use the "cut-and-try" method, varying both the spacing and length of the loading device to optimize the match. A hairpin at the feed point can be useful in achieving a 1:1 SWR at resonance.

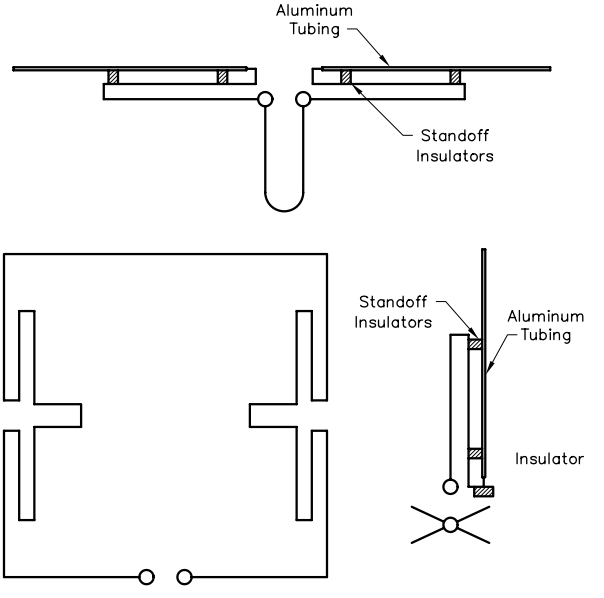

Fig 59—Some examples of linear loading. The small circles indicate the feed points of the antennas.

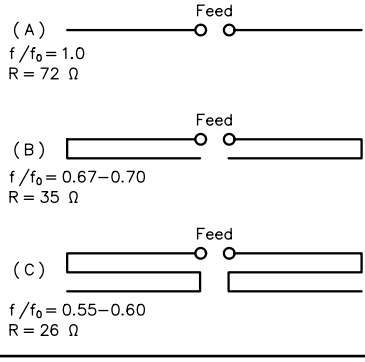

Fig 60—Wire dipole antennas. The ratio f/f_0 is the measured resonant frequency divided by frequency f_0 of a standard dipole of same length. R is radiation resistance in ohms. At A, standard single-wire dipole. At B, two-wire linear-loaded dipole, similar to folded dipole except that side opposite feed line is open. At C, three-wire linear-loaded dipole.

Linear-Loaded Short Wire Antennas

More detail on linear loading is provided in this section, which was originally presented in *The ARRL Antenna Compendium Vol 5* by John Stanford, NNØF. Linear loading can significantly reduce the required length for resonant antennas. For example, it is easy to make a resonant antenna that is as much as 30 to 40% shorter than an ordinary dipole for a given band. The shorter overall lengths come from bending back some of the wire. The increased self-coupling lowers the resonant frequency. These ideas are applicable to short antennas for restricted space or portable use.

Experiments

The results of the measurements are shown in **Fig 60** and are also consistent with values given by Rashed and Tai from an earlier paper. This shows several simple wire antenna configurations, with resonant frequencies and impedance (radiation resistance). The reference dipole has a resonant frequency f_0 and resistance R = 72 Ω. The f/f_0 values give the effective reduced frequency obtained with the linear loading in each case. For example, the two-wire linear-loaded dipole has its resonant frequency lowered to about 0.67 to 0.70 that of the simple reference dipole of the same length.

The three-wire linear-loaded dipole has its frequency reduced to 0.55 to 0.60 of the simple dipole of the same length. As you will see later, these values will vary with conductor diameter and spacing.

The two-wire linear-loaded dipole (Fig 60B) looks almost like a folded dipole but, unlike a folded dipole, it is open in the middle of the side opposite where the feed line is attached. Measurements show that this antenna structure has a resonant frequency lowered to about two-thirds that of the reference dipole, and R equal to about 35 Ω. A three-wire linear-loaded dipole (Fig 60C) has even lower resonant frequency and R about 25 to 30 Ω.

Linear-loaded monopoles (one half of the dipoles in Fig 60) working against a radial ground plane have similar resonant frequencies, but with only half the radiation resistance shown for the dipoles.

A Ladder-Line Linear-Loaded Dipole

Based on these results, NNØF next constructed a linear loaded dipole as in Fig 60B, using 24 feet of 1-inch ladder line (the black, 450-Ω plastic kind widely available) for the dipole length. He hung the system from a tree using nylon

fishing line, about 4 feet from the tree at the top, and about 8 feet from the ground on the bottom end. It was slanted at about a 60° angle to the ground. This antenna resonated at 12.8 MHz and had a measured resistance of about 35 Ω. After the resonance measurements, he fed it with 1-inch ladder open-wire line (a total of about 100 feet to the shack).

For brevity, this is called a vertical *LLSD* (linear-loaded short dipole). A tuner resonated the system nicely on 20 and 30 meters. On these bands the performance of the vertical LLSD seemed comparable to his 120-foot long, horizontal center-fed Zepp, 30 feet above ground. In some directions where the horizontal, all-band Zepp has nulls, such as toward Siberia, the vertical LLSD was definitely superior. This system also resonates on 17 and 40 meters. However, from listening to various signals, NNØF had the impression that this length LLSD is not as good on 17 and 40 meters as the horizontal 120-foot antenna.

Using Capacitance End Hats

He also experimented with an even shorter resonant length by trying an LLSD with capacitance end-hats. The hats, as expected, increased the radiation resistance and lowered the resonant frequency. Six-foot long, single-wire hats were used on each end of the previous 24-foot LLSD, as shown in **Fig 61**. The antenna was supported in the same way as the previous vertical dipole, but the bottom-end hat wire was only inches from the grass. This system resonated at 10.6 MHz with a measured resistance of 50 Ω.

If the dipole section were lengthened slightly, by a foot or so, to about 25 feet, it should hit the 10.1-MHz band and be a good match for 50-Ω coax. It would be suitable for a restricted space, shortened 30-meter antenna. Note that this antenna is only about half the length of a conventional 30-meter dipole, needs no tuner, and has no losses due to traps. It does have the loss of the extra wire, but this is essentially negligible.

Any of the linear-loaded dipole antennas can be mounted either horizontally or vertically. The vertical version can be used for longer skip contacts—beyond 600 miles or so—unless you have rather tall supports for horizontal antennas to give a low elevation angle. Using different diameter conductors in linear-loaded antenna configurations yields different results, depending on whether the larger or small diameter conductor is fed. NNØF experimented with a vertical ground-plane antenna using a 10-foot piece of electrical conduit pipe (⅝ inch OD) and #12 copper house wire.

Fig 62 shows the configuration. The radial ground system was buried a couple of inches under the soil and is not shown. Note that this is not a folded monopole, which would have either A or B grounded.

The two conductors were separated by 2 inches, using plastic spreaders held onto the pipe by stainless-steel hose clamps obtained from the local hardware store. Hose clamps intertwined at right angles were also used to clamp the pipe on electric fence stand-off insulators on a short 2×4 post set vertically in the ground.

The two different diameter conductors make the antenna characteristics change, depending on how they are configured. With the antenna bridge connected to the larger diameter conductor (point A in Fig 62), and point B unconnected, the system resonated at 16.8 MHz and had R = 35 Ω. With the bridge at B (the smaller conductor), and point A left unconnected, the resonance lowered to 12.4 MHz and R was found to be about 24 Ω.

The resonant frequency of the system in Fig 62 can be adjusted by changing the overall height, or for increasing the frequency, by reducing the length of the wire. Note that a 3.8-MHz resonant ground plane can be made with height only about half that of the usual 67 feet required, if the smaller conductor is fed (point B in Fig 62). In this case, the pipe would be left unconnected electrically. The lengths given above can be scaled to determine a first-try attempt for your favorite band. Resonant lengths will, however, depend on the conductor diameters and spacing.

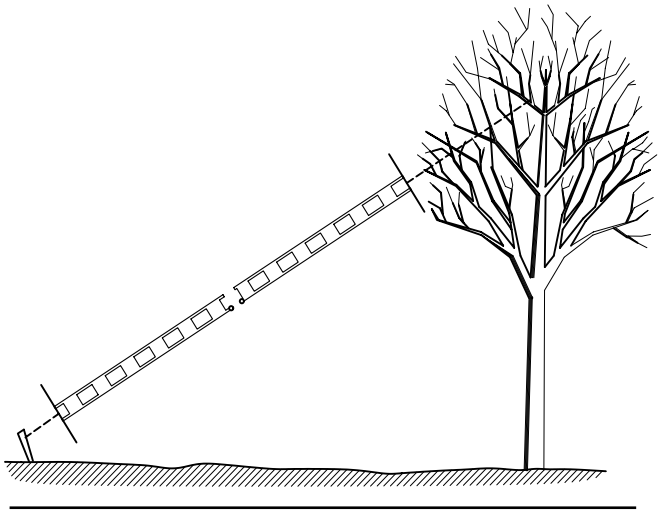

Fig 61—Two-wire linear-loaded dipole with capacitance end hats. Main dipole length was constructed from 24 feet of "windowed" ladder line. The end-hat elements were stiff wires 6 feet long. The antenna was strung at about a 60° angle from a tree limb using monofilament fishing line. Measured resonant frequency and radiation resistance were 10.6 MHz and 50 Ω.

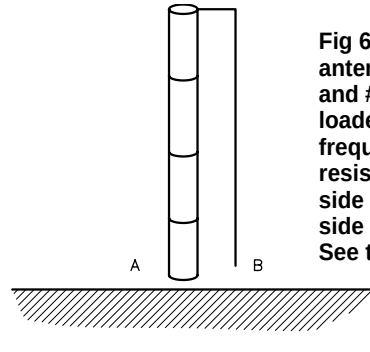

Fig 62—Vertical ground-plane antenna with a 10-foot pipe and #12 wire as the linear-loaded element. Resonant frequency and radiation resistance depend on which side (A or B) is fed. The other side (B or A) is *not* grounded. See text for details.

The same ideas hold for a dipole, except that the lengths should be doubled from those of the ground plane in Fig 62. The resistance will be twice that of the ground plane. Say, how about a shortened 40-meter horizontal beam to enhance your signal?!

COMBINED LOADING

As an antenna is shortened further the size of the top loading device will become larger and at some point will be impractical. In this situation inductive loading, usually placed directly between the capacitance "hat" and the top of the antenna, can be added to resonate the antenna. An alternative would be to use linear loading in place of inductive loading. The previous section contained an example of end loading combined with linear loading.

SHORTENING THE RADIALS

Very often the space required by full-length radials is simply not available. Like the vertical portion of the antenna, the radials can also be shortened and loaded in very much the same way. An example of end loaded radials is given in **Fig 63A**. Radials half the usual length can be used with little reduction in efficiency but, as in the case of top loading, the antenna Q will be higher and the bandwidth reduced. As shown in Fig 63B**,** inductive loading can also be used. As long as they are not made too short (down to 0.1λ) loaded radials can be efficient—with careful design.

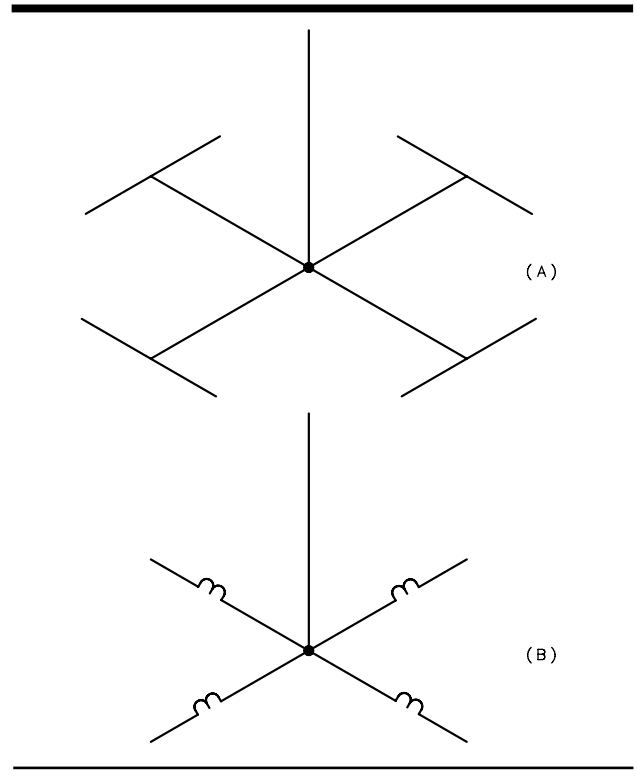

Fig 63—Radials may be shortened by using either capacitive (A) or inductive (B) loading. In extreme cases both may be used but the operating bandwidth will be limited.

GENERAL RULES

The steps in designing an efficient short vertical antenna system are:

- Make the vertical section as long as possible.
- Make the diameter of the vertical section as large as possible. Tubing or a cage of smaller wires will work well.
- Provide as much top and/or bottom loading as possible.
- If the top/bottom loading is insufficient, resonate the antenna with a high-Q inductor placed between the hat and the top of the antenna.
- For buried-ground systems, use as many radials (> 0.2 λ) as possible. 40 or more is best.
- If an elevated ground plane is used, use 4 to 8 radials, 5 or more feet above ground.
- If shortened radials must be used then capacitive loading is preferable to inductive loading.

EXAMPLES OF SHORT VERTICALS

A 6-Foot-High 7-MHz Vertical Antenna

Figs 64 through 67 give details for building short, effective vertical quarter-wavelength radiators. This information was originally presented by Jerry Sevick, W2FMI.

A short vertical antenna, properly designed and installed, approaches the efficiency of a full-size resonant quarter-wave antenna. Even a 6-foot vertical on 7 MHz can produce an exceptional signal. Theory tells us that this should be possible, but the practical achievement of such a result requires an understanding of the problems of ground losses, loading, and impedance matching.

The key to success with shortened vertical antennas lies in the efficiency of the ground system with which the antenna is used. A system of at least 60 radial wires is rec-

Fig 64—Jerry Sevick, W2FMI, adjusts the 6-foot high, 40-meter vertical.

ommended for best results, although the builder may elect to reduce the number at the expense of some performance. The radials can be tensioned and pinned at the far ends to permit on-the-ground installation, which will enable the amateur to mow the lawn without the wires becoming entangled in the mower blades. Alternatively, the wires can be buried in the ground, where they will not be visible. There is nothing critical about the wire size for the radials. Radials made of 28, 22, or even 16-gauge wire, will provide the same results. The radials should be at least 0.2 λ long (27 feet or greater on 7 MHz).

A top hat is formed as illustrated in **Fig 65**. The diameter is 7 feet, and a continuous length of wire is connected to the spokes around the outer circumference of the wheel. A loading coil consisting of 14 turns of B&W 3029 Miniductor stock (2½-inch dia, 6 TPI, #12 wire) is installed 6 inches below the top hat (see Fig 65). This antenna exhibits a feed-point impedance of 3.5 Ω at 7.21 MHz. For operation above or below this frequency, the number of coil turns must be decreased or increased, respectively. Matching is accomplished by increasing the feed-point impedance to 14 Ω through addition of a 4:1-transformer, then matching 14 Ω to 50 Ω (feeder impedance) by means of a pi network. The 2:1 SWR bandwidth for this antenna is approximately 100 kHz.

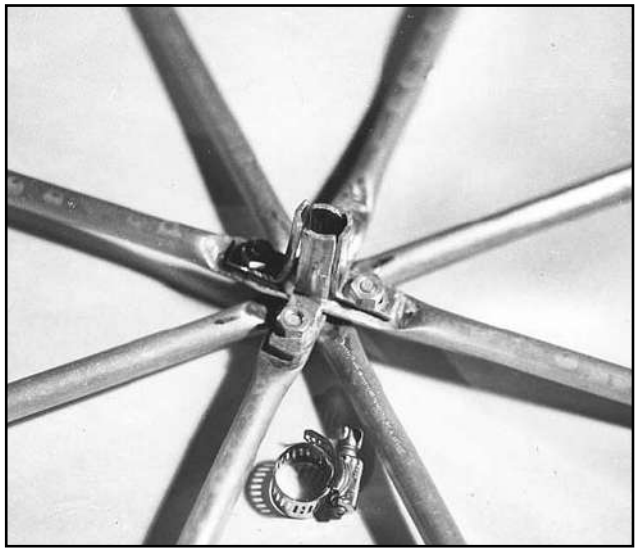

Fig 65—Construction details for the top hat. For a diameter of 7 feet, ½-in. aluminum tubing is used. The hose clamp is made of stainless steel and is available at Sears. The rest of the hardware is aluminum.

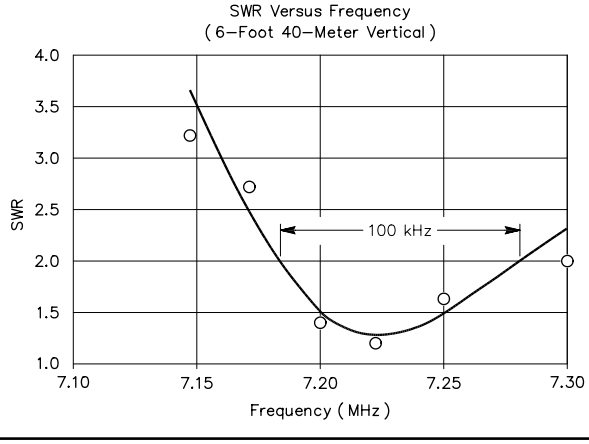

Fig 66—Standing-wave ratio of the 6-foot vertical using a 7-foot top hat and 14 turns of loading 6 inches below the top hat.

More than 200 contacts with the 6-foot antenna have indicated the efficiency and capability of a short vertical. Invariably at distances greater than 500 or 600 miles, the short vertical yields excellent signals. Similar antennas can be scaled and constructed for bands other than 7 MHz. The 7-foot-diameter-top hat was tried on a 3.5-MHz vertical, with an antenna height of 22 feet. The loading coil had 24 turns and was placed 2 feet below the top hat. On-the-air results duplicated those on 40-meters. The bandwidth was 65 kHz.

Short verticals such as these have the ability to radiate and receive almost as well as a full-size quarter-wave. Trade-offs are in lowered input impedances and bandwidths. However, with a good radial system and a proper design, these trade-offs can be made entirely acceptable.

Short Continuously Loaded Verticals

While there is the option of using lumped inductance to achieve resonance in a short antenna, the antenna can also be helically wound to provide the required inductance. This is shown in **Fig 68**. Shortened quarter-wavelength vertical antennas can be made by forming a helix on a long cylindrical insulator. The diameter of the helix must be small in terms of λ to prevent the antenna from radiating in the axial mode.

Acceptable form diameters for HF-band operation are from 1 inch to 10 inches when the practical aspects of antenna construction are considered. Insulating poles of fiberglass, PVC tubing, treated bamboo or wood, or phenolic are suitable for use in building helically wound radiators. If wood or bamboo is used the builder should treat the material with at least two coats of exterior spar varnish prior to winding the antenna element. The completed structure should be given two more coats of varnish, regardless of the material used for the coil form. Application of the varnish will help weatherproof the antenna and prevent the coil turns from changing position.

No strict rule has been established concerning how short a helically wound vertical can be before a significant drop in performance is experienced. Generally, one should use the greatest amount of length consistent with available space. A guideline might be to maintain an element length of 0.05 wavelength or more for antennas which are electrically a quarter wavelength long. Thus, use 13 feet or more of stock for an 80-meter antenna, 7 feet for 40 meters, and so on.

A quarter-wavelength helically wound vertical can be used in the same manner as a full-size vertical. That is, it can be worked against an above-ground wire radial system (four or more radials), or it can be ground-mounted with

Fig 67—Base of the vertical antenna showing the 60 radial wires. The aluminum disc is 15 inches in diameter and ¼ inches thick. Sixty tapped holes for ¼-20 aluminum hex-head bolts form the outer ring and 20 form the inner ring. The inner bolts were used for performance comparisons with more than 60 radials. The insulator is polystyrene material (phenolic or Plexiglas suitable) with a 1-inch diameter. Also shown is the impedance bridge used for measuring input resistance.

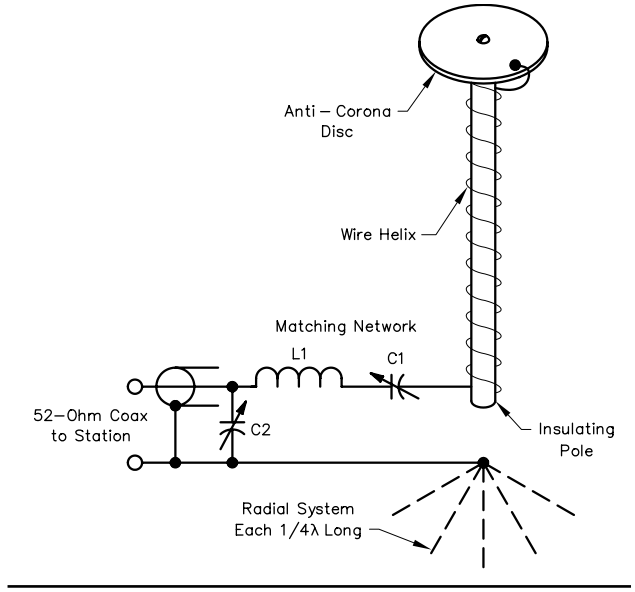

Fig 68—Helically wound ground-plane vertical. Performance from this type of antenna is comparable to that of many full-size λ/4 vertical antennas. The major design trade-off is usable bandwidth. All shortened antennas of this variety are narrow-band devices. At 7 MHz, in the example illustrated here, the bandwidth between the 2:1 SWR points will be on the order of 50 kHz, half that amount on 80 meters, and twice that amount on 20 meters. Therefore, the antenna should be adjusted for operation in the center of the frequency band of interest.

radials buried or lying on the ground. Some operators have reported good results when using antennas of this kind with four helically wound radials cut for resonance at the operating frequency. The latter technique should capture the attention of those persons who must use indoor antennas.

Winding Information

There is no hard-and-fast formula for determining the amount of wire needed to establish resonance in a helical antenna. The relationship between the length of wire needed for resonance and a full quarter wave at the desired frequency depends on several factors. Some of these are wire size, diameter of the turns, and the dielectric properties of the form material, to name a few. Experience has indicated that a section of wire approximately one half wavelength long, wound on an insulating form with a linear pitch (equal spacing between turns) will come close to yielding a resonant quarter wavelength. Therefore, an antenna for use on 160 meters would require approximately 260 feet of wire, spirally wound on the support.

No specific rule exists concerning the size or type of wire one should use in making a helix. Larger wire sizes are, of course, preferable in the interest of minimizing I^2R losses in the system. For power levels up to 1000 W it is wise to use a wire size of #16 or larger. Aluminum clothesline wire is suitable for use in systems where the spacing between turns is greater than the wire diameter. Antennas requiring close-spaced turns can be made from enameled magnet wire or #14 vinyl jacketed, single-conductor house wiring stock. Every effort should be made to keep the turn spacing as large as is practical to maximize efficiency.

A short rod or metal disc should be made for the top or high-impedance end of the vertical. This is a necessary part of the installation to assure reduction in antenna Q. This broadens the bandwidth of the system and helps prevent extremely high amounts of RF voltage from being developed at the top of the radiator. (Some helical antennas act like Tesla coils when used with high-power transmitters, and can actually catch fire at the high-impedance end when a stub or disc is not used.) Since the Q-lowering device exhibits some additional capacitance in the system, it must be in place before the antenna is tuned.

Tuning and Matching

Once the element is wound it should be mounted where it will be used, with the ground system installed. The feed end of the radiator can be connected temporarily to the ground system. Use a dip meter to check the antenna for resonance by coupling the dipper to the last few turns near the ground end of the radiator. Add or remove turns until the vertical is resonant at the desired operating frequency.

It is impossible to predict the absolute value of feed impedance for a helically wound vertical. The value will depend upon the length and diameter of the element, the ground system used with the antenna, and the size of the disc or stub atop the radiator. Generally speaking, the radiation resistance will be very low—approximately 3 to 10 Ω. An L

network of the kind shown in Fig 68 can be used to increase the impedance to 50 Ω. The Q_L (loaded Q) of the network inductors is low to provide reasonable bandwidth, consistent with the bandwidth of the antenna. Network values for other operating bands and frequencies can be determined by using the reactance values listed below. The design center for the network is based on a radiation resistance of 5 Ω. If the exact feed impedance is known, the following equations can be used to determine precise component values for the matching network. (See Chapter 25, Coupling the Transmitter to the Line, for additional information on L-network matching.)

XA QRL (Eq 7)

$$X_{C2} = 50\sqrt{\frac{R_L}{50 - R_L}} \quad \text{(Eq 8)}$$

$$X_{L1} = X_{C1} + \frac{R_L 50}{X_{C2}} \quad \text{(Eq 9)}$$

where

X_{C1} = capacitive reactance of C1
X_{C2} = capacitive reactance of C2
X_{L1} = inductive reactance of L1
Q = loaded Q of network
R_L = radiation resistance of antenna

Example: Find the network constants for a helical antenna with a feed impedance of 5 Ω at 7 MHz, Q = 3:

$$X_{C1} = 3 \times 5 = 15$$

$$X_{C2} = \sqrt{\frac{5}{50 - 5}} = 16.666$$

$$X_{L1} = 15 + \frac{250}{16.666} = 30$$

Therefore, C1 = 1500 pF, C2 = 1350 pF, and L1 = 0.7 μH. The capacitors can be made from parallel or series combinations of transmitting micas. L_1 can be a few turns of large Miniductor stock. At RF power levels of 100 W or less, large compression trimmers can be used at C1 and C2 because the maximum RMS voltage at 100 W (across 50 Ω) will be 50 V. At, say, 800 W there will be approximately 220 V RMS developed across 50 Ω. This suggests the use of small transmitting variables at C1 and C2, possibly connected in parallel with fixed values of capacitance to constitute the required amount of capacitance for the network.

By making some part of the network variable, it will be possible to adjust the circuit for an SWR of 1:1 without knowing precisely what the antenna feed impedance is. Actually, C1 is not required as part of the matching network. It is included here to bring the necessary value for L1 into a practical range.

Fig 68 illustrates the practical form a typical helically wound ground-plane vertical might take. Performance from this type antenna is comparable to that of many full-size quarter-wavelength vertical antennas. The major design trade-off is in usable bandwidth. All shortened antennas of this variety are narrow-band devices. At 7 MHz, in the example illustrated here, the bandwidth between the 2:1 SWR points will be on the order of 50 kHz, half that amount on 80 meters, and twice that amount on 20 meters. Therefore, the antenna should be adjusted for operation in the center of the frequency spread of interest.

SHORTENED DIPOLES

As shown in preceding sections, there are a number of ways to load antennas so they may be reduced in size without severe reductions in effectiveness. Loading is always a compromise; the best method is determined by the amount of space available and the band(s) to be worked.

The simplest way to shorten a dipole is shown in **Fig 69**. If you do not have sufficient length between the supports, simply hang as much of the center of the antenna as possible between the supports and let the ends hang down. The ends can be straight down or may be at an angle as indicated but in either case should be secured so that they do not move in the wind. As long as the center portion between the supports is at least ¼, the radiation pattern will be very nearly the same

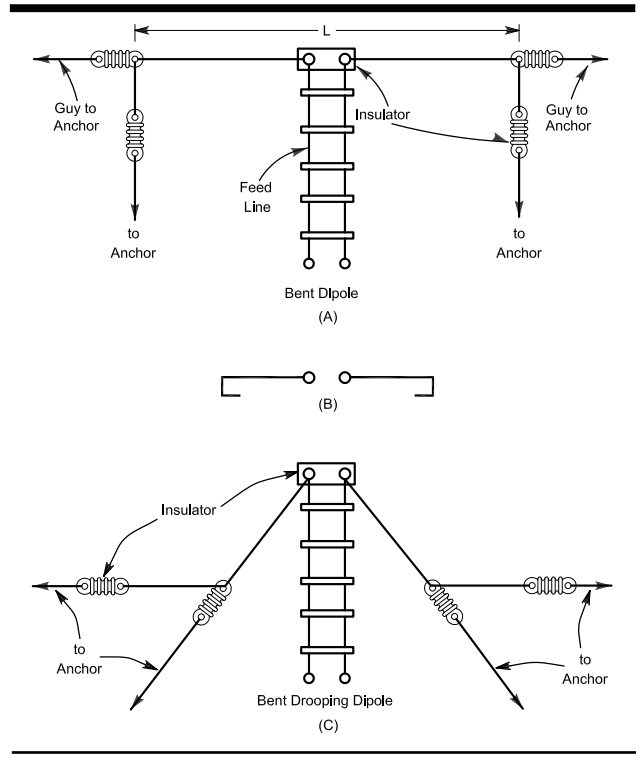

Fig 69—When space is limited, the ends may be bent downward as shown at A, or back on the radiator as shown at B. The bent dipole ends may come straight down or be led off at an angle away from the center of the antenna. An inverted V at C can be erected with the ends bent parallel to the ground when the support structure is not high enough.

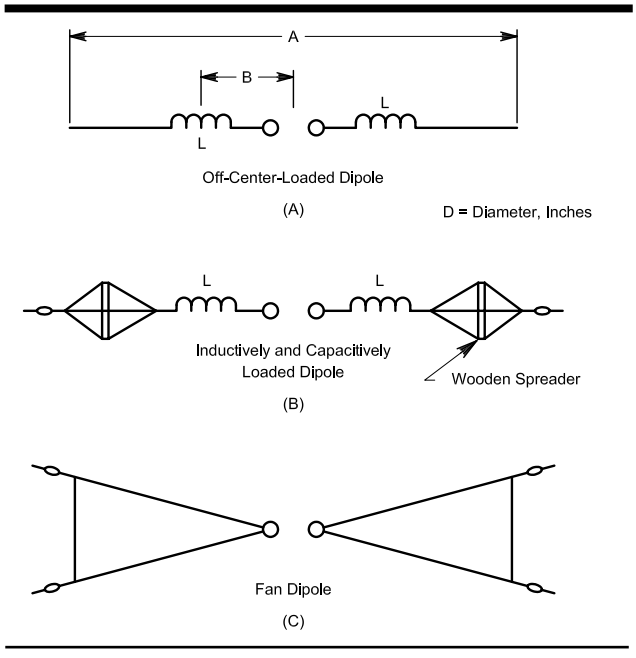

Fig 70—At A is a dipole antenna lengthened electrically with off-center loading coils. For a fixed dimension A, greater efficiency will be realized with greater distance B, but as B is increased, L must be larger in value to maintain resonance. If the two coils are placed at the ends of the antenna, in theory they must be infinite in size to maintain resonance. At B, capacitive loading of the ends, either through proximity of the antenna to other objects or through the addition of capacitance hats, will reduce the required value of the coils. At C, a fan dipole provides some electrical lengthening as well as broadbanding.

as a full-length dipole.

The resonant length of the wire will be somewhat shorter than a full-length dipole and can best be determined by experimentally adjusting the length of ends, which may be conveniently near ground. Keep in mind that there can be very high potentials at the ends of the wires and for safety the ends should be kept out of reach. Letting the ends hang down as shown is a form of capacitive end loading. While it is efficient, it will also reduce the matching bandwidth—as does any form of loading.

The most serious drawback associated with inductive loading is high loss in the coils themselves. It is important that you use inductors made from reasonably large wire or tubing to minimize this problem. Close winding of turns should also be avoided if possible. A good compromise is to use some off-center inductive loading in combination with capacitive end loading, keeping the inductor losses small and the efficiency as high as possible.

Some examples of off-center coil loading and capacitive-end loading are shown in **Fig 70**. This technique was described by Jerry Hall, K1TD in Sep 1974 *QST*. In the equation below, the diameter D is that of the wire used for the antenna, in inches. The frequency f is expressed in MHz.

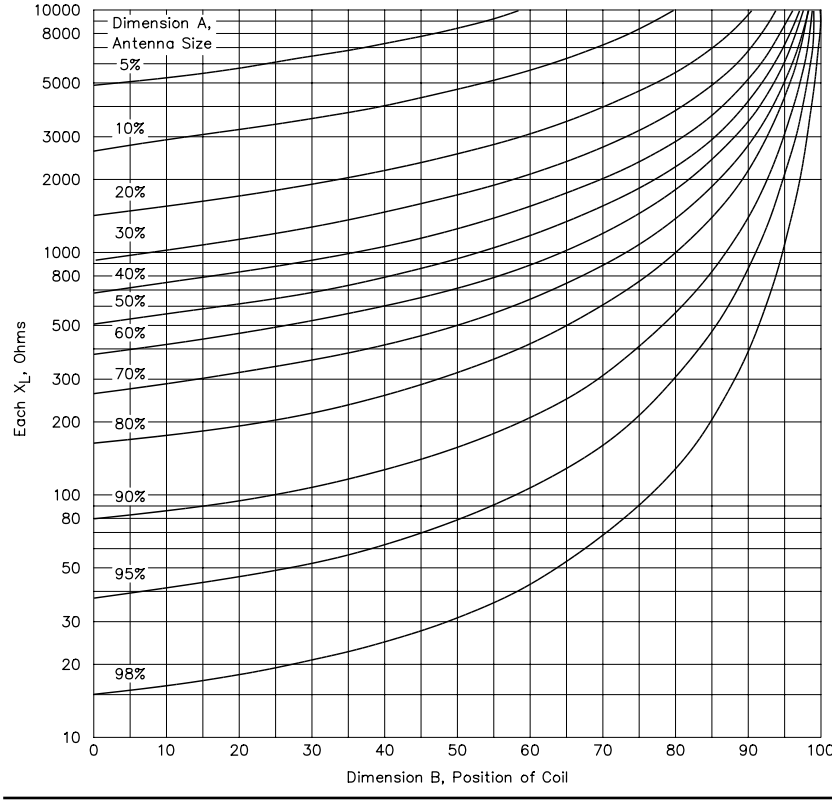

Fig 71—Chart for determining approximate inductance values for off-center-loaded dipoles. See Fig 70A. At the intersection of the appropriate curve from the body of the chart for dimension A and proper value for the coil position from the horizontal scale at the bottom of the chart, read the required inductive reactance for resonance from the scale at the left. Dimension A is expressed as percent length of the shortened antenna with respect to the length of a half-wave dipole of the same conductor material. Dimension B is expressed as the percentage of coil distance from the feed point to the end of the antenna. For example, a shortened antenna, which is 50% or half the size of a half-wave dipole (one-quarter wavelength overall) with loading coils positioned midway between the feed point and each end (50% out), would require coils having an inductive reactance of approximately 950 Ω at the operating frequency for antenna resonance.

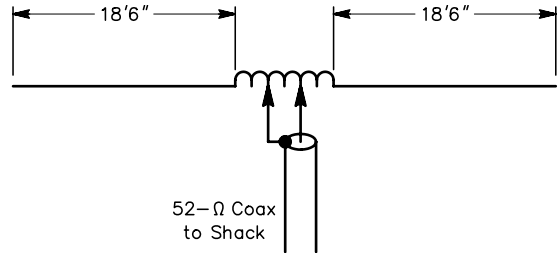

Fig 72—The WØSVM "Shorty Forty" center-loaded antenna. Dimensions given are for 7.0 MHz. The loading coil is 5 inches long and 2½ inches diameter. It has a total of 30 turns of #12 wire wound at 6 turns per inch (Miniductor 3029 stock).

For the antennas shown, the longer the overall length (dimension A, Fig 70A, in feet) and the farther the loading coils are from the center of the antenna (dimension B, also in feet), the greater the efficiency of the antenna. As dimension B is increased, however, the inductance required to resonate the antenna at the desired frequency increases.

Approximate inductive reactances for single-band resonance (for the antenna in Fig 70A only) may be determined with the aid of **Fig 71** or from Eq 10 below. The final values will depend on the proximity of surrounding objects in individual installations and must be determined experimentally. The use of high-Q low-loss coils is important for maximum efficiency.

A dip meter or SWR indicator is recommended for use during adjustment of the system. Note that the minimum inductance required is for a center-loaded dipole. If the inductive reactance is read from Fig 66 for a dimension B of zero, one coil having approximately twice this reactance can be used near the center of the dipole. **Fig 72** illustrates this idea. This antenna was conceived by Jack Sobel, WØSVM, who dubbed the 7-MHz version the "Shorty Forty."

$$X_L = \frac{10^6}{34\pi f}\left(\frac{\ln\frac{24\left(\frac{234}{f}\right)-B}{D}-1\left(\left(1-\frac{fB}{234}\right)^2-1\right)}{\frac{234}{f}-B} - \frac{\left(\ln\frac{24\left(\frac{A}{2}-B\right)}{D}-1\right)\left(\left(\frac{fA}{2}-fB\right)^2-1\right)}{\frac{A}{2}-B} \right) \quad \text{(Eq 10)}$$

Inverted-L Antennas

The antenna shown in **Fig 73** is called an *inverted-L* antenna. It is simple and easy to construct and is a good antenna for the beginner or the experienced 1.8-MHz DXer. Because the overall electrical length is made somewhat greater than λ/4, the feed-point resistance is on the order of 50 Ω, with an inductive reactance. That reactance is canceled by a series capacitor as indicated in the figure. For a vertical section length of 60 feet and a horizontal section length of 115 feet, the input impedance is ≈ 40 + *j* 300 Ω. Longer vertical or horizontal sections would increase the input impedance. The azimuthal radiation pattern is slightly asymmetrical with ≈1 to 2-dB increase in the direction opposite to the horizontal wire. This antenna requires a good buried ground system or elevated radials and will have a 2:1 SWR bandwidth of about 50 kHz.

This antenna is a form of top-loaded vertical, where the top loading is asymmetrical. This results in both vertical and horizontal polarization because the currents in the top wire do not cancel like they would in a symmetrical-T vertical. This is not necessarily a bad thing because it eliminates the zenith null present in a true vertical. This allows for good communication at short ranges as well as for DX.

A yardarm attached to a tower or a tree limb can be used to support the vertical section. As with any vertical, for best results the vertical section should be as long as possible. A good ground system is necessary for good results—the better the ground, the better the results.

If you don't have the space for the inverted L shown in Fig 73 (with its 115-foot horizontal section) and if you don't have a second tall supporting structure to make the top

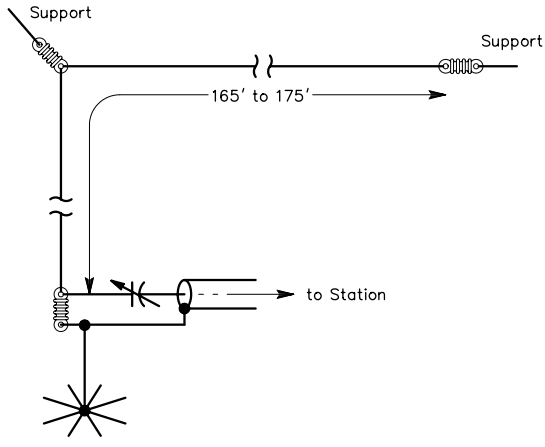

Fig 73—The 1.8-MHz inverted L. Overall wire length is 165 to 175 feet. The variable capacitor has a capacitance range from 100 to 800 pF, at 3 kV or more. Adjust antenna length and variable capacitor for lowest SWR.

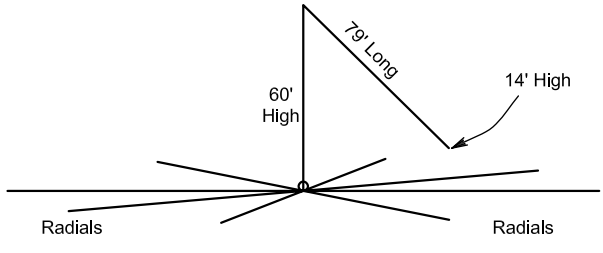

Fig 74—Sketch showing a modified 160-meter inverted L, with a single supporting 60-foot high tower and a 79-foot long slanted top-loading wire. The feed-point impedance is about 12 Ω in this system, requiring a quarter-wave matching transformer made of paralleled 50-Ω coaxes.

wire horizontal, consider sloping the top wire down towards ground. **Fig 74** illustrates such a setup, with a 60-foot high vertical section and a 79-foot sloping wire. As always, you will have to adjust the length of the sloping wire to fine-tune the resonant frequency. For a good ground radial system, the feed-point impedance is about 12 Ω, which may be transformed to 50 Ω with a 25-Ω quarter-wave transformer consisting of two paralleled 50-Ω quarter-wave coaxes. The peak gain will decrease about 1 dB compared to the inverted L shown in Fig 73. **Fig 75** overlays the elevation responses for average ground conditions. The 2:1 SWR bandwidth will be about 30 kHz, narrower than the larger system in Fig 73.

If the ground system suggested for Figs 73 and 74 is not practical, you can use a single elevated radial as shown in **Fig 76**. For the dimensions shown in the figure $Z_i = 50 + j\,498\ \Omega$, requiring a 175-pF series resonating capacitor. The azimuthal radiation pattern is shown in **Fig 77** compared to

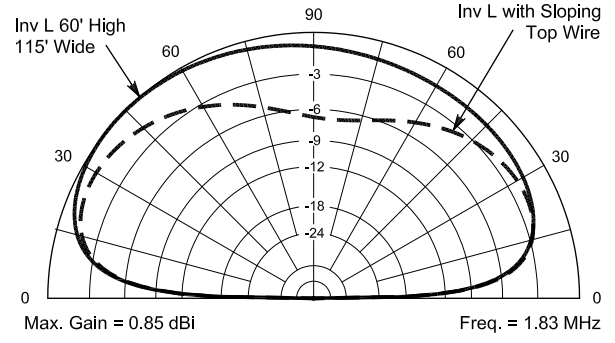

Fig 75—Overlay of the elevation responses for the inverted-L antennas in Fig 73 (solid line) and Fig 74 (dashed line). The gains are very close for these two setups, provided that the ground radial system for the antenna in Fig 74 is extensive enough to keep ground losses low.

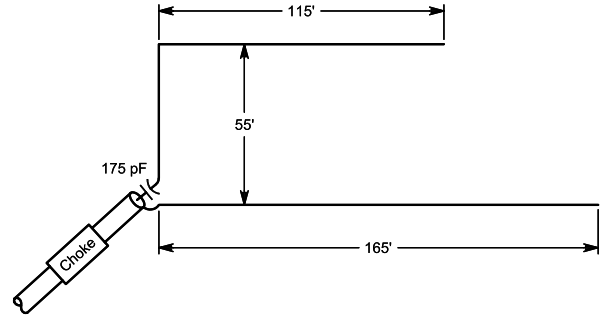

Fig 76—A single elevated radial can be used for the inverted-L. This changes the directivity slightly. The series tuning capacitor is approximately 175 pF for this system.

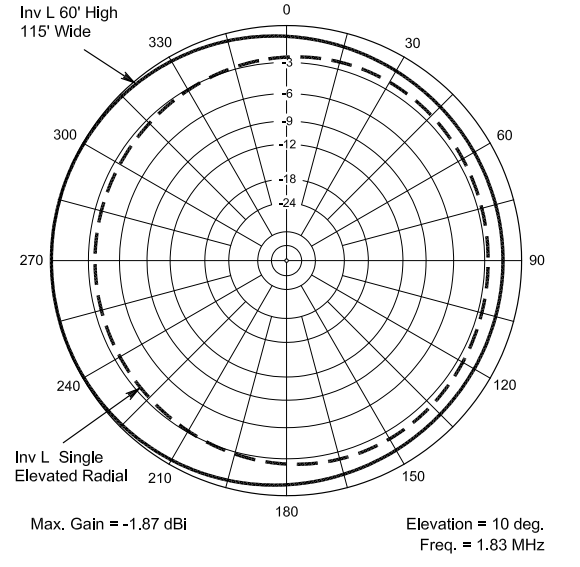

Fig 77—Azimuthal pattern comparison for inverted-L antennas shown in Fig 73 (solid line) and the compromise, single-radial system in Fig 76 (dashed line). This is for a takeoff angle of 10°.

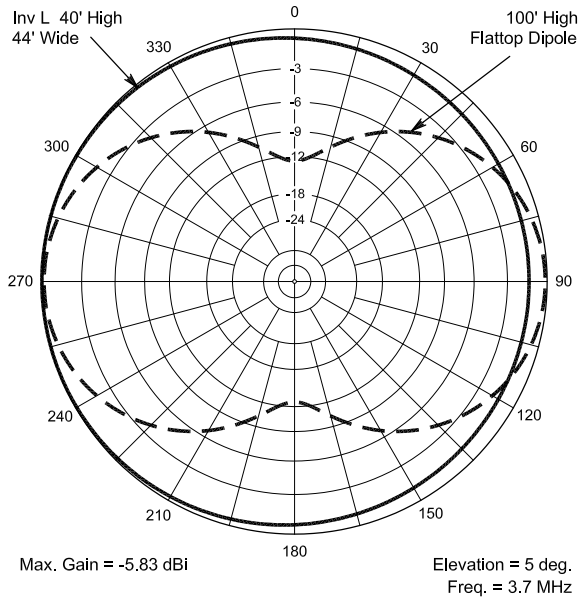

Fig 78—Azimuthal pattern at a takeoff angle of 5° for an 80-meter version of the inverted L (solid line) in Fig 73, compared to the response for a 100-foot high flattop dipole (dashed line).

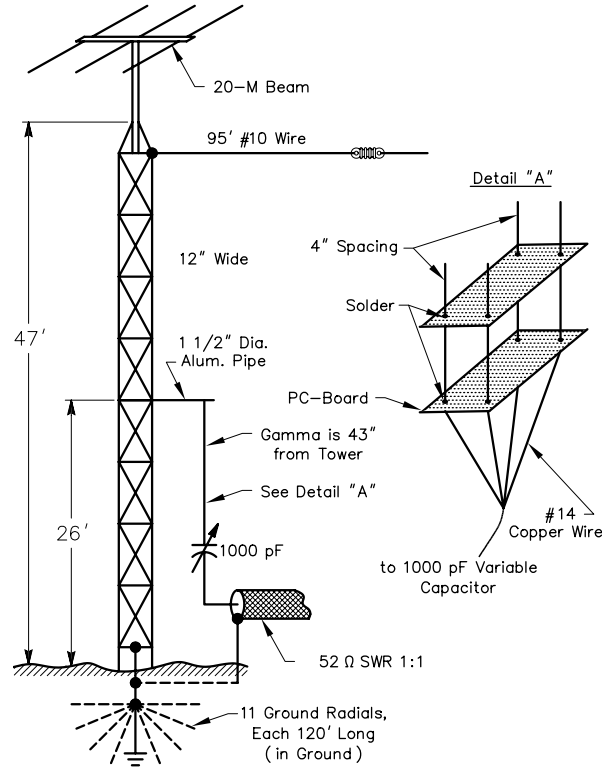

Fig 79—Details and dimensions for gamma-match feeding a 50-foot tower as a 1.8-MHz vertical antenna. The rotator cable and coaxial feed line for the 14-MHz beam is taped to the tower legs and run into the shack from ground level. No decoupling networks are necessary.

the inverted L in Fig 68. Note that the 1 to 2-dB asymmetry is now in the direction of the horizontal wires, just the opposite of that for a symmetrical ground system. The 2:1 SWR bandwidth is about 40 kHz, assuming that the series capacitor is adjusted at 1.83 MHz for minimum SWR.

Fig 78 shows the azimuthal response at a 5° elevation angle for an 80-meter version of the inverted L in Fig 73. The peak response occurs at an azimuth directly behind the direction in which the horizontal portion of the inverted L points. For comparison, the response for a 100-foot high flattop dipole is also shown. The top wire of this antenna is only 40 feet high and the 2:1 SWR bandwidth is about 150 kHz wide with a good, low-loss ground-radial system.

Fig 78 illustrates that the azimuth response of an inverted L is nearly omnidirectional. This gives such an antenna an advantage in certain directions compared to a flattop dipole, which is constrained by its supporting mounts (such as trees or towers) to favor fixed directions. For example, the flattop dipole in Fig 78 is at its weakest at azimuths of 90° and 270°, where it is down about 12 dB compared to the inverted L. Hams who are fortunate enough to have high rotary dipoles or rotatable low-band Yagis have found them to be very effective antennas indeed.

A DIFFERENT APPROACH

Fig 79 shows the method used by Doug DeMaw, W1FB, to gamma match his self-supporting 50-foot tower operating as an inverted L. A wire cage simulates a gamma rod of the proper diameter. The tuning capacitor is fashioned from telescoping sections of 1½ and 1½-inch aluminum tubing with polyethylene tubing serving as the dielectric. This capacitor is more than adequate for power levels of 100 W. The horizontal wire connected to the top of the tower provides the additional top loading.

Sloper Antennas

Sloping dipoles and λ/2 dipoles can be very useful antennas on the low bands. These antennas can have one end attached to a tower, tree or other structure and the other end near ground level, elevated high enough so that passersby can't contact them, of course. The following section gives a number of examples of these types of antennas.

THE HALF-WAVE SLOPING DIPOLE

If you have a sufficiently high support, you can install a halfwave dipole sloping downwards toward ground to provide vertical as well as horizontal polarization. This antenna is popularly known as a *sloper* or a *halfwave sloper*. The amount of slope from horizontal can vary from 0°, where the dipole is in a flattop configuration, all the way to 90°, where the dipole becomes fully vertical. The latter configuration is sometimes called a *Halfwave Vertical Dipole* (HVD).

The question arises when contemplating a vertical halfwave dipole or a halfwave sloping dipole about how to treat the feed line to make sure it doesn't accidentally become part of the radiating system. The ideal situation would be to bring the feed line out perpendicular to the vertical or sloping wire for an infinite distance. Obviously, that isn't very practical because the feed line eventually has to be connected to a transmitter located near the ground. An intensive modeling study on feeding an HVD was done for the book *Simple and Fun Antennas for Hams*. This study indicated that a slant angle down to the ground of as little as 30° from a vertical radiator can work with only minor interaction, provided that common-mode decoupling chokes were employed at the feed point and a quarter-wavelength down the line from the feed point. These common-mode chokes can consist of either discrete ferrite beads placed over the outer jacket of the coaxial line or multiple turns of the coax itself to form a choke.

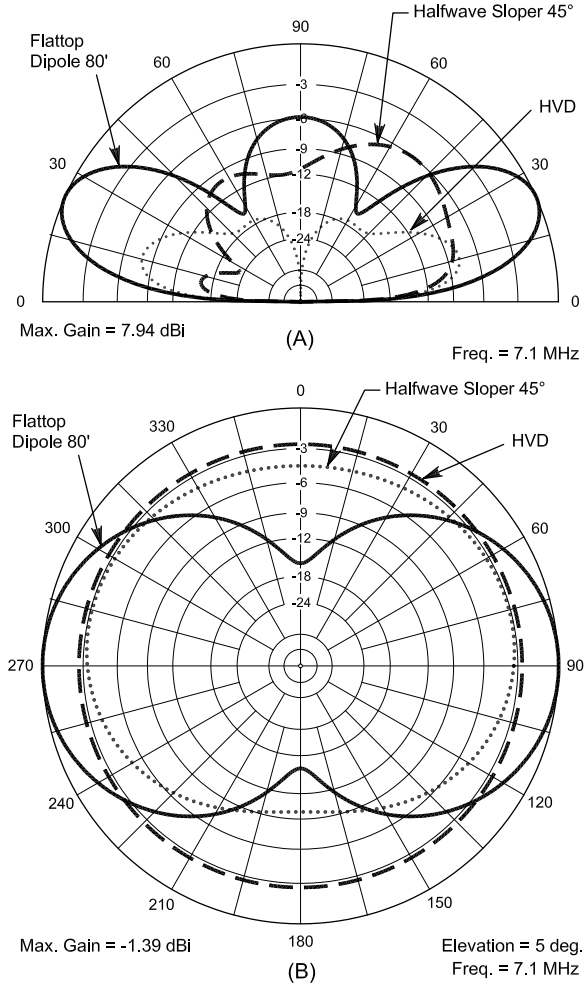

Fig 80—At A, the azimuthal responses for a flattop dipole (solid line), a dipole whose end has been tilted down 45° (dashed line), and a HVD (halfwave vertical dipole, dotted line). All these were modeled over average ground, with a conductivity of 5 mS/m and a dielectric constant of 13. Note that the tilted dipole exhibits about 5 dB front-to-back ratio, although its maximum gain is less than either the HVD or flattop dipole. At B, the elevation-plane patterns for the same antennas. Note that the tilted halfwave dipole (dashed line) has more energy at higher elevation angles than either the flattop dipole or HVD.

Fig 80A compares the 40-meter azimuthal patterns at a DX takeoff angle of 5° for three configurations: a flattop dipole, a dipole tilted down 45° and an HVD (halfwave vertical dipole). These are computed for ground with average conductivity and dielectric constant, and for a maximum height of 80 feet in each configuration. The sloping halfwave dipole exhibits about 5 dB of front-to-back ratio, although even at its most favored direction it doesn't quite have the same maximum gain as the HVD or the flattop dipole.

The reason why the maximum gain for the sloper is less than the other two configurations, even while still exhibiting some front-to-back pattern, is shown in Fig 80A, which shows the elevation-plane patterns for the same antennas, each at the azimuth of maximum gain. The halfwave sloper distributes much of its energy higher in elevation than the HVD, lowering the peak-gain potential of the sloper.

You can also see from Fig 80B that the 80-foot high horizontal dipole would perform much better than either the HVD or halfwave sloper for close-in local contacts, which occur at high elevation angles. On the other hand, except for the greater gain exhibited in the flattop dipole's most favored directions, the HVD has more gain than the other antennas at low elevation angles. While the HVD's omnidirectional pattern is a plus for transmitting, it may be a problem for receiving, where local noise may be coming from specific directions (such as power lines) and may also be predominantly vertically polarized. In such cases, a horizontally polarized flattop dipole may be a considerably better receiving antenna than a vertically polarized antenna of any sort. We've already mentioned the fact that a rotary flattop dipole high in the air can be a very effective antenna on the low bands.

THE QUARTER-WAVELENGTH "HALF SLOPER"

Perhaps one of the easiest antennas to install is the λ/4 sloper shown in **Fig 81**. As pointed out above, a sloping λ/2 dipole is known among radio amateurs as a *sloper* or sometimes as a *full sloper*. If only one half of it is used, it becomes a *half sloper*. The performance of the two types of sloping antennas is similar—They exhibit some directivity in the direction of the slope and radiate vertically polarized energy at low angles respective to the horizon. The amount of directivity will range from 3 to 6 dB, depending upon the individual installation, and will be observed in the slope direction.

The main advantage of the half sloper over the full half-wave-long sloping dipole is that its supporting tower needn't be as high. Both the half sloper and the full sloper place the feed point (the point of maximum current) high above lossy ground. But the half-sloper only needs half as much wire to build the antenna for a given amateur band. The disadvantage of the half sloper is that it is sometimes difficult or even impossible to obtain a low SWR when using coaxial-cable feed, especially without a good isolating choke balun. (See the section above on isolating ground-plane antennas.)

Other factors that affect the feed impedance are tower height, height of the attachment point, enclosed angle between the sloper and the tower, and what is mounted atop the tower (HF or VHF beams). Further, the quality of the ground under the tower (ground conductivity, radials, etc) has a marked effect on the antenna performance. The final SWR can vary (after optimization) from 1:1 to as high as 6:1. Generally speaking, the closer the low end of the slope wire is to ground, the more difficult it will be to obtain a good match.

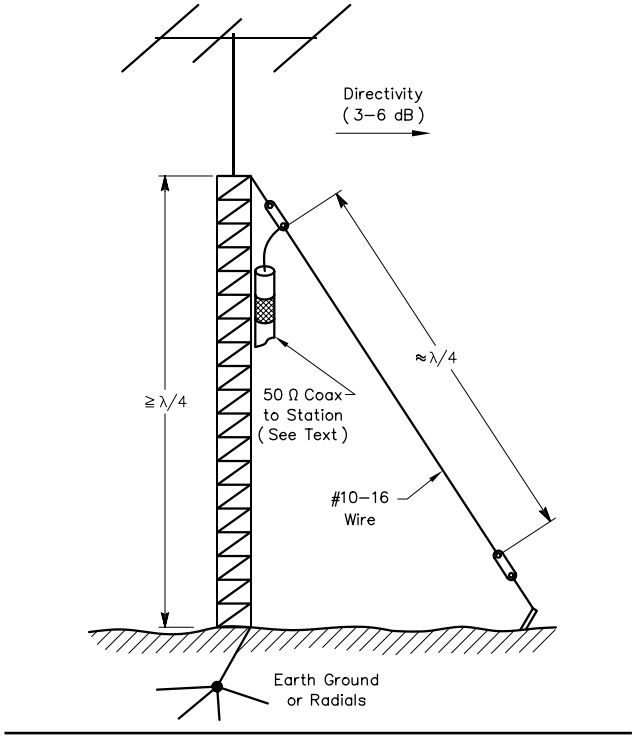

Fig 81—The λ/4 "half sloper" antenna.

Basic Recommendations for a Half Sloper

The half sloper can be an excellent DX type of antenna. Hams usually install theirs on a metal supporting structure such as a mast or tower. The support needs to be grounded at the lower end, preferably to a buried or on-ground radial system. If a nonconductive support is used, the outside of the coax braid becomes the return circuit and should be grounded at the base of the support. As a starting point you can attach the sloper so the feed point is approximately λ/4 above ground. If the tower is not high enough to permit this, the antenna should be fastened as high on the supporting structure as possible. Start with an enclosed angle of approximately 45°, as indicated in Fig 81. Cut the wire to the length determined from

$$\ell = \frac{260}{f_{MHz}} \qquad \text{(Eq 11)}$$

This will allow sufficient extra length for pruning the wire for the lowest SWR. A metal tower or mast becomes an operating part of the half sloper system. In effect, it and the slope wire function somewhat like an inverted-V dipole antenna. In other words, the tower operates as the missing half of the dipole. Hence its height and the top loading (beams) play a significant role.

Detailed modeling indicates that a sufficiently large

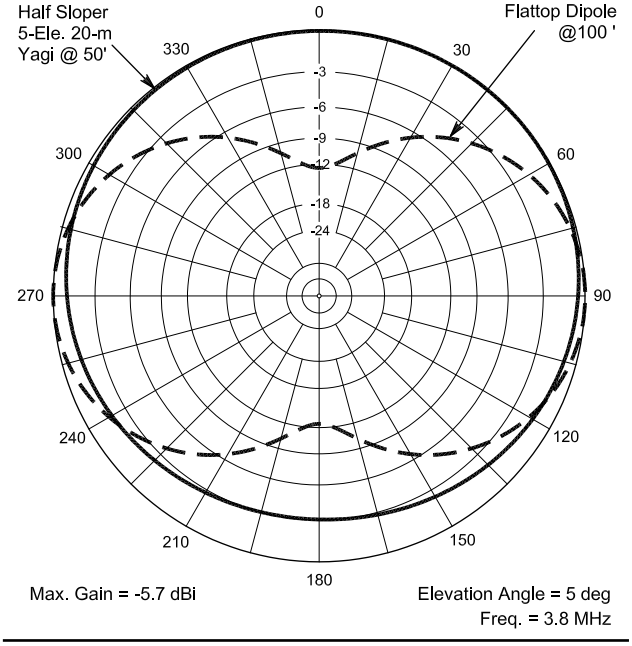

Fig 82—Radiation pattern for a typical half sloper (solid line) mounted on a 50-foot high tower with a large 5-element 20-meter beam on the top compared to that for a flattop dipole (dashed line) at 100 feet. At a 5° takeoff angle typical for DX work on 80 meters, the two antennas are pretty comparable in the directions favored by the high dipole. In other directions, the half sloper has an advantage of more than 10 dB.

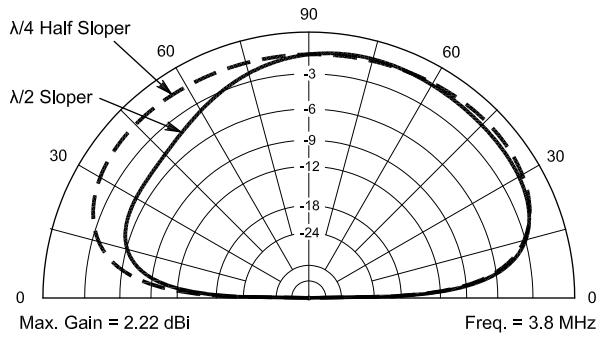

Fig 83—Comparison of elevation patterns for a full-sized halfwave sloper (solid line) on a 100-foot tower and a half sloper (dashed line) on a 50-foot tower with a 5-element 20-meter Yagi acting as a top counterpoise. The performance is quite comparable for these two systems.

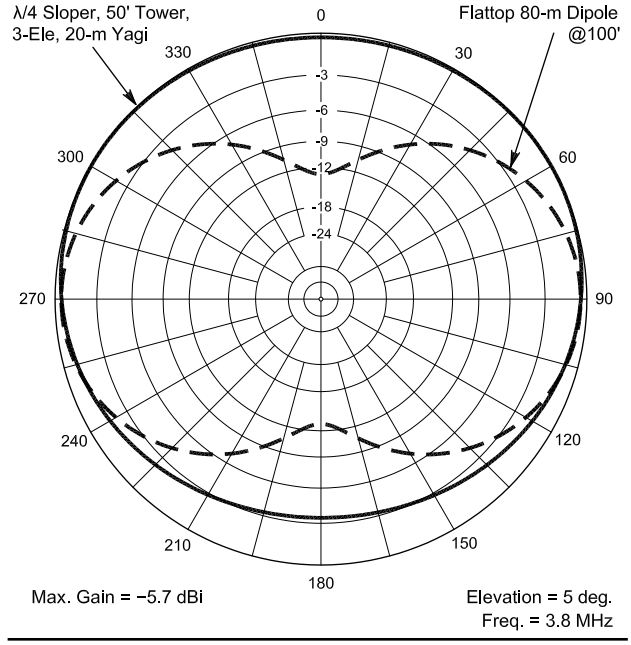

Fig 84—Comparing the azimuthal response of a half sloper (solid line) on a 50-foot tower with a 3-element 20-meter Yagi on top to that of a flattop dipole (dashed line) at 100 feet. The two are again quite comparable at a 5° takeoff angle.

mass of metal (that is, a large, "Plumber's Delight" Yagi) connected to the top of the tower acts like enough of a "top counterpoise" that the tower may be removed from the model with little change in the essential characteristics of the half-sloper system. Consider an installation using a freestanding 50-foot tower with a large 5-element 20-meter Yagi on top. This Yagi is assumed to have a 40-foot boom oriented 90° to the direction of the slanted 80-meter half-sloper wire. The best SWR that could be reached by changing the length and slant angle for this sloper is 1.67:1, representing a feed-point impedance of $30.1 - j\ 2.7\ \Omega$. The peak gain at 3.8 MHz is 0.97 dBi at an elevation angle of 70°. **Fig 82** shows the azimuth-plane pattern for this half sloper, compared to a 100-foot high flattop dipole for reference, at an elevation angle of 5°.

Removing the tower from the model resulted in a feed-point impedance of $30.1 - j\ 1.5\ \Omega$ and a peak gain of 1.17 dBi. The tower is obviously not contributing much in this setup, since the mass of the large 20-meter Yagi is acting like an elevated counterpoise all by itself. It's interesting to rotate the boom of the model Yagi and observe the change in SWR that occurs on the half-sloper antenna. With the boom turned 90°, the SWR falls to 1.38:1. This level of SWR change could be measured with amateur-type instrumentation.

On the other hand, substituting a smaller 3-element 20-meter Yagi with an 18-foot boom in the model does result in significant change in feed-point impedance and gain when the tower is removed from the model, indicating that the "counterpoise effect" of the smaller beam is insufficient by itself. Interestingly enough, the best SWR for the half sloper/tower and the 3-element Yagi (with its boom inline with the half sloper is 1.33:1), changing to 1.27:1 with the boom turned 90°. Such a small change in SWR would be difficult to measure using typical amateur instrumentation.

In any case, the 50-Ω transmission line feeding a half sloper should be taped to the tower leg at frequent intervals to make it secure. The best method is to bring it to earth level, then route it to the operating position along the surface of the ground if it can't be buried. This will ensure adequate RF decoupling, which will help prevent RF energy from affecting the equipment in the station. Rotator cable and other feed lines on the tower or mast should be treated in a similar manner.

Adjustment of the half sloper is done with an SWR indicator in the 50-Ω transmission line. A compromise can usually be found between the enclosed angle and wire length, providing the lowest SWR attainable in the center of the chosen part of an amateur band. If the SWR "bottoms out" at 2:1 or lower, the system will work fine without using an antenna tuner, provided the transmitter can work into the load. Typical optimum values of SWR for 3.5 or 7-MHz half slopers are between 1.3:1 and 2:1. A 100-kHz bandwidth is normal on 3.5 MHz, with 200 kHz being typical at 7 MHz.

If the lowest SWR possible is greater than 2:1, the attachment point can be raised or lowered to improve the match. Readjustment of the wire length and enclosed angle may be necessary when the feed-point height is changed. If the tower is guyed, the guy wires will need to be insulated from the tower and broken up with additional insulators to prevent resonance.

At this point you may be curious about which antenna is better—a full sloper or a half sloper. The peak gain for each antenna is very nearly identical. **Fig 83** overlays the elevation-plane pattern for the full-sized halfwave sloper on a 100-foot tower and for the half sloper shown in Fig 81 on a 50-foot tower with a 5-element 20-meter Yagi on top. The

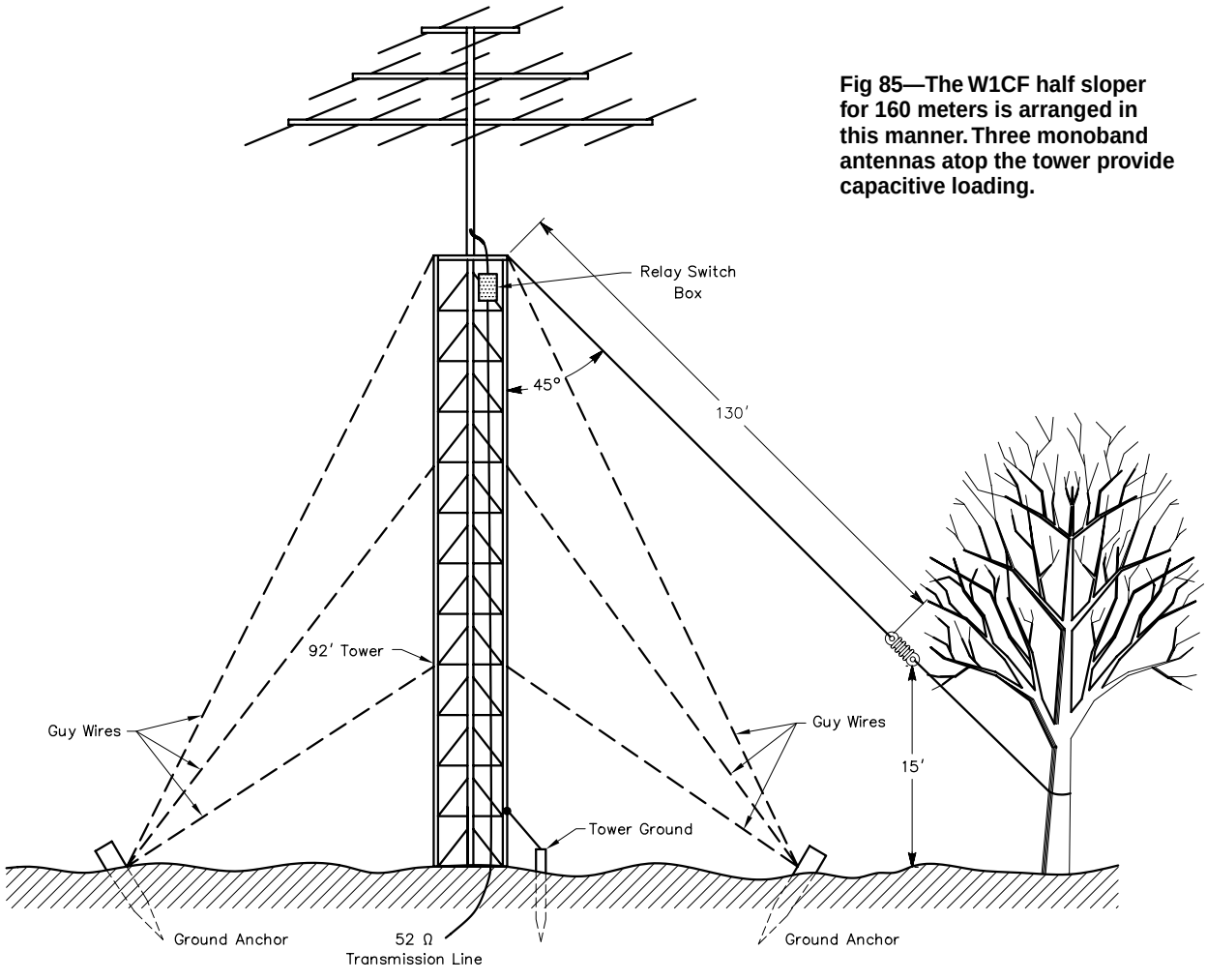

Fig 85—The W1CF half sloper for 160 meters is arranged in this manner. Three monoband antennas atop the tower provide capacitive loading.

full-sized halfwave sloper has more front-to-back ratio, but it is only a few dB more than the half sloper. **Fig 84** compares the azimuthal patterns at a 5° takeoff angle for a 100-foot high flattop dipole and a half-sloper system on a 50-foot tower with a 3-element 20-meter Yagi on top.

Despite the frustration some have experienced trying to achieve a low SWR with some half-sloper installations, many operators have found the half sloper to be an effective and low-cost antenna for DX work.

1.8-MHz ANTENNA SYSTEMS USING TOWERS

The half sloper discussed above for 80 or 40-meter operation will also perform well on 1.8 MHz where vertically polarized radiators can achieve the low takeoff angles needed on Topband. Prominent 1.8-MHz operators who have had success with the half sloper antenna suggest a minimum tower height of 50 feet. Dana Atchley, W1CF (SK), used the configuration sketched in **Fig 85**. He reported that the uninsulated guy wires act as an effective counterpoise for the sloping wire. In **Fig 86** is the feed system used by Doug

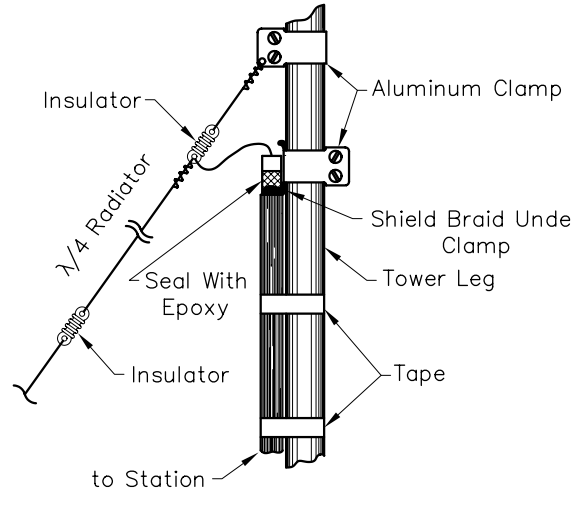

Fig 86—Feed system used by W1FB for 1.8 MHz half sloper on a 50-foot self-supporting tower.

DeMaw, W1FB (SK), on a 50-foot self-supporting tower. The ground for the W1FB system is provided by buried radials connected to the tower base.

As described previously, a tower can also be used as a true vertical antenna, provided a good ground system is used. The shunt-fed tower is at its best on 1.8 MHz, where a full λ/4 vertical antenna is rarely possible. Almost any tower height can be used. An HF beam at the top provides some top loading.

THE K1WA 7-MHz "SLOPER SYSTEM"

One of the more popular antennas for 3.5 and 7 MHz is the half-wave long sloping dipole described previously. David Pietraszewski, K1WA, made an extensive study of sloping dipoles at different heights with reflectors at the 3-GHz frequency range. From his experiments, he developed the novel 7-MHz antenna system described here. With several sloping dipoles supported by a single mast and a switching network, an antenna with directional characteristics and forward gain can be simply constructed. This 7-MHz system uses several "slopers" equally spaced around a common center support. Each dipole is cut to λ/2 and fed at the center with 50-Ω coax. The length of each feed line is 36 feet.

All of the feed lines go to a common point on the support (tower) where the switching takes place. The line length of 36 feet is just over 3λ/8, which provides a useful quality. At 7 MHz, the coax looks inductive to the antenna when the end at the switching box is open circuited. This has the effect of adding inductance at the center of the sloping dipole element, which electrically lengthens the element. The 36-foot length of feed line serves to increase the length of the element about 5%. This makes any unused element appear to be a reflector.

The array is simple and effective. By selecting one of the slopers through a relay box located at the tower, the system becomes a parasitic array that can be electrically rotated. All but the driven element of the array become reflectors.

The physical layout is shown in **Fig 87**, and the basic materials required for the sloper system are shown in **Fig 88**. The height of the support point should be about 70 feet, but can be less and still give reasonable results. The upper portion of the sloper is 5 feet from the tower, suspended by rope. The wire makes an angle of 60° with the ground.

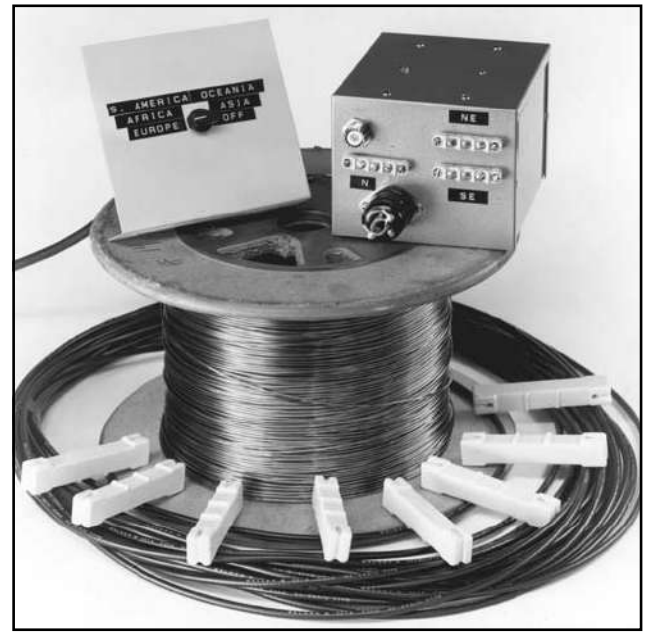

Fig 88—The basic materials required for the sloper system. The control box appears at the left, and the relay box at the right.

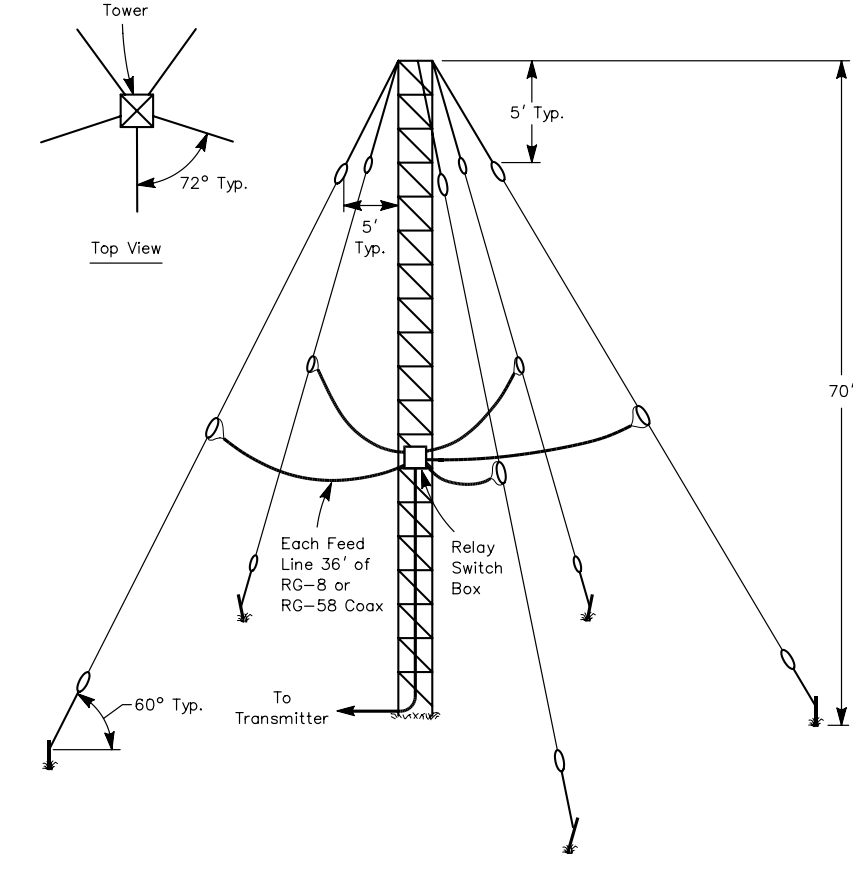

Fig 87—Five sloping dipoles suspended from one support. Directivity and forward gain can be obtained from this simple array. The top view shows how the elements should be spaced around the support.

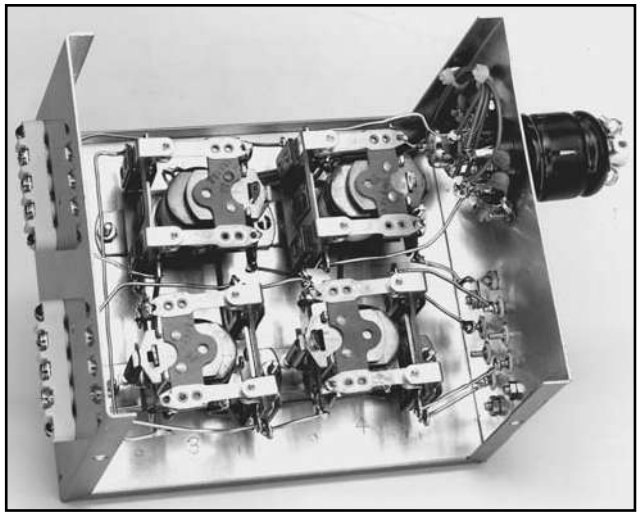

Fig 89—Inside view of relay box. Four relays provide control over five antennas. See text. The relays pictured here are Potter and Brumfeld type MR11D.

In **Fig 89**, the switch box is shown containing all the necessary relays to select the proper feed line for the desired direction. One feed line is selected at a time and the feed lines of those remaining are opened, **Fig 90**. In this way the array is electrically rotated. These relays are controlled from inside the shack with an appropriate power supply and rotary switch. For safety reasons and simplicity, 12-volt dc relays are used. The control line consists of a five conductor cable, one wire used as a common connection; the others go to the four relays. By using diodes in series with the relays and a dual-polarity power supply, the number of control wires can be reduced, as shown in Fig 90B.

Measurements indicate that this sloper array provides up to 20 dB front-to-back ratio and forward gain of about 4 dB over a single half-wave sloper. **Fig 91** shows the azimuthal pattern (at a 5° takeoff angle) for the K1WA array, compared to a 100-foot high flattop dipole and a full sloper suspended from a 50-foot tower. These patterns were calculated for average ground conditions. Just for fun, look at

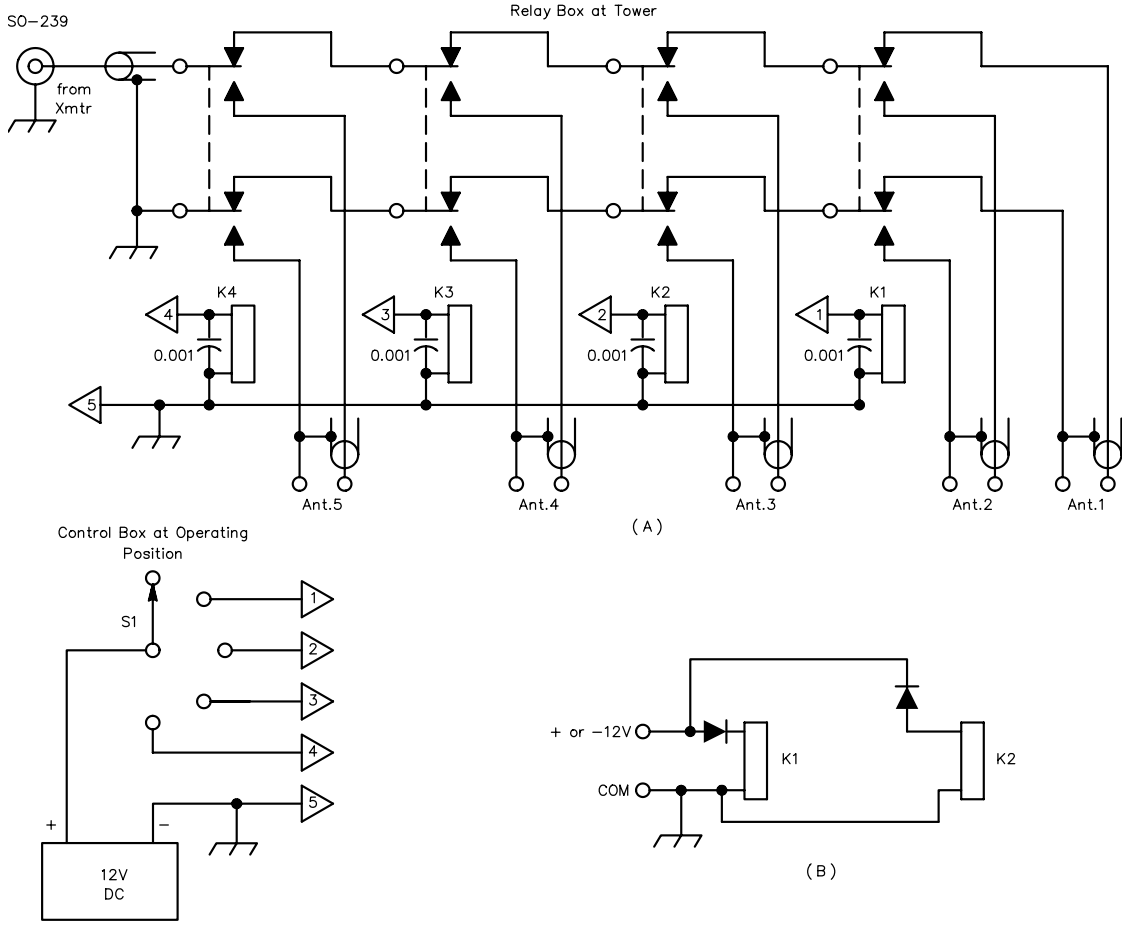

Fig 90—Schematic diagram for sloper control system. All relays are 12-volt dc, DPDT, with 8-A contact ratings. At A, the basic layout, excluding control cable and antennas. Note that the braid of the coax is also open-circuited when not in use. Each relay is bypassed with 0.001-μF capacitors. The power supply is a low current type. At B, diodes are used to reduce the number of control wires when using dc relays. See text.

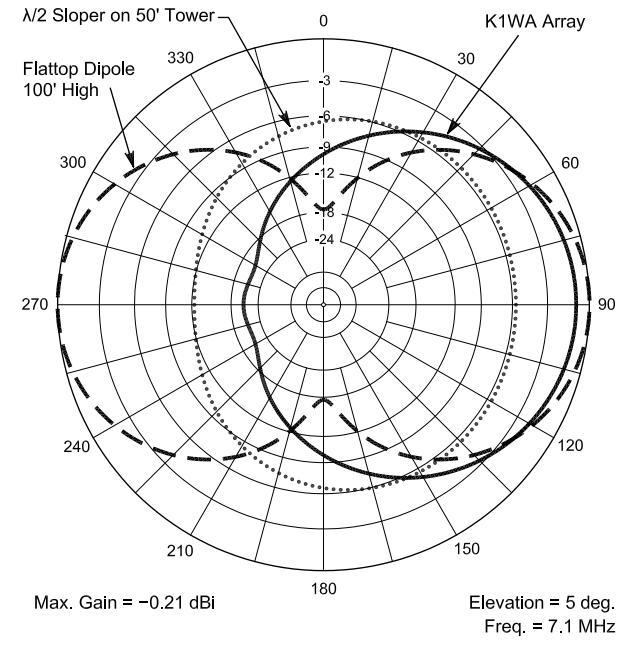

Fig 91—Azimuth pattern for K1WA 40-meter sloper array (solid line), compared to a flattop dipole (dashed line) at 100 feet and a halfwave full sloper on a 50-foot tower (dotted line). The K1WA array has an excellent front-to-back ratio and almost as much gain as the high flattop dipole. These patterns are for average ground.

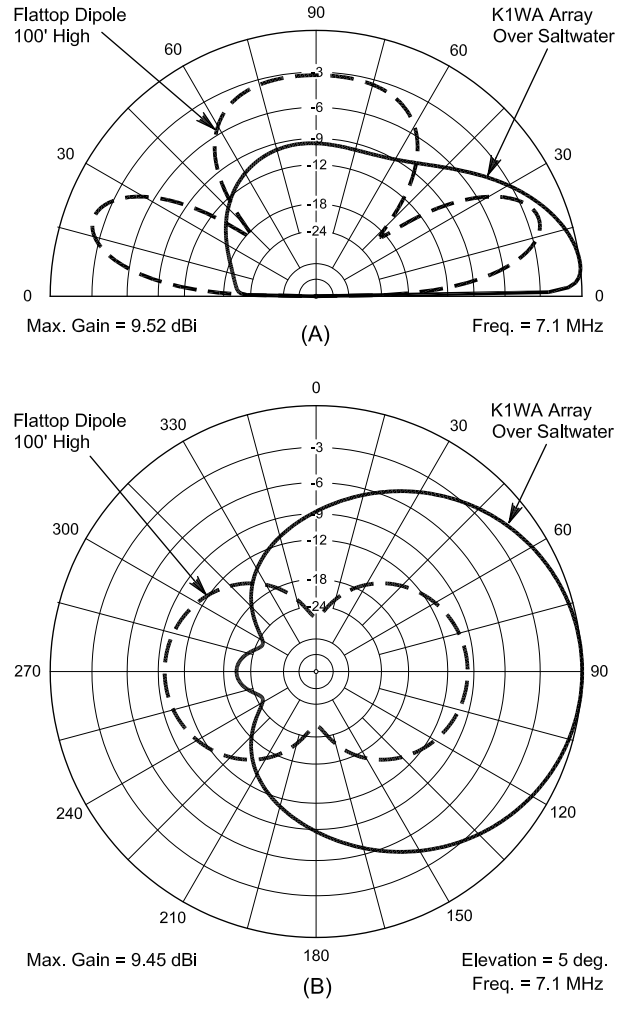

Fig 92—The K1WA 40-meter sloper array over saltwater, compared to a 100-foot high flattop dipole. At A, azimuth patterns. At B, elevation patterns. Now the sloper array really comes into its own!

Fig 92, which shows a comparison between a 100-foot high flattop dipole and a K1WA array placed over saltwater. Now that's a real barnburner at low takeoff angles! Such a seaside system would be very competitive with a rotatable 2-element "shorty-40" type of Yagi.

If one direction is the only concern, the switching system can be eliminated and the reflectors should be cut 5% longer than the resonant frequency. The feature worth noting is the good F/B ratio. By arranging the system properly, a null can be placed in an unwanted direction, thus making it an effective receiving antenna. In the tests conducted with this antenna, the number of reflectors used were as few as one and as many as five. The optimum combination appeared to occur with four reflectors and one driven element. No tests were conducted with more than five reflectors. This same array can be scaled to 3.5 MHz for similar results.

BIBLIOGRAPHY

Source material and more extended discussion of topics covered in this chapter can be found in the references given below.

D. Atchley, Jr., "Putting the Quarter-Wave Sloper to Work on 160," *QST*, Jul 1979, pp 19-20.

J. Belrose, "Transmission Line Low Profile Antennas," *QST*, Dec 1975, pp 19-25.

L. Braskamp, AA6GL, "*MOBILE*, a Computer Program for Short HF Verticals," *The ARRL Antenna Compendium Vol 4*, pp 92-96.

G. H. Brown, "The Phase and Magnitude of Earth Currents Near Radio Transmitting Antennas," *Proc. IRE*.

G. H. Brown, R. F. Lewis and J. Epstein, "Ground Systems as a Factor in Antenna Efficiency," *Proc. IRE* , Jun 1937, pp 753-787.

P. Carr, N4PC, "A Two Band Half-Square Antenna With Coaxial Feed," *CQ*, Sep 1992, pp 40-45.

P. Carr, N4PC, "A DX Antenna For 40 Meters," *CQ*, Sep 1994, pp 40-43.

A. Christman, KB8I, "Elevated Vertical Antennas for the Low Bands," *The ARRL Antenna Compendium Vol 5*, pp 11-18.

Curry Communications, PO Box 1884, Burbank, CA 91507, a kit manufacturer of lowfer CW transceivers.

D. DeMaw, "Additional Notes on the Half Sloper," *QST*, Jul 1979, p 20.

P. Dodd, *The LF Experimenter's Source Book* (RSGB, 1996).

A. C. Doty, Jr., J. A. Frey and H. J. Mills, "Efficient Ground Systems for Vertical Antennas," *QST*, Feb 1983, pp 9-12.

S. Ford, "*Low*fing on 1750 Meters," *QST*, Oct 1993, pp 67-68.

R. Fosberg, "Some Notes on Ground Systems for 160 Meters," *QST*, Apr 1965, pp 65-67.

J. Hall, "Off-Center-Loaded Dipole Antennas," *QST*, Sep 1974, pp 28-34.

G. Hubbell, "Feeding Grounded Towers as Radiators," *QST*, pp 32-33, 140, 142.

C. Hutchinson and R. D. Straw, *Simple and Fun Antennas for Hams* (Newington, Ct: ARRL, 2002).

P. H. Lee, *The Amateur Radio Vertical Antenna Handbook*, 1st edition (Port Washington, NY: Cowan Publishing Corp., 1974).

C. J. Michaels, "Some Reflections on Vertical Antennas," *QST*, July 1987, pp 15-19; feedback *QST*, Aug 1987, p 39.

Rashed and C. Tai, "A New Class of Wire Antennas," 1982 International Symposium Digest, *Antennas and Propagation*, Vol 2, IEEE.

T. Russell, N4KG, "Simple, Effective, Elevated Ground-Plane Antennas," *QST*, June 1994, pp 45-46

F. J. Schnell, "The Flagpole Deluxe," *QST*, Mar 1978, pp 29-32.

R. Severns, N6LF, "Using the Half-Square Antenna for Low-Band Dxing," *The ARRL Antenna Compendium Vol 5*, pp 35-42.

R. Severns, N6LF, "Broadbanding the Half-Square Antenna For 80-meter Dxing," *The ARRL Antenna Compendium Vol 5*, pp 43-44.

R. Severns, N6LF, "An Improved Double Extended Zepp," *The ARRL Antenna Compendium Vol 4*, pp 78-80.

J. Sevick, "The Ground-Image Vertical Antenna," *QST*, Jul 1971, pp 16-19, 22.

J. Sevick, "The W2FMI Ground-Mounted Short Vertical," *QST*, Mar 1973, pp 13-18, 41.

J. Sevick, "The Constant-Impedance Trap Vertical," *QST* , Mar 1974, pp 29-34.

J. Sevick, "Short Ground-Radial Systems for Short Verticals," *QST*, Apr 1978, pp 30-33.

J. Sevick, W2FMI, *Transmission Line Transformers* (Noble Publishing, Atlanta, 1996).

W. Smith, W6BCX, "Bet My Money On A Bobtail Beam," *CQ*, Mar 1948, pp 21-23, 92.

J. Stanford, NNØF, "Linear-Loaded Short Wire Antennas," *The ARRL Antenna Compendium Vol 5*, pp 105-107.

J. Swank, W8HXR, "The S-Meter Bender," *73*, Jun 1978, pp 170-173.

J. Tyskewicz, "The Heli-Rope Antenna," *QST*, Jun 1971.

B. Vester, K3BC, "The Half-Square Antenna," *QST*, Mar 1974, pp 11-14.

A. D. Watt, *VLF Radio Engineering* (Pergamon Press, 1967) (out of print).

Prediction of Sky-wave Field Strength at Frequencies Between About 150 and 1700 kHz, ITU Doc 3/14, Radiocommunication Study Groups, Feb 1995.

Chapter 7

Multiband Antennas

For operation in a number of bands, such as those between 3.5 and 30 MHz, it would be impractical for most amateurs to put up a separate antenna for each band. But this is not necessary—a dipole, cut for the lowest frequency band to be used, can be operated readily on higher frequencies. To do so, one must be willing to accept the fact that such harmonic-type operation leads to a change in the directional pattern of the antenna, both in the azimuth and the elevation planes (see Chapter 2, Antenna Fundamentals, and Chapter 3, The Effects of Ground).

You can see from discussions in Chapter 6, Low-Frequency Antennas, that you should carefully plan the height at which you install a multiband horizontally polarized antenna. This is one aspect of multiband antennas. Another important thing to consider is that you should be willing to use so-called *tuned feeders*. A center-fed single-wire antenna can be made to accept power and radiate it with high efficiency on any frequency higher than its fundamental resonant frequency and, with a reduction in efficiency and bandwidth, on frequencies as low as one half the fundamental.

In fact, it is not necessary for an antenna to be a full half-wavelength long at the lowest frequency. An antenna can be considerably shorter than ½ λ, even as short as ¼ λ, and still be a very efficient radiator. The use of such short antennas results in stresses, however, on other parts of the system, for example the antenna tuner and the transmission line. This will be discussed in some detail in this chapter.

Methods have been devised for making a single antenna structure operate on a number of bands while still offering a good match to a transmission line, usually of the coaxial type. It should be understood, however, that a multiband antenna is not *necessarily* one that will match a given line on all bands on which you intend to use it. Even a relatively short whip type of antenna can be operated as a multiband antenna with suitable loading for each band. Such loading may be in the form of a coil at the base of the antenna on those frequencies where loading is needed, or it may be incorporated in the tuned feeders running from the transmitter to the base of the antenna.

This chapter describes a number of systems that can be used on two or more bands. Beam antennas, such as Yagis or quads, are treated separately in later chapters.

Simple Wire Antennas

The simplest multiband antenna is a random length of #12 or #14 wire. Power can be fed to the wire on practically any frequency using one or the other of the methods shown in **Fig 1**. If the wire is made either 67 or 135 feet long, it can also be fed through a tuned circuit, as in **Fig 2**. It is advantageous to use an SWR bridge or other indicator in the coax line at the point marked "X."

If you have installed a 28- or 50-MHz rotary beam, in many cases it may be possible to use the beam's feed line as an antenna on the lower frequencies. Connecting the two wires of the feeder together at the station end will give a random-length wire that can be conveniently coupled to the transmitter as in Fig 1. The rotary system at the far end will serve only to *end-load* the wire and will not have much other effect.

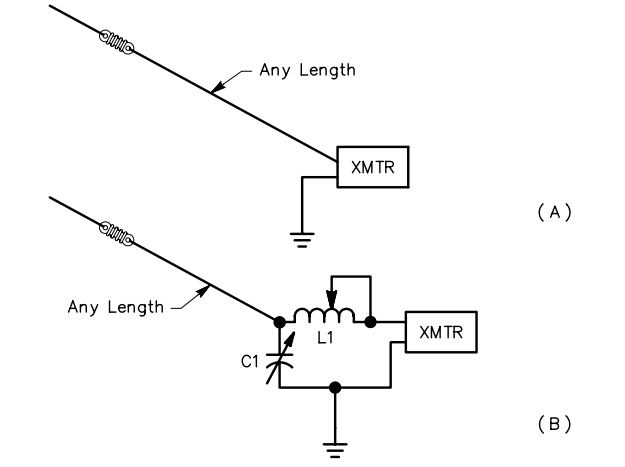

Fig 1—At A, a random-length wire driven directly from the pi-network output of a transmitter. At B, an L network for use in cases where sufficient loading cannot be obtained with the arrangement at A. C1 should have about the same plate spacing as the final tank capacitor in a vacuum-tube type of transmitter; a maximum capacitance of 100 pF is sufficient if L1 is 20 to 25 μH. A suitable coil would consist of 30 turns of #12 wire, 2½ inches diameter, 6 turns per inch. Bare wire should be used so the tap can be placed as required for loading the transmitter.

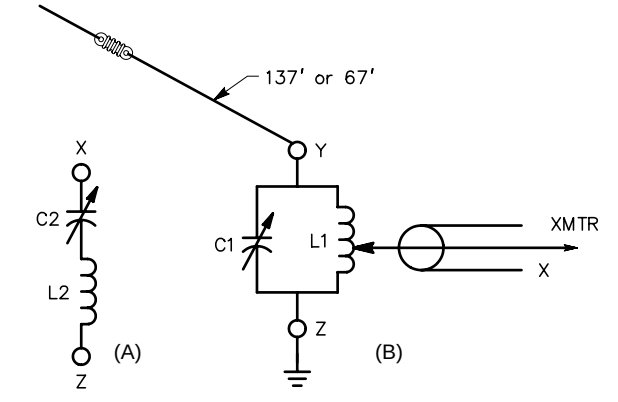

Fig 2—If the antenna length is 137 feet, a parallel-tuned coupling circuit can be used on each amateur band from 3.5 through 30 MHz, with the possible exception of the WARC 10-, 18- and 24-MHz bands. C1 should duplicate the final tank tuning capacitor and L1 should have the same dimensions as the final tank inductor on the band being used. If the wire is 67 feet long, series tuning can be used on 3.5 MHz as shown at the left; parallel tuning will be required on 7 MHz and higher frequency bands. C2 and L2 will in general duplicate the final tank tuning capacitor and inductor, the same as with parallel tuning. The L network shown in Fig 1B is also suitable for these antenna lengths.

One disadvantage of all such directly fed systems is that part of the antenna is practically within the station, and there is a good chance that you will have some trouble with RF feedback. RF within the station can often be minimized by choosing a length of wire so that the low feed-point impedance at a current loop occurs at or near the transmitter. This means using a wire length of λ/4 (65 feet at 3.6 MHz, 33 feet at 7.1 MHz), or an odd multiple of λ/4 (¾-λ is 195 feet at 3.6 MHz, 100 feet at 7.1 MHz). Obviously, this can be done for only one band in the case of even harmonically related bands, since the wire length that presents a current loop at the transmitter will present a voltage loop at two (or four) times that frequency.

When you operate with a random-length wire antenna, as in Figs 1 and 2, you should try different types of grounds on the various bands, to see what gives you the best results. In many cases it will be satisfactory to return to the transmitter chassis for the ground, or directly to a convenient metallic water pipe. If neither of these works well (or the metallic water pipe is not available), a length of #12 or #14 wire (approximately λ/4 long) can often be used to good advantage. Connect the wire at the point in the circuit that is shown grounded, and run it out and down the side of the house, or support it a few feet above the ground if the station is on the first floor or in the basement. It should not be connected to actual ground at any point.

END-FED ANTENNAS

When a straight-wire antenna is fed at one end with a two-wire transmission line, the length of the antenna portion becomes critical if radiation from the line is to be held to a minimum. Such an antenna system for multiband operation is the *end-fed Zepp* or *Zepp-fed* antenna shown in **Fig 3**. The antenna length is made λ/2 long at the lowest operating frequency. (This name came about because the first documented use of this sort of antennas was on the *Zeppelin* airships.) The feeder length can be anything that is convenient, but feeder lengths that are multiples of λ/4 generally give trouble with parallel currents and radiation from the feeder portion of the system. The feeder can be an open-wire line of #14 solid

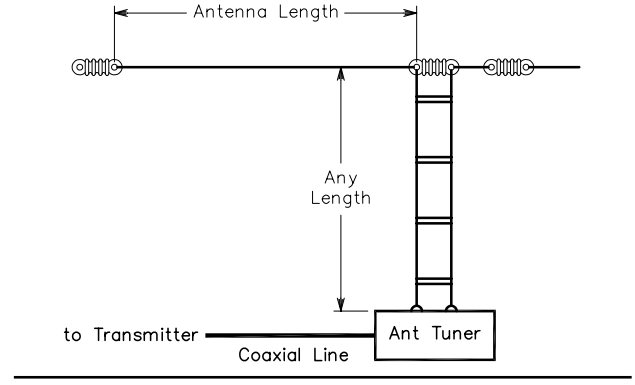

Fig 3—An end-fed Zepp antenna for multiband use.

copper wire spaced 4 or 6 inches with ceramic or plastic spacers. Open-wire TV line (not the type with a solid web of dielectric) is a convenient type to use. This type of line is available in approximately 300- and 450-Ω characteristic impedances.

If you have room for only a 67-foot flat top and yet want to operate in the 3.5-MHz band, the two feeder wires can be tied together at the transmitter end and the entire system treated as a random-length wire fed directly, as in Fig 1. The simplest precaution against parallel currents that could cause feed-line radiation is to use a feeder length that is not a multiple of λ/4. An antenna tuner can be used to provide multiband coverage with an end-fed antenna with any length of open-wire feed line, as shown in Fig 3.

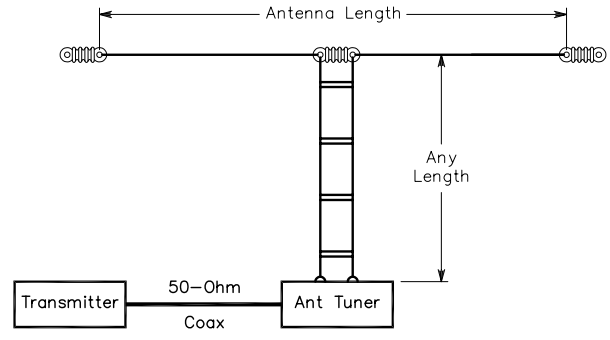

Fig 4—A center-fed antenna system for multiband use.

CENTER-FED ANTENNAS

The simplest and most flexible (and also least expensive) all-band antennas are those using open-wire parallel-conductor feeders to the center of the antenna, as in **Fig 4**. Because each half of the flat top is the same length, the feeder currents will be balanced at all frequencies unless, of course, unbalance is introduced by one half of the antenna being closer to ground (or a grounded object) than the other. For best results and to maintain feed-current balance, the feeder should run away at right angles to the antenna, preferably for at least λ/4.

Center feed is not only more desirable than end feed because of inherently better balance, but generally also results in a lower standing wave ratio on the transmission line, provided a parallel-conductor line having a characteristic impedance of 450 to 600 Ω is used. TV-type open-wire line is satisfactory for all but possibly high power installations (over 500 W), where heavier wire and wider spacing is desirable to handle the larger currents and voltages.

The length of the antenna is not critical, nor is the length of the line. As mentioned earlier, the length of the antenna can be considerably less than λ/2 and still be very effective. If the overall length is at least λ/4 at the lowest frequency, a quite usable system will result. The only difficulty that may exist with this type of system is the matter of coupling the antenna-system load to the transmitter. Most modern transmitters are designed to work into a 50-Ω coaxial load. With this type of antenna system a coupling network (an antenna tuner) is required.

Feed-Line Radiation

The preceding sections have pointed out means of reducing or eliminating feed-line radiation. However, it should be emphasized that any radiation from a transmission line is not "lost" energy and is not necessarily harmful. Whether or not feed-line radiation is important depends entirely on the antenna system being used. For example, feed-line radiation is not desirable when a directive array is being used. Such feed-line radiation can distort the desired pattern of such an array, producing responses in unwanted directions. In other words, you want radiation only from the directive array, rather than from the directive array and the feed line. See Chapter 26, Coupling the Line to the Antenna, for a detailed discussion of this topic.

On the other hand, in the case of a multiband dipole where general coverage is desired, if the feed line happens to radiate, such energy could actually have a desirable effect. Antenna purists may dispute such a premise, but from a practical standpoint where you are not concerned with a directive pattern, much time and labor can be saved by ignoring possible transmission-line radiation.

THE 135-FOOT, 80 TO 10-METER DIPOLE

As mentioned previously, one of the most versatile antennas around is a simple dipole, center-fed with open-wire transmission line and used with an antenna tuner in the shack. A 135-foot long dipole hung horizontally between two trees or towers at a height of 50 feet or higher works very well on 80 through 10 meters. Such an antenna system has significant gain at the higher frequencies.

Flattop or Inverted-V Configuration?

There is no denying that the inverted-V mounting configuration (sometimes called a *drooping dipole*) is very convenient, since it requires only a single support. The flattop configuration, however, where the dipole is mounted horizontally, gives more gain at the higher frequencies. **Fig 5** shows the 80-meter azimuth and elevation patterns for two 135-foot long dipoles. The first is mounted as a flattop at a height of 50 feet over flat ground with a conductivity of 5 mS/m and a dielectric constant of 13, typical for average soil. The second dipole uses the same length of wire, with the center apex at 50 feet and the ends drooped down to be suspended 10 feet off the ground. This height is sufficient so that there is no danger to passersby from RF burns.

At 3.8 MHz, the flattop dipole about 4 dB more peak gain than its drooping cousin. On the other hand, the inverted-V configuration gives a pattern that is more omnidirectional than the flattop dipole, which has nulls off the

ends of the wire. Omnidirectional coverage may be more important to net operators, for example, than maximum gain.

Fig 6 shows the azimuth and elevation patterns for the same two antenna configurations, but this time at 14.2 MHz. The flattop dipole has developed four distinct lobes at a 10° elevation angle, an angle typical for 20-meter skywave communication. The peak elevation angle gain of 9.4 dBi occurs at about 17° for a height of 50 feet above flat ground for the flattop dipole. The inverted-V configuration is again nominally more omnidirectional, but the peak gain is down some 6 dB from the flattop.

The situation gets even worse in terms of peak gain at 28.4 MHz for the inverted-V configuration. Here the peak gain is down about 8 dB from that produced by the flattop dipole, which exhibits eight lobes at this frequency with a maximum gain of 10.5 dBi at about 7° elevation. See the comparisons in **Fig 7**.

Whatever configuration you choose to mount the 135-foot dipole, you will want to feed it with some sort of low-loss open-wire transmission line. So-called *window* 450-Ω ladder line is popular for this application. Be sure to twist the line about three or four turns per foot to keep it from twisting excessively in the wind. Make sure also that you provide some mechanical support for the line at the junction with the dipole

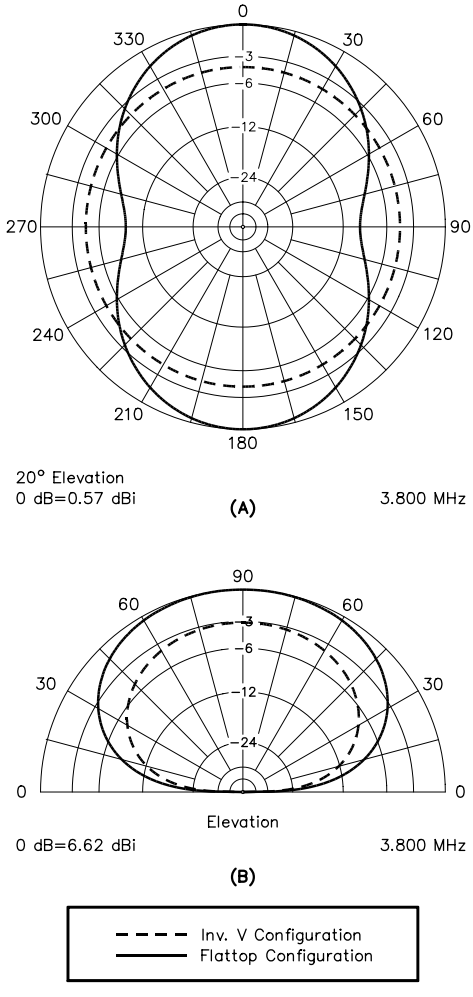

Fig 5—Patterns on 80 meters for 135-foot, center-fed dipole erected as a horizontal flattop dipole at 50 feet, compared with the same dipole installed as an inverted V with the apex at 50 feet and the ends at 10 feet. The azimuth pattern is shown at A, where the dipole wire lies in the 90° to 270° plane. At B, the elevation pattern, the dipole wire comes out of the paper at a right angle. On 80 meters, the patterns are not markedly different for either flattop or inverted-V configuration.

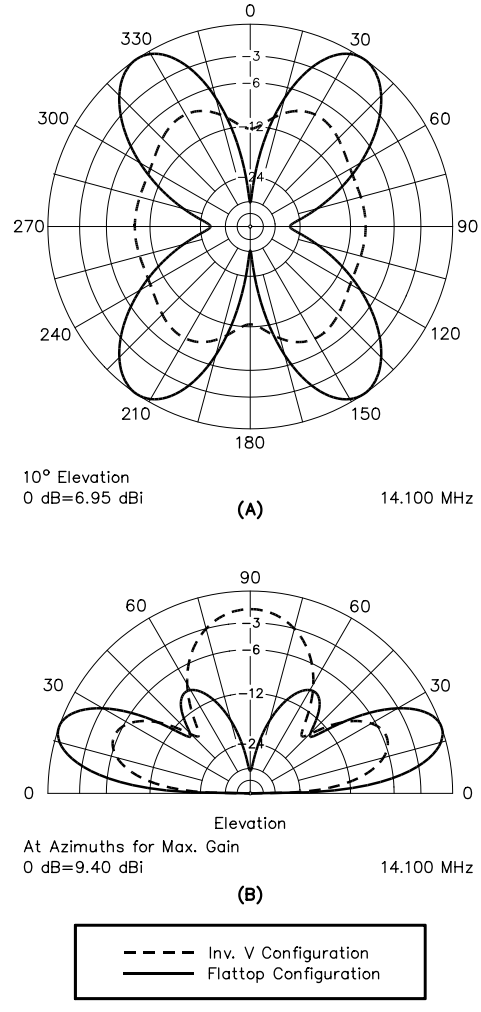

Fig 6—Patterns on 20 meters for two 135-foot dipoles. One is mounted horizontally as a flattop and the other as an inverted V with 120° included angle between the legs. The azimuth pattern is shown in A and the elevation pattern is shown in B. The inverted V has about 6 dB less gain at the peak azimuths, but has a more uniform, almost omnidirectional, azimuthal pattern. In the elevation plane, the inverted V has a fat lobe overhead, making it a somewhat better antenna for local communication, but not quite so good for DX contacts at low elevation angles.

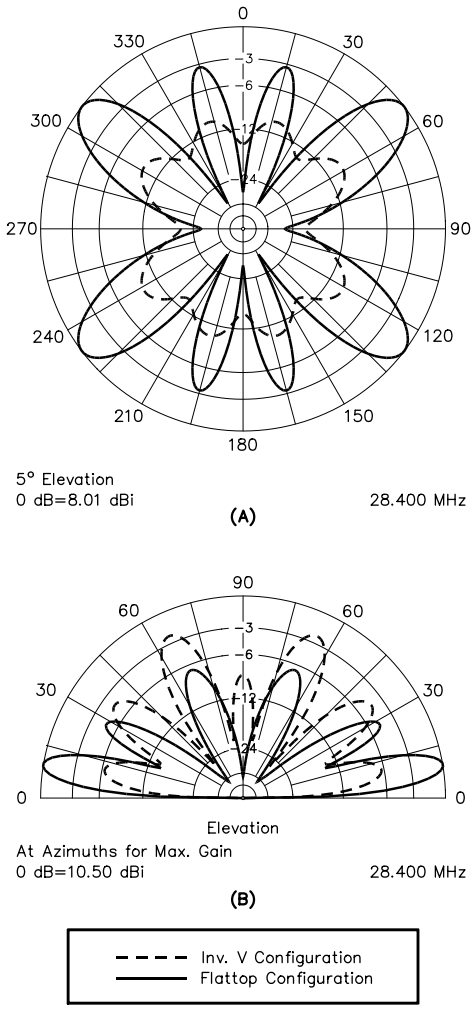

Fig 7—Patterns on 10 meters for same antenna configurations as in Figs 7 and 8. Once again, the inverted-V configuration yields a more omnidirectional pattern, but at the expense of almost 8 dB less gain than the flattop configuration at its strongest lobes.

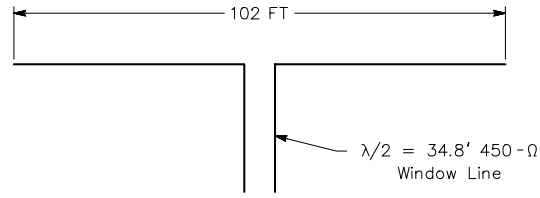

Fig 8—The G5RV multiband antenna covers 3.5 through 30 MHz. Although many amateurs claim it may be fed directly with 50-Ω coax on several amateur bands, Louis Varney, its originator, recommends the use of a matching network on bands other than 14 MHz.

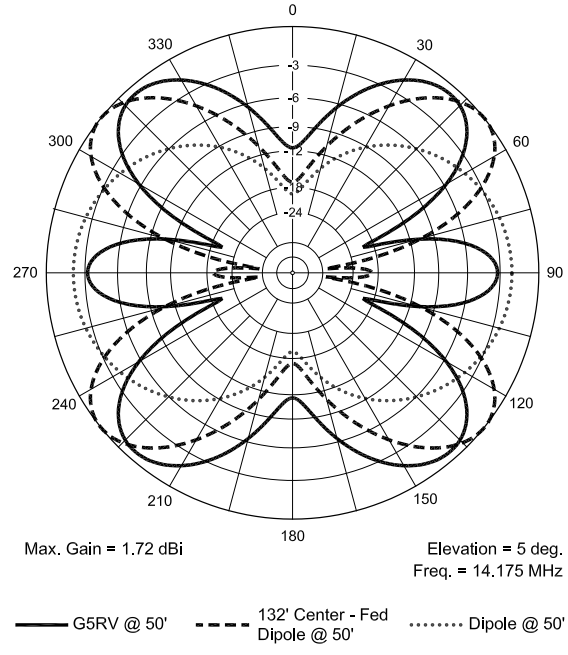

Fig 9—Azimuth pattern at a 5° takeoff angle for a 102-foot long, 50-foot high G5RV dipole (solid line). For comparison, the response for a 132-foot long, center-fed dipole at 50 feet height (dashed line) and a 33-foot long half wave 20-meter dipole at 50 feet (dotted line) are also shown. The longest antenna exhibits about 0.5 dB more gain than the G5RV, although the response is more omnidirectional for the G5RV—an advantage for a wire antenna that is not usually rotatable.

wires. This will prevent flexing of the transmission-line wire, since excessive flexing will result in breakage.

THE G5RV MULTIBAND ANTENNA

A multiband antenna that does not require a lot of space, is simple to construct, and is low in cost is the G5RV. Designed in England by Louis Varney (G5RV) some years ago, it has become quite popular in the US. The G5RV design is shown in **Fig 8**. The antenna may be used from 3.5 through 30 MHz. Although some amateurs claim it may be fed directly with 50-Ω coax on several amateur bands with a low SWR, Varney himself recommended the use of an antenna tuner on bands other than 14 MHz (see Bibliography). In fact, an analysis of the G5RV feed-point impedance shows there is *no* length of balanced line of *any* characteristic impedance that will transform the terminal impedance to the 50 to 75-Ω range on all bands. (Low SWR indication with coax feed and no matching network on bands other than 14 MHz may indicate excessive losses in the coaxial line.)

Fig 9 shows the 20-meter azimuthal pattern for a G5RV at a height of 50 feet over flat ground, at an elevation angle of 5° that is suitable for DX work. For comparison, the response for two other antennas is also shown in Fig 9—a standard half wave 20-meter dipole at 50 feet and a 132-foot long center-fed

dipole at 50 feet. The G5RV on 20 meters is, of course, longer than a standard half wave dipole and it exhibits about 2 dB more gain compared to that dipole. With four lobes making it look rather like a four-leaf clover, the azimuth pattern is more omnidirectional than the two-lobed dipole. The 132-foot center-fed dipole is longer than the G5RV and it has about 0.5 dB more gain than the G5RV, also exhibiting four major lobes, along with two strong minor lobes in the plane of the wire. Overall, the azimuthal response for the G5RV is more omnidirectional than the comparison antennas.

The G5RV patterns for other frequencies are similar to those shown for the 135-foot dipole previously for other frequencies. Incidentally, you may be wondering why a 132-foot dipole is shown in Fig 9, rather than the 135-foot dipole described earlier. The 132-foot overall length describes another antenna that we'll discus in the next section on Windom antennas.

The portion of the G5RV antenna shown as horizontal in Fig 8 may also be installed in an inverted-V dipole arrangement, subject to the same loss of peak gain mentioned above for the 135-foot dipole. Or instead, up to ⅙ of the total length of the antenna at each end may be dropped vertically, semi-vertically, or bent at a convenient angle to the main axis of the antenna, to cut down on the requirements for real estate.

THE WINDOM ANTENNA

An antenna that enjoyed popularity in the 1930s and into the 1940s was what we now call the *Windom*. It was known at the time as a "single-feeder Hertz" antenna, after being described in Sep 1929 *QST* by Loren G. Windom, W8GZ (see Bibliography).

The Windom antenna, shown in **Fig 10**, is fed with a single wire, attached approximately 14% off center. In theory, this location provides a match for the single-wire transmission line, which is worked against an earth ground. Because the single-wire feed line is not inherently well balanced and because it is brought to the operating position, "RF in the shack" and a potential radiation hazard may be experienced with this antenna.

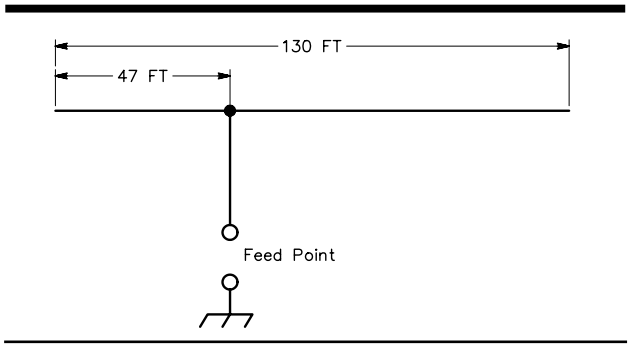

Fig 10—The Windom antenna, cut for a fundamental frequency of 3.75 MHz. The single-wire feeder, connected 14% off center, is brought into the station and the system is fed against ground. The antenna is also effective on its harmonics.

Later variations of the off-center fed Windom moved the attachment point slightly to accommodate balanced 300-Ω ribbon line. One relatively recent variation is called the "Carolina Windom," apparently because two of the designers, Edgar Lambert, WA4LVB, and Joe Wright, W4UEB, lived in coastal North Carolina (the third, Jim Wilkie, WY4R, lived

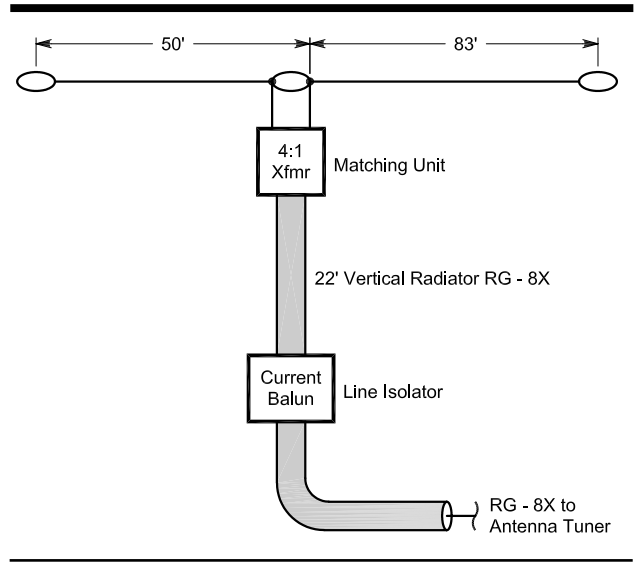

Fig 11—Layout for flattop "Carolina Windom" antenna.

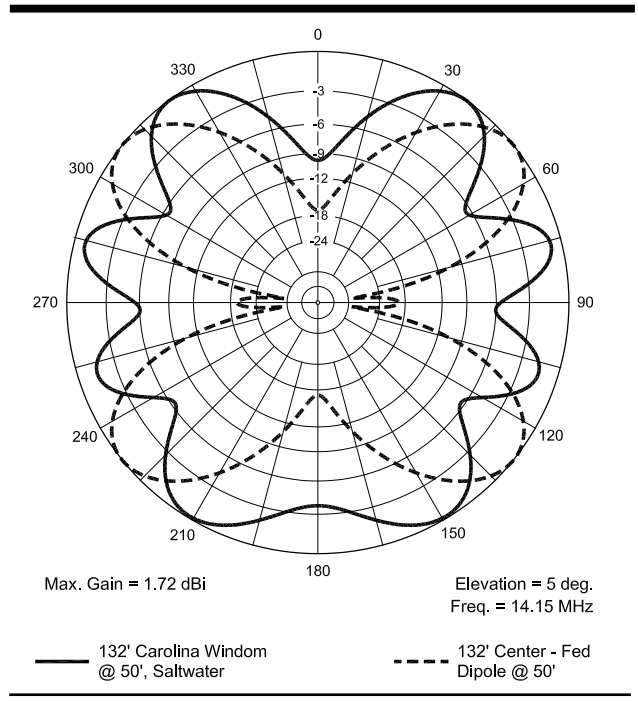

Fig 12—20-meter azimuth patterns for a 132-foot long off-center fed Carolina Windom and a 132-foot long center-fed flattop dipole on 20 meters, both at a height of 50 feet above saltwater. The response for the Carolina Windom is more omnidirectional because the vertically polarized radiation from the 22-foot long vertical RG-8X coax fills in the deep nulls.

in nearby Norfolk, Virginia). One of the interesting parts about the Carolina Windom is that it turns a potential disadvantage—feed line radiation—into a potential advantage.

Fig 11 is a diagram of a flattop Carolina Windom, which uses a 50-foot wire joined with an 83-foot wire at the feedpoint insulator. This resembles the layout shown in Fig 10 for the original W8GZ Windom. The "Vertical Radiator" for the Carolina Windom is a 22-foot piece of RG-8X coax, with a "Line Isolator" (current-type choke balun) at the bottom end and a 4:1 "Matching Unit" at the top. The system takes advantage of the asymmetry of the horizontal wires to induce current onto the braid of the vertical coax section. Note that the matching unit is a voltage-type balun transformer, which purposely does not act like a common-mode current choking balun. You must use an antenna tuner with this system to present a 1:1 SWR to the transmitter on the amateur bands from 80 through 10 meters.

The radiation resulting from current induced onto the 22-foot vertical coax section tends to fill in the deep nulls that would be present if the 132-feet of horizontal wire were symmetrically center fed. Over saltwater, the vertical radiator can give significant gain at the low elevation angles needed for DX work. Indeed, field reports for the Carolina Windom are most impressive for stations located near or on saltwater. Over average soil the advantage of the additional vertically polarized component is not quite so evident. **Fig 12** compares a 50-foot high Carolina Windom on 14 MHz over saltwater to a 50-foot high, 132-foot long, flattop center-fed dipole. The Carolina Windom has a more omnidirectional azimuthal pattern, a desirable characteristic in a 132-foot long wire antenna that is not normally rotated to favor different directions.

Another advantage of the Carolina Windom over a traditional Windom is that the coax feed line hanging below the common-mode current choke does not radiate, meaning that there will be less "RF in the shack." Since the feed line is not always operating at a low SWR on various ham bands, use the minimum length of feed coax possible to hold down losses in the coax.

Fig 13 shows the azimuth responses for a 50-foot long flattop Carolina Windom on 28.4 MHz over saltwater and over average soil. The pattern for a 50-foot high, flattop 20-meter dipole operated on 28.4 MHz is also shown, since this 20-meter dipole can also be used as a multiband antenna, when fed with open-wire transmission line rather than with coax. Again, the Carolina Windom exhibits a more omnidirectional pattern, even if the pattern is somewhat lopsided at the bottom.

MULTIPLE-DIPOLE ANTENNAS

The antenna system shown in **Fig 14** consists of a group of center-fed dipoles, all connected in parallel at the point where the transmission line joins them. The dipole elements are *stagger-tuned*. That is, they are individually cut to be λ/2 at different frequencies. Chapter 9, Broadband Antenna Matching, discusses stagger tuning of dipole antennas to attain a low SWR across a broad range of frequencies. An extension of the stagger tuning idea is to construct multiwire dipoles cut for different bands.

In theory, the 4-wire antenna of Fig 14 can be used with a coaxial feeder on five bands. The four wires are prepared as parallel-fed dipoles for 3.5, 7, 14, and 28 MHz. The 7-MHz dipole can be operated on its 3rd harmonic for 21-MHz operation to cover a fifth band. However, in practice it has been found difficult to get a good match to coaxial line

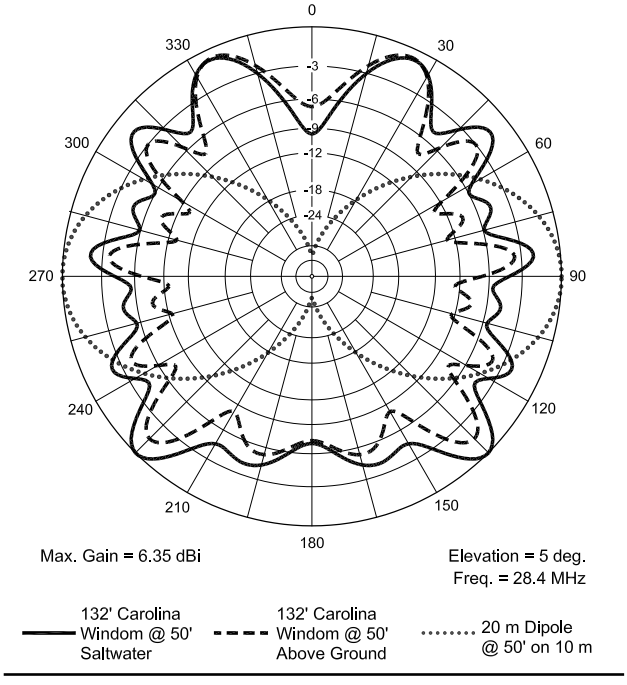

Fig 13—10-meter azimuthal responses for a 132-foot long, 50-foot high Carolina Windom over saltwater (solid line) and over average ground (dashed line), compared to that for a 20-meter half-wave dipole at 50 feet (dotted line).

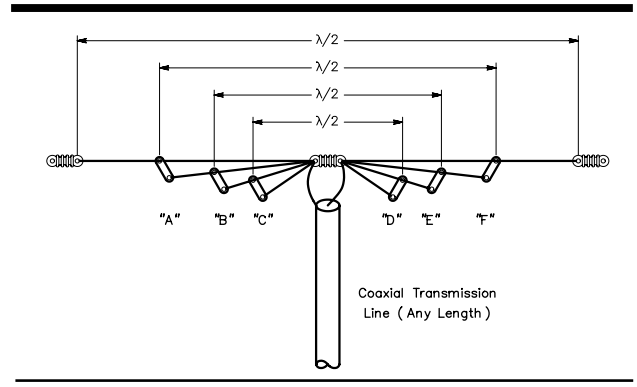

Fig 14—Multiband antenna using paralleled dipoles all connected to a common low-impedance transmission line. The half-wave dimensions may be either for the centers of the various bands or selected to fit favorite frequencies in each band. The length of a half wave in feet is 468/ frequency in MHz, but because of interaction among the various elements, some pruning for resonance may be needed on each band.

on all bands. The λ/2 resonant length of any one dipole in the presence of the others is not the same as for a dipole by itself due to interaction, and attempts to optimize all four lengths can become a frustrating procedure. The problem is compounded because the optimum tuning changes in a different antenna environment, so what works for one amateur may not work for another. Even so, many amateurs with limited antenna space are willing to accept the mismatch on some bands just so they can operate on those frequencies using a single coax feed line.

Since this antenna system is balanced, it is desirable to use a balanced transmission line to feed it. The most desirable type of line is 75-Ω transmitting twin-lead. However, either 52-Ω or 75-Ω coaxial line can be used. Coax line introduces some unbalance, but this is tolerable on the lower frequencies. An alternative is to use a balun at the feed point, fed with coaxial cable.

The separation between the dipoles for the various frequencies does not seem to be especially critical. One set of wires can be suspended from the next larger set, using insulating spreaders (of the type used for feeder spreaders) to give a separation of a few inches. Users of this antenna often run some of the dipoles at right angles to each other to help reduce interaction. Some operators use inverted-V-mounted dipoles as guy wires for the mast that supports the antenna system.

An interesting method of construction used successfully by Louis Richard, ON4UF, is shown in **Fig 15**. The antenna has four dipoles (for 7, 14, 21 and 28 MHz) constructed from 300-Ω ribbon transmission line. A single length of ribbon makes two dipoles. Thus, two lengths, as shown in the sketch, serve to make dipoles for four bands. Ribbon with copper-clad steel conductors (Amphenol type 14-022) should be used because all of the weight, including that of the feed line, must be supported by the uppermost wire.

Two pieces of ribbon are first cut to a length suitable for the two halves of the longest dipole. Then one of the conductors in each piece is cut to proper length for the next band higher in frequency. The excess wire and insulation is stripped away. A second pair of lengths is prepared in the same manner, except that the lengths are appropriate for the next two higher frequency bands.

A piece of thick polystyrene sheet drilled with holes for anchoring each wire serves as the central insulator. The shorter pair of dipoles is suspended the width of the ribbon below the longer pair by clamps also made of poly sheet. Intermediate spacers are made by sawing slots in pieces of poly sheet so they will fit the ribbon snugly.

The multiple-dipole principle can also be applied to vertical antennas. Parallel or fanned λ/4 elements of wire or tubing can be worked against ground or tuned radials from a common feed point.

OFF-CENTER-FED DIPOLES

Fig 16 shows an off-center-fed or *OCF* dipole. Because it is similar in appearance to the Windom of Fig 12, this antenna is often mistakenly called a "Windom," or sometimes a "coax-fed Windom." The two antennas are not the same, since the Windom is worked against its image in the ground, while one leg is worked against the other in the OCF dipole.

It is not necessary to feed a dipole antenna at its center, although doing so will allow it to be operated with a relatively low feed-point impedance on its fundamental and *odd* harmonics. (For example, a 7-MHz center-fed half-wave dipole can also be used for 21-MHz operation.) By contrast, the OCF dipole of Fig 16, fed ⅓ of its length from one end, may be used on its fundamental and *even* harmonics. Its free-space antenna-terminal impedance at 3.5, 7 and 14 MHz is on the order of 150 to 200 Ω. A 1:4 step-up transformer at the feed point should offer a reasonably good match to 50- or 75-Ω line, although some commercially made OCF dipoles use a 1:6 transformer.

At the 6th harmonic, 21 MHz, the antenna is three wavelengths long and fed at a voltage loop (maximum), instead of a current loop. The feed-point impedance at this frequency

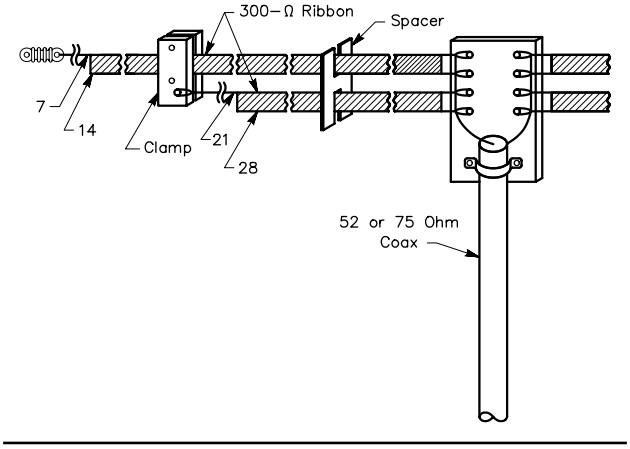

Fig 15—Sketch showing how the twin-lead multiple-dipole antenna system is assembled. The excess wire and insulation are stripped away.

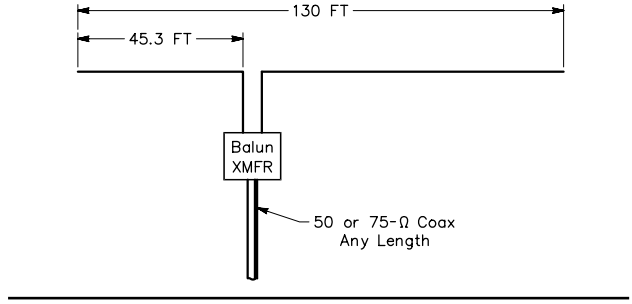

Fig 16—The off-center-fed (OCF) dipole for 3.5, 7 and 14 MHz. A 1:4 or 1:6 step-up current balun is used at the feed point.

is high, a few thousand ohms, so the antenna is unsuitable for use on this band.

Balun Requirements

Because the OCF dipole is not fed at the center of the radiator, the RF impedance paths of the two wires at the feed point are unequal. If the antenna is fed directly with coax (or a balanced line), or if a voltage step-up transformer is used, then voltages of equal magnitude (but opposite polarity) are applied to the wires at the feed point. Because of unequal impedances, the resulting antenna currents flowing in the two wires will not be equal. This also means that antenna current can flow on the feeder—on the *outside* of a coaxial line. (You may recall that this is how the Carolina Windom works, actually inducing current onto a carefully chosen length of coax, choked at its bottom end, so that it acts as a vertical radiator.)

How much current flows on the coax shield depends on the impedance of the RF current path down the outside of the feed line. In general, this is not a desirable situation. To prevent radiation, equal *currents* are required at the feed point, with the same current flowing in and out of the short leg as in and out of the long leg of the radiator. A *current* or *choke* type of balun provides just such operation. (Current baluns are discussed in detail in Chapter 26, Coupling the Line to the Antenna.)

Trap Antennas

By using tuned circuits of appropriate design strategically placed in a dipole, the antenna can be made to show what is essentially fundamental resonance at a number of different frequencies. The general principle is illustrated by **Fig 17**.

Even though a trap-antenna arrangement is a simple one, an explanation of how a trap antenna works can be elusive. For some designs, traps are resonated in our amateur bands, and for others (especially commercially made antennas) the traps are resonant far outside any amateur band.

A trap in an antenna system can perform either of two functions, depending on whether or not it is resonant at the operating frequency. A familiar case is where the trap is parallel-resonant in an amateur band. For the moment, let us assume that dimension A in Fig 17 is 32 feet and that each L/C combination is resonant in the 7-MHz band. Because of its parallel resonance, the trap presents a high impedance at that point in the antenna system. The electrical effect at 7 MHz is that the trap behaves as an insulator. It serves to divorce the outside ends, the B sections, from the antenna. The result is easy to visualize—we have an antenna system that is resonant in the 7-MHz band. Each 33-foot section (labeled A in the drawing) represents λ/4, and the trap behaves as an insulator. We therefore have a full-size 7-MHz antenna.

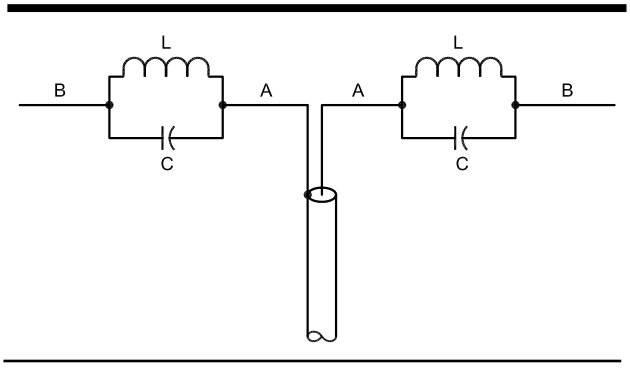

Fig 17—A trap dipole antenna. This antenna may be fed with 50-Ω coaxial line. Depending on the L/C ratio of the trap elements and the lengths chosen for dimensions A and B, the traps may be resonant either in an amateur band or at a frequency far removed from an amateur band for proper two-band antenna operation.

The second function of a trap, obtained when the frequency of operation is *not* the resonant frequency of the trap, is one of electrical loading. If the operating frequency is below that of trap resonance, the trap behaves as an inductor; if above, as a capacitor. Inductive loading will electrically lengthen the antenna, and capacitive loading will electrically shorten the antenna.

Let's carry our assumption a bit further and try using the antenna we just considered at 3.5 MHz. With the traps resonant in the 7-MHz band, they will behave as inductors when operation takes place at 3.5 MHz, electrically lengthening the antenna. This means that the total length of sections A and B (plus the length of the inductor) may be something less than a physical λ/4 for resonance at 3.5 MHz. Thus, we have a two-band antenna that is shorter than full size on the lower frequency band. But with the electrical loading provided by the traps, the overall electrical length is λ/2. The total antenna length needed for resonance in the 3.5-MHz band will depend on the L/C ratio of the trap elements.

The key to trap operation off resonance is its L/C ratio, the ratio of the value of L to the value of C. At resonance, however, within practical limitations the L/C ratio is immaterial as far as electrical operation goes. For example, in the antenna we've been discussing, it would make no difference for 7-MHz operation whether the inductor were 1 μH and the capacitor were 500 pF (the reactances would be just below 45 Ω at 7.1 MHz), or whether the inductor were 5 μH and the capacitor 100 pF (reactances of approximately 224 Ω at 7.1 MHz). But the choice of these values will make a significant difference in the antenna size for resonance at 3.5 MHz. In the first case, where the L/C ratio is 2000, the necessary length of section B of the antenna for resonance at 3.75 MHz would be approximately 28.25 feet. In the second case, where the L/C ratio is 50,000, this length need be only 24.0 feet, a difference of more than 15%.

The above example concerns a two-band antenna with

trap resonance at one of the two frequencies of operation. On each of the two bands, each half of the dipole operates as an electrical λ/4. However, the same band coverage can be obtained with a trap resonant at, say, 5 MHz, a frequency quite removed from either amateur band. With proper selection of the L/C ratio and the dimensions for A and B, the trap will act to shorten the antenna electrically at 7 MHz and lengthen it electrically at 3.5 MHz. Thus, an antenna that is intermediate in physical length between being full size on 3.5 MHz and full size on 7 MHz can cover both bands, even though the trap is not resonant at either frequency. Again, the antenna operates with electrical λ/4 sections. Note that such non-resonant traps have less RF current flowing in the trap components, and hence trap losses are less than for resonant traps.

Additional traps may be added in an antenna section to cover three or more bands. Or a judicious choice of dimensions and the L/C ratio may permit operation on three or more bands with just a pair of identical traps in the dipole.

An important point to remember about traps is this. If the operating frequency is below that of trap resonance, the trap behaves as an inductor; if above, as a capacitor. The above discussion is based on dipoles that operate electrically as λ/2 antennas. This is not a requirement, however. Elements may be operated as electrical 3/2 λ, or even 5/2 λ, and still present a reasonable impedance to a coaxial feeder. In trap antennas covering several HF bands, using electrical lengths that are odd multiples of λ/2 is often done at the higher frequencies.

To further aid in understanding trap operation, let's now choose trap L and C components that each have a reactance of 20 Ω at 7 MHz. Inductive reactance is directly proportional to frequency, and capacitive reactance is inversely proportional. When we shift operation to the 3.5-MHz band, the inductive reactance becomes 10 Ω, and the capacitive reactance becomes 40 Ω. At first thought, it may seem that the trap would become capacitive at 3.5 MHz with a higher capacitive reactance, and that the extra capacitive reactance would make the antenna electrically shorter yet. Fortunately, this is not the case. The inductor and the capacitor are connected in parallel with each other.

$$Z = \frac{-jX_L X_C}{X_L + X_C} \qquad \text{(Eq 1)}$$

where *j* indicates a reactive impedance component, rather than resistive. A positive result indicates inductive reactance, and a negative result indicates capacitive. In this 3.5-MHz case, with 40 Ω of capacitive reactance and 10 Ω of inductive, the equivalent series reactance is 13.3 Ω inductive. This inductive loading lengthens the antenna to an electrical λ/2 overall at 3.5 MHz, assuming the B end sections in Fig 17 are of the proper length.

With the above reactance values providing resonance at 7-MHz, X_L equals X_C, and the theoretical series equivalent is infinity. This provides the insulator effect, divorcing the ends.

At 14 MHz, where X_L = 40 Ω and X_C = 10 Ω, the resultant series equivalent trap reactance is 13.3 Ω capacitive. If the total physical antenna length is slightly longer than 3/2 λ at 14 MHz, this trap reactance at 14 MHz can be used to shorten the antenna to an electrical 3/2 λ. In this way, 3-band operation is obtained for 3.5, 7 and 14 MHz with just one pair of identical traps. The design of such a system is not straightforward, however, for any chosen L/C ratio for a given total length affects the resonant frequency of the antenna on both the 3.5 and 14-MHz bands.

Trap Losses

Since the tuned circuits have some inherent losses, the efficiency of a trap system depends on the unloaded Q values of the tuned circuits. Low-loss (high-Q) coils should be used, and the capacitor losses likewise should be kept as low as possible. With tuned circuits that are good in this respect—comparable with the low-loss components used in transmitter tank circuits, for example—the reduction in efficiency compared with the efficiency of a simple dipole is small, but tuned circuits of low unloaded Q can lose an appreciable portion of the power supplied to the antenna.

The commentary above applies to traps assembled from conventional components. The important function of a trap that is resonant in an amateur band is to provide a high isolating impedance, and this impedance is directly proportional to Q. Unfortunately, high Q restricts the antenna bandwidth, because the traps provide maximum isolation only at trap resonance.

FIVE-BAND W3DZZ TRAP ANTENNA

C. L. Buchanan, W3DZZ, created one of the first trap antennas for the five pre-1979 WARC amateur bands from 3.5 to 30 MHz. Dimensions are given in **Fig 18**. Only one set of traps is used, resonant at 7 MHz to isolate the inner (7-MHz) dipole from the outer sections. This causes the overall system to be resonant in the 3.5-MHz band. On 14, 21 and 28 MHz the antenna works on the capacitive-reactance principle just outlined. With a 75-Ω twin-lead feeder, the SWR with this antenna is under 2:1 throughout the three highest frequency

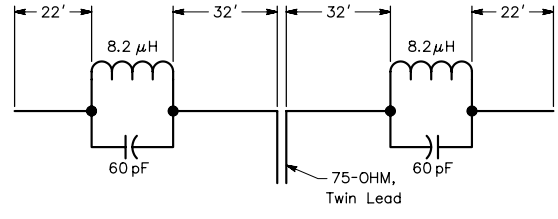

Fig 18—Five-band (3.5, 7, 14, 21 and 28 MHz) trap dipole for operation with 75-Ω feeder at low SWR (C. L. Buchanan, W3DZZ). The balanced (parallel-conductor) line indicated is desirable, but 75-Ω coax can be substituted with some sacrifice of symmetry in the system. Dimensions given are for resonance (lowest SWR) at 3.75, 7.2, 14.15 and 29.5 MHz. Resonance is very broad on the 21-MHz band, with SWR less than 2:1 throughout the band.

bands, and the SWR is comparable with that obtained with similarly fed simple dipoles on 3.5 and 7 MHz.

Trap Construction

Traps frequently are built with coaxial aluminum tubes (usually with polystyrene tubing in-between them for insulation) for the capacitor, with the coil either self-supporting or wound on a form of larger diameter than the tubular capacitor. The coil is then mounted coaxially with the capacitor to form a unit assembly that can be supported at each end by the antenna wires. In another type of trap devised by William J. Lattin, W4JRW (see Bibliography at the end of this chapter), the coil is supported inside an aluminum tube and the trap capacitor is obtained in the form of capacitance between the coil and the outer tube. This type of trap is inherently weatherproof.

A simpler type of trap, easily assembled from readily available components, is shown in **Fig 19**. A small transmitting-type ceramic "doorknob" capacitor is used, together with a length of commercially available coil material, these being supported by an ordinary antenna strain insulator. The circuit constants and antenna dimensions differ slightly from those of Fig 18, in order to bring the antenna resonance points closer to the centers of the various phone bands. Construction data are given in **Fig 20**. If a 10-turn length of inductor is used, a half turn from each end may be used to slip through the anchor holes in the insulator to act as leads.

The components used in these traps are sufficiently weatherproof in themselves so that no additional weatherproofing has been found necessary. However, if it is desired to protect them from the accumulation of snow or ice, a plastic cover can be made by cutting two discs of polystyrene slightly larger in diameter than the coil, drilling at the center to pass the antenna wires, and cementing a plastic cylinder on the edges of the discs. The cylinder can be made by wrapping two turns or so of 0.02-inch poly or Lucite sheet around the discs, if no suitable ready-made tubing is available. Plastic drinking glasses and 2-liter soft-drink plastic bottles are easily adaptable for use as impromptu trap covers.

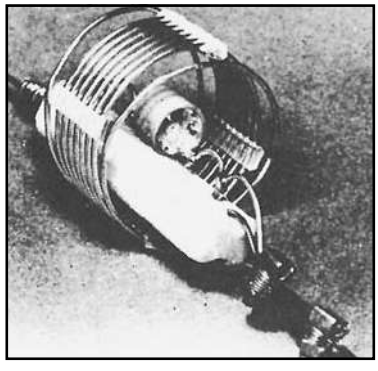

Fig 19—Easily constructed trap for wire antennas (A. Greenburg, W2LH). The ceramic insulator is 4¼ inches long (Birnback 688). The clamps are small service connectors available from electrical supply and hardware stores (Burndy KS90 servits).

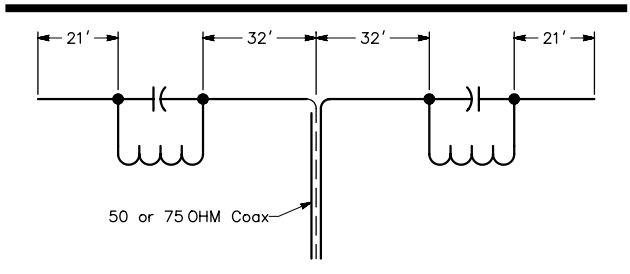

Fig 20—Layout of multiband antenna using traps constructed as shown in Fig 21. The capacitors are 100 pF each, transmitting type, 5000-volt dc rating (Centralab 850SL-100N). Coils are 9 turns of #12 wire, 2½ inches diameter, 6 turns per inch (B&W 3029) with end turns spread as necessary to resonate the traps to 7.2 MHz. These traps, with the wire dimensions shown, resonate the antenna at approximately the following frequencies on each band: 3.9, 7.25, 14.1, 21.5 and 29.9 MHz (based on measurements by W9YJH).

TWO W8NX MULTIBAND, COAX-TRAP DIPOLES

Over the last 60 or 70 years, amateurs have used many kinds of multiband antennas to cover the traditional HF bands. The availability of the 30, 17 and 12-meter bands has expanded our need for multiband antenna coverage.

Two different antennas are described here. The first covers the traditional 80, 40, 20, 15 and 10-meter bands, and the second covers 80, 40, 17 and 12 meters. Each uses the same type of W8NX trap—connected for different modes of operation—and a pair of short capacitive stubs to enhance coverage. The W8NX coaxial-cable traps have two different modes: a high- and a low-impedance mode. The inner-conductor windings and shield windings of the traps are connected in series for both modes. However, either the low- or high-impedance point can be used as the trap's output terminal. For low-impedance trap operation, only the center conductor turns of the trap windings are used. For high-impedance operation, all turns are used, in the conventional manner for a trap. The short stubs on each antenna are strategically sized and located to permit more flexibility in adjusting thc resonant frequencies of the antenna.

80, 40, 20, 15 and 10-Meter Dipole

Fig 21 shows the configuration of the 80, 40, 20, 15 and 10-meter antenna. The radiating elements are made of #14

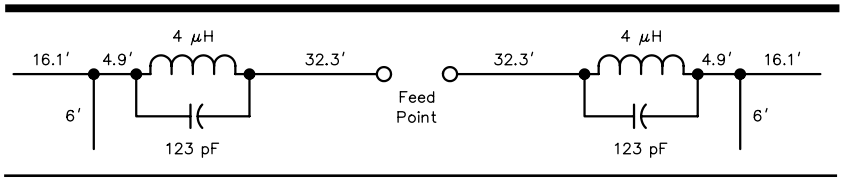

Fig 21—A W8NX multiband dipole for 80, 40, 20, 15 and 10 meters. The values shown (123 pF and 4 μH) for the coaxial-cable traps are for parallel resonance at 7.15 MHz. The low-impedance output of each trap is used for this antenna.

stranded copper wire. The element lengths are the wire span lengths in feet. These lengths do not include the lengths of the pigtails at the balun, traps and insulators. The 32.3-foot-long inner 40-meter segments are measured from the eyelet of the input balun to the tension-relief hole in the trap coil form. The 4.9-foot segment length is measured from the tension-relief hole in the trap to the 6-foot stub. The 16.l-foot outer-segment span is measured from the stub to the eyelet of the end insulator.

The coaxial-cable traps are wound on PVC pipe coil forms and use the low-impedance output connection. The stubs are 6-foot lengths of ⅛-inch stiffened aluminum or copper rod hanging perpendicular to the radiating elements. The first inch of their length is bent 90° to permit attachment to the radiating elements by large-diameter copper crimp connectors. Ordinary #14 wire may be used for the stubs, but it has a tendency to curl up and may tangle unless weighed down at the end. You should feed the antenna with 75-Ω coax cable using a good 1:1 balun.

This antenna may be thought of as a modified W3DZZ antenna due to the addition of the capacitive stubs. The length and location of the stub give the antenna designer two extra degrees of freedom to place the resonant frequencies within the amateur bands. This additional flexibility is particularly helpful to bring the 15 and 10-meter resonant frequencies to more desirable locations in these bands. The actual 10-meter resonant frequency of the original W3DZZ antenna is somewhat above 30 MHz, pretty remote from the more desirable low frequency end of 10 meters.

80, 40, 17 and 12-Meter Dipole

Fig 22 shows the configuration of the 80, 40, 17 and 12-meter antenna. Notice that the capacitive stubs are attached immediately outboard after the traps and are 6.5 feet long, ½ foot longer than those used in the other antenna. The traps are the same as those of the other antenna, but are connected for the high-impedance parallel-resonant output mode. Since only four bands are covered by this antenna, it is easier to fine tune it to precisely the desired frequency on all bands. The 12.4-foot tips can he pruned to a particular 17-meter frequency with little effect on the 12-meter frequency. The stub lengths can be pruned to a particular 12-meter frequency with little effect on the 17-meter frequency. Both such pruning adjustments slightly alter the 80-meter resonant frequency. However, the bandwidths of the antennas are so broad on 17 and 12 meters that little need for such pruning exists. The 40-meter frequency is nearly independent of adjustments to the capacitive stubs and outer radiating tip elements. Like the first antennas, this dipole is fed with a 75-Ω balun and feed line.

Fig 23 shows the schematic diagram of the traps. It explains the difference between the low and high-impedance modes of the traps. Notice that the high-impedance terminal is the output configuration used in most conventional trap applications. The low-impedance connection is made across only the inner conductor turns, corresponding to one-half of the total turns of the trap. This mode steps the trap's impedance down to approximately one-fourth of that of the high-impedance level. This is what allows a single trap design to be used for two different multiband antennas.

Fig 24 is a drawing of a cross-section of the coax trap shown through the long axis of the trap. Notice that the traps are conventional coaxial-cable traps, except for the added low-impedance output terminal. The traps are 8¾ close-spaced turns of RG-59 (Belden 8241) on a 2⅜-inch-OD PVC pipe (schedule 40 pipe with a 2-inch ID) coil form. The forms are 4⅛ inches long. Trap resonant frequency is very sensitive to the outer diameter of the coil form, so check it carefully. Unfortunately, not all PVC pipe is made with the same wall thickness. The trap frequencies should be checked with a dip meter and general-coverage receiver and adjusted to within 50 kHz of the 7150 kHz resonant frequency before installation. One inch is left over at each end of the coil forms to allow for the coax feed-through holes and holes for tension-relief attachment of the antenna radiating elements to the traps. Be sure to seal the ends of the trap coax cable with RTV sealant to prevent moisture from entering the coaxial cable.

Also, be sure that you connect the 32.3-foot wire element at the start of the inner conductor winding of the trap. This avoids detuning the antenna by the stray capacitance of the coaxial-cable shield. The trap output terminal (which has the shield stray capacitance) should be at the outboard side of

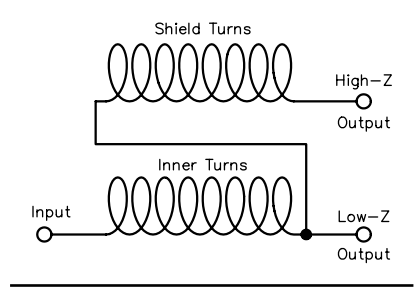

Fig 23—Schematic for the W8NX coaxial-cable trap. RG-59 is wound on a 2⅜-inch OD PVC pipe.

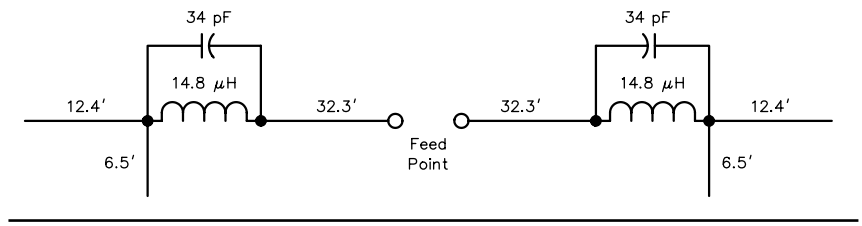

Fig 22—A W8NX multiband dipole for 80, 40, 17 and 12 meters. For this antenna, the high-impedance output is used on each trap. The resonant frequency of the traps is 7.15 MHz.

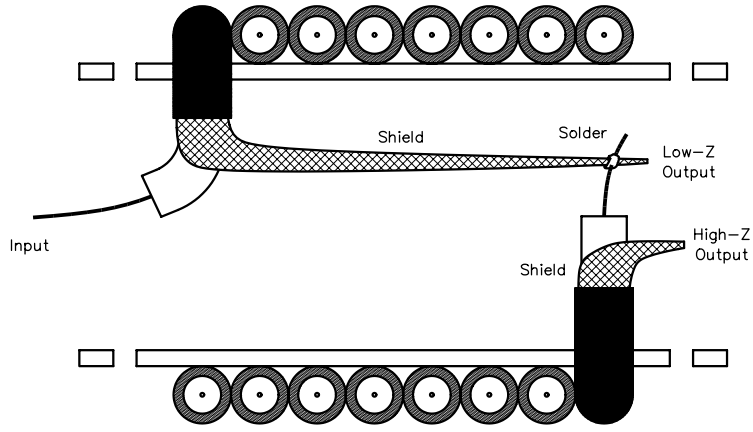

Fig 24—Construction details of the W8NX coaxial-cable trap.

the trap. Reversing the input and output terminals of the trap will lower the 40-meter frequency by approximately 50 kHz, but there will be negligible effect on the other bands.

Fig 25 shows a coaxial-cable trap. Further details of the trap installation are shown in **Fig 26**. This drawing applies specifically to the 80, 40, 20, 15 and l0-meter antenna, which uses the low-impedance trap connections. Notice the lengths of the trap pigtails: 3 to 4 inches at each terminal of the trap. If you use a different arrangement, you must modify the span lengths accordingly. All connections can be made using crimp connectors rather than by soldering. Access to the trap's interior is attained more easily with a crimping tool than with a soldering iron.

Performance

The performance of both antennas has been very satisfactory. W8NX uses the 80, 40, 17 and 12-meter version because it covers 17 and 12 meters. (He has a tribander for 20, 15 and 10 meters.) The radiation pattern on 17 meters is that of a ¾-wave dipole. On 12 meters, the pattern is that of a ⅝-wave dipole. At his location in Akron, Ohio, the antenna runs essentially east and west. It is installed as an inverted V, 40 feet high at the center, with a 120° included angle between the legs. Since the stubs are very short, they radiate little power and make only minor contributions to the radiation patterns. In theory, the pattern has four major lobes on 17 meters, with maxima to the northeast, southeast, southwest and northwest. These provide low-angle radiation into Europe, Africa, South Pacific, Japan and Alaska. A narrow pair of minor broadside lobes provides north and south coverage into Central America, South America and the polar regions.

There are four major lobes on 12 meters, giving nearly end-fire radiation and good low-angle east and west coverage. There are also three pairs of very narrow, nearly broadside, minor lobes on 12 meters, down about 6 dB from the major end-fire lobes. On 80 and 40 meters, the antenna has the usual figure-8 patterns of a half-wave-length dipole.

Both antennas function as electrical half-wave dipoles on 80 and 40 meters with a low SWR. They both function as odd-harmonic current-fed dipoles on their other operating frequencies, with higher, but still acceptable, SWR. The presence of the stubs can either raise or lower the input impedance of the antenna from those of the usual third and fifth harmonic dipoles. Again W8NX recommends that 75-Ω,

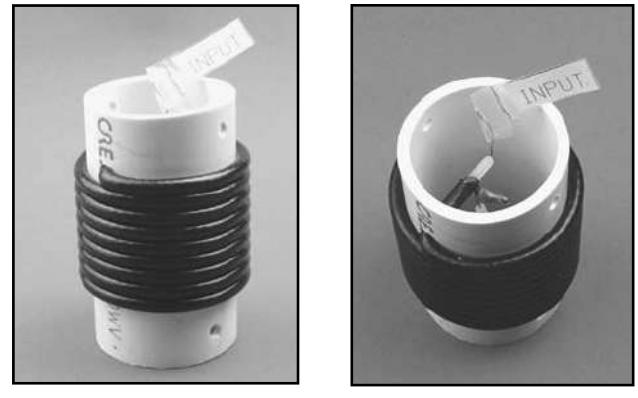

Fig 25—Other views of a W8NX coax-cable trap.

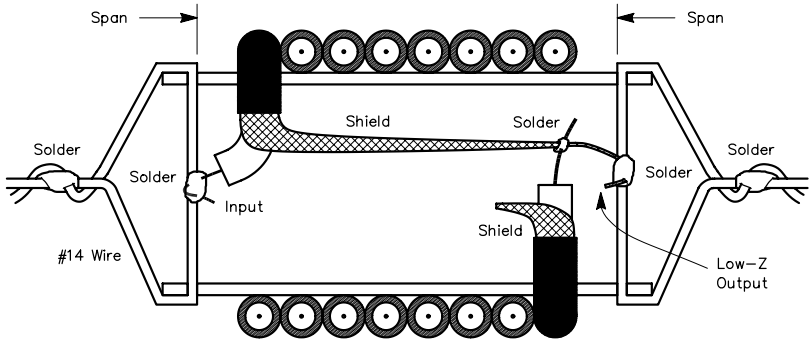

Fig 26—Additional construction details for the W8NX coaxial-cable trap.

rather than 50-Ω, feed line be used because of the generally higher input impedances at the harmonic operating frequencies of the antennas.

The SWR curves of both antennas were carefully measured using a 75 to 50-Ω transformer from Palomar Engineers inserted at the junction of the 75-Ω coax feed line and a 50-Ω SWR bridge. The transformer is required for accurate SWR measurement if a 50-Ω SWR bridge is used with a 75-Ω line. Most 50-Ω rigs operate satisfactorily with a 75-Ω line, although this requires different tuning and load settings in the final output stage of the rig or antenna tuner. The author uses the 75 to 50-Ω transformer only when making SWR measurements and at low power levels. The transformer is rated for 100 W, and when he runs his 1-kW PEP linear amplifier the transformer is taken out of the line.

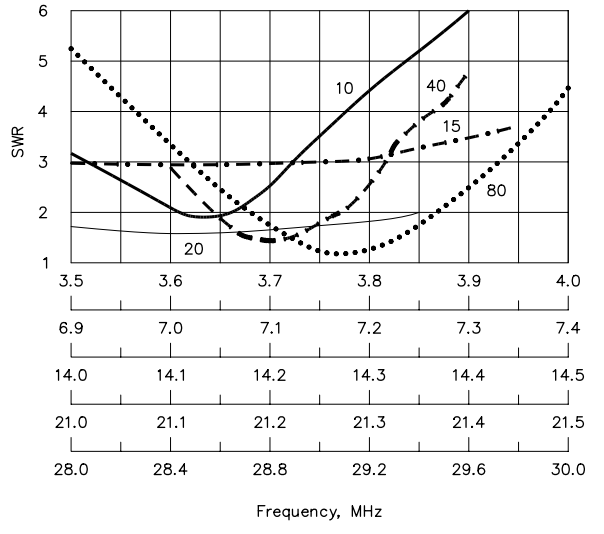

Fig 27—Measured SWR curves for an 80, 40, 20, 15 and 10-meter antenna, installed as an inverted-V with 40-ft apex and 120° included angle between legs.

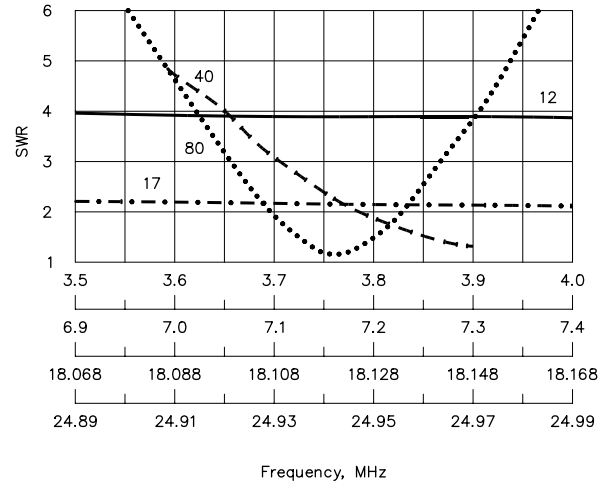

Fig 28—Measured SWR curves for an 80, 40, 17 and 12-meter antenna, installed as an inverted-V with 40-ft apex and 120° included angle between legs.

Fig 27 gives the SWR curves of the 80, 40, 20, 15 and 10-meter antenna. Minimum SWR is nearly 1:1 on 80 meters, 1.5:1 on 40 meters, 1.6:1 on 20 meters, and 1.5:1 on 10 meters. The minimum SWR is slightly below 3:1 on 15 meters. On 15 meters, the stub capacitive reactance combines with the inductive reactance of the outer segment of the antenna to produce a resonant rise that raises the antenna input resistance to about 220 Ω, higher than that of the usual 3/2-wavelength dipole. An antenna tuner may be required on this band to keep a solid-state final output stage happy under these load conditions.

Fig 28 shows the SWR curves of the 80, 40, 17 and 12-meter antenna. Notice the excellent 80-meter performance with a nearly unity minimum SWR in the middle of the band. The performance approaches that of a full-size 80-meter wire dipole. The short stubs and the low-inductance traps shorten the antenna somewhat on 80 meters. Also observe the good 17-meter performance, with the SWR being only a little above 2:1 across the band.

But notice the 12-meter SWR curve of this antenna, which shows 4:1 SWR across the band. The antenna input resistance approaches 300 Ω on this band because the capacitive reactance of the stubs combines with the inductive reactance of the outer antenna segments to give resonant rises in impedance. These are reflected back to the input terminals. These stub-induced resonant impedance rises are similar to those on the other antenna on 15 meters, but are even more pronounced.

Too much concern must not be given to SWR on the feed line. Even if the SWR is as high as 9:1 *no destructively high voltages will exist on the transmission line.* Recall that transmission-line voltages increase as the square root of the SWR in the line. Thus, 1 kW of RF power in 75-Ω line corresponds to 274 V line voltage for a 1:1 SWR. Raising the SWR to 9:1 merely triples the maximum voltage that the line must withstand to 822 V. This voltage is well below the 3700-V rating of RG-11, or the 1700-V rating of RG-59, the two most popular 75-Ω coax lines. Voltage breakdown in the traps is also very unlikely. As will be pointed out later, the operating power levels of these antennas are limited by RF power dissipation in the traps, not trap voltage breakdown or feed-line SWR.

Trap Losses and Power Rating

Table 1 presents the results of trap Q measurements and extrapolation by a two-frequency method to higher frequencies above resonance. W8NX employed an old, but recently calibrated, Boonton Q meter for the measurements. Extrapolation to higher-frequency bands assumes that trap resistance losses rise with skin effect according to the square root of frequency, and that trap dielectric loses rise directly with frequency. Systematic measurement errors are not increased by frequency extrapolation. However, random measurement

Table 1
Trap Q

Frequency (MHz)	*3.8*	*7.15*	*14.18*	*18.1*	*21.3*	*24.9*	*28.6*
High Z out (Ω)	101	124	139	165	73	179	186
Low Z out (Ω)	83	103	125	137	44	149	155

Table 2
Trap Loss Analysis: 80, 40, 20, 15, 10-Meter Antenna

Frequency (MHz)	*3.8*	*7.15*	*14.18*	*21.3*	*28.6*
Radiation Efficiency (%)	96.4	70.8	99.4	99.9	100.0
Trap Losses (dB)	0.16	1.5	0.02	0.01	0.003

Table 3
Trap Loss Analysis: 80, 40, 17, 12-Meter Antenna

Frequency (MHz)	*3.8*	*7.15*	*18.1*	*24.9*
Radiation Efficiency (%)	89.5	90.5	99.3	99.8
Trap Losses (dB)	0.5	0.4	0.03	0.006

errors increase in magnitude with upward frequency extrapolation. Results are believed to be accurate within 4% on 80 and 40 meters, but only within l0 to 15% at 10 meters. Trap Q is shown at both the high- and low-impedance trap terminals. The Q at the low-impedance output terminals is 15 to 20% lower than the Q at the high-impedance output terminals.

W8NX computer-analyzed trap losses for both antennas in free space. Antenna-input resistances at resonance were first calculated, assuming lossless, infinite-Q traps. They were again calculated using the Q values in Table 1. The radiation efficiencies were also converted into equivalent trap losses in decibels. **Table 2** summarizes the trap-loss analysis for the 80, 40, 20, 15 and 10-meter antenna and **Table 3** for the 80, 40,17 and 12-meter antenna.

The loss analysis shows radiation efficiencies of 90% or more for both antennas on all bands except for the 80, 40, 20, 15 and 10-meter antenna when used on 40 meters. Here, the radiation efficiency falls to 70.8%. A 1-kW power level at 90% radiation efficiency corresponds to 50-W dissipation per trap. In W8NX's experience, this is the trap's survival limit for extended key-down operation. SSB power levels of 1 kW PEP would dissipate 25 W or less in each trap. This is well within the dissipation capability of the traps.

When the 80, 40, 20, 15 and 10-meter antenna is operated on 40 meters, the radiation efficiency of 70.8% corresponds to a dissipation of 146 W in each trap when 1 kW is delivered to the antenna. This is sure to burn out the traps—even if sustained for only a short time. Thus, the power should be limited to leas than 300 W when this antenna is operated on 40 meters under prolonged key-down conditions. A 50% CW duty cycle would correspond to a 600-W power limit for normal 40-meter CW operation. Likewise, a 50% duty cycle for 40-meter SSB corresponds to a 600-W PEP power limit for the antenna.

The author knows of no analysis where the burnout wattage rating of traps has been rigorously determined. Operating experience seems to be the best way to determine trap burnout ratings. In his own experience with these antennas, he's had no traps burn out, even though he operated the 80, 40, 20, 15 and 10-meter antenna on the critical 40-meter band using his AL-80A linear amplifier at the 600-W PEP output level. He did not make a continuous, key-down, CW operating test at full power purposely trying to destroy the traps!

Some hams may suggest using a different type of coaxial cable for the traps. The dc resistance of 40.7 Ω per 1000 feet of RG-59 coax seems rather high. However, W8NX has found no coax other than RG-59 that has the necessary inductance-to-capacitance ratio to create the trap characteristic reactance required for the 80, 40, 20, 15 and 10-meter antenna. Conventional traps with wide-spaced, open-air inductors and appropriate fixed-value capacitors could be substituted for the coax traps, but the convenience, weatherproof configuration and ease of fabrication of coaxial-cable traps is hard to beat.

Multiband Vertical Antennas

There are two basic types of vertical antennas; either type can be used in multiband configurations. The first is the ground-mounted vertical and the second, the ground plane. These antennas are described in detail in Chapter 6, Low-Frequency Antennas.

The efficiency of any ground-mounted vertical depends a great deal on near-field earth losses. As pointed out in Chapter 3, The Effects of Ground, these near-field losses can be reduced or eliminated with an adequate radial system. Considerable experimentation has been conducted on this subject by Jerry Sevick, W2FMI, and several important results were obtained. It was determined that a radial system consisting of 40 to 50 radials, 0.2 λ long, would reduce the earth losses to about 2 Ω when a λ/4 radiator was being used. These radials should be on the earth's surface, or if buried, placed not more than an inch or so below ground. Otherwise, the RF current would have to travel through the lossy earth before reaching the radials. In a multiband vertical system, the radials should be 0.2 λ long for the lowest band, that is, 55 feet long for 3.5-MHz operation. Any wire size may be used for the radials. The radials should fan out in a circle, radiating from the base of the antenna. A metal plate, such as a piece of sheet copper, can be used at the center connection.

The other common type of vertical is the ground-plane antenna. Normally, this antenna is mounted above ground with the radials fanning out from the base of the antenna. The vertical portion of the antenna is usually an electrical λ/4, as is each of the radials. In this type of antenna, the system of radials acts somewhat like an RF choke, to prevent RF currents from flowing in the supporting structure, so the number of radials is not as important a factor as it is with a ground- mounted vertical system. From a practical standpoint, the customary number of radials is four or five. In a multiband configuration, λ/4 radials are required for each band of operation with the ground-plane antenna.

This is not so with the ground-mounted vertical antenna, where the ground plane is relied upon to provide an image of the radiating section. Note that even quarter-wave-long radials are greatly detuned by their proximity to ground—radial resonance is not necessary or even possible. In the ground-mounted case, so long as the ground-screen radials are approximately 0.2 λ long at the lowest frequency, the length will be more than adequate for the higher frequency bands.

Short Vertical Antennas

A short vertical antenna can be operated on several bands by loading it at the base, the general arrangement being similar to Figs 1 and 2. That is, for multiband work the vertical can be handled by the same methods that are used for random-length wires.

A vertical antenna should not be longer than about ¾ λ at the highest frequency to be used, however, if low-angle radiation is wanted. If the antenna is to be used on 28 MHz and lower frequencies, therefore, it should not be more than approximately 25 feet high, and the shortest possible ground lead should be used.

Another method of feeding is shown in **Fig 29**. L1 is a loading coil, tapped to resonate the antenna on the desired band. A second tap permits using the coil as a transformer for matching a coax line to the transmitter. C1 is not strictly necessary, but may be helpful on the lower frequencies, 3.5 and 7 MHz, if the antenna is quite short. In that case C1 makes it possible to tune the system to resonance with a coil of reasonable dimensions at L1. C1 may also be useful on other bands as well, if the system cannot be matched to the feed line with a coil alone.

The coil and capacitor should preferably be installed at the base of the antenna, but if this cannot be done a wire can be run from the antenna base to the nearest convenient location for mounting L1 and C1. The extra wire will of course be a part of the antenna, and since it may have to run through unfavorable surroundings it is best to avoid using it if at all possible.

This system is best adjusted with the help of an SWR indicator. Connect the coax line across a few turns of L1 and take trial positions of the shorting tap until the SWR reaches its lowest value. Then vary the line tap similarly; this should bring the SWR down to a low value. Small adjustments of both taps then should reduce the SWR to close to 1:1. If not, try adding C1 and go through the same procedure, varying C1 each time a tap position is changed.

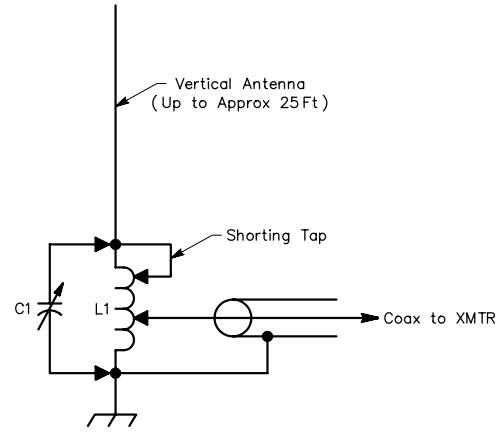

Fig 29—Multiband vertical antenna system using base loading for resonating on 3.5 to 28 MHz. L1 should be wound with bare wire so it can be tapped at every turn, using #12 wire. A convenient size is 2½ inches diameter, 6 turns per inch (such as B&W 3029). Number of turns required depends on antenna and ground lead length, more turns being required as the antenna and ground lead are made shorter. For a 25-foot antenna and a ground lead of the order of 5 feet, L1 should have about 30 turns. The use of C1 is explained in the text. The smallest capacitance that will permit matching the coax cable should be used; a maximum capacitance of 100 to 150 pF will be sufficient in any case.

Trap Verticals

The trap principle described in Fig 17 for center-fed dipoles also can be used for vertical antennas. There are two principal differences. Only one half of the dipole is used, the ground connection taking the place of the missing half, and the feed-point impedance is one half the feed-point impedance of a dipole. Thus it is in the vicinity of 30 Ω (plus the ground-connection resistance), so 52-Ω cable should be used since it is the commonly available type that comes closest to matching.

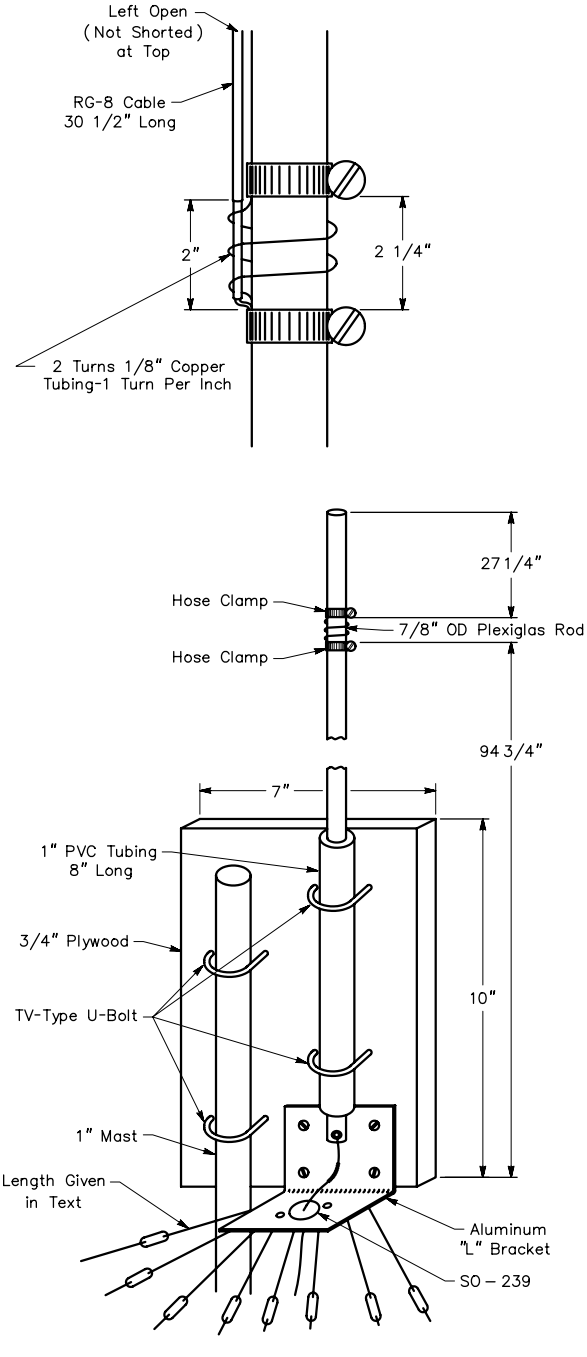

Fig 30—Constructional details of the 21- and 28-MHz dual-band antenna system.

A TRAP VERTICAL FOR 21 AND 28 MHZ

Simple antennas covering the upper HF bands can be quite compact and inexpensive. The two-band vertical ground plane described here is highly effective for long-distance communication when installed in the clear.

Figs 30, **31** and **32** show the important assembly details. The vertical section of the antenna is mounted on a ¾-inch thick piece of plywood board that measures 7 × 10 inches. Several coats of exterior varnish or similar material will help protect the wood from inclement weather. Both the mast and the radiator are mounted on the piece of wood by means of TV U-bolt hardware. The vertical is electrically isolated from the wood with a piece of 1-inch diameter PVC tubing. A piece approximately 8 inches long is required, and it is of the schedule-80 variety. To prepare the tubing, you must slit it along the entire length on one side. A hacksaw will work quite well. The PVC fits rather snugly on the aluminum tubing and

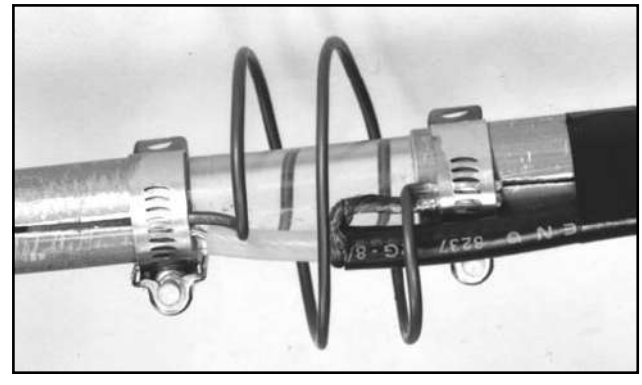

Fig 31—A close-up view of a trap. The coil is 3 inches in diameter. The leads from the coaxial-cable capacitor should be soldered directly to the pigtails of the coil. These connections should be coated with varnish after they have been secured under the hose clamps.

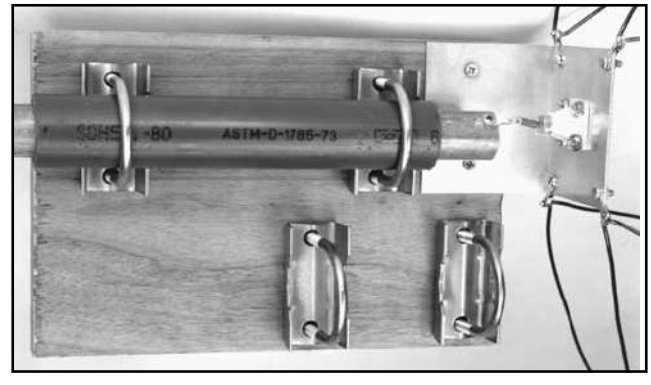

Fig 32—The base assembly of the 21- and 28-MHz vertical. The SO-239 coaxial connector and hood can be seen in the center of the aluminum L bracket. The U bolts are TV-type antenna hardware. The plywood should be coated with varnish or similar material.

will have to be "persuaded" with the aid of a hammer. Mount the mast directly on the wood with no insulation.

Use an SO-239 coaxial connector and four solder lugs on an L-shaped bracket made from a piece of aluminum sheet. Solder a short length of test probe wire, or inner conductor of RG-58 cable, to the inner terminal of the connector. A UG-106 connector hood is then slid over the wire and onto the coaxial connector. Then bolt the hood and connector to the aluminum bracket. Two wood screws are used to secure the aluminum bracket to the plywood, as shown in the drawing and photograph. Solder the free end of the wire coming from the connector to a lug mounted on the bottom of the vertical radiator. Fill any space between the wire and where it passes through the hood with GE silicone sealant or similar material to keep moisture out. The eight radials, four for each band, are soldered to the four lugs on the aluminum bracket. Separate the two sections of the vertical member with a piece of clear acrylic rod. Approximately 8 inches of ⅞-inch OD material is required. You must slit the aluminum tubing lengthwise for several inches so the acrylic rod may be inserted. The two pieces of aluminum tubing are separated by 2¼ inches.

The trap capacitor is made from RG-8 coaxial cable and is 30.5 inches long. RG-8 cable has 29.5 pF of capacitance per foot and RG-58 has 28.5 pF per foot. RG-8 cable is recommended over RG-58 because of its higher breakdown-voltage capability. The braid should be pulled back 2 inches on one end of the cable, and the center conductor soldered to one end of the coil. Solder the braid to the other end of the coil. Compression type hose clamps are placed over the capacitor/coil leads and put in position at the edges of the aluminum tubing. When tightened securely, the clamps serve a two-fold purpose—they keep the trap in contact with the vertical members and prevent the aluminum tubing from slipping off the acrylic rod. The coaxial-cable capacitor runs upward along the top section of the antenna. This is the side of the antenna to which the braid of the capacitor is connected. Place a cork or plastic cap in the very top of the antenna to keep moisture out.

Installation and Operation

The antenna may be mounted in position using a TV-type tripod, chimney, wall or vent mount. Alternatively, a telescoping mast or ordinary steel TV mast may be used, in which case the radials may be used as guys for the structure. The 28-MHz radials are 8 feet 5 inches long, and the 21-MHz radials are 11 feet 7 inches.

Any length of 50-Ω cable may be used to feed the antenna. The SWR at resonance should be on the order of 1.2:1 to 1.5:1 on both bands. The reason the SWR is not 1:1 is that the feed-point resistance is something other than 50 Ω—closer to 35 or 40 Ω.

The Open-Sleeve Antenna

Although only recently adapted for the HF and VHF amateur bands, the open-sleeve antenna has been around since 1946. The antenna was invented by Dr J. T. Bolljahn, of Stanford Research Institute. This section on sleeve antennas was written by Roger A. Cox, WBØDGF.

The basic form of the open-sleeve monopole is shown in **Fig 33**. The open-sleeve monopole consists of a base-fed central monopole with two parallel closely spaced parasitics, one on each side of the central element, and grounded at each base. The lengths of the parasitics are roughly one half that of the central monopole.

Impedance

The operation of the open sleeve can be divided into two modes, an antenna-mode and a transmission-line mode. This is shown in **Fig 34**.

The antenna-mode impedance, Z_A, is determined by the length and diameter of the central monopole. For sleeve lengths less than that of the monopole, this impedance is essentially independent of the sleeve dimensions.

The transmission-line mode impedance, Z_T, is determined by the characteristic impedance, end impedance, and length of the 3- wire transmission line formed by the central monopole and the two sleeve elements. The characteristic impedance, Z_c, can be determined by the element diameters and spacing if all element diameters are equal, and is found from

$$Z_c = 207 \log 1.59 (D/d) \qquad \text{(Eq 2)}$$

where

D = spacing between the center of each sleeve element and the center of the driven element

d = diameter of each element

This is shown graphically in **Fig 35**. However, since the end impedance is usually unknown, there is little need to know the characteristic impedance. The transmission-line mode impedance, Z_T, is usually determined by an educated guess and experimentation.

As an example, let us consider the case where the central monopole is λ/4 at 14 MHz. It would have an antenna mode impedance, Z_A, of approximately 52 Ω, depending upon the ground conductivity and number of radials. If two sleeve elements were added on either side of the central monopole, with each approximately half the height of the monopole and at a distance equal to their height, there would be very little

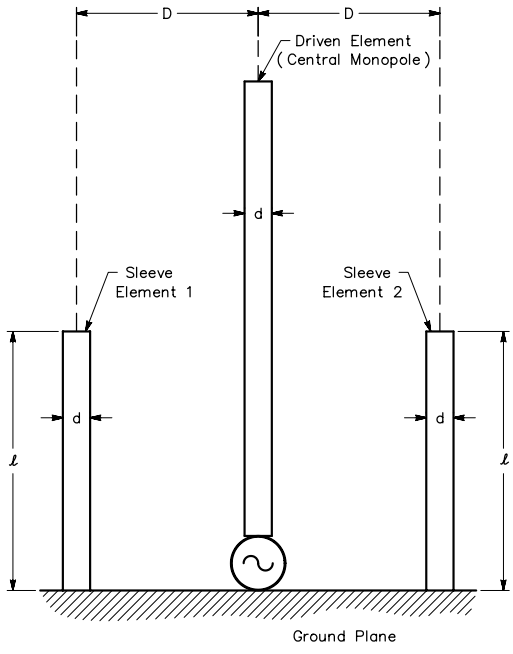

Fig 33—Diagram of an open-sleeve monopole.

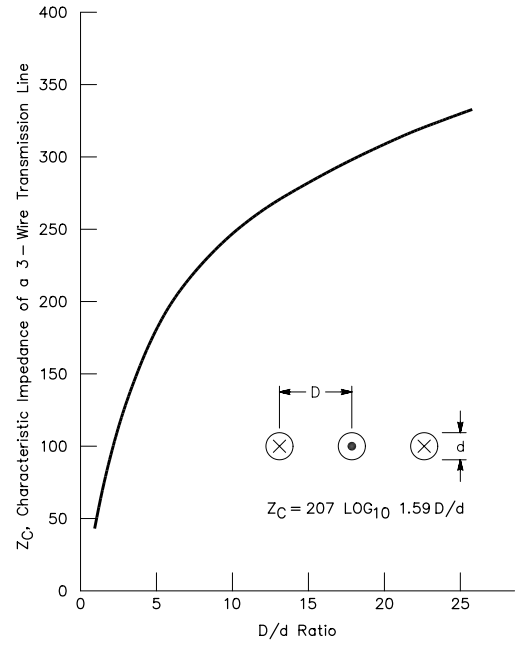

Fig 35—Characteristic impedance of transmission-line mode in an open-sleeve antenna.

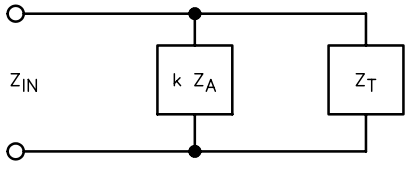

Fig 34—Equivalent circuit of an open-sleeve antenna.

effect on the antenna mode impedance, Z_A, at 14 MHz.

Also, Z_T at 14 MHz would be the end impedance transformed through a λ/8 section of a very high characteristic impedance transmission line. Therefore, Z_T would be on the order of 500-2000 Ω resistive plus a large capacitive reactance component. This high impedance in parallel with 52 Ω would still give a resultant impedance close to 52 Ω.

At a frequency of 28 MHz, however, Z_A is that of an end-fed half-wave antenna, and is on the order of 1000-5000 Ω resistive. Also, Z_T at 28 MHz would be on the order of 1000 to 5000 Ω resistive, since it is the end impedance of the sleeve elements transformed through a quarter-wave section of a very high characteristic impedance 3-wire transmission line. Therefore, the parallel combination of Z_A and Z_T would still be on the order of 500 to 2500 Ω resistive.

If the sleeve elements were brought closer to the central monopole such that the ratio of the spacing to element diameter was less than 10:1, then the characteristic impedance of the 3-wire transmission line would drop to less than 250 Ω. At 28 MHz, Z_A remains essentially unchanged, while Z_T begins to edge closer to 52 Ω as the spacing is reduced. At some particular spacing the characteristic impedance, as determined by the D/d ratio, is just right to transform the end impedance to exactly 52 Ω at some frequency. Also, as the spacing is decreased, the frequency where the impedance is purely resistive gradually increases.

The actual impedance plots of a 14/28-MHz open-sleeve monopole appear in **Figs 36** and **37**. The length of the central monopole is 195.5 inches, and of the sleeve elements 89.5 inches. The element diameters range from 1.25 inches at the bases to 0.875 inch at each tip. The measured impedance of the 14-MHz monopole alone, curve A of Fig 36, is quite high. This is probably because of a very poor ground plane under the antenna. The addition of the sleeve elements raises this impedance slightly, curves B, C and D.

As curves A and B in Fig 37 show, an 8-inch sleeve spacing gives a resonance near 27.8 MHz at 70 Ω, while a 6-inch spacing gives a resonance near 28.5 MHz at 42 Ω. Closer spacings give lower impedances and higher resonances. The optimum spacing for this particular antenna would be somewhere between 6 and 8 inches. Once the spacing is found, the lengths of the sleeve elements can be tweaked slightly for a choice of resonant frequency.

In other frequency combinations such as 10/21, 10/24, 14/21 and 14/24-MHz, spacings in the 6 to 10-inch range work very well with element diameters in the 0.5 to 1.25-inch range.

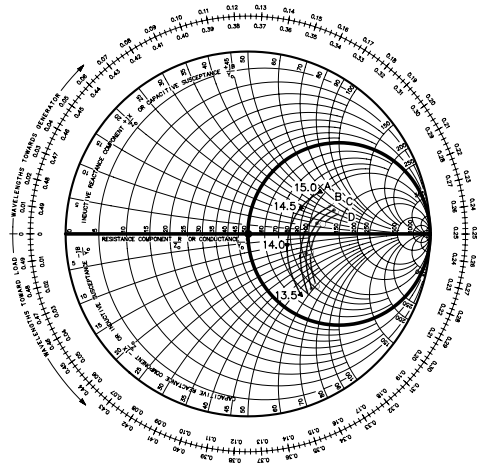

Fig 36—Impedance of an open-sleeve monopole for the frequency range 13.5-15 MHz. Curve A is for a 14 MHz monopole alone. For curves B, C and D, the respective spacings from the central monopole to the sleeve elements are 8, 6 and 4 inches. See text for other dimensions.

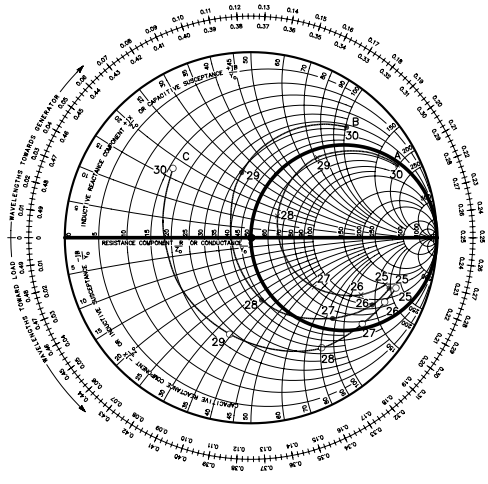

Fig 37—Impedance of the open-sleeve monopole for the range 25-30 MHz. For curves A, B and C the spacings from the central monopole to the sleeve elements are 8, 6 and 4 inches, respectively.

Bandwidth

The open-sleeve antenna, when used as a multiband antenna, does not exhibit broad SWR bandwidths unless, of course, the two bands are very close together. For example, **Fig 38** shows the return loss and SWR of a single 10-MHz vertical antenna. Its 2:1 SWR bandwidth is 1.5 MHz, from 9.8 to 11.3 MHz. Return loss and SWR are related as given by the following equation.

$$SWR = \frac{1+k}{1-k} \qquad \text{(Eq 3)}$$

where

$$k = 10^{\frac{R_L}{20}}$$

RL = return loss, dB

When sleeve elements are added for a resonance near 22 MHz, the 2:1 SWR bandwidth at 10 MHz is still nearly 1.5 MHz, as shown in **Fig 39**. The total amount of spectrum under 2:1 SWR increases, of course, because of the additional band, but the individual bandwidths of each resonance are virtually unaffected.

The open-sleeve antenna, however, can be used as a broadband structure, if the resonances are close enough to overlap. With the proper choices of resonant frequencies, sleeve and driven element diameters and sleeve spacing, the SWR "hump" between resonances can be reduced to a value less than 3:1. This is shown in **Fig 40**.

Current Distribution

According to H. B. Barkley (see Bibliography at the end of this chapter), the total current flowing into the base of the open-sleeve antenna may be broken down into two components, that contributed by the antenna mode, I_A, and that contributed by the transmission-line mode, I_T. Assuming that the sleeves are approximately half the height of the central monopole, the impedance of the antenna mode, Z_A, is very low at the resonant frequency of the central monopole, and

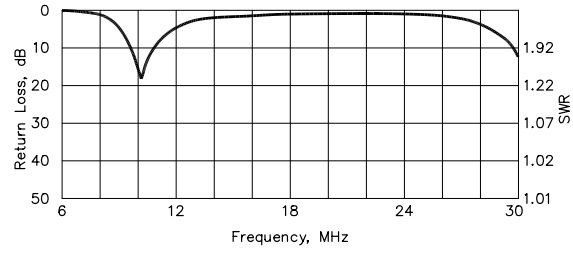

Fig 38—Return loss and SWR of a 10 MHz vertical antenna. A return loss of 0 dB represents an SWR of infinity. The text contains an equation for converting return loss to an SWR value.

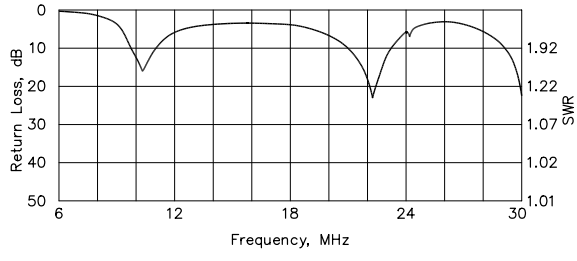

Fig 39—Return loss and SWR of a 10/22 MHz open-sleeve vertical antenna.

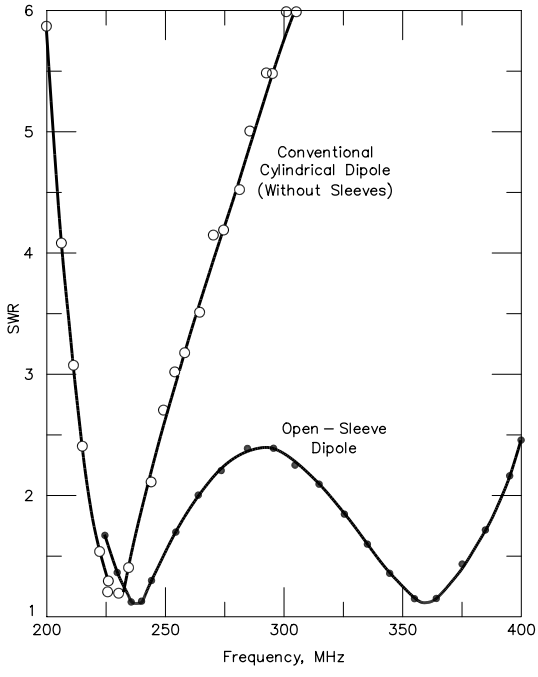

Fig 40—SWR response of an open-sleeve dipole and a conventional dipole.

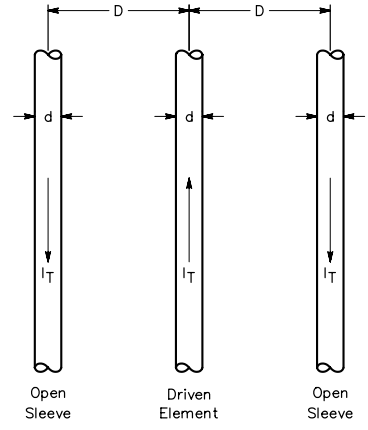

Fig 41—Current distribution in the transmission-line mode. The amplitude of the current induced in each sleeve element equals that of the current in the central element but the phases are opposite, as shown.

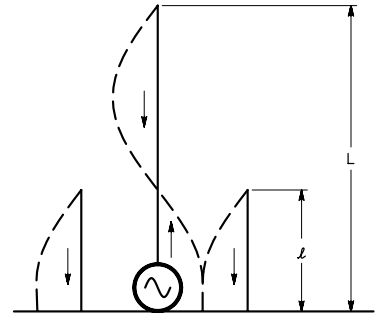

Fig 42—Total current distribution with λ= L/2.

the impedance of the transmission-line mode, Z_T, is very high. This allows almost all of the current to flow in the antenna mode, and I_A is very much greater than I_T. Therefore, the current on the central λ/4 monopole assumes the standard sinusoidal variation, and the radiation and gain characteristics are much like those of a normal λ/4 vertical antenna.

However, at the resonant frequency of the sleeves, the impedance of the central monopole is that of an end fed half-wave monopole and is very high. Therefore I_A is small. If proper element diameters and spacings have been used to match the transmission line mode impedance, Z_T, to 52 Ω, then I_T, the transmission line mode current, is high compared to I_A.

This means that very little current flows in the central monopole above the tops of the sleeve elements, and the radiation is mostly from the transmission-line mode current, I_T, in all three elements below the tops of the sleeve elements. The resulting current distribution is shown in **Figs 41** and **42** for this case.

Radiation Pattern and Gain

The current distribution of the open-sleeve antenna where all three elements are nearly equal in length is nearly that of a single monopole antenna. If, at a particular frequency, the elements are approximately λ/4 long, the current distribution is sinusoidal.

If, for this and other length ratios, the chosen diameters and spacings are such that the two sleeve elements approach an interelement spacing of λ/8, the azimuthal pattern will show directivity typical of two in-phase vertical radiators, approximately λ/8 apart. If a bi-directional pattern is needed, then this is one way to achieve it.

Spacings closer than this will produce nearly circular azimuthal radiation patterns. Practical designs in the 10 to 30 MHz range using 0.5 to 1.5-inch diameter elements will produce azimuthal patterns that vary less than ±1 dB.

If the ratio of the length of the central monopole to the length of the sleeves approaches 2:1, then the elevation pattern of the open-sleeve vertical antenna at the resonant frequency of the sleeves becomes slightly compressed. This is because of the in-phase contribution of radiation from the λ/2 central monopole.

As shown in **Fig 43**, the 10/21-Mhz open-sleeve vertical antenna produces a lower angle of radiation at 21.2 MHz with a corresponding increase in gain of 0.66 dB over that of the 10-MHz vertical alone. At length ratios approaching 3:1, the

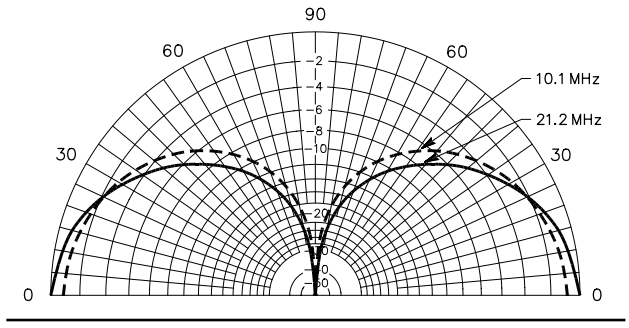

Fig 43—Vertical-plane radiation patterns of a 10/21-MHz open-sleeve vertical antenna on a perfect ground plane. At 10.1 MHz the maximum gain is 5.09 dBi, and 5.75 dBi at 21.2 MHz.

antenna mode and transmission-line mode impedance become nearly equal again, and the central monopole again carries a significant portion of the antenna current. The radiation from the top λ/2 combines constructively with the radiation from the λ/4 sleeve elements to produce gains of up to 3 dB more than just a quarter-wave vertical element alone.

Length ratios in excess of 3.2:1 produce higher level sidelobes and less gain on the horizon, except for narrow spots near the even ratios of 4:1, 6:1, 8:1, etc. These are where the central monopole is an even multiple of a half-wave, and the antenna-mode impedance is too high to allow much antenna-mode current.

Up to this point, it has been assumed that only λ/4 resonance could be used on the sleeve elements. The third, fifth, and seventh-order resonances of the sleeve elements and the central monopole element can be used, but their radiation patterns normally consist of high-elevation lobes, and the gain on the horizon is less than that of a λ/4 vertical.

Practical Construction and Evaluation

The open-sleeve antenna lends itself very easily to home construction. For the open-sleeve vertical antenna, only a feed-point insulator and a good supply of aluminum tubing are needed. No special traps or matching networks are required. The open-sleeve vertical can produce up to 3 dB more gain than a conventional λ/4 vertical. Further, there is no reduction in bandwidth, because there are no loading coils.

The open-sleeve design can also be adapted to horizontal dipole and beam antennas for HF, VHF and UHF. A good example of this is Telex/Hy-Gain's Explorer 14 triband beam which utilizes an open sleeve for the 10/15-meter driven element. The open-sleeve antenna is also very easy to model in computer programs such as *NEC* and *MININEC*, because of the open tubular construction and lack of traps or other intricate structures.

In conclusion, the open-sleeve antenna is an antenna experimenters delight. It is not difficult to match or construct, and it makes an ideal broadband or multiband antenna.

The Coupled-Resonator Dipole

A variation of the open-sleeve system above is the coupled-resonator system described by Gary Breed, K9AY, in an article in *The ARRL Antenna Compendium, Vol 5*, entitled "The Coupled-Resonator Principle: A Flexible Method for Multiband Antennas." The following is condensed from that article.

In 1995, *QST* published two antenna designs that use an interesting technique to get multiband coverage in one antenna. Rudy Severns, N6LF, described a wideband 80 and 75-meter dipole using this technique, and Robert Wilson, AL7KK, showed us how to make a three-band vertical. Both of these antennas achieve multi-frequency operation by placing resonant conductors very close to a driven dipole or vertical—with no physical connection.

The Coupled-Resonator Principle

As we all know, nearby conductors can interact with an antenna. Our dipoles, verticals and beams can be affected by nearby power lines, rain gutters, guy wires and other metallic materials. The antennas designed by Severns and Wilson use this interaction intentionally, to combine the resonances of several conductors at a single feed point. While other names have been used, I call the behavior that makes these antennas work the *coupled-resonator* (C-R) principle.

Take a look at **Fig 44**, which illustrates the general idea. Each figure shows the SWR at the feed point of a dipole, over a range of frequencies. When this dipole is all alone, it will have a very low SWR at its half-wave resonant frequency (Fig 44A). Next, if we take another wire or tubing conductor and start bringing it close to the dipole, we will see a "bump" in the dipole's SWR at the resonant frequency of this new wire. See Fig 44B. We are beginning to the see the effects of interaction between the two conductors. As we bring this new conductor closer, we reach a point where the SWR "bump" has grown to a very deep dip—a low SWR. We now have a good match at both the original dipole's resonant frequency and the frequency of the new conductor, as illustrated in Fig 44C.

We can repeat this process for several more conductors at other frequencies to get a dipole with three, four, five, six, or more resonant frequencies. The principle also applies to verticals, so any reference to a dipole can be considered to be valid for a vertical, as well.

We can write a definition of the C-R principle this

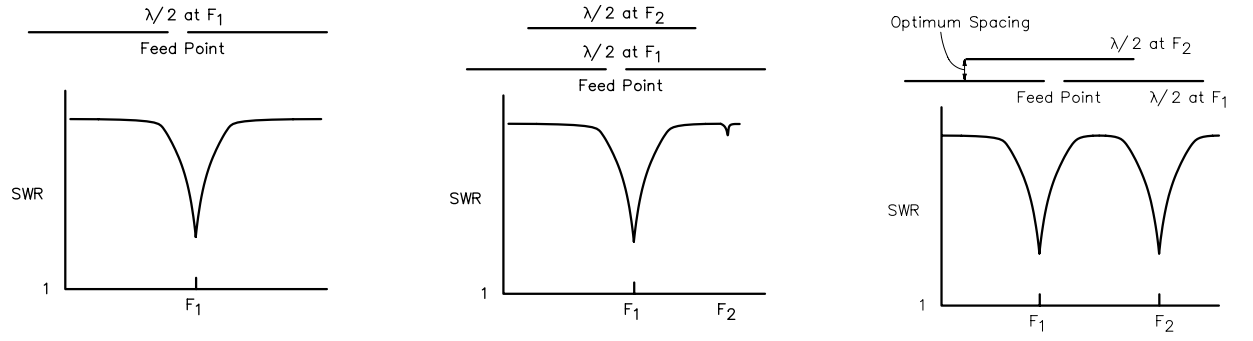

Fig 44—At A, the SWR of a dipole over a wide frequency range. At B, a nearby conductor is just close enough to interact with the dipole. At C, when the second conductor is at the optimum spacing, the combination is matched at both frequencies.

way: *Given a dipole (or vertical) at one frequency and an additional conductor resonant at another frequency, there is an optimum distance between them that results in the resonance of the additional conductor being imposed upon the original dipole, resulting in a low SWR at both resonant frequencies.*

Some History

In the late 1940s, the *coaxial sleeve* antenna was developed (**Fig 45A**), covering two frequencies by surrounding a dipole or monopole with a cylindrical tube resonant at the higher of the desired frequencies. In the 1950s, Gonset briefly marketed a two-band antenna based on this design. Other experimenters soon determined that two conductors at the second frequency, placed on either side of the main dipole or monopole, would make a skeleton representation of a cylinder (Fig 45B). This is called the *open-sleeve* antenna. The Hy-Gain Explorer tribander uses this method in its driven element to obtain resonance in the 10-meter band. Later on, a few antenna developers finally figured out that these extra conductors did not need to be added in pairs, and that a single conductor at each frequency could add the extra resonances (Fig 45C). This is the method used by Force 12 in some of their multiband antennas.

This is a perfect example of how science works. A specific idea is discovered, with later developments leading to an underlying general principle. The original coaxial-sleeve configuration is the most specific, being limited to two frequencies and requiring a particular construction method. The open-sleeve antenna is an intermediate step, showing that the sleeve idea is not limited to one configuration.

Finally, we have the coupled-resonator concept, which is the general principle, applicable in many different antenna configurations, for many different frequency combinations. Severns' antenna uses it with a folded dipole, and Wilson uses it with a main vertical that is off-center fed. The author K9AY used it with conventional dipoles and quarter-wave verticals. Other designers have used the principle more subtly, like putting the first director in a Yagi very close to the driven element, broadening the SWR bandwidth the same way Severns' design does with a dipole.

In the past, most antennas built with this single-conductor technique have also been called *open-sleeve* (or *multiple-open-sleeve*) antennas, a term taken from the history of their development. However, the term *sleeve* implies that one conductor must surround another. This is not really a physical or electrical description of the antenna's operation, therefore, K9AY suggests using the term *coupled-resonator,* which is the most accurate description of the general principle.

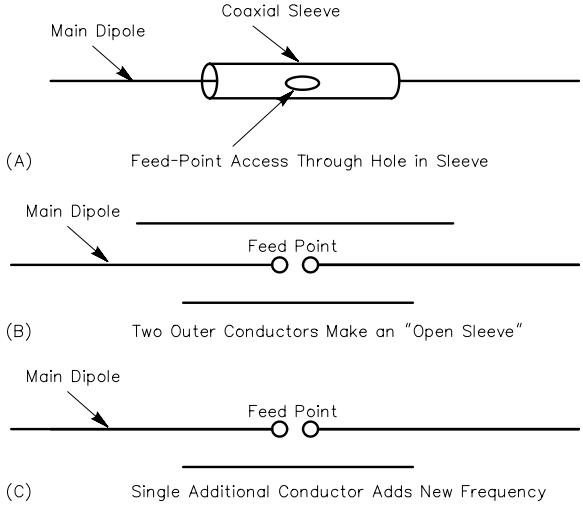

Fig 45—Evolution of coupled-resonator antennas: At A, the *coaxial-sleeve* dipole; at B, the *open-sleeve* dipole; and at C, a *coupled-resonator* dipole, the most universal configuration.

A Little Math

The interaction that makes the C-R principle work is not random. It behaves in a predictable, regular manner. K9AY

derived an equation that shows the relationship between the driven element and the additional resonators for ordinary dipoles and verticals:

$$\frac{\log_{10} d}{\log_{10}(D/4)} = 0.54 \qquad \text{(Eq 4)}$$

where

d = distance between conductors, measured in wavelengths at the frequency of the chosen additional resonator

D = the diameter of the conductors, also in wavelengths at the frequency of the additional resonator.

Eq 4 assumes they are both the same diameter and that the feed point impedance at both frequencies is the same as a dipole in free space (72 Ω) or a quarter-wave monopole over perfect ground (36 Ω).

The equation only describes the impedance due to the additional resonator. The main dipole element is always part of the antenna, and it may have a fairly low impedance at the additional frequency. This is the case when the frequencies are close together, or when the main element is operating at its third harmonic. At these frequencies, the spacing distance must be adjusted so that the parallel combination of dipole and resonator results in the desired feed-point impedance.

K9AY worked out two correction factors, one to cover a range of impedances and another for frequencies close together. These can be included in the basic equation, which is rearranged below to solve for the distance between the conductors:

$$d = 10^{0.54\log_{10}(D/4)} \times \frac{Z_0 + 35.5}{109} \times [1 + e^{-[((F_2/F_1)-1.1)\times 11.3)+0.1)]}] \qquad \text{(Eq 5)}$$

where

d and D are the same as above.

Z_0 = the desired feed point impedance at the frequency of the additional resonator (between 20 and 120 Ω). For a vertical, multiply the desired impedance by two to get Z_0. If you want a 50-Ω feed, use 100 Ω for Z_0.

F_1 = the resonant frequency of the main dipole or vertical.

F_2 = the resonant frequency of the additional conductor. The ratio F_2/F_1 is more than 1.1.

e = 2.7183, the base of natural logarithms.

Eq 5 does not directly allow for conductors of unequal diameters, but it can be used as a starting point if you use the diameter of the driven dipole or vertical element for D in the equation.

Characteristics of C-R Antennas

Here's the important stuff—what's different about C-R antennas, what are they good for and what are their drawbacks? The key points are:

- Multiband operation without traps, stubs or tuners

K9AY's Eq 5 above does indeed yield a good "first-cut" value for the spacing between coupled-resonator elements. **Fig A** shows the spacing, in inches, plotted against the ratio of frequencies, for two coupled resonator elements with different diameters, again expressed in inches. This is for an upper frequency of 28.4 MHz. Beyond a frequency ratio of about 1.5:1 (28.4:18.1 MHz), the spacing flattens out to a fixed distance between elements for each element diameter. For example, if $^1/_2$-inch elements are used at 28.4 and 18.1 MHz, the spacing between the elements is about 3.75 inches.

EZNEC verifies Eq 5's computations. Note that a large number of segments are necessary for each element when they are closely spaced from each other, and the segments on the elements must be closely aligned with each other. Be sure to run the Average Gain test, as well as Segmentation tests. The modeler should also be aware that if mutually coupled resonators are placed along a horizontal boom (as they would be on multiband Yagis using coupled resonators), the higher-frequency elements will act like retrograde directors, producing some gain (or lack of gain, depending on the azimuth being investigated).

For example, in the *EZNEC* file **K9AY C-R 28-21-14 MHz 1 In.EZ**, using 1-inch diameter elements spaced 6 inches apart, if the 28-MHz element is placed 6 inches behind the 14-MHz driven element (with the 21-MHz element placed 6 inches ahead), on 28 MHz the system will have a F/B of 2.6 dB, favoring the rearward direction. On 21 MHz, the system will exhibit a F/B of 1.6 dB, favoring the forward direction. Of course, there are systems where gain and F/B due to the C-R configuration may be put to good use, such as the multiband Yagis mentioned above. However, if the elements are spaced above/below the 14-MHz driven element there is no distortion of the dipole patterns.

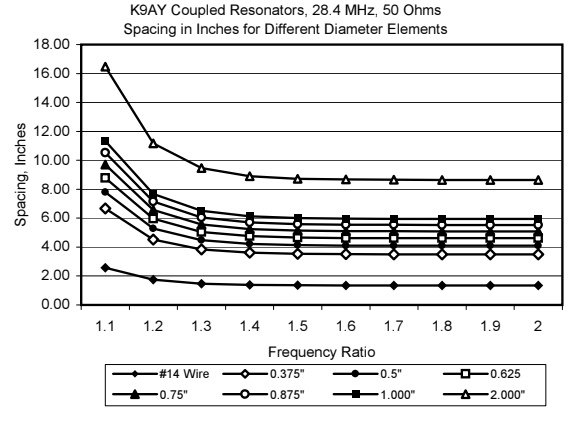

Fig A—Graph of the spacing versus frequency ratio for two Coupled-Resonator elements at 28.4 MHz, for 50-Ω feed-point impedance.

- Flexible impedance matching at each frequency
- Independent fine-tuning at each frequency (little interaction)
- Easily modeled using *MININEC* or *NEC*-based programs
- Pruning process same as a simple dipole
- Can accommodate many frequencies (seven or more)
- Virtually lossless coupling (high efficiency)
- Requires a separate wire or tubing conductor at each frequency
- Mechanical assembly requires a number of insulated supports
- Narrower bandwidth than equivalent dipole
- Capacitance requires slight lengthening of conductors

To begin with, the most obvious characteristic is that this principle can be used to add multiple resonant frequencies to an ordinary dipole or vertical, using additional conductors that are not physically connected. This gives us three variable factors: (1) the diameter of the conductor, (2) its length, and (3) its position relative to the main element.

Having the freedom to control these factors gives us the advantage of *flexibility*; we have a wide range of control over the impedance at each added frequency. Another advantage is that the behavior at each frequency is quite *independent*, once the basic design is in place. In other words, making fine-tuning adjustments at one frequency doesn't change the resonance or impedance at the other frequencies. A final advantage is *efficiency.* With conductors close together, and with a resonant target conductor, coupling is very efficient. Traps, stubs, and compensating networks found on other multiband antennas all introduce lossy reactive components.

There are two main disadvantages of C-R antennas. The first is the relative *complexity* of construction. Several conductors are needed, installed with some type of insulating spacers. Other multiband antennas have their complexities as well (such as traps that need to be mounted and tuned), but C-R antennas will usually be bulkier. The larger size generally means greater windload, which is a disadvantage to some hams.

The other significant disadvantage is *narrower bandwidth*, particularly at the highest of the operating frequencies. We can partially overcome this problem with large conductors that are naturally broad in bandwidth, and in some cases we might even use an extra conductor to put two resonances in one band. It is interesting to note that the pattern is opposite that of trapped antennas. The C-R antenna gets narrower at the highest frequencies of operation, while trap antennas generally have narrowest bandwidth at their lowest frequencies.

There are two special situations that should be noted. First, when the antenna has a resonance near the frequency where the driven dipole is 3/2 λ long (3/4 λ for a vertical), the dipole has a fairly low impedance. The spacing of the C-R element needs to be increased to raise its impedance so that the parallel combination of the main element and C-R element equals the desired impedance (usually 50 Ω). There is also significant antenna current in the part of the main dipole extending beyond the C-R section, contributing to the total radiation pattern. As a result, this particular arrangement radiates as three λ/2 sections in phase, and has about 3 dB gain and a narrower directional pattern compared to a dipole (**Fig 46**). This might be an advantage for antennas covering bands with a frequency ratio of about three, such as 3.5 and 10.1 MHz, 7 and 21 MHz, or 144 and 430 MHz.

The other special situation is when we want to add a new frequency very close to the resonant frequency of the main dipole. An antenna for 80 and 75 meters would be an example of this. Again, the driven dipole has a fairly low impedance at the new frequency. Add the fact that coupling is very strong between these similar conductors and we find that a wide spacing is required to make the antenna work. A dipole resonant at 3.5 MHz and another wire resonant at 3.8 MHz will need to be 3 or 4 feet apart, while a 3.5 MHz and 7 MHz combination might only need to be spaced 4 or 5 inches.

Another useful characteristic of C-R antennas is that they are easily and accurately modeled by computer programs based on either *MININEC* or *NEC*, as long as you stay within each program's limitations. For example, Severns points out that *MININEC* does not handle folded dipoles very well, and *NEC* modeling is required. With ease of computer modeling, a precise answer isn't needed for the design equation given above. An approximate solution will provide a starting point that can quickly be adjusted for optimum dimensions.

The added resonators have an effect on the lengths of all conductors, due to the capacitance between the conductors. Capacitance causes antennas to look electrically shorter, so

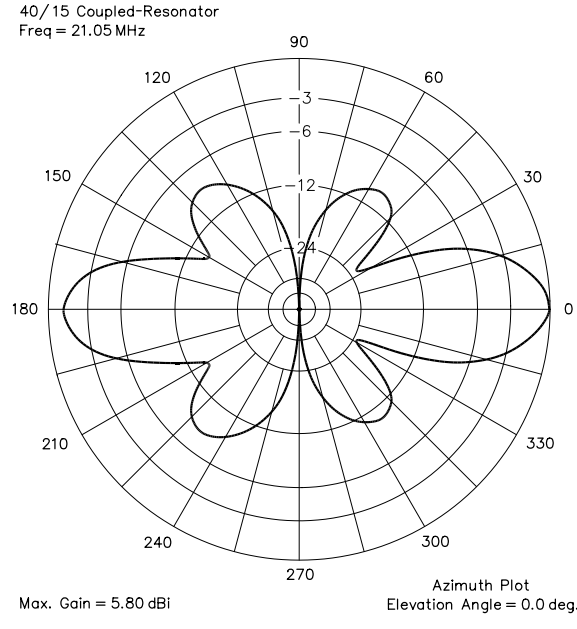

Fig 46—Radiation pattern for the special case of a C-R antenna with the additional frequency at the third harmonic of the main dipole resonant frequency.

each element needs to be about 1% or 2% longer than a simple dipole at the same frequency. As a rule of thumb, use 477/f (in feet) instead of the usual 468/f when calculating dipole length, and 239/f instead of 234/f for a λ/4 vertical.

A 30/17/12-Meter Dipole

To show how a C-R antenna is designed, let's build a dipole to cover all three WARC bands. We'll use #12 wire, which has a diameter of 0.08 inches, and the main dipole will be cut for the 10.1 MHz band. From the equation above, the spacing between the main dipole and the 18-MHz resonator should be 2.4 inches for 72 Ω, or 1.875 inches for 50 Ω. At 24.9 MHz, the spacing to the resonator for that band should be 2.0 inches for 72 Ω, or 1.62 inches for 50 Ω. Of course, this antenna will be installed over real ground, not in free space, so these spacing distances may not be exact. Plugging these numbers into your favorite antenna-modeling program will let you optimize the dimensions for installation at the height you choose.

For those of you who like to work with real antennas, not computer-generated ones, the predicted spacing is accurate enough to build an antenna with minimum trial-and-error. You should use a nice round number just larger than the calculated spacing for 50 Ω. For this antenna, K9AY decided that the right spacing for the desired height would be 2 inches for the 18 MHz resonator and 1.8 inches for the 24.9 MHz resonator. For simplicity of construction, he just used 2 inches for both, figuring that the worst he would get is a 1.2:1 SWR if the numbers were a little bit off. Like all dipoles, the impedance varies with height above ground, but the 2-inch spacing results in an excellent match on the two additional bands, at heights of more than 25 feet.

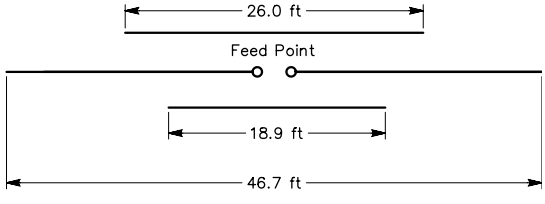

Fig 47—Dimensions of a C-R dipole for the 30, 17 and 12-meter bands.

The final dimensions of the dipole for 10.1, 18.068 and 24.89 MHz are shown in **Fig 47**. These are the final pruned lengths for a straight dipole installed at a height of about 40 feet. If you put up the antenna as an inverted V, you will need each wire to be a bit longer. Pruning this type of antenna is just like a dipole—if it's resonant too low in frequency, it's too long and the appropriate wire needs to be shortened. So, you can cut the wires just a little long to start with and easily prune them to resonance.

A final note: if you want to duplicate this antenna design, remember that the 2-inch spacing is just for #12 wire! The required spacing for a C-R antenna is related to the conductor diameter. This same antenna built with #14 wire needs under 1½-inch spacing, while a 1-inch aluminum-tubing version requires about 7-inch spacing.

Summary

The coupled-resonator principle is one more weapon in the antenna designer's arsenal. It's not the perfect method for all multiband antennas, but what the C-R principle offers is an alternative to traps and tuners, in exchange for using more wire or aluminum. Although a C-R antenna requires more complicated construction, its main attraction is in making a multiband antenna that can be built with no compromise in matching or efficiency.

HF Discone Antennas

The material in this section is adapted from an article by Daniel A. Krupp, W8NWF, in *The ARRL Antenna Compendium, Vol 5*. The name *discone* is a contraction of the words disc and cone. Although people often describe a discone by its design-center frequency (for example, a "20-meter discone"), it works very well over a wide frequency range, as much as several octaves. **Fig 48** shows a typical discone, constructed of sheet metal for UHF use. On lower frequencies, the sheet metal may be replaced with closely spaced wires and/or aluminum tubing.

The dimensions of a discone are determined by the lowest frequency of use. The antenna produces a vertically polarized signal at a low-elevation angle and it presents a good match for 50-Ω coax over its operating range. One advantage of the discone is that its maximum current area is near the top of the antenna, where it can radiate away from ground clutter. The cone-like skirt of the discone radiates the signal—radiation from the disc on top is minimal. This is because the currents flowing in the skirt wires essentially all go in the same direction, while the currents in the disc elements oppose each other and cancel out. The discone's omnidirectional characteristics make it ideal for roundtable QSOs or for a Net Control station.

Electrical operation of this antenna is very stable, with no changes due to rain or accumulated ice. It is a self-contained antenna—unlike a traditional ground-mounted vertical radiator, the discone does not rely on a ground-radial system for efficient operation. However, just like any other vertical

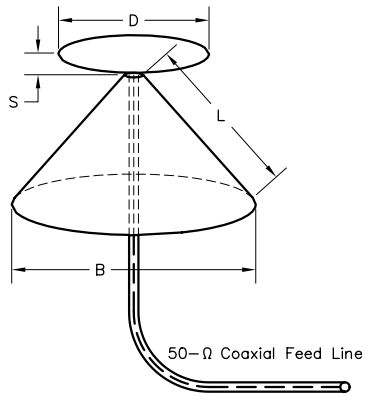

Fig 48—Diagram of VHF/UHF discone, using a sheet-metal disc and cone. It is fed directly with 50-Ω coax line. The dimensions L and D, together with the spacing S between the disc and cone, determine the frequency characteristics of the antenna. L = 246 / f_{MHz} for the lowest frequency to be used. Diameter D should be from 0.67 to 0.70 of dimension L. The diameter at the bottom of the cone B is equal to L. The space S between disc and cone can be 2 to 12 inches, with the wider spacing appropriate for larger antennas.

antenna, the quality of the ground in the Fresnel area will affect the discone's far-field pattern.

Both the disc and cone are inherently balanced for wind loading, so torque caused by the wind is minimal. The entire cone and metal mast or tower can be connected directly to ground for lightning protection.

Unlike a trap vertical or a triband beam, discone antennas are not adjusted to resonate at a particular frequency in a ham band or a group of ham bands. Instead, a discone functions as a sort of high-pass filter, efficiently radiating RF all the way from the low-frequency design cutoff to the high-frequency limits imposed by the physical design.

While VHF discones have been available out-of-the-box for many years, HF discones are rare indeed. Some articles have dealt with HF discones, where the number of disc elements and cone wires was minimized to cut costs or to simplify construction. While the minimalist approach is fine if the sought-after results really are obtained, W8NWF believes in building his discones without compromise.

History of the Discone

The July 1949 and July 1950 issues of *CQ* magazine both contained excellent articles on discones. The first article, by Joseph M. Boyer, W6UYH, said that the discone was developed and used by the military during World War II. (See Bibliography.) The exact configuration of the top disc and cone was the brainchild of Armig G. Kandonian. Boyer described three VHF models, plus information on how to build them, radiation patterns, and most importantly, a detailed description of how they work. He referred to the discone as a type of "coaxial taper transformer."

The July 1950 article was by Mack Seybold, W2RYI. He described an 11-MHz version he built on his garage roof. The mast actually fit through the roof to allow lowering the antenna for service. Seybold stated that his 11-MHz discone would load up on 2 meters but that performance was down 10 dB compared to his 100-MHz Birdcage discone. He commented that this was caused by the relatively large spacing between the disc and cone. Actually, the performance degradation he found was caused by the wave angle lifting upward at high frequencies. The cone wires were electrically long, causing them to act like long wire antennas. See **Fig 49**.

W8NWF's First Discone: the A-Frame Discone

The first discone was one designed to cover 20 through 10 meters without requiring an antenna tuner. The cone assembly uses 18-foot long wires, with a 60° included apex angle and a 12-foot diameter disc assembly. See **Fig 50** and **Fig 51**. The whole thing was assembled on the ground, with the feed coax and all guys attached. Then with the aid of some friends, it was pulled up into position.

The author used a 40-foot tall wooden "A-frame" mast, made of three 22-foot-long 2 × 4s. He primed the mast with sealer and then gave it two coats of red barn paint to make it look nice and last a long time. The disc hub was a 12-inch length of 3-inch schedule-40 PVC plumbing pipe. The PVC is very tough, slightly ductile, and easy to drill and cut. PVC is well suited for RF power at the feed point of the antenna.

Three 12-foot by 0.375-inch OD pieces of 6061 aluminum, with 0.058-inch wall thickness, were used for the 12-foot diameter top disc. These were cut in half to make the center portions of the six telescoping spreaders. Four twelve foot by 0.250-inch OD (0.035-inch wall thickness) tubes were cut into 12 pieces, each 40 inches long. This gave extension tips for each end of the six spreaders.

See **Fig 52** for details on the disc hub assembly. W8NWF started by drilling six holes straight through the PVC for the six spreaders, accurately and squarely, starting

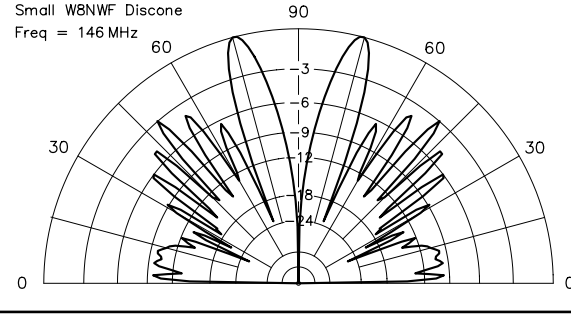

Fig49—Computed elevation plot over average ground for W8NWF's small discone at 146 MHz, ten times its design frequency range. The cone wires are acting as long-wire antennas, distorting severely the low-elevation angle response, even though the feed-point impedance is close to 50 Ω.

Fig 50—Photo of W8NWF's original A-frame mounted HF discone.

about two inches down from the top and spaced radially every 30°. Each hole is 0.375 inches below the plane of the previous one. Take great care in drilling—a poor job now will look bad from the ground up for a long time! It's a good idea to make up a paper template beforehand. Tape this to the PVC hub and then drill the holes, which should make for a close fit with the elements. If you goof, start over with a new piece of PVC—it's cheap.

Each six-foot spreader tube was secured exactly in the center to clear a 6-32 threaded brass rod that secured the elements mechanically and electrically. A two-foot long by ¼-inch OD wooden dowel was inserted into the middle of each six-foot length of tubing. The dowel added strength and also prevented crushing the element when the nuts on the threaded rod were tightened.

Insert the 40-inch long extensions four inches into each end of the six-foot spreaders. Mark and drill holes to pin the telescoping tips, plus holes big enough to clear #18 soft-drawn copper wire. This was for the inner circumferential wire for the disc. Drill a single hole for #18 wire about ¼ inch from each extension element tip, through which passes the outer circumferential wire. Finally, insert all 6-foot elements into the PVC hub and line up the holes in the center so the brass rod could be inserted through the middle to secure the elements.

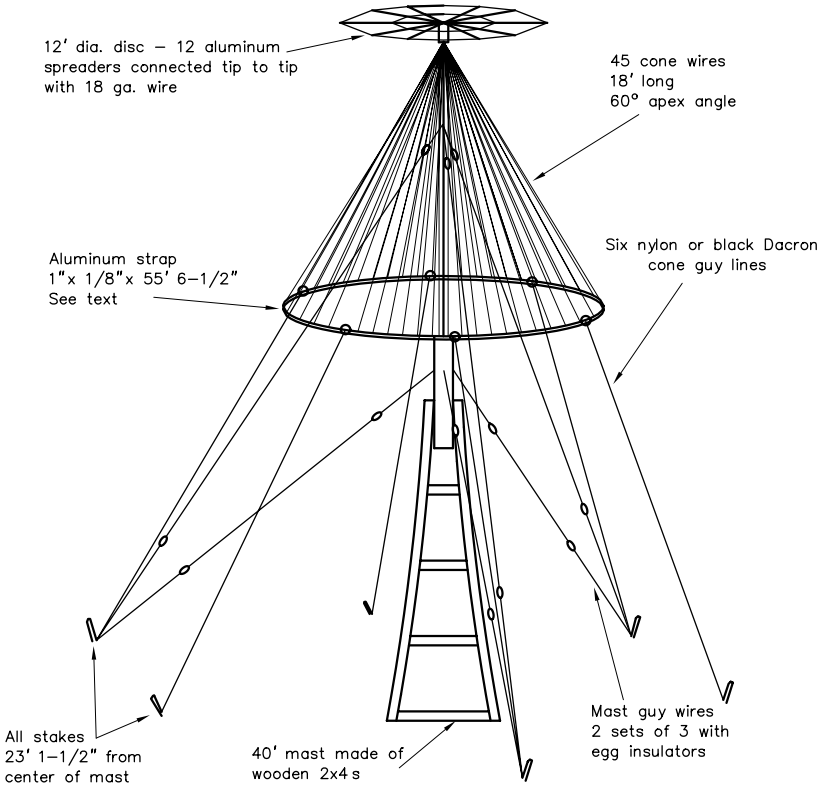

Fig 51—Detailed drawing of the A-frame discone for 14 to 30 MHz. The disc assembly at the top of the A-frame is 12 feet in diameter. There are 45 cone wires, each 18 feet long, making a 60° included angle of the cone. This antenna works very well over the design frequency range.

The next step is to "chisel to fit" the top of my wooden mast to allow the PVC to slide down on it about six or seven inches. For convenience, place the whole mast assembly in a horizontal position on top of two clothesline poles and one stepladder.

Place the disc head assembly over the top of the mast, but don't secure it yet. This allows for rotation while adding the disc spreader extensions. A tip for safety: tie white pieces of cloth to the ends of elements near eye level. Just remember to remove them before raising the antenna.

For a long-lasting installation, use an anti-corrosion compound, such as Penetrox, when assembling the aluminum antenna elements. As the extensions are added, secure them in the innermost of the two holes with a short piece of #18 wire. Then run a wire through the remaining holes looping each element as you go. This gives added support laterally to the elements. Next add a #18 wire to the tips of the extensions in the same fashion. This provides even more

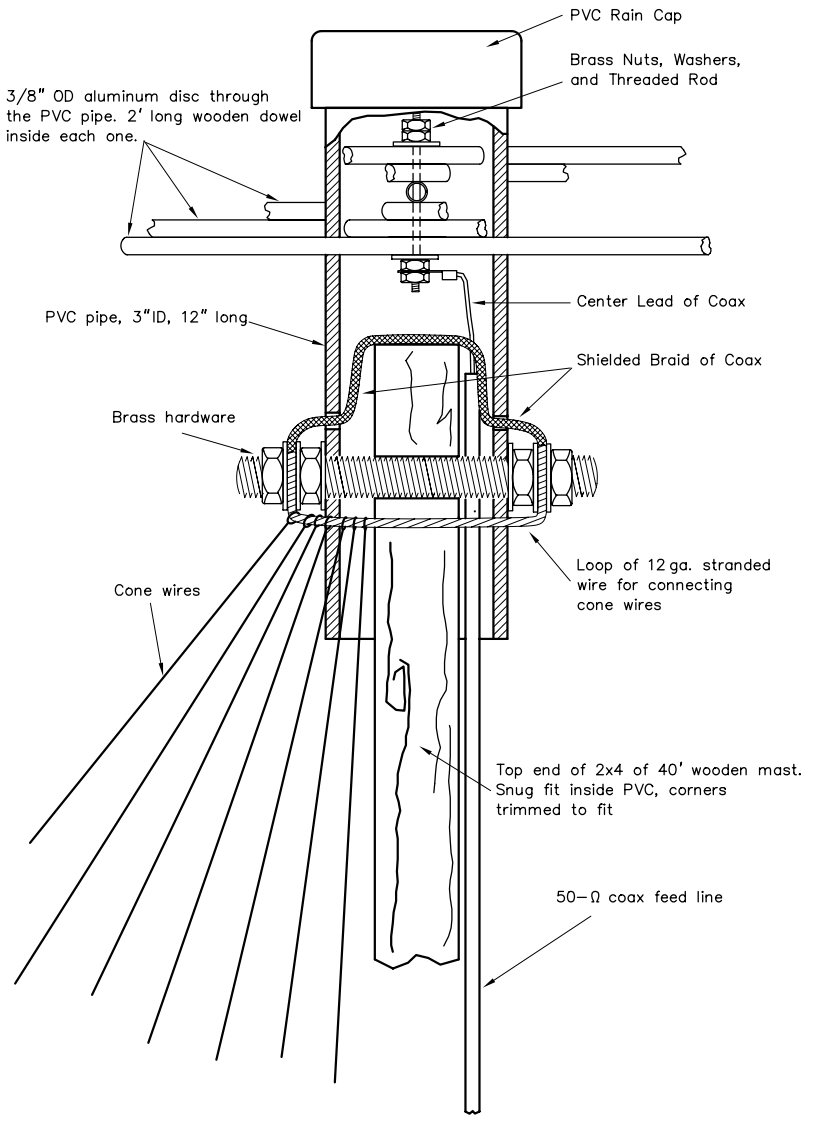

Fig 52—Details of the top hub for the A-frame discone. The three-inch PVC pipe was drilled to hold the six spreaders making up the top disc. Connections for the shield of the feed coax were made to the disc. The coax center conductor was connected to the cone-wire assembly by means of a loop of #12 stranded wire encircling the outside of the PVC hub.

physical stability as well as making electrical connections.

Next, pin the PVC disk hub to the wooden mast with a ⅜-inch threaded rod. This is also the point where the cone wires are attached, using a loop of #12 stranded copper wire around the PVC. Solder each cone wire to this loop, together with the coax shield braid. Make sure the loop of #12 wire is large enough to make soldering possible without burning the PVC with the soldering iron.

Connect the coax center conductor to the disc assembly by securing it with the same 6-32 threaded rod that ties all the disc elements together. Make sure to use coax-seal compound to keep moisture out of the coax. The coax is then fed down the mast and secured in a few places to provide strain relief and to keep it out of the way of the cone wires.

Use two sets of three guy wires. Break these up with egg insulators, just to be sure there won't be any interaction with the antenna. Use 45 wires of #18 soft-drawn copper wire for the cone, 18 feet long each. Cut them a little long so they can be soldered to the connecting loop.

A difficult task is now at hand—keeping all the cone wires from getting tangled! Solder each of the 45 cone wires to the loop of #12 wire, spacing each wire about ¼ inch from the last one for an even distribution all the way around.

The cone base is 18 feet in diameter to provide a 60° included angle. At the base of the cone, use five 12-foot long aluminum straps, 1 inche wide by ⅛ inch thick, overlapping 8¼ inches and fastened together with aluminum rivets. Drill holes along the strap every 15 inches to secure the cone wires.

Make sure to handle the aluminum strap carefully while fastening the cone wire ends; too sharp of a bend could possibly break it. Fasten six small-diameter nylon lines to the cone-base aluminum strap to stabilize the cone. These cone-guys share the same guy stakes as the mast guy lines.

After cutting the nylon lines, heat the frayed ends of each with a small flame to prevent unraveling. Apply several coats of clear protective spray to the disk head assembly, after checking that all hardware is tight. A rain cap at the top of the PVC disc hub completes construction.

Putting It All Up

You are going to need a lot of help now to raise this antenna. Have the whole process fully thought out before trying to raise it. You should have the spot selected for the base of the mast and some pipes driven into the ground to prevent the mast from slipping sideways as it is being pulled up. The three guy stakes should be in place, 23 feet, 1½ inches from mast center. Of course, the guys should have been cut to the correct length, with some extra. Be sure the coax transmission line will come off the mast where it should. A long length of rope to an upper and lower guy line is used to pull up the whole works.

The author used an old trick of standing an extension ladder vertically near the antenna base with the pull lines looped over the top rung to get a good lift angle. The weight added to the mast from the antenna disc assembly and cone wires is about 26 pounds, most of it from the cone assembly. Use two strong people to pull up the antenna slowly so that the other helpers on the guy wires and cone guy lines have time to move about as required. As the antenna rises to the vertical position, if there are no snafus, the guy lines can be secured. Then tie the six cone lines to stakes.

A Really Big Discone

When an opportunity arose to buy a 64-foot self-supporting TV tower, the author jumped at the chance to implement a full 7 to 30-MHz discone. His new tower had eight sections, each eight feet long. Counting the overlap between sections, the cone wires would come off the tower at about the 61.5-foot mark.

W8NWF took some liberties with the design of this larger discone compared to the first one, which he had done strictly "by the book." The first change was to make the cone wires 70 feet long, even though the formula said they should be 38 feet long. Further, the cone wires would not be connected together at the bottom. With the longer cone wires, he felt that 75 and 80-meter operation might be a possibility.

The second major change was to widen the apex angle out from 60° to about 78°. Modeling said this should produce a flatter SWR over the frequency spectrum and would also give a better guy system for the tower.

The topside disc assembly would be 27 feet in diameter and have 16 radial spreaders, using telescoping aluminum tubing tapering from ⅝ to ½ to ⅜ inches OD. All spreaders were made from 0.058-inch wall thickness 6063-T832 aluminum tubing, available from Texas Towers. A section of 10-inch PVC plumbing pipe would be used as the hub for construction of the disc assembly.

Construction Details for the Large Discone.

While installing the tower, the author had left the top section on the ground. This allowed him to fit the disc head assembly precisely to it. **Fig 53** shows the overall plan for the large discone. The 10-inch diameter PVC hub was designed to slip over the tower top section, but was a little too large. So a set of shims was installed on the three legs at the top of the tower for a just-right fit. Drilling the PVC pipe for the eight ⅝-inch OD elements was started about an inch down from the top. W8NWF purposely staggered the drilled holes in the same fashion as the hub for the smaller antenna. See **Fig 54**.

Again, three-foot sections of ½-inch wooden dowel were used to strengthen the ⅝-inch center portion of each spreader. Instead of using a loop of #12 wire for connecting the cone wires, as had been done on the smaller discone, he drilled 36 holes in the PVC hub. These holes are small enough so

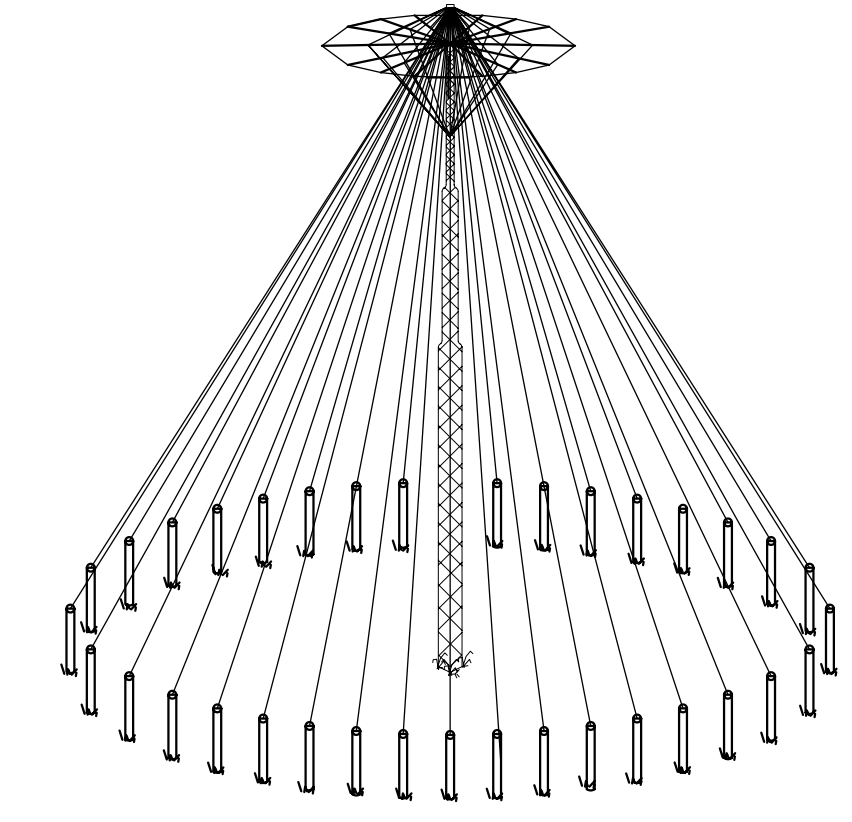

Fig 53—The large W8NWF discone, designed for operation from 7 to 14 MHz, but useable with a tuning network in the shack for 3.8 MHz.

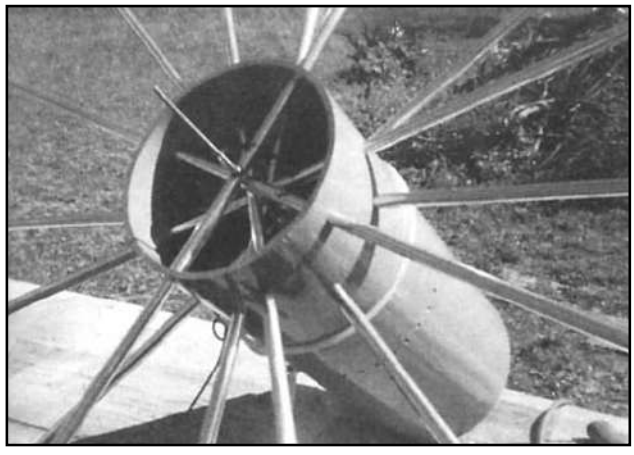

Fig 54—Photo showing details of the hub assembly for the large discone, including the threaded brass rod that connects the radial spreaders together. The 10-inch PVC pipe is drilled to accommodate the radial spreaders. Each spreader is reinforced with a three-foot long wooden dowel inside for crush resistance. Note the row of holes drilled below the lowest spreader. Each of the 36 cone wire passes through one of these holes.

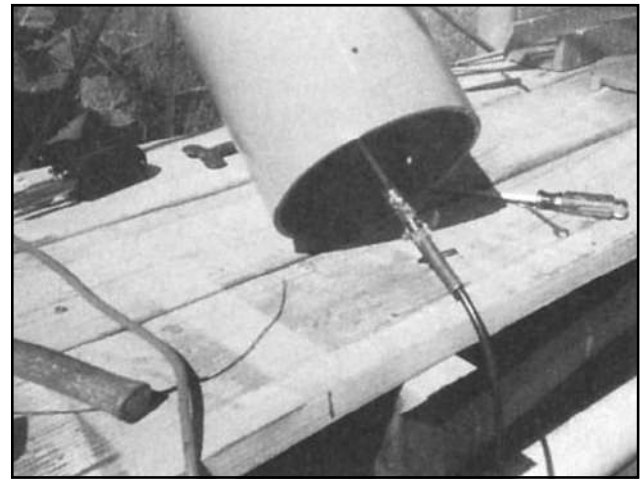

Fig 55—Details of the copper pipe slipped over the feed coax. The coax shield has been folded back over the copper pipe and secured with two stainless-steel hose clamps. The cone wires are also laid against the copper pipe and secured with additional hose clamps.

that the PVC hub would not be weakened appreciably. He drilled the circles of holes for the cone wires about 6 inches below the disc spreaders.

He prepared a three-foot long piece of RG-213 coax, permanently fastened on one end to the antenna, with a female type-N connector at the other end. Type-N fittings were used because of their superior waterproofing abilities. The coax center lead was connected with a terminal lug under a nut on the brass threaded rod securing the disc spreaders. The coax shield braid was folded back over a six-inch long copper pipe and clamped to it with a stainless-steel hose clamp. See **Fig 55** for details.

The plan was that after the top disc assembly had been hoisted up and attached at the top of the tower, individual cone wires would be fed, one at a time, through the small holes drilled in the PVC. They were to be laid against the copper pipe and secured with stainless-steel hose clamps.

The ½ and ⅜-inch OD spreader extension tips were secured in place with two aluminum pop-rivets at each joint. Again, the author used anti-oxidant compound on all spreader junctions. He drilled a hole horizontally near the tip of each ⅜-inch tip all around the perimeter to allow a #8 aluminum wire to circle the entire disc. A small stainless-steel sheet-metal screw was threaded into the end of each element to secure the wire.

In parallel with the aluminum wire, a length of small-diameter black Dacron line was run, securing it in a couple of places between each set of spreaders with UV-resistant plastic tie-wraps. The reason for doing this was to hold the aluminum wire in position and to prevent it from dangling, in case it should break some years in the future. Two coats of clear protective spray were applied for protection.

A truss system helps prevent the disc from sagging due to its own weight. See **Fig 56** for details. This shows the completed disk assembly mounted on the

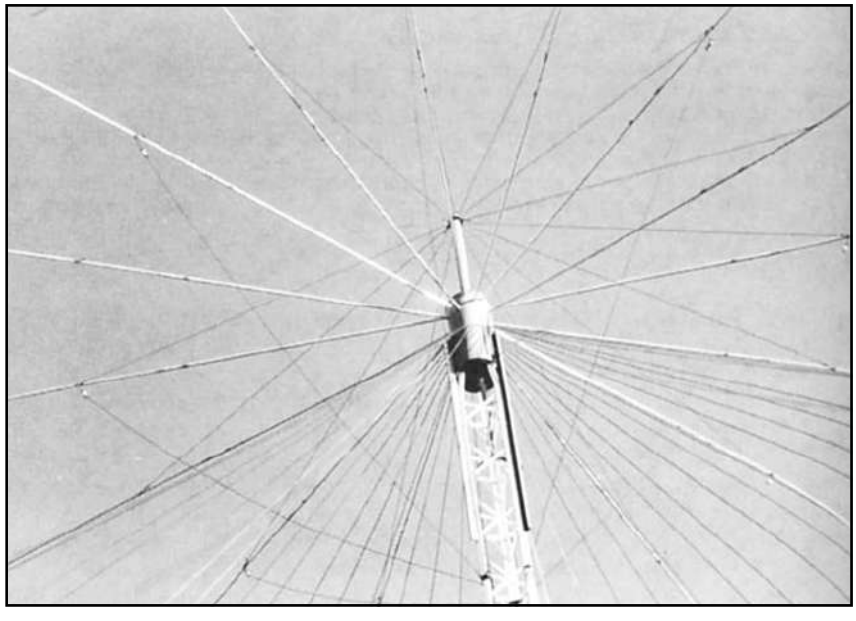

Fig 56—Photo of the spreader hub assembly, showing the truss ropes above and below the radial spreaders. This is a very rugged assembly!

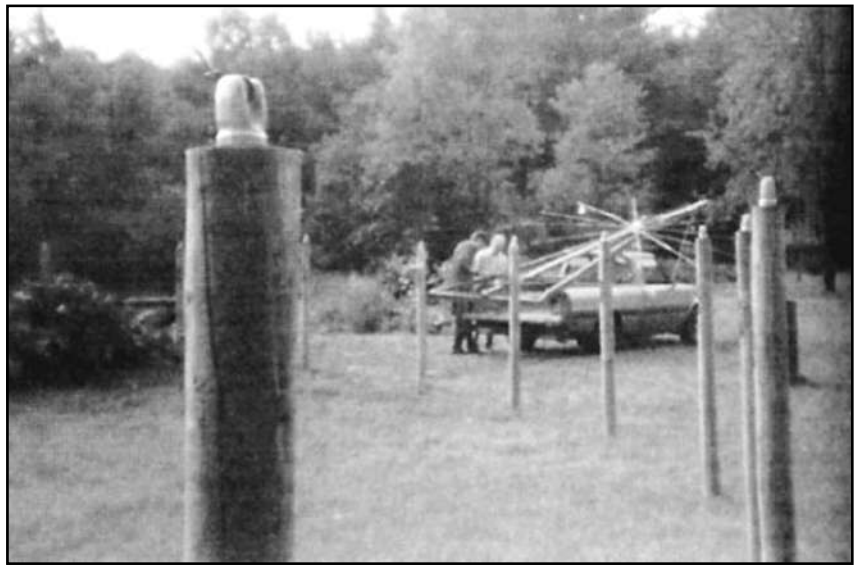

Fig 57—Photo showing some of the fence posts used to hold individual cone wires to keep them off the ground and out of harm's way. The truck in the background is carting away the A-frame discone for installation at KA8UNO's QTH.

top of the tower. A 3-foot length of 2-inch PVC pipe was used for a truss mast above the disc assembly, notching the bottom of the pipe so that it would form a saddle over the top couple of spreaders. This gave a good foothold. He cut a circle of thin sheet aluminum to fit over the 10-inch PVC to serve as a rain cap. The cap has a hole in the center for the two-inch PVC truss mast to pass through, thereby holding it down tight. The author sprayed a few light coats of paint over the PVC for protection from ultraviolet radiation from the sun.

Sixteen small-diameter black Dacron ropes were connected at the top of the truss support mast, with the other ends fastened to the disc spreaders, halfway out. Another rain cap was added to the top of the two-inch PVC truss mast. Eight lengths of the same small diameter Dacron rope were added halfway out the length of every other spreader. These ropes are meant to be tied back to the tower, to prevent updrafts from blowing the disc assembly upwards. Small egg insulators were used near the spot where the eight bottom trusses were tied to the disc spreaders, just to be sure there would be no RF leakage in rainy weather.

Hoisting the completed disc assembly to the top of the tower can be done easily, with the assistance of at least two others. The trickiest part is to get the disc assembly from its position sitting flat on the ground to the vertical position needed for hoisting it up the tower without damaging it. The disc assembly weighs about 35 pounds. Someone at the top of the tower will receive the disc as it is hoisted up by gin pole, and can mount it on the tower top.

You should prepare three 6-foot long metal braces going over the outside of the PVC to fasten to the tower legs. They really beef things up.

In plastic irrigation pipe buried between the house and tower base, the author ran 100 feet of 9086 low-loss coax to the shack. For cone wires, he was able to obtain some #18 copperclad steel wire, with heavy black insulation that looked a lot like neoprene. The cone system takes a lot of wire: 36 × 70 feet = 2520 feet, plus some extra at each end for termination. You'd be well advised to look around at hamfests to save money.

As each cone wire was connected at the top of the tower, a helper should place the other end at its proper spot below. The lower end of each cone wire is secured to an insulator screwed into a fencepost. See **Fig 57**. There are 36 treated-pine fenceposts, each standing about 5½ feet tall, 45 feet from the tower base to hold the lower end of the cone wires. This makes mowing the grass easier and the cone wires are less likely to be tripped over too.

On the final trip down the tower, the eight Dacron downward-truss lines were tied back to the tower about 6 feet below the disc assembly. The author's tower has three ground rods driven near the base, connected with heavy copper wire to the three tower legs.

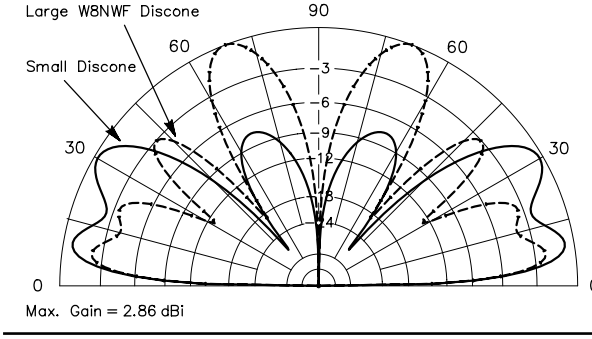

Fig 58—Computed patterns showing elevation response of small discone at 28.5 MHz compared to that of the larger discone at 28.5 MHz. The cone wires are clearly too long for efficient operation on 10 meters, producing unwanted high-angle lobes that rob power from the desirable low-elevation angles.

Performance Tests

On the air tests proved to be very satisfying. Loading up on 40 meters was easy—the SWR was 1:1 across the entire band. W8NWF can work all directions very well and receives excellent signal reports from DX stations. When he switches to his long (333 foot) center-fed dipole for comparison, he finds the dipole is much noisier and that received signals are weaker. During the daytime, nearby stations (less than about 300 to 500 miles) can be louder with the dipole, but the discone can work them just fine also.

The author happily reports that this antenna even works well on 75 meters. As you might expect, it doesn't present a 1:1 match. However, the SWR is between 3.5:1 and 5.5:1 across the band. W8NWF uses an antenna tuner to operate the discone on 75. It seems to get out as well on 75 as it does on 40 meters.

The SWR on 30 meters is about 1.1:1. On 20 meters the SWR runs from 1.05:1 at 14.0 MHz to 1.4:1 at 14.3 MHz. The SWR on the 17, 15, 12 and 10-meter bands varies, going up to a high of 3.5:1 on 12 meters.

Radiation Patterns for the Discones

From modeling using *NEC/Wires* by K6STI, W8NWF verified that the low-angle performance for the bigger antenna is worse than that for the smaller discone on the upper frequencies. See **Fig 58** for an elevation-pattern comparison on 10 meters for both antennas, with average ground constants. The azimuth patterns are simply circles. Radiation patterns produced by antenna modeling programs are very helpful to determine what to expect from an antenna.

The smaller discone, which was built by the book, displays good, low-angle lobes on 20 through 10 meters. The frequency range of 14 through 28 MHz is an octave's worth of coverage. It met his expectations in every way by covering this frequency span with low SWR and a low angle of radiation.

The bigger discone, with a modified cone suitable for use on 75 meters, presents a little different story. The low-angle lobe on 40 meters works well, and 75-meter performance also is good, although an antenna tuner is necessary on this band. The 30-meter band has a good low-angle lobe but secondary high-angle lobes are starting to hurt performance. Note that 30 meters is roughly three times the design frequency of the cone. On 20 and 17 meters there still are good low-angle lobes but more and more power is wasted in high-angle lobes.

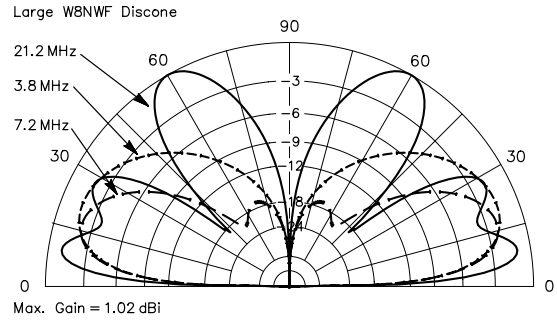

Fig 59—Computed elevation-response patterns for the larger W8NWF discone for 3.8, 7.2 and 21.2 MHz operation. Again, as in Fig 58, the pattern degrades at 21.2 MHz, although it is still reasonably efficient, if not optimal.

The operation on 15, 12, and 10 meters continues to worsen for the larger discone. The message here is that although a discone may have a decent SWR as high as 10 times the design frequency, its radiation pattern is not necessarily good for low-angle communications. See **Fig 59** for a comparison of elevation patterns for 3.8, 7.2 and 21.2 MHz on the larger discone.

A discone antenna built according to formula will work predictably and without any adjustments. One can modify the antenna's cone length and apex angle without fear of rendering it useless. The broadband feature of the discone makes it attractive to use on the HF bands. The low angle of radiation makes DX a real possibility, and the discone is also much less noisy on receive than a dipole.

Probably the biggest drawback to an HF discone is its bulky size. There is no disguising this antenna! However, if you live in the countryside you should be able to put up a nice one.

Harmonic Radiation from Multiband Antennas

Since a multiband antenna is intentionally designed for operation on a number of different frequencies, any harmonics or spurious frequencies that happen to coincide with one of the antenna resonant frequencies will be radiated with very little, if any, attenuation. Particular care should be exercised, therefore, to prevent such harmonics from reaching the antenna.

Multiband antennas using tuned feeders have a certain inherent amount of built-in protection against such radiation, since it is nearly always necessary to use a tuned coupling circuit (antenna tuner) between the transmitter and the feeder. This adds considerable selectivity to the system and helps to discriminate against frequencies other than the desired one.

Multiple dipoles and trap antennas do not have this feature, since the objective in design is to make the antenna show as nearly as possible the same resistive impedance in all the amateur bands the antenna is intended to cover. It is advisable to conduct tests with other amateur stations to determine whether harmonics of the transmitting frequency can be heard at a distance of, say, a mile or so. If they can, more selectivity should be added to the system since a harmonic that is heard locally, even if weak, may be quite strong at a distance because of propagation conditions.

BIBLIOGRAPHY

Source material and more extended discussion of topics covered in this chapter can be found in the references given below and in the textbooks listed at the end of Chapter 2, Antenna Fundamentals.

H. B. Barkley, *The Open-Sleeve As A Broadband Antenna*, Technical Report No. 14, U.S. Naval Postgraduate School, Monterey, CA, Jun 1955.

W. M. Bell, "A Trap Collinear Antenna," *QST*, Aug 1963, pp 30-31.

J. S. Belrose, "The HF Discone Antenna," *QST*, Jul 1975, pp 11-14, 56.

J. Belrose and P. Bouliane, "The Off-Center-Fed Dipole Revisited: A Broadband, Multiband Antenna," *QST*, Oct 1990, p 40.

H. J. Berg, "Multiband Operation with Paralleled Dipoles," *QST*, Jul 1956.

E. L. Bock, J. A. Nelson and A. Dorne, "Sleeve Antennas," *Very High Frequency Techniques*, H. J. Reich, ed. (New York: McGraw-Hill, 1947), Chap 5.

J. T. Bolljahn and J. V. N. Granger, "Omnidirectional VHF and UHF Antennas," *Antenna Engineering Handbook* , H. Jasik, ed. (New York: McGraw-Hill, 1961) pp 27-32 through 27-34.

J. M. Boyer, W6UYH, "Discone--40 to 500 Mc Skywire," *CQ*, July 1949, p 11.

G. A. Breed, K9AY, "Multi-Frequency Antenna Technique Uses Closely-Coupled Resonators," *RF Design*, November 1994. US Patent 5,489,914, "Method of Constructing Multiple-Frequency Dipole or Monopole Antenna Elements Using Closely-Coupled Resonators," Gary A. Breed, Feb 6, 1996.

G. H. Brown, "The Phase and Magnitude of Earth Currents Near Radio Transmitting Antennas," *Proc. IRE*, Feb 1935.

G. H. Brown, R. F. Lewis and J. Epstein, "Ground Systems as a Factor in Antenna Efficiency," *Proc. IRE* , Jun 1937, pp 753-787.

C. L. Buchanan, "The Multimatch Antenna System," *QST*, Mar 1955.

R. A. Cox, "The Open-Sleeve Antenna," *CQ*, Aug 1983, pp 13-19.

D. DeMaw, "Lightweight Trap Antennas—Some Thoughts," *QST*, Jun 1983, p 15.

W. C. Gann, "A Center-Fed 'Zepp' for 80 and 40," *QST*, May 1966.

D. Geiser, "An Inexpensive Multiband VHF Antenna," *QST*, Dec 1978, pp 28-29.

A. Greenberg, "Simple Trap Construction for the Multiband Antenna," *QST*, Oct 1956.

G. L. Hall, "Trap Antennas," Technical Correspondence, *QST*, Nov 1981, pp 49-50.

W. Hayward, "Designing Trap Antennas," Technical Correspondence, *QST*, Aug 1976, p 38.

R. H. Johns, "Dual-Frequency Antenna Traps," *QST*, Nov 1983, p 27.

A. G. Kandoian, "Three New Antenna Types and Their Applications," *Proc IEE*, Vol 34, Feb 1946, pp 70W-75W.

R. W. P. King, *Theory of Linear Antennas* (Cambridge, MA: Harvard Univ Press, 1956), pp 407-427.

W. J. Lattin, "Multiband Antennas Using Decoupling Stubs," *QST*, Dec 1960.

W. J. Lattin, "Antenna Traps of Spiral Delay Line," *QST*, Nov 1972, pp 13-15.

M. A. Logan, "Coaxial-Cable Traps," Technical Correspondence, *QST*, Aug 1985, p 43.

J. R. Mathison, "Inexpensive Traps for Wire Antennas," *QST*, Aug 1977, p 18.

L. McCoy, "An Easy-to-Make Coax-Fed Multiband Trap Dipole," *QST*, Dec 1964.

M. Mims, "The Mims Signal Squirter," *QST*, Dec 1939, p 12.

G. E. O'Neil, "Trapping the Mysteries of Trapped Antennas," *Ham Radio*, Oct 1981, pp 10-16.

B. Orr, W6SAI, "Radio FUNdamentals," The Open-Sleeve Dipole, *CQ*, February 1995.

E. W. Pappenfus, "The Conical Monopole Antenna," *QST*, Nov 1966, pp 21-24.

L. Richard, "Parallel Dipoles of 300-Ohm Ribbon," *QST*, Mar 1957.

R. Severns, N6LF, "A Wideband 80-Meter Dipole," *QST*, July 1995.

R. R. Shellenback, "Try the 'TJ'," *QST*, Jun 1982, p 18.

R. R. Shellenback, "The JF Array," *QST*, Nov 1982, p 26.

H. Scholle and R. Steins, "Eine Doppel-Windom Antenna fur Acht Bander," *cq-DL*, Sep 1983, p 427. (In English: *QST*, Aug 1990, pp 33-34.)

T. H. Schiller, N6BT, President, Force 12, US Patent 5,995,061, "No loss, multi-band, adaptable antenna," Nov 30, 1999.

M. Seybold, W2RYI, "The Low-Frequency Discone," *CQ*, July 1950, p 13.

D. P. Shafer, "Four-Band Dipole with Traps," *QST*, Oct 1958.

R. C. Sommer, "Optimizing Coaxial-Cable Traps," *QST*, Dec 1984, p 37.

L. Varney, "The G5RV Multiband Antenna . . . Up-to-Date," *The ARRL Antenna Compendium, Vol 1* (Newington: ARRL, 1985), pp 86.

R. Wilson, AL7KK, "The Offset Multiband Trapless Antenna (OMTA)," *QST*, October 1995.

L. G. Windom, "Notes on Ethereal Antennas," *QST*, Sep 1929, pp 19-22, 84.

W. I. Orr, W6SAI, editor, "The Low-Frequency Discone," *RADIO Handbook*, 14th Edition, (Editors and Engineers, 1956), p 369.

Chapter 8

Multielement Arrays

The gain and directivity offered by an array of elements represents a worthwhile improvement both in transmitting and receiving. *Power gain* in an antenna is the same as an equivalent increase in the transmitter power. But unlike increasing the power of your own transmitter, antenna gain works equally well on signals received from the favored direction. In addition, the directivity reduces the strength of signals coming from the directions not favored, and so helps discriminate against interference.

One common method of obtaining gain and directivity is to combine the radiation from a group of $\lambda/2$ dipoles to concentrate it in a desired direction. A few words of explanation may help make it clear how power gain is obtained.

In **Fig 1**, imagine that the four circles, A, B, C and D, represent four dipoles so far separated from each other that the coupling between them is negligible. Also imagine that point P is so far away from the dipoles that the distance from P to each one is exactly the same (obviously P would have to be much farther away than it is shown in this drawing). Under these conditions the fields from all the dipoles will add up at P if all four are fed RF currents in the same phase.

Let us say that a certain current, I, in dipole A will produce a certain value of field strength, E, at the distant point P. The same current in any of the other dipoles will produce the same field at P. Thus, if only dipoles A and B are operating, each with a current I, the field at P will be 2E. With A, B and C operating, the field will be 3E, and with all four operating with the same I, the field will be 4E. Since the power received at P is proportional to the square of the field strength, the relative power received at P is 1, 4, 9 or 16, depending on whether one, two, three or four dipoles are operating.

Now, since all four dipoles are alike and there is no coupling between them, the same power must be put into each in order to cause the current I to flow. For two dipoles the relative power input is 2, for three dipoles it is 3, for four dipoles 4, and so on. The actual gain in each case is the relative received (or output) power divided by the relative input power. Thus we have the results shown in **Table 1**. The power ratio is directly proportional to the number of elements used.

It is well to have clearly in mind the conditions under which this relationship is true:

1) The fields from the separate antenna elements must be in-phase at the receiving point.

2) The elements are identical, with equal currents in all elements.

3) The elements must be separated in such a way that the current induced in one by another is negligible; that is, the radiation resistance of each element must be the same as it would be if the other elements were not there.

Very few antenna arrays meet all these conditions exactly. However, the power gain of a directive array using dipole elements with optimum values of element spacing is approximately proportional to the number of elements.

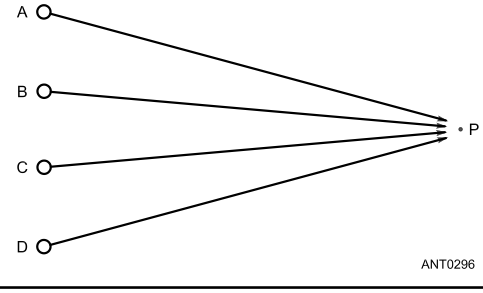

Fig 1—Fields from separate antennas combine at a distant point, P, to produce a field strength that exceeds the field produced by the same power in a single antenna.

Table 1
Comparison of Dipoles with Negligible Coupling (See Fig 1)

Dipoles	*Relative Output Power*	*Relative Input Power*	*Power Gain*	*Gain in dB*
A only	1	1	1	0
A and B	4	2	2	3
A, B and C	9	3	3	4.8
A, B, C and D	16	4	4	6

Another way to say this is that a gain of approximately 3 dB will be obtained each time the number of elements is doubled, assuming the proper element spacing is maintained. It is possible, though, for an estimate based on this rule to be in error by a ratio factor of two or more (gain error of 3 dB or more), especially if mutual coupling is *not* negligible.

DEFINITIONS

An *element* in a multi-element directive array is usually a λ/2 radiator or a λ/4 vertical element above ground. The length is not always an exact electrical half or quarter wavelength, because in some types of arrays it is desirable that the element show either inductive or capacitive reactance. However, the departure in length from resonance is ordinarily small (not more than 5% in the usual case) and so has no appreciable effect on the radiating properties of the element.

Antenna elements in multi-element arrays of the type considered in this chapter are always either *parallel*, as in **Fig 2A** , or *collinear* (end-to-end), as in Fig 2B. Fig 2C shows an array combining both parallel and collinear elements. The elements can be either horizontal or vertical, depending on whether horizontal or vertical polarization is desired. Except for space communications, there is seldom any reason for mixing polarization, so arrays are customarily constructed with all elements similarly polarized.

A *driven element* is one supplied power from the transmitter, usually through a transmission line. A *parasitic element* is one that obtains power solely through coupling to another element in the array because of its proximity to such an element.

A *driven array* is one in which all the elements are driven elements. A *parasitic array* is one in which one or more of the elements are parasitic elements. At least one element must be a driven element, since you must somehow introduce power into the array.

A *broadside array* is one in which the principal direction of radiation is perpendicular to the axis of the array and to the plane containing the elements, as shown in **Fig 3**. The elements of a broadside array may be collinear, as in Fig 3A, or parallel (two views in Fig 3B).

An *end-fire array* is one in which the principal direction of radiation coincides with the direction of the array axis. This definition is illustrated in **Fig 4**. An end-fire array must consist of parallel elements. They cannot be collinear, as λ/2 elements do not radiate straight off their ends. A Yagi is a familiar form of an end-fire array.

A *bidirectional array* is one that radiates equally well in either direction along the line of maximum radiation. A bidirectional pattern is shown in **Fig 5A**. A *unidirectional array* is one that has only one principal direction of radiation, as the pattern in Fig 5B shows.

The *major lobes* of the directive pattern are those in which the radiation is maximum. Lobes of lesser radiation intensity are called *minor lobes*. The *beamwidth* of a directive antenna is the width, in degrees, of the major lobe between the two directions at which the relative radiated power is equal to one half its value at the peak of the lobe. At these *half-power points* the field intensity is equal to 0.707 times its maximum value, or in other words, is down 3 dB from the maximum. **Fig 6** shows a lobe having a beamwidth of 30°.

Unless specified otherwise, the term *gain* as used in this

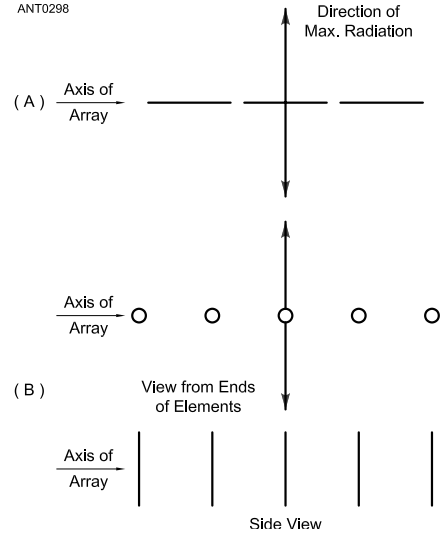

Fig 3—Representative broadside arrays. At A, collinear elements, with parallel elements at B.

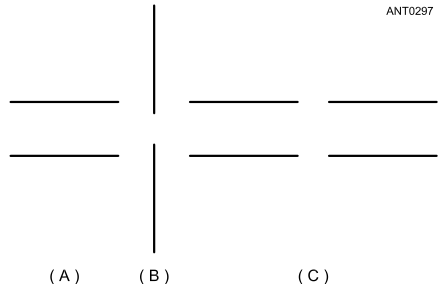

Fig 2—At A, parallel and at B, collinear antenna elements. The array shown at C combines both parallel and collinear elements.

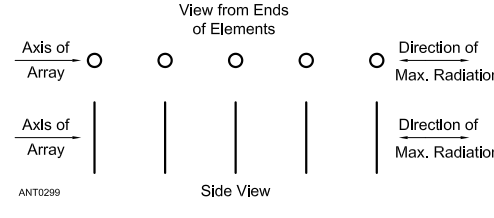

Fig 4—An end-fire array. Practical arrays may combine both broadside directivity (Fig 3) and end-fire directivity, including both parallel and collinear elements.

section is the power gain over an isotropic radiator in free space. The gain can also be compared with a λ/2 dipole of the same orientation and height as the array under discussion and having the same power input. Gain may either be measured experimentally or determined by calculation. Experimental measurement is difficult and often subject to considerable error, for two reasons. First, errors normally occur in measurement because the accuracy of simple RF measuring equipment is relatively poor—even high-quality instruments suffer in accuracy compared with their low-frequency and dc counterparts. And second, the accuracy depends considerably on conditions—the antenna site, including height, terrain characteristics, and surroundings—under which the measurements are made.

Calculations are frequently based on the measured or theoretical directive patterns of the antenna (see Chapter 2). The theoretical gain of an array may be determined approximately from:

$$G = 10 \log \frac{41{,}253}{\theta_H \, \theta_V} \qquad \text{(Eq 1)}$$

where

G = decibel gain over a dipole in its favored direction
θ_H = horizontal half-power beamwidth in degrees
θ_V = vertical half-power beamwidth in degrees.

This equation, strictly speaking, applies only to lossless antennas having approximately equal and narrow E- and H-plane beam widths—up to about 20°—and no large minor lobes. The E and H planes are discussed in Chapter 2. The error may be considerable when the formula is applied to simple directive antennas having relatively large beam widths. The error is in the direction of making the calculated gain larger than the actual gain.

Front-to-back ratio (F/B) is the ratio of the power radiated in the favored direction to the power radiated in the opposite direction. See Chapter 11 for a discussion of front-to-back ratio, and its close cousin, *worst-case front-to-rear ratio*.

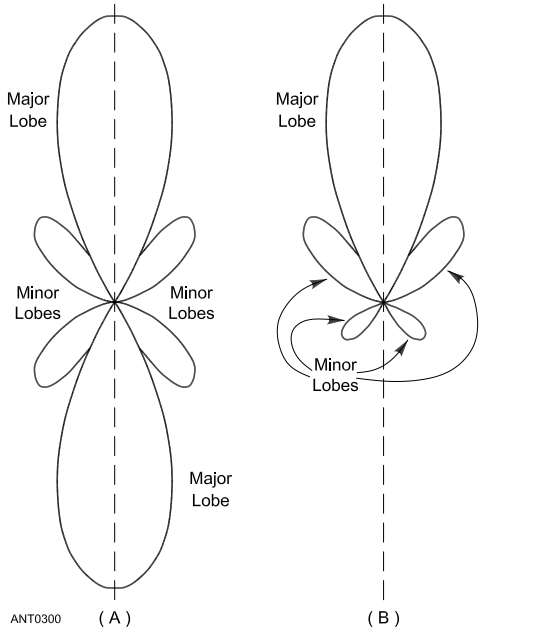

Fig 5—At A, typical bidirectional pattern and at B, unidirectional directive pattern. These drawings also illustrate the application of the terms *major* and *minor* to the pattern lobes.

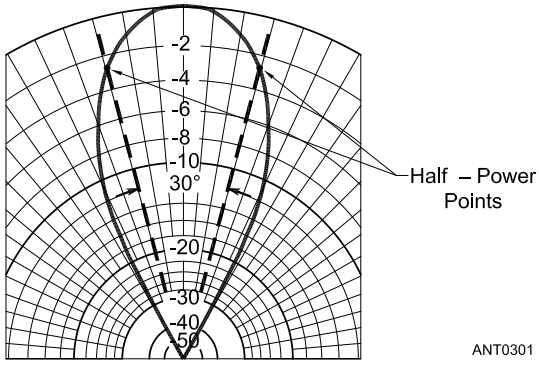

Fig 6—The width of a beam is the angular distance between the directions at which the received or transmitted power is half the maximum power (–3 dB). Each angular division of the pattern grid is 5°.

Phase

The term *phase* has the same meaning when used in connection with the currents flowing in antenna elements as it does in ordinary circuit work. For example, two currents are in-phase when they reach their maximum values, flowing in the same direction, at the same instant. The direction of current flow depends on the way in which power is applied to the element.

This is illustrated in **Fig 7**. Assume that by some means an identical voltage is applied to each of the elements at the ends marked A. Assume also that the coupling between the elements is negligible, and that the instantaneous polarity of the voltage is such that the current is flowing away from the point at which the voltage is applied. The arrows show the assumed current directions. Then the currents in elements 1 and 2 are in-phase, since they are flowing in the same direction in space and are caused by the same voltage. However, the current in element 3 is flowing in the *opposite* direction in space because the voltage is applied to the opposite end of the element. The current in element 3 is therefore 180° out-of-phase with the currents in elements 1 and 2.

The phasing of driven elements depends on the direction of the element, the phase of the applied voltage, and the point at which the voltage is applied. In many systems used by amateurs, the voltages applied to the elements are exactly

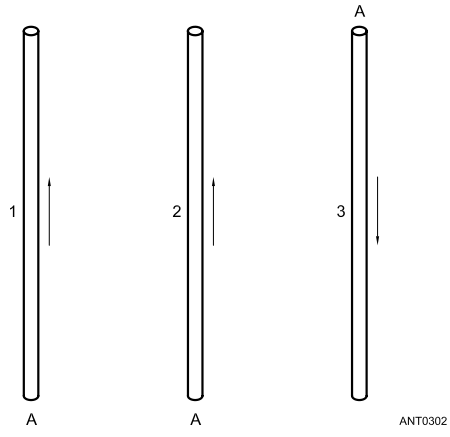

Fig 7—This drawing illustrates the phase of currents in antenna elements, represented by the arrows. The currents in elements 1 and 2 are in phase, while that in element 3 is 180° out of phase with 1 and 2.

in or exactly out-of-phase with each other. Also, the axes of the elements are nearly always in the same direction, since parallel or collinear elements are invariably used. The currents in driven elements in such systems therefore are usually either exactly in or exactly out-of-phase with the currents in other elements.

It is possible to use phase differences of less than 180° in driven arrays. One important case is where the current in one set of elements differs by 90° from the current in another set. However, making provision for proper phasing in such systems is considerably more complex than in the case of simple 0° or 180° phasing, as described in a later section of this chapter.

In parasitic arrays the phase of the currents in the parasitic elements depends on the spacing and tuning, as described later.

Ground Effects

The effect of the ground is the same with a directive antenna as it is with a simple dipole antenna. The reflection factors discussed in Chapter 3 may therefore be applied to the vertical pattern of an array, subject to the same modifications mentioned in that chapter. In cases where the array elements are not all at the same height, the reflection factor for the mean height of the array may be used for a close approximation. The mean height is the average of the heights measured from the ground to the centers of the lowest and highest elements.

MUTUAL IMPEDANCE

Consider two λ/2 elements that are fairly close to each other. Assume that power is applied to only one element, causing current to flow. This creates an electromagnetic field, which induces a voltage in the second element and causes current to flow in it as well. The current flowing in element 2 will in turn induce a voltage in element 1, causing additional current to flow there. The total current in 1 is then the sum (taking phase into account) of the original current and the induced current.

With element 2 present, the amplitude and phase of the resulting current in element 1 will be different than if element 2 were not there. This indicates that the presence of the second element has changed the impedance of the first. This effect is called *mutual coupling*. Mutual coupling results in a *mutual impedance* between the two elements. The mutual impedance has both resistive and reactive components. The actual impedance of an antenna element is the sum of its self-impedance (the impedance with no other antennas present) and its mutual impedances with all other antennas in the vicinity.

The magnitude and nature of the feed-point impedance of the first antenna depends on the amplitude of the current induced in it by the second, and on the phase relationship between the original and induced currents. The amplitude and phase of the induced current depend on the spacing between the antennas and whether or not the second antenna is tuned to resonance.

In the discussion of the several preceding paragraphs, power is applied to only one of the two elements. Do not interpret this to mean that mutual coupling exists only in parasitic arrays! It is important to remember that mutual coupling exists between any two conductors that are located near one another.

Amplitude of Induced Current

The induced current will be largest when the two antennas are close together and are parallel. Under these conditions the voltage induced in the second antenna by the first, and in the first by the second, has its greatest value and causes the largest current flow. The coupling decreases as the parallel antennas are moved farther apart.

The coupling between collinear antennas is comparatively small, and so the mutual impedance between such antennas is likewise small. It is not negligible, however.

Phase Relationships

When the separation between two antennas is an appreciable fraction of a wavelength, a measurable period of time elapses before the field from antenna 1 reaches antenna 2. There is a similar time lapse before the field set up by the current in number 2 gets back to induce a current in number 1. Hence the current induced in antenna 1 by antenna 2 will have a phase relationship with the original current in antenna 1 that depends on the spacing between the two antennas.

The induced current can range all the way from being completely in-phase with the original current to being completely out-of-phase with it. If the currents are in-phase, the total current is larger than the original current and the antenna feed-point impedance is reduced. If the currents are out-of-phase, the total current is smaller and the impedance

is increased. At intermediate phase relationships the impedance will be lowered or raised depending on whether the induced current is mostly in or mostly out-of-phase with the original current.

Except in the special cases when the induced current is exactly in or out-of-phase with the original current, the induced current causes the phase of the total current to shift with respect to the applied voltage. Consequently, the presence of a second antenna nearby may cause the impedance of an antenna to be reactive—that is, the antenna will be detuned from resonance—even though its self-impedance is entirely resistive. The amount of detuning depends on the magnitude and phase of the induced current.

Tuning Conditions

A third factor that affects the impedance of antenna 1 when antenna 2 is present is the tuning of number 2. If antenna 2 is not exactly resonant, the current that flows in it as a result of the induced voltage will either lead or lag the phase it would have if the antenna were resonant. This causes an additional phase advance or delay that affects the phase of the current induced back in antenna 1. Such a phase lag has an effect similar to a change in the spacing between self-resonant antennas. However, a change in tuning is not exactly equivalent to a change in spacing because the two methods do not have the same effect on the amplitude of the induced current.

MUTUAL IMPEDANCE AND GAIN

The mutual coupling between antennas is important because it can have a significant effect on the amount of current that will flow for a given amount of power supplied. And it is the amount of *current* flowing that determines the field strength from the antenna. Other things being equal, if the mutual coupling between two antennas is such that the currents are greater for the same total power than would be the case if the two antennas were not coupled, the power gain will be greater than that shown in Table 1.

On the other hand, if the mutual coupling is such as to reduce the current, the gain will be less than if the antennas were not coupled. The term *mutual coupling*, as used in this paragraph, assumes that the mutual impedance between elements is taken into account, along with the added effects of propagation delay because of element spacing and element tuning or phasing.

The calculation of mutual impedance between antennas is a complex problem. Data for two simple but important cases are graphed in Figs 8 and 9. These graphs do not show the mutual impedance, but instead show a more useful quantity—the feed-point resistance measured at the center of an antenna as it is affected by the spacing between two antennas.

As shown by the solid curve in **Fig 8**, the feed-point resistance at the center of either antenna, when the two are self-resonant, parallel, and operated in-phase, decreases as the spacing between them is increased until the spacing is about 0.7 λ. This is a broadside array. The maximum gain

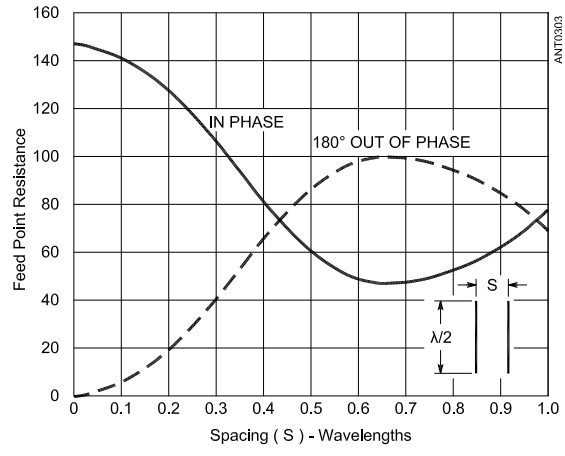

Fig 8—Feed-point resistance measured at the center of one element as a function of the spacing between two parallel ½-λ self-resonant antenna elements. For ground-mounted ¼-λ vertical elements, divide these resistances by two.

is achieved from a pair of such elements when the spacing is in this region, because the current is larger for the same power and the fields from the two arrive in-phase at a distant point placed on a line perpendicular to the line joining the two antennas.

The dashed line in Fig 8, representing two antennas operated 180° out-of-phase (end-fire), cannot be interpreted quite so simply. The feed-point resistance decreases with spacing decreasing less than about 0.6 λ in this case. However, for the range of spacings considered, only when the spacing is 0.5 λ do the fields from the two antennas add up exactly in phase at a distant point in the favored direction. At smaller spacings the fields become increasingly out-of-phase, so the total field is less than the simple sum of the two. Smaller spacings thus decrease the gain at the same time that

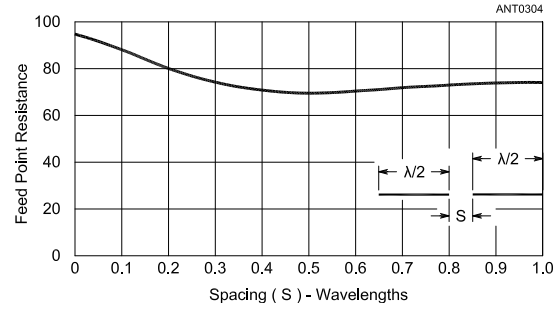

Fig 9—Feed-point resistance measured at the center of one element as a function of the spacing between the ends of two collinear self-resonant ½-λ antenna elements operated in phase.

the reduction in feed-point resistance is increasing it. For a lossless antenna, the gain goes through a maximum when the spacing is in the region of ⅛ λ.

The feed-point resistance curve for two collinear elements in-phase, **Fig 9**, shows that the feed-point resistance decreases and goes through a broad minimum in the region of 0.4 to 0.6-λ spacing between the adjacent ends of the antennas. As the minimum is not significantly less than the feed-point resistance of an isolated antenna, the gain will not exceed the gain calculated on the basis of uncoupled antennas. That is, the best that two collinear elements will give, even with optimum spacing, is a power gain of about 2 (3 dB). When the separation between the ends is very small—the usual method of operation—the gain is reduced.

GAIN AND ARRAY DIMENSIONS

The gain of an array is principally determined by the dimensions of the array, so long as there are a minimum number of elements. A good example of this is the relationship between boom length, gain and number of elements for an array such as a Yagi. **Fig 10** compares the gain versus boom length for Yagis with different numbers of elements. For given number of elements, notice that the gain increases as the boom length increases, up to a maximum. Beyond this point, longer boom lengths result in less gain for a given number of elements. This observation does not mean that it is always desirable to use only the minimum number of elements. Other considerations of array performance, such as front-to-back ratio, minor lobe amplitudes or operating bandwidth, may make it advantageous to use more than the minimum number of elements for a given array length. A specific example of this is presented in a later section in a comparison between a half-square, a bobtail curtain and a Bruce array.

In a broadside array the gain is a function of both the length and width of the array. The gain can be increased by adding more elements (with additional spacing) or by using longer elements (>λ/2), although the use of longer elements requires proper attention to current phase in the elements. In general, in a broadside array the element spacing that gives maximum gain for a minimum number of elements, is in the range of 0.5 to 0.7 λ. Broadside arrays with elements spaced

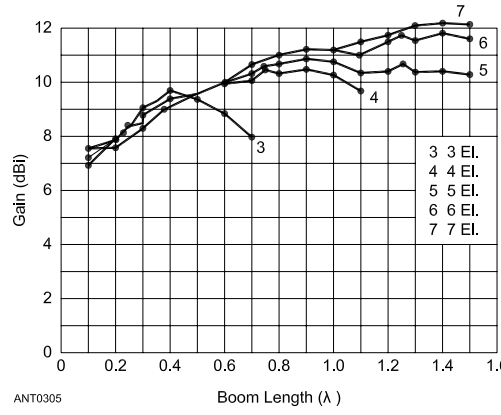

Fig 10—Yagi gain for 3, 4, 5, 6 and 7-element beams as a function of boom length. (From *Yagi Antenna Design*, J. Lawson, W2PV.)

for maximum gain will frequently have significant side lobes and associated narrowing of the main lobe beamwidth. Side lobes can be reduced by using more than the minimum number of elements, spaced closer than the maximum gain distance.

Additional gain can be obtained by expanding the array into a third dimension. An example of this is the stacking of endfire arrays in a broadside configuration. In the case of stacked short endfire arrays, maximum gain occurs with spacings in the region of 0.5 to 0.7 λ. However, for longer higher-gain end-fire arrays, larger spacing is required to achieve maximum gain. This is important in VHF and UHF arrays, which often use long-boom Yagis.

PARASITIC ARRAYS

The foregoing applies to multi-element arrays of both types, driven and parasitic. However, there are special considerations for driven arrays that do not necessarily apply to parasitic arrays, and vice versa. Such considerations for Yagi and quad parasitic arrays are presented in Chapters 11 and 12. The remainder of this chapter is devoted to driven arrays.

Driven Arrays

Driven arrays in general are either broadside or end-fire, and may consist of collinear elements, parallel elements, or a combination of both. From a practical standpoint, the maximum number of usable elements depends on the frequency and the space available for the antenna. Fairly elaborate arrays, using as many as 16 or even 32 elements, can be installed in a rather small space when the operating frequency is in the VHF range, and more at UHF. At lower frequencies the construction of antennas with a large number of elements is impractical for most amateurs.

Of course the simplest of driven arrays is one with just two elements. If the elements are collinear, they are always fed in-phase. The effects of mutual coupling are not great, as illustrated in Fig 9. Therefore, feeding power to each element in the presence of the other presents no significant problems. This may not be the case when the elements are parallel to each other. However, because the combination of spacing and phasing arrangements for parallel elements is infinite, the number of possible radiation patterns is endless.

This is illustrated in **Fig 11**. When the elements are fed

in-phase, a broadside pattern always results. At spacings of less than ⅝ λ with the elements fed 180° out-of-phase, an end-fire pattern always results. With intermediate amounts of phase difference, the results cannot be so simply stated. Patterns evolve that are not symmetrical in all four quadrants.

Because of the effects of mutual coupling between the two driven elements, for a given power input greater or lesser currents will flow in each element with changes in spacing and phasing, as described earlier. This, in turn, affects the gain of the array in a way that cannot be shown merely by plotting the *shapes* of the patterns, as has been done in Fig 11. Therefore, supplemental gain information is also shown in Fig 11, adjacent to the pattern plot for each combination of spacing and phasing. The gain figures shown are referenced to a single element. For example, a pair of elements fed 90° apart at a spacing of λ/4 will have a gain in the direction of maximum radiation of 3.1 dB over a single element.

Current Distribution in Phased Arrays

In the plots of Fig 11, the two elements are assumed to be identical and self-resonant. In addition, currents of equal amplitude are assumed to be flowing at the feed point of each element, a condition that most often will not exist in practice without devoting special consideration to the feeder system. Such considerations are discussed in the next section of this chapter.

Most literature for radio amateurs concerning phased arrays is based on the assumption that if all elements in the array are identical, the *current distribution* in all the elements will be identical. This distribution is presumed to be that of a single, isolated element, or nearly sinusoidal. However, information published in the professional literature as early as the 1940s indicates the existence of dissimilar current distributions among the elements of phased arrays. (See Harrison and King references in the Bibliography.) Lewallen, in July 1990 *QST*, pointed out the causes and effects of dissimilar current distributions.

In essence, even though the two elements in a phased array may be identical and have exactly equal currents of the desired phase flowing *at the feed point*, the amplitude and phase relationships degenerate with departure from the feed point. This happens any time the phase relationship is not 0° or 180°. Thus, the field strengths produced at a distant point by the individual elements may differ. This is because the field from each element is determined by the *distribution* of the current, as well as its magnitude and phase.

The effects are minimal with shortened elements—verticals less than λ/4 or dipoles less than λ/2 long. The effects on radiation patterns begin to show at the above resonant lengths, and become profound with longer elements—λ/2 or longer verticals and 1 λ or longer center-fed elements. These effects are less pronounced with thin elements. The amplitude and phase degeneration takes place because the currents in the array elements are not sinusoidal. Even in two-element arrays with phasing of 0° or 180°, the currents are not sinusoidal, but in these two special cases they do remain identical.

The pattern plots of Fig 11 take element current distributions into account. The visible results of dissimilar distributions are incomplete nulls in some patterns and the development of very small minor lobes in others. For example, the pattern for a phased array with 90° spacing and 90° phasing has traditionally been published in amateur literature as a cardioid with a perfect null in the rear direction. Fig 11, calculated for 7.15-MHz self-resonant dipoles of #12 wire in free space, shows a minor lobe at the rear and only a 33-dB front-to-back ratio.

It is characteristic of broadside arrays that the power gain is proportional to the length of the array but is substantially independent of the number of elements used, provided the optimum element spacing is not exceeded. This means, for example, that a five-element array and a six-element array will have the same gain, provided the elements in both are spaced so the overall array length is the same. Although this principle is seldom used for the purpose of reducing the number of elements because of complications introduced in feeding power to each element in the proper phase, it does illustrate the fact that there is nothing to be gained, in terms of more gain, by increasing the number of elements if the space occupied by the antenna is not increased proportionally.

Generally speaking, the maximum gain in the smallest linear dimensions will result when the antenna combines both broadside and end-fire directivity and uses both parallel and collinear elements. In this way the antenna is spread over a greater volume of space, which has the same effect as extending its length to a much greater extent in one linear direction.

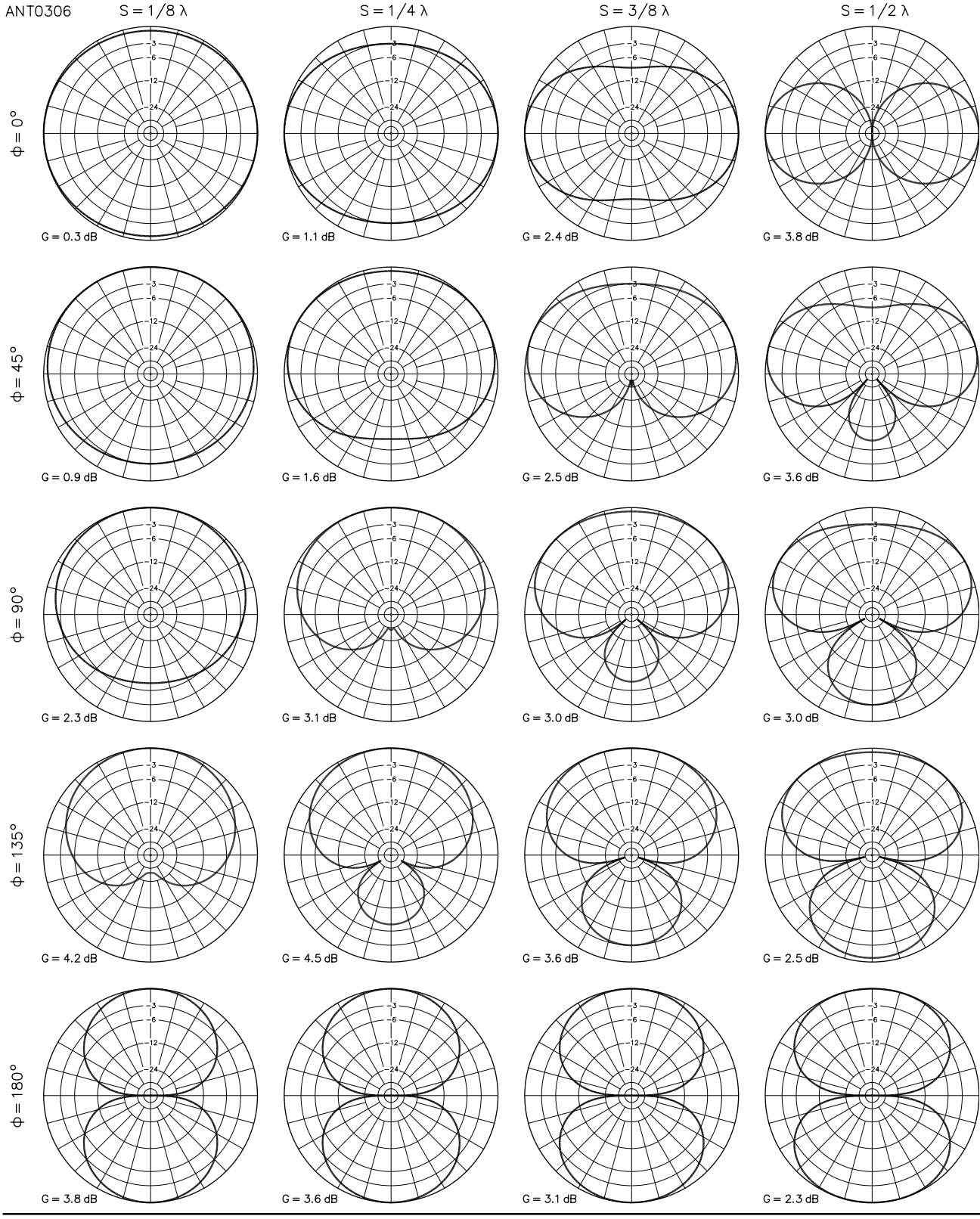

Fig 11—H-plane patterns of two identical parallel driven elements, spaced and phased as indicated (S = spacing, ϕ = phasing). The elements are aligned with the vertical (0°-180°) axis, and the element nearer the 0° direction (top of page) is of lagging phase at angles other than 0°. The two elements are assumed to be thin and self-resonant, with equal-amplitude currents flowing at the feed point. See text regarding current distributions. The gain figure associated with

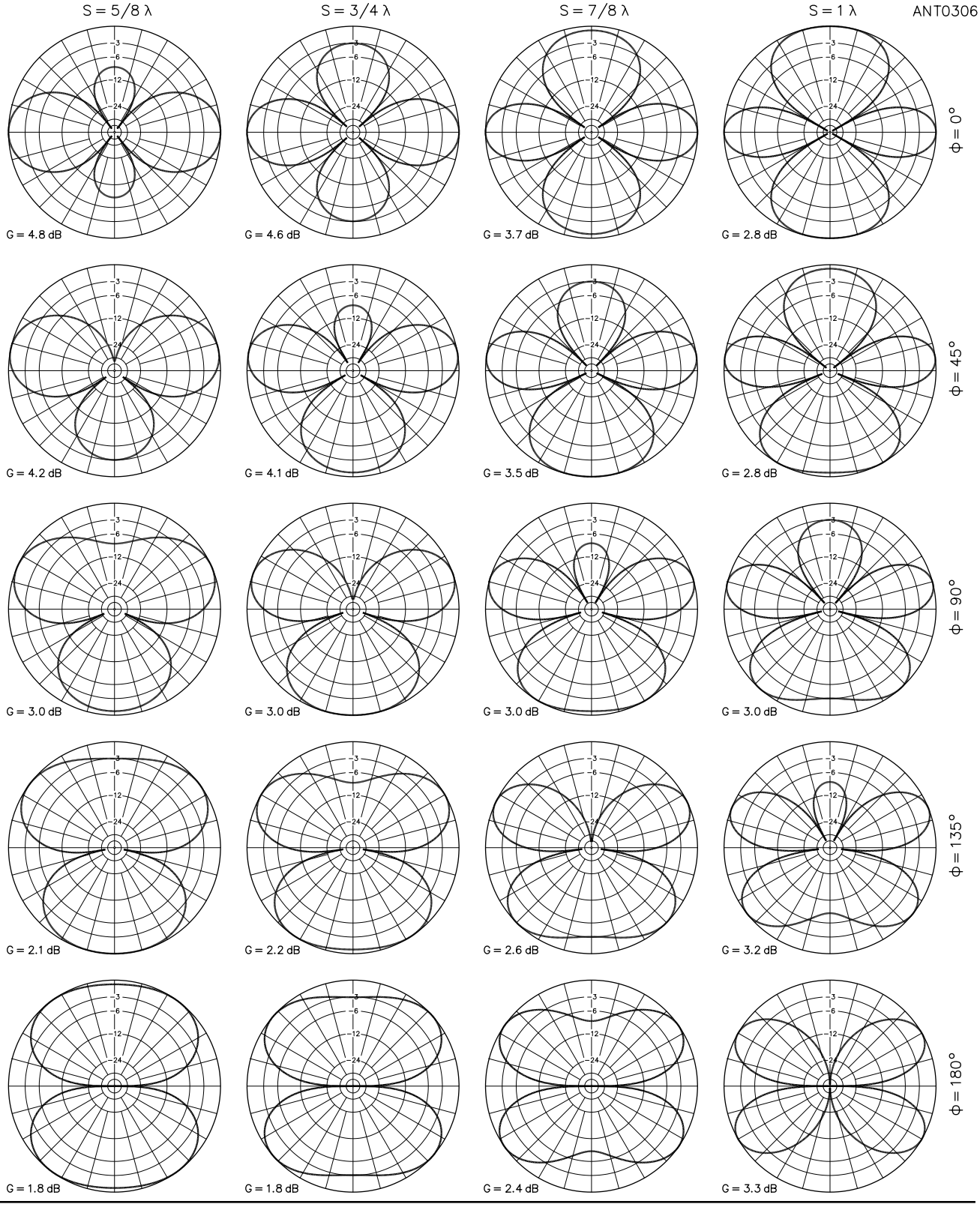

each pattern indicates that of the array over a single element. The plots represent the horizontal or azimuth pattern at a 0° elevation angle of two ¼-λ vertical elements over a perfect conductor, or the free-space vertical or elevation pattern of two horizontal ½-λ elements when viewed on end, with one element above the other. (Patterns computed with *ELNEC*—see Bibliography.)

Phased Array Techniques

Phased antenna arrays have become increasingly popular for amateur use, particularly on the lower frequency bands, where they provide one of the few practical methods to obtain substantial gain and directivity. This section on phased-array techniques was written by Roy Lewallen, W7EL.

The operation and limitations of phased arrays, how to design feed systems to make them work properly and how to make necessary tests and adjustments are discussed in the pages that follow. The examples deal primarily with vertical HF arrays, but the principles apply to VHF/UHF arrays and arrays made from other element types as well.

OVERVIEW

Much of this chapter is devoted to techniques for feeding phased arrays. Many people who have a limited acquaintance with phased array techniques believe this is a simple problem, consisting only of connecting array elements through "phasing lines" consisting of transmission lines of the desired electrical lengths. Unfortunately, except for a very few special cases, this approach won't achieve the desired array pattern.

Other proposed universal solutions, such as hybrid couplers or Wilkinson or other power dividers, also usually fail to achieve the necessary phasing. These approaches sometimes produce—often more by accident than design—results good enough to mislead the user into believing that the simple approach is working as planned. Confusion can result when an approach fails to work in different circumstances. This section will explain why the simple solutions don't work as often thought, and how to design feed systems that do consistently produce the desired results.

Very briefly, the reason why the simple phasing-line approach fails is that the delay of current or voltage in a transmission line equals the line's electrical length only if the line is terminated in its characteristic impedance. And in phased arrays, element feed-point impedances are profoundly affected by mutual coupling.

Consequently, even if each element has the correct impedance when isolated, it won't when all elements are excited. Furthermore, transmission lines that are not terminated in their characteristic impedance will transform both the voltage and current magnitude. The net result is that the array elements will have neither the correct magnitudes nor phases of current necessary for proper operation except in a few special cases. This isn't a minor effect of concern only to perfectionists, but often a major one that causes significant pattern distortion and poor or mislocated nulls. The problem is examined in greater depth later.

Power dividers and hybrid couplers also fail to achieve the desired result for different reasons, which will be discussed below, although in one common application hybrid couplers fortuitously provide results that are acceptable to many users. This chapter will show how to design array feed systems that *will* produce predicted element currents and array patterns.

Various *EZNEC* models are provided to illustrate concepts presented in this chapter. They can all be viewed with the *EZNEC-ARRL* software furnished on the CD included with this book. Step-by-step instructions for the examples are given in **Appendix A**.

FUNDAMENTALS OF PHASED ARRAYS

The performance of a phased array is determined by several factors. Most significant among these are the characteristics of a single element, reinforcement or cancellation of the fields from the elements and the effects of mutual coupling. To understand the operation of phased arrays, it is first necessary to understand the operation of a single antenna element.

Of primary importance is the strength of the field produced by the element. The field radiated from a linear (straight) element, such as a dipole or vertical monopole, is proportional to the sum of the elementary currents flowing in each part of the antenna element. For this discussion it is important to understand what determines the current in a single element.

The amount of current flowing at the base of a ground mounted vertical or ground-plane antenna is given by the familiar formula

$$I = \sqrt{\frac{P}{R}} \qquad \text{(Eq 2)}$$

where

P is the power supplied to the antenna

R is the feed-point resistance.

R consists of two parts, the loss resistance and the radiation resistance. The loss resistance, R_L, includes losses in the conductor, in the matching and loading components and dominantly (in the case of ground-mounted verticals) in ground losses. The power "dissipated" in the radiation resistance, R_R, is actually the power that is radiated, so maximizing the power dissipated by the radiation resistance is desirable. However, the power dissipated in the loss resistance truly is lost as heat, so resistive losses should be made as small as possible.

The radiation resistance of an element can be derived from electromagnetic field theory, being a function of antenna length, diameter and geometry. Graphs of radiation resistance versus antenna length are given in Chapter 2. The radiation resistance of a thin resonant $\lambda/4$ ground-mounted vertical is about 36 Ω. A resonant $\lambda/2$ dipole in free space has a radiation resistance of twice this amount, about 73 Ω. Reducing the antenna lengths by one half drops the radiation resistances to approximately 7 and 14 Ω, respectively.

The radiation resistance of a large variety of antennas can easily be determined by using *EZNEC-ARRL*, which is included on the CD in the back of this book. The radiation

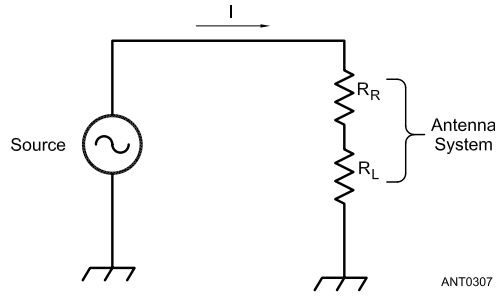

Fig 12—Simplified equivalent circuit for a single-element resonant antenna. R_R represents the radiation resistance, and R_L the ohmic losses in the total antenna system.

resistance is simply the feed-point resistance (the resistive part of the feed-point impedance) when all losses have been set to zero.

Radiation Efficiency

To generate a stronger field from a given radiator, it is necessary to increase the power P (the brute-force solution), decrease the loss resistance R_L (by putting in a more elaborate ground system for a vertical, for instance) or to somehow decrease the radiation resistance R_R so more current will flow with a given power input. This can be seen by expanding the formula for base current as

$$I = \sqrt{\frac{P}{R_R + R_L}} \qquad \text{(Eq 3)}$$

Splitting the feed-point resistance into components R_R and R_L easily leads to an understanding of element efficiency. The efficiency of an element is the proportion of the total power that is actually radiated. The roles of R_R and R_L in determining efficiency can be seen by analyzing a simple equivalent circuit, shown in **Fig 12**.

The power dissipated in R_R (the radiated power) equals I^2R_R. The total power supplied to the antenna system is

$$P = I^2 (R_R + R_L) \qquad \text{(Eq 4)}$$

so the efficiency (the fraction of supplied power that is actually radiated) is

$$\text{Eff} = \frac{I^2 R_R}{I^2 (R_R + R_L)} = \frac{R_R}{R_R + R_L} \qquad \text{(Eq 5)}$$

Efficiency is frequently expressed in percent, but expressing it in decibels relative to a 100%-efficient radiator gives a better idea of what to expect in the way of signal strength. The field strength of an element relative to a lossless but otherwise identical element, in dB, is

$$\text{FSG} = 10 \log \frac{R_R}{R_R + R_L} \qquad \text{(Eq 6)}$$

where FSG = field strength gain, dB.

For example, information presented by Sevick in March 1973 *QST* shows that a λ/4 ground-mounted vertical antenna with four 0.2-λ radials has a feed-point resistance of about 65 Ω (see the Bibliography at the end of this chapter). The efficiency of such a system is 36/65 = 55.4%. It is rather disheartening to think that, of 100 W fed to the antenna, only 55 W is being radiated, with the remainder literally warming up the ground. Yet the signal will be only 10 log (36/65) = –2.57 dB relative to the same vertical with a perfect ground system. In view of this information, trading a small reduction in signal strength for lower cost and greater simplicity may become an attractive consideration.

So far, only the current at the base of a resonant antenna has been discussed, but the field is proportional to the sum of currents in each tiny part of the antenna. The field is a function of not only the magnitude of current flowing at the feed point, but also the distribution of current along the radiator and the length of the radiator. Nothing can be done at the feed point to change the current distribution, so for a given element the field strength is proportional to the feed point current. However, changing the radiator length or loading it at some point other than the feed point will change the current distribution.

More information on shortened or loaded radiators may be found in Chapters 2 and 6 and in the Bibliography references of this chapter. The current distribution is also changed by mutual coupling to other array elements, although for most arrays this has only a minor effect on the pattern. This is discussed later in more detail. A few other important facts follow.

1) If there is no loss, the field from even an infinitesimally short radiator is less than ½ dB weaker than the field from a half-wave dipole or quarter-wave vertical. Without loss, all the supplied power is radiated regardless of the antenna length, so the only factor influencing gain is the slight difference in the patterns of very short and λ/2 antennas. The small pattern difference arises from different current distributions. A short antenna has a very low radiation resistance, resulting in a heavy current flow over its short length. In the absence of loss, this generates a field strength comparable to that of a longer antenna. Where loss is present—that is, in practical antennas—shorter radiators usually don't do so well, since the low radiation resistance leads to lower efficiency for a given loss resistance. If care is taken, reasonably short antennas can achieve good efficiency.

2) Care has to be taken in calculating the efficiency of folded antennas. (See Chapter 6.) Folding transforms both the radiation resistance and loss resistance by the same factor, so their ratio and therefore the efficiency remains the same. It's easy to show that in a ground-mounted vertical array, folding reduces the current flowing from the feed line to the ground system by a factor of two due to the impedance transformation. However, the folded antenna has an additional connection to ground, which also carries half the original ground current. The result is that the same amount of current flows

into the ground system, whether unfolded or folded, resulting in the same ground system loss. Analyses purporting to show otherwise invariably transform the radiation resistance but neglect to also transform the loss resistance and reach an incorrect conclusion.

3) The current flowing in an element with a given power input can be increased or decreased by mutual coupling to other elements. The effect is equivalent to changing the element radiation resistance. Mutual coupling is sometimes thought of as a minor effect, but often it is not minor!

Field Reinforcement and Cancellation

The mechanism by which phased arrays produce gain, and the role of mutual coupling in determining gain, were covered earlier in this chapter. One important point that can't be emphasized enough is that all antennas must abide by the law of *conservation of energy*. No antenna can radiate more power than supplied to it. The total amount of power it radiates is the amount it's supplied, less the amount lost as heat. This is true of all antennas, from the smallest "rubber ducky" to the most gigantic array.

Gain

Gain is strictly a relative measure, so the term is completely meaningless unless accompanied by a statement of just what it is relative to. One useful measure for phased array gain is *gain relative to a single similar element*. This is the increase in signal strength that would be obtained by replacing a single element by an array made from elements just like it. In some instances, such as investigating what happens to array performance when *all* elements become more lossy, it's useful to state gain relative to a more absolute, although unattainable standard: a lossless element.

And the most universal reference for gain is another unattainable standard, the *isotropic radiator*. This fictional antenna radiates absolutely equally in all directions. It's very useful because the field strength resulting from any power input is readily calculated, so if the gain relative to this standard is known, the field strength is also known for any radiated power. Gain relative to this reference is referred to as dBi, and it's the standard used by most modeling programs including *EZNEC-ARRL*. To find the gain of an array relative to a single element or other reference antenna such as a dipole, model both the array and the single element or other reference antenna in the same environment and subtract their dBi gains. Don't rely on some assumption about the gain of a single element—many people assume values that can be very wrong.

Nulls

Pattern nulls are very often more important to users of phased arrays than gain because of their importance in reducing both man-made and natural interference when receiving. Consequently, a good deal of emphasis is, and should be, placed on achieving good pattern nulls. Unfortunately, good nulls are much more difficult to achieve than gain and they are much more sensitive to array and feed-system imperfections.

As an illustration, consider two elements that each produce a field strength of, say, exactly 1 millivolt per meter (mV/m) at some distance many wavelengths from the array. In the direction in which the fields from the elements are in-phase, a total field of 2 mV/m results. In the direction in which they're out-of-phase, zero field results. The ratio of maximum to minimum field strength of this array is 2/0, or infinity.

Now suppose, instead, that one field is 10% high and the other 10% low—1.1 and 0.9 mV/m, respectively. In the forward direction, the field strength is still 2 mV/m, but in the canceling direction, the field will be 0.2 mV/m. The front-to-back ratio has dropped from infinity to 2/0.2, or 20 dB. (Actually, slightly more power is required to redistribute the field strengths this way, so the forward gain is reduced—but by only a small amount, less than 0.1 dB.) For most arrays, unequal fields from the elements have a minor effect on forward gain, but a major effect on pattern nulls. This is illustrated by ***EZNEC* Example: Nulls** in Appendix A.

Even with perfect current balance, deep nulls aren't assured. **Fig 13** shows the minimum spacing required for total field reinforcement or cancellation. If the element spacing isn't adequate, there may be no direction in which the fields are completely out-of-phase (see curve B of Fig 13). Slight physical and environmental differences between elements will invariably affect null depths, and null depths will also vary with elevation angle.

However, a properly designed and fed array can produce very impressive nulls. The key to producing good nulls, like producing gain, is controlling the strengths and phases of the fields from the elements. Just how to accomplish that is the subject of most of the remainder of this section. But be sure to keep in mind that producing good nulls is generally a much more difficult task than producing approximately the predicted gain.

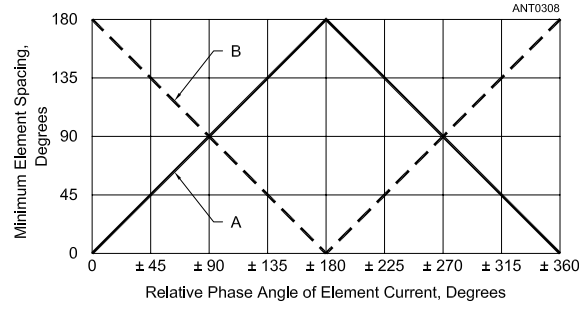

Fig 13—Minimum element spacing required for total field reinforcement, curve A, or total field cancellation, curve B. Total cancellation results in pattern nulls in one or more directions. Total reinforcement does not necessarily mean there is gain over a single element, as the effects of loss and mutual coupling must also be considered.

Mutual Coupling

Mutual coupling was discussed briefly earlier in this chapter. Because it has an important and profound effect on both the performance and feed system design of phased arrays, it will be covered in greater depth here.

Mutual coupling refers to the effects which the elements in an array have on each other. Mutual coupling can occur intentionally or entirely unintentionally. People with multiple antennas on a small lot (or car top) often discover that a better description of their system is a single antenna with multiple feed points. Current is induced in conductors in various antennas by mutual coupling, causing them to act like parasitic elements, which re-radiate and distort the antenna's pattern. The effects of mutual coupling are present whether or not the elements are driven.

Suppose that two driven elements are many wavelengths from each other. Each has some voltage and current at its feed point. For each element, the ratio of this voltage to current is the element self-impedance. If the elements are brought close to each other, the current in each element will change in magnitude and phase because of coupling with the field from the other element. The field from the first element changes the current in the second. This changes the field from the second, which alters the current in the first, and so forth until an equilibrium condition is reached in which the currents in all elements (hence, their fields) are totally interdependent.

The feed-point impedances of all elements also are changed from their values when far apart, and all are dependent on each other. In a driven array, the changes in feed-point impedances can cause additional changes in element currents, because the operation of many feed systems depends on the element feed-point impedances. Significant mutual coupling occurs at spacings as great as a wavelength or more.

Connecting the elements to a feed system to form a driven array does not eliminate the effects of mutual coupling. In fact, in many driven arrays the mutual coupling has a greater effect on antenna operation than the feed system does. All feed-system designs must account for the impedance changes caused by mutual coupling if the desired current balance and phasing are to be achieved.

Several general statements can be made regarding the effects of mutual coupling on phased-array systems.

1) The resistances and reactances of all elements of an array generally will be substantially different from the values when the elements are isolated (that is, very distant from other elements).

2) If the elements of a two-element array are identical and have equal currents that are in-phase or 180° out-of-phase, the feed-point impedances of the two elements will be equal. But they will be different than for an isolated element. If the two elements are part of a larger array, their impedances can be very different from each other.

3) If the elements of a two-element array have currents that are neither in-phase (0°) nor out-of-phase (180°), their feed-point impedances will not be equal. The difference will be considerable in typical amateur arrays.

4) The feed-point resistances of the elements in a closely spaced, 180° out-of-phase array will be very low, resulting in poor efficiency due to ohmic losses unless care is taken to minimize loss. This is also true for any other closely spaced array with significant predicted gain.

It's essential to realize that this is *not* a minor effect and one that can be overlooked or ignored. See ***EZNEC* Example—Mutual Coupling** in Appendix A for an illustration of these phenomena.

Loss Resistance, Mutual Coupling and Antenna Gain

Loss reduces the effects of mutual coupling because the feed-point impedance change resulting from mutual coupling is effectively in series with loss resistance. If the loss is great enough, two important results occur. First, the feed-point impedance becomes independent of the presence of nearby current-carrying elements. This greatly simplifies feed system design—the simple "phasing-line" or hybrid-coupler feed system described below is adequate *provided that all elements are physically identical and the feed point of each element is matched to the Z_0 of the feed line and, if used, the hybrid coupler.*

The impedance matching restrictions are necessary to insure that the phasing line or hybrid coupler performs as expected. Identical elements are needed so that equal element currents will result in equal fields from the elements.

In the absence of mutual coupling effects, the maximum gain of an array of identical elements relative to a single (similarly lossy) element is simply 10 log(N), where N is the number of elements—providing that spacing is adequate for the fields to fully reinforce in some direction. If spacing is less, maximum gain will also be less. Of course, the array gain relative to a single *lossless* element will be very low, most likely a sizeable negative number when expressed in dB. So intentionally introducing loss isn't a wise idea for a transmitting array. It is sometimes an advantageous thing to do for a receiving array, however, as explained in the following section.

High-gain close-spaced arrays, such as the W8JK phased array (see *EZNEC-ARRL* example file **ARRL_W8JK.EZ** and accompanying Antenna Notes file), and most parasitic arrays depend heavily on mutual coupling to achieve their gain. Introduction of any loss to these arrays, which reduces the mutual coupling effects, has a profound effect on the gain. Consequently, parasitic or close-spaced driven arrays often produce disappointing results when made from grounded vertical elements unless each has a fairly elaborate (and therefore very low-loss) ground system.

If you place two low-loss elements very close together and feed them in-phase, mutual coupling reduces the array gain to essentially that of a single element, so there's no advantage to this configuration over a single element. However, if you have a single lossy element, for example a short vertical having a relatively poor ground system, you can improve the gain by up to 3 dB by adding a second, close spaced, element and ground system and feeding the two in-phase. Another

way to look at this technique is that you're putting two equal ground system resistances in parallel, which effectively cuts the loss in half. The gain you can realize in practice depends on such things as the ground system overlap, but it might be a practical way to improve transmitting array performance in some situations.

FEEDING PHASED ARRAYS

The previous section explains why the fields from the elements must be very close to the ratios required by the array design. Since the field strengths are proportional to the currents in the elements, controlling the fields requires controlling the element currents. Since the desired current ratio is 1:1 for virtually all two-element and for most (but not all) larger amateur arrays, special attention is paid to methods of assuring equal element currents. But we will examine other current ratios also.

The Role of Element Currents

The field from a conductor is proportional to the current flowing on it. So if we're to control the relative strengths and phases of the fields from the elements, we have to control their currents. We usually do this by controlling the currents at the element feed points. But because the field from an element depends on the current everywhere along the element, elements having identical feed-point currents will produce different fields if they have different current distributions—that is, if the way the current varies along the lengths of the elements is different.

A previous section explained that mutual coupling alters the current distribution, so in many arrays the current distributions will be different on the elements and consequently the relationship between the overall fields won't be the same as that between the feed-point currents. Fortunately, this effect is relatively minor in thin, $\lambda/4$ monopole or $\lambda/2$ dipole elements. The most common arrays are made from elements in this category, so we can generally get very nearly the desired ratio of fields by effecting the same ratio of feed point currents. Exceptions are detailed immediately below.

Feed-point vs Element Current

For most antennas, environmental factors are likely to cause greater performance anomalies than current distribution differences, and both can be corrected with minor feed system adjustments. The difference between field and feed-point current ratios can become very significant, however, if the elements are very fat and/or close to $\lambda/2$ (monopole) or 1 λ (dipole) long. In those cases, most of the feed systems described here won't produce the desired field ratios without major adjustment or modification, except in the special cases of 2-element arrays with identical elements having feed point currents in-phase or 180° out-of-phase. In those special cases, the element current distributions are the same for the same reason the feed-point impedances are equal. This is explained later in the feed system sections.

To get an idea of just how large an element must be to disturb the pattern of an array with correct feed-point currents, a two-element cardioid array of quarter wave vertical elements was modeled at 10 MHz. With thin, 0.1-inch diameter elements, the front/back ratio was 35 dB, the very small reverse lobe caused by slightly unequal element current distributions. Increasing the element diameter to 20 inches decreased the front/back ratio to 20 dB. Returning the front/back ratio of the array of 20-inch elements to >35 dB required changing the feed-point current ratio from the nominal value of 1.0 at an angle of 90° to 0.88 at 83°.

The same array was first modeled with 0.1 inch diameter elements, where it has a front/back ratio of 35 dB, then the elements were lengthened. The front/back ratio dropped to 20 dB at an element length of 36 feet, or about 0.37 λ. In that case, adjustment of the feed-point current ratio to about 0.9 at about 83° restored a good front/back ratio.

In the discussion and development which follow, the assumption is made that the fields will be very nearly proportional to the feed-point currents. If the elements are fat or long enough to make this assumption untrue, some adjustment of feed-point current ratio will be necessary to achieve the desired pattern, particularly nulls. Most feed systems can be designed for any current ratio. Modeling will reveal the ratio required for the desired pattern, and then the feed system can be designed accordingly.

COMMON PHASED-ARRAY FEED SYSTEMS

This section will first describe several popular approaches to feeding phased arrays that often don't produce the desired results. It will describe why they don't work as well as hoped. It also briefly discusses systems that could be used, but that often aren't appropriate or optimum for amateur arrays.

This will be followed in the next section by detailed descriptions of array feed systems that *do* produce the predicted element current ratios and array patterns.

The "Phasing-Line" Approach

For an array to produce the desired pattern, the element currents must have the required magnitude and the required phase relationship. As explained above, this can generally be achieved well enough by causing the feed point currents to have that same relationship.

On the surface, this sounds easy—just make sure that the difference in electrical lengths of the feed lines to the elements equals the desired phase angle. Unfortunately, this approach doesn't necessarily achieve the desired result. The first problem is that the phase shift through the line is not equal to its electrical length. The current (or, for that matter, voltage) delay in a transmission line is equal to its electrical length in only a few special cases—cases which don't exist in most amateur arrays! The impedance of an element in an array is frequently very different from the impedance of an isolated element and the impedances of all the elements in an array can be different from each other.

See the ***EZNEC* Example—Mutual Coupling** in Appen-

dix A for a graphic illustration of the effect of mutual coupling on feed-point impedance. Also look at the Four-Square array example in the **Phased Array Design Examples** section. The array in that example has one element with a *negative* feed-point resistance, if ground loss is low. Without mutual coupling, the resistance of that same element would be about 36 Ω plus ground loss.

Because of mutual coupling, the elements seldom provide a matched load for the element feed lines. The effect of mismatch on phase shift can be seen in **Fig 14**. Observe what happens to the phase of the current and voltage on a line terminated by a purely resistive impedance that is lower than the characteristic impedance of the line (Fig 14A). At a point 45° from the load the current has advanced less than 45°, and the voltage more than 45°. At 90° from the load both are advanced 90°. At 135° the current has advanced more and the voltage less than 135°. This apparent slowing down and speeding up of the current and voltage waves is caused by interference between the forward and reflected waves. It occurs on any line that is not terminated with a pure resistance equal to its characteristic impedance. If the load resistance is greater than the characteristic impedance of the line, as shown in Fig 14B, the voltage and current exchange angles. Adding reactance to the load causes additional phase shift. The *only cases in which the current (or voltage) delay is equal to the electrical length of the line are*

1) When the line is flat; that is, terminated in a purely resistive load equal to its characteristic impedance;

2) When the line length is an integral number of half wavelengths;

3) When the line length is an odd number of quarter wavelengths and the load is purely resistive; and

4) When other specific lengths are used for specific load impedances.

Just how much phase error can be expected if two feed lines are simply hooked up to form an array? There is no simple answer. Some casually designed feed systems might deliver satisfactory results, but most will not. See the ***EZNEC* Example—"Phasing-Line" Feed** in Appendix A for the typical consequences of using this sort of feed system.

A second problem with simply connecting feed lines of different lengths to the elements is that the lines will change the *magnitudes* of the currents. The magnitude of the current (or voltage) out of a line does not equal the magnitude into that line, except in cases 1, 2 and 4 above. The feed systems presented later in this chapter assure currents that are correct in both magnitude and phase.

The elementary phasing-line approach *will* work in three very special but common situations. If the array consists of only two identical elements and those elements are fed in-phase, mutual coupling will modify the element impedances, but both will be modified exactly the same amount. Consequently, if the two elements are fed through equal-length transmission lines, the lines will transform and delay the currents by the same amount and result in equal, in-phase currents at the element feed points.

Similarly, an array of two identical elements fed 180° out-of-phase will have the same feed-point impedances and can be fed with two lines of any length so long as one line is an electrical half wavelength longer than the other. But this can't be extended to any two elements in a larger array, since mutual coupling to the other elements can result in different feed-point impedances. Methods will be described later which do assure a correct current ratio in this situation.

The third application in which the phasing-line approach works is in receiving arrays where the elements are very short in terms of wavelength and/or very lossy. In either of these cases, mutual coupling between elements is much less than an element's self-impedance. This allows the elements to be individually matched to the feed lines, with no significant change taking place when the elements are formed into an array. Under those conditions, the transmission lines can be matched and the lines used as simple delay lines with easily predictable phase shift and with no transformation of current or voltage magnitude other than cable loss. This is discussed in the later section on receiving antennas.

Many arrays *can* be correctly fed with a feed system consisting of only transmission lines, but the technique requires knowledge of the element feed-point impedances in a correctly fed array. Line lengths can then be computed that provide the correct ratio of currents into those particular load impedances. The line lengths generally differ by amount that's considerably different from the element phase angle

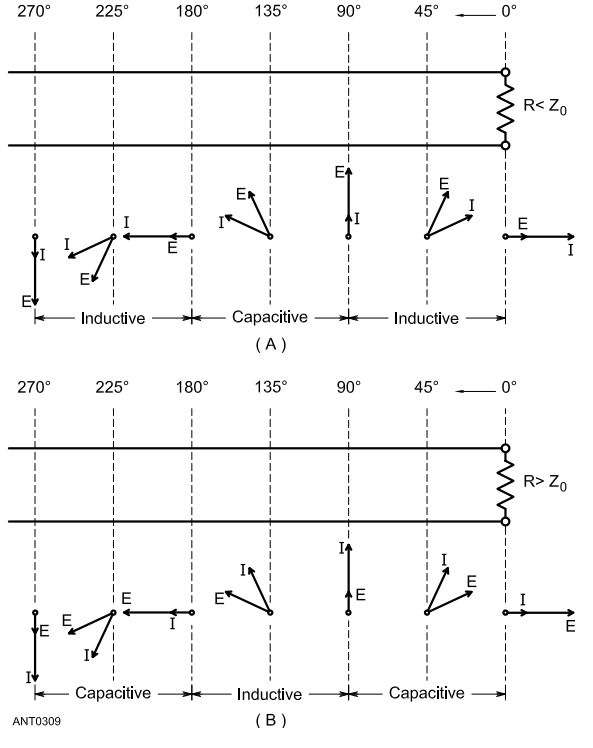

Fig 14—Resultant voltages and currents along a mismatched line. At A, R less than Z_0, and at B, R greater than Z_0.

difference, and appropriate line lengths can't always be found for all arrays. This technique is described more fully in the **"The Simplest Phased Array Feed System—That Works"** section later in the chapter and illustrated in the examples in **Phased Array Design Examples**.

The Wilkinson Divider

The *Wilkinson divider*, sometimes called the *Wilkinson power divider*, was once heavily promoted as a means to distribute power among the elements of a phased array. While it's a very useful device for other purposes, it won't produce the desired current ratios in antenna elements. In most phased arrays, element feed-point resistances are different and therefore require different amounts of power to achieve the desired equal magnitude currents. (See the section on mutual coupling above.) A Wilkinson divider is intended to deliver equal powers, not currents, to multiple loads. And it won't even do that when the load impedances are different.

The Hybrid Coupler

Hybrid couplers are promoted as solving the problem of achieving equal magnitude currents with a 90º phase difference between elements. Unfortunately, they provide equal magnitude, quadrature (90° phased) currents only when the load impedances are equal and correct. And this simply isn't true of arrays with quadrature-fed elements, except for arrays consisting of short and/or lossy elements, usually suitable only for receiving. In those arrays, the hybrid coupler can be useful for the same reasons as the phasing-line approach, discussed in an earlier section.

At the time of this writing, hybrid couplers are being used in a popular commercial product for phasing at least one type of array. Reports are that it works satisfactorily. However, this shouldn't be taken as proof that the hybrid coupler forces equal magnitude 90º phased currents in loads of arbitrary impedances. No passive network, including the hybrid coupler, is capable of doing that. See **The "Magic Bullet"** below for more information.

Large Array Feed Systems

The author once worked on a radar system where the transmit array consisted of over 5,000 separate dipole elements and the receive array over 4,000 pairs of crossed dipoles, all over a metal reflecting plane, which was the sloping side of a 140 foot high building. In such large arrays, each element is in essentially the same environment as every other element except near the array edges, so almost all elements have very nearly the same feed-point impedance. While producing the phase shifts and magnitude tapers is a considerable mathematical challenge, the problem of unequal element feed-point impedances can largely be ignored. Consequently, feed methods for these large arrays are generally not suitable for typical amateur arrays of a few elements.

The Broadcast Approach

Networks can be designed to transform the element base impedances from their values in an excited array to, say, 50 Ω resistive. Then another network can be inserted at the junction of the feed lines to properly divide the power among the elements (not necessarily equally!). And finally, additional networks must be added to correct for the phase shifts and magnitude transformations of the other networks. This general approach is used by the broadcast industry, in installations that are typically adjusted only once for a particular frequency and pattern.

Although this technique can be used to correctly feed any type of array, design is difficult and adjustment is tedious, since all adjustments interact. When the relative currents and phasings are adjusted, the feed-point impedances change, which in turn affect the element currents and phasings, and so on. A further disadvantage of using this method is that switching the array direction is generally impossible. Information on applying this technique to amateur arrays can be found in Paul Lee's book, listed in the Bibliography.

The "Magic Bullet"

For about 15 years prior to this writing, this *Antenna Book* section has contained a specification for a hypothetical passive circuit that would provide equal-magnitude, 90° phased currents into two loads without respect to the load impedances. This would be a circuit to which we could connect any two elements and guarantee that they'd have exactly the correct currents.

Along with the specifcation was a request that any person knowing of such a circuit would contact the author (Roy Lewallen, W7EL) or the book editors. During this time, only a single response was received, in 1996. It was from Kevin Schmidt, W9CF, who has formulated a mathematical proof that such a circuit—in fact, one resulting in any relative phase other than 0º or 180º—*cannot exist* if restricted to reciprocal elements. (That is, it can't exist unless directional components such as ferrite circulators are used.) This means that, in order to design a network to feed elements at any other phase angle other than 0 or 180º, we *must* know the impedance of at least one element, and correct feed system operation depends on that impedance. There's no way around this requirement. At the time of this writing, Schmidt's proof can be found at **fermi.la.asu.edu/w9cf/articles/magic/index.html**.

RECOMMENDED FEED METHODS FOR AMATEUR ARRAYS

The following feed methods are able to produce element feed-point currents having a desired magnitude and phase relationship, resulting in desirable and predictable patterns. Most methods require knowing the feed-point impedance of one or more array elements *when the array element currents are the correct values*. This isn't possible to measure directly, because if the element currents were correct, the feed system would already be working properly and no further design would be necessary.

By far the easiest way to get this information, if possible, is by computer modeling. Modeling programs such as *EZNEC-ARRL* (included on the CD in the back of this book)

allow you to construct an ideal array with perfect element currents, then look at the resulting feed-point impedances. Because of its simplicity and versatility, this approach is highly recommended and it's the one used for the array design examples in this chapter.

Some feed systems allow adjustment, so even an approximate result provides an adequate starting point on which to base the feed-system design. There are several other alternatives to computer modeling. One is to first eliminate the effects of coupling of the element to be measured from all other elements, usually by open circuiting the feed points of the other elements. Then the feed-point impedance of the element is measured. Next, the impedance change due to mutual coupling from all other elements has to be calculated, based on the intended currents in the other elements, their lengths and their distances from the element being measured. Mutual impedance (which is not the same as the impedance *change* due to mutual coupling) between each pair of elements must be known for this calculation and it can be determined by measurement, calculation or from a graph.

The latter two methods are possible only for the simplest element types and measurement is very difficult to do accurately because it involves resolving very small differences between two relatively large values. Accuracy of a calculated result will be reduced if any elements are relatively fat (that is, they have a large diameter, because this impacts the current distribution) or they aren't perfectly straight and parallel.

So the only situations where you're likely to get good results from approaches other than modeling are the very easiest ones to model! And modeling allows determination of the feed-point impedances of many antennas that areimpossible to calculate by manual or graphical methods. Therefore, the manual approach isn't discussed or used here. Appendix B, on the CD, contains equations and manual techniques from previous editions of *The ARRL Antenna Book*, for those who are interested. You can also find a great deal of additional information in many of the texts listed in the Bibliography, particularly Jasik and Johnson.

Current Forcing with λ/4 Lines—Elements In-Phase or 180° Out-of-Phase

The feed method introduced here has been used in its simplest form to feed television receiving antennas and other arrays, as presented by Jasik, pages 2-12 and 24-10 or Johnson, on his page 2-14. However, until first presented in *The ARRL Antenna Book*, this feed method was not widely applied to amateur arrays.

The method takes advantage of an interesting property of λ/4 transmission lines. (All references to lengths of lines are electrical length and lines are assumed to have negligible loss.) See **Fig 15**. The magnitude of the *current out* of a λ/4 transmission line is equal to the *input voltage* divided by the characteristic impedance of the line. This is independent of the load impedance. In addition, the phase of the output current lags the phase of the input voltage by 90°, also independent of the load impedance. These properties can be used to advantage in feeding arrays with certain phase angles between elements.

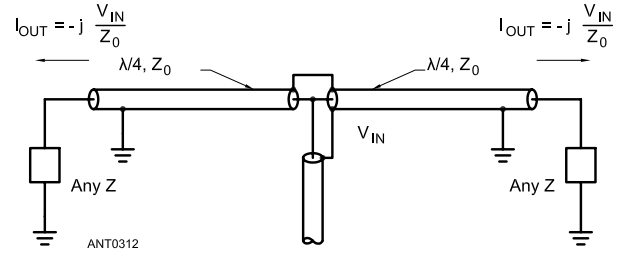

Fig 15—A useful property of λ/4 transmission lines; see text. This property is utilized in the "current-forcing" method of feeding an array of coupled elements.

If any number of loads are connected to a common driving point through λ/4 lines of equal impedance, the currents in the loads will be *forced* to be equal and in-phase, regardless of the load impedances. So any number of in-phase elements can be correctly fed using this method, regardless of how their impedances might have been changed by mutual coupling. Arrays that require unequal currents can be fed through λ/4 lines of unequal impedances to achieve other current ratios.

The properties of λ/2 lines also are useful. Since the current out of a λ/2 line equals the input current shifted 180°, regardless of the load impedance, any number of half wavelengths of line may be added to the basic λ/4, and the current and phase forcing property will be preserved. For example, if one element is fed through a λ/4 line and another element is fed from the same point through a 3λ/4 line of the same characteristic impedance, the currents in the two elements will be forced to be equal in magnitude and 180° out-of-phase, regardless of the feed-point impedances of the elements.

If an array of two, and only two, identical elements is fed in-phase or 180° out-of-phase with equal magnitude currents, both elements have the same feed-point impedance. The reason is that each element sees exactly the same thing when looking at the other. In an in-phase array, each sees another element with an identical current; in an out-of-phase array, each sees another element with an equal magnitude current that's 180° out-of-phase, the same distance away in both cases. This isn't true in something like a 90° fed array, where one element sees another with a current leading its current by 90°, while the other sees another element with a lagging current.

With arrays fed in-phase or 180° out-of-phase, feeding the elements through equal lengths of feed line (in-phase) or lengths differing by 180° (out-of-phase) will lead to the correct current magnitude ratio and phase difference, regardless of the line length and regardless of how much the element feed-point impedances depart from the lines' Z_0.

Unless the feed-point impedances equal the line Z_0 or the lines are an integral number of half wavelengths long, the magnitudes of the currents out of the lines will not be equal

to the input magnitudes, and the phase will not be shifted an amount equal to the electrical lengths of the lines. But both lines will produce the same transformation and phase shift because their load impedances are equal, resulting in a properly fed array. In practice, however, feed-point impedances of elements frequently are different even in these arrays, because of such things as different ground systems (for ground mounted vertical elements), proximity to buildings or other antennas, or different heights above ground (for horizontal or elevated vertical elements).

In many larger arrays, two or more elements must be fed either in-phase or out-of-phase with equal currents, but coupling to other elements can cause their impedances to change unequally—sometimes extremely so. Using the current-forcing method allows the feed system designer to ignore all these effects, while guaranteeing equal and correctly phased currents in any combination and number of 0° and 180° fed elements.

This method is used to develop feed systems for the Four Square and 4-element rectangular arrays in the **Practical Array Design** section. The front and rear elements of a Four-Square antenna provide a good example of elements having very different feed-point impedances that are forced to have equal out-of-phase currents.

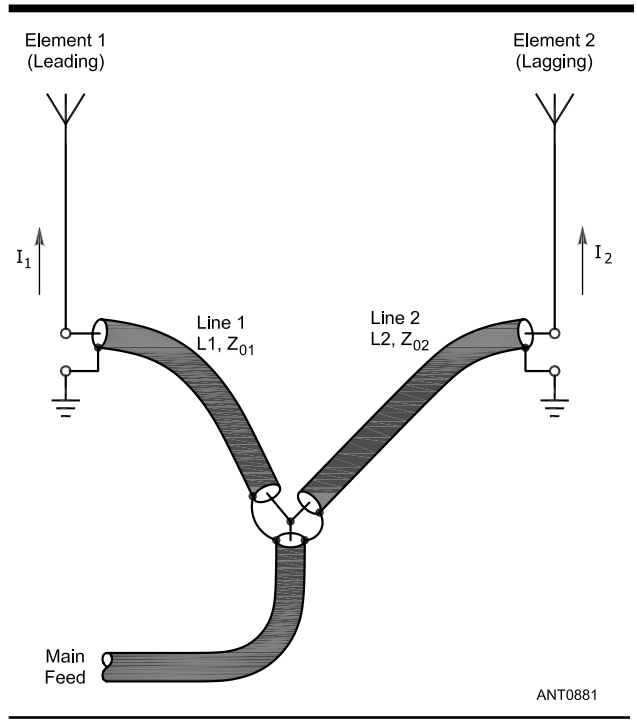

Fig 16—"Simplest" feed system for 2-element array. No matching or phasing network is used here, only transmission lines.

"The Simplest Phased Array Feed System—That Works"

This is the title of an article in *The ARRL Antenna Compendium, Vol 2*, which describes how arrays can be fed with a feed system consisting of only transmission lines. (The article is available for viewing at **eznec.com/Amateur/Articles/Simpfeed.pdf** and is also on the CD included in the back of this book, along with the program *Arrayfeed1*, which solves the equations presented in the article.)

As explained earlier in the Phasing Line section, this method requires knowing what the element feed-point impedances will be in a correctly fed array. Feed-line lengths can then be computed, for most but not all arrays. These lengths will produce the desired current ratio in array elements that do present those feed-point impedances. If you know the load impedances connected to transmission lines whose inputs are connected to a common source, it's simple to calculate the resulting load currents for any transmission line lengths. However, the reverse problem is much more difficult; that is, given the load impedances and desired currents to calculate the required cable lengths.

One way to solve the problem is to choose some feed-line lengths, solve for the currents, examine the answer, adjust the feed-line lengths, and try again until the desired currents are obtained. The author used this iterative approach, using first a programmable calculator and later a computer, for some time before developing a direct way of solving for the transmission-line lengths. The direct solution method is described briefly in the *Compendium* article.

Fig 16 shows the basic so-called "simplest" system applied to a two element array. Although it resembles an elementary phasing-line system as described earlier, the critical difference is that the lengths of Lines 1 and 2 are calculated to provide the correct current relative magnitude transformation and phase shift when terminated with the actual feed-point impedances.

The advantage to using this "simplest" feed system is indeed its simplicity. It's no more complicated than the elementary phasing-line approach but actually works as planned. The disadvantage over some other methods is that there's no convenient adjustment to compensate for environment factors, array imperfections or inaccurately known feed-point impedances.

Also, while unusual, it's possible that no suitable feedline lengths can be found for some arrays, or at least none with practical feed-line characteristic impedances. The difference in electrical feed-line lengths almost never equals the difference in phase angles between element currents. This is because of the different line delays resulting from different feed-point impedances.

Program *Arrayfeed1*, included on the CD included with this book, can do the calculations for any two elements (alone or in a larger array), a Four-Square array or a rectangular array in which two in-phase elements are driven at any current magnitude and phase relative to the other two in-phase elements. These possibilities cover a large number of common arrays.

Arrayfeed1 can also be applied to other types of arrays

using the method described in the **Feeding Larger Arrays** section in Appendix B (on the CD). The required knowledge of element feed-point impedances in a correctly fed array can be obtained using *EZNEC-ARRL*, also included on the CD. Examples of the design of a "simplest" feed system for several different arrays using *EZNEC-ARRL* and *Arrayfeed1* can be found in the **Phased Array Design Examples** section.

When a solution is possible for a given choice of line characteristic impedances, a second solution with different lengths is always available. See the comments in the introductory part of the **Phased Arrray Design Examples** section about choosing the solution to use.

An Adjustable L-Network Feed System

Adjustment of the current ratio of any two elements requires varying two independent quantities; for example the magnitude and phase of the current ratio. Two degrees of freedom—adjustments that are at least partially independent—are required. The "simplest" all-transmission line feed system described earlier adjusts the lengths of the two transmission lines to achieve the correct ratio.

But if the antenna characteristics aren't well known—for example, if the ground resistance isn't known even approximately—then the initial "simplest" design won't be optimum and adjustment can be difficult and tedious. The current-forcing method produces correct currents independently of the element characteristics, so it doesn't require adjustment as long as the elements are identical. But it's suitable only for feeding elements in-phase or 180° out-of-phase and a few fixed current-magnitude ratios.

The addition of a simple network as shown in **Fig 17** allows you to easily adjust feeding of element pairs at other relative phase angles and/or magnitude ratios. Any desired current ratio (magnitude and phase) can be obtained with two elements fed with any lengths of wire, equal or unequal, by adding a network.

However, calculations for the general case are complex. The problem becomes much simpler if the transmission lines are restricted to lengths of odd multiples of λ/4, forming a modified "forcing" system that includes an added network. There are at least three additional advantages of this scheme. One is that a λ/4 line is easy to measure, even if the velocity factor isn't known. This is described in the **Practical Aspects of Phased Array Design** section.

Second is that the feed system becomes completely insensitive to the feed-point impedance of one of the two elements. And the third is that the transmission lines of "forcing" systems feeding groups of elements in larger arrays can be used in place of the normal λ/4 lines. This greatly simplifies both the design of feed systems for larger arrays and the feed systems themselves. Note that both lines can be changed to 3λ/4 if necessary to span the physical distance between elements, but *both* lines must be the same 3λ/4 length.

This basic feed method can be used for any pair of elements, or for two groups of elements having forced equal currents. (See **Feeding Four Element and Larger Arrays** below.) Many networks can accomplish the desired function, but a simple L network is adequate for most feed systems. The network can be designed to produce a phase lead or phase lag. The basic two-element L-network feed system is shown in Fig 17. Many variations of this general method can be used, but the equations, program, and method to be discussed here apply only to the feed system shown.

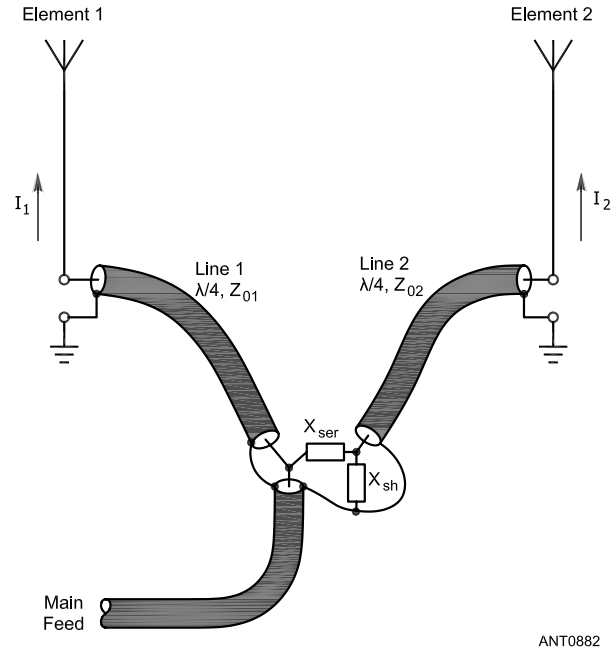

Fig 17— The addition of a simple L-network to Fig 16 allows you to easily adjust feeding of element pairs at other relative phase angles and/or magnitude ratios.

If the phase angle of I_2/I_1 is negative (element 2 is lagging element 1), the L network will usually resemble a low-pass network (X_{ser} is an inductor and X_{sh} is a capacitor). But if the phase angle is positive (element 2 lagging element 1), the L network will resemble a high-pass network (X_{ser} is a capacitor and X_{sh} is an inductor). However, some current ratios and feed-point impedances could result in both components being inductors or both being capacitors.

If it's desired to maintain symmetry in the feed system, X_{ser} can be divided into two components, each being inserted in series with a transmission line conductor. If X_{ser} is an inductor, the new components will each have half the value of the original X_{ser}, as shown in **Fig 18**. If X_{ser} is a capacitor, each of the new components will be twice the original value of X_{ser}.

Because of the current-forcing properties of λ/4 lines, we need to make the ratio of *voltages* at the inputs of the lines equal to the desired ratio of *currents* at the output ends of the lines; that is, at the element feed points. The job of the L network is to provide the desired voltage transformation. If the output-to-input voltage ratio of the network is, say, 2.0 at an angle of –60°, then the ratio of element currents (I_2/I_1)

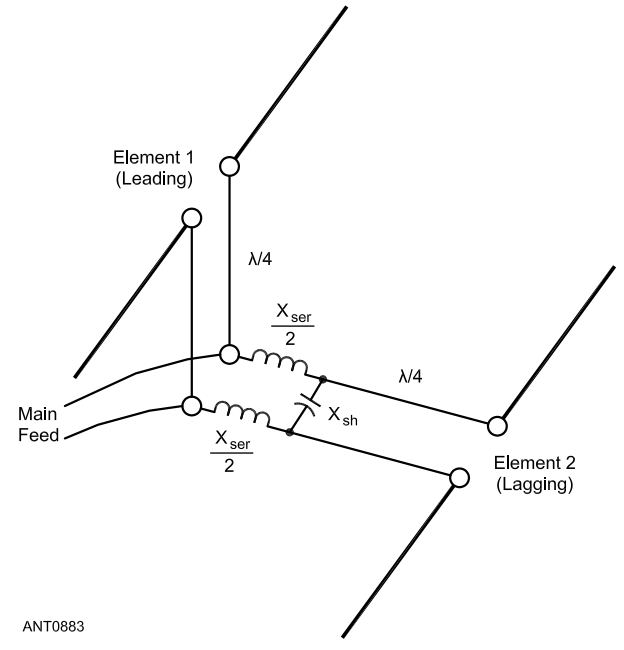

Fig 18—Symmetrical feed system similar to Fig 17, where feed network is split into two symmetrical parts.

will be 2.0 at an angle of –60°. The voltage transformation of the network is affected by the impedance of element 2, but not by the impedance of element 1. So only the impedance of element 2 must be known to design the feed system.

Equations for designing the L network are given in Appendix B, but the program *Arrayfeed1* is included on the CD to make it unnecessary to solve them. The feed-point impedance of the lagging element or group of elements must be known in order to design the network. This can best be determined by modeling the array with *EZNEC-ARRL*. The impedance can be manually calculated for some simple element and array types by using the equations in Appendix B, but those same types of element and array are simple to model.

Examples of the design of L-network feed systems for several different arrays using *EZNEC-ARRL* and *Arrayfeed1* can be found in the **Phased Array Design Examples** section. A similar application of this feed system and a spreadsheet program for calculation was developed by Robye Lahlum, W1MK, and described in *Low-Band DXing* (see the Bibliography). *Arrayfeed1* can be used for the applications of the feed system described in that book if desired.

Additional Considerations

Feeding 4-Element and Larger Arrays

Both the simplest and L-network feed systems described above can be extended to feeding larger arrays having two groups of elements in which all the elements in a group are in-phase or 180° out-of-phase with each other—basically, any group that can be fed with the current-forcing method. The elements in each group are connected to a common point with λ/4 or 3λ/4 lines to force the currents to be in the correct ratio within the group. Then the "simplest" or L-network feed system can be used to produce the correct phasing between the two groups, just as it does between two individual elements.

Two common arrays that fit this description are the Four Square and the 4-element rectangular array. But more elaborate arrays could be constructed and fed using this method, such as a pair of binomial arrays. (A single binomial array is described in the **Phased Array Design Example** section below.) The *Arrayfeed1* program incorporates additional calculations necessary for designing Four Square and 4-element rectangular arrays. The general procedure for adapting the feed methods to other larger arrays can be found in Appendix B.

What If the Elements Aren't Identical?

Getting the desired pattern requires getting the correct relative magnitude and phase of the *fields* from the elements. If the elements are identical, which we've generally assumed up to this point, then producing currents of the desired magnitude and phase will create the desired fields (neglecting mutual coupling current distribution effects, discussed elsewhere).

But what if the elements aren't identical? Fortunately, the feed systems described here can still be used for any 2-element array and some more complex arrays, provided that the system can be accurately modeled. But a slightly different approach is required than for identical elements.

The first step is to model the array with a current source at the feed point of each element. Next, the magnitudes and phases of the model source currents are varied until the desired pattern is achieved. Then the ratio of feed-point (source) currents is calculated and this value, along with the feed-point impedances reported by the model, are used for the feed system design. The feed system will produce the same ratio of currents as the model, resulting in the same pattern.

In general, this approach won't work with shunt fed towers or gamma-fed elements because of the difficulty of accurately modeling those structures. See **Shunt and Gamma Fed Towers and Elements** for more information.

Shunt and Gamma Fed Towers and Elements

In a shunt, gamma, or similarly fed tower or element, the feed-point current isn't the same as the main current flowing in the element. The ratio between the feed-point current and element current isn't a constant, but depends on a number of factors. The ratio of currents in shunt or gamma fed elements are typically different—often vastly different—from the currents at the feed points. This complicates the design of feed systems for arrays of these elements.

An even more limiting problem is that the feed-point impedances are difficult to determine. The feed-point impedances of one or more elements in a properly fed array must be known in order to design a feed system for anything but

2-element in-phase or 180° out-of-phase arrays.

The only practical way to get this information for a shunt or gamma fed array is by modeling an array having the desired element currents. But Cebik has pointed out ("Two Limitations of NEC-4"—see the Bibliography) that many common antenna analysis programs, including *EZNEC-ARRL*, have difficulty accurately modeling folded dipoles with unequal diameter wires. The same problem applies to shunt and gamma-fed elements when the element diameter is significantly different from the diameter of the shunt or gamma feed wire. Without accurate feed-point impedances, feed systems can't be designed to work without adjustment. It might be possible to get reasonably accurate results from a *MININEC*-based modeling program, but there are a number of issues which must be given great care when using one. (See Lewallen, "*MININEC*—The Other Edge of the Sword," listed in the Bibliography.)

If such a *MININEC* program is available, you would have to model the complete array including feed system, with sources at the normal feed points in the shunt or gamma wires. Next, you would have to adjust the magnitudes and phases of the sources to produce the desired pattern. The reported source impedances and currents would be the ones you would use to design the feed system. It's likely that some adjustment would be necessary, so an adjustable system such as the L-network feed system described later would be best.

Loading, Matching and Other Networks

Adding a component such as a loading inductor in series with an element or element feed point won't change the ratio of element current to feed-point current. As a result, a feed system designed to produce a particular ratio of element currents will still function properly if the elements contain series components. The extra feed-point impedance introduced by the loading component(s) must be considered when designing the feed system, however. Similarly, end or top loading won't alter the relationship between feed-point and element current, provided that the current distribution in the elements is essentially the same. (See **Feed-point vs Element Current** in a previous section.)

However, insertion of any *shunt* component, or a network containing a shunt component, *will* alter the relationship between feed-point and element current because it will divert part of the feed-line current that would otherwise flow into the antenna. As a result, a feed system designed to deliver correct currents at the feed points will produce incorrect element currents and therefore an incorrect pattern. Therefore, any components or networks other than a series loading component should be avoided at any place in the feed system on the antenna side of the point at which the feed system splits to go to the various elements.

There are a few exceptions to this rule. If the feed-point impedances of the elements when in the excited array are equal, then identical networks with or without shunt components can be put at the feed points of the elements and the proper element current ratio maintained—so long as the feed system is designed to deliver the proper feed-point current ratio with the networks in place. Equal element impedances occur in arrays having only two identical elements fed in-phase or 180º out-of-phase, or arrays of any number of elements where the elements are electrically short and/or very lossy.

Baluns in Phased Arrays

For purposes of achieving the correct array pattern, baluns aren't usually required when feeding grounded vertical elements with coaxial cable feed lines. However, a balun might be desirable if current induced onto the outside of the feed line by mutual coupling to the elements is causing RF in the shack. And with arrays of dipole or other elevated elements, baluns can be important to achieve the proper element current ratio, as explained below.

First, however, the general rules for using baluns in phased arrays will be stated. Here, "main feed line" means the feedline going from the transmitter or receiver to the common point where the system splits to feed the various elements. "Phasing-system lines" means any transmission lines between that common point and any element. The rules:

• **Rule 1:** A balun or baluns (more specifically, a current, sometimes called a choke balun) should be used as necessary to suppress unbalanced current on the main feed line. This usually isn't required when feeding grounded elements with coaxial feed line from an unbalanced rig or tuner. Unbalanced current can occur on either coax or parallel-conductor line.

"Baluns: What They Do and How They Do It", listed in the Bibliography, describes conducted-imbalance (common-mode) currents. Imbalance can also be caused by mutual coupling to the array elements. Common-mode currents have at least two undesirable effects on array performance. First, the imbalance current can flow from the main feed line to the phasing system lines, not necessarily splitting in the right proportion to maintain the correct element current ratio. This can affect the array pattern. In practice, however, this effect is likely to be small unless the common-mode current is unusually large. Even a small common-mode current, however, results in main feed-line radiation, and even a small amount of radiation can significantly degrade array pattern nulls. Any type of current balun can be used on the main feed line, at any place along the line, without any effect on the array pattern except to the extent that it reduces common mode current.

• **Rule 2:** No balun or any other component or network should be inserted in any phasing system line that will alter the line length or characteristic impedance. This means that baluns in phasing system lines must be of a type made from the phasing line itself. Options are the W2DU type balun, consisting of ferrite cores placed along the outside of the feed line; an air-core balun made by winding part of the line into an approximately self-resonant or otherwise high-impedance coil; or winding part of the line onto a ferrite core or rod to make a several-turn winding. When coaxial cable is used, the feed system characteristics are dictated by the inside of the cable. Any cores or winding of the outside prevents common-

mode current on the outside, but otherwise have no effect on the phasing performance. This rule applies equally to parallel wire line, where the balun affects only common-mode current (equivalent to current on the outside of coax) while the phasing performance depends on differential mode current (equivalent to the current on the inside of coax).

Baluns are important when feeding dipole or other elevated arrays, unless a fully balanced tuner is used. This is because common-mode current represents a diversion of some of the current that should be going to the array elements. The presence of common-mode current means that the element currents are being altered from the desired ratio and therefore the pattern won't as intended. A balun should be placed wherever a path for current exists other than along a parallel-line conductor or on the inside of a coaxial line. Such a path exists, for example, where a coaxial cable connects to a dipole, as shown in Fig 1 of the balun article referenced above. Or a path can exist where a parallel-conductor transmission line connects to an unbalanced tuner or to a coaxial line, as shown in Fig 2 of that article. In both those cases, a path exists for a common-mode current to flow on the outside of the coax cable. A balun creates a high impedance to this current, thereby reducing its magnitude. But remember that all baluns must conform to the rules above.

Fig19 shows recommended balun locations for a coax-fed dipole array using an L-network feed system.

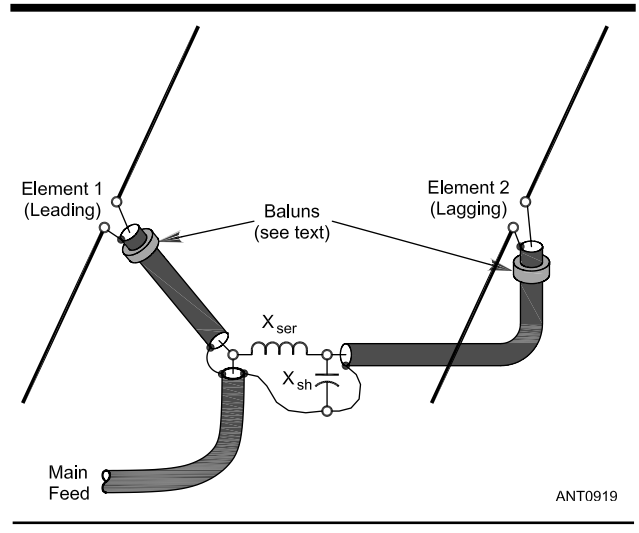

Fig 19—Adding choke baluns to a two-dipole feed system to get rid of common-mode currents radiated onto the coax shields.

Receiving Arrays

While it might not be entirely intuitive, an array designed for a particular gain and pattern for transmitting that considers mutual coupling, element currents, field reinforcement and cancellation, and so forth, will perform exactly the same when receiving. So a receiving array can be designed by approaching the problem as though the array were to be used for transmitting.

However, at HF and below, the system requirements for transmitting and receiving antennas are different, so receiving-only arrays can be designed that aren't suitable for transmitting but are perfectly adequate for receiving in that frequency range. The reason, described in more detail in Chapter 13 of this book, is that at HF and below atmospheric noise is typically much greater than a receiver's internally generated noise. Lowering a receiving antenna's gain and efficiency reduces the signal and atmospheric noise both by the same factor. Because the overall noise is for practical purposes all atmospheric noise, the signal/noise ratio isn't affected by antenna efficiency.

Of course, a point can be reached where the atmospheric noise is so reduced by inefficiency that the receiver itself becomes the dominant source of noise, but this typically doesn't happen until the antenna is extremely inefficient. When transmitting, reduced efficiency lowers the transmitted signal, but it has no effect on the receiving station's noise. So reduced efficiency of a transmitting antenna results in a reduced signal/noise ratio at the receiving end, and consequently should be avoided.

Mutual coupling effects can be minimized by increasing the loss (and therefore reducing the efficiency) of the elements, or by reducing the element sizes to a small fraction of a wavelength. Doing the second without the first isn't usually a good idea because the feed-point impedance tends to change rapidly with frequency for very small elements, making an antenna that works well over only a narrow bandwidth. But increasing loss broadens the bandwidth, even for small elements, as well as reducing mutual coupling effects. So this approach is often taken for designing a receiving-only array. With mutual coupling effects minimized because of loss, feed-system design becomes relatively simple, provided a few simple rules are followed. See **Loss Resistance, Mutual Coupling, and Antenna Gain**, above.

Phased Array Design Examples

This section, also written by Roy Lewallen, W7EL, presents examples of feed-system design for several kinds of array using the design principles given in previous sections. All but the last example array are assumed to be made of λ/4 vertical elements. The last example is for a halfwave-dipole array, which illustrates that exactly the same method can be used for arrays of any shape of elements, including dipole, square (quad) and triangular. Likewise, the methods shown here apply equally well to VHF and UHF arrays. The first example includes more detail than the remaining ones, so you should read it before the others.

General Array Design Considerations

If either the "simplest" feed system (Fig 16) or L-network feed system (Fig 17) is used, the feed-point impedance of one or more elements—*when the array elements all have the correct currents*—must be known. By far the best way to determine this is by modeling. If accurate modeling isn't practical for some reason, an estimation should be made from an approximate model, and you should expect to have to adjust the feed system after building and installing it.

Manual calculation methods for some simple configurations are given in Appendix B (on the CD), but calculation is tedious and, as stated earlier, the configurations for which this method works are the very ones which are easiest to model. *EZNEC-ARRL* (also included on the CD) is used in the following examples to determine feed-point impedance. Space doesn't permit detailed instructions here on creating the models, so they are included in complete form. They should provide a convenient starting point for any variations you might like to try. See the *EZNEC-ARRL* manual (accessed by clicking **Help/Contents** in the main *EZNEC-ARRL* window) for help in using this program.

In the following examples, vertical elements are close to λ/4 high and dipole elements close to λ/2, and their lengths have been adjusted for resonance when all other elements are absent or open circuited. There's actually no need in practice to make the elements self-resonant—it's simply used as a convenient reference point for these examples. You'll also find it interesting to see how much reactance is present at the feed points of the elements when in the arrays, knowing that it's very nearly zero when only one element is present.

In any real grounded vertical array, there is ground loss associated with each element. The amount of loss depends on the length and number of ground radials, and on the type and wetness of the ground under and around the antenna. This resistance becomes part of the feed-point resistance, so it must be included in the model used to determine feed-point impedance. The 90° Fed, 90° Spaced Array example below discusses how this is done. **Fig 20** gives resistance values for typical ground systems, based on measurements by Sevick (July 1971 and March 1973 *QST*). The values of feed system components based on Fig 20 will be reasonably close to correct, even if the ground characteristics are somewhat different than Sevick's.

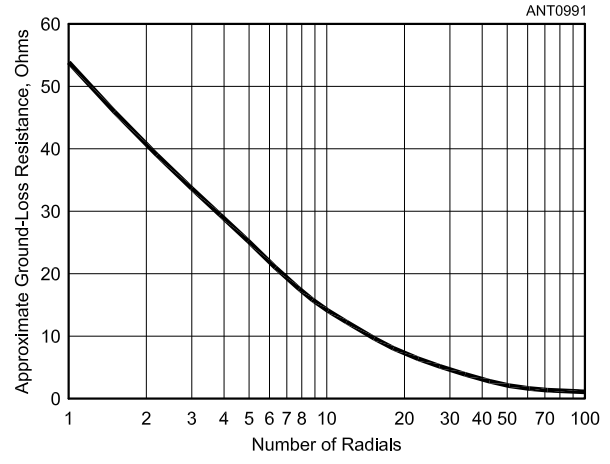

Fig 20—Approximate ground system loss resistance of a resonant λ/4 ground-mounted vertical element versus the number of radials, based on measurements by Jerry Sevick, W2FMI. Moderate length radials (0.2 to 0.4 λ) were used for the measurements. The exact resistance, especially for only a few radials, will depend on the nature of the soil under the antenna. Add 36 Ω for the approximate feed-point resistance of a thin resonant λ/4 vertical.

Feed systems for the design example arrays to follow are based on the resistance values given below.

Number of Radials	*Loss Resistance, Ω*
4	29
8	18
16	9
Infinite	0

Elevated radial systems also have some ground loss, although it can be considerably less than a system with the same number of buried radials. This loss will be automatically included in the feed-point impedance of a model which includes the elevated radials, so no further estimation is required. Be sure to use Perfect, High-Accuracy ground type when modeling an elevated radial system with *EZNEC-ARRL*. In other *NEC-2* based programs, this might be referred to as Sommerfeld type ground. More information can be found in the *EZNEC-ARRL* manual.

The matter of matching the array for the best SWR on the feed line to the station is not dealt with here, since it's a separate problem from that of the main topic, which is designing feed systems to produce a desired pattern. Some of the simpler arrays provide a match that is close to 50 or 75 Ω, so no further matching is required. However, as shown by program *Arrayfeed1*, many larger arrays present a less favorable impedance for direct connection and will require matching if a low SWR on the main feedline is required. If matching is necessary, the appropriate network should be

placed in the single feed line running to the station. Attempts to improve the match by adjustment of the phasing L network, individual element lengths, matching at the element feed points or individual element feeder lengths will usually ruin the current balance of the array. Program *TLW*, included on the CD, can be used for designing an appropriate matching network. Additional information on impedance matching may be found in Chapters 25 and 26 of this book.

Choosing Arrayfeed1 Solutions

When designing a feed system for a two element array, *Arrayfeed1* program allows you to choose the characteristic impedances of the two transmission lines going to the elements, which don't have to be equal, so you have your choice of more than one solution. However, directional array switching is much more difficult if the lines have different impedances, so in general you should use the same characteristic impedances.

For larger arrays, *Arrayfeed1* requires the feed lines to all elements to have the same impedance. In choosing the transmission line impedance values, usually you can simply use convenient impedances. But in general, you should avoid solutions where component reactance (X) values are vastly different (say, more than three times or less than one third as large) as the line characteristic impedances. Such networks will become more critical to adjust, and both the impedance and pattern will change more rapidly with changes in frequency. You can usually avoid this situation by choosing feed-line impedances that are in the same ballpark as the element feed-point impedances. The last example in the Practical Array Design section illustrates this problem and its solution.

When designing a "simplest" feed system, the most broadbanded and least critical system is usually one where the difference in electrical feed-line lengths is closest to the relative element phase angle. Here, "broadbanded" means that the pattern changes less with frequency, not necessarily that the SWR changes less. However, an array that's broadbanded in the pattern sense is usually also relatively broadbanded with respect to SWR.

Arrayfeed1 reports the impedance seen at the main array feed point. While it might be tempting to choose the solution producing the lowest SWR on the main feedline, you'll end up with a less critical and more broadbanded system if you base your choice on the criteria given above, and provide separate impedance matching at the array's main feed point when necessary.

90° Fed, 90° Spaced Vertical Array

This example illustrates the design of both "simplest" and L-network feed systems for a 2-element, 90° spaced and fed vertical array. The first task when using either feed system is to determine the feed-point impedances of the elements when placed in an array having the desired element currents. The "simplest" feed system method requires knowledge of both element impedances, while the L-network system requires you to know only one. Actually, it's equally easy to determine both as it is to find just one, using *EZNEC-ARRL*. (Appendix B contains equations for those interested in manual methods or for more insight as to how the impedances come about.) The first step is to specify the antenna we want. For this example, we'll specify:

- Frequency: 7.15 MHz.
- Two identical, one inch (2.54 cm) diameter, 33 feet (10.06 meter) long elements spaced 90 electrical degrees, with element currents equal in magnitude and 90° apart in-phase.
- 8 buried radial wires, 0.3 λ long, under each element.

A model of this antenna has been created and furnished with *EZNEC-ARRL*. So the next step is to start *EZNEC-ARRL*, click the **Open** button, enter **ARRL_Cardioid_Example** in the text box (or double-click it in the file list) to open example file **ARRL_Cardioid_Example.EZ**.

This *EZNEC* example model uses a *MININEC*-type ground, which is the same as perfect ground when calculating antenna currents and impedances. A real antenna would have some additional resistive loss due to the finite conductivity of the ground system. The only way to model a buried radial ground system with an *NEC-2* based program like *EZNEC* is to create radial wires just above the ground (using the Real, High-Accuracy ground type), because *NEC-2* can't handle buried conductors.

This provides only a moderate approximation of a buried system. Another way to estimate ground-system resistance is to measure the feed-point impedance of a single element, then subtract from that the resistance reported for a model of that element over perfect (or *MININEC*-type) ground. For most uses, however, an adequate approximation can be made by simply referring to the graph of Fig 20. As stated previously, the feed system design depends on the feed-point impedances of the elements, which in turn depend on the ground system resistance. So the ground system resistance must be known, approximately anyway, before designing the feed system. At the end of this example we'll investigate the effect of changes in the ground system or errors in estimating the resistance on the pattern.

For 8 radials, Fig 20 shows the ground system resistance to be about 18 Ω. This is included in the example model as a simple resistive load at the feed point of each element. Click the **Src Dat** button to see the feed-point impedances of the two elements. In this model, Source 1 is at the base of Wire 1 (element 1), and Source 2 is at the base of Wire 2 (element 2). Notice in the **Source Data** display that the Source 1 current has been specified at 1 amp at 0°, and Source 2 is 1 amp at –90°. So the Source 2 element is the lagging element. You should see impedances of 37.53 – *j*19.1 Ω for element 1 and 68.97 + *j*18.5 Ω for element 2. These are the feed-point impedances resulting when the array is ideally fed, with equal magnitude and 90° phased currents. Record these values for use in *Arrayfeed1*.

Click the **FF Plot** button to generate a plot of the azimuth pattern at an elevation angle of 10°. In the 2D Plot Window,

open the **File** menu and select **Save Trace As**. Enter **Cardioid_Ideal Feed** in the **File Name** box, then click **Save**. This saves the cardioid pattern plot so you can compare it later to the pattern you get with the transmission line feed system.

Now it's time to design the feed system. Refer to the appropriate subheading below for the design of each of the two kinds of feed systems. Both systems use program *Arrayfeed1* program.

"Simplest" (Transmission Line Only) Feed System

Start *Arrayfeed1*. In the **Array Type** frame, select **Two Element**. In Feed System Type, select **"Simplest."** In the **Inputs** frame, enter the following values:

Frequency MHz = 7.15; Feed-point impedances – Leading Element: R ohms = 37.53, X ohms = –19.1; Lagging Element: R ohms = 68.97, X ohms = 18.5 (these are the element R and X values from *EZNEC-ARRL*). We'll be discussing the array input impedance, so check the **Calc Zin** box near the lower left corner of the main window if it's not already checked.

We're free to choose any transmission-line characteristic impedances we want, so long as we can get cables with those impedances. And the two cables don't have to have the same characteristic impedances. Each choice will lead to a different set of solutions. But sometimes a solution isn't possible, which then requires choosing different line impedances. Let's try 50 Ω for both lines. Enter **50** in both **Z0** boxes.

Finally, enter **1** for the lagging:leading **I Mag**, and **–90** for the **Phase**. Click **Find Solutions**. The result is no solution! So enter **75** into both the line impedance boxes and click **Find Solutions** again. You should now see two sets of results in the **Solutions** frame, electrical lengths of 68.80° and 156.03° for the first solution and 131.69° and 185.00° for the second. (Notice that the difference in length between the two lines isn't 90° for either solution, although the first solution is quite close. It's normal for the feed-line length difference to be different than the phase difference, due to the unequal element feed-point impedances caused by mutual coupling.)

The solution with a line length difference closest to the element phase difference is usually preferable. Also, all else being equal, the solution with shortest lines is better providing that the lines will physically reach the elements. This is because the current magnitude and phase will change less with frequency than for a longer-length solution. However, there might be some cases where the change with frequency luckily compensates for the changing electrical distance between elements, so it's not a bad idea to model both solutions unless you plan on using the antenna over only a narrow frequency range.

In this case, the first solution looks best in all respects. The sum of the two lines in the first solution is about 225 electrical degrees. Assuming the lines have a velocity factor of 0.66, the total length of the lines will be more than 148 physical degrees. Since our two elements are spaced 90 physical degrees apart, the lines will comfortably reach. If they didn't, we could either use the second solution's lengths, use cable with a higher velocity factor or add a half wavelength to both the line lengths in the first solution.

The impedance **Zin** shown by *Arrayfeed1* is the impedance at the input to the feed system, so it's the impedance that will be seen by the main feed line. The second solution provides nearly a perfect match for a 50-Ω transmission line. But the first solution is good for nearly all applications. Also a 50-Ω line connected to the first solution's feed system would have an SWR of only 1.65:1, which wouldn't require any matching under most circumstances. Normal line loss would reduce the SWR even more at the transmitter end of the feed coax.

To find the required physical line lengths, enter the cable velocity factor and make your choice of units in the **Physical Lengths** frame. The design is now complete; all you have to do is cut two lines to the specified lengths and connect one from a common feed point to each element as shown in Fig 16, or the screen capture from *Arrayfeed1* shown in **Fig 21**.

Next, we'll design an L-network feed system for the same array.

L Network Feed System

In *Arrayfeed1*, select **L Network** in the **Feed System Type** frame. The program doesn't need to know the leading element impedance to calculate the L-network values, but it does need it to calculate the array input impedance. If you want to know the impedance, check the **Zin** box at the lower left corner of the main window, otherwise you can uncheck it and the input box for the leading element Z will disappear. The values from the "Simplest" analysis should still be present in the appropriate boxes; if not, refer to the "Simplest" feed system design above and re-enter the values. Again, we'll use 75 Ω for the line impedances, since that gave us a

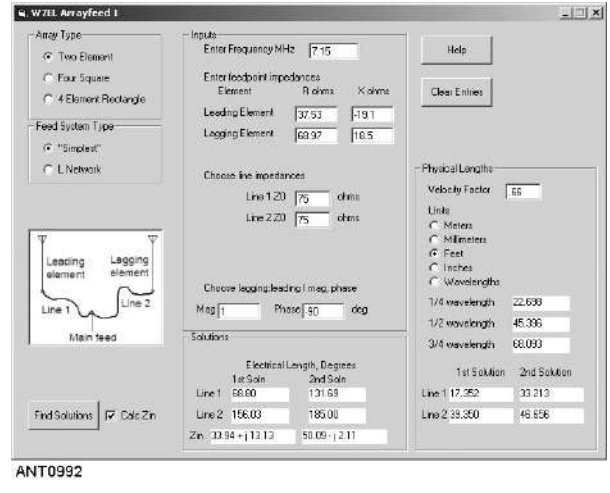

Fig 21—Screen capture from *Arrayfeed1* program for "Simplest" 2-element phased array shown in Fig 16 and whose feed-point impedances are modeled by *EZNEC-ARRL*.

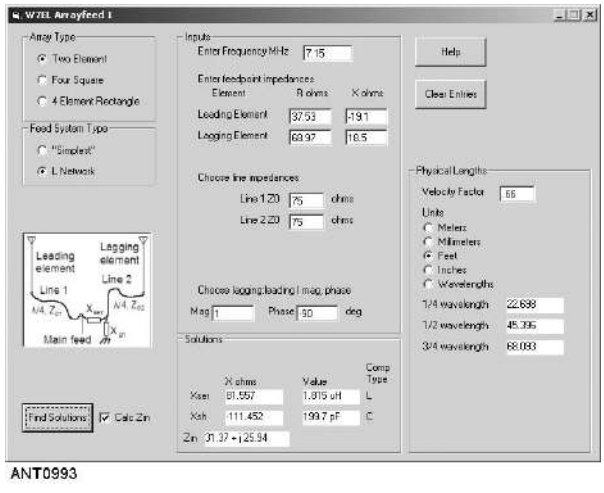

Fig 22—Screen capture from *Arrayfeed1* program for L-network feed system using "current-forcing" properties of λ/4 feed lines.

solution for the "Simplest" feed system. This feed system is more versatile, though, so we could use 50-Ω lines with this feed system if desired.

Click **Find Solution** and see the results in the **Solution** frame. See screen capture in **Fig 22**. With 75-Ω lines, the L network consists of a series inductor of 1.815 μH and a shunt capacitor of 199.7 pF, connected as shown in the diagram in the left part of the program window. To find the physical length of the λ/4 lines, enter the velocity factor and choice of units in the **Physical Lengths** frame.

The main feed-point impedance of 31.37 + *j*25.94 Ω would result in about a 2.2:1 SWR on a 50-Ω feed line, which would be acceptable for many applications. It could easily be reduced to 1.6:1 by the simple addition of a series capacitor of 25.94 Ω reactance (858 pF) at the main feed point or, of course, reduced to 1:1 with a simple L network or other matching system designed with the *TLW* program.

Pattern Verification and Effect of Loss Resistance—"Simplest" System

EZNEC-ARRL doesn't have the capability to model an L-network, so *EZNEC-ARRL* verification of the pattern and the effect of various modifications can be done only for the "simplest" feed system.

EZNEC model **ARRL_Cardioid_TL_Example.EZ** has been created to model the "simplest" feed system just designed. Open it with *EZNEC-ARRL*. In the View Antenna Display, you can see the transmission lines connecting to the source midway between the antennas. In *EZNEC*, the physical locations of the ends of transmission line models don't have to be the same as the physical locations, so the view isn't a precise representation of what the actual setup would look like. (You can find more about this in **ARRL_Cardioid_TL_Example.txt**, the Antenna Notes file that accompanies example file **ARRL_Cardioid_TL_Example.EZ.**)

Click **FF Plot** to generate a 2D pattern of the antenna. In the 2D Plot Window, open the **File** menu and select **Add Trace**. Select **Cardioid—Ideal Feed** (which you saved earlier) and click **Open**. The added plot overlays perfectly, indicating that the pattern using this feed system is identical to the pattern we got with perfect current sources at each feed point.

To check the feed-point currents, click the **Currents** button. In the resulting table, you can see that **Wire 1 Segment 1** current is 0.56467 A at a phase of –56.73° and **Wire 2 Segment 1** current is 0.56467 A at –146.7°. (If you get the correct phase angles but wrong magnitudes, open the main window **Options** menu, select **Power level**, and make sure the **Absolute V, I sources** box is checked.) The ratio is 1.0000 at an angle of –89.97°, which is within normal error bounds for the desired 1 at –90°.

As a check on *Arrayfeed1*, click the **Src Dat** button to find the impedance seen by the source. This would be the impedance at the main feedline connection in the real array. *EZNEC-ARRL* reports 33.96 + *j*13.11 Ω, very close to the 33.94 + *j*13.13 Ω given by *Arrayfeed1* in Fig 21. Small differences of this order are normal and to be expected. This provides a further check that the *EZNEC-ARRL* model is correctly analyzing the *Arrayfeed1* feed system.

This *EZNEC-ARRL* model uses lossless transmission lines of a fixed physical length rather than a fixed electrical length (number of degrees), so they'll behave like real lines as the frequency is changed. By changing the *EZNEC* frequency and re-running the 2D plot, you can see that the front-to-back ratio degrades at 7.0 and 7.3 MHz. A slight adjustment of one or more line lengths, or a new *Arrayfeed1* solution at a slightly different frequency might produce a better compromise for some uses.

Other things you can try are to evaluate the second *Arrayfeed1* solution, or to try using different line impedances. (Keep the two line impedances equal if you anticipate doing array direction switching.) The effect of varying ground system resistance can also be evaluated by clicking the **Loads** line in the main window and changing the load resistance values. For example, if the ground system resistance were 9 Ω instead of the 18 Ω we have assumed, the front/back ratio would drop from about 32 to about 20 dB. Note that changing the *EZNEC* ground conductivity in this model has no effect on the feed-point current ratio. With a *MININEC* type ground, it's used only for pattern calculation—the ground is assumed perfect during impedance and current calculations, and the only ground system loss resistance in the model is what we've specifically put in as loads.

Not surprisingly, the forward gain is affected very little by changes in frequency or ground system loss. To find the gain relative to a single element, compare the reported dBi gain of **ARRL_Cardioid_Example** with the same model with one of the elements deleted. You'll find it's very close to 3.0 dB. The 90° fed, 90° spaced array is a special case of array where the effects of mutual coupling on the two ele-

ments are opposite and cancel, resulting in the same gain as if mutual coupling didn't exist. But mutual coupling most certainly does exist!

The second solution presented a more favorable main feed-point impedance, so it would be tempting to use that one instead of the first solution. Replacing the feed-line lengths with the second solution lengths to model the second solution shows that the front/back ratio deteriorates more at the band edges when the second solution is used. This might be tolerable if restricted frequency use is anticipated. But it does illustrate that the solution with shorter lines is generally more broadbanded and that the choice of solution shouldn't in general be based on the one giving the most favorable impedance.

A Three-Element Binomial Broadside Array

An array of three in-line elements spaced λ/2 apart and fed in-phase gives a pattern that is generally bidirectional. If the element currents are equal, the resulting pattern has a forward gain of 5.7 dB (for lossless elements) compared to a single element, but it has substantial side lobes. If the currents are tapered in a binomial coefficient 1:2:1 ratio (twice the current in the center element as in the two end elements), the gain drops slightly to just under 5.3 dB, the main lobes widen and the side lobes disappear.

The array is shown in **Fig 23**, and an *EZNEC-ARRL* model of the antenna over perfect ground to show the ideal pattern is provided as **ARRL_Binomial_Example.EZ**. To obtain a 1:2:1 current ratio in the elements, each end element is fed through a 3λ/4 line of impedance Z_0. Line lengths of 3λ/4 are chosen because λ/4 lines will not physically reach. The center element is fed from the same point through two parallel 3λ/4 lines of the same characteristic impedance. This is equivalent to feeding it through a line of impedance $Z_0/2$. The currents are thus forced to be in-phase and to have the correct ratio. **ARRL_Binomial_TL_Example.EZ** is an *EZNEC-ARRL* model that shows this feed system with lossless transmission lines. The reader is encouraged to experiment with this model to see the effect of changes in frequency, the addition of loss resistance (as resistive loads at the element feed points) and other alterations on the array pattern and gain. You should also replace the perfect ground with *MININEC* type of ground to show how radiation patterns over real ground differ from the theoretical perfect-ground pattern.

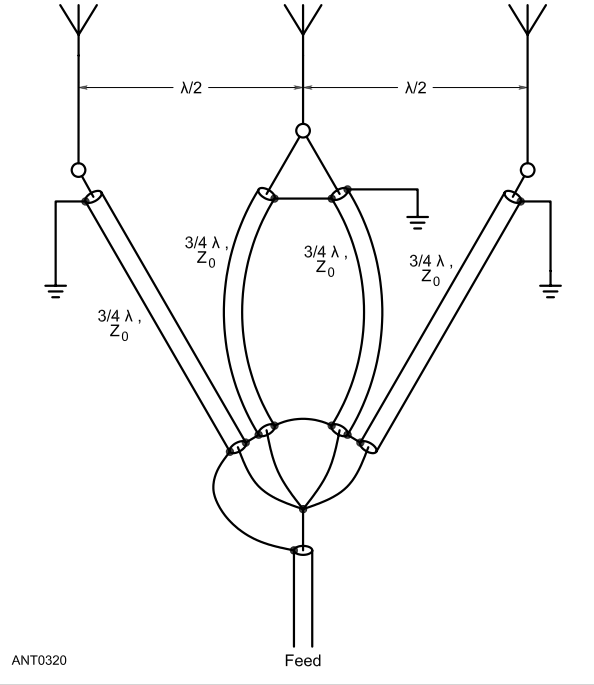

Fig 23—Feed system for the three element 1:2:1 binomial array. All feed lines are ¾ electrical wavelength long and have the same characteristic impedance.

A "Four Square" Array

Several types of feed system are used for feeding this popular array, and most share a common problem—they don't provide the correct element current ratio—although a number of them produce a workable approximation. The feed systems described here are capable of producing exactly the correct current ratio. The only significant variable is the element feed-point impedances, so the quality of the result depends on your ability to model the feed-point impedances of a correctly fed array. As in the examples above, *EZNEC-ARRL* will be used for that purpose and *Arrayfeed1* for the design of the feed system itself.

In this array (see **Fig 24**), four elements are placed in a square with λ/4 sides. (A variation of the Four Square uses wider spacing.) The rear and front elements (1 and 4) are 180° out-of-phase with each other. The side elements (2 and 3) are in phase with each other and 90° delayed from the front ele-

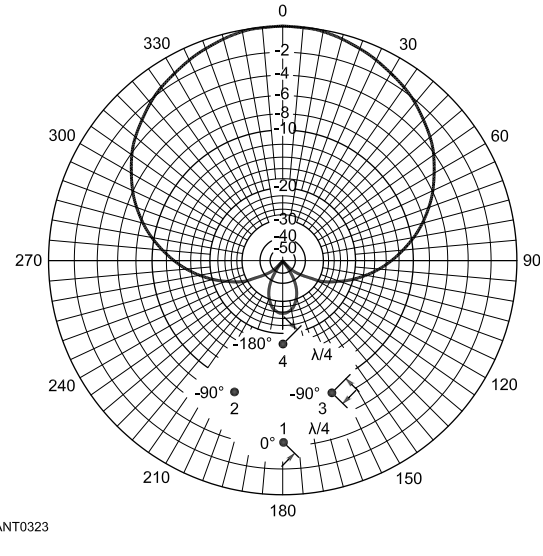

Fig 24—Pattern and layout of the four-element Four-Square array. Gain is referenced to a single similar element; add 5.5 dB to the scale values shown.

ment. The magnitudes of the currents in all four elements are equal. The front and rear elements can be forced to be 180° out-of-phase and to have equal currents by using the current-forcing method described earlier. One element is connected to a line that is either λ/4 or 3λ/4 long, the other to a line that is λ/2 longer, and the two lines to a common point.

Likewise, the two side element currents are forced to be equal by connecting them to a common point via λ/4 or 3λ/4 lines. **Fig 25** shows the basic current-forcing system.

If the pattern is to be electrically rotated, it is necessary to bring lines from all four elements to a common location. If solid-polyethylene dielectric coaxial cable, which has a dielectric constant of 0.66, is used, λ/4 lines won't reach the center of the array. So 3λ/4 lines must be used. Alternatively, you can use λ/4 lines with foam or other dielectric having a velocity factor of more than about 0.71 (plus a little extra margin). These will reach to the center. Whatever your choice, three of the lines must be the same length and the fourth must be λ/2 longer.

In this array, the side elements (2 and 3) have equal impedances, but the rear and front (1 and 4) are different from each other, and both are different from the side elements. We have to know the feed-point impedances of the front, rear and side elements in order to design the "simplest" feed system, but only the side element impedances are needed to design the L-network system. Knowledge of all feed-point impedances is necessary if the array main feedpoint impedance **Zin** is to be calculated. *EZNEC-ARRL* model **4Square_Example.EZ** shows a 40-meter Four Square array with 18 Ω of loss resistance at each element, to approximate an 8-radial per element ground system. (See the cardioid array example above for more information about modeling ground system loss.) Opening the file in *EZNEC-ARRL* and clicking the **Src Dat** button gives the following impedances:

Source 1: 16.4 – *j*15.85 Ω
Sources 2 and 3: 57.47 – *j*19.44 Ω
Source 4: 77.81 + *j* 54.8 Ω

It's interesting to note that the resistive part of source 1 is less than the 18 Ω of loss resistance we intentionally added to simulate ground system loss. That means that the element 1 feed-point resistance would be negative if the ground resistance were less than about an ohm and a half. This isn't uncommon in phased arrays and simply means that the element is feeding power *into* the feed system. This power is coming via mutual coupling from the other elements.

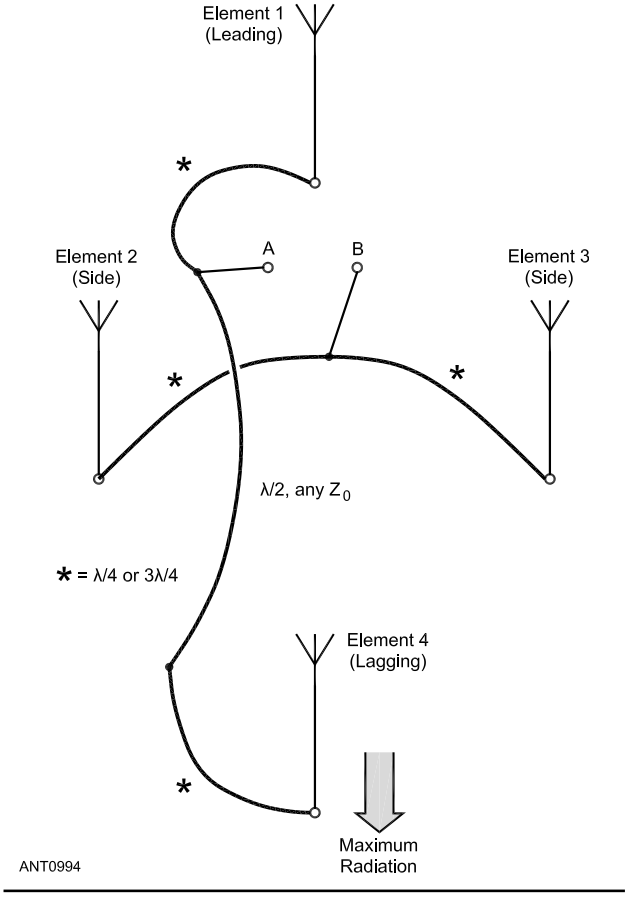

Fig 25—"Simplest" feed system for the Four-Square array in Fig 24. Grounds and cable shields have been omitted for clarity.

"Simplest" (Transmission Line Only) Feed System

To design a "simplest" feed system, start *Arrayfeed1*. In the **Array Type** frame, select **4 Square**, and select **"Simplest"** in the **Feed System Type** frame. In the **Inputs** frame, enter the frequency and the impedances from *EZNEC-ARRL*:

Frequency = 7.15 MHz
Leading Element: R = 16.4, X = –15.85
Side elements: R = 57.47, X = –19.44
Lagging Element: R = 77.81, X = 54.8

We'll try using 50 Ω for all lines, so enter **50** into the next three boxes.

Enter **1** for the lagging:leading I magnitude and **–90** for the phase.

Click **Find Solutions**.

The result is shown in the **Solutions** frame, shown in **Fig 26**. As always when any solution exists, there are two to choose from. The one with the shortest lines is generally preferable, so we'll choose it. For this example, we'll use λ/4 lines with velocity factor of 0.82. So enter **0.82** in the **Velocity Factor** box in the **Physical Lengths** frame, and read the physical lengths from the bottom of that frame. The λ/4 lines (marked in the *Arrayfeed1* diagram with an asterisk) are 28.2 feet, line 1 is 7.483 feet and line 2 is 51.668 feet. The "simplest" feed system is shown in Fig 26, and the complete feed system consists of this connected to the array of Fig 25.

EZNEC-ARRL model **ARRL_4Square_TL_Example.EZ** is simulates the array fed with this system. Comparison of the pattern plot to one from ideal-current model **ARRL_4Square_Example.EZ** and examination of

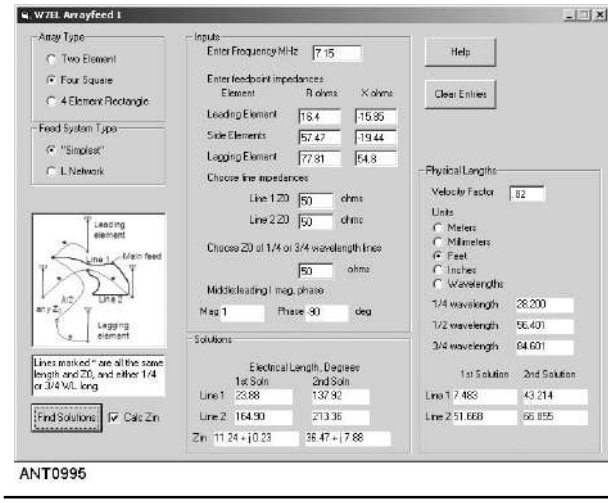

Fig 26—Screen capture from *Arrayfeed1* for "Simplest" feed system for Four Square feed system shown in Fig 25.

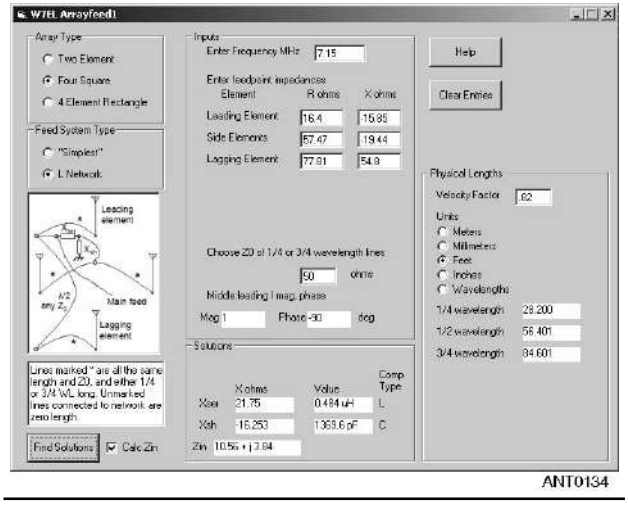

Fig 27—L-network setup for Four-Square array in Fig 25, fed with λ/4 (or 3λ/4) current-forcing feed system.

the element currents verify that the feed system is producing the desired pattern and element currents. You can use **ARRL_4Square_Example.EZ** to investigate the effect of frequency change, ground loss and other changes on the array gain and pattern.

L-Network Feed System

To design the L-network feed system, simply change the **Feed System Type** to **L Network** and click **Find Solutions**. The results you should see are a 0.484 μH inductor for the series component X_{ser}, and a 1369.6 pF capacitor for the shunt component X_{sh}. The L-network feed system is shown in **Fig 27**, and the complete feed system consists of this L network connected to the array of Fig 25.

EZNEC-ARRL doesn't have the ability to directly model

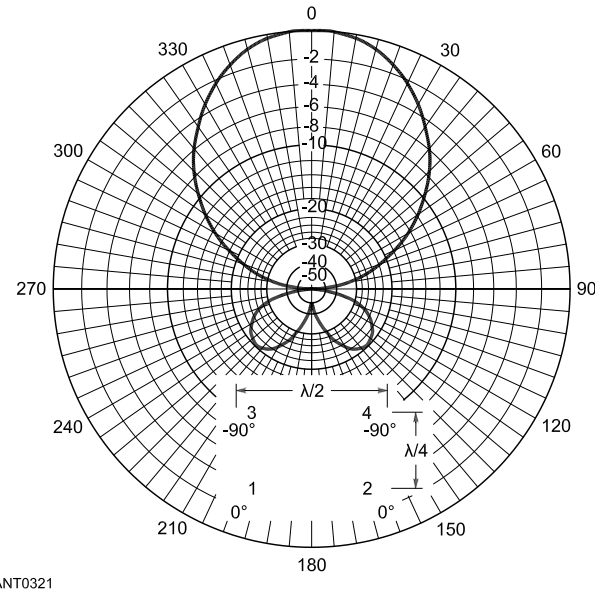

Fig 28—Pattern and layout of the four-element rectangular array. Gain is referenced to a single similar element; add 6.8 dB to the scale values shown.

the L network, so it's unable to model the complete system. However, the system has been modeled using the network capability of *EZNEC v.5* and found to work as designed. Arrays have also been built using this feed system and the element currents measured, with exactly the expected results.

This array is more sensitive to adjustment than the 2-element 90° fed, 90° spaced array. Adjustment procedures and a method of remotely switching the direction of this array are described in the **Practical Aspects of Phased Array Design** section that follows.

A 4-Element Rectangular Array

The 4-element rectangle array shown with its pattern in **Fig 28** has appeared numerous times in amateur publications. However, many of the accompanying feed systems fail to deliver currents in the proper amounts and phases to the various elements. The array can be correctly fed using the principles discussed in this chapter and the design methods that follow.

Elements 1 and 2 can be forced to be in-phase and to have equal currents by feeding them through 3λ/4 lines. (As in the binomial and Four Square array examples, 3λ/4 lines are chosen because λ/4 lines won't physically reach.) The currents in elements 3 and 4 can similarly be forced to be equal and in-phase. **Fig 29** shows the "current-forcing" feed system. Elements 3 and 4 are made to have currents of equal magnitude but of 90° phase difference from elements 1 and 2 by use of either a "simplest" all-transmission line feed system or an L-network feed system. Both will be designed in this example.

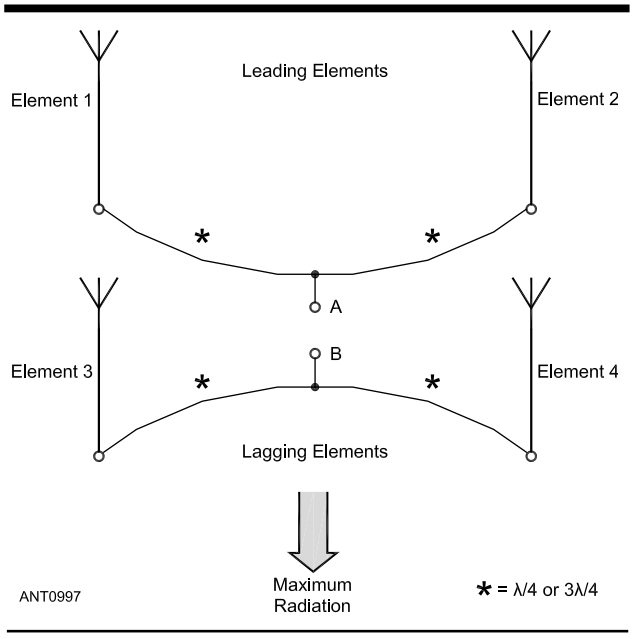

Fig 29—"Simplest" feed system for four-element rectangular array, using four equal-length λ/4 (or 3λ/4) cables.

For this array, we have to know the feed-point impedances of two elements (one of each pair) in order to design either type of feed system. *EZNEC-ARRL* model **Rectangular_Example.EZ** shows a 20-meter rectangular array with 18 Ω of loss resistance at each element, again to approximate an 8-radial per element ground system. (See the cardioid array example above for more information about modeling ground system loss.) Open the file in *EZNEC-ARRL* and click the **Src Dat** button to find the following feed-point impedances:

Sources 1 and 2: 21.44 – *j* 21.29 Ω
Sources 3 and 4: 70.81 – *j* 5.232 Ω

"Simplest" (Transmission- Line Only) Feed System

To design a "simplest" feed system, start program *Arrayfeed1*. In the **Array Type** frame, select **4 Element Rectangle**, and select **"Simplest"** in the **Feed System Type** frame. In the **Inputs** frame, enter the frequency and the impedances from *EZNEC-ARRL*:

Frequency = 14.15 MHz
Leading Elements R = 21.44, X = –21.29
Lagging Elements R = 70.81, X = –5.232

We'll use 50 Ω for all lines, so enter **50** into the next three boxes.

Enter **1** for the lagging:leading I magnitude and **–90** for the phase.

Click Find Solutions.

The result is "No Solution"—This combination of line impedances can't be used. Several other combinations also produce this result, but making lines 1 and 2 each 75 Ω and the 3λ/4 lines 50 Ω does produce a solution. Enter **75** into the **Line 1 Z0** and **Line 2 Z0** boxes, and leave **50** in the **Choose Z0 of ¼ or ¾ wavelength lines** box, then click the Find Solutions button. There won't be any problem making lines 1 and 2 reach, so we'll choose the first solution because the lines are shorter. The physical lengths of all the lines are shown in the **Physical Lengths** frame when the velocity factor is entered in the appropriate box. Assuming that we use coax with a velocity factor of 0.66 (and the example frequency of 14.15 MHz), the lengths are:

Line 1: 4.982 feet
Line 2: 20.153 feet
3λ/4 lines (marked with an asterisk in the *Arrayfeed1* diagram): 34.408 feet

The lines are connected following the diagram in the upper left part of the *Arrayfeed1* window. This completes the "simplest" feed system design. *EZNEC-ARRL* model **Rectangular_TL_Example.EZ** simulates an array fed with this system.

Comparison of the pattern plot to one from ideal-current **Rectangular_Example.EZ**, and examination of the element currents verify that the feed system is producing the desired pattern and element currents.

L-Network Feed System

To design the L-network feed system using *Arrayfeed1*, change the **Feed System Type** to **L Network** and click **Find Solutions**. The resulting L-network values are a 0.484 μH inductor for the series component X_{ser} and a 1369.6 pF capacitor for the shunt component X_{sh}.

120° Fed, 60° Spaced Dipole Array

This example shows the design of "simplest" and L network feed systems for a 2-element 20- meter dipole array, rather than a vertical array. No special accommodation is required for the array made from dipoles rather than vertical elements—the same methods can be used regardless of element shape. This example also shows that both the "simplest" and L-network feed systems can readily be applied to elements that use phase angles other than 90°.

Any 2-element array made with identical elements spaced λ/2 or closer and having equal magnitude currents with a relative phase angle of 180° minus the spacing will produce a unidirectional pattern with a good null to the rear. In practice, very close spacings lead to very low feed-point resistances, with consequent losses and very narrowband characteristics. But this 60° spaced array is well within the range of practical realization. File **ARRL_Dipole_Array_Example.EZ** is a model created for this array, with ideal element currents. Open this file in *EZNEC-ARRL* and click **FF Plot** to show the pattern at an elevation angle of 10°. You can save this pattern for later comparison to the pattern with a "simplest" feed system by opening the **File** menu in the **2D Plot** window, selecting **Save Trace As**, entering a name for the trace file and clicking **Save**.

Following the same procedure as in the previous examples, we begin the array design by finding the element feed-point impedances in the ideally fed array using *EZNEC-ARRL* numbers. Having already opened **ARRL_Dipole_Array_Example.EZ**, all that's needed is to click **Src Dat.** The results are:

Leading element (source 1) : 36.16 – *j* 46.05 Ω
Lagging element (source 2) : 49.56 + *j* 51.47 Ω

"Simplest" (Transmission Line Only) Feed System

Select **Two Element** for the **Array Type** in *Arrayfeed1* and **"Simplest"** for the **Feed System Type**. Enter the frequency of 14.15 MHz and enter the element feed-point impedances from *EZNEC-ARRL* into the appropriate boxes in the **Inputs** frame. For line impedances, the section describing the "simplest" feed system recommends against choosing one which is very different from the element feed-point impedances, but for fun let's try 300 Ω for the two lines and see what happens. Enter **300** in the **Line 1 Z0** and **Line 2 Z0** boxes. Finally, enter the **lagging:leading I mag, phase** of **1** for **Mag** and **–120** for **Phase**.

Click **Find Solutions**. For this example we'll assume that TV type twinlead with a velocity factor of 0.8 is being used. So enter **0.8** for the **Velocity Factor** and read the physical line lengths in the **Physical Lengths** frame. A model of the array using the first solution has been created as **ARRL_Dipole_Array_TL_Example.EZ**. Open this file in *EZNEC-ARRL* and click **FF Tab**. You should see that the plot is virtually identical to the one saved earlier from the ideal-current model. Note the gain and front/back ratio or 8.79 dBi and 31.01 dB respectively reported in the data box below the 2D plot.

Don't subtract 2.15 dB to find the gain relative to a single element! This isn't a free-space model, and the gain of a single dipole over ground is much greater than 2.15 dBi. Instead, delete one of the elements in **ARRL_Dipole_Array_Example.EZ** to find the gain of a single element and subtract that value from the array gain. You can use the undo feature or re-open the file to restore the array.

Now, go back to the model with the "simplest" feed system in *EZNEC-ARRL* and change the Frequency to **14.0** MHz. Click **FF Tab** again. The gain has decreased a little, to 8.54 dBi and the front/back ratio has also decreased, to 21.8 dB. At 14.3 MHz, the gain is slightly higher, 9.04 dBi, but the front/back is again worse, down to 18.64 dB. But this isn't bad overall.

Let's take a look at the second solution. Click the **Trans Lines** line in the main *EZNEC-ARRL* window to open the Transmission Lines Window. Change the length of the first line to **26.856** feet, the second to **28.356** feet, and press the **Enter** key to complete the change. Change the **Frequency** back to **14.15** MHz and click **FF Tab**. You should see exactly the same pattern as for both the first solution and for the ideal current model. But now change the **Frequency** to **14.0** MHz, click FF Tab, and look at the pattern.

What happened? The gain has dropped to 5.95 dBi and the front/back to only 3.1 dB. The array is now nearly bi-directional! It's almost as bad at 14.3 MHz. So we've created a terribly touchy system. The chance of its working correctly even at the design frequency is slim, because there are inevitably some differences between the model and real antenna.

We did have a clue this might happen. As stated in the section describing the "simplest" feed system, the best choices for line Z_0 and for the resulting solution give a difference in electrical line lengths about equal to the desired phase delay of the current. The difference in electrical line lengths for the first solution was about 152°—not as close to the 120° current phase difference as we'd like, but much better than the mere 9.7° difference of the lines for the second solution. While the 300-Ω line Z_0 is quite different from the element feed-point impedances, the first solution result is quite good. If desired, you can try other line impedance values into *Arrayfeed1* and evaluate the results with *EZNEC-ARRL*.

Please see the information about baluns in the **Baluns in Phased Arrays** section. Baluns are placed the same as in Fig 19, which shows the L-network feed system.

L-Network Feed System

To design an L network feed system, change the *Arrayfeed1* **Feed System Type** to **L Network** and click **Find Solutions**. The results aren't good ones to use. The component reactance magnitudes of about 1573 and 2619 Ω are more than five times the 300-Ω Z_0 of the feed lines. As explained in the section describing the L-network feed system, it's undesirable to have such a large ratio of component reactance to line Z_0. Among other problems, the inductor and capacitor values are quite extreme and capacitor stray inductance and inductor capacitance would have a significant impact on performance.

The problem occurs because the feed-line impedance we chose is much larger than the element feed-point impedances, so the λ/4 lines transform the feed-point impedances to much higher values at the L network and main feed point. This feed system would be extremely critical, narrowbanded and difficult to adjust. We can do better by choosing feed-line impedances that aren't too drastically different than the element feed-point impedances. In this case, 50 or 75 Ω would be a much better choice than 300. Let's try 75.

In *Arrayfeed1*, change the **Line 1 Z0** and **Line 2 Z0** impedances from **300** to **75** and click **Find Solutions**. L-network component reactance magnitudes are now about 98 and 164 Ω, much better than before. This will be a relatively uncritical and broadbanded feed system.

Again, be sure to read the information about baluns in the **Baluns in Phased Arrays** section. Fig 19 shows the completed feed system including baluns.

PRACTICAL ASPECTS OF PHASED ARRAY DESIGN

With almost any type of antenna system, there is much that can be learned from experimenting with, testing and using

various array configurations. In this section, Roy Lewallen, W7EL, shares the benefit of years of his experience from actually building, adjusting and using phased arrays. There is much more work to be done in most of the areas covered here, and Roy encourages the reader to build on this work.

Adjusting Phased Array Feed Systems

If a phased array is constructed only to achieve forward gain, adjusting it is seldom worthwhile. This is because the forward gain of most arrays is quite insensitive to either the magnitude or phase of the relative currents flowing in the elements. If, however, good rejection of unwanted signals is desired, adjustment may be required. And achieving very deep nulls will almost surely require some adjustment.

The in-phase and 180° out-of-phase current-forcing method supplies very well-balanced and well-phased currents to elements without adjustment. If the pattern of an array fed using this method is unsatisfactory, it's generally the result of environmental differences—where the elements, even though furnished with correct currents, aren't generating the correct fields. Such an array can be optimized in a single direction, but a more general approach than the current-forcing method must be taken. Some possibilities are described by Paul Lee and Forrest Gehrke (see Bibliography).

Unlike the current-forcing method, the "simplest" and L-network feed systems described earlier in this chapter are dependent on the self and mutual impedance of one or more elements. The required transmission-line lengths or L-network component values can be computed to a high level of precision, but the results are only as good as the knowledge of the relevant feed-point impedances.

While the simplest feed system doesn't readily lend itself to adjustment, the components of an L network can easily be made adjustable or can be experimentally changed in increments. A practical approach is to model the array as accurately as possible, design and build the feed system based on the model results and then adjust the network for the best performance.

Simple arrays such as the two-element 90° fed and spaced array can be adjusted as follows. Place a low-power signal source at a distance from the array (preferably several wavelengths), in the direction a null should be. While listening to the signal on a receiver connected to the array, alternately adjust the two L-network components for the best rejection of the signal.

This has proved to be a very good way to adjust 2-element arrays. However, variable results were obtained when a Four-Square array was adjusted using this technique. The probable reason is that more than one combination of current balance and phasing can produce a null in a given direction but each produces a different overall pattern. So a different method must be used for adjusting more complex arrays. This involves actually measuring the element currents in some way, and adjusting the network until the currents are correct. After adjusting the currents, small adjustments can be made to deepen the null(s) if desired.

Measuring Element Currents

You can measure the element currents two ways. One way is to measure them directly at the element feed points, as shown in **Fig 30**. A dual-channel oscilloscope is required to monitor the currents. This method is the most accurate and it provides a direct indication of the actual relative magnitudes and phases of the element currents. The current probe is shown in **Fig 31**.

Instead of measuring the element currents directly, you could measure them indirectly by measuring the voltages on the feed lines an electrical $\lambda/4$ or $3\lambda/4$ distance from the array. The voltages at these points are directly proportional to the element currents. This introduces additional variables that can reduce the accuracy of the result, but the method generally produces adequate performance. The 2-element arrays fed with the L-network system and all the four element arrays presented earlier have $\lambda/4$ or $3\lambda/4$ lines from all elements to a common location, making this second measurement method convenient. The voltages can be observed with a dual-channel oscilloscope, or, to adjust for equal-magnitude currents and 90° phasing, you can use the test circuit shown in **Fig 32**.

The test circuit is connected to the feed lines of two elements that are to be adjusted for 90° phasing (such as elements 1 and 2, or 2 and 4 of the Four-Square array of Figs 24 and 25). Adjust the L-network components alternately until both meters read zero. Proper operation of the test circuit can be verified by disconnecting one of the inputs. The *phase* output

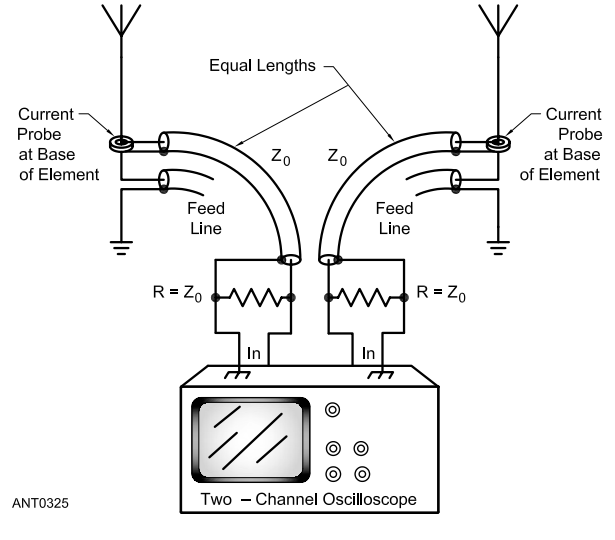

Fig 30—One method of measuring element currents in a phased array. Details of the current probe are given in Fig 31. Caution: Do not run high power to the antenna system for this measurement, or damage to the test equipment may result.

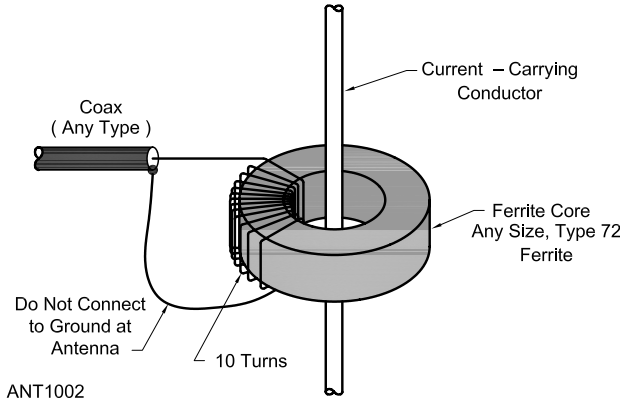

Fig 31—The current probe for use in the test setup of Fig 30. The ferrite core is of type 72 material, and may be any size. The coax line must be terminated at the opposite end with a resistor equal to its characteristic impedance. You should build this probe in a plastic or metal box to provide mechanical ruggedness.

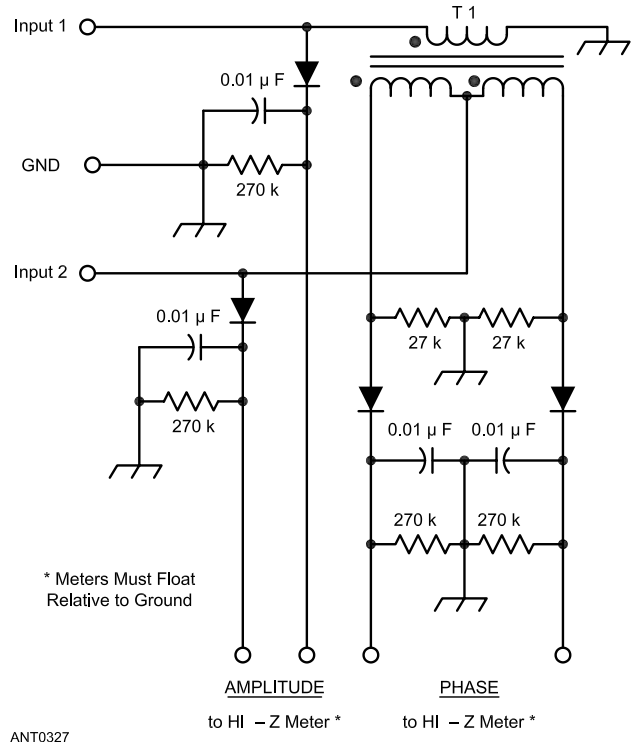

Fig 32—Quadrature test circuit. All diodes are germanium, such as 1N34A, 1N270, or equiv. Hot carrier or silicon diodes can be used at higher power levels. All resistors are ¼ or ½ W, 5% tolerance. Capacitors are ceramic. Alligator clips are convenient for making the input and ground connections to the array.

T1—7 trifilar turns on an Amidon FT-37-43, -75, -77, or equivalent ferrite toroid core.

should remain close to zero. If not, there is an undesirable imbalance in the circuit, which must be corrected. Another means of verification is to first adjust the L network so the tester indicates correct phasing (zero volts at the *phase* output). Then reverse the tester input connections to the elements. The *phase* output should remain close to zero.

Directional Switching of Arrays

One ideal directional-switching method would take the entire feed system, including the lines to the elements and physically rotate it. The smallest possible increment of rotation would depend on the symmetry of the array—the feed system would need to rotate until the array again *looks* the same to it. For example, any 2-element array can be rotated 180° (although that wouldn't accomplish anything if the array is bidirectional to begin with). The 4-element rectangular array of Figs 28 and 29 can also be reversed, and the Four-Square array of Figs 24 and 25 can be switched in 90° increments.

Smaller switching increments can be accomplished only by reconfiguring the feed system, including any network if used, effectively creating a different kind of array. Switching in smaller increments than dictated by symmetry will create a different pattern in some directions than in others, and must be thoughtfully done to maintain equal and properly phased element currents. The methods illustrated here will deal only with switching in increments related to the array symmetry, except for one: a 2-element broadside/end-fire array.

In all arrays, the success of directional switching depends on the elements and ground systems being identical so that equal element currents result in equal fields. It's even more important in arrays fed with any method other than current forcing, because the effectiveness of those methods depends on the element feed-point impedances. Few of us can afford the luxury of having an array many wavelengths away from all other conductors, so an array will nearly always perform somewhat differently in each direction. The array should be adjusted when steered in the direction requiring the most signal rejection in the nulls. Forward gain will, for all practical purposes, be equal in all the switched directions, since gain is much more tolerant of error than are nulls.

Basic Switching Methods

Following is a discussion of basic switching methods, how to power relays through the main feed line and other practical considerations. In diagrams, grounds are frequently omitted to aid clarity, but connections of the ground conductors must be carefully made. In fact, it is recommended that the ground conductors be switched just as the center conductors are, as explained in more detail in **Improving Array Switching Systems** below. In all cases, interconnecting lines must be very short.

A pair of elements spaced $\lambda/2$ apart can readily be switched between broadside and end-fire bidirectional pat-

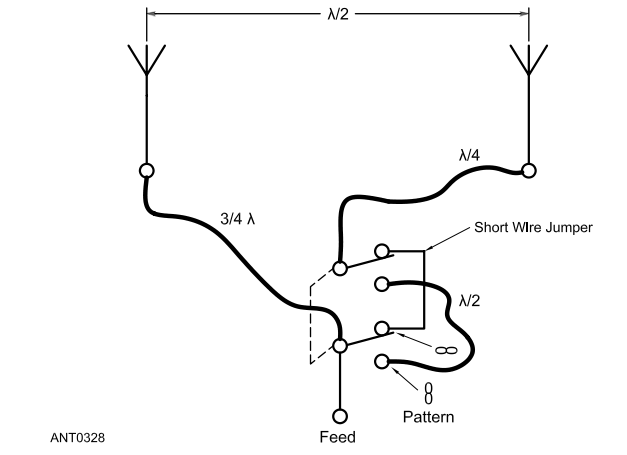

Fig 33—Two-element broadside/end-fire switching. All lines must have the same characteristic impedance. Grounds and cable shields have been omitted for clarity.

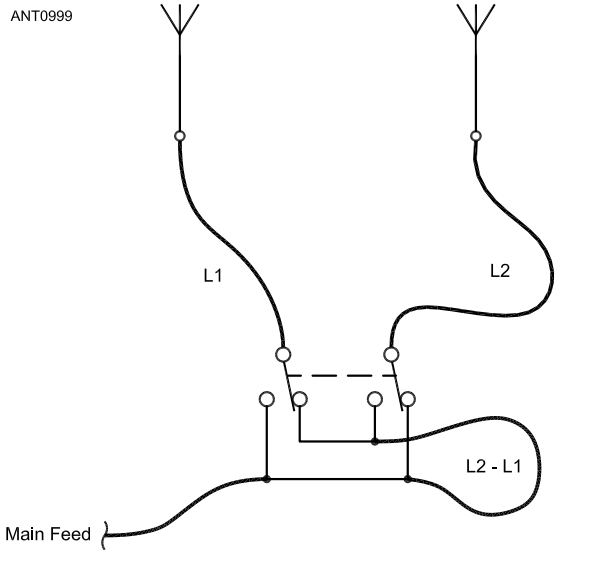

Fig 34—Directional switching for 90°, 90° spaced 2-element array fed with a "simplest" feed system.

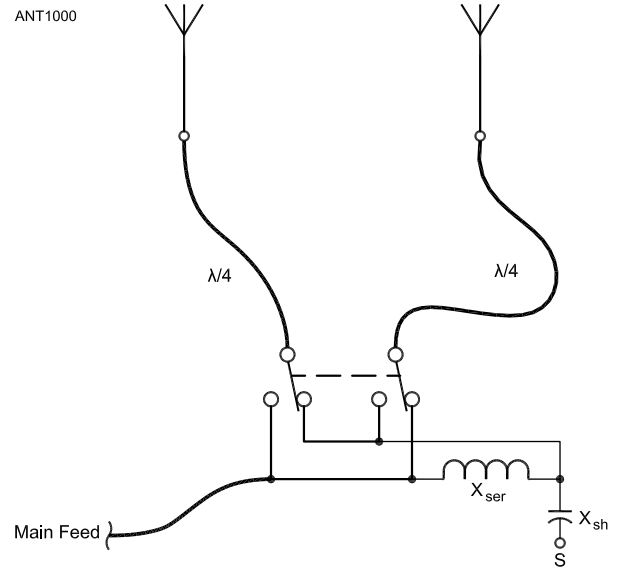

Fig 35—Directional switching for 90°, 90° spaced 2-element array fed with an L-network, current-forcing feed system.

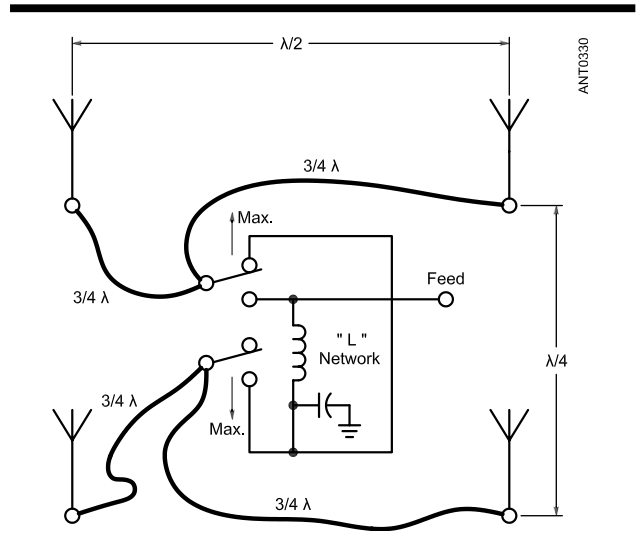

Fig 36—Directional switching of a four-element rectangular array. All interconnections must be very short. As usual, grounds and cable shields have been omitted for clarity.

terns, using the current-forcing properties of λ/4 lines. The method is shown in **Fig 33**. The switching device can be a relay powered via a separate cable or by dc sent along the main feed line.

Fig 34 shows directional switching of a 90° fed, 90° spaced array fed with a "simplest" feed system, where L1 and L2 are the required lengths of the two feed lines. **Fig 35** shows how to switch the same array when fed with an L-network, current-forcing system.

The rectangular array of Fig 28 can be switched in a similar manner, as shown in **Fig 36**. To switch a "simplest" fed rectangular array, use the switching circuit of Fig 34, but connect the two equal length lines to points A and B of Fig 29 in place of the two elements shown in Fig 34.

Switching the direction of an array in increments of 90°, when permitted by symmetry, requires at least two relays. A method of 90° switching of the Four-Square array with L-network feed is shown in **Fig 37**.

Powering Relays Through Feed Lines

All of the above switching methods can be implemented without additional wires to the switch box. A single-relay system is shown in **Fig 38A**, and a two-relay system in

Fig 38B. Small 12 or 24-V dc power relays can be used in either system at power levels up to at least a few hundred watts. Do not attempt to change directions while transmitting, however. Blocking capacitors C1 and C2 should be good quality ceramic or transmitting mica units of 0.01 to 0.1 μF. No problems have been encountered using 0.1 μF, 300-V monolithic ceramic units at RF output levels up to 300 W. C2 may be omitted if the antenna system is an open circuit at dc. C3 and C4 should be ceramic, 0.001 μF or larger.

In Fig 38B, capacitors C5 through C8 should be selected with the ratings of their counterparts in Fig 38A, as given above. Electrolytic capacitors across the relay coils, C9 and C10 in Fig 38B, should be large enough to prevent the relays from buzzing, but not so large as to make relay operation too slow. Final values for most relays will be in the range from 10 to 100 μF. They should have a voltage rating of at least double the relay coil voltage. Some relays do not require this capacitor. All diodes are 1N4001 or similar. A rotary switch may be used in place of the two toggle switches in the two-relay system to switch the relays in the desired sequence.

Improving Array-Switching Systems

The extra circuitry involved in switching arrays can degrade array performance by altering the relative currents fed to each element. One common cause is current sharing in common ground conductors, even when connections are kept very short. The author has seen a 30° phase shift in voltage along a 4-inch piece of #12 wire in a 40-meter array feed system.

When the two conductors of a feedline are physically separated from each other, the impedance increases. This is especially true when the main lines are coaxial cables. If currents from two elements share the ground conductor of a split line, a relatively large voltage drop results. Voltage changes λ/4 from the elements translate to current changes at the elements. Although keeping all leads extremely short is sometimes adequate, the best way to reduce current sharing problems is to keep the two conductors of each transmission line as close together as possible, and switch both conductors of each line rather than just a single or "hot" conductor.

An example of a carefully designed switching system is shown in **Fig 39**. It avoids the problem of shared ground conductor currents, as well as another common problem, namely that effective line lengths are often different along different switching paths. Notice how the path from the main feed point travels through a single line to each element with no common ground connections to other lines except at the

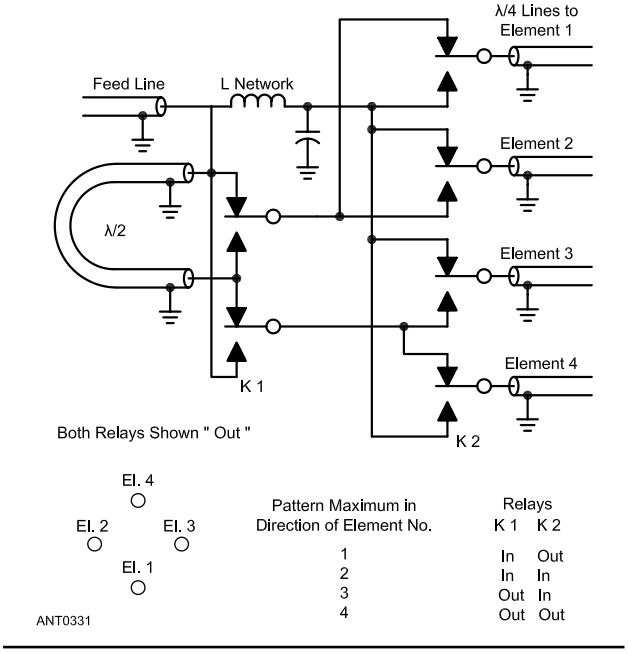

Fig 37—Directional switching of the four-square array. All interconnections must be very short.

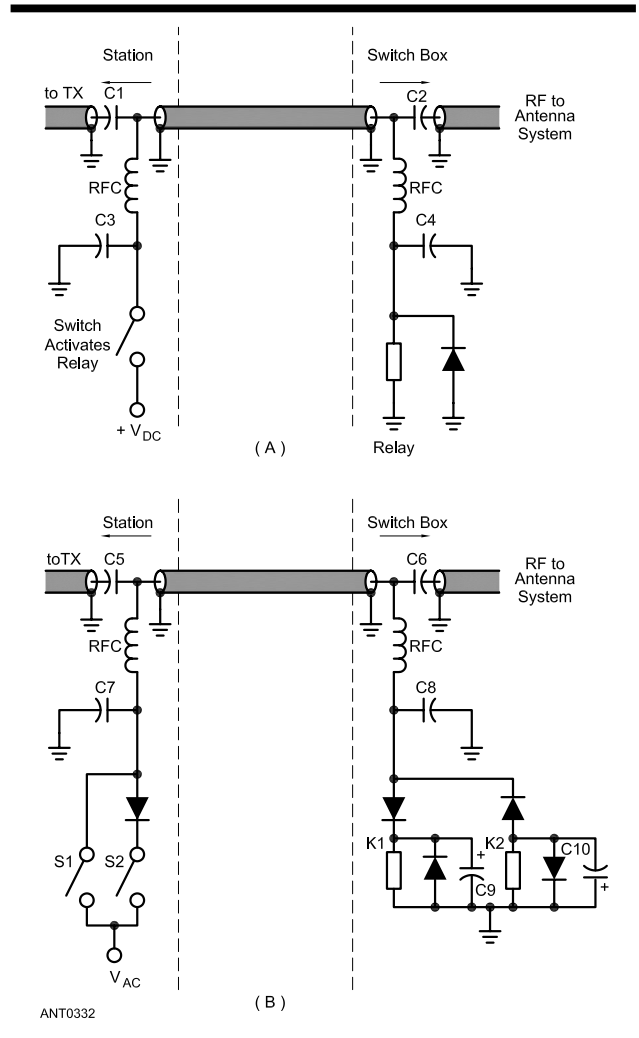

Fig 38—Remote switching of relays. See text for component information. A one-relay system is shown at A, and a two-relay system at B. In B, S1 activates K1, and S2 activates K2.

main feed point. Notice also that the distance doesn't change as the direction is switched. The λ/4 lines going to the two elements must be shortened by the length ℓ of the lines on the feed side of the relays, so that the total line length from the main feed point to each element is λ/4 (or 3λ/4).

You can see that in either relay position, there's an open ended stub of length ℓ connected at the main feed point and another at the output end of the L network. These will add capacitance at those points. Extra C at the main feed point will alter the overall impedance seen by a transmitter, but won't otherwise have any effect on the array or its performance. The one at the output of the L network will, however, change the transformation and phase shift properties of the network. But it's easy to compensate—the value of the shunt capacitor element is simply reduced by the amount of the C added by the stub. The amount of C for any kind of transmission line can be calculated from:

$$C(\text{pf/ft}) = \frac{1017}{Z_0 VF}$$

or

$$C(\text{pf/m}) = \frac{3336}{Z_0 VF}$$

where Z_0 = the characteristic impedance of the line and VF = the velocity factor. This works out to 31 pF/foot or 101 pF/meter for 50-Ω solid polyethylene insulated coax, which has a velocity factor of 0.66.

The general principles illustrated in Fig 39 can be extended to other switching systems. If switching the ground conductors as described above isn't practical, use of a metal box for the switching circuitry is recommended, so that the relatively large surface area of the box can be used for the common ground conductors, minimizing their inductance. Always keep leads extremely short.

Measuring the Electrical Length of Feed Lines

When using the feed methods described earlier the feed lines must be very close to the correct length. For best results, they should be correct within 1% or so. This means that a line that is intended to be, say, λ/4 at 7 MHz, should actually be λ/4 at some frequency within 70 kHz of 7 MHz. A simple but accurate method to determine at what frequency a line is λ/4 or λ/2 is shown in **Fig 40A**. The far end of the line is short circuited with a very short connection. A signal is applied to the input and the frequency is swept until the impedance at the input is a minimum. This is the frequency at which the

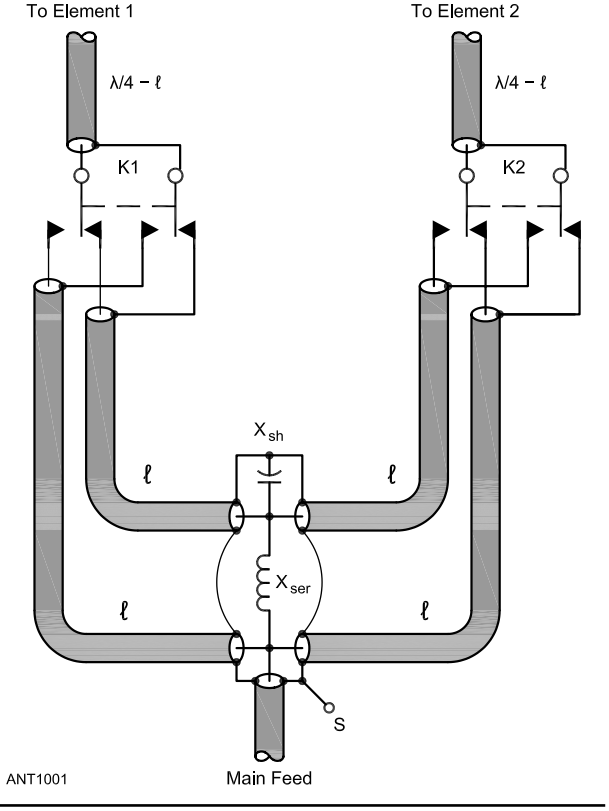

Fig 39—A carefully designed L-network, current-forcing switching system that switches both hot and shield conductors in feed coaxes.

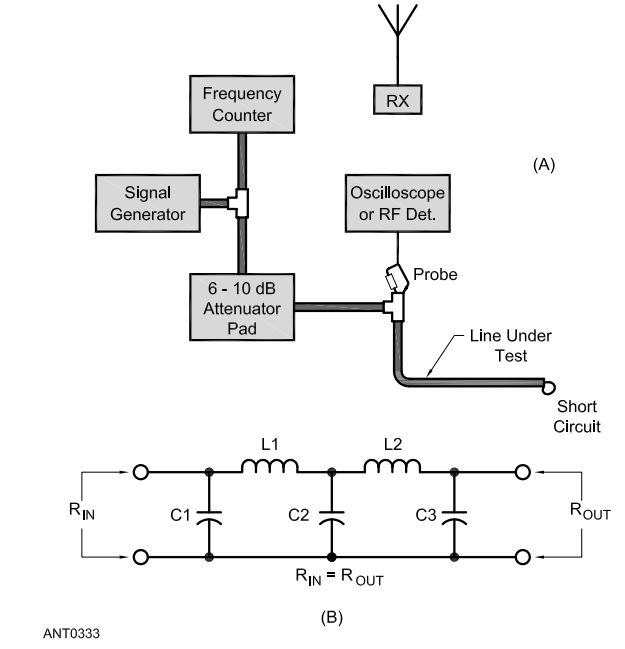

Fig 40—At A, the setup for measurement of the electrical length of a transmission line. The receiver may be used in place of the frequency counter to determine the frequency of the signal generator. The signal generator output must be free of harmonics; the half-wave harmonic filter at B may be used outboard if there is any doubt. It must be constructed for the frequency band of operation. Connect the filter between the signal generator and the attenuator pad.

C1, C3—Value to have a capacitive reactance = R_{IN}.
C2—Value to have a capacitive reactance = ½ R_{IN}.
L1, L2—Value to have an inductive reactance = R_{IN}.

line is λ/2. Either the frequency counter or the receiver may be used to determine this frequency. The line is, of course, λ/4 at one half the measured frequency.

The detector can be a simple diode detector or an oscilloscope may be used if available. A 6 to 10 dB attenuator pad is included to prevent the signal generator from looking into a short circuit at the measurement frequency. The signal generator output must be free of harmonics. If there is any doubt, an outboard low-pass filter, such as a half-wave harmonic filter, should be used. The half-wave filter circuit is shown in Fig 40B, and must be constructed for the frequency band of operation.

Another satisfactory method is to use a noise or resistance bridge or antenna analyzer at the input of the line, again looking for a low impedance at the input while the output is short circuited. Simple resistance bridges are described in Chapter 27.

Dip oscillators have been found to be unsatisfactory. The required coupling loop has too great an effect on measurements.

Measuring Element Self and Mutual Impedances

The need for measuring element self and mutual impedances has been made largely unnecessary with the ready availability of modeling software. Few amateurs appreciate the considerable difficulty of making accurate impedance measurements and accurate mutual impedance measurements are very difficult even with professional test equipment and skills. Despite the limitations of computer modeling, results very often are better than measured values because of the multiple factors affecting measurement accuracy.

Those who are interested in measuring self and mutual impedances can find more detailed information about doing so in Appendix B. The information there is from earlier editions of *The ARRL Antenna Book*.

Broadside Arrays

Broadside arrays can be made up of collinear or parallel elements or combinations of the two. This section was contributed by Rudy Severns, N6LF.

COLLINEAR ARRAYS

Collinear arrays are always operated with the elements in-phase. (If alternate elements in such an array are out-of-phase, the system simply becomes a harmonic type of antenna.) A collinear array is a broadside radiator, the direction of maximum radiation being at right angles to the line of the antenna.

POWER GAIN

Because of the nature of the mutual impedance between collinear elements, the feed-point resistance (compared to a single element, which is ≈73 Ω) is increased as shown earlier in this chapter (Fig 9). For this reason the power gain does not increase in direct proportion to the number of elements. The gain with two elements, as the spacing between them is varied, is shown by **Fig 41**. Although the gain is greatest when the end-to-end spacing is in the region of 0.4 to 0.6 λ, the use of spacings of this order is inconvenient constructionally and introduces problems in feeding the two elements. As a result, collinear elements are almost always operated with their ends

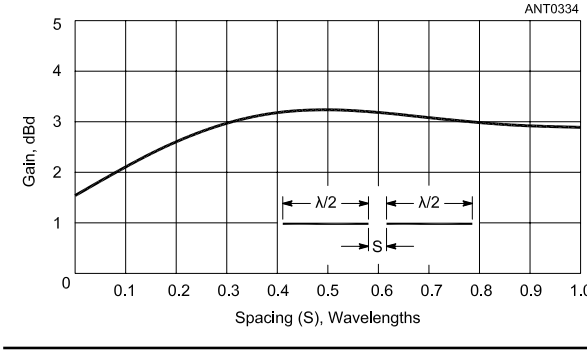

Fig 41—Gain of two collinear λ/2 elements as a function of spacing between the adjacent ends.

quite close together—in wire antennas, usually with just a strain insulator between.

With very small spacing between the ends of adjacent elements the theoretical power gain of collinear arrays, assuming the use of #12 copper wire, is approximately as follows over a dipole in free space:

2 collinear elements—1.6 dB
3 collinear elements—3.1 dB
4 collinear elements—3.9 dB

More than four elements are rarely used.

DIRECTIVITY

The directivity of a collinear array, in a plane containing the axis of the array, increases with its length. Small secondary lobes appear in the pattern when more than two elements are used, but the amplitudes of these lobes are low enough so that they are usually not important. In a plane at right angles to the array the directive diagram is a circle, no matter what the number of elements. Collinear operation, therefore, affects only E-plane directivity, the plane containing the antenna.

When a collinear array is mounted with the elements vertical, the antenna radiates equally well in all geographical directions. An array of such *stacked* collinear elements tends to confine the radiation to low vertical angles.

If a collinear array is mounted horizontally, the directive pattern in the vertical plane at right angles to the array is the same as the vertical pattern of a simple λ/2 antenna at the same height (Chapter 3).

TWO-ELEMENT ARRAYS

The simplest and most popular collinear array is one using two elements, as shown in **Fig 42**. This system is commonly known as *two half-waves in phase*. The directive pattern in a plane containing the wire axis is shown in **Fig 43**,

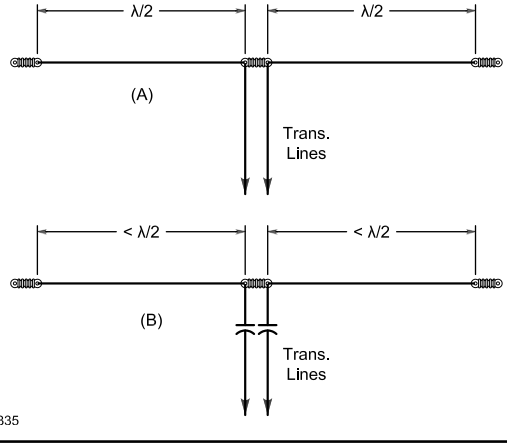

Fig 42—At A, two-element collinear array (two half-waves in phase). The transmission line shown would operate as a tuned line. A matching section can be substituted and a nonresonant line used if desired, as shown at B, where the matching section is two series capacitors.

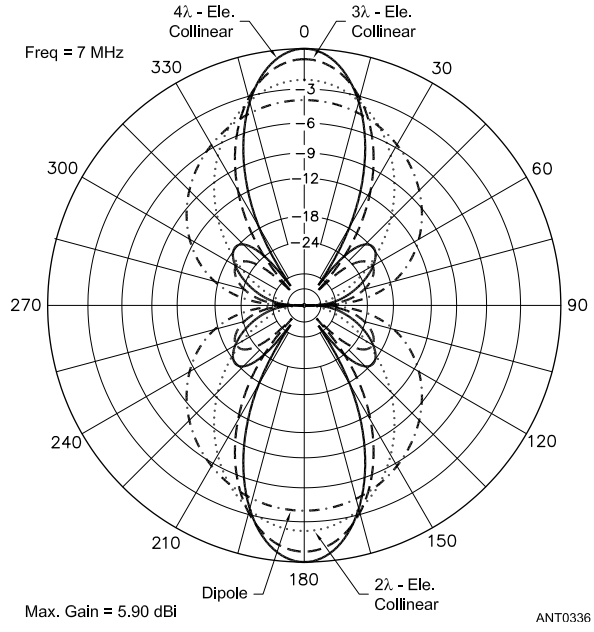

Fig 43—Free-space E-plane directive diagram for dipole, 2, 3 and 4-element collinear arrays. The solid line is a 4-element collinear; the dashed line is for a 3-element collinear; the dotted line is for a 2-element collinear and the dashed-dotted line is for a λ/2 dipole.

which shows superimposed patterns for a dipole and 2, 3 and 4-element collinear arrays. Depending on the conductor size, height, and similar factors, the impedance at the feed point can be expected to be in the range of 4 to 6 kΩ, for wire antennas. If the elements are made of tubing having a low λ/dia (wavelength to diameter) ratio, values as low as 1 kΩ are representative. The system can be fed through an open-wire tuned line with negligible loss for ordinary line lengths, or a matching section may be used if desired.

A number of arrangements for matching the feed line to this antenna are described in Chapter 26. If elements somewhat shorter than λ/2 are used, then additional matching schemes can be employed at the expense of a slight reduction in gain. When the elements are shortened two things happen—the impedance at the feed-point drops and the impedance has inductive reactance that can be tuned out with simple series capacitors, as shown in Fig 42B.

Note that these capacitors must be suitable for the power level. Small *doorknob* capacitors such as those frequently used in power amplifiers, are suitable. By way of an example, if each side of a 40-meter 2-element array is shortened from 67 to 58 feet, the feed-point impedance drops from nearly 6000 Ω to about 1012 Ω with an inductive reactance of 1800 Ω. The reactance can be tuned out by inserting 25 pF capacitors at the feed-point. The 1012 Ω resistance can be transformed to 200 Ω using a λ/4 matching section made of 450-Ω ladder line and then transformed to 50 Ω with a 4:1 balun. Shortening the array as suggested reduces the gain by about 0.5 dB.

Another scheme that preserves the gain is to use a 450-Ω

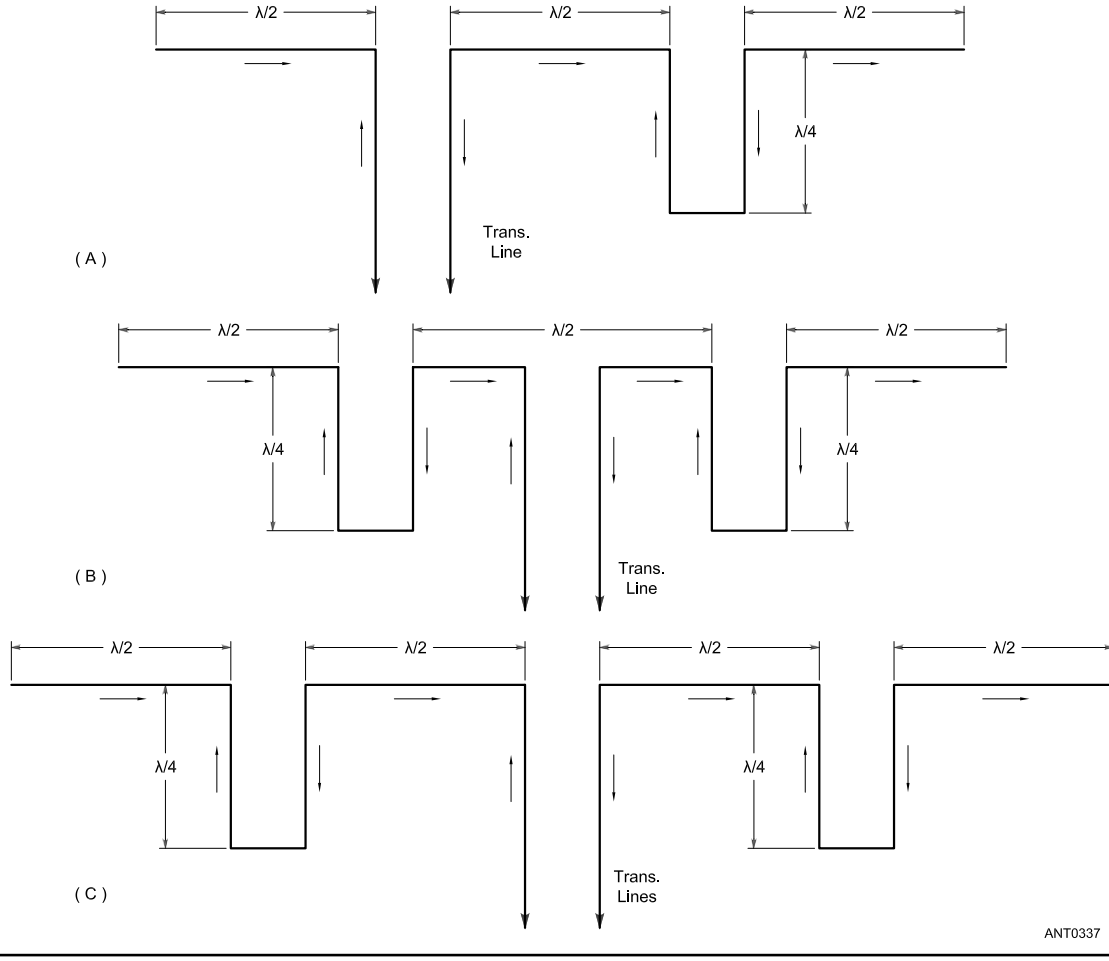

Fig 44—Layouts for 3- and 4-element collinear arrays. Alternative methods of feeding a 3-element array are shown at A and B. These drawings also show the current distribution on the antenna elements and phasing stubs. A matched transmission line can be substituted for the tuned line by using a suitable matching section.

λ/4 matching section and shorten the antenna only slightly to have a resistance of 4 kΩ. The impedance at the input of the matching section is then near 50 Ω and a simple 1:1 balun can be used. Many other schemes are possible. The free-space E-plane response for a 2-element collinear array is shown in Fig 43, compared with the responses for more elaborate collinear arrays described below.

THREE- AND FOUR-ELEMENT ARRAYS

In a long wire the direction of current flow reverses in each λ/2 section. Consequently, collinear elements cannot simply be connected end to end; there must be some means for making the current flow in the same direction in all elements. When more than two collinear elements are used it is necessary to connect *phasing* stubs between adjacent elements in order to bring the currents in all elements in-phase. In **Fig 44A** the direction of current flow is correct in the two left-hand elements because the shorted λ/4 transmission line (*stub*) is connected between them. This stub may be looked upon simply as the alternate λ/2 section of a long-wire antenna folded back on itself to cancel its radiation. In Fig 44A the part to the right of the transmission line has a total length of three half wavelengths, the center half wave being folded back to form a λ/4 phase-reversing stub. No data are available on the impedance at the feed point in this arrangement, but various considerations indicate that it should be over 1 kΩ.

An alternative method of feeding three collinear elements is shown in Fig 44B. In this case power is applied at the center of the middle element and phase-reversing stubs are used between this element and both of the outer elements. The impedance at the feed point in this case is somewhat over 300 Ω and provides a close match to 300 Ω line. The SWR will be less than 2:1 when 600-Ω line is used. Center feed of this type is somewhat preferable to the arrangement in Fig 44A because the system as a whole is balanced. This assures more uniform power distribution among the elements. In Fig 44A, the right-hand element is likely to receive somewhat less power than the other two because a portion of the input power is radiated by the middle element before it can reach the element located at the extreme right.

A four-element array is shown in Fig 44C. The system is symmetrical when fed between the two center elements as shown. As in the three-element case, no data are available on the impedance at the feed point. However, the SWR with a 600 Ω line should not be much over 2:1.

Fig 43 compares the directive patterns of 2, 3 and 4-element arrays. Collinear arrays can be extended to more than four elements. However, the simple 2-element collinear array is the type most frequently used, as it lends itself well to multi-band operation. More than two collinear elements are seldom used because more gain can be obtained from other types of arrays.

ADJUSTMENT

In any of the collinear systems described, the lengths of the radiating elements in feet can be found from the formula $468/f_{MHz}$. The lengths of the phasing stubs can be found from the equations given in Chapter 26 for the type of line used. If the stub is open-wire line (500 to 600 Ω impedance) you may assume a velocity factor of 0.975 in the formula for a λ/4 line. On-site adjustment is, in general, an unnecessary refinement. If desired, however, the following procedure may be used when the system has more than two elements.

Disconnect all stubs and all elements except those directly connected to the transmission line (in the case of feed such as is shown in Fig 44B leave only the center element connected to the line). Adjust the elements to resonance, using the still-connected element. When the proper length is determined, cut all other elements to the same length. Make the phasing stubs slightly long and use a shorting bar to adjust their length. Connect the elements to the stubs and adjust the stubs to resonance, as indicated by maximum current in the shorting bars or by the SWR on the transmission line. If more than three or four elements are used it is best to add elements two at a time (one at each end of the array), resonating the system each time before a new pair is added.

THE EXTENDED DOUBLE ZEPP

One method to obtain higher gain that goes with wider spacing in a simple system of two collinear elements is to make the elements somewhat longer than λ/2. As shown in **Fig 45**, this increases the spacing between the two in-phase λ/2 sections at the ends of the wires. The section in the center carries a current of opposite phase, but if this section is short the current will be small; it represents only the outer ends of a λ/2 antenna section. Because of the small current and short length, the radiation from the center is small. The optimum length for each element is 0.64 λ. At greater lengths the system tends to act as a long-wire antenna, and the gain decreases.

This system is known as the *extended double Zepp*. The gain over a λ/2 dipole is approximately 3 dB, as compared with about 1.6 dB for two collinear λ/2 dipoles. The directional pattern in the plane containing the axis of the antenna

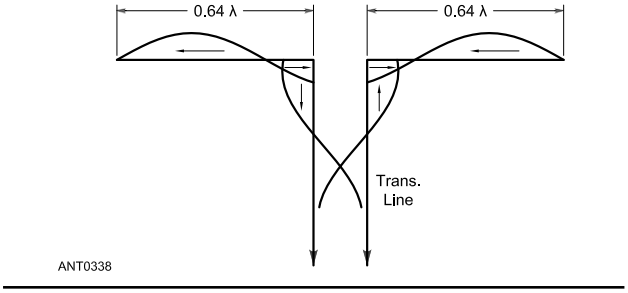

Fig 45—The extended double Zepp. This system gives somewhat more gain than two λ-sized collinear elements.

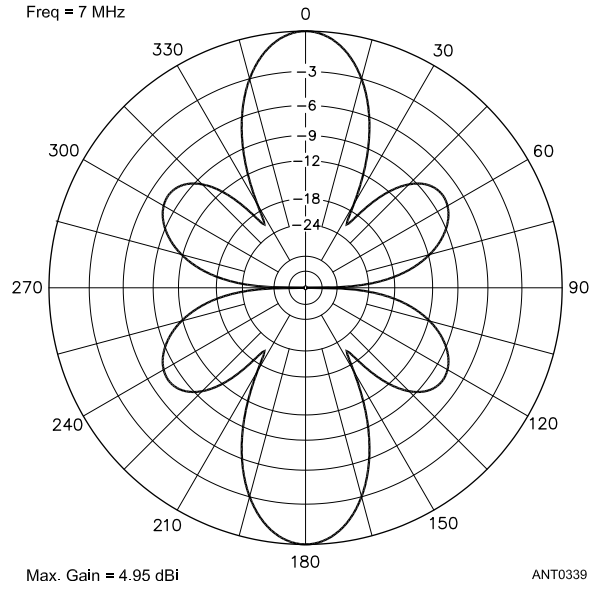

Fig 46—E-plane pattern for the extended double Zepp of Fig 45. This is also the horizontal directional pattern when the elements are horizontal. The axis of the elements lies along the 90°-270° line. The free-space array gain is approximately 4.95 dBi.

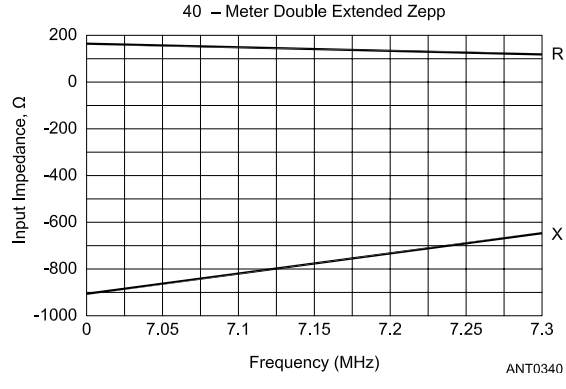

Fig 47—Resistive and reactive feed-point impedance of a 40-meter extended double Zepp in free space.

is shown in **Fig 46**. As in the case of all other collinear arrays, the free-space pattern in the plane at right angles to the antenna elements is the same as that of a λ/2 antenna—circular.

This antenna is not resonant at the operating frequency so that the feed-point impedance is complex ($R \pm jX$). A typical example of the variation of the feed-point impedance over the band for a 40-meter double-extended Zepp is shown in **Fig 47**. This antenna is normally fed with open-wire transmission line to an antenna tuner. Other matching arrangements are, of course, possible. A method for transforming the feed-point impedance to 450 Ω and eliminating the minor lobes is given in Chapter 6.

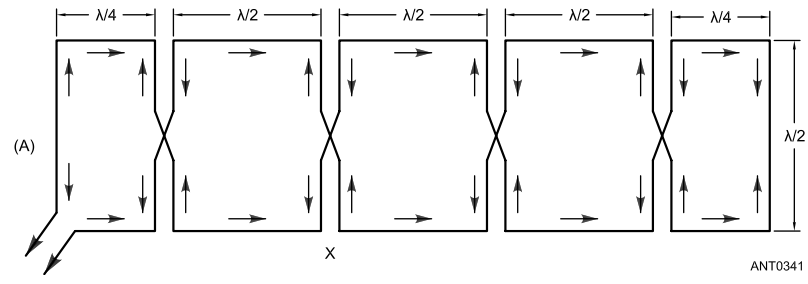

Fig 48—Typical Sterba array, an 8-element version.

THE STERBA ARRAY

Two collinear arrays can be combined to form the *Sterba array*, often called the *Sterba curtain*. An 8-element example of a Sterba array is shown in **Fig 48**. The four λ/4 elements joined on the ends are equivalent to two λ/2 elements. The two collinear arrays are spaced λ/2 and the λ/4 phasing lines connected together to provide λ/2 phasing lines. This arrangement has the advantage of increasing the gain for a given length and also increasing the E-plane directivity, which is no longer circular. An additional advantage of this array is that the wire forms a closed loop. For installations where icing is a problem a low voltage dc or low frequency (50 or 60 Hz) ac current can be passed through the wire to heat it for deicing. The heating current is isolated from RF by decoupling chokes. This is standard practice in commercial installations.

The number of sections in a Sterba array can be extended as far as desired but more than four or five are rarely used because of the slow increase in gain with extra elements, the narrow H-plane directivity and the appearance of multiple sidelobes. When fed at the point indicated the impedance is about 600 Ω. The antenna can also be fed at the point marked X. The impedance at this point will be about 1 kΩ. The gain of the 8-element array in Fig 48 will be between 7 to 8 dB over a single element.

Parallel Broadside Arrays

To obtain broadside directivity with parallel elements the currents in the elements must all be in-phase. At a distant point lying on a line perpendicular to the axis of the array and also perpendicular to the plane containing the elements, the fields from all elements add up in phase. The situation is like that pictured in Fig 1 in this chapter, where four parallel λ/2 dipoles were fed together a broadside array.

Broadside arrays of this type theoretically can have any number of elements. However, practical limitations of construction and available space usually limit the number of broadside parallel elements.

POWER GAIN

The power gain of a parallel-element broadside array depends on the spacing between elements as well as on the number of elements. The way in which the gain of a two-element array varies with spacing is shown in **Fig 49**. The greatest gain is obtained when the spacing is in the vicinity of 0.67 λ.

The theoretical gains of broadside arrays having more than two elements are approximately as follows:

No. of Parallel Elements	*dB Gain with λ/2 Spacing*	*dB Gain with 3λ/4 Spacing*
3	5.7	7.2
4	7.1	8.5
5	8.1	9.4
6	8.9	10.4

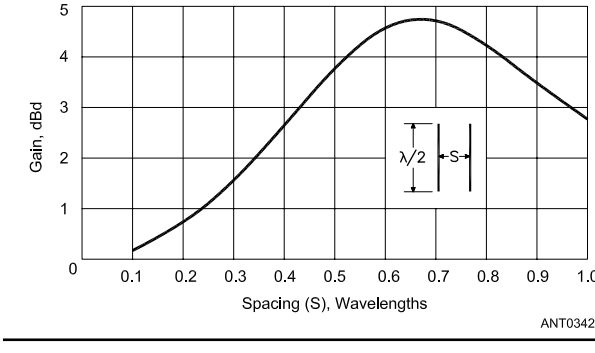

Fig 49—Gain as a function of the spacing between two parallel elements operated in-phase (broadside).

The elements must, of course, all lie in the same plane and all must be fed in-phase.

DIRECTIVITY

The sharpness of the directive pattern depends on spacing between elements and number of elements. Larger element spacing will sharpen the main lobe, for a given number of elements, up to a point as was shown in Fig 41. The two-element array has no minor lobes when the spacing is λ/2, but small minor lobes appear at greater spacings. When three or more elements are used the pattern always has minor lobes.

Other Forms Of Broadside Arrays

For those who have the available room, multi-element arrays based on the broadside concept have something to offer. The antennas are large but of simple design and non-critical dimensions; they are also very economical in terms of gain per unit of cost.

Large arrays can often be fed at several different points. However, the pattern symmetry may be sensitive to the choice of feed point within the array. Non-symmetrical feed points will result in small asymmetries in the pattern but these are not usually of great concern.

Arrays of three and four elements are shown in **Fig 50**. In the 3-element array with λ/2 spacing at A, the array is fed at the center. This is the most desirable point in that it tends to keep the power distribution among the elements uniform. However, the transmission line could alternatively be connected at either point B or C of Fig 50A, with only slight skewing of the radiation pattern.

When the spacing is greater than λ/2, the phasing lines must be 1 λ long and are not transposed between elements. This is shown Fig 50B. With this arrangement, any element spacing up to 1 λ can be used, if the phasing lines can be folded as suggested in the drawing.

The 2-element array at C is fed at the center of the system to make the power distribution among elements as uniform as possible. However, the transmission line could be connected at either point B, C, D or E. In this case the section of phasing line between B and D must be transposed to make the currents flow in the same direction in all elements. The 4-element array at C and the 3-element array at B have approximately the same gain when the element spacing in the array at B is 3λ/4.

An alternative feeding method is shown in Fig 50D. This system can also be applied to the 3-element arrays, and will result in better symmetry in any case. It is necessary only to move the phasing line to the center of each element, making connection to both sides of the line instead of one only.

The free-space pattern for a 4-element array with λ/2 spacing is shown in **Fig 51**. This is also approximately the pattern for a 3-element array with 3λ/4 spacing.

Larger arrays can be designed and constructed by following the phasing principles shown in the drawings. No accurate figures are available for the impedances at the various feed points indicated in Fig 50. You can estimate it to be in the vicinity of 1 kΩ when the feed point is at a junction between the phasing line and a λ/2 element, becoming smaller as the number of elements in the array is increased. When the feed point is midway between end-fed elements as in Fig 50C, the feed-point impedance of a 4-element array is in the vicinity of 200 to 300 Ω, with 600-Ω open-wire phasing lines. The impedance at the feed point with the antenna shown at D should be about 1.5 kΩ.

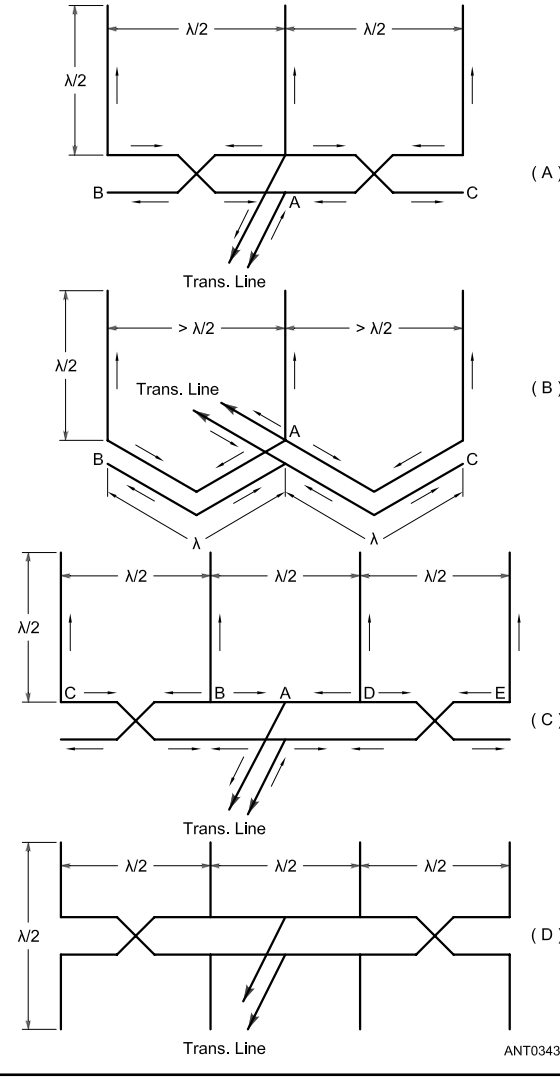

Fig 50—Methods of feeding 3- and 4-element broadside arrays with parallel elements.

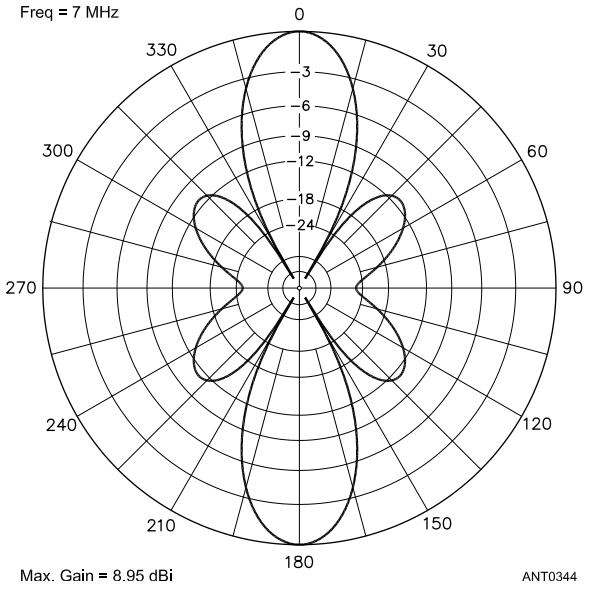

Fig 51—Free-space E-plane pattern of a 4-element broadside array using parallel elements (Fig 50). This corresponds to the horizontal directive pattern at low wave angles for a vertically polarized array over ground. The axis of the elements lies along the 90°-270° line.

NON-UNIFORM ELEMENT CURRENTS

The pattern for a 4-element broadside array shown in Fig 51 has substantial side lobes. This is typical for arrays more than λ/2 wide when equal currents flow in each element. Sidelobe amplitude can be reduced by using non-uniform current distribution among the elements. Many possible current amplitude distributions have been suggested. All of them have reduced current in the outer elements and greater current in the inner elements. This reduces the gain somewhat but can produce a more desirable pattern. One of the common current distributions is called *binomial current grading*. In this scheme the ratio of element currents is set equal to the coefficients of a polynomial. For example:

$$
\begin{aligned}
&1\,x+1, \quad \Rightarrow \; 1,1\\
&(x+1)^2 = 1x^2+2x+1, \quad \Rightarrow \; 1,\,2,\,1\\
&(x+1)^3 = 1x^3+3x^2+3x+1, \quad \Rightarrow \; 1,\,3,\,3,\,1\\
&(x+1)^4 = 1x^4+4x^3+6x^2+6x+1, \quad \Rightarrow \; 1,\,4,\,6,\,4,\,1
\end{aligned}
\qquad \text{(Eq 7)}
$$

In a 2-element array the currents are equal, in a 3-element array the current in the center element is twice that in the outer elements, and so on.

HALF-SQUARE ANTENNA

On the low-frequency bands (40, 80 and 160 meters) it becomes increasingly difficult to use λ/2 elements because of their size. The half-square antenna is a 2-element broadside array with λ/4-high vertical elements and λ/2 horizontal spacing. See **Fig 52**. The free-space H-plane pattern for this array is shown in **Fig 53**. The antenna gives modest (4.2 dBi) but useful gain and has the advantage of only λ/4 height. Like all vertically polarized antennas, real-world performance depends directly on the characteristics of the ground surrounding it.

The half-square can be fed either at the point indicated or at the bottom end of one of the vertical elements using a voltage-feed scheme, such as that shown in **Fig 54** for the bobtail curtain. The feed-point impedance is in the region of 50 Ω when fed at a corner as shown in Fig 52. A typical SWR plot is shown in **Fig 55**. Chapter 6 has a detailed discussion of the half-square antenna with several variations, together with practical considerations.

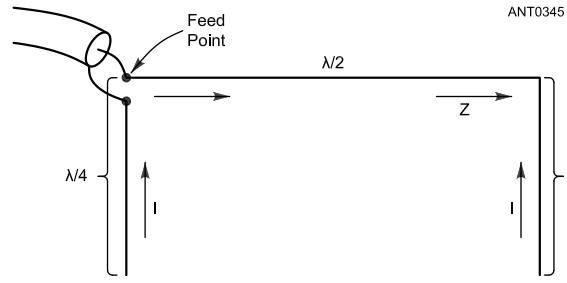

Fig 52—Layout for the half-square antenna.

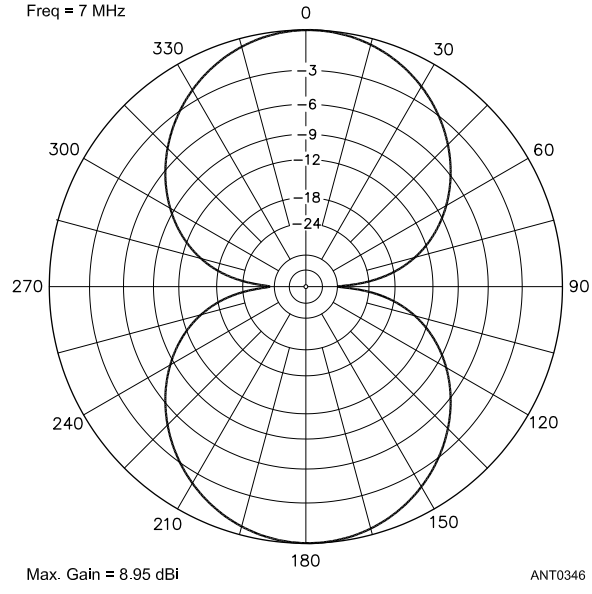

Fig 53—Free-space E-plane directive pattern for the half-square antenna.

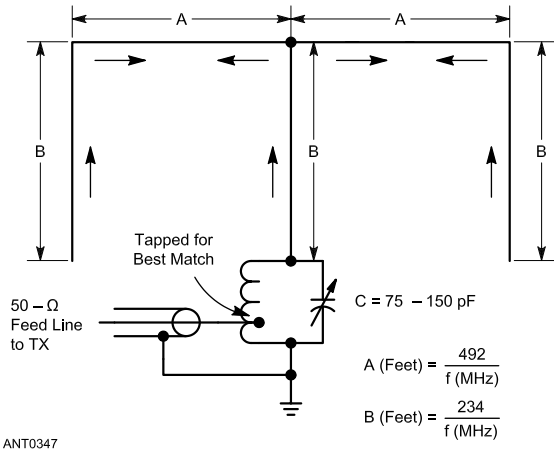

Fig 54—The bobtail curtain is an excellent low-angle radiator having broadside bidirectional characteristics. Current distribution is represented by the arrows. Dimensions A and B (in feet, for wire antennas) can be determined from the equations.

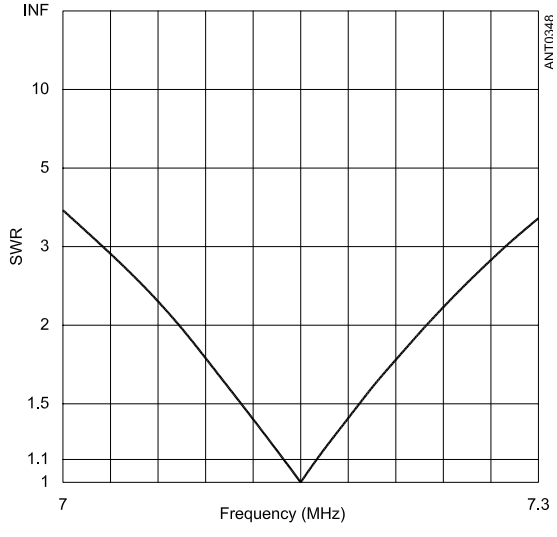

Fig 55—Typical SWR plot for a 40-meter half-square antenna fed at one corner. Antenna in free space.

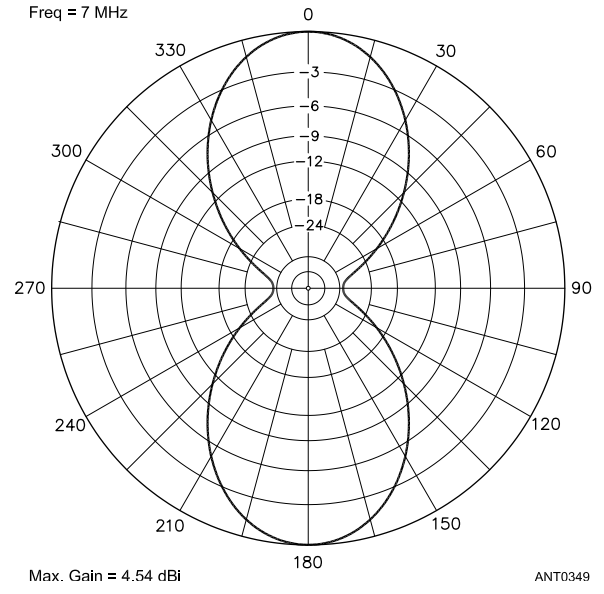

Fig 56—Calculated free-space E-plane directive diagram of the bobtail curtain shown in Fig 54. The array lies along the 90°-270° axis.

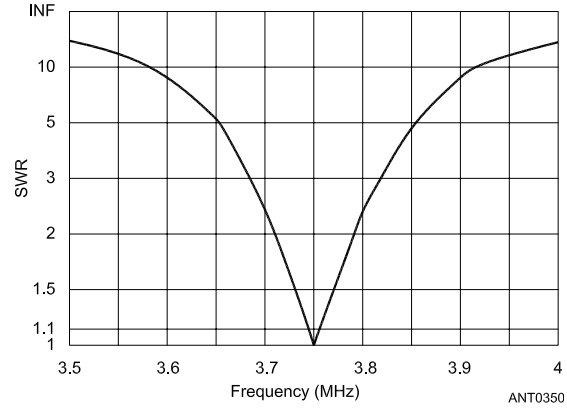

Fig 57—Typical SWR plot for an 80-meter bobtail curtain in free space. This is a narrow-band antenna.

BOBTAIL CURTAIN

The antenna system in Fig 54 uses the principles of co-phased verticals to produce a broadside, bidirectional pattern providing approximately 5.1 dB of gain over a single λ/4 element. The antenna performs as three in-phase, top-fed vertical radiators approximately λ/4 in height and spaced approximately λ/2. It is most effective for low-angle signals and makes an excellent long-distance antenna for 1.8, 3.5 or 7 MHz.

The three vertical sections are the actual radiating components, but only the center element is fed directly. The two horizontal parts, A, act as phasing lines and contribute very little to the radiation pattern. Because the current in the center element must be divided between the end sections, the current distribution approaches a binomial 1:2:1 ratio. The radiation pattern is shown in **Fig 56**.

The vertical elements should be as vertical as possible. The height for the horizontal portion should be slightly greater than B, as shown in Fig 54. The tuning network is resonant at the operating frequency. The L/C ratio should be fairly low to provide good loading characteristics. As a starting point, a maximum capacitor value of 75 to 150 pF is recommended, and the inductor value is determined by C and the operating frequency. The network is first tuned to resonance and then the

tap point is adjusted for the best match. A slight readjustment of C may be necessary. A link coil consisting of a few turns can also be used to feed the antenna.

A feeling for the matching bandwidth of this antenna can be obtained by looking at a feed point located at the top end of the center element. The impedance at this point will be approximately 32 Ω. An SWR plot (for Z_0 = 32 Ω) for an 80-meter bobtail curtain at this feed-point is shown in **Fig 57**. However, it is not advisable to actually connect a feed line at this point since it would detune the array and alter the pattern. This antenna is relatively narrow band. When fed at the bottom of the center element as shown in Fig 54, the SWR can be adjusted to be 1:1 at one frequency but the operating bandwidth for SWR < 2:1 may be even narrower than Fig 57 shows. For 80-meters, where operation is often desired in the CW DX window (3.510 MHz) and in the phone DX window (3.790 MHz), it will be necessary to retune the matching network as you change frequency. This can be done by switching a capacitor in or out, manually or remotely with a relay.

While the match bandwidth is quite narrow, the radiation pattern changes more slowly with frequency. **Fig 58** shows the variation in the pattern over the entire band (3.5 to 4.0 MHz). As would be expected, the gain increases with frequency because the antenna is larger in terms of wavelengths. The general shape of the pattern, however, is quite stable.

THE BRUCE ARRAY

Four variations of the Bruce array are shown in **Fig 59**. The Bruce is simply a wire folded so that the vertical sections carry large in-phase currents, while the horizontal sections carry small currents flowing in opposite directions with respect to the center of a section (indicated by dots). The radiation is vertically polarized. The gain is proportional to the length of the array but is somewhat smaller than you can obtain from a broadside array of λ/2 elements of the same length. This is because the radiating portion of the elements is only λ/4.

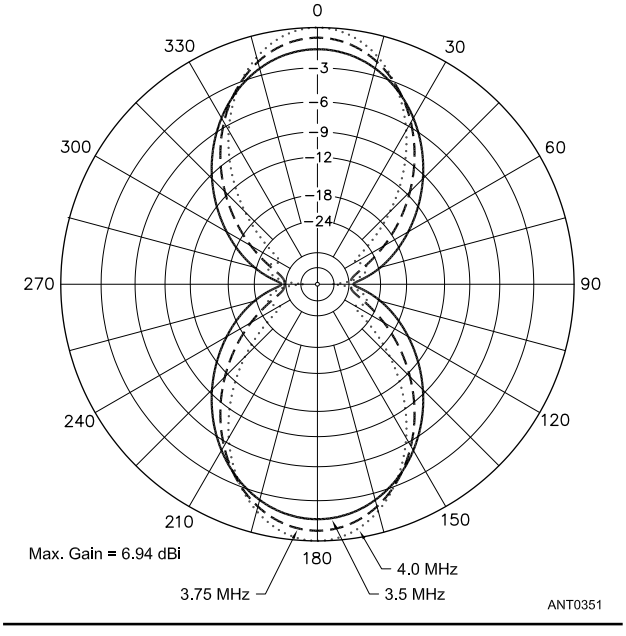

Fig 58—80-meter bobtail curtain's free-space E-plane pattern variation over the 80-meter band.

The Bruce array has a number of advantages:

1) The array is only λ/4 high. This is especially helpful on 80 and 160 meters, where the height of λ/2 supports becomes impractical for most amateurs.

2) The array is very simple. It is just a single piece of wire folded to form the array.

3) The dimensions of the array are very flexible. Depending on the available distance between supports, any number of elements can be used. The longer the array, the greater the gain.

4) The shape of the array does not have to be exactly 1.05 λ/4 squares. If the available height is short but the array can be made longer, then shorter vertical sections and longer horizontal sections can be used to maintain gain and resonance. Conversely, if more height is available but width is restricted then longer vertical sections can be used with shorter horizontal sections.

5) The array can be fed at other points more convenient for a particular installation.

6) The antenna is relatively low Q, so that the feed-point impedance changes slowly with frequency. This is very helpful on 80 meters, for example, where the antenna can be relatively broadband.

7) The radiation pattern and gain is stable over the width of an amateur band.

Note that the nominal dimensions of the array in Fig 59 call for section lengths = 1.05 λ/4. The need to use slightly longer elements to achieve resonance is common in large wire arrays. A quad loop behaves in the same manner. This is quite different from wire dipoles, which are typically *shortened* by 2-5% to achieve resonance.

Fig 60 shows the variations in gain and pattern for 2 to 5-element 80-meter Bruce arrays. **Table 2** lists the gain over a vertical λ/2 dipole, a 4-radial ground-plane vertical and the size of the array. The gain and impedance parameters listed are for free space. Over real ground the patterns and gain will depend on the height above ground and the ground characteristics. Copper loss using #12 conductors in included.

Worthwhile gain can be obtained from these arrays, especially on 80 and 160 meters, where any gain is hard to come by. The feed-point impedance is for the center of a vertical section. From the patterns in Fig 60 you can see that sidelobes start to appear as the length of the array is increased beyond 3λ/4. This is typical for arrays using equal currents in the elements.

It is interesting to compare the bobtail curtain (Fig 54) with a 4-element Bruce array. **Fig 61** compares the radiation patterns for these two antennas. Even though the Bruce is shorter (3λ/4) than the bobtail (1 λ), it has slightly more

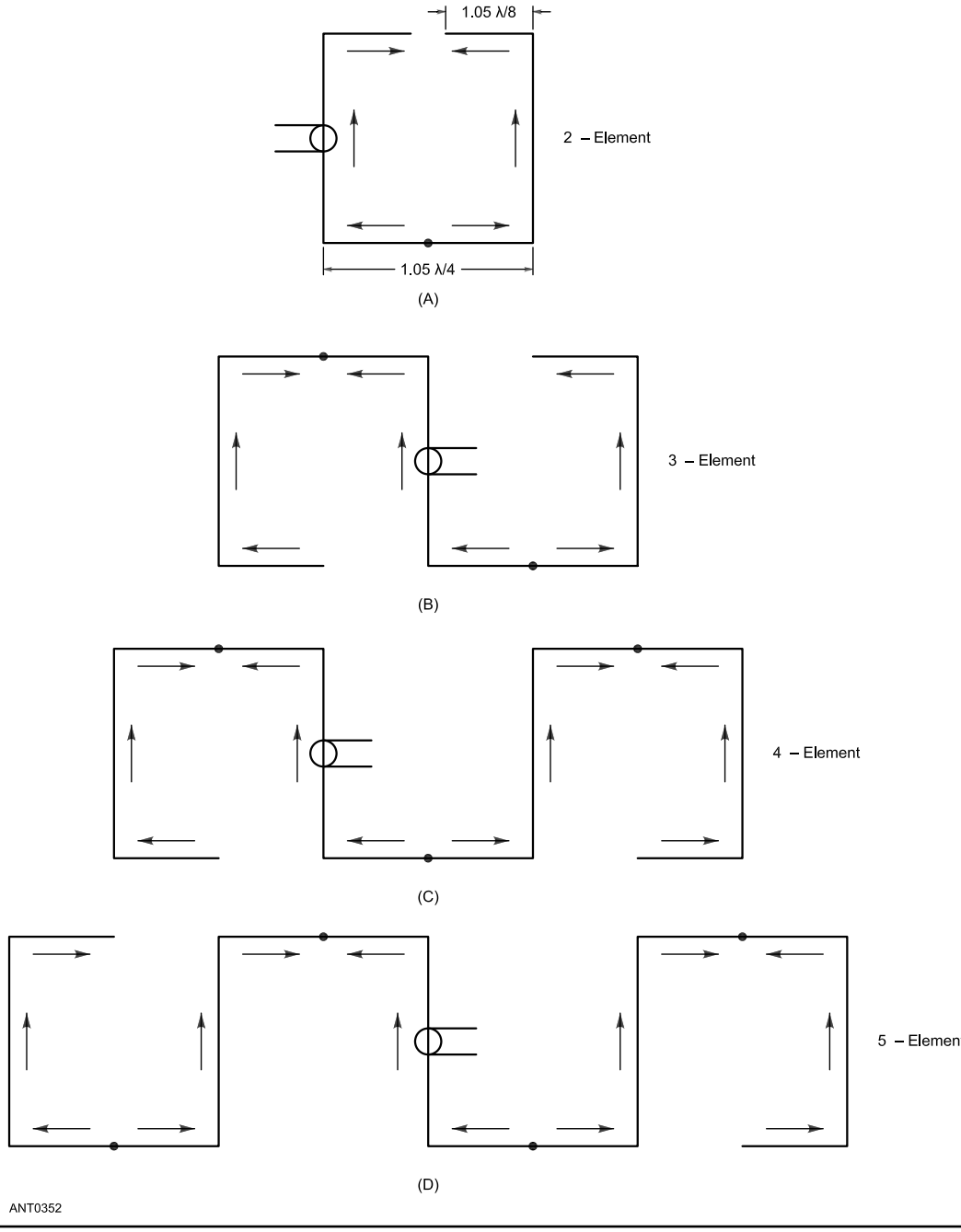

Fig 59—Various Bruce arrays: 2, 3, 4 and 5-element versions.

Table 2

Bruce array length, impedance and gain as a function of number of elements

Number Elements	*Gain Over λ/2 Vertical Dipole*	*Gain over λ/4 Ground-Plane*	*Array Length Wavelengths*	*Approx. Feed Z, Ω*
2	1.2 dB	1.9 dB	¼	130
3	2.8 dB	3.6 dB	½	200
4	4.3 dB	5.1 dB	¾	250
5	5.3 dB	6.1 dB	1	300

gain. The matching bandwidth is illustrated by the SWR curve in **Fig 62**. The 4-element Bruce has over twice the match bandwidth (200 kHz) than does the bobtail (75 kHz in Fig 57). Part of the gain difference is due to the binomial current distribution—the center element has twice the current as the outer elements in the bobtail. This reduces the gain slightly so that the 4-element Bruce becomes competitive. This is a good example of using more than the minimum number of elements to improve performance or to reduce size. On 160 meters the 4-element Bruce will be 140 feet shorter than the bobtail, a significant reduction. If additional space is available for the bobtail (1 λ) then a 5-element Bruce could

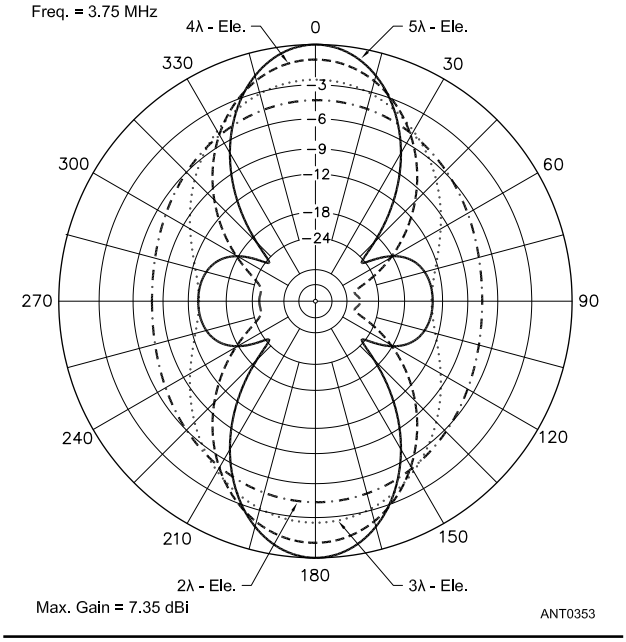

Fig 60—80-meter free-space E-plane directive patterns for the Bruce arrays shown in Fig 59. The 5-element's pattern is a solid line; the 4-element is a dashed line; the 3-element is a dotted line, and the 2-element version is a dashed-dotted line.

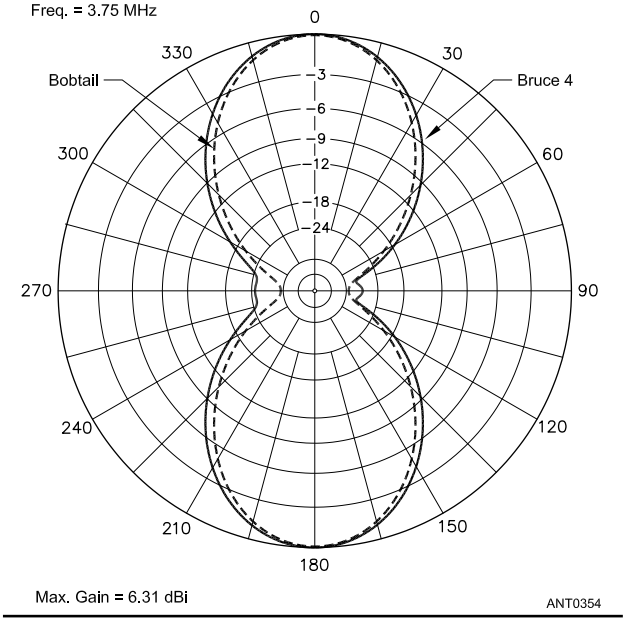

Fig 61—Comparison of free space patterns of a 4-element Bruce array (solid line) and a 3-element bobtail curtain (dashed line).

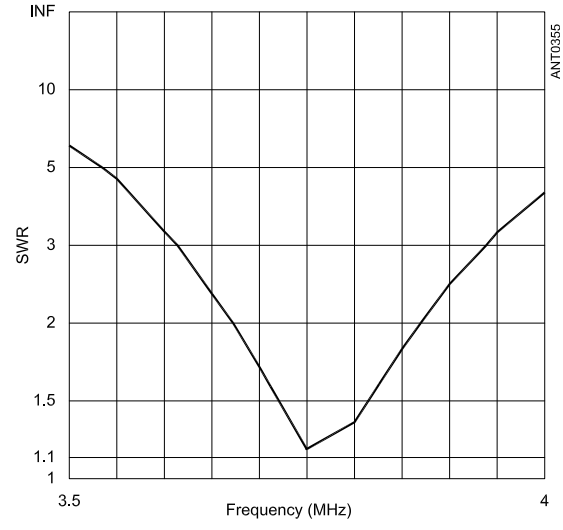

Fig 62—Typical SWR curve for a 4-element 80-meter Bruce array.

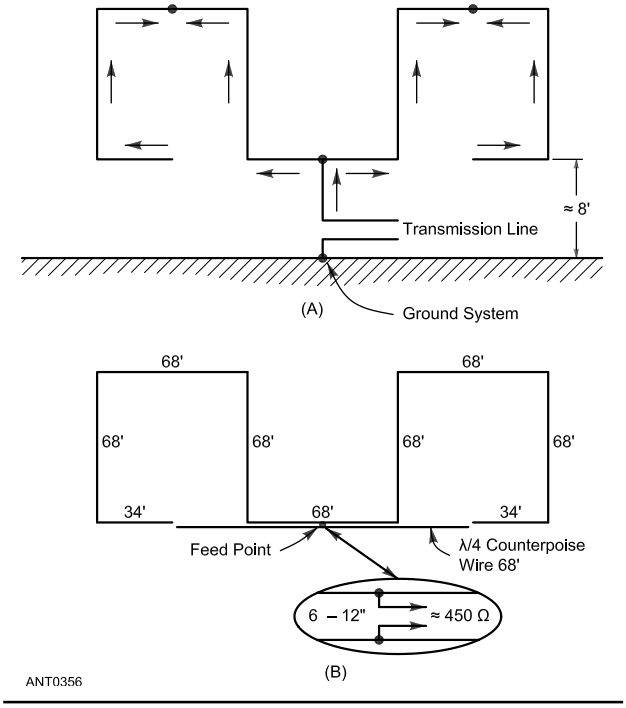

Fig 63—Alternate feed arrangements for the Bruce array. At A, the antenna is driven against a ground system and at B, it uses a two-wire counterpoise.

be used, with a small increase in gain but also introducing some sidelobes.

The 2-element Bruce and the half-square antennas are both 2-element arrays. However, since the spacing between radiators is greater in the half-square (λ/2) the gain of the half-square is about 1 dB greater. If space is available, the half-square would be a better choice. If there is not room for a half-square then the Bruce, which is only half as long (λ/4), may be a good alternative. The 3-element Bruce, which has the same length (λ/2) as the half-square, has about 0.6 dB more gain than the half-square and will have a wider match bandwidth.

The Bruce antenna can be fed at many different points and in different ways. In addition to the feed points indicated in Fig 59, you may connect the feed line at the center of any of the vertical sections. In longer Bruce arrays, feeding at one end will result in some current imbalance among the elements but the resulting pattern distortion is small. Actually, the feed-point can be anywhere along a vertical section. One very convenient point is at an outside corner. The feed-point impedance will be higher (about 600 Ω). A good match for 450-Ω ladder-line can usually be found somewhere on the vertical section. It is important to recognize that feeding the antenna at a voltage node (dots in Fig 59) by breaking the wire and inserting an insulator, completely changes the current distribution. This will be discussed in the section on endfire arrays.

A Bruce can be fed unbalanced against ground or against a counterpoise as shown in **Fig 63**. Because it is a vertically polarized antenna, the better the ground system, the better the performance. As few as two elevated radials can be used as shown in Fig 63B, but more radials can also be used to improve the performance, depending on local ground constants. The original development of the Bruce array in the late 1920s used this feed arrangement.

FOUR-ELEMENT BROADSIDE ARRAY

The 4-element array shown in **Fig 64** is commonly known as the *lazy H*. It consists of a set of two collinear elements and a set of two parallel elements, all operated in-phase to give broadside directivity. The gain and directivity will depend on the spacing, as in the case of a simple parallel-element broadside array. The spacing may be chosen between the limits shown on the drawing, but spacings below 3λ/8 are not worthwhile because the gain is small. Estimated gains compared to a single element are:

3λ/8 spacing—4.2 dB
λ/2 spacing—5.8 dB
5λ/8 spacing—6.7 dB
3λ/4 spacing—6.3 dB

Half-wave spacing is generally used. Directive patterns for this spacing are given in **Figs 65** and **66**. With λ/2 spacing between parallel elements, the impedance at the junction of the phasing line and transmission line is resistive and in the vicinity of 100 Ω. With larger or smaller spacing the impedance at this junction will be reactive as well as

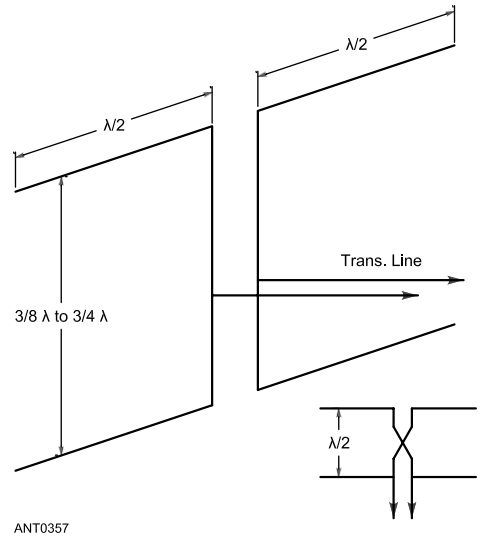

Fig 64—Four-element broadside array ("lazy H") using collinear and parallel elements.

resistive. Matching stubs are recommended in cases where a non-resonant line is to be used. They may be calculated and adjusted as described in Chapter 26.

The system shown in Fig 64 may be used on two bands having a 2-to-1 frequency relationship. It should be designed for the higher of the two frequencies, using 3λ/4 spacing between parallel elements. It will then operate on the lower frequency as a simple broadside array with 3λ/8 spacing.

An alternative method of feeding is shown in the small diagram in Fig 64. In this case the elements and the phasing line must be adjusted exactly to an electrical half wavelength. The impedance at the feed point will be resistive and on the order of 2 kΩ.

THE BI-SQUARE ANTENNA

A development of the lazy H, known as the *bi-square antenna*, is shown in **Fig 67**. The gain of the bi-square is somewhat less than that of the lazy-H, but this array is attractive because it can be supported from a single pole. It has a circumference of 2 λ at the operating frequency, and is horizontally polarized.

The bi-square antenna consists of two 1 λ radiators, fed 180° out-of-phase at the bottom of the array. The radiation resistance is 300 Ω, so it can be fed with either 300- or 600-Ω line. The free space gain of the antenna is about 5.8 dBi, which is 3.7 dB more than a single dipole element. Gain may be increased by adding a parasitic reflector or director. Two bi-square arrays can be mounted at right angles and switched to provide omnidirectional coverage. In this way, the antenna wires may be used as part of the guying system for the pole.

Although it resembles a loop antenna, the bi-square is not a true loop because the ends opposite the feed point

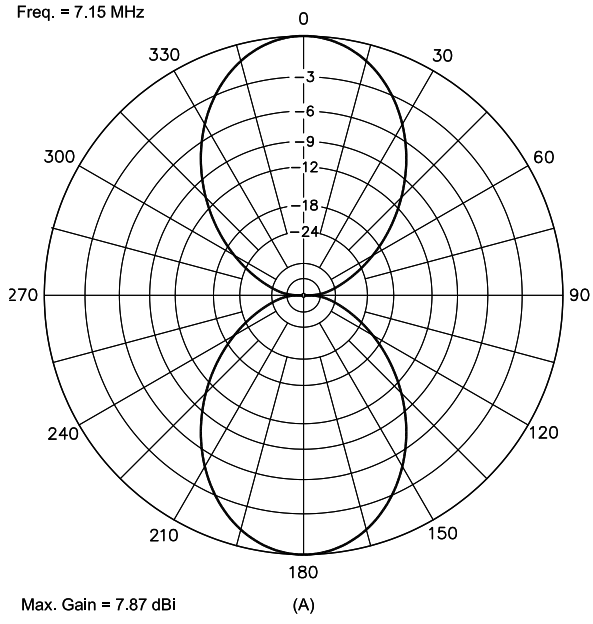

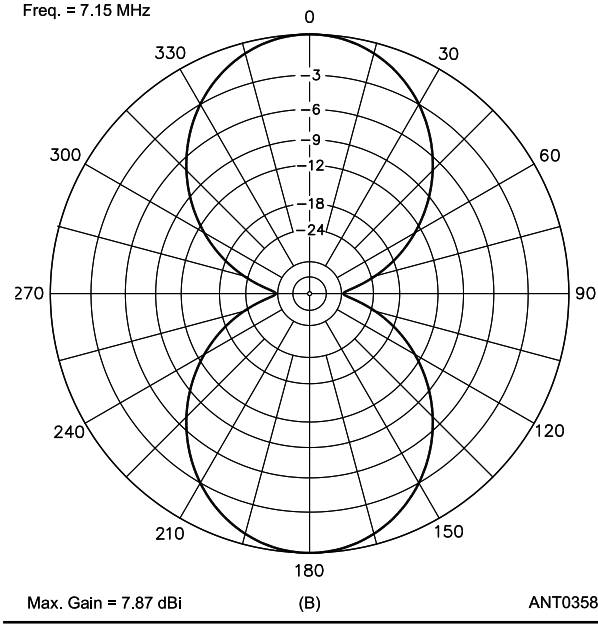

Fig 65—Free-space directive diagrams of the 4-element antenna shown in Fig 64. At A is the E-plane pattern. The axis of the elements lies along the 90°-270° line. At B is the free-space H-plane pattern, viewed as if one set of elements is above the other from the ends of the elements.

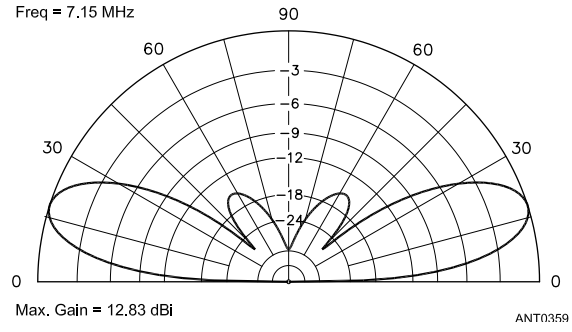

Fig 66—Vertical pattern of the 4-element broadside antenna of Fig 64, when mounted with the elements horizontal and the lower set λ/4 above flat ground. Stacked arrays of this type give best results when the lowest elements are at least λ/2 high. The gain is reduced and the wave angle raised if the lowest elements are too close to ground.

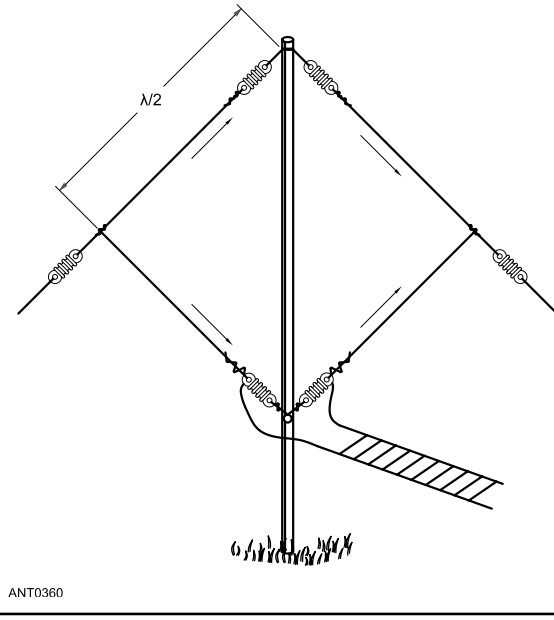

Fig 67—The bi-square array. It has the appearance of a loop, but is not a true loop because the conductor is open at the top. The length of each side, in feet, is 480/f (MHz).

are open. However, identical construction techniques can be used for the two antenna types. Indeed, with a means of remotely closing the connection at the top for lower frequency operation, the antenna can be operated on two harmonically related bands. As an example, an array with 17 feet per side can be operated as a bi-square at 28 MHz and as a full-wave loop at 14 MHz. For two-band operation in this manner, the side length should favor the higher frequency. The length of a closed loop is not as critical.

End-Fire Arrays

The term *end-fire* covers a number of different methods of operation, all having in common the fact that the maximum radiation takes place along the array axis, and that the array consists of a number of parallel elements in one plane. End-fire arrays can be either bidirectional or unidirectional. In the bidirectional type commonly used by amateurs there are only two elements, and these are operated with currents 180° out-of-phase. Even though adjustment tends to be complicated, unidirectional end-fire driven arrays have also seen amateur use, primarily as a pair of phased, ground-mounted λ/4 vertical elements. Extensive discussion of this array is contained in earlier sections of this chapter.

Horizontally polarized unidirectional end-fire arrays see little amateur use except in log-periodic arrays (described in Chapter 10). Instead, horizontally polarized unidirectional arrays usually have parasitic elements (described in Chapter 11) and are called Yagis.

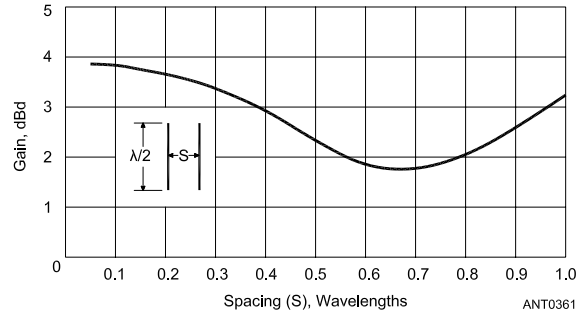

Fig 68—Gain of an end-fire array consisting of two elements fed 180° out-of-phase, as a function of the spacing between elements. Maximum radiation is in the plane of the elements and at right angles to them at spacings up to λ/2, but the direction changes at greater spacings.

TWO-ELEMENT END-FIRE ARRAY

In a 2-element array with equal currents out-of-phase, the gain varies with the spacing between elements as shown in **Fig 68**. The maximum gain occurs in the neighborhood of 0.1 λ spacing. Below that the gain drops rapidly due to conductor loss resistance.

The feed-point resistance for either element is very low at the spacings giving greatest gain, as shown in Fig 8 earlier in this chapter. The spacings most frequently used are λ/8 and λ/4, at which the resistances of center-fed λ/2 elements are about 9 and 32 Ω, respectively.

The effect of conductor resistance on gain for various spacings is shown in **Fig 69**. Because current along the element is not constant (it is approximately sinusoidal), the resistance shown is the equivalent resistance (R_{eq}) inserted at the center of the element to account for the loss distributed along the element.

The equivalent resistance of a λ/2 element is one half the ac resistance (R_{ac}) of the complete element. R_{ac} is usually >> R_{dc} due to skin effect. For example, a 1.84 MHz dipole using #12 copper wire will have the following R_{eq}:

Wire length = 267 feet
Rdc = 0.00159 [/foot] × 267 [feet] = 0.42
Fr = Rac/Rdc = 10.8
Req =(Rdc/2) × Fr = 2.29

For a 3.75 MHz dipole made with #12 wire, Req = 1.59 Ω. In Fig 69, it is clear that end-fire antennas made with #12 or smaller wire will limit the attainable gain because of losses. There is no point in using spacings much less than λ/4 if you use wire elements. If instead you use elements made of aluminum tubing then smaller spacings can be used to increase gain. However, as the spacing is reduced below λ/4 the increase in gain is quite small even with good conductors. Closer spacings give little gain increase but can drastically reduce the operating bandwidth due to the rapidly increasing Q of the array.

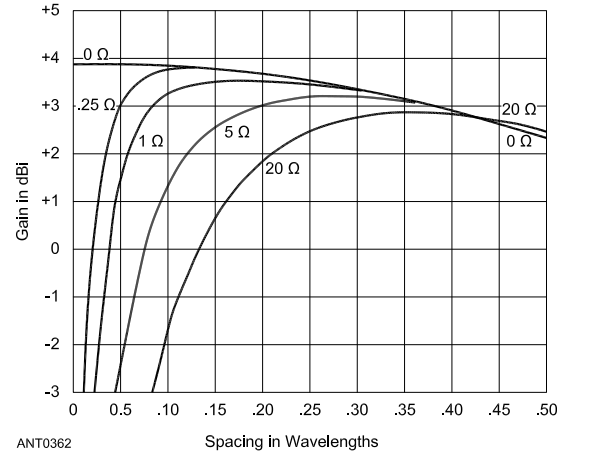

Fig 69—Gain over a single element of two out-of-phase elements in free space as a function of spacing for various loss resistances.

Unidirectional End-Fire Arrays

Two parallel elements spaced λ/4 apart and fed equal currents 90° out-of-phase will have a directional pattern in the plane at right angles to the plane of the array. See **Fig 70**. The maximum radiation is in the direction of the element in which the current lags. In the opposite direction the fields from the two elements cancel.

When the currents in the elements are neither in-phase nor 180° out-of-phase, the feed-point resistances of the elements are not equal. This complicates the problem of feeding equal currents to the elements, as discussed in earlier sections.

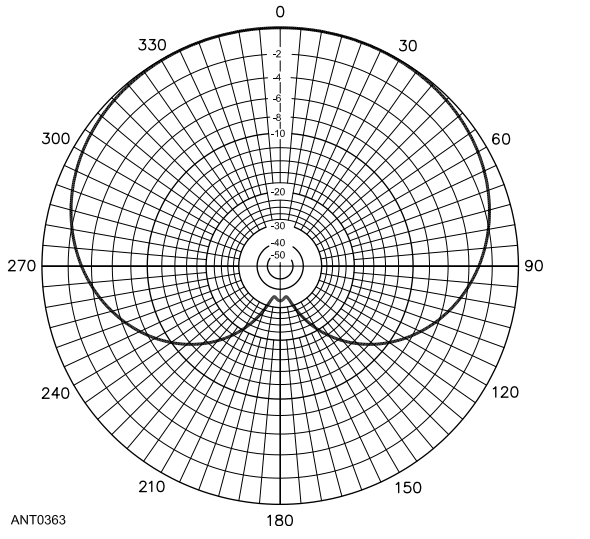

Fig 70—Representative H-plane pattern for a 2-element end-fire array with 90° spacing and phasing. The elements lie along the vertical axis, with the uppermost element the one of lagging phase. Dissimilar current distributions are taken into account. (Pattern computed with *ELNEC*.)

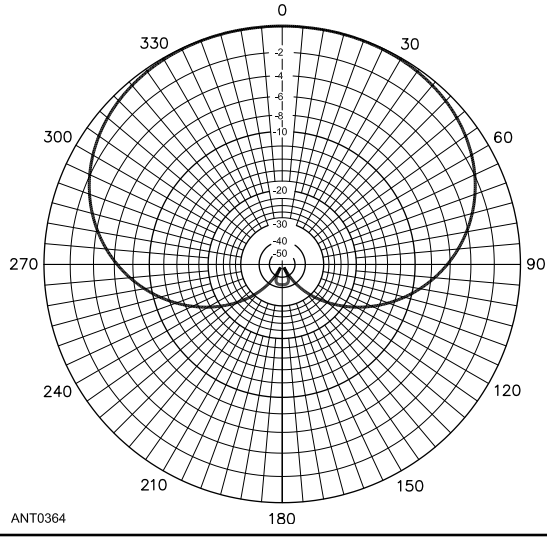

Fig 71—H-plane pattern for a 3-element end-fire array with binomial current distribution (the current in the center element is twice that in each end element). The elements are spaced λ/4 apart along the 0°-180° axis. The center element lags the lower element by 90°, while the upper element lags the lower element by 180° in phase. Dissimilar current distributions are taken into account. (Pattern computed with *ELNEC*.)

More than two elements can be used in a unidirectional end-fire array. The requirement for unidirectivity is that there must be a progressive phase shift in the element currents equal to the spacing, in electrical degrees, between the elements. The amplitudes of the currents in the various elements also must be properly related. This requires binomial current distribution. In the case of three elements, this requires that the current in the center element be twice that in the two outside elements, for 90° (λ/4) spacing and element current phasing. This antenna has an overall length of λ/2. The directive diagram is shown in **Fig 71**. The pattern is similar to that of Fig 70, but the 3-element binomial array has greater directivity, evidenced by the narrower half-power beamwidth (146° versus 176°). Its gain is 1.0 dB greater.

THE W8JK ARRAY

As pointed out earlier, John Kraus, W8JK, described his bidirectional flat-top W8JK beam antenna in 1940. See **Fig 72**. Two λ/2 elements are spaced λ/8 to λ/4 and driven 180° out-of-phase. The free-space radiation pattern for this antenna, using #12 copper wire, is given in **Fig 73**. The pattern is representative of spacings between λ/8 and λ/4 where the gain varies less than 0.5 dB. The gain over a dipole is about 3.3 dB (5.4 dBi referenced to an isotropic radiator), a worthwhile improvement. The feed-point impedance (including wire resistance) of *each* element is about 11 Ω for λ/8 spacing and 33 Ω for λ/4 spacing. The feed-point impedance at the center connection will depend on the length and Z_0 of the connecting transmission line.

Kraus gave a number of other variations for end-fire arrays, some of which are shown in **Fig 74**. The ones fed at the center (A, C and E) are usually horizontally polarized flat-top beams. The end-fed versions (B, D & F) are usually vertically polarized, where the feed point can be conveniently near ground.

A practical variation of Fig 74B is given in **Fig 75**. In this example, the height is limited to λ/4 so the ends can be bent over as shown, producing a 2-element Bruce array. This reduces the gain somewhat but allows much shorter supports, an important consideration on the low bands. If additional height is available, then you can achieve some additional gain. The upper ends can be bent over to fit the available height. The feed-point impedance will greater than 1 kΩ.

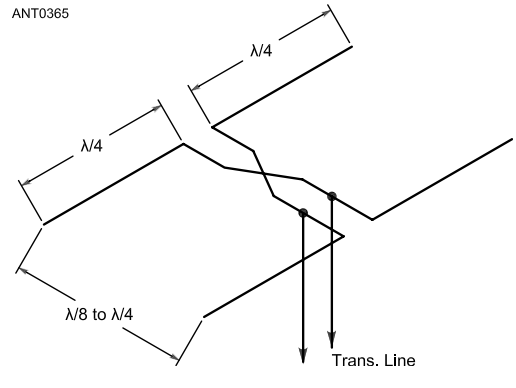

Fig 72—A 2-element W8JK array.

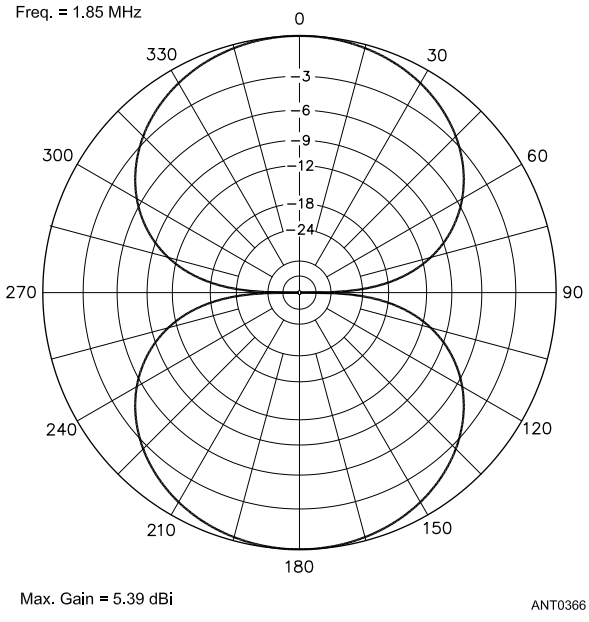

Fig 73—Free-space E-plane pattern for the 2-element W8JK array

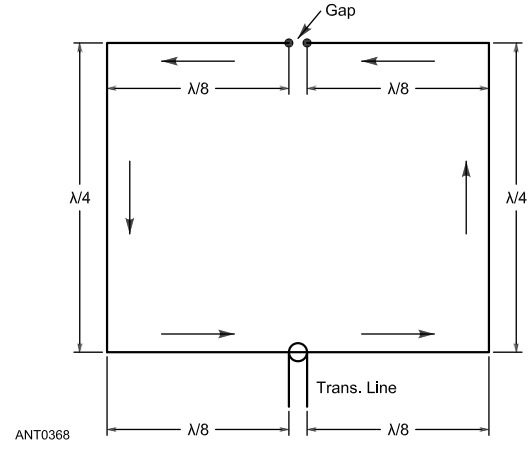

Fig 75—A 2-element end-fire array with reduced height.

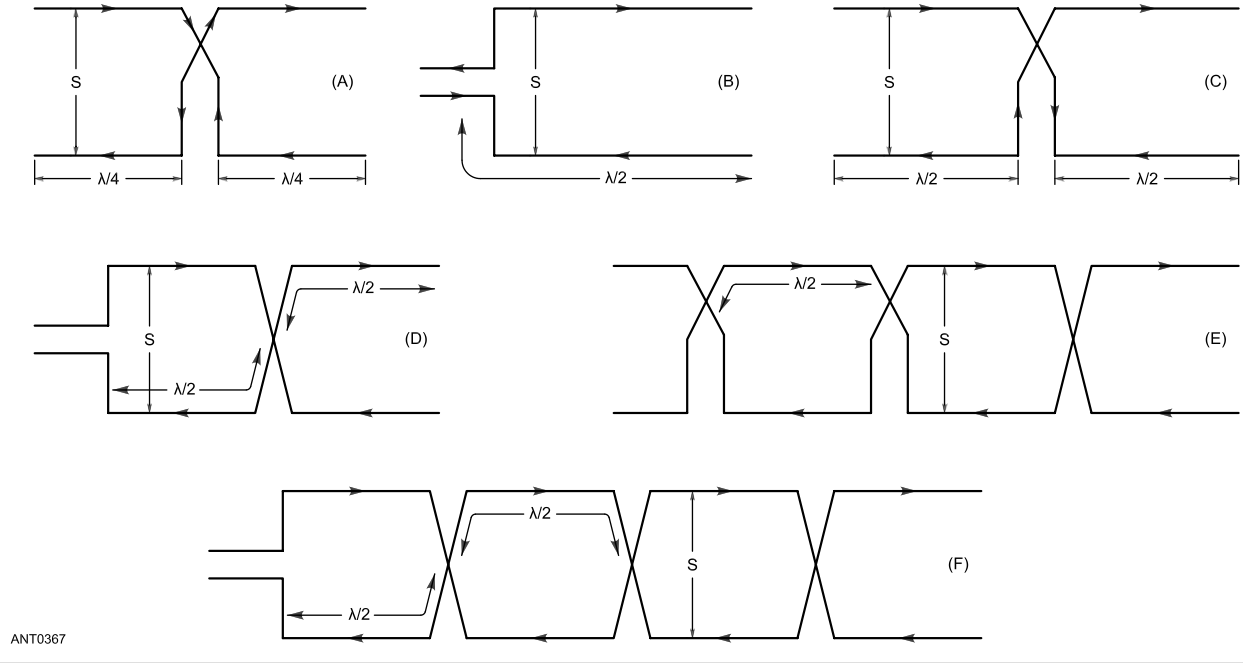

Fig 74—Six other variations of W8JK "flat-top beam" antennas.

FOUR-ELEMENT END-FIRE AND COLLINEAR ARRAYS

The array shown in **Fig 76** combines collinear in-phase elements with parallel out-of-phase elements to give both broadside and end-fire directivity. It is a *two-section W8JK*. The approximate free-space gain using #12 copper wire is 4.9 dBi with λ/8 spacing and 5.4 dBi with λ/4 spacing. Directive patterns are given in **Figs 77** for free space, and in **Fig 78** for heights of 1 λ and λ/2 above flat ground.

The impedance between elements at the point where the phasing line is connected is of the order of several thousand ohms. The SWR with an unmatched line consequently is quite high, and this system should be constructed with open-wire line (500 or 600 Ω) if the line is to be resonant. With λ/4 element spacing the SWR on a 600 Ω line is estimated to be in the vicinity of 3 or 4:1.

To use a matched line, you could connect a closed stub 3λ/16 long at the transmission-line junction shown in Fig 76. The transmission line itself can then be tapped on this matching section at the point resulting in the lowest line SWR. This point can be determined by trial.

This type of antenna can be operated on two bands having a frequency ratio of 2 to 1, if a resonant feed line is used. For example, if you design for 28 MHz with λ/4 spacing between elements, you can also operate on 14 MHz as a simple 2-element end-fire array having λ/8 spacing.

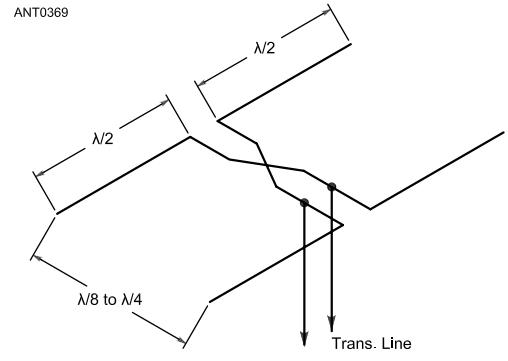

Fig 76—A 4-element array combining collinear broadside elements and parallel end-fire elements, popularly known as a two-section W8JK array.

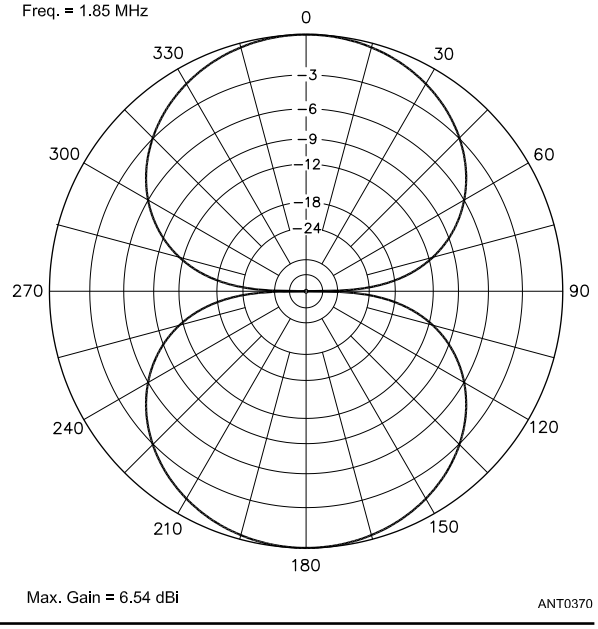

Fig 77—Free-space E-plane pattern for the antenna shown in Fig 76, with λ/8 spacing. The elements are parallel to the 90°-270° line in this diagram. Less than a 1° change in half-power beamwidth results when the spacing is changed from λ/8 to λ/4.

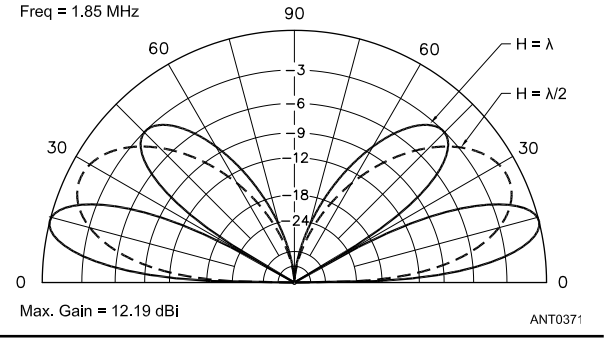

Fig 78—Elevation-plane pattern for the 4-element antenna of Fig 76 when mounted horizontally at two heights over flat ground. Solid line = 1 λ high; dashed line = λ/2 high.

Combination Driven Arrays

You can readily combine broadside, end-fire and collinear elements to increase gain and directivity, and this is in fact usually done when more than two elements are used in an array. Combinations of this type give more gain, in a given amount of space, than plain arrays of the types just described. Since the combinations that can be worked out are almost endless, this section describes only a few of the simpler types.

The accurate calculation of the power gain of a multielement array requires a knowledge of the mutual impedances between all elements, as discussed in earlier sections. For approximate purposes it is sufficient to assume that each set (collinear, broadside, end-fire) will have the gains as given earlier, and then simply add up the gains for the combination. This neglects the effects of cross-coupling between sets of elements. However, the array configurations are such that the mutual impedances from cross-coupling should be relatively small, particularly when the spacings are λ/4 or more, so the estimated gain should be reasonably close to the actual gain. Alternatively, an antenna modeling program, such as *EZNEC*, can give good estimates of all parameters for a real-world antenna, providing that you take care to model all applicable parameters.

FOUR-ELEMENT DRIVEN ARRAYS

The array shown in **Fig 79** combines parallel elements with broadside and end-fire directivity. The smallest array (physically)—3λ/8 spacing between broadside and λ/8 spacing between end-fire elements—has an estimated gain of 6.5 dBi and the largest—3λ/4 and λ/4 spacing, respectively—about 8.4 dBi. Typical directive patterns for a λ/4 × λ/2 array are given in **Figs 80** and **81**.

The impedance at the feed point will not be purely resistive unless the element lengths are correct and the phasing lines are exactly λ/2 long. (This requires somewhat less than λ/2 spacing between broadside elements.) In this case the impedance at the junction is estimated to be over 10 kΩ. With other element spacings the impedance at the junction will be reactive as well as resistive, but in any event the SWR will be quite large. An open-wire line can be used as a resonant line, or a matching section may be used for non-resonant operation.

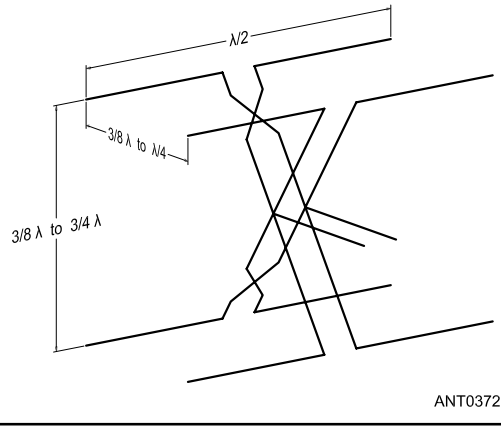

Fig 79—Four-element array combining both broadside and end-fire elements.

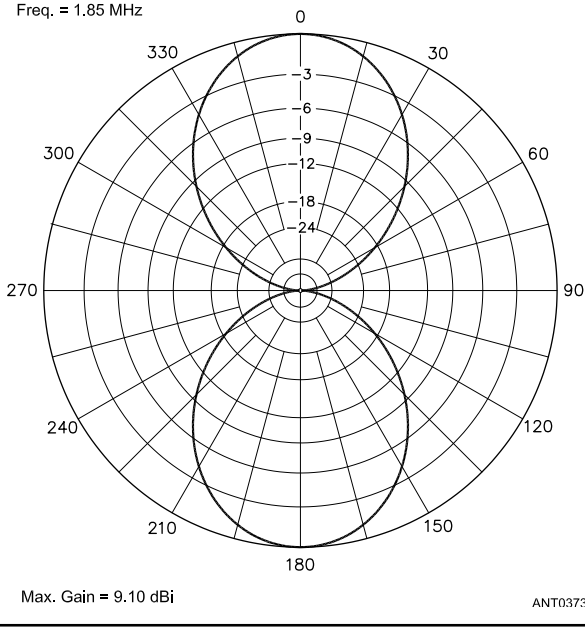

Fig 80—Free-space H-plane pattern of the 4-element antenna shown in Fig 79.

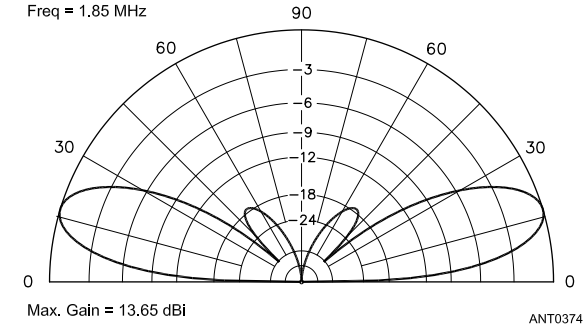

Fig 81—Vertical pattern of the antenna shown in Fig 79 at a mean height of 3λ/4 (lowest elements λ/2 above flat ground) when the antenna is horizontally polarized. For optimum gain and low wave angle the mean height should

EIGHT-ELEMENT DRIVEN ARRAYS

The array shown in **Fig 82** is a combination of collinear and parallel elements in broadside and end-fire directivity. Common practice in a wire antenna is to use λ/2 spacing for the parallel broadside elements and λ/4 spacing for the end-fire elements. This gives a free-space gain of about 9.1 dBi. Directive patterns for an array using these spacings are similar to those of Figs 80 and 81, but are somewhat sharper.

The SWR with this arrangement will be high. Matching stubs are recommended for making the lines non-resonant. Their position and length can be determined as described in Chapter 26.

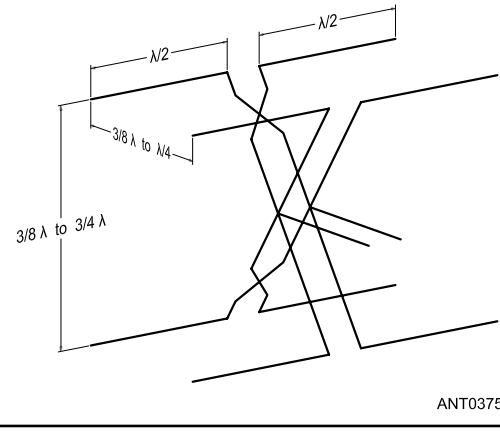

Fig 82—Eight-element driven array combining collinear and parallel elements for broadside and end-fire directivity.

This system can be used on two bands related in frequency by a 2-to-1 ratio, providing it is designed for the higher of the two, with 3λ/4 spacing between the parallel broadside elements and λ/4 spacing between the end-fire elements. On the lower frequency it will then operate as a 4-element antenna of the type shown in Fig 79, with 3λ/8 broadside spacing and λ/8 end-fire spacing. For two-band operation a resonant transmission line must be used.

PHASING ARROWS IN ARRAY ELEMENTS

In the antenna diagrams of preceding sections, the relative direction of current flow in the various antenna elements and connecting lines was shown by arrows. In laying out any antenna system it is necessary to know that the phasing lines are properly connected; otherwise the antenna may have entirely different characteristics than anticipated. The phasing may be checked either on the basis of current direction or polarity of voltages. There are two rules to remember:

1) In every λ/2 section of wire, starting from an open end, the current directions reverse. In terms of voltage, the polarity reverses at each λ/2 point, starting from an open end.
2) Currents in transmission lines always must flow in opposite directions in adjacent wires. In terms of voltage, polarities always must be opposite.

Examples of the use of current direction and voltage polarity are given at A and B, respectively, in **Fig 83**. The λ/2 points in the system are marked by small circles. When current in one section flows toward a circle, the current in the next section must also flow toward it, and vice versa. In the 4-element antenna shown at A, the current in the upper right-hand element cannot flow toward the transmission line because then the current in the right-hand section of the phasing line would have to flow upward and thus would be flowing in the same direction as the current in the left-hand wire. The phasing line would simply act like two wires in parallel in such a case. Of course, all arrows in the drawing could be reversed, and the net effect would be unchanged.

C shows the effect of transposing the phasing line. This transposition reverses the direction of current flow in the lower pair of elements, as compared with A, and thus changes the array from a combination collinear and end-fire arrangement into a collinear-broadside array.

The drawing at D shows what happens when the transmission line is connected at the center of a section of phasing line. Viewed from the main transmission line, the two parts of the phasing line are simply in parallel, so the half wavelength is measured from the antenna element along the upper section of phasing line and thence along the transmission line. The distance from the lower elements is measured in the same way. Obviously, the two sections of phasing line should be the same length. If they are not, the current distribution becomes quite complicated; the element currents are neither in-phase nor 180° out-of-phase, and the elements at opposite ends of the lines do not receive the same current. To change the element current phasing at D into the phasing at A, simply transpose the wires in one section of the phasing line. This reverses the direction of current flow in the antenna elements connected to that section of phasing line.

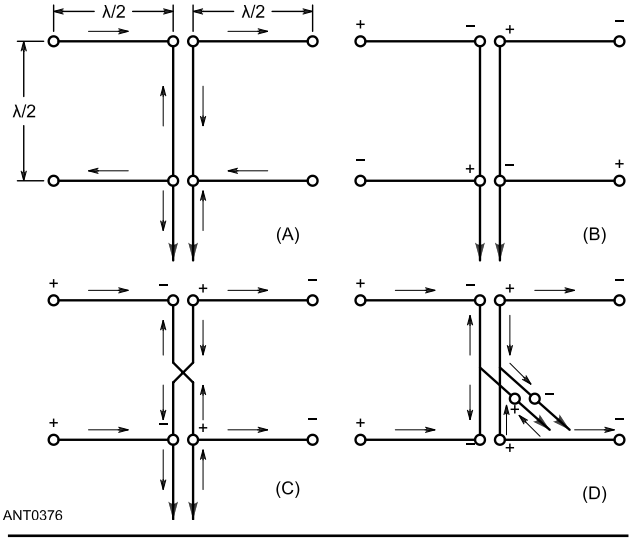

Fig 83—Methods of checking the phase of currents in elements and phasing lines.

BIBLIOGRAPHY

Source material and more extended discussion of topics covered in this chapter can be found in the references given below and in the textbooks listed at the end of Chapter 2.

D. W. Atchley, H. E. Stinehelfer, and J. F. White, "360°-Steerable Vertical Phased Arrays," *QST*, Apr 1976, pp 27-30.

G. H. Brown, "Directional Antennas," *Proc. IRE*, Vol 25, No. 1, Jan 1937, pp 78-145.

G. H. Brown, R. F. Lewis and J. Epstein, "Ground Systems as a Factor in Antenna Efficiency," *Proc. IRE*, Jun 1937, pp 753-787.

G. H. Brown and O. M. Woodward, Jr., "Experimentally Determined Impedance Characteristics of Cylindrical Antennas," *Proc. IRE*, Apr 1945.

L. B. Cebik, "Two Limitations of NEC-4", **www.cebik.com/model/fd.html**.

A. Christman, "Feeding Phased Arrays: An Alternate Method," *Ham Radio*, May 1985, pp 58-59, 61-64.

J. Devoldere, *ON4UN's Low-Band DXing*, 4th ed. (Newington, CT: ARRL, 2005).

EZNEC is an antenna-modeling computer program for Microsoft Windows. See **eznec.com** for full information.

F. Gehrke, "Vertical Phased Arrays," in six parts, *Ham Radio*, May-Jul, Oct and Dec 1983, and May 1984.

C. Harrison, Jr, and R. King, "Theory of Coupled Folded Antennas," *IRE Trans on Antennas and Propagation*, Mar 1960, pp131-135.

W. Hayward and D. DeMaw, *Solid State Design for the Radio Amateur* (Newington, CT: ARRL, 1977).

W. Hayward, *Radio Frequency Design* (Newington, CT: ARRL, 1994).
H. Jasik, *Antenna Engineering Handbook*, 1st ed. (New York: McGraw-Hill, 1961). Later editions are edited by Richard C. Johnson.
R. King and C. Harrison, Jr, "Mutual and Self-Impedance for Coupled Antennas," *Journal of Applied Physics* , Vol 15, Jun 1944, pp 481-495.
R. King, "Self- and Mutual Impedances of Parallel Identical Antennas," *Proc. IRE*, Aug 1952, pp 981-988.
R. W. P. King, *Theory of Linear Antennas* (Cambridge, MA: Harvard Univ Press, 1956), p 275ff.
H. W. Kohler, "Antenna Design for Field-Strength Gain," *Proc. IRE*, Oct 1944, pp 611-616.
J. D. Kraus, "Antenna Arrays with Closely Spaced Elements," *Proc. IRE*, Feb, 1940, pp 76-84.
J. D. Kraus, *Antennas*, 2nd ed. (New York: McGraw-Hill Book Co., 1988).
Johnson, Richard C., *Antenna Engineering Handbook*, 3rd ed. (New York: McGraw-Hill Inc., 1993). This is a later edition of the volume by the same name edited by H. Jasik.
E. A. Laport, *Radio Antenna Engineering* (New York: McGraw-Hill Book Co, 1952).
J. L. Lawson, "Simple Arrays of Vertical Antenna Elements," *QST*, May 1971, pp 22-27.
P. H. Lee, N6PL *The Amateur Radio Vertical Antenna Handbook*, 2nd ed. (Hicksville, NY: CQ Publishing, Inc., 1984).
R. W. Lewallen, "Baluns: What They Do and How They Do It," *The ARRL Antenna Compendium, Vol 1* (Newington: ARRL, 1985). Also available for viewing at **eznec.com/Amateur/Articles/Baluns.pdf**.
R. Lewallen, "The Impact of Current Distribution on Array Patterns," Technical Correspondence, *QST*, Jul 1990, pp 39-40. Also available for viewing at **eznec.com/Amateur/Articles/Current_Dist.pdf**.
R. Lewallen, "*MININEC*—The Other Edge of the Sword", *QST*, Feb 1991, pp 18-22. *ELNEC*, referenced in the article, is no longer available.
M. W. Maxwell, "Some Aspects of the Balun Problem," *QST*, Mar 1983, pp 38-40.
J. Sevick, "The Ground-Image Vertical Antenna," *QST*, Jul 1971, pp 16-19, 22.
J. Sevick, "The W2FMI Ground-Mounted Short Vertical," *QST*, Mar 1973, pp 13-28,41.
E. J. Wilkinson, "An N-Way Hybrid Power Divider," *IRE Transactions on Microwave Theory and Techniques*, Jan, 1960.
Radio Broadcast Ground Systems, available from Smith Electronics, Inc, 8200 Snowville Rd, Cleveland, OH 44141.

Appendix A—*EZNEC-ARRL* Examples

This appendix contains step-by-step procedures using *EZNEC-ARRL* (included on the *Antenna Book* CD) to illustrate various topics discussed in the main chapter. A standard *EZNEC* program type of v. 4.0 or later may also be used. Different versions, program types and calculating engines may give results that are slightly different from those shown in the examples. However, any differences should be insignificantly small.

EZNEC Example—Mutual Coupling

Illustrates the effect of mutual coupling on feed-point impedance. Open the **ARRL_Cardioid.EZ** file, which is mounted over "perfect" ground. Click the **View Ant** button to see a diagram of the antenna, a 2-element array of vertical elements. Click on the **Wires** line in the main window to open the Wires Window. Click the button at the left of the Wire 2 line, and then press the **Delete** key on your keyboard to delete wire #2. After clicking **Ok**, note that one of the verticals has disappeared from the View Antenna display, leaving a single element. Click **Src Dat** and note that the feed-point impedance of this single vertical is about $37 + j\ 1\ \Omega$--it's very nearly resonant.

Next, in the Wires Window, open the **Edit** menu at the top and click **Undo delete wire(s)** to restore the second element. Click **Src Dat** again and notice that the feed-point impedance of wire #1 is now about $21 - j\ 19\ \Omega$. The feed-point impedance of the second element, which is identical to the first, is about $52 + j\ 21\ \Omega$. This difference, and the change from the self-impedance of $37 + j\ 1\ \Omega$, is due to mutual coupling. As you see, it's not at all a minor effect.

As an additional exercise, change the magnitude or phase angle of the source at the base of wire #2 (click **Sources** in the main window), and see how this changes the feed-point impedances of both elements. You should be able to confirm each of the four points enumerated in the **MUTUAL COUPLING** section.

EZNEC Example—Nulls

Illustrates the effect of current magnitude on nulls and gain. Again, open the **ARRL_Cardioid.EZ** file. Click the **FF Plot** button to generate the azimuth pattern of an ideal array. Save the plot for future reference as follows: In the plot window, open the **File** menu and select **Save Trace As**. Enter the name **Cardioid** and click **Save**. Now, in the main window click on the **Sources** line to open the Sources Window. Change the magnitude of source 1 from 1 to 1.1, and of source 2 from 1 to 0.9 and press **Enter** on your keyboard so that *EZNEC-ARRL* will accept the last change.

Click **FF Plot** to generate a pattern with the new currents. In the plot window, open the File menu and select **Add**

Trace. Enter the name **Cardioid** and click Open. You should now see the original plot and new plot overlaid. Notice that the null is much less deep with the altered currents, but the forward patterns are nearly identical. By clicking on the names of the traces, **Primary** and **Cardioid**, you can see in turn the gain and front-to-back ratio of each of the traces. The original, **Cardioid**, has a front-to-back ratio of about 32 dB, while Primary, the new plot, has a ratio of about 22.5 dB. The forward gain, however, differs by only 0.02 dB, a completely insignificant amount.

EZNEC Example—"Phasing-Line" Feed

Illustrates the effect of using a "phasing-line" feed. Open the **ARRL_CardTL.EZ** file. This is a model of an array fed with transmission lines whose lengths were designed using the *Arrayfeed1* program to take into account the actual load impedances of elements in a phased array. This model is mounted over "perfect" ground.

Click the **View Ant** button to show the array. Note that the lengths of the lines from the source (circle) to the elements don't represent the actual physical lengths of the lines. In the main window, click on the **Trans Lines** line to open the Transmission Lines window. In it you can see that the lengths of the feed lines, both of which are connected to the same source, are about 81° and 155°, a difference of 74° rather than 90°.

In the main window, click the **Currents** button and take a look at the current shown for segment 1 of wires 1 and 2. These are the currents at the element feed points. The ratio of the magnitude of currents is 4.577/4.561 = 1.003, and the phase difference is –56.3°–(–147.5°) = 91.2°. (A more accurate determination of feed-line lengths with program *Arrayfeed1* gives lengths of 80.61° and 153.70°, resulting in a current ratio of 1.000 at a phase of 90.02°. But the resulting pattern is very nearly the same.) But let's see what happens when we make the lines exactly 90° different in length.

First, click the **FF Plot** button to generate the azimuth pattern of the original model. Save the plot for future reference as follows: In the plot window, open the **File** menu and select **Save Trace As**. Enter the name **CardTL** and click **Save**. Now in the Transmission Lines Window, change the length of line number 1 from 80.56° to 90°. *Important:* In the line 1 Length box, enter **90d** to make the line 90° long. If you omit the **d**, it will become 90 meters long! Similarly, change the length of line 2 to 180° by entering **180d** in the line 2 Length box, then press **Enter** on your keyboard so that *EZNEC* will accept the last change.

Click **FF Plot** to generate a pattern with the new line lengths. In the plot window, open the **File** menu and select **Add Trace**. Enter the name **CardTL** and click **Open**. You should now see the original plot and new plot overlaid together. Notice that the gain of the modified model is about 1 dB greater than the original, but the front-to-back ratio has deteriorated to about 10 dB.

Experiment with different combinations of line lengths that differ by 90°--for example, 45° and 135° (don't forget the '**d**'!), or change the impedance of one or both lines and you'll see that you can get a wide variety of patterns. None, however, are likely to be as close to the ideal cardioid pattern as the original.

Chapter 9

Broadband Antenna Matching

Antenna systems that provide a good impedance match to the transmitter over a wide frequency range have been a topic of interest to hams for many years. Most emphasis has been focused on the 80-meter band since a conventional half-wave dipole will provide better than 2:1 SWR over only about one-third of the 3.5 to 4.0 MHz band. The advantage of a broadband match is obvious—fewer adjustments during tune-up and an antenna tuner may not be required.

This chapter was written by Frank Witt, AI1H, who has written numerous articles in *QST* and in *The ARRL Antenna Compendium* series on this subject. See the Bibliography for details.

The term *broadband antennas* has frequently been used to describe antenna systems that provide a wideband impedance match to the transmitter. This is something of a misnomer, since most antennas are good radiators over a wide range of frequencies and are therefore "broadband antennas" by definition. The problem is getting the energy to the antenna so it can be radiated. Antenna tuners solve this problem in some cases, although losses in transmission lines, baluns and the antenna tuner itself can be excessive. Also worthy of mention is that antenna directional properties are usually frequency dependent. In this chapter, we discuss broadbanding the impedance match to the transmitter only.

GENERAL CONCEPTS

The Objective

Fig 1 shows a simplified system: the transmitter, an SWR meter and the transmitter load impedance. Modern transceivers are designed to operate properly into a 50-Ω load and they will deliver full power into the load impedance, at their rated level of distortion, when the SWR is less than about 1.5:1. Loads beyond this limit may cause the transceiver to protect itself by lowering the output power.

Many transceivers have built-in automatic antenna tuners that permit operation for loads outside the 1.5:1 SWR range, but the matching range is often limited, particularly on the lower-frequency bands. In practice, barefoot operation is simplified if the load SWR is held to less than 2:1.

For high-power amplifiers, it is also best to keep the load SWR to less than about 2:1, since output tuning components are commonly rated to handle such loads. You can see that the primary function of the SWR meter in Fig 1 is to measure the suitability of the load impedance so far as the transmitter is concerned. Henceforth, we will use the term *load SWR* as a description of the transmitter's load.

The SWR meter is actually reading a circuit condition at a single point in the system. In fact, the meter really measures magnitude of the reflection coefficient, but is calibrated in SWR. The relationships between the complex load impedance, Z_L, the magnitude of the reflection coefficient, $|\rho|$, and the load SWR are as follows:

$$|\rho| = \left|\frac{Z_L - 50}{Z_L + 50}\right| \qquad \text{(Eq 1)}$$

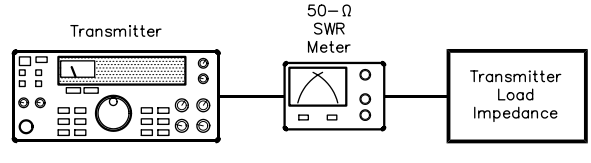

Fig 1—Basic antenna system elements at the output of a transmitter.

$$SWR = \frac{1 + |\rho|}{1 - |\rho|} \qquad \text{(Eq 2)}$$

where 50 Ω is used as the reference impedance, since the design load impedance for the transmitter is assumed to be 50 Ω.

An important point is that you need not know the output impedance of the transmitter to design a broadband matching network. The issue of the actual value of the output impedance of typical RF power amplifiers is a matter of continuing controversy in amateur circles. Fortunately, this issue is not important for the design of broadband matching networks, since the load SWR is independent of the output impedance of the transmitter. Our objective is to design the matching network so that the load SWR (with a 50-Ω reference resistance) is less than some value, say 2:1, over as wide a band as possible.

Resonant Antennas

The broadband matching techniques described here apply to antennas operating near resonance. Typical resonant antennas include half-wave dipoles, quarter-wave verticals over a ground plane and full-wave loops. To design a broadband matching network, you must know the antenna feed-point impedance near resonance. **Fig 2** shows the antenna-impedance equivalent circuit near resonance. Although the series RLC circuit is an approximation, it is good enough to allow us to design matching networks that significantly increase the band over which a good match to the transmitter is achieved.

Note that the impedance is defined by F_0, the resonant frequency, R_A, the antenna resistance at resonance, and Q_A, the antenna Q. R_A is actually the sum of the radiation resistance and any loss resistance, including conductor losses and losses induced by surrounding objects, such as the ground below the antenna. R_A is frequency dependent, but it is sufficient to assume it is fixed during the matching network design process. Minor adjustments to the matching network will correct for the frequency dependence of R_A.

The antenna resistance and Q depend on the physical properties of the antenna itself, the properties of ground and the height above ground. Consider as an example an 80-meter horizontal half-wave dipole made from #12 wire located over average ground (dielectric constant = 13 and conductivity = 5 mS/m). **Figs 3** and **4** show how feed-point resistance and Q vary with height. It is clear from these figures that there are wide gyrations in antenna parameters. The better these parameters are known, the more successful we will be at designing the broadband matching network. For horizontal dipoles, Figs 3 and 4 may be used to get a good idea of antenna resistance and Q, so long as the height is scaled in proportion to wavelength. For example, a 160-meter dipole at a height of 100 feet would have about the same resistance and Q as an 80-meter dipole at 50 feet.

For optimum results, the resistance and Q can be

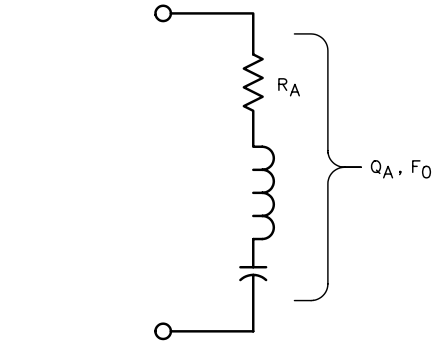

Fig 2—The equivalent circuit of a resonant antenna. The simple series RLC approximation applies to many resonant antenna types, such as dipoles, monopoles, and loops. R_A, Q_A and F_0 are properties of the entire antenna, as discussed in the text.

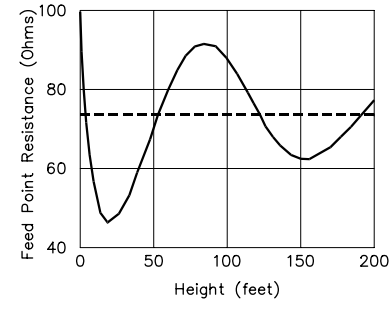

Fig 3—Feed-point resistance (solid line) for 80-meter horizontal dipole at resonance versus height over ground. The free-space value is shown as a dashed line.

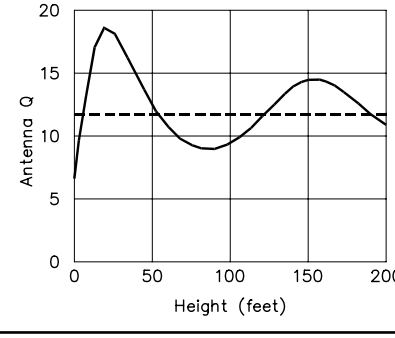

Fig 4—Antenna Q for 80-meter horizontal dipole (solid line) versus height. The free-space value is shown as a dashed line.

determined from computer simulation (using a program like *EZNEC*, for example) or measurement (using a low power SWR/Z meter such as the MFJ-259B or the Autek Research VA1 or RF-1). R_A can be computed using SWR measurements at resonance. **Fig 5** shows the typical bowl-shaped SWR curve as a function of frequency for a resonant antenna. S_0 is the SWR at resonance. You must take into account the loss of the feed line if the measurement must be made at the end of a long 50-Ω transmission line. If the line loss is low or if the measurement is made at the antenna terminals, the formulas given below apply.

For $R_A > 50\ \Omega$

$$R_A = S_0 \times 50 \qquad \text{(Eq 3)}$$

For $R_A < 50\ \Omega$

$$R_A = \frac{50}{S_0} \qquad \text{(Eq 4)}$$

There is an ambiguity, since we do not know if R_A is greater than or less than 50 Ω. A simple way of resolving this ambiguity is to take the same SWR measurement at resonance with a 10-Ω non-inductive resistor added in series with the antenna impedance. If the SWR goes up, $R_A > 45\ \Omega$. If the SWR goes down, $R_A < 45\ \Omega$. This will resolve the ambiguity.

Q_A may be determined by measuring the SWR bandwidth. Define BW_2 as the bandwidth over which the resonant antenna SWR is less than 2:1 (in the same units as F_0). See Fig 5.

For $R_A > 50\ \Omega$

$$Q_A = \frac{F_0}{BW_2}\sqrt{2.5S_0 - S_0^{\,2} - 1} \qquad \text{(Eq 5)}$$

For $R_A < 50\ \Omega$

$$Q_A = \frac{F_0}{BW_2 \times S_0}\sqrt{2.5S_0 - S_0^{\,2} - 1} \qquad \text{(Eq 6)}$$

Again, you must take into account the loss of the feed line if you make the measurement at the end of a long 50-Ω transmission line.

For horizontal and inverted-V half-wave dipoles, a very good approximation for the antenna Q when R_A is known is given by:

$$Q_A = \frac{93.9\left[1n\,\frac{8110}{D\,F_0} - 1\right]}{R_A} \qquad \text{(Eq 7)}$$

where D = the diameter of wire, in inches.

Loss

When you build a resonant antenna with some matching scheme designed to increase the bandwidth, you might overlook the loss introduced by the broadband matching components. Loss in dB is calculated from:

$$\text{Loss} = -10\log\frac{\text{Power radiated by antenna}}{\text{Total power from transmitter}} \qquad \text{(Eq 8)}$$

or, alternatively, define efficiency in % as

$$\text{Efficiency} = \frac{100 \times \text{Power radiated by antenna}}{\text{Total power from transmitter}} \qquad \text{(Eq 9)}$$

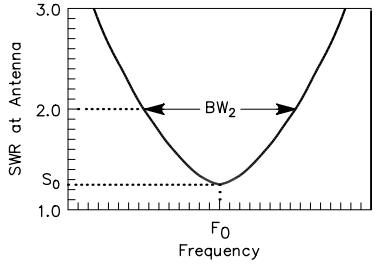

Fig 5—SWR at the antenna versus frequency in the vicinity of resonance.

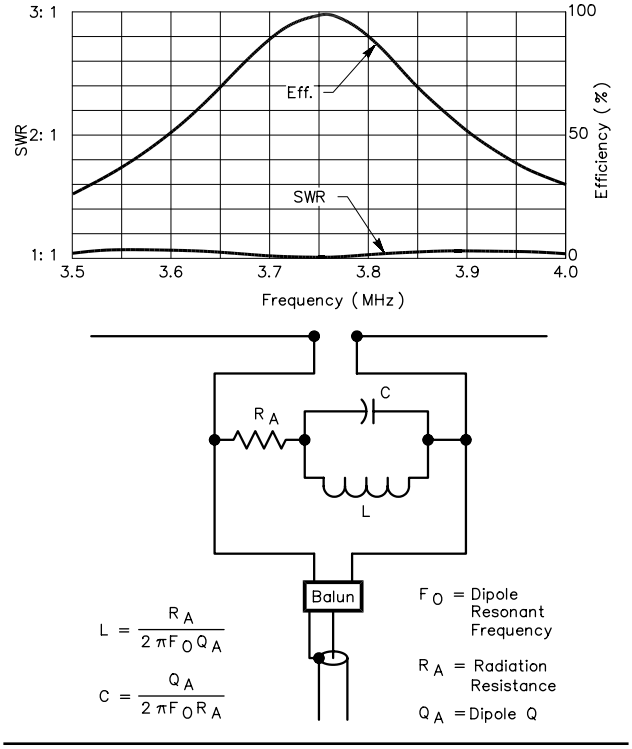

Fig 6—Matching the dipole with a complementary RLC network greatly improves the SWR characteristics, nearly 1:1 across the 3.5-MHz band. However, the relative loss at the band edges is greater than 5 dB.

An extreme degree of bandwidth broadening of an 80-meter dipole is illustrated in **Fig 6**. This approach is not recommended, but it is offered here to make a point. The broadening is accomplished by adding resistive losses. From network theory we obtain the RLC (resistor, inductor, capacitor) matching network shown. The network provides the complement of the antenna impedance. Note that the SWR is virtually 1:1 over the entire band (and beyond), but the efficiency falls off dramatically away from resonance.

The band-edge efficiency of 25 to 30% shown in Fig 6 means that the antenna has about 5 to 6 dB of loss relative to an ideal dipole. At the band edges, 70 to 75% of the power delivered down the transmission line from the transmitter is heating up the matching-network resistor. For a 1-kW output level, the resistor must have a power rating of at least 750 W! Use of an RLC complementary network for broadbanding is not recommended, but it does illustrate how resistance (or losses) in the matching network can significantly increase the apparent antenna SWR bandwidth.

The loss introduced by any broadband matching approach must be taken into consideration. Lossy matching networks will usually provide more match bandwidth improvement than less lossy ones.

SIMPLE BROADBAND MATCHING TECHNIQUES

The Cage Dipole

You can increase the match bandwidth of a single-wire dipole by using a thick radiator, one with a large diameter. The gain and radiation pattern are essentially the same as that of a thin-wire dipole. The radiator does not necessarily have to be solid; open construction such as shown in **Fig 7** may be used.

The theoretical SWR response of an 80-meter cage dipole having a 6-inch diameter is shown in **Fig 8**. BW_2 for this antenna fed with 50-Ω line is 287 kHz, and the Q is approximately 8. Its 2:1-SWR frequency range is 1.79 times broader than a dipole with a Q of 13, typical for thin-wire dipoles.

There are other means of creating a thick radiator, thereby gaining greater match bandwidth. The bow-tie and the fan dipole make use of the same Q-lowering principle as the cage for increased match bandwidth. The broadbanding techniques described below are usually more practical than the unwieldy cage dipole.

Stagger-Tuned Dipoles

A single-wire dipole exhibits a relatively narrow bandwidth in terms of coverage for the 3.5 to 4.0-MHz band. A technique that has been used for years to cover the entire band is to use two dipoles, one cut for the CW portion and one for the phone portion. The dipoles are connected in parallel at the feed point and use a single feeder. This technique is known as *stagger tuning*.

Fig 9 shows the theoretical SWR response of a pair of stagger-tuned dipoles fed with 50-Ω line. No mutual coupling between the wires is assumed, a condition

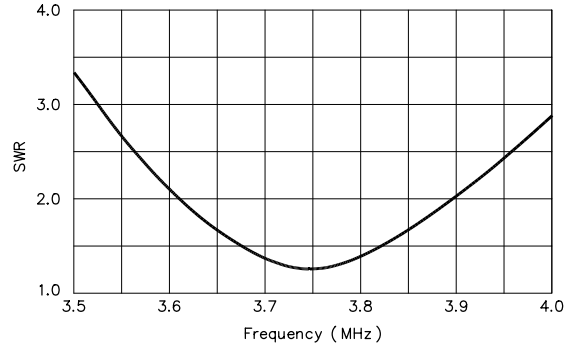

Fig 8—Theoretical SWR versus frequency response for a cage dipole of length 122 feet 6 inches and a spreader diameter of 6 inches, fed with 50-Ω line. The 2:1-SWR bandwidth frequencies are 3.610 and 3.897 MHz, with a resulting BW_2 of 287 kHz.

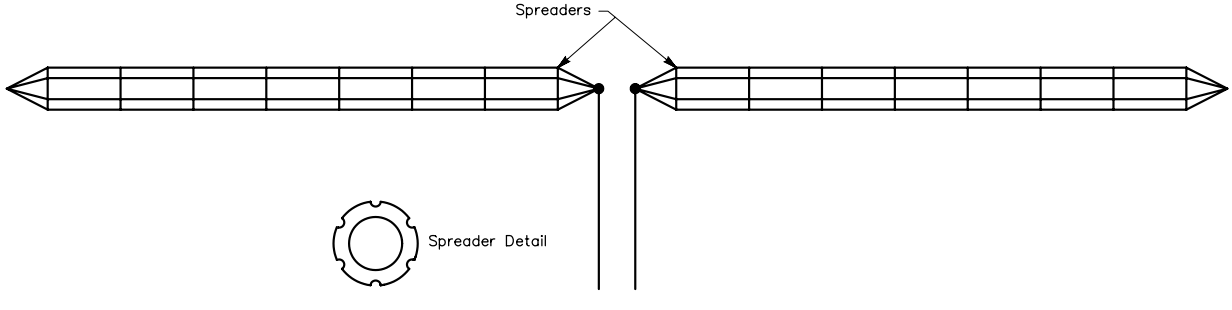

Fig 7—Construction of a cage dipole, which has some resemblance to a round birdcage. The spreaders need not be of conductive material, and should be lightweight. Between adjacent conductors, the spacing should be 0.02 λ or less. The number of spreaders and their spacing should be sufficient to maintain a relatively constant separation of the radiator wires.

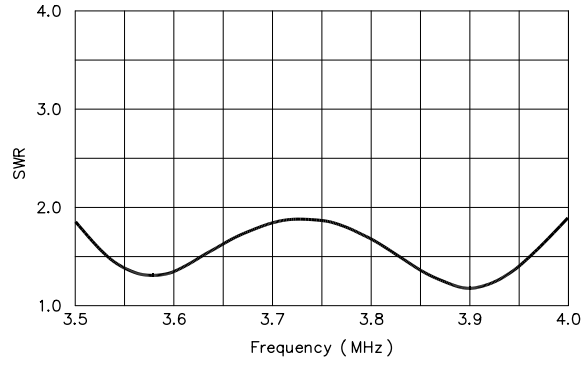

Fig 9—Theoretical SWR response of two stagger-tuned dipoles. They are connected in parallel at the feed point and fed with 50-Ω line. The dipoles are of wire such as #12 or #14, with total lengths of 119 and 132 feet.

that would exist if the two antennas were mounted at right angles to one another. As Fig 9 shows, the SWR response is less than 1.9:1 across the entire band.

A difficulty with such crossed dipoles is that four supports are required for horizontal antennas. A more common arrangement is to use inverted V dipoles with a single support, at the apex of each element. The radiator wires can also act as guy lines for the supporting mast.

When the dipoles are mounted at something other than a right angle, mutual coupling between them comes into play. This causes interaction between the two elements—tuning of one by length adjustment will affect the tuning of the other. The interaction becomes most critical when the two dipoles are run parallel to each other, suspended by the same supports, and the wires are close together. Finding the optimum length for each dipole for total band coverage can become a tedious and frustrating process.

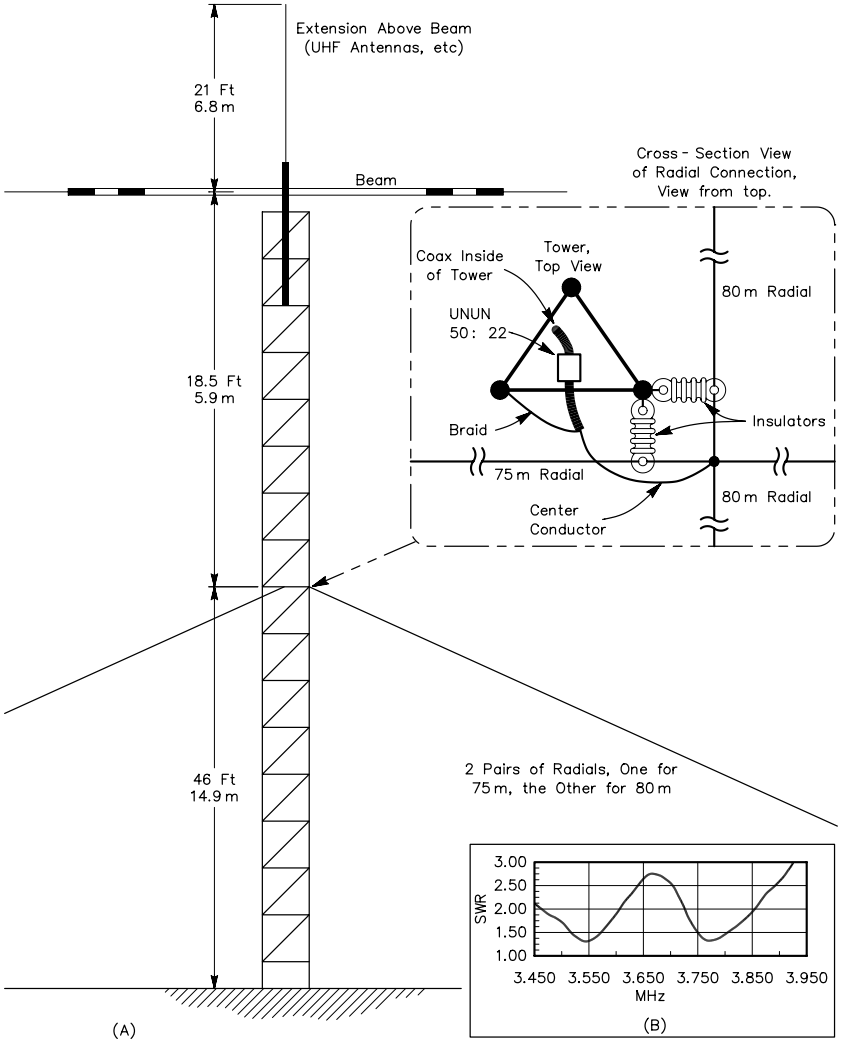

Fig 10—At A, details of the inverse-fed ground-plane at W4PK. The inset shows the feed-point details. Keep the two sets of radials as close to 90· as possible. Don't try to resonate the antenna by adjusting radial lengths. At B, SWR curve of the inverse-fed ground plane antenna with stagger-tuned radials. The objective is to have a low SWR for both the CW and SSB 80/75-meter DX windows.

Stagger-Tuned Radials

A variation of the use of stagger tuning has been applied by Sam Leslie, W4PK. See his article entitled "Broadbanding the Elevated, Inverse-Fed Ground Plane Antenna" in *The ARRL Antenna Compendium, Vol 6*. An existing tower with a large beam and VHF/UHF antennas on top is used as an 80-meter monopole. See **Fig 10A**. The feed point is part way up the tower, at a point where the metal above it makes up an electrical quarter wavelength. Four elevated quarter-wave radials are used as a ground plane. The radials droop away from the tower. They are joined together at the tower but not connected to the tower. The antenna is fed with 50-Ω coax and an impedance step-down autotransformer (50:22 Ω unun) located at the tower. The shield of the coax is carried through the transformer and connected to the tower. The coax "hot side" is connected to the junction of the radials. A Q-section made from two paralleled RG-59 coax cables (Z_0 = 75/2 = 37.5 Ω) may be used instead of the autotransformer.

The broadband match is achieved by cutting two opposing radials for one end of the desired match range (75 meters) and cutting the other two for the other end of the range (80 meters). See Fig 10B for the resultant SWR versus frequency characteristic.

FEED-LINE IMPEDANCE MISMATCHING

The simplest broadband matching network is a transformer at the junction of the transmission line and the antenna. See Frank Witt's article entitled "Match Bandwidth of Resonant Antenna Systems" in October 1991 *QST*. Observe that the impedance of the series RLC resonant antenna model of Fig 2 increases at frequencies away from resonance. The result is that more bandwidth is achieved when SWR at resonance is not exactly 1:1. For example, if the antenna is fed with a low-loss 50-Ω transmission line, the maximum SWR bandwidth is obtained if the effective R_A = 50/1.25 = 40 Ω. The improvement in BW_2, the 2:1 SWR bandwidth, over a perfect match at resonance is only 6%, however. This condition of R_A = 40 Ω can be achieved by installing a transformer at the junction of the feed line and the antenna.

If the line loss is larger, you can gain more benefit in terms of bandwidth by deliberately mismatching at the antenna. If the matched-line loss is 2 dB, the improvement rises to 18%. To achieve this requires an R_A = 28.2 Ω. Again, the improvement over a perfect match at resonance is modest.

It is interesting to compare the 2:1 SWR bandwidth (at the transmitter end of the line) for the case of a lossless line versus the case of 2-dB matched-line loss. BW_2 for the lossy line case is 1.95 times that of the lossless line case, so substantial match bandwidth improvement occurs, but at the cost of considerable loss. The band edge loss for the lossy-line case is 3 dB!

This example is provided mostly as a reference for comparison with the more desirable broadbanding techniques below. It also explains why some installations with long feed lines show large match bandwidths.

PARALLEL-TUNED CIRCUITS AT THE ANTENNA TERMINALS

As mentioned previously, a resonant antenna has an equivalent circuit that may be represented as a series RLC circuit. We can cancel out some of the antenna reactance away from resonance with a parallel-tuned circuit connected across the antenna terminals. The impedance level of the parallel-tuned circuit must be low enough to be effective and must have the same resonant frequency as the antenna. You can use a parallel-tuned circuit made with lumped LC components or with transmission-line segments. A quarter-wave transmission line with a short at the far end, or a half-wave line with an open at the far end, each behave like a parallel-tuned LC circuit.

The Double Bazooka

The response of the controversial *double bazooka* antenna is shown in **Fig 11**. This antenna actually consists of a dipole with two quarter-wave coaxial resonator stubs connected in series. The stubs are connected across the antenna terminals.

Not much bandwidth enhancement is provided by this resonator connection because the impedance of the matching network is too high. The antenna offers a 2:1-SWR bandwidth frequency range that is only 1.14 times that of a simple dipole with the same feeder. And the bandwidth enhancement is partially due to the "fat" antenna wires composed mostly of the coax shield. No

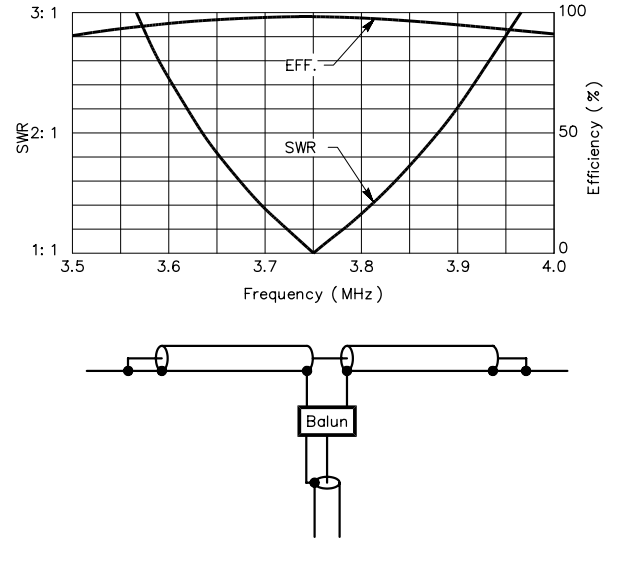

Fig 11—The double bazooka, sometimes called a coaxial dipole. The antenna is self-resonant at 3.75 MHz. The resonator stubs are 43.23-foot lengths of RG-58A coax.

improvement in antenna gain or pattern over a thin-wire dipole can be expected from this antenna.

The Crossed Double Bazooka

A modified version of the double-bazooka antenna is shown in **Fig 12**. In this case, the impedance of the matching network is reduced to one-fourth of the impedance of the standard double-bazooka network. The lower impedance provides more reactance correction, and hence increases the bandwidth frequency range noticeably, to 1.55 times that of a simple dipole. Notice, however, that the efficiency of the antenna drops to about 80% at the 2:1-SWR points. This amounts to a loss of approximately 1 dB. The broadbanding, in part, is caused by the losses in the coaxial resonator stubs (made of RG-58A coax), which have a remarkably low Q (only 20).

MATCHING NETWORK DESIGN

Optimum Matching

You can improve the match bandwidth by using a transformer or a parallel-tuned circuit at the antenna terminals. A combination of these two techniques can yield a very effective match bandwidth enhancement. Again, you can make the impedance transformation and implement the tuned circuit using lumped-circuit elements (transformers, inductors and capacitors) or with distributed-circuit elements (transmission lines).

In 1950, an article by R. M. Fano presented the theory of broadband matching of arbitrary impedances. This classic work was limited to lossless matching networks. Unfortunately, matching networks realized with transmission lines have enough loss to render the Fano results useful as only a starting point in the design process. A theory of optimum matching with lossy matching networks was presented in an article by Frank Witt entitled "Optimum Lossy Broadband Matching Networks for Resonant Antennas" that appeared in April 1990 *RF Design* and was summarized and extended in "Broadband Matching with the Transmission Line Resonator," in *The ARRL Antenna Compendium Vol 4*.

Using a matching network, the 2:1 SWR bandwidth can be increased by a factor of about 2.5. Instead of the familiar bowl-shaped SWR versus frequency characteristic seen in Fig 5, the addition of the matching network yields the W-shaped characteristic of **Fig 13**. The maximum SWR over the band is S_M. The band edges are F_L and F_H. Thus the bandwidth, BW, and the center frequency, F_0, are

$$BW = F_H - F_L \quad \text{(Eq 10)}$$

$$F_0 = \sqrt{F_H \times F_L} \quad \text{(Eq 11)}$$

Fig 14 shows the pertinent equivalent circuit for a typical broadband antenna system. The parallel LC matching network is defined by its resonant frequency, F_0 (which is the same as the resonant frequency of the antenna), its Q and its impedance level. The impedance level is the reactance of either the matching network inductance or capacitance at F_0. The optimum transmitter load resistance,

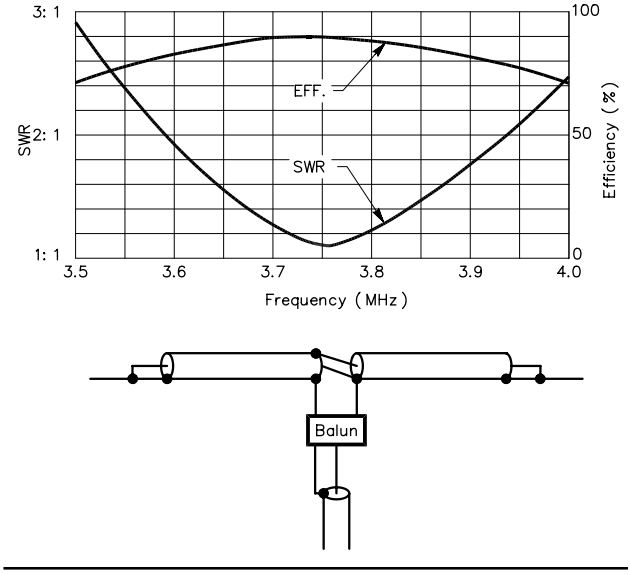

Fig 12—The crossed double bazooka yields bandwidth improvement by using two quarter-wave resonators, parallel connected, as a matching network. As with the double bazooka, the resonator stubs are 43.23-foot lengths of RG-58A coax.

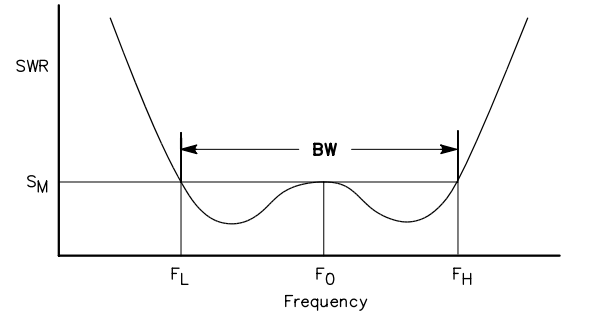

Fig 13—W-shaped SWR versus frequency characteristic that results when a transformer and parallel LC matching network are used.

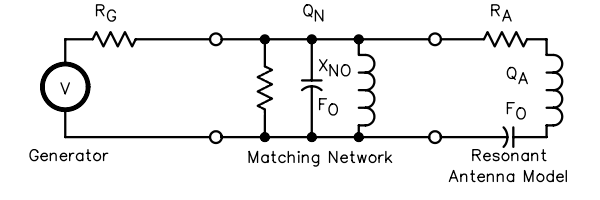

Fig 14—Assumed equivalent circuit for the broadband matching system. The antenna and the matching network have the same resonant frequency.

R_G, is achieved using an impedance transformer between the transmitter and the input to the parallel-tuned circuit. Thus for a transmitter whose optimum load resistance is 50 Ω, the required impedance transformer would have an impedance transformation ratio of 50:R_G.

The goal is to keep the SWR over the band as low as possible. There is a best or minimum value of S_M that may be achieved over the entire band. It depends on the desired match bandwidth and the Q's of the antenna and matching network and is given by the following formula:

$$S_{M\,min} = \frac{\sqrt{B_N{}^2 + 1} + \sqrt{B_N{}^2 + 1 + \frac{2Q_A}{Q_N}\left(1 + \frac{Q_A}{2Q_N}\right)}}{2\left(1 + \frac{Q_A}{2Q_N}\right)} \qquad \text{(Eq 12)}$$

where $B_N = \frac{BW}{F_0}$ and

Q_A = antenna Q

Q_N = matching network Q.

The reactance at resonance of the parallel tuned LC matching network is given by:

$$X_{N0} = \frac{R_A}{Q_A}\left[\left(1 + \frac{Q_A}{2Q_N}\right)S_{M\,min}{}^2 - \frac{Q_A}{2Q_N}\right] \qquad \text{(Eq 13)}$$

where R_A = antenna resistance in Ω.

The transmitter load resistance is calculated from:

$$R_G = \frac{S_{M\,min}\,R_A\,Q_N\,X_{N0}}{R_A + Q_N\,X_{N0}} \qquad \text{(Eq 14)}$$

The loss of the matching network is always greatest at the edges of the band. This loss, L_{MNE}, in dB, is given by:

$$L_{MNE} = 10\log\left[1 + \frac{R_A}{Q_N\,X_{N0}}\left(B_N{}^2 + 1\right)\right] \qquad \text{(Eq 15)}$$

Now you have all the information needed to design an optimal broadband matching network. An 80-meter dipole will serve as an example to illustrate the procedure. The following parameters are assumed:

F_L = 3.5 MHz
F_H = 4.0 MHz
R_A = 57.2 Ω
Q_A = 13
Q_N = 40.65

The values of R_A and Q_A are reasonable values for an 80-meter inverted V with an apex 60 feet above ground. Q_N = 40.65 is the calculated value of the Q of a resonator made from RG-213 or similar cable in the middle of the 80-meter band. The results are:

BW = 0.5 MHz (from Eq 10)
F_0 = 3.742 MHz (from Eq 11)
S_{Mmin} = 1.8 (from Eq 12)
X_{N0} = 15.9 Ω (from Eq 13)
R_G = 94.8 Ω (from Eq 14)
L_{MNE} = 1.32 dB (from Eq 15)

Shown in **Fig 15** is the plot of SWR and matching-network loss versus frequency for this example. The reference resistance for the SWR calculation is R_G or 94.8 Ω. Since the desired load resistance for the transmitter is 50 Ω, we need some means to transform from 94.8 Ω to 50 Ω. The examples given in the rest of this chapter will show a variety of ways of achieving the necessary impedance transformation.

The meaning of X_{N0} = 15.9 Ω is that the inductor and the capacitor in the matching network would each have a reactance of 15.9 Ω at 3.742 MHz. Methods for obtaining a particular value of X_{N0} are shown in the fol-

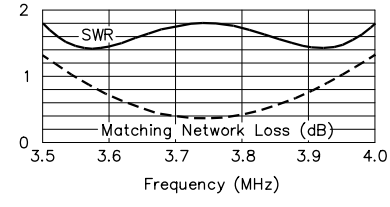

Fig 15—SWR and matching-network loss for example. Note that S_M is exactly 1.8 and the band-edge loss is exactly 1.32 dB, as calculated.

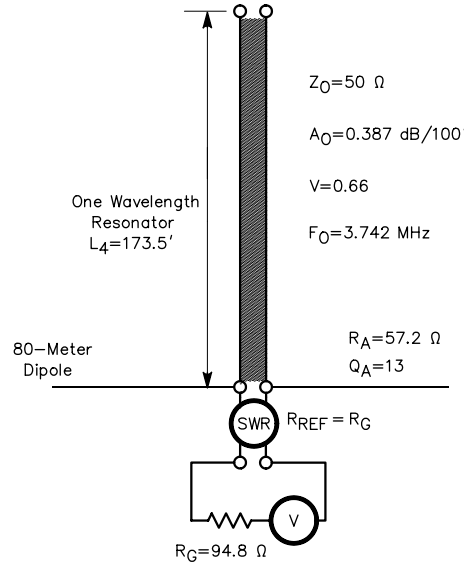

Fig 16—80-meter dipole example with a 1-λ resonator as the matching network.

lowing examples as well. The particular value of X_{N0} of this example may be obtained with a one-wavelength resonator (open-circuited at the far end) made from RG-213. The system described in this example is shown in **Fig 16**.

The broadband antenna system shown in Fig 16 has a desirable SWR characteristic, but the feed line to the transmitter is not yet present. Fortunately, the same cable segment that makes up the resonator may be used as the feed line. A property of a feed line whose length is a multiple of λ/2 (an even multiple of λ/4) is that its input impedance is a near replica of the impedance at the far end. This is exactly true for lossless lines at the frequencies where the λ/2 condition is true. Fortunately, practical lines have low-enough loss that the property mentioned above is true at the resonant frequency. Off resonance, the desired reactance cancellation we are looking for from the resonant line takes place. The very same design equations apply.

In **Fig 17**, the antenna shown in Fig 16 is moved to the far end of the 1λ resonator. The SWR and loss for this case are shown in **Fig 18**, which should be compared with Fig 15. The SWR is only slightly degraded, but the loss is about the same at the band edges. We have picked up a feed line that is 1λ long (173.5 feet) *and* broadband matching. You can make the SWR curve virtually the same as that of Fig 15 if the transmitter load resistance is increased from 94.8 Ω to 102 Ω. From a practical point of view, this degree of design refinement is unnecessary, but is instructive to know how the SWR characteristic may be controlled. You may apply the same approach when the resonator is an odd multiple of a wavelength, but in that case the transmitter or antenna must be connected λ/4 from the shorted end.

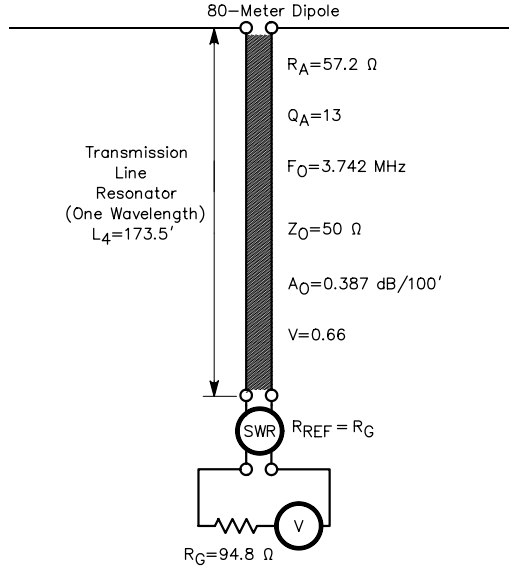

Fig 17—The antenna is at the far end of the 1-λ line. The line does double duty—broadband matching and signal transport.

Chebyshev Matching

Although it is not as efficient from the standpoint of bandwidth improvement and loss, Chebyshev matching is useful for some purposes. This arrangement yields a transmitter load impedance of 50 + *j* 0 Ω at two frequencies in the band. The matching network circuit is the same as the optimum matching case, but the parameters are different. In this case, we assume that the antenna parameters, F_0, R_A and Q_A, the network Q and the maximum SWR over the band are specified. The bandwidth, impedance level and generator resistance are given by:

$$BW = \frac{F_0}{Q_A Q_N} \left\{ \frac{(Q_A + Q_N)\left[(Q_A + 2Q_N)S_M - Q_A\right](S_M - 1)}{S_M} \right\}^{\frac{1}{2}} \quad \text{(Eq 16)}$$

$$X_{N0} = \frac{R_A}{Q_A}\left[S_M + \frac{Q_A}{Q_N}(S_M - 1)\right] \quad \text{(Eq 17)}$$

$$R_G = R_A\left(S_M - \frac{Q_A}{Q_A + Q_N}\right) \quad \text{(Eq 18)}$$

The loss at the band edges is given by Eq 15. The frequencies where the transmitter load is 50 + *j* 0 Ω, F_L and F_H, are given by:

$$F_L = \sqrt{F_0^{\,2} + F_M^{\,2}} - F_M \quad \text{(Eq 19)}$$

where

$$F_M = \frac{F_0}{2Q_A}\left[(S_M - 1)\left(1 + \frac{Q_A}{Q_N}\right)\right]^{\frac{1}{2}} \quad \text{(Eq 20)}$$

$$F_H = \frac{F_0^{\,2}}{F_L} \quad \text{(Eq 21)}$$

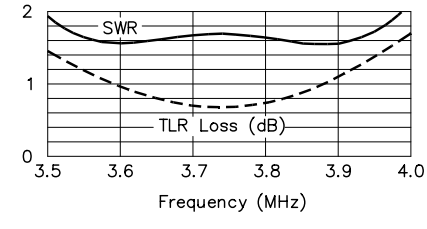

Fig 18—SWR and loss for a 1-λ 50-Ω feed line. The antenna system model is the one shown in Fig 17.

LC-MATCHING NETWORKS

Before the theory of optimal matching above was developed, Frank Witt, AI1H, described in his article "Broadband Dipoles—Some New Insights" in October 1986 *QST* the basic principle and some applications of LC matching networks. **Fig 19** shows an LC matching network that is a modified version of one originally proposed by Alan Bloom, N1AL. Note that the basic ingredients are present: the parallel-tuned circuit for reactance cancellation and a transformer.

The network also functions as a voltage balun by connecting the shield of the coaxial feed line to the center tap of the inductor. The capacitor is connected across the entire coil to obtain practical element values. The SWR response and efficiency offered by a network of lumped components is shown in **Fig 20**. The 2:1-SWR bandwidth with 50-Ω line is 460 kHz. The design is a Chebyshev match, where SWR = 1:1 is achieved at two frequencies. For the same configuration, more match bandwidth and less loss could have been realized if the optimal-match theory had been applied.

The efficiency at the band edges for the antenna system shown in Fig 20 is 90% (Loss = 0.5 dB). This low loss is due to the high Q of the LC matching network ($Q_N \approx 200$). The very low-impedance level required ($X_{N0} = 12.4\ \Omega$) cannot be easily realized with practical inductor-capacitor values. It is for this reason that the coil is tapped and serves as an autotransformer with multiple taps. The required impedance transformation ratio of 1:2.8 is easily achieved with this arrangement.

80-Meter DXer's Delight

A version of an antenna system with an LC broadbanding network is dubbed the *80-meter DXer's Delight*. This antenna has SWR minima near 3.5 and 3.8 MHz. A single antenna permits operation with a transmitter load impedance of about 50 Ω in the DX portions of the band, both CW and phone. The efficiency and SWR characteristic are shown in **Fig 21**.

Fig 22 shows the method of construction. The selection of a capacitor for this application must be made carefully, especially if high power is to be used. For the capacitor described in the caption of Fig 22, the allowable peak power (limited by the breakdown voltage) is 2450 W. However, the allowable average power (limited by the RF current rating of 4 A) is only 88 W! These limits apply at the 1.8:1 SWR points.

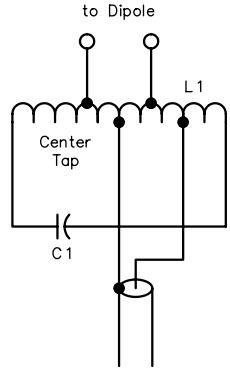

Fig 19—A practical LC matching network that provides reactance compensation, impedance transformation and balun action.

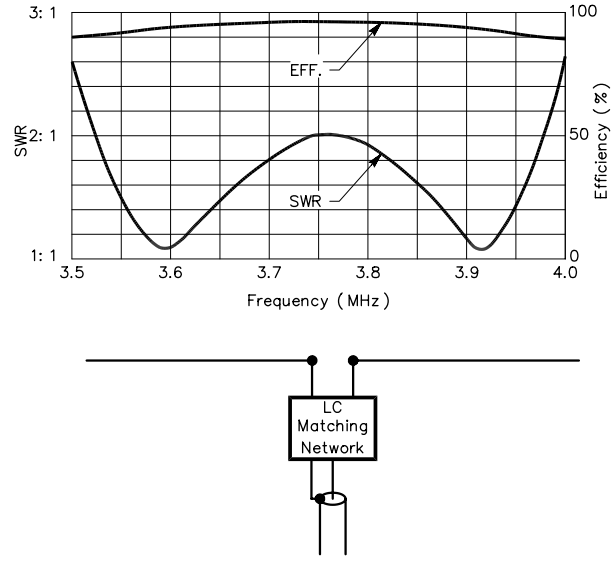

Fig 20—Efficient broadband matching with a lumped element LC network. The antenna in this example has a resistance of 72 Ω and a Q of 12. The matching network has an impedance level of 12.4 Ω, and a Q of 200. The feed line is 50-Ω coax, and the matching network provides an impedance step-up ratio of 2.8:1.

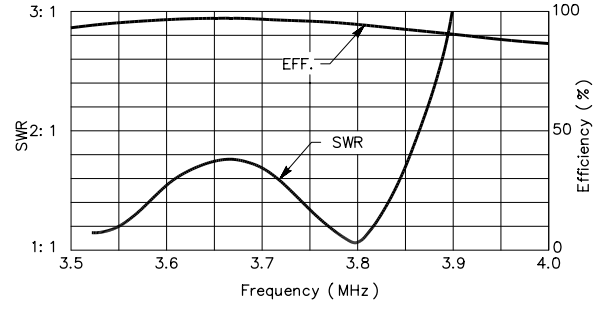

Fig 21—The 80-meter DXer's Delight permits operation with a 50-Ω transmitter load in the DX portions of the band, both CW and phone. This network was designed to provide a broadband match for an inverted V with F_0 = 3.67 MHz, an antenna resistance of 60 Ω and a Q of 13. The matching network has an impedance level of 9 Ω, and a Q of 220. The feed line is 50-Ω coax, and the matching network provides an impedance step-up ratio of 2.0:1.

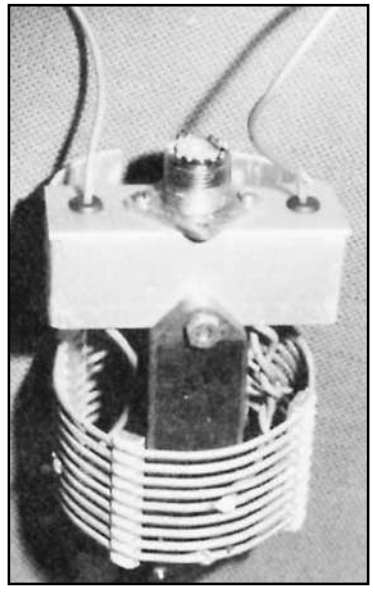

Fig 22—A method of constructing the LC broadband matching network. Components must be chosen for high Q and must have adequate voltage and current ratings. The network is designed for use at the antenna feed point, and should be housed in a weather-resistant package. The component values are as follows:
C1—400 pF transmitting mica rated at 3000 V, 4 A (RF)
L1—4.7 µH, 8 1/2 turns of B&W coil stock, type 3029 (6 turns per in., 2 1/2-in. dia, #12 wire).
The LC circuit is brought to midband resonance by adjusting an end tap on the inductor. The primary and secondary portions of the coil have 1 3/4 and 2 1/2 turns, respectively.

PROPERTIES OF TRANSMISSION-LINE RESONATORS

One way around the power limitations of LC broadband matching networks is to use a transmission line as the resonator. Transmission line resonators, TLRs, typically have higher power-handling capability because the losses, though higher, are distributed over the length of the line instead of being concentrated in the lumped-LC components. Transmission-line resonators must be multiples of a quarter wavelength. For a parallel-tuned circuit, the odd-multiple λ/4 lines must be shorted at the far end and the even-multiple λ/4 lines must be open circuited.

The length of the matching network resonator is n electrical quarter wavelengths. The impedance level, Q, and line length are given by:

$$X_{N0} = \frac{4 Z_0}{n \pi}$$

or, solving for Z_0,

$$Z_0 = \frac{n \pi X_{N0}}{4} \qquad \text{(Eq 22)}$$

$$Q_N = \frac{2.774 F_0}{A_0 V} \qquad \text{(Eq 23)}$$

$$L_N = \frac{245.9 n V}{F_0} \qquad \text{(Eq 24)}$$

where

Z_0 = line characteristic impedance in Ω
A_0 = matched line loss in dB per 100 feet
V = velocity factor, and
L_N = line length in feet.

These equations may be used to find the properties of the transmission line resonator in the systems shown in Figs 16 and 17. The line is RG-213 with the following properties:

Z_0 = 50 Ω
V = 0.66
A_0 = 0.4 dB/100 feet at 4 MHz

We need the matched loss at 3.742 MHz. Since the line loss is approximately proportional to $\sqrt{\text{frequency}}$,

$$A_{0F2} = A_{0F1} \sqrt{\frac{F_2}{F_1}} \qquad \text{(Eq 25)}$$

where A_{0F1} and A_{0F2} are the matched line losses at frequencies F_1 and F_2, respectively. Hence,

A_0 = 0.387 dB/100 feet at 3.742 MHz
Q_N = 40.65 (from Eq 23)

This is the Q of any resonator made from RG-213 for a frequency of 3.742 MHz. It does not matter how many quarter wavelengths (n) make up the cable segment. Earlier we calculated that the required impedance level, X_{N0}, is 15.9 Ω. Therefore, the required impedance level is:

$$Z_0 = \frac{n \pi \times 15.9}{4} = 12.5 n \Omega \qquad \text{(from Eq 22)}$$

This means that you could use a quarter-wavelength segment with a short at the far end if Z_0 = 12.5 Ω, or a half-wavelength segment with a open at the far end if Z_0 = 25 Ω. Our example used an open-circuited full-wavelength resonator (n = 4) with a Z_0 of 50 Ω. This example was crafted to make this happen (so that it fits RG-213 properties), but it illustrates that some juggling is required to obtain the right resonator properties when it is made from a transmission line, since we are stuck with the cable's characteristic impedance.

The TLR Transformer

A way around the limitation created by available characteristic impedance values is to use the *transmission-line resonator transformer*. The basic idea is to make the connection to the TLR at an intermediate point along the line instead of at the end of the line. It is analogous to using taps on a parallel-tuned LC resonant circuit to achieve transformer action (See Fig 19). The nature of the transformer action is seen in **Fig 23**, where the ends of the transformer are designated 1-1 and 2-2. The impedance ratio of the transformer, N_Z, is approximated by

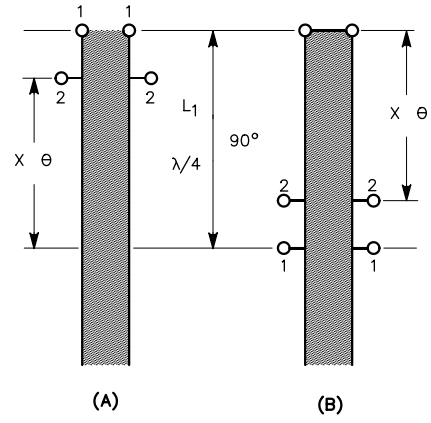

Fig 23—Transformer action in the TLR. The definition of transformer terminals depends on whether the TLR end is open- or short-circuited. θ is the distance between the minimum of the voltage standing wave (at resonance) and the connection point, expressed as an electrical angle. The distance x is that same distance expressed in feet.

$$N_Z = \sin^2 \theta \qquad \text{(Eq 26)}$$

The distance in feet, x, is given by

$$x = \frac{\theta}{90} \times \frac{\lambda}{4} = \frac{\theta}{90} \times \frac{245.9\ \text{V}}{F_0} \qquad \text{(Eq 27)}$$

This approach may be used for the connection of the TLR to the transmitter or to the antenna or both. An example will help make the power of the TLR transformer clear. We want to broadband match an 80-meter dipole (where F_0 is 3.742 MHz, R_A is 65 Ω and Q_A is 13). The feed line is RG-213 50-Ω cable, and the total distance between the antenna and transmitter is less than 100 feet.

Since we know that Z_0 = 50 Ω, we will design a prototype system with a ¾ λ TLR (n=3). Since n is odd, the TLR must be shorted at one end, and we will place the short at the transmitter end of the line. The intermediate step of using a prototype system will enable us to design a system with the final TLR, but without transformer action. Then we'll calculate the proper connection points along the TLR. **Fig 24** shows the prototype system and the system with built-in transformers.

Note that the prototype antenna is connected to the open end of the TLR. The prototype generator (transmitter) is connected at a multiple of λ/2 from the antenna. Here, at resonance, an approximate replica of the antenna will appear. We will use primed variables to indicate prototype antenna system elements. The prototype antenna differs from the actual antenna in impedance level, so only R_A will change. F_0 and Q_A remain the same.

Starting with the ¾ λ TLR, we have:

X_{N0} = 21.2 Ω (from Eq 22)

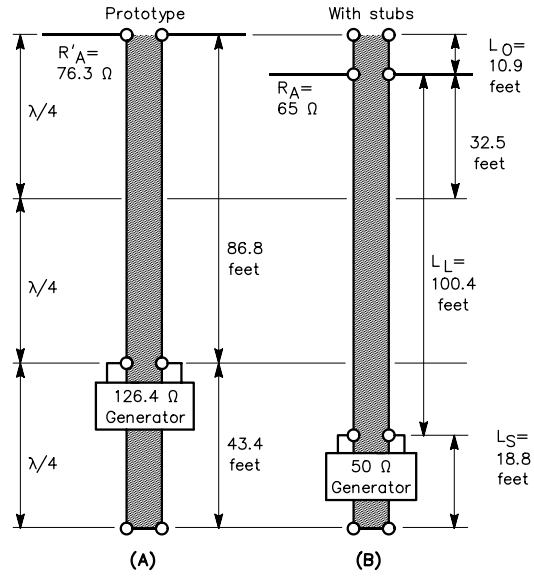

Fig 24—An optimized antenna system with a ¾ λ TLR made from RG-213 coaxial cable. The prototype system at A is a convenient intermediate step in the design process. At B is the configuration with TLR transformers. It has an open stub, L_O, a link, L_L (which serves as the feed line), and a shorted stub, L_S.

The prototype antenna resistance at resonance, R'_A, is calculated by rearranging Eq 13.

$$R'_G = \frac{X_{N0}\, Q_A}{\left(1 + \frac{Q_A}{2Q_N}\right) S_{M\,min}^{\,2} - \frac{Q_A}{2\,Q_N}} \qquad \text{(Eq 28)}$$

Earlier we calculated that Q_N = 40.65 and S_{Mmin} = 1.8. Now we find

R'_A = 76.3 Ω (from Eq 28)
R'_G = 126.4 Ω (from Eq 14)

The electrical angles (in degrees) and connection locations (in feet) are given by

$$\theta_A = \sin^{-1}\sqrt{\frac{R_A}{R'_A}} \qquad \text{(Eq 29)}$$

$$\theta_G = \sin^{-1}\sqrt{\frac{R_G}{R'_G}} \qquad \text{(Eq 30)}$$

$$X_A = \frac{\theta_A}{90} L_1 \qquad \text{(Eq 31)}$$

$$X_G = \frac{\theta_G}{90} L_1 \qquad \text{(Eq 32)}$$

where

$$L_1 = \frac{\lambda}{4} = \frac{245.9\ V}{F_0}$$

The lengths of the stubs and link of Fig 24 are given by

$L_O = L_1 = x_A$ (Eq 33)

$L_S = x_G$ (Eq 34)

$L_L = 3L_1 - L_O - L_S$ (Eq 35)

Since L_1 = 43.4 feet,

$\theta_A = 67.4°$ (from Eq 29)

$\theta_G = 39.0°$ (from Eq 30)

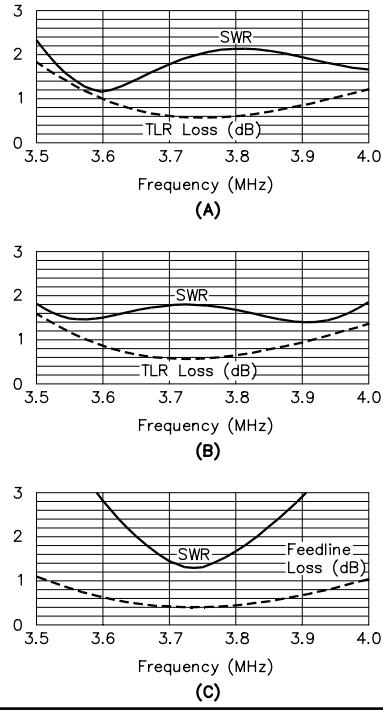

Fig 25—The SWR and loss of the TLR transformer antenna system. At A, the results are shown with the calculated line lengths. At B, the improvement after the lengths were optimized is shown in Table 1. At C, for comparison, SWR and loss for the same setup as at A, but with the stubs removed.

Table 1

Calculated and Optimized Parameters Using TLR Transformers

	Calculated	*Optimized*
Dipole resonant frequency (F_0)	3.742 MHz	3.710 MHz
Open stub (L_O)	10.9 feet	13.1 feet
Shorted stub (L_S)	18.8 feet	20.1 feet
Link (L_L)	100.4 feet	101.0 feet

L_O = 10.9 feet (from Eq 33)

L_S = 18.8 feet (from Eq 34)

L_L = 100.4 feet (from Eq 35)

These dimensions are summarized in Fig 24. If required, additional 50-Ω cable may be added between the transmitter and the junction of the shorted stub and the link. A remarkable aspect of the TLR transformer, as demonstrated in this example, is that it is a transformer with multiple taps distributed over a great distance, in this case over 100 feet.

The calculated SWR and loss of the antenna system with the TLR transformer are shown in **Fig 25A**. We mentioned earlier that the stub calculations are an approximation. Fig 25 bears this out, but the changes necessary to achieve the optimized results are relatively small. By changing the lengths and dipole resonant frequency slightly, the target optimized SWR characteristic of Fig 25B results. See **Table 1** for a summary of the changes required.

To demonstrate the significant improvement in match bandwidth that the TLR transformer provides, the SWR and loss of the same dipole fed with 100.4 feet of RG-213 cable is shown in Fig 25C. The loss added by the two stubs used to obtain match bandwidth enhancement is negligible (0.2 to 0.5 dB).

A TLR transformer may be used by itself to achieve a low-loss narrow-band impedance transformation, functioning like a λ/4 Q-section. It is different in nature from a Q-section, in that it is a true impedance transformer, while a Q section is an *impedance inverter*. The TLR transformer may be designed into the antenna system and is a useful tool when a narrow-band impedance transformation is needed.

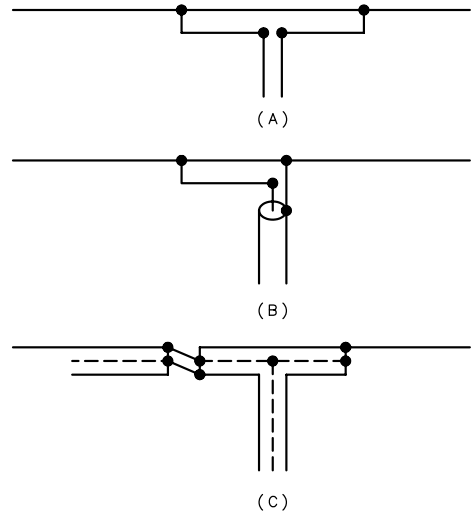

Fig 26—Dipole matching methods. At A, the T match; at B, the gamma match; at C, the coaxial resonator match.

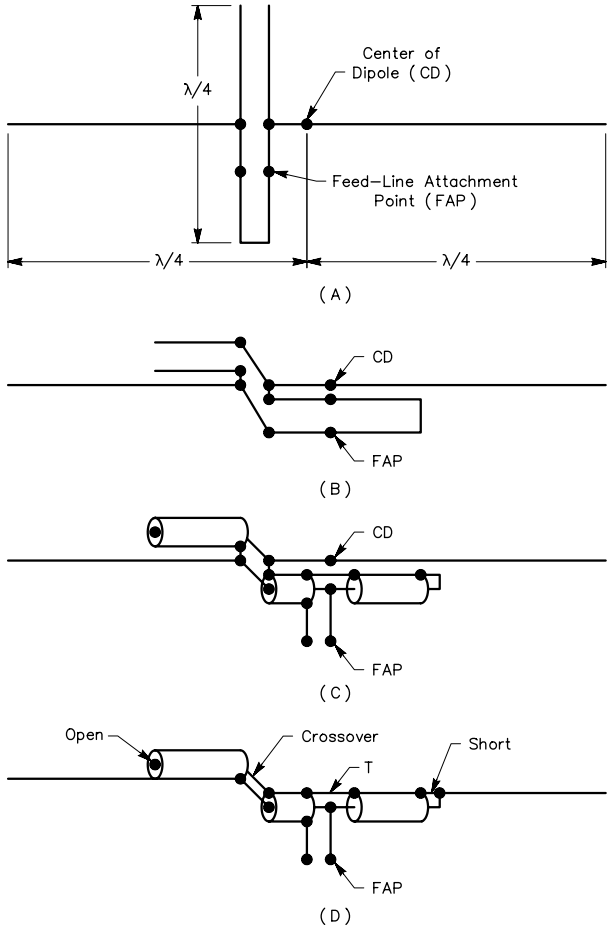

Fig 27—Evolution of the coaxial-resonator-match broadband dipole. At A, a TLR transformer is used to match the feed line to the off-center-fed dipole. The match and dipole are made collinear at B. At C, the balanced transmission-line TLR transformer of A and B is replaced by a coaxial version. Because the shield of the coax can serve as a part of the dipole radiator, the wire adjacent to the coax match may be eliminated, D.

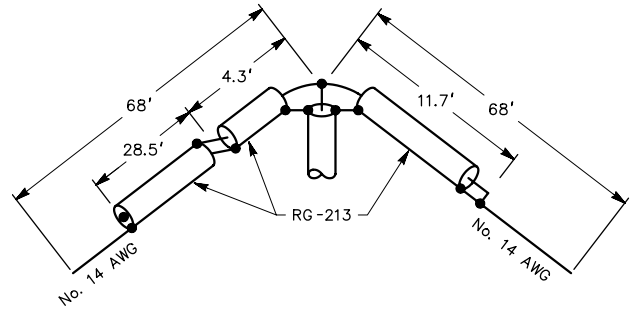

Fig 28—Dimensions for the 80-Meter MHz DX Special, an antenna optimized for the phone and CW DX portions of the 3.5-MHz band. The coax segment lengths total to one quarter-wavelength. The overall length is the same as that of a conventional inverted V dipole.

TRANSMISSION-LINE RESONATORS AS PART OF THE ANTENNA

The Coaxial-Resonator Match

This material is condensed from articles that appeared in April 1989 *QST* and *The ARRL Antenna Compendium, Vol 2*. The coaxial-resonator match, a concept based on the TLR transformer, performs the same function as the T match and the gamma match, that is, matching a transmission line to a resonant dipole. These familiar matching devices as well as the coaxial resonator match are shown in **Fig 26**. The coaxial resonator match has some similarity to the gamma match in that it allows connection of the shield of the coaxial feed line to the center of the dipole, and it feeds the dipole off center. The coaxial resonator match has a further advantage: It can be used to broadband the antenna system while providing an impedance match.

The coaxial resonator match is a resonant transformer made from a quarter-wave long piece of coaxial cable. **Fig 27** shows the evolution of the coaxial-resonator match. Now it becomes clear why coaxial cable is used for the quarter-wave TLR transformer—interaction between the dipole and the matching network is minimized. The effective dipole feed point is located at the crossover, which is an off-center feed point. In effect, the match is physically located "inside" the dipole. Currents flowing on the inside of the shield of the coax are associated with the resonator; currents flowing on the outside of the shield of the coax are the usual dipole currents. Skin effect provides a degree of isolation and allows the coax to perform its dual function. The wire extensions at each end make up the remainder of the dipole, making the overall length equal to one half-wavelength.

A useful feature of an antenna using the coaxial-resonator match is that the entire antenna is at the same dc potential as the feed-line potential, thereby avoiding charge buildup on the antenna. Hence, noise and the potential of lightning damage are reduced.

Fig 28 shows the detailed dimensions of an 80-meter inverted-V dipole using a coaxial-resonator match. This design provides a load SWR better than 1.6:1 from 3.5 to 3.825 MHz and has been named the *80-Meter DX Special*. The coax is an electrical quarter wavelength, has a short at one end, an open at the other end, a strategically placed crossover, and is fed at a tee junction. (The crossover is made by connecting the shield of one coax segment to the center conductor of the adjacent segment and by connecting the remaining center conductor and shield in a similar way.) The antenna is constructed as an inverted-V dipole with a 110° included angle and an apex at 60 feet. The measured SWR versus frequency is shown in **Fig 29**. Also in Fig 29

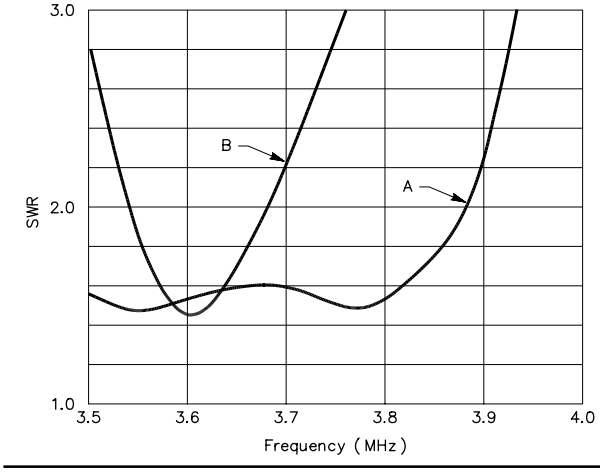

Fig 29—Measured SWR performance of the 80-Meter DX Special, curve A. Note the substantial broadbanding relative to a conventional uncompensated dipole, curve B.

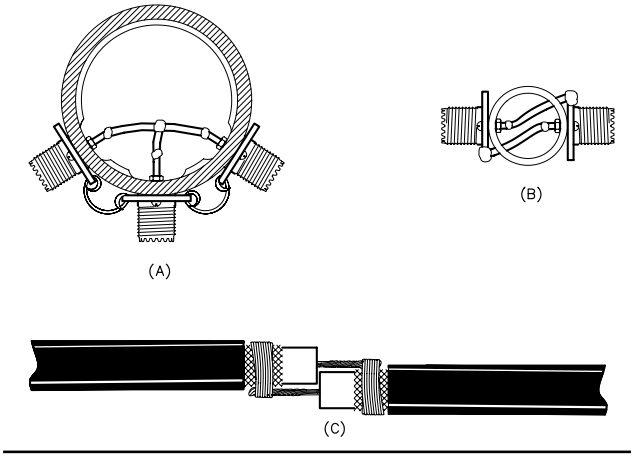

Fig 30—T and crossover construction. At A, a 2-inch PVC pipe coupling can be used for the T, and at B, a 1-inch coupling for the crossover. These sizes are the nominal inside diameters of the PVC pipe that is normally used with the couplings. The T could be made from standard UHF hardware (an M-358 T and a PL-258 coupler). An alternative construction for the crossover is shown at C, where a direct solder connection is made.

is the SWR characteristic for an uncompensated inverted-V dipole made from the same materials and positioned exactly like the broadband version.

The 80-Meter DX Special is made from RG-213 coaxial cable and #14 AWG wire, and is fed with 50-Ω coax. The coax forming the antenna should be cut so that the stub lengths of Fig 28 are within $^1/_2$ inch of the specified values. PVC plastic-pipe couplings and SO-239 UHF chassis connectors can be used to make the T and crossover connections, as shown in **Fig 30A** and 30B. Alternatively, a standard UHF T connector and coupler can be used for the T, and the crossover may be a soldered connection (Fig 30C). RG-213 is used because of its ready availability, physical strength, power handling capability, and moderate loss.

Cut the wire ends of the dipole about three feet longer than the lengths given in Fig 28. If there is a tilt in the SWR-frequency curve when the antenna is first built, it may be flattened to look like the shape given in Fig 29 by increasing or decreasing the wire length. Each end should be lengthened or shortened by the same amount.

A word of caution: If the coaxial cable chosen is not RG-213 or equivalent, the dimensions will have to be modified. The following cable types have about the same characteristic impedance, loss and velocity factor as RG-213 and could be substituted: RG-8, RG-8A, RG-10, RG-10A and RG-215. If the Q of the dipole is particularly high or the radiation resistance is unusually low because of different ground characteristics, antenna height, surrounding objects and so on, then different segment lengths will be required.

What is the performance of this broadband antenna relative to that of a conventional inverted-V dipole? Aside from the slight loss (about 0.75 dB at band edges, less elsewhere) because of the non-ideal matching network, the broadband version will behave essentially the same as a dipole cut for the frequency of interest. That is, the radiation patterns for the two cases will be virtually the same.

The Snyder Dipole

A commercially manufactured antenna utilizing the principles described in the Matching Network Design section is the Snyder dipole. Patented by Richard D. Snyder in late 1984 (see Bibliography), it immediately received much public attention through an article that Snyder published. Snyder's claimed performance for the antenna is a 2:1 SWR bandwidth of 20% with high efficiency.

The configuration of the Snyder antenna is like that of the crossed-double bazooka of Fig 12, with 25-Ω line used for the cross-connected resonators. In addition, the antenna is fed through a 2:1 balun, and exhibits a W-shaped SWR characteristic like that of Fig 13. The SWR at band center, based on information in the patent document, is 1.7 to 1. There is some controversy in professional circles regarding the claims for the Snyder antenna.

The Improved Crossed-Double Bazooka

The following has been condensed from an article by Reed Fisher, W2CQH, that appeared in *The ARRL Antenna Compendium Volume 2*. The antenna is shown in **Fig 31**. Note that the half-wave flat-top is constructed of sections of RG-58 coaxial cable. These sections of coaxial cable serve as quarter-wave shunt stubs that are essentially connected *in parallel* at the feed point in the crossed double-bazooka fashion. At an electrical quarter

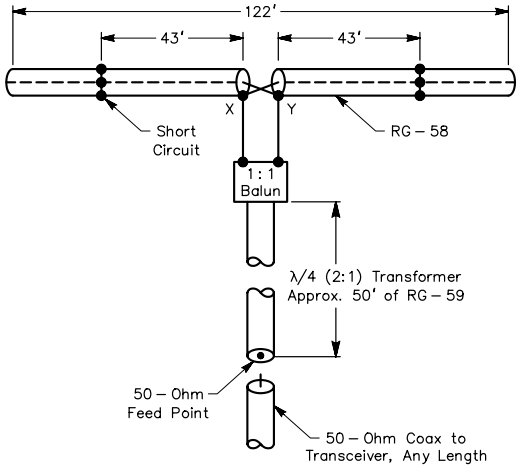

Fig 31—Details of the W2CQH broadband-matched 80-meter dipole.

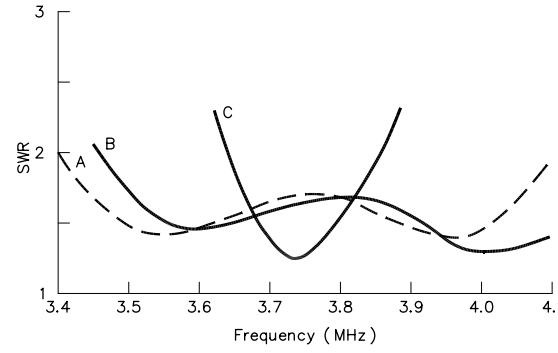

Fig 32—SWR curves for the improved double bazooka. Curve A, the theoretical curve with 50-Ω stubs and a λ/4, 75-Ω matching transformer. Curve B, measured response of the same antenna, built with RG-58 stubs and an RG- 59 transformer. Curve C, measurements from a dipole without broadbanding. Measurements were made at W2CQH with the dipole horizontal at 30 feet.

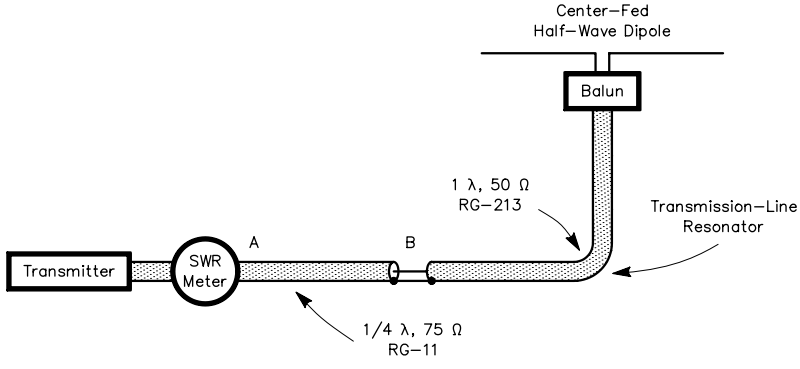

Fig 33—This simple broadband antenna system resembles a conventional 80-meter dipole except for the λ/4-wavelength 75-Ω segment. The lengths of the Q-section, TLR (including balun) and dipole are 43.3 feet, 170.5 feet, and 122.7 feet, respectively.

wavelength (43 feet) from each side of the feed point X-Y, the center conductor is shorted to the braid of the coaxial cable.

The parallel stubs provide reactance compensation. The necessary impedance transformation at the antenna feed point is provided by the quarter-wave Q-section constructed of a 50-foot section of 75-Ω coaxial cable (RG-59). A W2DU 1:1 current balun is used at the feed point. See **Fig 32** for the SWR versus frequency for this antenna with and without the broadband matching network.

This antenna is essentially that of the crossed double bazooka antenna shown in Fig 12, with the addition of the 75-Ω Q-section. The improvement in match bandwidth is substantial. The antenna at W2CQH is straight and nearly horizontal with an average height of about 30 feet.

TRANSMISSION-LINE RESONATORS AS PART OF THE FEED LINE

A Simple Broadband Dipole for 80 Meters

This system was described in an article in September 1993 *QST*. It has the advantage that the radiator is the same as that of a conventional half-wave wire dipole. Thus the antenna is light weight, easy to support and has small wind and ice loading. The broadband matching network is integrated into the feed line.

The system is shown in **Fig 33**. It is a variation of the example shown in the Matching Network Design section of this chapter as shown in Fig 17. The TLR is a 1λ length of RG-213 50-Ω coax and the impedance transformation is accomplished with a 75-Ω Q-section

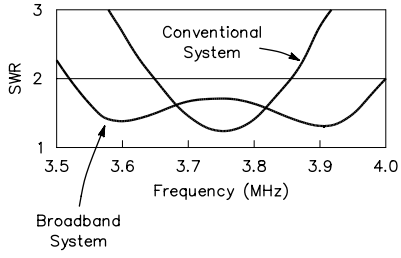

Fig 34—Measured SWR versus frequency for the broadband and conventional antenna systems.

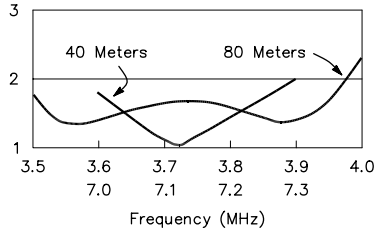

Fig 35—Measured SWR for the 80- and 40-meter multiband antenna system.

made of RG-11. The antenna is an inverted-V with a 140° included angle and an apex height of 60 feet. The wire size is #14, but is not critical. The balun is a W2DU 1:1 current type. It easily handles the legal power limit over the entire 80-meter band. The measured SWR is shown in **Fig 34**.

A unique advantage of this antenna is that by paralleling a 40-meter dipole at the feed point and sharing the feed line, operation on both 80 and 40 meters is possible. The reason for this is that the lengths of the Q-section and the TLR are multiples of a half-wavelength on 40 meters. To minimize the interaction, the two dipoles should be spaced from each other away from the feed point. First tune the 80-meter antenna and then the 40-meter one. **Fig 35** shows the result of adding a 40-meter dipole to the system shown in Fig 33. Each 40-meter dipole leg is 34.4 feet long. Note that the SWR on 80 meters changes very little compared to Fig 34. No change was made to the 80-meter dipole or to the transmission line.

80-Meter Dipole with the TLR Transformer

The total length of the feed line in the system just described above in Fig 33 is quite long, about 214 feet. For installations with shorter runs, the TLR transformer concept may be employed to advantage. An example provided in "Optimizing the 80-Meter Dipole" in *The ARRL Antenna Compendium, Vol 4* is shown in **Fig 36**. Here the TLR is $^3/_4$ λ long overall and is made from RG-213 50-Ω cable. The design applies for an 80-meter horizontal dipole, 80 feet above average ground, with an

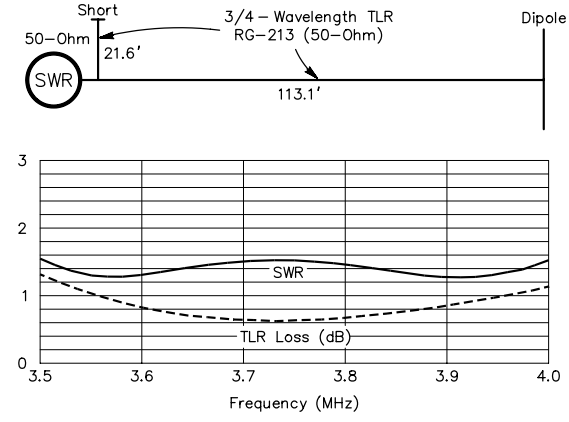

Fig 36—Broadbanding with the TLR transformer. The dimensions shown apply for an 80-meter horizontal dipole 80 feet above average ground.

assumed antenna F_0, R_A, and Q_A of 3.72 MHz, 92 Ω and 9, respectively. (See Figs 3 and 4). The lengths must be revised for other dipole parameters.

For this design, the feed line is 113.1 feet long and the shorted stub at the transmitter end is 21.6 feet long. You can add any length of 50-Ω cable between the transmitter and the junction of the shorted stub and the feed line. The shorted stub gives a dc path to ground for both sides of the dipole, preventing charge buildup and some lightning protection. For multiband operation with an antenna tuner, the stub should be removed.

The general application of the TLR transformer concept has a tap at both the transmitter end and a tap at the antenna end. (See Fig 24.) In this case, the concept was applied only at the transmitter end, since very little impedance transformation was required at the antenna end. The location of the TLR transformer is not obvious. Consider a $^3/_4$ λ TLR with a short at one end, and an open at the other end where the antenna is connected. The generator for no impedance transformation would be located λ/4 (43.6 feet @ 3.72 MHz) from the short. By connecting the transmitter 21.6 feet from the short, the required impedance transformation for a transmitter optimized for 50-Ω loads is achieved.

BIBLIOGRAPHY

Source material and more extended discussion of the topics covered in this chapter can be found in the references given below and in the textbooks listed at the end of Chapter 2.

A. Bloom, "Once More with the 80-Meter Dipole," Technical Correspondence, *QST*, Jun 1985, p 42.

R. E. Fisher, "A Simple, Broadband 80-Meter Dipole Antenna," *The ARRL Antenna Compendium, Vol 2* (Newington, CT: ARRL, 1989), pp 119-123.

R. M. Fano, "Theoretical Limitations on the Broadband Matching of Arbitrary Impedances," *Journal of the Franklin Inst*, Jan 1950, pp 57-83, and Feb 1950, pp 139-155.

J. Hall, "The Search for a Simple, Broadband 80-Meter Dipole," *QST*, Apr 1983, pp 22-27.

J. Hall, "Maxcom Antenna Matcher and Dipole Cable Kit," Product Review, *QST*, Nov 1984, pp 53-54.

R. C. Hansen, "Evaluation of the Snyder Dipole," *IEEE Trans on Antennas and Prop*, Vol AP-35, No. 2, Feb 1987, pp 207-210.

A. Harbach, "Broadband 80-Meter Antenna," *QST*, Dec 1980, pp 36-37 (presentation of a cage antenna).

S. Leslie, "Broadbanding the Elevated, Inverse-Fed Ground Plane Antenna," *The ARRL Antenna Compendium, Vol 6* (Newington, CT: 1999), pp 209-211.

R. D. Snyder, "The Snyder Antenna," *RF Design*, Sep/Oct 1984, pp 49-51.

R. D. Snyder, "Broadband Antennae Employing Coaxial Transmission Line Sections," United States Patent no. 4,479,130, issued Oct 23, 1984.

C. Whysall, "The 'Double Bazooka' Antenna," *QST*, Jul 1968, pp 38-39.

F. Witt, "A Simple Broadband Dipole for 80 Meters," *QST*, Sept 1993, pp 27-30, 76.

F. J. Witt, "Broadband Dipoles—Some New Insights," *QST*, Oct 1986, pp 27-37.

F. Witt, "Broadband Matching with the Transmission Line Resonator," *The ARRL Antenna Compendium, Vol 4*, (Newington, CT: 1995), pp 30-37.

F. Witt, "How to Design Off-Center-Fed Multiband Wire Antennas Using that Invisible Transformer in the Sky," *The ARRL Antenna Compendium, Vol 3,* (Newington, CT: ARRL, 1992), p 74.

F. Witt, "Match Bandwidth of Resonant Antenna Systems," *QST*, Oct 1991, pp 21-25

F. Witt, "Optimizing the 80-Meter Dipole," *The ARRL Antenna Compendium, Vol 4* (Newington, CT: 1995), pp 38-48.

F. Witt, "Optimum Lossy Broadband Matching Networks for Resonant Antennas," *RF Design*, Apr 1990, pp 44-51 and Jul 1990, p 10.

F. Witt, "The Coaxial Resonator Match and the Broadband Dipole," *QST*, Apr 1989, pp 22-27.

F. Witt, "The Coaxial Resonator Match, *The ARRL Antenna Compendium, Vol 2* (Newington, CT: ARRL, 1989), pp 110-118.

Chapter 10

Log Periodic Arrays

This chapter was contributed by L. B. Cebik, W4RNL. The *Log Periodic Dipole Array* (*LPDA*) is one of a family of frequency-independent antennas. Alone, an LPDA forms a directional antenna with relatively constant characteristics across a wide frequency range. It may also be used with parasitic elements to achieve specific characteristic within a narrow frequency range. Common names for such hybrid arrays are the *log-cell Yagi* or the *Log-Yag*. We shall look at the essential characteristics of both types of arrays in this chapter.

The LPDA is the most popular form of log-periodic systems, which also include zig-zag, planar, trapezoidal, slot, and V forms. The appeal of the LPDA version of the log periodic antenna owes much to its structural similarity to the Yagi-Uda parasitic array. This permits the construction of directional LPDAs that can be rotated—at least within the upper HF and higher frequency ranges. Nevertheless, the LPDA has special structural as well as design considerations that distinguish it from the Yagi. A number of different construction techniques for both wire and tubular elements are illustrated later in this chapter.

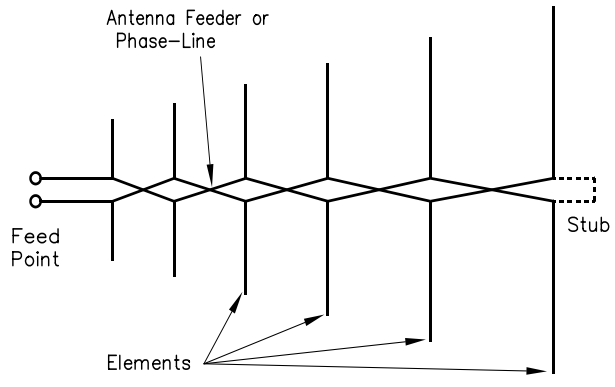

Fig 1—The basic components of a log periodic dipole array (LPDA). The forward direction is to the left in this sketch. Many variations of the basic design are possible.

The LPDA in its present form derives from the pioneering work of D. E. Isbell at the University of Illinois in the late 1950s. Although you may design LPDAs for large frequency ranges—for example, from 3 to 30 MHz or a little over 3 octaves—the most common LPDA designs that radio amateurs use are limited to a one-octave range, usually from 14 to 30 MHz. Amateur designs for this range tend to consist of linear elements. However, experimental designs for lower frequencies have used elements shaped like inverted Vs, and some versions use vertically oriented $^1/_4\ \lambda$ elements over a ground system.

Fig 1 shows the parts of a typical LPDA. The structure consists of a number of linear elements, the longest of which is approximately $^1/_2\ \lambda$ long at the lowest design frequency. The shortest element is usually about $^1/_2\ \lambda$ long at a frequency well above the highest operating frequency. The antenna feeder, also informally called the *phase-line*, connects the center points of each element in the series, with a phase reversal or *cross-over* between each element. A stub consisting of a shorted length of parallel feed line is often added at the back of an LPDA.

The arrangement of elements and the method of feed yield an array with relatively constant gain and front-to-back ratio across the designed operating range. In addition, the LPDA exhibits a relatively constant feed-point impedance, simplifying matching to a transmission line.

BASIC DESIGN CONSIDERATIONS

For the amateur designer, the most fundamental facets of the LPDA revolve around three interrelated design variables: α (alpha), τ (tau), and σ (sigma). Any one of the three variables may be defined by reference to the other two.

Fig 2 shows the basic components of an LPDA. The angle α defines the outline of an LPDA and permits every dimension to be treated as a radius or the consequence of a radius (R) of a circle. The most basic structural dimensions are the element lengths (L), the distance (R) of each element from the apex of angle α, and the distance between elements (D). A single design constant, τ, defines all of these relationships in the following manner:

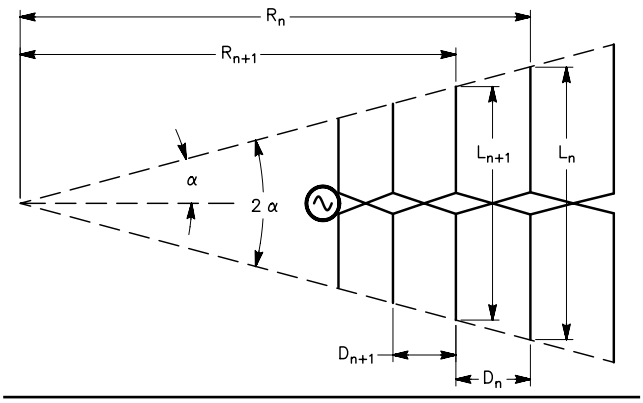

Fig 2—Some fundamental relationships that define an array as an LPDA. See the text for the defining equations.

$$\tau = \frac{R_{n+1}}{R_n} = \frac{D_{n+1}}{D_n} = \frac{L_{n+1}}{L_n} \qquad \text{(Eq 1)}$$

where element n and n+1 are successive elements in the array working toward the apex of angle α. The value of τ is always less than 1.0, although effective LPDA design requires values as close to 1.0 as may be feasible.

The variable τ defines the relationship between successive element spacings but it does not itself determine the initial spacing between the longest and next longest elements upon which to apply τ successively. The initial spacing also defines the angle α for the array. Hence, we have two ways to determine the value of σ, the relative spacing constant:

$$\sigma = \frac{1-\tau}{4\tan\alpha} = \frac{D_n}{2L_n} \qquad \text{(Eq 2)}$$

where D_n is the distance between any two elements of the array and L_n is the length of the longer of the two elements. From the first of the two methods of determining the value of σ, we may also find a means of determining α when we know both τ and σ.

For any value of τ, we may determine the optimal value of σ:

$$\sigma_{opt} = 0.243\tau - 0.051 \qquad \text{(Eq 3)}$$

The combination of a value for τ and its corresponding optimal value of σ yields the highest performance of which an LPDA is capable. For values of τ from 0.80 through 0.98, the value of optimal σ varies from 0.143 to 0.187, in increments of 0.00243 for each 0.01 change in τ. However, using the optimal value of σ usually yields a total array length that is beyond ham construction or tower/mast support capabilities. Consequently, amateur LPDAs usually employ compromise values of τ and σ that yield lesser but acceptable performance.

For a given frequency range, increasing the value of τ increases both the gain and the number of required elements. Increasing the value of σ increases both the gain and the overall boom length. A τ of 0.96—which approaches the upper maximum recommended value for τ—yields an optimal σ of about 0.18, and the resulting array grows to over 100 feet long for the 14 to 30 MHz range. The maximum free space gain is about 11 dBi, with a front-to-back ratio that approaches 40 dB. Normal amateur practice, however, uses values of τ from about 0.88 to 0.95 and values of σ from about 0.03 to 0.06.

Standard design procedures usually set the length of the rear element for a frequency about 7% lower than the lowest design frequency and use the common dipole formula ($L_{feet} = 468/f_{MHz}$) to determine its length (5% lower than a free-space half wavelength, where $L_{feet} = 493.56/f_{MHz}$). The upper frequency limit of the design is ordinarily set at about 1.3 times the highest design frequency. Since τ and σ set the increment between successive element lengths, the number of elements becomes a function of when the shortest element reaches the dipole length for the adjusted upper frequency.

The adjusted upper frequency limit results from the behavior of LPDAs with respect to the number of active elements. See **Fig 3**, which shows an edge view of a 10-element LPDA for 20 through 10 meters. The vertical lines represent the peak relative current magnitude for each element at the specified frequency. At 14 MHz, virtually every element of the array shows a significant cur-

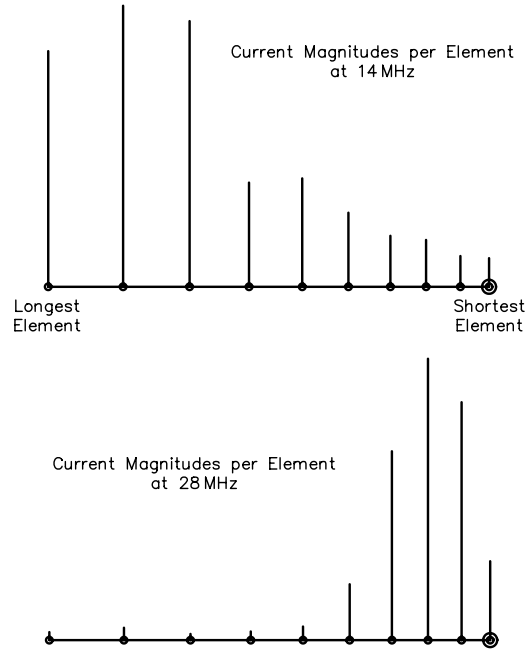

Fig 3—The relative current magnitude on the elements of an LPDA at the lowest and highest operating frequencies for a given design. Compare the number of "active" elements, that is, those with current levels at least 1/10 of the highest level.

rent magnitude. However, at 28 MHz, only the forward 5 elements carry significant current. Without the extended design range to nearly 40 MHz, the number of elements with significant current levels would be severely reduced, along with upper frequency performance.

The need to extend the design equations below the lowest proposed operating frequency varies with the value of τ. In **Fig 4**, we can compare the current on the rear elements of two LPDAs, both with a σ value of 0.04. The upper design uses a τ of 0.89, while the lower design uses a value of 0.93. The most significant current-bearing element moves forward with increases in τ, reducing (but not wholly eliminating) the need for elements whose lengths are longer than a dipole for the lowest operating frequency.

LPDA Design and Computers

Originally, LPDA design proceeded through a series of design equations intended to yield the complete specifications for an array. More recent techniques available to radio amateurs include basic LPDA design software and antenna modeling software. One good example of LPDA design software is *LPCAD28* by Roger Cox, WBØDGF. A copy of this freeware program is on the CD-ROM that accompanies this volume. The user begins by specifying the lowest and highest frequencies in the design. He then enters either his selected values for τ and σ or his choices for the number of elements and the total length of the array. With this and other input data, the program provides a table of element lengths and spacings, using the adjusted upper and lower frequency limits described earlier.

The program also requests the diameters of the longest and shortest elements in the array, as well as the diameter of average element. From this data, the program calculates a recommended value for the phase-line connecting the elements and the approximate resistive value of the input impedance. Among the additional data that *LPCAD28* makes available is the spacing of conductors to achieve the desired characteristic impedance of the phase-line. These conductors may be round—as we would use for a wire phase-line—or square—as we might use for double-boom construction.

An additional vital output from *LPCAD28* is the conversion of the design into antenna modeling input files of several formats, including versions for *AO* and *NEC4WIN* (both *MININEC*-based programs), and a version in the standard *.NEC format usable by many implementations of *NEC-2* and *NEC-4*, including *NECWin Plus*, *GNEC*, and *EZNEC Pro*. Every proposed LPDA design should be verified and optimized by means of antenna modeling, since basic design calculations rarely provide arrays that require no further work before construction. A one-octave LPDA represents a segment of an arc defined by α that is cut off at both the upper and the lower frequency limits. Moreover, some of the design equations are based upon approximations and do not completely predict LPDA behavior. Despite these limitations, most of the sample LPDA designs shown later in this chapter are based directly upon the fundamental calculations. Therefore, the procedure will be outlined in detail before turning to hybrid log-cell Yagi concepts.

Modeling LPDA designs is most easily done on a version of *NEC*. The transmission line (TL) facility built into *NEC-2* and *NEC-4* alleviates the problem of modeling the phase-line as a set of physical wires, each section of which has a set of constraints in *MININEC* at the right-angle junctions with the elements. Although the *NEC* TL facility does not account for losses in the lines, the losses are ordinarily low enough to neglect.

NEC models do require some careful construction to obtain the most accurate results. Foremost among the cautions is the need for careful segmentation, since each element has a different length. The shortest element should have about 9 or 11 segments, so that it has sufficient segments at the highest modeling frequency for the design. Each element behind the shortest one should have a greater number of segments than the preceding element by the inverse of the value of τ. However, there is a further limitation. Since the transmission line is at the center of each

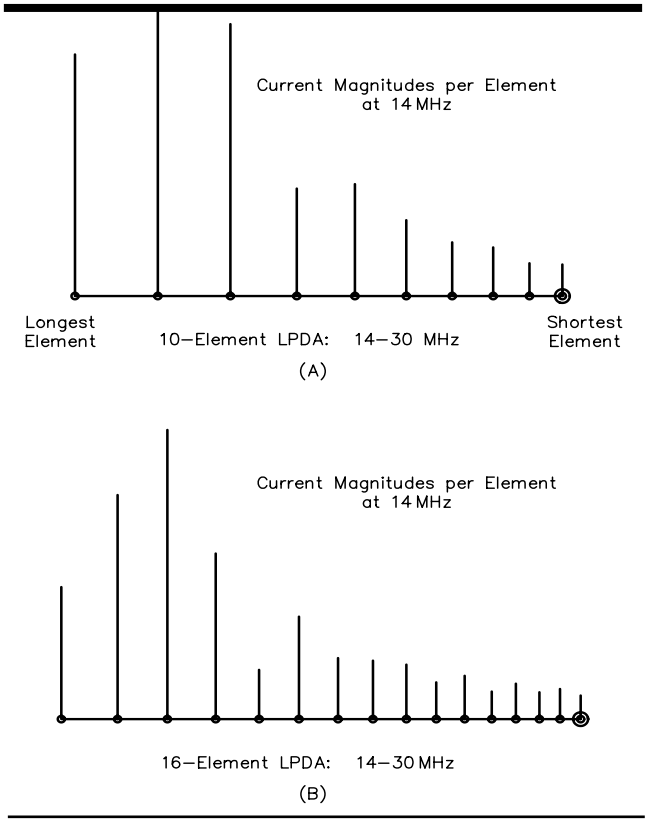

Fig 4—Patterns of current magnitude at the lowest operating frequency of two different LPDA designs: a 10-element low-τ design and a 16-element higher-τ design.

element, *NEC* elements should have an odd number of segments to hold the phase-line centered. Hence, each segmentation value calculated from the inverse of τ must be rounded up to the nearest odd integer.

Initial modeling of LPDAs in *NEC-2* should be done with uniform-diameter elements, with any provision for stepped-diameter element correction turned off. Since these correction factors apply only to elements within about 15% of dipole resonance at the test frequency, models with stepped-diameter elements will correct for only a few elements at any test frequency. The resulting combination of corrected and uncorrected elements will not yield a model with assured reliability.

Once one has achieved a satisfactory model with uniform-diameter elements, the modeling program can be used to calculate stepped-diameter substitutes. Each uniform-diameter element, when extracted from the larger array, will have a resonant frequency. Once this frequency is determined, the stepped-diameter element to be used in final construction can be resonated to the same frequency. Although *NEC-4* handles stepped diameter elements with much greater accuracy than *NEC-2*, the process just described is also applicable to *NEC-4* models for the greatest precision.

LPDA Behavior

Although LPDA behavior is remarkably uniform over a wide frequency range compared to narrow-band designs, such as the Yagi-Uda array, it nevertheless exhibits very significant variations within the design range. **Fig 5** shows several facets of these behaviors. Fig 5 shows the free-space gain for three LPDA designs using 0.5-inch diameter aluminum elements. The designations for each model list the values of τ (0.93, 0.89, and 0.85) and of σ (0.02, 0.04, and 0.06) used to design each array. The resultant array lengths are listed with each designator. The total number of elements varies from 16 for "9302" to 10 for "8904" to 7 for "8504."

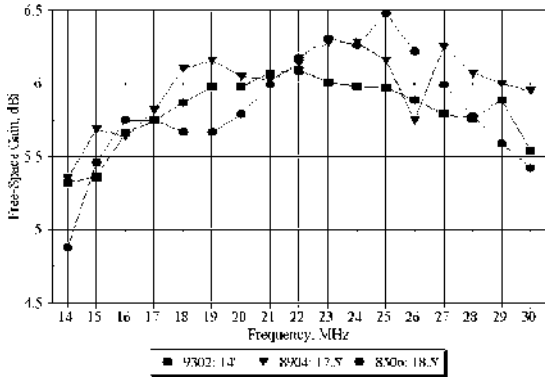

Fig 5—The modeled free-space gain of 3 relatively small LPDAs of different design. Note the relationship of the values of τ and of σ for these arrays with quite similar performance across the 14-30 MHz span.

First, the gain is never uniform across the entire frequency span. The gain tapers off at both the low and high ends of the design spectrum. Moreover, the amount of gain undulates across the spectrum, with the number of peaks dependent upon the selected value of τ and the resultant number of elements. The front-to-back ratio tends to follow the gain level. In general, it ranges from less than 10 dB when the free-space gain is below 5 dBi to over 20 dB as the gain approaches 7 dBi. The front-to-back ratio may reach the high 30s when the free-space array gain exceeds 8.5 dBi. Well-designed arrays, especially those with high values of τ and σ, tended to have well-controlled rear patterns that result in only small differences between the 180° front-to-back ratio and the averaged front-to-rear ratio.

Since array gain is a mutual function of both τ and σ, average gain becomes a function of array length for any given frequency range. Although the gain curves in Fig 5 interweave, there is little to choose among them in terms of average gain for the 14 to 18-foot range of array lengths. Well-designed 20- to 10-meter arrays in the 30-foot array length region are capable of about 7 dBi free-space gain, while 40-foot arrays for the same frequency range can achieve about 8 dBi free-space gain.

Exceeding an average gain of 8.5 dBi requires at least a 50-foot array length for this frequency range. Long arrays with high values of τ and σ also tend to show smaller excursions of gain and of front-to-back ratio in the overall curves. In addition, high-τ designs tend to show higher gain at the low frequency end of the design spectrum.

The frequency sweeps shown in Fig 5 are widely spaced at 1 MHz intervals. The evaluation of a specific design for the 14 to 30-MHz range should decrease the interval between check points to no greater than 0.25 MHz in order to detect frequencies at which the array may show a *performance weakness*. Weaknesses are frequency regions in the overall design spectrum at which the array shows unexpectedly lower values of gain and front-to-back ratio. In Fig 5 note the unexpected decrease in gain of model "8904" at 26 MHz. The other designs also have weak points, but they fall between the frequencies sampled.

In large arrays, these regions may be quite small and may occur in more than one frequency region. The weakness results from the harmonic operation of longer elements to the rear of those expected to have high current levels. Consider a 7-element LPDA about 12.25-foot long for 14 to 30 MHz using 0.5-inch aluminum elements. At 28 MHz, the rear elements operate in a harmonic mode, as shown by the high relative current magnitude curves in **Fig 6**. The result is a radical decrease in gain, as shown in the "No Stub" curve of **Fig 7**. The front-to-back ratio also drops as a result of strong radiation from the long

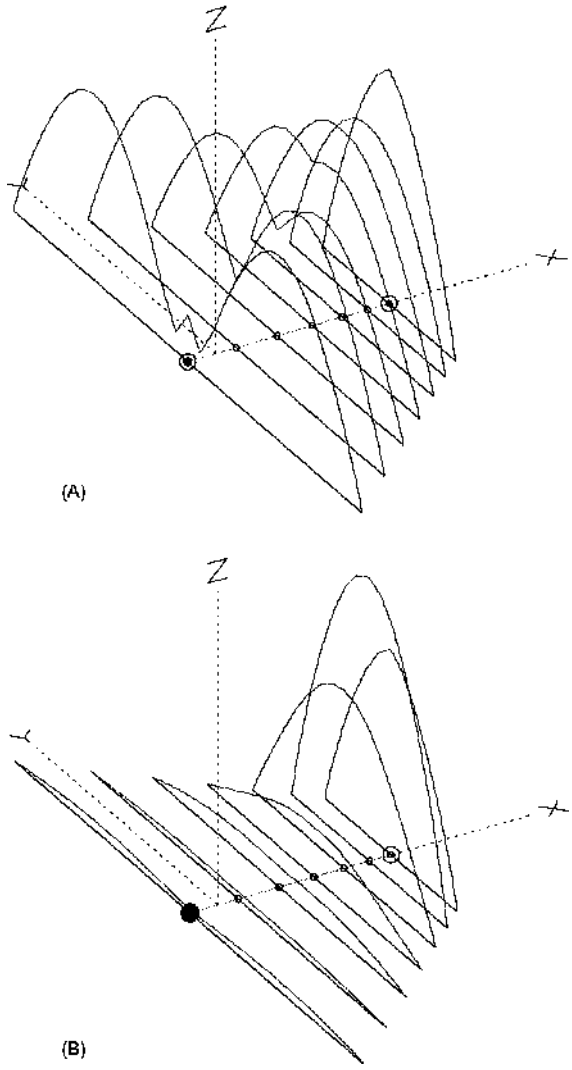

Fig 6—The relative current magnitude on the elements of model "8504" at 28 MHz without and with a stub. Note the harmonic operation of the rear elements before a stub is added to suppress such operation.

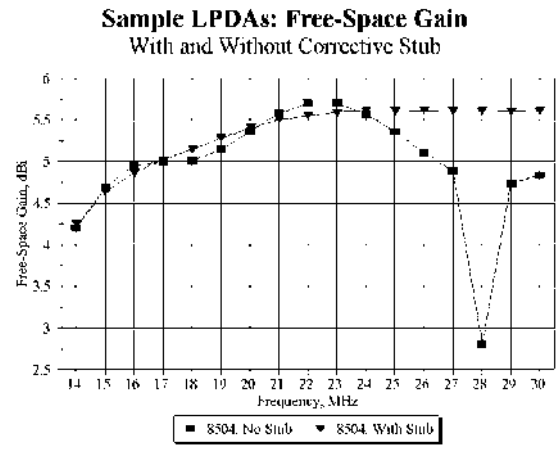

Fig 7—A graph of the gain of model "8504" showing the frequency region in which a "weakness" occurs and its absence once a suitable stub is added to the array.

elements to the rear of the array.

Early designs of LPDAs called for terminating transmission-line stubs as standard practice to help eliminate such weak spots in frequency coverage. In contemporary designs, their use tends to be more specific for eliminating or moving frequencies that show gain and front-to-back weakness. (Stubs have the added function of keeping both sides of each element at the same level of static charge or discharge.) The model dubbed "8504" was fitted (by trial and error) with an 18-inch shorted stub of 600-Ω transmission line. As Fig 6B shows, the harmonic operation of the rear elements is attenuated. The "stub" curve of Fig 7 shows the smoothing of the gain curve for the array throughout the upper half of its design spectrum. In some arrays showing multiple weaknesses, a single stub may not eliminate all of them. However, it may move the weaknesses to unused frequency regions. Where full-spectrum operation of an LPDA is necessary, additional stubs located at specific elements may be needed.

Most LPDA designs benefit (with respect to gain and front-to-back ratio) from the use of larger-diameter elements. Elements with an average diameter of at least 0.5-inch are desirable in the 14 to 30 MHz range. However, standard designs usually presume a constant element length-to-diameter ratio. In the case of *LPCAD28*, this ratio is about 125:1, which assumes an even larger diameter. To achieve a relatively constant length-to-diameter ratio in the computer models, you can set the diameter of the shortest element in a given array design and then increase the element diameter by the inverse of τ for each succeeding longer element. This procedure is often likely to result in unreasonably large element diameters for the longest elements, relative to standard amateur construction practices.

Since most amateur designs using aluminum tubing for elements employ stepped-diameter (tapered) elements, roughly uniform element diameters will result unless the LPDA mechanical design tries to lighten the elements at the forward end of the array. This practice may not be advisable, however. Larger elements at the high end of the design spectrum often counteract (at least partially) the natural decrease in high-frequency gain and show improved performance compared to smaller diameter elements.

An alternative construction method for LPDAs uses wire throughout. At every frequency, single-wire elements reduce gain relative to larger-diameter tubular elements. An alternative to tubular elements appears in **Fig 8**. For each element of a tubular design, there is a roughly equivalent 2-wire element that may be substituted. The

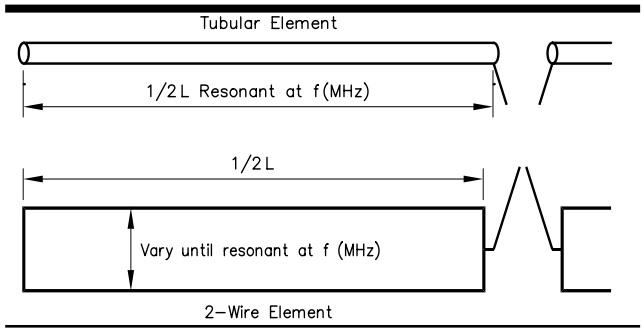

Fig 8—A substitute for a large-diameter tubular element composed of two wires shorted at both the outer ends and at the center junction with the phase-line.

spacing between the wire is determined by taking one of the modeled tubular elements and finding its resonant frequency. A two-wire element of the same length is then constructed with shorts at the far ends and at the junctions with the phase-line. The separation of the two wires is adjusted until the wire element is resonant at the same frequency as the original tubular element. The required separation will vary with the wire chosen for the element. Models used to develop these substitutes must pay close attention to segmentation rules for *NEC* due to the short length of segments in the end and center shorts, and to the need to keep segment junctions as exactly parallel as possible with close-spaced wires.

Feeding and Constructing the LPDA

Original design procedures for LPDAs used a single, ordinarily fairly high, characteristic impedance for the phase-line (antenna feeder). Over time, designers realized that other values of impedance for the phase line offered both mechanical and performance advantages for LPDA performance. Consequently, for the contemporary designer, phase-line choice and construction techniques are almost inseparable considerations.

High-impedance phase lines (roughly 200 Ω and higher) are amenable to wire construction similar to that used with ordinary parallel-wire transmission lines. They require careful placement relative to a metal boom used to support individual elements (which themselves must be insulated from the support boom). Connections also require care. If the phase-line is given a half-twist between each element, the construction of the line must ensure constant spacing and relative isolation from metal supports to maintain a constant impedance and to prevent shorts.

Along with the standard parallel-wire line, shown in **Fig 9A**, there are a number of possible LPDA structures using booms. The booms serve both to support the elements and to create relatively low-impedance (under 200 Ω) phase-lines. Fig 9B shows the basics of a twin circular tubing boom with the elements cross-supported by insulated rods. Fig 9C shows the use of square tubing with the elements attached directly to each tube by through-bolts. Fig 9D illustrates the use of L-stock, which may be practical at VHF frequencies. Each of these sketches is incomplete, however, since it omits the necessary stress analyses that determine the mechanical feasibility of a structure for a given LPDA project.

The use of square boom material requires some adjustment when calculating the characteristic impedance of the phase-line. For conductors with a circular cross-section,

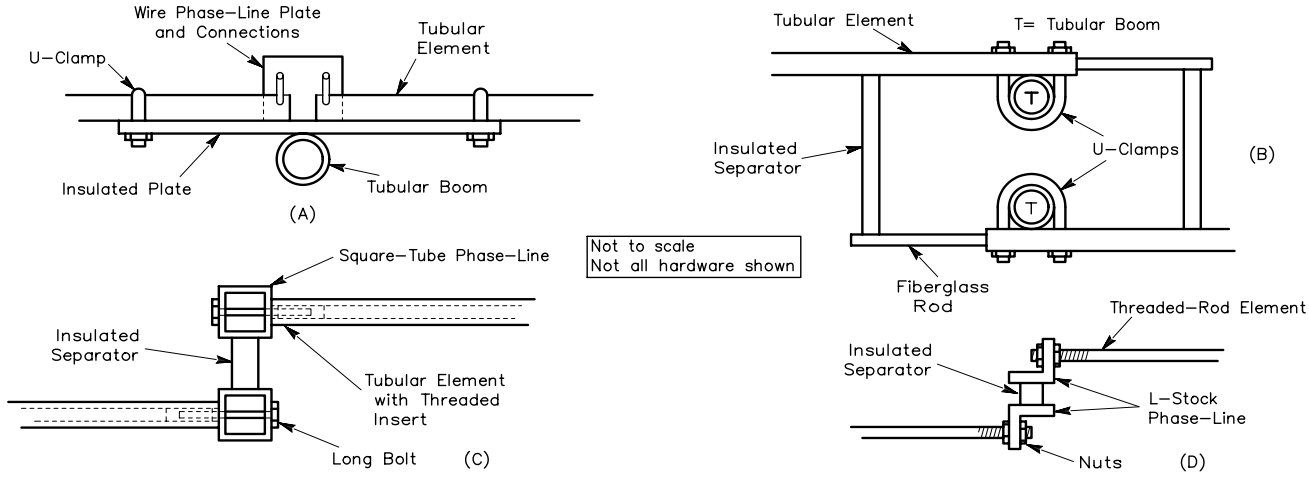

Fig 9—Four (of many) possible construction techniques, shown from the array end. In A, an insulated plate supports and separates the wires of the phase-line, suitable with wire or tubular elements. A dual circular boom phase-line also supports the elements, which are cross-supported for boom stability. Square tubing is used in C, with the elements joined to the boom/phase-line with through-bolts and an insert in each half element. The L-stock shown in D is useful for lighter VHF and UHF arrays.

$$Z_0 = 120 \cosh^{-1} \frac{D}{d} \quad \text{(Eq 4)}$$

where D is the center-to-center spacing of the conductors and d is the outside diameter of each conductor, both expressed in the same units of measurement. Since we are dealing with closely spaced conductors, relative to their diameters, the use of this version of the equation for calculating the characteristic impedance (Z_0) is recommended. For a square conductor,

$$d \approx 1.18\ w \quad \text{(Eq 5)}$$

where d is the approximate equivalent diameter of the square tubing and w is the width of the tubing across one side. Thus, for a given spacing, a square tube permits you to achieve a lower characteristic impedance than round conductors. However, square tubing requires special attention to matters of strength, relative to comparable round tubing.

Electrically, the characteristic impedance of the LPDA phase-line tends to influence other performance parameters of the array. Decreasing the phase-line Z_0 also decreases the feed-point impedance of the array. For small designs with few elements, the decrease is not fully matched by a decrease in the excursions of reactance. Consequently, using a low impedance phase-line may make it more difficult to achieve a 2:1 or less SWR for the entire frequency range. However, higher-impedance phase-lines may result in a feed-point impedance that requires the use of an impedance-matching balun.

Decreasing the phase-line Z_0 also tends to increase LPDA gain and front-to-back ratio. There is a price to be paid for this performance improvement—weaknesses at specific frequency regions become much more pronounced with reductions in the phase-line Z_0. For a specific array you must weigh carefully the gains and losses, while employing one or more transmission line stubs to get around performance weaknesses at specific frequencies.

Depending upon the specific values of τ and σ selected for a design, you can sometimes select a phase-line Z_0 that provides either a 50-Ω or a 75-Ω feed-point impedance, holding the SWR under 2:1 for the entire design range of the LPDA. The higher the values of τ and σ for the design, the lower the reactance and resistance excursions around a central value. Designs using optimal values of σ with high values of τ show a very slight capacitive reactance throughout the frequency range. Lower design values obscure this phenomenon due to the wide range of values taken by both resistance and reactance as the frequency is changed.

At the upper end of the frequency range, the source resistance value decreases more rapidly than elsewhere in the design spectrum. In larger arrays, this can be overcome by using a variable Z_0 phase-line for approximately the first 20% of the array length. This technique is, however, difficult to implement with anything other than wire phase-lines. Begin with a line impedance about half of the final value and increase the wire spacing evenly until it reaches its final and fixed spacing. This technique can sometimes produce smoother impedance performance across the entire frequency span and improved high-frequency SWR performance.

Designing an LPDA requires as much attention to designing the phase-line as to element design. It is always useful to run models of the proposed design through several iterations of possible phase-line Z_0 values before freezing the structure for construction.

Special Design Corrections

The curve for the sample 8504 LPDA in Fig 7 revealed several deficiencies in standard LPDA designs. The weakness in the overall curve was corrected by the use of a stub to eliminate or move the frequency at which rearward elements operated in a harmonic mode. In the course of describing the characteristics of the array, we have noted several other means to improve performance. Fattening elements (either uniformly or by increasing their diameter in step with τ) and reducing the characteristic impedance of the phase-line are capable of small improvements in performance. However, they cannot wholly correct the tendency of the array gain and front-to-back ratio to fall off at the upper and lower limits of the LPDA frequency range.

One technique sometimes used to improve performances near the frequency limits is to design the LPDA for upper and lower frequency limits much higher and lower than the frequencies of use. This technique unnecessarily increases the overall size of the array and does not eliminate the downward performance curves. Increasing the values of τ and σ will usually improve perfor-

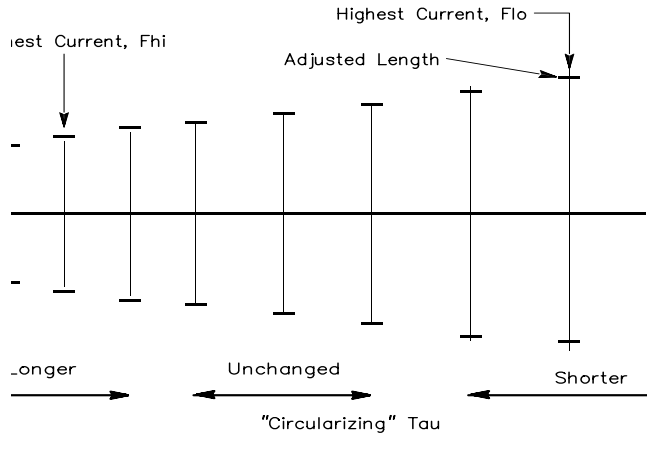

Fig 10—A before and after sketch of an LPDA, showing the original lengths of the elements and their adjustments from diminishing the value of τ at both ends of the array. See the text for the amount of change applicable to each element.

mance at no greater cost in size than extending the frequency range. Increasing the value of τ is especially effective in improving the low frequency performance of an LPDA.

Working within the overall size limits of a standard design, one may employ a technique of *circularizing* the value of τ for the rear-most and forward-most elements. See **Fig 10**, which is not to-scale relative to overall array length and width. Locate (using an antenna-modeling program) the element with the highest current at the lowest operating frequency, and the element with the highest current at the highest operating frequency. The adjustments to element lengths may begin with these elements or—at most—one element further toward the array center. For the first element (counting from the center) to be modified, reduce the value of τ by about 0.5%. For a rearward element, use the inverse of the adjusted value of τ to calculate the new length of the element relative to the unchanged element just forward of the change. For a forward element, use the new value of τ to calculate the new length of the element relative to the unchanged element immediately to the rear of it.

For succeeding elements outward, calculate new values of τ from the adjusted values, increasing the increment of decrease with each step. Second adjusted elements may use values of τ about 0.75% to 1.0% lower than the values just calculated. Third adjusted elements may use an increment of 1.0% to 1.5% relative to the preceding value.

Not all designs require extensive treatment. As the values of τ and σ increase, fewer elements may require adjustment to obtain the highest possible gain at the frequency limits, and these will always be the most outward elements in the array. A second caution is to check the feed-point impedance of the array after each change to ensure that it remains within design limits.

Fig 11 shows the free-space gain curves from 14 to 30 MHz for a 10-element LPDA with an initial τ of 0.89 and a σ of 0.04. The design uses a 200-Ω phase-line, 0.5-inch aluminum elements, and a 3-inch 600-Ω stub. The lowest curve shows the modeled performance across the design frequency range with only the stub. Performance at the frequency limits is visibly lower than within the peak performance region. The middle curve shows the effects of circularizing τ. Average performance levels have improved noticeably at both ends of the spectrum.

In lieu of, or in addition to, the adjustment of element lengths, you may also add a parasitic director to an LPDA, as shown in **Fig 12**. The director is cut roughly for the highest operating frequency. It may be spaced between 0.1 λ and 0.15 λ from the forward-most element of the LPDA. The exact length and spacing should be determined experimentally (or from models) with two factors in mind. First, the element should not adversely effect the feed-point impedance at the highest operating frequencies. Close spacing of the director has the greatest effect on this impedance. Second, the exact spacing and element length should be set to have the most desired effect on the overall performance curve of the array. The mechanical impact of adding a director is to increase overall array length by the spacing selected for the element.

The upper curve in Fig 11 shows the effect of adding a director to the circularized array already equipped with a stub. The effect of the director is cumulative, increasing the upper range gain still further. Note that the added parasitic director is not just effective at the highest

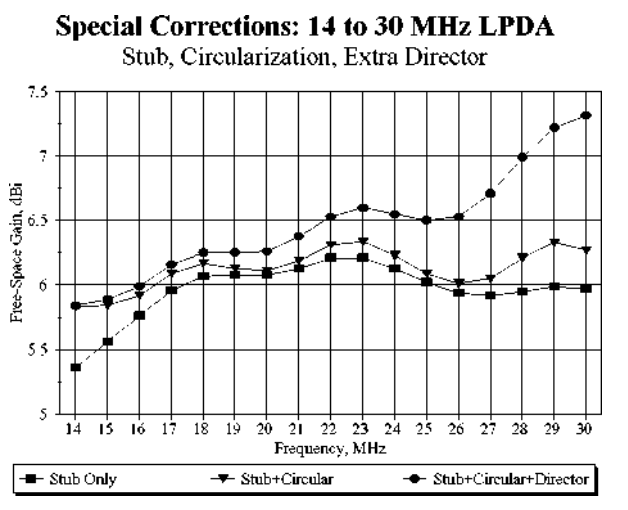

Fig 11—The modeled free space gain from 14 to 30 MHz of an LPDA with τ of 0.89 and σ of 0.04. Squares: just a stub to eliminate a weakness; Triangles: with a stub and circularized elements, and Circles: with a stub, circularized elements and a parasitic director.

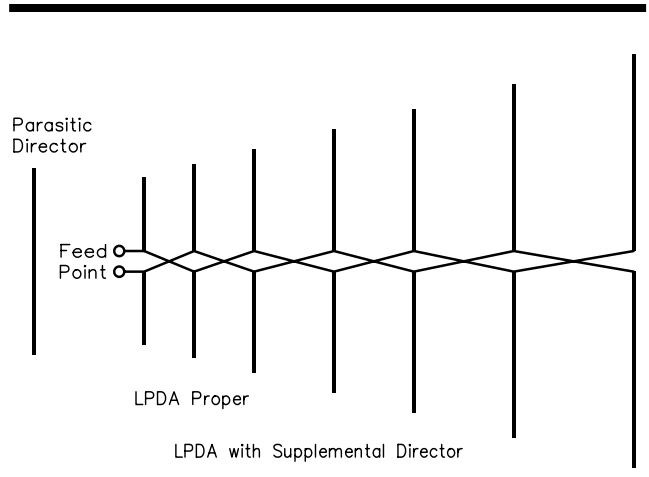

Fig 12—A generalized sketch of an LPDA with the addition of a parasitic director to improve performance at the higher frequencies within the design range.

frequencies within the LPDA design range. It has a perceptible effect almost all the way across the frequency span of the array, although the effect is smallest at the low-frequency end of the range.

The addition of a director can be used to enhance upper frequency performance of an LPDA, as in the illustration, or simply to equalize upper frequency performance with mid-range performance. High-τ designs, with good low-frequency performance, may need only a director to compensate for high-frequency gain decrease. One potential challenge to adding a director to an LPDA is sustaining a high front-to-back ratio at the upper frequency range.

Throughout the discussion of LPDAs, the performance curves of sample designs have been treated at all frequencies alike, seeking maximum performance across the entire design frequency span. Special compensations are also possible for ham-band-only LPDA designs. They include the insertion of parasitic elements within the array as well as outside the initial design boundaries. In addition, stubs may be employed not so much to eliminate weaknesses, but only to move them to frequencies outside the range of amateur interests.

A DESIGN PROCEDURE FOR AN LPDA

The following presents a systematic step-by-step design procedure for an LPDA with any desired bandwidth. The procedure requires some mathematical calculations, but a common calculator with square-root, logarithmic, and trigonometric functions is completely adequate. The notation used in this section may vary slightly from that used earlier in this chapter.

1) Decide on an operating bandwidth B between f_1, lowest frequency and f_n, highest frequency:

$$B = \frac{f_n}{f_1} \qquad \text{(Eq 6)}$$

2) Choose τ and σ to give the desired estimated average gain.

$$0.8 \le \tau \le 0.98 \text{ and } 0.03 \le \sigma \le \sigma_{opt} \qquad \text{(Eq 7)}$$

where σ_{opt} is calculated as noted earlier in this chapter.

3)Determine the value for the cotangent of the apex half-angle α from

$$\cot \alpha = \frac{4\sigma}{1-\tau} \qquad \text{(Eq 8)}$$

Although α is not directly used in the calculations, cot α is used extensively.

4) Determine the bandwidth of the active region B_{ar} from

$$B_{ar} = 1.1 + 7.7(1-\tau)^2 \cot \alpha \qquad \text{(Eq 9)}$$

5) Determine the structure (array) bandwidth B_s from

$$B_S = B \times B_{ar} \qquad \text{(Eq 10)}$$

6) Determine the boom length L, number of elements N, and longest element length ℓ_1.

$$L_n = \left(1 - \frac{1}{B_S}\right) \cot \alpha \times \frac{\lambda_{max}}{4} \qquad \text{(Eq 11)}$$

$$\lambda_{max} = \frac{984}{f_1} \qquad \text{(Eq 12)}$$

$$N = 1 + \frac{\log B_s}{\log \frac{1}{\tau}} = 1 + \frac{\ln B_S}{\ln \frac{1}{\tau}} \qquad \text{(Eq 13)}$$

$$\lambda_{1ft} = \frac{492}{f_1} \qquad \text{(Eq 14)}$$

Usually the calculated value for N will not be an integral number of elements. If the fractional value is more than about 0.3, increase the value of N to the next higher integer. Increasing the value of N will also increase the actual value of L over that obtained from the sequence of calculations just performed.

Examine L, N and l_1 to determine whether or not the array size is acceptable for your needs. If the array is too large, increase f_1 or decrease σ or τ and repeat steps 2 through 6. Increasing f_1 will decrease all dimensions. Decreasing σ will decrease the boom length. Decreasing τ will decrease both the boom length and the number of elements.

7) Determine the terminating stub Z_t. (Note: For many HF arrays, you may omit the stub, short out the longest element with a 6-inch jumper, or design a stub to overcome a specific performance weakness.) For VHF and UHF arrays calculate the stub length from

$$Z_t = \frac{\lambda_{max}}{8} \qquad \text{(Eq 15)}$$

8) Solve for the remaining element lengths from

$$\ell_n = \tau \, \ell_{n-1} \qquad \text{(Eq 16)}$$

9) Determine the element spacing d_{1-2} from

$$d_{1-2} = \frac{(\ell_1 - \ell_2)\cot \alpha}{2} \qquad \text{(Eq 17)}$$

where ℓ_1 and ℓ_2 are the lengths of the rearmost elements, and d_{1-2} is the distance between the elements with the lengths ℓ_1 and ℓ_2. Determine the remaining element-to-element spacings from

$$d_{(n-1)-n} = \tau \, d_{(n-2)-(n-1)} \qquad \text{(Eq 18)}$$

10) Choose R_0, the desired feed-point resistance, to give the lowest SWR for the intended balun ratio and feedline impedance. R_0, the mean radiation resistance level of the LPDA input impedance, is approximated by:

$$R_0 = \frac{Z_0}{\sqrt{1 + \frac{Z_0}{4\sigma' Z_{AV}}}} \qquad \text{(Eq 19)}$$

where the component terms are defined and/or calculated in the following way.

From the following equations, determine the necessary antenna feeder (phase-line) impedance, Z_0:

$$Z_0 = \frac{{R_0}^2}{8\sigma' Z_{AV}} + R_0 \sqrt{\left(\frac{R_0}{8\sigma' Z_{AV}}\right)^2 + 1} \qquad \text{(Eq 20)}$$

σ' is the mean spacing factor and is given by

$$\sigma' = \frac{\sigma}{\sqrt{\tau}} \qquad \text{(Eq 21)}$$

Z_{AV} is the average characteristic impedance of a dipole and is given by

$$Z_{AV} = 120\left[1n\left(\frac{\ell_n}{diam_n}\right) - 2.25\right] \qquad \text{(Eq 22)}$$

The ratio, $l_n/diam_n$ is the length-to-diameter ratio of the element n.

11) Once Z_0 has been determined, select a combination of conductor size and spacing to achieve that impedance, using the appropriate equation for the shape of the conductors. If an impractical spacing results for the antenna feeder, select a different conductor diameter and repeat step 11. In severe cases it may be necessary to select a different R_0 and repeat steps 10 and 11. Once a satisfactory feeder arrangement is found, the LPDA design is complete.

A number of the LPDA design examples at the end of this chapter make use of this calculation method. However, the resultant design should be subjected to extensive modeling tests to determine whether there are performance deficiencies or weaknesses that require modification of the design before actual construction.

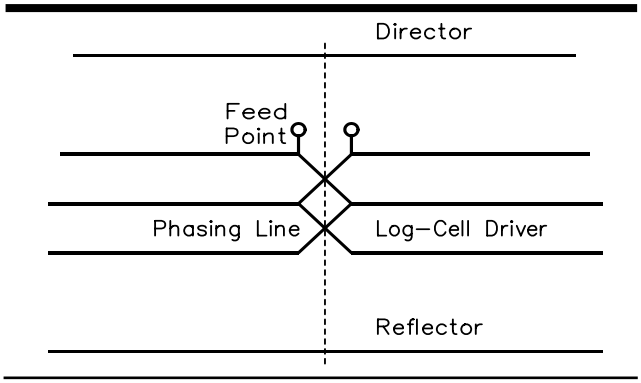

Fig 13—A sketch of a typical monoband log-cell Yagi. The reflector is, in principle, optional. The log-cell may have from 2 to 5 (or more elements). There may be one or more directors.

Log-Cell Yagis

Fig 12 showed an LPDA with an added parasitic director. Technically, this converts the original design into a hybrid Log-Yag. However, the term *Log-Yag* (or more generally the *log-cell Yagi*) is normally reserved for monoband designs that employ two or more elements in a single-band LPDA arrangement, together with (usually) a reflector and one or more directors. The aim is to produce a monoband directive array with superior directional qualities over a wider bandwidth than can be obtained from many Yagi-Uda designs. Log-cells have also been successfully used as wide-band driver sections for multiband Yagi beams.

Fig 13 illustrates the general outline of a typical log-cell Yagi. The driver section consists of a log periodic array designed for the confines of a single amateur band or other narrow range of frequencies. The parasitic reflector is usually spaced about 0.085 λ behind the rear element of the log cell, while the parasitic director is normally placed between 0.13 and 0.15 λ ahead of the log cell.

Early log-cell Yagis tended to be casually designed. Most of these designs have inferior performance compared with present-day computer-optimized Yagis of the same boom length. Some were designed by adding one or more parasitic directors to simple phased pairs of elements. Although good performance is possible, the operating bandwidth of these designs is small, suitable only for the so-called WARC bands. However, when the log-cell is designed as a narrowly spaced monoband log periodic array, the operating bandwidth increases dramatically. Operating bandwidth here refers not just to the SWR bandwidth, but also to the gain and front-to-back bandwidth.

The widest operating bandwidths require log cells of 3 to 4 elements for HF bands like 20 meters, and 4 to 5 elements for bands as wide as 10 meters. (The bandwidth of the 20-meter band is approximately 2.4% of the center frequency, while the bandwidth of the 10-meter band approaches 9.4% of the center frequency.) A practical limit to σ for log cells used within parasitic arrays is about 0.05. Slightly higher gain may be obtained from higher values of σ, but at the cost of a much longer log cell. The limiting figure for σ results in a practical value for τ between 0.94 and 0.95 to achieve a cell with the desired bandwidth characteristics.

An array designed according to these principles has an overall length that varies with the size of the log cell. A typical array with a 4-element log-cell and single parasitic elements fore and aft is a bit over 0.35 λ long, while a 5-element log-cell Yagi will be between 0.4 and 0.45 λ long. Spacing the reflector more widely (for example, up

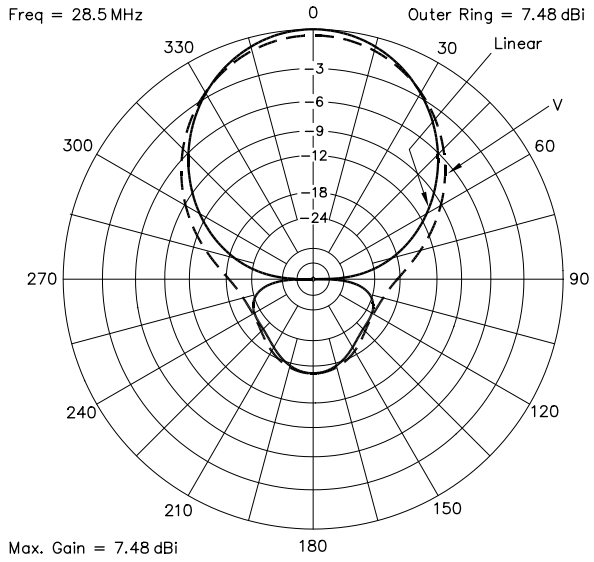

Fig 14—Overlaid free-space azimuth patterns for virtually identical 5-element log-cell Yagis (with 3-element log-cells), one having the elements V'd forward at 40° from linear (dashed), the other with linear elements (solid).

to 0.25 λ) has little effect on either gain or front-to-back ratio. Wider spacing of the director will also have only a small effect on gain, since the arrangement is already close to the boom-length limit recommended for director-driver-reflector arrays. Further lengthening of the boom should be accompanied by the addition of one or more directors to the array, if additional gain is desired from the design.

Compared to a modern-day Yagi of the same boom length, the log-cell Yagi is considerably heavier and exhibits a higher wind load due to the requirements of the log-cell driver. Yagis with 3- and 4-elements within the boom lengths just given are capable of peak free-space gain values of 8.2 to 8.5 dBi, while sustaining a high front-to-back ratio. Peak front-to-back ratios are typically in the vicinity of 25 dB. However, Yagi gain tends to decrease below the design frequency (and increase above it), while the front-to-back ratio tends to taper off as one moves away from the design frequency. For the largest log-cell sizes, log-cell Yagis of the indicated boom lengths are capable of sustaining at least 8.2 dBi free-space gain over the entire band, with front-to-back ratios of over 30 dB across the operating bandwidth.

The feed-point impedance of a log-cell Yagi is a function of both the cell design and the influence of the parasitic elements. However, for most cell designs and common phase-line designs, you can achieve a very low variation of resistance and reactance across a desired band. In many cases, the feed impedance will form a direct match for the standard 50-Ω coaxial cable used by most amateur installations. (In contrast, the high-gain, high-front-to-back Yagis used for comparison here have feed-point impedances ranging from 20 to 25 Ω.)

A common design technique used in some LPDA and log-cell Yagi designs is to bend the elements forward to form a series of Vs. A forward angle on each side of the array centerline of about 40° relative to a linear element has been popular. In some instances, the mechanical design of the array may dictate this element formation. However, this arrangement has no special benefits and possibly may degrade performance.

Fig 14 shows the free-space azimuth patterns of a single 5-element log-cell Yagi in two versions: with the elements linear and with the elements bent forward 40°. The V-array loses about $^1/_2$ dB gain, but more significantly, it loses considerable signal rejection from the sides. Similar comparisons can be obtained from pure LPDA designs and from Yagi-Uda designs when using elements in the vicinity of $^1/_2$ λ. Unless mechanical considerations call for arranging the elements in a V, the technique is not recommended.

Ultimately, the decision to build and use a log-cell Yagi involves balancing the additional weight and wind-load requirements of this design against the improvements in operating bandwidth for all of the major operating parameters, especially with respect to the front-to-back ratio and the feed-point impedance.

Wire Log-Periodic Dipole Arrays for 3.5 or 7 MHz

These wire log-periodic dipole arrays for the lower HF bands are simple in design and easy to build. They are designed to have reasonable gain, be inexpensive and lightweight, and may be assembled with stock items found in large hardware stores. They are also strong—they can withstand a hurricane! These antennas were first described by John J. Uhl, KV5E, in *QST* for August, 1986. **Fig 15** shows one method of installation. You can use the information here as a guide and point of reference for building similar LPDAs.

If space is available, the antennas can be rotated or repositioned in azimuth after they are completed. A 75-foot tower and a clear turning radius of 120 feet around the base of the tower are needed. The task is simplified

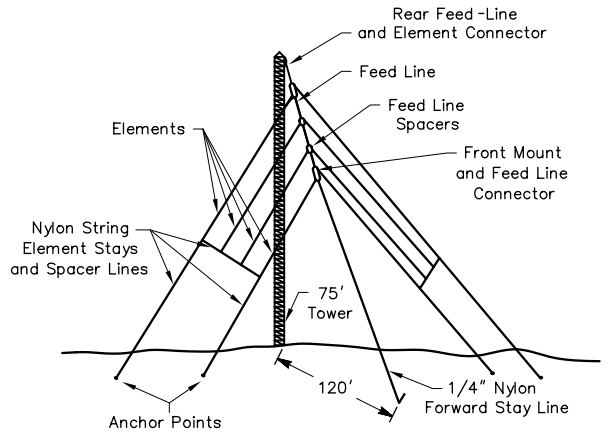

Fig 15—Typical lower-HF wire 4-element log periodic dipole array erected on a tower.

if you use only three anchor points, instead of the five shown in Fig 15. Omit the two anchor points on the forward element, and extend the two nylon strings used for element stays all the way to the forward stay line.

DESIGN OF THE LOG-PERIODIC DIPOLE ARRAYS

Design constants for the two arrays are listed in **Tables 1** and **2**. The preceding sections of this chapter contain the design procedure for arriving at the dimensions and other parameters of these arrays. The primary differences between these designs and one-octave upper HF arrays are the narrower frequency ranges and the use of wire, rather than tubing, for the elements. As design examples for the LPDA, you may wish to work through the step-by-step procedure and check your results against the values in Tables 1 and 2. You may also wish to compare these results with the output of an LPDA design software package such as *LPCAD28*.

From the design procedure, the feeder wire spacings for the two arrays are slightly different, 0.58 inch for the 3.5-MHz array and 0.66 inch for the 7-MHz version. As a compromise toward the use of common spacers for both bands, a spacing of $^5/_8$ inch is quite satisfactory. Surprisingly, the feeder spacing is not at all critical here from a matching standpoint, as may be verified from Z_0 = 276 log (2S/diam) and from Eq 4. Increasing the spacing to as much as $^3/_4$ inch results in an R_0 SWR of less than 1.1:1 on both bands.

Constructing the Arrays

Construction techniques are the same for both the 3.5 and the 7-MHz versions of the array. Once the designs are completed, the next step is to fabricate the fittings; see **Fig 16** for details. Cut the wire elements and feed lines to the proper sizes and mark them for identification. After the wires are cut and placed aside, it will be difficult to remember which is which unless they are marked. When you have finished fabricating the connectors and cutting all of the wires, the antenna can be assembled. Use your ingenuity when building one of these antennas; it isn't necessary to duplicate these LPDAs precisely.

The elements are made of standard #14 stranded cop-

Table 1
Design Parameters for the 3.5-MHz Single-Band LPDA

f1 = 3.3 MHz	Element lengths:
f_n = 4.1 MHz	ℓ1 = 149.091 feet
B = 1.2424	ℓ2 = 125.982 feet
τ = 0.845	ℓ3 = 106.455 feet
σ = 0.06	ℓ4 = 89.954 feet
Gain = 5.9 dBi = 3.8 dBd	Element spacings:
cot α = 1.5484	d_{12}=17.891 feet
B_{ar} = 1.3864	d_{23} = 15.118 feet
B_s = 1.7225	d_{34} = 12.775 feet
L = 48.42 feet	Element diameters
N = 4.23 elements (decrease to 4)	All = 0.0641 inches
Zt = 6-inch short jumper	ℓ/diameter ratios:
R_0 = 208 Ω	ℓ/$diam_4$ = 16840
Z_{AV} = 897.8 Ω	ℓ/$diam_3$ = 19929
σ' = 0.06527	ℓ/$diam_2$ = 23585
Z_0 = 319.8 Ω	ℓ/$diam_1$ = 27911
Antenna feeder:	
#12 wire spaced 0.58 inches	
Balun: 4:1	
Feed line: 52-Ω coax	

Table 2
Design Parameters for the 7-MHz Single-Band LPDA

f1 = 6.9 MHz	Element lengths:
f_n = 7.5 MHz	ℓ1 = 71.304 feet
B = 1.0870	ℓ2 = 60.252 feet
τ = 0.845	ℓ3 = 50.913 feet
σ = 0.06	ℓ4 = 43.022 feet
Gain = 5.9 dBi = 3.8 dBd	Element spacings:
cot α = 1.5484	d_{12} = 8.557 feet
B_{ar} = 1.3864	d_{23} = 7.230 feet
B_s = 1.5070	d_{34} = 6.110 feet
L = 18.57 feet	Element diameters:
N = 3.44 elements (increase to 4)	All = 0.0641 inches
Z_t = 6-inch short jumper	ℓ/diameter ratios:
R_0 = 208 Ω	ℓ4/$diam_4$ = 8054
Z_{AV} = 809.3 Ω	ℓ3/$diam_3$ = 9531
σ' = 0.06527	ℓ2/$diam_2$ = 11280
Z_0 = 334.2 Ω	ℓ1/$diam_1$ = 13349
Antenna feeder:	
#12 wire spaced 0.66 inches	
Balun: 4:1	
Feed line: 52-Ω coax	

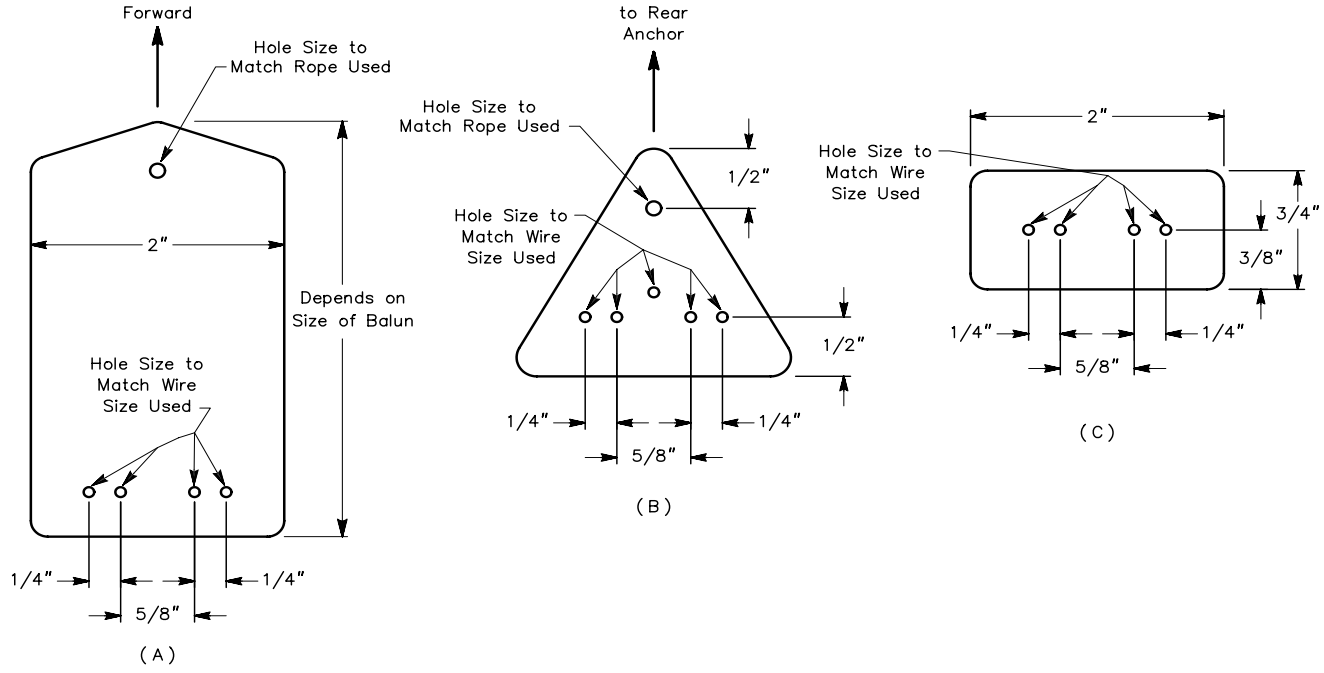

Fig 16—Pieces for the LPDA that require fabrication. At A is the forward connector, made from 1/2-inch Lexan (polycarbonate). At B is the rear connector, also made from 1/2-inch Lexan. At C is the pattern for the phase-line spacers, made from 1/4-inch Plexiglas. Two spacers are required for the array.

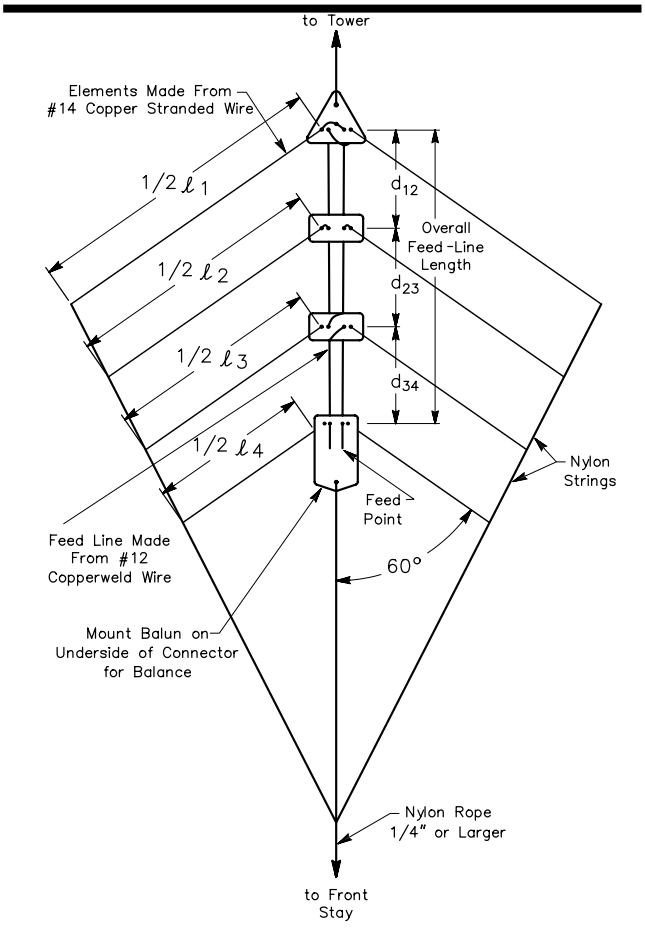

Fig 17—The generic layout for the lower HF wire LPDA. Use a 4:1 balun on the forward connector. See Tables 1 and 2 for dimensions.

per wire. The two parallel feed lines are made of #12 solid copper-coated steel wire, such as Copperweld. Copperweld will not stretch when placed under tension. The front and rear connectors are cut from 1/2-inch thick Lexan sheeting, and the feed-line spacers from 1/4-inch Plexiglas sheeting.

Study the drawings carefully and be familiar with the way the wire elements are connected to the two feed lines, through the front, rear and spacer connectors. Details are sketched in **Figs 17** and **18**. Connections made in the way shown in the drawings prevent the wire from breaking. All of the rope, string, and connectors must be made of materials that can withstand the effects of tension and weathering. Use nylon rope and strings, the type that yachtsmen use. Fig 15 shows the front stay rope coming down to ground level at a point 120 feet from the base of a 75-foot tower. Space may not be available for this arrangement in all cases. An alternative installation technique is to put a pulley 40 feet up in a tree and run the front stay rope through the pulley and down to ground level at the base of the tree. The front stay rope will have to be tightened with a block and tackle at ground level.

Putting an LPDA together is not difficult if it is assembled in an orderly manner. It is easier to connect the elements to the feeder lines when the feed-line

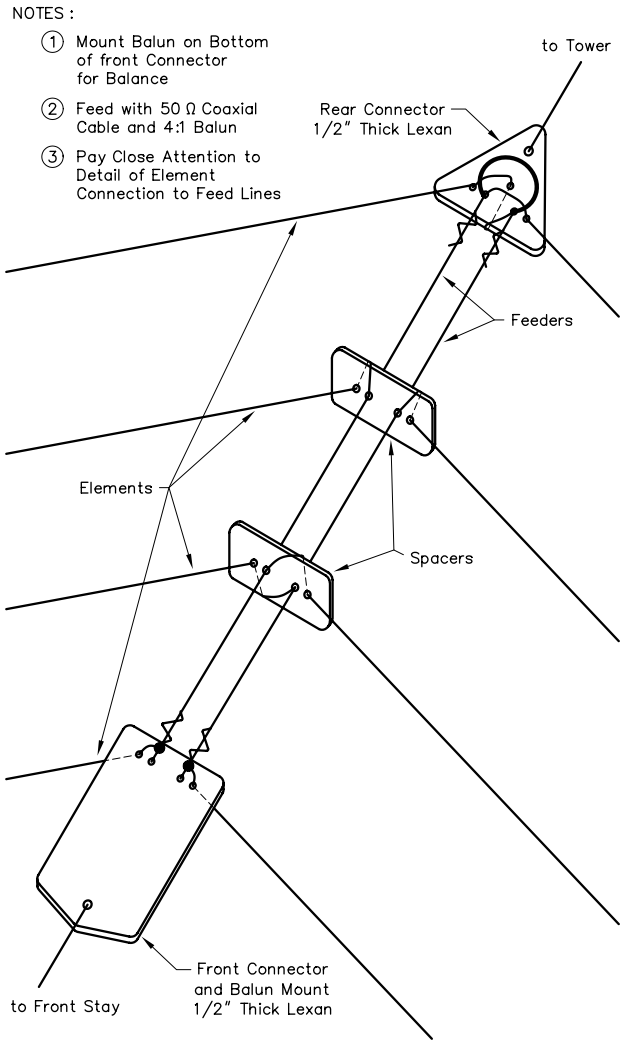

Fig 18—Details of the electrical and mechanical connections of the elements to the phase-line. Knots in the nylon rope stay line are not shown.

assembly is stretched between two points. Use the tower and a block and tackle. Attaching the rear connector to the tower and assembling the LPDA at the base of the tower makes raising the antenna into place a much simpler task. Tie the rear connector securely to the base of the tower and attach the two feeder lines to it. Then thread the two feed-line spacers onto the feed line. The spacers will be loose at this time, but will be positioned properly when the elements are connected. Now connect the front connector to the feed lines. A word of caution: Measure accurately and carefully! Double-check all measurements before you make permanent connections.

Connect the elements to the feeder lines through their respective plastic connectors, beginning with element 1, then element 2, and so on. Keep all of the element wires securely coiled. If they unravel, you will have a tangled mess of kinked wire. Recheck the element-to-feeder connections to ensure proper and secure junctions. (See Figs 17 and 18.) Once you have completed all of the element connections, attach the 4:1 balun to the underside of the front connector. Connect the feeder lines and the coaxial cable to the balun.

You will need a separate piece of rope and a pulley to raise the completed LPDA into position. First secure the eight element ends with nylon string, referring to Figs 15 and 17. The string must be long enough to reach the tie-down points. Connect the front stay rope to the front connector, and the completed LPDA is now ready to be raised into position. While raising the antenna, uncoil the element wires to prevent their getting away and tangling up into a mess. Use care! Raise the rear connector to the proper height and attach it securely to the tower, then pull the front stay rope tight and secure it. Move the elements so they form a 60° angle with the feed lines, in the direction of the front, and space them properly relative to one another. By adjusting the end positions of the elements as you walk back and forth, you will be able to align all the elements properly. Now it is time to hook your rig to the system and make some contacts.

Performance

The reports received from these LPDAs were compared with an inverted-V dipole. All of the antennas are fixed; the LPDAs radiate to the northeast, and the dipole to the northeast and southwest. The apex of the dipole is at 70 feet, and the 40- and 80-meter LPDAs are at 60 and 50 feet, respectively. Basic array gain was apparent from many of the reports received. During pileups, it was possible to break in with a few tries on the LPDAs, yet it was impossible to break in the same pileups using the dipole. The gain of the LPDAs is several dB over the dipole. For additional gain, experimenters may wish to try a parasitic director about $^1/_8\ \lambda$ ahead of the array. Director length and spacing from the forward LPDA element should be field-adjusted for maximum performance while maintaining the impedance match across each of the bands.

Wire LPDA systems offer many possibilities. They are easy to design and to construct: real advantages in countries where commercially built antennas and parts are not available at reasonable cost. The wire needed can be obtained in all parts of the world, and cost of construction is low. If damaged, the LPDAs can be repaired easily with pliers and solder. For those who travel on DXpeditions where space and weight are large considerations, LPDAs are lightweight but sturdy, and they perform well.

5-Band Log Periodic Dipole Array

A rotatable log periodic array designed to cover the frequency range from 13 to 30 MHz is pictured in **Fig 19**. This is a large array having a free-space gain that varies from 6.6 to over 6.9 dBi, depending upon the operating portion of the design spectrum. This antenna system was originally described by Peter D. Rhodes, WA4JVE, in Nov 1973 *QST*. A measured radiation pattern for the array appears in **Fig 20**.

The characteristics of this array are:

1) Half-power beamwidth, 43° (14 MHz)
2) Design parameter $\tau = 0.9$
3) Relative element spacing constant $\sigma = 0.05$
4) Boom length, L = 26 feet
5) Longest element $\lambda 1$ = 37 feet 10 inches. (A tabulation

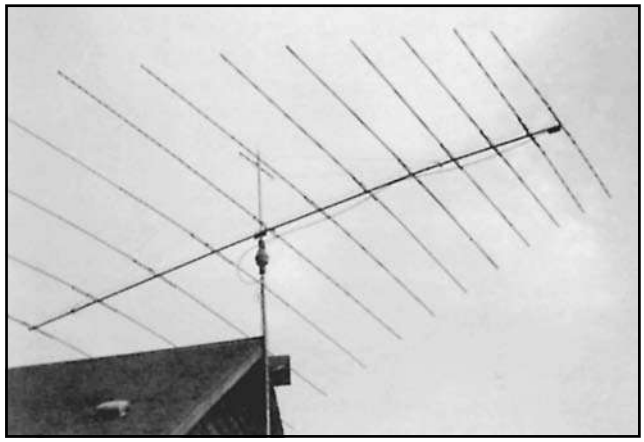

Fig 19—The 13-30 MHz log periodic dipole array.

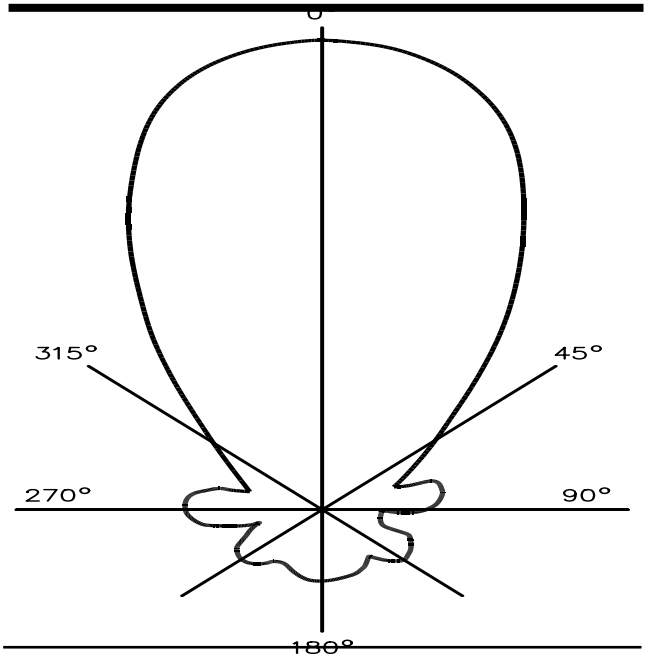

Fig 20—Measured radiation pattern of the 13-30 MHz LPDA. The front-to-back ratio is about 14 dB at 14 MHz and increases to 21 dB at 28 MHz.

Table 3
13-30 MHz LPDA Dimensions, feet

Ele. No.	*Length*	*$d_{n-1,n}$ (spacing)*	*Nearest Resonant*
1	37′ 10.2″	—	
2	34′ 0.7″	3′ 9.4″ = d_{12}	14 MHz
3	30′ 7.9″	3′ 4.9″ = d_{23}	
4	27′ 7.1″	3′ 0.8″ = d_{34}	
5	24′ 10.0″	2′ 9.1″ = d_{45}	18 MHz
6	22′ 4.2″	2′ 5.8″ = d_{56}	21 MHz
7	20′ 1.4″	2′ 2.8″ = d_{67}	
8	18′ 1.2″	2′ 0.1″ = d_{78}	24.9 MHz
9	16′ 3.5″	1′ 9.7″ = d_{89}	28 MHz
10	14′ 7.9″	1′ 7.5″ = $d_{9,10}$	
11	13′ 2.4″	1′ 5.6″ = $d_{10,11}$	
12	11′ 10.5″	1′ 3.8″ = $d_{11,12}$	

Table 4
Materials list: 13-30 MHz LPDA

Material Description	*Quantity*
1) Aluminum tubing—0.047″ wall thickness	
1″—12′ or 6′ lengths	126 lineal feet
7/8″—12′ lengths	96 lineal feet
7/8″—6′ or 12′ lengths	66 lineal feet
3/4″—8′ lengths	16 lineal feet
2) Stainless-steel hose clamps—2″ max	48 ea
3) Stainless-steel hose clamps—1 1/4″ max	26 ea
4) TV type U bolts	14 ea
5) U bolts, galv. type	
5/16″ × 1 1/2″	4 ea
1/4″ × 1″	2 ea
6) 1″ ID polyethylene water-service pipe 160 lb/in.^{2} test, approx. 1 1/4″ OD	20 lineal feet
A) 1 1/4″ × 1 1/4 × 1/8″ aluminum Angle—6' lengths	30 lineal feet
B) 1″ × 1/4″ aluminum bar—6′ lengths	12 lineal feet
7) 1 1/4″ top rail of chain-link fence	26 lineal feet
8) 1:1 toroid balun	1 ea
9) 6-32 × 1″ stainless steel screws	24 ea
6-32 stainless steel nuts	48 ea
#6 solder lugs	24 ea
10) #12 copper feeder wire	60 lineal feet
11A) 12″ × 8″ × 1/4″ aluminum plate	1 ea
B) 6″ × 4″ × 1/4″ aluminum plate	1 ea
12A) 3/4″ galv. Pipe	3 lineal feet
B) 1″ galv. pipe-mast	5 lineal feet
13) Galv. guy wire	50 lineal feet
14) 1/4″ × 2″ turnbuckles	4 ea
15) 1/4″ × 1 1/2″ eye bolts	2 ea
16) TV guy clamps and eye bolts	2 ea

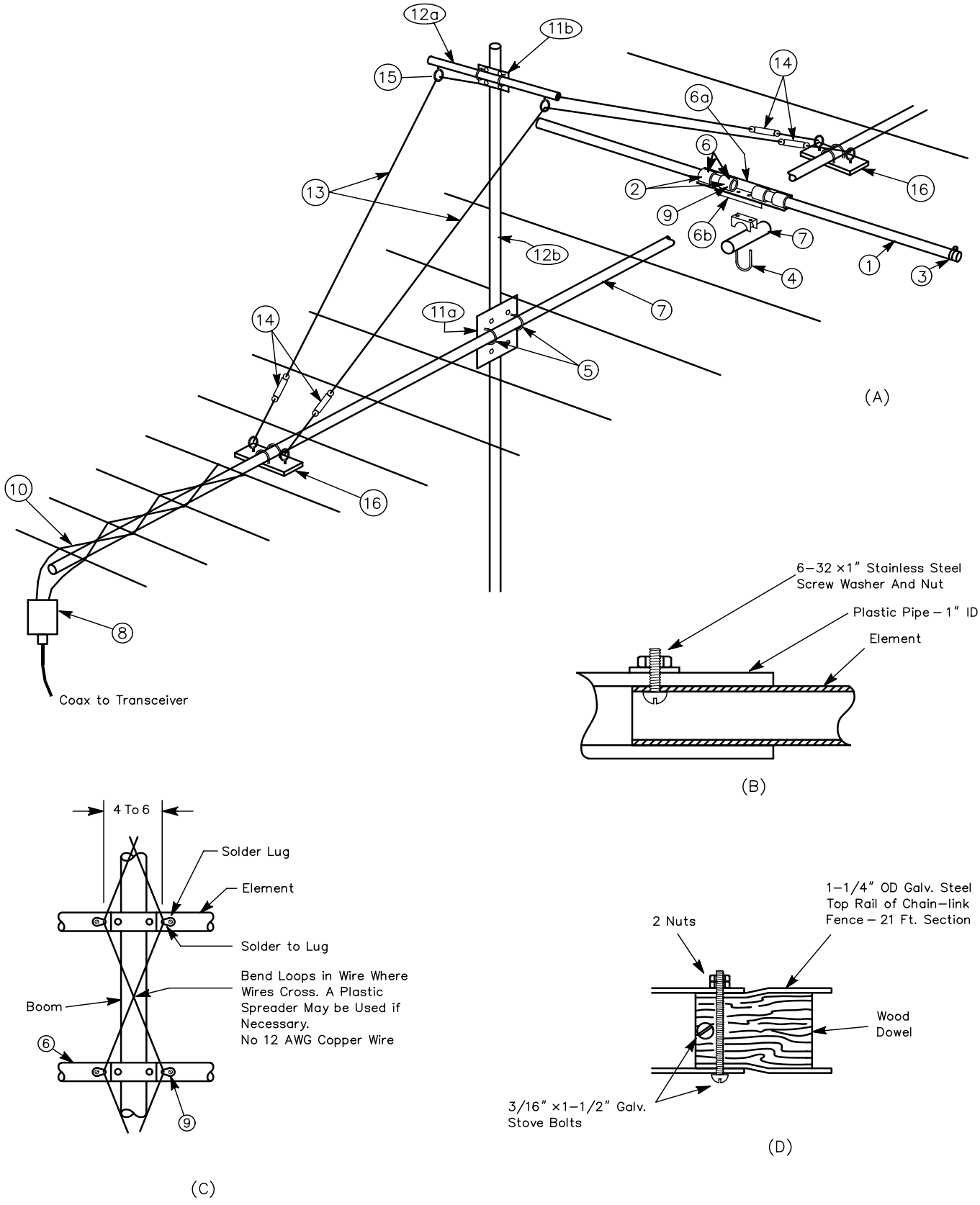

Fig 21—Construction diagrams of the 13-30 MHz LPDA. B and C show the method of making electrical connection between the phase-line and each half-element. D shows how the boom sections are joined.

Table 5
Element Material Requirements: 13-30 MHz LPDA

Ele. No.	1″ Tubing		7/8″ Tubing		3/4″ Tubing		1 1/4″ Angle	1″ Bar
	Len.	Qty	Len.	Qty	Len.	Qty	Len.	Len.
1	6′	2	6′	2	8′	2	3′	1′
2	6′	2	12′	2	—	—	3′	1′
3	6′	2	12′	2	—	—	3′	1′
4	6′	2	8.5′	2	—	—	3′	1′
5	6′	2	7′	2	—	—	3′	1′
6	6′	2	6′	2	—	—	3′	1′
7	6′	2	5′	2	—	—	2′	1′
8	6′	2	3.5′	2	—	—	2′	1′
9	6′	2	2.5′	2	—	—	2′	1′
10	3′	2	5′	2	—	—	2′	1′
11	3′	2	4′	2	—	—	2′	1′
12	3′	2	4′	2	—	—	2′	1′

of element lengths and spacings appears in **Table 3**.)
6) Total weight, 116 pounds
7) Wind-load area, 10.7 square feet
8) Required input impedance (mean resistance), R_0 = 72 Ω, Z_t = 6-inch jumper #18 wire
9) Average characteristic dipole impedance, Z_{AV}: 337.8 Ω
10) Impedance of the feeder, Z_0: 117.1 Ω
11) Feeder: #12 wire, close spaced
12) With a 1:1 toroid balun at the input terminals and a 72-Ω coax feed line, the maximum SWR is 1.4:1.

The mechanical assembly uses materials readily available from most local hardware stores or aluminum supply houses. The materials needed are given in **Table 4**. In the construction diagram, **Fig 21**, the materials are referenced by their respective material list numbers. The photograph shows the overall construction, and the drawings show the details. **Table 5** gives the required tubing lengths to construct the elements.

Experimenters may wish to improve the performance of the array at both the upper and lower frequency ends of the design spectrum so that it more closely approaches the performance in the middle of the design frequency range. The most apt general technique for raising both the gain and the front-to-back ratio at the frequency extremes would be to circularize τ as described earlier in this chapter. However, other techniques may also be applied.

The Telerana

The Telerana (Spanish for *spider web*) is a rotatable log periodic antenna that is lightweight, easy to construct and relatively inexpensive to build. Designed to cover 12.1 to 30 MHz, it was co-designed by George Smith, W4AEO, and Ansyl Eckols, YV5DLT, and first described by Eckols in *QST* for Jul 1981. Some of the design parameters are as follow.
1) τ = 0.9
2) σ = 0.05
3) Gain = 4.5 to 5.5 dBi (free-space) depending upon frequency
4) Feed arrangement: 400-Ω feeder line with 4:1 balun, fed with 52-Ω coax. The SWR is 1.5:1 or less in all amateur bands.

The array consists of 13 dipole elements, properly spaced and transposed, along an open wire feeder having an impedance of approximately 400 Ω. See **Figs 22** and **23**. The array is fed at the forward (smallest) end with a 4:1 balun and RG-8 cable placed inside the front arm and leading to the transmitter. An alternative feed method is to use open wire or ordinary TV ribbon and a tuner, eliminating the balun.

The frame that supports the array (**Fig 24**) consists of four 15-foot fiberglass vaulting poles slipped over short nipples at the hub, appearing like wheel spokes (**Fig 25**). Instead of being mounted directly into the fiberglass, the hub mounts into short metal tubing sleeves that are inserted into the ends of each arm to prevent crushing and splitting the fiberglass. The necessary holes are drilled to receive the wires and nylon.

A shopping list is provided in **Table 6**. The center hub is made from a 1 1/4-inch galvanized four-outlet cross or X and four 8-inch nipples (Fig 25). A 1-inch diameter X may be used alternatively, depending on the diameter of the fiberglass. A hole is drilled in the bottom of the hub to allow the cable to be passed through after welding the hub to the rotator mounting stub.

All four arms of the array must be 15 feet long. They should be strong and springy to maintain the tautness of the array. If vaulting poles are used, try to obtain all of them with identical strength ratings.

The forward spreader should be approximately 14.8 feet long. It can be much lighter than the four main arms, but must be strong enough to keep the lines rigid.

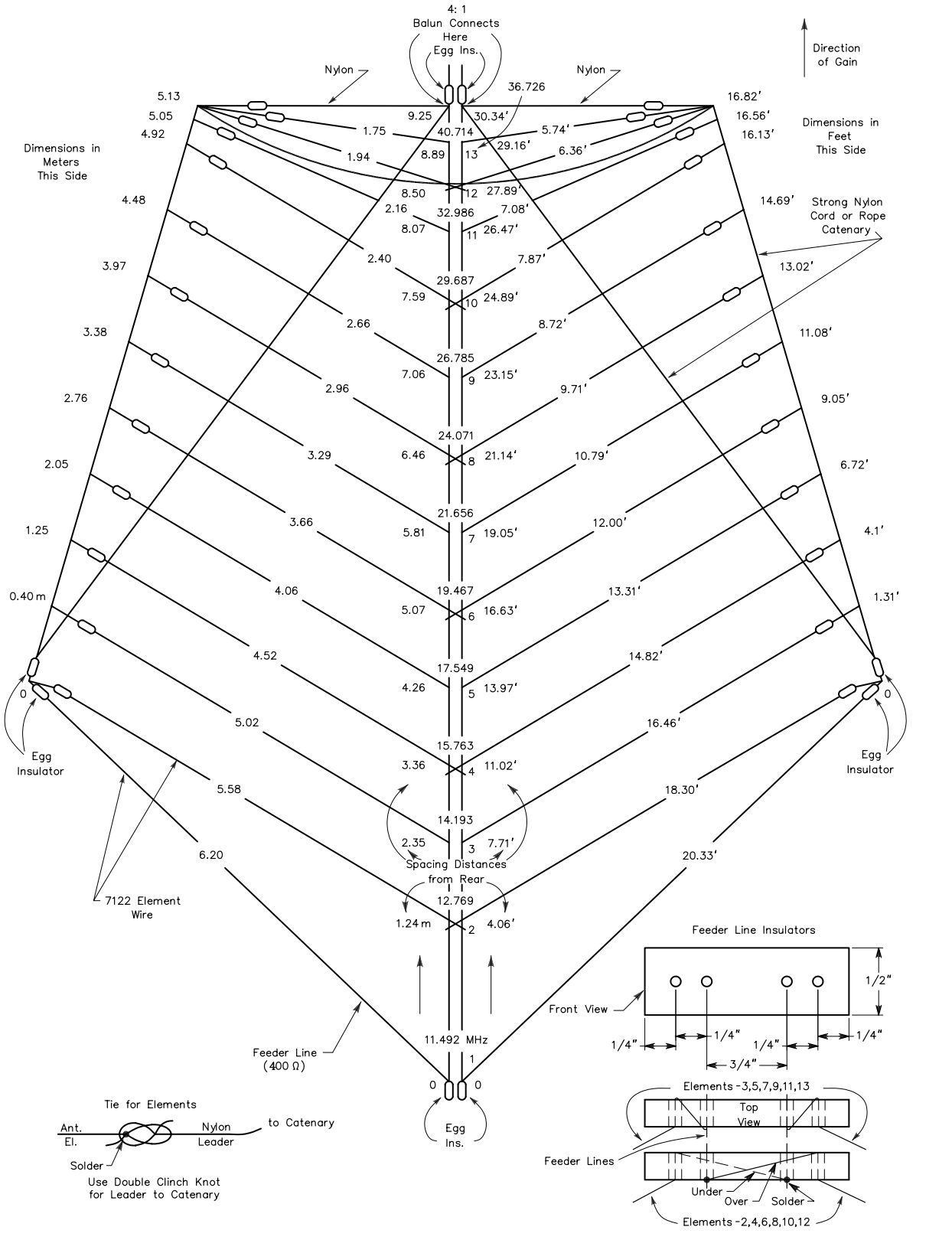

Fig 22—The overall configuration of the spider web antenna. Nylon monofilament line is used from the ends of the elements to the nylon cords. Use nylon line to tie every point where lines cross. The forward fiberglass feeder lies on the feeder line and is tied to it. Both metric and English measurements are shown, except for the illustration of the feed-line insulator. Use soft-drawn copper or stranded wire for elements 2 through 12. Element 1 should use 7/22 flexible wire or #14 AWG Copperweld.

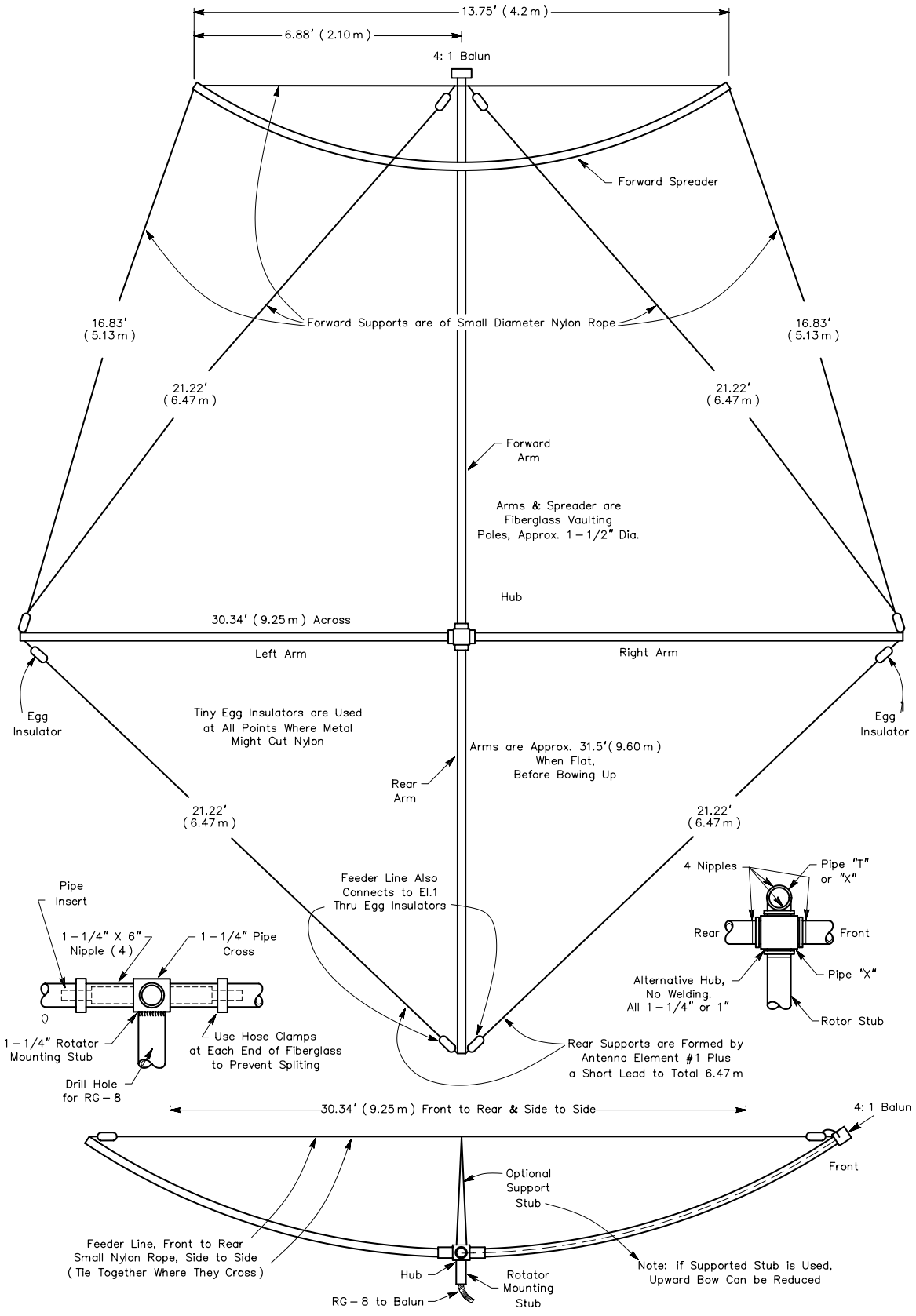

Fig 23—The frame construction of the spider web antenna. Two different hub arrangements are illustrated.

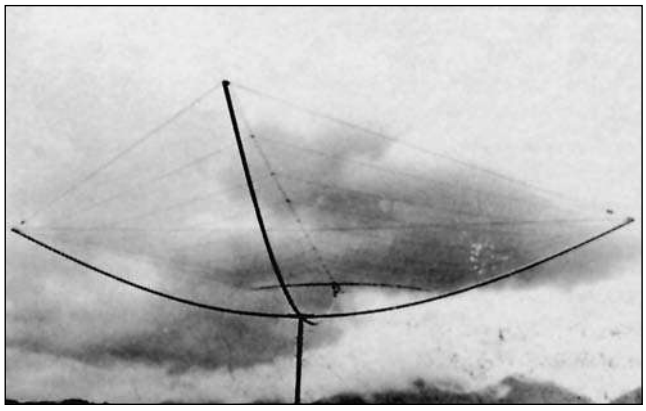

Fig 24—Although the spider web antenna resembles a rotatable clothes line, it is much larger, as indicated by Figs 22 and 23. However, the antenna can be lifted by hand.

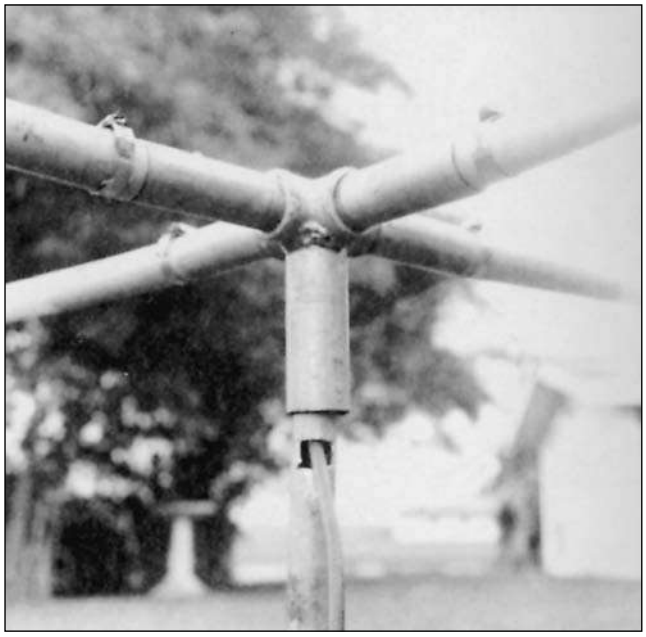

Fig 25—The simple arrangement of the spider web antenna hub. See Fig 23 and the text for details.

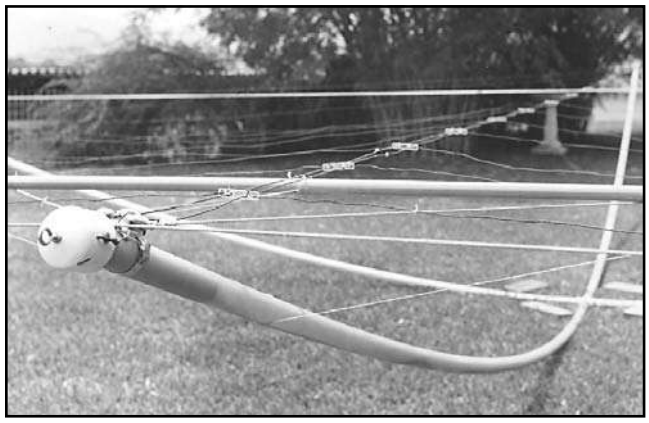

Fig 26—The elements, balun, transmission line and main bow of the spider web antenna.

Table 6
Shopping List for the Telerana

1—1 1/4-inch galvanized, 4-outlet cross or X.
4—8-inch nipples.
4—15-foot long arms. Vaulting poles suggested. These must be strong and all of the same strength (150 lb) or better.
1—Spreader, 14.8 foot long (must not be metal).
1—4:1 balun unless open-wire or TV cable is used.
12—Feed-line insulators made from Plexiglas or fiberglass.
36—Small egg insulators.
328 feet copper wire for elements; flexible 7/22 is suggested.
65.6 feet (20 m) #14 Copperweld wire for interelement feed line.
164 feet (50 m) strong 1/8-inch dia cord.
1—Roll of nylon monofilament fishing line, 50 lb test or better.
4—Metal tubing inserts go into the ends of the fiberglass arms.
2—Fiberglass fishing-rod blanks.
4—Hose clamps.

If tapered, the spreader should have the same measurements from the center to each end. *Do not use metal for this spreader*.

Building the frame for the array is the first construction step. Once the frame is prepared, then everything else can be built onto it. Begin by assembling the hub and the four arms, letting them lie flat on the ground with the rotator stub inserted in a hole in the ground. The tip-to-tip length should be about 31.5 feet each way. A hose clamp is used at each end of the arms to prevent splitting. Place the metal inserts in the outer ends of the arms, with 1 inch protruding. The mounting holes should have been drilled at this point. If the egg insulators and nylon cords are mounted to these tube inserts, the whole antenna can be disassembled simply by bending up the arms and pulling out the inserts with everything still attached.

Choose the arm to be at the front end. Mount two egg insulators at the front and rear to accommodate the inter-element feeder. These insulators should be as close as possible to the ends.

At each end of the cross-arm on top, install a small pulley and string nylon cord across and back. Tighten the cord until the upward bow reaches 3 feet above the hub. All cords will require retightening after the first few days because of stretching. The cross-arm can be laid on its side while preparing the feeder line. For the front-to-rear bowstring it is important to use a wire that will not stretch, such as #14 Copperweld. This bowstring is actually the inter-element transmission line. See **Fig 26**.

Secure the rear ends of the feeder to the two rear insulators, soldering the wrap. Before securing the fronts, slip the 12 insulators onto the two feed lines. A rope can be used temporarily to form the bow and to aid in mounting the feeder line. The end-to-end length of the feeder

Improving the Telerana

In *The ARRL Antenna Compendium, Vol 4*, Markus Hansen, VE7CA, described how he modified the Telerana to improve the front-to-back ratio on 20 and 15 meters. In addition, he added a trapped 30/40-meter dipole that functions as a top truss system to stabilize the modified Telerana in strong uprising winds that otherwise could turn the antenna into an "inside-out umbrella."

Fig A shows the layout for the modified Telerana, and Table A lists the lengths and spacings for the #14 wire elements. Note that VE7CA used tuning stubs to tweak the 15 and 20-meter reflector wires for best rearward pattern. The construction techniques used by VE7CA are the same as for the original Telerana. Fig B shows a side view of the additional 40/30-meter-dipole truss sytem.

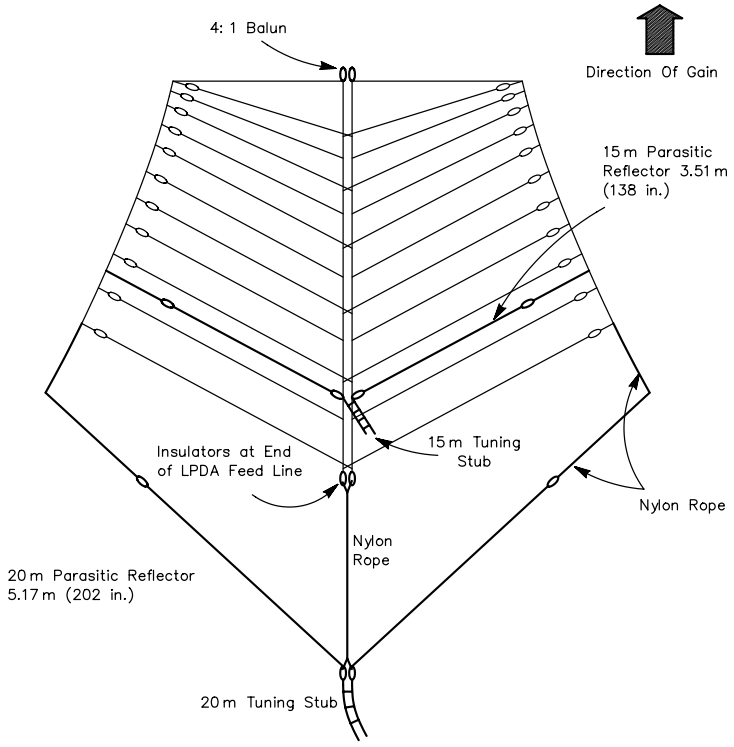

Table A

Element Lengths and Spacings, in Inches

Element Number	*½ Element Length (inches)*	*Total Distance (inches)*
R1	202.0	0.0
L1	210.1	102.0
L2	191.2	140.7
R2	138.0	158.3
L3	174.0	175.9
L4	158.3	207.9
L5	144.1	237.0
L6	131.1	261.5
L7	119.3	285.6
L8	108.6	307.6
L9	98.8	327.6
L10	89.9	345.8
L11	82.4	364.5

Note: the reflector lengths do not include the length of the tuning stubs.

Fig A—Physical layout of modified Telerana with 20 and 15-meter reflectors added (in place of first two elements in original Telerana). Note the tuning stubs for the added reflectors.

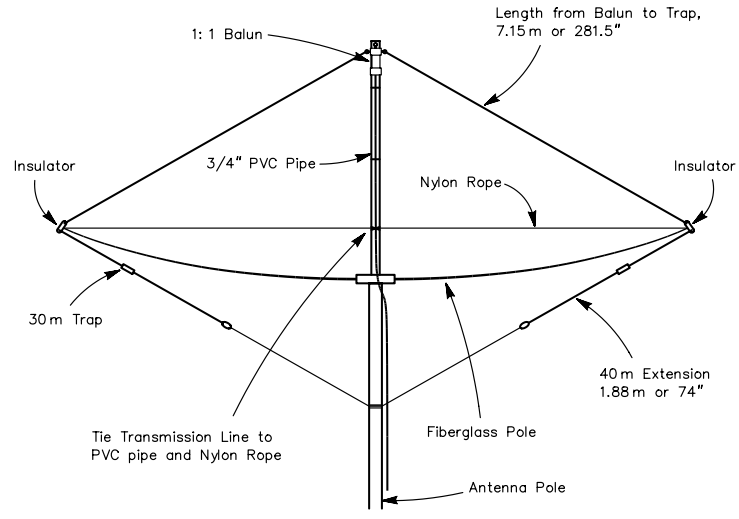

Fig B—Side view of 30/40-meter addition to the modified Telerana, using ¾-inch PVC pipe as a vertical stabilizer and support for the 30/40-meter trapped dipole.

should be 30.24 feet.

Now lift both bows to their upright position and tie the feeder line and the cross-arm bowstring together where they cross, directly over and approximately 3 feet above the hub.

The next step is to install the number 1 rear element from the rear egg insulators to the right and left cross-arms using other egg insulators to provide the proper element length. Be sure to solder the element halves to the transmission line. Complete this portion of the construction by installing the nylon cord catenaries from the front arm to the cross-arm tips. Use egg insulators where needed to prevent cutting the nylon cords.

When preparing the fiberglass forward spreader, keep in mind that it should be 14.75 feet long before bowing and is approximately 13.75 feet across when bowed. Secure the center of the bowstring to the end of the front arm. Lay the spreader on top of the feed line, then tie the feeder to the spreader with nylon fish line. String the catenary from the spreader tips to the cross-arm tips.

At this point of assembly, prepare antenna elements 2 through 13. There will be two segments for each element. At the outer tip make a small loop and solder the wrap. The loop will be for the nylon leader. Measure the length plus 0.4 inch for wrapping and soldering the element segment to the feeder. Seven-strand #22 antenna wire is suggested for the element wires. Slide the feedline insulators to their proper position and secure them temporarily.

The drawings show the necessary transposition scheme. Each element half of elements 1, 3, 5, 7, 9, 11 and 13 is connected to its own side of the feeder, while elements 2, 4, 6, 8, 10 and 12 cross over to the opposite side of the transmission line.

There are four holes in each of the transmission-line insulators (see Fig 22). The inner holes are for the transmission line, and the outer ones are for the elements. Since the array elements are slanted forward, they should pass through the insulator from front to back, then back over the insulator to the front side and be soldered to the transmission line. The small drawings of Fig 22 show the details of the element transpositions.

Everywhere that lines cross, tie them together with nylon line, including all copper-nylon and nylon-nylon junctions. Careful tying makes the array much more rigid. However, all elements should be mounted loosely before you try to align the whole thing. Tightening any line or element affects all the others. There will be plenty of walking back and forth before the array is aligned properly. Expect the array to be firm but not extremely taut.

The Pounder: A Single-Band 144-MHz LPDA

The 4-element Pounder LPDA pictured in **Fig 27** was developed by Jerry Hall, K1TD, for the 144-148 MHz band. Because it started as an experimental antenna, it utilizes some unusual construction techniques. However, it gives a very good account of itself, exhibiting a theoretical free-space gain of about 7.2 dBi and a front-to-back ratio of 20 dB or better. The Pounder is small and light. It weighs just 1 pound, and hence its name. In addition, as may be seen in **Fig 28**, it can be disassembled and reassembled quickly, making it an excellent antenna for portable use. This array also serves well as a fixed-station antenna, and may be changed easily to either vertical or horizontal polarization.

The antenna feeder consists of two lengths of $^1/_2 \times ^1/_2 \times ^1/_{16}$-inch angle aluminum. The use of two facing flat surfaces permits the builder to obtain a lower characteristic impedance than can be obtained from round conductors with the same spacing. The feeder also serves as the boom for the Pounder. In the first experimental model, the array contained only two elements with a spacing of 1 foot, so a boom length of 1 foot was the primary design requirement for the 4-element version. **Table 7** gives the calculated design data for the 4-element array.

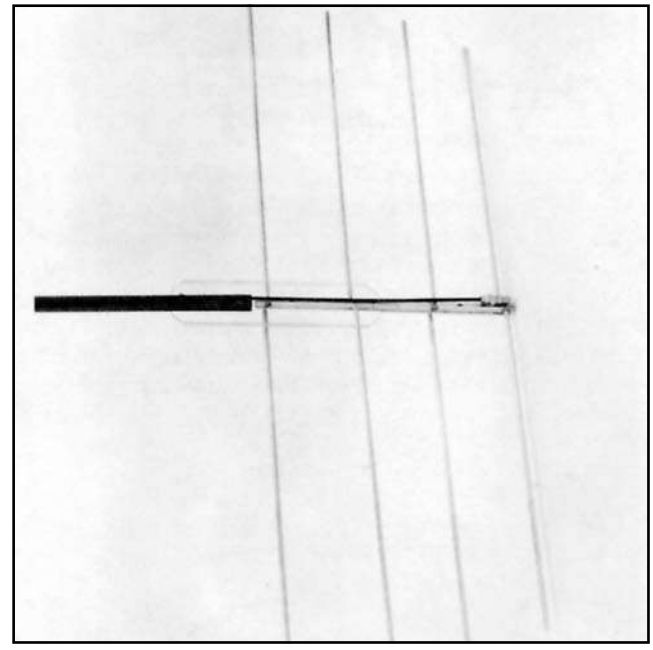

Fig 27—The 144 MHz Pounder. The boom extension at the left of the photo is a 40-inch length of slotted PVC tubing, $^7/_8$-inch outer diameter. The tubing may be clamped to the side of a tower or attached to a mast with a small boom-to-mast plate. Rotating the tubing at the clamp will provide for either vertical or horizontal polarization.

Construction

You can see the general construction approach for

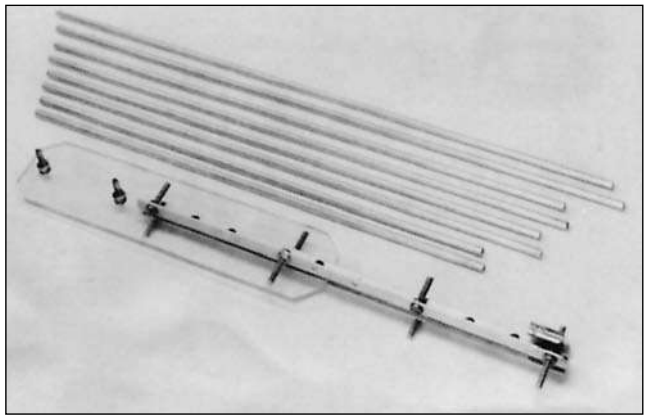

Fig 28—One end of each half element is tapped to fasten onto boom-mounted screws. Disassembly of the array consists of merely unscrewing 8 half elements from the boom. The entire disassembled array creates a small bundle only 21 inches long.

Table 7

Design Parameters for the 144-MHz Pounder

f1 = 143 MHz	Element lengths:
f_n = 148 MHz	ℓ1 = 3.441 feet
B = 1.0350	ℓ2 = 3.165 feet
τ = 0.92	ℓ3 = 2.912 feet
σ = 0.053	ℓ4 = 2.679 feet
Gain = 7.2 dBi = 5.1 dBd	Element spacings:
cot α = 2.6500	d_{12} = 0.365 feet
B_{ar} = 1.2306	d_{23} = 0.336 feet
B_s = 1.2736	d_{34} = 0.309 feet
L = 0.98 feet	Element diameters:
N = 3.90 elements (increase to 4)	All = 0.25 inches
Zt = none	ℓ/diameter ratios:
R_0 = 52 Ω	$\ell 4/diam_4$ = 128.6
Z_{AV} = 312.8 Ω	$\ell 3/diam_3$ = 139.8
σ' = 0.05526	$\ell 2/diam_2$ = 151.9
Z_0 = 75.1 Ω	$\ell 1/diam_1$ = 165.1

Antenna feeder: $^1/_2 \times {}^1/_2 \times {}^1/_{16}$″ angle aluminum spaced $^1/_4$″
Balun: 1:1 (see text)
Feed line: 52-Ω coax (see text)

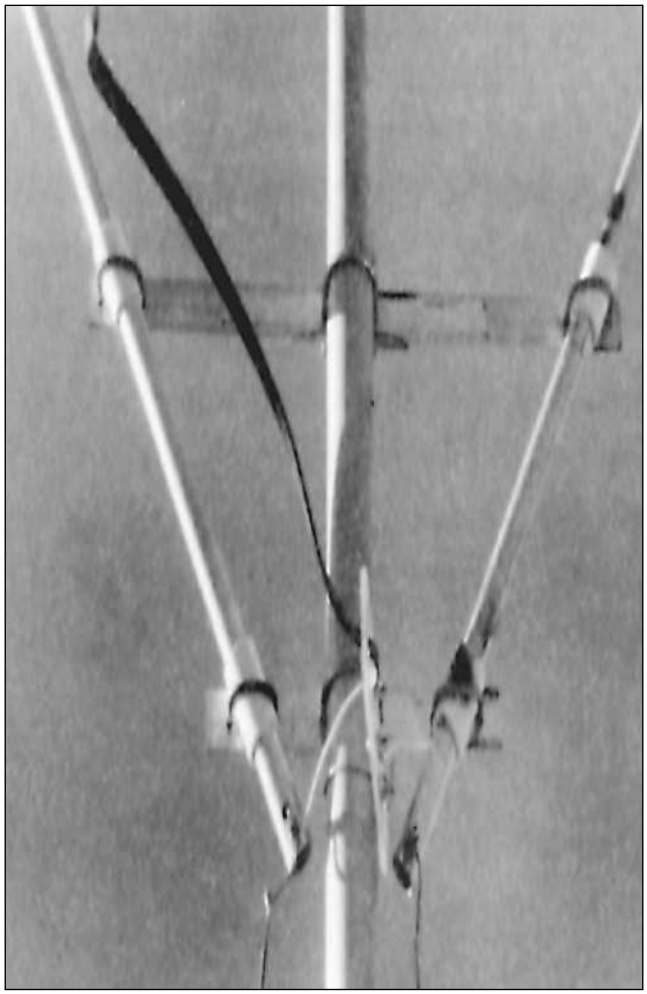

Fig 29—A close-up view of the boom, showing an alternative mounting scheme. This photo shows an earlier 2-element array, but the boom construction is the same for 2 or 4 elements. See the text for details.

Fig 30—The feed arrangement, using a right-angle chassis-mounted BNC connector, modified by removing a portion of the flange. A short length of bus wire connects the center pin to the opposite feeder conductor.

the Pounder in the photographs. Drilled and tapped pieces of Plexiglas sheet, 1/4-inch thick, serve as insulating spacers for the angle aluminum feeder. Two spacers are used, one near the front and one near the rear of the array. Four #6-32 × 1/4-inch pan head screws secure each aluminum angle section to the Plexiglas spacers, as shown in **Figs 29** and **30**. Use flat washers with each screw to prevent it from touching the angle stock on the opposite side of the spacer. Be sure the screws are not so long as to short out the feeder! A clearance of about 1/16 inch is sufficient. If you have doubts about the screw lengths, check the assembled boom for a short with your ohmmeter on a Megohm range.

Either of two mounting techniques may be used for the Pounder. As shown in Figs 27 and 28, the rear spacer measures 10 × 2 1/2 inches, with 45° corners to avoid sharp points. This spacer also accommodates a boom extension of PVC tubing, which is attached with two #10-32 × 1-inch screws. This tubing provides for side mounting the Pounder away from a mast or tower.

An alternative support arrangement is shown in Fig 29. Two 1/2 × 3-inch Plexiglas spacers are used at the front and rear of the array. Each spacer has four holes drilled 5/8 inch apart and tapped with #6-32 threads. Two screws enter each spacer from either side to make a tight aluminum-Plexiglas-aluminum sandwich. At the center of the boom, secured with only two screws, is a 2 × 18-inch strip of 1/4-inch Plexiglas. This strip is slotted about 2 inches from each end to accept hose clamps for mounting the Pounder atop a mast. As shown, the strip is attached for vertical polarization. Alternate mounting holes, visible on the now-horizontal lip of the angle stock, provide for horizontal polarization. Although sufficient, this mounting arrangement is not as sturdy as that shown in Fig 27.

The elements are lengths of thick-wall aluminum tubing, 1/4-inch OD. The inside wall conveniently accepts a #10-32 tap. The threads should penetrate the tubing to a depth of at least 1 inch. Eight #10-32 × 1-inch screws are attached to the boom at the proper element spacings and held in place with #10-32 nuts, as shown in Fig 28. For assembly, the elements are then simply screwed into place.

Note that with this construction arrangement, the two halves of any individual element are not precisely collinear; their axes are offset by about 3/4 inch. This offset does not seem to affect performance.

The Feed Arrangement

Use care initially in mounting and cutting the elements to length. To obtain the 180° crossover feed arrangement, the element halves from a single section of the feeder/boom must alternate directions. That is, for half-elements attached to one of the two pieces of angle stock, elements 1 and 3 will point to one side, and elements 2 and 4 to the other. This arrangement may be seen by observing the element-mounting screws in Fig 28. Because of this mounting scheme, the length of tubing for an element "half" is not simply half of the length given in Table 7. After final assembly, halves for elements 2 and 4 will have a slight overlap, while elements 1 and 3 are extended somewhat by the boom thickness. The best procedure is to cut each assembled element to its final length by measuring from tip to tip.

The Pounder may be fed with RG-58 or RG-59 coax and a BNC connector. A modified right-angle chassis-mount BNC connector is attached to one side of the feeder/boom assembly for cable connection, Fig 30. The modification consists of cutting away part of the mounting flange that would otherwise protrude from the boom assembly. This leaves only two mounting-flange holes, but these are sufficient for a secure mount. A short length of small bus wire connects the center pin to the opposite side of the feeder, where it is secured under the mounting-screw nut for the shortest element.

For operation, you may secure the coax to the PVC boom extension or to the mast with electrical tape. You should use a balun, especially if the Pounder is operated with vertical elements. A choke type of balun is satisfactory, formed by taping 6 turns of the coax into a coil of 3 inches diameter, but a bead balun is preferred (see Chapter 26). The balun should be placed at the point where the coax is brought away from the boom. If the mounting arrangement of Fig 29 is used with vertical polarization, a second balun should be located approximately 1/4 wavelength down the coax line from the first. This will place it at about the level of the lower tips of the elements. For long runs of coax to the transmitter, a transition from RG-58 to RG-8 or from RG-59 to RG-9 is suggested, to reduce line losses. Make this transition at some convenient point near the array.

No shorting feeder termination is used with the array described here. The antenna feeder (phase-line) Z_0 of this array is in the neighborhood of 120 Ω, and with a resulting feed-point impedance of about 72 Ω. The theoretical mean SWR with 52 Ω line is 72/52 or 1.4 to 1. Upon array completion, the measured SWR (52-Ω line) was found to be relatively constant across the band, with a value of about 1.7 to 1. The Pounder offers a better match to 72-Ω coax.

Being an all-driven array, the Pounder is more immune to changes in feed-point impedance caused by nearby objects than is a parasitic array. This became obvious during portable use when the array was operated near trees and other objects… the SWR did not change noticeably with antenna rotation toward and away from those objects. Consequently, the Pounder should behave well in a restricted environment, such as an attic. Weighing just one pound, this array indeed does give a good account of itself.

Log Periodic-Yagi Arrays

Several possibilities exist for constructing high-gain arrays that use the log periodic dipole array concept. One technique is to add parasitic elements to the LPDA to increase both the gain and the front-to-back ratio for a specific frequency within the passband of the LPDA. The LPDA-Yagi combination is simple in concept. It utilizes an LPDA group of driven elements, along with parasitic elements at normal Yagi spacings from the active elements of the LPDA.

The LPDA-Yagi combinations are endless. An example of a single-band high-gain design is a 2- or 3-element LPDA for 21.0 to 21.45 MHz with the addition of two or three parasitic directors and one parasitic reflector. The name Log-Yag (log-cell Yagi) array has been coined for these hybrid antennas. The LPDA portion of the array is of the usual design to cover the desired bandwidth, and standard Yagi design procedures are used for the parasitic elements. Information in this section is based on a Dec 1976, *QST* article by P. D. Rhodes, K4EWG, and J. R. Painter, W4BBP, "The Log-Yag Array."

THE LOG-YAG ARRAY

The Log-Yag array, with its added parasitic elements, provides higher gain and greater directivity than would be realized with the LPDA alone. Yagi arrays require a long boom and wide element spacing for wide bandwidth and high gain, because the Q of the Yagi system increases as the number of elements is increased or as the spacing between adjacent elements is decreased. An increase in the Q of the Yagi array means that the total operating bandwidth of the array is decreased, and the gain and front-to-back ratio specified in the design are obtainable only over small portions of the band. [Older Yagi designs did indeed exhibit the limitations mentioned here. But modern, computer-aided design has resulted in wideband Yagis, provided that sufficient elements are used on the boom to allow stagger tuning for wide-band coverage. See Chapter 11.—*Ed.*]

The Log-Yag system overcomes this difficulty by using a multiple driven element cell designed in accordance with the principles of the log periodic dipole array. Since this log cell exhibits both gain and directivity by itself, it is a more effective wide-band radiator than a simple dipole driven element. The front-to-back ratio and gain of the log cell can then be improved with the addition of a parasitic reflector and director.

It is not necessary for the parasitic element spacings to be large with respect to wavelength, since the log cell is the determining factor in the array bandwidth. As well, the element spacings within the log cell may be small with respect to a wavelength without appreciable deterioration of the cell gain. For example, decreasing the relative spacing constant (σ) from 0.1 to 0.05 will decrease the array gain by less than 1 dB.

A Practical Example

The photographs and figures show a Log-Yag array for the 14-MHz amateur band. The array design takes the form of a 4-element log cell, a parasitic reflector spaced at 0.085 λ_{max}, and a parasitic director spaced at 0.15 λ_{max} (where λ_{max} is the longest free-space wavelength within the array passband). Array gain is almost unaffected with reflector spacings from 0.08 λ to 0.25 λ, and the increase in boom length is not justified. The function of the reflector is to improve the front-to-back ratio of the log cell, while the director sharpens the forward lobe and decreases the half-power beamwidth. As the spacing between the parasitic elements and the log cell decreases, the parasitic elements must increase in length.

The log cell is designed to meet upper and lower band limits with σ = 0.05. The design parameter τ is dependent on the structure bandwidth, B_s. When the log periodic design parameters have been found, the element length and spacings can be determined.

Array layout and construction details can be seen in Figs 31 through 34. Characteristics of the array are given in **Table 8**.

The method of feeding the antenna is identical to that of feeding the log periodic dipole array without the parasitic elements. As shown in **Fig 31**, a balanced feeder is required for each log-cell element, and all adjacent elements are fed with a 180° phase shift by alternating connections. Since the Log-Yag array will be covering a relatively small bandwidth, the radiation resistance of the narrow-band log cell will vary from 80 to 90 Ω (tubing

Table 8
Log-Yag Array Characteristics

1) Frequency range	14 to 14.35 MHz
2) Operating bandwidth	B = 1.025
3) Design parameter	τ = 0.946657
4) Apex half angle	α = 14.921°; cot α = 3.753
5) Half-power beamwidth	42° (14 to 14.35 MHz)
6) Bandwidth of structure	Bs = 1.17875
7) Free-space wavelength	λ_{max} = 70.28 feet
8) Log cell boom length	L = 10.0 feet
9) Longest log element	ℓ1 = 35.14 feet (a tabulation of element lengths and spacings is given in Table 9)
10) Forward gain (free space)	8.2 dBi
11) Front-to-back ratio	32 dB (theoretical)
12) Front-to-side ratio	45 dB (theoretical)
13) Input impedance	Z_0 = 37 Ω
14) SWR	1.3 to 1 (14 to 14.35 MHz)
15) Total weight	96 pounds
16) Wind-load area	8.5 sq feet
17) Reflector length	36.4 feet at 6.0 foot spacing
18) Director length	32.2 feet at 10.5 foot spacing
19) Total boom length	26.5 feet

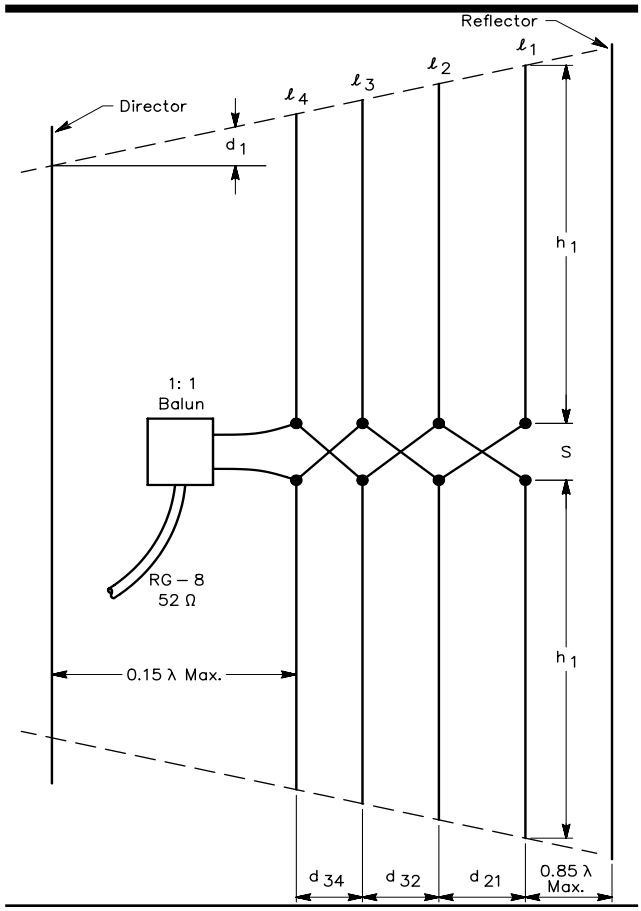

Fig 31—Layout of the Log-Yag array.

Table 9
Log-Yag Array Dimensions

Element	*Length*	*Spacing*
	Feet	*Feet*
Reflector	36.40	6.00 (Ref. to ℓ1)
ℓ1	35.14	3.51 (d_{12})
ℓ2	33.27	3.32 (d_{23})
ℓ3	31.49	3.14 (d_{34})
ℓ4	29.81	10.57 (ℓ4 to dir.)
Director	32.20	

elements) depending on the operating bandwidth. The addition of parasitic elements lowers the log-cell radiation resistance. Hence, it is recommended that a 1:1 balun be connected at the log-cell input terminals and 50-Ω coaxial cable be used for the feed line.

The measured radiation resistance of the 14-MHz Log-Yag is 37 Ω over the frequency range from 14.0 to 14.35 MHz. It is assumed that tubing elements will be used. However, if a wire array is used, then the radiation resistance R_0 and antenna-feeder input impedance Z_0 must be calculated so that the proper balun and coax may be used. The procedure is outlined in detail in an earlier part of this chapter. However, programs such as *LPCAD28* are also suitable to automate the calculations.

Table 9 has array dimensions. **Tables 10** and **11** contain lists of the materials necessary to build the Log-Yag array.

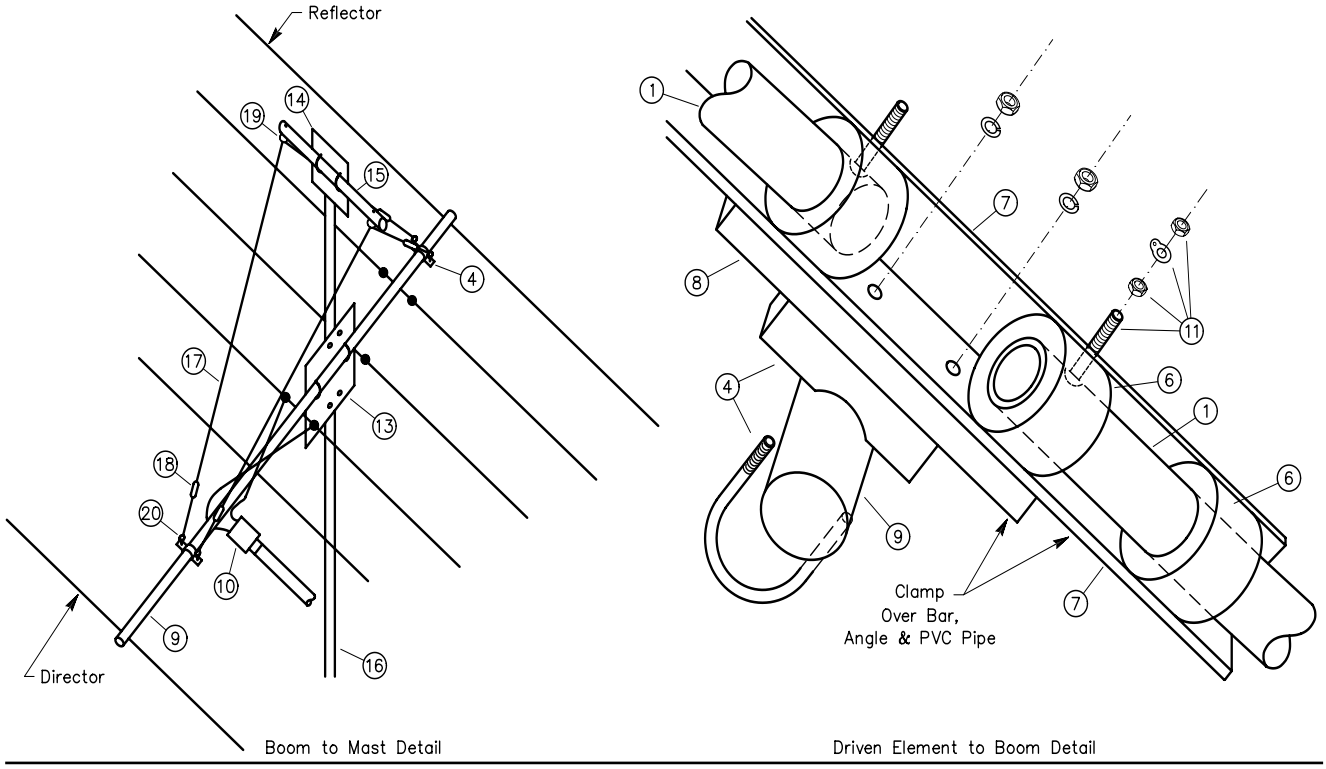

Fig 32—Assembly details. The numbered components refer to Table 11.

Table 10
Element Material Requirements: Log-Yag Array

	1-in. Tubing		*7/8-in. Tubing*		*3/4-in. Tubing*		*1 1/4-in. Angle*	*1 1/4-in. Bar*
	Len. Feet	*Qty*	*Len. Feet*	*Qty*	*Len. Feet*	*Qty*	*Len. Feet*	*Len. Feet*
Reflector	12	1	6	2	8	2	None	None
ℓ1	6	2	6	2	8	2	3	1
ℓ2	6	2	6	2	8	2	3	1
ℓ3	6	2	6	2	6	2	3	1
ℓ4	6	2	6	2	6	2	3	1
Director	12	1	6	2	6	2	None	None

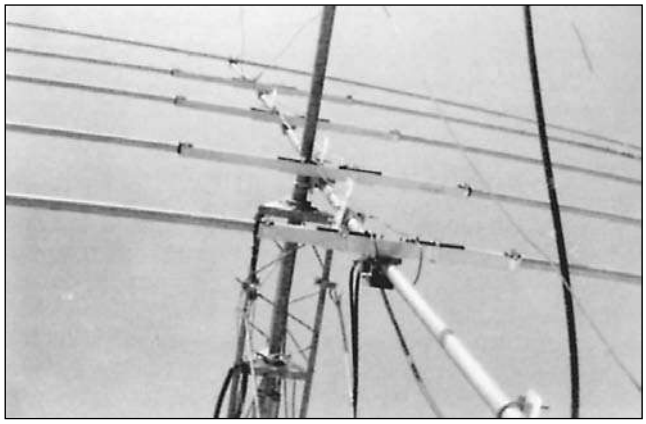

Fig 33—The attachment of the elements to the boom.

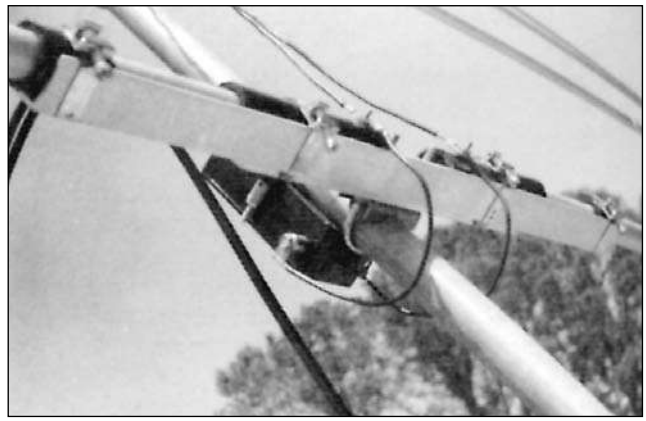

Fig 34—Looking from the front to the back of the Log-Yag array. A truss provides lateral and vertical support.

Table 11
Materials List, Log-Yag Array

1) Aluminum tubing—0.047 in. wall thickness
   1 in.—12 ft lenths, 24 lin. ft
   1 in.—12 ft or 6 ft lengths, 48 lin. ft
   7/8 in.—12 ft or 6 ft lengths, 72 lin. ft
   3/4 in.—8 ft lengths, 48 lin. ft
   3/4 in.—6 ft lengths, 36 lin. ft
2) Stainless steel hose clamps—2 in. max, 8 ea
3) Stainless steel hose clamps—1 1/4 in. max, 24 ea
4) TV-type U bolts—1 1/2 in., 6 ea
5) U bolts, galv. type: 5/16 in. × 1 1/2 in., 6 ea
5A) U bolts, galv. type: 1/4 in. × 1 in., 2 ea
6) 1 in. ID water-service polyethylene pipe 160 lb/in.^{2} test, approx. 1 3/8 in. OD, 7 lin. ft
7) 1 1/4 in. × 1 1/4 in. × 1/8 in. aluminum angle—6 ft lengths, 12 lin. ft
8) 1 in. × 1/4 in. × 1/4 in. aluminum angle—6 ft lengths, 6 lin. ft
9) 1 1/4 in. top rail of chain-link fence, 26.5 lin. ft
10) 1:1 toroid balun, 1 ea
11) No. 6-32 × 1 in. stainless steel screws, 8 ea
    No. 6-32 stainless steel nuts, 16 ea
    No. 6 solder lugs, 8 ea
12) #12 copper feed wire, 22 lin. ft
13) 12 in. × 6 in. × 1/4 in. aluminum plate, 1 ea
14) 6 in. × 4 in. × 1/4 in. aluminum plate, 1 ea
15) 3/4 in. galv. pipe, 3 lin. ft
16) 1 in. galv. pipe—mast, 5 lin. ft
17) Galv. guy wire, 50 lin. ft
18) 1/4 in. × 2 in. turnbuckles, 4 ea
19) 1/4 in. × 1 1/2 in. eye bolts, 2 ea
20) TV guy clamps and eyebolts, 2 ea

BIBLIOGRAPHY

Source material and more extended discussion of the topics covered in this chapter can be found in the references listed below and in the textbooks listed at the end of Chapter 2.

D. Allen, "The Log Periodic Loop Array (LPLA) Antenna," *The ARRL Antenna Compendium, Vol 3*, pp 115-117.

C. A. Balanis, *Antenna Theory, Analysis and Design*, 2nd Ed. (New York: John Wiley & Sons, 1997) Chapter 9.

P. C. Butson and G. T. Thompson, "A Note on the Calculation of the Gain of Log-Periodic Dipole Antennas," *IEEE Trans on Antennas and Propagation*, Vol AP-24, No. 1, Jan 1976, pp 105-106.

R. L. Carrel, "The Design of Log-Periodic Dipole Antennas," *1961 IRE International Convention Record*.

L. B. Cebik, "The Monoband Log-Cell Yagi Revisited," (4-part series) *National Contest Journal*, Jan-Jul 2000.

L. B. Cebik, "Some Preliminary Notes on Standard Design LPDAs for 3-30 MHz," (2-part series), *QEX*, Mar-May 2000.

R. H. DuHamel and D. E. Isbell, "Broadband Logarithmically Periodic Antenna Structures," *1957 IRE National Convention Record*, Part 1.

A. Eckols, "The Telerana: A Broadband 13- to 30-MHz Directional Antenna," *QST*, Jul 1981, pp 24-27.

J. Fisher, "Development of the W8JF Waveram: A Planar Log-Periodic Quad Array," *The ARRL Antenna Compendium, Vol 1*, pp 50-54.

M. Hansen, "The Improved Telerana, with Bonus 30/40 meter Coverage," *The ARRL Antenna Compendium, Vol 4*, pp 112-117.

K. Heitner, "A Wide-Band, Low-Z Antenna—New Thoughts on Small Antennas," *The ARRL Antenna Compendium, Vol 1*, pp 48-49.

D. E. Isbell, "Log-Periodic Dipole Arrays," *IRE Transactions on Antennas and Propagation*, Vol. AP-8, No. 3, May 1960.

J. D. Kraus, *Antennas*, 2nd Ed. (New York: McGraw-Hill, 1988), Chapter 15.

R. A. Johnson, ed., *Antenna Engineering Handbook*, 3rd Ed. (New York: McGraw-Hill, 1993), Chapters 14 and 26.

K. Luetzelschwab, "Log Periodic Dipole Array Improvements," *The ARRL Antenna Compendium, Vol 6*, pp 74-76.

D. A. Mack, "A Second-Generation Spiderweb Antenna," *The ARRL Antenna Compendium, Vol 1*, pp 55-59.

P. E. Mayes and R. L. Carrel, "Log Periodic Resonant-V Arrays," *IRE Wescon Convention Record*, Part 1, 1961.

P. E. Mayes, G. A. Deschamps, and W. T. Patton, "Backward Wave Radiation from Periodic Structures and Application to the Design of Frequency Independent Antennas," *Proc. IRE*.

J. J. Meyer, "A Simple Log-Yag Array for 50 MHz," *The ARRL Antenna Compendium, Vol 1*, pp 62-63.

C. T. Milner, "Log Periodic Antennas," *QST*, Nov 1959, pp 11-14.

W. I. Orr and S. D. Cowan, *Beam Antenna Handbook*, pp 251-253.

P. D. Rhodes, "The Log-Periodic Dipole Array," *QST*, Nov 1973, pp 16-22.

P. D. Rhodes and J. R. Painter, "The Log-Yag Array," *QST*, Dec 1976, pp 18-21.

P. D. Rhodes, "The Log-Periodic V Array," *QST*, Oct 1979, pp 40-43.

P. D. Rhodes, "The K4EWG Log Periodic Array," *The ARRL Antenna Compendium, Vol 3*, pp 118-123

V. H. Rumsey, *Frequency Independent Antennas* (New York: Academic Press, 1966).

F. Scholz, "A 14-30 MHz LPDA for Limited Space," *The ARRL Antenna Compendium, Vol 2*, pp 96-99

W. L. Stutzman and G. A. Thiele, *Antenna Theory and Design*, 2nd Ed. (New York: John Wiley & Sons, 1998), Chapter 6.

J. J. Uhl, "Construct a Wire Log-Periodic Dipole Array for 80 or 40 Meters," *QST*, Aug 1976, pp 21-24.

R. F. Zimmer, "Three Experimental Antennas for 15 Meters," *CQ*, Jan 1983, pp 44-45.

R. F. Zimmer, "Development and Construction of 'V' Beam Antennas," *CQ*, Aug 1983, pp 28-32.

Chapter 11

HF Yagi Arrays

Along with the dipole and the quarter-wave vertical, radio amateurs throughout the world make extensive use of the Yagi array. Hidetsugu Yagi and Shintaro Uda, two Japanese university professors, invented the Yagi in the 1920s. Uda did much of the developmental work, while Yagi introduced the array to the world outside Japan through his writings in English. Although the antenna should properly be called a *Yagi-Uda* array, it is commonly referred to simply as a *Yagi*.

The Yagi is a type of endfire multielement array. At the minimum, it consists of a single driven element and a single parasitic element. These elements are placed parallel to each other, on a supporting boom spacing them apart. This arrangement is known as a 2-element Yagi. The parasitic element is termed a *reflector* when it is placed behind the driven element, opposite to the direction of maximum radiation, and is called a *director* when it is placed ahead of the driven element. See **Fig 1**. In the VHF and UHF spectrum, Yagis employing 30 or more elements are not uncommon, with a single reflector and multiple directors. See Chapter 18, VHF and UHF Antenna Systems, for details on VHF and UHF Yagis. Large HF arrays may employ 10 or more elements, and will be covered in this chapter.

The gain and directional pattern of a Yagi array is determined by the relative amplitudes and phases of the currents induced into all the parasitic elements. Unlike the directly driven multielement arrays considered in Chapter 8, Multielement Arrays, where the designer must compensate for mutual coupling between elements, proper Yagi operation *relies on* mutual coupling. The current in each parasitic element is determined by its spacing from both the driven element and other parasitic elements, and by the tuning of the element itself. Both length and diameter affect element tuning.

For about 50 years amateurs and professionals created Yagi array designs largely by "cut and try" experimental techniques. In the early 1980s, Jim Lawson, W2PV, described in detail for the amateur audience the fundamental mathematics involved in modeling Yagis. His book *Yagi Antenna Design* is highly recommended for serious antenna designers. The advent of powerful microcomputers and sophisticated computer antenna modeling software in the mid 1980s revolutionized the field of Yagi design for the radio amateur. In a matter of minutes, a computer can

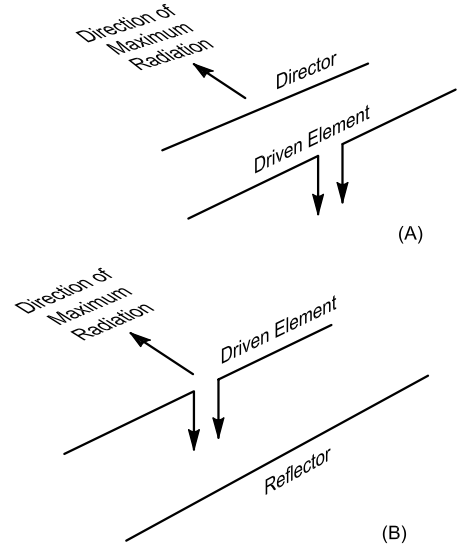

Fig 1—Two-element Yagi systems using a single parasitic element. At A the parasitic element acts as a director, and at B as a reflector. The arrows show the direction in which maximum radiation takes place.

try 100,000 or more different combinations of element lengths and spacings to create a Yagi design tailored to meet a particular set of high-performance parameters. To explore this number of combinations experimentally, a human experimenter would take an unimaginable amount of time and dedication, and the process would no doubt suffer from considerable measurement errors. With the computer tools available today, an antenna can be designed, constructed and then put up in the air, with little or no tuning or pruning required.

Yagi Performance Parameters

There are three main parameters used to characterize the performance of a particular Yagi—*forward gain*, *pattern* and *drive impedance/SWR*. Another important consideration is *mechanical strength*. It is very important to recognize that each of the three electrical parameters should be characterized over the frequency band of interest in order to be meaningful. Neither the gain, SWR nor the pattern measured at a single frequency gives very much insight into the overall performance of a particular Yagi.

Poor designs have been known to reverse their directionality over a frequency band, while other designs have excessively narrow SWR bandwidths, or overly "peaky" gain response. Finally, an antenna's ability to survive the wind and ice conditions expected in one's geographical location is an important consideration in any design. Much of this chapter will be devoted to describing detailed Yagi designs that are optimized for a good balance between gain, pattern and SWR over various amateur bands, and that are designed to survive strong winds and icing.

YAGI GAIN

Like any other antenna, the gain of a Yagi must be stated in comparison to some standard of reference. Designers of phased vertical arrays often state gain referenced to a single, isolated vertical element. See the section on "Phased Array Techniques" in Chapter 8, Multielement Arrays.

Many antenna designers prefer to compare gain to that of an *isotropic radiator in free space*. This is a theoretical antenna that radiates equally well in all directions, and by definition, it has a gain of 0 *dBi* (dB isotropic). Many radio amateurs, however, are comfortable using a dipole as a standard reference antenna, mainly because it is *not* a theoretical antenna.

In free space, a dipole does not radiate equally well in all directions—it has a figure-eight azimuth pattern, with deep nulls off the ends of the wire. In its favored directions, a free-space dipole has 2.15 dB gain compared to the isotropic radiator. You may see the term *dBd* in amateur literature, meaning gain referenced to a dipole in free space. Subtract 2.15 dB from gain in dBi to convert to gain in dBd.

Assume for a moment that we take a dipole out of "free space," and place it one wavelength over the ocean, whose saltwater makes an almost perfect ground. At an elevation angle of 15°, where sea water-reflected radiation adds in phase with direct radiation, the dipole has a gain of about 6 dB, compared to its gain when it was in free space, isolated from any reflections. See Chapter 3, The Effects of the Earth.

It is perfectly legitimate to say that this dipole has a gain of 6 dBd, although the term "dBd" (meaning "dB dipole") makes it sound as though the dipole somehow has gain over itself! Always remember that gain expressed in dBd (or dBi) refers to the *counterpart antenna in free space*. The gain of the dipole over saltwater in this example can be rated at either 6 dBd (over a dipole in free space), or as 8.15 dBi (over an isotropic radiator in free space). Each frame of reference is valid, as long as it is used consistently and clearly. In this chapter we will often switch between Yagis in free space and Yagis over ground. To prevent any confusion, gains will be stated in dBi.

Yagi free-space gain ranges from about 5 dBi for a small 2-element design to about 20 dBi for a 31-element long-boom UHF design. The length of the boom is the main factor determining the gain a Yagi can deliver. Gain as a function of boom length will be discussed in detail after the sections below defining antenna response patterns and SWR characteristics.

RESPONSE PATTERNS— FRONT-TO-REAR RATIO

As discussed in Chapter 2, Antenna Fundamentals, for an antenna to have gain, it must concentrate energy radiated in a particular direction, at the expense of energy radiated in other directions. Gain is thus closely related to an antenna's directivity pattern, and also to the losses in the antenna. **Fig 2** shows the *E-plane* (also called *E-field*, for electric field) and *H-plane* (also called *H-field*, for magnetic field) pattern of a 3-element Yagi in free space, compared to a dipole, and an isotropic radiator. These patterns were generated using the computer program *NEC-2*, which is highly regarded by antenna professionals for its accuracy and flexibility.

In free space there is no Earth reference to determine whether the antenna polarization is horizontal or vertical, and so its response patterns are labeled as E-field (electric) or H-field (magnetic). For a Yagi mounted over ground rather than in free space, if the

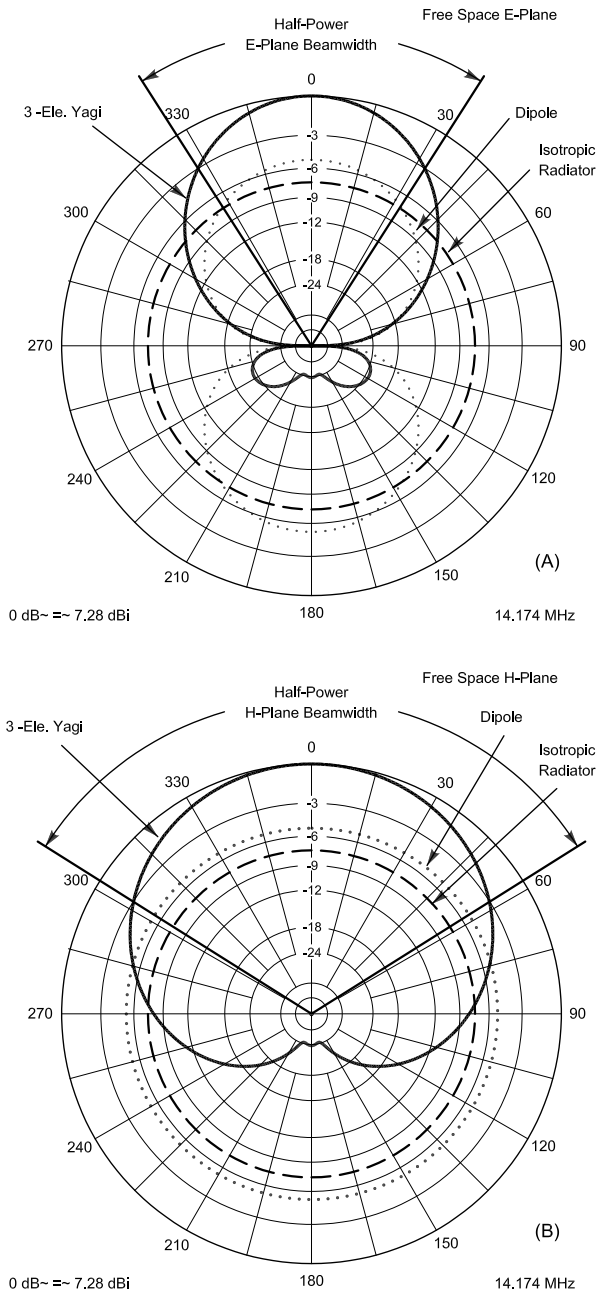

Fig 2—E-Plane (electric field) and H-Plane (magnetic field) response patterns for 3-element 20-meter Yagi in free space. At A the E-Plane pattern for a typical 3-element Yagi is compared with a dipole and an isotropic radiator. At B the H-Plane patterns are compared for the same antennas. The Yagi has an E-Plane half-power beamwidth of 66°, and an H-Plane half-power beamwidth of about 120°. The Yagi has 7.28 dBi (5.13 dBd) of gain. The front-to-back ratio, which compares the response at 0° and at 180°, is about 35 dB for this Yagi. The front-to-rear ratio, which compares the response at 0° to the largest lobe in the rearward 180° arc behind the antenna, is 24 dB, due to the lobes at 120° and 240°.

E-field is parallel to the earth (that is, the elements are parallel to the earth) then the antenna polarization is horizontal, and its E-field response is then usually referred to as its *azimuth* pattern. Its H-field response is then referred to as its *elevation* pattern.

Fig 2A demonstrates how this 3-element Yagi in free space exhibits 7.28 dBi of gain (referenced to isotropic), and has 5.13 dB gain over a free-space dipole. The gain is in the forward direction on the graph at 0° azimuth, and the forward part of the lobe is called the *main lobe*. For this particular antenna, the angular width of the E-plane main lobe at the half power, or 3 dB points compared to the peak, is about 66°. This performance characteristic is called the antenna's azimuthal *half-power beamwidth*.

Again as seen in Fig 2A, this antenna's response in the reverse direction at 180° azimuth is 34 dB less than in the forward direction. This characteristic is called the antenna's *front-to-back ratio*, and it describes the ability of an antenna to discriminate, for example, against interfering signals coming directly from the rear, when the antenna is being used for reception. In Fig 2A there are two sidelobes, at 120° and at 240° azimuth, which are about 24 dB down from the peak response at 0°. Since interference can come from any direction, not only directly off the back of an antenna, these kinds of sidelobes limit the ability to discriminate against rearward signals. The term *worst-case front-to-rear ratio* is used to describe the worst-case rearward lobe in the 180°-wide sector behind the antenna's main lobe. In this case, the worst-case front-to-rear ratio is 24 dB.

In the rest of this chapter the worst-case front-to-rear ratio will be used as a performance parameter, and will be abbreviated as "F/R." For a dipole or an isotropic radiator, Fig 2A demonstrates that F/R is 0 dB. Fig 2B depicts the H-field response for the same 3-element Yagi in free space, again compared to a dipole and an isotropic radiator in free space. Unlike the E-field pattern, the H-field pattern for a Yagi does not have a null at 90°, directly over the top of the Yagi. For this 3-element design, the H-field half-power beamwidth is approximately 120°.

Fig 3 compares the azimuth and elevation patterns for a horizontally polarized 6-element 14-MHz Yagi, with a 60-foot boom mounted one wavelength over ground, to a dipole at the same height. As with any horizontally polarized antenna, the height above ground is the main factor determining the peaks and nulls in the elevation pattern of each antenna. Fig 3A shows the E-field pattern, which has now been labeled as the Azimuth pattern. This antenna has a half-power azimuthal beamwidth of about 50°, and at an elevation angle of 12° it exhibits a forward gain of 16.02 dBi, including about 5 dB of ground reflection gain over relatively poor ground, with a dielectric constant of 13 and conductivity of 5 mS/m. In free space this Yagi has a gain of 10.97 dBi.

The H-field elevation response of the 6-element Yagi has a half-power beamwidth of about 60° in free space,

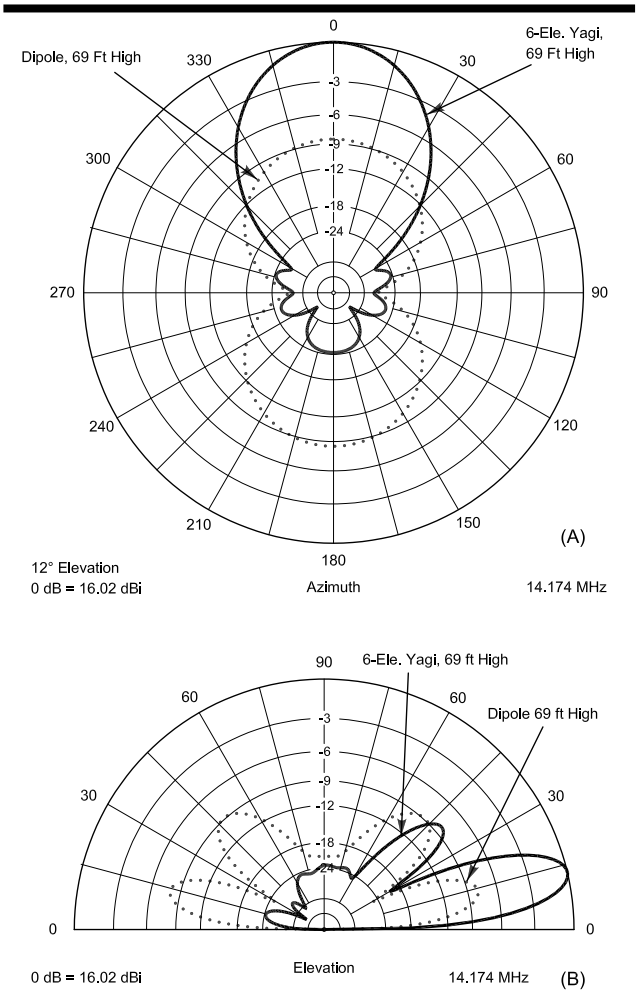

Fig 3—Azimuth pattern for 6-element 20-meter Yagi on 60-foot long boom, mounted 60 feet over ground. At A, the azimuth pattern at 12° elevation angle is shown, compared to a dipole at the same height. Peak gain of the Yagi is 16.04 dBi, or just over 8 dB compared to the dipole. At B, the elevation pattern for the same two antennas is shown. Note that the peak elevation pattern of the Yagi is compressed slightly lower compared to the dipole, even though they are both at the same height over ground. This is most noticeable for the Yagi's second lobe, which peaks at about 40°, while the dipole's second lobe peaks at about 48°. This is due to the greater free-space directionality of the Yagi at higher angles.

but as shown in Fig 3B, the first lobe (centered at 12° in elevation) has a half-power beamwidth of only 13° when the antenna is mounted one wavelength over ground. The dipole at the same height has a very slightly larger first-lobe half-power elevation beamwidth of 14°, since its free-space H-field response is omnidirectional.

Note that the free-space H-field directivity of the Yagi suppresses its second lobe over ground (at an elevation angle of about 40°) to 8 dBi, while the dipole's response at its second lobe peak (at about 48°) is at a level of 9 dBi.

The shape of the azimuthal pattern for a Yagi operated over real ground will change slightly as the Yagi is placed closer and closer to earth. Generally, however, the azimuth pattern doesn't depart significantly from the free-space pattern until the antenna is less than 0.5 λ high. This is just over 17 feet high at 28.4 MHz, and just under 35 feet at 14.2 MHz, heights that are not difficult to achieve for most amateurs. Some advanced computer programs can optimize Yagis at the exact installation height.

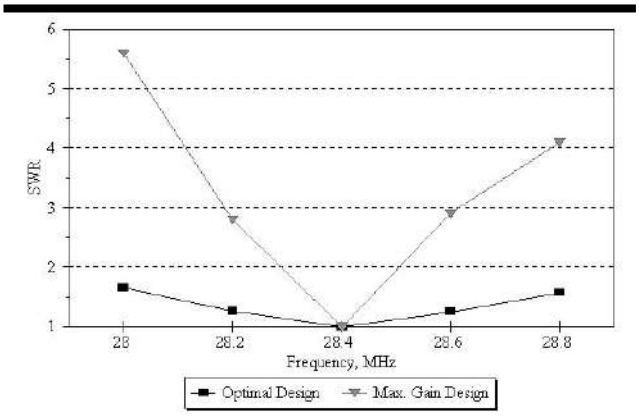

Fig 4—SWR over the 28.0 to 28.8 MHz portion of the 10-meter band for two different 3-element Yagi designs. One is designed strictly for maximum gain, while the second is optimized for F/R pattern and SWR over the frequency band. A Yagi designed only for maximum gain usually suffers from a very narrow SWR bandwidth.

DRIVE IMPEDANCE AND SWR

The impedance at the driven element in a Yagi is affected not only by the tuning of the driven element itself, but also by the spacing and tuning of nearby parasitic elements, and to a lesser extent by the presence of ground. In some designs that have been tuned solely for maximum gain, the driven-element impedance can fall to very low levels, sometimes less than 5 Ω. This can lead to excessive losses due to conductor resistance, especially at VHF and UHF. In a Yagi that has been optimized solely for gain, conductor losses are usually compounded by large excursions in impedance levels with relatively small changes in frequency. The SWR can thus change dramatically over a band and can create additional losses in the feed cable. **Fig 4** illustrates the SWR over the 28 to 28.8 MHz portion of the 10-meter amateur band for a 5-element Yagi on a 24-foot boom, which has been tuned for maximum forward gain at a spot frequency of 28.4 MHz. Its SWR curve is contrasted to that of a Yagi designed for a good compromise of gain, SWR and F/R.

Even professional antenna designers have difficulty accurately measuring forward gain. On the other hand, SWR can easily be measured by professional and amateur alike. Few manufacturers would probably want to advertise an antenna with the narrow-band SWR curve shown in Fig 4!

Monoband Yagi Performance Optimization

DESIGN GOALS

The previous section discussing driven-element impedance and SWR hinted at possible design trade-offs among gain, pattern and SWR, especially when each parameter is considered over a frequency band rather than at a spot frequency. Trade-offs in Yagi design parameters can be a matter of personal taste and operating style. For example, one operator might exclusively operate the CW portions of the HF bands, while another might only be interested in the Phone portions. Another operator may want a good pattern in order to discriminate against signals coming from a particular direction; someone else may want the most forward gain possible, and may not care about responses in other directions.

Extensive computer modeling of Yagis indicates that the parameter that must be compromised most to achieve wide bandwidths for front-to-rear ratio and SWR is forward gain. However, not much gain must be sacrificed for good F/R and SWR coverage, especially on long-boom Yagis. Although 10 and 7-MHz Yagis are not rare, the HF bands from 14 to 30 MHz are where Yagis are most often found, mainly due to the mechanical difficulties involved with making sturdy antennas for lower frequencies. The highest HF band, 28.0 to 29.7 MHz, represents the largest percentage bandwidth of the upper HF bands, at almost 6%. It is difficult to try to optimize in one design the main performance parameters of gain, worst-case F/R ratio and SWR over this large a band. Many commercial designs thus split up their 10-meter designs into antennas covering one of two bands: 28.0 to 28.8 MHz, and 28.8 to 29.7 MHz. For the amateur bands below 10 meters, optimal designs that cover the entire band are more easily achieved.

DESIGN VARIABLES

There are only a few variables available when one is designing a Yagi to meet certain design goals. The variables are:

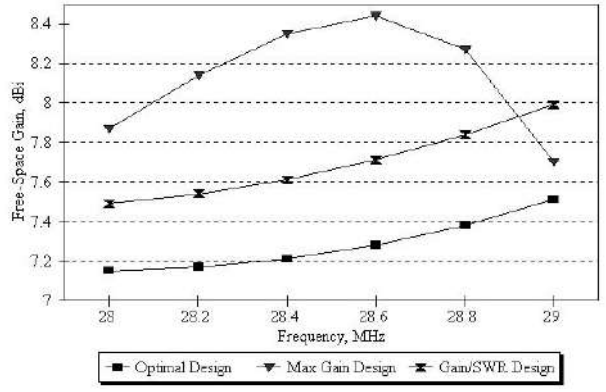

(A)

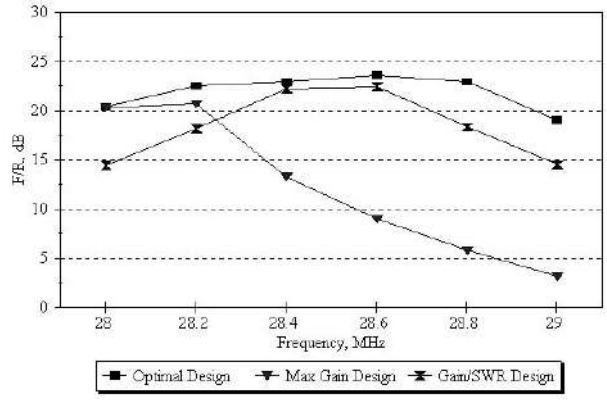

(B)

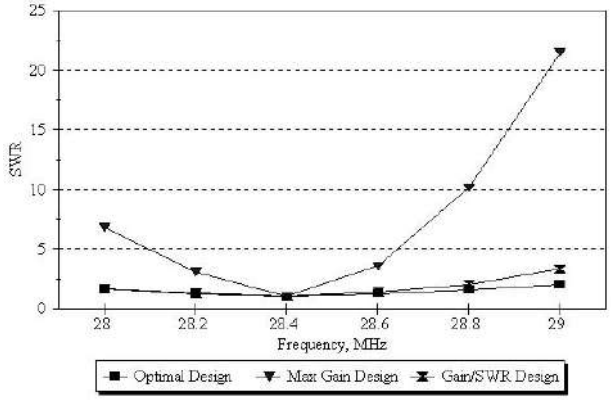

(C)

Fig 5—Comparisons of three different 3-element 10-meter Yagi designs using 8-foot booms. At A, gain comparisons are shown. The Yagi designed for the best compromise of gain and SWR sacrifices an average of about 0.5 dB compared to the antenna designed for maximum gain. The Yagi designed for optimal F/R, gain and SWR sacrifices an average of 1.0 dB compared to the maximum-gain case, and about 0.4 dB compared to the compromise gain and SWR case. At B, the front-to-rear ratio is shown for the three different designs. The antenna designed for optimal combination of gain, F/R and SWR maintains a F/R higher than 20 dB across the entire frequency range, while the antenna designed strictly for gain has a F/R of 3 dB at the high end of the band. At C, the three antenna designs are compared for SWR bandwidth. At the high end of the band, the antenna designed strictly for gain has a very high SWR.

1. The physical length of the boom
2. The number of elements on the boom
3. The spacing of each element along the boom
4. The tuning of each element
5. The type of matching network used to feed the array.

GAIN AND BOOM LENGTH

As pointed out earlier, the gain of a Yagi is largely a function of the length of the boom. As the boom is made longer, the maximum gain potential rises. For a given boom length, the number of elements populating that boom can be varied, while still maintaining the antenna's gain, provided of course that the elements are tuned properly. In general, putting more elements on a boom gives the designer added flexibility to achieve desired design goals, especially to spread the response out over a frequency band.

Fig 5A is an example illustrating gain versus frequency for three different types of 3-element Yagis on 8-foot booms. The three antennas were designed for the lower end of the 10-meter band, 28.0 to 28.8 MHz, based on the following different design goals:

Antenna 1: Maximum mid-band gain, regardless of F/R or SWR across the band

Antenna 2: SWR less than 2:1 over the frequency band; best compromise gain, with no special consideration for F/R over the band.

Antenna 3: "Optimal" case: F/R greater than 20 dB, SWR less than 2:1 over the frequency band; best compromise gain.

Fig 5B shows the F/R over the frequency band for these three designs, and Fig 5C shows the SWR curves over the frequency band. Antenna 1, the design that strives strictly for maximum gain, has a poor SWR response over the band, as might be expected after the previous section discussing SWR. The SWR is 10:1 at 28.8 MHz and rises to 22:1 at 29 MHz. At 28 MHz, at the low end of the band, the SWR of the maximum-gain design is more than 6:1. Clearly, designing for maximum gain alone produces an unacceptable design in terms of SWR bandwidth. The F/R for Antenna 1 reaches a high point of about 20 dB at the low-frequency end of the band, but falls to only 3 dB at the high-frequency end.

Antenna 2, designed for the best compromise of gain while the SWR across the band is held to less than 2:1, achieves this goal, but at an average gain sacrifice of 0.7 dB compared to the maximum gain case. The F/R for this design is just under 15 dB over the band. This design is fairly typical of many amateur Yagi designs before the advent of computer modeling and optimization programs. SWR can easily be measured, and experimental optimization for forward gain is a fairly straightforward procedure. By contrast, overall pattern optimization is not a trivial thing to achieve experimentally, particularly for antennas with more than four or five elements.

Antenna 3, designed for an optimum combination of F/R, SWR and gain, compromises forward gain an average of 1.0 dB compared to the maximum gain case, and about 0.4 dB compared to the compromise gain/SWR case. It achieves its design objectives of more than 20 dB F/R over the 28.0 to 28.8 MHz portion of the band, with an SWR less than 2:1 over that range.

Fig 6A shows the free-space gain versus frequency for the same three types of designs, but for a bigger 5-element 10-meter Yagi on a 20-foot boom. Fig 6B shows the variation in F/R, and Fig 6C shows the SWR curves versus frequency. Once again, the design that concentrates solely on maximum gain has a poor SWR curve over the band, reaching just over 6:1 toward the high end of the band. The difference in gain between the maximum gain case and the optimum design case has narrowed for this size of boom to an average of under 0.5 dB. This comes about because the designer has access to more variables in a 5-element design than he does in a 3-element design, and he can stagger-tune the various elements to spread the response out over the whole band.

Fig 7A, **B** and **C** show the same three types of designs, but for a 6-element Yagi on a 36-foot boom. The SWR bandwidth of the antenna designed for maximum gain has improved compared to the previous two shorter-boom examples, but the SWR still rises to more than 4:1 at 28.8 MHz, while the F/R ratio is pretty constant over the band, at a mediocre 11 dB average level. While the antenna designed for gain and SWR does hold the SWR below 2:1 over the band, it also has the same mediocre level of F/R performance as does the maximum-gain design.

The optimized 36-foot boom antenna achieves an excellent F/R of more than 22 dB over the whole 28.0 to 28.8 MHz band. Again, the availability of more elements and more space on the 36-foot long boom gives the designer more flexibility in broadbanding the response over the whole band, while sacrificing only 0.3 dB of gain compared to the maximum-gain design.

Fig 8A, **B**, and **C** show the same three types of 10-meter designs, but now for a 60-foot boom, populated with eight elements. With eight elements and a very long boom on which to space them out, the antenna designed solely for maximum gain can achieve a much better SWR response across the band, although the SWR does rise to more than 7:1 at the very high end of the band. The SWR remains less than 2:1 from 28.0 to 28.7 MHz, much better than for shorter-boom, maximum-gain designs. The worst-case F/R ratio is never better than 19 dB, however, and remains around 10 dB over much of the band. The antenna designed for the best compromise gain and SWR loses only about 0.1 dB of gain compared to the maximum-gain design, but does little better in terms of F/R across the band.

Contrasted to these two designs, the antenna optimized for F/R, SWR and gain has an outstanding pattern, exhibiting an F/R of more than 24 dB across the entire

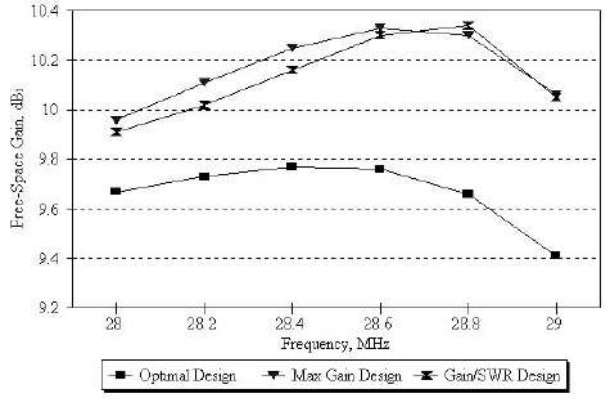

(A)

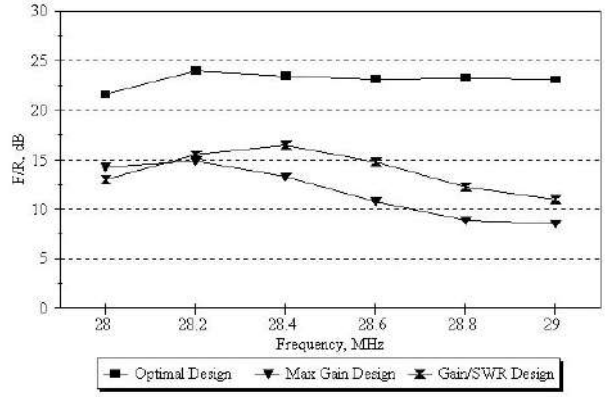

(B)

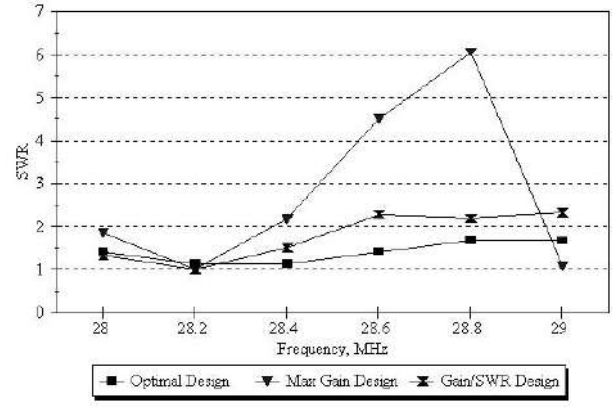

(C)

Fig 6—Comparisons of three different designs for 5-element 10-meter Yagis on 20-foot booms. At A, the gain of three different 5-element 10-meter Yagi designs are graphed. The difference in gain between the three antennas narrows because the elements can be stagger-tuned to spread the response out better over the desired frequency band. The average gain reduction for the fully optimized antenna design is about 0.5 dB. At B, the optimal antenna displays better than 22 dB F/R over the band, while the Yagi designed for gain and SWR displays on average 10 dB less F/R throughout the band. At C, the SWR bandwidth is compared for the three Yagis. The antenna designed strictly for forward gain has a poor SWR bandwidth and a high peak SWR of 6:1 at 28.8 MHz.

band, while keeping the SWR below 2:1 from 28.0 to 28.9 MHz. It must sacrifice an average of only 0.4 dB compared to the maximum gain design at the low end of the band, and actually has more gain than the maximum gain and gain/SWR designs at the high-frequency end of the band.

The conclusion drawn from these and many other detailed comparisons is that designing strictly for maximum mid-band gain yields an inferior design when the antenna is examined over an entire frequency band, especially in terms of SWR. Designing a Yagi for both gain and SWR will yield antennas that have mediocre rearward patterns, but that lose relatively little gain compared to the maximum gain case, at least for designs with more than three elements.

However, designing a Yagi for an optimal combination of F/R, SWR and gain results in a loss of gain less than 0.5 dB compared to designs designed only for gain and SWR. **Fig 9** summarizes the forward gain achieved for the three different design types versus boom length, as expressed in wavelength.

Except for the 2-element designs, the Yagis described in the rest of this chapter have the following design goals over a desired frequency band:

1. Front-to-rear ratio over the frequency band of more than 20 dB
2. SWR over the frequency band less than 2:1
3. Maximum gain consistent with points 1 and 2 above

Just for fun, **Fig 10** shows the gain versus boom length for theoretical 20-meter Yagis that have been designed to meet the three design goals above. The 31-element design for 14 MHz would be wondrous to behold. Sadly, it is unlikely that anyone will build one, considering that the boom would be 724 feet long! However, such a design *does* become practical when scaled to 432 MHz. In fact, a K1FO 22-element and a K1FO 31-element Yagi are the prototypes for the theoretical 14-MHz long-boom designs. See Chapter 18, VHF and UHF Antenna Systems.

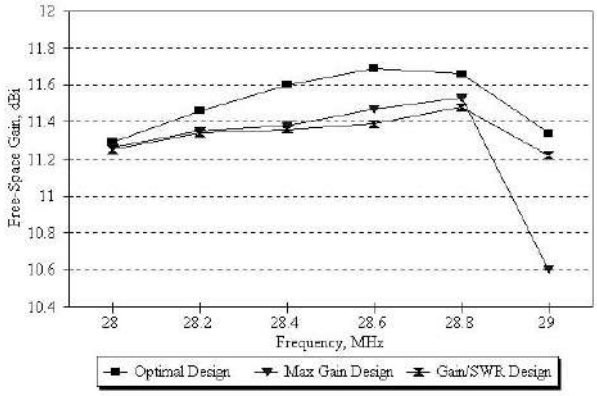

(A)

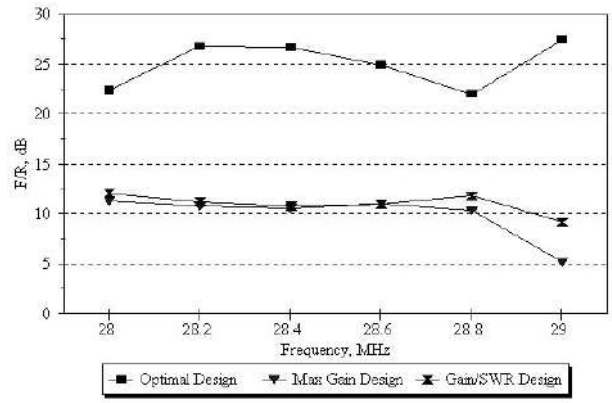

(B)

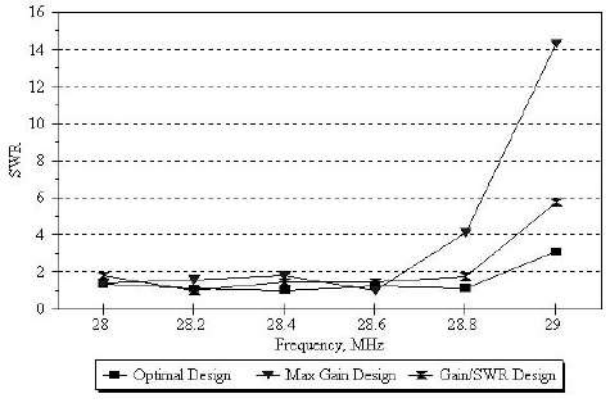

(C)

Fig 7—Comparisons of three different 6-element 10-meter Yagi designs on 36-foot booms. At A, gain is shown over the band. With more elements and a longer boom, the tuning can be staggered even more to make the antenna gain more uniform over the band. This narrows the gain differential between the antenna designed strictly for maximum gain and the antenna designed for an optimal combination of F/R, SWR and gain. The average difference in gain is about 0.2 dB throughout the band. At B, the F/R performance over the band is shown for the three antenna designs. The antenna designed for optimal performance maintains an average of almost 15 dB better F/R over the whole band compared to the other designs. At C, the SWR bandwidth is compared. Again, the antenna designed strictly for maximum gain exhibits a high SWR of 4:1 at 28.8 MHz, and rises to more than 14:1 at 29.0 MHz.

OPTIMUM DESIGNS AND ELEMENT SPACING

Two-Element Yagis

Many hams consider a 2-element Yagi to give "the most bang for the buck" among various Yagi designs, particularly for portable operations such as Field Day. A 2-element Yagi has about 4 dB of gain over a simple dipole (sometimes jokingly called a "one-element Yagi") and gives a modest F/R of about 10 dB to help with rejection of interference on receive. By comparison, going from a 2-element to a 3-element Yagi increases the boom length by about 50% and adds another element, a 50% increase in the number of elements—for a gain increase of about 1 dB and another 10 dB in F/R.

Element Spacing in Larger Yagis

One of the more interesting results of computer modeling and optimization of high-performance Yagis with four or more elements is that a distinct pattern in the element spacings along the boom shows up consistently. This pattern is relatively independent of boom length, once the boom is longer than about 0.3 λ.

The reflector, driven element and first director of these optimal designs are typically bunched rather closely together, occupying together only about 0.15 to 0.20 λ of the boom. This pattern contrasts sharply with older designs, where the amount of boom taken up by the reflector, driven element and first director was typically more than 0.3 λ. **Fig 11** shows the element spacings for an optimized 6-element, 36-foot boom, 10-meter design, compared to a W2PV 6-element design with constant spacing of 0.15 λ between all elements.

A problem arises with such a bunching of elements toward the reflector end of the boom—the wind loading of the antenna is not equal along the boom. Unless properly compensated, such new-generation Yagis will act like windvanes, punishing, and often breaking, the rotators trying to turn, or hold, them in the wind. One successful solution to windvaning has been to employ "dummy elements" made of PVC piping. These nonconducting elements are placed on the boom close to the last director so

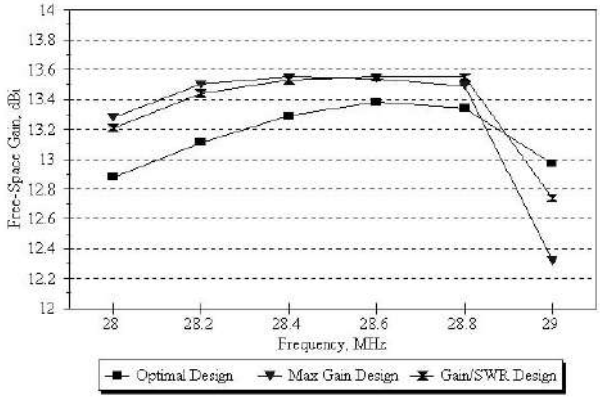

(A)

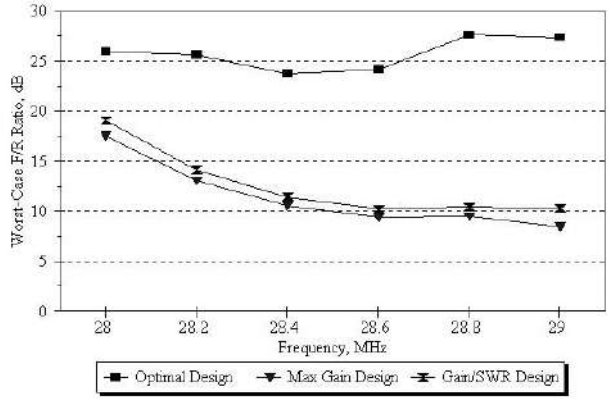

(B)

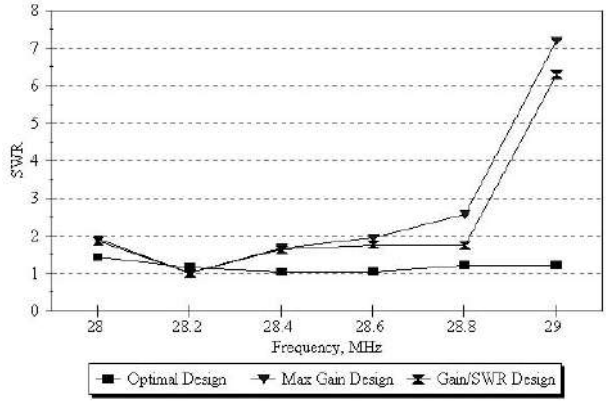

(C)

Fig 8—Comparisons of three different 8-element 10-meter Yagi designs using 60-foot booms. At A, gain is shown over the frequency band. With even more freedom to stagger-tune elements and a very long boom on which to place them, the average antenna gain differential over the band is now less than 0.2 dB between the three design cases. At B, an excellent 24 dB F/R for the optimal design is maintained over the whole band, compared to the average of about 12 dB for the other two designs. At C, the SWR differential over the band is narrowed between the three designs, again because there are more variables available to broaden the bandwidth.

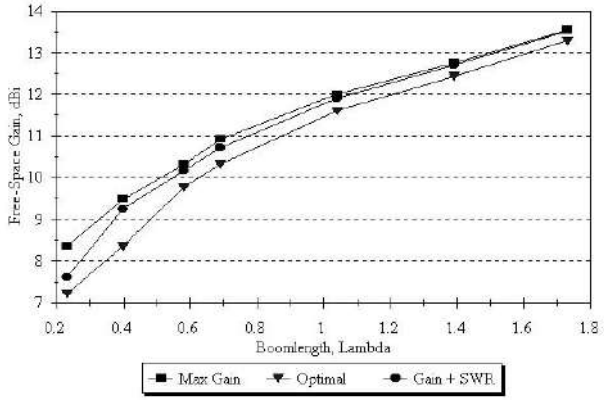

Fig 9—Gain versus boom length for three different 10-meter design goals. The goals are: (1) designed for maximum gain across band, (2) designed for a compromise of gain and SWR, and (3) designed for optimal F/R, SWR and gain across 28.0 to 28.8 MHz portion of 10-meter band. The gain difference is less than 0.5 dB for booms longer than approximately 0.5 λ.

the windload is equalized at the mast-to-boom bracket. In addition, it may be necessary to insert a small amount of lead weight at one end of the boom in order to balance the antenna weight.

Despite the relatively close spacing of the reflector, driven element and first director, modern optimal Yagi designs are not overly sensitive to small changes in either element length or spacing. In fact, these antennas can be constructed from design tables without excessive concern about close dimensional tolerances. In the HF range up to 30 MHz, building the antennas to the nearest $^1/_8$-inch results in performance remarkably consistent with the computations, without any "tweaking" or fine-tuning when the Yagi is on the tower.

ELEMENT TUNING

Element tuning (or *self-impedance*) is a complex function of the effective electrical length of each element and the effective diameter of the element. In turn, the effective length and diameter of each element is related to

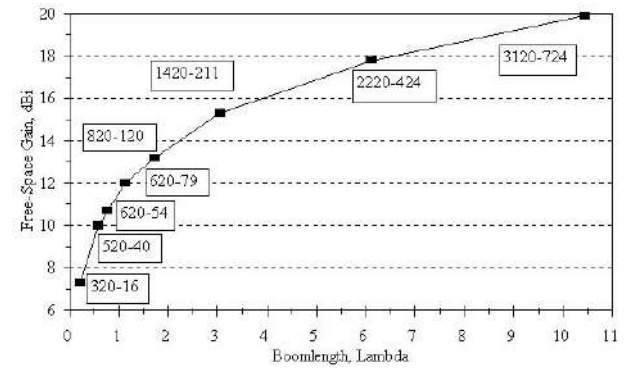

Fig 10—Theoretical gain versus boom length for 20-meter Yagis designed for optimal combination of F/R, SWR and gain across the entire 14.0 to 14.35 MHz band. The theoretical gain approaches 20 dBi for a gigantic 724-foot boom, populated with 31 elements. Such a design on 20 meters is not too practical, of course, but can readily be achieved on a 24-foot boom on 432 MHz.

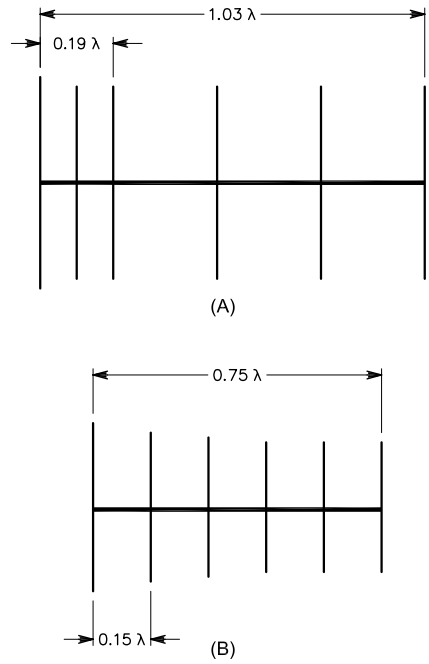

Fig 11—Tapering spacing versus constant element spacing. At A, illustration of how the spacing of the reflector, driven element and first director (over the first 0.19 λ of the boom) of an optimally designed Yagi is bunched together compared to the Yagi at B, which uses constant 0.15 λ spacing between all elements. The optimally designed antenna has more than 22 dB F/R and an SWR less than 1.5:1 over the frequency band 28.0 to 28.8 MHz.

the taper schedule (if telescoping aluminum tubing is used, the most common method of construction), the length of each telescoping section, the type and size of mounting bracket used to secure the element to or through the boom, and the size of the Yagi boom itself. See the section entitled "Antenna Frequency Scaling," and "Tapered Elements" in Chapter 2, Antenna Fundamentals, of this book for details about element tuning as a function of tapering and element diameter. Note especially that Yagis constructed using wire elements will perform very differently compared to the same antenna constructed with elements made of telescoping aluminum tubing.

The process by which a modern Yagi is designed usually starts out with the selection of the longest boom possible for a given installation. A suitable number of elements of a given taper schedule are then placed on this boom, and the gain, pattern and SWR are calculated over the entire frequency band of interest to the operator. Once an electrical design is chosen, the designer must then ensure the mechanical integrity of the antenna design. This involves verifying the integrity of the boom and each element in the face of the wind and ice loading expected for a particular location. The section entitled "Construction with Aluminum Tubing" in Chapter 20, Antenna Materials and Accessories, of this book shows details of tapered telescoping aluminum elements for the upper HF bands. In addition, the ARRL book *Physical Design of Yagi Antennas*, by Dave Leeson, W6NL (ex-W6QHS), describes the mechanical design process for all portions of a Yagi antenna very thoroughly, and is highly recommended for serious Yagi builders.

Specific Monoband Yagi Designs

The detailed Yagi design tables that follow are for two taper schedules for HF Yagis covering the 14 through 30-MHz amateur bands. The heavy-duty elements are designed to survive at least 120-mph winds without icing, or 85-mph winds with 1/4-inch radial ice. The medium-duty elements are designed to survive winds greater than 80 mph, or 60-mph winds with 1/4-inch radial ice.

For 10.1 MHz, the elements shown are capable of surviving 105-mph winds, or 93-mph winds with 1/4-inch radial ice. For 7.1 MHz the elements shown can survive 93-mph winds, or 69-mph winds with 1/4-inch radial ice. For these two lower frequency bands, the elements and the booms needed are very large and heavy. Mounting, turning and keeping such antennas in the air is not a trivial task.

Each element is mounted above the boom with a heavy rectangular aluminum plate, by means of U-bolts with saddles, as shown in Fig 35 in Chapter 18, VHF and UHF Antenna Systems for a 6-meter Yagi. This method of element mounting is rugged and stable, and because the element is mounted away from the boom, the amount of element detuning due to the presence of the boom is minimal. The element dimensions given in each table already take into account any element detuning due to the boom-to-element mounting plate. For each element, the length of the tip determines the tuning, since the inner tubes are fixed in diameter and length.

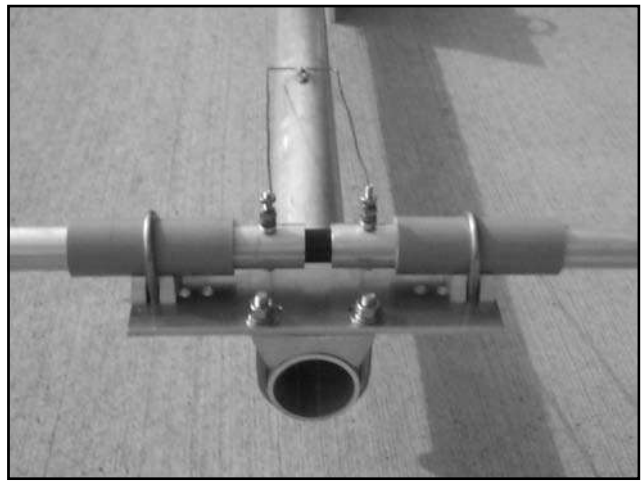

Fig 12—Typical construction techniques for an HF Yagi. This photo shows a hairpin match on a driven element that uses a fiberglass insulator (wrapped in black vinyl tape for protection against UV). Muffler clamps and saddles mount the element to the boom, while U-bolts and saddles mount the element to the boom-to-element plate. The gray PVC sleeves insulate the element from the plate. The feed coax is connected to the two bolts that also connect to the hairpin wire. Note that the hairpin is grounded at its opposite end to dissipate static charges that might otherwise build up.

Half Elements

Each design shows the dimensions for *one-half* of each element, mounted on *one side* of the boom. The other half of each element is symmetrical, mounted on the other side of the boom. The use of a tubing sleeve inside the center portion of the element is recommended, so that the element is not crushed by the mounting U-bolts. Unless otherwise noted, each section of tubing is made of 6061-T6 aluminum tubing, with a 0.058-inch wall thickness. This wall thickness ensures that the next standard size of tubing can telescope with it. Each telescoping section is inserted 3 inches into the larger tubing, and is secured by one of the methods shown in Fig 11 in Chapter 20, Antenna Materials and Accessories.

Matching System

Each antenna is designed with a driven-element length appropriate for a hairpin type of matching network. The driven-element's length may require slight readjustment for best match, particularly if a different matching network is used. *Do not change* either the lengths or the telescoping tubing schedule of the parasitic elements—they have been optimized for best performance and will not be affected by tuning of the driven element!

Fig 12 is a photograph of the driven element for a 2-element 17-meter Yagi built by Chuck Hutchinson, K8CH, for the ARRL book *Simple and Fun Antennas for Hams*. The aluminum tubing on each side of the boom was 1-inch OD, and the two pieces were mechanically joined together with a 3/4-inch OD fiberglass insulator. Chuck wound electrical tape over the insulator to protect the fiberglass from the sun's UV.

Chuck used 3-inch lengths of 1-inch sunlight-resistant PVC conduit, split lengthwise, to make the grey outer insulators for the driven element. The aluminum plates came from DX Engineering, as did the stainless-steel U-bolts and saddle clamps. These saddles ensured that the elements don't rotate on the 2-inch OD boom in the heavy winds in his part of rural Michigan.

You can see the bolts used to pin the center fiberglass insulator to the aluminum tubing, while also providing an electrical connection for the #12 hairpin wire and for the feed-line coax, which uses ferrite beads over the coax's outer vinyl jacket to make a common-mode current-type of balun (not shown in Fig 12). Note that the center of the hairpin is connected to the boom using a grounding lug for some measure of protection from static buildup.

10-METER YAGIS

Fig 13 describes the electrical performance of eight optimized 10-meter Yagis with boom lengths between 6 to 60 feet. The end of each boom includes 3 inches of space for the reflector and last-director (or driven element for the 2-element designs) mounting plates. Fig 13A shows the free-space gain versus frequency for each antenna; 13B shows the front-to-rear ratio, and 13C shows the SWR versus frequency. Each antenna with three or more elements was designed to cover the lower half of the 10-meter band from 28.0 to 28.8 MHz, with SWR less than 2:1 and F/R better than 20 dB over that range.

Fig 13D shows the taper schedule for two types of 10-meter elements. The heavy-duty design can survive 125-mph winds with no icing, and 88-mph winds with 1/4-inch of radial ice. The medium-duty design can handle 96-mph winds with no icing, and 68-mph winds with 1/4-inch of radial ice. The element-to-boom mounting plate for these Yagis is a 0.250-inch thick flat aluminum plate, 4 inches wide by 4 inches long. Each element except for the insulated driven element, is centered on the plate, held by two stainless-steel U-bolts with saddles. Another set

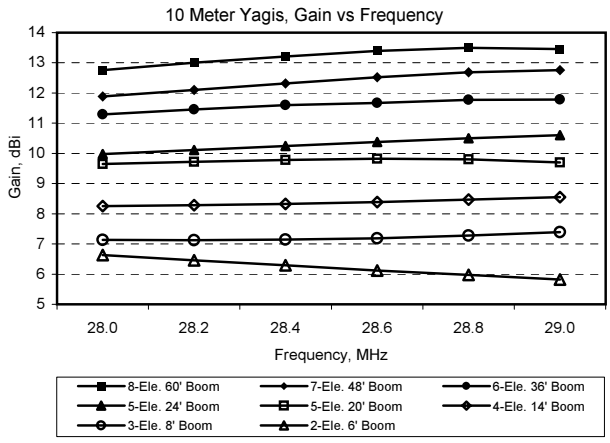

(A)

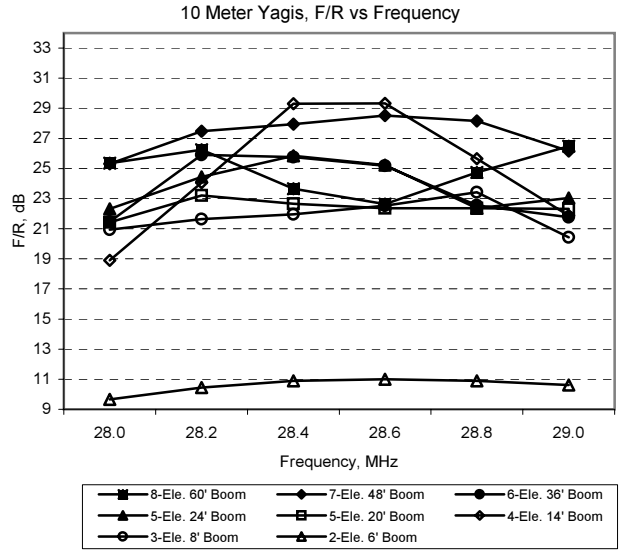

(B)

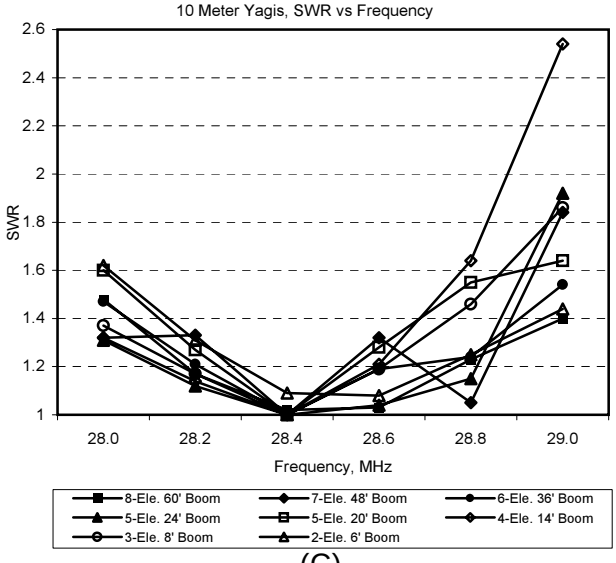

(C)

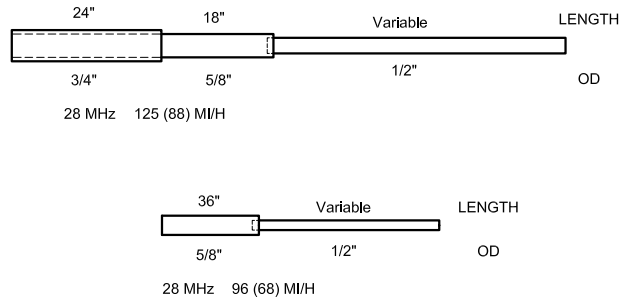

(D)

Fig 13—Gain, F/R and SWR performance versus frequency for optimized 10-meter Yagis. At A, gain is shown versus frequency for eight 10-meter Yagis whose booms range from 6 feet to 60 feet long. Except for the 2-element design, these Yagis have been optimized for better than 20 dB F/R and less than 2:1 SWR over the frequency range 28.0 to 28.8 MHz. At B, front-to-rear ratio for these antennas is shown versus frequency, and at C, SWR is shown over the frequency range. At D, the taper schedule is shown for heavy-duty and for medium-duty 10-meter elements. The heavy-duty elements can withstand 125-mph winds without icing, and 88-mph winds with 1/4-inch radial ice. The medium-duty elements can survive 96-mph winds without icing, and 68-mph winds with 1/4-inch radial ice. The wall thickness for each telescoping section of 6061-T6 aluminum tubing is 0.058 inches, and the overlap at each telescoping junction is 3 inches.

Table 1

Optimized 10-Meter Yagi Designs

Two-element 10-meter Yagi, 6 foot boom

Element	*Spacing*	*Heavy-Duty Tip*	*Medium-Duty Tip*
File Name		210-06H.YW	210-06M.YW
Reflector	0.000"	66.000"	71.500"
Driven Element	66.000"	57.625"	63.000"

Three-element 10-meter Yagi, 8 foot boom

Element	*Spacing*	*Heavy-Duty Tip*	*Medium-Duty Tip*
File Name		310-08H.YW	310-08M.YW
Reflector	0.000"	66.750"	71.875"
Driven Element	36.000"	57.625"	62.875"
Director 1	54.000"	53.125"	58.500"
Compensator	12" behind Dir. 1	19.000"	18.125"

Four-element 10-meter Yagi, 14 foot boom

Element	*Spacing*	*Heavy-Duty Tip*	*Medium-Duty Tip*
File Name		410-14H.YW	410-14M.YW
Reflector	0.000"	66.000"	72.000"
Driven Element	36.000"	58.625"	63.875"
Director 1	36.000"	57.000"	62.250"
Director 2	90.000"	47.750"	53.125"
Compensator	12" behind Dir. 2	22.000"	20.500"

Five-element 10-meter Yagi, 24 foot boom

Element	*Spacing, inches*	*Heavy-Duty Tip*	*Medium-Duty Tip*
File Name		510-24H.YW	510-24M.YW
Reflector	0.000"	65.625"	70.750"
Driven Element	36.000"	58.000"	63.250"
Director 1	36.000"	57.125"	62.375"
Director 2	99.000"	55.000"	60.250"
Director 3	111.000"	50.750"	56.125"
Compensator	12" behind Dir. 3	28.750"	26.750"

Six-element 10-meter Yagi, 36 foot boom

Element	*Spacing, inches*	*Heavy-Duty Tip*	*Medium-Duty Tip*
File Name		610-36H.YW	610-36M.YW
Reflector	0.000"	66.500"	71.500"
Driven Element	37.000"	58.500"	64.000"
Director 1	43.000"	57.125"	62.375"
Director 2	98.000"	54.875"	60.125"
Director 3	127.000"	53.875"	59.250"
Director 4	121.000"	49.875"	55.250"
Compensator	12" behind Dir. 4	32.000"	29.750"

Seven-element 10-meter Yagi, 48 foot boom

Element	*Spacing, inches*	*Heavy-Duty Tip*	*Medium-Duty Tip*
File Name		710-48H.YW	710-48M.YW
Reflector	0.000"	65.375"	70.500"
Driven Element	37.000"	59.000"	64.250"
Director 1	37.000"	57.500"	62.750"
Director 2	96.000"	54.875"	60.125"
Director 3	130.000"	52.250"	57.625"
Director 4	154.000"	52.625"	58.000"
Director 5	116.000"	49.875"	55.250"
Compensator	12" behind Dir. 5	35.750"	33.750"

Eight-element 10-meter Yagi, 60 foot boom

Element	*Spacing, inches*	*Heavy-Duty Tip*	*Medium-Duty Tip*
File Name		810-60H.YW	810-60M.YW
Reflector	0.000"	65.000"	70.125"
Driven Element	42.000"	58.000"	63.500"
Director 1	37.000"	57.125"	62.375"
Director 2	87.000"	55.375"	60.625"
Director 3	126.000"	53.250"	58.625"
Director 4	141.000"	51.875"	57.250"
Director 5	157.000"	52.500"	57.875"
Director 6	121.000"	50.125"	55.500"
Compensator	12" behind Dir. 6	59.375"	55.125"

These 10-meter Yagi designs are optimized for > 20 dB F/R, and SWR < 2:1 over frequency range from 28.000 to 28.800 MHz, for heavy-duty elements (125 mph wind survival) and for medium-duty (96 mph wind survival). For coverage from 28.8 to 29.7 MHz, subtract 2.000 inches from end of each element, but leave element spacings the same as shown here. Only element tip dimensions are shown, and all dimensions are inches. See Fig 13D for element telescoping tubing schedule. Torque compensator element is made of 2.5" OD PVC water pipe placed 12 inches behind last director. Dimensions shown for compensators is one-half of total length, centered on boom.

of U-bolts with saddles is used to secure the mounting plate to the boom.

Electrically each mounting plate is equivalent to a cylinder, with an effective diameter of 2.405 inches for the heavy-duty element, and 2.310 inches for the medium-duty element. The equivalent length on each side of the boom is 2 inches. These dimensions are incorporated in the files for the *YW* (Yagi for Windows) computer modeling program on the CD-ROM accompanying this book to simulate the effect of the mounting plate.

The second column in **Table 1** shows the spacing of each element relative to the next element in line on the boom, starting at the reflector, which itself is defined as being at the 0.000-inch reference point on the boom. The boom for antennas less than 30 feet long can be constructed of 2-inch OD tubing with 0.065-inch wall thickness. Designs larger than 30 feet long should use 3-inch OD heavy-wall tubing for the boom. Because each boom has extra space at each end, the reflector is actually placed 3 inches from the end of the boom. For example, in the 310-08H.YW design (3 elements on an 8-foot boom), the driven element is placed 36 inches ahead of the reflector, and the director is placed 54 inches ahead of the driven element.

The next columns give the lengths for the variable tips for the heavy-duty and then the medium-duty elements. In the example above for the 310-08H.YW Yagi, the heavy-duty reflector tip, made out of 1/2-inch OD tubing, sticks out 66.750 inches from the 5/8-inch OD tubing. Note that each telescoping piece of tubing overlaps 3 inches inside the piece into which it fits, so the overall length of 1/8-inch OD tubing is 69.750 inches long for the reflector. The medium-duty reflector tip has 71.875 inches protruding from the 5/8-inch OD tube, and is 74.875 inches long overall. As previously stated, the dimensions are not extremely critical, although measurement accu-

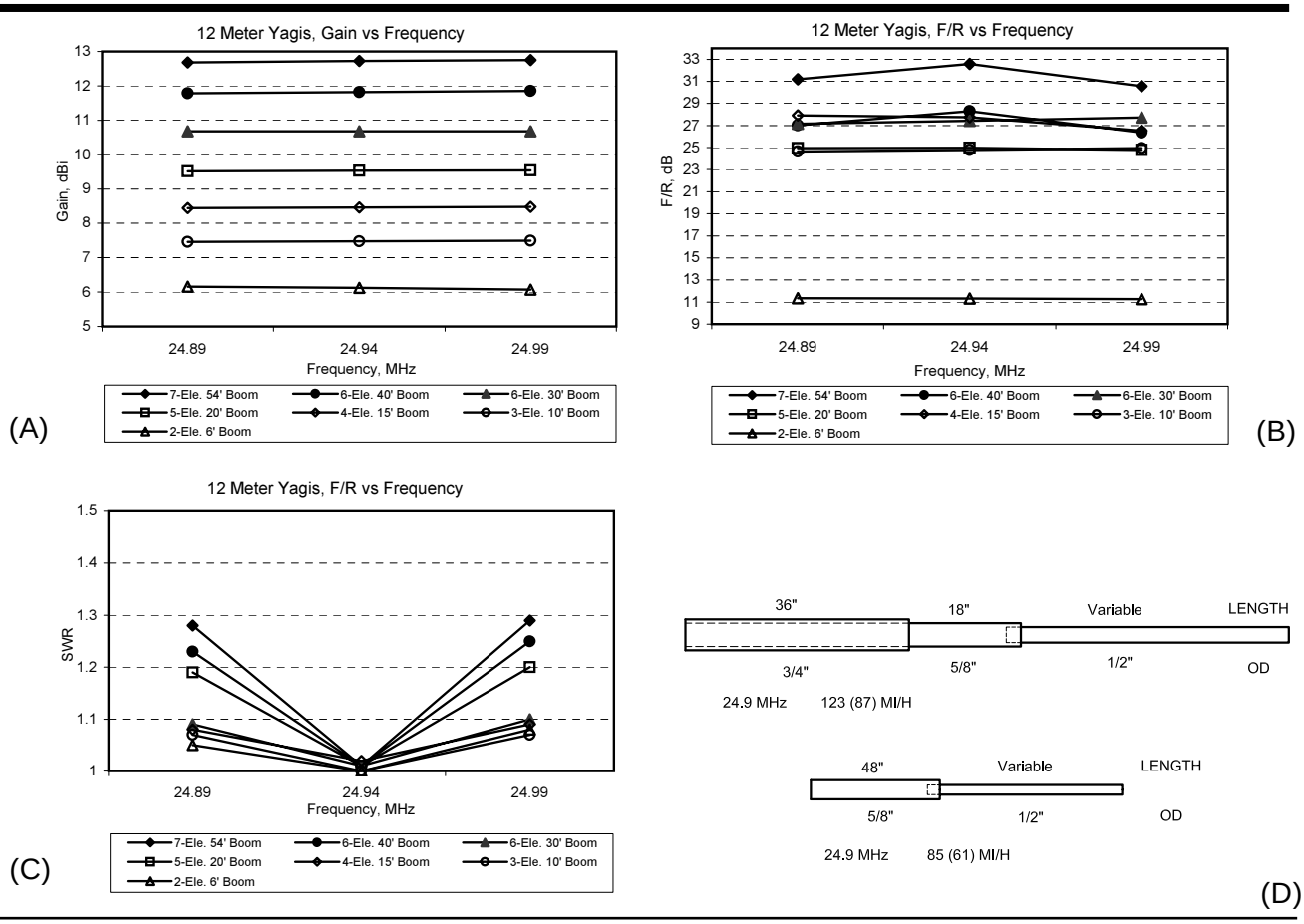

Fig 14—Gain, F/R and SWR performance versus frequency for optimized 12-meter Yagis. At A, gain is shown versus frequency for seven 12-meter Yagis whose booms range from 6 feet to 54 feet long. Except for the 2-element design, these Yagis have been optimized for better than 20 dB F/R and less than 2:1 SWR over the narrow 12-meter band 24.89 to 24.99 MHz. At B, front-to-rear ratio for these antennas is shown versus frequency, and at C, SWR over the frequency range is shown. At D, the taper schedule for heavy-duty and for medium-duty 12-meter elements is shown. The heavy-duty elements can withstand 123-mph winds without icing, and 87-mph winds with 1/4-inch radial ice. The medium-duty elements can survive 85-mph winds without icing, and 61-mph winds with 1/4-inch radial ice. The wall thickness for each telescoping section of 6061-T6 aluminum tubing is 0.058 inches, and the overlap at each telescoping junction is 3 inches.

Table 2

Optimized 12-Meter Yagi Designs

Two-element 12-meter Yagi, 6 foot boom

Element	*Spacing*	*Heavy-Duty Tip*	*Medium-Duty Tip*
File Name		212-06H.YW	212-06M.YW
Reflector	0.000"	67.500"	72.500"
Driven Element	66.000"	59.500"	65.000"

Three-element 12-meter Yagi, 10 foot boom

Element	*Spacing, inches*	*Heavy-Duty Tip*	*Medium-Duty Tip*
File Name		312-10H.YW	312-10M.YW
Reflector	0.000"	69.000"	73.875"
Driven Element	40.000"	60.250"	65.250"
Director 1	74.000"	54.000"	59.125"
Compensator	12" behind Dir. 1	13.625"	12.000"

Four-element 12-meter Yagi, 15 foot boom

Element	*Spacing, inches*	*Heavy-Duty Tip*	*Medium-Duty Tip*
File Name		412-15H.YW	412-15M.YW
Reflector	0.000"	66.875"	71.875"
Driven Element	46.000"	61.000"	66.000"
Director 1	46.000"	58.625"	63.750"
Director 2	82.000"	50.875"	56.125"
Compensator	12" behind Dir. 2	16.375"	14.500"

Five-element 12-meter Yagi, 20 foot boom

Element	*Spacing, inches*	*Heavy-Duty Tip*	*Medium-Duty Tip*
File Name		512-20H.YW	512-20M.YW
Reflector	0.000"	69.750"	74.625"
Driven Element	46.000"	62.250"	67.000"
Director 1	46.000"	60.500"	65.500"
Director 2	48.000"	55.500"	60.625"
Director 3	94.000"	54.625"	59.750"
Compensator	12" behind Dir. 3	22.125"	19.625"

Six-element 12-meter Yagi, 30 foot boom

Element	*Spacing, inches*	*Heavy-Duty Tip*	*Medium-Duty Tip*
File Name		612-30H.YW	612-30M.YW
Reflector	0.000"	68.125"	73.000"
Driven Element	46.000"	61.750"	66.750"
Director 1	46.000"	60.250"	65.250"
Director 2	73.000"	52.375"	57.625"
Director 3	75.000"	57.625"	62.750"
Director 4	114.000"	53.625"	58.750"
Compensator	12" behind Dir. 4	30.000"	26.250"

Six-element 12-meter Yagi, 40 foot boom

Element	*Spacing, inches*	*Heavy-Duty Tip*	*Medium-Duty Tip*
File Name		612-40H.YW	612-40M.YW
Reflector	0.000"	67.000"	71.875"
Driven Element	46.000"	60.125"	65.500"
Director 1	46.000"	57.375"	62.500"
Director 2	91.000"	57.375"	62.500"
Director 3	157.000"	57.000"	62.125"
Director 4	134.000"	54.375"	59.500"
Compensator	12" behind Dir. 4	36.500"	31.625"

Seven-element 12-meter Yagi, 54 foot boom

Element	*Spacing, inches*	*Heavy-Duty Tip*	*Medium-Duty Tip*
File Name		712-54H.YW	712-54M.YW
Reflector	0.000"	68.000"	73.000"
Driven Element	46.000"	60.500"	65.500"
Director 1	46.000"	56.750"	61.875"
Director 2	75.000"	58.000"	63.125"
Director 3	161.000"	55.625"	60.750"
Director 4	174.000"	56.000"	61.125"
Director 5	140.000"	53.125"	58.375"
Compensator	12" behind Dir. 5	43.125"	37.500"

These 12-meter Yagi designs were optimized for > 20 dB F/R, and SWR < 2:1 over frequency range from 24.890 to 24.990 MHz, for heavy-duty elements (123 mph wind survival) and for medium-duty (85 mph wind survival). Only element tip dimensions are shown, and all dimensions are inches. See Fig 14D for element telescoping tubing schedule. Torque compensator element is made of 2.5" OD PVC water pipe placed 12" behind last director. Dimensions shown for compensators is one-half of total length, centered on boom.

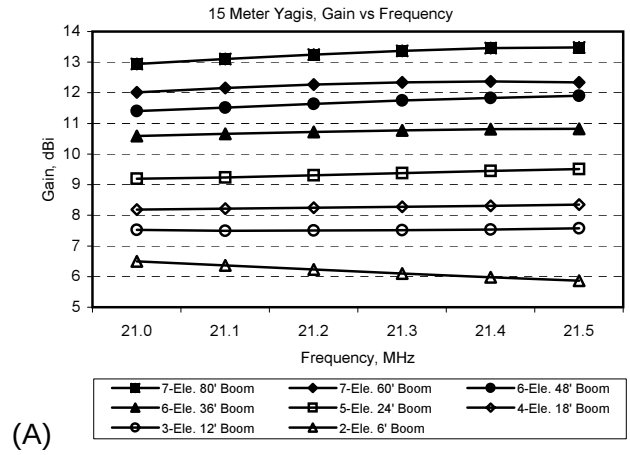

(A)

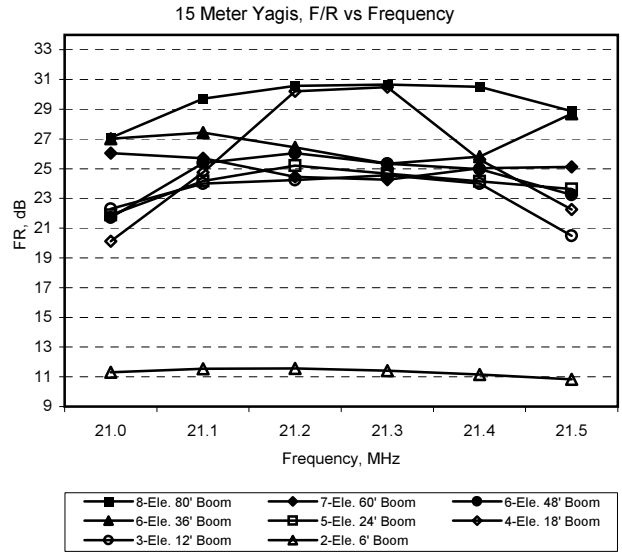

(B)

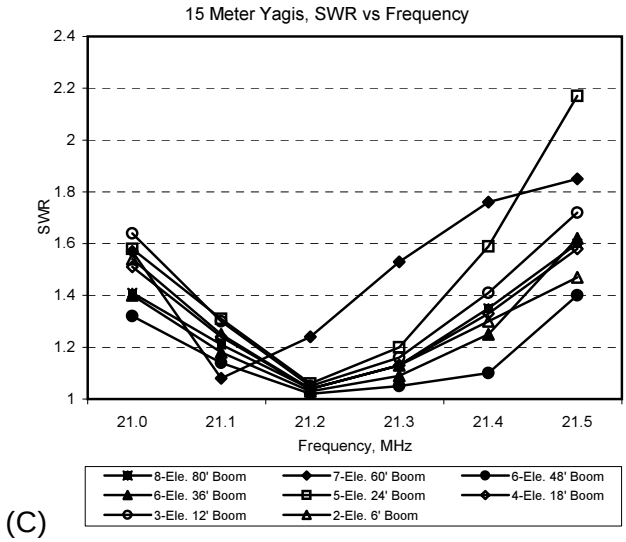

(C)

Fig 15—Gain, F/R and SWR performance versus frequency for optimized 15-meter Yagis. At A, gain versus frequency is shown for eight 15-meter Yagis whose booms range from 6 feet to 80 feet long. Except for the 2-element design, these Yagis have been optimized for better than 20 dB F/R and less than 2:1 SWR over the frequency range 21.0 to 21.45 MHz. At B, front-to-rear ratio for these antennas is shown versus frequency, and at C, SWR over the frequency range is shown. At D, the taper schedule for heavy-duty and for medium-duty 15-meter elements is shown. The heavy-duty elements can withstand 124-mph winds without icing, and 90-mph winds with 1/4-inch radial ice. The medium-duty elements can survive 86-mph winds without icing, and 61-mph winds with 1/4-inch radial ice. The wall thickness for each telescoping section of 6061-T6 aluminum tubing is 0.058 inches, and the overlap at each telescoping junction is 3 inches.

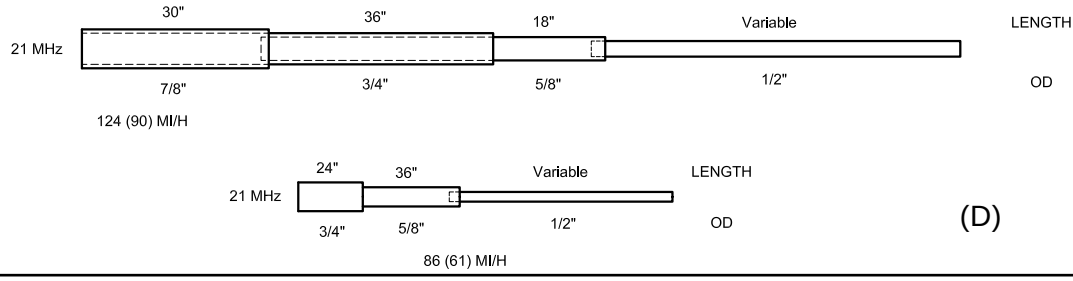

(D)

racy to 1/8 inch is desirable.

The last row in each variable tip column shows the length of one-half of the "dummy element" torque compensator used to correct for uneven wind loading along the boom. This compensator is made from 2.5 inches OD PVC water pipe mounted to an element-to-boom plate like those used for each element. The compensator is mounted 12 inches behind the last director, the first director in the case of the 3-element 310-08H.YW antenna. Note that the heavy-duty elements require a correspondingly longer torque compensator than do the medium-duty elements.

12-METER YAGIS

Fig 14 describes the electrical performance of seven optimized 12-meter Yagis with boom lengths between 6 to 54 feet. The end of each boom includes 3 inches of space for the reflector and last director (or driven element) mounting plates. The narrow frequency width of the 12-meter band allows the performance to be optimized easily. Fig 14A shows the free-space gain versus frequency for each antenna; 14B shows the front-to-rear ratio, and 14C shows the SWR versus frequency. Each antenna with three or more elements was designed to

Table 3
Optimized 15-Meter Yagi Designs

Two-element 15-meter Yagi, 6 foot boom

Element	*Spacing*	*Heavy-Duty Tip*	*Medium-Duty Tip*
File Name		215-06H.YW	215-06M.YW
Reflector	0.000"	62.000"	85.000"
Driven Element	66.000"	51.000"	74.000"

Three-element 15-meter Yagi, 12 foot boom

Element	*Spacing*	*Heavy-Duty Tip*	*Medium-Duty Tip*
File Name		315-12H.YW	315-12M.YW
Reflector	0.000"	62.000"	84.250"
Driven Element	48.000"	51.000"	73.750"
Director 1	92.000"	43.500"	66.750"
Compensator	12" behind Dir. 1	34.750"	37.625"

Four-element 15-meter Yagi, 18 foot boom

Element	*Spacing*	*Heavy-Duty Tip*	*Medium-Duty Tip*
File Name		415-18H.YW	415-18M.YW
Reflector	0.000"	61.000"	83.500"
Driven Element	56.000"	51.500"	74.500"
Director 1	56.000"	48.000"	71.125"
Director 2	98.000"	36.625"	60.250"
Compensator	12" behind Dir. 2	20.875"	18.625"

Five-element 15-meter Yagi, 24 foot boom

E*lement*	*Spacing*	*Heavy-Duty Tip*	*Medium-Duty Tip*
File Name		515-24H.YW	515-24M.YW
Reflector	0.000"	62.000"	84.375"
Driven Element	48.000"	52.375"	75.250"
Director 1	48.000"	47.875"	71.000"
Director 2	52.000"	47.000"	70.125"
Director 3	134.000"	41.000"	64.375"
Compensator	12" behind Dir. 3	40.250"	35.125"

Six-element 15-meter Yagi, 36 foot boom

Element	*Spacing*	*Heavy-Duty Tip*	*Medium-Duty Tip*
File Name		615-36H.YW	615-36M.YW
Reflector	0.000"	61.000"	83.375"
Driven Element	53.000"	52.000"	75.000"
Director 1	56.000"	49.125"	72.125"
Director 2	59.000"	45.125"	68.375"
Director 3	116.000"	47.875"	71.000"
Director 4	142.000"	42.000"	65.375"
Compensator	12" behind Dir. 4	45.500"	39.750"

Seven-element 15-meter Yagi, 48 foot boom

Element	*Spacing*	*Heavy-Duty Tip*	*Medium-Duty Tip*
File Name		615-48H.YW	615-48M.YW
Reflector	0.000"	62.000"	84.000"
Driven Element	48.000"	52.000"	75.000"
Director 1	48.000"	51.250"	74.125"
Director 2	125.000"	48.000"	71.125"
Director 3	190.000"	45.500"	68.750"
Director 4	161.000"	42.000"	65.375"
Compensator	12" behind Dir. 4	51.500"	45.375"

Seven-element 15-meter Yagi, 60 foot boom

Element	*Spacing*	*Heavy-Duty Tip*	*Medium-Duty Tip*
File Name		715-60H.YW	715-60M.YW
Reflector	0.000"	59.750"	82.250"
Driven Element	48.000"	52.000"	75.000"
Director 1	48.000"	52.000"	74.875"
Director 2	93.000"	49.500"	72.500"
Director 3	173.000"	44.125"	67.375"
Director 4	197.000"	45.500"	68.750"
Director 5	155.000"	41.750"	65.125"
Compensator	12" behind Dir. 5	58.500"	51.000"

Eight-element 15-meter Yagi, 80 foot boom

Element	*Spacing*	*Heavy-Duty Tip*	*Medium-Duty Tip*
File Name		815-80H.YW	815-80M.YW
Reflector	0.000"	62.000"	84.000"
Driven Element	56.000"	52.500"	75.500"
Director 1	48.000"	51.500"	74.375"
Director 2	115.000"	48.375"	71.500"
Director 3	164.000"	45.750"	69.000"
Director 4	202.000"	43.125"	66.500"
Director 5	206.000"	44.750"	68.000"
Director 6	163.000"	40.875"	64.250"
Compensator	12" behind Dir. 6	95.000"	83.375"

These 15-meter Yagi designs are optimized for > 20 dB F/R, and SWR < 2:1 over entire frequency range from 21.000 to 21.450 MHz, for heavy-duty elements (124 mph wind survival) and for medium-duty (86 mph wind survival). Only element tip dimensions are shown. See Fig 15D for element telescoping tubing schedule. All dimensions are in inches. Torque compensator element is made of 2.5" OD PVC water pipe placed 12" behind last director, and dimensions shown for compensators is one-half of total length, centered on boom.

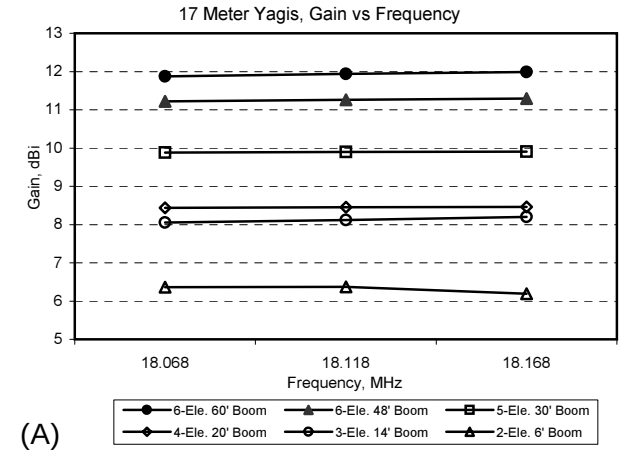

(A)

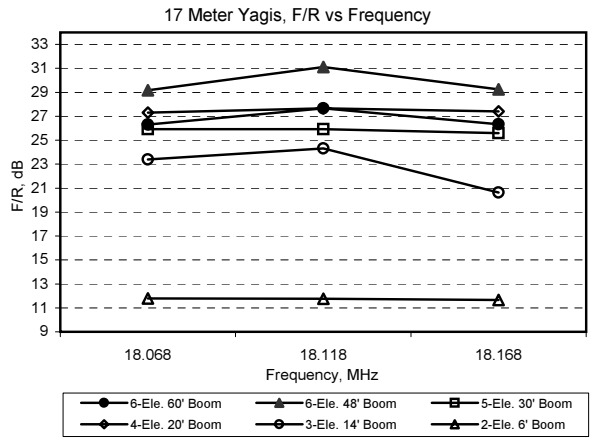

(B)

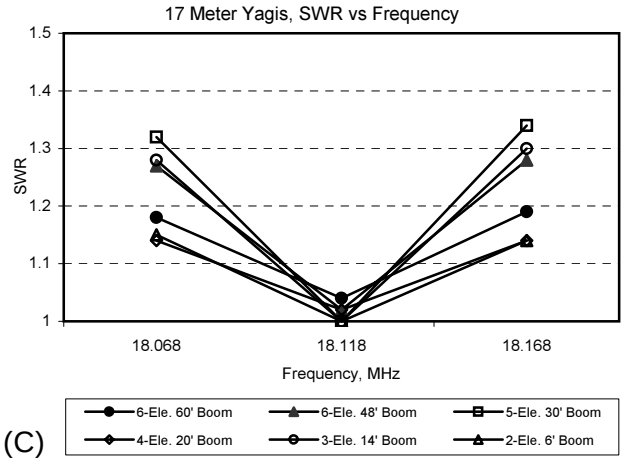

(C)

Fig 16—Gain, F/R and SWR performance versus frequency for optimized 17-meter Yagis. At A, gain versus frequency is shown for six 17-meter Yagis whose booms range from 6 feet to 60 feet long. Except for the 2-element design, these Yagis have been optimized for better than 20 dB F/R and less than 2:1 SWR over the narrow 17-meter band 18.068 to 18.168 MHz. At B, front-to-rear ratio for these antennas is shown versus frequency, and at C, SWR over the frequency range is shown. At D, the taper schedule for heavy-duty and for medium-duty 10-meter elements is shown. The heavy-duty elements can withstand 123-mph winds without icing, and 89-mph winds with 1/4-inch radial ice. The medium-duty elements can survive 83-mph winds without icing, and 59-mph winds with 1/4-inch radial ice. The wall thickness for each telescoping section of 6061-T6 aluminum tubing is 0.058 inches, and the overlap at each telescoping junction is 3 inches.

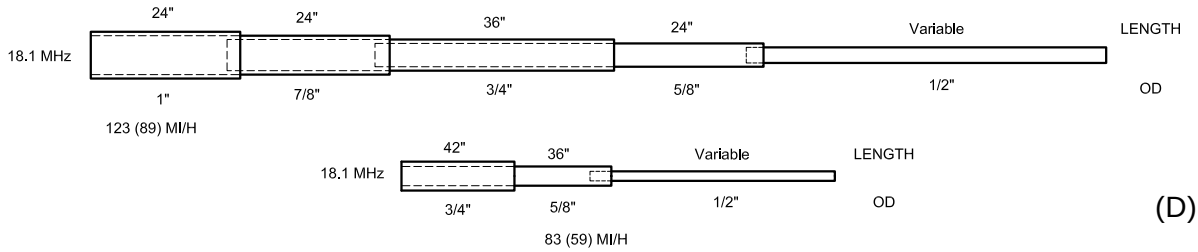

(D)

cover the narrow 12-meter band from 24.89 to 24.99 MHz, with SWR less than 2:1 and F/R better than 20 dB over that range.

Fig 14D shows the taper schedule for two types of 12-meter elements. The heavy-duty design can survive 123-mph winds with no icing, and 87-mph winds with 1/4 inch of radial ice. The medium-duty design can handle 85-mph winds with no icing, and 61-mph winds with 1/4 inch of radial ice. The element-to-boom mounting plate for these Yagis is a 0.375 inch thick flat aluminum plate, 5 inches wide by 6 inches long.

Electrically, each mounting plate is equivalent to a cylinder, with an effective diameter of 2.945 inches for the heavy-duty element, and 2.857 inches for the medium-duty element. The equivalent length on each side of the boom is 3 inches. As usual, the torque compensator is mounted 12 inches behind the last director.

15-METER YAGIS

Fig 15 describes the electrical performance of eight optimized 15-meter Yagis with boom lengths between 6 feet to a spectacular 80 feet. The end of each boom includes 3 inches of space for the reflector and last-director (or driven element) mounting plates. Fig 15A shows the free-space gain versus frequency for each antenna; 15B shows the worst-case front-to-rear ratio, and 15C shows the SWR versus frequency. Each antenna with three or more elements was designed to cover the full 15-meter band from

Table 4
Optimized 17-meter Yagi Designs

Two-element 17-meter Yagi, 6 foot boom

Element	*Spacing*	*Heavy-Duty Tip*	*Medium-Duty Tip*
File Name		217-06H.YW	217-06M.YW
Reflector	0.000"	61.000"	89.000"
Driven Element	66.000"	48.000"	76.250"

Three-element 17-meter Yagi, 14 foot boom

Element	*Spacing*	*Heavy-Duty Tip*	*Medium-Duty Tip*
File Name		317-14H.YW	317-14M.YW
Reflector	0.000"	61.500"	91.500"
Driven Element	65.000"	52.000"	79.500"
Director 1	97.000"	46.000"	73.000"
	12" behind Dir. 1	12.625"	10.750"

Four-element 17-meter Yagi, 20 foot boom

Element	*Spacing*	*Heavy-Duty Tip*	*Medium-Duty Tip*
File Name		417-20H.YW	417-20M.YW
Reflector	0.000"	61.500"	89.500"
Driven Element	48.000"	54.250"	82.625"
Director 1	48.000"	52.625"	81.125"
Director 2	138.000"	40.500"	69.625"
Compensator	12" behind Dir. 2	42.500"	36.250"

Five-element 17-meter Yagi, 30 foot boom

Element	*Spacing*	*Heavy-Duty Tip*	*Medium-Duty Tip*
File Name		517-30H.YW	517-30M.YW
Reflector	0.000"	61.875"	89.875"
Driven Element	48.000"	52.250"	80.500"
Director 1	52.000"	49.625"	78.250"
Director 2	93.000"	49.875"	78.500"
Director 3	161.000"	43.500"	72.500"
Compensator	12" behind Dir. 3	54.375"	45.875"

Six-element 17-meter Yagi, 48 foot boom

Element	*Spacing*	*Heavy-Duty Tip*	*Medium-Duty Tip*
File Name		617-48H.YW	617-48M.YW
Reflector	0.000"	63.000"	90.250"
Driven Element	52.000"	52.500"	80.500"
Director 1	51.000"	45.500"	74.375"
Director 2	87.000"	47.875"	76.625"
Director 3	204.000"	47.000"	75.875"
Director 4	176.000"	42.000"	71.125"
Compensator	12" behind Dir. 4	68.250"	57.500"

Six-element 17-meter Yagi, 60 foot boom

Element	*Spacing*	*Heavy-Duty Tip*	*Medium-Duty Tip*
File Name		617-60H.YW	617-60M.YW
Reflector	0.000"	61.250"	89.250"
Driven Element	54.000"	54.750"	83.125"
Director 1	54.000"	52.250"	80.750"
Director 2	180.000"	46.000"	74.875"
Director 3	235.000"	44.625"	73.625"
Director 4	191.000"	41.500"	70.625"
Compensator	12" behind Dir. 4	62.875"	53.000"

These 17-m Yagi designs are optimized for > 20 dB F/R, and SWR < 2:1 over entire frequency range from18.068 to 18.168 MHz, for heavy-duty elements (123 mph wind survival) and for medium-duty (83 mph wind survival). Only element tip dimensions are shown. All dimensions are in inches. Torque compensator element is made of 2.5" OD PVC water pipe placed 12" behind last director, and dimensions shown for compensators is one-half of total length, centered on boom.

21.000 to 21.450 MHz, with SWR less than 2:1 and F/R ratio better than 20 dB over that range.

Fig 15D shows the taper schedule for two types of 15-meter elements. The heavy-duty design can survive 124-mph winds with no icing, and 90-mph winds with 1/4 inch of radial ice. The medium-duty design can handle 86-mph winds with no icing, and 61-mph winds with 1/4 inch of radial ice. The element-to-boom mounting plate for these Yagis is a 0.375-inch thick flat aluminum plate, 5 inches wide by 6 inches long.

Electrically, each mounting plate is equivalent to a cylinder, with an effective diameter of 3.0362 inches for

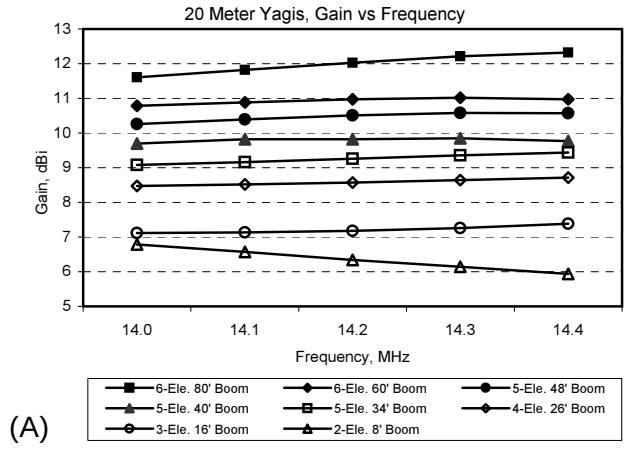

(A)

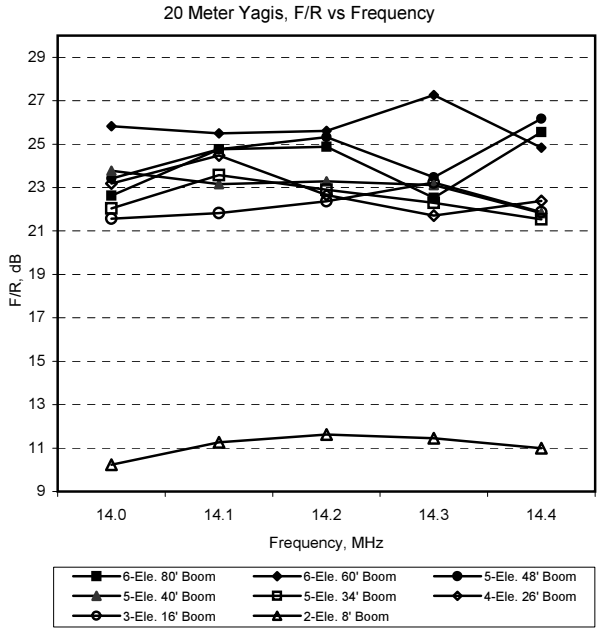

(B)

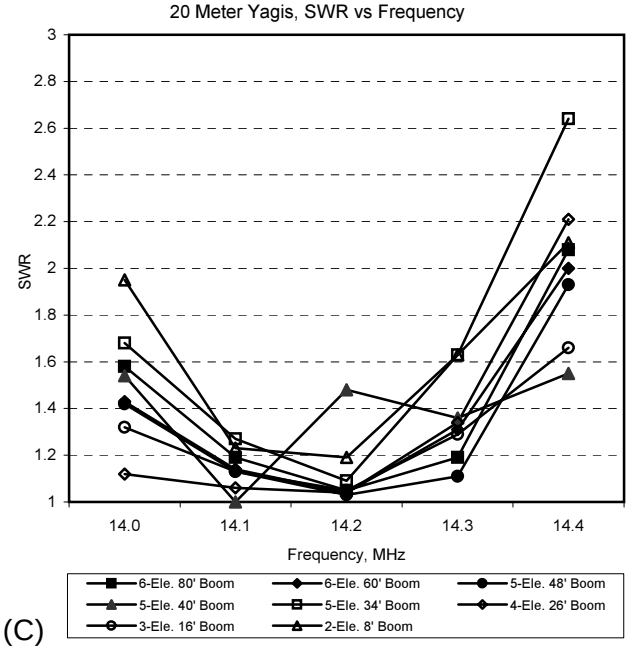

(C)

Fig 17—Gain, F/R and SWR performance versus frequency for optimized 20-meter Yagis. At A, gain versus frequency is shown for eight 20-meter Yagis whose booms range from 8 feet to 80 feet long. Except for the 2-element design, these Yagis have been optimized for better than 20 dB F/R and less than 2:1 SWR over the frequency range 14.0 to 14.35 MHz. At B, front-to-rear ratio for these antennas is shown versus frequency, and at C, SWR over the frequency range is shown. At D, the taper schedule for heavy-duty and for medium-duty 20-meter elements is shown. The heavy-duty elements can withstand 122-mph winds without icing, and 89-mph winds with 1/4-inch radial ice. The medium-duty elements can survive 82-mph winds without icing, and 60-mph winds with 1/4-inch radial ice. The wall thickness for each telescoping section of 6061-T6 aluminum tubing is 0.058 inches, and the overlap at each telescoping junction is 3 inches.

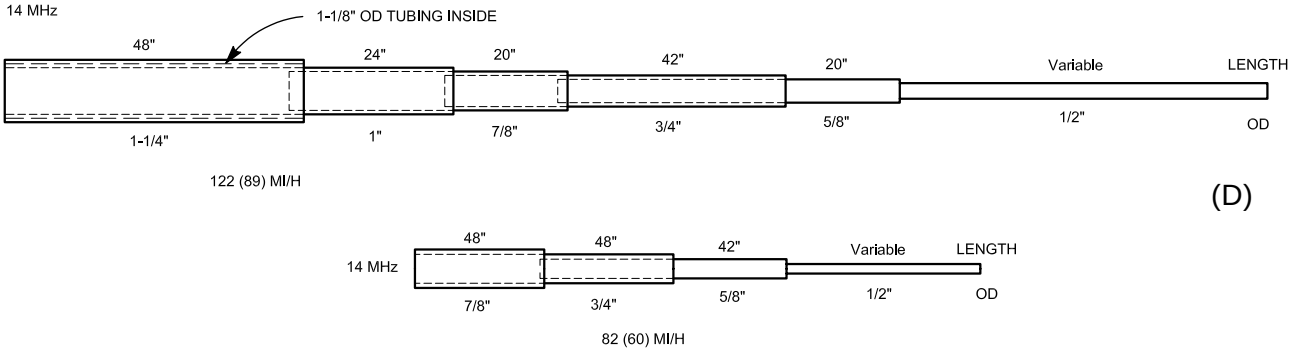

(D)

the heavy-duty element, and 2.9447 inches for the medium-duty element. The equivalent length on each side of the boom is 3 inches. As usual, the torque compensator is mounted 12 inches behind the last director.

17-METER YAGIS

Fig 16 describes the electrical performance of six optimized 17-meter Yagis with boom lengths between 6 to a heroic 60 feet. As usual, the end of each boom includes 3 inches of space for the reflector and last director (or driven element) mounting plates. Fig 16A shows the free-space gain versus frequency for each an-

Table 5

Optimized 20-Meter Yagi Designs

Two-element 20-meter Yagi, 8 foot boom

Element	*Spacing*	*Heavy-Duty Tip*	*Medium-Duty Tip*
File Name		220-08H.YW	220-08M.YW
Reflector	0.000"	66.000"	80.000"
Driven Element	90.000"	46.000"	59.000"

Three-element 20-meter Yagi, 16 foot boom

Element	*Spacing*	*Heavy-Duty Tip*	*Medium-Duty Tip*
File Name		320-16H.YW	320-16M.YW
Reflector	0.000"	69.625"	81.625"
Driven Element	80.000"	51.250"	64.500"
Director 1	106.000"	42.625"	56.375"
Compensator	12" behind Dir. 1	33.375"	38.250"

Four-element 20-meter Yagi, 26 foot boom

Element	*Spacing*	*Heavy-Duty Tip*	*Medium-Duty Tip*
File Name		420-26H.YW	420-26M.YW
Reflector	0.000"	65.625"	78.000"
Driven Element	72.000"	53.375"	65.375"
Director 1	60.000"	51.750"	63.875"
Director 2	174.000"	38.625"	51.500"
Compensator	12" behind Dir. 2	54.250"	44.250"

Five-element 20-meter Yagi, 34 foot boom

Element	*Spacing*	*Heavy-Duty Tip*	*Medium-Duty Tip*
File Name		520-34H.YW	520-34M.YW
Reflector	0.000"	68.625"	80.750"
Driven Element	72.000"	52.250"	65.500"
Director 1	71.000"	45.875"	59.375"
Director 2	68.000"	45.875"	59.375"
Director 3	191.000"	37.000"	51.000"
Compensator	12" behind Dir. 3	69.250"	56.250"

Five-element 20-meter Yagi, 40 foot boom

Element	*Spacing*	*Heavy-Duty Tip*	*Medium-Duty Tip*
File Name		520-40H.YW	520-40M.YW
Reflector	0.000"	68.375"	80.500"
Driven Element	72.000"	53.500"	66.625"
Director 1	72.000"	51.500"	64.625"
Director 2	139.000"	48.375"	61.750"
Director 3	191.000"	38.000"	52.000"
Compensator	12" behind Dir. 3	69.750"	56.750"

Five-element 20-meter Yagi, 48 foot boom

Element	*Spacing*	*Heavy-Duty Tip*	*Medium-Duty Tip*
File Name		520-48H.YW	520-48M.YW
Reflector	0.000"	66.250"	78.500"
Driven Element	72.000"	53.000"	66.000"
Director 1	88.000"	50.500"	63.750"
Director 2	199.000"	47.375"	60.875"
Director 3	211.000"	39.750"	53.625"
Compensator	12" behind Dir. 3	70.325"	57.325"

Six-element 20-meter Yagi, 60 foot boom

Element	*Spacing*	*Heavy-Duty Tip*	*Medium-Duty Tip*
File Name		620-60H.YW	620-60M.YW
Reflector	0.000"	67.000"	79.250"
Driven Element	84.000"	51.500"	65.000"
Director 1	91.000"	45.125"	58.750"
Director 2	130.000"	41.375"	55.125"
Director 3	210.000"	46.875"	60.375"
Director 4	199.000"	39.125"	53.000"
Compensator	12" behind Dir. 4	72.875"	59.250"

Six-element 20-meter Yagi, 80 foot boom

Element	*Spacing*	*Heavy-Duty Tip*	*Medium-Duty Tip*
File Name		620-80H.YW	620-80M.YW
Reflector	0.000"	66.125"	78.375"
Driven Element	72.000"	52.375"	65.500"
Director 1	122.000"	49.125"	62.500"
Director 2	229.000"	44.500"	58.125"
Director 3	291.000"	42.625"	56.375"
Director 4	240.000"	38.750"	52.625"
Compensator	12" behind Dir. 4	78.750"	64.125"

These 20-meter Yagi designs are optimized for > 20 dB F/R, and SWR < 2:1 over entire frequency range from 14.000 to 14.350 MHz, for heavy-duty elements (122 mph wind survival) and for medium-duty (82 mph wind survival). Only element tip dimensions are shown. See Fig 17 for element telescoping tubing schedule. All dimensions are in inches. Torque compensator element is made of 2.5" OD PVC water pipe placed 12" behind last director, and dimensions shown for compensators is one-half of total length, centered on boom.

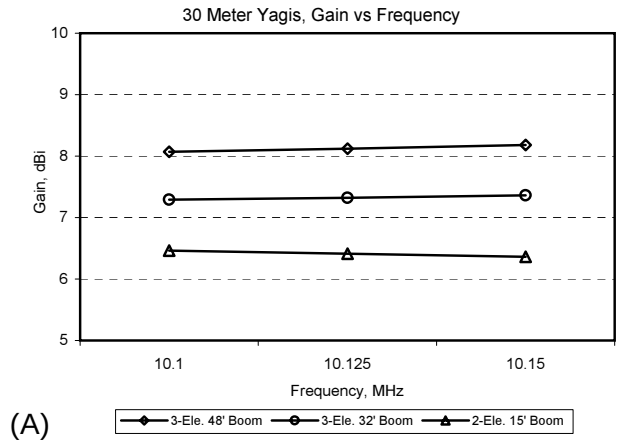

(A)

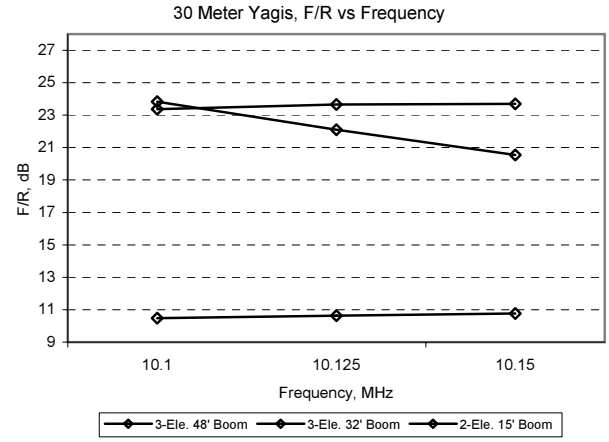

(B)

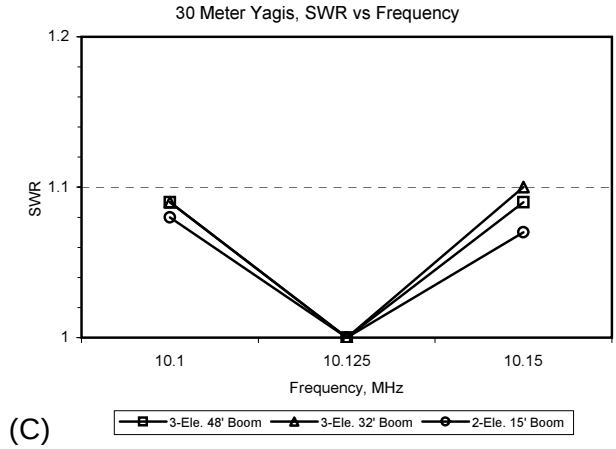

(C)

Fig 18—Gain, F/R and SWR performance versus frequency for optimized 30-meter Yagis. At A, gain versus frequency is shown for three 30-meter Yagis whose booms range from 15 feet to 34 feet long, and which have been optimized for better than 10 dB F/R and less than 2:1 SWR over the frequency range 10.1 to 10.15 MHz. At B, front-to-rear ratio for these antennas is shown versus frequency, and at C, SWR over the frequency range is shown. At D, the taper schedule is shown for heavy-duty 30-meter elements, which can withstand 107-mph winds without icing, and 93-mph winds with $^1/_4$-inch radial ice. Except for the 2$^1/_4$-inch and 2-inch sections, which have 0.083 inch thick walls, the wall thickness for the other telescoping sections of 6061-T6 aluminum tubing is 0.058 inches, and the overlap at the 1 inch telescoping junction with the $^7/_8$-inch section is complete. The 2-inch section utilizes two machined aluminum reducers to accommodate the 1-inch tubing.

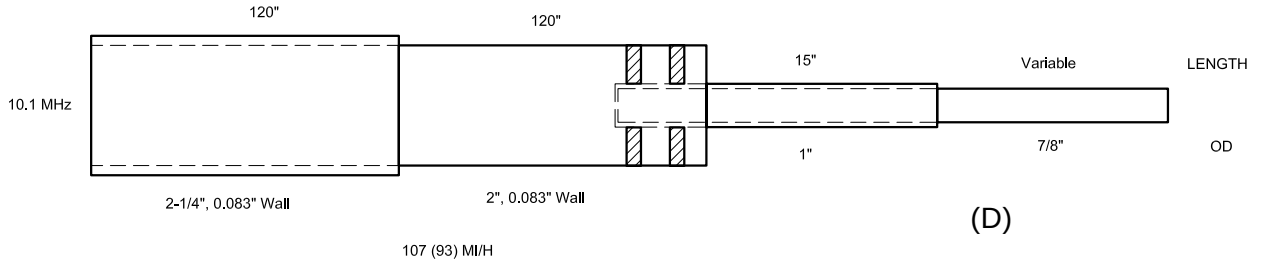

(D)

tenna; 16B shows the worst-case front-to-rear ratio, and 16C shows the SWR versus frequency. Each antenna with three or more elements was designed to cover the narrow 17-meter band from 18.068 to 18.168 MHz, with SWR less than 2:1 and F/R ratio better than 20 dB over that range.

Fig 16D shows the taper schedule for two types of 17-meter elements. The heavy-duty design can survive 123-mph winds with no icing, and 83-mph winds with $^1/_4$-inch of radial ice. The medium-duty design can handle 83-mph winds with no icing, and 59-mph winds with ¼ inch of radial ice.

The element-to-boom mounting plate for these Yagis is a 0.375-inch thick flat aluminum plate, 6 inches wide by 8 inches long. Electrically, each mounting plate is equivalent to a cylinder, with an effective diameter of 3.5122 inches for the heavy-duty element, and 3.3299 inches for the medium-duty element. The equivalent length on each side of the boom is 4 inches. As usual, the torque compensator is mounted 12 inches behind the last director.

20-METER YAGIS

Fig 17 describes the electrical performance of eight optimized 20-meter Yagis with boom lengths between 8 to a giant 80 feet. As usual, the end of each boom includes 3 inches of space for the reflector and last director (driven element) mounting plates. Fig 17A shows the free-space gain versus frequency for each antenna; 17B shows the front-to-rear ratio, and 17C shows the SWR versus frequency. Each antenna with three or more ele-

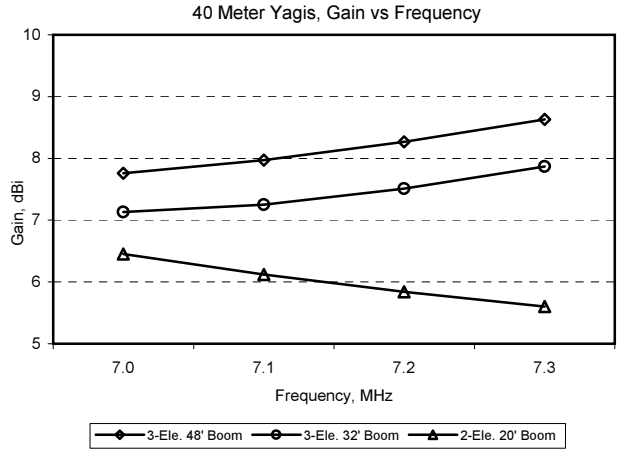

(A)

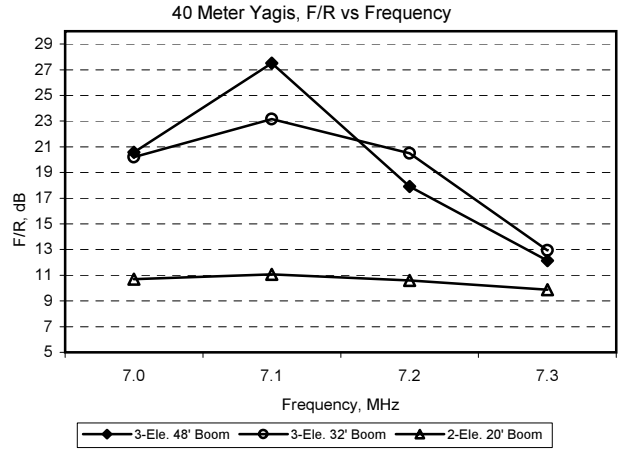

(B)

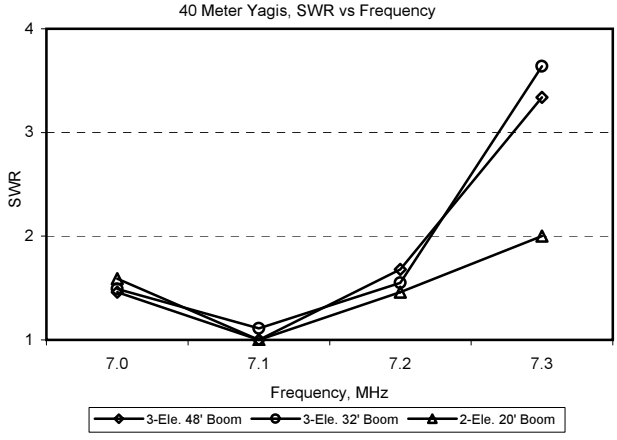

(C)

Fig 19—Gain, F/R and SWR performance versus frequency for optimized 40-meter Yagis. At A, gain versus frequency is shown for three 40-meter Yagis whose booms range from 20 feet to 48 feet long, and which have been optimized for better than 10 dB F/R and less than 2:1 SWR over the frequency range 7.0 to 7.2 MHz. At B, front-to-rear ratio for these antennas is shown versus frequency, and at C, SWR over the frequency range is shown. At D, the taper schedule is shown for heavy-duty 40-meter elements, which can withstand 107-mph winds without icing, and 93-mph winds with 1/4-inch radial ice. Except for the 2 1/4-inch and 2-inch sections, which have 0.083 inch thick walls, the wall thickness for the other telescoping sections of 6061-T6 aluminum tubing is 0.058 inches, and the overlap at the end telescoping junction is 3 inches. The 2-inch section utilizes two machined aluminum reducers to accommodate the 1-inch tubing.

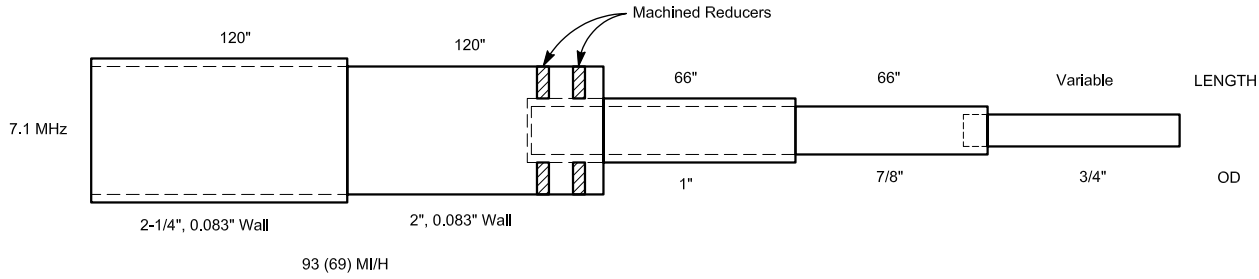

(D)

ments was designed to cover the complete 20-meter band from 14.000 to 14.350 MHz, with SWR less than 2:1 and F/R ratio better than 20 dB over that range.

Fig 17D shows the taper schedule for two types of 20-meter elements. The heavy-duty design can survive 122-mph winds with no icing, and 89-mph winds with 1/4 inch of radial ice. The medium-duty design can handle 82-mph winds with no icing, and 60-mph winds with 1/4 inch of radial ice. The element-to-boom mounting plate for these Yagis is a 0.375-inch thick flat aluminum plate, 6 inches wide by 8 inches long. Electrically, each mounting plate is equivalent to a cylinder, with an effective diameter of 3.7063 inches for the heavy-duty element, and 3.4194 inches for the medium-duty element. The equivalent length on each side of the boom is 4 inches. As usual, the torque compensator is mounted 12 inches behind the last director.

30-METER YAGIS

Fig 18 describes the electrical performance of three

Table 6
Optimized 30-Meter Yagi Designs

Two-element 30-meter Yagi, 15 foot boom

Element	*Spacing*	*Heavy-Duty Tip*
File Name		230-15H.YW
Reflector	0.000"	50.250"
Driven Element	174.000"	14.875"

3-element 30-meter Yagi, 22 foot boom

Element	*Spacing*	*Heavy-Duty Tip*
File Name		330-22H.YW
Reflector	0.000	59.375
Driven Element	135.000	35.000
Director 1	123.000	19.625

Three-element 30-meter Yagi, 34 foot boom

Element	*Spacing*	*Heavy-Duty Tip*
File Name		330-34H.YW
Reflector	0.000"	53.750"
Driven Element	212"	29.000"
Director 1	190"	14.500"

These 30-m Yagi designs are optimized for > 10 dB F/R, and SWR < 2:1 over entire frequency range from 10.100 to 10.150 MHz for heavy-duty elements (105 mph wind survival). Only element tip dimensions are shown. See Fig 18D for element telescoping tubing schedule. All dimensions are in inches. No torque compensator element is required.

Table 7
Optimized 40-Meter Yagi Designs

Two-element 40-meter Yagi, 20 foot boom

Element	*Spacing*	*Heavy-Duty Tip*
File Name		240-20H.YW
Reflector	0.000"	85.000"
Driven Element	234.000"	35.000"

Three-element 40-meter Yagi, 32 foot boom

Element	*Spacing*	*Heavy-Duty Tip*
File Name		340-32H.YW
Reflector	0.000"	90.750"
Driven Element	196.000"	55.875"
Director 1	182.000"	33.875"

Three-element 40-meter Yagi, 48 foot boom

Element	*Spacing*	*Heavy-Duty Tip*
File Name		340-48H.YW
Reflector	0.000"	81.000"
Driven Element	300.000"	45.000"
Director 1	270.000"	21.000"

These 40-m Yagi designs are optimized for > 10 dB F/R, and SWR < 2:1 over low-end of frequency range from 7.000 to 7.200 MHz, for heavy-duty elements (95 mph wind survival). Only element tip dimensions are shown. See Fig 19D for element telescoping tubing schedule. All dimensions are in inches. No wind torque compensator is required.

optimized 30-meter Yagis with boom lengths between 15 to 34 feet. Because of the size and weight of the elements alone for Yagis on this band, only 2-element and 3-element designs are described. The front-to-rear ratio requirement for the 2-element antenna is relaxed to be greater than 10 dB over the band from 10.100 to 10.150 MHz, while that for the 3-element designs is kept at greater than 20 dB over that frequency range.

As usual, the end of each boom includes 3 inches of space for the reflector and last director mounting plates. Fig 18A shows the free-space gain versus frequency for each antenna; 18B shows the worst-case front-to-rear ratio, and 18C shows the SWR versus frequency.

Fig 18D shows the taper schedule for the 30-meter elements. Note that the wall thickness of the first two sections of tubing is 0.083 inches, rather than 0.058 inches. This heavy-duty element design can survive 107-mph winds with no icing, and 93-mph winds with 1/4 inch of radial ice. The element-to-boom mounting plate for these Yagis is a 0.500-inch thick flat aluminum plate, 6 inches wide by 24 inches long. Electrically, each mounting plate is equivalent to a cylinder, with an effective diameter of 4.684 inches. The equivalent length on each side of the boom is 12 inches. These designs require no torque compensator.

40-METER YAGIS

Fig 19 describes the electrical performance of three optimized 40-meter Yagis with boom lengths between 20 to 48 feet. Like the 30-meter antennas, because of the size and weight of the elements for a 40-meter Yagi, only 2-element and 3-element designs are described. The front-to-rear ratio requirement for the 2-element antenna is relaxed to be greater than 10 dB over the band from 7.000 to 7.300 MHz, while the goal for the 3-element designs is 20 dB over the frequency range of 7.000 to 7.200 MHz. It is exceedingly difficult to hold the F/R greater than 20 dB over the entire 40-meter band without sacrificing excessive gain with a 3-element design.

As usual, the end of each boom includes 3 inches of space for the reflector and last director mounting plates. Fig 19A shows the free-space gain versus frequency for each antenna; 19B shows the front-to- rear ratio, and 19C shows the SWR versus frequency.

Fig 19D shows the taper schedule for the 40-meter elements. Note that the wall thickness of the first two sections of tubing is 0.083 inches, rather than 0.058 inches. This element design can survive 93-mph winds with no icing, and 69-mph winds with 1/4 inch of radial ice. The element-to-boom mounting plate for these Yagis is a 0.500-inch thick flat aluminum plate, 6 inches wide by 24 inches long. Electrically each mounting plate is equivalent to a cylinder, with an effective diameter of 4.684 inches. The equivalent length on each side of the boom is 12 inches. These designs require no torque compensator.

Modifying Monoband Hy-Gain Yagis

Enterprising amateurs have long used the Telex Communications Hy-Gain "Long John" series of HF monobanders as a source of top-quality aluminum and hardware for customized Yagis. Often-modified older models include the 105BA for 10 meters, the 155BA for 15 meters, and the 204BA and 205BA for 20 meters. Newer Hy-Gain designs, the 105CA, 155CA and 205CA, have been redesigned by computer for better performance.

Hy-Gain antennas have historically had an excellent reputation for superior mechanical design, and Hy-Gain proudly points out that many of their monobanders are still working after more than 30 years. In the older designs the elements were purposely spaced along the boom to achieve good weight balance at the mast-to-boom bracket, with electrical performance as a secondary goal. Thus, the electrical performance was not necessarily optimum, particularly over an entire amateur band. Newer Hy-Gain designs are electrically superior to the older ones, but because of their strong concern for weight-balance are still not optimal by the definitions used in this chapter.

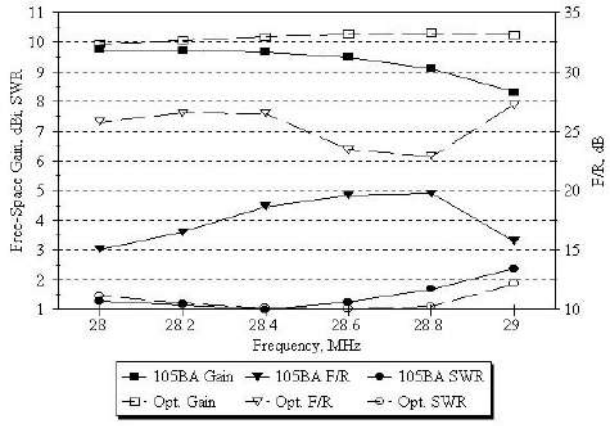

Fig 20—Gain, F/R and SWR over the 28.0 to 28.8 MHz range for original and optimized Yagis using Hy-Gain hardware. Original 105BA design provided excellent weight balance at boom-to-mast bracket, but compromised the electrical performance somewhat because of non-optimum spacing of elements. Optimized design requires wind torque-balancing compensator element, and compensating weight at director end of boom to rebalance weight. The F/R ratio over the frequency range for the optimized design is more than 23 dB. Each element uses the original Hy-Gain taper schedule and element-to-boom clamp, but the length of the tip is changed per Table 8.

Table 8

Optimized Hy-Gain 20-Meter Yagi Designs

Optimized 204BA, Four-element 20-meter Yagi, 26 foot boom

Element	*Spacing*	*Element Tip*
File Name		BV204CA.YW
Reflector	0.000"	56.000"
Driven Element	85.000"	52.000"
Director 1	72.000"	61.500"
Director 2	149.000"	50.125"

Optimized 205CA, Five-element 20-meter Yagi, 34 foot boom

Element	*Spacing*	*Element Tip*
File Name		BV205CA.YW
Reflector	0.000"	62.625"
Driven Element	72.000"	53.500"
Director 1	72.000"	63.875"
Director 2	74.000"	61.625"
Director 3	190.000"	55.000"

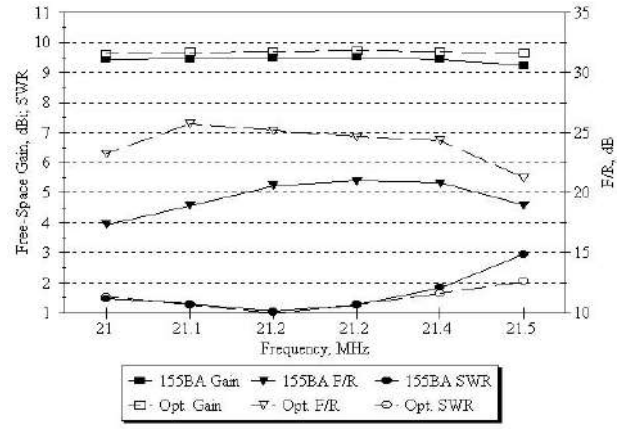

Fig 21—Gain, F/R and SWR over the 21.0 to 21.45 MHz band for original and optimized Yagis using Hy-Gain hardware. Original 155BA design provided excellent weight balance at boom-to-mast bracket, but compromised the electrical performance somewhat because of non-optimum spacing of elements. Optimized design requires wind torque-balancing compensator element, and compensating weight at director end of boom to rebalance weight. The F/R ratio over the frequency range for the optimized design is more than 22 dB. Each element uses the original Hy-Gain taper schedule and element-to-boom clamp, but the length of the tip is changed per Table 9.

Table 9

Optimized Hy-Gain 15-Meter Yagi Designs

Optimized 155BA, Five-element 15-meter Yagi, 24 foot boom

Element	*Spacing*	*Element Tip*
File Name		BV155CA.YW
Reflector	0.000"	64.000"
Driven Element	48.000"	65.500"
Director 1	48.000"	63.875"
Director 2	82.750"	61.625"
Director 3	127.250"	55.000"

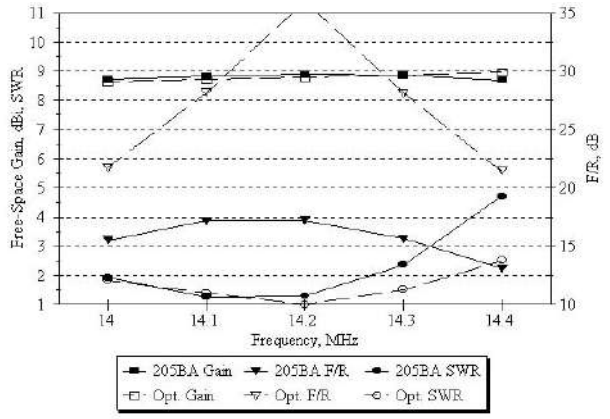

Fig 22—Gain, F/R and SWR over the 14.0 to 14.35 MHz band for original and optimized Yagis using Hy-Gain hardware. Original 205BA design provided good weight balance at boom-to-mast bracket, but compromised the electrical performance because of non-optimum spacing of elements. Optimized design requires wind torque-balancing compensator element, and compensating weight at director end of boom to rebalance weight. The F/R ratio over the frequency range for the optimized design is more than 23 dB, while the original design never went beyond 17 dB of F/R. Each element uses the original Hy-Gain taper schedule and element-to-boom clamp, but the length of the tip is changed per Table 10.

Table 10
Optimized Hy-Gain 10-Meter Yagi Designs

Optimized 105BA, Five-element 10-meter Yagi, 24 foot boom

Element	*Spacing, inches*	*Element Tip*
File Name		BV105CA.YW
Reflector	0.000"	44.250"
Driven Element	40.000"	53.625"
Director 1	40.000"	52.500"
Director 2	89.500"	50.500"
Director 3	112.250"	44.750"

With the addition of wind torque-compensation dummy elements, and with extra lead weights, where necessary, at the director end of the boom for weight-balance, the electrical performance can be enhanced, using the same proven mechanical parts.

Fig 20 shows the computed gain, F/R ratio and SWR for a 24-foot boom, 10-meter optimized Yagi (modified 105BA) using Hy-Gain hardware. **Fig 21** shows the same for a 26-foot boom 15-meter Yagi (modified 155BA), and **Fig 22** shows the same for a 34-foot boom (modified 205BA) 20-meter Yagi. **Tables 8** through **10** show dimensions for these designs. The original Hy-Gain taper schedule is used for each element. Only the length of the end tip (and the spacing along the boom) is changed for each element.

Multiband Yagis

So far, this chapter has discussed monoband Yagis—that is, Yagis designed for a single Amateur-Radio frequency band. Because hams have operating privileges on more than one band, multiband coverage has always been very desirable.

INTERLACING ELEMENTS

In the late 1940s, some experimenters tried interlacing Yagi elements for different frequencies on a single boom, mainly to cover the 10 and 20-meter bands (at that time the 15-meter band wasn't yet available to hams). The experimenters discovered, to their considerable chagrin, that the mutual interactions between different elements tuned to different frequencies are very difficult to handle.

Adjusting a lower-frequency element usually results in interaction with higher-frequency elements near it. In effect, the lower-frequency element acts like a retrograde reflector, throwing off the effectiveness of the higher-frequency directors nearby. Element lengths and the spacing between elements can be changed to improve performance of the higher-frequency Yagi, but the resulting compromise is rarely equal to that of an optimized monoband Yagi. A reasonable compromise for portable operation may be found in Chapter 15, Portable Antennas, by VE7CA.

TRAPPED MULTIBANDERS

Multiband Yagis using a single boom can also be made using traps. Traps allow an element to have multiple resonances. See Chapter 7, Multiband Antennas, for details on trap designs. Commercial vendors have sold trapped antennas to hams since the 1950s and surveys show that after simple wire dipoles and multiband verticals, trapped triband Yagis are the most popular antennas in the Amateur Radio service.

The originator of the trapped tribander was Chester Buchanan, W3DZZ, in his Mar 1955 *QST* article, "The Multimatch Antenna System." On 10 meters this rather unusual tribander used two reflectors (one dedicated and one with traps) and two directors (one dedicated and one with traps). On 20 and 15 meters three of the five elements were active using traps. The W3DZZ tribander employed 12 traps overall, made with heavy wire and concentric tubular capacitors to hold down losses in the traps. Each trap was individually fine tuned after con-

struction before mounting it on an element.

Another example of a homemade tribander was the 26-foot boom 7-element 20/15/10-meter design described by Bob Myers, W1XT (ex-W1FBY) in Dec 1970 *QST*. The W1FBY tribander used only two sets of traps in the driven element, with dedicated reflectors and directors for each frequency band. Again, the traps were quite robust in this design to minimize trap losses, using $^{7}/_{16}$-inch aluminum tubing for the coils and short pieces of RG-8 coax as high-voltage tuning capacitors.

Only a relatively few hams actually built tribanders for themselves, mainly because of the mechanical complexity and the close tolerances required for such antennas. The traps themselves must be constructed quite accurately for reproducible results, and they must be carefully weatherproofed for long life in rain, snow, and often polluted or corrosive atmospheres.

Christmas Tree Stacks

Another possible method for achieving multiband coverage using monoband Yagis is to stack them in a "Christmas tree" arrangement. See **Fig 23**. For an installation covering 20, 15 and 10 meters, you could mount on the rotating mast just at the top of the tower the 20-meter monobander. Then perhaps 9 feet above that you would mount the 15-meter monobander, followed by the 10-meter monoband Yagi 7 feet further up on the mast. Another configuration would be to place the 10-meter Yagi in between the lower 20-meter and upper 15-meter Yagis. Whatever the arrangement, the antenna in the middle of such a Christmas-tree always suffers the most interaction from the lowest-frequency Yagi.

Dave Leeson, W6NL (ex-W6QHS), mentions that the 10-meter Yagi in his closely stacked Christmas Tree (15 meters at the top, 10 meters in the middle, and 20 meters at the bottom of the rotating mast) loses "substantial gain" because of serious interaction with the 20-meter antenna. (N6BV and K1VR calculated that the free-space gain in the W6NL stack drops to 5 dBi, compared to about 9 dBi with no surrounding antennas.) Monobanders are *definitely not* universally superior to tribanders in multiband installations. In private conversations, W6NL has indicated that he would not repeat this kind of short Christmas Tree installation again.

Forward Staggering

Some hams have built multiband Yagis on a common boom, using a technique called *forward staggering*. This means that that most (or all) of the higher-frequency elements are placed in front of any lower-frequency elements—in other words, most of the elements are not interlaced. Richard Fenwick, K5RR, described his triband Yagi design in Sep 1996 *QEX* magazine. This uses forward-stagger and open-sleeve design techniques and was optimized using several sophisticated modeling programs.

Fenwick's tribander used a 57-foot, 3-inch OD boom

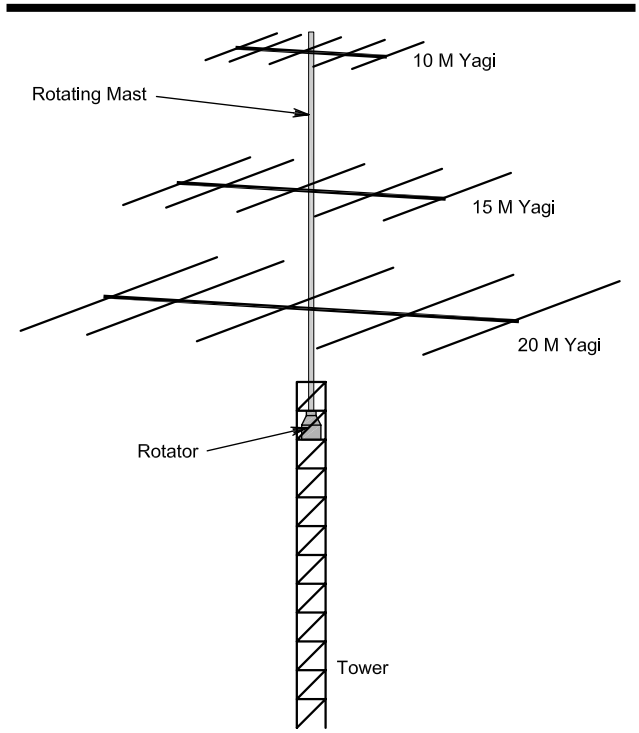

Fig 23—"Christmas Tree" stack of 20/15/10-meter Yagis spaced vertically on a single rotating mast.

to hold 4 elements on 20 meters, 4 elements on 15 meters and 5 elements on 10 meters. **Fig 24** shows the element placement for the K5RR tribander. Most hams, of course, don't have the real-estate or the large rotator needed to turn such a large, but elegant solution to the interaction problem!

Force 12 C3 "Multi-Monoband" Triband Yagi

Antenna manufacturer Force 12 also uses forward-stagger layouts and patented combinations of open- and closed-sleeve drive techniques extensively in their product line of multiband antennas, which they call "multi-monoband Yagis." **Fig 25** shows the layout for the popular Force 12 C3 triband Yagi. The C3 uses no traps, thereby avoiding any losses due to traps. The C3 consists of three 2-element Yagis on an 18-foot boom, using full-sized elements designed to withstand high winds.

The C3 feed system employs open-sleeves, where the 20-meter driver element is fed with coax through a common-mode current balun and parasitically couples to the closely spaced 15-meter driver and the two 10-meter drivers to yield a feed-point impedances close to 50 Ω on all three bands. See the section on open-sleeve dipoles in Chapter 7, Multiband Antennas.

Note the use of the forward-stagger technique in the C3, especially on 10 meters. To reduce interaction with

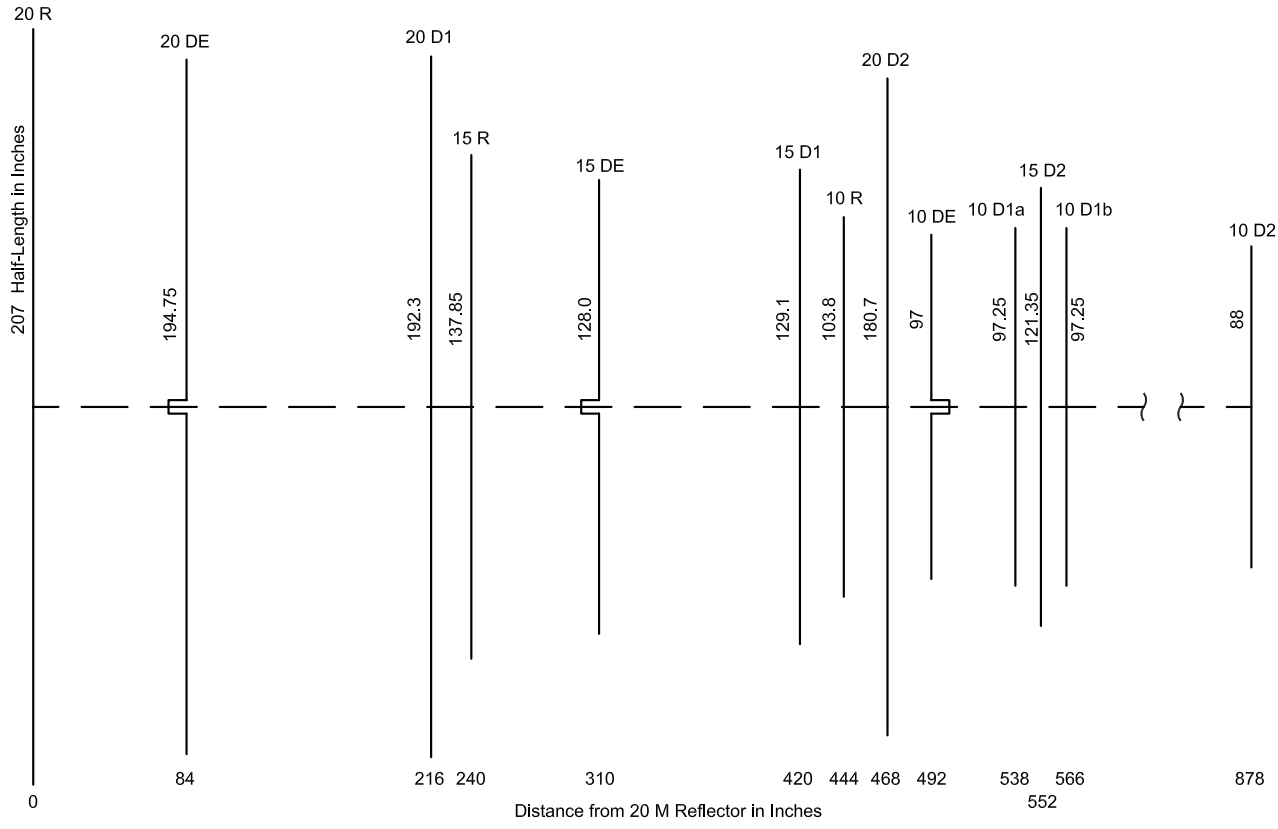

Fig 24—Dimensions of K5RR's trapless tribander using "forward stagger" and open-sleeve techniques to manage interaction between elements for different frequencies.

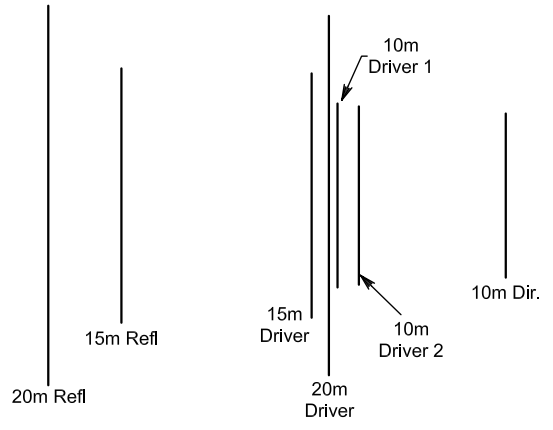

Fig 25—Layout of Force 12 C3 multiband Yagi. Note that the 10-meter (driver/director) portion of the antenna is "forward staggered" ahead of the 15-meter (reflector/driver) portion, which in turn is placed ahead of the 20-meter (reflector/driver) portion. The antenna is fed at the 20-meter driver, which couples parasitically to the 15-meter driver and the two 10-meter drivers.

the lower-frequency elements behind it, the 10-meter portion of the C3 is mounted on the boom ahead of all the lower-frequency elements, with the main 10-meter parasitic element (#7) acting as a director. The lower-frequency elements behind the 10-meter section act as retrograde reflectors, gaining some improvement of the gain and pattern compared to a monoband 2-element Yagi. A simplified *EZNEC* model of the C3 is included on the CD-ROM accompanying this book.

On 15 meters, the main parasitic element (#2) is a dedicated reflector, but the other elements ahead on the boom act like retrograde directors to improve the gain and pattern somewhat over a typical 2-element Yagi with a reflector. On 20 meters, the C3 is a 2-element Yagi with a dedicated reflector (#1) at the back end of the boom.

The exact implementation of any Yagi, of course, depends on the way the elements are constructed using telescoping aluminum tubing. The C3 type of design is no exception.

Stacked Yagis

Monoband parasitic arrays are commonly stacked either in broadside or collinear fashion to produce additional directivity and gain. In HF amateur work, the most common broadside stack is a vertical stack of identical Yagis on a single tower. This arrangement is commonly called a *vertical stack*. At VHF and UHF, amateurs often employ collinear stacks, where identical Yagis are stacked side-by-side at the same height. This arrangement is called a *horizontal stack*, and is not usually found at HF, because of the severe mechanical difficulties involved with large, rotatable side-by-side arrays.

Fig 26 illustrates the two different stacking arrangements. In either case, the individual Yagis making up the stack are generally fed in phase. There are times, however, when individual antennas in a stacked array are purposely fed out of phase in order to emphasize a particular elevation pattern. See Chapter 17, Repeater Antenna Systems, for such a case where elevation pattern steering is implemented for a repeater station.

Let's look at the reasons hams stack Yagis:

- For more gain
- For a wider elevation footprint in a target geographical area
- For azimuthal diversity—two or more directions at once
- For less fading
- For less precipitation static

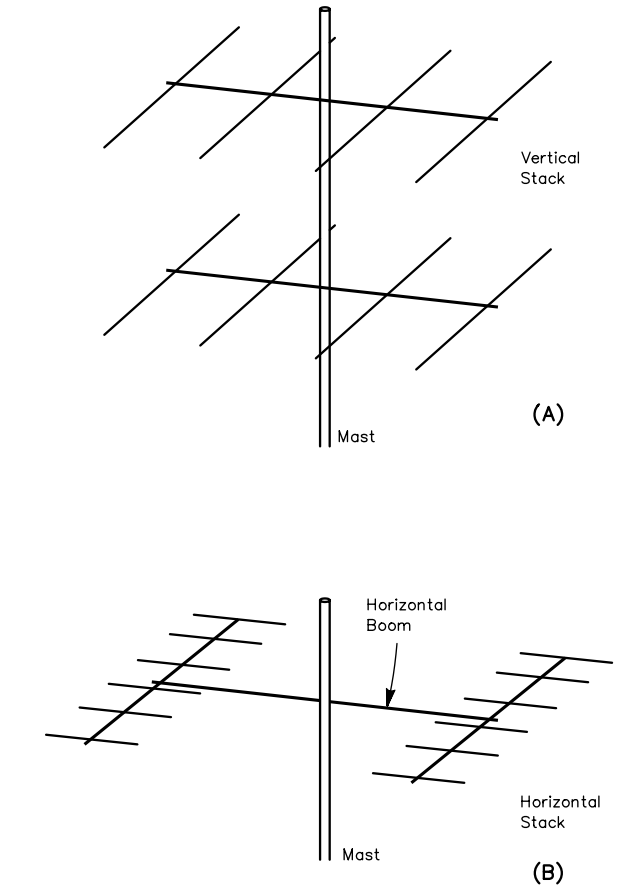

Fig 26—Stacking arrangements. At A, two Yagis are stacked vertically (broadside) on the same mast. At B, two Yagis are stacked horizontally (collinear) side-by-side. At HF the vertical stack is more common because of mechanical difficulties involved with large HF antennas stacked side-by-side, whereas at VHF and UHF the horizontal stack is common.

STACKS AND GAIN

Fig 27 compares the elevation responses for three antenna systems of 4-element 15-meter Yagis. The response for the single Yagi at a height of 120 feet peaks at an elevation of about 5°, with a second peak at 17° and a third at 29°. When operated by itself, the 60-foot high Yagi has its first peak at about 11° and its second peak beyond 34°.

The basic principle of a vertically stacked HF array is that it takes energy from higher-angle lobes and concentrates that energy into the main elevation lobe. The main lobe of the 120/60-foot stack peaks about 7° and is about 2 dB stronger than either the 60- or 120-foot antenna by itself. The shape of the left-hand side of the stack's main lobe is determined mainly by the 120-foot antenna's response. The right-hand side of the stack's main lobe is "stretched" rightwards (toward higher angles) mainly by the 60-foot Yagi, while the shape follows the curve of the 120-foot Yagi.

Look at the second and third lobes of the stack, which appear about 18° and 27°. These are about 14 dB down from the stack's peak gain, showing that energy has indeed been extracted from them. By contrast, look at the levels of the second and third lobes for the individual Yagis at 60 and 120 feet. These higher-angle lobes are almost as strong as the first lobes.

The stack squeezes higher-angle energy into its main elevation lobe, while maintaining the frontal lobe azimuth pattern of a single Yagi. This is the reason why many state-of-the-art contest stations are stacking arrays of relatively short-boom antennas, rather than stacking long-boom, higher-gain Yagis. A long-boom HF Yagi narrows the azimuthal pattern (and the elevation pattern too), making pointing the antenna more critical and making it more difficult to spread a signal over a wide azimuthal area, such as all of Europe and Asiatic Russia at one time.

STACKS AND WIDE ELEVATION FOOTPRINTS

Detailed studies using sophisticated computer models of the ionosphere have revealed that coverage

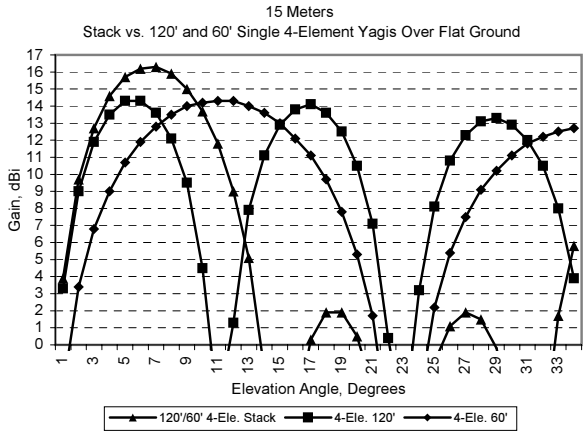

Fig 27—Comparison of elevation patterns on 15 meters for a stack of 4-element Yagis at 120 and 60 feet and individual Yagis at those two heights. The shape of the stack's response is determined mainly by that of the top antenna.

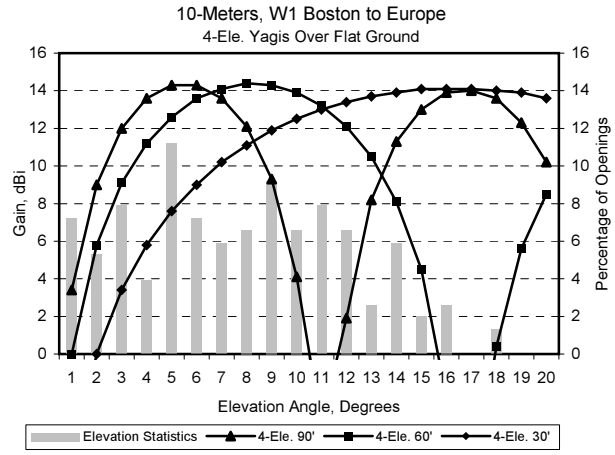

Fig 28—Comparison of elevation patterns and elevation-angle statistics for individual 10-meter TH7DX tribanders mounted over flat ground aiming from New England to Europe. No single antenna can cover the wide range of angles needed—from 1° to 18°.

of a wide range of elevation angles is necessary to ensure consistent DX or contest coverage on the HF bands. These studies have been conducted over all phases of the 11-year solar cycle, and for numerous transmitting and receiving QTHs throughout the world.

Chapter 23, Radio Wave Propagation, covers these studies in more detail, and the CD-ROM accompanying this book contains a huge number of elevation-angle statistical tables for locations all around the world. The *HFTA* (HF Terrain Assessment) program on the CD-ROM can not only compute antenna elevation patterns over irregular local terrain, but it can compare them directly to the elevation-angle statistics for a particular target geographic area.

A 10-Meter Example

Fig 28 shows the 10-meter elevation-angle statistics for the New England path from Boston, Massachusetts, to all of the continent of Europe. The statistics are overlaid with the computed elevation response for three individual 4-element Yagis, at three heights: 90, 60 and 30 feet above flat ground. In terms of wavelength, these heights are 2.60 λ, 1.73 λ and 0.86 λ high.

You can see that the 90-foot high Yagi covers the lower elevation angles best, but it has a large null in its response centered at about 11°. This null puts a big hole in the coverage for some 22% of all the times the 10-meter band is open to Europe. At those angles where the 90-foot Yagi exhibits a null, the 60-foot Yagi would be effective, and so would the 30-foot Yagi. If that is the only antenna you have, the 90-foot high Yagi would be too high for good coverage of Europe from New England.

The peak statistical elevation angle into Europe is 5°, and this occurs about 11% of all the times the 10-meter band is open to Europe from Boston. At an elevation of 5° the 30-foot high Yagi would be down almost 7 dB compared to the 90-foot high Yagi, but at 11° the 90-foot Yagi would be more than 22 dB down from the 30-foot Yagi. There is no single height at which one Yagi can optimally cover all the necessary elevation angles, especially to a large geographic area such as Europe—although the 60-foot high antenna is arguably the best compromise for a single height. To cover all the possibilities to Europe, however, you need a 10-meter antenna system that can cover equally well the entire range of elevation angles from 1° to 18°.

Fig 29 compares elevation-angle statistics for two 10-meter paths from New England to Europe and to Japan. The elevation angles needed for communications with the Far East are very low. Overlaid on Fig 29 for comparison are the elevation responses over flat ground for three different antenna systems, using identical 4-element Yagis:

- Three Yagis, stacked at 90, 60 and 30 feet
- Two Yagis, stacked at 70 and 40 feet
- One Yagi at 90 feet.

The best coverage of all the necessary angles on 10 meters to Europe is with the stack of three Yagis at 90/60/30 feet. The two-Yagi stack at 70 and 40 feet comes in a close second to Europe, and for elevation angles higher than about 9° the 70/40-foot stack is actually superior to the 90/60/30-foot stack.

Both of the stacks illustrated here give a wider *elevation footprint* than any single antenna, so that all the angles can be covered automatically without having to switch from higher to lower antennas manually. This is perhaps the major benefit of using stacks, but not the only

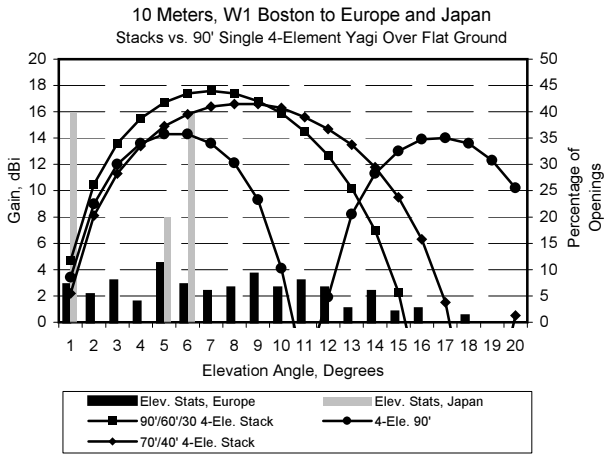

Fig 29—Combinations of 4-element Yagis over flat ground. The elevation-angle statistics into Japan from New England (Boston) are represented by the black vertical bars, while the grey vertical bars represent the elevation-angle statistics to Europe. The 90/60/30-foot stack has the best *elevation footprint* into Japan, although the 70/40-foot stack performs well also.

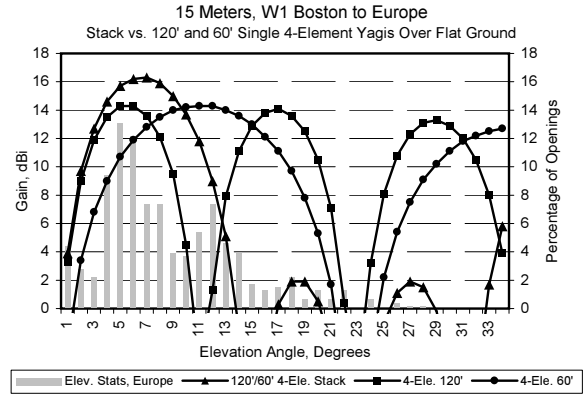

Fig 30—Comparison of elevation patterns for K1EA's illustration about 15-meter Yagis mounted over flat ground, with elevation-angle statistics to Europe added. The stack at 120 and 60 feet yields a better footprint over the range of 3° to 11° at its half-power points, better than either antenna by itself.

one, as we'll see.

To Japan, the necessary range of elevation angles is considerably smaller than that needed to a larger geographic target area like Europe. The 90/60/30-foot stack is still best on the basis of having higher gain at low angles, although the two-Yagi stack at 70 and 40 feet is a good choice too. Note that the single 90-foot high Yagi's performance is very close to the 70/40-foot stack of two Yagis at low angles, but the two-Yagi stack is superior to the single 90-foot antenna for angles higher than about 5° on 10 meters.

A 15-Meter Example

The situation is similar on 15 meters from New England to Europe. On 15 meters, the range of angles needed to fully cover Europe is 1° to 28°. This large range of angles makes covering all the angles even more challenging. Ken Wolff, K1EA, a devoted contest operator and the author of the famous *CT* contest logging program, put it very clearly when he wrote in the bulletin for the Yankee Clipper Contest Club:

"Suppose you have 15-meter Yagis at 120 feet and 60 feet, but can feed only one at a time. A 15-meter beam at 120 feet has its first maximum at roughly 5° and the first minimum at 10°. The Yagi at 60 feet has a maximum at 10° and a minimum at 2°. At daybreak, the band is just opening, signals are arriving at 3° or less and the high Yagi outperforms the low one by 5-10 dB. Late in the morning, western Europeans are arriving at angles of 10° or more, while UA6 is still arriving at 4-5°. Western Europe can be 20-30 dB louder on the low antenna than the high! What to do? Stack em!"

Fig 30 illustrates K1EA's scenario, showing the elevation statistics to Europe from Massachusetts and the elevation responses for a 120- and a 60-foot high, 4-element Yagi, both over flat ground, together with the response for both antennas operated as vertical stack. The half-power beamwidth of the stack's main lobe is 6.9°, while that for the 120-foot antenna by itself is 5.5° and that for the 60-foot antenna by itself is 11.1°. The half-power beamwidth numbers by themselves can be deceiving, mainly because the stack starts out with a higher gain. A more meaningful observation is that the stack has equal to or more gain than either of the two individual antennas from 1° to about 10°.

Is such a stack of 15-meter Yagis at 120 and 60 feet optimal for the New England to Europe path? No, it isn't, as we'll explore later, but the stack is clearly better than either antenna by itself for the scenario K1EA outlined above.

A 20-Meter Example

Take a look now at **Fig 31**, which overlays elevation-angle statistics for Europe (gray vertical bars) and Japan (black vertical bars) from Boston on 20 meters, plus the elevation responses for four different sets of antennas mounted over flat ground. Just for emphasis, the highest antenna is a 200-foot high 4-Element Yagi. It is clearly too high for complete coverage of all the needed angles into Europe. A number of New England operators have verified that this is true—a really high Yagi will open the 20-meter band to Europe in the morning and may shut it down in the afternoon, but during the middle of the day the high antenna gets soundly beaten by lower antennas.

To Japan, however, from New England the range of angles needed narrows considerably on 20 meters,

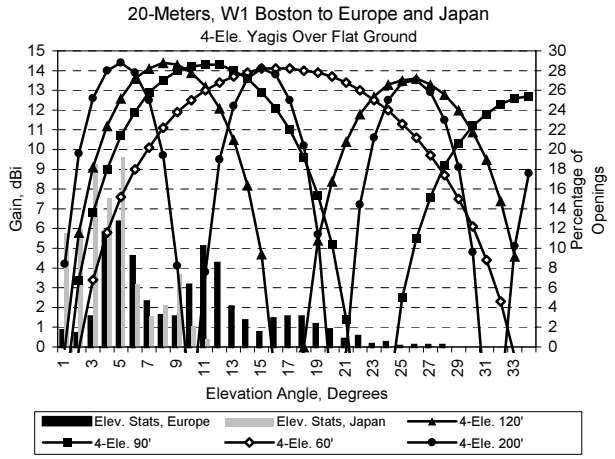

Fig 31—Comparison of elevation patterns for individual 20-meter Yagis over flat ground, compared with the range of elevation angles needed on this band from New England to Europe (gray bars) and to Japan (black bars). For fun, the response of a 200-foot high Yagi is included—this antenna is far too high to cover the needed range of angles to Europe because of its deep nulls at critical angles, like 10°. But the 200 footer is great into Japan!

from 1° to only 11°. For these angles, the 200-foot Yagi is the best antenna to work Japan from New England on 20 meters.

This is true provided that the antenna is aiming out over flat ground. The actual, generally irregular, terrain in various directions can profoundly modify the takeoff angles favored by an antenna system, particularly on steep hills. There will be more discussion on this important topic later on.

SPARE ME THE NULLS!

Now, let's look closely at some other 20-meter antennas in Fig 28, the ones at 120 and 60 feet. At an elevation angle of 8° the difference in elevation response between the 60- and 120-foot high Yagis is just over 3 dB. Can you really notice a change of 3 dB on the air? Signals on the HF bands often rise and fall quickly due to fading, so differences of 2 or 3 dB are difficult to discern. Consequently, the difference between a Yagi at 120 feet and one at 60 feet may be difficult to detect at elevation angles covered well by both antennas. But a *deep null* in the elevation response is very noticeable.

Back in 1990, when editor Dean Straw, N6BV, put up his 120-foot tower in Windham, New Hampshire, his first operational antenna was a 5-element triband Yagi, with 3 elements on 40 and 4 elements on both 20 and 15 meters. Just as the sun was going down on a late August day Straw finished connecting the feed line in the shack. The antenna seemed to be playing like it should, with a good SWR curve and a good pattern when it was rotated. So N6BV/1 called a nearby friend, John Dorr, K1AR, on the telephone and asked him to get on the air to make some signal comparisons on 20 meters into Europe.

Straw was shocked that every European they worked that evening said his signal was several S units weaker than K1AR's. Dorr was using a 4-element 20-meter monobander at 90 feet, which at first glance should have been comparable to Straw's 4-element antenna at 120 feet. But N6BV really shouldn't have been so shocked—in New England, the elevation angles from Europe late in the day on 20 meters are almost always higher than 11°, and that is true for the entire solar cycle.

The N6BV/1 station was located on a small hill, while K1AR was located on flat terrain towards Europe. The elevation response for N6BV/1's 120-foot high Yagi fell right into a deep null at 11°. This was later confirmed many times in the following eight years that the N6BV/1 station was operational. During the early morning opening on 20 meters into Europe, the top antenna was always very close to or equal to the stack of three TH7DX tribanders at 90/60/30 feet on the same tower. But in the afternoon the top antenna was *always* decidedly worse than the stack, so much so that Straw often wondered whether something had gone wrong with the top antenna!

So what's the moral to this short tale? It's simple: *The gain you can achieve, while useful, is not so important as the deep nulls you can avoid by using a stack.*

STACKING DISTANCES BETWEEN YAGIS

So far, we've examined stacks as a means of achieving more gain over an individual Yagi, while also matching the antenna system's response to the range of elevation angles needed for particular propagation paths. Most importantly, we seek to avoid nulls in the elevation response. Earlier we asked whether a 120/60-foot stack was optimal for the path from New England to Europe on 15 meters. Let's examine how the stacking distance between individual antennas affects the performance of a stack.

Fig 32 shows overlays of various combinations of 15-meter Yagis. Just for reference, a plot for a single 60-foot high Yagi is also included. Let's start by looking at the most widely spaced stack in the group: the 120/30-foot stack. Here, the spacing is obviously too large, since the second lobe is actually stronger than the first lobe. In terms of wavelength, the 90-foot spacing between antennas in this stack is 1.94 λ, a large spacing indeed.

There is a great deal of folklore and superstition among amateurs about stacking distances for HF arrays. For years, high-performance stacked Yagi arrays have been used for weak-signal DXing on the VHF and UHF bands. The most extreme example of weak-signal work is EME work (Earth-Moon-Earth, also called *moonbounce*) because of the huge path losses incurred on the way to and from the Moon. The most successful arrays used for

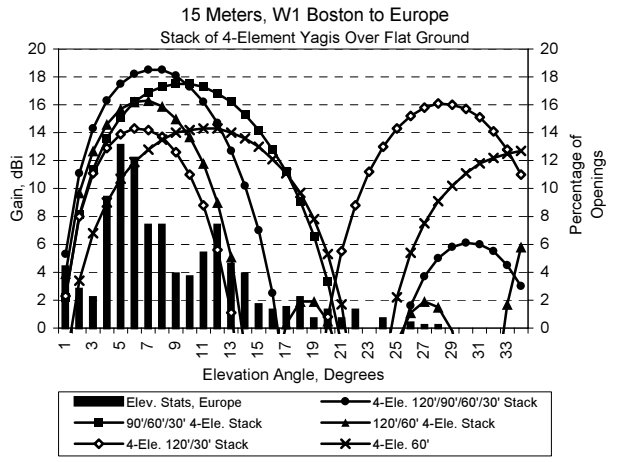

Fig 32—Various stacks towards Europe from New England for 15-meters. The stack at 120 and 30 feet is clearly suboptimal, since the second lobe is higher than the first lobe. The 120/60-foot stack is better in this regard, but is still not as good a performer as the 90/60/30-foot stack. It's debatable whether going to four Yagis in the 120/90/60/30-foot stack is a good idea because it drops below the performance of the 90/60/30-foot stack at about 10° in elevation. The exact distance between practical HF Yagis is not critical to obtain the benefits of stacking. For a stack of tribanders at 90, 60 and 30 feet, the distance in wavelengths between individual antennas is 0.87 λ at 28.5 MHz, 0.65 λ at 21.2 MHz, and 0.43 λ at 14.2 MHz.

moonbounce have low sidelobe levels and very narrow frontal lobes that give huge amounts of gain. The low sidelobes help minimize received noise, since the receive levels for signals that do manage to bounce off the Moon and return to Earth are exceedingly weak.

But HF work is different from moonbounce in that rigorously trying to minimize high-angle lobes is far less crucial at HF, where we've already shown that the main goal is to achieve gain over a wide elevation-plane footprint without any disastrous nulls in the pattern. The gain gradually increases as spacing in terms of wavelength is increased between individual Yagis in a stack, and then decreases slowly once the spacing is greater than about 1.0 λ. The difference in gain between spacings of 0.5 λ to 1.0 λ for a stack of typical HF Yagis amounts to only a fraction of a decibel. Stacking distances on the order of 0.6 λ to 0.75 λ give best gain commensurate with good patterns.

While the stack at 120/60 feet in Fig 32 doesn't have the second-lobe-stronger problem the 120/30-foot stack has, 60 feet between antennas is 1.29 λ, again outside the normal range of HF stack spacings. As a consequence, the 120/60-foot stack doesn't cover the range of elevation angles as well as it could, and is inferior to both the 90/60/30-foot stack and the 120/90/60/30-foot stack. The 120/60-foot two-Yagi stack needs at least one more antenna placed in-between to spread out the elevation-range coverage and to provide more gain.

It could be debated, but the 90/60/30-foot stack seems optimal for coverage of all the angles into Europe from New England on 15 meters. Note that the 30-foot spacing between Yagis is 0.65 λ on 21.2 MHz, right in the middle of the range of typical stack spacings.

Switching Out Yagis in the Stack

Still, the extra gain that is available at low elevation angles from a 120/90/60/30-foot high, four-Yagi stack in Fig 32 is alluring. For those statistically possible, but less likely, occasions when the elevation angle is higher than about 12°, it would be advantageous to switch out the top 120-foot Yagi and operate with only the lower three Yagis in a stack. (This also allows the top antenna to be rotated in another direction, an aspect we'll explore later.) There are even times when the incoming angles are really high and when the top two antennas might be switched out to create a 60/30-foot stack. Later in this chapter we'll explore flexible circuitry for such stack switching.

Stacking Distance and Lobes at HF

Let's look a little more closely at how a stack achieves gain and a wide elevation footprint. **Fig 33** shows a rectangular X-Y graph of the elevation response from 0° to 180° for two 3-element 15-meter Yagis (with 12-foot booms) spaced 30 feet apart (0.65 λ at 21.2 MHz), but mounted at two different heights: 95/65 and 85/55 feet. The rectangular plot gives more resolution than is possible on a polar plot. Note that the heights shown represent typical stacking heights on 15 meters—there's nothing magic about these choices. The free-space H-Plane pattern for the 30-foot spaced stack is also shown for reference.

The worst-case overhead elevation lobe, which ranges from about 60° to 120° in elevation (±30° from straight overhead at 90°), is about 14.7 dB down for the 95/65-foot stack. The overhead lobe peaks broadly at an elevation angle of about 82°. The overhead lobe for the lower 85/55-foot stack occurs at an elevation of about 64°, where it is 19 dB down.

The F/B for both 3-element sets of heights is about 15 dB, well down from the excellent 32 dB F/B for each Yagi by itself. The degradation of F/B is mainly due to mutual coupling to its neighbor in the stack.

The ground-reflection pattern in effect "modulates" the free-space pattern of the individual Yagi, but in a complex and not always intuitive manner. This is quite evident for the 85/55-foot stack at near-overhead angles. In this region things become complicated indeed, because the fourth and fifth lobes due to ground reflections are interacting with the free-space pattern of the stack.

Because the spacing remains constant at 30 feet for

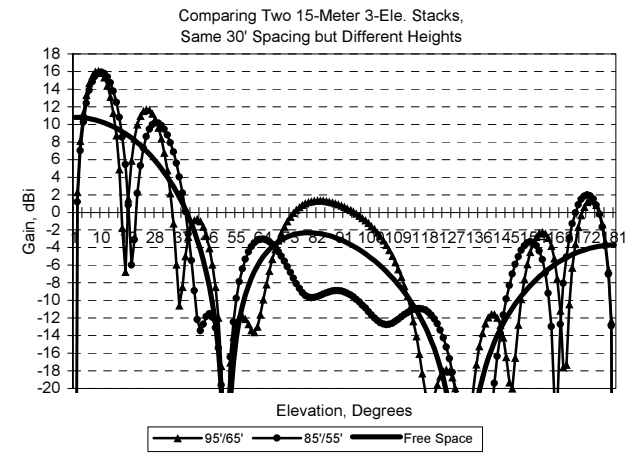

Fig 33—Rectangular plot comparing two 15-meter stacks of 3-element Yagis—each antenna is spaced 30 feet from its partner, but at different heights. The lobes are a complicated function of the antenna height, not the spacing, since that remains constant.

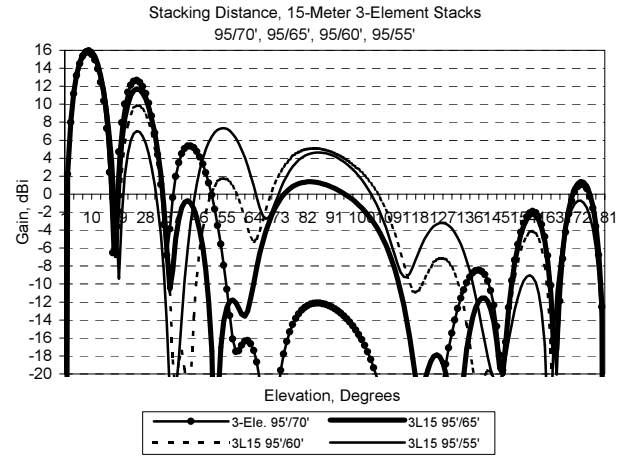

Fig 34—Four spacing scenarios for two 3-element 15-meter Yagis. Things get very complicated. The optimal spacing in terms of stacking gain is 30 feet, which is 0.65 λ. The near-overhead lobes turn out to be ugly looking, but unimportant for skywave propagation.

these pairs of antennas, however, the main determinant for the upper-elevation angle lobes is the distance of the horizontally polarized antennas above the ground, not the spacing between them.

Changing the Stack Spacing

Fig 34 demonstrates just how complicated things get for four different spacing scenarios. Here, the lower Yagi in the stack is moved down in 5-foot increments from the 95/70 feet level, to 95/65, 95/60 and 95/55 feet. The closest spacing, 25 feet in the 95/70-foot stack, yields nominally the "cleanest" pattern in the overhead region from 60° to 120°. The worst-case overhead lobe for the 95/70-foot stack is down 28 dB from peak. The F/B is again about 15 dB.

The worst case overhead lobe for the widest spacing, 40 feet in the 95/55-foot stack, is about 11 dB down from peak. The F/B has increased marginally, but is still only about 16 dB. It is difficult to pinpoint directly whether the spacing or the height above ground is the major determinant for the various lobe amplitudes for the 3-element stack. We'll soon look closely at whether the overhead lobe is important or not for HF work.

Longer Boom Length and Stack Spacing

Fig 35 shows the same type overlay of elevation plots, but this time for two 7-element 15-meter Yagis on gigantic 64-foot booms. These Yagis are also spaced 30 feet apart (0.65 λ at 21.2 MHz), mounted at the same four sets of heights in Fig 34. As you'd expect, the free-space elevation pattern for a stacked pair of 7-element Yagis on 64-foot booms is narrower than that for a stacked pair of 3-element Yagis on 12-foot booms. The intrinsic

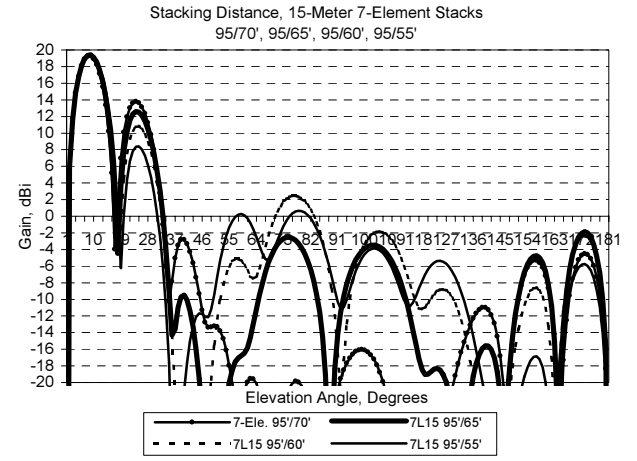

Fig 35—Four spacing scenarios for two large 7-element 15-meter Yagis (on 64-foot booms). Again, a 0.65 λ spacing (30 feet) provides the most stacking gain.

F/B of the longer Yagi is also better than the F/B of the shorter antenna. As a result, all lobes beyond the main lobe of the stacked 7-element pair are lower for both sets of heights than their 3-element counterparts. The worst-case overhead lobe for the 7-element 95/65-foot pair is about 22 dB down at 76° and the F/B at 172° is greater than 21 dB for all four sets of heights.

Table 11 summarizes the main performance characteristics for four sets of stacked Yagis. The first entry for each boom length is for the Yagi by itself at a height of 95 feet. Stacked configurations are next listed in order of gain. The column labeled "Worst lobe, dB re Peak" is the

Table 11
Example, Spacing Between 15–Meter Yagis

Antenna	*Peak Gain dBi*	*Worst Lobe dB re Peak*	*Worst Lobe Angle,°*	*F/B dB*	*Overhead Lobe dB re Peak*
3–Ele., 12' boom					
By itself 95'	13.2	–0.9	21	28.8	–17.5
95'/65' (Δ 30')	16.08	–4.5	25	14.9	–14.7
95'/60' (Δ 35')	16.01	–6.2	24	15.1	–10.9
95'/70' (Δ 25')	15.81	–3.2	24	14.8	–28
95'/55' (Δ 40')	15.71	–8.7	24	16.4	–11
95'/75' (Δ 20')	15.34	–2.3	23	16.3	–17.2
4–Ele., 18' boom					
By itself 95'	13.92	–1	21	28.3	–20.4
95'/65' (Δ 30')	16.63	–4.5	23	18.5	–17.3
95'/60' (Δ 35')	16.6	–6.2	24	18.2	–13.1
95'/55' (Δ 40')	16.36	–8.7	24	19.8	–13.2
95'/70' (Δ 25')	16.36	–3.3	24	20.4	–31.8
95'/75' (Δ 20')	15.92	–2.5	23	25.9	–19
5–Ele., 23' boom					
By itself 95'	14.26	–1.1	21	27.9	–22.3
95'/65' (Δ 30')	16.86	–4.6	24	20.8	–19
95'/60' (Δ 35')	16.86	–6.3	24	20.7	–14.4
95'/55' (Δ 40')	16.67	–8.8	24	23.5	–14.4
95'/70' (Δ 25')	16.59	–3.4	24	24.9	–34.4
95'/75' (Δ 20')	16.18	–2.6	23	34.3	–20.2
7–Ele., 64' boom					
By itself 95'	17.93	–2.2	21	28.9	–17.1
95'/65' (Δ 30')	19.39	–6.9	24.3	21.4	–21.9
95'/60' (Δ 35')	19.38	–8.6	24	21.4	–16.9
95'/55' (Δ 40')	19.29	–10.9	24	25.0	–18.6
95'/70' (Δ 25')	19.26	–5.5	23	24	–35.3
95'/75' (Δ 20')	19.08	–4.6	23	27	–23.4

amplitude of the second lobe due to ground reflections, and the elevation angle of that second lobe is listed as well.

Besides the 3- and 7-element designs discussed above, we've also added 4- and 5-element designs in Table 11. Over the range of stacking distances between 20 and 40 feet on 15 meters (0.43 λ to 0.86 λ), the peak gain for the 3-element stacks changes less than 0.75 dB, with the 30-foot spacing exhibiting the highest gain. The differences between peak gains versus stacking distance become smaller as the boom length increases. For example, for the 64-foot boom Yagi, the gain varies 19.39 – 19.08 = 0.31 dB for stack spacings from 20 to 40 feet.

In other words, changing the spacing from 20 to 40 feet (0.43 λ to 0.86 λ) doesn't change the gain significantly for boom lengths from 12 to 64 feet (0.26 λ to 1.38 λ). From the point of view of gain, the vertical spacing between individual antennas in an HF stack is not critical.

The worst-case lobes (generally speaking, the second lobe due to ground reflections) are highest for a Yagi operated by itself. After all, a single Yagi doesn't benefit from the redistribution of energy from higher-angle lobes into the main lobe that a stack gives. Thus, the 3-element, 12-foot boom Yagi by itself at 95 feet would have a second lobe at 21° that is only 0.9 dB down from the main lobe, while the stack of two such antennas at a 30-foot (0.65 λ) spacing at 95/65 feet would have a second lobe down 4.5 dB. As the spacing between antennas in a vertical stack increases, the second lobe is suppressed more, up to 8.7 dB at a 40-foot (0.86 λ) spacing.

Since the free-space elevation pattern for a 3-element Yagi is wider than that for a 7-element Yagi, the second lobe due to ground reflection will be somewhat reduced. This is true for all longer-boom antennas operating by themselves over ground. Used in stacks, the second lobe's amplitude will vary depending on spacing between antennas, but they range only about 6 dB.

The front-to-back ratio will also tend to increase with longer boom lengths on a properly designed Yagi. Table 11 shows that the F/B is somewhat better for closer spacings between antennas in a stack, a rather non-intuitive result, considering that the mutual coupling should be greater for closer antennas. For example, the 5-ele-

ment Yagi stack with a 20-foot spacing has a exceptional F/B of 34.3 dB, compared to a F/B of 21.4 dB with the 30-foot spacing distance that gives nominally the most gain. High values of F/B, however, rarely hold over a wide frequency range because of the very critical phasing relationships necessary to get a deep null, so the difference between 34.3 and 21.4 dB would rarely be noticeable in practice.

The near-overhead lobe structure (between 60º to 120º in elevation) tends also to be lower for smaller stack spacings—for all boom lengths—peaking in this example at a spacing of 25 feet for the boom lengths considered here. Since the peak gain actually occurs with smaller spacing between Yagis in this 7-element stack, even relatively large and messy looking overhead lobes are not subtracting from the stacking gain. In the next section we'll now examine whether this overhead lobe is important or not.

Are Higher-Angle Lobes Important?

We've already shown that the exact spacing between HF Yagis is not critical for stacking gain. Further, the heights (and hence spacing) of the individual Yagis in a stack interact in a complicated fashion to determine higher-angle lobes.

Let's examine the relevance of such higher-angle lobes for stacked HF Yagis, this time in terms of interference reduction on receive. As Chapter 23, Radio Wave Propagation, points out, few DX signals arrive at elevation angles greater than about 30°. In fact, DX signals only propagate at elevation angles in the range from 1° to 30° on all the bands where operators might reasonably expect to stack Yagis—nominally from 7 to 29.7 MHz.

You should remember that the definition of the *critical frequency* for HF propagation is the highest frequency for which a wave launched directly overhead at 90° elevation is reflected back down to Earth, rather than being lost into outer space. The maximum critical frequency for extremely high levels of solar flux is about 15 MHz. In other words, high overhead angles do not propagate signals on the upper HF bands.

However, some domestic signals do arrive at relatively high elevation angles. Let's look at some scenarios where higher angles might be encountered and how the elevation patterns of typical HF stacks affect these signals. Let's examine a situation where a medium-range interfering station is on the same heading as a more distant target station.

We'll examine a typical scenario involving stations in Atlanta, Boston and Paris. The heading from Atlanta to Paris is 49º, the same heading as Atlanta to Boston. In other words, the Atlanta station would have to transmit over (and listen through) a Boston station for communication with Paris. The distance between Atlanta and Boston is about 940 miles, while the distance from Atlanta to Paris is about 4350 miles. Ground wave signals obviously cannot travel either of these distances at 21 MHz (ground wave coverage is less than about 10 miles at this frequency), and so the propagation between Atlanta to Boston and Atlanta to Paris will be entirely by means of the ionosphere.

Let's evaluate the situation on 15 meters in the month of October. We'll assume a smoothed sunspot number (SSN) of 100 and that each station puts 1500 W of power into theoretical isotropic antennas that have +10 dBi of gain at all elevation and azimuth angles. [We use such theoretical isotropic antennas because they make it easier to work in *VOACAP*. We will factor in real-world stacks later.] *VOACAP* predicts that the signal from Boston will be S9 + 8 dB in Atlanta at 1400 UTC, arriving at an elevation angle of 21.3º on a single F_2 hop. This elevation angle is higher than commonly encountered angles for DX signals, but it is still far away from near-overhead angles.

The signal from Paris into Atlanta is predicted to be about S6 for the same theoretical isotropic antennas, at an incoming elevation angle of 6.4º on three F_2 hops. The S6 level validates the rule-of-thumb that each extra hop loses approximately 10 dB of signal strength, assuming that each S unit is about 4 dB, typical for modern receivers.

Now look at **Fig 36**, which shows the response for a stack of 3-element Yagis at 90/60/30 feet over flat ground, along with the response for a similar stack of 7-element Yagis. Again, we'll assume that all three stations are using such 3-element 90/60/30-foot stacks. The stations in Atlanta and Boston point their stacks into Europe and the Parisian station points his stack towards the USA. The gain of the Atlanta array at 6.4º into Paris will be about 16 dBi, or 6 dB more than the isotropic array with its +10 dBi of gain selected for use in *VOACAP*. Similarly, the French station's transmitted signal will enjoy a 6 dB gain advantage over the isotropic array used in the *VOACAP* calculation, and thus the French signal into Atlanta will now be S6 + 12 dB, or about S9.

By comparison, the interfering signal from Boston into Atlanta will be reduced by the rearward pattern of his array, which will launch a signal at 180º – 21.3º = 158.7º in elevation at the single F_2 mode from Boston to Atlanta. From Fig 33, the Boston station's gain at this rearward elevation is going to drop from the isotropic's +10 dBi of gain down to –11 dBi, a drop of 21 dB. The signal into the Atlanta receiver will also be reduced by the pattern of the Atlanta array on receive, which has a gain of about 0 dBi at 21.3º, compared to the isotropic's +10 dBi gain at 6.4º, a net drop of 10 dB.

Thus, the Boston station's signal will drop by about 21 + 10 = 31 dB, bringing the interfering signal from Boston, which would be S9 + 8 dB for isotropic antennas, down to about S3 due to the combined effects of the arrays. This is a very significant reduction in interference. But you will note that the reduction has nothing to

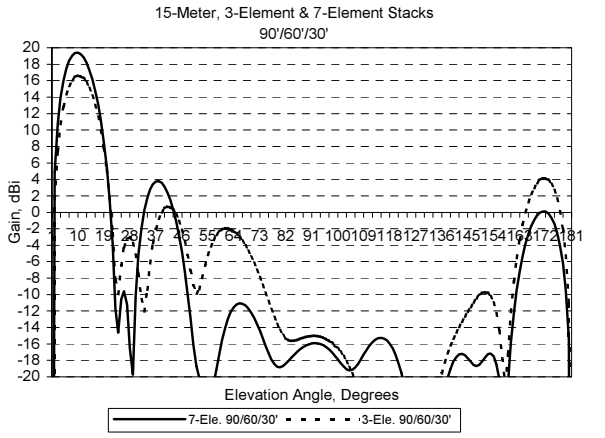

Fig 36—Stacks of three 3-element and 7-element Yagis on 15 meters at 90/60/30 feet heights. The F/B for the 7-element stack is superior to the 3-element stack mainly because the F/B is intrinsically better for the long-boom design.

do with the near-overhead lobes, dealing as it does with the trailing edge of the main lobe and the F/B lobe.

Even Higher Elevation Angles

Now let's evaluate a station that is even closer to Boston, say a station in Philadelphia. The heading from Philadelphia to Paris is 53º and the distance is 3220 miles. On the same day in October as above, *VOACAP* predicts a signal strength of S8 from Paris to Philadelphia, at a 2.7º elevation angle on two F_2 hops. Again, the *VOACAP* computations assume isotropic antennas with +10 dBi gain at all three stations. The gain of the 3-element stacks at both ends of the circuit at 2.7º is also about +10 dBi, so the signal level from Paris to Philadelphia would be S8 with the 3-element stacks.

Now *VOACAP* computes the elevation angle from Philadelphia to Boston as 56.3º, on one F_2 hop launched at an azimuth of 53º, well within the azimuthal beamwidth of the stack. *VOACAP* says the predicted signal strength for isotropic antennas with +10 dBi of gain is less than S1!

What's happening here? Boston and Philadelphia are within the "skip" region on 21 MHz and signals are skipping right over Boston from Philadelphia (and vice versa). Actual signals would be much weaker than they would be with theoretical isotropic antennas because of the actual patterns of the transmitting and receiving stacks. At an elevation angle of 56.3º the receiving stack would have a gain of –10 dBi, while at an elevation of 180º – 56.3º = 123.7º the transmitting stack would be down to –10 dBi as well. The net reduction for the stacks compared to isotropics with +10 dBi gain each would be 40 dB, putting the interfering signal well into the receiver noise.

You can safely say that near-overhead angles don't enter into the picture, simply because signals at intermediate distances are in the ionospheric skip zone and interfering signals are very weak in that zone already.

Even in situations where having a poor front-to-back ratio might be beneficial—because it alerts stations tuning across your signal that you are occupying that frequency—the ionosphere doesn't cooperate for intermediate-distance signals that are in the skip zone. Often two stations may be on the same frequency without either knowing that the other is there.

Ground Wave?

What happens, you might wonder, for ground-wave signals? Let's look at a situation where the interfering station is in the same direction as the desired target, but is only 5 miles away. Unfortunately, his signal is S9 + 50 dB. Even reducing the level by 30 dB, a huge number, is still going to make his signal 20 dB stronger than signals from your desired target location! There is not much you can do about ground-wave signals and fretting about optimizing stack heights to discriminate against local signals is generally futile.

Stacking Distances for Multiband Yagis

By definition, a stack of multiband Yagis (such as a "tribander" covering 20/15/10 meters) has a constant vertical spacing between antennas in terms of feet or meters, but not in terms of wavelength. Tribanders are no different than monobanders in terms of optimal spacing between individual antennas. Again, the difference in gain between spacings of 0.5 λ and 1.0 λ for a stack of triband Yagis amounts to only a fraction of a decibel. Furthermore, the main practical constraint that limits choice of stacking distances between any kind of Yagis, multiband or monoband, is the spacing between guy wire sets on the tower itself.

Summary, Stacking Distances

In short, let us summarize that there is nothing magical about stacking distances for practical HF Yagis—a good rule-of-thumb is a stacking distance of 0.65 λ. This is 23 feet on 10 meters, 30 feet on 15 meters and 45 feet on 20 meters for monoband stacks. Practically speaking, however, you've only got limited places where you can mount antennas on the tower—mainly where guy wires allow you to place them. This is especially applicable if you wish to rotate lower antennas on the tower, where you must clear the guys from up above.

STACKS AND FADING

The following is derived from an article by Fred Hopengarten, K1VR, and Dean Straw, N6BV, in a Feb 1994 *QST* article. Using stacked Hy-Gain TH7DXs or TH6DXXs at their respective stations, they have solicited a number of reports from stations, mainly in Europe,

to compare various combinations of antennas in stacks and as single antennas. The peak gain of the stack is usually just a little bit higher than that for the best of the single antennas, which is not surprising. Even a large stack has no more than about 6 dB of gain over a single Yagi at a height favoring the prevailing elevation angle. Fading on the European path can easily be 20 dB or more, so it is very confusing to try to make definitive comparisons. They have noticed over many tests that the stacks are much less susceptible to fading compared to single Yagis. Even within the confines of a typical SSB bandwidth, frequency-selective fading occasionally causes the tonal quality of a voice to change on both receive and transmit, often dramatically becoming fuller on the stacks, and tinnier on the single antennas. This doesn't happen all the time, but is often seen. They have also observed often that the depth of a fade is less, and the period of fading is longer, on the stacks compared to single antennas.

Exactly *why* stacks exhibit less fading is a fascinating subject, for which there exist a number of speculative ideas, but little hard evidence. Some maintain that stacks outperform single antennas because they can afford *space diversity* effects, where by virtue of the difference in physical placement one antenna will randomly pick up signals that another one in another physical location might not hear.

This is difficult to argue with, and equally difficult to prove scientifically. A more plausible explanation about why stacked Yagis exhibit superior fading performance is that their narrower frontal elevation lobes can discriminate against undesired propagation modes. Even when band conditions favor, for example, a very low 3° elevation angle on 10 or 15 meters from New England to Western Europe, there are signals, albeit weaker ones, that arrive at higher elevation angles. These higher-angle signals have traveled longer distances on their journey through the ionosphere, and thus their signal levels and their phase angles are different from the signals traversing the primary propagation mode. When combined with the dominant mode, the net effect is that there is both destructive and constructive fading. If the elevation response of a stacked antenna can discriminate against signals arriving at higher elevation angles, then in theory the fading will be reduced. Suffice it to say: In practice, stacks do reduce fading.

STACKS AND PRECIPITATION STATIC

The top antenna in a stack is often much more affected by rain or snow precipitation static than is the lower antenna. N6BV and K1VR have observed this phenomenon, where signals on the lower antenna by itself are perfectly readable, while S9+ rain static is rendering reception impossible on the higher antenna or on the stack. This means that the ability to select individual antennas in a stack can sometimes be extremely important.

STACKS AND AZIMUTHAL DIVERSITY

Azimuthal diversity is a term coined to describe the situation where one of the antennas in a stack is purposely pointed in a direction different from the main direction of the stack. During most of the time in a DX contest from the East Coast, the lower antennas in a stack are pointed into Europe, while the top antenna is often rotated toward the Caribbean or Japan. In a stack of three identical Yagis, the first-order effect of pointing one antenna in a different direction is that one-third of the transmitter power is diverted from the main target area. This means that the peak gain is reduced by 1.8 dB, not a very large amount considering that signals are often 10 to 20 dB over S9 anyway when the band is open from New England to Europe.

Fig 37 shows the 3D pattern of a pair of 4-element Yagis fed in-phase at 95 and 65 feet, but where the lower antenna has been rotated 180° to fire in the –X direction. The backwards lobe peaks at a higher elevation angle because the antenna doing the radiating in this direction is lower on the tower. The forward lobe peaks at a lower angle because its main radiator is higher.

THE N6BV/1 ANTENNA SYSTEM—BRUTE FORCE FEEDING

The N6BV/1 system in Windham, New Hampshire, was located on the crest of a small hill about 40 miles from Boston, and could be characterized as a good, but not dominant, contesting station. A number of top-10 contest results were achieved from that station in the 1990s before N6BV returned to California.

There was a single 120-foot high Rohn 45 tower, guyed at 30-foot intervals, with a 100-foot horizontal spread from tower base to each guy point so there was sufficient room for rotation of individual Yagis on the tower. Each set of guy wires employed heavy-duty insulators at 57-foot intervals, to avoid resonances in the 80 through 10-meter amateur bands. There were five Yagis on the tower. A heavy-duty 12-foot long steel mast with 0.25-inch walls was at the top of the tower, turned by an Orion 2800 rotator. Two thrust bearings were used above the rotator, one at the top plate of the tower itself, and the other about 2 feet down in the tower on a modified rotator shelf plate. The two thrust bearings allowed the rotator to be removed for service.

At the top of the mast, 130 feet high, was a 5-element, computer-optimized 10-meter Yagi, which was a modified Create design on a 24-foot boom. The element tuning was modified from the stock antenna in order to achieve higher gain and a better pattern over the band. At the top of the tower (120-foot level) was mounted a Create 714X-3 triband Yagi. This was a large tribander, with a 32-foot boom and five elements. Three elements were active on 40 meters, four were active on 20 meters and four were active on 15 meters. The 40-meter elements were loaded with coils, traps and

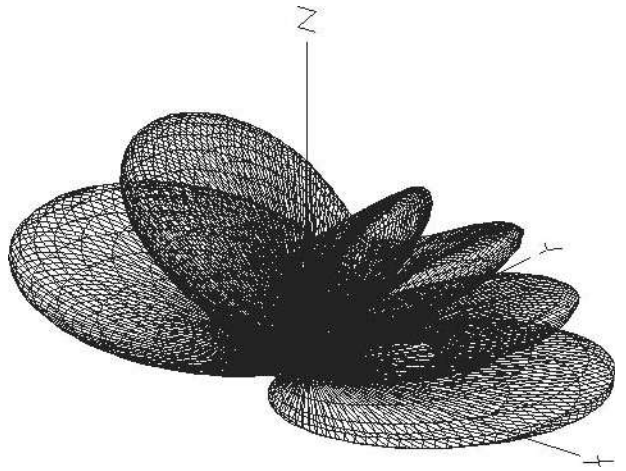

Fig 37—3D representation of the pattern for two 4-element 15-meter Yagis, with the top antenna at 95 and the bottom at 65 feet, but pointed in the opposite direction.

capacitance hats, and were approximately 46 feet long. A triband 20/15/10-meter Hy-Gain TH7DX tribander was fixed into Europe at the 90-foot level on the tower, just above the third set of guys.

At the 60-foot level on the tower, just above the second set of guys, there was a "swinging-gate" side-mount bracket, made by DX Engineering of Oregon. A Hy-Gain *Tailtwister* rotator turned a TH7DX on this side mount. (Note that both the side mount and the element spacings of the TH7DX itself prevented full rotation around the tower—about 280° of rotation was achieved with this system.) At the 30-foot level, just above the first set of guys, was located the third TH7DX, also fixed on Europe.

All five Yagis were fed with equal lengths of Belden 9913 low-loss coaxial cable, each measured with a noise bridge to ensure equal electrical characteristics. At each feed point a ferrite-bead choke balun (using seven large beads) was placed on the coax. All five coaxial cables went to a relay switch box mounted at the 85-foot level on the tower. **Fig 38** shows the schematic for the switch box, which was fed with 250 feet of 75-Ω, 0.75-inch OD Hardline coaxial cable.

The stock DX Engineering remote switch box was modified by adding relay K6, so that either the 130-foot or the 120-foot rotating antenna could be selected through a second length of 0.75-inch Hardline going to the shack. This created a *Multiplier* antenna, independent of the *Main* antennas. A second band could be monitored in this fashion while calling CQ using the main antennas on another band. Band-pass filters were required at the multiplier receiver to prevent overload from the main transmitter.

The 0.75-inch Hardline had very low losses, even when presented with a significant amount of SWR at the switch-box end. This was important, because unlike K1VR's system, no attempt was made at N6BV to maintain a constant SWR when relays K1 through K5 were switched in or out. This seemingly cavalier attitude came about because of several factors. First, there were many

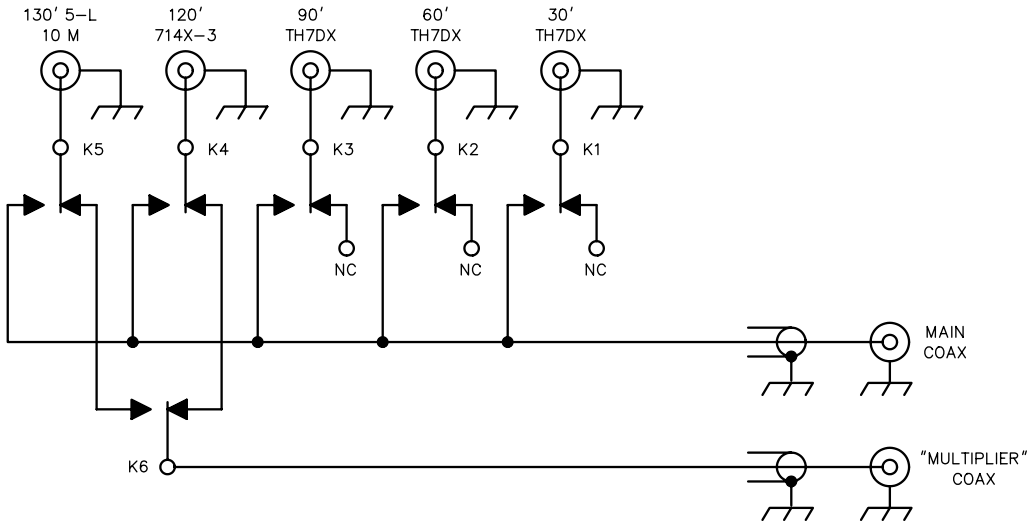

Fig 38—N6BV/1 switch box system. This uses a modified DX Engineering remote switch box, with relay K6 added to allow selection of either of the two top antennas (5-element 10-meter Yagi or 40/20/15-meter triband 714X-3) as a "multiplier" antenna. There is no special provision for SWR equalization when any or all of the Yagis are connected in parallel as a stack fed by the Main coaxial cable. Each of the five Yagis is fed with equal lengths of flexible Belden 9913 coax, so phasing can be maintained on any band. The Main and "Multiplier" coaxes going to the shack are 0.75" OD 75-Ω Hardline cables.

different combinations of antennas that could be used together in this system. Each relay coil was independently controlled by a toggle switch in the shack. N6BV was unable to devise a matching system that did not become incredibly complex because of the numerous impedance combinations used over all the five bands.

Second, the worst-case additional transmission line loss due to a 4:1 SWR mismatch when four antennas were connected in parallel on 10 meters was only 0.5 dB. It was true that the linear amplifier had to be retuned slightly when combinations of antennas were switched in and out, but this was a small penalty to pay for the reduced complexity of the switching and matching networks. The 90/60/30-foot stack into Europe was used for about 95% of the time during DX contests, so the small amount of amplifier retuning for other antenna combinations was considered only a minor irritation.

WHY TRIBANDERS?

Without a doubt, the most common question K1VR and N6BV have been asked is: "Why did you pick *tribanders* for your stacks?" Triband antennas were chosen with full recognition that they are compromise antennas. Other enterprising amateurs have built stacked tribander arrays. Bob Mitchell, N5RM, is a prominent example, with his so-called *TH28DX* array of four TH7DX tribanders on a 145-foot-high rotating tower. Mitchell employed a rather complex system of relay-selected tuned networks to choose either the upper stacked pair, the lower stacked pair or all four antennas in stack. Others in Texas have also had good results with their tribander stacks. Contester Danny Eskenazi, K7SS, has very successfully used a pair of stacked KT-34XA tribanders for years.

A major reason why tribanders were used is that over the years both authors have had good results using TH6DXX or TH7DX antennas. They are ruggedly built, mechanically and electrically. They are able to withstand New England winters without a whimper, and their 24-foot long booms are long enough to produce significant gain, despite trap-loss compromises. Amateurs speculating about trap losses in tribanders freely bandy about numbers between 0.5 and 2 dB. Both N6BV and K1VR are comfortable with the lower figure, as are the Hy-Gain engineers.

Consider this: If 1500 W of transmitter power is going into an antenna, a loss of 0.5 dB amounts to 163 W. This would create a significant amount of heat in the six traps that are on average in use on a TH6DXX, amounting to 27 W per trap. If the loss were as high as 1 dB, this would be 300 W total, or 50 W per trap. Common sense says that if the overall loss were greater than about 0.5 dB, the traps would act more like big *firecrackers* than resonant circuits! A long-boom tribander like the TH6DXX or TH7DX also has enough space to employ elements dedicated to different bands, so the compromises in element spacing usually found on short-boom 3 or 4-element tribanders can be avoided.

Another factor in the conscious choice of tribanders was first-hand frustration with the serious interaction that can result from stacking monoband antennas closely together on one mast in a Christmas Tree configuration. N6BV's worst experience was with the ambitious 10 through 40-meter Christmas Tree at W6OWQ in the early 1980s. This installation used a Tri-Ex SkyNeedle tubular crankup tower with a rotating 10-foot-long heavy-wall mast. The antenna suffering the greatest degradation was the 5-element 15-meter Yagi, sandwiched 5 feet below the 5-element 10-meter Yagi at the top of the mast, and 5 feet above the full-sized 3-element 40-meter Yagi, which also had five 20-meter elements interlaced on its 50-foot boom.

The front-to-back ratio on 15 meters was at best about 12 dB, down from the 25+ dB measured with the bottom 40/20-meter Yagi removed. No amount of fiddling with element spacing, element tuning or even orientation of the 15-meter boom with respect to the other booms (at 90° or 180°, for example) improved its performance. Further, the 20-meter elements had to be lengthened by almost a foot *on each end of each element* in order to compensate for the effect of the interlaced 40-meter elements. It was a lucky thing that the tower was a motorized crankup, because it went up and down hundreds of times as various experiments were attempted!

Interaction due to close proximity to other antennas in a short Christmas Tree can definitely destroy carefully optimized patterns of individual Yagis. Nowadays, such interaction can be modeled using a computer program such as *EZNEC* or *NEC*. A gain reduction of as much as 2 to 3 dB can easily result due to close vertical spacing of monobanders, compared to the gain of a single monoband antenna mounted in the clear. Curiously enough, at times such a reduction in gain can be found even when the front-to-back ratio is not drastically degraded, or when the front-to-back occasionally is actually *improved*.

If you plan on stacking monoband Yagis—for example, putting only 15-meters Yagis on a single tower, with your other monoband stacks on other towers—do make sure you model the system to see if any interactions occur. You may be quite surprised.

Finally, in the N6BV/1 installation, triband antennas were chosen because the system was meant to be as simple as possible, given a certain desired level of performance, of course. Triband antennas make for less mechanical complexity than do an equivalent number of monobanders. There were five Yagis on the N6BV/1 tower, yielding gain from 40 to 10 meters, as opposed to using 12 or 13 monobanders on the tower.

THE K1VR ARRAY: A MORE ELEGANT APPROACH TO MATCHING

The K1VR stacked array is on a 100-foot high Rohn

25 tower, with sets of guy wires at 30, 60 and 90 feet, made of nonconducting Phillystran. Phillystran is a nonmetallic Kevlar rope covered by black polyethylene to protect against the harmful effects of the sun's ultraviolet rays. A caution about Phillystran: Don't allow tree branches to rub against it. It is designed to work in tension, but unlike steel guy wire, it does not tolerate abrasion well.

Both antennas are Hy-Gain TH6DXX tribanders, with the top one at 97 feet and the bottom one at 61 feet. The lower antenna is rotated by a Telex Ham-M rotator on a homemade swinging-gate side mount, which allows it to be rotated 300° around the tower without hitting any guy wires or having an element swing into the tower. At the 90-foot point on the tower, a 2-element 40-meter Cushcraft Yagi has been mounted on a RingRotor so it can be rotated 360° around the tower.

After several fruitless attempts trying to match the TH6DXX antennas so that either could be used by itself or together in a stack, K1VR settled on using a relay-selected broadband toroidal matching transformer. When both triband antennas are fed together in parallel as a stack, it transforms the resulting 25-Ω impedance to 50 Ω. The transformer is wound on a T-200A powdered-iron core, available from Amidon, Palomar Engineering or Ocean State Electronics. Two lengths of twin RG-59 coax (sometimes called Siamese or WangNet), four turns each, are wound on the core. Two separate RG-59 cables could be used, but the Siamese-twin cable makes the assembly look much more tidy. The shields of the RG-59 cables are connected in series, and the center conductors are connected in parallel. See **Fig 39** for details.

Fig 40 shows the schematic of the K1VR switch box, which is located in the shack. Equal electrical lengths of 50-Ω Hardline are brought from the antennas into the shack and then to the switch box. Inside the box, the relay contacts were soldered directly to the SO-239 chassis connectors to keep the wire lengths down to the absolute minimum. K1VR used a metal box that was larger than

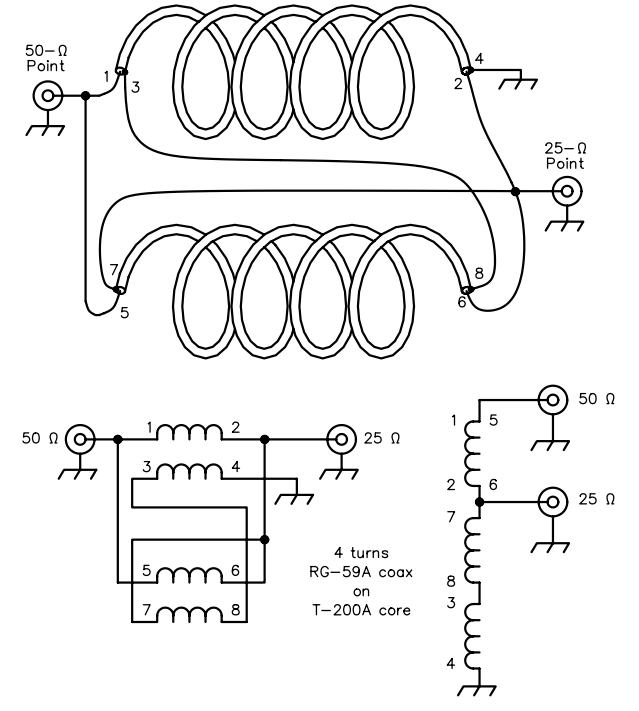

Fig 39—Diagram for matching transformer for K1VR stacked tribander system. The core is powdered iron-core T-200A, with four turns of two RG-59A or "Siamese" coax cables. Center conductors are connected in parallel and shields are connected in series to yield 0.667:1 turns ratio, close to desired 25-Ω to 50-Ω transformation.

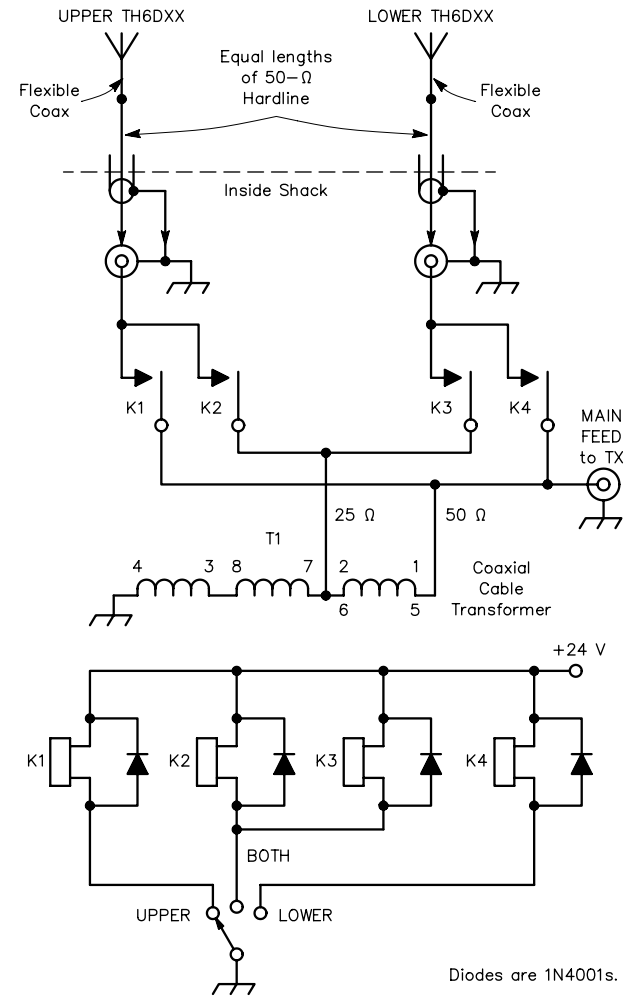

Fig 40—Relay switch box for K1VR stacked tribander system. Equal lengths of 50-Ω Hardline (with equal lengths of flexible 50-Ω cable at each antenna to allow rotation) go to the switch box in the shack. The SWR on all three bands for Upper, Lower or Both switch positions is very close to constant.

might appear necessary because he wanted to mount the toroidal transformer with plenty of clearance between it and the box walls. The toroid is held in place with a piece of insulation foam board. Before placing the switch box in service, the system was tested using two 50-Ω dummy loads, with equal lengths of cable connected in parallel to yield 25 Ω. The maximum SWR measured was 1.25:1 at 14 MHz, 1.3:1 at 21 MHz and 1.15:1 at 28 MHz, and the core remained cold with 80 W of continuous output power.

One key to the system performance is that K1VR made the electrical lengths of the two hardlines the same (within 1 inch) by using a borrowed TDR (time domain reflectometer). Almost as good as Hardline, K1VR points out, would be to cut exactly the same length of cable from the same 500-foot roll of RG-213. This eliminates manufacturing tolerances between different rolls of cable.

K1VR's experience over the last 10 years has been that at the beginning of the 10 or 15-meter morning opening to Europe the upper antenna is better. Once the band is wide open, both antennas are fed in phase to cast a bigger shadow, or footprint, on Europe. By mid-morning, the lower antenna is better for most Europeans, although he continues to use the stack in case someone is hearing him over a really long distance path throughout Europe. He reports that it is always very pleasant to be called by a 4S7 or HSØ or VU2 when he is working Europeans at a fast clip!

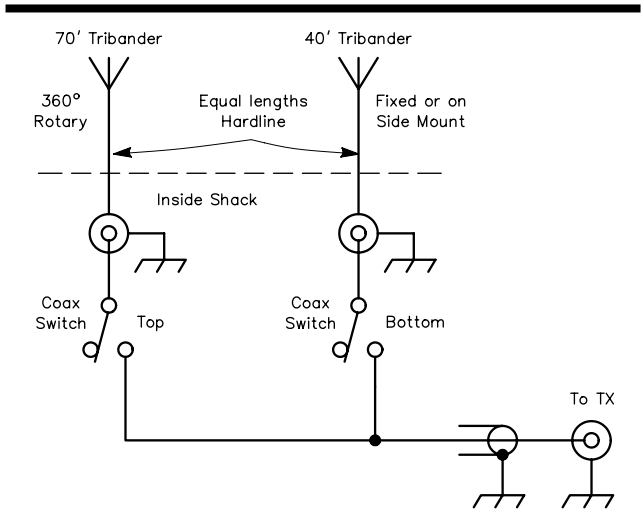

Fig 41—Simple feed system for 70/40-foot stack of tribanders. Each tribander is fed with equal lengths of 0.5-inch 75-Ω Hardline cables (with equal lengths of flexible coax at the antenna to allow rotation), and can be selected singly or in parallel at the operator's position in the shack. Again, no special provision is made in this system to equal SWR for any of the combinations.

SOME SUGGESTIONS FOR STACKING TRIBANDERS

It is unlikely that many amateurs will try to duplicate exactly K1VR's or N6BV's contest setups. However, many hams already have a tribander on top of a moderately tall tower, typically at a height of about 70 feet. It is not terribly difficult to add another, identical tribander at about the 40-foot level on such a tower. The second tribander can be pointed in a fixed direction of particular interest (such as Europe or Japan), or it can be rotated around the tower on a side mount or a Ring Rotor. If guy wires get in the way of rotation, the antenna can usually be arranged so that it is fixed in a single direction.

Insulate the guy wires at intervals to ensure that they don't shroud the lower antenna electrically. A simple feed system consists of equal-length runs of surplus 0.5-inch 75-Ω Hardline (or more expensive 50-Ω Hardline, if you are really obsessed by SWR) from the shack up the tower to each antenna. Each tribander is connected to its respective Hardline feeder by means of an equal length of flexible coaxial cable, with a ferrite choke balun, so that the antenna can be rotated.

Down in the shack, the two hardlines can simply be switched in and out of parallel to select the upper antenna only, the lower antenna only, or the two antennas as a stack. See **Fig 41**. Any impedance differences can be handled as stated previously, simply by retuning the linear amplifier, or by means of the internal antenna tuner (included in most modern transceivers) when the transceiver is run barefoot. The extra performance experienced in such a system will be far greater than the extra decibel or two that modeling calculates.

THE WXØB APPROACH TO STACK MATCHING AND FEEDING

Earlier we mentioned how useful it would be to switch various antennas in or out of a stack, depending on the elevation angles that need to be emphasized at that moment. Jay Terleski, WXØB, of Array Solutions has designed switchable matching systems, called *StackMatches*, for stacks of monoband or multiband Yagis.

The StackMatch uses a 50-Ω to 22.25-Ω broadband transmission-line transformer to match combinations of up to three Yagis in a stack. See **Fig 42** for a schematic of the StackMatch. For selection of any 50-Ω Yagi by itself, no matching transformer is needed and Relay IN routes RF directly to the common bus going to Relay 1, 2 and 3. For selection of two Yagis together the parallel impedance is 50/2 = 25 Ω and Relay IN routes RF to the matching transformer. The SWR is 25/22.25 = 1.1:1. For three Yagis used together, the parallel impedance is 50/3 = 16.67 Ω, and the SWR is 22.25/16.67 = 1.3:1.

The broadband transformer consists of four trifilar turns of #12 enamel-insulated wire wound on a Ferrite Corporation FT-240 2.4-inch OD core made of #61

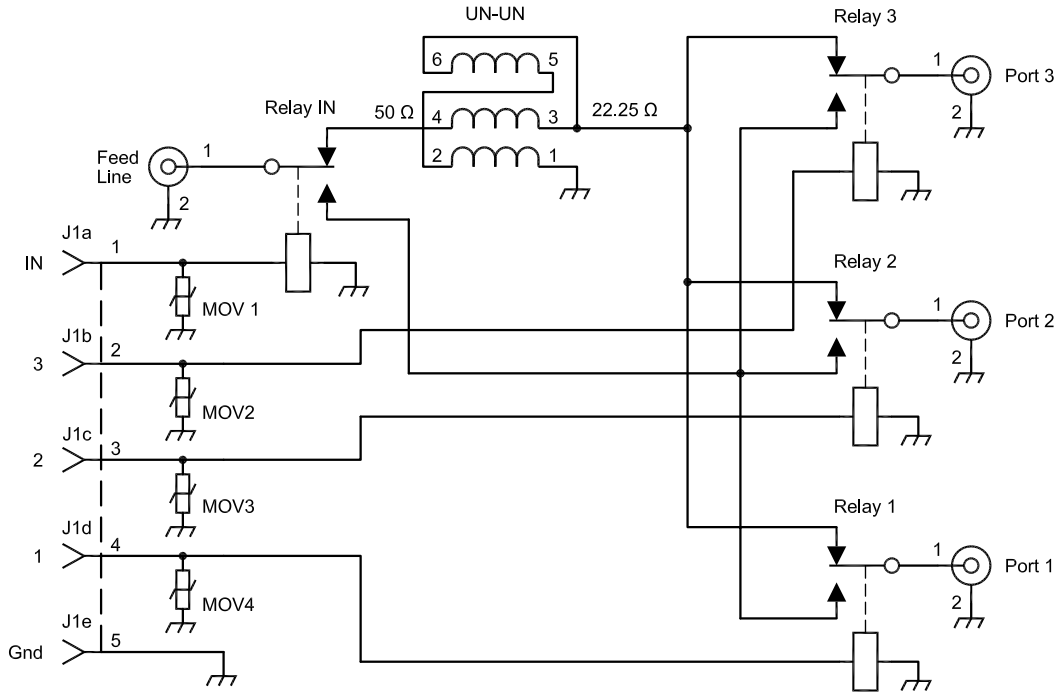

Fig 42—Schematic of WXØB's StackMatch 2000 switchbox, which uses a broadband transmission line transformer using trifilar #12 enamel-insulated wires. (*Courtesy Array Solutions.*)

material (μ = 125). WXØB uses 10-A relays enclosed in plastic cases to do the RF switching, selected by a control box at the operating position. (10-A relays can theoretically handle 10 $A^2 \times 50\ \Omega$ = 5000 W.) **Fig 43** shows a photo of the transmission-line transformer and StackMaster PCB.

The control/indicator box uses a diode matrix to switch various combinations of antennas in/out of the stack. Three LEDs lined up vertically on the front panel indicate which antennas in a stack are selected.

"BIP/BOP" OPERATION

The contraction "BIP" means "both in-phase," while "BOP" means "both out-of-phase." BIP/BOP refer to stacks containing two Yagis, although the term is commonly used for stacks containing more than two Yagis. In theory, feeding a stack with the antennas out-of-phase will shift the elevation response higher than in-phase feeding.

Fig 44 shows a rectangular plot comparing BIP/BOP operation of two 3-element 15-meter Yagis at heights of 2 λ and 1 λ (93 and 46 feet) over flat ground. The BOP pattern is the higher-angle lobe and the two lobes cross over about 14°. The maximum amplitude of the BOP stack's gain is about ½ dB less than the BIP pair. For reference, the pattern of a single 46-foot high Yagi is overlaid on the pattern for the stacks.

The most common method for feeding one Yagi 180° out-of-phase is to include an extra electrical half wavelength of feed-line coax going to one of the antennas. This method obviously works on a single frequency band and thus is not applicable to stacks of multiband Yagis, such as tribanders. For such multiband stacks, feeding only the lower antenna(s)—by switching out higher antenna(s) in the stack—is a practical method for achieving better coverage at medium or high elevation angles.

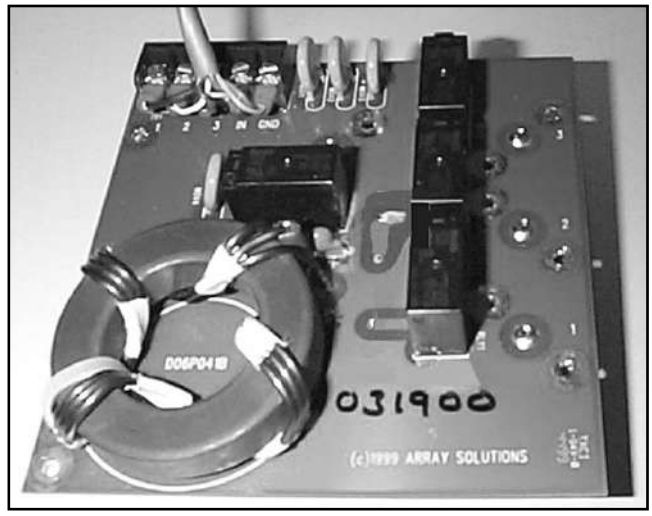

Fig 43—Inside view of StackMatch. (*Photo courtesy Array Solutions.*)

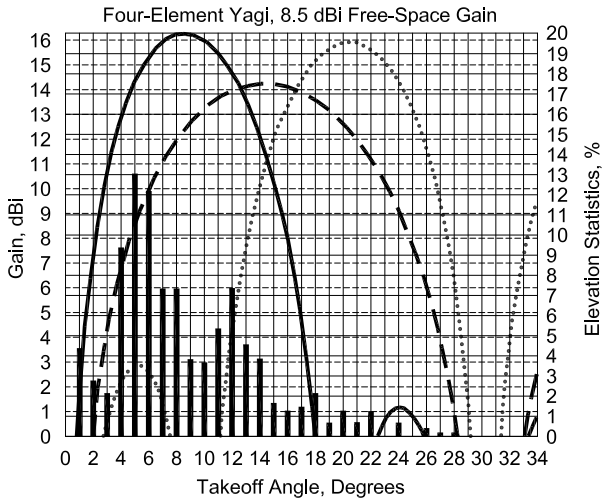

Fig 44—*HFTA* screen shot of "BIP/BOP" operation of two 4-element 15-meter Yagis at 93 and 46 feet above flat ground. The elevation response in BOP (both out-of-phase) operation is shifted higher, peaking at about 21°, compared to the BIP (both in-phase) operation where the peak is at 8°. The dashed line is response of single Yagi at 46 feet.

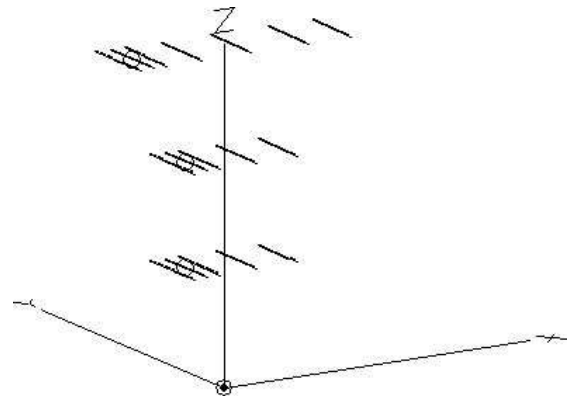

Fig 45—Stacking dissimilar Yagis. In this case a 7-element 10-meter Yagi is stacked over two 5-element Yagis. Note the displacement of the 7-element Yagi's driven element compared to the position of the two 5-element Yagis. This leads to an undesired phase shift for the higher antenna.

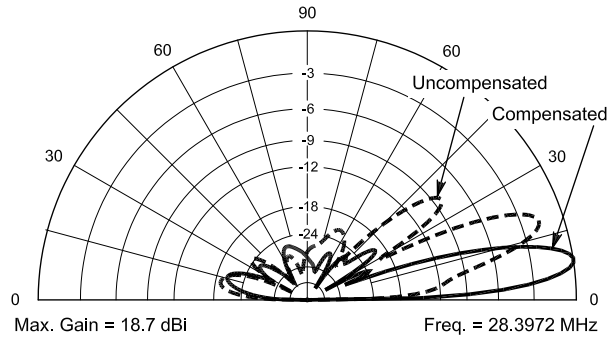

Fig 46—Comparison of elevation responses for 7/5/5-element 10-meter stacks, with and without compensation for driven-element offset.

STACKING DISIMILAR YAGIS

So far we have been discussing vertical stacks of identical Yagis. Less commonly, hams have successfully stacked dissimilar Yagis. For example, consider a case where two 5-element 10-meter Yagis are placed 46 and 25 feet above flat ground, with a 7-element 10-meter Yagi at 68 feet on the same tower. See **Fig 45**, which is a schematic of the layout for this stack. Note that the driven element for the top 7-element Yagi is well behind the vertical plane of the driven elements for the two 5-element Yagis. This offset distance must be compensated for with a phase shift in the drive system for the top Yagi.

Fig 46 shows the elevation-pattern responses for uncompensated (equal-length feed lines) and the compensated (additional 150° of phase shift to top Yagi) stacks. These patterns were computed using *EZNEC ARRL*, which is included with this book. Not only is about 1.7 dB of maximum gain lost, but the peak elevation angle is shifted upwards by 11° from the optimal takeoff angle of 8°—where some 10 dB of gain is also lost. Without compensation, this is a severe distortion of the stack's elevation pattern.

For RG-213 coax, the extra length needed to provide an additional 150° of phase shift = 150°/360° λ = 0.417 λ = 9.53 feet at 28.4 MHz. This was computed using the program *TLW* (Transmission Line for Windows) included on the CD-ROM accompanying this book.

It is not always possible to compensate for dissimilar Yagis in a stack with a simple length of extra coax, so you should be sure to model such combinations to make sure that they work properly. A safe alternative, of course, is to stack only identical Yagis, feeding all of them with equal lengths of coax to ensure in-phase operation.

Real-World Terrain and Stacks

So far, the stacking examples shown have been for flat ground. Things can become a lot more complicated when you deal with real-world irregular terrains! See Chapter 3, The Effects of Ground, for a description of the *HFTA* (High Frequency Terrain Assessment) program that is included with this book.

Fig 47 shows the *HFTA*-computed 20-meter elevation responses towards Europe (at an azimuth of 45°) for three antennas at the N6BV/1 location in Windham, New Hampshire. Overlaid as a bar graph are the elevation-angle statistics for the path to all of Europe from New England (Massachusetts). The stack at 90/60/30 feet clearly covers all the angles needed best at 14 MHz. The N6BV 120-foot Yagi has a severe null in the region from about 7° to about 20°, with the deepest part of that null occurring at about 13° and is roughly comparable to the 90/60/30-foot stack between 2° to 7°.

In practice, the 120-foot Yagi was indeed comparable to the stack during morning openings to Europe on 20 meters, when the elevation angles are typically about 5°. In the New England afternoon, when the elevation angles typically rise to about 11°, the 120-foot Yagi was always distinctly inferior to the stack.

For reference, the response of a single 120-foot high Yagi over flat ground is also shown. Note that the N6BV 120-foot high Yagi has about 3 dB more gain at a 5° takeoff angle than does its flatland counterpart. This additional gain is due to the focusing effects of the local terrain, which had about a 3° downwards slope towards Europe.

Fig 48 shows the *HFTA*-computed 15-meter elevation responses towards Europe for the 90/60/30-foot stack at 90/60/30 feet at N6BV/1, compared to the same 120-foot high Yagi and a 90/60/30-foot stack, but this time over flat ground. Again, the N6BV/1 terrain towards Europe has a significant effect on the gain of the stack compared to that of an identical stack over flat ground. In fact, the peak gain of 20.1 dBi at a 4° elevation angle is close to moon-bounce levels.

OPTIMIZING OVER LOCAL TERRAIN

There are only a small number of possibilities to optimize an installation over local terrain:

- Change the antenna height(s) above ground.
- Stack two (or more) Yagis.
- Change the spacing between stacked Yagis.
- Move the tower back from a cliff (or a hill).
- BIP/BOP (Both In Phase/Both Out of Phase).

The *HFTA* program on the CD-ROM accompanying this book can be used, together with Digital Elevation Model (DEM) topographic data available on the Internet, to evaluate all these options.

SO NEAR, YET SO FAR

It is sometimes very surprising to compare elevation responses for different towers located at various points on the same property, particularly when that prop-

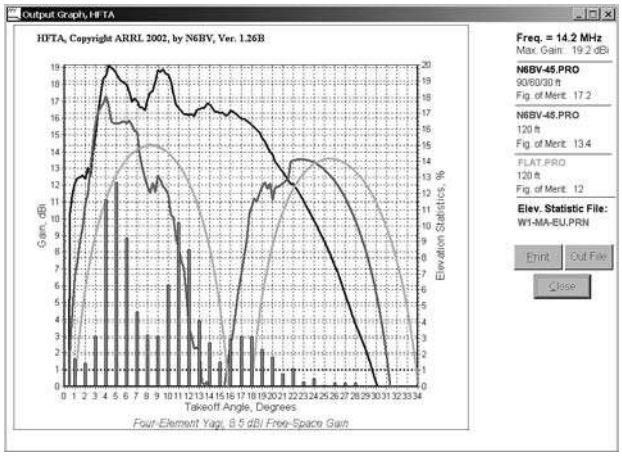

Fig 47—*HFTA* screen shot showing how complicated things become when real-world irregular terrain is analyzed. This is the 20-meter elevation pattern for the N6BV/1 station location in Windham, NH, for the 90/60/30-foot stack of triband TH7DX Yagis and a 4-element Yagi at 120 feet on the same tower. For comparison, the response of a 120-foot Yagi over flat ground is also included.

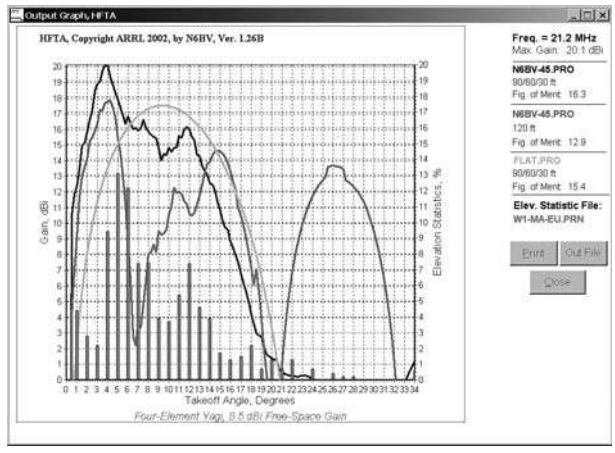

Fig 48—*HFTA* screen shot showing the 15-meter elevation pattern for the N6BV/1 station location in Windham, NH, for the 90/60/30-foot stack of triband TH7DX Yagis and a 4-element Yagi at 120 feet on the same tower. For comparison, the response of a 120-foot Yagi over flat ground is also included.

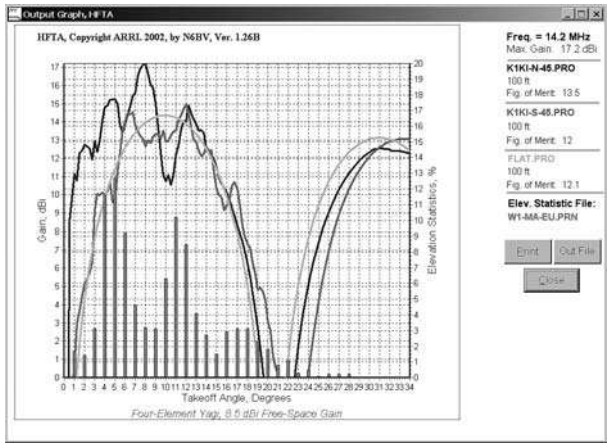

Fig 49—*HFTA* screen shot showing the 20-meter elevation pattern for K1KI's North and South towers, with 100-foot high 4-element Yagis pointing into Europe at an azimuth of 45°. The responses are surprisingly different for two towers separated by only 600 feet.

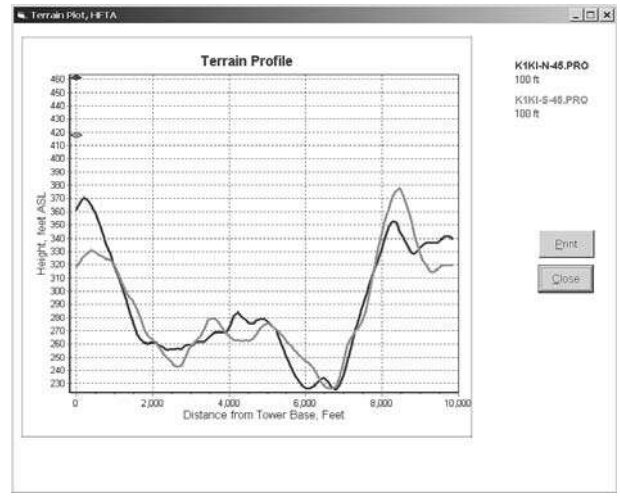

Fig 50—K1KI's terrain profiles for the North and South towers at an azimuth of 45° into Europe.

erty is located in the mountains. **Fig 49** shows the computed elevation responses for three 100-foot high 14-MHz Yagis over three terrains towards Europe: from the North tower at K1KI's location in West Suffield, Connecticut, from the South tower at K1KI, and over flat ground. The elevation response from the South tower follows that over flat ground well, while the response from the North tower is quite a bit stronger at low elevation angles—about 1.5 dB on average, as the Figure of Merit shows from *HFTA*.

Fig 50 shows the reason why this happens—the terrain from the North tower slopes down quickly towards Europe, while the terrain from the South tower goes out almost 900 feet before starting to fall off. These two towers are about 600 feet apart.

Moxon Rectangle Beams

LB Cebik, W4RNL, has written extensively about the *Moxon rectangle*, an antenna invented by Les Moxon, G6XN, derived from a design by VK2ABQ. The Moxon rectangle beam takes less space horizontally than a conventional 2-element Yagi design, yet it offers nearly the same amount of gain and a superior front-to-back ratio. And as an additional benefit, the drive-point impedance is close to 50 Ω, so that it doesn't need a matching section.

For example, rather than a "wingspan" of 17 feet for the reflector in a conventional 2-element 10-meter Yagi, the Moxon rectangle is 13 feet wide, a saving of almost 25%. The Moxon rectangle W4RNL created for *The ARRL Antenna Compendium, Vol 6*, had an SWR less than 2:1 from 28.0 to 29.7 MHz, with a gain over ground of 11 dBi. It had a F/B of 15 dB at 28.0 MHz, more than 20 dB at 28.4 MHz, and 12 dB at 29.7 MHz.

The Moxon rectangle relies on controlling the spacing (hence controlling the coupling) between the ends of the driven element tips and the ends of the reflector tips, which are both bent toward each other. See **Fig 51**, which shows the general outline for W4RNL's 10-meter aluminum Moxon rectangle. The tips of the elements are kept a fixed distance from each other by PVC spacers. The closed rectangular mechanical assembly gives some rigidity to the design, keeping it stable in the wind. W4RNL described other Moxon rectangle designs using wire elements in June 2000 *QST*.

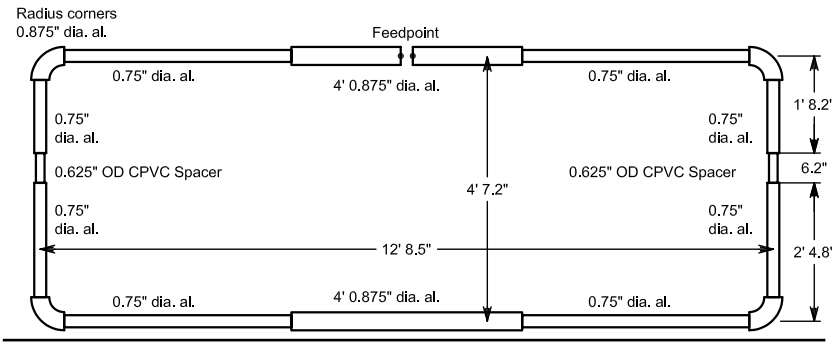

Fig 51—General outline of the 10-meter aluminum Moxon rectangle, showing tubing dimensions.

Chapter 12

Quad Arrays

Chapter 11, HF Yagi Arrays, discussed Yagi arrays as systems of approximately half-wave dipole elements that are coupled together mutually. You can also employ other kinds of elements using the same basic principles of analysis. For example, loops of various types may be combined into directive arrays. A popular type of parasitic array using loops is the *quad antenna*, in which loops having a perimeter of about one wavelength are used in much the same way as half-wave dipole elements in the Yagi antenna.

Clarence Moore, W9LZX, created the quad antenna in the early 1940s while he was at the Missionary Radio Station HCJB in Quito, Ecuador. He developed the quad to combat the effects of corona discharge at high altitudes. The problem at HCJB was that their large Yagi was literally destroying itself by melting its own element tips. This occurred due to the huge balls of corona it generated in the thin atmosphere of the high Andes mountains. Moore reasoned correctly that closed loop elements would generate less high voltage—and hence less corona—than would the high impedances at the ends of a half-wave dipole element.

Fig 1 shows the original version of the two-element quad, with a driven element and a parasitic reflector. The square loops may be mounted either with the corners lying on horizontal and vertical lines, as shown at the left, or with two sides horizontal and two vertical (right). The feed points shown for these two cases will result in horizontal polarization, which is commonly used.

Since its inception, there has been controversy whether the quad is a better performer than a Yagi. Chapter 11 showed that the three main electrical performance parameters of a Yagi are gain, response patterns (front-to-rear ratio, F/R) and drive impedance/SWR. Proper analysis of a quad also involves checking all these parameters across the entire frequency range over which you intend to use it. Both a quad and a Yagi are classified as "parasitic, end-fire arrays." Modern antenna modeling by computer shows that monoband Yagis and quads with the same boom lengths and optimized for the same performance parameters have gains within about 1 dB of each other, with the quad slightly ahead of the Yagi.

Fig 2 plots the three parameters of gain, front-to-

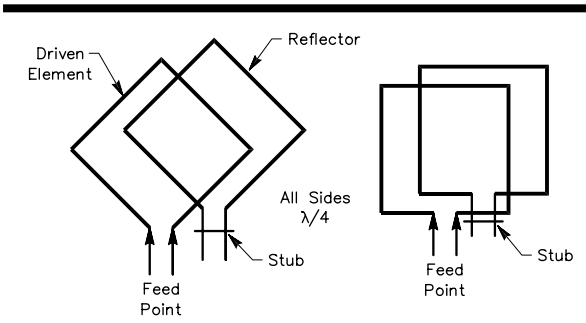

Fig 1—The basic two-element quad antenna, with driven-element loop and reflector loop. The driven loops are electrically one wavelength in circumference (1/4 wavelength on a side); the reflectors are slightly longer. Both configurations shown give horizontal polarization. For vertical polarization, the driven element should be fed at one of the side corners in the arrangement at the left, or at the center of a vertical side in the "square" quad at the right.

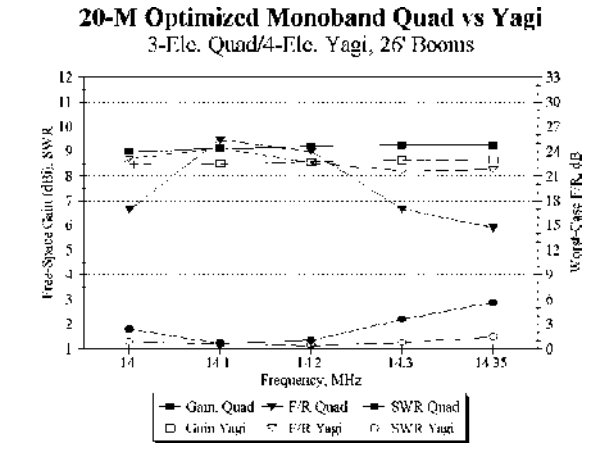

Fig 2—Comparison of gain, F/R and SWR over the 14.0 to 14.35-MHz range for an optimized three-element quad and an optimized three-element Yagi, both on 26-foot booms. The quad exhibits almost 0.5 dB more gain for the same boom length, but doesn't have as good a rearward pattern over the whole frequency range compared to the Yagi. This is evidenced by the F/R curve. The quad's SWR curve is also not quite as flat as the Yagi. The quad's design emphasizes gain more than the other two parameters.

rear ratio (F/R) and SWR over the 14.0 to 14.35-MHz band for two representative antennas—a monoband three-element quad and a monoband four-element Yagi. Both of these have 26-foot booms and both are optimized for the best compromise of gain, F/R and SWR across the whole band.

While the quad in Fig 2 consistently exhibits about 0.5 dB more gain over the whole band, its F/R pattern toward the rear isn't quite as good as the Yagi's over that span of frequencies. This quad attains a maximum F/R of 25 dB at 14.1 MHz, but it falls to 17 dB at the bottom end of the band and 15 dB at the top. On the other hand, the Yagi's F/R stays consistently above 21 dB across the whole 20-meter band. The quad's SWR rises to just under 3:1 at the top end of the band, but stays below 2:1 from 14.0 to almost 14.3 MHz. The Yagi's SWR remains lower than 1.5:1 over the whole band.

The reason the Yagi in Fig 2 has more consistent responses for gain, F/R and SWR across the whole 20-meter band is that it has an additional parasitic element, giving two additional variables to play with—that is, the length of that additional element and the spacing of that element from the others on the boom.

Yagi advocates point out that it is easier to add extra elements to a Yagi, given the mechanical complexities of adding another element to a quad. Extra parasitic elements give a designer more flexibility to tailor all performance parameters over a wide frequency range. Quad designers have historically opted to optimize strictly for gain and, as stated before, they can achieve as much as 1 dB more gain than a Yagi with the same length boom. But in so doing, a quad designer typically has to settle for front-to-rear patterns that are peaked over more narrow frequency ranges. The 20-meter quad plots in Fig 2 actually represent an even-handed approach, where the gain is compromised slightly to obtain a more consistent pattern and SWR across the whole band.

Fig 3 plots gain, F/R and SWR for two 10-meter monoband designs: a five-element quad and a five-element Yagi, both placed on 26-foot booms. The quad now has the same degrees of freedom as the Yagi, and as a consequence the pattern and SWR are more consistent across the range from 28.0 to 28.8 MHz. The quad's F/R remains above about 18.5 dB from 28.0 to 28.8 MHz. Meanwhile, the Yagi maintains an F/R of greater than 22 dB over the same range, but has almost 0.8 dB less gain compared to the quad at the low end of the band, eventually catching up at the high end of the band. The SWR for the quad is just over 2:1 at the bottom of the band, but remains less than 2:1 up to 28.8 MHz. The SWR on the Yagi remains less than 1.6:1 over the whole band.

Fig 4 shows the performance parameters for two 15-meter monoband designs: a five-element quad and a five-element Yagi, both on 26-foot booms. The quad is still the leader in gain, but has a less optimal rearward pattern and a somewhat less flat SWR curve than the Yagi. One thing should be noted in Figs 2 through 4. The F/R pattern on the

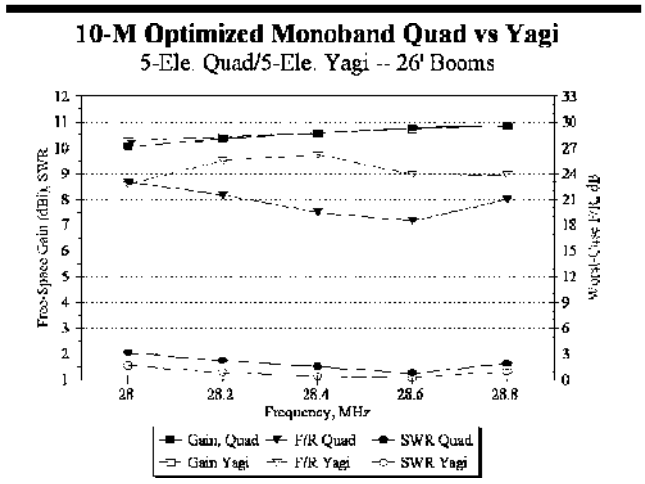

Fig 3—Comparison of gain, F/R and SWR over the 28.0 to 28.8-MHz range for an optimized five-element quad and an optimized five-element Yagi, both on 26-foot booms. The gain advantage of the quad is about 0.25 dB at the low end of the band. The F/R is more peaked in frequency for the quad, however, than the Yagi.

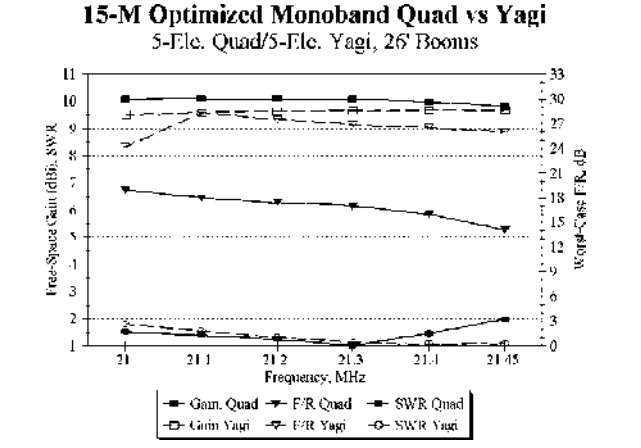

Fig 4—Comparison of gain, F/R and SWR over the 21.0 to 21.45-MHz range for an optimized 5-element quad and optimized 5-element Yagi, both on 26-foot booms. The quad enjoys a gain advantage of about 0.5 dB over most of the band. Its rearward pattern is not as good as the Yagi, which remains higher than 24 dB across the whole range, compared to the quad, which remains in the 16-dB average range.

Yagi is largely determined by the response at the 180° point, directly in back of the frontal lobe. This point is usually referred to when discussing the "front-to-back ratio."

The quad on the other hand has what a sailor might term "quartering lobes" (referring to the direction back towards the "quarterdeck" at the stern of a sailing vessel) in the rearward pattern. These quartering lobes are often

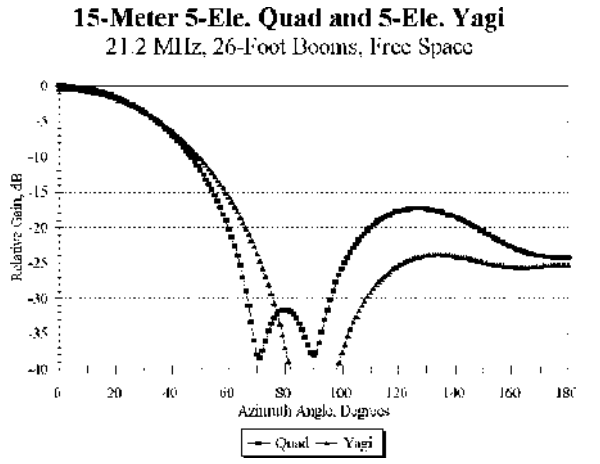

Fig 5—Comparing the pattern of the 15-meter quad and Yagi shown in Fig 4. The quad has a slightly narrower frontal beamwidth (it has 0.5 dB more gain than the Yagi), but has higher "rear quartering" sidelobes at about 125° (with a twin sidelobe, not shown, at 235°). These sidelobes limit the worst-case front-to-rear (F/R) to about 17 dB, while the F/B (at 180°, directly at the back of the quad) is more than 24 dB for each antenna.

Table 1
Dimensions for Optimized Monoband Quads in Figs 2, 3 and 4, on 26-Foot Booms

	14.2 MHz	*21.2 MHz*	*28.4 MHz*
Reflector	73′ 9"	49′ 6"	37′ 3"
R-DE Spacing	17′ 8"	7′	6′ 4"
Driven Element	71′ 8"	47′ 6"	35′ 9"
DE-D1 Spacing	8′ 3"	5′	5′ 6"
Director 1	68′ 7"	46′ 8"	34′ 8"
D1-D2 Spacing	—	6′ 8"	6′ 9"
Director 2	—	46′ 10"	35′ 2"
D2-D3 Spacing	—	7′ 4"	7′ 5"
Director 3	—	45′ 8"	34′ 2"
Feed method	Direct 50 Ω	Direct 50 Ω	Direct 50 Ω

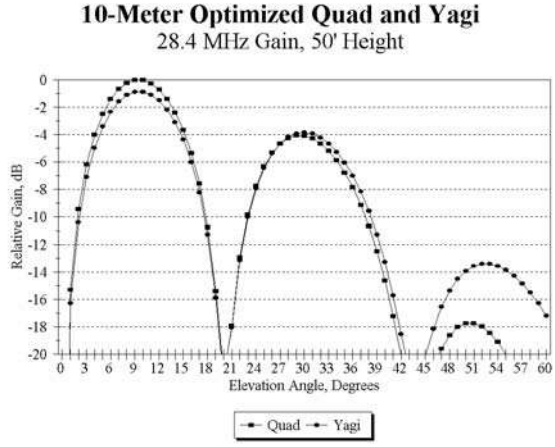

Fig 6—A comparison on 10 meters between an optimized five-element quad and an optimized five-element Yagi, both mounted 50 feet high over flat ground and both employing 26-foot booms. There is no appreciable difference in the peak elevation angle for either antenna. In other words, a quad does not have an appreciable elevation-angle advantage over a Yagi mounted at the same boom height. Note that the quad achieves its slightly higher gain by taking energy from higher-angle lobes and concentrating that energy in the main elevation lobe. This is a process that is similar to what happens with stacked Yagis.

worse than the response at 180°, directly in back of the main beam. **Fig 5** overlays the free-space E-Field responses of the 15-meter quad and Yagi together. At 21.2 MHz, the quad actually has a front-to-back ratio (F/B) of about 24 dB, excellent in anyone's book. The Yagi at 180° has a F/B of about 25 dB, again excellent.

However, at an azimuth angle of about 125° (and at 235° azimuth on the other side of the main lobe) the quad's "quartering lobe" is down only some 17 dB, setting the worst-case F/R at 17 dB also. As explained in Chapter 11, the reason F/R is more important than just the F/B is that on receive signals can come from any direction, not just from directly behind the main beam.

Table 1 lists the dimensions for the three computer-optimized monoband quads shown in Figs 2, 3 and 4.

Is a Quad Better at Low Heights than a Yagi?

Another belief held by some quads enthusiasts is that they need not be mounted very high off the ground to give excellent DX performance. Quads are somehow supposed to be greatly superior to a Yagi at the same height above ground. Unfortunately, this is mainly wishful thinking.

Fig 6 compares the same two 10-meter antennas as in Fig 3, but this time with each one mounted on a 50-foot tower over flat ground, rather than in theoretical free space. The quad does indeed have slightly more gain than a Yagi with the same boom length, as it has in free space. This is evidenced by the very slight compression of the quad's main lobe, but is more obvious when you look at the third lobe, which peaks at about 53° elevation. In effect, the quad squeezes some energy out of its second and third lobes and adds that to the first lobe. However, the difference in gain compared to the Yagi is only 0.8 dB for this particular quad design at a 9° elevation angle. And while it's true that every dB counts, you can also be certain that on the air you wouldn't be able to tell the difference between the two antennas. After all, a 10- to 20-dB variation in the level of signals is pretty common because of fading at HF.

Multiband Quads

On the other hand, one of the valid reasons quads have remained popular over the years is that antenna homebrewers

can build multiband quads far more easily than they can construct multiband Yagis. In effect, all you have to do with a quad is add more wire to the existing support arms. It's not quite as simple as that, of course, but the idea of ready expandability for other bands is very appealing to experimenters.

Like the Yagi, the quad does suffer from interactions between wires of different frequencies, but the degree of interaction between bands is usually less for a quad. The higher-frequency bands are the ones that often suffer most from any interaction, for both Yagis and quads. For example, the 10- and 15-meter bands are usually the ones affected most by nearby 20-meter wires in a triband quad, while the 20-meter elements are not affected by the 10- or 15-meter elements.

Modern computer modeling software can help you counteract at least some of the interaction by allowing you to do virtual "retuning" of the quad on the computer screen — rather than clinging precariously to your tower fiddling with wires. However, the programs (such as *NEC-2* or *EZNEC*) that can model three-dimensional wire antennas such as quads typically run far more slowly than those designed for monoband Yagis (such as *YW* included with this book). This makes optimizing rather tedious, but you use the same considerations for tradeoffs between gain, pattern (F/R) and SWR over the operating bandwidth as you do with monoband Yagis.

CONSTRUCTING A QUAD

The parasitic element shown in Fig 1 is tuned in much the same way as the parasitic element in a Yagi antenna. That is, the parasitic loop is tuned to a lower frequency than the driven element when the parasitic is to act as a reflector, and to a higher frequency when it is to act as a director. Fig 1 shows the parasitic element with an adjustable tuning stub, a convenient method of tuning since the resonant frequency can be changed simply by changing the position of the shorting bar on the stub. In practice, it has been found that the length around the loop should be approximately 3.5% greater than the self-resonant length if the element is a reflector, and about 3.0% shorter than the self-resonant length if the parasitic element is a director. Approximate formulas for the loop lengths in feet are:

$$\text{Driven Element} = \frac{1008}{f_{MHz}}$$

$$\text{Reflector} = \frac{1045}{f_{MHz}}$$

$$\text{Director} = \frac{977}{f_{MHz}}$$

These are valid for quad antennas intended for operation below 30 MHz and using uninsulated #14 stranded copper wire. At VHF, where the ratio of loop circumference to conductor diameter is usually relatively small, the circumference must be increased in comparison to the wavelength. For example, a one-wavelength loop constructed of $^1/_4$-inch tubing for 144 MHz should have a circumference about 2% greater than in the above equation for the driven element.

Element spacings on the order of 0.14 to 0.2 free-space wavelengths are generally used. You would employ the smaller spacings for antennas with more than two elements, where the structural support for elements with larger spacings tends to become challenging. The feed-point impedances of antennas having element spacings on this order have been found to be in the 40- to 60-Ω range, so the driven element can be fed directly with coaxial cable with only a small mismatch.

For spacings on the order of 0.25 wavelength (physically feasible for two elements, or for several elements at 28 MHz) the impedance more closely approximates the impedance of a driven loop alone—that is, 80 to 100 Ω. The feed methods described in Chapter 26 can be used, just as in the case of the Yagi.

Making It Sturdy

The physical sturdiness of a quad is directly proportional to the quality of the material used and the care with which it is constructed. The size and type of wire selected for use with a quad antenna is important because it will determine the capability of the spreaders to withstand high winds and ice. One of the more common problems confronting the quad owner is that of broken wires. A solid conductor is more apt to break than stranded wire under constant flexing conditions. For this reason, stranded copper wire is recommended. For 14-, 21- or 28-MHz operation, #14 or #12 stranded wire is a good choice. Soldering of the stranded wire at points where flexing is likely to occur should be avoided.

You may connect the wires to the spreader arms in many ways. The simplest method is to drill holes through the fiberglass at the appropriate points on the arms and route the wires through the holes. Soldering a wire loop across the spreader, as shown later, is recommended. However, you should take care to prevent solder from flowing to the corner point where flexing could break it.

While a boom diameter of 2 inches is sufficient for smaller quads using two or even three elements for 14, 21 and 28 MHz, when the boom length reaches 20 feet or longer a 3-inch diameter boom is highly recommended. Wind creates two forces on the boom, vertical and horizontal. The vertical load on the boom can be reduced with a guy-wire truss cable. The horizontal forces on the boom are more difficult to relieve, so 3-inch diameter tubing is desirable.

Generally speaking, three grades of material can be used for quad spreaders. The least expensive material is bamboo. Bamboo, however, is also the weakest material normally used for quad construction. It has a short life, typically only three or four years, and will not withstand a harsh climate very well. Also, bamboo is heavy in con-

trast to fiberglass, which weighs only about a pound per 13-foot length. Fiberglass is the most popular type of spreader material, and will withstand normal winter climates. One step beyond the conventional fiberglass arm is the pole-vaulting arm. For quads designed to be used on 7 MHz, surplus "rejected" pole-vaulting poles are highly recommended. Their ability to withstand large amounts of bending is very desirable. The cost of these poles is high, and they are difficult to obtain. See Chapter 21 for dealers and manufacturers of spreaders.

Diamond or Square?

The question of how to orient the spreader arms has been raised many times over the years. Should you mount the loops in a diamond or a square configuration? Should one set of spreaders be horizontal to the earth as shown in Fig 1 (right), or should the wire itself be horizontal to the ground (spreaders mounted in the fashion of an X) as shown in Fig 1 (left)? From the electrical point of view, there is not enough difference in performance to worry about.

From the mechanical point of view there is no question which version is better. The diamond quad, with the associated horizontal and vertical spreader arms, is capable of holding an ice load much better than a system where no vertical support exists to hold the wire loops upright. Put another way, the vertical poles of a diamond array, if sufficiently strong, will hold the rest of the system erect. When water droplets are accumulating and forming into ice, it is very reassuring to see water running down the wires to a corner and dripping off, rather than just sitting there on the wires and freezing. The wires of a loop (or several loops, in the case of a multiband antenna) help support the horizontal spreaders under a load of ice. A square quad will droop severely under heavy ice conditions because there is nothing to hold it up straight.

Of course, in climates where icing is not a problem, many amateurs point out that they like the aesthetics of the square configuration. There are thousands of square-configuration quads in temperate areas around the world.

Another consideration will enter into your choice of orientation for a quad. You must mount a diamond quad somewhat higher on the mast or tower than for an equivalent square array, just to keep the bottom spreader away from the tower guys when you rotate the antenna.

Two Multiband Quads

This section describes two multiband quad designs. The first is a large triband 20/15/10-meter quad built on a 26-foot boom made of 3-inch irrigation tubing. This antenna has three elements on 20 meters, four elements on 15 meters, and five elements on 10 meters. **Fig 7** shows a photograph of the five-element triband quad.

The second project is a compact two-element triband quad on an 8-foot boom that covers 20, 17, 15, 12 and 10 meters. We call this a "pentaband" quad since it covers five bands. This antenna uses five concentric wire loops mounted on each of the two sets of spreaders. Either antenna may be constructed in a diamond or square configuration.

While the same basic construction techniques are employed for both multiband quads, the scale of the larger triband antenna makes it a far more ambitious undertaking! The large quad requires a strong tower and a rugged rotator. It also requires a fair amount of real estate in order to raise the quad to the top of the tower without entangling trees or other antennas.

A FIVE-ELEMENT, 26-FOOT BOOM TRIBAND QUAD

Five sets of element spreaders are used to support the three elements used on 14 MHz, four elements on 21 MHz and five elements on 28-MHz. We chose to use four elements on 15 meters in this design (rather than the five we could have been employed on this length of boom) because the difference in optimized performance wasn't great enough to warrant the extra complexity of using five elements. The dimensions are listed in **Table 2**, and are designed for center frequencies of 14.175, 21.2 and 28.4 MHz.

The spacing between elements has been chosen to provide good compromises in performance consistent with boom length and mechanical construction. You can see that the element spacings for 20 meters are quite different from those for the optimized monoband design. This is because the same set of spreaders is used for all

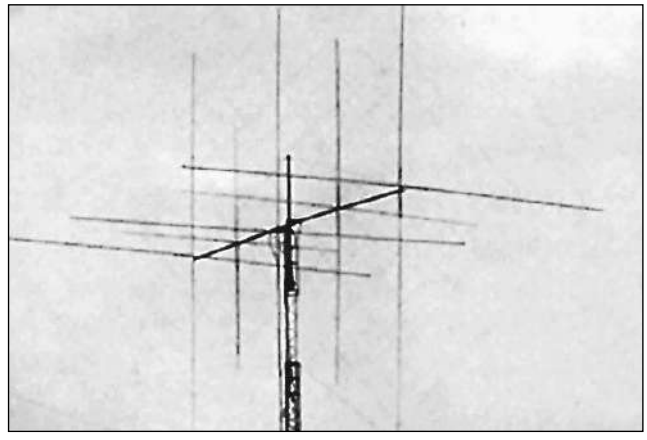

Fig 7—Photo of the three-band, five-element quad antenna.

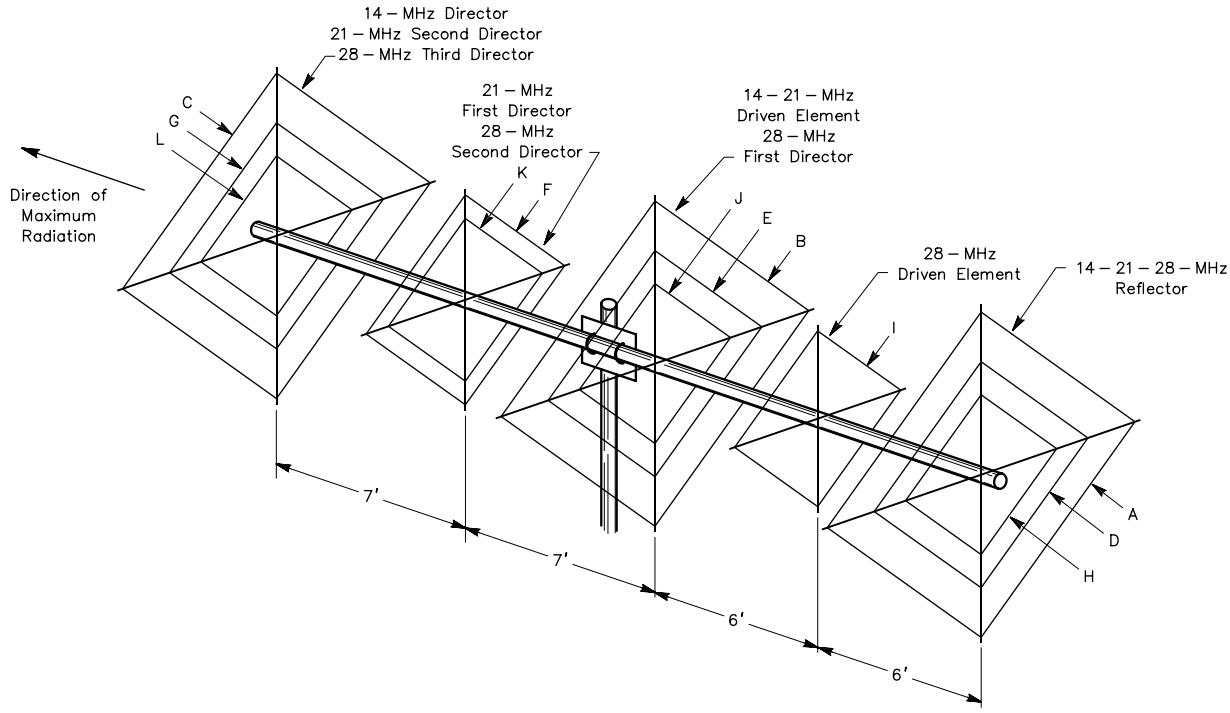

Fig 8—Layout for the three-band, five-element quad, not drawn to scale. See Table 2 for dimensions.

three bands on three out of the five elements, and the higher-frequency bands dictate the spacing because they are more critical.

Each of the parasitic loops is closed (ends soldered together) and requires no tuning. **Fig 8** shows the physical layout of the triband quad. **Fig 9** plots the computed free-space gain, front-to-rear ratio and SWR response across the 20-meter band. With only a few degrees of freedom in tuning and spacing of the three elements, it is impossible to spread the response out to cover the entire 20-meter band. The compromise design results in a rearward pattern that varies from a worst-case of just under 10 dB at the high end of the band, to a peak F/R of just under 19 dB at 14.2 MHz, in the phone portion of the band. The F/R is about 11 dB at the low end of the band.

The SWR remains under 3:1 for the entire 20-meter band, rising to 2.8:1 at the high end. The feed system for this triband quad consists of three separate 50-Ω coax

Table 2
Three-Band Five-Element Quad on 26-Foot Boom

	14.15 MHz	*21.2 MHz*	*28.4 MHz*
Reflector	72′ 6"	49′ 4"	36′ 8"
R-DE Spacing	12′	12′	6′
Driven Element	71′	47′ 6"	35′ 4"
DE-D1 Spacing	14′	7′	6′
Director 1	68′ 6"	46′ 8"	34′ 8"
D1-D2 Spacing	—	14′	7′
Director 2	—	46′ 5"	34′ 8"
D2-D3 Spacing	—	—	7′
Director 3	—	—	34′
Feed method	Direct 50 Ω	Direct 50 Ω	Direct 50 Ω

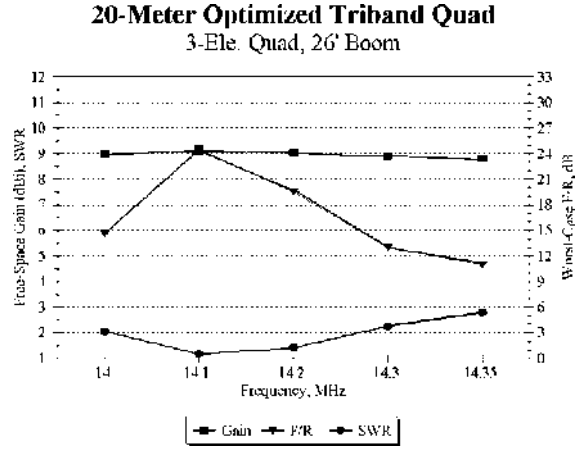

Fig 9—Computed performance of the triband, five-element quad over the 20-meter band. The direct 50-Ω feed system holds the SWR below 2.8: 1 across the whole band. This could be improved with a gamma-match system tuned to 14.1 MHz if the builder really desires a low SWR. The F/R peaks at 14.1 MHz and remains above 10 dB across the whole band.

lines, one per driven element, together with a relay switchbox mounted to the boom so that a single coax can be used back to the operating position. Each feed line uses a ferrite-bead balun to control common-mode currents and preserve the radiation pattern and each coax going to the switchbox is cut to be an electrical three-quarter wavelength on 15 meters. This presents a short at the unused driven elements since modeling indicated that the 15-meter band is adversely affected by the presence of the 20-meter driven element if it is left open-circuited. If you use RG-213 coax, the $^3/_4$-λ electrical length of each feed line is 23 feet long at 21.2 MHz. This is sufficient physical length to reach each driven element from the switchbox.

Fig 10 shows the free-space response for the 15-meter band. The rearward response is roughly 15 dB across the band. This is a result of the residual interaction between the 20-meter elements on 15 meters, and no further tuning could improve the F/R. Note how flat the SWR curve is. This SWR characteristic is what gives the quad the reputation of being "wideband." A flat SWR curve, however, is not necessarily a good indicator of optimal performance for directional antennas like quads or Yagis, particularly multiband designs where compromises must be made by physical necessity.

Fig 11 shows the characteristics of the 10-meter portion of the two-element triband quad. The response favors the low-phone band, with the F/R falling to about 12 dB at the low end of the frequency range and rising to just about 23 dB at 28.4 MHz. The SWR curve is once again relatively flat across the major portion of the band up to 28.8 MHz.

Construction

The most obvious problem related to quad antennas is the ability to build a structurally sound system. If high winds or heavy ice are a normal part of the environment, special precautions are necessary if the antenna is to survive a winter season. Another stumbling block for would-be quad builders is the installation of a three-dimensional system (assuming a Yagi has only two important dimensions) on top of a tower—especially if the tower needs guy wires for support. With proper planning, however, many of these obstacles can be overcome. For example, a tram system may be used.

Both multiband quad arrays use fiberglass spreaders (see Chapter 21 for suppliers). Bamboo is a suitable substitute (if economy is of great importance). However, the additional weight of the bamboo spreaders over fiberglass is an important consideration. A typical 12-foot bamboo pole weighs about 2 pounds; the fiberglass type weighs less than a pound. By multiplying the difference times 8 for a two-element array, times 12 for a three-element antenna, and so on, it quickly becomes apparent that fiberglass is worth the investment if weight is an important factor. Properly treated, bamboo has a useful life of three or four years, while fiberglass life is probably 10 times longer.

Spreader supports (sometimes called *spiders*) are available from many different manufacturers. If the builder is keeping the cost at a minimum, he should consider building his own. The expense is about half that of a commercially manufactured equivalent and, according to some authorities, the homemade arm supports described below are less likely to rotate on the boom as a result of wind pressure.

A 3-foot length of steel angle stock, 1 inch per side, is used to interconnect the pairs of spreader arms. The steel is drilled at the center to accept a muffler clamp of sufficient size to clamp the assembly to the boom. The fiberglass is clamped to the steel angle stock with auto-

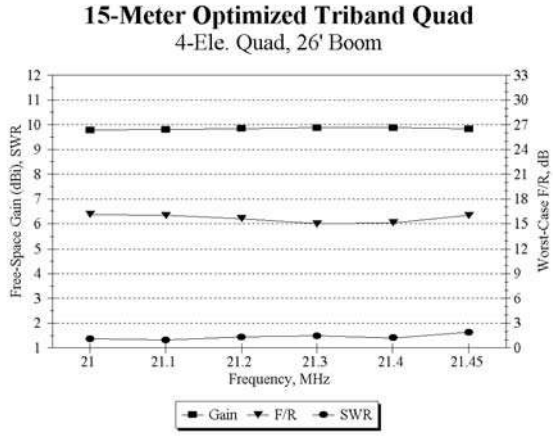

Fig 10—Computed performance of the triband, five-element quad over the 15-meter band. There is some degree of interaction with the 20-meter elements, limiting the worst-case F/R to about 15 dB. The gain and SWR curves are relatively flat across the band.

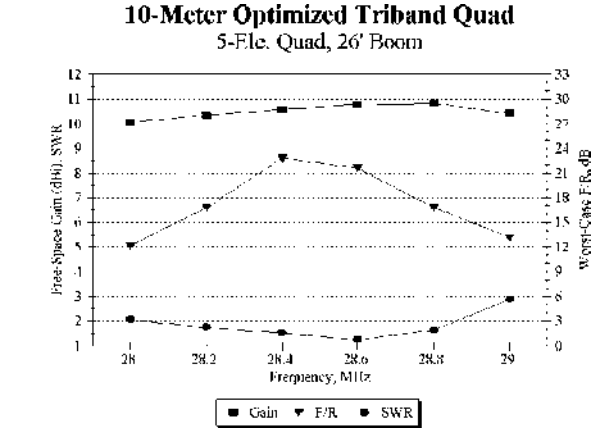

Fig 11—Computed performance of the triband, five-element quad over the 10-meter band. The F/R is higher than 12 dB across the band from 28.0 to 29.0 MHz, but the SWR rises at the top end of the band beyond 2:1. The free-space gain is higher than 10 dBi across the band.

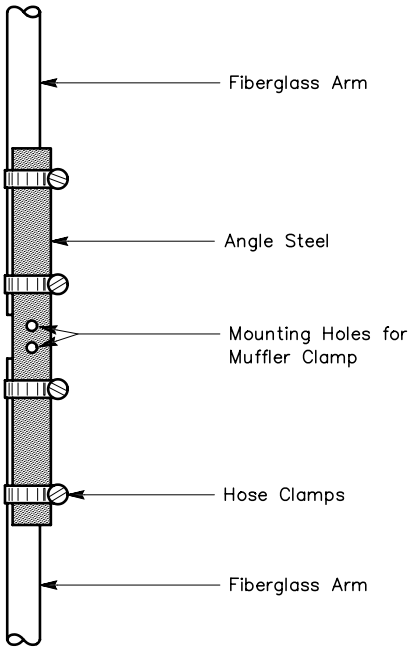

Fig 12—Details of one of two assemblies for a spreader frame. The two assemblies are joined back-to-back to form an X with a muffler clamp mounted at the position shown.

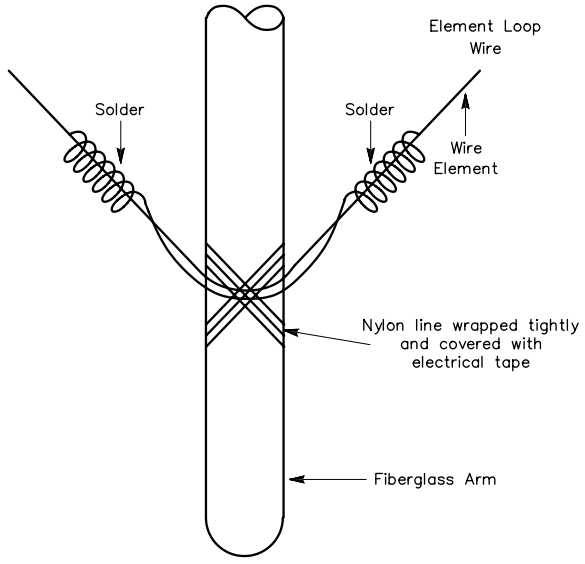

Fig 14—An alternative method of assembling the wire of a quad loop to the spreader arm.

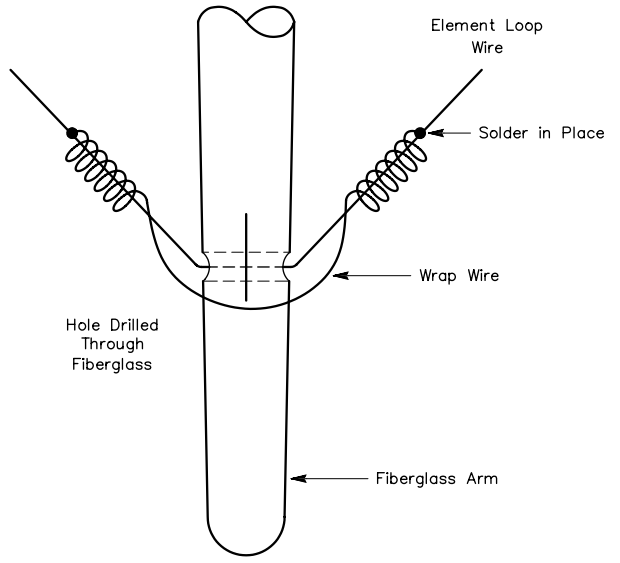

Fig 13—A method of assembling a corner of the wire loop of a quad element to the spreader arm.

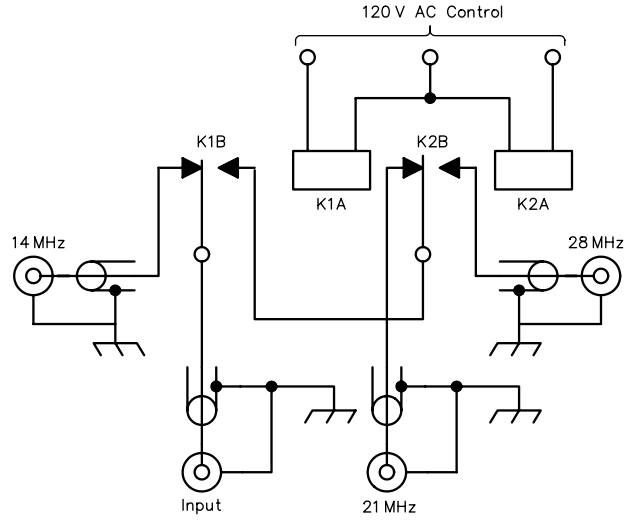

Fig 15—Suitable circuit for relay switching of bands for the three-band quad. A three-wire control cable is required. K1, K2—any type of relay suitable for RF switching, coaxial type not required (Potter and Brumfeld MR11A acceptable; although this type has double-pole contacts, mechanical arrangements of most single-pole relays make them unacceptable for switching of RF).

motive hose clamps, two per pole. Each quad-loop spreader frame consists of two assemblies of the type shown in **Fig 12**.

Connecting the wires to the fiberglass can be done in a number of different ways. Holes can be drilled at the proper places on the spreader arms and the wires run through them. A separate wrap wire should be included at the entry/exit point to prevent the loop from slipping. Details are presented in **Fig 13**. Some amateurs have experienced cracking of the fiberglass, which might be a result of drilling holes through the material. However, this seems to be the exception rather than the rule. The model described here has no holes in the spreader arms; the wires are attached to each arm with a few layers of

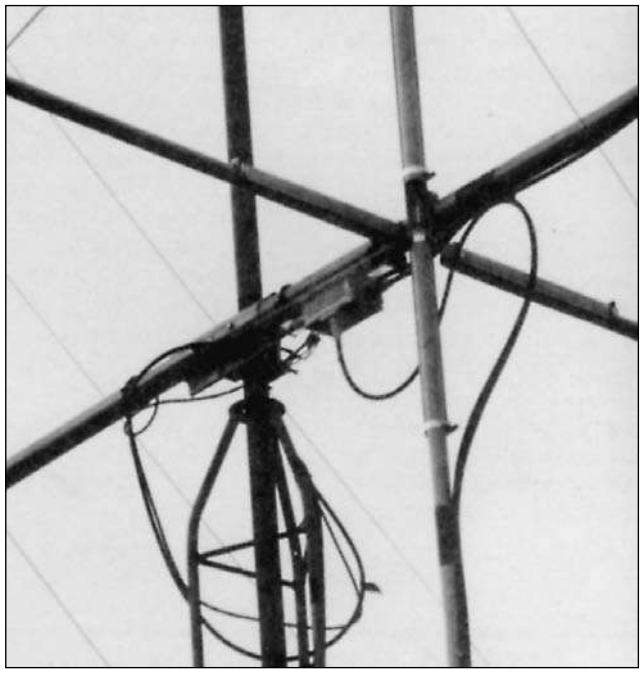

Fig 16—The relay box is mounted on the boom near the center. Each of the spreader-arm fiberglass poles is attached to steel angle stock with hose clamps.

plastic electrical tape and then wrapped approximately 20 times in a crisscross fashion with 1/8-inch diameter nylon string, followed by more electrical tape for UV protection, as shown in **Fig 14**.

The wire loops are left open at the bottom of each driven element where the feed-line coaxes are attached. All of the parasitic elements are continuous loops of wire; the solder joint is at the base of the diamond.

Although you could run three separate coax cables down to the shack, we suggest that you install a relay box at the center of the boom. A three-wire control system may be used to apply power to the proper relay for changing bands. The circuit diagram of a typical configuration is presented in **Fig 15** and its installation is shown in **Fig 16**.

Every effort must be placed upon proper construction if you want to have freedom from mechanical problems. Hardware must be secure or vibration created by the wind may cause separation of assemblies. Solder joints should be clamped in place to keep them from flexing, which might fracture a connection point.

A TWO-ELEMENT, 8-FOOT BOOM PENTABAND QUAD

This two-element pentaband (20/17/15/12/10-meter) quad uses the same construction techniques as its big brother above. Since only two elements are used, the boom can be less robust for this antenna, at 2 inches diameter rather than 3 inches. Those who like really rugged antennas can still use the 3-inch diameter boom, of course.

Table 3 lists the element dimensions for the pentaband quad. The following plots show the performance for each of the five bands covered. The feed system for the pentaband quad uses five, direct 50-Ω coaxes, one to each driven element. These five coaxes are cut to be 3/4-λ electrically on 10 meters (17 feet, 2 inches for RG-213 at 28.4 MHz). In this design the 10-meter band is the one most affected by the presence of the other driven elements if they are left unshorted. The 3/4-λ lines open-circuited at the switchbox are long enough physically to reach all elements from a centrally mounted switchbox. This length assumes that the switchbox open-circuits the unused coaxes. If the switchbox short-circuits unused coaxes (as several commercial switchboxes do), then use 1/2-λ long lines to feed all five driven elements (11 feet,

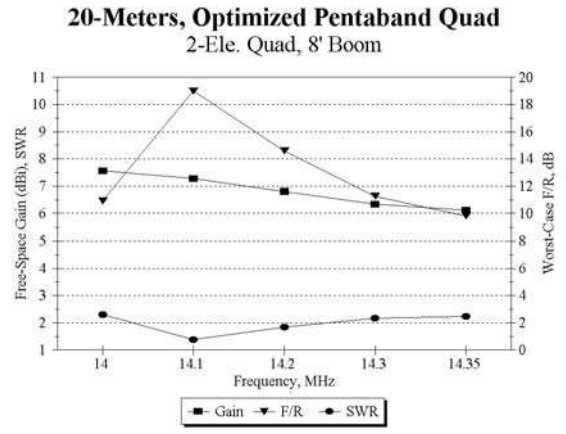

Fig 17—Computed performance of the pentaband two-element quad on 20 meters. With the simple direct-feed system, the SWR rises to about 2.3:1 at the low end of the band. A gamma match can bring the SWR down to 1:1 at 14.1 MHz, if desired.

Table 3
Five-Band Two-Element Quad on 8-Foot Boom

	14.2 MHz	*18.1 MHz*	*21 MHz*	*24.9 MHz*	*28.4 MHz*
Reflector	72′ 4"	56′ 4"	48′ 6"	40′ 11 1/4"	37′ 5 1/2"
R-DE Spacing	8′	8′	8′	8′	8′
Driven Element	69′ 10 1/2"	54′ 10 1/2"	46′ 7"	39′ 10 1/2"	34′ 6"

5 inches for RG-213 at 28.4 MHz).

The SWR curves do not necessarily go down to 1:1 because of this simple, direct feed system. If anyone is bothered by this, of course they can always implement individual matching systems, such as gamma matches. Most amateurs would agree that such a degree of complexity is not warranted. The worst-case SWR is less than 2.3:1 on each band, even with direct feed on 20 meters. With typical lengths of coaxial feed line from the shack to the switchbox at the antenna, say 100 feet of RG-213, the SWR at the transmitter would be less than 2.0:1 on all bands due to losses in the feed line.

Fig 17 shows the computed responses for the pentaband quad over the 20-meter band. With only two degrees of freedom (spacing and element tuning) there is not much that can be done to spread the response out over the entire 20-meter band. Nonetheless, the performance over the band is still pretty reasonable for an antenna this small. The F/R pattern peaks at 19 dB at 14.1 MHz and falls to about 10 dB at either end of the band. The free-space gain varies from about 7.5 dBi to just above 6 dBi, comparable to a short-boom three-element Yagi. The SWR curve remains below 2.3:1 across the band. If you were to employ a gamma match tuned at 14.1 MHz, you could limit the peak SWR to less than 2.0:1, and this would still occur at 14.0 MHz.

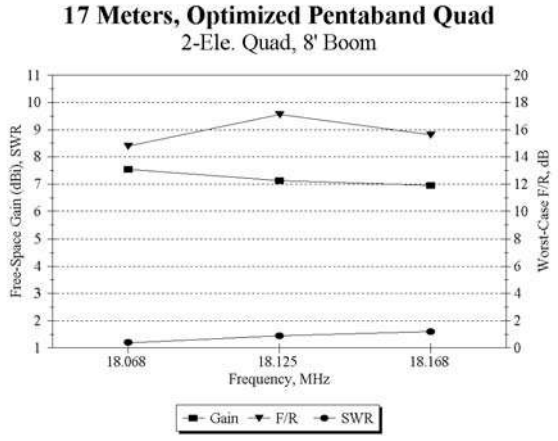

Fig 18—Computed performance of the pentaband two-element quad on 17 meters. There is some interaction with the other elements, but overall the performance is satisfactory on this band.

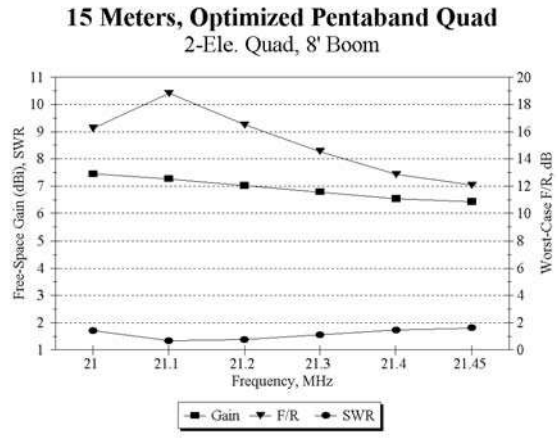

Fig 19—Computed performance of the pentaband two-element quad on 15 meters. The performance is acceptable across the whole band.

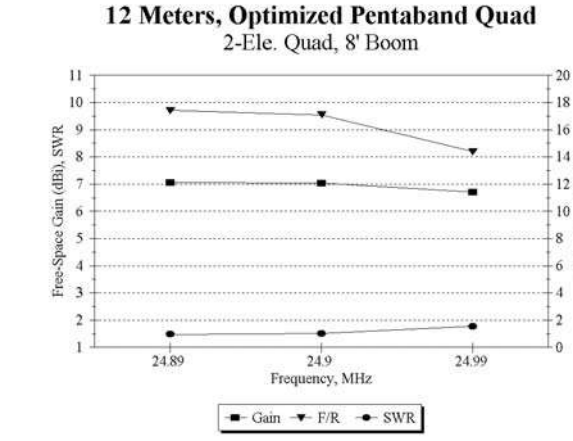

Fig 20—Computed performance of the pentaband two-element quad on 12 meters.

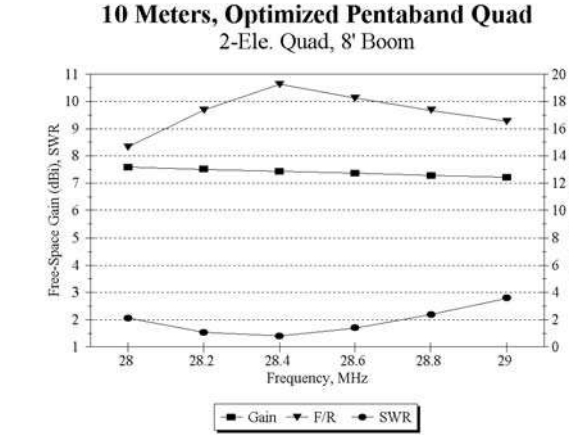

Fig 21—Computed performance of the pentaband two-element quad on 10 meters. The SWR curve is slightly above the target 2:1 at the low end of the band and rises to about 2.2:1 at 28.8 MHz. This unlikely to be a problem, even with rigs with automatic power-reduction due to SWR, since the SWR at the input of a typical coax feed line will be lower than that at the antenna due to losses in the line.

On 17 meters, **Fig 18** shows that the other elements are affecting 18 MHz, even with element-length optimization. Careful examination of the current induced on the other elements shows that the 20-meter driven element is interacting on 18 MHz, deteriorating the pattern and gain slightly. Even still, the performance on 17 meters is reasonable, especially for a five-band quad on an 8-foot boom.

On 15 meters, the interactions seems to have been contained, as **Fig 19** demonstrates. The F/R peaks at 21.1 MHz, at 19 dB and remains better than 12 dB past the top of the band. The SWR curve is low across the whole band.

On 12 meters, the interaction between bands is minor, leading to the good results shown in **Fig 20**. The SWR change across this band is quite flat, which isn't surprising given the narrow bandwidth of the 12-meter band.

On 10 meters, the interaction seems to have been tamed well by computer-tuning of the elements. The F/R remains higher than about 14 dB from 28 to 29 MHz. The SWR remains below 2.2:1 up to about 28.8 MHz, while the gain is relatively flat across the band at more than 7.2 dBi in free space. See **Fig 21**.

Overall, this pentaband quad is physically compact and yet it provides good performance across all five bands. It is competitive with commercial Log Periodic Dipole Array (LPDA) designs and triband Yagi designs that employ longer booms.

BIBLIOGRAPHY

Source material and more extended discussions of the topics covered in this chapter can be found in the references given below and in the textbooks listed at the end of Chapter 2.

P. S. Carter, C. W. Hansell and N. E. Lindenblad, "Development of Directive Transmitting Antennas by R.C.A. Communications," *Proc. IRE*, Oct 1931.

C. Cleveland, "More'n One Way to Switch an Antenna," Technical Correspondence, *QST*, Nov 1986.

D. Cutter, "Simple Switcher," *73*, May 1980.

D. DeMaw, "A Remote Antenna Switcher for HF," *QST*, Jun 1986.

M. G. Knitter, Ed., *Loop Antennas—Design and Theory* (Cambridge, WI: National Radio Club, 1983).

H. Landskov, W7KAR, "Evolution of a Quad Array," *QST*, Mar 1977.

J. Lindsay, "Quads and Yagis," *QST*, May 1968.

F. E. Terman, *Radio Engineering*, 3rd ed. (New York: McGraw-Hill Book Co, 1947).

E. M. Williams, "Radiating Characteristics of Short-Wave Loop Aerials," *Proc. IRE*, Oct 1940.

Chapter 13

Long-Wire and Traveling-Wave Antennas

The power gain and directive characteristics of electrically long wires (that is, wires that are long in terms of wavelength), as described in Chapter 2, make them useful for long-distance transmission and reception on the higher frequencies. Long wires can be combined to form antennas of various shapes that increase the gain and directivity over a single wire. The term *long wire*, as used in this chapter, means any such configuration, not just a straight-wire antenna.

Long Wires Versus Multielement Arrays

In general, the gain obtained with long-wire antennas is not as great, when the space available for the antenna is limited, as you can obtain from the multielement phased arrays in Chapter 8 or from a parasitic array such as a Yagi or quad (Chapters 11 or 12). However, the long-wire antenna has advantages of its own that tend to compensate for this deficiency. The construction of long-wire antennas is simple both electrically and mechanically, and there are no especially critical dimensions or adjustments. The long-wire antenna will work well and give satisfactory gain and directivity over a 2-to-1 frequency range. In addition, it will accept power and radiate well on any frequency for which its overall length is not less than about a half wavelength. Since a wire is not electrically long, even at 28 MHz, unless its physical length is equal to at least a half wavelength on 3.5 MHz, any long-wire can be used on all amateur bands that are useful for long-distance communication.

Between two directive antennas having the same theoretical gain, one a multielement array and the other a long-wire antenna, many amateurs have found that the long-wire antenna seems more effective in reception. One possible explanation is that there is a *diversity effect* with a long-wire antenna because it is spread out over a large distance, rather than being concentrated in a small space, as would be the case with a Yagi, for example. This may raise the average level of received energy for ionospheric-propagated signals. Another factor is that long-wire antennas have directive patterns that can be extremely sharp in the horizontal (azimuthal) plane. This is an advantage that other types of multielement arrays do not have, but it can be a double-edged sword too. We'll discuss this aspect in some detail in this chapter.

General Characteristics of Long-Wire Antennas

Whether the long-wire antenna is a single wire running in one direction or is formed into a V-beam, rhombic, or some other configuration, there are certain general principles that apply and some performance features that are common to all types. The first of these is that the power gain of a long-wire antenna as compared with a half-wave dipole is not considerable until the antenna is really long (its length measured in wavelengths rather than in a specific number of feet). The reason for this is that the fields radiated by elementary lengths of wire along the antenna do not combine, at a distance, in as simple a fashion as the fields from half-wave dipoles used in other types of directive arrays.

There is no point in space, for example, where the distant fields from all points along the wire are exactly in phase (as they are, in the optimum direction, in the case of two or more collinear or broadside dipoles when fed with in-phase currents). Consequently, the field strength at a distance is always less than would be obtained if the same length of wire were cut up into properly phased and sepa-

rately driven dipoles. As the wire is made longer, the fields combine to form increasingly intense main lobes, but these lobes do not develop appreciably until the wire is several wavelengths long. See **Fig 1**.

The longer the antenna, the sharper the lobes become, and since it is really a hollow cone of radiation about the wire in free space, it becomes sharper in both planes. Also, the greater the length, the smaller the angle with the wire at which the maximum radiation lobes occur. There are four main lobes to the directive patterns of long-wire antennas; each makes the same angle with respect to the wire.

Fig 2A shows the azimuthal radiation pattern of a 1-λ long-wire antenna, compared with a $^1/_2$-λ dipole. Both antennas are mounted at the same height of 1 λ above flat ground (70 feet high at 14 MHz, with a wire length of 70 feet) and both patterns are for an elevation angle of 10°, an angle suitable for long-distance communication on 20 meters. The long-wire in Fig 2A is oriented in the 270° to 90° direction, while the dipole is aligned at right angles so that its characteristic figure-8 pattern goes left-to-right. The 1-λ long-wire has about 0.6 dB more gain than the dipole, with four main lobes as compared to the two lobes from the dipole.

You can see that the two lobes on the left side of Fig 2A are about 1 dB down compared to the two lobes on the right side. This is because the long-wire here is fed at the left-hand end in the computer model. Energy is radiated as a wave travels down the wire and some energy is also lost to ohmic resistance in the wire and the ground. The forward-going wave then reflects from the open-circuit at the right-hand end of the wire and reverses direction, traveling toward the left end, still radiating as it

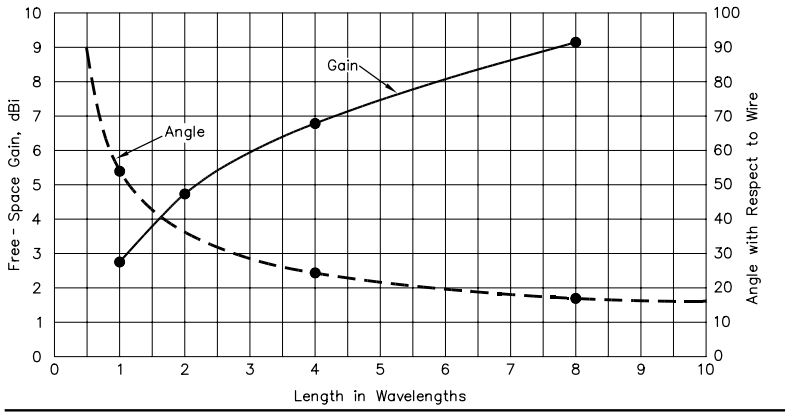

Fig 1—Theoretical gain of a long-wire antenna, in dBi, as a function of wire length. The angle, with respect to the wire, at which the radiation intensity is maximum also is shown.

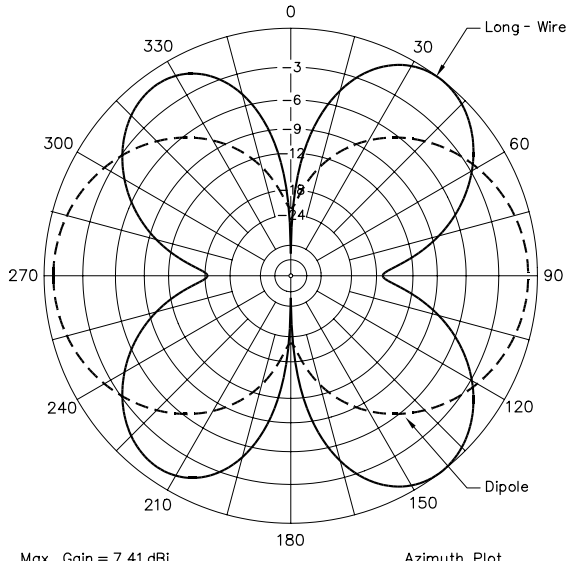

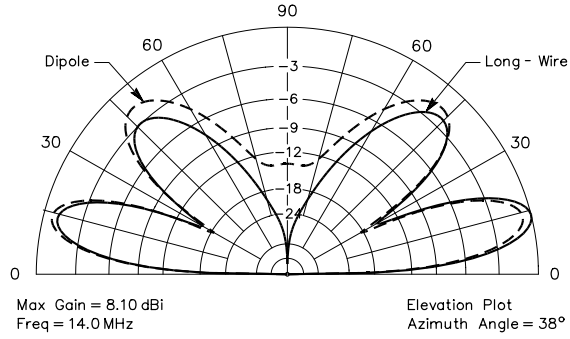

(B)

Fig 2—At A, comparison of azimuthal patterns for a 1-λ long-wire antenna (solid line) and a ½-λ dipole (dashed line) at an elevation angle of 10°. Each antenna is located 1 λ (70 feet) over flat ground at 14 MHz. At B, the elevation-plane patterns at peak azimuth angles for each antenna. The long-wire has about 0.6 dB more gain than the dipole.

chap 13.pmd 2 2/12/2007, 9:50 AM

travels. An antenna operating in this way has much the same characteristics as a transmission line that is terminated in an open circuit—that is, it has standing waves on it. Unterminated long-wire antennas are often referred to as *standing wave antennas*. As the length of a long-wire antenna is increased, a moderate front-to-back ratio results, about 3 dB for very long antennas.

Fig 2B shows the elevation-plane pattern for the long-wire and for the dipole. In each case the elevation pattern is at the azimuth of maximum gain—at an angle of 38° with respect to the wire-axis for the long-wire and at 90° for the dipole. The peak elevation for the long-wire is very slightly lower than that for the dipole at the same height above ground, but not by much. In other words, the height above ground is the main determining factor for the shape of the main lobe of a long-wire's elevation pattern, as it is for most horizontally polarized antennas.

The shape of the azimuth and elevation patterns in Fig 2 might lead you to believe that the radiation pattern is simple. **Fig 3** is a 3-D representation of the pattern from a 1-λ long-wire that is 1 λ high over flat ground. Besides the main low-angle lobes, there are strong lobes at higher angles. Things get even more complicated when the length of the long-wire increases.

Directivity

Because many points along a long wire are carrying currents in different phases (with different current amplitudes as well), the field pattern at a distance becomes more complex as the wire is made longer. This complexity is manifested in a series of minor lobes, the number of which increases with the wire length. The intensity of radiation from the minor lobes is frequently as great as, and sometimes greater than, the radiation from a half-wave dipole. The energy radiated in the minor lobes is not available to improve the gain in the major lobes, which is another reason why a long-wire antenna must be long to give appreciable gain in the desired directions.

Fig 4 shows an azimuthal-plane comparison between a 3-λ (209 feet long) long-wire and the comparison $^1/_2$-λ dipole. The long-wire now has 8 minor lobes besides the four main lobes. Note that the angle the main lobes make with respect to the axis of the long-wire (also left-to-right in Fig 4) becomes smaller as the length of the long-wire increases. For the 3-λ long-wire, the main lobes occur 28° off the axis of the wire itself.

Other types of simple driven and parasitic arrays do not have minor lobes of any great consequence. For that reason they frequently seem to have much better directivity than long-wire antennas, because their responses in undesired directions are well down from their response in the desired direction. This is the case even if a multielement array and a long-wire antenna have the same peak gain in the favored direction. **Fig 5** compares the same 3-λ long-wire with a 4-element Yagi and a ½-λ dipole, again both at the same height as the long-wire. Note that the Yagi has only a single backlobe, down about 21 dB from its broad main lobe, which has a 3-dB beamwidth of 63°. The 3-dB beamwidth of the long-wire's main lobes (at a 28° angle from the wire axis) is far more narrow, at only 23°.

For amateur work, particularly with directive antennas that cannot be rotated, the minor lobes of a long-wire antenna have some advantages. Although the nulls in the

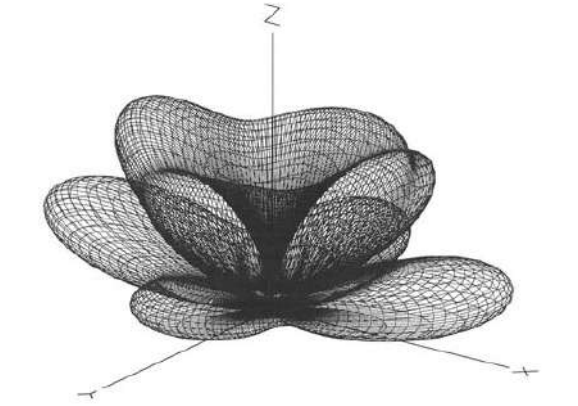

Fig 3—A 3-D representation of the radiation pattern for the 1-λ long-wire shown in Fig 2. The pattern is obviously rather complex. It gets even more complicated for wires longer than 1 λ.

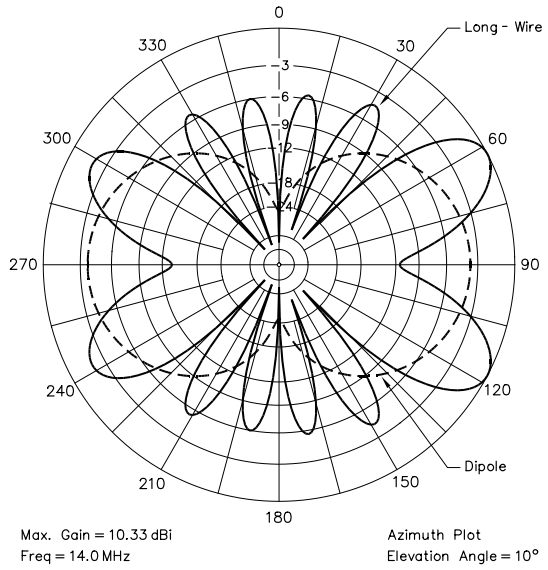

Fig 4—An azimuthal-plane comparison between a 3-λ (209 feet long) long-wire (solid line) and the comparison ½-λ dipole (dashed line) at 70 feet high (1 λ) at 14 MHz.

chap 13.pmd 3 2/12/2007, 9:50 AM

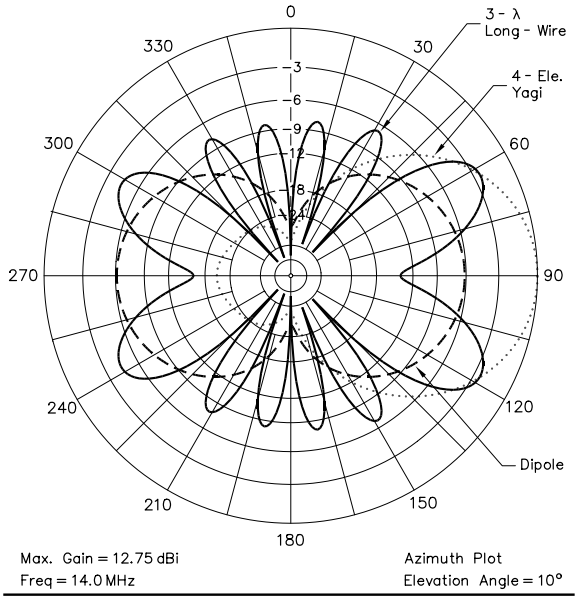

Fig 5—A comparison between the 3-λ long-wire (solid line) in Fig 4, a 4-element 20-meter Yagi on a 26-foot boom (dotted line), and a ½-λ dipole (dashed line), again at a height of 70 feet. The main lobes of the long-wire are very narrow compared to the wide frontal lobe of the Yagi. The long-wire exhibits an azimuthal pattern that is more omnidirectional in nature than a Yagi, particularly when the narrow, deep nulls in the long-wire's pattern are filled-in due to irregularities in the terrain under its long span of wire.

computer model in Fig 5 are deeper than 30 dB, they are not so dramatic in actual practice. This is due to irregularities in the terrain that inevitably occur under the span of a long wire. In most directions the long-wire antenna will be as good as a half-wave dipole, and in addition will give high gain in the most favored directions, even though that is over narrow azimuths.

Fig 6A compares the azimuth responses for a 5-λ long-wire (350 feet long at 14 MHz) to the same 4-element Yagi and dipole. The long-wire now exhibits 16 minor lobes in addition to its four main lobes. The peaks of these sidelobes are down about 8 dB from the main lobes and they are stronger than the dipole, making this long-wire antenna effectively omnidirectional. Fig 6B shows the elevation pattern of the 5-λ long-wire at its most effective azimuth compared to a dipole. Again, the shape of the main lobe is mainly determined by the long-wire's height above ground, since the peak angle is only just a bit lower than the peak angle for the dipole. The long-wire's elevation response breaks up into numerous lobes above the main lobes, just as it does in the azimuth plane.

For the really ambitious, **Fig 7** compares the performance for an 8-λ (571 feet) long-wire antenna with a 4-element Yagi and the $^1/_2$-λ dipole. Again, in actual practice, the nulls would tend to be filled in by terrain irregularities, so a very long antenna like this would be a pretty potent performer.

Calculating Length

In this chapter, lengths are discussed in terms of wave-

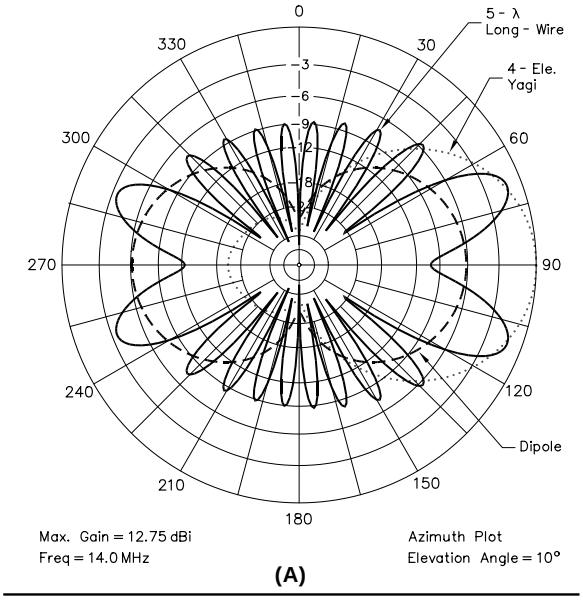

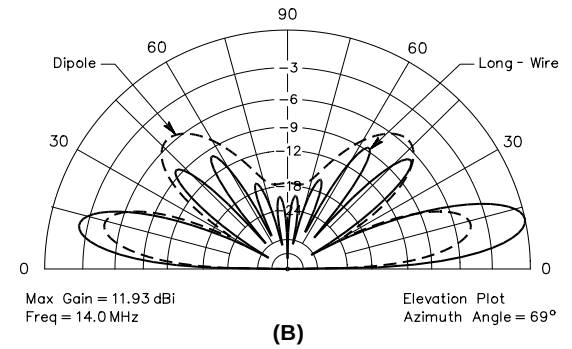

Fig 6—At A, the azimuth responses for a 5-λ long-wire (350 feet long at 14 MHz—solid line) to the same 4-element Yagi (dotted line) and dipole (dashed line) as in Fig 5. At B, the elevation-plane responses for the long-wire (solid line) and the dipole (dashed line) by themselves. Note that the elevation angle giving peak gain for each antenna is just about the same. The long-wire achieves gain by compressing mainly the azimuthal response, squeezing the gain into narrow lobes; not so much by squeezing the elevation pattern for gain.

chap 13.pmd 4 2/12/2007, 9:50 AM

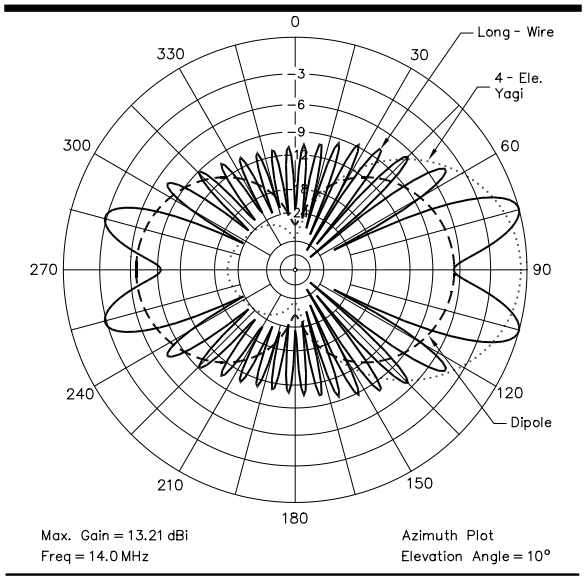

Fig 7—The azimuthal-plane performance for an 8-λ (571 feet) long-wire antenna (solid line), compared with a 4-element Yagi (dotted line) and a ½-λ dipole (dashed line).

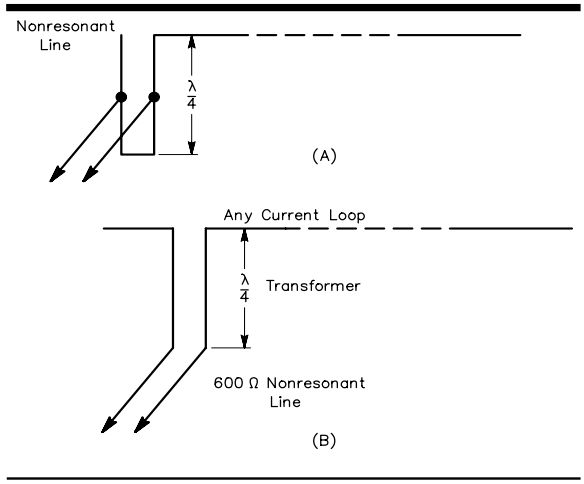

Fig 8—Methods for feeding long single-wire antennas.

lengths. Throughout the preceding discussion the frequency in the models was held at 14 MHz. Remember that a long-wire that is 4 λ long at 14 MHz is 8 λ long at 28 MHz.

There is nothing very critical about wire lengths in an antenna system that will work over a frequency range including several amateur bands. The antenna characteristics change very slowly with length, except when the wires are short (around one wavelength, for instance). There is no need to try to establish exact resonance at a particular frequency for proper antenna operation.

The formula for determining the lengths for harmonic wires is:

$$\text{Length}\,(\text{feet}) = \frac{984\,(\text{N} - 0.025)}{\text{f}\,(\text{MHz})} \qquad \text{(Eq 1)}$$

where N is the antenna length in wavelengths. In cases where precise resonance is desired for some reason (for obtaining a resistive load for a transmission line at a particular frequency, for example) it is best established by trimming the wire length until the standing-wave ratio on the line is minimum.

Tilted Wires

In theory, it is possible to maximize gain from a long-wire antenna by tilting it to favor a desired elevation take-off angle. Unfortunately, the effect of real ground under the antenna negates the possible advantages of tilting, just as it does when a Yagi or other type of parasitic array is tilted from horizontal. You would do better keeping a long-wire antenna horizontal, but raising it higher above ground, to achieve more gain at low takeoff angles.

Feeding Long Wires

A long-wire antenna is normally fed at the end or at a current loop. Since a current loop changes to a node when the antenna is operated at any even multiple of the frequency for which it is designed, a long-wire antenna will operate as a true long wire on all bands only when it is fed at the end.

A common method of feeding a long-wire is to use a resonant open-wire line. This system will work on all bands down to the one, if any, at which the antenna is only a half wave long. Any convenient line length can be used if you match the transmitter to the line's input impedance using an antenna tuner, as described in Chapter 25.

Two arrangements for using nonresonant lines are given in **Fig 8**. The one at A is useful for one band only since the matching section must be a quarter wave long, approximately, unless a different matching section is used for each band. In B, the λ/4 transformer (Q-section) impedance can be designed to match the antenna to the line, as described in Chapter 26. You can determine the value of radiation resistance using a modern modeling program or you can actually measure the feed-point impedance. Although it will work as designed on only one band, the antenna can be used on other bands by treating the line and matching transformer as a resonant line. In this case, as mentioned earlier, the antenna will not radiate as a true long wire on even multiples of the frequency for which the matching system is designed.

The end-fed arrangement, although the most convenient when tuned feeders are used, suffers the disadvantage that there is likely to be a considerable antenna current on the line. In addition, the antenna reactance changes rap-

chap 13.pmd 5 2/12/2007, 9:50 AM

idly with frequency. Consequently, when the wire is several wavelengths long, a relatively small change in frequency—a fraction of the width of a band—may require major changes in the adjustment of the antenna tuner. Also, the line becomes unbalanced at all frequencies between those at which the antenna is resonant. This leads to a considerable amount of radiation from the line. The unbalance can be overcome by using multiple long wires in a V or rhombic shape, as described below.

COMBINATIONS OF LONG WIRES

The directivity and gain of long wires may be increased by using two wires placed in relation to each other such that the fields from both combine to produce the greatest possible field strength at a distant point. The principle is similar to that used in designing the multielement arrays described in Chapter 8.

Parallel Wires

One possible method of using two (or more) long wires is to place them in parallel, with a spacing of $^1/_2$ λ or so, and feed the two in phase. In the direction of the wires the fields will add in phase. However, the takeoff angle is high directly in the orientation of the wire, and this method will result in rather high-angle radiation even if the wires are several wavelengths long. With a parallel arrangement of this sort the gain should be about 3 dB over a single wire of the same length, at spacings in the vicinity of $^1/_2$ wavelength.

The V-Beam Antenna

Instead of using two long wires parallel to each other, they may be placed in the form of a horizontal V, with the included angle between the wires equal to twice the angle made by the main lobes referenced to the wire axis for a single wire of the same physical length. For example, for a leg length of 5 λ, the angle between the legs of a V should be about 42°, twice the angle of 21° of the main lobe referenced to the long-wire's axis. See Fig 6A.

The plane directive patterns of the individual wires combine along a line in the plane of the antenna and bisecting the V, where the fields from the individual wires reinforce each other. The sidelobes in the azimuthal pattern are suppressed by about 10 dB, so the pattern becomes essentially bidirectional. See **Fig 9**.

The included angle between the legs is not particularly critical. This is fortunate, especially if the same antenna is used on multiple bands, where the electrical length varies directly with frequency. This would normally require different included angles for each band. For multiband V-antennas, a compromise angle is usually chosen to equalize performance. **Fig 10** shows the azimuthal pattern for a V-beam with 1-λ legs, with an included angle of 75° between the legs, mounted 1 λ above flat ground. This is for a 10° elevation angle. At 14 MHz the antenna has two 70-foot high, 68.5-foot long legs, separated at their far ends by 83.4 feet. For comparison the azimuthal patterns for the same 4-element Yagi and ½-λ dipole used previously for the long-wires are overlaid on the same plot. The V has about 2 dB more gain than the dipole but is down some 4 dB compared to the Yagi, as expected for relatively short legs.

Fig 11 shows the azimuthal pattern for the same antenna in Fig 10, but at 28 MHz and at an elevation angle of 6°. Because the legs are twice as long electrically at 28 MHz, the V-beam has compressed the main lobe into a narrow beam that now has a peak gain equal to the Yagi, but with a 3-dB beamwidth of only 18.8°. Note that you could obtain about 0.7 dB more gain at 14 MHz, with a 1.7-dB degradation of gain at 28 MHz, if you increase the included angle to 90° rather than 75°.

Fig 12 shows the azimuthal pattern for a V-beam with 2-λ legs (137 feet at 14 MHz), with an included angle of 60° between them. As usual, the assumed height is 70 feet, or 1 λ at 14 MHz. The peak gain for the V-beam is just about equal to that of the 4-element Yagi, although the 3-dB

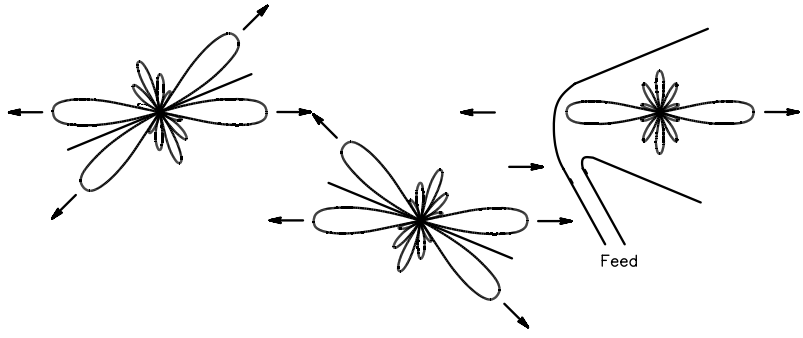

Fig 9—Two long wires and their respective patterns are shown at the left. If these two wires are combined to form a V with an angle that is twice that of the major lobes of the wires and with the wires excited out of phase, the radiation along the bisector of the V adds and the radiation in the other directions tends to cancel.

chap 13.pmd 6 2/12/2007, 9:50 AM

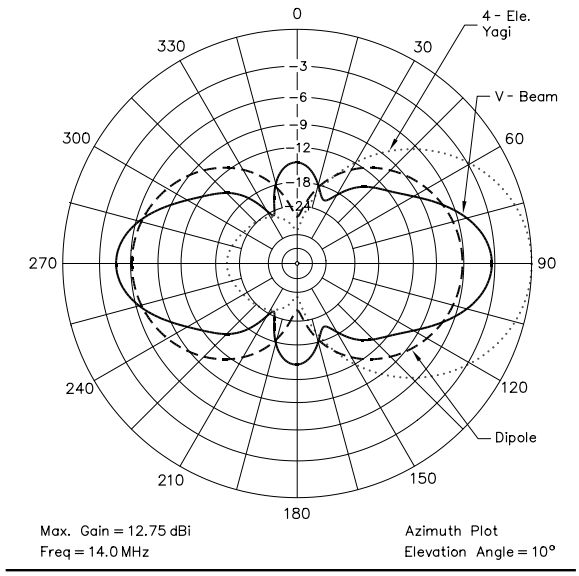

Fig 10— Azimuthal-plane pattern at 10° elevation angle for a 14-MHz V-beam (solid line) with 1-λ legs (68.5 feet long), using an included angle of 75° between the legs. The V-beam is mounted 1 λ above flat ground, and is compared with a ½-λ dipole (dashed line) and a 4-element 20-meter Yagi on a 26-foot boom (dotted line).

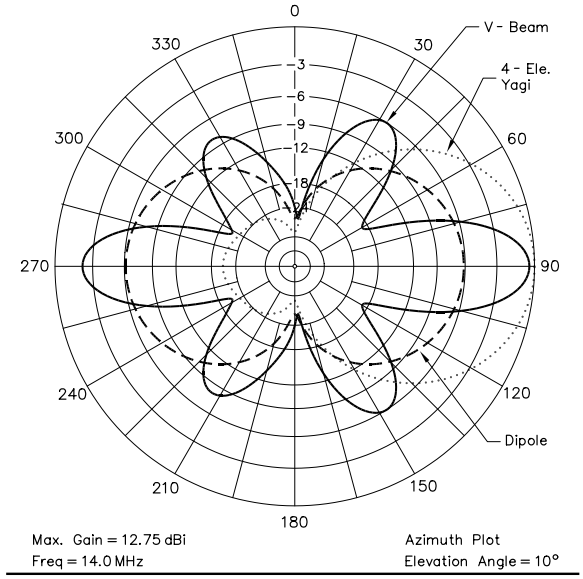

Fig 12—Azimuthal pattern for a V-beam (solid line) with 2-λ legs (137 feet at 14 MHz), with an included angle of 60° between them. The height is 70 feet, or 1 λ, over flat ground. For comparison, the response for a 4-element Yagi (dotted line) and a dipole (dashed line) are shown. The 3-dB beamwidth has decreased to 23.0°.

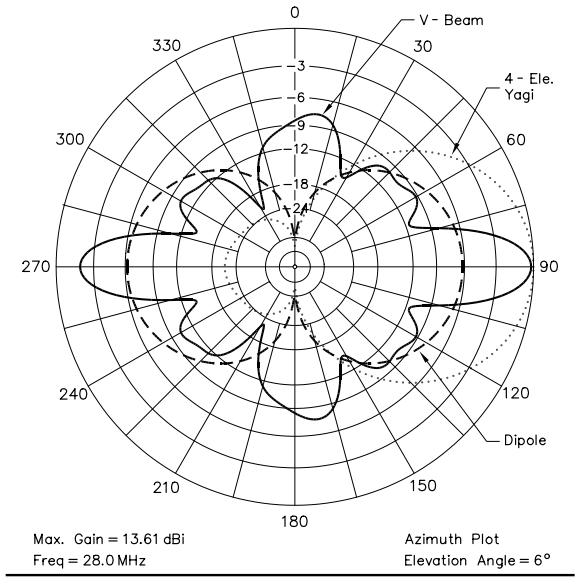

Fig 11—The same V-beam as in Fig 10 at 28 MHz (solid line), at an elevation angle of 6°, compared to a 4-element Yagi (dotted line) and a dipole (dashed line). The V-beam's pattern is very narrow, at 18.8° at the 3-dB points, requiring accurate placement of the supports poles to aim the antenna at the desired geographic target.

nose beamwidth is narrow, at 23°. This makes setting up the geometry critical if you want to maximize gain into a particular geographic area. While you might be able to get away with using convenient trees to support such an antenna, it's far more likely that you'll have to use carefully located towers to make sure the beam is aimed where you expect it to be pointed.

For example, in order to cover all of Europe from San Francisco, an antenna must cover from about 11° (to Moscow) to about 46° (to Portugal). This is a range of 35° and signals from the V-beam in Fig 12 would be down some 7 dB over this range of angles, assuming the center of the beam is pointed exactly at a heading of 28.5°. The 4-element Yagi on the other hand would cover this range of azimuths more consistently, since its 3-dB beamwidth is 63°.

Fig 13 shows the same V-beam as in Fig 12, but this time at 28 MHz. The peak gain of the main lobe is now about 1 dB stronger than the 4-element Yagi used as a reference, and the main lobe has two nearby sidelobes that tend to broaden out the azimuthal response. At this frequency the V-beam would cover all of Europe better from San Francisco.

Fig 14 shows a V-beam with 3-λ (209 feet at 14 MHz) legs with an included angle of 50° between them. The peak gain is now greater than that of a 4-element Yagi, but the 3-dB beamwidth has been reduced to 17.8°, making aim-

chap 13.pmd 7 2/12/2007, 9:50 AM

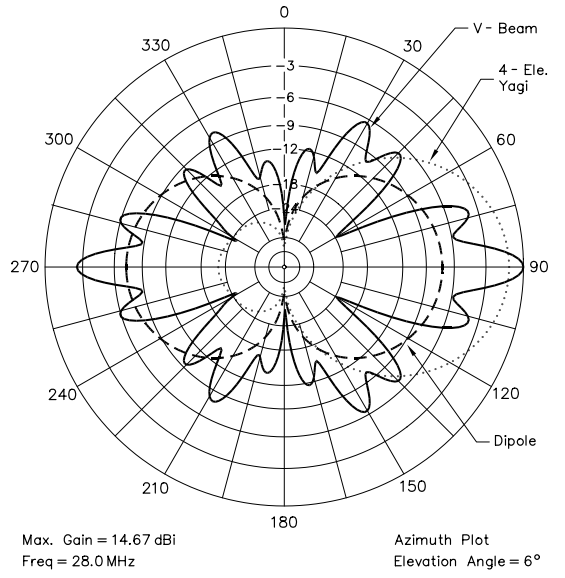

Fig 13—The same 2-λ per leg V-beam (solid line) as in Fig 12, but at 28 MHz and at a 6° takeoff elevation angle. Two sidelobes have appeared flanking the main lobe, making the effective azimuthal pattern wider at this frequency.

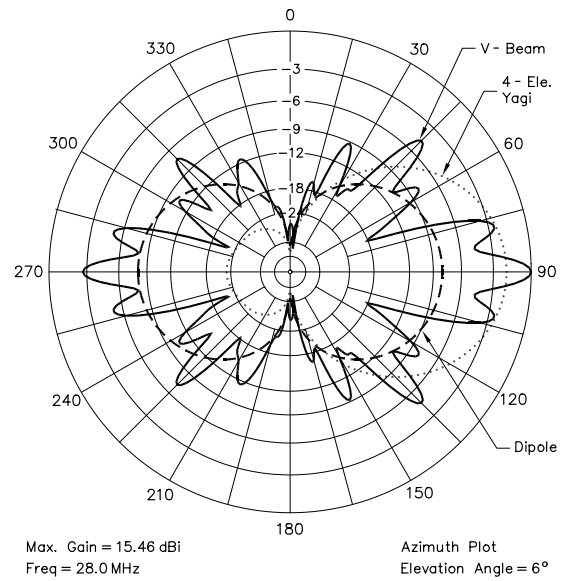

Fig 15—The same 209-foot/leg V-beam as Fig 14, but at 28 MHz. Again, the two close-in sidelobes tend to spread out the azimuthal response some at 28 MHz.

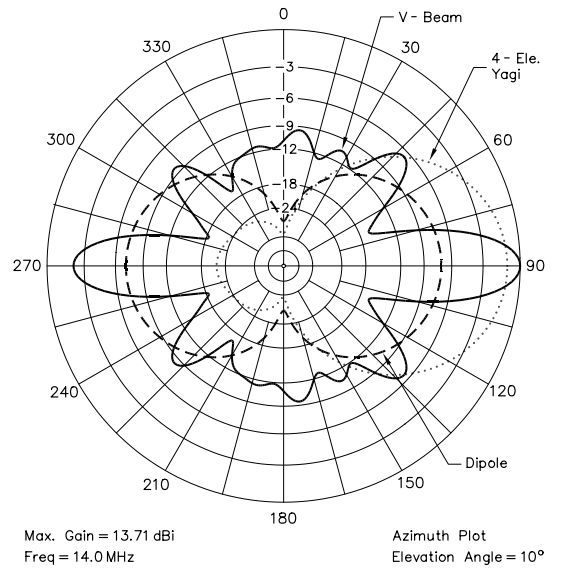

Fig 14—A V-beam (solid line) with 3-λ (209 feet at 14 MHz) legs using an included angle of 50° between them, compared to a 4-element Yagi (dotted line) and a dipole (dashed line). The 3-dB beamwidth has now decreased to 17.8°.

ing the antenna even more critical. **Fig 15** shows the same V-beam at 28 MHz. Here again, the main lobe has nearby sidelobes that broaden the effective azimuth to cover a wider area.

Fig 16 shows the elevation-plane response for the same 209-foot leg V-beam at 28 MHz (3-λ at 14 MHz), compared to a dipole at the same height of 70 feet. The higher-gain V-beam suppresses higher-angle lobes, essentially stealing energy from them and concentrating it in the main beam at 6° elevation.

The same antenna can be used at 3.5 and 7 MHz. The gain will not be large, however, because the legs are not very long at these frequencies. **Fig 17** compares the V-beam versus a horizontal ½-λ 40-meter dipole at 70 feet. At low elevation angles there is about 2 dB of advantage on 40 meters. **Fig 18** shows the same type of comparison for 80 meters, where the 80-meter dipole is superior at all angles.

Other V Combinations

A gain increase of about 3 dB can be had by stacking two V-beams one above the other, a half wavelength apart, and feeding them with in-phase currents. This will result in a lowered angle of radiation. The bottom V should be at least a quarter wavelength above the ground, and preferably a half wavelength. This arrangement will narrow the

chap 13.pmd 8 2/12/2007, 9:50 AM

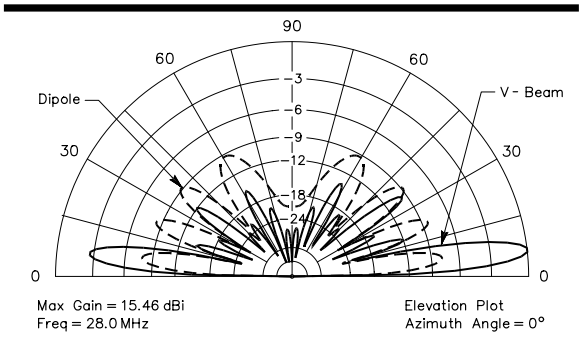

Fig 16—The elevation-plane of the 209-foot/leg V-beam (solid line) compared to the dipole (dashed line). Again, the elevation angle for peak gain corresponds well to that of the simple dipole at the same height.

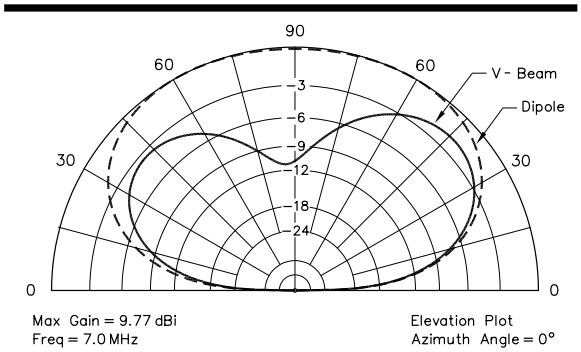

Fig 18—Elevation pattern for the same 209-foot-per-leg V-beam (solid line), at 3.5 MHz, compared to an 80-meter dipole at 70 feet (dashed line).

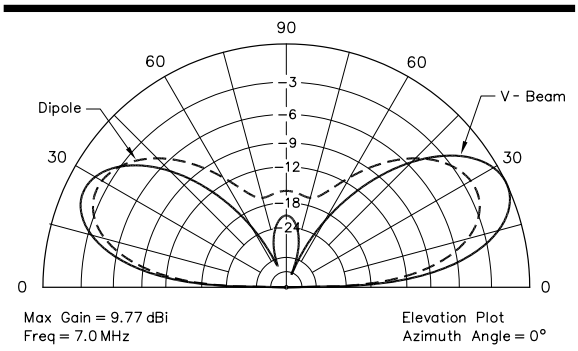

Fig 17—Elevation pattern for the same 209-foot-per-leg V-beam (solid line), at 7 MHz, compared to a 40-meter dipole (dashed line) at the same height of 70 feet.

elevation pattern and it will also have a narrow azimuthal pattern.

The V antenna can be made unidirectional by using a second V placed an odd multiple of a quarter wavelength in back of the first and exciting the two with a phase difference of 90º. The system will be unidirectional in the direction of the antenna with the lagging current. However, the V reflector is not normally employed by amateurs at low frequencies because it restricts the use to one band and requires a fairly elaborate supporting structure. Stacked Vs with driven reflectors could, however, be built for the 200- to 500-MHz region without much difficulty.

Feeding the V Beam

The V-beam antenna is most conveniently fed with tuned open-wire feeders with an antenna tuner, since this permits multiband operation. Although the length of the wires in a V-beam is not at all critical, it is important that both wires be the same electrical length. If a single band matching solution is desired, probably the most appropriate matching system is that using a stub or quarter-wave matching section. The adjustment of such a system is described in Chapter 26.

THE RESONANT RHOMBIC ANTENNA

The diamond-shaped or rhombic antenna shown in **Fig 19** can be looked upon as two acute-angle V-beams placed end-to-end. This arrangement is called a *resonant rhombic*. The leg lengths of the resonant rhombic must be an integral number of half wavelengths to avoid reactance at its feed point.

The resonant rhombic has two advantages over the simple V-beam. For the same total wire length it gives somewhat greater gain than the V-beam. A rhombic with 3 λ on a leg, for example, has about 1 dB gain over a V antenna with 6 wavelengths on a leg. **Fig 20** compares the azimuthal pattern at a 10° elevation for a resonant rhombic with 3 λ legs on 14 MHz, compared to a V-beam with 6 λ legs at the same height of 70 feet. The 3-dB nose beamwidth of the resonant rhombic is only 12.4° wide, but the gain is very high at 16.26 dBi.

The directional pattern of the rhombic is less frequency sensitive than the V when the antenna is used over a wide frequency range. This is because a change in frequency causes the major lobe from one leg to shift in one direction while the lobe from the opposite leg shifts the other way. This automatic compensation keeps the direction the same over a considerable frequency range. The disadvantage of the rhombic as compared with the V-beam is that an additional support is required.

The same factors that govern the design of the V-beam apply in the case of the resonant rhombic. The optimal apex angle A in Fig 19 is the same as that for a V having an equal leg length. The diamond-shaped antenna also can be operated as a terminated antenna, as described later in this chapter, and much of the discus-

chap 13.pmd 9 2/12/2007, 9:50 AM

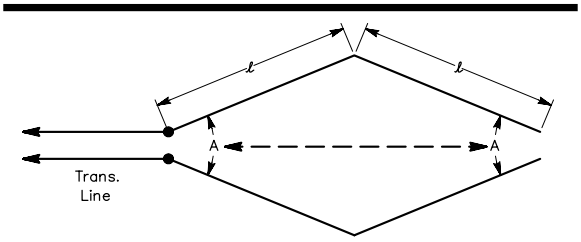

Fig 19—The resonant rhombic or diamond-shaped antenna. All legs are the same length, and opposite angles of the diamond are equal. Length ℓ is an integral number of half wavelengths for resonance.

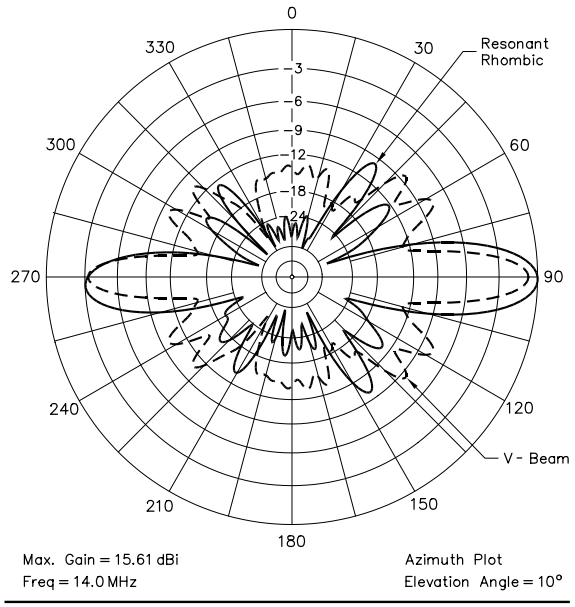

Fig 20—Azimuthal-plane pattern of resonant (unterminated) rhombic (solid line) with 3-λ legs on 14 MHz, at a height of 70 feet above flat ground, compared with a 6-λ per leg V-beam (dashed line) at the same height. Both azimuthal patterns are at a takeoff angle of 10°. The sidelobes for the resonant rhombic are suppressed to a greater degree than those for the V-beam.

sion in that section applies to the resonant rhombic as well.

The resonant rhombic has a bidirectional pattern, with minor lobes in other directions, their number and intensity depending on the leg length. In general, these sidelobes are suppressed better with a resonant rhombic than with a V-beam. When used at frequencies below the VHF region, the rhombic antenna is always mounted with the plane containing the wires horizontal. The polarization in this plane, and also in the perpendicular plane that bisects the rhombic, is horizontal. At 144 MHz and above, the dimensions are such that the antenna can be mounted with the plane containing the wires vertical if vertical polarization is desired.

When the rhombic antenna is to be used on several HF amateur bands, it is advisable to choose the apex angle, A, on the basis of the leg length in wavelengths at 14 MHz. Although the gain on higher frequency bands will not be quite as favorable as if the antenna had been designed for the higher frequencies, the system will still work well at the low angles that are necessary at such frequencies.

The resonant rhombic has lots of gain, but you must not forget that this gain comes from a radiation pattern that is very narrow. This requires careful placement of the supports for the resonant rhombic to cover desired geographic areas. This is definitely not an antenna that allows you to use just any convenient trees as supports!

The resonant rhombic antenna can be fed in the same way as the V-beam. Resonant feeders are necessary if the antenna is to be used in several amateur bands.

TERMINATED LONG-WIRE ANTENNAS

All the antenna systems considered so far in this chapter have been based on operation with standing waves of current and voltage along the wire. Although most hams use antenna designs based on using resonant wires, resonance is by no means a necessary condition for the wire to radiate and intercept electromagnetic waves efficiently, as discussed in Chapter 2. The result of using nonresonant wires is reactance at the feed point, unless the antenna is terminated with a resistive load.

In **Fig 21**, suppose that the wire is parallel with the ground (horizontal) and is terminated by a load Z equal to its characteristic impedance, Z_{ANT}. The wire and its image in the ground create a transmission line. The load Z can represent a receiver matched to the line. The *terminating resistor* R is also equal to the Z_{ANT} of the wire. A wave coming from direction X will strike the wire first at its far end and sweep across the wire at some angle until it reaches the end at which Z is connected. In so doing, it will induce voltages in the antenna, and currents will flow as a result. The current flowing toward Z is the useful output of the antenna, while the current flowing backwards toward R will be absorbed in R. The same thing is true of a wave coming from the direction X'. In such an antenna there are no standing waves, because all received power is absorbed at either end.

The greatest possible power will be delivered to the load Z when the individual currents induced as the wave sweeps across the wire all combine properly on reaching the load. The currents will reach Z in optimum phase when the time required for a current to flow from the far end of the antenna to Z is exactly one-half cycle longer than the time taken by the wave to sweep over the antenna. A half cycle is equivalent to a half wavelength greater than the distance traversed by the wave from the instant it strikes

chap 13.pmd 10 2/12/2007, 9:50 AM

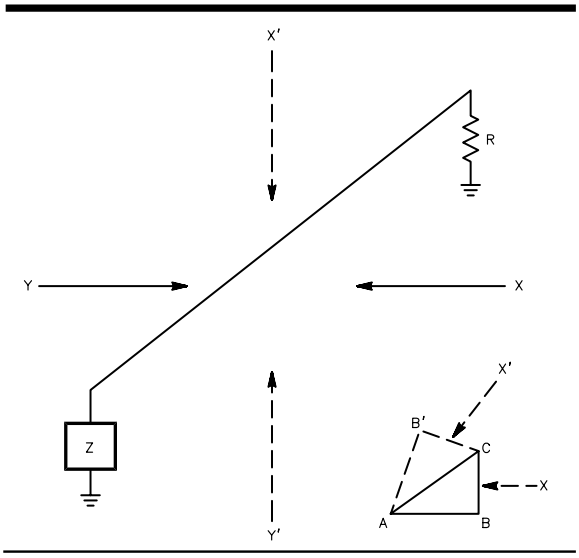

Fig 21—Layout for a terminated long-wire antenna.

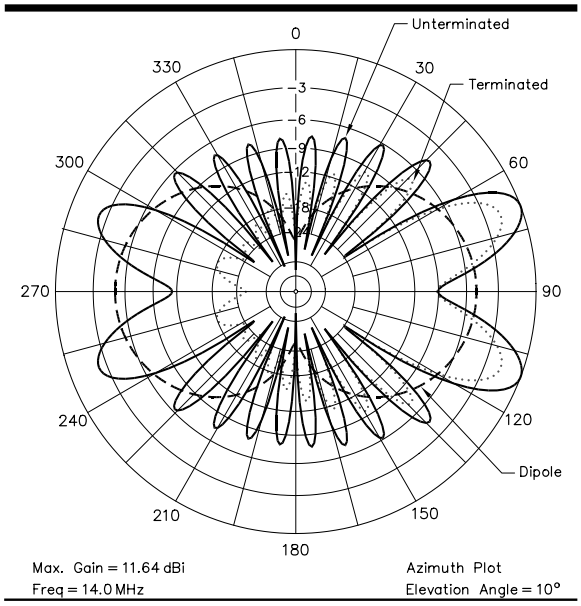

Fig 22—Azimuthal-plane pattern for 5-λ long-wire antenna at 14 MHz and 70 feet above flat ground. The solid line shows the long-wire terminated with 600-Ω to ground, while the dashed line is for the same antenna unterminated. For comparison, the response for a ½-λ dipole is overlaid with the two other patterns. You can see that the terminated long-wire has a good front-to-back pattern, but it loses about 2 dB in forward gain compared to the unterminated long-wire.

the far end of the antenna to the instant that it reaches the near end. This is shown by the small drawing, where AC represents the antenna, BC is a line perpendicular to the wave direction, and AB is the distance traveled by the wave in sweeping past AC. AB must be one-half wavelength shorter than AC. Similarly, AB' must be the same length as AB for a wave arriving from X'.

A wave arriving at the antenna from the opposite direction Y (or Y'), will similarly result in the largest possible current at the far end. However, since the far end is terminated in R, which is equal to Z, all the power delivered to R by the wave arriving from Y will be absorbed in R. The current traveling to Z will produce a signal in Z in proportion to its amplitude. If the antenna length is such that all the individual currents arrive at Z in such phase as to add up to zero, there will be no current through Z. At other lengths the resultant current may reach appreciable values. The lengths that give zero amplitude are those which are odd multiples of $^1/_4$ λ, beginning at $^3/_4$ λ. The response from the Y direction is greatest when the antenna is any even multiple of $^1/_2$ λ long; the higher the multiple, the smaller the response.

Directional Characteristics

Fig 22 compares the azimuthal pattern for a 5-λ long 14-MHz long-wire antenna, 70 feet high over flat ground, when it is terminated and when it is unterminated. The rearward pattern when the wire is terminated with a 600 Ω resistor is reduced about 15 dB, with a reduction in gain in the forward direction of about 2 dB.

For a shorter leg length in a terminated long-wire antenna, the reduction in forward gain is larger—more energy is radiated by a longer wire before the forward wave is absorbed in the terminating resistor. The azimuthal patterns for terminated and unterminated V-beams with 2-λ legs are overlaid for comparison in **Fig 23**. With these relatively short legs the reduction in forward gain is about 3.5 dB due to the terminations, although the front-to-rear ratio approaches 20 dB for the terminated V-beam. Each leg of this terminated V-beam use a 600-Ω non-inductive resistor to ground. Each resistor would have to dissipate about one-quarter of the transmitter power. For average conductor diameters and heights above ground, the Z_{ANT} of the antenna is of the order of 500 to 600 Ω.

THE TERMINATED RHOMBIC ANTENNA

The highest development of the long-wire antenna is the *terminated rhombic*, shown schematically in **Fig 24**. It consists of four conductors joined to form a diamond, or *rhombus*. All sides of the antenna have the same length and the opposite corner angles are equal. The antenna can be considered as being made up of two V antennas placed end to end and terminated by a noninductive resistor to produce a unidirectional pattern. The terminating resistor is connected between the far ends of the two sides, and is made approximately equal to the characteristic impedance of the antenna as a unit. The rhombic may be constructed either horizontally or vertically, but is practically always constructed horizontally at frequencies below 54 MHz,

chap 13.pmd 11 2/12/2007, 9:50 AM

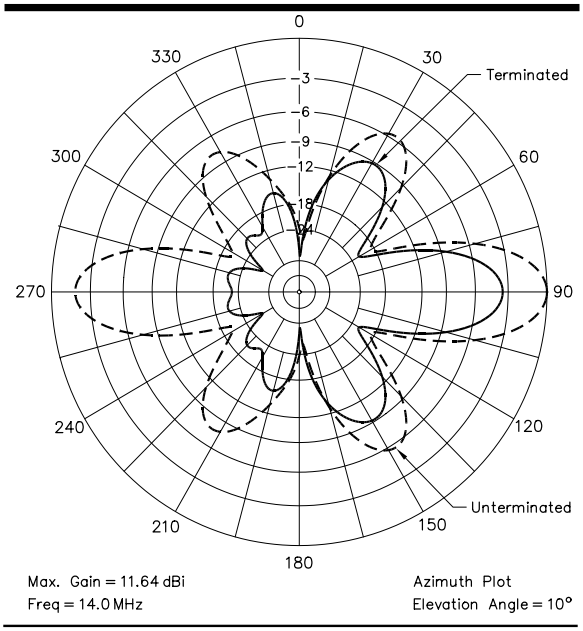

Fig 23—The azimuthal patterns for a shorter-leg V-beam (2-λ legs) when it is terminated (solid line) and unterminated (dashed line). With shorter legs, the terminated V-beam loses about 3.5 dB in forward gain compared to the unterminated version, while suppressing the rearward lobes as much as 20 dB.

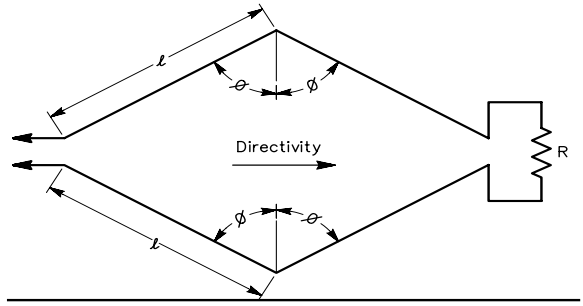

Fig 24—The layout for a terminated rhombic antenna.

since the pole height required is considerably less. Also, horizontal polarization is equally, if not more, satisfactory at these frequencies over most types of soil.

The basic principle of combining lobes of maximum radiation from the four individual wires constituting the rhombus or diamond is the same in either the terminated type or the resonant type described earlier in this chapter.

Tilt Angle

In dealing with the terminated rhombic, it is a matter of custom to talk about the *tilt angle* (ϕ in Fig 24), rather than the angle of maximum radiation with respect to an individual wire. **Fig 25** shows the tilt angle as a function of the antenna leg length. The curve marked "0°" is used for a takeoff elevation angle of 0°; that is, maximum radiation in the plane of the antenna. The other curves show the proper tilt angles to use when aligning the major lobe with a desired takeoff angle. For a 5° takeoff angle, the difference in tilt angle is less than 1° for the range of lengths shown.

The broken curve marked "optimum length" shows the leg length at which maximum gain is obtained at any given takeoff angle. Increasing the leg length beyond the optimum will result in less gain, and for that reason the curves do not extend beyond the optimum length. Note that the optimum length becomes greater as the desired takeoff angle decreases. Leg lengths over 6 λ are not recommended because the directive pattern becomes so sharp that the antenna performance is highly variable with small changes in the angle, both horizontal and vertical, at which an incoming wave reaches the antenna. Since these angles vary to some extent in ionospheric propagation, it does not pay to attempt to try for too great a degree of directivity.

Multiband Design

When a rhombic antenna is to be used over a considerable frequency range, a compromise must be made in the tilt angle. **Fig 26** gives the design dimensions of a suitable compromise for a rhombic that covers the 14 to 30 MHz range well. **Fig 27** shows the azimuth and elevation patterns for this antenna at 14 MHz, at a height of 70 feet over flat ground. The comparison antenna in this case is a 4-element Yagi on a 26-foot boom, also 70 feet above flat ground. The rhombic has about 2.2 dB more gain, but its azimuthal pattern is 17.2° wide at the 3 dB points, and only 26° at the –20 dB points! On the other hand, the Yagi has a 3-dB beamwidth of 63°, making it far easier to aim at a distant geographic location. Fig 27B shows the elevation-plane patterns for the same antennas above. As usual, the peak angle for either horizontally polarized antenna is determined mainly by the height above ground.

The peak gain of a terminated rhombic is less than that of an unterminated resonant rhombic. For the rhombic of Fig 26, the reduction in peak gain is about 1.5 dB. **Fig 28** compares the azimuthal patterns for this rhombic with and without an 800-Ω termination.

Fig 29 shows the azimuth and elevation patterns for the terminated rhombic of Fig 26 when it is operated at 28 MHz. The main lobe becomes very narrow, at 6.9° at the 3-dB points. However, this is partially compensated for by the appearance of two sidelobes each side of the main beam. These tend to spread out the main pattern some. Again, a 4-element Yagi at the same height is used for comparison.

chap 13.pmd 12 2/12/2007, 9:50 AM

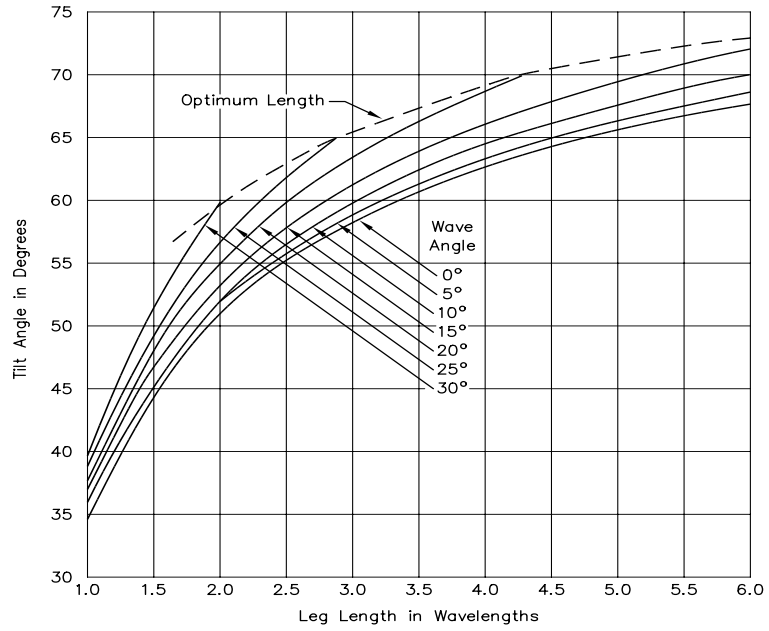

Fig 25—Rhombic-antenna design chart. For any given leg length, the curves show the proper tilt angle to give maximum radiation at the selected takeoff angle. The broken curve marked "optimum length" shows the leg length that gives the maximum possible output at the selected takeoff angle. The optimum length as given by the curves should be multiplied by 0.74 to obtain the leg length for which the takeoff angle and main lobe are aligned.

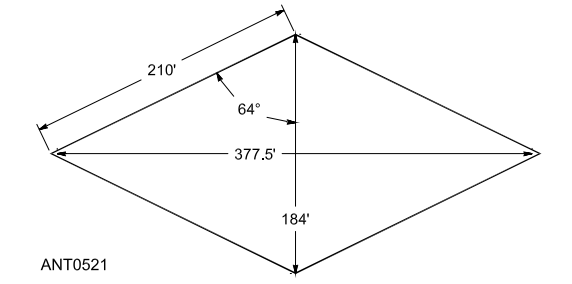

Fig 26—Rhombic antenna dimensions for a compromise design between 14- and 28-MHz requirements, as discussed in the text. The leg length is 6 λ at 28 MHz, 3 λ at 14 MHz.

Termination

Although the difference in the gain is relatively small with terminated or unterminated rhombics of comparable design, the terminated antenna has the advantage that over a wide frequency range it presents an essentially resistive and constant load to the transmitter. In a sense, the power dissipated in the terminating resistor can be considered power that would have been radiated in the other direction had the resistor not been there. Therefore, the fact that some of the power (about one-third) is used up in heating the resistor does not mean that much actual loss in the desired direction.

The characteristic impedance of an ordinary rhombic antenna, looking into the input end, is in the order of 700 to 800 Ω when properly terminated in a resistance at the far end. The terminating resistance required to bring about the matching condition usually is slightly higher than the input impedance because of the loss of energy through radiation by the time the far end is reached. The correct value usually will be found to be of the order of 800 Ω, and should be determined experimentally if the flattest possible antenna is desired. However, for average work a noninductive resistance of 800 Ω can be used with the assurance that the operation will not be far from optimum.

The terminating resistor must be practically a pure resistance at the operating frequencies; that is, its inductance and capacitance should be negligible. Ordinary wire-wound resistors are not suitable because they have far too much inductance and distributed capacitance. Small carbon resistors have satisfactory electrical characteristics but will not dissipate more than a few watts and so cannot be used, except when the transmitter power does not exceed 10 or 20 watts or when the antenna is to be used for reception only. The special resistors designed either for use as dummy antennas or for terminating rhombic antennas should be used in other cases. To allow a factor of safety, the total rated power dissipation of the resistor or resistors should be equal to half the power output of the transmitter.

To reduce the effects of stray capacitance it is desirable to use several units, say three, in series even when one alone will safely dissipate the power. The two end units should be identical and each should have one fourth to one third the total resistance, with the center unit making up the difference. The units should be installed in a weather-

chap 13.pmd 13 2/12/2007, 9:50 AM

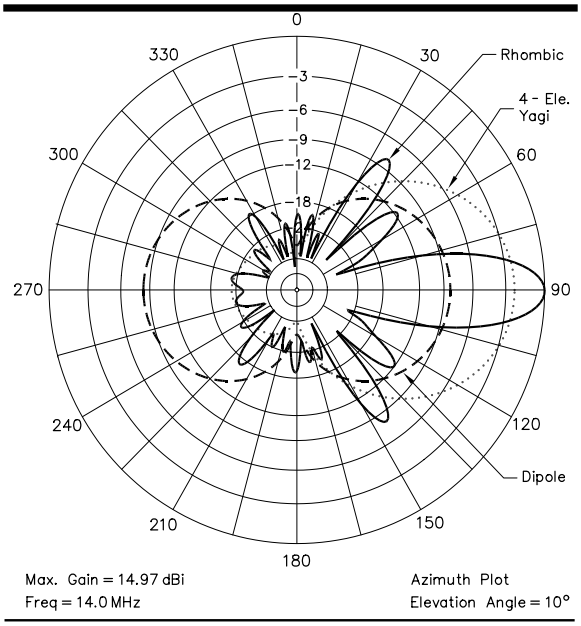

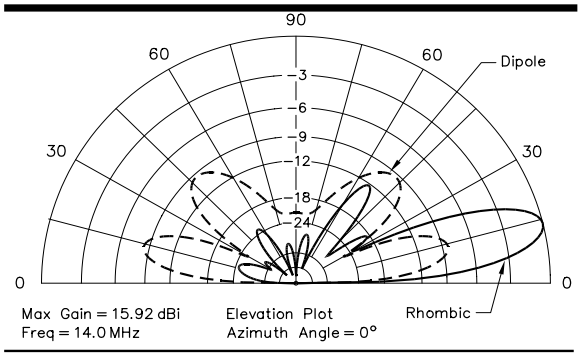

Fig 27—At left, azimuthal pattern for 3-λ (at 14 MHz) terminated rhombic (solid line) shown in Fig 26, compared with 4-element 20-meter Yagi (dotted line) on a 26-foot boom and a 20-meter dipole (dashed line). All antennas are mounted 70 feet (1 λ) above flat ground. The rearward pattern of the terminated rhombic is good and the forward gain exceeds that of the Yagi, but the frontal lobe is very narrow. Above, elevation-plane pattern of terminated rhombic compared to that of a simple dipole at the same height.

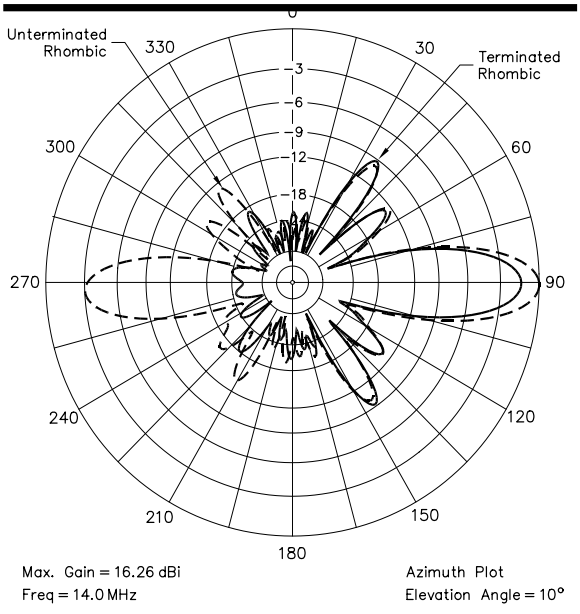

Fig 28—Comparison of azimuthal patterns for terminated (solid line) and unterminated (dashed line) rhombic antennas, using same dimensions as Fig 26 at a frequency of 14 MHz. The gain tradeoff is about 1.5 dB in return for the superior rearward pattern of the terminated antenna.

proof housing at the end of the antenna to protect them and to permit mounting without mechanical strain. The connecting leads should be short so that little extraneous inductance is introduced.

Alternatively, the terminating resistance may be placed at the end of an 800-Ω line connected to the end of the antenna. This will permit placing the resistors and their housing at a point convenient for adjustment rather than at the top of the pole. Resistance wire may be used for this line, so that a portion of the power will be dissipated before it reaches the resistive termination, thus permitting the use of lower wattage lumped resistors.

Multiwire Rhombics

The input impedance of a rhombic antenna constructed as in Fig 26 is not quite constant as the frequency is varied. This is because the varying separation between the wires causes the characteristic impedance of the antenna to vary along its length. The variation in Z_{ANT} can be minimized by a conductor arrangement that increases the capacitance per unit length in proportion to the separation between the wires.

The method of accomplishing this is shown in **Fig 30**. Three conductors are used, joined together at the ends but with increasing separation as the junction between legs is approached. For HF work the spacing between the wires at the center is 3 to 4 feet, which is similar to that used in commercial installations using legs several wavelengths long. Since all three wires should have the same length, the top and bottom wires should be slightly farther from the support than the middle wire. Using three wires in this way reduces the Z_{ANT} of the antenna to approximately 600 Ω, thus providing a better match for practical open-wire line, in addition to smoothing out the impedance variation over the frequency range.

A similar effect (although not quite as favorable) is obtained by using two wires instead of three. The 3-wire system has been found to increase the gain of the

chap 13.pmd 14 2/12/2007, 9:50 AM

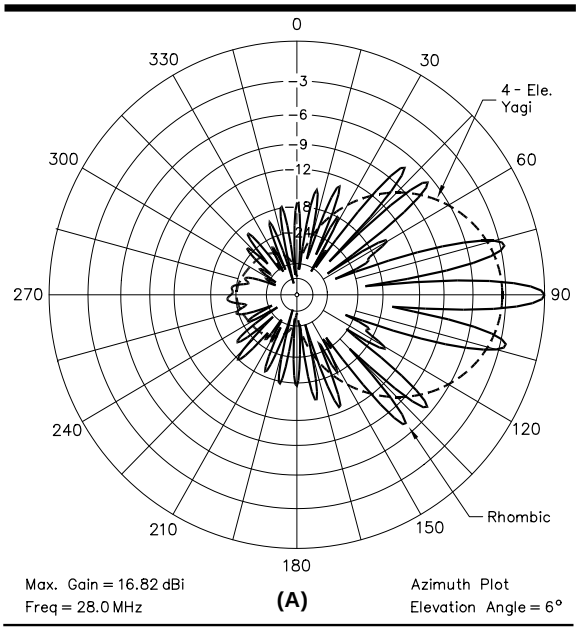

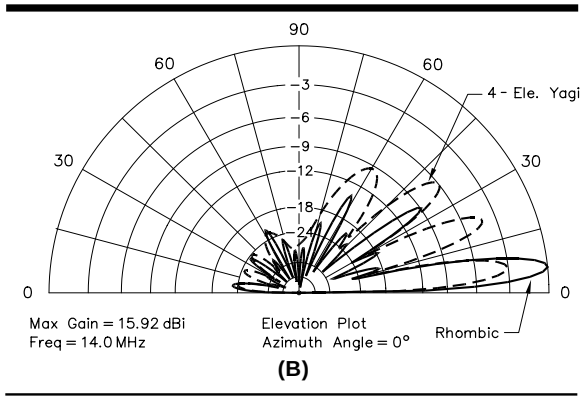

Fig 29—At A, the azimuthal pattern for the same terminated antenna in Fig 26, but now at 28 MHz compared to a 4-element 10-meter Yagi. At B, the elevation-plane pattern comparison for these antennas.

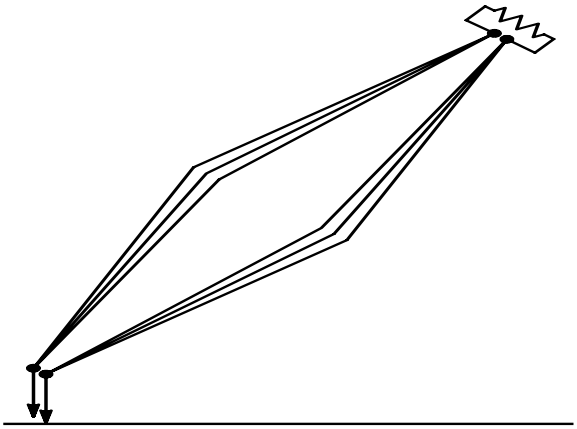

Fig 30—Three-wire rhombic antenna. Use of multiple wires improves the impedance characteristic of a terminated rhombic and increases the gain somewhat.

antenna by about 1 dB over that of a single-conductor version.

Front-to-Back Ratio

It is theoretically possible to obtain an infinite front-to-back ratio with a terminated rhombic antenna, and in practice very large values can be had. However, when the antenna is terminated in its characteristic impedance, the infinite front-to-back ratio can be obtained only at frequencies for which the leg length is an odd multiple of a quarter wavelength. The front-to-back ratio is smallest at frequencies for which the leg length is a multiple of a half wavelength.

When the leg length is not an odd multiple of a quarter wave at the frequency under consideration, the front-to-back ratio can be made very high by decreasing the value of terminating resistance slightly. This permits a small reflection from the far end of the antenna, which cancels out the residual response at the input end. With large antennas, the front-to-back ratio may be made very large over the whole frequency range by experimental adjustment of the terminating resistance. Modification of the terminating resistance can result in a splitting of the back null into two nulls, one on either side of a small lobe in the back direction. Changes in the value of terminating resistance thus permit steering the back null over a small horizontal range so that signals coming from a particular spot not exactly to the rear of the antenna may be minimized.

Methods of Feed

If the broad frequency characteristic of the terminated rhombic antenna is to be utilized fully, the feeder system must be similarly broadbanded. Open-wire transmission line of the same characteristic impedance as that shown at the antenna input terminals (approximately 700 to 800 Ω) may be used. Data for the construction of such lines is given in Chapter 24. While the usual matching stub can be used to provide an impedance transformation to more satisfactory line impedances, this limits the operation of the antenna to a comparatively narrow range of frequencies centering about that for which the stub is adjusted. Probably a more satisfactory arrangement would be to use a coaxial transmission line and a broadband transformer balun at the antenna feed point.

chap 13.pmd 15 2/12/2007, 9:50 AM

Receiving Wave Antennas

Perhaps the best known type of wave antenna is the *Beverage*. Many 160-meter enthusiasts have used Beverage antennas to enhance the signal-to-noise ratio while attempting to extract weak signals from the often high levels of atmospheric noise and interference on the low bands. Alternative antenna systems have been developed and used over the years, such as loops and long spans of unterminated wire on or slightly above the ground, but the Beverage antenna seems to be the best for 160-meter weak-signal reception. The information in this section was prepared originally by Rus Healy, K2UA (ex-NJ2L).

THE BEVERAGE ANTENNA

A Beverage is simply a directional wire antenna, at least one wavelength long, supported along its length at a fairly low height and terminated at the far end in its characteristic impedance. This antenna is shown in **Fig 31A**. It takes its name from its inventor, Harold Beverage, W2BML.

Many amateurs choose to use a single-wire Beverage because they are easy to install and they work well. The drawback is that Beverages are physically long and they do require that you have the necessary amount of real estate to install them. Sometimes, a neighbor will allow you to put up a temporary Beverage for a particular contest or DXpedition on his land, particularly during the winter months.

Beverage antennas can be useful into the HF range, but they are most effective at lower frequencies, mainly on 160 through 40 meters. The antenna is responsive mostly to low-angle incoming waves that maintain a constant (vertical) polarization. These conditions are nearly always satisfied on 160 meters, and most of the time on 80 meters. As the frequency is increased, however, the polarization and arrival angles are less and less constant and favorable, making Beverages less effective at these frequencies. Many amateurs have, however, reported excellent performance from Beverage antennas at frequencies as high as 14 MHz, especially when rain or snow (precipitation) static prevents good reception on the Yagi or dipole transmitting antennas used on the higher frequencies.

Beverage Theory

The Beverage antenna acts like a long transmission line with one lossy conductor (the earth), and one good conductor (the wire). Beverages have excellent directivity if erected properly, but they are quite inefficient because they are mounted close to the ground. This is in contrast with the terminated long-wire antennas described earlier, which are typically mounted high off the ground. Beverage antennas are not suitable for use as transmitting antennas.

Because the Beverage is a traveling wave, terminated antenna, it has no standing waves resulting from radio signals. As a wave strikes the end of the Beverage from the desired direction, the wave induces voltages along the antenna and continues traveling in space as well. Fig 31B shows part of a wave on the antenna resulting from a desired signal. This diagram also shows the tilt of the wave. The signal induces equal voltages in both directions. The resulting currents are equal and travel in both directions; the component traveling toward the termination end moves *against* the wave and thus builds down to a very low level at the termination end. Any residual signal resulting from this direction of current flow will be absorbed in the termination (if the termination is equal to the antenna impedance). The component of the signal flowing in the other direction, as we will see, becomes a key part of the received signal.

As the wave travels along the wire, the wave in space travels at approximately the same velocity. (There is some phase delay in the wire, as we shall see.) At any given point in time, the wave traveling along in space induces a voltage in the wire in addition to the wave already travel-

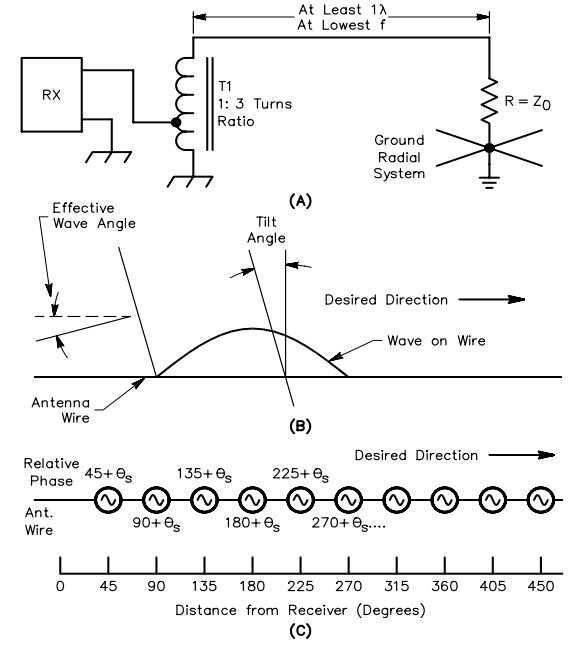

Fig 31—At A, a simple one-wire Beverage antenna with a variable termination impedance and a matching 9:1 autotransformer for the receiver impedance. At B, a portion of a wave from the desired direction is shown traveling down the antenna wire. Its tilt angle and effective takeoff angle are also shown. At C, a situation analogous to the action of a Beverage on an incoming wave is shown. See text for discussion.

chap 13.pmd 16 2/12/2007, 9:50 AM

ing on the wire (voltages already induced by the wave). Because these two waves are nearly in phase, the voltages add and build toward a maximum at the receiver end of the antenna.

This process can be likened to a series of signal generators lined up on the wire, with phase differences corresponding to their respective spacings on the wire (Fig 31C). At the receiver end, a maximum voltage is produced by these voltages adding in phase. For example, the wave component induced at the receiver end of the antenna will be in phase (at the receiver end) with a component of the same wave induced, say, 270° (or any other distance) down the antenna, after it travels to the receiver end.

In practice, there is some phase shift of the wave on the wire with respect to the wave in space. This phase shift results from the velocity factor of the antenna. (As with any transmission line, the signal velocity on the Beverage is somewhat less than in free space.) Velocity of propagation on a Beverage is typically between 85 and 98% of that in free space. As antenna height is increased to a certain optimum height (which is about 10 feet for 160 meters), the velocity factor increases. Beyond this height, only minimal improvement is afforded, as shown in **Fig 32**. These curves are the result of experimental work done in 1922 by RCA, and reported in a *QST* article (November 1922) entitled "The Wave Antenna for 200-Meter Reception," by H. H. Beverage. The curve for 160 meters was extrapolated from the other curves.

Phase shift (per wavelength) is shown as a function of velocity factor in **Fig 33**, and is given by:

$$\theta = 360\left(\frac{100}{k} - 1\right) \qquad \text{(Eq 2)}$$

where k = velocity factor of the antenna in percent.

The signals present on and around a Beverage antenna are shown graphically in A through D of **Fig 34**. These curves show relative voltage levels over a number of periods of the wave in space and their relative effects in terms of the total signal at the receiver end of the antenna.

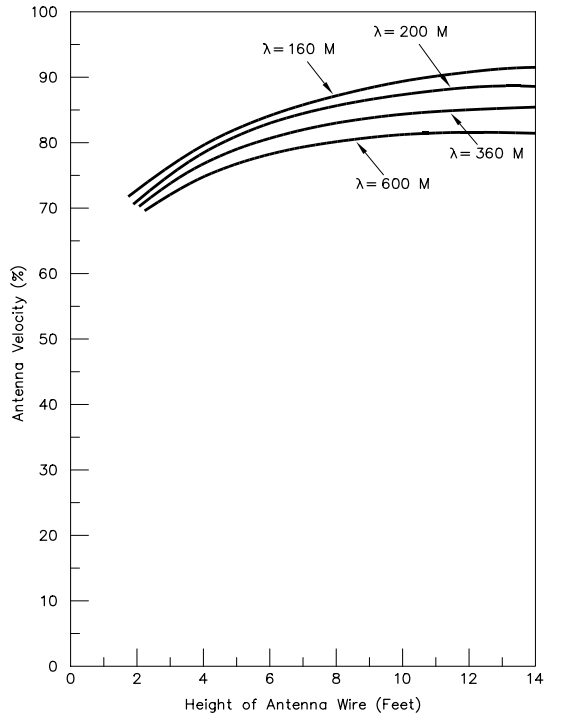

Fig 32—Signal velocity on a Beverage increases with height above ground, and reaches a practical maximum at about 10 feet. Improvement is minimal above this height. (The velocity of light is 100%.)

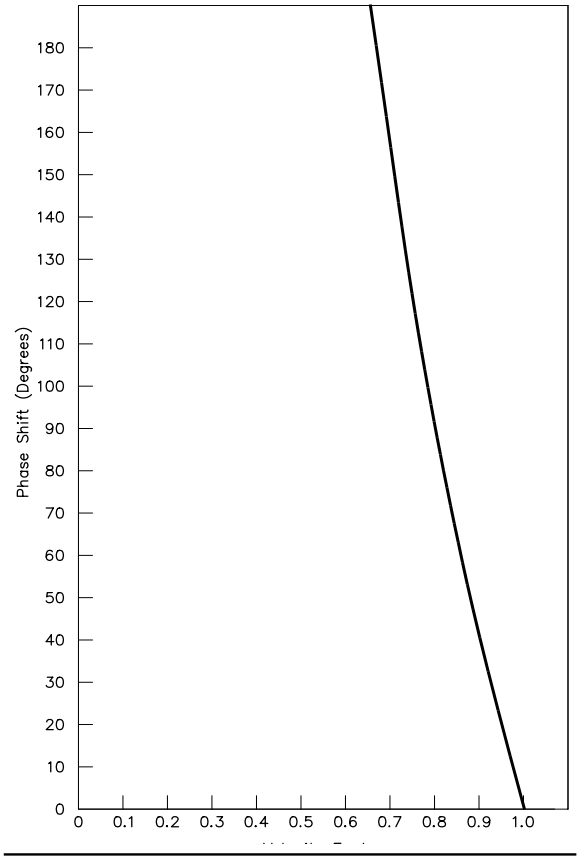

Fig 33—This curve shows phase shift (per wavelength) as a function of velocity factor on a Beverage antenna. Once the phase shift for the antenna goes beyond 90°, the gain drops off from its peak value, and any increase in antenna length will decrease gain.

chap 13.pmd 17 2/12/2007, 9:50 AM

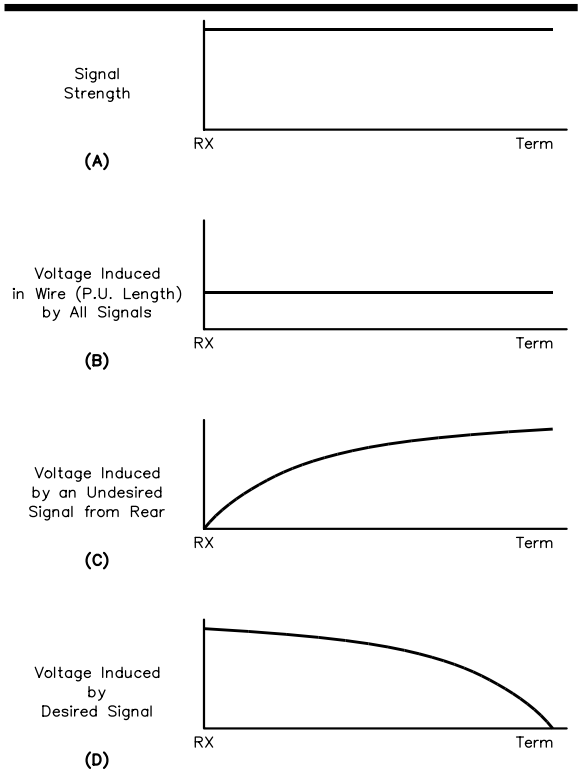

Fig 34—These curves show the voltages that appear in a Beverage antenna over a period of several cycles of the wave. Signal strength (at A) is constant over the length of the antenna during this period, as is voltage induced per unit length in the wire (at B). (The voltage induced in any section of the antenna is the same as the voltage induced in any other section of the same size, over the same period of time.) At C, the voltages induced by an undesired signal from the rearward direction add in phase and build to a maximum at the termination end, where they are dissipated in the termination (if $Z_{term} = Z_0$). The voltages resulting from a desired signal are shown at D. The wave on the wire travels closely with the wave in space, and the voltages resulting add in phase to a maximum at the receiver end of the antenna.

Performance in Other Directions

The performance of a Beverage antenna in directions other than the favored one is quite different than previously discussed. Take, for instance, the case of a signal arriving perpendicular to the wire (90° either side of the favored direction). In this case, the wave induces voltages along the wire that are essentially *in phase*, so that they arrive at the receiver end more or less out of phase, and thus cancel. (This can be likened to a series of signal generators lined up along the antenna as before, but having no progressive phase differences.)

As a result of this cancellation, Beverages exhibit deep nulls off the sides. Some minor sidelobes will exist, as with other long-wire antennas, and will increase in number with the length of the antenna.

In the case of a signal arriving from the rear of the antenna, the behavior of the antenna is very similar to its performance in the favored direction. The major difference is that the signal from the rear adds in phase at the termination end and is absorbed by the termination impedance. **Fig 35** compares the azimuth and elevation patterns for a 2-λ (1062 foot) and a 1-λ (531 foot) Beverage at 1.83 MHz. The wire is mounted 8 feet above flat ground (to keep it above deer antlers and away from humans too) and is terminated with a 500-Ω resistor in each case, although the exact value of the terminating resistance is not very critical. The ground constants assumed in this computer model are conductivity of 5 mS/m and a dielectric constant of 13. Beverage dielectric performance tends to decrease as the ground becomes better. Beverages operated over saltwater do not work as well as they do over poor ground.

For most effective operation, the Beverage should be terminated in an impedance equal to the characteristic impedance Z_{ANT} of the antenna. For maximum signal transfer to the receiver you should also match the receiver's input impedance to the antenna. If the termination impedance is not equal to the characteristic impedance of the antenna, some part of the signal from the rear will be reflected back toward the receiver end of the antenna.

If the termination impedance is merely an open circuit (no terminating resistor), total reflection will result and the antenna will exhibit a bidirectional pattern (still with very deep nulls off the sides). An unterminated Beverage will not have the same response to signals in the rearward direction as it exhibits to signals in the forward direction because of attenuation and reradiation of part of the reflected wave as it travels back toward the receiver end. **Fig 36** compares the response from two 2-λ Beverages, one terminated and the other unterminated. Just like a terminated long-wire transmitting antenna (which is mounted higher off the ground than a Beverage, which is meant only for receiving), the terminated Beverage has a reduced forward lobe compared to its unterminated sibling. The unterminated Beverage exhibits about a 5 dB front-to-back ratio for this length because of the radiation and wire and ground losses that occur before the forward wave gets to the end of the wire.

If the termination is between the extremes (open circuit and perfect termination in Z_{ANT}), the peak direction and intensity of signals off the rear of the Beverage will change. As a result, an adjustable reactive termination can be employed to *steer* the nulls to the rear of the antenna (see **Fig 37**). This can be of great help in eliminating a local interfering signal from a rearward direction (typically 30° to 40° either side of the back direction). Such a scheme doesn't help much for interfering skywave signals because of variations encountered in the ionosphere that constantly shift polarity, amplitude, phase and

chap 13.pmd 18 2/12/2007, 9:50 AM

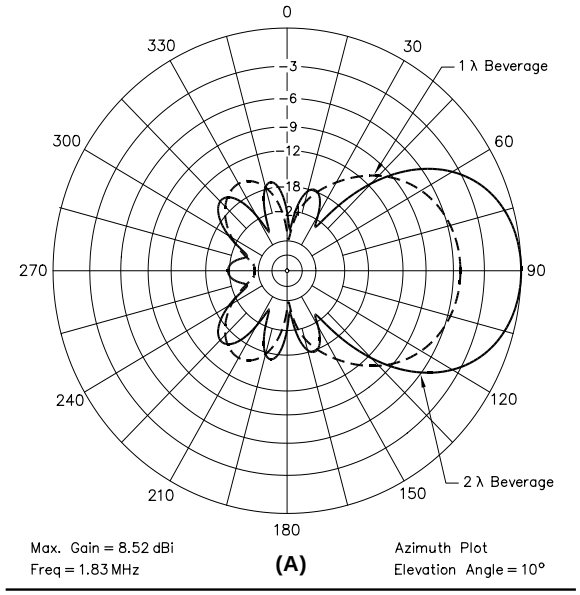

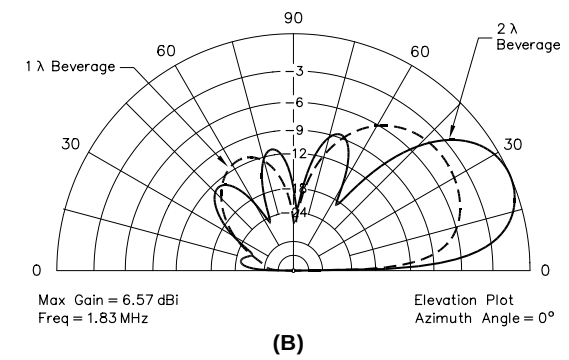

Fig 35—At A, azimuthal patterns of a 2-λ (solid line) and a 1-λ (dashed line) Beverage antenna, terminated with 550-Ω resistor at 1.83 MHz, at an elevation angle of 10°. The rearward pattern around 180° is more than 20 dB down from the front lobe for each antenna. At B, the elevation-plane patterns. Note the rejection of very high-angle signals near 90°.

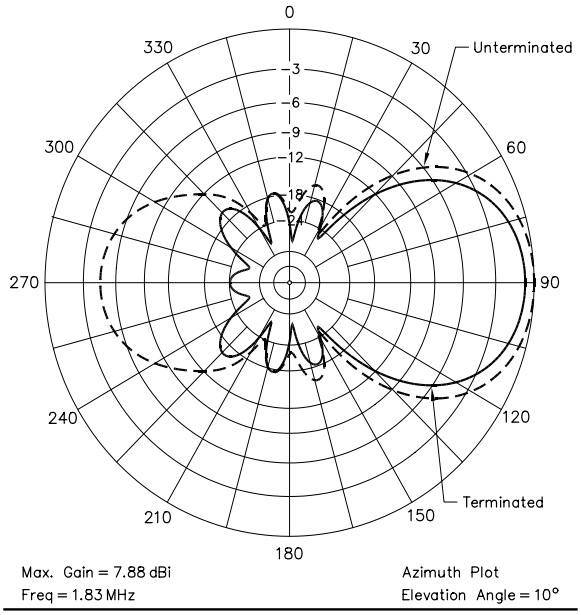

Fig 36—Comparing the azimuthal patterns for a 2-λ Beverage, terminated (solid line) and unterminated (dashed line).

incoming elevation angles.

To determine the appropriate value for a terminating resistor, you need to know the characteristic impedance (surge impedance), Z_{ANT}, of the Beverage. It is interesting to note that Z_{ANT} is not a function of the length, just like a transmission line.

$$Z_{ANT} = 138 \times \log\left(\frac{4h}{d}\right) \qquad \text{(Eq 3)}$$

where

Z_{ANT} = characteristic impedance of the Beverage = terminating resistance needed

h = wire height above ground

d = wire diameter (in the same units as h)

Another aspect of terminating the Beverage is the quality of the RF ground used for the termination. For most types of soil a ground rod is sufficient, since the optimum value for the termination resistance is in the range of 400 to 600 Ω for typical Beverages and the ground-loss resistance is in series with this. Even if the ground-loss resistance at the termination point is as high as 40 or 50 Ω, it still is not an appreciable fraction of the overall terminating resistance. For soil with very poor conductivity, however, (such as sand or rock) you can achieve a better ground termination by laying radial wires on the ground at both the receiver and termination ends. These wires need not be resonant quarter-wave in length, since the ground detunes them anyway. Like the ground counterpoise for a vertical antenna, a number of short radials is better than a few long ones. Some amateurs use chicken-wire ground screens for their ground terminations.

As with many other antennas, improved directivity and gain can be achieved by lengthening the antenna and by arranging several antennas into an array. One item that must be kept in mind is that by virtue of the velocity factor of the antenna, there is some phase shift of the wave on the antenna with respect to the wave in space. Because of this phase shift, although the directivity will continue to sharpen with increased length, there will be some optimum length at which the gain of the antenna will peak. Beyond this

chap 13.pmd 19 2/12/2007, 9:50 AM

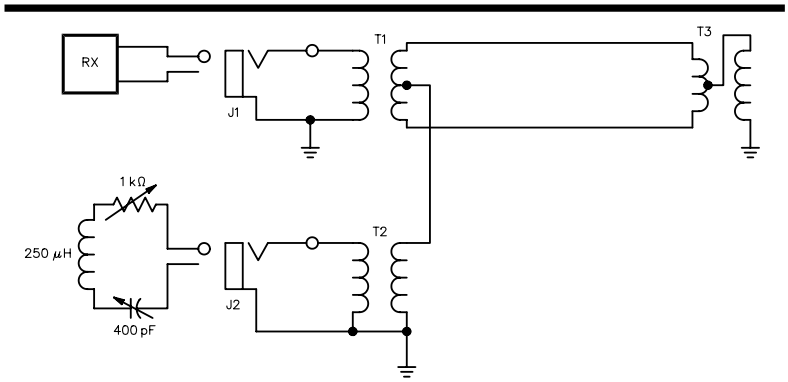

Fig 37—A two-wire Beverage antenna that has provisions for direction switching and null steering in the rear quadrant. Performance improves with height to a point, and is optimum for 1.8-MHz operation at about 10 to 12 feet. Parts identifications are for text reference.

length, the current increments arriving at the receiver end of the antenna will no longer be in phase, and will not add to produce a maximum signal at the receiver end. This optimum length is a function of velocity factor and frequency, and is given by:

$$L = \frac{\lambda}{4\left(\frac{100}{k} - 1\right)} \qquad \text{(Eq 4)}$$

where

L = maximum effective length

λ = signal wavelength in free space (same units as L)

k = velocity factor of the antenna in percent

Because velocity factor increases with height (to a point, as mentioned earlier), optimum length is somewhat longer if the antenna height is increased. The maximum effective length also increases with the number of wires in the antenna system. For example, for a two-wire Beverage like the bidirectional version shown in Fig 37, the maximum effective length is about 20% longer than the single-wire version. A typical length for a single-wire 1.8-MHz Beverage (made of #16 wire and erected 10 feet above ground) is about 1200 feet.

Feed-Point Transformers for Single-Wire Beverages

Matching transformer T1 in Fig 31 is easily constructed. Small toroidal ferrite cores are best for this application, with those of high permeability (μ_i = 125 to 5000) being the easiest to wind (requiring fewest turns) and having the best high-frequency response (because few turns are used). Trifilar-wound autotransformers are most convenient.

Most users are not concerned with a small amount of SWR on the transmission line feeding their Beverages. For example, let us assume that the Z_{ANT} of a particular Beverage is 525 Ω and the terminating resistance is made equal to that value. If a standard 3:1 turns-ratio autotransformer is used at the input end of the antenna, the nominal impedance transformation 50 Ω × 3^2 = 450 Ω. This leads to the terminology often used for this transformer as a *9:1 transformer*, referring to its impedance transformation. The resulting SWR on the feed line going back to the receiver would be 525/450 = 1.27:1, not enough to be concerned about. For a Z_{ANT} of 600 Ω, the SWR is 600/450 = 1.33:1, again not a matter of concern.

Hence, most Beverage users use standard 9:1 (450:50 Ω) autotransformers. You can make a matching transformer suitable for use from 160 to 40 meters using eight trifilar turns of #24 enameled wire wound over a stack of two Amidon FT-50-75 or two MN8-CX cores. See **Fig 38**.

Make your own trifilar cable bundle by placing three 3-foot lengths of the #24 wire side-by-side and twisting them in a hand drill so that there is a uniform twist about one twist-per-inch. This holds the three wires together in a bundle that can be passed through the two stacked cores, rather like threading a needle. Remember that each time you put the bundle through the center of the cores counts as one turn.

After you finish winding, cut the individual wires to leave about $^3/_4$-inch leads, sand off the enamel insulation and tin the wires with a soldering iron. Identify the individual wires with an ohmmeter and then connect them together following Fig 38. Coat the transformer with Q-dope (liquid polystyrene) to finalize the transformer. White glue will work also. See Chapters 25 and 26 and *The ARRL Handbook* for more information on winding toroidal transformers or see Chapter 7 (Special Receiving Antennas) of *ON4UN's Low-Band DXing* book.

The Two-Wire Beverage

The two-wire antenna shown in Fig 37 has the major advantage of having signals from both directions available at the receiver at the flip of a switch between J1 and J2. Also, because there are two wires in the system (equal amounts of signal voltage are induced in both wires), greater signal voltages will be produced.

chap 13.pmd 20 2/12/2007, 9:50 AM

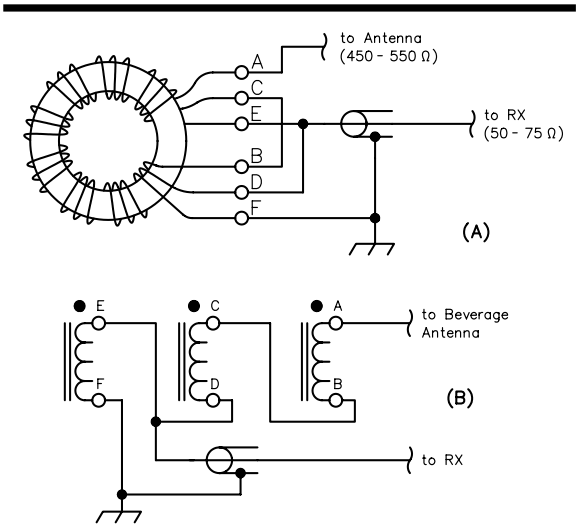

Fig 38—Constructing the feed-point transformer for a single-wire Beverage. See text for details.

A signal from the left direction in Fig 37 induces equal voltages in both wires, and equal in-phase currents flow as a result. The *reflection transformer* (T3 at the right-hand end of the antenna) then inverts the phase of these signals and reflects them back down the antenna toward the receiver, using the antenna wires as a balanced open-wire transmission line. This signal is then transformed by T1 down to the input impedance of the receiver (50 Ω) at J1.

Signals traveling from right to left also induce equal voltages in each wire, and they travel in phase toward the receiver end, through T1, and into T2. Signals from this direction are available at J2.

T1 and T2 are standard 9:1 wideband transformers capable of operating from 1.8 to at least 10 MHz. Like any two parallel wires making up a transmission line, the two-wire Beverage has a certain characteristic impedance—we'll call it Z_1 here—depending on the spacing between the two wires and the insulation between them. T3 transforms the terminating resistance needed at the end of the line to Z_1. Keep in mind that this terminating resistance is equal to the characteristic impedance Z_{ANT} of the Beverage—that is, the impedance of the parallel wires over their images in the ground below. For example, if Z_1 of the Beverage wire is 300 Ω (that is, you used TV twin-lead for the two Beverage wires), T3 must transform the balanced 300 Ω to the unbalanced 500 Ω Z_{ANT} impedance used to terminate the Beverage.

The design and construction of the reflection transformer used in a two-wire Beverage is more demanding than that for the straightforward matching transformer T1 because the exact value of terminating impedance is more critical for good F/B. See Chapter 7 (Special Receiving Antennas) in *ON4UN's Low-Band DXing* for details on winding the reflection transformers for a two-wire Beverage.

Another convenient feature of the two-wire Beverage is the ability to steer the nulls off either end of the antenna while receiving in the opposite direction. For instance, if the series RLC network shown at J2 is adjusted while the receiver is connected to J1, signals can be received from the left direction while interference coming from the right can be partially or completely nulled. The nulls can be steered over a 60° (or more) area off the right-hand end of the antenna. The same null-steering capability exists in the opposite direction with the receiver connected at J2 and the termination connected at J1.

The two-wire Beverage is typically erected at the same height as a single-wire version. The two wires are at the same height and are spaced uniformly—typically 12 to 18 inches apart for discrete wires. Some amateurs construct two-wire Beverages using "window" ladder-line, twisting the line about three twists per foot for mechanical and electrical stability in the wind.

The characteristic impedance Z_{ANT} of a Beverage made using two discrete wires with air insulation between them depends on the wire size, spacing and height and is given by:

$$Z_{ANT} = \frac{69}{\sqrt{\varepsilon}} \times \log\left[\frac{4h}{d}\sqrt{1+\left(\frac{2h}{S}\right)^2}\right] \qquad \text{(Eq 5)}$$

where

Z_{ANT} = Beverage impedance = desired terminating resistance
S = wire spacing
h = height above ground
d = wire diameter (in same units as S and h)
ε = 2.71828

Beverages in Echelon

The pattern of a Beverage receiving antenna is dependent on the terminating resistance used for a particular antenna, as was demonstrated at the extremes by Fig 36. This compared the patterns for a terminated and an unterminated Beverage. The pattern of even a poorly terminated Beverage can be significantly improved by the addition of a second Beverage. The additional Beverage is installed so that it is operated *in echelon*, a word deriving from the fact that the two wires look like the parallel rungs on a ladder. For a practial 160- and 80-meter setup the second Beverage wire is parallel to the first Beverage, spaced from it by about 5 meters, and also staggered 30 meters ahead. See **Fig 38**.

The forward Beverage is fed with a phase difference of +125° such that the total phase, including that due to the forward staggering, is 180°. This forms the equivalent of an end-fire array fed out-of-phase, but it takes advantage of the natural directivity of each Beverage. **Fig 39** compares the pattern of a single 1-λ 160-meter Beverage that is sloppily terminated with two Beverages fed in echelon. The

chap 13.pmd 21 2/12/2007, 9:50 AM

Beverages in echelon gives a modest additional gain of almost 2 dB. But where the two Beverages in echelon really shine is how they cleans up the rearward pattern—from an average about 15 dB for the single Beverage to more than 25 dB for the two Beverages.

Even at a spacing of 5 meters, there is very little mutual coupling between the two Beverage wires because of their inherently small radiation resistance when they are mounted low above lossy ground. If you adjust for a low SWR (using proper transformers to match the feed-line coaxes), the phase difference will depend solely on the difference in length of the two coaxes feeding the Beverage wires. **Fig 40** shows a wideband feed system designed by Tom Rauch, W8JI, as a "cross-fire" feed system. The 180° wideband phase-inverting transformer allows the system to work on two bands, say 160 and 80 meters. See Chapter 7, Receiving Antennas, in *ON4UN's Low-Band DXing* book, 4th Edition for transformer details.

Practical Considerations

Even though Beverage antennas have excellent directive patterns if terminated properly, gain never exceeds about –3 dBi in most practical installations. However, the directivity that the Beverage provides results in a much higher signal-to-noise ratio for signals in the desired direction than almost any other real-world antenna used at low frequencies.

A typical situation might be a station located in the US Northeast (W1), trying to receive Topband signals from Europe to the northeast, while thunderstorms behind him in the US Southeast (W4) are creating huge static crashes. Instead of listening to an S7 signal with 10-dB over S9 noise and interference on a vertical, the directivity of a Beverage will typically allow you to copy the same signal at perhaps S5 with only S3 (or lower) noise and interference. This is certainly a worthwhile improvement. However, if you are in the middle of a thunderstorm, or if there is a thunderstorm in the direction from which you are trying to receive a signal, no Beverage is going to help you!

There are a few basic principles that must be kept in mind when erecting Beverage antennas if optimum performance is to be realized.

1) Plan the installation thoroughly, including choosing an antenna length consistent with the optimum length values discussed earlier.
2) Keep the antenna as straight and as nearly level as possible over its entire run. Avoid following the terrain under the antenna too closely—keep the antenna level with the average terrain.
3) Minimize the lengths of vertical downleads at the ends of the antenna. Their effect is detrimental to the directive pattern of the antenna. It is best to slope the antenna wire from ground level to its final height (over a distance of 50 feet or so) at the feed-point end. Similar action should be taken at the termination end. Be sure to seal the transformers against weather.

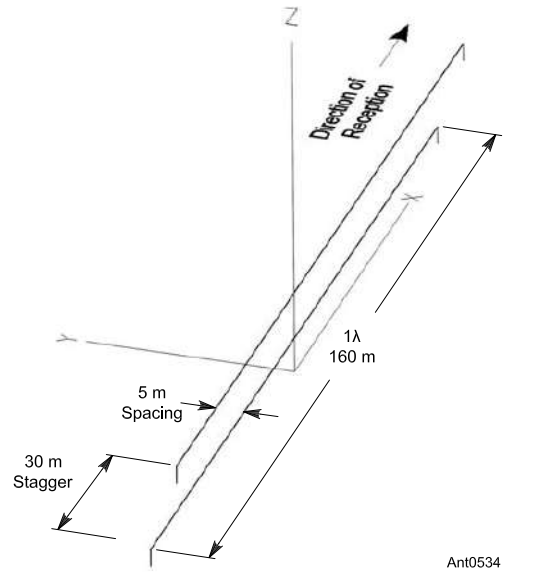

Fig 39—Layout of two 160-meter 1-λ long Beverages in echelon, spaced 5 meters apart, with 30 meter forward stagger. The upper antenna has a 125° phase shift in its feed system.

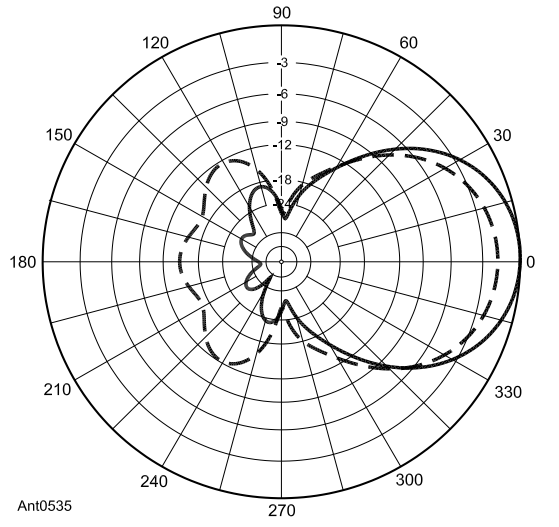

Fig 40—Azimuth pattern at 10° takeoff angle for single Beverage (dashed line) and two Beverages in an echelon end-fire array. The rearward pattern is considerably cleaner on the echelon. Thus, two closely spaced, short Beverages can give considerable improvement over a single short Beverage.

chap 13.pmd 22 2/12/2007, 9:50 AM

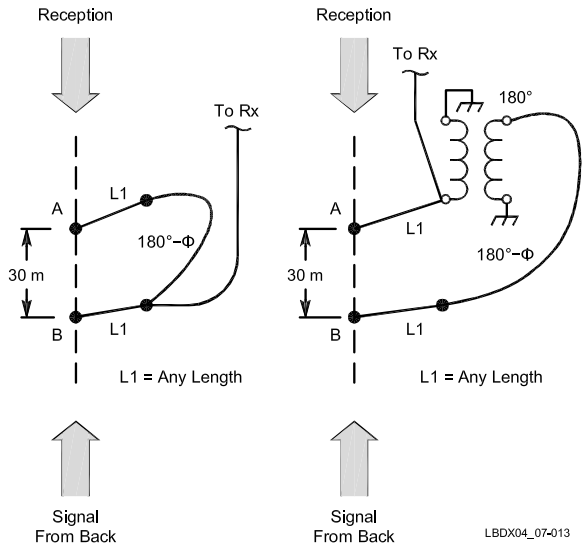

Fig 41—Two ways of feeding the two-Beverage echelon array in Fig 39. On the left, a feed system good for one frequency; on the right, a "cross-fire" feed system good for 1.8 and 3.6 MHz. For this system we want a phase shift due to the coax length of +116° at the back Beverage A. The angle ϕ is thus 180°–116° = 64° long on 160 meters. In the system on the right, a 64° length on 160 meters becomes 128° long on 80 meters. So with the phase-inverting transformer the net phase shift becomes 53° on 80 meters, a reasonable compromise. (*Courtesy W8JI and ON4UN.*)

4) Use a noninductive resistor for terminating a single-wire Beverage. If you live in an area where lightning storms are common, use 2-W terminating resistors, which can survive surges due to nearby lightning strikes.
5) Use high-quality insulators for the Beverage wire where it comes into contact with the supports. Plastic insulators designed for electric fences are inexpensive and effective.
6) Keep the Beverage away from parallel conductors such as electric power and telephone lines for a distance of at least 200 feet. Perpendicular conductors, even other Beverages, may be crossed with relatively little interaction, but do not cross any conductors that may pose a safety hazard.
7) Run the coaxial feed line to the Beverage so that it is not directly under the span of the wire. This prevents common-mode currents from appearing on the shield of the coax. It may be necessary to use a ferrite-bead choke on the feed line if you find that the feed line itself picks up signals when it is temporarily disconnected from the Beverage. See Chapter 26 for details on common-mode chokes.
8) If you use elevated radials in your transmitting antenna system, keep your Beverage feed lines well away from them to avoid stray pickup that will ruin the Beverage's directivity.

BIBLIOGRAPHY

Source material and more extended discussion of topics covered in this chapter can be found in the references given below.

A. Bailey, S. W. Dean and W. T. Wintringham, "The Receiving System for Long-Wave Transatlantic Radio Telephony," *The Bell System Technical Journal*, Apr 1929.

J. S. Belrose, "Beverage Antennas for Amateur Communications," Technical Correspondence, *QST*, Sep 1981.

H. H. Beverage, "Antennas," *RCA Review*, Jul 1939.

H. H. Beverage and D. DeMaw, "The Classic Beverage Antenna Revisited," *QST* , Jan 1982.

B. Boothe, "Weak-Signal Reception on 160—Some Antenna Notes," *QST*, Jun 1977.

E. Bruce, "Developments in Short-Wave Directive Antennas," *Proc IRE*, Aug 1931.

E. Bruce, A. C. Beck and L. R. Lowry, "Horizontal Rhombic Antennas," *Proc IRE*, Jan 1935.

P. S. Carter, C. W. Hansel and N. E. Lindenblad, "Development of Directive Transmitting Antennas by R.C.A. Communications," *Proc IRE*, Oct 1931.

J. Devoldere, *Low-Band DXing* (Newington: ARRL, 1987).

J. Devoldere, *ON4UN's Low-Band DXing* (Newington: ARRL, 1999). See in particular Chapter 7, "Special Receiving Antennas," for many practical details on Beverage antennas.

A. E. Harper, *Rhombic Antenna Design* (New York: D. Van Nostrand Co, Inc).

E. A. Laport, "Design Data for Horizontal Rhombic Antennas," *RCA Review*, Mar 1952.

G. M. Miller, *Modern Electronic Communication* (Englewood Cliffs, NJ: Prentice Hall, 1983).

V. A. Misek, *The Beverage Antenna Handbook* (Wason Rd., Hudson, NH: W1WCR, 1977).

F. E. Terman, *Radio Engineering*, Second Edition (New York: McGraw-Hill, 1937).

chap 13.pmd 23 2/12/2007, 9:50 AM

Chapter 14

Direction Finding Antennas

The use of radio for direction-finding purposes (RDF) is almost as old as its application for communications. Radio amateurs have learned RDF techniques and found much satisfaction by participating in hidden-transmitter hunts. Other hams have discovered RDF through an interest in boating or aviation, where radio direction finding is used for navigation and emergency location systems.

In many countries of the world, the hunting of hidden amateur transmitters takes on the atmosphere of a sport, as participants wearing jogging togs or track suits dash toward the area where they believe the transmitter is located. The sport is variously known as *fox hunting*, *bunny hunting*, ARDF (Amateur Radio direction finding) or simply transmitter hunting. In North America, most hunting of hidden transmitters is conducted from automobiles, although hunts on foot are gaining popularity.

There are less pleasant RDF applications as well, such as tracking down noise sources or illegal operators from unidentified stations. Jammers of repeaters, traffic nets and other amateur operations can be located with RDF equipment. Or sometimes a stolen amateur rig will be operated by a person who is not familiar with Amateur Radio, and by being lured into making repeated transmissions, the operator unsuspectingly permits himself to be located with RDF equipment. The ability of certain RDF antennas to reject signals from selected directions has also been used to advantage in reducing noise and interference. Through APRS, radio navigation is becoming a popular application of RDF. The locating of downed aircraft is another, and one in which amateurs often lend their skills. Indeed, there are many useful applications for RDF.

Although sophisticated and complex equipment pushing the state of the art has been developed for use by governments and commercial enterprises, relatively simple equipment can be built at home to offer the Radio Amateur an opportunity to RDF. This chapter deals with antennas suitable for that purpose.

RDF by Triangulation

It is impossible, using amateur techniques, to pinpoint the whereabouts of a transmitter from a single receiving location. With a directional antenna you can determine the direction of a signal source, but not how far away it is. To find the distance, you can then travel in the determined direction until you discover the transmitter location. However, that technique can be time consuming and often does not work very well.

A preferred technique is to take at least one additional direction measurement from a second receiving location. Then use a map of the area and plot the bearing or direction measurements as straight lines from points on the map representing the two locations. The approximate location of the transmitter will be indicated by the point where the two bearing lines cross. Even better results can be obtained by taking direction measurements from three locations and using the mapping technique just described. Because absolutely precise bearing measurements are difficult to obtain in practice, the three lines will almost always cross to form a triangle on the map, rather than at a single point. The transmitter will usually be located inside the area represented by the triangle. Additional information on the technique of triangulation and much more on RDF techniques may be found in recent editions of *The ARRL Handbook*.

DIRECTION FINDING SY\STEMS

Required for any RDF system are a directive antenna and a device for detecting the radio signal. In amateur applications the signal detector is usually a transceiver and for convenience it will usually have a meter to indicate signal strength. Unmodified, commercially available portable or mobile receivers are generally quite satisfac-

tory for signal detectors. At very close ranges a simple diode detector and dc microammeter may suffice for the detector.

On the other hand, antennas used for RDF techniques are not generally the types used for normal two-way communications. Directivity is a prime requirement, and here the word *directivity* takes on a somewhat different meaning than is commonly applied to other amateur antennas. Normally we associate directivity with gain, and we think of the ideal antenna pattern as one having a long, thin main lobe. Such a pattern may be of value for coarse measurements in RDF work, but precise bearing measurements are not possible. There is always a spread of a few (or perhaps many) degrees on the *nose* of the lobe, where a shift of antenna bearing produces no detectable change in signal strength. In RDF measure-ments, it is desirable to correlate an exact bearing or compass direction with the position of the antenna. In order to do this as accurately as possible, an antenna exhibiting a *null* in its pattern is used. A null can be very sharp in directivity, to within a half degree or less.

Loop Antennas

A simple antenna for HF RDF work is a small loop tuned to resonance with a capacitor. Several factors must be considered in the design of an RDF loop. The loop must be small in circumference compared with the wavelength. In a single-turn loop, the conductor should be less than 0.08 λ long. For 28 MHz, this represents a length of less than 34 inches (a diameter of approximately 10 inches). Maximum response from the loop antenna is in the plane of the loop, with nulls exhibited at right angles to that plane.

To obtain the most accurate bearings, the loop must be balanced electrostatically with respect to ground. Otherwise, the loop will exhibit two modes of operation. One is the mode of a true loop, while the other is that of an essentially nondirectional vertical antenna of small dimensions. This second mode is called the *antenna effect*. The voltages introduced by the two modes are seldom in phase and may add or subtract, depending upon the direction from which the wave is coming.

The theoretical true loop pattern is illustrated in **Fig 1A**. When properly balanced, the loop exhibits two nulls that are 180° apart. Thus, a single null reading with a small loop antenna will not indicate the exact direction toward the transmitter—only the line along which the transmitter lies. Ways to overcome this ambiguity are discussed later.

When the antenna effect is appreciable and the loop is tuned to resonance, the loop may exhibit little directivity, as shown in Fig 1B. However, by detuning the loop to shift the phasing, a pattern similar to 1C may be obtained. Although this pattern is not symmetrical, it does exhibit a null. Even so, the null may not be as sharp as that obtained with a loop that is well balanced, and it may not be at exact right angles to the plane of the loop.

By suitable detuning, the unidirectional cardioid pattern of Fig 1D may be approached. This adjustment is sometimes used in RDF work to obtain a unidirectional bearing, although there is no complete null in the pattern. A cardioid pattern can also be obtained with a small loop antenna by adding a *sensing element*. Sensing elements are discussed in a later section of this chapter.

An electrostatic balance can be obtained by shielding the loop, as **Fig 2** shows. The shield is represented by the broken lines in the drawing, and eliminates the antenna effect. The response of a well-constructed shielded loop is quite close to the ideal pattern of Fig 1A.

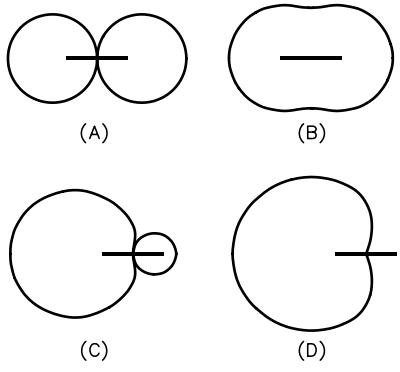

Fig 1—Small-loop field patterns with varying amounts of antenna effect—the undesired response of the loop acting merely as a mass of metal connected to the receiver antenna terminals. The straight lines show the plane of the loop.

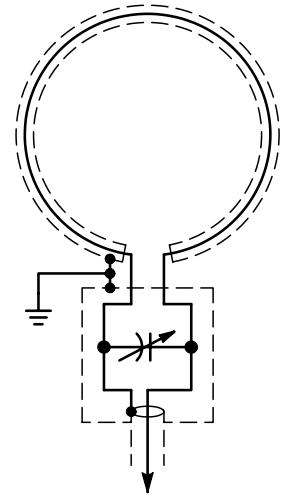

Fig 2—Shielded loop for direction finding. The ends of the shielding turn are not connected, to prevent shielding the loop from magnetic fields. The shield is effective against electric fields.

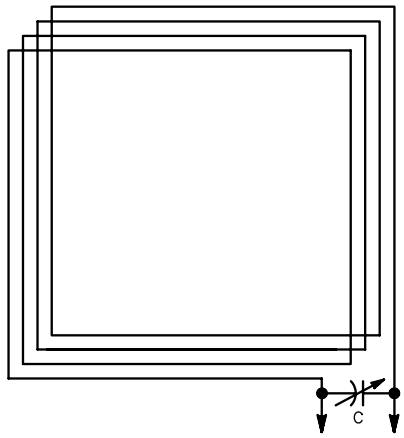

Fig 3—Small loop consisting of several turns of wire. The total conductor length is very much less than a wavelength. Maximum response is in the plane of the loop.

For the low-frequency amateur bands, single-turn loops of convenient physical size for portability are generally found to be unsatisfactory for RDF work. Therefore, multiturn loops are generally used instead. Such a loop is shown in **Fig 3**. This loop may also be shielded, and if the total conductor length remains below 0.08 λ, the directional pattern is that of Fig 1A. A sensing element may also be used with a multiturn loop.

Loop Circuits and Criteria

No single word describes a direction-finding loop of high performance better than *symmetry*. To obtain an undistorted response pattern from this type of antenna, you must build it in the most symmetrical manner possible. The next key word is *balance*. The better the electrical balance, the deeper the loop null and the sharper the maxima.

The physical size of the loop for 7 MHz and below is not of major consequence. A 4-foot diameter loop will exhibit the same electrical characteristics as one which is only an inch or two in diameter. The smaller the loop, however, the lower its efficiency. This is because its aperture samples a smaller section of the wave front. Thus, if you use loops that are very small in terms of a wavelength, you will need preamplifiers to compensate for the reduced efficiency.

An important point to keep in mind about a small loop antenna oriented in a vertical plane is that it is vertically polarized. It should be fed at the bottom for the best null response. Feeding it at one side, rather than at the bottom, will not alter the polarization and will only degrade performance. To obtain horizontal polarization from a small loop, it must be oriented in a horizontal plane, parallel to the earth. In this position the loop response is essentially omnidirectional.

The earliest loop antennas were of the *frame antenna* variety. These were unshielded antennas built on a wooden frame in a rectangular format. The loop conductor could be a single turn of wire (on the larger units) or several turns if the frame was small. Later, shielded versions of the frame antenna became popular, providing electrostatic shielding—an aid to noise reduction from such sources as precipitation static.

Ferrite Rod Antennas

With advances in technology, magnetic-core loop antennas came into use. Their advantage was reduced size, and this appealed especially to the designers of aircraft and portable radios. Most of these antennas contain ferrite bars or cylinders, which provide high inductance and Q with a relatively small number of coil turns.

Magnetic-core antennas consist essentially of turns of wire around a ferrite rod. They are also known as *loopstick* antennas. Probably the best-known example of this type of antenna is that used in small portable AM broadcast receivers. Because of their reduced-size advantage, ferrite-rod antennas are used almost exclusively for portable work at frequencies below 150 MHz.

As implied in the earlier discussion of shielded loops in this chapter, the true loop antenna responds to the magnetic field of the radio wave, and not to the electrical field. The voltage delivered by the loop is proportional to the amount of magnetic flux passing through the coil, and to the number of turns in the coil. The action is much the same as in the secondary winding of a transformer. For a given size of loop, the output voltage can be increased by increasing the flux density, and this is done with a ferrite core of high permeability. A 1/2-inch diameter, 7-inch rod of Q2 ferrite (m_i = 125) is suitable for a loop core from the broadcast band through 10 MHz. For increased output, the turns may be wound on two rods that are taped together, as shown in **Fig 4**. Loopstick antennas for con-

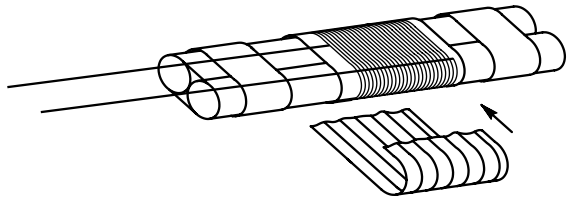

Fig 4—A ferrite-rod or loopstick antenna. Turns of wire may be wound on a single rod, or to increase the output from the loop, the core may be two rods taped together, as shown here. The type of core material must be selected for the intended frequency range of the loop. To avoid bulky windings, fine wire such as #28 or #30 is often used, with larger wire for the leads.

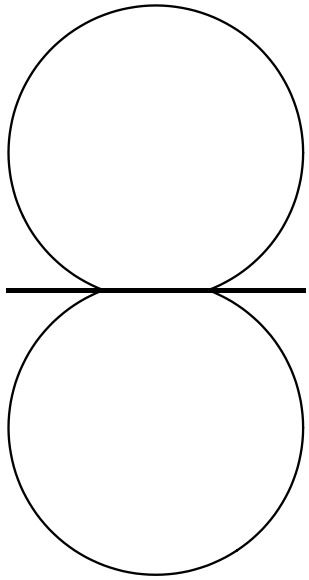

Fig 5—Field pattern for a ferrite rod antenna. The dark bar represents the rod on which the loop turns are wound.

struction are described later in this chapter.

Maximum response of the loopstick antenna is broadside to the axis of the rod as shown in **Fig 5**, whereas maximum response of the ordinary loop is in a direction at right angles to the plane of the loop. Otherwise, the performances of the ferrite-rod antenna and of the ordinary loop are similar. The loopstick may also be shielded to eliminate the antenna effect, such as with a U-shaped or C-shaped channel of aluminum or other form of *trough*. The length of the shield should equal or slightly exceed the length of the rod.

Sensing Antennas

Because there are two nulls that are 180° apart in the directional pattern of a loop or a loopstick, an ambiguity exists as to which one indicates the true direction of the station being tracked. For example, assume you take a bearing measurement and the result indicates the transmitter is somewhere on a line running approximately east and west from your position. With this single reading, you have no way of knowing for sure if the transmitter is east of you or west of you.

If more than one receiving station takes bearings on a single transmitter, or if a single receiving station takes bearings from more than one position on the transmitter, the ambiguity may be worked out by triangulation, as described earlier. However, it is sometimes desirable to have a pattern with only one null, so there is no question about whether the transmitter in the above example would be east or west from your position.

A loop or loopstick antenna may be made to have a

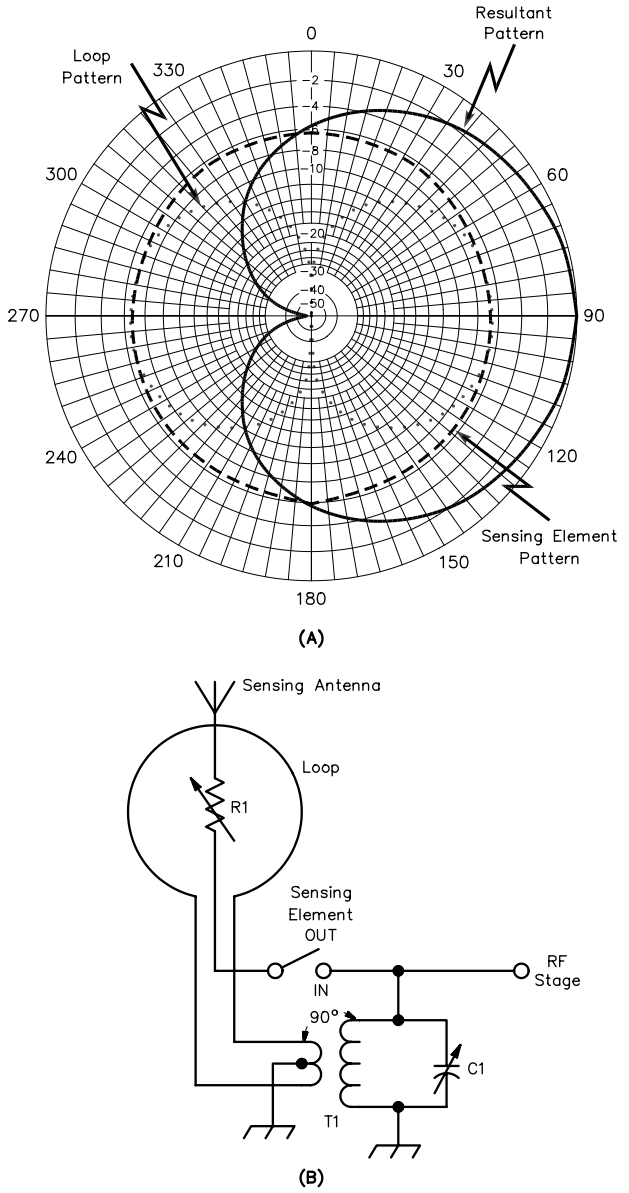

Fig 6—At A, the directivity pattern of a loop antenna with sensing element. At B is a circuit for combining the signals from the two elements. C1 is adjusted for resonance with T1 at the operating frequency.

single null if a second antenna element is added. The element is called a *sensing antenna*, because it gives an added sense of direction to the loop pattern. The second element must be omnidirectional, such as a short vertical. When the signals from the loop and the vertical element are combined with a 90° phase shift between the two, a cardioid pattern results. The development of the pattern is shown in **Fig 6A**.

Fig 6B shows a circuit for adding a sensing antenna to a loop or loopstick. R1 is an internal adjustment and is used to set the level of the signal from the sensing

antenna. For the best null in the composite pattern, the signals from the loop and the sensing antenna must be of equal amplitude, so R1 is adjusted experimentally during setup. In practice, the null of the cardioid is not as sharp as that of the loop, so the usual measurement procedure is to first use the loop alone to obtain a precise bearing reading, and then to add the sensing antenna and take another reading to resolve the ambiguity. (The null of the cardioid is 90° away from the nulls of the loop.) For this reason, provisions are usually made for switching the sensing element in an out of operation.

PHASED ARRAYS

Phased arrays are also used in amateur RDF work. Two general classifications of phased arrays are end-fire and broadside configurations. Depending on the spacing and phasing of the elements, end-fire patterns may exhibit a null in one direction along the axis of the elements. At the same time, the response is maximum off the other end of the axis, in the opposite direction from the null. A familiar arrangement is two elements spaced $^1/_4$ λ apart and fed 90° out of phase. The resultant pattern is a *cardioid*, with the null in the direction of the leading element. Other arrangements of spacing and phasing for an end-fire array are also suitable for RDF work. One of the best known is the *Adcock array*, discussed in the next section.

Broadside arrays are inherently bidirectional, which means there are always at least two nulls in the pattern. Ambiguity therefore exists in the true direction of the transmitter, but depending on the application, this may be no handicap. Broadside arrays are seldom used for amateur RDF applications however.

The Adcock Antenna

Loops are adequate in RDF applications where only the ground wave is present. The performance of an RDF system for sky-wave reception can be improved by the use of an Adcock antenna, one of the most popular types of end-fire phased arrays. A basic version is shown in **Fig 7**.

This system was invented by F. Adcock and patented in 1919. The array consists of two vertical elements fed 180° apart, and mounted so the system may be rotated. Element spacing is not critical, and may be in the range from 0.1 to 0.75 λ. The two elements must be of identical lengths, but need not be self-resonant. Elements that are shorter than resonant are commonly used. Because neither the element spacing nor the length is critical in terms of wavelengths, an Adcock array may be operated over more than one amateur band.

The response of the Adcock array to vertically polarized waves is similar to a conventional loop, and the directive pattern is essentially the same. Response of the array to a horizontally polarized wave is considerably different from that of a loop, however. The currents induced in the horizontal members tend to balance out regardless of the orientation of the antenna. This effect has been verified in practice, where good nulls were obtained with an experimental Adcock under sky-wave conditions. The same circumstances produced poor nulls with small loops (both conventional and ferrite-loop models).

Generally speaking, the Adcock antenna has attractive properties for amateur RDF applications. Unfortunately, its portability leaves something to be desired, making it more suitable to fixed or semi-portable applications. While a metal support for the mast and boom could be used, wood, PVC or fiberglass are preferable because they are nonconductors and would therefore cause less pattern distortion.

Since the array is balanced, an antenna tuner is required to match the unbalanced input of a typical receiver. **Fig 8** shows a suitable link-coupled network. C2 and C3 are null-balancing capacitors. A low-power signal source is placed some distance from the Adcock

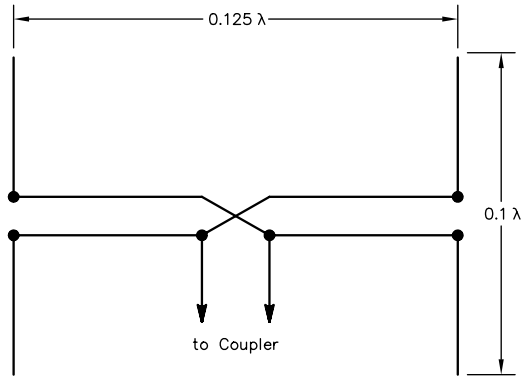

Fig 7—A simple Adcock antenna.

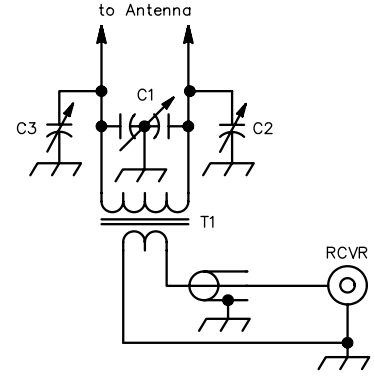

Fig 8—A suitable coupler for use with the Adcock antenna.

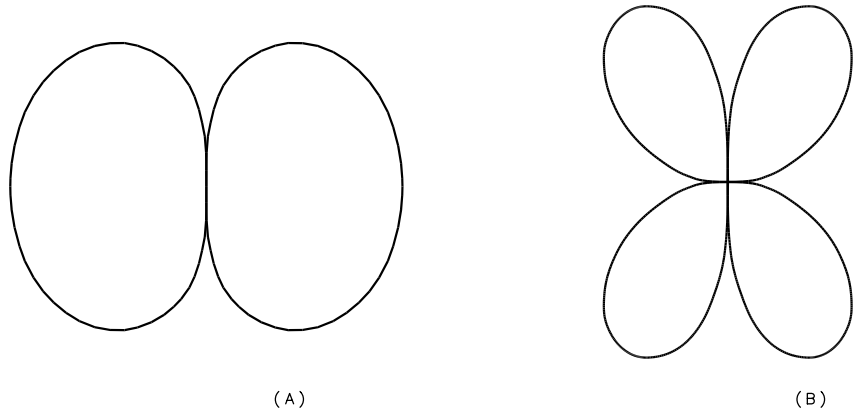

Fig 9—At A, the pattern of the Adcock array with an element spacing of $^1/_2$ wavelength. In these plots the elements are aligned with the horizontal axis. As the element spacing is increased beyond $^3/_4$ wavelength, additional nulls develop off the ends of the array, and at a spacing of 1 wavelength the pattern at B exists. This pattern is unsuitable for RDF work.

antenna and broadside to it. C2 and C3 are then adjusted until the deepest null is obtained. The tuner can be placed below the wiring-harness junction on the boom. Connection can be made by means of a short length of 300-Ω twin-lead.

The radiation pattern of the Adcock is shown in **Fig 9A**. The nulls are in directions broadside to the array, and become sharper with greater element spacings. However, with an element spacing greater than 0.75 λ, the pattern begins to take on additional nulls in the directions off the ends of the array axis. At a spacing of 1 λ the pattern is that of Fig 9B, and the array is unsuitable for RDF applications.

Short vertical monopoles are often used in what is sometimes called the *U-Adcock*, so named because the elements with their feeders take on the shape of the letter U. In this arrangement the elements are worked against the earth as a ground or counterpoise. If the array is used only for reception, earth losses are of no great consequence. Short, elevated vertical dipoles are also used in what is sometimes called the *H-Adcock*.

The Adcock array, with two nulls in its pattern, has the same ambiguity as the loop and the loopstick. Adding a sensing element to the Adcock array has not met with great success. Difficulties arise from mutual coupling between the array elements and the sensing element, among other things. Because Adcock arrays are used primarily for fixed-station applications, the ambiguity presents no serious problem. The fixed station is usually one of a group of stations in an RDF network.

LOOPS VERSUS PHASED ARRAYS

Although loops can be made smaller than suitable phased arrays for the same frequency of operation, the phased arrays are preferred by some for a variety of reasons. In general, sharper nulls can be obtained with phased arrays, but this is also a function of the care used in constructing and feeding the individual antennas, as well as of the size of the phased array in terms of wavelengths. The primary constructional consideration is the shielding and balancing of the feed line against unwanted signal pickup, and the balancing of the antenna for a symmetrical pattern.

Loops are not as useful for skywave RDF work because of random polarization of the received signal. Phased arrays are somewhat less sensitive to propagation effects, probably because they are larger for the same frequency of operation and therefore offer some space diversity. In general, loops and loopsticks are used for mobile and portable operation, while phased arrays are used for fixed-station operation. However, phased arrays are used successfully above 144 MHz for portable and mobile RDF work. Practical examples of both types of antennas are presented later in this chapter.

THE GONIOMETER

Most fixed RDF stations for government and commercial work use antenna arrays of stationary elements, rather than mechanically rotatable arrays. This has been true since the earliest days of radio. The early-day device that permits finding directions without moving the elements is called a *radiogoniometer*, or simply a *goniometer*. Various types of goniometers are still used today in many installations, and offer the amateur some possibilities.

The early style of goniometer is a special form of RF transformer, as shown in **Fig 10**. It consists of two fixed coils mounted at right angles to one another. Inside the fixed coils is a movable coil, not shown in Fig 10 to

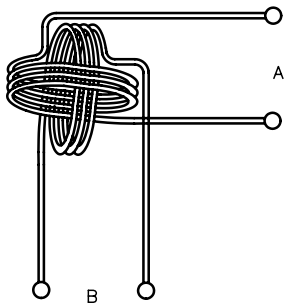

Fig 10—An early type of goniometer that is still used today in some RDF applications. This device is a special type of RF transformer that permits a movable coil in the center (not shown here) to be rotated and determine directions even though the elements are stationary.

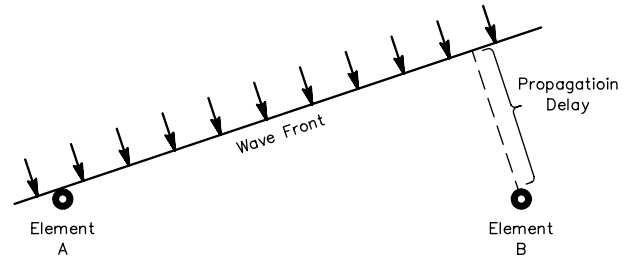

Fig 11—This diagram illustrates one technique used in electronic beam forming. By delaying the signal from element A by an amount equal to the propagation delay, the two signals may be summed precisely in phase, even though the signal is not in the broadside direction. Because this time delay is identical for all frequencies, the system is not frequency sensitive.

avoid cluttering the diagram. The pairs of connections marked A and B are connected respectively to two elements in an array, and the output to the detector or receiver is taken from the movable coil. As the inner coil is rotated, the coupling to one fixed coil increases while that to the other decreases. Both the amplitude and the phase of the signal coupled into the pickup winding are altered with rotation in a way that corresponds to actually rotating the array itself. Therefore, the rotation of the inner coil can be calibrated in degrees to correspond to bearing angles from the station location.

In the early days of radio, the type of goniometer just described saw frequent use with fixed Adcock arrays. A refinement of that system employed four Adcock elements, two arrays at right angles to each other. With a goniometer arrangement, RDF measurements could be taken in all compass directions, as opposed to none off the ends of a two-element fixed array. However, resolution of the 4-element system was not as good as with a single pair of elements, probably because of mutual coupling among the elements. To overcome this difficulty a few systems of eight elements were installed.

Various other types of goniometers have been developed over the years, such as commutator switching to various elements in the array. A later development is the diode switching of capacitors to provide a commutator effect. As mechanical action has gradually been replaced with electronics to "rotate" stationary elements, the word goniometer is used less frequently these days. However, it still appears in many engineering reference texts. The more complex electronic systems of today are called *beam-forming networks*.

Electronic Antenna Rotation

With an array of many fixed elements, beam rotation can be performed electronically by sampling and combining signals from various individual elements in the array. Contingent upon the total number of elements in the system and their physical arrangement, almost any desired antenna pattern can be formed by summing the sampled signals in appropriate amplitude and phase relationships. Delay networks are used for some of the elements before the summation is performed. In addition, attenuators may be used for some elements to develop patterns such as from an array with binomial current distribution.

One system using these techniques is the *Wullenweber* antenna, employed primarily in government and military installations. The Wullenweber consists of a very large number of elements arranged in a circle, usually outside of (or in front of) a circular reflecting screen. Depending on the installation, the circle may be anywhere from a few hundred feet to more than a quarter of a mile in diameter. Although the Wullenweber is not one that would be constructed by an amateur, some of the techniques it uses may certainly be applied to Amateur Radio.

For the moment, consider just two elements of a Wullenweber antenna, shown as A and B in **Fig 11**. Also shown is the wavefront of a radio signal arriving from a distant transmitter. As drawn, the wavefront strikes element A first, and must travel somewhat farther before it strikes element B. There is a finite time delay before the wavefront reaches element B.

The propagation delay may be measured by delaying the signal received at element A before summing it with that from element B. If the two signals are combined directly, the amplitude of the resultant signal will be maximum when the delay for element A exactly equals the propagation delay. This results in an in-phase condition at the summation point. Or if one of the signals is inverted and the two are summed, a null will exist when the element-A delay equals the propagation delay; the signals will combine in a 180° out-of-phase relationship. Either way, once the time delay is known, it may be converted to distance. Then the direction from which the wave

is arriving may be determined by trigonometry.

By altering the delay in small increments, the peak of the antenna lobe (or the null) can be steered in azimuth. This is true without regard to the frequency of the incoming wave. Thus, as long as the delay is less than the period of one RF cycle, the system is not frequency sensitive, other than for the frequency range that may be covered satisfactorily by the array elements themselves. Surface acoustic wave (SAW) devices or lumped-constant networks can be used for delay lines in such systems if the system is used only for receiving. Rolls of coaxial cable of various lengths are used in installations for transmitting. In this case, the lines are considered for the time delay they provide, rather than as simple phasing lines. The difference is that a phasing line is ordinarily designed for a single frequency (or for an amateur band), while a delay line offers essentially the same time delay at all frequencies.

By combining signals from other Wullenweber elements appropriately, the broad beamwidth of the pattern from the two elements can be narrowed, and unwanted sidelobes can be suppressed. Then, by electronically switching the delays and attenuations to the various elements, the beam so formed can be rotated around the compass. The package of electronics designed to do this, including delay lines and electronically switched attenuators, is the beam-forming network. However, the Wullenweber system is not restricted to forming a single beam. With an isolation amplifier provided for each element of the array, several beam-forming networks can be operated independently. Imagine having an antenna system that offers a dipole pattern, a rhombic pattern, and a Yagi beam pattern, all simultaneously and without frequency sensitivity. One or more may be rotating while another is held in a particular direction. The Wullenweber was designed to fulfill this type of requirement.

One feature of the Wullenweber antenna is that it can operate 360° around the compass. In many government installations, there is no need for such coverage, as the areas of interest lie in an azimuth sector. In such cases an in-line array of elements with a backscreen or curtain reflector may be installed broadside to the center of the sector. By using the same techniques as the Wullenweber, the beams formed from this array may be slewed left and right across the sector. The maximum sector width available will depend on the installation, but beyond 70° to 80° the patterns begin to deteriorate to the point that they are unsatisfactory for precise RDF work.

RDF SYSTEM CALIBRATION AND USE

Once an RDF system is initially assembled, it should be calibrated or checked out before actually being put into use. Of primary concern is the balance or symmetry of the antenna pattern. A lop-sided figure-8 pattern with a loop, for example, is undesirable; the nulls are not 180° apart, nor are they at exact right angles to the plane of the loop. If you didn't know this fact in actual RDF work, measurement accuracy would suffer.

Initial checkout can be performed with a low-powered transmitter at a distance of a few hundred feet. It should be within visual range and must be operating into a vertical antenna. (A quarter-wave vertical or a loaded whip is quite suitable.) The site must be reasonably clear of obstructions, especially steel and concrete or brick buildings, large metal objects, nearby power lines, and so on. If the system operates above 30 MHz, you should also avoid trees and large bushes. An open field makes an excellent site.

The procedure is to find the transmitter with the RDF equipment as if its position were not known, and compare the RDF null indication with the visual path to the transmitter. For antennas having more than one null, each null should be checked.

If imbalance is found in the antenna system, there are two options available. One is to correct the imbalance. Toward this end, pay particular attention to the feed line. Using a coaxial feeder for a balanced antenna invites an asymmetrical pattern, unless an effective balun is used. A balun is not necessary if the loop is shielded, but an asymmetrical pattern can result with misplacement of the break in the shield itself. The builder may also find that the presence of a sensing antenna upsets the balance slightly, due to mutual coupling. Experiment with its position with respect to the main antenna to correct the error. You will also note that the position of the null shifts by 90° as the sensing element is switched in and out, and the null is not as deep. This is of little concern, however, as the intent of the sensing antenna is only to resolve ambiguities. The sensing element should be switched out when accuracy is desired.

The second option is to accept the imbalance of the antenna and use some kind of indicator to show the true directions of the nulls. Small pointers, painted marks on the mast, or an optical sighting system might be used. Sometimes the end result of the calibration procedure will be a compromise between these two options, as a perfect electrical balance may be difficult or impossible to attain.

The discussion above is oriented toward calibrating portable RDF systems. The same general suggestions apply if the RDF array is fixed, such as an Adcock. However, it won't be possible to move it to an open field. Instead, the array must be calibrated in its intended operating position through the use of a portable or mobile transmitter. Because of nearby obstructions or reflecting objects, the null in the pattern may not appear to indicate the precise direction of the transmitter. Do not confuse this with imbalance in the RDF array. Check for imbalance by rotating the array 180° and comparing readings.

Once the balance is satisfactory, you should make a table of bearing errors noted in different compass directions. These error values should be applied as corrections when actual measurements are made. The mobile or por-

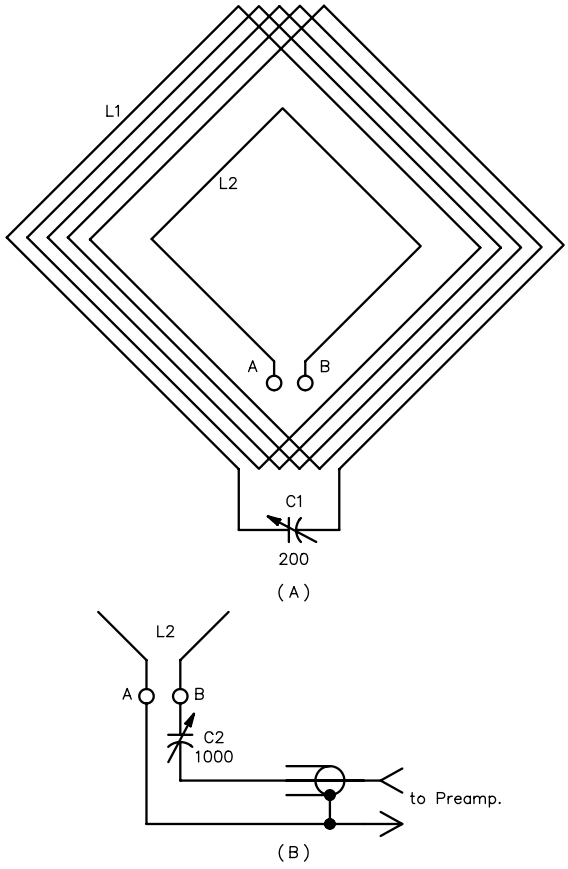

Fig 12—A multiturn frame antenna is shown at A. L2 is the coupling loop. The drawing at B shows how L2 is connected to a preamplifier.

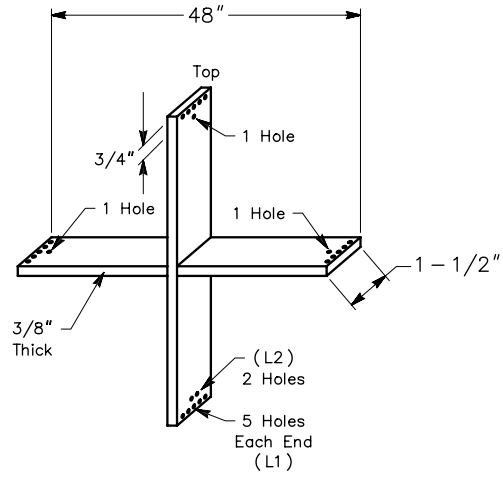

Fig 13—A wooden frame can be used to contain the wire of the loop shown in Fig 12.

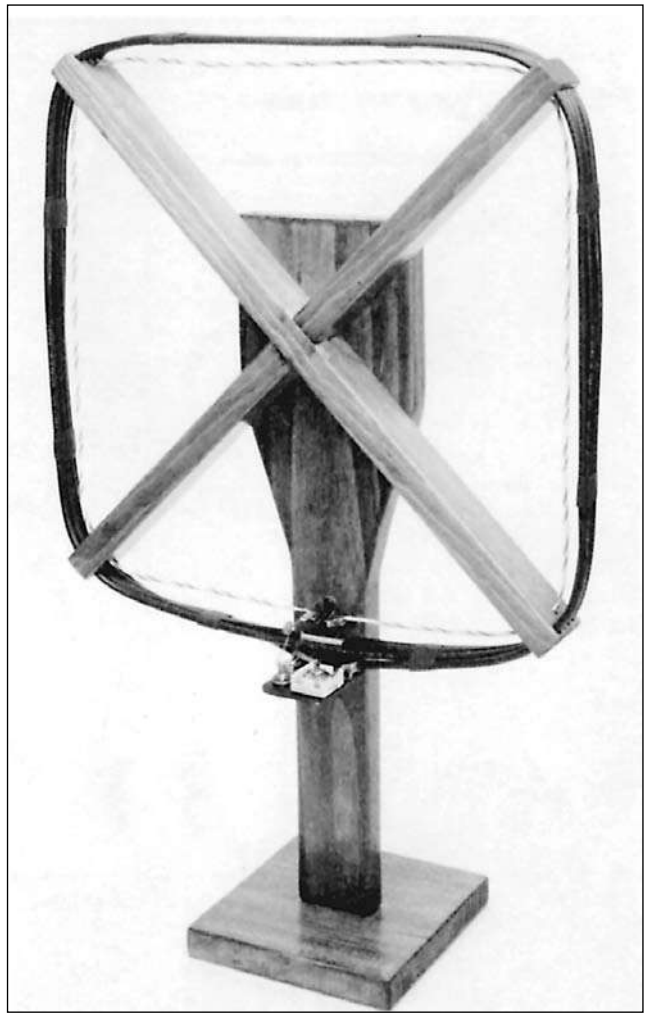

Fig 14—An assembled table-top version of the electrostatically shielded loop. RG-58 cable is used in its construction.

table transmitter should be at a distance of two or three miles for these measurements, and should be in as clear an area as possible during transmissions. The idea is to avoid conduction of the signal along power lines and other overhead wiring from the transmitter to the RDF site. Of course the position of the transmitter must be known accurately for each transmission.

FRAME LOOPS

It was mentioned earlier that the earliest style of receiving loops was the frame antenna. If carefully constructed, such an antenna performs well and can be built at low cost. **Fig 12** illustrates the details of a practical frame type of loop antenna. This antenna was designed by Doug DeMaw, W1FB, and described in *QST* for July 1977. (See the Bibliography at the end of this chapter.) The circuit in Fig 12A is a 5-turn system tuned to resonance by C1. If the layout is symmetrical, good balance should be obtained. L2 helps to achieve this objective by eliminating the need for direct coupling to the feed ter-

minals of L1. If the loop feed were attached in parallel with C1, a common practice, the chance for imbalance would be considerable.

L2 can be situated just inside or slightly outside of L1; a 1-inch separation works nicely. The receiver or preamplifier can be connected to terminals A and B of L2, as shown in Fig 12B. C2 controls the amount of coupling between the loop and the preamplifier. The lighter the coupling, the higher is the loop Q, the narrower is the frequency response, and the greater is the gain requirement from the preamplifier. It should be noted that no attempt is being made to match the extremely low loop impedance to the preamplifier.

A supporting frame for the loop of Fig 12 can be constructed of wood, as shown in **Fig 13**. The dimensions given are for a 1.8-MHz frame antenna. For use on 75 or 40 meters, L1 of Fig 12A will require fewer turns, or the size of the wooden frame should be made somewhat smaller than that of Fig 13.

SHIELDED FRAME LOOPS

If electrostatic shielding is desired, the format shown in **Fig 14** can be adopted. In this example, the loop conductor and the single-turn coupling loop are made from RG-58 coaxial cable. The number of loop turns should be sufficient to resonate with the tuning capacitor at the operating frequency. Antenna resonance can be checked by first connecting C1 (Fig 12A) and setting it at midrange. Then connect a small 3-turn coil to the loop feed terminals, and couple to it with a dip meter. Just remember that the pickup coil will act to lower the frequency slightly from actual resonance.

In the antenna photographed for Fig 14, the 1-turn coupling loop was made of #22 plastic-insulated wire. However, electrostatic noise pickup occurs on such a coupling loop, noise of the same nature that the shield on the main loop prevents. This can be avoided by using RG-58 for the coupling loop. The shield of the coupling loop should be opened for about 1 inch at the top, and each end of the shield grounded to the shield of the main loop.

Larger single-turn frame loops can be fashioned from aluminum-jacketed Hardline, if that style of coax is available. In either case, the shield conductor must be opened at the electrical center of the loop, as shown in **Fig 15** at A and B. The design example is for 1.8-MHz operation.

To realize the best performance from an electrostatically shielded loop antenna, you must operate it near to and directly above an effective ground plane. An automobile roof (metal) qualifies nicely for small shielded loops. For fixed-station use, a chicken-wire ground screen can be placed below the antenna at a distance of 1 to 6 feet.

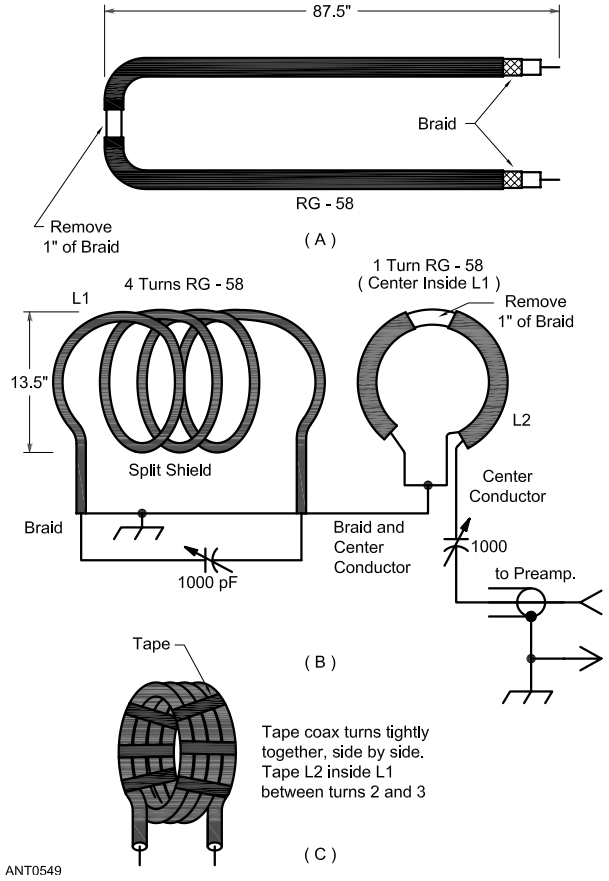

Fig 15—Components and assembly details of the shielded loop shown in Fig 14.

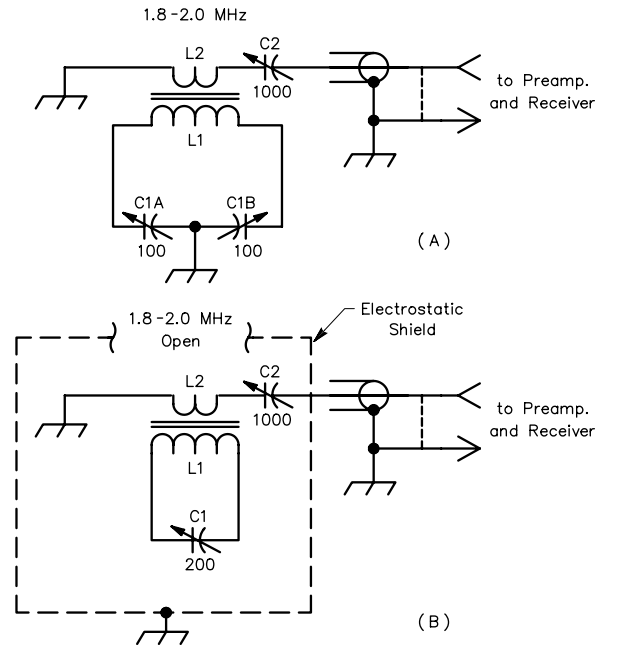

Fig 16—At A, the diagram of a ferrite loop. C1 is a dual-section air-variable capacitor. The circuit at B shows a rod loop contained in an electrostatic shield channel (see text). A suitable low-noise preamplifier is shown in Fig 19.

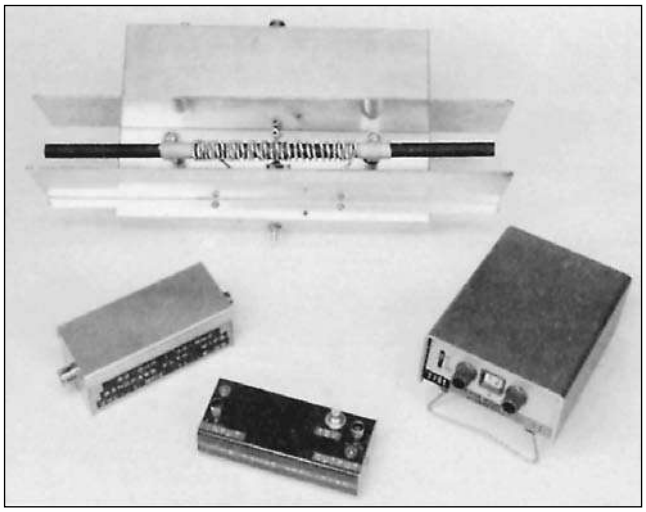

Fig 17—The assembly at the top of the picture is a shielded ferrite-rod loop for 160 meters. Two rods have been glued end to end (see text). The other units in the picture are a low-pass filter (lower left), broadband preamplifier (lower center) and a Tektronix step attenuator (lower right). These were part of the test setup used when the antenna was evaluated.

FERRITE-CORE LOOPS

Fig 16 contains a diagram for a rod loop (loopstick antenna). This antenna was also designed by Doug DeMaw, W1FB, and described in *QST* for July 1977. The winding (L1) has the appropriate number of turns to permit resonance with C1 at the operating frequency. L1 should be spread over approximately 1/3 of the core center. Litz wire will yield the best Q, but Formvar magnet wire can be used if desired. A layer of 3M Company glass tape (or Mylar tape) is recommended as a covering for the core before adding the wire. Masking tape can be used if nothing else is available.

L2 functions as a coupling link over the exact center of L1. C1 is a dual-section variable capacitor, although a differential capacitor might be better toward obtaining optimum balance. The loop Q is controlled by means of C2, which is a mica-compression trimmer.

Electrostatic shielding of rod loops can be effected by centering the rod in a U-shaped aluminum, brass or copper channel, extending slightly beyond the ends of the rod loop (1 inch is suitable). The open side (top) of the channel can't be closed, as that would constitute a shorted turn and render the antenna useless. This can be proved by shorting across the center of the channel with a screwdriver blade when the loop is tuned to an incoming signal. The shield-braid gap in the coaxial loop of Fig 15 is maintained for the same reason.

Fig 17 shows the shielded rod loop assembly. This antenna was developed experimentally for 160 meters and uses two 7-inch ferrite rods, glued together end-to-end with epoxy cement. The longer core resulted in improved sensitivity for weak-signal reception. The other items in the photograph were used during the evaluation tests and are not pertinent to this discussion. This loop and the frame loop discussed in the previous section have bidirectional nulls, as shown in Fig 1A.

Obtaining a Cardioid Pattern

Although the bidirectional pattern of loop antennas

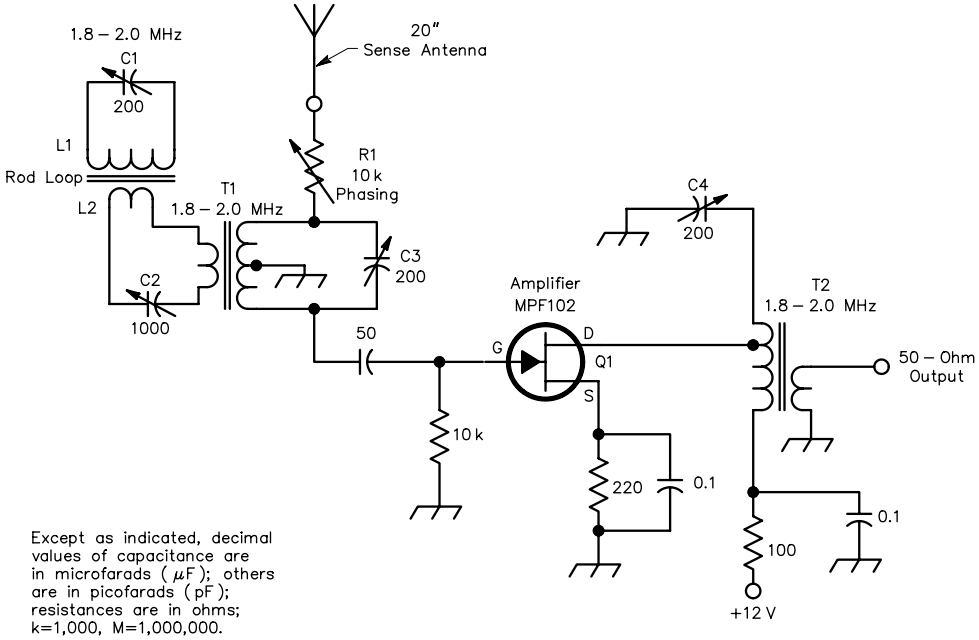

Fig 18—Schematic diagram of a rod-loop antenna with a cardioid response. The sensing antenna, phasing network and a preamplifier are shown also. The secondary of T1 and the primary of T2 are tuned to resonance at the operating frequency of the loop. T-68-2 to T-68-6 Amidon toroid cores are suitable for both transformers. Amidon also sells ferrite rods for this type of antenna.

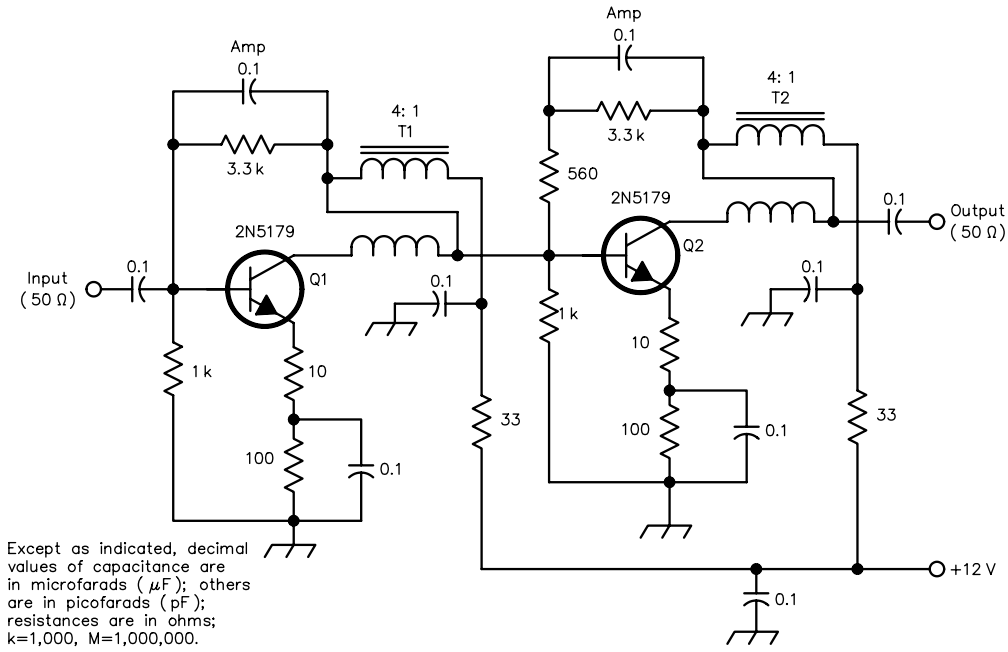

Fig 19—Schematic diagram of a two-stage broadband amplifier patterned after a design by Wes Hayward, W7ZOI. T1 and T2 have a 4:1 impedance ratio and are wound on FT-50-61 toroid cores (Amidon) which have a μ_i of 125. They contain 12 turns of #24 enamel wire, bifilar wound. The capacitors are disc ceramic. This amplifier should be built on double-sided circuit board for best stability.

can be used effectively in tracking down signal sources by means of triangulation, an essentially unidirectional loop response will help to reduce the time spent finding the fox. Adding a sensing antenna to the loop is simple to do, and it will provide the desired cardioid response. The theoretical pattern for this combination is shown in Fig 1D.

Fig 18 shows how a sensing element can be added to a loop or loopstick antenna. The link from the loop is connected by coaxial cable to the primary of T1, which is a tuned toroidal transformer with a split secondary winding. C3 is adjusted for peak signal response at the frequency of interest (as is C4), then R1 is adjusted for minimum back response of the loop. It will be necessary to readjust C3 and R1 several times to compensate for the interaction of these controls. The adjustments are repeated until no further null depth can be obtained. Tests at ARRL Headquarters showed that null depths as great as 40 dB could be obtained with the circuit of Fig 18 on 75 meters. A near-field weak-signal source was used during the tests.

The greater the null depth, the lower the signal output from the system, so plan to include a preamplifier with 25 to 40 dB of gain. Q1 shown in Fig 18 will deliver approximately 15 dB of gain. The circuit of **Fig 19** can be used following T2 to obtain an additional 24 dB of gain. In the interest of maintaining a good noise figure, even at 1.8 MHz, Q1 should be a low-noise device. A 2N4416, an MPF102, or a 40673 MOSFET would be satisfactory. The sensing antenna can be mounted 6 to 15 inches from the loop. The vertical whip need not be more than 12 to 20 inches long. Some experimenting may be necessary in order to obtain the best results. Optimization will also change with the operating frequency of the antenna.

A SHIELDED LOOP WITH SENSING ANTENNA FOR 28 MHz

Fig 20 shows the construction and mounting of a simple shielded 10-meter loop. The loop was designed by Loren Norberg, W9PYG, and described in *QST* for April 1954. (See the Bibliography at the end of this chapter.) It is made from an 18-inch length of RG-11 coax (either solid or foam dielectric) secured to an aluminum box of any convenient size, with two coaxial cable hoods (Amphenol 83-1HP). The outer shield must be broken at the exact center. C1 is a 25-pF variable capacitor, and is connected in parallel with a 33-pF fixed mica padder capacitor, C3. C1 must be tuned to the desired frequency while the loop is connected to the receiver in the same way as it will be used for RDF. C2 is a small differential capacitor used to provide electrical symmetry. The lead-in to the receiver is 67 inches of RG-59 (82 inches if the cable has a foamed dielectric).

The loop can be mounted on the roof of the car with a rubber suction cup. The builder might also fabricate some kind of bracket assembly to mount the loop tempo-

rarily in the window opening of the automobile, allowing for loop rotation. Reasonably true bearings may be obtained through the windshield when the car is pointed in the direction of the hidden transmitter. More accurate bearings may be obtained with the loop held out the window and the signal coming toward that side of the car.

Sometimes the car broadcast antenna may interfere with accurate bearings. Disconnecting the antenna from the broadcast receiver may eliminate this trouble.

Sensing Antenna

A sensing antenna can be added to Norberg's loop above to determine which of the two directions indicated by the loop is the correct one. Add a phono jack to the top of the aluminum case shown in Fig 20. The insulated center terminal of the jack should be connected to the side of the tuning capacitors that is common to the center conductor of the RG-59 coax feed line. The jack then takes a short vertical antenna rod of the diameter to fit the jack, or a piece of #12 or #14 solid wire may be soldered to the center pin of a phono plug for insertion in the jack. The sensing antenna can be plugged in as needed. Starting with a length of about four times the loop diameter, the length of the sensing antenna should be pruned until the pattern is similar to that of Fig 1D.

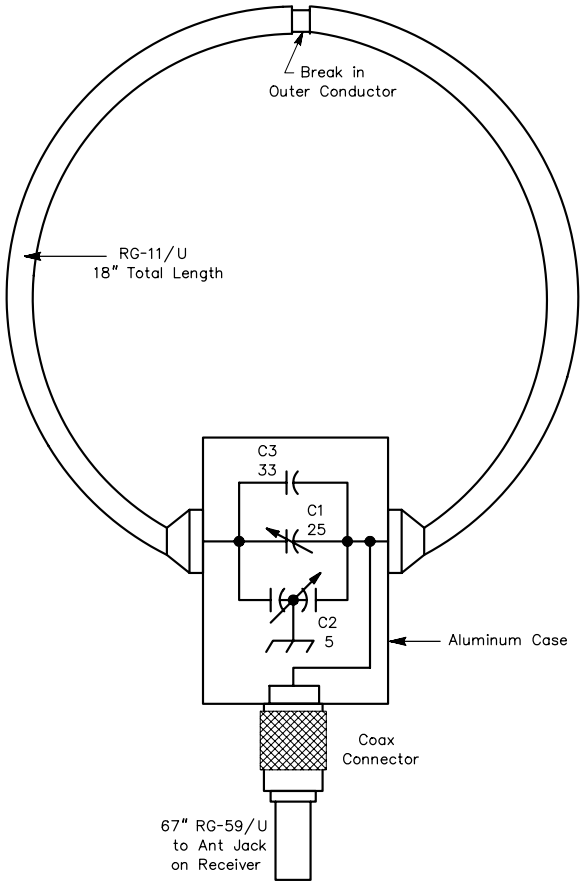

Fig 20—Sketch showing the constructional details of the 28-MHz RDF loop. The outer braid of the coax loop is broken at the center of the loop. The gap is covered with waterproof tape, and the entire assembly is given a coat of acrylic spray.

THE SNOOP LOOP—FOR CLOSE-RANGE HF RDF

Picture yourself on a hunt for a hidden 28-MHz transmitter. The night is dark, very dark. After you take off at the start of the hunt, heading in the right direction, the signal gets stronger and stronger. Your excitement increases with each additional S unit on the meter. You follow your loop closely, and it is working perfectly. You're getting out of town and into the countryside. The roads are unfamiliar. Now the null is beginning to swing rather rapidly, showing that you are getting close.

Suddenly the null shifts to give a direction at right angles to the car. With your flashlight you look carefully across the deep ditch beside the road and into the dark field where you know the transmitter is hidden. There are no roads into the field as far as you can see in either direction. You dare not waste miles driving up and down the road looking for an entrance, for each tenth of a mile counts. But what to do?—Your HF transceiver is mounted in your car and requires power from your car battery.

In a brief moment your decision is made. You park

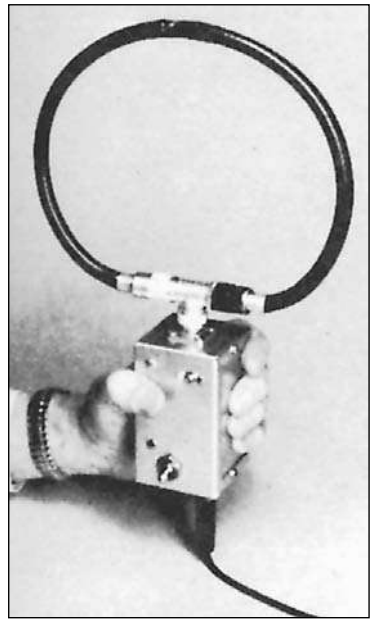

Fig 21—The box containing the detector and amplifier is also the "handle" for the Snoop Loop. The loop is mounted with a coax T as a support, a convenience but not an essential part of the loop assembly. The loop tuning capacitor is screwdriver adjusted. The on-off switch and the meter sensitivity control may be mounted on the bottom.

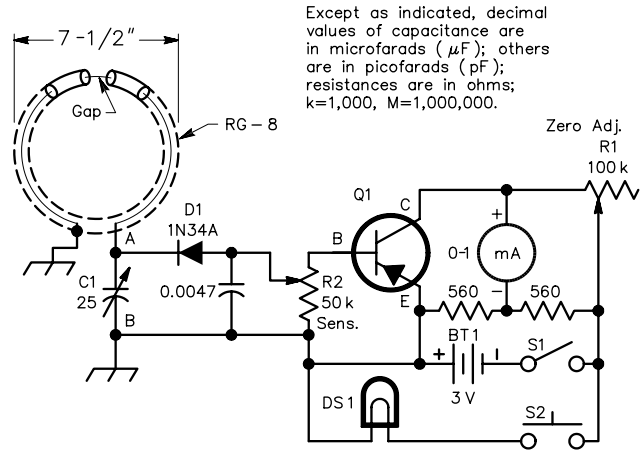

Fig 22—The Snoop Loop circuit for 28-MHz operation. The loop is a single turn of RG-8 inner conductor, the outer conductor being used as a shield. Note the gap in the shielding; about a 1-inch section of the outer conductor should be cut out. Refer to Fig 23 for alternative connection at points A and B for other frequencies of operation.

BT1—Two penlight cells.
C1—25-pF midget air padder.
D1—Small-signal germanium diode such as 1N34A or equiv.
DS1—Optional 2-cell penlight lamp for meter illumination, such as no. 222.
Q1—PNP transistor such as ECG102 or equiv.
R1—100-kΩ potentiometer, linear taper. May be PC-mount style.
R2—50-kΩ potentiometer, linear taper.
S1—SPST toggle.
S2—Optional momentary push for illuminating meter.

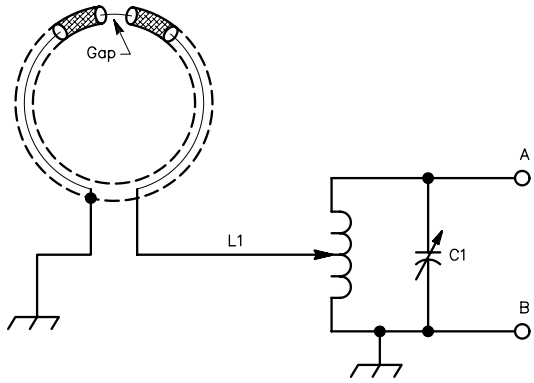

Fig 23—Input circuit for lower frequency bands. Points A and B are connected to corresponding points in the circuit of Fig 22, substituting for the loop and C1 in that circuit. L1-C1 should resonate within the desired amateur band, but the L/C ratio is not critical. After construction is completed, adjust the position of the tap on L1 for maximum signal strength. Instead of connecting the RDF loop directly to the tap on L1, a length of low impedance line may be used between the loop and the tuned circuit, L1-C1.

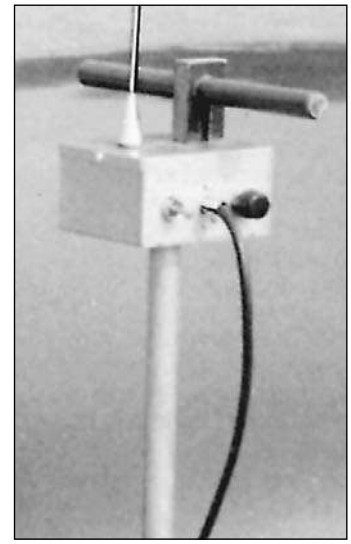

Fig 24—Unidirectional 3.5-MHz RDF using ferrite-core loop with sensing antenna. Adjustable components of the circuit are mounted in the aluminum chassis supported by a short length of tubing.

beside the road, take your flashlight, and plunge into the veldt in the direction your loop null clearly indicated. But after taking a few steps, you're up to your armpits in brush and can't see anything forward or backward. You stumble on in hopes of running into the hidden transmitter—you're probably not more than a few hundred feet from it. But away from your car and radio equipment, it's like the proverbial hunt for the needle in the haystack. What you really need is a portable setup for hunting at close range, and you may prefer something that is inexpensive. The Snoop Loop was designed for just these requirements by Claude Maer, Jr, WØIC, and was described in *QST* for February 1957. (See the Bibliography at the end of this chapter.)

The Snoop Loop is pictured in **Fig 21**. The loop itself is made from a length of RG-8 coax, with the shield broken at the top. A coax T connector is used for convenience and ease of mounting. One end of the coax loop is connected to a male plug in the conventional way, but the center conductor of the other end is shorted to the shield so the male connector at that end has no connection to the center prong. This results in an unbalanced circuit, but seems to give good bidirectional null readings, as well as an easily detectable maximum reading when the grounded end of the loop is pointed in the direction of the transmitter. Careful tuning with C1 will improve this maximum reading. Don't forget to remove one inch of shielding from the top of the loop. You won't get much signal unless you do.

The detector and amplifier circuit for the Snoop Loop

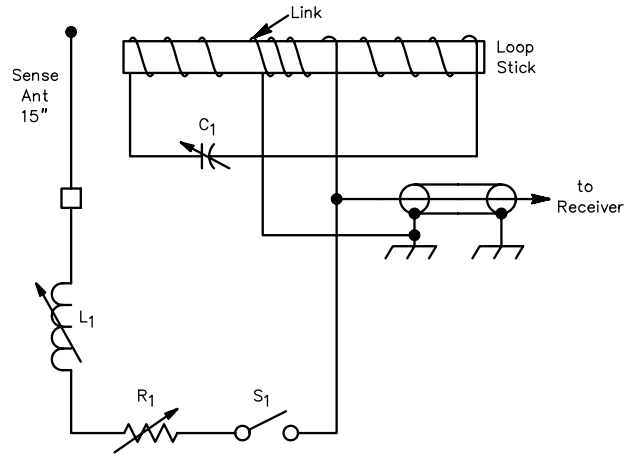

Fig 25—Circuit of the 3.5-MHz direction finder loop.
C1—140 pF variable (125-pF ceramic trimmer in parallel with 15-pF ceramic fixed.
L1—Approximately 140 µH adjustable (Miller No. 4512 or equivalent.
R1—1-kΩ carbon potentiometer.
S1—SPST toggle.
Loopstick—Approximately 15 µH (Miller 705-A, with original winding removed and wound with 20 turns of #22 enamel). Link is two turns at center. Winding ends secured with Scotch electrical tape. This type of ferrite rod may also be found in surplus transistor AM radios.

is shown in **Fig 22**. The model photographed does not include the meter, as it was built for use only with high-impedance headphones. The components are housed in an aluminum box. Almost any size box of sufficient size to contain the meter can be used. At very close ranges, reduction of sensitivity with R2 will prevent pegging the meter.

The Snoop Loop is not limited to the 10-meter band or to a built-in loop. **Fig 23** shows an alternative circuit for other bands and for plugging in a separate loop connected by a low-impedance transmission line. Select coil and capacitor combinations that will tune to the desired frequencies. Plug-in coils could be used. It is a good idea to have the RF end of the unit fairly well shielded, to eliminate signal pickup except through the loop. This little unit should certainly help you on those dark nights in the country. (Tip to the hidden-transmitter operator—if you want to foul up some of your pals using these loops, just hide near the antenna of a 50-kW broadcast transmitter!)

A LOOPSTICK FOR 3.5 MHz

Figs 24 through 26 show an RDF loop suitable for the 3.5-MHz band. It uses a construction technique that has had considerable application in low-frequency marine direction finders. The loop is a coil wound on a ferrite rod from a broadcast-antenna loopstick. The loop was designed by John Isaacs, W6PZV, and described in *QST* for June 1958. Because you can make a coil with high Q using a ferrite core, the sensitivity of such a loop is comparable to a conventional loop that is a foot or so in diameter. The output of the vertical-rod sensing antenna, when properly combined with that of the loop, gives the system the cardioid pattern shown in Fig 1D.

To make the loop, remove the original winding on the ferrite core and wind a new coil, as shown in **Fig 25**. Other types of cores than the one specified may be substituted; use the largest coil available and adjust the winding so that the circuit resonates in the 3.5-MHz band within the range of C1. The tuning range of the loop may be checked with a dip meter.

The sensing system consists of a 15-inch whip and an adjustable inductor that resonates the whip as a quarter-wave antenna. It also contains a potentiometer to control the output of the antenna. S1 is used to switch the sensing antenna in and out of the circuit.

The whip, the loopstick, the inductance L1, the capacitor C1, the potentiometer R1, and the switch S1 are all mounted on a $4 \times 5 \times 3$-inch box chassis, as shown in **Fig 26**. The loopstick may be mounted and protected inside a piece of $^1/_2$-inch PVC pipe. A section of $^1/_2$-inch electrical conduit is attached to the bottom of the chassis box and this supports the instrument.

To produce an output having only one null there must a 90° phase difference between the outputs of the loop and sensing antennas, and the signal strength from each must be the same. The phase shift is obtained by tuning the sensing antenna slightly off frequency, using the slug in L1. Since the sensitivity of the whip antenna is greater than that of the loop, its output is reduced by adjusting R1.

Adjustment

To adjust the system, enlist the aid of a friend with a mobile transmitter and find a clear spot where the transmitter and RDF receiver can be separated by several hundred feet. Use as little power as possible at the transmitter. (Make very sure you don't transmit into the loop if you are using a transceiver as a detector.) With the test transmitter operating on the proper frequency, disconnect the sensing antenna with S1, and peak the loopstick using C1, while watching the S meter on the transceiver. Once the loopstick is peaked, no further adjustment of C1 will be necessary. Next, connect the sensing antenna and turn R1 to minimum resistance. Then vary the adjustable slug of L1 until a maximum reading of the S meter is again obtained. It may be necessary to turn the unit a bit during this adjustment to obtain a higher reading than with the loopstick alone. The last turn of the slug is quite critical, and some hand-capacitance effect may be noted.

Now turn the instrument so that one side (not an end) of the loopstick is pointed toward the test transmitter. Turn R1 a complete revolution and if the proper side was chosen a definite null should be observed on the S meter for one particular position of R1. If not, turn the RDF 180° and try again. This time leave R1 at the setting producing

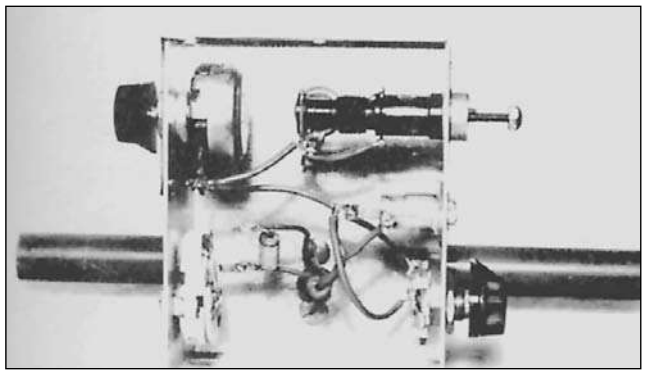

Fig 26—Components of the 3.5-MHz RDF are mounted on the top and sides of a channel-lock type box. In this view R1 is on the left wall at the upper left and C1 is at the lower left. L1, S1 and the output connector are on the right wall. The loopstick and whip mount on the outside.

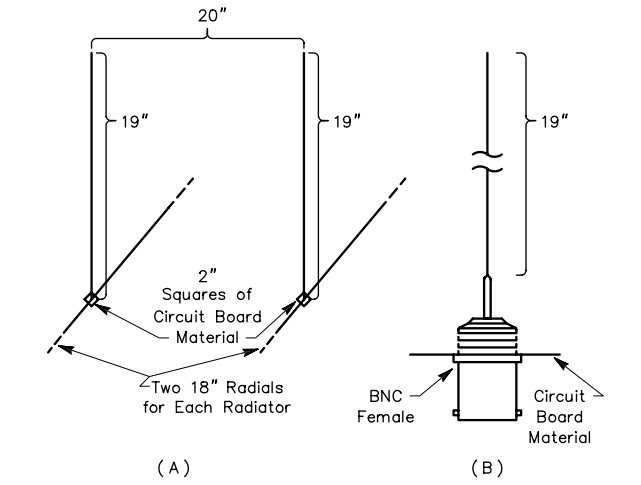

Fig 27—At A is a simple configuration that can produce a cardioid pattern. At B is a convenient way of fabricating a sturdy mount for the radiator using BNC connectors.

the minimum reading. Now adjust L1 very slowly until the S-meter reading is reduced still further. Repeat this several times, first R1, and then L1, until the best minimum is obtained.

Finally, as a check, have the test transmitter move around the RDF and follow it by turning the RDF. If the tuning has been done properly the null will always be broadside to the loopstick. Make a note of the proper side of the RDF for the null, and the job is finished.

A 144-MHZ CARIOID-PATTERN RDF ANTENNA

Although there may be any number of different VHF antennas that can produce a cardioid pattern, a simple design is depicted in **Fig 27**. Two $^1/_4$-wavelength vertical elements are spaced one $^1/_4$-λ apart and are fed 90° out of phase. Each radiator is shown with two radials approximately 5% shorter than the radiators. This array was designed by Pete O'Dell, KB1N, and described in *QST* for March 1981.

Computer modeling showed that slight alterations in the size, spacing and phasing of the elements strongly impact the pattern. The results suggest that this system is a little touchy and that the most significant change comes at the null. Very slight alterations in the dimensions caused the notch to become much more shallow and, hence, less usable for RDF. Early experience in building a working model bore this out.

This means that if you build this antenna, you will find it advantageous to spend a few minutes to tune it carefully for the deepest null. If it is built using the techniques presented here, then this should prove to be a small task, well worth the extra effort. Tuning is accomplished by adjusting the length of the vertical radiators, the spacing between them and, if necessary, the lengths of the phasing harness that connects them. Tune for the deepest null on your S meter when using a signal source such as a moderately strong repeater.

This should be done outside, away from buildings and large metal objects. Initial indoor tuning on this project was tried in the kitchen, which revealed that reflections off the appliances were producing spurious readings. Beware too of distant water towers, radio towers, and large office or apartment buildings. They can reflect the signal and give false indications.

Construction is simple and straightforward. Fig 27B shows a female BNC connector (RadioShack 278-105) that has been mounted on a small piece of PC-board material. The BNC connector is held upside down, and the vertical radiator is soldered to the center solder lug. A 12-inch piece of brass tubing provides a snug fit over the solder lug. A second piece of tubing, slightly smaller in diameter, is telescoped inside the first. The outer tubing is crimped slightly at the top after the inner tubing is installed. This provides positive contact between the two tubes. For 146 MHz the length of the radiators is calculated to be about 19 inches. You should be able to find small brass tubing at a hobby store. If none is available in your area, consider brazing rods. These are often available in hardware sections of discount stores. It will probably be necessary to solder a short piece to the top since these come in 18-inch sections. Also, tuning will not be quite as convenient. Two 18-inch radials are added to each element by soldering them to the board. Two 36-inch pieces of heavy brazing rod were used in this project.

The Phasing Harness

As shown in **Fig 28**, a T connector is used with two different lengths of coaxial line to form the phasing harness. This method of feeding the antenna is superior over

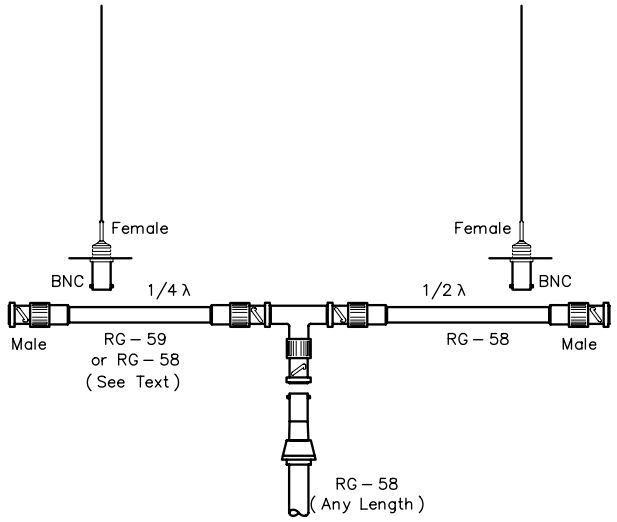

Fig 28—The phasing harness for the phased 144-MHz RDF array. The phasing sections must be measured from the center of the T connector to the point that the vertical radiator emerges from the shielded portion of the upside-down BNC female. Don't forget to take the length of the connectors into account when constructing the harness. If care is taken and coax with solid polyethylene dielectric is used, you should not have to prune the phasing line. With this phasing system, the null will be in a direction that runs along the boom, on the side of the 1/4-wavelength section.

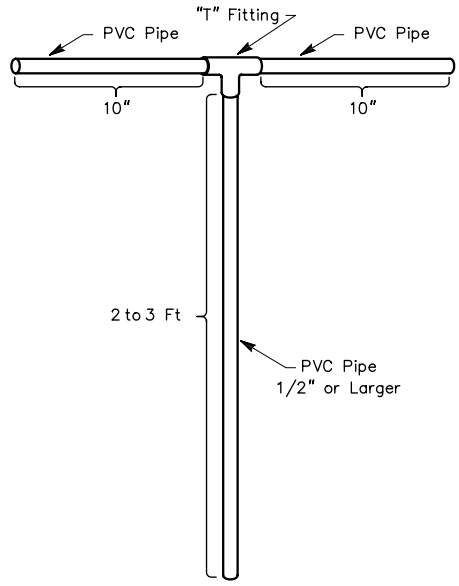

Fig 29—A simple mechanical support for the DF antenna, made of PVC pipe and fittings.

other simple systems to obtain equal currents in the two radiators. Unequal currents tend to reduce the depth of the null in the pattern, all other factors being equal.

The 1/2-wavelength section can be made from either RG-58 or RG-59, because it should act as a 1:1 transformer. With no radials or with two radials perpendicular to the vertical element, it was found that a 1/4-wavelength section made of RG-59 75-Ω coax produced a deeper notch than a 1/4-wavelength section made of RG-58 50-Ω line. However, with the two radials bent downward somewhat, the RG-58 section seemed to outperform the RG-59. Because of minor differences in assembly techniques from one antenna to another, it will probably be worth your time and effort to try both types of coax and determine what works best for your antenna. You may also want to try bending the radials down at slightly different angles for the best null performance.

The most important thing about the coax for the harness is that it be of the highest quality (well-shielded and with a polyethylene dielectric). The reason for avoiding foam dielectric is that the velocity factor can vary from one roll to the next—some say that it varies from one foot to the next. Of course, it can be used if you have test equipment available that will allow you to determine its electrical length. Assuming that you do not want to or cannot go to that trouble, stay with coax having a solid polyethylene dielectric. Avoid coax that is designed for the CB market or do-it-yourself cable-TV market. (A good choice is Belden 8240 for the RG-58 or Belden 8241 for the RG-59.)

Both RG-58 and RG-59 with polyethylene dielectric have a velocity factor of 0.66. Therefore, for 146 MHz a quarter wavelength of transmission line will be 20.2 inches × 0.66 = 13.3 inches. A half-wavelength section will be twice this length or 26.7 inches. One thing you must take into account is that the transmission line is the total length of the cable *and the connectors*. Depending on the type of construction and the type of connectors that you choose, the actual length of the coax by itself will vary somewhat. You will have to determine that for yourself.

Y connectors that mate with RCA phono plugs are widely available and the phono plugs are easy to work with. Avoid the temptation, however, to substitute these for the T and BNC connectors. Phono plugs and a Y connector were tried. The results with that system were not satisfactory. The performance seemed to change from day to day and the notch was never as deep as it should have been. Although they are more difficult to find, BNC T connectors will provide superior performance and are well worth the extra cost. If you must make substitutions, it would be preferable to use UHF connectors (type PL-259).

Fig 29 shows a simple support for the antenna. PVC tubing is used throughout. Additionally, you will need a T fitting, two end caps, and possibly some cement. (By not cementing the PVC fittings together, you will have the option of disassembly for transportation.) Cut the PVC for the dimensions shown, using a saw or a tubing cutter.

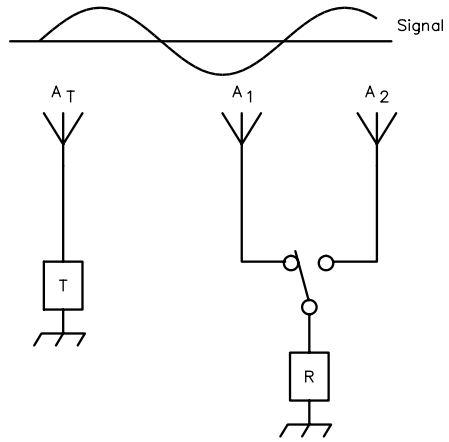

Fig 30—At the left, A_T represents the antenna of the hidden transmitter, T. At the right, rapid switching between antennas A_1 and A_2 at the receiver samples the phase at each antenna, creating a pseudo-Doppler effect. An FM detector detects this as phase modulation.

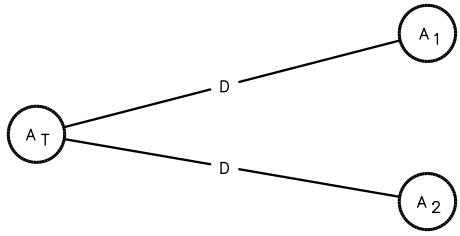

Fig 31—If both receiving antennas are an equal distance (D) from the transmitting antenna, there will be no difference in the phase angles of the signals in the receiving antennas. Therefore, the detector will not detect any phase modulation, and the audio tone will disappear from the output of the detector.

A tubing cutter is preferred because it produces smooth, straight edges without making a mess. Drill a small hole through the PC board near the female BNC of each element assembly. Measure the 20-inch distance horizontally along the boom and mark the two end points. Drill a small hole vertically through the boom at each mark. Use a small nut and bolt to attach each element assembly to the boom.

Tuning

The dimensions given throughout this section are those for approximately 146 MHz. If the signal you will be hunting is above that frequency, then the measurements should be a bit shorter. If you wish to operate below that frequency, then they will need to be somewhat longer. Once you have built the antenna to the rough size, the fun begins. You will need a signal source near the frequency that you will be using for your RDF work. Adjust the length of the radiators and the spacing between them for the deepest null on your S meter. Make changes in increments of $^1/_4$ inch or less. If you must adjust the phasing line, make sure that the $^1/_4$-wavelength section is exactly one-half the length of the half-wavelength section. Keep tuning until you have a satisfactorily deep null on your S meter.

THE DOUBLE-DUCKY DIRECTION FINDER

For direction finding, most amateurs use antennas having pronounced directional effects, either a null or a peak in signal strength. FM receivers are designed to eliminate the effects of amplitude variations, and so they are difficult to use for direction finding without looking at an S meter. Most modern HT transceivers do not have S meters.

This classic "Double-Ducky" direction finder (DDDF) was designed by David Geiser, WA2ANU, and was described in *QST* for July 1981. It works on the principle of switching between two nondirectional antennas, as shown in **Fig 30**. This creates phase modulation on the incoming signal that is heard easily on the FM receiver. When the two antennas are exactly the same distance (phase) from the transmitter, as in **Fig 31**, the tone disappears. (This technique is also known in the RDF literature as *Time-Difference-of-Arrival*, or TDOA, since signals arrive at each antenna at slightly different times, and hence at slightly different phases, from any direction except on a line perpendicular to and halfway in-between the two antennas. Another general term for this kind of two-antenna RDF technique is *interferometer*. —*Ed.*)

In theory the antennas may be very close to each other, but in practice the amount of phase modulation increases directly with the spacing, up to spacings of a half wavelength. While a half-wavelength separation on 2 meters (40 inches) is pretty large for a mobile array, a quarter wavelength gives entirely satisfactory results, and even an eighth wavelength (10 inches) is acceptable.

Think in terms of two antenna elements with fixed spacing. Mount them on a ground plane and rotate that ground plane. The ground plane held above the hiker's head or car roof reduces the needed height of the array and the directional-distorting effects of the searcher's body or other conducting objects.

The DDDF is bidirectional and, as described, its tone null points both toward and away from the signal origin. An L-shaped search path would be needed to resolve the ambiguity. Use the techniques of triangulation described earlier in this chapter.

Specific Design

It is not possible to find a long-life mechanical switch operable at a fairly high audio rate, such as 1000 Hz. Yet we want an audible tone, and the 400- to 1000-Hz range is perhaps most suitable considering audio amplifiers and average hearing. Also, if we wish to use the transmit function of a transceiver, we need a switch that will carry per-

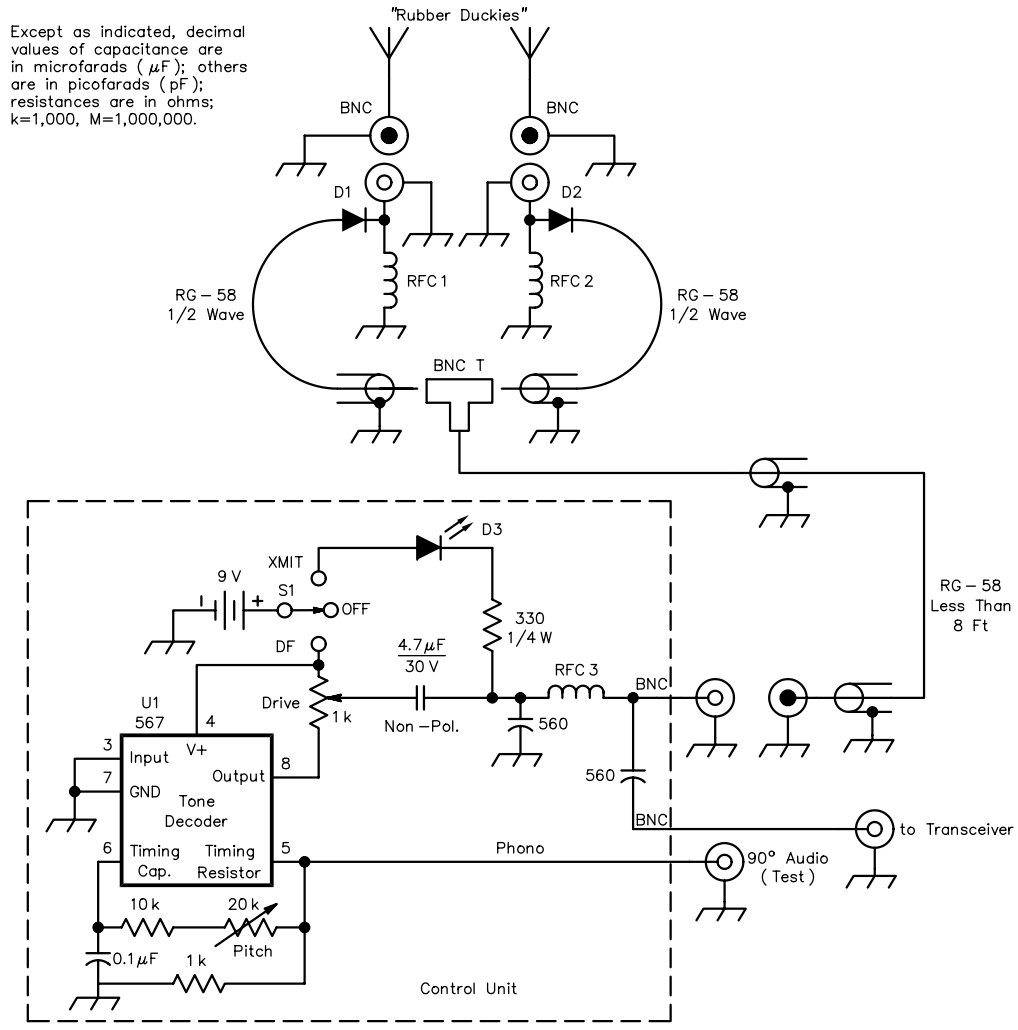

Fig 32—Schematic diagram of the DDDF circuit. Construction and layout are not critical. Components inside the broken lines should be housed inside a shielded enclosure. Most of the components are available from RadioShack, except D1, D2, the antennas and RFC1-RFC3. These components are discussed in the text. S1—See text.

haps 10 W without much problem.

A solid-state switch, the PIN diode is used. The intrinsic region of this type of diode is ordinarily bare of current carriers and, with a bit of reverse bias, looks like a low-capacitance open space. A bit of forward bias (20 to 50 mA) will load the intrinsic region with current carriers that are happy to dance back and forth at a 148-MHz rate, looking like a resistance of an ohm or so. In a 10-W circuit, the diodes do not dissipate enough power to damage them.

Because only two antennas are used, the obvious approach is to connect one diode *forward* to one antenna, to connect the other *reverse* to the second antenna and to drive the pair with square-wave audio-frequency ac. **Fig 32** shows the necessary circuitry. RF chokes (Ohmite Z144, J. W. Miller RFC-144 or similar vhf units) are used to let the audio through to bias the diodes while blocking RF. Of course, the reverse bias on one diode is only equal to the forward bias on the other, but in practice this seems sufficient.

A number of PIN diodes were tried in the particular setup built. These were the Hewlett-Packard HP5082-3077, the Alpha LE-5407-4, the KSW KS-3542 and the Microwave Associates M/A-COM 47120. All worked well, but the HP diodes were used because they provided a slightly lower SWR (about 3:1).

A type 567 IC is used as the square-wave generator. The output does have a dc bias that is removed with a nonpolarized coupling capacitor. This minor inconvenience is more than rewarded by the ability of the IC to work well with between 7 and 15 volts (a nominal 9-V minimum is recommended).

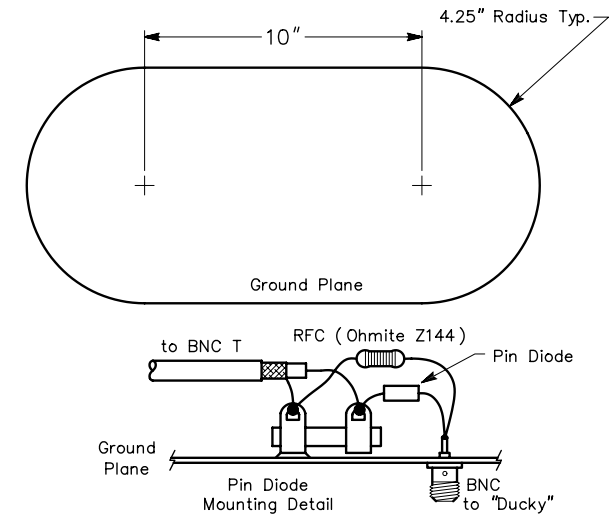

Fig 33—Ground-plane layout and detail of parts at the antenna connectors.

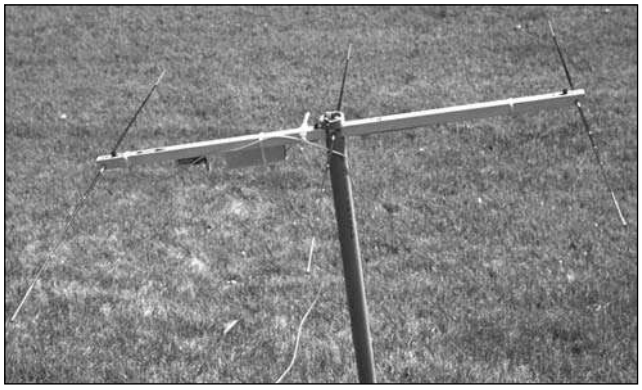

Fig 34—Photo of Fox-Hunting DF Twin 'Tenna set up as a horizontally polarized, 3-element Yagi.

The nonpolarized capacitor is also used for dc blocking when the function switch is set to XMIT. D3, a light-emitting diode (LED), is wired in series with the transmit bias to indicate selection of the XMIT mode. In that mode there is a high battery current drain (20 mA or so). S1 should be a center-off locking type toggle switch. An ordinary center-off switch may be used, but beware. If the switch is left on XMIT you will soon have dead batteries.

Cables going from the antenna to the coaxial T connector were cut to an electrical 1/2 wavelength to help the open circuit, represented by the reverse-biased diode, look open at the coaxial T. (The length of the line within the T was included in the calculation.)

The length of the line from the T to the control unit is not particularly critical. If possible, keep the total of the cable length from the T to the control unit to the transceiver under 8 feet, because the capacitance of the cable does shunt the square-wave generator output.

Ground-plane dimensions are not critical. See **Fig 33**. Slightly better results may be obtained with a larger ground plane than shown. Increasing the spacing between the pickup antennas will give the greatest improvement. Every doubling (up to a half wavelength maximum) will cut the width of the null in half. A 1° wide null can be obtained with 20-inch spacing.

DDDF Operation

Switch the control unit to DF and advance the drive potentiometer until a tone is heard on the desired signal. Do not advance the drive high enough to distort or "hash up" the voice. Rotate the antenna for a null in the fundamental tone. Note that a tone an octave higher may appear.

If the incoming signal is quite out of the receiver linear region (10 kHz or so off frequency), the off-null antenna aim may present a fairly symmetrical AF output to one side, **Fig 35A**. It may also show instability at a sharp null position, indicated by the broken line on the display in Fig 35B. Aimed to the other side of a null, it will give a greatly increased AF output, Fig 35C. This is caused by the different parts of the receiver FM detector curve used. The sudden tone change is the tip-off that the antenna null position is being passed.

The user should practice with the DDDF to become acquainted with how it behaves under known situations of signal direction, power and frequency. Even in difficult nulling situations where a lot of second-harmonic AF exists, rotating the antenna through the null position causes a very distinctive tone change. With the same frequencies and amplitudes present, the quality of the tone (timbre) changes. It is as if a note were first played by a violin, and then the same note played by a trumpet. (A good part of this is the change of phase of the fundamental and odd harmonics with respect to the even harmonics.) The listener can recognize differences (passing through the null) that would give an electronic analyzer indigestion.

A FOX-HUNTING DF TWIN 'TENNA

Interferometers give sharp bearings, but they lack sensitivity for distant work. Yagis are sensitive, but they provide relatively broad bearings. This project yields an antenna that blends both on a single boom to cover both ends of the hunt. This is a condensation of a October 1998 *QST* article by R. F. Gillette, W9PE.

A good fox-hunting antenna must meet a number of criteria: (1) small size, (2) gain to detect weak signals and (3) high directivity to pinpoint the fox. Small antennas, however, do not normally yield both gain and direc-

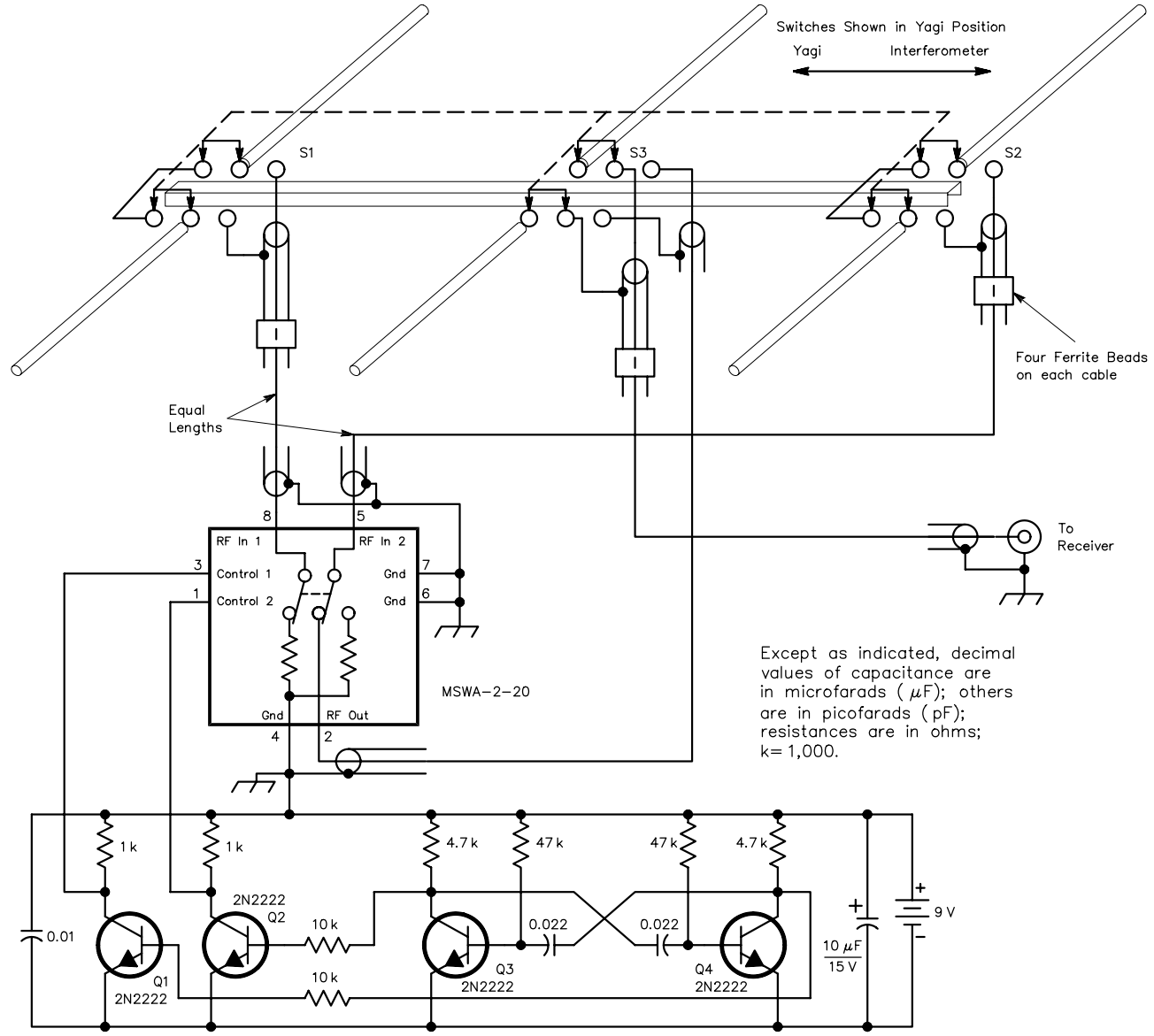

Fig 35—Schematic of the Yagi/interferometer antenna system.

Table 1
Yagi Design

Item	*Overall Length (Inches)*	*Boom to Element Tip (Inches)*
Director length	34.75	17.00
Director to Driven El. spacing	15.75	16.00
Driven El. length	37.75	18.50
Driven El. to Reflector spacing	15.75	16.00
Reflector length	40.75	20.00

*SWR less than 1.3:1 from 144.5 to 148 MHz

tivity. By combining two antennas, all three requirements are satisfied in a way that makes a nice build-it-yourself project.

This antenna uses slide switches to configure it as either a Yagi or a single-channel interferometer. When used as an interferometer, a GaAs RF microcircuit switches the FM receiver between two matched dipoles at an audio frequency. To make the antenna compact W9PE used hinged, telescopic whips as the elements; they collapse and fold parallel to the boom for storage.

The Yagi

The Yagi is a standard three-element design, based on 0.2-λ spacing between the director, the driven element

and the reflector. It yields about 7 dBi gain and a front-to-back ratio of over 15 dB. Because a slide switch is used at the center of each element and the elements have small diameters, their resonant lengths are different from typical ones. **Table 1** shows the sizes used and **Fig 34** shows the Yagi.

To make sure that radiation from the coax does not affect the pattern, the author used some ferrite beads as coaxial choke-baluns. This also prevents objects near the coax from affecting signal-strength readings. The Yagi also has a low SWR; with uncalibrated equipment, he measured less than 1.3:1 over most of the 2-meter band.

This Yagi has a lot more gain than a "rubber ducky," but we need more directivity for fox hunting. That's where the interferometer comes in.

An Interferometer

To form the interferometer, the two end elements are converted to dipoles and the center element is disabled. When the three switches in **Fig 35** are thrown to the right, the feed line to the receiver is switched from the center element to the RF switch output, and the end elements are connected via feed lines to the RF switch inputs. With the Yagi's feed point open and the driven element equidistant from both interferometer antennas, the center element should have no effect on the interferometer. Nonetheless, it's easier to collapse the driven-element whips and get them out of the way than to worry about spacing.

Now if both interferometer coax cables are of equal length (between the antennas and switch) and the two antennas are the same distance from the transmitter (broadside to it), the signals from both antennas will be in phase. Switching from one antenna to the other will have no effect on the received signal. If one antenna is a little closer to the transmitter than the other, however, there will be a phase shift when we switch antennas.

When the antenna switch is at an audio rate, say 700 Hz, the repeated phase shifts result in a set of 700 Hz sidebands. At this point, all that was needed was a circuit to switch from one antenna to the other at an audio rate. W9PE chose a low-cost Mini-Circuits MSWA-2-20 GaAs RF switch driven by a simple multivibrator and buffer. The GaAs switch is rated to 2.0 GHz, hence this switching concept can easily be scaled to other ham bands. The PC board should work through the 440 MHz ham band. The author suggests adding a ground plane under the RF portion of the PC board and testing it before using it at a higher frequency.

The RF switch is controlled by a set of equal-amplitude, opposite-phase square waves: 0 V at one control port and –8 to –12 V at the other. (Mini Circuits is unclear about maximum voltages for this device. For safety, don't power it with more than 9 V.—*Ed*.) The opposite controls the other switch position. A 9-V battery was used as the power supply, with the positive terminal grounded. This results in a 0 V control signal to the RF switch when the buffer transistor is off and a Vsat (about 0.2 V less than the –9 V battery: –8.8 V) signal when the buffer transistor is saturated. The multi-vibrator has two outputs, and each drives a buffer resulting in the required equal-and-opposite-phase drive signals.

Table 2
Bill of Materials

Quantity	*Item*
3 ft	3/4-inch aluminum U channel
6 sets	insulated shoulder washers for elements
1	9 V battery
1	9 V battery connector
1	10 µF, 16 V electrolytic capacitor
1	0.01 µF, 25 V capacitor
2	0.022 µF, 25 V capacitor
2	1 kΩ 1/8 W resistor
2	4.7 kΩ 1/8 W resistor
2	10 kΩ 1/8 W resistor
2	47 kΩ 1/8 W resistor
2	1 kΩ 1/8 W resistor
4	2N2222 transistors
1	Mini-Circuits MSWA-2-20 (Mini-Circuits Labs, 13 Neptune Ave, Brooklyn, NY 11235; tel 718-934-4500, 417-335-5935, fax 718-332-4661; e-mail **sales@minicircuits.com**; URL **www.minicircuits.com**)
3	DPDT slide switch (1 1/8-inch, 29 mm, mounting centers), Stackpole, 3 A, 125 V used
10 ft	50 Ω coax (0.140-inch maximum OD)
1	coaxial connector (receiver dependent)
1	lot, mounting hardware
1	lot, heat-shrink tubing or equal
4	cable ties
1	2 × 3.5-inch single-sided fiberglass PC board
1	1-inch PVC conduit
12	#FB-20 ferrite beads 0.14-inch ID, 0.5-inch long (All Electronics Corp: PO Box 567, Van Nuys, CA 91408-0567; tel 888-826-5432, fax 818-781-2653, e-mail: **allcorp@allcorp.com**; URL **www.allcorp.com/**.)
6	20 1/2-inch telescoping antenna elements (Nebraska Surplus, tel 402-346-4750; e-mail **grinnell@probe.net**)
1	Special resist film (Techniks Inc, PO Box 463, Ringoes, NJ 08551; tel 908-788-8249, fax 908-788-8837; e-mail **techniks@idt.net**; URL **www.techniks.com/**)

Circuit Construction

After he selected the Mini-Circuits RF switch, W9PE realized that its small size would be best handled with a simple PC board. He made the prototype boards with a photocopy transparency technique.

A power on-off switch was not used, as the 9-V bat-

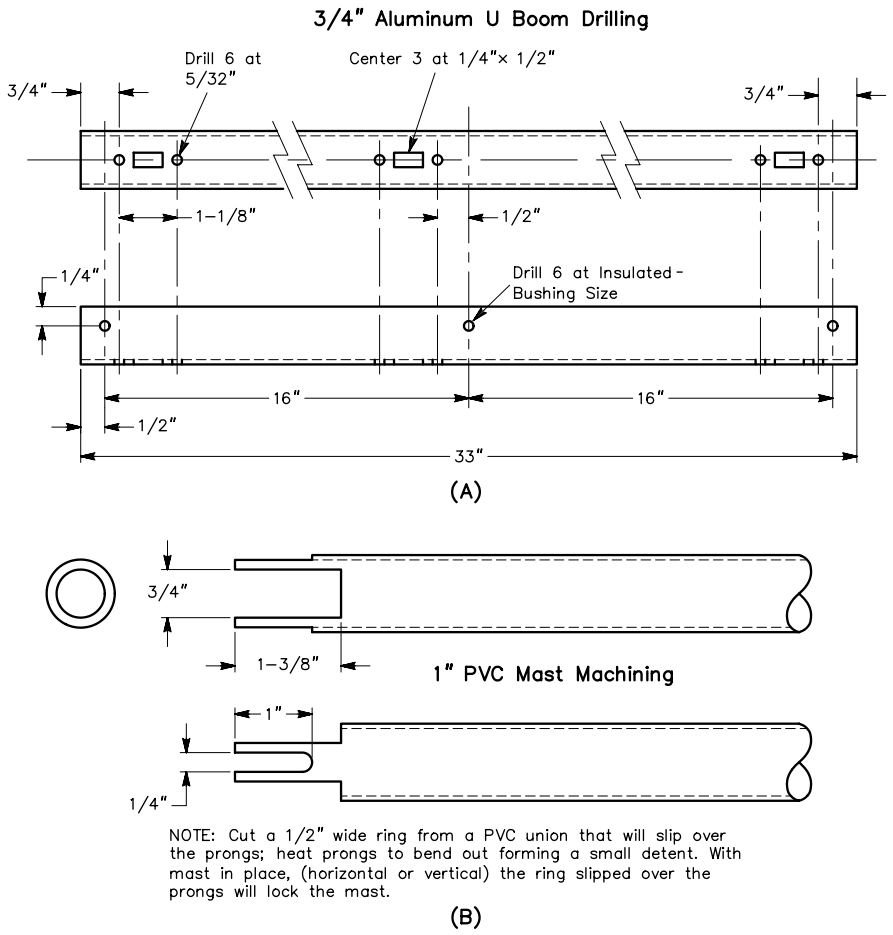

Fig 36—Boom-drilling and mast-machining details.

tery connector serves the same function. The battery fits tightly in the 3/4-inch U channel. W9PE covered the circuit board with a plastic-lined aluminum cover, but plastic film and some aluminum foil, provide the same function. A cable tie will strap either into the U channel.

Table 2 is a complete bill of materials. You can use any telescoping elements, providing that they extend to over 20 inches and have a mounting stud long enough to accommodate the insulated washers. As an alternate to the stud, they can have ends tapped to receive a screw for the insulated mounting. The author picked up his elements at a hamfest from the vendor listed; they are also available from most electronic parts houses. The Mini-Circuit RF switch is a currently available part.

Antenna Construction

Fig 35 shows the antenna schematic. It shows all three switches in the Yagi position; each would slide to the right for interferometer use. Slide switches work pretty well at 2 meters. Each of the elements is mounted to the boom with insulating washers, and a strip of copper stock connects each element to its slide switch. (You can substitute copper braid, solder wick, coax shield or any short, low resistance, low inductance conductor for the copper stock.) This switching arrangement allows you to switch the reflector and director from being parasitic elements (electrically continuous) to being dipoles (center fed).

Because the elements telescope, you can adjust the interferometer dipoles to exactly equal lengths each time you switch the antenna configuration from Yagi to interferometer. Again, choke baluns block RF on the outside of each element's coax.

Caution: Do not transmit when the RF switch is selected. Transmit only when in the Yagi configuration. RF power will destroy the Mini-Circuits RF switch. To be safe, lock out your transmit function. Most HTs have this capability. When using a mobile radio, disconnect the microphone. It is, however, safe to transmit in the Yagi configuration—which is nice for portable operating.

Fig 36 gives dimensions for drilling a standard 3/4-inch aluminum U channel for the boom and shows how the author cut a 1-inch PVC pipe (plastic conduit) for a mast and a mast locking ring. If PVC conduit is not available in your area, PVC water pipe (and a PVC union for

the locking ring) will work. This mast allows mounting the antenna for either vertical or horizontal polarization.

Be sure to test the plastic pipe you use for low RF loss. Do this by heating a sample in a microwave oven. Place a pipe sample and a glass of water in the oven. (The sample is not placed in the glass of water; the water keeps the microwave from operating without a load.) Bring the water to a boil, and then carefully check the sample's temperature. If the sample is not hot, its RF loss is low, and the plastic can be used.

Using the Antenna

When starting a hunt, set up the Yagi antenna by placing all switches in the Yagi position. Swing all of the telescoping elements perpendicular to the boom and set the whip lengths to achieve the proper element lengths, while keeping each element symmetrical about the boom. The cables or boom can be marked with the length data.

While the signal is weak, use the Yagi. It has 7 dBi gain, but its bearing resolution is only about 20°. When the signal gets stronger, use the interferometer. It has less gain, but its bearing resolution is better than 1°. If the fox transmitter begins overloading your receiver, collapse the whips (equally) to reduce the gain and continue triangulating. Near the transmitter, you should triangulate both horizontally (azimuth) and vertically (elevation). The antenna works both ways, and the transmitter may be located above or below you.

Antenna Alternative

As an alternative to the telescoping elements, George Holada, K9GLJ, suggested using fixed-length elements with banana plugs matched to banana jacks on the boom. Three pairs would be used for the Yagi, an extra driven-element pair for the interferometer mode and two short-element pairs to reduce the received signal level if an overload condition occurs. He also suggested a PVC boom allowing the elements to be stored inside the boom.

THE FOUR-WAY MOBILE DF SYSTEM

This innovative, yet simple, RDF antenna system was described in an article by Malcolm C. Mallette, WA9BVS, in November 1995 *QST*. It is derived from the TDOA design shown earlier in this chapter by David T. Geiser, WA2ANU, and by a design by Paul Bohrer, W9DUU. (See Bibliography.)

Direction-finding often involves two different activities: DFing on foot and DFing from a vehicle. Often, you must track the signal using a vehicle, then finish the hunt on foot. Whether on foot or in a vehicle, the primary problem you'll encounter when trying to locate the transmitter is multipath reception. Multipath reception involves receiving the same signal by more than one path, one signal from the true direction of the transmitter and others by reflected paths that may come from widely different directions. VHF and UHF signals bounce off almost any object and hide the true source of a signal. For example, if there's a large metal building north of you, a signal from the south may arrive from the north because the signal bounces off the building and back to you.

Multipath reception effects can be defeated by taking a number of readings from different positions and arriving at an average direction. While moving at road speeds in a vehicle, it's possible to take a number of readings from different positions and average them, and it's also possible to average a number of readings over a distance of travel by electronic means. The true bearing to the transmitter can usually be found by either method.

DFing equipment for use on foot is simpler than systems for use on a vehicle. While afoot, you can turn at will or easily rotate an antenna. Turning a vehicle while going down a street may result in a fender-bender if you're not careful!

The simplest DFing system to use while on foot consists of an S-meter-equipped hand-held receiver and a small, hand-held Yagi with an attenuator in line between the antenna and receiver. The attenuator keeps the S meter from pinning. The direction in which the beam points when the strongest signal is received is the direction of the transmitter. Of course, you'll want to take readings at several locations at least a wavelength apart to obtain an average heading, as multipath reception can still cause false readings in some locations.

Another approach that many hams have taken is the simple WA2ANU DDFF—it is now commonly known simply as the "buzzbox." Various commercial versions of the hand-held buzzbox system are available. Some sys-

Fig 37—Front panel of the Four-Way DFer. At the extreme left of the front panel is the VOLUME control. Immediately to the right is the RCV/OFF/DF center-off toggle switch, with the damping (DMP) control switch nearby. Four LEDs mounted in a diamond pattern indicate signal direction: front (yellow), right (green), back (orange) and left (red). The horizontally mounted zero-center meter indicates left/right signal reception, the vertically mounted meter displays front/back signal reception. A small speaker is mounted on the top cover.

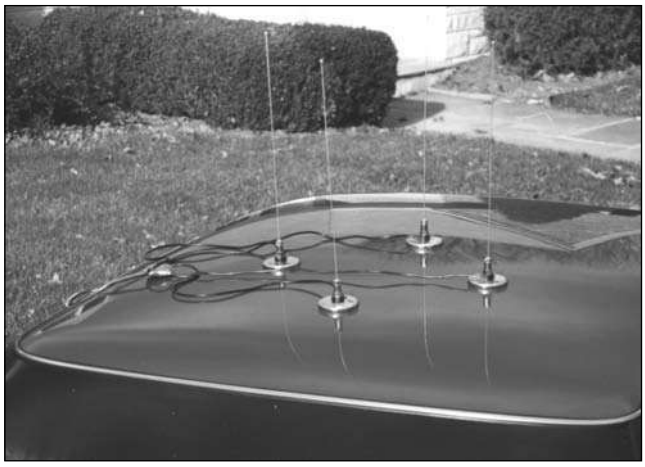

Fig 38—Placement of the four antennas on the author's car roof. The small object to the left of the antennas is the switch board.

tems have been upgraded to indicate whether the signal is arriving from the left or right of your position. The main drawback, however, to the buzzbox is that it's not as sensitive as a simple dipole and not nearly as sensitive as a beam.

In theory, you could take a buzzbox or Yagi/attenuator system in a car, stop periodically, get out and check the direction to the transmitter, then climb back in and drive off. Although this procedure works, it isn't very practical—it takes a long time to find the transmitter.

This design is for a left-right, front-back box (LRFB box) that indicates whether the received signal is to the left or right and whether it is to the front or back of the receiver. The location display consists of four LEDs arranged in a diamond pattern (see the title-page photo). When the top LED is on, the signal is coming from the front. When the top and right LEDs are on, the transmitter is between the front and the right. When only the right LED is on, the signal is directly to the right. When the bottom LED and right LED are on, the transmitter is to the right and to the back. The same pattern occurs around the clock. Therefore, four LEDs indicate eight directions. As most highways and streets have intersections that force a driver to choose moving straight ahead, right or left, the indication is sufficiently precise for practical transmitter hunting.

If the four-LED display is used alone, all parts can be obtained from your local Radio Shack store. Two zero-center 50-μA meters (50-0-50)—M1 and M2—can be used in addition to, or in place of, the LEDs, but RadioShack does not stock such meters. **Fig 37** shows the front panel layout of the LRFB.

The LRFB box uses four mag-mount $^1/_4$-λ antennas placed on the vehicle roof as shown in **Fig 38**. The whips in the mag mounts can be changed to $^1/_4$-λ 440-MHz whips and the antennas placed closer together when switching from 144-MHz to 440-MHz operation.

Circuit Description

See **Fig 39** in the following discussion (pages 26 and 27). U2, a 555 timer, generates a string of square-wave pulses at pin 3. The pulse frequency is determined by the setting of R4. The pulses are fed to the clock input (pin 14) of U3, a 4017 decade counter. On the first pulse, a positive voltage appears at U3, pin 3. On receipt of the second pulse from U2, pin 3 of U3 goes to ground and a positive voltage appears on pin 2. This sequence continues on successive pulses from U2 as pins 3, 2, 4, 7, 10, 1, 5, 6, 9 and 11 go positive in succession.

D1 through D5, and D6 through D10, OR the pulses. The result is that TP3 goes positive on the first pulse from U2, while TP2 is at 0 V. The next pulse of U2 results in TP2 going positive and TP3 going to 0 V. This sequence repeats as the counter goes around to make pin 3 positive again, and recycles.

Antenna Switching

U2 and U3 produce alternating pulses at TP2 and TP3. If we wanted only to alternately turn on and off two antennas, we could use the pulses at TP2 and TP3. The design ensures that the pulses at TP2 are the same length as the pulses at TP3. For the LRFB box, however, we need to switch between the left-right antennas many times, then switch between the front-back antennas many times.

Pin 12 of U3, CARRY OUT, emits a pulse every time U3 counts through its cycle of 10 pulses. The carry pulses from U3 go to U4, pin 14, the clock input of that 4017 counter. As U4 cycles, its output pins pulse; those pulses are, in effect, directed by D11 through D20.

As a result, TP4 is positive during the first 50 pulses from U2 and TP5 is positive during the second 50 pulses of U2. Q1 through Q6 form a quad AND gate. They AND the pulses at TP4 and TP5 with the alternating pulses at TP2 and TP3 so that the result is a pulse at the base of Q9, followed by a pulse at the base of Q10, a pulse at the base of Q9, and so on. The pulses alternate 25 times between Q9 and Q10. Then, as TP4 goes to 0 V, TP5 rises from 0 V to some positive voltage and the alternating pulses appear at the bases of Q7 and Q8. The pulses alternately go to the bases of Q7 and Q8 25 times. Then they alternate between the bases of Q9 and Q10 25 times. This pattern continues as long as the unit is in DF operation.

In **Fig 40**, two leads of a four-conductor-plus-ground cable to the antenna-switch board are connected to points A and B. The same pulses that turn Q7 and Q8 off and on turn on and off the left and right antennas. One of those two antennas is turned on and off in phase with Q7 and the other is turned on and off in phase with Q8. The PHASE switch, S3, determines which antenna is in phase with which transistor. Similarly, the two front/back antennas are turned on and off in phase with Q9 and Q10, and S4 determines which antenna is in phase with which transistor.

The pulses arriving at points A and B turn on and off the diodes connecting the coax of the left and right

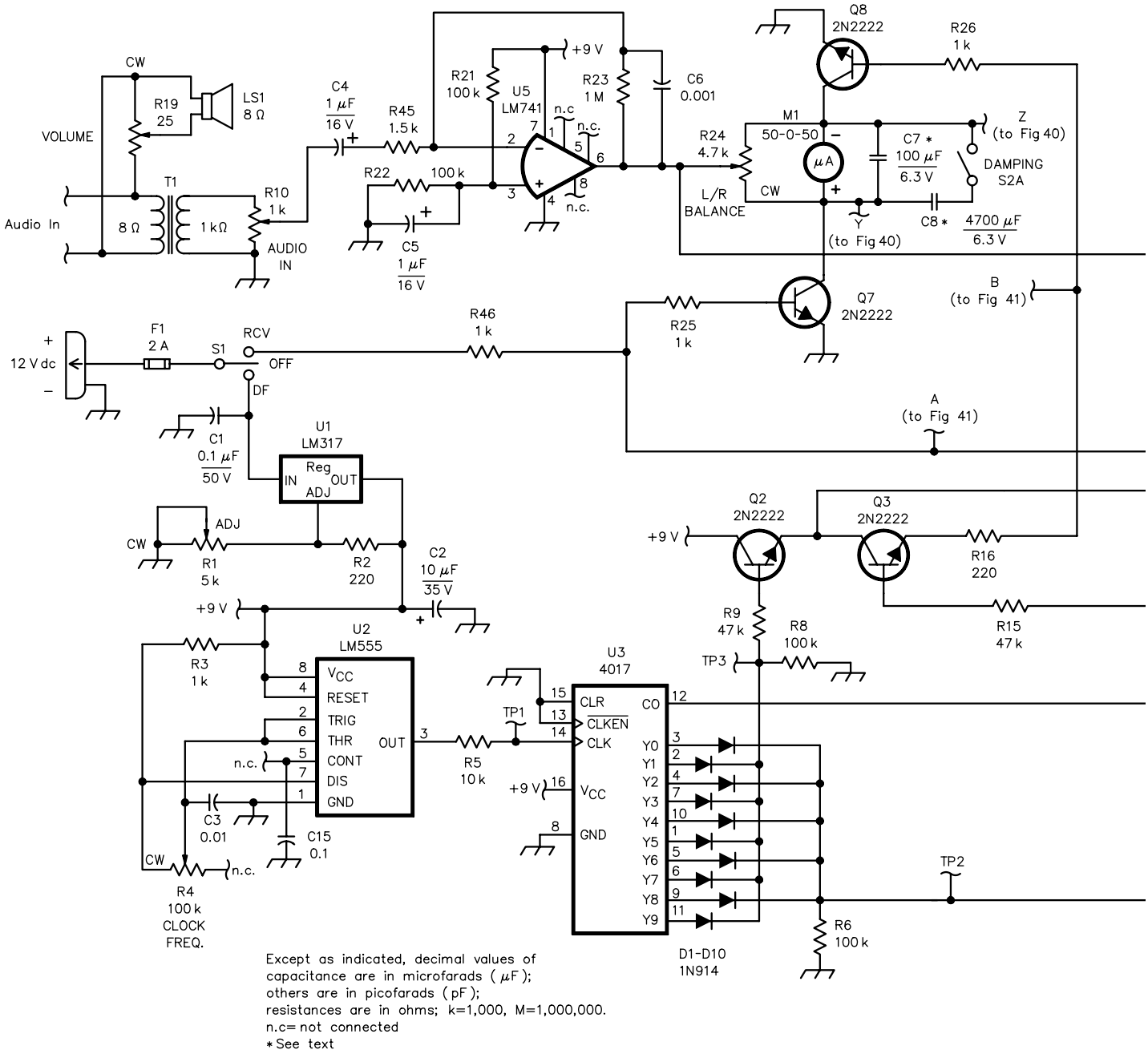

Except as indicated, decimal values of capacitance are in microfarads (μF); others are in picofarads (pF); resistances are in ohms; k=1,000, M=1,000,000.
n.c= not connected
*See text

Fig 39—Unless otherwise specified, part numbers in parentheses are RadioShack. All fixed-value resistors are 1/4-W, 5%-tolerance units. Equivalent parts can be substituted.

C1, C15—0.1-μF, 50-V (272-1069)
C2—10-μF, 35-V electrolytic capacitor (272-1025)
C3—0.01-μF, 25-V disc-ceramic capacitor (272-131)
C4, C5—1-μF, 16-V electrolytic capacitor (272-1434)
C6—0.001-μF, 25-V disc-ceramic capacitor (272-126)
C7, C9—100-μF, 6.3-V bipolar (nonpolarized) capacitor; Digi-Key P-1102, available from Digi-Key Corp, 701 Brooks Ave S, PO Box 677, Thief River Falls, MN 56701-0677, tel 800-344-4539, 218-681-6674; fax: 218-681-3880; RadioShack stocks 100-μF, 35-V axial (272-1016) and radial-lead (272-1028) electrolytic capacitors.
C8, C10—4700-μF, 6.3-V bipolar capacitor (made of five 1000-μF, 6.3-V bipolar capacitors), Digi-Key P1106. Standard 1000-μF, 35-V radial and axial-lead electrolytic capacitors are available from RadioShack; a 4700-μF, 35-V axial-lead electrolytic capacitor is also available (272-1022). Note that C7, C8, C9 and C10 are non-polarized capacitors because a small reverse voltage can appear across the meter and capacitors when the system is in use. Standard polarized electrolytics have been used in a number of units using this circuit (the same detector circuit used in W9DUU's unit) without any known ill effects, however.
D1-D20—1N914 silicon switching diode (276-1620 or 276-1122)
F1—2-A fuse (270-1007)
LS1—8-W speaker (40-245)

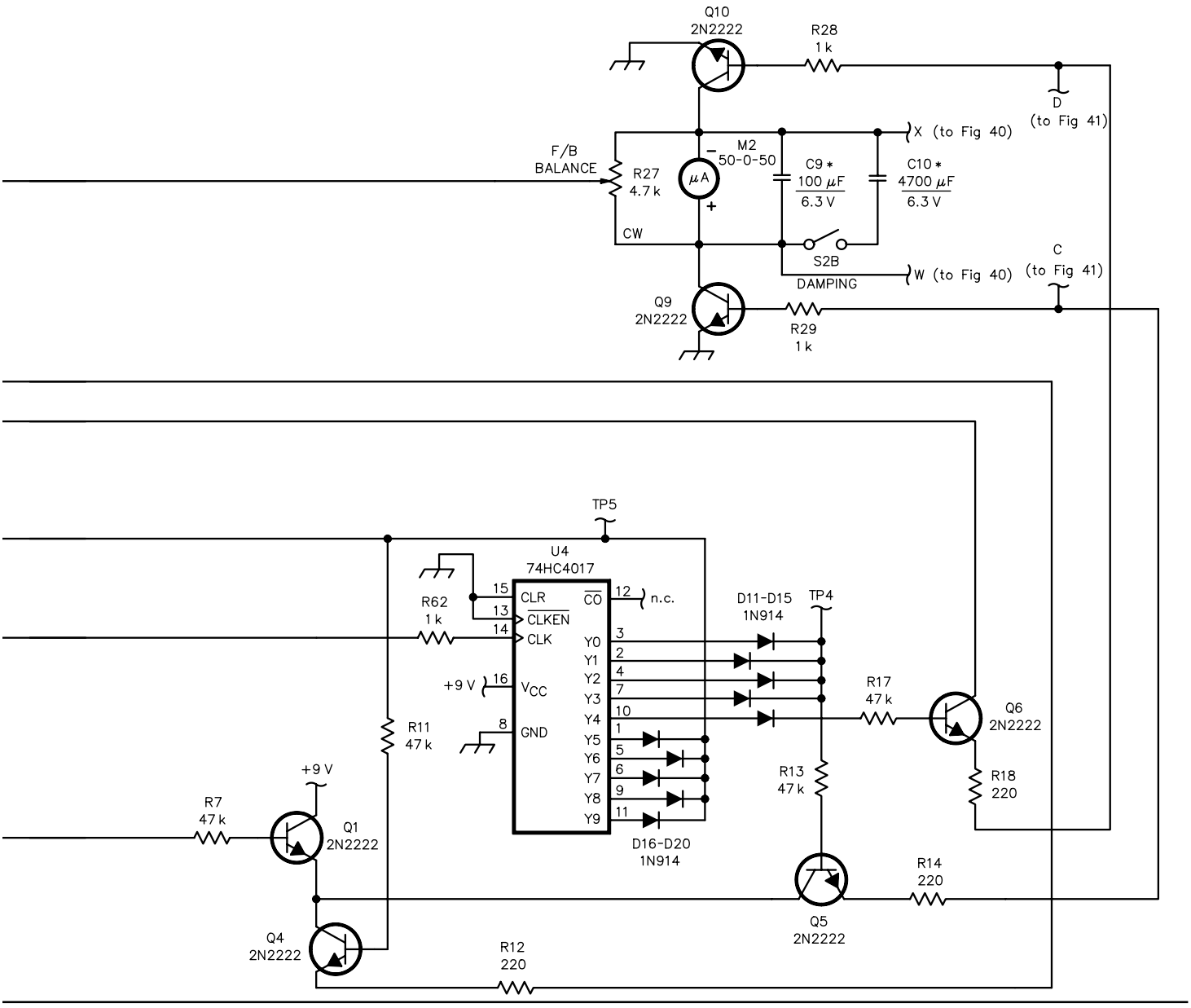

M1, M2—Zero-center, 50-µA meter; optional—see text
Q1-Q10—MPS2222 or 2N2222 NPN silicon general-purpose transistors (276-2009)
R1, R24, R27—4.7 kΩ (271-281); note: many of the fixed-value resistors can be found in RadioShack resistor assortment packages 271-308 and 271-312.
R2, R12, R14, R16, R18—220 Ω (271-1330)
R3, R25, R26, R28, R29—1 kΩ (271-1321)
R4—100-kΩ trimmer potentiometer (271-284)
R5—10 kΩ (271-1335)
R6, R8, R21, R22—100 kΩ (271-1347)
R7, R9, R11, R13, R15, R17—47 kΩ (271-1342)
R10—1-kΩ trimmer potentiometer (271-280)
R19—25-Ω panel-mount potentiometer (271-265A)
R23—1 MΩ (271-1134)
R45—1.5 kΩ (part of 271-312 assortment)
S1—SPDT, center-off switch (275-325)
S2—DPDT switch (275-626)
T1—8-Ω to 1-kΩ audio-output transformer (273-1380)
U1—LM317T, 1.5-A, three-terminal, adjustable voltage regulator (276-1778)
U2—555 timer (276-1723)
U3, U4—4017 decade counter (276-2417)
U5—LM741 op amp (276-007)
Misc: two 8-pin IC sockets (276-1995); two 16-pin IC sockets (276-1992); experimenter's PC board (276-148) or FAR Circuits PC board set; enclosure; four mag-mount antennas, four-conductor shielded cable; in-line fuse holder (270-1281).

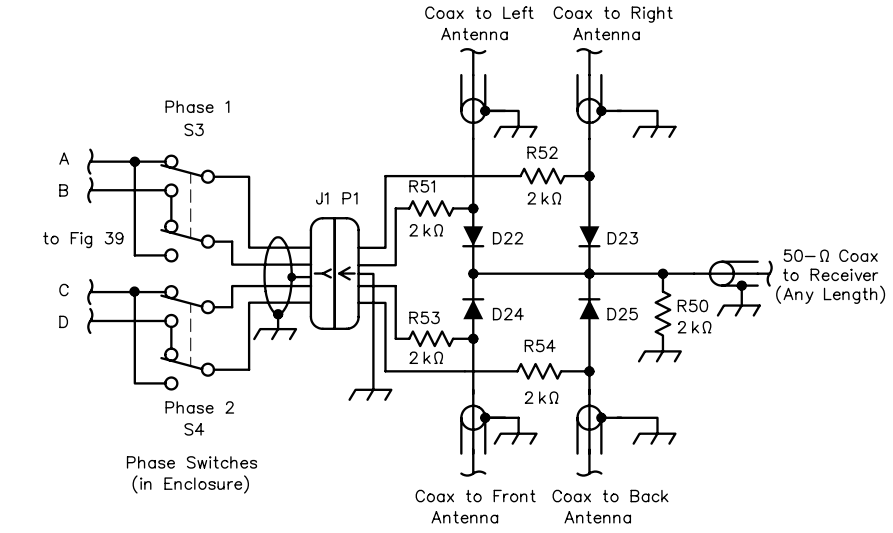

Fig 40—Schematic of the antenna switch board. Part numbers in parentheses are RadioShack. All fixed-value resistors are 1/4-W, 5%-tolerance units. Equivalent parts can be substituted.

D22-D25—1N914 silicon switching diode (276-1620 or 276-1122)
J1—Six-pin female Molex connector (274-236 or 274-155)
P1—Six-pin male Molex connector (274-226 or 274-152)
R50-R54—2.2 kΩ (can be found in RadioShack resistor assortment packages 271-308 and 271-312); also available in pack of five (271-1325)
S3, S4—DPDT switch (275-626)

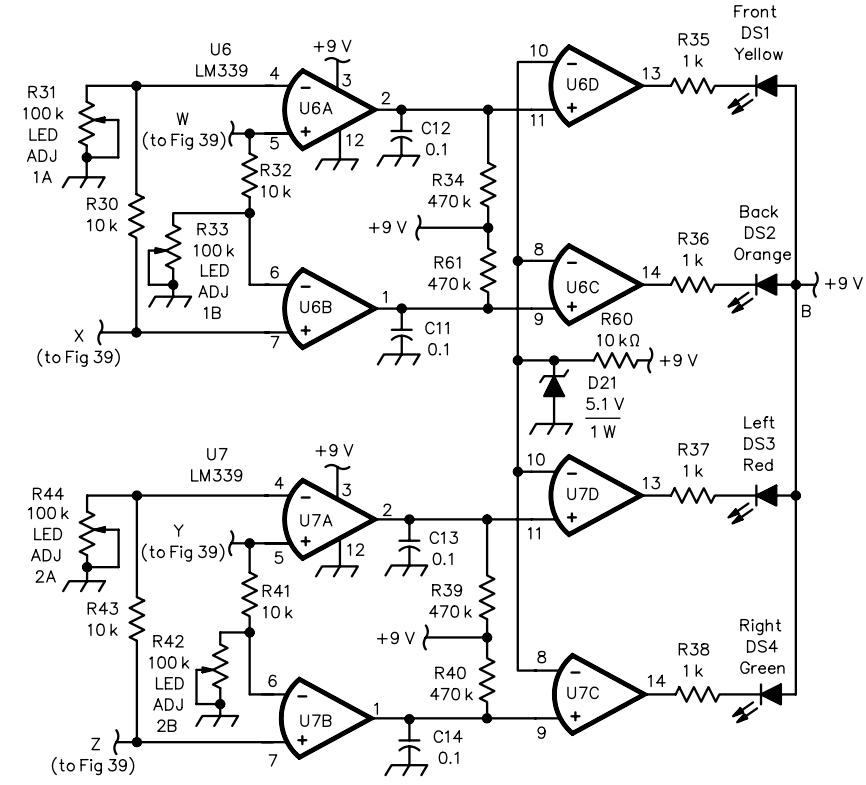

Fig 41—Schematic of the LED driver circuit. Part numbers in parentheses are RadioShack. All fixed-value resistors are 1/4-W, 5%-tolerance units. Equivalent parts can be substituted.

C11-C14—0.1-µF, 25-V disc-ceramic capacitor (272-135)
D21—1N4733, 5.1-V, 1-W Zener diode (276-565)
DS1-DS4—LEDs; one each red (276-066); green (276-022); yellow (276-021); orange (276-012)
R30, R32, R41, R43—10 kΩ (271-1335)
R34, R39, R40, R61—470 kΩ (271-1354)
R35-R38—1 kΩ (271-1321)
R31, R33, R42, R44—100-kΩ trimmer potentiometer (271-284)
U6, U7—LM339 quad comparator (276-1712)
Misc: two 14-pin IC sockets (276-1999)

antennas to the receiver coax. This occurs 25 times, thereby switching the receiver between the left and right antennas 25 times. Similar switching then occurs between the front and the back antennas from pulses arriving at points C and D.

Detector Circuit

The detector circuit (back again in Fig 39) starts with U5, a 741 op amp that amplifies the receiver's audio output. The audio is fed into R24 and R27, two 4.7-kΩ pots. The zero-center, 50-µA meters across R24 and R27 are optional. The meters, as well as the LEDs, indicate front/back and left/right. Such meters can be expensive unless you find surplus meters, and they're not really necessary.

When the left/right antennas are active, one end of R24 is grounded by Q7 and Q8 on each alternate pulse.

If Q7 is conducting, Q8 is not conducting. On each pulse, one of the left/right antennas is turned on and one end of R24 is grounded. On the next pulse, the other left/right antenna is turned on and the other end of R24 is grounded. If there is a phase difference between the signal received by the left antenna and the signal received by the right antenna, a dc voltage is built up across R24. That voltage causes the quad comparator, U7 in **Fig 41** to turn on DS3 (red) or DS4 (green) L/R LEDs. If the optional left/right meter is installed, it deflects to indicate the direction as do the LEDs.

After 25 cycles, the left and right antennas are both turned off and the front and back antennas are cycled on and off 25 times with the same detection process, producing a voltage across R27 if there is a phase difference between the RF received by the front and the back antennas. That voltage across R27 causes quad comparator U6 to turn on DS1 or DS2.

C9 and C10, for the F/B detector, and C7 and C8, for the L/R detector, damp the voltage swings caused by multipath reception. To control damping, S2A and S2B switch the 4700-µF capacitors in or out of the circuit. You want the greatest amount of damping when you drive through an area with a lot of multipath propagation (as from buildings); a lot of damping helps under those circumstances.

Construction

The prototype was built using a pad-per-hole RadioShack board. However, a PC board makes construction a lot faster. Far Circuits offers a printed-circuit project on their Web site: **www.cl.ais.net/farcir**). Except for the optional meters and the nonpolarized capacitors, most parts are available from RadioShack.

First build the power supply so you can power the unit from your car or another 12-V source. Apply 12 V to the DFer and adjust R1 until U1's output is +9 V. (You can use a 9-V battery and omit the power-supply section, but you'd better take along a spare battery when you go DFing.)

Install U2 and its associated parts. Power up and turn on S1. A string of pulses should appear at TP1. If you have a frequency counter, set R4 for a pulse frequency of 2200 Hz at TP1. If you don't have a counter, connect a 0.1-µF capacitor from TP1 to headphones or a small speaker and set R4 for a tone of about 2 kHz. Later, you'll adjust the clock so the unit works with the passband of your receiver.

Turn off S1 and remove the power source. Install U3 and its diodes. Pin 12 of U3 need not be connected yet. Apply power and turn on S1. At TP2 and TP3, you should find alternating 1100-Hz pulses. If you have a dual-trace scope, you can see that the pulses alternate. If you have a single-trace scope, connect TP3 to TP2 and to the scope input and the trace will appear as a solid line as there is a pulse at either TP2 or TP3 at all times. If you don't have a scope, the tone in a speaker or earphones from TP2 or TP3 will sound half as high (about 1 kHz) as the tone at TP1.

Turn off S1. Install U4 and its diodes. Note that pin 12 of U3 is connected to pin 14 of U4. At TP4 and TP5, there should be long pulses—five times longer than the pulses at TP1, and the pulses should alternate between TP4 and TP5. The pulse frequency should be about 44 Hz. Power down and turn off S1. Install the remaining circuit components. When you power up, 25 alternating pulses should appear at A and B, then 25 alternating pulses should appear at C and D. Use a scope to verify that.

If you're not using the optional panel meters, connect a voltmeter across R24 (L/R BALANCE), using the lowest dc-voltage range. Note that neither end of R24 is grounded. With no audio input, adjust R24 until there is no voltage across it. Do the same with R27 (F/B BALANCE). If you use the optional meters, adjust R24 and R27 so there's no current shown on either meter.

Power down and assemble the rest of the circuit. With power applied, but with no audio input, adjust R31, 33, 42 and 44 so that the four LEDs (DS1 through DS4) are off. The objective of the following adjustments is to get the red and green LEDs to turn on with the same voltage amplitude, but opposite polarity, across R24. Move R24's wiper so a low positive voltage appears across R24, as indicated by the voltmeter connected across R24 or movement of the panel-meter needle. Adjust R44 (LED ADJ 1A) and R42 (LED ADJ 1B) so that the green LED (DS4) comes on when the voltage goes positive at one end of

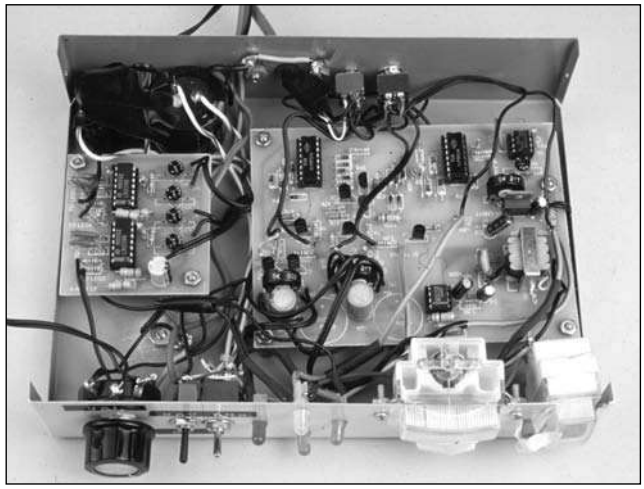

Fig 42—An inside view of one DF unit built into a 2 × 8 × 5¾-inch (HWD) box. Because of the height restriction, the two 4700-µF damping capacitors (C8 and C10) are not mounted on the PC board, but near the rear panel behind the smaller of the two PC boards. One of the 4700-µF damping capacitors is a standard electrolytic, the other is a parallel combination of five 1000-µF, 6.3-V bipolar (nonpolarized) capacitors wrapped in electrical tape.

Fig 43—The rear panel of the DF unit supports the two DPDT PHASE toggle switches. Grommets in the panel holes allow abrasion-free passage of the antenna, dc-power and audio cables. The dc power cord is outfitted with an inline fuse holder and a male Jones plug. A six-pin female Molex connector (five pins are used) feeds the four antennas. The audio-input cable is terminated in a 1/8-inch diameter male plug.

R24, but goes off when R24 is adjusted for 0 V across R24.

Next, adjust R24 for a slight negative-voltage indication and adjust R42 and R44 so that the red LED (DS3) comes on, but extinguishes when the voltage across R24 is 0 V. When you're done, adjusting R24's wiper slightly one way should illuminate the red LED. Both LEDs should be off when there's no voltage across R24; rotating R24's wiper slightly in the opposite direction should turn on the green LED.

Connect the voltmeter across R27 or use the panel meter as an indicator. With no audio input, adjust R27 so that there's no voltage across R27. Adjust R31 (F/B LED ADJ 1A) and R33 (F/B LED 1B) so that a F/B LED (DS1) is on when there is a slight positive voltage across R27 and the other F/B LED (DS2) is on when there is a negative voltage across R27.

Switch Board

Assemble the switch board for the four mag-mount antennas (see Fig 40). You can use half of a RadioShack dual pad-per-hole PC board (RS 276-148) as a platform. Lead length is critical only on this board and in the length of the coax from the switching board to the antennas, so avoid wire-wrap construction here.

Feed Lines

The coax lines from the switch board to each of the four antennas must be of equal length. The coax lengths should be long enough to permit each antenna to be placed slightly less than 1/4 λ from its counterpart, at the lowest frequency of operation. (There's a local belief that 27 1/2 inches is the best length. The author used that length and it works, but other lengths might work as well.) An attempt to locate the switch board inside the vehicle and run equal-length 12-foot-long cables to the antennas failed. Keep the switch board on the vehicle's roof.

Use the same type of coax for all lines—that is, don't mix foam and polyethylene dielectric coax on the antenna lines. If the velocity factor of the lines is not equal, a phase shift in the signals will exist even when the transmitter is dead ahead and it will lead you astray.

Solder the coax from the antennas directly to the board—don't use connectors. From the switch board to the receiver, use 50-Ω coax of any type and length. Equip the receiver end of the line with a connector that mates with your receiver's antenna-input jack. Make the four-conductor shielded cable from the main DFer box to the switch board long enough to reach from the LRFB box's operating position to the roof of the car. Construct the antennas so that the whips can be changed easily for use on any frequency in which you're interested.

Mechanical Assembly

Mount the finished PC boards in a metal box of your choice. You can follow the construction method used in the prototype (see **Fig 42** and **Fig 43**), but do ensure that R4 can be adjusted easily with a tuning tool from outside the box. A hole drilled in the box at the right point will suffice. Arrange the LEDs in a diamond pattern on the front panel, with the left LED (red) to the left, the right LED (green) on the right, and the front and back LEDs at the top and the bottom.

Wrap the switch board with tape to waterproof it, or place it in a watertight box. Arrange the mag-mount antennas on top of the vehicle in a diamond shape. The distance between each antenna pair should be less than 1/4 λ at the operating frequency. (In limiting the distance between antennas in a pair—F/B or L/R—to less than 1/4 λ, the author followed W9DUU's example.)

Final Adjustments

It's best to start on 2 meters. Install the 2-meter whips in the antenna bases. Mount the antennas on the top of your vehicle. Identify the left and right antenna bases with L and R, and mark the front and back antenna bases, too.

A good way to find out if the antennas are properly installed is to short either the left or right antenna with a clip lead from the whip to the metal base; the L/R meter will deflect one way and the left or right LED will light. If you short one of the front and back antennas with a clip lead, the front or back LED will come on. If you short one of the L/R antennas and it makes the meter go to the right, it does not necessarily mean you have the PHASE switch in the proper position. That depends on the relative phase determined by the number of audio stages in your receiver, each of which may contribute a shift of 180°.

Connect the coax from the switch board to your FM receiver. It must be an FM receiver; an AM VHF or AM aircraft receiver won't suffice. Connect the audio output

of your 2-meter receiver to the LRFB box audio input. If you're using a transceiver, disable its transmit function by removing the mike. You don't want to transmit into the switch board!

Turn on the receiver and place the LRFB box in receive by setting S1 to the RCV position. Center R10. Only one of the antennas will be turned on and the DF operation will be disabled. Back off the squelch and notice that you hear the audio from the speaker of the LRFB box. Switch to an unused simplex channel. Have a friend with an HT stand 20 feet or so in front of the vehicle. With the receiver in the car turned off, turn S1 to DF. The four LEDs should be off. If an LED lights, adjust R24 and R27 for zero voltage. If the LED is still on, readjust R31 and R33, or R42 and R44 as explained earlier. When all four LEDs are off with the antennas connected, no audio from the receiver and no RF input signal, you're ready. Turn on your receiver and have your friend transmit on the 2-meter frequency (simplex) that your receiver is set to. When he transmits, one or more of the LEDs should illuminate. Ignore the front/back LEDs, but check to see if the right or left LED is on. If the right LED is on and your friend is standing to the right of the center of the vehicle front, all is well. Have him walk back and forth in front of the vehicle and notice that when he is to the right, the green LED turns on, and when he's to the left, the red LED glows. If the indications are reversed, that is, if the LRFB box indicates left when your friend is to your right, reverse the position of PHASE switch S3.

When the L/R indicators are working properly, have your friend walk back and forth between a position 20 feet to the front and right of the car and a position 20 feet away to the rear and right of the car. The right LED should stay on, but the front LED should be on when the HT is in front of the antennas, and the back LED should be on when the HT is behind the antennas. If the front/back indications are reversed, reverse the position of PHASE switch S4.

While receiving a signal from your friend's HT, adjust R4 for maximum deflection on any one of the two optional meters, or on a voltmeter (set on the lowest dc voltage range) connected across R24 or R27. Look for the maximum deflection of the meter needle as the meter swings both ways while the signal source moves from back to front or left to right (depending, of course, on which panel meter you're looking at or which resistor—R24 or R27—your voltmeter is across). The audio passband of FM receivers varies, and if you switch from an ICOM IC-27 to an ICOM IC-W2A, for example, you'll have to change U2's master clock frequency. You may encounter receivers that don't require readjusting R4, but such readjustment should be expected. When changing receivers, you may also need to change the position of PHASE switches S3 and S4. This may also be necessary when changing from UHF to VHF, or VHF to UHF on the same receiver, as the number of receiver stages (and, hence, the audio phase) may change from band to band.

Audio Level Adjustments

With meter damping (S2) off, adjust R10 so that you have full deflection of one of the two meters (or your multimeter) with the signal source at a 45° angle from the vehicle (halfway between ahead and right), and a reasonable audio level from the speaker. Turn the rig's volume control all the way up to ensure that the audio circuit doesn't overload. If it overloads, the meters won't deflect. From zero to full blast, the meter should deflect more and more (unless the signal is straight ahead or exactly left or right). If you're using an H-T, maximum deflection of the meter should occur before the volume control is $^3/_4$ of maximum, or before the volume control is at $^1/_2$ of maximum if you're using a mobile rig. If R10 is properly adjusted, turning the volume control to maximum won't cause the meter to fall back toward zero. If increasing the volume causes the meter to deflect less, then R10's setting is too high.

Now have your friend walk around the vehicle with the HT transmitting and notice that the LEDs indicate the signal direction. On 2 meters in a clear field, the indications should be correct 80 or 90% of the time. The erroneous readings that occasionally occur are due to multipath propagation caused by the irregular shape of the vehicle. Slight adjustments in the positions of the L/R and F/B antennas may be necessary to make the zero points fall directly in front of the vehicle (neither left nor right LED on) and at the center of the antennas (neither front nor back LED on).

Try the same procedure on 440 MHz. You may have to flip the PHASE switches when you move to another band, even when using the same receiver. Remember that the total length of the 440-MHz antennas must be $^1/_4$ λ or less, and the antennas must be placed less than $^1/_4$ λ apart. The results on 440 MHz probably won't be as consistent as the results on 2 meters, as there is likely to be a lot more multipath propagation caused by the irregular shape of the vehicle.

Fox Hunting

Before heading out to find the fox, check to be certain the LRFB box is working properly. Tune to the fox's frequency and drive off. Turning on the DAMPING switch stabilizes the indication as you drive along. Follow indications generated as you travel over the road or street. If an indication is constant for 15 or 20 seconds while you're moving down the road, it's probably the true direction to the fox. It's possible to have a reflection from a mountain over a long distance down the road, however. When you can hear the fox with no antenna, it's time to get out of the car, switch to the hand-held system and hunt for the fox on foot.

If you switch to a new receiver, you may have to readjust R4, CLOCK FREQ. That's because both receivers may not have the same audio bandwidth. Author WA9BVS forgot this while chasing a balloon once and

the results were comical. When chasing balloons with ham radio transmitters, the readings you get are likely to be confusing when the balloon is at a high angle with respect to the plane of the car top. Use a hand-held Yagi to verify the balloon location. Even with a simple buzzbox, you should be able to find a keyed transmitter.

A TAPE-MEASURE BEAM FOR RDFING

Joe Leggio, WB2HOL, designed this antenna while searching for a beam with a really great front-to-back ratio to use in hidden transmitter hunts. It exhibits a very clean pattern and is perfect for RDF use. You can construct this beam using only simple hand tools, and it has been duplicated many times.

WB2HOL's first design requirement was to be able to get in and out of his car easily when hunting for a hidden transmitter. He accomplished this by using steel "tape-measure" elements, which fold easily when putting the antenna into a car and yet are self supporting. They also hold up well while crashing through the underbrush on a fox hunt.

WB2HOL decided to use three elements to keep the boom from getting too long. He used inexpensive

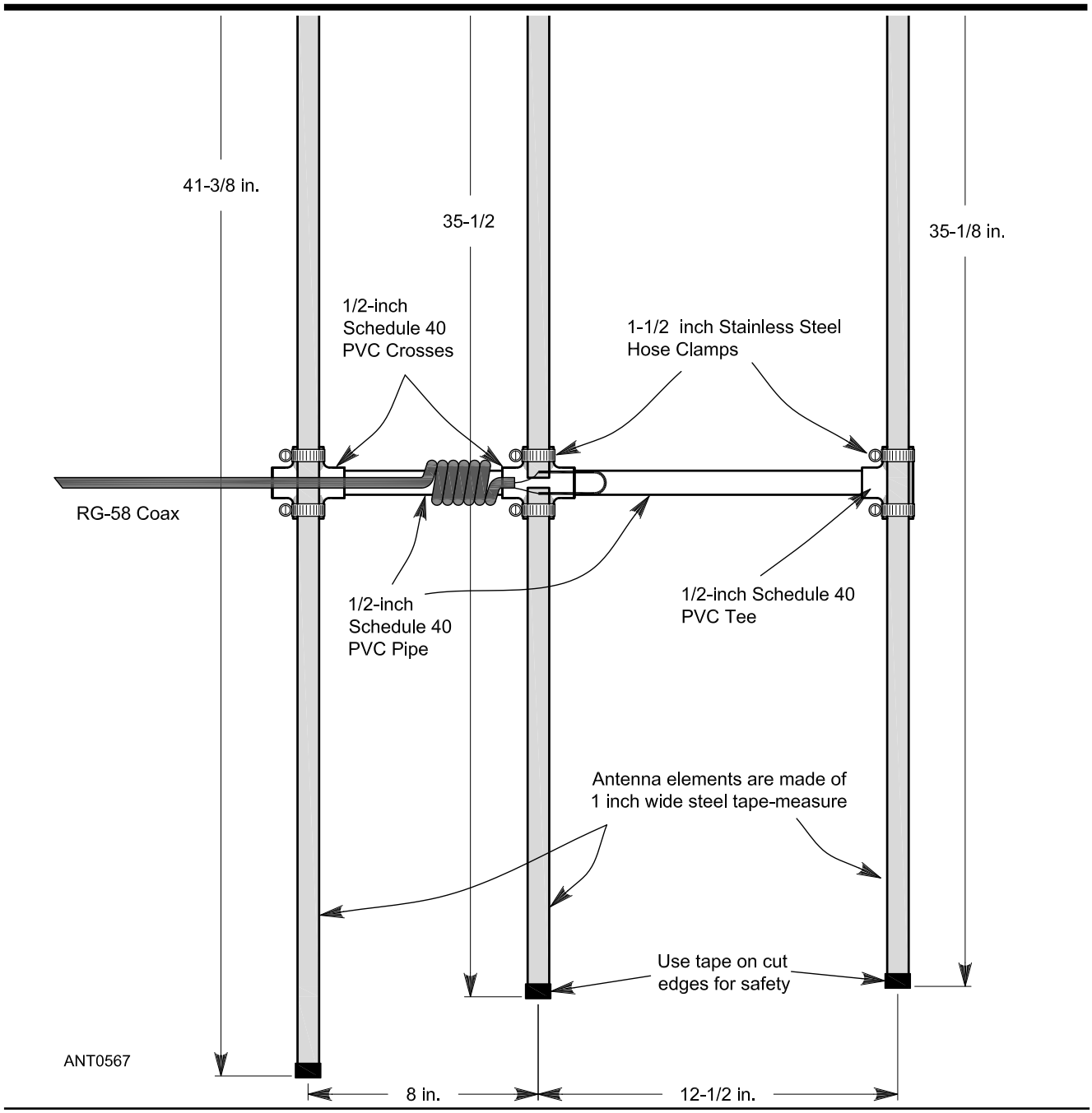

Fig 44—Tape-measure beam dimensions.

Fig 45—Photo of driven-element mounted to PVC tee using hose clamps. The hairpin match wires is shown here soldered to the tape-measure elements, along with the RG-58 feed line.

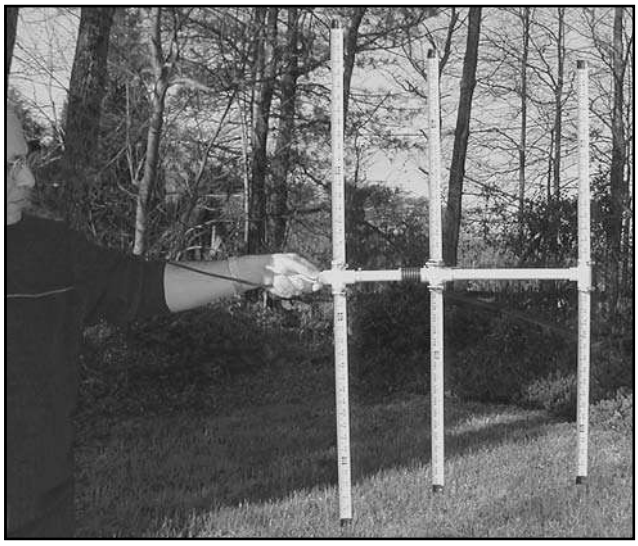

Fig 46—Photo of complete tape-measure beam, ready to hunt foxes!

Schedule-40 PVC pipe, crosses and tees that can be found at any hardware store for the boom and element supports.

He used a simple hairpin match, consisting of a 5-inch length of #14 solid wire bent into the shape of a U, with the two legs about 3/4 inch apart. This gave in a very good match across the 2-meter band after he tweaked the distance (1-inch on his prototype) between the halves of the driven element for minimum SWR.

You can cut the 1-inch wide tape-measure elements with a pair of shears, chamfering the ends of the elements. Be very careful—the edges are very sharp and will inflict a nasty cut if you are careless. Use some sandpaper to remove the sharp edges and burrs and put some vinyl electrical tape on the ends of the elements to protect yourself from getting cut. Wear safety glasses while cutting the elements. See **Fig 44** for dimensions.

The RG-58 coax feed line is wound into a 8-turn coil along the boom to form a choke balun. The coil is covered with vinyl black tape to secure it to the boom. Make sure you scrape or sand the paint off the tape-measure elements where the feed line is attached. Most tape measures have a very durable paint finish designed to stand up to heavy use. You do not want the paint to insulate your feed-line connection!

If you are careful, you can solder the feed line to the element halves, but take care since the steel tape measure does not solder easily and the PVC supports can be easily melted. Tin the tape-measure elements before mounting them to the PVC cross if you decide to connect the feed line in this fashion.

If you decide not to solder to the tape-measure elements, you can use two other methods to attach the feed line. One method employs ring terminals on the end of the coax. The ring terminals are then secured under self-tapping screws or with 6-32 bolts and nuts into holes drilled in the driven-element halves. However, with this method you cannot fine-tune the antenna by moving the halves of the driven element in and out.

The simplest method is simply to slide the ends of the feed line under the driven element hose clamps and tighten the clamps to hold the ends of the coax. This is low-tech but it works just fine.

WB2HOL used 1 1/2-inch stainless-steel hose clamps to attach each driven-element half to the PVC cross that acts as its support. This allowed him to fine-tune his antenna for lowest SWR simply by loosening the hose clamps and sliding the halves of the driven element in or out to lengthen or shorten the element. He achieved a 1:1 SWR at 146.565 MHz (the local fox-hunt frequency) when the two elements were spaced about 1 inch apart. **Fig 45** shows the hose-clamp method for attaching the driven element to the PVC cross, along with the hairpin wire and feed-line coax.

Some builders have used rubber faucet washers between the tape-measure elements and the PVC-cross fittings on the director and reflector. These allow for the tape to fit the contour of the PVC fitting better and will make the antenna look nicer. It is normal for the reflector and director elements to buckle a bit as they are tightened to the PVC tee and cross if you don't use faucet washers. You can also eliminate the buckling if you use self-tapping screws to attach these elements instead of hose clamps. The beam will not be as rugged, however, as when you use hose clamps.

This beam has been used on fox hunts, on mountain tops, at local public-service events, outdoors, indoors in attics—just about everywhere. The SWR is typically very close to 1:1 once adjusted. Front-to-back performance is exactly as predicted. The null in the rear of the pattern is perfect for transmitter hunts.

BIBLIOGRAPHY

Source material and more extended discussion of topics covered in this chapter can be found in the references given below and in the textbooks listed at the end of Chapter 2.

W. U. Amphar, "Unidirectional Loops for Transmitter Hunting," *QST*, Mar 1955.

G. Bonaguide, "HF DF—A Technique for Volunteer Monitoring," *QST*, Mar 1984.

D. S. Bond, *Radio Direction Finders*, 1st edition (New York: McGraw-Hill Book Co).

R. E. Cowan and T. A. Beery, "Direction Finding with the Interferometer," *QST*, Nov 1985.

D. DeMaw, "Beat the Noise with a Scoop Loop," *QST*, Jul 1977.

D. DeMaw, "Maverick Trackdown," *QST*, Jul 1980.

T. Dorbuck, "Radio Direction-Finding Techniques," *QST*, Aug 1975.

D. T. Geiser, "Double-Ducky Direction Finder," *QST*, Jul 1981.

D. T. Geiser, "The Simple Seeker," *The ARRL Antenna Compendium, Vol 3*, p 126.

N. K. Holter, "Radio Foxhunting in Europe," Parts 1 and 2, *QST*, Aug and Nov 1976.

J. Isaacs, "Transmitter Hunting on 75 Meters," *QST*, Jun 1958.

H. Jasik, *Antenna Engineering Handbook*, 1st edition (New York: McGraw-Hill, 1961).

R. Keen, *Wireless Direction Finding*, 3rd edition (London: Wireless World).

J. Kraus, *Antennas*, 2nd edition (New York: McGraw-Hill Book Co, 1988).

J. Kraus, *Electromagnetics*, 4th edition (New York: McGraw-Hill Book Co, 1992).

C. M. Maer, Jr., "The Snoop-Loop," *QST*, Feb 1957.

M. C. Mallette, "The Four-Way DFer," *QST*, Nov 1995. A set of two PC boards is available from FAR Circuits for the "Four-Way DFer" project. 18N640 Field Ct, Dundee, IL 60118-9269, tel 708-576-3540 (voice and fax). Note: No component pads for C15 exist. Mount C15 between U2 pin 5 and ground on the bottom (foil) side of the board. A PC-board template package is available from the ARRL free of charge. Send your request for the MALLETTE 4-WAY DFER, along with a business size SASE, to the Technical Department Secretary, 225 Main St, Newington, CT 06111-1494.

L. R. Norberg, "Transmitter Hunting with the DF Loop," *QST*, Apr 1954.

P. O'Dell, "Simple Antenna and S-Meter Modification for 2-Meter FM Direction Finding," Basic Amateur Radio, *QST*, Mar 1981.

Ramo and Whinnery, *Fields and Waves in Modern Radio* (New York: John Wiley & Sons, 1944).

F. Terman, *Electronic and Radio Engineering* (New York: McGraw-Hill Book Co, 1955).

Radio Direction Finding , published by the Happy Flyer, 1811 Hillman Ave, Belmont, CA 94002.

For more information on direction finding, see *The ARRL Handbook* and *Transmitter Hunting: Radio Direction Finding Simplified*, by Joe Moell, KØOV, and Thomas Curlee, WB6UZZ. These books are available from your local dealer or can be ordered directly from ARRL.

Chapter 15

Portable Antennas

For many amateurs, the words *portable antennas* may conjure visions of antenna assemblies that can be broken down and carried in a backpack, suitcase, golf bag, or what-have-you, for transportation to some out-of-the way place where they will be used. Or the vision could be of larger arrays that can be disassembled and moved by pickup truck to a Field Day site, and then erected quickly on temporary supports. Portable antennas come in a wide variety of sizes and shapes, and can be used on any amateur frequency.

Strictly speaking, the words "portable antenna" really means *transportable antenna*—one that is moved to some (usually temporary) operating position for use. As such, portable antennas are not placed into service when they are being transported. This puts them in a different class from mobile antennas, which are intended to be used while in motion. Of course this does not mean that mobile antennas cannot be used during portable operation. Rather, true portable antennas are designed to be packed up and moved, usually with quick reassembly being one of the design requisites. This chapter describes antennas that are designed for portability. However, many of these antennas can also be used in more permanent installations.

Any of several schemes can be employed to support an antenna during portable operation. For HF antennas made of wire, probably the most common support is a conveniently located tree at the operating site. Temporary, lightweight masts are also used. An aluminum extension ladder, properly guyed, can serve as a mast for Field Day operation. Such supports are discussed in Chapter 22, Antenna Supports.

A SIMPLE TWIN-LEAD ANTENNA FOR HF PORTABLE OPERATION

The typical portable HF antenna is a random-length wire flung over a tree and end-fed through an antenna tuner. Low-power antenna tuners can be made quite compact, but each additional piece of necessary equipment makes portable operation less attractive. The station can be simplified by using resonant impedance-matched antennas for the bands of interest. Perhaps the simplest antenna of this type is the half-wave dipole, center-fed with 50- or 75-Ω coax. Unfortunately, RG-58, RG-59 or RG-8 cable is quite heavy and bulky for backpacking, and the miniature cables such as RG-174 are too lossy.

A practical solution to the coax problem, developed by Jay Rusgrove, W1VD, and Jerry Hall, K1TD, is to use folded dipoles made from lightweight TV twin-lead. The characteristic impedance of this type of dipole is near 300 Ω, but this can easily be transformed to a 50-Ω impedance. The transformation is obtained by placing a lumped capacitive reactance at a strategic distance from the input end of the line. **Fig 1** illustrates the construction method and gives important dimensions for the twin-lead dipole.

A silver-mica capacitor is shown for the reactive element, but an open-end stub of twin-lead can serve as well, provided it is dressed at right angles to the transmission line for some distance. The stub method has the advantage of easy adjustment of the system resonant frequency.

The dimensions and capacitor values for twin-lead dipoles for the HF bands are given in **Table 1**. To pre-

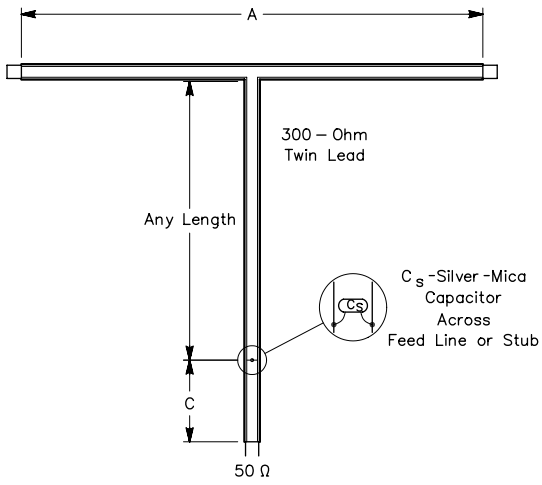

Fig 1—A twin-lead folded dipole makes an excellent portable antenna that is easily matched to 50-Ω equipment. See text and Table 1 for details.

Table 1
Twin-Lead Dipole Dimensions and Capacitor Values

Frequency	*Length A*	*Length C*	C_s	*Stub Length*
3.75 MHz	124' 9½"	13' 0"	289 pF	37' 4"
7.15	65' 5½"	6' 10"	151 pF	19' 7"
10.125	46' 2½"	4' 10"	107 pF	13' 10"
14.175	33' 0"	3' 5½"	76 pF	9' 10½"
18.118	25' 10"	2' 8½"	60 pF	7' 9"
21.225	22' ½"	2' 3½"	51 pF	6' 7"
24.94	18' 9"	1' 11½"	43 pF	5' 7½"
28.5	16' 5"	1' 8½"	38 pF	4' 11"

serve the balance of the feeder, a 1:1 balun must be used at the end of the feed line. In most backpack QRP applications the balance is not critical, and the twin-lead can be connected directly to a coaxial output jack—one lead to the center contact, and one lead to the shell.

Because of the transmission-line effect of the shorted-radiator sections, a folded dipole exhibits a wider bandwidth than a single-conductor type. The antennas described here are not as broad as a standard folded dipole because the impedance-transformation mechanism is frequency selective. However, the bandwidth should be adequate. An antenna cut for 14.175 MHz, for example, will present an SWR of less than 2:1 over the entire 14-MHz band.

ZIP-CORD ANTENNAS

Zip cord is readily available at hardware and department stores, and it's not expensive. The nickname, *zip cord*, refers to that parallel-wire electrical cord with brown or white insulation used for lamps and many small appliances. The conductors are usually #18 stranded copper wire, although larger sizes may also be found. Zip cord is light in weight and easy to work with.

For these reasons, zip cord can be pressed into service as both the transmission line and the radiator section for an emergency dipole antenna system. This information by Jerry Hall, K1TD, appeared in *QST* for March 1979. The radiator section of a zip-cord antenna is obtained simply by "unzipping" or pulling the two conductors apart for the length needed to establish resonance for the operating frequency band. The initial dipole length can be determined from the equation $\ell = 468/f$, where ℓ is the length in feet and f is the frequency in MHz. (It would be necessary to unzip only half the length found from the formula, since each of the two wires becomes half of the dipole.) The insulation left on the wire will have some loading effect, so a bit of length trimming may be needed for exact resonance at the desired frequency.

For installation, you may want to use the electrician's knot shown in **Fig 2** at the dipole feed point. This is a balanced knot that will keep the transmission-line part of the system from unzipping itself under the tension of dipole suspension. This way, if zip cord of sufficient length for both the radiator and the feed line is obtained, a solder-free installation can be made right down to the input end of the line.

(Purists may argue that knots at the feed point will create an impedance mismatch or other complications, but as will become evident in the next section, this is not a major consideration.) Granny knots (or any other variety) can be used at the dipole ends with cotton cord to suspend the system. You end up with a lightweight, low-cost antenna system that can serve for portable or emergency use.

But just how efficient is a zip-cord antenna system? Since it is easy to locate the materials and simple to install, how about using such for a more permanent installation? Upon casual examination, zip cord looks about like 72-Ω balanced feed line. Does it work as well?

Zip Cord as a Transmission Line

To determine the electrical characteristics of zip cord as a radio-frequency transmission line, a 100-foot roll was subjected to tests in the ARRL laboratory with an RF impedance bridge. Zip cord is properly called *parallel power cord*. The variety tested was manufactured for GC Electronics, Rockford, IL, being 18-gauge, brown, plastic-insulated type SPT-1, GC cat. no. 14-118-2G42. Undoubtedly, minor variations in the electrical-characteristics will occur among similar cords from different manufacturers, but the results presented here are probably typical.

The characteristic impedance was determined to be 107 Ω at 10 MHz, dropping in value to 105 Ω at 15 MHz and to a slightly lower value at 29 MHz. The nominal

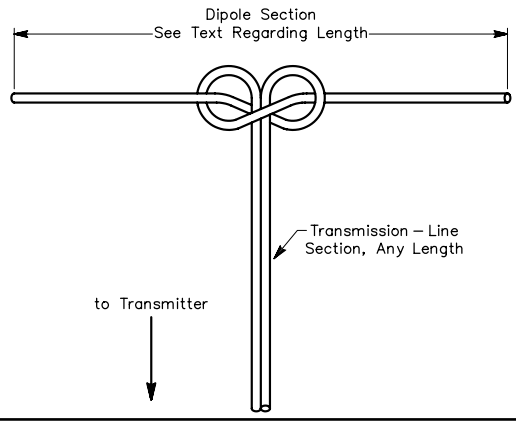

Fig 2—This electrician's knot, often used inside lamp bases and appliances in lieu of a plastic grip, can also serve to prevent the transmission-line section of a zip-cord antenna from unzipping itself under the tension of dipole suspension. To tie the knot, first use the right-hand conductor to form a loop, passing the wire behind the unseparated zip cord and off to the left. Then pass the left-hand wire of the pair behind the wire extending off to the left, in front of the unseparated pair, and thread it through the loop already formed. Adjust the knot for symmetry while pulling on the two dipole wires.

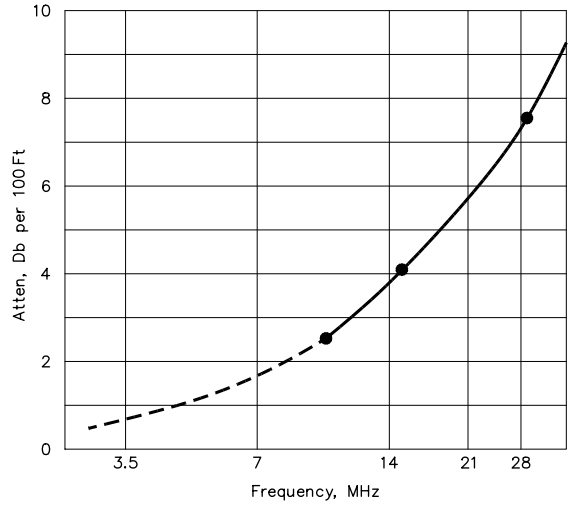

Fig 3—Attenuation of zip cord in decibels per hundred feet when used as a transmission line at radio frequencies. Measurements were made only at the three frequencies where plot points are shown, but the curve has been extrapolated to cover all high-frequency amateur bands.

value is 105 Ω at HF. The velocity factor of the line was determined to be 69.5%.

Who needs a 105-Ω line, especially to feed a dipole? A dipole in free space exhibits a feed-point resistance of 73 Ω, and at heights above ground of less than 1/4 wavelength the resistance can be even lower. An 80-meter dipole at 35 feet over average soil, for example, will exhibit a feed-point resistance of about 35 Ω. Thus, for a resonant antenna, the SWR in the zip-cord transmission line can be 105/35 or 3:1, and maybe even higher in some installations. Depending on the type of transmitter in use, the rig may not like working into the load presented by the zip-cord antenna system.

But the really bad news is still to come—line loss! **Fig 3** is a plot of line attenuation in decibels per hundred feet of line versus frequency. Chart values are based on the assumption that the line is perfectly matched (sees a 105-Ω load as its terminating impedance).

In a feed line, losses up to about 1 decibel or so can be tolerated, because at the receiver a 1-dB difference in signal strength is just barely detectable. But for losses above about 1 dB, beware. Remember that if the total losses are 3 dB, half of your power will be used just to heat the transmission line. Additional losses over those charted in Fig 3 will occur when standing waves are present. (See Chapter 24, Transmission Lines.) The trouble is, you can't use a 50- or 75-Ω SWR instrument to measure the SWR in zip-cord line accurately.

Based on this information, we can see that a hundred feet or so of zip-cord transmission line on 80 meters might be acceptable, as might 50 feet on 40 meters. But for longer lengths and higher frequencies, the losses become appreciable.

Zip Cord Wire as the Radiator

For years, amateurs have been using ordinary copper house wire as the radiator section of an antenna, erecting it without bothering to strip the plastic insulation. Other than the loading effects of the insulation mentioned earlier, no noticeable change in performance has been noted with the insulation present. And the insulation does offer a measure of protection against the weather. These same statements can be applied to single conductors of zip cord.

The situation in a radiating wire covered with insulation is not quite the same as in two parallel conductors, where there may be a leaky dielectric path between the two conductors. In the parallel line, it is the current leakage that contributes to line losses. This leakage current is set up by the voltage potential that exists on the two adjacent wires. The current flowing through the insulation on a single radiating wire is quite small by comparison, and so as a radiator the efficiency is high.

In short, communications can certainly be established with a zip-cord antenna in a pinch on 160, 80, 40, 30 and perhaps 20 meters. For higher frequencies, especially with long line lengths for the feeder, the efficiency of the system is so low that its value becomes questionable.

A TREE-MOUNTED HF GROUND-PLANE ANTENNA

A tree-mounted, vertically polarized antenna may sound silly. But is it really? Perhaps engineering references do not recommend it, but such an antenna does not cost much, is inconspicuous, and it works. This idea was described by Chuck Hutchinson, K8CH, in *QST* for September 1984.

The antenna itself is simple, as shown in **Fig 4**. A piece of RG-58 cable runs to the feed point of the antenna, and is attached to a porcelain insulator. Two radial wires are soldered to the coax-line braid at this point. Another piece of wire forms the radiator. The top of the radiator section is suspended from a tree limb or other convenient support, and in turn supports the rest of the antenna.

The dimensions for the antenna are given in **Fig 5**. All three wires of the antenna are ¼ wavelength long. This generally limits the usefulness of the antenna for portable operation to 7 MHz and higher bands, as temporary supports higher than 35 or 40 feet are difficult to come by. Satisfactory operation might be had on 3.5 MHz with an inverted-L configuration of the radiator, if you can overcome the accompanying difficulty of erecting the antenna at the operating site.

The tree-mounted vertical idea can also be used for fixed station installations to make an invisible antenna. Shallow trenches can be slit for burying the coax feeder and the radial wires. The radiator itself is difficult to see unless you are standing right next to the tree.

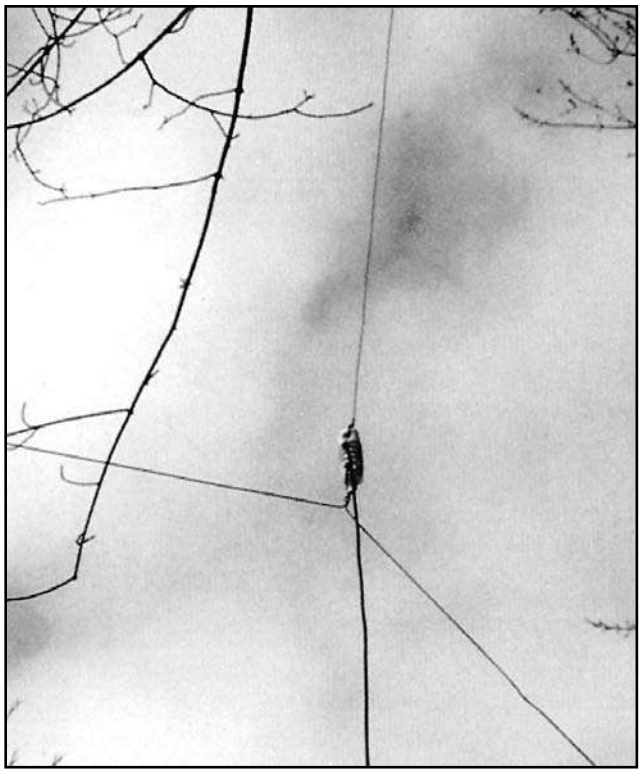

Fig 4—The feed point of the tree-mounted ground-plane antenna. The opposite ends of the two radial wires may be connected to stakes or other convenient points.

A PORTABLE DIPOLE FOR 80 TO 2 METERS

This dipole antenna, described by Robert Johns, W3JIP, in August 1998 *QST*, can be used for any band from 80 through 2 meters. One half of the dipole is an inductively loaded aluminum tube. Its length is adjustable from 4 to 11 feet, depending on how much room is available. The other half is flexible insulated wire that can be spooled out as necessary. The tube is supported by a flagpole bracket attached to a long carpenter's clamp. The clamp mounts the antenna to practically anything: a windowsill, railing, a chair or post. If there is no structure to mount the antenna (a parking lot or the beach), the clamp attaches to two light wooden legs to form a tripod, as shown in **Fig 6**.

The key to mounting flexibility is the large clamp. The key to electrical flexibility is a large adjustable coil that lets you resonate the tube on many bands. The coil is wound with #8 aluminum ground wire from RadioShack. The form is a four-inch ($4^1/_2$-inch OD) styrene drain coupling from the Home Depot or a large plumbing supply store. A movable tap adjusts the inductance to tune the upright tube to the desired band. The wire half of the antenna is always a bit less than $\lambda/4$ on each band. Hang it from any convenient support or drape it over bushes to keep it off the ground.

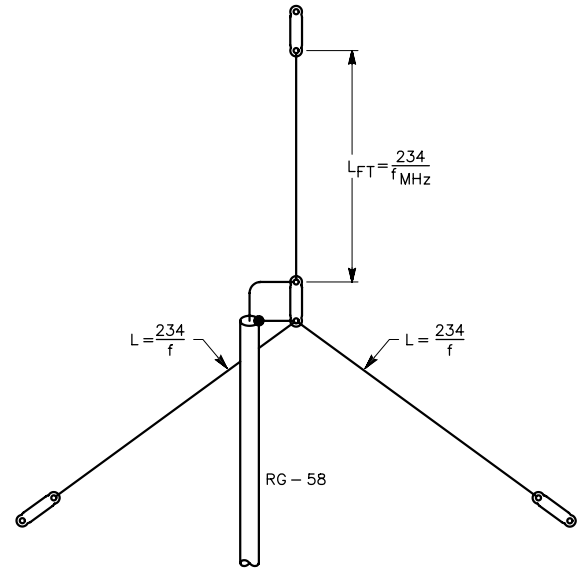

Fig 5—Dimensions and construction of the tree-mounted ground-plane antenna.

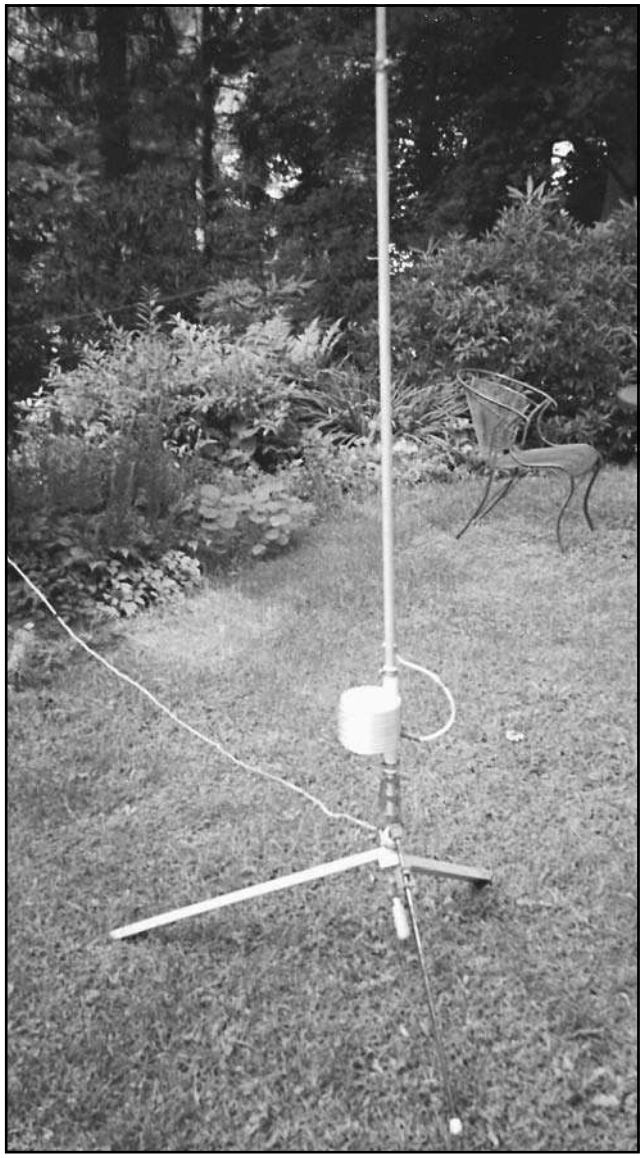

Fig 6—At top, the portable antenna in some of the many places it may be mounted around the house, porch and yard. At bottom, the simple ground-mounted legs that make a tripod.

Construction

The 18-inch carpenter's clamp (sometimes called a *bar clamp*, such as Jorgensen's No. 3718) and flagpole bracket that takes a $^3/_4$-inch pole are common hardware items. Insulate the bracket from the clamp jaw with a $1^1/_2$-inch length of 1-inch PVC pipe (see **Fig 7**). Hammer the PVC over the end clamp jaw to make it take the shape of the jaw. Secure the flagpole bracket to PVC with a large ground clamp (for $^1/_2$ or 1-inch conduit). The ground clamp includes $^1/_4$-inch bolts; enlarge the flagpole bracket holes to accept them. Some flagpole brackets have an integral cleat; the author hammered the cleat ears flat on his.

Mount an SO-239 chassis connector on the flagpole bracket using RadioShack insulated standoffs (276-1381). The standoffs tightly press the center pin of the SO-239 against the bracket surface; no other connection is needed. Other mounting hardware may require a connection from the coax center conductor to the bracket. The spooled wire's inner end wraps around a standoff and connects to a ring terminal under a screw holding the SO-239 flange to the standoff.

The 1 × 2-inch wooden legs for the tripod are each 30 inches long. Bolt them together at one end with a 1 or $1^1/_4$-inch-long bolt. Countersink the bolt head and nut below the surface of the wood so they don't interfere with the clamp jaws.

Aluminum Element

You can make this element from three lengths of telescoping aluminum tubing ($^3/_4$, $^5/_8$ and $^1/_2$ inch, 0.058-inch walls). The author used tubing with thinner walls for less weight and easier handling. A 45-inch-long, $^3/_4$-inch tube fits the flagpole bracket. He chose this length because it and the flagpole bracket make $\lambda/4$ on 6 meters. The two outer tubes are both $^5/_8$ inch, made by cutting a seven-foot aluminum clothesline pole in halves. They are

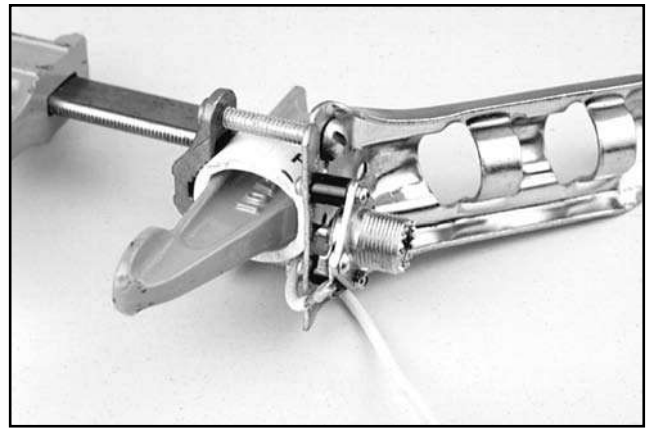

Fig 7—The flagpole bracket that supports the tubing elements is clamped to the long carpenter's clamp, but insulated from it by a small section of 1-inch PVC pipe. A coax connector is mounted to the bracket and the spool of wire is attached to the coax connector.

joined together with a copper coupling (5/8 inch ID) for 1/2-inch copper pipe. The coupling is bolted to one of the 5/8-inch sections, and a slot is cut in the free half of the coupling. The remaining 5/8-inch tube is inserted there and secured with a hose clamp. See **Fig 8**.

One 5/8-inch tube slides into the 3/4-inch tube to provide a continuously variable element length from about 4 to 7 1/2 feet. This extends from 7 1/2 to 11 feet when the two 5/8-inch sections are joined together.

Loading Coil

The loading coil has 12 turns of bare aluminum wire spaced to fill the 3 1/2-inch length of the drain coupling. Drill 9/64-inch holes at the ends of the coil form to accept the ends of the coil wire. (See **Fig 9**.) To wind the coil, feed four inches of wire through the form, make a sharp bend in the wire and start winding away from the nearby mounting hole. Wind 12 turns on the form, spacing them only approximately. Cut the wire for a 4-inch lead and feed it through the other hole in the form. Tighten the wire as best you can and bend it into another acute angle where it passes into the form. Space the turns about equally, but don't fuss with them. Final spacing will be set after the wire is tightened.

Tighten the coil wire by putting a screwdriver or a needle-nose pliers jaw under one turn, and pry the wire up and away from the surface of the coil form. While this can be done anywhere, it's best to put these kinks on the backside, away from the mounting shaft. Put kinks in every other turn, removing any slack from the coil and holding the turns in place. Should the coil ever loosen, simply retighten it with a screwdriver. If you prefer, glue the coil turns in place with epoxy or coil dope. Use a thin bead of glue that won't interfere with the clip that connects to the coil.

The coil form mounts on a nine-inch-long 3/4-inch PVC pipe. (See Fig 9 and **Fig 10**.) The inside diameter is slightly larger than the 3/4-inch aluminum, but slotting the PVC and tightening it with a hose clamp secures the tube. (Use a wide saw to cut these slots, not a hacksaw.) The coil form mounts to the PVC pipe with #6-32 × 1 1/2-inch bolts. A five-inch long, 3/4-inch aluminum tube permanently attaches to one end of the coil assembly and slides into the flagpole bracket. One end of the coil wire connects to this short tube. Flatten the wire end by hammering it on something hard, then drill a 9/64-inch hole in the flattened end and attach it to the short tube with a #6-32 × 1-inch bolt. Tighten the bolt until the 1/2-inch tube starts to flatten. This will keep pressure on the aluminum-to-aluminum joint.

The aluminum element slides into the opposite end of the coil assembly. The hose clamp there can be tightened until the element just slides in snugly.

A 12-inch clip lead connects the aluminum element to the coil. Bolt the plain wire end to the 3/4-inch tube three inches from its end. Many alligator clips will fit in the space between the turns of the coil (about 3/16 inch), but W3JIP preferred using a solid-copper clip (Mueller TC-1). Cut off most of the jaws, so that only the part close to the hinge grabs the coil. This shorter lever grips very tightly.

Wire and Spool

The lower half of the antenna is insulated wire that is about λ/4 on the band of operation. The wire is pulled from the spool, and the remaining wire forms an inductance that doesn't add much to the antenna length. The Home Depot sells #12 and #14 insulated stranded copper wire in 50 and 100-foot lengths, on plastic spools. (See **Fig 11**.) A 1/2-inch dowel fits into the spool to make a

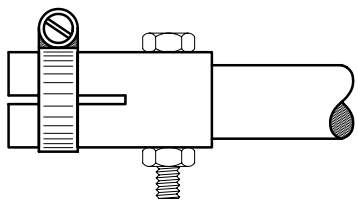

Fig 8—The joint between two sections of 5/8-inch tubing is made from a 1/2-inch copper pipe coupling, bolted to one section and hose clamped to the other.

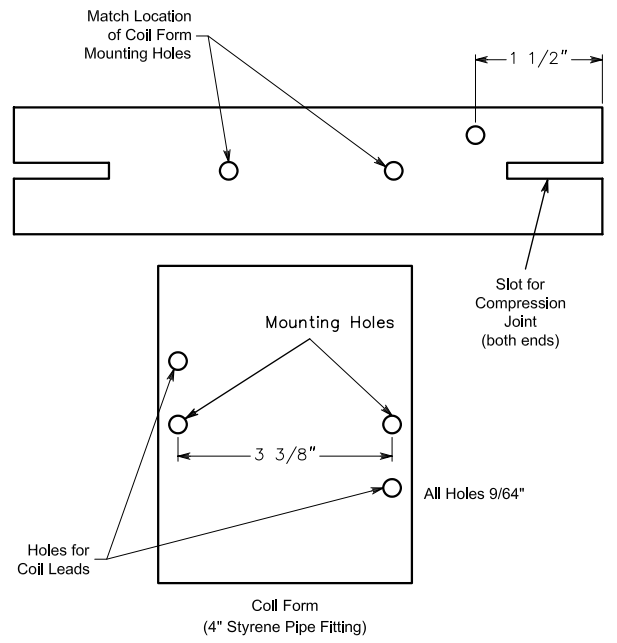

Fig 9—Holes to be drilled in the styrene coupling and the 3/4-inch PVC pipe. All holes are 9/64-inch diameter, to provide clearance for #6-32 bolts. The hole 1 1/2 inches from one end holds a bolt that serves as a stop, so that the antenna tube does not slide in too far. Space the holes for coil leads far enough from the mounting holes to clear the 3/4-inch pipe.

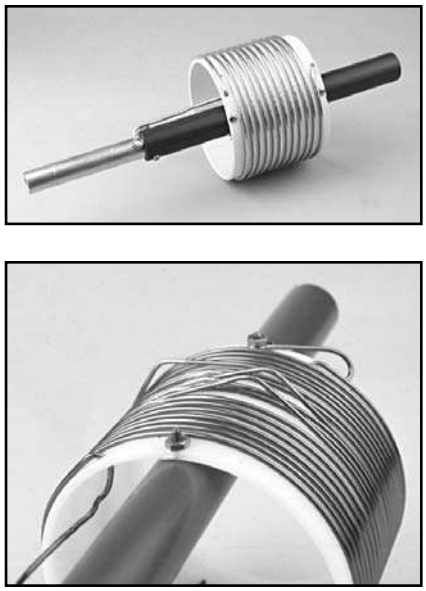

Fig 10—Top photo shows the loading coil for the 20, 30, and 40-meter band coverage. The short aluminum tube on the coil slides into the flagpole bracket, and the tubing element slides into the other end of the PVC pipe. The wire and clip connect the element to the coil. Bottom photo shows the coil for operating the antenna on 80 meters. This is placed in the flagpole bracket and the 40-meter aluminum coil plus the tubing element is inserted into it.

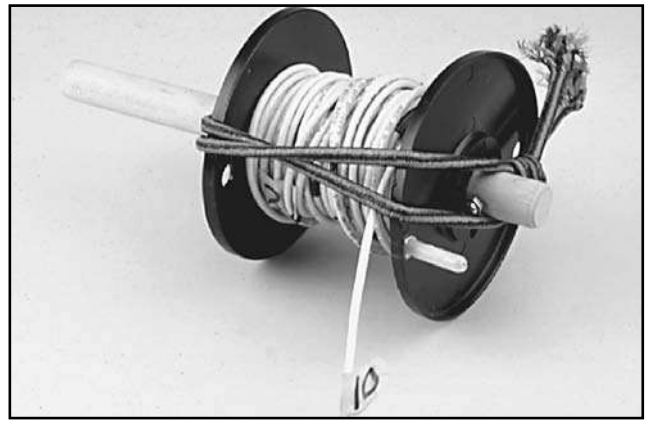

Fig 11—The wire spool has a wooden axle/handle and small handle for winding the wire. A bungee cord stretched over the spool and around the axle prevents the wire from unwinding.

Table 2

	Tubing Length (feet)	*Coil Turns*	*Wire Length (feet)*
6 meters	4	0	4
10 meters	7	0	8
	4	1.7	7
12 meters	8	0	8.3
	4	1.8	9
15 meters	10	0	10.3
	8	1.8	10
	4	3.5	10
17 meters	11	0	13
	8	2.2	13
	4	4.2	13
20 meters	11	1	16
	8	4	16
	4	6.2	16
30 meters	11	4	24
	8	7	24
	4	10.5	24
40 meters	11	9	32
	8	12	32

handle and spool axle. Bolts through the dowel on either side of the spool hold it in place. A crank handle is made by putting a one-inch-long bolt through the spool flange.

The author calibrates the wire on the spool with markers and electrical-tape flags. There's a mark (from a permanent marking pen) at each foot, a black flag every five feet and a length-marked colored flag every 10 feet. Simply mark the length for each band, if you like.

Make sure you prevent the wire from unspooling, especially when it's hanging from a window mounting. A heavy rubber band works, but it doesn't last long. A better solution is a loop of light bungee cord, preferably with a knot for grip. The bungee loop runs from the axle/handle around the spool making a half twist on the way, and then passes over the axle end on the other side of the spool. (See Fig 11.)

Operation

Table 2 lists element length, wire length and coil tap point for various bands. When the number of turns shown is zero, the coil is not needed. On all bands except 6 meters, you can simply bypass the coil with the clip lead—the extra length just lowers the frequency a bit. For 6 meters, the coil *must* be removed. The location of the unspooled wire greatly affects the settings, so these numbers are only starting points. The lengths in the table were taken with the wire one to three feet above ground, draped over and through bushes and flowerbeds. The antenna will still work if the wire is lying on the ground, but it will require less unspooled wire to resonate. A balun is not needed, and an SWR analyzer is very helpful while adjusting this antenna.

The SWR is less than 1.5:1 on all bands, and it's usually below 1.2:1. Occasionally, a band shows a higher SWR (still less than 2:1), but that can always be lowered by adjusting the length or location of the lower wire. Never set up the antenna where it could fall and injure someone, or where the unwary could get an RF burn by touching it.

The author's results with this antenna have been excellent, both from home and on vacation. If you haven't

yet operated from a seashore location, be prepared for a pleasant surprise! The good ground afforded by the salt water really makes a difference.

80 Meters

It's easy to add this lower frequency band. Fig 10 shows a 35 μH coil for 80 meters. It's constructed and tightened just like the 40-meter coil, but has 20 turns of #12 magnet wire.

To operate on 75/80 meters, insert the new coil into the flagpole bracket and plug the 40-meter coil into it. Tune across the band with the movable tap on the 40-meter coil. This varies antenna resonance from below 3.5 to above 4.0 MHz, with the full 11 feet of tubing extended. If your version doesn't achieve this tuning range, adjust the spacing of the turns on the 80-meter coil.

The 80-meter coil has a five-inch length of $^3/_4$-inch aluminum tube inserted into one end of the $^1/_2$-inch PVC pipe that supports the coil form. One end of the coil is connected to this aluminum tube. The other end is secured under the bolt that holds the coil form to the PVC pipe. A second clip lead connects the base of the 40-meter coil to the outer end of the larger coil. The length of wire on the spool must also be increased to about 64 feet.

2 Meters

A λ/2 dipole for 2 meters can be made with about 15 inches of $^1/_2$-inch aluminum tubing in the flagpole bracket, and 18 inches of wire. The tubing element is shorter than normal for 2 meters because the bracket is also part of the antenna. You can also shorten the 6-meter wire a bit and operate the 6-meter antenna as a 3λ/2 on 2 meters, with a somewhat higher SWR.

Continuous Coverage

With easily changed element lengths and a continuously variable loading coil, you may operate the antenna on any frequency from 6.5 to 60 MHz, if coverage for other services is needed. With taps in the 80-meter coil at 8, 11 and 14 turns, the antenna will also tune from 4 to 7 MHz.

THE HF CABOVER ANTENNA

If you have ever had the pleasure of traveling across the country with an HF mobile in a camper, trailer or motor home you may want to duplicate this antenna for use when you park. This antenna was described in *The ARRL Antenna Compendium, Vol* 5, by Jim Ford, N6JF.

The author's camper has limited spots on which to mount an HF mobile antenna. The back ladder is a convenient place to mount a small mobile whip. However, the efficiency of typical mobile center-loaded antennas, depending on coil Q and other assumptions, is often less than 2% for 80 meters and 10% for 40 meters. (These numbers come from the excellent, easy-to-use *MOBILE* antenna design program by Leon Braskamp, AA6GL, which is on the CD-ROM bundled with this book.)

At some locations, N6JF used an 80-meter dipole, which was very efficient and worked great on all bands when fed with open-wire line and an antenna tuner. However, it took over 40 minutes to set up and about 20 minutes to tear down, working with a sling shot and many tree snags. This is too much time to make a schedule or for an early morning departure, although it's OK if you plan to stay for a while. Even more important, there were often too many trees or other barriers (perhaps some even social) to allow putting up the dipole at a campsite.

When this happened he was stuck with the mobile antenna with poor efficiency. There had to be a better antenna for camper operation. The author decided on a large vertical.

A telescoping aluminum extension pole used for roller painting would make a good bottom section for the loaded vertical. These are available at many local home supply centers. The author's was 1 inch in diameter and 6 feet long, telescoping to almost 12 feet. He disassembled both sections and cross-cut a 1-inch slot in the top of the bottom section with a hacksaw to allow compression clamping with a hose clamp. The tip of the top section was fitted with an aluminum plug that had a 3/8-24 hole tapped in it. This procedure was a simple machine-shop operation. The plug was pounded into the top section and is quite snug. He tapped some set screws through the pole into the plug, however, just to be sure. An insulated, lay-down marine antenna mount fit perfectly into the bottom of the aluminum base and was secured with a bolt that also served as the electrical connection from the capacitor matching box. See **Fig 12** showing the aluminum base plate, the laydown mount and the antenna

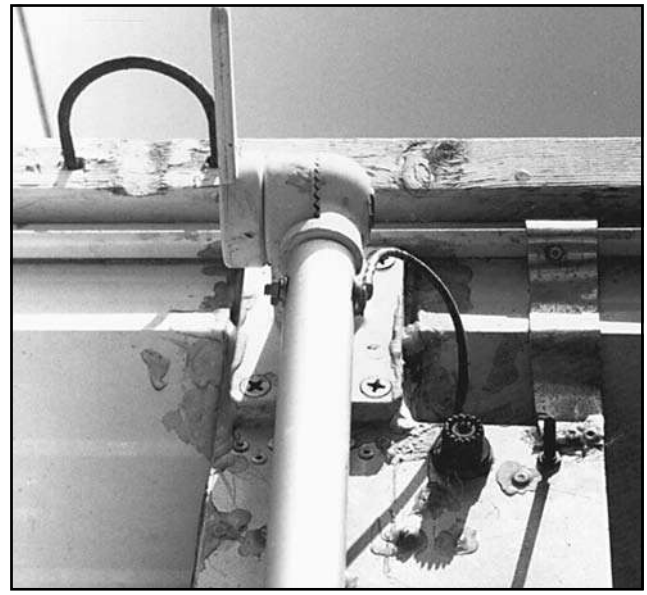

Fig 12—Photo of aluminum base plate, showing details of mounting to the camper. The four banana-plug jacks on the bottom are for extra radials, if desired.

Fig 13—Photo showing the back of the camper, with the antenna in the lowered position, parallel to the ladder. The "Outback" standby mobile antenna is shown clamped to the left side of the ladder.

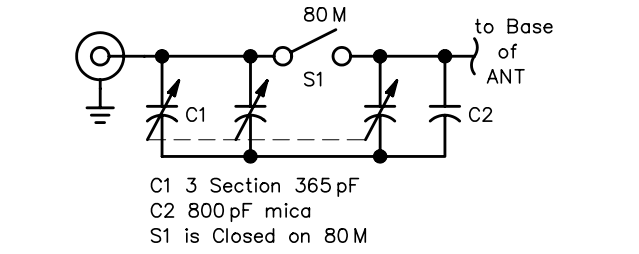

Fig 14—Schematic of tuning capacitor at base plate. C2 is an 800 pF transmitting mica capacitor. C1 is a three-section 365 pF broadcast tuning capacitor. S1 is closed for 80-meter operation.

mast itself lowered down the back of the camper. **Fig 13** shows the layout of the back of the camper, with the antenna on the right-hand side, laid down for travel.

The variable capacitor in the matching box is a surplus three-section 365-pF broadcast tuning capacitor. Two of three sections are connected in parallel and a switch parallels in the third section, along with an extra 800 pF mica capacitor for use on 80 meters. See the schematic in **Fig 14**.

The capacitor assembly was put in a custom-glued Plexiglas box to keep out the weather and mounted to a piece of plate aluminum, along with an SO-239 connector. The aluminum plate was riveted to the camper shell using a lot of aluminum rivets. Do not use steel. N6JF peeled back about a 4-inch wide section of the side of the camper for this direct aluminum-to-aluminum connection. People who are hesitant to modify their campers like this need to find an alternate low-resistance connection method. His camper was old enough not to be an issue.

For an extra low-resistance connection a $1^1/_2$-inch aluminum strip was added from the top of the base plate to the camper, as shown in Fig 12 near the 80-meter

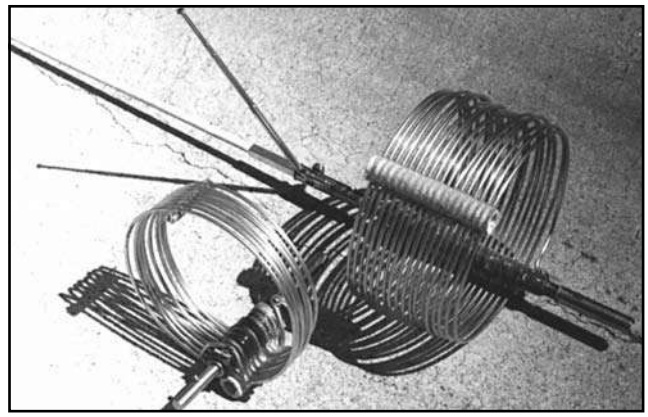

Fig 15—Close-up photo of 80 and 40-meter coils, with top section and telescoping whip antenna with swivel bracket for tuning the top section for the higher bands. Note quick-disconnect connectors at top and bottom of both coils. The top whip is a Fiberglas CB whip, used on 80 and 40 meters.

switch. The tuning knob protrudes from the side of the Plexiglas box. The four bottom holes in the plate are for banana plugs to connect ground radials if extra efficiency is desired. However, the roof of a camper is one of the better places for a mobile antenna, so the author seldom hooks up the radials. When he does use them, the tuning changes only a little.

To keep losses down, N6JF used coils wound with aluminum clothes-line wire on old mobile coil center sections with quick disconnect fittings. See **Fig 15**, which shows both the 80 and 40 meter coils, together with the top portion of the antenna. An article by Robert Johns, W3JIP, in October 1992 *QST* described techniques for building your own loading coils. The coils ended with a little more inductance than calculated and the author had to remove some turns. Both coils are spaced at 4 turns per inch. The 8-inch long 80-meter coil has 18 turns. The 7-inch long 40-meter coil has 8 turns.

The matching network is actually an L-section step-up match, using the net inductive reactance of the antenna plus the center loading coil. The PVC coil construction technique was described in W3JIP's *QST* article and a follow-up Technical Correspondence piece in October 1992 *QST*. Basically, it consists of drilling an accurate row of slightly undersized holes along a length of $^1/_2$-inch PVC pipe and then carefully sawing down the center of the row of holes with a hack saw. Then, you trap the coil wires in the grooves between the two sawed halves and tie the two halves together with string. When you are satisfied that everything is proper, you then tighten the string and apply epoxy glue to make it strong and permanent.

One advantage of aluminum clothes line wire is that it is already coiled at the approximate diameter needed when you buy it and it is easy to position on the coil form.

The clothes line wire had a plastic coating, which wasn't removed except at the contact points. Once the epoxy dries, this method of construction does a good job of holding the finished coil together and it is lightweight.

The computed coil Q from the *MOBILE* antenna program is about 800 for the 80-meter coil and about 400 for the 40-meter coil. The author accidentally made the 40-meter coil 7 inches in diameter instead of a higher-Q 6 inch diameter. Even so, the whole antenna system with a 9-foot top section calculates as being 56% efficient on 80 meters and 85% for 40 meters.

The removable top section for 80 and 40 meters is a full-size fiberglass CB whip from RadioShack. The fiberglass whip has about a #16 hole in the center of it. Be sure to sand and paint the whip for protection against UV and to protect yourself against fiberglass spurs in the hands. N6JF tried a full-size stainless steel CB whip to get a slightly higher capacitance to ground because of larger conductor size but discovered it was far too heavy. That experience reinforced his decision that aluminum was a far more practical coil and base section material for this project.

Quick-disconnect connectors found years ago at a hamfest were used for both coil forms and for the top section. Bands higher than 40 meters don't need any loading coils and the antenna length can be telescoped to get a $^1/_4$ wavelength. Ten meters doesn't require any top section. Be sure to use some NOALOX or similar compound to prevent corrosion and poor connections at all aluminum joints. This is especially true for the telescoping sections and the aluminum rivets. The matching capacitor is in the circuit at all times but when the 80-meter switch is off you can set the capacitor at minimum (about 14 pF) and it is effectively out of the circuit, even at 10 meters. The author has not tried this antenna on power levels greater than about 100 W but the weakest link would probably be the matching capacitor. The voltage at the matching capacitor is low, so 200 W should be no problem.

You can achieve a 1:1 SWR match for 80 or 40 meters and a good SWR is obtained without retuning the base matching capacitor for approximately 100 kHz on 80 meters and most of 40 meters. The top section, however, does not have such low Q and needs to be tuned. The 2:1 SWR bandwidth on 80 meters is about 25 kHz and 150 kHz for 40 meters. Tuning is accomplished by using a telescoping FM portable radio antenna connected to the top-section whip with a stainless steel hose clamp. The maximum length of the telescoping section used was 29 inches, and it collapses down to 7 inches. A whip with an elbow was used to adjust the angle of the whip as well. A telescoping whip half the length would still be long enough for the full adjustment of both bands.

Adjustment of the top section is one of the penalties paid to achieve high efficiency for operation on 80 and 40 meters. Substituting an automatic antenna tuner would likely lose efficiency, particularly on 80 meters since the base resistance calculates to about 10 Ω. N6JF has not tried to make the antenna work on 160 meters. The SWR for the higher bands was good enough without any matching network.

As light as the antenna is, it still won't hold up in a moderate wind without some support guys. N6JF used $^3/_4$-inch and $^1/_2$-inch PVC support pipes in a telescoping arrangement for storage, but expanding to give an approximate 45° support at the top of the bottom section from both directions. One end of the telescoping section was connected to the camper roof with a hinge. The other end formed a snap-fit out of a PVC barrel that was cut lengthwise. See **Fig 16** and **Fig 17** for details. Even though it formed a good snap fit, N6JF didn't trust the joint for strong winds so he glued a piece of Velcro to the joint to close up the open end. Be careful, though, because Velcro deteriorates with exposure.

Another hose clamp near the top of the bottom section holds an $^1/_8$-inch line taken up the ladder to pull up the antenna without the need of an assistant. The disadvantage is you have to climb the roof. Use a non-slip floor mat or something similar to spread the load on the roof and to avoid slipping. Once on the roof, however, the coil is at a height for easy adjustment when the telescoping section is in the down position.

An advantage of being able to assemble the whole antenna on the roof is that you don't need a lot of swing-up room and you can clear trees easily. You can put calibration marks on the upper aluminum section for resonant lengths on the higher bands but just raise the top section up all the way for 80 or 40 meters. Mark also the small

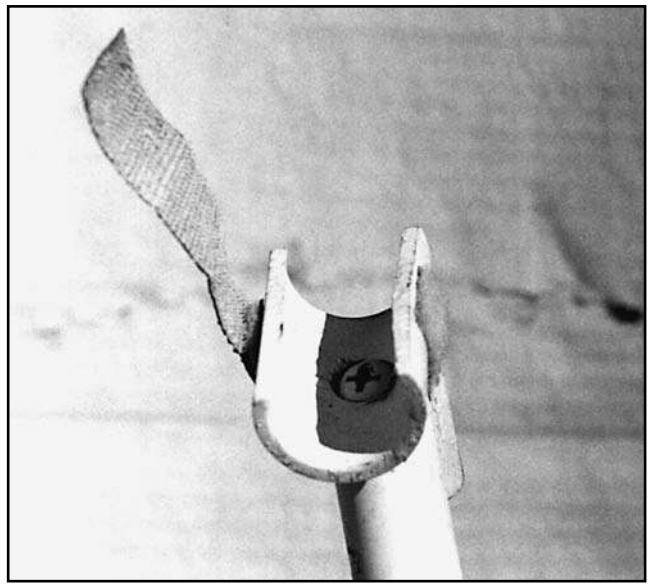

Fig 16—Close-up of one of the snap-on support brackets used to brace the antenna. Note the Velcro pieces used to ensure that the antenna doesn't pop out of the bracket in the wind.

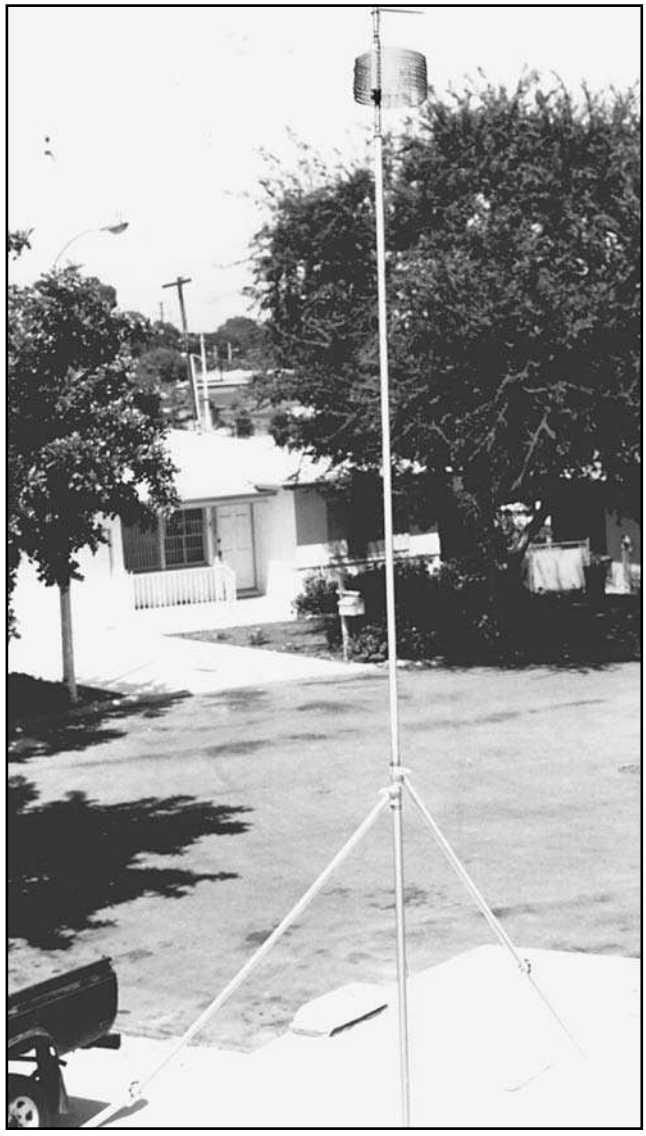

Fig 17—Photo showing the two support bracket poles bracing the bottom section of the antenna. The top tuning whip is evident above the homemade loading coil at the top of the bottom section.

coil tuning whip for 80 or 40 meters, although different locations may require slightly different settings due to detuning from nearby metal objects.

The overall length is about 21 feet. The top of the author's camper is about 10 feet high when on the truck, putting the tip at 31 feet. This antenna is definitely designed for use when you are parked at a fixed location. N6JF can put up this antenna in less than 5 minutes and can take it down in half the time. The success of this project has as much to do with knowing how and where you operate as it does paying attention to mechanical and electrical details. The antenna has been a good compromise between efficiency and convenience.

TWO PORTABLE 6-METER ANTENNAS

These antennas were described by Markus Hansen, VE7CA, in *The ARRL Antenna Compendium, Vol 5*. After years of HF operation, he became enthusiastic about VHF/UHF operation when he found a used Yaesu FT-726R VHF/UHF all-mode transceiver at a reasonable price.

But he became really enthused when he got on 6 meters and discovered the joys of driving to high mountain peaks to operate. Not only does an antenna have to be portable for this kind of operation, it must be easily assembled and disassembled, just in case you have to move quickly to a better location.

A Portable Two-Element Six-Meter Quad

VE7CA's primary objective was to construct a two-element quad using material found in any small town. It should not use a complicated matching network. The Gamma matches commonly used on quads do not hold up well when you are setting up and taking down these antennas in the field. The final design adjusted the distance between the driven and the reflector elements so that the intrinsic feed-point impedance was 50 Ω.

Fig 18 shows the dimensions for the boom and the boom-to-mast bracket. The boom is made from a $27\frac{1}{4}$-inch length of 2×2. (The actual dimension of 2×2 is closer to $1\frac{3}{4}$ by $1\frac{3}{4}$ inches but it is commonly known in lumber yards as a 2×2.) Use whatever material is available in your area, but lightweight wood is preferred, so clear cedar or pine is ideal. Drill the four $\frac{1}{2}$-inch holes for the spreaders with a wood bit, two at each end, through one of the faces of the 2×2 and the other through the other face. The boom-to-mast bracket is made from $\frac{1}{4}$-inch fir plywood.

The spreaders are $\frac{1}{2}$-inch dowel. The local lumberyard had a good supply of fir dowels but other species of wood are available. The exact material is not important. Maple is stronger but expensive. Fiberglass would be ideal but it is not always available locally. Cut two of the $\frac{1}{2}$-inch dowels to a length of $83\frac{5}{8}$ inches for the driven element spreaders and two to 88 inches for the reflector spreaders. **Fig 19** shows one end of the boom with the two spreaders inserted. The mast was made from two six-foot lengths of $1\frac{3}{4}$-inch fir dowel. Again, use whatever you may have available. Waterproof all wooden parts with at least two coats of exterior varnish.

While you are at the lumberyard or hardware store look for plastic pipe that fits over the end of the $\frac{1}{2}$-inch spreaders. You will need a one-foot length, with some to spare. Cut it into seven equal lengths, approximately one inch long, and one to a length of $1\frac{1}{2}$ inches. Drill a $\frac{1}{16}$-inch hole through the seven equal lengths $\frac{1}{4}$ inch from the ends, and two holes one above the other $\frac{1}{4}$-inch apart on the $1\frac{1}{2}$-inch sleeve. VE7CA used #14 hard-drawn stranded bare copper wire for the elements. Do not use insulated wire unless you are willing to experimentally

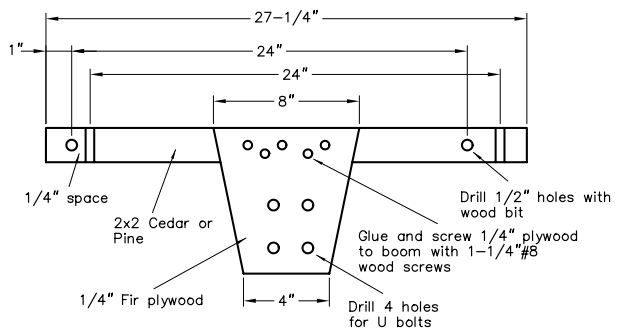

Fig 18—Dimensions for the boom-to-mast bracket for VE7CA's portable two-element 6-meter quad.

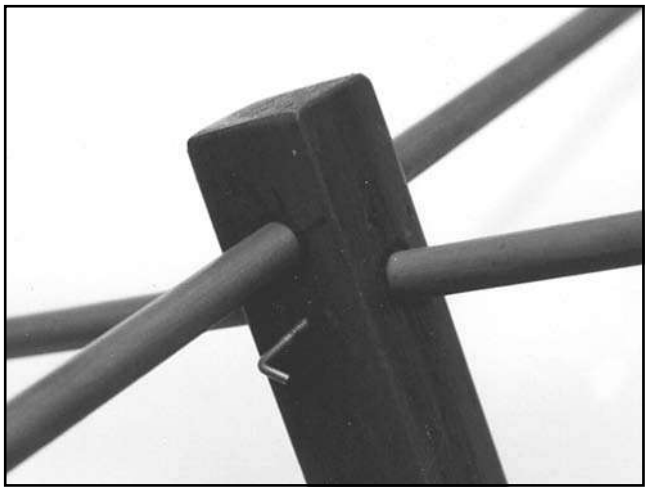

Fig 19—Photo of one end of the VE7CA quad with the two spreaders inserted.

determine the element lengths, since the insulation detunes each element slightly.

Cut the reflector element 251 inches long and slip one end of the wire through the holes you drilled in four of the plastic sleeves. Don't attempt to secure the wire to the plastic sleeves at this point. Cross the end of the reflector elements one inch from their respective ends and twist and solder together. The total circumference of the reflector element should be 249 inches when the ends are connected together.

Cut the driven element wire to 241 inches and slip three of the 1-inch sleeves onto the wire. Again, don't secure the wires to the sleeves yet. Then the ends are passed through the two holes in the $1^1/_2$-inch pipe. Wrap the ends around the pipe and twist them back onto themselves to secure the wire. The coax feed line is attached directly to the two ends at this point. The circumference of the driven-element loop from the points where the coax is attached should be $236^5/_8$ inches. Solder the coax feed line to the driven element and waterproof the coax with silicone seal. The author used RG-58, as it is lightweight. The length required for a portable installation is typically not very long, maybe 20 feet, so the loss in the small cable is not excessive. Near the feed point, coil the coax into six turns with an inside diameter of two inches. This is an effective method of choking any RF from flowing on the outside of the coax shield.

Begin assembling the quad by pushing the two reflector spreaders, without wires attached, through one end of the boom and the two shorter driven-element spreaders through the holes in the other end of the boom. Center the spreaders and mark the spreaders with a black felt-tip pen next to the boom. Now insert a $1^1/_2$ #8 wood screw or a threaded L-hook into the boom so that it just touches one of the spreaders. Take the screw or L-hook out and file the end flat, then reinsert it so that it is just snug against the spreaders. The author only used two L-hooks for the two vertical spreaders; the horizontal spreaders are held in the proper position by the tension of the wire loops. If you use an L-hook, you can unscrew it with your hands—you won't have to worry about leaving the screwdriver at home.

You are now ready to assemble the wire loops. Take the reflector loop and place the four plastic caps over the ends of the reflector spreaders. Equalize the wire lengths between the spreader so that the loop is square. Now, secure the plastic sleeve pipes by tightly wrapping wire around the sleeve and the wire element and soldering the wire in place. See **Fig 20**, a photo showing one of the plastic sleeves slipped over one of the spreader ends, with the wire element through the hole and fastened in place. Follow the same procedure with the driven element.

Fig 21 shows the quad's boom, with the plywood boom-to-mast bracket fastened with wood screws and glue. Two U-bolts are used to attach to the mast. When the quad is raised, the shape of the loop is commonly known as a diamond configuration. The mast consists of two six-foot lengths of doweling joined together with a two-foot length of PVC plastic pipe, held together with wood screws.

Make a slot the width of a #8 wood screw about one inch deep from the top of the plastic PVC pipe and then put the top mast into the plastic pipe. Insert a one inch #8 wood screw into the bottom of the slot you cut into the top of the pipe and tighten only enough so that the top mast can be removed without unscrewing it. VE7CA drove a nail into the end of the lower mast and left it exposed an inch or more. This end is placed in the ground and the nail holds the pole in place. A strip of wood approximately 1×3 and long enough to cross over the roof rack of the family van is used to hold the center of the antenna mast to the roof rack of the van with small diameter rope. See **Fig 22** for a photo of the quad in action next to the family van.

To disassemble the quad, lay it on its side, slip the plastic sleeves off the ends of the spreaders and roll up

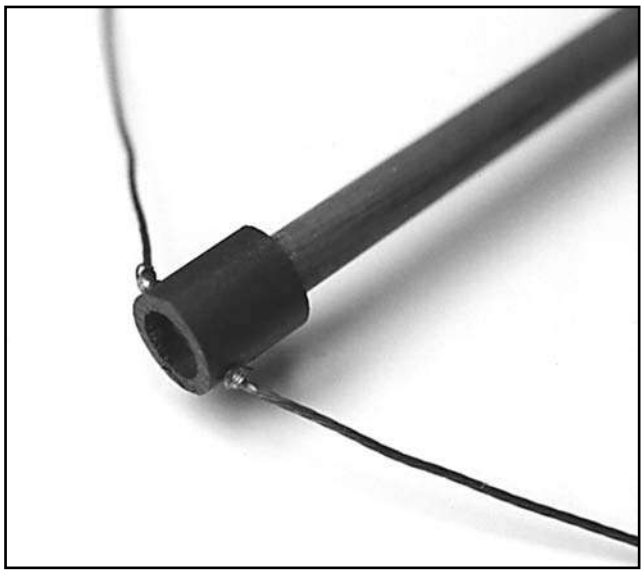

Fig 20—Photo showing one of the plastic sleeves slipped over end of a spreader to provide a mechanical mounting point and support for the wires.

Fig 21—Photo of the two-element quad's boom, with the plywood boom-to-mast bracket secured with wood screws and glue.

Fig 22—Ready for action! VE7CA has set up his quad next to the family van.

the wire loops. Loosen the L-hooks holding the vertical spreaders in place. Push the spreaders out of the boom, loosen the U-bolts and free the mast from the boom.

That is all there is to it. It takes about two minutes to put it up, or take it down. It is quite sturdy and has survived several high-wind storms.

A Three-Element Portable 6-Meter Yagi

The idea to build a Yagi antenna resulted when the author traded the family van for a compact car. He needed something that would fit into the trunk of the car. At close to 7-feet long, the quad spreaders were too long. Computer modeling showed that a three-element Yagi on a five-foot boom also could pick up about 1.5 dB gain over the short-boom two-element quad. A five-foot boom fits into the trunk or across the back seat of the car, but something had to be done about the nine-foot elements!

One day VE7CA noticed a box of portable-radio telescoping antenna elements at the radio parts store. They were 54 inches long when fully extended. He next found a 60-inch length of aluminum tubing that fit over the end of the telescoping elements. There are many different sizes of telescoping antenna elements, with different diameters. This is where you will have to use your scrounging skills! **Fig 23** shows how the tubing is used as a center section to join two telescoping elements together. It also serves to extend the total length of each element, since two telescoping elements themselves are not long enough to resonate on six meters. See **Table 3** for dimensions and element spacings. Each center section is slotted at both ends with a hacksaw, and stainless-steel hose clamps are used to secure the telescoping elements.

Fig 24 shows the center sections of the three elements with their mounting brackets. A square boom was used to obtain a flat surface to work with. **Fig 25** shows how the reflector is attached to the end of the boom with two $1^1/_2$-inch 10-32 bolts and wingnuts. **Fig 26A** provides the dimensions and details for the reflector and director element-to-boom brackets, which are formed from $^1/_{16}$-inch plate aluminum. The driven element is split in the center and is insulated from the boom. Fig 26B shows details for the driven-element bracket. **Fig 27** is a photo

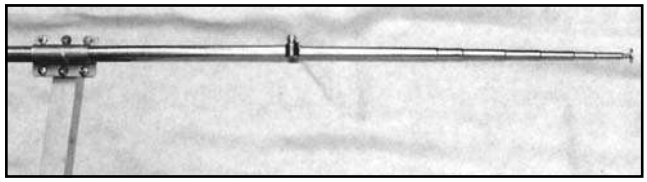

Fig 23—Photo showing a piece of aluminum tubing used as a center section to join the two telescoping tips together.

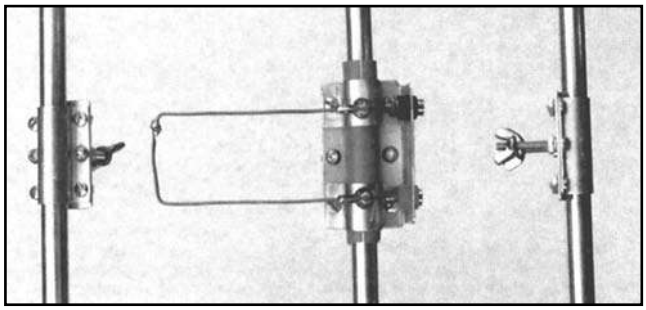

Fig 24—A view of the center sections of the three Yagi elements with their mounting brackets.

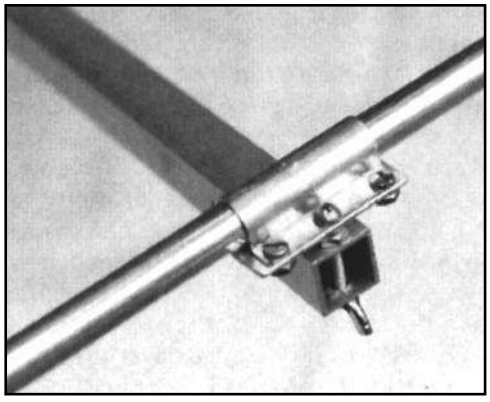

Fig 25—Photo detailing attachment of the reflector to the square-section boom, using two #10 bolts and wingnuts.

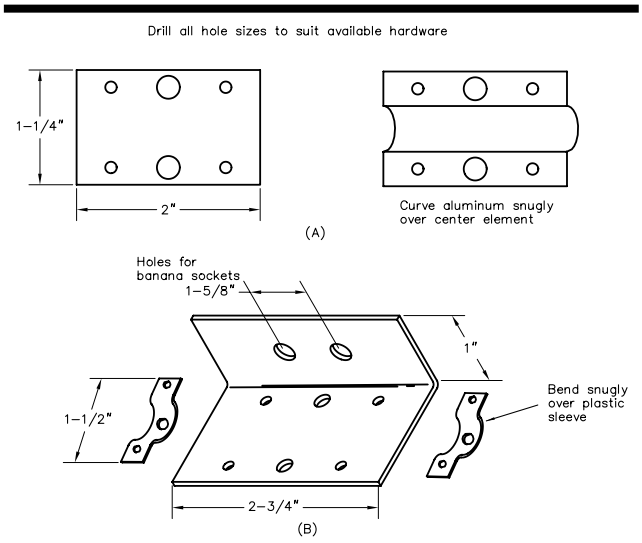

Fig 26—At A, details for the reflector and director element-to-boom brackets, made of 1/16-inch plate aluminum. At B, details for the driven-element bracket. These are screwed to the square boom.

of the driven element with the hairpin matching wire and the banana plugs used to connect the coax to the driven element. You could use a female PL-259 connector if you wish. VE7CA used #14 solid bare copper wire for the hairpin. It is very durable—even after being severely warped in the car trunk, it can be bent back into shape quickly and easily.

The boom is 3/4-inch square aluminum, 65 inches long. The material was found at a local hardware store. To detach the elements, just loosen the wing nuts and remove the elements from the boom. A similar method was used to attach the support mast to the boom.

As with the quad, a choke balun was used, consisting of a coil of 6 turns of coax with an inside diameter of 2 inches. To tune the hairpin match, assemble the Yagi on its mast and extend the elements. Spray switch contact solution on a cloth and wipe any dirt and grease from the elements. Push the elements together and apart a

Table 3
Three-Element Yagi, Element Lengths and Spacing Along the Boom, and Hairpin Dimensions

Element Along Boom	Spacing Section Ele. (inches)	Center Length (inches)	Telescoping (inches)	Total Length (inches)
Reflector	0	22 3/4	51 1/2	125 3/4
Driven	28	9 3/4 *	48 5/8	58 3/16
Director	63 3/8	14 1/2	51 1/4	117
Hairpin	#14 wire	4 long	1 5/8 spacing	

* Driven-element uses 2 sections insulated at center

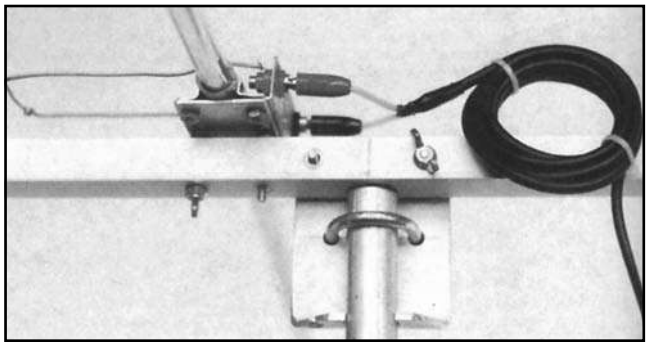

Fig 27—Photo of the driven element, complete with hairpin match and the banana plugs used to connect the coax cable to the driven element.

couple of times so that the contact solution cleans the elements thoroughly. Attach the antenna mast to your vehicle or use whatever method of support you intend to use in the field. Connect an SWR meter and a transmitter to the coax feeding the antenna. VE7CA used two alligator clips soldered together to slide along the two hairpin wires to find the position for the lowest SWR. The dimensions computed by computer were correct! The SWR was below 1.16:1 from 50.05 to 50.2 MHz.

You can take this antenna out of the trunk of the car and assemble it in less than two minutes. One caution: the telescoping elements when fully extended are quite fragile. VE7CA has not broken one as yet, but carrying a spare element just in case would be a good idea.

VE7CA 2-Element Portable HF Triband Yagis

These portable HF wire Yagis were described by Markus Hansen, VE7CA, in November 2001 *QST* and in *The ARRL Antenna Compendium, Vol 7*.

A 20/15/10-Meter Triband 2-Element Yagi

VE7CA wanted a simple 2-element wire Yagi for 20/15/10 meters that could be stored in the ski boot of his car. The basic concept comprises three individual dipole driven elements, one each for 20, 15 and for 10 meters tied to a common feed point, plus three separate reflector elements. The elements are strung between two 2.13-meter (7-foot) long, 2 × 2-inch wood spreaders, each just long enough to fit into the ski boot of his car.

By playing with the reflector-to-driven element spacing and the initial driven-element lengths, VE7CA was able to come up with a feed-point impedance on each band that allowed the use of a single setting for the shorting bar on a hairpin match. The result was a very acceptable match over the lower portions of each band. The layout of the 20/15/10-meter triband wire Yagi is shown in **Fig 28**, with the dimensions provided in **Table 4**.

The dimensions shown in Table 4 are what resulted after tuning for the lowest SWR in the middle of the lower portion of each band. VE7CA set his system up by hanging one end of the antenna from a tree and sloped it downwards at 45°, tying the lower end to a peg in the ground. The height at the feed point was 30 feet.

The feed-point impedance of an antenna is affected by many environmental factors. The presence of a reflector relatively close to the driven element has a major effect, since the impedance at the driven element in a Yagi is affected by the tuning of the driven element itself, by the spacing and length of the reflector element and to a lesser extent the height of the antenna above ground and the character of the soil itself. The real challenge in a multiband Yagi with a single feed line is to obtain a low SWR on all the bands.

The hairpin match is one of the easiest matching systems to make. It is easy to adjust and since wire is the only ingredient, it can be coiled up with the rest of the antenna when the antenna is disassembled. The feed-point impedance of the Yagi with a reflector element spaced 0.1 λ behind the driven element typically produces a resistance around 20 Ω. By shortening the driven element from its resonant length, capacitive reactance is added to the feed-point resistance. This can be cancelled by shunting the feed point with an inductor in the shape of a wire loop resembling a *hairpin*. This causes a step up of the 20-Ω feed-point resistance to 50 Ω.

Table 4
Dimensions for 20/15/10-Meter Tribander

Frequency MHz	*Spacing DE to Refl cm (feet)*	*Driven Element Half Length cm (feet)*	*Reflector Length cm (feet)*	*Hairpin Length cm (inches)*
14.1	213 (6.99)	488 (16.01)	1065 (34.94)	43 (14.9)
21.1	175 (5.74)	335 (10.99)	708 (23.23)	
28.25	125 (4.1)	254 (8.33)	531 (17.42)	

Spacing between hairpin wires is 10 cm (4 inches).

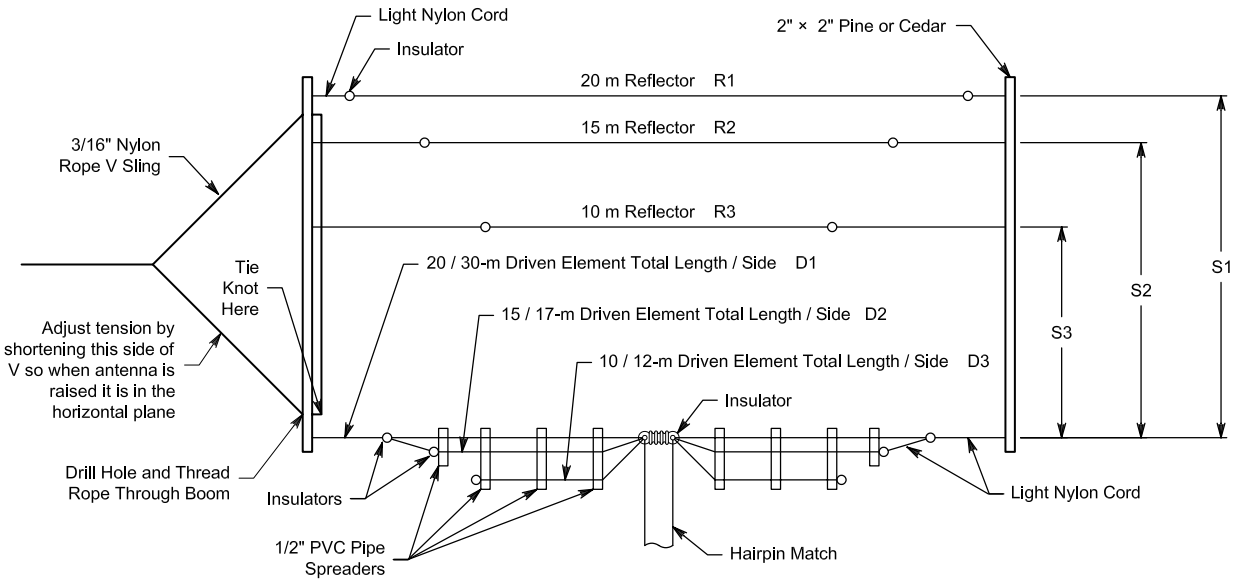

Fig 28—Dimensions for VE7CA's 2-element 20/15/10-meter triband Yagi.

The Balun

Fig 29 shows the hairpin match and the common-mode choke balun for the 10/15/20-meter triband wire Yagi. You should let the coax drop straight down from the center insulator and attach it to the center of the hairpin shorting bar. Continue by making a coil using the coax of 8 turns, with a diameter of about 4 inches. This balun will choke off RF flowing along the outside of the coax shield that would otherwise distort the radiation pattern of the antenna. The center of the shorting bar is at a neutral potential, so there is no harm in attaching the coax feed line at that point.

Flattop or Tilted?

If DX is your main interest, then you want to tilt the antenna towards the vertical to emphasize the lower elevation angles. Remember that the radiation pattern is quite dependent on ground conductivity and dielectric constant for a vertically polarized antenna. A location close to saltwater will yield the highest gain and the lowest radiation angle. With very poor soil in the near and far field, the peak radiation angle will be higher and the gain less.

VE7CA has had numerous opportunities to test this out while operating portable at his favorite location. Using two trees as supports he can pull the antenna to horizontal with the feed line about 7 meters above the ground. In this position, with 20 meters open to Europe, he found it difficult to work DX on CW with 3 W of output power. However, when he changed the slope of the antenna so that it is nearly vertical he not only heard more DX stations, but he found it relatively easy to work DX. The sloping antenna always performs much better for working DX than a low horizontal antenna.

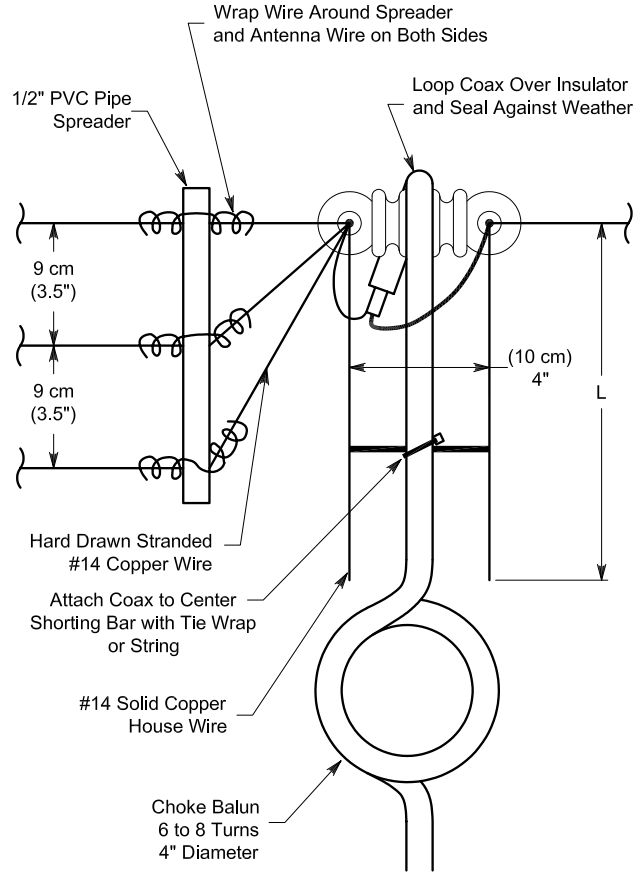

Fig 29—Details of feed point for 20/15/10-meter triband Yagi. The same mechanical support is provided for the balun and feed coax for the 30/17/12-meter tribander.

A 30/17/12-Meter Triband 2-Element Yagi

When the author attempted to add 17 and 12 meter elements to the existing 20/15/10-meter Yagi model he became exasperated. Adding two more driven elements and reflectors brings many more variables into the equation! It became clear that there was serious interaction between the elements. He could not obtain a workable feed-point impedance on all five bands that could be transformed to 50 Ω using a single hairpin match. There was also serious pattern distortion on 12 meters.

Even building a WARC-only triband Yagi for 30/17/12 meters turned out to be a real challenge. VE7CA had difficulty finding a combination that would allow him to use a single matching system to transform the feed-point impedance of the combined driven elements to 50 Ω. He couldn't create a 30/17/12 triband Yagi using the same design principles as his 20/15/10-meter version. The main problem occurred on 12 meters. Not only was the feed-point impedance unmanageable, but the radiation pattern had four lobes, not the single lobe you'd like from a Yagi.

He decided to try the *Modified Coaxial-Sleeve* method, more aptly termed by K9AY the *Coupled-Resonator (C-R)* in his article in *The ARRL Antenna Compendium, Vol 5*. The K9AY method uses a single driven element, with other elements placed in very close proximity (but not physically connected) to the driven element. By starting with the dimensions suggested by K9AY for a triband 30/17/12-meter dipole, VE7CA was able to develop a 2-element Yagi with acceptable feed-point impedances on all three bands using a single hairpin match. Notice that this WARC design uses a 2 × 2-inch wooden boom length that is 230 cm (7.5 feet) long. Of course, the antenna can't fit into a typical ski boot anymore, so VE7CA had to put it on a roof rack for transportation.

The space between the tightly coupled driven elements is only 3.7 cm (1.5 inches), so you need to use more PVC pipe spreaders than in the 20/15/10 design to make sure the driven-element wires stay as close as possible to the desired spacing without physically touching each other. The driven elements lie in the horizontal plane and the hairpin match and feed line hang down vertically from the center of the 30-meter driven element.

The spacing between the 30-meter driven elements and the other two conductors and the size of the wire all played a part in developing this antenna for a single feed line with the common hairpin match. Do not change the wire size from the recommended #14 for the driven elements unless you are willing to spend a considerable amount of time with a *NEC*-based modeling program retweaking the antenna. This is not the case with the 20/15/10 tri-band Yagi, where any convenient sized wire is acceptable.

Using #14 gauge wire allows all the Yagi antennas in this article to be used at the maximum power levels allowed in North America. The only limiting factor is the power handling capability of the feed line. However, even RG-58 should work for the relatively short length from the feed point down to ground level, where you can change to RG-8 or some other higher-power, lower-loss coaxial cable if you wish. **Fig 30** is a detailed drawing of the 30/17/12-meter driven element. The other dimensions for the 30/17/12-meter triband Yagi are shown in **Table 5**.

Assembly

When you are ready to assemble your wire Yagi, start by attaching the longest reflector element and the driven element assembly to the wood end booms. Do this with the wires and the booms on the ground. Next attach the V slings to both of the booms and with ropes attached to the V slings pull the array up off the ground between two supports (perhaps two trees). A height of 1.5 meters (5 feet) above the ground makes it easy to work on the antenna while you add the other reflector elements and adjust the V slings. Pull them tight so that the array is fairly flat. It won't stay horizontal, because the driven elements are heavier than a single reflector element. So you will need to support the 2 × 2-inch spreaders so they are horizontal. Lean the booms on something at a convenient height, such as the rungs of two step ladders. Now add the two other reflector elements, but don't pull them as tight as the longest reflector. Next attach the feed line.

Table 5
Dimensions for 30/17/12-Meter Tribander

Frequency MHz	*Spacing DE to Refl cm (feet)*	*Driven Element Length cm (feet)*	*Reflector Length cm (feet)*	*Hairpin Length cm (inches)*
10.12	230 (7.5)	713 (23.4) Half	1476 (48.4)	24.5 (9.5)
18.11	165 (5.4)	808 (26.5)	822 (27.0)	
24.91	120 (3.9)	570 (18.7)	606 (19.9)	

Spacing between hairpin wires is 10 cm (4 inches). Note that dimensions for 17 and 12-meter driven elements are full lengths, since they are not broken with insulator in the middle, unlike all driven elements for 20/15/10-meter triband design in Table 4.

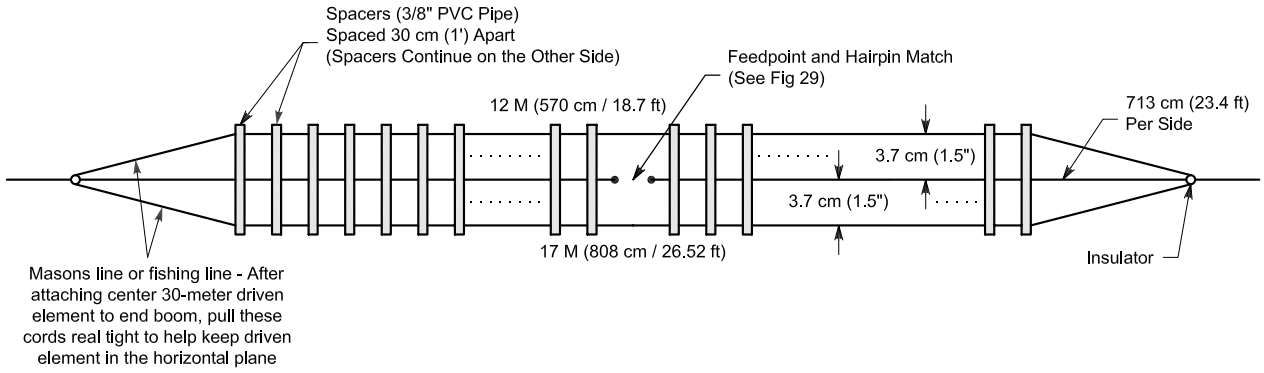

Fig 30—Layout of 30-meter driven element with coupled resonators for 17 and 12 meters.

V Slings

Since the author wanted to be able to raise the 30/17/12-meter triband antenna by himself, he again used only one rope on either end of the array. One end goes over a tree limb and the other end is tied to a stake in the ground or some other nearby support, perhaps a tree trunk. Using only one attachment rope on either end makes it very easy to change beam direction by walking the antenna around the antenna support tree or tower. To accomplish this he used two V slings, one on each end attached to the 2 × 2-inch spreaders.

The secret to keeping the antenna level in the horizontal plane is that the V slings are not equilateral in shape. The combined weight of driven elements, balun and feed line is heavier than the reflectors. If the length of the sides of the V are equal, the array will rotate downwards. The driven elements will end up facing the ground, with the reflectors facing up. Adjust the V slings so that the antenna will stay level in the horizontal plane by shortening the length of the side of the V attached to the driven elements. It is quite easy to adjust in the field, and once you have it adjusted it stays balanced.

Once you raise the antenna to its operating position and in the horizontal plane, you can change direction 180° by pulling on the feed line. As you pull, the whole array will slowly turn over. Stop it from turning by holding onto the feed line once the array has swung over to face the opposite direction.

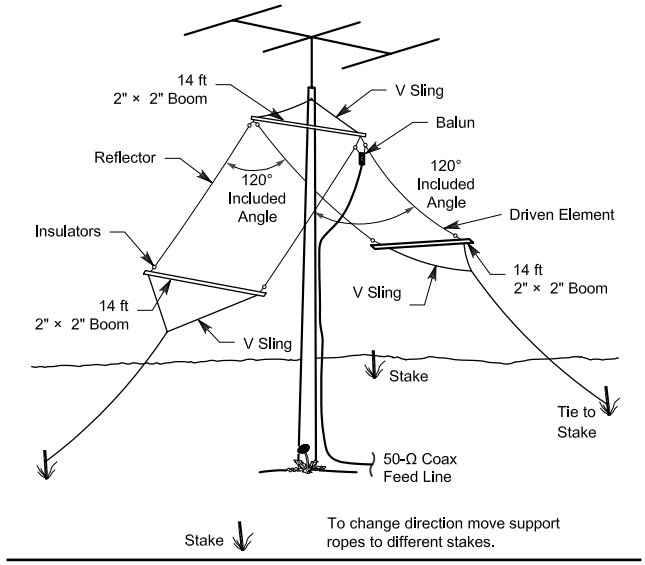

Fig 31—Layout for inverted-V 40-meter portable wire Yagi suspended from tower.

SWR Adjustment

Since you may situate your antenna in an entirely different position than VE7CA did, you may need to fine tune your antenna. Begin with the dimensions in Table 5 as a starting point. Make a temporary shorting bar using two alligator clips joined by a piece of wire and attach them at the recommended position. Next raise the antenna to the desired final position. Using an antenna analyzer (or transmitter and SWR meter) plot the SWR over all three bands. Start with the lowest band, 30 meters and adjust the shorting bar up or down to find the lowest SWR point in the portion of the band you plan to operate in. (This procedure also works if you wish to adjust the 20/15/10-meter tribander. Start with the lowest frequency.)

You shouldn't have to move the shorting bar very far from the suggested length. Now that you have determined the right shorting-bar position, adjust the other two driven element lengths for the lowest SWR in the portion of those bands in which you plan to operate. You may have to compromise with the position of the shorting bar to find a satisfactory range where the SWR is acceptable on all three bands. After satisfying himself with the position of the shorting bar, VE7CA replaced the alligator clips simply by folding one side of the parallel hair-pin

wire lengths over to the other side and soldering it in the position where the alligator clips had been attached. The author does not recommend changing the reflector element lengths unless you are familiar with antenna modeling programs and are willing to model different spacing or element lengths.

40-Meter Wire Yagis

After his November 2001 *QST* article, VE7CA received several requests for a 40-meter wire Yagi. One ham mentioned that he wanted to be able to pull up a 40-meter Yagi between two towers and to be able to flip it over to change direction. Another wanted a 40-meter Yagi he could pull up on a single tower for the winter DX contests and then put it away during the summer. So VE7CA ran four different 40-meter scenarios in his computer models:

1. A horizontal 2-element wire Yagi at 65 feet.
2. A sloping 2-element wire Yagi, with one end at 65 feet and sloping downward 30° from vertical.
3. A sloping 2-element wire Yagi, with one end at 65 feet and sloping downward 65° from vertical.
4. An inverted-V 2-element wire Yagi with the apex at 65 feet and an included angle between the wires of 120°.

Fig 31 shows the layout for an inverted-V system and **Table 6** lists the element and hairpin lengths. Elevation patterns for the 40 meter antennas are compared in **Fig 32**, with a reference antenna of a single flattop dipole at 65 feet. As they say, a picture is worth a thousand words. If your interest is DX, it is very clear that horizontal and high is a very good rule of thumb for most antennas.

Yes, a $^1/_4$ wave vertical over salt water or 120 $^1/_4$-wave radials over good ground will produce very low radiation angles, but such systems are not exactly portable and we don't all live near the ocean. Mind you, if you can manage to locate antenna Number 3 (the most vertically oriented wire Yagi) next to the ocean, you would be very happy.

The point here is that if you have two towers and you're not fortunate enough to be located on a saltwater marsh, you should pull the 40-meter array up as high and as horizontal as you can. If you have only one tower and don't need to change direction often, then try the inverted-V configuration. You can still change the direction by walking each end around the tower.

However, even the sloping 40-meter Yagi with one end at 65 feet up a tower (or tree) and the other end attached with a long rope as far as possible from the tower will still put out a very respectable signal. It is directional, and you can walk it around the tower to change direction or you can

Table 6
40-Meter Wire Yagi Configurations

Configuration	*Driven Element cm (feet)*	*Reflector cm (feet)*	*Hairpin Length cm (feet)*
1. Horizontal	1978 (64.90)	2098 (68.83)	Approx 50 cm
2. –30° Sloper	1978 (64.90)	2113 (69.32)	(22 inches)
3. –65° Sloper	1978 (64.90)	2101 (68.93)	
4. Inverted V	2040 (66.93)	2126 (69.75)	

Spacing between driven element and reflector is 427 cm (14 feet). Spacing between parallel hairpin wires is 10 cm (4 inches). The lengths shown above are the total wire length for each element.

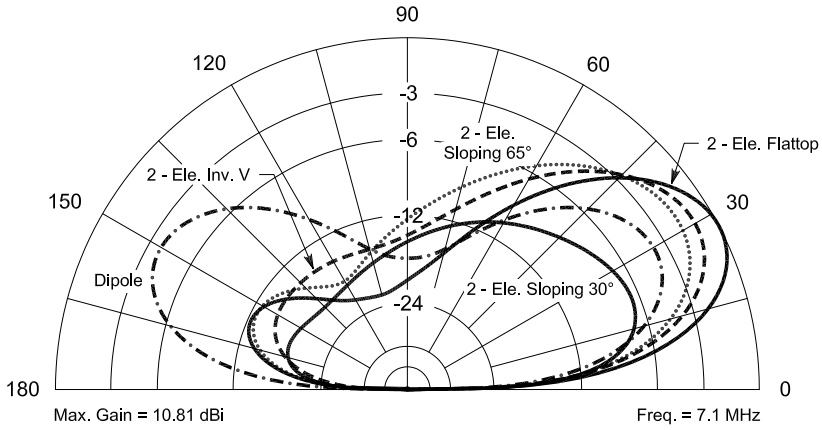

Fig 32—Comparisons of elevation patterns for five 40-meter antennas: a 2-element flattop Yagi at 65 feet; a 2-element inverted-V Yagi at 65 feet; a 2-element Yagi sloped 65° from the vertical plane; a 2-element Yagi sloped 30° from the vertical plane; and a horizontal dipole at 65 feet.

Fig 33 — VE7CA portable 2-element 20/15/10-meter wire Yagi installed at Plimoth Plantation in Plymouth, Massachusetts. (*Photo courtesy K1HTN*).

flip the antenna over and change direction 180° very quickly.

Summary

You don't need a 10-meter (60-foot) high tower, a commercial triband Yagi and a rotator to put out a good signal on the HF bands. Wire Yagis work very well and they can be inexpensive and easy-to-build, using components found at your local hardware store. **Fig 33** is a photograph of a successful portable installation in Massachusetts.

BIBLIOGRAPHY

Source material and more extended discussion of topics covered in this chapter can be found in the references given below.

G. Breed, K9AY, "The Coupled-Resonator Principle: A Flexible Method for Multiband Antennas," *The ARRL Antenna Compendium, Vol 5* (Newington: ARRL, 1996), p 109ff.

R. J. Decesari, "A Portable Quad for 2 Meters," *QST*, Oct 1980, and "Portable Quad for 2 Meters, Part 2," Technical Correspondence, *QST*, Jun 1981, p 39ff.

D. DeMaw, "A Traveling Ham's Trap Vertical," *QST*, Oct 1980, p 28ff.

J. Hall, "Zip-Cord Antennas—Do They Work?" *QST*, Mar 1979, p 31ff.

M. Hansen, "A Portable 2-Element Triband Yagi," *QST*, Nov 2001, p 35ff.

M. Hansen, "Some More VE7CA 2-Element Portable Yagis," *The ARRL Antenna Compendium, Vol7* (Newington: ARRL, 2002, p 183ff.

C. L. Hutchinson, "A Tree-Mounted 30-Meter Ground-Plane Antenna," *QST*, Sep 1974, p 16ff.

C. W. Schecter, "A Deluxe RV 5-Band Antenna," *QST*, Oct 1980, p 38.

Chapter 16

Mobile and Maritime Antennas

Mobile antennas are those designed for use while antennas, most amateurs think of a whip mounted on an automobile or other highway vehicle, perhaps on a recreational vehicle (RV) or maybe on an off-road vehicle. While it is true that most mobile antennas are vertical whips, mobile antennas can also be found in other places. For example, antennas mounted aboard a boat or ship are mobile, and are usually called *maritime antennas*. **Fig 1** shows yet another type of mobile antenna—those for use on handheld transceivers. Because they may be used while in motion, even these antennas are mobile by literal definition.

Pictured in Fig 1 is a telescoping full-size quarter-wave antenna for 144 MHz, and beside it a *stubby* antenna for the same band. The stubby is a helically wound radiator, made of stiff copper wire enclosed in a protective covering of rubber-like material. The inductance of the helical windings provides electrical loading for the antenna. For frequencies above 28 MHz, most mobile installations permit the use of a full-size antenna, but sometimes smaller, loaded antennas are used for convenience. The stubby, for example, is convenient for short-range communications, avoiding the problems of a lengthier, cumbersome antenna attached to a handheld radio.

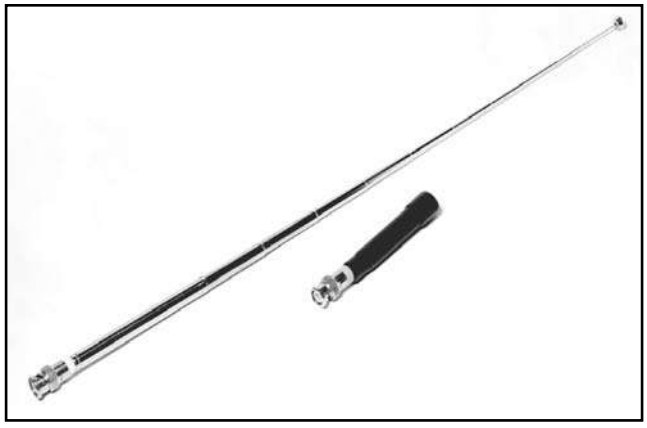

Fig 1—Two mobile antennas—mobile because they may be used while in motion. Shown here are a telescoping $^1/_4$-λ antenna and a "stubby" antenna, both designed for use at 144 MHz. The $^1/_4$-λ antenna is 19 inch long, while the stubby antenna is only $3^1/_2$ inch long. (Both dimensions exclude the length of the BNC connectors. The stubby is a helically wound radiator.

Below 28 MHz, physical size becomes a problem with full-size whips, and some form of electrical loading (as with the stubby) is usually employed. Commonly used loading techniques are to place a coil at the base of the whip (base loading), or at the center of the whip (center loading). These and other techniques are discussed in this chapter.

Few amateurs construct their own antennas for HF mobile and maritime use, since safety reasons dictate very sound mechanical construction. Several construction projects are included, however, in this chapter for those who may wish to build their own mobile antenna. Even if commercially made antennas are installed, most require some adjustment for the particular installation and type of operation desired and the information given here may provide a better understanding of the optimization requirements.

HF-MOBILE FUNDAMENTALS

Fig 2 shows a typical bumper-mounted center-loaded whip suitable for operation in the HF range. Jack Schuster, W1WEF, operates 80 through 2 meters from his car. The antenna could also be mounted on the car body itself (such as a fender), and mounts are available for this purpose. The base spring and tennis ball act as shock absorbers for the bottom of the whip, as the continual flexing while in motion would otherwise weaken the antenna. A short heavy mast section is mounted between the base spring and loading coil. Some models have a mechanism that allows the antenna to be tipped over for adjustment or for fastening to the roof of the car when not in use.

It is also advisable to extend a couple of guy lines from the base of the loading coil to clips or hooks fastened to the roof gutter on the car, or to the trunk and

Fig 2—A typical bumper-mounted HF mobile antenna, as used by W1WEF. Note the nylon guy lines and the tennis ball used as a shock absorber. (*Photo courtesy W1WEF.*)

rear bumper, as W1WEF has done. Nylon fishing line (about 40-pound test) is suitable for this purpose. The guy lines act as safety cords and also reduce the swaying motion of the antenna considerably. The feed line to the transmitter is connected to the bumper and base of the antenna. Good low-resistance connections are important here.

Tune-up of the antenna is usually accomplished by changing the height of the adjustable whip section above the precut loading coil. First, tune the receiver and try to determine where the signals seem to peak up. Once this frequency is found, check the SWR with the transmitter on, and find the frequency where the SWR is lowest. Shortening the adjustable section will increase the resonant frequency, and making it longer will lower the frequency. It is important that the antenna be away from surrounding objects such as overhead wires by ten feet or more, as considerable detuning can occur. Once the setting is found where the SWR is lowest at the center of the desired frequency range, the length of the adjustable section should be recorded.

Propagation conditions and ignition noise are usually the limiting factors for mobile operation on 10 through 28 MHz. Antenna size restrictions affect operation somewhat on 7 MHz and much more on 3.5 and 1.8 MHz. From this standpoint, perhaps the optimum band for HF-mobile operation is 7 MHz. The popularity of the regional mobile nets on 7 MHz is perhaps the best indication of its suitability. For local work, 28 MHz is also useful, as antenna efficiency is high and relatively simple antennas without loading coils are easy to build.

As the frequency of operation is lowered, an antenna of fixed length looks (at its feed point) like a decreasing resistance in series with an increasing capacitive reactance. The capacitive reactance must be tuned out, necessitating the use of an equivalent series inductive reactance or loading coil. The amount of inductance required will be determined by the placement of the coil in the antenna system.

Base loading requires the lowest value of inductance for a fixed-length antenna, and as the coil is placed farther up the whip, the necessary value increases. This is because the capacitance of the shorter antenna section (above the coil) to the car body is now lower (higher capacitive reactance), requiring more inductance to tune the antenna to resonance. The advantage is that the current distribution on the whip is improved, increasing the radiation resistance. The disadvantage is that requirement of a larger coil also means the coil size and losses increase. Center loading has been generally accepted as a good compromise with minimal construction problems. Placing the coil $^2/_3$ the distance up the whip seems to be about the optimum position.

For typical antenna lengths used in mobile work, the difficulty in constructing suitable loading coils increases as the frequency of operation is lowered. Since the required resonating inductance gets larger and the radiation resistance decreases at lower frequencies, most of the power is dissipated in the coil's loss resistance and in other ohmic losses. This is one reason why it is advisable to buy a commercially made loading coil with the highest power rating possible, even if only low-power operation is planned.

Coil losses in the higher-power loading coils are usually less (percentage-wise), with subsequent improvement in radiation efficiency, regardless of the power level used. Of course, the above philosophy also applies to homemade loading coils, and design considerations will be considered in a later section.

Once the antenna is tuned to resonance, the input impedance at the antenna terminals will look like a pure resistance. Neglecting losses, this value drops from nearly 15 Ω at 21 MHz to 0.1 Ω at 1.8 MHz for an 8-foot whip. When coil and other losses are included, the input resistance increases to approximately 20 Ω at 1.8 MHz and 16 Ω at 21 MHz. These values are for relatively high-efficiency systems. From this it can be seen that the radiation efficiency is much poorer at 1.8 MHz than at 21 MHz under typical conditions.

Since most modern gear is designed to operate with a 50-Ω transmission line, a matching network is usually necessary, especially with the high-efficiency antennas previously mentioned. This can take the form of either a broadband transformer, a tapped coil, or an LC matching network. With homemade or modified designs, the tapped-coil arrangement is perhaps the easiest one to build, while the broadband transformer requires no adjustment. As the losses go up, so does the input resis-

tance, and in less efficient systems the matching network may not be needed.

The Equivalent Circuit of a Typical Mobile Antenna

In the previous section, some of the general considerations were discussed, and these will now be taken up in more detail. It is customary in solving problems involving electric and magnetic fields (such as antenna systems) to try to find an equivalent network with which to replace the antenna for analysis reasons. In many cases, the network may be an accurate representation over only a limited frequency range. However, this is often a valuable method in matching the antenna to the transmission line.

Antenna resonance is defined as the frequency at which the input impedance at the antenna terminals is purely resistive. The shortest length at which this occurs for a vertical antenna over a ground plane is when the antenna is an electrical quarter wavelength at the operating frequency; the impedance value for this length (neglecting losses) is about 36 Ω. The idea of resonance can be extended to antennas shorter (or longer) than a quarter wave, and means only that the input impedance is purely resistive. As pointed out previously, when the frequency is lowered, the antenna looks like a series RC circuit, as shown in **Fig 3**. For the average 8-foot whip, the capacitive reactance of C_A may range from about −150 Ω at 21 MHz to as high as −8000 Ω at 1.8 MHz, while the radiation resistance R_R varies from about 15 Ω at 21 MHz to as low as 0.1 Ω at 1.8 MHz.

For an antenna less than 0.1 λ long, the approximate radiation resistance may be determined from the following:

$$R_R = 273 \times (\ell f)^2 \times 10^{-8} \qquad \text{(Eq 1)}$$

where ℓ is the length of the whip in inches, and f is the frequency in megahertz.

Since the resistance is low, considerable current must flow in the circuit if any appreciable power is to be dissipated in the form of radiation in R_R. Yet it is apparent that little current can be made to flow in the circuit as long as the comparatively high series reactance remains.

Antenna Capacitance

Capacitive reactance can be canceled by connecting an equivalent inductive reactance, (coil L_L) in series, as shown in **Fig 4**, thus tuning the system to resonance.

The capacitance of a vertical antenna shorter than a quarter wavelength is given by:

$$C_A = \frac{17\ell}{\left[\left(\ln\frac{24\ell}{D}\right)-1\right]\left[1-\left(\frac{f\ell}{234}\right)^2\right]} \qquad \text{(Eq 2)}$$

where

C_A = capacitance of antenna in pF
ℓ = antenna height in feet
D = diameter of radiator in inches
f = operating frequency in MHz

$$\ln\frac{24\ell}{D} = 2.3\log_{10}\frac{24\ell}{D}$$

Fig 5 shows the approximate capacitance of whip antennas of various average diameters and lengths. For 1.8, 4 and 7 MHz, the loading coil inductance required (when the loading coil is at the base) would be approximately the inductance required to resonate in the desired band (with the whip capacitance taken from the graph). For 10 through 21 MHz, this rough calculation will give more than the required inductance, but it will serve as a

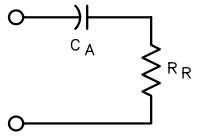

Fig 3—At frequencies below resonance, the whip antenna will show capacitive reactance as well as resistance. R_R is the radiation resistance, and C_A represents the antenna capacitance.

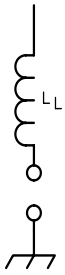

Fig 4—The capacitive reactance at frequencies below the resonant frequency of the whip can be canceled by adding an equivalent inductive reactance in the form of a loading coil in series with the antenna.

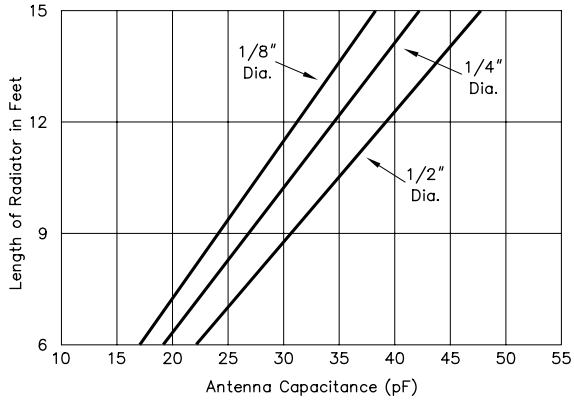

Fig 5—Graph showing the approximate capacitance of short vertical antennas for various diameters and lengths. These values should be approximately halved for a center-loaded antenna.

starting point for the final experimental adjustment that must always be made.

LOADING COIL DESIGN

To minimize loading coil loss, the coil should have a high ratio of reactance-to-resistance (that is, a high unloaded Q). A 4-MHz loading coil wound with small wire on a small-diameter solid form of poor quality, and enclosed in a metal protector, may have a Q as low as 50, with a loss resistance of 50 Ω or more. High-Q coils require a large conductor, air-wound construction, large spacing between turns, and the best insulating material available. A diameter not less than half the length of the coil (not always mechanically feasible) and a minimum of metal in the field of the coil are also necessities for optimum efficiency. Such a coil for 4 MHz may show a Q of 300 or more, with a resistance of 12 Ω or less.

The coil could then be placed in series with the feed line at the base of the antenna to tune out the unwanted capacitive reactance, as shown in Fig 4. Such a method is often referred to as *base-loading*, and many practical mobile antenna systems have been built using this scheme.

Over the years, the question has come up as to whether or not more efficient designs are possible compared with simple base loading. While many ideas have been tried with varying degrees of success, only a few have been generally accepted and incorporated into actual systems. These are center loading, continuous loading, and combinations of the latter with more conventional antennas.

Base Loading and Center Loading

If a whip antenna is short compared to a wavelength *and the current is uniform along the length* ℓ, the electric field strength E, at a distance d, away from the antenna is approximately:

$$E = \frac{120\pi I\ell}{d\lambda} \qquad \text{(Eq 3)}$$

where

I is the antenna current in amperes

λ is the wavelength in the same units as D and ℓ.

A uniform current flowing along the length of the whip is an idealized situation, however, since the current is greatest at the base of the antenna and goes to a minimum at the top. In practice, the field strength will be less than that given by the above equation, because it is a function of the current distribution on the whip.

The reason that the current is not uniform on a whip antenna can be seen from the circuit approximation shown in **Fig 6**. A whip antenna over a ground plane is similar in many respects to a tapered coaxial cable where the center conductor remains the same diameter along its length, but with an increasing diameter outer conductor. The inductance per unit length of such a cable would increase along the line, while the capacitance per unit length would decrease. In Fig 6 the antenna is represented by a series of LC circuits in which C1 is greater than C2, which is greater than C3, and so on. L1 is less than L2, which is less than succeeding inductances. The net result is that most of the antenna current returns to ground near the base of the antenna, and very little near the top.

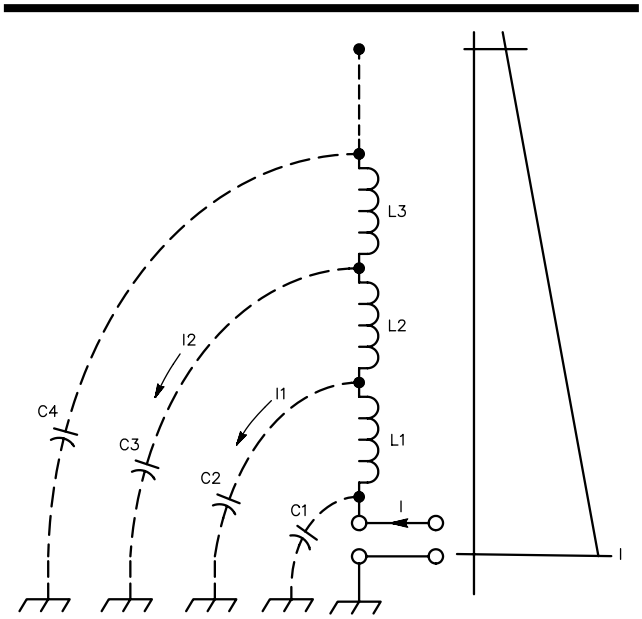

Fig 6—A circuit approximation of a simple whip over a perfectly conducting ground plane. The shunt capacitance per unit length gets smaller as the height increases, and the series inductance per unit length gets larger. Consequently, most of the antenna current returns to the ground plane near the base of the antenna, giving the current distribution shown at the right.

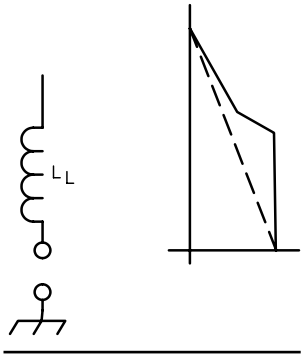

Fig 7—Improved current distribution resulting from center loading.

Two things can be done to improve this distribution and make the current more uniform. One would be to increase the capacitance of the top of the antenna to ground through the use of top loading or a capacitance hat, as discussed in Chapter 6. Unfortunately, the wind resistance of the hat makes it somewhat unwieldy for mobile use. The other method is to place the loading coil farther up the whip, as shown in **Fig 7**, rather than at the base. If the coil is resonant (or nearly so) with the

Table 1
Approximate Values for 8-ft Mobile Whip

f(MHz)	Loading L μH	R_C(Q50) Ω	R_C(Q300) Ω	R_R Ω	Feed R* Ω	Matching L μH
Base Loading						
1.8	345	77	13	0.1	23	3
3.8	77	37	6.1	0.35	16	1.2
7.2	20	18	3	1.35	15	0.6
10.1	9.5	12	2	2.8	12	0.4
14.2	4.5	7.7	1.3	5.7	12	0.28
18.1	3.0	5.0	1.0	10.0	14	0.28
21.25	1.25	3.4	0.5	14.8	16	0.28
24.9	0.9	2.6	—	20.0	22	0.25
29.0	—	—	—	—	36	0.23
Center Loading						
1.8	700	158	23	0.2	34	3.7
3.8	150	72	12	0.8	22	1.4
7.2	40	36	6	3.0	19	0.7
10.1	20	22	4.2	5.8	18	0.5
14.2	8.6	15	2.5	11.0	19	0.35
18.1	4.4	9.2	1.5	19.0	22	0.31
21.25	2.5	6.6	1.1	27.0	29	0.29

R_C = loading coil resistance; R_R = radiation resistance.
*Assuming loading coil Q = 300, and including estimated ground-loss resistance.

Table 2
Suggested Loading Coil Dimensions

Req'd L(μH)	Turns	Wire Size	Dia. Inches	Length Inches
700	190	22	3	10
345	135	18	3	10
150	100	16	2 1/2	10
77	75	14	2 1/2	10
77	29	12	5	4 1/4
40	28	16	2 1/2	2
40	34	12	2 1/2	4 1/4
20	17	16	2 1/2	1 1/4
20	22	12	2 1/2	2 3/4
8.6	16	14	2	2
8.6	15	12	2 1/2	3
4.5	10	14	2	1 1/4
4.5	12	12	2 1/2	4
2.5	8	12	2	2
2.5	8	6	2 3/8	4 1/2
1.25	6	12	1 3/4	2
1.25	6	6	2 3/8	4 1/2

capacitance to ground of the section above the coil, the current distribution is improved as also shown in Fig 7. The result with both top loading and center loading is that the radiation resistance is increased, offsetting the effect of losses and making matching easier.

Table 1 shows the approximate loading coil inductance for the various amateur bands. Also shown in the table are approximate values of radiation resistance to be expected with an 8-foot whip, and the resistances of loading coils—one group having a Q of 50, the other a Q of 300. A comparison of radiation and coil resistances will show the importance of reducing the coil resistance to a minimum, especially on the three lower frequency bands. **Table 2** shows suggested loading-coil dimensions for the inductance values given in Table 1.

OPTIMUM DESIGN OF SHORT COIL-LOADED HF MOBILE ANTENNAS

Optimum design of short HF mobile antennas results from a careful balance of the appropriate loading coil Q-factor, loading coil position in the antenna, ground loss resistance, and the length-to-diameter ratio of the antenna. The optimum balance of these parameters can be realized only through a thorough understanding of how they interact. This section presents a mathematical approach to designing mobile antennas for maximum radiation efficiency. Bruce Brown, W6TWW, in *The ARRL Antenna Compendium Volume 1*, first presented this approach. (See the Bibliography at the end of this chapter.)

The optimum location for a loading coil in an antenna can be found experimentally, but it requires many hours of designing and constructing models and making measurements to ensure the validity of the design. A faster and more reliable way of determining optimum coil location is through the use of a personal computer. This approach allows the variation of any single variable, while observing the cumulative effects on the system. When plotted graphically, the data reveals that the placement of the loading coil is critical if maximum radiation efficiency

Table 3
Variables used in Eqs 4 through 20

A = area in degree-amperes
a = antenna radius in English or metric units
dB = signal loss in decibels
E = efficiency in percent
f (MHz) = frequency in megahertz
H = height in English or metric units
h = height in electrical degrees
h_1 = height of base section in electrical degrees
h_2 = height of top section in electrical degrees
$I = I_{base}$ = 1 ampere base current
k = 0.0128
k_m = mean characteristic impedance
k_{m1} = mean characteristic impedance of base section
k_{m2} =mean characteristic impedance of top section
L = length or height of the antenna in feet
P_I = power fed to the antenna
P_R = power radiated
Q = coil figure of merit
R_C = coil loss resistance in Ω
R_G = ground loss resistance in Ω
R_R = radiation resistance in Ω
X_L = loading-coil inductive reactance

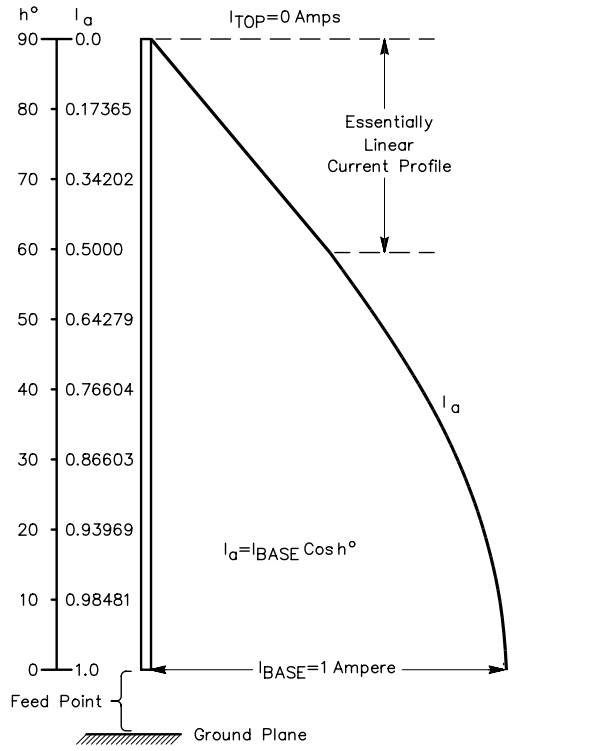

Fig 8—Relative current distribution on a vertical antenna of height h = 90 electrical degrees.

is to be realized. (See the program *MOBILE.EXE*, which is included on the CD-ROM in the back of this book.)

Radiation Resistance

The determination of radiation efficiency requires the knowledge of resistive power losses and radiation losses. Radiation loss is expressed in terms of radiation resistance. Radiation resistance is defined as the resistance that would dissipate the same amount of power that is radiated by the antenna. The variables used in the equations that follow are defined once in the text, and are summarized in **Table 3**. Radiation resistance of vertical antennas shorter than 45 electrical degrees (1/8 wavelength) is approximately:

$$R_R = \frac{h^2}{312} \qquad \text{(Eq 4)}$$

where

R_R = radiation resistance in Ω
h = antenna length in electrical degrees.

Antenna height in electrical degrees is expressed by:

$$h = \frac{\ell}{984} \times f\left(MHz\right) \times 360 \qquad \text{(Eq 5)}$$

where

ℓ = antenna length in feet
f (MHz) = operating frequency in megahertz.

End effect is purposely omitted to ensure that an antenna is electrically long. This is so that resonance at the design frequency can be obtained easily by removing a turn or two from the loading coil.

Eq 4 is valid only for antennas having a sinusoidal current distribution and no reactive loading. However, it can be used as a starting point for deriving an equation that is useful for shortened antennas with other than sinusoidal current distributions.

Refer to **Fig 8**. The current distribution on an antenna 90° long electrically (1/4 wavelength) varies with the cosine of the length in electrical degrees. The current distribution of the top 30° of the antenna is essentially linear. It is this linearity that allows for derivation of a simpler, more useful equation for radiation resistance.

The radiation resistance of an electrically short base-loaded vertical antenna can be conveniently defined in terms of a geometric figure, a triangle, as shown in **Fig 9**. The radiation resistance is given by:

$$R_R = KA^2 \qquad \text{(Eq 6)}$$

where

K is a constant (to be derived shortly)
A = area of the triangular current distribution in degree-amperes.

Degree-ampere area is expressed by

$$A = \frac{1}{2} h \times I_{base} \qquad \text{(Eq 7)}$$

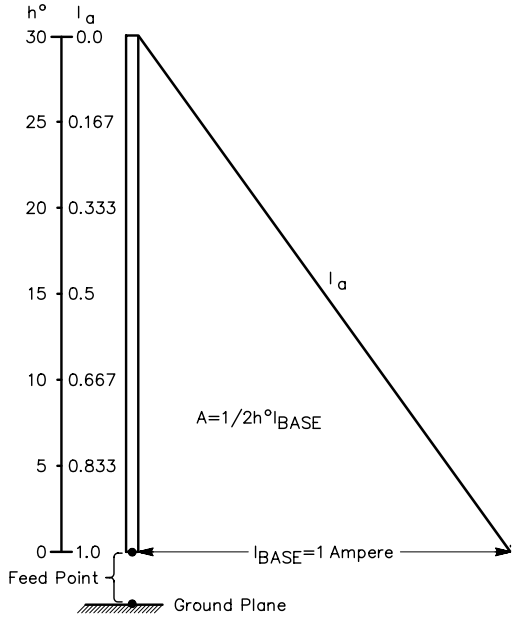

Fig 9—Relative current distribution on a base-loaded vertical antenna of height H = 30 electrical degrees (linearized). The base loading coil is not shown here.

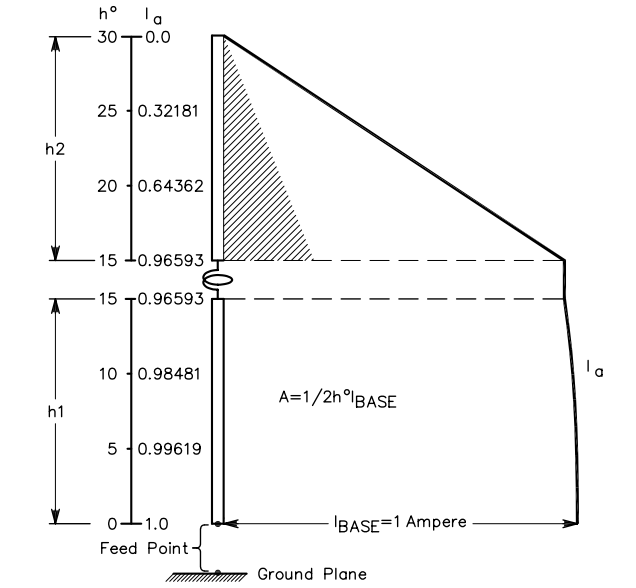

Fig 10—Relative current distribution on a center-loaded antenna with base and top sections each equal to 15 electrical degrees in length. The cross-hatched area shows the current distribution that would exist in the top 15° of a 90°-high vertical fed with 1 ampere at the base.

By combining Eqs 4 and 6 and solving for K, we get

$$K = \frac{h^2}{312 \times A^2} \qquad \text{(Eq 8)}$$

By substituting the values from Fig 9 into Eq 8 we get

$$K = \frac{30^2}{312 \times \left(0.5 \times 30 \times 1\right)^2} = 0.0128$$

and by substituting the derived value of K into Eq 6 we get

$$R_R = 0.0128 \times A^2 \qquad \text{(Eq 9)}$$

Eq 9 is useful for determining the radiation resistance of coil-loaded vertical antennas less than 30° in length. The derived constant differs slightly from that presented by Laport (see Bibliography), as he used a different equation for radiation resistance Eq 4.

When the loading coil is moved up an antenna (away from the feed point), the current distribution is modified as shown in **Fig 10**. The current varies with the cosine of the height in electrical degrees at any point in the base section. Therefore, the current flowing into the bottom of the loading coil is less than the current flowing at the base of the antenna.

But what about the current in the top section of the antenna? The loading coil acts as the lumped constant that it is, and disregarding losses and coil radiation, maintains the same current flow throughout. As a result, the current at the top of a high-Q coil is essentially the same as that at the bottom of the coil. This is easily verified by installing RF ammeters immediately above and below the loading coil in a test antenna. Thus, the coil "forces" much more current into the top section than would flow in the equivalent section of a full 90° long antenna. This occurs as a result of the extremely high voltage that appears at the top of the loading coil. This higher current flow results in more radiation than would occur from the equivalent section of a quarter-wave antenna. (This is true for conventional coils. However, radiation from long thin coils allows coil current to decrease, as in helically wound antennas.)

The cross-hatched area in Fig 10 shows the current that would flow in the equivalent part of a 90° high antenna, and reveals that the degree-ampere area of the whip section of the short antenna is greatly increased as a result of the modified current distribution. The current flow in the top section decreases almost linearly to zero at the top. This can be seen in Fig 10.

The degree-ampere area of Fig 10 is the sum of the triangular area represented by the current distribution in the top section, and the nearly trapezoidal current distribution in the base section. Radiation from the coil is not included in the degree-ampere area because it is small and difficult to define. Any radiation from the coil can be considered a bonus.

The degree-ampere area is expressed by:

$$A = \frac{1}{2}\left[h_1\left(1 + \cos h_1\right) + h_2\left(\cos h_1\right)\right] \qquad \text{(Eq 10)}$$

where

h_1 = electrical length in degrees of the base section

h_2 = electrical height in degrees of the top section.

The degree-ampere area (calculated by substituting Eq 10 into Eq 9) can be used to determine the radiation resistance when the loading coil is at any position other than the base of the antenna. Radiation resistance has been calculated with these equations and plotted against loading coil position at three different frequencies for 8- and 11-foot antennas, **Fig 11**. Eight feet is a typical length for commercial antennas, and 11-foot antennas are about the maximum practical length that can be installed on a vehicle.

In Fig 11, the curves reveal that the radiation resistance rises almost linearly as the loading coil is moved up the antenna. They also show that the radiation resistance rises rapidly as the frequency is increased. If the analysis were stopped at this point, one might conclude that the loading coil should be placed at the top of the antenna. This is not so, and will become apparent shortly.

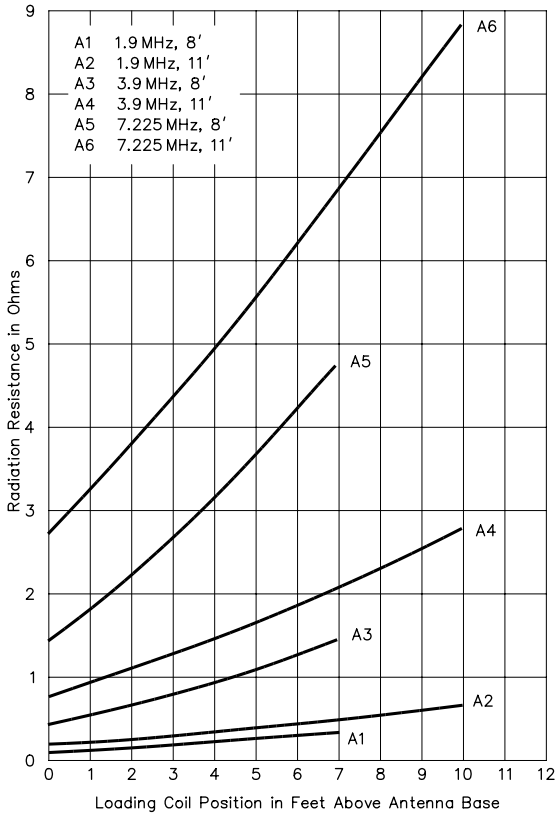

Fig 11—Radiation resistance plotted as a function of loading coil position.

Required Loading Inductance

Calculation of the loading coil inductance needed to resonate a short antenna can be done easily and accurately by using the antenna transmission-line analog described by Boyer in *Ham Radio*. For a base-loaded antenna, Fig 9, the loading coil reactance required to resonate the antenna is given by

$$X_L = -j\, K_m \cot h \qquad \text{(Eq 11)}$$

where

X_L = inductive reactance required

K_m = mean characteristic impedance (defined in Eq 12).

The $-j$ term indicates that the antenna presents capacitive reactance at the feed point. A loading coil must cancel this reactance.

The mean characteristic impedance of an antenna is expressed by

$$K_m = 60\left[\left(\ln \frac{2H}{a}\right) - 1\right] \qquad \text{(Eq 12)}$$

where

H = physical antenna height (excluding the length of the loading coil)

a = radius of the antenna in the same units as H.

From Eq 12 you can see that decreasing the height-to-diameter ratio of an antenna by increasing the radius results in a decrease in K_m. With reference to Eq 11, a decrease in K_m decreases the inductive reactance required to resonate an antenna. As will be shown later, this will increase radiation efficiency. In mobile applications, we quickly run into wind-loading problems if we attempt to use an antenna that is physically large in diameter.

If the loading coil is moved away from the base of the antenna, the antenna is divided into a base and top section, as depicted in Fig 10. The loading coil reactance required to resonate the antenna when the coil is away from the base is given by

$$X_L = j\, K_{m2} (\cot h_2) - j\, K_{m1} (\tan h_1) \qquad \text{(Eq 13)}$$

In mobile-antenna design and construction, the top section is usually a whip with a much smaller diameter than the base section. Because of this, it is necessary to compute separate values of K_m for the top and base sections. K_{m1} and K_{m2} are the mean characteristic impedances of the base and top sections, respectively.

Loading coil reactance curves for the 3.8-MHz antennas of Fig 11 have been calculated and plotted in **Fig 12**. These curves show the influence of the loading coil position on the reactance required for resonance. The curves in Fig 12 show that the required reactance decreases with longer antennas. The curves also reveal that the required loading coil reactance grows at an increasingly rapid rate after the coil passes the center of the antenna. Because the highest possible loading coil Q

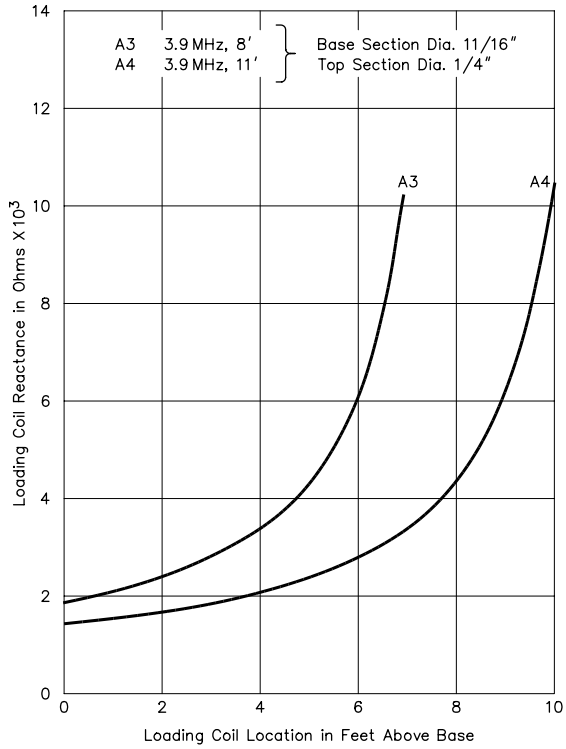

Fig 12—Loading coil reactance required for resonance, plotted as a function of coil height above the antenna base. The resonant frequency is 3.9 MHz.

factor is needed, and because optimum Q is attained when the loading coil diameter is twice the loading coil length, the coil would grow like a smoke ring above the center of the antenna, and would quickly reach an impractical size. It is for this reason that the highest loading coil position is limited to one foot from the top of the antenna in all computations.

Loading Coil Resistance

Loading coil resistance constitutes one of the losses that consumes power that could otherwise be radiated by the antenna. Heat loss in the loading coil is not of any benefit, so it should be minimized by using the highest possible loading coil Q. Loading coil loss resistance is a function of the coil Q and is given by

$$R_C = \frac{X_L}{Q} \qquad \text{(Eq 14)}$$

where

R_C = loading coil loss resistance in Ω
X_L = loading coil reactance
Q = coil figure of merit

Inspection of Eq 14 reveals that, for a given value of inductive reactance, loss resistance will be lower for higher Q coils. Measurements made with a Q meter show that typical, commercially manufactured coil stock produces a Q between 150 and 160 in the 3.8-MHz band.

Higher Q values can be obtained by using larger diameter coils having a diameter-to-length ratio of two, by using larger diameter wire, by using more spacing between turns, and by using low-loss polystyrene supporting and enclosure materials. In theory, loading coil turns should not be shorted for tuning purposes because shorted turns somewhat degrade Q. Pruning to resonance should be done by removing turns from the coil.

In fairness, it should be pointed out that many practical mobile antennas use large-diameter loading coils with shorted turns to achieve resonance. The popular "Texas Bug Catcher" coils come to mind here. Despite general proscriptions against shorting turns, these systems are often more efficient than antennas with small, relatively low-Q, fixed loading coils.

Radiation Efficiency

The ratio of power radiated to power fed to an antenna determines the radiation efficiency. It is given by:

$$E = \frac{P_R}{P_I} \times 100\% \qquad \text{(Eq 15)}$$

where

E = radiation efficiency in percent
P_R = power radiated
P_I = power fed to the antenna at the feed point.

In a short, coil-loaded mobile antenna, a large portion of the power fed to the antenna is dissipated in ground and coil resistances. A relatively insignificant amount of power is also dissipated in the antenna conductor resistance and in the leakage resistance of the base insulator. Because these last two losses are both very small and difficult to estimate, they are here neglected in calculating radiation efficiency.

Another loss worth noting is matching network loss. Because we are concerned only with power fed to the antenna in the determination of radiation efficiency, matching network loss is not considered in any of the equations. Suffice it to say that matching networks should be designed for minimum loss in order to maximize the transmitter power available at the antenna.

The radiation efficiency equation may be rewritten and expanded as follows:

$$E = \frac{I^2 R_R \times 100}{I^2 R_R + I^2 R_G + \left(I \cos h_1\right)^2 R_C} \qquad \text{(Eq 16)}$$

where

I = antenna base current in amperes
R_G = ground loss resistance in Ω
R_C = coil loss resistance in Ω.

Each term of Eq 16 represents the power dissipated in its associated resistance. All the current terms cancel,

simplifying this equation to

$$E = \frac{R_R \times 100}{R_R + R_G + R_C \left(\cos^2 h_1\right)} \qquad \text{(Eq 17)}$$

For base-loaded antennas the term $\cos^2 h_1$ drops to unity and may be omitted.

Ground Loss

Eq 14 shows that the total resistive losses in the antenna system are:

$$R_T = R_R + R_G + R_c (\cos^2 h_1) \qquad \text{(Eq 18)}$$

where R_T is the total resistive loss. Ground loss resistance can be determined by rearranging Eq 18 as follows:

$$R_G = R_T - R_R - R_C \cos^2 h_1 \qquad \text{(Eq 19)}$$

R_T may be measured in a test antenna installation on a vehicle using an R-X noise bridge or an SWR analyzer. You can then calculate R_R and R_C.

Ground loss is a function of vehicle size, placement of the antenna on the vehicle, and conductivity of the ground over which the vehicle is traveling. Only the first two variables can be feasibly controlled. Larger vehicles provide better ground planes than smaller ones. The vehicle ground plane is only partial, so the result is considerable RF current flow (and ground loss) in the ground around and under the vehicle.

By raising the antenna base as high as possible on the vehicle, ground losses are decreased. This results from a decrease in antenna capacitance to ground, which increases the capacitive reactance to ground. This, in turn, reduces ground currents and ground losses.

This effect has been verified by installing the same antenna at three different locations on two different vehicles, and by determining the ground loss from Eq 19. In the first test, the antenna was mounted 6 inches below the top of a large station wagon, just behind the left rear window. This placed the antenna base 4 feet 2 inches above the ground, and resulted in a measured ground loss resistance of 2.5 Ω. The second test used the same antenna mounted on the left rear fender of a mid-sized sedan, just to the left of the trunk lid. In this test, the measured ground loss resistance was 4 Ω. The third test used the same mid-sized car, but the antenna was mounted on the rear bumper. In this last test, the measured ground loss resistance was 6 Ω.

The same antenna therefore sees three different ground loss resistances as a direct result of the antenna mounting location and size of the vehicle. It is important to note that the measured ground loss increases as the antenna base nears the ground. The importance of minimizing ground losses in mobile antenna installations cannot be overemphasized.

Efficiency Curves

With the equations defined previously, a computer

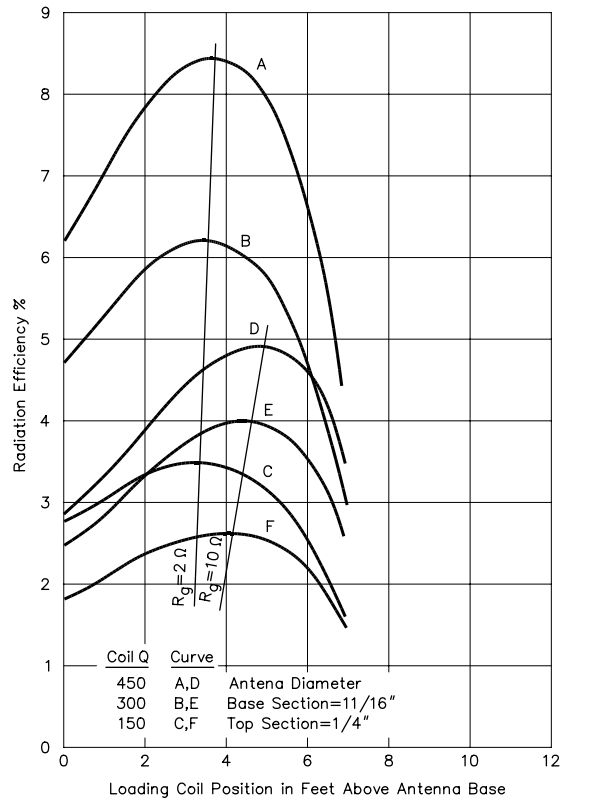

Fig 13—Radiation efficiency of 8-foot antennas at 3.9 MHz.

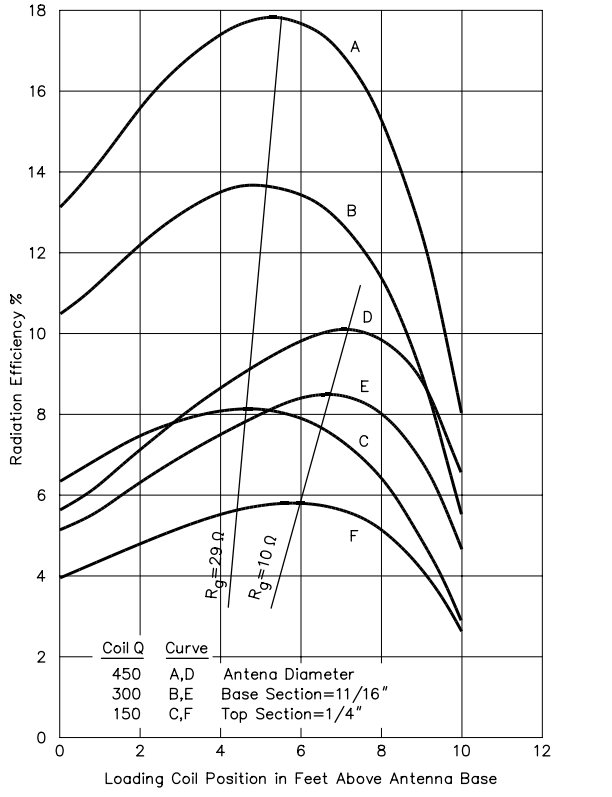

Fig 14—Radiation efficiency of 11-foot antennas at 3.9 MHz.

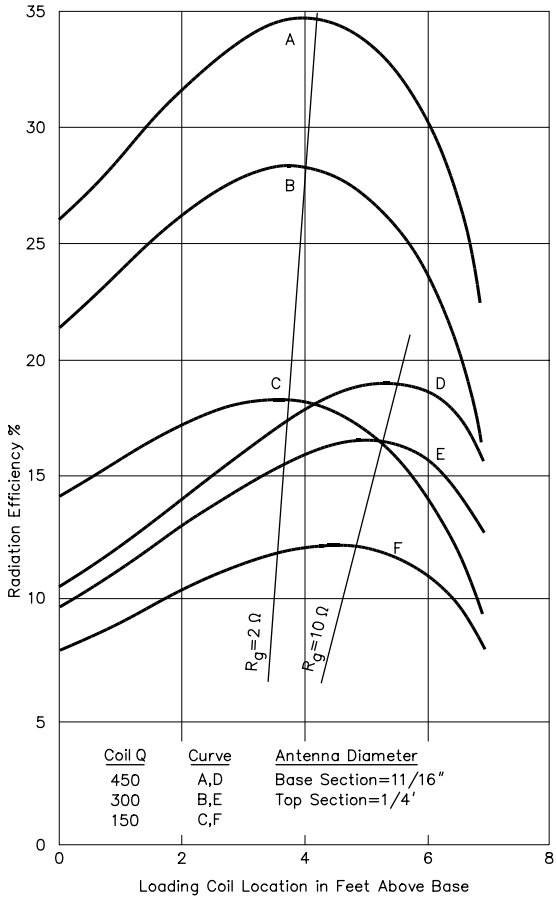

Fig 15—Radiation efficiency of 8-foot antennas at 7.225 MHz.

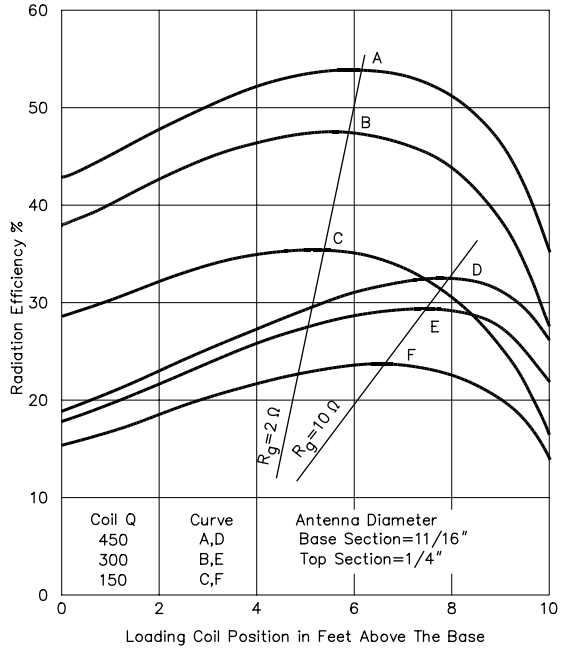

Fig 16—Radiation efficiency of 11-foot antennas at 7.225 MHz.

was used to calculate the radiation efficiency curves depicted in **Figs 13** through **16**. These curves were calculated for 3.8- and 7-MHz antennas of 8- and 11-foot lengths. Several values of loading coil Q were used, for both 2 and 10 Ω of ground loss resistance. For the calculations, the base section is $^1/_2$-inch diameter electrical EMT, which has an outside diameter of $^{11}/_{16}$ inch. The top section is fiberglass bicycle-whip material covered with Belden braid. These are readily available materials, which can be used by the average amateur to construct an inexpensive but rugged antenna.

Upon inspection, these radiation-efficiency curves reveal some significant information:

1) Higher coil Q produces higher radiation efficiencies,
2) longer antennas produce higher radiation efficiencies,
3) higher frequencies produce higher radiation efficiencies,
4) lower ground loss resistances produce higher radiation efficiencies,
5) higher ground loss resistances force the loading coil above the antenna center to reach a crest in the radiation-efficiency curve, and
6) higher coil Q sharpens the radiation-efficiency curves, resulting in the coil position being more critical for optimum radiation efficiency.

Note that the radiation efficiency curves reach a peak and then begin to decline as the loading coil is raised farther up the antenna. This is because of the rapid increase in loading coil reactance required above the antenna center. Refer to Fig 12. The rapid increase in coil size required for resonance results in the coil loss resistance increasing much more rapidly than the radiation resistance. This results in decreased radiation efficiency, as shown in Fig 11.

A slight reverse curvature exists in the curves between the base-loaded position and the one-foot coil-height position. This is caused by a shift in the curve resulting from insertion of a base section of larger diameter than the whip when the coil is above the base.

The curves in Figs 13 through 16 were calculated with constant (but not equal) diameter base and whip sections. Because of wind loading, it is not desirable to increase the diameter of the whip section. However, the base-section diameter can be increased within reason to further improve radiation efficiency. **Fig 17** was calculated for base-section diameters ranging from $^{11}/_{16}$ inch to 3 inches. The curves reveal that a small increase in radiation efficiency results from larger diameter base sections.

The curves in Figs 13 through 16 show that radiation efficiencies can be quite low in the 3.8-MHz band compared to the 7-MHz band. They are lower yet in the 1.8-MHz band. To gain some perspective on what these low efficiencies mean in terms of signal strength, **Fig 18** was calculated using the following equation:

$$dB = \log \frac{100}{E} \qquad \text{(Eq 20)}$$

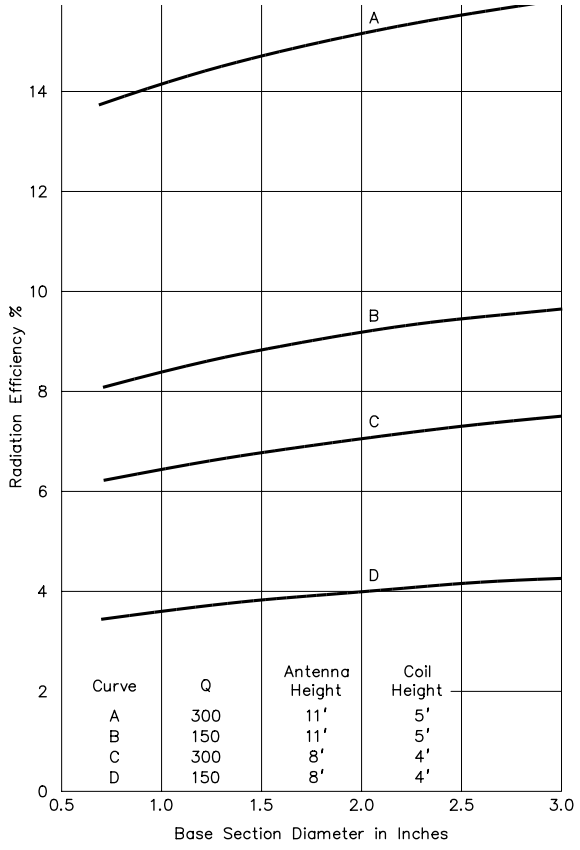

Fig 17—Radiation efficiency plotted as a function of base section diameter. Frequency = 3.9 MHz, ground loss resistance = 2 Ω, and whip section = 1/4-inch diameter.

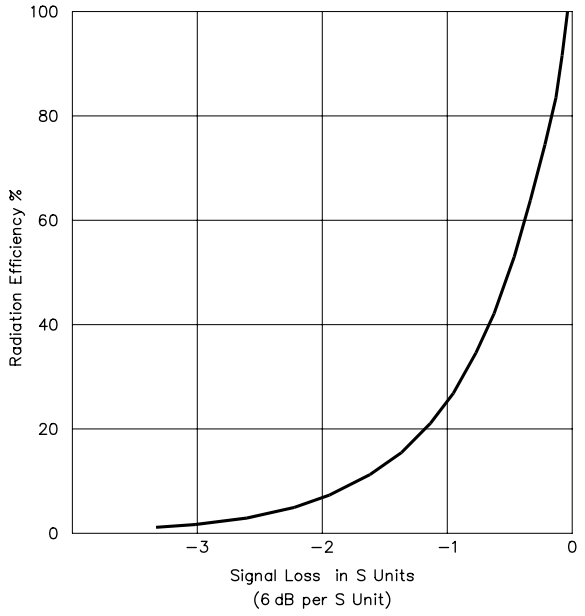

Fig 18—Mobile antenna signal loss as a function of radiation efficiency, compared to a quarter-wave vertical antenna over perfect ground.

where

dB = signal loss in decibels
E = efficiency in percent.

The curve in Fig 18 reveals that an antenna having 25% efficiency has a signal loss of 6 dB (approximately one S unit) below a quarter-wave vertical antenna over perfect ground. An antenna efficiency in the neighborhood of 6% will produce a signal strength on the order of two S units or about 12 dB below the same quarter-wave reference vertical. By careful optimization of mobile-antenna design, signal strengths from mobiles can be made fairly competitive with those from fixed stations using comparable power. And don't forget: Moving your car near saltwater, with its high conductivity, can result in surprisingly strong signals from a mobile station!

Impedance Matching

The input impedance of short, high-Q coil-loaded antennas is quite low. For example, an 8-foot antenna optimized for 3.9 MHz with an unloaded coil Q of 300 and a ground-loss resistance of 2 Ω has a base input impedance of about 13 Ω. This low impedance value causes a standing wave ratio of 4:1 on a 50-Ω coaxial line at resonance. This high SWR is not compatible with the requirements of solid-state transmitters. Also, the bandwidth of shortened vertical antennas is very narrow. This severely limits the capability to maintain transmitter loading over even a small frequency range.

Impedance matching can be accomplished by means of L networks or impedance-matching transformers, but the narrow bandwidth limitation remains. A more elegant solution to the impedance matching and narrow bandwidth problem is to install an automatic tuner at the antenna base. Such a device matches the antenna and coaxial line automatically, and permits operation over a wide frequency range.

The tools are now available to tailor a mobile antenna design to produce maximum radiation efficiency. Mathematical modeling with a personal computer reveals that loading coil Q factor and ground loss resistance greatly influence the optimum loading coil position in a short vertical antenna. It also shows that longer antennas, higher coil Q, and higher operating frequencies produce higher radiation efficiencies.

End effect has not been included in any of the equations to assure that the loading coil will be slightly larger than necessary. Pruning the antenna to resonance should be done by removing coil turns, rather than by shorting turns or shortening the whip section excessively. Shortening the whip reduces radiation efficiency, by both shortening the antenna and moving the optimum coil position. Shorting turns in the loading coil degrades the Q of the coil.

Shortened Dipoles

Mathematical modeling techniques can be applied to shortened dipoles by using zero ground loss resistance

and by doubling the computed values of radiation resistance and feed-point impedance. Radiation efficiency, however, does not double. Rather, it remains unchanged, because a second loading coil is required in the other leg of the dipole. The addition of the second coil offsets the gain in efficiency that occurs when the feed-point impedance and radiation resistance are doubled. There is a gain in radiation efficiency over a vertical antenna worked against ground, though, because the dipole configuration allows ground loss resistance to be eliminated from the calculations.

CONTINUOUSLY LOADED ANTENNAS

The design of high-Q air core inductors for RF work is complicated by the number of parameters that must be optimized simultaneously. One of these factors affecting coil Q adversely is radiation from a discrete loading coil. Therefore, the possibility of cutting down other losses while incorporating the coil radiation into that from the rest of the antenna system is an attractive one.

The general approach has been to use a coil made from heavy wire (#14 or larger), with length-to-diameter ratios as high as 21. British experimenters have reported good results with 8-foot overall lengths on the 1.8- and 3.5-MHz bands. The idea of making the entire antenna out of one section of coil has also been tried with some success. This technique is referred to as linear loading. Further information on linear-loaded antennas can be found in Chapter 6.

While going to extremes trying to find a perfect loading arrangement may not improve antenna performance very much, a poor system with lossy coils and high-resistance connections must be avoided if a reasonable signal is to be radiated.

MATCHING TO THE TRANSMITTER

Most modern transmitters require a 50-Ω output load, and because the feed-point impedance of a mobile whip is quite low, a matching network is usually necessary. Although calculations are helpful in the initial design, considerable experimenting is often necessary in final tune-up. This is particularly true for the lower bands, where the antenna is electrically short compared with a quarter-wave whip. The reason is that the loading coil is required to tune out a very large capacitive reactance, and even small changes in component values result in large reactance variations. Since the feed-point resistance is low to begin with, the problem is even more aggravated.

You can transform the low resistance of the whip to a value suitable for a 50-Ω system with an RF transformer or with a shunt-feed arrangement, such as an L network. The latter may only require a shunt coil or shunt capacitor at the base of the whip, since the net series capacitive or inductive reactance of the antenna and its loading coil may be used as part of the network. The following example illustrates the calculations involved.

Assume that a center-loaded whip antenna, 8.5 feet in overall length, is to be used on 7.2 MHz. From Table 1, earlier in this chapter, we see that the feed-point resistance of the antenna will be approximately 19 Ω, and from Fig 5 that the capacitance of the whip, as seen at its base, is approximately 24 pF. Since the antenna is to be center loaded, the capacitance value of the section above the coil will be cut approximately in half, to 12 pF. From this, it may be calculated that a center-loading inductor of 40.7 μH is required to resonate the antenna, that is, to cancel out the capacitive reactance. (This figure agrees with the approximate value of 40 μH shown in Table 1. The resulting feed-point impedance would then be 19 + *j* 0 Ω—a good match, *if* one happens to have a supply of 19-Ω coax.)

Solution: The antenna can be matched to a 52-Ω line such as RG-8 by tuning it either above or below reso-

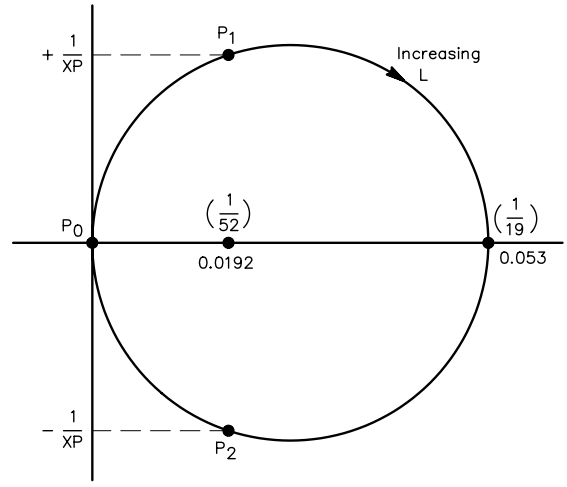

Fig 19—Admittance diagram of the RLC circuit consisting of the whip capacitance, radiation resistance and loading coil discussed in text. The horizontal axis represents conductance, and the vertical axis susceptance. The point P_0 is the input admittance with no whip loading inductance. Points P1 and P2 are described in the text. The conductance equals the reciprocal of the resistance, if no reactive components are present. For a series RX circuit, the conductance is given by

$$G = \frac{R}{R^2 + X^2}$$

and the susceptance is given by

$$B = \frac{-X}{R^2 + X^2}$$

Consequently, a parallel equivalent GB circuit of the series RX one can be found which makes computations easier. This is because conductances and susceptances add in parallel the same way resistances and reactances add in series.

nance and then canceling out the undesired component with an appropriate shunt element, capacitive or inductive. The way in which the impedance is transformed up can be seen by plotting the admittance of the series RLC circuit made up of the loading coil, antenna capacitance, and feed-point resistance. Such a plot is shown in **Fig 19** for a constant feed-point resistance of 19 Ω. There are two points of interest, P1 and P2, where the input conductance is 19.2 millisiemens, corresponding to 52 Ω. The undesired susceptance is shown as $1/X_P$ and $-1/X_P$, which must be canceled with a shunt element of the opposite sign, but with the same magnitude. The value of the canceling shunt reactance, X_P, may be found from the formula:

$$X_p = \frac{R_f\ Z_0}{\sqrt{R_f\ (Z_0 - R_f)}} \qquad \text{(Eq 21)}$$

where X_p is the reactance in Ω, R_f is the feed-point resistance, and Z_0 is the feed-line impedance. For Z_0 = 52 Ω and R_f = 19 Ω, X_p = ±39.5 Ω. A coil or good quality mica capacitor may be used as the shunt element. With the tune-up procedure described later, the value is not critical, and a fixed-value component may be used.

To arrive at point P1, the value of the center loading-coil inductance would be less than that required for resonance. The feed-point impedance would then appear capacitive, and an inductive shunt matching element would then be required. To arrive at point P2, the center loading coil should be more inductive than required for resonance, and the shunt element would need to be capacitive.

The value of the center loading coil required for the shunt-matched and resonated condition may be determined from the equation:

$$L = \frac{10^6}{4\pi^2\ f^2\ C} \pm \frac{X_S}{2\pi f} \qquad \text{(Eq 22)}$$

where addition is performed if a capacitive shunt is to be used, or subtraction performed if the shunt is inductive, and where L is in μH, f is the frequency in MHz, C is the capacitance of the antenna section being matched in pF, and

$$X_S = \sqrt{R_f\ (Z_0 - R_f)} \qquad \text{(Eq 23)}$$

For the example given, where Z_0 = 52 Ω, R_f = 19 Ω, f = 7.2 MHz, and C = 12 pF, X_S is found to be 25.0 Ω. The required antenna loading inductance is either 40.2 μH or 41.3 μH, depending on the type of shunt. Various matching possibilities for this example are shown in **Fig 20**. At A, the antenna is shown as tuned to resonance with L_L, a 40.7 μH coil, but with no provisions included for matching the resulting 19-Ω impedance to the 52-Ω line. At B, L_L has been reduced to 40.2 μH to make the antenna appear net capacitive, and L_M, having a reactance of 39.5 Ω, is added in shunt to cancel the capacitive reactance and transform the feed-point impedance to 50 Ω. The arrangement at C is similar to that at B except that L_L has been increased to 41.3 μH, and C_M (a shunt capacitor having a negative reactance of 39.5 Ω) is added, which also results in a 52-Ω nonreactive termination for the feed line.

The values determined for the loading coil in the above example point out an important consideration concerning the matching of short antennas—relatively small changes in values of the loading components will have a greatly magnified effect on the matching requirements. A change of less than 3% in the loading coil inductance value necessitates a completely different matching network! Likewise, calculations show that a 3% change in antenna capacitance will give similar results, and the value of the precautions mentioned earlier becomes clear. The sensitivity of the circuit with regard to frequency variations is also quite critical, and an excursion around practically the entire circle in Fig 19 may represent only 600 kHz, centered around 7.2 MHz, for the above example. This is why tuning up a mobile antenna can be very frustrating unless a systematic procedure is followed.

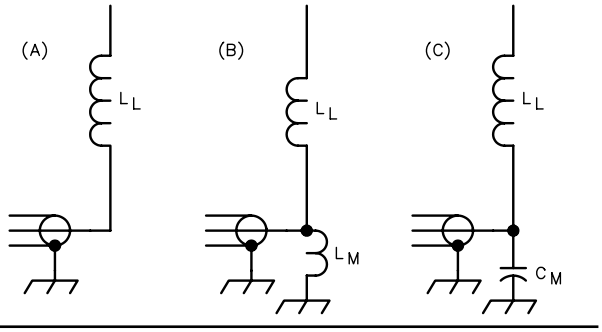

Fig 20—At A, a whip antenna that is resonated with a center loading coil. At B and C, the value of the loading coil has been altered slightly to make the feed-point impedance appear reactive, and a matching component is added in shunt to cancel the reactance. This provides an impedance transformation to match the Z_0 of the feed line. An equally acceptable procedure, rather than altering the loading coil inductance, is to adjust the length of the top section above the loading coil for the best match, as described in the tune-up section of the text.

Tune-Up

Assume that inductive shunt matching is to be used with the antenna in the previous example, Fig 20B, where 39.5 Ω is needed for L_M. This means that at 7.2 MHz, a coil of 0.87 μH will be needed across the whip feed-point terminal to ground. With a 40-μH loading coil in place, the adjustable whip section above the loading coil should be set for minimum height. Signals in the receiver will sound weak and the whip should be lengthened a bit at a time until signals start to peak. Turn the transmitter on and check the SWR at a few frequencies to find where a

minimum occurs. If it is below the desired frequency, shorten the whip slightly and check again. It should be moved approximately 1/4 inch at a time until the SWR is minimum at the center of the desired range. If the frequency where the minimum SWR occurs is above the desired frequency, repeat the procedure above, but lengthen the whip only slightly.

If a shunt capacitance is to be used, as in Fig 20C, a value of 560 pF would correspond to the required –39.5 Ω of reactance at 7.2 MHz. With a capacitive shunt, start with the whip in its longest position and shorten it until signals peak up.

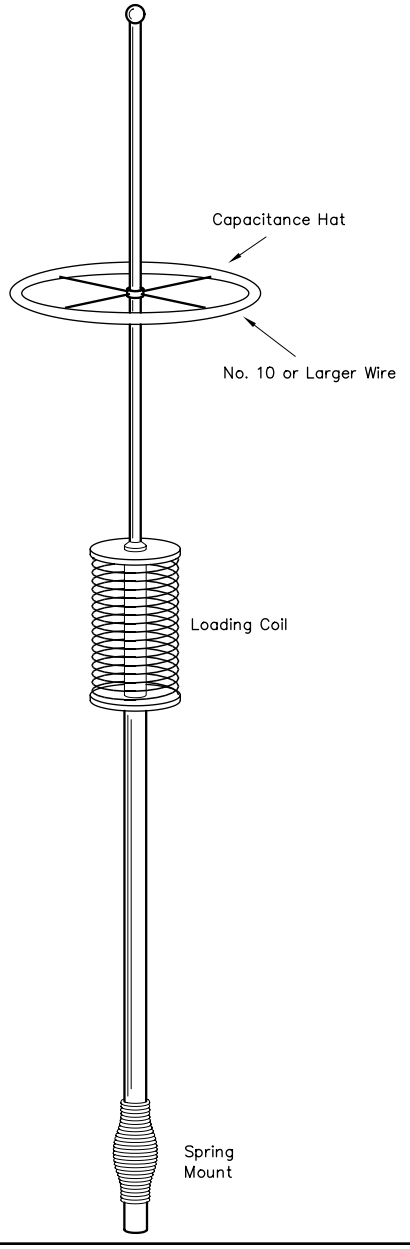

Fig 21—A capacitance hat can be used to improve the performance of base- or center-loaded whips. A solid metal disc can be used in place of the skeleton disc shown here.

TOP-LOADING CAPACITANCE

Because the loss resistance varies with the inductance of the loading coil, the resistance can be reduced by removing turns from the coil. This must be compensated by adding capacitance to the portion of the mobile antenna that is *above* the loading coil (**Fig 21**). *Capacitance hats*, as they are called, can consist of a single stiff wire, two wires or more, or a disc made up of several wires like the spokes of a wheel. A solid metal disc could also be used, but is less practical for mobile work. The larger the capacitance hat (physically), the greater is the capacitance. The greater the capacitance, the less is the inductance required for resonance at a given frequency.

Capacitance-hat loading is applicable in either base-loaded or center-loaded systems. Since more inductance is required for center-loaded whips to make them resonant at a given frequency, capacitance hats are particularly useful in improving their efficiency.

TAPPED-COIL MATCHING NETWORK

Some of the drawbacks of the L-network can be eliminated by the use of the tapped-coil arrangement shown in **Fig 22**. Tune-up still remains critical, however, although somewhat more straightforward than for an L-network.

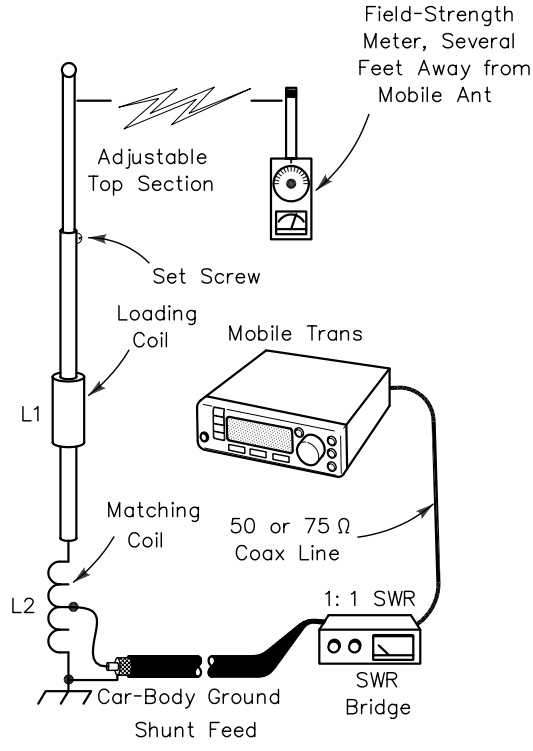

Fig 22—A mobile antenna using shunt-feed matching. Overall antenna resonance is determined by the combination of L1 and L2. Antenna resonance is set by pruning the turns of L1, or adjusting the top section of the whip, while observing the field-strength meter or SWR indicator. Then adjust the tap on L2 for the lowest SWR.

Coil L2 can be inside the car body, at the base of the antenna, or at the base of the whip. As L2 helps determine the resonance of the antenna, L1 should be tuned to resonance in the desired part of the band with L2 in the circuit. The top section of the whip can be telescoped until a field-strength maximum is found. The tap on L2 is then adjusted for the lowest reflected power. Repeat these two adjustments until no further increase in field strength can be obtained; this point should coincide with the lowest SWR. The number of turns needed for L2 will have to be determined experimentally.

THE "SCREWDRIVER" MOBILE ANTENNA

Imagine QSYing from the bottom of 80 meters to the top of 10 meters, right from the driver's seat. With this antenna you will enjoy a very high Q antenna that has no taps or external adjustments, and that exhibits an SWR under 1.5:1 on all bands. Max Bloodworth, KO4TV, described this antenna in *The ARRL Antenna Compendium, Vol 7*.

The Screwdriver type of antenna was the brainchild of Don Johnson, W6AAQ, who developed it after many years of experimenting with mobile antennas. **Fig 23** is a photo of the completed antenna mounted on KO4TV's truck.

Fig 23—The completed Screwdriver antenna mounted on KO4TV's truck rear bumper. (*Photo courtesy of Gary Pearce, KN4AQ.*)

THE LOADING COIL

The general concept for the Screwdriver is that of a center-loaded antenna with an adjustable loading coil. This is an old idea; however, most previous multi-band antennas required multiple coil taps and an adjustable top whip section, as well as an impedance-matching unit at the base.

The problem of tapping a coil is well known. If you leave one end of the coil open, you have a miniature Tesla Coil, which can cause corona discharge and arcing. If you short the turns, the Q of the loading coil usually drops drastically. The Screwdriver is remarkable in that it does not have any coil taps and yet it can cover a wide range of frequencies with very high Q.

The secret is in the manner of adjusting the coil. It simply slides up or down into a metal tube (the base section), and makes contact with the top of the tube by means of "finger stock," which is made of spring-like Beryllium Copper. The coil is pushed up or down by an ordinary cordless screwdriver; hence the name, Screwdriver. This turns a section of threaded rod and moves the coil form up or down. The section of coil above the finger stock is the active loading coil, and the part of the coil just below the finger stock simply "disappears" into the base tube and is totally out of the circuit. No taps, no loose ends—just a high-Q coil in the middle of two solid metal tubes. Although this antenna is available ready-made from several commercial sources, making one is well within the capabilities of any ham who is relatively handy with ordinary hand tools, and who has access to either a small lathe or a common $1^1/_4$-inch pipe die.

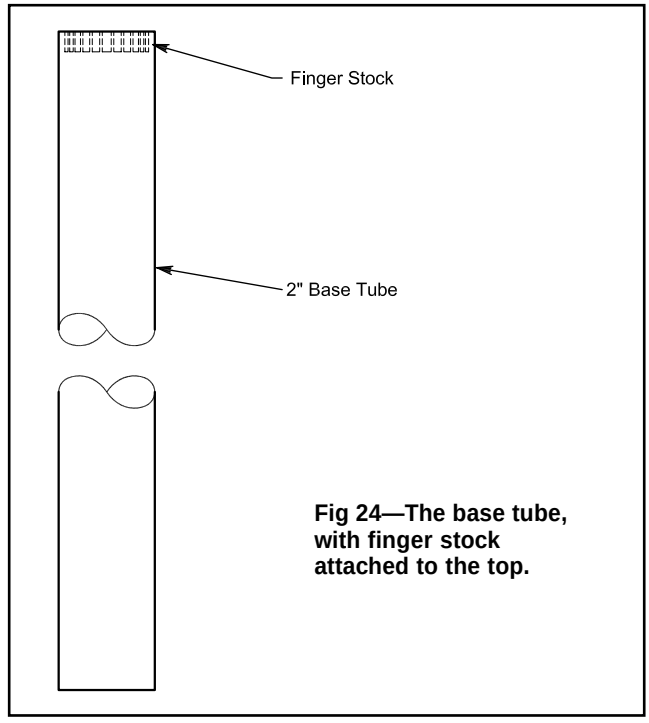

Fig 24—The base tube, with finger stock attached to the top.

CONSTRUCTING YOUR SCREWDRIVER ANTENNA

Construction begins by locating a 2-inch inside-diameter tube, about 3 to 3 1/2 feet long. See **Fig 24**. The author had used such diverse materials as:

- Aluminum irrigation pipe
- Schedule-20 copper tubing
- A stainless-steel hydraulic cylinder
- A section of aluminum from a 6-meter beam that was damaged by a tornado
- And even a brass bedpost salvaged from the local garbage dump.

The brass bedpost looked especially good on his vehicle, which was Burgundy with gold trim. Whatever material you use for the bottom tube, you can either leave it unfinished or painted to your taste.

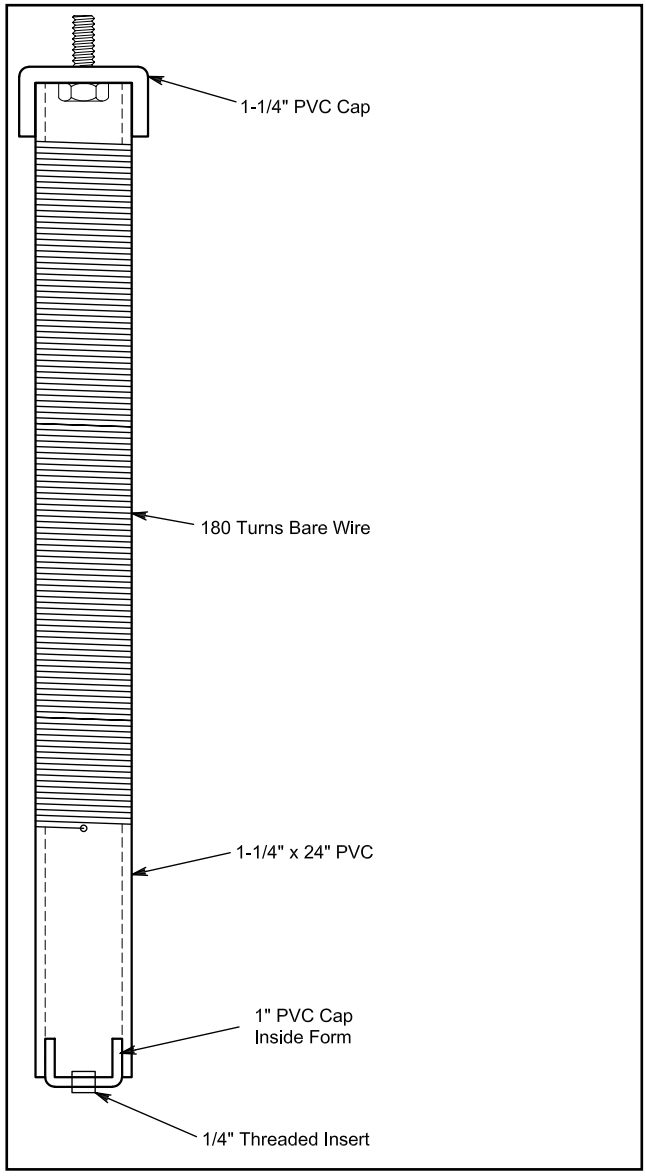

Fig 25—The coil form, with a threaded insert inserted into the bottom PVC cap inside the coil form.

The other essential item is a cordless screwdriver, minus its batteries and switch. You can often find one at yard sales or flea markets for a dollar or so, usually with dead batteries, since it is often just as cheap to buy another one new as it is to buy new batteries. So long as it will fit snugly inside the base tube, the brand name is immaterial. KO4TV has used Skil, Black & Decker, or even a Wal-Mart $8 special, all with equal success. The most difficult part of the job will be making the coil form and winding the loading coil, but with a little patience you should be able to do this satisfactorily.

Bear in mind that it is *not* a "Heathkit" type project, and it will require some innovation and ingenuity on your part. Next, obtain a 2-foot long piece of 1 1/4-inch PVC pipe (*not* CPVC, which is vulnerable to ultraviolet rays from the sun). With either a lathe or a pipe die, thread approximately 20 inches from one end, at 10 to 12 threads per inch (See **Fig 25**). If you use a pipe die, it helps to loosen the cutters slightly, to make the grooves shallower.

When using a lathe, temporarily insert a piece of 1-inch water pipe inside the coil form to hold it steady in the lathe. The grooves should be just deep enough to comfortably hold the wire in place when it is wound. The choice of coil wire is up to you. The author has used #16 or #18 tinned copper, bare copper, or best yet, 17-gauge aluminum electric fence wire. This is available from any

Fig 26—Photo of the top of the loading coil. (*Photo courtesy of Gary Pearce, KN4AQ.*)

farm supply store at a very reasonable cost. It will take about 65 to 70 feet of wire.

Begin by drilling a 1/16-inch hole through the PVC pipe at the bottom end of the threaded portion. Slip the end of the wire through this hole and tie a knot in it to serve as a stop. You could also insert a nut and bolt through a loop in the wire. Then carefully wind the coil to within an inch of the end of the threaded portion. The preferred method of winding is to put a stick or pipe through the holes of the wire reel and hold it between your feet and the floor, to provide the necessary tension to allow tight winding.

About an inch below the top of the coil, drill a 1/16-inch hole and thread about 6 or 8 inches of wire through it. This will be the top connection from the coil to the whip. The bottom of the coil has no electrical connection.

The method of attaching the whip to the top of the coil form is up to you. I usually drill a 3/8-inch hole through a 1 1/4-inch PVC pipe cap and place a 3/8 × 1 1/2-inch SAE bolt through the hole, with a matching washer and nut on top. The bolt can be drilled and tapped for mounting the whip, which should be about 5 to 6 feet long. (It will be pruned for resonance later.) See **Fig 26**, a photo showing the top of the coil.

A more elegant way of connecting the whip is to obtain a swivel or quick-disconnect antenna fitting from your nearest truck stop. These are widely available for use with CB antennas and are threaded 3/8-inch SAE. Do not attach the cap to the coil form until after the coil is inserted in the base tube.

Now that you have a coil form and a base tube, the next step will be to plug the bottom of the PVC coil form with a 1-inch PVC pipe cap, which fits snugly inside the coil form. Drill a hole directly in the center of this cap, and install a 1/4-20 threaded insert, available at most hardware stores for about 25 or 30 cents. These are commonly used in wooden furniture to provide a thread for attaching bolts to wood. See **Fig 27**.

It is imperative that you install this insert squarely. The best method is to screw a short bolt into it and chuck the bolt in a drill press, placing the pipe cap

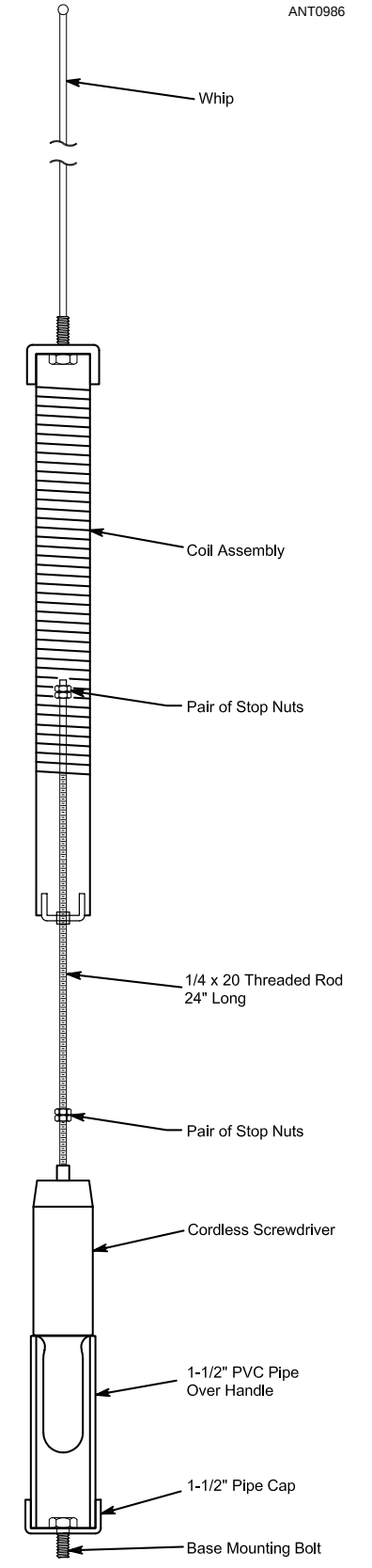

Fig 27—The coil assembly and cordless screwdriver drive assembly.

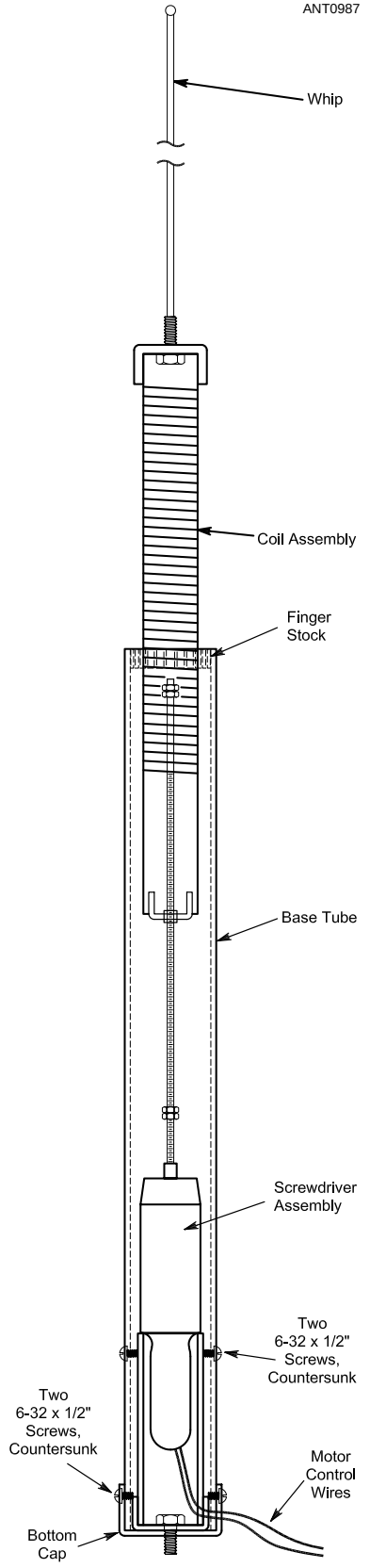

Fig 28—The complete antenna assembly.

squarely on the drill press table. Carefully turn the drill chuck by hand until the insert is properly seated.

The Motor

Now prepare the cordless drill by removing the dead batteries and the switch. Install a pair of 1 or 1.5-Ω, 10-W resistors in series with each motor lead. Connect a 0.1 μF 50-V disc ceramic capacitor across the motor leads to suppress motor noise.

Connect a pair of wires, about a foot long, to the other ends of the resistors. These will power the screwdriver from your car's 12-V system. Next, procure a 20-inch long piece of 1/4-20 threaded rod (also called "all-thread"). Insert one end of this into the cordless screwdriver chuck, and drill a 1/16-inch or 3/32-inch hole through both the chuck and the rod. Secure the rod in place with either a roll or cotter pin, and install a pair of 1/4-inch nuts on the rod near the screwdriver chuck. This will be the lower stop for the coil travel and will be adjusted later.

Thread the rod into the threaded insert at the bottom of the coil form, and install another pair of stop nuts on the top side of the rod. It will be easier to do this before attaching the bottom plug to the coil form. Again, these nuts will be adjusted later for proper coil travel.

Place the bottom plug into the coil form, drill a couple of holes through the form and the plug and tap them for 6-32 flat head bolts. Countersink the form so that the heads will be flush with the outside. Again, see **Fig 27**.

Finger Stock

Now, let's go back to the base tube. You must install a circle of finger-stock strip on the top of the tube to make contact with the coil, as shown in Fig 24. This can either be soldered or riveted, depending on your choice of tube material. Next, insert the coil and screwdriver assembly through the bottom of the tube, making sure that the coil clears the finger stock without deforming or bending it.

The best method I have found for attaching the screwdriver to the bottom tube is to fit a piece of 1 1/2-inch PVC pipe, about 8 or 10 inches long, over the handle of the screwdriver and attach it with a couple of flat-head 6-32 bolts. You may have to either grind some material off the handle or wrap it with some duct tape to make a snug fit inside the 1 1/2-inch PVC pipe, which should slip snugly into the base tube.

Place a matching 1 1/2-inch PVC pipe cap on the bottom of the pipe, and secure it with a couple of 6-32 screws. Drill a 1/4-inch hole through one side of the cap, which will serve to pass the wires from the screwdriver motor. Drill a 3/8-inch hole directly in the center of this cap for the base mount. See **Fig 28**, which is a drawing of the completed antenna assembly.

MOUNTING THE ANTENNA

At this point you must determine exactly how you wish to mount the antenna on your vehicle. You could fasten it to a standard mobile antenna mount, but *do not* use a spring! I prefer to fasten the assembly to a thick metal plate about 6 × 18 inches in size. I mount this to the frame of the car, protruding about 4 or 5 inches from the lower car body, just behind the rear wheel. You could also fasten such a plate to the lower fender sheet metal with large sheet-metal screws. The SO-239 connector is mounted to this plate also. See **Fig 29**.

An upper bracket, made from Plexiglas or similar insulating material, can be mounted from the trunk lip with an L-angle and used to support the top of the lower tube. See **Fig 30**. With a Plexiglas bracket about 4-inches wide, a 2-inch hole can be drilled in it to pass the tube. This will make a snug and rigid fit at the top. Under no circumstances use a metal band around the tube, as this will form a shorted turn and drastically lower the antenna Q.

With a little care, this type of mounting will leave no visible holes in the vehicle, which will likely enhance its trade-in value. If you mount the antenna on a pickup truck, it can be mounted directly on the rear safety bumper with a 1 1/2 inch pipe floor flange and matching adaptor on the bottom of the tube.

Electrical Connections

After mounting the base, your next job is to connect the wires from the screwdriver to a DPDT, spring-return center-off switch, mounted in a convenient location in your car. See the schematic in **Fig 31**. Connect the coax from the radio to the base tube, with the center conductor going to the base tube and the shield connected to ground at the base of the antenna.

If you like, you could install a simple base-matching network to give a perfect match on the lower bands. Even with no matching unit, SWR is usually under 2:1 on all

Fig 29—Base-mounting plate for Screw-driver installation on KO4TV's truck. Note the quick-disconnect dc motor con-nections and the SO-239 coax connector.

Fig 30—The support Plexiglas plate. (*Photo courtesy of Gary Pearce, KN4AQ.*)

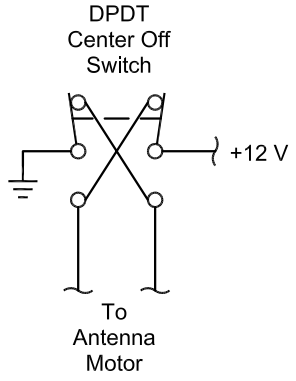

Fig 31—The DPDT center-off spring-loaded switch used to control the screwdriver motor.

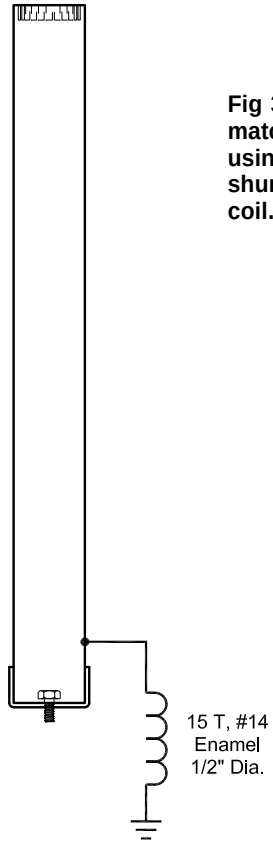

Fig 33—Alternative matching scheme using a single shunt matching coil.

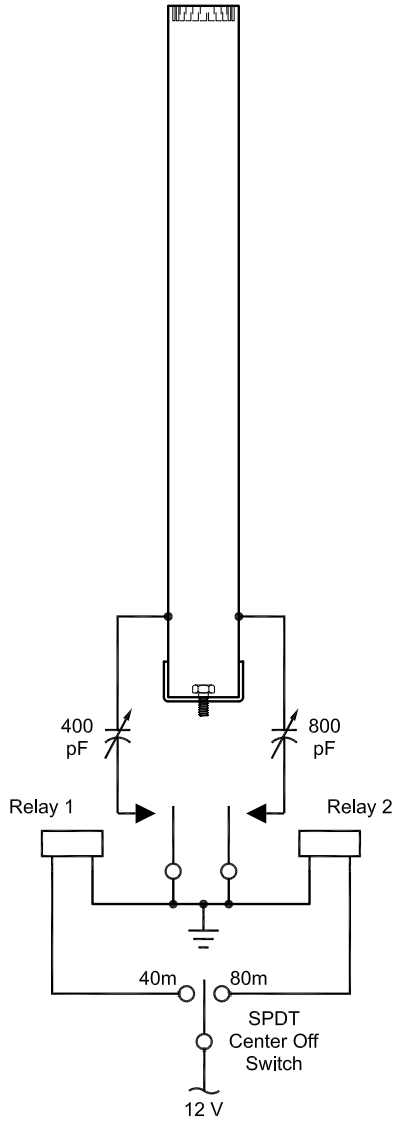

Fig 32—Relay-switched matching capacitors for 40 and 80 meters.

bands. See **Fig 32**. One matching network consists of a couple of trimmer capacitors switched from the bottom of the base tube to ground using a pair of small relays. For 80 meters, approximately 800 pF is required, and for 40 meters about 400 pF. No matching is required for 30 meters or higher.

An alternative matching method is to install a 15-turn coil made from #14 enamel wire, about 1/2 inch diameter, from the base to ground. See **Fig 33**. In either case, adjust the whip length for proper resonance at both ends of the HF spectrum over the range of movement of your coil.

This antenna may have different matching requirements, depending on the vehicle type and mounting location, so you may need to do some experimentation to obtain optimum results. If it doesn't work exactly right at first, be prepared to do a little experimenting.

A COIL COVER

Most builders will want to provide a coil cover, both for protection and appearance. KO4TV's favorite cover is made from a plastic mailing tube, about 24 to 30 inches long and about 1/2 inches in diameter. You can find these at an office supply store. They have a screw-on cap on one end, which can be mounted to the top of the loading coil.

Fig 34—Remote control by the rear-view mirror—tuning by the stripes! (*Photo courtesy of Gary Pearce, KN4AQ.*)

You trim the bottom of the cover to the proper length to allow the coil to be fully retracted into the base tube while still clearing the top bracket. Other builders have used such diverse materials as:

- Several 1-liter soft drink bottles cut off, swaged and glued together
- Sections of Schedule 20 PVC pipe with matching cap
- Empty beef jerky tubes (usually available for the asking at convenience stores)
- Wands from a shop vacuum cleaner, fitted with the cap from an aerosol spray can.

Just let your imagination run wild and you may be surprised at your own ingenuity. Whatever material you do use, paint it to match your vehicle. Just be sure to use non-metallic paint.

TUNING BY THE STRIPES

The author used different colored vinyl tapes to mark the tuning points for the amateur bands along the tuning coil. The lower edge of the supporting Plexiglas middle support acts as a pointer, which he can spot from his rear-view mirror. See **Fig 34**. This may be low-tech tuning method, but it works!

THE PROOF IS IN THE PUDDING

Now, you are ready to enjoy some real mobile communications on all bands, without even stopping the vehicle to QSY. KO4TV's antenna has contacted over 100 DX countries, from as far away as Tasmania and Japan from the East Coast. He enjoys regular contacts with Israel and other stations in the Mid-East, running 100 W or less.

A MOBILE J ANTENNA FOR 144 MHz

The J antenna is a mechanically modified version of the Zepp (Zeppelin) antenna. It consists of a half-wavelength radiator fed by a quarter-wave matching stub. This antenna exhibits an omnidirectional pattern with little high-angle radiation, but does not require the ground plane that $^1/_4$-wave and $^5/_8$-wave antennas do to work properly. The material in this section was prepared by Domenic Mallozzi, N1DM, and Allan White, W1EYI.

Fig 35 shows two common configurations of the J antenna. Fig 35A shows the shorted-stub version that is usually fed with 200- to 600-Ω open-wire line. Some have attempted to feed this antenna directly with coax without a balun, and this usually leads to less than optimum results. Among the problems with such a configuration are a lack of reproducibility and heavy coupling with nearby objects. To eliminate these problems, many

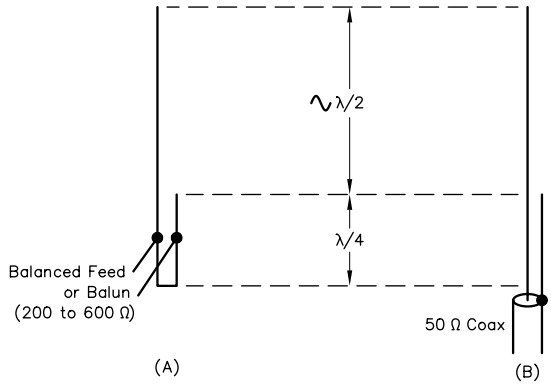

Fig 35—Two configurations of the J antenna.

Fig 36—The mount for the mobile J is made from stainless-steel angle stock and secured to the bumper with stainless-steel hardware. Note the $^1/_2$-inch pipe plug and a PL-259 (with a copper disc soldered in its unthreaded end). These protect the mount and connector threads when the antenna is not in use.

Fig 37—The J antenna, ready for use. Note the bakelite insulator and the method of feed. Tie wraps are used to attach the balun to the mounting block and to hold the coax to the support pipe. Clamps made of flashing copper are used to connect the balun to the J antenna just above the insulating block. The ends of the balun should be weatherproofed.

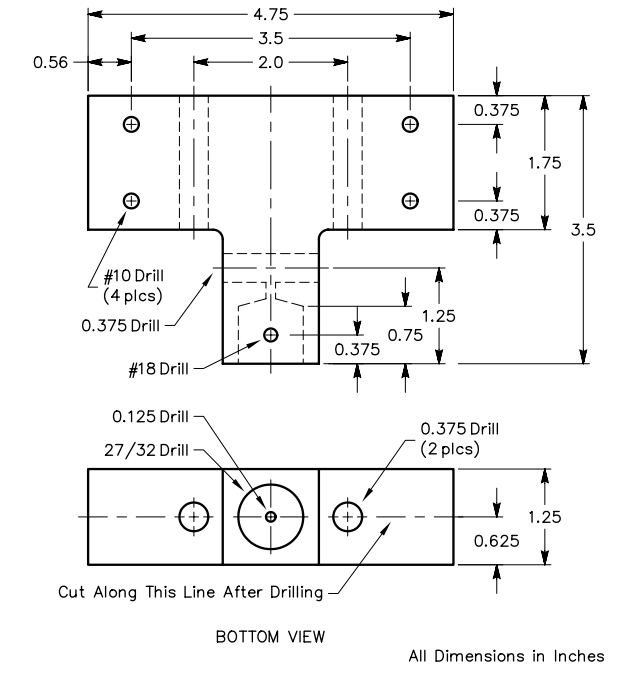

Fig 38—Details of the insulated mounting block. The material is bakelite.

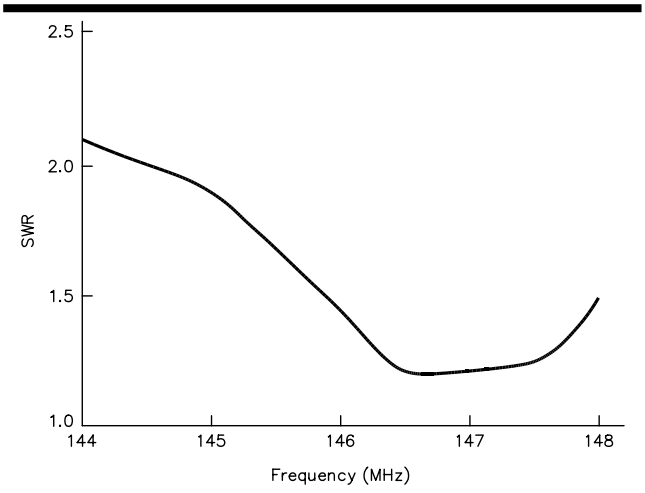

Fig 39—Measured SWR of the mobile J antenna.

amateurs have used a 4:1 half-wave balun between the feed point and a coaxial feed line. This simple addition results in an antenna that can be easily reproduced and that does not interact so heavily with surrounding objects. The bottom of the stub may be grounded (for mechanical or other reasons) without impairing the performance of the antenna.

The open-stub-fed J antenna shown in Fig 35B can be connected directly to low-impedance coax lines with good results. The lack of a movable balun (which allows some impedance adjustment) may make this antenna a bit more difficult to adjust for minimum SWR, however.

The Length Factor

Dr. John S. Belrose, VE2CV, noted in *The Canadian Amateur* that the diameter of the radiating element is important to two characteristics of the antenna—its bandwidth and its physical length. (See Bibliography at the end of this chapter.) As the element diameter is increased, the usable bandwidth increases, while the physical length of the radiating element decreases with respect to the free-space half-wavelength. The increased diameter makes the end effect more pronounced, and also slows the velocity of propagation on the element. These two effects are related to resonant antenna lengths by a factor, "k." This factor is expressed as a decimal fraction giving the equivalent velocity of propagation on the antenna wire as a function of the ratio of the element diameter to a wavelength. The k factor is discussed at length in Chapter 2.

The length of the radiating element is given by

$$\ell = \frac{5904 \times k}{f} \qquad \text{(Eq 25)}$$

where

ℓ = length in inches
f = frequency in MHz
k = k factor.

The k factor can have a significant effect. For example, if you use a $^5/_8$-inch diameter piece of tubing for the radiator at 144 MHz, the k value is 0.907 (9.3% shorter than a free-space half wavelength).

The J antenna gives excellent results for both mobile and portable work. The mobile described here is similar to an antenna described by W. B. Freely, K6HMS, in April 1977 *QST*. This design uses mechanical components that are easier to obtain. As necessary with all mobile antennas, significant attention has been paid to a strong, reliable, mechanical design. It has survived not only three New England winters, but also two summers of 370-mile weekend commutes. During this time, it has maintained consistent electrical performance with no noticeable deterioration.

The mechanical mount to the bumper is a 2 × 2-inch stainless steel angle iron, 10 inches long. It is secured to the bumper with stainless steel hardware, as shown in **Fig 36**. A stainless steel $^1/_2$-inch pipe coupling is welded to the left side of the bracket, and an SO-239 connector is mounted at the right side of the bracket. The bracket is mounted to the bumper so a vertical pipe inserted in the coupling will allow the hatchback of the vehicle to be opened with the antenna installed, **Fig 37**.

A $^1/_2$-inch galvanized iron pipe supports the antenna so the radiating portion of the J is above the vehicle roof line. This pipe goes into a bakelite insulator block, visible in Fig 37. The insulator block also holds the bottom of the stub. This block was first drilled and then split with a band saw, as shown in **Fig 38**. After splitting, the two portions are weatherproofed with varnish and rejoined with 10-32 stainless hardware. The corners of the insulator are cut to clear the L sections at the shorted end of the stub.

The quarter-wave matching section is made of $^1/_4$-inch type L copper tubing ($^5/_{16}$ inch ID, $^3/_8$ inch OD). The short at the bottom of the stub is made from two copper L-shaped sections and a short length of $^1/_4$-inch tubing. Drill a $^1/_8$-inch hole in the bottom of this piece of tubing to drain any water that may enter or condense in the stub.

A $^5/_{16}$-inch diameter brass rod, $1^1/_2$ to 2 inches long, is partially threaded with a $^5/_{16} \times 24$ thread to accept a Larsen whip connector. This rod is then sweated into one of the legs of the quarter-wave matching section. A 40-inch whip is then inserted into the Larsen connector.

The antenna is fed with 50-Ω coaxial line and a coaxial 4:1 half-wave balun. This balun is described at the end of Chapter 26. As with any VHF antenna, use high-quality coax for the balun. Seal all open cable ends and the rear of the SO-239 connector on the mount with RTV sealant.

Adjustment is not complicated. Set the whip so that its tip is 41 inches above the open end of the stub, and adjust the balun position for lowest SWR. Then adjust the height of the whip for the lowest SWR at the center frequency you desire. **Fig 39** shows the measured SWR of the antenna after adjustments are completed.

THE SUPER-J MARITIME ANTENNA

This 144-MHz vertical antenna doesn't have stringent grounding requirements and can be made from easy to find parts. The material in this section was prepared by Steve Cerwin, WA5FRF, who developed the Super-J for use on his boat.

Antennas for maritime use must overcome difficulties that other kinds of mobile antennas normally do not encounter. For instance, the transom of a boat is the logical place to mount an antenna. But the transoms of many boats are composed mostly of fiberglass, and they ride some distance out of the water—from several inches to a few feet, depending on the size of the vessel. Because the next best thing to a ground plane (the water surface) is more than an appreciable fraction of a wavelength away at 144 MHz, none of the popular gain-producing antenna designs requiring a counterpoise are suitable. Also, since a water surface does a good job of assuming the earth's lowest mean elevation (at least on a calm day), anything that can be done to get the radiating part of the antenna up in the air is helpful.

One answer is the venerable J-pole, with an extra in-phase half-wave section added on top—the Super-J antenna. The two vertical half waves fed in phase give outstanding omnidirectional performance for a portable antenna. Also, the J-pole feed arrangement provides the desired insensitivity to height above ground (or water) plus added overall antenna height. Best of all, a $^1/_4$-wave CB whip provides enough material to build the whole driven element of the antenna, with a few inches to spare. The antenna has enough bandwidth to cover the entire 144-MHz band, and affords a measure of lightning protection by being a grounded design.

Antenna Operation

The antenna is represented schematically in **Fig 40**. The classic J-pole antenna is the lower portion shown between points A and C. The half-wave section between points B and C does most of the radiating. The added half-wave section of the Super-J version is shown between points C and E. The side-by-side quarter-wave elements between points A and B comprise the J feed arrangement.

At first glance, counterproductive currents in the J section between points A and B may seem a waste of element material, but it is through this arrangement that

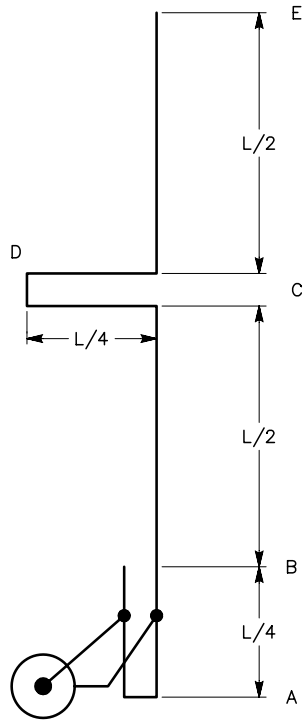

Fig 40—Schematic representation of the Super-J maritime antenna. The radiating section is two half waves in phase.

the antenna is able to perform well in the absence of a good ground. The two halves of the J feed arrangement, side by side, provide a loading mechanism regardless of whether or not a ground plane is present.

The radiation resistance of any antenna fluctuates as a function of height above ground, but the magnitude of this effect is small compared to the wildly changing impedance encountered when the distance from a ground plane element to its counterpoise is varied. Also, the J section adds 1/4 wavelength of antenna height, reducing the effect of ground height variations even further. Reducing ground-height sensitivity is particularly useful in maritime operation on those days when the water is rough.

The gain afforded by doubling the aperture of a J-pole with the extra half-wave section can be realized only if the added section is excited in phase with the half-wave element B-C. This is accomplished in the Super-J in a conventional manner, through the use of the quarter-wave phasing stub shown between C and D.

Construction and Adjustment

The completed Super-J is shown in **Fig 41**. Details of the individual parts are given in **Fig 42**. The driven element can be liberated from a quarter-wave CB whip antenna and cut to the dimensions shown. All other metal stock can be obtained from metal supply houses or machine shops. Metal may even be scrounged for little or nothing as scraps or remnants, as were the parts for the antenna shown here.

The center insulator and the two J stub spacers are made of 1/2-inch fiberglass and stainless steel stock, and the end caps are bonded to the insulator sections with epoxy. If you don't have access to a lathe to make the end caps, a simpler one-piece insulator design of wood or fiberglass could be used. However, keep in mind that good electrical connections must be maintained at all joints, and strength is a consideration for the center insulator.

The quarter-wave phasing stub is made of 1/8-inch stainless steel tubing, **Fig 43**. The line comprising this stub is bent in a semicircular arc to narrow the vertical profile and to keep the weight distribution balanced. This makes for an attractive appearance and keeps the antenna from leaning to one side.

Fig 41—Andy and the assembled Super-J antenna.

The bottom shorting bar and base mounting plate are made of 1/4-inch stainless steel plate, shown in **Fig 44**. The J stub is made of 3/16-inch stainless-steel rod stock. The RF connector may be mounted on the shorting bar as shown, and connected to the adjustable slider with a short section of coaxial cable. RTV sealant should be used at the cable ends to keep out moisture. The all-stainless construction looks nice and weathers well in maritime mobile applications.

The antenna should work well over the whole 144-MHz band if cut to the dimensions shown. The only tuning required is adjustment of the sliding feed point for minimum SWR in the center of the band segment you use most. Setting the slider 2 13/16 inch above the top of the shorting bar gave the best match for this antenna and may be used for a starting point. Four turns of coax made into a coil at the feed point or a ferrite-sleeve balun act as a common-mode choke balun to ensure satisfactory performance.

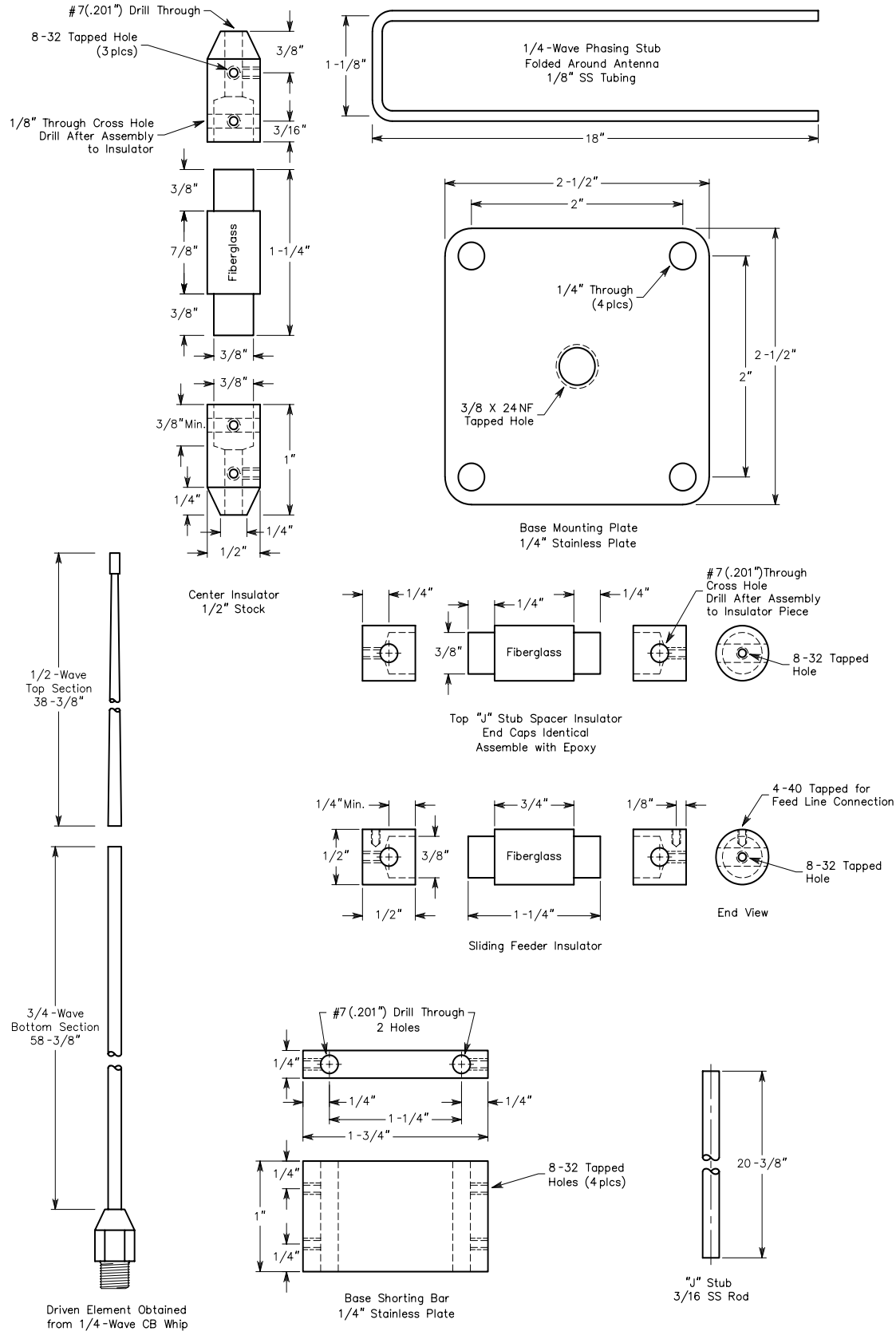

Fig 42—Details of parts used in the construction of the 144-MHz Super-J. Not to scale.

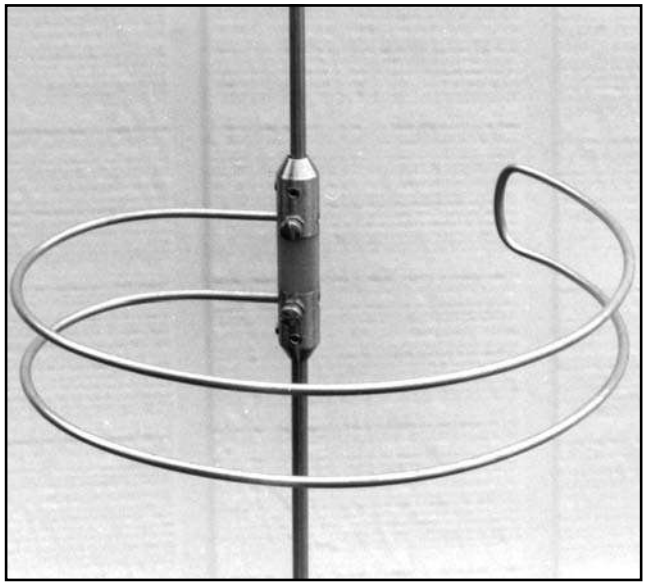

Fig 43—A close-up look at the $^1/_4$-λ phasing section of the Super-J. The insulator fitting is made of stainless-steel end caps and fiberglass rod.

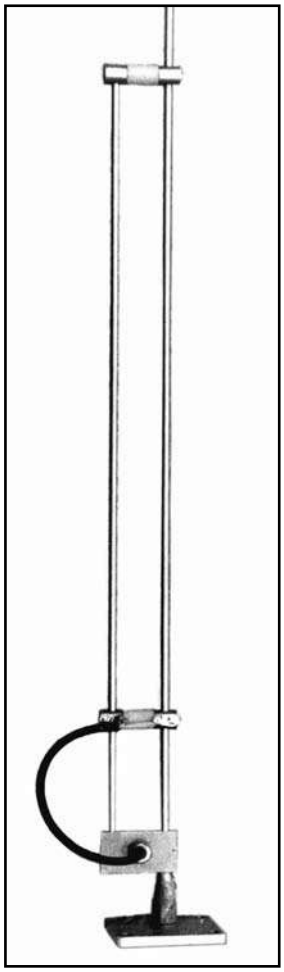

Fig 44—The bottom shorting bar and base mounting plate assembly.

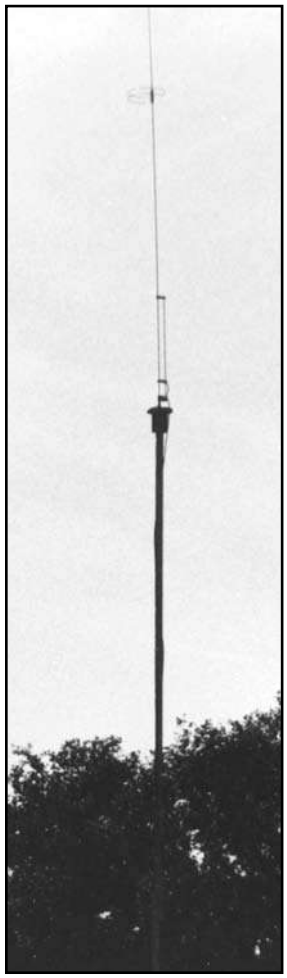

Fig 45—The Super-J in portable use at a field site.

Performance

Initial tests of the Super-J were performed in portable use and were satisfactory, if not exciting. **Fig 45** shows the Super-J mounted on a wooden mast at a portable site. Simplex communication with a station 40 miles away with a 10-W mobile rig was full quieting both ways. Stations were worked through distant repeaters that were thought inaccessible from this location.

Comparative tests between the Super-J and a commercial $^5/_8$-wave antenna mounted on the car showed the Super-J to give superior performance, even when the Super-J was lowered to the same height as the car roof. The mast shown in Fig 45 was made from two 8-foot lengths of 1 × 2-inch pine. (The two mast sections and the Super-J can be easily transported in most vehicles.)

The Super-J offers a gain of about 6 dB over a quarter-wave whip and around 3 dB over a $^5/_8$-wave antenna. Actual performance, especially under less-than-ideal or variable ground conditions, is substantially better than other vertical antennas operated under the same conditions. The freedom from ground-plane radials proves to be a real benefit in maritime mobile operation, especially for those passengers in the back of the boat with sensitive ribs!

A TOP-LOADED 144-MHz MOBILE ANTENNA

Earlier in this chapter, the merits of various loading schemes for shortened whip antennas were discussed. Quite naturally, one might be considering HF mobile operation for the application of those techniques. But the principles may be applied at any frequency. **Fig 46** shows a 144-MHz antenna that is both top and center loaded. This antenna is suitable for both mobile and portable operation, being intended for use on a handheld transceiver. This antenna was devised by Don Johnson, W6AAQ, and Bruce Brown, W6TWW.

Fig 46—This 144-MHz antenna uses a combination of top and center loading. It offers low construction cost and improved efficiency over continuously loaded rubber-ducky antennas.

A combination of top and center loading offers improved efficiency over continuously loaded antennas such as the "stubby" pictured at the beginning of this chapter. This antenna also offers low construction cost. The only materials needed are a length of stiff wire and a scrap of circuit-board material, in addition to the appropriate connector.

Construction

The entire whip section with above-center loading coil is made of one continuous length of material. An 18-inch length of brazing rod or #14 Copperweld wire is suitable.

In the antenna pictured in Fig 46, the top loading disk was cut from a scrap of circuit-board material, but flashing copper or sheet brass stock could be used instead. Aluminum is not recommended.

The dimensions of the antenna are given in **Fig 47**. First wind the center loading coil. Use a 1/2-inch bolt, wood dowel, or other cylindrical object for a coil form. Begin winding at a point 3 inches from one end of the wire, and wrap the wire tightly around the coil form. Wind 5 1/2 turns, with just enough space between turns so they don't touch.

Remove the coil from the form. Next, determine the length necessary to insert the wire into the connector you'll be using. Cut the long end of the wire to this length plus 4 inches, measured from the center of the coil. Solder the wire to the center pin and assemble the connector. A tight-fitting sleeve made of Teflon or Plexiglas rod may be used to support and insulate the antenna wire inside the shell. An alternative is to fill the shell with epoxy cement, and allow the cement to set while the wire is held centered in the shell.

The top loading disk may be circular, cut with a hole saw. A circular disk is not required, however—it may be of any shape. Just remember that with a larger disk, less coil inductance will be required, and vice versa. Drill a hole at the center of the disk for mounting it to the wire. For a more rugged antenna, reinforce the hole with a brass eyelet. Solder the disk in place at the top of the antenna, and construction is completed.

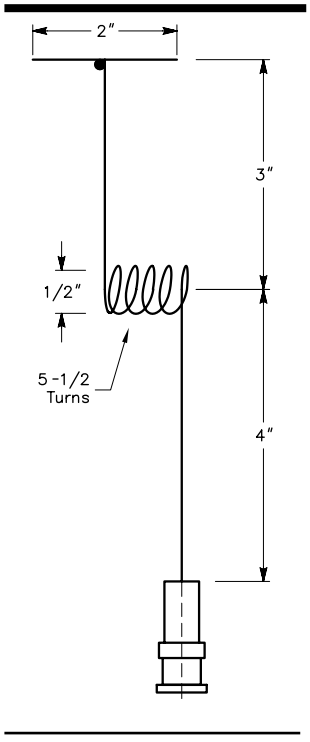

Fig 47—Dimensions for the top-loaded 144-MHz antenna. See text regarding coil length.

Tune-Up

Adjustment consists of spreading the coil turns for the correct amount of inductance. Do this at the center frequency of the range you'll normally be using. Optimum inductance is determined with the aid of a field strength meter at a distance of 10 or 15 feet.

Attach the antenna to a handheld transceiver operating on low power, and take a field-strength reading. With the transmitter turned off, spread the coil turns slightly, and then take another reading. By experiment, spread or compress the coil turns for the maximum field-strength reading. Very little adjustment should be required. There is one precaution, however. You must keep your body, arms, legs, and head in the same relative position for each field-strength measurement. It is suggested that the transceiver be placed on a nonmetal table and operated at arm's length for these checks.

Once the maximum field-strength reading is obtained, adjustments are completed. With this antenna in operation, you'll likely find it possible to access repeaters that are difficult to reach with other shortened antennas. W6AAQ reports that in distant areas his antenna even outperforms a 5/8-λ vertical.

VHF QUARTER-WAVELENGTH VERTICAL

Ideally, a VHF vertical antenna should be installed over a perfectly flat reflector to assure uniform omnidirectional radiation. This suggests that the center of the automobile roof is the best place to mount it for mobile use. Alternatively, the flat portion of the trunk deck can be used, but will result in a directional pattern because of car-body obstruction.

Fig 48 illustrates how a Millen high-voltage connector can be used as a roof mount for a VHF whip. The hole in the roof can be made over the dome light, thus providing accessibility through the upholstery. RG-59 and the 1/4-wave matching section, L (Fig 48C), can be routed between the car roof and the ceiling upholstery and brought into the trunk compartment, or down to the dashboard of the car. Instead of a Millen connector, some operators install an SO-239 coax connector on the roof for mounting the whip. The method is similar to that shown in Fig 48.

It has been established that in general, 1/4-λ vertical antennas for mobile repeater work are not as effective as 5/8-λ verticals are. With a 5/8-λ antenna, more of the transmitted signal is directed at a low wave angle, toward the horizon, offering a gain of about 1 dB over the 1/4-λ vertical. However, in areas where the repeater is located nearby on a very high hill or a mountain top, the 1/4-λ antenna will usually offer more reliable per-

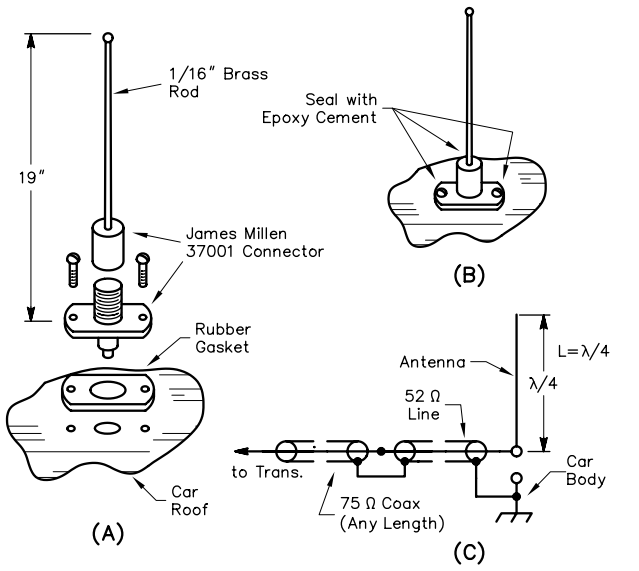

Fig 48—At A and B, an illustration of how a quarter-wavelength vertical antenna can be mounted on a car roof. The whip section should be soldered into the cap portion of the connector and then screwed into the base socket. This arrangement allows for the removal of the antenna when desired. Epoxy cement should be used at the two mounting screws to prevent the entry of moisture through the screw holes. Diagram C is discussed in the text.

formance than a $^5/_8$-λ antenna. This is because there is more power in the lobe of the $^1/_4$-λ vertical at higher angles.

144-MHz 5/8-WAVELENGTH VERTICAL

Perhaps the most popular antenna for 144-MHz FM mobile and fixed-station use is the $^5/_8$-wavelength vertical. As compared to a $^1/_4$-wavelength vertical, it has 1 dB of gain.

This antenna is suitable for mobile or fixed-station use because it is small, omnidirectional, and can be used with radials or a solid-plane ground (such as a car body). If radials are used, they need be only $^1/_4$ wavelength long.

Construction

The antenna shown here is made from low-cost materials. **Fig 49** shows the base coil and aluminum mounting plate. The coil form is a piece of low-loss solid rod, such as Plexiglas or phenolic. The dimensions for this and other parts of the antenna are given in **Fig 50**. A length of brazing rod is used as the whip section.

The whip should be 47 inches long. However, brazing rod comes in standard 36-inch lengths, so if used, it is necessary to solder an 11-inch extension to the top of the whip. A piece of #10 copper wire will suffice. Alternatively, a stainless-steel rod can be purchased to

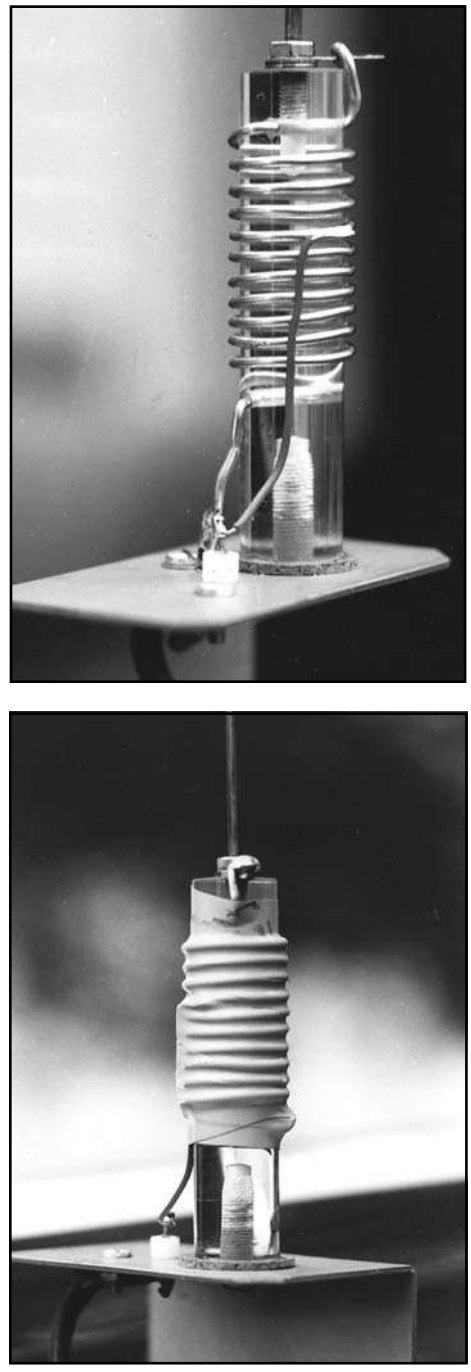

Fig 49—At top, a photograph of the $^5/_8$-λ vertical base section. The matching coil is affixed to an aluminum bracket that screws onto the inner lip of the car trunk. Above, the completed assembly. The coil has been wrapped with vinyl electrical tape to keep out dirt and moisture.

make a 47-inch whip. Shops that sell CB antennas should have such rods for replacement purposes on base-loaded antennas. The limitation one can expect with brazing rod is the relative fragility of the material, especially when the threads are cut for screwing the rod into the base coil form. Excessive stress can cause the rod to break where it enters the form. The problem is compli-

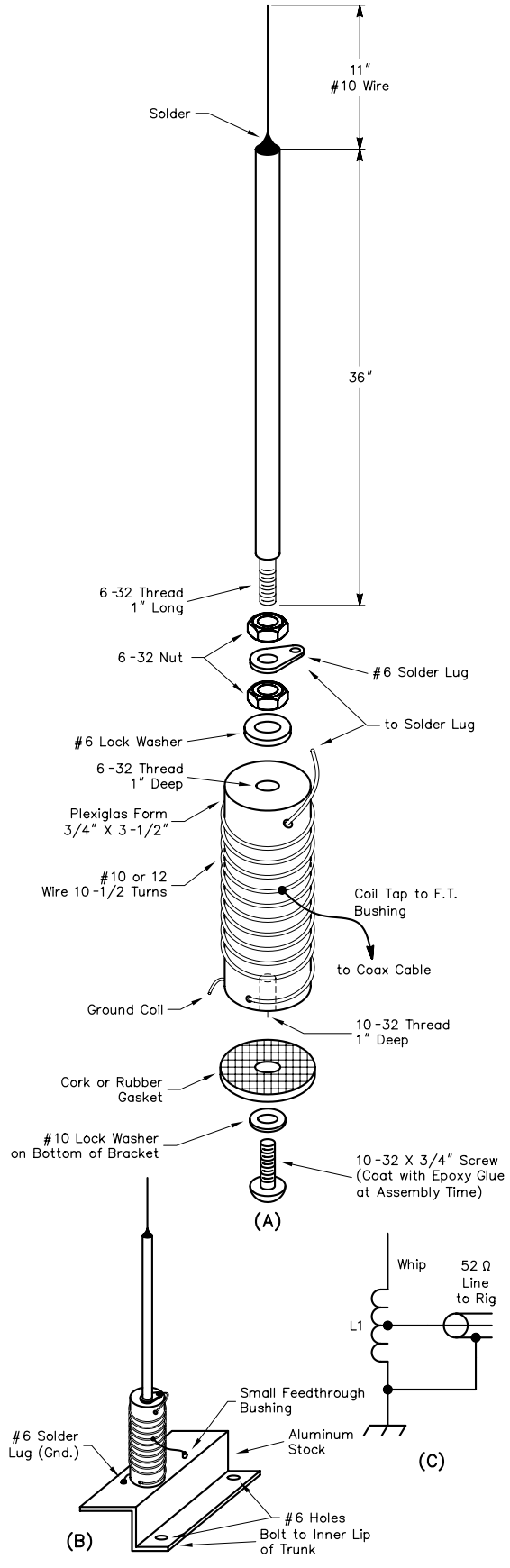

Fig 50—Structural details for the 2-meter $^5/_8$-λ antenna are provided at A. The mounting bracket is shown at B and the equivalent circuit is given at C.

cated somewhat in this design because a spring is not used at the antenna mounting point. Builders of this antenna can find all kinds of solutions to the problems just outlined by changing the physical design and using different materials when constructing the antenna. The main purpose of this description is to provide dimensions and tune-up information.

The aluminum mounting bracket must be shaped to fit the car with which it will be used. The bracket can be used to effect a no-holes mount with respect to the exterior portion of the car body. The inner lip of the vehicle trunk (or hood) can be the point where the bracket is attached by means of no. 6 or no. 8 sheet-metal screws. The remainder of the bracket is bent so that when the trunk lid or car hood is raised and lowered, there is no contact between the bracket and the moving part. Details of the mounting unit are given in Fig 50B. A 14-gauge metal (or thicker) is recommended for rigidity.

Wind $10^1/_2$ turns of #10 or #12 copper wire on the $^3/_4$-inch diameter coil form. The tap on L1 is placed approximately four turns below the whip end. A secure solder joint is imperative.

Tune-Up

After the antenna has been mounted on the vehicle, connect an SWR indicator in the 50-Ω transmission line. Key the 144-MHz transmitter and experiment with the coil tap placement. If the whip section is 47 inches long, an SWR of 1:1 can be obtained when the tap is at the right location. As an alternative method of adjustment, place the tap at four turns from the top of L1, make the whip 50 inches long, and trim the whip length until an SWR of 1:1 occurs. Keep the antenna well away from other objects during tune-up, as they may detune the antenna and yield false adjustments for a match.

A 5/8-WAVELENGTH 220-MHz MOBILE ANTENNA

The antenna shown in **Figs 51** and **52** was developed to fill the gap between a homemade $^1/_4$-λ mobile antenna and a commercially made $^5/_8$-λ model. While antennas can be made by modifying CB models, that presents the problem of cost in acquiring the original antenna. The major cost in this setup is the whip portion. This can be any tempered rod that will spring easily.

Construction

The base insulator portion is made of $^1/_2$-inch Plexiglas rod. A few minutes' work on a lathe is sufficient to shape and drill the rod. (The innovative builder can use an electric drill and a file for the lathe work.)

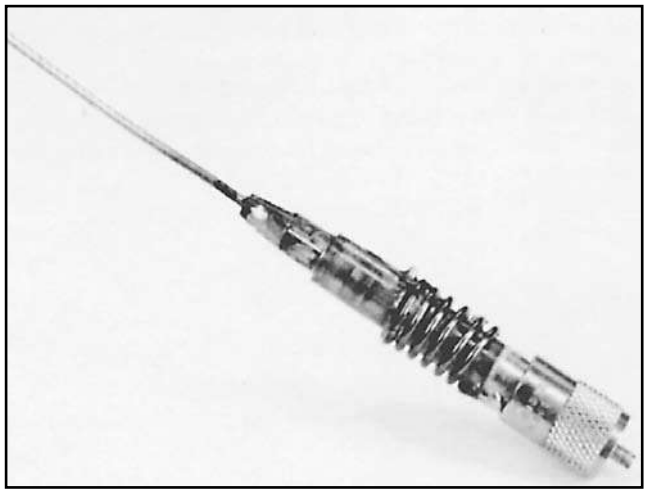

Fig 51—The 220-MHz $^{5}/_{8}$-λ mobile antenna. The coil turns are spaced over a distance of 1 inch, and the bottom end of the coil is soldered to the coax connector.

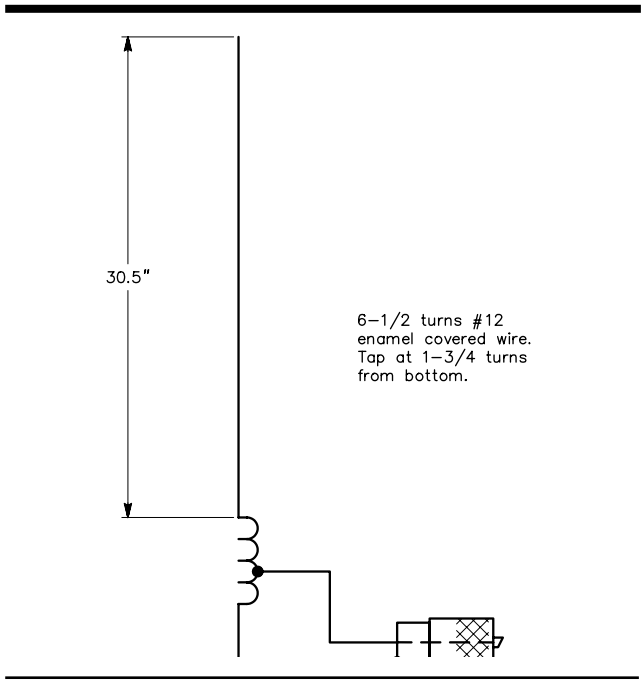

Fig 52—Diagram of the 220-MHz mobile antenna.

The bottom $^{1}/_{2}$ inch of the rod is turned down to a diameter of $^{3}/_{8}$ inch. This portion will now fit into a PL-259 UHF connector. A $^{1}/_{8}$-inch diameter hole is drilled through the center of the rod. This hole will hold the wires that make the connections between the center conductor of the connector and the coil tap. The connection between the whip and the top of the coil is also run through this opening. A stud is force-fitted into the top of the Plexiglas rod. This allows for removal of the whip from the insulator.

The coil should be initially wound on a form slightly smaller than the base insulator. When the coil is transferred to the Plexiglas rod, it will keep its shape and will not readily move. After the tap point has been determined, a longitudinal hole is drilled into the center of the rod. A #22 wire can then be inserted through the center of the insulator into the connector. This method is also used to attach the whip to the top of the coil. After the whip has been fully assembled, a coating of epoxy cement is applied. This seals the entire assembly and provides some additional strength. During a full winter's use there was no sign of cracking or other mechanical failure. The adjustment procedure is the same as for the 144-MHz version described previously.

HF Antennas For Sailboats

This material was contributed by Rudy Severns, N6LF. Many of the antenna ideas appearing earlier in this chapter can be applied to sailboats. However, the presence of the mast and the rigging, plus the prevalence of non-conducting fiberglass hulls complicates the issue. There are many possibilities for antennas aboard sailboats. This includes both permanently installed antennas and antennas that can be hoisted for temporary use at anchor:

1. ***Permanent***
   Commercial or home-brew automobile-type verticals
   Backstay verticals and slopers
   Shunt feed of uninsulated rigging

2. ***Temporary***
   Sloping dipoles
   Inverted V's
   Yagis

You should remember some basic facts of life on a sailboat:

1) On most boats the spars, standing rigging and some running rigging will be conductors. Stainless steel wire is usually used for the rigging and aluminum for the spars.
2) Topping lifts, running backstays and jackstays all may be made of conducting materials and may often change position while the boat is underway. This changes the configuration of the rigging and may affect radiation patterns and feed-point impedances.
3) Shipboard antennas will always be close to the mast and rigging, in terms of electrical wavelength. Some antennas may in fact be part of the rigging.
4) The feed-point impedance and radiation pattern can be strongly influenced by the presence of the rigging.
5) Because of the close proximity, the rigging is an integral part of the antenna and should be viewed as such.
6) The behavior of a given antenna will depend on the details of the rigging on a particular vessel. The performance of a given antenna can vary widely on different boats, due to differences in dimensions and arrangement of the rigging.
7) Even though you may be floating on a sea of salt water, grounding still requires careful attention!

ANTENNA MODELING

Because of the strong interaction between the rigging and the antenna, accurate prediction of radiation patterns and a reasonable guess at expected feed-point impedance requires that you model both the antenna and the rigging. Unless you do accurately model the system, considerable cut-and-try may be needed. This can be expensive when it has to be done in 1 × 19 stainless steel wire with $300 swaged insulator fittings!

In fact, when your antenna is going to be part of standing rigging, it's a very good idea to try your designs out at the dock. You could temporarily use Copperweld wire and inexpensive insulators in place of the stainless rigging wire and the expensive insulators. This approach can save a good deal of money and aggravation. A wide variety of modeling programs are available and can be very helpful in designing a new antenna but they have to be used with some caution:

1) The rigging will have many small intersection angles and radically different conductor diameters, this can cause problems for *NEC* and *MININEC* programs.
2) You must usually taper the segment lengths near the junctions. This is done automatically in programs like *ELNEC* and *EZNEC*.
3) It is usually necessary to use one wire size for the mast, spars and rigging. Some improvement in accuracy can be obtained by modeling the mast as a cage of 3 or 4 wires.

The predicted radiation patterns will be quite good but the feed-point impedance predictions should be viewed as preliminary. Some final adjustment will usually be required. Because of the wide variation between boats, even those of the same class, each new installation is unique and should be analyzed separately.

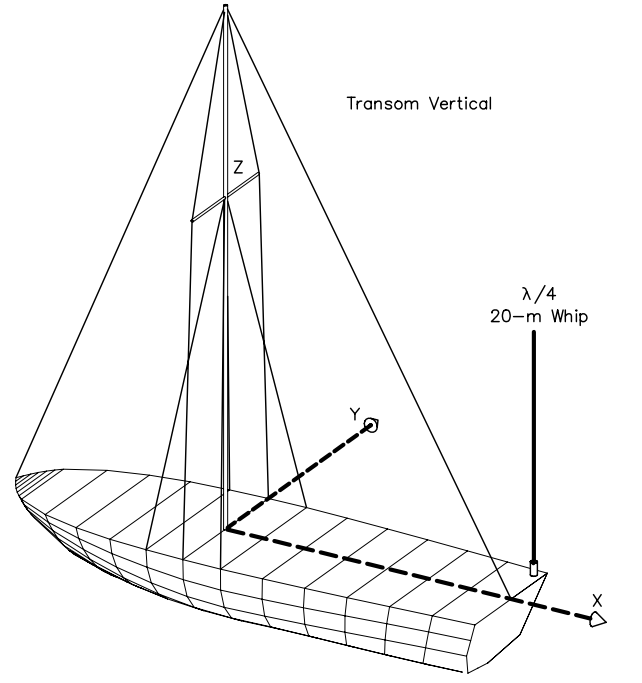

Fig 53—An example of a 20-meter λ/4 whip mounted on the transom. A local ground system must also be provided, as described in the section on grounding.

A SAFETY NOTE

Ungrounded rigging endpoints near deck level can have high RF potentials on them when you transmit. For example, the shrouds on a fiberglass boat connect to chainplates that are bolted to the hull, but are not grounded. These can inflict painful RF burns on the unwary, even while operating at low power! As a general rule all rigging, spars and lifelines near deck level should be grounded. This also makes good sense for lightning protection. For a backstay antenna with its feed point near deck level, a sleeve of heavy wall PVC pipe can be placed over the lower end of the stay as a protective shield.

TRANSOM AND MASTHEAD MOUNTED VERTICALS

A very common antenna for boats is a vertical, either a short mobile antenna or a full λ/4, placed on the transom, as shown in **Fig 53**. Note that in this example the antenna is mounted off to one side—it could also be mounted in the center of the transom. The 20-meter radiation pattern for this antenna as shown in **Fig 54**. Unlike a free standing vertical, this antenna doesn't have an omnidirectional pattern. It is asymmetrical, with a front-to-back ratio of about 13 dB. Further, the angle for maximum gain is offset in the direction the antenna is placed on the transom.

This is a very good example of the profound effect the rigging can have on any antenna used on board a sailboat. Not only is the pattern affected but the feed-point impedance will be reduced from a nominal 36 Ω to 25 to 30 Ω.

The directive gain can be useful—if you point the boat in the right direction! Usually, however, a more uniform omnidirectional pattern is more desirable. It is tempting to suggest putting the vertical at the masthead, perhaps using a 6-foot loaded automobile whip, with the mast and rigging acting as a ground plane. **Fig 55** shows such a system. Unfortunately, this usually doesn't work very well because the overall height of the mast and antenna will very likely be > 5/8 λ. This will result in high-angle lobes, as shown in **Fig 56**. Depending on the mast height, this idea may work reasonably well on 40 or 80 meters, but

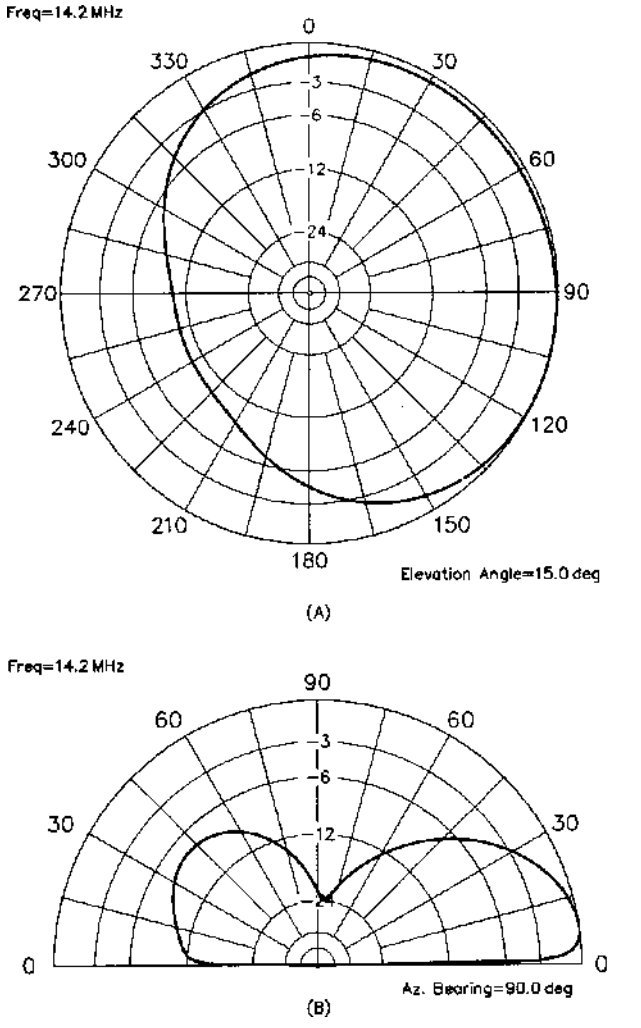

Fig 54—Typical radiation pattern for the λ/4 transom mounted whip in Fig 53.

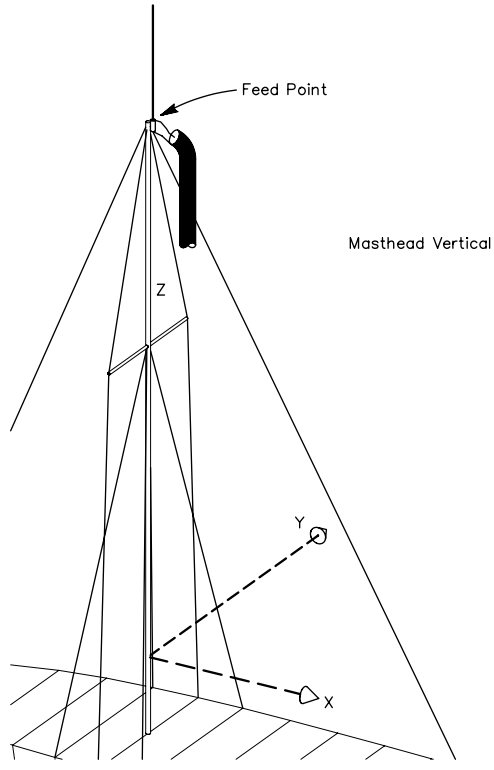

Fig 55—A whip mounted at the masthead. The feed line is fed back down the mast either inside or outside. The base of the mast and the rigging is assumed to be properly grounded.

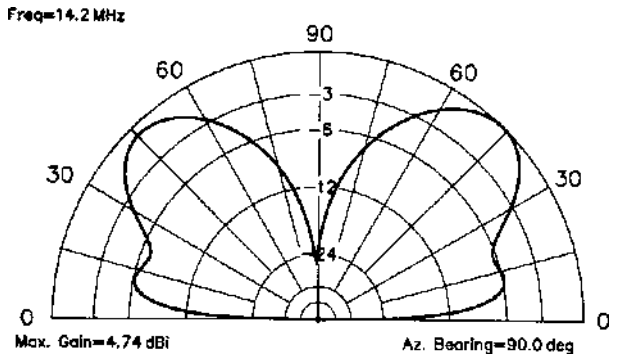

Fig 56—Typical radiation pattern for a masthead-mounted vertical. The multiple vertical lobes are due to the fact the antenna is higher than λ/2.

you will still be faced with severe mechanical stress due to magnified motion at the masthead in rough sea. The masthead is usually reserved to VHF antennas, with their own radial ground plane.

THE BACKSTAY VERTICAL

A portion of the backstay can be insulated and used as a vertical as shown in **Fig 57**. The length of the insulated section will be λ/4 on the lowest band of interest. Typically, due to the loading effect of the rest of the rigging, the resonant length of the insulated section will be shorter than the classic 234/f (MHz) relation, although it can in some case actually be longer. Either modeling or trial adjustment can be used to determine the actual length needed. On a typical 35 to 40-foot sailboat, the lowest band for λ/4 resonance will be 40 meters due to the limited length of the backstay. Examples of the radiation patterns on several bands for such an an-

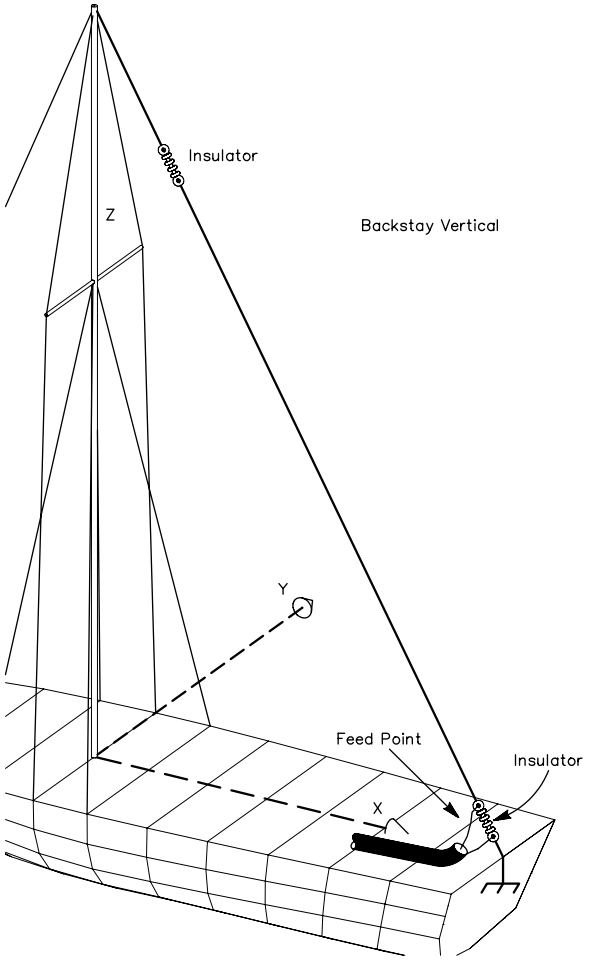

Fig 57—An example of a backstay vertical. A local ground point must be established on the transom next to the base of the backstay.

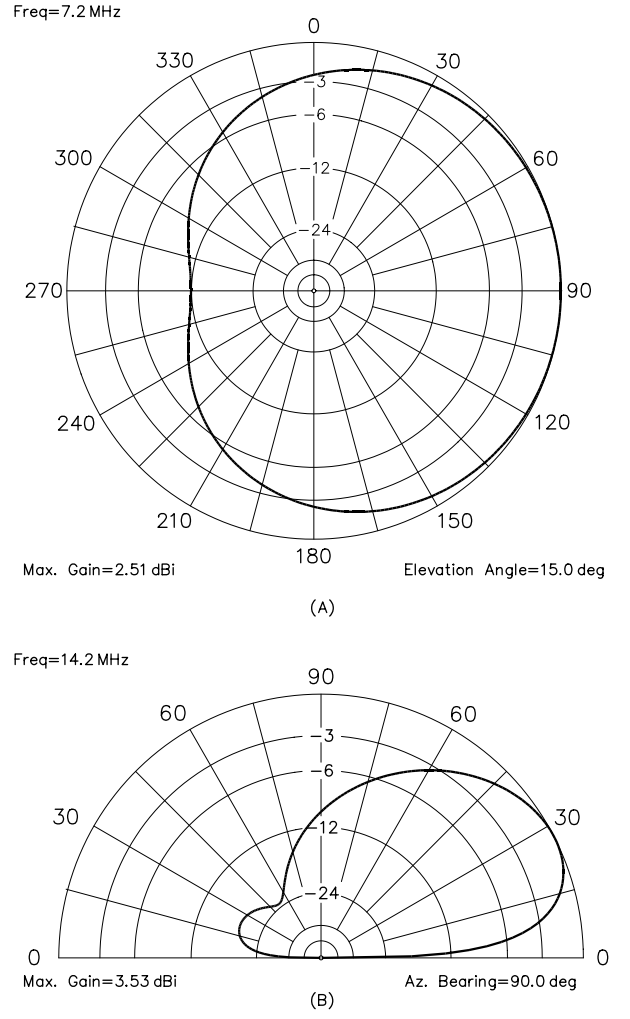

Fig 58—Typical radiation patterns on 40 meters for the backstay vertical in Fig 57.

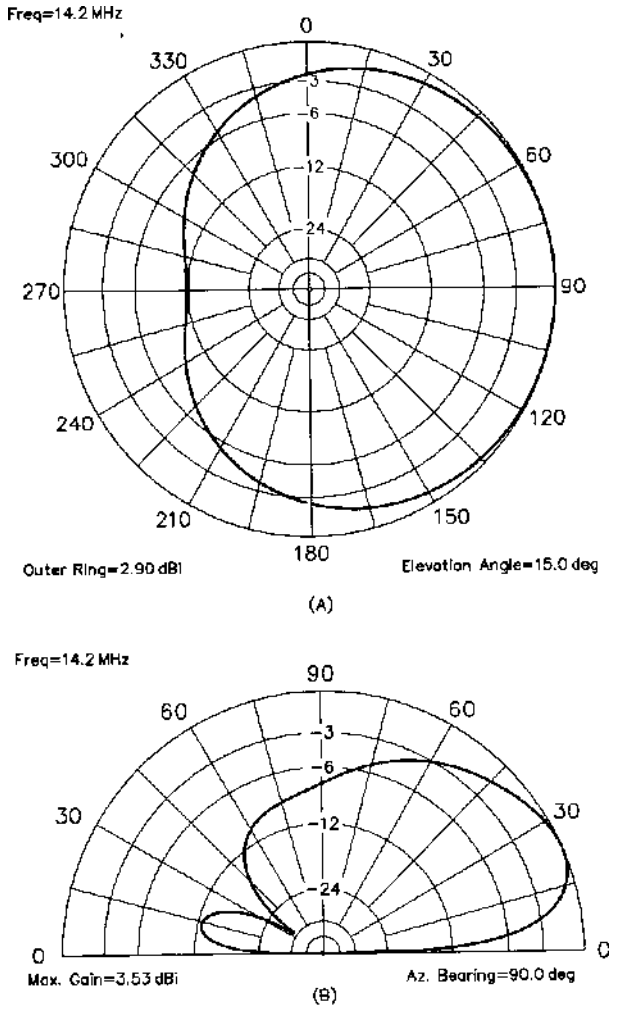

Fig 59—Typical radiation patterns on 20 meters for the backstay vertical in Fig 57.

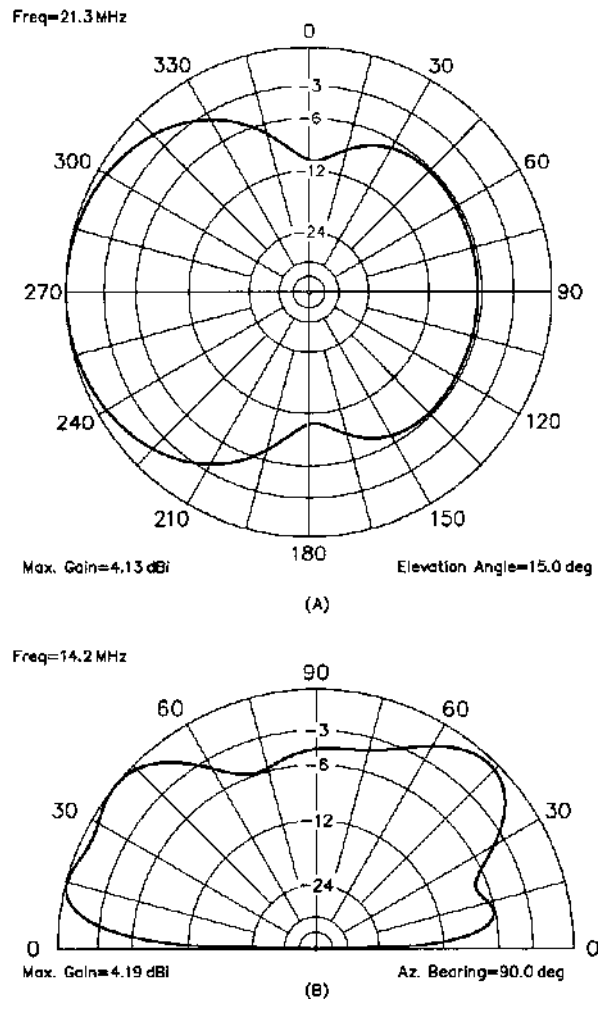

Fig 60—Typical radiation patterns on 15 meters for the backstay vertical in Fig 57.

tenna are given in **Figs 58** through **60**.

The pattern is again quite directional due to the presence of the mast and rigging. On 15 meters, where the antenna is approximately $^3/_4$ λ, higher angle lobes appear. On 40 and 15 meters, the feed point is near a current maximum and is in the range of 30 to 50 Ω. On 20 meters, however, the feed point is a very high impedance because the antenna is near λ/2 resonance. One way to get around this problem for multiband use is to make the antenna longer than λ/4 on the lowest band. If the lowest band is 40 meters then on 20 meters the feed-point impedance will be much lower. This antenna is non-resonant on any of the bands but can be conveniently fed with a tuner because the feed-point impedances are within the range of commonly available commercial tuners. Tuners specifically intended for marine applications frequently can accommodate very high input impedances, but they tend to be quite expensive.

The sensitivity of the radiation pattern to small details of the mast and rigging is illustrated in **Fig 61**. This is the same antenna as shown in Fig 57 with the exception that the forestay is assumed to be ungrounded. In this particular example, ungrounding the forestay drastically increases the front-to-back ratio. With slightly different dimensions, however, the pattern could have changed in other ways.

High-quality insulators for rigging wire can be quite expensive and represent a potential weak point—if they fail the mast may come down. It is not absolutely necessary to use two insulators in a backstay vertical. As shown in **Fig 62**, the upper insulator may be omitted. The radiation patterns are shown in **Figs 63** and **64**. In this case

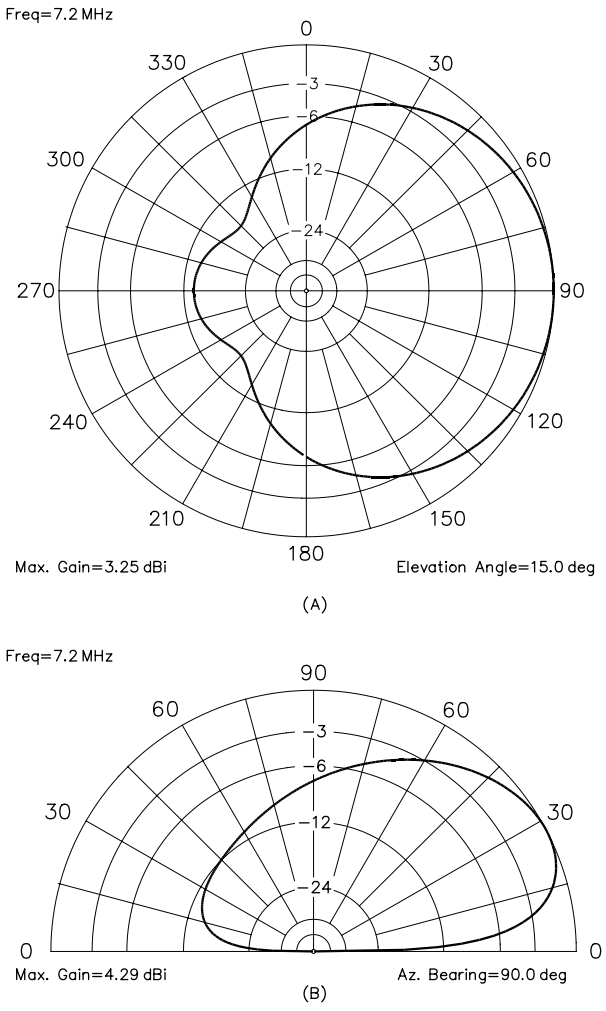

Fig 61—The effect of ungrounding the forestay on the radiation pattern. This is for 40-meter operation.

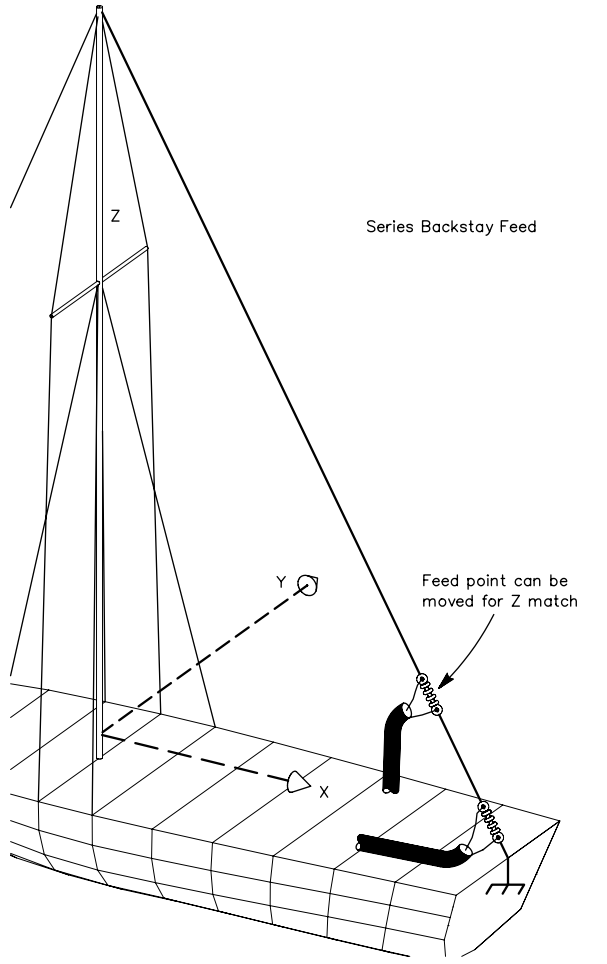

Fig 62—Feeding the backstay without an insulator at the top. The feed point may be moved along the antenna to find a point with a better match on a particular band or to provide a better range of impedances for the tuner to match. The coaxial feed line is taped to the lower portion of the backstay. Again, a good local ground is needed at the base of the backstay.

the pattern is actually more symmetrical than it was with an upper insulator—but this may not hold true for other rigging dimensions. The feed point does not have to be at the bottom of the backstay. As indicated in Fig 62, the feed point can be moved up into the backstay to achieve a better match or a more desirable feed-point impedance variation with frequency. In that case, the center of the coaxial feed line is connected to the upper section and the shield to the lower section. The cable is then taped to the lower portion of the backstay.

If single-band operation is all you want, even the lower insulator can be omitted by using shunt feed. A gamma match would be quite effective for this purpose, as discussed in Chapter 6 when driving a grounded tower.

A 40-METER BACKSTAY HALF SLOPER

A half-sloper antenna can be incorporated into the backstay, as shown in **Fig 65**. This will behave very much the same as the slopers described in Chapter 6. The advantage of this antenna for a sailboat installation is that you don't need to create a good ground connection at the stern, as you would have to do for a transom-mounted vertical or the backstay vertical just described. This may be more convenient. The mast, shrouds and stays must still be grounded for the half-sloper but the arrangement is somewhat simpler.

TEMPORARY ANTENNAS

Not everyone needs permanent antennas. A variety

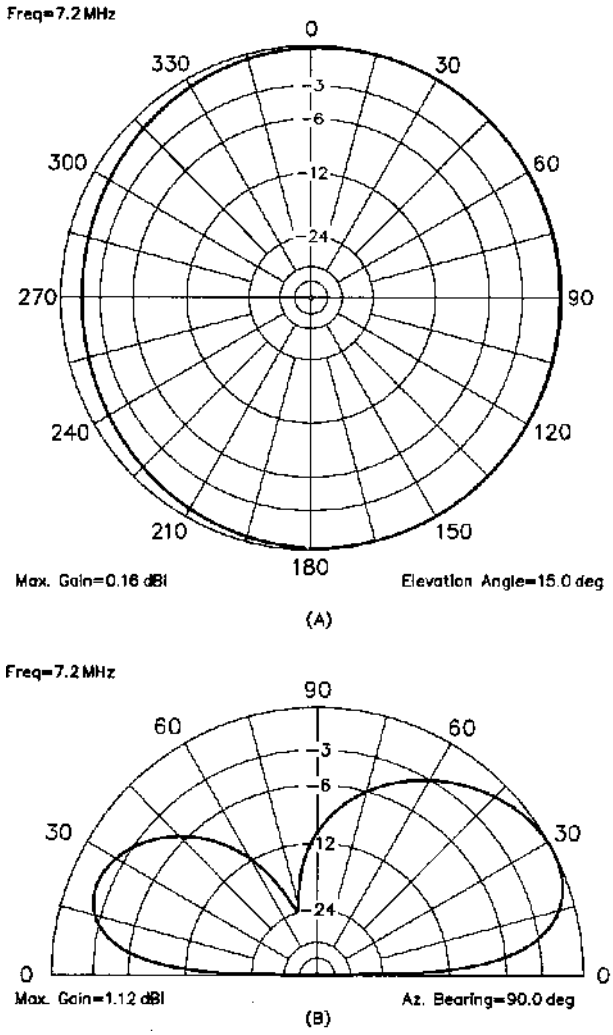

Fig 63—Typical 40-meter radiation pattern in Fig 62.

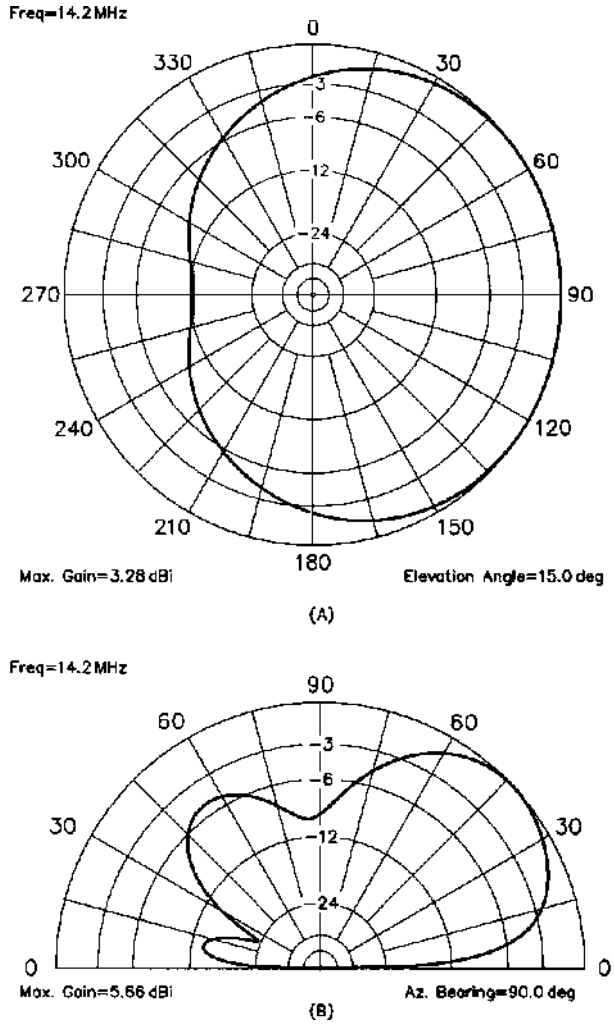

Fig 64—Typical 20-meter radiation pattern in Fig 62.

of temporary antennas can be arranged. A few of these are shown in **Figs 66** through **68**. Of all of these the rigid dipole (Fig 66) will provide the best operation and will have a pattern close to that expected from a freestanding dipole. The other two examples will be strongly affected by their close proximity to the rigging.

GROUNDING SYSTEMS

You may be sitting in the middle of a thousand miles of saltwater. This is great for propagation but you will still have to connect to that ground if you want to use a vertical. There are many possibilities, but the scheme shown in **Fig 69** is representative. First a bonding wire, or better yet a copper strap (it can be very thin!), is connected from bow-to-stern on each side, connecting the forestay, lifeline stanchions, chainplates, bow and stern pulpits and the backstay. Other bonding wires are run from the bow, stern and chainplates on both sides to a common connection at the base of the mast. The fore-and-aft bonding can be attached to the engine and to the keel bolts. The question arises: "What about electrolysis between the keel and propeller if you bond them together?" This has to be dealt with on a case-by-case basis. If your protective zincs are depleting more rapidly after you install a bonding scheme, change it by disconnecting something, the engine-shaft-propeller, for example.

Grounding will vary in every installation and has to be customized to each vessel. However, just as on shore, the better the ground system, the better the performance of the vertical!

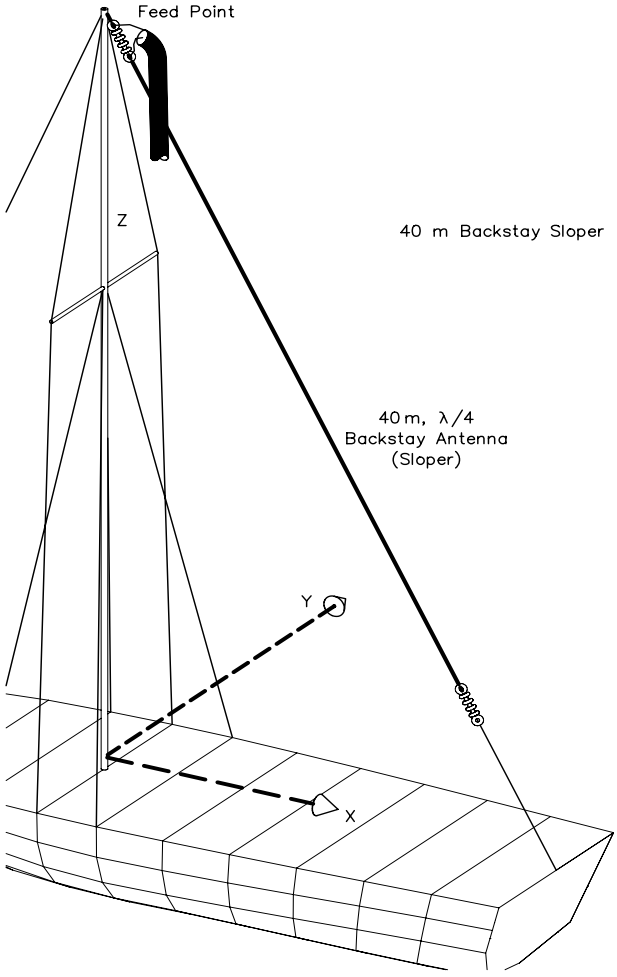

Fig 65—A 40-meter half-sloper fed at the masthead.

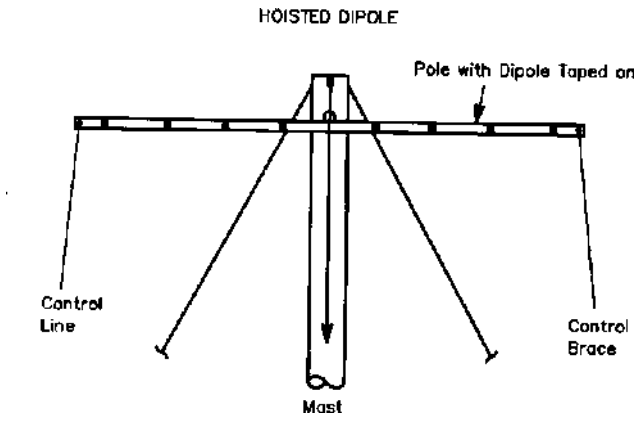

Fig 66—A dipole can be taped to a wood or bamboo pole and hoisted to the masthead with the main halyard while at anchor. It is possible to make this a multiband dipole.

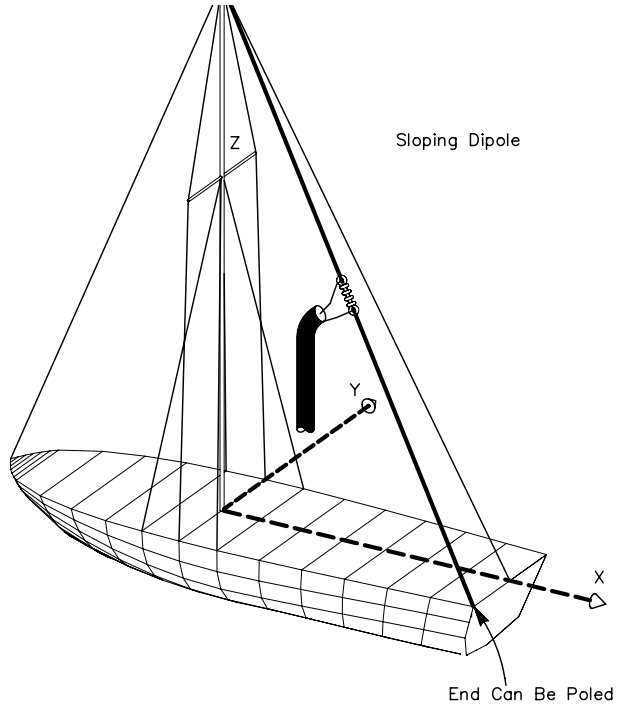

Fig 67—One end of dipole can be attached to the main halyard and pulled up to the masthead. The bottom end of the dipole should be pulled out away from the rigging as much as possible to reduce the impact of the rigging on the impedance.

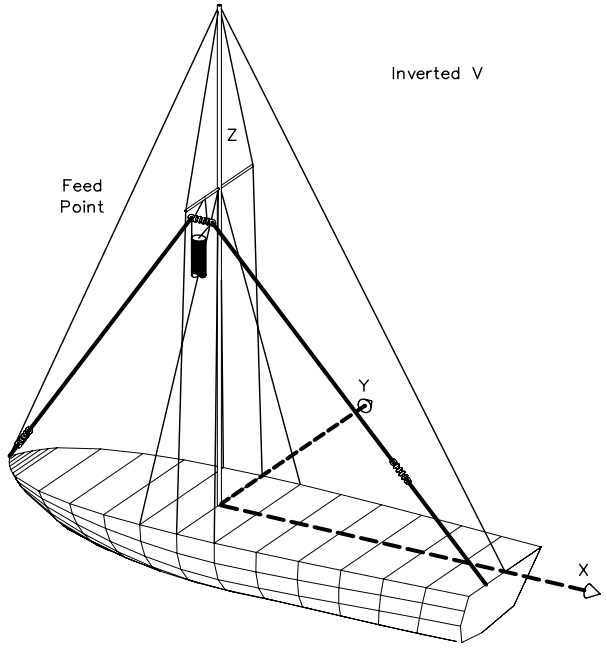

Fig 68—The flag halyard can be used to hoist the center of an inverted V to the spreaders, or alternatively, the main halyard can be used to hoist the center of the antenna to the masthead. Interaction between the rigging and the antenna will be very pronounced and the length of the antenna will have to be adjusted on a cut-and-try basis.

Antennas for Power Boats

Powerboaters are not usually faced with the problems and opportunities created by the mast and rigging on a sailboat. A powerboat may have a small mast, but usually not on the same scale as a sailboat. Antennas for power boats have much more in common with automotive mobile operation, but with some important exceptions:

1) In an automobile, the body is usually metal and it provides a groundplane or counterpoise for a whip antenna. Most modern powerboats, however, have fiberglass hulls. These are basically insulators, and will not work as counterpoises. (On the other hand, metal-hulled power boats can provide nearly ideal grounding!)
2) A height restriction on automotive mobile whips is imposed by clearance limits on highway overpasses and also by the need to sustain wind speeds of up to 80 miles per hour on the highway.
3) In general, powerboats can have much taller antennas that can be lowered for the occasional low bridge.
4) The motion on a powerboat, especially in rough seas, can be quite severe. This places additional mechanical strain on the antennas.
5) On both powerboats and sailboats, operation in a saltwater marine environment is common. This means that a careful choice of materials must be made for the antennas to prevent corrosion and premature failure.

The problem of a ground plane for vertical antennas can be handled in much the same manner as shown in **Fig 69** for sailboats. Since there will most likely not be a large keel structure to connect to and provide a large surface area, additional copper foil can be added inside the hull to increase the counterpoise area. Because of the small area of the propeller, it may be better not to connect to the engine, but to rely instead on increasing the area of the counterpoise and operate it as a true counterpoise—that is, isolated from ground. Sometimes a number of radial wires are used for a vertical, much like that for a ground-plane antenna. This is not a very good idea unless the "wires" are actually wide copper-foil strips that can lower the Q substantially.

The problem is the high voltage present at the ends of normal ground-plane antenna radials. For a boat these radials are likely to be in close proximity to the cabin, which in turn contains both people and electronic equipment. The high potential at the ends of the radials is both a safety hazard and can result in RF coupling back into the equipment, including ham gear, navigational instruments and entertainment devices. The cook is not likely to be happy if he or she gets an RF burn after touching the galley stove! Decoupling the counterpoise from the transmission line, as discussed in Chapter 6, can be very helpful to keep RF out of other equipment.

One way to avoid many of the problems associated with grounding is to use a rigid dipole antenna. On 20 meters and higher, a rigid dipole made up from aluminum tubing, fiberglass poles or some combination of these, can be effective. As shown in **Fig 70A** the halves of the dipole can be slanted upward like rabbit ears to reduce the wingspan and increase the feed-point impedance for a better match to common coax lines. On the lower bands a pair of mobile whips can be used, as shown in Fig 70B. Home-brew coils could also be used.

For short-range communication, a relatively low dipole over saltwater can be effective. However, if long-range communication is needed, then a well-designed vertical, operating over seawater, will work much better. For these to work, of course, you must solve the ground problems associated with a vertical.

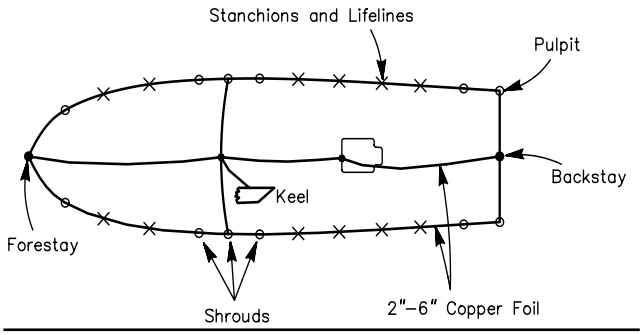

Fig 69—A typical sailboat grounding scheme.

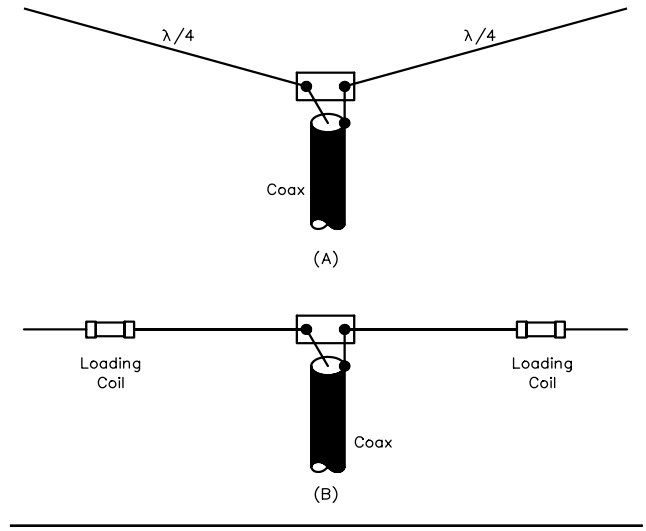

Fig 70—At A, a rigid dipole made from aluminum tubing, fiberglass poles or a combination of these. At B, a pair of mobile whips used as a dipole.

It is not uncommon for large powerboats to have a two or three-element multiband Yagi installed on a short mast. While these can be effective, if they are not mounted high (> λ/2) they may be disappointing for longer-range communication. Over saltwater, vertical polarization is very effective for longer distances. A simpler, but well-designed, vertical system on a boat may outperform a low Yagi.

The combination of a good ground system and one of the high-quality, motor-tuned multiband mobile whips now available commercially can also be very effective.

BIBLIOGRAPHY

Source material and more extended discussions of topics covered in this chapter can be found in the references given below and in the textbooks listed at the end of Chapter 2.

J. S. Belrose, "Short Antennas for Mobile Operation," *QST*, Sep 1953.

J. S. Belrose, "Vertical J Antenna for 2 meters," *The Canadian Amateur*, Jul/Aug 1979, pp 23-26.

J. M. Boyer, "Antenna-Transmission Line Analog," *Ham Radio*, May 1977.

B. F. Brown, "Tennamatic: An Auto-Tuning Mobile Antenna System," *73*, Jul 1979.

B. F. Brown, "Optimum Design of Short Coil-Loaded High-Frequency Mobile Antennas," *ARRL Antenna Compendium Volume 1* (Newington: ARRL, 1985), p 108.

W. B. Freely, "A Two-meter J Antenna," *QST*, Apr 1977, pp 35-36.

E. A. Laport, *Radio Antenna Engineering* (New York: McGraw-Hill Book Co., 1952), p 23.

C. E. Smith and E. M. Johnson, "Performance of Short Antennas," Proceedings of the IRE, Oct 1947.

F. E. Terman, *Radio Engineering Handbook*, 3rd edition (New York: McGraw-Hill Book Co., 1947), p 74.

Chapter 17

Repeater Antenna Systems

There is an old adage in Amateur Radio that goes, "If your antenna did not fall down last winter, it wasn't big enough." This adage might apply to antennas for MF and HF work, but at VHF things are a bit different, at least as far as antenna size is concerned. VHF antennas are smaller than their HF counterparts, but yet the theory is the same—a dipole is a dipole, and a Yagi is a Yagi, regardless of frequency. A 144-MHz Yagi may pass as a TV antenna, but most neighbors can easily detect a radio hobbyist if a 14-MHz Yagi looms over his property.

Repeater antennas are discussed in this chapter. Because the fundamental operation of these antennas is no different than presented in earlier chapters, there is no need to delve into any exotic theory. Certain considerations must be made and certain precautions must be observed, however, since most repeater operations—amateur and commercial—take place at VHF and UHF.

Basic Concepts

The antenna is a vital part of any repeater installation. Because the function of a repeater is to extend the range of communications between mobile and portable stations, the repeater antenna should be installed in the best possible location to provide the desired coverage. This usually means getting the antenna as high above average terrain as possible. In some instances, a repeater may need to have coverage only in a limited area or direction. When this is the case, antenna installation requirements will be completely different, with certain limits being set on height, gain and power.

Horizontal and Vertical Polarization

Until the upsurge in FM repeater activity in the 1970s, most antennas used in amateur VHF work were horizontally polarized. These days, very few repeater groups use horizontal polarization. (One of the major reasons for using horizontal polarization is to allow separate repeaters to share the same input and/or output frequencies with closer-than-normal geographical spacing.) The vast majority of VHF and UHF repeaters use vertically polarized antennas, and all the antennas discussed in this chapter are of that type.

Transmission Lines

Repeaters provide the first venture into VHF and UHF work for many amateurs. The uninitiated may not be aware that the transmission lines used at VHF become very important because feed-line losses increase with frequency.

The characteristics of feed lines commonly used at VHF are discussed in Chapter 24, Transmission Lines. Although information is provided there for small-diameter RG-58 and RG-59 coaxes, these should not be used except for very short feed lines (25 feet or less). These cables are very lossy at VHF. In addition, the losses can be much higher if fittings and connections are not carefully installed.

The differences in loss between solid-polyethylene dielectric types (RG-8 and RG-11) and those using foam polyethylene are significant at VHF and UHF. If you can afford the line with the least loss, buy it.

If you must bury coaxial cable, check with the cable manufacturer before doing so. Many popular varieties of coaxial cable should not be buried, since the dielectric can become contaminated from moisture and soil chemicals. Some coaxial cables are labeled as non-contaminating. Such a label is the best way to be sure your cable can be buried without damage.

Matching

Losses are lowest in transmission lines that are matched to their characteristic impedances. If there is a

mismatch at the end of the line, the losses increase. The *only way* to reduce the SWR on a transmission line is by matching the line *at the antenna*. Changing the length of a transmission line does not reduce the SWR. The SWR is established by the impedance of the line and the impedance of the antenna, so matching must be done at the antenna end of the line.

The importance of matching, so far as feed-line losses are concerned, is sometimes overstressed. But under some conditions, it is necessary to minimize feed-line losses related to SWR if repeater performance is to be consistent. It is important to keep in mind that most VHF/UHF equipment is designed to operate into a 50-Ω load. The output circuitry will not be loaded properly if connected to a mismatched line. This leads to a loss of power, and in some cases, damage to the transmitter.

Repeater Antenna System Design

Choosing a repeater or remote-base antenna system is as close as most amateurs come to designing a commercial-grade antenna system. The term *system* is used because most repeaters utilize not only an antenna and a transmission line, but also include duplexers, cavity filters, circulators or isolators in some configuration. Assembling the proper combination of these items in constructing a reliable system is both an art and a science. In this section prepared by Domenic Mallozzi, N1DM, the functions of each component in a repeater antenna system and their successful integration are discussed. While every possible complication in constructing a repeater cannot be foreseen at the outset, this discussion should serve to steer you along the right lines in solving any problems encountered.

COMPUTING THE COVERAGE AREA FOR A REPEATER

Modern computer programs can show the coverage of a repeater using readily available topographic data from the Internet. In Chapter 3, The Effects of Ground, we described the *MicroDEM* program supplied on the CD-ROM accompanying this book. Dr Peter Guth, the author of *MicroDEM*, built into it the ability to generate terrain profiles that can be used with ARRL's *HFTA* (HF Terrain Assessment) program (also included on the CD-ROM).

MicroDEM has a wide range of capabilities beyond simply making terrain profiles. It can do *LOS* (line of sight) computations, based on visual or radio-horizon considerations. **Fig 1** shows a *MicroDEM* map for the area around Glastonbury, Connecticut. This is somewhat hilly terrain, and as a result the coverage for a repeater placed here on a 30-meter (100-foot) high tower would be somewhat spotty. Fig 1 shows a "Viewshed" on the map, in the form of the white terrain profile strokes in 5° increments around the tower.

Fig 2 shows the LOS for an azimuth of 80°, from a 30-meter high tower out to a distance of 8000 meters. The light-shaded areas on the profile are those that are illuminated directly by the antenna on the tower, while the dark portions of the profile are those that cannot be seen directly from the tower. This profile assumes that the mobile station is 2 meters high—the height of a 6-foot high person with a handheld radio.

The terrain at an 80° azimuth allows direct radio view from the top of the tower out to about 1.8 km. From here, the downslope prevents direct view until about 2.5 km,

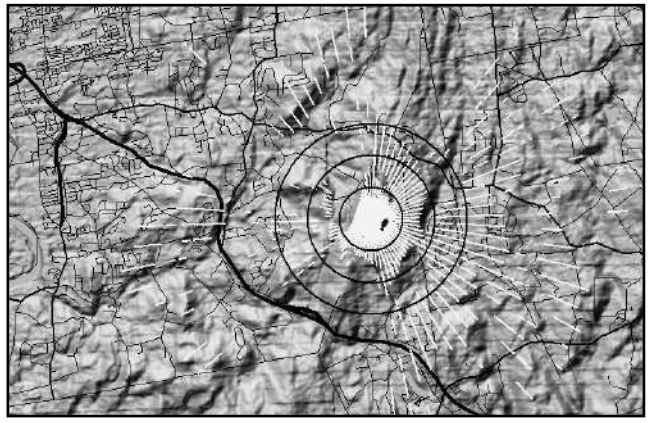

Fig 1—*MicroDEM* topographic map, showing the coverage for a repeater placed on a 30-meter high tower in Glastonbury, CT. The white radial lines indicate the coverage in 5° increments of azimuth around the tower. The range circles are 1000 meters apart.

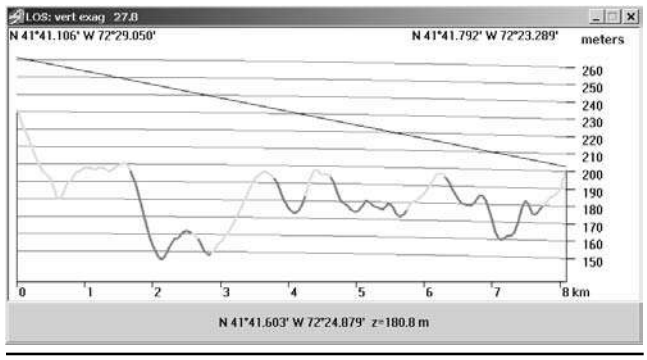

Fig 2—An "LOS" (line of sight) profile at an azimuth of 80° from the tower in Fig 1. The light-gray portions of the terrain profile are visible from the top of the tower, while the dark portions are blocked by the terrain.

where the terrain is briefly visible again from several hundred meters, disappearing from radio view until about 2.8 km, after which it becomes visible until about 3.6 km. Note that other than putting the repeater antenna on a higher tower, there is nothing that can be done to improve repeater coverage over this hilly terrain, although knife-edge diffraction off the hill tops will help fill in coverage gaps.

The Repeater Antenna

The most important part of the system is the antenna itself. As with any antenna, it must radiate and collect RF energy as efficiently as possible. Many repeaters use omnidirectional antennas, but this is not always the best choice. For example, suppose a group wishes to set up a repeater to cover towns A and B and the interconnecting state highway shown in **Fig 3**. The available repeater site is marked on the map. No coverage is required to the west or south, or over the ocean. If an omnidirectional antenna is used in this case, a significant amount of the radiated signal goes in undesired directions. By using an antenna with a cardioid pattern, as shown in Fig 1, the coverage is concentrated in the desired directions. The repeater will be more effective in these locations, and signals from low-power portables and mobiles will be more reliable.

In many cases, antennas with special patterns are more expensive than omnidirectional models. This is an obvious consideration in designing a repeater antenna system. Over terrain where coverage may be difficult in some direction from the repeater site, it may be desirable to skew the antenna pattern in that direction. This can be accomplished by using a phased-vertical array or a com-

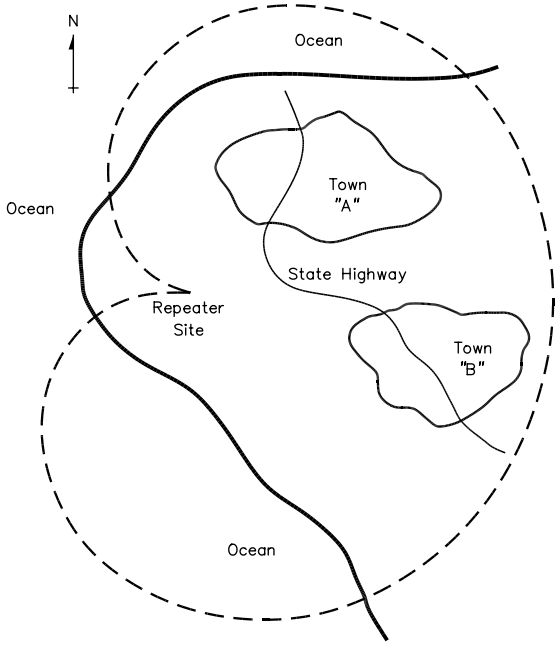

Fig 3—There are many situations where equal repeater coverage is not desired in all directions from the "machine." One such situation is shown here, where the repeater is needed to cover only towns A and B and the interconnecting highway. An omnidirectional antenna would provide coverage in undesired directions, such as over the ocean. The broken line shows the radiation pattern of an antenna that is better suited to this circumstance.

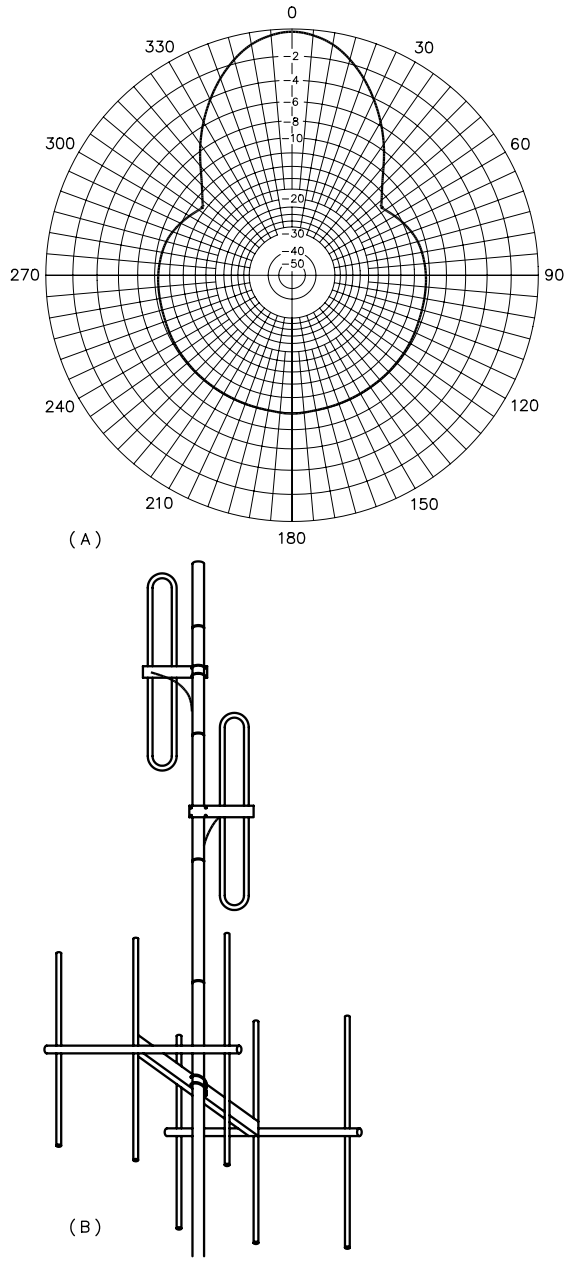

Fig 4—The "keyhole" horizontal radiation pattern at A is generated by the combination of phased Yagis and vertical elements shown at B. Such a pattern is useful in overcoming coverage blockages resulting from local terrain features. (*Based on a design by Decibel Products, Inc.*)

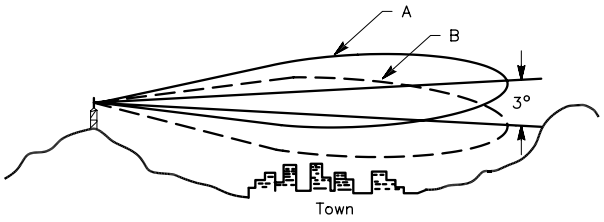

Fig 5—Vertical-beam downtilt is another form of radiation-pattern distortion useful for improving repeater coverage. This technique can be employed in situations where the repeater station is at a greater elevation than the desired coverage area, when a high-gain omnidirectional antenna is used. Pattern A shows the normal vertical-plane radiation pattern of a high-gain omnidirectional antenna with respect to the desired coverage area (the town). Pattern B shows the pattern tilted down, and the coverage improvement is evident.

bination of a Yagi and a phased vertical to produce a "keyhole" pattern. See **Fig 4**.

Repeaters are common on 440 MHz and above, and many groups invest in high-gain omnidirectional antennas. A consequence of getting high gain from an omnidirectional antenna is vertical beamwidth reduction. In most cases, these antennas are designed to radiate their peak gain at the horizon, resulting in optimum coverage when the antenna is located at a moderate height over normal terrain. Unfortunately, in cases where the antenna is located at a very high site (overlooking the coverage area) this may not be the most desirable pattern. The vertical pattern of the antenna can be tilted downward, however, to facilitate coverage of the desired area. This is called *vertical-beam downtilt*.

An example of such a situation is shown in **Fig 5**. The repeater site overlooks a town in a valley. A 450-MHz repeater is needed to serve low-power portable and mobile stations. Constraints on the repeater dictate the use of an antenna with a gain of 11 dBi. (An omnidirec-

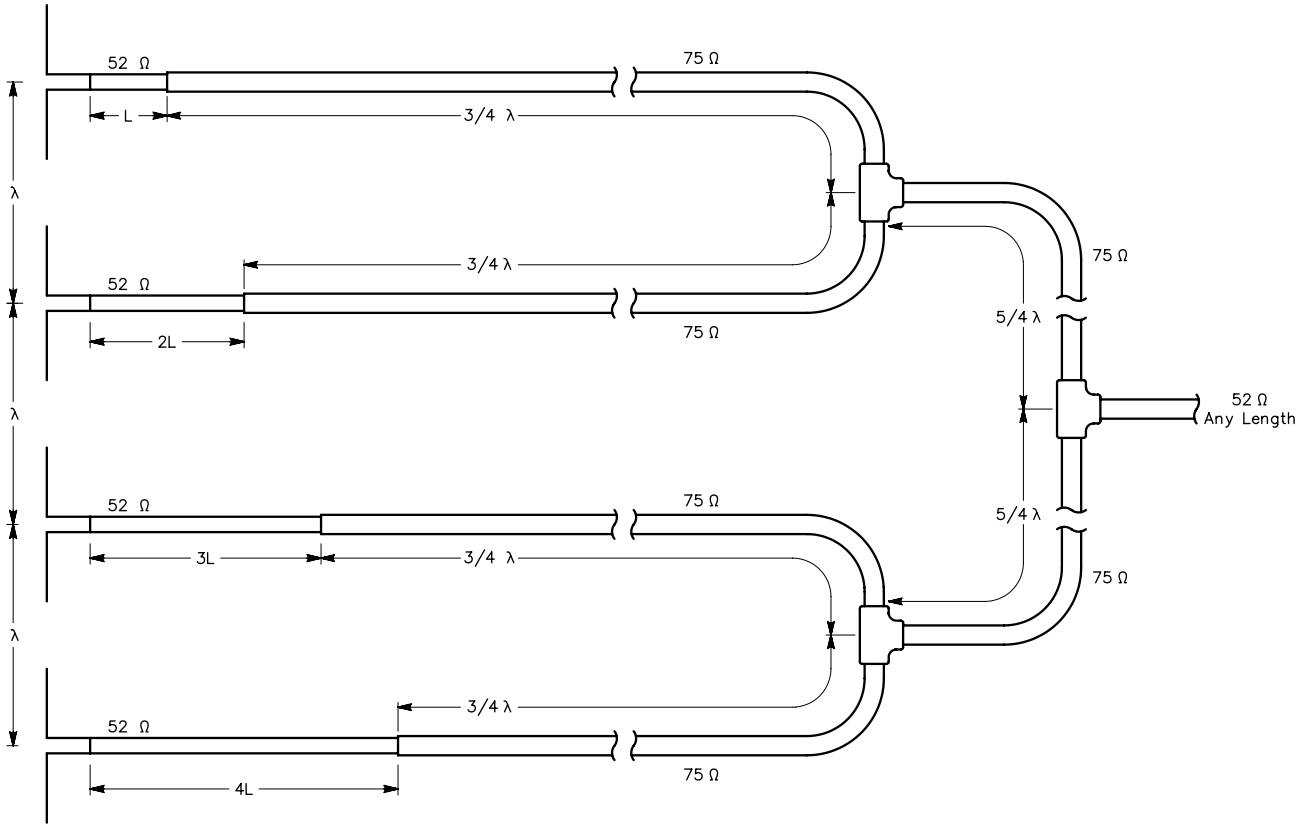

Fig 6—Vertical-beam downtilt can be facilitated by inserting 52-Ω delay lines in series with the 75-Ω feed lines to the collinear elements of an omnidirectional antenna. The delay lines to each element are progressively longer so the phase shift between elements is uniform. Odd $^1/_4$-λ coaxial transformers are used in the main (75-Ω) feed system to match the dipole impedances to the driving point. Tilting the vertical beam in this way often produces minor lobes in the vertical pattern that do not exist when the elements are fed in phase.

tional antenna with this gain has a vertical beamwidth of approximately 6°.) If the repeater antenna has its peak gain at the horizon, a major portion of the transmitted signal and the best area from which to access the repeater exists *above* the town. By tilting the pattern down 3°, the peak radiation will occur in the town.

Vertical-beam downtilt is generally produced by feeding the elements of a collinear vertical array slightly out of phase with each other. Lee Barrett, K7NM, showed such an array in *Ham Radio* magazine. (See the Bibliography at the end of this chapter.) Barrett gives the geometry and design of a four-pole array with progressive phase delay, and a computer program to model it. The technique is shown in **Fig 6**, with a free-space elevation plot showing downtilting in **Fig 7**.

Commercial antennas are sometimes available (at extra cost) with built-in downtilt characteristics. Before ordering such a commercial antenna, make sure that you really require it—they generally are special-order items and are not returnable.

There are disadvantages to improving coverage by means of vertical-beam downtilt. When compared to a standard collinear array, an antenna using vertical-beam downtilt will have somewhat greater extraneous lobes in the vertical pattern, resulting in reduced gain (usually less than 1 dB). Bandwidth is also slightly reduced. The reduction in gain, when combined with the downtilt characteristic, results in a reduction in total coverage area. These trade-offs, as well as the increased cost of a commercial antenna with downtilt, must be compared to the improvement in total performance in a situation where vertical-beam downtilt is contemplated.

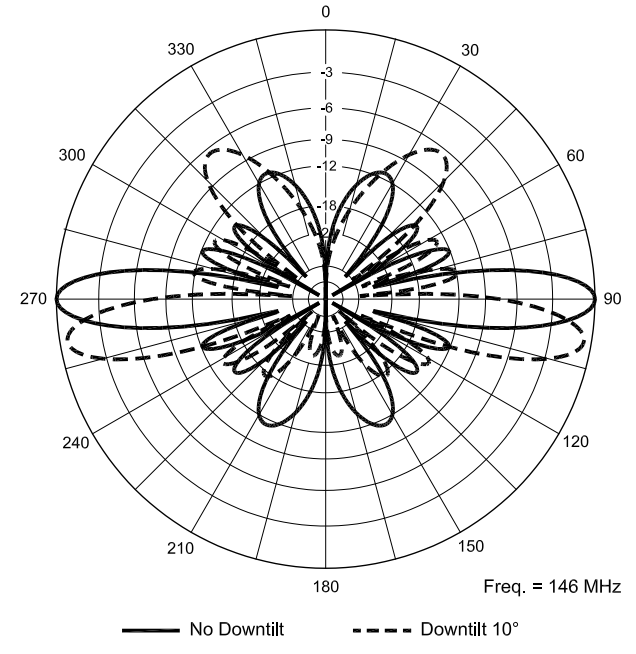

Fig 7—Free-space elevation-plane patterns showing downtilting that results from progressive phase shifts for the feed currents for the dipole in Fig 6.

Top Mounting and Side Mounting

Amateur repeaters often share towers with commercial and public service users. In many of these cases, other antennas are at the top of the tower, so the amateur antenna must be side mounted. A consequence of this arrangement is that the free-space pattern of the repeater antenna is distorted by the tower. This effect is especially noticeable when an omnidirectional antenna is side mounted on a structure.

The effects of supporting structures are most pronounced at close antenna spacings to the tower and with large support dimensions. The result is a measurable increase in gain in one direction and a partial null in the other direction (sometimes 15 dB deep). The shape of the supporting structure also influences pattern distortion. Many antenna manufacturers publish radiation patterns showing the effect of side mounting antennas in their catalogs.

Side mounting is not always a disadvantage. In cases where more (or less) coverage is desired in one direction, the supporting structure can be used to advantage. If pattern distortion is not acceptable, a solution is to mount antennas around the perimeter of the structure and feed them with the proper phasing to synthesize an omnidirectional pattern. Many manufacturers make antennas to accommodate such situations.

The effects of different mounting locations and arrangements can be illustrated with an array of exposed dipoles, **Fig 8**. Such an array is a very versatile antenna because, with simple rearrangement of the elements, it can develop either an omnidirectional pattern or an offset pattern. Drawing A of Fig 8 shows a basic collinear array of four vertical ½-λ elements. The vertical spacing between adjacent elements is 1 λ. All elements are fed in phase. If this array is placed in the clear and supported by a nonconducting mast, the calculated radiation resistance of each dipole element is on the order of 63 Ω. If the feed line is completely decoupled, the resulting azimuth pattern is omnidirectional. The vertical-plane pattern is shown in **Fig 9**.

Fig 8B shows the same array in a side-mounting arrangement, at a spacing of ¼ λ from a conducting mast. In this mounting arrangement, the mast takes on the role of a reflector, producing an F/B on the order of 5.7 dB. The azimuth pattern is shown in **Fig 10**. The vertical pattern is not significantly different from that of Fig 9, except the four small minor lobes (two on either side of the vertical axis) tend to become distorted. They are not as "clean," tending to merge into one minor lobe at some mast heights. This apparently is a function of currents in the supporting mast. The proximity of the mast also alters the feed-point impedance. For elements that

are resonant in the configuration of Fig 8A, the calculated impedance in the arrangement of Fig 8B is in the order of 72 + *j* 10 Ω.

If side mounting is the only possibility and an omnidirectional pattern is required, the arrangement of Fig 8C may be used. The calculated azimuth pattern takes on a slight cloverleaf shape, but is within 1.5 dB of being circular. However, gain performance suffers, and the idealized vertical pattern of Fig 9 is not achieved. See **Fig 11**. Spacings other than 1/4-λ from the mast were not investigated.

One very important consideration in side mounting an antenna is mechanical integrity. As with all repeater components, reliability is of great importance. An antenna hanging by the feed line and banging against the tower provides far from optimum performance and reliability. Use a mount that is appropriately secured to the tower and the antenna. Also use good hardware, preferably stainless steel (or bronze). If your local hardware store does not carry stainless steel hardware, try a boating supplier.

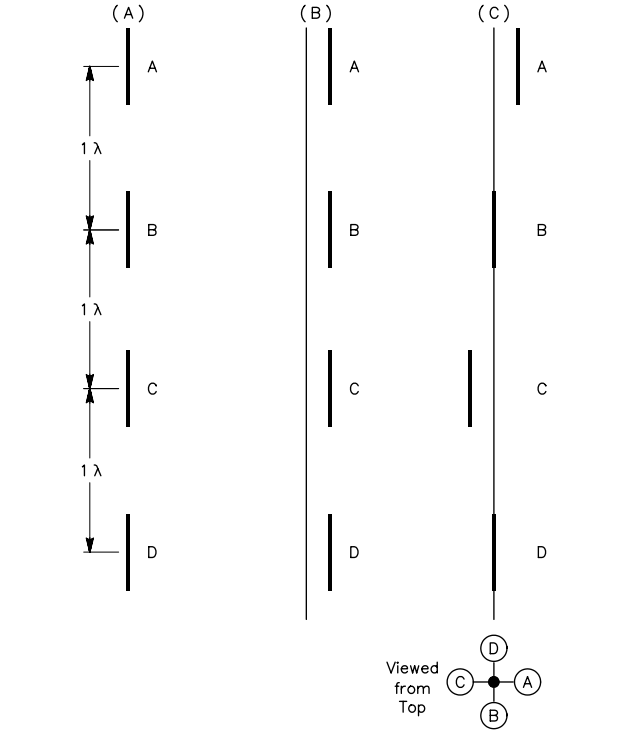

Fig 8—Various arrangements of exposed dipole elements. At A is the basic collinear array of four elements. B shows the same elements mounted on the side of a mast, and C shows the elements in a side-mounted arrangement around the mast for omnidirectional coverage. See text and Figs 9 through 11 for radiation-pattern information.

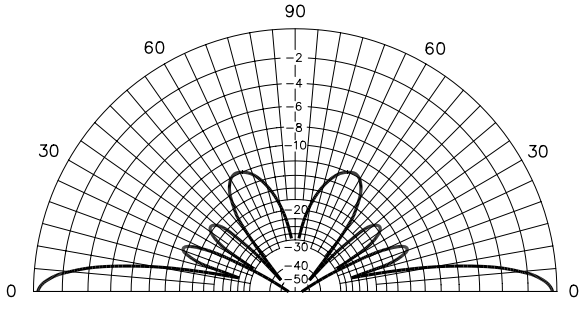

Fig 9—Calculated vertical-plane pattern of the array of Fig 8A, assuming a nonconducting mast support and complete decoupling of the feeder. In azimuth the array is omnidirectional. The calculated gain of the array is 8.6 dBi at 0° elevation; the –3 dB point is at 6.5°.

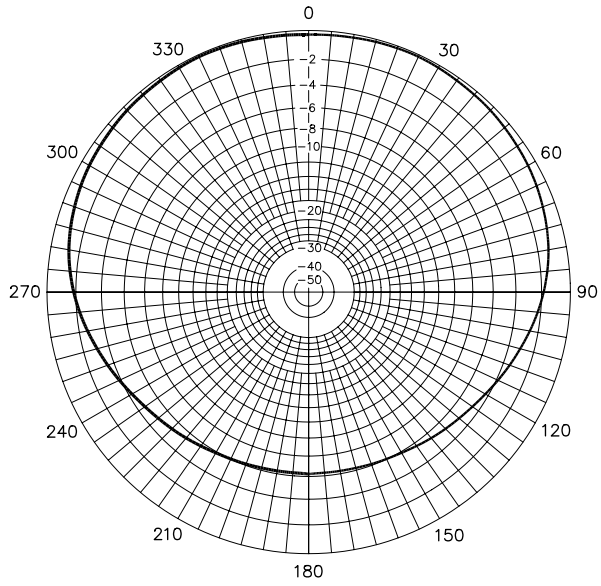

Fig 10—Calculated azimuth pattern of the side-mounted array of Fig 8B, assuming 1/4-λ spacing from a 4-inch mast. The calculated gain in the favored direction, away from the mast and through the elements, is 10.6 dBi.

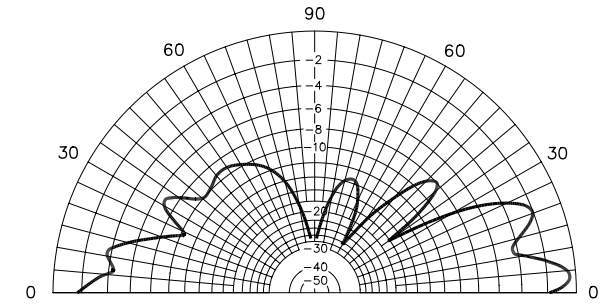

Fig 11—Calculated vertical pattern of the array of Fig 8C, assuming 1/4-λ element spacing from a 4-inch mast. The azimuth pattern is circular within 1.5 dB, and the calculated gain is 4.4 dBi.

Be certain that the feed line is properly supported along its length. Long lengths of cable are subject to contraction and expansion with temperature from season to season, so it is important that the cable not be so tight that contraction causes it to stress the connection at the antenna. This can cause the connection to become intermittent (and noisy) or, at worst, an open circuit. This is far from a pleasant situation if the antenna connection is 300 feet up a tower, and it happens to be the middle of the winter!

Effects of Other Conductors

Feed-line proximity and tower-access ladders or cages also have an effect on the radiation patterns of side-mounted antennas. This subject was studied by Connolly and Blevins, and their findings are given in *IEEE Conference Proceedings* (see the Bibliography at the end of this chapter). Those considering mounting antennas on air-conditioning evaporators or maintenance penthouses on commercial buildings should consult this article. It gives considerable information on the effects of these structures on both unidirectional and omnidirectional antennas.

Metallic guy wires also affect antenna radiation patterns. Yang and Willis studied this and reported the results in *IRE Transactions on Vehicular Communications*. As expected, the closer the antenna is to the guy wires, the greater the effect on the radiation patterns. If the antennas are near the point where the guy wires meet the tower, the effect of the guy wires can be minimized by breaking them up with insulators every 0.75 λ for 2.25 λ to 3.0 λ.

ISOLATION REQUIREMENTS IN REPEATER ANTENNA SYSTEMS

Because repeaters generally operate in full *duplex* (the transmitter and receiver operate simultaneously), the antenna system must act as a filter to keep the transmitter from blocking the receiver. The degree to which the transmitter and receiver must be isolated is a complex problem. It is quite dependent on the equipment used and the difference in transmitter and receiver frequencies (offset). Instead of going into great detail, a simplified example can be used for illustration.

Consider the design of a 144-MHz repeater with a 600-kHz offset. The transmitter has an RF output power of 10 watts, and the receiver has a squelch sensitivity of 0.1 μV. This means there must be at least 1.9×10^{-16} watts at the 52-Ω receiver-antenna terminals to detect a signal. If both the transmitter and receiver were on the same frequency, the isolation (attenuation) required between the transmitter and receiver antenna jacks to keep the transmitter from activating the receiver would be

$$\text{Isolation} = 10 \log \frac{10 \text{ watts}}{1.9 \times 10^{-16} \text{ watts}} = 167 \text{ dB}$$

Obviously there is no need for this much attenuation, because the repeater does not transmit and receive on the same frequency.

If the 10-watt transmitter has noise 600 kHz away from the carrier frequency that is 45 dB below the carrier power, that 45 dB can be subtracted from the isolation requirement. Similarly, if the receiver can detect a 0.1 μV on-frequency signal in the presence of a signal 600 kHz away that is 40 dB greater than 0.1 μV, this 40 dB can also be subtracted from the isolation requirement. Therefore, the isolation requirement is

167 dB – 45 dB – 40 dB = 82 dB

Other factors enter into the isolation requirements as well. For example, if the transmitter power is increased by 10 dB (from 10 to 100 watts), this 10 dB must be added to the isolation requirement. Typical requirements for 144- and 440-MHz repeaters are shown in **Fig 12**.

Obtaining the required isolation is the first problem to be considered in constructing a repeater antenna system. There are three common ways to obtain this isolation:

1) Physically separate the receiving and transmitting antennas so the combination of path loss for the spacing and the antenna radiation patterns results in the required isolation.
2) Use a combination of separate antennas and high-Q filters to develop the required isolation. (The high-Q filters serve to reduce the physical distance required between antennas.)
3) Use a combination filter and combiner system to

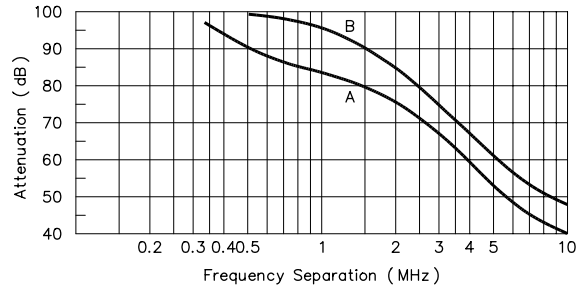

Fig 12—Typical isolation requirements for repeater transmitters and receivers operating in the 132-174 MHz band (Curve A), and the 400-512 MHz band (Curve B). Required isolation in dB is plotted against frequency separation in MHz. These curves were developed for a 100-W transmitter. For other power levels, the isolation requirements will differ by the change in decibels relative to 100 W. Isolation requirements will vary with receiver sensitivity. (The values plotted were calculated for transmitter-carrier and receiver-noise suppression necessary to prevent more than 1 dB degradation in receiver 12-dB SINAD sensitivity.)

allow the transmitter and receiver to share one antenna. Such a filter and combiner is called a *duplexer*.

Repeaters operating on 28 and 50 MHz generally use separate antennas to obtain the required isolation. This is largely because duplexers in this frequency range are both large and very expensive. It is generally less expensive to buy two antennas and link the sites by a committed phone line or an RF link than to purchase a duplexer. At 144 MHz and higher, duplexers are more commonly used. Duplexers are discussed in greater detail in a later section.

Separate Antennas

Receiver desensing (gain limiting caused by the presence of a strong off-frequency signal) can be reduced, and often eliminated, by separation of the transmitting and receiving antennas. Obtaining the 55 to 90 dB of isolation required for a repeater antenna system requires separate antennas to be spaced a considerable distance apart (in wavelengths).

Fig 13 shows the distances required to obtain specific values of isolation for vertical dipoles having horizontal separation (at A) and vertical separation (at B). The isolation gained by using separate antennas is subtracted from the total isolation requirement of the system. For example, if the transmitter and receiver antennas for a 450-MHz repeater are separated horizontally by 400 feet, the total isolation requirement in the system is reduced by about 64 dB.

Note from Fig 13B that a vertical separation of only about 25 feet also provides 64 dB of isolation. Vertical separation yields much more isolation than does horizontal separation. Vertical separation is also more practical than horizontal, since only a single support is required.

An explanation of the significant difference between the two graphs is in order. The vertical spacing requirement for 60 dB attenuation (isolation) at 150 MHz is about 43 feet. The horizontal spacing for the same isolation level is on the order of 700 feet. **Fig 14** shows why this difference exists. The radiation patterns of the antennas at A overlap; each antenna has gain in the direction of the other. The path loss between the antennas is given by

$$\text{Path loss (dB)} = 20 \log \frac{4\pi d}{\lambda} \qquad \text{(Eq 1)}$$

where

d = distance between antennas

λ = wavelength, in the same units as d.

The isolation between the antennas in Fig 14A is the path loss less the antenna gains. Conversely, the antennas at B share pattern nulls, so the isolation is the path loss added to the depth of these nulls. This significantly reduces the spacing requirement for vertical sepa-

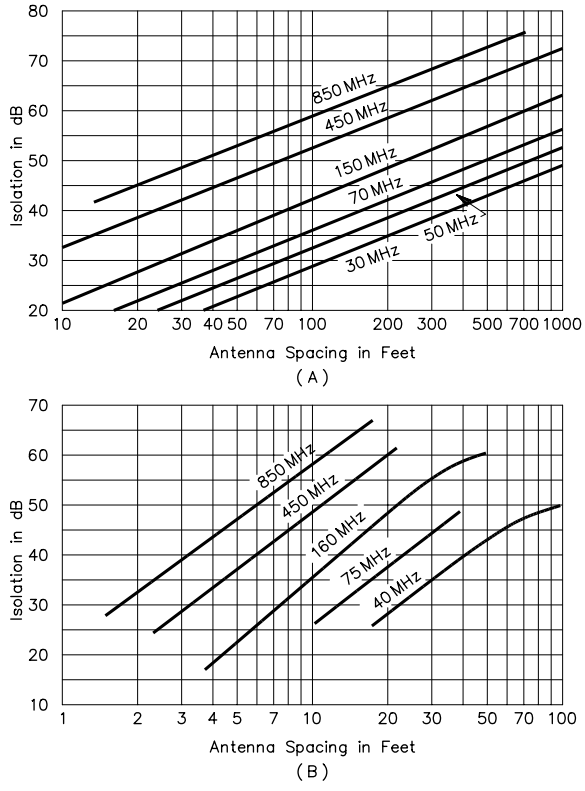

Fig 13—At A, the amount of attenuation (isolation) provided by horizontal separation of vertical dipole antennas. At B, isolation afforded by vertical separation of vertical dipoles.

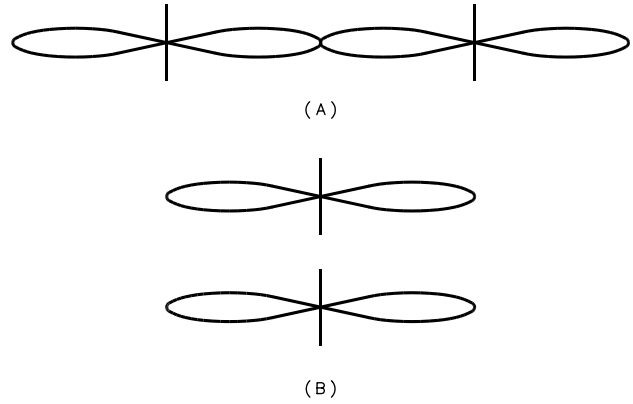

Fig 14—A relative representation of the isolation advantage afforded by separating antennas horizontally (A) and vertically (B) is shown. A great deal of isolation is provided by vertical separation, but horizontal separation requires two supports and much greater distance to be as effective. Separate-site repeaters (those with transmitter and receiver at different locations) benefit much more from horizontal separation than do single-site installations.

ration. Because the depth of the pattern nulls is not infinite, some spacing is required. Combined horizontal and vertical spacing is much more difficult to quantify because the results are dependent on both radiation patterns and the positions of the antennas relative to each other.

Separate antennas have one major disadvantage: They create disparity in transmitter and receiver coverage. For example, say a 50-MHz repeater is installed over average terrain with the transmitter and repeater separated by 2 miles. If both antennas had perfect omnidirectional coverage, the situation depicted in **Fig 15** would exist. In this case, stations able to hear the repeater may not be able to access it, and vice versa. In practice, the situation can be considerably worse. This is especially true if the patterns of both antennas are not omnidirectional. If this disparity in coverage cannot be tolerated, the solution involves skewing the patterns of the antennas until their coverage areas are essentially the same.

Cavity Resonators

As just discussed, receiver desensing can be reduced by separating the transmitter and receiver antennas. But the amount of transmitted energy that reaches the receiver input must often be decreased even farther. Other nearby transmitters can cause desensing as well. A *cavity resonator* (cavity filter) can be helpful in solving these problems. When properly designed and constructed, this type of resonator has very high Q. A commercially made cavity is shown in **Fig 16**.

A cavity resonator placed in series with a transmission line acts as a band-pass filter. For a resonator to operate in series, it must have input and output coupling loops (or probes). A cavity resonator can also be connected across (in parallel with) a transmission line. The cavity then acts as a band-reject (notch) filter, greatly attenuating energy at the frequency to which it is tuned. Only one coupling loop or probe is required for this method of filtering. This type of cavity could be used in the receiver line to "notch" the transmitter signal. Several cavities can be connected in series or parallel to increase the attenuation in a given configuration. The graphs of **Fig 17** show the attenuation of a single cavity (A) and a pair of cavities (B).

The only situation in which cavity filters would not help is the case where the off-frequency noise of the transmitter was right on the receiver frequency. With cavity resonators, an important point to remember is that addition of a cavity across a transmission line may change the impedance of the system. This change can be compensated by adding tuning stubs along the transmission line.

Duplexers

The material in this section was prepared by Domenic Mallozzi, N1DM. Most amateur repeaters in the 144-, 220- and 440-MHz bands use duplexers to obtain the necessary transmitter to receiver isolation. Duplexers have been commonly used in commercial repeaters for many years. The duplexer consists of two high-Q filters. One filter is used in the feed line from the transmitter to the antenna, and another between the antenna and the receiver. These filters must have low loss at the frequency to which they are tuned while having very high attenuation at the surrounding frequencies. To meet the high attenuation requirements at frequencies within as little as 0.4% of the frequency to which they are tuned, the filters usually take the form of cascaded transmission-line cavity filters. These are either band-pass filters, or band-pass filters with a rejection notch. (The rejection notch is tuned to the center frequency of the other filter.) The number of cascaded filter sections is determined by the frequency separation and the ultimate attenuation requirements.

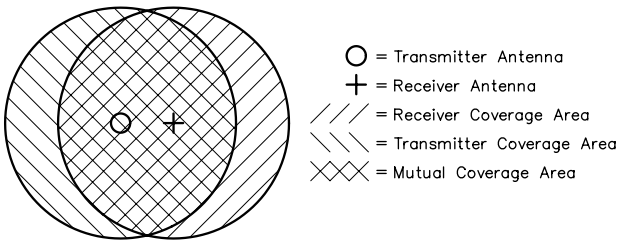

Fig 15—Coverage disparity is a major problem for separate-site repeater antennas. The transmitter and receiver coverage areas overlap, but are not entirely mutually inclusive. Solving this problem requires a great deal of experimentation, as many factors are involved. Among these factors are terrain features and distortion of the antenna radiation patterns from supports.

Fig 16—A coaxial cavity filter of the type used in many amateur and commercial repeater installations. Center-conductor length (and thus resonant frequency) is varied by adjustment of the knob (top).

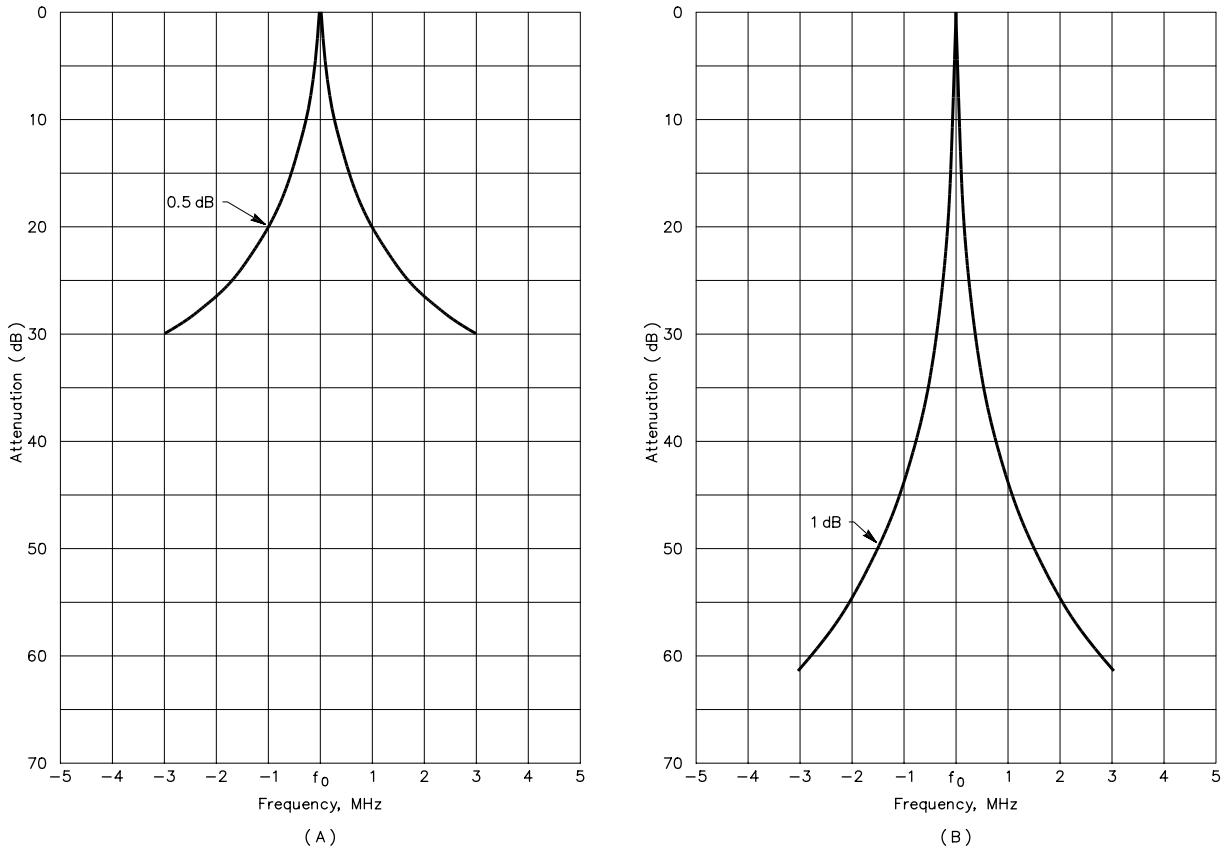

Fig 17—Frequency response curves for a single cavity (A) and two cavities cascaded (B). These curves are for cavities with coupling loops, each having an insertion loss of 0.5 dB. (The total insertion loss is indicated in the body of each graph.) Selectivity will be greater if lighter coupling (greater insertion loss) can be tolerated.

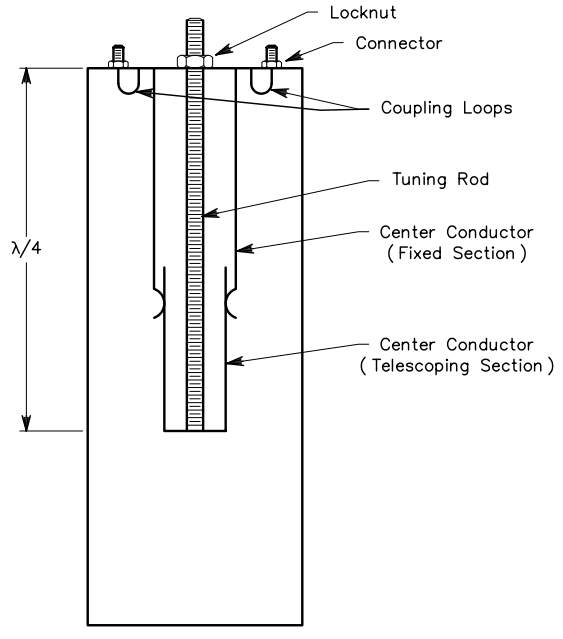

Duplexers for the amateur bands represent a significant technical challenge, because in most cases amateur repeaters operate with significantly less frequency separation than their commercial counterparts. Information on home construction of duplexers is presented in a later section of this chapter. Many manufacturers market high-quality duplexers for the amateur frequencies.

Duplexers consist of very high-Q cavities whose resonant frequencies are determined by mechanical components, in particular the tuning rod. **Fig 18** shows the cutaway view of a typical duplexer cavity. The rod is usually made of a material that has a limited thermal expansion coefficient (such as Invar). Detuning of the cavity by environmental changes introduces unwanted losses in the antenna system. An article by Arnold in *Mobile Radio Technology* considered the causes of drift in the

Fig 18—Cutaway view of a typical cavity. Note the relative locations of the coupling loops to each other and to the center conductor of the cavity. A locknut is used to prevent movement of the tuning rod after adjustment.

cavity (see the Bibliography at the end of this chapter). These can be broken into four major categories.

1) Ambient temperature variation (which leads to mechanical variations related to the thermal expansion coefficients of the materials used in the cavity).
2) Humidity (dielectric constant) variation.
3) Localized heating from the power dissipated in the cavity (resulting from its insertion loss).
4) Mechanical variations resulting from other factors (vibration, etc).

In addition, because of the high-Q nature of these cavities, the insertion loss of the duplexer increases when the signal is not at the peak of the filter response. This means, in practical terms, that less power is radiated for a given transmitter output power. Also, the drift in cavities in the receiver line results in increased system noise figure, reducing the sensitivity of the repeater.

As the frequency separation between the receiver and the transmitter decreases, the insertion loss of the duplexer reaches certain practical limits. At 144 MHz, the minimum insertion loss for 600 kHz spacing is 1.5 dB per filter.

Testing and using duplexers requires some special considerations (especially as frequency increases). Because duplexers are very high-Q devices, they are very sensitive to the termination impedances at their ports. A high SWR on any port is a serious problem, because the apparent insertion loss of the duplexer will increase, and the isolation may appear to decrease. Some have found that when duplexers are used at the limits of their isolation capabilities, a small change in antenna SWR is enough to cause receiver desensitization. This occurs most often under ice-loading conditions on antennas with open-wire phasing sections.

The choice of connectors in the duplexer system is important. BNC connectors are good for use below 300 MHz. Above 300 MHz, their use is discouraged because even though many types of BNC connectors work well up to 1 GHz, older style standard BNC connectors are inadequate at UHF and above. Type N connectors should be used above 300 MHz. It is false economy to use marginal quality connectors. Some commercial users have reported deteriorated isolation in commercial UHF repeaters when using such connectors. The location of a bad connector in a system is a complicated and frustrating process. Despite all these considerations, the duplexer is still the best method for obtaining isolation in the 144- to 925 MHz range.

ADVANCED TECHNIQUES

As the number of available antenna sites decreases and the cost of various peripheral items (such as coaxial cable) increases, amateur repeater groups are required to devise advanced techniques if repeaters are to remain effective. Some of the techniques discussed here have been applied in commercial services for many years, but until recently have not been economically justified for amateur use.

One technique worth consideration is the use of *cross-band couplers*. To illustrate a situation where a cross-band coupler would be useful, consider the following example. A repeater group plans to install 144- and 902-MHz repeaters on the same tower. The group intends to erect both antennas on a horizontal cross arm at the 325-foot level. A 325-foot run of $^{7}/_{8}$-inch Heliax costs approximately $2000. If both antennas are to be mounted at the top of the tower, the logical approach would require two separate feed lines. A better solution involves the use of a single feed line for both repeaters, along with a cross-band coupler at each end of the line.

The use of the cross-band coupler is shown in **Fig 19**. As the term implies, the coupler allows two signals on different bands to share a common transmission line. Such couplers cost approximately $300 each. In our hypothetical example, this represents a saving of $1400 over the cost of using separate feed lines. But, as with all compromises, there are disadvantages. Cross-band cou-

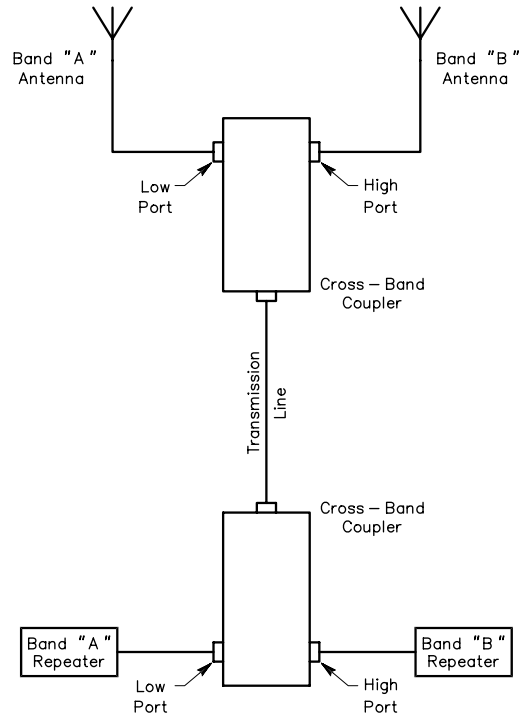

Fig 19—Block diagram of a system using cross-band couplers to allow the use of a single feed line for two repeaters. If the feeder to the antenna location is long (more than 200 feet or so), cross-band couplers may provide a significant saving over separate feed lines, especially at the higher amateur repeater frequencies. Cross-band couplers cannot be used with two repeaters on the same band.

plers have a loss of about 0.5 dB per unit. Therefore, the pair required represents a loss of 1.0 dB in *each* transmission path. If this loss can be tolerated, the cross-band coupler is a good solution.

Cross-band couplers do not allow two repeaters *on the same band* to share a single antenna and feed line. As repeater sites and tower space become more scarce, it may be desirable to have two repeaters on the same band share the same antenna. The solution to this problem is the use of a *transmitter multicoupler*. The multicoupler is related to the duplexers discussed earlier. It is a cavity filter and combiner that allows multiple transmitters and receivers to share the same antenna. This is a common commercial practice. A block diagram of a multicoupler system is shown in **Fig 20**.

The multicoupler, however, is a very expensive device, and has the disadvantage of even greater loss per transmission path than the standard duplexer. For example, a well-designed duplexer for 600 kHz spacing at 146 MHz has a loss per transmission path of approximately 1.5 dB. A four-channel multicoupler (the requirement for two repeaters) has an insertion loss per transmission path on the order of 2.5 dB or more. Another constraint of such a system is that the antenna must present a good match to the transmission line at all frequencies on which it will be used (both transmitting and receiving). This becomes difficult for the system with two repeaters operating at opposite ends of a band.

If you elect to purchase a commercial base-station antenna that requires you to specify a frequency to which the antenna must be tuned, be sure to indicate to the manufacturer the intended use of the antenna and the frequency extremes. In some cases, the only way the manufacturer can accommodate your request is to provide an antenna with some vertical-beam uptilt at one end of the band and some downtilt at the other end of the band. In the case of antennas with very high gain, this in itself may become a serious problem. Careful analysis of the situation is necessary before assembling such a system.

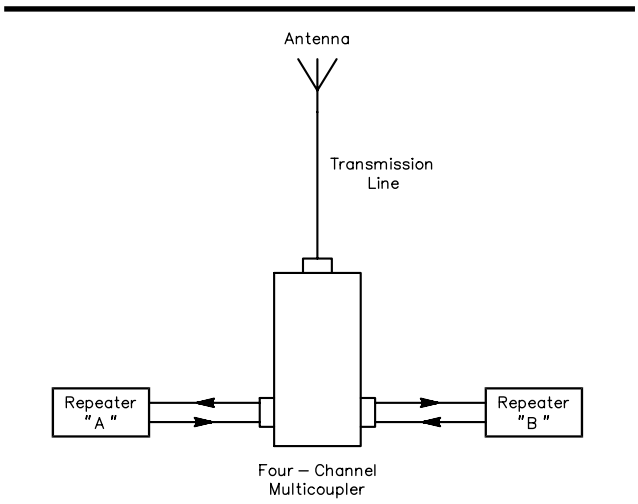

Fig 20—Block diagram of a system using a transmitter multicoupler to allow a single feed line and antenna to be used by two repeaters on one band. The antenna must be designed to operate at all frequencies that the repeaters utilize. More than two repeaters can be operated this way by using a multicoupler with the appropriate number of input ports.

Diversity Techniques for Repeaters

Mobile flutter, "dead spots" and similar problems are a real problem for the mobile operator. The popularity of hand-held transceivers using low power and mediocre antennas causes similar problems. A solution to these difficulties is the use of some form of *diversity reception*. Diversity reception works because signals do not fade at the same rate when received by antennas at different locations (space diversity) or of different polarizations (polarization diversity).

Repeaters with large transmitter coverage areas often have difficulty "hearing" low power stations in peripheral areas or in dead spots. Space diversity is especially useful in such a situation. Space diversity utilizes separate receivers at different locations that are linked to the repeater. The repeater uses a circuit called a *voter* that determines which receiver has the best signal, and then selects the appropriate receiver from which to feed the repeater transmitter. This technique is helpful in urban areas where shadowing from large buildings and bridges causes problems. Space-diversity receiving, when properly executed, can give excellent results. But with the improvement come some disadvantages: added initial cost, maintenance costs, and the possibility of failure created by the extra equipment required. If installed and maintained carefully, problems are generally minimal.

A second improvement technique is the use of *circularly polarized* repeater antennas. This technique has been used in the FM broadcast field for many years, and has been considered for use in the mobile telephone service as well. Some experiments by amateurs have proved very promising, as discussed by Pasternak and Morris (see the Bibliography at the end of this chapter).

The improvement afforded by circular polarization is primarily a reduction in *mobile flutter*. The flutter on a mobile signal is caused by reflections from large buildings (in urban settings) or other terrain features. These reflections cause measurable polarization shifts, sometimes to the point where a vertically polarized signal at the transmitting site may appear to be primarily horizontally polarized after reflection.

A similar situation results from *multipath propagation*, where one or more reflected signals combine with the direct signal at the repeater, having varying effects on the signal. The multipath signal is subjected to large amplitude and phase variations at a relatively rapid rate.

In both of the situations described here, circular polarization can offer considerable improvement. This is because circularly polarized antennas respond equally to all linearly polarized signals, regardless of the plane of polarization. At this writing, there are no known sources of commercial circularly polarized omnidirectional antennas for the amateur bands. Pasternak and Morris describe a circularly polarized antenna made by modifying two commercial four-pole arrays.

EFFECTIVE ISOTROPIC RADIATED POWER (EIRP)

It is useful to know effective isotropic radiated power (EIRP) in calculating the coverage area of a repeater. The FCC formerly required EIRP to be entered in the log of every amateur repeater station. Although logging EIRP is no longer required, it is still useful to have this information on hand for repeater-coordination purposes and so system performance can be monitored periodically.

Calculation of EIRP is straightforward. The PEP output of the transmitter is simply multiplied by the gains and losses in the transmitting antenna system. (These gains and losses are best added or subtracted in decibels and then converted to a multiplying factor.) The following worksheet and example illustrates the calculations.

Feed-line loss	____	dB
Duplexer loss	____	dB
Isolator loss	____	dB
Cross-band coupler loss	____	dB
Cavity filter loss	____	dB
Total losses (L)	____	dB

G (dB) = antenna gain (dBi) –L

where G = antenna system gain. (If antenna gain is specified in dBd, add 2.14 dB to obtain the gain in dBi.)

$M = 10^{G/10}$

where M = multiplying factor

EIRP (watts) = transmitter output (PEP)×M

Example

A repeater transmitter has a power output of 50 W PEP (50-W FM transmitter). The transmission line has 1.8 dB loss. The duplexer used has a loss of 1.5 dB, and a circulator on the transmitter port has a loss of 0.3 dB. There are no cavity filters or cross-band couplers in the system. Antenna gain is 5.6 dBi.

Feed-line loss	1.8 dB
Duplexer loss	1.5 dB
Isolator loss	0.3 dB
Cross-band coupler loss	0 dB
Cavity filter loss	0 dB
Total losses (L)	3.6 dB

Antenna system gain in dB = G = antenna gain (dBi) –L

G = 5.6 dBi – 3.6 dB = 2 dB

Multiplying factor = $M = 10^{G/10}$

$M = 10^{2/10} = 1.585$

EIRP (watts) = transmitter output (PEP) × M

EIRP = 50 W × 1.585 = 79.25 W

If the antenna system is lossier than this example, G may be *negative*, resulting in a multiplying factor less than one. The result is an EIRP that is less than the transmitter output power. This situation can occur in practice, but for obvious reasons is not desirable.

Assembling a Repeater Antenna System

This section will aid you in planning and assembling your repeater antenna system. The material was prepared by Domenic Mallozzi, N1DM. Consult Chapter 23, Radio Wave Propagation, for information on propagation for the band of your interest.

First, a repeater antenna selection checklist such as this will help you in evaluating the antenna system for your needs.

Gain needed _____ dBi

Pattern required _____ Omnidirectional
_____ Offset
_____ Cardioidal
_____ Bidirectional
_____ Special pattern (specify)
_____

Mounting _____ Top of tower
_____ Side of tower

(Determine effects of tower on pattern. Is the result consistent with the pattern required?)

Is downtilt required? _____ Yes
_____ No

Type of RF connector _____ UHF
_____ N
_____ BNC
_____ Other (specify)

Size (length) _____

Weight _____

Maximum cost $_____

Table 1 (see next page) has been compiled to provide general information on commercial components available for repeater and remote-base antenna systems. The various components are listed in a matrix format by manufacturer, for equipment designed to operate in the various amateur bands. See Chapter 21, Antenna Products Suppliers, for further information for these components. Although every effort has been made to make this data complete, the ARRL is not responsible for omissions or errors. The listing of a product in Table 1 does not constitute an endorsement by ARRL. Manufacturers are urged to contact the editors with updating information.

Even though almost any antenna can be used for a repeater, the companies indicated in the *Antennas* column in Table 1 are known to have produced heavy-duty antennas to commercial standards for repeater service. Many of these companies offer their antennas with special features for repeater service (such as vertical-beam downtilt). It is best to obtain catalogs of current products from the manufacturers listed, both for general information and to determine which special options are available on their products.

A 144 MHz Duplexer

Obtaining sufficient isolation between the transmitter and receiver of a repeater can be difficult. Many of the solutions to this problem compromise receiver sensitivity or transmitter power output. Other solutions create an imbalance between receiver and transmitter coverage areas. When a duplexer is used, insertion loss is the compromise. But a small amount of insertion loss is more than offset by the use of one antenna for both the transmitter and receiver. Using one antenna assures equal antenna patterns for both transmitting and receiving, and reduces cost, maintenance and mechanical complexity.

As mentioned earlier in this chapter, duplexers may be built in the home workshop. Bob Shriner, WAØUZO, presented a small, mechanically simple duplexer for low-power applications in April 1979 *QST*. Shriner's design is unique, as the duplexer cavities are constructed of circuit-board material. Low cost and simplicity are the result, but with a trade-off in performance. A silver-plated version of Shriner's design has an insertion loss of approximately 5 dB at 146 MHz. The loss is greater if the copper is not plated, and increases as the inner walls of the cavities tarnish.

This duplexer construction project by John Bilodeau, W1GAN, represents an effective duplexer. The information originally appeared in July 1972 *QST*. It is a time-proven project used by many repeater groups, and can be duplicated relatively easily. Its insertion loss is just 1.5 dB.

Fig 21 will help you visualize the requirements for a duplexer, which can be summed up as follows. The duplexer must attenuate the transmitter carrier to avoid overloading the receiver and thereby reducing its sensitivity. It must also attenuate any noise or spurious frequencies from the transmitter on or near the receiver frequency. In addition, a duplexer must provide a proper impedance match between transmitter, antenna, and receiver.

Table 1
Product Matrix Showing Repeater Equipment and Manufacturer by Frequency Band

	Antennas							*Duplexers*				*Cavity Filters*			
Source	*28*	*50*	*144*	*220*	*450*	*902*	*1296*	*144*	*220*	*450*	*902*	*144*	*220*	*450*	*902*
Austin	S	S	S	S	S	S	S								
Celwave	C	C	C	C	C	C		C	C	C	C	C	C	C	C
Comet															
Cushcraft		C	C	C	C										
Dec Prod		C	C	C	C	C		C	C		C	C		C	
MA/COM												C		C	
RF Parts			C		C	C	C								
Sinclair	C	C	C					C		C		C		C	C
TX/RX								C	C	C		C		C	C
Wacom															

	Isolators/Circulators						*Transmitter Combiners*				*Cross-Band Couplers*			
Source	*28*	*50*	*144*	*220*	*450*	*902*	*144*	*220*	*450*	*902*	*0-174 450-512*	*0-512 800-960*	*59-174 806-960*	*406-512 806-960*
Celwave			C	C	C	C	C	C	C	C		S		
Dec Prod			C		C	C		C	C	C				
Sinclair			C		C	C								
TX/RX			C		C	C	C	C	C	C	C	C	C	C
Wacom			C	C	C	C	C	C	C	C		C		C

Abbreviated names above are for the following manufacturers: Austin Antennas, Celwave RF Inc, Cushcraft Corp, Decibel Products Inc, RF Parts, Sinclair Radio Laboratories Inc, TX/RX Systems Inc and Wacom Inc. A manufacturer's contact list appears in Chapter 21.

Key to codes used:
C = catalog (standard) item
S = special-order item

Note: Coaxial cable is not listed, because most manufacturers sell only to dealers.

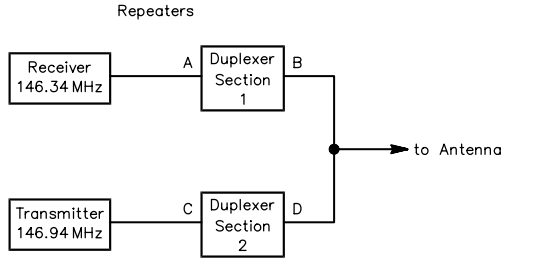

Fig 21—Duplexers permit using one antenna for both transmitting and receiving in a repeater system. Section 1 prevents energy at the transmitter frequency from interfering with the receiver, while section 2 attenuates any off-frequency transmitter energy that is at or near the receiver frequency.

As shown in Fig 21, transmitter output on 146.94 MHz going from point C to D should not be attenuated. However, the transmitter energy should be greatly attenuated between points B and A. Duplexer section 2 should attenuate any noise or signals that are on or near the receiver input frequency of 146.34 MHz. For good reception the noise and spurious signal level must be less than –130 dBm (0 dBm = 1 milliwatt into 50 Ω). Typical transmitter noise 600 kHz away from the carrier frequency is 80 dB below the transmitter power output. For 60 watts of output (+48 dBm), the noise level is –32 dBm. The duplexer must make up the difference between –32 dBm and –130 dBm, or 98 dB.

The received signal must go from point B to A with a minimum of attenuation. Section 1 of the duplexer must also provide enough attenuation of the transmitter energy to prevent receiver overload. For an average receiver, the transmitter signal must be less than –30 dBm to meet this requirement. The difference between the transmitter output of +48 dBm and the receiver overload point of –30 dBm, 78 dB, must be made up by duplexer section 1.

THE CIRCUIT

Fig 22 shows the completed 6-cavity duplexer, and **Fig 23** shows the assembly of an individual cavity. A $^1/_4$-λ resonator was selected for this duplexer design. The length of the center conductor is adjusted by turning a

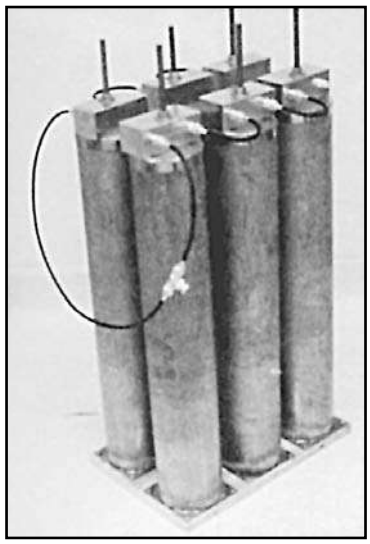

Fig 22—A six-cavity duplexer for use with a 144-MHz repeater. The cavities are fastened to a plywood base for mechanical stability. Short lengths of double-shielded cable are used for connections between individual cavities. An insertion loss of less than 1.5 dB is possible with this design.

threaded rod, which changes the resonant frequency of the cavity. Energy is coupled into and out of the tuned circuit by the coupling loops extending through the top plate.

The cavity functions as a series resonant circuit. When a reactance is connected across a series resonant circuit, an anti-resonant notch is produced, and the resonant frequency is shifted. If a capacitor is added, the notch appears below the resonant frequency. Adding inductance instead of capacitance makes the notch appear above the resonant frequency. The value of the added component determines the spacing between the notch and the resonant frequency of the cavity.

Fig 24 shows the measured band-pass characteristics of the cavity with shunt elements. With the cavity tuned to 146.94 MHz and a shunt capacitor connected from input to output, a 146.34-MHz signal is attenuated

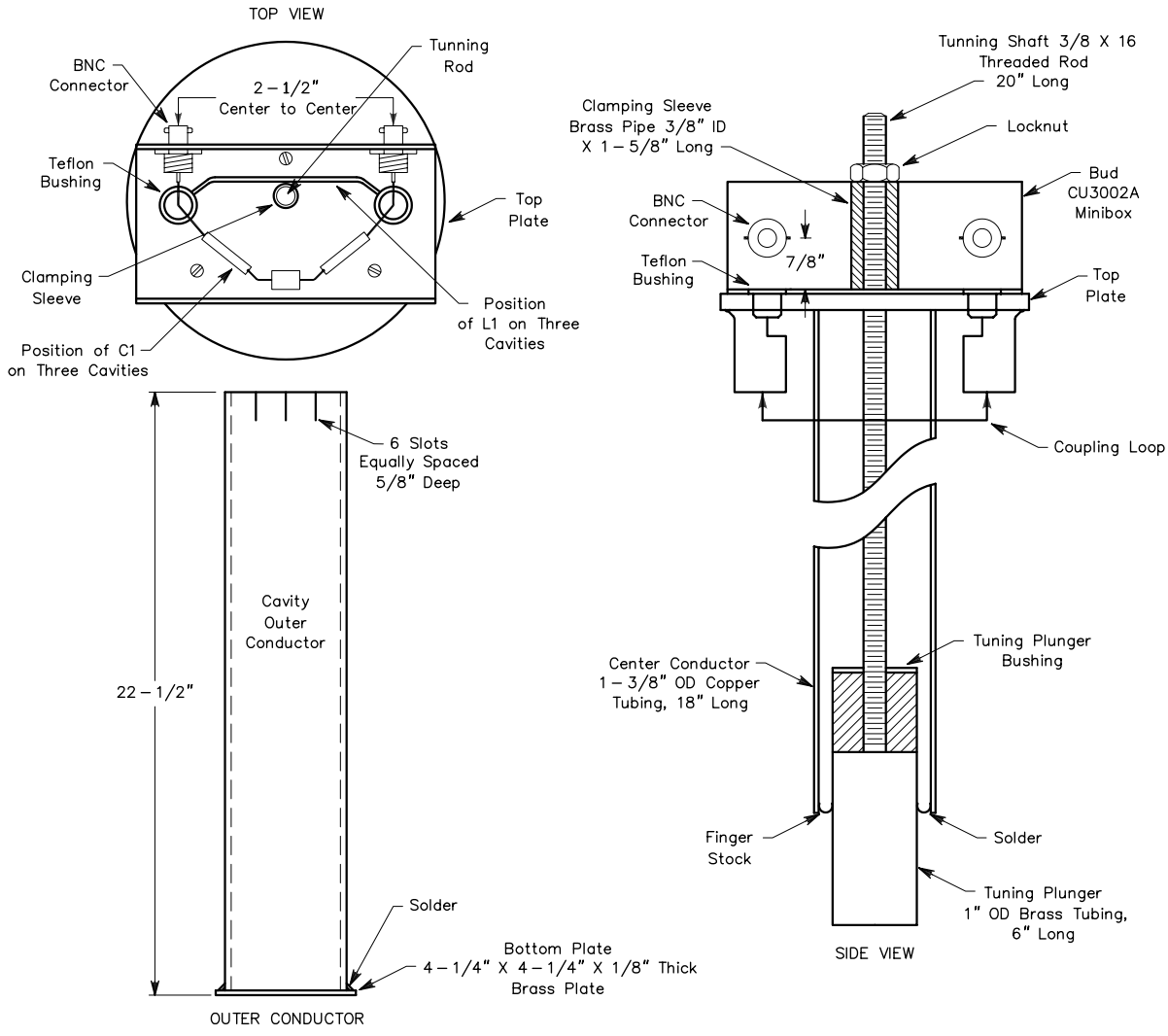

Fig 23—The assembly of an individual cavity. A Bud Minibox is mounted on the top plate with three screws. A clamping sleeve made of brass pipe is used to prevent crushing the box when the locknut is tightened on the tuning shaft. Note that the positions of both C1 and L1 are shown, but that three cavities will have C1 installed and three will have L1 in place.

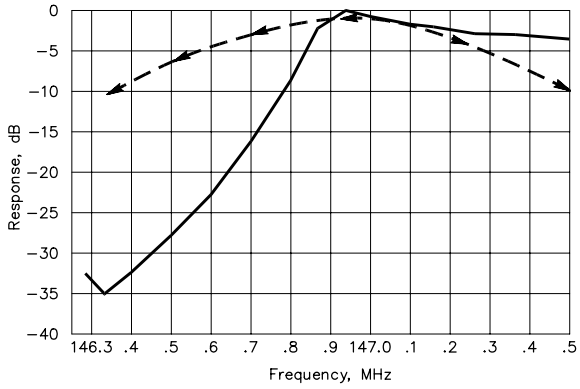

Fig 24—Typical frequency response of a single cavity of the type used in the duplexer. The dotted line represents the passband characteristics of the cavity alone; the solid line for the cavity with a shunt capacitor connected between input and output. An inductance connected in the same manner will cause the rejection notch to be above the frequency to which the cavity is tuned.

by 35 dB. If an inductance is placed across the cavity and the cavity is tuned to 146.34 MHz, the attenuation at 146.94 MHz is 35 dB. Insertion loss in both cases is 0.4 dB. Three cavities with shunt capacitors are tuned to 146.94 MHz and connected together in cascade with short lengths of coaxial cable. The attenuation at 146.34 MHz is more than 100 dB, and insertion loss at 146.94 MHz is 1.5 dB. Response curves for a six-cavity duplexer are given in **Fig 25**.

Construction

The schematic diagram for the duplexer is shown in **Fig 26**. Three parts for the duplexer must be machined; all others can be made with hand tools. A small lathe can be used to machine the brass top plate, the threaded tuning plunger bushing and the Teflon insulator bushing. The dimensions of these parts are given in **Fig 27**.

Type DWV copper tubing is used for the outer conductor of the cavities. The wall thickness is 0.058 inch, with an outside diameter of $4^1/_8$ inches. You will need a tubing cutter large enough to handle this size (perhaps borrowed or rented). The wheel of the cutter should be tight and sharp. Make slow, careful cuts so the ends will be square. The outer conductor is $22^1/_2$ inches long.

The inner conductor is made from type M copper tubing having an outside diameter of $1^3/_8$ inches. A 6-inch length of 1-inch OD brass tubing is used to make the tuning plunger.

The tubing types mentioned above are designations used in the plumbing and steam-fitting industry. Other types may be used in the construction of a duplexer, but you should check the sizes carefully to assure that the parts will fit each other. A greater wall thickness will make the assembly heavier, and the expense will increase accordingly. Soft solder is used throughout the assembly. Unless you have experience with silver solder, do not use it. Eutectic type 157 solder with paste or acid

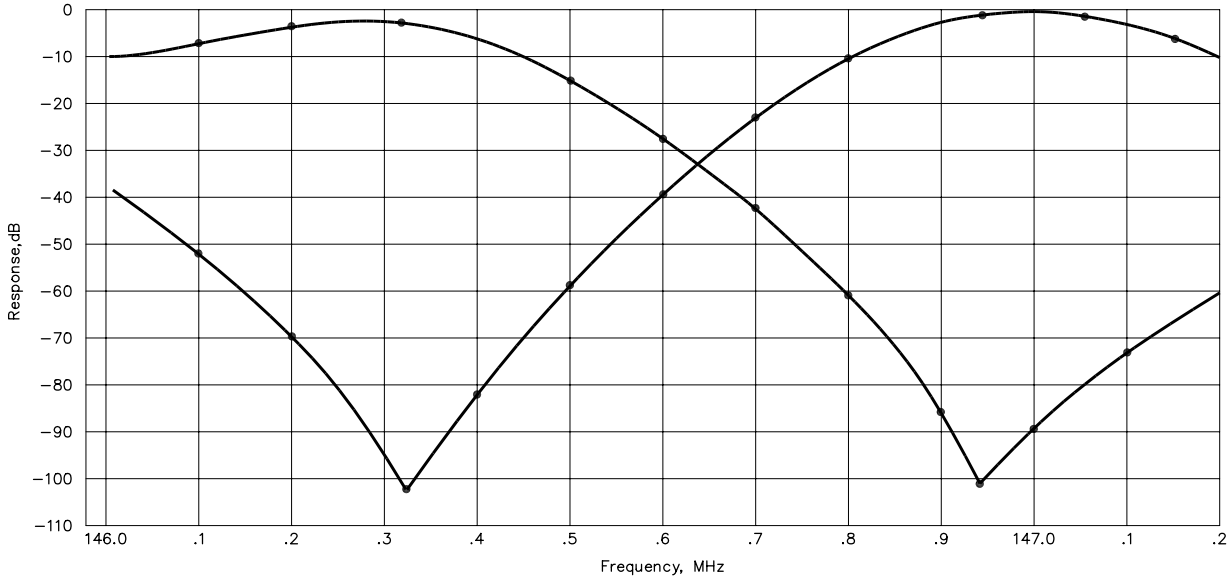

Fig 25—Frequency response of the six-cavity duplexer. One set of three cavities is tuned to pass 146.34 MHz and notch 146.94 MHz (the receiver leg). The remaining set of three cavities is tuned to pass 146.94 MHz and notch 146.34 MHz. This duplexer provides approximately 100 dB of isolation between the transmitter and receiver when properly tuned.

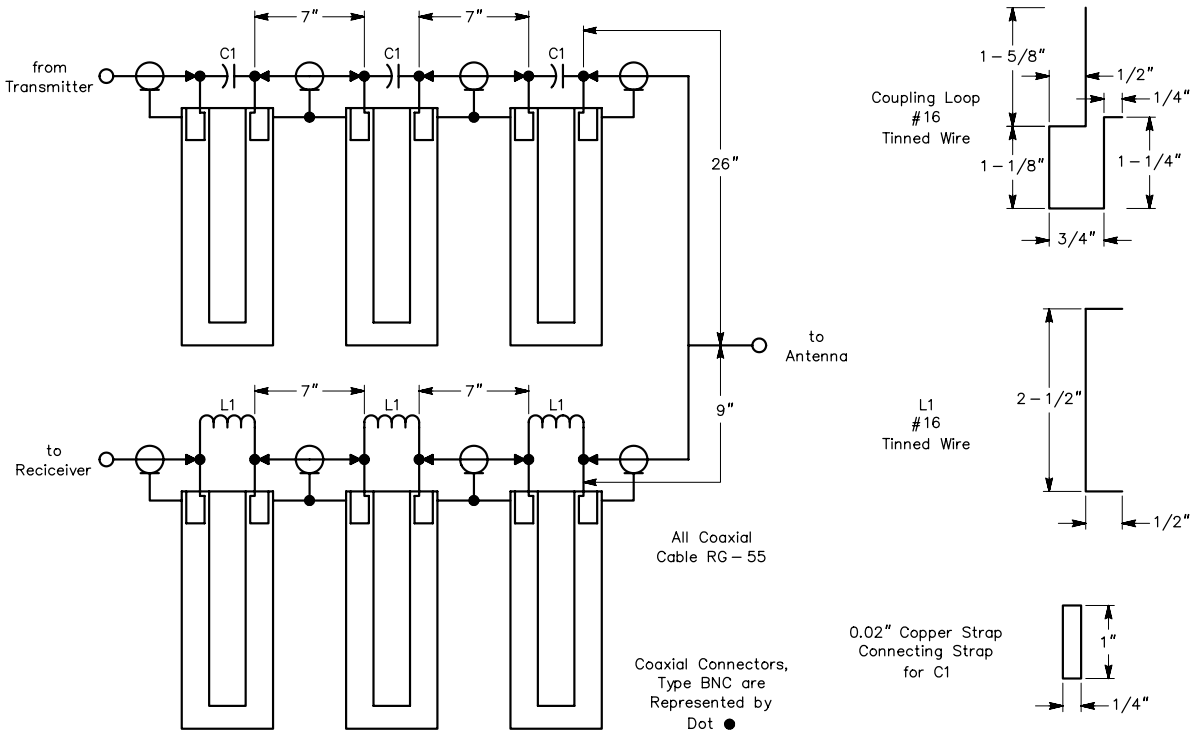

Fig 26—Diagram of the six-cavity duplexer. Coaxial cable lengths between cavities are critical and must be followed closely. Double shielded cable and high quality connectors should be used throughout. The sizes and shapes of the coupling loops, L1, and the straps for connecting C1 should be observed.
C1—1.7-11 pF circuit-board mount, E. F. Johnson 189-5-5 or equiv. Set at 3/4 closed for initial alignment.

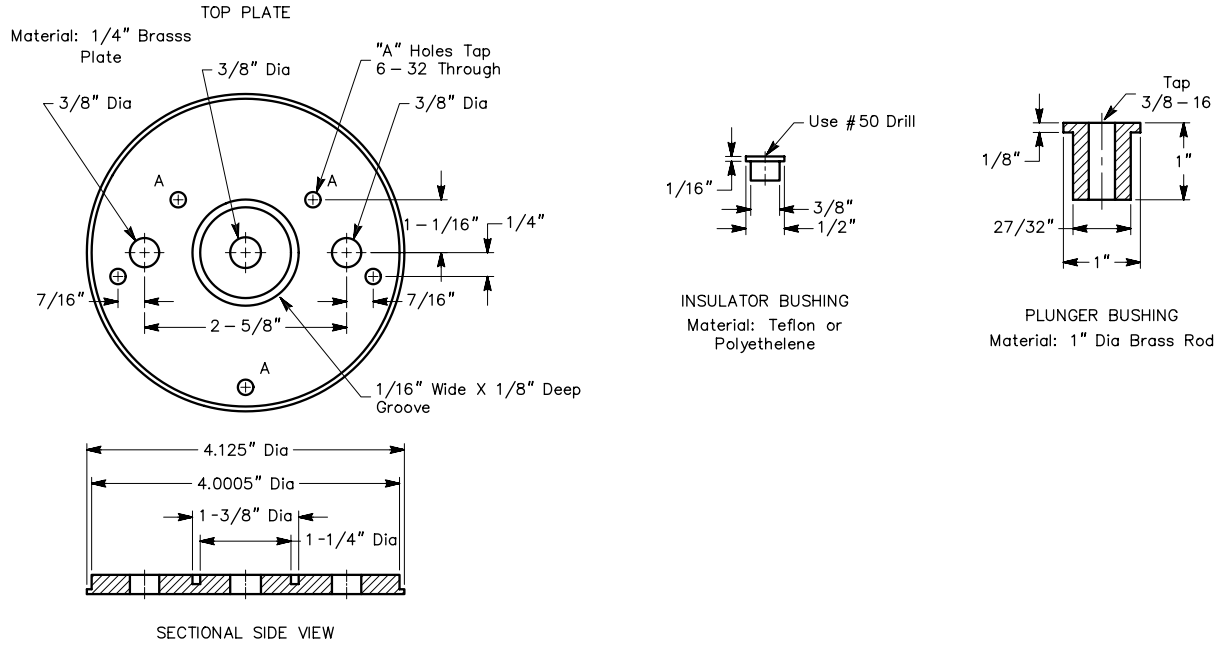

Fig 27—Dimensions for the three parts that require machining. A small metal-working lathe should be used for making these parts.

flux makes very good joints. This type has a slightly higher melting temperature than ordinary tin-lead alloy, but has considerably greater strength.

First solder the inner conductor to the top plate (**Fig 28**). The finger stock can then be soldered inside the lower end of the inner conductor, while temporarily held in place with a plug made of aluminum or stainless steel. While soldering, do not allow the flame from the torch to overheat the finger stock. The plunger bushing is soldered into the tuning plunger and a 20-inch length of threaded rod is soldered into the bushing.

Cut six slots in the top of the outer conductor. They should be $^5/_8$ inch deep and equally spaced around the tubing. The bottom end of the 4-inch tubing is soldered to the square bottom plate. The bottom plates have holes in the corners so they can be fastened to a plywood base by means of wood screws. Because the center conductor has no support at one end, the cavities must be mounted vertically.

The size and position of the coupling loops are critical. Follow the given dimensions closely. Both loops should be $^1/_8$ inch away from the center conductor on opposite sides. Connect a solder lug to the ground end of the loop, then fasten the lug to the top plate with a screw. The free end of the loop is insulated by Teflon bushings where it passes through the top plate for connection to the BNC fittings.

Before final assembly of the parts, clean them thoroughly. Soap-filled steel wool pads and hot water work well for this. Be sure the finger stock makes firm contact with the tuning plunger. The top plate should fit snugly in the top of the outer conductor—a large hose clamp tightened around the outer conductor will keep the top plate in place.

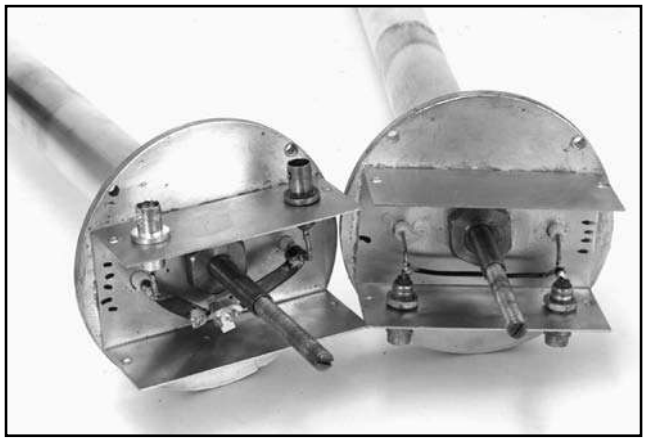

Fig 28—Two of the center conductor and top plate assemblies. In the assembly at the left, C1 is visible just below the tuning shaft, mounted by short straps made from sheet copper. The assembly on the right has L1 in place between the BNC connectors. The Miniboxes are fastened to the top plate by a single large nut in these units. Using screws through the Minibox into the top plate, as described in the text, is preferred.

ADJUSTMENT

After the cavities have been checked for band-pass characteristics and insertion loss, install the anti-resonant elements, C1 and L1. (See Fig 24.) It is preferable to use laboratory test equipment when tuning the duplexer. An option is to use a low-power transmitter with an RF probe and an electronic voltmeter. Both methods are shown in **Fig 29**.

With the test equipment connected as shown in Fig 29A, adjust the signal generator frequency to the desired repeater input frequency. Connect a calibrated step attenuator between points X and Y. With no attenuation, adjust the HP-415 for 0 on the 20-dB scale. You can check the calibration of the 415 by switching in different amounts of attenuation and noting the meter reading. You may note a small error at either high or very low signal levels.

Next, remove the step attenuator and replace it with a cavity that has the shunt inductor, L1, in place. Adjust the tuning screw for maximum reading on the 415 meter. Remove the cavity and connect points X and Y. Set the

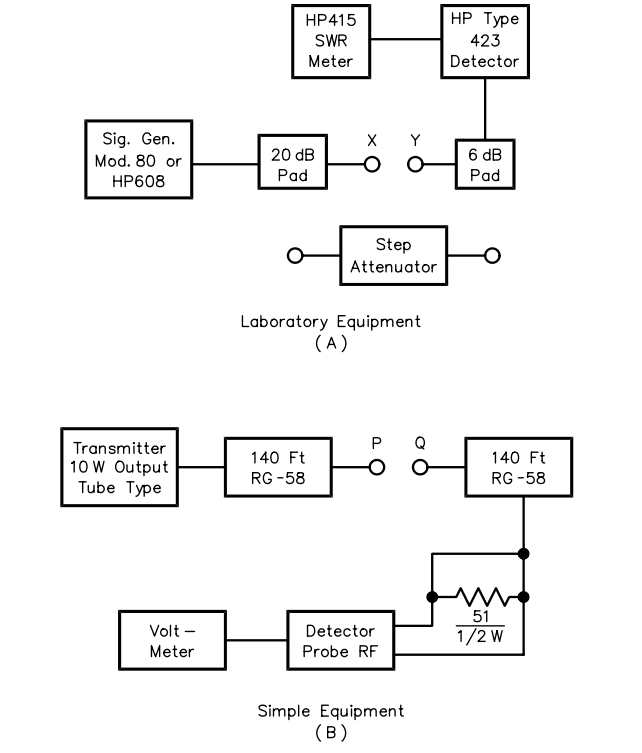

Fig 29—The duplexer can be tuned by either of the two methods shown here, although the method depicted at A is preferred. The signal generator should be modulated by a 1-kHz tone. If the setup shown at B is used, the transmitter should not be modulated, and should have a minimum of noise and spurious signals. The cavities to be aligned are inserted between X and Y in the setup at A, and between P and Q in B.

signal generator to the repeater output frequency and adjust the 415 for a 0 reading on the 20-dB scale.

Reinsert the cavity between X and Y and adjust the cavity tuning for minimum reading on the 415. The notch should be sharp and have a depth of at least 35 dB. It is important to maintain the minimum reading on the meter while tightening the locknut on the tuning shaft.

To check the insertion loss of the cavity, the output from the signal generator should be reduced, and the calibration of the 415 meter checked on the 50-dB expanded scale. Use a fixed 1-dB attenuator to make certain the error is less than 0.1 dB. Replace the attenuator with the cavity and read the loss. The insertion loss should be 0.5 dB or less. The procedure is the same for tuning all six cavities, except that the frequencies are reversed for those having the shunt capacitor installed.

Adjustment with Minimum Equipment

A transmitter with a minimum of spurious output is required. Most modern transmitters meet this requirement. The voltmeter in use should be capable of reading 0.5 volt (or less), full scale. The RF probe used should be rated to 150 MHz or higher. Sections of RG-58 cable are used as attenuators, as shown in Fig 29B. The loss in these 140-foot lengths is nearly 10 dB, and helps to isolate the transmitter in case of mismatch during tuning.

Set the transmitter to the repeater input frequency and connect P and Q. Obtain a reading between 1 and 3 volts on the voltmeter. Insert a cavity with shunt capacitors in place between P and Q and adjust the cavity tuning for a minimum reading on the voltmeter. (This reading should be between 0.01 and 0.05 volt.) The rejection in dB can be calculated by

$$dB = 20 \log (V1/V2)$$

This should be at least 35 dB. Check the insertion loss by putting the receiver on the repeater output frequency and noting the voltmeter reading with the cavity out of the circuit. A 0.5-dB attenuator can be made from a 7-foot length of RG-58. This 7-foot cable can be used to check the calibration of the detector probe and the voltmeter.

Cavities with shunt inductance can be tuned the same way, but with the frequencies reversed. If two or more cavities are tuned while connected together, transmitter noise can cause the rejection readings to be low. In other words, there will be less attenuation.

Results

The duplexer is conservatively rated at 150 watts input, but if constructed carefully should be able to handle as much as 300 watts. Silver plating the interior surfaces of the cavities is recommended if input power is to be greater than 150 watts. A duplexer of this type with silver-plated cavities has an insertion loss of less than 1 dB, and a rejection of more than 100 dB. Unplated cavities should be disassembled at least every two years, cleaned thoroughly, and then retuned.

Miscellaneous Notes

1) Double shielded cable and high quality connectors are *required* throughout the system.
2) The SWR of the antenna should not exceed 1.2:1 for proper duplexer performance.
3) Good shielding of the transmitter and receiver at the repeater is essential.
4) The antenna should have four or more wavelengths of vertical separation from the repeater.
5) Conductors in the near field of the antenna should be well bonded and grounded to eliminate noise.
6) The feed line should be electrically bonded and mechanically secured to the tower or mast.
7) Feed lines and other antennas in the near field of the repeater antenna should be well bonded and as far from the repeater antenna as possible.
8) Individual cavities can be used to improve the performance of separate antenna or separate site repeaters.
9) Individual cavities can be used to help solve intermodulation problems.

BIBLIOGRAPHY

Source material and more extended discussions of the topics covered in this chapter can be found in the references below.

P. Arnold, "Controlling Cavity Drift in Low-Loss Combiners," *Mobile Radio Technology*, Apr 1986, pp 36-44.

L. Barrett, "Repeater Antenna Beam Tilting," *Ham Radio*, May 1983, pp 29-35. (See correction, *Ham Radio*, Jul 1983, p 80.)

W. F. Biggerstaff, "Operation of Close Spaced Antennas in Radio Relay Systems," *IRE Transactions on Vehicular Communications*, Sep 1959, pp 11-15.

J. J. Bilodeau, "A Homemade Duplexer for 2-Meter Repeaters," *QST*, Jul 1972, pp 22-26, 47.

W. B. Bryson, "Design of High Isolation Duplexers and a New Antenna for Duplex Systems," *IEEE Transactions on Vehicular Communications*, Mar 1965, pp 134-140.

K. Connolly and P. Blevins, "A Comparison of Horizontal Patterns of Skeletal and Complete Support Structures," *IEEE 1986 Vehicular Technology Conference Proceedings*, pp 1-7.

S. Kozono, T. Tsuruhara and M. Sakamoto, "Base Station Polarization Diversity Reception for Mobile Radio," *IEEE Transactions on Vehicular Technology*, Nov 1984, pp 301-306.

J. Kraus, *Antennas*, 2nd ed. (New York: McGraw-Hill Book Co., 1988).

W. Pasternak and M. Morris, *The Practical Handbook of Amateur Radio FM & Repeaters*, (Blue Ridge Summit, PA: Tab Books Inc., 1980), pp 355-363.

M. W. Scheldorf, "Antenna-To-Mast Coupling in Com-

munications," *IRE Transactions on Vehicular Communications*, Apr 1959, pp 5-12.

R. D. Shriner, "A Low Cost PC Board Duplexer," *QST*, Apr 1979, pp 11-14.

W. V. Tilston, "Simultaneous Transmission and Reception with a Common Antenna," *IRE Transactions on Vehicular Communications*, Aug 1962, pp 56-64.

E. P. Tilton, "A Trap-Filter Duplexer for 2-Meter Repeaters," *QST*, Mar 1970, pp 42-46.

R. Wheeler, "Fred's Advice solves Receiver Desense Problem," *Mobile Radio Technology*, Feb 1986, pp 42-44.

R. Yang and F. Willis, "Effects of Tower and Guys on Performance of Side Mounted Vertical Antennas," *IRE Transactions on Vehicular Communications*, Dec 1960, pp 24-31.

Chapter 18

VHF and UHF Antenna Systems

A good antenna system is one of the most valuable assets available to the VHF/UHF enthusiast. Compared to an antenna of lesser quality, an antenna that is well designed, is built of good quality materials, and is well maintained, will increase transmitting range, enhance reception of weak signals and reduce interference problems. The work itself building antennas is by no means the least attractive part of the job. Even with high-gain antennas, experimentation is greatly simplified at VHF and UHF because the antennas are a physically manageable size. Setting up a home antenna range is within the means of most amateurs, and much can be learned about the nature and adjustment of antennas. No large investment in test equipment is necessary.

The Basics

Selecting the best VHF or UHF antenna for a given installation involves much more than scanning gain figures and prices in a manufacturer's catalog. There is no one "best" VHF or UHF antenna design for all purposes. The first step in choosing an antenna is figuring out what you want it to do.

Gain

At VHF and UHF, it is possible to build Yagi antennas with very high gain—15 to 20 dBi—on a physically manageable boom. Such antennas can be combined in arrays of two, four, six, eight or more antennas. These arrays are attractive for EME, tropospheric scatter or other weak-signal communications modes.

Radiation Patterns

Antenna radiation can be made omnidirectional, bidirectional, practically unidirectional, or anything between these conditions. A VHF net operator may find an omnidirectional system almost a necessity, but it may be a poor choice otherwise. Noise pickup and other interference problems are greater with such omnidirectional antennas, and omnidirectional antennas having some gain are especially bad in these respects. Maximum gain and low radiation angle are usually prime interests of the weak-signal DX aspirant. A clean pattern, with lowest possible pickup and radiation off the sides and back, may be important in high-activity areas, or where the noise level is high.

Frequency Response

The ability to work over an entire VHF band may be important in some types of work. Modern Yagis can achieve performance over a remarkably wide frequency range, providing that the boom length is long enough and enough elements are used to populate the boom. Modern Yagi designs in fact are competitive with directly driven collinear arrays of similar size and complexity. The primary performance parameters of gain, front-to-rear ratio and SWR can be optimized over all the VHF or UHF amateur bands readily, with the exception of the full 6meter band from 50.0 to 54.0 MHz, which is an 8% wide bandwidth. A Yagi can be easily designed to cover any 2.0 MHz portion of the 6-meter band with superb performance.

Height Gain

In general, higher is better in VHF and UHF antenna installations. Raising the antenna over nearby obstructions may make dramatic improvements in coverage. Within reason, greater height is almost always worth its cost, but height gain (see Chapter 23, Radio Wave Propagation) must be balanced against increased transmission-line loss. This loss can be considerable, and it increases with frequency. The best available line may not be very good if the run is long in terms of wavelengths. Line loss considerations (see Chapter 24, Transmission Lines) are important in antenna planning.

Physical Size

A given antenna design for 432 MHz has the same gain as the same design for 144 MHz, but being only one-third as large intercepts only one-ninth as much energy in receiving. In other words, the antenna has less pickup efficiency at 432 MHz. To be equal in communication effectiveness, the 432-MHz array should be at least equal in *size* to the 144-MHz antenna, which requires roughly three times as many elements. With all the extra difficulties involved in using the higher frequencies effectively, it is best to keep antennas as large as possible for these bands.

DESIGN FACTORS

With the objectives sorted out in a general way, decisions on specifics, such as polarization, type of transmission line, matching methods and mechanical design must be made.

Polarization

Whether to position antenna elements vertically or horizontally has been widely debated since early VHF pioneering days. Tests have shown little evidence about which polarization sense is most desirable. On long propagation paths there is no consistent advantage either way. Shorter paths tend to yield higher signal levels with horizontally polarized antennas over some kinds of terrain. Man-made noise, especially ignition interference, also tends to be lower with horizontal antennas. These factors make horizontal polarization somewhat more desirable for weak-signal communications. On the other hand, vertically polarized antennas are much simpler to use in omnidirectional systems and in mobile work.

Vertical polarization was widely used in early VHF work, but horizontal polarization gained favor when directional arrays started to become widely used. The major use of FM and repeaters, particularly in the VHF/UHF bands, has tipped the balance in favor of vertical antennas in mobile and repeater use. Horizontal polarization predominates in other communication on 50 MHz and higher frequencies. An additional loss of 20 dB or more can be expected when cross-polarized antennas are used.

TRANSMISSION LINES

Transmission line principles are covered in detail in Chapter 24, Transmission Lines. Techniques that apply to VHF and UHF operation are dealt with in greater detail here. The principles of carrying RF from one location to another via a feed line are the same for all radio frequencies. As at HF, RF is carried principally via open wire lines and coaxial cables at VHF/UHF. Certain aspects of these lines characterize them as good or bad for use above 50 MHz.

Properly built open-wire line can operate with very low loss in VHF and UHF installations. A total line loss under 2 dB per 100 feet at 432 MHz can easily be obtained. A line made of #12 wire, spaced $^3/_4$ inch or more with Teflon spreaders and run essentially straight from antenna to station, can be better than anything but the most expensive coax. Such line can be home made or purchased at a fraction of the cost of coaxial cables, with comparable loss characteristics. Careful attention must be paid to efficient impedance matching if the benefits of this system are to be realized. A similar system for 144 MHz can easily provide a line loss under 1 dB.

Small coax such as RG-58 or RG-59 should never be used in VHF work if the run is more than a few feet. Lines of $^1/_2$-inch diameter (RG-8 or RG-11) work fairly well at 50 MHz, and are acceptable for 144-MHz runs of 50 feet or less. These lines are somewhat better if they employ foam instead of ordinary PE dielectric material. Aluminum-jacket *hardline* coaxial cables with large inner conductors and foam insulation are well worth their cost, and can sometimes be obtained for free from local Cable TV operators as "end runs"—pieces at the end of a roll. The most common CATV cable is $^1/_2$-inch OD 75-Ω hardline. Matched-line loss for this cable is about 1.0 dB/100 feet at 146 MHz and 2.0 dB/100 feet at 432 MHz. Less commonly available from CATV companies is the $^3/_4$-inch 75Ω hardline, sometimes with a black self-healing hard plastic covering. This line has 0.8 dB of loss per 100 feet at 146 MHz, and 1.6 dB loss per 100 feet at 432 MHz. There will be small additional losses for either line if 75-to-50Ω transformers are used at each end.

Commercial connectors for hardline are expensive but provide reliable connections with full waterproofing. Enterprising amateurs have homebrewed low-cost connectors. If they are properly water proofed, connectors and hardline can last almost indefinitely. Hardline must not be bent too sharply, because it will kink. See Chapter 24, Transmission Lines, for details on hardline connectors.

Beware of any "bargains" in coax for VHF or UHF use. Feed-line loss can be compensated to some extent by increasing transmitter power, but once lost, a weak signal can never be recovered in the receiver. Effects of weather on transmission lines should not be ignored. Well-constructed open-wire line works optimally in nearly any weather, and it stands up well. Twin-lead is almost useless in heavy rain, wet snow or icing. The best grades of

coax are completely impervious to weather—they can be run underground, fastened to metal towers without insulation and bent into any convenient position with no adverse effects on performance.

WAVEGUIDES

Above 2 GHz, coaxial cable is a losing proposition for communications work. Fortunately, at this frequency the wavelength is short enough to allow practical, efficient energy transfer by an entirely different means. A *waveguide* is a conducting tube through which energy is transmitted in the form of electromagnetic waves. The tube is not considered as carrying a current in the same sense that the wires of a two-conductor line do, but rather as a *boundary* that confines the waves in the enclosed space. Skin effect prevents any electromagnetic effects from being evident outside the guide. The energy is injected at one end, either through capacitive or inductive coupling or by radiation, and is removed from the other end in a like manner. Waveguide merely confines the energy of the fields, which are propagated through it to the receiving end by means of reflections against its inner walls.

Analysis of waveguide operation is based on the assumption that the guide material is a perfect conductor of electricity. Typical distributions of electric and magnetic fields in a rectangular guide are shown in **Fig 1**. The intensity of the electric field is greatest (as indicated by closer spacing of the lines of force) at the center along the X dimension (Fig 1C), diminishing to zero at the end walls. The fields must diminish in this manner, because the existence of any electric field parallel to the walls at the surface would cause an infinite current to flow in a perfect conductor. Waveguides, of course, cannot carry RF in this fashion.

Modes of Propagation

Fig 1 represents the most basic distribution of the electric and magnetic fields in a waveguide. There are an infinite number of ways in which the fields can arrange themselves in a waveguide (for frequencies above the low cutoff frequency of the guide in use). Each of these field configurations is called a *mode*.

The modes may be separated into two general groups. One group, designated *TM* (transverse magnetic), has the magnetic field entirely transverse to the direction of propagation, but has a component of the electric field in that direction. The other type, designated *TE* (transverse electric) has the electric field entirely transverse, but has a component of magnetic field in the direction of propagation. TM waves are sometimes called *E waves*, and TE waves are sometimes called *H waves*, but the TM and TE designations are preferred.

The mode of propagation is identified by the group letters followed by two subscript numerals. For example, TE_{10}, TM_{11}, etc. The number of possible modes increases with frequency for a given size of guide, and there is only one possible mode (called the *dominant mode*) for the lowest frequency that can be transmitted. The dominant mode is the one generally used in amateur work.

Waveguide Dimensions

In rectangular guide the critical dimension is X in Fig 1. This dimension must be more than $^1/_2$ λ at the lowest frequency to be transmitted. In practice, the Y dimension usually is made about equal to $^1/_2$ X to avoid the possibility of operation in other than the dominant mode.

Cross-sectional shapes other than a rectangle can be used, the most important being the circular pipe. Much the same considerations apply as in the rectangular case.

Wavelength dimensions for rectangular and circular guides are given in **Table 1**, where X is the width of a rectangular guide and r is the radius of a circular guide. All figures apply to the dominant mode.

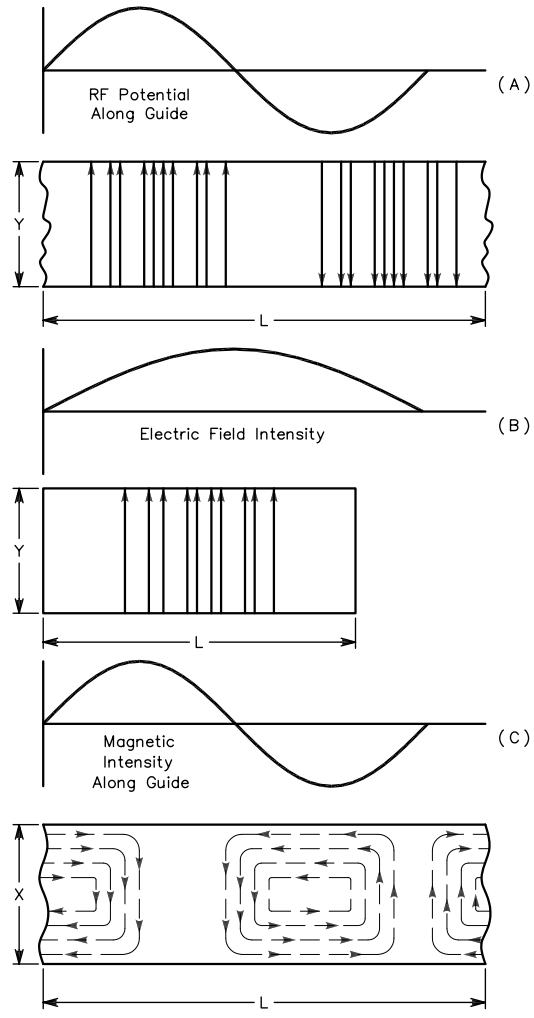

Fig 1—Field distribution in a rectangular waveguide. The TE10 mode of propagation is depicted.

Coupling to Waveguides

Energy may be introduced into or extracted from a waveguide or resonator by means of either the electric or magnetic field. The energy transfer frequently is through a coaxial line. Two methods for coupling to coaxial line are shown in **Fig 2**. The probe shown at A is simply a short extension of the inner conductor of the coaxial line, oriented so that it is parallel to the electric lines of force. The loop shown at B is arranged so that it encloses some of the magnetic lines of force. The point at which maximum coupling is obtained depends upon the mode of propagation in the guide or cavity. Coupling is maximum when the coupling device is in the most intense field.

Coupling can be varied by turning the probe or loop through a 90° angle. When the probe is perpendicular to the electric lines the coupling is minimum. Similarly, when the plane of the loop is parallel to the magnetic lines the coupling is minimum.

If a waveguide is left open at one end it will radiate energy. This radiation can be greatly enhanced by flaring the waveguide to form a pyramidal horn antenna. The horn acts as a transition between the confines of the waveguide and free space. To effect the proper impedance transformation the horn must be at least $^1/_2\ \lambda$ on a side. A horn of this dimension (cutoff) has a unidirectional radiation pattern with a null toward the waveguide transition. The gain at the cutoff frequency is 3 dB, increasing 6 dB with each doubling of frequency. Horns are used extensively in microwave work, both as primary radiators and as feed elements for more elaborate focusing systems. Details for constructing 10-GHz horn antennas are given later in this chapter.

Evolution of a Waveguide

Suppose an open-wire line is used to carry RF energy from a generator to a load. If the line has any appreciable length it must be mechanically supported. The line must be well insulated from the supports if high losses are to be avoided. Because high-quality insulators are difficult to construct at microwave frequencies, the logical alternative is to support the transmission line with $^1/_4\ \lambda$ stubs, shorted at the end opposite the feed line. The open end of such a stub presents an infinite impedance to the transmission line, provided the shorted stub is nonreactive. However, the shorting link has a finite length, and therefore some inductance. The effect of this inductance can be removed by making the RF current flow on the surface of a plate rather than a thin wire. If the plate is large enough, it will prevent the magnetic lines of force from encircling the RF current.

An infinite number of these $^1/_4\ \lambda$ stubs may be connected in parallel without affecting the standing waves of voltage and current. The transmission line may be supported from the top as well as the bottom, and when an infinite number of supports are added, they form the walls of a waveguide at its cutoff frequency. **Fig 3** illustrates how a rectangular waveguide evolves from a two-wire parallel transmission line as described. This simplified analysis also shows why the cutoff dimension is $^1/_2\ \lambda$.

Table 1
Waveguide Dimensions

	Rectangular	*Circular*
Cutoff wavelength	2X	3.41r
Longest wavelength transmitted with little attenuation	1.6X	3.2r
Shortest wavelength before next mode becomes possible	1.1X	2.8r

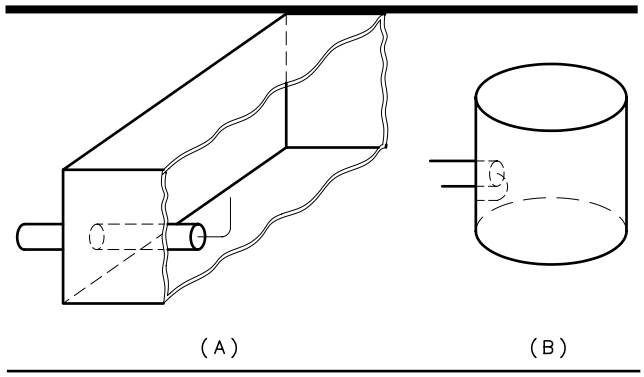

Fig 2—Coupling coaxial line to waveguide and resonators.

While the operation of waveguides is usually described in terms of fields, current does flow on the inside walls, just as on the conductors of a two-wire transmission line. At the waveguide cutoff frequency, the current is concentrated in the center of the walls, and disperses toward the floor and ceiling as the frequency increases.

IMPEDANCE MATCHING

Impedance matching is covered in detail in Chapter 25, Coupling the Transmitter to the Line, and Chapter 26, Coupling the Line to the Antenna. The theory is the same for frequencies above 50 MHz. Practical aspects are similar, but physical size can be a major factor in the choice of methods. Only the matching devices used in practical construction examples later in this chapter are discussed in detail here. This should not rule out consideration of other methods, however, and you should read the relevant portions of both Chapters 25 and 26.

Universal Stub

As its name *universal stub* implies, the double-adjustment stub of **Fig 4A** is useful for many matching purposes. The stub length is varied to resonate the system and the transmission-line attachment point is varied until the transmission line and stub impedances are equal. In practice this involves moving both the sliding short and

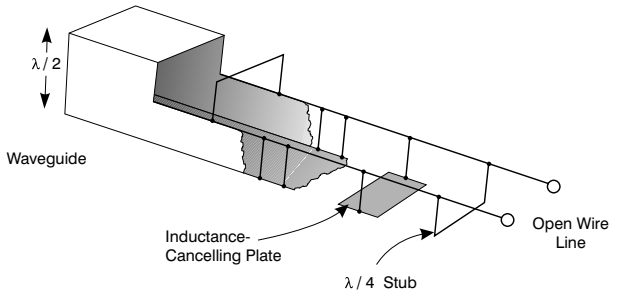

Fig 3—At its cutoff frequency a rectangular waveguide can be thought of as a parallel two-conductor transmission line supported from top and bottom by an infinite number of $^1/_4$-λ stubs.

the point of line connection for zero reflected power, as indicated on an SWR bridge connected in the line.

The universal stub allows for tuning out any small reactance present in the driven part of the system. It permits matching the antenna to the line without knowledge of the actual impedances involved. The position of the short yielding the best match gives some indication of the amount of reactance present. With little or no reactive component to be tuned out, the stub must be approximately $^1/_2$ λ from load toward the short.

The stub should be made of stiff bare wire or rod, spaced no more than $^1/_{20}$ λ apart. Preferably it should be mounted rigidly, on insulators. Once the position of the short is determined, the center of the short can be grounded, if desired, and the portion of the stub no longer needed can be removed.

It is not necessary that the stub be connected directly to the driven element. It can be made part of an open-wire line as a device to match coaxial cable to the line. The stub can be connected to the lower end of a delta match or placed at the feed point of a phased array. Examples of these uses are given later.

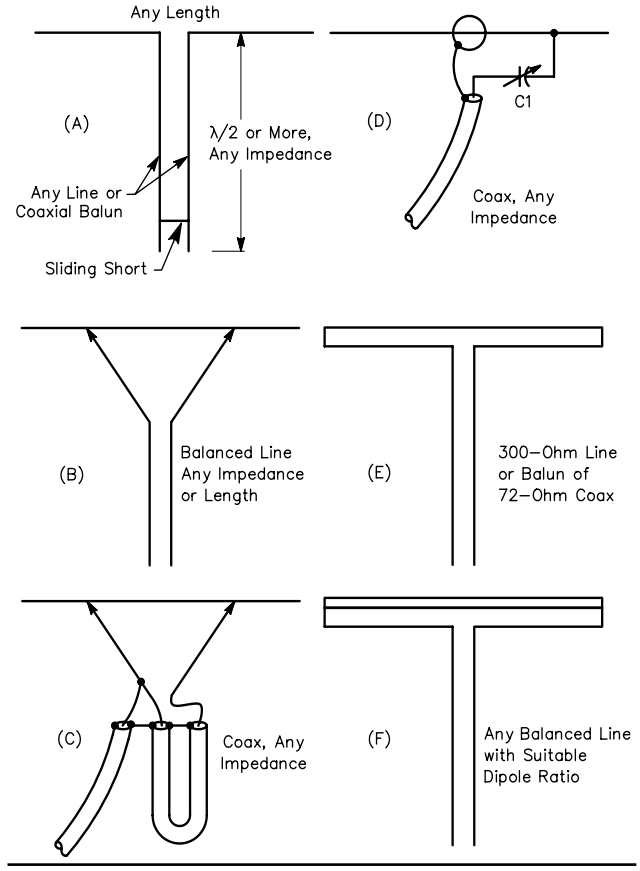

Fig 4—Matching methods commonly used at VHF. The universal stub, A, combines tuning and matching. The adjustable short on the stub and the points of connection of the transmission line are adjusted for minimum reflected power on the line. In the delta match, B and C, the line is fanned out and connected to the dipole at the point of optimum impedance match. Impedances need not be known in A, B or C. The gamma match, D, is for direct connection of coax. C1 tunes out inductance in the arm. A folded dipole of uniform conductor size, E, steps up antenna impedance by a factor of four. Using a larger conductor in the unbroken portion of the folded dipole, F, gives higher orders of impedance transformation.

Delta Match

Probably the most basic impedance matching device is the *delta match*, fanned ends of an open-wire line tapped onto a $^1/_2$ λ antenna at the point of the most-efficient power transfer. This is shown in Fig 4B. Both the side length and the points of connection either side of the center of the element must be adjusted for minimum reflected power on the line, but as with the universal stub, you needn't know the impedances. The delta match makes no provision for tuning out reactance, so the universal stub is often used as a termination for it.

At one time, the delta match was thought to be inferior for VHF applications because of its tendency to radiate if improperly adjusted. The delta has come back into favor now that accurate methods are available for measuring the effects of matching. It is very handy for phasing multiple-bay arrays with open-wire lines, and its dimensions in this use are not particularly critical. It should be checked out carefully in applications like that of Fig 4C, where no tuning device is used.

Gamma and T Matches

An application of the same principle allowing direct connection of coax is the *gamma match*, Fig 4D. Because the RF voltage at the center of a $^1/_2$ λ dipole is zero, the outer conductor of the coax is connected to the element at this point. This may also be the junction with a metallic or wooden boom. The inner conductor, carrying the RF current, is tapped out on the element at the matching point. Inductance of the arm is tuned out by

means of C1, resulting in electrical balance. Both the point of contact with the element and the setting of the capacitor are adjusted for zero reflected power, with a bridge connected in the coaxial line.

The capacitance can be varied until the required value is found, and the variable capacitor replaced with a fixed unit of that value. C1 can be mounted in a waterproof box. The maximum required value should be about 100 pF for 50 MHz and 35 to 50 pF for 144 MHz.

The capacitor and arm can be combined in one coaxial assembly, with the arm connected to the driven element by means of a sliding clamp and the inner end of the arm sliding inside a sleeve connected to the center conductor of the coax. An assembly of this type can be constructed from concentric pieces of tubing, insulated by plastic or heat-shrink sleeving. RF voltage across the capacitor is low when the match is adjusted properly, so with a good dielectric, insulation presents no great problem. The initial adjustment should be made with low power. A clean, permanent high-conductivity bond between arm and element is important, since the RF current is high at this point.

Because it is inherently somewhat unbalanced, the gamma match can sometimes introduce pattern distortion, particularly on long-boom, highly directive Yagi arrays. The *T-match*, essentially two gamma matches in series creating a balanced feed system, has become popular for this reason. A coaxial balun like that shown in **Fig 5** is used from the 200 Ω balanced T-match to the unbalanced 50 Ω coaxial line going to the transmitter. See the K1FO Yagi designs later in this chapter for details on practical use of a T-match.

Folded Dipole

The impedance of a $^1/_2$ λ dipole broken at its center is about 70 Ω. If a single conductor of uniform size is folded to make a $^1/_2$ λ dipole as shown in Fig 4E, the impedance is stepped up four times. Such a folded dipole can be fed directly with 300Ω line with no appreciable mismatch. If a 4:1 balun is used, the antenna can be fed with 75Ω coaxial cable. (See balun information presented below.) Higher step-up impedance transformation can be obtained if the unbroken portion is made larger in cross-section than the fed portion, as shown in Fig 4F.

Hairpin Match

The feed-point resistance of most multielement Yagi arrays is less than 50 Ω. If the driven element is split and fed at the center, it may be shortened from its resonant length to add capacitive reactance at the feed point. Then, shunting the feed point with a wire loop resembling a *hairpin* causes a step-up of the feed-point resistance. The hairpin match is used together with a 4:1 coaxial balun in the 50 MHz arrays described later in this chapter. See Chapter 26, Coupling the Line to the Antenna, for details on the hairpin match.

BALUNS AND ANTENNA TUNERS

Conversion from balanced loads to unbalanced lines (or vice versa) can be performed with electrical circuits, or their equivalents made of coaxial cable. A balun made from flexible coax is shown in Fig 5A. The looped portion is an electrical $^1/_2$ λ. The physical length depends on the velocity factor of the line used, so it is important to check its resonant frequency as shown in Fig 5B. The two ends are shorted, and the loop at one end is coupled to a dip meter coil. This type of balun gives an impedance step-up of 4:1 (typically 50 to 200 Ω, or 75 to 300 Ω).

Coaxial baluns that yield 1:1 impedance transformations are shown in **Fig 6**. The coaxial sleeve, open at the top and connected to the outer conductor of the line at the lower end (A) is the preferred type. At B, a conductor of approximately the same size as the line is used with the outer conductor to form a $^1/_4$ λ stub. Another piece of coax, using only the outer conductor, will serve this purpose. Both baluns are intended to present an infi-

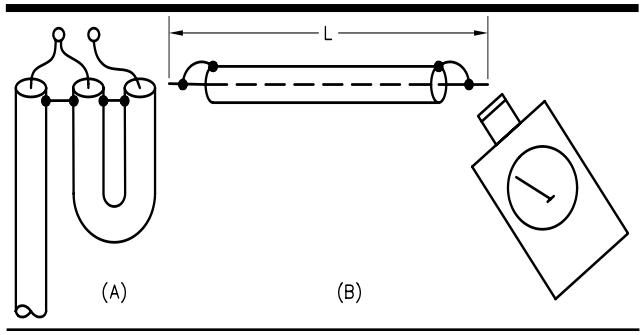

Fig 5—Conversion from unbalanced coax to a balanced load can be done with a ½-λ, coaxial balun at A. Electrical length of the looped section should be checked with a dip meter, with the ends shorted, as at B. The $^1/_2$-λ balun gives a 4:1 impedance step-up.

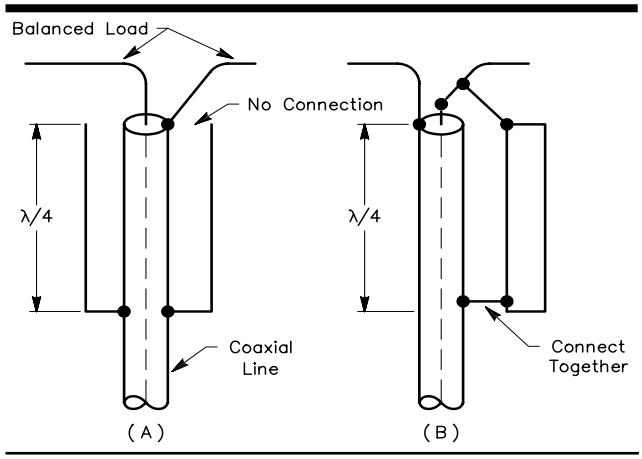

Fig 6—The balun conversion function, with no impedance transformation, can be accomplished with ¼-λ lines, open at the top and connected to the coax outer conductor at the bottom. The coaxial sleeve at A is preferred.

nite impedance to any RF current that might otherwise flow on the outer conductor of the coax.

The functions of the balun and the impedance transformer can be handled by various tuned circuits. Such a device, commonly called an *antenna tuner* or a *Transmatch*, can provide a wide range of impedance transformations. Additional selectivity inherent in the antenna tuner can reduce RFI problems.

THE YAGI AT VHF AND UHF

Without doubt, the Yagi is king of home-station antennas these days. Today's best designs are computer optimized. For years amateurs as well as professionals designed Yagi arrays experimentally. Now we have powerful (and inexpensive) personal computers and sophisticated software for antenna modeling. These have brought us antennas with improved performance, with little or no element pruning required. Chapter 11, HF Yagi Arrays, describes the parameters associated with Yagi-Uda arrays. Except for somewhat tighter dimensional tolerances needed at VHF and UHF, the properties that make a good Yagi at HF also are needed on the higher frequencies. See the end of this chapter for practical Yagi designs.

STACKING YAGIS

Where suitable provision can be made for supporting them, two Yagis mounted one above the other and fed in phase can provide better performance than one long Yagi with the same theoretical or measured gain. The pair occupies a much smaller turning space for the same gain, and their wider elevation coverage can provide excellent results. The wide azimuthal coverage for a vertical stack often results in QSOs that might be missed with a single narrow-beam long-boom Yagi pointed in a different direction. On long ionospheric paths, a stacked pair occasionally may show an *apparent* gain much greater than the measured 2 to 3 dB of stacking gain. (See also the extensive section on stacking Yagis in Chapter 11, HF Yagi Arrays.)

Optimum vertical spacing for Yagis with boom longer than 1 λ or more is about 1 λ (984/50.1 = 19.64 feet), but this may be too much for many builders of 50-MHz antennas to handle. Worthwhile results can be obtained with as little as $^1/_2$ λ (10 feet), but $^5/_8$ λ (12 feet) is markedly better. The difference between 12 and 20 feet, however, may not be worth the added structural problems involved in the wider spacing, at least at 50 MHz. The closer spacings give lower measured gain, but the antenna patterns are cleaner in both azimuth and elevation than with 1 λ spacing. Extra gain with wider spacings is usually the objective on 144 MHz and higher-frequency bands, where the structural problems are not as severe.

Yagis can also be stacked in the same plane (collinear elements) for sharper azimuthal directivity. A spacing of $^5/_8$ λ between the ends of the inner elements yields the maximum gain within the main lobe of the array.

If individual antennas of a stacked array are properly designed, they look like noninductive resistors to the phasing system that connects them. The impedances involved can thus be treated the same as resistances in parallel.

Three sets of stacked dipoles are shown in **Fig 7**. Whether these are merely dipoles or the driven elements of Yagi arrays makes no difference for the purpose of these examples. Two 300 Ω antennas at A are 1 λ apart, resulting in a paralleled feed-point impedance of 150 Ω at the center. (Actually it is slightly less than 150 Ω because of coupling between bays, but this can be neglected for illustrative purposes.) This value remains the same regardless of the impedance of the phasing line. Thus, any convenient line can be used for phasing, as long as the *electrical* length of each line is the same.

The velocity factor of the line must be taken into account as well. As with coax, this is subject to so much variation that it is important to make a resonance check on the actual line used. The method for doing this is shown in Fig 5B. A $^1/_2$ λ line is resonant both open and shorted, but the shorted condition (both ends) is usually the more convenient test condition.

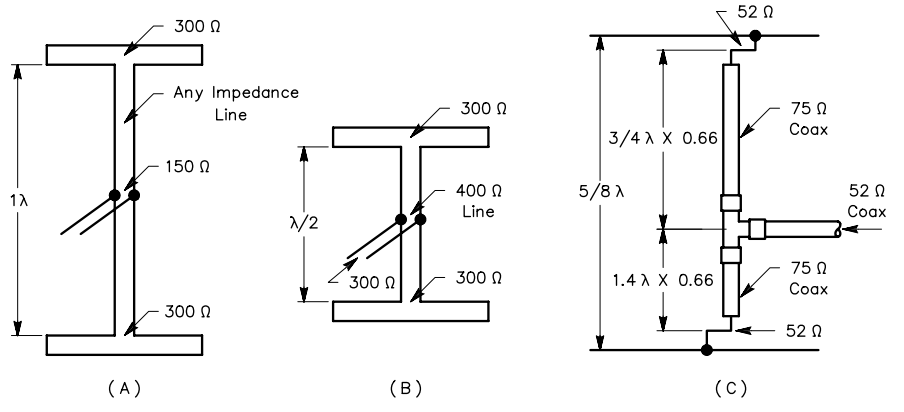

Fig 7—Three methods of feeding stacked VHF arrays. A and B are for bays having balanced driven elements, where a balanced phasing line is desired. Array C has an all-coaxial matching and phasing system. If the lower section is also $^3/_4$ λ no transposition of line connections is needed.

The impedance transforming property of a 1/4 λ line section can be used in combination matching and phasing lines, as shown in Fig 7B and C. At B, two bays spaced 1/2 λ apart are phased and matched by a 400-Ω line, acting as a double-Q section, so that a 300-Ω main transmission line is matched to two 300-Ω bays. The two halves of this phasing line could also be 3/4-λ or 5/4-λ long, if such lengths serve a useful mechanical purpose. (An example is the stacking of two Yagis where the desirable spacing is more than 1/2 λ.)

A double-Q section of coaxial line is illustrated in Fig 7C. This is useful for feeding stacked bays that were designed for 50-Ω feed. A spacing of 5/8 λ is useful for small Yagis, and this is the equivalent of a full electrical wavelength of solid-dielectric coax such as RG-11.

If one phasing line is electrically 1/4 λ and 3/4 λ on the other, the connection to one driven element should be reversed with respect to the other to keep the RF currents in the elements in phase—the gamma match is located on opposite sides of the driven elements in Fig 7C. If the number of 1/4 λ lengths is the same on either side of the feed point, the two connections should be in the same position, and not reversed. Practically speaking however, you can ensure proper phasing by using exactly equal lengths of line from the same roll of coax. This ensures that the velocity factor for each line is identical.

One marked advantage of coaxial phasing lines is that they can be wrapped around the vertical support, taped or grounded to it, or arranged in any way that is mechanically convenient. The spacing between bays can be set at the most desirable value, and the phasing lines placed anywhere necessary.

Stacking Yagis for Different Frequencies

In stacking horizontal Yagis one above the other on a single rotating support, certain considerations apply when the bays are for different bands. As a very general rule of thumb, the minimum desirable spacing is half the boom length of the higher frequency Yagi.

For example, assume the stacked two-band array of **Fig 8A** is for 50 and 144 MHz. This vertical arrangement is commonly referred to as a *Christmas tree*, because it resembles one. The 50MHz Yagi has 5elements on a 12-foot boom. It tends to look like "ground" to the 8-element 144 MHz Yagi on a 12-foot boom directly above it. [The exact Yagi designs for the examples used in this section are located on the CD-ROM accompanying this book. They may be evaluated as monoband Yagis using the *YW* (Yagi for Windows) program also supplied on the CD-ROM. In each case the bottom Yagi in the stack (at the top of the tower) is assumed to be 20 feet high.]

SWR Change in a Multi-Frequency Stack

Earlier editions of *The ARRL Antenna Book* stated that the feed-point impedance of the higher-frequency antenna would likely be affected the most by the proxim-

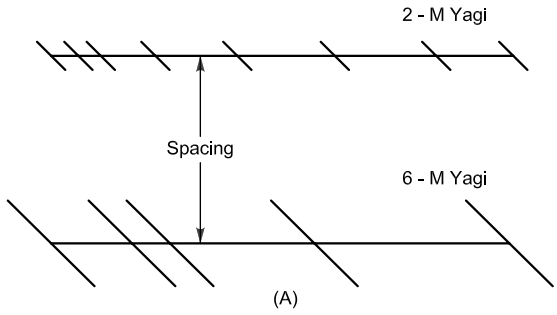

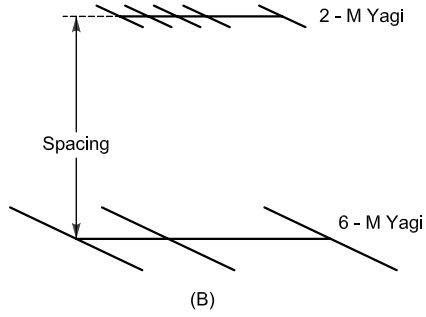

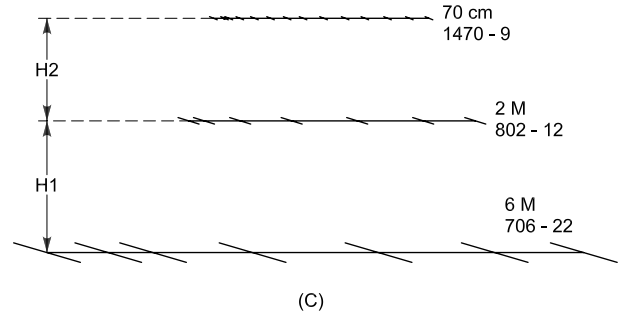

Fig 8—In stacking Yagi arrays one above the other, the minimum spacing between bays (S) should be about half the boom length of the smaller array. Wider spacing is desirable, in which case it should be ½ λ or some multiple thereof, at the frequency of the smaller array. At A, stack of 8-element 2-meter Yagi on a 12-foot boom over a 5-element 6-meter Yagi, also on a 12-foot boom. At B, 5-element 2-meter beam on a 6-foot boom over a 3-element 6-meter beam on a 4-foot boom. At C, a 14-element 70-cm beam on a 9-foot boom, mounted over a 8-element 2-meter beam on a 12-foot boom and a 7-element 6-meter beam on a 22-foot boom.

ity of the lower-frequency Yagi. Modern computer modeling programs reveal that while the feed-point SWR can indeed be affected, by far the greatest degradation is in the forward gain and rearward pattern of the higher-frequency Yagi when the booms are closely spaced. In fact, the SWR curve is usually not affected enough to make it a good diagnostic indicator of interaction between the two Yagis.

Fig 9 shows an overlay of the SWR curves across the 2-meter band for four configurations: an 8-element 2-meter Yagi by itself, and then over a 5-element 6-meter Yagi with spacings between the booms of 1, 2, 4 and 6 feet. The SWR curves are similar—it would be difficult to see any difference between these configurations using typical amateur SWR indicators for anything but the very closest (1-foot) spacing. For example, the SWR curve for the 2-foot spacing case is virtually indistinguishable from that of the Yagi by itself, while the forward gain has dropped more than 0.6 dB because of interactions with the 6-meter Yagi below it.

Gain and Pattern Degradation Due to Stacking

Fig 10 shows four overlaid rectangular plots of the azimuth response from 0° to 180° for the 8-element 2-meter Yagi described above, spaced 1, 2, 4 and 6 feet over a 5-element 6-meter beam. The rectangular presentation gives more detail than a polar plot. The most closely spaced configuration (with 1-foot spacing between the booms) shows the largest degradation in the forward gain, a drop of 1.7 dB. The worst-case front-to-rear ratio for the 6-foot spacing is 29.0 dB, while it is 36.4 dB for the 1-foot spacing—actually better than the F/R for the 8-element 2-meter Yagi by itself. Performance change due to the nearby presence of other Yagis can be enormously complicated (and sometimes is non-intuitive as well).

What happens when a different kind of 6-meter Yagi is mounted below the 8-element 2-meter Yagi? **Fig 11** compares the change in forward gain and the worst-case F/R performance as a function of spacing between the booms for two varieties of 6-meter Yagis: the 5-element design on a 12-foot boom and a 7-element Yagi on a

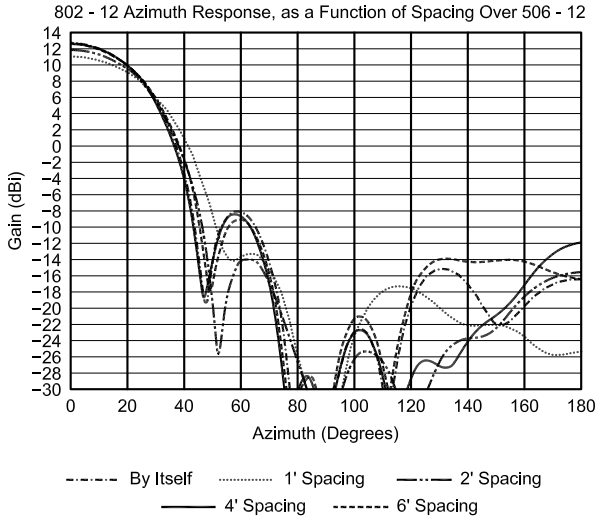

Fig 10—Plots of the 8-element 2-meter Yagi's azimuth response from 0° to 180° for spacing distances from 1 to 6 feet. The sidelobe at about 60° varies about 6 dB over the range of boom spacings, while the shape of worst-case F/R curve varies considerably due to interactions with the lower 6-meter beam. The gain for the 1-foot spacing is degraded by more than 3 dB compared to the 2-meter antenna by itself.

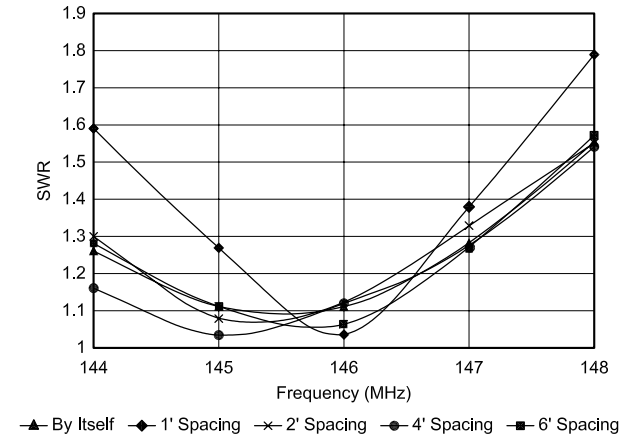

Fig 9—SWR curves for different boom spacing between 8-element 2-meter Yagi on 12-foot boom, over a 5-element 6-meter Yagi on a 12-foot boom. For spacings greater than 1 foot between the booms, differences between the SWR curves are difficult to discern.

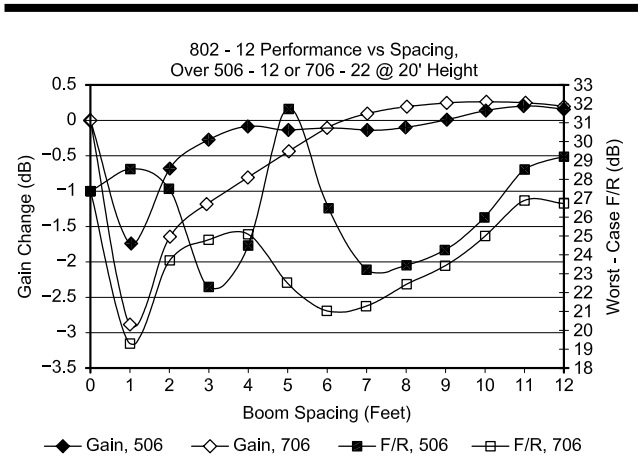

Fig 11—Plot of 8-element 2-meter Yagi's gain and worst-case F/R as a function of distance over two types of 6-meter beams, one on a 12-foot boom and the other on a 22-foot boom. Beyond a spacing of about 5 feet the performance is degraded a minimal amount.

22-foot boom. The spacing of "0 feet" represents the 8-element 2-meter Yagi when it is used alone, with no other antenna nearby. This sets the reference expectations for gain and F/R.

The most severe degradation occurs for the 1-foot spacing, as you might imagine, for both the 12 and 22-foot boom lengths. Over the 5-element 6-meter Yagi, the 2-meter gain doesn't recover to the reference level of the 8-element 2-meter beam by itself until the spacing is greater than 9 feet. However, the gain is within 0.25 dB of the reference level for spacings of 3 feet or more. Interestingly, the F/R is higher than that of the 2-meter antenna by itself for the 1, 2 and 5-foot spacings and for spacings greater than 11 feet. The 2-meter F/R in the presence of the 12-foot 5-element 6-meter Yagi remains above 20 dB for spacings beyond 1 feet.

Overall, the 2-meter beam performs reasonably well for spacings of 3 feet or more over the 5-element 6-meter Yagi. Put another way, the 2-meter beam's performance is degraded only slightly for boom spacings greater than 3 feet. A spacing of 3 feet is less than the old rule of thumb that the minimum spacing between booms be greater than one-half the boomlength of the higher-frequency Yagi, which in this case is 6 feet long.

For the 7-element 6-meter Yagi, the 2-meter gain recovers to the reference level for spacings beyond 7 feet, but the F/R is degraded below the reference level for all spacings shown in Fig 11. If we use a gain reduction criterion of less than 0.25 dB and a 20-dB F/R level as the minimum acceptable level, then the spacing must be 5 feet or more over the larger 6-meter Yagi. Again, this is less than the rule of thumb that the minimum spacing between booms be greater than one-half the boomlength of the higher-frequency Yagi.

Now, let's try a smaller setup of 2- and 6-meter Yagis stacked vertically in a Christmas-tree configuration to see if the rule of thumb for spacing the booms still holds. **Fig 12** shows the performance curves versus boom spacing for a 5-element 2-meter Yagi on a 4-foot boom stacked over a 3-element 6-meter Yagi on a 6-foot boom. Again, the 1-foot spacing produces a substantial gain reduction of about 1.3 dB compared to the reference gain when the 2-meter Yagi is used by itself. Beyond a boom spacing of 3 feet the 2-meter gain drops less than 0.25 dB from the reference level of the 2-meter Yagi by itself and the F/R remains above about 20 dB. In this example, the simple rule of thumb that the minimum spacing between booms be greater than half the boom length (half of 4 feet) of the higher-frequency Yagi does not hold up. However, the same minimum spacing of 3 feet we found for the larger 2-meter Yagi remains true. Three feet spacing is almost 0.5 λ between the booms at the higher frequency.

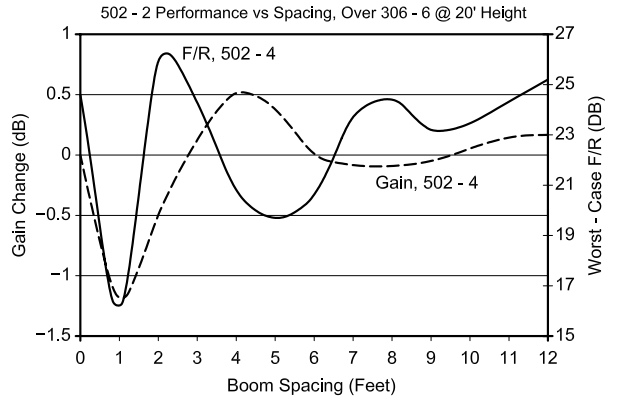

Fig 12— Plot of gain and worst-case F/R of a 5-element 2-meter Yagi on a 4-foot boom as a function of distance over a 3-element 6-meter beam on a 6-foot boom. Beyond a spacing of about 3 feet the performance is degraded a minimal amount.

Adding a 70-cm Yagi to the Christmas Tree

Let's get more ambitious and set up a larger VHF/UHF Christmas tree, with a 14-element 70-cm Yagi on a 9-foot boom at the top, mounted 5 feet over an 8-element 2-meter Yagi on a 12-foot boom. At the bottom of the stack (at the top of the tower) is either the 5-element 6-meter beam on a 12-foot boom, or a 7-element 6-meter beam on a 22-foot boom. See Fig 8C. As before, we will vary the spacing between the 70-cm Yagi and the 2-meter Yagi below it to assess the interactions that degrade the 70-cm performance.

Fig 13 compares the change in gain and F/R curves as a function of boom spacings between the 70-cm and 2-meter Yagis for the two different 6-meter Yagis (with a fixed distance of 5 feet between the 2-meter and 6-meter Yagis). In this example, the 70-cm Yagi was designed to be an intrinsic 50-Ω feed, where the F/R has been compromised to some extent. Still, the F/R is greater than 20 dB when the 70-cm Yagi is used by itself.

For spacings greater than 4 feet between the 70-cm and 2-meter booms, the 70-cm gain is equal to or even slightly greater than that of the 70-cm antenna by itself. The increase of gain indicates that the elevation pattern of the 70-cm antenna is slightly compressed by the presence of the other Yagis below it. The F/R stays above at 19.5 dB for spacings greater than or equal to 4 feet. This falls just below our desired lower limit of 20 dB, but it is highly doubtful that anyone would notice this 0.5-dB drop in actual operation. A spacing of 4 feet between booms falls under the rule of thumb that the minimum spacing be at least half the boomlength of the higher-frequency Yagi, which in this case is 9 feet.

What should be obvious in this discussion is that you should model the exact configuration you plan to build to avoid unnecessary performance degradation.

Stacking Same-Frequency Yagis

This subject has been examined in some detail in Chapter 11, HF Yagi Arrays. The same basic principles

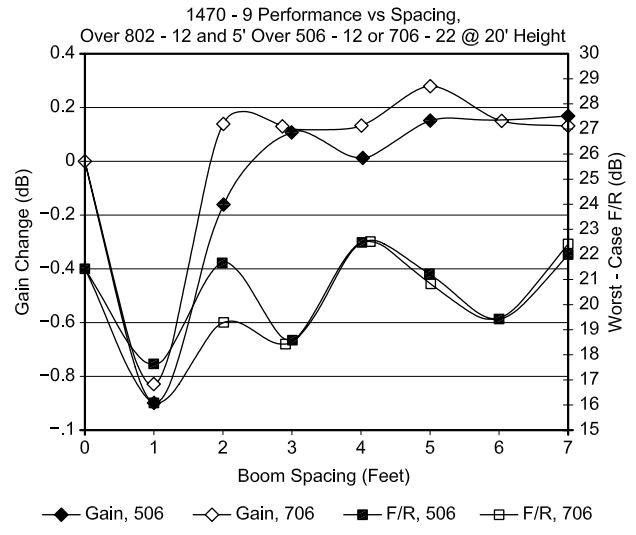

Fig 13—Performance of a 14-element 70-cm Yagi on a 9-foot boom, mounted a variable distance over an 8-element 2-meter Yagi on a 12-foot boom, which is mounted 5 feet above either a 5-element 6-meter Yagi on a 12-foot boom or a 7-element 6-meter Yagi on a 22-foot boom. Beyond a spacing of about 4 feet, the performance of the 70-cm beam is degraded a minimal amount.

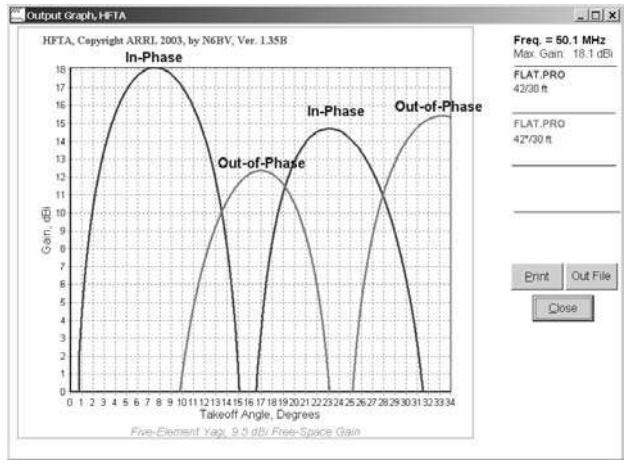

Fig 14—*HFTA* comparison plots of the elevation responses for two 5-element 6-meter Yagis mounted at 42 and 30 feet above flat ground, when they are fed in-phase and out-of-phase. By switching the phasing (adding a half-wavelength of coax to one of the antennas), the elevation angle can be controlled to enhance performance when a Sporadic-E cloud is nearly overhead.

hold at VHF and UHF as they do on HF. That is, the gain increases gradually with increasing spacing between the booms, and then falls off gradually past a certain spacing distance.

At HF, Chapter 11 emphasizes that you should avoid nulls in the antenna's elevation response—so that you can cover all the angles needed for geographic areas of interest. At VHF/UHF, propagation is usually at low elevation angles for most propagation modes, and signals are often extremely weak. Thus, achieving maximum gain is the most common design objective for a VHF/UHF stack. Of secondary importance is the cleanliness of the beam pattern, to discriminate against interference and noise sources.

Six-meter Sporadic-E can sometimes occur at high elevation angles, especially if the E_s cloud is overhead, or nearly overhead. Since Sporadic-E is exactly that, *sporadic*, it's not a good design practice to try to cover a wide range of elevation angles, as you must often do at HF to cover large geographic areas. On 6 meters, you can change to high-angle coverage when necessary. For example, you might switch to a separate Yagi mounted at a low height, or you might provide means to feed stacked antennas out-of-phase. **Fig 14** shows an *HFTA* (HF Terrain Assessment) plot of two 5-element 6-meter Yagis, fed either in-phase or out-of-phase to cover a much wider range of elevation angles than the in-phase stack alone.

Fig 15A shows the change in gain for four 2-meter stacked designs, as a function of the spacing in wavelengths between the booms. The 3-element Yagi is mounted on a 2-foot boom (occupying 0.28 λ of that boom). The 5-element Yagi is on a 4-foot boom (0.51 λ of the boom), while the 8-element Yagi is on a 12-foot boom (1.72 λ of boom). The biggest antenna in the group has 16 elements, on a 27-foot boom (4.0 λ of boom). This range of boom lengths pretty much covers the practical range of antennas used by hams.

The stack of two 3-element Yagis peaks at 3.2 dB of additional gain over a single Yagi for 0.75 λ spacing between the booms. Further increases in spacing see the gain change gradually drop off. Fig 15B shows the worst-case F/R of the four stacks, again as a function of boom length. The F/R of a single 3-element Yagi is just over 24 dB, but in the presence of the second 3-element Yagi in the stack, the F/R of the pair oscillates between 15 to 26 dB, finally remaining consistently over the desired 20-dB level for spacings greater than about 1.7 λ, where the gain has fallen about 0.6 dB from the peak possible gain. A boom spacing of 1.7 λ at 146 MHz is 11.5 feet. Thus you must compromise in choosing the boom spacing between achieving maximum gain and the best pattern.

The increase in gain of the stack of two 5-element Yagis peaks at a spacing of about 1 λ (6.7 feet), where the F/R is an excellent 25 dB. Having more elements on a particular length of boom aids in holding a more consistent F/R in the presence of the second antenna.

The gain increase for the bigger stack of 8-element Yagis peaks at a spacing of about 1.5 λ (10.1 feet), where the F/R is more than 27 dB. The 16-element Yagi's gain

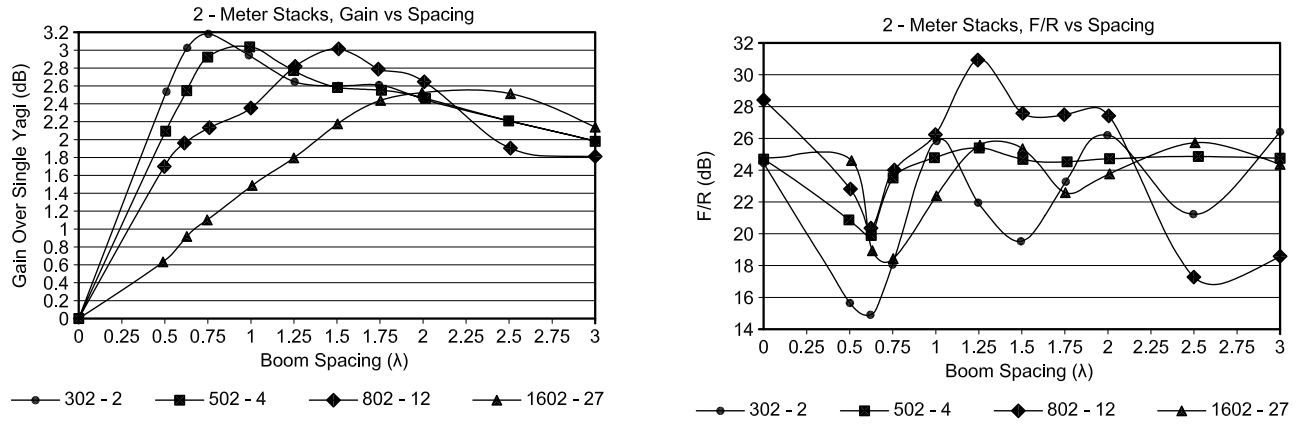

Fig 15—Performance of two different 2-meter Yagis (5-elements on 4-foot boom and 8-elements on 12-foot boom) fed in-phase, as a function of spacing between the booms. Note that the distance is measured in wavelengths.

increase is 2.6 dB for a spacing of about 2.25 λ (15.2 feet), where the F/R remains close to 25 dB. The stacking distance of 15.2 feet for an antenna with a 27-foot long boom may be a real challenge physically, requiring a very sturdy rotating mast to withstand wind pressures without bending.

These examples show that the exact spacing between booms is not overly critical, since the gain varies relatively slowly around the peak. Fig 15A shows that the boom spacing needed to achieve peak gain from a stack increases when higher-gain (longer-boom) individual antennas are used in that stack. It also shows that the increase in maximum gain from stacking decreases for long-boom antennas. Fig 15B shows that beyond boom spacings of about 1 λ, the F/R pattern holds well for Yagi designs with booms longer than about 0.5 λ, which is about 4 feet at 146 MHz.

The plots in Fig 15 are representative of typical modern Yagis. You could simply implement these designs as is, and you'll achieve good results. However, we recommend that you model any specific stack you design, just to make sure. Since the boom spacings are displayed in terms of wavelength, you can extend the results for 2 meters to other bands, provided that you use properly scaled Yagi designs to the other bands too.

You can even tweak the element dimensions and spacings of each Yagi used in a stack to optimize the rearward pattern for a particular stacking distance. This strategy can work out well at VHF/UHF, where stacks are often configured for best gain (and pattern) and are "hard-wired" with fixed lengths of feed lines permanently junctioned together.

This is in contrast to the situation at HF (and even on 6 meters). The HF operator usually wants flexibility to select individual Yagis (or combinations of Yagis) from the stack, to match the array's takeoff angle with ionospheric propagation conditions. See Chapter 11, HF Yagi Arrays. The designer of a flexible HF stack thus usually doesn't try to redo the element lengths and spacings of the Yagis to optimize a particular stack.

Stacking Stacks of Different-Frequency Yagis

The investment in a tower is usually substantial, and most hams want to put as many antennas as possible on a tower, provided that interaction between the antennas can be held to a reasonable level. Really ambitious weak-signal VHF/UHF enthusiasts may want "stacked stacks"—sets of stacked Yagis that cover different bands. For example, a VHF contester might want a stack of two 8-element 2-meter Yagis mounted on the same rotating mast as a stack of two 5-element 6-meter Yagis. Let's assume that the boom length of the 8-element 2-meter Yagis is 12 feet (1.78 λ). We'll assume a boom length of 12 feet (0.61 λ) for the 5-element 6-meter Yagis.

From Fig 15, we find the stacking distance between the 8-element 2-meter beams for peak gain and good pattern is 1.5 λ, or 10 feet, but adequate performance can be had for a boom spacing of 0.75 λ, which is 5 feet on 2 meters.

The boom spacing for two 5-element 6-meter beams is 1 λ for peak stacking gain, but a compromise of 0.625 λ (12 feet) still yields an acceptable gain increase of 2 dB over a single Yagi. The overall height of the rotating mast sticking out of the top of the tower is thus set by the 0.625 λ stacking distance on 6 meters, at 12 feet. In-between the 6-meter Yagis at the bottom and top of the rotating mast we will mount the 2-meter Yagi stack. With only 12 feet available on the mast, the spacing for symmetric placement of the two 2-meter Yagis in-between the 6-meter Yagis dictates a distance of only 4 feet between the 2-meter beams. This is less than optimal.

The performance of the 2-meter stack in this "stack within a stack" is affected by the close spacing, but the

interactions are not disastrous. The stacking gain is 1.62 dB more than the gain for a single 8-element 2-meter Yagi and the F/R remains above 20 dB across the 2-meter band.

On 6 meters, the stacking gain for two 5-element 6-meter Yagis spaced 12 feet apart is 2.2 dB more than the gain of a single Yagi, while the F/R pattern remains about 20 dB over the weak-signal portion of the 6-meter band. As described in Chapter 11, HF Yagi Arrays, stacking gives more advantages than merely a gain increase, and 6-meter propagation does require coverage of a range of elevation angles because much of the time ionospheric modes are involved.

Increasing the length of the rotating mast to 18 feet sticking out of the top of the tower will increase performance, particularly on 2 meters. The stacking gain on 6 meters will increase to 2.3 dB while the F/R decreases to 18.5 dB, modest changes both. The 18-foot mast allows the 2-meter Yagis to be spaced 6 feet from each other and 6 feet away from both top and bottom 6-meter antennas. The stacking gain goes to 2.14 dB and the F/R approaches 27 dB in the weak-signal portion of the 2-meter band.

Whether the modest increase in stacking gain is worth the cost and mechanical complexity of stacking two 2-meter Yagis in-between a stack of 6-meter Yagis is a choice left to the operator. Certainly the cost and weight of a rotating mast that is 20 feet long (18 feet out of the top of the tower and 2 feet down inside the tower), a mast that must be sturdy enough to support the antennas in high winds without bending, should give pause to even the most enthusiastic 6-meter weak-signal operator.

QUADS FOR VHF

The quad antenna can be built with inexpensive materials, yet its performance is comparable to other arrays of its size. Adjustment for resonance and impedance matching can be accomplished readily. Quads can be stacked horizontally and vertically to provide high gain, without sharply limiting frequency response. Construction of quad antennas for VHF use is covered later in this chapter.

Stacking Quads

Quads can be mounted side by side or one above the other, or both, in the same general way as other beam antennas. Sets of driven elements can also be mounted in front of a screen reflector. The recommended spacing between adjacent element sides is $^1/_2$ λ. Phasing and feed methods are similar to those employed with other antennas described in this chapter.

Adding Quad Directors

Parasitic elements ahead of the driven element work in a manner similar to those in a Yagi array. Closed loops can be used for directors by making them 5% shorter than the driven element. Spacings are similar to those for conventional Yagis. In an experimental model the reflector was spaced 0.25 λ and the director 0.15 λ. A square array using four 3element bays worked extremely well.

VHF AND UHF QUAGIS

At higher frequencies, especially 420 MHz and above, Yagi arrays using dipole-driven elements can be difficult to feed and match, unless special care is taken to keep the feed-point impedance relatively high by proper element spacing and tuning. The cubical quad described earlier overcomes the feed problems to some extent. When many parasitic elements are used, however, the loops are not nearly as convenient to assemble and tune as are straight cylindrical ones used in conventional Yagis. The *Quagi*, designed and popularized by Wayne Overbeck, N6NB, is an antenna having a full-wave loop driven element and reflector, and Yagi type straight rod directors. Construction details and examples are given in the projects later in this chapter.

COLLINEAR ANTENNAS

The information given earlier in this chapter pertains mainly to parasitic arrays, but the collinear array is worthy of consideration in VHF/UHF operations. This array tends to be tolerant of construction tolerances, making it easy to build and adjust for VHF applications. The use of many collinear driven elements was once popular in very large phased arrays, such as those required in moonbounce (EME) communications, but the advent of computer-optimized Yagis has changed this.

Large Collinear Arrays

Bidirectional curtain arrays of four, six, and eight half waves in phase are shown in **Fig 16**. Usually reflector elements are added, normally at about 0.2 λ behind each driven element, for more gain and a unidirectional pattern. Such parasitic elements are omitted from the sketch in the interest of clarity.

The feed-point impedance of two half waves in phase is high, typically 1000 Ω or more. When they are combined in parallel and parasitic elements are added, the feed impedance is low enough for direct connection to open wire line or twin-lead, connected at the points indicated by black dots. With coaxial line and a balun, it is suggested that the universal stub match, Fig 4A, be used at the feed point. All elements should be mounted at their electrical centers, as indicated by open circles in Fig 16. The framework can be metal or insulating material. The metal supporting structure is entirely behind the plane of the reflector elements. Sheet-metal clamps can be cut from scraps of aluminum for this kind of assembly. Collinear elements of this type should be mounted at their centers (where the RF voltage is zero), rather than at their ends, where the voltage is high and insulation losses and detuning can be harmful.

Collinear arrays of 32, 48, 64 and even 128 elements can give outstanding performance. Any collinear array

should be fed at the center of the system, to ensure balanced current distribution. This is very important in large arrays, where sets of six or eight driven elements are treated as "sub arrays," and are fed through a balanced harness. The sections of the harness are resonant lengths, usually of open wire line. The 48-element collinear array for 432 MHz in **Fig 17** illustrates this principle.

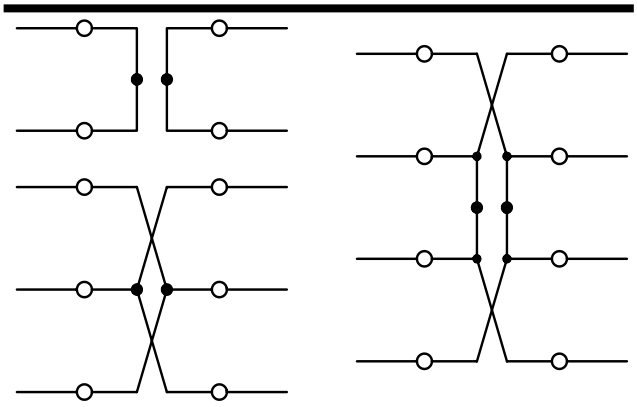

Fig 16—Element arrangements for 8-, 12- and 16-element collinear arrays. Elements are ½ λ long and spaced ½ λ. Parasitic reflectors, omitted here for clarity, are 5% longer and 0.2 λ behind the driven elements. Feed points are indicated by black dots. Open circles show recommended support points. The elements can run through wood or metal booms, without insulation, if supported at their centers in this way. Insulators at the element ends (points of high RF voltage) detune and unbalance the system.

A reflecting plane, which may be sheet metal, wire mesh, or even closely spaced elements of tubing or wire, can be used in place of parasitic reflectors. To be effective, the plane reflector must extend on all sides to at least $^1/_4$ λ beyond the area occupied by the driven elements. The plane reflector provides high F/B ratio, a clean pattern, and somewhat more gain than parasitic elements, but large physical size limits it to use above 420 MHz. An interesting space-saving possibility lies in using a single plane reflector with elements for two different bands mounted on opposite sides. Reflector spacing from the driven element is not critical. About 0.2 λ is common.

THE CORNER REFLECTOR

When a single driven element is used, the reflector screen may be bent to form an angle, giving an improvement in the radiation pattern and gain. At 222 and 420 MHz its size assumes practical proportions, and at 902 MHz and higher, practical reflectors can approach ideal dimensions (very large in terms of wavelengths), resulting in more gain and sharper patterns. The corner reflector can be used at 144 MHz, though usually at much less than optimum size. For a given aperture, the corner reflector does not equal a parabola in gain, but it is simple to construct, broadbanded, and offers gains from about 9 to 14 dBi, depending on the angle and size. This section was written by Paul M. Wilson, W4HHK.

The corner angle can be 90, 60 or 45°, but the side length must be increased as the angle is narrowed. For a 90° corner, the driven element spacing can be anything from 0.25 to 0.7 λ, 0.35 to 0.75 λ for 60°, and 0.5 to

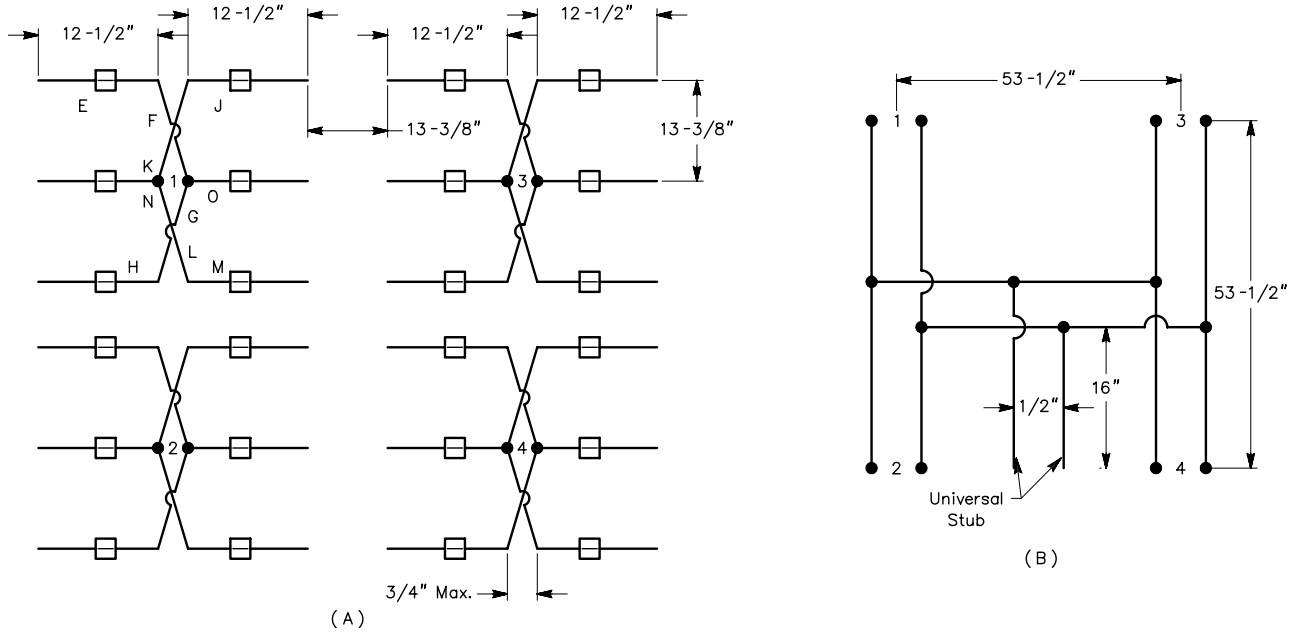

Fig 17—Large collinear arrays should be fed as sets of no more than eight driven elements each, interconnected by phasing lines. This 48-element array for 432 MHz (A) is treated as if it were four 12-element collinear antennas. Reflector elements are omitted for clarity. The phasing harness is shown at B. Squares represent insulators.

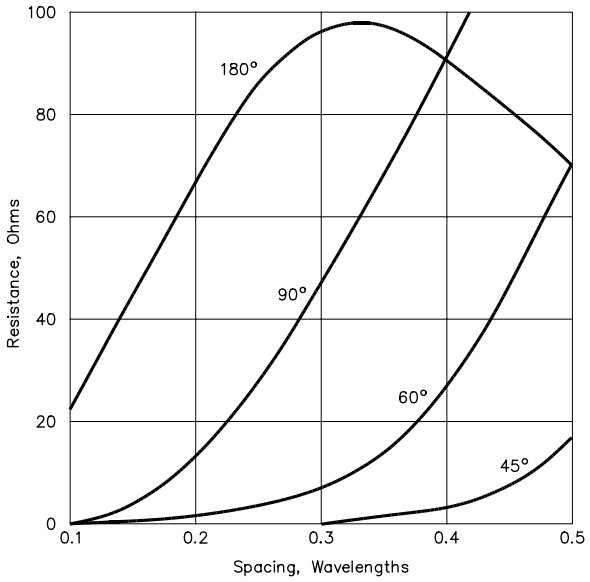

Fig 18—Radiation resistance of the driven element in a corner reflector array for corner angles of 180° (flat sheet), 90°, 60° and 45° as a function of spacing D, as shown in Fig 19.

0.8 λ for 45°. In each case the gain variation over the range of spacings given is about 1.5 dB. Because the spacing is not very critical to gain, it may be varied for impedance-matching purposes. Closer spacings yield lower feed-point impedances, but a folded dipole radiator could be used to raise this to a more convenient level.

Radiation resistance is shown as a function of spacing in **Fig 18**. The maximum gain obtained with minimum spacing is the primary mode (the one generally used at 144, 222 and 432 MHz to maintain reasonable side lengths). A 90° corner, for example, should have a minimum side length (S, **Fig 19**) equal to twice the dipole spacing, or 1 λ long for 0.5-λ spacing. A side length greater than 2 λ is ideal. Gain with a 60° or 90° corner reflector with 1-λ sides is about 10 dB. A 60° corner with 2-λ sides has about 13 dBi gain, and a 45° corner with 3-λ sides has about 14 dBi gain.

Reflector length (L, Fig 19) should be a minimum of 0.6 λ. Less than that spacing causes radiation to increase to the sides and rear, and decreases gain.

Spacing between reflector rods (G, Fig 19) should not exceed 0.06 λ for best results. A spacing of 0.06 λ results in a rear lobe that is about 6% of the forward lobe

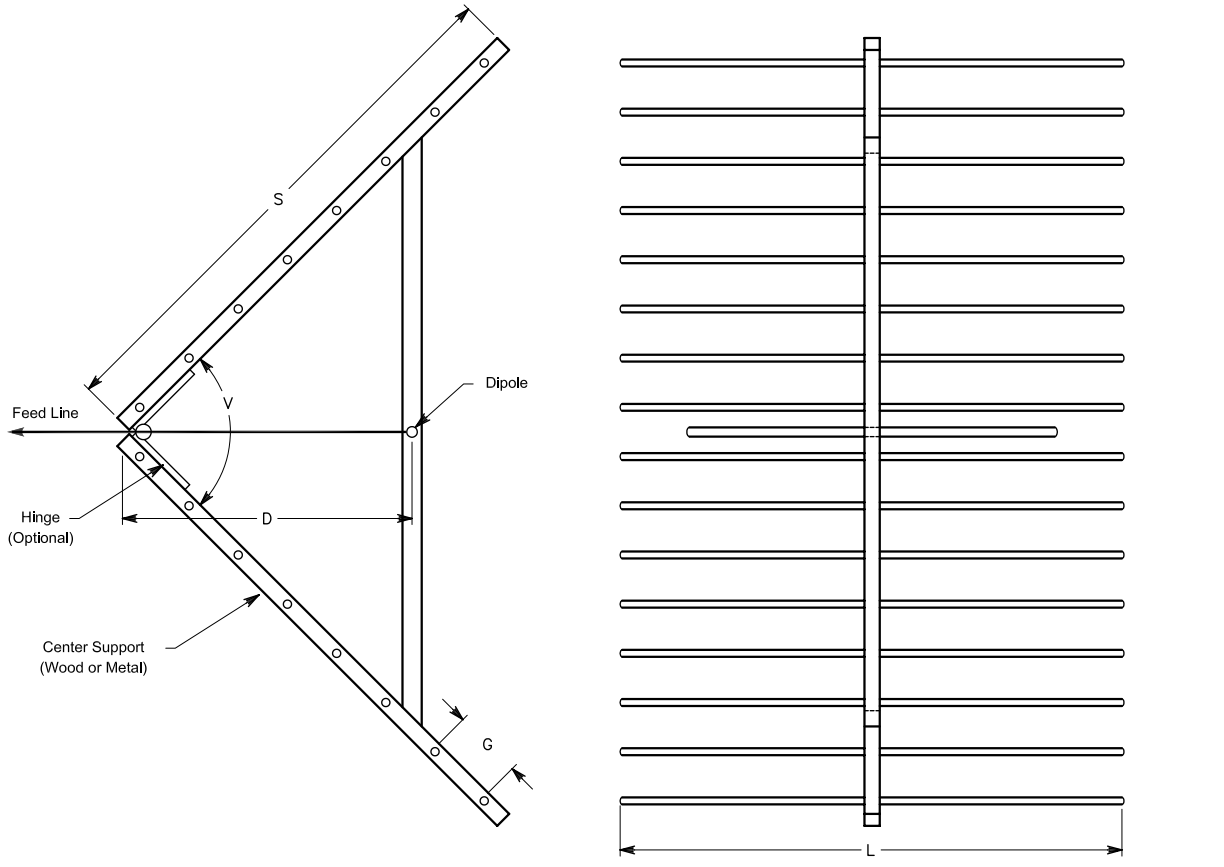

Fig 19—Construction of a corner reflector array. The frame can be wood or metal. Reflector elements are stiff wire or tubing. Dimensions for several bands are given in Table 2. Reflector element spacing, G, is the maximum that should be used for the frequency; closer spacings are optional. The hinge permits folding for portable use.

(down 12 dB). A small mesh screen or solid sheet is preferable at the higher frequencies to obtain maximum efficiency and highest F/B ratio, and to simplify construction. A spacing of 0.06 λ at 1296 MHz, for example, requires mounting reflector rods about every 1/2 inch along the sides. Rods or spines may be used to reduce wind loading. The support used for mounting the reflector rods may be of insulating or conductive material. Rods or mesh weave should be parallel to the radiator.

A suggested arrangement for a corner reflector is shown in Fig 19. The frame may be made of wood or metal, with a hinge at the corner to facilitate portable work or assembly atop a tower. A hinged corner is also useful in experimenting with different angles. **Table 2** gives the principal dimensions for corner reflector arrays for 144 to 2300 MHz. The arrays for 144, 222 and 420 MHz have side lengths of twice to four times the driven element spacing. The 915 MHz corner reflectors use side lengths of three times the element spacing, 1296 MHz corners use side lengths of four times the spacing, and 2304 MHz corners employ side lengths of six times the spacing. Reflector lengths of 2, 3, and 4 wavelengths are used on the 915, 1296 and 2304 MHz reflectors, respectively. A 4 × 6 λ reflector closely approximates a sheet of infinite dimensions.

A corner reflector may be used for several bands, or for UHF television reception, as well as amateur UHF work. For operation on more than one frequency, side length and reflector length should be selected for the lowest frequency, and reflector spacing for the highest frequency. The type of driven element plays a part in determining bandwidth, as does the spacing to the corner. A fat cylindrical element (small λ/dia ratio) or triangular dipole (bow tie) gives more bandwidth than a thin driven element. Wider spacings between driven element and corner give greater bandwidths. A small increase in gain can be obtained for any corner reflector by mounting collinear elements in a reflector of sufficient size, but

Table 2
Dimensions of Corner Reflector Arrays for VHF and UHF

Freq, MHz	*Side Length S, in.*	*Dipole to Vertex D, in.*	*Reflector Length L, in.*	*Reflector Spacing G, in.*	*Corner Angle, Vo*	*Radiation Resistance, Ω*
144*	65	27½	48	7¾	90	70
144	80	40	48	4	90	150
222*	42	18	30	5	90	70
222	52	25	30	3	90	150
222	100	25	30	Screen	60	70
420	27	8¾	16¼	2 5/8	90	70
420	54	13½	16¼	Screen	60	70
915	20	6½	25¾	0.65	90	70
915	51	16¾	25¾	Screen	60	65
915	78	25¾	25¾	Screen	45	70
1296	18	4½	27½	½	90	70
1296	48	11¾	27½	Screen	60	65
1296	72	18¼	27½	Screen	45	70
2304	15½	2½	20½	¼	90	70
2304	40	6¾	20½	Screen	60	65
2304	61	10¼	20½	Screen	45	70

*Side length and number of reflector elements somewhat below optimum—slight reduction in gain.

Notes:

915 MHz
Wavelength is 12.9 in.
Side length S is 3 × D, dipole to vertex distance
Reflector length L is 2.0 λ
Reflector spacing G is 0.05 λ

1296 MHz
Wavelength is 9.11 in.
Side length S is 4 × D, dipole to vertex distance
Reflector length L is 3.0 λ
Reflector spacing G is 0.05 λ

2304 MHz
Wavelength is 5.12 in.
Side length S is 6 × D, dipole to vertex distance
Reflector length L is 4.0 λ
Reflector spacing G is 0.05 λ

the simple feed of a dipole is lost if more than two elements are used.

A dipole radiator is usually employed with a corner reflector. This requires a balun between the coaxial line and the balanced feed-point impedance of the antenna. Baluns are easily constructed of coaxial line on the lower VHF bands, but become more difficult at the higher frequencies. This problem may be overcome by using a ground-plane corner reflector, which can be used for vertical polarization. A ground-plane corner with monopole driven element is shown in **Fig 20**. The corner reflector and a $^1/_4$ λ radiator are mounted on the ground plane, permitting direct connection to a coaxial line if the proper spacing is used. The effective aperture is reduced, but at the higher frequencies, second- or third-mode radiator spacing and larger reflectors can be employed to obtain more gain and offset the loss in effective aperture. A J antenna could be used to maintain the aperture area and provide a match to a coaxial line.

For vertical polarization work, four 90° corner reflectors built back-to-back (with common reflectors) could be used for scanning 360° of horizon with modest gain. Feed-line switching could be used to select the desired sector.

TROUGH REFLECTORS

To reduce the overall dimensions of a large corner reflector the vertex can be cut off and replaced with a plane reflector. Such an arrangement is known as a *trough reflector*. See **Fig 21**. Performance similar to that of the large corner reflector can thereby be had, provided that the dimensions of S and T as shown in Fig 21 do not exceed the limits indicated in the figure. This antenna provides performance very similar to the corner reflector, and presents fewer mechanical problems because the plane center portion is relatively easy to mount on the mast. The sides are considerably shorter, as well.

The gain of both corner reflectors and trough reflectors may be increased by stacking two or more and arranging them to radiate in phase, or alternatively by

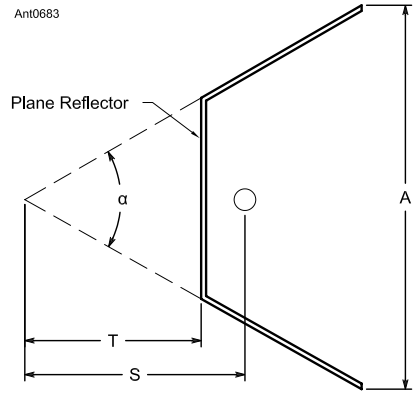

Angle α	*Value of S for maximum gain*	*Gain*	*Value of T*
90°	1.5 λ	13.5 dB	1λ - 1.25 λ
60°	1.75 λ	15 dB	1.0 λ
45°	2.0 λ	16 dB	1.9 λ

Fig 21—The trough reflector. This is a useful modification of the corner reflector. The vertex has been cut off and replaced by a simple plane section. The tabulated data shows the gain obtainable for greater values of S than those covered in Table 2, assuming that the reflector is of adequate size.

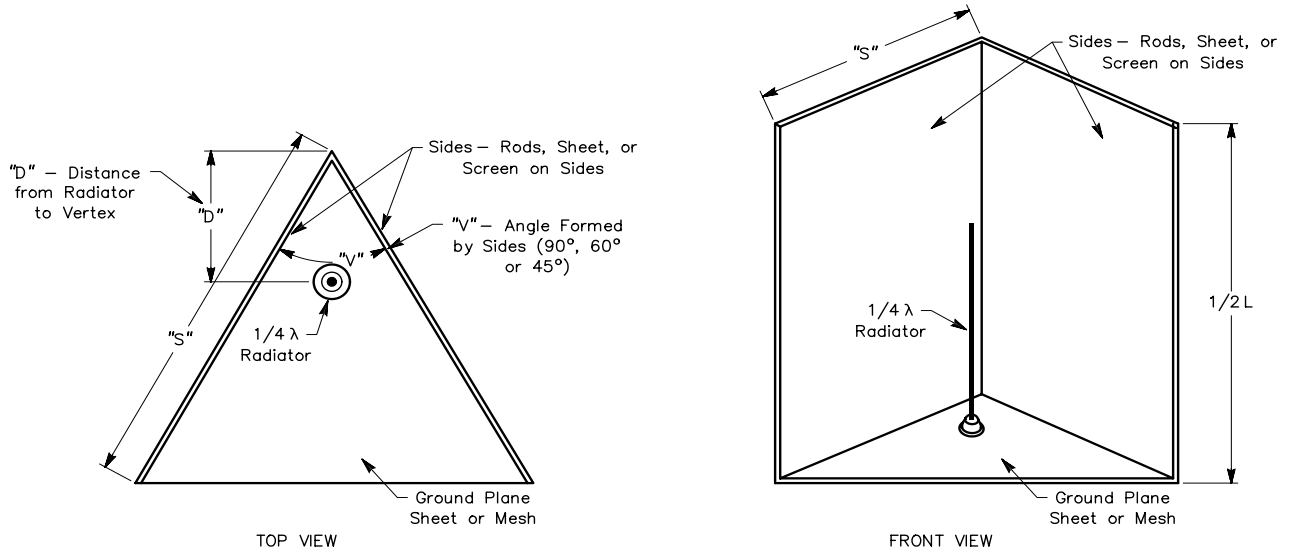

Fig 20—A ground-plane corner reflector antenna for vertical polarization, such as FM communications or packet radio. The dimension ½ λ in the front view refers to data in Table 2.

adding further collinear dipoles (fed in phase) within a wider reflector. Not more than two or three radiating units should be used, because the great virtue of the simple feeder arrangement would then be lost.

HORN ANTENNAS FOR THE MICROWAVE BANDS

Horn antennas were briefly introduced in the section on coupling energy into and out of waveguides. For amateur purposes, horns begin to show usable gain with practical dimensions in the 902 MHz band.

It isn't necessary to feed a horn with waveguide. If only two sides of a pyramidal horn are constructed, the antenna may be fed at the apex with a two-conductor transmission line. The impedance of this arrangement is on the order of 300 to 400 Ω. A 60° two-sided pyramidal horn with 18 inch sides is shown in **Fig 22**. This antenna has a theoretical gain of 15 dBi at 1296 MHz, although the feed system detailed in **Fig 23** probably degrades this value somewhat. A 1/4 λ, 150-Ω matching section made from two parallel lengths of twin-lead connects to a bazooka balun made from RG-58 cable and a brass tube. This matching system was assembled strictly for the purpose of demonstrating the two-sided horn in a 50-Ω system. In a practical installation the horn would be fed with open-wire line and matched to 50 Ω at the station equipment.

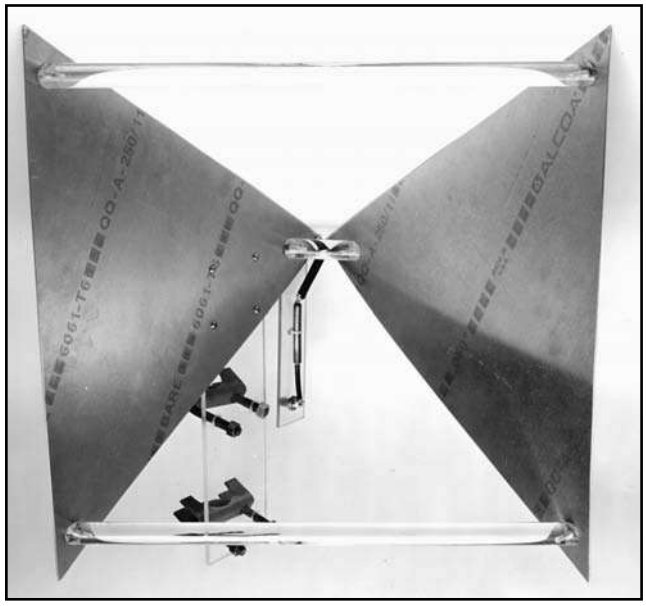

Fig 22—An experimental two-sided pyramidal horn constructed in the ARRL laboratory. A pair of muffler clamps allows mounting the antenna on a mast. This model has sheet-aluminum sides, although window screen would work as well. Temporary elements could be made from cardboard covered with aluminum foil. The horizontal spreaders are Plexiglas rod. Oriented as shown here, the antenna radiates horizontally polarized waves.

PARABOLIC ANTENNAS

When an antenna is located at the focus of a parabolic reflector (dish), it is possible to obtain considerable gain. Furthermore, the beamwidth of the radiated energy will be very narrow, provided all the energy from the driven element is directed toward the reflector. This section was written by Paul M. Wilson, W4HHK.

Gain is a function of parabolic reflector diameter, surface accuracy and proper illumination of the reflector by the feed. Gain may be found from

$$G = 10 \log k \left(\frac{\pi D}{\lambda} \right)^2 \qquad \text{(Eq 1)}$$

where

G = gain over an isotropic antenna, dBi (subtract 2.15 dB for gain over a dipole)
k = efficiency factor, usually about 55%
D = dish diameter in feet
λ = wavelength in feet

See **Table 3** for parabolic antenna gain for the bands 420 MHz through 10 GHz and diameters of 2 to 30 feet.

A close approximation of beamwidth may be found from

$$\psi = \frac{70\lambda}{D} \qquad \text{(Eq 2)}$$

where

ψ = beamwidth in degrees at half-power points (3 dB down)
D = dish diameter in feet
λ = wavelength in feet

At 420 MHz and higher, the parabolic dish becomes a practical antenna. A simple, single feed point eliminates phasing harnesses and balun requirements. Gain is dependent on good surface accuracy, which is more difficult to achieve with increasing frequency. Surface

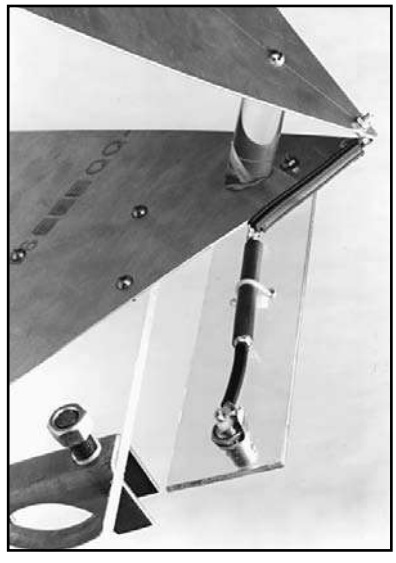

Fig 23—Matching system used to test the horn. Better performance would be realized with open wire line. See text.

Table 3
Gain, Parabolic Antennas*

	Dish Diameter (Feet)						
Frequency	*2*	*4*	*6*	*10*	*15*	*20*	*30*
420 MHz	6.0	12.0	15.5	20.0	23.5	26.0	29.5
902	12.5	18.5	22.0	26.5	30.0	32.5	36.0
1215	15.0	21.0	24.5	29.0	32.5	35.0	38.5
2300	20.5	26.5	30.0	34.5	38.0	40.5	44.0
3300	24.0	30.0	33.5	37.5	41.5	43.5	47.5
5650	28.5	34.5	38.0	42.5	46.0	48.5	52.0
10 GHz	33.5	39.5	43.0	47.5	51.0	53.5	57.0

*Gain over an isotropic antenna (subtract 2.1 dB for gain over a dipole antenna). Reflector efficiency of 55% assumed.

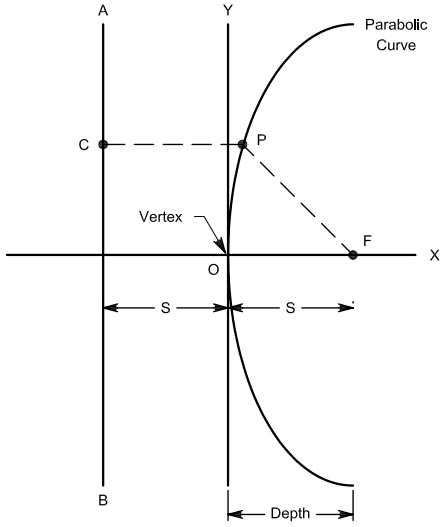

Fig 24—Details of the parabolic curve, $Y^2 = 4SX$. This curve is the locus of points that are equidistant from a fixed point, the focus (F), and a fixed line (AB) that is called the *directrix*. Hence, FP = PC. The focus (F) is located at coordinates S,0.

errors should not exceed $^1/_8$ λ in amateur work. At 430 MHz $^1/_8$ λ is 3.4 inches, but at 10 GHz it is 0.1476 inch! Mesh can be used for the reflector surface to reduce weight and wind loading, but hole size should be less than $^1/_{12}$ λ. At 430 MHz the use of 2-inch hole diameter poultry netting (chicken wire) is acceptable. Fine mesh aluminum screening works well as high as 10 GHz.

A support form may be fashioned to provide the proper parabolic shape by plotting a curve (**Fig 24**) from

$$Y^2 = 4SX$$

as shown in the figure.

Optimum illumination occurs when power at the reflector edge is 10 dB less than that at the center. A circular waveguide feed of correct diameter and length for the frequency and correct beamwidth for the dish focal length to diameter (f/D) ratio provides optimum illumination at 902 MHz and higher. This, however, is impractical at 432 MHz, where a dipole and plane reflector are often used. An f/D ratio between 0.4 and 0.6 is considered ideal for maximum gain and simple feeds.

The focal length of a dish may be found from

$$f = \frac{D^2}{16d} \qquad \text{(Eq 3)}$$

where

f = focal length
D = diameter
d = depth distance from plane at mouth of dish to vertex (see Fig 17)

The units of focal length f are the same as those used to measure the depth and diameter. **Table 4** gives the subtended angle at focus for dish f/D ratios from 0.2 to 1.0. A dish, for example, with a typical f/D of 0.4 requires a 10-dB beamwidth of 130°. A circular waveguide feed with a diameter of approximately 0.7 λ provides nearly optimum illumination, but does not uniformly illuminate the reflector in both the magnetic (TM) and electric (TE) planes. **Fig 25** shows data for plotting radiation patterns from circular guides. The waveguide feed aperture can be modified to change the beamwidth.

One approach used successfully by some experimenters is the use of a disc at a short distance behind the aperture as shown in **Fig 26**. As the distance between the aperture and disc is changed, the TM plane patterns become alternately broader and narrower than with an unmodified aperture. A disc about 2 λ in diameter appears to be as effective as a much larger one. Some experimenters have noted a 1 to 2 dB increase in dish gain with this modified feed. Rectangular waveguide feeds can also be used, but dish illumination is not as uniform as with round guide feeds.

The circular feed can be made of copper, brass, aluminum or even tin in the form of a coffee or juice can, but the latter must be painted on the outside to prevent rust or corrosion. The circular feed must be within a proper size (diameter) range for the frequency being used.

This feed operates in the dominant circular waveguide mode known as the TE_{11} mode. The guide must be large enough to pass the TE_{11} mode with no attenuation, but smaller than the diameter that permits the next higher TM_{01} mode to propagate. To support the desirable TE_{11} mode in circular waveguide, the cutoff frequency, F_C, is given by

$$F_C\,(TE_{11}) = \frac{6917.26}{d\,(\text{inches})} \qquad \text{(Eq 4)}$$

where

F_C = cutoff frequency in MHz for TE_{11} mode
d = waveguide inner diameter

Circular waveguide will support the TM_{01} mode having a cutoff frequency

$$F_C\,(TM_{01}) = \frac{9034.85}{d\,(\text{inches})} \qquad \text{(Eq 5)}$$

The wavelength in a waveguide always exceeds the free-space wavelength and is called guide wavelength, λ_g. It is related to the cutoff frequency and operating frequency by the equation

$$\lambda_g = \frac{11802.85}{\sqrt{f_0^{\,2} - f_C^{\,2}}} \qquad \text{(Eq 6)}$$

where

λ_g = guide wavelength, inches
f_0 = operating frequency, MHz
f_C = TE_{11} waveguide cutoff frequency, MHz

An inside diameter range of about 0.66 to 0.76 l is

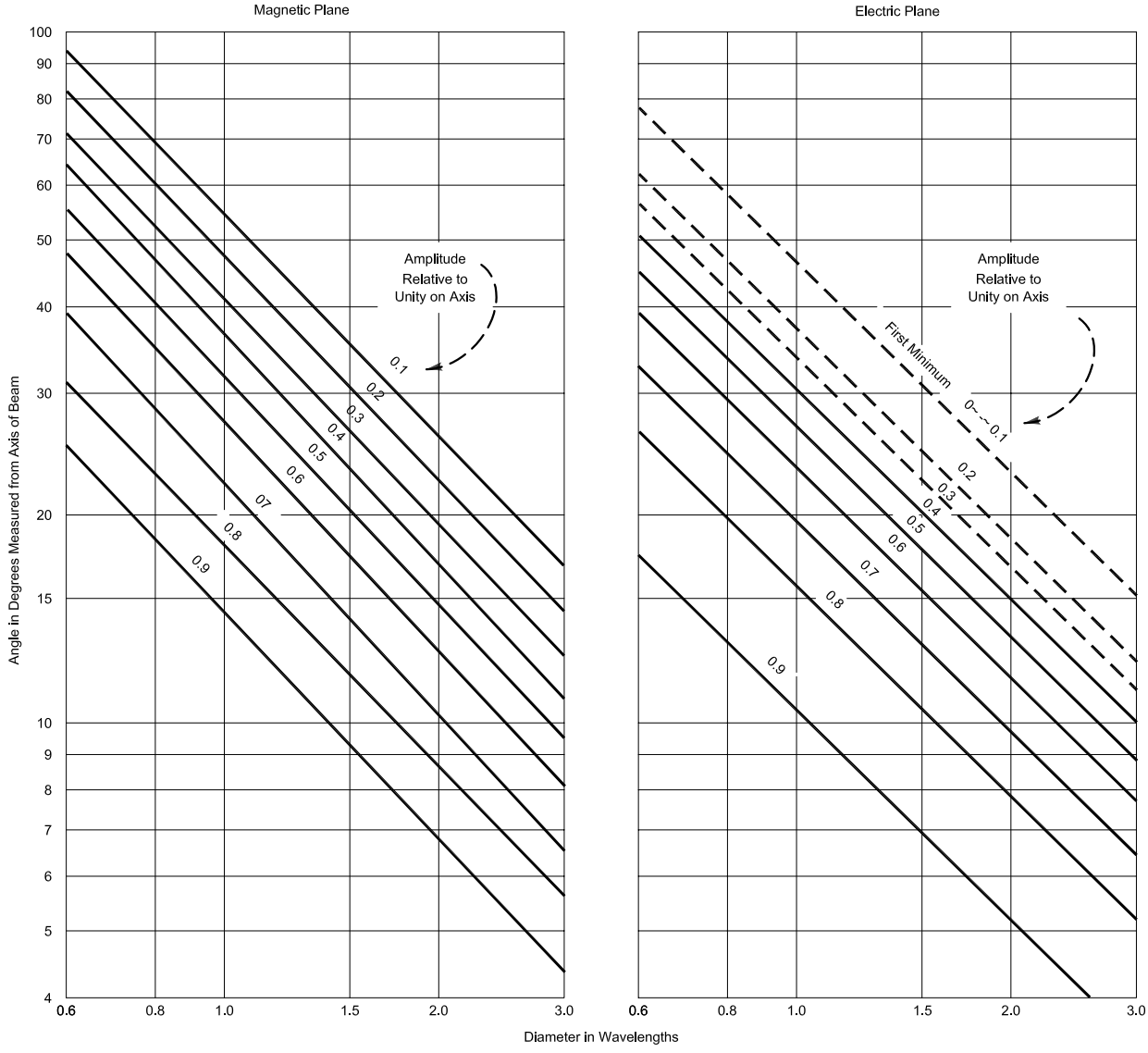

Fig 25—This graph can be used in conjunction with Table 4 for selecting the proper diameter waveguide to illuminate a parabolic reflector.

Table 4

f/D Versus Subtended Angle at Focus of a Parabolic Reflector Antenna

f/D	Subtended Angle (Deg.)	f/D	Subtended Angle (Deg.)
0.20	203	0.65	80
0.25	181	0.70	75
0.30	161	0.75	69
0.35	145	0.80	64
0.40	130	0.85	60
0.45	117	0.90	57
0.50	106	0.95	55
0.55	97	1.00	52
0.60	88		

Taken from graph "f/D vs Subtended Angle at Focus," page 170 of the 1966 *Microwave Engineers' Handbook and Buyers Guide*. Graph courtesy of K. S. Kelleher, Aero Geo Astro Corp, Alexandria, Virginia

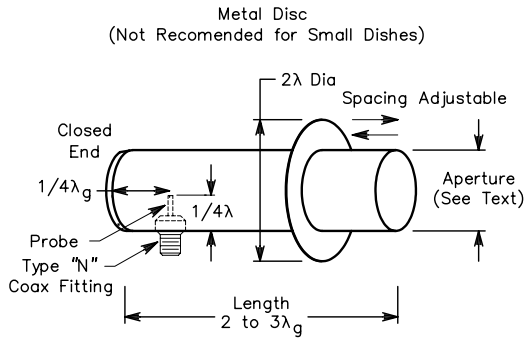

Fig 26—Details of a circular waveguide feed.

suggested. The lower frequency limit (longer dimension) is dictated by proximity to the cutoff frequency. The higher frequency limit (shorter dimension) is dictated by higher order waves. See **Table 5** for recommended inside diameter dimensions for the 902- to 10,000-MHz amateur bands.

The probe that excites the waveguide and makes the transition from coaxial cable to waveguide is 1/4 λ long and spaced from the closed end of the guide by 1/4 guide wavelength. The length of the feed should be two to three guide wavelengths. The latter is preferred if a second probe is to be mounted for polarization change or for polaplexer work where duplex communication (simultaneous transmission and reception) is possible because of the isolation between two properly located and oriented probes. The second probe for polarization switching or polaplexer work should be spaced 3/4 guide wavelength from the closed end and mounted at right angles to the first probe.

The feed aperture is located at the focal point of the dish and aimed at the center of the reflector. The feed

Table 5

Circular Waveguide Dish Feeds

Freq. (MHz)	Inside Diameter Circular Waveguide Range (in.)
915	8.52-9.84
1296	6.02-6.94
2304	3.39-3.91
3400	2.29-2.65
5800	1.34-1.55
10,250	0.76-0.88

mounts should permit adjustment of the aperture either side of the focal point and should present a minimum of blockage to the reflector. Correct distance to the dish center places the focal point about 1 inch inside the feed aperture. The use of a nonmetallic support minimizes blockage. PVC pipe, fiberglass and Plexiglas are commonly used materials. A simple test by placing a material in a microwave oven reveals if it is satisfactory up to 2450 MHz. PVC pipe has tested satisfactorily and appears to work well at 2300 MHz. A simple, clean looking mount for a 4-foot dish with 18 inches focal length, for example, can be made by mounting a length of 4-inch PVC pipe using a PVC flange at the center of the dish. At 2304 MHz the circular feed is approximately 4 inches ID, making a snug fit with the PVC pipe. Precautions should be taken to keep rain and small birds from entering the feed.

Never look into the open end of a waveguide when power is applied, or stand directly in front of a dish while transmitting. Tests and adjustments in these areas should be done while receiving or at extremely low levels of transmitter power (less than 0.1 watt). The US Government has set a limit of 10 mW/cm^2 averaged over a 6-minute period as the safe maximum. Other authorities believe even lower levels should be used. Destructive thermal heating of body tissue results from excessive exposure. This heating effect is especially dangerous to the eyes. The accepted safe level of 10 mW/cm^2 is reached in the near field of a parabolic antenna if the level at $2D^2/\lambda$ is 0.242 mW/cm^2. The equation for power density at the far-field boundary is

$$\text{Power density} = \frac{137.8\ P}{D^2}\ \text{mW/cm}^2 \qquad \text{(Eq 7)}$$

where

P = average power in kilowatts
D = antenna diameter in feet
λ = wavelength in feet

New commercial dishes are expensive, but surplus ones can often be purchased at low cost. Some amateurs build theirs, while others modify UHF TV dishes or circular metal snow sleds for the amateur bands. **Fig 27** shows a dish using the homemade feed just described.

Fig 27—Coffee-can 2304 MHz feed described in text and Fig 26 mounted on a 4-ft dish.

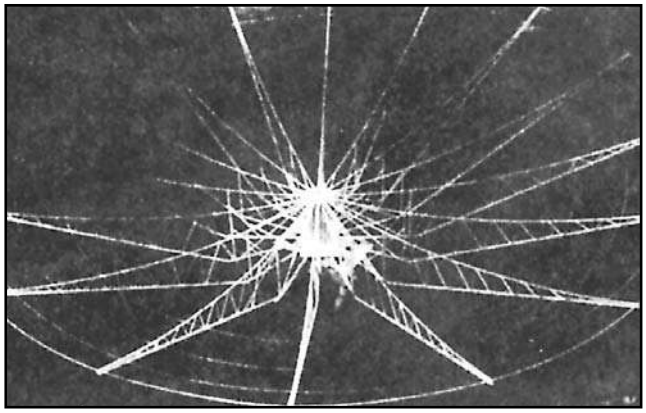

Fig 28—Aluminum framework for a 23-foot dish under construction by ZL1BJQ.

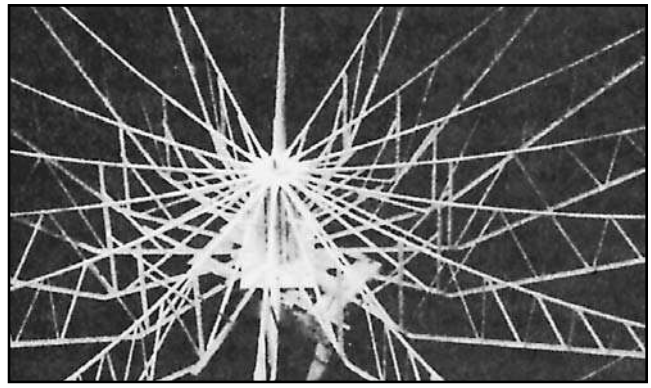

Fig 29—Detailed look at the hub assembly for the ZL1BJQ dish. Most of the structural members are made from ¾-inch T section.

Photos showing a highly ambitious dish project under construction by ZL1BJQ appear in **Figs 28** and **29**. Practical details for constructing this type of antenna are given in Chapter 19. Dick Knadle, K2RIW, described modern UHF antenna test procedures in February 1976 *QST* (see Bibliography). Also see Chapter 19.

OMNIDIRECTIONAL ANTENNAS FOR VHF AND UHF

Local work with mobile stations requires an antenna with wide coverage capabilities. Most mobile work is on FM, and the polarization used with this mode is generally vertical. Some simple vertical systems are described below. Additional material on antennas of this type is presented in Chapter 16, Mobile and Maritime Antennas.

Ground-plane Antennas for 144, 222 and 440 MHz

For the FM operator living in the primary coverage area of a repeater, the ease of construction and low cost of a 1/4 λ ground-plane antenna make it an ideal choice. Three different types of construction are detailed in Figs 30 through 43; the choice of construction method depends upon the materials at hand and the desired style of antenna mounting.

The 144-MHz model shown in **Fig 30** uses a flat piece of sheet aluminum, to which radials are connected with machine screws. A 45° bend is made in each of the radials. This bend can be made with an ordinary bench vise. An SO239 chassis connector is mounted at the center of the aluminum plate with the threaded part of the connector facing down. The vertical portion of the

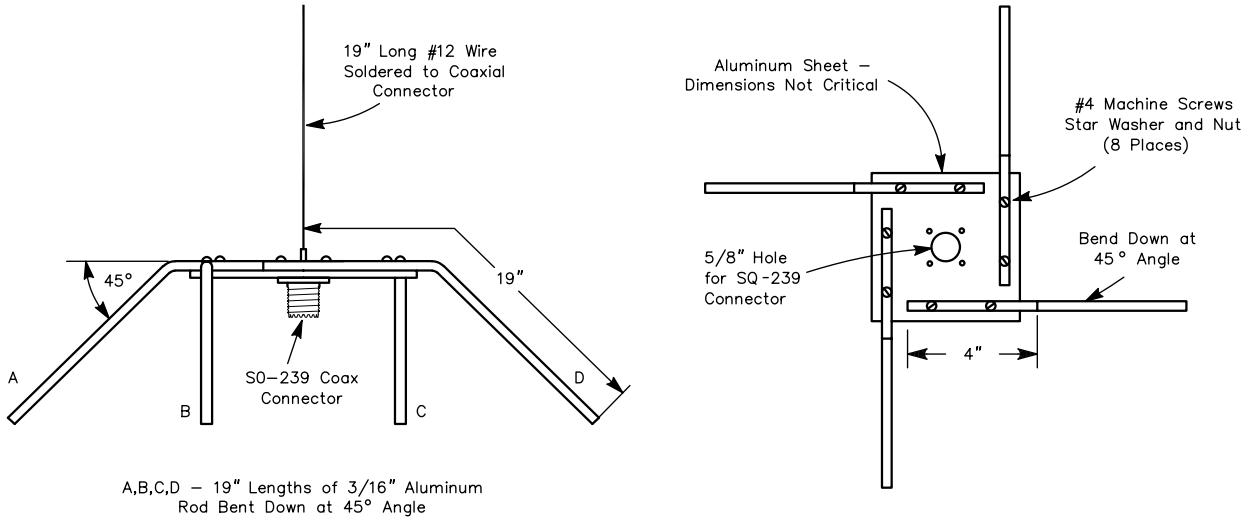

Fig 30—These drawings illustrate the dimensions for the 144-MHz ground-plane antenna. The radials are bent down at a 45° angle.

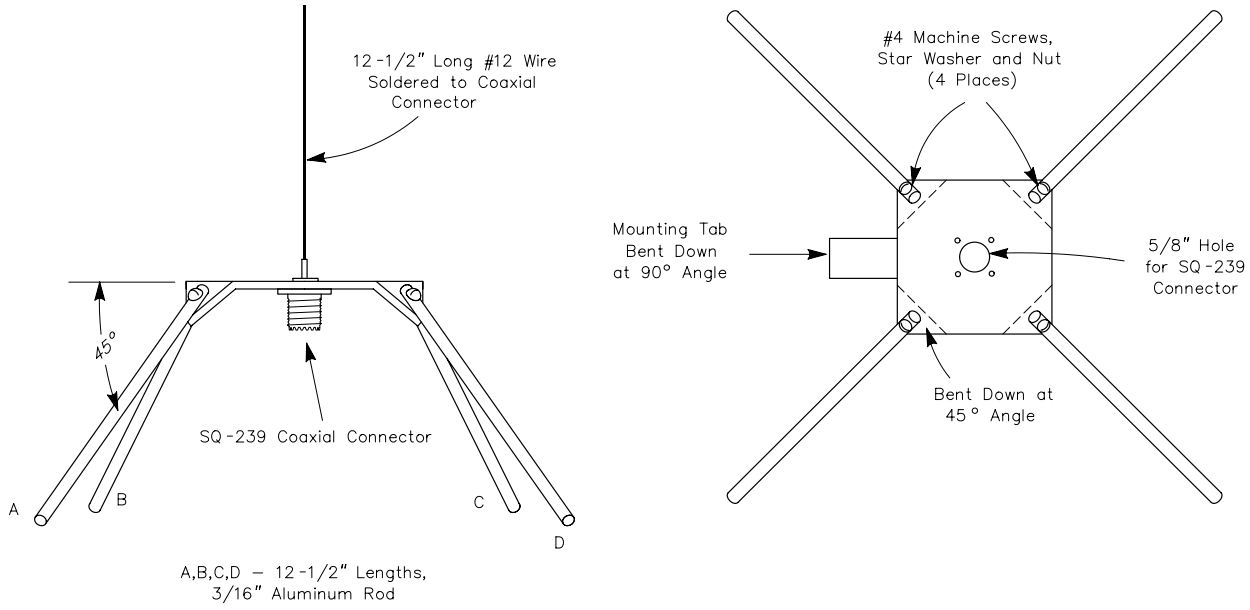

Fig 31—Dimensional information for the 222-MHz ground-plane antenna. Lengths for A, B, C and D are the total distances measured from the center of the SO-239 connector. The corners of the aluminum plate are bent down at a 45° angle rather than bending the aluminum rod as in the 144-MHz model. Either method is suitable for these antennas.

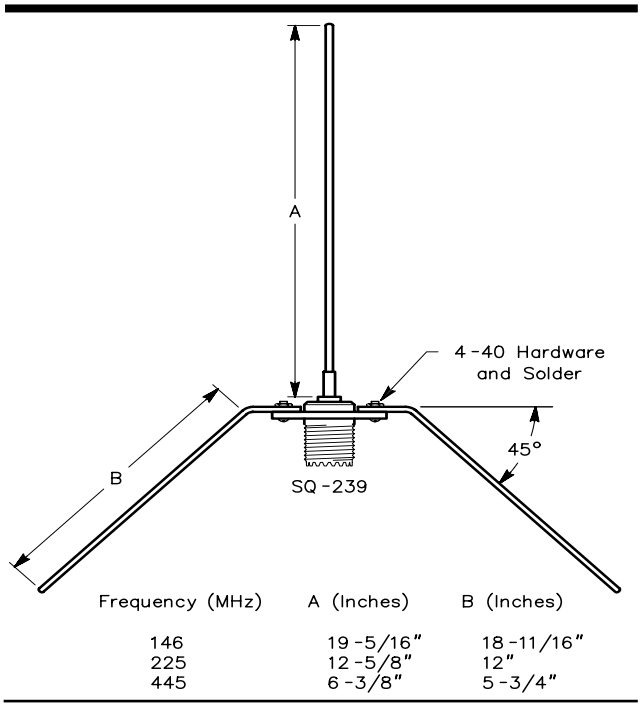

Fig 32—Simple ground-plane antenna for the 144-, 222- and 440-MHz bands. The vertical element and radials are 3/32- or 1/16-in. brass welding rod. Although 3/32-in. rod is preferred for the 144-MHz antenna, #10 or #12 copper wire can also be used.

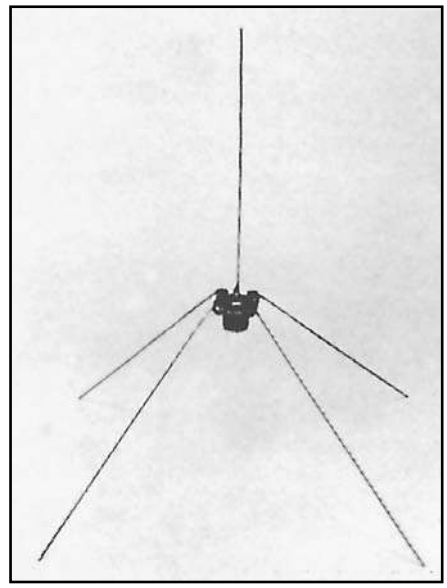

Fig 33—A 440-MHz ground-plane constructed using only an SO-239 connector, no. 4-40 hardware and 1/16-in. brass welding rod.

antenna is made of #12 copper wire soldered directly to the center pin of the SO-239 connector.

The 222-MHz version, **Fig 31**, uses a slightly different technique for mounting and sloping the radials. In this case the corners of the aluminum plate are bent down at a 45° angle with respect to the remainder of the plate. The four radials are held to the plate with machine screws, lock washers and nuts. A mounting tab is included in the design of this antenna as part of the aluminum base. A compression type of hose clamp could be used to secure the antenna to a mast. As with the 144-MHz version, the vertical portion of the antenna is soldered directly to the SO-239 connector.

A very simple method of construction, shown in **Figs 32** and **33**, requires nothing more than an SO-239 connector and some no. 4-40 hardware. A small loop formed at the inside end of each radial is used to attach the radial directly to the mounting holes of the coaxial connector. After the radial is fastened to the SO-239 with no. 4-40 hardware, a large soldering iron or propane torch is used to solder the radial and the mounting hardware to the coaxial connector. The radials are bent to a 45° angle and the vertical portion is soldered to the center pin to complete the antenna. The antenna can be mounted by passing the feed line through a mast of ¾-inch ID plastic or aluminum tubing. A compression hose clamp can be used to secure the PL-259 connector, attached to the feed line, in the end of the mast. Dimensions for the 144-, 222- and 440-MHz bands are given in Fig 32.

If these antennas are to be mounted outside it is wise to apply a small amount of RTV sealant or similar material around the areas of the center pin of the connector to prevent the entry of water into the connector and coax line.

The J-Pole Antenna

The J-Pole is a half-wave antenna that is end-fed at its bottom. Since the radiator is longer than that of a $^1/_4$-wave ground-plane antenna, the vertical lobe is compressed down toward the horizon and it has about 1.5 dB of gain compared to the ground-plane configuration. The stub-matching section used to transform the high impedance seen looking into a half-wave to 50 Ω coax is shorted at the bottom, making the antenna look like the letter "J," and giving the antenna its name.

Rigid copper tubing, fittings and assorted hardware can be used to make a really rugged J-pole antenna for 2 meters. When copper tubing is used, the entire assembly can be soldered together, ensuring electrical integrity, and making the whole antenna weatherproof. This

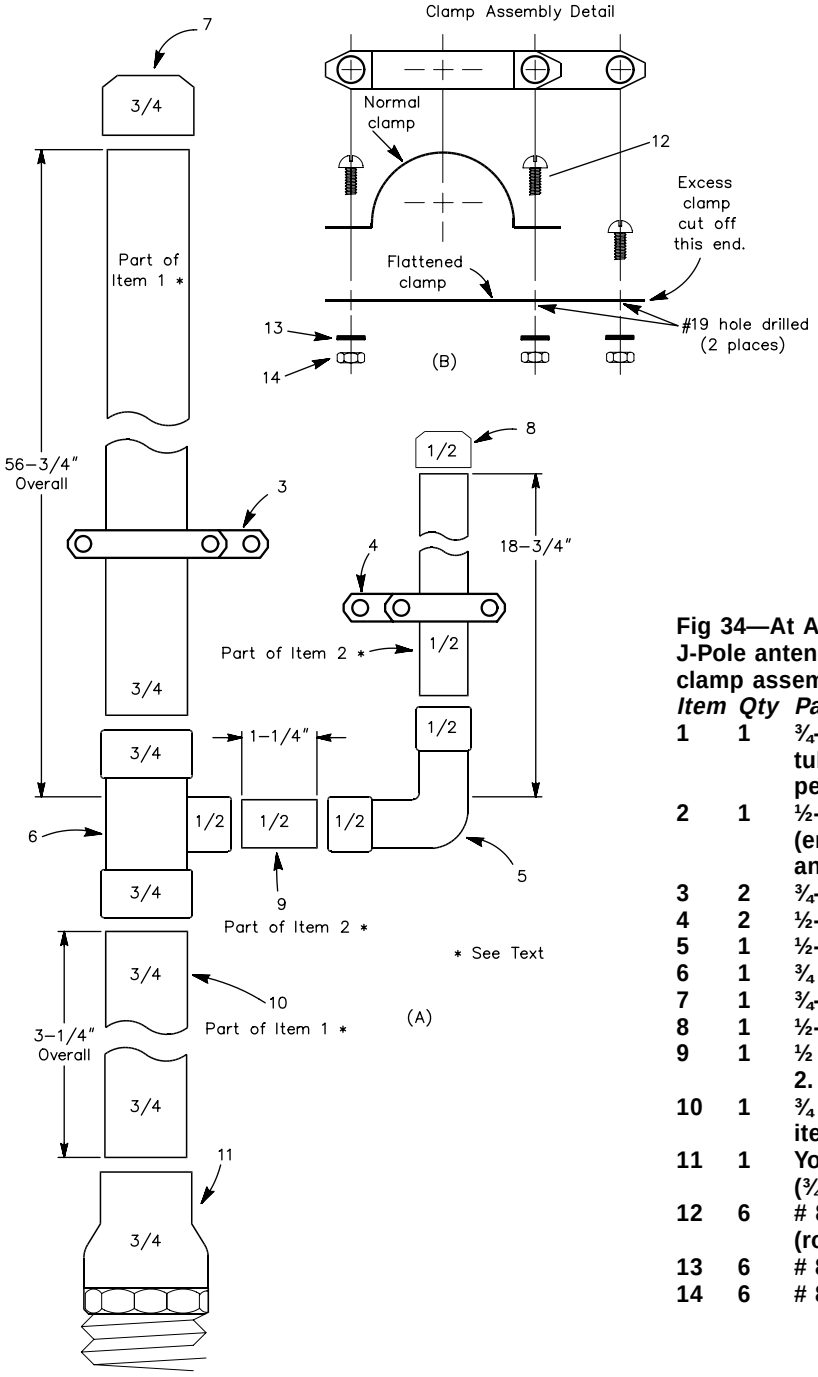

Fig 34—At A, exploded assembly diagram of all-copper J-Pole antenna. At B, detail of clamp assemblies. Both clamp assemblies are the same.

Item	*Qty*	*Part or Material Name*
1	1	¾-inch × 10 foot length of rigid copper tubing (enough for 2 antennas, 60 inches per antenna)
2	1	½-inch × 10 ft length of rigid copper tubing (enough for 6 antennas, 20 inches per antenna)
3	2	¾-inch copper pipe clamps
4	2	½-inch copper pipe clamps
5	1	½-inch copper elbow
6	1	¾ × ½-inch copper tee
7	1	¾-inch copper end cap
8	1	½-inch copper end cap
9	1	½ × 1¼-inch copper nipple (Make from item 2. See text)
10	1	¾ × 3 ¼-inch copper nipple (Make from item 1. See text)
11	1	Your choice of coupling to mast fitting (¾ × 1 inch NPT used at KD8JB)
12	6	# 8-32 × ½-inch brass machine screws (round, pan, or binder head)
13	6	# 8 brass flat washers
14	6	# 8-32 brass hex nuts

material came from an article by Michael Hood, KD8JB, in *The ARRL Antenna Compendium,Vol. 4*.

No special hardware or machined parts are used in this antenna, nor are insulating materials needed, since the antenna is always at dc ground. Best of all, even if the parts aren't on sale, the antenna can be built for less than $15. If you only build one antenna, you'll have enough tubing left over to make most of a second antenna.

Construction

Copper and brass is used exclusively in this antenna. These metals get along together, so dissimilar metal corrosion is eliminated. Both metals solder well, too. See **Fig 34**. Cut the copper tubing to the lengths indicated. Item 9 is a 1 1/4-inch nipple cut from the 20-inch length of 1/2-inch tubing. This leaves 18 3/4 inches for the 1/4-matching stub. Item 10 is a 3 1/4-inch long nipple cut from the 60-inch length of 3/4-inch tubing. The 3/4-wave element should measure 56 3/4-inches long. Remove burrs from the ends of the tubing after cutting, and clean the mating surfaces with sandpaper, steel wool, or emery cloth.

After cleaning, apply a very thin coat of flux to the mating elements and assemble the tubing, elbow, tee, end caps and stubs. Solder the assembled parts with a propane torch and rosin-core solder. Wipe off excess solder with a damp cloth, being careful not to burn yourself. The copper tubing will hold heat for a long time after you've finished soldering. After soldering, set the assembly aside to cool.

Flatten one each of the 1/2-inch and 3/4-inch pipe clamps. Drill a hole in the flattened clamp as shown in Fig 34A. Assemble the clamps and cut off the excess metal from the flattened clamp using the unmodified clamp as a template. Disassemble the clamps.

Assemble the 1/2-inch clamp around the 1/4-wave element and secure with two of the screws, washers, and nuts as shown in Fig 34B. Do the same with the 3/4-inch clamp around the 3/4-wave element. Set the clamps initially to a spot about 4 inches above the bottom of the "J" on their respective elements. Tighten the clamps only finger tight, since you'll need to move them when tuning.

Tuning

The J-Pole can be fed directly from 50-Ω coax through a choke balun (3 turns of the feed coax rolled into a coil about 8 inches in diameter and held together with electrical tape). Before tuning, mount the antenna vertically, about 5 to 10 feet from the ground. A short TV mast on a tripod works well for this purpose. When tuning VHF antennas, keep in mind that they are sensitive to nearby objects—such as your body. Attach the feed line to the clamps on the antenna, and make sure all the nuts and screws are at least finger tight. It really doesn't matter to which element (¾-wave element or stub) you attach the coaxial center lead. The author has done it both ways with no variation in performance. Tune the antenna by moving the two feed-point clamps equal distances a small amount each time until the SWR is minimum at the desired frequency. The SWR will be close to 1:1.

Final Assembly

The final assembly of the antenna will determine its long-term survivability. Perform the following steps with care. After adjusting the clamps for minimum SWR, mark the clamp positions with a pencil and then remove the feed line and clamps. Apply a very thin coating of flux to the inside of the clamp and the corresponding surface of the antenna element where the clamp attaches. Install the clamps and tighten the clamp screws.

Solder the feed line clamps where they are attached to the antenna elements. Now, apply a small amount of solder around the screw heads and nuts where they contact the clamps. Don't get solder on the screw threads! Clean away excess flux with a non-corrosive solvent. After final assembly and erecting/mounting the antenna in the desired location, attach the feed line and secure with the remaining washer and nut. Weather-seal this joint with RTV. Otherwise, you may find yourself repairing the feed line after a couple years.

On-the-Air Performance

Years ago, prior to building the first J-Pole antenna for this station, the author used a standard 1/4-wave ground plane vertical antenna. While he had no problem working various repeaters around town with a 1/4-wave antenna, simplex operation left a lot to be desired. The J-Pole performs just as well as a Ringo Ranger, and significantly better than the 1/4-wave ground-plane vertical.

Practical 6-Meter Yagis

Boom length often proves to be the deciding factor when one selects a Yagi design. **Table 6** shows three 6-meter Yagis designed for convenient boom lengths (6, 12 and 22 feet). The 3-element, 6-foot boom design has 8.0 dBi gain in free space; the 12 foot boom, 5-element version has 10.1 dBi gain, and the 22-foot, 7 element Yagi has a gain of 11.3 dBi. All antennas exhibit better than 22 dB front-to-rear ratio and cover 50 to 51 MHz with better than 1.7:1 SWR.

Half-element lengths and spacings are given in the table. Elements can be mounted to the boom as shown in **Fig 35**. Two muffler clamps hold each aluminum plate to the boom, and two U bolts fasten each element to the plate, which is 0.25 inches thick and 4 × 4 inches square. Stainless steel is the best choice for hardware, however, galvanized hardware can be substituted. Automotive muffler clamps do not work well in this application, because they are not galvanized and quickly rust once exposed to the weather. Please note that the element lengths shown in Table 6 are half the overall element lengths. See page 20-7 to 20-11 in Chapter 20 for practical details of telescoping aluminum elements.

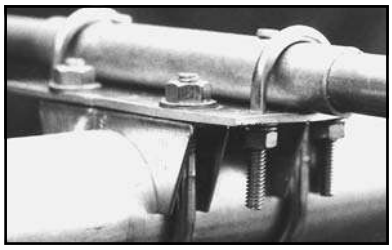

Fig 35—The element to boom clamp. U bolts are used to hold the element to the plate, and 2-in. galvanized muffler clamps hold the plates to the boom.

The driven element is mounted to the boom on a Bakelite or G-10 fiberglass plate of similar dimension to the other mounting plates. A 12-inch piece of Plexiglas rod is inserted into the driven element halves. The Plexiglas allows the use of a single clamp on each side of the element and also seals the center of the elements against moisture. Self-tapping screws are used for electrical connection to the driven element.

Refer to **Fig 36** for driven-element and hairpin match details. A bracket made from a piece of aluminum is used to mount the three SO239 connectors to the driven element plate. A 4:1 transmission-line balun connects the two element halves, transforming the 200 Ω resistance at the hairpin match to 50 Ω at the center connector. Note

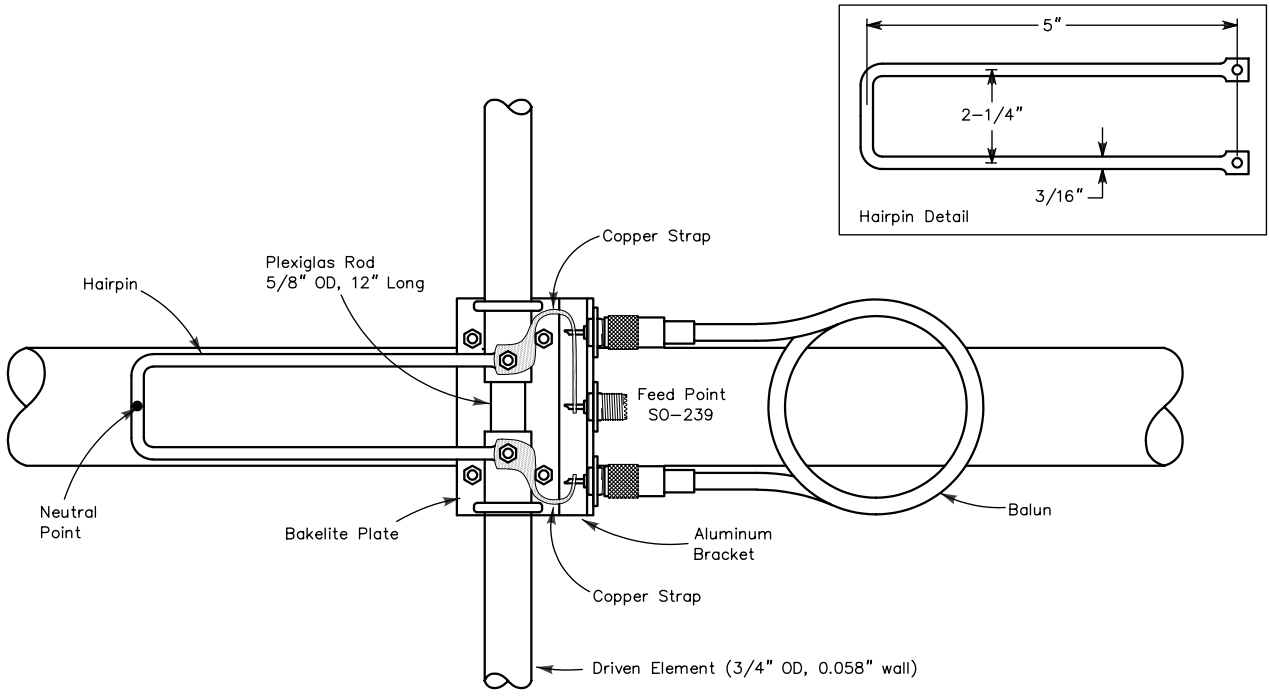

Fig 36—This shows how the driven element and feed system are attached to the boom. The phasing line is coiled and taped to the boom. The center of the hairpin loop may be connected to the boom electrically and mechanically if desired.
Phasing-line lengths:
For cable with 0.80 velocity factor – 7 ft, $10^3/_8$ in.
For cable with 0.66 velocity factor – 6 ft, $5^3/_4$ in.

Table 6
Optimized 6-Meter Yagi Designs

	Spacing Between Elements inches	*Seg 1 OD* Length inches*	*Seg2 OD* Length inches*	*Midband Gain F/R*
306-06				
OD		0.750	0.625	
Refl.	0	36	23.500	7.9 dBi
D.E.	24	36	16.000	27.2 dB
Dir. 1	66	36	15.500	
506-12				
OD		0.750	0.625	
Refl.	0	36	24.000	10.1 dBi
D.E.	24	36	17.125	24.7 dB
Dir. 1	12	36	19.375	
Dir. 2	44	36	18.250	
Dir. 3	58	36	15.375	

	Spacing Between Elements inches	*Seg 1 OD* Length inches*	*Seg2 OD* Length inches*	*Midband Gain F/R*
706-22				
OD		0.750	0.625	
Refl.	0	36	25.000	11.3 dBi
D.E.	27	36	17.250	29.9 dB
Dir. 1	16	36	18.500	
Dir. 2	51	36	15.375	
Dir. 3	54	36	15.875	
Dir. 4	53	36	16.500	
Dir. 5	58	36	12.500	

*See pages 20-7 to 20-11 for telescoping aluminum tubing details.

that the electrical length of the balun is λ/2, but the physical length will be shorter due to the velocity factor of the particular coaxial cable used. The hairpin is connected directly across the element halves. The exact center of the hairpin is electrically neutral and should be fastened to the boom. This has the advantage of placing the driven element at dc ground potential.

The hairpin match requires no adjustment as such. However, you may have to change the length of the driven element slightly to obtain the best match in your preferred portion of the band. Changing the driven-element length will not adversely affect antenna performance. *Do not adjust the lengths or spacings of the other elements—they are optimized already*. If you decide to use a gamma match, add 3 inches to each side of the driven element lengths given in the table for all antennas.

High-Performance Yagis for 144, 222 and 432 MHz

This construction information is presented as an introduction to the three high-performance VHF/UHF Yagis that follow. All were designed and built by Steve Powlishen, K1FO. For years the design of long Yagi antennas seemed to be a mystical black art. The problem of simultaneously optimizing 20 or more element spacings and element lengths presented an almost unsolvable set of simultaneous equations. With the unprecedented increase in computer power and widespread availability of antenna analysis software, we are now able to quickly examine many Yagi designs and determine which approaches work and which designs to avoid.

At 144 MHz and above, most operators desire Yagi antennas two or more wavelengths in length. This length (2λ) is where most classical designs start to fall apart in terms of gain per boom length, bandwidth and pattern quality. Extensive computer and antenna range analysis has proven that the best possible design is a Yagi that has both varying element spacings and varying element lengths.

This design approach starts with closely spaced directors. The director spacings gradually increase until a constant spacing of about 0.4 λ is reached. Conversely, the director lengths start out longest with the first director and decrease in length in a decreasing rate of change until they are virtually constant in length. This method of construction results in a wide gain bandwidth. A bandwidth of 7% of the center frequency at the –1 dB forward-gain points is typical for these Yagis even when they are longer than 10 λ. The log-taper design also reduces the rate of change in driven-element impedance vs frequency. This allows the use of simple dipole driven elements while still obtaining acceptable driven-element SWR over a wide frequency range. Another benefit is that the resonant frequency of the Yagi changes very little as the boom length is increased.

The driven-element impedance also changes moderately with boom length. The tapered approach creates a Yagi with a very clean radiation pattern. Typically, first side lobe levels of ~17 dB in the E plane, ~15 dB in the H plane, and all other lobes at ~20 dB or more are possible on designs from 2 λ to more than 14 λ.

The actual rate of change in element lengths is determined by the diameter of the elements (in wavelengths). The spacings can be optimized for an individual boom length or chosen as a best compromise for most boom lengths.

The gain of long Yagis has been the subject of much debate. Recent measurements and computer analysis by both amateurs and professionals indicates that given an optimum design, doubling a Yagi's boom length will result in a maximum theoretical gain increase of about 2.6 dB. In practice, the real gain increase may be less because of escalating resistive losses and the greater possibility of construction error. **Fig 37** shows the maximum possible gain per boom length expressed in decibels, referenced to an isotropic radiator. The actual number of directors does not play an important part in determining the gain vs boom length as long as a reasonable number of directors are used. The use of more directors per boom length will normally give a wider gain bandwidth, however, a point exists where too many directors will adversely affect all performance aspects.

While short antennas (< 1.5 λ) may show increased gain with the use of quad or loop elements, long Yagis (> 2 λ) will not exhibit measurably greater forward gain or pattern integrity with loop-type elements. Similarly, loops used as driven elements and reflectors will not significantly change the properties of a long log-taper Yagi. Multiple-dipole driven-element assemblies will also not result in any significant gain increase per given boom length when compared to single-dipole feeds.

Once a long-Yagi director string is properly tuned, the reflector becomes relatively non critical. Reflector spacings between 0.15 λ and 0.2 λ are preferred. The spacing can be chosen for best pattern and driven element impedance. Multiple-reflector arrangements will not significantly increase the forward gain of a Yagi which has its directors properly optimized for forward gain. Many multiple-reflector schemes such as tri-reflectors and corner reflectors have the disadvantage of lowering the driven element impedance compared to a single optimum-length reflector. The plane or grid reflector, shown in **Fig 38**, may however reduce the intensity of unwanted rear lobes. This can be used to reduce noise pickup on EME or satellite arrays. This type of reflector will usually increase the driven-element impedance compared to a single reflector. This sometimes makes driven-element matching easier. Keep in mind that even for EME, a plane reflector will add considerable wind load and weight for

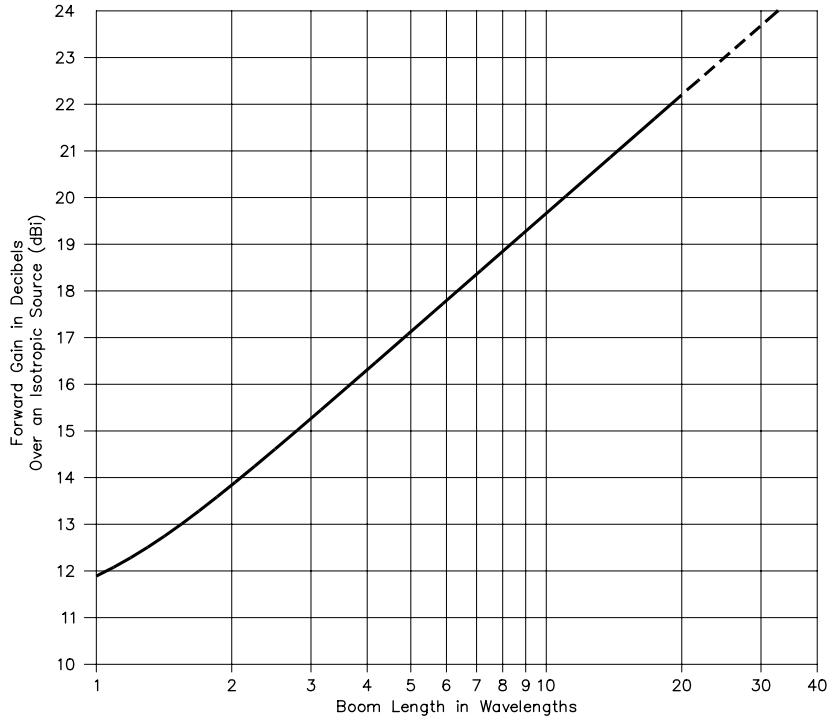

Fig 37—This chart shows maximum gain per boom length for optimally designed long Yagi antennas.

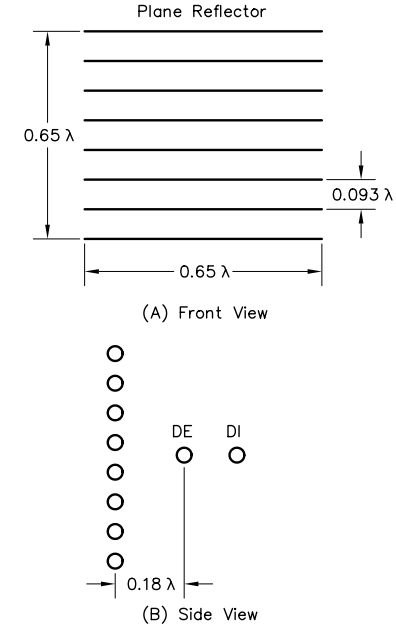

Fig 38—Front and side views of a plane-reflector antenna.

only a few tenths of a decibel of receive signal-to-noise improvement.

Yagi Construction

Normally, aluminum tubing or rod is used for Yagi elements. Hard-drawn enamel-covered copper wire can also be used on Yagis above 420 MHz. Resistive losses are inversely proportional to the square of the element diameter and the square root of its conductivity.

Element diameters of less than $^3/_{16}$ inch or 4 mm should not be used on any band. The size should be chosen for reasonable strength. Half-inch diameter is suitable for 50 MHz, $^3/_{16}$ to $^3/_8$ inch for 144 MHz and $^3/_{16}$ inch is recommended for the higher bands. Steel, including stainless steel and unprotected brass or copper wire, should not be used for elements.

Boom material may be aluminum tubing, either square or round. High-strength aluminum alloys such as 6061-T6 or 6063-T651 offer the best strength-to-weight advantages. Fiberglass poles have been used (where available as surplus). Wood is a popular low-cost boom material. The wood should be well seasoned and free from knots. Clear pine, spruce and Douglas fir are often used. The wood should be well treated to avoid water absorption and warping.

Elements may be mounted insulated or uninsulated, above or through the boom. Mounting uninsulated elements through a metal boom is the least desirable method unless the elements are welded in place. The Yagi elements will oscillate, even in moderate winds. Over several years this element oscillation will work open the boom holes. This will allow the elements to move in the boom. This will create noise (in your receiver) when the wind blows, as the element contact changes. Eventually the element-to-boom junction will corrode (aluminum oxide is a good insulator). This loss of electrical contact between the boom and element will reduce the boom's effect and change the resonant frequency of the Yagi.

Noninsulated elements mounted above the boom will perform fine as long as a good mechanical connection is made. Insulating blocks mounted above the boom will also work, but they require additional fabrication. One of the most popular construction methods is to mount the elements through the boom using insulating shoulder washers. This method is lightweight and durable. Its main disadvantage is difficult disassembly, making this method of limited use for portable arrays.

If a conductive boom is used, element lengths must be corrected for the mounting method used. The amount of correction is dependent upon the boom diameter in

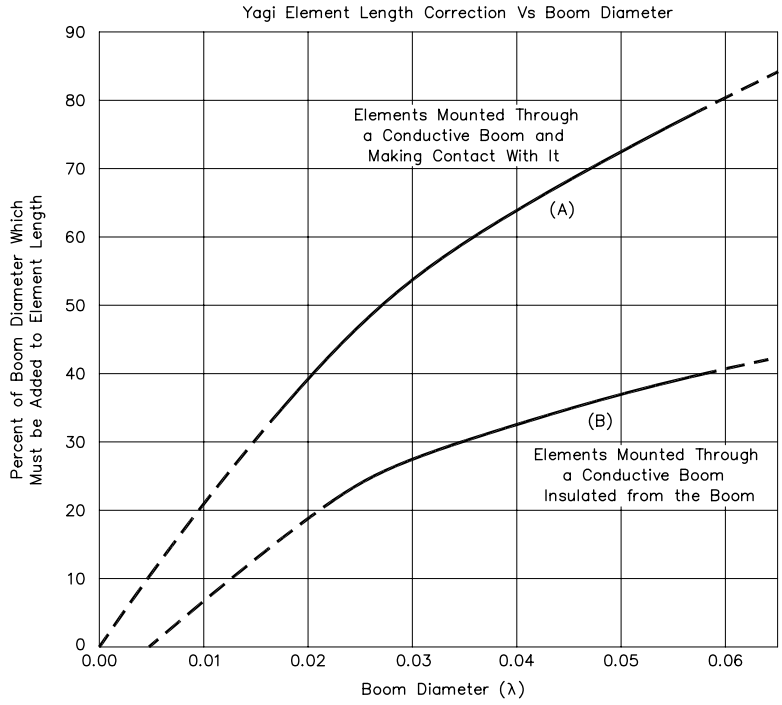

Fig 39—Yagi element correction vs boom diameter. Curve A is for elements mounted through a round or square conductive boom, with the elements in mechanical contact with the boom. Curve B is for insulated elements mounted through a conductive boom, and for elements mounted on top of a conductive boom (elements make electrical contact with the boom). The patterns were corrected to computer simulations to determine Yagi tuning. The amount of element correction is not affected by element diameter.

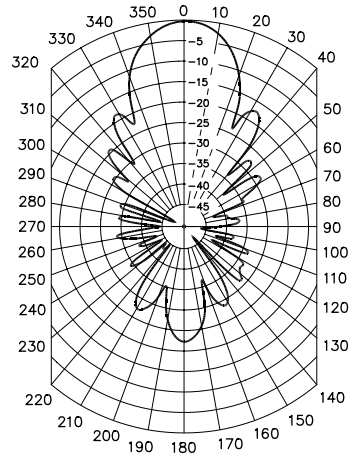

Fig 40—Measured E-plane pattern for the 22-element Yagi. Note: This antenna pattern is drawn on a linear dB grid, rather than on the standard ARRL log-periodic grid, to emphasize low sidelobes.

wavelengths. See **Fig 39**. Elements mounted through the boom and not insulated require the greatest correction. Mounting on top of the boom or through the boom on insulated shoulder washers requires about half of the through-the-boom correction. Insulated elements mounted at least one element diameter above the boom require no correction over the free-space length.

The three following antennas have been optimized for typical boom lengths on each band.

A HIGH-PERFORMANCE 432-MHz YAGI

This 22-element, 6.1-λ, 432-MHz Yagi was originally designed for use in a 12-Yagi EME array built by K1FO. A lengthy evaluation and development process preceded its construction. Many designs were considered and then analyzed on the computer. Next, test models were constructed and evaluated on a home-made antenna range. The resulting design is based on WlEJ's computer-optimized spacings.

The attention paid to the design process has been worth the effort. The 22-element Yagi not only has exceptional forward gain (17.9 dBi), but has an unusually clean radiation pattern. The measured E-plane pattern is shown in **Fig 40**. Note that a 1-dB-per-division axis is used to show pattern detail. A complete description of the design process and construction methods appears in December 1987 and January 1988 *QST*.

Like other log-taper Yagi designs, this one can easily be adapted to other boom lengths. Versions of this Yagi have been built by many amateurs. Boom lengths ranged between 5.3 λ (20 elements) and 12.2 λ (37 elements).

The size of the original Yagi (169 inches long, 6.1 λ) was chosen so the antenna could be built from small-diameter boom material ($^7/_8$-inch and 1 inch round 6061-T6 aluminum) and still survive high winds and ice loading. The 22-element Yagi weighs about 3.5 pounds and has a wind load of approximately 0.8 square feet. This allows a high-gain EME array to be built with manageable wind load and weight. This same low wind load and weight lets the tropo operator add a high-performance 432-MHz array to an existing tower without sacrificing antennas on other bands.

Table 7 lists the gain and stacking specifications for the various length Yagis. The basic Yagi dimensions are shown in **Table 8**. These are free-space element lengths for $^3/_{16}$-inch-diameter elements. Boom corrections for the element mounting method must be added in. The element-length correction column gives the length that must be added to keep the Yagi's center frequency optimized for use at 432 MHz. This correction is required to use the same spacing pattern over a wide range of boom lengths. Although any length Yagi will work well, this design is at its best when made with 18 elements or more (4.6 λ). Element material of less than $^3/_{16}$-inch diameter is not recommended because resistive losses will reduce the gain by about 0.1 dB, and wet-weather performance will be worse.

Quarter-inch-diameter elements could be used if all elements are shortened by 3 mm. The element lengths are intended for use with a slight chamfer (0.5 mm) cut into the element ends. The gain peak of the array is centered at 437 MHz. This allows acceptable wet-weather performance, while reducing the gain at 432 MHz by only 0.05 dB.

The gain bandwidth of the 22-element Yagi is 31 MHz (at the –1 dB points). The SWR of the Yagi is less than l.4: l between 420 and 440 MHz. **Fig 41** is a network analyzer plot of the driven-element SWR vs frequency. These numbers indicate just how wide the frequency response of a log-taper Yagi can be, even with a simple dipole driven element. In fact, at one antenna gain contest, some ATV operators conducted gain vs frequency measurements from 420 to 440 MHz. The 22-element Yagi beat all entrants including those with so-called broadband feeds.

To peak the Yagi for use on 435 MHz (for satellite use), you may want to shorten all the elements by 2 mm. To peak it for use on 438 MHz (for ATV applications), shorten all elements by 4 mm. If you want to use the Yagi

Table 7
Specifications for 432-MHz Yagi Family

No. of Ele.	*Boom length(λ)*	*Gain (dBi)**	*F/B ratio (dB)*	*DE imped (Ω)*	*Beamwidth E/H (°)*	*Stacking E/H (inches)*
15	3.4	15.67	21	23	30/32	53/49
16	3.8	16.05	19	23	29/31	55/51
17	4.2	16.45	20	27	28/30	56/53
18	4.6	16.8	25	32	27/29	58/55
19	4.9	17.1	25	30	26/28	61/57
20	5.3	17.4	21	24	25.5/27	62/59
21	5.7	17.65	20	22	25/26.5	63/60
22	6.1	17.9	22	25	24/26	65/62
23	6.5	18.15	27	30	23.5/25	67/64
24	6.9	18.35	29	29	23/24	69/66
25	7.3	18.55	23	25	22.5/23.5	71/68
26	7.7	18.8	22	22	22/23	73/70
27	8.1	19.0	22	21	21.5/22.5	75/72
28	8.5	19.20	25	25	21/22	77/75
29	8.9	19.4	25	25	20.5/21.5	79/77
30	9.3	19.55	26	27	20/21	80/78
31	9.7	19.7	24	25	19.6/20.5	81/79
32	10.2	19.8	23	22	19.3/20	2/80
33	10.6	9.9	23	23	19/19.5	83/81
34	11.0	20.05	25	22	18.8/19.2	84/82
35	11.4	20.2	27	25	18.5/19.0	85/83
36	11.8	20.3	27	26	18.3/18.8	86/84
37	12.2	20.4	26	26	18.1/18.6	87/85
38	12.7	20.5	25	25	18.9/18.4	88/86
39	13.1	20.6	25	23	18.7/18.2	89/87
40	13.5	20.8	26	21	17.5/18	90/88

*Gain is approximate real gain based on gain measurements made on six different-length Yagis.

Table 8

Free-Space Dimensions for 432-MHz Yagi Family

*Element correction is the amount to shorten or lengthen all elements when building a Yagi of that length.
Element lengths are for $^{3}/_{16}$-inch diameter material.

Ele. No.	*Element Position (mm from reflector)*	*Element Length (mm)*	*Element Correction**
Refl	0	340	
DE	104	334	
D1	146	315	
D2	224	306	
D3	332	299	
D4	466	295	
D5	622	291	
D6	798	289	
D7	990	287	
D8	1196	285	
D9	1414	283	
D10	1642	281	–2
D11	1879	279	–2
D12	2122	278	–2
D13	2373	277	–2
D14	2629	276	–2
D15	2890	275	–1
D16	3154	274	–1
D17	3422	273	–1
D18	3693	272	0
D19	3967	271	0
D20	4242	270	0
D21	4520	269	0
D22	4798	269	0
D23	5079	268	0
D24	5360	268	+1
D25	5642	267	+1
D26	5925	267	+1
D27	6209	266	+1
D28	6494	266	+1
D29	6779	265	+2
D30	7064	265	+2
D31	7350	264	+2
D32	7636	264	+2
D33	7922	263	+2
D34	8209	263	+2
D35	8496	262	+2
D36	8783	262	+2
D37	9070	261	+3
D38	9359	261	+3

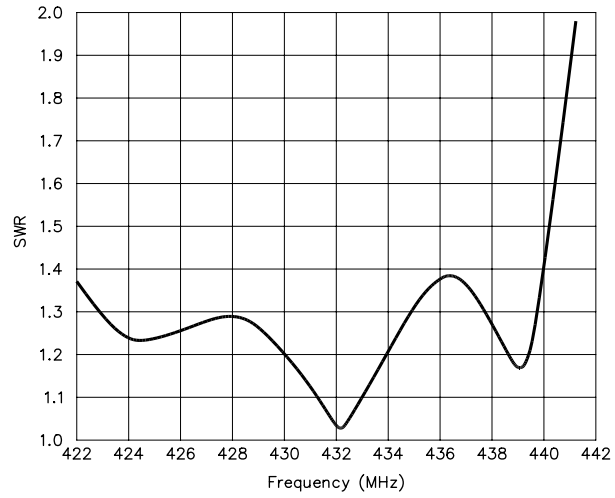

Fig 41—SWR performance of the 22-element Yagi in dry weather.

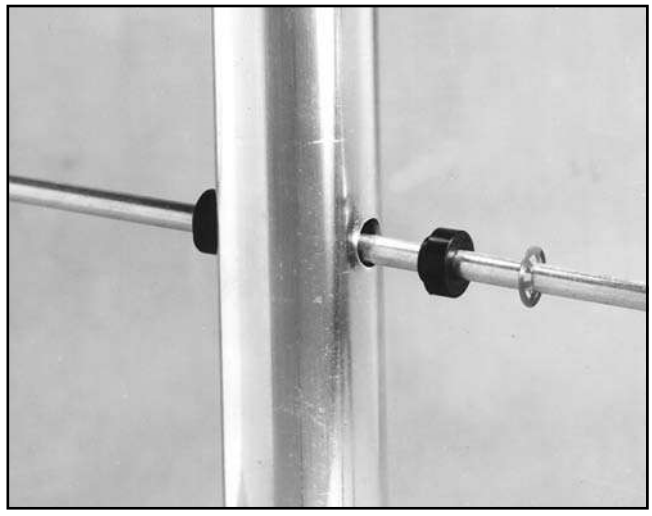

Fig 42—Element-mounting detail. Elements are mounted through the boom using plastic insulators. Stainless steel push-nut retaining rings hold the element in place.

on FM between 440 MHz and 450 MHz, shorten all the elements by 10 mm. This will provide 17.6 dBi gain at 440 MHz, and 18.0 dBi gain at 450 MHz. The driven element may have to be adjusted if the element lengths are shortened.

Although this Yagi design is relatively broadband, it is suggested that close attention be paid to copying the design exactly as built. Metric dimensions are used because they are convenient for a Yagi sized for 432 MHz. Element holes should be drilled within ±2 mm. Element lengths should be kept within ±0.5 mm. Elements can be accurately constructed if they are first rough cut with a hack saw and then held in a vise and filed to the exact length.

The larger the array, the more attention you should pay to making all Yagis identical. Elements are mounted on shoulder insulators and run through the boom (see **Fig 42**). The element retainers are stainless-steel push nuts. These are made by several companies, including Industrial Retaining Ring Co in Irvington, New Jersey, and AuVeco in Ft Mitchell, Kentucky. Local industrial hardware distributors can usually order them for you. The element insulators

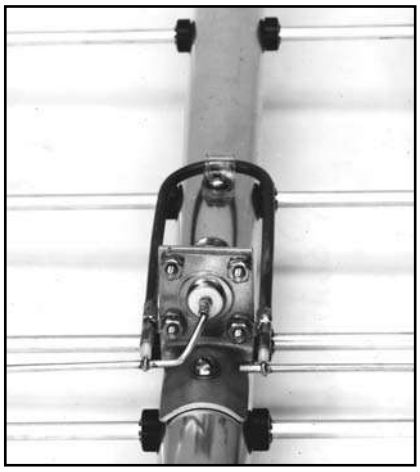

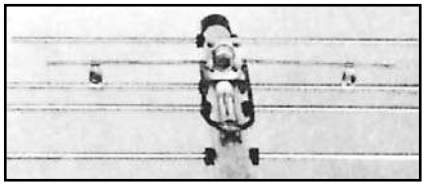

Fig 43—Several views of the driven element and T match.

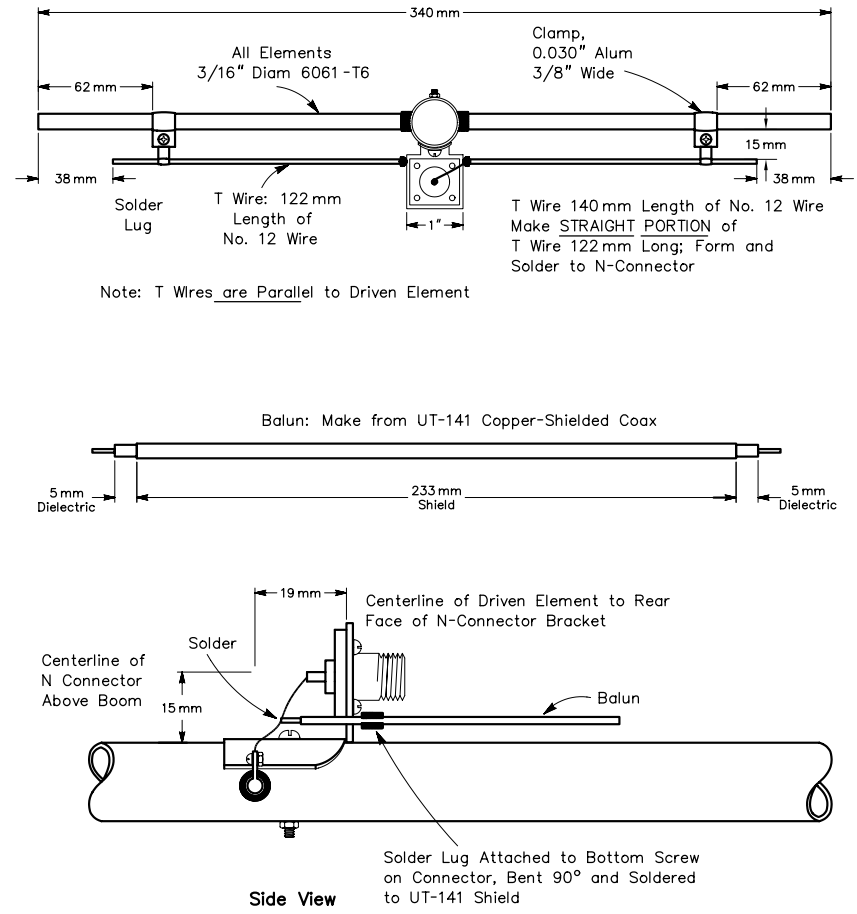

Fig 44—Details of the driven element and T match for the 22-element Yagi. Lengths are given in millimeters to allow precise duplication of the antenna. See text.

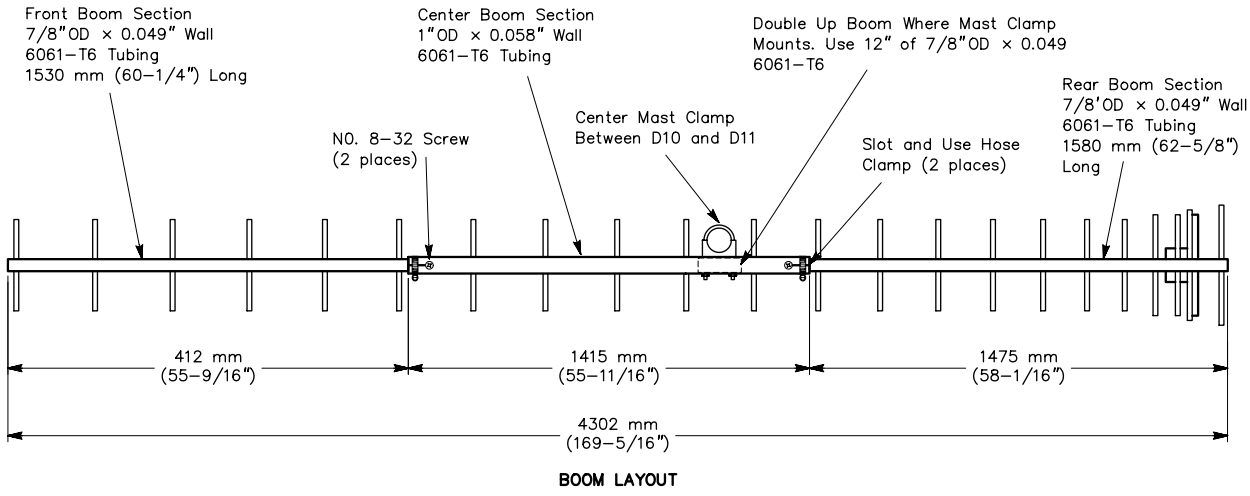

Fig 45—Boom-construction information for the 22-element Yagi Lengths are given in millimeters to allow precise duplication of the antenna. See text.

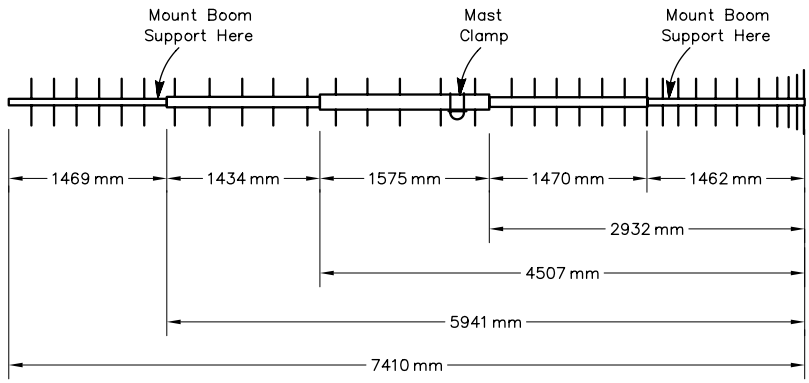

Fig 46—Boom-construction information for the 33-element Yagi. Lengths are given in millimeters to allow precise duplication of the antenna.

are not critical. Teflon or black polyethylene are probably the best materials. The Yagi in the photographs is made with black Delryn insulators, available from C3i in Washington, DC.

The driven element uses a UG-58A/U connector mounted on a small bracket. The UG58A/U should be the type with the press-in center pin. UG-58s with center pins held in by "C" clips will usually leak water. Some connectors use steel retaining clips, which will rust and leave a conductive stripe across the insulator. The T-match wires are supported by the UT-141 balun. RG-303/U or RG-142/U Tefloninsulated cable could be used if UT-141 cannot be obtained. **Fig 43A** and Fig 42B show details of the driven-element construction. Driven element dimensions are given in **Fig 44**.

Dimensions for the 22-element Yagi are listed in **Table 9**. **Fig 45** details the Yagi's boom layout. Element material can be either $^3/_{16}$ inch 6061-T6 aluminum rod or hard aluminum welding rod.

A 24-foot-long, 10.6-λ, 33-element Yagi was also built. The construction methods used were the same as the 22-element Yagi. Telescoping round boom sections of 1, $1^1/_8$, and $1^1/_4$ inches in diameter were used. A boom support is required to keep boom sag acceptable. At 432 MHz, if boom sag is much more than two or three inches, H-plane pattern distortion will occur. Greater amounts of boom sag will reduce the gain of a Yagi. **Table 10** lists the proper dimensions for the antenna when built with the previously given boom diameters. The boom layout is shown in **Fig 46**, and the driven element is described in **Fig 47**. The 33-element Yagi exhibits the same clean pattern traits as the 22-element Yagi (see **Fig 48**). Measured gain of the 33-element Yagi is 19.9 dBi at 432 MHz. A measured gain sweep of the 33-element Yagi gave a –1 dB gain bandwidth of 14 MHz with the –1 dB points at 424.5 MHz and 438.5 MHz.

A HIGH-PERFORMANCE 144MHZ YAGI

This 144MHz Yagi design uses the latest log-tapered element spacings and lengths. It offers near theoretical gain per boom length, an extremely clean pattern and wide bandwidth. The design is based upon the spacings used in a 4.5-λ 432-MHz computerdeveloped design by W1EJ. It is quite similar to the 432MHz Yagi described elsewhere in this chapter. Refer to that project for additional construction diagrams and photographs.

Mathematical models do not always directly translate into real working examples. Although the computer design provided a good starting point, the author, Steve Powlishen, K1FO, built several test models before the final working Yagi was obtained. This hands-on tuning included changing the element-taper rate in order to obtain the flexibility that allows the Yagi to be built with different boom lengths.

The design is suitable for use from 1.8 λ (10 elements) to 5.1 λ (19 elements). When elements are added to a Yagi, the center frequency, feed impedance and front-to-back ratio will range up and down. A modern tapered design will minimize this effect and allow the builder to select any desired boom length. This Yagi's design capabilities per boom length are listed in **Table 11**.

The gain of any Yagi built around this design will be within 0.1 to 0.2 dB of the maximum theoretical gain at the design frequency of 144.2 MHz. The design is intentionally peaked high in frequency (calculated gain peak is about 144.7 MHz). It has been found that by doing this, the SWR bandwidth and pattern at 144.0 to 144.3 MHz will be better, the Yagi will be less affected by weather and its performance in arrays will be more predictable. This design starts to drop off in performance if built with fewer than 10 elements. At less than 2 λ, more traditional designs perform well.

Table 12 gives free-space element lengths for $^1/_4$ inch-diameter elements. The use of metric notation allows for much easier dimensional changes during the design stage. Once you become familiar with the metric system, you'll probably find that construction is easier without the burden of cumbersome English fractional units. For $^3/_{16}$ inch-diameter elements, lengthen all parasitic elements by 3 mm. If $^3/_8$ inch diameter elements are used, shorten all of the

Table 9

Dimensions for the 22-Element 432-MHz Yagi

Element Number	*Element Position (mm from reflector)*	*Element Length (mm)*	*Boom Diam (in)*
Refl	30	346	
DE	134	340	
D1	176	321	
D2	254	311	7/8
D3	362	305	
D4	496	301	
D5	652	297	
D6	828	295	
D7	1020	293	
D8	1226	291	
D9	1444	289	
D10	1672	288	
D11	1909	286	
D12	2152	285	1
D13	2403	284	
D14	2659	283	
D15	2920	281	
D16	3184	280	
D17	3452	279	7/8
D18	3723	278	
D19	3997	277	
D20	4272	276	

directors and the reflector by 6 mm. The driven element will have to be adjusted for the individual Yagi if the 12-element design is not adhered to.

For the 12-element Yagi, 1/4-inch diameter elements were selected because smaller-diameter elements become rather flimsy at 2 meters. Other diameter elements can be used as described previously. The 2.5-λ boom was chosen because it has an excellent size and wind load vs gain and pattern trade-off. The size is also convenient; three 6-foot-long pieces of aluminum tubing can be used without any waste. The relatively large-diameter boom sizes ($1^1/_4$ and $1^3/_8$ inches) were chosen, as they provide an extremely rugged Yagi that does not require a boom support. The 12-element 17-foot-long design has a calculated wind survival of close to 120 mph! The absence of a boom support also makes vertical polarization possible.

Table 10

Dimensions for the 33-Element 432-MHz Yagi

Element Number	*Element Position (mm from reflector)*	*Element Length (mm)*	*Boom Diam (in)*
REF	30	348	
DE	134	342	
D1	176	323	
D2	254	313	
D3	362	307	
D4	496	303	1
D5	652	299	
D6	828	297	
D7	1020	295	
D8	1226	293	
D9	1444	291	
D10	1672	290	
D11	1909	288	
D12	2152	287	$1^1/_8$
D13	2403	286	
D14	2659	285	
D15	2920	284	
D16	3184	284	
D17	3452	283	
D18	3723	282	1¼
D19	3997	281	
D20	4272	280	
D21	4550	278	
D22	4828	278	
D23	5109	277	$1^1/_8$
D24	5390	277	
D25	5672	276	
D26	5956	275	
D27	6239	274	
D28	6524	274	1
D29	6809	273	
D30	7094	273	
D31	7380	272	

Longer versions could be made by telescoping smaller-size boom sections into the last section. Some sort of boom support will be required on versions longer than 22 feet. The elements are mounted on shoulder insulators and mounted through the boom. However, elements may

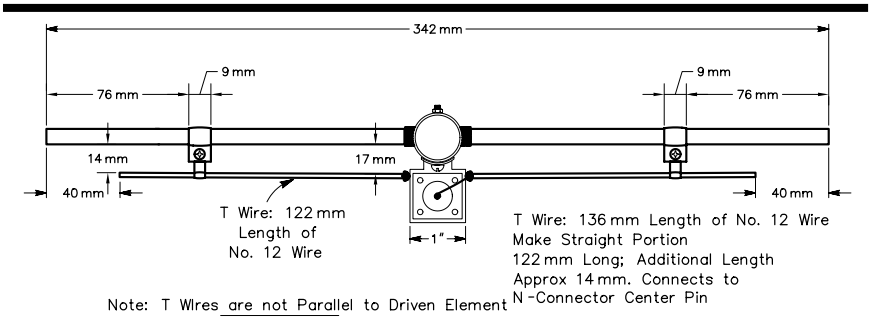

Fig 47—Details of the driven element and T match for the 33-element Yagi. Lengths are given in millimeters to allow precise duplication of the antenna.

Table 11
Specifications for the 144-MHz Yagi Family

No. of Ele.	Boom Length(λ)	Gain (dBd)	DE Imped (Ω)	FB Ratio (dB)	Beamwidth E/H (°)	Stacking E/H (°)
10	1.8	11.4	27	17	39/42	10.2/9.5
11	2.2	12.0	38	19	36/40	11.0/10.0
12	2.5	12.5	28	23	34/37	11.7/10.8
13	2.9	13.0	23	20	32/35	12.5/11.4
14	3.2	13.4	27	18	31/33	12.8/12.0
15	3.6	13.8	35	20	30/32	13.2/12.4
16	4.0	14.2	32	24	29/30	13.7/13.2
17	4.4	14.5	25	23	28/29	14.1/13.6
18	4.8	14.8	25	21	27/28.5	14.6/13.9
19	5.2	15.0	30	22	26/27.5	15.2/14.4

Table 12
Free-Space Dimensions for the 144-MHz Yagi Family
Element diameter is ¼ inch

Element No.	Element Position (mm from reflector)	Element Length
Refl.	0	1038
DE	312	955
D1	447	956
D2	699	932
D3	1050	916
D4	1482	906
D5	1986	897
D6	2553	891
D7	3168	887
D8	3831	883
D9	4527	879
D10	5259	875
D11	6015	870
D12	6786	865
D13	7566	861
D14	8352	857
D15	9144	853
D16	9942	849
D17	10744	845

be mounted, insulated or uninsulated, above or through the boom, as long as appropriate element length corrections are made. Proper tuning can be verified by checking the depth of the nulls between the main lobe and first side lobes. The nulls should be 5 to 10 dB below the first sidelobe level at the primary operating frequency. The boom layout for the 12-element model is shown in **Fig 49**. The actual corrected element dimensions for the 12-element 2.5-λ Yagi are shown in **Table 13**.

The design may also be cut for use at 147 MHz. There is no need to change element spacings. The element lengths should be shortened by 17 mm for best operation between 146 and 148 MHz. Again, the driven element will have to be adjusted as required.

The driven-element size ($^1/_2$-inch diameter) was chosen to allow easy impedance matching. Any reasonably sized driven element could be used, as long as appropriate length and T-match adjustments are made. Different driven-element dimensions are required if you change the boom length. The calculated natural driven-element impedance is given as a guideline. A balanced T-match was chosen because it's easy to adjust for best SWR and provides a balanced radiation pattern. A 4:1 half-wave coaxial balun is used, although impedance-transforming quarter-wave sleeve baluns could also be used. The cal-

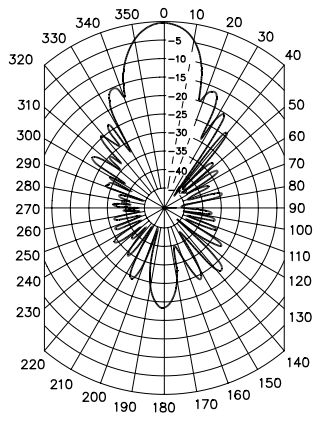

Fig 48—E-plane pattern for the 33-element Yagi. This pattern is drawn on a linear dB grid scale, rather than the standard ARRL log-periodic grid, to emphasize low sidelobes.

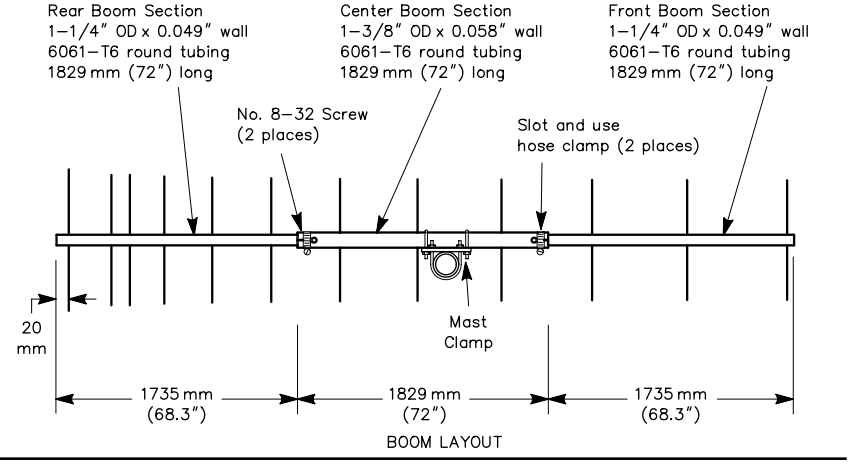

Fig 49—Boom layout for the 12-element 144-MHz Yagi. Lengths are given in millimeters to allow precise duplication.

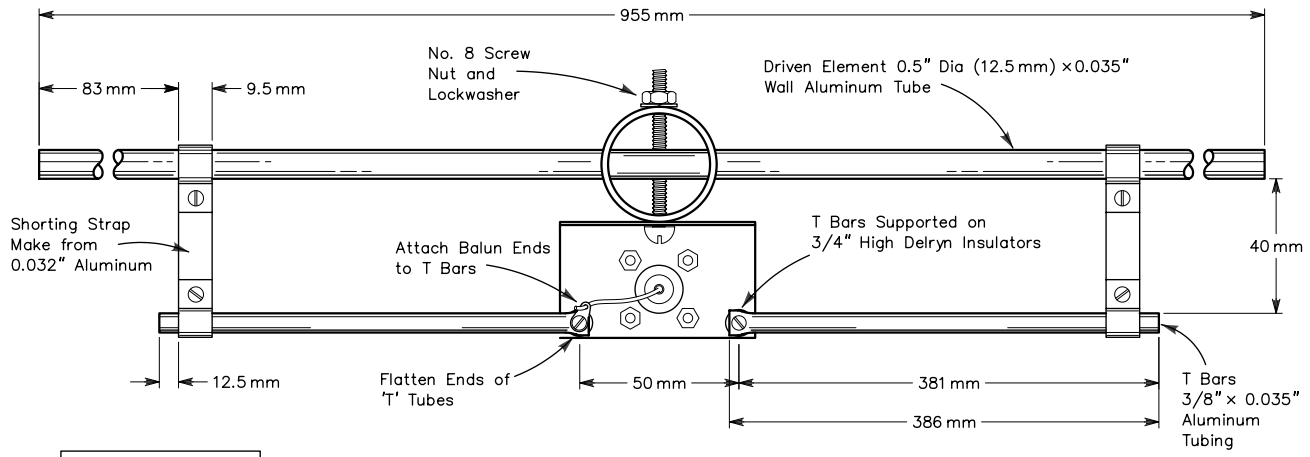

Driven Element Detail 12—Element 144 MHz Yagi

(A)

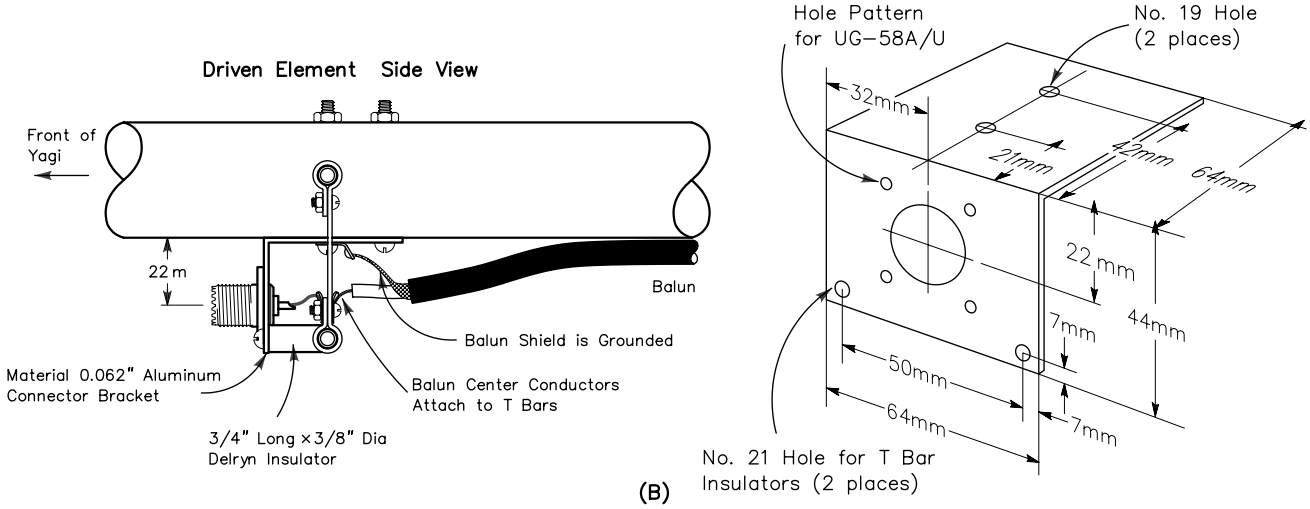

(B)

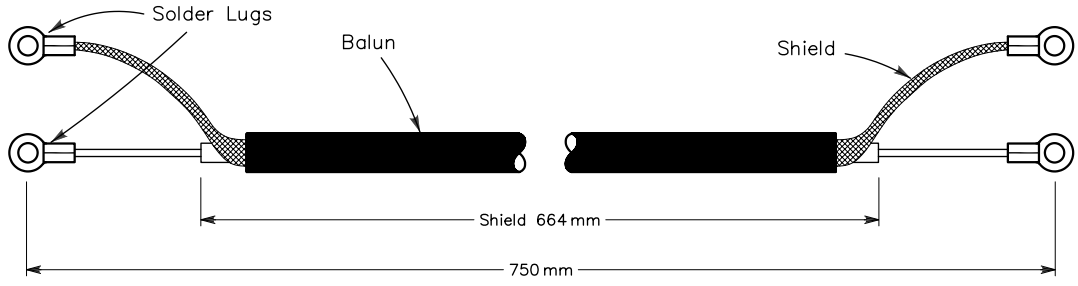

Material: RG—142/U or RG—303/U Teflon—Insulated Coaxial Cable

Ant18—50

(C)

Fig 50—Driven-element detail for the 12-element 144-MHz Yagi. Lengths are given in millimeters to allow precise duplication.

Table 13

Dimensions for the 12-Element 2.5-λ Yagi

Element Number	*Element Position (mm from reflector)*	*Element Length (mm)*	*Boom Diam (in)*
Refl.	0	1044	
DE	312	955	
D1	447	962	1 1/4
D2	699	938	
D3	1050	922	
D4	1482	912	
D5	1986	904	
D6	2553	898	1 3/8
D7	3168	894	
D8	3831	889	
D9	4527	885	1 1/4
D10	5259	882	

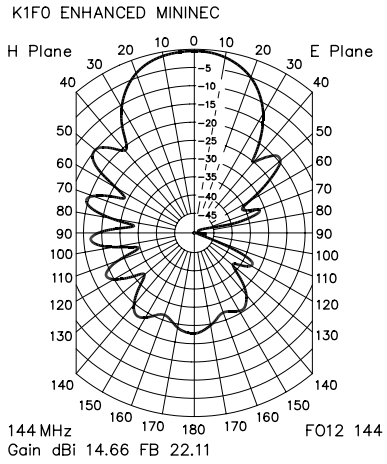

Fig 51—H- and E-plane pattern for the 12-element 144-MHz Yagi.

culated natural impedance will be useful in determining what impedance transformation will be required at the 200-Ω balanced feed point. Chapter 26, Coupling the Line to the Antenna, contains information on calculating folded-dipole and T-match driven-element parameters. A balanced feed is important for best operation on this antenna. Gamma matches can severely distort the pattern balance. Other useful driven-element arrangements are the Delta match and the folded dipole, if you're willing to sacrifice some flexibility. **Fig 50** details the driven-element dimensions.

A noninsulated driven element was chosen for mounting convenience. An insulated driven element may also be used. A grounded driven element may be less affected by static build-up. On the other hand, an insulated driven element allows the operator to easily check his feed lines for water or other contamination by the use of an ohmmeter from the shack.

Table 14

Free-Space Dimensions for the 222-MHz Yagi Family

Element diameter is 3/16-inch.

Element No.	*Element Position (mm from reflector)*	*Element Length (mm)*
Refl.	0	676
DE	204	647
D1	292	623
D2	450	608
D3	668	594
D4	938	597
D5	1251	581
D6	1602	576
D7	1985	573
D8	2395	569
D9	2829	565
D10	3283	562
D11	3755	558
D12	4243	556
D13	4745	554
D14	5259	553
D15	5783	552
D16	6315	551
D17	6853	550
D18	7395	549
D19	7939	548
D20	8483	547

Fig 51 shows computer-predicted E- and H-plane radiation patterns for the 12-element Yagi. The patterns are plotted on a l-dB-per-division linear scale instead of the usual ARRL polar-plot graph. This expanded scale plot is used to show greater pattern detail. The pattern for the 12-element Yagi is so clean that a plot done in the standard ARRL format would be almost featureless, except for the main lobe and first sidelobes.

The excellent performance of the 12-element Yagi is demonstrated by the reception of Moon echoes from several of the larger 144MHz EME stations with only one 12-element Yagi. Four of the 12-element Yagis will make an excellent starter EME array, capable of working many EME QSOs while being relatively small in size. The advanced antenna builder can use the information in Table 11 to design a dream array of virtually any size.

A HIGH-PERFORMANCE 222-MHz YAGI

Modern tapered Yagi designs are easily applied to 222 MHz. This design uses a spacing progression that is in between the 12-element 144-MHz design, and the 22-element 432-MHz design presented elsewhere in this chapter. The result is a design with maximum gain per boom length, a clean, symmetrical radiation pattern, and wide bandwidth. Although it was designed for weak-signal work (tropospheric scatter and EME), the design is

Table 15
Specifications for the 222-MHz Yagi Family

No of Ele.	Boom Length(λ)	Gain (dBd)	FB Ratio (dB)	DE Imped (Ω)	Beamwidth E/H (°)	Stacking E/H (feet)
12	2.4	12.3	22	23	37/39	7.1/6.7
13	2.8	12.8	19	28	33/36	7.8/7.2
14	3.1	13.2	20	34	32/34	8.1/7.6
15	3.5	13.6	24	30	30/33	8.6/7.8
16	3.9	14.0	23	23	29/31	8.9/8.3
17	4.3	14.35	20	24	28/30.5	9.3/8.5
18	4.6	14.7	20	29	27/29	9.6/8.9
19	5.0	15.0	22	33	26/28	9.9/9.3
20	5.4	15.3	24	29	25/27	10.3/9.6
21	5.8	15.55	23	24	24.5/26.5	10.5/9.8
22	6.2	15.8	21	23	24/26	10.7/10.2

suited to all modes of 222-MHz operation, such as packet radio, FM repeater operation and control links.

The spacings were chosen as the best compromise for a 3.9-λ 16-element Yagi. The 3.9-λ design was chosen, like the 12-element 144-MHz design, because it fits perfectly on a boom made from three 6-foot-long aluminum tubing sections. The design is quite extensible, and models from 12 elements (2.4 λ) to 22 elements (6.2 λ) can be built from the dimensions given in **Table 14**. Note that free-space lengths are given. They must be corrected for the element-mounting method. Specifications for various boom lengths are shown in **Table 15**.

Construction

Large-diameter ($1^1/_4$- and $1^3/_8$-inch diameter) boom construction is used, eliminating the need for boom supports. The Yagi can also be used vertically polarized. Three-sixteenths-inch-diameter aluminum elements are used. The exact alloy is not critical; 6061-T6 was used, but hard aluminum welding rod is also suitable. Quarter-inch-diameter elements could also be used if all elements are shortened by 3 mm. Three-eighths-inch-diameter elements would require 10-mm shorter lengths. Elements smaller than $^3/_{16}$ inch-diameter are not recommended. The elements are insulated and run through the boom. Plastic shoulder washers and stainless steel retainers are used to hold the elements in place. The various pieces needed to build the Yagi may be obtained from C3i in Washington, DC. **Fig 52** details the boom layout for the 16-element Yagi. **Table 16** gives the dimensions for the 16-element Yagi as built. The driven element is fed with a T match and a 4:1 balun. See **Fig 53** for construction details. See the 432-MHz Yagi project elsewhere in this chapter for additional photographs and construction diagrams.

The Yagi has a relatively broad gain and SWR curve, as is typical of a tapered design, making it usable over a wide frequency range. The example dimensions are intended for use at 222.0 to 222.5 MHz. The 16-element Yagi is quite usable to more than 223 MHz. The best compromise for covering the entire band is to shorten all parasitic elements by 4 mm. The driven element will have to be adjusted in length for best match. The position of the T-wire shorting straps may also have to be moved.

The aluminum boom provides superior strength, is lightweight, and has a low wind-load cross section. Aluminum is doubly attractive, as it will long outlast wood and fiberglass. Using state-of-the-art designs, it is unlikely that significant performance increases will be achieved in the next few years. Therefore, it's in your best interest to build an antenna that will last many years. If suitable wood or fiberglass poles are readily available, they may be used without any performance degradation, at least when the wood is new and dry. Use the free-space element lengths given in Table 16 for insulated-boom construction.

The pattern of the 16-element Yagi is shown in **Fig 54**. Like the 144-MHz Yagi, a l-dB-per-division plot is used to detail the pattern accurately. This 16-element design makes a good building block for EME or tropo DX arrays. Old-style narrow-band Yagis often perform

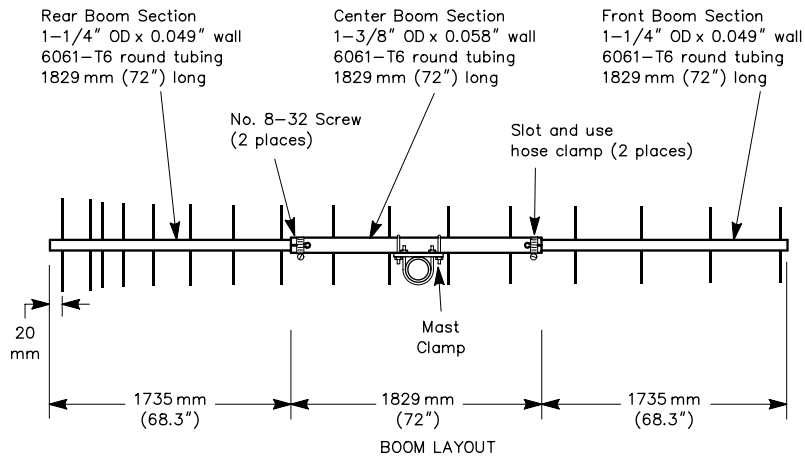

Fig 52—Boom layout for the 16-element 222-MHz Yagi. Lengths are given in millimeters to allow precise duplication.

Table 16

Dimensions for 16-Element 3.9-λ 222-MHz Yagi

Element Number	*Element Position (mm from reflector)*	*Element Length (mm)*	*Boom Diam (in)*
Refl.	0	683	
DE	204	664	
D1	292	630	
D2	450	615	
D3	668	601	$1^1/_4$
D4	938	594	
D5	1251	588	
D6	1602	583	
D7	1985	580	
D8	2395	576	
D9	2829	572	$1^3/_8$
D10	3283	569	
D11	3755	565	
D12	4243	563	
D13	4745	561	$1^1/_4$
D14	5259	560	

unpredictably when used in arrays. The theoretical 3.0-dB stacking gain is rarely observed. The 16-element Yagi (and other versions of the design) reliably provides stacking gains of nearly 3 dB. (The spacing dimensions listed in Table 15 show just over 2.9 dB stacking gain.) This has been found to be the best compromise between gain, pattern integrity and array size. Any phasing line losses will subtract from the possible stacking gain. Mechanical misalignment will also degrade the performance of an array.

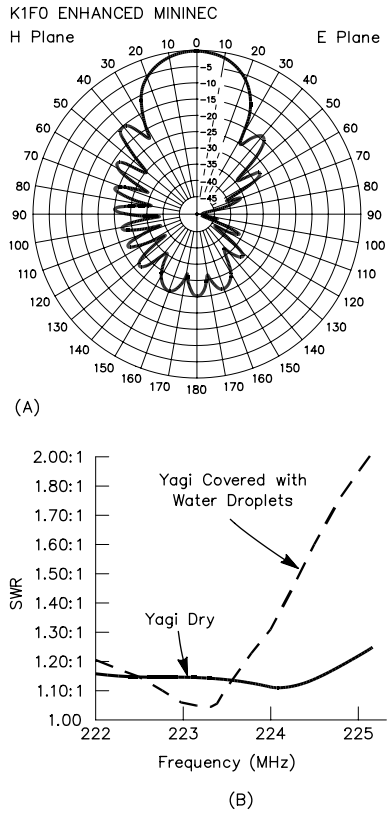

Fig 54—H- and E-plane patterns for the 16-element 222-MHz Yagi at A. The driven-element T-match dimensions were chosen for the best SWR compromise between wet and dry weather conditions. The SWR vs frequency curve shown at B demonstrates the broad frequency response of the Yagi design.

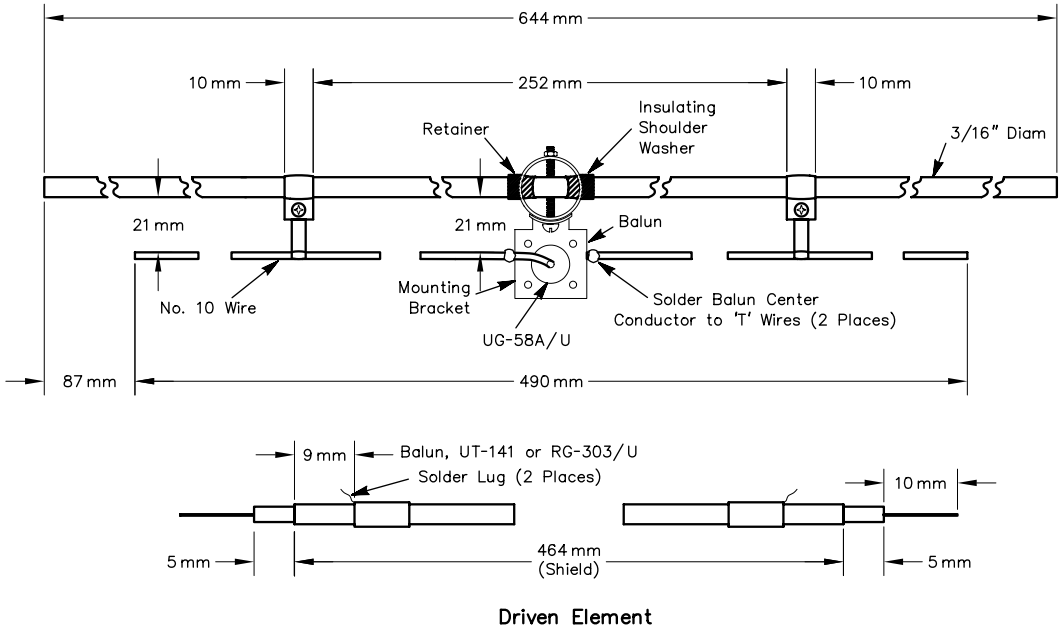

Fig 53—Driven-element detail for the 16-element 222-MHz Yagi. Lengths are given in millimeters to allow precise duplication.

A 144 MHz 2-Element Quad

The basic 2-element quad array for 144 MHz is shown in **Fig 55**. The supporting frame is 1 × 1-inch wood, of any kind suitable for outdoor use. Elements are #8 aluminum wire. The driven element is 1 λ (83 inches) long, and the reflector five percent longer (87 inches). Dimensions are not critical, as the quad is relatively broad in frequency response.

The driven element is open at the bottom, its ends fastened to a plastic block. The block is mounted at the bottom of the forward vertical support. The top portion of the element runs through the support and is held firmly by a screw running into the wood and then bearing on the aluminum wire. Feed is by means of 50-Ω coax, connected to the driven-element loop.

The reflector is a closed loop, its top and bottom portions running through the rear vertical support. It is held in position with screws at the top and bottom. The loop can be closed by fitting a length of tubing over the element ends, or by hammering them flat and bolting them together as shown in the sketch.

The elements in this model are not adjustable, though this can easily be done by the use of stubs. It would then be desirable to make the loops slightly smaller to compensate for the wire in the adjusting stubs. The driven element stub would be trimmed for length and the point of connection for the coax would be adjustable for best match. The reflector stub can be adjusted for maximum gain or maximum F/B ratio, depending on the builder's requirements.

In the model shown only the spacing is adjusted, and this is not particularly critical. If the wooden supports are made as shown, the spacing between the elements can be adjusted for best match, as indicated by an SWR meter connected in the coaxial line. The spacing has little effect on the gain (from 0.15 to 0.25 λ), so the variation in impedance with spacing can be used for matching. This also permits use of either 50- or 75-Ω coax for the transmission line.

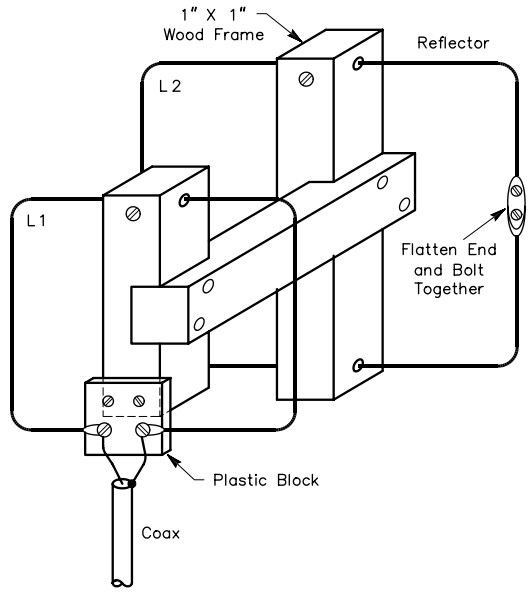

Fig 55—Mechanical details of a 2-element quad for 144 MHz. The driven element, L1, is one wavelength long; reflector L2 is 5% longer. With the transmission line connected as shown here, the resulting radiation is horizontally polarized. Sets of elements of this type can be stacked horizontally and vertically for high gain with broad frequency response. Recommended bay spacing is ½ λ between adjacent element sides. The example shown may be fed directly with 50-Ω coax.

A Portable 144 MHz 4-Element Quad

Element spacing for quad antennas found in the literature ranges from 0.14 λ to 0.25 λ. Factors such as the number of elements in the array and the parameters to be optimized (F/B ratio, forward gain, bandwidth, etc), determine the optimum element spacing within this range. The 4-element quad antenna described here was designed for portable use, so a compromise between these factors was chosen. This antenna, pictured in **Fig 56**, was designed and built by Philip D'Agostino, W1KSC.

Based on several experimentally determined correction factors related to the frequency of operation and the wire size, optimum design dimensions were found to be as follows.

$$\text{Reflector length (ft)} = \frac{1046.8}{f_{MHz}} \qquad \text{(Eq 8)}$$

$$\text{Driven element (ft)} = \frac{985.5}{f_{MHz}} \qquad \text{(Eq 9)}$$

$$\text{Directors (ft)} = \frac{937.3}{f_{MHz}} \qquad \text{(Eq 10)}$$

Cutting the loops for 146 MHz provides satisfactory performance across the entire 144MHz band.

Fig 56—The 4-element 144-MHz portable quad, assembled and ready for operation. Sections of clothes closet poles joined with pine strips make up the mast. (*Photo by Adwin Rusczek, W1MPO)*

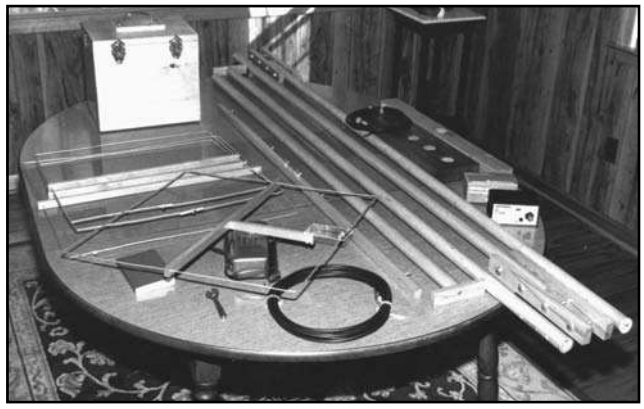

Fig 57—The complete portable quad, broken down for travel. Visible in the foreground is the driven element. The pine box in the background is a carrying case for equipment and accessories. A hole in the lid accepts the mast, so the box doubles as a base for a short mast during portable operation. *(W1MPO photo)*

Materials

The quad was designed for quick and easy assembly and disassembly, as illustrated in **Fig 57**. Wood (clear trim pine) was chosen as the principal building material because of its light weight, low cost, and ready availability. Pine is used for the boom and element supporting arms. Round wood clothes closet poles comprise the mast material. Strips connecting the mast sections are made of heavier pine trim. Elements are made of no. 8 aluminum wire. Plexiglas is used to support the feed point. **Table 17** lists the hardware and other parts needed to duplicate the quad.

Construction

The elements of the quad are assembled first. The mounting holes in the boom should be drilled to accommodate $1^1/_2$ inch no. 8 hardware. Measure and mark the locations where the holes are to be drilled in the element spreaders, **Fig 58**. Drill the holes in the spreaders just

Table 17

Parts List for the 144 MHz 4-element Quad

Boom: ¾ × ¾ ×48-in. pine

Driven element support (spreader):
½ × ¾ × 21¼ in. pine

Driven element feed point strut: ½ × ¾ × 7½ in. pine

Reflector support (spreader): ½ × ¾ × 22½ in. pine

Director supports (spreaders):
½ × ¾ × 20¼ in. pine, 2 req'd

Mast brackets: ¾ × 1½ × 12 in. heavy pine trim, 4 req'd

Boom to mast bracket: ½ × $1^5/_8$ × 5 in. pine

Element wire: Aluminum ground wire
(Radio Shack no. 15-035)

Wire clamps: ¼in. electrician's copper or zinc plated steel clamps, 3 req'd

Boom hardware:
- 6 no. 8-32 × 1½ in. stainless steel machine screws
- 6 no. 8-32 stainless steel wing nuts
- 12 no. 8 stainless steel washers

Mast hardware:
- 8 hex bolts, ¼-20 × 3½ in.
- 8 hex nuts, ¼-20
- 16 flat washers

Mast material: $1^5/_{16}$ in. × 6 ft wood clothes closet poles, 3 req'd

Feed point support plate: 3½ × 2½ in. Plexiglas sheet

Wood preparation materials:
Sandpaper, clear polyurethane, wax

Feed line: 52-W RG-8 or RG-58 cable

Feed line terminals: Solder lugs for no. 8 or larger hardware, 2 req'd

Miscellaneous hardware:
4 small machine screws, nuts, washers; 2 flat-head wood screws

large enough to accept the #8 wire elements. It is important to drill all the holes straight so the elements line up when the antenna is assembled.

Construction of the wire elements is easiest if the directors are made first. A handy jig for bending the elements can be made from a piece of 2 × 3-inch wood cut to the side length of the directors. It is best to start with about 82 inches of wire for each director. The excess can be cut off when the elements are completed. (The total length of each director is 77 inches.) Two bends should initially be made so the directors can be slipped into the spreaders before the remaining corners are bent. See **Fig 59**. Electrician's copper-wire clamps can be used to join the wires after the final bends are made, and they facilitate adjustment of element length. The reflector is made the same way as the directors, but the total length is 86 inches.

The driven element, total length 81 inches, requires special attention, as the feed attachment point needs to be adequately supported. An extra hole is drilled in the driven element spreader to support the feed-point strut, as shown in **Fig 60**. A Plexiglas plate is used at the feed point to support the feed- point hardware and the feed line. The feed-point support strut should be epoxied to the spreader, and a wood screw used for extra mechanical strength.

For vertical polarization, locate the feed point in the center of one side of the driven element, as shown in Fig 60. Although this arrangement places the spreader supports at voltage maxima points on the four loop conductors, D'Agostino reports no adverse effects during operation. However, if the antenna is to be left exposed to the weather, the builder may wish to modify the design to provide support for the loops at current maxima points, such as shown in Fig 60. (The element of Fig 60 should be rotated 90° for horizontal polarization.)

Orient the driven element spreader so that it mounts properly on the boom when the antenna is assembled. Bend the driven element the same way as the reflector and directors, but do not leave any overlap at the feed point. The ends of the wires should be 3/4 inch apart where they mount on the Plexiglas plate. Leave enough excess that small loops can be bent in the wire for attachment to the coaxial feed line with stainless steel hardware.

Drill the boom as shown in **Fig 61**. It is a good idea to use hardware with wing nuts to secure the element spreaders to the boom. After the boom is drilled, clean all the wood parts with denatured alcohol, sand them, and give them two coats of glossy polyurethane. After the polyurethane dries, wax all the wooden parts.

The boom to mast attachment is made next. Square the ends of a 6-foot section of clothes closet pole (a miter box is useful for this). Drill the center holes in both the boom

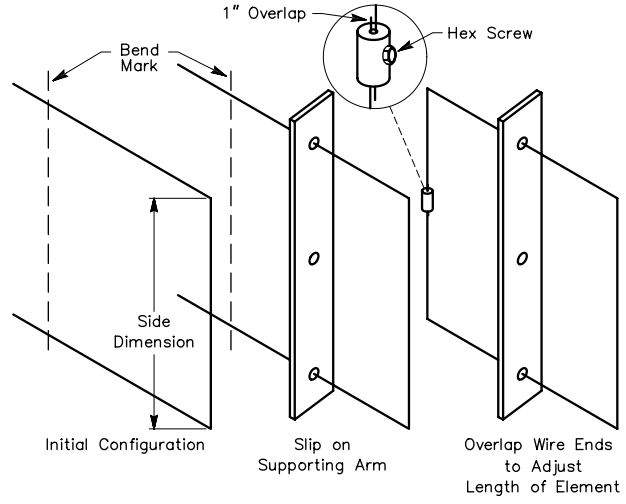

Fig 59—Illustration showing how the aluminum element wires are bent. The adjustment clamp and its location are also shown.

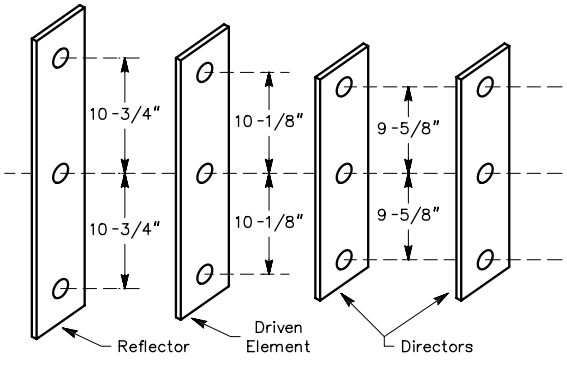

Fig 58—Dimensions for the pine element spreaders for the 144-MHz 4-element quad.

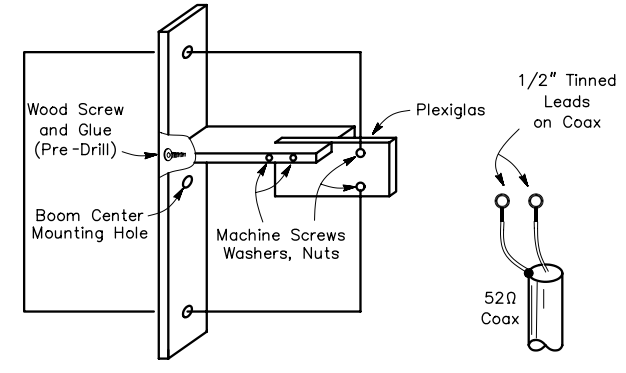

Fig 60—Layout of the driven element of the 144-MHz quad. The leads of the coaxial cable should be stripped to ½ in. and solder lugs attached for easy connection and disconnection. See text regarding impedance at loop support points.

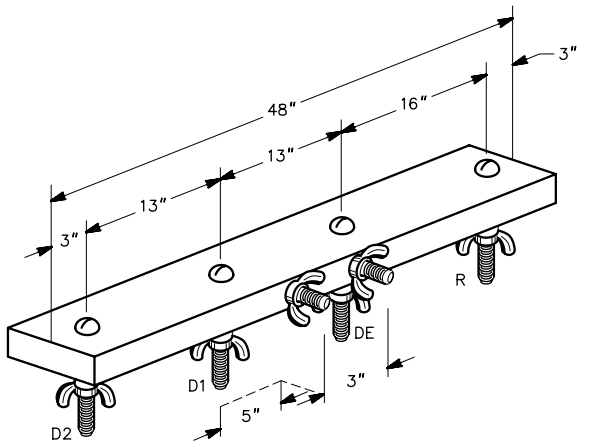

Fig 61—Detail of the boom showing hole center locations and boom to mast connection points.

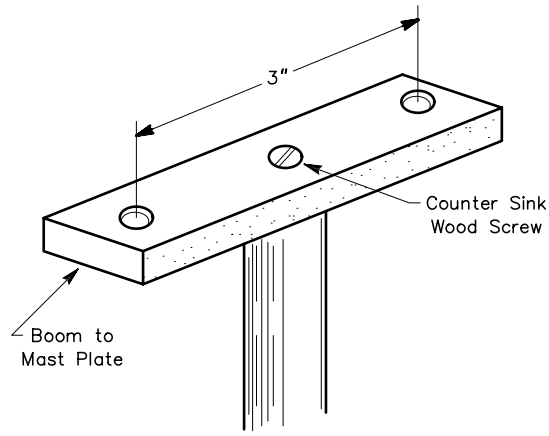

Fig 62—Boom to mast plate for the 144-MHz quad. The screw hole in the center of the plate should be countersunk so the wood screw attaching it to the mast does not interfere with the fit of the boom.

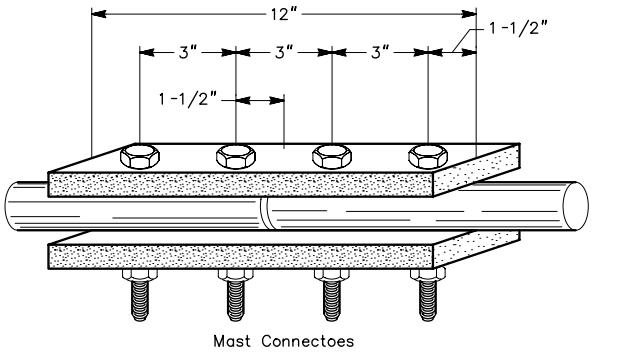

Fig 63—Mast coupling connector details for the portable quad. The plates should be drilled two at a time to ensure the holes line up.

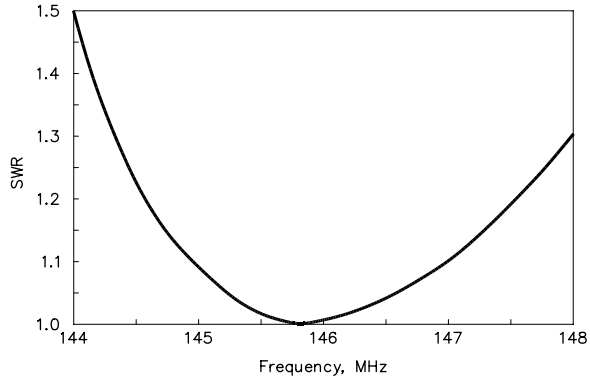

Fig 64—Typical SWR curve for the 144MHz portable quad. The large wire diameter and the quad design provide excellent bandwidth.

attachment piece and one end of the mast section (**Fig 62**). Make certain that the mast hole is smaller than the flat-head screw to be used to ensure a snug fit. Accurately drill the holes for attachment to the boom as shown in Fig 62.

Countersink the hole for the flat-head screw to provide a smooth surface for attachment to the boom. Apply epoxy cement to the surfaces and screw the boom attachment piece securely to the mast section. One 6 foot mast is used for attachment to the other mast sections.

Two additional 6-foot mast sections are prepared next. This brings the total mast height to 18 feet. It is important to square the ends of each pole so the mast stands straight when assembled. Mast-section connectors are made of pine as shown in **Fig 63**. Using $3^1/_2 \times {}^1/_4$-inch hex bolts, washers, and nuts, sections may be attached as needed, for a total height of 6, 12 or 18 feet. Drill the holes in two connectors at a time. This ensures good alignment of the holes. A drill press is ideal for this job, but with care a hand drill can be used if necessary.

Line up two mast sections end to end, being careful that they are perfectly straight. Use the predrilled connectors to maintain pole straightness, and drill through the poles, one at a time. If good alignment is maintained, a straight 18-foot mast section can be made. Label the connectors and poles immediately so they are always assembled in the same order.

When assembling the antenna, install all the elements on the boom before attaching the feed line. Connect the coax to the screw connections on the driven element support plate and run the cable along the strut to the boom. From there, the cable should be routed directly to the mast and down. Assemble the mast sections to the desired height. The antenna provides good performance, and has a reasonable SWR curve over the entire 144 MHz band (**Fig 64**).

Building Quagi Antennas

The Quagi antenna was designed by Wayne Overbeck, N6NB. He first published information on this antenna in 1977 (see Bibliography). There are a few tricks to Quagi building, but nothing very difficult or complicated is involved. In fact, Overbeck mass produced as many as 16 in one day. **Tables 18** and **19** give the dimensions for Quagis for various frequencies up to 446 MHz.

For the designs of Tables 18 and 19, the boom is *wood* or any other nonconductor (such as, fiberglass or Plexiglas). If a metal boom is used, a new design and new element lengths will be required. Many VHF antenna builders go wrong by failing to follow this rule: If the original uses a metal boom, use the same size and shape metal boom when you duplicate it. If it calls for a wood boom, use a nonconductor. Many amateurs dislike wood booms, but in a salt air environment they outlast aluminum (and surely cost less). Varnish the boom for added protection.

The 144-MHz version is usually built on a 14 foot, 1×3 inch boom, with the boom tapered to 1 inch at both ends. Clear pine is best because of its light weight, but construction grade Douglas fir works well. At 222 MHz the boom is under 10 feet long, and most builders use 1×2 or (preferably) $^3/_4 \times 1^1/_4$ inch pine molding stock. At 432 MHz, except for long-boom versions, the boom should be $^1/_2$ inch thick or less. Most builders use strips of $^1/_2$-inch exterior plywood for 432 MHz.

The quad elements are supported at the current maxima (the top and bottom, the latter beside the feed point) with Plexiglas or small strips of wood. See **Fig 65**. The quad elements are made of #12 copper wire, commonly used in house wiring. Some builders may elect to use #10 wire on 144 MHz and #14 on 432 MHz, although this changes the resonant frequency slightly. Solder a type N connector (an SO-239 is often used at 144 MHz) at the midpoint of the driven element bottom side, and close the reflector loop.

Table 19

432MHz, 15-Element, Long Boom Quagi Construction Data

Element Lengths, Inches	*Interelement Spacing, Inches*
R—28	R-DE7
DE—$26^5/_8$	DE-D1—$5^1/_4$
D1—$11^3/_4$	D1-D2—11
D21—$^{11}/_{16}$	D2-D3—$5^7/_8$
D3—$11^5/_8$	D3-D4—$8^3/_4$
D4—$11^9/_{16}$	D4-D5—$8^3/_4$
D5—$11^1/_2$	D5-D6—$8^3/_4$
D6—$11^7/_{16}$	D6-D7—12
D7—$11^3/_8$	D7-D8—12
D8—$11^5/_{16}$	D8-D9—$11^1/_4$
D9—$11^5/_{16}$	D9-D10—$11^1/_2$
D10—$11^1/_4$	D10-D11—$9^3/_{16}$
D11—$11^3/_{16}$	D11-D12—$12^3/_8$
D12—$11^1/_8$	D12-D13—1-$^3/_4$
D13—$11^1/_{16}$	

Boom: 1×2in. $\times$ 12-ft Douglas fir, tapered to $^5/_8$ in. at both ends.
Driven element: #12 TW copper wire loop in square configuration, fed at bottom center with type N connector and 52-Ω coax.
Reflector: #12 TW copper wire loop, closed at bottom.
Directors: $^1/_8$ in. rod passing through boom.

Table 18

Dimensions, Eight-Element Quagi

Element Lengths	*144.5 MHz*	*147 MHz*	*Frequency 222 MHz*	*432 MHz*	*446 MHz*
Reflector[1]	$86^5/_8$"	85"	$56^3/_8$"	28"	$27^1/_8$"
Driven[2]	82"	80"	53½"	$26^5/_8$"	$25^7/_8$"
Directors	$35^{15}/_{16}$" to 35" in $^3/_{16}$" steps	$35^5/_{16}$" to $34^3/_8$" in $^3/_{16}$" steps	$23^3/_8$" to 23¾" in $^1/_8$" steps	11¾" to $11^7/_{16}$" in $^1/_{16}$" steps	$11^3/_8$" to $11^1/_{16}$" in $^1/_{16}$" steps
Spacing					
R-DE	21"	20½"	$13^5/_8$"	7"	6.8"
DE-D1	15¾"	$15^3/_8$"	10¼"	5¼"	5.1"
D1-D2	33"	32½"	21½"	11"	10.7"
D2-D3	17½"	$17^1/_8$"	$11^3/_8$"	5.85"	5.68"
D3-D4	26.1"	$25^5/_8$"	17"	8.73"	8.46"
D4-D5	26.1"	$25^5/_8$"	17"	8.73"	8.46"
D5-D6	26.1"	$25^5/_8$"	17"	8.73"	8.46"
Stacking Distance Between Bays					
	11'	10' 10"	7' 1½"	3'7"	3' $5^5/_8$"

[1] All #12 TW (electrical) wire, closed loops.
[2] All #12 TW wire loops, fed at bottom.

The directors are mounted through the boom. They can be made of almost any metal rod or wire of about 1/8-inch diameter. Welding rod or aluminum clothesline wire works well if straight. (The designer uses 1/8-inch stainless-steel rod obtained from an aircraft surplus store.)

A TV type U bolt mounts the antenna on a mast. A single machine screw, washers and a nut are used to secure the spreaders to the boom so the antenna can be quickly "flattened" for travel. In permanent installations two screws are recommended.

Construction Reminders

Based on the experiences of Quagi builders, the following hints are offered. First, remember that at 432 MHz even a 1/8-inch measurement error results in performance deterioration. Cut the loops and elements as carefully as possible. No precision tools are needed, but accuracy is necessary. Also make sure to get the elements in the right order. The longest director goes closest to the driven element.

Finally, remember that a balanced antenna is being fed with an unbalanced line. Every balun the designer tried introduced more trouble in terms of losses than the feed imbalance caused. Some builders have tightly coiled several turns of the feed line near the feed point to limit line radiation. In any case, the feed line should be kept at right angles to the antenna. Run it from the driven element directly to the supporting mast and then up or down perpendicularly for best results.

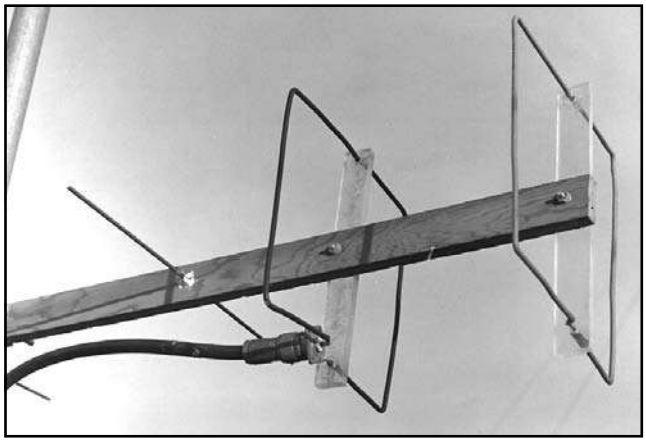

Fig 65—A close-up view of the feed method used on a 432-MHz Quagi. This arrangement produces a low SWR and gain in excess of 13 dBi with a 4-ft 10-in. boom! The same basic arrangement is used on lower frequencies, but wood may be substituted for the Plexiglas spreaders. The boom is ½-in. exterior plywood.

QUAGIS FOR 1296 MHz

The Quagi principle has recently been extended to the 1296-MHz band, where good performance is extremely difficult to obtain from homemade conventional Yagis. **Fig 66** shows the construction and **Table 20** gives the design information for antennas with 10, 15 and 25 elements.

At 1296 MHz, even slight variations in design or building materials can cause substantial changes in performance. The 1296 MHz antennas described here work every time—but only if the same materials are used and the antennas are built *exactly* as described. This is not to discourage experimentation, but if modifications to these 1296-MHz antenna designs are contemplated, consider building one antenna as described here, so a reference is available against which variations can be compared.

The Quagis (and the cubical quad) are built on 1/4-inch thick Plexiglas booms. The driven element and reflector (and also the directors in the case of the cubical quad) are made of insulated #18 AWG solid copper bell wire, available at hardware and electrical supply stores. Other types and sizes of wire work equally well, but the dimensions vary with the wire diameter. Even removing the insulation usually necessitates changing the loop lengths.

Quad loops are approximately square (**Fig 67**), although the shape is relatively uncritical. The element lengths, however, *are* critical. At 1296 MHz, variations

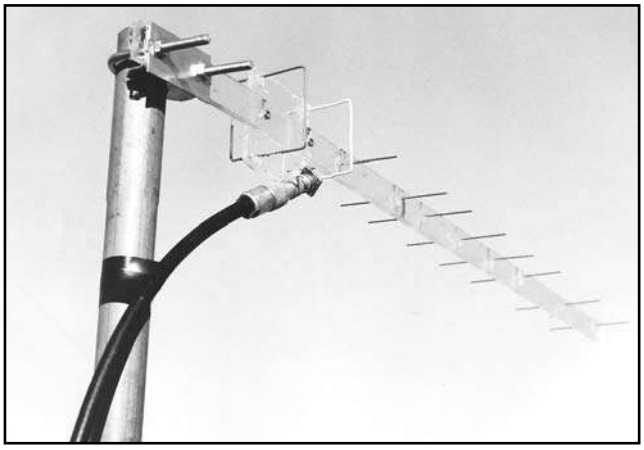

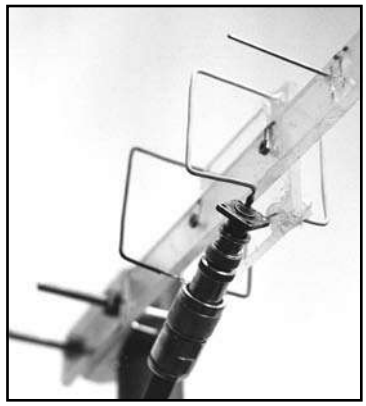

Fig 66—A view of the 10-element version of the 1296-MHz Quagi. It is mounted on a 30-in. Plexiglas boom with a 3 × 3-in. square of Plexiglas to support the driven element and reflector. Note how the driven element is attached to a standard UG-290 BNC connector. The elements are held in place with silicone sealing compound.

of 1/16 inch alter the performance measurably, and a 1/8 inch departure can cost several decibels of gain. The loop lengths given are *gross* lengths. Cut the wire to these lengths and then solder the two ends together. There is a 1/8-inch overlap where the two ends of the reflector (and director) loops are joined, as shown in Fig 67.

The driven element is the most important of all. The #18 wire loop is soldered to a standard UG-290 chassis-mount BNC connector as shown in the photographs. This exact type of connector must be used to ensure uniformity in construction. Any substitution may alter the driven element electrical length. One end of the 9 1/4 inch driven loop is pushed as far as it can go into the center pin, and is soldered in that position. The loop is then shaped and threaded through small holes drilled in the Plexiglas support. Finally, the other end is fed into one of the four mounting holes on the BNC connector and soldered. In most cases, the best SWR is obtained if the end of the wire just passes through the hole so it is flush with the opposite side of the connector flange.

Table 20

Dimensions, 1296-MHz Quagi Antennas

Note: All lengths are gross lengths. See text and photos for construction technique and recommended overlap at loop junctions. All loops are made of #18 AWG solid-covered copper bell wire. The Yagi type directors are 1/16-in. brass brazing rod. See text for a discussion of director taper.

Feed: Direct with 52-Ω coaxial cable to UG-290 connector at driven element; run coax symmetrically to mast at rear of antenna.

Boom: 1 1/4-in. thick Plexiglas, 30 in. long for 10-element quad or Quagi and 48 in. long for 15-element Quagi; 84 in. for 25-element Quagi.

10-Element Quagi for 1296 MHz

Element	*Length, Inches*	*Construction*	*Element*	*Interelement Spacing, In.*
Reflector	9.5625	Loop	R-DE	2.375
Driven	9.25	Loop	DE-D1	2.0
Director 1	3.91	Brass rod	D1-D2	3.67
Director 2	3.88	Brass rod	D2-D3	1.96
Director 3	3.86	Brass rod	D3-D4	2.92
Director 4	3.83	Brass rod	D4-D5	2.92
Director 5	3.80	Brass rod	D5-D6	2.92
Director 6	3.78	Brass rod	D6-D7	4.75
Director 7	3.75	Brass rod	D7-D8	3.94
Director 8	3.72	Brass rod		

15-Element Quagi for 1296 MHz

The first 10 elements are the same lengths as above, but the spacing from D6 to D7 is 4.0 in.; 07 to D8 is also 4.0 in.

Director 9	3.70	D8-D9	3.75
Director 10	3.67	D9-D10	3.83
Director 11	3.64	D10-D11	3.06
Director 12	3.62	D11-D12	4.125
Director 13	3.59	D12-D13	4.58

25-Element Quagi for 1296 MHz

The first 15 elements use the same element lengths and spacings as the 15-element model. The additional directors are evenly spaced at 3.0-in. intervals and taper in length successively by 0.02 in. per element. Thus, D23 is 3.39 in.

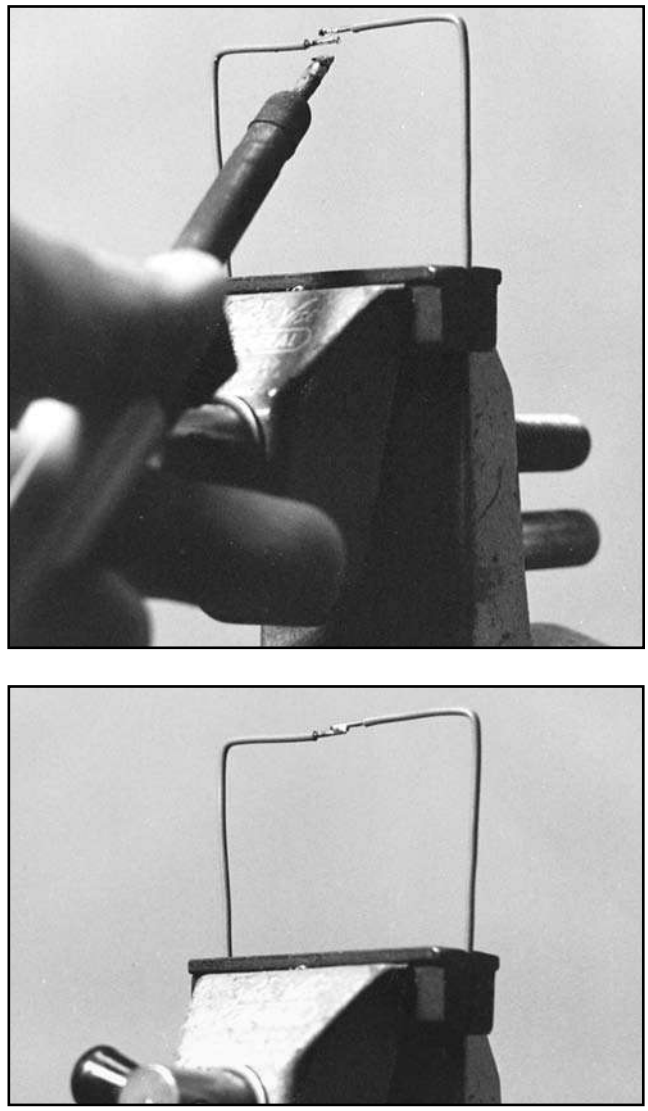

Fig 67—These photos show the construction method used for the 1296-MHz quad type parasitic elements. The two ends of the #18 bell wire are brought together with an overlap of 1/8 in. and soldered.

Loop Yagis for 1296 MHz

Described here are loop Yagis for the 1296-MHz band. The loop Yagi fits into the quad family of antennas, as each element is a closed loop with a length of approximately 1 λ. Several versions are described, so the builder can choose the boom length and frequency coverage desired for the task at hand. Mike Walters, G3JVL, brought the original loop-Yagi design to the amateur community in the 1970s. Since then, many versions have been developed with different loop and boom dimensions. Chip Angle, N6CA, developed the antennas shown here.

Three sets of dimensions are given. Good performance can be expected if the dimensions are carefully followed. Check all dimensions before cutting or drilling anything. The 1296-MHz version is intended for weak-signal operation, while the 1270-MHz version is optimized for FM and mode L satellite work. The 1283-MHz antenna provides acceptable performance from 1280 to 1300 MHz.

These antennas have been built on 6- and 12-foot booms. Results of gain tests at VHF conferences and by individuals around the country show the gain of the 6-foot model to be about 18 dBi, while the 12-foot version provides about 20.5 dBi. Swept measurements indicate that gain is about 2 dB down from maximum gain at ±30 MHz from the design frequency. The SWR, however, deteriorates within a few megahertz on the low side of the design center frequency.

The Boom

The dimensions given here apply only to a ¾-inch OD boom. If a different boom size is used, the dimensions must be scaled accordingly. Many hardware stores

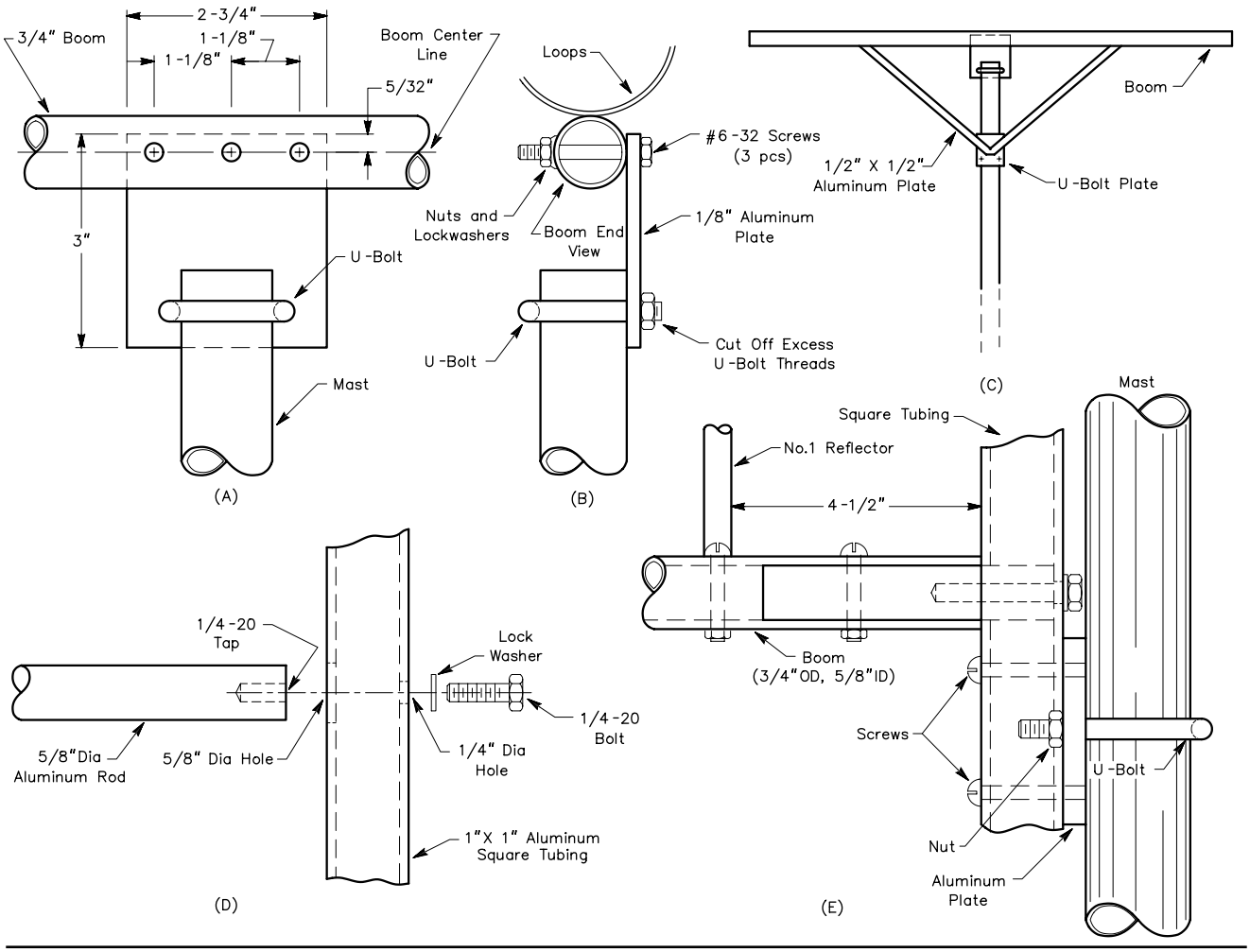

Fig 68—Loop Yagi boom-to-mast plate details are given at A. At B, the mounting of the antenna to the mast is detailed. A boom support for long antennas is shown at C. The arrangement shown in D and E may be used to rear-mount antennas up to 6 or 7 ft long.

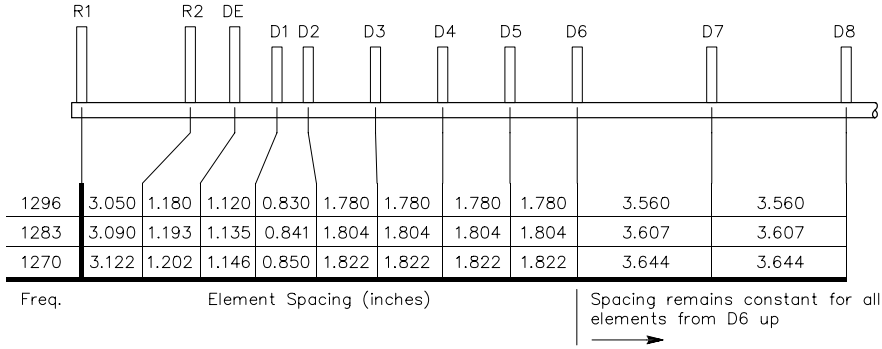

Freq.	D1	D2	D3	D4	D5	D6	D7	D8
1296	3.050	1.180	1.120	0.830	1.780	1.780	1.780	1.780	3.560	3.560
1283	3.090	1.193	1.135	0.841	1.804	1.804	1.804	1.804	3.607	3.607
1270	3.122	1.202	1.146	0.850	1.822	1.822	1.822	1.822	3.644	3.644

Fig 69—Boom drilling dimensions. These dimensions must be carefully followed and the same materials used if performance is to be optimum. Element spacings are the same for all directors after D6—use as many as necessary to fill the boom.

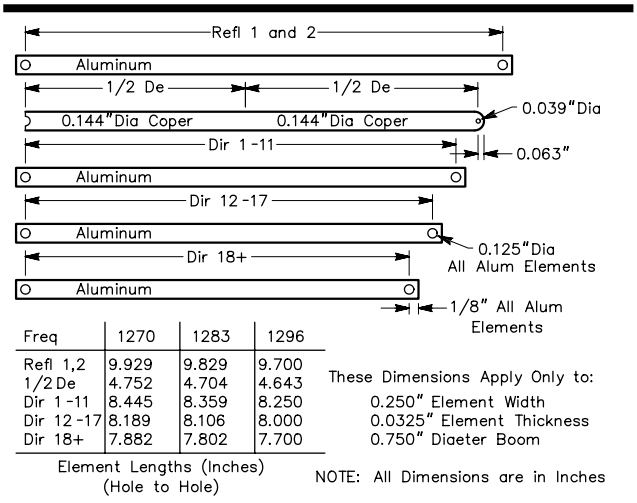

Freq	1270	1283	1296
Refl 1,2	9.929	9.829	9.700
1/2 De	4.752	4.704	4.643
Dir 1-11	8.445	8.359	8.250
Dir 12-17	8.189	8.106	8.000
Dir 18+	7.882	7.802	7.700

Fig 70—Parasitic elements for the loop Yagi are made from aluminum sheet, the driven element from copper sheet. The dimensions given are for ¼-in. wide by 0.0325-in. thick elements only. Lengths specified are hole to hole distances; the holes are located 1/8 in. from each element end.

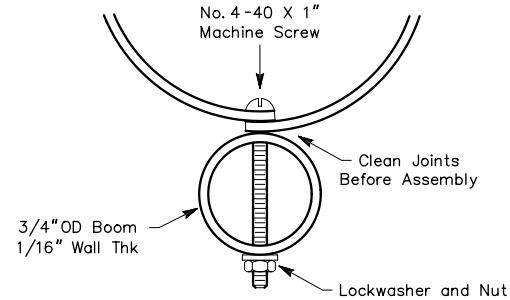

Fig 71—Element-to-boom mounting details.

carry aluminum tubing in 6- and 8-foot lengths, and that tubing is suitable for a short Yagi. If a 12-foot antenna is planned, find a piece of more rugged boom material, such as 6061-T6 grade aluminum. Do not use anodized tubing. The 12foot antenna must have additional boom support to minimize boom sag. The 6 foot version can be rear mounted. For rear mounting, allow $4^1/_2$ inches of boom behind the last reflector to eliminate SWR effects from the support.

The antenna is attached to the mast with a gusset plate. This plate mounts at the boom center. See **Fig 68**. Drill the plate mounting holes perpendicular to the element mounting holes (assuming the antenna polarization is to be horizontal).

Elements are mounted to the boom with no. 4-40 machine screws, so a series of no. 33 (0.113inch) holes must be drilled along the center of the boom to accommodate this hardware. **Fig 69** shows the element spacings for different parts of the band. Dimensions should be followed as closely as possible.

Parasitic Elements

The reflectors and directors are cut from 0.032-inch thick aluminum sheet and are $^1/_4$ inch wide. **Fig 70** indicates the lengths for the various elements. These lengths apply only to elements cut from the specified material. For best results, the element strips should be cut with a shear. If the edges are left sharp, birds won't sit on the elements.

Drill the mounting holes as shown in Fig 70 after carefully marking their locations. After the holes are drilled, form each strap into a circle. This is easily done by wrapping the element around a round form. (A small juice can works well.)

Mount the loops to the boom with no. 4-40 × 1-inch machine screws, lock washers and nuts. See **Fig 71**. It is best to use only stainless steel or plated-brass hardware. Although the initial cost is higher than for ordinary plated-steel hardware, stainless or brass hardware will not rust and need replacement after a few years. Unless the antenna

is painted, the hardware will definitely deteriorate.

Driven Element

The driven element is cut from 0.032-inch copper sheet and is 1/4 inch wide. Drill three holes in the strap as detailed in Fig 69. Trim the ends as shown and form the strap into a loop similar to the other elements. This antenna is like a quad; if the loop is fed at the top or bottom, it is horizontally polarized.

Driven element mounting details are shown in **Fig 72**. A mounting fixture is made from a 1/4-20 × 1 1/4 inch brass bolt. File the bolt head to a thickness of 1/8 inch. Bore a 0.144-inch (no. 27 drill) hole lengthwise through the center of the bolt. A piece of 0.141 inch semi-rigid Hardline (UT-141 or equivalent) mounts through this hole and is soldered to the driven loop feed point. The point at which the UT-141 passes through the copper loop and brass mounting fixture should be left unsoldered at this time to allow for matching adjustments when the antenna is completed, although the range of adjustment is not very large.

The UT-141 can be any convenient length. Attach the connector of your choice (preferably type N). Use a short piece of low-loss RG-8 size cable (or 1/2-inch Hardline) for the run down the boom and mast to the main feed line. For best results, the main feed line should be the lowest loss 50-Ω cable obtainable. Good 7/8-inch Hardline has 1.5 dB of loss per 100 feet and virtually eliminates the need for remote mounting of the transmit converter or amplifier.

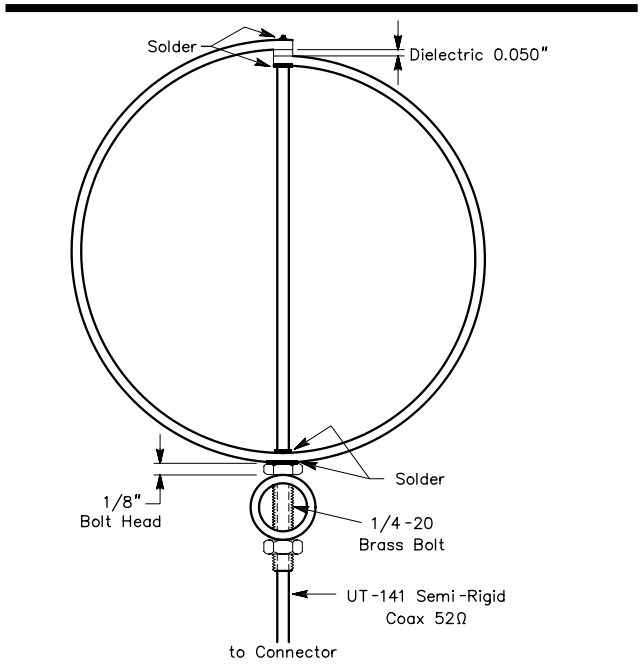

Fig 72—Driven-element details. See Fig 70 and the text for additional information.

Tuning the Driven Element

If the antenna is built carefully to the dimensions given, the SWR should be close to 1:1. Just to be sure, check the SWR if you have access to test equipment. Be sure the signal source is clean, however; wattmeters respond to "dirty" signals and can give erroneous readings. If problems are encountered, recheck all dimensions. If they look good, a minor improvement may be realized by changing the shape of the driven element. Slight bending of reflector 2 may also improve the SWR. When the desired match has been obtained, solder the point where the UT-141 jacket passes through the loop and brass bolt.

Tips for 1296-MHz Antenna Installations

Construction practices that are common on lower frequencies cannot be used on 1296 MHz. This is the most important reason why all who venture to these frequencies are not equally successful. First, when a proven design is used, copy it exactly¾don't change *anything*. This is especially true for antennas.

Use the best feed line you can get. Here are some realistic measurements of common coaxial cables at 1296 MHz (loss per 100 feet).

RG-8, 213, 214: 11 dB
1/2 in. foam/copper Hardline: 4 dB
7/8 in. foam/copper Hardline: 1.5 dB

Mount the antennas to keep feed line losses to an absolute minimum. Antenna height is less important than keeping the line losses low. *Do not* allow the mast to pass through the elements, as is common on antennas for lower frequencies. Cut all U-bolts to the minimum length needed; 1/4 λ at 1296 MHz is only a little over 2 inches. Avoid any unnecessary metal around the antenna.

Trough Reflectors for 432 and 1296 MHz

Dimensions are given in **Fig 73** for 432- and 1296-MHz trough reflectors. The gain to be expected is 16 dBi and 15 dBi, respectively. A very convenient arrangement, especially for portable work, is to use a metal hinge at each angle of the reflector. This permits the reflector to be folded flat for transit. It also permits experiments to be carried out with different apex angles.

A housing is required at the dipole center to prevent the entry of moisture and, in the case of the 432-MHz antenna, to support the dipole elements. The dipole may be moved in and out of the reflector to get either minimum SWR or, if this cannot be measured, maximum gain. If a two-stub tuner or other matching device is used, the dipole may be placed to give optimum gain and the matching device adjusted to give optimum match. In the case of the 1296-MHz antenna, the dipole length can be adjusted by means of the brass screws at the ends of the elements. Locking nuts are essential.

The reflector should be made of sheet aluminum for 1296 MHz, but can be constructed of wire mesh (with twists parallel to the dipole) for 432 MHz. To increase the gain by 3 dB, a pair of these arrays can be stacked so the reflectors are barely separated (to prevent the formation of a slot radiator by the edges). The radiating dipoles must then be fed in phase, and suitable feeding and matching must be arranged. A two-stub tuner can be used for matching either a single- or double-reflector system.

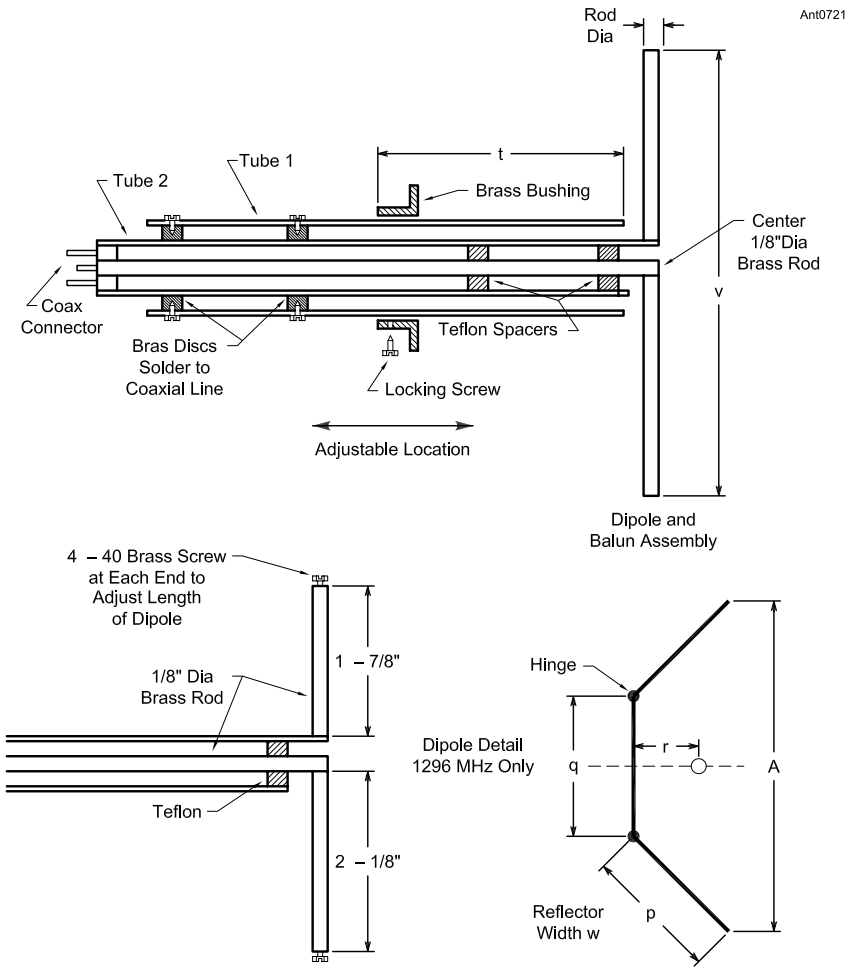

Dimensions in Inches

Band	A	p	q	r	w	t	u	v	Tube 1 Brass or Copper	Tube 2 Brass or Copper	Gain
432	120	100	50	7 – 1/2	60	6 – 1/2	1/4	12 – 3/4	1 – 1/2" ID 1/16" Wall	5/8" OD 1/16" Wall	16 dBi
1296	45	36	9 – 1/2	2 – 1/2	20	2 – 1/8	1/8	4 – 1/4	3/4" ID	3/8" OD 20 s.w.g.	15 dBi

Fig 73—Practical construction information for trough reflector antennas for 432 and 1296 MHz.

A Horn Antenna for 10 GHz

The horn antenna is the easiest antenna for the beginner on 10 GHz to construct. It can be made out of readily available flat sheet brass. Because it is inherently a broadband structure, minor constructional errors can be tolerated. The one drawback is that horn antennas become physically cumbersome at gains over about 25 dBi, but for most line-of-sight work this much gain is rarely necessary. This antenna was designed by Bob Atkins, KA1GT, and appeared in *QST* for April and May, 1987.

Horn antennas are usually fed by waveguide. When operating in its normal frequency range, waveguide propagation is in the TE_{10} mode. This means that the electric (E) field is across the short dimension of the guide and the magnetic (H) field is across the wide dimension. This is the reason for the E-plane and H-plane terminology shown in **Fig 74**.

There are many varieties of horn antennas. If the waveguide is flared out only in the H-plane, the horn is called an H-plane sectoral horn. Similarly, if the flare is only in the E-plane, an Eplane sectoral horn results. If the flare is in both planes, the antenna is called a pyramidal horn.

For a horn of any given aperture, directivity (gain along the axis) is maximum when the field distribution across the aperture is uniform in magnitude and phase. When the fields are not uniform, side lobes that reduce the directivity of the antenna are formed. To obtain a uniform distribution, the horn should be as long as possible with minimum flare angle. From a practical point of view, however, the horn should be as short as possible, so there is an obvious conflict between performance and convenience.

Fig 75 illustrates this problem. For a given flare angle and a given side length, there is a path-length difference from the apex of the horn to the center of the aperture (L), and from the apex of the horn to the edge of the aperture (L'). This causes a phase difference in the field across the aperture, which in turn causes formation of side lobes, degrading directivity (gain along the axis) of the antenna. If L is large this difference is small, and the field is almost uniform. As L decreases however, the phase difference increases and directivity suffers. An optimum (shortest possible) horn is constructed so that this phase difference is the maximum allowable before side lobes become excessive and axial gain markedly decreases.

The magnitude of this permissible phase difference is different for E-plane and H-plane horns. For the E-plane horn, the field intensity is quite constant across the aperture. For the H-plane horn, the field tapers to zero at the edge. Consequently, the phase difference at the edge of the aperture in the E-plane horn is more critical and should be held to less than 90° ($^1/_4$ λ). In an H-plane horn, the allowable phase difference is 144° (0.4 λ). If the aperture of a pyramidal horn exceeds one wavelength in both planes, the Eplane and Hplane patterns are essentially independent and can be analyzed separately.

The usual direction for orienting the waveguide feed is with the broad face horizontal, giving vertical polarization. If this is the case, the H-plane sectoral horn has a narrow horizontal beamwidth and a very wide vertical beamwidth. This is not a very useful beam pattern for most amateur applications. The E-plane sectoral horn has a narrow vertical beamwidth and a wide horizontal beamwidth. Such a radiation pattern could be useful in a beacon system where wide coverage is desired.

The most useful form of the horn for general applications is the optimum pyramidal horn. In this configuration the two beamwidths are almost the same. The E-plane (vertical) beamwidth is slightly less than the H-plane (horizontal), and also has greater side lobe intensity.

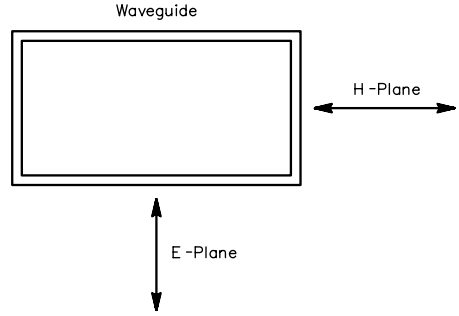

Fig 74—10-GHz antennas are usually fed with waveguide. See text for a discussion of waveguide propagation characteristics.

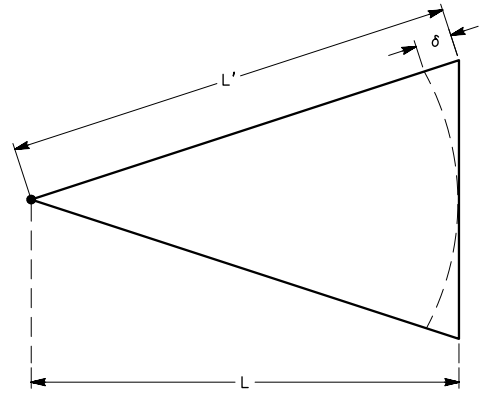

Fig 75—The path-length (phase) difference between the center and edge of a horn antenna is δ.

Building the Antenna

A 10-GHz pyramidal horn with 18.5 dBi gain is shown in **Fig 76**. The first design parameter is usually the required gain, or the maximum antenna size. These are of course related, and the relationships can be approximated by the following:

L = H-plane length (λ) = 0.0654 × gain (Eq 1)
A = H-plane aperture (λ) = 0.0443 × gain (Eq 2)
B = E-plane aperture (λ) = 0.81 A (Eq 3)

where

gain is expressed as a *ratio*; 20 dBi gain = 100
L, A and B are dimensions shown in **Fig 77.**

From these equations, the dimensions for a 20-dBi gain horn for 10.368 GHz can be determined. One wavelength at 10.368 GHz is 1.138 inches. The length (L) of such a horn is 0.0654 × 100 = 6.54 λ. At 10.368 GHz, this is 7.44 inches. The corresponding H-plane aperture (A) is 4.43 λ (5.04 inches), and the E-plane aperture (B), 4.08 inches.

The easiest way to make such a horn is to cut pieces from brass sheet stock and solder them together. Fig 77 shows the dimensions of the triangular pieces for the sides and a square piece for the waveguide flange. (A standard commercial waveguide flange could also be used.) Because the E-plane and H-plane apertures are different, the horn opening is not square. Sheet thickness is unimportant; 0.02 to 0.03 inch works well. Brass sheet is often available from hardware or hobby shops.

Note that the triangular pieces are trimmed at the apex to fit the waveguide aperture (0.9 × 0.4 inch). This necessitates that the length, from base to apex, of the smaller triangle (side B) is shorter than that of the larger (side A). Note that the length, S, of the two different sides of the horn must be the same if the horn is to fit together! For such a simple looking object, getting the parts to fit together properly requires careful fabrication.

The dimensions of the sides can be calculated with simple geometry, but it is easier to draw out templates on a sheet of cardboard first. The templates can be used to build a mock antenna to make sure everything fits together properly before cutting the sheet brass.

First, mark out the larger triangle (side A) on cardboard. Determine at what point its width is 0.9 inch and draw a line parallel to the base as shown in Fig 77. Measure the length of the side S; this is also the length of the sides of the smaller (side B) pieces.

Mark out the shape of the smaller pieces by first drawing a line of length B and then constructing a second line of length S. One end of line S is an end of line B, and the other is 0.2 inch above a line perpendicular to the center of line B as shown in Fig 76. (This procedure is much more easily followed than described.) These smaller pieces are made slightly oversize (shaded area in Fig 77) so you can construct the horn with solder seams on the outside of the horn during assembly.

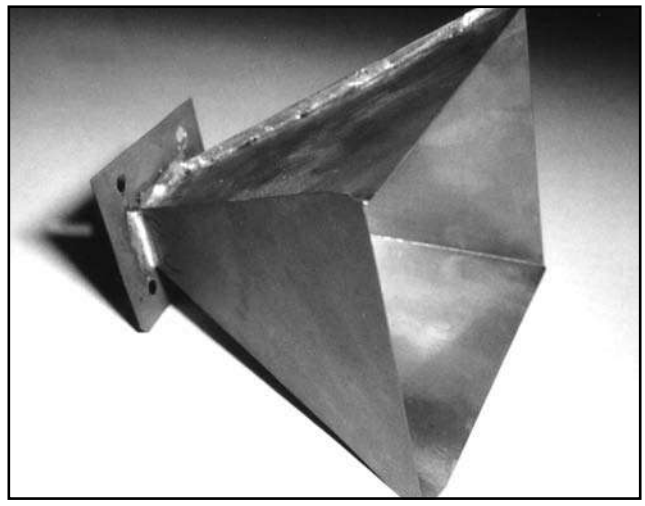

Fig 76—This pyramidal horn has 18.5 dBi gain at 10 GHz. Construction details are given in the text.

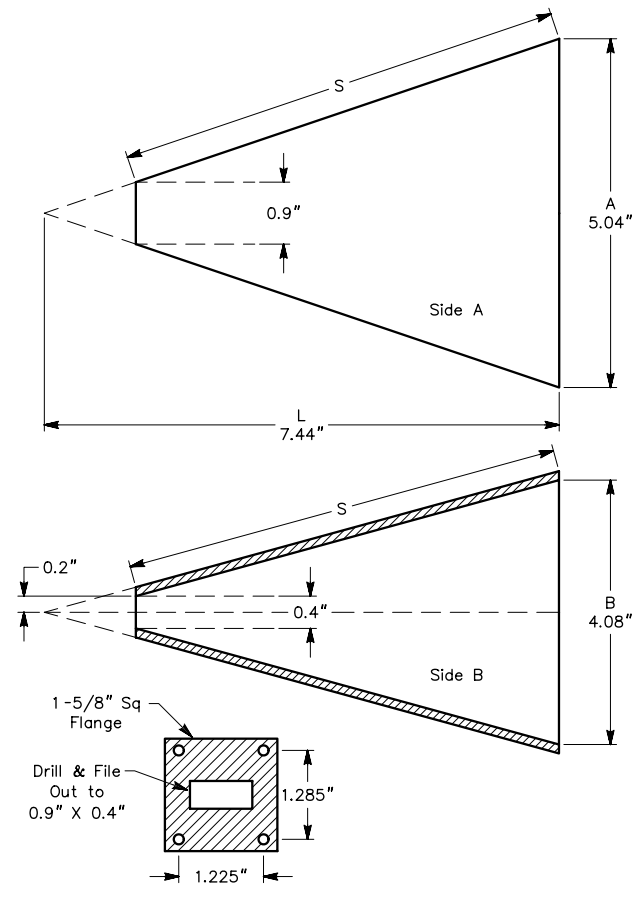

Fig 77—Dimensions of the brass pieces used to make the 10-GHz horn antenna. Construction requires two of each of the triangular pieces (side A and side B).

Cut out two cardboard pieces for side A and two for side B and tape them together in the shape of the horn. The aperture at the waveguide end should measure 0.9 × 0.4 inch and the aperture at the other end should measure 5.04 × 4.08 inches.

If these dimensions are correct, use the cardboard templates to mark out pieces of brass sheet. The brass sheet should be cut with a bench shear if one is available, because scissors type shears tend to bend the metal. Jig the pieces together and solder them on the *outside* of the seams. It is important to keep both solder and rosin from contaminating the inside of the horn; they can absorb RF and reduce gain at these frequencies.

Assembly is shown in **Fig 78**. When the horn is completed, it can be soldered to a standard waveguide flange, or one cut out of sheet metal as shown in Fig 77. The transition between the flange and the horn must be smooth. This antenna provides an excellent performance-to-cost ratio (about 20 dBi gain for about five dollars in parts).

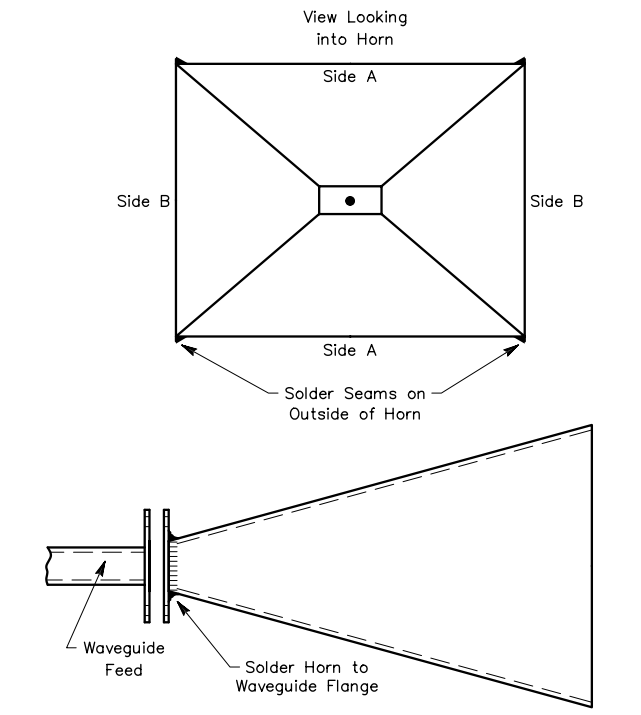

Fig 78—Assembly of the 10-GHz horn antenna.

Periscope Antenna Systems

One problem common to all who use microwaves is that of mounting an antenna at the maximum possible height while trying to minimize feed-line losses. The higher the frequency, the more severe this problem becomes, as feeder losses increase with frequency. Because parabolic dish reflectors are most often used on the higher bands, there is also the difficulty of waterproofing feeds (particularly waveguide feeds). Inaccessibility of the dish is also a problem when changing bands. Unless the tower is climbed every time and the feed changed, there must be a feed for each band mounted on the dish. One way around these problems is to use a periscope antenna system (sometimes called a "flyswatter antenna").

The material in this section was prepared by Bob Atkins, KA1GT, and appeared in *QST* for January and February 1984. **Fig 79** shows a schematic representation of a periscope antenna system. A plane reflector is mounted at the top of a rotating tower at an angle of 45°. This reflector can be elliptical with a major to minor axis ratio of 1.41, or rectangular. At the base of the tower is mounted a dish or other type of antenna such as a Yagi, pointing straight up. The advantage of such a system is that the feed antenna can be changed and worked on easily. Additionally, with a correct choice of reflector size, dish size, and dish to reflector spacing, feed losses can be made small, increasing the effective system gain. In fact, for some particular system configurations, the gain of the overall system can be greater than that of the feed antenna alone.

Gain of a Periscope System

Fig 80 shows the relationship between the effective gain of the antenna system and the distance between the reflector and feed antenna for an elliptical reflector. At first sight, it is not at all obvious how the antenna system can have a higher gain than the feed alone. The reason lies in the fact that, depending on the feed to reflector spacing, the reflector may be in the near field (Fresnel) region of the antenna, the far field (Fraunhöffer) region, or the transition region between the two.

In the far field region, the gain is proportional to the reflector area and inversely proportional to the distance between the feed and reflector. In the near field region, seemingly strange things can happen, such as decreasing gain with decreasing feed to reflector separation. The reason for this gain decrease is that, although the reflec-

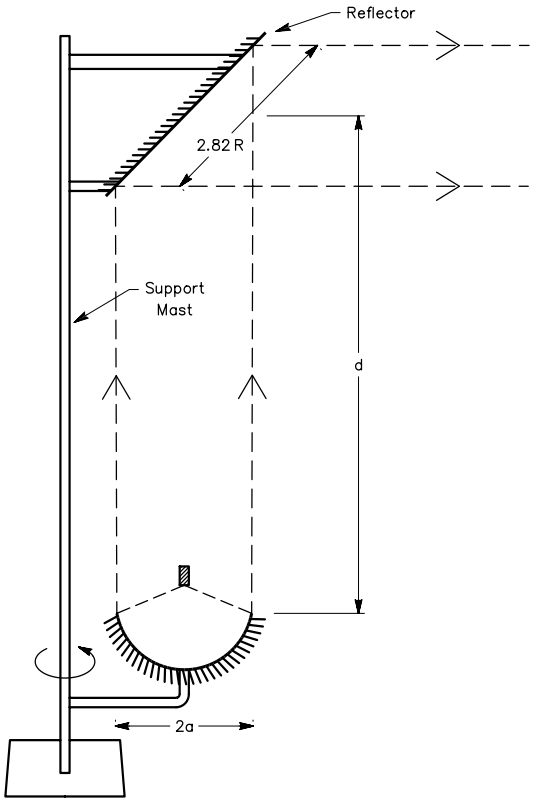

Fig 79—The basic periscope antenna. This design makes it easy to adjust the feed antenna.

tor is intercepting more of the energy radiated by the feed, it does not all contribute in phase at a distant point, and so the gain decreases.

In practice, rectangular reflectors are more common than elliptical. A rectangular reflector with sides equal in length to the major and minor axes of the ellipse will, in fact, normally give a slight gain increase. In the far field region, the gain will be proportional to the area of the reflector. To use Fig 80 with a rectangular reflector, R^2 may be replaced by A / π, where A is the projected area of the reflector. The antenna pattern depends in a complicated way on the system parameters (spacing and size of the elements), but **Table 21** gives an approximation of what to expect. R is the radius of the projected circular area of the elliptical reflector (equal to the minor axis radius), and b is the length of the side of the projected square area of the rectangular reflector (equal to the length of the short side of the rectangle).

For those wishing a rigorous mathematical analysis of this type of antenna system, several references are given in the Bibliography at the end of this chapter.

Mechanical Considerations

There are some problems with the physical construction of a periscope antenna system. Since the antenna gain of a microwave system is high and, hence, its beamwidth narrow, the reflector must be accurately aligned. If the reflector does not produce a beam that is horizontal, the

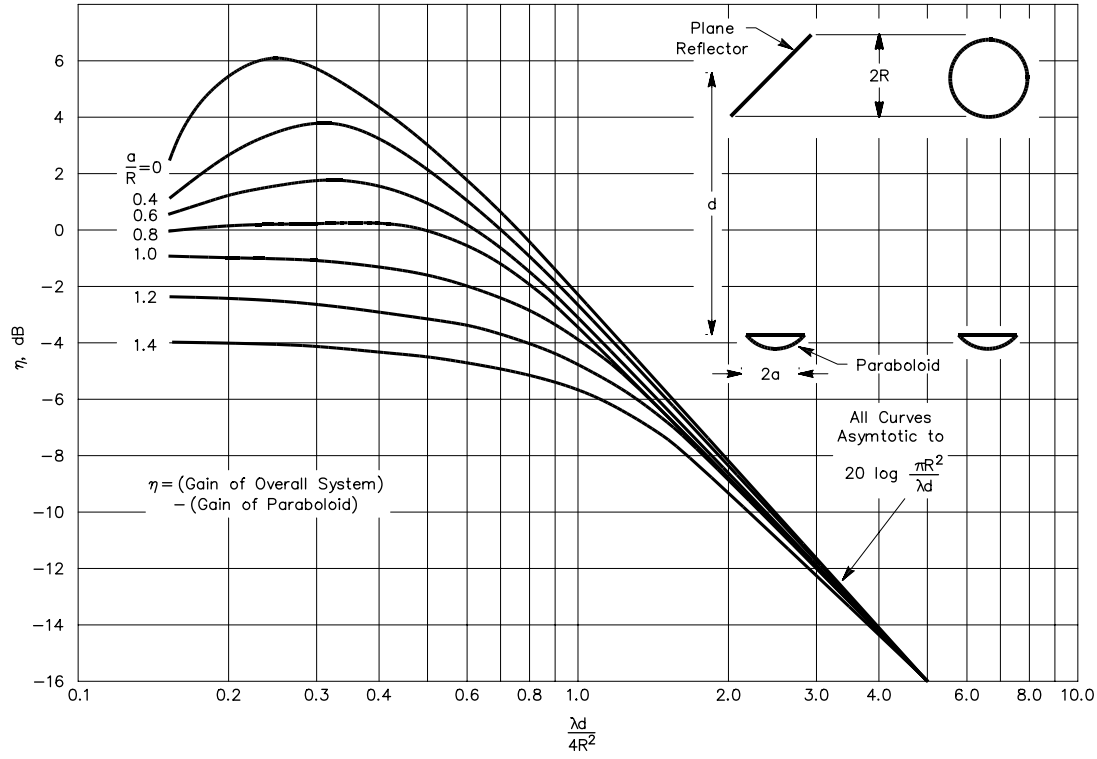

Fig 80—Gain of a periscope antenna using a plane elliptical reflector (after Jasik—see Bibliography).

Table 21
Radiation Patterns of Periscope Antenna Systems

	Elliptical Reflector	*Rectangular Reflector*
3-dB beamwidth, degrees	60 λ/2R	52 λ/b
6-dB beamwidth, degrees	82 λ/2R	68 λ/b
First minimum, degrees from axis	73 λ/2R	58 λ/b
First maximum, degrees from axis	95 λ/2R	84 λ/b
Second minimum, degrees from axis	130 λ/2R	116 λ/b
Second maximum, degrees from axis	156 λ/2R	142 λ/b
Third minimum, degrees from axis	185 λ/2R	174 λ/b

Fig 81—Commercial periscope antennas, such as this one, are often used for point-to-point communication.

useful gain of the system will be reduced. From the geometry of the system, an angular misalignment of the reflector of X degrees in the vertical plane will result in an angular misalignment of 2X degrees in the vertical alignment of the antenna system pattern. Thus, for a dish pointing straight up (the usual case), the reflector must be at an angle of 45° to the vertical and should not fluctuate from factors such as wind loading.

The reflector itself should be flat to better than $^1/_{10}$ λ for the frequency in use. It may be made of mesh, provided that the holes in the mesh are also less than $^1/_{10}$ λ in diameter. A second problem is getting the support mast to rotate about a truly vertical axis. If the mast is not vertical, the resulting beam will swing up and down from the horizontal as the system is rotated, and the effective gain at the horizon will fluctuate. Despite these problems, amateurs have used periscope antennas successfully on the bands through 10 GHz. Periscope antennas are used frequently in commercial service, though usually for point-to-point transmission. Such a commercial system is shown in **Fig 81**.

Circular polarization is not often used for terrestrial work, but if it is used with a periscope system there is an important point to remember. The circularity sense changes when the signal is reflected. Thus, for right hand circularity with a periscope antenna system, the feed arrangement on the ground should produce left hand circularity. It should also be mentioned that it is possible (though more difficult for amateurs) to construct a periscope antenna system using a parabolically curved reflector. The antenna system can then be regarded as an offset fed parabola. More gain is available from such a system at the added complexity of constructing a parabolically curved reflector, accurate to $^1/_{10}$ λ.

BIBLIOGRAPHY

Source material and more extended discussion of topics covered in this chapter can be found in the references given below and in the textbooks listed at the end of Chapter 2, Antenna Fundamentals.

B. Atkins, "Periscope Antenna Systems," The New Frontier, *QST*, Jan and Feb 1984.

B. Atkins, "Horn Antennas for 10 GHz," The New Frontier, *QST*, Apr and May 1987.

J. Drexler, "An Experimental Study of a Microwave Periscope," *Proc. IRE*, Correspondence, Vol 42, Jun 1954, p 1022.

D. Evans and G. Jessop, *VHF-UHF Manual*, 3rd ed. (London: RSGB), 1976.

N. Foot, "WA9HUV 12foot Dish for 432 and 1296 MHz," The World Above 50 Mc., *QST*, Jun 1971, pp 98-101, 107.

N. Foot, "Cylindrical Feed Horn for Parabolic Reflectors," *Ham Radio*, May 1976.

G. Gobau, "Single-Conductor Surface-Wave Transmission Lines," *Proc. IRE*, Vol 39, Jun 1951, pp 619-624; also see *Journal of Applied Physics*, Vol 21 (1950), pp 1119-1128.

R. E. Greenquist and A. J. Orlando, "An Analysis of Passive Reflector Antenna Systems," *Proc. IRE*, Vol 42, Jul 1954, pp 1173-1178.

G. A. Hatherell, "Putting the G Line to Work," *QST*, Jun 1974, pp 11-15, 152, 154, 156.

D. L. Hilliard, "A 902MHz Loop Yagi Antenna," *QST*, Nov 1985, pp 30-32.

W. C. Jakes, Jr., "A Theoretical Study of an Antenna-Reflector Problem," *Proc. IRE*, Vol 41, Feb 1953, pp 272-274.

H. Jasik, *Antenna Engineering Handbook*, 1st ed. (New York: McGraw-Hill, 1961).

R. T. Knadle, "UHF Antenna Ratiometry," *QST*, Feb 1976, pp 22-25.
T. Moreno, *Microwave Transmission Design Data* (New York: McGraw- Hill, 1948).
W. Overbeck, "The VHF Quagi," *QST*, Apr 1977, pp 11-14.
W. Overbeck, "The Long-Boom Quagi," *QST*, Feb 1978, pp 20-21.
W. Overbeck, "Reproducible Quagi Antennas for 1296 MHz," *QST*, Aug 1981, pp 11-15.
G. Southworth, *Principles and Applications of Waveguide Transmission* (New York: D. Van Nostrand Co, 1950).
P. P. Viezbicke, "Yagi Antenna Design," *NBS Technical Note 688* (U. S. Dept. of Commerce/National Bureau of Standards, Boulder, CO), Dec 1976.
D. Vilardi, "Easily Constructed Antennas for 1296 MHz," *QST*, Jun 1969.
D. Vilardi, "Simple and Efficient Feed for Parabolic Antennas," *QST*, Mar 1973.
Radio Communication Handbook, 5th ed. (London: RSGB, 1976).

Chapter 19

Antenna Systems for Space Communications

When we consider amateur space communications, we usually think about two basic modes: satellite and earth-moon-earth (EME—also referred to as *moonbounce*). At their essence, both modes communicate using one of the Earth's satellites—our natural satellite (the Moon) or one of a variety of manmade satellites.

There are two main differences between these satellites. The first is one of distance. The Moon is about 250,000 miles from Earth, while man-made satellites can be as far as 36,000 miles away. This 7:1 difference in distance makes a huge difference in the signals that arrive at the satellite, since transmission loss varies as the square of the distance. In other words, the signal arriving at the Moon is 20 dB weaker than that arriving at a geo-synchronous satellite 25,000 miles high, due to distance alone.

The second difference between the Moon and a man-made satellite is that the Moon is a *passive reflector*—and not a very good one at that, since it has a craggy and rather irregular surface, at least when compared to a flat mirror-like surface that would make an ideal reflector. Signals scattered by the Moon's irregular surface are thus weaker than for better reflecting surfaces. By comparison, a man-made satellite is an *active* system, where the satellite receives the signal coming from Earth, amplifies it and then retransmits the signal (usually at a different frequency) using a high-gain antenna. Think of a satellite as an ideal reflector, with gain.

The net result of these differences between a man-made satellite and the Earth's natural satellite is that moonbounce (EME) operation challenges the station builder considerably more than satellite operation, particularly in the area of antennas. Successful EME requires high transmitting power, superb receiver sensitivity and excellent operators capable of pulling weak signals out of the noise. This chapter will first explore antennas suitable for satellite operations and then describe techniques needed for EME work.

Common Ground

There are areas of commonality between satellite and EME antenna requirements, of course. Both require consideration of the effects of polarization and elevation angle, along with the azimuth directions of transmitted and received signals.

On the HF bands, signal polarization is generally of little concern, since the original polarization sense is lost after the signal passes through the ionosphere. At HF, vertical antennas receive sky-wave signals emanating from horizontal antennas, and vice versa. It is not beneficial to provide a means of varying the polarization at HF. With satellite communications, however, because of polarization changes, a signal that would disappear into the noise on one antenna may be S9 on one that is not sensitive to polarization direction. Elevation angle is also important from the standpoint of tracking and avoiding indiscriminate ground reflections that may cause nulls in signal strength.

Antennas for Satellite Work

We have amateur satellites providing links from 2 meters and up, and these provide opportunities to use antennas of many types—from the very simple to some pretty complex ones. This section was written by Dick Jansson, WD4FAB. It covers descriptions of a wide range of satellite antennas and points operators to source material for construction of many of them.

Antennas for LEO Satellites

Antenna design and construction requirements for use with Amateur satellites vary from low-gain antennas for low-earth-orbit (LEO) satellites to higher-gain antennas for the high-altitude elliptical-orbit satellites. You can operate the FM LEO satellites with a basic dual-band VHF/UHF FM transceiver or even a good FM H-T, as some amateurs have managed. Assuming that the transceiver is reasonably sensitive, you can even use a good "rubber duck" antenna. Some amateurs manage to work the FM birds with H-Ts and a multi-element directional antenna such as the popular Arrow Antenna, **Fig 1**. Of course, this means they must aim their antennas at the satellites, even as they cross overhead.

High-quality omnidirectional antennas for LEO service come in quite a number of forms and shapes. M^2 Enterprises has their EB-144 and EB-432 Eggbeater antennas, which have proven to be very useful and do not require any rotators for control. See **Fig 2**. The turnstile-over-reflector antenna has been around for a long time, as shown in **Fig 3**. Other operators have done well using low-gain Yagi antennas, such as those shown in **Fig 4**.

For even better performance, at the modest cost of a single, simple TV antenna rotator, check out the fixed-elevation *Texas Potato Masher* antenna by K5OE, **Fig 5.** This antenna provides a dual-band solution for medium-gain directional antennas for LEO satellites. This is a considerable improvement over omnidirectional antennas and does not require an elevation rotator for good performance.

There are still two LEO satellites that work on the 10-meter band, RS-15 and the newly resurrected AO-7. Both have 10-meter downlinks in the range of 29.3 to 29.5 MHz. Low-gain 10-meter antennas, such as dipoles or long-wire antennas, are used to receive these satellites.

Antennas for High-Altitude Satellites

The high-altitude, Phase-3 satellites, such as AO-10 (and the late AO-13), have been around for quite a number of years. The greater distances to the Phase-3 satellites mean that more transmitted power is needed to access them and weaker signals are received on the ground. Successful stations usually require ground-station antennas with significant gain (12 dBi or more), such as a set of high-gain Yagi antennas. See **Fig 6**. Note the use of two Yagi antennas mounted on each boom to provide *circular polarization*, usually referred to as CP.

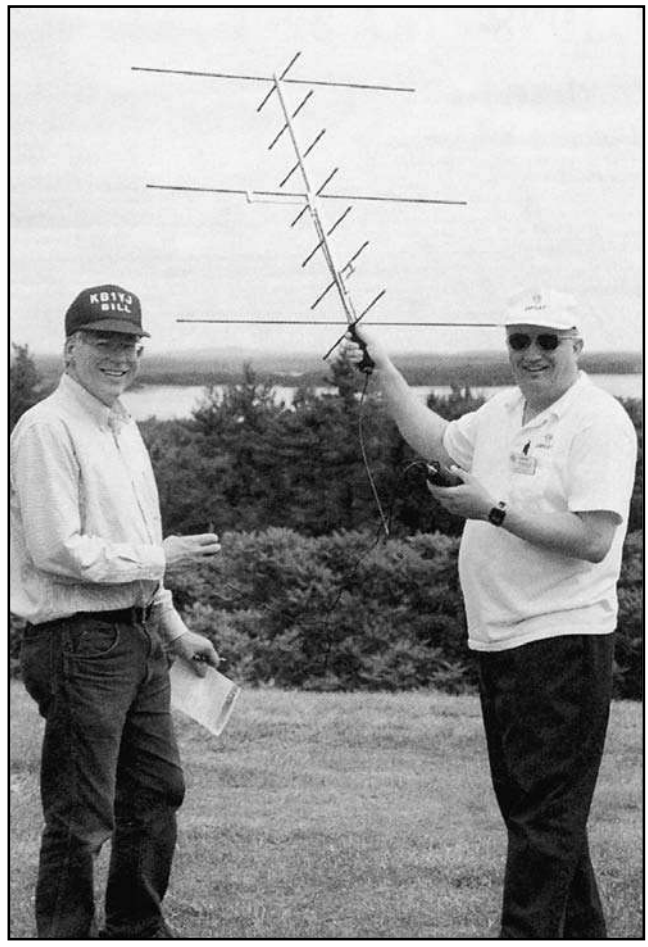

Fig 1—The hand-held "Arrow" gain antenna is popular for LEO FM operations. (*Photo courtesy* The AMSAT Journal, *Sept/Oct 1998.*)

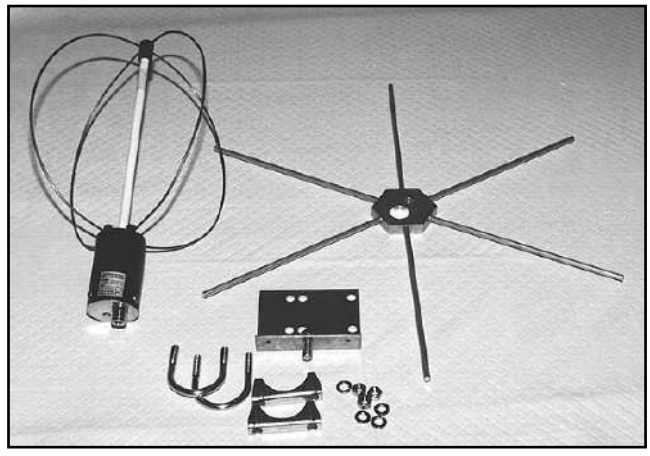

Fig 2—Eggbeater antennas are popular for base station LEO satellite operations. This EB-432 eggbeater antenna for 70 cm is small enough to put in an attic. Antenna gain pattern is helped with the radials placed below the antenna.

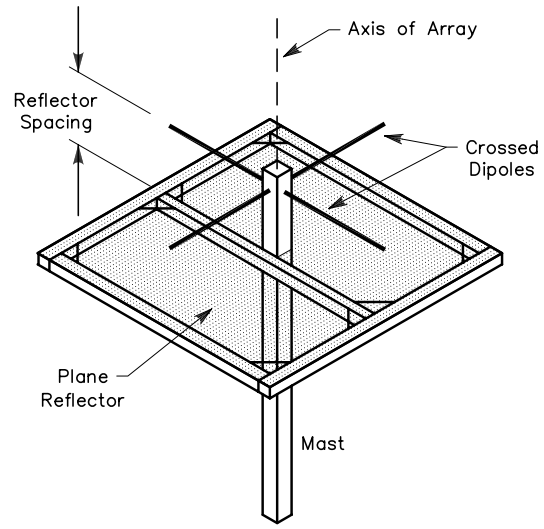

Fig 3—The Turnstile Over Reflector antenna has served well for LEO satellite service for a number of years.

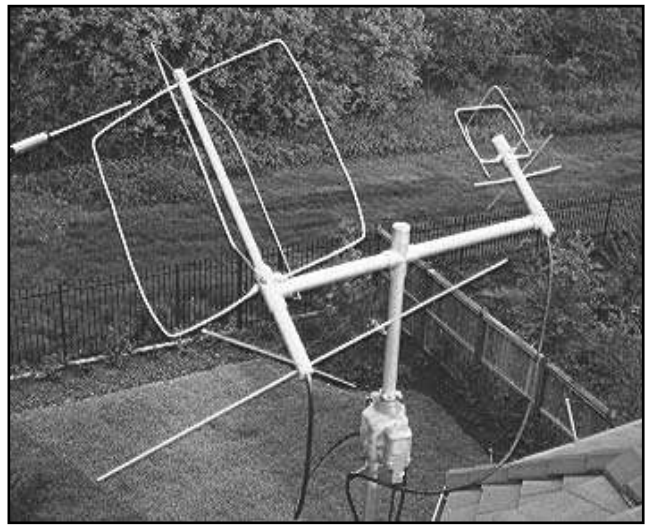

Fig 5—Jerry Brown, K5OE, uses his Texas Potato Masher antennas to work LEO satellites.

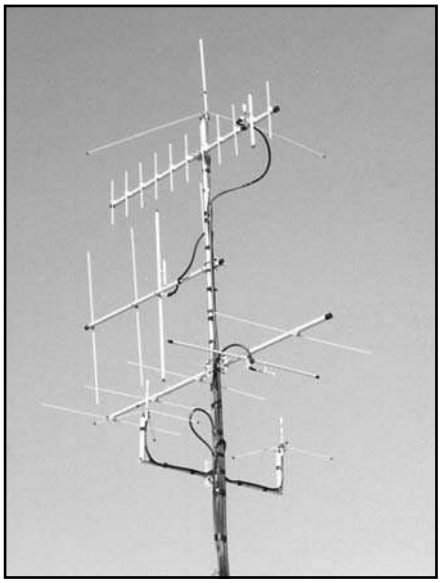

Fig 4—Simple ground plane and Yagi antennas can be used for LEO satellite contacts.

Fig 6—Dick Jansson, WD4FAB, used these 2-meter and 70-cm crossed Yagi's in RHCP for AO-10 and AO-13 operations. The satellite antennas are shown mounted above a 6-meter long-boom Yagi.

CIRCULAR POLARIZATION

Linearly polarized antennas are horizontal or vertical in terms of the antenna's position relative to the surface of the Earth, a reference that loses its meaning in space. The need to use circularly polarized (CP) antennas for space communications is well established. If spacecraft antennas used linear polarization, ground stations would not be able to maintain polarization alignment with the spacecraft because of changing orientations. The ideal antenna for random satellite polarizations is one with a circularly polarized radiation pattern.

There are two commonly used methods for obtaining circular polarization. One is with crossed linear elements such as dipoles or Yagis, as Fig 6 shows. The second popular CP method uses a helical antenna, described below. Other methods also exist, such as with the omnidirectional quadrifilar helix, **Fig 7**.

Polarization *sense* is a critical factor, especially in EME and satellite work. The IEEE standard uses the term "clockwise circular polarization" for a *receding* wave. Amateur technology follows the IEEE standard, calling clockwise polarization for a receding wave as right-hand, or RHCP. Either clockwise or a counter-clockwise (LHCP) sense can be selected by reversing the phasing harness of a crossed-Yagi antenna, see **Fig 8**. The sense of a helical antenna is fixed, determined by its physical construction.

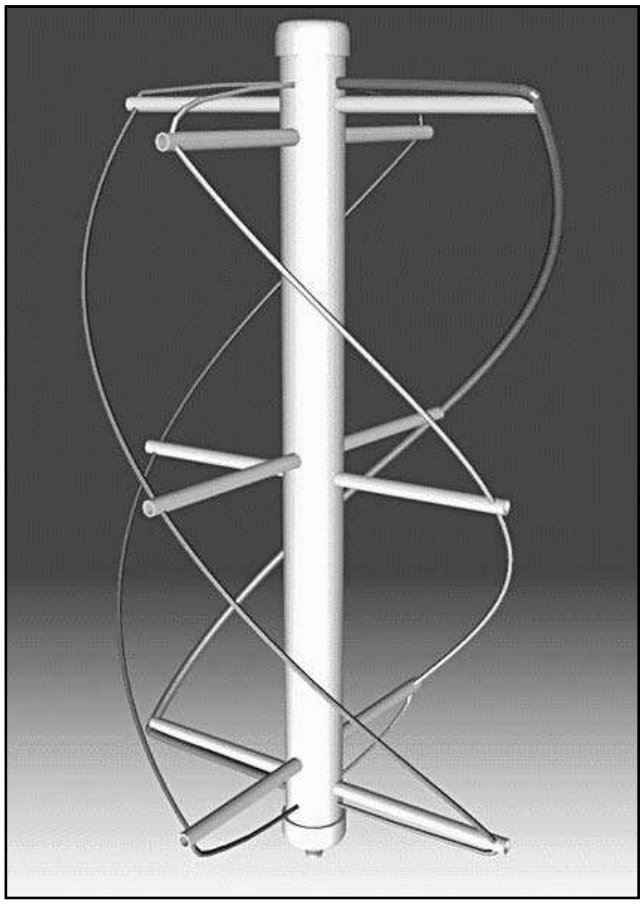

Fig 7—W3KH suggests that quadrifilar antennas can serve well for omnidirectional satellite-station antenna service.

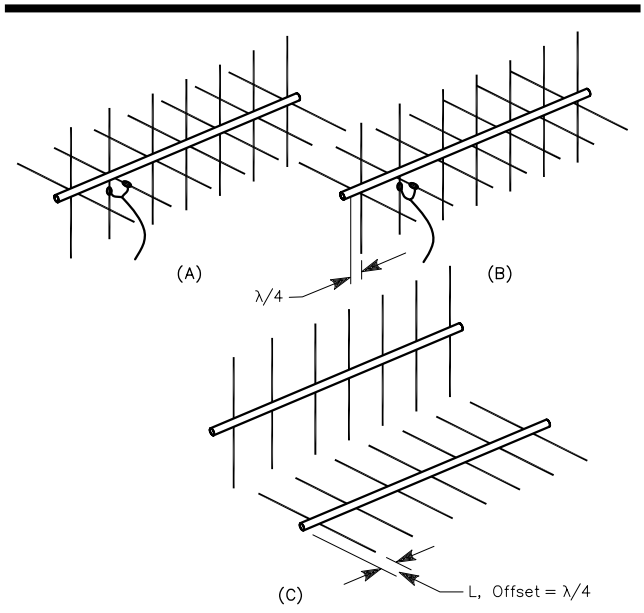

Fig 8—Evolution of the circularly polarized Yagi. The simplest form of crossed Yagi, A, is made to radiate circularly by feeding the two driven elements 90° out of phase. Antenna B has the driven elements fed in phase, but has the elements of one bay mounted 1/4 λ forward from those of the other. Antenna C offers elliptical (circular) polarization using separate booms. The elements in one set are perpendicular to those of the other and are 1/4 λ forward from those of the other.

See **Fig 9** for construction details.

In working through a satellite with a circularly polarized antenna, it is often convenient to have the capability of switching polarization sense. This is because the sense of the received signal of some of the LEO satellites reverses when the satellite passes its nearest point to you. If the received signal has right-hand circular polarization as the satellite approaches, it may have left-hand circularity as the satellite recedes. There is a sense reversal in EME work, as well, because of a phase reversal of the signal as it is reflected from the surface of the moon. A signal transmitted with right-hand circularity will be returned to the Earth with left-hand circularity. Similarly, the polarization is reversed as it is reflected from a dish antenna, so that for an overall RHCP performance, the feed antenna for the dish needs to be LHCP.

Crossed Linear Antennas

Dipoles radiate linearly polarized signals, and the polarization direction depends on the orientation of the antenna. It two dipoles are arranged for horizontal and vertical dipoles, and the two outputs are combined with the correct phase difference (90°), a circularly polarized wave results. Because the electric fields are identical in magnitude, the power from the transmitter will be equally divided between the two fields. Another way of looking at this is to consider the power as being divided between the two antennas; hence the gain of each is decreased by 3 dB when taken alone in the plane of its orientation.

A 90° phase shift must exist between the two antennas and the simplest way to obtain this shift is to use two feed lines to a coplanar pair of crossed-Yagi antennas. One feed-line section is 1/4 λ longer than the other, as shown in Fig 8A. These separate feed lines are then paralleled to a common transmission line to the transmitter or receiver. Therein lies one of the headaches of this system. Assuming negligible coupling between the crossed antennas, the impedance presented to the common transmission line by the parallel combination is one half that of either section alone. (This is not true when there is mutual coupling between the antennas, as in phased arrays.) A practical construction method for implementing a RHCP/LHCP coplanar switched system is shown in **Fig 10**.

Another example of a coplanar crossed-Yagi antenna is shown in **Fig 11**. With this phasing-line method, any mismatch at one antenna will be magnified by the extra 1/4 λ of transmission line. This upsets the current balance between the two antennas, resulting in a loss of polarization circularity. Another factor to consider is the attenuation of the cables used in the harness, along with the

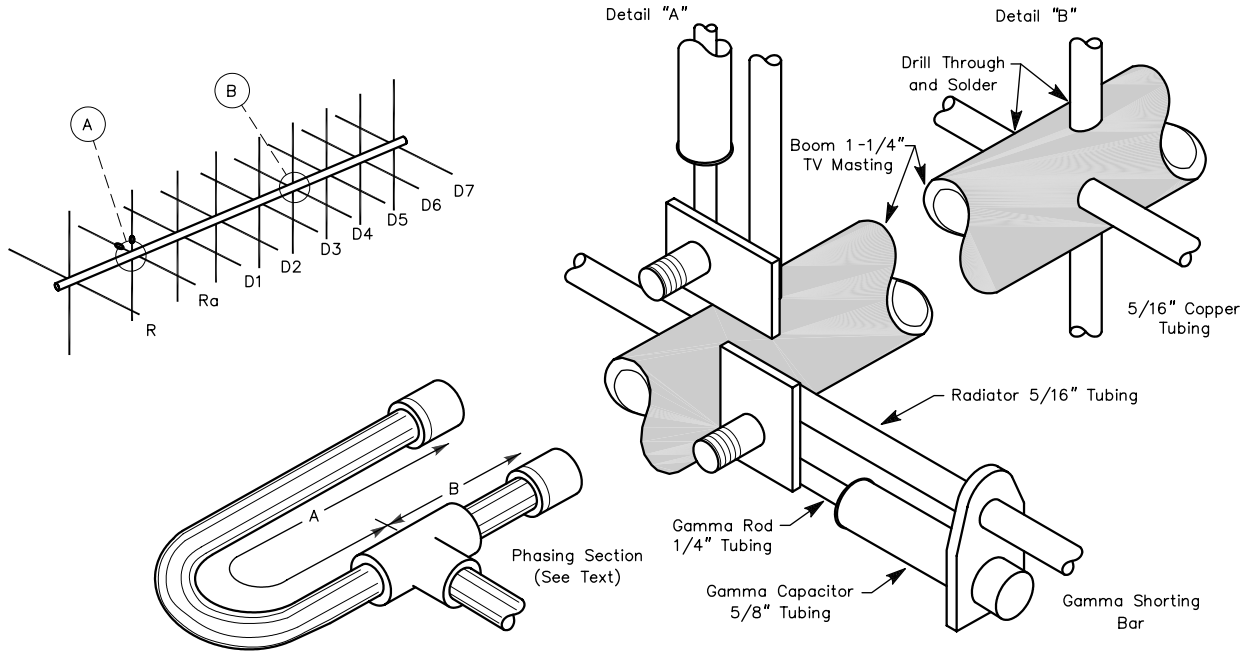

Fig 9—Construction details of a co-planar crossed-Yagi antenna.

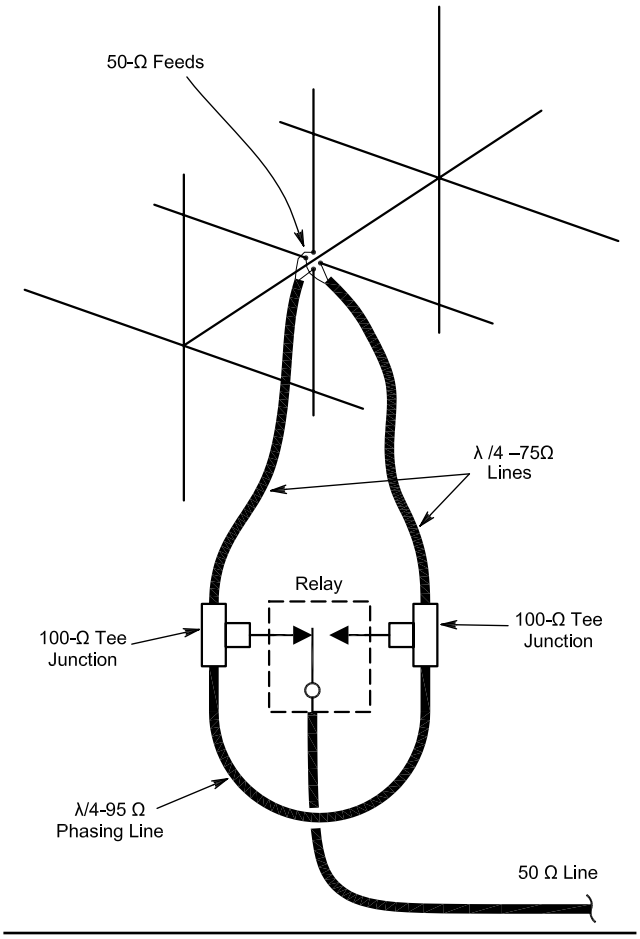

Fig 10—Co-planar crossed Yagi, circularly polarized antenna with switchable polarization phasing harness.

connectors. Good low-loss coaxial line should be used. Type-N or BNC connectors are preferable to the UHF variety.

Another method to obtain circular polarization is to use equal-length feed lines and place one antenna 1/4 λ ahead of the other. This offset pair of Yagi-crossed antennas is shown in Fig 8B. The advantage of equal-length feed lines is that identical load impedances will be presented to the common feeder, as shown in **Fig 12**, which shows a fixed circularity sense feed. To obtain a switchable sense feed with the offset Yagi pair, you can use a connection like that of **Fig 13**, although you must compensate for the extra phase added by the relay and connectors.

Fig 8C diagrams a popular method of mounting two separate off-the-shelf Yagis at right angles to each other. The two Yagis may be physically offset by 1/4 λ and fed in parallel, as shown in Fig 8C, or they may be mounted with no offset and fed 90° out of phase. Neither of these arrangements on two separate booms produces true circular polarization. Instead, *elliptical* polarization results from such a system. **Fig 14** is a photo of this type of mounting of Yagis on two booms for elliptical operation.

Helical Antennas

As mentioned, the second method to create a circularly polarized signal is by means of a helical antenna. The axial-mode helical antenna was introduced by Dr John Kraus, W8JK, in the 1940s. **Fig 15** shows examples of S-band (2400-MHz), V-band (145-MHz), and U-band (435-MHz) helical antennas, all constructed by WD4FAB for satellite service.

This antenna has two characteristics that make it

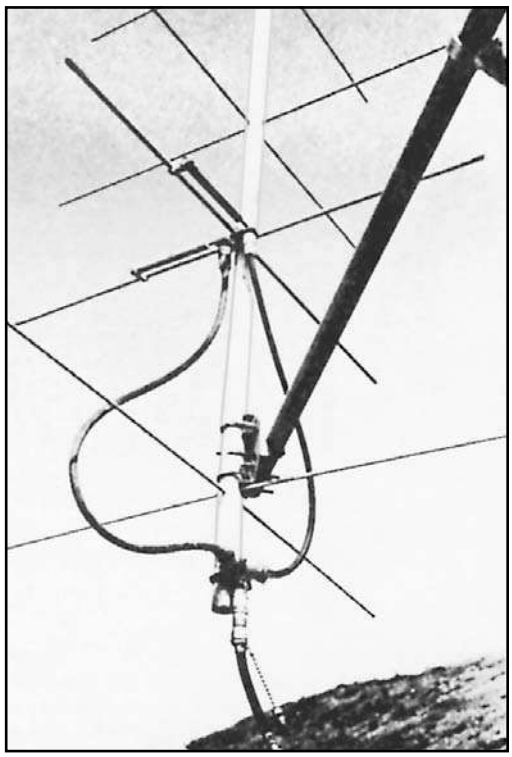

Fig 11—This VHF crossed Yagi design by KH6IJ (Jan 1973 *QST*) illustrates the co-planar, fixed-circularity Yagi.

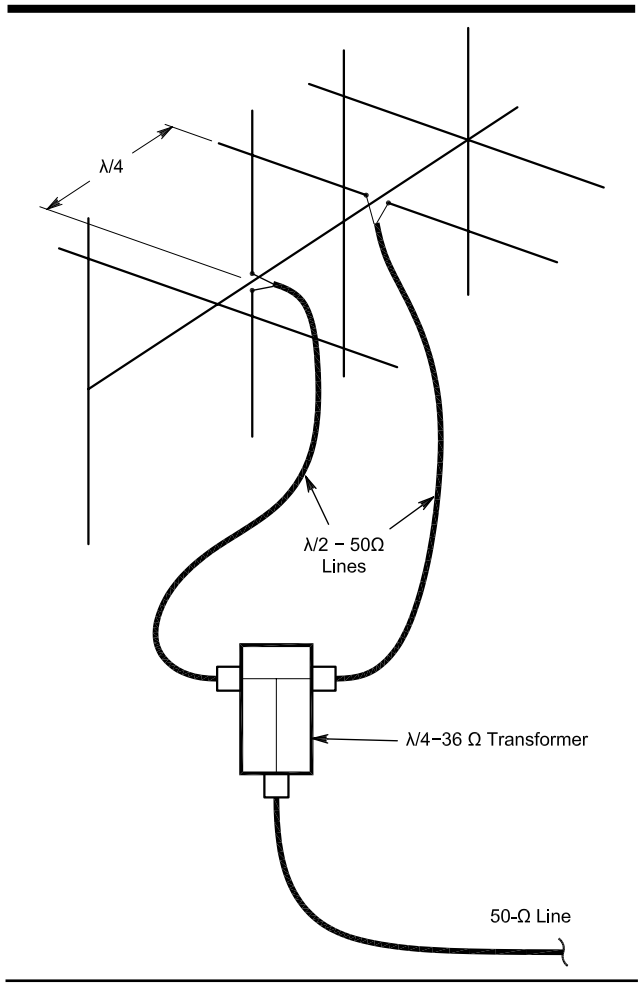

Fig 12—Offset crossed-Yagi circularly polarized antenna-phasing harness with fixed polarization.

especially interesting and useful in many applications. First, the helix is circularly polarized. As discussed earlier, circular polarization is simply linear polarization that continually rotates as it travels through space. In the case of a helical antenna, this rotation is about the axis of the antenna. This can be pictured as the second hand of a watch moving at the same rate as the applied frequency, where the position of the second hand can be thought of as the instantaneous polarization of the signal.

The second interesting property of the helical antenna is its predictable pattern, gain and impedance characteristics over a wide frequency range. This is one of the few antennas that has both broad bandwidth and high gain. The benefit of this property is that, when used for narrow-band applications, the helical antenna is very forgiving of mechanical inaccuracies.

Probably the most common amateur use of the helical antenna is in satellite communications, where the spinning of the satellite antenna system (relative to the earth) and the effects of Faraday rotation cause the polarization of the satellite signal to be unpredictable. Using a linearly polarized antenna in this situation results in deep fading, but with the helical antenna (which responds equally to linearly polarized signals), fading is essentially eliminated.

This same characteristic makes helical antennas useful in polarization-diversity systems. The advantages of circular polarization have been demonstrated on VHF voice schedules over non-optical paths, in cases where linearly polarized beams did not perform satisfactorily.

Another use for the helical antenna is the transmission of color ATV signals. Many beam antennas (when adjusted for maximum gain) have far less bandwidth than the required 6 MHz, or have non-uniform gain over this frequency range. The result is significant distortion of the transmitted and received signals, affecting color reproduction and other features. This problem becomes more aggravated over non-optical paths. The helix exhibits maximum gain (within 1 dB) more than 20 MHz anywhere above 420 MHz.

The helical antenna can be used to advantage with multimode rigs, especially above 420 MHz. Not only does the helix give high gain over an entire amateur band, but it also allows operation on FM, SSB and CW without the need for separate vertically and horizontally polarized antennas.

Helical Antenna Basics

The helical antenna is an unusual specimen in the antenna world, in that its physical configuration gives a

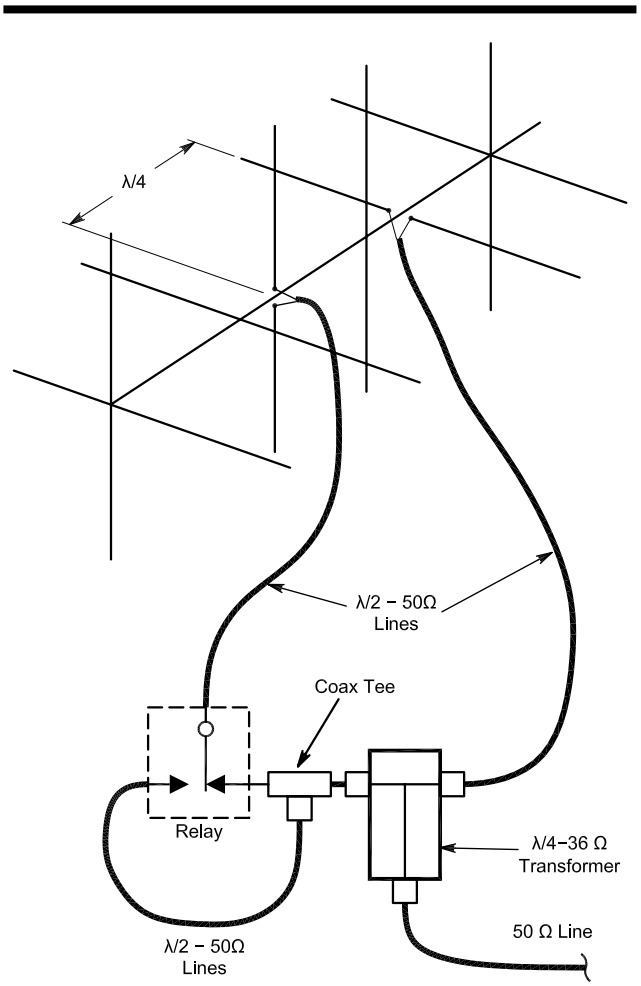

Fig 13—Offset crossed-Yagi circularly polarized antenna-phasing harness with switchable polarization.

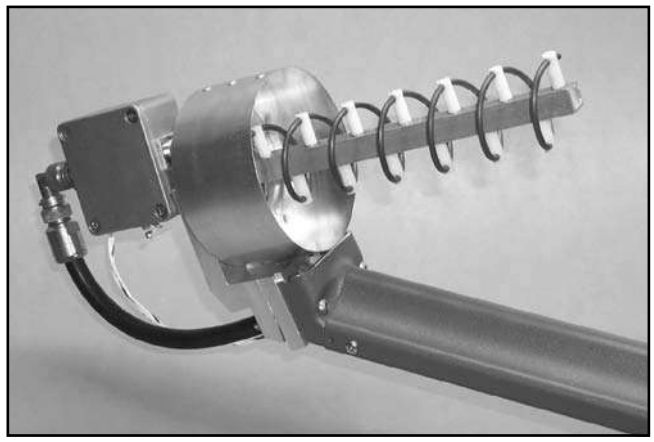

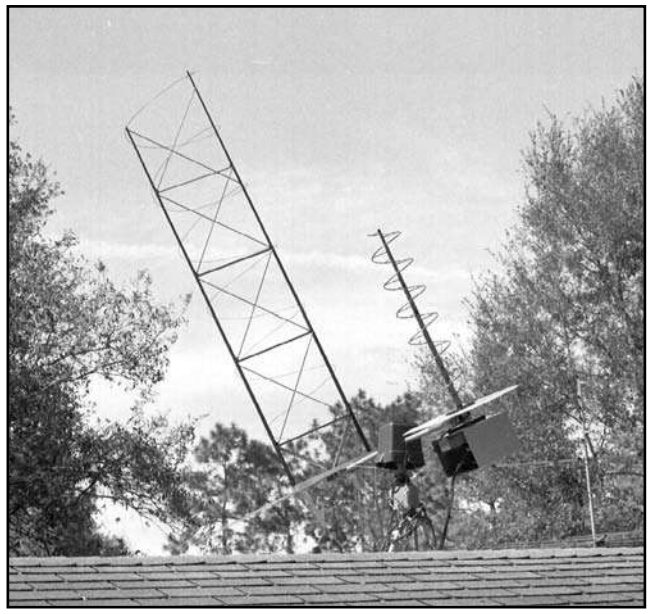

Fig 15—At top, a seven-turn LHCP helical antenna for S-band dish feed for AO-40 service. This helical antenna uses a cupped reflector and has a preamplifier mounted directly to the antenna feed point. At bottom, a pair of helical antennas for AO-10 service on 2 meters and 70 cm. The 2-meter helical antenna is not small! (*WD4FAB photos.*)

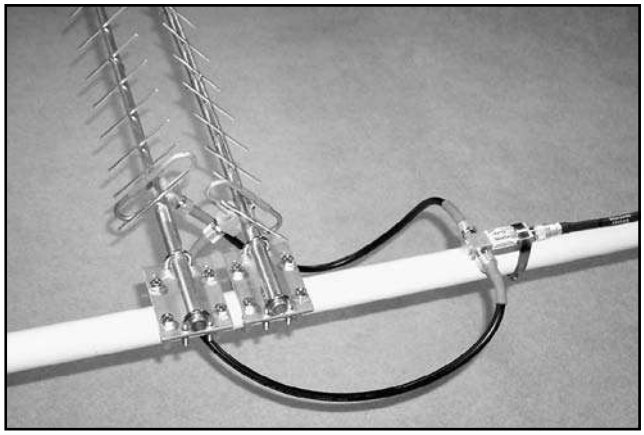

Fig 14—An example of offset crossed-Yagi circularly polarized antennas with fixed polarization. This example is a pair of M² 23CM22EZA antennas, for L band (1269 MHz), mounted on an elevation boom. (*WD4FAB photo.*)

hint to its electrical performance. A helix looks like a large air-wound coil with one of its ends fed against a ground plane, as shown in **Fig 16**. The ground plane is a screen of 0.8 λ to 1.1 λ diameter (or on a side for a square ground plane). The circumference (C_λ) of the coil form must be between 0.75 λ and 1.33 λ for the antenna to radiate in the axial mode. The coil should have at least three turns to radiate in this mode. The ratio of the spacing between turns (in wavelengths), S_λ to C_λ, should be in the range of 0.2126 to 0.2867. This ratio range results from the requirement that the pitch angle, α, of the helix be between 12° and 16°, where:

$$\alpha = \arctan \frac{S_\lambda}{C_\lambda} \qquad \text{(Eq 1)}$$

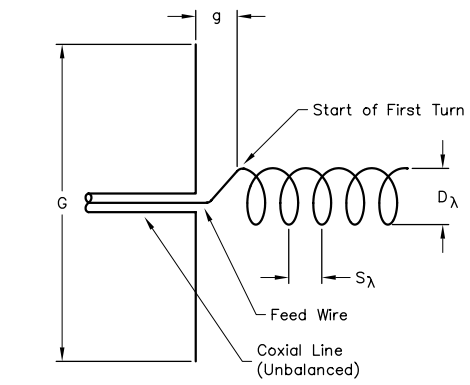

Fig 16—The basic helical antenna and design equations.

These constraints result in a single main lobe along the axis of the coil. This is easily visualized from Fig 15A. The winding of the helix comes away from the cupped reflector with a counterclockwise winding direction for a LHCP. (The winding can also be a clockwise—this results in a RHCP polarization sense.)

A helix with a C_λ of 1λ has a wave propagating from one end of the coil (at the ground plane), corresponding to an instantaneous dipole "across" the helix. The electrical rotation of this dipole produces circularly polarized radiation. Because the wave is moving along the helix conductor at nearly the speed of light, the rotation of the electrical dipole is at a very high rate, and true circular polarization results.

The IEEE definition, in simple terms, is that when viewing the antenna from the feed-point end, a clockwise wind results in right-hand circular polarization (RHCP), and a counterclockwise wind results in left-hand circular polarization (LHCP). This is important, because when two stations use helical antennas over a nonreflective path, both must use antennas with the same polarization sense. If antennas of opposite sense are used, a signal loss of at least 20 dB results from the cross polarization alone.

As mentioned previously, circularly polarized antennas can be used in communications with any linearly polarized antenna (horizontal or vertical), because circularly polarized antennas respond equally to all linearly polarized signals. The gain of a helix is 3 dB less than the theoretical gain in this case, because the linearly polarized antenna does not respond to linear signal components that are orthogonally polarized relative to it.

The response of a helix to all polarizations is indicated by a term called *axial ratio*, also known as *circularity*. Axial ratio is the ratio of amplitude of the polarization that gives maximum response to the amplitude of the polarization that gives minimum response. An ideal circularly polarized antenna has an axial ratio of 1.0. A well-designed practical helix exhibits an axial ratio of 1.0 to 1.1. The axial ratio of a helix is:

$$AR = \frac{2n + 1}{2n} \qquad \text{(Eq 2)}$$

where:

AR = axial ratio
n = the number of turns in the helix

Axial ratio can be measured in two ways. The first is to excite the helix and use a linearly polarized antenna with an amplitude detector to measure the axial ratio directly. This is done by rotating the linearly polarized antenna in a plane perpendicular to the axis of the helix and comparing the maximum and minimum amplitude values. The ratio of maximum to minimum is the axial ratio.

The impedance of the helix is easily predicted. The terminal impedance of a helix is unbalanced, and is defined by:

$$Z = 140 \times C_\lambda \qquad \text{(Eq 3)}$$

where Z is the impedance of the helix in ohms.

The gain of a helical antenna is determined by its physical characteristics. Gain can be calculated from:

$$\text{Gain}\,(\text{dBi}) = 11.8 + 10\log\left(C_\lambda^{\,2}\, nS_\lambda\right) \qquad \text{(Eq 4)}$$

In practice, helical antennas do not deliver the gain in Eq 4 for antennas with turns count greater than about twelve. There will be more discussions in this area when practical antennas are discussed.

The beamwidth of the helical antenna (in degrees) at the half-power points is:

$$BW = \frac{52}{C_\lambda \sqrt{nS_\lambda}} \qquad \text{(Eq 5)}$$

The diameter of the helical antenna conductor should be between 0.006 λ and 0.05 λ, but smaller diameters have been used successfully at 144 MHz. The previously noted diameter of the ground plane (0.8 λ to 1.1 λ) should not be exceeded if you desire a clean radiation pattern. As the ground plane size is increased, the sidelobe levels also increase. Cupped ground planes have been used according to Kraus, as in Fig 15. (The ground plane need not be solid; it can be in the form of a spoked wheel or a frame covered with hardware cloth or screen.)

50-Ω Helix Feed

Joe Cadwallader, K6ZMW, presented this feed method in June 1981 *QST*. Terminate the helix in an N connector mounted on the ground screen at the periphery of the helix. See **Fig 17**. Connect the helix conductor to the N connector as close to the ground screen as possible (**Fig 18**). Then adjust the first quarter turn of the helix to a close spacing from the reflector.

This modification goes a long way toward curing a deficiency of the helix—the 140-Ω nominal feed-point

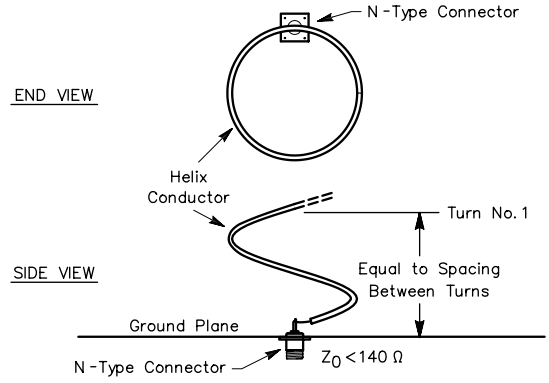

Fig 17—End view and side view of peripherally fed helix.

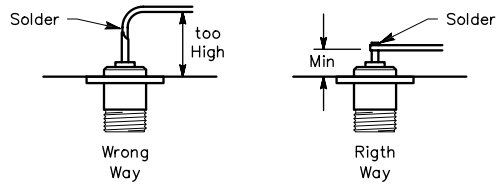

Fig 18—Wrong and right ways to attach helix to a type N connector for 50-Ω feed.

impedance. The traditional λ/4 matching section has proved difficult to fabricate and maintain. But if the helix is fed at the periphery, the first quarter turn of the helix conductor (leaving the N connector) acts much like a transmission line—a single conductor over a perfectly conducting ground plane. The impedance of such a transmission line is:

$$Z_0 = 138 \log \frac{4h}{d} \qquad \text{(Eq 6)}$$

where:

Z_0 = line impedance in ohms
h = height of the center of the conductor above the ground plane
d = conductor diameter (in the same units as h).

The impedance of the helix is 140 Ω a turn or two away from the feed point. But as the helix conductor swoops down toward the feed connector (and the ground plane), h gets smaller, so the impedance decreases. The 140-Ω nominal impedance of the helix is transformed to a lower value. For any particular conductor diameter, an optimum height can be found that will produce a feed-point impedance equal to 50 Ω. The height should be kept very small, and the diameter should be large. Apply power to the helix and measure the SWR at the operating frequency. Adjust the height for an optimum match.

Typically, the conductor diameter may not be large

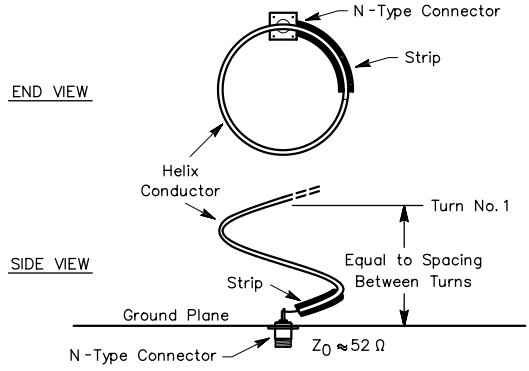

Fig 19—End view and side view of peripherally fed helix with metal strip added to improve transformer action.

enough to yield a 50-Ω match at practical (small) values of h. In this case, a strip of thin brass shim stock or flashing copper can be soldered to the first quarter turn of the helix conductor (**Fig 19**). This effectively increases the conductor diameter, which causes the impedance to decrease further yet. The edges of this strip can be slit every 1/2 inch or so, and the strip bent up or down (toward or away from the ground plane) to tune the line for an optimum match.

This approach yields a perfect match to nearly any coax. The usually wide bandwidth of the helix (70% for less than 2:1 SWR) will be reduced slightly (to about 40%) for the same conditions. This reduction is not enough to be of any consequence for most amateur work. The improvements in performance, ease of assembly and adjustment are well worth the effort in making the helix more practical to build and tune.

ANTENNAS FOR AO-40 OPERATIONS

Antennas for successful operations on AO-40 come in many shapes and sizes. AO-40 has provided amateurs the opportunity to broadly experiment with antennas.

Fig 20 shows the satellite antennas at WD4FAB. The Yagi antennas are used for the U- and L-band AO-40 uplinks and the V-band AO-10 downlink, while the S-band dish antenna is for the AO-40 downlink. These satellite antennas are tower mounted at 63 feet (19 meters) to avoid pointing into the many nearby trees and suffering from the resulting "green attenuation." Of course, satellite antennas do not always need to be mounted high on a tower if dense foliage is not a problem. If satellite antennas are mounted lower down, feed-line length and losses can reduced.

Another benefit, however, to tower mounting of satellite antennas is that they can be used for terrestrial ham communications and contests. The fact that the antennas are set up for CP does not really degrade these other operating activities.

Experience with AO-40 has clearly shown the advan-

Fig 20—Details of WD4FAB's tower cluster of satellite antennas including a home-brew elevation rotator. Top to bottom: M² 436-CP30, a CP U-band antenna; two M² 23CM22EZA antennas in a CP array for L band; "FABStar" dish antenna with helix feed for S band; M² 2M-CP22, a CP V-band antenna (only partially shown.) To left of dish antenna is a NEMA4 equipment box with an internal 40-W L-band amplifier, and also hosts externally mounted preamplifiers. (*WD4FAB photo*)

Fig 21—Domenico, I8CVS, has this cluster of satellite antennas for AO-40. Left to right: array of 4 × 23-element Yagi horizontally polarized for L band; 1.2-meter dish with 3-turn helix feed for S band; 15-turn RHCP helical antenna for U band; 60-cm dish for X band. All microwave preamplifiers and power amplifiers are homebrew and are mounted on this antenna cluster. (*I8CVS photo.*)

tages of using RHCP antennas for both the uplink and downlink communications. The antennas shown in Fig 20 are a single-boom RHCP Yagi antenna for U band, a pair of closely spaced Yagi antennas phased for RHCP for L band (see Fig 14), and a helix-fed dish antenna for S band. The antenna gain requirements for U band can easily be met with the gain of a 30-element crossed Yagi. Antennas of this size have boom lengths of 4 to 4$^1/_2$ wavelengths. The enterprising constructor can build a Yagi antenna from one of several references, however most of us prefer to purchase well-tested antennas from commercial sources as M² or Hy-Gain. In the past, KLM (now out of business) had offered a 40-element CP Yagi for U-band satellite service, and many of these are still in satisfactory use today.

U-band uplink requirements for AO-40 have clearly demonstrated the need for gain less than 16 to 17 dBic RHCP, with an RF power of less than 50 W PEP at the antenna (≈ 2,500 W-PEP EIRP with a RHCP antenna) depending upon the *squint angle*. (The squint angle is the angle at which the main axis of the satellite is pointed away from your antenna on the ground. If the squint angle is less than half of the half-power beamwidth, the ground station will be within the spacecraft antenna's nominal beam width.)

A gain of 16 to 17 dBic RHCP can be obtained from a 30-element crossed Yagi, AO-13 type antenna, and is good news, considering that the satellite may be over 60,000 km (37,000 miles) from your station. Success on the U-band uplinks to AO-40 is easier than those for L band at wider squint angles more than 20°. At squint angles less than 10°, U-band uplink operation can even be done with 1-5 W power outputs to a RHCP antenna (≈ 200 W-PEP EIRP with RHCP). These lower levels mean that smaller antennas can be used. In practice, these uplinks will produce downlink signals that are 10 to 15 dB above the noise floor, or S7 signals over an S3 noise floor. The beacon will give a downlink S9 signal for these same conditions.

WD4FAB's experience with the AO-40 L-band uplink has demonstrated that 40 W-PEP delivered to an antenna with a gain of ≈ 19dBic (3,000 W-PEP EIRP with RHCP) is needed for operations at the highest altitudes of AO-40 and with squint angles ≤ 15°. This is the pretty com-

pact L-band antenna arrangement with two 22-element antennas in a RHCP array shown in Fig 14 and 20. Other operators have experience that using a 1.2-meter L-band dish antenna and 40 W of RF power (6,100 W-PEP EIRP with RHCP) can also provide a superb uplink for squint angles even up to 25°. A dish antenna can have a practical gain of about 21 to 22 dBic. These uplinks will provide the user a downlink that is 10 to 18 dB above the transponder noise floor. In more practical terms, this is an S7 to 8 signal over a S3 transponder noise floor, a very comfortable armchair copy.

Fig 22—Wilfred Carey, ZS6JT, constructed this cluster of satellite and EME antennas. Left to right: 2 × 23-element offset feed Yagi for U band; 1.64-meter dish with $2^1/_4$-turn helix feed for S band; 2 × 11-element coplanar feed Yagi for V band. (*ZS6JT photo.*)

Using the L-band uplink for AO-40, instead of the U-band uplink, allows the use of Yagi antennas that more manageable, since their size for a given gain is only one third of those for U-band. With L band there is a narrower difference between using a dish antenna and a Yagi, since a 21- to 22-dBic dish antenna would be only about 1.2 meters (4 feet) in diameter. However, some of us may not have such "real estate" available on our towers and may seek a lower wind-loading solution offered by Yagis. Long-boom rod-element Yagi, or loop-Yagi antennas are commercially offered by M^2 and DEM, although this band is about the highest for practical Yagis. The example shown in Fig 20 is a pair of rod-element Yagi antennas from M^2 in a CP arrangement with a gain of 18 to 19 dBic.

Other amateurs have successful AO-40 operation with different arrangements. **Fig 21** shows I8CVS's 4 × 23-element linear array for a 1270 MHz, a 1.2-meter solid dish for 2400 MHz, a 15-turn helical antenna for 435 MHz, and a 60-cm dish for 10,451 MHz. This arrangement clearly shows the advantage and accessibility of having a roof-mounted antenna.

Fig 22 shows ZS6JT's setup, with a 1.64-meter home-built mesh dish for 2400 MHz and two home-built crossed Yagi antennas, one for 435 MHz and the other for 145 MHz. Note that in these examples, the antennas permit terrestrial communication as well as satellite service. Two of these stations have also maintained the capability to operate the LEO satellites with U- and V-band antennas.

A number of amateurs have taken advantage of the availability of surplus C-band TVRO dishes, since most users of satellite television have moved up to the more

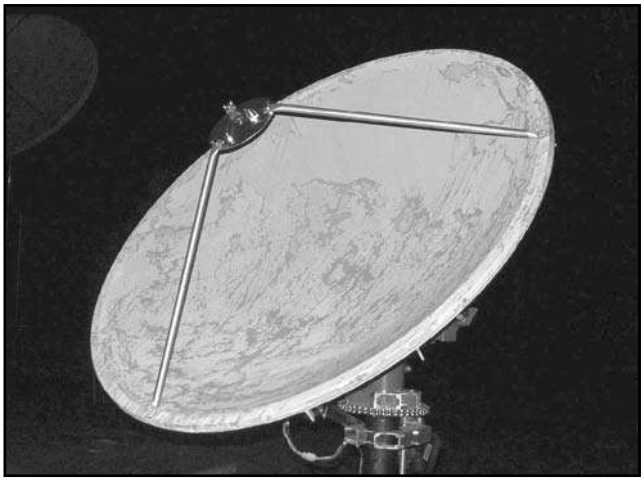

Fig 23—Robert Suding, WØLMD, modified this 4-foot dish antenna with a patch feed for S band and an Az-El mount. (*WØLMD photo.*)

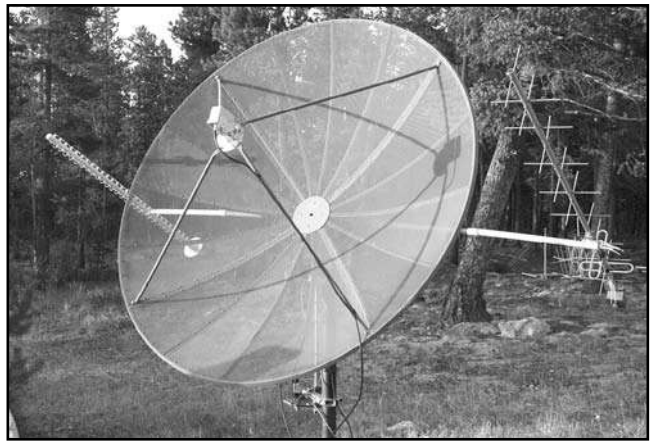

Fig 24—WØLMD graduated to this 8-foot dish with patch feed for S band for AO-40. On the left is a helical antenna for L band and on the right is a 2 × 9-element offset-feed Yagi for U band. A home-brew Az-El mount is provided. (*WØLMD photo.*)

Fig 25—WØLMD increased to this 10-foot dish for AO-40 operations, with a triband patch feed for U, L, and S bands on an Az-El mount. (*WØLMD photo.*)

Fig 26—WØLMD found the ultimate in this 14-foot dish for AO-40, with a triband patch feed and Az-El mount. (*WØLMD photo.*)

convenient K band using 0.5-meter dishes. Some examples of these dish conversions for satellite communications are shown in **Fig 23**, a WØLMD 4-foot dish with patch feed and Az-El mount. **Fig 24** shows a WØLMD 8-foot dish with patch feed, Az-El mount, a U-band Yagi, and an L-band helical antenna.

Fig 25 is a WØLMD 10-foot dish with tri-band patch feed and Az-El mount; and **Fig 26** is also a WØLMD

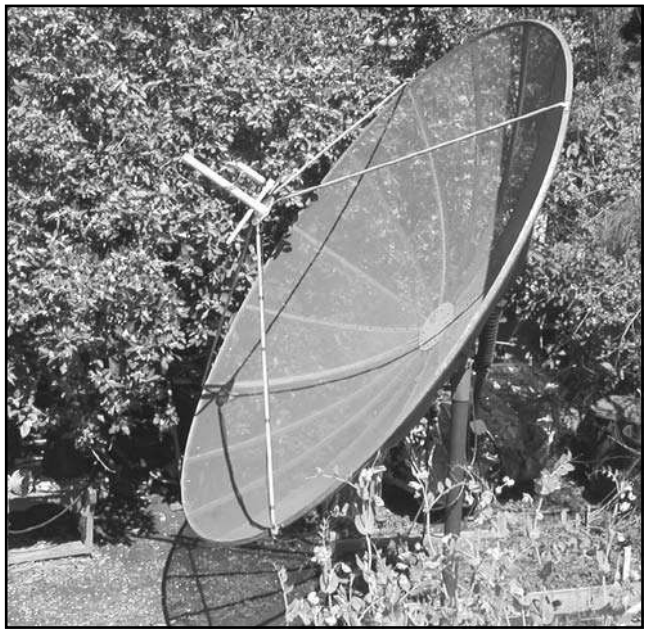

Fig 27—Clair E. Cessna, K6LG, has this 10-foot dish with S-band patch feed. This dish uses the original polar-mounting system and offsets the patch feed to compensate for AO-40's deviation from the Clarke belt. (*K6LG photo.*)

Fig 28—K5GNA's "circularized" mesh modification of an MMDS dish antenna with a helix-CP feed and DEP preamp. The dish modification reduces the spillover loss by making the antenna fully circular. (*K5OE photo.*)

14-foot dish with tri-band patch feed and Az-El mounting. Other operators, like K6LG, have been able to use TVRO dishes, **Fig 27**, with multiband patch feeds and still use, within limits, their polar-mounting system, as will be explained later.

Other hams have taken advantage of other surplus dish situations. **Fig 28** shows modified MMDS dishes, by K5GNA, and **Fig 29**, by K5OE, both using helix feeds. **Fig 30** shows a 75-cm high modified PrimeStar offset feed dish, by WD4FAB, using a longer helical feed antenna because of the higher f/D ratio of this dish configuration. This dish provides 5 dB of Sun noise, which is good performance. These efforts have rewarded their users with superb service on AO-40. Many have experimented with different feed and mounting systems. These experiments will be further illustrated.

One very popular spun-aluminum dish antenna seen in use on AO-40 has been the G3RUH-ON6UG 60-cm unit with its S-band patch feed, **Fig 31**. A kit, complete with a CP-patch feed is available from SSB-USA and has a gain of 21 dBic. It provides a 2.5-dB Sun noise signal. Surplus dishes have not been the only source for antennas for AO-40 operations, since some ingenious operators have even turned to the use of cardboard boxes. See **Figs 32** to **35**.

Fig 29—Mesh modification of an MMDS dish antenna by Jerry Brown, K5OE, with a helix-CP feed and DEM preamplifier mounted directly to the helix feed point. (*K5OE photo.*)

Fig 30—PrimeStar offset-fed dish with WD4FAB's helix-feed antenna. NØNSV was so pleased with the modification that he renamed the dish "FABStar," and made a new label! (*NØNSV photo.*)

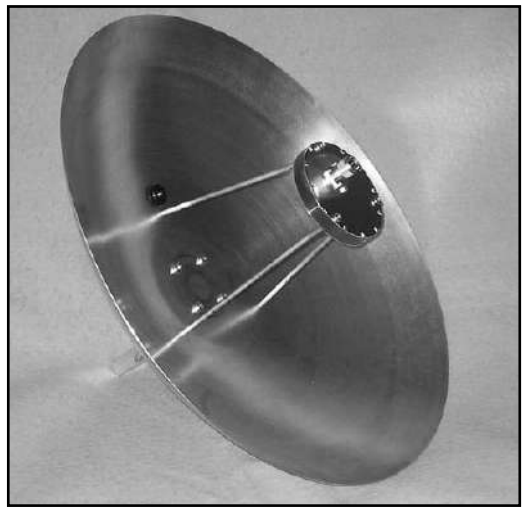

Fig 31—G3RUH's 60-cm spun-aluminum dish with CP-patch feed is available as a kit. This antenna has been popular with many AO-40 operators all over the world.

Fig 32—A complete satellite station with the tracking laptop, FT-847 transceiver, and both downlink and uplink cardboard-box antennas.

Parabolic Reflector Antennas

The satellite S-band downlinks have become very popular for a variety of reasons:

- Good performance with physically small downlink antennas
- Availability of good-quality downconverters
- Availability of preamps at reasonable prices.

A number of people advocate S-band operation, including Bill McCaa, KØRZ, who led the team that designed and built the AO-13 S-band transponder and James Miller, G3RUH, who operates one of the AO-40 command stations. Ed Krome, K9EK, and James Miller have published a number of articles detailing construction of preamps, downconverters and antennas for S band.

Some access AO-40's S-band downlink using compact S-band helical antennas. See **Fig 36**. With the demise of AO-40's S1 transmitter and its high-gain downlink antenna, enthusiasts have had to employ high-gain parabolic-dish antennas to use AO-40's S2 downlink, with its lower-gain helical antenna.

WØLMD notes that like a bulb in a flashlight, the

Fig 33—The completed high-performance corner-reflector uplink antenna for U band. Note how the box corners hold the reflectors and dipole feed in place. The rear legs set the antenna elevation to 20°—this gives good coverage at the design latitude but will need modification for other stations.

Fig 35—Side view of the downlink pyramidal horn showing the elevation control supports and how the downconverter is attached to the horn. The downconverter is pulled forward by the tape to align the probe wire parallel to the rear surface of the horn.

Fig 34—Front view of the downlink pyramidal horn showing how it is mounted in the support carton. Notice the coax probe at the back of the horn.

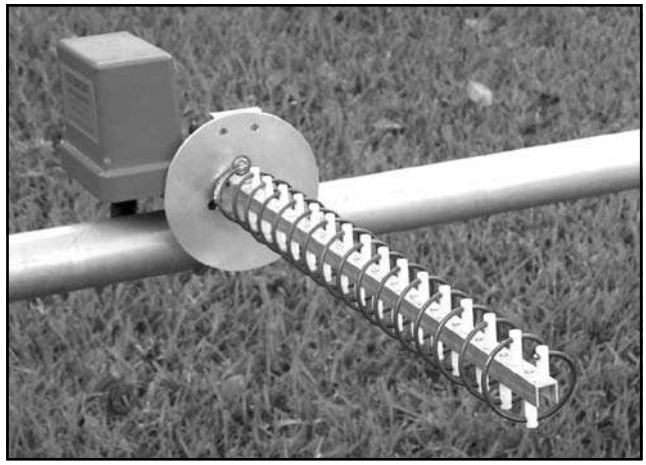

Fig 36—WD4FAB's example of a 16-turn S-band helical antenna for AO-40. This is about the maximum length of any practical helix. Note the SSB UEK2000 down-converter mounted behind the reflector of the antenna. (*WD4FAB photo.*)

parabolic reflector or dish antenna must have a feed source looking into the surface of the dish. Some dishes are designed so that the feed source is mounted directly in front of the dish. This is referred to as a *center-fed dish*. Other dishes are designed so that the feed source is off to one side, referred to as an *off-center-fed dish*, or just offset-fed dish, as shown in Fig 30. The offset-fed dish may be considered a side section of a center-fed dish. The center-fed dish experiences some signal degradation due to blockage of the feed system, but this is usually an insignificantly small amount. The offset-fed dish is initially more difficult to aim, since the direction of reception is not the center axis, as it is for center-fed dishes.

The basic design precepts of parabolic-dish antennas are covered in more detail in the EME Antenna section of this chapter. Dish antenna properties specific to satellite operations are covered here. The dish's parabola can be designed so the focus point is closer to the surface of the dish, referred to a *short-focal-length* dish, or further away from the dish's surface, referred to as a *long-focal-length* dish. To determine the exact focal length, measure the diameter of the dish and the depth of the dish.

$$f = \frac{D^2}{16d} \qquad \text{(Eq 7)}$$

The focal length divided by the diameter of the dish gives the *focal ratio*, commonly shown as f/D. Center-fed dishes usually have short-focal ratios in the range of f/D = 0.3 to 0.45. Offset-fed dishes usually have longer focal lengths, with f/D = 0.45 to 0.80. If you attach two small mirrors to the outer front surface of a dish and then point the dish at the Sun, you can easily find the focus point of the dish. Put the reflector of the patch or helix feed just beyond this point of focus.

An alternate method for finding a dish's focal length is suggested by W1GHZ (ex-N1BWT), who provides a computer program called *HDL_ANT*, available at: **www.w1ghz.org/10g/10g_home.htm**. The method literally measures a solid-surface dish by the dimensions of the bowl of water that it will form when properly positioned. (See: **www.qsl.net/n1bwt/chap5.pdf**.) WD4FAB used this method on the dish of Fig 30, carefully leveling the bowl, plugging bolt holes, and filling it with water to measure the data needed by the W1GHZ Web-site calculation.

While many of us enjoy building our own antennas, surplus-market availability of these small dish antennas makes their construction unproductive. Many AO-40 operators have followed the practices of AO-13 operators using a surplus MMDS linear-screen parabolic reflector antenna, Figs 28 and 29. These grid-dish antennas are often called *barbeque dishes*. K5OE and K5GNA have shown how to greatly improve these linearly polarized reflectors by adapting them for the CP service desired for AO-40. Simple methods can be used to *circularize* a linear dish and to further add to its gain using simple methods to increase the dish area and feed efficiency.

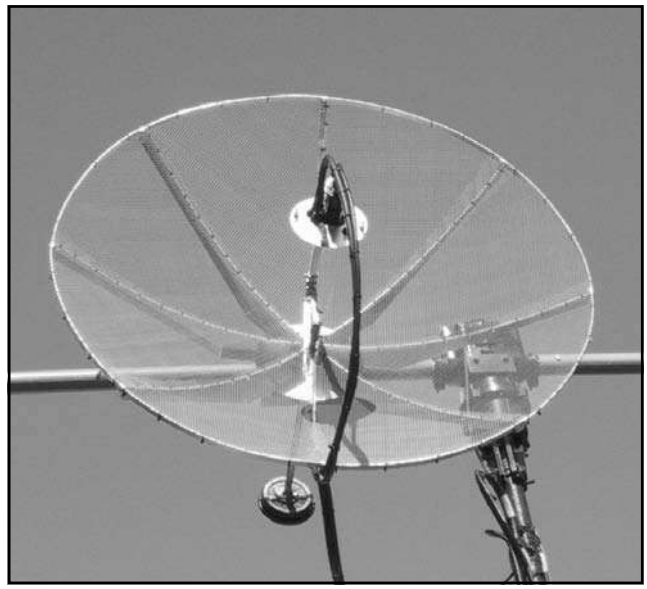

Fig 37—Prototype 1.2-meter dish by Rick Fletcher, KG6IAL, using a dual-band (L and S) patch-feed antenna for AO-40. See text. This kit dish is covered with 1/4-inch mesh. (*KG6IAL photo.*)

Another approach is the construction of a kit-type dish antenna, just becoming available in 1.2-meter and 1.8-meter diameters. This ingenious design by KG6IAL is available from his Web site **www.teksharp.com/**. **Fig 37** shows the prototype of the 1.2-meter dish with an f/D of 0.30. The 1.2-meter dish is fed with a dual-band patch feed for L and S bands. The 1.8-meter dish is designed for up to three bands using a tri-band patch feed for the U, L and S bands. This dish will permit U-band operation. A Central States VHF Society measurement on a similar sized dish (by WØLMD) with a patch feed showed a gain of about 17.1 dBic (actual measurement was 12.0 dBd linearly fed). This performance along with a small V-band (145 MHz) Yagi would permit a very modest satellite antenna assembly for all of the VHF/UHF LEO satellites, as well as AO-40.

The ingenuity of the design of the KG6IAL antenna is that it is constructed of robust, 1/8-inch-thick aluminum sheet that is numerically machined for the parabolic shape of the ribs. The backsides of the ribs are stiffened by a bent flange edge. The panel mesh is attached by using small tie-wraps or small aluminum wire through the mesh and holes provided along the parabolic edge. KG6IAL used 1/4-inch mesh in the prototype antenna to reduce wind loading. A single formed conduit post is provided in the kit for mounting the patch-feed assembly. The post extends rearward to permit the attachment of a counterweight, if needed.

AO-40 has also provided some additional challenges to the ham operator. Besides its well-known S-band downlink, AO-40 also has a K-band downlink in the range of

24.05 GHz. This quite low-powered transmitter has provided a substantial challenge to some operators, such as N1JEZ, K5OE, W5LUA, G3WDG and others. N1JEZ documented his work in *QST* while K5OE shows his K-band work on his Web site and in the *Proceedings of the AMSAT Space Symposium*. See **Fig 38**.

Parabolic Dish Antenna Construction

In the USA large numbers of dishes can be obtained either free or at low cost. But in some parts of the world dishes are not so plentiful, so hams make their own. **Fig 39** shows G3RUH's S-band dish antenna. There are three parts to the dish antenna—the parabolic reflector, the boom and the feed. There are as many ways to construct this as there are constructors. You need not slavishly replicate every nuance of the design. The only critical dimensions occur in the feed system. After construction, you will have a 60-cm diameter S-band RHCP dish antenna with a gain of about 20 dBi and a 3-dB beamwidth of 18°. Coupled with the proper downconverter, performance will be more than adequate for S-band downlink.

The parabolic reflector used for the original antenna was intended to be a lampshade. Several of these aluminum reflectors were located in department-store surplus. The dish is 585 mm in diameter and 110 mm deep, corresponding to an f/D ratio of 585/110/16 = 0.33 and a focal length of 0.33 × 585 = 194 mm. The f/D of 0.33 is a bit too concave for a simple feed to give optimal performance but the price was right, and the under-illumination keeps ground noise pickup to a minimum. The reflector already had a 40-mm hole in the center with three 4-mm holes around it in a 25-mm radius circle.

The boom passes through the center of the reflector and is made from 12.7-mm square aluminum tube. The boom must be long enough to mount to the rotator boom on the backside of the dish. The part of the boom extending through to the front of the dish must be long enough

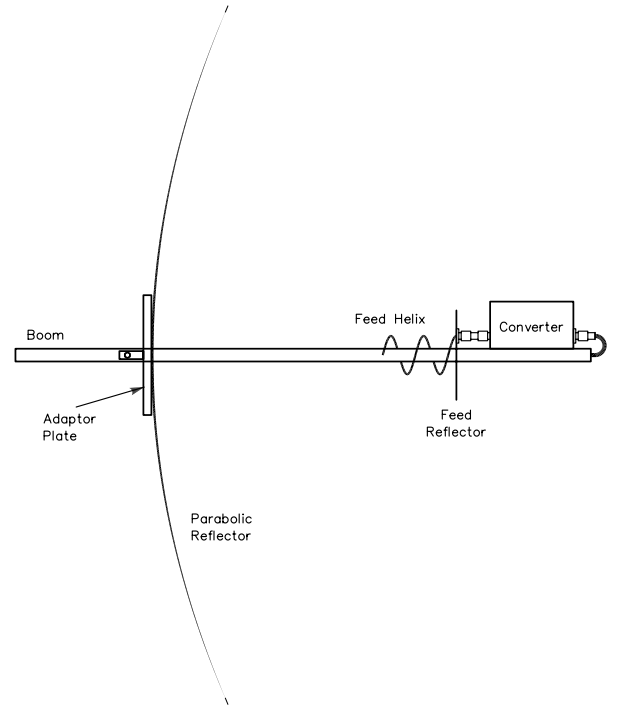

Fig 39—Detail of 60-cm S-band dish antenna with feed.

Fig 38—K5OE found this K-band dish on the Web and has set it up for the AO-40 K-band downlink. (*K5OE photo.*)

to mount the feed at the focus. If you choose to mount the downconverter or a preamp near the feed, some additional length will be necessary. Carefully check the requirements for your particular setup.

A 3-mm thick piece of aluminum, 65 mm in diameter, supports the boom at the center of the reflector. Once the center mounting plate is installed, the center boom is attached using four small angle brackets—two on each side of the reflector. See Fig 39 for details of reflector and boom assembly.

A small helix is used for the S-band antenna feed. The reflector for the helix is made from a 125-mm square piece of 1.6-mm thick aluminum. The center of the reflector has a 13-mm hole to accommodate the square center boom described above. The type-N connector is mounted to the reflector about 21.25 mm from the middle. This distance from the middle is, of course, the radius of a helical antenna for S-band. Mount the N connector with spacers so that the back of the connector is flush with the reflector surface. The helix feed assembly is shown in **Fig 40**.

Copper wire, or tubing, about 3.2 mm in diameter is used to form the helix. Wind four turns around a 40-mm diameter form. The turns are wound counterclockwise. This is because the polarization sense is reversed from RHCP when reflected from the dish surface. The wire helix will spring out slightly when winding is complete.

Once the helix is wound, carefully stretch it so that the turns are spaced 28 mm (±1 mm). Make sure the finished spacing of the turns is nice and even. Cut off the first half turn. Carefully bend the first quarter turn about 10° so it will be parallel to the reflector surface once the helix is attached to the N connector. This quarter turn will form part of the matching section.

Cut a strip of brass, 0.2 mm thick and 6 mm wide, and match the curvature of the first quarter turn of the helix, using a paper pattern. Be careful to get this pattern and subsequent brass cutting done exactly right. Using a large soldering iron and working on a heatproof surface, solder the brass strip to the first 1/4 turn of the helix. Unless you are experienced at this type of soldering, getting the strip attached just right will require some practice. If it doesn't turn out right, just dismantle, wipe clean and try again.

After tack soldering the end of the helix to the type-N connector, the first 1/4 turn, with its brass strip in place, should be 1.2 mm above the reflector at its start (at the N connector) and 3.0 mm at its end. Be sure to line up the helix so its axis is perpendicular to the reflector. Cut off any extra turns to make the finished helix have 2 1/4 turns total. Once you are satisfied, apply a generous amount of solder at the point the helix attaches to the N connector. Remember this is all that supports the helix.

Once the feed assembly is completed, pass the boom through the middle hole and complete the mounting by any suitable method. The middle of the helix should be at the geometric focus of the dish. In the figures shown here, the feed is connected directly to the downconverter and then the downconverter is attached to the boom. You may require a slightly different configuration depending on whether you are attaching a downconverter, preamp or just a cable with connector. Angle brackets may be used to secure the feed to the boom in a manner similar to the boom-to-reflector mounting. Be sure to use some method of waterproofing if needed for your preamp and/or downconverter.

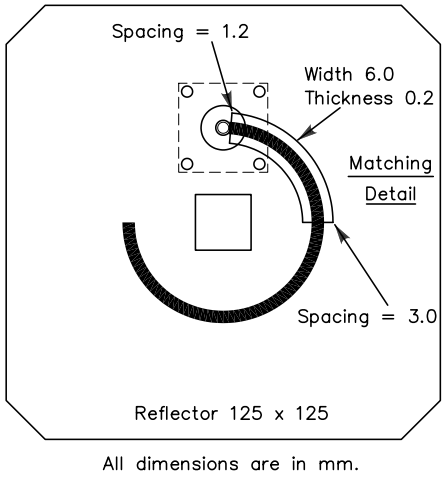

Fig 40—Details of helix feed for S-band dish antennas. The type-N connector is fixed with three screws and is mounted on a 1.6-mm spacer to bring the PTFE molding flush with the reflector. An easier mounting can be using a smaller TNC connector. Reflectors should be 95 to 100 mm in diameter.

Dish Feeds

WØLMD describes in **www.ultimatecharger.com/** that feeding a dish has two major factors that determine the efficiency. Like a flashlight bulb, the feed source should evenly illuminate the entire dish, and none of the feed energy should spillover outside the dish's reflecting surface. No feed system is perfect in illuminating a dish. Losses affect the gain from either under-illuminating or over-illuminating the dish (spillover losses). Typical dish efficiency is 50%. That's 3 dB of lost gain. A great feed system for one dish can be a real lemon on another. A patch feed system is very wide angle, but a helix feed system is narrow angle.

WØLMD has experimented with helical feeds for low f/D antennas ("deep" dishes) shown in **Fig 41**. A short-focal-ratio center-fed dish requires a wide-angle feed system to fully illuminate the dish, making the CP patch the preferred feed system. When used with an offset-fed dish, a patch-type feed system will result in a considerable spillover, or over-illumination loss, with an increased sensitivity to off-axis QRM, due to the higher f/D of this dish. Offset-fed

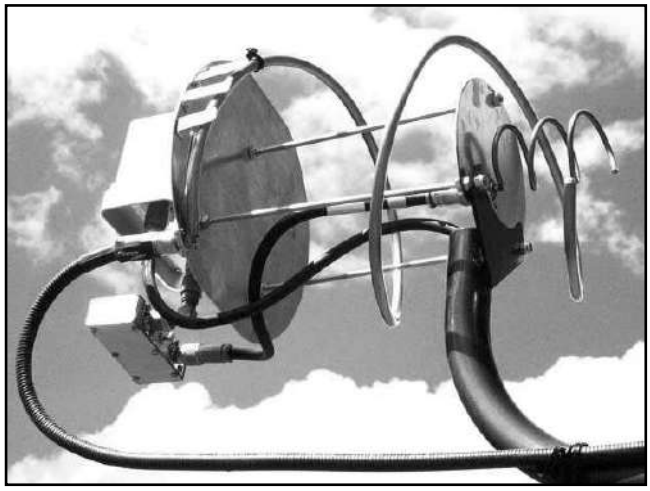

Fig 41—WØLMD's dual helix-dish feed for U and S bands. This early experimental feed was found to be wanting and he then turned to patch feeds for dishes. (*WØLMD photo.*)

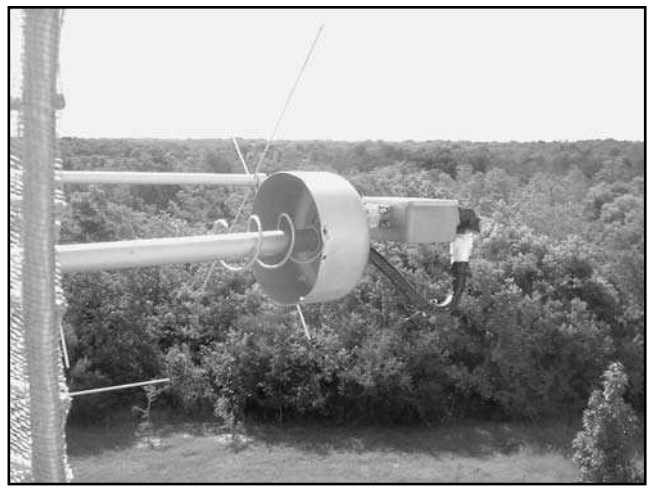

Fig 42—K5OE's helix feed for his MMDS S-band dish antenna. (*K5OE photo.*)

dishes do much better when fed with a helix antenna.

A helix feed is simplicity personified. Mount a type N connector on a flat reflector plate and solder a couple of turns wire to the inner terminal. Designs are anywhere from 2 to 6 turns. The two-turn helices are used for very short-focal-length dishes in the f/D = 0.3 region, and the 6-turn helices are used with longer-focal-length (f/D ~ 0.6) dishes, typically offset-fed dishes. Since AO-40 is right circular and the dish reflection will reverse the polarity, the helix should be wound left circular, looking forward from the connector. Helix feeds work poorly on the short-focal-length dishes but really perform well on the longer-focal-length offset-fed dishes. K5OE shows us the helix feed for his modified MMDS dish in **Fig 42**. This design employs the cupped reflector of W8JK.

A Helix Feed for an Offset-Dish Antenna

This section describes WD4FAB's surplus PrimeStar offset-fed dish antenna with a 7-turn helical feed antenna, shown in Fig 30. This S-band antenna can receive Sun noise 5 dB above sky noise. (Don't try to receive Sun noise with the antenna looking near the horizon, since terrestrial noise will be greater than 5 dB, at least in a big-city environment.) WD4FAB received the dish from NØNSV, who renamed the finished product the "FABStar."

The dish's reflector is a bit out of the ordinary, with the shape of a horizontal ellipse. It is still a single paraboloid, illuminated with an unusual feed horn. At 2401 MHz (S band) we can choose to under-illuminate the sides of the dish while properly feeding the central section, or over-illuminate the center while properly feeding the sides. WD4FAB chose to under-illuminate. The W1GHZ water-bowl measurements showed this to be a dish with a focal point of 500.6 mm and requiring a feed for an f/D = 0.79. The total illumination angle of the feed is 69.8° in the vertical direction and a feed horn with a 3-dB beamwidth of 40.3°. At 50% efficiency this antenna was calculated to provide a gain of 21.9 dBi. A 7-turn helical feed antenna was estimated to provide the needed characteristics for this dish and is shown in **Fig 43**.

The helix is basically constructed as described for the G3RUH parabolic dish above. A matching section for the first λ/4 turn of the helix is spaced from the reflector at 2 mm at the start and 8 mm at the end of that fractional turn. Modifications of the G3RUH design include the addition of a cup reflector, a design feature used by the originator of the helical antenna, John Kraus, W8JK. For the reflector, a 2-mm thick circular plate is cut for a 94 mm (0.75 λ) diameter with a thin aluminum sheet metal cup, formed with a depth of 47 mm. Employment of the cup enhances the performance of the reflector for a dish feed, as shown by K5OE. (See the K5OE material on the CD-ROM accompanying this book.)

The important information for this 7-turn helical antenna is:

- Boom: 12.7-mm square tube or "C" channel.
- Element: $^1/_8$-inch diameter copper wire or tubing.

Close wind the element on a circular 1.50-inch tube or rod; the finished winding is 40 mm in diameter and spaced to a helical angle of 12.3°, or 28 mm spacing. These dimensions work out for an element circumference of 1.0 λ about the center of the wire.

When WD4FAB tackled this antenna, he felt that the small number of helical element supports used by G3RUH would be inadequate, in view of the real-life bird traffic on the antennas at his QTH. He chose to use PTFE (Teflon) support posts every $^1/_2$ turn. This closer spacing of posts permitted a careful control of the helix-winding diameter and spacing and also made the antenna very

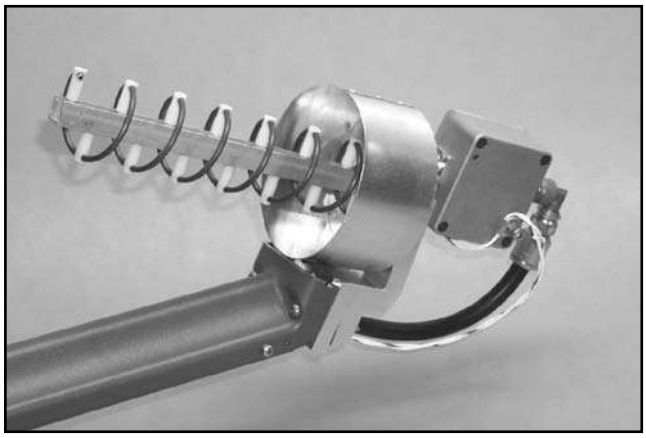

Fig 43—Seven-turn LHCP helix feed for an offset dish, long f/D, antenna, with DEM preamp. (*WD4FAB photo.*)

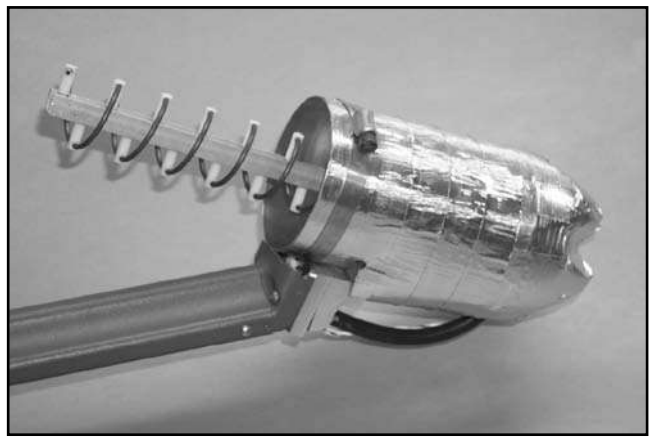

Fig 45—Rain cover for preamp using a two-liter soft-drink bottle with aluminum foil tape for protection from sun damage. (*WD4FAB photo.*)

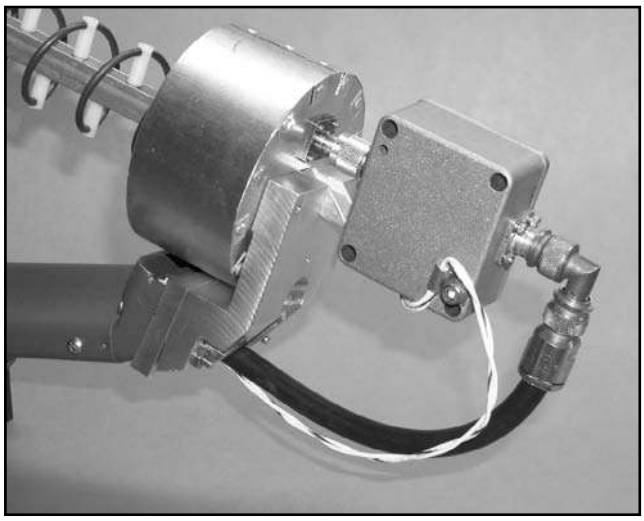

Fig 44—Mounting details of seven-turn helix and preamp. (*WD4FAB photo.*)

robust. He set up a fixture on the drill press to uniformly predrill the holes for the element spacers and boom. Attachment of the reflector is through three very small aluminum angle brackets on the element side of the boom.

Mounting of the helix to the dish requires modification of the dish's receiver-mounting boom. **Fig 44** shows these modifications using a machined mount. NM2A constructed one of these antennas and showed that a machine shop is not needed for this construction. He made a "Z" shaped mount from aluminum-angle plate and then used a spacer from a block of acrylic sheet. The key here is to get the dish focal point at the 1.5-turn point of the feed antenna, which is also at about the lip of the reflector cup.

The W1GHZ data for this focal point is 500.6 mm from the bottom edge of the dish and 744.4 mm from the top edge. A two-string measurement of this point can confirm the focal point, as shown by Wade in his writings. When mounting this feed antenna the constructor must be cautious to aim the feed at the beam-center of the dish, and not the geometric center, as the original microwave horn antenna was constructed. Taking the illumination angle information noted above, the helical feed antenna should be aimed 5.5° down from the geometric center of the dish.

As illustrated in Fig 44, a DEM preamp was directly mounted to the feed helix, using a TNC female connector on the helix, chosen for this case, since N connectors are quite large for this antenna. A male chassis connector should be mounted on the preamp so that the preamp can be directly connected to the antenna without any adaptors. This photo also illustrates how the reflector cup walls were riveted to the reflector plate.

Exposed connectors must be protected from rainwater. Commonly materials such as messy Vinyl Mastic Pads (3M 2200) or Hand Moldable Plastic (Coax Seal) are used. Since this is a tight location for such mastic applications, a rain cover was made instead from a 2-liter soft-drink bottle, **Fig 45**. Properly cutting off the top of the bottle allows it to be slid over the helix reflector cup and secured with a large hose clamp. You must provide UV protection for the plastic bottle and that was done with a wrapping of aluminum foil pressure-sensitive adhesive tape.

There are many methods for mounting this dish antenna to your elevation boom. You must give consideration to the placement of the dish to reduce the wind loading and off-balance to the rotator system. In WD4FAB's FABStar installation, the off-balance issue was not a major factor, as the dish was placed near the center of the elevation boom, between the pillow-block bearing supports. Since there is already a sizeable aluminum plate for these bearings, the dish was located to "cover" part of that plate, so as to not add measurably to the existing wind-loading area of the overall assembly.

A mounting bracket provided with the stock dish clamps to the end of a standard 2-inch pipe stanchion (actual measure: 2.38 inches in diameter). This bracket was turned around on the dish and clamped to the leg of a welded-pipe Tee assembly. See **Fig 46**. Pipe-reducing fittings were machined and fitted in the Tee-top bar, which was sawn in half for clamping over the 1½ inch pipe used for the elevation boom. Bolts were installed through drilled holes and used to clamp this assembly.

Patch Feeds for Dish Antennas

Patch feeds are almost as simple as helix feeds. A patch is typically an N connector on a flat reflector plate with a tuned flat-metal plate soldered to the inner terminal. Sometimes the flat plate is square; sometimes it is rectangular; sometimes it is round. It could have two feed points, 90° out of phase for circular polarization, as used in the construction of the AO-40 U-band antennas. Some patches are rectangular with clipped corners to create a circular radiation pattern.

On 2401 MHz, the plate is 57 mm square and spaced 3 mm away from the reflector. The point of attachment is about halfway between the center and the edge. A round patch for 2401 MHz is about 66 mm in diameter. These patches work well on the shorter focal length center-fed MMDS and TVRO dishes. G3RUH made a CP patch feed for these short f/D dishes, shown in Fig 31 and **Fig 47**.

Robert, WØLMD, has done a considerable amount of experimenting with patch feeds for his dish antennas. One tri-band feed is shown in **Fig 48**. These are circular patches that have CP properties through the arrangement of the feed point and a small piston-variable capacitor that is offset from the feed point. **Fig 49** shows some of the many patches that Robert has created for his trials.

Fig 46—Welded pipefitting mount bracket for FABStar dish antenna. (*WD4FAB photo.*)

A No-Tune Dual-Band Feed for Mode L/S

Jerry, K5OE, notes that the AO-40 transponder has two uplink receivers active most of the time for CW/SSB activity. Most operators use U band at 435 MHz (70 cm). Also available, however, are two L-band (23-cm) receivers: L1 at 1269 MHz and L2 at 1268 MHz. The reasons for going to L band can be varied, but there is no arguing the benefits in reduced antenna size and AGC suppression. The types of L-band antennas are varied as well. Many use helices. Others use beams and arrays of beams. Still others use dishes, small and large.

K5OE recently acquired an old UHF TV dish measuring 1.2 meters in diameter. He wanted to use it both to receive on S band at 2401 MHz (13cm) and to transmit on the uplink on L band. He covered it with aluminum mesh and built a dual-helix feed for it, but was unhappy with the L-band performance. It seems the concentric helices interacted with each other substantially. Having had good success with patch feeds on S band, he designed, built and installed a dual-patch feed on a 1.5-meter solid dish for Field Day 2002. This arrangement worked superbly on uplink (with 25 W), but was embarrassingly deaf on receive. This second dual-band feed failure led him to experiment for months with different configurations, leading ultimately to the design presented here. The project goals were:

- Good performance on both S-band receive and L-band uplink.
- An easy-to-produce model using common hardware and simple hand tools.

Patches are better than helices as dish feeds. This revelation came to K5OE while doing investigation and

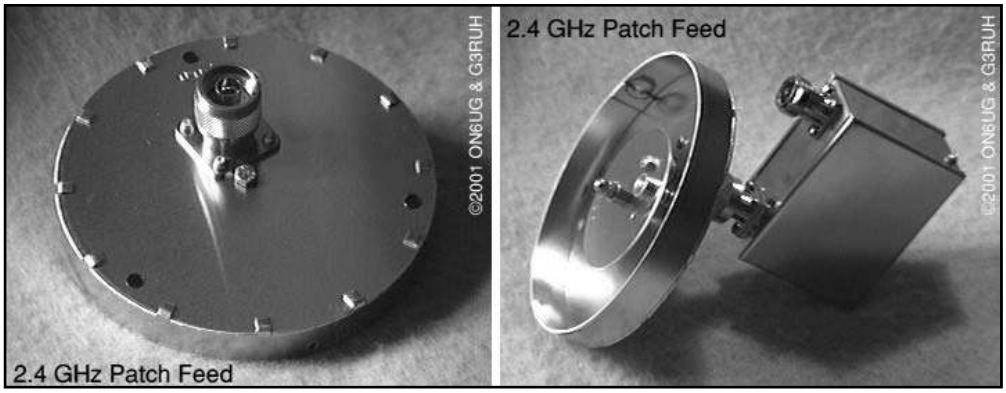

Fig 47—Details of CP-patch feed for short f/D dish antennas by G3RUH and ON6UG.

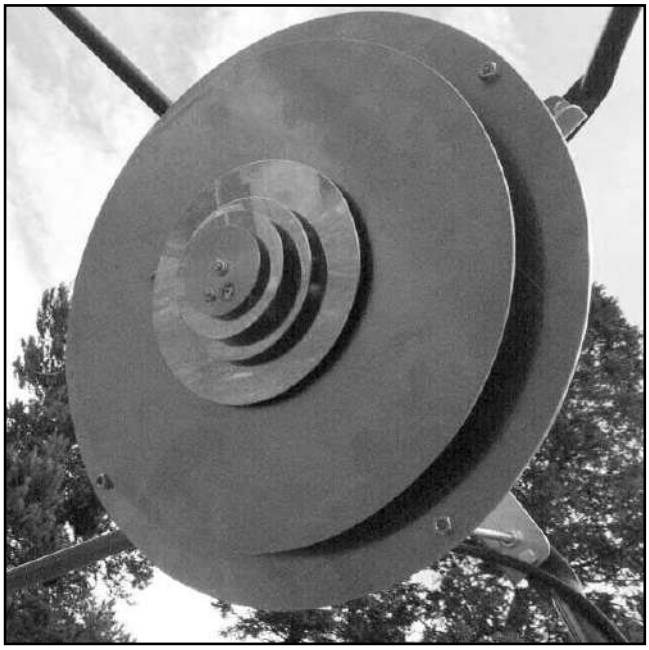

Fig 48—A triband (U, L and S bands) patch-CP feed for large dish antennas for AO-40 service. (*WØLMD photo.*)

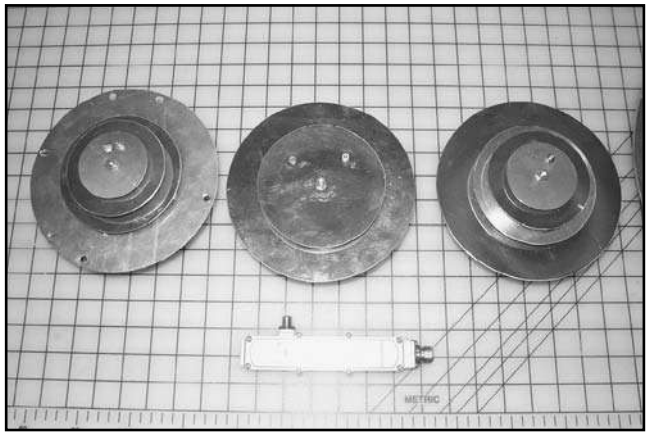

Fig 49—Some of the many experimental CP-patch-feed antennas by WØLMD. (*WØLMD photo.*)

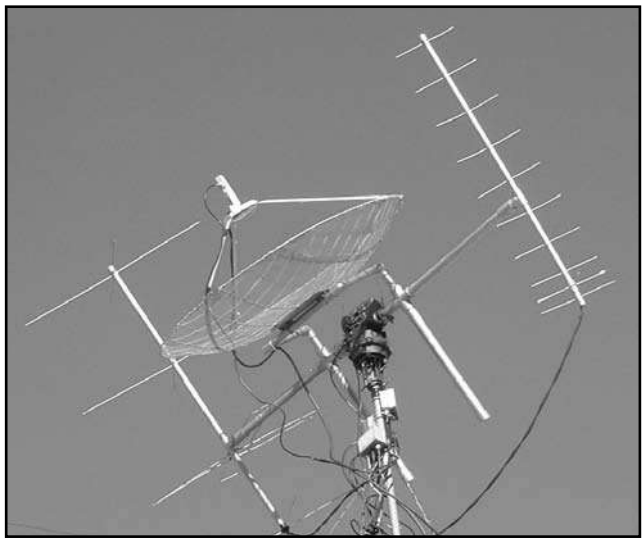

Fig 50—The 1.2-meter dish with dual-band patch feed installed. (*K5OE photo; courtesy of* The AMSAT Journal.)

experimenting with helix antennas. In the middle of this investigative foray, he saw the radiation pattern for the G3RUH patch feed published on James Miller's web site. When he modeled that pattern and input it into the W1GHZ feed pattern program, it produced an amazing 72% efficiency. The best helix he ever modeled has about 60% efficiency. I8CVS recently ran his own antenna range tests of a design similar to the G3RUH patch and produced a similarly impressive pattern.

Then K5OE came across the *truncated corners* square patch design popularized by K3TZ. This AO-40 design here is attributed to 7N1JVW, JF6BCC and JG1IIK. There are references in the literature going back over a decade for this now-common commercial design. The first model K5OE built outperformed his best helix-in-cup design by a full S unit (delta over the noise) on his FT-100 portable setup. Compared to a helix, the patch simply has better illumination efficiency with less spillover from side lobes.

Patch theory is beyond the scope of this article, but can be summarized as building a shape that resonates at the desired frequency, compensated in size by the capacitive inductance between itself and the reflector. A patch can be practically any shape since it basically acts like a parallel-plate transmission line. Current in the patch flows from the feed point to the outer edge(s), where all the radiation occurs. The reputed, but often disputed, circularity of the truncated corner patch is accomplished by effectively designing two antennas into the patch element (of two different diagonal lengths) and feeding them 90º out of phase.

For K5OE's 1.2-meter dish, shown in **Fig 50**, computations predicted 21-dBi gain on L band and almost 27 dBi on S band, with an assumed 50% efficiency:

$$G = 10\log_{10}\left[\eta A\left(\frac{4\pi}{\lambda^2}\right)\right] \qquad \text{(Eq 8)}$$

where

η = efficiency

λ = wavelength in meters.

A = aperture of the dish in meters = $\pi \times r^2$

r = dish radius in meters = diameter/2 in meters = 0.6 meters

At 1269 MHz, λ= 300/1269 = 0.236 meters:

$$G = 10\log_{10}\left[0.50 \times \left(3.14 \times 0.6^2\right) \times \frac{4 \times 3.14}{0.236^2}\right] = 21.1\,\text{dBi}$$

At 2401.5 MHz, λ = 300/2401.5 = 0.125 meters:

$$G = 10\log_{10}\left[0.50 \times \left(3.14 \times 0.6^2\right) \times \frac{4 \times 3.14}{0.125^2}\right] = 26.6\,\text{dB}^2$$

Where does the feed get mounted? The *focal point* is where the parabolic shape of the dish concentrates the reflected signal. In K5OE's case the antenna was placed flat on the garage floor to measure the depth:

$f = D^2 / 16d$ (Eq 9)

where

D = diameter of the dish in inches
d = depth of the dish in inches
$f = 48^2 / (16 \times 7.25) = 19.8$ inches (50.5 cm)

This is just one example of countless combinations of hardware and patch designs. Inherent in this design, however, are five key design and construction features developed from building and empirical testing of a number of patch feeds.

1. The specified dimensions are critical for no-tune operation. **Fig 51** shows the dimensions necessary to build the dual-feed patch. (K5OE recommends you reproduce this sketch accurately on graph paper. When you cut your patches you can lay them on the paper template for checking.) Repeat: These dimensions are critical. Even a 0.5-mm error will throw your resonance off considerably—patches are not broadband.
2. The reflector must be rigid. Spacing between the driven element (patch) and the reflector affects the resonant frequency. K5OE found 0.025-inch aluminum sheet and 26-gauge copper sheet acceptable for a single S-band patch feed, but too flimsy for an L-band reflector. Use more rigid material or provide additional stiffening for the L-band reflector, as shown in Figs **52**, **53** and **54**.
3. The patches must be electrically isolated from each other. A metallic center support works for a single patch but creates harmonic-coupling problems when patches are stacked for multiband use. The use of nylon machine screws and nuts helps solve the vexing problem of the S-band patch coupling to the L-band patch.
4. The "straight corners" of the truncated corner patch must be kept clear of any nearby metal. This includes the edges of the feed support or cup, if used. See Fig 54.
5. Feeding the patches at 90° to each other minimizes the electromagnetic interaction between the two antenna fields.

One final design issue deals with the first harmonic of the L-band antenna. You must significantly reduce the potentially destructive effect from the 1269-MHz signal's second harmonic. Severe desense of your receive signal could occur and potentially even overload and damage the first active device in your system. Sensitive preamps and downconverters without a pre-RF-amplifier filter will need an external filter. K5OE has used a G3WDG stub filter rated at 100-dB rejection with good success ahead of his preamp. His current setup, however, uses a AIDC-3731AA downconverter with its internal combline filter providing adequate filtering. Using the downconverter directly at the

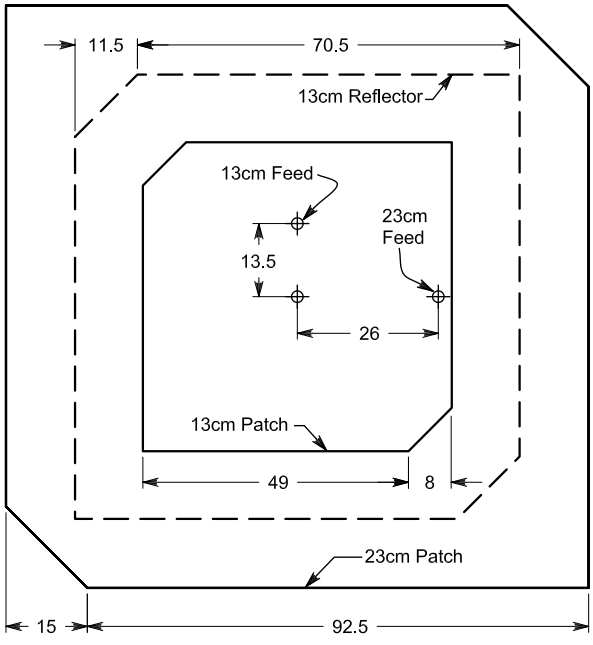

Fig 51—Dual-band patch feed dimensions, in millimeters. (*K5OE diagram; courtesy of* The AMSAT Journal.)

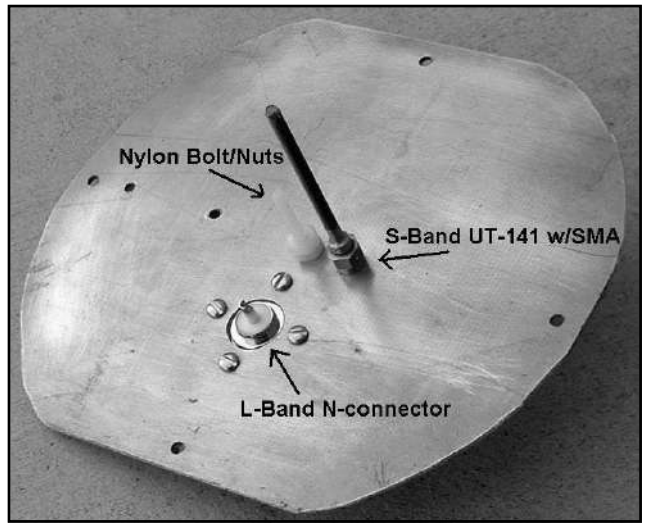

Fig 52—Assembly of the L band reflector. (*K5OE photo; courtesy of* The AMSAT Journal.)

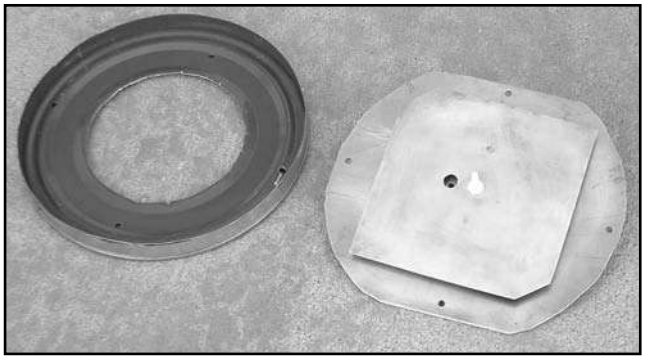

Fig 53—The support, L-band reflector and patch. (*K5OE photo; courtesy of* The AMSAT Journal.)

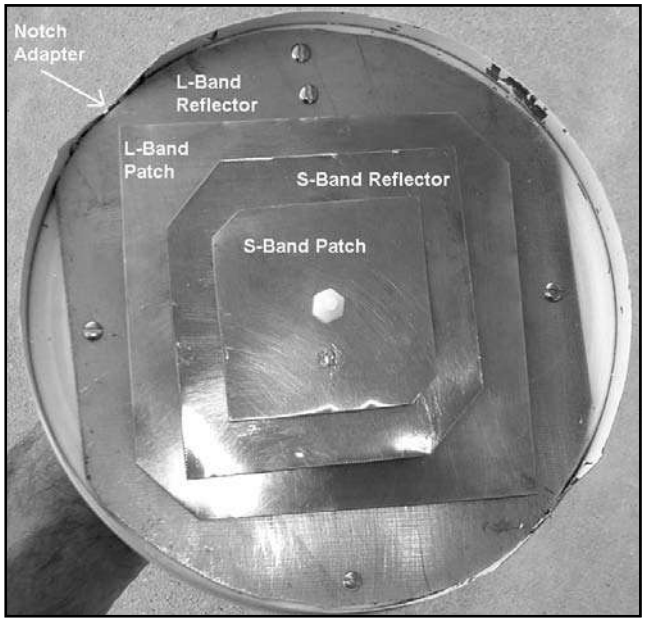

Fig 54—The completed dual-band patch feed. (*K5OE photo; courtesy of* The AMSAT Journal.)

feed point has a noise figure (NF) of 1.0 dB, compared to the cumulative NF of 1.6 dB using a filter and a preamp.

Construction of the feed begins with selection of material for both the electrical parts (the antennas) and the mechanical parts (the support structure). The L-band antenna is constructed using a 6 × 6-inch double-sided circuit board for the reflector and a piece of 26-gauge copper sheet for the driven element (patch). A flanged female type-N connector is used for the feed connection. The S-band antenna is constructed of two pieces of 26-gauge copper sheeting and the feed connection is made with a short piece of UT-141 (0.141-inch copper-clad semirigid coax) terminated in a male SMA fitting. Fig 52 illustrates the assembly of the L-band reflector with the nylon-center support bolt, the L-band N-connector, and the S-band semirigid coax terminated onto an SMA-to-N adapter through the circuit board.

The support structure began life as a paint can, measuring 155 mm in diameter. It was cut down to a 15-mm depth. Cut a hole in the middle of the bottom of the can and trim the PC board to fit inside the can bottom. Use stainless-steel $^3/_8$-inch 4-40 bolts, washers and nuts to secure the PC board to the can bottom. A $1^1/_2$-inch 6-32 nylon bolt is secured through the center of the PC board with two nylon nuts to provide the 6-mm spacing for the L-band patch. Fig 53 shows the L-band patch in position and ready to be soldered to the N-connector. Note the hole through the L-band patch allowing the S-band UT-141 coax to pass (without making contact).

The remainder of the antenna is then assembled in order: First the L-band patch is secured with two nylon nuts and soldered to the N-connector. Then the S-band reflector is secured with one nylon nut to provide 3-mm spacing, and the UT-141 coax shield is soldered to the S-band reflector. Finally, the S-band patch is secured with a single nylon nut (3-mm spacing) and soldered to the center conductor of the UT-141 coax. To summarize the overall order of assembly: L-band reflector, two nylon nuts, L-band patch, two nylon nuts, S-band reflector, one nylon nut, S-band patch, and one nylon nut.

An electrical check with an ohmmeter of the completed feed should show the two reflectors connected, with the patches isolated from the reflectors and from each other. Fig 54 shows the completed feed. Note how the sides of the support are cut out to avoid proximity to the L-band patch and how the L-band and S-band patches are at 90º to each other. **Fig 55** shows the back of the feed, complete with an angle support for the downconverter. The flanged N-connector is for the L-band coax and the male-N adapter is secured from the other side of the feed with the SMA fitting on the UT-141 coax.

For those who are tempted to tune the patch, K5OE recommends doing it with the feed installed on the antenna—since the dish surface affects the feed-point impedance slightly. The feed-point impedance, and thus the resonant frequency, can be changed quite a bit by adjustment of the spacing of just the straight corners. There is no need to change the spacing at the center or the feed—just a slight up or down bending of the straight corners will change the tuning. Do this carefully: a little bit goes a long way. This patch design is very repeatable and will work adequately (an SWR below 1.5:1) with no adjustments.

The antenna performs to the calculated predictions above. On receive, this antenna is 4 S units better than K5OE's 45-cm dish and 3 S units above his 65-cm dish (both other dishes have similar patch feeds and the same downconverter). It also clearly outperforms his previous dual-helix arrangement on the 1.2-meter dish, but he was unable to do a side-by-side comparison.

On transmit, it does equally well, with a decent signal into the satellite with only 10 W measured at the

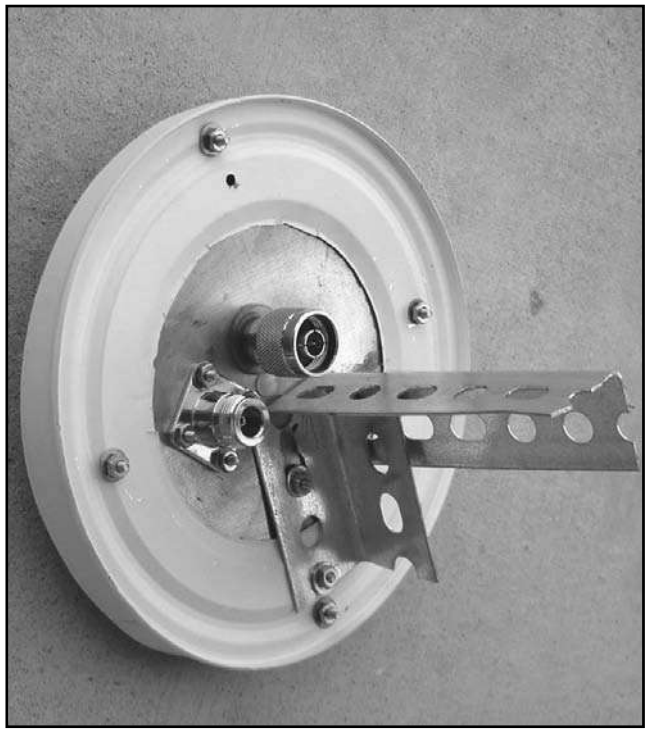

Fig 55—Rear of the completed feed. (K5OE photo; courtesy of *The AMSAT Journal*.)

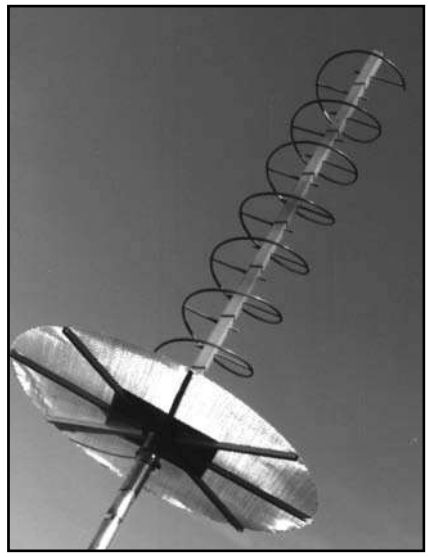

Fig 56—The portable 435-MHz helix assembled and ready for operation. (*WØCY photo*.)

antenna. The L band is noticeably improved over the helix predecessor. At low squint angles K5OE finds the L-band uplink to be about 1 S unit weaker than his U-band uplink. He later added a small plastic hat to extend over the top of the patches to keep the rain and bird droppings off—both detune the patches when built up between the patch and the reflector.

Though simple and effective, this is merely one way to construct a dual feed. Cookie-tin lids also make excellent supports. Tin snips are a good investment and much easier to use than a hacksaw. Use a flat file to remove burrs from the edges of the patches. Use stainless-steel hardware, most notably $^3/_8$-inch 4-40 machine bolts and nuts for the antenna hardware and $^1/_2$-inch 6-32 for the support-structure connections to the support arms ($^1/_2$-inch aluminum tubing). The copper sheet is much easier to solder to than aluminum. Once completed, the feed received a few coats of white enamel paint to protect the copper and to minimize the visual reflections.

This is not the only dual-band antenna on AO-40. There are many varied, innovative designs available, including G6LVB's simple and effective 1.2-meter homebrew stressed *chicken wire* dish with a dual-G3RUH helix feed. G3WDG has a 3-meter dish with L/S-band helices and a K-band (1.3-cm) feed horn, and WØLMD has developed some popular dual- and tri-band "round" patch feeds. (See the Notes and References, as well as the CD-ROM bundled with this book.)

For additional information on constructing antennas, feeds and equipment techniques for use at microwave frequencies, see *The ARRL UHF/Microwave Experimenter's Manual* and *The ARRL UHF/Microwave Projects Manual*. Both of these books have a wealth of information for the experimenter.

PORTABLE HELIX FOR 435 MHZ

Helical antennas for 435 MHz are excellent uplinks for U-band satellite communications. The true circular polarization afforded by the helix minimizes signal *spin fading* that is so predominant in these applications. The antenna shown in **Fig 56** fills the need for an effective portable uplink antenna for OSCAR operation. Speedy assembly and disassembly and light weight are among the benefits of this array. This antenna was designed by Jim McKim, WØCY.

As mentioned previously, the helix is about the most tolerant of any antenna in terms of dimensions. The dimensions given here should be followed as closely as possible, however. Most of the materials specified are available in any well supplied do-it-yourself hardware or building supply store. The materials required to construct the portable helix are listed in **Table 1**.

The portable helix consists of eight turns of $^1/_4$-inch soft-copper tubing spaced around a 1-inch fiberglass tube or maple dowel rod 4 feet, 7 inches long. Surplus aluminum jacket Hardline can be used instead of the copper tubing if necessary. The turns of the helix are supported by 5-inch lengths of $^1/_4$-inch maple dowel mounted through the 1-inch rod in the center of the antenna. **Fig 57A** shows the overall dimensions of the antenna. Each of these support dowels has a V-shaped notch in the end to locate the tubing, as shown in Fig 57B.

The rod in the center of the antenna terminates at the feed-point end in a 4-foot piece of 1-inch ID galva-

Table 1

Parts List for the Portable 435-MHz Helix

Qty	*Item*
1	Type N female chassis mount connector
18 feet	1/4-in. soft copper tubing
4 feet	1-inch ID galvanized steel pipe
1	5 feet × 1-inch fiberglass tube or maple dowel
14	5-inch pieces of 1/4-inch maple dowel (6 feet total)
1	1/8-inch aluminum plate, 10 inches diameter
3	2 × 3/4-inch steel angle brackets
1	30 × 30-inch (round or square) aluminum screen or hardware cloth
8 feet	1/2 × 1/2 × 1/2-inch aluminum channel stock or old TV antenna element stock
3	Small scraps of Teflon or polystyrene rod (spacers for first half turn of helix)
1	1/8 × 5 × 5-inch aluminum plate (boom-to-mast plate)
4	1½-inch U bolts (boom-to-mast mounting)
3 feet	#22 bare copper wire (helix turns to maple spacers)

Assorted hardware for mounting connector, aluminum plate and screen, etc.

nized steel pipe. The pipe serves as a counterweight for the heavier end of the antenna. The 1-inch rod material inside the helix must be nonconductive. Near the point where the nonconductive rod and the steel pipe are joined, a piece of aluminum screen or hardware cloth is used as a reflector screen.

If you have trouble locating the 1/4-inch soft copper tubing, try a refrigeration supply house. The perforated aluminum screening can be cut easily with tin snips. This material is usually supplied in 30 × 30-inch sheets, making this size convenient for a reflector screen. Galvanized 1/4-inch hardware cloth or copper screen could also be used for the screen, but aluminum is easier to work with and is lighter.

A 1/8-inch-thick aluminum sheet is used as the support plate for the helix and the reflector screen. Surplus rack panels provide a good source of this material. **Fig 58** shows the layout of this plate.

Fig 59 shows how aluminum channel stock is used to support the reflector screen. (Aluminum tubing also works well for this. Discarded TV antennas provide plenty of this material if the channel stock is not available.) The screen is mounted on the bottom of the 10-inch aluminum center plate. The center plate, reflector screen and channel stock are connected together with plated hardware or pop rivets. This support structure is very sturdy. Fiberglass tubing is the best choice for the center rod material although maple dowel can be used.

Mount the type-N connector on the bottom of the center plate with appropriate hardware. The center pin should be exposed enough to allow a flattened end of the copper tubing to be soldered to it. Tin the end of the tubing after it is flattened so that no moisture can enter it. If the helix is to be removable from the ground-plane screen, do not solder the copper tubing to the connector. Instead, prepare a small block of brass, drilled and tapped at one side for a 6-32 screw. Drill another hole in the brass block to accept the center pin of the type-N connector, and solder this connection. Now the connection to the copper tubing helix can be made in the field with a 6-32 screw instead of with a soldering iron.

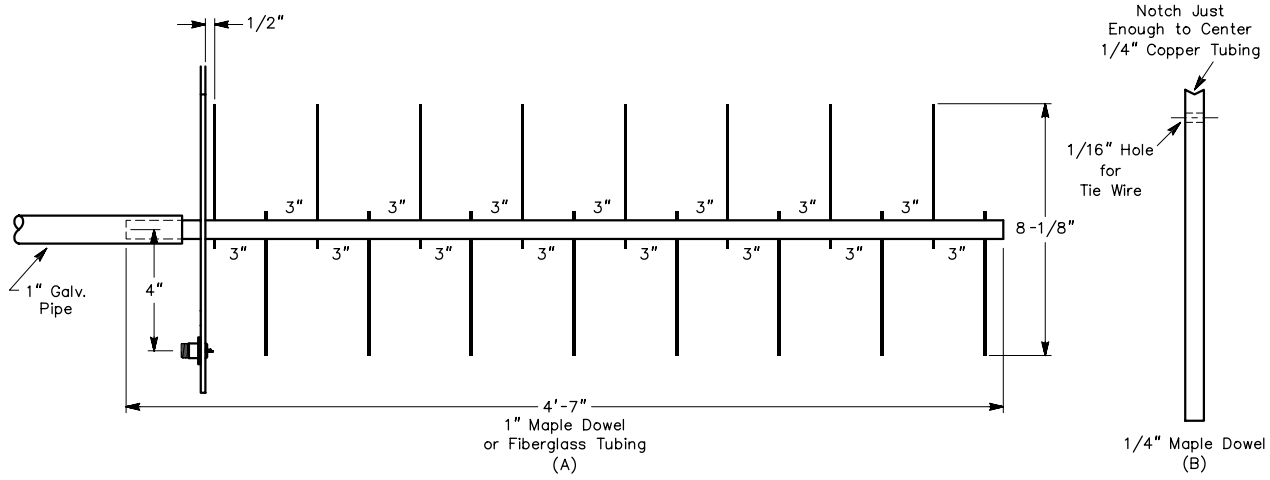

Fig 57—At A, the layout of the portable 435-MHz helix is shown. Spacing between the first 5-inch winding-support dowel and the ground plane is 1/2 inch; all other dowels are spaced 3 inches apart. At B, the detail of notching the winding-support dowels to accept the tubing is shown. As indicated, drill a 1/16-inch hole below the notch for a piece of small wire to hold the tubing in place.

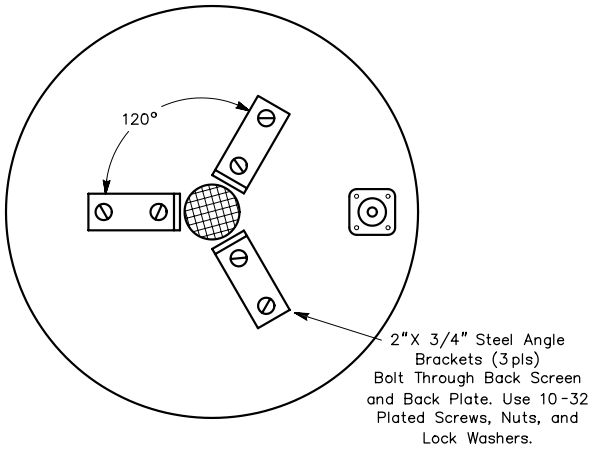

Fig 58—The ground plane and feed-point support assembly are shown. The circular piece is a 10-inch diameter, 1/8-inch thick piece of aluminum sheet. (A square plate may be used instead.) Three 2 × 3/4-inch angle brackets are bolted through this plate to the backside of the reflector screen to support the screen on the pipe. The type-N female chassis connector is mounted in the plate 4 inches from the 1-inch diameter center hole.

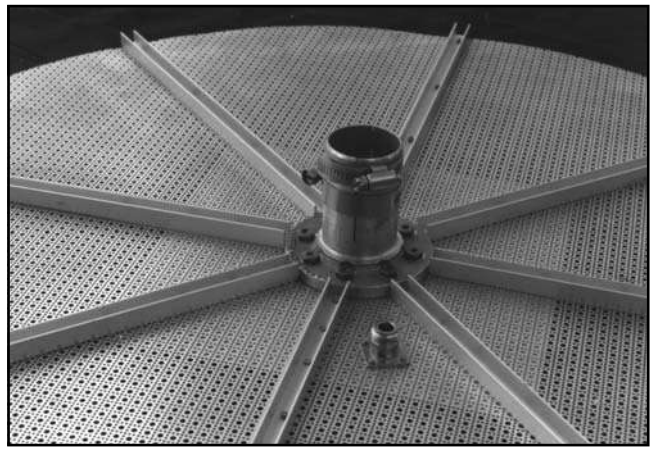

Fig 59—At top, the method of reinforcing the reflector screen with aluminum channel stock is shown. In this version of the antenna, the three angle brackets of Fig 58 have been replaced with a surplus aluminum flange assembly. (*WØCY photo.*) At bottom, this helix view shows the details of a 1/4-turn matching transformer, as discussed in the text. (*K9EK photo.*)

Refer to Fig 57A. Drill the fiberglass or maple rod at the positions indicated to accept the 5-inch lengths of 1/2-inch dowel. (If maple doweling is used, the wood must be weatherproofed as described below before drilling.) Drill a 1/16-inch hole near the notch of each 5-inch dowel to accept a piece of #22 bare copper wire. (The wire is used to keep the copper tubing in place in the notch.) Sand the ends of the 5-inch dowels so the glue will adhere properly, and epoxy them into the main support rod.

Begin winding the tubing in a clockwise direction from the reflector screen end. First drill a hole in the flattened end of the tubing to fit over the center pin of the type-N connector. Solder it to the connector, or put the screw into the brass block described earlier. Carefully proceed to bend the tubing in a circular winding from one support to the next.

See the earlier section entitled "50-Ω Helix Feed" and Figs 19 and 20 to see how the first half-turn of the helix tubing must be positioned close above the reflector assembly. **Fig 59B** shows also an excellent example by K9EK on matching his U-band helical antenna to a 52-Ω feed line. It is important to maintain this spacing, since extra capacitance between the tubing and ground is required for impedance-matching purposes.

Insert a piece of #22 copper wire in the hole in each support as you go. Twist the wire around the tubing and the support dowel. Solder the wire to the tubing and to itself to keep the tubing in the notches. Continue in this way until all eight turns have been wound. After winding the helix, pinch the far end of the tubing together and solder it closed.

Weatherproofing the Wood

A word about preparing the maple doweling is in order. Wood parts must be protected from the weather to ensure long service life. A good way to protect wood is to boil it in paraffin for about half an hour. Any holes to be drilled in the wooden parts should be drilled after the paraffin is applied, since epoxy does not adhere well to wood after it has been coated with paraffin. The small dowels can be boiled in a saucepan. Caution must be exercised here—the wood can be scorched if the paraffin is too hot. Paraffin is sold for canning purposes at most grocery stores. Wood parts can also be protected with three or four coats of spar varnish. Each coat must be allowed to dry fully before another coat is applied.

The fiberglass tube or wood dowel must fit snugly

with the steel pipe. The dowel can be sanded or turned down to the appropriate diameter on a lathe. If fiberglass is used, it can be coupled to the pipe with a piece of wood dowel that fits snugly inside the pipe and the tubing. Epoxy the dowel splice into the pipe for a permanent connection.

Drill two holes through the pipe and dowel and bolt them together. The pipe provides a solid mount to the boom of the rotator, as well as most of the weight needed to counterbalance the antenna. More weight can be added to the pipe if the assembly is "front-heavy." (Cut off some of the pipe if the balance is off in the other direction.)

The helix has a nominal impedance of about 105 Ω in this configuration. By varying the spacing of the first half turn of tubing, a good match to 52-Ω coax should be obtainable. When the spacing has been established for the first half turn to provide a good match, add pieces of polystyrene or Teflon rod stock between the tubing and the reflector assembly to maintain the spacing. These can be held in place on the reflector assembly with silicone sealant. Be sure to seal the type-N connector with the same material.

Exposed Antenna Relays and Preamplifiers

For stations using crossed Yagi antennas for CP operation, one feature that has been quite helpful for communicating through most of the LEO satellites, has been the ability to switch polarization from RHCP to LHCP. In some satellite operation this switchable CP ability has been essential. Operation through AO-40 has not shown a great need for such CP agility, since if the satellite is seriously off-pointed the signals are not particularly useable. When AO-40's squint angle is less than 25° the need for LHCP has not been observed. For those using helical antennas or helical-fed dish antennas, we just would not have the choice to switch CP unless an entirely new antenna is added to the cluster for that purpose. Not many of us have the luxury of that kind of space available on our towers.

For stations with switchable-circularity Yagi antennas, experience with exposed circularity switching relays and preamplifiers mounted on antennas have shown that they are prone to failure caused by an elusive mechanism known as *diurnal pumping*. Often these relays are covered with a plastic case, and the seam between the case and PC board is sealed with a silicone sealant. Preamps may also have a gasket seal for the cover, while the connectors can easily leak air. None of these methods create a true hermetic seal and as a result the day/night temperature swings pump air and moisture in and out of the relay or preamp case. Under the right conditions of temperature and moisture content, moisture from the air will condense inside the case when the outside air cools down. Condensed water builds up inside the case, promoting extensive corrosion and unwanted electrical conduction, seriously degrading component performance in a short time.

A solution for those antennas with "sealed" plastic relays, such as the KLM CX series; you can avoid problems by making the modifications shown in **Fig 60**. Relocate the 4:1 balun as shown and place a clear polystyrene plastic refrigerator container over the relay. Notch the container edges for the driven element and the boom so the container will sit down over the relay, sheltering it from the elements. Bond the container in place with a few dabs of RTV adhesive sealant. Position the antenna in an "X" orientation, so neither set of elements is parallel to the ground. The switcher board should now be canted at an angle, and one side of the relay case should be lower than the other. An example for the protective cover for an S-band preamp can be seen in the discussion on feeds for parabolic antennas.

For both the relay and preamp cases, carefully drill a 3/32-inch hole through the low side of the case to provide the needed vent. The added cover keeps rainwater off the

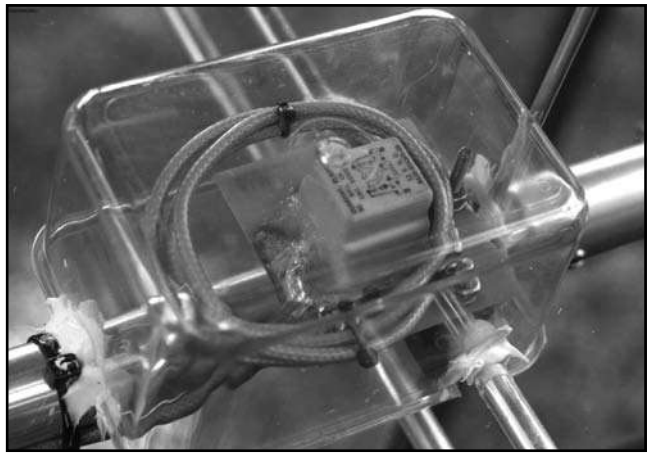

Fig 60—KLM 2M-22C antenna CP switching relay with relocated balun. The protective cover is needed for rain protection, be sure to use a polystyrene kitchen box, see text. (*WD4FAB photo.*)

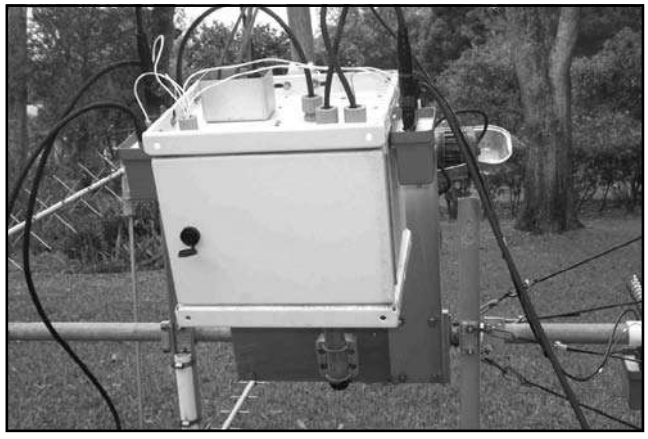

Fig 61—A NEMA4 box is used to shelter the L-band electronics and power supply. The box flanges are convenient for mounting preamplifiers. The box is shown inverted since it is on a tilt-over tower. (*WD4FAB photo.*)

relay and preamp, and the holes will prevent any buildup of condensation inside the relay case. Relays and preamplifiers so treated have remained clean and operational over periods of years without problems.

Another example for the protection of remotely, tower-mounted equipment is shown in Fig 50, illustrating the equipment box and mast-mounted preamplifiers at the top of WD4FAB's tower. The commercial NEMA4-rated equipment box, detailed in **Fig 61** (shown inverted), is used to protect the 23-cm power amplifier and its power supply, as well as a multitude of electrical connections. This steel box is very weather resistant, with an exceptionally good epoxy finish, but it is not sealed and so it will not trap moisture to be condensed with temperature changes. Be sure to use a box with at least a NEMA3 rating for rainwater and dust protection. The NEMA4 rating is just a little better protection than the NEMA3 rating. Using a well-rated equipment box is very well worth the expense of the box. As you can see, the box also provides some pretty good flanges to mount the mast-mounted preamplifiers for three bands. This box is an elegant solution for the simple need of rain shelter for your equipment. See **Fig 62**.

Elevation Control

Satellite antennas need to have elevation control to point up to the sky. This is the "El" part of Az-El control of satellite antennas. Generally, elevation booms for CP satellite antennas need to be non-conducting so that the boom does not affect the radiation pattern of the antenna. In the example shown next, the elevation boom center section is a piece of extra-heavy-wall $1^1/_2$-inch pipe (for greater strength) coupled with a tubular fiberglass-epoxy boom extension on the 70-cm end and a home-brew long extension on the 2-meter end. This uses large PVC pipe reinforced with four braces of Phillystran non-metallic guy cable. (PVC pipe is notoriously flexible, but the Phillystran cables make a quite stiff and strong boom of the PVC pipe.) For smaller installations, a continuous piece of fiberglass-epoxy boom can be placed directly through the elevation rotator.

Elevation boom motion needs to be powered, and one solution by WD4FAB, shown in **Fig 63**, uses a surplus jackscrew drive mechanism. I8CVS has also built his own robust elevation mechanism. See **Fig 64**. Note in each of these applications the methods used to provide bearings for the elevation mechanism. In WD4FAB's case, the elevation axis is a piece of heavy-duty $1^1/_2$-inch pipe,

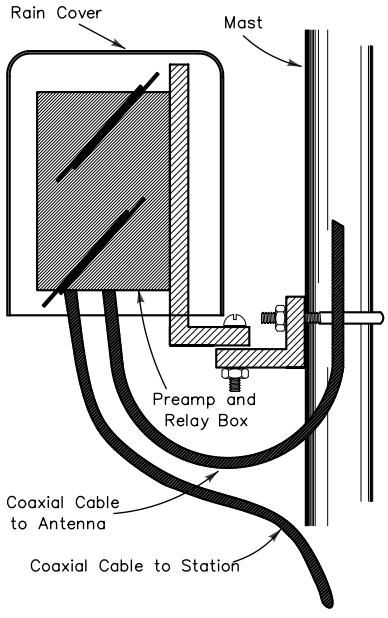

Fig 62—Protection for tower-mounted equipment need not be elaborate. Be sure to dress the cables as shown so that water drips off the cable jacket before it reaches the enclosure. One hazard for such open-bottom enclosures is that of animals liking the cable insulation as a delicacy. Flying insects also like to build their houses in these enclosures.

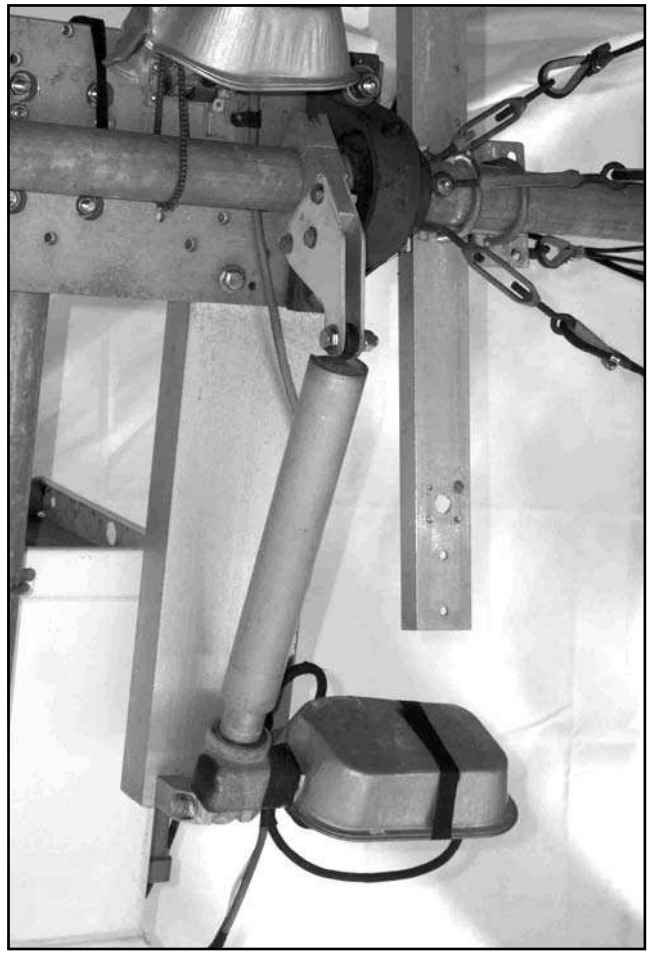

Fig 63—WD4FAB's homebrew elevation rotator drive using a surplus-store drive screw mechanism. Note also the large journal bearing supporting the elevation axis pipe shaft. (*WD4FAB photo.*)

($1^{15}/_{16}$-inch OD) and large 2 inch journal bearings are used for the motion. I8CVS uses a very large hinge to allow his motion.

Robust commercial solutions for Az-El rotators have given operators good service over the years. **See Fig 65**. Manufacturers such as Yaesu and M^2 are among these suppliers. One operator, VE5FP, found a solution for his Az-El needs by using two low-cost, lightweight TV rotators. See Fig 65B.

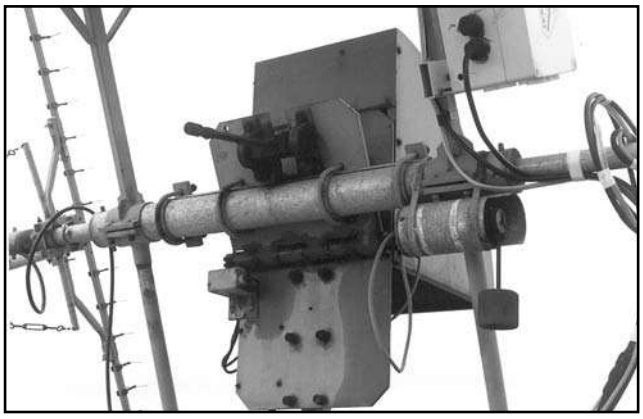

Fig 64—I8CVS's homebrew elevation mechanism using a very large, industrial hinge as the pivot and a jackscrew drive. (*I8CVS photo.*)

CONVERTED C-BAND TVRO DISHES

In working with larger, converted C-band TVRO dishes for AO-40, some operators have used only the polar mount with its jack-screw mechanism. See **Fig 66**. This dish is called *Big Ugly Dish* or just "BUD" by their users. Only using the polar mount mechanism limits the operator in the range of motion, as previously discussed. WØLMD provides for a greater degree of articulation of these dishes through several mechanisms. One of these is a sector-gear elevation drive, shown in **Fig 67**.

For the azimuth motion of our satellite antennas, most use motorized rotator drives, mainly the commercial sources previously mentioned. Most antennas are tower-mounted, allowing the placement of the rotator inside the tower. For the large wind loads of satellite antennas, these commercial rotators become rather expensive.

High loads are also prominent with the use of BUD

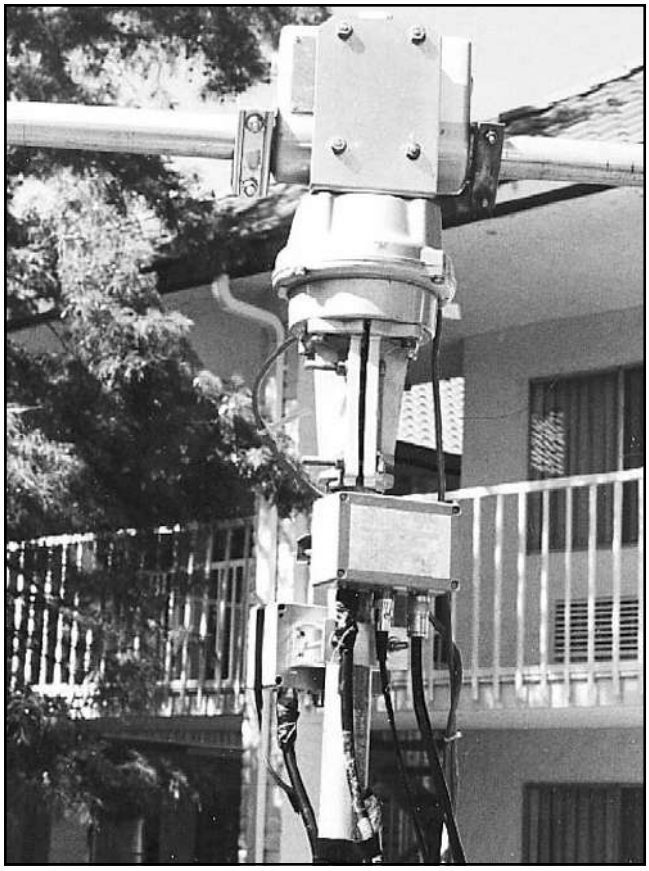

Fig 65—At left, Yaesu Az-El antenna-rotator mounting system is shown. Note that antenna loads must be more carefully balanced on this rotator than in the previously shown systems. At right, VE5FP has a solution for his Az-El rotators by bolting two of them together in his "An Inexpensive Az-El Rotator System", *QST*, December 1998.

Fig 66—A TVRO dish-drive system is shown on its polar mount, using a protected drive-screw mechanism. (*WØLMD photo.*)

Fig 67—A modified TVRO dish mount is shown using an Az-El mount and a sector-gear drive for the elevation. (*WØLMD photo.*)

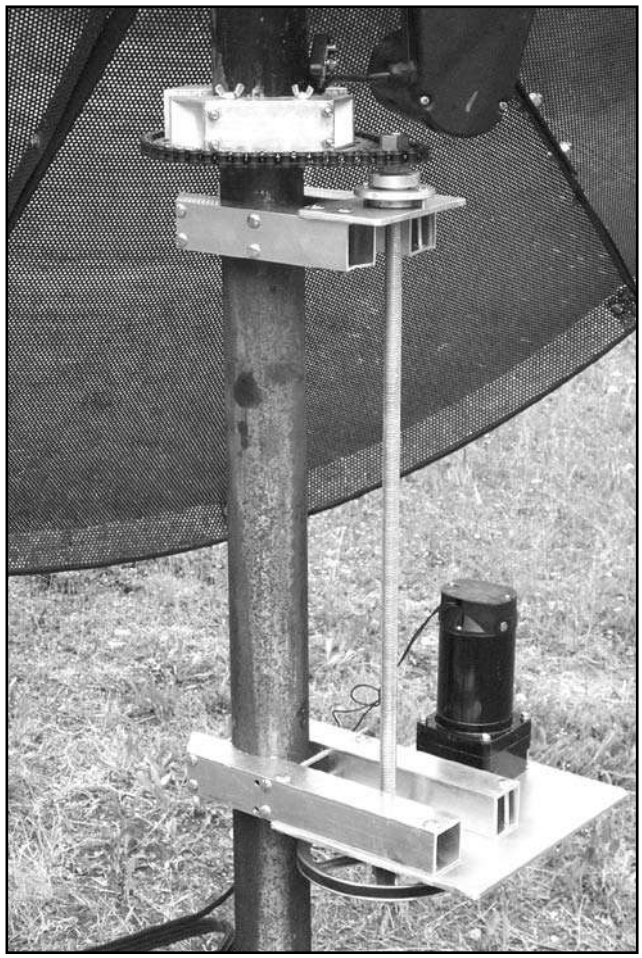

Fig 68—WØLMD constructed a very robust and low-cost Az drive mechanism. (*WØLMD photo.*)

antennas, and WØLMD has again engineered some very robust mechanisms using combinations of motorcycle-chain drives, V-belt drives and gear-head motors, as seen in **Fig 68**. An overall view of one of his BUD antennas is shown in **Fig 69**, showing the Az drive with an El drive that uses a jackscrew mechanism.

Operators through the years have employed many methods for the control of their antenna positions, ranging from true *arm-strong* manual positioning, to manual operation of the powered antenna azimuth and elevation rotators, to fully automated computer control of the rotators. While computer control of the rotators is not essential, life is greatly assisted with their use. For many years, one of the keystone control units for rotators has been the *Kansas City Tracker* (KCT) board installed in your computer. Most satellite-tracking programs can connect to the KCT with ease. One difficulty with the KCT unit is that they are 8-bit digital units, providing positioning precision of 0.35° in elevation and 1.41° in azimuth. For the larger dishes, with their narrow beamwidths, these values of precision are unacceptable. There are other options to replace the KCT unit.

A recent trend for amateur antenna control has been evolving in the form of a standalone controller that translates computer antenna-position information into controller commands with an understanding of antenna-position limits. These boxes, represented by the *EasyTrak* unit, **Fig 70**, from the Tucson Amateur Packet Radio (TAPR) group, have made this capability readily available for many amateurs. This unit is a 10-bit encoder, providing precisions of 0.09° in elevation and 0.35° in azimuth. The computer can also control the operation of your station transceiver through the radio interface provided in *EasyTrak*; you will not need any other radio interface.

Other position readout and control options are available. For many years ham operators have employed synchros, or *selsyns*, for their position readouts. These are

Fig 69—A completed TVRO dish Az-El mounting system is shown, using a jackscrew elevation drive. (*WØLMD photo.*)

Fig 70—The EasyTrak automated antenna rotator and radio controller by TAPR. (*WD4FAB photo.*)

specialized transformers, using principles developed over sixty years ago and employed in such devices as surplus "radio compass" steering systems for aircraft. While the position readout of these devices can be quite precise, in general they only provide a visual position indication, one that is not easily adapted to computer control. I8CVS employs such a system at his station and his elevation synchro can be seen in Fig 64, using a weighted arm on the synchro to provide a constant reference to the Earth's gravity vector.

The more up-to-date, computer-friendly position readout methods used these days are usually based on precision potentiometers or digital code wheels. **Fig 71** shows such a digital code-wheel system employed by WØLMD. He notes that such systems, while providing a very high precision of angular position, they are not absolute systems and that once calibrated, they must be continually powered so they do not lose their calibration. Precision potentiometers, on the other hand, provide an absolute position reference, but with a precision that is limited to the quality of the potentiometer, typically 0.5% (0.45° in El and 1.80° in Az) to 1.0%. So the choices have their individual limits, unless a lot of money is spent for very precise commercial systems.

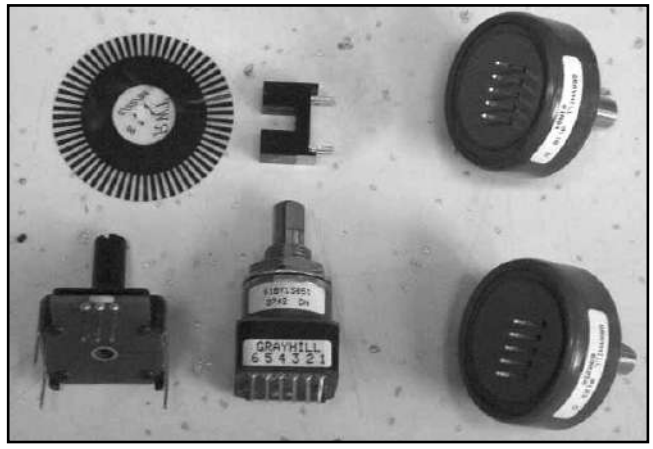

Fig 71—WØLMD has experimented with highly precise optical encoders for his antenna position systems. See text. (*WØLMD photo.*)

NOTES AND REFERENCES, SATELLITE ANTENNAS

AO-40 frequencies, "Official Transponder Frequency Bandplan for P-3D"; **www.amsat-dl.org/p3dqrg.html**.

Brown, Gerald R., K5OE, "A Helix Feed for Surplus MMDS, Antennas" *Proceedings of the 2001AMSAT-NA Symposium*, October 2001, pp 89-94, also: **members.aol.com/k5oe**.

Brown, Jerry, K5OE, "A K-Band Receiver for AO-40", *Proceedings for the AMSAT-NA Space Symposium, 2002*.

Brown, Gerald R., K5OE, "Build This No-Tune Dual-Band Feed for Mode L/S" *The AMSAT Journal*, Vol 26, No 1, Jan/Feb 2003.

Brown, Gerald R., K5OE, "Dual-Band Dish Feeds for 13/23 cm," *Proceedings of the 2002AMSAT-NA Symposium*, October 2002, pp 123-131.

Brown, Jerry, K5OE, **members.aol.com/k5oe/** MMDS Dishes.

Brown, Gerald R., K5OE, "Patch Feeds," **members.aol.com/k5oe**.

Brown, Jerry, K5OE, "The Texas Potato Masher: A Medium-Gain Directional Satellite Antenna For

LEOs," *The AMSAT Journal*, Vol 22, No. 1, Jan/Feb 1999.
Jansson, Dick, WD4FAB, *QST*, Sep 2002, "Product Review", "M² 23CM22EZA 1.2 GHz Antenna", p 59.
Kingery, Mike, KE4AZN, "Setting Up for AO-40 L-Band Uplink," *The AMSAT Journal*, May/Jun 2002, pp 14-16, also: **web.infoave.net/~mkmk518/**.
Koehler, Jim, VE5FP, "An Inexpensive Az-El Rotator System", *QST*, Dec 1998.
Kraus, John D., "The Helical Antenna", Chapter 7, *Antennas*, McGraw-Hill Book Company, 1988.
Kraus, John D., W8JK, "16-12, Patch or Microstrip Antennas," *Antennas*, 1988, pp 745-749.
Krome, Ed, K9EK, "Development of a Portable Mode S Ground Station." *The AMSAT Journal*, Vol 16, No. 6, Nov/Dec 1993, pp 25-28.
Krome, Ed, K9EK, "S band Reception: Building the DEM Converter and Preamp Kits," *The AMSAT Journal*, Vol 16, No. 2, Mar/Apr 1993, pp 4-6.
Krome, Ed., K9EK, *Mode S—The Book*, p 96, 109.
Krome, Ed, K9EK, "Mode S: Plug and Play!" *The AMSAT Journal*, Vol 14, No. 1, Jan 1991, pp 21-23, 25.
Long, Howard, G6LVB, "My Shack Configuration—Spring 2002": **www.g6lvb.com/g6lvb_shack_spring_2002.htm**.
McCaa, William D., K0RZ, "Hints on Using the AMSAT-OSCAR 13 Mode S Transponder," *The AMSAT Journal*, Vol 13, No. 1, Mar 1990, pp 21-22.
MacAllister, Andy, W5ACM, "Field Day 2002," *73 Amateur Radio Today*, Sept. 2002, pp 48-52.
Miller, James, G3RUH, "Mode S — Tomorrow's Downlink?" *The AMSAT Journal*, Vol 15, No. 4, Sep/Oct 1992, pp 14-15.
Miller, James S., G3RUH, "'Patch' Feed For S-Band Dish Antennas"; **www.jrmiller.demon.co.uk/products/patch.html**.
Miller, James, G3RUH, "A 60-cm S-Band Dish Antenna," *The AMSAT Journal*, Vol 16 No. 2, Mar/Apr 1993, pp 7-9.
Miller, James, G3RUH, "Small is Best," *The AMSAT Journal*, Vol 16, No. 4, Jul/Aug 1993, p 12.
Monteiro, Anthony, "Work OSCAR 40 with Cardboard-box Antennas!," *QST*, Mar 2003, pp 57-62.
Orban Microwave, "The Basics of Patch Antennas: **www.orbanmicrowave.com/antenna_application_notes.htm**.
Seguin, Mike, N1JEZ, "OSCAR 40 on 24GHz", *QST*, Dec 2002, pp 55-56.
Seydler, Robert, K5GNA,"Modifications of the AIDC 3731 Downconverters", **members.aol.com/k5gna/AIDC3731modifications.doc**.
Suckling, Charles, G3WDG, "K-Band Results From AO-40": **www.g3wdg.free-online.co.uk/kband.htm**.
Suckling, Charles, G3WDG "Notch Filters for AO-40 Mode L/S": **www.g3wdg.free-online.co.uk.notch.htm**.
Suding, Dr. Robert, WØLMD, "Converting TVRO Dish & Dishes For Amateurs" **www.ultimatecharger.com/dish.html**.
Thiel, David & Smith, Staphani, *Switched Parasitic Antennas for Cellular Communications*, Artech House, 2002, "Chapter 3, Patch Antennas," pp 79-96.
Wade, Paul, N1BWT (W1GHZ), *Online Microwave Antenna Handbook*, "Chapter 4, Parabolic Dish Antennas," **www.w1ghz.cx/antbook/chap4.pdf**, Mar. 98. (See CD-ROM bundled with this book.)
Zibrat,Timothy S, K3TZ, "2.4 GHz Patch Design": **www.qsl.net/k3tz/**.

Antenna Systems for EME Communications

This section was updated by David Hallidy, K2DH. As mentioned earlier, the tremendous path loss incurred over an EME circuit places stringent requirements on Earth-station performance. Low-noise receiving equipment, maximum available power and high-gain antenna arrays are required for successful EME operation. Although it is possible to copy some of the better-equipped stations with a low-gain antenna, it is unlikely that such an antenna can provide reliable two-way communications. Antenna gain of at least 20 dBi is required for reasonable EME success. Generally speaking, more antenna gain yields the most noticeable improvement in station performance, since the increased gain improves both the received and transmitted signals.

VHF/UHF EME ANTENNAS

Several types of antennas for 2 meters and 70 cm are popular among EME enthusiasts. Perhaps the most popular antenna for 144-MHz work is an array of either 4 or 8 long-boom (14 to 15 dBi gain) Yagis. The 4-Yagi array provides approximately 20 dB gain, and an 8-Yagi array gives an approximate 3 dB increase over the 4-antenna array. **Fig 72** shows the computed response at a 30° tilt above the horizon for a stack of four 14-element 2-meter Yagis, each with a boomlength of 3.1 λ (22 feet).

At 432 MHz, EME enthusiasts often use 8 or 16 long-boom Yagis in an array. Such Yagis are commercially available or they can be constructed from readily available materials. Chapter 18, VHF and UHF Antenna Systems,

has details on some popular Yagi designs.

The main disadvantage of Yagi arrays is that the polarization plane of the individual Yagis cannot be conveniently changed. One way around this is to use cross-polarized Yagis and a relay switching system to select the desired polarization, as described in the previous section. This represents a considerable increase in system complexity to select the desired polarization. Some amateurs have gone so far as to build complicated mechanical systems to allow constant polarization adjustment of all the Yagis in a large array. **Fig 73** shows the K1FO 70-cm EME 16-Yagi array with full polarization control, described in *The ARRL Antenna Compendium, Vol 3*. This 432-MHz EME array uses open-wire phasing lines to minimize feed-line losses. **Fig 74** shows the computed response for this array, which employs rugged but lightweight 14-element Yagis on 3.1 λ (7.1 foot) booms. Feed-line losses are not explicitly accounted for in the *EZNEC Professional* computer model, but are estimated to be less than 0.25 dB.

Polarization shift of EME signals at 144 MHz is fairly rapid, and the added complexity of a relay-controlled cross-polarized antenna system or a mechanical polarization adjustment scheme is probably not worth the effort. At 432 MHz, however, where the polarization shifts at a much slower rate, an adjustable polarization system does offer a definite advantage over a fixed one.

The Yagi antenna system used by Ed Stallman, N5BLZ, is shown in **Fig 75**. His system employs twelve 144-MHz long-boom 17-element Yagi antennas. The monster 48-Yagi 2-meter array of Gerald Williamson, K5GW, is shown in **Fig 76**, and the huge 48-Yagi 70-cm EME array of Frank Potts, NC1I, is shown in **Fig 77**.

Although not as popular as Yagis, Quagi antennas (made from both quad and Yagi elements) are sometimes used for EME work. Slightly more gain per unit boom length is possible as compared to the conventional Yagi, at the expense of some robustness. Additional information on the Quagi is presented in Chapter 18, VHF and UHF Antenna Systems.

The collinear array is an older type of antenna for EME work. A 40-element collinear array has approximately

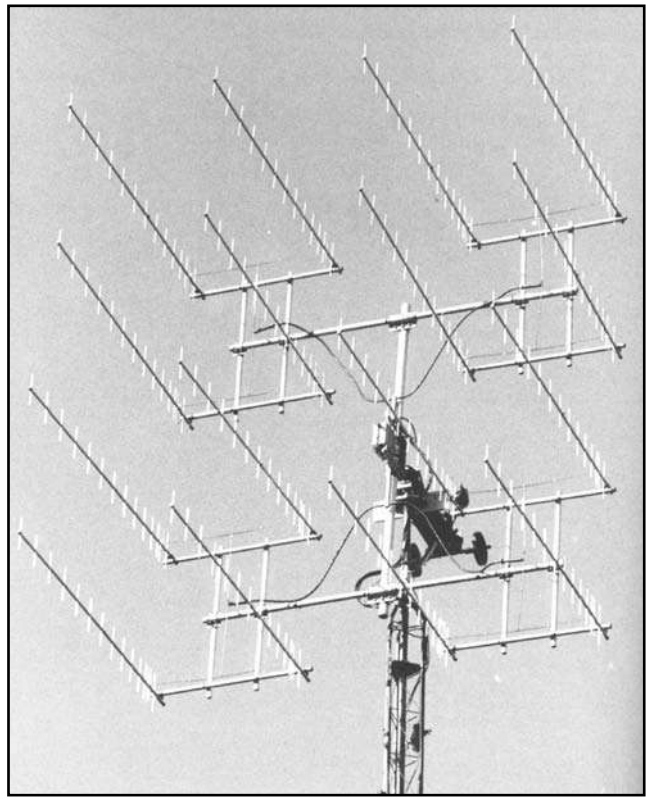

Fig 73—K1FO's variable polarization 16 × 14-element (3.6-λ boom lengths) 432-MHz EME array shown at 2° elevation and vertical polarization. (See *The ARRL Antenna Compendium, Vol 3.*)

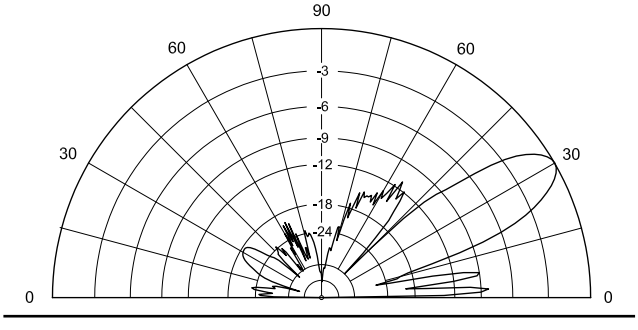

Fig 72—*EZNEC Pro* elevation pattern for four 14-element 2-meter Yagis (3.6-λ boom lengths) at an elevation angle of 30° above the horizon. The computed system gain is 21.5 dBi, suitable for 2-meter EME. This assumes that the phasing system is made of open-wire transmission lines so that feed-line losses can be kept below 0.25 dB.

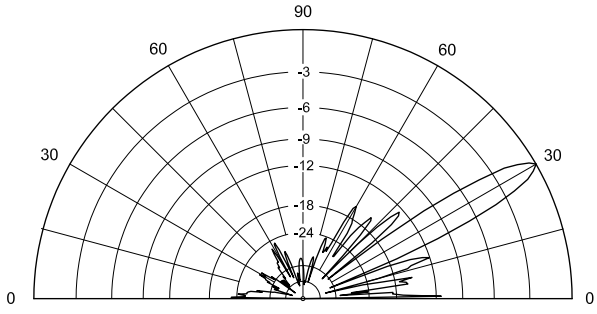

Fig 74—Computed elevation response for K1FO 16-Yagi 432-MHz array shown in Fig 73. (The *EZNEC Pro* model required 2464 segments!) With assumed phasing harness feed-line losses of 0.25 dB, the overall gain exceeds 27.5 dBi.

the same frontal area as an array of four Yagis, but produces approximately 1 to 2 dB less gain. One attraction to a collinear array is that the depth dimension is considerably less than the long-boom Yagis. An 80-element collinear is marginal for EME communications, providing approximately 19 dB gain. As with Yagi and Quagi antennas, the collinear cannot be adjusted easily for polarity changes. From a construction standpoint, there is little difference in complexity and material costs between the collinear and Yagi arrays.

DISH ANTENNAS FOR EME

On 2 meters the minimum antenna gain for reliable EME communications is about 20 dBi. While a few amateurs have had access to parabolic dishes large enough for EME work at 144 and 222 MHz, at those frequencies an array of four long Yagis is equal in gain to a dish 24 feet in diameter! To achieve truly high-gain performance from a dish on 2 meters would require a reflector diameter of nearly 96 feet (providing 32 dBi gain). Such undertakings are generally beyond amateur means, so there has been little work done with dishes at low frequencies, except for the occasional expedition to one of the large radio telescopes that have accommodated amateur EME work.

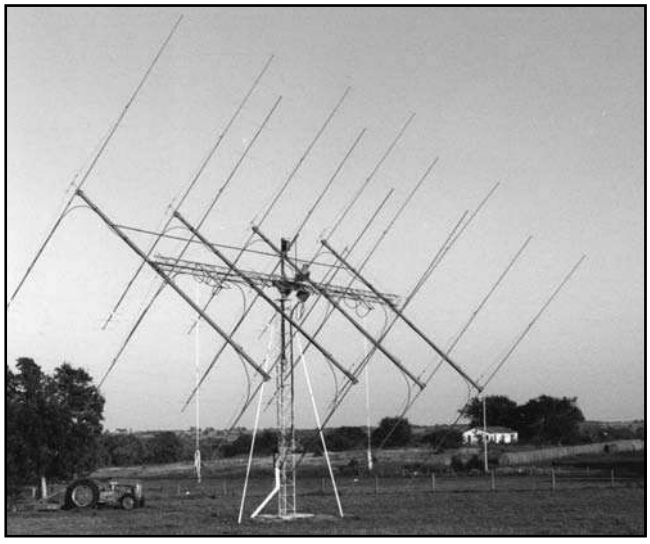

Fig 75—The EME array used at N5BLZ consists of twelve long-boom 144-MHz Yagis. The tractor, lower left, really puts this array into perspective! (*Photo courtesy N5BLZ.*)

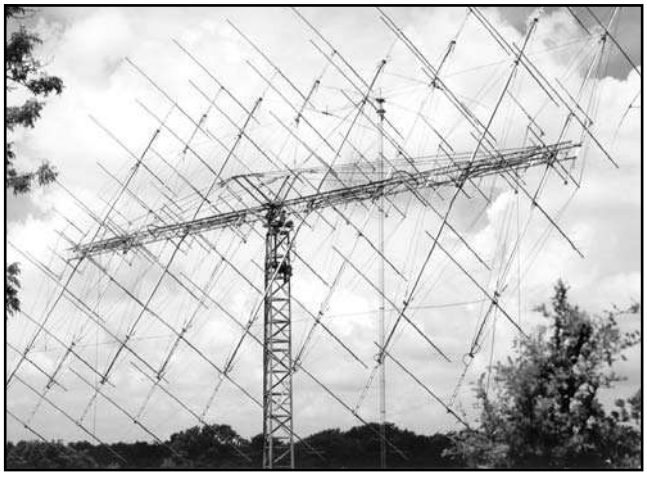

Fig 76—K5GW's huge 48-Yagi 2-meter EME array. (*Photo courtesy K5GW.*)

Microwave Parabolic Dish Antennas

The major problems associated with parabolic dish antennas are mechanical ones. A dish of about 16 feet in diameter is the minimum size required for successful EME operation on 432 MHz. With wind and ice loading, structures of this size place a real strain on the mounting and positioning system. Extremely rugged mounts are required for large dish antennas, especially when used in windy locations. **Fig 78** shows the impressive 7-meter diameter

Fig 77—NC1I's magnificent 48-Yagi 70-cm EME array. (*Photo courtesy NC1I.*)

dish built by David Wardley, ZL1BJQ.

Several aspects of parabolic dish antennas make the extra mechanical problems worth the trouble, however. For example, the dish antenna is inherently broadband, and may be used on several different amateur bands by simply changing the feed. An antenna that is suitable for 432 MHz work will most likely be usable on several of the higher amateur bands too. Increased gain is available as the frequency of operation is increased.

Another advantage of a dish is the flexibility of the feed system. The polarization of the feed, and therefore the polarization of the antenna, can be changed with little difficulty. It is a relatively easy matter to devise a system to rotate the feed remotely from the shack to change polarization. Because polarization changes can account for as much as 30 dB of signal attenuation, the rotatable feed can make the difference between consistent communications and no communications at all. Further information on Parabolic Antennas can be found in Chapter 18, VHF and UHF Antenna Systems as well as in the section below.

A 12-FOOT STRESSED HOMEBREW PARABOLIC DISH

Very few antennas evoke as much interest among UHF amateurs as the parabolic dish, and for good reason. First, the parabola and its cousins—Cassegrain, hog horn and Gregorian—are probably the ultimate in high-gain antennas. One of the highest-gain antennas in the world (148 dB) is a parabola. This is the 200-inch Mt. Palomar telescope. (The very short wavelength of light rays causes such a high gain to be realizable.)

Second, the efficiency of the parabola does not change as size increases. With Yagis and collinear arrays, the losses in the phasing harness increase as the array size increases. The corresponding component of the parabola is lossless air between the feed horn and the reflecting surface. If there are a few surface errors, the efficiency of the system stays constant regardless of antenna size. This project was presented by Richard Knadle, K2RIW, in August 1972 *QST*.

Some amateurs reject parabolic antennas because of the belief that they are all heavy, hard-to-construct, have large wind-loading surfaces and require precise surface accuracy. However, with modern construction techniques, a prudent choice of materials and an understanding of accuracy requirements, these disadvantages can be largely overcome. A parabola may be constructed with a 0.6 f/D (focal length/diameter) ratio, producing a rather flat dish, which makes it easy to surface and allows the use of recent advances in high-efficiency feed horns. This results in greater gain for a given dish size over conventional designs.

Such an antenna is shown in **Fig 79**. This parabolic dish is lightweight, portable, easy to build, and can be used for 432 and 1296-MHz mountain topping, as well as on 2304, 3456 and 5760 MHz. Disassembled, it fits into the trunk of a car, and can be assembled in 45 minutes.

The usually heavy structure that supports the surface of most parabolic dish antennas has been replaced in this design by aluminum spokes bent into a near parabolic shape by string. These strings serve the triple function of guying the focal point, bending the spokes and reducing the error at the dish perimeter (as well as at the center) to nearly zero. By contrast, in conventional designs, the dish perimeter (which has a greater surface area than the center) is farthest from the supporting center hub. For these reasons, it often has the greatest error. This error becomes more severe when the wind blows.

Here, each of the spokes is basically a cantilevered beam with end loading. The equations of beam bending

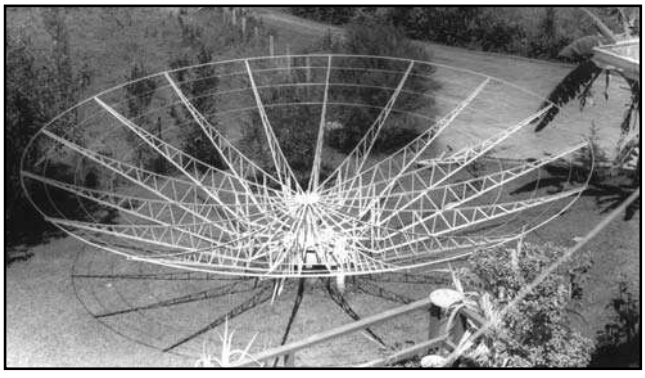

Fig 78—ZL1BJQ's homemade 7-meter (23-foot) parabolic dish, just prior to adding 1/2-inch wire mesh. (*Photo courtesy ZL1BJQ.*)

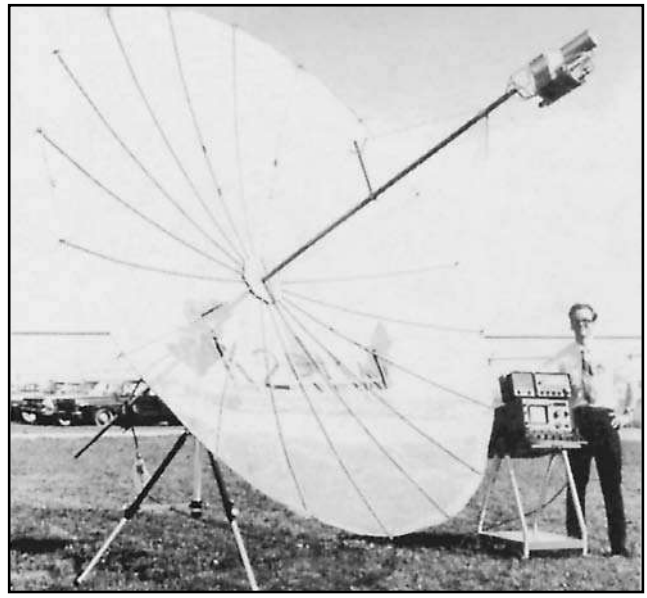

Fig 79—A 12-foot stressed parabolic dish set up for satellite signals near 2280 MHz. A preamplifier is shown taped below the feed horn. The dish was designed by K2RIW, standing at the right. From *QST*, August 1972.

predict a near-perfect parabolic curve for extremely small deflections. Unfortunately the deflections in this dish are not that small and the loading is not perpendicular. For these reasons, mathematical prediction of the resultant curve is quite difficult. A much better solution is to measure the surface error with a template and make the necessary correction by bending each of the spokes to fit. This procedure is discussed later.

The uncorrected surface is accurate enough for 432 and 1296-MHz use. Trophies taken by this parabola in antenna-gain contests were won using a completely natural surface with no error correction. By placing the transmission line inside the central pipe that supports the feed horn, the area of the shadows or blockages on the reflector surface is much smaller than in other feeding and supporting systems, thus increasing gain. For 1296 MHz, a backfire feed horn may be constructed to take full advantage of this feature. At 432 MHz, a dipole and reflector assembly produces 1.5 dB additional gain over a corner-reflector feed system. Because the preamplifier is located right at the horn on 2300 MHz, a conventional feed horn may be used.

Construction

Table 2 is a list of materials required for construction. Care must be exercised when drilling holes in the connecting center plates so assembly problems will not be experienced later. See **Fig 80**. A notch in each plate allows them to be assembled in the same relative positions. The two plates should be clamped together and drilled at the same time. Each of the 18 1/2-inch diameter aluminum spokes has two no. 28 holes drilled at the base to accept no. 6-32 machine screws that go through the center plates. The 6-foot long spokes are cut from standard 12-foot lengths of tubing. A fixture built from a block of aluminum assures that the holes are drilled in exactly the same position in each spoke. The front and back center plates constitute an I-beam type of structure that gives the dish center considerable rigidity.

A side view of the complete antenna is shown in **Fig 81**. Aluminum alloy (6061-T6) is used for the spokes, while 2024-T3 aluminum alloy sheet, 1/8 inch thick, is used for the center plates. (Aluminum has approximately three times the strength-to-weight ratio of wood, and aluminum cannot warp or become water logged.) The end of each of the 18 spokes has an eyebolt facing the dish focal point, which serves a dual purpose:

1) To accept the #9 galvanized fence wire that is routed through the screw eyes to define the dish perimeter, and
2) To facilitate rapid assembly by accepting the S hooks which are tied to the end of each of the lengths of 130-pound test Dacron fishing string.

The string bends the spokes into a parabolic curve; the dish may be adapted for many focal lengths by tightening or slackening the strings. Dacron was chosen because it has the same chemical formula as Mylar. This is a low-stretch material that keeps the dish from changing shape. The galvanized perimeter wire has a 5-inch overlap area that is bound together with baling wire after the spokes have been hooked to the strings.

The aluminum window screening is bent over the perimeter wire to hold it in place on the back of the spokes. Originally, there was concern that the surface perturbations (the spokes) in front of the screening might decrease the gain. The total spoke area is so small, however, that

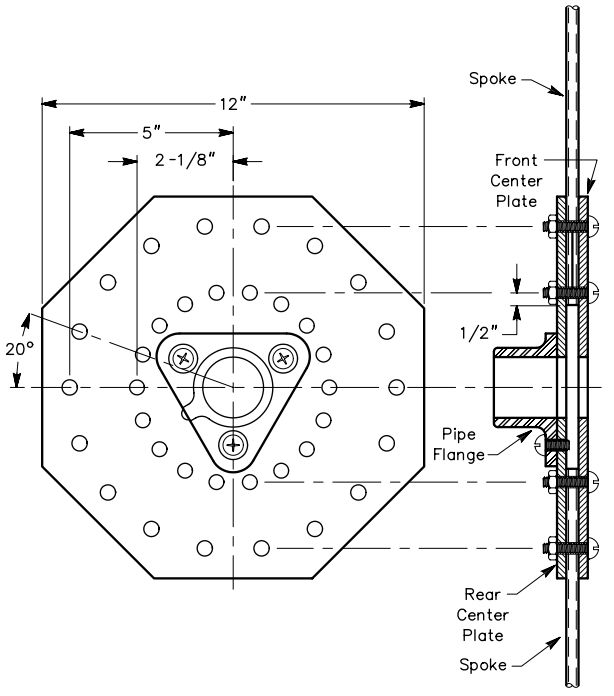

Fig 80—Center plate details. Two center plates are bolted together to hold the spokes in place.

Table 2

Materials List for the 12-Foot Stressed Parabolic Dish

1) Aluminum tubing, 12 ft × 1/2 in. OD × 0.049-in. wall, 6061-T6 alloy, 9 required to make 18 spokes.
2) Octagonal mounting plates 12 × 12 × 1/8 in., 2024-T3 alloy, 2 required.
3) 1 1/4 in. ID pipe flange with setscrews.
4) 1 1/4 in. × 8 ft TV mast tubing, 2 required.
5) Aluminum window screening, 4 × 50 ft.
6) 130-pound test Dacron trolling line.
7) 38 ft #9 galvanized fence wire (perimeter).
8) Two hose clamps, 1 1/2 in.; two U bolts; 1/2 × 14 in. Bakelite rod or dowel; water-pipe grounding clamp; 18 eye bolts; 18 S hooks.

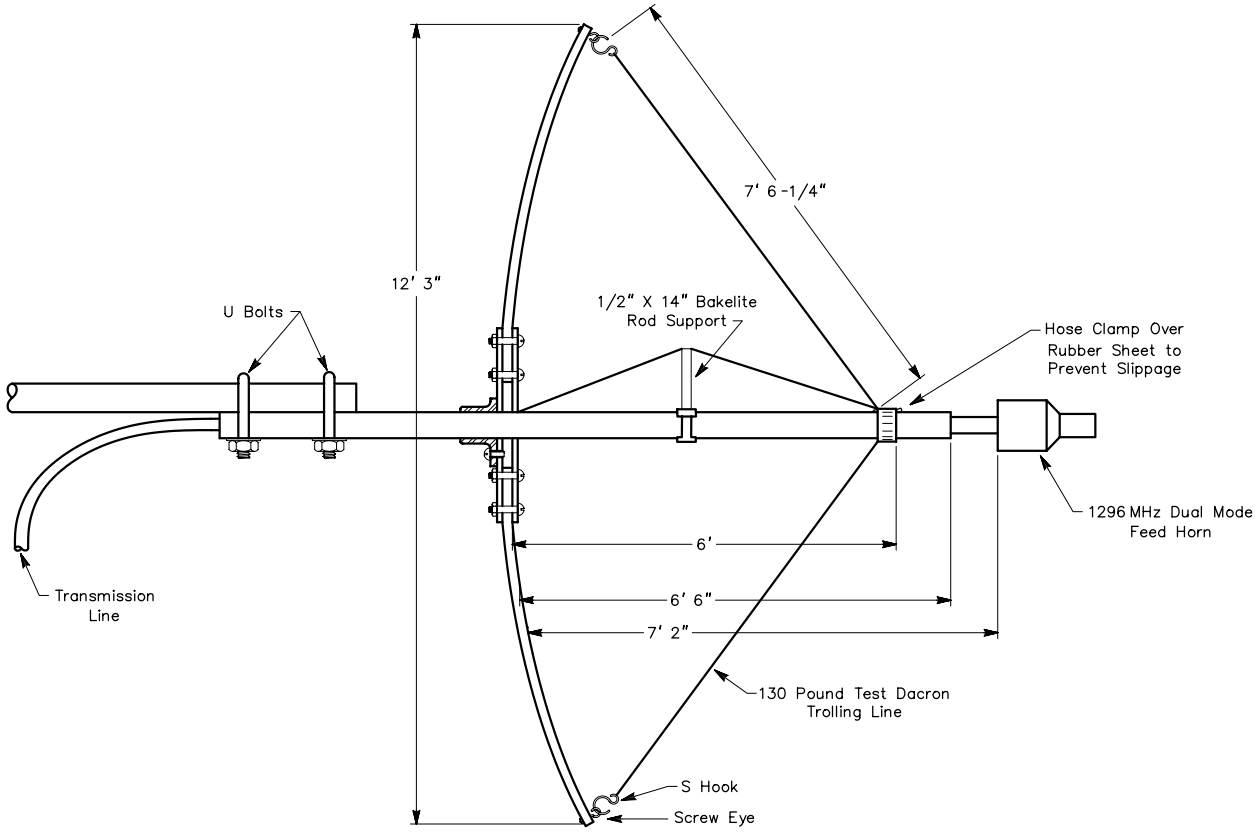

Fig 81—Side view of the stressed parabolic dish.

this fear proved unfounded.

Placing the aluminum screening in front of the spokes requires the use of 200 pieces of baling wire to hold the screening in place. This would increase the assembly time by at least an hour. For contest and mountaintop operation (when the screening is on the back of the spokes) no fastening technique is required other than bending the screen to overlap the wire perimeter.

The Parabolic Surface

A 4-foot wide roll of aluminum screening 50 feet long is cut into appropriate lengths and laid parallel, with a 3-inch overlap between the top of the unbent spokes and hub assembly. The overlap seams are sewn together on one half of the dish using heavy Dacron thread and a sailmaker's curved needle. Every seam is sewn twice; once on each edge of the overlapped area. The seams on the other half are left open to accommodate the increased overlap that occurs when the spokes are bent into a parabola. The perimeter of the screening is then trimmed. Notches are cut in the 3-inch overlap to accept the screw eyes and S hooks.

The first time the dish is assembled, the screening strips are anchored to the inside surface of the dish and the seams sewn in this position. It is easier to fabricate the surface by placing the screen on the back of the dish frame with the structure inverted. The spokes are sufficiently strong to support the complete weight of the dish when the perimeter is resting on the ground.

The 4-foot wide strips of aluminum screening conform to the compound bend of the parabolic shape very easily. If the seams are placed parallel to the E-field polarization of the feed horn, minimum feedthrough will occur. This feedthrough, even if the seams are placed perpendicular to the E field, is so small that it is negligible. Some constructors may be tempted to cut the screening into pie-shaped sections. This procedure will increase the seam area and construction time considerably. The dish surface appears most pleasing from the front when the screening perimeter is slipped between the spokes and the perimeter wire, and is then folded back over the perimeter wire. In disassembly, the screening is removed in one piece, folded in half, and rolled.

The Horn and Support Structure

The feed horn is supported by $1^1/_4$-inch aluminum television mast. The Hardline that is inserted into this tubing is connected first to the front of the feed horn, which then slides back into the tubing for support. A setscrew assures that no further movement of the feed horn occurs. During antenna-gain competition the setscrew is omit-

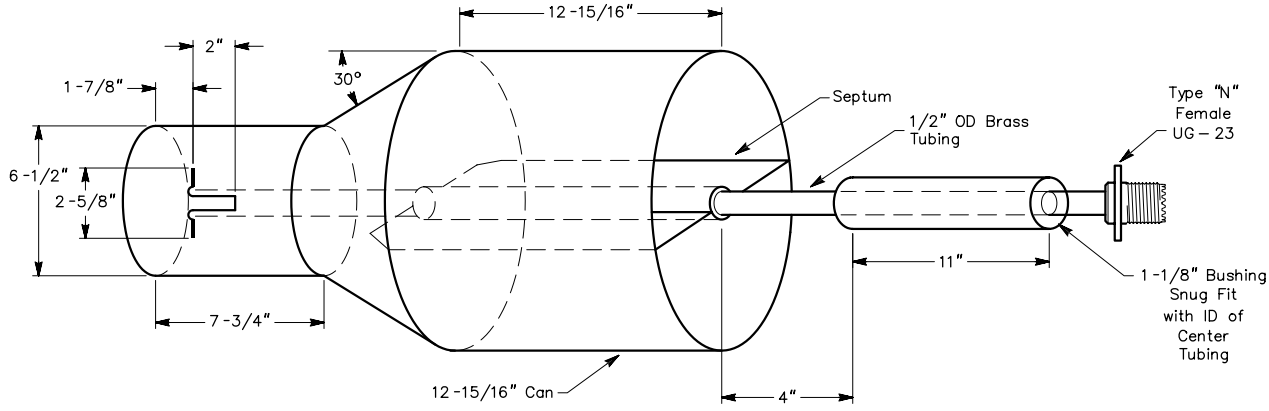

Fig 82—Backfire type 1296-MHz feed horn, linear polarization only. The small can is a Quaker State oil container; the large can is a 50-pound shortening container (obtained from a restaurant, Gold Crisp brand). Brass tubing, 1/2-inch OD extends from UG-23 connector to dipole. Center conductor and dielectric are obtained from 3/8-inch Alumafoam coaxial cable. The dipole is made from 3/32-inch copper rod. The septum and 30° section are made from galvanized sheet metal. Styrofoam is used to hold the septum in position. The primary gain is 12.2 dBi.

ted, allowing the 1/2-inch semirigid CATV transmission line to move in or out while adjusting the focal length for maximum gain. The TV mast is held firmly at the center plates by two setscrews in the pipe flange that is mounted on the rear plate. At 2300 MHz, the dish is focused for best gain by loosening these setscrews on the pipe flange and sliding the dish along the TV mast tubing. (The dish is moved instead of the feed horn.)

The fishing strings are held in place by attaching them to a hose clamp that is permanently connected to the TV tubing. A piece of rubber sheet under the hose clamp prevents slippage and keeps the hose clamp from cutting the fishing string. A second hose clamp is mounted below the first as extra protection against slippage.

The high-efficiency 1296-MHz dual mode feed horn, detailed in **Fig 82**, weighs 5 3/4 pounds. This weight causes some bending of the mast tubing, but this is corrected by a 1/2-inch diameter bakelite support, as shown in Fig 81. This support is mounted to a pipe grounding clamp with a no. 8-32 screw inserted in the end of the rod. The bakelite rod and grounding clamp are mounted midway between the hose clamp and the center plates on the mast. A double run of fishing string slipped over the notched upper end of the bakelite rod counteracts bending.

The success of high-efficiency parabolic antennas is primarily determined by feed horn effectiveness. The multiple diameter of this feed horn may seem unusual. This patented dual-mode feed, designed by Dick Turrin, W2IMU, achieves efficiency by launching two different kinds of waveguide modes simultaneously. This causes the dish illumination to be more constant than conventional designs.

Illumination drops off rapidly at the perimeter, reducing spillover. The feed backlobes are reduced by at least 35 dB because the current at the feed perimeter is almost zero; the phase center of the feed system stays constant across the angles of the dish reflector. The larger diameter section is a phase corrector and should not be changed in length. In theory, almost no increase in dish efficiency can be achieved without increasing the feed size in a way that would increase complexity, as well as blockage.

The feed is optimized for a 0.6 f/D dish. The dimensions of the feeds are slightly modified from the original design in order to accommodate the cans. Either feed type can be constructed for other frequencies by changing the scale of all dimensions.

Multiband Use

Many amateurs construct multiband antenna arrays by putting two dishes back to back on the same tower. This is cost inefficient. The parabolic reflector is a completely frequency independent surface, and studies have shown that a 0.6 f/D surface can be steered seven beamwidths by moving the feed horn from side to side before the gain diminishes by 1 dB. Therefore, the best dual-band antenna can be built by mounting separate horns side by side. At worst, the antenna may have to be moved a few degrees (usually less than a beamwidth) when switching between horns, and the unused horn increases the shadow area only slightly. In fact, the same surface can function simultaneously on multiple frequencies, making crossband duplex operation possible with the same dish.

Order of Assembly

1) A single spoke is held upright behind the rear center plate with the screw eye facing forward. Two no. 6-

32 machine screws are pushed through the holes in the rear center plate, through the two holes of the spoke, and into the corresponding holes of the front center plate. Lock washers and nuts are placed on the machine screws and hand tightened.

2) The remaining spokes are placed between the machine screw holes. Make sure that each screw eye faces forward. Machine screws, lock washers and nuts are used to mount all 18 spokes.
3) The no. 6-32 nuts are tightened using a nut driver.
4) The mast tubing is attached to the spoke assembly, positioned properly, and locked down with the setscrews on the pipe flange at the rear center plate. The S hooks of the 18 Dacron strings are attached to the screw eyes of the spokes.
5) The ends of two pieces of fishing string (which go over the bakelite rod support) are tied to a screw eye at the forward center plate.
6) The dish is laid on the ground in an upright position and #9 galvanized wire is threaded through the eyebolts. The overlapping ends are lashed together with baling wire.
7) The dish is placed on the ground in an inverted position with the focus downward. The screening is placed on the back of the dish and the screening perimeter is fastened as previously described.
8) The extension mast tubing (with counterweight) is connected to the center plate with U bolts.
9) The dish is mounted on a support and the transmission line is routed through the tubing and attached to the horn.

Parabola Gain Versus Errors

How accurate must a parabolic surface be? This is a frequently asked question. According to the Rayleigh limit for telescopes, little gain increase is realized by making the mirror accuracy greater than $\pm$ $^1/_8$ λ peak error. John Ruze of the MIT Lincoln Laboratory, among others, has derived an equation for parabolic antennas and built models to verify it. The tests show that the tolerance loss can be predicted within a fraction of a decibel, and less than 1 dB of gain is sacrificed with a surface error of $\pm^1/_8$ λ. (A $^1/_8$ λ is 3.4 inches at 432 MHz, 1.1 inches at 1296 MHz and 0.64 inch at 2300 MHz.)

Some confusion about requirements of greater than $^1/_8$-λ accuracy may be the result of technical literature describing highly accurate surfaces. Low sidelobe levels are the primary interest in such designs. Forward gain is a much greater concern than low sidelobe levels in amateur work; therefore, these stringent requirements do not apply.

When a template is held up against a surface, positive and negative ($\pm$) peak errors can be measured. The graphs of dish accuracy requirements are frequently plotted in terms of RMS error, which is a mathematically derived function much smaller than $\pm$ peak error (typically $^1/_3$). These small RMS accuracy requirements have discouraged many constructors who confuse them with $\pm$ peak errors.

Fig 83 may be used to predict the resultant gain of various dish sizes with typical errors. There are a couple of surprises, as shown in **Fig 84**. As the frequency is increased for a given dish, the gain increases 6 dB per octave until the tolerance errors become significant. Gain deterioration then increases rapidly. Maximum gain is realized at the frequency where the tolerance loss is 4.3 dB. Notice that at 2304 MHz, a 24-foot dish with $\pm$2-inch peak errors has the same gain as a 6-foot dish with $\pm$1-inch peak errors. This is quite startling, when it is realized that a 24-foot dish has 16 times the area of a 6-foot dish. Each time the diameter or frequency is doubled or halved, the gain changes by 6 dB. Each time all the errors are halved, the frequency of maximum gain is doubled. With this information, the gain of other dish sizes with other tolerances can be predicted.

These curves are adequate for predicting gain, assuming a high-efficiency feed horn is used (as described earlier), which realizes 60% aperture efficiency. At frequencies below 1296 MHz where the horn is large and causes considerable blockage, the curves are somewhat optimistic. A properly built dipole and splasher feed will have about 1.5 dB less gain when used with a 0.6 f/D dish than the dual-mode feed system described.

The worst kind of surface distortion is where the surface curve in the radial direction is not parabolic but gradually departs in a smooth manner from a perfect parabola. The decrease in gain can be severe, because a large area is involved. If the surface is checked with a template, and if reasonable construction techniques are employed, deviations are controlled and the curves represent an upper limit to the gain that can be realized.

If a 24-foot dish with $\pm$2-inch peak errors is being used with 432 and 1296-MHz multiple feed horns, the constructor might be discouraged from trying a 2300-MHz feed because there is 15 dB of gain degradation. The dish will still have 29 dBi of gain on 2300 MHz, however, making it worthy of consideration.

The near-field range of this 12-foot stressed dish (actually 12 feet 3 inches) is 703 feet at 2300 MHz. By using the sun as a noise source and observing receiver noise power, it was found that the antenna had two main lobes about 4° apart. The template showed a surface error (insufficient spoke bending at $^3/_4$ radius), and a correction was made. A recheck showed one main lobe, and the solar noise was almost 3 dB stronger.

Other Surfacing Materials

The choice of surface materials is a compromise between RF reflecting properties and wind loading. Aluminum screening, with its very fine mesh (and weight of 4.3 pounds per 100 square feet) is useful beyond 10 GHz because of its very close spacing. This screening is easy to roll up and is therefore ideal for a portable dish. This close spacing causes the screen to be a 34% filled aperture, bring-

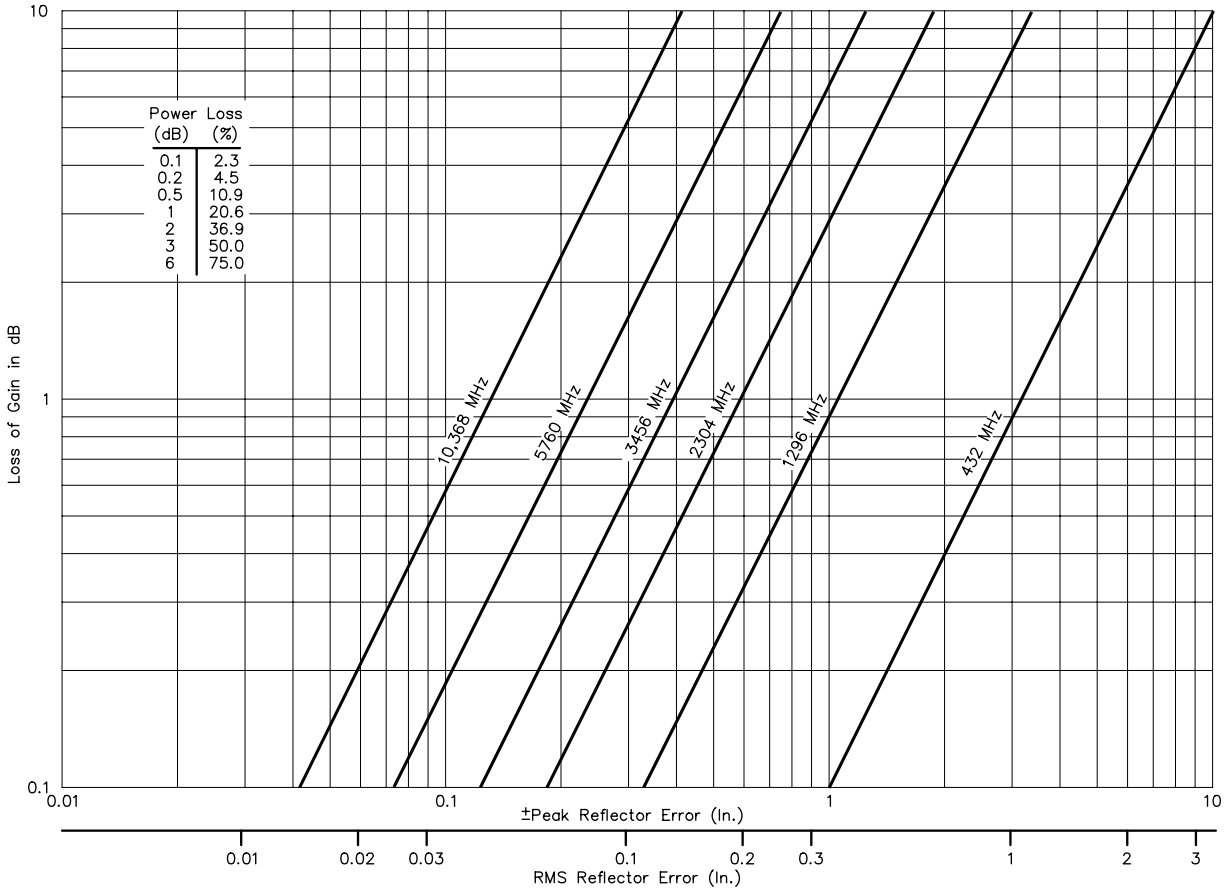

Fig 83—Gain deterioration versus reflector error. By Richard Knadle, K2RIW.

ing the wind force at 60 mph to more than 400 *pounds* on this 12-foot dish. Those considering a permanent installation of this dish should investigate other surfacing materials.

Hexagonal 1-inch poultry netting (chicken wire), which is an 8% filled aperture, is nearly ideal for 432-MHz operation. It weighs 10 pounds per 100 square feet, and exhibits only 81 pounds of force with 60 mph winds. Measurement on a large piece reveals 6 dB of feedthrough at 1296 MHz, however. Therefore, on 1296 MHz, one fourth of the power will feed through the surface material. This will cause a loss of only 1.3 dB of forward gain. Since the low-wind loading material will provide a 30-dBi gain potential, it is still a very good tradeoff.

Poultry netting is very poor material for 2300 MHz and above, because the hole dimensions approach $^1/_2\ \lambda$. As with all surfacing materials, minimum feedthrough occurs when the E-field polarization is parallel to the longest dimension of the surfacing holes.

Hardware cloth with $^1/_2$-inch mesh weighs 20 pounds per 100 square feet and has a wind loading characteristic of 162 pounds with 60 mph winds. The filled aperture is 16%, and this material is useful to 2300 MHz.

A rather interesting material worthy of investigation is $^1/_4$-inch reinforced plastic. It weighs only 4 pounds per 100 square feet. The plastic melts with many universal solvents such as lacquer thinner. If a careful plastic-melting job is done, what remains is the $^1/_4$-inch spaced aluminum wires with a small blob of plastic at each junction to hold the matrix together.

There are some general considerations to be made in selecting surface materials:

1) Joints of screening do not have to make electrical contact. The horizontal wires reflect the horizontal wave. Skew polarizations are merely a combination of horizontal and vertical components which are thus reflected by the corresponding wires of the screening. To a horizontally polarized wave, the spacing and diameter of only the horizontal wires determine the reflection coefficient (see **Fig 85**). Many amateurs have the mistaken impression that screening materials that do not make electrical contact at their junctions are poor reflectors.
2) By measuring wire diameter and spacings between the wires, a calculation of percentage of aperture that is filled can be made. This will be one of the major determining factors of wind pressure when the surfacing material is dry.

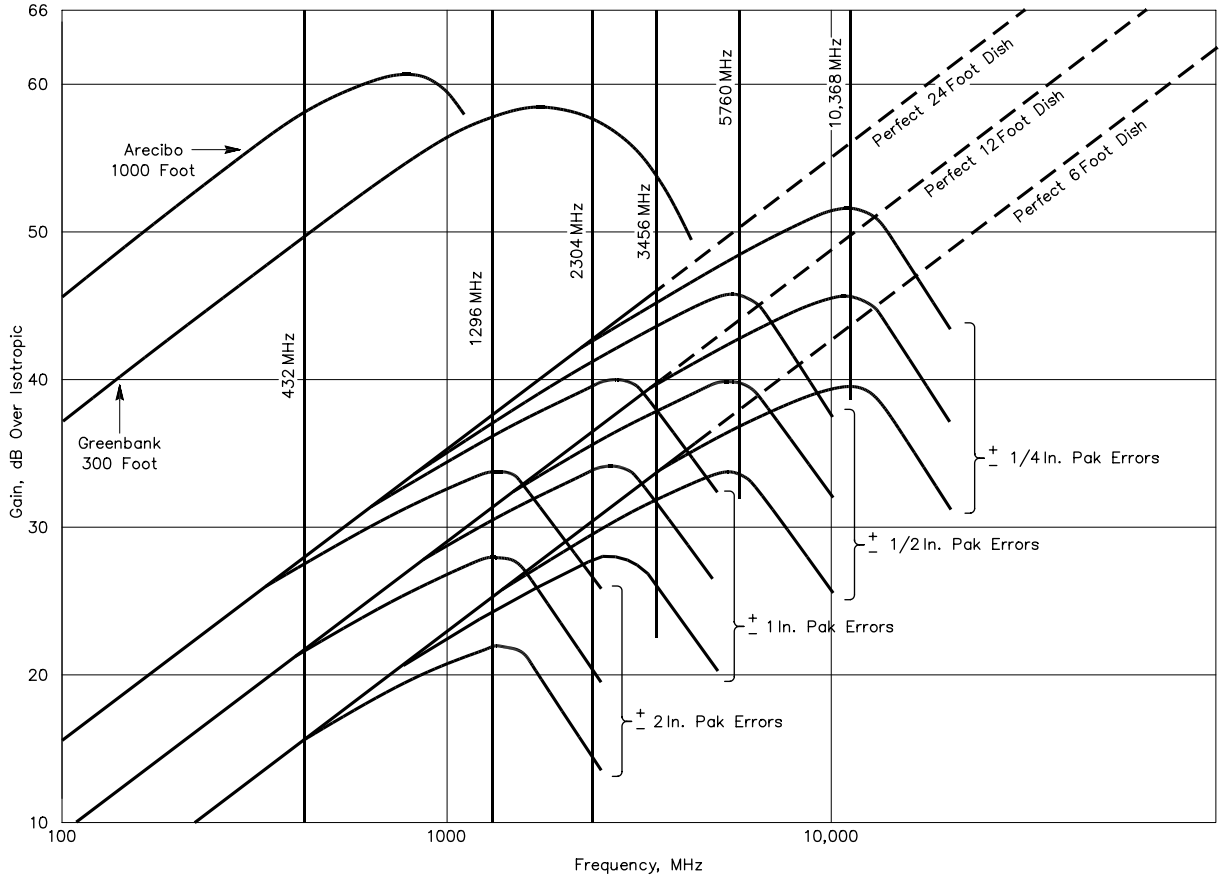

Fig 84—Parabolic-antenna gain versus size, frequency and surface errors. All curves assume 60% aperture efficiency and 10-dB power taper. Graph by K2RIW for ham bands, using display technique of J. Ruze, British IEE.

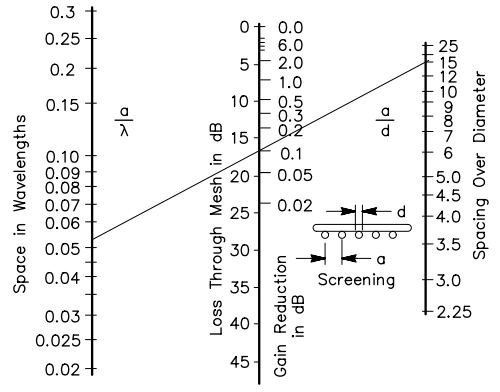

Fig 85—Surfacing material quality.

A Parabolic Template

At and above 2300 MHz (where high surface accuracy is required), a parabolic template should be constructed to measure surface errors. A simple template may be constructed (see **Fig 86**) by taking a 12-foot 3-inch length of 4-foot wide tar paper and drawing a parabolic shape on it with chalk. The points for the parabolic shape are calculated at 6-inch intervals and these points are connected with a smooth curve. For those who wish to use the template with the surface material installed, the template should be cut along the chalk line and stiffened by cardboard or a wood lattice frame. Surface error measurements should take place with all spokes installed and deflected by the fishing lines, as some bending of the center plates does take place. **Fig 87** shows the 12-foot stressed dish built by Franco Marcelo, N2UO.

Variations

All the possibilities of the stressed parabolic antenna have not been explored. For instance, a set of fishing lines or guy wires can be set up behind the dish for error correction, as long as this does not cause permanent bending of the aluminum spokes. This technique also protects the dish against wind loading from the rear. An extended piece of TV mast is an ideal place to hang a counterweight and attach the rear guys. This strengthens the structure considerably.

EME USING SURPLUS TVRO DISH ANTENNAS

Since the 1990s, there has been a significant change

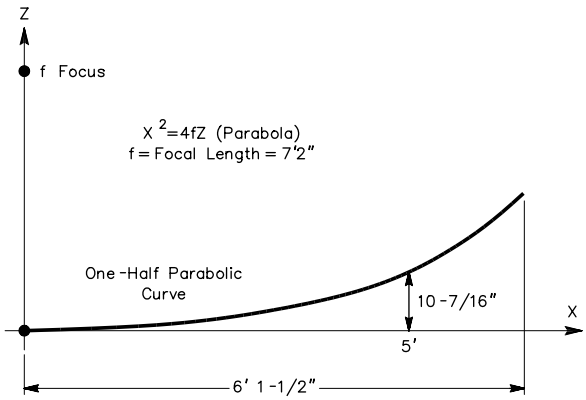

X	Z	(to Nearest 1/16")	X	Z
0.5'	1/8"		3.5'	5-1/8"
1.0'	7/16"		4.0'	6-11/16"
1.5'	15/16"		4.5'	8-1/2"
2.0'	1-11/16"		5.0'	10-7/16"
2.5'	2-5/8"		5.5'	12-11/16"
3.0'	3-3/4"		6.0'	15-1/16"

Fig 86—Parabolic template for 12-foot, 3-inch dish.

Fig 87—N2UO's homemade 12-foot stressed dish. (*Photo courtesy N2UO.*)

in the systems people use to watch satellite TV broadcasts. Formerly, C-band satellite receivers were used, along with parabolic dish antennas in the 3- to 5-meter diameter range. Now, Ku-band (12-GHz) receivers are the norm, with their associated small (usually 18-inch) dish antennas. This has provided a large body of surplus C-band dishes, which can be used for EME—certainly on the bands at 33 cm and above, and for the larger dishes (5 meters), even at 70 cm. Many times, these dishes and their mounts can be had for the asking, so they truly become an inexpensive way to build a multi-band EME antenna.

This updated article, first presented by David Hallidy, K2DH (ex-KD5RO) in the ARRL *UHF/Microwave Projects Manual*, describes the use of a 3-meter (10-foot) TVRO antenna in such an application. (Also see earlier in this chapter the section describing converted C-Band TVRO Dishes for satellite work.)

Background

Calculations show that a 3-meter dish will have about 30 dBi gain at 1296 MHz. With a state-of-the-art LNA (Low-Noise Amplifier or preamp) at the feed, an efficient feed horn illuminating the dish surface, and 200 W at 1296 MHz, lunar echoes should be easily detected and many stations can be worked. The biggest challenges to such a system are assembling the dish to its mount and steering it to track the Moon. As much as possible, the KISS ("Keep It Simple, Stupid") principle was used to accomplish this task.

In 1987, WA5TNY, KD5RO, KA5JPD, and W7CNK proved that such an EME system could work, even as high as 3.4 and 5.7 GHz, to provide the first EME contacts on those bands. An additional advantage to this (or any) small dish is its ability to be mounted to a trailer and taken out on EME expeditions. It can also be easily disassembled and stored, if necessary.

As can be seen from **Fig 88**, the entire setup is very simple, using a standard amateur tower as the main support for the dish.

Azimuth Drive

In azimuth, direct drive of the main rotating shaft was selected, and a small prop-pitch motor was used. These motors, while not as plentiful as they were some years ago, still turn up with some regularity at flea markets for very little money. The beauty of the prop-pitch motor is that it turns slowly, is reversible, provides very high torque, and requires no braking system (the gear reduction, on the order of 4000:1, provides the necessary braking). Prop-pitch motors are dc motors, and were designed to vary the pitch of propeller blades at start-up, take-off and landing of older large airplanes. Thus, they can be run at different speeds merely by varying the dc voltage to the motor, and can be reversed by reversing the polarity of the dc voltage. By mounting a thrust bearing of the appropriate size at the top of the tower, and mounting the motor directly below it at the end of the rotating shaft that turns the antenna, a simple direct-drive system can be constructed.

The dc power supply and control relays are located in a weatherproof box on the side of the tower, next to the motor. This system requires only 9 V dc at about 5 A to adequately start, turn and stop the prop-pitch motor, and this voltage turns the antenna through 360° of rotation in about $2^1/_2$ minutes. Azimuth position sensing is also a simple task. See **Fig 89**. A linear multi-turn potentiometer is driven by the rotating shaft, using a simple friction drive.

A strip of rubber is attached to the rotating shaft and a wheel is connected to the shaft of the pot. The pot is then mounted so that it presses against the rubber strip, and as the shaft turns so does the pot. If a ten-turn pot is used, and the system is aligned such that the pot is at the center of its rotation when the antenna is pointed approximately south, the pot will not rotate past the end at either extreme of the antenna's rotation (CW/CCW north), and absolute alignment is a simple task of calibrating the change in resistance (change in voltage, when the pot is fed from a constant voltage source) with degrees of rotation (see the discussion on Position Readout for details).

Elevation Drive

The elevation drive is also very simple. Most (nearly all) TVRO setups have a means of moving the dish across the sky to align it with various satellites. To do this, most companies use a device called a *Linear Actuator*. This is a dc motor to which is attached a long lead screw that pulls (or pushes) the outer shell of the actuator in or out to make it longer or shorter. The movable end of the actuator is attached to the dish and the motor end is fixed to the mount. The dish rests on pivots, which allow it to move as the actuator extends/retracts. To convert this type of mount (called a *Polar Mount*) to an Az/El mount is usually very simple.

Fig 90 shows how this can be done. Simply breaking the welds that held the mount in a polar fashion allows the mount to be turned on its side and used to pivot the dish vertically with the linear actuator. Another feature of linear actuators is that they also have some means of feeding their relative position to the satellite receiver. This is usually just a multi-turn potentiometer geared to the lead screw. All we have to do is connect this pot to a readout system, and we can calibrate the lift of the actuator in degrees. We thus have a simple means of rotating the dish and elevating it—but how do we know that it's pointed at the Moon?

Position Readout

Readout of the position of the antenna, in both azimuth and elevation is also a relatively simple task. On the

Fig 88—View of K2DH's (ex-KD5RO) complete TVRO antenna installation. (*K2DH photo.*)

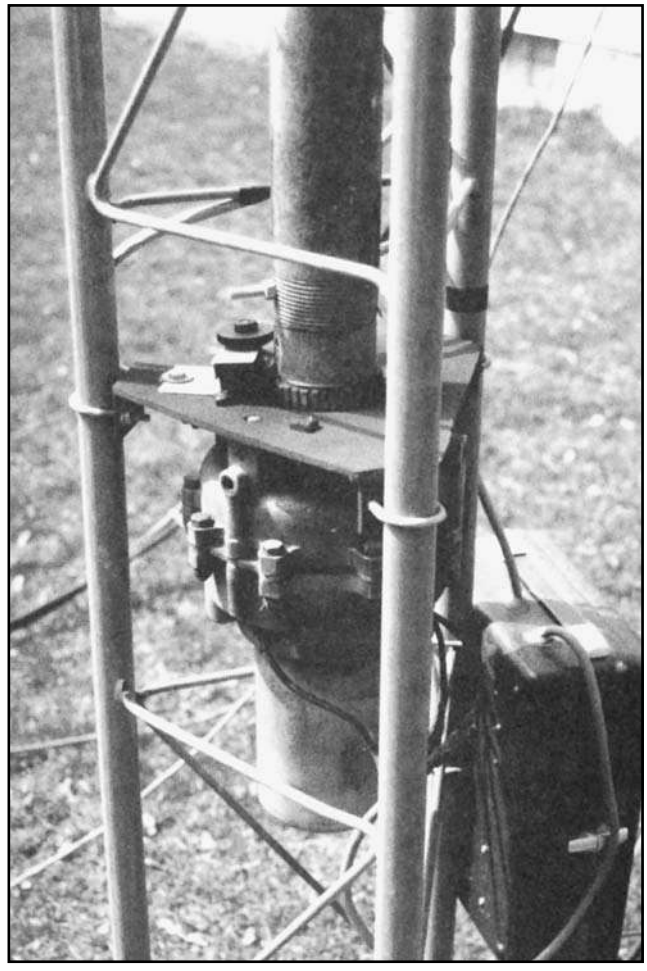

Fig 89—Azimuth rotation systems, showing prop-pitch motor and position sensor.

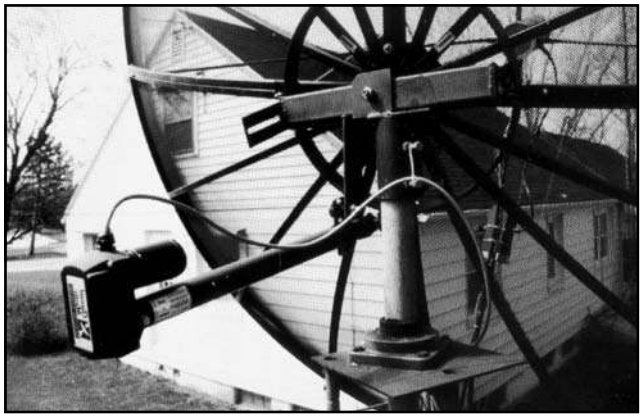

Fig 90—Elevation system, showing modified TVRO mount.

surplus market there are available Digital Volt Meters (DVMs) using LED or LCD displays that can do this job nicely, and that have more precision than is probably necessary for a dish (or Yagi array) of small size. As mentioned earlier, a multi-turn potentiometer on the elevation-drive mechanism can be used to readout elevation, and the same technique can be used for azimuth readout—a potentiometer coupled to the main rotating shaft that turns the antenna.

When using a pot for readout, the most important thing to know is how many degrees of antenna position change occur (in Az or El) for each turn of the pot. This then can be used to calibrate a voltmeter to read volts directly as degrees—for example, 3.60 V could correspond to 360° azimuth (Clockwise North), and 9.0 V could correspond

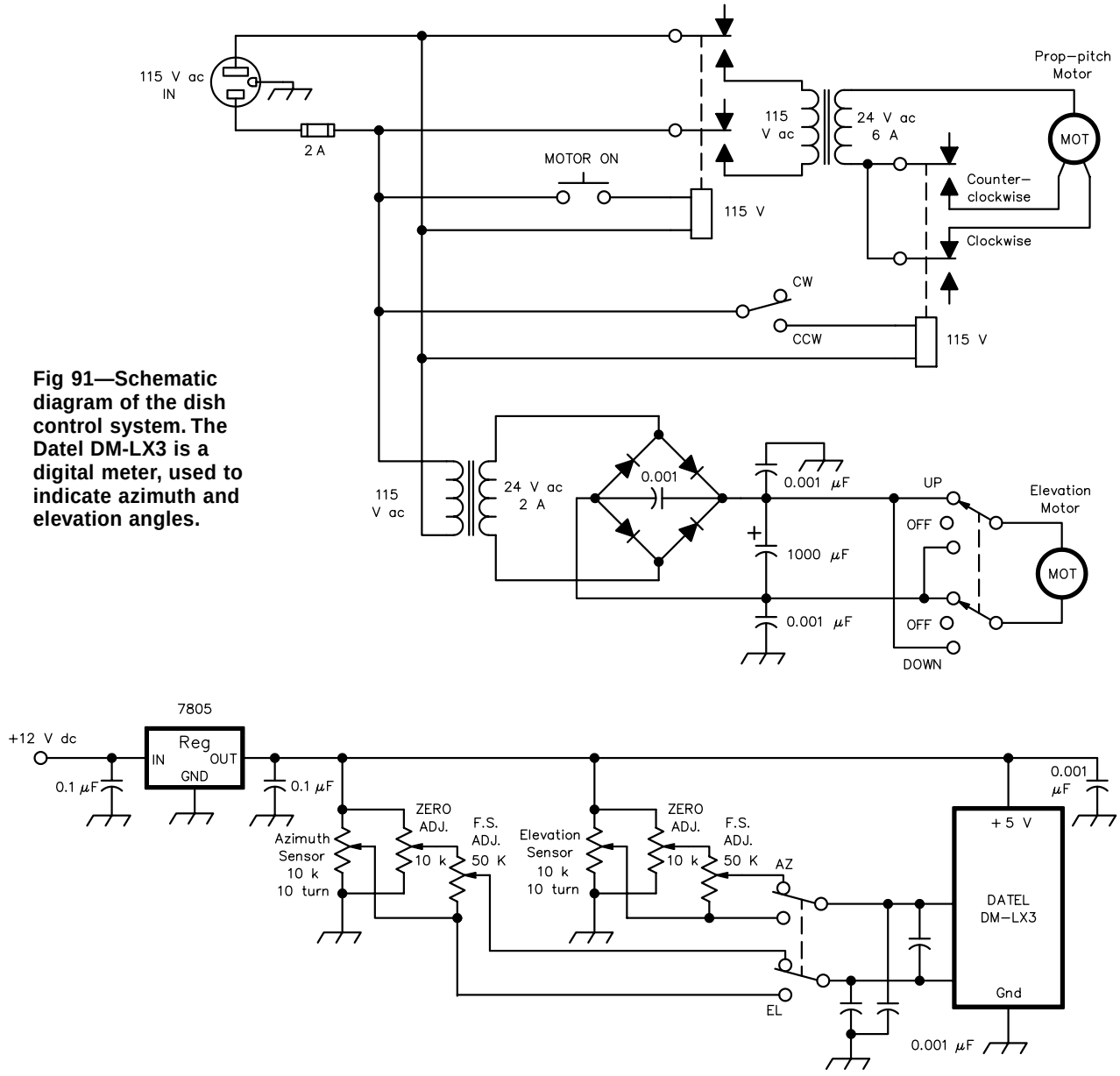

Fig 91—Schematic diagram of the dish control system. The Datel DM-LX3 is a digital meter, used to indicate azimuth and elevation angles.

to 90° elevation (straight up).

A resistance bridge circuit is best used in this application, since it is less sensitive to changes in the supply voltage. The only thing to be careful about is that the DVM must have both the positive (high) and negative (low) inputs isolated from ground (assuming the power supply used to power the DVM is grounded). You could also use a pair of small, cheap Digital Multi-Meters (DMMs), which can sometimes be found for under $10. Because they are battery powered, the isolation issue just discussed is eliminated.

Please see **Fig 91** for a complete schematic of the azimuth, elevation and readout electronics for this antenna-drive system. Also note that while this discussion is geared towards the use of a small dish, the same positioning and readout systems could be used in a Yagi array for 2 meters or 70 cm.

Now that we know where the dish is pointed, how do we know where the Moon is? There are several software programs available to the Amateur for tracking celestial bodies such as the Moon, the Sun, certain stars (usable as noise sources), and even Amateur Satellites. Programs by W9IP, VK3UM, F1EHN and others can be obtained very reasonably and these work well to provide highly accurate position information for tracking.

Feeding the Surplus TVRO Dish

An area that needs particular attention when attempting EME with a small dish is an efficient feed system. An efficient feed system can be a real challenge with TVRO dishes, because many are "deep"—that is, their f/D (focal length to Diameter ratio) is small.

The satellite TV industry used deep dishes because they tend to be quieter, picking up less Earth noise due to spillover effects. A deep dish has a short focal length, and therefore, the feed is relatively close to the surface of the dish. To properly illuminate the reflector out to its edges, a feed horn of relatively wide beamwidth must be used. The feeds designed several years ago by Barry Malowanchuk, VE4MA, are intended for use with just such dishes, and have the advantage of being adjustable to optimize their pattern to the dish in use.

The feed that was used with this dish was modeled after VE4MA's 1296-MHz feed, and a version was even scaled for use at 2304 MHz that worked as well as the original. See **Fig 92** and also see the Notes and References section at the end of this chapter. (Also see the earlier section in the satellite portion of this chapter describing patch feeds for small dishes.)

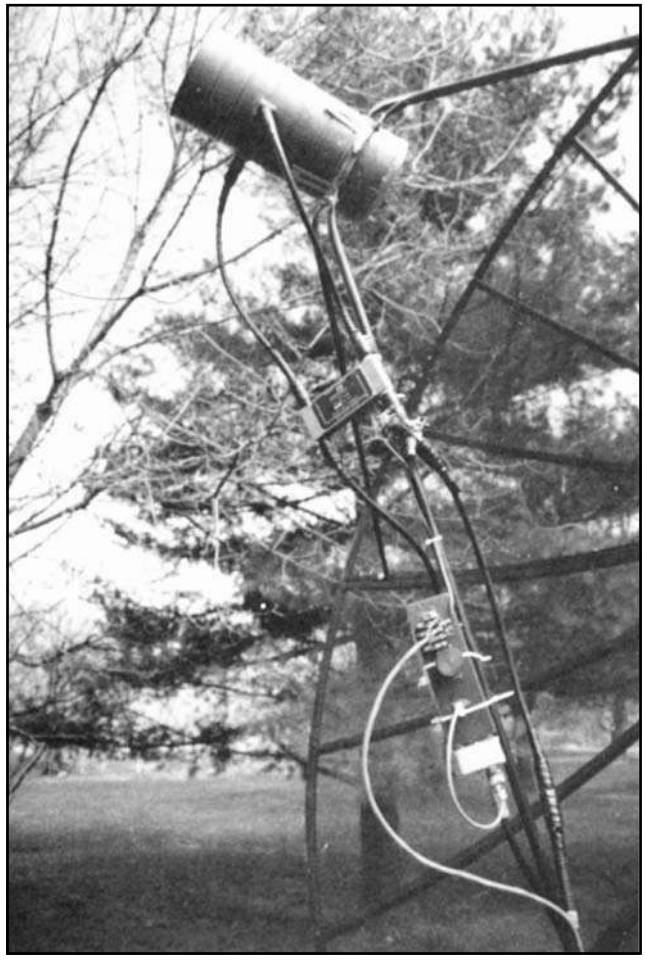

Fig 92—View of feed, showing coffee-can feed horn and hybrid coupler.

SHF EME CHALLENGES

The challenges met when successfully building a station for EME at 900 MHz to 5.7 GHz only become more significant on the SHF bands at 10 GHz and above. Absolute attention to detail is the primary requirement, and this extends to every aspect of the EME antenna system. The dish surface is probably the most difficult problem to solve. As was discussed earlier in this chapter, the shape and accuracy of the reflector contribute directly to the overall gain of the antenna.

But where slight errors in construction can be tolerated at the lower frequencies, the same cannot be said at millimetric wavelengths. Those who have attempted EME on 10 and 24 GHz have discovered that the weight of the dish reflector itself will distort its shape enough to lower the gain to the point where echoes are degraded. Stiffening structures at the back of such dishes are often found necessary. **Fig 93** illustrates the back struts added by Al Ward, W5LUA, to strengthen his dish.

Pointing accuracy is also paramount—a 16-foot dish at 10 GHz has a beamwidth about equal to the diameter of the Moon—0.5°. This means that the echo degradation due to the Moon's movement away from where the dish is pointed is almost immediate, and autotracking systems become more of a necessity than a luxury. At these frequencies, most amateurs actually peak their antennas on

Fig 93—Strengthening struts W5LUA added to the back of his dish to hold down distortion. (*Photo courtesy W5LUA.*)

Moon Noise—the black-body Radiation from the Moon that becomes the dominant source of noise in space.

At these frequencies, the elevation of the Moon above the horizon also plays a role in the ability to communicate, since tropospheric absorption due to water vapor is greatest at low elevation angles (the signal must pass through a greater portion of the troposphere than when the Moon is highly elevated). It is beyond the abilities of most Amateurs to construct their own dishes for these frequencies, so surplus dishes for Ku-band satellite TV (typically 3 meters in diameter) are usually employed, as have high-performance dishes designed for millimetric radar and point-to-point communications at 23 and 38 GHz.

NOTES AND REFERENCES, EME ANTENNAS

W. Allen, "A Mode J Helix," *AMSAT Newsletter*, Jun 1979, pp 30-31.

D. J. Angelakos and D. Kajfez, "Modifications on the Axial-Mode Helical Antenna," *Proc. IEEE*, Apr 1967, pp 558-559.

A. L. Bridges, "Really Zap OSCAR With this Helical Antenna," *73*, in three parts, Jul, Aug and Sep 1975.

K. R. Carver, "The Helicone—A Circularly Polarized Antenna with Low Sidelobe Level," *Proc. IEEE*, Apr 1967, p 559.

M. R. Davidoff, "A Simple 146-MHz Antenna for Oscar Ground Stations," *QST*, Sep 1974, pp 11-13.

M. R. Davidoff, *The Radio Amateur's Satellite Handbook* (Newington: ARRL, 1998-2000).

D. DeMaw, "The Basic Helical Beam," *QST*, Nov 1965, pp 20-25, 170.

D. Evans and G. Jessop, *VHF-UHF Manual, 3rd ed.* (London: RSGB), 1976.

N. Foot, "WA9HUV 12-Foot Dish for 432 and 1296 MHz," The World Above 50 Mc., *QST*, Jun 1971, pp 98-101, 107.

N. Foot, "Cylindrical Feed horn for Parabolic Reflectors," *Ham Radio*, May 1976.

O. J. Glasser and J. D. Kraus, "Measured Impedances of Helical Beam Antennas," *Journal of Applied Physics*, Feb 1948, pp 193-197.

D. Hallidy, "Microwave EME Using A Ten-Foot TVRO Antenna," *The ARRL UHF/Microwave Projects Manual*, 1994 pp 10-9 to 10-13.

G. R. Isely and W. G. Smith, "A Helical Antenna for Space Shuttle Communications," *QST*, Dec 1984, pp 14-18.

H. Jasik, *Antenna Engineering Handbook*, 1st ed. (New York: McGraw-Hill, 1961).

R. T. Knadle, "A Twelve-Foot Stressed Parabolic Dish," *QST*, Aug 1972, pp 16-22.

J. D. Kraus, "Helical Beam Antenna," *Electronics*, Apr 1947, pp 109-111.

J. D. Kraus and J. C. Williamson, "Characteristics of Helical Antennas Radiating in the Axial Mode," *Journal of Applied Physics*, Jan 1948, pp 87-96.

J. D. Kraus, "Helical Beam Antenna for Wide Band Applications," *Proc of the IRE*, Oct 1948, pp 1236-1242.

J. D. Kraus, *Antennas* (New York: McGraw-Hill Book Co., 1950).

J. D. Kraus, "A 50-Ohm Input Impedance for Helical Beam Antenna," *IEEE Transactions on Antennas and Propagation*, Nov 1977, p 913.

J. D. Kraus, *Big Ear* (Powell, OH: Cygnus-Quasar Books, 1976).

T. S. M. MacLean, "Measurements on High-Gain Helical Aerial and on Helicals of Triangular Section," *Proc. of IEE* (London), Jul 1964, pp 1267-1270.

D. M. Mallozzi, "The Tailored Helical," *AMSAT Newsletter*, Mar 1978, pp 8-9.

B. Malowanchuk, "Use of Small TVRO Dishes for EME," *Proceedings of the 21st Conference of The Central States VHF Society*, 1987 pp 68-77.

B. Malowanchuk, "Selection of An Optimum Dish Feed," *Proceedings of the 23rd Conference of The Central States VHF Society*, 1989 pp 35-43.

M. W. Maxwell, *Reflections—Transmission Lines and Antennas* (Newington, CT: ARRL, 1990) [out of print].

T. Moreno, *Microwave Transmission Design Data* (New York: McGraw-Hill, 1948).

K. Nose, "Crossed Yagi Antennas for Circular Polarization," *QST*, Jan 1973, pp 11-12.

K. Nose, "A Simple Az-El Antenna System for Oscar," *QST*, Jun 1973, pp 11-12.

S. Powlishen, K1FO, "432-MHz EME 1990s Style," Parts 1 and 2, *Communications Quarterly*, Oct 1990, pp 29-39; Oct 1991, pp 33-48.

S. Powlishen, K1FO, "Rear-Mount Yagi Arrays for 432-MHz EME: Solving the EME Polarization Problem," *The ARRL Antenna Compendium, Vol 3* (Newington:

ARRL, 1992), pp 79-98.
C. Richards, "The 10 Turn Chopstick Helical (Mk2) for OSCAR 10 432 MHz Uplink," *Radio Communication*, Oct 1984, pp 844-845.
S. Sander and D. K. Cheng, "Phase Center of Helical Beam Antennas," *IRE National Convention Record Part 6*, 1958, pp 152-157.
E. A. Scott and H. E. Banta, "Using the Helical Antenna at 1215 Mc.," *QST*, Jul 1962, pp 14-16.
R. Soifer, W2RS, "More 'QRP' EME on 144 MHz," *QST*, Oct 1990, pp 36-38.
G. Southworth, *Principles and Applications of Waveguide Transmission* (New York: D. Van Nostrand Co., 1950).
B. Sykes, "Circular Polarization and Crossed-Yagi Antennas," Technical Topics, *Radio Communication*, Feb 1985, p 114.
H. E. Taylor and D. Fowler, "A V-H-F Helical Beam Antenna," *CQ*, Apr 1949, pp 13-16.
G. Tillitson, "The Polarization Diplexer—A Polaplexer," *Ham Radio*, Mar 1977.
P. P. Viezbicke, "Yagi Antenna Design," *NBS Technical Note 688* (U. S. Dept. of Commerce/National Bureau of Standards, Boulder, CO), Dec 1976.
D. Vilardi, "Easily Constructed Antennas for 1296 MHz," *QST*, Jun 1969.
D. Vilardi, "Simple and Efficient Feed for Parabolic Antennas," *QST*, Mar 1973.
J. L. Wong and H. E. King, "Broadband Quasi-Tapered Helical Antenna," *IEEE Transactions on Antennas and Propagation*, Jan 1979, pp 72-78.

Chapter 20

Antenna Materials and Accessories

This chapter contains information on materials amateurs use to construct antennas—what types of material to look for in a particular application, tips on working with and using various materials. Chapter 21 contains information on where to purchase these materials.

Basically, antennas for MF, HF, VHF and the lower UHF range consist simply of one or more conductors that radiate (or receive) electromagnetic waves. However, an antenna system must also include some means to support those conductors and maintain their relative positions—the boom for a Yagi antenna and the halyards for a wire dipole, for example. In this chapter we'll look at materials for those applications, too. Structural supports such as towers, masts, poles, etc. are discussed in Chapter 22.

There are two main types of material used for antenna conductors, wire and tubing. Wire antennas are generally simple and therefore easier to construct, although some arrays of wire elements can become rather complex. When tubing is required, aluminum tubing is used most often because of its light weight. Aluminum tubing is discussed in a subsequent section of this chapter.

Wire Antennas

Although wire antennas are relatively simple, they can constitute a potential hazard unless properly constructed. Antennas should never be run under or over public utility (telephone or power) lines. Several amateurs have lost their lives by failing to observe this precaution.

The National Electric Code® of the National Fire Protection Association contains a section on amateur stations in which a number of recommendations are made concerning minimum size of antenna wire and the manner of bringing the transmission line into the station. Chapter 1 contains more information about this code. The code in itself does not have the force of law, but it is frequently made a part of local building regulations, which are enforceable. The provisions of the code may also be written into, or referred to, in fire and liability insurance documents.

The RF resistance of copper wire increases as the size of the wire decreases. However, in most types of antennas that are commonly constructed of wire (even quite small wire), the radiation resistance will be much higher than the RF resistance, and the efficiency of the antenna will still be adequate. Wire sizes as small as #30, or even smaller, have been used quite successfully in the construction of "invisible" antennas in areas where more conventional antennas cannot be erected. In most cases, the selection of wire for an antenna will be based primarily on the physical properties of the wire, since the suspension of wire from elevated supports places a strain on the wire.

WIRE TYPES

Wire having an enamel coating is preferable to bare wire, since the coating resists oxidation and corrosion. Several types of wire having this type of coating are available, depending on the strength needed. "Soft-drawn" or annealed copper wire is easiest to handle; unfortunately, it stretches considerably under stress. Soft-drawn wire should be avoided, except for applications where the wire will be under little or no tension, or where some change in length can be tolerated. (For example, the length of a horizontal antenna fed at the center with open-wire line is not critical, although a change in length may require some readjustment of coupling to the transmitter.)

"Hard-drawn" copper wire or copper-clad steel wire

(also known as Copperweld™) is harder to handle, because it has a tendency to spiral when it is unrolled. These types of wire are ideal for applications where significant stretch cannot be tolerated. Care should be exercised in using this wire to make sure that kinks do not develop—the wire will have a far greater tendency to break at a kink. After the coil has been unwound, suspend the wire a few feet above ground for a day or two before using it. The wire should not be recoiled before it is installed.

Several factors influence the choice of wire type and size. Most important to consider are the length of the unsupported span, the amount of sag that can be tolerated, the stability of the supports under wind pressure, and whether or not an unsupported transmission line is to be suspended from the span. **Table 1** shows the wire diam, current-carrying capacity and resistance of various sizes of copper wire. **Table 2** shows the maximum rated working tensions of hard-drawn and copper-clad steel wire of various sizes. These two tables can be used to select the appropriate wire size for an antenna.

Table 1
Copper-Wire Table

Wire Size AWG (B&S)	*Dia in Mils*[1]	*Dia in mm*	*Turns per Linear Inch Enamel*	*Feet per Pound Bare*	*Ohms per 1000 ft 25°C*	*Cont.-duty current*[2] *Single Wire in Open Air*
1	289.3	7.348	—	3.947	0.1264	—
2	257.6	6.544	—	4.977	0.1593	—
3	229.4	5.827	—	6.276	0.2009	—
4	204.3	5.189	—	7.914	0.2533	—
5	181.9	4.621	—	9.980	0.3195	—
6	162.0	4.115	—	12.58	0.4028	—
7	144.3	3.665	—	15.87	0.5080	—
8	128.5	3.264	7.6	20.01	0.6405	73
9	114.4	2.906	8.6	25.23	0.8077	—
10	101.9	2.588	9.6	31.82	1.018	55
11	90.7	2.305	10.7	40.12	1.284	—
12	80.8	2.053	12.0	50.59	1.619	41
13	72.0	1.828	13.5	63.80	2.042	—
14	64.1	1.628	15.0	80.44	2.575	32
15	57.1	1.450	16.8	101.4	3.247	—
16	50.8	1.291	18.9	127.9	4.094	22
17	45.3	1.150	21.2	161.3	5.163	—
18	40.3	1.024	23.6	203.4	6.510	16
19	35.9	0.912	26.4	256.5	8.210	—
20	32.0	0.812	29.4	323.4	10.35	11
21	28.5	0.723	33.1	407.8	13.05	—
22	25.3	0.644	37.0	514.2	16.46	—
23	22.6	0.573	41.3	648.4	20.76	—
24	20.1	0.511	46.3	817.7	26.17	—
25	17.9	0.455	51.7	1031	33.00	—
26	15.9	0.405	58.0	1300	41.62	—
27	14.2	0.361	64.9	1639	52.48	—
28	12.6	0.321	72.7	2067	66.17	—
29	11.3	0.286	81.6	2607	83.44	—
30	10.0	0.255	90.5	3287	105.2	—
31	8.9	0.227	101	4145	132.7	—
32	8.0	0.202	113	5227	167.3	—
33	7.1	0.180	127	6591	211.0	—
34	6.3	0.160	143	8310	266.0	—
35	5.6	0.143	158	10480	335	—
36	5.0	0.127	175	13210	423	—
37	4.5	0.113	198	16660	533	—
38	4.0	0.101	224	21010	673	—
39	3.5	0.090	248	26500	848	—
40	3.1	0.080	282	33410	1070	—

[1]A mil is 0.001 inch.
[2]Max wire temp of 212° F and max ambient temp of 135° F.

Table 2
Stressed Antenna Wire

American Wire Gauge	***Recommended Tension[1] (pounds)***		***Weight (pounds per 1000 feet)***	
	Copper-clad steel[2]	*Hard-drawn copper*	*Copper-clad steel[2]*	*Hard-drawn copper*
4	495	214	115.8	126.0
6	310	130	72.9	79.5
8	195	84	45.5	50.0
10	120	52	28.8	31.4
12	75	32	18.1	19.8
14	50	20	11.4	12.4
16	31	13	7.1	7.8
18	19	8	4.5	4.9
20	12	5	2.8	3.1

[1]Approximately one-tenth the breaking load. Might be increased 50% if end supports are firm and there is no danger of ice loading.
[2]Copperweld,™ 40% copper.

Wire Tension

If the tension on a wire can be adjusted to a known value, the expected sag of the wire (**Fig 1**) may be determined before installation using Table 2 and the nomograph of **Fig 2**. Even though there may be no convenient method to determine the tension in pounds, calculation of the expected sag for practicable working tensions is often desirable. If the calculated sag is greater than allowable it may be reduced by any one or a combination of the following:

1) Providing additional supports, thereby decreasing the span
2) Increasing the tension in the wire if less than recommended
3) Decreasing the size of the wire

Instructions for Using the Nomograph

1) From Table 2, find the weight (pounds/1000 feet) for the particular wire size and material to be used.
2) Draw a line from the value obtained above, plotted on the weight axis, to the desired span (feet) on the span axis, Fig 2. Note in Fig 1 that the span is one half the distance between the supports.
3) Choose an operating tension level (in pounds) consistent with the values presented in Table 2 (preferably less than the recommended wire tension).
4) Draw a line from the tension value chosen (plotted on the tension axis) through the point where the work axis crosses the original line constructed in step 2, and continue this new line to the sag axis.
5) Read the sag in feet on the sag axis.

Example:

Weight = 11 pounds/1000 feet
Span = 210 feet
Tension = 50 pounds
Answer: Sag = 4.7 feet

These calculations do not take into account the weight of a feed line supported by the antenna wire.

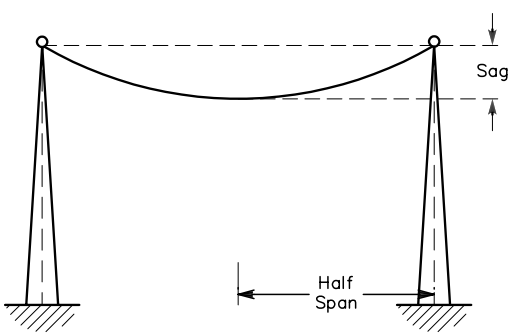

Fig 1—The half span and sag of a long-wire antenna.

Wire Splicing

Wire antennas should preferably be made with unbroken lengths of wire. In instances where this is not feasible, wire sections should be spliced as shown in **Fig 3**. The enamel insulation should be removed for a distance of about 6 inches from the end of each section by scraping with a knife or rubbing with sandpaper until the copper underneath is bright. The turns of wire should be brought up tight around the standing part of the wire by twisting with broad-nose pliers.

The crevices formed by the wire should be completely filled with rosin-core solder. An ordinary soldering iron or gun may not provide sufficient heat to melt solder outdoors; a propane torch is desirable. The joint should be heated sufficiently so the solder flows freely into the joint when the source of heat is removed momentarily. After the joint has cooled completely, it should be wiped clean with a cloth, and then sprayed generously with acrylic to prevent corrosion.

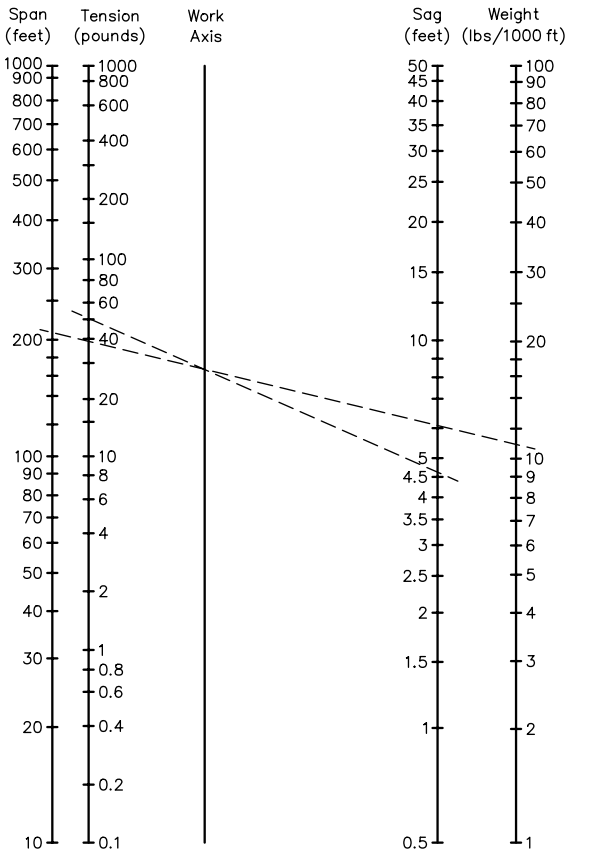

Fig 2—Nomograph for determining wire sag. (John Elengo, Jr, K1AFR)

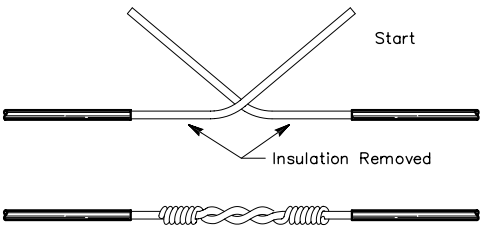

Fig 3—Correct method of splicing antenna wire. Solder should be flowed into the wraps after the connection is completed. After cooling, the joint should be sprayed with acrylic to prevent oxidation and corrosion.

ANTENNA INSULATION

To prevent loss of RF power, the antenna should be well insulated from ground, unless of course it is a shunt-fed system. This is particularly important at the outer end or ends of wire antennas, since these points are always at a comparatively high RF potential. If an antenna is to be installed indoors (in an attic, for instance) the antenna may be suspended directly from the wood rafters without additional insulation, if the wood is permanently dry. Much greater care should be given to the selection of proper insulators when the antenna is located outside where it is exposed to wet weather.

Insulator Leakage

Antenna insulators should be made of material that will not absorb moisture. The best insulators for antenna use are made of glass or glazed porcelain. Depending on the type of material, plastic insulators may be suitable. The length of an insulator relative to its surface area is indicative of its comparative insulating ability. A long thin insulator will have less leakage than a short thick insulator. Some antenna insulators are deeply ribbed to increase the surface leakage path without increasing the physical length of the insulator. Shorter insulators can be used at low-potential points, such as at the center of a dipole. If such an antenna is to be fed with open-wire line and used on several bands, however, the center insulator should be the same as those used at the ends, because high RF potential may exist across the center insulator on some bands.

Insulator Stress

As with the antenna wire, the insulator must have sufficient physical strength to support the stress of the antenna without danger of breakage. Long elastic bands or lengths of nylon fishing line provide long leakage paths and make satisfactory insulators within their limits to resist mechanical strain. They are often used in antennas of the "invisible" type mentioned earlier.

For low-power work with short antennas not subject to appreciable stress, almost any small glass or glazed-porcelain insulator will do. Homemade insulators of Lucite rod or sheet will also be satisfactory. More care is required in the selection of insulators for longer spans and higher transmitter power.

For a given material, the breaking tension of an insulator will be proportional to its cross-sectional area. It should be remembered, however, that the wire hole at the end of the insulator decreases the effective cross-sectional area. For this reason, insulators designed to carry heavy strains are fitted with heavy metal end caps, the eyes being formed in the metal cap, rather than in the insulating material itself. The following stress ratings of antenna insulators are typical:

$^5/_8$ in. square by 4 in. long—400 lb
1 in. diameter by 7 or 12 in. long—800 lb
$1^1/_2$ in. diameter by 8, 12 or 20 in. long, with special metal end caps—5000 lb

These are rated breaking tensions. The actual working tensions should be limited to not more than 25% of the breaking rating.

The antenna wire should be attached to the insulators as shown in **Fig 4**. Care should be taken to avoid sharp angular bends in the wire when it is looped through the insulator eye. The loop should be generous enough in size that it will not bind the end of the insulator tightly. If the

length of the antenna is critical, the length should be measured to the outward end of the loop, where it passes through the eye of the insulator. The soldering should be done as described earlier for the wire splice.

Strain Insulators

Strain insulators have their holes at right angles, since they are designed to be connected as shown in **Fig 5**. It can be seen that this arrangement places the insulating material under compression, rather than tension. An insulator connected this way can withstand much greater stress. Furthermore, the wire will not collapse if the insulator breaks, since the two wire loops are inter-locked. Because the wire is wrapped around the insulator, however, the leakage path is reduced drastically, and the capacitance between the wire loops provides an additional leakage path. For this reason, the use of the strain insulator is usually confined to such applications as breaking up resonances in guy wires, where high levels of stress prevail, and where the RF insulation is of less importance. Such insulators might be suitable for use at low-potential points on an antenna, such as at the center of a dipole. These insulators may also be fastened in the conventional manner if the wire will not be under sufficient tension to break out the eyes.

Insulators for Ribbon-Line Antennas

Fig 6A shows the sketch of an insulator designed to be used at the ends of a folded dipole or a multiple dipole made of ribbon line. It should be made approximately as shown, out of Lucite or bakelite material about 1/4 inch thick. The advantage of this arrangement is that the strain of the antenna is shared by the conductors and the plastic webbing of the ribbon, which adds considerable strength. After soldering, the screw should be sprayed with acrylic.

Fig 6B shows a similar arrangement for suspending one dipole from another in a stagger-tuned dipole system. If better insulation is desired, these insulators can be wired to a conventional insulator.

PULLEYS AND HALYARDS

Pulleys and halyards commonly used to raise and lower a wire antenna must also be capable of taking the

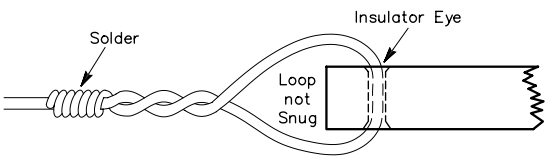

Fig 4—When fastening antenna wire to an insulator, do not make the wire loop too snug. After the connection is complete, flow solder into the turns. Then when the joint has cooled completely, spray it with acrylic.

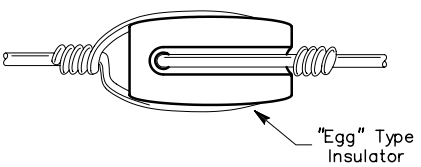

Fig 5—Conventional manner of fastening wire to a strain insulator. This method decreases the leakage path and increases capacitance, as discussed in the text.

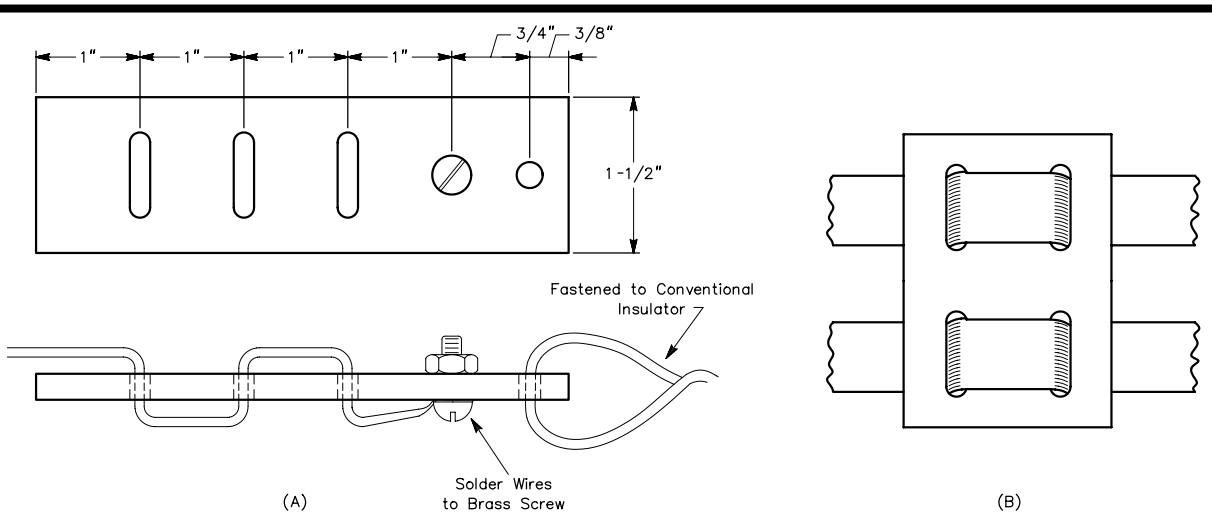

Fig 6—At A, an insulator for the ends of folded dipoles, or multiple dipoles made of 300-ohm ribbon. At B, a method of suspending one ribbon dipole from another in a multiband dipole system.

same strain as the antenna wire and insulators. Unfortunately, little specific information on the stress ratings of most pulleys is available. Several types of pulleys are readily available at almost any hardware store. Among these are small galvanized pulleys designed for awnings and several styles and sizes of clothesline pulleys. Heavier and stronger pulleys are those used in marine work. The factors that determine how much stress a pulley will handle include the diameter of the shaft, how securely the shaft is fitted into the sheath and the size and material of the frame.

Another important factor to be considered in the selection of a pulley is its ability to resist corrosion. Galvanized awning pulleys are probably the most susceptible to corrosion. While the frame or sheath usually stands up well, these pulleys usually fail at the shaft. The shaft rusts out, allowing the grooved wheel to break away under tension.

Most good-quality clothesline pulleys are made of alloys which do not corrode readily. Since they are designed to carry at least 50 feet of line loaded with wet clothing in stiff winds, they should be adequate for normal spans of 100 to 150 feet between stable supports. One type of clothesline pulley has a 4-inch diameter plastic wheel with a ¼-inch shaft running in bronze bearings. The sheath is made of cast or forged corrosion-proof alloy. Some look-alike low-cost pulleys of this type have an aluminum shaft with no bearings. For antenna work, these cheap pulleys are of little long-term value.

Marine pulleys have good weather-resisting qualities, since they are usually made of bronze, but they are comparatively expensive and are not designed to carry heavy loads. For extremely long spans, the wood-sheathed pulleys used in "block and tackle" devices and for sail hoisting should work well.

Table 3
Approximate Safe Working Tension for Various Halyard Materials

Material	*Dia, In.*	*Tension, Lb*
Manila hemp rope	1/4	120
	3/8	270
	1/2	530
	5/8	800
Polypropylene rope	1/4	270
	3/8	530
	1/2	840
Nylon rope	1/4	300
	3/8	660
	1/2	1140
7×11 galvanized sash cord	1/16	30
	1/8	125
	3/16	250
	1/4	450
High-strength stranded galvanized steel guy wire	1/8	400
	3/16	700
	1/4	1200
Rayon-filled plastic clothesline	7/32	60 to 70

Halyards

Table 3 shows the recommended maximum tensions for various sizes and types of line and rope suitable for hoisting halyards. Probably the best type for general amateur use for spans up to 150 or 200 feet is ¼-inch nylon rope. Nylon is somewhat more expensive than ordinary rope of the same size, but it weathers much better. Nylon also has a certain amount of elasticity to accommodate gusts of wind, and is particularly recommended for antennas using trees as supports. A disadvantage of new nylon rope is that it stretches by a significant percentage. After an installation with new rope, it will be necessary to repeatedly take up the slack created by stretching. This process will continue over a period of several weeks, at which time most of the stretching will have taken place. Even a year after installation, however, some slack may still arise from stretching.

Most types of synthetic rope are slippery, and some types of knots ordinarily used for rope will not hold well. **Fig 7** shows a knot that should hold well, even in nylon rope or plastic line.

For exceptionally long spans, stranded galvanized steel sash cord makes a suitable support. Cable advertised as "wire rope" usually does not weather well. A boat winch, sold at marinas and at Sears, is a great convenience in antenna hoisting (and usually a necessity with metal halyards).

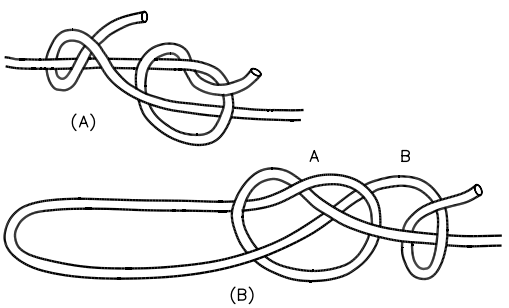

Fig 7—This is one type of knot that will hold with smooth rope, such as nylon. Shown at A, the knot for splicing two ends. B shows the use of a similar knot in forming a loop, as might be needed for attaching an insulator to a halyard. Knot A is first formed loosely 10 or 12 in. from the end of the rope; then the end is passed through the eye of the insulator and knot A. Knot B is then formed and both knots pulled tight. (Richard Carruthers, K7HDB)

Antennas of Aluminum Tubing

Aluminum is a malleable, ductile metal with a mass density of 2.70 grams per cubic centimeter. The density of aluminum is approximately 35% that of iron and 30% that of copper. Aluminum can be polished to a high brightness, and it will retain this polish in dry air. In the presence of moisture, aluminum forms an oxide coating (Al_2O_3) that protects the metal from further corrosion. Direct contact with certain metals, however (especially ferrous metals such as iron or steel), in an outdoor environment can bring about galvanic corrosion of aluminum and its alloys. Some protective coating should be applied to any point of contact between two dissimilar metals. Much of this information about aluminum and aluminum tubing was prepared by Ralph Shaw, K5CAV.

Aluminum is non-toxic; it is used in cooking utensils and to hold and cover "TV dinners" and other frozen foods, so it is certainly safe to work with. The ease with which it can be drilled or sawed makes it a pleasure to work with. Aluminum products lend themselves to many and varied applications.

Aluminum alloys can be used to build amateur antennas, as well as for towers and supports. Light weight and high conductivity make aluminum ideal for these applications. Alloying lowers the conductivity ratings, but the tensile strength can be increased by alloying aluminum with one or more metals such as manganese, silicon, copper, magnesium or zinc. Cold rolling can be employed to further increase the strength.

A four-digit system is used to identify aluminum alloys, such as 6061. Aluminum alloys starting with a 6 contain di-magnesium silicide (Mg_2Si). The second digit indicates modifications of the original alloy or impurity limits. The last two digits designate different aluminum alloys within the category indicated by the first digit.

In the 6000 series, the 6061 and 6063 alloys are a commonly used for antenna applications. Both types have good resistance to corrosion and medium strength. A further designation like T-6 denotes thermal treatment (heat tempering). More information on the available aluminum alloys can be found in **Table 4**.

Table 4

Aluminum Numbers for Amateur Use

	Common Alloy Numbers
Type	*Characteristic*
2024	Good formability, high strength
5052	Excellent surface finish, excellent corrosion resistance, normally not heat treatable for high strength
6061	Good machinability, good weldability
6063	Good machinability, good weldability
7075	Good formability, high strength
	Common Tempers
Type	*Characteristics*
T0	Special soft condition
T3	Hard
T6	Hardest, possibly brittle
TXXX	Three digit tempers—usually specialized high strength heat treatments, similar to T6
	General Uses
Type	*Uses*
2024-T3	Chassis boxes, antennas, anything that will be bent or
7075-T3	Flexed repeatedly
6061-T6	Tubing and pipe; angle channel and bar stock
6063-T832	Tubing and pipe; angle channel and bar stock

SELECTING ALUMINUM TUBING

Table 5 shows the standard sizes of aluminum tubing that are stocked by most aluminum suppliers or distributors in the United States and Canada. Note that all tubing comes in 12-foot lengths (local hardware stores sometimes stock 6- and 8-foot lengths) and larger-diameter sizes may be available in lengths up to 24 feet. Note also that any diameter tubing will fit snugly into the next larger size, if the larger size has a 0.058-inch wall thickness. For example, $^5/_8$-inch tubing has an outside diameter of 0.625 inch. This will fit into $^3/_4$-inch tubing with a 0.058-inch wall, which has an inside diameter of 0.634 inch. A clearance of 0.009 inch is just right for a slip fit or for slotting the tubing and then using hose clamps. Always get the next larger size and specify a 0.058-inch wall to obtain the 0.009-inch clearance.

A little figuring with Table 5 will give you all the information you need to build a beam, including what the antenna will weigh. The 6061-T6 type of aluminum has a relatively high strength and has good workability. It is highly resistant to corrosion and will bend without taking a "set."

SOURCES FOR ALUMINUM

Aluminum can be purchased new, and suppliers are listed in Chapter 21. But don't overlook the local metal scrap yard. The price varies, but between 35 and 60 cents per pound is typical for scrap aluminum. Some aluminum items to look for include aluminum vaulting poles, tent poles, tubing and fittings from scrapped citizen's band antennas, and aluminum angle stock. The scrap yard may even have a section or two of triangular aluminum tower.

Aluminum vaulting poles are 12 or 14 feet long and range in diameter from $1^1/_2$ to $1^3/_4$ inches. These poles are suitable for the center-element sections of large 14-MHz beams or as booms for smaller antennas. Tent poles range in length from 2½ to 4 feet. The tent poles are

Table 5

Aluminum Tubing Sizes

6061-T6 (61S-T6) Round Aluminum Tube In 12-Foot Lengths

Tubing Diameter	Wall Thickness Inches	Stubs Ga.	ID, Inches	Approximate Weight Pounds Per Foot	Pounds Per Length
3/16 in.	0.035	(#20)	0.117	0.019	0.228
	0.049	(#18)	0.089	0.025	0.330
1/4 in.	0.035	(#20)	0.180	0.027	0.324
	0.049	(#18)	0.152	0.036	0.432
	0.058	(#17)	0.134	0.041	0.492
5/16 in.	0.035	(#20)	0.242	0.036	0.432
	0.049	(#18)	0.214	0.047	0.564
	0.058	(#17)	0.196	0.055	0.660
3/8 in.	0.035	(#20)	0.305	0.043	0.516
	0.049	(#18)	0.277	0.060	0.720
	0.058	(#17)	0.259	0.068	0.816
	0.065	(#16)	0.245	0.074	0.888
7/16 in.	0.035	(#20)	0.367	0.051	0.612
	0.049	(#18)	0.339	0.070	0.840
	0.065	(#16)	0.307	0.089	1.068
1/2 in.	0.028	(#22)	0.444	0.049	0.588
	0.035	(#20)	0.430	0.059	0.708
	0.049	(#18)	0.402	0.082	0.984
	0.058	(#17)	0.384	0.095	1.040
	0.065	(#16)	0.370	0.107	1.284
5/8 in.	0.028	(#22)	0.569	0.061	0.732
	0.035	(#20)	0.555	0.075	0.900
	0.049	(#18)	0.527	0.106	1.272
	0.058	(#17)	0.509	0.121	1.452
	0.065	(#16)	0.495	0.137	1.644
3/4 in.	0.035	(#20)	0.680	0.091	1.092
	0.049	(#18)	0.652	0.125	1.500
	0.058	(#17)	0.634	0.148	1.776
	0.065	(#16)	0.620	0.160	1.920
	0.083	(#14)	0.584	0.204	2.448
7/8 in.	0.035	(#20)	0.805	0.108	1.308
	0.049	(#18)	0.777	0.151	1.810
	0.058	(#17)	0.759	0.175	2.100
	0.065	(#16)	0.745	0.199	2.399
1 in.	0.035	(#20)	0.930	0.123	1.476
	0.049	(#18)	0.902	0.170	2.040
	0.058	(#17)	0.884	0.202	2.424
	0.065	(#16)	0.870	0.220	2.640
	0.083	(#14)	0.834	0.281	3.372
1 1/8 in.	0.035	(#20)	1.055	0.139	1.668
	0.058	(#17)	1.009	0.228	2.736
1 1/4 in.	0.035	(#20)	1.180	0.155	1.860
	0.049	(#18)	1.152	0.210	2.520
	0.058	(#17)	1.134	0.256	3.072
	0.065	(#16)	1.120	0.284	3.408
	0.083	(#14)	1.084	0.357	4.284
1 3/8 in.	0.035	(#20)	1.305	0.173	2.076
	0.058	(#17)	1.259	0.282	3.384
1 1/2 in.	0.035	(#20)	1.430	0.180	2.160
	0.049	(#18)	1.402	0.260	3.120
	0.058	(#17)	1.384	0.309	3.708
	0.065	(#16)	1.370	0.344	4.128
	0.083	(#14)	1.334	0.434	5.208
	*0.125	1/8 in.	1.250	0.630	7.416
	*0.250	1/4 in.	1.000	1.150	14.832
1 5/8 in.	0.035	(#20)	1.555	0.206	2.472
	0.058	(#17)	1.509	0.336	4.032
1 3/4 in.	0.058	(#17)	1.634	0.363	4.356
	0.083	(#14)	1.584	0.510	6.120
1 7/8 in.	0.058	(#17)	1.759	0.389	4.668
2 in.	0.049	(#18)	1.902	0.350	4.200
	0.065	(#16)	1.870	0.450	5.400
	0.083	(#14)	1.834	0.590	7.080
	*0.125	1/8 in.	1.750	0.870	9.960
	*0.250	1/4 in.	1.500	1.620	19.920
2 1/4 in.	0.049	(#18)	2.152	0.398	4.776
	0.065	(#16)	2.120	0.520	6.240
	0.083	(#14)	2.084	0.660	7.920
2 1/2 in.	0.065	(#16)	2.370	0.587	7.044
	0.083	(#14)	2.334	0.740	8.880
	*0.125	1/8 in.	2.250	1.100	12.720
	*0.250	1/4 in.	2.000	2.080	25.440
3 in.	0.065	(#16)	2.870	0.710	8.520
	*0.125	1/8 in.	2.700	1.330	15.600
	*0.250	1/4 in.	2.500	2.540	31.200

*These sizes are extruded. All other sizes are drawn tubes.

usually tapered; they can be split on the larger end and then mated with the smaller end of another pole of the same diameter. A small stainless-steel hose clamp (sometimes also available at scrap yards!) can be used to fasten the poles at this junction. A 14- or 21-MHz element can be constructed from several tent poles in this fashion. If a longer continuous piece of tubing is available, it can be used for the center section to decrease the number of junctions and clamps.

Other aluminum scrap is sometimes available, such as US Army aluminum mast sections designated AB-85/GRA-4 (J&H Smith Mfg). These are 3 foot sections with a 1 5/8 inch diameter. The ends are swaged so they can be assembled one into another. These are ideal for making a portable mast for a 144-MHz beam or for Field Day applications.

CONSTRUCTION WITH ALUMINUM TUBING

Most antennas built for frequencies of 14 MHz and above are made to be rotated. Constructing a rotatable antenna requires materials that are strong, lightweight and easy to obtain. The materials required to build a suitable antenna will vary, depending on many factors. Perhaps the most important factor that determines the type of hardware needed is the weather conditions normally encountered.

High winds usually don't cause as much damage to an antenna as does ice, especially ice along with high winds. Aluminum element and boom sizes should be selected so the various sections of tubing will telescope to provide the necessary total length.

The boom size for a rotatable Yagi or quad should be selected to provide stability to the entire system. The best diameter for the boom depends on several factors; most important are the element weight, number of elements and overall length. Tubing of 1-¼-inch diameter can easily support three-element 28-MHz arrays and perhaps a two-element 21-MHz system. A 2-inch diameter boom will be adequate for larger 28-MHz antennas or for harsh weather conditions, and for antennas up to three elements on 14 MHz or four elements on 21 MHz. It is not recommended that 2-inch diameter booms be made any longer than 24 feet unless additional support is given to reduce both vertical and horizontal bending forces. Suitable rein-forcement for a long 2-inch boom can consist of a truss or a truss and lateral support, as shown in **Fig 8**.

A boom length of 24 feet is about the point where a 3-inch diameter begins to be very worthwhile. This dimension provides a considerable improvement in overall mechanical stability as well as increased clamping surface area for element hardware. Clamping surface area is extremely important if heavy icing is common and rotation of elements around the boom is to be avoided. Pinning an element to the boom with a large bolt helps in this regard. On smaller diameter booms, however, the elements sometimes work loose and tend to elongate the pinning holes in both the element and the boom. After some time the elements shift their positions slightly (sometimes from day to day!) and give a rather ragged appearance to the system, even though this doesn't generally harm the electrical performance.

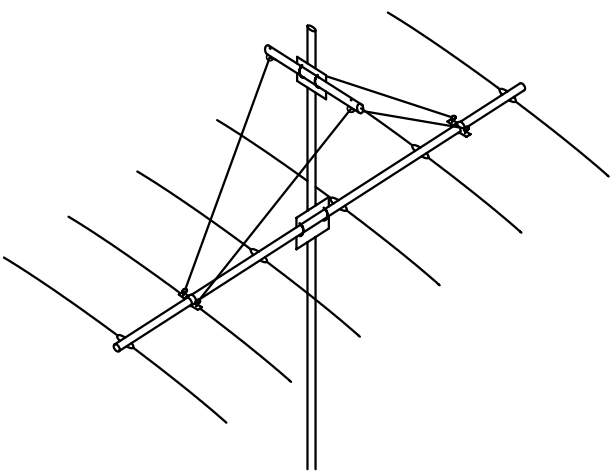

Fig 8—A long boom needs both vertical and horizontal support. The cross bar mounted above the boom can support a double truss to help keep the antenna in position.

A 3-inch diameter boom with a wall thickness of 0.065 inch is satisfactory for antennas up to about a five-element, 14-MHz array that is spaced on a 40-foot long boom. A truss is recommended for any boom longer than 24 feet.

There is no RF voltage at the center of a parasitic element, so no insulation is required in mounting elements that are centered on the boom (driven elements excepted). This is true whether the boom is metal or a nonconducting material. Metal booms have a small "shortening effect" on elements that run through them. With materials sizes commonly employed, this is not more than one percent of the element length, and may not be noticeable in many applications. It is just perceptible with ½-inch tubing booms used on 432 MHz, for example. Design-formula lengths can be used as given, if the matching is adjusted in the frequency range one expects to use. The center frequency of an all-metal array will tend to be 0.5 to 1 percent higher than a similar system built of wooden supporting members.

Element Assembly

While the maximum safe length of an antenna element depends to some extent on its diameter, the only laws that specify the minimum diameter of an element are the laws of nature. That is, the element must be rugged enough to survive whatever weather conditions it will encounter.

Fig 9 shows tapered Yagi element designs that will survive winds in excess of 80 mi/h. With a ¼-inch thickness of radial ice, these designs will withstand winds up to approximately 60 mi/h. (Ice increases the wind area but does not increase the strength of the element.) More rugged designs are shown in **Fig 10**. With no ice loading, these elements will survive in 120-mi/h winds, and in winds exceeding 85 mi/h with ¼ inch of radial ice. If you lose an antenna made with elements like these, you'll have plenty of company among your neighbors with commercially made antennas!

Figs 9 and 10 show only half elements. When the element is assembled, the largest size tubing for each element should be double the length shown in the drawing, with its center being the point of attachment to the boom. These designs are somewhat conservative, in that they are self-resonant slightly below the frequency indicated for each design. Telescoping the outside end sections to shorter lengths for resonance will increase the survival wind speeds. Conversely, lengthening the outside end sections will reduce the survival wind speeds. [See Bibliography listing for David Leeson (W6NL, ex-W6QHS) at the end of this chapter.]

Fig 11 shows several methods of fastening antenna element sections together. The slot and hose clamp method shown in Fig 11A is probably the best for joints where adjustments are required. Generally, one adjustable joint per element half is sufficient to tune the antenna. Stainless-steel hose clamps (beware—some "stainless

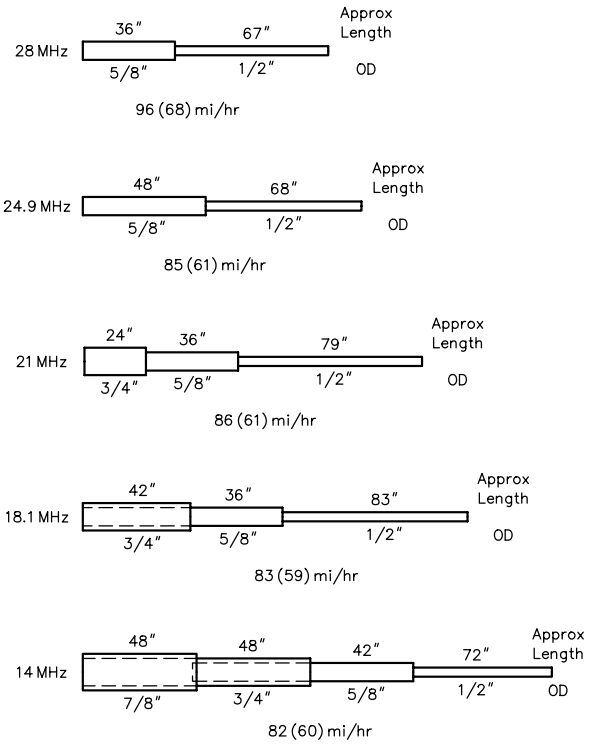

Fig 9—Half-element designs for Yagi antennas. The other side of the element is identical, and the center section should be a single piece twice as long as the length shown here for the largest diameter section. Use 0.058-in.-wall aluminum tubing throughout. Broken lines indicate double tubing thickness, where one tube is inserted into another. The overlap insertion depth into a tube two sizes larger, where shown, should be at least two inches. Maximum survival wind speeds without ice are shown adjacent to each design; values enclosed in parentheses are survival speeds for ¼ inch of radial ice.

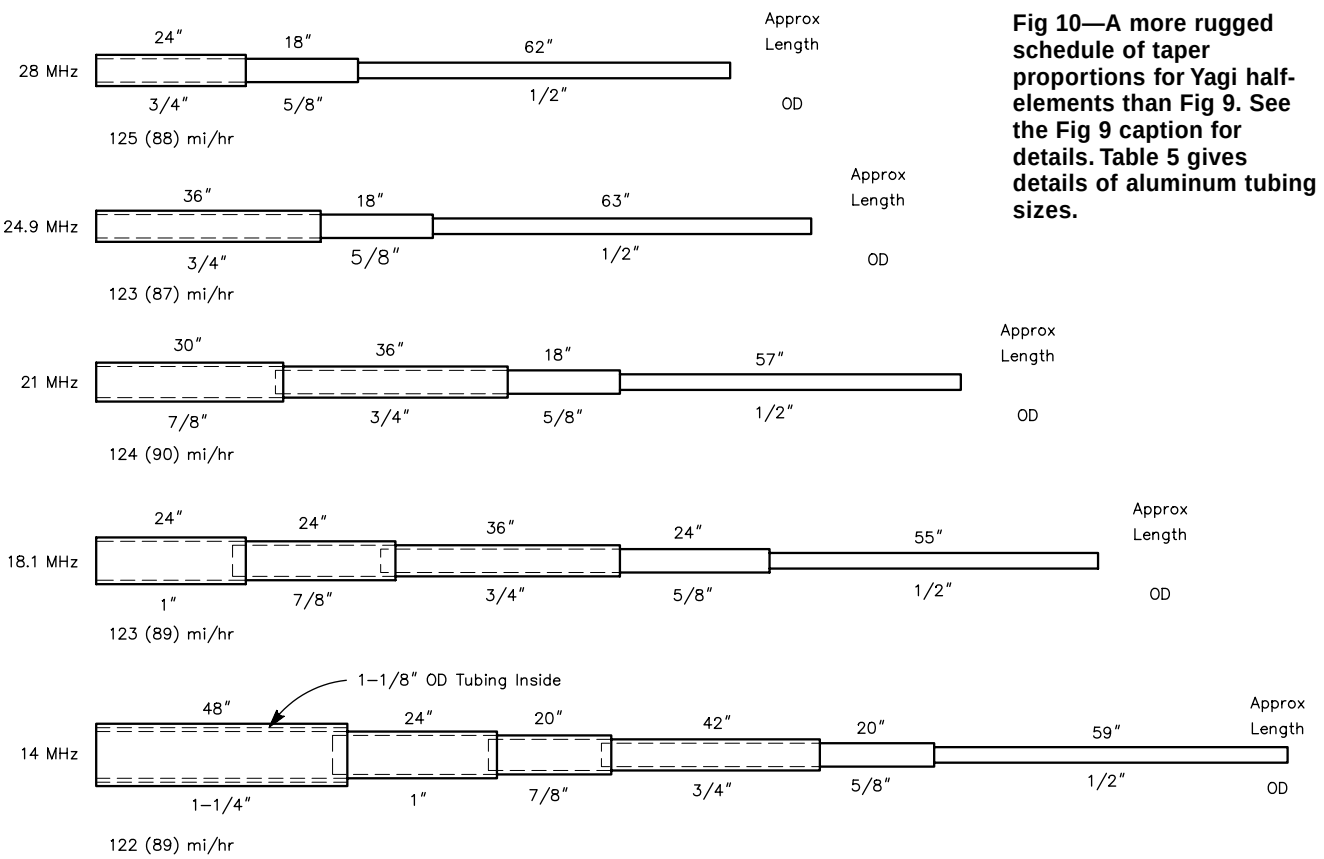

Fig 10—A more rugged schedule of taper proportions for Yagi half-elements than Fig 9. See the Fig 9 caption for details. Table 5 gives details of aluminum tubing sizes.

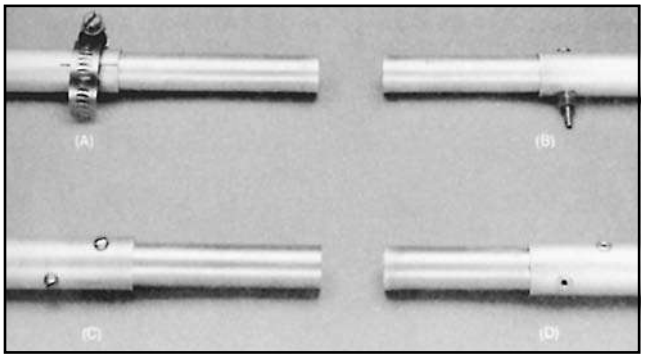

Fig 11—Methods of connecting telescoping tubing sections to build beam elements. See text for a discussion of each method.

Table 6
Hose-Clamp Diameters

	Clamp Diameter (In.)	
Size No.	*Min*	*Max*
06	7/16	7/8
08	7/16	1
10	1/2	1 1/8
12	5/8	1 1/4
16	3/4	1 1/2
20	7/8	1 3/4
24	1 1/8	2
28	1 3/8	2 1/4
32	1 5/8	2 1/2
36	1 7/8	2 3/4
40	2 1/8	3
44	2 5/16	3 1/4
48	2 5/8	3 1/2
52	2 7/8	3 3/4
56	3 1/8	4
64	3 1/2	4 1/2
72	4	5
80	4 1/2	5 1/2
88	5 1/8	6
96	5 5/8	6 1/2
104	6 1/8	7

steel" models do not have a stainless screw and will rust) are recommended for longest antenna life. **Table 6** shows available hose-clamp sizes.

Figs 11B, 11C and 11D show possible fastening methods for joints that do not require adjustment. At B, machine screws and nuts hold the elements in place. At C, sheet metal screws are used. At D, rivets secure the tubing. If the antenna is to be assembled permanently, rivets are the best choice. Once in place, they are permanent. They will never work free, regardless of vibration or wind. If aluminum rivets with aluminum mandrels are used, they will never rust. In addition, there is no danger of dissimilar-metal corrosion with aluminum rivets and aluminum antenna elements. If the antenna is to be disassembled and moved periodically, either B or C will work. If machine screws are used, however, take all possible precautions to keep the nuts from vibrating free. Use lock washers, lock nuts and flexible sealant such as silicone bathtub sealant to keep the hardware in place.

Very strong elements can be made by using a double thickness of tubing, made by telescoping one size inside another for the total length. This is usually done at the center of an element where more element strength is desired at at the boom support point, as in the 14-MHz element in Fig 10. Other materials can be used as well, such as wood dowels, fiberglass rods, and so forth.

In each case where a smaller diameter length of tubing is telescoped inside a larger diameter one, it's a good idea to coat the inside of the joint with Penetrox or a similar substance to ensure a good electrical bond. Antenna elements have a tendency to vibrate when they are mounted on a tower, and one way to dampen the vibrations is by running a piece of clothesline rope through the length of the element. Cap or tape the end of the element to secure the clothesline. If mechanical requirements dictate (a U-bolt going through the center of the element, for instance), the clothesline may be cut into two pieces.

Antennas for 50 MHz need not have elements larger than 1/2-inch diameter, although up to 1 inch is used occasionally. At 144 and 220 MHz the elements are usually 1/8 to 1/4 inch in diameter. For 420 MHz, elements as small as 1/16 inch diameter work well, if made of stiff rod. Aluminum welding rod of 3/32 to 1/8 inch diameter is fine for 420-MHz arrays, and 1/8 inch or larger is good for the 220-MHz band. Aluminum rod or hard-drawn wire works well at 144 MHz.

Tubing sizes recommended in the paragraph above are usable with most formula dimensions for VHF/UHF antennas. Larger diameters broaden the frequency response; smaller ones sharpen it. Much smaller diameters than those recommended will require longer elements, especially in 50-MHz arrays.

Element Taper and Electrical Length

The builder should be aware of one important aspect of telescoping or tapered elements. When the element diameters are tapered, as shown in Figs 9 and 10, the electrical length is not the same as it would be for a cylindrical element of the same total length. Length corrections for tapered elements are discussed in Chapter 2.

Other Materials for Antenna Construction

Wood is very useful in antenna work. It is available in a great variety of shapes and sizes. Rug poles of wood or bamboo make fine booms. Bamboo is quite satisfactory for spreaders in quad antennas.

Round wood stock (doweling) is found in many hardware stores in sizes suitable for small arrays. Wood is good for the framework of multibay arrays for the higher bands, as it keeps down the amount of metal in the active area of the array. Square or rectangular boom and frame materials can be cut to order in most lumber yards if they are not available from the racks in suitable sizes.

Wood used for antenna construction should be well seasoned and free of knots or damage. Available materials vary, depending on local sources. Your lumber dealer can help you better than anyone else in choosing suitable materials. Joining wood members at right angles can be done with gusset plates, as shown in **Fig 12**. These can be made of thin outdoor-grade plywood or Masonite. Round materials can be handled in ways similar to those used with metal components, with U clamps and with other hardware.

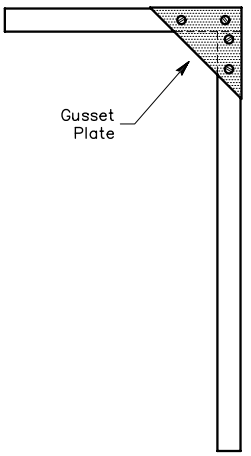

Fig 12—Wood members can be joined at right angles using gusset plates.

In the early days of Amateur Radio, hardwood was used as insulating material for antennas, such as at the center and ends of dipoles, or for the center insulator of a driven element made of tubing. Wood dowels cut to length were the most common source. To drive out moisture and prevent the subsequent absorption of moisture into the wood, it was treated before use by boiling it in paraffin. Of course today's technology has produced superior materials for insulators in terms of both strength and insulating qualities. However, the technique is worth consideration in an emergency situation or if low cost is a prime requirement. "Baking" the wood in an oven for a short period at 200° F should drive out any moisture. Then treatment as described in the next paragraph should prevent moisture absorption. The use of wood insulators should be avoided at high-voltage points if high power is being used.

All wood used in outdoor installations should be protected from the weather with varnish or paint. A good grade of marine spar varnish or polyurethane varnish will offer protection for years in mild climates, and one or more seasons in harsh climates. Epoxy-based paints also offer good protection.

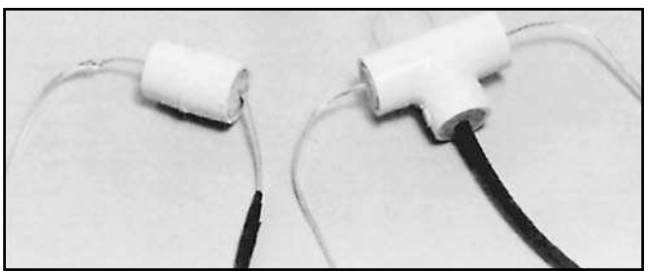

Fig 13—Plastic plumbing parts can be used as antenna center and end insulators.

Plastics

Plastic tubing and rods of various sizes are available from many building-supplies stores. The uses for the available plastic materials are limited only by your imagination. Some amateurs have built beam antennas for VHF using wire elements run inside thin PVC plumbing pipe. The pipe gives the elements a certain amount of physical strength. Other hams have built temporary antennas by wrapping plastic pipe with aluminum foil or other conductive material. Plastic plumbing pipe fittings can also be used to enclose baluns and as the center insulator or end insulators of a dipole, as shown in **Fig 13**. Plastic or Teflon rod can be used as the core of a loading coil for a mobile antenna (**Fig 14**) but the material for this use should be selected carefully. Some plastics become quite warm in the presence of a strong RF field, and the loading-coil core might melt or catch fire!

Fiberglass

Fiberglass poles are the preferred material for spreaders for quad antennas. They are lightweight, they withstand harsh weather well, and their insulating qualities are excellent. One disadvantage of fiberglass poles is that they may be crushed rather easily. Fracturing occurs at the point where the pole is crushed, causing it to lose its strength. A crushed pole is next to worthless. Some amateurs have repaired crushed poles with fiberglass cloth and epoxy, but the original strength is

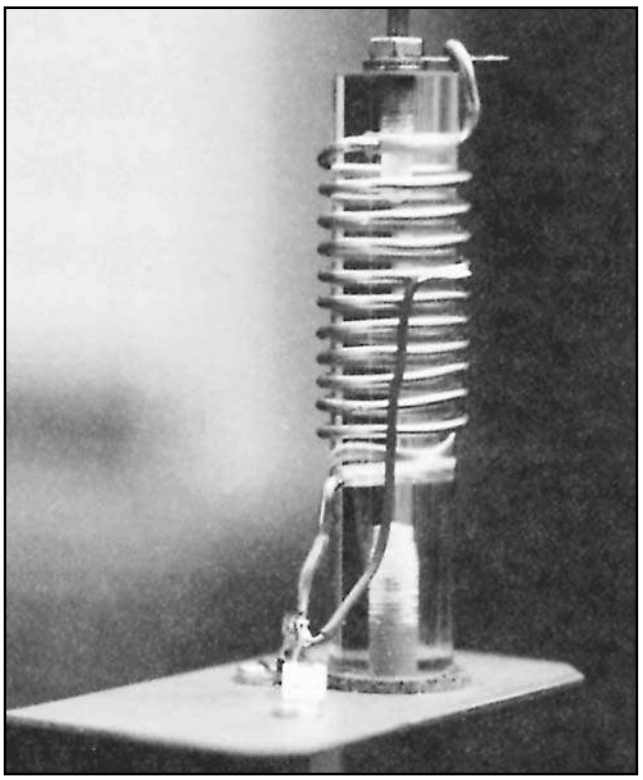

Fig 14—A mobile-antenna loading coil wound on a polystyrene rod.

nearly impossible to regain.

Fiberglass poles can also be used to construct other types of antennas. Examples are helically wound Yagi elements or verticals, where a wire is wound around the pole.

CONCLUSION

The antenna should be put together with good quality hardware. Stainless steel is best for long life. Rust will quickly attack plated steel hardware, making nuts difficult, if not impossible, to remove. If stainless-steel muffler clamps and hose clamps are not available, the next best thing is to have them plated. If you can't have them plated, at least paint them with a good zinc-chromate primer and a finish coat or two.

Galvanized steel generally has a longer life than plated steel, but this depends on the thickness of the galvanizing coat. Even so, in harsh climates rust will usually develop on galvanized fittings in a few years. For the ultimate in long-term protection, galvanized steel should be further protected with zinc-chromate primer and then paint or enamel before exposing it to the weather.

Good quality hardware is expensive initially, but if you do it right the first time, you won't have to take the antenna down in a few years and replace the hardware. When the time does come to repair or modify the antenna, nothing is more frustrating than fighting rusty hardware at the top of the tower.

Basically any conductive material can be used as the radiating element of an antenna. Almost any insulating material can be used as an antenna insulator. The materials used for antenna construction are limited mainly by physical considerations (required strength and resistance to outdoor exposure) and by the availability of materials. Don't be afraid to experiment with radiating materials and insulators.

BIBLIOGRAPHY

Source Material and more extended discussion of topics covered in this chapter can be found in the reference given below.

J. J. Elengo, Jr., "Predicting Sag in Long Wire Antennas," *QST*, Jan 1966, pp 57-58.

D. B. Leeson, *Physical Design of Yagi Antennas* (Newington, CT: ARRL).

Chapter 21

Antenna Products Suppliers

Antenna Manufacturers Products

Finding parts can be the most difficult aspect of an antenna project. Suppliers of aluminum exist in most major metropolitan areas. They can be found in the Yellow Pages of the phone book. Some careful searching of the Yellow Pages may also reveal sources of other materials and accessories. If you live away from a metropolitan area, try using telephone books for the nearest large metropolitan area; they may be available in the reference section of your local library.

Many dealers and distributors will ship their products by freight or by mail. Tables 1 through 7 list several categories of antenna products and some suppliers of them. Company names have been abbreviated where necessary. Table 8 is an address list arranged alphabetically by company name.

Product lines change often; we recommend that you

Table 1
VHF/UHF/Microwave Antenna Suppliers

Manufacturer	Yagi	Quad	Loop Yagi	Vertical	Mobile	HT	Microwave	Helical	Satellite
Antennaco	✓								
Ant Specialists				✓	✓				
Austin Antenna				✓	✓	✓			
Butternut				✓					
Centurion						✓			
Comet				✓	✓	✓			
Create Design	✓								
Cubex		✓							
Cushcraft	✓		✓	✓	✓				✓
Diamond	✓		✓	✓	✓				
Down East	✓		✓				✓		✓
Eur-AM				✓	✓	✓			
Force 12	✓			✓					
Hustler	✓			✓	✓				
Hy-Gain (MFJ)	✓			✓					✓
Kilo-Tec				✓					
Lakeview				✓	✓	✓			
Larsen				✓	✓				
M^2	✓	✓		✓					
Maldol					✓				
MFJ	✓			✓	✓	✓			
Mosley	✓			✓					
Pro-Am Valor					✓				
RadioShack				✓	✓	✓			
Radio Works					✓				
Sommer	✓								
Spectrum Intl	✓		✓				✓	✓	✓
Tennadyne	LPDA								
Tonna	✓						✓		

Chap 21.pmd 1 3/13/2007, 3:25 PM

request current catalogs from those manufacturers who interest you. In addition, all indications of sales policies and prices for catalogs are given for general information only and are subject to change without notice.

Antenna products for repeaters are listed separately, in Chapter 17.

Table 2
HF Antenna Suppliers

Manufacturer	Yagi	Quad	LPDA	Vertical	Dipole	Mobile	Small Xmtg	Active (RX only)
Alpha Delta				✔	✔	✔		
B & W				✔	✔			
Bilal							✔	
Butternut/Bencher	✔			✔			✔	
Create Design	✔		✔	✔	✔		✔	
Cubex		✔						
Cushcraft	✔		✔	✔	✔			
Flytecraft				✔		✔		
Force 12	✔		✔	✔	✔	✔	✔	
GAP				✔				
Gem Quad		✔						
Grove					✔	✔		✔
High Sierra				✔	✔	✔		
Hustler				✔		✔		
Hy-Gain (MFJ)	✔			✔	✔			
Lakeview/Hamstick						✔		
Lightning Bolt		✔						
M^2	✔				✔			
MFJ	✔	✔	✔	✔	✔	✔	✔	✔
Mosley	✔			✔	✔			
Palomar								✔
Pro-Am Valor						✔		
Roadrunner						✔		
Sommer	✔			✔				
Spi-Ro				✔	✔			
Tennadyne			✔					
Texas Radio					✔	✔		
Radio Works				✔	✔			
Van Gorden				✔	✔			
W1JC					✔		✔	
W9INN					✔			

Chap 21.pmd 2 3/13/2007, 3:25 PM

Table 3
Antenna Parts

Manufacturer	Hardware	Insulators	Traps	Aluminum Tubing	Wire	Transmission Lines
Alexanderson AeroPlane Co				✔		
Barker & Williamson		✔	✔			
Cable X-Perts	✔	✔			✔	✔
Hy-Gain (MFJ)	✔	✔				
Metal & Cable, Inc	✔			✔	✔	
Ocean State Electronics	✔	✔			✔	✔
Spi-Ro		✔	✔		✔	✔
Texas Towers				✔	✔	✔
Radio Works	✔	✔			✔	✔
Van Gorden	✔	✔			✔	✔
The Wireman	✔	✔			✔	✔
W1JC		✔			✔	
W9INN					✔	

Table 4
Suppliers of Quad Antenna Parts

Company	*Material Size*
Cubex Co., Inc.	$1^1/_4$-$^1/_2$ in. × 13 ft; $1^1/_2$ in. × 13 ft cast spiders, boom-to-mast mounts.
Lightning Bolt	Custom-made fiberglass spreaders; any length.
Max-Gain Systems, Inc.	Quad spreaders; fiberglass insulators.

Table 5
Towers, Masts and Accessories

Towers
Aluma
Champion Radio
Create Design
Force 12
Glen Martin Engineering
Heights Tower
Hy-Gain (MFJ)
National Tower
RadioShack (masts only)
Rohn
Rotating Tower Systems
Tashjian Towers Corporation
Texas Tower
Trylon
Universal Manufacturing
US Tower

Climbing and Safety Equipment
Champion Radio Products
ONV
Texas Towers

Rotators
Create Design
Hy-Gain (MFJ)
M^2
RadioShack
The Rotor Doctor
Yaesu

Stacking Frames
(Unless otherwise noted these frames are for use in stacking the manufacturer's own antennas in pairs or in quads. These stacking kits are for VHF or UHF antennas only.)
C3i
Cushcraft
Down East
IIX
Spectrum International

Combiners, Power Dividers and Phasing Harnesses
Byers
C3i
Down East
Spectrum International
Tonna

Table 6
Transmission Lines

Source	Coax	Hardline	Ladder Line
Belden	✓	✓	
Cable X-Perts	✓	✓	✓
International Wire & Cable	✓		
Nemal	✓	✓	
The Radio Works	✓	✓	✓
W1JC			✓
W9INN			✓
The Wireman	✓	✓	✓

Chap 21.pmd 3 3/13/2007, 3:25 PM

Table 7
Transmission Line Instruments and Accessories

Matching Networks
Ameritron
Barker & Williamson
Cubex
ICOM (mobile & fixed)
Kenwood
MFJ
Nye
SGC
Ten-Tec
Texas Radio (mobile only)
Vectronics
XMatch

Ferrite Cores and Rods
Amidon
Palomar
The Wireman

Filters—TVI (Low Pass & High Pass)
K-Com
MFJ

Lightning Arresters
Alpha Delta
Ameritron
Comet
Cushcraft
Hy-Gain (MFJ)
Polyphaser
Radioware
Rohn
The Wireman
Zero Surge Inc

Switches (Manual, Coax)
Alpha Delta
Barker & Williamson
MFJ

Switches (Remote, Coax)
Ameritron
MFJ

SWR and Wattmeters
Autek
Bird
Coaxial Dynamics
MFJ
Nye
Palomar
RF Parts
Texas Radio

Table 8
Suppliers Addresses

We have made every effort to ensure that this list is complete and accurate as of mid 2003. The ARRL takes no responsibility for errors or omissions. Similarly, a listing here does not represent an endorsement of a manufacturer or products by the ARRL. Refer to the product reviews in *QST* for descriptions of particular products that interest you. To the best of our knowledge the suppliers listed are willing to sell products to amateurs by mail unless indicated otherwise. This listing will be updated with each edition of *The Antenna Book* and *The ARRL Handbook* in the TISFIND manufacturer database. Check ads in *QST* and other Amateur Radio publications for any changes to this information. Suppliers who wish to be listed or update their information are urged to contact the editors.

Advanced Composites
1154 S. 300 W.
Salt Lake City, UT 84101
801-467-1204
fax 801-467-4367
e-mail
info@advancedcomposites.com

Advanced Specialties
114 Essex Street
Lodi, NJ 07644
USA
Tel: 800-926-9426
Email: advanspec@aol.com
http://advancedspec.freeyellow.com/

AEA—Div. Tempo Research Corporation
1221 Liberty Way
Vista, CA 92083
760-598-9677
fax 760-598-4898
e-mail tempo@inetworld.com
web www.aea-wireless.com

AFT
132 Boulevard Dauphinot
F-51100 Reims, France
+33 326 070 047
fax +33 326 023 654
e-mail Antennes-ft@wanadoo.fr
web www.f9ft.com

Alexander Aeroplane Co
PO Box 909
Griffin, GA 30224
800-831-2949; 404-229-2329

Alan Broadband Company (Zap Checker)
93 Arch Street
Redwood City, CA 94062
USA
Tel: 888-369-9627 (orders)
650-369-9627
Fax: 650-369-3788
Email: ABCom@prodigy.net
http://www.alanbroadband.com/

Alpha Delta Communications
PO Box 620
Manchester, KY 40962
606-598-2029
fax 606-598-4413

Aluma Tower Co, Inc
PO Box 2806-AL
Vero Beach, FL 32961-2806
772-567-3423
fax 772-567-3432
e-mail atc-t@alumatower.com
web www.alumatower.com/index.html

Amateur Electronic Supply
5710 W Good Hope Rd
Milwaukee, WI 53223
800-558-0411
web www.aesham.com/

Ameritron Division
116 Willow Road
Starkville, MS 39759
662-323-8211 (Tech)
fax 662-323-6551
e-mail
ameritron@ameritron.com
web www.ameritron.com/ameritron

Amidon Associates, Inc.
1510 E. Edinger Avenue, Unit B
Santa Ana CA 92705
800-898-1883; 714-547-4494
fax 714-547-4433
e-mail sales@amidon-inductive.com
web www.amidon-inductive.com/

Antennaco Inc
102 Armory Road
PO Box 218
Milford, NH 03055-0218
603-673-3153
fax 603-673-4347

Allen Telecom Group
Antenna Specialists Mobile Division
30500 Bruce Industrial Parkway
Cleveland, OH 44139-3996
USA
440-349-8400
fax 440-349-8404
web www.antenna.com/

Array Solutions
350 Gloria Rd
Sunnyvale, Tx 75182
USA
Tel: 972-203-8810
Fax: 972-203-8811
Email: wx0b@arrysolutions.com
http://www.arraysolutions.com

ASA Antenna Sales
PO Box 3461
Myrtle Beach, SC 29578
800-772-2681

Associated Radio Communications
8012 Conser
Overland Park, KS 66204
913-381-5900; 800-497-1457
fax 913-648-3020
e-mail assocrad@tfs.net
web www.associatedradio.com

Austin Amateur Radio Supply
5310 Cammeron Road
Austin, TX 78723
800-423-2604; 512-454-2994
fax 512-454-3069

Austin Antenna, Ltd
10 Main St
Gonic, NH 03839
603-336-6339
fax 603-335-1756

Chap 21.pmd 4 3/13/2007, 3:25 PM

Autek Research
PO Box 7556
Wesley Chapel, FL 33544
813-994-2199
e-mail
Mailbox@autekresearch.com
web www.autekresearch.com/
index.htm

Barker & Williamson Co
603 Cidco Rd
Cocoa, FL 32926
321-639-2545
fax 321-639-2545
e-mail
custsrvc@bwantennas.com
web www.bwantennas.com

Barry Electronics Corp
540 Broadway
New York, NY 10012
212-925-7000
fax 212-925-7001

Belden Wire & Cable
PO Box 1980
Richmond, IN 47374
317-983-5257
fax 317-983-5257
web www.belden.com

Bencher Inc.
831 North Central Avenue
Wood Dale, IL 60191
630-238-1183
fax 630-238-1186
e-mail bencher@bencher.com
web www.bencher.com/

Bilal Company
137 Manchester Dr
Florissant, CO 81816
719-687-0650
web www.isotronantennas.com/

Bird Electronics Corporation
30303 Aurora Rd.
Solon, OH 44139
866-695-4569
e-mail sales@bird-
technologies.com
web www.bird-electronic.com/

Brian Beezley, K6STI
3532 Linda Vista Dr
San Marcos, CA 92069
619-599-4962
e-mail k6sti@n2.net

Burghardt Amateur Center, Inc.
710 10th Street SW
PO Box 73
Watertown, SD 57201
800-927-4261
605-886-7314 (Service)
605-886-6914 (Fax-back
product info)
fax 605-886-3444
e-mail burghart@daknet.com
web www.burghardt-
amateur.com/

Butternut Electronics Co
See Bencher Inc.

Byers Chassis Kits
5120 Harmony Grove Road
Dover, PA 17315
717-292-4901
(6p-9p EST M-F, 8a-4p Sat)
717-292-4901 (24 hrs)

Cable X-Perts Inc.
225 Larkin Drive Suite #6
Wheeling, IL 60090-7209
800-828-3340 (orders only)
847-520-3003 (Tech. Info.)
fax 847-520-3444
e-mail cxp@cablexperts.com
web www.cablexperts.com/

CAL-AV Labs, Inc.
1802 w. Grant road, Ste. 116
Tucson, AZ 85745
USA
Tel: 520-624-1300
888-815-0400 (orders only)
Fax: 520-624-1311
Email: info@cal-av.com
http://www.cal-av.com/

Cardwell Condenser Corp
80 East Montauk Hwy
Lindenhurst, NY 11757
516-957-7200
fax 516-957-7203
web www.cardwellcondenser.com

C.A.T.S.
Formerly known as: Rotor Doctor
7368 SR 105
Pemberville, OH 43450
419-353-2287
fax 419-354-7746
e-mail mailto:craig@rotor-doc.com
web www.rotordoc.com

C-Comm
6115 15th NW
Seattle, WA 98107
206-784-7337; 800-426-6528
fax 206-784-0541

C3i
1401 K Street NW Suite 900
Washington DC 20005
(800) 224-5137
fax (202) 362-8481
e-mail info@C3iusa.com
web www.c3iusa.com/
corpover.html

Centurion International
PO Box 82846
Lincoln, NE 68501-2846
402-467-4491
fax 800-848-3825

Champion Radio Products
Box 572
Woodinville, WA 98072
425-485-7913
206-890-4188 Cell Phone
fax 360-668-1447
e-mail championradio@aol.com
web www.championradio.com/

Coaxial Dynamics
15210 Industrial Parkway
Cleveland, Ohio 44135-3308
800-262-9425
fax 216-267-3142
e-mail cdi-sales@coaxial.com
web www.coaxial.com/
home_frames.htm

Comet North America Inc.
394 Wards Corner Road
Suite 130
Cincinnati, Ohio, 45140
513-831-5000
fax 513-831-7889
e-mail
info@CometNorthAmerica.com
web www.cometnorthamerica.com/

Comet Antenna
See NCG

Comm-Pute
7946 State Street
Midvale, UT 84047
801-567-9944
fax 801-567-9494
e-mail bobwood@xmission.com
web www.comm-pute.com/

Communication Headquarters Inc.
3832 Oleander Drive
Wilmington, NC 28403
910-791-8885
800-688-0073 (orders)
fax 910-452-3891 (orders)
web www.chq-inc.com/

Communications Data Corp
1051 Main St
St Joseph, MI 49085
269-982-0404
fax 269-982-0433
e-mail mailto:did@gtm.net

Comtelco Industries Inc
501 Mitchell Rd
Glendale Heights, IL 60139
800-634-4622; 708-7790-9894
fax 708-798-9799

Create
4-8 Asano-Cho
Kawasaki-Ku
Kawasaki-City, Japan
044 (333) 6681
fax 044 (333) 6598
e-mail email@cd-corp.com

Cubex Co.
228 Hibiscus St, #9
Jupiter, FL 33458
561-748-2830
fax 561-748-2831
e-mail CubexCo@aol.com
web www.cubex.com/

Cushcraft Corp
48 Perimeter Rd.
Manchester, NH 03108
603-627-7877
e-mail sales@cushcraft.com
web www.cushcraft.com/

Dave's Hobby Shop
600 Main St.
Van Buren, AK 72956
USA
Tel: 479-471-0750
Web www.daveswebshop.com

Davis RF Co
See Radioware (distributor)
PO Box 730
Carlisle, MA 01741
978-371-1356
978-369-1738
800-328-4773 (Orders only)
fax 978-369-3484
e-mail davisrfinc@aol.com
web www.davisRF.com

Diamond Antennas
See RF Parts

Down East Microwave
954 Rt 519
Frenchtown, NJ 08825
908-996-3584
fax 908-996-3702
web downeastmicrowave.com/

Dressler Hochfrequenztechnik
GMBH
Werther Strasse 14-16
W-5190 Stolberg
Germany

DX Engineering
POB 440
Peninsula, Ohio 44264
USA
Fax: 330-657-2168
Email:
dxengineering@dxengineering.com
http://www.dxengineering.com/

EDCO - Electronic Distributors
Company
325 Mill Street
Vienna, VA 22180
703-938-8105
fax 703-938-6911
e-mail web www.elecdist.com/
index.html

EUR-AM Antennas
PO Box 225
Moultonboro, NH 03254-0225
603-476-5113
fax 603-476-5113
e-mail info@eur-am.com
web www.eur-am.com/

EZ Hang, Inc.
8645 Tower Dr.
Code C
Laurel, MD 20723
Tel: 540-286-0176
Fax: 202-260-3797
http://www.ezhang.com

Fluidmotion Incorporated
14135 233rd Place SE
Issaquah, WA 98027
425-456-0200; 800-885-8700
fax 425-391-6031
e-mail sales@steppir.com
web www.steppir.com/

Flytecraft
PO Box 3141
Simi Valley, CA 93093
805-583-8173

Force 12
PO Box 1349
Paso Robles, CA 93447
800-248-1985
805-227-1680 (Tech)
fax 805-227-1684
e-mail
mailto:force12e@lightlink.com
web force12inc.com/

GAP Antenna Products
99 North Willow St
Fellsmere, FL 32948
772-571-9922
Email: contact@gapantenna.com
web www.gapantenna.com

Gem Quad Products Ltd
PO Box 291
Boissevain, MB R0K 0E0
Canada
204-534-6184
fax 204-534-6492
e-mail
mailto:gemquad@escape.ca
web www.escape.ca/~gemquad/

Chap 21.pmd 5 3/13/2007, 3:25 PM

GLA Systems
PO Box 425
Caddo Mills, TX 75135
903-527-4163
800-588-2841
fax 214-381-2895
web www.texasbugcatcher.com/

Grove Enterprises Inc.
PO Box 98
Brasstown, NC 28902
800-438-8155 (orders)
704-837-9200 (BBS)
fax 704-837-2216
e-mail nada@grove.net
web www.grove-ent.com/

Ham Radio Outlet
1702 W. Camelback Rd
Phoenix, AZ 85015
web www.hamradio.com/
800-444-4799 Mid Atlantic
800-444-9476 Mountain
800-444-0047 New England
800-644-4476 Northeast
800-444-7927 Southeast
800-854-6046 West

The Ham Station
220 North Fulton Avenue
PO Box 6522
Evansville, IN 47719-0522
800-729-4373 (orders)
812-422-0231 (Tech)
812-422-0252 (Service)
fax 812-422-4253
e-mail sales@hamstation.com
web www.hamstation.com/

Hamtronics, Inc
65-Q Moul Rd
Hilton, NY 14468
716-392-9430
fax 716-392-9420
web www.hamtronics.com

Hamware.de
Int'l: Klaus Bemmerer
Tel: +49 4371 869145
e-mail service@hamware.de
Web www.hamware.de
US: Dillon RF Systems
Email dillonel@mtaonline.net

Heights Tower Systems
1529 Gulf Beach Hwy
Pensacola, FL 32507
850-455-1210
fax 850-455-4355
e-mail info@heightstowers.com
web www.heightstowers.com/

Hi-Q Antennas
21085 Cielo Vista Way
Wildomar, CA 92595
909-674-4862
fax 909-245-2031
e-mail sales@hiqantennas.com
web www.hiqantennas.com/

High Sierra Antennas
Box 2389
Nevada City, CA 95959
888-273-3415; 530-273-3415
fax 530-273-7561
e-mail heath@hsantennas.com
web www.hsantennas.com

Hustler Antennas
see New-Tronics Antenna Corp.

Hy-Gain (also see MFJ)
308 Industrial Park Road
Starkville, MS 39759
800-647-1800 (Sales)
662-323-9358 (Tech)
fax 662-323-6551
web www.hy-gain.com/

ICOM America, Inc.
2380 116th Ave, NE, Suite S
Bellevue, WA 98004
USA
Tel: 800 872-4266
Fax: 425 454-1509
Web www.icomamerica.com

Industrial Communications
Engineers (ICE)
Array Solutions
350 Gloria Rd.
Sunnyvale, TX 75182
972-203-2008; 800-423-2666
fax 972-203-8811
e-mail wx0b@arraysolutions.com
web www.iceradioproducts.com/

IIX Equipment, Ltd
PO Box 9
Oak Lawn, IL 60454
708-423-0605
fax 708-423-1691
web www.w9iix.com/

International Radio
13620 Tyee Road
Umpqua, OR 97486
541-459-5623 9AM-1PM PDT,
Tues-Sat
fax 541-459-5632
e-mail inrad@rosenet.net
web www.qth.com/inrad/

Kenwood USA Corporation
3975 Johns Creek Court,
Suite 300
Suwanee, GA 30024
USA
Tel: 678 474-4700
Fax: 678 474-4730
Web www.kenwoodusa.com

KØXG Systems
1117 Highland Park Drive
Bettendorf, IA 52722
USA
Tel: 563 355-7451
Email KØXG@KØXG.com
Web www.k0xg.com

Kilo-Tec
PO Box 10
Oakview, CA 93022
805-646-9645

K-Com
PO Box 82
Randolph OH 44265
330-325-2110
fax 330-325-2525
e-mail k-com@worldnet.att.net
web www.k-comfilters.com/
howtoget.asp

Lakeview Co Inc
3620-9A Whitehall Rd
Anderson, SC 29626
(864) 226-6990
fax (864) 225-4565
web www.hamstick.com

Larsen Electronics, Inc
See Radial/Larsen

LDG Electronics
1445 Parran Road
St Leonard, MD 20685
877-890-3003 Toll-Free Orders
410-586-2177 Tech Support
fax 410-586-8475
e-mail ldg@ldgelectronics.com
web www.ldgelectronics.com

Lentini Communications
21 Garfield St
Newington, CT 06111
860-666-6227
800-666-0908 (outside CT)
fax 860-667-3561
e-mail radio@lentinicomm.com
web www.lentinicomm.com

Roy Lewallen, W7EL
PO Box 6658
Beaverton, OR 97007
503-646-2885
fax 503-671-9046
e-mail w7el@eznec.com
web www.eznec.com

Lightning Bolt Antennas
RD #2, RT 19
Volant, PA 16156
724-530-7396
fax 724-530-6796
e-mail lbaquads@ztrain.com
web
www.lightningboltantennas.com/

M² Antenna Systems Inc.
4202 N. Selland
Fresno CA, 93722
559-432-8873
fax 559-432-3059
e-mail wyatt@m2inc.com
web www.m2inc.com/

M/A-COM, Inc
(an AMP Company)
1011 Pawtucket Blvd
PO Box 3295
Lowell, MA 01853-3295
508-442-4500
fax 508-442-4436
e-mail sales@macom.com
web www.amp.com

Maldol USA
4711 NE 50th St
Seattle, WA 98105
Answerfax 206-525-1896
fax 206-524-7826
e-mail transtec@cyberquest.com

Glen Martin Engineering
13620 Old Highway 40
Boonville, MO 65233
660-882-2734; 800-486-1223
fax 660-882-7200
web www.glenmartin.com

The Mast Company
Henry Pollock - K4TMC
P.O. Box 1932
Raleigh, NC 27602
Email: k4tmc@aol.com
http://www.geocities.com/tmastco/

MCM Electronics
650 Congress Park Dr
Centerville, OH 45459-4072
800-543-4330
fax 800-765-6960
web www.i-mcm.com

Memphis Amateur Electronics
1465 Wells Station Rd
Memphis, TN 38108
901-683-9125; 800-238-6168
fax 901-682-7165

Metal and Cable Corp, Inc
9241 Ravenna Road, Unit C-10
PO Box 117
Twinsburg, OH 44087
330-425-8455
fax 330-425-3504
web www.metal-cable.com/

MFJ Enterprises
300 Industrial Park Rd
Starkville, MS 39759
662-323-5869
Email
mfjcustserv@mfjenterprises.com
web www.mfjenterprises.com/

MGS (Max-Gain Systems, Inc.)
221 Greencrest Court
Marietta, GA 30068-3825
770-973-6251 (before 9 PM
eastern)
fax 815) 461-7730
e-mail info@mgs4u.com
web www.mgs4u.com/

Michigan Radio
26014 Groesbeck Hwy
Warren, MI 48089
810-771-4711
800-TRU-HAMM (800-878-4266)
Orders only
810-771-4712 (Service)
fax 810-771-6546
web www.michiganradio.com/

Mirage Communications
116 Willow Road
Starkville, MS 39759
662-323-8287
fax 662-323-6551
web www.mirageamp.com/

James Millen Electronics
PO Box 4215BV
Andover, MA 01810-4215
978-975-2711
fax 978-474-8949
e-mail info@jamesmillenco.com
web www.jamesmillenco.com/
millen/millmain.htm

Mosley Electronics
1325 Style Master Drive
Union, MO 63084
800-325-4016 (Orders)
800-9MOSLEY (966-7539)
314-994-7872 (Technical)
fax 314-994-7873
web www.mosley-electronics.com/

Multi-band Antennas (originally
Spider Antennas)
7131 Ownesmouth Avenue -
Suite 563C
Canoga Park, CA 91303
818-341-5460
web www.spiderantenna.com/

Multi-tech Industries, Inc. (MTI)
(formally Radio Switch)
64 South Main Street
PO Box 159
Marlboro, NJ 07746-0159
800-431-3223; 732-431-0550
732-462-6100
fax 732-409-6695
e-mail multitech@sprynet.com
web www.multi-tech-industries.com

Chap 21.pmd 6 3/13/2007, 3:25 PM

National RF, Inc.
7969 Engineer Road, Suite 102
San Diego, CA 92111
858-565-1319
fax 858-571-5909
web www.nationalrf.com/

National Tower Co
PO Box 15417
Shawnee Mission, KS 66285
800-762-5049; 913-888-8864

NCG Companies—Comet Antenna
1275 North Grove St
Anaheim, CA 92806
714-630-4541; 800-962-2611
fax 714-630-7024
web www.cometantenna.com
web www.natcommgroup.com/

Nemal Electronics Inc.
12240 NE 14th Avenue
North Miami, FL 33161
305-893-3924; 305-849-0900
800-522-2253
fax 305-895-8178
e-mail info@nemal.com
web www.nemal.com/

New-Tronics Antenna Corp. - Hustler
1 Newtronics Place
Mineral Wells, TX 76067-9563
877-994-9499 Sales
940-325-1386 Service
fax 940-328-1409
e-mail sales@new-tronics.com
web www.new-tronics.com/main/index.html

Nittany Scientific
1733 West 12600 South
Suite 420
Riverton, UT 84065
Phone/fax (801) 446-1426
e-mail sales@nittany-scientific.com
web www.nittany-scientific.com/

William M. Nye Co
PO Box 1877
Priest River, ID 83856
208-448-1762
fax 208-448-1832

Ocean State Electronics
PO Box 1458
6 Industrial Dr
Westerly, RI 02891
401-596-3080; 800-866-6626
fax 401-596-3590
web www.oselectronics.com

ONV Safety Belt Co.
Box 404
Ramsey, NJ 07446
800-345-5634; 201-327-2462
fax 201-327-2462

OptiBeam
Thomas Schmenger DF2BO
Rastatter Straße 37
D-75179 Pforzheim
Tel./Fax: (0049) 07231 / 45 31 53
Email: Info@optibeam.de

OptiBeam NorthAmerica
Array Solutions
350 Gloria Rd
Sunnyvale, Tx 75182 USA
Tel: 972-203-8810
Fax: 972-203-8811
Email: wx0b@arrysolutions.com
http://www.arraysolutions.com

Orion now sold by M²

Outbacker Antenna Sales
330 Cedar Glen Circle
Chattanooga, TN 37412
615-899-3390
fax 615-899-6536

Palomar Engineers
PO Box 462222
Escondido, CA 92046
619-747-3343
fax 619-747-3346
e-mail palomar@compuserve.com
web www.palomar-engineers.com/

Palstar, Inc.
9676 N Looney Rd
P O Box 1136-1482
Piqua, Ohio 45356
USA
Tel: 937-773-6255
Fax: 937-773-8003
Email: Palstar@erinet.com
http://www.palstarinc.com/

Phillystran, Inc
151 Commerce Dr
Montgomeryville, PA 18936
215-368-6611
fax 215-362-7956
web www.phillystran.com/

PolyPhaser Corp
2225 Park Place
PO Box 9000
Minden, NV 89423-9000
702-782-2511
fax 702-782-4476
e-mail info@polyphaser.com
web www.polyphaser.com

Quicksilver Radio Products
30 Tremont St.
Meriden, CT 06450
USA
Tel: 203-440-4468
http://www.qsradio.com

Radiall/Larsen Antenna Technologies
3611 NE 112th Avenue
Vancouver, WA 98682
800-ANTENNA (800-268-3662)
360-944-7551
FAX 360-944-7556
fax 800-525-6749
e-mail info@radialllarsen.com
web www.radialllarsen.com/default.htm

Radio Bookstore (Radioware)
PO Box 209
Rindge, NH 03461-0209
603-899-6957
800-457-7373 (10am-6pm EST)
fax 603-899-6826
e-mail radware@radio-ware.com
web www.radiobooks.com/

Radio Center USA
1242 Howell
N. Kansas City, MO 64116
816-459-8832; 800-821-7323

Radio City
2663 County Rd I
Mounds View, MN 55112
612-786-4475; 800-426-2891
fax 612-786-6513
web www.radioinc.com

Radio Engineers/Technitron (see National RF, Inc.)

Radio Shack
(Contact your local store)

Radio Switch Corp
See Multi-tech Industries

Radio Works
PO Box 6159
Portsmouth, VA 23703
757-484-0140
800-280-8327 (Orders)
fax 757-483-1873
e-mail jim@radioworks.com
web radioworks.com/

Raibeam Antennas, Int'l
5638 West Alice Avenue
Glendale, AZ 85302
800-530-1913 (orders)
602-931-9135
e-mail wa7rai@raibeam.com
web www.raibeam.com/

RF Parts Co
435 South Pacific St
San Marcos, CA 92069
760-744-0700; 800-737-2787
760-744-0750 (Tech)
fax 760-744-1943; 888-744-1943
e-mail rfp@rfparts.com
web www.rfparts.com

RF TEC Manufacturing
256 Commerce Rd, Suite 517
Peachtree, GA 30269
770-251-2235
fax 770-502-9827
web www.rftec.com/

Roadrunner Resonator
1850 Swanson, #A20
Lake Havasu, AZ 86403
520-453-7211

ROHN Industries, Inc.
PO Box 2000
Peoria, IL 61656
309-697-4400
fax 309-697-5612
e-mail mail@rohnnet.com
web www.rohnnet.com/Index.htm

Ross Distributing Co
78 South State St
Preston, ID 83263
208-852-0830
fax 208-852-0833
web www.rossdist.com

Rotating Tower Sytems, Inc.
Box 44
Prosper, TX 75058
214-347-2560

Rotor Doctor
See C.A.T.S.

SGC Inc
13737 SE 26th St
Bellevue, WA 98005
425-746-6310
fax 425-746-6384
e-mail sgc@sgcworld.com
web www.sgcworld.com/

Shoestring Antennas
PO Box 425
Keyport, WA 98345
360-697-5399
fax 360-697-8416
e-mail jacksa@juno.com
web www.qth.com/shoestring/

Sky-Pole Manufacturing, Inc
1922 Placentia Ave
Costa Mesa, CA 92627
949-548-5596
fax 949-548-5598

Sommer Antennas
PO Box 710
Geneva, FL 32732
407-349-9114
fax 407-349-2485
e-mail sommer1@ix.netcom.com
web www.sommerantennas.com

Spectrum International, Inc
PO Box 1084
Concord, MA 01742
508-263-2145
fax 508-263-7008

Spi-Ro Manufacturing, Inc.
P.O. Box 189
Jonesborough, TN 37659
800-728-7594
423-913-1615 Tech Support
fax 423-913-2131
e-mail mailto:contact@spiromfg.com
web www.spiromfg.com/

Surplus Sales of Nebraska
1502 Jones St
Omaha, NE 68102-3112
402-346-4750
800-244-4567 (Orders only)
fax 402-346-2939
e-mail grinnell@surplussales.com
web www.surplussales.com/

Tarheel Antennas
913 Old Honeycutt Rd
Fuquay-Varina, NC 27256
919-552-8788
fax 919-552-4970
e-mail tarheelantennas@aol.com
web www.tarheelantennas.com/

Tashjian Towers Corporation
(used to be Tri-Ex Towers)
2183 S Highland Ave.
Sanger, CA 93657
559-495-0307
559-284-9707 Mobile
fax 559-495-0557
e-mail tashjian@MSN.com
web www.karltashjian.com/

Telex Communications, Inc
Hy-Gain (see MFJ)

Ten-Tec, Inc
1185 Dolly Parton Parkway
Sevierville, TN 37862
865-453-7172
865-428-0364 (Repairs)
fax 865-428-4483
web www.tentec.com/

Chap 21.pmd 7 3/13/2007, 3:25 PM

Tennadyne Corp
PO Box 34202
San Antonio, TX 78265-4202
210-599-9064
fax 210-599-9064
(same as voice)
e-mail tennadyn@satx.net
web www.tennadyne.com/

Teri Software
PO Box 277
Lincoln, TX 78948
979-542-7952
e-mail
support@antennamodel.com
web www.antennamodel.com

Texas Radio Products
5 E Upshaw
Temple, TX 76501
817-771-1188

Texas Towers
1108 Summit Ave, Suite 4
Plano, TX 75074
800-272-3467
972-422-7306 (Tech)
fax 972-881-0776
e-mail sales@texastowers.com
web www.texastowers.com/

T.G.M. Communications
121 Devon Street
Stratford, Ontario, N5A 2Z8
Canada
519-271-5928
e-mail tgmc@sympatico.ca
web www3.sympatico.ca/tgmc/
index.html

TIC General
PO Box 1 - 1110 Airport Rd
Thief River Falls, MN 56701
218-681-1119
fax 218-681-8509

Timewave Technology, Inc.
1025 Selby Ave, Suite 101
St Paul, MN 55104
USA
Tel: 651-489-5080
Email: sales@timewave.com
http://www.timewave.com

Traffie Technology
421 Jones Hill Road
Ashby, MA 01431-1801
888-599-BEAM (888-599-2326)
978-386-7900
fax 978-386-7900 (same as voice)

Trylon Manufacturing Co, Ltd
21 South Field Dr
PO Box 186
Elmira, Ontario
N3B 2Z6 Canada
519-669-5421
fax 519-669-8912
e-mail info@trylon.com
web www.trylon.com/home.asp

Tucker Electronics and Computers
1717 Reserve St.
PO Box 551419
Garland, TX 75355-1419
800-527-4642 (Test equipment
and catalog requests)
214-348-8800 (x332)
fax 214-340-5460
web www.tucker.com/

Unadilla Antenna Manufacturing
PO Box 4215
Andover, MA 01810-4215
978-975-2711
978-475-7831 (Office)
fax 978-474-8949
e-mail info@unadilla.com
web www.unadilla.com/

Universal Manufacturing Co
43900 Groesbeck Hwy
Clinton Township, MI 48036
810-463-2560
fax 810-463-2964

Universal Radio
6830 Americana Parkway
Reynoldsburg, OH 43068-4113
USA
Tel: 800-431-3939 (Orders)
614-866-4267 (Technical Info)
Fax: 614-866-2339
Email: dx@universal-radio.com
http://www.universal-radio.com/

US Tower Corp
1220 Marcin St
Visalia, CA 93291
559-733-2438
fax 559-733-7194
web www.ustower.com

Valor Enterprises
1711 Commerce Drive
PO Box 601
Piqua, OH 45356-0601
513-778-0074; 800-543-2197
fax 513-778-0259
web www.valorantenna.com/

Van Gorden Engineering
PO Box 21305
South Euclid, OH 44121

Van Valzah Co
38 W 111 Horseshoe Dr
Batavia, IL 60515-9730
708-406-9210

Vectronics
300 Industrial Park Road
Starkville, MS 39759
800-363-2922; 662-323-5800
fax 662-323-6551
e-mail jshurden@vectronics.com
web www.vectronics.com

XMatch
Paul Schrader, N4XM
7001 Briscoe Lane
Louisville, KY 40228
web http://n4xm.myiglou.com/

XX Towers
814 Hurricane Hill Road
Mason, NH 03048
603-878-1102
fax 603-878-4200
e-mail kc1xx@kc1xx.mv.com
web www.xxtowers.com/

W1JC—TV Evans
113 Stratton Brook Rd
Simsbury, CT 06070
860-658-5579
web pages.prodigy.com/w1jc

W3FF Antennas
2390 Templeton Dr.
Redding, CA 96002
USA
Tel: 530-226-8446
Email: sales@buddipole.com
http://www.buddipole.com

W7FG Vintage Manuals
3300 Wayside Drive
Bartlesville, OK 74006
USA
Tel: 800-807-6146 (orders)
918-333-3754
Email: w7fg@eigen.net
http://www.w7fg.com/

W9INN Antennas
PO Box 393
Mt Prospect, IL 60056
847-394-3414

Wacom Products
PO Box 21145
Waco, TX 76702
716-549-4700
e-mail sales@txrx.com

WBØW, Inc
PO Box 8547
Saint Joseph, MO 64508
USA
Tel: 816-364-2691
Email: WB0W@WB0W.com

The Wireman Inc.
261 Pittman Road
Landrum, SC 29356-9544
800-727-WIRE (800-727-9473)
Orders only
864-895-4195 Technical
fax 803-895-5811
e-mail N8UG@earthlink.net
web thewireman.com/

Yaesu U.S.A. (Vertex Standard)
10900 Walker St.
Cypress, CA 90630
714-827-7600
e-mail
amateurtech@vxstdusa.com
web www.yaesu.com/amateur/
amateur.html

YagiStress
Kurt Andress, K7NV
2835 Wade Street
Minden, NV 89423
702-267-5290
e-mail K7NV@contesting.com
web yagistress.freeyellow.com/

Zero Surge Inc
944 State Rt 12
Frenchtown, NJ 08825
908-996-7700
fax 908-996-7773
e-mail zerosurge1@aol.com
web www.zerosurge.com/

Chap 21.pmd 8 3/13/2007, 3:25 PM

Chapter 22

Antenna Supports

A prime consideration in the selection of a support for an antenna is that of structural safety. Building regulations in many localities require that a permit be obtained in advance of the erection of certain structures, often including antenna poles or towers. In general, localities having such requirements also have building safety codes that must be observed. Such regulations may govern the method and materials used in construction of, for example, a self-supporting tower. Checking with your local government building department before putting up a tower may save a good deal of difficulty later, because a tower would have to be taken down or modified if not approved by the building inspector on safety grounds.

Municipalities have the right and duty to enforce any reasonable regulations having to do with the safety of life or property. The courts generally have recognized, however, that municipal authority does not extend to aesthetic questions. The fact that someone may object to the mere presence of a pole, tower or other antenna structure because in his opinion it detracts from the beauty of the neighborhood is not grounds for refusing to issue a permit for a safe structure to be erected. Since the introduction of PRB-1 (federal preemption of unnecessarily restrictive antenna ordinances), this principle has been borne out in many courts. Permission for erecting amateur towers is more easily obtained than in the recent past because of this legislation.

Even where local regulations do not exist or are not enforced, the amateur should be careful to select a location and a type of support that contribute as much safety as possible to the installation. If collapse occurs, the chances of personal injury or property damage should be minimized by careful choice of design and erection methods. A single injury can be far more costly than the price of a more rugged support, in terms of both monetary loss and damage to the public respect for amateur radio.

This chapter has been reviewed and rewritten by Kurt Andress, K7NV.

TREES AS ANTENNA SUPPORTS

From the beginning of Amateur Radio, trees have been used widely for supporting wire antennas. Trees cost noth-

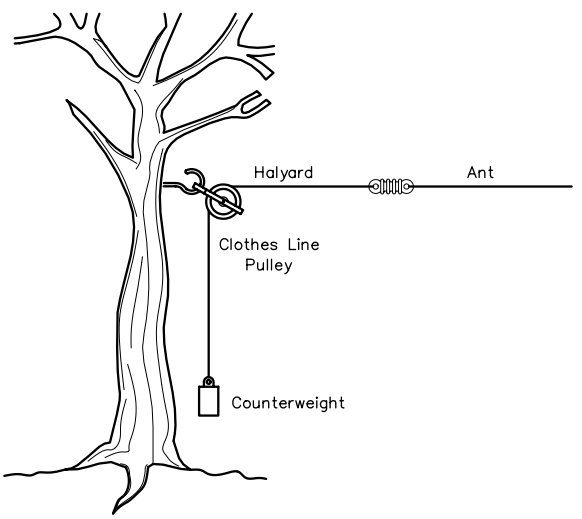

Fig 1—A method of counter weighting to minimize antenna movement and avoid its breaking from tree movement in the wind. The antenna may be lowered without climbing the tree by removing the counterweight and tying additional rope at the bottom end of the halyard. Excess rope may be left at the counterweight for this purpose, as the knot at the lower end of the halyard will not pass through the pulley.

ing to use, and often provide a means of supporting a wire antenna at considerable height. As antenna supports, trees are unstable in the presence of wind, except in the case of very large trees used to support antennas well down from the top branches. As a result, tree-supported antennas must be constructed much more sturdily than is necessary with stable supports. Even with rugged construction, it is unlikely that an antenna suspended from a tree, or between trees, will stand up indefinitely. Occasional repair or replacement usually must be expected.

There are two general methods of securing a pulley to a tree. If the tree can be climbed safely to the desired level, a pulley can be attached to the trunk of the tree, as shown in **Fig 1**. To clear the branches of the tree, the antenna end of the halyard can be tied temporarily to the tree at the pulley level. Then the remainder of the halyard is coiled up, and the coil thrown out horizontally from this level, in the direction in which the antenna runs. It may help to have the antenna end of the halyard weighted.

After attaching the antenna to the halyard, the other end is untied from the tree, passed through the pulley, and brought to ground along the tree trunk in as straight a line as possible. The halyard need only be long enough to reach the ground after the antenna has been hauled up. (Additional rope can be tied to the halyard when it becomes necessary to lower the antenna.)

The other method consists of passing a line over the tree from ground level, and using this line to haul a pulley up into the tree and hold it there. Several ingenious methods have been used to accomplish this. The simplest method employs a weighted pilot line, such as fishing line or mason's chalk line. By grasping the line about two feet from the weight, the weight is swung back and forth, pendulum style, and then heaved with an underhand motion in the direction of the treetop.

Several trials may be necessary to determine the optimum size of the weight for the line selected, the distance between the weight and the hand before throwing, and the point in the arc of the swing where the line released. The weight, however, must be sufficiently large to carry the pilot line back to ground after passing over the tree. Flipping the end of the line up and down so as to put a traveling wave on the line often helps to induce the weight to drop down if the weight is marginal. The higher the tree, the lighter the weight and the pilot line must be. A glove should be worn on the throwing hand, because a line running swiftly through the bare hand can cause a severe burn.

If there is a clear line of sight between ground and a particularly desirable crotch in the tree, it may eventually be possible to hit the crotch after a sufficient number of tries. Otherwise, it is best to try to heave the pilot line completely over the tree, as close to the centerline of the tree as possible. If it is necessary to retrieve the line and start over again, the line should be drawn back very slowly; otherwise the swinging weight may wrap the line around a small limb, making retrieval impossible.

Stretching the line out straight on the ground before throwing may help to keep the line from snarling, but it places extra drag on the line, and the line may snag on obstructions overhanging the line when it is thrown. Another method is to make a stationary reel by driving eight nails, arranged in a circle, through a 1-inch board. After winding the line around the circle formed by the nails, the line should reel off readily when the weighted end of the line is thrown. The board should be tilted at approximately right angles to the path of the throw.

Other devices that have been used successfully to pass a pilot line over a tree are a bow and arrow with heavy thread tied to the arrow, and a short casting rod and spinning reel used by fishermen. The Wrist Rocket slingshot made from surgical rubber tubing and a metal frame has proved highly effective as an antenna-launching device. Still another method that has been used where sufficient space is available is flying a kite to sufficient altitude, walking around the tree until the kite string lines up with the center of the tree, and paying out string until the kite falls to the earth. This method can be used to pass a line over a patch of woods between two higher supports, which may be impossible using any other method.

The pilot line can be used to pull successively heavier lines over the tree until one of adequate size to take the strain of the antenna has been reached. This line is then used to haul a pulley up into the tree after the antenna halyard has been threaded through the pulley. The line that holds the pulley must be capable of withstanding considerable chafing where it passes through the crotch, and at points where lower branches may rub against the standing part. For this reason, it may be advisable to use galvanized sash cord or stranded guy wire for raising the pulley.

Larger lines or cables require special attention when they must be spliced to smaller lines. A splice that minimizes the chances of coming undone when coaxed through the tree crotch must be used. One type of splice is shown in **Fig 2**.

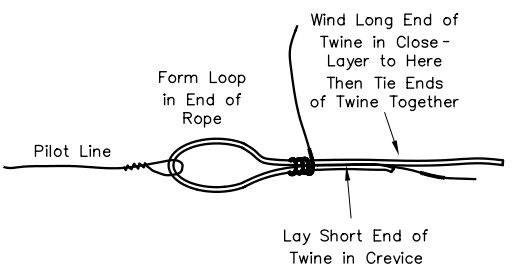

Fig 2—In connecting the halyard to the pilot line, a large knot that might snag in the crotch of a tree should be avoided, as shown.

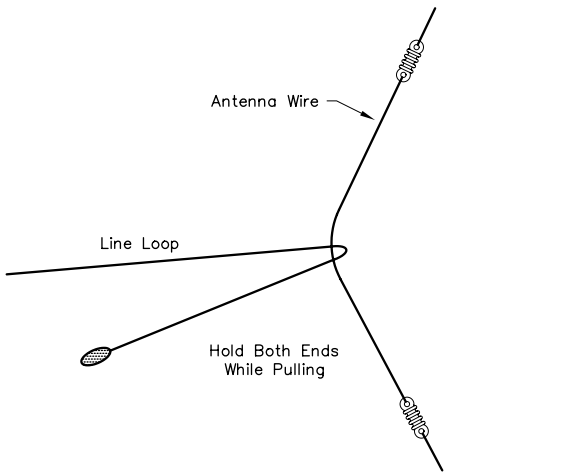

Fig 3—A weighted line thrown over the antenna can be used to pull the antenna to one side of overhanging obstructions, such as tree branches, as the antenna is pulled up. When the obstruction has been cleared, the line can be removed by releasing one end.

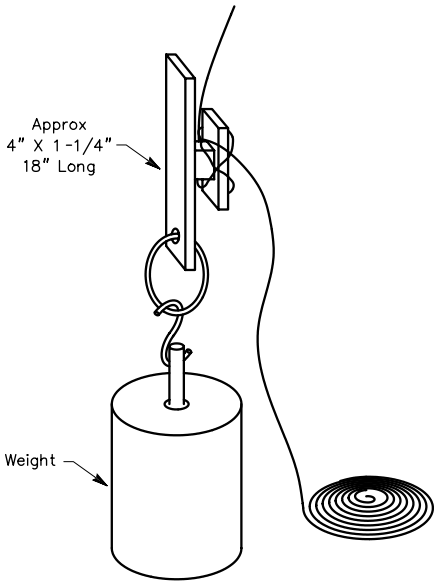

Fig 4—The cleat eliminates the need to untie a knot that may be weather hardened.

The crotch in which the line first comes to rest may not be sufficiently strong to stand up under the tension of the antenna. If, however, the line has been passed over (or close to) the center line of the tree, it will usually break through the lighter crotches and come to rest in a stronger one lower in the tree.

Needless to say, any of the suggested methods should be used with due respect to persons or property in the immediate vicinity. A child's sponge-rubber ball (baseball size) makes a safe weight for heaving a heavy thread line or fishing line.

If the antenna wire snags in the lower branches of the tree when the wire is pulled up, or if other trees interfere with raising the antenna, a weighted line thrown over the antenna and slid to the appropriate point is often helpful in pulling the antenna wire to one side to clear the interference as the antenna is being raised. This is shown in **Fig 3**.

Wind Compensation

The movement of an antenna suspended between supports that are not stable in the wind can be reduced by the use of heavy springs, such as screen-door springs under tension, or by a counterweight at the end of one halyard. This is shown in Fig 1. The weight, which may be made up of junkyard metal, window sash weights, or a galvanized pail filled with sand or stone, should be adjusted experimentally for best results under existing conditions. **Fig 4** shows a convenient way of fastening the counterweight to the halyard. It eliminates the necessity for untying a knot in the halyard, which may have hardened under tension and exposure to the weather.

TREES AS SUPPORTS FOR VERTICAL WIRE ANTENNAS

Trees can often be used to support vertical as well as horizontal antennas. If the tree is tall and has overhanging branches, the scheme of **Fig 5** may be used. The top end of the antenna is secured to a halyard passed over the limb, brought back to ground level, and fastened to the trunk of the tree.

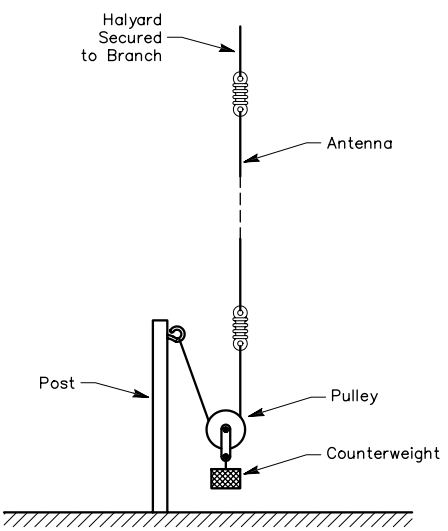

Fig 5—Counterweight for a vertical antenna suspended from an overhanging tree branch.

MAST MATERIALS

Where suitable trees are not available, or a more stable support is desired, light-duty guyed masts are suitable for wire antennas of reasonable span length. At one time, most amateur masts were constructed of lumber, but the TV industry has brought out metal masts that are inexpensive and much more durable than wood. However, there are some applications where wood is necessary or desirable.

A Ladder Mast

A temporary antenna support is sometimes needed for an antenna system for antenna testing, site selection, emergency exercises or Field Day. Ordinary aluminum extension ladders are ideal candidates for this service. They are strong, light, extendable, weatherproof and easily transported. Additionally, they are readily available and can be returned to normal use once the project is concluded. A ladder tower will support a lightweight triband beam and rotator.

With patience and ingenuity one person can erect this assembly. One of the biggest problems is holding the base down while "walking" the ladder to a vertical position. The ladder can be guyed with 1/4-inch polypropylene rope. Rope guys are arranged in the standard fashion with three at each level. If help is available, the ladder can be walked up in its retracted position and extended after the antenna and rotator are attached. The lightweight pulley system on most extension ladders is not strong enough to lift the ladder extension. This mechanism must be replaced (or augmented) with a heavy-duty pulley and rope. Make sure when attaching the guy ropes that they do not foul the operation of the sliding upper section of the ladder.

There is one hazard in this system that must be avoided: Do not climb or stand on the ladder when it is being extended—even as much as one rung. Never stand on the ladder and attempt to raise or lower the upper section. Do all the extending and retracting with the heavy-duty rope and pulley!

If the ladder is to be raised by one person, use the following guidelines. First, make sure the rung-latching mechanism operates properly before beginning. The base must be hinged so that it does not slip along the ground during erection. The guy ropes should be tied and positioned in such a way that they serve as safety constraints in the event that control of the assembly is lost. Have available a device (such as another ladder) for supporting the ladder during rest periods. (See **Fig 6**.)

After the ladder is erect and the lower section guys tied and tightened, raise the upper portion one rung at a time. Do not raise the upper section higher than it is designed to go; safety is far more important than a few extra feet of height.

For a temporary installation, finding suitable guy anchors can be an exercise in creativity. Fence posts, trees, and heavy pipes are all possibilities. If nothing of sufficient strength is available, anchor posts or pipes can be driven into the soil. Sandy soil is the most difficult to work with because it does a very poor job of holding anchors. A discarded car axle can be driven into the ground as an anchor, as its mass and strength are substantial. A chain and car-bumper jack can be used to remove the axle when the operation is done.

Fig 6—Walking the ladder up to its vertical position. Keith, VE2AQU, supports the mast with a second ladder while Chris, VE2FRJ, checks the ropes. (*Photo by Keith Baker, VE2XL.*)

Above all else, keep the tower and antenna away from power lines. Make sure that nothing can touch the lines if the assembly falls. Disassemble by reversing the process. Ladder towers are handy for "quickie" antenna supports, but as with any improvisation of support materials, care must be taken to ensure safe construction.

The A-Frame Mast

A light and relatively inexpensive mast is shown in **Fig 7**. In lengths up to 40 feet it is very easy to erect and will stand the pull of ordinary wire antenna systems. The lumber used is 2 × 2-inch straight-grained pine (which many lumber yards know as hemlock) or even fir stock. The uprights can be as long as 22 feet each (for a mast slightly over 40 feet high) and the cross pieces are cut to fit. Four pieces of 2 × 2 lumber, each 22 feet long, provides more than enough. The only other materials required are five 1/4-inch carriage bolts 5 1/2 inches long, a few spikes, about 300 feet of stranded or solid galvanized wire for guying, enough glazed porcelain compression ("egg") insulators to break up the guys into sections, and the usual pulley and halyard rope. If the strain insulators are put in every 20 feet, approximately 15 of them will be enough.

After selecting and purchasing the lumber—which should be straight-grained and knot-free—sawhorses or boxes should be set up and the mast assembled as shown

in **Fig 8**. At this stage it is wise to give the mast a coat of primer and a coat of outside white latex paint.

After the coat of paint is dry, attach the guys and rig the pulley for the antenna halyard. The pulley anchor should be at the point where the top stays are attached so the backstay will assume the greater part of the load tension. It is better to use wire wrapped around the mast with a small through-bolt to prevent sliding down than to use eyebolts.

If the mast is to stand on the ground, a couple of stakes should be driven to keep the bottom from slipping. At this point the mast may be "walked up" by a helper. If it is to go on a roof, first stand it up against the side of the building and then hoist it, from the roof, keeping it vertical. The whole assembly is light enough for two men to perform the complete operation—lifting the mast, carrying it to its permanent berth, and fastening the guys with the mast vertical. It is entirely practical to put up such a mast on a flat area of roof that would be too small to erect a regular tower installation, one that had to be raised vertically on the same spot.

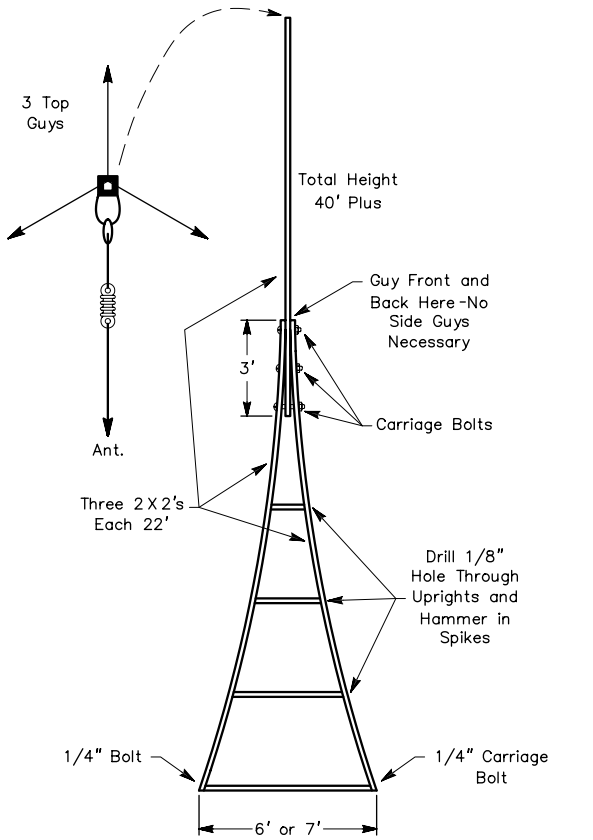

Fig 7—The A-frame mast is lightweight and easily constructed and erected.

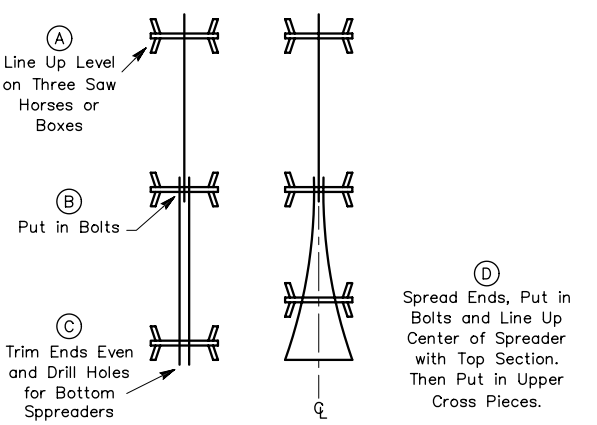

Fig 8—Method of assembling the A-frame mast on sawhorses.

TV Mast Material

TV mast is available in 5- and 10-foot lengths, $1^{1}/_{4}$ inches diameter, in both steel and aluminum. These sections are crimped at one end to permit sections to be joined together. A form that is usually more convenient is the telescoping mast available from many electronic supply houses. The masts may be obtained with three, four or five 10-foot sections, and come complete with guying rings and a means of locking the sections in place after they have been extended. These masts are inherently more suitable for guyed mast installations than the non-telescoping type because the diameters of the sections increase toward the bottom of the mast. For instance, the top section of a 50-foot mast is $1^{1}/_{4}$ inches diameter, and the bottom section is $2^{1}/_{2}$ inches diameter.

Guy rings are provided at 10-foot intervals, but guys may not be required at every point. Guying is essential at the top and at least one other place near the center of the mast. If the mast has any tendency to whip in the wind, or to bow under the load of a horizontal wire antenna, additional guys should be added at the appropriate points.

MAST GUYING

Three guy wires in each set are usually adequate for a mast. These should be spaced equally round the mast. The required number of sets of guys depends on the height of the mast, its natural sturdiness (or stiffness), and the required antenna tension. A 30-foot-high mast usually requires two sets of guys, and a 50-foot mast needs at least three sets. One guy of the top set should be anchored to a point directly opposing the force exerted by the wire antenna. The other two guys of the same set should be spaced 120° with respect to the first, as shown in the inset in Fig 7.

Generally, the top guys should be anchored at distances from the base of the mast at least 60% of the mast height. The distance of the guy anchors from the mast determines the guy loads and the vertical load compressing the mast. At a 60% distance, the load on the guy wire

opposite the wire antenna is approximately twice the antenna tension. The compression in the mast will be 1.66 times the antenna tension. With the anchors out 80% of the mast height, the guy tension will be 1.6 times larger than the antenna load and the mast compression will be 1.25 times larger.

Whenever possible, the largest available anchor spacing should be used. The additional compression on the mast, due to closer anchor spacing, increases the tendency of the mast to buckle. Buckling occurs when the compression on the unsupported spans between guys become too great for the unsupported length. The section then bows out laterally and will usually fold over, collapsing the mast. Additional sets of guys reduce the tendency for the mast to buckle under the compression by decreasing the unsupported span lengths and stabilizing the mast, keeping it in a straight line.

A natural phenomenon, called *vortex shedding*, can occur when the wind passes over the sections of a guyed mast. For every section size, shape, and length, there is a wind speed that can cause the sections to oscillate mechanically. When all the sections of an antenna support mast are close to the same size and length, it is possible for all of the mast sections to vibrate simultaneously between the guys. To reduce the potential for this, you can place the guys at locations along the mast that will result in different span lengths. This creates different mechanical resonant frequencies for each span, eliminating the possibility of all sections oscillating at the same time.

When determining the guy locations along the mast to treat this problem, you also need to consider the mast buckling requirements. Since the compression in the mast is greatest in the bottom span, and the least in the top span, the guys should be placed to make the bottom span the shortest and the top span the longest. A general guide for determining the different span lengths is to make the unguyed lengths change by 10 to 20%.

Example: For a 30-foot high mast with three guy sets, the equal-guy locations would be every 10 feet. We can make the center span, 10 feet long, and then make the lower span 15% shorter and the top span 15% longer. While this is not an exact technical method to determine the best solution, the approach will create different mechanical resonant frequencies for the spans, with the span lengths approximately adjusted for the varying buckling requirements.

You can eliminate electrical resonance from conductive guy materials that might cause distortion of the antenna radiation pattern by breaking each guy into nonresonant lengths using strain insulators (see **Figs 9** and **10**). This subject is covered in detail later in this chapter.

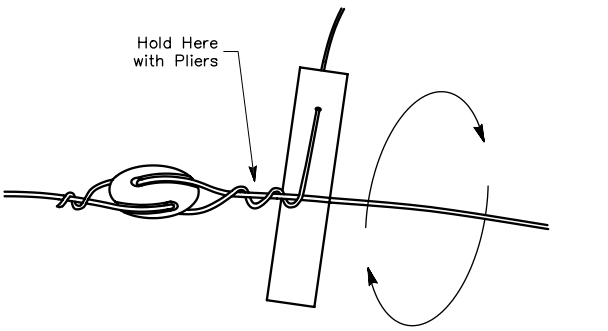

Fig 9—Simple lever for twisting solid guy wires when attaching strain insulators.

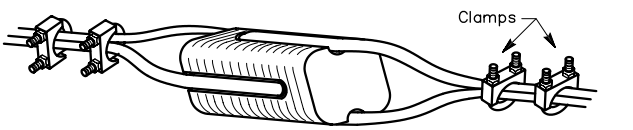

Fig 10—Stranded guy wire should be attached to strain insulators by means of standard cable clamps made to fit the size of wire used.

Guy Material

When used within their safe load ratings, you may use any of the halyard materials listed in Chapter 20 for the mast guys. Nonmetallic materials have the advantage that there is no need to break them up into sections to avoid unwanted resonant interactions. All of these materials are subject to *stretching*, however, which causes mechanical problems in permanent installations. At rated working loads, dry manila rope stretches about 5%, while nylon rope stretches about 20%. Usually, after a period of wind load and wet/dry cycles, the lines will become fairly stable and require less frequent adjustment.

Solid galvanized steel wire is also widely used for guying. This wire has approximately twice the load ratings of similar sizes of copper-clad wire, but it is more susceptible to corrosion. Stranded galvanized wire sold for guying TV masts is also suitable for light-duty applications, but is also susceptible to corrosion. It is prudent to inspect the guys every six months for signs of deterioration or damage.

Guy Anchors

Figs 11 and **12** show two different kinds of guy anchors. In Fig 11, one or more pipes are driven into the ground at right angles to the guy wire. If a single pipe proves to be inadequate, another pipe can be added in tandem, as shown, and connected with a galvanized steel cable. Heavy-gauge galvanized pipe is preferred for corrosion resistance. Steel fence posts may be used in the same manner. Fig 12 shows a *dead-man* type of

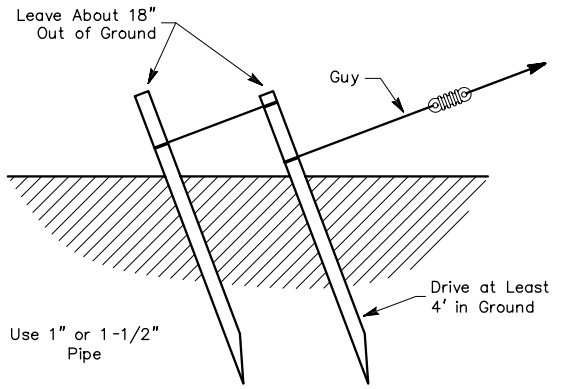

Fig 11—Driven guy anchors. One pipe is usually sufficient for a small mast. For added strength, a second pipe may be added, as shown.

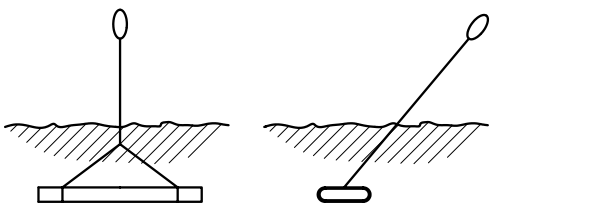

Fig 12—Buried *dead-man* guy anchor (see text).

anchor. The buried anchor may consist of one or more pipes 5 or 6 feet long, or scrap automobile parts, such as bumpers or wheels. The anchors should be buried 3 or 4 feet in the ground. The cable connecting the dead-man to the guys should be galvanized wire rope, like EHS guy cable. You should coat the buried part of the cable with roofing tar, and thoroughly dry it prior to burial to enhance resistance to corrosion.

Also available are some heavy auger-type anchors that screw into the earth. These anchors are usually heavier than required for guying a mast, although they may be more convenient to install. You should conduct annual inspections of the anchors by digging several inches below grade around the anchor to inspect for corrosion.

Trees and buildings may also be used as guy anchors if they are located appropriately. Care should be exercised, however, to make sure that the tree is of adequate size and that any fastening to a building can be made sufficiently secure.

Guy Tension

Many troubles encountered in mast guying are a result of pulling the guy wires too tight. Guy-wire tension should never be more than necessary to correct for obvious bowing or movement under wind pressure. Approximately 10% to 15% of the working load is sufficient. In most cases, the tension needed does not require the use of turnbuckles, with the possible exception of the guy opposite a wire antenna. If any great difficulty is experienced in eliminating bowing from the mast, the guy tension should be reduced or additional sets of guys are required. The mast should be checked periodically, especially after large wind events, to ensure the guys and anchors have not stretched or moved, allowing the mast to get away from the required straight alignment.

ERECTING A MAST OR OTHER SUPPORT

Masts less than 30 feet high usually can be simply walked up after blocking the bottom end securely. Blocking must be done so that the base can neither slip along the ground nor upend when the mast is raised. An assistant should be stationed at each guy wire, and may help by pulling the proper guy wire as the mast nears the vertical position. Halyards can be used in the same manner.

As the mast is raised, it may be helpful to follow the underside of the mast with a scissors rest (**Fig 13**), should a pause in the hoisting become necessary. The rest may also be used to assist in the raising if an assistant mans each leg.

As the mast nears the vertical position, those holding the guy wires should be ready to temporarily fasten the guys to prevent the mast from falling. The guys can then be adjusted until the mast is perfectly straight.

For masts over 30 feet long, a *gin pole* of some form may be required, as shown in Fig 13. Several turns of

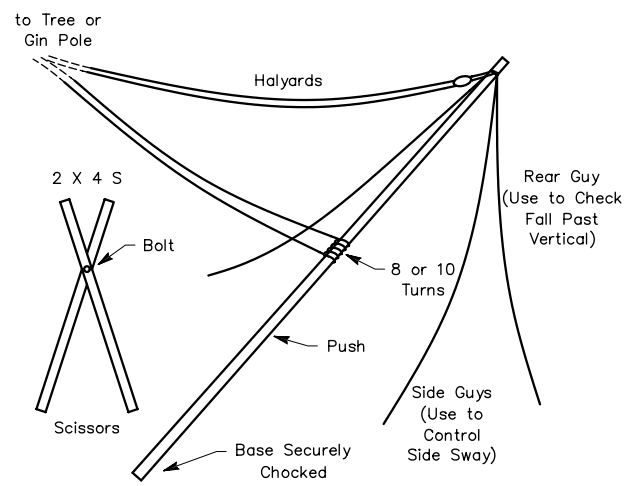

Fig 13—Pulling on a gin line fastened slightly above the center point of the mast and on the halyards can assist in erecting a tall mast. The tensions should be just enough to keep the mast in as straight a line as possible. The "scissors" may be used to push on the under side and to serve as a rest if a pause in raising becomes necessary.

rope are wound around a point on the mast above center. The ends of the rope are then brought together and passed over a tree limb. The rope should be pulled as the mast is walked up to keep the mast from bending at the center. If a tree is not available, a post, such as a 2×4, temporarily erected and guyed, can be used. After the mast has been erected, the assisting rope can be removed by walking one end around the mast (inside the guy wires).

Telephone poles and towers are much sturdier supports. Such supports may require no guying, but they are not often used solely for the support of wire antennas because of their relatively high cost. For antenna heights in excess of 50 feet, however, they are usually a most practical form of support.

Tower And Antenna Selection and Installation

The selection of a tower, its height, and the type of antennas and rotator is probably one of the more complex issues faced by station builders. All aspects of the tower, antenna, and rotator system are interrelated, and you should consider the overall system before making any decisions regarding specific system components.

Perhaps the most important consideration for many amateurs is the effect of the antenna system on the surrounding environment. If plenty of space is available for a tower installation and if there is little chance of causing esthetic distress on the part of family members or the neighbors, the amateur is indeed fortunate. Often, the primary considerations are purely financial. For most, however, the size of the property, the effect of the system on others, local ordinances, and the proximity of power lines and poles influence the selection of the tower/antenna system considerably.

The amateur must consider the practical limitations for installation. Some points for consideration are given below:

1) A tower should not be installed in a position where it could fall onto a neighbor's property.
2) The antenna must be located in such a position that it cannot possibly tangle with power lines, either during normal operation or if the structure should fall.
3) Sufficient yard space must be available to position a guyed tower properly. The guy anchors should be between 60% and 80% of the tower height in distance from the base of the tower on level ground—sloping terrain may require larger areas.
4) Provisions must be made to keep children from climbing the support. (Poultry netting around the tower base will serve this need.)
5) Local ordinances should be checked to determine if any legal restrictions affect the proposed installation.

Other important considerations are (1) the total dollar amount to be invested, (2) the size and weight of the antenna desired, (3) the climate, and (4) the ability of the owner to climb a fixed tower.

Most tower manufacturers provide catalogues or data packages that represent engineered tower configurations. These are provided as a convenience for users to help determine the most suitable tower configurations. The most commonly used design specifications for towers are EIA (Electronic Industries Assoc.) RS-222 and UBC (Uniform Building Code). These specifications define how the tower, antenna, and guy loads are determined and applied to the system, and establish general design criteria for the analysis of the tower. Local authorities often require the review and approval of the installation by a state licensed Professional Engineer (P.E.) to obtain building permits. All local authorities in the United States do not subscribe to the same design standards, so often the manufacturers' general-purpose engineering is not applicable.

One of the first things you need to determine in the tower selection process is the type of specification required by the local authorities, if any. Then, you must determine the *Basic Wind Speed* appropriate for the site. The *Basic Wind Speed* used in most specifications is the average wind speed for one mile of wind passing across the structure. It will be a lower value than the peak readings from an anemometer (wind gauge) installed at the site. For example, a Basic Wind Speed of 70 mph could have a maximum value of 80 mph and a minimum of 60 mph, equally distributed during the passage of the mile of wind. Basic wind speeds can be found in tables or maps contained in the appropriate specifications. Often, the basic wind speed used for the location may be obtained from the local permit authority. Check out the Web site at **www.championradio.com**, which contains EIA basic wind speed tables for every county in the USA. UBC speeds are available at almost every local library.

Antenna manufacturers also provide antenna data to assist in the selection process. Unfortunately, antenna mechanical designs do not always follow the same design standards used for towers. Proper antenna selection often means that you must determine the antenna surface areas yourself to avoid overloading the tower. More discussion about this follows later in this chapter.

It is often very helpful to the novice tower installer to visit other local amateurs who have installed towers. Look over their hardware and ask questions. If possible, have a few local experienced amateurs look over your plans—before you commit yourself. They may be able to offer a great deal of help. If someone in your area is planning to install a tower and antenna system, be sure to offer your assistance. There is no substitute for experience when it comes to tower work, and your experience there may prove invaluable to you later.

THE TOWER

Towers for supporting antennas come in a variety of different types. Each type has its own set of benefits and limitations, or conditions and requirements. Often, you can choose a particular tower type by considering issues other than pure mechanical performance. Understanding how each type of tower functions, and what its respective requirements are, are the first steps in making the best tower selection for your own situation.

Guyed Towers

The most common variety of tower is the *guyed tower* made of identical stacked sections, supported by guy cables attached to ground anchors placed symmetrically around the tower. These towers are the most economical, in terms of feet per dollar investment, and are more efficient for carrying antenna loads than non-guyed towers.

The guys resist the lateral loads on the system created by the wind. Since the guys slope down to the ground, horizontal loads due to the wind result in vertical loads applied to the tower at each tower/guy connection. The tower becomes a compression member, trying to resist the column compression generated by the guy reactions. A tower in compression can buckle, so the distance between guy connections along the tower is important.

Tower Bases for Guyed Towers

Another important phenomenon in a guyed tower is stretching of the guy cables. All guys stretch under load and when the wind blows the elongated guys allow the tower to lean over somewhat. If the tower base is buried in the concrete footing—as is commonly done in amateur installations—the bending stress at the tower base can become a significant factor. Towers that have been installed with tapered pier-pin bases much more freely absorb tower leaning, and they are far less sensitive to guy-elongation problems.

The tapered pier-pin tower installation is not without some drawbacks. These installations often require torque-arm guy brackets or six-guy torque-arm assemblies to control tower rotation due to antenna torque. They also require temporary guys when they are being installed to hold the base steady until the permanent guys are mounted. Some climbers also don't like the flexing when they start to climb these types of towers.

On the positive side, pier-pin base towers have all structural members above the concrete footing, eliminating concerns about hidden corrosion that can occur with buried towers. Most decisions regarding the type of base installation are made according to the preference of the tower builder/maintainer. While either type of base configuration can be successfully used, you would be wise to do the stress calculations (or have a professional engineer do them) to ensure safety, particularly when large antenna loads are contemplated and particularly if guys that can easily stretch are used, such as Phillystran guys.

The configuration shown in **Fig 14A** is taken from an older (1983) Unarco-Rohn catalog. This configuration has the top set of guys placed at the top of the tower with the lower set halfway up the tower. This configuration is best for most amateur installations, which usually have the antennas mounted on a rotatable mast extending

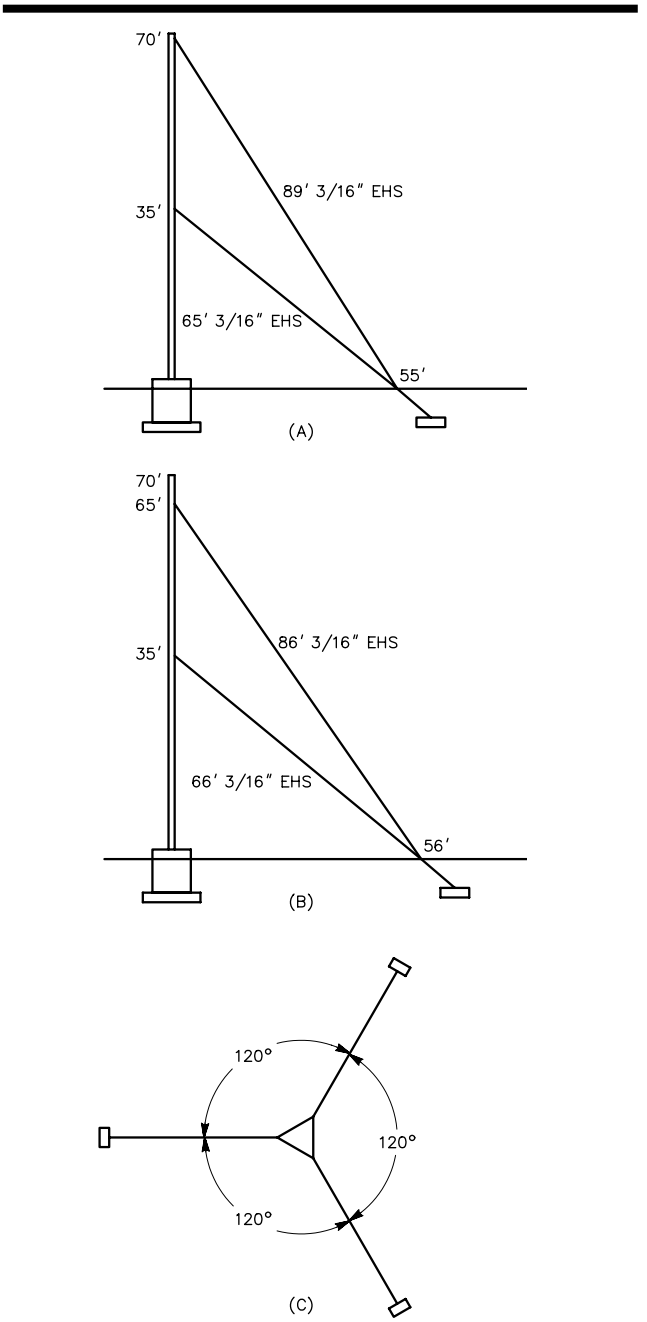

Fig 14—The proper method of installation of a guyed tower. At A, the method recommended for most amateur installations. At B, the method shown in later Rohn catalogs. This places considerable strain on the top section of the tower when large antennas are mounted on the tower.

out the top of the tower—thereby placing the maximum lateral loads when the wind blows at the top of the tower (and the bottom of the rotating mast).

The configuration shown in Fig 14B is from a newer (1998) Rohn catalog. It has 5 feet of unsupported tower extending above the top guy set. The lower guy set is approximately halfway between the top guys and the base. The newer configurations are tailored for commercial users who populate the top region of the tower with fixed arrays and/or dishes. The installation in Fig 14B cannot safely withstand the same amount of horizontal top load as can the configuration shown in Fig 14A, simply because the guys start farther down from the top of the tower.

An overhead view of a guyed tower is given in Fig 14C. Common practice is to use equal angular spacings of 120° between guy wires. If you must deviate from this spacing, the engineering staff of the tower manufacturer or a civil engineer should be contacted for advice.

Amateurs should understand that most catalogs show generic examples of tower configurations that work within the cited design specifications. They are by no means the only solution for any specific tower/antenna configuration. You can usually substantially change the load capability of any given tower by varying the size and number of guys. Station builders are encouraged to utilize the services of professional engineers to get the most out of their guyed towers. Those interested in more generic information about guyed tower behavior can find it at **www.freeyellow.com/members3/yagistress/**.

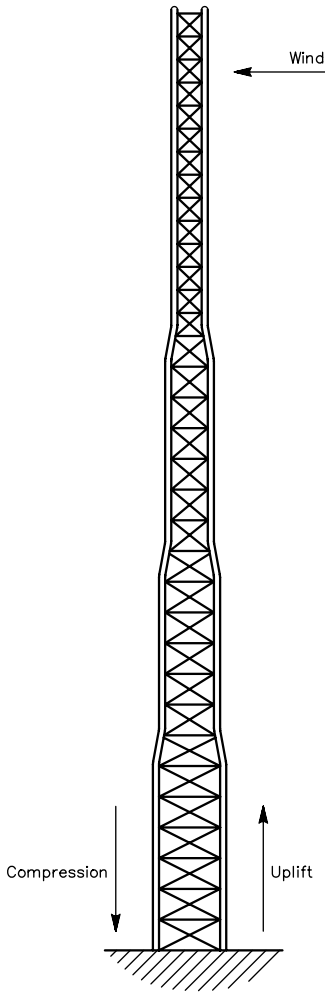

Fig 15—Typical freestanding (unguyed) tower. Arrows indicate the directions of the forces acting upon the structure. See text for discussion.

Unguyed Towers

Another commonly used type of tower is not normally guyed—these are usually referred to as *freestanding* or *self-supporting* towers. Unguyed towers come in three different styles.

One style is comprised of stacked lengths of identical tower sections, just like those used for guyed towers. The only difference is that no guys are used. Manufacturers provide the recommended configurations and allowable loads for this type of installation in their catalogs. Unguyed towers are vastly less capable of supporting antenna loads than their guyed counterparts, but have great utility for light-duty applications—when configured within their capabilities.

The second style utilizes different tower section sizes, varying from large sections at the base and tapering down to smaller sections at the top. This style is more much more efficient for freestanding applications, because the tower is sized for the varying bending loads along the tower length, and is shown in **Fig 15**.

The third style of unguyed towers is commonly called a *crank-up tower*. It is a freestanding tower with telescoping sections that can be extended or retracted with a winch, cable, and pulley mechanism. This allows the tower to be raised and lowered for maintenance and antenna work. It is usually necessary to retract such towers for moderate to heavy winds. Some consider this a disadvantage because they can't operate their antennas at full height when it is windy. Two different forms of the crank-up style, freestanding tower are shown in **Fig 16**. Fig 16A shows the tubular version; Fig 16B shows the triangular space-frame version.

Some crank-up towers are used with guys and are only retracted for maintenance and antenna work. These towers are specially designed with locking mechanisms between the tower sections to carry the vertical compression created by the guys. *Do not* use guys with normal crank-up towers (those that have no locking devices between sections)! The increased tower compression will be carried by the hoisting cable, which will eventually cause it to fail.

Never climb a crank-up tower unless it is properly nested, with all load removed from the hoisting cable. For general antenna work, this can be accomplished by completely retracting it until the cable becomes loose. When servicing the rotator, the tower must be left partially extended. In this case every tower section must be

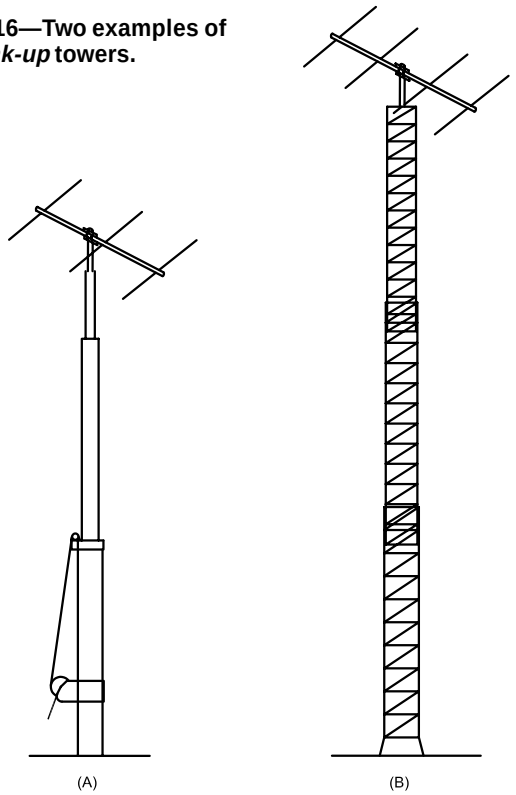

Fig 16—Two examples of *crank-up* towers.

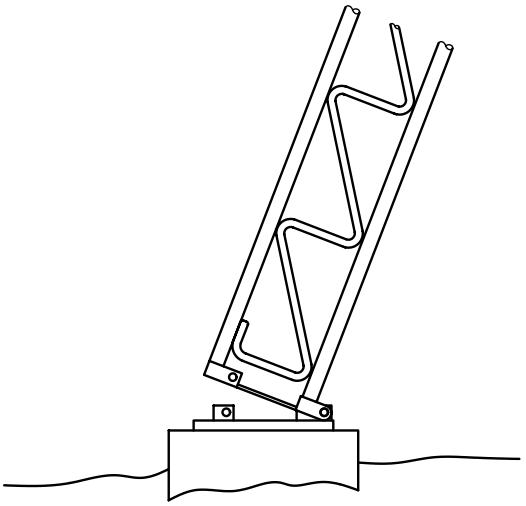

Fig 17—Fold-over or tilting base. There are several different kinds of hinged sections permitting different types of installation. Great care should be exercised when raising or lowering a tilting tower.

blocked with heavy timber or thick-wall tubes, installed through the tower bracing, until all sections are resting on the blocks and the hoisting cable becomes slack. Safely installing the blocks in an extended crank-up tower can be challenging. The object is to get all the blocks installed without a climber having to scale the unblocked tower, risking loss of limbs should the hoisting cable fail. An extension ladder, capable of reaching the required block elevations is the safest approach. If the necessary equipment or expertise is not available, the tower can be retracted, antennas removed, and leaned over, with the base tilt-over assembly, before extending it to access the rotator. Failure to properly block the tower before climbing can result in serious injury should the cable slip or break!

All freestanding towers share some unique characteristics. Each must support antenna and tower loads only by virtue of the bending strength of the tower sections and the tower footing connection to earth. Because of the large overturning moment at the tower base, freestanding towers require larger concrete footings than guyed towers. They are usually more expensive for the same load capability compared to guyed towers, simply because they require larger heavier tower sections and a larger footing to get the job done. The telescoping mechanisms in crank-up tower require more maintenance too.

Freestanding towers are quite popular, and are often the best solutions for sites with limited space and ascetic concerns. When cranked down, a telescoping tower can maintain a low-profile system, out of sight of the neighbors and family.

Tilt-Over Towers

Some towers have another convenience feature—a hinged section that permits the owner to fold over all or a portion of the tower. The primary benefit is in allowing antenna work to be done close to ground level, without the necessity of removing the antenna and lowering it for service. **Fig 17** shows a hinged base used with stacked, guyed tower sections. The hinged section can be designed for portions of the tower above the base. These are usually referred to as *guyed tilt-over towers*, where a conventional guyed tower can be tilted over for installing and servicing antennas. Many crank-up towers come with optional tilt-over base fixtures that are equipped with a winch and cable system for tilting the fully nested tower from horizontal to vertical positions.

Misuse of hinged sections during tower erection is a dangerously common practice among radio amateurs. Unfortunately, these episodes can end in accidents. If you do not have a good grasp of the fundamentals of physics, it might be wise to avoid hinged towers or to consult an expert if there are any questions about safely installing and using such a tower. It is often far easier (and safer) to erect a regular guyed tower or self-supporting tower with gin pole and climbing belt than it is to try to walk up an unwieldy hinged tower.

The AB-577 Military Surplus Tower

Another light duty tower has found acceptance among many amateurs. Available from assorted military surplus dealers is the AB-577 system. This was designed to be a portable, rapid deployment antenna support for field communications. It is a guyed mast that goes up somewhat like a crank-up. The system consists of several short sections of aluminum tubing, with special end connections for joining them. These can be erected from the base fixture, which has a crank-up type winch-driven elevator platform. The tubing sections are installed in the base fixture and connected to the section above it with an over-center locking *Marmon*-style clamp. Then, the elevator platform is raised with the winch and the new tube is locked in place, high on the base fixture. Then the elevator is lowered to accept the next section. While the tower is extended, the supporting guys are adjusted via the unique *snubber* assemblies at the anchor connection. One person can erect this system, even in windy conditions, when special care is given to keeping the guys properly adjusted during each extension.

Fig 18—Installation of surplus AB-577 tower with tribander at 45 feet at K7NV. (*Photo by Kurt Andress, K7NV.*)

The standard AB-577 system, with 3 sets of guys, will support a modest triband Yagi at 45 feet. **Fig 18A** shows an installation with a Hy-Gain TH7DX at 45 feet.

TOWER BASES

Tower manufacturers can provide customers with detailed plans for properly constructing tower bases. **Fig 19** is an example of one such plan. This plan calls for a hole that is $3^1/_2 \times 3^1/_2 \times 6$ feet. Steel reinforcement bars are lashed together and placed in the hole. The bars are positioned so that they will be completely embedded in the concrete, yet will not contact any metallic object in the base itself. This is done to minimize the possibility of a direct discharge path for lightning through the base. Should such a lightning discharge occur, the concrete base could be damaged.

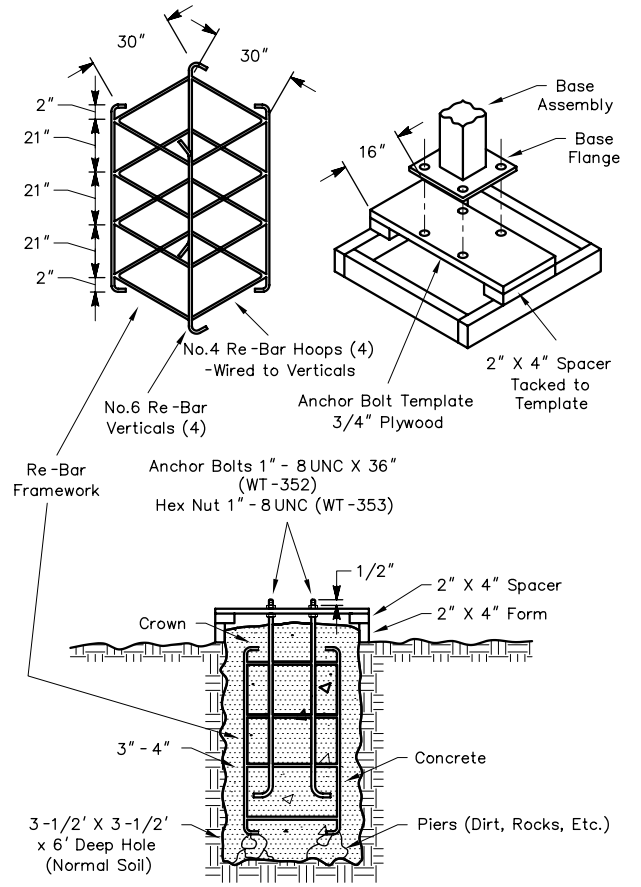

Fig 19—Plans for installing concrete base for Wilson ST-77B tower. Although the instructions and dimensions vary from tower to tower, this is representative of the type of concrete base specified by most manufacturers.

Providing suitable paths for the discharge of lightning energy safely for towers is a complex subject. Several companies offer products and guidance. The basic requirements for providing controlled discharge paths for lightning-induced current is to supply a low-impedance grid of conductors from the tower and feed lines to a field of interconnected ground rods around the base of the tower. Generally, the tower, station, and electrical service grounds need to be connected to prevent damaging potential differences from developing between the various components in the system.

A strong wooden form is constructed around the top of the hole. The hole and the wooden form are filled with concrete so that the resultant block will be 4 inches above grade. The anchor bolts are embedded in the concrete, and aligned with the plywood template, before it hardens. The template serves to align the anchor bolts to properly mate with the tower itself. Once the concrete has

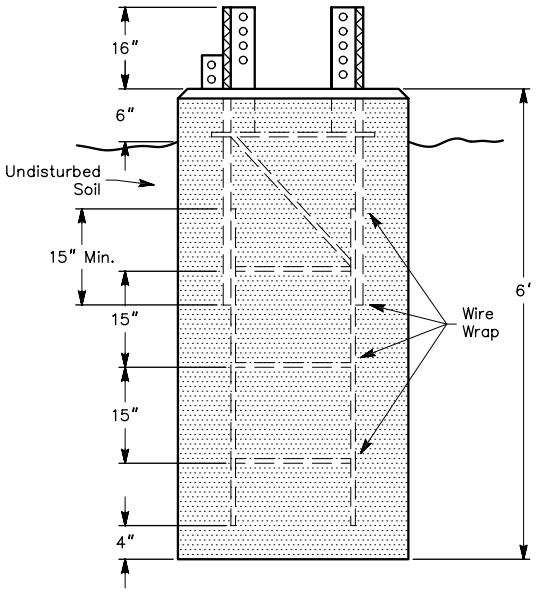

Fig 20—Another example of a concrete base (Tri-Ex LM-470).

cured, the tower base is installed on the anchor bolts and the base connection is adjusted to bring the tower into vertical alignment.

For a tower that bolts to a flat base plate mounted to the footing bolts (as shown in Fig 19), you can bolt the first tower section on the base plate to ensure that the base is level and properly aligned. Use temporary guys to hold things exactly vertical while the concrete cures. (The use of such temporary guys also works well when you place the first tower section in the base hole and plumb it vertically before pouring in the concrete.) Manufacturers can provide specific, detailed instructions for the proper mounting procedure. **Fig 20** shows a slightly different design for a tower base.

The one assumption so far is that *normal* soil is predominant in the area in which the tower is to be installed. Normal soil is a mixture of clay, loam, sand and small rocks. More conservative design parameters for the tower base should be adopted (usually, using more concrete) if the soil is sandy, swampy or extremely rocky. If there are any doubts about the soil, the local agricultural extension office can usually provide specific technical information about the soil in a given area. When this information is in hand, contact the engineering department of the tower manufacturer or a civil engineer for specific recommendations with regard to compensating for any special soil characteristics.

TOWER INSTALLATION

The installation of a tower is not difficult when the proper techniques are used. A guyed tower, in particular, is not hard to erect, because each of the individual sections is relatively lightweight and can be handled with only a few helpers and some good quality rope.

The Gin Pole and Tips on Tower Building

An essential piece of hardware for working on towers is a *gin pole*. This section came from the ARRL book *Simple and Fun Antennas for Hams*. The dictionary describes a gin pole as "a device for moving heavy objects." See **Fig 21**, which shows a drawing of the Rohn "Erection Fixture" EF2545. This gin pole was designed to work with the nominal 10-foot long sections of Rohn 25 or 45 towers.

We're going to assume in the following discussion that you are installing Rohn 45, which weighs about 70 pounds. This is a lot of weight, and you must refrain from adding to that during installation. That means, for example, that you *do not* attempt to lift a 10-foot section with the guy wires attached! Neither should you attempt to lift the top section with the rotator and rotor shelf installed. The gin pole (and your ground crew) will not appreciate all that strain.

The main working part of the gin pole is the pulley

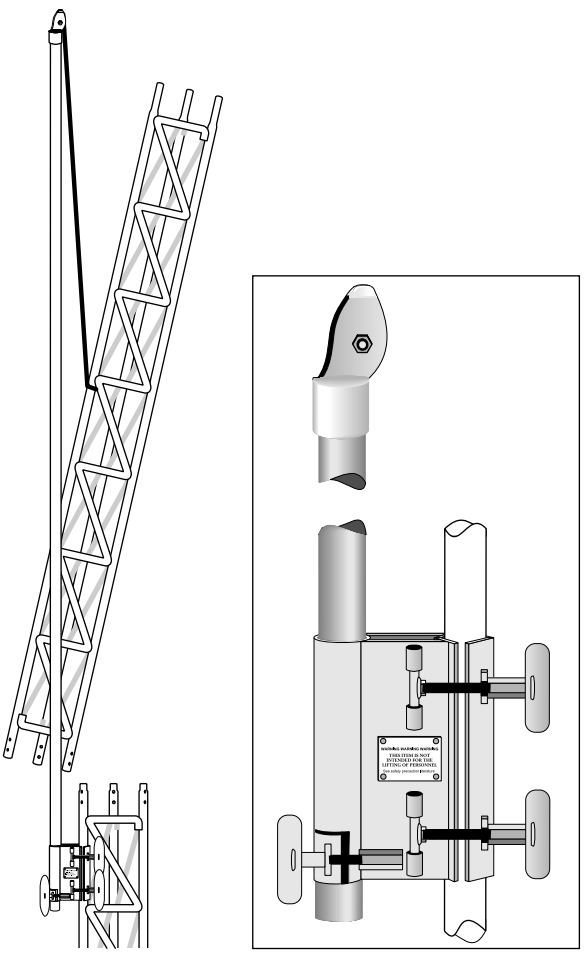

Fig 21—Drawing of Rohn "Erection Fixture" EF2545, also known commonly as a "gin pole."

mounted at the top of the 12-foot long heavy-wall aluminum tubing. This pulley has a rope going down to the ground crew through the center of the aluminum tube. At the base of the tower, the pull rope should be run through a *snatch block* attached to the tower just above ground level. This block allows the pull rope to be pulled out horizontally away from the tower base. That helps protect ground crew should a tool be dropped by the people on the tower.

An adjustable, sliding clamp towards the bottom of the aluminum tubing is clamped to the tower using a swinging L-bracket-type clamp with two clamping bolts. These have T-bar handles that can be tightened by hand. In fact, this gin pole can be moved and deployed without any tools. The clamp is positioned on the top of the tower section onto which the next tower section is to be installed. Once clamped to the top of the tower, you would loosen the T-bar handle that tightens the clamp against the sliding aluminum tube and slide the tubing up to its maximum extent.

In practice, the following steps are taken as each 10-foot section of tower is installed, one-by-one. We're assuming here that the gin pole starts out on the ground, with at least one person belted in at the top of the tower. We're also assuming that the pull rope has been threaded through the aluminum tube and the top pulley, with a knot tied to prevent it from falling back down the tube.

1. The clamp holding the aluminum tubing is loosened so that the pulley on the tube can be lowered to where it is just above the bottom clamp. Then the T-bar handle for the tube clamp is tightened.
2. The climber lowers a tag rope for the ground crew to tie to the gin-pole pull rope. (This tag rope has been looped through a temporary pulley clipped to the top of the tower. It is also used to pull up tools and other materials.) The ground crew then pulls the gin pole up to the climber, using the tag line rope. Friction of the rope against the top of the pulley-head assembly will prevent the gin-pole assembly from slipping down. [Note that some climbers prefer to "walk" the gin-pole up the tower rather than having it pulled up from the ground below. They free up their hands for climbing and temporarily holding the gin pole by using their belt lanyard looped around the tower as they climb.]
3. Once the gin-pole head reaches the top of the tower, the climber clamps the gin pole clamp securely to the top of the tower.
4. The T-bar handle for the tube clamp is loosened, and the aluminum tube is extended to its maximum height, as shown in Fig 21. Make sure you have tied the free end of the rope coming through the top pulley temporarily to the top of the tower, or else you'll have to lower the gin pole and go through this step again.
5. The free end of the pulley rope is then dropped to the ground, often using a weight such as a medium Crescent wrench or perhaps a hammer to keep the rope from waving about as it dangles down the tower, tangling with every imaginable thing as it proceeds downwards. It's amazing how even a tiny breeze can make an unweighted rope dance like that.
6. The ground crew then ties the free end of the rope *above* the balance point of the tower. For Rohn 25 or 45 there are eight horizontal cross braces per section. You want the crew to tie the rope to the fifth horizontal brace from the bottom. Please remember that you want the bottoms of the tower sections' legs to be pointed downwards, not flipped over, when the bottom of these legs approach you at the top of the tower section the climber is standing on.
7. Once the bottom of the rising tower section is just above the top of the legs of the bottom tower section, the climber guides the tower down onto the top of the three legs, while calling out to the ground crew instructions about *slowly lowering* the new section down onto the legs. See **Fig 22**, which shows the climber guiding the new section of Rohn HBX tower onto the previous section's legs. This process is considerably easier to accomplish if each section of tower has been put together on the ground to make sure that the legs fit together easily. There's nothing more frustrating that trying to manually force-fit tower sections together at the top of a tower.

Fig 22—Climber is guiding the new section onto the top of the existing one. The gin pole attached to the left leg is bearing the weight, as the climber gives verbal instructions to the ground crew pulling on the gin-pole rope. (*Photo courtesy Mike Hammer, N2VR.*)

It seems that freight companies don't always handle heavy tower sections very gently and legs easily get bent out of alignment. A careful installer numbers tower sections in the order they've been test-fitted together on the ground, marking them with a laundry marker pen. You should also spray a small amount of WD-40 up inside mating tower legs after test-assembling them to help prevent galling and to ease fitting sections together. [Don't do this to excess—WD-40 is slippery and messy when it runs out of the bottom of tower legs.]

Another caution: Make sure before you start installing any tower that the correct ends of the bottom

section's legs, "male" rather than "female," are pointed upwards. A prominent amateur (who will go unnamed) had to have Rohn make and send him a special "gender-bender" flange to turn females into males, since he had installed the base upside-down in the concrete base. You don't want to do that.

8. Once the new tower section has been guided down onto the male ends, the six pinning bolts are inserted and tightened with nuts. Note that Rohn uses two different sized bolts, with the larger diameter one on the bottom.
9. If this section of tower is one where guy wires are to be placed, they can be brought up using the gin pole rope and positioned on the tower. The maximum spacing for Rohn 25 is 30 feet between guy-wire sets, and 40 feet for Rohn 45. Thirty feet of unguyed Rohn 25 tower is wobbly, though safe. Many installers prefer to come down off the tower when setting guy-wire tension, since they do not like to be on a wobbly tower when the ground crew is moving around yanking on guy wires. Many also greatly prefer working on Rohn 45 tower, which is substantially more secure feeling and easier to stand on, with its legs 18 inches apart, while Rohn 25 legs are only 12 inches apart.
10. Finally, you reposition the gin pole for the next section of tower. The T-bar at the clamp is loosened, the tube is dropped down to the level of the clamp, and the climber walks the gin pole up to the top of the section just installed and clamps it there, ready to pull up the next tower section.

Tower Safety

One of the most important aspects of any tower installation project is the safety of all persons involved. See Chapter 1 for details on important safety issues. The use of hard hats is highly recommended for all assistants helping from the ground. Helpers should always stand clear of the tower base to prevent being hit by a dropped tool or hardware. Each person working on the tower must use a good climber's safety belt.

When climbing the tower, if more than one person is involved, one should climb into position before the other begins climbing. The same procedure is required for climbing down a tower after the job is completed. The purpose is to have the non-climbing person stand still so as not to drop any tools or objects on the climbing person, or unintentionally obstruct his movements. When two persons are working on top of a tower, only one should change position (unbelt and move) at a time.

For most installations, a good-quality $^1/_2$-inch diameter Manila hemp rope can adequately handle the workload for the hoisting tasks. The rope must be periodically inspected to assure that no tearing or chafing has developed, and if the rope should get wet from rain, it should be hung out to dry at the first opportunity. The knots used for connecting hoisting lines and hardware are critical to executing any safe installation, and special attention should be given to this detail for any work party.

Here is an important point regarding safety—the person who climbs the tower should be in charge of what happens with the ground crew. Not only does the person on the tower have a better overall view of the situation below, but also any confusion on the ground can result in serious injury to the climber.

GUY WIRES

In typical guyed tower installations, guy wires may experience loads in excess of 1000 pounds. Since the guys are the primary means of carrying the horizontal wind loads, great care should be taken in their selection and installation.

Guys come in a variety of materials and constructions. Normally, the tower manufacturer or professional engineer will specify the size and type of cable to be used. The most common type of cable used for tower guying is the EHS (Extra High Strength) galvanized steel cable. The EHS cables are very stiff and are the highest strength

Table 1
Guy Cable Comparisons

Cable	*Nominal Dia. Inches*	*Breaking Strength Lbs*	*Weight Lbs/100'*	*Elongation Inches/100'*	*%Elongation*
$^3/_{16}$" 1 × 7 EHS	0.188	3990	7.3	6.77	0.56%
$^1/_4$" 1 × 7 EHS	0.250	6700	12.1	3.81	0.32%
HPTG6700	0.220	6700	3.1	13.20	1.10%
HPTG8000	0.290	8000	3.5	8.90	0.74%
$^5/_{16}$" 1 × 7 EHS	0.313	11200	20.5	2.44	0.20%
HPTG11200	0.320	11200	5.5	5.45	0.45%
$^3/_8$" Fiberglass Rod	0.375	13000	9.7	5.43	0.45%

EHS steel cable information is taken from ASTM A 475-89, the industry standard specification for steel wire rope. The HPTG listings are for *Phillystran* aramid cables, and are based on the manufacturers' data sheets. The elongation (stretch) values are for 100 feet of cable with a 3000-pound load.

cables in the wire rope family. Other steel cables are made to be more flexible for running around pulleys. While these are easier to work with when assembling, they are not as strong as the EHS type, and should be avoided for tower guying. Non-conductive guys, such as *Phillystran* or *pultruded* fiberglass rod have become popular for eliminating resonant interaction with antennas.

Do not attempt to use cheaper cables that don't meet or exceed the criteria for those specified for your installation. Using the wrong cable, or failing to install the cable properly can have disastrous results! **Table 1** shows data for several cables commonly used for tower guying. It is important to note that the minimum breaking strength of the various cables are independent of their elongation (stretch) under load.

Guy Cable Installation

Figs 23 and **24** show methods for tensioning and safety wiring guy-wire turnbuckles. **Fig 25** shows the traditional method for fixing the end of a steel guy wire. A thimble is used to prevent the wire from breaking because of a sharp bend at the point of intersection. Conventional wisdom strongly recommends the use of thimbles that are at least one wire size larger than the cable to provide a more gentle wire bend radius. Three cable clamps follow to hold the wire securely. Be sure to follow the note in Fig 25 for which part of the clip bears against the live (loaded) cable. As a final backup measure, the individual strands of the free end are unraveled and wrapped around the guy wire. It is a lot of work, but it is necessary to ensure a safe and permanent connection.

Fig 26 shows the use of a device that replaces the clamps and twisted strands of wire. These devices are known as *dead ends, preformed guy grips,* or *Big Grips* and are commonly used on electrical power poles. They are far more convenient to use than are clamps, and are the recommended method for terminating Phillystran and

Fig 23—Proper tension can be placed on the guy wires with the aid of a block-and-tackle system. (*Photo by K1WA*)

Fig 24—A length of guy cable is used to assure that the turnbuckles remain in place after they are tightened. This procedure is an absolute requirement in guyed tower systems. (*Photo by N4QX*)

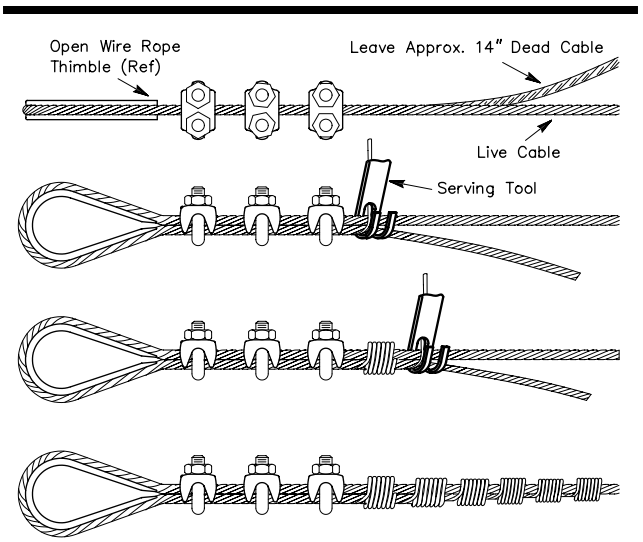

Fig 25—Traditional method for securing the end of a guy wire.

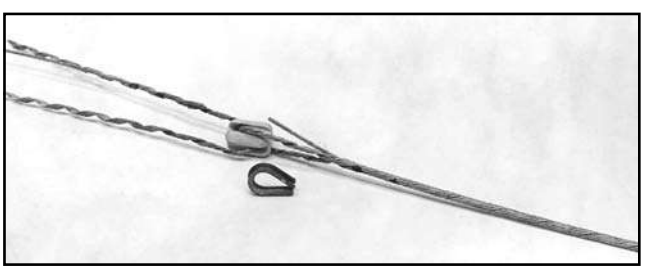

Fig 26—Alternative method for attaching guy wires using *dead ends*. The dead end on the right is completely assembled (the end of the guy wire extends beyond the grip for illustrative purposes). On the left, one side of the dead end is partially attached to the guy wire. In front, a thimble is used where a sharp bend might cause the guy wire or dead end to break.

fiberglass-rod guys. When using the guy grips, it is imperative that the recommended end sleeves are installed over the free end of the grip to prevent ice and falling hardware from sliding down the guy and unraveling the grip connection to the guy. The guy wires must be cut to the proper length. The dead end of each wire is installed into the object to which the guy wire is being attached (use a thimble, if needed to eliminate sharp cable bends). One side of the dead end is then wrapped around the guy wire. The other side of the dead end follows. Using dead ends saves time and trouble, more than making up for their slightly higher cost.

When using the non-conductive guy materials, it is highly recommended that a 25-foot length of EHS steel cable be used at the bottom for connection to the anchor. This serves a valuable purpose. The steel cable is more resistant to damage from ground activity and brush fires, and it is the preferred material for measuring cable pretension with commonly available devices.

Fig 27 shows two different methods for attaching guy wires to towers. At Fig 27A, the guy wire is simply looped around the tower leg and terminated in the usual manner. At Fig 27B, a *guy bracket*, with *torque arms* has been added. Even if the torque arms are not required, it is preferred to use the guy bracket to distribute the load from the tower/guy connection to all three tower legs, instead of just one. The torque bracket is more effective resisting torsional loads on the tower than the simpler installation. Rohn offers another guy attachment bracket, called a *Torque Arm Assembly*, that allows six guys to be connected between the bracket and anchors. This is by far the best method of stabilizing a tower against high torque loads, and is recommended for installations with large antennas.

There are two types of commonly used guy anchors. **Fig 28A** depicts an *earth screw*. These are usually 4 to 6 feet long. The screw blade at the bottom typically measures 6 to 8 inches diameter. Fig 28B illustrates two people installing the anchor. The shaft is tilted so that it will be in line with the mean angle of all the guys connecting to the anchor. Earth screws are suitable for use in normal soil where permitted by local building codes. Information about *screw anchors* is available from the manufacturers of these devices. Information from a supplier specializing in this type of anchor can be found at **www.abchance.com**.

The alternative to earth screws is the concrete block anchor. Fig 28C shows the installation of this type of anchor; it is suitable for any soil condition, with the possible exception of a bed of lava rock or coral. Consult the instructions from the manufacturer, or your tower designer, for the precise anchor configuration.

Turnbuckles and associated hardware are used to attach guy wires to anchors and to provide a convenient method for adjusting tension. **Fig 29A** shows a turnbuckle with a single guy wire attached to the eye of the anchor. Turnbuckles are usually fitted with either two eyes, or one eye and one jaw. The eyes are the oval ends, while the jaws are U-shaped with a bolt through each tip.

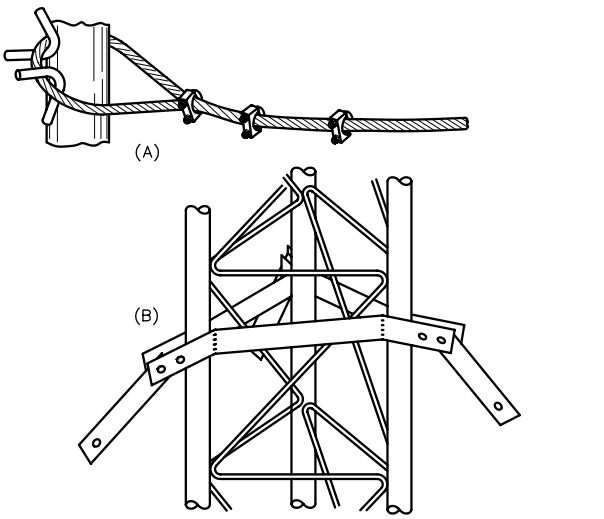

Fig 27—Two methods of attaching guy wires to tower. See text for discussion.

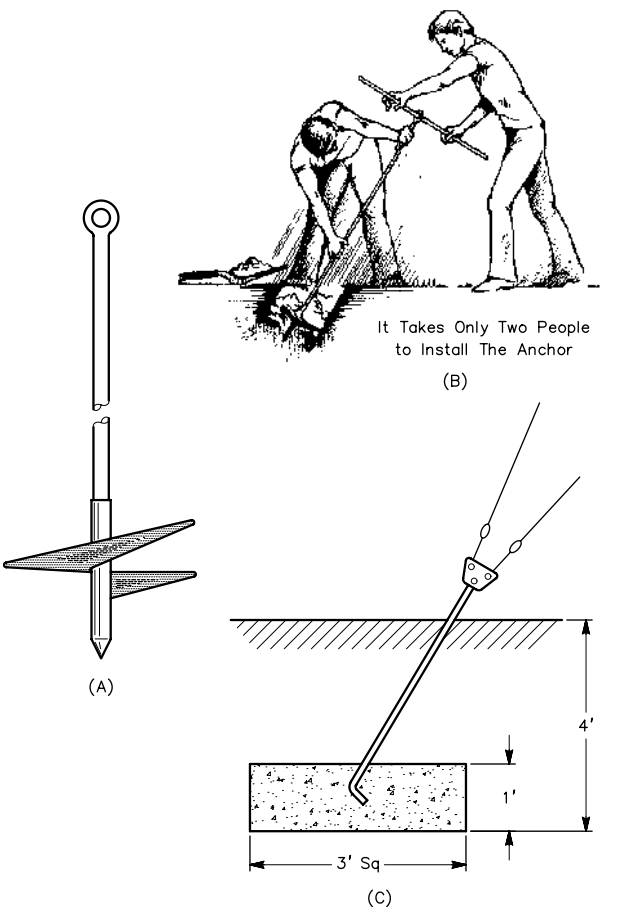

Fig 28—Two standard types of guy anchors. The earth screw shown at A is easy to install and widely available, but may not be suitable for use in certain soils. The concrete anchor is more difficult to install properly, but it is suitable for use with a wide variety of soil conditions and will satisfy most building code requirements.

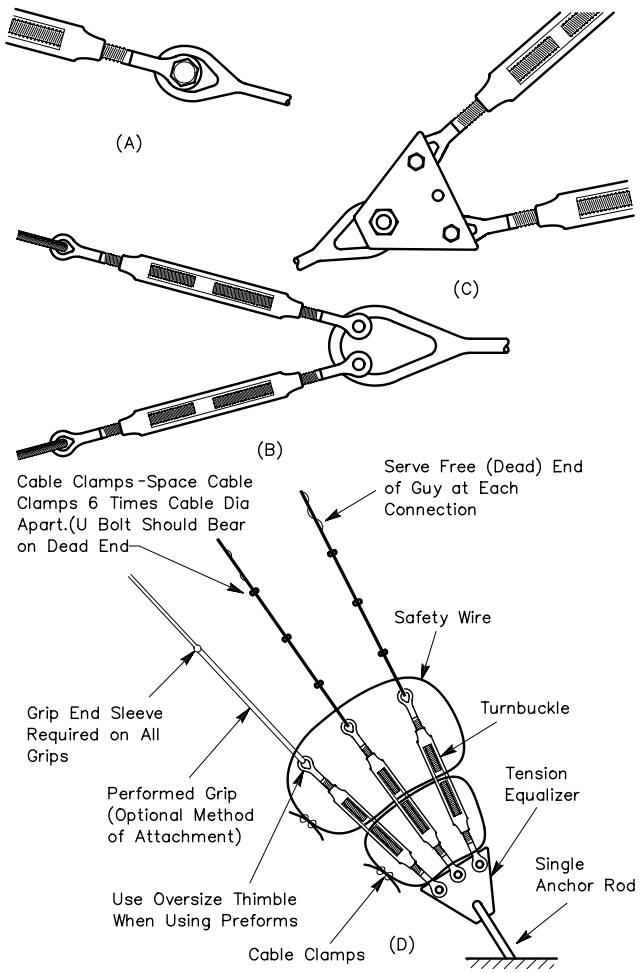

Fig 29—Variety of means available for attaching guy wires and turnbuckles to anchors.

Fig 29B shows two turnbuckles attached to the eye of an anchor. The procedure for installation is to remove the bolt from the jaw, pass the jaw over the eye of the anchor and reinstall the bolt through the jaw, through the eye of the anchor and through the other side of the jaw.

If two or more guy wires are attached to one anchor, *equalizer plates* should be installed (Fig 29C). In addition to providing a convenient point to attach the turnbuckles, the plates pivot slightly to equalize the various guy loads and produce a single load applied to the anchor. Once the installation is complete, a safety wire should be passed through the turnbuckles in a figure-eight fashion to prevent the turnbuckles from turning and getting out of adjustment (Fig 29D).

All guyed towers require the guys to be installed with a certain amount of pre-tension. The tower manufacturer or designer specifies the required pre-tension values, which are usually 10% of the cable breaking strength. Pre-tension is necessary to eliminate looseness in the cable caused by the spiral wire construction and to eliminate excessive dynamic guy and tower motion under wind loading. The recommended method for adjusting the guys is to use a cable tension-measuring device such as the popular *Loos Guy Wire Tensioner*. The guy is gripped with a special clamp, such as the *Klein Cable Grip*, which is connected to the anchor below the eye (or equalizer plate) with a block and tackle arrangement (Fig 23) or a ratcheting come-along. Then the turnbuckle is adjusted to take up the load, the cable grip is released and the final guy tension is adjusted and checked.

When you adjust the guys at each level, you should check the tower for vertical alignment and straightness. This is often done with a transit from two ground points located 90° from each other.

Resonance in Guy Wires

If guy wires are resonant at or near the operating frequency, they can receive and reradiate RF energy. By behaving as parasitic elements, the guy wires may alter and thereby distort the radiation pattern of a nearby antenna. For low frequencies where a dipole or other simple antenna is used, this is generally of little or no consequence. But at the higher frequencies where a unidirectional antenna is installed, it is desirable to avoid pattern distortion if at all possible. The symptoms of re-radiating guy wires are usually a lower front to back ratio and a lower front to side ratio than the antenna is capable of producing. The gain of the antenna and the feed-point impedance will usually not be significantly affected, although sometimes changes in SWR can be noted as the antenna is rotated. (Of course other conductors in the vicinity of the antenna can also produce these same symptoms.)

The amount of re-radiation from a guy wire depends on two factors—its resonant frequency, and the degree of coupling to the antenna. Resonant guy wires near the antenna will have a greater effect on performance than those that are farther away. Therefore, the upper portion of the top level of guy wires should warrant the most attention with horizontally polarized arrays. The lower guy wires are usually closer to horizontal than the top level, but by virtue of their increased distance from the antenna, are not coupled as tightly to the antenna.

To avoid resonance, the guys should be broken up by means of egg or strain insulators. **Fig 30** shows wire lengths that fall within 10% of $^1/_2$-λ resonance (or a multiple of $^1/_2$ λ) for all the HF amateur bands. Unfortunately, no single length greater than about 14 feet avoids resonance in all bands. If you operate just a few bands, you can locate greater lengths from Fig 30 that will avoid resonance. For example, if you operate only the 14-, 21- and 24-MHz bands, guy wire lengths of 27 feet or 51 feet would be suitable, along with any length less than 16 feet.

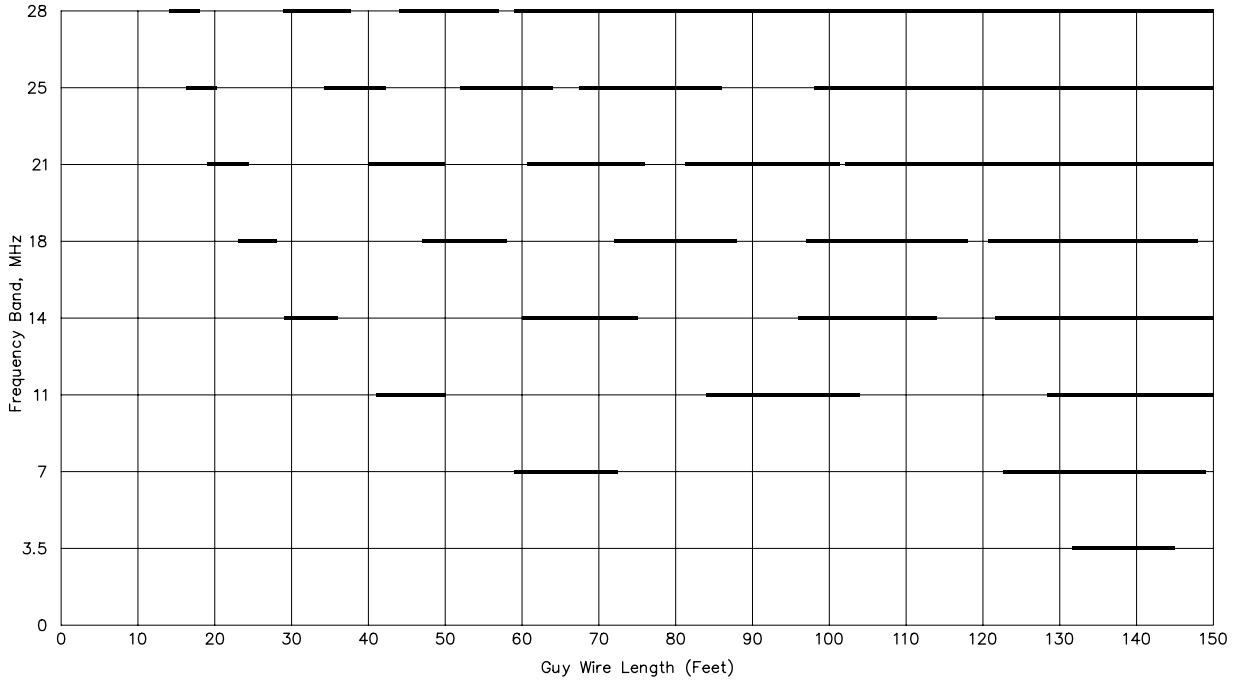

Fig 30—The black bars indicate ungrounded guy wire lengths to avoid for the eight HF amateur bands. This chart is based on resonance within 10% of any frequency in the band. Grounded wires will exhibit resonance at odd multiples of a quarter wavelength. (*By Jerry Hall, K1TD.*)

THE RIGHT TOWER FOR YOUR ANTENNA

Most manufacturers rate their towers in terms of the maximum allowable antenna load that can safely be carried at a specific wind speed. Ensuring that the specific antennas you plan to install meet the tower's design criteria, however, may not always be a straightforward task.

For most towers, the manufacturer assumes that the allowable antenna load is a horizontal force applied at the top of the tower. The allowable load represents a defined amount of exposed antenna area, at a specified wind velocity. Most tower manufacturers rate the load in terms of *Flat Projected Area* (FPA). This is simply the equivalent area of a flat rectangular surface at right angles to the wind. The FPA is not related to the actual shape of the antenna itself, only its rectangular projected area. Some manufacturers provide separate FPAs for antennas made from cylindrical sections and those made from rectangular sections.

In the realm of antenna manufacturers, however, you may encounter another wind load rating called the *Effective Projected Area* (EPA). This attempts to take into account the actual shape of antenna elements. The problem is that there is no agreed-upon standard for the conversion from EPA to load numbers. Different manufacturers may use different conversion factors.

Since most tower manufacturers have provided FPA figures for their towers—allowing us in effect to ignore design-specification details—it would be easiest for us to work only with FPA values for our antennas. This would be fine, if indeed we had good FPA figures for the specific antennas we plan to use! Unfortunately, FPAs are rarely specified for commercially built amateur antennas. Instead, most antenna manufacturers provide effective areas in their specification sheets. You may need to contact the antenna manufacturer directly for the FPA antenna area or for the antenna dimensions so that you can do your own FPA calculations.

Determining Antenna Areas

The method for determining the flat projected area of an antenna is quite simple. We'll use a Yagi antenna as an example. There are two worst-case areas that should be considered here. The first is the FPA of all the elements when the wind blows in the direction along the boom; that is, at right angles to the elements. The second FPA for a Yagi is when the wind is at right angles to the boom. One of these two orientations produces the worst-case exposed antenna area—all other wind angles present lower exposed areas. The idea is to take the highest of the FPAs for these two wind directions and call that the FPA of the antenna structure. See **Fig 31A**.

The element FPA is calculated by multiplying each element's dimension of length by its diameter and then

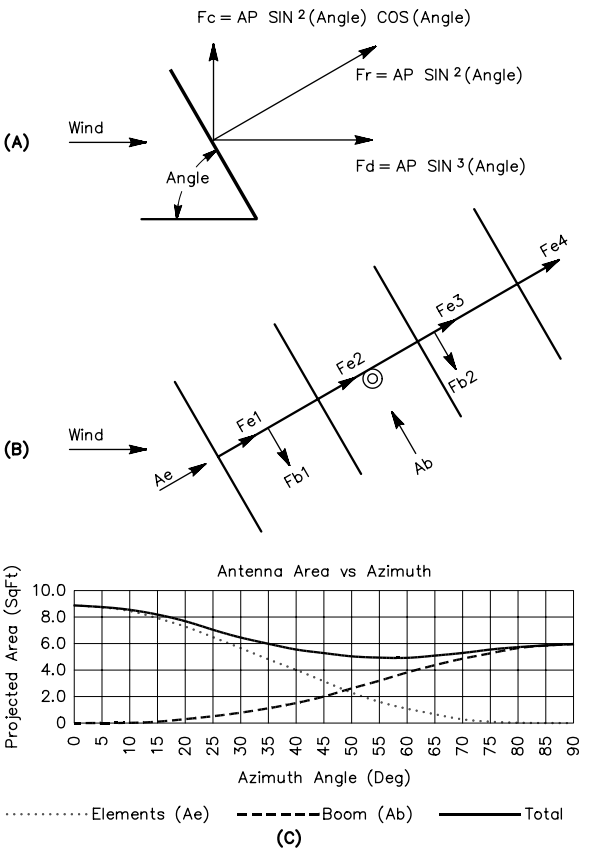

Fig 31—Description of how loads are developed on a Yagi. At A, Fr is the resultant force from the wind load on a generalized member. Fd is the load acting downwind (drag) that creates the load on the tower. Fc is the lateral component of the wind load. The term A is the flat projected area (FPA), which is the broadside area normal to the wind. The term P is the wind pressure. At B, Ae is the total element area, while Ab is the total boom area. All the loads due to the wind act normal to the antenna sections—the force on element #1 (Fe1) acts along the axis of the boom, for example. At C, a plot of the *effective FPA* as a function of the azimuthal wind direction for a Yagi, ignoring drag coefficients. The Yagi in this example has 9.0 square feet of element FPA and 6.0 square feet of boom FPA. The worst-case FPAs occur with the beam pointed in the wind and with the boom broadside to the wind. To determine the actual tower loading, the actual drag coefficients and wind pressures must be used.

summing the FPAs for all elements. The boom's FPA is computed by multiplying the boom's length by its diameter.

The reason for considering two potential peak-load orientations becomes clear when different frequency antennas are stacked on a mast or tower. Some antennas produce peak loads when the elements are broadside to the wind. This is typical of low-frequency Yagis, where the elements are long lengths of aluminum tubing. On the other hand, the boom can dominate the surface area computations in higher-frequency Yagis.

The fundamentals responsible for the need to examine both potential FPAs for Yagis relates to how wind flows over a structure and develops loads. Called *The Cross-Flow Principle*, this was introduced to the communications industry by Dick Weber, K5IU, in 1993. The principle is based on the fact that the loads created by wind flowing across an antenna member only produce forces that are normal to (or perpendicular to) the major axis of the member. The resultant and component load calculations for this method are shown in Fig 31A.

For a Yagi, this means that wind forces on the elements act in-line with the boom, while forces on the boom act in-line with the elements. Fig 31B shows a force diagram for a typical Yagi. Fig 31C shows the FPA for a Yagi rotated through 90° of azimuth.

Antenna Placement on the Mast/Tower

Another important consideration is where the antenna(s) will be placed on the tower. As mentioned before, most generic tower specifications assume that the entire antenna load is applied at the top of the tower. Most amateur installations have a tubular mast extending above the tower top, turned by a rotator mounted down inside the tower. Multiple Yagi antennas are often placed on the mast above the tower top, and you must make sure that both the tower and the mast can withstand the wind forces on the antennas.

For freestanding towers, you can determine how a proposed antenna configuration compares to the tower manufacturer's rating by using an *Equivalent Moment* method. The method computes the bending moment generated at the base of the tower by wind loads on the tower's rated antenna area located right at the top of the tower and compares that to the case when the antenna is mounted on a mast sticking out of the top of the tower.

The exact value of wind pressure is not important, so long as it is the same for both comparisons. The wind load on the tower itself can be ignored because it is the same in both comparisons and the drag coefficients for the antennas can also be ignored if all calculations are performed using flat projected antenna areas, as we've recommended previously.

Keep in mind that this approach does not calculate *actual* loads and moments relevant to any specific tower design standard, but it does allow equivalent comparisons when the wind pressure is constant and all the antenna areas are of the same type. An example is in order.

Fig 32A shows a generic tower configuration, with a concentrated antenna load at the top of the tower. We'll assume that the tower manufacturer rates this tower at 20 square feet of flat projected antenna area. Fig 32B shows a typical amateur installation with a rotating mast and an antenna mounted 7 feet above the top of the tower. To make the calculations easy, we select a wind pressure

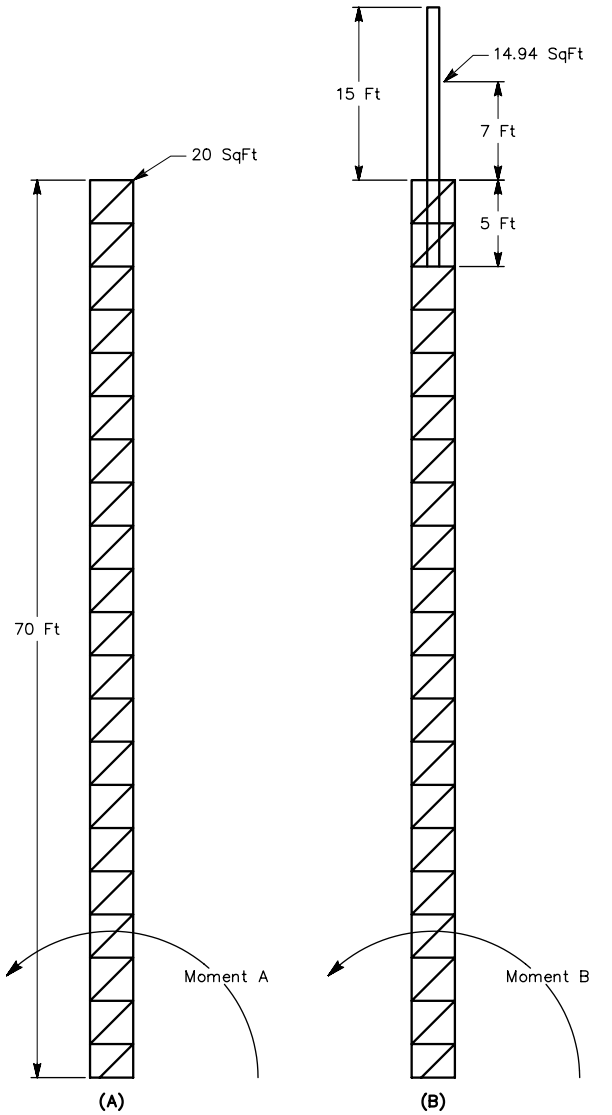

Fig 32—At A, a 70-foot tower rated for 20 square feet of antenna load at the top. At B, the same tower with a 2-inch OD × 20-foot long mast, with an antenna mounted 7 feet above the top of the tower. Both configurations produce the same tower load.

of 1 pound per square foot (1 psf). This makes the tower base moment calculation for Fig 32A:

Antenna load = 20 feet^2 × 1 psf = 20 pounds
Base moment = 70 feet × 20 pounds =
1400 foot-pounds.

This is the target value for the comparison. An equivalent configuration would produce the same base moment. For the configuration in Fig 32B, we assume a tubular 2-inch diameter mast that is 20 feet long, mounted 5 feet down inside the tower. Note that the lattice structure of the tower allows the wind to "see" the whole length of the mast and that we can consider the force distributed along the mast as being a single force concentrated at the mast's center. The flat projected area of the mast by itself, without the antenna, is:

Mast area = 20 feet × 2 inches / 12 inches/foot =
3.33 square feet

The center of the mast is located at a height of 75 feet. Using the same 1-psf-wind load, the base bending moment due to the mast alone is:

Base moment (due to mast) = 3.33 feet^2 × 1 psf ×
75 feet = 249.75 foot-pounds

Including the mast in the configuration reduces the allowable antenna load. The remaining target base moment left for the antenna is found by subtracting the moment due to the mast from the original target value:

New base target moment = 1400 - 249.75 foot-pounds
= 1150.25 foot-pounds.

The antenna in Fig 32B is located at a height of 77 feet. To obtain the allowable antenna area at this elevation we divide the new base target moment by the antenna height, yielding an allowable antenna load of:

1150.25 foot-pounds / 77 feet = 14.94 pounds.

Since we chose a wind load of 1 psf, the allowable antenna FPA has been reduced to 14.94 square feet from 20 square feet. If the projected area of the antenna we are planning to mount in the new configuration is less than or equal to this value, we have satisfied the requirements of the original design. You can use this equivalent-moment method to evaluate different configurations, even ones involving multiple antennas on the mast or situations with additional antennas placed along the tower below the tower top.

For guyed towers, the analyses become much more rigorous to solve. Because the guys and their behaviors are such a significant portion of the tower support mechanism, these designs can become very sensitive to antenna load placements. A general rule of thumb for guyed towers is never to exceed the original tower-top load rating, regardless of distributed loads along its length. Once you redistribute the antenna load placements along a guyed tower, you should do a fresh analysis, just to be sure.

You can run evaluations using the above method for antennas placed on the mast above a guyed tower top. The use of the Equivalent-Moment method for antennas mounted below the top of a guyed tower, however, can become quite suspect, since many generic tower designs have their intermediate guys sized for zero antenna loads lower down the tower. The proper approach in this case is to have a qualified mechanical engineer check the configuration, to see if guy placement and strength is adequate for the additional antennas down the tower.

Mounting the mast and antenna as shown in Fig 32B

increases tower loads in the region of the mast. You should investigate these loads to ensure that the tower bracing in that area is sufficient. Now we will consider the problem of bending the rotating mast.

Mast Strength

When you mount antennas on a mast above the tower top, you should examine the bending loads on the mast to ensure that it will be strong enough. This section explains how to perform mast stress calculations for a single sustained wind speed. This procedure does not include height, exposure and gust-response factors found in most tower design standards.

Here are some fundamental formulas and values used to calculate the bending stress in a mast mounted in the top of a tower. The basic formula for wind pressure is:

$$P = .00256\ V^2 \qquad \text{(Eq 1)}$$

where

P is the wind pressure is in pounds per square foot (psf)
V = wind speed in miles per hour (mph)

This assumes an air density for standard temperature and atmospheric pressure at sea level. The wind speed is not the Basic Wind Speed discussed in other sections of this chapter. It is simply a steady state (static) wind velocity.

The formula for calculating the force created by the wind on a structure is:

$$F = P \times A \times C_d \qquad \text{(Eq 2)}$$

where

P = the wind pressure from Eq (1)
A = the flat projected area of the structure (square feet)
C_d = drag coefficient for the shape of the structure's members.

The commonly accepted *drag coefficient* for long cylindrical members like the tubing used for the mast and antenna is 1.20. The coefficient for a flat plate is 2.0.

The formula used to find the *bending stress* in a simple beam like our mast is:

$$\sigma = \frac{M \times c}{I} \qquad \text{(Eq 3)}$$

where

σ = the stress in pounds per square inch (psi)
M = *bending moment* at the base of the mast (inch-pounds)
c = ½ of the mast outside diameter (inches)
I = *moment of inertia* of the mast section (inches^4)

In this equation you must make sure that all values are in the same units. To arrive at the mast stress in pounds per square inch (psi), the other values need to be in inches and pounds also. The equation used to find the moment of inertia for the round tubing mast section is:

$$I = \frac{\pi}{4}(R^4 - r^4) \qquad \text{(Eq 4)}$$

where

I = Moment of Inertia of the section (inches^4)
R = Radius of tube outside diameter (inches)
r = Radius of tube inside diameter (inches)

This value describes the distribution of material about the mast *centroid*, which determines how it behaves under load. The equation used to compute the *bending moment* at the base of the mast (where it is supported by the tower) is:

$$M = (F_M \times L_M) + (F_A \times L_M) \qquad \text{(Eq 5)}$$

where

F_M = wind force from the mast (pounds)
L_M = Distance from tower top to center of mast (inches)
F_A = Wind force from the antenna (pounds)
L_A = Distance from tower top to antenna attachment (inches)

L_M is the distance to the center of the portion of the mast extending above the tower top. Additional antennas can be added to this formula by including their F × L. In the installation shown in Fig 32B, a wind speed of 90 mph, and a mast that is 2 inches OD, with a 0.250-inch wall thickness, the steps for calculating the mast stress are:

1. Calculate the wind pressure for 90 mph, from Eq 1:

$P = .00256\ V^2 = .00256 \times (90)^2 = 20.736$ psf

2. Determine the flat projected area of the mast. The portion of the mast above the tower is 15 feet long and has an outside diameter of 2 inches, which is 2/12 feet.

Mast FPA, A_M = 15 feet × (2 inches / 12 inches/feet) = 2.50 square feet.

3. Calculate the wind load on the mast, from Eq 2:

Mast Force, $F_M = P \times A \times C_d$ = 20.736 psf × 2.50 feet^2 × 1.20 = 62.21 pounds

4. Calculate the wind load on the antenna: From Eq 2

Antenna Force, $F_A = P \times A \times C_d$ = 20.736 psf × 14.94 feet^2 × 1.20 = 371.76 pounds

5. Calculate the mast *Bending Moment*, from Eq 5:

$M = (F_M \times L_M) + (F_A \times L_A)$
= (62.21 pounds × 90 inches) + (371.76 pounds × 84 inches) = 36827 inch-pounds

where L_M = 7.5 feet × 12 inches/foot = 90 inches and L_A = 7.0 feet × 12 inches/foot = 84 inches.

6. Calculate the mast *Moment of Inertia*, from Eq 4:

$$I = \frac{\pi}{4}(R^4 - r^4) = \frac{\pi}{4}(1.0^4 - 0.75^4) = 0.5369 \text{ inches}^4$$

where, for a 2.0-inch OD and 0.250-inch wall thickness tube, R= 1.0 and r = 0.75.

7. Calculate the mast *Bending Stress*, from Eq 3:

$$\sigma = \frac{M \times c}{I} = \frac{36827 \text{ inch - pounds} \times 1.0 \text{ inches}}{0.5369} = 68592 \text{ psi}$$

If the yield strength of the mast material is greater than the calculated bending stress, the mast is considered safe for this configuration and wind speed. If the calculated stress is higher than the mast yield strength, a stronger alloy, or a larger mast, or one with a thicker wall is required.

There are many different materials and manufacturing processes for tubing that may be used for a mast. Yield strengths range from 25,000 psi to nearly 100,000 psi. Knowing the minimum yield strength of the material used for a mast is an important part of determining if it will be safe. Using unknown materials renders efforts from the preceding calculations useless!

When evaluating a mast with multiple antennas attached to it, special care should be given to finding the worst-case condition (wind direction) for the system. What may appear to be the worst load case, by virtue of the combined flat projected antenna areas, may not always be the exposure that creates the largest mast bending moment. Masts with multiple stacked antennas should always be examined to find the exposure that produces the largest mast bending moment. The antenna flat projected areas at 0° and 90° azimuths are particularly useful for this evaluation.

ANTENNA INSTALLATION

All antenna installations are different in some respects. Therefore, thorough planning is the most important first step in installing any antenna. Before anyone climbs the tower, the whole process should be discussed to be sure each crewmember understands what is to be done. And remember that the person on the tower is in charge! Coordinate beforehand what signals and commands are used: “Up” or “Up Slowly” for raising something from the ground; “Down” or “Down Slowly” for the opposite.

“Watch Out!” or ‘Watch Out Below!” works for dropped hardware or tools to alert the ground crew below. Remember, once someone is on the tower, no one should be allowed to stand near the base of the tower!

Consider what tools and parts must be assembled and what items must be taken up the tower, and plan alternative actions for possible trouble spots. Extra trips up and down the tower can be avoided by careful planning.

If done properly, the actual work of getting the antenna into position can be executed quite easily with only one person at the top of the tower. The ground crew should do all the heavy work and leave the person on the tower free to guide the antenna into position. Because the ground crew does all the lifting, a large pulley, preferably on a gin pole placed at the top of the tower, is essential. Local radio clubs often have gin poles available for use by their members. Stores that sell tower materials frequently rent gin poles as well.

A gin pole should be placed along the side of the tower so the pulley is no more than 2 feet above the top of the tower (or the point at which the antenna is to be placed). Normally this height is sufficient to allow the antenna to be positioned easily. An important reason that the pulley is placed at this level is that there can be considerable strain on the gin pole when the antenna is pulled away from the tower to maneuver past guy wires.

Sometime the mast to which the antenna will be mounted is used as a place to hang the pulley. You should take care that you don’t end up bending the mast by placing the pulley too high on the mast. It may be necessary to back-guy the mast on the opposite side of the tower from which the antenna is raised.

The rope (halyard) through the pulley must be somewhat longer than twice the tower height so that the ground crew can raise the antenna from ground level. The rope should be ½ or ⅝ inch diameter for both strength and ease of handling. Smaller diameter rope is less easily manipulated; it has a tendency to jump out of the pulley track and foul pulley operation.

The first person to climb the tower should carry an end of the halyard so that the gin pole can be lifted and secured to the tower. Those climbing the tower must have safety belts. Belts provide safety and convenience; it is simply impossible to work effectively while hanging onto the tower with one hand.

Once positioned, the gin pole and pulley allow parts and tools to be sent up the tower. A useful trick for sending up small items like bolts and pliers is for a ground crew member to slide them through the rope strands where they are held by the rope for the trip to the top of the tower. Items that might be dislodged by contact with the tower should either be taped or tied to the halyard.
Ever present is the hazard of falling tools or hardware. It is foolish to stand near a tower when someone is working above. Ground crew member should wear hard-hats as extra insurance.

Raising the Antenna Alongside the Tower

A technique that can save much effort in raising the antenna is outlined here. First, the halyard is passed through the gin-pole pulley or the pulley mounted to the mast, and the leading end of the rope is returned to the ground crew, where it is tied to the antenna. The assembled antenna should be placed in a clear area of the yard (or the roof) so the boom points toward the tower. The halyard is then passed *under* the front elements of the beam to a position past the midpoint of the antenna, where it is securely tied

to the boom (**Fig 33A**).

Note that once the antenna is installed, the tower worker must be able to reach and untie the halyard from the boom; the rope must be tied less than an arm's length along the boom from the mounting point. If necessary, a large loop may be placed around the first element located beyond the midpoint of the boom, with the knot tied near the center of the antenna. The rope may then be untied easily after completion of the installation. The halyard should be tied temporarily to the boom at the front of the antenna by means of a short piece of light rope or twine.

While the antenna is being raised, the ground crew does all the pulling. As soon as the front of the antenna reaches the top of the mast, the person atop the tower unties the light rope and prevents the front of the antenna from falling, as the ground crew continues to lift the antenna (Fig 33B). When the center of the antenna is even with the top of the tower, the tower worker puts one bolt through the mast and the antenna-mounting bracket on the boom. The single bolt acts as a pivot point and the ground crew continues to lift the back of the antenna with the halyard (Fig 33C). After the antenna is horizontal, the tower worker secures the rest of the mounting bolts and unties the halyard. By using this technique, the tower worker performs no heavy lifting.

Avoiding Guy Wires

Although the same basic methods of installing a Yagi apply to any tower, guyed towers pose a special problem. Steps must be taken to avoid snagging the antenna on the guy wires. With proper precautions, however, even large antennas can be pulled to the top of a tower, even if the

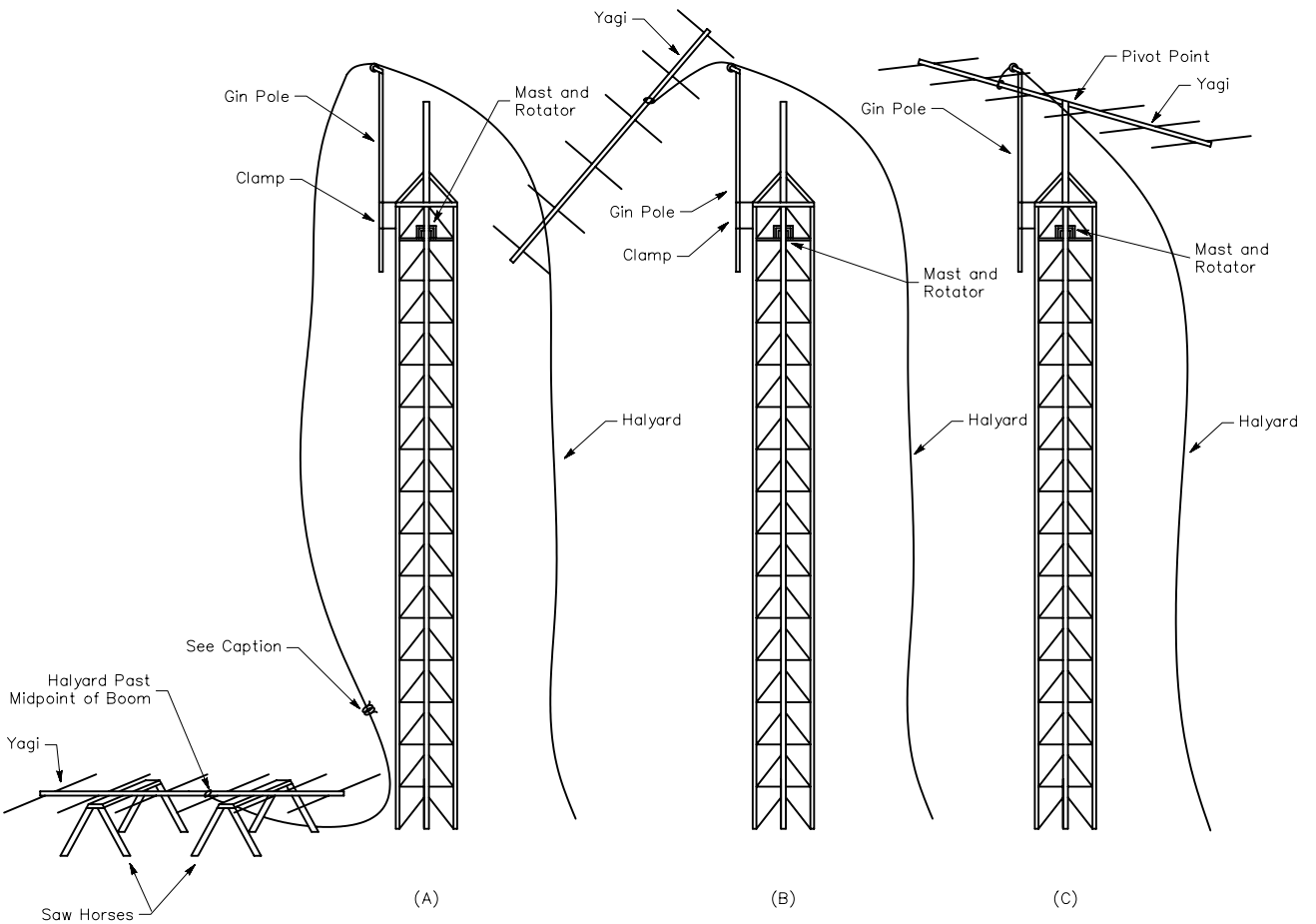

Fig 33—Raising a Yagi antenna alongside the tower. At A the Yagi is placed in a clear area, with the boom pointing toward the tower. The halyard is passed under the elements, then is secured to the boom beyond the midpoint. B shows the antenna approaching the top of the mast. The person on the tower guides it after the lifting rope has been untied from the front of the antenna. At C the antenna is pulled into a horizontal position by the ground crew. The tower worker inserts the pivot bolt and secures it. Note: A short piece of rope is tied around the halyard and the boom at the front of the antenna to stabilize the beam as it is being raised. The tower worker removes it when the boom reaches him at the top of the tower.

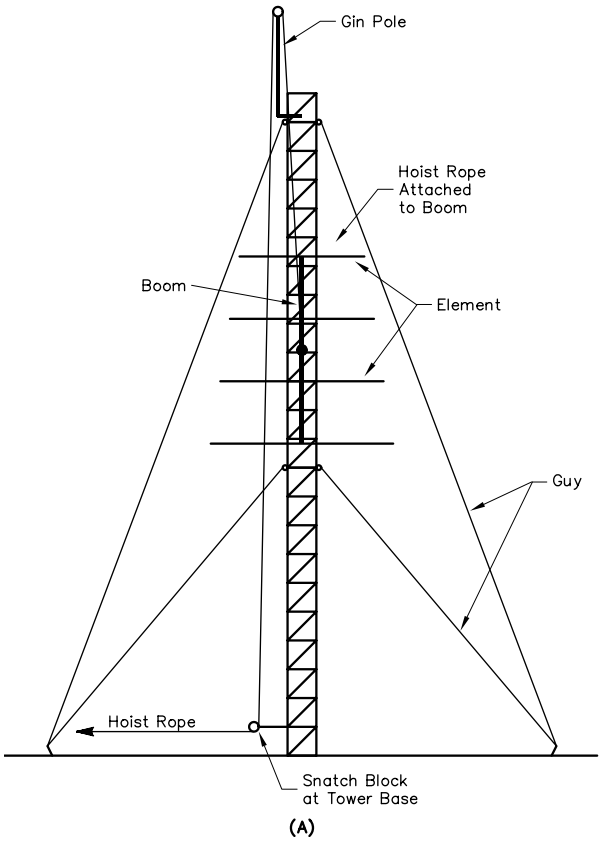

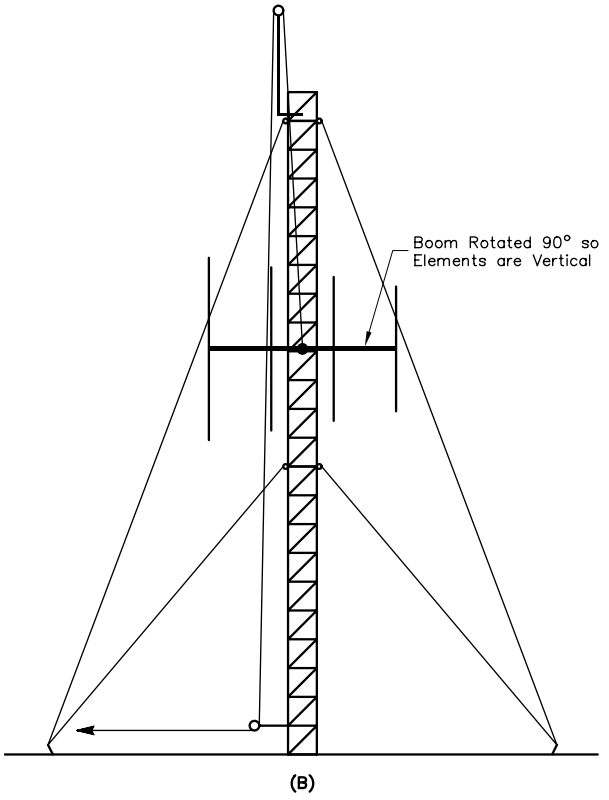

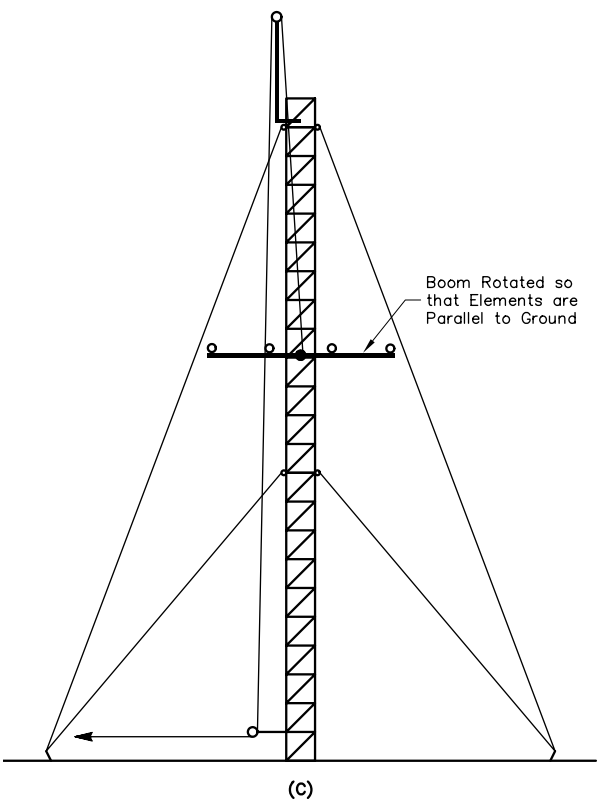

Fig 34—Building a Yagi partway down the tower. At A, the boom is lashed temporarily to the tower and elements are added, starting at the bottom. At B, the temporary rope securing the boom to the tower is removed and the boom is rotated 90° so that the elements are vertical. At C, the boom is rotated another 90°, "weaving through" guy wires if necessary, until the elements are parallel with the ground, whereupon the boom is secured to the tower.

mast is guyed at several levels.

Sometimes one of the top guys can provide a *track* to support the antenna as it is pulled upward. Insulators in the guys, however, may obstruct the movement of the antenna. A better track made with rope is an alternative. One end of the rope is secured outside the guy anchors. The other end is passed over the top of the tower and back down to an anchor near the first anchor. So arranged, the rope forms a narrow V-track strung outside the guy wires. Once the V-track is secured, the antenna may simply be pulled up, resting on the track.

Another method is to tie a rope to the back of the antenna (but within reach of the center). The ground crews then pull the antenna out away from the guys as the antenna is raised. With this method, some crewmembers are pulling up the antenna to raise it while others are pulling down and out to keep the beam clear of the guys. Obviously, the opposing crews must act in coordination to avoid damaging the antenna. The beam is especially vulnerable when it begins to tip into the horizontal posi-

tion. If the crew continues to pull out and down against the antenna, the boom can be broken. Another problem with this approach is that the antenna may rotate on the axis of the boom as it is raised. To prevent such rotation, long lengths of twine may be tied to outer elements, one piece on each side of the boom. Ground personnel may then use these *tag lines* to stabilize the antenna. Where this is done, provisions must be made for untying the twine once the antenna is in place.

A third method is to tie the halyard to the center of the antenna. A crewmember, wearing a safety belt, walks the antenna up the tower as the crew on the ground raises it. Because the halyard is tied at the balance point, the tower worker can rotate the elements around the guys. A tag line can be tied to the bottom end of the boom so that a ground worker can help move the antenna around the guys. The tag line must be removed while the antenna is still vertical.

A fourth method is to build the antenna on the tower and then swing it into position. (See also the section below on the PVC Mount.) Building the Yagi on the tower works particularly well for Yagis mounted partway up the tower, as you might do in a stacked array. The technique works best when the vertical spacing between the guys is greater than the length of the Yagi boom.

Fig 34 illustrates the steps involved. A pull rope through a gin-pole or tower-mounted pulley is secured to the boom at the final balance point and the ground crew raises the boom in a vertical position up the tower. A tie rope is used to temporarily secure the upper end of the boom to keep it stable while the boom is being raised. The tower person removes the tie-rope once the boom is raised to the right level and has been temporarily secured to the tower.

The elements are then brought up one at a time and mounted to the boom. It helps if you have a 2- or 3-foot long *spotting mast* temporarily attached to the boom to form a 90° frame of reference. This allows the ground crew to spot from below so that the elements are all lined up in the same plane. After all the elements are mounted and aligned properly, the temporary rope securing the boom to the tower is released, suspending the antenna on the pull rope. The tower person then rotates the boom 90° so that the elements are vertical. Next the elements are rotated 90° into the tower so that they are parallel to the ground. The ground crew then moves the boom up or down using the pull rope to the final point where it is mounted to the tower.

A modification of this technique also works for building a medium-sized Yagi on the top of the tower. This technique will work if the length of the gin pole at maximum safe extension is long enough. See **Fig 35**.

As usual, the gin-pole pull rope is attached to the balance point of the boom and the boom is pulled up the tower in the vertical position, using a rope to temporarily tie the pull rope to the top end of the boom for stability.

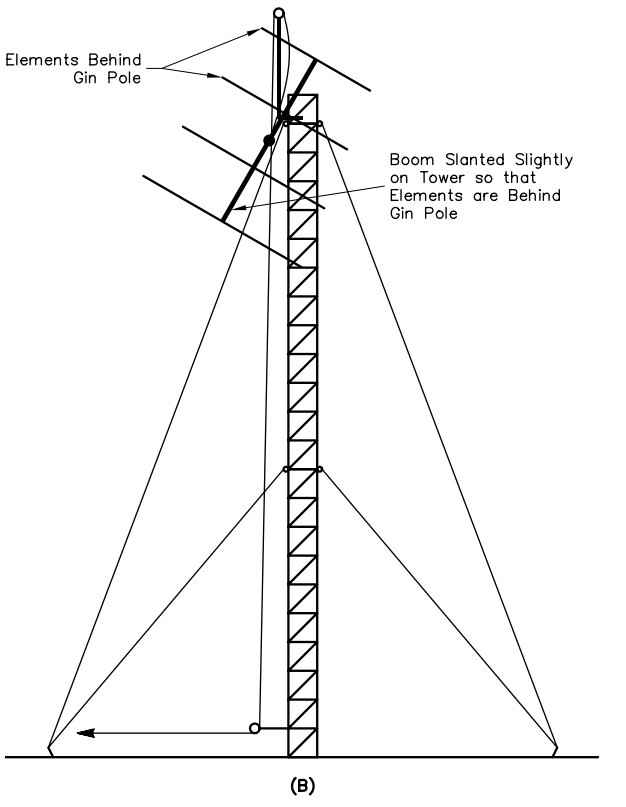

Fig 35—Building a Yagi at the top of the tower. The length of the gin pole must be longer than $^1/_2$ the boom so that the boom can be hoisted upwards to the place where it is mounted to the mast. Usually the boom is initially lashed to the tower slanted slightly from vertical so that the top element ends up *behind* the gin pole. The elements are mounted at the bottom end of the boom first to provide stability. Then the element at the top of the boom is mounted and the boom is moved upwards using the gin-pole hoist rope so that the next-to-top element may be mounted, again behind the gin pole. This process is repeated until all elements are mounted (save possibly the middle element if it can be reached easily from the tower once the beam has been mounted to the mast). Then the boom is tilted to the final position, weaving the elements to clear guy wires if necessary.

The boom is temporarily secured to the tower with rope in the vertical position so that the top end is just higher than the top of the tower. In order to clear the gin pole when the elements are mounted and the boom is raised higher to mount the next element, you must tilt the boom slightly so that the element mounted to the top end of the boom will be *behind* the mast. This is very important!

The elements are first mounted to the bottom side of the boom to provide weight down below for stability. Then the top-most element is mounted to the boom. The tower person removes the temporary rope securing the boom to the tower and the ground crew uses the pull rope

to move the mast vertically upwards to the point where the next element from the top can be mounted. Once all the elements are mounted and aligned in the same plane (with perhaps the center element closest to the mast-to-boom bracket left on the ground until later), the temporary securing rope is removed. The boom is now swung so that the elements can be maneuvered to clear the top guy wires. Once the elements are horizontal the boom is secured to the mast and the center element is mounted.

Using a Tram

Another method to get a large Yagi to the top of the tower safely is a *tram*. A tram supports the antenna *under* the tram wire, using a pulley riding on the tram wire. The antenna can thus move more freely—without the friction it would have riding on top of a track rope, as described previously. This puts considerably less strain on the tram wire itself and on the mast to which it is tied on the tower. Some installers prefer to use a wire-rope tramline for its reduced sag.

The tram method uses an easily constructed fixture mounted to the boom of the Yagi to stabilize it from rotating away from the desired attitude as the antenna is raised. A guy-wire cable or heavy rope is fixed to the mast about two feet above the point where the antenna will mount to the mast. A come-along is often used at the ground end to tension the tram wire properly. It is often necessary to back-guy the mast to make sure it doesn't get bent, since the horizontal forces acting on the mast can be considerable in any tram (or track) operation. (Note that the tram technique works well for side-mounted antennas also, where back-guying is not necessary if you are reasonably close to a guy set, as is usually the case.)

Fig 36 is a photograph of a tram fixture built by Kurt Andress, K7NV. This consists of a pulley riding on top of the tramline. This pulley is attached using a caribiner or shackle to two equal-length wires connected to the boom to make an inverted-V shaped *sling*. The two sling wires are secured to the boom using angle irons and muffler clamps so that the antenna is perfectly balanced in the horizontal plane. Balance is very important to make sure the antenna rises properly on the tram without having the boom rotate downward on one end or the other.

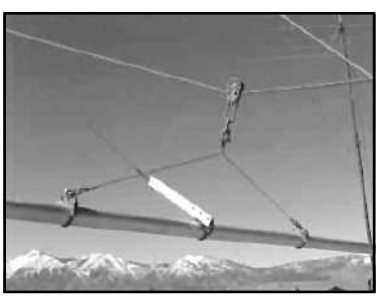

Fig 36—Photo of the tram system used by Kurt Andress, K7NV. (*Photo by K7NV.*)

The hoisting rope running through the tower-mounted gin-pole pulley (and used by the ground crew to pull the antenna up to the tower on the tram line) is attached to a 2-foot piece of angle iron. This is attached to the boom with a muffler clamp. Note that the angle iron is rotated slightly from horizontal so that the plane of the elements is tilted upwards—this allows the elements to clear the guy wires as the antenna is raised. (While the antenna is close to the ground, the angle iron is adjusted so that the elements remain horizontal. Once they are clear of the ground, the angle iron is readjusted to align the elements in the proper direction to clear the guy wires on the tower.) The force of the pull rope along the angle iron also stabilizes the antenna from yawing from side-to-side. Note in Fig 36 that the angle iron is mounted just off-center from where the boom-to-mast plate will be attached so that it clears the mast as the antenna nears the top of the tower. **Fig 37** diagrams how the tram and hoisting line are rigged to the mast.

The tower person directs the activity of the ground crew below and guides the antenna to the mast. Once the end of the pull rope reaches the mast, the tower man ties the boom temporarily to the mast so that he can undo the pull rope from the tram-fixture angle iron and retie it around the boom. Then the antenna can be raised to the point where it can be mounted to the mast.

This technique has been employed to raise Yagis with booms as long as 42 feet at the N6RO contest station on towers as high as 130 feet. As with the track, the tram system requires a good deal of open real estate. While it sounds complicated to set up, you can raise some rather large antennas in less than an hour, once you get the hang of the operation.

THE PVRC MOUNT

The methods described above for hoisting antennas are sometimes not satisfactory for really large, heavy arrays. The best way to handle large Yagis is to assemble them on top of the tower. One way to do this easily is by using the *PVRC Mount*. Many members of the Potomac Valley Radio Club have successfully used this method to install large antennas. Simple and ingenious, the idea involves offsetting the boom from the mast to permit the boom to tilt 360° and rotate axially 360°. This permits the entire length of the boom to be brought alongside the tower, allowing the elements to be attached one by one. (It also allows any part of the antenna to be brought alongside the tower for antenna maintenance.)

See **Figs 38** through **42**. The mount itself consists of a short length of pipe of the same diameter as the rotating mast (or greater), a steel plate, eight U bolts and four pinning bolts. The steel plate is the larger, horizontal one shown in Fig 38. Four U bolts attach the plate to the rotating mast, and four attach the horizontal pipe to the plate. The horizontal pipe provides the offset between the antenna boom and the tower. The antenna boom-to-mast plate is mounted at the outer end of the short pipe. Four bolts are used to ensure that the antenna ends up parallel to the ground, two pinning each plate to the short pipe. When the mast plate pinning bolts are removed and the

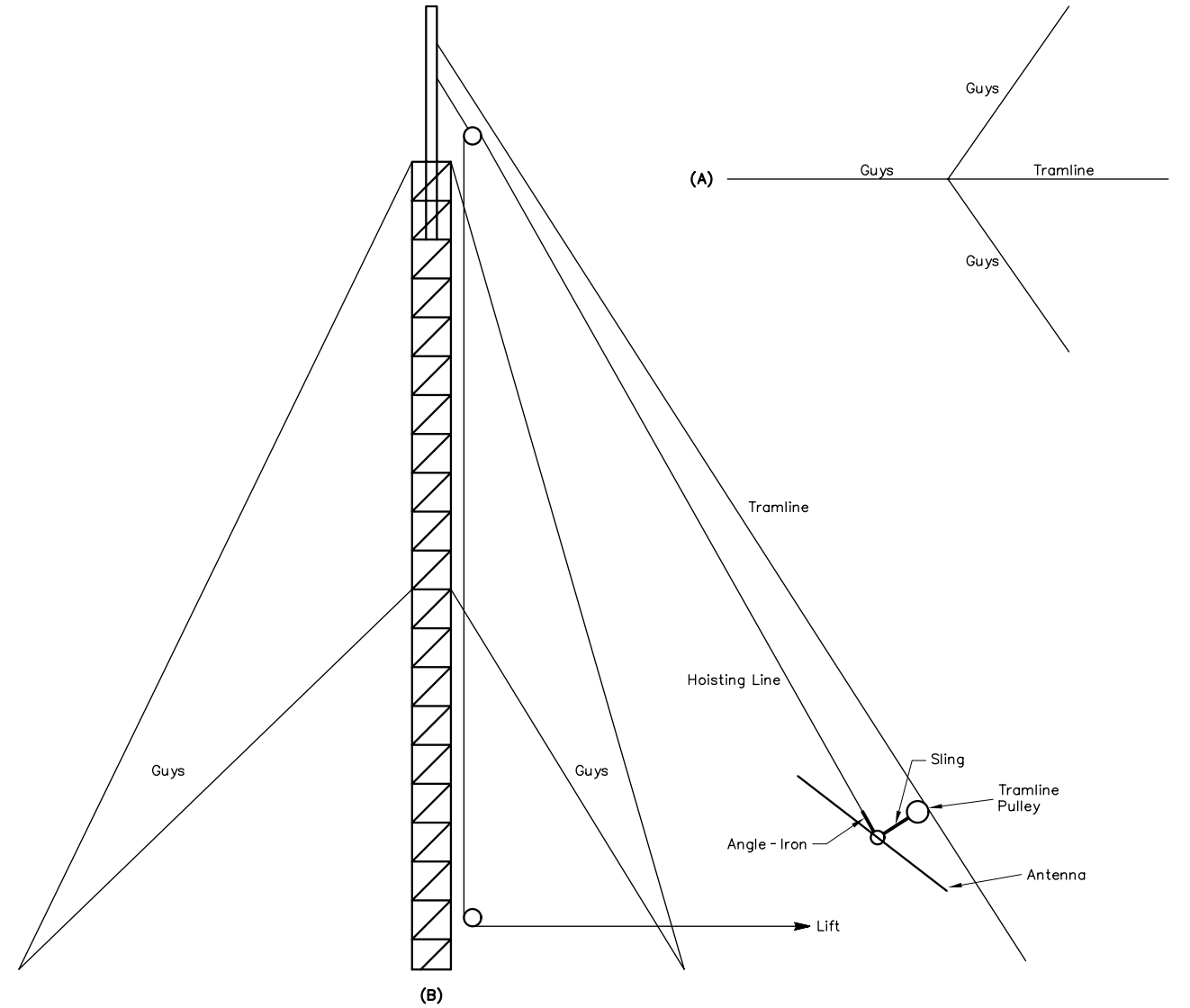

Fig 37—At A, bird's-eye view of tram system used to bring large Yagi antennas from the ground to the top of the tower. At B, side view of rigging used for tramline and hoisting line, along with the sling and tram fixture used to hold the Yagi on the tramline.

four U bolts loosened, the short pipe and boom plate can be rotated through 360°, allowing either half of the boom to come alongside the tower.

First assemble the antenna on the ground. Carefully mark all critical dimensions, and then remove the antenna elements from the boom. Once the rotator and mast have been installed on the tower, a gin pole is used to bring the mast plate and short pipe to the top of the tower. There, the top crew unpins the horizontal pipe and tilts the antenna boom plate to place it in the vertical plane. The boom is attached to the boom plate at the final balance point of the assembled antenna. It is important that the boom be rotated axially so the bottom side of the boom is closest to the tower. This will allow the boom to be tilted without the elements striking the tower.

During installation it may be necessary to loosen one guy wire temporarily to allow for tilting of the boom. As a safety precaution, a temporary guy should be attached to the same leg of the tower just low enough so the assembled antenna will clear it.

The elements are assembled on the boom, starting with those closest to the center of the boom, working out alternately to the farthest director and reflector. This procedure must be followed. If all the elements are put first on one half of the boom, it will be dangerous (if not impossible) to put on the remaining elements. By start-

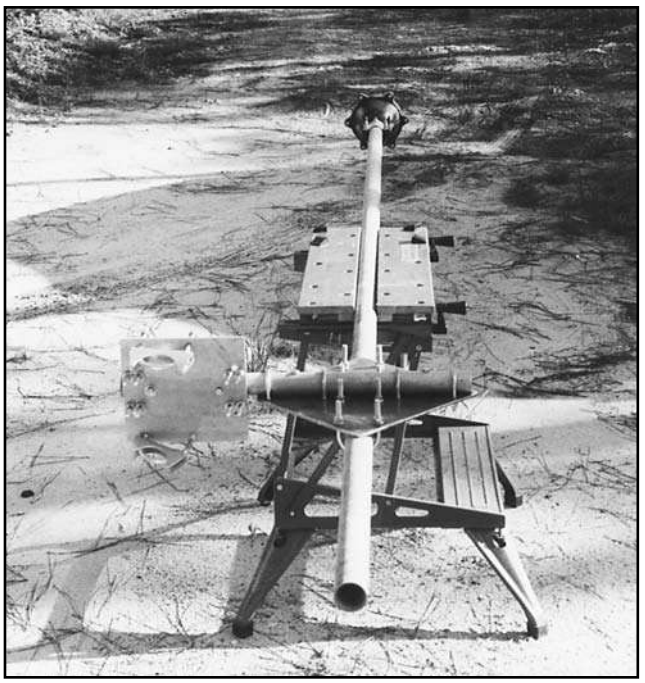

Fig 38—The PVRC mount, boom plate, mast and rotator ready to go. The mast and rotator are installed on the tower first.

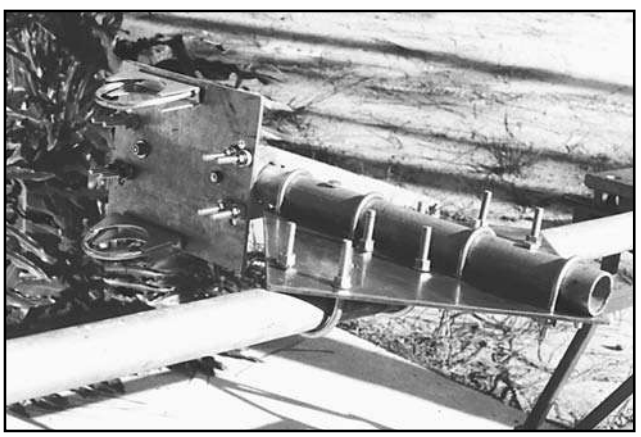

Fig 39—Close-up of the PVRC mount. The long pipe (horizontal in this photo) is the rotating mast. The U bolts in the vertical plate at the left are ready to accept the antenna boom. The heads of two locking pins (bolts) are visible at the midline of the boom plate. The other two pins help secure the horizontal pipe to the large steel mast plate. (The head of the bolt nearest the camera blends in with the right hand leg of the U bolt behind it.)

ing at the middle and working outward, the balance point of the partly assembled antenna will never be so far removed from the tower that tilting of the boom becomes impossible.

When the last element is attached, the boom is brought parallel to the ground, the horizontal pipe is

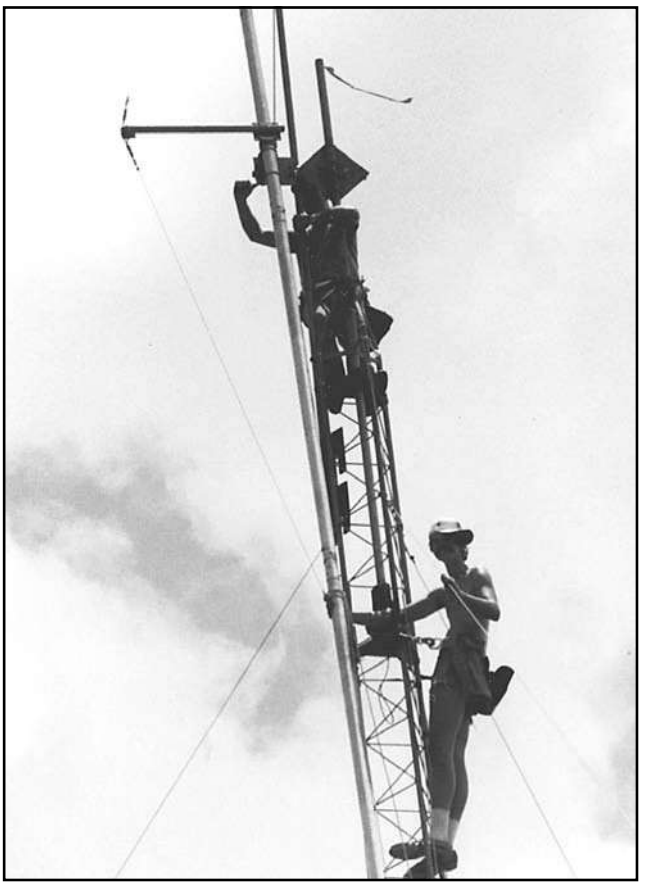

Fig 40—Working at the 70-foot level. A gin pole makes pulling up and mounting the boom to the boom plate a safe and easy procedure.

pinned to the mast plate, and the mast plate U bolts tightened. At this point, all the antenna elements will be positioned vertically. Next, loosen the U bolts that hold the boom and rotate the boom axially 90°, bringing the elements parallel to the ground. Tighten the boom bolts and double check all the hardware.

Many long-boom Yagis employ a truss to prevent boom sag. With the PVRC mount, the truss must be attached to a pipe that is independent of the rotating mast. A short length of pipe is attached to the boom as close as possible to the balance point. The truss then moves with the boom whenever the boom is tilted or twisted.

A precaution: Unless you have a really strong rotator, you should consider using this mount mainly for assembling the antenna on the tower. The offset between the boom and the mast with this assembly can generate high torque loads on the rotator. Mounting the boom as close as possible to the mast will minimize the torque when the antenna is pointed into the wind.

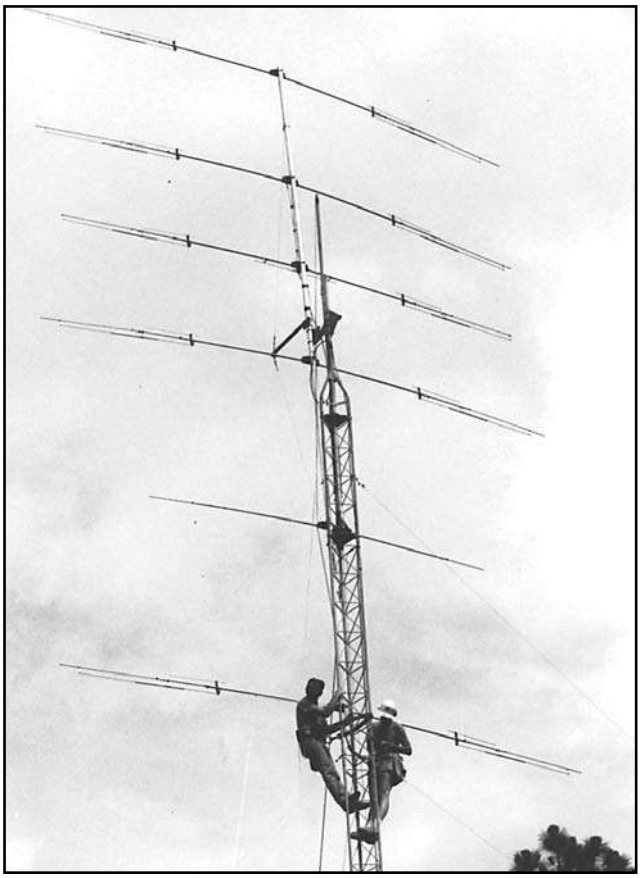

Fig 41—Mounting the last element prior to positioning the boom in a horizontal plane.

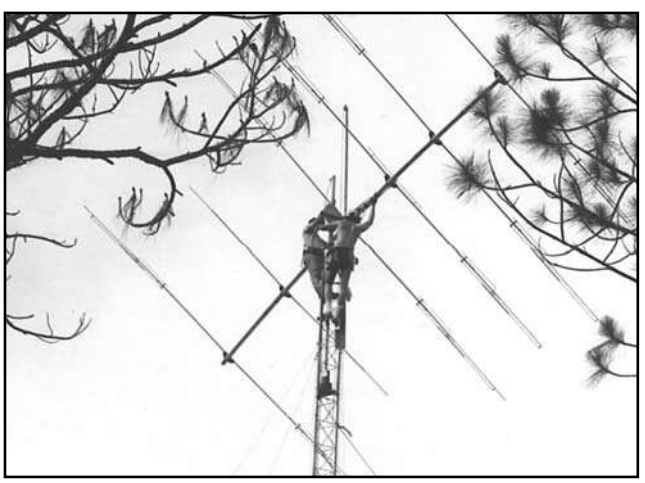

Fig 42—The U bolts securing the short pipe to the mast plate are loosened and the boom is turned to a horizontal position. This puts the elements in a vertical plane. Then the pipe U bolts are tightened and pinning bolts secured. The boom U bolts are then loosened and the boom turned axially 90°.

THE TOWER ALTERNATIVE

A cost saving alternative to the ground-mounted tower is the roof-mounted tripod. Units suitable for small HF or VHF antennas are commercially available. Perhaps the biggest problem with a tripod is determining how to fasten it securely to the roof.

One method of mounting a tripod on a roof is to nail 2 × 6 boards to the undersides of the rafters. Bolts can be extended from the leg mounts through the roof and the 2 × 6s. To avoid exerting too much pressure on the area of the roof between rafters, place another set of 2 × 6s on top of the roof (a mirror image of the ones in the attic). Installation details are shown in **Figs 43** through **46**.

The 2 × 6s are cut 4 inches longer than the outside distance between two rafters. Bolts are cut from a length of ¼-inch-threaded rod. Nails are used to hold the boards in place during installation, and roofing tar is used to seal the area to prevent leaks.

Find a location on the roof that will allow the antenna to turn without obstruction from such things as trees, TV antennas and chimneys. Determine the rafter locations. (Chimneys and vent pipes make good reference points.) Now the tower is set in place atop three 2 × 6s. A plumb line run from the top center of the tower can be used to center it on the peak of the roof. Holes for the mounting bolts can now be drilled through the roof.

Before proceeding, the bottom of the 2 × 6s and the area of the roof under them should be given a coat of roofing tar. Leave about $^1/_8$ inch of clear area around the holes to ensure easy passage of the bolts. Put the tower back in place and insert the bolts and tighten them. Apply tar to the bottom of the legs and the wooden supports, including the bolts. For added security the tripod can be guyed. Guys should be anchored to the frame of the house.

If a rotator is to be mounted above the tripod, pressure will be applied to the bearings. Wind load on the antenna will be translated into a "pinching" of one side of the bearings. Make sure that the rotator is capable of handling this additional stress.

ROTATOR SYSTEMS

There are not that many choices when it comes to antenna rotators for the amateur antenna system. Making the correct decision as to how much capacity the rotator must have is very important to ensure trouble-free operation. Manufacturers generally provide an antenna surface-area rating to help the purchase choose a suitable rotator. The maximum antenna area is linked to the rotator's torque capability.

Some rotator manufacturers provide additional information to help you select the right size of rotator for the antennas you plan to use. Hy-Gain provides an *Effective Moment* value. Yaesu calls theirs a *K-Factor*. Both of these ratings are torque values in foot-pounds. You can compute the effective moment of your antenna by multiplying the antenna turning radius by its weight. So long

Fig 43—This tripod tower supports a rotary beam antenna. In addition to saving yard space, a roof-mounted tower can be more economical than a ground-mounted tower. A ground lead fastened to the lower part of the frame is for lightning protection. The rotator control cable and the coaxial line are dressed along two of the legs. (*Photo courtesy of Jane Wolfert.*)

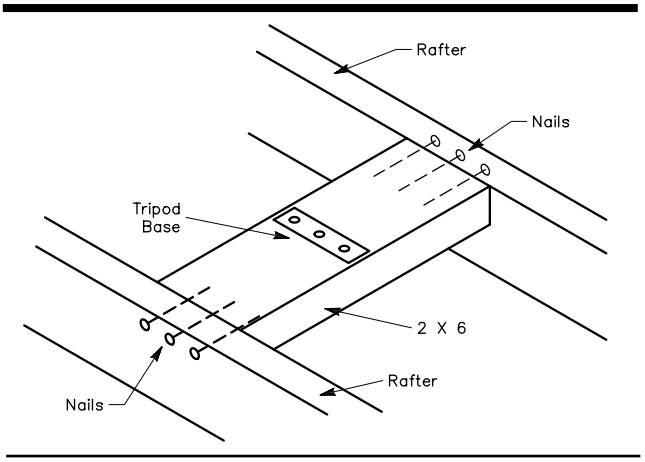

Fig 44—This cutaway view illustrates how the tripod tower is secured to the roof rafters. The leg to be secured to the crosspiece is placed on the outside of the roof. Another cross member is fastened to the underside of the rafters. Bolts, inserted through the roof and the two cross pieces, hold the inner cross member in place because of pressure applied. The inner crosspiece can be nailed to the rafter for added strength.

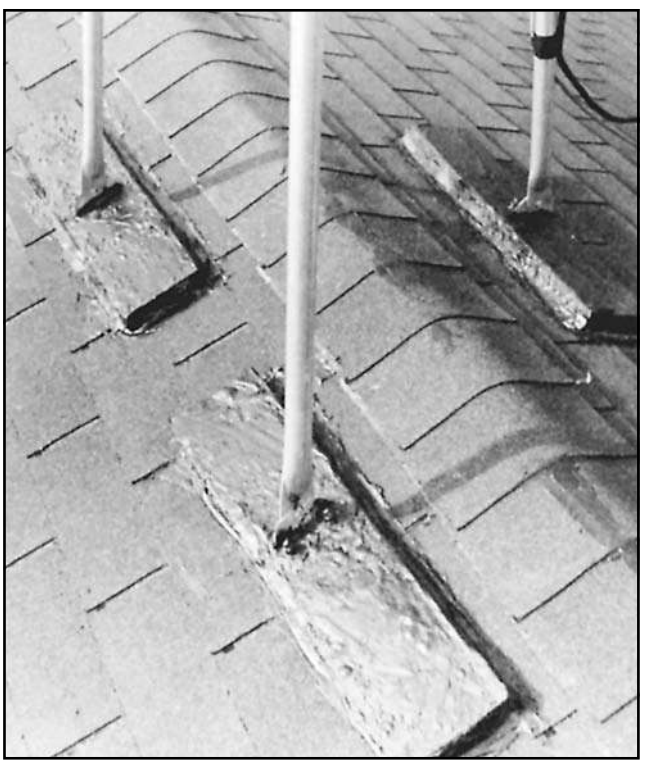

Fig 45—Three lengths of 2 × 6 wood mounted on the outside of the roof and reinforced under the roof by three identical lengths provide a durable means for anchoring the tripod. A thick coat of roofing tar guards against weathering and leaks.

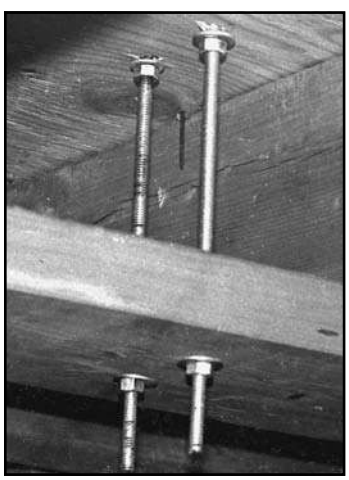

Fig 46—The strengthened anchoring for the tripod. Bolts are placed through two 2 × 6s on the underside of the roof and through the 2 × 6 on the top of the roof, as shown in Fig 43.

as the effective moment rating of the rotator is greater than or equal to the antenna value, the rotator can be expected to provide a useful service life.

There are basically four grades of rotators available to the amateur. The lightest-duty rotator is the type typically used to turn TV antennas. Without much difficulty, these rotators will handle a small 3-element tribander array (14, 21 and 28 MHz) or a single 21- or 28-MHz monoband three-element antenna. The important consideration with a TV rotator is that it lacks braking or holding capability. High winds turn the rotator motor via the gear train in a reverse fashion. Broken gears sometimes result.

The next grade up from the TV class of rotator usually includes a braking arrangement, whereby the antenna is held in place when power is not applied to the rotator. Generally speaking, the brake prevents gear damage on windy days. If adequate precautions are taken, this group of rotators is capable of holding and turning stacked monoband arrays, or up to a five-element 14-MHz system. The next step up in rotator strength is more expensive. This class of rotator will turn just about anything the most demanding amateur might want to install.

A description of antenna rotators would not be complete without the mention of the *prop pitch* class. The prop pitch rotator system consists of a surplus aircraft propeller blade pitch motor coupled to an indicator system and a power supply. There are mechanical problems of installation, however, resulting mostly from the size and weight of these motors. It has been said that a prop pitch rotator system, properly installed, is capable of turning a house. Perhaps in the same class as the prop pitch motor (but with somewhat less capability) is the electric motor of the type used for opening garage doors. These have been used successfully in turning large arrays.

Proper installation of the antenna rotator can provide many years of trouble-free service; sloppy installation can cause problems such as a burned out motor, slippage, binding and casting breakage. Most rotators are capable of accepting mast sizes of different diameters, and suitable precautions must be taken to shim an undersized mast to ensure dead-center rotation. It is very desirable to mount the rotator inside and as far below the top of the tower as possible. The mast absorbs the torsion developed by the antenna during high winds, as well as during starting and stopping.

Some amateurs have used a long mast from the top to the base of the tower. Rotator installation and service can be accomplished at ground level. A mast length of 10 feet or more between the rotator and the antenna will add greatly to the longevity of the entire system by allowing the mast to act as a torsion shock absorber. Another benefit of mounting the rotator 10 feet or more below the antenna is that any misalignment among the rotator, mast and the top of the tower is less significant. A tube at the top of the tower (a sleeve bearing) through which the mast protrudes almost completely eliminates any lateral forces on the rotator casing. All the rotator must do is support the downward weight of the antenna system and turn the array.

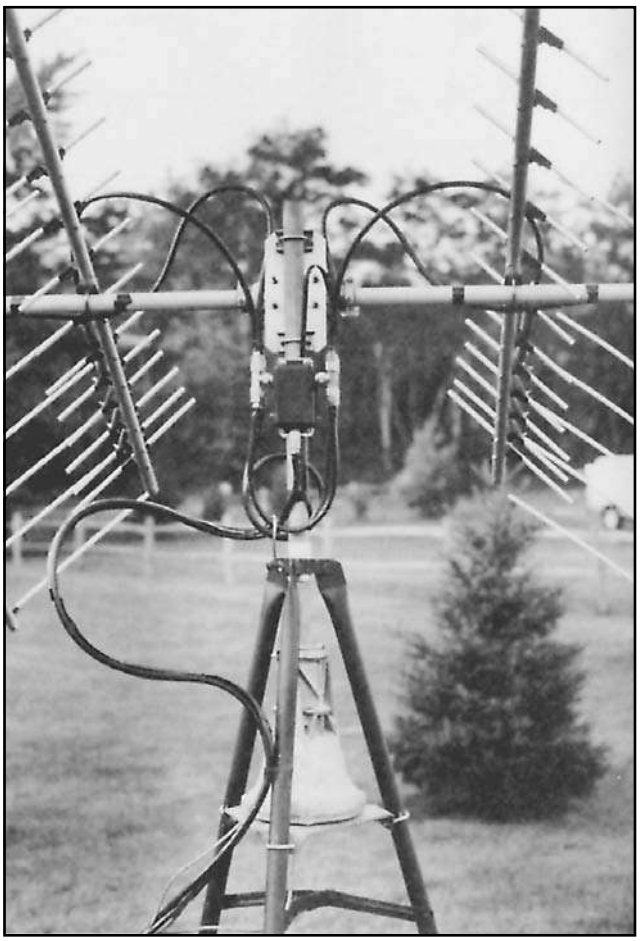

Fig 47—Rotator loop for UHF Yagi array. The feed coax is bundled with a control cable for the polarization relay. The coax/control-cable loop is taped to the rotating mast and to the top of the tower with vinyl electric tape to allow the array to be rotated.

While the normal weight of the antenna and the mast is usually not more than a couple of hundred pounds, even with a large system, one can ease this strain on the rotator by installing a thrust bearing at the top of the tower. The bearing is then the component that holds the weight of the antenna system, and the rotator need perform only the rotating task.

Don't forget to provide a loop of coax to allow your beam to rotate properly. Make sure you position the rotator loop so that it doesn't snag on anything. **Fig 47** shows a rotator loop for an elliptically polarized UHF Yagi array. Note that the coax loop is taped to the rotating mast above the top of the tower and to the tower itself.

Indicator Alignment

A problem often encountered in amateur installations is that of misalignment between the direction indicator in the rotator control box and the heading of the antenna. With a light duty rotator, this happens frequently when the wind blows the antenna to a different heading. With no brake, the force of the wind can move the gear train and motor of the rotator, while the indicator remains fixed. Such rotator systems have a mechanical stop to prevent continuous rotation during operation, and provision is usually included to realign the indicator against the mechanical stop from inside the shack. During installation, the antenna must be oriented correctly for the mechanical stop position, which is usually north.

In larger rotator systems with an adequate brake, indicator misalignment is caused by mechanical slippage in the antenna boom-to-mast hardware. Many texts suggest that the boom be pinned to the mast with a heavy-duty bolt and the rotator be similarly pinned to the mast. There is a trade-off here. If there is sufficient wind to cause slippage in the couplings without pins, with pins the wind could break a rotator casting. The slippage will act as a clutch release, which may prevent serious damage to the rotator. On the other hand, the amateur might not like to climb the tower and realign the system after each heavy windstorm.

BIBLIOGRAPHY

Source material and more extended discussions of the topics covered in this chapter can be found in the references listed below and in the texts listed at the end of Chapter 2.

L. H. Abraham, "Guys for Guys Who Have To Guy," *QST*, Jun 1955.

K. Baker, "A Ladder Mast," *QST*, Jun 1981, p 24.

W. R. Gary, "Toward Safer Antenna Installations," *QST*, Jan 1980, p 56.

S. F. Hoerner, "Fluid Dynamic Drag," published by author, Bricktown, New Jersey, 1965, pp 1-10.

C. L. Hutchinson, "A Tree-Mounted 30-Meter Ground-Plane Antenna," *QST*, Sep 1984, pp 16-18.

C. L. Hutchinson, R. D. Straw, *Simple and Fun Antennas for Hams* (Newington: ARRL, 2002).

M. P. Keown and L. L. Lamb, "A Simple Technique for Tower-Section Separation," *QST*, Sep 1979, pp 37-38.

P. O'Dell, "The Ups and Downs of Towers," *QST*, Jul 1981, p 35.

S. Phillabaum, "Installation Techniques for Medium and Large Yagis," *QST*, Jun 1979, p 23.

C. J. Richards, "Mechanical Engineering in Radar and Communications" (London: Van Nostrand Reinhold Co., 1969) pp 162-165.

D. Weber "Determination of Yagi Wind Loads Using the Cross-Flow Principle," *Communications Quarterly*, Spring 1993.

A. B. White, "A Delayed Brake Release for the Ham-II," *QST*, Aug 1977, p 14.

B. White, E. White and J. White, "Assembling Big Antennas on Fixed Towers," *QST*, Mar 1982, pp 28-29

L. Wolfert, "The Tower Alternative," *QST*, Nov 1980, p 36.

W. C. Young., "Roark's Formulas for Stress & Strain" (New York: McGraw-Hill Co., 1989), pp 67, 96

Structural Standards for Steel Antenna Towers and Antenna Supporting Structures, TIA/EIA Standard TIA/EIA-222-F, Electronic Industries Association, Mar 1996. May be purchased from Telecommunications Industry Association (TIA), Standards and Technology Department, 2500 Wilson Boulevard, Arlington VA, 22201 or Global Engineering Documents, 15 Inverness Way East, Englewood, CO, 80112-5704, 1-800-854-7179.

Chapter 23

Radio Wave Propagation

Because radio communication is carried on by means of electromagnetic waves traveling through the Earth's atmosphere, it is important to understand the nature of these waves and their behavior in the propagation medium. Most antennas will radiate the power applied to them efficiently, but no antenna can do all things equally well, under all circumstances. Whether you design and build your own antennas, or buy them and have them put up by a professional, you'll need propagation know-how for best results, both during the planning stages and while operating your station.

For station planning, this chapter contains detailed new information on elevation angles from transmitting locations throughout the world to important areas throughout the world. With this information in hand, you can design your own antenna installation for optimum capabilities possible within your budget. See the CD-ROM in back of this book.

The Nature of Radio Waves

You probably have some familiarity with the concept of electric and magnetic fields. A radio wave is a combination of both, with the energy divided equally between them. If the wave could originate at a point source in free space, it would spread out in an ever-growing sphere, with the source at the center. No antenna can be designed to do this, but the theoretical *isotropic antenna* is useful in explaining and measuring the performance of practical antennas we *can* build. It is, in fact, the basis for any discussion or evaluation of antenna performance.

Our theoretical spheres of radiated energy would expand very rapidly at the same speed as the propagation of light, approximately 186,000 miles or 300,000,000 meters per second. These values are close enough for practical purposes, and are used elsewhere in this book. If one wishes to be more precise, light propagates in a vacuum at the speed of 299.7925 meters per microsecond, and slightly slower in air.

The path of a *ray* traced from its source to any point on a spherical surface is considered to be a straight line—a radius of the sphere. An observer on the surface of the sphere would think of it as being flat, just as the Earth seems flat to us. A radio wave far enough from its source to appear flat is called a *plane wave*. From here on, we will be discussing primarily plane waves.

It helps to understand the radiation of electromagnetic energy if we visualize a plane wave as being made up of electric and magnetic forces, as shown in **Fig 1**. The nature of wave propagation is such that the electric and magnetic lines of force are always perpendicular. The plane containing the sets of crossed lines represents the wave front. The direction of travel is always perpendicular to the wave front; *forward* or *backward* is determined by the relative directions of the electric and magnetic forces.

The speed of travel of a wave through anything but a vacuum is always less than 300,000,000 meters per second. How much less depends on the medium. If it is air, the reduction in propagation speed can be ignored in most discussions of propagation at frequencies below 30 MHz. In the VHF range and higher, temperature and moisture content of the medium have increasing effects on the communication range, as will be discussed later. In solid insulating materials the speed is considerably less. In distilled water (a good insulator) the speed is $^1/_9$ that in free space. In good conductors the speed is so low that the opposing fields set up by the wave front occupy practically the same space as the wave itself, and thus cancel it out. This is the reason for "skin effect" in conductors at high frequencies, making metal enclosures good shields for electrical circuits working at radio frequencies.

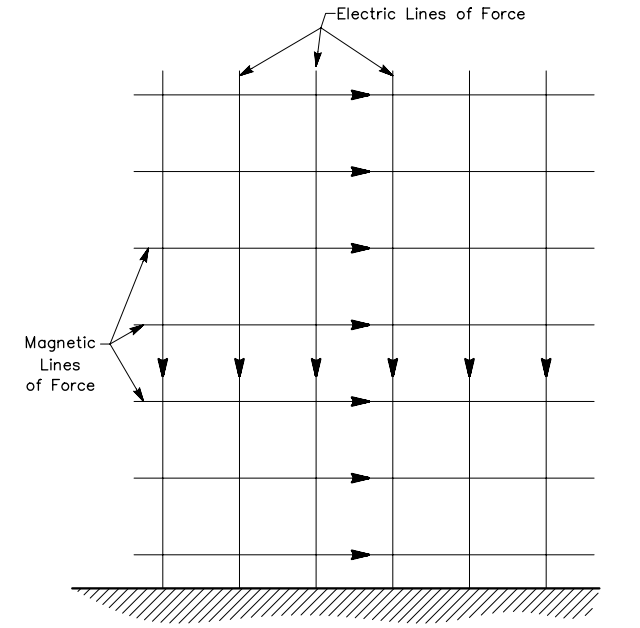

Fig 1—Representation of the magnetic and electric fields of a vertically polarized plane wave traveling along the ground. The arrows indicate instantaneous directions of the fields for a wave traveling perpendicularly out of the page toward the reader. Reversal of the direction of one set of lines reverses the direction of travel. There is no change in direction when both sets are reversed. Such a dual reversal occurs in fact once each half cycle.

Phase and Wavelength

Because the velocity of wave propagation is so great, we tend to ignore it. Only $^1/_7$ of a second is needed for a radio wave to travel around the world—but in working with antennas the *time* factor is extremely important. The wave concept evolved because an alternating current flowing in a wire (antenna) sets up moving electric and magnetic fields. We can hardly discuss antenna theory or performance at all without involving travel time, consciously or otherwise.

Waves used in radio communication may have frequencies from about 10,000 to several billion Hz. Suppose the frequency is 30 MHz. One cycle, or period, is completed in 1/30,000,000 second. The wave is traveling at 300,000,000 meters per second, so it will move only 10 meters during the time that the current is going through one complete period of alternation. The electromagnetic field 10 meters away from the antenna is caused by the current that was flowing one period earlier in time. The field 20 meters away is caused by the current that was flowing two periods earlier, and so on.

If each period of the current is simply a repetition of the one before it, the currents at corresponding instants in each period will be identical. The fields caused by those currents will also be identical. As the fields move outward from the antenna they become more thinly spread over larger and larger surfaces. Their amplitudes decrease with distance from the antenna but they do not lose their identity with respect to the instant of the period at which they were generated. They are, and they remain, *in phase*. In the example above, at intervals of 10 meters measured outward from the antenna, the phase of the waves at any given instant is identical.

From this information we can define both *wave front* and *wavelength*. Consider the wave front as an imaginary surface. On every part of this surface, the wave is in the same phase. The wavelength is the distance between two wave fronts having the same phase at any given instant. This distance must be measured perpendicular to the wave fronts along the line that represents the direction of travel. The abbreviation for wavelength is the Greek letter lambda, λ, which is used throughout this book.

The wavelength will be in the same length units as the velocity when the frequency is expressed in the same time units as the velocity. For waves traveling in free space (and near enough for waves traveling through air) the wavelength is

$$\lambda_{meters} = \frac{299.7925}{F(MHz)} \qquad \text{(Eq 1)}$$

There will be few pages in this book where phase, wavelength and frequency do not come into the discussion. It is essential to have a clear understanding of their meaning in order to understand the design, installation, adjustment or use of antennas, matching systems or transmission lines in detail. In essence, *phase* means *time*. When something goes through periodic variations, as an alternating current does, corresponding instants in succeeding periods are *in phase*.

The points A, B and C in **Fig 2** are all in phase. They are corresponding instants in the current flow, at 1-λ intervals. This is a conventional view of a sine-wave alternating current, with time progressing to the right. It also represents a *snapshot* of the intensity of the traveling fields, if distance is substituted for time in the horizontal axis. The distance between A and B or between B and C is one wavelength. The field-intensity distribution follows the sine curve, in both amplitude and polarity, corresponding exactly to the time variations in the current that produced the fields. Remember that this is an *instantaneous* picture—the wave moves outward, much as a wave created by a rock thrown into water does.

Polarization

A wave like that in Fig 1 is said to be *polarized* in the direction of the electric lines of force. The polarization here is vertical, because the electric lines are perpendicular to the surface of the Earth. It is one of the laws of electromagnetics that electric lines touching the surface of a perfect conductor must do so perpendicularly, or else they would have to generate infinite currents in the conductor, an obvious impossibility. Most ground is a rather good conductor at frequencies below about 10 MHz, so waves at these

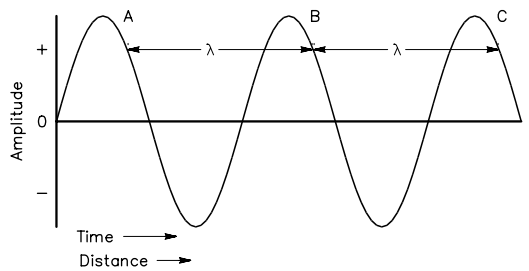

Fig 2—The instantaneous amplitude of both fields (electric and magnetic) varies sinusoidally with time as shown in this graph. Since the fields travel at constant velocity, the graph also represents the instantaneous distribution of field intensity along the wave path. The distance between two points of equal phase such as A-B and B-C is the length of the wave.

frequencies, traveling close to good ground, are mainly vertically polarized. Over partially conducting ground there may be a forward tilt to the wave front; the tilt in the electric lines of force increases as the energy loss in the ground becomes greater.

Waves traveling in contact with the surface of the Earth, called *surface waves*, are of little practical use in amateur communication. This is because as the frequency is raised, the distance over which they will travel without excessive energy loss becomes smaller and smaller. The surface wave is most useful at low frequencies and through the standard AM broadcast band. The surface wave will be covered later. At high frequencies a wave reaching a receiving antenna has had little contact with the ground, and its polarization is not necessarily vertical.

If the electric lines of force are horizontal, the wave is said to be *horizontally polarized*. Horizontally and vertically polarized waves may be classified generally under *linear polarization*. Linear polarization can be anything between horizontal and vertical. In free space, "horizontal" and "vertical" have no meaning, since the reference of the seemingly horizontal surface of the Earth has been lost.

In many cases the polarization of waves is not fixed, but rotates continually, somewhat at random. When this occurs the wave is said to be *elliptically polarized*. A gradual shift in polarization in a medium is known as *Faraday rotation*. For space communication, circular polarization is commonly used to overcome the effects of Faraday rotation. A circularly polarized wave rotates its polarization through 360° as it travels a distance of one wavelength in the propagation medium. The direction of rotation as viewed from the transmitting antenna defines the direction of circularity—right-hand (clockwise) or left-hand (counterclockwise). Linear and circular polarization may be considered as special cases of elliptical polarization.

Field Intensity

The energy from a propagated wave decreases with distance from the source. This decrease in strength is caused by the spreading of the wave energy over ever-larger spheres as the distance from the source increases.

A measurement of the strength of the wave at a distance from the transmitting antenna is its *field intensity*, which is synonymous with *field strength*. The strength of a wave is measured as the voltage between two points lying on an electric line of force in the plane of the wave front. The standard of measure for field intensity is the voltage developed in a wire that is 1 meter long, expressed as volts per meter. (If the wire were 2 meters long, the voltage developed would be divided by two to determine the field strength in volts per meter.)

The voltage in a wave is usually low, so the measurement is made in millivolts or microvolts per meter. The voltage goes through time variations like those of the current that caused the wave. It is measured like any other ac voltage—in terms of the effective value or, sometimes, the peak value. It is fortunate that in amateur work it is not necessary to measure actual field strength, as the equipment required is elaborate. We need to know only if an adjustment has been beneficial, so relative measurements are satisfactory. These can be made easily with home-built equipment.

Wave Attenuation

In free space, the field intensity of the wave varies inversely with the distance from the source, once you are in the radiating far field of the antenna. If the field strength at 1 mile from the source is 100 millivolts per meter, it will be 50 millivolts per meter at 2 miles, and so on. The relationship between field intensity and power density is similar to that for voltage and power in ordinary circuits. They are related by the impedance of free space, which is approximately 377 Ω. A field intensity of 1 volt per meter is therefore equivalent to a power density of

$$P = \frac{E^2}{Z} = \frac{1(\text{volt/m})^2}{377\,\Omega} = 2.65\,\text{mW/m}^2 \qquad \text{(Eq 2)}$$

Because of the relationship between voltage and power, the power density therefore varies with the square root of the field intensity, or inversely with the *square* of the distance. If the power density at 1 mile is 4 mW per square meter, then at a distance of 2 miles it will be 1 mW per square meter.

It is important to remember this so-called *spreading loss* when antenna performance is being considered. Gain can come only from narrowing the radiation pattern of an antenna, which concentrates the radiated energy in the desired direction. There is no "antenna magic" by which the total energy radiated can be increased.

In practice, attenuation of the wave energy may be much greater than the inverse-distance law would indicate. The wave does not travel in a vacuum, and the receiving antenna seldom is situated so there is a clear line of sight.

The Earth is spherical and the waves do not penetrate its surface appreciably, so communication beyond visual distances must be by some means that will bend the waves around the curvature of the Earth. These means involve additional energy losses that increase the path attenuation with distance, above that for the theoretical spreading loss in a vacuum.

Bending of Radio Waves

Radio waves and light waves are both propagated as electromagnetic energy. Their major difference is in wavelength, since radio-reflecting surfaces are usually much smaller in terms of wavelength than those for light. In material of a given electrical conductivity, long waves penetrate deeper than short ones, and so require a thicker mass for good reflection. Thin metal however is a good reflector of even long-wavelength radio waves. With poorer conductors, such as the Earth's crust, long waves may penetrate quite a few feet below the surface.

Reflection occurs at any boundary between materials of differing dielectric constant. Familiar examples with light are reflections from water surfaces and window panes. Both water and glass are transparent for light, but their dielectric constants are very different from that of air. Light waves, being very short, seem to bounce off both surfaces. Radio waves, being much longer, are practically unaffected by glass, but their behavior upon encountering water may vary, depending on the purity of that medium. Distilled water is a good insulator; salt water is a relatively good conductor.

Depending on their wavelength (and thus their frequency), radio waves may be reflected by buildings, trees, vehicles, the ground, water, ionized layers in the upper atmosphere, or at boundaries between air masses having different temperatures and moisture content. Ionospheric and atmospheric conditions are important in practically all communication beyond purely local ranges.

Refraction is the bending of a ray as it passes from one medium to another at an angle. The appearance of bending of a straight stick, where it enters water at an angle, is an example of light refraction known to us all. The degree of bending of radio waves at boundaries between air masses increases with the radio frequency. There is slight atmospheric bending in our HF bands. It becomes noticeable at 28 MHz, more so at 50 MHz, and it is much more of a factor in the higher VHF range and in UHF and microwave propagation.

Diffraction of light over a solid wall prevents total darkness on the far side from the light source. This is caused largely by the spreading of waves around the top of the wall, due to the interference of one part of the beam with another. The dielectric constant of the surface of the obstruction may affect what happens to our radio waves when they encounter terrestrial obstructions—but the radio *shadow area* is never totally dark. See Chapter 3, The Effects of Ground, for more information on diffraction.

The three terms, reflection, refraction and diffraction, were in use long before the radio age began. Radio propagation is nearly always a mix of these phenomena, and it may not be easy to identify or separate them while they are happening when we are on the air. This book tends to rely on the words *bending* and *scattering* in its discussions, with appropriate modifiers as needed. The important thing to remember is that any alteration of the path taken by energy as it is radiated from an antenna is almost certain to affect on-the-air results—which is why this chapter on propagation is included in an antenna book.

GROUND WAVES

As we have already seen, radio waves are affected in many ways by the media through which they travel. This has led to some confusion of terms in earlier literature concerning wave propagation. Waves travel close to the ground in several ways, some of which involve relatively little contact with the ground itself. The term *ground wave* has had several meanings in antenna literature, but it has come to be applied to any wave that stays close to the Earth, reaching the receiving point without leaving the Earth's lower atmosphere. This distinguishes the ground wave from a *sky wave*, which utilizes the ionosphere for propagation between the transmitting and receiving antennas.

The ground wave could be traveling in actual contact with the ground, as in Fig 1, where it is called the *surface wave*. Or it could travel directly between the transmitting and receiving antennas, when they are high enough so they can "see" each other—this is commonly called the *direct wave*. The ground wave also travels between the transmitting and receiving antennas by reflections or diffractions off intervening terrain between them. The ground-influenced wave may interact with the direct wave to create a vector-summed resultant at the receiver antenna.

In the generic term ground wave, we also will include ones that are made to follow the Earth's curvature by bending in the Earth's lower atmosphere, or *troposphere*, usually no more than a few miles above the ground. Often called *tropospheric bending*, this propagation mode is a major factor in amateur communications above 50 MHz.

THE SURFACE WAVE

The surface wave travels in contact with the Earth's surface. It can provide coverage up to about 100 miles in the standard AM broadcast band during the daytime, but attenuation is high. As can be seen from **Fig 3**, the attenuation increases with frequency. The surface wave is of little value in amateur communication, except possibly at 1.8 MHz. Vertically polarized antennas must be used, which tends to limit amateur surface-wave communication to where large vertical systems can be erected.

THE SPACE WAVE

Propagation between two antennas situated within line of sight of each other is shown in **Fig 4**. Energy traveling directly between the antennas is attenuated to about the same degree as in free space. Unless the antennas are very high or

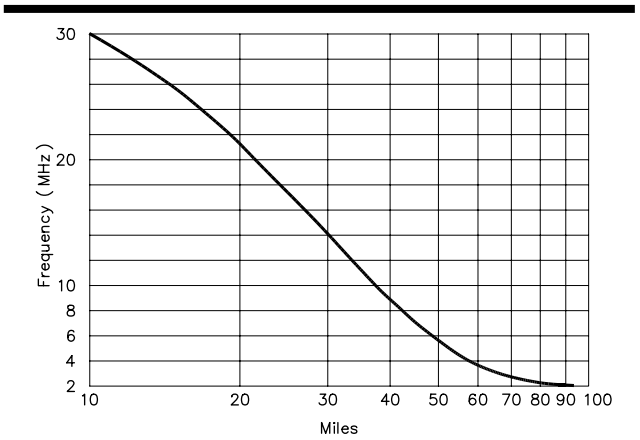

Fig 3—Typical HF ground-wave range as a function of frequency.

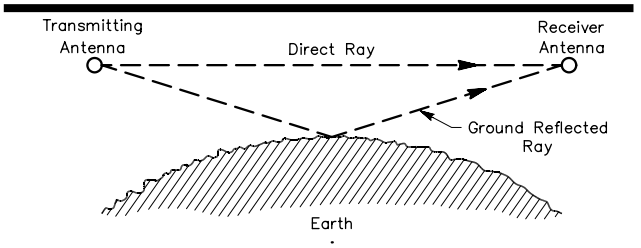

Fig 4—The ray traveling directly from the transmitting antenna to the receiving antenna combines with a ray reflected from the ground to form the space wave. For a horizontally polarized signal a reflection as shown here reverses the phase of the ground-reflected ray.

quite close together, an appreciable portion of the energy is reflected from the ground. This reflected wave combines with direct radiation to affect the actual signal received.

In most communication between two stations on the ground, the angle at which the wave strikes the ground will be small. For a horizontally polarized signal, such a reflection reverses the phase of the wave. If the distances traveled by both parts of the wave were the same, the two parts would arrive out of phase, and would therefore cancel each other. The ground-reflected ray in Fig 4 must travel a little further, so the phase difference between the two depends on the lengths of the paths, measured in wavelengths. The wavelength in use is important in determining the useful signal strength in this type of communication.

If the difference in path length is 3 meters, the phase difference with 160-meter waves would be only 360° × 3/160 = 6.8°. This is a negligible difference from the 180° shift caused by the reflection, so the effective signal strength over the path would still be very small because of cancellation of the two waves. But with 6-meter radio waves the phase length would be 360° × 3/6 = 180°. With the additional 180° shift on reflection, the two rays would add. Thus, the space wave is a negligible factor at low frequencies, but it can be increasingly useful as the frequency is raised. It is a dominant factor in local amateur communication at 50 MHz and higher.

Interaction between the direct and reflected waves is the principle cause of *mobile flutter* observed in local VHF communication between fixed and mobile stations. The flutter effect decreases once the stations are separated enough so that the reflected ray becomes inconsequential. The reflected energy can also confuse the results of field-strength measurements during tests on VHF antennas.

As with most propagation explanations, the space-wave picture presented here is simplified, and practical considerations dictate modifications. There is always some energy loss when the wave is reflected from the ground. Further, the phase of the ground-reflected wave is not shifted exactly 180°, so the waves never cancel completely. At UHF, ground-reflection losses can be greatly reduced or eliminated by using highly directive antennas. By confining the antenna pattern to something approaching a flashlight beam, nearly all the energy is in the direct wave. The resulting energy loss is low enough that microwave relays, for example, can operate with moderate power levels over hundreds or even thousands of miles. Thus we see that, while the space wave is inconsequential below about 20 MHz, it can be a prime asset in the VHF realm and higher.

VHF/UHF PROPAGATION BEYOND LINE OF SIGHT

From Fig 4 it appears that use of the space wave depends on direct line of sight between the antennas of the communicating stations. This is not literally true, although that belief was common in the early days of amateur communication on frequencies above 30 MHz. When equipment became available that operated more efficiently and after antenna techniques were improved, it soon became clear that VHF waves were actually being bent or scattered in several ways, permitting reliable communication beyond visual distances between the two stations. This was found true even with low power and simple antennas. The average communication range can be approximated by assuming the waves travel in straight lines, but with the Earth's radius increased by one-third. The distance to the *radio horizon* is then given as

$$D_{miles} = 1.415\sqrt{H_{feet}} \qquad \text{(Eq 3)}$$

or

$$D_{km} = 4.124\sqrt{H_{meters}} \qquad \text{(Eq 4)}$$

where H is the height of the transmitting antenna, as shown in **Fig 5**. The formula assumes that the Earth is smooth out to the horizon, so any obstructions along the path must be taken into consideration. For an elevated receiving antenna the communication distance is equal to D + D1, that is, the sum of the distances to the horizon of both

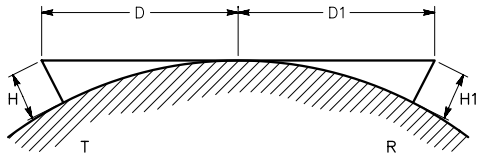

Fig 5—The distance D to the horizon from an antenna of height H is given by equations in the text. The maximum line-of-sight distance between two elevated antennas is equal to the sum of their distances to the horizon as indicated here.

antennas. Radio horizon distances are given in graphic form in **Fig 6**. Two stations on a flat plain, one with its antenna 60 feet above ground and the other 40 feet, could be up to about 20 miles apart for strong-signal line-of-sight communication (11 + 9 mi). The terrain is almost never completely flat, however, and variations along the way may add to or subtract from the distance for reliable communication. Remember that energy is absorbed, reflected or scattered in many ways in nearly all communication situations. The formula or the chart will be a good guide for estimating the potential radius of coverage for a VHF FM repeater, assuming the users are mobile or portable with simple, omnidirectional antennas. Coverage with optimum home-station equipment, high-gain directional arrays, and SSB or CW is quite a different matter. A much more detailed method for estimating coverage on frequencies above 50 MHz is given later in this chapter.

For maximum use of the ordinary space wave it is important to have the antenna as high as possible above nearby buildings, trees, wires and surrounding terrain. A hill that rises above the rest of the countryside is a good location for an amateur station of any kind, and particularly so for extensive coverage on the frequencies above 50 MHz. The highest point on such an eminence is not necessarily the best location for the antenna. In the example shown in **Fig 7**, the hilltop would be a good site in all directions. But if maximum performance to the right is the objective, a point just below the crest might do better. This would involve a trade-off with reduced coverage in the opposite direction. Conversely, an antenna situated on the left side, lower down the hill, might do well to the left, but almost certainly would be inferior in performance to the right.

Selection of a home site for its radio potential is a complex business, at best. A VHF enthusiast dreams of the highest hill. The DX-minded HF ham may be more attracted by a dry spot near a salt marsh. A wide saltwater horizon, especially from a high cliff, just smells of DX. In shopping for ham radio real estate, a mobile or portable rig for the frequencies you're most interested in can provide useful clues.

ANTENNA POLARIZATION

If effective communication over long distances were the only consideration, we might be concerned mainly with

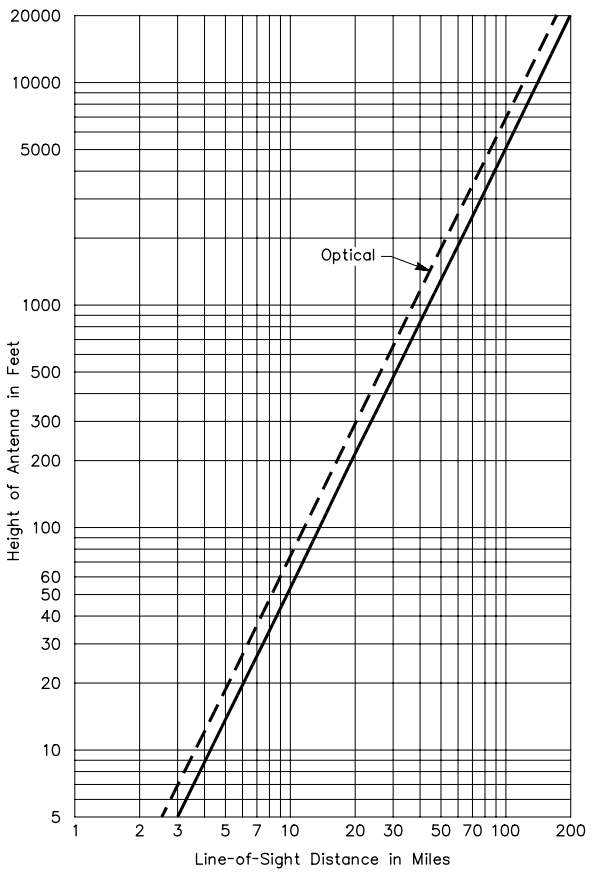

Fig 6—Distance to the horizon from an antenna of given height. The solid curve includes the effect of atmospheric retraction. The optical line-of-sight distance is given by the broken curve.

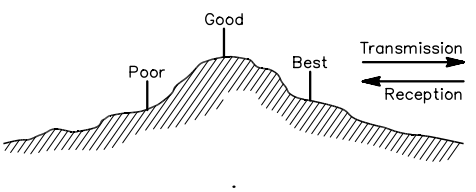

Fig 7—Propagation conditions are generally best when the antenna is located slightly below the top of a hill on the side facing the distant station. Communication is poor when there is a sharp rise immediately in front of the antenna in the direction of communication.

radiation of energy at the lowest possible angle above the horizon. However, being engaged in a residential avocation often imposes practical restrictions on our antenna projects. As an example, our 1.8 and 3.5-MHz bands are used primarily for short-distance communication because they serve that purpose with antennas that are not difficult or expensive to put up. Out to a few hundred miles, simple wire

antennas for these bands do well, even though their radiation is mostly at high angles above the horizon. Vertical systems might be better for long-distance use, but they require extensive ground systems for good performance.

Horizontal antennas that radiate well at low angles are most easily erected for 7 MHz and higher frequencies—horizontal wires and arrays are almost standard practice for work on 7 through 29.7 MHz. Vertical antennas, such as a single omnidirectional antenna of multiband design, are also used in this frequency range. An antenna of this type may be a good solution to the space problem for a city dweller on a small lot, or even for the resident of an apartment building.

High-gain antennas are almost always used at 50 MHz and higher frequencies, and most of them are horizontal. The principal exception is mobile communication with FM through repeaters, discussed in Chapter 17, Repeater Antenna Systems. The height question is answered easily for VHF enthusiasts—the higher the better.

The theoretical and practical effects of height above ground at HF are treated in detail in Chapter 3, The Effects of Ground. Note that it is the height in *wavelengths* that is important—a good reason to think in the metric system, rather than in feet and inches.

In working locally on any amateur frequency band, best results will be obtained with the same polarization at both stations, except on rare occasions when polarization shift is caused by terrain obstructions or reflections from buildings. Where such a shift is observed, mostly above 100 MHz or so, horizontal polarization tends to work better than vertical. This condition is found primarily on short paths, so it is not too important. Polarization shift may occur on long paths where tropospheric bending is a factor, but here the effect tends to be random. Long-distance communication by way of the ionosphere produces random polarization effects, so polarization matching is of little or no importance. This is fortunate for the HF mobile enthusiast, who will find that even his short, inductively loaded whips work very well at all distances other than local.

Because it responds to all plane polarizations equally, circular polarization may pay off on circuits where the arriving polarization is random, but it exacts a 3-dB penalty when used with a single-plane polarization of any kind. Circular systems find greatest use in work with orbiting satellites. It should be remembered that "horizontal" and "vertical" are meaningless terms in space, where the plane-Earth reference is lost.

Polarization Factors Above 50 MHz

In most VHF communication over short distances, the polarization of the space wave tends to remain constant. Polarization discrimination is high, usually in excess of 20 dB, so the same polarization should be used at both ends of the circuit. Horizontal, vertical and circular polarization all have certain advantages above 50 MHz, so there has never been complete standardization on any one of them.

Horizontal systems are popular, in part because they tend to reject man-made noise, much of which is vertically polarized. There is some evidence that vertical polarization shifts to horizontal in hilly terrain, more readily than horizontal shifts to vertical. With large arrays, horizontal systems may be easier to erect, and they tend to give higher signal strengths over irregular terrain, if any difference is observed.

Practically all work with VHF mobiles is now handled with vertical systems. For use in a VHF repeater system, the vertical antenna can be designed to have gain without losing the desired omnidirectional quality. In the mobile station a small vertical whip has obvious aesthetic advantages. Often a telescoping whip used for broadcast reception can be pressed into service for the 144-MHz FM rig. A car-top mount is preferable, but the broadcast whip is a practical compromise. Tests with at least one experimental repeater have shown that horizontal polarization can give a slightly larger service area, but mechanical advantages of vertical systems have made them the almost unanimous choice in VHF FM communication. Except for the repeater field, horizontal is the standard VHF system almost everywhere.

In communication over the Earth-Moon-Earth (EME) route the polarization picture is blurred, as might be expected with such a diverse medium. If the moon were a flat target, we could expect a 180° phase shift from the moon reflection process. But it is not flat. This plus the moon's *libration* (its slow oscillation, as viewed from the Earth), and the fact that waves must travel both ways through the Earth's entire atmosphere and magnetic field, provide other variables that confuse the phase and polarization issue. Building a huge array that will track the moon, and give gains in excess of 20 dB, is enough of a task that most EME enthusiasts tend to take their chances with phase and polarization problems. Where rotation of the element plane has been tried it has helped to stabilize signal levels, but it is not widely employed.

PROPAGATION OF VHF WAVES

The wave energy of VHF stations does not simply disappear once it reaches the radio horizon. It is scattered, but it can be heard to some degree for hundreds of miles, well beyond line-of-sight range. Everything on Earth, and in the regions of space up to at least 100 miles, is a potential forward-scattering agent.

Tropospheric scatter is always with us. Its effects are often hidden, masked by more effective propagation modes on the lower frequencies. But beginning in the VHF range, scatter from the lower atmosphere extends the reliable range markedly if we make use of it. Called *troposcatter*, this is what produces that nearly flat portion of the curves that will be described later (in the section where you can compute reliable VHF coverage range). With a decent station, you can consistently make troposcatter contacts out to 300 miles out on the VHF and even UHF bands, especially if you don't mind weak signals and something less than 99% reliability. As long ago as the early 1950s, VHF enthusiasts found that VHF contests could be won with high power, big antennas and a good ear for signals deep in the noise. They still can.

Ionospheric scatter works much the same as the tropo version, except that the scattering medium is higher up, mainly the E region of the ionosphere but with some help from the D and F layers too. Ionospheric scatter is useful mainly above the MUF, so its useful frequency range depends on geography, time of day, season, and the state of the Sun. With near maximum legal power, good antennas and quiet locations, ionospheric scatter can fill in the skip zone with marginally readable signals scattered from ionized trails of meteors, small areas of random ionization, cosmic dust, satellites and whatever may come into the antenna patterns at 50 to 150 miles or so above the Earth. It's mostly an E-layer business, so it works all E-layer distances. Good antennas and keen ears help.

Transequatorial propagation (TE) was an amateur 50-MHz discovery in the years 1946-1947. Amateurs of all continents observed it almost simultaneously on three separate north-south paths. These amateurs tried to communicate at 50 MHz, even though the predicted MUF was around 40 MHz for the favorable daylight hours. The first success came at night, when the MUF was thought to be even lower. A remarkable research program inaugurated by amateurs in Europe, Cyprus, Zimbabwe and South Africa eventually provided technically sound theories to explain the then-unknown mode.

It has been known for years that the MUF is higher and less seasonally variable on transequatorial circuits, but the full extent of the difference was not learned until amateur work brought it to light. As will be explained in a later section in more detail, the ionosphere over equatorial regions is higher, thicker and more dense than elsewhere. Because of its more constant exposure to solar radiation, the equatorial belt has high nighttime-MUF possibilities. TE can often work marginally at 144 MHz, and even at 432 MHz on occasion. The potential MUF varies with solar activity, but not to the extent that conventional F-layer propagation does. It is a late-in-the-day mode, taking over about when normal F-layer propagation goes out.

The TE range is usually within about 4000 km (2500 miles) either side of the geomagnetic equator. The Earth's magnetic axis is tilted with respect to the geographical axis, so the TE belt appears as a curving band on conventional flat maps of the world. See **Fig 8**. As a result, TE has a different latitude coverage in the Americas from that from Europe to Africa. The TE belt just reaches into the southern continental US. Stations in Puerto Rico, Mexico and even the northern parts of South America encounter the mode more often than those in favorable US areas. It is no accident that TE was discovered as a result of 50-MHz work in Mexico City and Buenos Aires.

Within its optimum regions of the world, the TE mode extends the usefulness of the 50-MHz band far beyond that of conventional F-layer propagation, since the practical TE MUF runs around 1.5 times that of normal F_2. Both its seasonal and diurnal characteristics are extensions of what is considered normal for 50-MHz propagation. In that part of the Americas south of about 20° North latitude, the existence of TE affects the whole character of band usage, especially in years of high solar activity.

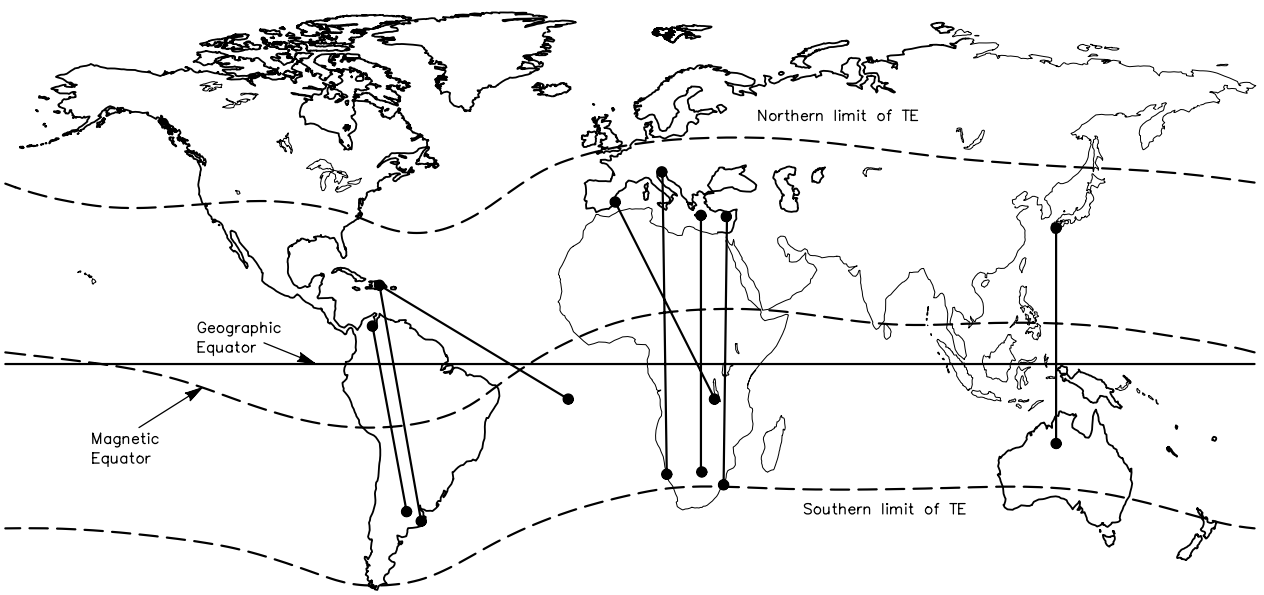

Fig 8—Transequatorial spread-F propagation takes place between stations equidistant across the geomagnetic equator. Distances up to 8000 km (5000 miles) are possible on 28 through 432 MHz. Note that the geomagnetic equator is considerably south of the geographic equator in the Western Hemisphere. (*Figure courtesy of The ARRL Handbook.*)

Weather Effects on VHF/UHF Tropospheric Propagation

Changes in the dielectric constant of the medium can affect propagation. Varied weather patterns over most of the Earth's surface can give rise to boundaries between air masses of very different temperature and humidity characteristics. These boundaries can be anything from local anomalies to air-circulation patterns of continental proportions.

Under stable weather conditions, large air masses can retain their characteristics for hours or even days at a time. See **Fig 9**. Stratified warm dry air over cool moist air, flowing slowly across the Great Lakes region to the Atlantic Seaboard, can provide the medium for east-west communication on 144 MHz and higher amateur frequencies over as much as 1200 miles. More common, however, are communication distances of 400 to 600 miles under such conditions.

A similar inversion along the Atlantic Seaboard as a result of a tropical storm air-circulation pattern may bring VHF and UHF openings extending from the Maritime Provinces of Canada to the Carolinas. Propagation across the Gulf of Mexico, sometimes with very high signal levels, enlivens the VHF scene in coastal areas from Florida to Texas. The California coast, from below the San Francisco Bay Area to Mexico, is blessed with a similar propagation aid during the warmer months. Tropical storms moving west, across the Pacific below the Hawaiian Islands, may provide a transpacific long-distance VHF medium. Amateurs first exploited this on 144, 220 and 432 MHz, in 1957. It has been used fairly often in the summer months since, although not yearly.

The examples of long-haul work cited above may occur infrequently, but lesser extensions of the minimum operating range are available almost daily. Under minimum conditions there may be little more than increased signal strength over paths that are workable at any time.

There is a diurnal effect in temperate climates. At sunrise the air aloft is warmed more rapidly than that near the Earth's surface, and as the Sun goes lower late in the day the upper air is kept warm, while the ground cools. In fair, calm weather such sunrise and sunset temperature inversions can improve signal strength over paths beyond line of sight as much as 20 dB over levels prevailing during the hours of high sun. The diurnal inversion may also extend the operating range for a given strength by some 20 to 50%. If you would be happy with a new VHF antenna, try it first around sunrise!

There are other short-range effects of local atmospheric and topographical conditions. Known as *subsidence*, the flow of cool air down into the bottom of a valley, leaving warm air aloft, is a familiar summer-evening pleasure. The daily inshore-offshore wind shift along a seacoast in summer sets up daily inversions that make coastal areas highly favored as VHF sites. Ask any jealous 144-MHz operator who lives more than a few miles inland.

Tropospheric effects can show up at any time, in any season. Late spring and early fall are the most favored periods, although a winter warming trend can produce strong and stable inversions that work VHF magic almost equal to that of the more familiar spring and fall events.

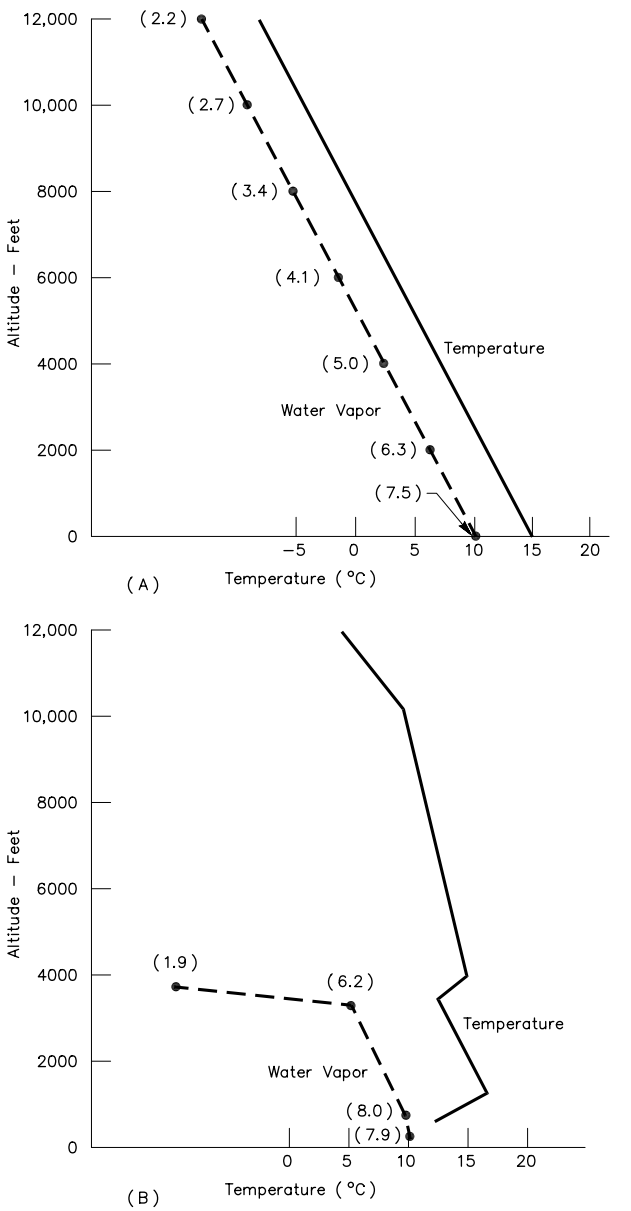

Fig 9—Upper air conditions that produce extended-range communication on the VHF bands. At the top is shown the US Standard Atmosphere temperature curve. The humidity curve (dotted) is what would result if the relative humidity were 70%, from ground level to 12,000 feet elevation. There is only slight refraction under this standard condition. At the bottom is shown a sounding that is typical of marked refraction of VHF waves. Figures in parentheses are the "mixing ratio"—grams of water vapor per kilogram of dry air. Note the sharp break in both curves at about 3500 feet.

Regions where the climate is influenced by large bodies of water enjoy the greatest degree of tropospheric bending. Hot, dry desert areas see little of it, at least in the forms described above.

Tropospheric Ducting

Tropospheric propagation of VHF and UHF waves can influence signal levels at all distances from purely local to something beyond 4000 km (2500 miles). The outer limits are not well known. At the risk of over simplification, we will divide the modes into two classes—extended local and long distance. This concept must be modified depending on the frequency under consideration, but in the VHF range the extended-local effect gives way to a form of propagation much like that of microwaves in a waveguide, called *ducting*. The transition distance is ordinarily somewhere around 200 miles. The difference lies in whether the atmospheric condition producing the bending is localized or continental in scope. Remember, we're concerned here with frequencies in the VHF range, and perhaps up to 500 MHz. At 10 GHz, for example, the scale is much smaller.

In VHF propagation beyond a few hundred miles, more than one weather front is probably involved, but the wave is propagated between the inversion layers and ground, in the main. On long paths over the ocean (two notable examples are California to Hawaii and Ascension Island to Brazil), propagation is likely to be between two atmospheric layers. On such circuits the communicating station antennas must be in the duct, or capable of propagating strongly into it. Here again, we see that the positions and radiation angles of the antennas are important. As with microwaves in a waveguide, the low-frequency limit for the duct is critical. In long-distance ducting it is also very variable. Airborne equipment has shown that duct capability exists well down into the HF region in the stable atmosphere west of Ascension Island. Some contacts between Hawaii and Southern California on 50 MHz are believed to have been by way of tropospheric ducts. Probably all contact over these paths on 144 MHz and higher bands is because of duct propagation.

Amateurs have played a major part in the discovery and eventual explanation of tropospheric propagation. In recent years they have shown that, contrary to beliefs widely held in earlier times, long-distance communication using tropospheric modes is possible to some degree on all amateur frequencies from 50 to at least 10,000 MHz.

RELIABLE VHF COVERAGE

In the preceding sections we discussed means by which amateur bands above 50 MHz may be used intermittently for communication far beyond the visual horizon. In emphasizing distance we should not neglect a prime asset of the VHF band: reliable communication over relatively short distances. The VHF region is far less subject to disruption of local communication than are frequencies below 30 MHz. Since much amateur communication is essentially local in nature, our VHF assignments can carry a great load, and such use of the VHF bands helps solve interference problems on lower frequencies.

Because of age-old ideas, misconceptions about the coverage obtainable in our VHF bands persist. This reflects the thoughts that VHF waves travel only in straight lines, except when the DX modes described above happen to be present. However, let us survey the picture in the light of modern wave-propagation knowledge and see what the bands above 50 MHz are good for on a day-to-day basis, ignoring the anomalies that may result in extensions of normal coverage.

It is possible to predict with fair accuracy how far you should be able to work consistently on any VHF or UHF band, provided a few simple facts are known. The factors affecting operating range can be reduced to graph form, as described in this section. The information was originally published in November 1961 *QST* by D. W. Bray, K2LMG (see the Bibliography at the end of this chapter).

To estimate your station's capabilities, two basic numbers must be determined: station gain and path loss. Station gain is made up of seven factors: receiver sensitivity, transmitted power, receiving antenna gain, receiving antenna height gain, transmitting antenna gain, transmitting antenna height gain and required signal-to-noise ratio. This looks complicated but it really boils down to an easily made evaluation of receiver, transmitter, and antenna performance. The other number, path loss, is readily determined from the nomogram, **Fig 10**. This gives path loss over smooth Earth, for 99% reliability.

For 50 MHz, lay a straightedge from the distance between stations (left side) to the appropriate distance at the right side. For 1296 MHz, use the full scale, right center. For 144, 222 and 432, use the dot in the circle, square or triangle, respectively. Example: At 300 miles the path loss for 144 MHz is 214 dB.

To be meaningful, the losses determined from this nomograph are necessarily greater than simple free-space path losses. As described in an earlier section, communication beyond line-of-sight distances involves propagation modes that increase the path attenuation with distance.

VHF/UHF Station Gain

The largest of the eight factors involved in station design is receiver sensitivity. This is obtainable from **Fig 11**, if you know the approximate receiver noise figure and transmission-line loss. If you can't measure noise figure, assume 3 dB for 50 MHz, 5 for 144 or 222, 8 for 432 and 10 for 1296 MHz, if you know your equipment is working moderately well. These noise figures are well on the conservative side for modern solid-state receivers.

Line loss can be taken from information in Chapter 24 for the line in use, if the antenna system is fed properly. Lay a straightedge between the appropriate points at either side of Fig 11, to find effective receiver sensitivity in decibels below 1 watt (dBW). Use the narrowest bandwidth that is practical for the emission intended, with the receiver you will be using. For CW, an average value for effective work

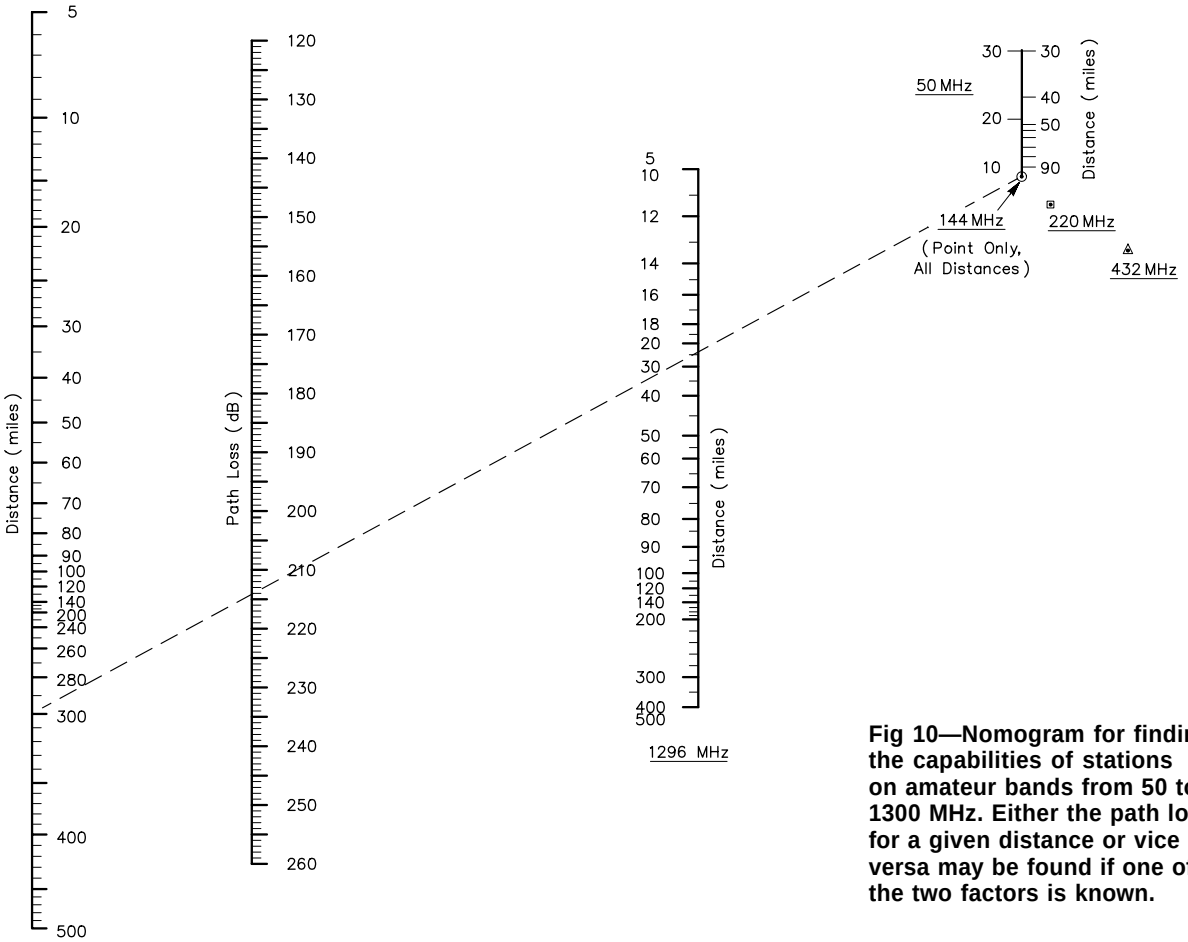

Fig 10—Nomogram for finding the capabilities of stations on amateur bands from 50 to 1300 MHz. Either the path loss for a given distance or vice versa may be found if one of the two factors is known.

is about 500 Hz. Phone bandwidth can be taken from the receiver instruction manual, but it usually falls between 2.1 to 2.7 kHz.

Antenna gain is next in importance. Gains of amateur antennas are often exaggerated. For well-designed Yagis the gain (over isotropic) run close to 10 times the boom length in wavelengths. (Example: A 24-foot Yagi on 144 MHz is 3.6 wavelengths long; 3.6 x 10 = 36, and 10 $\log_{10}$ 36 = 15.5 dBi in free space.) Add 3 dB for stacking, where used properly. Add 4 dB more for ground reflection gain. This varies in amateur work, but averages out near this figure.

We have one more plus factor—antenna height gain, obtained from **Fig 12**. Note that this is greatest for short distances. The left edge of the horizontal center scale is for 0 to 10 miles, the right edge for 100 to 500 miles. Height gain for 10 to 30 feet is assumed to be zero. For 50 feet the height gain is 4 dB at 10 miles, 3 dB at 50 miles, and 2 dB at 100 miles. At 80 feet the height gains are roughly 8, 6 and 4 dB for these distances. Beyond 100 miles the height gain is nearly uniform for a given height, regardless of distance.

Transmitter power output must be stated in decibels above 1 watt. If you have 500 W output, add 10 log (500/1), or 27 dB, to your station gain. The transmission-line loss must be subtracted from the station gain. So must the required signal-to-noise ratio. The information is based on CW work, so the additional signal needed for other modes must be subtracted. Use a figure of 3 dB for SSB. Fading losses must be accounted for also. It has been shown that for distances beyond 100 miles, the signal will vary plus or minus about 7 dB from the average level, so 7 dB must be subtracted from the station gain for high reliability. For distances under 100 miles, fading diminishes almost linearly with distance. For 50 miles, use –3.5 dB for fading.

What It All Means

Add all the plus and minus factors to get the station gain. Use the final value to find the distance over which you can expect to work reliably from the nomogram, Fig 10. Or work it the other way around: Find the path loss for the distance you want to cover from the nomogram and then figure out what station changes will be needed to overcome it.

The significance of all this becomes more obvious when we see path loss plotted against frequency for the various bands, as in **Fig 13**. At the left this is done for 50% reliability. At the right is the same information for 99% reliability.

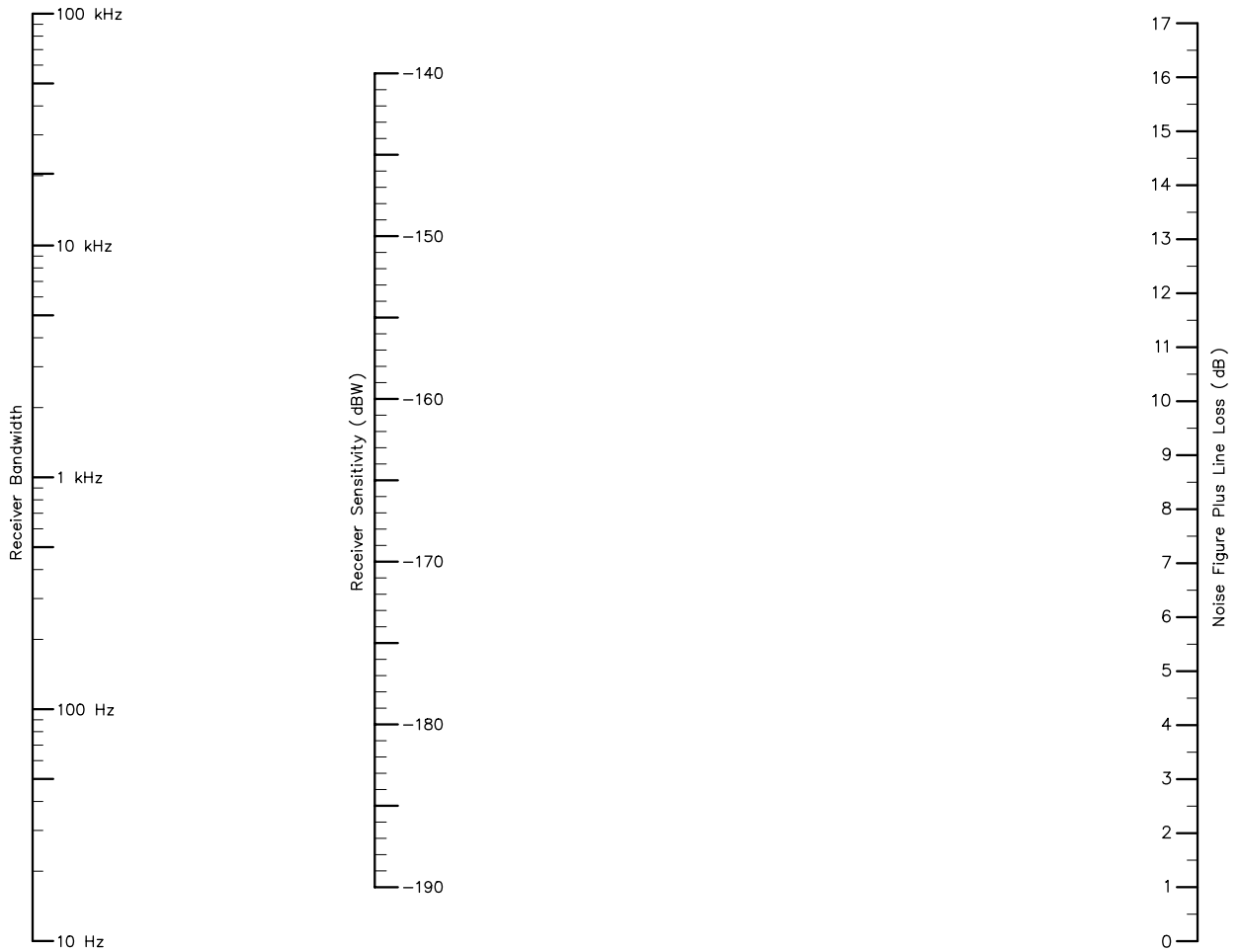

Fig 11—Nomogram for finding effective receiver sensitivity.

For near-perfect reliability, a path loss of 195 dB (easily encountered at 50 or 144 MHz) is involved in 100-mile communication. But look at the 50% reliability curve: The same path loss takes us out to well over 250 miles. Few amateurs demand near-perfect reliability. By choosing our times, and by accepting the necessity for some repeats or occasional loss of signal, we can maintain communication out to distances far beyond those usually covered by VHF stations.

Working out a few typical amateur VHF station setups with these curves will show why an understanding of these factors is important to any user of the VHF spectrum. Note that path loss rises very steeply in the first 100 miles or so. This is no news to VHF operators; locals are very strong, but stations 50 or 75 miles away are much weaker. What happens beyond 100 miles is not so well known to many of us.

From the curves of Fig 13, we see that path loss levels off markedly at what is the approximate limit of working range for average VHF stations using wideband modulation modes. Work out the station gain for a 50-W station with an average receiver and antenna, and you'll find that it comes out around 180 dB. This means you'd have about a 100-mile working radius in average terrain, for good but not perfect reliability. Another 10 dB may extend the range to as much as 250 miles. Just changing from AM phone to SSB and CW makes a major improvement in daily coverage on the VHF bands.

A bigger antenna, a higher one if your present beam is not at least 50 feet up, an increase in power to 500 W from 50 W, an improvement in receiver noise figure if it is presently poor—any of these things can make a big improvement in reliable coverage. Achieve all of them, and you will have very likely tripled your sphere of influence, thanks to that hump in the path-loss curves. This goes a long way toward explaining why using a 10-W packaged station with a small antenna, fun though it may be, does not begin to show what the VHF bands are really good for.

Terrain at VHF/UHF

The coverage figures derived from the above procedure are for average terrain. What of stations in mountainous country? Although an open horizon is generally desirable for the VHF station site, mountain country should not be

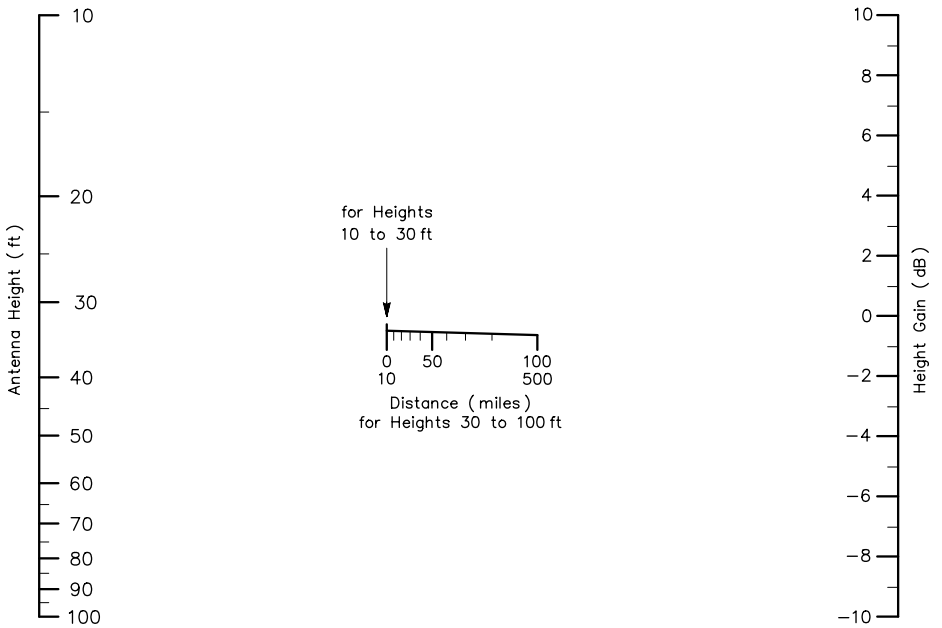

Fig 12—Nomogram for determining antenna-height gain.

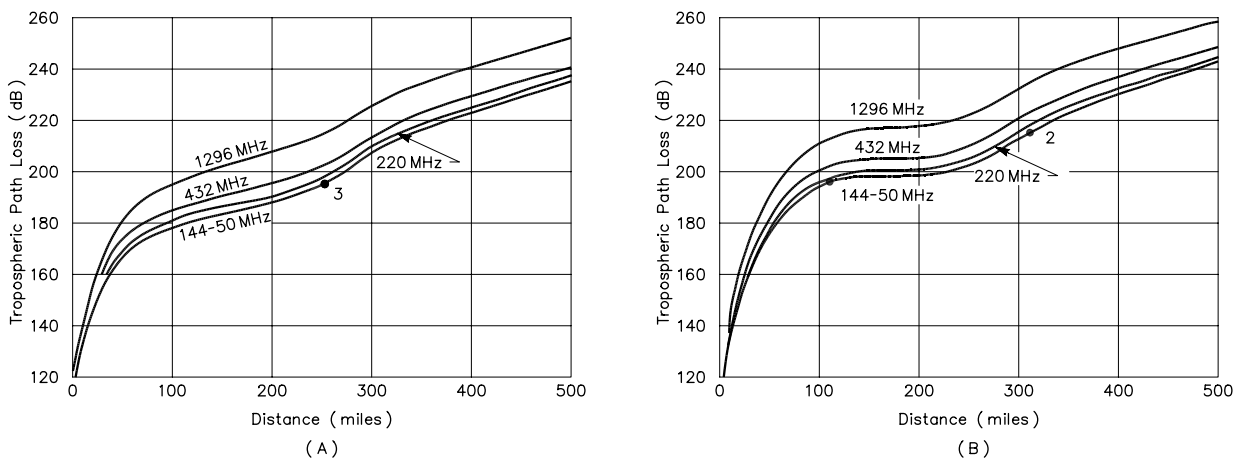

Fig 13—Path loss versus distance for amateur frequencies above 50 MHz. At A are curves for 50% of the time; at B, for 99%. The curves at A are more representative of Amateur Radio requirements.

considered hopeless. Help for the valley dweller often lies in the optical phenomenon known as *knife-edge diffraction*. A flashlight beam pointed at the edge of a partition does not cut off sharply at the partition edge, but is diffracted around it, partially illuminating the shadow area. A similar effect is observed with VHF waves passing over ridges; there is a shadow effect, but not a complete blackout. If the signal is strong where it strikes the mountain range, it will be heard well in the bottom of a valley on the far side. (See Chapter 3, The Effects of Ground, for a more thorough discussion of the theory of diffraction.)

This is familiar to all users of VHF communications equipment who operate in hilly terrain. Where only one ridge lies in the way, signals on the far side may be almost as good as on the near side. Under ideal conditions (a very high and sharp-edged obstruction near the midpoint of a long-enough path so that signals would be weak over average terrain), knife-edge diffraction may yield signals even stronger than would be possible with an open path.

The obstruction must project into the radiation patterns of the antennas used. Often mountains that look formidable to the viewer are not high enough to have an appreciable

effect, one way or the other. Since the normal radiation pattern from a VHF array is several degrees above the horizontal, mountains that are less than about three degrees above the horizon, as seen from the antenna, are missed by the radiation from the array. Moving the mountains out of the way would have substantially no effect on VHF signal strength in such cases.

Rolling terrain, where obstructions are not sharp enough to produce knife-edge diffraction, still does not exhibit a complete shadow effect. There is no complete barrier to VHF propagation—only attenuation, which varies widely as the result of many factors. Thus, even valley locations are usable for VHF communication. Good antenna systems, preferably as high as possible, the best available equipment, and above all, the willingness and ability to work with weak signals may make outstanding VHF work possible, even in sites that show little promise by casual inspection.

AURORAL PROPAGATION

The Earth has a *magnetosphere* or magnetic field surrounding it. NASA scientists have described the magnetosphere as a sort of protective "bubble" around the Earth that shields us from the solar wind. Under normal circumstances, there are lots of electrons and protons moving in our magnetosphere, traveling along magnetic lines of force that trap them and keep them in place, neither bombarding the earth nor escaping into outer space.

Sudden bursts of activity on the Sun are sometimes accompanied by the ejection of charged particles, often from so-called Coronal Mass Ejections (CME) because they originate from the Sun's outer coronal region. These charged particles can interact with the magnetosphere, compressing and distorting it. If the orientation of the magnetic field contained in a large blast of solar wind or in a CME is aligned opposite to that of the Earth's magnetic field, the magnetic bubble can partially collapse and the particles normally trapped there can be deposited into the Earth's atmosphere along magnetic lines near the North or South poles. This produces a visible or radio *aurora*. An aurora is visible if the time of entry is after dark.

The visible aurora is, in effect, fluorescence at E-layer height—a curtain of ions capable of refracting radio waves in the frequency range above about 20 MHz. D-region absorption increases on lower frequencies during auroras. The exact frequency ranges depend on many factors: time, season, position with relation to the Earth's auroral regions, and the level of solar activity at the time, to name a few.

The auroral effect on VHF waves is another amateur discovery, this one dating back to the 1930s. The discovery came coincidentally with improved transmitting and receiving techniques then. The returning signal is diffused in frequency by the diversity of the auroral curtain as a refracting (scattering) medium. The result is a modulation of a CW signal, from just a slight burbling sound to what is best described as a "keyed roar." Before SSB took over in VHF work, voice was all but useless for auroral paths. A sideband signal suffers, too, but its narrower bandwidth helps to retain some degree of understandability. Distortion induced by a given set of auroral conditions increases with the frequency in use. 50-MHz signals are much more intelligible than those on 144 MHz on the same path at the same time. On 144 MHz, CW is almost mandatory for effective auroral communication.

The number of auroras that can be expected per year varies with the geomagnetic latitude. Drawn with respect to the Earth's magnetic poles instead of the geographical ones, these latitude lines in the US tilt upward to the northwest. For example, Portland, Oregon, is 2° farther north (geographic latitude) than Portland, Maine. The Maine city's geomagnetic latitude line crosses the Canadian border before it gets as far west as its Oregon namesake. In terms of auroras intense enough to produce VHF propagation results, Portland, Maine, is likely to see about 10 times as many per year. Oregon's auroral prospects are more like those of southern New Jersey or central Pennsylvania.

The antenna requirements for auroral work are mixed. High gain helps, but the area of the aurora yielding the best returns sometimes varies rapidly, so sharp directivity can be a disadvantage. So could a very low radiation angle, or a beam pattern very sharp in the vertical plane. Experience indicates that few amateur antennas are sharp enough in either plane to present a real handicap. The beam heading for maximum signal can change, however, so a bit of scanning in azimuth may turn up some interesting results. A very large array, such as is commonly used for moonbounce (with azimuth-elevation control), should be worthwhile.

The incidence of auroras, their average intensity, and their geographical distribution as to visual sightings and VHF propagation effects all vary to some extent with solar activity. There is some indication that the peak period for auroras lags the sunspot-cycle peak by a year or two. Like sporadic E, an unusual auroral opening can come at any season. There is a marked diurnal swing in the number of auroras. Favored times are late afternoon and early evening, late evening through early morning, and early afternoon, in about that order. Major auroras often start in early afternoon and carry through to early morning the next day.

HF Sky-Wave Propagation

As described earlier, the term *ground wave* is commonly applied to propagation that is confined to the Earth's lower atmosphere. Now we will use the term *sky wave* to describe modes of propagation that use the Earth's ionosphere. First, however, we must examine how the Earth's ionosphere is affected by the Sun.

THE ROLE OF THE SUN

Everything that happens in radio propagation, as with all life on Earth, is the result of radiation from the Sun. The variable nature of radio propagation here on Earth reflects the ever-changing intensity of ultraviolet and X-ray radiation, the primary ionizing agents in solar energy. Every day, solar nuclear reactions are turning hydrogen into helium, releasing an unimaginable blast of energy into space in the process. The total power radiated by the Sun is estimated at 4×10^{23} kW—that is, the number four followed by 23 zeroes. At its surface, the Sun creates about 60 *megawatts* per square meter. That is a very potent transmitter!

The Solar Wind

The Sun is constantly ejecting material from its surface in all directions into space, making up the so-called *solar wind*. Under relatively quiet solar conditions the solar wind blows around 200 miles per second—675,000 miles per hour—taking away about two million tons of solar material each second from the Sun. You needn't worry—the Sun is not going to shrivel up anytime soon. It's big enough that it will take many billions of years before that happens.

A 675,000 mile/hour wind sounds like a pretty stiff breeze, doesn't it? Lucky for us, the density of the material in the solar wind is very small by the time it has been spread out into interplanetary space. Scientists calculate that the density of the particles in the solar wind is less than that of the best vacuum they've ever achieved on Earth. Despite the low density of the material in the solar wind, the effect on the Earth, especially its magnetic field, is very significant.

Before the advent of sophisticated satellite sensors, the Earth's magnetic field was considered to be fairly simple, modeled as if the Earth were a large bar magnet. The axis of this hypothetical bar magnet is oriented about 11° away from the geographic north-south pole. We now know that the solar wind alters the shape of the Earth's magnetic field significantly, compressing it on the side facing the Sun and elongating it on the other side—in the same manner as the tail of a comet is stretched out radially in its orientation from the Sun. In fact, the solar wind is also responsible for the shape of a comet's tail.

Partly because of the very nature of the nuclear reactions going on at the Sun itself, but also because of variations in the speed and direction of the solar wind, the interactions between the Sun and our Earth are incredibly complex. Even scientists who have studied the subject for years do not completely understand everything that happens on the Sun. Later in this chapter, we'll investigate the effects of the solar wind when conditions on the Sun are *not* "quiet." As far as amateur HF skywave propagation is concerned, the results of disturbed conditions on the Sun are not generally beneficial.

Sunspots

The most readily observed characteristic of the Sun, other than its blinding brilliance, is its tendency to have grayish black blemishes, seemingly at random times and at random places, on its fiery surface. (See **Fig 14**.) There are written records of naked-eye sightings of *sunspots* in the Orient back to more than 2000 years ago. As far as is known, the first indication that sunspots were recognized as part of the Sun was the result of observations by Galileo in the early 1600s, not long after he developed one of the first practical telescopes.

Galileo also developed the projection method for observing the Sun safely, but probably not before he had suffered severe eye damage by trying to look at the Sun di-

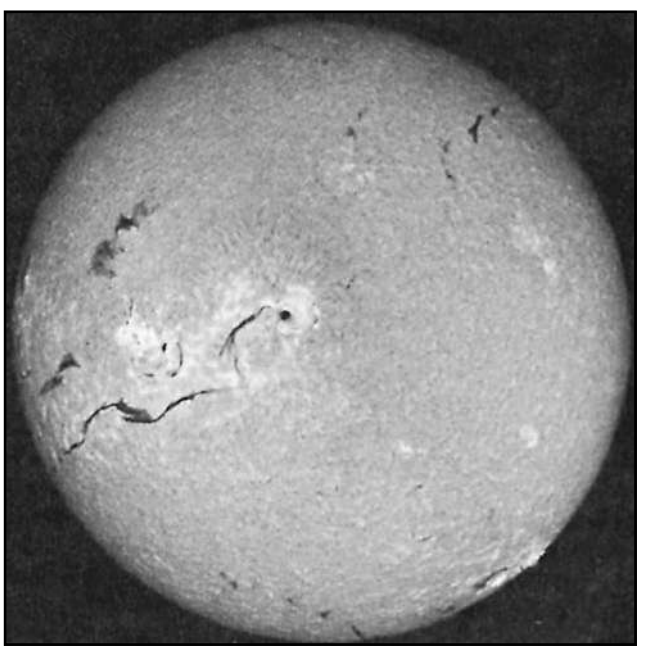

Fig 14—Much more than sunspots can be seen when the sun is viewed through selective optical filters. This photo was taken through a hydrogen-alpha filter that passes a narrow light segment at 6562 angstroms. The bright patches are active areas around and often between sunspots. Dark irregular lines are filaments of activity having no central core. Faint magnetic field lines are visible around a large sunspot group near the disc center. (*Photo courtesy of Sacramento Peak Observatory, Sunspot, New Mexico*).

rectly. (He was blind in his last years.) His drawings of sunspots, indicating their variable nature and position, are the earliest such record known to have been made. His reward for this brilliant work was immediate condemnation by church authorities of the time, which probably set back progress in learning more about the Sun for generations.

The systematic study of solar activity began about 1750, so a fairly reliable record of sunspot numbers goes back that far. (There are some gaps in the early data.) The record shows clearly that the Sun is always in a state of change. It never looks exactly the same from one day to the next. The most obvious daily change is the movement of visible activity centers (sunspots or groups thereof) across the solar disc, from east to west, at a constant rate. This movement was soon found to be the result of the rotation of the Sun, at a rate of approximately four weeks for a complete round. The average is about 27.5 days, the Sun's *synodic* rotation speed, viewed from the perspective of the Earth, which is also moving around the Sun in the same direction as the Sun's rotation.

Sunspot Numbers

Since the earliest days of systematic observation, our traditional measure of solar activity has been based on a count of sunspots. In these hundreds of years we have learned that the average number of spots goes up and down in cycles very roughly approximating a sine wave. In 1848, a method was introduced for the daily measurement of sunspot numbers. That method, which is still used today, was devised by the Swiss astronomer Johann Rudolph Wolf. The observer counts the total number of spots visible on the face of the Sun and the number of groups into which they are clustered, because neither quantity alone provides a satisfactory measure of sunspot activity. The observer's sunspot number for that day is computed by multiplying the number of groups he sees by 10, and then adding to this value the number of individual spots. Where possible, sunspot data collected prior to 1848 have been converted to this system.

As can readily be understood, results from one observer to another can vary greatly, since measurement depends on the capability of the equipment in use and on the stability of the Earth's atmosphere at the time of observation, as well as on the experience of the observer. A number of observatories around the world cooperate in measuring solar activity. A weighted average of the data is used to determine the *International Sunspot Number* or ISN for each day. (Amateur astronomers can approximate the determination of ISN values by multiplying their values by a correction factor determined empirically.)

A major step forward was made with the development of various methods for observing narrow portions of the Sun's spectrum. Narrowband light filters that can be used with any good telescope perform a visual function very similar to the aural function of a sharp filter added to a communications receiver. This enables the observer to see the actual area of the Sun doing the radiating of the ionizing energy, in addition to the sunspots, which are more a by-product than a cause. The photo of Fig 14 was made through such a filter. Studies of the ionosphere with instrumented probes, and later with satellites, manned and unmanned, have added greatly to our knowledge of the effects of the Sun on radio communication.

Daily sunspot counts are recorded, and monthly and yearly averages determined. The averages are used to see trends and observe patterns. Sunspot records were formerly kept in Zurich, Switzerland, and the values were known as *Zurich Sunspot Numbers*. They were also known as Wolf sunspot numbers. The official international sunspot numbers are now compiled at the Sunspot Index Data Center in Bruxelles, Belgium.

The yearly means (averages) of sunspot numbers from 1700 through 2002 are plotted in **Fig 15**. The cyclic nature of solar activity becomes readily apparent from this graph. The duration of the cycles varies from 9.0 to 12.7 years, but averages approximately 11.1 years, usually referred to as the 11-year solar cycle. The first complete cycle to be observed systematically began in 1755, and is numbered Cycle 1. Solar cycle numbers thereafter are consecutive. Cycle 23 began in October, 1996.

The "Quiet" Sun

For more than 60 years it has been well known that radio propagation phenomena vary with the number and size of sunspots, and also with the position of sunspots on the surface of the Sun. There are daily and seasonal variations in the Earth's ionized layers resulting from changes in the amount of ultraviolet light received from the Sun. The 11-year sunspot cycle affects propagation conditions because there is a direct correlation between sunspot activity and ionization.

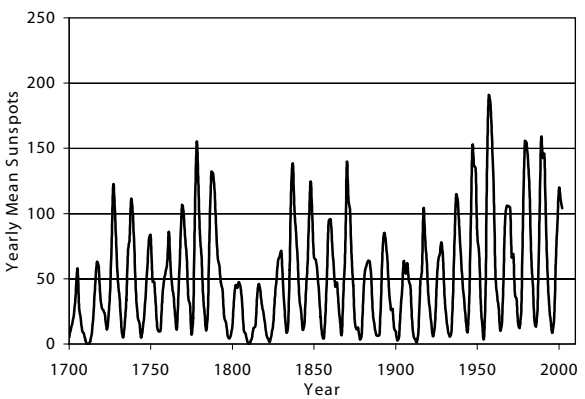

Fig 15—Yearly means of smoothed sunspot numbers from data for 1700 through 2002. This plot clearly shows that sunspot activity takes place in cycles of approximately 11 years duration. There is also a longer-term periodicity in this plot, the Gleissberg 88-year cycle. Cycle 1, the first complete cycle to be examined by systematic observation, began in 1755.

Activity on the surface of the Sun is changing continually. In this section we want to describe the activity of the so-called *quiet Sun*, meaning those times when the Sun is not doing anything more spectacular than acting like a "normal" thermonuclear ball of flaming gases. The Sun and its effects on Earthly propagation can be described in *statistical* terms—that's what the 11-year solar cycle does. You may experience vastly different conditions on any particular day compared to what a long-term average would suggest.

An analogy may be in order here. Have you ever gazed into a relatively calm campfire and been surprised when suddenly a flaming ember or a large spark was ejected in your direction? The Sun can also do unexpected and sometimes very dramatic things. Disturbances of propagation conditions here on Earth are caused by disturbed conditions on the Sun. More on this later.

Individual sunspots may vary in size and appearance, or even disappear totally, within a single day. In general, larger active areas persist through several rotations of the Sun. Some active areas have been identified over periods up to about a year. Because of these continual changes in solar activity, there are continual changes in the state of the Earth's ionosphere and resulting changes in propagation conditions. A short-term burst of solar activity may trigger unusual propagation conditions here on Earth lasting for less than an hour.

Smoothed Sunspot Numbers (SSN)

Sunspot data are averaged or smoothed to remove the effects of short-term changes. The sunspot values used most often for correlating propagation conditions are *Smoothed Sunspot Numbers* (SSN), often called 12-month running average values. Data for 13 consecutive months are required to determine a smoothed sunspot number.

Long-time users have found that the upper HF bands are reliably open for propagation only when the average number of sunspots is above certain minimum levels. For example, between mid 1988 to mid 1992 during Cycle 22, the SSN stayed higher than 100. The 10-meter band was open then almost all day, every day, to some part of the world. However, by mid 1996, few if any sunspots showed up on the Sun and the 10-meter band consequently was rarely open. Even 15 meters, normally a workhorse DX band when solar activity is high, was closed most of the time during the low point in Cycle 22. So far as propagation on the upper HF bands is concerned, the higher the sunspot number, the better the conditions.

Each smoothed number is an average of 13 monthly means, centered on the month of concern. The 1st and 13th months are given a weight of 0.5. A monthly mean is simply the sum of the daily ISN values for a calendar month, divided by the number of days in that month. We would commonly call this value a monthly average.

This may all sound very complicated, but an example should clarify the procedure. Suppose we wished to calculate the smoothed sunspot number for June 1986. We would require monthly mean values for six months prior and six months after this month, or from December 1985 through December 1986. The monthly mean ISN values for these months are

Dec	85	17.3	Jul	86	18.1
Jan	86	2.5	Aug	86	7.4
Feb	86	23.2	Sep	86	3.8
Mar	86	15.1	Oct	86	35.4
Apr	86	18.5	Nov	86	15.2
May	86	13.7	Dec	86	6.8
Jun	86	1.1			

First we find the sum of the values, but using only one-half the amounts indicated for the first and 13th months in the listing. This value is 166.05. Then we determine the smoothed value by dividing the sum by 12: 166.05/12 = 13.8. (Values beyond the first decimal place are not warranted.) Thus, 13.8 is the smoothed sunspot number for June 1986. From this example, you can see that the smoothed sunspot number for a particular month cannot be determined until six months afterwards.

Generally the plots we see of sunspot numbers are averaged data. As already mentioned, smoothed numbers make it easier to observe trends and see patterns, but sometimes this data can be misleading. The plots tend to imply that solar activity varies smoothly, indicating, for example, that at the onset of a new cycle the activity just gradually increases. But this is definitely not so! On any one day, significant changes in solar activity can take place within hours, causing sudden band openings at frequencies well above the MUF values predicted from smoothed sunspot number curves. The durations of such openings may be brief, or they may recur for several days running, depending on the nature of the solar activity.

Solar Flux

Since the late 1940s an additional method of determining solar activity has been put to use—the measurement of *solar radio flux*. The quiet Sun emits radio energy across a broad frequency spectrum, with a slowly varying intensity. Solar flux is a measure of energy received per unit time, per unit area, per unit frequency interval. These radio fluxes, which originate from atmospheric layers high in the Sun's chromosphere and low in its corona, change gradually from day to day, in response to the activity causing sunspots. Thus, there is a degree of correlation between solar flux values and sunspot numbers.

One solar flux unit equals 10^{-22} joules per second per square meter per hertz. Solar flux values are measured daily at 2800 MHz (10.7 cm) at The Dominion Radio Astrophysical Observatory, Penticton, British Columbia, where daily data have been collected since 1991. (Prior to June 1991, the Algonquin Radio Observatory, Ontario, made the measurements.) Measurements are also made at other observatories around the world, at several frequencies. With some variation, the daily measured flux values increase with

increasing frequency of measurement, to at least 15.4 GHz. The daily 2800 MHz Penticton value is sent to Boulder, Colorado, where it is incorporated into WWV propagation bulletins (see later section). Daily solar flux information can be of some value in determining current propagation conditions, as sunspot numbers on a given day do not relate directly to maximum usable frequency. Solar flux values are much more reliable for this purpose, when it is averaged over time, as will be discussed later in the section on computer-prediction programs.

Correlating Sunspot Numbers and Solar Flux Values

Based on historical data, an exact mathematical relationship does not exist to correlate sunspot data and solar flux values. Comparing daily values yields almost no correlation. Comparing monthly mean values (often called monthly averages) produces a degree of correlation, but the spread in data is still significant. This is indicated in **Fig 16**, a scatter diagram plot of monthly mean sunspot numbers versus the monthly means of solar flux values adjusted to one astronomical unit. (This adjustment applies a correction for differences in distance between the Sun and the Earth at different times of the year.)

A closer correlation exists when smoothed (12-month running average) sunspot numbers are compared with smoothed (12-month running average) solar flux values adjusted to one astronomical unit. A scatter diagram for smoothed data appears in **Fig 17**. Note how the plot points establish a better defined pattern in Fig 17. The correlation is still no better than a few percent, for records indicate a given smoothed sunspot number does not always correspond with the same smoothed solar flux value, and vice versa.

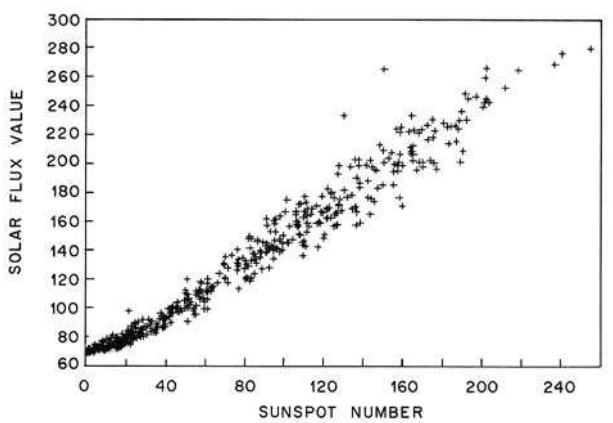

Fig 16—Scatter diagram or X-Y plot of monthly mean sunspot numbers and monthly mean 2800MHz solar flux values. Data values are from February 1947 through February 1987. Each "+" mark represents the intersection of data for a given month. If the correlation between sunspot number and flux values were consistent, all the marks would align to form a smooth curve.

Table 1 illustrates some of the inconsistencies that exist in the historical data. Smoothed or 12-month running average values are shown.

Even though there is no precise mathematical relationship between sunspot numbers and solar flux values, it is helpful to have some way to convert from one to the other. The primary reason is that sunspot numbers are valuable as a long-term link with the past, but the great usefulness of solar flux values are their immediacy, and their direct bearing on our field of interest. (Remember, a smoothed sunspot number will not be calculated until six months after the fact.)

The following mathematical approximation has been derived to convert a smoothed sunspot number to a solar flux value.

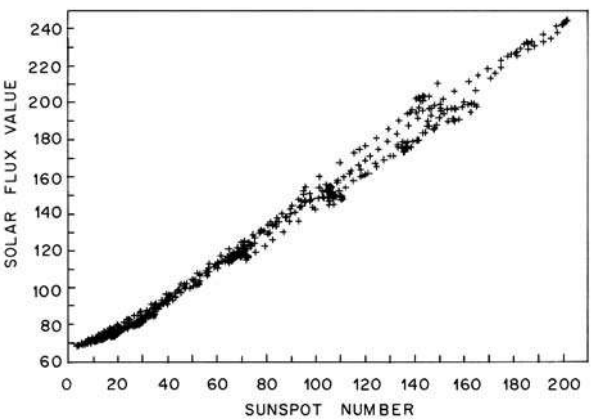

Fig 17—Scatter diagram of smoothed, or 12-month running averages, sunspot numbers versus 2800MHz solar flux values. The correlation of smoothed values is better than for monthly means, shown in Fig 16.

Table 1

Selected Historical Data Showing Inconsistent Correlation Between Sunspot Number and Solar Flux

Month	*Smoothed Sunspot Number*	*Smoothed Solar Flux Value*
May 1953	17.4	75.6
Sept 1965	17.4	78.5
Jul 1985	17.4	74.7
Jun 1969	106.1	151.4
Jul 1969	105.9	151.4
Dec 1982	94.6	151.4
Aug 1948	141.1	180.5
Oct 1959	141.1	192.3
Apr 1979	141.1	180.4
Aug 1981	141.1	203.3

$$F = 63.75 + 0.728S + 0.00089S^2 \quad \text{(Eq 5)}$$

where

F = solar flux number

S = smoothed sunspot number

A graphic representation of this equation is given in **Fig 18**. Use this chart to make conversions graphically, rather than by calculations. With the graph, solar flux and sunspot number conversions can be made either way. The equation has been found to yield errors as great as 10% when historical data was examined. (Look at the August 1981 data in Table 1.) Therefore, conversions should be rounded to the nearest whole number, as additional decimal places are unwarranted. To make conversions from flux to sunspot number, the following approximation may be used.

$$S = 33.52\sqrt{85.12 + F} - 408.99 \quad \text{(Eq 6)}$$

THE IONOSPHERE

There will be inevitable "gray areas" in our discussion of the Earth's atmosphere and the changes wrought in it by the Sun and by associated changes in the Earth's magnetic field. This is not a story that can be told in neat equations, or values carried out to a satisfying number of decimal places. The story must be told, and understood—with its well-known limitations—if we are to put up good antennas and make them serve us well.

Thus far in this chapter we have been concerned with what might be called our "above-ground living space"—that portion of the total atmosphere wherein we can survive without artificial breathing aids, or up to about 6 km (4 miles). The boundary area is a broad one, but life (and radio propagation) undergo basic changes beyond this zone. Somewhat farther out, but still technically within the Earth's atmosphere, the role of the Sun in the wave-propagation picture is a dominant one.

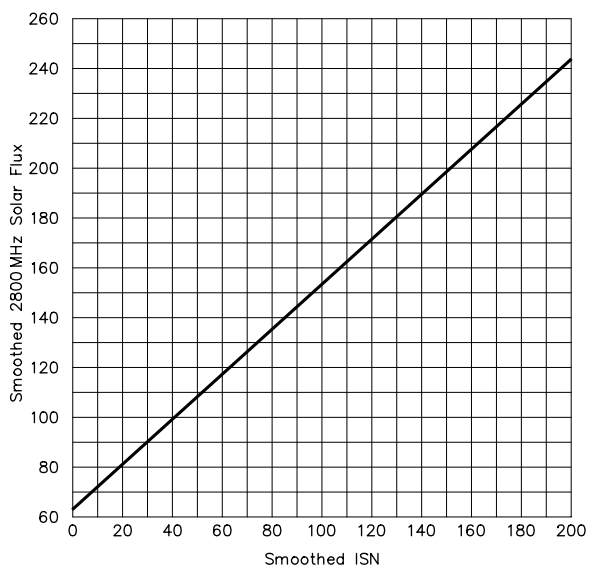

Fig 18—Chart for conversions between smoothed International Sunspot Numbers and smoothed 2800MHz solar flux. This curve is based on the mathematical approximation given in the text.

This is the *ionosphere*—a region where the air pressure is so low that free electrons and ions can move about for some time without getting close enough to recombine into neutral atoms. A radio wave entering this rarefied atmosphere, a region of relatively many free electrons, is affected in the same way as in entering a medium of different dielectric constant—its direction of travel is altered.

Ultraviolet (UV) radiation from the Sun is the primary cause of ionization in the outer regions of the atmosphere, the ones most important for HF propagation. However, there are other forms of solar radiation as well, including both hard and soft x-rays, gamma rays and extreme ultraviolet (EUV). The radiated energy breaks up, or *photoionizes*, atoms and molecules of atmospheric gases into electrons and positively charged ions. The degree of ionization does not increase uniformly with distance from the Earth's surface. Instead there are relatively dense regions (layers) of ionization, each quite thick and more or less parallel to the Earth's surface, at fairly well-defined intervals outward from about 40 to 300 km (25 to 200 miles). These distinct layers are formed due to complex photochemical reactions of the various types of solar radiation with oxygen, ozone, nitrogen and nitrous oxide in the rarefied upper atmosphere.

Ionization is not constant within each layer, but tapers off gradually on either side of the maximum at the center of the layer. The total ionizing energy from the Sun reaching a given point, at a given time, is never constant, so the height and intensity of the ionization in the various regions will also vary. Thus, the practical effect on long-distance communication is an almost continuous variation in signal level, related to the time of day, the season of the year, the distance between the Earth and the Sun, and both short-term and long-term variations in solar activity. It would seem from all this that only the very wise or the very foolish would attempt to predict radio propagation conditions, but it is now possible to do so with a fair chance of success. It is possible to plan antenna designs, particularly the choosing of antenna heights, to exploit known propagation characteristics.

Ionospheric Layer Characteristics

The lowest known ionized region, called the *D layer* (or the *D region*), lies between 60 and 92 km (37 to 57 miles) above the Earth. In this relatively low and dense part of the atmosphere, atoms broken up into ions by sunlight recombine quickly, so the ionization level is directly related to sunlight. It begins at sunrise, peaks at local noon and disappears at sundown. When electrons in this dense medium are set in motion by a passing wave, collisions between particles are so frequent that a major portion of their energy may be used up as heat, as the electrons and disassociated ions recombine.

The probability of collisions depends on the distance an electron travels under the influence of the wave—in other words, on the wavelength. Thus, our 1.8- and 3.5-MHz bands, having the longest wavelengths, suffer the highest daytime absorption loss as they travel through the D layer, particularly for waves that enter the medium at the lowest angles. At times of high solar activity (peak years of the solar cycle) even waves entering the D layer vertically suffer almost total energy absorption around midday, making these bands almost useless for communication over appreciable distances during the hours of high sun. They "go dead" quickly in the morning, but come alive again the same way in late afternoon. The diurnal (daytime) D-layer effect is less at 7 MHz (though still marked), slight at 14 MHz and inconsequential on higher amateur frequencies.

The D region is ineffective in bending HF waves back to Earth, so its role in long-distance communication by amateurs is largely a negative one. It is the principal reason why our frequencies up through the 7-MHz band are useful mainly for short-distance communication during the high-sun hours.

The lowest portion of the ionosphere useful for long-distance communication by amateurs is the *E layer* (also known as the *E region*) about 100 to 115 km (62 to 71 miles) above the Earth. In the E layer, at intermediate atmospheric density, ionization varies with the Sun angle above the horizon, but solar ultraviolet radiation is not the sole ionizing agent. Solar X-rays and meteors entering this portion of the Earth's atmosphere also play a part. Ionization increases rapidly after sunrise, reaches maximum around noon local time, and drops off quickly after sundown. The minimum is after midnight, local time. As with the D layer, the E layer absorbs wave energy in the lower-frequency amateur bands when the Sun angle is high, around mid-day. The other varied effects of E-region ionization will be discussed later.

Most of our long-distance communication capability stems from the tenuous outer reaches of the Earth's atmosphere known as the *F layer*. At heights above 100 miles, ions and electrons recombine more slowly, so the observable effects of the Sun develop more slowly. Also, the region holds its ability to reflect wave energy back to Earth well into the night. The *maximum usable frequency* (MUF) for F-layer propagation on east-west paths thus peaks just after noon at the midpoint, and the minimum occurs after midnight. We'll examine the subject of MUF in more detail later.

Judging what the F layer is doing is by no means that simple, however. The layer height may be from 160 to more than 500 km (100 to over 310 miles), depending on the season of the year, the latitudes, the time of day and, most capricious of all, what the Sun has been doing in the last few minutes and in perhaps the last three days before the attempt is made. The MUF between Eastern US and Europe, for example, has been anything from 7 to 70 MHz, depending on the conditions mentioned above, plus the point in the long-term solar-activity cycle at which the check is made.

During a summer day the F layer may split into two layers. The lower and weaker *F_1 layer*, about 160 km (100 miles) up, has only a minor role, acting more like the E than the *F_2 layer*. At night the F_1 region disappears and the F_2 region height drops somewhat.

Propagation information tailored to amateur needs is transmitted in all information bulletin periods by the ARRL Headquarters station, W1AW. Finally, solar and geomagnetic field data, transmitted hourly and updated eight times daily, are given in brief bulletins carried by the US Time Standard stations, WWV and WWVH, and also on Internet Web sites. But more on these services later.

Bending in the Ionosphere

The degree of bending of a wave path in an ionized layer depends on the density of the ionization and the length of the wave (inversely related to its frequency). The bending at any given frequency or wavelength will increase with increased ionization density and will bend away from the region of most-intense ionization. For a given ionization density, bending increases with wavelength (that is, it decreases with frequency).

Two extremes are thus possible. If the intensity of the ionization is sufficient and the frequency is low enough, even a wave entering the layer perpendicularly will be reflected back to Earth. Conversely, if the frequency is high enough or the ionization decreases to a low-enough density, a condition is reached where the wave angle is not affected enough by the ionosphere to cause a useful portion of the wave energy to return to the Earth. The frequency at which this occurs is called the vertical-incidence *critical frequency.* Each region in the ionosphere has a critical frequency associated with it, and this critical frequency will change depending on the date, time and state of the 11-year solar cycle.

Fig 19 shows a simplified graph of the electron density (in electrons per cubic meter) versus height in the ionosphere (in km) for a particular set of daytime and nighttime conditions. Free electrons are what return the signals you launch into the ionosphere back down to the Earth at some distance from your transmitter—The more free electrons in the ionosphere, the better propagation will be, particularly at higher frequencies.

Electron-density profiles are extremely complicated and vary greatly from one location to the next, depending on a bewildering variety of factors. Of course, this sheer variability makes it all the more interesting and challenging for hams to work each other on ionospheric HF paths!

The following discussion about sounding the ionosphere provides some background information about the scientific instruments used to decipher the highly intricate mechanisms behind ionospheric HF propagation.

SOUNDING THE IONOSPHERE

For many years scientists have *sounded* the ionosphere to determine its communication potential at various elevation angles and frequencies. The word "sound" stems from

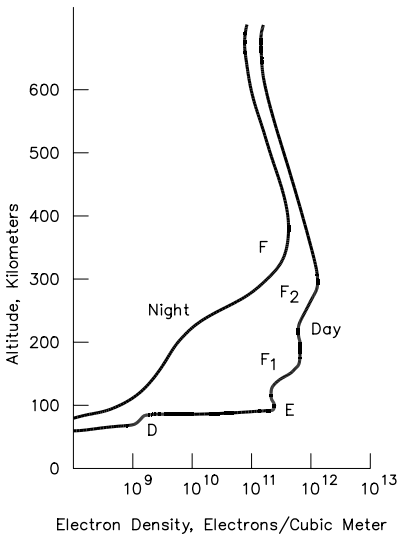

Fig 19—Typical electron densities for nighttime and daytime conditions in the various ionospheric regions.

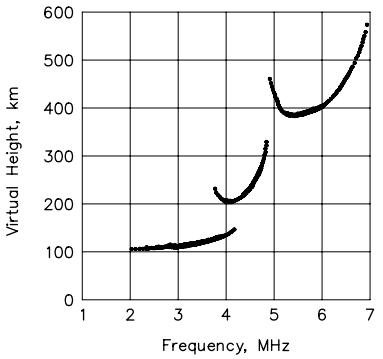

Fig 20—Very simplified ionogram from a vertical-incidence sounder. The lowest trace is for the E region; the middle for the F_1 and the upper trace for the F_2 region.

an old idea—one that has nothing to do with the audio waves that we can hear as "sounds." Long ago, sailors sounded the depths beneath their boats by dropping weighted ropes, calibrated in fathoms, into the water. In a similar fashion, the instrument used to probe the height of the ionosphere is called an *ionosonde*, or ionospheric sounder. It measures distances to various layers by launching a calibrated electronic signal directly up into the ionosphere.

Radar uses the same techniques as ionospheric sounding to detect targets such as airplanes. An ionosonde sends precisely timed pulses into the ionosphere over a range of MF and HF frequencies. The time of reception of an echo reflected from a region in the ionosphere is compared to the time of transmission. The time difference is multiplied by the speed of light to give the apparent distance that the wave has traveled from the transmitter to the ionosphere and back to the receiver. (It is an *apparent* or *virtual distance* because the speed of a wave slows very slightly in the ionosphere, just as the speed of propagation through any medium other than a vacuum slows down because of that medium.)

Another type of ionosonde sweeps the frequency of transmission, from low to high. This is called an "FM-CW," or more colorfully, a "chirp" sounder. Since a received echo takes time to travel from the transmitter up to the reflection point and then back again to the receiver, the echo will be at a lower frequency than the still-moving frequency of the transmitter. The frequency difference is an indication of the height of the echo's reflection off the various ionospheric layers.

Vertical-Incidence Sounders

Most ionosondes are *vertical-incidence sounders*, bouncing their signals perpendicularly off the various ionized regions above it by launching signals straight up into the ionosphere. The ionosonde frequency is swept upwards until echos from the various ionospheric layers disappear, meaning that the critical frequencies for those layers have been exceeded, causing the waves to disappear into space.

Fig 20 shows a highly simplified ionogram for a typical vertical-incidence sounder. The echos at the lowest height at the left-hand side of the plot show that the E region is about 100 km high. The F_1 region shown in the middle of the plot varies from about 200 to 330 km in this example, and the F_2 region ranges from just under 400 km to almost 600 km in height. You can see that the F_1 and F_2 ionospheric regions take a "U" shape, indicating that the electron density varies throughout the layer. In this example, the peak in electron density is at a virtual height of the F_2 region of about 390 km, the lowest point in the F_2 curve.

Scientists can derive a lot of information from a vertical-incidence ionogram, including the critical frequencies for each region, where raising the frequency any higher causes the signals to disappear into space. In Fig 20, the E-region critical frequency (abbreviated f_oE) is about 4.1 MHz. The F_1-region critical frequency (abbreviated f_oF_1) is 4.8 MHz. The F2-region critical frequency (abbreviated f_oF_2) is this simplified diagram is 6.8 MHz.

The observant reader may well be wondering what the subscripted "o" in the abbreviations f_oE, f_oF_1 and f_oF_2 mean. The abbreviation "o" means "ordinary." When an electromagnetic wave is launched into the ionosphere, the Earth's magnetic field splits the wave into two independent waves—the "ordinary" (o) and the "extraordinary" (x) components. The ordinary wave reaches the same height in the ionosphere whether the Earth's magnetic field is present or not, and hence is called "ordinary." The extraordinary wave, however, is greatly affected by the presence of the Earth's magnetic field, in a very complex fashion.

Fig 21 shows an example of an actual ionogram from the vertical Lowell Digisonde at Millstone Hill in Massa-

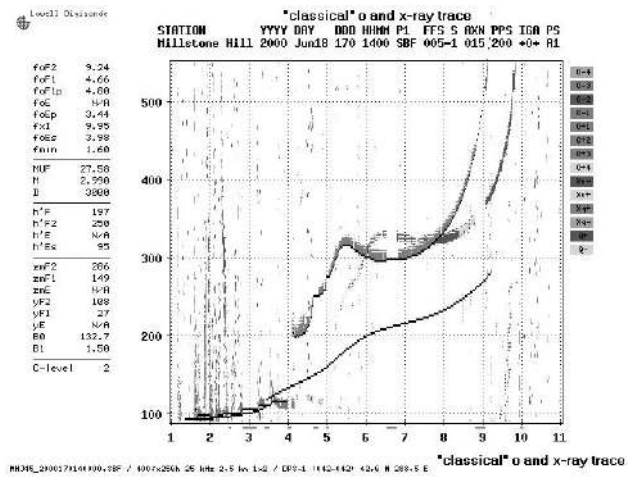

Fig 21—Actual vertical-incidence ionogram from the Lowell Digisonde, owned and operated at Millstone Hill in Massachusetts by MIT. The ordinary (o) and extraordinary (x) traces are shown for heights greater than about 300 km. At the upper left are listed the computer-determined ionospheric parameters, such as f_oF_2 of 9.24 MHz and f_oF_1 at 4.66 MHz.

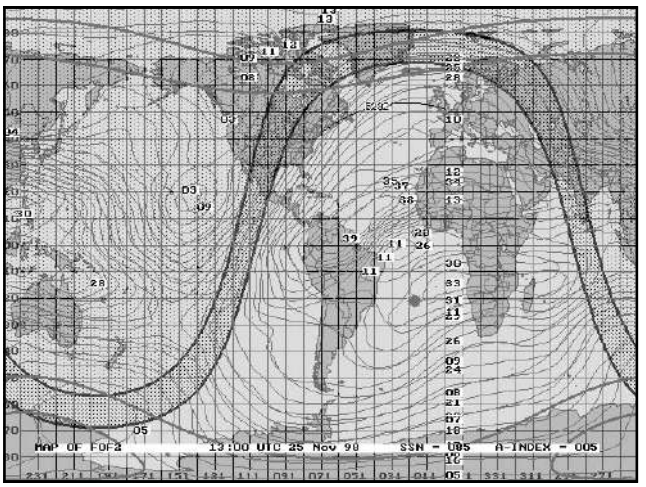

Fig 22—Computer simulation of the f_oF_2 contours for 25 November 1998, for an SSN of 85 and a quiet planetary A_p index of 5. Note the two regions of high f_oF_2 values off the upper and lower west coast of Africa. These are the "equatorial anomalies," regions of high electronic density in the F_2 region that often allow chordal-hop north-south propagation. See also Fig 8. (*PropLab Pro simulation, courtesy of Solar Terrestrial Dispatch.*)

chusetts, owned and operated by the Massachusetts Institute of Technology. This ionogram was made on June 18, 2000, and shows the conditions during a period of very high solar activity. The black-and-white rendition in Fig 21 of the actual color ionogram unfortunately loses some information. However, you can still see that a real ionogram is a lot more complicated looking than the simple simulated one in Fig 20.

The effects of noise and interference from other stations are shown by the many speckled dots appearing in the ionogram. The critical frequencies for various ionospheric layers are listed numerically at the left-hand side of the plot and the signal amplitudes are color-coded by the color bars at the right-hand side of the plot. The x-axis is the frequency, ranging from 1 to 11 MHz.

Compared to the simplified ionogram in Fig 20, Fig 21 shows another trace that appears on the plot from about 5.3 to 9.8 MHz, a trace shifted to the right of the darker ordinary trace. This second trace is the extraordinary (x) wave mentioned above. Since the x and o waves are created by the Earth's magnetic field, the difference in the ordinary and extraordinary traces is about $^1/_2$ the *gyro frequency*, the frequency at which an electron will spiral down a particular magnetic field line. The electron gyro frequency is different at various places around the Earth, being related to the Earth's complicated and changing magnetic field. The extraordinary trace always has a higher critical frequency than the ordinary trace on a vertical-incidence ionogram, and it is considerably weaker than the ordinary trace, especially at frequencies below about 4 MHz because of heavy absorption.

The Big Picture Overhead

There are about 150 vertical-incidence ionosondes around the world. Ionosondes are located on land, even on a number of islands. There are gaps in sounder coverage, however, mainly over large expanses of open ocean. The compilation of all available vertical-incidence data from the worldwide network of ionospheric sounders results in global f_oF_2 maps, such as the map shown in **Fig 22**, a simulation from the highly sophisticated *PropLab Pro* computer program.

This simulation is for 1300 UTC, several hours after East Coast sunrise on Nov 25, 1998, with a high level of solar activity of 85 and a planetary A_p index of 5, indicating calm geomagnetic conditions. The contours of f_oF_2 peak over the ocean off the west coast of Africa at 38 MHz. Over the southern part of Africa, f_oF_2 peaks at 33 MHz.

These two "humps" in f_oF_2 form what is known as the "equatorial anomaly" and are caused by upwelling "fountains" of high electron concentration located in daylight areas about ±20° from the Earth's magnetic dip equator. The equatorial anomaly is important in transequatorial propagation. Those LU stations in Argentina that you can hear on 28 MHz from the US in the late afternoon, even during low portions of the solar cycle when other stations to the south are not coming through, are benefiting from transequatorial propagation, sometimes called "chordal hop" propagation, because signals going through this area remain in the ionosphere without lossy intermediate hops to the ground.

From records of f_oF_2 profiles, the underlying electron densities along a path can be computed. And from the electron density profiles computerized "ray tracing" may be done

throughout the ionosphere to determine how a wave propagates from a transmitter to a particular receiver location. *PropLab Pro* can do complex ray tracings that explicitly include the effect of the Earth's magnetic field, even taking into effect ionospheric stormy conditions.

Oblique-Angle Ionospheric Sounding

A more elaborate form of ionospheric sounder is the *oblique ionosonde*. Unlike a vertical-incidence ionospheric sounder, which sends its signals directly overhead, an oblique sounder transmits its pulses obliquely through the ionosphere, recording echos at a receiver located some distance from the transmitter. The transmitter and distant receiver are precisely coordinated in GPS-derived time in modern oblique sounders.

Interpretation of ionograms produced by oblique sounders is considerably more difficult than for vertically incident ones. An oblique ionosonde purposely transmits over a continuous range of elevation angles simultaneously and hence cannot give explicit information about each elevation angle it launches. **Fig 23** shows a typical HF oblique-sounder ionogram for the path from Hawaii to California in March of 1973, during a period of medium-level sunspot activity. The y-axis is calibrated in time delay, in milliseconds. Longer distances involve longer time delays between the start of a transmitted pulse and the reception of the echo. The x-axis in this ionogram is the frequency, just like a vertical-incidence ionogram. Note that the frequency range for this plot extends to 32 MHz, while vertical-incidence ionograms usually don't sweep higher than about 12 MHz.

Six possible modes are shown in this ionogram: $1F_2$, $2F_2$, $3F_2$, $4F_2$ and $5F_2$. These involve multiple modes of propagation (commonly called *hops*) between the ionosphere and reflections from the Earth. For example, at an operating frequency of 14 MHz, there are three modes open during the mid-morning: $2F_2$, $3F_2$ and $4F_2$. We'll discuss multiple hops later in more detail.

The lowest mode, $1F_2$ in Fig 23, employs a single F_2 hop to cover the 3900-km long path from Hawaii to California, but it is only open on 28-MHz. (Note that 3900 km is close to the maximum possible single-hop length for the F_2 region. We'll look at this in more detail later too.) In general, each mode that involves more than a single hop is weaker than a single hop. For example, you can see that the received $5F_2$ echo is weak and broken up because of the accumulation of losses at each ground-level reflection in its five hops, with absorption in the ionosphere all along its complicated path to the receiver.

The trace labeled "FOT" is the *frequency of optimum traffic*, considered the most reliable frequency for communications on this particular circuit and date/time. In this example, the FOT would be near the 21-MHz amateur band.

Another interesting point in Fig 23 is labeled "High Angle Ray." This refers to the Pedersen ray. Before we go into more details about the Pedersen high-angle wave, we need to examine how launch angles affect the way waves are propagated through the ionosphere.

Fig 24 shows a highly simplified situation, with a single ionospheric layer and a smooth Earth. This illustrates several important facts about antenna design for long-distance communication. In Fig 24, Wave #1 is launched at the lowest elevation angle (that is, most nearly horizontal to the horizon). Wave #1 manages to travel from the transmitter to the receiving location at point C in a single hop.

Wave #2 is launched at a higher elevation angle than Wave #1, and penetrates further into the ionospheric layer before it is refracted enough to return to Earth. The ground distance covered from the transmitter to point B is less for

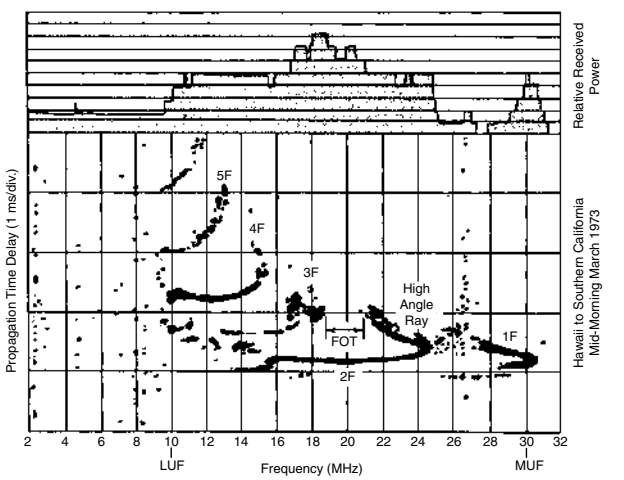

Fig 23—HF oblique-sounder ionogram. This is a typical chirpsounder measurement on a 2500-mile path from Hawaii to southern California during midmorning in March at a medium level of solar activity. Six possible modes (hops) are shown. The "FOT" is the frequency of optimum traffic, considered most reliable for this path/time.

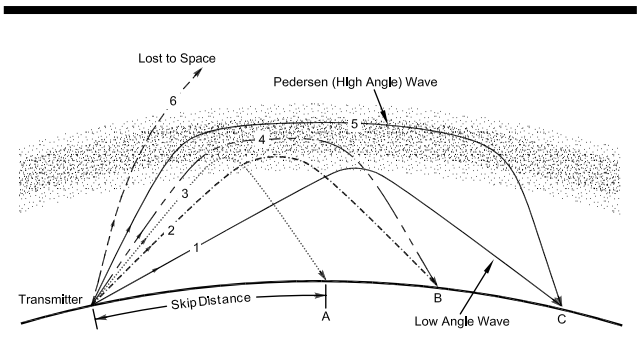

Fig 24—Very simplified smooth-Earth/ionosphere diagram showing how the ground range from transmitter to receiver can vary as the elevation angle is gradually raised. The Pedersen wave, launched at a relatively high angle, has the same ground range as the low-angle wave #1, but is weaker because it travels for a long distance in the ionosphere.

Wave #2 than for lower-angle Wave #1. Wave #3 is launched at a still-higher elevation angle. Like Wave #2 before it, Wave #3 penetrates further into the ionosphere and covers less ground downrange than #2.

Now, we see something very interesting happening for Wave #4, whose launch elevation angle is still higher than #3. Wave #4 penetrates even higher into the ionosphere than #3, reaching the highest level of ionization in our theoretical ionospheric layer, where it is finally refracted sufficiently to bend down to Earth. Wave #4 manages to arrive at the same point B as Wave #2, which was launched at a much lower elevation angle.

In other words, in the sequence from #1 to #3 we have been continually *increasing* the elevation launch angle and the ground range covered from the transmitter to the return of the signal back to Earth has been continually *decreasing*. However, starting with Wave #4, the ground range starts to *increase* with increased elevation angle. A further increase in the elevation angle causes Wave #5 to travel for an even longer distance through the ionosphere, exiting finally at point C, the same ground distance as lowest-angle Wave #1.

Finally, increasing the elevation angle even further results in Wave #6 being lost to outer space because the ionization in the layer is insufficient to bend the wave back to Earth. In other words, Wave #6 has exceeded the *critical angle* for this hypothetical ionospheric layer and this frequency of operation.

Both Waves #4 and #5 in Fig 24 are called "high-angle" or Pedersen waves. Because Wave #5 has traveled a greater distance through the ionosphere, it is always weaker than Wave #1, the one launched at the lowest elevation angle. Pedersen waves are usually not very stable, since small changes in elevation angle can result in large changes in the ground range that these high-angle waves cover.

SKIP DISTANCE

Fig 24 shows that we can communicate with the point on the Earth labeled "A" (where Wave #3 arrives), but not any closer to our transmitter site. When the critical angle is less than 90° (that is, directly overhead) there will always be a region around the transmitting site where an ionospherically propagated signal cannot be heard, or is heard weakly. This area lies between the outer limit of the ground-wave range and the inner edge of energy return from the ionosphere. It is called the *skip zone*, and the distance between the originating site and the beginning of the ionospheric return is called the skip distance. This terminology should not to be confused with ham jargon such as "the skip is in," referring to the fact that a band is open for sky-wave propagation.

The signal may often be heard to some extent within the skip zone, through various forms of scattering (discussed in detail later), but it will ordinarily be marginal in strength. When the skip distance is short, both ground-wave and sky-wave signals may be received near the transmitter. In such instances the sky wave frequently is stronger than the ground wave, even as close as a few miles from the transmitter. The ionosphere is an efficient communication medium under favorable conditions. Comparatively, the ground wave is not.

If the radio wave leaves the Earth at a radiation angle of zero degrees, just at the horizon, the maximum distance that may be reached under usual ionospheric conditions in the F_2 region is about 4000 km (2500 miles).

MULTI-HOP PROPAGATION

As mentioned previously in the discussion about Fig 24, the Earth itself can act as a reflector for radio waves, resulting a multiple hops. Thus, a radio signal can be reflected from the reception point on the Earth back into the ionosphere, reaching the Earth a second time at a still more-distant point. This effect is illustrated in **Fig 25**, where a single ionospheric layer is depicted, although this time we show both the layer and the Earth beneath it as curved rather than flat. The wave identified as "Critical Angle" travels from the transmitter via the ionosphere to point A, in the center of the drawing, where it is reflected upwards and travels through the ionosphere to point B, at the right. This shows a two-hop signal.

As in the simplified case in Fig 24, the distance at which a ray eventually reaches the Earth depends on the launch elevation angle at which it left the transmitting antenna. You have some control of the launch angle by adjusting the height of the antennas you use, as described in Chapter 3, The Effects of Ground.

The information in Fig 25 is greatly simplified. On actual communication paths the picture is complicated by many factors. One is that the transmitted energy spreads over a considerable area after it leaves the antenna. Even with an antenna array having the sharpest practical beam pattern, there is what might be described as a *cone of radiation* centered on the wave lines (rays) shown in the drawing. The reflection/refraction in the ionosphere is also highly variable, and is the cause of considerable spreading and scattering.

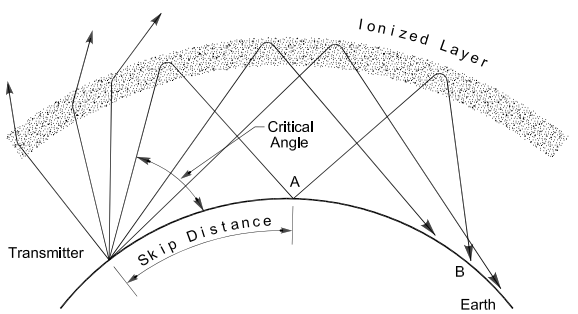

Fig 25—Behavior of waves encountering a simple curved ionospheric layer over a curved Earth. Rays entering the ionized region at angles above the critical angle are not bent enough to be returned to Earth, and are lost to space. Waves entering at angles below the critical angle reach the Earth at increasingly greater distances as the launch angle approaches the horizontal. The maximum distance that may normally be covered in a single hop is 4000 km. Greater distances are covered with multiple hops.

Under some conditions it is possible for as many as four or five signal hops to occur over a radio path, as illustrated by the oblique ionogram in Fig 23. But no more than two or three hops is the norm. In this way, HF communication can be conducted over thousands of miles.

An important point should be recognized with regard to signal hopping. A significant loss of signal occurs with each hop. The D and E layers of the ionosphere absorb energy from signals as they pass through, and the ionosphere tends to scatter the radio energy in various directions, rather than confining it in a tight bundle. The roughness of the Earth's surface also scatters the energy at a reflection point.

Assuming that both waves do reach point B in Fig 25, the low-angle wave will contain more energy at point B. This wave passes through the lower layers just twice, compared to the higher-angle route, which must pass through these layers four times, plus encountering an Earth reflection. Measurements indicate that although there can be great variation in the relative strengths of the two signals—the one-hop signal will generally be from 7 to 10 dB stronger. The nature of the terrain at the mid-path reflection point for the two-hop wave, the angle at which the wave is reflected from the Earth, and the condition of the ionosphere in the vicinity of all the refraction points are the primary factors in determining the signal-strength ratio.

The loss per hop becomes significant at greater distances. It is because of these losses that no more than four or five propagation hops are useful; the received signal becomes too weak to be usable over more hops. Although modes other than signal hopping also account for the propagation of radio waves over thousands of miles, backscatter studies of actual radio propagation have displayed signals with as many as five hops. So the hopping mode is arguably the most prevalent method for long-distance communication.

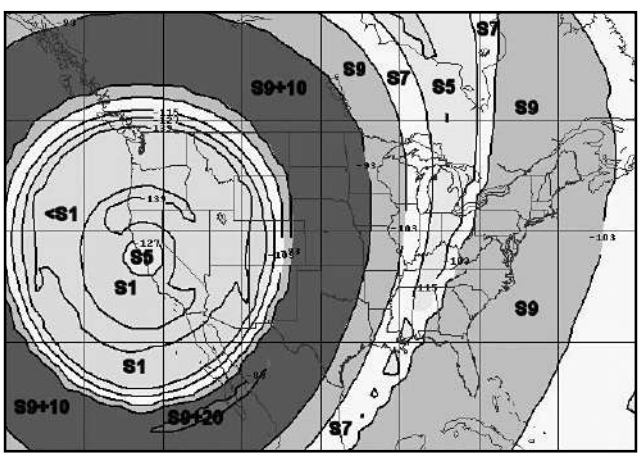

Fig 26—Modified *VOAAREA* plot for 21.2 MHz from San Francisco to the rest of the US, annotated with signal levels in S units, as well as signal contours in dBW (dB below a watt). Antennas are assumed to be 3-element Yagis at 55 feet above flat ground; the transmitter power is 1500 W; the month is November with SSN = 50, a moderate level of solar activity, at 22 UTC. The most obvious feature is the large "skip zone" centered on the transmitter in San Francisco, extending almost a 1/3 of the distance across the US.

Fig 26 shows another way of looking at propagation—a *geographic area* look. Fig 26 shows 15-meter signal levels across the US as they propagate from a transmitting station in San Francisco. This simulation of propagation conditions is for the month of November, with a medium level of solar activity (SSN = 50) at 22 UTC. Fig 26 was created using the *VOAAREA* software program, part of the *VOACAP* software suite. Transmitter power is assumed to be 1500 W, with 3-element Yagis, 55 feet high, at the transmitter and at each receiving location.

From the transmitter out to about 50 miles, signals are moderate, at about S5 on an S meter. Beyond that coverage area to almost 1/3 of the way across the country (to Colorado), there is a large and distinctive skip zone, where only very weak signals return to Earth (S1 or less). Beyond Colorado, signals rapidly build up to S9+10 dB across the middle of the US, falling to S9 and then to S7 in the vicinity of Chicago, Illinois. Beyond Chicago, the signals drop to S5 in a swath from Michigan and part of Ohio down to Alabama. All along the US East Coast, signals come back strong at S9.

The reason why the signals in Fig 26 drop down to S5 in the Midwest is that the necessary elevation angles to cover this region in a single F2 hop are extremely low even at a moderate level of solar activity. To achieve launch angles as low as 1° requires either very high antenna heights or a high mountaintop location. Beyond the Midwest, out to the US East Coast, two F2 hops are required, with higher elevation angles and hence greater antenna gain for moderate antenna heights.

Non-Hopping Propagation Modes

Present propagation theory holds that for communication distances of many thousands of kilometers, signals do not always hop in relatively short increments from ionosphere-to-Earth-to-ionosphere and so forth along the entire path. Instead, the wave is thought to propagate *inside* the ionosphere throughout some portion of the path length, tending to be *ducted* in the ionized layer.

As was shown in Fig 24, the high-angle Pedersen ray can also penetrate an ionospheric layer farther than lower-angle rays. In the less-densely ionized upper edge of the layer, the amount of refraction is less, nearly equaling the curvature of the layer itself as it encircles the Earth.

Non-hopping theory of long-distance propagation is further supported by studies of travel times for signals that go completely around the world. The time required is significantly less than would be necessary to hop between the Earth and the ionosphere 10 or more times while circling the Earth.

Propagation between two points thousands of kilometers apart may in fact consist of a combination of ducting and hopping. It may involve combinations of refractions from the E layer and the F layer. Despite all the complex factors involved, most long-distance propagation can be seen to follow certain general rules. Thus, much commercial and military point-to-point communication over long distances

employs antennas designed to make maximum use of known radiation angles and layer heights, even on paths where multihop propagation is assumed.

In amateur work, however, we usually try for the lowest practical radiation angle, hoping to keep reflection losses to a minimum. Years of amateur experience have shown this to be a decided advantage under all usual conditions.

The geometry of propagation by means of the F_2 layer limits our maximum distance along the Earth's surface to about 4000 km (2500 miles) for a single hop. For higher radiation angles, this same distance may require two or more hops (with higher reflection loss). And fewer hops are better, in most cases. If you have a nearby neighbor who consistently outperforms you on the longer paths, a radiation angle difference in his favor is probably the reason.

MAXIMUM USABLE FREQUENCY

The vertical-incidence critical frequency is the *maximum usable frequency* for local sky-wave high-angle communication. It is also useful in the selection of optimum working frequencies and the determination of the maximum usable frequency for distant points at a given time. The abbreviation "MUF" for maximum usable frequency will be used hereafter.

In geographic middle latitudes, the vertical-incident critical frequency ranges between about 1 and 4 MHz for the E layer, and between 2 and 13 MHz for the F_2 layer. The lowest figures are for nighttime conditions in the lowest years of the solar cycle. The highest are for the daytime hours in the years of high solar activity. These are average figures. Critical frequencies have reached as high as 20 MHz briefly during exceptionally high solar activity in the middle latitudes. As was pointed out earlier in Fig 22, $f_o F_2$ levels approaching 40 MHz are possible at low latitudes.

While vertical-incidence critical frequencies are interesting from a scientific point of view, hams are far more concerned about how we can exploit propagation conditions to communicate, preferably at long distances. The MUF for a 4000-km (2500 miles) distance is about 3.5 times the vertical-incidence critical $f_o F_2$ frequency existing at the path midpoint. For one-hop signals, if a uniform ionosphere is assumed, the MUF decreases with shorter distances along the path. This is true because the higher-frequency waves must be launched at higher elevation angles for shorter ranges, and at these launch angles they are not bent sufficiently to reach the Earth. Thus, a lower frequency (where more bending occurs) must be used.

Precisely speaking, a maximum usable frequency or MUF is defined for communication between two specific points on the Earth's surface, for the conditions existing at the time, including the minimum elevation angle that the station can launch at the frequency in use. (This practical form of MUF is sometimes called the *operational MUF*). At the same time and for the same conditions, the MUF from either of these two points to a third point may be different.

Table 2
Time and Frequency Stations Useful for Propagation Monitoring

Call	*Frequency (MHz)*	*Location*
WWV	2.5, 5, 10, 15, 20	Ft Collins, Colorado
WWVH	Same as WWV but no 20	Kekaha, Kauai, Hawaii
CHU	3.330, 7.335, 14.670	Ottawa, Ontario, Canada
RID	5.004, 10.004, 15.004	Irkutsk, USSR*
RWM	4.996, 9.996, 14.996	Novosibirsk, USSR
VNG	2.5, 5, 8.634, 12.984, 16	Lyndhurst, Australia
BPM	5, 5.43, 9.351, 10, 15	Xiang, China
BSF	15	Taoyuan, Taiwan
JJY	2.5, 5, 8, 10, 15	Tokyo, Japan
LOL	5, 10, 15	Buenos Aires, Argentina

*The call, taken from an international table, may not be the one used during actual transmission. Locations and frequencies appear to be accurate as provided.

Therefore, the MUF cannot be expressed broadly as a single frequency, even for any given location at a particular time. The ionosphere is never uniform, and in fact at a given time and for a fixed distance, the MUF changes significantly with changes in compass direction for almost any point on the Earth. Under usual conditions, the MUF will always be highest in the direction toward the Sun—to the east in the morning, to the south at noon (from northern latitudes), and to the west in the afternoon and evening.

For the strongest signals at the greatest distance, especially where the limited power levels of the Amateur Radio Service are concerned, it is important to work fairly near the MUF. It is at these frequencies where signals suffer the least loss. The MUFs can be estimated with sufficient accuracy by using the prediction charts that appear on the ARRL Web site (**www.arrl.org/qst/propcharts/**) or by using a computer prediction program. The CD-ROM bundled in the back of this book contains detailed and summary tables for more than 175 transmitting locations around the world. (See section on "What HF Bands Are Open—Where and When?" later in this chapter.)

MUFs can also be observed, with the use of a continuous coverage communications receiver. Frequencies up to the MUFs are in round-the-clock use today. When you "run out of signals" while tuning upward in frequency from your favorite ham band, you have a pretty good clue as to which band is going to work well, right then. Of course, it helps to know the direction to the transmitters whose signals you are hearing. Shortwave broadcasters know what frequencies to use, and you can hear them anywhere, if conditions are good. Time-and-frequency stations are also excellent indicators, since they operate around the clock. See **Table 2**. WWV is also a reliable source of propagation data, hourly, as discussed in more detail later in this chapter.

The value of working near the MUF is two-fold. Under undisturbed conditions, the absorption loss decreases proportional to the square of a change in frequency. For example, the absorption loss is four times higher at 14 MHz than it is at 28 MHz. Perhaps more important, the hop distance is considerably greater as the MUF is approached. A transcontinental contact is thus much more likely to be made on a single hop on 28 MHz than on 14 MHz, so the higher frequency will give the stronger signal most of the time. The strong-signal reputation of the 28-MHz band is founded on this fact.

LOWEST USABLE FREQUENCY

There is also a lower limit to the range of frequencies that provide useful communication between two given points by way of the ionosphere. *Lowest usable frequency* is abbreviated LUF. If it were possible to start near the MUF and work gradually lower in frequency, the signal would decrease in strength and eventually would disappear into the ever-present "background noise." This happens because signal absorption increases proportional to the square of the lowering of the frequency. The frequency nearest the point where reception became unusable would be the LUF. It is not likely that you would want to work at the LUF, although reception could be improved if the station could increase power by a considerable amount, or if larger antennas could be used at both ends of the path.

For example, when solar activity is very high at the peak of a solar cycle, the LUF often rises higher than 14 MHz on the morning Eastern US-to-Europe path on 20 meters. Just before sunrise in the US, the 20-meter band will be first to open to Europe, followed shortly by 15 meters, and then 10 meters as the Sun rises further. By mid-morning, however, when 10 and 15 meters are both wide open, 20 meters will become very marginal to Europe, even when both sides are running maximum legal power levels. By contrast, stations on 10 meters can be worked readily with a transmitter power of only 1 or 2 watts, indicating the wide range between the LUF and the MUF.

Frequently, the *window* between the LUF and the MUF for two fixed points is very narrow, and there may be no amateur frequencies available inside the window. On occasion the LUF may be higher than the MUF between two points. This means that, for the highest possible frequency that will propagate through the ionosphere for that path, the absorption is so great as to make even that frequency unusable. Under these conditions it is impossible to establish amateur sky-wave communication between those two points, no matter what frequency is used. (It would normally be possible, however, to communicate between either point and other points on some frequency under the existing conditions.) Conditions when amateur sky-wave communication is impossible between two fixed points occur commonly for long distances where the total path is in darkness, and for very great distances in the daytime during periods of low solar activity.

Fig 27 shows a typical propagation prediction from the ARRLWeb members-only site (**www.arrl.org/qst/propcharts/**, previously from the "How's DX" column in *QST*). In this instance, the MUF and the LUF lines are blurred together at about 10 UTC, meaning that the statistical likelihood of any amateur frequency being open for that particular path at that particular time was not very good. Later on, after about 11 UTC, the gap between the MUF and LUF increased, indicating that the higher bands would be open on that path.

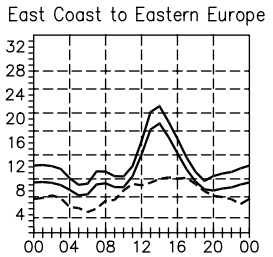

Fig 27—Propagation prediction chart for East Coast of US to Europe. This appeared in December 1994 *QST*, where an average 2800-MHz (10.7-cm) solar flux of 83 was assumed for the mid-December to mid-January period. On 10% of these days, the highest frequency propagated was predicted at least as high as the uppermost curve (the Highest Possible Frequency, or HPF, approximately 21 MHz), and for 50% of the days as high as the middle curve, the MUF. The broken lines show the Lowest Usable Frequency (LUF) for a 1500-W CW transmitter.

DISTURBED IONOSPHERIC CONDITIONS

So far, we have discussed the Earth's ionosphere when conditions at the Sun are undisturbed. There are three general types of major disturbances on the Sun that can affect radio propagation here on the Earth. On the air, you may hear people grousing about *Solar Flares*, *Coronal Holes* or *Sudden Disappearing Filaments*, especially when propagation conditions are not good. Each of these disturbances causes both electromagnetic radiation and ejection of material from the Sun.

Solar Flares

Solar flares are cataclysmic eruptions that suddenly release huge amounts of energy, including sustained, high-energy bursts of radiation from VLF to X-ray frequencies and vast amounts of solar material. Most solar flares occur around the peak of the 11-year solar cycle.

The first Earthly indication of a huge flare is often a visible brightness near a sunspot group, along with increases in UV, X-ray radiation and VHF radio noise. If the geometry between the Sun and Earth is right, intense X-ray radiation takes eight minutes, traveling the 93 million miles to Earth at the speed of light. The sudden increase in X-ray

energy can immediately increase RF absorption in the Earth's lowest ionospheric layers, causing a phenomenon known as a *Sudden Ionospheric Disturbance* (SID).

An SID affects all HF communications on the sunlit side of the Earth. Signals in the 2 to 30-MHz range may disappear entirely, and even most background noise may cease in extreme cases. When you experience a big SID, your first inclination may be to look outside to see if your antenna fell down! SIDs may last up to an hour before ionospheric conditions temporarily return to normal.

Between 45 minutes and 2 hours after an SID begins, particles from the mass eruption on the Sun may begin to arrive. These high-energy particles are mainly protons and they can penetrate the ionosphere at the Earth's magnetic poles, where intense ionization can occur, with attendant absorption of HF signals propagating through the polar regions. This is called a *Polar Cap Absorption* (PCA) event and it may last for several days. A PCA results in spectacular auroral displays at high latitudes.

Coronal Holes

As described earlier in the section dealing with auroral propagation at VHF, a second major solar disturbance is a so-called "coronal hole" in the Sun's outer layer (the *corona*). Temperatures in the corona can be more than four million °C over an active sunspot region but more typically are about two million °C. A coronal hole is an area of somewhat lower temperature. Solar-terrestrial scientists have a number of competing theories about how coronal holes are formed.

Matter ejected through this "hole" takes the form of a *plasma*, a highly ionized gas made up of electrons, protons and neutral particles, traveling at speeds up to 1,000 km per second (2 million miles per hour). The plasma becomes part of the solar wind and can affect the Earth's magnetic field, but only if the Sun-Earth geometry is right. A plasma has a very interesting and somewhat bizarre ability. It can lock-in the orientation of the magnetic field where it originates and carry it outwards into space. However, unless the locked-in magnetic field orientation is aligned properly with the Earth's magnetic field, even a large plasma mass may not severely disrupt our magnetosphere, and thence our ionosphere.

Presently, we don't have the ability to predict very long in advance when the Sun might erupt in a disturbance that results in Earthly propagation problems. The SOHO satellite can help determine whether a mass ejection is heading towards Earth, and the ACE satellite about 1 million miles away from Earth can give about an hour's warning whether the imbedded magnetic field in a mass ejection from the Sun might impact the Earth's magnetosphere, causing propagation problems for hams.

Statistically, coronal holes tend to occur most often during the declining phase of the 11-year solar cycle and they can last for a number of solar rotations. This means that a coronal hole can be a "recurring coronal hole," disrupting communications for several days about the same time each month for as long as a year, or even more.

Sudden Disappearing Filaments

A sudden disappearing filament (SDF) is the third major category of solar disturbance that can affect propagation. SDFs take their names from the manner in which they suddenly arch upward from the Sun's surface, spewing huge amounts of matter as plasma out into space in the solar wind. They tend to occur mostly during the rising phase of the 11-year solar cycle.

IONOSPHERIC STORMS

When the conditions are right, a flare, coronal hole or an SDF can launch a plasma cloud into the solar wind, resulting in an *ionospheric storm* here on Earth. Unlike a hurricane or a winter Nor'easter storm in New England, an ionospheric storm is not something we can see with our eyes or feel on our skins. We can't easily measure things occurring in the ionosphere some 200 miles overhead. However, we can see the indirect effects of an ionospheric storm on magnetic instruments located on the Earth's surface, because disturbances in the ionosphere are closely related to the Earth's magnetic field. The term *Geomagnetic Storm* ("Geo" means "Earth" in Greek) is used almost synonymously with ionospheric storm.

During a ionospheric storm, we may experience extraordinary radio noise and interference, especially at HF. You may hear solar radio emissions as increases of noise at VHF. A geomagnetic storm generally adds noise and weakens or disrupts ionospheric propagation for several days. Transpolar signals at 14 MHz or higher may be particularly weak, with a peculiar hollow sound or flutter—even more than normal for transpolar signals.

Depending on the severity of the disturbance to the Earth's geomagnetic field and the consequent disturbance of the ionosphere, propagation may be disrupted completely or it might be at least degraded for a period of time that ranges from a day to three or four days before returning to normal propagation conditions.

What can we do about the solar disturbances and related disturbed ionospheric propagation on Earth? The truth is that we are powerless faced with the truly awesome forces of solar disturbances like flares, coronal holes or sudden disappearing filaments. Perhaps there is some comfort, however, in understanding what has happened to cause our HF bands to be so poor. And as a definite consolation, conditions on the VHF bands are often exceptionally good just when HF propagation is remarkably poor due to solar disturbances. VHF operators enthusiastically look forward to conditions when they can engage in auroral communications—exactly the kind of conditions that have HF operators scratching their heads, wondering where the ionosphere went.

ELEVATION ANGLES FOR HF COMMUNICATION

It was shown in connection with Fig 25 that the distance at which a ray returns to Earth depends on the eleva-

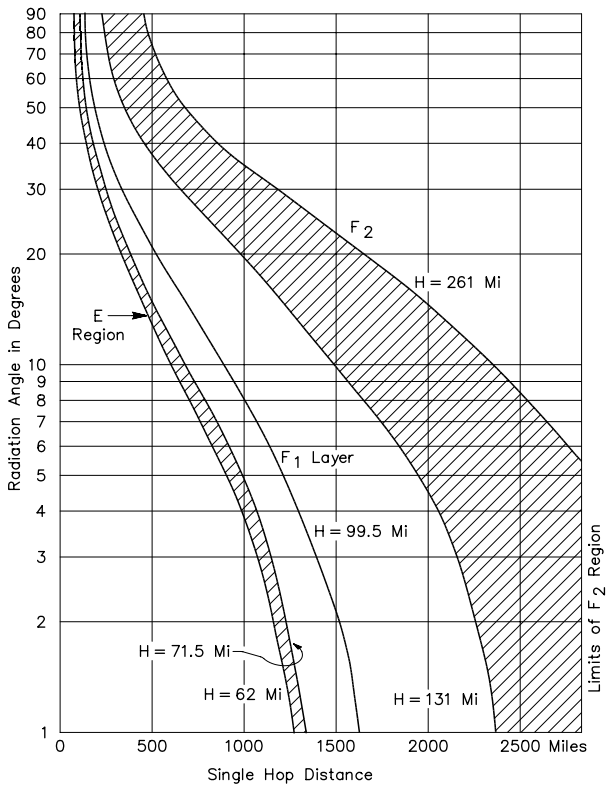

Fig 28—Distance plotted against wave angle (one-hop transmission) for the nominal range of heights for the E and F2 layers, and for the F1 layer.

tion angle at which it left the Earth (also known by other names: takeoff, launch or wave angle). Chapter 3, The Effects of Ground, in this book deals with the effects of local terrain, describing how the elevation angle of a horizontally polarized antenna is determined mainly by its height above the ground.

Although it is not shown specifically in Fig 25, propagation distance also depends on the layer height at the time, as well as the elevation angle. As you can probably imagine, the layer height is a very complex function of the state of the ionosphere and the Earth's geomagnetic field. There is a large difference in the distance covered in a single hop, depending on the height of the E or the F_2 layer. The maximum single-hop distance by the E layer is about 2000 km (1250 miles) or about half the maximum distance via the F_2 layer. Practical communicating distances for single-hop E or F layer work at various wave angles are shown in graphic form in **Fig 28**.

Actual communication experience usually does not fit the simple patterns shown in Fig 25. Propagation by means of the ionosphere is an enormously complicated business (which makes it all the more intriguing and challenging to radio amateurs, of course), even when the Sun is not in a disturbed state. Until the appearance of sophisticated computer models of the ionosphere, there was little definitive information available to guide the radio amateur in the design of his antenna systems for optimal performance over all portions of the 11-year solar cycle. Elevation angle information that had appeared for many years in *The ARRL Antenna Book* was measured for only one transmitting path, during the lowest portion of Solar Cycle 17 in 1934.

The *IONCAP* Computer Propagation Model

Since the 1960s several agencies of the US government have been working on a detailed computer program that models the complex workings of the ionosphere. The program has been dubbed *IONCAP*, short for "Ionospheric Communications Analysis and Prediction Program." *IONCAP* was originally written for a mainframe computer, but later versions have been rewritten to allow them to be run by high-performance personal computers. *IONCAP* incorporates a detailed database covering almost three complete solar cycles. The program allows the operator to specify a wide range of parameters, including detailed antenna models for multiple frequency ranges, noise models tailored to specific local environments (from low-noise rural to noisy residential QTHs), minimum elevation angles suitable for a particular location and antenna system, different months and UTC times, maximum levels of multipath distortion, and finally solar activity levels, to name the most significant of a bewildering array of options.

While *IONCAP* has a well-justified reputation for being very *unfriendly* to use, due to its mainframe, noninteractive background, it is also the one ionospheric model most highly regarded for its accuracy and flexibility, both by amateurs and professionals alike. It is the program used for many years to produce the long-term MUF charts formerly included in the "How's DX" monthly column of *QST* and now available on the Members Only ARRLWeb page.

IONCAP is not well suited for short-term forecasts of propagation conditions based on the latest solar indices received from WWV. It is an excellent tool, however, for long-range, detailed planning of antenna systems and shortwave transmitter installations, such as that for the Voice of America, or for radio amateurs. See the section later in this chapter describing other computer programs that can be used for short-term, interactive propagation predictions.

IONCAP/VOACAP Parameters

The elevation-angle statistical information contained in this section was compiled from thousands of *VOACAP* runs (an improved version of *IONCAP* developed by scientists from VOA, the Voice of America). These runs were done for a number of different transmitting locations throughout the world to important DX locations throughout the world.

Some assumptions were needed for setting *VOACAP* parameters. The transmitting and receiving sites were all assumed to be located on flat ground, with "average" ground conductivity and dielectric constant. Each site was assumed to have a clear shot to the horizon, with a minimum elevation angle less than or equal to 1°. Electrical noise at each

Table 3

Boston, Massachusetts, to All of Europe

Elev	80 m	40 m	30 m	20 m	17 m	15 m	12 m	10 m
1	4.1	9.6	4.6	1.7	2.1	4.4	5.5	7.2
2	0.8	2.3	7.2	1.4	2.8	2.8	3.7	5.3
3	0.3	0.7	4.3	3.1	2.4	2.2	4.4	7.9
4	0.5	4.1	8.7	11.6	12.2	9.4	8.1	3.9
5	4.6	4.8	7.5	12.7	14.3	13.1	9.2	11.2
6	7.1	8.9	5.5	9.2	9.6	12.2	9.2	7.2
7	8.5	6.9	7.2	4.6	7.9	7.4	10.0	5.9
8	5.1	7.0	5.4	3.2	5.9	7.4	4.8	6.6
9	3.3	5.6	3.2	3.1	2.1	3.9	8.1	9.2
10	1.0	4.0	7.9	6.3	5.1	3.7	11.1	6.6
11	1.9	3.8	9.7	10.2	7.2	5.4	3.7	7.9
12	5.6	3.4	4.8	8.5	6.9	7.4	4.8	6.6
13	11.0	3.0	2.4	4.1	5.9	4.6	3.3	2.6
14	7.6	4.8	2.0	2.7	3.8	3.9	6.3	5.9
15	5.3	7.9	2.0	1.5	2.4	1.7	1.5	2.0
16	2.8	6.4	3.8	2.9	1.5	1.3	2.6	2.6
17	5.0	3.4	4.5	3.1	1.0	1.5	0.0	0.0
18	4.2	2.0	3.1	3.1	2.0	2.2	1.8	1.3
19	5.7	1.4	1.4	2.3	1.3	0.7	0.0	0.0
20	6.6	1.4	1.2	1.8	1.1	1.3	0.7	0.0
21	4.4	1.4	0.5	0.8	0.7	0.7	0.4	0.0
22	2.3	2.4	1.0	1.1	0.6	1.3	0.7	0.0
23	1.3	1.8	0.1	0.3	0.1	0.0	0.0	0.0
24	0.6	1.0	0.5	0.5	0.4	0.7	0.0	0.0
25	0.3	0.8	0.3	0.1	0.4	0.0	0.0	0.0
26	0.0	0.5	0.7	0.2	0.1	0.4	0.0	0.0
27	0.1	0.1	0.1	0.2	0.1	0.2	0.0	0.0
28	0.0	0.3	0.1	0.2	0.0	0.2	0.0	0.0
29	0.1	0.0	0.2	0.0	0.0	0.0	0.0	0.0
30	0.0	0.1	0.0	0.0	0.0	0.0	0.0	0.0
31	0.0	0.0	0.0	0.0	0.0	0.0	0.0	0.0
32	0.0	0.0	0.1	0.0	0.0	0.0	0.0	0.0
33	0.1	0.0	0.0	0.0	0.0	0.0	0.0	0.0
34	0.0	0.0	0.0	0.0	0.0	0.0	0.0	0.0
35	0.0	0.0	0.0	0.0	0.0	0.0	0.0	0.0

Percentage of time a particular frequency band is open on this specific propagation path.

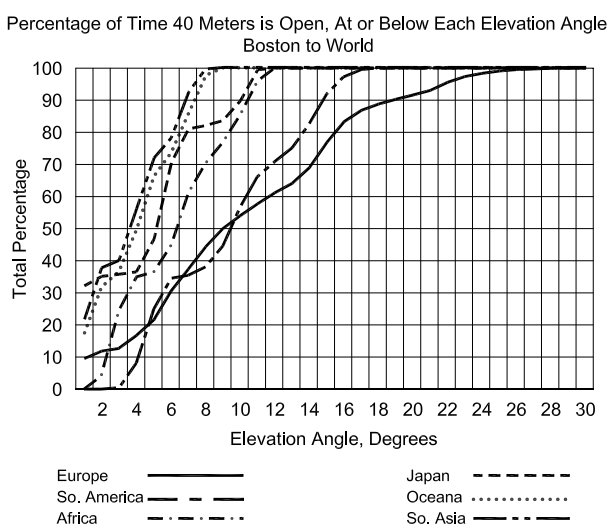

Fig 29—The cumulative distribution function showing the total percentage of time that 40 meters is open, at or below each elevation angle, from Boston to the world. For example, 50% of the time the band is open to Europe from Boston, it is at 10° or less. The angles for DX work are indeed low.

receiving location was also assumed to be very low.

Transmitting and receiving antennas for the 3.5 to 30-MHz frequency range were specified to be isotropic-type antennas, but with +6 dBi gain, representing a good amateur antenna on each frequency band. These theoretical antennas radiate uniformly from the horizon, up to 90° directly overhead. With response patterns like this, these are obviously not real-world antennas. They do, however, allow the computer program to explore all possible modes and elevation angles.

Looking at the Elevation-Angle Statistical Data

Table 3 shows detailed statistical elevation informa-

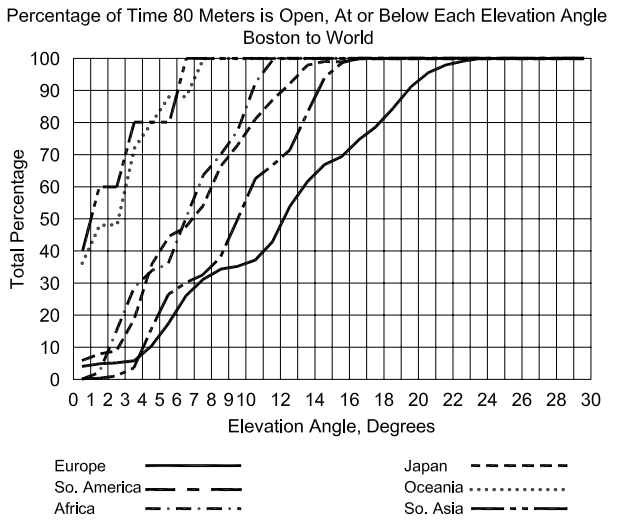

Fig 30—The cumulative distribution function showing the total percentage of time that 80 meters is open, at or below each elevation angle, from Boston to the world. For example, 50% of the time the band is open to Europe from Boston, it is at 13° or less.

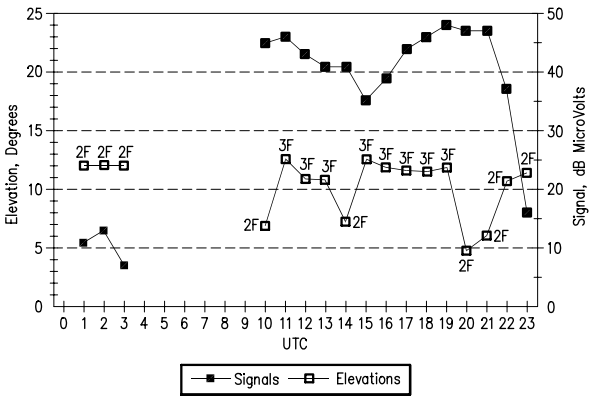

Fig 31—Overlay of signals and elevation angles, together with hop-mode information. This is for one month, October, at one level of solar activity, SSN=70, for the path from Newington, CT, to London, England. The mode of propagation does not closely follow the elevation angle. From 15 to 19 UTC the mode is 3F2 hops, and the elevation angle is approximately 12°. The same elevation angle is required from 23 to 03 UTC, but here the mode is 2F2 hops.

tion for the path from Boston, Massachusetts, near ARRL HQ in Newington, Connecticut, to all of Europe. The data incorporated into Table 3 shows the percentage of time versus elevation angle for all HF bands from 80 meters to 10 meters, over all portions of the 11-year solar cycle. The CD-ROM accompanying this book contains more tables such as this for more than 150 transmitting sites around the world. These tables are used by the *HFTA* program (and earlier *YT* program) and can also be imported into many programs, such as word processors or spreadsheets. Six important areas throughout the world are covered, one per table: all of Europe (from London, England, to Kiev, Ukraine), the Far East (centered on Japan), South America (Paraguay), Oceania (Melbourne, Australia), Southern Africa (Zambia) and South Asia (New Delhi, India).

You may be surprised to see in Table 3 that angles lower than 10° dominate the possible range of incoming angles for this moderate-distance path from New England to Europe. In fact, 1.7% of all the times when the 20-meter band is open to Europe, the takeoff angle is as low as 1°. You should recognize that very few real-world 20-meter antennas achieve much gain at such an extremely low angle—unless they just happen to be mounted about 400 feet high over flat ground or else are located on the top of a tall, steep mountain.

The situation is even more dramatic on 40 and 80 meters. **Fig 29** shows the "cumulative distribution function" of the total percentage of time (derived from Table 3) when 40 meters is open from Boston to the rest of the world, plotted against the elevation angle. For example, into Europe from Boston, 50% of the time when the band is open, it is at 10° or less. Into Japan from Boston, the statistics are even more revealing: 50% of the time when the band is open, the angle is 6° or less, and 90% of the time the angle is 13° or less!

Fig 30 shows the same sort of information for 80 meters from Boston to the world. For 50% of the time from Boston to Europe the elevation angle is 13° or less; at the 90% level the angle is 20° or less. For the path to Japan on 80 meters from Boston, 50% of the time the angle is 8° or less; at the 90% level, the angle is 13° or less. Now, to achieve peak gain on 80 meters at an elevation angle of 8° over flat land, a horizontally polarized antenna must be 500 feet high. You can begin to see why verticals can do very well on long-distance contacts on 80 meters, even when they are mounted over poorly conducting, rocky ground. Clearly, low angles are very important for successful DXing.

The Ionosphere Controls Propagation

You should always remember that it is the *ionosphere* that controls the elevation angles, *not* the transmitting antenna. The elevation response of a particular antenna only determines how strong or weak a signal is, at whatever angle (or angles) the ionosphere is supporting at that particular instant, for that propagation path and for that frequency.

If only one propagation mode is possible at a particular time, and if the elevation angle for that one mode happens to be 5°, then your antenna will have to work satisfactorily at that very low angle or else you won't be able to communicate. For example, if your low dipole has a gain of –10 dBi at 5°, compared to your friend's Yagi on a mountain top with +10 dBi gain at 5°, then you will be down 20 dB compared to his signal. It's not that the elevation angle is somehow *too low*—the real problem here is that you don't have *enough gain* at that particular angle where the ionosphere is supporting propagation. Many "flatlanders" can

vividly recall the times when their mountain-top friends could easily work DX stations, while they couldn't even hear a whisper.

Looking at the Data—Further Cautions

A single propagation mode is quite common at the opening and the closing of daytime bands like 20, 15 or 10 meters, when the elevation angle is often lower (but not always) than when the band is wide open. The lower-frequency bands tend to support multiple propagation modes simultaneously. For example, **Fig 31** plots the signal strength (in dBμV) and the elevation angle for the dominant mode (with the strongest signal) over a 24-hour period from Newington to London in October, for a medium-level SSN = 70. The morning opening at 10 UTC starts out with a two-hop $2F_2$ mode (labeled 2F) at an elevation angle of 6°. By 11 UTC the mode has changed to a three-hop $3F_2$ (labeled 3F) at a 12° elevation angle. The band starts to close down with weaker signals after about 23 UTC. Note that this path actually supports both $2F_2$ and $3F_2$ modes most of the time. Either mode may be stronger than the other, depending on the particular time of day.

It is tempting to think that two-hop signals always occur at lower elevation launch angles, while three-hop signals require higher elevation angles. In reality, the detailed workings of the ionosphere are enormously complicated. From 22 UTC to 03 UTC, the elevation angles are higher than 11° for $2F_2$ hops. During much of the morning and early afternoon in Newington (from 11 to 13 UTC, and from 15 to 19 UTC), the angles are also higher than 11°. However, $3F_2$ hops are involved during these periods of time. The number of hops is not directly related to the elevation angles needed—changing layer heights account for this.

Note that starting around 15 UTC, the mid-morning 20-meter "slump" (down some 10 dB from peak signal level) is caused by higher levels of mainly E-layer absorption when the Sun is high overhead. This condition favors higher elevation angles, since signals launched at lower angles must travel for a longer time through the lossy lower layer.

How does the situation change with different levels of solar activity? **Fig 32** overlays predicted signals and elevation angles for three levels of solar activity in October, again for the Newington-London path. Fig 32 shows the mid-morning slump dramatically when the solar activity is at

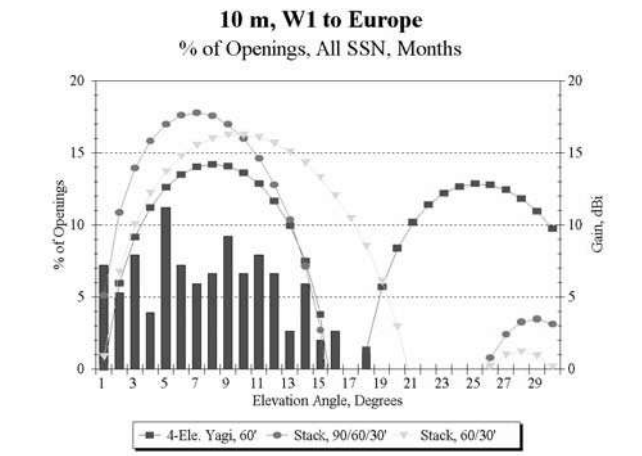

Fig 33—10-meter graph of the percentage of all openings versus elevation angles, together with overlay of elevation patterns over flat ground for three 10-meter antenna systems. Stacked antennas have wider "footprints" in elevation angle coverage for this example from New England to Europe.

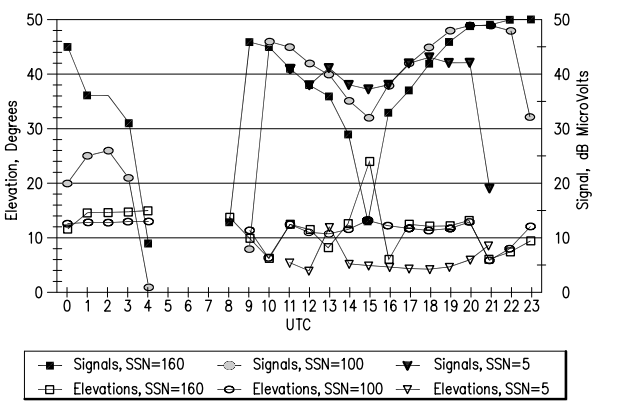

Fig 32—October 20-meter signals and elevation angles for the full range of solar activity, from W1 to England. The elevation angle does not closely follow the level of solar activity. What is important in designing a station capable of covering all levels of solar activity is to have flexibility in antenna elevation pattern response — to cover a wide range of possible angles.

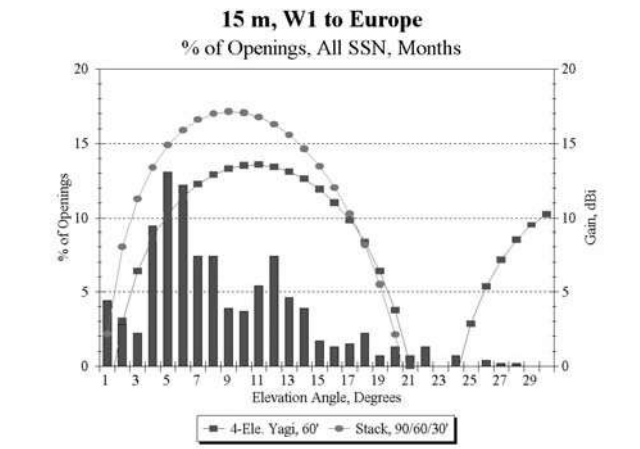

Fig 34—15-meter graph of the percentage of all openings versus elevation angles, together with overlay of elevation patterns over flat ground for two 15-meter antenna systems. Like 10 meters, 15-meter stacked antennas have wider footprints in elevation angle coverage for this example from New England to Europe.

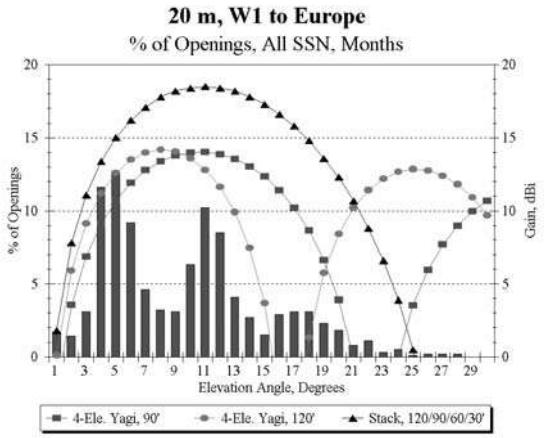

Fig 35—20-meter graph of the percentage of all openings from New England to Europe versus elevation angles, together with overlay of elevation patterns over flat ground for three 20-meter antenna systems.

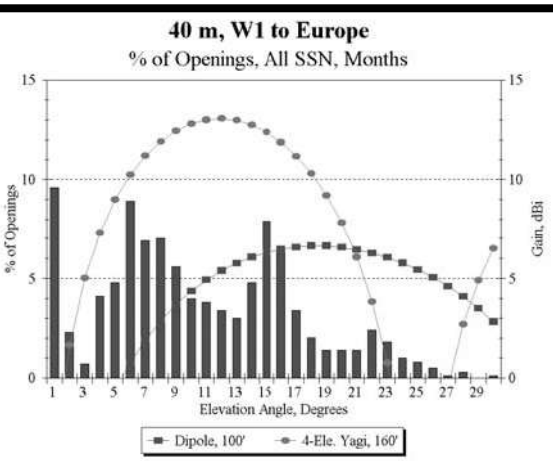

Fig 36—40-meter graph of the percentage of all openings from New England to Europe versus elevation angles, together with overlays of elevation patterns over flat ground for a 100-foot high dipole and a large 4-element Yagi at 160 feet. Achieving gain at very low elevation angles requires very high heights above ground.

a very high level, represented by SSN = 160. At 15 UTC, the signal level drops 35 dB from peak level, and the elevation angle rises all the way to 24°. By the way, as a percentage of all possible openings, the 24° angle occurs only rarely, 0.5% of the time. It barely shows up as a blip in Table 3. Elevation angles are *not* closely related to the level of solar activity.

IONCAP/VOACAP demonstrates that elevation angles do not follow neat, easily identified patterns, even over a 24-hour period—much less over all portions of the solar cycle. Merely looking at the percentage of all openings versus elevation angle, as shown in Table 3, does not tell the whole

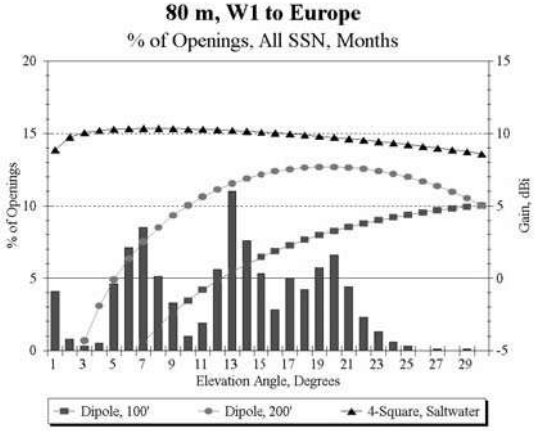

Fig 37—80-meter graph of the percentage of all openings from New England to Europe versus elevation angles, together with overlay of elevation patterns over flat ground for dipoles at two different heights. The 200-foot-high dipole clearly covers the necessary elevation angles better than does the 100-foot-high dipole, although a Four Square vertical array located over saltwater is even better for all angles needed.

story, although it is probably the most statistically valid approach to station design, and possibly the most emotionally satisfying approach too. Neither is the whole story revealed by looking only at a snapshot of elevation angles versus time for one particular month, or for one solar activity level.

What is important to recognize is that the most effective antenna system will be one that can cover the *full range* of elevation angles, over the whole spectrum of solar activity, even if the actual angle in use at any one moment in time may not be easy to determine. For this particular path, from New England to all of Europe, an ideal antenna would have equal response over the full range of angles from 1° to 28°. Unfortunately, real-world antennas have a tough time covering such a wide range of elevation angles equally well.

Antenna Elevation Patterns

Figs 33 through **37** show overlays of the same sort of elevation angle information listed in Table 3, together with the elevation response patterns for typical antennas for the HF amateur bands 80, 40, 20, 15 and 10 meters. For example, Fig 34 shows an overlay for 20 meters, with three different types of 20-meter antennas. These are a 4-element Yagi at 90 feet, a 4-element Yagi at 120 feet and a large stack of four 4-element Yagis located at 120, 90, 60 and 30 feet. Each antenna is assumed to be mounted over flat ground. Placement on a hill with a long slope in the direction of interest would lower the required elevation angle by the amount of the hill's slope. For example, if a 10° launch angle is desired, and the antenna is placed on a hill with a slope of –5°, the antenna itself should be designed for a height that would optimize the response at 15° over flat ground—one wavelength high.

In Fig 35, the large stack of four 20-meter Yagis over flat ground comes closest to being ideal, but even this large array will not work well for that very small percentage of time when the angle needed is higher than about 20°. Some hams might conclude that the tiny percentage of time when the angles are very high doesn't justify an antenna tailored for that response. However, when that new DX country pops up on a band, or when a rare multiplier shows up in a contest, doesn't it always seem that the desired signal only comes in at some angle your antenna doesn't cover well? What do you do then, if your only antenna happens to be a large stack?

The answer to this, perhaps unique, high-angle problem lies in switching to using only the top antenna in the stack. In this example, the second elevation lobe of the 120-foot high antenna would cover the angles from 20° to 30° well, much better than the stack does. Note that the top antenna by itself would not be ideal for all conditions. It is simply too high much of the time when the elevation angles are higher than about 12°. The experience of many amateurs on the US East Coast with high 20-meter antennas bears this out—they find that 60 to 90-foot high antennas are far more consistent performers into Europe.

ONE-WAY PROPAGATION

On occasion a signal may be started on the way back toward the Earth by reflection from the F region, only to come down onto the top of the E region and be reflected back up again. This set of conditions is one possible explanation for the often-reported phenomenon called *one-way skip*. The reverse path may not necessarily have the same multilayer characteristic. The effect is more often a difference in the signal strengths, rather than a complete lack of signal in one direction, and many times there may be local noises that mask signals at one end of the path. It is important to remember these sorts of possibilities when a long-distance test with a new antenna system yields apparently conflicting results. Even many tests, on paths of different lengths and headings, may provide data that are difficult to understand. Communication by way of the ionosphere is not always a source of consistent answers to antenna questions.

Fig 37 shows the 80-meter path from New England to Europe with three different antennas. A really high dipole at a height of 200 feet above flat ground would certainly be an impressive antenna. But it would still be overshadowed dramatically by a Four-Square vertical array, at least at the low elevation angles needed often on this path. This is predicated on the Four Square being located over salt water, which provides a virtually perfect RF ground. At an elevation angle of 7°, the Four Square has 7 dB more gain than the 200-foot high dipole.

SHORT OR LONG PATH?

Propagation between any two points on the Earth's surface is usually by the shortest direct route—the *great-circle path* found by stretching a string tightly between the two points on a globe. If an elastic band going completely around the globe in a straight line is substituted for the string, it will show another great-circle path, going "the long way around." The long path may serve for communication over the desired circuit when conditions are favorable along the longer route. There may be times when communication is possible over the long path but not possible at all over the short path. Especially if there is knowledge of this potential at both ends of the circuit, long-path communication may work very well. Cooperation is almost essential, because both the aiming of directional antennas and the timing of the attempts must be right for any worthwhile result. The *IONCAP/VOACAP* computations in the preceding tables were made for short-path azimuths only.

Sunlight is a required element in long-haul communication via the F layer above about 10 MHz. This fact tends to define long-path timing and antenna aiming. Both are essentially the reverse of the "normal" for a given circuit. We know also that salt-water paths work better than overland ones. This can be significant in long-path work.

We can better understand several aspects of long-path propagation if you become accustomed to thinking of the Earth as a ball. This is easy if you use a globe frequently. A

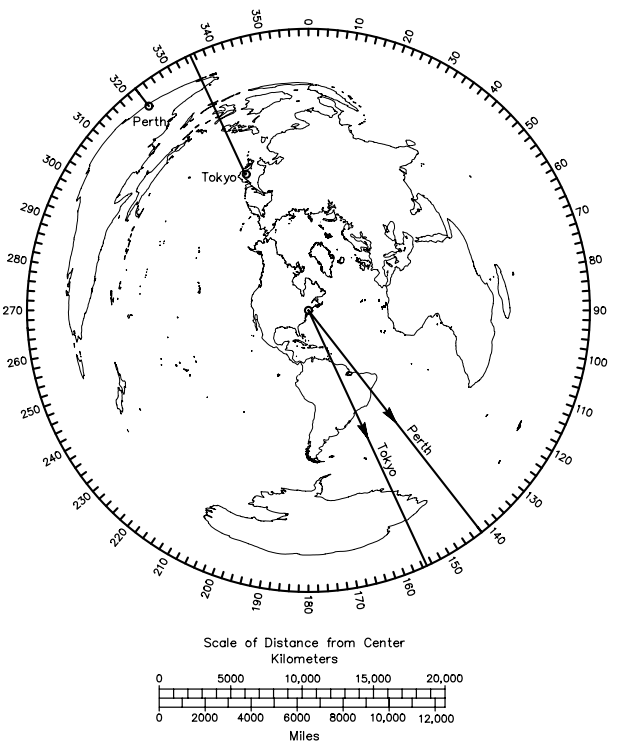

Fig 38—K5ZI's computer-generated azimuthal-equidistant projection centered on Newington, Connecticut. (See Bibliography for ordering information.) Land masses and information showing long paths to Perth and Tokyo have been added. Notice that the paths in both cases lie almost entirely over water, rather than over land masses.

flat map of the world, of the azimuthal-equidistant projection type, is a useful substitute. The ARRL World Map is one, centered on Wichita, Kansas. A similar world map prepared by K5ZI and centered on Newington, Connecticut, is shown in **Fig 38**. These help to clarify paths involving those areas of the world.

Long-Path Examples

There are numerous long-path routes well known to DX-minded amateurs. Two long paths that work frequently and well when 28 MHz is open from the northeastern US are New England to Perth, Western Australia, and New England to Tokyo. Although they represent different beam headings and distances, they share some favorable conditions. By the long path, Perth is close to halfway around the world; Tokyo is about three-quarters of the way. On 28 MHz, both areas come through in the early daylight hours, Eastern Time, but not necessarily on the same days. Both paths are at their best around the equinoxes. (The sunlight is more uniformly distributed over transequatorial paths at these times.) Probably the factor that most favors both is the nature of the first part of the trip at the US end. To work Perth by way of long path, northeastern US antennas are aimed southeast, out over salt water for thousands of miles—the best low-loss start a signal could have. It is salt water essentially all the way, and the distance, about 13,000 miles, is not too much greater than the "short" path.

The long path to Japan is more toward the south, but still with no major land mass at the early reflection points. It is much longer, however, than that to Western Australia. Japanese signals are more limited in number on the long path than on the short, and signals on the average somewhat weaker, probably because of the greater distance.

On the short path, an amateur in the Perth area is looking at the worst conditions—away from the ocean, and out across the huge land mass of North America, unlikely to provide strong ground reflections. The short paths to both Japan and Western Australia, from most of the eastern half of North America, are hardly favorable. The first hop comes down in various western areas likely to be desert or mountains, or both, and not favored as reflection points.

A word of caution: Don't count on the long-path signals always coming in on the same beam heading. There can be notable differences in the line of propagation via the ionosphere on even relatively short distances. There can be more variations on long path, especially on circuits close to halfway around the world. Remember, for a point exactly halfway around, all directions of the compass represent great-circle paths.

FADING

When all the variable factors in long-distance HF communication are taken in account, it is not surprising that signals vary in strength during almost every contact beyond the local range. In VHF communication we can also encounter some fading at distances greater than just to the visible horizon. These are mainly the result of changes in the temperature and moisture content of the air in the first few thousand feet above the ground.

On paths covered by HF ionospheric modes, the causes of fading are very complex—constantly changing layer height and density, random polarization shift, portions of the signal arriving out of phase, and so on. The energy arriving at the receiving antenna has components that have been acted upon differently by the ionosphere. Often the fading is very different for small changes in frequency. With a signal of a wideband nature, such as high-quality FM, or even double-sideband AM, the sidebands may have different fading rates from each other, or from the carrier. This causes severe distortion, resulting in what is termed *selective fading*. The effects are greatly reduced (but still present to some extent) when single-sideband (SSB) is used. Some immunity from fading during reception (but not to the distortion induced by selective fading) can be had by using two or more receivers on separate antennas, preferably with different polarizations, and combining the receiver outputs in what is known as a *diversity* receiving system.

OTHER PROPAGATION MODES

In propagation literature there is a tendency to treat the various propagation modes as if they were separate and distinct phenomena. This they may be at times, but often there is a shifting from one to another, or a mixture of two or more kinds of propagation affecting communication at one time. In the upper part of the usual frequency range for F-region work, for example, there may be enough tropospheric bending at one end (or both ends) to have an appreciable effect on the usable path length. There is the frequent combination of E and F-region propagation in long-distance work. And in the case of the E region, there are various causes of ionization that have very different effects on communication. Finally, there are weak-signal variations of both tropospheric and ionospheric modes, lumped under the term "scatter." We look at these phenomena separately here, but in practice we have to deal with them in combination, more often than not.

Sporadic E (E_s)

First, note that this is *E-subscript-s*, a usefully descriptive term, wrongly written "Es" so often that it is sometimes called "ease," which is certainly not descriptive. *Sporadic E* is ionization at E-layer height, but of different origin and communication potential from the E layer that affects mainly our lower amateur frequencies.

The formative mechanism for sporadic E is believed to be wind shear. This explains ambient ionization being distributed and compressed into a ledge of high density, without the need for production of extra ionization. Neutral winds of high velocity, flowing in opposite directions at slightly different altitudes, produce shears. In the presence of the Earth's magnetic field, the ions are collected at a particular altitude, forming a thin, overdense layer. Data from rockets entering E_s regions confirm the electron density, wind velocities and height parameters.

The ionization is formed in clouds of high density, lasting only a few hours at a time and distributed randomly. They vary in density and, in the middle latitudes in the Northern Hemisphere, move rapidly from southeast to northwest. Although E_s can develop at any time, it is most prevalent in the Northern Hemisphere between May and August, with a minor season about half as long beginning in December (the summer and winter solstices). The seasons and distribution in the Southern Hemisphere are not so well known. Australia and New Zealand seem to have conditions much like those in the US, but with the length of the seasons reversed, of course. Much of what is known about E_s came as the result of amateur pioneering in the VHF range.

Correlation of E_s openings with observed natural phenomena, including sunspot activity, is not readily apparent, although there is a meteorological tie-in with high-altitude winds. There is also a form of E_s, mainly in the northern part of the north temperate zone, that is associated with auroral phenomena.

At the peak of the long E_s season, most commonly in late June and early July, ionization becomes extremely dense and widespread. This extends the usable range from the more common "single-hop" maximum of about 1400 miles to "double-hop" distances, mostly 1400 to 2500 miles. With 50-MHz techniques and interest improving in recent years, it has been shown that distances considerably beyond 2500 miles can be covered. There is also an E_s "link-up" possibility with other modes, believed to be involved in some 50-MHz work between antipodal points, or even long-path communication beyond 12,500 miles.

When E_s is particularly strong and widespread, even the HF bands can suddenly go *short skip* producing exceptionally strong signals from distances that would normally be in the no-signal "skip zone." Editor N6BV distinctly remembers a spectacular 20-meter E_s opening in September 1994, during the "Hiram Percy Maxim/125" anniversary celebration, when he was living in New Hampshire. Signals on 20 meters were 30 to 40 dB over S9 from all along the Eastern Seaboard, from W2 to W4. One exasperated W3 complained that he had been calling in the huge pileup for 20 minutes. N6BV glanced at the S meter and saw that the W3 was 20 dB over S9, normally a very strong 20-meter SSB signal, but not when almost everybody else was 40 dB over S9!

Such short-skip conditions caused by Sporadic E are more common on 10 meters than they are on 15 or 20 meters. They can result in excellent transAtlantic 10-meter openings during the summer months—when 10 meters is not normally open for F_2 ionospheric propagation.

The MUF for E_s is not known precisely. It was long thought to be around 100 MHz, but in the last 25 years or so there have been thousands of 144-MHz contacts during the summer E_s season. Presumably, the possibility also exists at 222 MHz. The skip distance at 144 MHz does average much longer than at 50 MHz, and the openings are usually brief and extremely variable.

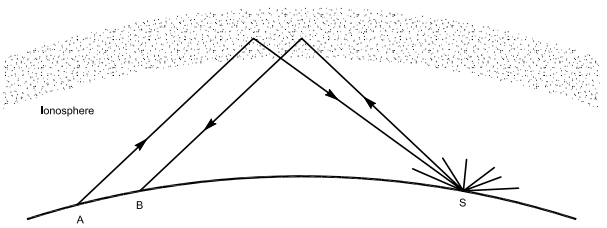

Fig 39—Schematic of a simple backscatter path. Stations A and B are too close to make contact via normal F-layer ionospheric refraction. Signals scattered back from a distant point on the Earth's surface (S), often the ocean, may be accessible to both A and B to create a backscatter circuit. (*Courtesy of The ARRL Handbook.*)

The terms "single" and "double" hop may not be accurate technically, since it is likely that cloud-to-cloud paths are involved. There may also be "no-hop" E_s. At times the very high ionization density produces critical frequencies up to the 50-MHz region, with no skip distance at all. It is often said that the E_s mode is a great equalizer. With the reflecting region practically overhead, even a simple dipole close to the ground may do as well over a few hundred miles as a large stacked antenna array designed for low-angle radiation. It's a great mode for low power and simple antennas on 28 and 50 MHz.

HF Scatter Modes

The term "skip zone" (where no signals are heard) should not be taken too literally. Two stations communicating over a single ionospheric hop can be heard to some degree by other stations at almost any point along the way, unless the two are running low power and using simple antennas. Some of the wave energy is *scattered* in all directions, including back to the starting point and farther.

Backscatter functions like a sort of HF ionospheric radar. **Fig 39** shows a schematic for a simple backscatter path. The signal launched from point A travels through the ionosphere back to earth at Point S, the scattering point. Here, the rough terrain of the land scatters signals in many directions, one of which propagates a weak signal back through the ionosphere to land at point B. Point B would normally be in the no-signal skip zone between A and S. Because backscatter signals arrive from multiple directions, through various paths through the ionosphere, they have a characteristic "hollow" sound, much like you get when you talk into a paper tube with its many internal reflections.

Because backscatter involves mainly scattering from the Earth at the point where the strong ionospherically propagated signal comes down, it is a part of HF over-the-horizon radar techniques. (The infamous 1970s-era "woodpecker" was an over-the-horizon HF radar.) Amateurs using sounding techniques have shown that you can tell to what part of the world a band is usable (single-hop F) by probing

the backscatter with a directive antenna and high transmitter power, even when the Earth contact point is open ocean. In fact, that's where the mode is at its best, because ocean waves can be efficient backscatter reflectors.

Backscatter is very useful on 28 MHz, particularly when that band seems dead simply because nobody is active in the right places. The mode keeps the 10-meter band lively in the low years of the solar cycle, thanks to the never-say-die attitude of some users. The mode is also an invaluable tool of 50-MHz DX aspirants, in the high years of the sunspot cycle, for the same reasons. On a high-MUF morning, hundreds of 6-meter beams may zero in on a hot spot somewhere in the Caribbean or South Atlantic, where there is no land, let alone other 6-meter stations—keeping in contact while they wait for the band to open to a place where there is somebody.

Sidescatter is similar to backscatter, except the ground scatter zone is off the direct line between participants. A typical example, often observed during the lowest years of the solar cycle, is communication on 28 MHz between the eastern US (and adjacent areas of Canada) and much of the European continent. Often, this may start as "backscatter chatter" between Europeans whose antennas are turned toward the Azores. Then suddenly the North Americans join the fun, perhaps for only a few minutes, but sometimes much longer, with beams also pointed toward the Azores. Duration of the game can be extended, at times, by careful reorientation of antennas at both ends, as with backscatter. The secret, of course, is to keep hitting the highest-MUF area of the ionosphere and the most favorable ground-reflection points.

The favorable route is usually, but not always, south of the great-circle heading (for stations in the Northern Hemisphere). There can also be sidescatter from the auroral regions. Sidescatter signals are stronger than backscatter signals using the same general area of ground scattering.

Sidescatter signals have been observed frequently on the l4-MHz band, and can take place on any band where there is a large window between the MUF and the LUF. For sidescatter communications to occur, the thing to look for is a common area to which the band is open from both ends of the path (the Azores, in the above example), when there is no direct-path opening. It helps if the common area is in the open ocean, where there is less scattering loss than over land.

GRAY-LINE PROPAGATION

The *gray line*, sometimes called the *twilight zone*, is a band around the Earth between the Sunlit portion and darkness. Astronomers call this the *terminator*. The terminator is a somewhat diffused region because the Earth's atmosphere tends to scatter the light into the darkness. **Fig 40** illustrates the gray line. Notice that on one side of the Earth, the gray line is coming into daylight (sunrise), and on the other side it is coming into darkness (sunset).

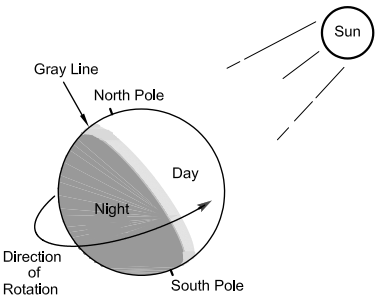

Fig 40—The gray line or terminator is a transition region between daylight and darkness. One side of the Earth is coming into sunrise, and the other is just past sunset.

Propagation along the gray line is very efficient, particularly on the lower bands, especially on 80 or 160 meters, so greater distances can be covered than might be expected for the frequency in use. One major reason for this is that the D layer, which absorbs HF signals, disappears rapidly on the sunset side of the gray line, and has not yet built up on the sunrise side.

The gray line runs generally north and south, but varies as much as 23° either side of the north-south line. This variation is caused by the tilt of the Earth's axis relative to its orbital plane around the Sun. The gray line will be exactly north and south at the equinoxes (March 21 and September 21). On the first day of Northern Hemisphere summer, June 21, it is tilted to the maximum of 23° one way, and on December 21, the first day of winter, it is tilted 23° the other way.

To an observer on the Earth, the direction of the terminator is always at right angles to the direction of the Sun at sunrise or sunset. It is important to note that, except at the equinoxes, the gray-line direction will be different at sunrise from that at sunset. This means you can work different areas of the world in the evening than you worked in the morning.

It isn't necessary to be located inside the twilight zone in order to take advantage of gray-line propagation. The effects can be used to advantage before sunrise and after sunset. This is because the Sun "rises" earlier and "sets" later on the ionospheric layers than it does on the Earth below.

What HF Bands Are Open—Where and When?

The CD-ROM included at the back of this book includes summary and detailed propagation predictions for more than 150 transmitting locations around the world. This propagation data was calculated using *CapMAN*, an upgraded variety of the mainframe propagation program *IONCAP*. The predictions were done for default antennas and powers that are representative of a "big-gun" station. Of course, not everyone has a big-gun station in his/her backyard, but this represents what the ultimate possibilities are, statistically speaking. After all, if the bands aren't open for the big guns, they are unlikely to be open for the "little pistols" too.

Let's see how propagation is affected if the smoothed sunspot number is 0 (corresponding to a smoothed solar flux of about 65), which is classified as a "Very Low" level of solar activity. And we'll examine the situation for a sunspot number of 100 (a smoothed solar flux of 150), which is typical of a "Very High" portion of the solar cycle.

Five-Band Summary Predictions

Tables 4 and **5** are Summary tables showing the predicted signal levels (in S units) from Boston, Massachusetts, to the rest of the world for the month of January. The Boston transmitting site is representative of the entire New England area of the USA. The target geographic receiving regions for the major HF bands from 80 through 10 meters are tabulated versus UTC (Universal Coordinated Time) in hours. Table 4 represents a Very Low level of solar activity, while Table 5 is for a Very High level of solar activity.

Each transmitting location is organized by six levels of solar activity over the whole 11-year solar cycle:

- VL (Very Low: SSN between 0 to 20)
- LO (Low: SSN between 20 to 40)
- ME (Medium: SSN between 40 to 60)
- HI (High: SSN between 60 to 100)
- VH (Very High: SSN between 100 to 150)
- UH (Ultra High: SSN greater than 150)

The receiving geographic regions for each frequency band are abbreviated:

Table 4

Printout of summary propagation table for Boston to the rest of the world, for a Very Low level of solar activity in the month of January. The abbreviations for the target geographic areas are: EU = Europe, FE = Far East, SA = South America, AF = Africa, AS = south Asia, OC = Oceania, and NA = North America.

Jan., MA (Boston), for SSN = Very Low, Sigs in S-Units. By N6BV, ARRL.

	80 Meters							40 Meters							20 Meters							15 Meters							10 Meters							
UTC	EU	FE	SA	AF	AS	OC	NA	EU	FE	SA	AF	AS	OC	NA	EU	FE	SA	AF	AS	OC	NA	EU	FE	SA	AF	AS	OC	NA	EU	FE	SA	AF	AS	OC	NA	UTC
0	9	-	9+	9	9	-	9+	9	8	9+	9+	9	2	9+	-	8	9+	7	4	8	9+	-	-	-	-	-	-	1	-	-	-	-	-	-	2	0
1	9	-	9+	9	9	-	9+	9	6	9+	9+	9+	6	9+	-	4	9	4	2	6	9+	-	-	-	-	-	-	1	-	-	-	-	-	-	2	1
2	9	-	9+	9+	8	1	9+	9	6	9+	9+	9	8	9+	-	1	8	1	2	3	9+	-	-	-	-	-	-	1	-	-	-	-	-	-	2	2
3	9	-	9+	9+	8	6	9+	9	6	9+	9+	9	8	9+	-	-	8	2	2	-	9+	-	-	-	-	-	-	1	-	-	-	-	-	-	2	3
4	9	-	9+	9+	1	8	9+	9	8	9+	9+	9	9	9+	-	1	8	7	2	-	9+	-	-	-	-	-	-	1	-	-	-	-	-	-	2	4
5	9	-	9+	9+	-	9	9+	9	8	9+	9+	8	9	9+	-	1	9	8	2	-	9	-	-	-	-	-	-	1	-	-	-	-	-	-	2	5
6	9+	-	9+	9+	-	9	9+	7	8	9+	9+	8	9	9+	-	1	9+	8	-	-	9	-	-	-	-	-	-	1	-	-	-	-	-	-	2	6
7	9	7	9+	9	-	9	9+	7	8	9+	9	8	9	9+	-	1	9+	1	-	1	8	-	-	-	-	-	-	1	-	-	-	-	-	-	2	7
8	9	8	9+	9	-	9	9+	8	9	9+	9	8	9+	9+	-	1	9+	-	-	5	9	-	-	-	-	-	-	1	-	-	-	-	-	-	2	8
9	8	8	9+	7	6	9	9+	8	9	9+	9	9	9+	9+	-	-	9	1	-	7	9	-	-	-	-	-	-	1	-	-	-	-	-	-	2	9
10	5	8	9+	4	6	9	9+	9	9	9+	9	9	9+	9+	-	3	9	5	-	6	9	-	-	-	-	-	-	1	-	-	-	-	-	-	2	10
11	3	8	9+	-	5	9	9+	8	9	9+	7	9	9+	9+	5	-	9+	9	5	1*	8	-	-	-	-	-	-	1	-	-	-	-	-	-	2	11
12	1	8	9	-	4	9	9+	7	9	9+	4	8	9	9+	9	5	9+	9+	9	2*	8	-	-	5	6	-	-	1	-	-	-	-	-	-	2	12
13	-	6	1	-	-	7	9+	6	8	9+	1	8	9	9+	9+	9	9+	9	9	7	8	4	-	9+	9	7	-	1	-	-	-	-	-	-	1	13
14	-	-	-	-	-	1	9+	5	7	8	-	8	8	9+	9+	9	9+	9	9	9	9+	7	2*	9+	9	9	-	8	-	-	5	-	-	-	1	14
15	-	-	-	-	-	-	9+	4	6	5	-	6	7	9+	9+	9	9+	9	9	9	9+	7	5	9+	9	2	2	5	-	-	5	-	-	-	-	15
16	-	-	-	-	-	-	9+	5	6	4	2	5	4	9+	9+	8	9+	9+	9	9	9+	5	1	9+	8	2*	2	9	-	-	5	-	-	-	1	16
17	-	-	-	-	-	-	9+	6	5	5	5	6	1	9+	9+	5	9+	9+	3	9	9+	-	-	9+	9	-	3	9+	-	-	5	-	-	-	1	17
18	1	-	-	-	-	-	9+	8	6	6	7	6	-	9+	9+	6	9+	9+	4	9	9+	-	-	9+	9	-	7	9+	-	-	5	-	-	-	1	18
19	3	-	-	2	-	-	9+	9	7	8	8	8	-	9+	6	6	9+	9+	6	9	9+	-	-	9+	9	-	9	9+	-	-	2	-	-	-	1	19
20	5	-	7	5	-	-	9+	9	8	9+	9	8	4	9+	1	7	9+	9+	8	9	9+	-	-	9+	4	-	9	9	-	-	-	-	-	-	1	20
21	8	3	9	8	6	-	9+	9	8	9+	9+	9	7	9+	-	8	9+	9	8	9	9+	-	-	9+	-	-	9	6	-	-	-	-	-	-	1	21
22	9	3	9+	9	8	-	9+	9	8	9+	9+	9	5	9+	-	9+	9+	9	8	9	9+	-	-	9	-	-	7	1	-	-	-	-	-	-	1	22
23	9	2	9+	9	9	-	9+	9	8	9+	9+	9	4	9+	-	9+	9+	9	5	9	9+	-	1	6	-	-	2	3	-	-	-	-	-	-	2	23
	EU	FE	SA	AF	AS	OC	NA	EU	FE	SA	AF	AS	OC	NA	EU	FE	SA	AF	AS	OC	NA	EU	FE	SA	AF	AS	OC	NA	EU	FE	SA	AF	AS	OC	NA	

Table 5

Printout of summary propagation table for Boston to the rest of the world, for a Very High level of solar activity in the month of January.

Jan., MA (Boston), for SSN = Very High, Sigs in S-Units. By N6BV, ARRL.

	80 Meters							40 Meters							20 Meters							15 Meters							10 Meters							
UTC	EU	FE	SA	AF	AS	OC	NA	EU	FE	SA	AF	AS	OC	NA	EU	FE	SA	AF	AS	OC	NA	EU	FE	SA	AF	AS	OC	NA	EU	FE	SA	AF	AS	OC	NA	UTC
0	9+	-	9+	9+	8	-	9+	9+	5	9+	9+	9	-	9+	1	9+	9+	9+	9+	9	9+	-	9	9+	2	2	9+	9+	-	1	8	-	-	8	9+	0
1	9+	-	9+	9+	8	-	9+	9+	4	9+	9+	9	2	9+	1	9	9+	8	9+	9+	9+	-	3	9	-	7	9+	9	-	-	-	-	-	4	2	1
2	9+	-	9+	9+	7	-	9+	9+	4	9+	9+	9	7	9+	1	9	9+	8	9	9+	9+	-	-	3	-	-	7	9	-	-	-	-	-	-	2	2
3	9+	-	9+	9+	1	2	9+	9+	4	9+	9+	9	9	9+	-	7	9+	7	8	9+	9	-	-	-	-	-	-	-	-	-	-	-	-	-	2	3
4	9+	-	9+	9+	-	7	9+	9+	5	9+	9+	8	9	9+	-	5	9+	9	9	9	9+	-	-	1	-	-	-	-	-	-	-	-	-	-	2	4
5	9+	-	9+	9+	-	8	9+	9+	6	9+	9+	7	9	9+	-	5	9+	9	9	5	9+	-	-	-	-	-	-	-	-	-	-	-	-	-	2	5
6	9+	-	9+	9+	-	8	9+	9+	7	9+	9+	7	9	9+	-	8	9+	8	9	5	9+	-	-	-	-	-	-	-	-	-	-	-	-	-	2	6
7	9+	-	9+	9+	-	8	9+	9	8	9+	9+	7	9+	9+	-	9	9+	-	7	9	9+	-	-	1	-	-	-	-	-	-	-	-	-	-	2	7
8	9	7	9+	9	-	8	9+	9	8	9+	9+	8	9+	9+	-	9	9+	-	4	9+	9+	-	-	1	-	-	-	2	-	-	-	-	-	-	2	8
9	8	7	9+	7	-	8	9+	9	9	9+	9	8	9+	9+	-	6	9+	-	1	9+	9+	-	-	-	-	-	-	1	-	-	-	-	-	-	2	9
10	5	8	9+	2	3	8	9+	9	9	9+	8	8	9	9+	4	-	9+	9+	1	5	9	-	-	-	-	-	-	-	-	-	-	-	-	-	2	10
11	1	8	9+	-	4	9	9+	8	9	9+	5	8	9	9+	9+	4*	9+	9+	7	-	8	-	-	9	9	-	-	-	-	-	-	-	-	-	2	11
12	-	7	8	-	1	9	9+	6	9	9+	1	8	9	9+	9+	9	9+	9	9	1*	9+	9	8*	9+	9+	9	5*	-	-	2*	9	9	1	1*	2	12
13	-	-	-	-	-	2	9+	4	8	8	-	7	9	9+	9+	9	9+	9	9	9+	9+	9+	7	9+	9+	9+	3*	9	9	5*	9+	9+	9	6*	2	13
14	-	-	-	-	-	-	9+	2	7	4	-	5	8	9+	9+	9	9+	8	9	9	9+	9+	9	9+	9+	9+	9	9+	9	6*	9+	9+	9	1*	1	14
15	-	-	-	-	-	-	9	1	5	-	-	4	5	9+	9+	9	9+	9	9	9	9+	9+	9+	9+	9+	9+	9	9+	9	5	9+	9+	6	6	8	15
16	-	-	-	-	-	-	8	3	4	-	-	3	1	9+	9+	8	9	9	9	9	9+	9+	9+	9+	9+	9	9+	9+	9	8	9+	9+	-	8	9	16
17	-	-	-	-	-	-	8	5	3	-	2	4	-	9+	9+	8	9+	9+	9	9	9+	9+	9	9+	9+	1*	9+	9+	-	8	9+	9+	-	8	9+	17
18	-	-	-	-	-	-	9	7	4	2	5	5	-	9+	9+	9	9+	9+	9	9	9+	9+	9	9+	9+	1	9+	9+	-	7	9+	9+	-	9+	9+	18
19	1	-	-	1	-	-	9+	8	5	6	8	7	-	9+	9+	9	9+	9+	9	9	9+	-	9+	9+	9+	2	9	9+	-	6	9+	9+	-	9+	9+	19
20	4	-	2	5	-	-	9+	9	6	9	9	8	-	9+	9+	9	9+	9+	9	9	9+	-	8	9+	9+	3	9	9+	-	1	9+	9	-	9	9+	20
21	7	-	8	7	1	-	9+	9+	7	9+	9+	8	1	9+	8	9	9+	9+	9	9	9+	-	6	9+	9+	3	9	9+	-	-	9+	5*	-	9+	9+	21
22	9	2	9+	9	8	-	9+	9+	7	9+	9+	9	4	9+	2	9+	9+	9+	9	9	9+	-	9+	9+	9	1	9+	9+	-	5	9+	4*	-	9	6	22
23	9	-	9+	9	8	-	9+	9+	7	9+	9+	9	-	9+	1	9+	9+	9+	9	9	9+	-	9+	9+	6	-	9	9+	-	7	9+	2*	-	9	2	23
	EU	FE	SA	AF	AS	OC	NA	EU	FE	SA	AF	AS	OC	NA	EU	FE	SA	AF	AS	OC	NA	EU	FE	SA	AF	AS	OC	NA	EU	FE	SA	AF	AS	OC	NA	

- EU All of Europe
- FE The Far East, centered on Japan
- SA South America, centered on Paraguay
- AF All of Africa, centered on Zambia
- AS South Asia, centered on India
- OC Oceania, centered on Sydney, Australia
- NA North America, all across the USA

These propagation files show the highest predicted signal strength (in S-units) throughout the generalized receiving area, for a 1500-W transmitter and rather good antennas on both sides of the circuit. The standard antennas are:

- 100-foot high inverted-V dipoles for 80 and 40 meters
- 3-element Yagi at 100 feet for 20 meters
- 4-element Yagi at 60 feet for 15 and 10 meters.

For example, Summary Table 4 shows that in January during a period of Very Low solar activity, 15 meters is open to somewhere in Europe from Boston for only 4 hours, from 13 to 16 UTC, with a peak signal level between S4 and S7. Now look at Table 5, where 15 meters is predicted to be open to Europe during a period of Very High solar activity for 7 hours, from 12 to 18 UTC, with peak signals ranging from S9 to S9+.

Both Tables 4 and 5 represent *snapshots* of predicted signal levels to generalized receiving locations—that is, they are computed for a particular month, from a particular transmitting location, and for a particular level of solar activity. These tables provide summary information that is particularly valuable for someone planning for an operating event such as a DXpedition or a contest.

What happens if you don't have a big-gun station with high antennas or the 1500-W power assumed in the analyses above? You can discount the S-Meter readings to reflect a smaller station:

- Subtract 2 S units for a dipole instead of a Yagi at same height on 20/15/10 meters.
- Subtract 3 S units for a dipole at 50 feet instead of a Yagi at 100 feet on 20 meters.
- Subtract 1 S unit for a dipole at 50 feet rather than a dipole at 100 feet on 40/80 meters.
- Subtract 3 S units for 100 W rather than 1500 W.
- Subtract 6 S units for 5 W (QRP) rather than 1500 W.

For example, Table 4 predicts an S7 signal into Boston from Europe on 15 meters at 14 UTC. If a European station is using a dipole at 50 feet, with 100 W of power, what

20 Meters: Jan., MA (Boston), for SSN = Very High, Sigs in S-Units. By N6BV, ARRL.

		UTC -->																						
Zone		00	01	02	03	04	05	06	07	08	09	10	11	12	13	14	15	16	17	18	19	20	21	22	23
KL7 = 01		9+	9+	9+	7	-	-	-	-	-	-	-	-	-	-	-	3	9+	9+	9+	9+	9+	9+	9+	9+
VO2 = 02		9+	9	9	9	9	9	8	7	5	3	2	1	5	9+	9+	9+	9+	9+	9+	9+	9+	8	9+
W6 =	03	9+	9+	9+	7	7	1	1	5	8	8	3	-	-	1	9	9+	9+	9+	9+	9	9	9+	9+	9+
W0 =	04	9+	9+	9+	8	5	5	5	5	3	2	1	-	-	9+	9+	9+	9+	9+	9+	9+	9+	9+	9+	9+
W3 =	05	4	2	2	2	2	2	2	3	3	3	3	2	1	1	8	9+	9+	9+	9+	9+	9+	9+	9+	9
XE1 = 06		9+	9+	7	9	9+	9+	9+	9+	9+	9+	9	8	9+	9+	9+	9+	9	9	9	9	9+	9+	9+	9+
TI =	07	9+	9+	8	9	9	9	9	9	9	9+	9	9+	9+	9+	9+	9+	9	8	9	9	9+	9+	9+	9+
VP2 = 08		9+	9+	9+	9+	9+	9+	9+	9+	9+	8	9	9+	9+	9+	9+	9+	9	9+	9+	9+	9+	9+	9+	9+
P4 =	09	9+	9+	9+	9+	9+	9+	9+	9+	9+	9+	9+	9+	9+	9+	9+	9	9	9	9	9+	9+	9+	9+	9+
HC =	10	9+	8	9+	9	9	9	9	9	7	3	1	7	9+	9+	9	5	5	5	7	8	9+	9+	9+	9+
PY1 = 11		9+	9+	9+	9	9	9+	9+	9	8	6	9	9+	8	2	1	-	-	1	4	8	9	9+	9+	9+
CE =	12	9+	9+	9+	9+	9+	9+	9+	9+	9	8	8	9+	9	8	2	1	1	-	1	3	7	9	9+	9+
LU =	13	9+	9+	9+	9+	9+	9+	9+	9+	8	8	8	9+	8	4	2	1	-	-	1	4	8	9	9+	9+
G =	14	-	-	-	-	-	-	-	-	-	-	-	9+	9+	9+	9+	9+	9+	9+	9+	9+	9+	8	2	-
I =	15	-	-	-	-	-	-	-	-	-	-	4	9	9	9	9	9	9	9+	9+	9	8	2	-	-
UA3 = 16		1	1	1	-	-	-	-	-	-	-	-	8	9	9+	9+	9+	9	8	5	-	-	-	-	1
UN =	17	1	-	-	8	7	7	7	1	-	-	-	2	9	9	9	6	-	-	2	4	8	9	5	4
UA9 = 18		6	7	6	6	9	9	9	7	4	1	-	-	8	8	6	6	5	6	7	8	9	9	8	7
UA0 = 19		9+	9	9	6	5	5	8	8	8	4	-	-	2	6	8	8	8	7	4	4	7	9	9+	9+
4X =	20	8	6	3	1	-	3	4	-	-	-	1	8	8	8	8	8	9	9	9+	9	9	8	7	7
HZ =	21	9+	9	4	3	8	8	2	-	-	-	1	7	8	9	8	8	9	9	9	9	9	9	9	9
VU =	22	7	5	8	7	6	7	5	-	-	-	-	6	9	9	9	9	3	2	2	2	8	8	9	8
JT =	23	9	9+	9	5	7	8	8	6	3	-	-	2*	8	8	5	6	8	8	8	8	9	7	5	6
VS6 = 24		9	9	9	5	4	5	7	8	6	1	-	1*	5	7	1	1	1	1	4	2	-	-	-	9
JA1 = 25		9	9	8	7	5	5	8	9	9	6	-	1	1	2	7	7	6	2	-	-	7	9	9+	9
HS =	26	9	9	6	4	2	-	-	2	1	-	-	2*	9	9	9	9	8	7	5	4	5	-	1*	1
DU =	27	9	8	7	-	-	-	5	7	7	1	-	-	1*	9	9	7	6	4	5	3	1*	1*	8	9
YB =	28	9	8	1	-	-	-	-	-	-	-	-	4*	8	9	9	9	8	8	9	9	9	9	9+	9+
VK6 = 29		3*	4*	-	-	-	-	-	-	5	3	-	-	-	5	9	9	9	8	9	9	9	9	9	8
VK3 = 30		1*	-	-	-	-	-	1	3	9	9	4	-	-	9+	9	8	2	1	-	-	1	2*	5*	4*
KH6 = 31		9	9+	9+	9+	8	2	2	6	4	-	-	-	-	-	-	-	9	9	8	7	6	4	6	7
KH8 = 32		-	2	9	9	9	5	5	9	9+	9+	5	-	-	9+	9	9	8	5	3	1	-	-	-	-
CN =	33	-	-	-	-	-	-	-	-	-	-	9	9+	9	9	8	9	9	9+	9+	9+	9+	9+	9+	7
SU =	34	9	8	3	3	-	1	4	-	-	-	2	7	8	8	8	8	9	9	9+	9+	9+	9+	8	8
6W =	35	9+	8	-	-	2	7	5	-	-	-	9+	9+	8	5	4	3	7	9	9+	9+	9+	9+	9+	9+
D2 =	36	9+	9+	5	3	9	9	8	-	-	-	3	-	-	-	-	4	4	7	8	9	9+	9+	9+	9+
5Z =	37	9+	9	2	4	8	8	1	-	-	-	2	-	-	3	5	5	7	8	9	9	9+	9+	9+	9+
ZS6 = 38		9+	9+	8	7	8	9	6	-	-	-	-	-	-	-	1*	1	2	6	8	9	9+	9+	9+	9+
FR =	39	9+	8	2	1	4	1	-	-	-	-	-	-	-	2*	3*	1*	1	3	8	9	9+	9+	9+	9+
FJL = 40		9+	9+	7	4	7	8	7	1	-	-	-	1*	8	9	9	9	9	9	9	9	9+	9+	9+	9+
Zone		00	01	02	03	04	05	06	07	08	09	10	11	12	13	14	15	16	17	18	19	20	21	22	23
		UTC -->																							

Expected signal levels using 1500 W and 3-element Yagis at 100 feet at each station.

Fig 41—The 20-meter page from Detailed propagation-prediction for the month of January, during Very High solar conditions, from Boston to 40 CQ Zones throughout the world. There are similar pages for each month/SSN level for 160, 80, 40, 20, 15 and 10 meters. These Detailed tables are very useful for planning DX work.

would this do to the predicted signal level in Boston? You would compute: S7 – 2 S units (for a dipole instead of Yagi) – 3 S units (100 W rather than 1500 W) = an S2 signal in Boston. A QRP station with a 4-element 15-meter Yagi at 60 feet would yield: S7 – 6 S units = an S1 signal in Boston.

More Detailed Predictions

Let's now look at table in **Fig 41**, which is the Detailed 20-meter page for the same conditions in Table 5: January at a Very High level of solar activity from Boston to the world. There are six such pages per month/SSN level, covering 160, 80, 40, 20, 15 and 10 meters.

In a Detailed prediction table, the world is divided into the 40 CQ Zones, with a particular sample location in each zone. For example, Zone 14 in Western Europe is represented by a location in London, England (call sign G), while Zone 25 is represented by a location in Tokyo, Japan (call sign JA1). Note that Zones with large ham populations are highlighted with dark shadowing for easy identification. For example, Zones 3, 4 and 5 cover the USA, while Zones 14, 15 and 16 cover the majority of Europe. Zone 25 covers the big ham population in Japan.

Let's revisit the example above for computing the signal strength for a station in London, but this time on 20 meters. Again, we'll assume that the G station has a dipole at 50 feet and 100 W of transmitter power. At 14 UTC in Zone 14, the table in Fig 40 predicts a very healthy signal for the reference big-gun station, at S9+. This is a signal at least S9 + 10 dB. Here, we're going to round off the plus 10 dB to 2 S units, giving a fictional 11 S units to start. We discount this for the smaller station: S11 – 3 S units (for a dipole at 50 feet instead of a 3-element Yagi at 100 feet) – 3 S units (100 W rather than 1500 W) = S5 signal in Boston. This is a respectable signal and will probably get through, in the absence of stronger signals calling the Boston station at the same time, of course.

Here's another example of how to use the Detailed propagation-prediction tables. Let's say that at 1230 UTC in January you work a VU2 station in New Delhi on 15 meters from Boston, where the local time is 7:30 AM.

You need a 20-meter contact also for the 5-Band DXCC award, so you quickly check the table in Fig 40 for Zone 22 (VU) and find that the predicted signal strength is S9. Your new VU2 friend is willing to jump to 20 meters and so you QSY to make the contact.

But perhaps you are late leaving for work and so you ask your new VU2 friend to make a schedule with you later that evening. Again, you consult the Detailed prediction table for 20 meters and find that signals are predicted to be S8 or stronger from 20 to 23 UTC, dropping to S7 at 00 UTC. You quickly ask your new friend whether he minds waking up at 4:30 AM his time to make a schedule with you at 2300 UTC, because New Delhi is 5½ hours ahead of UTC. You determined this using the program *GeoClock*, which is included with the software on the CD-ROM in the back of this book and which you run in the background on *Windows*. Luckily, he's a very gracious fellow and agrees to meet you on a specific frequency at that time.

The Detailed propagation-prediction tables give you all the information needed to plan your operations to maximize your enjoyment chasing DX. You can use these tables to plan a 48-hour contest next month, or next year—or you can use them to plan a schedule with your ham cousin on the West Coast on Saturday afternoon.

THE PROPAGATION BIG PICTURE

A newcomer to the HF bands could easily be overwhelmed with the sheer amount of data available in the Summary (and particularly the Detailed) prediction tables on the CD-ROM included with this book. So here's a long-term, "big-picture" view of HF propagation that might help answer some common questions. For example, what month really is the best for working DX around the clock? Or what level of solar activity is necessary to provide an opening between your QTH and somewhere in the South Pacific?

Table 6 is a table showing the number of hours in a day during each month when each major HF band is open to the same receiving areas shown in Tables 4 and 5. The listing is for New England, for three levels of solar activity: Very Low, Medium and Very High. The number of hours are separated in Table 6 by slashes. (Versions of Table 6 for other areas around the US are on the CD-ROM that accompanies this book in **Fig6Tab.PDF**.)

Let's examine the conditions for New England to Europe on 15 meters for October. The entry shows "7/11/17," meaning that for a Very Low level of solar activity, 15 meters is open for 7 hours; for a Medium level, it is open for 11 hours and for a Very High level of solar activity it is open for 17 hours a day.

Even for a Very Low level of solar activity, the month with the most hours available per day from Boston to somewhere in Europe is October, with 7 hours, followed by the next largest month of March, with 6 hours. For a Very High level of solar activity, however, the 15-meter band is open to Europe for 18 hours in April, followed by 17 hours availability in September and October. Arguably, the CQ World Wide Contest Committee picked the very best month for higher-frequency propagation when they chose October for the Phone portion of that contest.

You can easily see that even at a Very High level of solar activity, the summer months are not very good to work DX, particularly on east-west paths. For example, the 10-meter band is very rarely open from New England to Europe after the month of April, even when solar activity is at the highest levels possible. Things pick up after September, even for a Medium level of solar activity. Again, October looks like the most fruitful month in terms of the number of hours 10 meters is open to Europe under all levels of solar conditions.

Ten meters is open more regularly on north-south paths, such as from New England to South America or to southern Africa. It is open as much as 10 hours a day during March and October to deep South America, and 7 hours a day in October to Africa—even during the lowest parts of the solar cycle. (Together with the sporadic-E propagation that 10 meters enjoys during the summer, this band can often be a lot of fun even during the sunspot doldrums. You just have to *be operating* on the band, rather than avoiding it because you know the sunspots are "spotty!")

Now, look at the 20-meter band in Table 6. From New England, twenty is open to somewhere in South America for 24 hours a day, no matter the level of solar activity. Note that Table 6 doesn't predict the level of signals available; it just shows that the band is open with a signal strength greater than 0 on the S meter. Look back at Summary Table 4 for the predicted signal strengths in January at a Very Low level of solar activity. There, you can see that the signal strength from New England into deep South America is always S8 or greater for a big gun station. A lot of the time during the night the band sounds dead, simply because everyone is either asleep or operating on a lower frequency.

For the 40-meter band in Table 6, during the month of January the band is open to Europe for 24 hours a day, whatever the level of solar activity is. Look now at Table 4, and you'll see that the predicted level for Very Low solar activity varies from S4 to S9. Local QRM or QRN would probably disrupt communications on 40 meters in Europe for stateside signals weaker than perhaps S3 or S4. Even though you might well be able to hear Europeans from New England during the day, they probably won't hear you because of local conditions, including local S9+ European stations and atmospheric noise from nearby thunderstorms. New England stations with big antennas can often hear Europeans on 40 meters as early as noontime, but must wait until the late afternoon before the Europeans can hear them above their local noise and QRM.

Let's say that you want to boost your country total on 80 meters by concentrating on stations in the South Pacific. The best months would be from November to

Table 6

The number of hours per day when a particular band is open to the target geographic areas in Table 4, as related to the level of solar activity (Very Low, Medium and Very High). This table is customized for Boston to the rest of the world. Some paths are open 24 hours a day, plus or minus QRM and local QRN, no matter what the level of solar activity is. See CD-ROM for other transmitting locations.

MA (Boston)
Hours Open to Each Region for Very-Low/Medium/Very-High SSNs

80 Meters:

Month	Europe	Far East	So. Amer.	Africa	So. Asia	Oceania	No. Amer.
Jan	17/17/16	5/ 4/ 3	17/17/16	16/16/15	8/ 7/ 5	11/10/ 9	24/24/24
Feb	17/16/15	3/ 3/ 2	17/16/16	15/15/14	6/ 4/ 4	10/ 9/ 9	24/24/24
Mar	15/15/14	3/ 2/ 1	16/16/15	15/13/13	4/ 4/ 3	9/ 8/ 7	24/24/24
Apr	13/13/12	1/ 0/ 0	16/16/14	13/13/13	3/ 3/ 1	9/ 8/ 7	24/24/24
May	12/11/10	0/ 0/ 0	16/15/14	12/11/10	2/ 1/ 1	7/ 6/ 6	24/24/24
Jun	10/ 9/ 8	0/ 0/ 0	14/14/14	11/10/10	1/ 1/ 0	6/ 5/ 5	24/24/24
Jul	11/11/ 9	0/ 0/ 0	15/14/14	11/11/11	2/ 1/ 1	7/ 6/ 5	24/24/24
Aug	13/11/11	0/ 0/ 0	16/16/14	13/12/11	3/ 2/ 1	7/ 7/ 6	24/24/24
Sep	14/13/11	2/ 1/ 0	17/16/14	13/13/12	4/ 4/ 2	9/ 8/ 8	24/24/24
Oct	15/15/13	3/ 2/ 1	17/17/16	14/14/13	5/ 4/ 4	9/ 9/ 7	24/24/24
Nov	17/17/15	4/ 4/ 2	17/17/16	16/15/14	8/ 7/ 4	11/10/ 9	24/24/24
Dec	19/18/17	7/ 6/ 4	18/18/17	16/16/16	11/ 9/ 7	12/11/11	24/24/24

40 Meters:

Month	Europe	Far East	So. Amer.	Africa	So. Asia	Oceania	No. Amer.
Jan	24/24/24	15/16/15	24/24/21	21/20/19	21/21/19	19/18/15	24/24/24
Feb	24/24/21	13/11/11	24/23/20	20/19/18	19/19/17	16/15/14	24/24/24
Mar	23/22/19	10/ 9/ 7	24/21/18	19/17/17	17/17/13	13/13/13	24/24/24
Apr	21/19/18	8/ 6/ 4	22/20/18	17/16/15	16/11/ 8	13/13/11	24/24/24
May	19/17/17	5/ 4/ 3	22/18/17	17/16/14	9/ 8/ 5	12/11/10	24/24/24
Jun	17/15/13	4/ 2/ 2	22/18/16	16/15/14	7/ 5/ 5	11/10/ 9	24/24/24
Jul	18/16/15	5/ 4/ 2	24/18/17	17/15/14	8/ 7/ 5	12/11/10	24/24/24
Aug	19/17/16	7/ 5/ 4	24/19/18	18/16/15	11/10/ 6	13/12/11	24/24/24
Sep	22/21/17	9/ 8/ 5	23/20/18	18/17/16	14/11/ 7	13/13/12	24/24/24
Oct	24/23/20	12/11/ 8	24/23/19	20/18/17	17/16/14	16/13/13	24/24/24
Nov	24/24/22	14/13/12	24/24/20	21/19/18	21/20/17	17/17/13	24/24/24
Dec	24/24/24	18/19/22	24/24/21	23/21/19	24/23/22	21/19/18	24/24/24

February in terms of the number of hours per day when the 80-meter band is open to Oceania. You can see by reading across the line for each month that the level of solar activity is not hugely important on 80 meters to any location. Common experience (backed by the statistical information in Table 6) is that the 80-meter band is open only marginally longer when sunspots are low.

This is true to a greater extent on 40 meters. Thus you may hear the generalization that the low bands tend to be better during periods of low solar activity, while the upper HF bands (above 10 MHz) tend to be better when the sun is more active.

Table 6 can give you a good handle on what months are the most productive for DXing and contesting. It should be no surprise to most veteran operators that the fall and winter months are the best times to work DX.

20 Meters:

Month	Europe	Far East	So. Amer.	Africa	So. Asia	Oceania	No. Amer.
Jan	13/16/22	15/22/22	24/24/24	20/21/21	18/20/22	18/23/22	24/24/24
Feb	12/18/23	13/21/24	24/24/24	22/22/24	15/21/24	18/23/24	24/24/24
Mar	15/18/24	17/20/24	24/24/24	22/24/24	18/21/24	16/24/24	24/24/24
Apr	15/20/24	19/22/24	24/24/24	21/24/24	19/22/24	18/24/24	24/24/24
May	19/23/24	22/24/24	24/24/24	23/24/24	23/24/24	21/24/24	24/24/24
Jun	22/24/24	24/24/24	24/24/24	24/24/24	24/24/24	24/24/24	24/24/24
Jul	19/24/24	24/24/24	24/24/24	21/24/24	24/24/24	23/24/24	24/24/24
Aug	15/20/24	20/24/24	24/24/24	20/24/24	20/24/24	19/24/24	24/24/24
Sep	16/19/24	17/21/24	24/24/24	21/24/24	18/21/24	17/24/24	24/24/24
Oct	15/21/24	16/20/24	24/24/24	22/24/24	19/22/24	17/24/24	24/24/24
Nov	14/20/23	14/22/24	24/24/24	20/24/24	17/21/24	19/23/24	24/24/24
Dec	11/17/24	13/22/24	24/24/24	17/23/24	12/22/24	16/24/24	24/24/24

15 Meters:

Month	Europe	Far East	So. Amer.	Africa	So. Asia	Oceania	No. Amer.
Jan	4/ 6/ 7	2/ 9/13	12/15/16	9/13/13	3/ 4/ 7	9/12/13	24/15/16
Feb	4/ 7/12	4/10/14	13/18/23	11/13/16	3/ 7/13	8/13/15	22/16/19
Mar	6/ 9/14	2/13/15	14/21/24	13/17/22	5/11/17	10/14/17	15/16/23
Apr	0/10/18	3/13/18	15/23/24	15/18/24	9/15/19	11/15/21	16/16/24
May	1/13/16	6/10/19	17/20/24	14/18/24	13/17/18	10/16/19	20/19/24
Jun	0/ 2/16	0/ 9/15	16/21/24	14/18/24	5/15/18	10/12/20	24/22/22
Jul	0/ 2/16	0/ 5/18	15/19/24	12/18/24	0/12/18	4/12/20	24/22/21
Aug	0/ 2/14	0/ 8/17	14/18/22	13/16/22	0/12/17	6/10/19	22/19/21
Sep	1/10/17	6/13/17	14/16/24	13/17/22	9/14/17	9/14/17	16/16/22
Oct	7/11/17	10/13/17	12/16/22	12/15/22	7/12/17	12/13/15	18/15/22
Nov	5/ 8/14	8/11/14	12/16/22	11/14/17	3/ 7/16	10/13/15	20/16/21
Dec	3/ 6/ 9	2/10/13	12/15/23	8/13/15	2/ 4/12	9/12/14	24/15/18

10 Meters:

Month	Europe	Far East	So. Amer.	Africa	So. Asia	Oceania	No. Amer.
Jan	0/ 1/ 4	0/ 1/ 8	6/11/13	0/ 7/10	0/ 1/ 3	0/ 3/11	23/24/24
Feb	0/ 2/ 7	0/ 2/10	8/12/14	0/ 9/13	0/ 3/ 5	0/ 7/13	24/24/24
Mar	0/ 0/ 8	0/ 1/10	10/14/20	1/11/14	0/ 0/ 8	0/ 7/13	23/24/24
Apr	0/ 0/ 8	0/ 0/ 8	7/14/21	0/12/17	0/ 0/13	0/ 5/11	18/24/24
May	0/ 0/ 0	0/ 0/ 1	7/12/20	1/10/17	0/ 1/12	0/ 2/11	17/20/22
Jun	0/ 0/ 0	0/ 0/ 0	7/11/18	0/ 3/17	0/ 0/ 0	0/ 0/ 2	21/19/23
Jul	0/ 0/ 0	0/ 0/ 0	2/ 9/19	0/ 2/18	0/ 0/ 7	0/ 0/ 6	16/16/24
Aug	0/ 0/ 0	0/ 0/ 0	2/10/17	0/ 1/16	0/ 0/10	0/ 0/ 8	17/17/24
Sep	0/ 0/ 8	0/ 1/10	7/13/18	0/11/16	0/ 0/10	0/ 2/ 9	19/24/24
Oct	0/ 5/ 9	0/ 2/11	10/12/16	7/12/14	0/ 5/ 9	0/ 8/12	24/24/24
Nov	0/ 4/ 8	0/ 3/11	9/12/15	5/10/13	0/ 3/ 6	4/10/12	24/24/24
Dec	0/ 3/ 6	0/ 1/ 8	8/11/13	1/ 8/12	0/ 1/ 4	2/ 7/12	23/23/24

Do-It-Yourself Propagation Prediction

Very reliable methods of determining the MUF for any given radio path have been developed over the last 50 years. As discussed previously, these methods are all based on the smoothed sunspot number (SSN) as the measure of solar activity. It is for this reason that smoothed sunspot numbers hold so much meaning for radio amateurs and others concerned with radio-wave propagation—they are the link to past (and future) propagation conditions.

Early on, the prediction of propagation conditions required tedious work with numerous graphs, along with charts of frequency contours overlaid, or overprinted, on world maps. The basic materials were available from an agency of the US government. Monthly publications provided the frequency-contour data a few months in advance. Only rarely did amateurs try their hand at predicting propagation conditions using these hard-to-use methods.

Today's powerful PCs have given the amateur wonderful tools to make quick-and-easy HF propagation predictions, whether for a contest or a DXpedition. The summary and detailed prediction tables described earlier in this chapter were generated using *CAPMan*, a modernized version of the mainframe *IONCAP* program, on a PC.

While tremendously useful to setting up schedules and for planning strategy for contests, both the Summary and Detailed prediction tables located on the CD-ROM accompanying this book show signal strength. They do not show

Table 7
Features and Attributes of Propagation Prediction Programs

	ASAPS V. 4	*CAPMan*	*VOACAP Windows*	*ACE-HF*	*W6ELProp V. 2.70*	*WinCAP Wizard 2*	*PropLab Pro*
User Friendliness	Good	Good	Good	Excellent	Good	Good	Poor
Operating System	Windows	DOS	Windows	Windows	Windows	Windows	DOS
Uses k or A index	No	Yes	No	No	Yes	Yes	Yes
User library of QTHs	Yes	Yes	Yes	Yes-RX	Yes	Yes	No
Bearings, distances	Yes	Yes	Yes	Yes	Yes	Yes	Yes
MUF calculation	Yes	Yes	Yes	Yes	Yes	Yes	Yes
LUF calculation	Yes	Yes	Yes	Yes	No	Yes	Yes
Wave angle calculation	Yes	Yes	Yes	Yes	Yes	Yes	Yes
Vary minimum wave angle	Yes	Yes	Yes	Yes	Yes	Yes	Yes
Path regions and hops	Yes	Yes	Yes	Yes	Yes	Yes	Yes
Multipath effects	Yes	Yes	Yes	Yes	No	Yes	Yes
Path probability	Yes	Yes	Yes	Yes	Yes	Yes	Yes
Signal strengths	Yes	Yes	Yes	Yes	Yes	Yes	Yes
S/N ratios	Yes	Yes	Yes	Yes	No	Yes	Yes
Long-path calculation	Yes	Yes	Yes	Yes	Yes	Yes	Yes
Antenna selection	Yes	Yes	Yes	Yes	Indirectly	Isotropic	Yes
Vary antenna height	Yes	Yes	Yes	Yes	Indirectly	No	Yes
Vary ground characteristics	Yes	Yes	Yes	Yes	No	No	No
Vary transmit power	Yes	Yes	Yes	Yes	Indirectly	Yes	Yes
Graphic displays	Yes	Yes	Yes	Yes	Yes	Yes	2D/3D
UT-day graphs	Yes	Yes	Yes	Yes	Yes	Yes	Yes
Area Mapping	No	Yes	Yes	Yes	Yes	No	Yes
Documentation	Yes	Yes	On-line	Yes	Yes	Yes	Yes
Price class	$275+	$89	free†	$99	free§	$29.95+	$150††

Price classes are for late 2003 and subject to change.
†Available on the World Wide Web: **elbert.its.bldrdoc.gov/hf.html**
§Available on the World Wide Web at: **www.qsl.net/w6elprop/**
+ Shipping and handling extra.
††Available on the World Wide Web: **www.spacew.com/www/proplab.html**

other information that is also in the underlying databases used to generate them. They don't, for example, show the dominant elevation angles and neither do they show reliability statistics. You may want to run propagation-prediction software yourself to get into the really "nitty-gritty" details.

Modern programs are designed for quick-and-easy predictions of propagation parameters. See **Table 7** for a listing of a number of popular programs. The basic input information required is the smoothed sunspot number (SSN) or smoothed solar flux, the date (month and day), and the latitudes and longitudes at the two ends of the radio path. The latitude and longitude, of course, are used to determine the great-circle radio path. Most commercial programs tailored for ham use allow you to specify locations by the call sign. The date is used to determine the latitude of the Sun, and this, with the sunspot number, is used to determine the properties of the ionosphere at critical points on the path.

Of course, just because a computer program predicts that a band will be open on a particular path, it doesn't follow that the Sun and the ionosphere will always cooperate! A sudden solar flare can result in a major geomagnetic storm, taking out HF communication anywhere from hours to days. There is still art, as well as a lot of science, in predicting propagation. In times of quiet geomagnetic activity, however, the prediction programs are good at forecasting band openings and closings.

Obtaining Sunspot Number/Solar Flux Data

After you have chosen and then set up a computer program for evaluation of a particular path, you will still need the sunspot number or solar flux level for the period in question. A caution must be stated here—for best accuracy and consistency, use the average of solar flux values taken from actual observations, perhaps from WWV/WWVH, over the previous three or four days. Many amateur packet systems archive WWV flux numbers (plus planetary k_p and A_p indices). Solar flux numbers can vary dramatically from day to day, but the Earth's ionosphere is relatively slow to respond to instantaneous changes in solar radiation. This caveat also

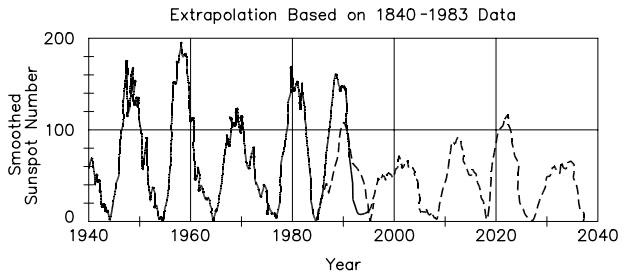

Fig 42—Smoothed sunspot number, with predictions, from 1940 to 2040. This was extrapolated based on data from 1840 to 1983. Cycle 22 actually peaked in Nov 1989, at a monthly smoothed sunspot number of 158. Propagation on the higher frequencies throughout the peak of Cycle 22 was good to excellent, since the monthly smoothed sunspot number stayed at 100 or above from July 1988 through May 1992. (*Courtesy of Naval Ocean Systems Center,* San Diego.)

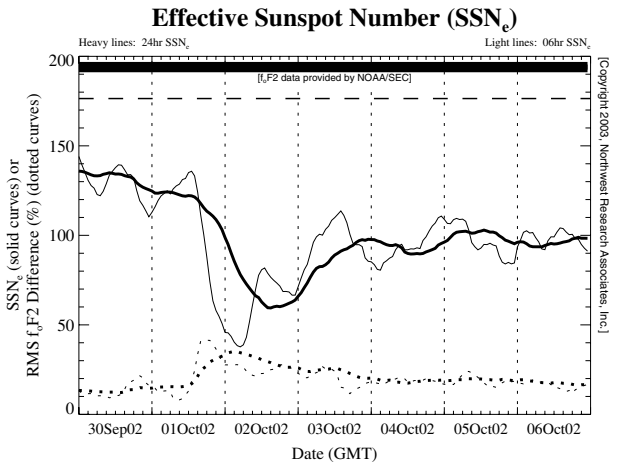

Fig 43—Effective Sunspot Number (SSN$_e$) produced by NWRA. Note large drop in effective SSN due to a geomagnetic storm commencing Oct 1, 2002. (*Courtesy of Northwest Research Associates.*)

holds for sunspot numbers derived, using Fig 18, from WWV/WWVH solar flux numbers.

Fig 42 shows a graph produced in the early 1980s of smoothed sunspot numbers for Solar Cycles 17 through 21, with predictions for Cycles 22 through 26. The graph covers a period of 100 years, from 1940 to 2040, and may be used for making long-term or historical calculations. Just remember that the graph shows smoothed numbers. The solar activity at any given time can be significantly lower or significantly higher than the graph indicates. In fact, Cycle 22 peaked at the end of 1989, as predicted, but with a monthly smoothed sunspot level of 158, quite a bit higher than predicted. Cycle 23 peaked in early 2002 at a level of about 115, a considerably higher level than the predicted value.

WWV PROPAGATION DATA

For the most current data on what the Sun is doing, National Institute of Standards and Technology stations WWV and WWVH broadcast information on solar activity at 18 and 45 minutes past each hour, respectively. These propagation bulletins give the solar flux, geomagnetic A-Index, Boulder K-Index, and a brief statement of solar and geomagnetic activity in the past and coming 24-hour periods, in that order. The solar flux and A-Index are changed daily with the 2118 UT bulletin, the rest every three hours—0018, 0318, 0618 UT and so on. On the Web, up-to-date WWV information can be found at: **ftp://ftp.sel.noaa.gov/pub/latest/wwv.txt** or on the NOAA Web page **www.sec.noaa.gov/**.

Some other useful Web sites are: **dx.qsl.net/propagation/**, **www.dxlc.com/solar**, **hfradio.org/propagation.html**. The Solar Terrestrial Dispatch page contains a wealth of propagation-related information: **www.spacew.com/**. You may also access propagation information on your local PacketCluster. Use the command SH/WWV/*n*, where *n* is the number of spots you wish to see (five is the default).

Another excellent method for obtaining an "equivalent sunspot number" (SSN$_e$) is to go to the Space Weather site of Northwest Research Services: **www.nwra-az.com/spawx/ssne24.html**. NWRA compares real-time ionospheric sounder data around the world with predictions using various levels of SSN looking for the best match. They thus "back into" the actual effective sunspot number. **Fig 43** is a typical NWRA graph, which covers the week ending 6 October 2002. Note the sudden decrease in SSN$_e$ after a geomagnetic storm depressed SSN$_e$ by more than 50%.

The A-Index

The WWV/WWVH A-Index is a daily figure for the state of activity of the Earth's magnetic field. It is updated with the 2118/2145 UT bulletin. The A-Index tells you mainly how yesterday was, but it is very revealing when charted regularly, because geomagnetic disturbances nearly always recur at four-week intervals.

The K-Index

The K-Index (new every three hours) reflects Boulder readings of the Earth's geomagnetic field in the hours just preceding the bulletin data changes. It is the nearest thing to current data on radio propagation available. With new data every three hours, K-Index trend is important. Rising is bad news; falling is good, especially related to propagation on paths involving latitudes above 30° north. Because this is a Boulder, Colorado, reading of geomagnetic activity, it may not correlate closely with conditions in other areas.

The K-Index is also a timely clue to aurora possibilities. Values of 4, and rising, warn that conditions associated with

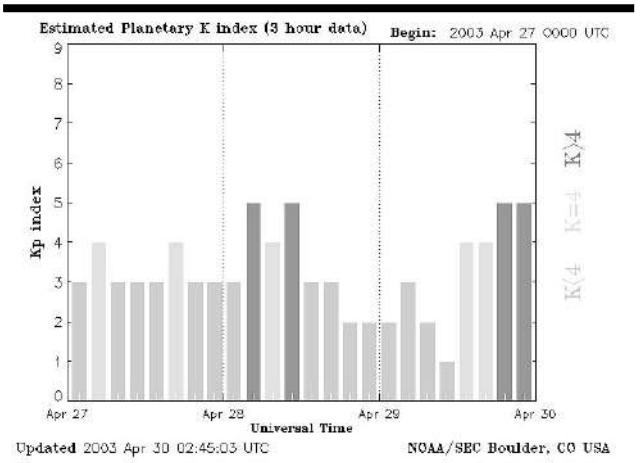

Fig 44—Plot of the estimated planetary k index, K_p, for the last four days. (*Courtesy NOAA/SEC.*)

auroras and degraded HF propagation are present in the Boulder area at the time of the bulletin's preparation. A NOAA Web site that carries up-to-date planetary K_p data is: **www.sel.noaa.gov/ftpmenu/plots/2003_plots/kp.html**. **Fig 44** is a graph from this Web site for four days starting 27 April 2003 to 30 April 2003. This was a period of significant geomagnetic activity, indicated by K_p indices of 5 and 4.

BIBLIOGRAPHY

Source material and more extended discussion of topics covered in this chapter can be found in the references given below.

E. V. Appleton and W.R. Piggott, "Ionospheric Absorption Measurements during a Sunspot Cycle," *J. Atmos. Terr. Phys.*, Vol 3, p 141, 1954.

D. Bilitiza, *International Reference Ionosphere (IRI 90)*, National Space Science Data Center, Greenbelt, MD, 1990.

D. Bray, "Method of Determining VHF/HF Station Capabilities," *QST*, Nov 1961.

A. Brekke, "Physics of the Upper Polar Atmosphere," (John Wiley and Sons: New York, 1997).

R. R. Brown, "Demography, DXpeditions and Magneto-Ionic Theory," *The DX Magazine*, Vol. X, No. 2, p 44, Mar/Apr 1998.

R. R. Brown, *The Little Pistol's Guide to HF Communication* (Sacramento: WorldRadio Books, 1996).

R. R. Brown, "Signal Ducting on the 160 Meter Band," *Communications Quarterly*, p 65, Spring 1998.

R. R. Brown, "Unusual Low-Frequency Signal Propagation at Sunrise," *Communications Quarterly*, p 67, Fall 1998.

R. R. Brown,, "Atmospheric Ozone, a Meteorological Factor in Low-Frequency and 160 Meter Propagation," *Communications Quarterly*, Spring 1999.

K. Davies, *Ionospheric Radio* (London: Peter Peregrinus Ltd, 1990). Excellent technical reference.

R. Garcia, S. Solomon, S. Avery, G. C. Reid, "Transport of Nitric Oxide and the D-Region Winter Anomaly," *J. Geophys. Res.*, Vol 92, p 977, 1987.

J. Hall, "Propagation Predictions and Personal Computers," Technical Correspondence, *QST*, Dec 1990, pp 58-59 (description of *IONCAP* as used for ARRL. publications).

E . Harper, *Rhombic Antenna Design* (New York: D. Van Nostrand Co, Inc, 1941).

H. Hertz, *Electric Waves*, translated by D. E. Jones (London: MacMillan, 1893).

R. D. Hunsucker, *Radio Techniques for Probing the Terrestrial Ionosphere* (New York: Springer-Verlag).

R. D. Hunsucker, J. K. Hargreaves, *The High Latitude Ionosphere and Its Effects on Radio Propagation* (Cambridge: Cambridge University Press, 2003).

W. D. Johnston, Computer-calculated and computer-drawn great-circle maps are offered. An 11 × 14-inch map is custom made for your location. Write to K5ZI, PO Box 640, Organ, NM 88052, tele 505-382-7804.

T.L. Killeen, R.M. Johnsson, "Upper Atmospheric Waves, Turbulence, and Winds: Importance for Mesospheric and Thermospheric Studies," **earth.agu.org/revgeophys/killee00/killee00.html**.

J. L. Lynch, "The Maunder Minimum," *QST*, Jul 1976, pp 24-26.

J. C. Maxwell, *A Treatise on Electricity and Magnetism*, Vols I and II (Oxford: Oxford University Press, 1873).

M. W. Maxwell, *Reflections—Transmission Lines and Antennas* (Newington, CT: ARRL, 1990) [out of print].

M. W. Maxwell, *Reflections II—Transmission Lines and Antennas* (Sacramento, CA: 2001).

L. F. McNamara, *The Ionosphere: Communications, Surveillance, and Direction Finding* (Malabar, FL: Krieger Publishing Company, 1991). Another excellent technical reference on propagation.

L. F. McNamara, *Radio Amateur's Guide to the Ionosphere* (Malabar, FL: Krieger Publishing Company, 1994). Excellent, quite-readable text on HF propagation.

A. K. Paul, "Medium Scale Structure of the F Region," *Radio Science*, Volume 24, No. 3, p. 301, 1989.

W. R. Piggott, K. Rawer, "URSI Handbook of Ionogram Interpretation and Reduction," Report UAG-50. World Data Center A for Solar-Terrestrial Physics, Boulder, CO, 1975.

E. Pocock, "Sporadic-E Propagation at VHF: A Review of Progress and Prospects," *QST*, Apr 1988, pp 33-39.

E. Pocock, "Auroral-E Propagation at 144 MHz," *QST*, Dec 1989, pp 28-32.

E. Pocock, "Propagation Forecasting During Solar Cycle 22," *QST*, Jun 1989, pp 18-20.

G. C. Reid, "Ion Chemistry of the D-region," *Advances in Atomic and Molecular Physics*, Vol 12, Academic Press, 1976.

R. B. Rose, "MINIMUF: A Simplified MUF-Prediction Program for Microcomputers," *QST*, Dec 1982, pp 36-38

M. L. Salby, "Fundamentals of Atmospheric Physics," (Academic Press: Boulder, CO, 1996).

S. C. Shallon, W6EL: *MINIPROP PLUS*, a commercially prepared program written for Amateur Radio users; 11058 Queensland St, Los Angeles, CA 90034-3029.

R. D. Straw, *All the Right Angles* (New Bedford, PA: LTA, 1993). Out of print.

R. D. Straw, "*ASAPS* and *CAPMAN*: HF Propagation-Prediction Software for the IBM PC," *QST*, Dec 1994, pp 79-81.

R. D. Straw, "Heavy-Duty HF Propagation-Prediction/Analysis Software," Part 1: *QST*, Sep 1996, pp 28-32; Part 2: *QST*, Oct 1996, pp 28-30.

Chapter 27

Antenna and Transmission-Line Measurements

The principal quantities measured on transmission lines are line current or voltage, and standing-wave ratio (SWR). You make measurements of current or voltage to determine the power input to the line. SWR measurements are useful in connection with the design of coupling circuits and the adjustment of the match between the antenna and transmission line, as well as in the adjustment of these matching circuits.

For most practical purposes a relative measurement is sufficient. An uncalibrated indicator that shows when the largest possible amount of power is being put into the line is just as useful, in most cases, as an instrument that measures the power accurately. It is seldom necessary to know the actual number of watts going into the line unless the overall efficiency of the system is being investigated. An instrument that shows when the SWR is close to 1:1 is all you need for most impedance-matching adjustments. Accurate measurement of SWR is necessary only in studies of antenna characteristics such as bandwidth, or for the design of some types of matching systems, such as a stub match.

Quantitative measurements of reasonable accuracy demand good design and careful construction in the measuring instruments. They also require intelligent use of the equipment, including a knowledge not only of its limitations but also of stray effects that often lead to false results. Until you know the complete conditions of the measurements, a certain amount of skepticism regarding numerical data resulting from amateur measurements with simple equipment is justified. On the other hand, purely qualitative or relative measurements are easy to make and are reliable for the purposes mentioned above.

LINE CURRENT AND VOLTAGE

A current or voltage indicator that can be used with coaxial line is a useful piece of equipment. It need not be elaborate or expensive. Its principal function is to show when the maximum power is being taken from the transmitter; for any given set of line conditions (length, SWR, etc). This will occur when you adjust the transmitter coupling for maximum current or voltage into the transmission line. Although the final-amplifier plate or collector current meter is frequently used for this purpose, it is not always a reliable indicator. In many cases, particularly with a screen-grid tube in the final stage, minimum loaded plate current does not occur simultaneously with maximum power output.

RF VOLTMETER

You can put together a germanium diode in conjunc-

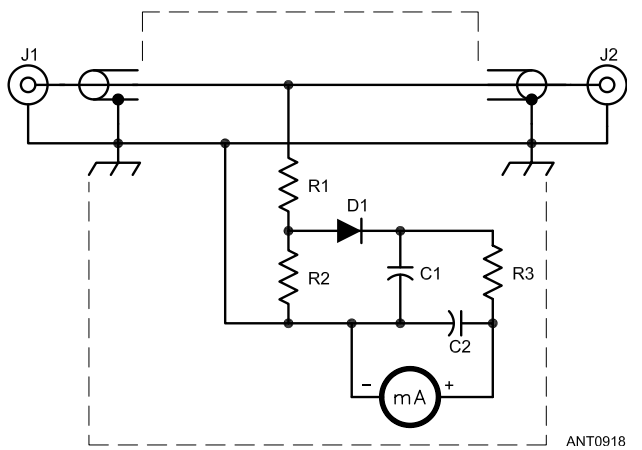

Fig 1—RF voltmeter for coaxial line.
C1, C2—0.005- or 0.01-µF ceramic.
D1—Germanium diode, 1N34A.
J1, J2—Coaxial fittings, chassis-mounting type.
M1—0-1 milliammeter (more sensitive meter may be used if desired; see text).
R1—6.8 kΩ, composition, 1 W for each 100 W of RF power.
R2—680 Ω, 1/2 or 1 W composition.
R3—10 kΩ, 1/2 W (see text).

tion with a low-range milliammeter and a few resistors to form an RF voltmeter suitable for connecting across the two conductors of a coaxial line, as shown in **Fig 1**. It consists of a voltage divider, R1-R2, having a total resistance about 100 times the Z_0 of the line (so the power consumed will be negligible) with a diode rectifier and milliammeter connected across part of the divider to read relative RF voltage. The purpose of R3 is to make the meter readings directly proportional to the applied voltage, as nearly as possible, by swamping the resistance of D1, since the diode resistance will vary with the amplitude of the current through the diode.

You may construct the voltmeter in a small metal box, indicated by the dashed line in the drawing, and fitted with coax receptacles. R1 and R2 should be carbon-composition resistors. The power rating for R1 should be 1 W for each 100 W of carrier power in the matched line; separate 1- or 2-W resistors should be used to make up the total power rating required, to the total resistance as given. Any type of resistor can be used for R3; the total resistance should be such that about 10 V dc will be developed across it at full scale. For example, a 0-1 milliammeter would require 10 kΩ, a 0-500 microammeter would take 20 kΩ, and so on. For comparative measurements only, R3 may be a variable resistor so the sensitivity can be adjusted for various power levels.

In constructing such a voltmeter, you should exercise care to prevent inductive coupling between R1 and the loop formed by R2, D1 and C1, and between the same loop and the line conductors in the assembly. With the lower end of R1 disconnected from R2 and grounded to the enclosure, but without changing its position with respect to the loop, there should be no meter indication when full power is going through the line.

If more than one resistor is used for R1, the units should be arranged end-to-end with very short leads. R1 and R2 should be kept 1/2 inch or more from metal surfaces parallel to the body of the resistor. If you observe these precautions the voltmeter will give consistent readings at frequencies up to 30 MHz. Stray capacitance and stray coupling limit the accuracy at higher frequencies but do not affect the utility of the instrument for comparative measurements.

Calibration

You may calibrate the meter for RF voltage by comparison with a standard such as an RF ammeter. This requires that the line be well matched so the impedance at the point of measurement is equal to the actual Z_0 of the line. Since in that case $P = I^2Z_0$, the power can be calculated from the current. Then $E=\sqrt{PZ_0}$. By making current and voltage measurements at a number of different power levels, you can obtain enough points to draw a calibration curve for your particular setup.

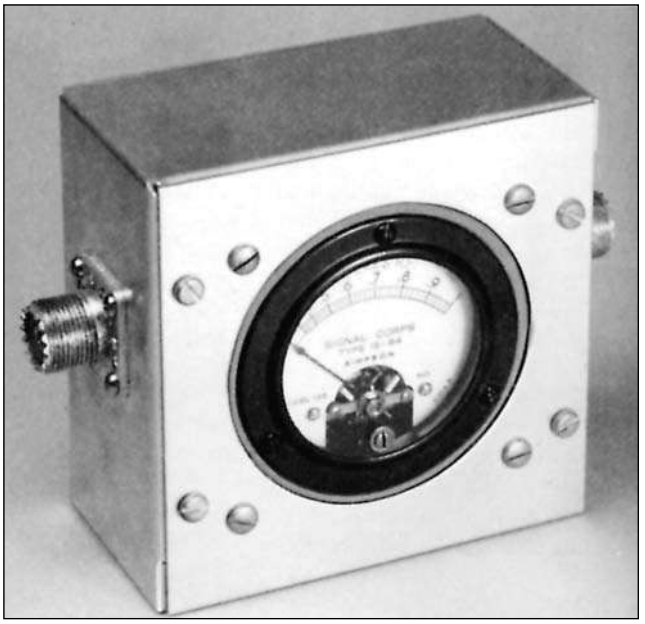

Fig 2—A convenient method of mounting an RF ammeter for use in a coaxial line. This is a metal-case instrument mounted on a thin bakelite panel. The cutout in the metal clears the edge of the meter by about 1/8 inch.

RF AMMETERS

Although they are not as widely available as they used to be, if you can find one on the surplus market or at a hamfest, an RF ammeter is a good way to gauge output power. You can mount an RF ammeter in any convenient location at the input end of the transmission line, the principal precaution being that the capacitance to ground, chassis, and nearby conductors should be low. A bakelite-case instrument can be mounted on a metal panel without introducing enough shunt capacitance to ground to cause serious error up to 30 MHz. When installing a metal-case instrument on a metal panel, you should mount it on a separate sheet of insulating material so that there is 1/8 inch or more separation between the edge of the case and the metal.

A 2-inch instrument can be mounted in a 2 × 4 × 4-inch metal box, as shown in **Fig 2**. This is a convenient arrangement for use with coaxial line. Installed this way, a good quality RF ammeter will measure current with an accuracy that is entirely adequate for calculating power in the line. As discussed above in connection with calibrating RF voltmeters, the line must be closely matched by its load so the actual impedance is resistive and equal to Z_0. The scales of such instruments are cramped at the low end, however, which limits the range of power that can be measured by a single meter. The useful current range is about 3 to 1, corresponding to a power range of about 9 to 1.

SWR Measurements

On parallel-conductor lines it is possible to measure the standing-wave ratio by moving a current (or voltage) indicator along the line, noting the maximum and minimum values of current (or voltage) and then computing the SWR from these measured values. This cannot be done with coaxial line since it is not possible to make measurements of this type inside the cable. The technique is, in fact, seldom used with open lines because it is not only inconvenient but sometimes impossible to reach all parts of the line conductors. Also, the method is subject to considerable error from antenna currents flowing on the line.

Present-day SWR measurements made by amateurs practically always use some form of *directional coupler* or RF-bridge circuit. The indicator circuits themselves are fundamentally simple, but they require considerable care in construction to ensure accurate measurements. The requirements for indicators used only for the adjustment of impedance-matching circuits, rather than actual SWR measurement, are not so stringent, and you can easily make an instrument for this purpose.

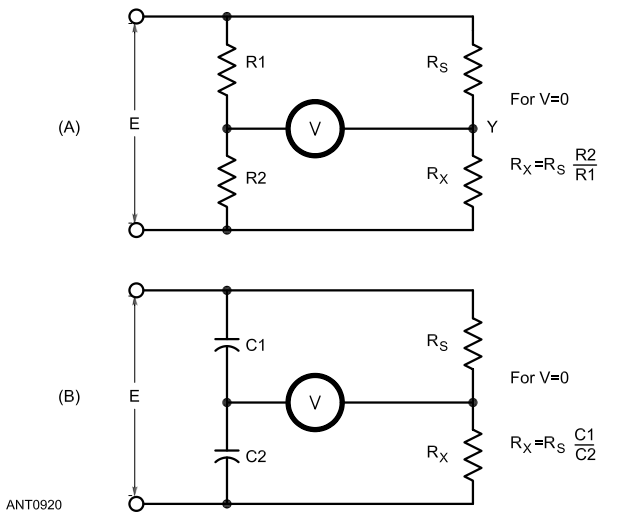

Fig 3—Bridge circuits suitable for SWR measurement. At A, Wheatstone type using resistance arms. At B, capacitance-resistance bridge ("Micromatch"). Conditions for balance are independent of frequency in both types.

BRIDGE CIRCUITS

Two commonly used bridge circuits are shown in **Fig 3**. The bridges consist essentially of two voltage dividers in parallel, with a voltmeter connected between the junctions of each pair of *arms*, as the individual elements are called. When the equations shown to the right of each circuit are satisfied there is no potential difference between the two junctions, and the voltmeter indicates zero voltage. The bridge is then said to be in *balance*.

Taking Fig 3A as an illustration, if R1 = R2, half the applied voltage, E, will appear across each resistor. Then if $R_S = R_X$, $^1/_2$E will appear across each of these resistors and the voltmeter reading will be zero. Remember that a matched transmission line has essentially a purely resistive input impedance. Suppose that the input terminals of such a line are substituted for R_X. Then if R_S is a resistor equal to the Z_0 of the line, the bridge will be balanced.

If the line is not perfectly matched, its input impedance will not equal Z_0 and hence will not equal R_S, since you chose the latter to be equal to Z_0. There will then be a difference in potential between points X and Y, and the voltmeter will show a reading. Such a bridge therefore can be used to show the presence of standing waves on the line, because the line input impedance will be equal to Z_0 only when there are no standing waves.

Considering the nature of the incident and reflected components of voltage that make up the actual voltage at the input terminals of the line, as discussed in Chapter 24, it should be clear that when $R_S = Z_0$, the bridge is always in balance for the incident component. Thus the voltmeter does not respond to the incident component at any time but reads only the reflected component (assuming that R2 is very small compared with the voltmeter impedance). The incident component can be measured across either R1 or R2, if they are equal resistances. The standing-wave ratio is then

$$SWR = \frac{E1+E2}{E1-E2} \qquad \text{(Eq 1)}$$

where E1 is the incident voltage and E2 is the reflected voltage. It is often simpler to normalize the voltages by expressing E2 as a fraction of E1, in which case the formula becomes

$$SWR = \frac{1+k}{1-k} \qquad \text{(Eq 2)}$$

where k = E2/E1.

The operation of the circuit in Fig 3B is essentially the same, although this circuit has arms containing reactance as well as resistance.

It is not necessary that R1 = R2 in Fig 3A; the bridge can be balanced, in theory, with any ratio of these two resistances provided R_S is changed accordingly. In practice, however, the accuracy is highest when the two are equal; this circuit is most commonly used.

A number of types of bridge circuits appear in **Fig 4**, many of which have been used in amateur products or amateur construction projects. All except that at G can have the generator and load at a common potential. At G, the generator and detector are at a common potential. You may interchange the positions of the detector and trans-

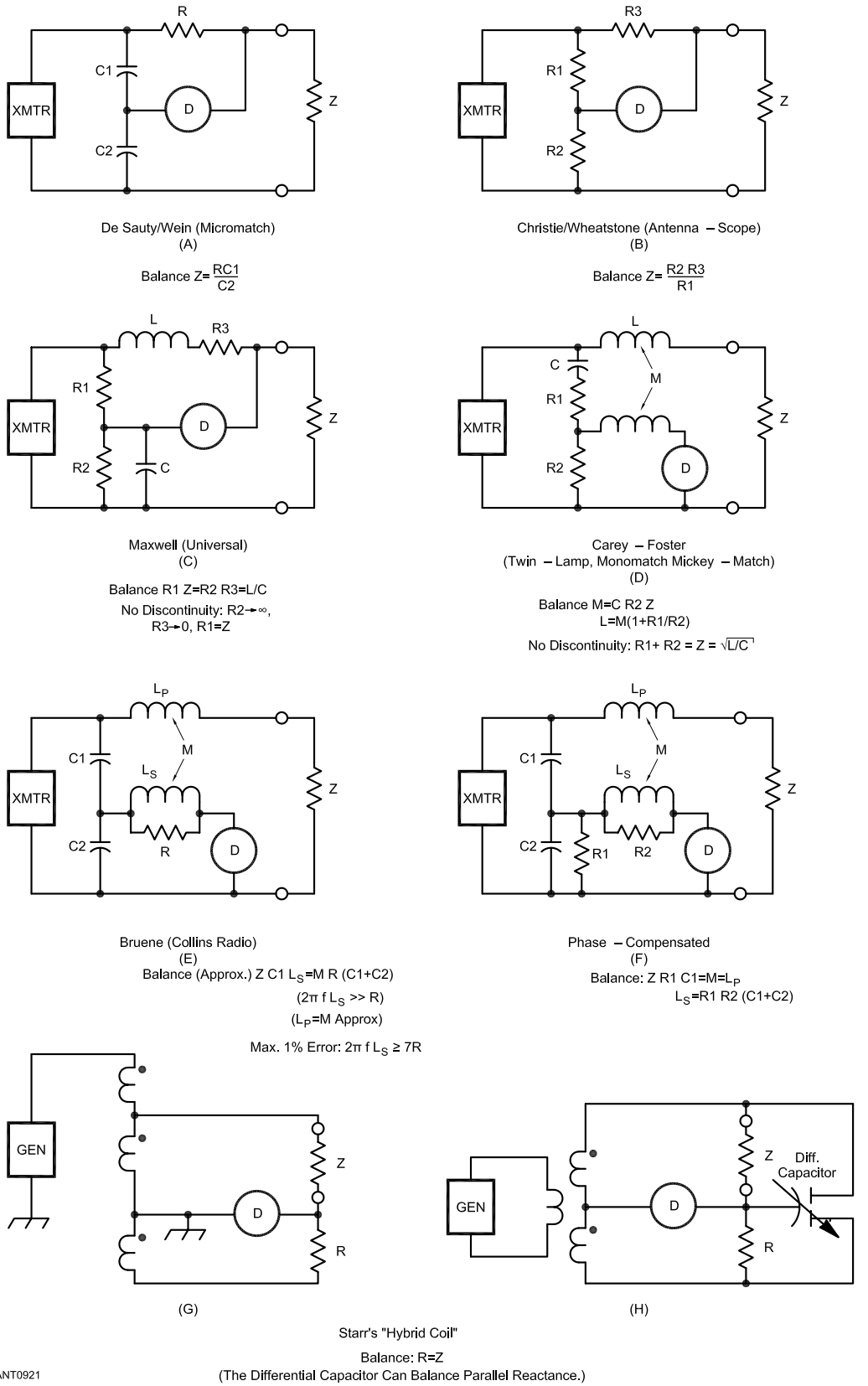

Fig 4—Various types of SWR indicator circuits and commonly known names of bridge circuits or devices in that they have been used. Detectors (D) are usually semiconductor diodes with meters, isolated with RF chokes and capacitors. However, the detector may be a radio receiver. In each circuit, Z represents the load being measured. (*This information provided by David Geiser, WA2ANU*)

mitter (or generator) in the bridge, and this may be advantageous in some applications.

The bridges shown at D, E, F and H may have one terminal of the generator, detector and load common. Bridges at A, B, E, F, G and H have constant sensitivity over a wide frequency range. Bridges at B, C, D and H may be designed to show no discontinuity (impedance lump) with a matched line, as shown in the drawing. Discontinuities with A, E and F may be small.

Bridges are usually most sensitive when the detector bridges the midpoint of the generator voltage, as in G or H, or in B when each resistor equals the load impedance. Sensitivity also increases when the currents in each leg are equal.

Resistance Bridge

The basic bridge configuration shown in Fig 3B may be home constructed and is reasonably accurate for SWR measurement. A practical circuit for such a bridge is given in **Fig 5** and a representative layout is shown in **Fig 6**. Properly built, a bridge of this design can be used for measurement of SWRs up to about 15:1 with good accuracy.

You should observe these important construction points:

1) Keep leads in the RF circuit short, to reduce stray inductance.
2) Mount resistors two or three times their body diameter away from metal parts, to reduce stray capacitance.
3) Place the RF components so there is as little inductive and capacitive coupling as possible between the bridge arms.

In the instrument shown in Fig 6, the input and line connectors, J1 and J2, are mounted fairly close together so the standard resistor, R_S, can be supported with short leads directly between the center terminals of the connectors. R2 is mounted at right angles to R_S, and a shield partition is used between these two components and the others.

The two 47-kΩ resistors, R5 and R6 in Fig 5, are voltmeter multipliers for the 0-100 microammeter used as an indicator. This is sufficient resistance to make the voltmeter linear (that is, the meter reading is directly proportional to the RF voltage) and no voltage calibration curve is needed. D1 is the rectifier for the reflected volt-

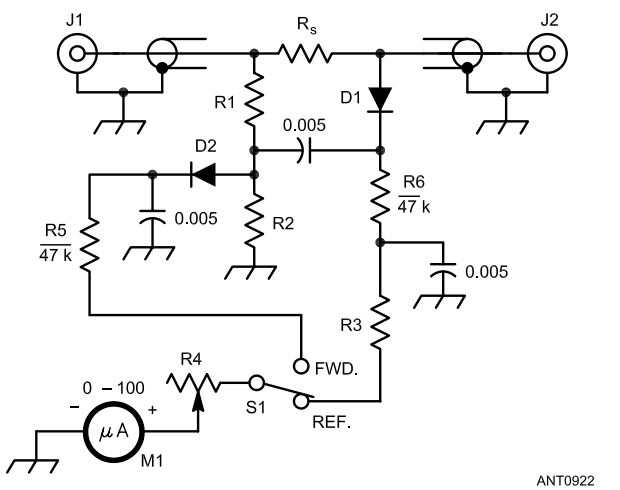

Fig 5—Resistance bridge for SWR measurement. Capacitors are disc ceramic. Resistors are ½-watt composition except as noted below.
D1, D2—Germanium diode, high back resistance type (1N34A, 1N270, etc).
J1, J2—Coaxial connectors, chassis-mounting type.
M1—0-100 dc microammeter.
R1, R2—47 Ω, ½-W composition (see text).
R3—See text.
R4—50-kΩ volume control.
R_S—Resistance equal to line Z_0 (½ or 1 W composition).
S1—SPDT toggle.

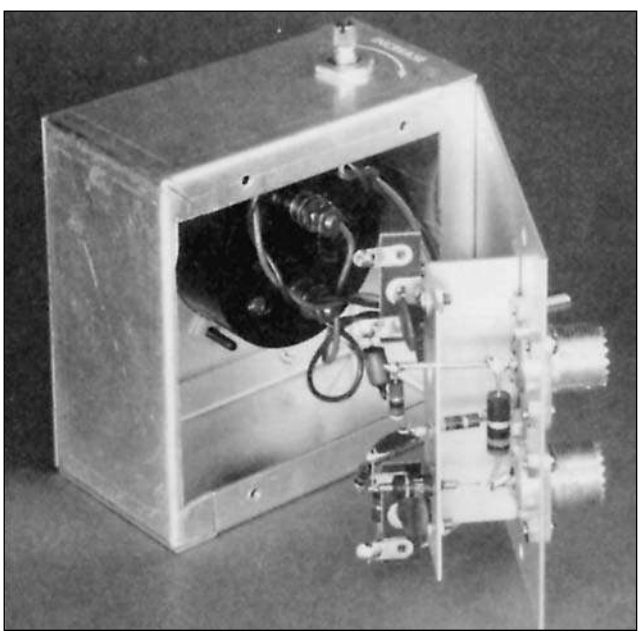

Fig 6—A 2 × 4 × 4-inch aluminum box is used to house this SWR bridge, which uses the circuit of Fig 5. The variable resistor, R4, is mounted on the side. The bridge components are mounted on one side plate of the box and a subchassis formed from a piece of aluminum. The input connector is at the top in this view. R_S is connected directly between the two center posts of the connectors. R2 is visible behind it and perpendicular to it. One terminal of D1 projects through a hole in the chassis so the lead can be connected to J2. R1 is mounted vertically to the left of the chassis in this view, with D2 connected between the junction of R1-R2 and a tie point.

age and D2 is for the incident voltage. Because of manufacturing variations in resistors and diodes, the readings may differ slightly with two multipliers of the same nominal resistance value, so a correction resistor, R3, is included in the circuit. You should select its value so that the meter reading is the same with S1 in either position, when RF is applied to the bridge with the line connection open. In the instrument shown, a value of 1000 Ω was required in series with the multiplier for reflected voltage; in other cases different values probably would be needed and R3 might have to be put in series with the multiplier for the incident voltage. You can determine this by experiment.

The value used for R1 and R2 is not critical, but you should match the two resistors within 1% or 2% if possible. Keep the resistance of R_S as close as possible to the actual Z_0 of the line you use (generally 50 or 75 Ω). Select the resistor by actual measurement with an accurate resistance bridge, if you have one available.

R4 is for adjusting the incident-voltage reading to full scale in the measurement procedure described below. Its use is not essential, but it offers a convenient alternative to exact adjustment of the RF input voltage.

Testing

Measure R1, R2 and R_S with a reliable digital ohmmeter or resistance bridge after completing the wiring. This will ensure that their values have not changed from the heat of soldering. Disconnect one side of the microammeter and leave the input and output terminals of the unit open during such measurements to avoid stray shunt paths through the rectifiers.

Check the two voltmeter circuits as described above, applying enough RF (about 10 V) to the input terminals to give a full-scale reading with the line terminals open. If necessary, try different values for R3 until the reading is the same with S1 in either position.

With J2 open, adjust the RF input voltage and R4 for full-scale reading with S1 in the incident-voltage position. Then switch S1 to the reflected-voltage position. The reading should remain at full scale. Next, short-circuit J2 by touching a screwdriver between the center terminal and the frame of the connector to make a low-inductance short. Switch S1 to the incident-voltage position and readjust R4 for full scale, if necessary. Then throw S1 to the reflected-voltage position, keeping J2 shorted, and the reading should be full scale as before. If the readings differ, R1 and R2 are not the same value, or there is stray coupling between the arms of the bridge. You must read the reflected voltage at full scale with J2 either open or shorted, when the incident voltage is set to full scale in each case, to make accurate SWR measurements.

The circuit should pass these tests at all frequencies at which it is to be used. It is sufficient to test at the lowest and highest frequencies, usually 1.8 or 3.5 and 28 or 50 MHz. If R1 and R2 are poorly matched but the bridge construction is otherwise good, discrepancies in the readings will be substantially the same at all frequencies. A difference in behavior at the low and high ends of the frequency range can be attributed to stray coupling between bridge arms, or stray inductance or capacitance in the arms.

To check the bridge for balance, apply RF and adjust R4 for full scale with J2 open. Then connect a resistor identical with R_S (the resistance should match within 1% or 2%) to the line terminals, using the shortest possible leads. It is convenient to mount the test resistor inside a cable connector (PL-259), a method of mounting that also minimizes lead inductance. When you connect the test resistor the reflected-voltage reading should drop to zero. The incident voltage should be reset to full scale by means of R4, if necessary. The reflected reading should be zero at any frequency in the range to be used. If a good null is obtained at low frequencies but some residual current shows at the high end, the trouble may be the inductance of the test resistor leads, although it may also be caused by stray coupling between the arms of the bridge itself.

If there is a constant low (but not zero) reading at all frequencies the problem is poor matching of the resistance values. Both effects can be present simultaneously. You should make sure you obtain a good null at all frequencies before using your bridge.

Bridge Operation

You must limit the RF power input to a bridge of this type to a few watts at most, because of the power-dissipation ratings of the resistors. If the transmitter has no provision for reducing power output to a very low value—less than 5 W—a simple power-absorber circuit can be made up, as shown in **Fig 7**. Lamp DS1 tends to maintain constant current through the resistor over a fairly

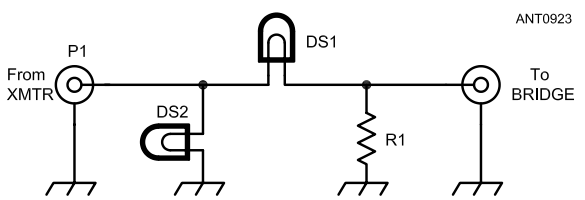

Fig 7—Power-absorber circuit for use with resistance-type SWR bridges when the transmitter has no special provisions for power reduction. For RF powers up to 50 W, DS1 is a 117-V 40-W incandescent lamp and DS2 is not used. For higher powers, use sufficient additional lamp capacity at DS2 to load the transmitter to about normal output; for example, for 250 W output DS2 may consist of two 100-W lamps in parallel. R1 is made from three 1-W 68-Ω resistors connected in parallel. P1 and P2 are cable-mounting coaxial connectors. Leads in the circuit formed by the lamps and R1 should be kept short, but convenient lengths of cable may be used between this assembly and the connectors.

wide power range, so the voltage drop across the resistor also tends to be constant. This voltage is applied to the bridge, and with the constants given is in the right range for resistance-type bridges.

To make a measurement, connect the unknown load to J2 and apply sufficient RF voltage to J1 to give a full-scale incident-voltage reading. Use R4 to set the indicator to exactly full scale. Then throw S1 to the reflected voltage position and note the meter reading. The SWR is then found by using these readings in Eq 1.

For example, if the full-scale calibration of the dc instrument is 100 μA and the reading with S2 in the reflected-voltage position is 40 μA, the SWR is

$$SWR = \frac{100+40}{100-40} = \frac{140}{60} = 2.33:1$$

Instead of calculating the SWR value, you could use the voltage curve in **Fig 8**. In this example the ratio of reflected to forward voltage is 40/100 = 0.4, and from Fig 8 the SWR value is about 2.3:1.

You may calibrate the meter scale in any arbitrary units, so long as the scale has equal divisions. It is the ratios of the voltages, and not the actual values, that determine the SWR.

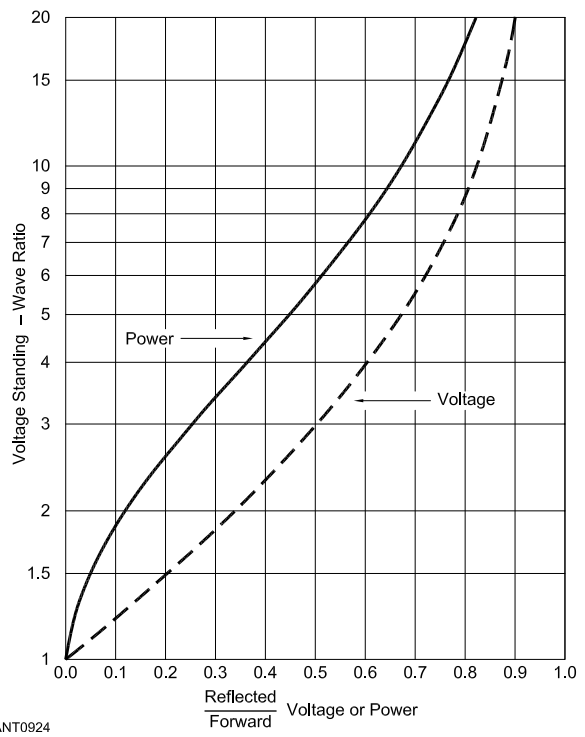

Fig 8—Chart for finding voltage standing-wave ratio when the ratio of reflected-to-forward voltage or reflected-to-forward power is known.

AVOIDING ERRORS IN SWR MEASUREMENTS

The principal causes of inaccuracies within the bridge are differences in the resistances of R1 and R2, stray inductance and capacitance in the bridge arms, and stray coupling between arms. If the checkout procedure described above is followed carefully, the bridge in Fig 5 should be amply accurate for practical use. The accuracy is highest for low standing-wave ratios because of the nature of the SWR calculation; at high ratios the divisor in the equation above represents the difference between two nearly equal quantities, so a small error in voltage measurement may mean a considerable difference in the calculated SWR.

The standard resistor R_S must equal the actual Z_0 of the line. The actual Z_0 of a sample of line may differ by a few percent from the nominal figure because of manufacturing variations, but this has to be tolerated. In the 50- to 75-Ω range, the RF resistance of a composition resistor of $^1/_2$- or 1-W rating is essentially identical with its dc resistance.

Common-Mode Currents

As explained in Chapter 26, there are two ways in which unwanted *common-mode* (sometimes called *antenna*) currents can flow on the outside of a coaxial line—currents radiated onto the line because of its spatial relationship to the antenna and currents that result from the direct connection between the coax outer conductor and (usually) one side of the antenna. The radiated current usually will not be troublesome if the bridge and the transmitter (or other source of RF power for operating the bridge) are shielded so that any RF currents flowing on the outside of the line cannot find their way into the bridge. This point can be checked by inserting an additional section of line ($^1/_8$ to $^1/_4$ electrical wavelength preferably) of the same Z_0. The SWR indicated by the bridge should not change except for a slight decrease because of the additional line loss. If there is a marked change, you may need better shielding.

Parallel-type currents caused by the connection to the antenna without using a common-mode choke balun will change the SWR with variations in line length, even though the bridge and transmitter are well-shielded and the shielding is maintained throughout the system by the use of coaxial fittings. Often, merely moving the transmission line around will cause the indicated SWR to change. This is because the outside of the coax becomes part of the antenna system—being connected to the antenna at the feed point. The outside shield of the line thus constitutes a load, along with the desired load represented by the antenna itself. The SWR on the line then is determined by the composite load of the antenna and the outside of the coax. Since changing the line length (or position) changes one component of this composite load, the SWR changes too.

The remedy for such a situation is to use a good balun

or to detune the outside of the line by proper choice of length. Note that this is not a *measurement error*, since what the instrument reads is the actual SWR on the line. However, it is an undesirable condition since the line is usually operating at a higher SWR than it should—and would if the parallel-type current on the outside of the coax were eliminated.

Spurious Frequencies

Off-frequency components in the RF voltage applied to the bridge may cause considerable error. The principal components of this type are harmonics and low-frequency subharmonics that may be fed through the final stage of the transmitter driving the bridge. The antenna is almost always a fairly selective circuit, and even though the system may be operating with a very low SWR at the desired frequency, it is almost always mismatched at harmonic and subharmonic frequencies. If such spurious frequencies are applied to the bridge in appreciable amplitude, the SWR indication will be very much in error. In particular, it may not be possible to obtain a null on the bridge with any set of adjustments of the matching circuit. The only remedy is to filter out the unwanted components by increasing the selectivity of the circuits between the transmitter final amplifier and the bridge.

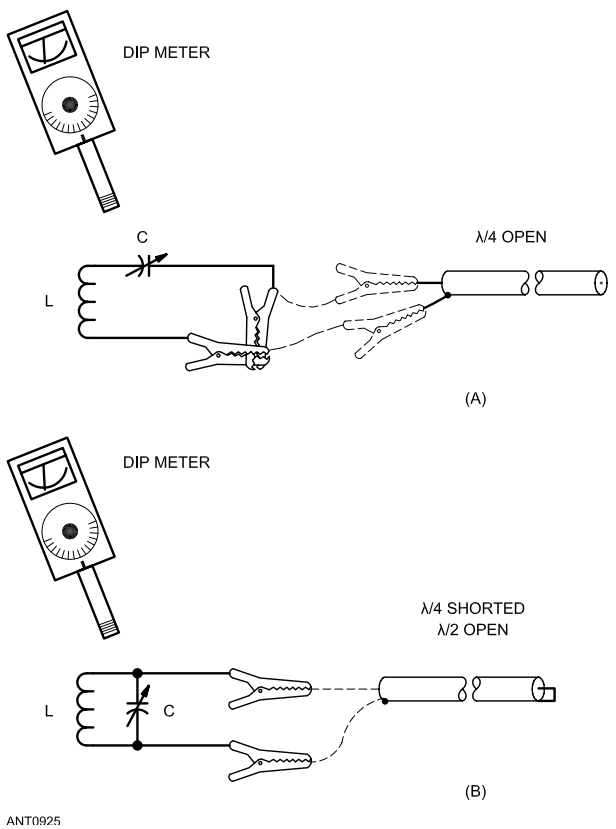

Fig 9—Methods of determining $^1/_4$ and $^1/_2$-λ line lengths. At A, $^1/_4$-λ open-circuited line; at B, $^1/_4$-λ shorted and $^1/_2$-λ open-circuited line.

MEASURING LINE LENGTH

The following material is taken from information in September 1985 *QST* by Charlie Michaels, W7XC (see Bibliography).

There is a popular myth that one may prepare an open quarter-wave line by connecting a loop of wire to one end and trimming the line to resonance (as indicated by a dip meter). This actually yields a line with capacitive reactance equal to the inductive reactance of the loop: a 4-inch wire loop yields a line 82.8º line at 18 MHz; a 2-inch loop yields an 86º line. As the loop size is reduced, line length approaches—but never equals—90º.

To make a quarter-wave open line, parallel connect a coil and capacitor that resonate at the required frequency (see **Fig 9A**). After adjusting the network to resonance, do not make further network adjustments. Open the connection between the coil and capacitor and series connect the line to the pair. Start with a line somewhat longer than required, and trim it until the circuit again resonates at the desired frequency. For a shorted quarter-wave line or an open half-wave line, connect the line in parallel with the coil and capacitor (see Fig 9B).

Another method to accurately measure a coaxial transmission line length uses one of the popular "SWR analyzers," portable hand-held instruments with a tunable low-power signal generator and an SWR bridge. While an SWR analyzer cannot compute the very high values of SWR at the input of a shorted quarter-wave line at the fundamental frequency, most include another readout showing the magnitude of the impedance. This is very handy for finding a low-impedance dip, rather than a high-impedance peak.

At the operating frequency, a shorted quarter-wave line results in a high-impedance open-circuit at the input to that line. At twice the frequency, where the line is now one-half wave long electrically, the instrument shows a low-impedance short-circuit. However, when you are pruning a line to length by cutting off short pieces at the end, it is inconvenient to have to install a short before measuring the response. It is far easier to look for the dip in impedance when a quarter-wave line is terminated in an open circuit.

Again, the strategy is to start with a line physically a little longer than a quarter-wave length. A good rule of thumb is to cut the line 5% longer to take into account the variability in the velocity factor of a typical coax cable. Compute this using:

Length (feet) = 0.25 × 1.05 × VF × 984/Freq = VF/Freq

where

Freq is in MHz

VF is the velocity factor in %.

Plug the coax connector installed at one end of the line into the SWR analyzer and find the frequency for the

impedance dip. Prune the line by snipping off short pieces at the end. Once you've pruned the line to the desired frequency, connect the short at the end of the line and recheck for a short circuit at twice the fundamental frequency. Seal the shorted end of the coax and you're done.

REFLECTOMETERS

Low-cost *reflectometers* that do not have a guaranteed wattmeter calibration are not ordinarily reliable for accurate numerical measurement of standing-wave ratio. They are, however, very useful as aids in the adjustment of matching networks, since the objective in such adjustment is to reduce the reflected voltage or power to zero. Relatively inexpensive devices can be used for this, since only good bridge balance is required, not actual calibration of SWR. Bridges of this type are usually frequency-sensitive that is, the meter response increase with increasing frequency for the same applied voltage. When matching and line monitoring, rather than SWR measurement, is the principal use of the device, this is not a serious handicap.

Various simple reflectometers, useful for matching and monitoring, have been described from time to time in *QST* and in *The ARRL Handbook*. Because most of these are frequency sensitive, it is difficult to calibrate them accurately for power measurement, but their low cost and suitability for use at moderate power levels, combined with the ability to show accurately when a matching circuit has been properly adjusted, make them a worthwhile addition to the amateur station.

The Tandem Match—An Accurate Directional Wattmeter

Most SWR meters are not very accurate at low power levels because the detector diodes do not respond to low voltage in a linear fashion. This design uses a compensating circuit to cancel diode nonlinearity. It also provides peak detection for SSB operation and direct SWR readout that does not vary with power level. The following information is condensed from an article by John Grebenkemper, KI6WX, in January 1987 *QST*.

DESIGN PRINCIPLES

Directional wattmeters for Amateur Radio use consist of three basic elements: a directional coupler, a detector and a signal-processing and display circuit. A directional coupler samples forward and reflected-power components on a transmission line. An ideal directional coupler would provide signals proportional to the forward and reflected voltages (independent of frequency), which could then be used to measure forward and reflected power over a wide frequency range. The best contemporary designs work over two decades of frequency.

The detector circuit provides a dc output voltage proportional to the ac input voltage. Most directional wattmeters use a single germanium diode as the detector element. A germanium, rather than silicon, diode is used to minimize diode nonlinearity at low power levels. Diode non-linearity still causes SWR measurement errors unless it is compensated ahead of the display circuit. Most directional wattmeters do not work well at low power levels because of diode nonlinearity.

The signal-processing and display circuits compute and display the SWR. There are a number of ways to perform this function. Meters that display only the forward and reflected power require the operator to compute the SWR manually. Many instruments require that the operator adjust the meter to a reference level while measuring forward power, then switch to measure reflected power on a special scale that indicates SWR. Meters that directly compute the SWR using analog signal-processing circuits have been described by Fayman, Perras,

Table 1

Performance Specifications for the Tandem Match

Power range: 1.5 to 1500 W
Frequency range: 1.8 to 54 MHz
Power accuracy: Better than ± 10% (± 0.4 dB)
SWR accuracy: Better than ± 5%
Minimum SWR: Less than 1.05:1
Power display: Linear, suitable for use with either analog or digital meters
Calibration: Requires only an accurate voltmeter

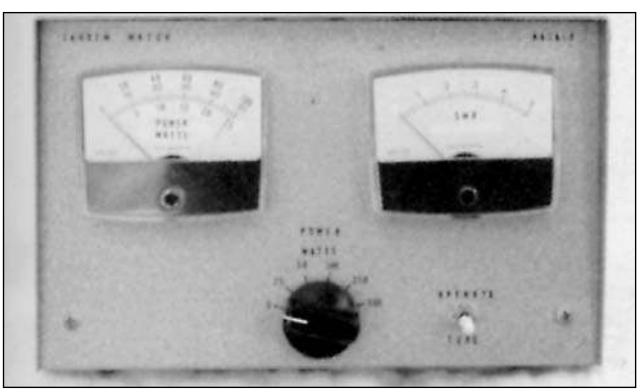

Fig 10—The Tandem Match uses a pair of meters to display net forward power and true SWR simultaneously.

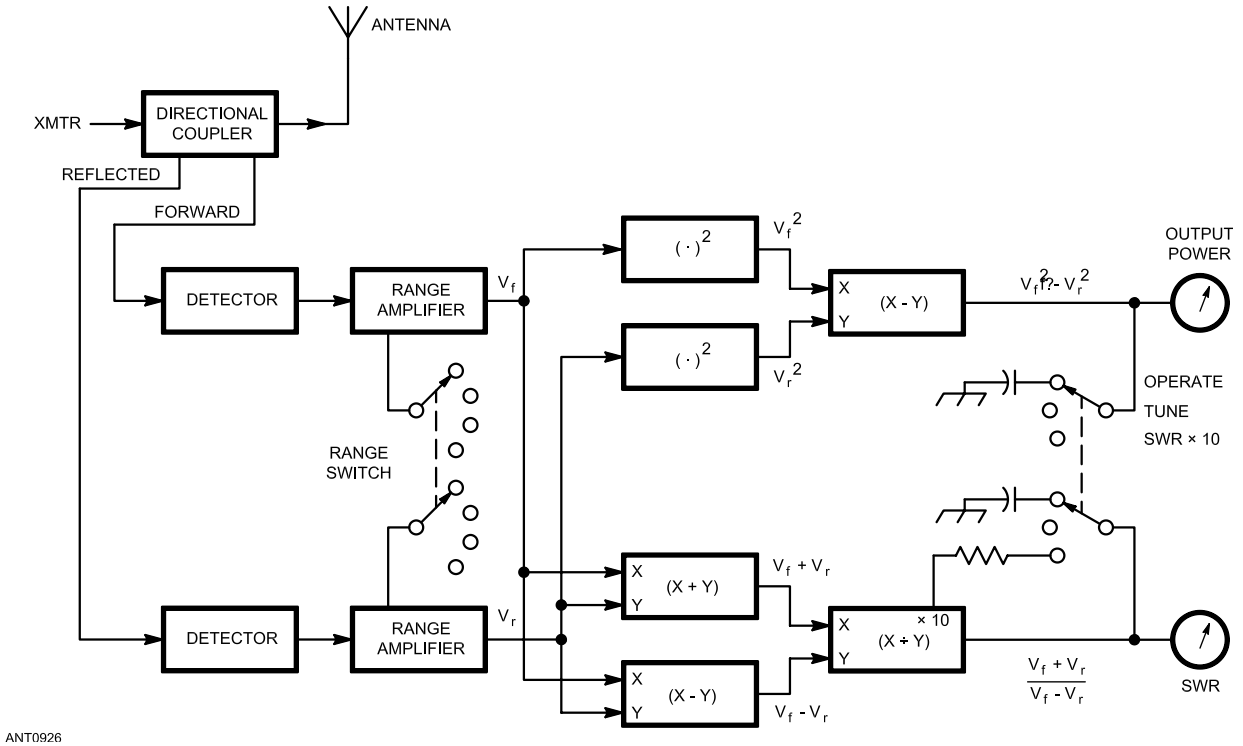

Fig 11—Block diagram of the Tandem Match.

Leenerts and Bailey (see the Bibliography at the end of this chapter).

The next section takes a brief look at several popular circuits that accomplish the functions above and compares them to the circuits used in the Tandem Match. The design specifications of the Tandem Match are shown in **Table l**, and a block diagram is shown in **Fig 11**.

CIRCUIT DESCRIPTION

A directional coupler consists of an input port, an output port and a coupled port. The device takes a portion of the power flowing from the input port to the output port and directs it to the coupled port, but *none* of the power flowing from the output port to the input port is directed to the coupled port.

There are several terms that define the performance of a directional coupler:

1) *Insertion loss* is the amount of power that is lost as the signal flows from the input port to the output port. Insertion loss should be minimized so the coupler doesn't dissipate a significant amount of the transmitted power.

2) *Coupling factor* is the amount of power (or voltage) that appears at the coupled port relative to the amount of power (or voltage) transferred from the input port to the output port. The "flatness" (with frequency) of the coupling factor determines how accurately the directional wattmeter can determine forward and reflected power over a range of frequencies.

3) *Isolation* is the amount of power (or voltage) that appears at the coupled port relative to the amount of power (or voltage) transferred from the output port to the input port.

4) *Directivity* is the isolation less the coupling factor. Directivity dictates the minimum measurable SWR. A directional coupler with 20 dB of directivity measures a 1:1 SWR as l.22:l, but one with 30 dB measures a 1:1 SWR as 1.07:1.

The directional coupler most commonly used in amateur radio was first described in 1959 by Bruene in *QST* (see Bibliography). The coupling factor was fairly flat (± l dB), and the directivity was about 20 dB for a Bruene coupler measured from 3 to 30 MHz. Both factors limit the accuracy of the Bruene coupler for measuring low values of power and SWR. It is a simple directional coupler, however, and it works well over a wide frequency range if great precision is not required.

The coupler used in the Tandem Match (see **Fig 12**) consists of a pair of toroidal transformers connected in tandem. The configuration was patented by Carl G. Sontheimer and Raymond E. Fredrick (US Patent no. 3,426,298, issued February 4, 1969). It has been described by Perras, Spaulding (see Bibliography) and others. With coupling factors of 20 dB or greater, this coupler is suitable for sampling both forward and reflected power.

The configuration used in the Tandem Match works well over the frequency range of 1.8 to 54 MHz, with a

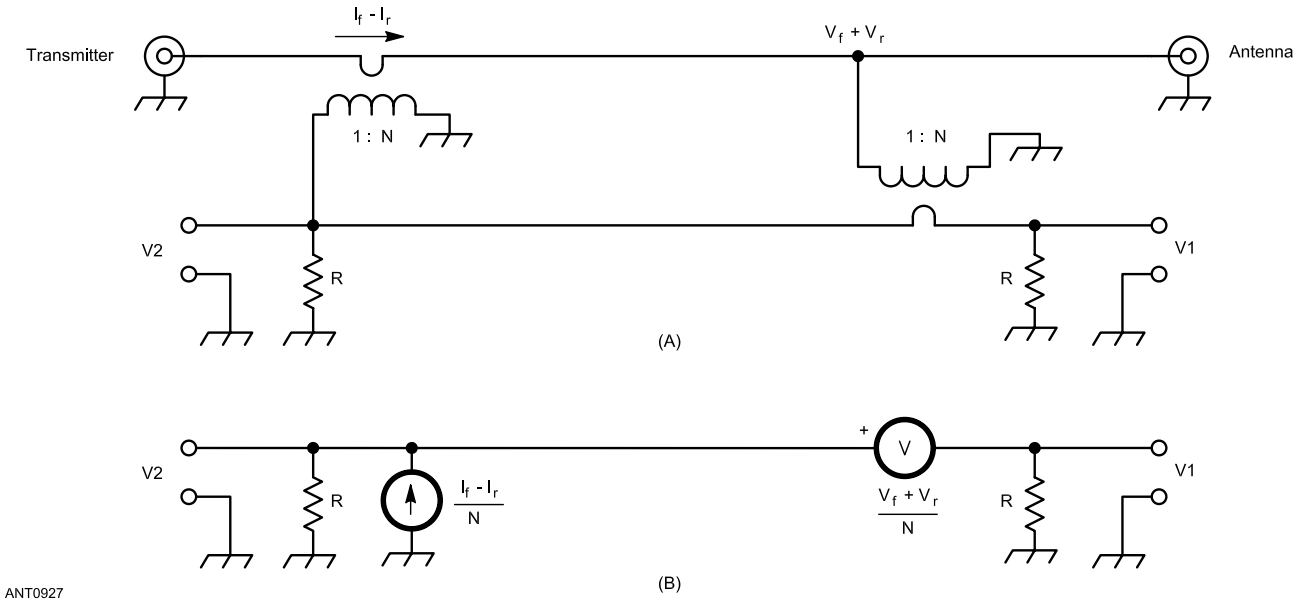

Fig 12—Simplified diagram of the Tandem Match directional coupler. At A, a schematic of the two transformers. At B, an equivalent circuit.

nominal coupling factor of 30 dB. Over this range, insertion loss is less than 0.1 dB. The coupling factor is flat to within ± 0.1 dB from 1.8 to 30 MHz, and increases to only ±0.3 dB at 50 MHz. Directivity exceeds 35 dB from 1.8 to 30 MHz and exceeds 26 dB at 50 MHz.

The low-frequency limit of this directional coupler is determined by the inductance of the transformer secondary windings. The inductive reactance should be greater than 150 Ω (three times the line characteristic impedance) to reduce insertion loss. The high-frequency limit of this directional coupler is determined by the length of the transformer windings. When the winding length approaches a significant fraction of a wavelength, coupler performance deteriorates.

The coupler described here may overheat at 1500 W on 160 meters (because of the high circulating current in the secondary of T2). The problem could be corrected by using a larger core or one with greater permeability. A larger core would require longer windings; that option would decrease the high-frequency limit.

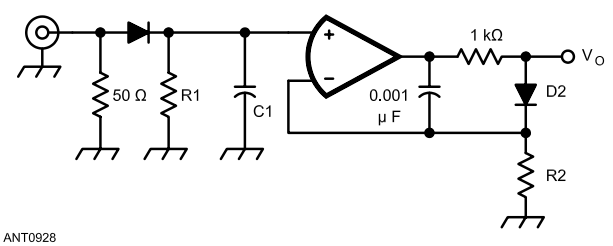

Fig 13—Simplified diagram of the detector circuit used in the Tandem Match. The output voltage, V_o is approximately equal to the input voltage. D1 and D2 must be a matched pair (see text). The op amp should have a low offset voltage (less than 1 mV), a low leakage current (less than 1 nA), and be stable over time and temperature. The resistor and capacitor in the feedback path assure that the op amp will be stable.

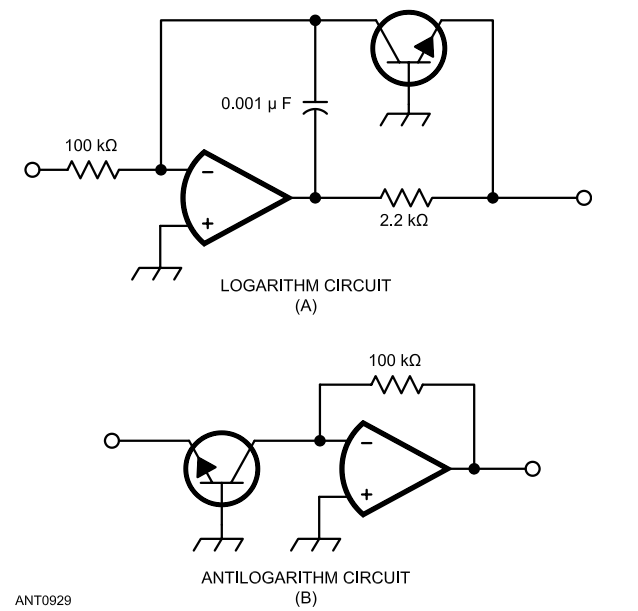

Fig 14—Simplified diagrams of the log circuit at A and the antilog circuit at B.

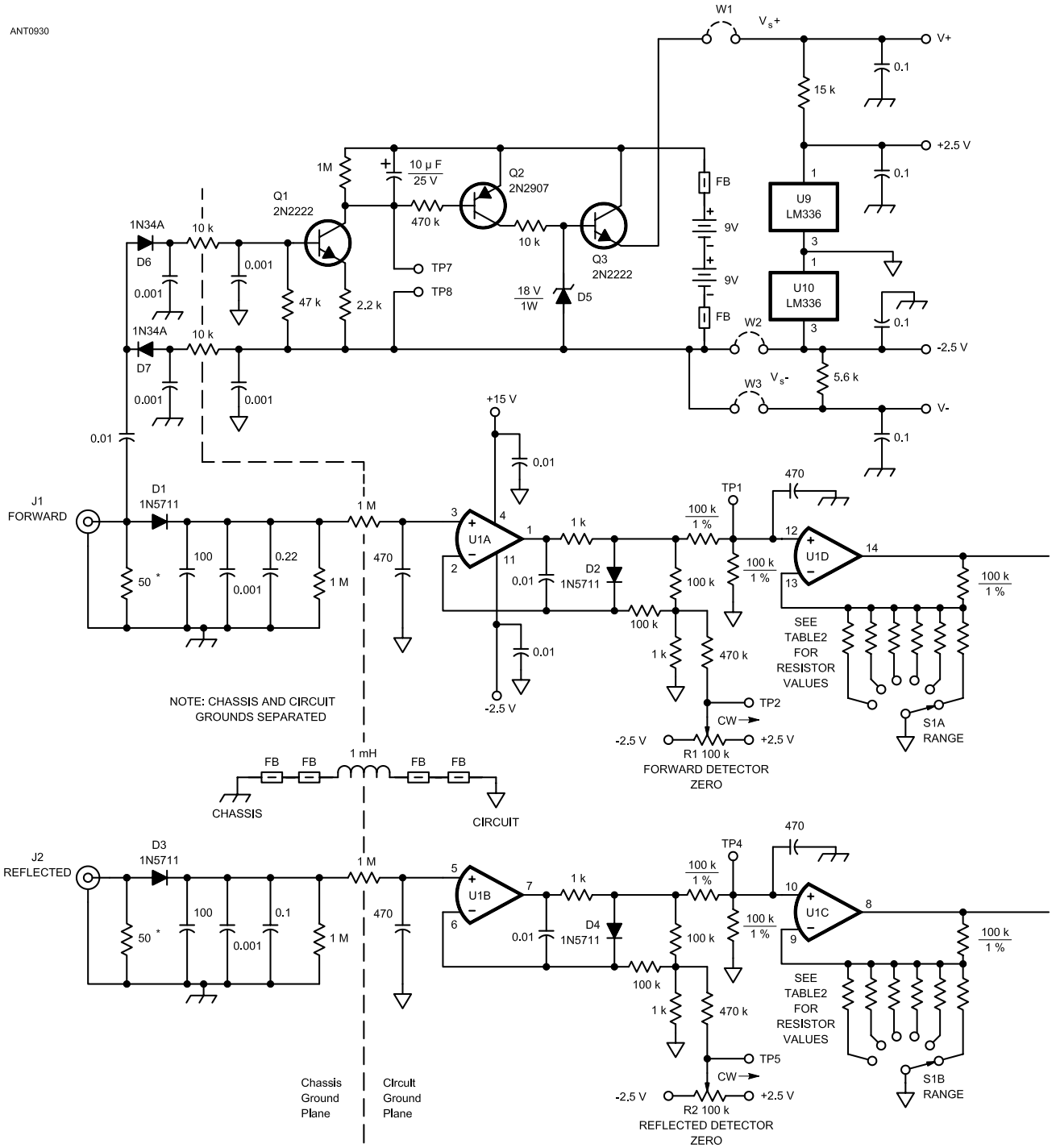

Fig 15—Schematic diagram for the Tandem Match directional wattmeter. Parts identified as RS are from RadioShack. For other parts sources, see Table 3. See Fig 17 for construction of 50-Ω loads at J1 and J2.

D1, D2—Matched pair 1N5711, or equivalent.
D3, D4—Matched pair 1N5711, or equivalent.
D6, D7—1N34A.
D8-D14—1N914.
FB—Ferrite bead, Amidon FB-73-101 or equiv.
J1, J2—SO-239 connector.
J3, J4—Open-circuit jack.
M1, M2—50 µA panel meter, RS 270-1751.
Q1, Q3, Q4—2N2222 or equiv.
Q2—2N2907 or equiv.

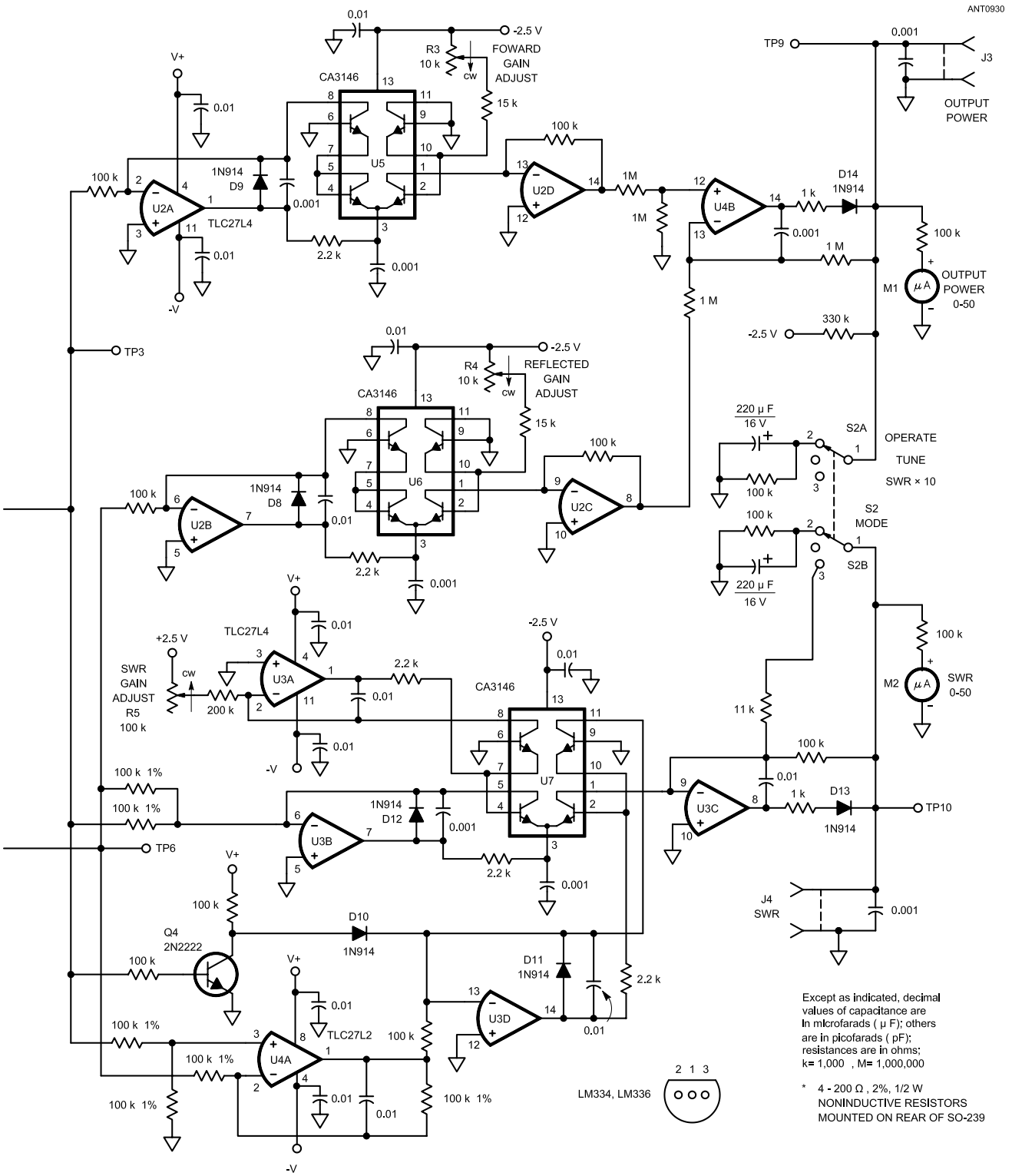

R1, R2, R5—100 kΩ, 10-turn, cermet Trimpot.
R3, R4—10 kΩ, 10-turn, cermet Trimpot.
U1-U3—TLC27L4 or TLC27M4 quad op amp (Texas Instruments).
U4—TLC27L2 or TLC27M2 dual op amp.
U5-U7—CA3146 quad transistor array.
U8—LM334 adjustable current source.
U9-U10—LM336 2.5-V reference diode. See text.

Detector Circuits

Most amateur directional wattmeters use a germanium diode detector to minimize the forward voltage drop. Detector voltage drop is still significant, however, and an uncompensated diode detector does not respond to small signals in a linear fashion. Many directional wattmeters compensate for diode nonlinearity by adjusting the meter scale.

The effect of underestimating detected power worsens at low power levels. Under these conditions, the ratio of the forward power to the reflected power is overestimated because the reflected power is always less than the forward power. This results in an instrument that underestimates SWR, particularly as power is reduced. A directional wattmeter can be checked for this effect by measuring SWR at several power levels: the SWR should be independent of power level.

The Tandem Match uses a feedback circuit to compensate for diode nonlinearity. A simplified diagram of the compensated detector is shown in **Fig 13**. When used with the 30-dB directional coupler, the output voltage of this circuit tracks the square root of power over a range from 10 mW to 1.5 kW. The compensated diode detector tracks the peak input voltage down to 30 mV, while an uncompensated germanium-diode detector shows significant errors at peak inputs of 1 V and less. More information about compensated detectors appears in Grebenkemper's *QEX* article, "Calibrating Diode Detectors" (see Bibliography).

The compensation circuit uses the voltage across a feedback diode, D2, to compensate for the voltage drop across the detector diode, D1. (The diodes must be a matched pair.) The average current through D1 is determined by the detector diode load resistor, R1. The peak current through this diode is several times larger than the average current; therefore, the current through D2 must be several times larger than the average current through D1 to compensate adequately for the peal voltage drop across D1. This is accomplished by making the feedback-diode load resistor, R2, several times smaller than R1. The voltage at the output of the compensated detector approximates the peak RF voltage at the input. For Schottky barrier diodes and a 1 MΩ detector-diode load resistor, a 5:1 ratio of R1 to R2 is nearly optimal.

Signal-Processing and Display Circuits

The signal-processing circuitry calculates and displays transmission-line power and SWR. When measuring forward power, most directional wattmeters display the actual forward power present in the transmission line, which is the sum of forward and reflected power if a match exists at the input end of the line. Transmission-line forward power is very close to the net forward power (the actual power delivered to the line) so long as the SWR is low. As the SWR increases, however, forward power becomes an increasingly poor measure of the power delivered to the load. At an SWR of 3:1, a forward power reading of 100 W implies that only 75 W is delivered to the load (the reflected power is 25 W), assuming the transmission-line loss is zero.

The Tandem Match differs from most wattmeters in that *it displays the net forward power, rather than the sum of forward and reflected power.* This is the quantity that must be optimized to result in maximum radiated power (and which concerns the FCC).

The Tandem Match directly computes and displays the transmission-line SWR on a linear scale. As the displayed SWR is not affected by changes in transmitter power, a matching network can be simply adjusted to minimize SWR. Transmatch adjustment requires only a few watts.

The heart of the Tandem Match signal-processing circuit is the analog logarithm and antilogarithm circuitry shown in **Fig 14**. The circuit is based on the fact that collector current in a silicon transistor is proportional to the exponential (antilog) of its base-emitter voltage over a range of collector currents from a few nanoamperes to a few milliamperes when the collector-base voltage is zero (see Gibbons and Horn reference in the Bibliography). Variations of this circuit are used in the squaring circuits to convert voltage to power and in the divider circuit used to compute the SWR. With good op amps, this circuit will work well for input voltages from less than 100 mV to greater than 10 V.

(For the Tandem Match, "good" op amps are quad-packaged, low-power-consumption, unity-gain-stable parts with input bias less than 1 nA and offset voltage less than 5 mV. Op amps that consume more power than those shown may require changes to the power supply.)

CONSTRUCTION

The schematic diagram for the Tandem Match is shown in **Fig 15** (see pages 14 and 15). The circuit is designed to operate from batteries and draw very little power. Much of the circuitry is of high impedance, so take care to isolate it from RF fields. House it in a metal case. Most problems in the prototype were caused by stray RF in the op-amp circuitry.

Directional Coupler

The directional coupler is constructed in its own small ($2^3/_4 \times 2^3/_4 \times 2^1/_4$-inch) aluminum box (see **Fig 16**). Two pairs of S0-239 connectors are mounted on opposite sides of the box. A piece of PC board is run diagonally across the box to improve coupler directivity. The pieces of RG-8X coaxial cable pass through holes in the PC board.

(Note: Some brands of "mini 8" cable have extremely low breakdown voltage ratings and are unsuitable to carry even 100 W when the SWR exceeds 1:1. See the subsequent section, "High-Power Operation," for details of a coupler made with RG-8 cable.)

Begin by constructing T1 and T2, which are identi-

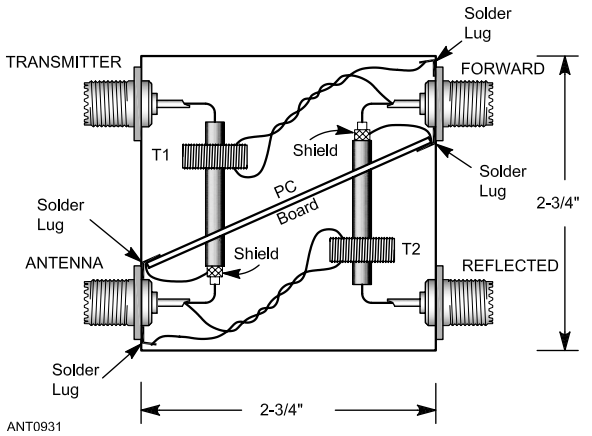

Fig 16—Construction details for the directional coupler.

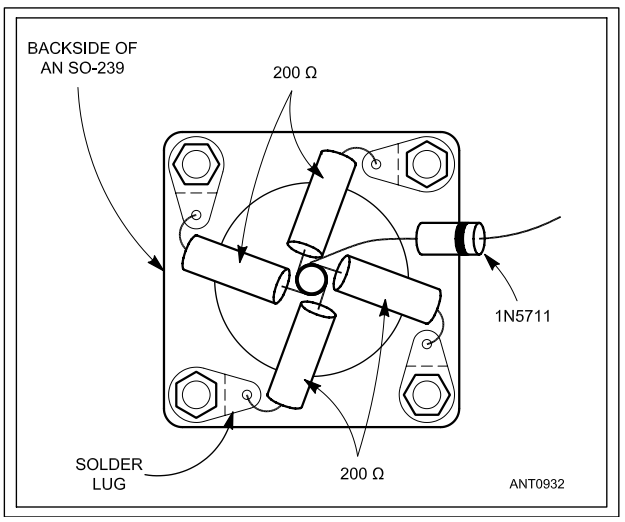

Fig 17—The parallel load resistors mounted on an SO-239 connector. Four 200-Ω, 2%, 1/2-W resistors are mounted in parallel to provide a 50-Ω detector load.

cal except for their end connections. Refer to Fig 16. The primary for each transformer is the center conductor of a length of RG-8X coaxial cable. Cut two cable lengths sufficient for mounting as shown in the figure. Strip the cable jacket, braid and dielectric as shown. The cable braid is used as a Faraday shield between the transformer windings, so it is only grounded at one end. *Important—connect the braid only at one end or the directional-coupler circuit will not work properly!* Wind two transformer secondaries, each 31 turns of #24 enameled wire on an Amidon T50-3 or equivalent powdered-iron core.

Slip each core over one of the prepared cable pieces (including both the shield and the outer insulation). Mount and connect the transformers as shown in Fig 16, with the wire running through separate holes in the copper-clad PC board. The directional coupler can be mounted separately

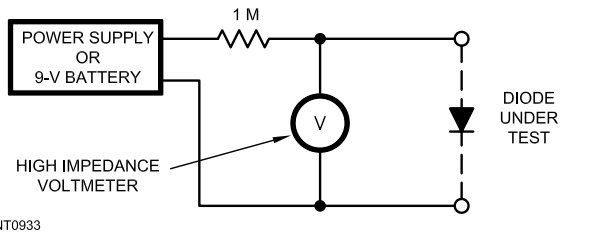

Fig 18—Diode matching test setup.

from the rest of the circuitry if desired. If so, use two coaxial cables to carry the forward and reflected-power signals from the directional coupler to the detector inputs. Be aware, however that any losses in the cables will affect power readings.

This directional coupler has not been used at power levels in excess of 100 W. For more information about using the Tandem Match at high power levels, see the section, "High-Power Operation."

Detector and Signal-Processing Circuits

The detector and signal-processing circuits were constructed on a perforated, copper-clad circuit board. These circuits use two separate grounds—*it is extremely important that the grounds be isolated as shown in the circuit diagram.* Failure to do so may result in faulty circuit operation. Separate grounds prevent RF currents on the cable braid from affecting the op-amp circuitry.

The directional coupler requires good 50-Ω loads. They are constructed on the back of female UHF chassis connectors where the cables from the directional coupler enter the wattmeter housing. Each load consists of four 200-Ω resistors connected from the center conductor of the UHF connector to the four holes on the mounting flange, as shown in **Fig 17**. The detector diode is then run from the center conductor of the connector to the 100-pF and 1000-pF bypass capacitors, which are mounted next to the connector. The response of this load and detector combination measures flat to beyond 500 MHz.

Schottky-barrier diodes (type 1N5711) were used in this design because they were readily available. Any RF-detector diode with a low forward voltage drop (less than 300 mV) and reverse break-down voltage greater than 30 V could be used. (Germanium diodes could be used in this circuit, but performance will suffer. If germanium diodes are used, reduce the resistance values for the detector-diode and feedback-diode load resistors by a factor of 10.)

The detector diodes must be matched. This can be done with dc, using the circuit shown in **Fig 18**. Use a high-impedance voltmeter (10 MΩ or greater). For this project, diodes are matched when their forward voltage drops are equal (within a few millivolts). Diodes from the same batch will probably be sufficiently matched.

Table 2
Range-Switch Resistor Values

Full-Scale Power Level (W)	*Range Resistor (1% Precision) (kΩ)*
1	2.32
2	3.24
3	4.02
5	5.23
10	7.68
15	9.53
20	11.0
25	12.7
30	14.0
50	18.7
100	28.7
150	37.4
200	46.4
250	54 9
300	63.4
500	100.0
1000	237.0
1500	649.0
2000	Open

The rest of the circuit layout is not critical, but keep the lead lengths of the 0.001 and 0.01-pF bypass capacitors short. The capacitors provide additional bypassing for the op-amp circuitry. D6 and D7 form a voltage doubler to detect the presence of a carrier. When the forward power exceeds 1.5 W, Q3 switches on and stays on until about 10 seconds after the carrier drops. (A connection from TP7 to TP9 forces the unit on, even with no carrier present.) The regulated references of +2.5 V and –2.5 V generated by the LM334 and two LM336s are critical. Zener-diode substitutes would significantly degrade performance.

The four op amps in U1 compensate for the nonlinearity of the detector diodes. D1-D2 and D3-D4 are the matched diode pairs discussed above. A RANGE switch selects the meter range. (A six-position switch was used here because it was handy.) The resistor values for the RANGE switch are shown in **Table 2**. Full-scale input power gives an output at U1C or U1D of 7.07 V. The forward and reflected-power detectors are zeroed with R1 and R2.

The forward and reflected-detector voltages are squared by U2, U5 and U6 so that the output voltages are proportional to forward and reflected power. The gain constants are adjusted using R3 and R4 so that an input of 7.07 V to the squaring circuit gives an output of 5 V. The difference between these two voltages is used by U4B to yield an output that is proportional to the power delivered to the transmission line. This voltage is peak detected (by an RC circuit connected to the OPERATE position of the MODE switch) to hold and indicate the maximum power during CW or SSB transmissions. SWR is computed from the forward and reflected voltages by U3, U4 and U7. When no carrier is present, Q4 forces the SWR reading to be zero (that is, when the forward power is less than 2% of the full-scale setting of the RANGE switch). The SWR computation circuit gain is adjusted by R5. The output is peak detected in the OPERATE mode to steady the SWR reading during CW or SSB transmissions.

Transistor arrays (U5, U6 and U7) are used for the log and antilog circuits to guarantee that the transistors will be well matched. Discrete transistors may be used, but accuracy may suffer. A three-position toggle switch selects the three operating modes. In the OPERATE mode, the power and SWR outputs are peak detected and held for a few seconds to allow meter reading during actual transmissions. In the TUNE mode, the meters display instantaneous output power and SWR.

A digital voltmeter is used to obtain more precise readings than are possible with analog meters. The output power range is 0 to 5 V (0 V = 0 W and 5 V = full scale). SWR output varies from 1 V (SWR = 1:1) to 5 V (SWR = 5:1). Voltages above 5 V are unreliable because of voltage limiting in some of the op amp circuits.

Calibration

The directional wattmeter can be calibrated with an accurate voltmeter. All calibration is done with dc voltages. The directional-coupler and detector circuits are inherently accurate if correctly built. To calibrate the wattmeter, use the following procedure:

1) Set the MODE switch to TUNE and the RANGE switch to 100 W or less.
2) Jumper TP7 to TP8. This turns the unit on.
3) Jumper TP1 to TP2. Adjust R1 for 0 V at TP3.
4) Jumper TP4 to TP5. Adjust R2 for 0 V at TP6.
5) Adjust R1 for 7.07 V at TP3.
6) Adjust R3 for 5.00 V at TP9, or a full-scale reading on M1.
7) Adjust R2 for 7.07 V at TP6.
8) Adjust R4 for 0 V at TP9, or a zero reading on M1.
9) Adjust R2 for 4.71 V at TP6.
10) Adjust R5 for 5.00 V at TP10, or a full-scale reading on M2.
11) Set the RANGE switch to its most sensitive scale.
12) Remove the jumpers from TP1 to TP2 and TP4 to TP5.
13) Adjust R1 for 0 V at TP3.
14) Adjust R2 for 0 V at TP6.
15) Remove the jumper from TP7 to TP8.

This completes the calibration procedure. This procedure has been found to equal calibration with expensive laboratory equipment. The directional wattmeter should now be ready for use.

ACCURACY

Performance of the Tandem Match has been compared to other well-known directional couplers and laboratory test equipment, and it equals any amateur directional wattmeter tested. Power measurement accuracy compares well to a Hewlett-Packard HP-436A power meter. The HP meter has a specified measurement error of less than ± 0.05 dB. The Tandem Match tracked the HP436A within +0.5 dB from 10 mW to 100 W, and within ± 0.1 dB from 1 W to 100 W. The unit was not tested above 100 W because a transmitter with a higher power rating was not available.

SWR performance was equally good when compared to the SWR calculated from measurements made with the HP436A and a calibrated directional coupler. The Tandem Match tracked the calculated SWR within ± 5% for SWR values from 1:1 to 5:1. SWR measurements were made at 8 W and 100 W.

OPERATION

Connect the Tandem Match in the 50-Ω line between the transmitter and the antenna matching network (or antenna if no matching network is used). Set the RANGE switch to a range greater than the transmitter output rating and the MODE switch to TUNE. When the transmitter is keyed, the Tandem Match automatically switches on and indicates both power delivered to the antenna and SWR on the transmission line. When no carrier is present, the OUTPUT POWER and SWR meters indicate zero.

The OPERATE mode includes RC circuitry to momentarily hold the peak-power and SWR readings during CW or SSB transmissions. The peak detectors are not ideal, so there could be about 10% variation from the actual power peaks and the SWR reading. The SWR ×10 mode increases the maximum readable SWR to 50:1. This range should be sufficient to cover any SWR value that occurs in amateur use. (A 50-foot open stub of RG-8 yields a measured SWR of only 43:1, or less, at 2.4 MHz because of cable loss. Higher frequencies and longer cables exhibit a lesser maximum SWR.)

It is easy to use the Tandem Match to adjust an antenna matching network: Adjust the transmitter for minimum output power (at least 1.5 W). With the carrier on and the MODE switch set to TUNE or SWR ×10, adjust the matching network for minimum SWR. Once the minimum SWR is obtained, set the transmitter to the proper operating mode and output power. Place the Tandem Match in the OPERATE mode.

DESIGN VARIATIONS

There are several ways in which this design could be enhanced. The most important is to add UHF capability. This would require a new directional-coupler design for the band of interest. (The existing detector circuit should work to at least 500 MHz.)

Those who desire a low-power directional wattmeter can build a directional coupler with a 20-dB coupling factor by decreasing the transformer turns ratio to 10:1. That version should be capable of measuring output power from 1 mW to about 150 W (and it should switch on at about 150 mW).

This change should also increase the maximum operating frequency to about 150 MHz (by virtue of the shorter transformer windings). If you desire 1.8-MHz operation, it may be necessary to change the toroidal core material for sufficient reactance (low insertion loss).

The Tandem Match circuit can accommodate coaxial cable with a characteristic impedance other than 50 Ω. The detector terminating resistors, transformer secondaries and range resistors must change to match the new design impedance.

The detector circuitry can be used (without the directional coupler) to measure low-level RF power in 50-Ω circuits. RF is fed directly to the forward detector (J1, Fig 15), and power is read from the output power meter. The detector is quite linear from 10 μW to 1.5 W.

HIGH-POWER OPERATION

This material was condensed from information by Frank Van Zant, KL7IBA, in July 1989 *QST*. In April 1988, Zack Lau, W1VT, described a directional-coupler circuit (based on the same principle as Grebenkemper's circuit) for a QRP transceiver (see the Bibliography at the end of this chapter). The main advantage of Lau's circuit is a very low parts count.

Grebenkemper used complex log-antilog amplifiers to provide good measurement accuracy. This application gets away from complex circuitry, but retains reasonable measurement accuracy over the 1 to 1500-W range. It also forfeits the SWR-computation feature. Lau's coupler uses ferrite toroids. It works well at low power levels, but the ferrite toroids heat excessively with high power, causing erratic meter readings and the potential for burned parts.

The Revised Design

Powdered-iron toroids are used for the transformers in this version of Lau's basic circuit. The number of turns on the secondaries was increased to compensate for the lower permeability of powdered iron.

Two meters display reflected and forward power (see **Fig 19**). The germanium detector diodes (D1 and D2—1N34) provide fairly accurate meter readings, particularly if the meter is calibrated (using R3, R4 and R5) to place the normal transmitter output at mid scale. If the winding sense of the transformers is reversed, the meters are transposed (the forward-power meter becomes the reflected-power meter, and vice versa).

Construction

Fig 20 shows the physical layout of the coupler. The pickup unit is mounted in a $3^1/_2 \times 3^1/_2 \times$ 4-inch box. The meters, PC-mount potentiometers and HIGH/LOW power

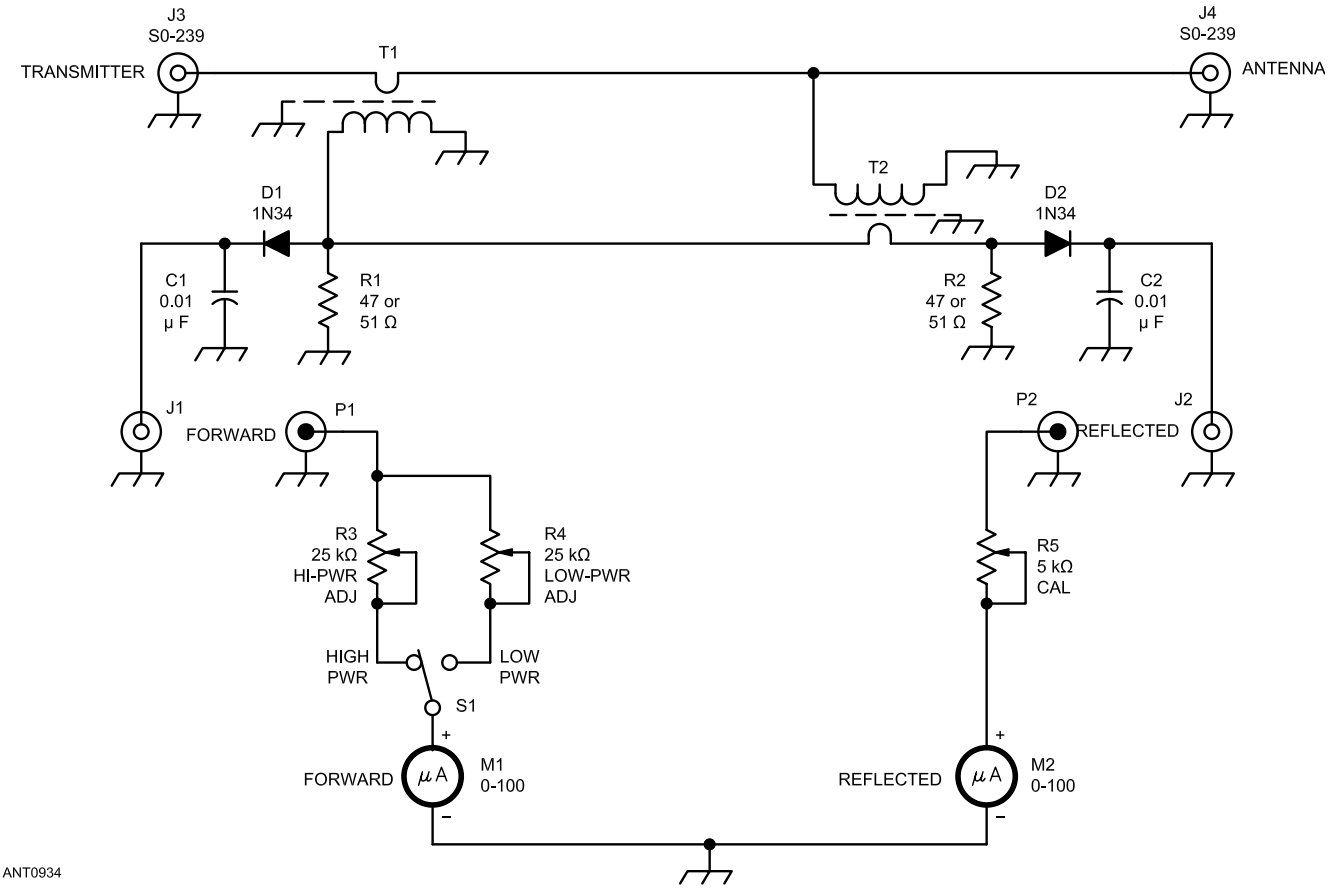

Fig 19—Schematic diagram of the high-power directional coupler. D1 and D2 are germanium diodes (1N34 or equiv). R1 and R2 are 47 or 51-Ω, 1/2-W resistors. C1 and C2 have 500-V ratings. The secondary windings of T1 and T2 each consist of 40 turns of #26 to #30 enameled wire on T-68-2 powdered-iron toroid cores. If the coupler is built into an existing antenna tuner, the primary of T1 can be part of the tuner coaxial output line. The remotely located meters (M1 and M2) are connected to the coupler box at J1 and J2 via P1 and P2.

switch are mounted in a separate box or a compartment in an antenna tuner. Parts for this project are available from the suppliers listed in **Table 3**.

The primary windings of Tl and T2 are constructed much as Grebenkemper described, but use RG-8 with its jacket removed so that the core and secondary winding may fit over the cable. The braid is wrapped with fiberglass tape to insulate it from the secondary winding. An excellent alternative to fiberglass tape—with even higher RF voltage-breakdown characteristics—is ordinary plumber's Teflon pipe tape, available at most hardware stores.

The transformer secondaries are wound on T-68-2 powdered-iron toroid cores. They are 40 turns of #26 to #30 enameled wire spread evenly around each core. By using #26 to #30 wire on the cores, the cores slip over the tape-wrapped RG-8 lines. With #26 wire on the toroids, a single layer of tape (slightly more with Teflon tape) over the braid provides an extremely snug fit for the core. Use care when fitting the cores onto the RG-8 assemblies.

After the toroids are mounted on the RG-8 sections,

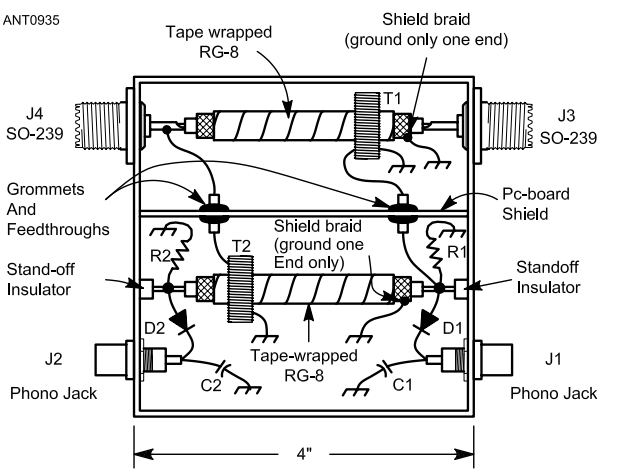

Fig 20—Directional-coupler construction details. Grommets or feedthrough insulators can be used to route the secondary winding of T1 and T2 through the PC board shield. A 3 1/2 × 3 1/2 × 4-inch box serves as the enclosure.

Table 3
Parts Sources
(Also see Chapter 21)

Components	*Source*
TLC-series and CA3146 ICs	Newark Electronics 4801 N Ravenswood St Chicago, IL 60640 773-784-5100
LM334, LM336, 1% resistors, trimmer potentiometers	Digi-Key Corporation 701 Brooks Ave S PO Box 677 Thief River Falls, MN 56701 800-344-4539
Toroid cores, Fiberglass tape	Amidon Associates 240 & 250 Briggs Ave Costa Mesa, CA 92626 714-850-4660
Meters	Fair Radio Sales PO Box 1105 Lima, OH 45804 419-227-6573
Toroid cores	Palomar Engineers PO Box 462222 Escondido, CA 92046 760-747-3343
0-150/1500-W-scale meters, A&M model no. 255-138, 1N5711 diodes	Surplus Sales of Nebraska 1502 Jones St Omaha, NE 68102 402-346-4750

coat the assembly with General Cement Corp Polystyrene Q Dope, or use a spot or two of RTV sealant to hold the windings in place and fix the transformers on the RG-8 primary windings.

Mount a PC-board shield in the center of the box, between T1 and T2, to minimize coupling between the transformers. Suspend T1 between the SO-239 connectors and T2 between two standoff insulators. The detector circuits (C1, C2, D1, D2, R1 and R2) are mounted inside the coupler box as shown.

Calibration, Tune Up and Operation

The coupler has excellent directivity. Calibrate the meters for various power levels with an RF ammeter and a 50-Ω dummy load. Calculate I^2R for each power level, and mark the meter faces accordingly. Use R3, R4 and R5 to adjust the meter readings within the ranges. Diode nonlinearities are thus taken into account, and Grebenkemper's signal-processing circuits are not needed for relatively accurate power readings. Start the tune-up process using about 10 W, adjust the antenna tuner for minimum reflected power, and increase power while adjusting the tuner to minimize reflected power.

This circuit has been built into several antenna tuners with good success. The instrument works well at 1.5-kW output on 1.8 MHz. It also works well from 3.5 to 30 MHz with 1.2 and 1.5-kW output.

The antenna is easily tuned for a 1:1 SWR using the null indication provided. Amplifier settings for a matched antenna, as indicated with the wattmeter, closely agreed with those for a 50-Ω dummy load. Checks with a Palomar noise bridge and a Heath Antenna Scope also verified these findings. This circuit should handle more than 1.5 kW, as long as the SWR on the feed line through the wattmeter is kept at or near 1:1. (On one occasion high power was applied while the antenna tuner was not coupled to a load. Naturally the SWR was extremely high, and the output transformer secondary winding opened like a fuse. This resulted from the excessively high voltage across the secondary. The damage was easily and quickly repaired.)

An Inexpensive VHF Directional Coupler

Precision in-line metering devices capable of reading forward and reflected power over a wide range of frequencies are very useful in amateur VHF and UHF work, but their rather high cost puts them out of the reach of many VHF enthusiasts. The device shown in Figs 14 through 16 is an inexpensive adaptation of their basic principles. It can be made for the cost of a meter, a few small parts, and bits of copper pipe and fittings that can be found in the plumbing stocks at many hardware stores.

Construction

The sampler consists of a short section of handmade coaxial line, in this instance, of 50 Ω impedance, with a reversible probe coupled to it. A small pickup loop built into the probe is terminated with a resistor at one end and a diode at the other. The resistor matches the impedance of the loop, not the impedance of the line section. Energy picked up by the loop is rectified by the diode, and the resultant current is fed to a meter equipped with a calibration control.

The principal metal parts of the device are a brass plumbing T, a pipe cap, short pieces of $^3/_4$-inch ID and $^5/_{16}$-inch OD copper pipe, and two coaxial fittings. Other available tubing combinations for 50-Ω line may be usable. The ratio of outer conductor ID to inner conductor OD should be 2.4/1. For a sampler to be used with other

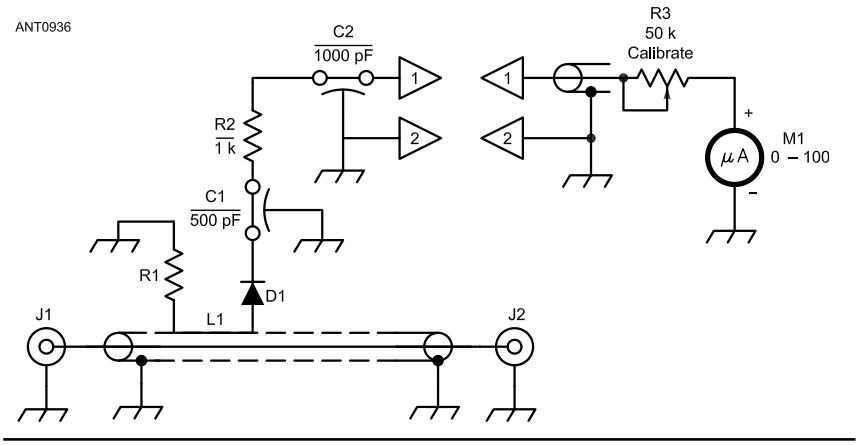

Fig 21—Circuit diagram for the line sampler.
C1—500-pF feedthrough capacitor, solder-in type.
C2—1000-pF feedthrough capacitor, threaded type.
D1—Germanium diode 1N34, 1N60, 1N270, 1N295, or similar.
J1, J2—Coaxial connector, type N (UG-58A).
L1—Pickup loop, copper strap 1-inch long × 3/16-inch wide. Bend into "C" shape with flat portion 5/8-inch long.
M1—0-100 μA meter.
R1—Composition resistor, 82 to 100 Ω. See text.
R3—50-kΩ composition control, linear taper.

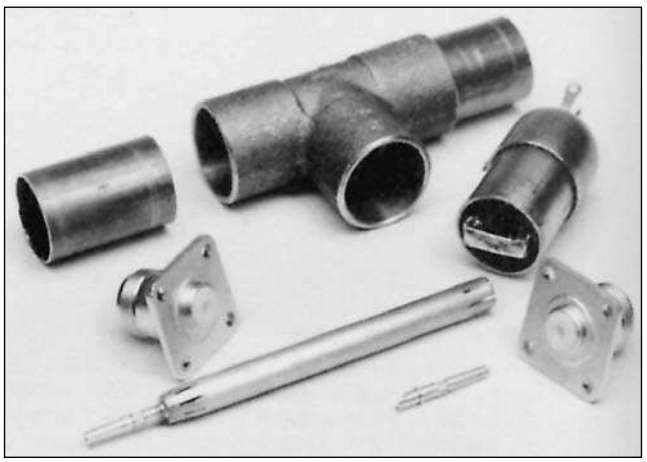

Fig 22—Major components of the line sampler. The brass T and two end sections are at the upper left in this picture. A completed probe assembly is at the right. The N connectors have their center pins removed. The pins are shown with one inserted in the left end of the inner conductor and the other lying in the right foreground.

impedances of transmission line, see Chapter 24 for suitable ratios of conductor sizes. The photographs and **Fig 21** show construction details.

Soldering of the large parts can be done with a 300-watt iron or a small torch. A neat job can be done if the inside of the T and the outside of the pipe are tinned before assembling. When the pieces are reheated and pushed together, a good mechanical and electrical bond will result. If a torch is used, go easy with the heat, as an overheated and discolored fitting will not accept solder well.

Coaxial connectors with Teflon or other heat-resistant insulation are recommended. Type N, with split-ring retainers for the center conductors, are preferred. Pry the split-ring washers out with a knife point or small screwdriver. Don't lose them, as they'll be needed in the final assembly.

The inner conductor is prepared by making eight radial cuts in one end, using a coping saw with a fine-toothed blade, to a depth of 1/2 inch. The fingers so made are then bent together, forming a tapered end, as shown in **Figs 22** and **23**. Solder the center pin of a coaxial fitting into this, again being careful not to overheat the work.

In preparation for soldering the body of the coax connector to the copper pipe, it is convenient to use a similar fitting clamped into a vise as a holding fixture. Rest the T assembly on top, held in place by its own weight. Use the partially prepared center conductor to assure that the coax connector is concentric with the outer conductor. After being sure that the ends of the pipe are cut exactly perpendicular to the axis, apply heat to the coax fitting, using just enough so a smooth fillet of solder can be formed where the flange and pipe meet.

Before completing the center conductor, check its length. It should clear the inner surface of the connector by the thickness of the split ring on the center pin. File to length; if necessary, slot as with the other end, and solder the center pin in place. The fitting can now be soldered onto the pipe, to complete the 50-Ω line section.

The probe assembly is made from a 1 1/2 inch length of the copper pipe, with a pipe cap on the top to support the upper feedthrough capacitor, C2. The coupling loop is mounted by means of small Teflon standoffs on a copper disc, cut to fit inside the pipe. The disc has four small tabs around the edge for soldering inside the pipe. The diode, D1, is connected between one end of the loop and

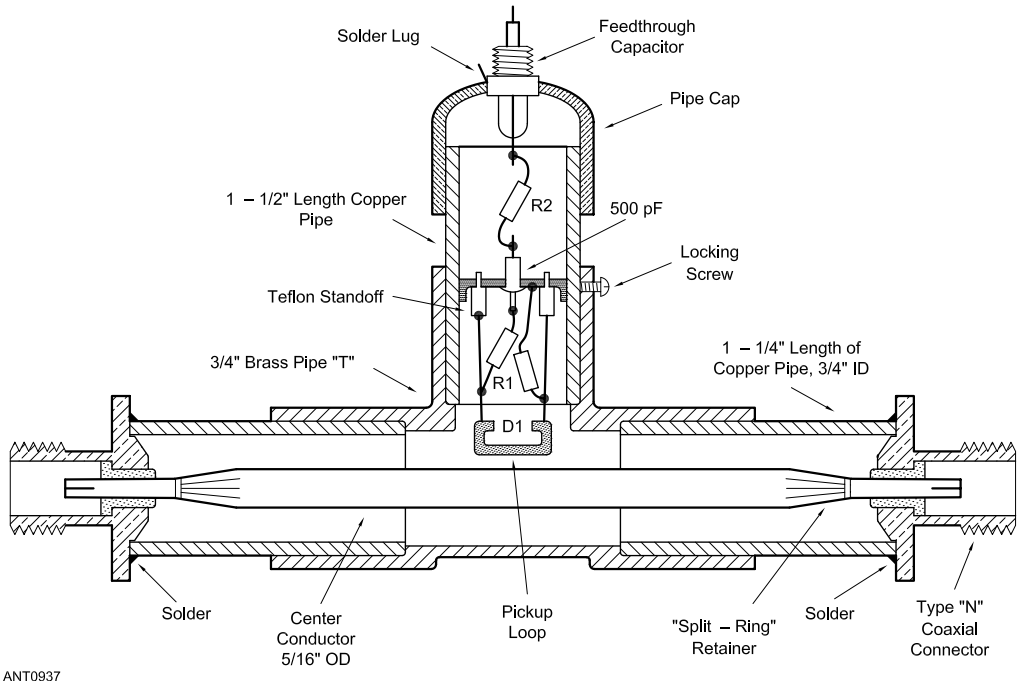

Fig 23—Cross-section view of the line sampler. The pickup loop is supported by two Teflon standoff insulators. The probe body is secured in place with one or more locking screws through holes in the brass T.

a 500-pF feedthrough capacitor, C1, soldered into the disc. The terminating resistor, R1, is connected between the other end of the loop and ground, as directly as possible.

When the disc assembly is completed, insert it into the pipe, apply heat to the outside, and solder the tabs in place by melting solder into the assembly at the tabs. The position of the loop with respect to the end of the pipe will determine the sensitivity of a given probe. For power levels up to 200 watts the loop should extend beyond the face of the pipe about $^{5}/_{32}$ inch. For use at higher power levels the loop should protrude only $^{3}/_{32}$ inch. For operation with very low power levels the best probe position can be determined by experiment.

The decoupling resistor, R2, and feedthrough capacitor, C2, can be connected, and the pipe cap put in place. The threaded portion of the capacitor extends through the cap. Put a solder lug over it before tightening its nut in place. Fasten the cap with two small screws that go into threaded holes in the pipe.

Calibration

The sampler is very useful for many jobs even if it is not accurately calibrated, although it is desirable to calibrate it against a wattmeter of known accuracy. A good 50-Ω VHF dummy load is required.

The first step is to adjust the inductance of the loop, or the value of the terminating resistor, for lowest reflected power reading. The loop is the easier to change. Filing it to reduce its width will increase its impedance. Increasing the cross-section of the loop will lower the impedance, and this can be done by coating it with solder. When the reflected power reading is reduced as far as possible, reverse the probe and calibrate for forward power by increasing the transmitter power output in steps and making a graph of the meter readings obtained. Use the calibration control, R3, to set the maximum reading.

Variations

Rather than to use one sampler for monitoring both forward and reflected power by repeatedly reversing the

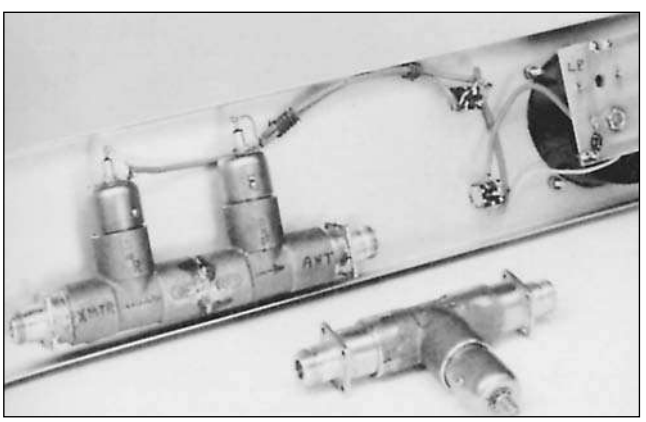

Fig 24—Two versions of the line sampler. The single unit described in detail here is in the foreground. Two sections in a single assembly provide for monitoring forward and reflected power without probe reversal.

probe, it is better to make two assemblies by mounting two T fittings end-to-end, using one for forward and one for reflected power. The meter can be switched between the probes, or two meters can be used.

The sampler described was calibrated at 146 MHz, as it was intended for repeater use. On higher bands the meter reading will be higher for a given power level, and it will be lower for lower frequency bands. Calibration for two or three adjacent bands can be achieved by making the probe depth adjustable, with stops or marks to aid in resetting for a given band. Of course more probes can be made, with each probe calibrated for a given band, as is done in some of the commercially available units.

Other sizes of pipe and fittings can be used by making use of information given in Chapter 24 to select conductor sizes required for the desired impedances. (Since it is occasionally possible to pick up good bargains in 75-Ω line, a sampler for this impedance might be desirable.)

Type-N fittings were used because of their constant impedance and their ease of assembly. Most have the split-ring retainer, which is simple to use in this application. Some have a crimping method, as do apparently all BNC connectors. If a fitting must be used and cannot be taken apart, drill a hole large enough to clear a soldering-iron tip in the copper-pipe outer conductor. A hole of up to $^3/_8$-inch diameter will have very little effect on the operation of the sampler.

A Calorimeter For VHF And UHF Power Measurements

A quart of water in a Styrofoam ice bucket, a roll of small coaxial cable and a thermometer are all the necessary ingredients for an accurate RF wattmeter. Its calibration is independent of frequency. The wattmeter works on the calorimeter principle: A given amount of RF energy is equivalent to an amount of heat, which can be determined by measuring the temperature rise of a known quantity of thermally insulated material. This principle is used in many of the more accurate high-power wattmeters. This procedure was developed by James Bowen, WA4ZRP, and was first described in December 1975 *QST*.

The roll of coaxial cable serves as a dummy load to convert the RF power into heat. RG-174 cable was chosen for use as the dummy load in this calorimeter because of its high loss factor, small size, and low cost. It is a standard 50-Ω cable of approximately 0.11 inch diameter. A prepackaged roll marked as 60 feet long, but measured to be 68 feet, was purchased at a local electronics store. A plot of measured RG-174 loss factor as a function of frequency is shown in **Fig 25**.

In use, the end of the cable not connected to the transmitter is left open-circuited. Thus, at 50 MHz, the reflected wave returning to the transmitter (after making a round trip of 136 feet through the cable) is 6.7 dB × 1.36 = 9.11 dB below the forward wave. A reflected wave 9.11 dB down represents an SWR to the transmitter of 2.08:1. While this value seems larger than would be desired, keep in mind that most 50-MHz transmitters can be tuned to match into an SWR of this magnitude efficiently. To assure accurate results, merely tune the transmitter for maximum power into the load before making

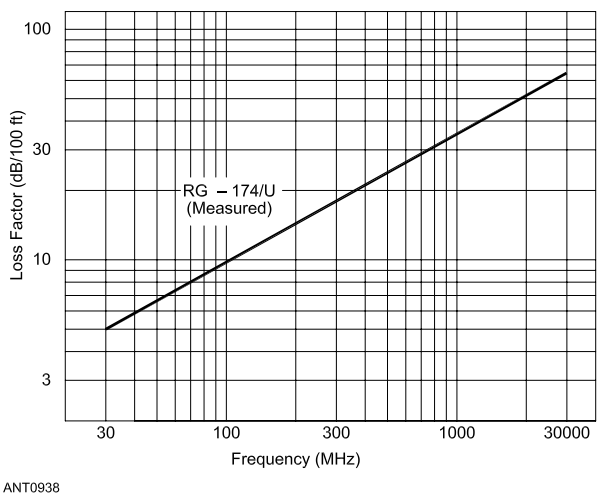

Fig 25—Loss factor of RG-174 coax used in the calorimeter.

Table 4
Calculated Input SWR for 68 Feet of Unterminated RG-174 Cable

Freq. (MHz)	*SWR*
50	2.08
144	1.35
220	1.20
432	1.06
1296	1.003
2304	1.0003

the measurement. At higher frequencies the cable loss increases so the SWR goes down. **Table 4** presents the calculated input SWR values at several frequencies for 68 feet of RG-174. At 1000 MHz and above, the SWR caused by the cable connector will undoubtedly exceed the very low cable SWR listed for these frequencies.

In operation, the cable is submerged in a quart of water and dissipated heat energy flows from the cable into the water, raising the water temperature. See **Fig 26**. The calibration of the wattmeter is based on the physical fact that one calorie of heat energy will raise one gram of liquid water 1° Celsius. Since one quart of water contains 946.3 grams, the transmitter must deliver 946.3 calories of heat energy to the water to raise its temperature 1° C. One calorie of energy is equivalent to 4.186 joules and a joule is equal to 1 W for 1 second. Thus, the heat capacitance of 1 quart of water expressed in joules is 946.3 × 4.186 = 3961 joules/° C.

The heat capacitance of the cable is small with respect to that of the water, but nevertheless its effect should be included for best accuracy. The heat capacitance of the cable was determined in the manner described below. The 68-foot roll of RG-174 cable was raised to a uniform temperature of 100° C by immersing it in a pan of boiling water for several minutes. A quart of tap water was poured into the Styrofoam ice bucket and its temperature was measured at 28.7° C. the cable was then transferred quickly from the boiling water to the water in the ice bucket. After the water temperature in the ice bucket had ceased to rise, it measured 33.0° C. Since the total heat gained by the quart of water was equal to the total heat lost from the cable, we can write the following equation:

$$(\Delta T_{WATER})(C_{WATER}) = -(\Delta T_{CABLE})(C_{CABLE})$$

where

ΔT_{WATER} = the change in water temperature
C_{WATER} = the water heat capacitance
Δ_{CABLE} = the change in cable temperature
C_{CABLE} = the cable heat capacitance

Substituting and solving:

$$(33.0 - 28.7)(3961) = -(33.0 - 100)(C_{CABLE})$$

Thus, the total heat capacitance of the water and cable in the calorimeter is 3961 + 254 = 4215 joules/° C. Since 1° F = 5/9° C, the total heat capacitance can also be expressed as 4215 × 5/9 = 2342 joules/° F.

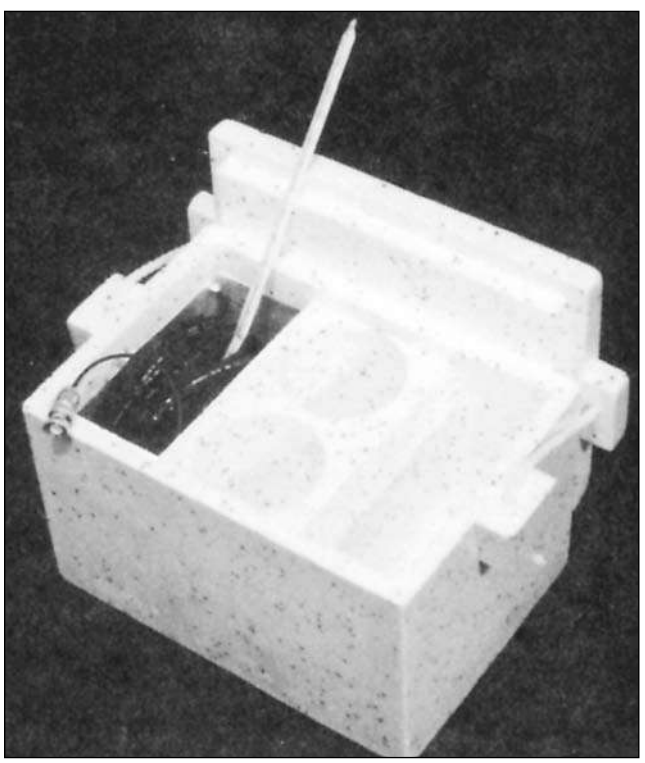

Fig 26—The calorimeter ready for use. The roll of coaxial cable is immersed in one quart of water in the left-hand compartment of the Styrofoam container. Also shown is the thermometer, which doubles as a stirring rod.

Materials and Construction

The quart of water and cable must be thermally insulated to assure that no heat is gained from or lost to the surroundings. A Styrofoam container is ideal for this purpose since Styrofoam has a very low thermal conductivity and a very low thermal capacitance. A local variety store was the source of a small Styrofoam cold chest with compartments for carrying sandwiches and drink cans. The rectangular compartment for sandwiches was found to be just the right size for holding the quart of water and coax.

The thermometer can be either a Celsius or Fahrenheit type, but try to choose one that has divisions for each degree spaced wide enough so that the temperature can be estimated readily to one-tenth degree. Photographic supply stores carry darkroom thermometers, which are ideal for this purpose. In general, glass bulb thermometers are more accurate than mechanical dial-pointer types.

The RF connector on the end of the cable should be a constant-impedance type. A BNC type connector especially designed for use on 0.11-inch diameter cable was located through surplus channels. If you cannot locate one of these, wrap plastic electrical tape around the cable near its end until the diameter of the tape wrap is the same as that of RG-58. Then connect a standard BNC connector for RG-58 in the normal fashion. Carefully seal the opposite open end of the cable with plastic tape or silicone caulking compound so no water can leak into the cable at this point.

Procedure for Use

Pour 1 quart of water (4 measuring cups) into the Styrofoam container. As long as the water temperature is not very hot or very cold, it is unnecessary to cover the top of the Styrofoam container during measurements. Since the transmitter will eventually heat the water sev-

eral degrees, water initially a few degrees cooler than air temperature is ideal because the average water temperature will very nearly equal the air temperature and heat transfer to the air will be minimized.

Connect the RG-174 dummy load to the transmitter through the shortest possible length of lower loss cable such as RG-8. Tape the connectors and adapter at the RG-8 to RG-174 joint carefully with plastic tape to prevent water from leaking into the connectors and cable at this point. Roll the RG-174 into a loose coil and submerge it in the water. Do not bind the turns of the coil together in any way, as the water must be able to freely circulate among the coaxial cable turns. All the RG-174 cable must be submerged in the water to ensure sufficient cooling. Also submerge part of the taped connector attached to the RG-174 as an added precaution.

Upon completing the above steps, quickly tune up the transmitter for maximum power output into the load. Cease transmitting and stir the water slowly for a minute or so until its temperature has stabilized. Then measure the water temperature as precisely as possible. After the initial temperature has been determined, begin the test transmission, measuring the total number of seconds of key-down time accurately. Stir the water slowly with the thermometer and continue transmitting until there is a significant rise in the water temperature, say 5° to 10°. The test may be broken up into a series of short periods, as long as you keep track of the total key-down time. When the test is completed, continue to stir the water slowly and monitor its temperature. When the temperature ceases to rise, note the final indication as precisely as possible.

To compute the transmitter power output, multiply the calorimeter heat capacitance (4215 for C or 2342 for F) by the difference in initial and final water temperature. Then divide by the total number of seconds of key-down time. The resultant is the transmitter power in watts. A nomogram that can also be used to find transmitter power output is given in **Fig 27**. With a straight line, connect the total number of key-down seconds in the time column to the number of degrees change (F or C) in the temperature rise column, and read off the transmitter power output at the point where the straight line crosses the power-output column.

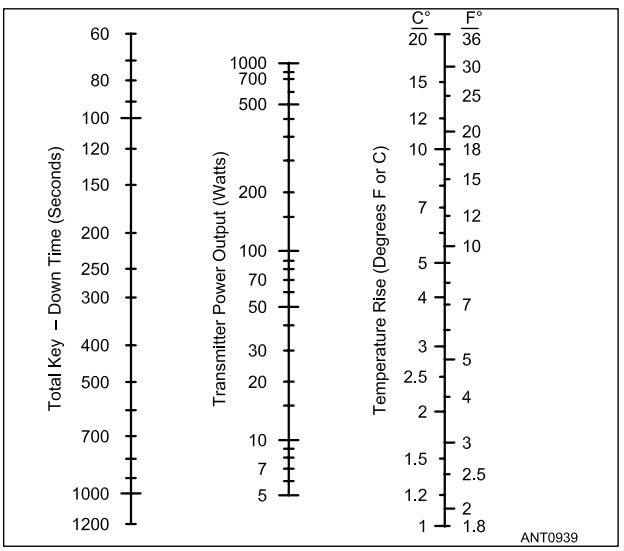

Fig 27—Nomogram for finding transmitter power output for the calorimeter.

Power Limitation

The maximum power handling capability of the calorimeter is limited by the following. At very high powers the dielectric material in the coaxial line will melt because of excessive heating or the cable will arc over from excessive voltage. As the transmitter frequency gets higher, the excessive-heating problem is accentuated, as more of the power is dissipated in the first several feet of cable. For instance, at 1296 MHz, approximately 10% of the transmitting power is dissipated in the first foot of cable. Overheating can be prevented when working with high power by using a low duty cycle to reduce the average dissipated power. Use a series of short transmissions, such as two seconds on, ten seconds off. Keep count of the total key-down time for power calculation purposes. If the cable arcs over, use a larger-diameter cable, such as RG-58, in place of the RG-174. The cable should be long enough to assure that the reflected wave will be down 10 dB or more at the input. It may be necessary to use more than one quart of water in order to submerge all the cable conveniently. If so, be sure to calculate the new value of heat capacitance for the larger quantity of water. Also you should measure the new coaxial cable heat capacitance using the method previously described.

A Noise Bridge For 1.8 Through 30 MHz

The noise bridge, sometimes referred to as an antenna (RX) noise bridge, is an instrument for measuring the impedance of an antenna or other electrical circuits. The unit shown here in **Fig 28**, designed for use in the 1.8 through 30-MHz range, provides adequate accuracy for most measurements. Battery operation and small physical size make this unit ideal for remote-location use. Tone modulation is applied to the wide-band noise generator as an aid for obtaining a null indication. A detector, such as the station receiver, is required for operation.

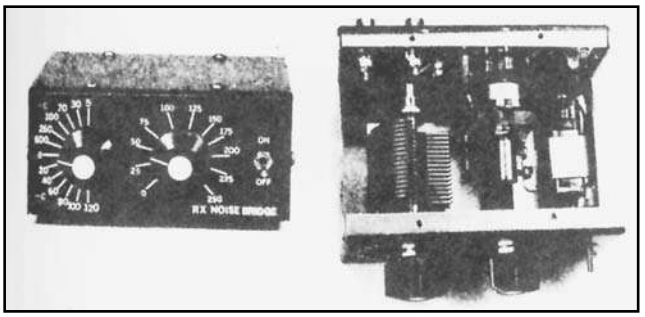

Fig 28—Exterior and interior views of the noise bridge. The unit is finished in red enamel. Press-on lettering is used for the calibration marks. Note that the potentiometer must be isolated from ground.

The noise bridge consists of two parts—the noise generator and the bridge circuitry. See **Fig 29**. A 6.8-V

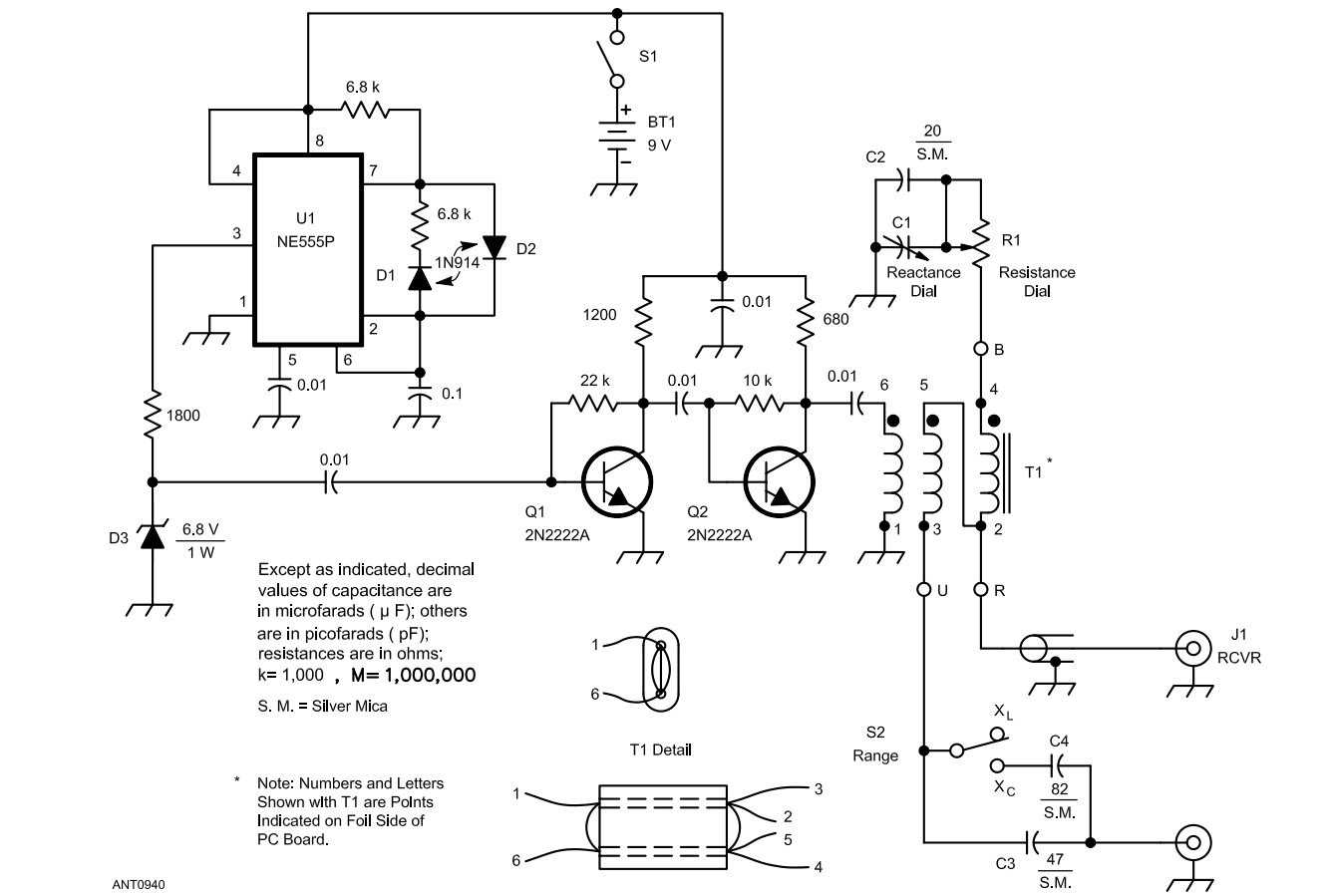

Fig 29—Schematic diagram of the noise bridge. Use 1/4 W composition resistors. Capacitors are miniature ceramic units unless indicated otherwise. Component designations indicated in the schematic but not called out in the parts list are for text and parts-placement reference only.

BT1—9-V battery, NEDA 1604A or equiv.
C1—15- to 150-pF variable
C2—20-pF mica.
C3—47-pF mica.
C4—82-pF mica.
J1, J2—Coaxial connector.
R1—Linear, 250 Ω, AB type. Use a good grade of resistor.
S1, S2—Toggle, SPST.
T1—Transformer; 3 windings on an Amidon BLN-43-2402 ferrite binocular core. Each winding is three turns of #30 enameled wire. One turn is equal to the wire passing once through both holes in the core. The primary winding starts on one side of the transformer, and the secondary and tertiary windings start on the opposite side.
U1—Timer, NE555 or equiv.

Zener diode serves as the noise source. U1 generates an approximate 50% duty cycle, 1000-Hz square wave signal which is applied to the cathode of the Zener diode. The 1000-Hz modulation appears on the noise signal and provides a useful null detection enhancement effect. The broadband-noise signal is amplified by Q1, Q2 and associated components to a level that produces an approximate S9 signal in the receiver. Slightly more noise is available at the lower end of the frequency range, as no frequency compensation is applied to the amplifier. Roughly 20 mA of current is drawn from the 9-V battery, thus ensuring long battery life—providing the power is switched off after use!

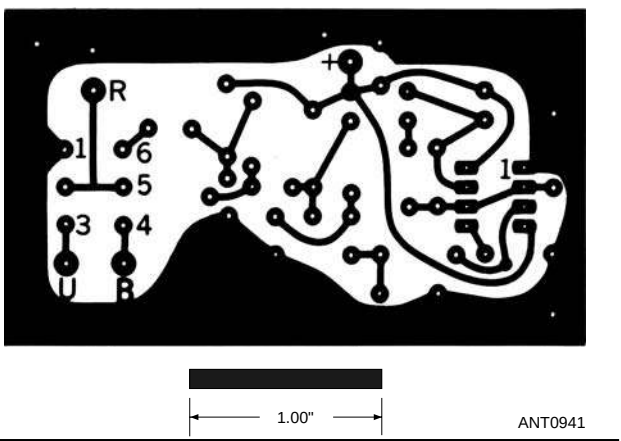

Fig 30—Etching pattern for the noise bridge PC board, at actual size. Black represents copper. This is the pattern for the bottom side of the board. The top side of the board is a complete ground plane with a small amount of copper removed from around the component holes.

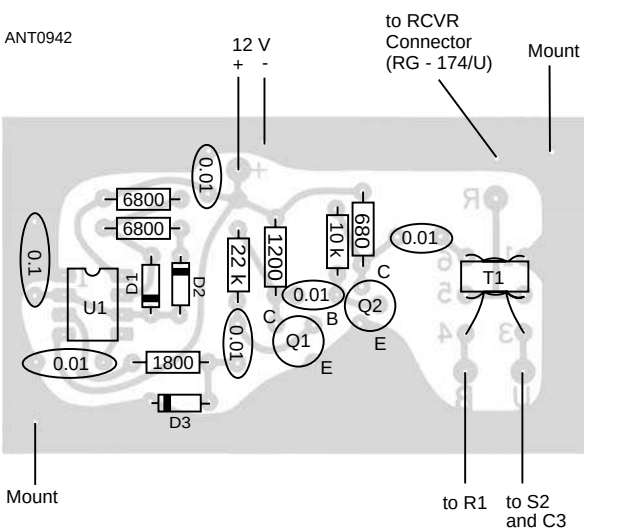

Fig 31—Parts-placement guide for the noise bridge as viewed from the component or top side of the board. Mounting holes are located in two corners of the board, as shown.

The bridge portion of the circuit consists of T1, C1, C2 and R1. T1 is a trifilar wound transformer with one of the windings used to couple noise energy into the bridge circuit. The remaining two windings are arranged so that each one is in an arm of the bridge. C1 and R1 complete one arm and the UNKNOWN circuit, along with C2, comprise the remainder of the bridge. The terminal labeled RCVR is for connection to the detector.

The reactance range of a noise bridge is dependent on several factors, including operating frequency, value of the series capacitor (C3 or C3 plus C4 in Fig 29) and the range of the variable capacitor (C1 in Fig 29). The RANGE switch selects reactance measurements weighted toward either capacitance or inductance by placing C4 in parallel with C3. The zero-reactance point occurs when C1 is either nearly fully meshed or fully unmeshed. The RANGE switch nearly doubles the resolution of the reactance readings.

CONSTRUCTION

The noise bridge is contained in a homemade aluminum enclosure that measures $5 \times 2^{3}/_{8} \times 3^{3}/_{4}$ inches. Many of the circuit components are mounted on a circuit board that is fastened to the rear wall of the cabinet. The circuit-board layout is such that the lead lengths to the board from the bridge and coaxial connectors are at a minimum. An etching pattern and a parts-placement guide for the circuit board are shown in **Figs 30** and **31**.

Care must be taken when mounting the potentiometer, R1. For accurate readings the potentiometer must be well insulated from ground. In the unit shown this was accomplished by mounting the control on a piece of plexiglass, which in turn was fastened to the chassis with a piece of aluminum angle stock.

Additionally, a $^{1}/_{4}$-inch control-shaft coupling and a length of phenolic rod were used to further isolate the control from ground where the shaft passes through the front panel. A high-quality potentiometer is required if good measurement results are to be obtained.

There is no such problem when mounting the variable capacitor because the rotor is grounded. Use a high-quality capacitor; do not try to save money on that component. Two RF connectors on the rear panel are connected to a detector (receiver) and to the UNKNOWN circuit. Do not use plastic-insulated phono connectors (they might influence bridge accuracy at higher frequencies). Use miniature coaxial cable (RG-174) between the RCVR connector and circuit board. Attach one end of C3 to the circuit board and the other directly to the UNKNOWN circuit connector.

Bridge Compensation

Stray capacitance and inductance in the bridge circuit can affect impedance readings. If a very accurate bridge is required, use the following steps to counter the effects of stray reactance. Because the physical location

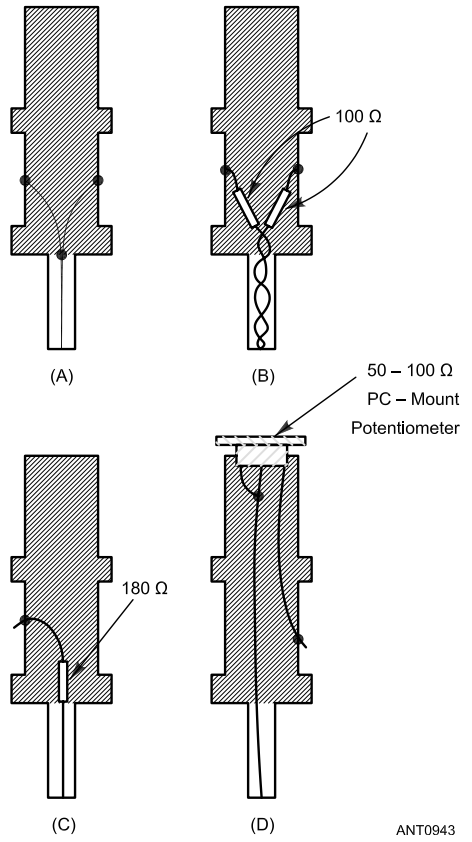

Fig 32—Construction details of the resistive loads used to check and calibrate the noise bridge. Each of the loads is constructed inside a coaxial connector that matches those on the bridge. (Views shown are cross-sections of PL-259 bodies; the sleeves are not shown.) Leads should be kept as short as possible to minimize parasitic inductance. A is a 0-Ω load; B depicts a 50-Ω load; C is a 180-Ω load; D shows a variable-resistance load used to determine the loss in a coaxial cable.

of the board, connectors and controls in the cabinet determine where compensation is needed, there is no provision for the compensation components on the printed circuit board.

Good calibration loads are necessary to check the accuracy of the noise bridge. Four are needed here: a 0-Ω (short-circuit) load, a 50-Ω load, a 180-Ω load, and a variable-resistance load. The short-circuit and fixed-resistance loads are used to check the accuracy of the noise bridge; the variable-resistance load is used when measuring coaxial-cable loss.

Construction details of the loads are shown in **Fig 32**. Each load is constructed inside a connector. When building the loads, keep leads as short as possible to minimize parasitic effects. The resistors must be noninductive (*not* wirewound).

Quarter-watt, carbon-composition resistors should work fine. The potentiometer in the variable-resistance load is a miniature PC-mount unit with a maximum resistance of 100 Ω or less. The potentiometer wiper and one of the end leads are connected to the center pin of the connector; the other lead is connected to ground.

Stray Capacitance

Stray capacitance on the variable-resistor side of the bridge tends to be higher than that on the unknown side. This is so because the parasitic capacitance in the variable resistor, R1, is comparatively high.

The effect of parasitic capacitance is most easily detected using the 180-Ω load. Measure and record the actual resistance of the load, R_L. Connect the load to the UNKNOWN connector, place S2 in the X_L position, tune the receiver to 1.8 MHz, and null the bridge. (See the section, "Finding the Null" for tips.) Use an ohmmeter across R1 to measure its dc resistance. The magnitude of the stray capacitance can be calculated by

$$C_P = C3\left(\sqrt{\frac{R1}{R2}} - 1\right) \qquad \text{(Eq 4)}$$

where

R_L = load resistance (as measured)
R1 = resistance of the variable resistor
C3 = series capacitance.

You can compensate for C_P by placing a variable capacitor, C_C, in the side of the bridge with lesser stray capacitance. If R1 is greater than R_L, stray capacitance is greater on the variable resistor side of the bridge: Place C_C between point U (on the circuit board) and ground. If R1 is less than R_L, stray capacitance is greater on the unknown side: Place C_C between point B and ground. If the required compensating capacitance is only a few picofarads, you can use a gimmick capacitor (made by twisting two short pieces of insulated, solid wire together) for C_C. A gimmick capacitor is adjusted by trimming its length.

Stray Inductance

Parasitic inductance, if present, should be only a few tens of nanohenries. This represents a few ohms of inductive reactance at 30 MHz. The effect is best observed by reading the reactance of the 0-Ω test load at 1.8 and 30 MHz; the indicated reactance should be the same at both frequencies.

If the reactance reading decreases as frequency is increased, parasitic inductance is greater in the known arm, and compensating inductance is needed between point U and C3. If the reactance increases with frequency, the unknown-arm inductance is greater, and compensating inductance should be placed between point B and R1.

Compensate for stray inductance by placing a single-turn coil, made from a 1 to 2-inch length of solid wire, in the appropriate arm of the bridge. Adjust the size of this coil until the reactance reading remains constant from 1.8 to 30 MHz.

Calibration

Good calibration accuracy is necessary for accurate noise-bridge measurements. Calibration of the resistance scale is straightforward. To do this, tune the receiver to a frequency near 10 MHz. Attach the 0-Ω load to the UNKNOWN connector and null the bridge. This is the zero-resistance point; mark it on the front-panel resistance scale. The rest of the resistance range is calibrated by adjusting R1, measuring R1 with an accurate ohmmeter, calculating the increase from the zero point and marking the increase on the front panel.

Most bridges have the reactance scale marked in capacitance because capacitance does not vary with frequency. Unfortunately, that requires calibration curves or non-trivial calculations to arrive at the load reactance. An alternative method is to mark the reactance scale in *ohms* at a reference frequency of 10 MHz. This method calibrates the bridge near the center of its range and displays reactance directly, but it requires a simple calculation to scale the reactance reading for frequencies other than 10 MHz. The scaling equation is:

$$X_{u(f)} = X_{u(10)} \frac{10}{f} \qquad \text{(Eq 5)}$$

where

f = frequency in MHz

$X_{u(10)}$ = reactance of the unknown load at 10 MHz

$X_{u(f)}$ = reactance of the unknown load at f.

A shorted piece of coaxial cable serves as a reactance source. (The reactance of a shorted, low-loss coaxial cable is dependent only on the cable length, the measurement frequency and the cable characteristic impedance.) Radio Shack RG-8M is used here because it is readily available, has relatively low loss and has an almost purely resistive characteristic impedance.

Prepare the calibration cable as follows:

1) Cut a length of coaxial cable that is slightly longer than ¼ λ at 10 MHz (about 20 feet for RG-8M). Attach a suitable connector to one end of the cable; leave the other end open-circuited.
2) Connect the 0-Ω load to the noise bridge UNKNOWN connector and set the receiver frequency to 10 MHz. Adjust the noise bridge for a null. Do not adjust the reactance control after the null is found.
3) Connect the calibration cable to the bridge UNKNOWN terminal. Null the bridge by adjusting *only* the variable resistor and the receiver frequency. The receiver frequency should be less than 10 MHz; if it is above 10 MHz, the cable is too short, and you need to prepare a longer one.
4) Gradually cut short lengths from the end of the coaxial cable until you obtain a null at 10 MHz by adjusting only the resistance control. Then connect the cable center and shield conductors at the open end with a short length of braid. Verify that the bridge nulls with zero reactance at 20 MHz.
5) The reactance of the coaxial cable (normalized to 10 MHz) can be calculated from:

$$X_{i(10)} = R_0 \frac{f}{10} \tan\left(2\pi \frac{f}{40}\right) \qquad \text{(Eq 6)}$$

where

$X_{i(10)}$ = cable reactance at 10 MHz

R_0 = characteristic resistance of the coaxial cable (52.5 Ω for Radio Shack RG-8M)

f = frequency in MHz

The results of Eq 6 have less than 5% error for reactances less than 500 Ω, so long as the test-cable loss is less than 0.2 dB. This error becomes significantly less at lower reactances (2% error at 300 Ω for a 0.2-dB-loss cable). The loss in 18 feet of RG-8M is 0.13 dB at 10 MHz. Reactance data for Radio Shack RG-8M is given in **Table 5**.

Table 5

Noise Bridge Calibration Data: Coaxial-Cable Method

This data is for Radio Shack RG-8M cable (R_0 =52.5 Ω) cut to exactly ¼ λ at 10 MHz; the reactances and capacitances shown correspond to this frequency.

Reactance				Capacitance	
X_i	f(MHz)	X_i	f(MHz)	C(pF)	f(MHz)
10	3.318	–10	19.376	10	9.798
20	4.484	–20	18.722	20	9.612
30	5.262	–30	18.048	30	9.440
40	5.838	–40	17.368	40	9.280
50	6.286	–50	16.701	50	9.130
60	6.647	–60	16.062	60	8.990
70	6.943	–70	15.471	70	8.859
80	7.191	–80	14.936	80	8.735
90	7.404	–90	14.462	90	8.618
100	7.586	–100	14.044	100	8.508
110	7.747	–110	13.682	110	8.403
120	7.884	–120	13.369	120	8.304
130	8.009	–130	13.097	130	8.209
140	8.119	–140	12.861	140	8.119
150	8.217	–150	12.654		
160	8.306	–160	12.473		
170	8.387	–170	12.313		
180	8.460	–180	12.172		
190	8.527	–190	12.045		
200	8.588	–200	11.932	C(pF)	f(MHz)
210	8.645	–210	11.831	–10	10.219
220	8.697	–220	11.739	–20	10.459
230	8.746	–230	11.655	–30	10.721
240	8.791	–240	11.579	–40	11.010
250	8.832	–250	11.510	–50	11.328
260	8.872	–260	11.446	–60	11.679
270	8.908	–270	11.387	–70	12.064
280	8.942	–280	11.333	–80	12.484
290	8.975	–290	11.283	–90	12.935
300	9.005	–300	11.236	–100	13.407
350	9.133	–350	11.045	–110	13.887
400	9.232	–400	10.905	–120	14.357
450	9.311	–450	10.798	–130	14.801
500	9.375	–500	10.713	–140	15.211

With the prepared cable and calibration values on hand, proceed to calibrate the reactance scale. Tune the receiver to the appropriate frequency for the desired reactance (given in Table 5, or found using Eq 6). Adjust the resistance and reactance controls to null the bridge. Mark the reactance reading on the front panel. Repeat this process until all desired reactance values have been marked. The resistance values needed to null the bridge during this calibration procedure may be significant (more than 100 Ω) at the higher reactances.

This calibration method is much more accurate than using fixed capacitors across the UNKNOWN connector. Also, you can calibrate a noise bridge in less than an hour using this method.

Finding the Null

In use, a receiver is attached to the RCVR connector and some load of unknown value is connected to the UNKNOWN terminal. The receiver allows us to hear the noise present across the bridge arms at the frequency of the receiver passband. The strength of the noise signal depends on the strength of the noise-bridge battery, the receiver bandwidth/sensitivity and the impedance difference between the known and unknown bridge arms. The noise is stronger and the null more obvious with wide receiver passbands. Set the receiver to the widest bandwidth AM mode available.

The noise-bridge output is heard as a 1000-Hz tone. When the impedances of the known and unknown bridge arms are equal, the voltage across the receiver is minimized; this is a null. In use, the null may be difficult to find because it appears only when both bridge controls approach the values needed to balance the bridge.

To find the null, set C1 to mid-scale, sweep R1 slowly through its range and listen for a reduction in noise (it's also helpful to watch the S meter). If no reduction is heard, set R1 to mid-range and sweep C1. If there is still no reduction, begin at one end of the C1 range and sweep R1. Increment C1 about 10% and sweep R1 with each increment until some noise reduction appears. Once noise reduction begins, adjust C1 and R1 alternately for minimum signal.

MEASURING COAXIAL-CABLE PARAMETERS WITH A NOISE BRIDGE

Coaxial cables have a number of properties that affect the transmission of signals through them. Generally, radio amateurs are concerned with cable attenuation and characteristic impedance. If you plan to use a noise bridge or SWR analyzer to make antenna-impedance measurements, however, you need to accurately determine not just cable impedance and attenuation, but also electrical length. Fortunately, all of these parameters are easy to measure with an accurate noise bridge or SWR analyzer.

Cable Electrical Length

With a noise bridge and a general-coverage receiver, you can easily locate frequencies at which the line in question is a multiple of $^1/_2$ λ, because a shorted $^1/_2$ λ line has a 0-Ω impedance (neglecting line loss). By locating two adjacent null frequencies, you can solve for the length of line in terms of $^1/_2$ λ at one of the frequencies and calculate the line length (overall accuracy is limited by bridge accuracy and line loss, which broadens the nulls). As an interim variable, you can express cable length as the frequency at which a cable is 1 λ long. This length will be represented by f λ. Follow these steps to determine f λ for a coaxial cable.

1) Tune the receiver to the frequency range of interest. Attach the short-circuit load to the noise bridge UNKNOWN connector and null the bridge.
2) Disconnect the far end of the coaxial cable from its load (the antenna) and connect it to the 0-Ω test load. Connect the near end of the cable to the bridge UNKNOWN connector.
3) Adjust the receiver frequency and the noise-bridge resistance control for a null. *Do not change the noise bridge reactance-control setting during this procedure*. Note the frequency at which the null is found; call this frequency f_n. The noise-bridge resistance at the null should be relatively small (less than 20 Ω).
4) Tune the receiver upward in frequency until the next null is found. Adjust the resistance control, if necessary, to improve the null, *but do not adjust the reactance control*. Note the frequency at which this second null is found; this is f_{n+2}.
5) Solve Eq 7 for n and the electrical length of the cable.

$$n = \frac{2f_n}{f_{n+2} - f_n} \qquad \text{(Eq 7)}$$

$$f_\lambda = \frac{4f_n}{n} \qquad \text{(Eq 8)}$$

where

n = cable electrical length in quarter waves, at f_n
f_l = frequency at which the cable is 1λ
ℓ = cable electrical length, in λ

For example, consider a 74-foot length of Columbia 1188 foam-dielectric cable (velocity factor = 0.78) to be used on the 10-meter band. Based on the manufacturer's specification, the cable is 2.796 λ at 29 MHz. Nulls were found at 24.412 (f_n) and 29.353 (f_{n+2}) MHz. Eq 7 yields n = 9.88, which produces 9.883 MHz from Eq 8 and 2.934 l for Eq 9. If the manufacturer's specification is correct, the measured length is off by less than 5%, which is very reasonable. Ideally, n would yield an integer. The difference between n and the closest integer indicates that there is some error.

This procedure also works for lines with an open circuit as the termination (n will be close to an odd number). End effects from the PL-259 increase the effective length of the coaxial cable; however, this decreases the calculated f_λ.

Cable Characteristic Impedance

The characteristic impedance of the coaxial cable is found by measuring its input impedance at two frequencies separated by $^1/_4\ f_\lambda$. This must be done when the cable is terminated in a resistive load.

Characteristic impedance changes slowly as a function of frequency, so this measurement must be done near the frequency of interest. The measurement procedure is as follows.

1) Place the 50-Ω load on the far end of the coaxial cable and connect the near end to the UNKNOWN connector of the noise bridge. (Measurement error is minimized when the load resistance is close to the characteristic impedance of the cable. This is the reason for using the 50-Ω load.)
2) Tune the receiver approximately $^1/_8$ f below the frequency of interest. Adjust the bridge resistance and reactance controls to obtain a null, and note their readings as R_{f1} and X_{f1}. Remember, the reactance reading must be scaled to the measurement frequency.
3) Increase the receiver frequency by exactly $^1/_4\ f\lambda$. Null the bridge again, and note the readings as R_{f2} and X_{f2}.
4) Calculate the characteristic impedance of the coaxial cable using Eqs 10 through 15. A scientific calculator is helpful for this.

$$\ell = \frac{f_0}{f_\lambda} \qquad \text{(Eq 9)}$$

$$R = R_{f1} \times F_{f2} - X_{f1} \times X_{f2} \qquad \text{(Eq 10)}$$

$$X = R_{f1} \times X_{f2} + X_{f1} \times R_{f2} \qquad \text{(Eq 11)}$$

$$Z = \sqrt{R^2 + X^2} \qquad \text{(Eq 12)}$$

$$R_0 = \sqrt{Z}\cos\left[\frac{1}{2}\tan^{-1}\left(\frac{X}{R}\right)\right] \qquad \text{(Eq 13)}$$

$$X_0 = \sqrt{Z}\sin\left[\frac{1}{2}\tan_{-1}\left(\frac{X}{R}\right)\right] \qquad \text{(Eq 14)}$$

$$Z_0 = R_0 + jX_0 \qquad \text{(Eq 15)}$$

Let's continue with the example used earlier for cable length. The measurements are:

f1 = 29.000 – (9.883 / 8) = 27.765 MHz
R_{f1} = 64 Ω
X_{f1} = –22 Ω × (10 / 27.765) = –7.9 Ω
f2 = 27.765 + (9.883/4) = 30.236 MHz
R_{f2} = 50 Ω
X_{f2} = –24 Ω × (10 / 30.236) = –7.9 Ω

When used in Eqs 10 through 15, these data yield:

R = 3137.59
X = –900.60
Z = 3264.28
R_0 = 56.58 Ω
X_0 = –7.96 Ω

Cable Attenuation

Cable loss can be measured once the cable electrical length and characteristic resistance are known. The measurement must be made at a frequency where the cable presents no reactance. Reactance is zero when the cable electrical length is an integer multiple of λ/4. You can easily meet that condition by making the measurement frequency an integer multiple of $^1/_4\ f\lambda$. Loss at other frequencies can be interpolated with reasonable accuracy. This procedure employs a resistor-substitution method that provides much greater accuracy than is achieved by directly reading the resistance from the noise-bridge scale.

1) Determine the approximate frequency at which you want to make the loss measurement by using

$$n = \frac{4f_0}{f_\lambda} \qquad \text{(Eq 16A)}$$

Round n to the nearest integer, then

$$f1 = \frac{n}{4}\ f_\lambda \qquad \text{(Eq 16B)}$$

2) If n is odd, leave the far end of the cable open; if n is even, connect the 0-Ω load to the far end of the cable. Attach the near end of the cable to the UNKNOWN connector on the noise bridge.
3) Set the noise bridge to zero reactance and the receiver to f1. Fine tune the receiver frequency and the noise-bridge resistance to find the null.
4) Disconnect the cable from the UNKNOWN terminal, and connect the variable-resistance calibration load in its place. Without changing the resistance setting on the bridge, adjust the load resistor and the bridge reactance to obtain a null.
5) Remove the variable-resistance load from the bridge UNKNOWN terminal and measure the load resistance using an ohmmeter that's accurate at low resistance levels. Refer to this resistance as R_i.
6) Calculate the cable loss in decibels using

$$a\ell = 8.69\ \frac{R_i}{R_0} \qquad \text{(Eq 17)}$$

To continue this example, Eq 16A gives n = 11.74, so measure the attenuation at n = 12. From Eq 16B, f1 = 29.649 MHz. The input resistance of the cable measures 12.1 Ω with 0-Ω load on the far end of the cable; this corresponds to a loss of 1.86 dB.

USING A BRIDGE TO MEASURE THE IMPEDANCE OF AN ANTENNA

The impedance at the end of a transmission line can be easily measured using a noise bridge or SWR analyzer. In many cases, however, you really want to measure the impedance of an antenna—that is, the impedance of the load at the far end of the line. There are several ways to handle this.

1) Measurements can be made with the bridge at the antenna. This is usually not practical because the antenna must be in its final position for the measurement to be accurate. Even if it can be done, making such a measurement is certainly not very convenient.
2) Measurements can be made at the source end of a coaxial cable—if the cable length is an exact integer multiple of $^1/_2$ λ. This effectively restricts measurements to a single frequency.
3) Measurements can be made at the source end of a coaxial cable and corrected using a Smith Chart as shown in Chapter 28. This graphic method can result in reasonable estimates of antenna impedance—as long as the SWR is not too high and the cable is not too lossy. However, it doesn't compensate for the complex impedance characteristics of real-world coaxial cables. Also, compensation for cable loss can be tricky to apply. These problems, too, can lead to significant errors.
4) Last, measurements can be corrected using the transmission-line equation. The *TLW* program included on the CD-ROM in the back of this book, can do these complicated computations for you. This is the best method for calculating antenna impedances from measured parameters, but it requires that you measure the feed-line characteristics beforehand—measurements for which you need access to both ends of the feed line.

The procedure for determining antenna impedance is to first measure the electrical length, characteristic impedance, and attenuation of the coaxial cable connected to the antenna. After making these measurements, connect the antenna to the coaxial cable and measure the input impedance of the cable at a number of frequencies. Then use these measurements in the transmission-line equation to determine the actual antenna impedance at each frequency.

Table 6 and **Fig 33** give an example of such a calculation. The antenna used for this example is a 10-meter inverted V about 30 feet above the ground. The arms of the antenna are separated by a 120° angle. Each arm is exactly 8 feet long, and the antenna is made of #14 wire. The feed line is the 74-foot length of Columbia 1188 characterized earlier.

See Fig 33A. From this plot of impedance measurements, it is very difficult to determine anything about the antenna. Resistance and reactance vary substantially over this frequency range, and the antenna appears to be resonant at 27.7, 29.0 and 29.8 MHz.

The plot in Fig 33B shows the true antenna imped-

Table 6
Impedance Data for Inverted-V Antenna

Freq (MHz)	*R_u (Ω)*	*X_u @ 10 MHz (Ω)*	*X_u (Ω)*	*R_L (Ω)*	*X_L (Ω)*
27.0	44	85	31.5	24	–65
27.2	60	95	34.9	26	–56
27.4	75	85	31.0	30	–51
27.6	90	40	14.5	32	–42
27.8	90	–20	–7.2	35	–34
28.0	75	–58	–20.7	38	–24
28.2	65	–65	–23.0	40	–19
28.4	56	–52	–18.3	44	–12
28.6	50	–40	–14.0	44	–6
28.8	48	–20	–6.9	47	1
29.0	50	0	0.0	52	8
29.2	55	20	6.8	57	15
29.4	64	30	10.2	63	21
29.6	78	20	6.8	75	26
29.8	85	0	0	78	30
30.0	90	–50	–16.7	89	33

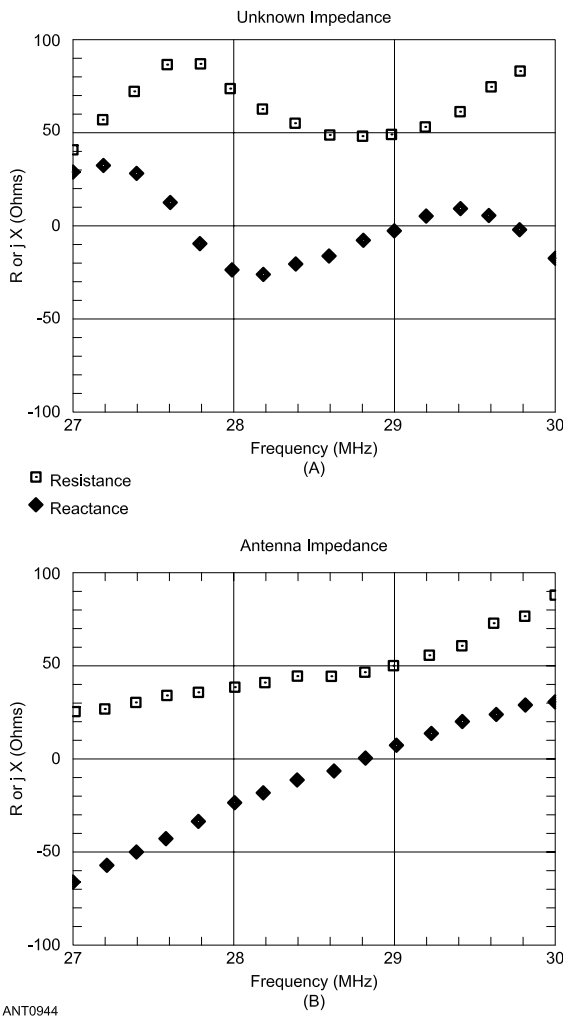

Fig 33–Impedance plot of an inverted-V antenna cut for 29 MHz. At A, a plot of resistances and reactances, measured using the noise bridge, at the end of a 74-foot length of Columbia 1188 coaxial cable. At B, the actual antenna-impedance plot (found using the transmission-line equation to remove the effects of the transmission line).

ance. This plot has been corrected for the effects of the cable using the transmission-line equation. The true antenna resistance and reactance both increase smoothly with frequency. The antenna is resonant at 28.8 MHz, with a radiation resistance at resonance of 47 Ω. This is normal for an inverted V.

When doing the conversions, be careful not to make measurement errors. Such errors introduce more errors into the corrected data. This problem is most significant when the transmission line is near an odd multiple of a $^1/_4$ λ and the line SWR and/or attenuation is high. Measurement errors are probably present if small changes in the input impedance or transmission-line characteristics appear as large changes in antenna impedance. If this effect is present, it can be minimized by making the measurements with a transmission line that is approximately an integer multiple of $^1/_2$ λ.

A Practical Time-Domain Reflectometer

A time-domain reflectometer (TDR) is a simple but powerful tool used to evaluate transmission lines. When used with an oscilloscope, a TDR displays impedance "bumps" (open and short circuits, kinks and so on) in transmission lines. Commercially produced TDRs cost from hundreds to thousands of dollars each, but you can add the TDR described here to your shack for much less. This material is based on a *QST* article by Tom King, KD5HM (see Bibliography), and supplemented with information from the references.

How a TDR Works

A simple TDR consists of a square-wave generator and an oscilloscope. See **Fig 34**. The generator sends a train of dc pulses down a transmission line, and the oscilloscope lets you observe the incident and reflected waves from the pulses (when the scope is synchronized to the pulses).

A little analysis of the scope display tells the nature and location of any impedance changes along the line. The nature of an impedance disturbance is identified by comparing its pattern to those in **Fig 35**. The patterns are based on the fact that the reflected wave from a disturbance is determined by the incident-wave magnitude and the reflection coefficient of the disturbance. (The patterns shown neglect losses; actual patterns may vary somewhat from those shown.)

The location of a disturbance is calculated with a simple proportional method: The round-trip time (to the disturbance) can be read from the oscilloscope screen (graticule). Thus, you need only read the time, multiply it by the velocity of the radio wave (the speed of light adjusted by the velocity factor of the transmission line) and divide by two. The distance to a disturbance is given by:

$$\ell = \frac{983.6 \times VF \times t}{2} \qquad \text{(Eq 18)}$$

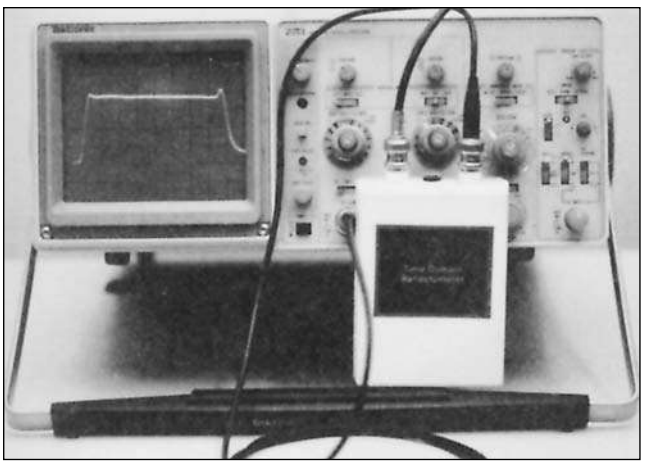

Fig 34—The time-domain reflectometer shown here is attached to a small portable oscilloscope.

where

ℓ = line length in feet
VF = velocity factor of the transmission line (from 0 to 1.0)
t = time delay in microseconds (μs).

The Circuit

The time-domain reflectometer circuit in **Fig 36** consists of a CMOS 555 timer configured as an astable multivibrator, followed by an MPS3646 transistor acting as a 15-ns-risetime buffer. The timer provides a 71-kHz square wave. This is applied to the 50-Ω transmission line under test (connected at J2). The oscilloscope is connected to the circuit at J1.

Construction

An etching pattern for the TDR is shown in **Fig 37**. **Fig 38** is the part-placement diagram. The TDR is

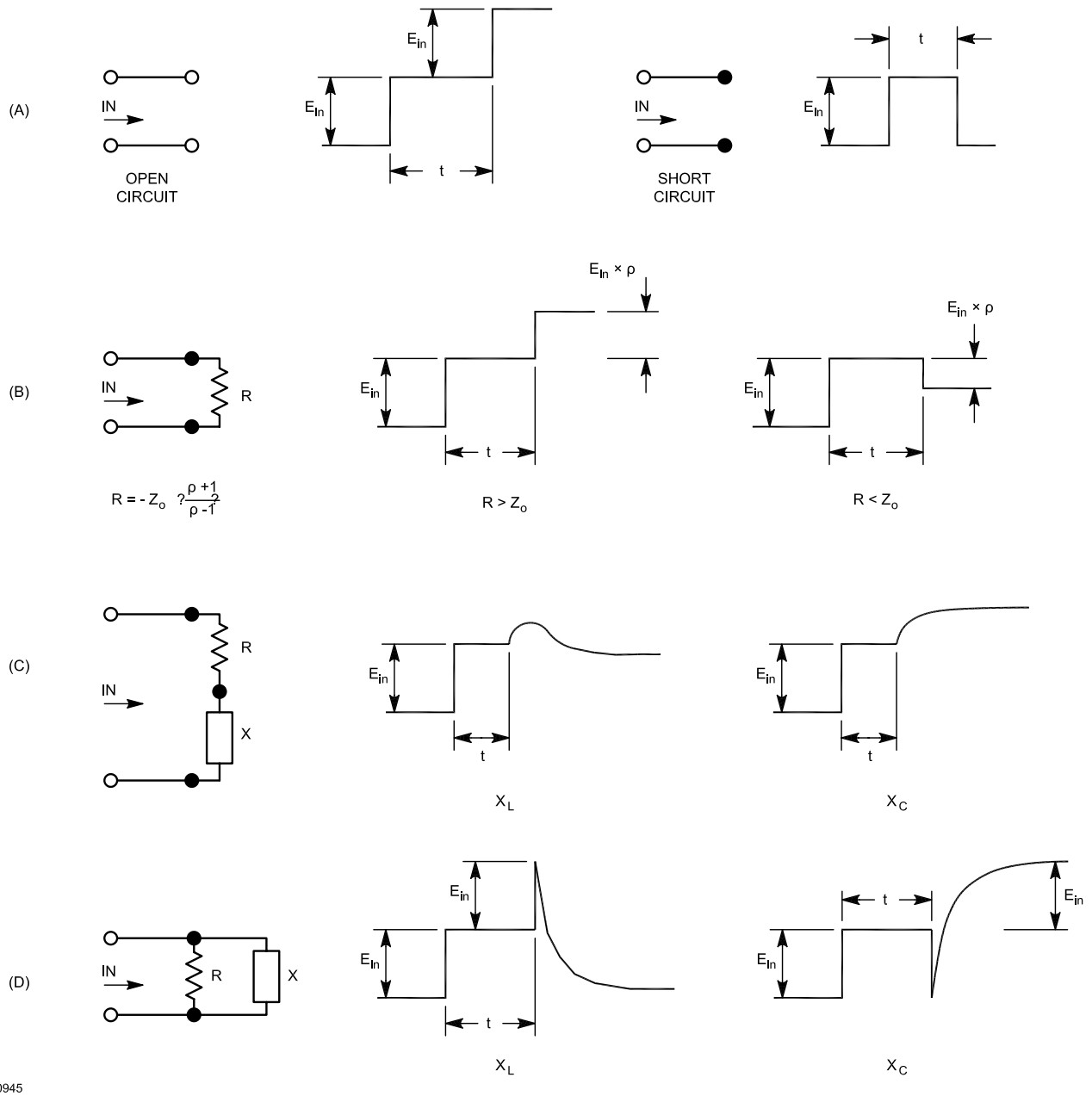

Fig 35—Characteristic TDR patterns for various loads. The location of the load can be calculated from the transit time, t, which is read from the oscilloscope (see text). R values can be calculated as shown (for purely resistive loads only—$\rho < 0$ when $R < Z_0$; $\rho < 0$ when $R > Z_0$). Values for reactive loads cannot be calculated simply.

designed for a 4 × 3 × 1-inch enclosure (including the batteries). Sl, Jl and J2 are right-angle-mounted components. Two aspects of construction are critical. First use *only* an MPS3646 for Q1. This type was chosen for its good performance in this circuit. If you substitute another transistor, the circuit may not perform properly.

Second, for the TDR to provide accurate measurements, the cable connected to J1 (between the TDR and the oscilloscope) must not introduce impedance mismatches in the circuit. *Do not make this cable from ordinary coaxial cable.* Oscilloscope-probe cable is the best thing to use for this connection.

(It took the author about a week and several phone calls to determine that scope-probe cable isn't "plain old coax." Probe cable has special characteristics that prevent undesired ringing and other problems.)

Mount a binding post at J1 and connect a scope probe to the binding post when testing cables with the TDR. R5 and C2 form a compensation network—much like the networks in oscilloscope probes—to adjust for effects of

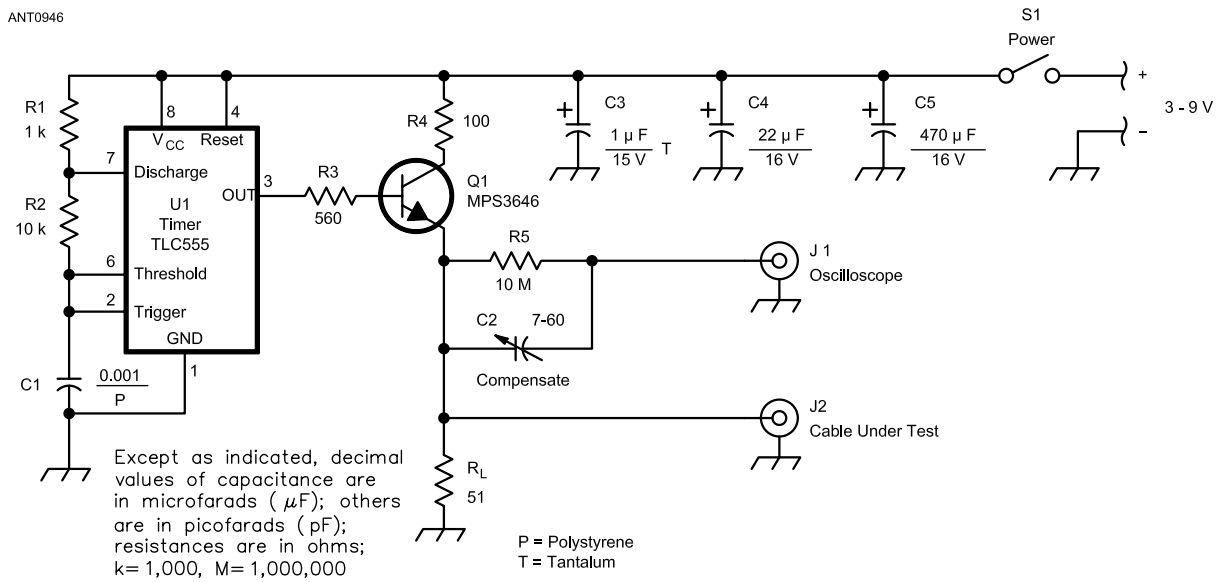

Fig 36—Schematic diagram of the time-domain reflectometer. All resistors are 1/4-W, 5% tolerance. U1 is a CMOS 555 timer. Circuit current drain is 10 to 25 mA. When building the TDR, observe the construction cautions discussed in the text. C2 is available from Mouser Electronics, part no. ME242-8050. Right-angle BNC connectors for use at J1 and J2 can be obtained from Newark Electronics, part no. 89N1578. S1 can be obtained from All Electronics, part no. NISW-1. An SPST toggle switch can also be used at S1.

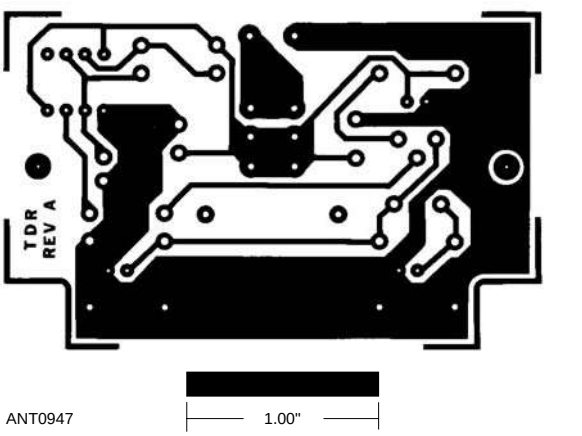

Fig 37—Full-size PC-board etching pattern for the TDR. Black areas represent unetched copper foil.

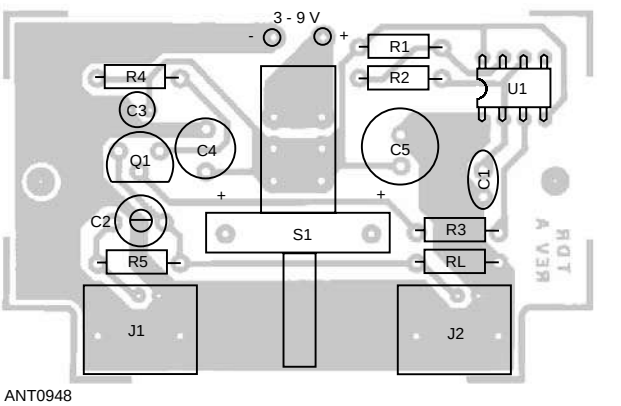

Fig 38—Part-placement diagram for the TDR. Parts are mounted on the nonfoil side of the board; the shaded area represents an X-ray view of the copper pattern. Be sure to observe the polarity markings of C3, C4 and C5.

the probe wire.

The TDR is designed to operate from dc between 3 and 9 V. Two C cells (in series—3 V) supply operating voltage in this version. The circuit draws only 10 to 25 mA, so the cells should last a long time (about 200 hours of operation). U1 can function with supply voltages as low as 2.25 to 2.5.

If you want to use the TDR in transmission-line systems with characteristic impedances other than 50 Ω, change the value of R_L to match the system impedance as closely as possible.

Calibrating and Using the TDR

Just about any scope with a bandwidth of at least 10 MHz should work fine with the TDR, but for tests in short-length cables, a 50-MHz scope provides for much more accurate measurements. To calibrate the TDR, terminate CABLE UNDER TEST connector, J2, with a 51-Ω

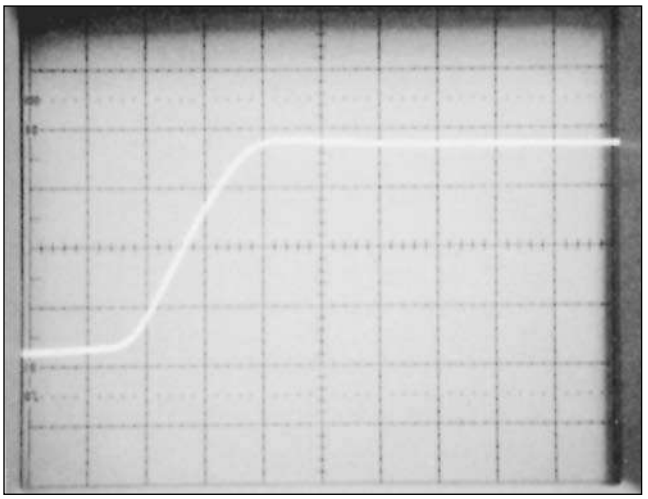

Fig 39—TDR calibration trace as shown on an oscilloscope. Adjust C2 (See Figs 36 and 38) for maximum deflection and sharpest waveform corners during calibration. See text.

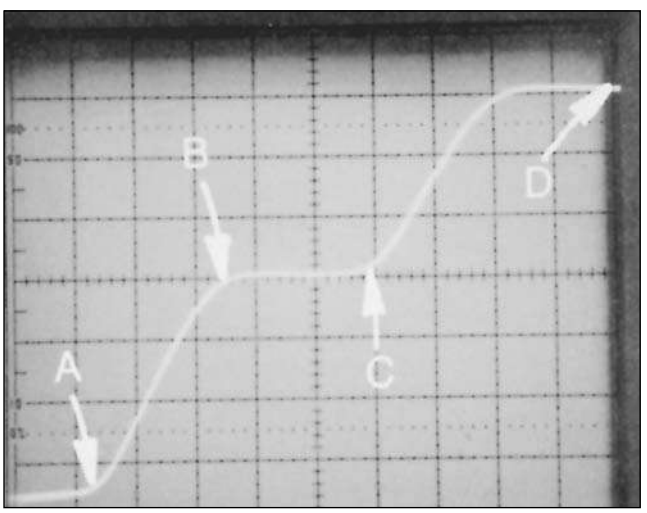

Fig 40—Open-circuited test cable. The scope is set for 0.01 ms per division. See text for interpretation of the waveform.

resistor. Connect the scope vertical input to J1. Turn on the TDR, and adjust the scope timebase so that one square-wave cycle from the TDR fills as much of the scope display as possible (without uncalibrating the timebase). The waveform should resemble **Fig 39**. Adjust C2 to obtain maximum amplitude and sharpest corners on the observed waveform. That's all there is to the calibration process!

To use the TDR, connect the cable under test to J2, and connect the scope vertical input to J1. If the waveform you observe is different from the one you observed during calibration, there are impedance variations in the load you're testing. See **Fig 40**, showing an unterminated test cable connected to the TDR. The beginning of the cable is shown at point A. (AB represents the TDR output-pulse rise time.)

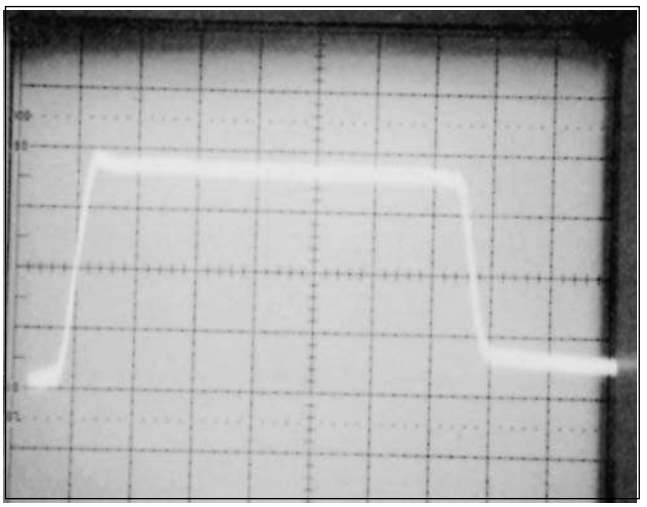

Fig 41—TDR display of the impedance characteristics of the 142-foot Hardline run to the 432-MHz antenna at KD5HM. The scope is set for 0.05 ms per division. See text for discussion.

Segment AC shows the portion of the transmission line that has a 50-Ω impedance. Between points C and D, there is a mismatch in the line. Because the scope trace is higher than the 50-Ω trace, the impedance of this part of the line is higher than 50 Ω—in this case, an open circuit.

To determine the length of this cable, read the length of time over which the 50-Ω trace is displayed. The scope is set for 0.01 μs per division, so the time delay for the 50-Ω section is (0.01 μs × 4.6 divisions) = 0.046 μs. The manufacturer's specified velocity factor (VF) of the cable is 0.8. Eq 1 tells us that the 50-Ω section of the cable is

$$\ell = \frac{983.6 \times 0.8 \times 0.046\,\mu s}{2} = 18.1\,\text{feet}$$

The TDR provides reasonable agreement with the actual cable length—in this case, the cable is really 16.5 feet long. (Variations in TDR-derived calculations and actual cable lengths can occur as a result of cable VFs that can vary considerably from published values. Many cables vary as much as 10% from the specified values.)

A second example is shown in **Fig 41**, where a length of $^3/_4$-inch Hardline is being tested. The line feeds a 432-MHz vertical antenna at the top of a tower. Fig 41 shows that the 50-Ω line section has a delay of (6.6 divisions × 0.05 μs) = 0.33 μs. Because the trace is straight and level at the 50-Ω level, the line is in good shape. The trailing edge at the right-hand end shows where the antenna is connected to the feed line.

To determine the actual length of the line, use the same procedure as before: Using the published VF for the Hardline (0.88) in Eq 1, the line length is

$$\ell = \frac{983.6 \times 0.88 \times 0.33\ \mu s}{2} = 142.8\ \text{feet}$$

Again, the TDR-derived measurement is in close agreement with the actual cable length (142 feet).

Final Notes

The time-domain reflectometer described here is not frequency specific; its measurements are not made at the frequency at which a system is designed to be used. Because of this, the TDR cannot be used to verify the impedance of an antenna, nor can it be used to measure cable loss at a specific frequency. Just the same, in two years of use, it has never failed to help locate a transmission-line problem. The vast majority of transmission-line problems result from improper cable installation or connector weathering.

Limitations

Certain limitations are characteristic of TDRs because the signal used to test the line differs from the system operating frequency and because an oscilloscope is a broadband device. In the instrument described here, measurements are made with a 71-kHz square wave. That wave contains components at 71 kHz and odd harmonics thereof, with the majority of the energy coming from the lower frequencies. The leading edge of the trace indicates that the response drops quickly above 6 MHz. (The leading edge in Fig 40 is 0.042 µs, corresponding to a period of 0.168 µs and a frequency of 5.95 MHz.) The result is dc pulses of approximately 7 µs duration. The scope display combines the circuit responses to all of those frequencies. Hence, it may be difficult to interpret any disturbance which is narrowband in nature (affecting only a small range of frequencies, and thus a small portion of the total power), or for which the travel time plus pattern duration exceeds 7 µs. The 432-MHz vertical antenna in Fig 41 illustrates a display error resulting from narrow-band response.

The antenna shows as a major impedance disturbance because it is mismatched at the low frequencies that dominate the TDR display, yet it is matched at 432 MHz. For an event that exceeds the observation window, consider a l-µF capacitor across a 50-Ω line. You would see only part of the pattern shown in Fig 35C because the time constant ($1 \times 10^{-6} \times 50 = 50$ ms) is much larger than the 7-µs window.

In addition, TDRs are unsuitable for measurements where there are major impedance changes inside the line section to be tested. Such major changes mask reflections from additional changes farther down the line.

Because of these limitations, TDRs are best suited for spotting faults in dc-continuous systems that maintain a constant impedance from the generator to the load. Happily, most amateur stations would be ideal subjects for TDR analysis, which can conveniently check antenna cables and connectors for short and open-circuit conditions and locate the position of such faults with fair accuracy.

Ground Parameters for Antenna Analysis

This section is taken from an article in *The ARRL Antenna Compendium, Vol 5* by R. P. Haviland, W4MB. In the past, amateurs paid very little attention to the characteristics of the earth (ground) associated with their antennas. There are two reasons for this. First, these characteristics are not easy to measure—even with the best equipment, extreme care is needed. Second, almost all hams have to put up with what they have—there are very few who can afford to move because their location has poor ground conditions! Further, the ground is not a dominant factor in the most popular antennas—a tri-band Yagi at 40 feet or higher, or a 2-meter vertical at roof height, for example.

Even so, there has been a desire and even a need for ground data and for ways to use it. It is very important for vertically polarized antennas. Ground data is useful for antennas mounted at low heights generally, and for such specialized ones as Beverages. The performance of such antennas change a lot as the ground changes.

Importance of Ground Conditions

To see why ground conditions can be important, let us look at some values. For a frequency of 10 MHz, *CCIR Recommendation 368*, gives the distance at which the signal is calculated to drop 10 dB below its free-space level as:

Conductivity (mS/meter)	*Distance for 10 dB Drop (km)*
5000	100
30	15
3	0.3

The high-conductivity condition is for sea-water. Inter-island work in the Caribbean on 40 and 80 meters is easy, whereas 40-meter ground-wave contact is difficult for much of the USA, because of much lower ground conductivity. On the other hand, the Beverage works because of poor ground conductivity.

Fig 42 shows a typical set of expected propagation curves for a range of frequencies. This data is also from *CCIR Recommendation 368* for relatively poor ground, with a dielectric constant of 4 and a conductivity of 3 mS/m (one milliSiemens/meter is 0.001 mho/meter). The same data is available in the *Radio Propagation Handbook*. There are equivalent FCC curves, found in the book *Reference Data for Radio Engineers*, but only the ones near 160 meters are useful. In Florida the author has difficulty hearing stations across town on ground

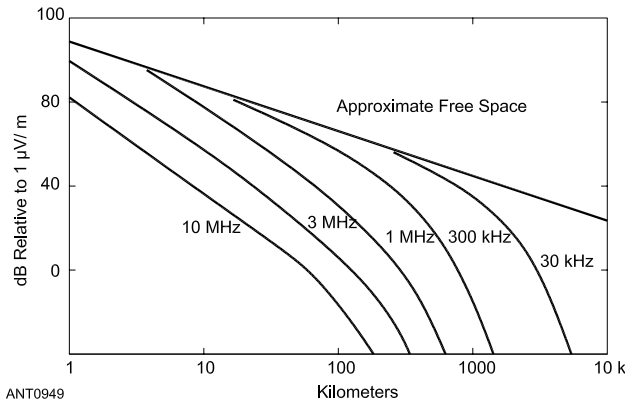

Fig 42—Variation of field strength with distance. Typical field strengths for several frequencies are shown. This is from CCIR data for fairly poor soil, with dielectric constant of 4 and conductivity of 3 mS/m. The curves for good soil are closer to the free-space line, and those for sea water are much closer to the free-space line.

wave, an indication of the poor soil conditions—reflected sky-wave signals are often stronger.

Securing Ground Data

There are only two basic ways to approach this matter of ground data. One is to use generic ground data typical to the area. The second is to make measurements, which haven't really gotten easier. For most amateurs, the best approach seems to be a combination of these—use some simple measurements, and then use the generic data to make a better estimate. Because of equipment costs and measurement difficulties, none of these will be highly accurate for most hams. But they will be much better than simply taking some condition preset into an analysis program. Having a good set of values to plug into an analysis can help you evaluate the true worth of a new antenna project.

Generic Data

In connection with its licensing procedure for broadcast stations, the FCC has published generic data for the

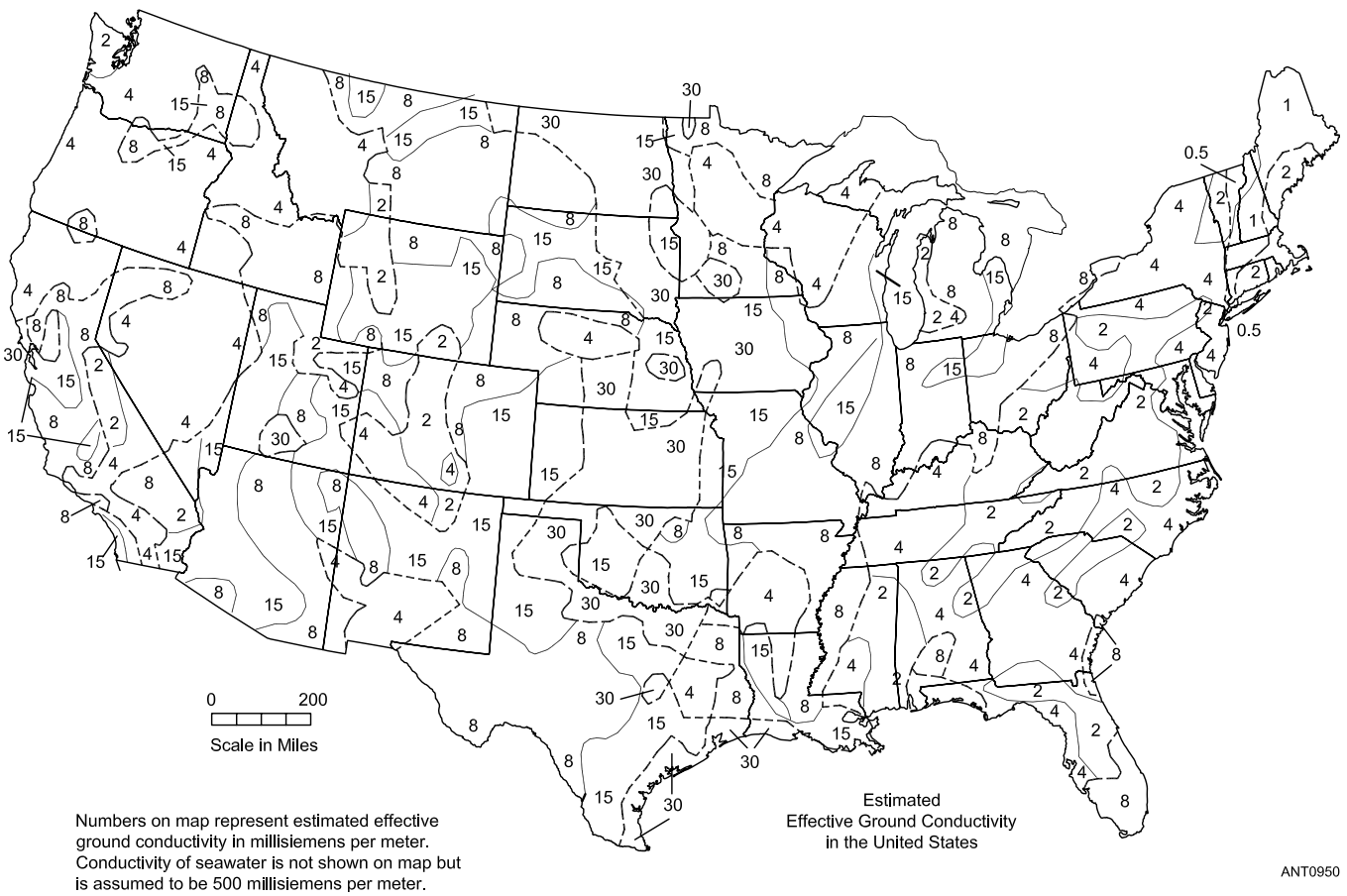

Fig 43—Estimated effective ground conductivity in the United States. FCC map prepared for the Broadcast Service, showing typical conductivity for continental USA. Values are for the band 500 to 1500 KHz. Values are for flat, open spaces and often will not hold for other types of commonly found terrain, such as seashores, river beds, etc.

entire country. This is reproduced in **Fig 43**, a chart showing the "estimated effective ground conductivity in the United States." A range of 30:1 is shown, from 1 to 30 mS/m. An equivalent chart for Canada has been prepared, originally by DOT, now DOC.

Of course, some judgment is needed when trying to use this data for your location. Broadcast stations are likely to be in open areas, so the data should not be assumed to apply to the center city. And a low site near the sea is likely to have better conductivity than the generic chart for, say, the coast of Oregon. Other than such factors, this chart gives a good first value, and a useful cross-check if some other method is used.

Still another FCC-induced data source is the license application of your local broadcast station. This includes calculated and measured coverage data. This may include specific ground data, or comparison of the coverage curves with the CCIR or FCC data to give the estimated ground conductivity. Another set of curves for ground conditions are those prepared by SRI. These give the conductivity and dielectric constant versus frequency for typical terrain conditions. These are reproduced as **Fig 44** and **Fig 45**. By inspecting your own site, you may select the curve most appropriate to your terrain. The curves are based on measurements at a number of sites across the USA, and are averages of the measured values.

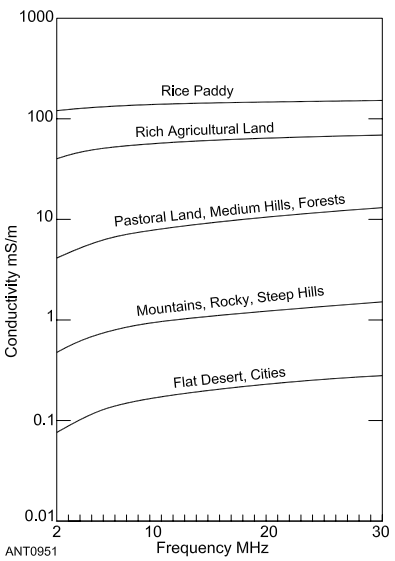

Fig 44—Typical terrain conductivities versus frequency for 5 types of soils. This was measured by SRI. Units are mS/m. Conductivity of seawater is usually taken as 5000 mS/m. Conductivity of fresh water depends on the impurities present, and may be very low. To extrapolate conductivity values (for 500 to 1500 KHz) shown in Fig 43 for a particular geographic area to a different frequency, move from the conductivity at the left edge of Fig 44 to the desired frequency. For example, in rocky New Hampshire, with a conductivity of 1 mS/m at BC frequencies, the effective conductivity at 14 MHz would be approximately 4 mS/m.

Figs 46 through 48 are data derived from these measurements. **Fig 46** gives the ground-dissipation factor. Sea water has low loss (a high dissipation factor), while soil in the desert or in the city is very lossy, with a low dissipation factor. **Fig 47** gives the skin depth, the distance for the signal to decease to 63% of its value at the surface. Penetration is low in high-conductivity areas and deep in low-conductivity soil. Finally, **Fig 48** shows the wavelength in the earth. For example, at 10 meters (30 MHz), the wavelength in sea water is less than 0.3 meters. Even in the desert, the wavelength has been reduced to about 6 meters at this frequency. This is one reason why buried antennas have peculiar properties. Lacking other data, it is suggested that the values of Figs 44 and 45 be used in computer antenna modeling programs.

Measuring Ground Conditions

W2FNQ developed a simple technique to measure low-frequency earth conductivity, which has been used by W2FMI. The test setup is drawn in **Fig 49**, and uses a very old technique of 4-terminal resistivity measurements. For probes of $^{9}/_{16}$-inch diameter, spaced 18 inches and pene-trating 12 inches into the earth, the conductivity is:

$$C = 21\ V_1/V_2 \quad \text{mS/m} \qquad \text{(Eq 19)}$$

The voltages are conveniently measured by a digital voltmeter, to an accuracy of about 2%. In soil suitable for farming, the probes can be copper or aluminum. The strength of iron or copperweld may be needed in hard soils. A piece of 2×4 or 4×4 with guide holes drilled through it will help maintain proper spacing and vertical alignment of the probes. Use care when measuring—there is a shock hazard. An isolating transformer with a 24-V secondary instead of 115 V will reduce the danger.

Ground conditions vary quite widely over even small

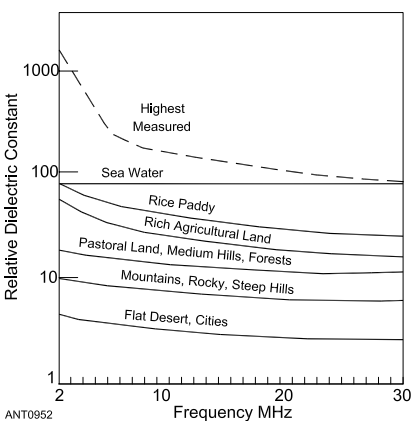

Fig 45—Typical terrain relative dielectric constant for the 5 soil types of Fig 44, plus sea water. The dashed curve shows the highest measured values reported, and usually indicates mineralization.

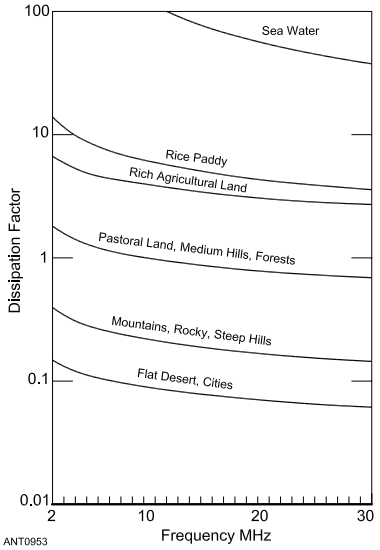

Fig 46—Typical values of dissipation factor. The soil behaves as a leaky dielectric. These curves showing the dimensionless dissipation factor versus frequency for various types of soils and for sea water. The dissipation factor is inversely related to soil conductivity. Among other things, a high dissipation factor indicates that a signal penetrating the soil or water will decrease in strength rapidly with depth.

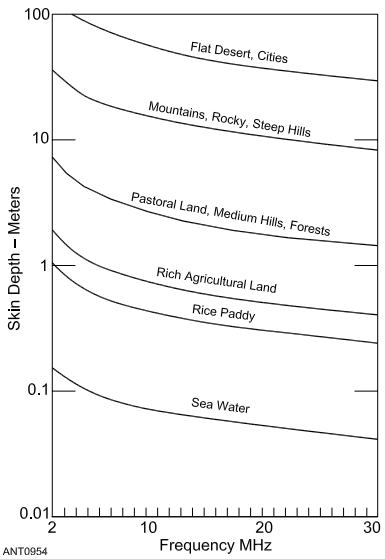

Fig 47—Typical values of skin depth. The skin depth is the depth at which a signal will have decreased to 1/e of its value at the surface (to about 30%). The effective height above ground is essentially the same as the physical height for sea water, but may be much greater for the desert. For practical antennas, this may increase low-angle radiation, but at the same time will increase ground losses.

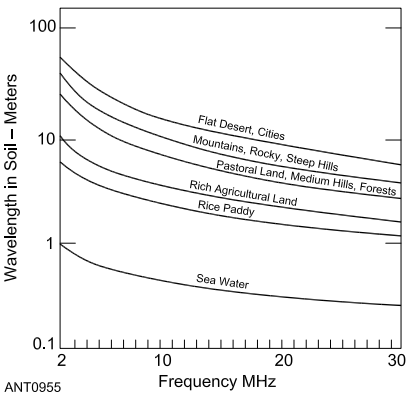

Fig 48—Typical values of wavelength in soil. Because of its dielectric constant, the wavelength in soils and water will be shorter than that for a wave traveling in air. This can be important, since in a Method of Moment the accuracy is affected by the number of analysis segments per wavelength. Depending on the program being used, adjust the number of segments for antennas wholly or partly in the earth, for ground rods, and for antennas very close to earth.

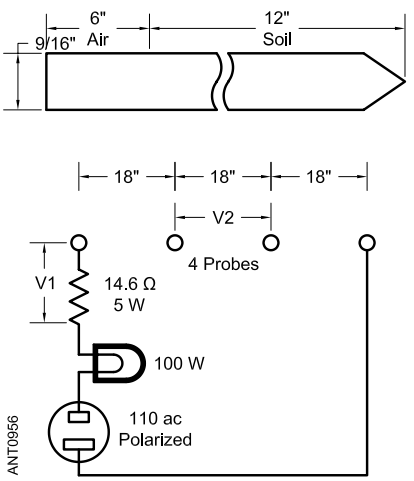

Fig 49—Low-frequency conductivity measurement system. A 60-Hz measuring system devised by W2FNQ and used by W2FMI. The basic system is widely used in geophysics. Use care to be certain that the plug connection is correct. A better system would use a lower voltage and an isolation transformer. Measure the value of V_2 with no power applied—there may be stray ground currents present, especially if there is a power station or an electric railway close.

areas. It is best to make a number of measurements around the area of the antenna, and average the measured values.

While this measurement gives only the low-frequency conductivity, it can be used to select curves in Fig 44 to give an estimate of the conductivity for the common ham bands. Assume that the 60 Hz value is valid at 2 MHz, and find the correct value on the left axis. Move parallel to the curves on the figure to develop the estimated curve for other soil conditions.

A small additional refinement is possible. If the dielectric constant from Fig 45 is plotted against the conductivity from Fig 44 for a given frequency, a scatter plot develops, showing a trend to higher dielectric constant as conductivity increases. At 14 MHz, the relation is:

$$k = \sqrt{1000/C} \qquad \text{(Eq 20)}$$

where k is the dielectric constant and C is the measured conductivity. Using these values in *MININEC* or *NEC* calculations should give better estimates than countrywide average values.

Direct Measurement of Ground Properties

For really good values, both the conductivity and dielectric constant should be measured at the operating frequency. One way of doing this is the two-probe technique described in George Hagn's article (see Bibliography). This was the technique used to secure the data for Figs 44 through 48. The principle is sketched in **Fig 50**. In essence, the two probes form a short, open-circuited, two-wire transmission line. As shown by the equations for such lines, the input impedance is a function of the conductivity and dielectric constant of the medium. A single measurement is difficult to calculate, since the end effect of the two probes must be determined, a complex task if they are pointed for easy driving. The calculation is greatly simplified if a set of measurements is made with several sets of probes that vary in length by a fixed ratio, since the measured difference is largely due to the increased two-wire length, with some change due to the change in soil moisture with depth.

The impedance to be measured is high because of the short line length, so impedance bridges are not really suitable. An RF vector impedance meter, such as the HP-4193A, is probably the best instrument to use, with a RF susceptance bridge, such as the GR-821A, next best. With care, a Q-meter can be substituted. Because of the rarity of these instruments among amateurs, this method of measurement is not explored further here.

Indirect Measurement

Since the terminal impedance and resonant frequency of an antenna change as the antenna approaches earth, measurement of an antenna at one or more heights permits an analysis of the ground characteristics. The technique is to calculate the antenna drive impedance for an assumed ground condition, and compare this with

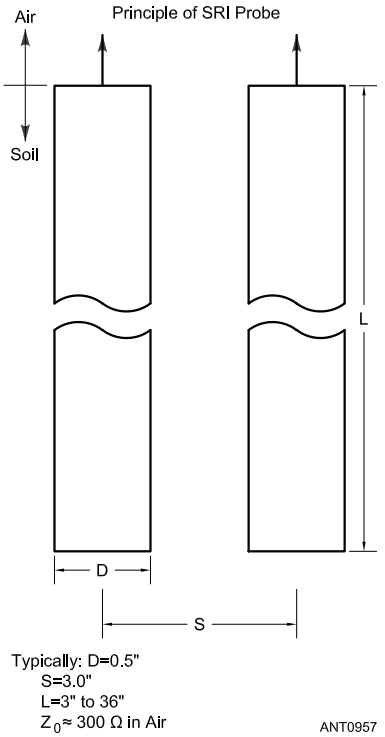

Fig 50—High-frequency conductivity/dielectric constant measurement system. System for measuring ground conditions at frequencies up to about 100 MHz, devised by SRI and used to obtain the data in Figs 44 through 48. Basically, this is a section of transmission line with soil as the dielectric. Requires measurement of high impedances to good accuracy.

measured values. If not the same, another set of ground conditions is assumed, and the process is repeated. It is best to have a plan to guide the assumptions.

In connection with his studies of transmission lines, Walt Maxwell, W2DU, made such measurements on 20, 40 and 80 meters. Some of the data was included in his book *Reflections*. The following example is based on his 80-meter data. Data came from his Table 20-1, for a 66-foot, 2-inch dipole of #14 wire at 40 feet above ground. His table gives an antenna impedance of 72.59 + *j* 1.38 Ω at 7.15 MHz.

Table 7 shows calculated antenna impedances for ground conductivities of three different ground conductivities: 10, 1 and 0.1 mS/m, and for dielectric constants of 3, 15 and 80. The nearest value to the measured drive impedance is for a conductivity of 0.1 mS/m and a dielectric constant of 3. Figs 44 and 45 indicate that these are typical of flat desert and city land. The effect on antenna performance is shown in **Fig 51**. The maximum lobe gain for soil typical of a city is over 2 dB lower than that for the high-conductivity, high-dielectric constant value. Note that the maximum lobe occurs for a radiation angle that is directly overhead.

Table 7

Calculated values of drive resistance, in ohms, for an 40 meter dipole at 40 feet elevation versus conductivity and dielectric constant.

Conductivity	*Dielectric Constant*		
(mS/m)	*3*	*15*	*50*
10	89.78 – *j* 12.12	88.53 – *j* 10.69	88.38 – *j* 7.59
1	80.05 – *j* 17.54	83.72 – *j* 10.23	87.33 – *j* 6.98
0.1	76.44 – *j* 15.69	83.18 – *j* 9.85	97.30 – *j* 6.46

The value measured by W2DU was 72.59 – *j* 1.28 Ω, and compares closest to the poor soil condition of dielectric constant of 3 and conductivity of 0.1 mS/m.

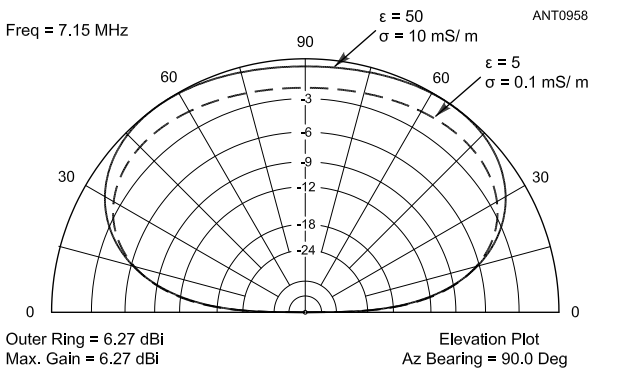

Fig 51—Plot showing computed elevation patterns for 40-foot high, 40-meter dipole for two different ground conditions: poor ground, with dielectric constant of 3 and conductivity of 0.1 mS/m, and good ground, with dielectric constant of 50 and conductivity of 10 mS/m. Note that for a low horizontal antenna, high-angle radiation is most affected by poor ground, with low-angle radiation least affected by ground characteristics.

The ground at the W2DU QTH is a suburban Florida lot, covered with low, native vegetation. The ground is very sandy (a fossil sand dune), and is some 60-70 feet above sea-level. Measurements were made near the end of the Florida dry season. The water table is estimated to be 20 to 30 feet below the surface. Thus the calculated and measured values are reasonably consistent.

In principle, a further analysis, using values around 0.1 mS/m conductivity and 3 for dielectric constant, will give a better ground parameter estimate. However, the results should be taken with a grain of salt, because the opportunities for error in the computer modeling must be considered. The antenna should have no sag, and its length and height should be accurate. The measurement must be with accurate equipment, free from strays, such as current on the outer conductor of the coax. The feed-point gap effect must be estimated. Further, the ground itself under the antenna must be flat and have constant characteristics for modeling to be completely accurate.

Finally, the feed-line length and velocity constant of the transmission line must be accurately measured for transfer of the measured values at the feeding end of the transmission line to the antenna itself. Because of all the possibilities for error, most attempts at precision should be based on measured values at two or three frequencies, and preferably at two or three heights. Orienting the antenna to right angles for another set of measurements may be useful. Obviously, this can involve a lot of detailed work.

The author was not been able to find any guidelines for the best height or frequency. The data in the book *Exact Image Method for Impedance Computation of Antennas Above the Ground* suggests that a height of 0.3 λ will give good sensitivity to ground conditions. Very low heights may give confusing results, since several combinations of ground parameters can give nearly the same drive impedance. Both this data and experience suggest that sensitivity to ground for heights above 0.75 λ is small or negligible.

If an overall conclusion about ground characteristics is needed, we can just restate from the first paragraph—it is not greatly important for the most common horizontally polarized antenna installations. But it's worth taking a look when you need to depart from typical situations, or when the performance of a vertically polarized antenna is contemplated. Then the techniques outlined here can be helpful.

A Switchable RF Attenuator

A switchable RF attenuator is helpful for making antenna-gain comparisons or for plotting antenna radiation patterns. You may switch attenuation in or out of the line leading to the receiver to obtain an initial reference reading on a signal strength meter. Some form of attenuator is also helpful for locating hidden transmitters, where the real trick is pinpointing the signal source from within a few hundred feet. At such a close distance, strong signals may overload the front end of the receiver, making it impossible to obtain any indication of a bearing.

The attenuator of **Figs 52** and **53** is designed for low power levels, not exceeding 1/4 watt. If for some reason the attenuator will be connected to a transceiver, a means of bypassing the unit during transmit periods must be devised. An attenuator of this type is commonly called a *step attenuator*, because any amount of attenuation from 0 dB to the maximum available (81 dB for this particular instrument) may be obtained in steps of 1 dB. As each switch is successively thrown from the OUT to the IN position, the attenuation sections add in cascade to yield the total of the attenuator steps switched in. The maximum attenuation of any single section is limited to 20 dB because leak-through would probably degrade the accuracy of higher values. The tolerance of resistor values also becomes more significant regarding accuracy at higher attenuation values.

A good quality commercially made attenuator will cost upwards from $150, but for less than $25 in parts and a few hours of work, you can build an attenuator at home. It will be suitable for frequencies up to 450 MHz. Double-sided pc board is used for the enclosure. The version of the attenuator shown in Fig 52 has identification lettering etched into the top surface (or front panel) of the unit. This adds a nice touch and is a permanent means of labeling. Of course rub-on transfers or Dymo tape labels could be used as well.

Female BNC single-hole, chassis-mount connectors are used at each end of the enclosure. These connectors

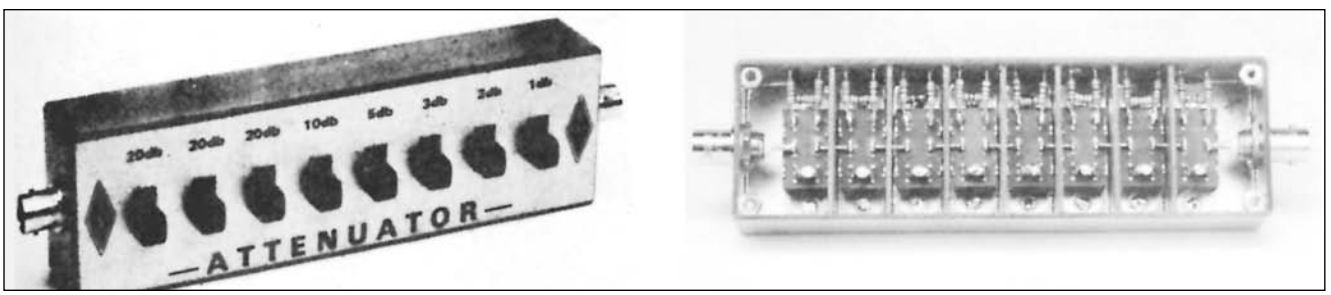

Fig 52—A construction method for a step attenuator. Double-sided circuit-board material, unetched (except for panel identification), is cut to the desired size and soldered in place. Flashing copper may also be used, although it is not as sturdy. Shielding partitions between sections are necessary to reduce signal leakage. Brass nuts soldered at each of the four corners allow machine screws to secure the bottom cover. The practical limit for total attenuation is 80 or 90 dB, as signal leakage around the outside of the attenuator will defeat attempts to obtain much greater amounts.

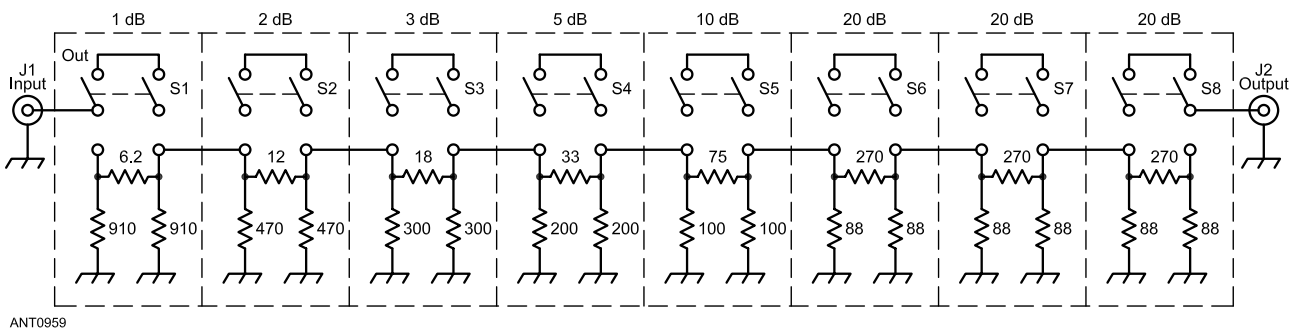

Fig 53—Schematic diagram of the step attenuator, designed for a nominal impedance of 50 Ω. Resistance values are in ohms. Resistors are 1/4-watt, carbon-composition types, 5% tolerance. Broken lines indicate walls of circuit-board material. A small hole is drilled through each partition wall to route bus wire. Keep all leads as short as possible. The attenuator is bilateral; that is, the input and output ends may be reversed.

J1, J2—Female BNC connectors, Radio Shack 278-105 or equiv.

S1-S8, incl.—DPDT slide switches, standard size. (Avoid subminiature or toggle switches.) Stackpole S-5022CD03-0 switches are used here.

provide a means of easily connecting and disconnecting the attenuator.

Construction

After all the box parts are cut to size and the necessary holes made, scribe light lines to locate the inner partitions. Carefully tack-solder all partitions in position. A 25-W pencil type of iron should provide sufficient heat. Dress any pc board parts that do not fit squarely. Once everything is in proper position, run a solder bead all the way around the joints. Caution! Do not use excessive amounts of solder, as the switches must later be fit flat inside the sections. Complete the top, sides, ends and partitions. Dress the outside of the box to suit your taste. For instance, you might wish to bevel the box edges. Buff the copper with steel wool, add lettering, and finish off the work with a coat of clear lacquer or polyurethane varnish.

Using a little lacquer thinner, soak the switches to remove the grease that was added during their manufacture. When they dry, spray the inside of the switches lightly with a TV tuner cleaner/lubricant. Use a sharp drill bit (about $^3/_{16}$ inch will do), and countersink the mounting holes on the actuator side of the switch mounting plate. This ensures that the switches will fit flush against the top plate. At one end of each switch, bend the two lugs over and solder them together. Cut off the upper halves of the remaining switch lugs. (A close look at Fig 52 will help clarify these steps.)

Solder the series-arm resistors between the appropriate switch lugs. Keep the lead lengths as short as possible and do not overheat the resistors. Now solder the switches in place to the top section of the enclosure by flowing solder through the mounting holes and onto the circuit-board material. Be certain that you place the switches in their proper positions; correlate the resistor values with the degree of attenuation. Otherwise, you may wind up with the 1-dB step at the wrong end of the box how embarrassing!

Once the switches are installed, thread a piece of #18 bare copper wire through the center lugs of all the switches, passing it through the holes in the partitions. Solder the wire at each switch terminal. Cut the wire between the poles of each individual switch, leaving the wire connecting one switch pole to that of the neighboring one on the other side of the partition, as shown in Fig 52. At each of the two end switch terminals, leave a wire length of approximately $^1/_8$ inch. Install the BNC connectors and solder the wire pieces to the connector center conductors.

Now install the shunt-arm resistors of each section. Use short lead lengths. Do not use excessive amounts of heat when soldering. Solder a no. 4-40 brass nut at each inside corner of the enclosure. Recess the nuts approximately $^1/_{16}$-inch from the bottom edge of the box to allow sufficient room for the bottom panel to fit flush. Secure the bottom panel with four no. 4-40, $^1/_4$-inch machine screws and the project is completed. Remember to use caution, always, when your test setup provides the possibility of transmitting power into the attenuator.

A Portable Field Strength Meter

Few amateur stations, fixed or mobile, are without need of a field-strength meter. An instrument of this type serves many useful purposes during antenna experiments and adjustments. When work is to be done from many wavelengths away, a simple wavemeter lacks the necessary sensitivity. Further, such a device has a serious fault because its linearity leaves much to be desired. The information in this section is based on a January 1973 *QST* article by Lew McCoy, W1ICP.

The field-strength meter described here takes care of these problems. Additionally, it is small, measuring only 4 × 5 × 8 inches. The power supply consists of two 9-volt batteries. Sensitivity can be set for practically any amount desired. However, from a usefulness standpoint, the circuit should not be too sensitive or it will respond to unwanted signals. This unit also has excellent linearity with regard to field strength. (The field strength of a received signal varies inversely with the distance from the source, all other things being equal.) The frequency range includes all amateur bands from 3.5 through

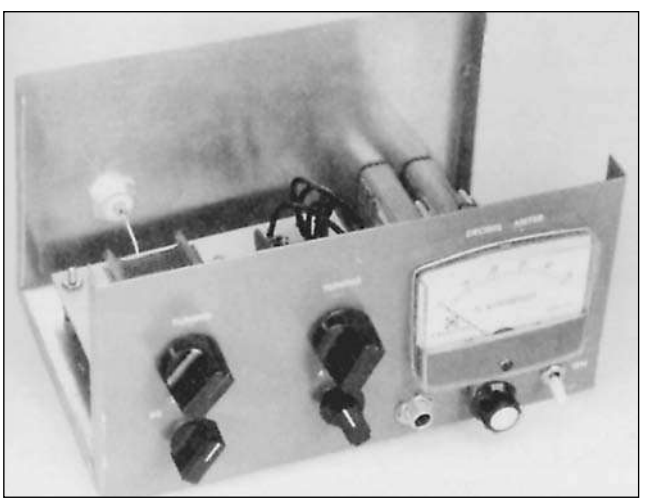

Fig 54—The linear field strength meter. The control at the upper left is for C1 and the one to the right for C2. At the lower left is the band switch, and to its right the sensitivity switch. The zero-set control for M1 is located directly below the meter.

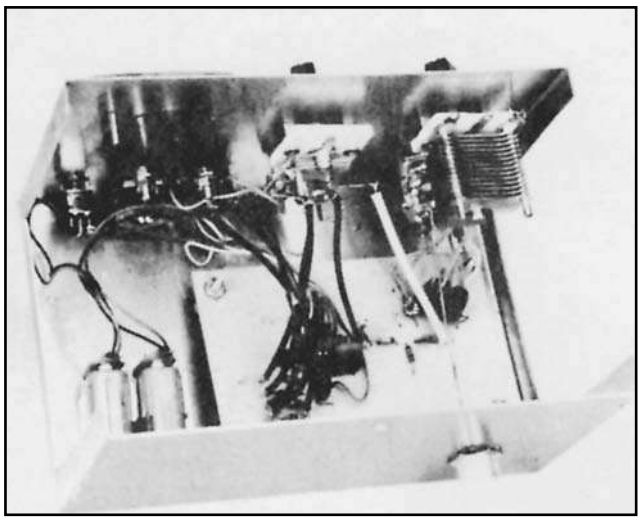

Fig 55—Inside view of the field-strength meter. At the upper right is C1 and to the left, C2. The dark leads from the circuit board to the front panel are the shielded leads described in the text.

148 MHz, with band-switched circuits, thus avoiding the use of plug-in inductors. All in all, it is a quite useful instrument.

The unit is pictured in **Figs 54** and **55**, and the schematic diagram is shown in **Fig 56**. A type 741 op-amp IC is the heart of the unit. The antenna is connected to J1, and a tuned circuit is used ahead of a diode detector. The rectified signal is coupled as dc and amplified in the op amp. Sensitivity of the op amp is controlled by inserting resistors R3 through R6 in the circuit by means of S2.

With the circuit shown, and in its most sensitive setting, M1 will detect a signal from the antenna on the order of 100 µV. Linearity is poor for approximately the first 1/5 of the meter range, but then is almost straight-line from there to full-scale deflection. The reason for the poor linearity at the start of the readings is because of nonlinearity of the diodes at the point of first conduction. However, if gain measurements are being made this is of no real importance, as accurate gain measurements can be made in the linear portion of the readings.

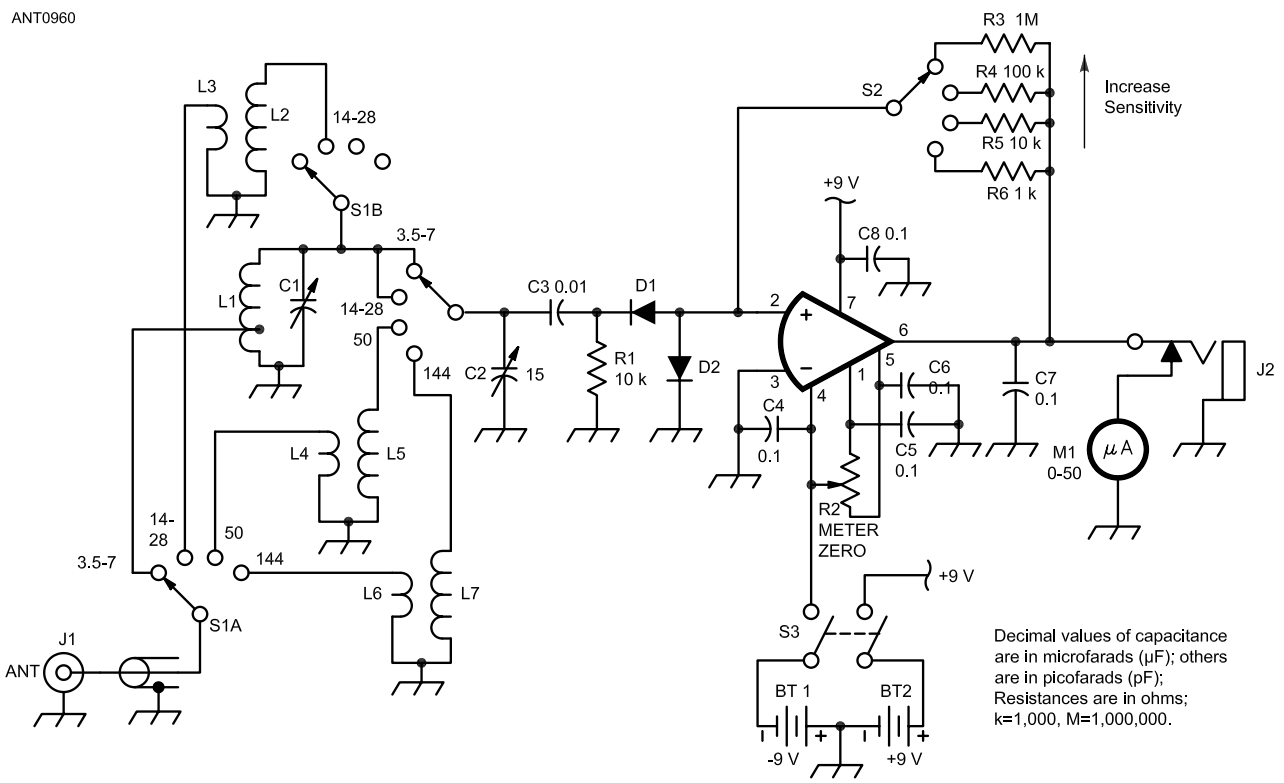

Fig 56—Circuit diagram of the linear field strength meter. All resistors are 1/4- or 1/2-W composition types.

C1 — 140 pF variable.
C2 — 15-pF variable
D1, D2 — 1N914 or equiv.
L1 — 34 turns #24 enam. wire wound on an Amidon T-68-2 core, tapped 4 turns from ground end.
L2 — 12 turns #24 enam. wire wound on T-68-2 core.
L3 — 2 turns #24 enam. wire wound at ground end of L2.
L4 — 1 turn #26 enam. wire wound at ground end of L5.
L5 — 12 turns #26 enam. wire wound on T-25-12 core.
L6 — 1 turn #26 enam. wire wound at ground end of L7.
L7 — 1 turn #18 enam. wire wound on T-25-12 core.
M1 — 50 or 100 µA dc.
R2 — 10-kΩ control, linear taper.
S1 — Rotary switch, 3 poles, 5 positions, 3 sections.
S2 — Rotary switch, 1 pole, 4 positions.
S3 — DPST toggle.
U1 — Type 741 op amp. Pin numbers shown are for a 14-pin package.

The 741 op amp requires both a positive and a negative voltage source. This is obtained by connecting two 9-volt batteries in series and grounding the center. One other feature of the instrument is that it can be used remotely by connecting an external meter at J2. This is handy if you want to adjust an antenna and observe the results without having to leave the antenna site.

L1 is the 3.5/7 MHz coil and is tuned by C1. The coil is wound on a toroid form. For 14, 21 or 28 MHz, L2 is switched in parallel with L1 to cover the three bands. L5 and C2 cover approximately 40 to 60 MHz, and L7 and C2 from 130 MHz to approximately 180 MHz. The two VHF coils are also wound on toroid forms.

Construction Notes

The majority of the components may be mounted on an etched circuit board. A shielded lead should be used between pin 4 of the IC and S2. The same is true for the leads from R3 through R6 to the switch. Otherwise, parasitic oscillations may occur in the IC because of its very high gain.

In order for the unit to cover the 144-MHz band, L6 and L7 should be mounted directly across the appropriate terminals of S1, rather than on a circuit board. The extra lead length adds too much stray capacitance to the circuit. It isn't necessary to use toroid forms for the 50- and 144-MHz coils. They were used in the version described here simply because they were available. You may substitute air-wound coils of the appropriate inductance.

Calibration

The field strength meter can be used *as is* for a relative-reading device. A linear indicator scale will serve admirably. However, it will be a much more useful instrument for antenna work if it is calibrated in decibels, enabling the user to check relative gain and front-to-back ratios. If you have access to a calibrated signal generator, connect it to the field-strength meter and use different signal levels fed to the device to make a calibration chart. Convert signal-generator voltage ratios to decibels by using the equation

$$dB = 20 \log (V1/V2) \qquad \text{(Eq 21)}$$

where

V1/V2 is the ratio of the two voltages

log is the common logarithm (base 10)

Let's assume that M1 is calibrated evenly from 0 to 10. Next, assume we set the signal generator to provide a reading of 1 on M1, and that the generator is feeding a 100-μV signal into the instrument. Now we increase the generator output to 200 μV, giving us a voltage ratio of 2:1. Also let's assume M1 reads 5 with the 200-μV input. From the equation above, we find that the voltage ratio of 2 equals 6.02 dB between 1 and 5 on the meter scale. M1 can be calibrated more accurately between 1 and 5 on its scale by adjusting the generator and figuring the ratio. For example, a ratio of 126 μV to 100 μV is 1.26, corresponding to 2.0 dB. By using this method, all of the settings of S2 can be calibrated. In the instrument shown here, the most sensitive setting of S2 with R3, 1 MΩ, provides a range of approximately 6 dB for M1. Keep in mind that the meter scale for each setting of S1 must be calibrated similarly for each band. The degree of coupling of the tuned circuits for the different bands will vary, so each band must be calibrated separately.

Another method for calibrating the instrument is using a transmitter and measuring its output power with an RF wattmeter. In this case we are dealing with power rather than voltage ratios, so this equation applies:

$$dB = 10 \log (P1/P2) \qquad \text{(Eq 22)}$$

where P1/P2 is the power ratio.

With most transmitters the power output can be varied, so calibration of the test instrument is rather easy. Attach a pickup antenna to the field-strength meter (a short wire a foot or so long will do) and position the device in the transmitter antenna field. Let's assume we set the transmitter output for 10 W and get a reading on M1. We note the reading and then increase the output to 20 W, a power ratio of 2. Note the reading on M1 and then use Eq 2. A power ratio of 2 is 3.01 dB. By using this method the instrument can be calibrated on all bands and ranges.

With the tuned circuits and coupling links specified in Fig 56, this instrument has an average range on the various bands of 6 dB for the two most sensitive positions of S2, and 15 dB and 30 dB for the next two successive ranges. The 30-dB scale is handy for making front-to-back antenna measurements without having to switch S2.

An RF Current Probe

The RF current probe of **Figs 57** through **59** operates on the magnetic component of the electromagnetic field, rather than the electric field. Since the two fields are precisely related, as discussed in Chapter 23, the relative field strength measurements are completely equivalent. The use of the magnetic field offers certain advantages, however. The instrument may be made more compact for the same sensitivity, but its principal advantage is that it may be used near a conductor to measure the current flow without cutting the conductor.

In the average amateur location there may be substantial currents flowing in guy wires, masts and towers, coaxial-cable braids, gutters and leaders, water and gas pipes, and perhaps even drainage pipes. Current may be flowing in telephone and power lines as well. All of these RF currents may have an influence on antenna patterns or can be of significance in the case of RFI.

The circuit diagram of the current probe appears in Fig 58, and construction is shown in the photo, Fig 59. The winding data given here apply only to a ferrite rod of the particular dimensions and material specified. Almost any microammeter can be used, but it is usually convenient to use a rather sensitive meter and provide a series resistor to swamp out nonlinearity arising from diode conduction characteristics. A control is also used to adjust instrument sensitivity as required during operation. The tuning capacitor may be almost anything that will cover the desired range.

Fig 57—The RF current probe. The sensitivity control is mounted at the top of the instrument, with the tuning and band switches on the lower portion of the front panel. Frequency calibration of the tuning control was not considered necessary for the intended use of this particular instrument, but marks identifying the various amateur bands would be helpful. If the unit is provided with a calibrated dial, it can also be used as an absorption wavemeter.

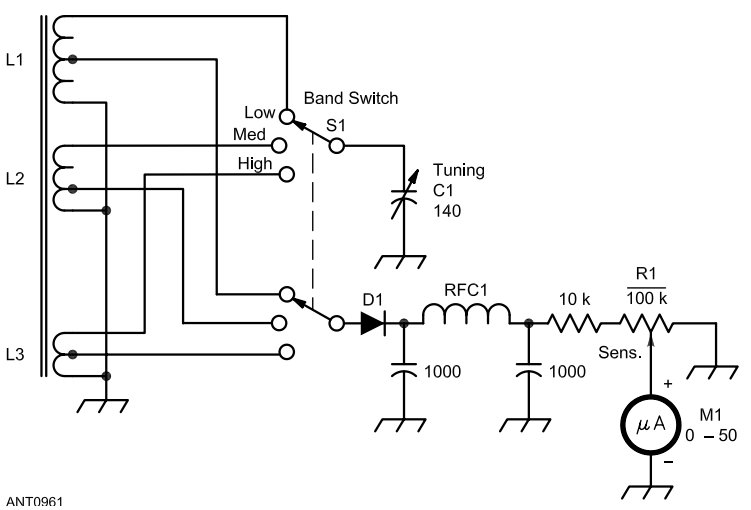

Fig 58—Schematic diagram of the RF current probe. Resistances are in ohms; k = 1000. Capacitances are in picofarads; fixed capacitors are silver mica. Be sure to ground the rotor of C1, rather than the stator, to avoid hand capacitance. L1, L2 and L3 are each close-wound with #22 enameled wire on a single ferrite rod, 4 inch long and $^1/_2$ inch diameter, with μ = 125 (Amidon R61-50-400). Windings are spaced approximately $^1/_4$ inch apart.

C1—Air variable, 6-140 pF; Hammarlund HF140 or equiv.
D1—Germanium diode; 1N34A, 1N270 or equiv.
L1—1.6-5 MHz; 30 turns, tapped at 3 turns from grounded end.
L2—5-20 MHz; 8 turns, tapped at 2 turns from grounded end.
L3—17-39 MHz; 2 turns, tapped at 1 turn.
M1—Any microammeter may be used. The one pictured is a Micronta meter, RadioShack no. 270-1751.
R1—Linear taper.
RFC1—1 mH; Miller no. 4642 or equiv. Value is not critical.
S1—Ceramic rotary switch, 1 section, 2 poles, 2 to 6 positions; Centralab PA2002 or PA2003 or equiv.

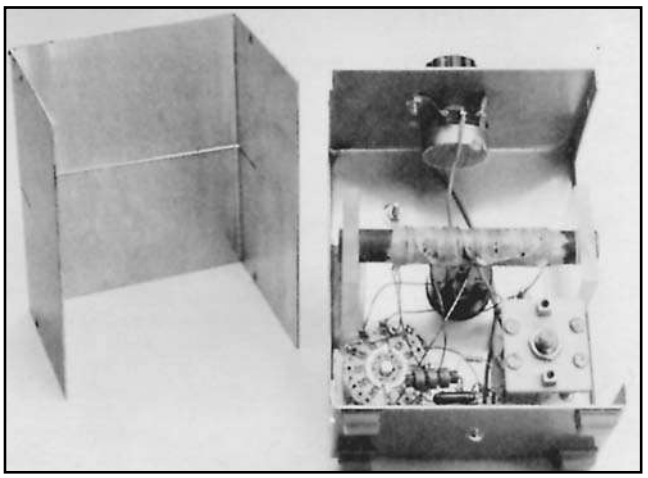

Fig 59—The current probe just before final assembly. Note that all parts except the ferrite rod are mounted on a single half of the 3 × 4 × 5-inch Minibox (Bud CU-2105B or equiv.). Rubber grommets are fitted in holes at the ends of the slot to accept the rod during assembly of the enclosure. Leads in the RF section should be kept as short as possible, although those from the rod windings must necessarily be left somewhat long to facilitate final assembly.

As shown in the photos, the circuit is constructed in a metal box. This enclosure shields the detector circuit from the electric field of the radio wave. A slot must be cut with a hacksaw across the back of the box, and a thin file may be used to smooth the cut. This slot is necessary to prevent the box from acting as a shorted turn.

Using the Probe

In measuring the current in a conductor, the ferrite rod should be kept at right angles to the conductor, and at a constant distance from it. In its upright or vertical position, this instrument is oriented for taking measurements in vertical conductors. It must be laid horizontal to measure current in horizontal conductors.

Numerous uses for the instrument are suggested in an earlier paragraph. In addition, the probe is an ideal instrument for checking the current distribution in antenna elements. It is also useful for measuring RF ground currents in radial systems. A buried radial may be located easily by sweeping the ground. Current division at junctions may be investigated. *Hot spots* usually indicate areas where additional radials would be effective.

Stray currents in conductors not intended to be part of the antenna system may often be eliminated by bonding or by changing the physical lengths involved. Guy wires and other unwanted parasitic elements will often give a tilt to the plane of polarization and can make a marked difference in front-to-back ratios. When the ferrite rod is oriented parallel to the electric field lines, there will be a sharp null reading that may be used to locate the plane of polarization quite accurately. When using the meter, remember that the magnetic field is at right angles to the electric field.

You may also use the current probe as a relative signal strength meter. When making measurements on a vertical antenna, locate the meter at least two wavelengths away, with the rod in a horizontal position. For horizontal antennas, hold the instrument at approximately the same height as the antenna, with the rod vertical.

Antenna Measurements

Of all the measurements made in Amateur Radio systems, perhaps the most difficult and least understood are various measurements of antennas. For example, it is relatively easy to measure the frequency and CW power output of a transmitter, the response of a filter, or the gain of an amplifier. These are all what might be called *bench measurements* because, when performed properly, all the factors that influence the accuracy and success of the measurement are under control. In making antenna measurements, however, the "bench" is probably your backyard. In other words, the environment surrounding the antenna can affect the results of the measurement.

Control of the environment is not at all as simple as it was for the bench measurement, because now the work area may be rather spacious. This section describes antenna measurement techniques that are closely allied to those used in an antenna measuring event or contest. With these procedures you can make measurements successfully and with meaningful results. These techniques should provide a better understanding of the measurement problems, resulting in a more accurate and less difficult task. The information in this section was provided by Dick Turrin, W2IMU, and was originally published in November 1974 *QST*.

SOME BASIC IDEAS

An antenna is simply a transducer or coupler between a suitable feed line and the environment surrounding it. In addition to the efficient transfer of power from feed line to environment, an antenna at VHF or UHF is most frequently required to concentrate the radiated power into a particular region of the environment.

To be consistent while comparing different antennas, you must standardize the environment surrounding the antenna. Ideally, you want to make measurements with the measured antenna so far removed from any objects causing environmental effects that it is literally in outer space—a very impractical situation. The purpose of the measurement techniques is therefore to simulate, under practical conditions, a *controlled environment*. At VHF

and UHF, and with practical-size antennas, the environment can be controlled so that successful and accurate measurements can be made in a reasonable amount of space.

The electrical characteristics of an antenna that are most desirable to obtain by direct measurement are: (1) gain (relative to an isotropic source, which by definition has a gain of unity); (2) space-radiation pattern; (3) feed-point impedance (mismatch) and (4) polarization.

Polarization

In general the polarization can be assumed from the geometry of the radiating elements. That is to say, if the antenna consists of a number of linear elements (straight lengths of rod or wire that are resonant and connected to the feed point) the polarization of the electric field will be linear and polarized parallel to the elements. If the elements are not consistently parallel with each other, then the polarization cannot easily be assumed. The following techniques are directed to antennas having polarization that is essentially linear (in one plane), although the method can be extended to include all forms of elliptic (or mixed) polarization.

Feed-Point Mismatch

The feed-point mismatch, although affected to some degree by the immediate environment of the antenna, does not affect the gain or radiation characteristics of an antenna. If the immediate environment of the antenna does not affect the feed-point impedance, then any mismatch intrinsic to the antenna tuning reflects a portion of the incident power back to the source. In a receiving antenna this reflected power is reradiated back into the environment, and can be lost entirely.

In a transmitting antenna, the reflected power travels back down the feed line to the transmitter, where it changes the load impedance presented to that transmitter. The amplifier output controls are customarily altered during the normal tuning procedure to obtain maximum power transfer to the antenna. You can still use a mismatched antenna to its full gain potential, provided the mismatch is not so severe as to cause heating losses in the system, especially the feed line and matching devices. (See also the discussion of additional loss caused by SWR in Chapter 24.)

Similarly, a mismatched receiving antenna may be matched into the receiver front end for maximum power transfer. In any case you should clearly keep in mind that the feed-point mismatch does not affect the radiation characteristics of an antenna. It can only affect the system efficiency when heating losses are considered.

Why then do we include feed-point mismatch as part of the antenna characteristics? The reason is that for efficient system performance, most antennas are resonant transducers and present a reasonable match over a relatively narrow frequency range. It is therefore desirable to design an antenna, whether it be a simple dipole or an array of Yagis, such that the final single feed-point impedance is essentially resistive and matched to the feed line. Furthermore, in order to make accurate, absolute gain measurements, it is vital that the antenna under test accept all the power from a matched-source generator, or that the reflected power caused by the mismatch be measured and a suitable error correction for heating losses be included in the gain calculations. Heating losses may be determined from information contained in Chapter 24.

While on the subject of feed-point impedance, mention should be made of the use of *baluns* in antennas. A balun is simply a device that permits a lossless transition between a balanced system feed line or antenna and an unbalanced feed line or system. If the feed point of an antenna is symmetric, such as with a dipole, and it is desired to feed this antenna with an unbalanced feed line such as coax, you should provide a balun between the line and the feed point. Without the balun, current will be allowed to flow on the outside of the coax. The current on the outside of the feed line will cause radiation, and thus the feed line will become part of the antenna radiation system. In the case of beam antennas, where it is desired to concentrate the radiated energy is a specific direction, this extra radiation from the feed line will be detrimental, causing distortion of the expected antenna pattern. See Chapter 26 for additional details on this problem.

ANTENNA TEST SITE SET-UP AND EVALUATION

Since an antenna is a reciprocal device, measurements of gain and radiation patterns can be made with the test antenna used either as a transmitting or as a receiving antenna. In general and for practical reasons, the test antenna is used in the receiving mode, and the source or transmitting antenna is located at a specified fixed remote site and unattended. In other words the source antenna, energized by a suitable transmitter, is simply required to illuminate or flood the receiving site in a controlled and constant manner.

As mentioned earlier, antenna measurements ideally should be made under free-space conditions. A further restriction is that the illumination from the source antenna be a *plane wave* over the effective aperture (capture area) of the test antenna. A plane wave by definition is one in which the magnitude and phase of the fields are uniform, and in the test-antenna situation, *uniform over the effective area plane of the test antenna*. Since it is the nature of all radiation to expand in a spherical manner at great distance from the source, it would seem to be most desirable to locate the source antenna as far from the test site as possible. However, since for practical reasons the test site and source location will have to be near the earth and not in outer space, the environment must include the effects of the ground surface and other obstacles in the vicinity of both antennas. These effects almost always

dictate that the test range (spacing between source and test antennas) be as short as possible consistent with maintaining a nearly error-free plane wave illuminating the test *aperture*.

A nearly error-free plane wave can be specified as one in which the phase and amplitude, from center to edge of the illuminating field over the test aperture, do not deviate by more than about 30° and 1 decibel, respectively. These conditions will result in a gain-measurement error of no more than a few percent less than the true gain. Based on the 30° phase error alone, it can be shown that the minimum range distance is approximately

$$S_{min} = 2\frac{D^2}{\lambda} \qquad \text{(Eq 23)}$$

where D is the largest aperture dimension and λ is the free-space wavelength in the same units as D. The phase error over the aperture D for this condition is $^1/_{16}$ wavelength.

Since aperture size and gain are related by

$$\text{Gain} = \frac{4\pi A_e}{\lambda^2} \qquad \text{(Eq 24)}$$

where A_e is the effective aperture area, the dimension D may be obtained for simple aperture configurations. For a square aperture

$$D_2 = G\frac{\lambda^2}{4\pi} \qquad \text{(Eq 25)}$$

that results in a minimum range distance for a square aperture of

$$S_{min} = G\frac{\lambda}{2\pi} \qquad \text{(Eq 26)}$$

and for a circular aperture of

$$S_{min} = G\frac{2\lambda}{\pi^2} \qquad \text{(Eq 27)}$$

For apertures with a physical area that is not well defined or is much larger in one dimension that in other directions, such as a long thin array for maximum directivity in one plane, it is advisable to use the maximum estimate of D from either the expected gain or physical aperture dimensions.

Up to this point in the range development, only the conditions for minimum range length, S_{min}, have been established, as though the ground surface were not present. This minimum S is therefore a necessary condition even under free-space environment. The presence of the ground further complicates the range selection, not in the determination of S but in the exact location of the source and test antennas above the earth.

It is always advisable to select a range whose intervening terrain is essentially flat, clear of obstructions, and of uniform surface conditions, such as all grass or all pavement. The extent of the range is determined by the illumination of the source antenna, usually a Yagi, whose gain is no greater than the highest gain antenna to be measured. For gain measurements the range consists essentially of the region in the beam of the test antenna. For radiation-pattern measurements, the range is considerably larger and consists of all that area illuminated by the source antenna, especially around and behind the test site. Ideally you should choose a site where the test-antenna location is near the center of a large open area and the source antenna is located near the edge where most of the obstacles (trees, poles, fences, etc.) lie.

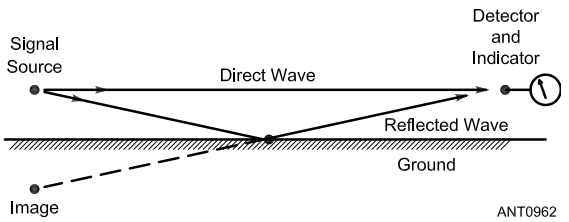

Fig 60—On an antenna test range, energy reaching the receiving equipment may arrive after being reflected from the surface of the ground, as well as by the direct path. The two waves may tend to cancel each other, or may reinforce one another, depending on their phase relationship at the receiving point.

The primary effect of the range surface is that some of the energy from the source antenna will be reflected into the test antenna, while other energy will arrive on a direct line-of-sight path. This is illustrated in **Fig 60**. The use of a flat, uniform ground surface assures that there will be essentially a mirror reflection, even though the reflected energy may be slightly weakened (absorbed) by the surface material (ground). In order to perform an analysis you should realize that horizontally polarized waves undergo a 180° phase reversal upon reflection from the earth. The resulting illumination amplitude at any point in the test aperture is the vector sum of the electric fields arriving from the two directions, the direct path and the reflected path.

If a perfect mirror reflection is assumed from the ground (it is nearly that for practical ground conditions at VHF/UHF) and the source antenna is isotropic, radiating equally in all directions, then a simple geometric analysis of the two path lengths will show that at various point in the vertical plane at the test-antenna site the waves will combine in different phase relationships. At some points the arriving waves will be in phase, and at other points they will be 180° out of phase. Since the field amplitudes are nearly equal, the resulting phase change caused by path length difference will produce an ampli-

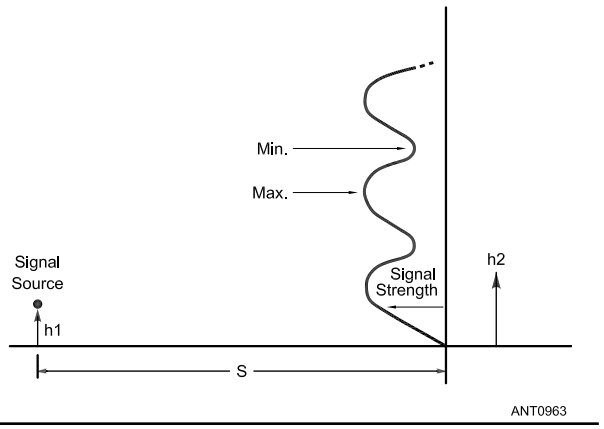

Fig 61—The vertical profile, or plot of signal strength versus test-antenna height, for a fixed height of the signal source above ground and at a fixed distance. See text for definitions of symbols.

tude variation in the vertical test site direction similar to a standing wave, as shown in **Fig 61**.

The simplified formula relating the location of h2 for maximum and minimum values of the two-path summation in terms of h1 and S is

$$h2 = n\frac{\lambda}{4} \times \frac{S}{h1} \qquad \text{(Eq 28)}$$

with n = 0, 2, 4, . . . for minimums and n = 1, 3, 5, . . . for maximums, and S is much larger than either h1 or h2.

The significance of this simple ground reflection formula is that it permits you to determine the approximate location of the source antenna to achieve a nearly plane-wave amplitude distribution *in the vertical direction* over a particular test *aperture size*. It should be clear from examination of the height formula that as h1 is decreased, the vertical distribution pattern of signal at the test site, h2, expands. Also note that the signal level for h2 equal to zero is always zero on the ground regardless of the height of h1.

The objective in using the height formula then is, given an effective antenna aperture to be illuminated from which a minimum S (range length) is determined and a suitable range site chosen, to find a value for h1 (source antenna height). The required value is such that the *first* maximum of vertical distribution at the test site, h2, is at a practical distance above the ground, and at the same time the signal amplitude over the aperture in the vertical direction does not vary more than about 1 dB. This last condition is not sacred but is closely related to the particular antenna under test.

In practice these formulas are useful only to initialize the range setup. A final check of the vertical distribution at the test site must be made by direct measurement. This measurement should be conducted with a small low-gain but unidirectional probe antenna such as a corner reflector or 2-element Yagi that you move along a vertical line over the intended aperture site. Care should be exercised to minimize the effects of local environment around the probe antenna and that the beam of the probe be directed at the source antenna at all times for maximum signal. A simple dipole is undesirable as a probe antenna because it is susceptible to local environmental effects.

The most practical way to instrument the vertical distribution measurement is to construct some kind of vertical track, preferably of wood, with a sliding carriage or platform that may be used to support and move the probe antenna. It is assumed of course that a stable source transmitter and calibrated receiver or detector are available so variations of the order of $^1/_2$ dB can be clearly distinguished.

Once you conduct these initial range measurements successfully, the range is now ready to accommodate any aperture size less in vertical extent than the largest for which S_{min} and the vertical field distribution were selected. Place the test antenna with the center of its aperture at the height h2 where maximum signal was found. Tilt the test antenna tilted so that its main beam is pointed in the direction of the source antenna. The final tilt is found by observing the receiver output for maximum signal. This last process must be done empirically since the apparent location of the source is somewhere between the actual source and its image, below the ground.

An example will illustrate the procedure. Assume that we wish to measure a 7-foot diameter parabolic reflector antenna at 1296 MHz (λ = 0.75 foot). The minimum range distance, S_{min}, can be readily computed from the formula for a circular aperture.

$$S_{min} = 2\frac{D^2}{\lambda} = 2 \times \frac{49}{0.75} = 131 \text{ feet}$$

Now a suitable site is selected based on the qualitative discussion given before.

Next determine the source height, h1. The procedure is to choose a height h1 such that the first minimum above ground (n = 2 in formula) is at least two or three times the aperture size, or about 20 feet.

$$h1 = n\frac{\lambda}{4}\frac{S}{h1} = 2 \times \frac{0.75}{4} \times \frac{131}{20} = 2.5 \text{ feet}$$

Place the source antenna at this height and probe the vertical distribution over the 7-foot aperture location, which will be about 10 feet off the ground.

$$h2 = n\frac{\lambda}{4}\frac{S}{h1} = 1 \times \frac{0.75}{4} \times \frac{131}{2.5} = 9.8 \text{ feet}$$

Plot the measured profile of vertical signal level versus height. From this plot, empirically determine whether the 7-foot aperture can be fitted in this profile such that the 1-dB variation is not exceeded. If the variation exceeds

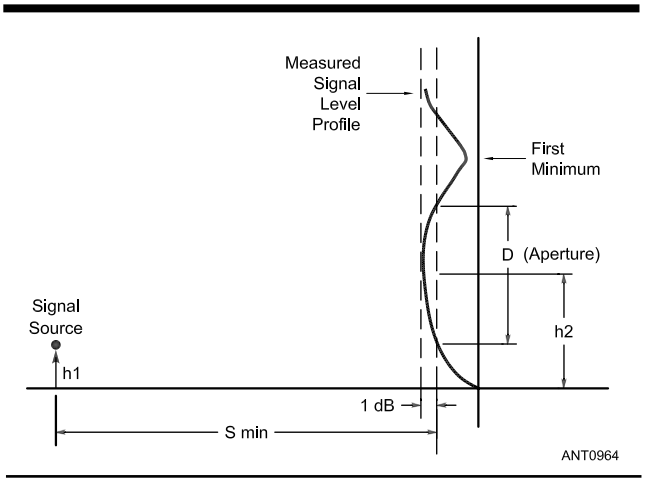

Fig 62—Sample plot of a measured vertical profile.

1 dB over the 7-foot aperture, the source antenna should be lowered and h2 raised. Small changes in h1 can quickly alter the distribution at the test site. **Fig 62** illustrates the points of the previous discussion.

The same set-up procedure applies for either horizontal or vertical linear polarization. However, it is advisable to check by direct measurement at the site for each polarization to be sure that the vertical distribution is satisfactory. Distribution probing in the horizontal plane is unnecessary as little or no variation in amplitude should be found, since the reflection geometry is constant. Because of this, antennas with apertures that are long and thin, such as a stacked collinear vertical, should be measured with the long dimension parallel to the ground.

A particularly difficult range problem occurs in measurements of antennas that have depth as well as cross-sectional aperture area. Long end-fire antennas such as long Yagis, rhombics, V-beams, or arrays of these antennas, radiate as *volumetric arrays* and it is therefore even more essential that the illuminating field from the source antenna be reasonably uniform in depth as well as plane wave in cross section. For measuring these types of antennas it is advisable to make several vertical profile measurements that cover the depth of the array. A qualitative check on the integrity of the illumination for long end-fire antennas can be made by moving the array or antenna axially (forward and backward) and noting the change in received signal level. If the signal level varies less than 1 or 2 dB for an axial movement of several wavelengths then the field can be considered satisfactory for most demands on accuracy. Large variations indicate that the illuminating field is badly distorted over the array depth and subsequent measurements are questionable. It is interesting to note in connection with gain measurements that any illuminating field distortion will always result in measurements that are lower than true values.

ABSOLUTE GAIN MEASUREMENT

Having established a suitable range, the measure-

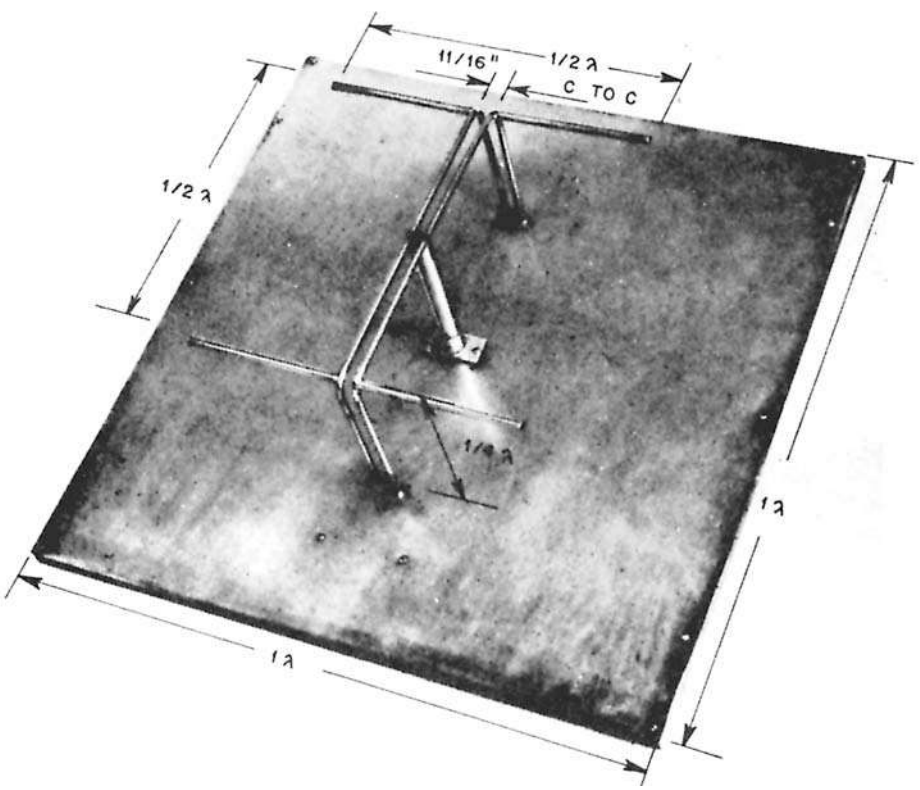

Fig 63—Standard-gain antenna. When accurately constructed for the desired frequency, this antenna will exhibit a gain of 7.7 dB over a dipole radiator, plus or minus 0.25 dB. In this model, constructed for 432 MHz, the elements are $^{3}/_{8}$-inch diameter tubing. The phasing and support lines are of $^{5}/_{16}$-inch diameter tubing or rod.

ment of gain relative to an isotropic (point source) radiator is almost always accomplished by direct comparison with a calibrated standard-gain antenna. That is, the signal level with the test antenna in its optimum location is noted. Then you remove the test antenna and place the standard-gain antenna with its aperture at the center of location where the test antenna was located. Measure the difference in signal level between the standard and the test antennas and add to or subtract from the gain of the standard-gain antenna to obtain the absolute gain of the test antenna. Here, *absolute* means with respect to a point source with a gain of unity, by definition. The reason for using this reference rather than a dipole, for instance, is that it is more useful and convenient for system engineering. We assume that both standard and test antennas have been carefully matched to the appropriate impedance and an accurately calibrated and matched detecting device is being used.

A standard-gain antenna may be any type of unidirectional, preferably planar-aperture, antenna, which has been calibrated either by direct measurement or in special cases by accurate construction according to computed dimensions. A standard-gain antenna has been suggested by Richard F. H. Yang (see Bibliography). Shown in **Fig 63**, it consists of two in-phase dipoles $^1/_2$ λ apart and backed up with a ground plane 1 λ square.

In Yang's original design, the stub at the center is a balun formed by cutting two longitudinal slots of $^1/_8$-inch width, diametrically opposite, on a $^1/_4$-λ section of $^7/_8$-inch rigid 50-Ω coax. An alternative method of feeding is to feed RG-8 or RG-213 coax through slotted $^7/_8$-inch copper tubing. Be sure to leave the outer jacket on the coax to insulate it from the copper-tubing balun section. When constructed accurately to scale for the frequency of interest, this type of standard will have an absolute gain of 9.85 dBi (7.7 dBd gain over a dipole in free space) with an accuracy of ± 0.25 dB.

RADIATION-PATTERN MEASUREMENTS

Of all antenna measurements, the radiation pattern is the most demanding in measurement and the most difficult to interpret. Any antenna radiates to some degree in all directions into the space surrounding it. Therefore, the radiation pattern of an antenna is a three-dimensional representation of the magnitude, phase and polarization. In general, and in practical cases for Amateur Radio communications, the polarization is well defined and only the magnitude of radiation is important.

Furthermore, in many of these cases the radiation in one particular plane is of primary interest, usually the plane corresponding to that of the Earth's surface, regardless of polarization. Because of the nature of the range setup, measurement of radiation pattern can be successfully made only in a plane nearly parallel to the earth's surface. With beam antennas it is advisable and usually sufficient to take two radiation pattern measurements, one in the polarization plane and one at right angles to the plane of polarization. These radiation patterns are referred to in antenna literature as the principal E-plane and H-plane patterns, respectively. *E-plane* means parallel to the electric field that is the polarization plane and *H-plane* means parallel to the magnetic field in free space. The electric field and magnetic field are always perpendicular to each other in a plane wave as it propagates through space.

When the antenna is located over real earth, the terms *Azimuth* and *elevation* planes are commonly used, since the frame of reference is the Earth itself, rather than the electric and magnetic fields in free space. For a horizontally polarized antenna such as a Yagi mounted with its elements parallel to the ground, the azimuth plane is the E-plane and the elevation plane is the H-plane.

The technique to obtain these patterns is simple in procedure but requires more equipment and patience than does making a gain measurement. First, a suitable mount is required that can be rotated in the azimuth plane (horizontal) with some degree of accuracy in terms of azimuth-angle positioning. Second, a signal-level indicator calibrated over at least a 20-dB dynamic range with a readout resolution of at least 2 dB is required. A dynamic range of up to about 40 dB would be desirable but does not add greatly to the measurement significance.

With this much equipment, the procedure is to locate first the area of maximum radiation from the beam antenna by carefully adjusting the azimuth and elevation positioning. These settings are then arbitrarily assigned an azimuth angle of zero degrees and a signal level of zero decibels. Next, without changing the elevation setting (tilt of the rotating axis), the antenna is carefully rotated in azimuth in small steps that permit signal-level readout of 2 or 3 dB per step. These points of signal level corresponding with an azimuth angle are recorded and plotted on polar coordinate paper. A sample of the results is shown on ARRL coordinate paper in **Fig 64**.

On the sample radiation pattern the measured points are marked with an X and a continuous line is drawn in, since the pattern is a continuous curve. Radiation patterns should preferably be plotted on a logarithmic radial scale, rather than a voltage or power scale. The reason is that the log scale approximates the response of the ear to signals in the audio range. Also many receivers have AGC systems that are somewhat logarithmic in response; therefore the log scale is more representative of actual system operation.

Having completed a set of radiation-pattern measurements, one is prompted to ask, "Of what use are they?" The primary answer is as a diagnostic tool to determine if the antenna is functioning as it was intended to. A second answer is to know how the antenna will discriminate against interfering signals from various directions.

Consider now the diagnostic use of the radiation patterns. If the radiation beam is well defined, then there is an approximate formula relating the antenna gain to the

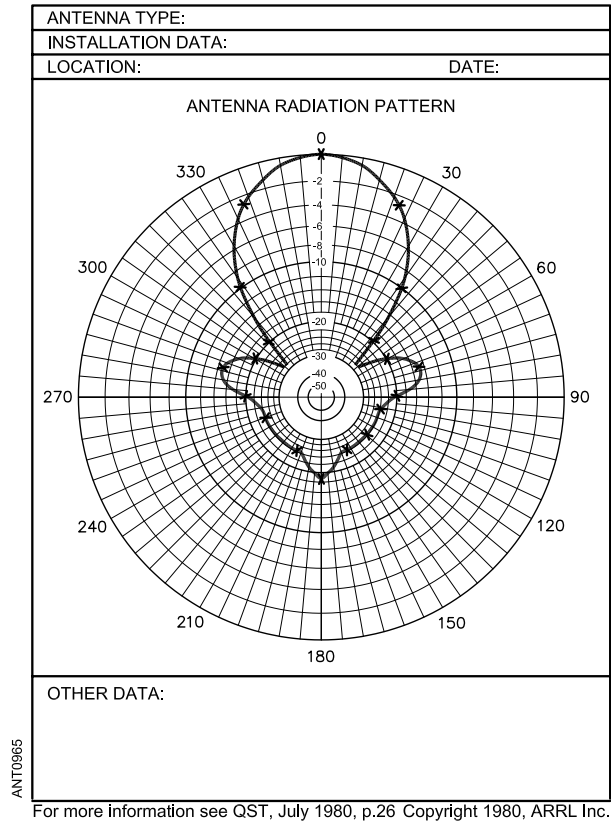

Fig 64—Sample plot of a measured radiation pattern, using techniques described in the text. The plot is on coordinate paper available from ARRL HQ. The form provides space for recording significant data and remarks.

measured half-power beamwidth of the E- and H-plane radiation patterns. The half-power beamwidth is indicated on the polar plot where the radiation level falls to 3 dB below the main beam 0-dB reference on either side. The formula is

$$\text{Gain}\,(\text{dBi}) \cong \frac{41{,}253}{\theta_E \phi_H} \qquad \text{(Eq 29)}$$

where θ_E and ϕ_H are the half-power beamwidths in degrees of the E- and H-plane patterns, respectively. This equation assumes a lossless antenna system, where any side-lobes are well suppressed.

To illustrate the use of this equation, assume that we have a Yagi antenna with a boom length of two wavelengths. From known relations (described in Chapter 11) the expected free-space gain of a Yagi with a boom length of 2 λ is about 13 dBi; its gain, G, equals 20. Using the above relationship, the product of $\theta_E \times \phi_H \approx 2062$ square degrees. Since a Yagi produces a nearly symmetric beam shape in cross section, $\theta_E = \phi_H = 45^\circ$. Now if the measured values of θ_E and ϕ_H are much larger than 45°, then the gain will be much lower than the expected 13 dBi.

As another example, suppose that the same antenna (a 2-wavelength-boom Yagi) gives a measured gain of 9 dBi but the radiation pattern half power beamwidths are approximately 45°. This situation indicates that although the radiation patterns seem to be correct, the low gain shows inefficiency somewhere in the antenna, such as lossy materials or poor connections.

Large broadside collinear antennas can be checked for excessive phasing-line losses by comparing the gain computed from the radiation patterns with the direct-measured gain. It seems paradoxical, but it is indeed possible to build a large array with a very narrow beamwidth indicating high gain, but actually having very low gain because of losses in the feed distribution system.

In general, and for most VHF/UHF Amateur Radio communications, gain is the primary attribute of an antenna. However, radiation in other directions than the main beam, called *sidelobe radiation*, should be examined by measurement of radiation patterns for effects such as nonsymmetry on either side of the main beam or excessive magnitude of sidelobes. (Any sidelobe that is less than 10 dB below the main beam reference level of 0 dB should be considered excessive.) These effects are usually attributable to incorrect phasing of the radiating elements or radiation from other parts of the antenna that was not intended, such as the support structure or feed line.

The interpretation of radiation patterns is intimately related to the particular type of antenna under measurement. Reference data should be consulted for the antenna type of interest, to verify that the measured results are in agreement with expected results.

To summarize the use of pattern measurements, if a beam antenna is first checked for gain (the easier measurement to make) and it is as expected, then pattern measurements may be academic. However, if the gain is lower than expected it is advisable to make pattern measurements to help determine the possible causes for low gain.

Regarding radiation pattern measurements, remember that the results measured under proper range facilities will not necessarily be the same as observed for the same antenna at a home-station installation. The reasons may be obvious now in view of the preceding information on the range setup, ground reflections, and the vertical-field distribution profiles. For long paths over rough terrain where many large obstacles may exist, the effects of ground reflection tend to become diffused, although they still can cause unexpected results. For these reasons it is usually unjust to compare VHF/UHF antennas over long paths.

Vector Network Analyzers

The process of building and properly tuning a phased array often involves making a number of different measurements to achieve a desired level of performance, as was pointed out in Chapter 8, Multielement Arrays. This section was written by Rudy Severns, N6LF.

After erecting an array we would like to measure the resonant frequency of each element, the self-impedances of each element and the mutual impedances between the elements. We will also want to know these impedances over the whole operating band to help design a feed network. When building the feed network, we may need to check the values and Qs of the network elements and we will want to determine the electrical lengths of transmission lines.

Final tuning of the array requires that the relative current amplitudes and phases in each element be measured and adjusted, if necessary. We also will want to determine the SWR at the feed point. Doing all of this even moderately well can require quite a bit of equipment, some of which is heavy and requires ac line power. This can be a nuisance in the field, especially if the weather is not cooperating.

Professionals make these measurements by employing a *vector network analyzer* (VNA) or the somewhat simpler, *reflection-transmission test set*. These instruments can make all the necessary measurements quickly and with great accuracy. However, in the past VNAs have been very expensive, out of reach for general amateur use. But thanks to modern digital technology VNAs that work with a laptop computer are now becoming available at prices an amateur might consider. It's even possible to homebrew a VNA[1] with performance that approaches a professional instrument. Considering the cost of even a simple array, investment in a VNA makes sense.

VNAs are based on reflection and transmission measurements. To use a VNA it is very helpful to have a basic understanding of *Scattering Parameters* (S-parameters). Microwave engineers have long used these because they have to work with circuits that are large in terms of wavelength, where measurements of forward and reflected power are easy.

HF arrays are also large in terms of wavelength. The techniques for measuring forward and reverse powers work well even at 160 meters. For example, even though the array elements may be 100 feet apart, you can place your instruments in a central location and run cables out to each element. The effect of the cables from the VNA to the elements can be absorbed in the initial calibration procedure so the measurements read out at the VNA are effectively those at each element. In other words, the measurement reference points can be placed electrically at the base of the element, regardless of the physical location of the instrumentation and the interconnecting cables.

In a completed array with its feed network, the network can be excited by the VNA at the feed point and the relative current amplitudes and phases at each element can be measured over a frequency band. Then, adjustments can be made as needed. When the final values for the current amplitudes and phases are known, these values can be put back into an array model in a program like *EZNEC* to determine the pattern of the array across the whole frequency band.

S-PARAMETERS

In Chapter 24, Transmission Lines, the reflection coefficient rho (ρ) is defined as the ratio of the reflected voltage (V_r) to the incident voltage (V_i):

$$\rho = \frac{V_r}{V_i} \qquad \text{(Eq 30)}$$

If we know the load impedance (Z_L) and the transmission line impedance (Z_0) we can calculate ρ from:

$$\rho = \frac{Z_L - Z_0}{Z_L + Z_0} \qquad \text{(Eq 31)}$$

Keep in mind that ρ is a complex number (a vector), which we represent by either amplitude and phase ($|Z|$, θ) or by real and imaginary parts ($R \pm j\,X$). The two representations are equivalent. From ρ we can then calculate SWR. That's very handy, but here we want to do something different. If we have an instrument that measures ρ and we know Z_0 then we can determine Z_L from:

$$Z_L = Z_0\left(\frac{1+\rho}{1-\rho}\right) \qquad \text{(Eq 32)}$$

Measuring ρ is one of the things that VNAs do very well. With a VNA, the measurement can be made at one end of a long transmission line with the load at the other end. The effect of the line can be calibrated out, as mentioned above, so that we are in effect measuring right at the load.

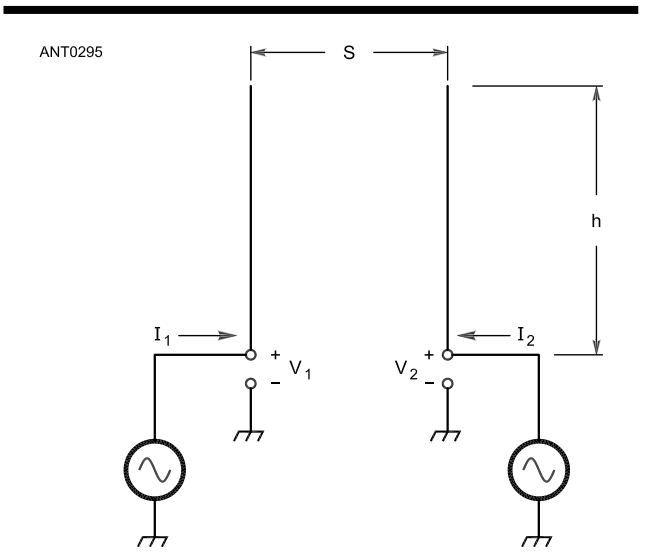

Fig 65—A 2-element array, where h is the element height and S is the spacing between the elements.

This approach can be used directly to measure the impedance and resonant frequency of a single element. By open and short circuiting elements in an array we can determine the mutual as well as self impedances for, and between, all the elements. We can also use this approach to measure component values, inductor Qs, etc.

This is an example of a *one-port* measurement; that is, a load at the end of a transmission line. However, a multi-element array actually behaves as a multi-port network, so to get the most out of a VNA, you need to generalize the above procedure. This is where S-parameters come into play. To illustrate the principles we will use a simple 2-element array like that shown in **Fig 65**.

To design a feed network to drive this array we need to know the input impedance of each element (Z_1 and Z_2) as a function of the drive currents (I_1 and I_2). The input impedances will depend on the self impedance of each element, the coupling between them (the mutual impedance) and the drive currents in each element. To manage this problem we can represent a 2-element array as a two-port network, as shown in **Fig 66**. And we can relate the port voltages, currents and impedances with Eq 33:

$$V_1 = Z_{11}I_1 + Z_{12}I_2$$
$$V_2 = Z_{21}I_1 + Z_{22}I_2 \qquad \text{(Eq 33)}$$

Normally we know I_1 and I_2 from the design of the array, but we need to determine the resulting element impedances. That's the challenge. Fortunately, an array is a linear network, so $Z_{12} = Z_{21}$, which means we need only determine three variables: the self impedances Z_{11} and Z_{22} and the mutual impedance, Z_{12}.

Once we know Z_{11}, Z_{12}, Z_{22} and are given I_1 and I_2, we can determine the feed-point impedances at each element from:

$$Z_1 = Z_{11} + \left(\frac{I_2}{I_1}\right) Z_{12}$$
$$Z_2 = Z_{22} + \left(\frac{I_1}{I_2}\right) Z_{12} \qquad \text{(Eq 34)}$$

This is the conventional approach. However, there are some problems here. We have to be able to accurately measure either voltages and currents or impedances in multiple elements that may be separated by large fractions of a wavelength. In addition, accurate measurements of current, voltage and impedance become increasingly more difficult as we go up in frequency.

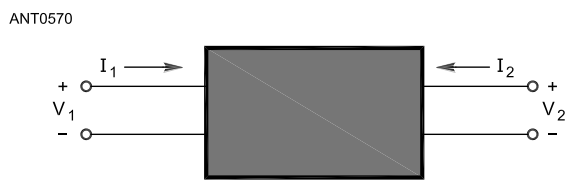

Fig 66—Two-port representation of currents and voltages in the 2-element array in Fig 65.

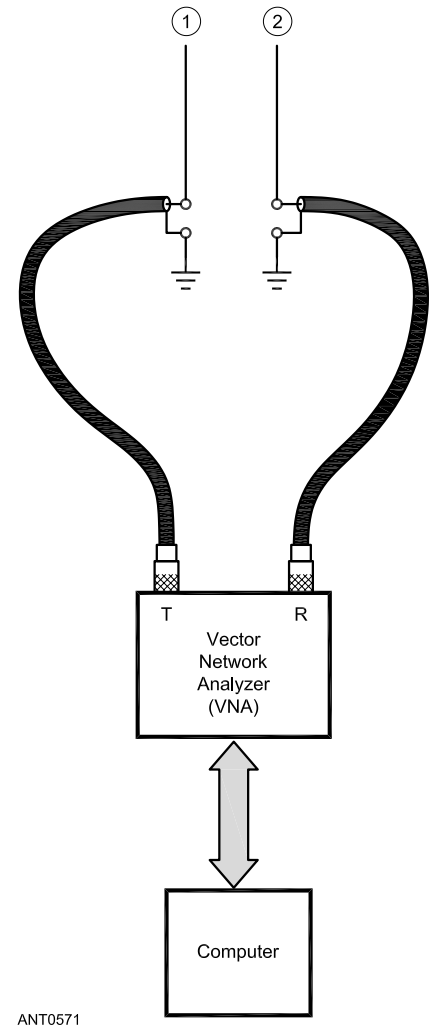

Fig 67—Test setup to measure a 2-element array using a VNA.

It turns out that we can get the information more easily by measuring incident and reflected voltages at the ports and from those measurements determine the feed-point impedances. A VNA is an instrument for measuring these voltages. It turns out to be easier to measure the ratios of two voltages rather than their absolute values.

The measurement setup using a VNA for a 2-element array is shown in **Fig 67**. VNAs usually have at least two RF connections: the transmit port (T) and the receive port (R). Professional units may have more RF connections. The T output provides an signal from a 50-Ω source and the R port is a detector with a 50-Ω input impedance. Basically we have a transmitter and a receiver. The transmit port uses a directional coupler to provide measurements of the forward and reflected signals at that output. The receive port measures the signal transmitted through the network. Transmission lines usually have Z_0 = 50 Ω and may be of any length required by the size of the array.

Using incident and reflected voltages, the two-port network representation is now changed, as shown in **Fig 68**, where:

V_{1i} = incident voltage at port 1
V_{1r} = reflected voltage at port 1
V_{2i} = incident voltage at port 2
V_{2r} = reflected voltage at port 2

In a manner analogous to Eq 33, we can write an expression in terms of the incident and reflected voltages:

$$b_1 = S_{11}a_1 + S_{12}a_2$$
$$b_2 = S_{21}a_1 + S_{22}a_2 \qquad \text{(Eq 35)}$$

where:

$$a_1 \frac{V_{1i}}{\sqrt{Z_0}} \qquad b_1 \frac{V_{1r}}{\sqrt{Z_0}}$$
$$a_2 = \frac{V_{2i}}{\sqrt{Z_0}} \qquad b_2 = \frac{V_{2r}}{\sqrt{Z_0}} \qquad \text{(Eq 36)}$$

We see that the a_n and b_n are simply the incident and reflected voltages at the two ports divided by $\sqrt{Z_o}$. Because this is a linear network, $S_{21} = S_{12}$.

What are the S_{ij} quantities? These are called the *S-parameters*, which are defined by:

$$S_{11} \equiv \left.\frac{b_1}{a_1}\right|_{a_2=0} = \left.\frac{V_{1r}}{V_{1i}}\right|_{V_{2i}=0}$$
$$S_{21} \equiv \left.\frac{b_2}{a_1}\right|_{a_2=0} = \left.\frac{V_{2r}}{V_{1i}}\right|_{V_{2i}=0}$$
$$S_{12} \equiv \left.\frac{b_1}{a_2}\right|_{a_1=0} = \left.\frac{V_{1r}}{V_{2i}}\right|_{V_{1i}=0} \qquad \text{(Eq 37)}$$
$$S_{22} \equiv \left.\frac{b_2}{a_2}\right|_{a_1=0} = \left.\frac{V_{2r}}{V_{2i}}\right|_{V_{1i}=0}$$

Note that the S_{ij} parameters are all ratios of reflected and incident voltages, and they are usually complex numbers. The condition that $a_2 = 0 = V_{2i}$ is the same as saying that port 2 is terminated in a load equal to Z_0 and the network is excited at port 1. This means there is no reflection from the load on port 2, which makes $V_{2i} = 0$. Similarly, if we terminate port 1 with Z_0 and excite port 2, then $V_{1i} = 0 = a_1$.

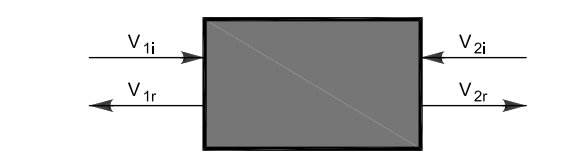

Fig 68—Two-port network with incident and reflected waves.

If we compare Eq 30 to the first line of Eq 37 we see that $S_{11} = \rho_1$, the reflection coefficient at port 1. We can now restate Eq 32 in terms of S_{11}:

$$Z = Z_0\left(\frac{1+S_{11}}{1-S_{11}}\right) \qquad \text{(Eq 38)}$$

where Z is the impedance looking into port 1 with port 2 terminated in Z_0. In the case where port 2 does not exist—that is, you are measuring a single element (for example, measuring element 1 with element 2 open-circuited) or a component, then Z is simply the self impedance (Z_{11} in Eq 33). Since S_{11} is a standard measurement for VNAs you can calculate Z using Eq 38. In many cases the VNA software will do this calculation for you automatically. You can also measure element 2 with element 1 open and determine Z_{22}.

S_{21} represents the ratio of the signal coming out of port 2 (V_{2r}) to the input signal on port 1 (V_{1i}) and is another standard VNA measurement. S_{21} is a measurement of the signal transmission between the ports through the network, or in the case of an array, the signal transmission due to the coupling between the elements. Again, port 2 is terminated in Z_0.

A full-feature VNA will measure all the S_{ij} parameters at once, but most of the lower-cost units of interest to amateurs are what we call *reflection-transmission test sets*. What this means is that they only measure S_{11} and S_{21}. To obtain S_{22} and S_{12} we have to interchange the test cables at the array elements (see Fig 67) and run the measurements again. Normally the software will accommodate this as a second entry and we end up with the full set of S_{ij} parameters.

If we do run a full set of S_{ij} parameters then we can transform these to Z_{ij} (Eq 33) using the following expressions, assuming that $S_{21} = S_{12}$:

$$Z_{11} = \frac{(1+S_{11})(1-S_{22})+S_{12}^2}{(1-S_{11})(1-S_{22})-S_{12}^2}$$
$$Z_{22} = \frac{(1-S_{11})(1+S_{22})+S_{12}^2}{(1-S_{11})(1-S_{22})-S_{12}^2} \qquad \text{(Eq 39)}$$
$$Z_{12} = \frac{(2S_{12})}{(1-S_{11})(1-S_{22})-S_{12}^2}$$

The example to this point has been for a 2-element array. The S-parameters can be determined for an array with any number of elements. In an n-port S-parameter measurement, all ports are terminated in Z_0 at the same time. Measurements are made between one set of ports at a time and repeated until all pairs of ports are measured.

ARRAY MEASUREMENT EXAMPLE

A good way to illustrate the use of a VNA for array measurements is to work through an example with a real array. **Fig 69** is a picture of a 2-element 20-meter phased

array built by Mark Perrin, N7MQ.

Each element is λ/4 (self resonant at 14.150 MHz) and spaced λ/4 (17 feet 5 inches). In the ideal case, both elements would have the same current amplitude with a 90° phase difference. This gives the cardioid pattern shown in Chapter 8, Multielement Arrays. There are many schemes for correctly feeding such an array. The one used in this example uses two different 75-Ω transmission lines (one λ/4 and the other λ/2, electrically), as described by Roy Lewallen, W7EL.[2,3]

The first task is to resonate the elements individually. With the VNA set to measure S_{11} phase, we will get a graph like that shown in **Fig 70**.

At the λ/4 resonant frequency (f_r) we will see a sharp phase transition as we go from −180° to +180°. This is typical of any series resonant circuit. The length of each element is adjusted until the desired f_r is achieved. This is a very sensitive measurement. You can see the shift in f_r due to the wind blowing, the length of the element changing as it heats up in the sun or any interactions between the feed line and the antenna as you move the feed line around. In fact this is very good point in the process to make sure everything is mechanically stable and free of unexpected couplings. Usually you will find it necessary place choke baluns on each element to reduce stray coupling.

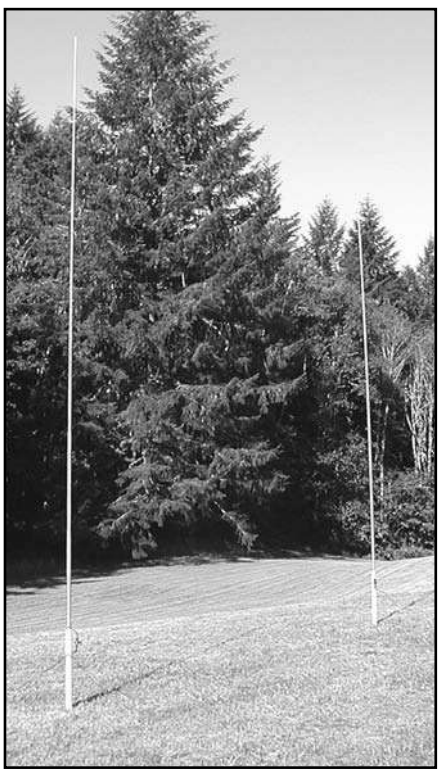

Fig 69—2-element 20-meter phased array (*Photo courtesy N7MQ*).

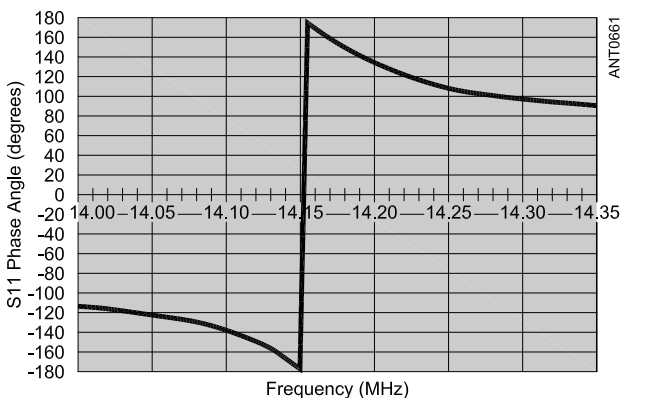

Fig 70—S_{11} phase plot for an individual element.

The next step is to determine the self (Z_{11} and Z_{22}) and mutual (Z_{12}) impedances from which the actual driving point impedances present when the array is excited can be determined. See Chapter 8, Multielement Arrays. There are two ways to go.

First, we can simply use the VNA as an impedance bridge—ie, make two S_{11} measurements at one element, first with the other element open (Z_{11} or Z_{22}) and then with it shorted (Z_1 or Z_2). We can convert the S_{11} measurements to impedances using Eq 38. The value for Z_{12} can be obtained from Eq 40:

$$Z_{12} = \pm\sqrt{Z_{11}\left(Z_{11} - Z_1\right)}$$
$$Z_{12} = \pm\sqrt{Z_{22}\left(Z_{22} - Z_2\right)} \qquad \text{(Eq 40)}$$

The second approach is to do a full two-port S-parameter measurement (S_{11}, S_{21}, S_{12} and S_{22}) and derive the impedances using Eq 38. Both approaches will work but the second approach has the advantage that the ± ambiguity in Eq 40 is eliminated.

For this example, the impedance values from the measurements at 14.150 MHz, turn out to be:

$$Z_{11} = 51.4 + j\,0.35$$
$$Z_{22} = 50.3 + j\,0.299$$
$$Z_{12} = 15.06 - j\,19.26 \qquad \text{(Eq 41)}$$

With these values we can now determine the feed-point impedances from:

$$Z_1' = Z_{11} + \frac{I_2}{I_1} Z_{12}$$
$$Z_2' = Z_{22} + \frac{I_1}{I_2} Z_{12}$$
$$\frac{I_1}{I_2} = -j \qquad \text{(Eq 42)}$$

Note that $-j$ represents the 90° phase shift between the currents. Substituting the values from Eq 41 into Eq 42:

$$Z_1' = 32.09 - j\,14.7$$
$$Z_2' = 69.6 + j\,15.32 \qquad \text{(Eq 43)}$$

With these impedances in hand we can now design the feed network. In this particular example however, we have decided to use the λ/4 and λ/2 cables as described by Lewallen[2,3] and accept the results. So we now proceed to cut and trim the two cables to length.

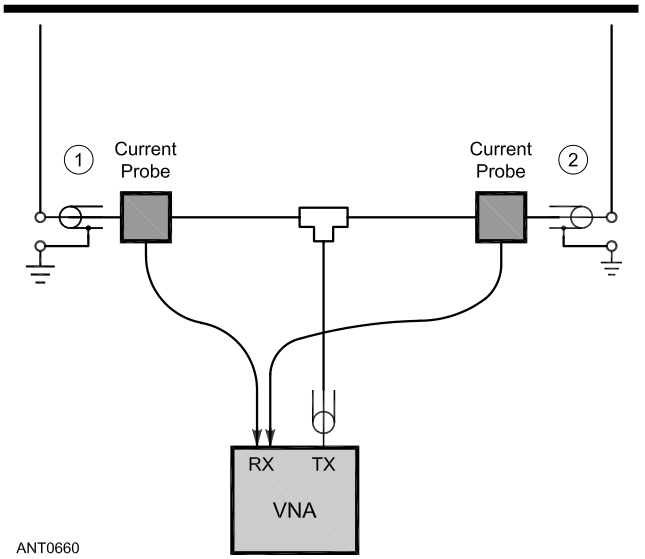

Fig 71—Current phase and amplitude ratio test setup.

Again, there are two ways to go. First we can determine the frequency at which each cable is λ/4 long. At this point the input impedance of the cable will be equivalent to a series-resonant circuit and we can simply measure the phase of S_{11} as we did earlier for f_r and get a plot like that shown in Fig 70. In this example the λ/4 resonant frequencies of the two cables are 7.075 MHz and 14.150 MHz.

The second approach would be to measure S_{21} for each cable at 14.150 MHz. The phase shift in S_{21} tells you how long the cable is, in degrees, at a given frequency. Because there is a small variation in cable characteristics with frequency (dispersion) this approach is slightly more accurate since it is done at the desired operating frequency. But this is not very large effect at HF.

This brings us down to the final measurements, which are to check that the relative current amplitudes and phases between the two elements are correct. We can then determine

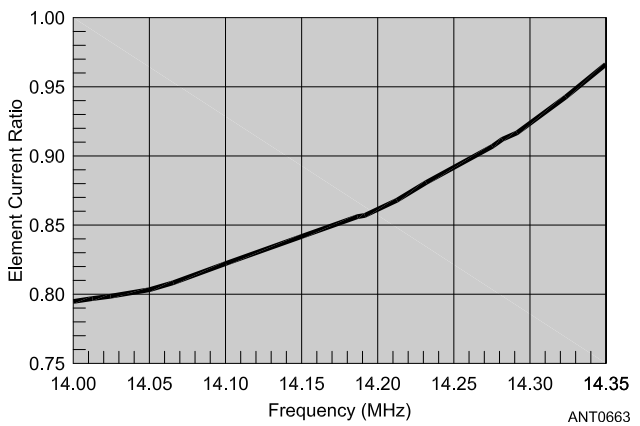

Fig 72—Measured element current ratio over the 20-meter band.

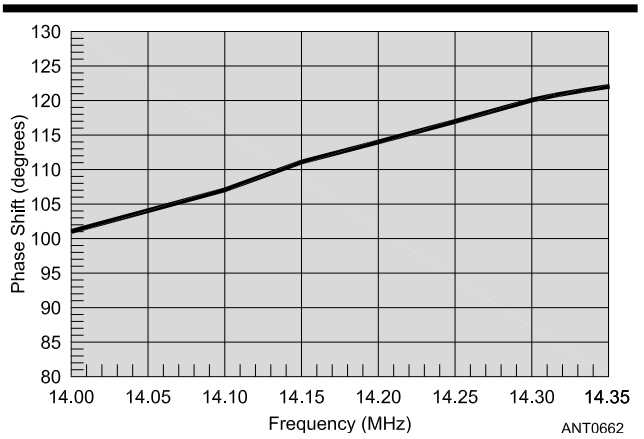

Fig 73—Measured relative current phase shift over the 20-meter band.

the feed-point SWR. The phase and amplitude ratios are made using the S_{12} capability of the VNA and the test setup shown in **Fig 71**.

The VNA transmit port is connected to the normal feed point. A current sensor (see Chapter 8, Multielement Arrays, for a discussion of current sensors) is inserted at the base of element 1 and the output of the sensor is returned to the detector or receive port of the VNA. A calibration run is then made to normalize this path. That makes it the reference.

Next, the current sensor is shifted to element 2. The amplitude and phase plots for S_{12} obtained at this point will be the desired relative phase shift and amplitude ratio between the currents in the array when driven at the normal feed point. **Figs 72** and **73** show the behavior of the example array over the 20-meter band. Note that the amplitude ratio has been converted from dB. We can now use these values in a *EZNEC* model of the array to determine the actual radiation pattern.

Obviously the W7EL feed scheme is not perfect, but it has a definite advantage of simplicity. If better performance is desired we can use the values of Z_1' and Z_2' determined earlier to design and fabricate a new feed network and then proceed to evaluate its performance in the same way.

The final measurement is to connect the transmit port of the VNA to the feed point and measure S_{11}. From this we can calculate the SWR:

$$SWR = \frac{1+|S_{11}|}{1-|S_{11}|} \qquad \text{(Eq 44)}$$

In this example, the return loss, $|S_{11}|$, is about −19 dB over the entire 20-meter band. This corresponds to SWR= 1.25:1.

Notes

[1]Paul Kiciak, N2PK, **http://n2pk.com**.

[2]Roy Lewallen, W7EL, *QST*, Aug 1979, Technical Correspondence, pp 42-43.

[3]Orr and Cowan, *Vertical Antennas*, Radio Amateur Call Book, 1986, pp 148-150.

BIBLIOGRAPHY

Source material and more extended discussion of topics covered in this chapter can be found in the references given below.

A. Bailey, "The Antenna Lab, Parts 1 and 2," *Radio Communication*, Aug and Sep 1983.

L. Blake, *Transmission Lines and Waveguides* (New York: John Wiley & Sons, 1969), pp 244-251.

J. H. Bowen, "A Calorimeter for VHF and UHF Power Measurements, *QST*, Dec 1975, pp 11-13.

W. Bruene, "An Inside Picture of Directional Wattmeters," *QST*, Apr 1959.

CCIR Recommendation 368, Documents of the CCIR XII Plenary assembly, ITU, Geneva, 1967.

J. Carr, "Find Fault with Your Coax," *73*, Oct 1984, pp 10-14.

D. DeMaw, "In-Line RF Power Metering," *QST*, Dec 1969.

D. Fayman, "A Simple Computing SWR Meter," *QST*, Jul 1973, pp 23-33.

J. Gibbons and H. Horn, "A Circuit With Logarithmic Response Over Nine Decades," *IEEE Transactions on Circuit Theory*, Vol CT-11, No. 3, Sep 1964, pp 378-384.

J. Grebenkemper, "Calibrating Diode Detectors," *QEX*, Aug 1990.

J. Grebenkemper, "The Tandem Match—An Accurate Directional Wattmeter," *QST*, Jan 1987.

J. Grebenkemper, "Improving and Using R-X Noise Bridges," *QST*, Aug 1989; Feedback, *QST*, Jan 1990, p 27.

G. H. Hagn, SRI, "HF Ground Measurements at the Lawrence Livermore National Laboratory (LLNL) Field Site," *Applied Computational Electromagnetics Society Journal and Newsletter*, Vol 3, Number 2, Fall 1988.

T. King, "A Practical Time-Domain Reflectometer," *QST*, May 1989, pp 22-24.

Z. Lau and C. Hutchinson, "Improving the HW-9 Transceiver," *QST*, Apr 1988, pp 26-29.

V. G. Leenerts, "Automatic VSWR and Power Meter," *Ham Radio*, May 1980, pp 34-43.

J. Lenk, *Handbook of Oscilloscopes* (Englewood Cliffs, NJ: Prentice-Hall, 1982), pp 288-292.

I. Lindell, E. Alanen, K. Mannerslo, "Exact Image Method for Impedance Computation of Antennas Above the Ground," *IEEE Trans. On Antennas and Propagation*, AP-33, Sep 1985.

L. McCoy, "A Linear Field-Strength Meter," *QST*, Jan 1973.

T. McMullen, "The Line Sampler, an RF Power Monitor for VHF and UHF," *QST*, Apr 1972.

M. Walter Maxwell, W2DU, *Reflections* (Newington: ARRL, 1990), p 20-3. [Out of print.]

C. Michaels, "Determining Line Lengths," Technical Correspondence, *QST*, Sep 1985, pp 43-44.

H. Perras, "Broadband Power-Tracking VSWR Bridge," *Ham Radio*, Aug 1979, pp 72-75.

S. Ramo, J. Whinnery and T. Van Duzer, *Fields and Waves in Communication Electronics* (New York: John Wiley & Sons, 1967), Chap 1.

Reference Data for Radio Engineers, 5th edition (Indianapolis: Howard W. Sams, 1968), Chapter 28.

P. N. Saveskie, *Radio Propagation Handbook* (Blue Ridge Summit, PA: TAB Books, 1960).

J. Sevick, "Short Ground-Radial Systems for Short Verticals," *QST*, Apr 1978, pp 30-33.

J. Sevick, "Measuring Soil Conductivity," *QST*, Mar 1981, pp 38- 39.

W. Spaulding, "A Broadband Two-Port S-Parameter Test Set," *Hewlett-Packard Journal*, Nov 1984.

D. Turrin, "Antenna Performance Measurements," *QST*, Nov 1974, pp 35-41.

F. Van Zant, "High-Power Operation with the Tandem Match Directional Coupler," Technical Correspondence, *QST*, Jul 1989, pp 42-43.

R. F. H. Yang, "A Proposed Gain Standard for VHF Antennas," *IEEE Transactions on Antennas and Propagation*, Nov 1966.

Chapter 28

Smith Chart Calculations

The Smith Chart is a sophisticated graphic tool for solving transmission line problems. One of the simpler applications is to determine the feed-point impedance of an antenna, based on an impedance measurement at the input of a random length of transmission line. By using the Smith Chart, the impedance measurement can be made with the antenna in place atop a tower or mast, and there is no need to cut the line to an exact multiple of half wavelengths. The Smith Chart may be used for other purposes, too, such as the design of impedance-matching networks. These matching networks can take on any of several forms, such as L and pi networks, a stub matching system, a series-section match, and more. With a knowledge of the Smith Chart, the amateur can eliminate much "cut and try" work.

Named after its inventor, Phillip H. Smith, the Smith Chart was originally described in *Electronics* for January 1939. Smith Charts may be obtained at most university book stores. Smith Charts are also available from ARRL HQ. (See the caption for Fig 3.)

It is stated in Chapter 24 that the input impedance, or the impedance seen when "looking into" a length of line, is dependent upon the SWR, the length of the line, and the Z_0 of the line. The SWR, in turn, is dependent upon the load which terminates the line. There are complex mathematical relationships which may be used to calculate the various values of impedances, voltages, currents, and SWR values that exist in the operation of a particular transmission line. These equations can be solved with a personal computer and suitable software, or the parameters may be determined with the Smith Chart. Even if a computer is used, a fundamental knowledge of the Smith Chart will promote a better understanding of the problem being solved. And such an understanding might lead to a quicker or simpler solution than otherwise. If the terminating impedance is known, it is a simple matter to determine the input impedance of the line for any length by means of the chart. Conversely, as indicated above, with a given line length and a known (or measured) input impedance, the load impedance may be determined by means of the chart—a convenient method of remotely determining an antenna impedance, for example.

Although its appearance may at first seem somewhat formidable, the Smith Chart is really nothing more than a specialized type of graph. Consider it as having curved, rather than rectangular, coordinate lines. The coordinate system consists simply of two families of circles—the resistance family, and the reactance family. The resistance circles, **Fig 1**, are centered on the resistance axis (the only straight line on the chart), and are tangent to the outer circle at the right of the chart. Each circle is assigned a value of resistance, which is indicated at the point where the circle crosses the resistance axis. All points along any one circle have the same resistance value.

The values assigned to these circles vary from zero at the left of the chart to infinity at the right, and actually represent a *ratio* with respect to the impedance value assigned to the center point of the chart, indicated 1.0. This center point is called prime center. If prime center is assigned a value of 100 Ω, then 200 Ω resistance is represented by the 2.0 circle, 50 Ω by the 0.5 circle, 20 Ω by the 0.2 circle, and so on. If, instead, a value of 50 is assigned to prime center,

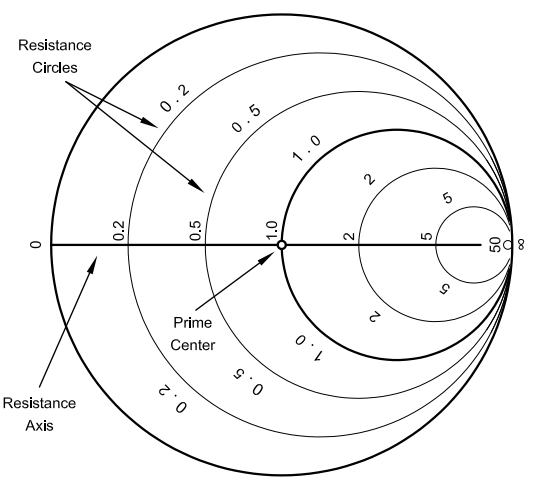

Fig 1—Resistance circles of the Smith Chart coordinate system.

the 2.0 circle now represents 100 Ω, the 0.5 circle 25 Ω, and the 0.2 circle 10 Ω. In each case, it may be seen that the value on the chart is determined by dividing the actual resistance by the number assigned to prime center. This process is called normalizing.

Conversely, values from the chart are converted back to actual resistance values by multiplying the chart value times the value assigned to prime center. This feature permits the use of the Smith Chart for any impedance values, and therefore with any type of uniform transmission line, whatever its impedance may be. As mentioned above, specialized versions of the Smith Chart may be obtained with a value of 50 Ω at prime center. These are intended for use with 50-Ω lines.

Now consider the reactance circles, **Fig 2**, which appear as curved lines on the chart because only segments of the complete circles are drawn. These circles are tangent to the resistance axis, which itself is a member of the reactance family (with a radius of infinity). The centers are displaced to the top or bottom on a line tangent to the right of the chart. The large outer circle bounding the coordinate portion of the chart is the reactance axis.

Each reactance circle segment is assigned a value of reactance, indicated near the point where the circle touches the reactance axis. All points along any one segment have the same reactance value. As with the resistance circles, the values assigned to each reactance circle are normalized with respect to the value assigned to prime center. Values to the top of the resistance axis are positive (inductive), and those to the bottom of the resistance axis are negative (capacitive).

When the resistance family and the reactance family of circles are combined, the coordinate system of the Smith Chart results, as shown in **Fig 3**. Complex impedances (R + *j*X) can be plotted on this coordinate system.

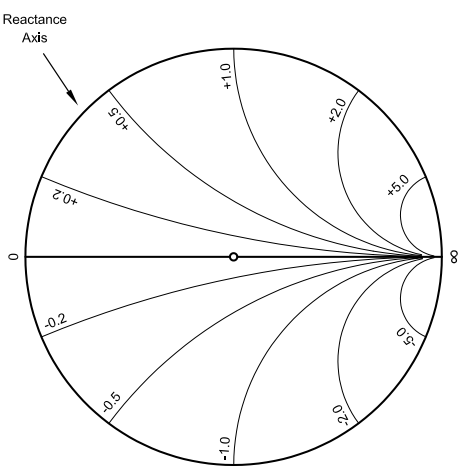

Fig 2—Reactance circles (segments) of the Smith Chart coordinate system.

IMPEDANCE PLOTTING

Suppose we have an impedance consisting of 50 Ω resistance and 100 Ω inductive reactance (Z = 50 + *j* 100). If we assign a value of 100 Ω to prime center, we normalize the above impedance by dividing each component of the impedance by 100. The normalized impedance is then 50/100 + *j* (100/100) = 0.5 + *j* 1.0. This impedance is plotted on the Smith Chart at the intersection of the 0.5 resistance circle and the +1.0 reactance circle, as indicated in Fig 3. Calculations may now be made from this plotted value.

Now say that instead of assigning 100 Ω to prime center, we assign a value of 50 Ω. With this assignment, the 50 + *j* 100 Ω impedance is plotted at the intersection of the 50/50 = 1.0 resistance circle, and the 100/50 = 2.0 positive reactance circle. This value, 1 + *j* 2, is also indicated in Fig 3. But now we have *two* points plotted in Fig 3 to represent the same impedance value, 50 + *j* 100 Ω. How can this be?

These examples show that the same impedance may be plotted at different points on the chart, depending upon the value assigned to prime center. But two plotted points cannot represent the same impedance *at the same time*! It is customary when solving transmission-line problems to assign to prime center a value equal to the characteristic impedance, or Z_0, of the line being used. This value should always be recorded at the start of calculations, to avoid possible confusion later. (In using the specialized charts with the value of 50 at prime center, it is, of course, not necessary to normalize impedances when working with 50-Ω line. The resistance and reactance values may be read directly from the chart coordinate system.)

Prime center is a point of special significance. As

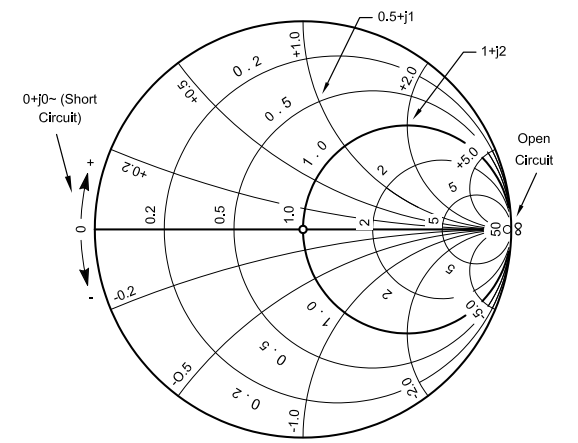

Fig 3—The complete coordinate system of the Smith Chart. For simplicity, only a few divisions are shown for the resistance and reactance values. Various types of Smith Chart forms are available from ARRL HQ. At the time of this writing, five 8½ × 11 inch Smith Chart forms are available for $2.

ch28.pmd 2 3/9/2007, 4:25 PM

just mentioned, is is customary when solving problems to assign the Z_0 value of the line to this point on the chart—50 Ω for a 50-Ω line, for example. What this means is that the center point of the chart now represents 50 +*j* 0 ohms–a pure resistance equal to the characteristic impedance of the line. If this were a load on the line, we recognize from transmission-line theory that it represents a perfect match, with no reflected power and with a 1.0 to 1 SWR. Thus, prime center also represents the 1.0 SWR circle (with a radius of zero). SWR circles are also discussed in a later section.

Short and Open Circuits

On the subject of plotting impedances, two special cases deserve consideration. These are short circuits and open circuits. A true short circuit has zero resistance and zero reactance, or 0 + *j* 0). This impedance is plotted at the left of the chart, at the intersection of the resistance and the reactance axes. By contrast, an open circuit has infinite resistance, and therefore is plotted at the right of the chart, at the intersection of the resistance and reactance axes. These two special cases are sometimes used in matching stubs, described later.

Standing-Wave-Ratio Circles

Members of a third family of circles, which are not printed on the chart but which are added during the process of solving problems, are standing-wave-ratio or SWR circles. See **Fig 4**. This family is centered on prime center, and appears as concentric circles inside the reactance axis. During calculations, one or more of these circles may be added with a drawing compass. Each circle represents a value of SWR, with every point on a given circle representing the same SWR. The SWR value for a given circle may be determined directly from the chart coordinate system, by reading the resistance value where the SWR circle crosses the resistance axis to the right of prime center. (The reading where the circle crosses the resistance axis to the left of prime center indicates the inverse ratio.)

Consider the situation where a load mismatch in a length of line causes a 3-to-1 SWR ratio to exist. If we temporarily disregard line losses, we may state that the SWR remains constant throughout the entire length of this line. This is represented on the Smith Chart by drawing a 3:1 constant SWR circle (a circle with a radius of 3 on the resistance axis), as in **Fig 5**. The design of the chart is such that any impedance encountered *anywhere* along the length of this mismatched line will fall on the SWR circle. The impedances may be read from the coordinate system merely by the progressing around the SWR circle by an amount corresponding to the length of the line involved.

This brings into use the wavelength scales, which appear in Fig 5 near the perimeter of the Smith Chart. These scales are calibrated in terms of portions of an electrical wavelength along a transmission line. Both scales start from 0 at the left of the chart. One scale, running

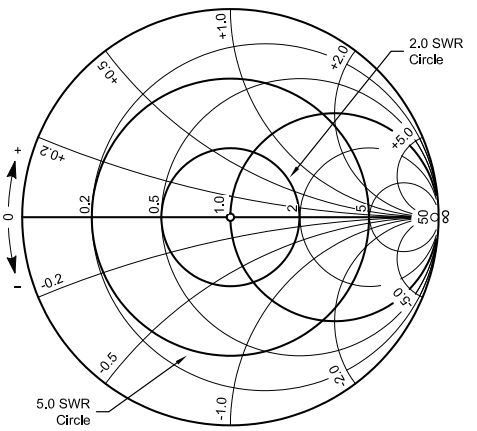

Fig 4—Smith Chart with SWR circles added.

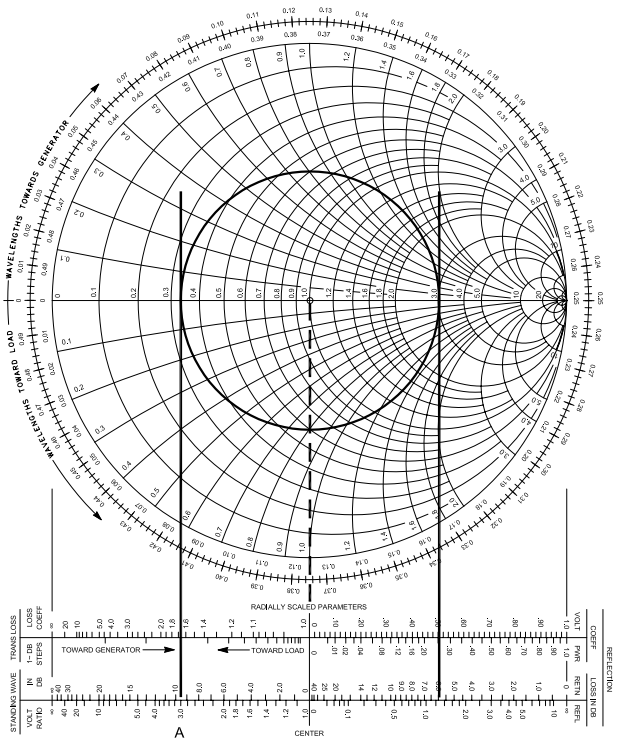

Fig 5—Example discussed in text.

ch28.pmd 3 3/9/2007, 4:25 PM

counterclockwise, starts at the generator or input end of the line and progresses toward the load. The other scale starts at the load and proceeds toward the generator in a clockwise direction. The complete circle around the edge of the chart represents $^1/_2$ λ. Progressing once around the perimeter of these scales corresponds to progressing along a transmission line for $^1/_2$ λ. Because impedances repeat themselves every $^1/_2$ λ along a piece of line, the chart may be used for any length of line by disregarding or subtracting from the line's total length an integral, or whole number, of half wavelengths.

Also shown in Fig 5 is a means of transferring the radius of the SWR circle to the external scales of the chart, by drawing lines tangent to the circle. Another simple way to obtain information from these external scales is to transfer the radius of the SWR circle to the external scale with a drawing compass. Place the point of a drawing compass at the center or 0 line, and inscribe a short arc across the appropriate scale. It will be noted that when this is done in Fig 5, the external STANDING-WAVE VOLTAGE-RATIO scale indicates the SWR to be 3.0 (at A)—our condition for initially drawing the circle on the chart (and the same as the SWR reading on the resistance axis).

SOLVING PROBLEMS WITH THE SMITH CHART

Suppose we have a transmission line with a characteristic impedance of 50 Ω and an electrical length of 0.3 λ. Also, suppose we terminate this line with an impedance having a resistive component of 25 Ω and an inductive reactance of 25 Ω (Z = 25 + *j* 25). What is the input impedance to the line?

The characteristic impedance of the line is 50 Ω, so we begin by assigning this value to prime center. Because the line is not terminated in its characteristic impedance, we know that standing waves will exist on the line, and that, therefore, the input impedance to the line will not be exactly 50 Ω. We proceed as follows. First, normalize the load impedance by dividing both the resistive and reactive components by 50 (Z_0 of the line being used). The normalized impedance in this case is 0.5 + *j* 0.5. This is plotted on the chart at the intersection of the 0.5 resistance and the +0.5 reactance circles, as in **Fig 6**. Then draw a constant SWR circle passing through this point. Transfer the radius of this circle to the external scales with the drawing compass. From the external STANDING-WAVE VOLTAGE-RATIO scale, it may be seen (at A) that the voltage ratio of 2.62 exists for this radius, indicating that our line is operating with an SWR of 2.62 to 1. This figure is converted to decibels in the adjacent scale, where 8.4 dB may be read (at B), indicating that the ratio of the voltage maximum to the voltage minimum along the line is 8.4 dB. (This is mathematically equivalent to 20 times the log of the SWR value.)

Next, with a straightedge, draw a radial line from prime center through the plotted point to intersect the wavelengths scale. At this intersection, point C in Fig 6, read a value from the wavelengths scale. Because we are starting from the load, we use the TOWARD GENERATOR or outermost calibration, and read 0.088 λ.

To obtain the line input impedance, we merely find the point on the SWR circle that is 0.3 λ toward the generator from the plotted load impedance. This is accomplished by adding 0.3 (the length of the line in wavelengths) to the reference or starting point, 0.088; 0.3 + 0.088 = 0.388. Locate 0.388 on the TOWARD GENERATOR scale (at D). Draw a second radial line from this point to prime center. The intersection of the new radial line with the SWR circle represents the normalized line input impedance, in this case 0.6 – *j* 0.66.

To find the unnormalized line impedance, multiply by 50, the value assigned to prime center. The resulting value is 30 – *j* 33, or 30 Ω resistance and 33 Ω capacitive reactance. *This* is the impedance that a transmitter must match if such a system were a combination of antenna

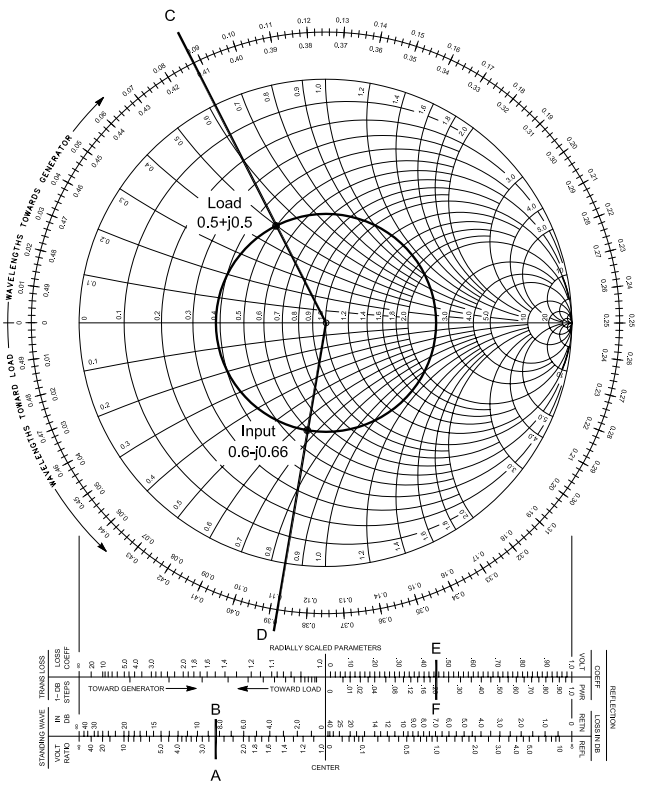

Fig 6—Example discussed in text.

ch28.pmd 4 3/9/2007, 4:25 PM

and transmission line. This is also the impedance that would be measured on an impedance bridge if the measurement were taken at the line input.

In addition to the line input impedance and the SWR, the chart reveals several other operating characteristics of the above system of line and load, if a closer look is desired. For example, the voltage reflection coefficient, both magnitude and phase angle, for this particular load is given. The phase angle is read under the radial line drawn through the plot of the load impedance, where the line intersects the ANGLE OF REFLECTION COEFFICIENT scale. This scale is not included in Fig 6, but will be found on the Smith Chart just inside the wavelengths scales. In this example, the reading is 116.6 degrees. This indicates the angle by which the reflected voltage wave leads the incident wave at the load. It will be noted that angles on the bottom half, or capacitive-reactance half, of the chart are negative angles, a "negative" lead indicating that the reflected voltage wave actually lags the incident wave.

The magnitude of the voltage-reflection-coefficient may be read from the external REFLECTION COEFFICIENT VOLTAGE scale, and is seen to be approximately 0.45 (at E) for this example. This means that 45 percent of the incident voltage is reflected. Adjacent to this scale on the POWER calibration, it is noted (at F) that the power reflection coefficient is 0.20, indicating that 20 percent of the incident power is reflected. (The amount of reflected power is proportional to the square of the reflected voltage.)

ADMITTANCE COORDINATES

Quite often it is desirable to convert impedance information to admittance data—conductance and susceptance. Working with admittances greatly simplifies determining the resultant when two complex impedances are connected in parallel, as in stub matching. The conductance values may be added directly, as may be the susceptance values, to arrive at the overall admittance for the parallel combination. This admittance may then be converted back to impedance data, if desired.

On the Smith Chart, the necessary conversion may be made very simply. The equivalent admittance of a plotted impedance value lies diametrically opposite the impedance point on the chart. In other words, an impedance plot and its corresponding admittance plot will lie on a straight line that passes through prime center, and each point will be the same distance from prime center (on the same SWR circle). In the above example, where the normalized line input impedance is $0.6 - j\ 0.66$, the equivalent admittance lies at the intersection of the SWR circle and the extension of the straight line passing from point D though prime center. Although not shown in Fig 6, the normalized admittance value may be read as $0.76 + j\ 0.84$ if the line starting at D is extended.

In making impedance-admittance conversions, remember that capacitance is considered to be a positive susceptance and inductance a negative susceptance. This corresponds to the scale identification printed on the chart. The admittance in siemens is determined by dividing the normalized values by the Z_0 of the line. For this example the admittance is $0.76/50 + j\ 0.84/50 = 0.0152 + j\ 0.0168$ siemen. Of course admittance coordinates may be converted to impedance coordinates just as easily—by locating the point on the Smith Chart that is diametrically opposite that representing the admittance coordinates, on the same SWR circle.

DETERMINING ANTENNA IMPEDANCES

To determine an antenna impedance from the Smith Chart, the procedure is similar to the previous example. The electrical length of the feed line must be known and the impedance value at the input end of the line must be determined through measurement, such as with an impedance-measuring or a good quality noise bridge. In this case, the antenna is connected to the far end of the line and becomes the load for the line. Whether the

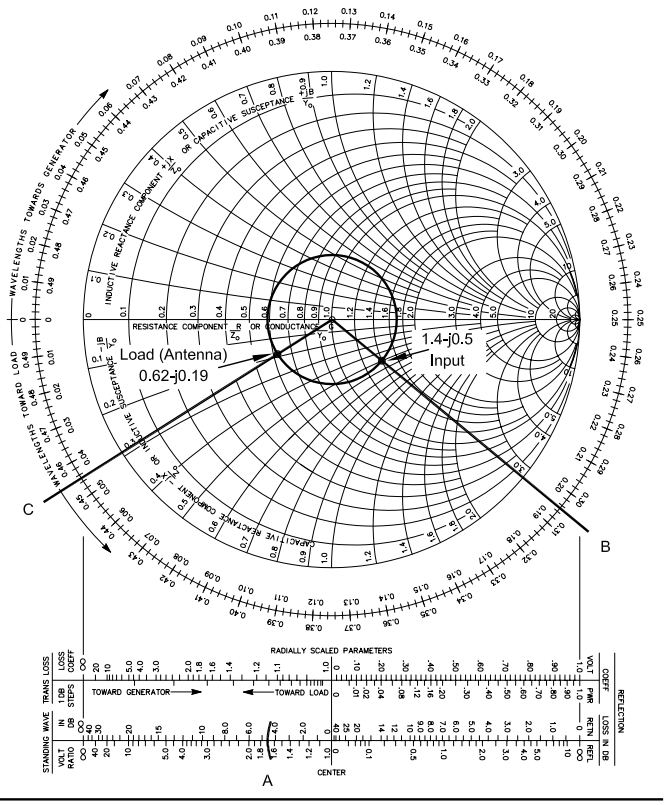

Fig 7—Example discussed in text.

ch28.pmd 5 3/9/2007, 4:25 PM

antenna is intended purely for transmission of energy, or purely for reception makes no difference; the antenna is still the terminating or load impedance on the line as far as these measurements are concerned. The input or generator end of the line is that end connected to the device for measurement of the impedance. In this type of problem, the measured impedance is plotted on the chart, and the TOWARD LOAD wavelengths scale is used in conjunction with the electrical line length to determine the actual antenna impedance.

For example, assume we have a measured input impedance to a 50-Ω line of 70 – *j* 25 Ω. The line is 2.35 λ long, and is terminated in an antenna. What is the antenna feed impedance? Normalize the input impedance with respect to 50 Ω, which comes out 1.4 – *j* 0.5, and plot this value on the chart. See **Fig 7**. Draw a constant SWR circle through the point, and transfer the radius to the external scales. The SWR of 1.7 may be read from the VOLTAGE RATIO scale (at A). Now draw a radial line from prime center through this plotted point to the wavelengths scale, and read a reference value (at B). For this case the value is 0.195, on the TOWARD LOAD scale. Remember, we are starting at the generator end of the transmission line.

To locate the load impedance on the SWR circle, add the line length, 2.35 λ, to the reference value from the wavelengths scale; 2.35 + 0.195 = 2.545. Locate the new value on the TOWARD LOAD scale. But because the calibrations extend only from 0 to 0.5, we must first subtract a number of half wavelengths from this value and use only the remaining value. In this situation, the largest integral number of half wavelengths that can be subtracted with a positive result is 5, or 2.5 λ. Thus, 2.545 – 2.5 = 0.045. Locate the 0.045 value on the TOWARD LOAD scale (at C). Draw a radial line from this value to prime center. Now, the coordinates at the intersection of the second radial line and the SWR circle represent the load impedance. To read this value closely, some interpolation between the printed coordinate lines must be made, and the value of 0.62 – *j* 0.19 is read. Multiplying by 50, we get the actual load or antenna impedance as 31 – *j* 9.5 Ω, or 31 Ω resistance with 9.5 Ω capacitive reactance.

Problems may be entered on the chart in yet another manner. Suppose we have a length of 50-Ω line feeding a base-loaded resonant vertical ground-plane antenna which is shorter than 1/4 λ. Further, suppose we have an SWR monitor in the line, and that it indicates an SWR of 1.7 to 1. The line is known to be 0.95 λ long. We want to know both the input and the antenna impedances.

From the information available, we have no impedances to enter into the chart. We may, however, draw a circle representing the 1.7 SWR. We also know, from the definition of resonance, that the antenna presents a purely resistive load to the line, that is, no reactive component. Thus, the antenna impedance must lie on the resistance axis. If we were to draw such an SWR circle and observe the chart with only the circle drawn, we would see two points which satisfy the resonance requirement for the load. These points are 0.59 + *j* 0 and 1.7 + *j* 0. Multiplying by 50, we see that these values represent 29.5 and 85 Ω resistance. This may sound familiar, because, as was discussed in Chapter 24, when a line is terminated in a pure resistance, the SWR in the line equals Z_R/Z_0 or Z_0/Z_R, where Z_R=load resistance and Z_0=line impedance.

If we consider antenna fundamentals described in Chapter 2, we know that the theoretical impedance of a 1/4-λ ground-plane antenna is approximately 36 Ω. We therefore can quite logically discard the 85-Ω impedance figure in favor of the 29.5-Ω value. This is then taken as the load impedance value for the Smith Chart calculations. To find the line input impedance, we subtract 0.5 λ from the line length, 0.95, and find 0.45 λ on the TOWARD GENERATOR scale. (The wavelength-scale starting point in this case is 0.) The line input impedance is found to be 0.63 – *j* 0.20, or 31.5 – *j* 10 Ω.

DETERMINATION OF LINE LENGTH

In the example problems given so far in this chapter, the line length has conveniently been stated in wavelengths. The electrical length of a piece of line depends upon its physical length, the radio frequency under consideration, and the velocity of propagation in the line. If an impedance-measurement bridge is capable of quite reliable readings at high SWR values, the line length may be determined through line input-impedance measurements with short- or open-circuit line terminations. Information on the procedure is given later in this chapter. A more direct method is to measure the physical length of the line and calculate its electrical length from

$$N = \frac{Lf}{984VF} \qquad \text{(Eq 1)}$$

where

N = number of electrical wavelengths in the line
L = line length in feet
f = frequency, MHz
VF = velocity or propagation factor of the line

The velocity factor may be obtained from transmission-line data tables in Chapter 24.

ch28.pmd 6 3/9/2007, 4:25 PM

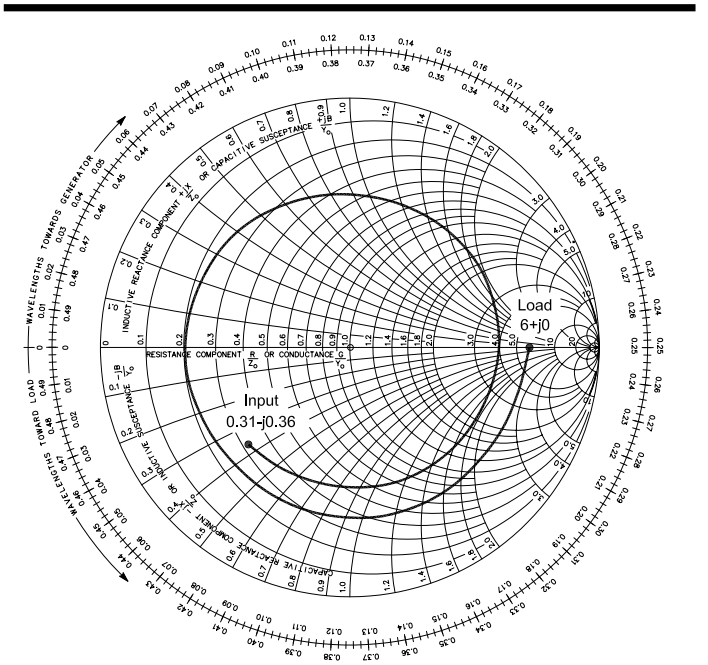

Fig 8—This spiral is the actual "SWR circle" when line losses are taken into account. It is based on calculations for a 16-ft length of RG-174 coax feeding a resonant 28-MHz 300-Ω antenna (50-Ω coax, velocity factor = 66%, attenuation = 6.2 dB per 100 ft). The SWR at the load is 6:1, while it is 3.6:1 at the line input. When solving problems involving attenuation, two constant SWR circles are drawn instead of a spiral, one for the line input SWR and one for the load SWR.

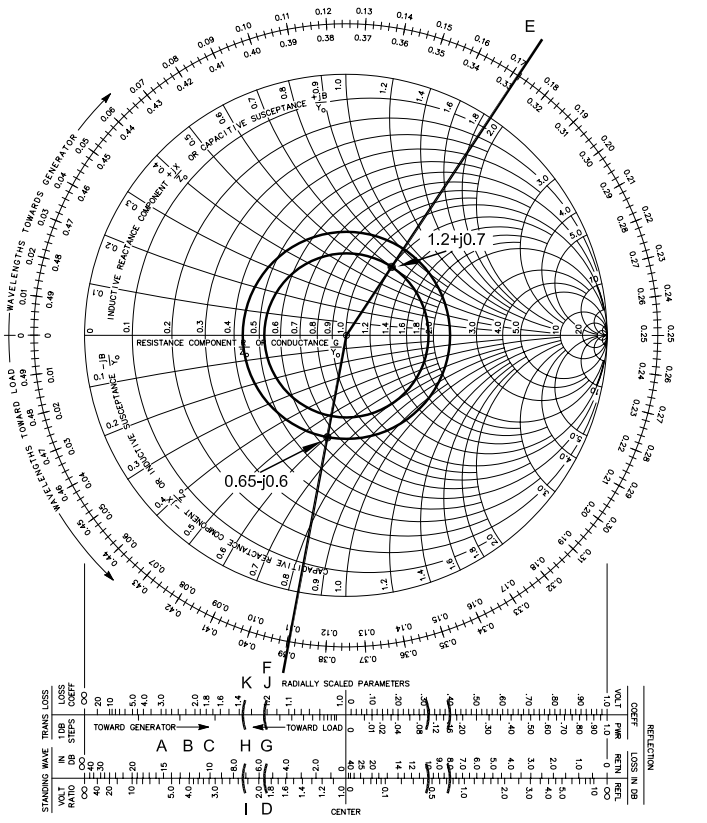

Fig 9—Example of Smith Chart calculations taking line losses into account.

LINE-LOSS CONSIDERATIONS WITH THE SMITH CHART

The example Smith Chart problems presented in the previous section ignored attenuation, or line losses. Quite frequently it is not even necessary to consider losses when making calculations; any difference in readings obtained are often imperceptible on the chart. However, when the line losses become appreciable, such as for high-loss lines, long lines, or at VHF and UHF, loss considerations may become significant in making Smith Chart calculations. This involves only one simple step, in addition to the procedures previously presented.

Because of line losses, as discussed in Chapter 24 the SWR does not remain constant throughout the length of the line. As a result, there is a decrease in SWR as one progresses away from the load. To truly present this situation on the Smith Chart, instead of drawing a constant SWR circle, it would be necessary to draw a spiral inward and clockwise from the load impedance toward the generator, as shown in **Fig 8**. The rate at which the curve spirals toward prime center is related to the attenuation in the line. Rather than drawing spiral curves, a simpler method is used in solving line-loss problems, by means of the external scale TRANSMISSION LOSS 1-DB STEPS. This scale may be seen in **Fig 9**. Because this is only a relative scale, the decibel steps are not numbered.

If we start at the left end of this external scale and proceed in the direction indicated TOWARD GENERATOR, the first dB step is seen to occur at a radius from center corresponding to an SWR of about 9 (at A); the second dB step falls at an SWR of about 4.5 (at B), the third at 3.0 (at C), and so forth, until the

ch28.pmd 7 3/9/2007, 4:25 PM

15th dB step falls at an SWR of about 1.05 to 1. This means that a line terminated in a short or open circuit (infinite SWR), and having an attenuation of 15 dB, would exhibit an SWR of only 1.05 at its input. It will be noted that the dB steps near the right end of the scale are very close together, and a line attenuation of 1 or 2 dB in this area will have only slight effect on the SWR. But near the left end of the scale, corresponding to high SWR values, a 1 or 2 dB loss has considerable effect on the SWR.

Using a Second SWR Circle

In solving a problem using line-loss information, it is necessary only to modify the radius of the SWR circle by an amount indicated on the TRANSMISSION-LOSS 1-DB STEPS scale. This is accomplished by drawing a second SWR circle, either smaller or larger than the first, depending on whether you are working toward the load or toward the generator.

For example, assume that we have a 50-Ω line that is 0.282 λ long, with 1-dB inherent attenuation. The line input impedance is measured as 60 + *j* 35 Ω. We desire to know the SWR at the input and at the load, and the load impedance. As before, we normalize the 60 + *j* 35-Ω impedance, plot it on the chart, and draw a constant SWR circle and a radial line through the point. In this case, the normalized impedance is 1.2 + *j* 0.7. From Fig 9, the SWR at the line input is seen to be 1.9 (at D), and the radial line is seen to cross the TOWARD LOAD scale, first subtract 0.500, and locate 0.110 (at F); then draw a radial line from this point to prime center.

To account for line losses, transfer the radius of the SWR circle to the external 1-DB STEPS scale. This radius crosses the external scale at G, the fifth decibel mark from the left. Since the line loss was given as 1 dB, we strike a new radius (at H), one "tick mark" to the left (toward load) on the same scale. (This will be the fourth decibel tick mark from the left of the scale.) Now transfer this new radius back to the main chart, and scribe a new SWR circle of this radius. This new radius represents the SWR at the load, and is read as 2.3 on the external VOLTAGE RATIO scale. At the intersection of the new circle and the load radial line, we read 0.65 – *j* 0.6. This is the normalized load impedance. Multiplying by 50, we obtain the actual load impedance as 32.5 – *j* 30 Ω. The SWR in this problem was seen to increase from 1.9 at the line input to 2.3 (at I) at the load, with the 1-dB line loss taken into consideration.

In the example above, values were chosen to fall conveniently on or very near the "tick marks" on the 1-dB scale. Actually, it is a simple matter to interpolate between these marks when making a radius correction. When this is necessary, the relative distance between marks for each decibel step should be maintained while counting off the proper number of steps.

Adjacent to the 1-DB STEPS scale lies a LOSS COEFFICIENT scale. This scale provides a factor by which the matched-line loss in decibels should be multiplied to account for the increased losses in the line when standing waves are present. These added losses do not affect the SWR or impedance calculations; they are merely the additional dielectric copper losses of the line caused by the fact that the line conducts more average voltage in the presence of standing waves. For the above example, from Fig 9, the loss coefficient at the input end is seen to be 1.21 (at J), and 1.39 (at K) at the load. As a good approximation, the loss coefficient may be averaged over the length of line under consideration; in this case, the average is 1.3. This means that the total losses in the line are 1.3 times the matched loss of the line (1 dB), or 1.3 dB. This is the same result that may be obtained from procedures given in Chapter 24 for this data.

Smith Chart Procedure Summary

To summarize briefly, any calculations made on the Smith Chart are performed in four basic steps, although not necessarily in the order listed.

1) Normalize and plot a line input (or load) impedance, and construct a constant SWR circle.
2) Apply the line length to the wavelengths scales.
3) Determine attenuation or loss, if required, by means of a second SWR circle.
4) Read normalized load (or input) impedance, and convert to impedance in ohms.

The Smith Chart may be used for many types of problems other than those presented as examples here. The transformer action of a length of line—to transform a high impedance (with perhaps high reactance) to a purely resistive impedance of low value—was not mentioned. This is known as "tuning the line," for which the chart is very helpful, eliminating the need for "cut and try" procedures. The chart may also be used to calculate lengths for shorted or open matching stubs in a system, described later in this chapter. In fact, in any application where a transmission line is not perfectly matched, the Smith Chart can be of value.

ATTENUATION AND Z_0 FROM IMPEDANCE MEASUREMENTS

If an impedance bridge is available to make accurate measurements in the presence of very high SWR values, the attenuation, characteristic impedance and velocity factor of any random length of coaxial transmission line can be determined. This section was written by Jerry Hall, K1TD.

Homemade impedance bridges and noise bridges will seldom offer the degree of accuracy required to use this technique, but sometimes laboratory bridges can be found as industrial surplus at a reasonable price. It may also be possible for an amateur to borrow a laboratory type of bridge for the purpose of making some weekend measurements. Making these determinations is not difficult, but the procedure is not commonly known among

ch28.pmd 8 3/9/2007, 4:25 PM

amateurs. One equation treating complex numbers is used, but the math can be handled with a calculator supporting trig functions. Full details are given in the paragraphs that follow.

For each frequency of interest, two measurements are required to determine the line impedance. Just one measurement is used to determine the line attenuation and velocity factor. As an example, assume we have a 100-foot length of unidentified line with foamed dielectric, and wish to know its characteristics. We make our measurements at 7.15 MHz. The procedure is as follows.

1) Terminate the line in an open circuit. The best "open circuit" is one that minimizes the capacitance between the center conductor and the shield. If the cable has a PL-259 connector, unscrew the shell and slide it back down the coax for a few inches. If the jacket and insulation have been removed from the end, fold the braid back along the outside of the line, away from the center conductor.
2) Measure and record the impedance at the input end of the line. If the bridge measures admittance, convert the measured values to resistance and reactance. Label the values as $R_{oc} + j\,X_{oc}$. For our example, assume we measure $85 + j179\ \Omega$. (If the reactance term is capacitive, record it as negative.)
3) Now terminate the line in a short circuit. If a connector exists at the far end of the line, a simple short is a mating connector with a very short piece of heavy wire soldered between the center pin and the body. If the coax has no connector, removing the jacket and center insulation from a half inch or so at the end will allow you to tightly twist the braid around the center conductor. A small clamp or alligator clip around the outer braid at the twist will keep it tight.
4) Again measure and record the impedance at the input end of the line. This time label the values as $R_{sc} \pm j\,X$. Assume the measured value now is $4.8 - j\,11.2\ \Omega$.

This completes the measurements. Now we reach for the calculator.

As amateurs we normally assume that the characteristic impedance of a line is purely resistive, but it can (and does) have a small capacitive reactance component. Thus, the Z_0 of a line actually consists of $R_0 + j\,X_0$. The basic equation for calculating the characteristic impedance is

$$Z_0 = \sqrt{Z_{oc} \times Z_{sc}} \qquad \text{(Eq 2)}$$

where

$Z_{oc} = R_{oc} + jX_{oc}$

$Z_{sc} = R_{sc} + jX_{sc}$

From Eq 2 the following working equation may be derived.

$$Z_0 = \sqrt{\left(R_{oc}R_{sc} - X_{oc}X_{sc}\right) + j\left(R_{oc}X_{sc} + R_{sc}X_{oc}\right)} \qquad \text{(Eq 3)}$$

The expression under the radical sign in Eq 3 is in the form of $R + j\,X$. By substituting the values from our example into Eq 3, the R term becomes $85 \times 4.8 - 179 \times (-11.2) = 2412.8$, and the X term becomes $85 \times (-11.2) + 4.8 \times 179 = -92.8$. So far, we have determined that

$$Z_0 = \sqrt{2412.8 - j\,92.8}$$

The quantity under the radical sign is in rectangular form. Extracting the square root of a complex term is handled easily if it is in polar form, a vector value and its angle. The vector value is simply the square root of the sum of the squares, which in this case is

$$\sqrt{2412.8^2 + 92.8^2} = \sqrt{2414.58}$$

The tangent of the vector angle we are seeking is the value of the reactance term divided by the value of the resistance term. For our example this is arctan –92.8/2412.8 = arctan –0.03846. The angle is thus found to be –2.20°. From all of this we have determined that

$$Z_0 = \sqrt{2414.58\ \angle -2.20°}$$

Extracting the square root is now simply a matter of finding

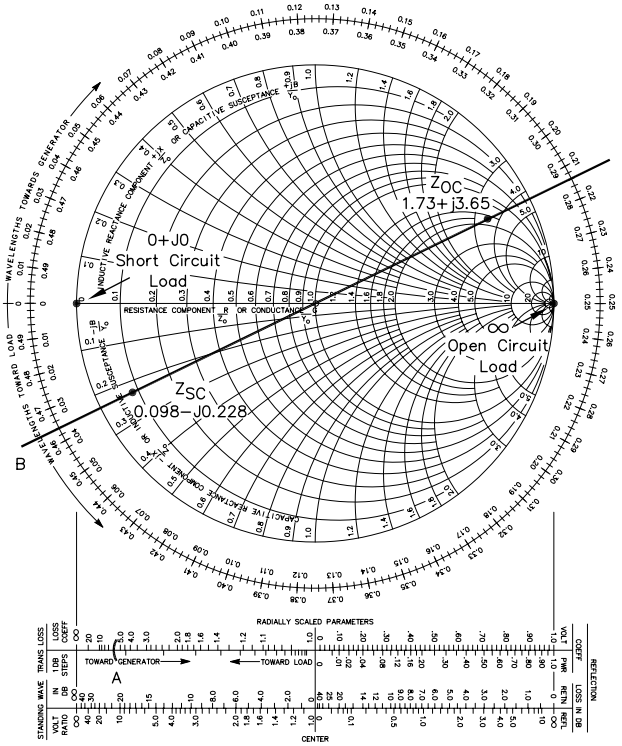

Fig 10—Determining the line loss and velocity factor with the Smith Chart from input measurements taken with open-circuit and short-circuit terminations.

ch28.pmd 9 3/9/2007, 4:25 PM

the square root of the vector value, and taking half the angle. (The angle is treated mathematically as an exponent.)

Our result for this example is $Z_0 = 49.1/\underline{-1.1°}$. The small negative angle may be ignored, and we now know that we have coax with a nominal 50-Ω impedance. (Departures of as much as 6 to 8% from the nominal value are not uncommon.) If the negative angle is large, or if the angle is positive, you should recheck your calculations and perhaps even recheck the original measurements. You can get an idea of the validity of the measurements by normalizing the measured values to the calculated impedance and plotting them on a Smith Chart as shown in **Fig 10** for this example. Ideally, the two points should be diametrically opposite, but in practice they will be not quite 180° apart and not quite the same distance from prime center. Careful measurements will yield plotted points that are close to ideal. Significant departures from the ideal indicates sloppy measurements, or perhaps an impedance bridge that is not up to the task.

Determining Line Attenuation

The short circuit measurement may be used to determine the line attenuation. This reading is more reliable than the open circuit measurement because a good short circuit is a short, while a good open circuit is hard to find. (It is impossible to escape some amount of capacitance between conductors with an "open" circuit, and that capacitance presents a path for current to flow at the RF measurement frequency.)

Use the Smith Chart and the 1-DB STEPS external scale to find line attenuation. First normalize the short circuit impedance reading to the calculated Z_0, and plot this point on the chart. See Fig 10. For our example, the normalized impedance is $4.8/49.1 - j\ 11.2 / 49.1$ or $0.098 - j\ 0.228$. After plotting the point, transfer the radius to the 1-DB STEPS scale. This is shown at A of Fig 10.

Remember from discussions earlier in this chapter that the impedance for plotting a short circuit is $0 + j\ 0$, at the left edge of the chart on the resistance axis. On the 1-DB STEPS scale this is also at the left edge. The total attenuation in the line is represented by the number of dB steps from the left edge to the radius mark we have just transferred. For this example it is 0.8 dB. Some estimation may be required in interpolating between the 1-dB step marks.

Determining Velocity Factor

The velocity factor is determined by using the TOWARD GENERATOR wavelength scale of the Smith Chart. With a straightedge, draw a line from prime center through the point representing the short-circuit reading, until it intersects the wavelengths scale. In Fig 10 this point is labeled B. Consider that during our measurement, the short circuit was the load at the end of the line. Imagine a spiral curve progressing from $0 + j\ 0$ clockwise and inward to our plotted measurement point. The wavelength scale, at B, indicates this line length is 0.464 λ. By rearranging the terms of Eq 1 given early in this chapter, we arrive at an equation for calculating the velocity factor.

$$VF = \frac{Lf}{984N} \qquad \text{(Eq 4)}$$

where

VF = velocity factor
L = line length, feet
f = frequency, MHz
N = number of electrical wavelengths in the line

Inserting the example values into Eq 4 yields $VF = 100 \times 7.15/(984 \times 0.464) = 1.566$, or 156.6%. Of course, this value is an impossible number—the velocity factor in coax cannot be greater than 100%. But remember, the Smith Chart can be used for lengths greater than ½ λ. Therefore, that 0.464 value could rightly be 0.964, 1.464, 1.964, and so on. When using 0.964 λ, Eq 4 yields a velocity factor of 0.753, or 75.3%. Trying successively greater values for the wavelength results in velocity factors of 49.6 and 37.0%. Because the cable we measured had foamed dielectric, 75.3% is the probable velocity factor. This corresponds to an electrical length of 0.964 λ. Therefore, we have determined from the measurements and

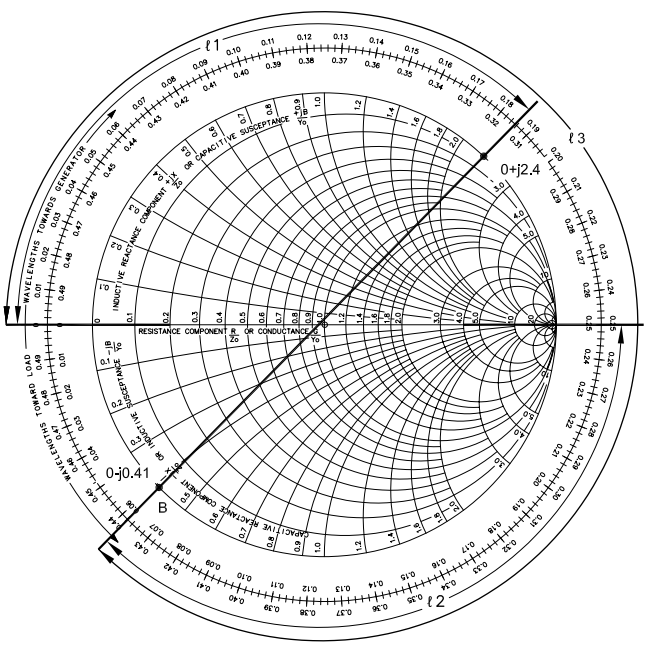

Fig 11—Smith Chart determination of input impedances for short- and open-circuited line sections, disregarding line losses.

ch28.pmd 10 3/9/2007, 4:25 PM

calculations that our unmarked coax has a nominal 50-Ω impedance, an attenuation of 0.8 dB per hundred feet at 7.15 MHz, and a velocity factor of 75.3%.

It is difficult to use this procedure with short lengths of coax, just a few feet. The reason is that the SWR at the line input is too high to permit accurate measurements with most impedance bridges. In the example above, the SWR at the line input is approximately 12:1.

The procedure described above may also be used for determining the characteristics of balanced lines. However, impedance bridges are generally unbalanced devices, and the procedure for measuring a balanced impedance accurately with an unbalanced bridge is complicated.

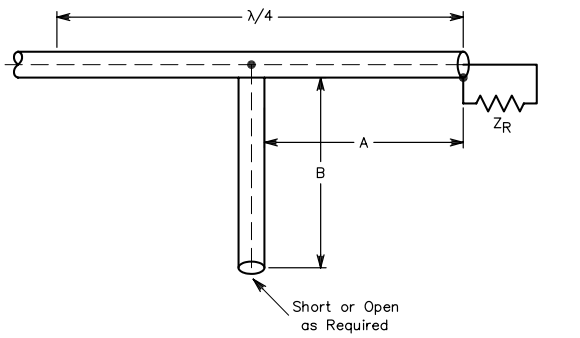

Fig 12—The method of stub matching a mismatched load on coaxial lines.

LINES AS CIRCUIT ELEMENTS

Information is presented in Chapter 24 on the use of transmission-line sections as circuit elements. For example, it is possible to substitute transmission lines of the proper length and termination for coils or capacitors in ordinary circuits. While there is seldom a practical need for that application, lines are frequently used in antenna systems in place of lumped components to tune or resonate elements. Probably the most common use of such a line is in the hairpin match, where a short section of stiff open-wire line acts as a lumped inductor.

The equivalent "lumped" value for any "inductor" or "capacitor" may be determined with the aid of the Smith Chart. Line losses may be taken into account if desired, as explained earlier. See **Fig 11**. Remember that the top half of the Smith Chart coordinate system is used for impedances containing inductive reactances, and the bottom half for capacitive reactances. For example, a section of 600-Ω line $^3/_{16}$-λ long (0.1875 λ) and short-circuited at the far end is represented by ℓ1, drawn around a portion of the perimeter of the chart. The "load" is a short-circuit, 0 + *j* 0 Ω, and the TOWARD GENERATOR wavelengths scale is used for marking off the line length. At A in Fig 11 may be read the normalized impedance as seen looking into the length of line, 0 + *j* 2.4. The reactance is therefore inductive, equal to 600 × 2.4 = 1440 Ω. The same line when open-circuited (termination impedance = ∞, the point at the right of the chart) is represented by ℓ2 in Fig 11. At B the normalized line-input impedance may be read as 0 – *j* 0.41; the reactance in this case is capacitive, 600 × 0.41 = 246 Ω. (Line losses are disregarded in these examples.) From Fig 11 it is easy to visualize that if ℓ1 were to be extended by $^1/_4$ λ, the total length represented by ℓ3, the line-input impedance would be identical to that obtained in the case represented by ℓ2 alone. In the case of ℓ2, the line is open-circuited at the far end, but in the case of ℓ3 the line is terminated in a short. The added section of line for ℓ3 provides the "transformer action" for which the $^1/_4$-λ line is noted.

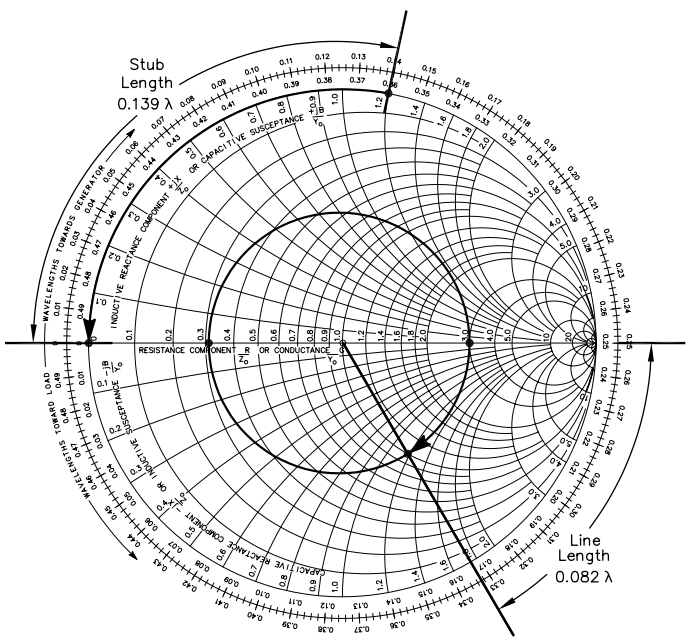

Fig 13—Smith Chart method of determining the dimensions for stub matching.

The equivalent inductance and capacitance as determined above can be found by substituting these values in the equations relating inductance and capacitance to reactance, or by using the various charts and calculators available. The frequency corresponding to the line length in degrees must be used, of course. In this example, if the frequency is 14 MHz

ch28.pmd 11 3/9/2007, 4:25 PM

the equivalent inductance and capacitance in the two cases are 16.4 μH and 46.2 pF, respectively. Note that when the line length is 45° (0.125 λ), the reactance in either case is numerically equal to the characteristic impedance of the line. In using the Smith Chart it should be kept in mind that the electrical length of a line section depends on the frequency and velocity of propagation, as well as on the actual physical length.

At lengths of line that are exact multiples of $^1/_4$ λ, such lines have the properties of resonant circuits. At lengths where the input reactance passes through zero at the left of the Smith Chart, the line acts as a series-resonant circuit. At lengths for which the reactances theoretically pass from "positive" to "negative" infinity at the right of the Smith Chart, the line simulates a parallel-resonant circuit.

Designing Stub Matches with the Smith Chart

The design of stub matches is covered in detail in Chapter 26. Equations are presented there to calculate the electrical lengths of the main line and the stub, based on a purely resistive load and on the stub being the same type of line as the main line. The Smith Chart may also be used to determine these lengths, without the requirements that the load be purely resistive and that the line types be identical.

Fig 12 shows the stub matching arrangement in coaxial line. As an example, suppose that the load is an antenna, a close-spaced array fed with a 52-Ω line. Further suppose that the SWR has been measured as 3.1:1. From this information, a constant SWR circle may be drawn on the Smith Chart. Its radius is such that it intersects the right portion of the resistance axis at the SWR value, 3.1, as shown at point B in **Fig 13**.

Since the stub of Fig 12 is connected in parallel with the transmission line, determining the design of the matching arrangement is simplified if Smith Chart values are dealt with as admittances, rather than impedances. (An admittance is simply the reciprocal of the associated impedance. Plotted on the Smith Chart, the two associated points are on the same SWR circle, but diametrically opposite each other.) Using admittances leaves less chance for errors in making calculations, by eliminating the need for making series-equivalent to parallel-equivalent circuit conversions and back, or else for using complicated equations for determining the resultant value of two complex impedances connected in parallel.

A complex impedance, Z, is equal to $R + j X$, as described in Chapter 24. The equivalent admittance, Y, is equal to $G - j B$, where G is the conductive component and B the susceptance. (Inductance is taken as negative susceptance, and capacitance as positive.) Conductance and susceptance values are plotted and handled on the Smith Chart in the same manner as resistance and reactance.

Assuming that the close-spaced array of our example has been resonated at the operating frequency, it will present a purely resistive termination for the load end of the 52-Ω line. From information in Chapter 24, it is known that the impedance of the antenna equals $Z_0/SWR = 52/3.1 = 16.8$ Ω. (We can logically discard the possibility that the antenna impedance is SWR × Z_0, or 0.06 Ω.) If this 16.8-Ω value were to be plotted as an impedance on the Smith Chart, it would first be normalized (16.8/52 = 0.32) and then plotted as $0.32 + j\ 0$. Although not necessary for the solution of this example, this value is plotted at point A in Fig 13. What is necessary is a plot of the admittance for the antenna as a load. This is the reciprocal of the impedance; 1/16.8 Ω equals 0.060 siemen. To plot this point it is first normalized by multiplying the conductance and susceptance values by the Z_0 of the line. Thus, $(0.060 + j\ 0) \times 52 = 3.1 + j\ 0$. This admittance value is shown plotted at point B in Fig 13. It may be seen that points A and B are diametrically opposite each other on the chart. Actually, for the solution of this example, it wasn't necessary to compute the values for either point A or point B as in the above paragraph, for they were both determined from the known SWR value of 3.1. As may be seen in Fig 13, the points are located on the constant SWR circle which was already drawn, at the two places where it intersects the resistance axis. The plotted value for point A, 0.32, is simply the reciprocal of the value for point B, 3.1. However, an understanding of the relationship between impedance and admittance is easier to gain with simple examples such as this.

In stub matching, the stub is to be connected at a point in the line where the conductive component equals the Z_0 of the line. Point B represents the admittance of the load, which is the antenna. Various admittances will be encountered along the line, when moving in a direction indicated by the TOWARD GENERATOR wavelengths scale, but all admittance plots must fall on the constant SWR circle. Moving clockwise around the SWR circle from point B, it is seen that the line input conductance will be 1.0 (normalized Z_0 of the line) at point C, 0.082 λ toward the transmitter from the antenna. Thus, the stub should be connected at this location on the line.

The normalized admittance at point C, the point representing the location of the stub, is $1 - j\ 1.2$ siemens, having an inductive susceptance component. A capacitive susceptance having a normalized value of $+ j\ 1.2$ siemens is required across the line at the point of stub connection, to cancel the inductance. This capacitance is to be obtained from the stub section itself; the problem now is to determine its type of termination (open or shorted), and how long the stub should be. This is done by first plotting the susceptance required for cancellation, $0 + j\ 1.2$, on the chart (point D in Fig 13). This point represents the input admittance as seen looking into the stub. The "load" or termination for the stub section is found by moving in the TOWARD LOAD direction around the chart, and will appear at the closest point on the resistance/conductance axis, either at the left or the right

ch28.pmd 12 3/9/2007, 4:25 PM

of the chart. Moving counterclockwise from point D, this is located at E, at the left of the chart, 0.139 λ away. From this we know the required stub length. The "load" at the far end of the stub, as represented on the Smith Chart, has a normalized admittance of 0 + *j* 0 siemen, which is equivalent to an open circuit.

When the stub, having an input admittance of 0 + *j* 1.2 siemens, is connected in parallel with the line at a point 0.082 λ from the load, where the line input admittance is 1.0 – *j* 1.2, the resultant admittance is the sum of the individual admittances. The conductance components are added directly, as are the susceptance components. In this case, 1.0 – *j* 1.2 + *j* 1.2 = 1.0 + *j* 0 siemen. Thus, the line from the point of stub connection to the transmitter will be terminated in a load which offers a perfect match. When determining the physical line lengths for stub matching, it is important to remember that the velocity factor for the type of line in use must be considered.

MATCHING WITH LUMPED CONSTANTS

It was pointed out earlier that the purpose of a matching stub is to cancel the reactive component of line impedance at the point of connection. In other words, the stub is simply a reactance of the proper kind and value shunted across the line. It does not matter what physical shape this reactance takes. It can be a section of transmission line or a "lumped" inductance or capacitance, as desired. In the above example with the Smith Chart solution, a capacitive reactance was required. A capacitor having the same value of reactance can be used just as well. There are cases where, from an installation standpoint, it may be considerably more convenient to connect a capacitor in place of a stub. This is particularly true when open-wire feeders are used. If a variable capacitor is used, it becomes possible to adjust the capacitance to the exact value required.

The proper value of reactance may be determined from Smith Chart information. In the previous example, the required susceptance, normalized, was +*j* 1.2 siemens. This is converted into actual siemens by dividing by the line Z_0; 1.2/52 = 0.023 siemen, capacitance. The required capacitive reactance is the reciprocal of this latter value, 1/0.023 = 43.5 Ω. If the frequency is 14.2 MHz, for instance, 43.5 Ω corresponds to a capacitance of 258 pF. A 325-pF variable capacitor connected across the line 0.082 λ from the antenna terminals would provide ample adjustment range. The RMS voltage across the capacitor is

$$E = \sqrt{P \times Z_0}$$

For 500 W, for example, E = the square root of 500 × 52 = 161 V. The peak voltage is 1.41 times the RMS value, or 227 V.

The Series-Section Transformer

The series-section transformer is described in Chapter 26, and equations are given there for its design. The transformer can be designed graphically with the aid of a Smith Chart. This information is based on a *QST* article by Frank A. Regier, OD5CG. Using the Smith Chart to design a series-section match requires the use of the chart in its less familiar off-center mode. This mode is described in the next two paragraphs.

Fig 14 shows the Smith Chart used in its familiar centered mode, with all impedances normalized to that of the transmission line, in this case 75 Ω, and all constant SWR circles concentric with the normalized value r = 1 at the chart center. An actual impedance is recovered by multiplying a chart reading by the normalizing impedance of 75 Ω. If the actual (unnormalized) impedances represented by a constant SWR circle in Fig 14 are instead divided by a normalizing impedance of 300 Ω, a different picture results. A Smith Chart shows all possible impedances, and so a closed path such as a constant SWR circle in Fig 14 must again be represented by a closed path. In fact, it can be shown that the path remains a circle, but that the constant SWR circles are no longer concentric. **Fig 15** shows the circles that result when the impedances along a mismatched 75-Ω line are normalized by dividing by 300 Ω instead of 75. The constant SWR circles still surround the point corresponding to the characteristic impedance of the line (r = 0.25) but are no longer concentric with it. Note that the normalized impedances read from corresponding points on Figs 14 and 15 are different but that the actual, unnormalized, impedances are exactly the same.

An Example

Now turn to the example shown in **Fig 16**. A complex load of Z_L = 600 + *j* 900 Ω is to be fed with 300-Ω line, and a 75-Ω series section is to be used. These characteristic impedances agree with those used in Fig 15, and thus Fig 15 can be used to find the impedance variation along the 75-Ω series section. In particular, the constant SWR circle which passes through the Fig 15 chart center, SWR = 4 in this case, passes through all the impedances (normalized to 300 Ω) which the 75-Ω series section is able to match to the 300-Ω main line. The length $\ell 1$ of 300-Ω line has the job of transforming the load impedance to some impedance on this matching circle.

Fig 17 shows the whole process more clearly, with all

ch28.pmd 13 3/9/2007, 4:25 PM

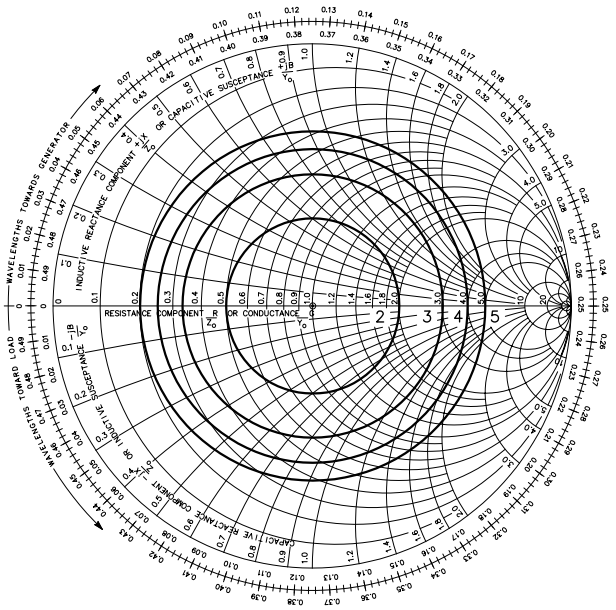

Fig 14—Constant SWR circles for SWR = 2, 3, 4 and 5, showing impedance variation along 75-Ω line, normalized to 75 Ω. The actual impedance is obtained by multiplying the chart reading by 75 Ω.

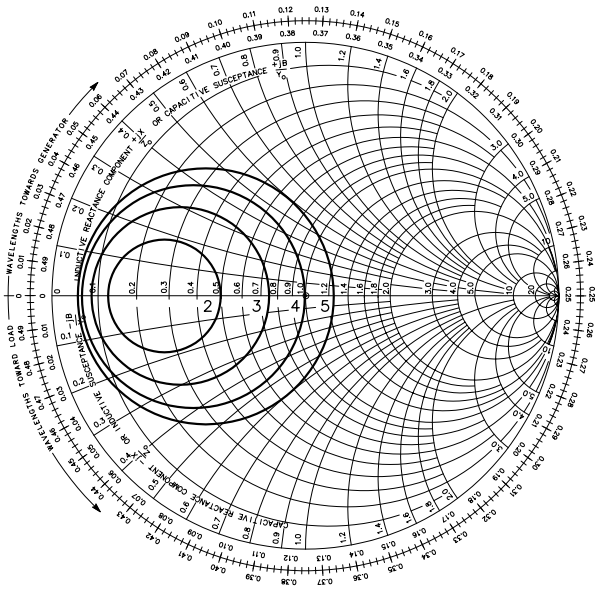

Fig 15—Paths of constant SWR for SWR = 2, 3, 4 and 5, showing impedance variation along 75-Ω line, normalized to 300 Ω. Normalized impedances differ from those in Fig 14, but actual impedances are obtained by multiplying chart readings by 300 Ω and are the same as those corresponding in Fig 14. Paths remain circles but are no longer concentric. One, the matching circle, SWR = 4 in this case, passes through the chart center and is thus the locus of all impedances which can be matched to a 300-Ω line.

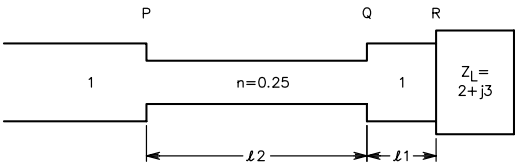

Fig 16—Example for solution by Smith Chart. All impedances are normalized to 300 Ω.

impedances normalized to 300 Ω. Here the normalized load impedance $Z_L = 2 + j\,3$ is shown at R, and the matching circle appears centered on the resistance axis and passing through the points r = 1 and $r = n^2 = (75/300)^2 = 0.0625$. A constant SWR circle is drawn from R to an intersection with the matching circle at Q or Q′ and the corresponding length $\ell 1$ (or $\ell 1'$) can be read directly from the Smith Chart. The clockwise distance around the matching circle represents the length of the matching line, from either Q′ to P or from Q to P. Because in this example the distance QP is the shorter of the two for the matching section, we choose the length $\ell 1$ as shown. By using values from the TOWARD GENERATOR scale, this length is found as 0.045 – 0.213, and adding 0.5 to obtain a positive result yields a value of 0.332 λ.

Although the impedance locus from Q to P is shown in Fig 17, the length $\ell 2$ cannot be determined directly from this chart. This is because the matching circle is not concentric with the chart center, so the wavelength scales do not apply to this circle. This problem is overcome by forming **Fig 18**, which is the same as Fig 17 except that all normalized impedances have been divided by n = 0.25, resulting in a Smith Chart normalized to 75 Ω instead of 300. The matching circle and the chart center are now concentric, and the series-section length $\ell 2$, the distance between Q and P, can be taken directly from the chart. By again using the TOWARD GENERATOR scale, this length is found as 0.250 – 0.148 = 0.102 λ.

In fact it is not necessary to construct the entire impedance locus shown in Fig 18. It is sufficient to plot Z_Q/n (Z_Q is read from Fig 17) and $Z_p/n = 1/n$, connect them by a circular arc centered on the chart center, and to determine the arc length $\ell 2$ from the Smith Chart.

Procedure Summary

The steps necessary to design a series-section transformer by means of the Smith Chart can now be listed:

1) Normalize all impedances by dividing by the characteristic impedance of the main line.
2) On a Smith Chart, plot the normalized load impedance Z_L at R and construct the matching circle

ch28.pmd 14 3/9/2007, 4:25 PM

so that its center is on the resistance axis and it passes through the points r = 1 and r = n^2.

3) Construct a constant SWR circle centered on the chart center through point R. This circle should intersect the matching circle at two points. One of these points, normally the one resulting in the shorter clockwise distance along the matching circle to the chart center, is chosen as point Q, and the clockwise distance from R to Q is read from the chart and taken to be $\ell 1$.
4) Read the impedance Z_Q from the chart, calculate Z_Q/n and plot it as point Q on a second Smith Chart. Also plot r = 1/n as point P.
5) On this second chart construct a circular arc, centered on the chart center, clockwise from Q to P. The length of this arc, read from the chart, represents $\ell 2$. The design of the transformer is now complete, and the necessary physical line lengths may be determined.

The Smith Chart construction shows that two design solutions are usually possible, corresponding to the two intersections of the constant SWR circle (for the load) and the matching circle. These two values correspond to positive and negative values of the square-root radical in the equation for a mathematical solution of the problem. It may happen, however, that the load circle misses the matching circle completely, in which case no solution is possible. The cure is to enlarge the matching circle by choosing a series section whose impedance departs more from that of the main line.

A final possibility is that, rather than intersecting the matching circle, the load circle is tangent to it. There is then but one solution—that of the $^1/_4$-λ transformer.

BIBLIOGRAPHY

Source material and more extended discussion of topics covered in this chapter can be found in the references given below and in the textbooks listed at the end of Chapter 2.

W. N. Caron, *Antenna Impedance Matching* (Newington: ARRL, 1989).

C. MacKeand, "The Smith Chart in BASIC," *QST*, Nov 1984, pp 28-31.

M. W. Maxwell, *Reflections—Transmission Lines and Antennas* (Newington: ARRL, 1990).

F. A. Regier, Series-Section Transmission-Line Impedance Matching," *QST*, Jul 1978, pp 14-16.

P. H. Smith, *Electronic Applications of the Smith Chart*, reprint ed. (Malabar, FL: Krieger Pub Co, Inc, 1983).

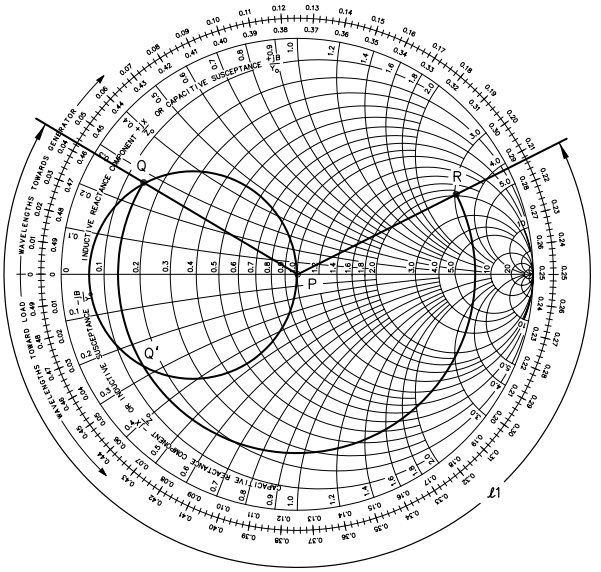

Fig 17—Smith Chart representation of the example shown in Fig 16. The impedance locus always takes a clockwise direction from the load to the generator. This path is first along the constant SWR circle from the load at R to an intersection with the matching circle at Q or Q′, and then along the matching circle to the chart center at P. Length $\ell 1$ can be determined directly from the chart, and in this example is 0.332 λ.

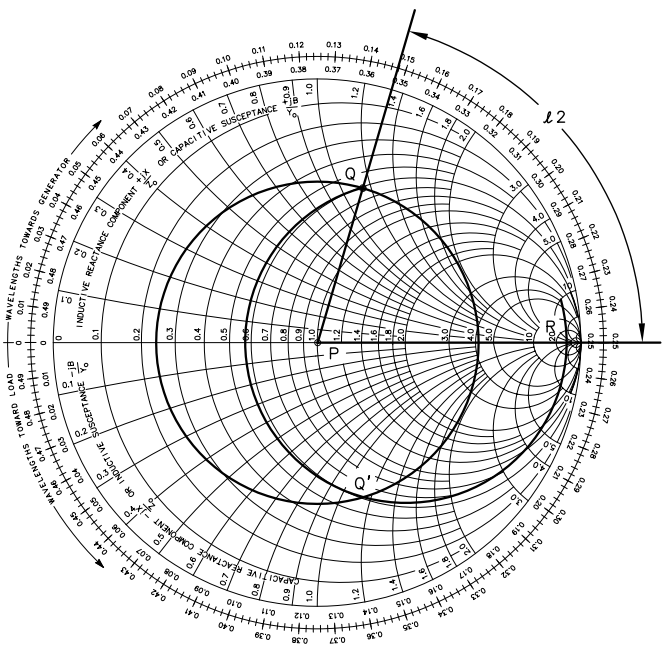

Fig 18—The same impedance locus as shown in Fig 17 except normalized to 75 Ω instead of 300. The matching circle is now concentric with the chart center, and $\ell 2$ can be determined directly from the chart, 0.102 λ in this case.

ch28.pmd 15 3/9/2007, 4:25 PM

Appendix

This appendix contains a glossary of terms, a list of common abbreviations, length conversion information (feet and inches), metric equivalents and antenna-gain-reference data.

Glossary of Terms

This glossary provides a handy list of terms that are used frequently in Amateur Radio conversation and literature about antennas. With each item is a brief definition of the term. Most terms given here are discussed more thoroughly in the text of this book, and may be located by using the index.

Actual ground—The point within the earth's surface where effective ground conductivity exists. The depth for this point varies with frequency and the condition of the soil.

Antenna—An electrical conductor or array of conductors that radiates signal energy (transmitting) or collects signal energy (receiving).

Antenna tuner—A device containing variable reactances (and perhaps a balun). It is connected between the transmitter and the feed point of an antenna system, and adjusted to "tune" or resonate the system to the operating frequency.

Aperture, effective—An area enclosing an antenna, on which it is convenient to make calculations of field strength and antenna gain. Sometimes referred to as the "capture area."

Apex—The feed-point region of a V type of antenna.

Apex angle—The included angle between the wires of a V, an inverted-V dipole, and similar antennas, or the included angle between the two imaginary lines touching the element tips of a log periodic array.

Balanced line—A symmetrical two-conductor feed line that has uniform voltage and current distribution along its length.

Balun—A device for feeding a balanced load with an unbalanced line, or vice versa. May be a form of choke, or a transformer that provides a specific impedance transformation (including 1:1). Often used in antenna systems to interface a coaxial transmission line to the feed point of a balanced antenna, such as a dipole.

Base loading—A lumped reactance that is inserted at the base (ground end) of a vertical antenna to resonate the antenna.

Bazooka—A transmission-line balancer. It is a quarter-wave conductive sleeve (tubing or flexible shielding) placed at the feed point of a center-fed element and grounded to the shield braid of the coaxial feed line at the end of the sleeve farthest from the feed point. It permits the use of unbalanced feed line with balanced feed antennas.

Beamwidth—Related to directive antennas. The width, in degrees, of the major lobe between the two directions at which the relative radiated power is equal to one half its value at the peak of the lobe (half power = –3 dB).

Beta match—A form of hairpin match. The two conductors straddle the boom of the antenna being matched, and the closed end of the matching-section conductors is strapped to the boom.

Bridge—A circuit with two or more ports that is used in measurements of impedance, resistance or standing waves in an antenna system. When the bridge is adjusted for a balanced condition, the unknown factor can be determined by reading its value on a calibrated scale or meter.

Capacitance hat—A conductor of large surface area that is connected at the high-impedance end of an antenna to effectively increase the electrical length. It is sometimes mounted directly above a loading coil to reduce the required inductance for establishing resonance. It usually takes the form of a series of wheel spokes or a solid circular disc. Sometimes referred to as a "top hat."

Capture area—See aperture.

Center fed—Transmission-line connection at the electrical center of an antenna radiator.

Center loading—A scheme for inserting inductive reactance (coil) at or near the center of an antenna element for the purpose of lowering its resonant frequency. Used with elements that are less than 1/4 wavelength at the operating frequency.

Coax—See coaxial cable.

Coaxial cable—Any of the coaxial transmission lines that have the outer shield (solid or braided) on the same axis as the inner or center conductor. The insulating material can be air, helium or solid-dielectric compounds.

Collinear array—A linear array of radiating elements (usually dipoles) with their axes arranged in a straight line. Popular at VHF and above.

Conductor—A metal body such as tubing, rod or wire that permits current to travel continuously along its length.

Counterpoise—A wire or group of wires mounted close to ground, but insulated from ground, to form a low-impedance, high-capacitance path to ground. Used at MF and HF to provide an RF ground for an antenna. Also see ground plane.

Current loop—A point of current maxima (antipode) on an antenna.

Current node—A point of current minima on an antenna.

Decibel—A logarithmic power ratio, abbreviated dB. May also represent a voltage or current ratio if the voltages or currents are measured across (or through) identical impedances. Suffixes to the abbreviation indicate references: dBi, isotropic radiator; dBic, isotropic radiator circular; dBm, milliwatt; dBW, watt.

Delta loop—A full-wave loop shaped like a triangle or delta.

Delta match—Center-feed technique used with radiators that are not split at the center. The feed line is fanned near the radiator center and connected to the radiator symmetrically. The fanned area is delta shaped.

Dielectrics—Various insulating materials used in antenna systems, such as found in insulators and transmission lines.

Dipole—An antenna that is split at the exact center for connection to a feed line, usually a half wavelength long. Also called a "doublet."

Direct ray—Transmitted signal energy that arrives at the receiving antenna directly rather than being reflected by any object or medium.

Directivity—The property of an antenna that concentrates the radiated energy to form one or more major lobes.

Director—A conductor placed in front of a driven element to cause directivity. Frequently used singly or in multiples with Yagi or cubical-quad beam antennas.

Doublet—See dipole.

Driven array—An array of antenna elements which are all driven or excited by means of a transmission line, usually to achieve directivity.

Driven element—A radiator element of an antenna system to which the transmission line is connected.

Dummy load—Synonymous with dummy antenna. A nonradiating substitute for an antenna.

E layer—The ionospheric layer nearest earth from which radio signals can be reflected to a distant point, generally a maximum of 2000 km (1250 ml).

E plane—Related to a linearly polarized antenna, the plane containing the electric field vector of the antenna and its direction of maximum radiation. For terrestrial antenna systems, the direction of the E plane is also taken as the polarization of the antenna. The E plane is at right angles to the H plane.

Efficiency—The ratio of useful output power to input power, determined in antenna systems by losses in the system, including in nearby objects.

EIRP—Effective isotropic radiated power. The power radiated by an antenna in its favored direction, taking the gain of the antenna into account as referenced to isotropic.

Elements—The conductive parts of an antenna system that determine the antenna characteristics. For example, the reflector, driven element and directors of a Yagi antenna.

End effect—A condition caused by capacitance at the ends of an antenna element. Insulators and related support wires contribute to this capacitance and lower the resonant frequency of the antenna. The effect increases with conductor diameter and must be considered when cutting an antenna element to length.

End fed—An end-fed antenna is one to which power is applied at one end, rather than at some point between the ends.

F layer—The ionospheric layer that lies above the E layer. Radio waves can be refracted from it to provide communications distances of several thousand miles by means of single- or double-hop skip.

Feed line—See feeders.

Feeders—Transmission lines of assorted types that are used to route RF power from a transmitter to an antenna, or from an antenna to a receiver.

Field strength—The intensity of a radio wave as measured at a point some distance from the antenna. This measurement is usually made in microvolts per meter.

Front to back—The ratio of the radiated power off the front and back of a directive antenna. For example, a dipole would have a ratio of 1, which is equivalent to 0 dB.

Front to rear—Worst-case rearward lobe in the 180°-wide sector behind an antenna's main lobe, in dB.

Front to side—The ratio of radiated power between the major lobe and that 90° off the front of a directive antenna.

Gain—The increase in effective radiated power in the desired direction of the major lobe.

Gamma match—A matching system used with driven antenna elements to effect a match between the transmission line and the feed point of the antenna. It consists of a series capacitor and an arm that is mounted close to the driven element and in parallel with it near the feed point.

Ground plane—A system of conductors placed beneath an elevated antenna to serve as an earth ground. Also see counterpoise.

Ground screen—A wire mesh counterpoise.

Ground wave—Radio waves that travel along the earth's surface.

H plane—Related to a linearly polarized antenna. The plane containing the magnetic field vector of an antenna and its direction of maximum radiation. The H plane is at right angles to the E plane.

HAAT—Height above average terrain. A term used mainly in connection with repeater antennas in determining coverage area.

Hairpin match—A U-shaped conductor that is connected to the two inner ends of a split dipole for the purpose of creating an impedance match to a balanced feeder.

Harmonic antenna—An antenna that will operate on its fundamental frequency and the harmonics of the fundamental frequency for which it is designed. An end-fed half-wave antenna is one example.

Helical—A helically wound antenna, one that consists of a spiral conductor. If it has a very large winding length to diameter ratio it provides broadside radiation. If the length-to-diameter ratio is small, it will operate in the axial mode and radiate off the end opposite the feed point. The polarization will be circular for the axial mode, with left or right circularity, depending on whether the helix is wound clockwise or counterclockwise.

Helical hairpin—"Hairpin" match with a lumped inductor, rather than parallel-conductor line.

Image antenna—The imaginary counterpart of an actual antenna. It is assumed for mathematical purposes to be located below the earth's surface beneath the antenna, and is considered symmetrical with the antenna above ground.

Impedance—The ohmic value of an antenna feed point, matching section or transmission line. An impedance may contain a reactance as well as a resistance component.

Inverted V—A misnomer, as the antenna being referenced does not have the characteristics of a V antenna. See inverted-V dipole.

Inverted-V dipole—A half-wavelength dipole erected in the form of an upside-down V, with the feed point at the apex. Its radiation pattern is similar to that of a horizontal dipole.

Isotropic—An imaginary or hypothetical point-source antenna that radiates equal power in all directions. It is used as a reference for the directive characteristics of actual antennas.

Lambda—Greek symbol (λ) used to represent a wavelength with reference to electrical dimensions in antenna work.

Line loss—The power lost in a transmission line, usually expressed in decibels.

Line of sight—Transmission path of a wave that travels directly from the transmitting antenna to the receiving antenna.

Litz wire—Stranded wire with individual strands insulated; small wire provides a large surface area for current flow, so losses are reduced for the wire size.

Load—The electrical entity to which power is delivered. The antenna system is a load for the transmitter.

Loading—The process of a transferring power from its source to a load. The effect a load has on a power source.

Lobe—A defined field of energy that radiates from a directive antenna.

Log periodic antenna—A broadband directive antenna that has a structural format causing its impedance and radiation characteristics to repeat periodically as the logarithm of frequency.

Long wire—A wire antenna that is one wavelength or greater in electrical length. When two or more wavelengths long it provides gain and a multilobe radiation pattern. When terminated at one end it becomes essentially unidirectional off that end.

Marconi antenna—A shunt-fed monopole operated against ground or a radial system. In modern jargon, the term refers loosely to any type of vertical antenna.

Matching—The process of effecting an impedance match between two electrical circuits of unlike impedance. One example is matching a transmission line to the feed point of an antenna. Maximum power transfer to the load (antenna system) will occur when a matched condition exists.

Monopole—Literally, one pole, such as a vertical radiator operated against the earth or a counterpoise.

Nichrome wire—An alloy of nickel and chromium; not a good conductor; resistance wire. Used in the heating elements of electrical appliances; also as conductors in transmission lines or circuits where attenuation is desired.

Null—A condition during which an electrical unit is at a minimum. A null in an antenna radiation pattern is a point in the 360-degree pattern where a minima in field intensity is observed. An impedance bridge is said to be "pulled" when it has been brought into balance, with a null in the current flowing through the bridge arm.

Octave—A musical term. As related to RF, frequencies having a 2:1 harmonic relationship.

Open-wire line—A type of transmission line that resembles a ladder, sometimes called "ladder line." Consists of parallel, symmetrical wires with insulating spacers at regular intervals to maintain the line spacing. The dielectric is principally air, making it a low-loss type of line.

Parabolic reflector—An antenna reflector that is a portion of a parabolic revolution or curve. Used mainly at UHF and higher to obtain high gain and a relatively narrow beamwidth when excited by one of a variety of driven elements placed in the plane of and perpendicular to the axis of the parabola.

Parasitic array—A directive antenna that has a driven element and at least one independent director or reflector, or a combination of both. The directors and reflectors are not connected to the feed line. Except for VHF and UHF arrays with long booms (electrically), more than one reflector is seldom used. A Yagi antenna is one example of a parasitic array.

Phasing lines—Sections of transmission line that are used to ensure the correct phase relationship between the elements of a driven array, or between bays of an array of antennas. Also used to effect impedance transformations while maintaining the desired phase.

Polarization—The sense of the wave radiated by an antenna. This can be horizontal, vertical, elliptical or circular (left or right hand circularity), depending on the design and application. (See H plane.)

Q section—Term used in reference to transmission-line matching transformers and phasing lines.

Quad—A parasitic array using rectangular or diamond shaped full-wave wire loop elements. Often called the "cubical quad." Another version uses delta-shaped elements, and is called a delta loop beam.

Radiation pattern—The radiation characteristics of an antenna as a function of space coordinates. Normally, the pattern is measured in the far-field region and is represented graphically.

Radiation resistance—The ratio of the power radiated by an antenna to the square of the RMS antenna current, referred to a specific point and assuming no losses. The effective resistance at the antenna feed point.

Radiator—A discrete conductor that radiates RF energy in an antenna system.

Random wire—A random length of wire used as an antenna and fed at one end by means of an antenna tuner. Seldom operates as a resonant antenna unless the length happens to be correct.

Reflected ray—A radio wave that is reflected from the earth, ionosphere or a man-made medium, such as a passive reflector.

Reflector—A parasitic antenna element or a metal assembly that is located behind the driven element to enhance forward directivity. Hillsides and large man-made structures such as buildings and towers may act as reflectors.

Refraction—Process by which a radio wave is bent and returned to earth from an ionospheric layer or other medium after striking the medium.

Resonator—In antenna terminology, a loading assembly consisting of a coil and a short radiator section. Used to lower the resonant frequency of an antenna, usually a vertical or a mobile whip.

Rhombic—A rhomboid or diamond-shaped antenna consisting of sides (legs) that are each one or more wavelengths long. The antenna is usually erected parallel to the ground. A rhombic antenna is bidirectional unless terminated by a resistance, which makes it unidirectional. The greater the electrical leg length, the greater the gain, assuming the tilt angle is optimized.

Shunt feed—A method of feeding an antenna driven element with a parallel conductor mounted adjacent to a low-impedance point on the radiator. Frequently used with grounded quarter-wave vertical antennas to provide an impedance match to the feeder. Series feed is used when the base of the vertical is insulated from ground.

Stacking—The process of placing similar directive antennas atop or beside one another, forming a "stacked array." Stacking provides more gain or directivity than a single antenna.

Stub—A section of transmission line used to tune an antenna element to resonance or to aid in obtaining an impedance match.

SWR—Standing-wave ratio on a transmission line in an antenna system. More correctly, VSWR, or voltage standing-wave ratio. The ratio of the forward to reflected voltage on the line, and not a power ratio. A VSWR of 1:1 occurs when all parts of the antenna system are matched correctly to one another.

T match—Method for matching a transmission-line to an unbroken driven element. Attached at the electrical center of the driven element in a T-shaped manner. In effect it is a double gamma match.

Tilt angle—Half the angle included between the wires at the sides of a rhombic antenna.

Top hat—See capacitance hat.

Top loading—Addition of a reactance (usually a capacitance hat) at the end of an antenna element opposite the feed point to increase the electrical length of the radiator.

Transmatch—An antenna tuner.

Trap—Parallel L-C network inserted in an antenna element to provide multiband operation with a single conductor.

Unipole—See monopole.

Velocity factor—The ratio of the velocity of radio wave propagation in a dielectric medium to that in free space. When cutting a transmission line to a specific electrical length, the velocity factor of the particular line must be taken into account.

VSWR—Voltage standing-wave ratio. See SWR.

Wave—A disturbance or variation that is a function of time or space, or both, transferring energy progressively from point to point. A radio wave, for example.

Wave angle—The angle above the horizon of a radio wave as it is launched from or received by an antenna. Also called elevation angle.

Wave front—A surface that is a locus of all the points having the same phase at a given instant in time.

Yagi—A directive, gain type of antenna that utilizes a number of parasitic directors and a reflector. Named after one of the two Japanese inventors (Yagi and Uda).

Zepp antenna—A half-wave wire antenna that operates on its fundamental and harmonics. It is fed at one end by means of open-wire feeders. The name evolved from its popularity as an antenna on Zeppelins. In modern jargon the term refers loosely to any horizontal antenna.

Abbreviations

Abbreviations and acronyms that are commonly used throughout this book are defined in the list below. Periods are not part of an abbreviation unless the abbreviation otherwise forms a common English word. When appropriate, abbreviations as shown are used in either singular or plural construction.

-A-
A—ampere
ac—alternating current
AF—audio frequency
AFSK—audio frequency-shift keying
AGC—automatic gain control
AM—amplitude modulation
ANT—antenna
ARRL—American Radio Relay League
ATV—amateur television
AWG—American wire gauge
az-el—azimuth-elevation

-B-
balun—balanced to unbalanced
BC—broadcast
BCI—broadcast interference
BW—bandwidth

-C-
ccw—counterclockwise
cm—centimeter
coax—coaxial cable
CT—center tap
cw—clockwise
CW—continuous wave

-D-
D—diode
dB—decibel
dBd—decibels referenced to a dipole
dBi—decibels referenced to isotropic
dBic—decibels referenced to isotropic, circular
dBm—decibels referenced to one milliwatt
dBW—decibels referenced to one watt
dc—direct current
deg—degree
DF—direction finding
dia—diameter
DPDT—double pole, double throw
DPST—double pole, single throw
DVM—digital voltmeter
DX—long distance communication

-E-
E—ionospheric layer, electric field
ed.—edition
Ed.—editor
EIRP—effective isotropic radiated power
ELF—extremely low frequency
EMC—electromagnetic compatibility
EME—earth-moon-earth
EMF—electromotive force
ERP—effective radiated power
E_S—ionospheric layer (sporadic E)

-F-
f—frequency
F—ionospheric layer, farad
F/B—front to back (ratio)
F/R—worst-case front to rear (ratio)
FM—frequency modulation
FOT—frequency of optimum transmission
ft—foot or feet (unit of length)
F_1—ionospheric layer
F_2—ionospheric layer

-G-
GDO—grid- or gate-dip oscillator
GHz—gigahertz
GND—ground

-H-
H—magnetic field, henry
HAAT—height above average terrain
HF—high frequency (3-30 MHz)
Hz—hertz (unit of frequency)

-I-
I—current
ID—inside diameter
IEEE—Institute of Electrical and Electronic Engineers
in.—inch
IRE—Institute of Radio Engineers (now IEEE)

-J-
j—vector notation

-K-
kHz—kilohertz
km—kilometer
kW—kilowatt
kW—kilohm

-L-
L—inductance
lb—pound (unit of mass)
LF—low frequency (30-300 kHz)
LHCP—left-hand circular polarization
ln—natural logarithm
log—common logarithm
LP—log periodic
LPDA—log periodic dipole array
LPVA—log periodic V array
LUF—lowest usable frequency

-M-
m—meter (unit of length)
m/s—meters per second
mA—milliampere
max—maximum
MF—medium frequency (0.3-3 MHz)
mH—millihenry
MHz—megahertz
mi—mile
min—minute
mm—millimeter
ms—millisecond
mS—millisiemen
MS—meteor scatter
MUF—maximum usable frequency
mW—milliwatt
MW—megohm

-N-
NC—no connection, normally closed
NiCd—nickel cadmium
NIST—National Institute of Standards and Technology
NO—normally open
no.—number

-O-
OD—outside diameter

-P-
p—page (bibliography reference)
P-P—peak to peak
PC—printed circuit
PEP—peak envelope power
pF—picofarad
pot—potentiometer
pp—pages (bibliography reference)
Proc—Proceedings

-Q-
Q—figure of merit

-R-
R—resistance, resistor
RF—radio frequency
RFC—radio frequency choke
RFI—radio frequency interference
RHCP—right-hand circular polarization
RLC—resistance-inductance-capacitance
r/min—revolutions per minute
RMS—root mean square
r/s—revolutions per second
RSGB—Radio Society of Great Britain
RX—receiver

-S-
s—second
S—siemen
S/NR—signal-to-noise ratio
SASE—self-addressed stamped envelope
SINAD—signal-to-noise and distortion
SPDT—single pole, double throw
SPST—single pole, single throw
SWR—standing wave ratio
sync—synchronous

-T-
tpi—turns per inch
TR—transmit-receive
TVI—television interference
TX—transmitter

-U-
UHF—ultra-high frequency (300-3000 MHz)
US—United States
UTC—Universal Time, Coordinated

-V-
V—volt
VF—velocity factor
VHF—very-high frequency (30-300 MHz)
VLF—very-low frequency (3-30 kHz)
Vol—volume (bibliography reference)
VOM—volt-ohm meter
VSWR—voltage standing-wave ratio
VTVM—vacuum-tube voltmeter

-W-
W—watt
WPM—words per minute
WRC—World Radio Conference
WVDC—working voltage, direct current

-X-
X—reactance
XCVR—transceiver
XFMR—transformer
XMTR—transmitter

-Z-
Z—impedance

-Other symbols and Greek letters-
°—degrees
λ—wavelength
λ/dia—wavelength to diameter (ratio)
μ—permeability
μF—microfarad
μH—microhenry
μV—microvolt
Ω—ohm
ϕ—angles
π—3.14159
θ—angles

Length Conversions

Throughout this book, equations may be found for determining the design length and spacing of antenna elements. For convenience, the equations are written to yield a result in feet. (The answer may be converted to meters simply by multiplying the result by 0.3048.) If the result in feet is not an integral number, however, it is necessary to make a conversion from a decimal fraction of a foot to inches and fractions before the physical distance can be determined with a conventional tape measure. Table 1 may be used for this conversion, showing inches and fractions for increments of 0.01 foot. The table deals with only the fractional portion of a foot. The integral number of feet remains the same.

For example, say a calculation yields a result of 11.63 feet, and we wish to convert this to a length we can find on a tape measure. For the moment, consider only the fractional part of the number, 0.63 foot. In Table 1 1ocate the line with "0.6" appearing in the left column. (This is the 7th line down in the body of the table.) Then while staying on that line, move over to the column headed "0.03." Note here that the sum of the column and line heads, 0.6 + 0.03, equals the value of 0.63 that we want to convert. In the body of the table for this column and line we read the equivalent fraction for 0.63 foot, $7^{9}/_{16}$ inches. To that value, add the number of whole feet from the value being converted, 11 in this case. The total length equivalent of 11.63 feet is thus 11 feet $7^{9}/_{16}$ inches.

Similarly, Table 2 may be used to make the conversion from inches and fractions to decimal fractions of a foot. This table is convenient for using measured distances in equations. For example, say we wish to convert a length of 19 feet $7^{3}/_{4}$ inches to a decimal fraction. Considering only the fractional part of this value, $7^{3}/_{4}$ inches, locate the decimal value on the line identified as "7-" and in the column headed "$^{3}/_{4}$," where we read 0.646. This decimal value is equivalent to $7 + {}^{3}/_{4} = 7^{3}/_{4}$ inches. To this value add the whole number of feet from the value being converted for the final result, 19 in this case. In this way, 19 feet $7^{3}/_{4}$ inches converts to 19 + 0.646 = 19.646 feet.

Table 2
Conversion, Inches and Fractions to Decimal Feet

	Fractional Increments							
	0	*1/8*	*1/4*	*3/8*	*1/2*	*5/8*	*3/4*	*7/8*
0-	0.000	0.010	0.021	0.031	0.042	0.052	0.063	0.073
1-	0.083	0.094	0.104	0.115	0.125	0.135	0.146	0.156
2-	0.167	0.177	0.188	0.198	0.208	0.219	0.229	0.240
3-	0.250	0.260	0.271	0.281	0.292	0.302	0.313	0.323
4-	0.333	0.344	0.354	0.365	0.375	0.385	0.396	0.406
5-	0.417	0.427	0.438	0.448	0.458	0.469	0.479	0.490
6-	0.500	0.510	0.521	0.531	0.542	0.552	0.563	0.573
7-	0.583	0.594	0.604	0.615	0.625	0.635	0.646	0.656
8-	0.667	0.677	0.688	0.698	0.708	0.719	0.729	0.740
9-	0.750	0.760	0.771	0.781	0.792	0.802	0.813	0.823
10-	0.833	0.844	0.854	0.865	0.875	0.885	0.896	0.906
11-	0.917	0.927	0.938	0.948	0.958	0.969	0.979	0.990

Table 1
Conversion, Decimal Feet to Inches (Nearest 16th)

	Decimal Increments									
	0.00	*0.01*	*0.02*	*0.03*	*0.04*	*0.05*	*0.06*	*0.07*	*0.08*	*0.09*
0.0	0-0	$0^{1}/_{8}$	$0^{1}/_{4}$	$0^{3}/_{8}$	$0^{1}/_{2}$	$0^{5}/_{8}$	$0^{3}/_{4}$	$0^{13}/_{16}$	$0^{15}/_{16}$	$1^{1}/_{16}$
0.1	$1^{3}/_{16}$	$1^{5}/_{16}$	$1^{7}/_{16}$	$1^{9}/_{16}$	$1^{11}/_{16}$	$1^{13}/_{16}$	$1^{15}/_{16}$	$2^{1}/_{16}$	$2^{3}/_{16}$	$2^{1}/_{4}$
0.2	$2^{3}/_{8}$	$2^{1}/_{2}$	$2^{5}/_{8}$	$2^{3}/_{4}$	$2^{7}/_{8}$	3-0	$3^{1}/_{8}$	$3^{1}/_{4}$	$3^{3}/_{8}$	$3^{1}/_{2}$
0.3	$3^{5}/_{8}$	$3^{3}/_{4}$	$3^{13}/_{16}$	$3^{15}/_{16}$	$4^{1}/_{16}$	$4^{3}/_{16}$	$4^{5}/_{16}$	$4^{7}/_{16}$	$4^{9}/_{16}$	$4^{11}/_{16}$
0.4	$4^{13}/_{16}$	$4^{15}/_{16}$	$5^{1}/_{16}$	$5^{3}/_{16}$	$5^{1}/_{4}$	$5^{3}/_{8}$	$5^{1}/_{2}$	$5^{5}/_{8}$	$5^{3}/_{4}$	$5^{7}/_{8}$
0.5	6-0	$6^{1}/_{8}$	$6^{1}/_{4}$	$6^{3}/_{8}$	$6^{1}/_{2}$	$6^{5}/_{8}$	$6^{3}/_{4}$	$6^{13}/_{16}$	$6^{15}/_{16}$	$7^{1}/_{16}$
0.6	$7^{3}/_{16}$	$7^{5}/_{16}$	$7^{7}/_{16}$	$7^{9}/_{16}$	$7^{11}/_{16}$	$7^{13}/_{16}$	$7^{15}/_{16}$	$8^{1}/_{16}$	$8^{3}/_{16}$	$8^{1}/_{4}$
0.7	$8^{3}/_{8}$	$8^{1}/_{2}$	$8^{5}/_{8}$	$8^{3}/_{4}$	$8^{7}/_{8}$	9-0	$9^{1}/_{8}$	$9^{1}/_{4}$	$9^{3}/_{8}$	$9^{1}/_{2}$
0.8	$9^{5}/_{8}$	$9^{3}/_{4}$	$9^{13}/_{16}$	$9^{15}/_{16}$	$10^{1}/_{16}$	$10^{3}/_{16}$	$10^{5}/_{16}$	$10^{7}/_{16}$	$10^{9}/_{16}$	$10^{11}/_{16}$
0.9	$10^{13}/_{16}$	$10^{15}/_{16}$	$11^{1}/_{16}$	$11^{3}/_{16}$	$11^{1}/_{4}$	$11^{3}/_{8}$	$11^{1}/_{2}$	$11^{5}/_{8}$	$11^{3}/_{4}$	$11^{7}/_{8}$

Metric Equivalents

Throughout this book, distances and dimensions are usually expressed in English units—the mile, the foot, and the inch. Conversions to metric units may be made by using the following equations:

km = mi × 1.609

m = ft (′) × 0.3048

mm = in. (″) × 25.4

An inch is $^{1}/_{12}$ of a foot. Tables in the previous section provide information for accurately converting inches and fractions to decimal feet, and vice versa, without the need for a calculator.

Gain Reference

Throughout this book, gain is referenced to an isotropic radiator (dBi) or to an isotropic radiator with circular polarization (dBic).

THE ARRL

$4.00

ANTENNA ANTHOLOGY

The best
of recent QST
hf antenna articles
and theory presentations

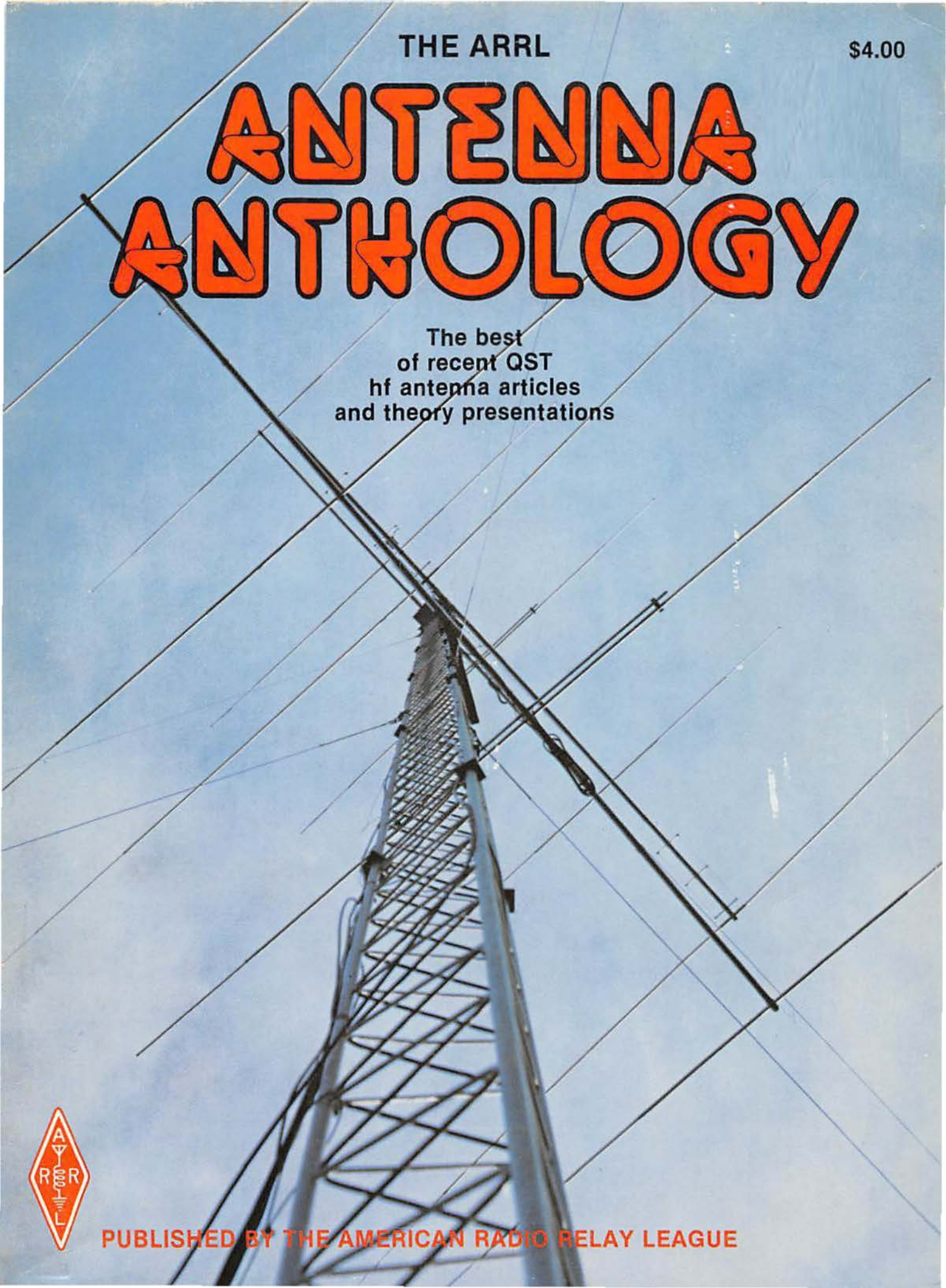

PUBLISHED BY THE AMERICAN RADIO RELAY LEAGUE

The ARRL Antenna Anthology

Edited by
Marian S. Anderson, WB1FSB

American Radio Relay League, Inc.
Newington, CT 06111

Copyright © 1978 by

The American Radio Relay League, Inc.

Copyright secured under the Pan-American Convention

International Copyright secured

This work is Publication No. 36 of the Radio Amateur's Library, published by the League. All rights reserved. No part of this work may be reproduced in any form except by written permission of the publisher. All rights of translation are reserved.

Printed in USA

Quedan reservados todos los derechos

Library of Congress Catalog Card Number: 78-71955

$4.00 in USA
$4.50 elsewhere

Foreword

What type of amateur antenna best suits your needs? Does the available space on your property permit the installation of an effective DX antenna? Is there a compromise antenna system that will provide acceptable results over short and long distances while being reasonable in price and modest in complexity? No doubt you have come to grips with these matters repeatedly since obtaining your amateur license. So, where does one turn to find the answers to these sometimes perplexing questions? What one pre-eminent source might one consult among all of the antenna booklets published for amateurs? Why, *QST*, naturally!

This anthology contains what the ARRL hq. staff considers the best of the *QST* antenna articles and theory presentations in recent years. The contributions of numerous amateur authors and designers are contained in this volume for your convenience. This publication was developed not only to serve as a compilation of good articles, but to reach those amateurs who do not have access to past issues of the League's official monthly journal, *QST*.

The editors of this booklet have attempted to select the types of antennas that have greatest appeal to those who like to construct their own radiators, and for the many amateurs who can't justify the expense of purchasing commercial counterparts. A book of this type contains something for everyone who enjoys building and experimenting with antennas. But, if you aren't a builder you will still enjoy the hours of interesting reading provided by these works.

We wish to extend our gratitude to those *QST* authors whose articles have been selected for publication in this volume. Their enthusiasm, ability and generosity typifies clearly what Amateur Radio is all about. Should you have some original antenna ideas of proven performance, send an article to the ARRL, describing your work. Not only may your story be published in *QST* — it might appear in a future edition of this book.

Richard L. Baldwin, W1RU
General Manager

Contents

1 Vertical Antennas
Page 7

2 Yagi Antennas
Page 41

3 Quad Antennas
Page 53

4 Miscellaneous Antenna Types
Page 76

5 Antenna Theory and Test Methods
Page 100

Index
Page 150

Chapter 1

Vertical Antennas

One of the most practical antennas for use where limited space exists is the vertical. This type of antenna is particularly useful to amateurs who live in dense urban areas where city lots are traditionally small. The same general restriction prevails for those who dwell in apartment buildings. In such locations it is often easier to go "up" with an antenna than to erect one horizontally. But the virtues of vertical antennas extend beyond the foregoing considerations: "Verticals," as they often are called, are relatively inexpensive, easy to erect and are capable of performing well for local (stateside) and DX work. A vertical antenna exhibits a low angle of radiation when worked against a good ground system. This makes it an effective DX type of antenna.

This chapter contains reprints of some popular vertical-antenna systems that have appeared in *QST* during recent years. For the most part, the presentations contained herein have been "lifted" in their entirety, thus making it unnecessary for the reader to research the original articles for additional information.

A Two-Band Vertical for the Novice

Build this inexpensive Novice antenna. It is easy to construct and is made from readily available materials.

Knowing of a Novice who had space problems, the author set out to design an antenna for him that could be used on 40 and 15 meters. His previous antenna was a horizontal "V" whose performance wasn't worth the time it took to put it up. Because of his narrow property, the angle between the two wires was only around 40 degrees, no doubt causing considerable signal cancelation. Horizontal antennas were ruled out, so the best antenna for him was a vertical.

Knowing (or caring) little about multiband trap-loaded antennas, it was decided the simplest antenna would be a quarter-wavelength vertical on 40 meters. After a little paper work, and using formulas given in *The ARRL Antenna Book,* the correct length would be 31 feet 10 inches (9.70 m) for 7.175 MHz. This length would also work as a 3/4-wavelength antenna on 15 meters, providing two-band coverage. However, a 32-foot (9.75-m) vertical antenna made roof-mounting too difficult! Mounting the vertical to the side of the house alleviated many guying and support problems.

Materials

The first concern was what to use for antenna materials. Being almost 32 feet high, the vertical would need strength, so the writer thought of steel tubing, but that was much too expensive. With conduit there aren't enough sizes offered, and that left only one more material — aluminum tubing. The latter comes in just about any size desired, and the author had no trouble in finding just what he wanted. Going to the nearest aluminum dealer, the author found his stock to be more than ample.[1]

In order to keep the cost minimal, the author decided to make the base piece from 1-inch (25-mm) diameter thin-wall tubing. Into 12 feet (3.66 m) of this was inserted a 12-foot piece of 7/8-inch (22-mm) diameter thin-wall tubing. This piece was telescoped 2 feet (0.610 m), then bolted and clamped (after the end had been slit twice by a pair of tin snips). It was necessary to use hose clamps on the tubing because the galvanized bolts didn't provide a good bond between the pieces. The top section was 13-1/2-foot (4.11-m) piece of 3/4-inch (19-mm) diameter thin-wall tubing inserted far enough into the lower piece to make the overall antenna length about 31 feet, 10 inches (9.70 m). Because of its large size, all the work must be done while the antenna is

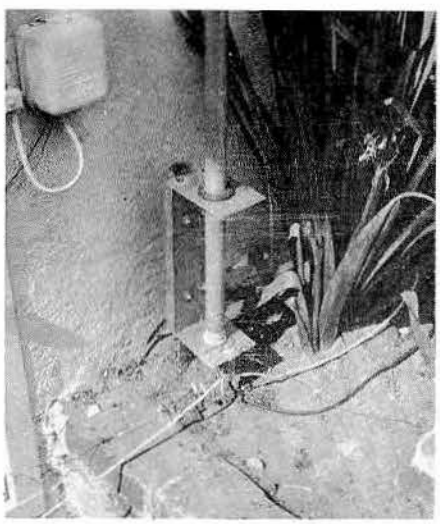

Here is the base mount, installed on the side of the house. The two white wires coming out from the base are the radials.

[1][Editor's Note: TV mast material is also well suited for verticals and comes in 10-foot (3.05-m) lengths, either steel or, preferably, aluminum.]

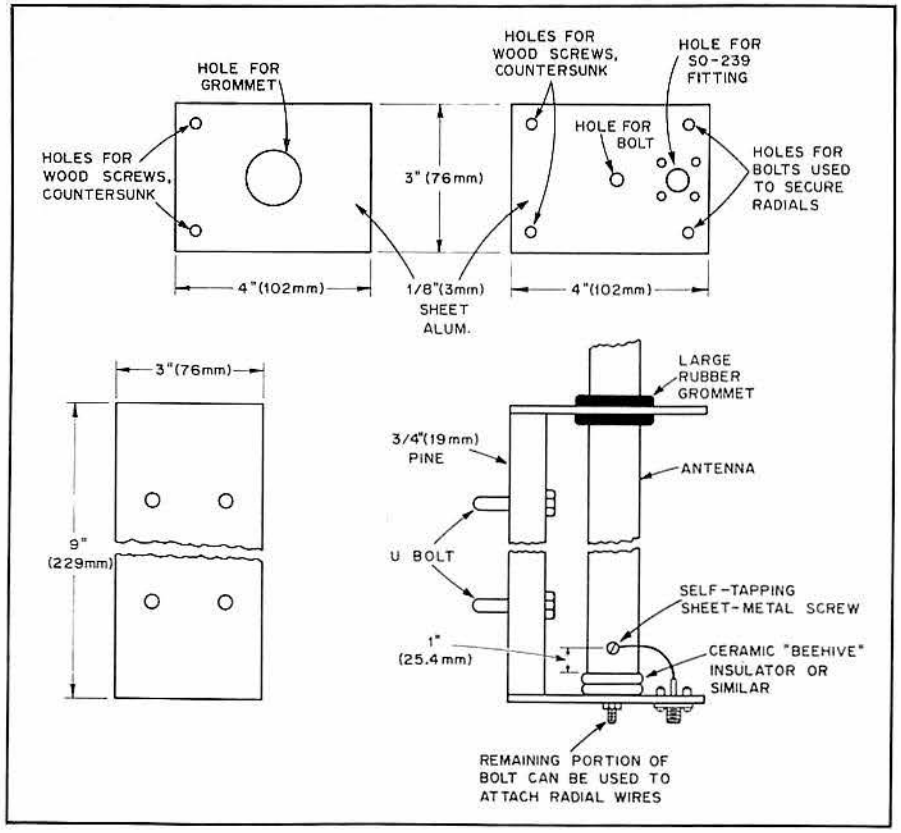

Fig. 1 — Details for making the base-mounting section of the vertical.

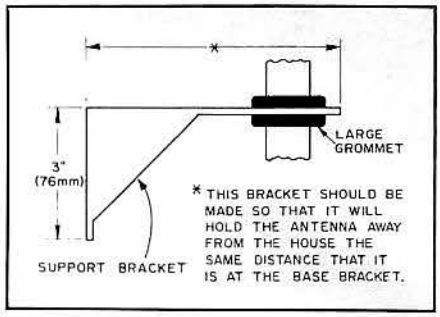

Fig. 2 — Details for the support bracket.

lying on the ground. Then, the antenna must be disassembled and put up piece by piece. (Do not attempt to put the antenna up in one piece! While the weight isn't excessive, the tubing cannot stand the strain.)

Putting It Up

The original base bracket was made from 3/4-inch (19-mm) pine, but during the first rain the wood got wet and the bracket turned out to be a very poor insulator. So the unit was redesigned to use two pieces of 1/8-inch (3-mm) thick sheet aluminum, a large grommet, and a ceramic standoff insulator (see Fig. 1).

Assembling the two-band vertical was quite simple. First, a 4-foot (1.22-m) stake was driven into the ground about 2-1/2 feet (0.76 m), and about four or five inches (102 or 127 mm) away from the side of the house. Next, the bottom section (with the bracket attached) was slipped over the stake and tightened in place with the U bolts. Then the second section was inserted into the first, clamped and bolted in place. A support bracket was made from scrap aluminum, and a large grommet was installed on it to insulate the antenna from the brace (see Fig. 2). This assembly was then attached to the side of the house (near the gable) with wood screws. Last, the third section was forced through the grommet in the second bracket, and was then inserted into the second piece and clamped. (If adjustment of resonance is desired, it is better not to bolt the final section). A suitable cap was mounted on top of the antenna to keep out moisture.

Tune Up

RG-58/U coax was then connected between the transmitter and antenna with an SWR bridge in the line, and power was applied at 7175 kHz. The SWR was found to be 3:1. This was without any ground system on the antenna. In order to obtain a better match and reduce the SWR, it was apparent that a ground system was required.

According to *The ARRL Antenna Book,* two methods of making a suitable ground system can be used. One way is to connect the coax outer shield directly to ground at the base of the antenna, via a ground rod. However, this doesn't work too well unless the soil is extremely conductive (his wasn't). The other method is to make up some sort of artificial ground in the form of radials.

The author cut a radial from some surplus wire to the same length as the vertical section, attached the radial to the base plate and the SWR dropped to 2:1. Unknown to the author at the time, *The Antenna Book* says that the radials should be 2.5 percent longer than the vertical itself, so actually, they should have been made 32-feet 7-3/4-inches (9.95-m) long. A second radial, similar to the first, was attached and the SWR dropped further (to about 1.4:1). When the soil was wet, such as after a rain or after watering, the SWR takes a nose dive to less than 1.2:1. Since the property space was limited, two radials were all that could be used. Ideally, the most perfect system would consist of a metal disk, one quarter wavelength in radius, buried a few inches below the earth's surface, but this approach is rather impractical! But if the antenna was to be erected in an area *away* from buildings, and guyed, a ground system could be made of chicken wire or other similar material. However, the more radials, the better the artificial ground. Also, they should be laid out in as nearly a spoke-like pattern as possible. Hy-Gain recommended for their AVQ series antennas that a radial system be used consisting of at least two radials for *each* band used. However, for this installation the 40-meter radials operate on their third harmonic at 15 meters, requiring but one set of wires.[2]

The length specified makes the antenna resonant at about 7175 kHz on 40 meters. On 15 meters, at the third harmonic, the antenna is resonant at about 21,425 kHz, but power was applied as low as 21,105 kHz,

[2][Editor's note: Actually, *any* radials, regardless of length, will help the performance of the system. Also when used on 15 meters, the antenna would be three quarter wavelengths long with low-impedance feed, approximately 50 ohms. However, the angle of radiation from the antenna will be higher than that of a quarter-wavelength vertical.]

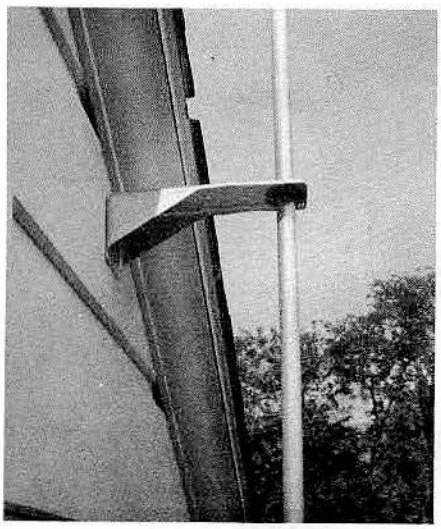

The support bracket, as described in Fig. 2.

and the SWR appeared to be only 1.4:1, well within tolerable limits. Bandwidth on both Novice bands was essentially flat.

Additional Information

Total cost will depend greatly on the individual's ability to scrounge parts. If the builder prefers to purchase the principal materials, this list will be useful.

3 — pieces thin-wall aluminum tubing, 1- (25-mm), 7/8- (22-mm), and 3/4-inch (19-mm) diameters. 12 (3.66 m), 12 (3.66 m) and 13-1/2 feet (4.11 m) long, respectively.

2 — U bolts.

1 —SO-239 connector.

The other material, including three bolts and nuts, six wood screws, two grommets, two hose clamps, wood and aluminum for brackets, ground stake, and cap will vary from no cost to a few dollars, dependent on available materials. If used or surplus tubing is available one could save a substantial amount of money.

In this instance, the top of the antenna extends about 16 feet (4.88 m) above the peak of the roof, but because of the bracing no guy wires were necessary. If the antenna is to be erected in a high-wind area, guys made from nonconducting monofilament fishing line (or other nonconducting line) could be used.

The owner has received nothing but glowing reports so far. Running about 70 watts input, the first CQ on 40 meters raised W9SVJ in northern Indiana from Glendale, CA. His report, RST 589. On 15 meters the owner has worked ZL3JC, AX7SM and JH1EZZ, and received very good reports.

This vertical has no gain, and probably couldn't come near a Yagi or a quad in performance, but for an antenna costing less than $10 it does one heck of an FB job. This material was originally presented in *QST* by Jerry Arnold, WA6MBP.

Build This Novice Four-Band Vertical

Putting your first amateur station together can be an expensive proposition. One way to cut costs is to keep the antenna simple. Here's how to shave the price and provide four-band operation.

Is operation with one antenna acceptable if it covers the 80-, 40-, 15- and 10-meter bands? For a new Novice that's a reasonable approach. The author's backyard is smaller than that of most urban homes, so full-size dipole or inverted-V antennas were out of the question. Not owning a tower (yet!), it seemed that a ground-mounted vertical antenna would be worth trying.

After reading *The ARRL Antenna Book*, it was decided that a ground-mounted vertical antenna would be easiest to build. Some radial wires could be buried, and the metal fence which encloses the backyard could also be hooked up to enlarge the ground system. The author preferred this type of antenna to one installed above ground, because radials of specific lengths for each of the four bands would have been needed for a roof-mounted, groundplane type of vertical. The buried wires for the ground-mounted antenna could be any convenient length, as long as the available space would permit. From what was read about these antennas, the author believed that reasonable performance could be had even if the ground radials weren't numerous and long, although generally the more, the better.

With the help of W1FB some used aluminum tubing was purchased that would telescope together and give the author a 25-foot (7.62-meter) antenna. The wall thickness of the tubing is 0.058 inch (1.5 mm). Three 10-foot (3.05 m) sections are used. The largest diameter is 1 inch (25 mm). The center telescoping section has a diameter of 7/8 inch (22 mm) and the top piece of tubing has a 3/4-inch (19-mm) diameter. This material, plus hose clamps for holding the sections together, came to $8. An old ceramic rotary switch, a coaxial connector, a feed-through bushing, and a piece of Air Dux coil stock were acquired at a flea market for an additional $3. Two medium-size, ceramic standoff insulators were donated by W1FB. He said they cost him 50 cents each at a swap session. All that remained to collect was a weatherproof box for the loading coil, some 50-ohm coaxial cable and six U bolts. The author's OM, Bob, found some used 1-1/2-inch (38-mm) steel pipe which is 7 feet (2.13 m) long. It is used as a support for the vertical.

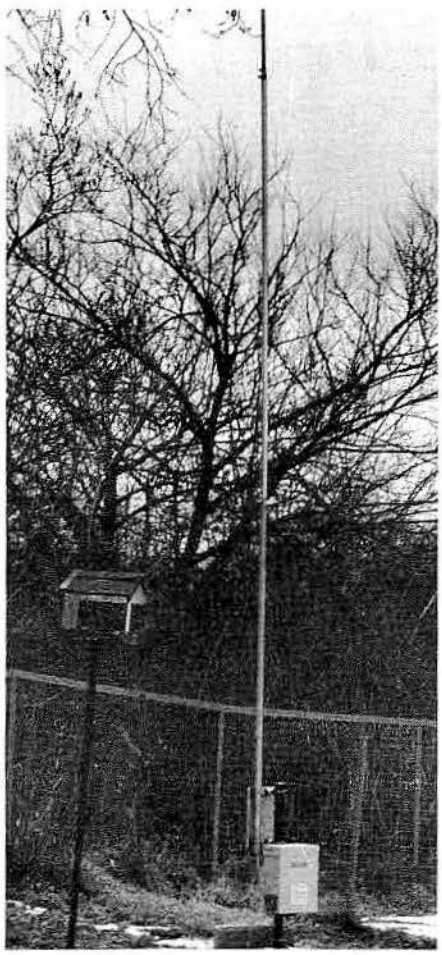

The completed 4-band vertical antenna used at WB1FSB. The box at the base of the antenna contains a loading coil.

Constructing the Antenna

A lawn-edger tool was used to make slits in the lawn, out from the base of the antenna toward the edges of the backyard. The slits were cut to a depth of 2 inches (51 mm). A total of 10 radials were buried in the slits. Some are only 15 feet (4.57 m) in length, while others are 25 feet (7.62 m) long. The metal yard fence was bonded together as needed, using wire jumpers between the fence sections. A single buried wire joined the fence to the common ground point at the base of the antenna.

The OM drove the steel pipe into the ground to a depth of 4 feet (1.22 m), leaving 3 feet (0.91 m) above ground for attaching the vertical antenna and weatherproof box. Construction details are shown in Fig. 3.

Although a wooden box could have been used to house the loading coil, switch and other hardware, an old electrical housing that the author's OM had in his junk box was used (Fig. 4.). It was drilled and

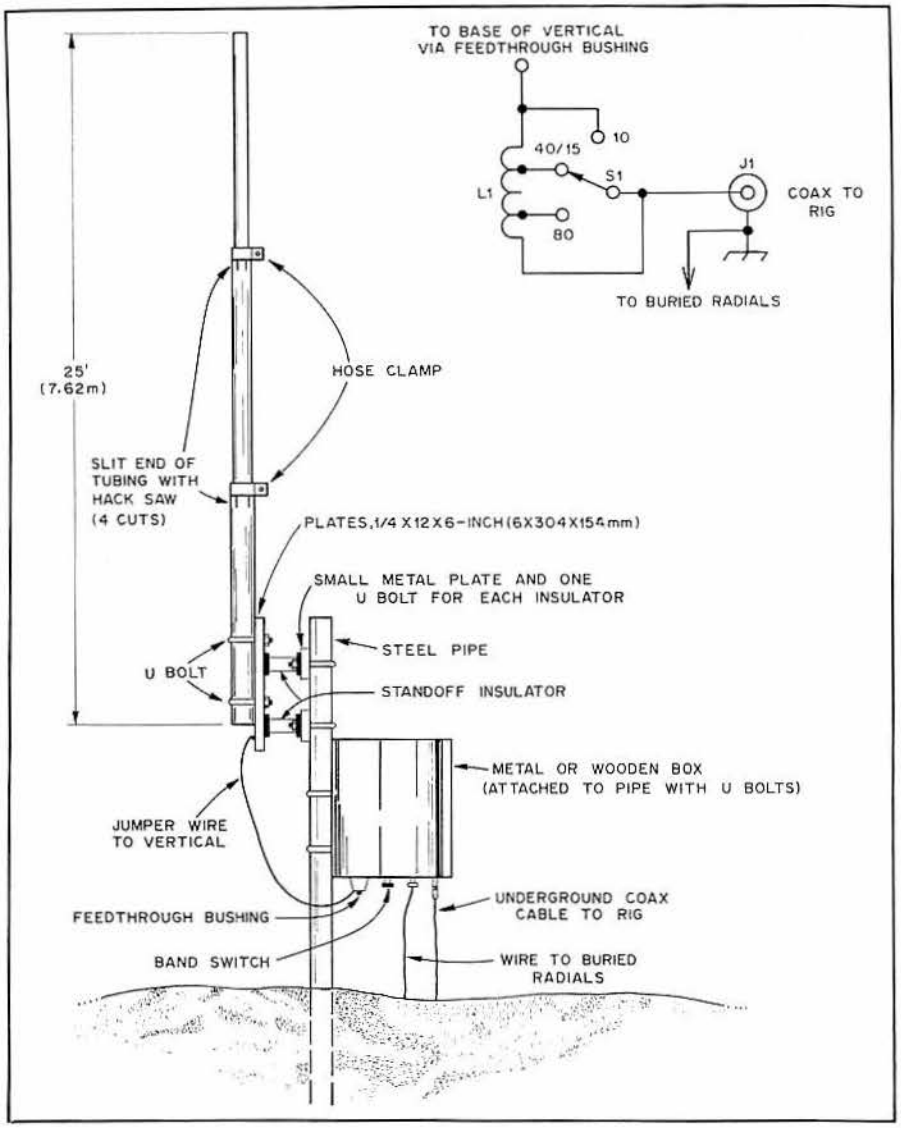

Fig. 3 — Dimensional drawing of the four-band Novice antenna. The top ends of the two lower tubing sections are slit four times each by means of a hack saw. This permits a tight joint when the hose clamp is compressed. The vertical is attached to one metal plate with U bolts. The large standoff insulators with metal feet connect this plate to a pair of small ones. The latter are attached to the steel support pipe by means of two U bolts. The metal box is also affixed to the steel pipe with two U bolts. The band switch is a single-pole three-position ceramic wafer type. L1 can be a 5-inch (127-mm) length of B & W 3029 Miniductor, 2-1/2 inches (64 mm) in diameter, 6 turns per inch of no. 12 wire. See text for alternative mounting methods.

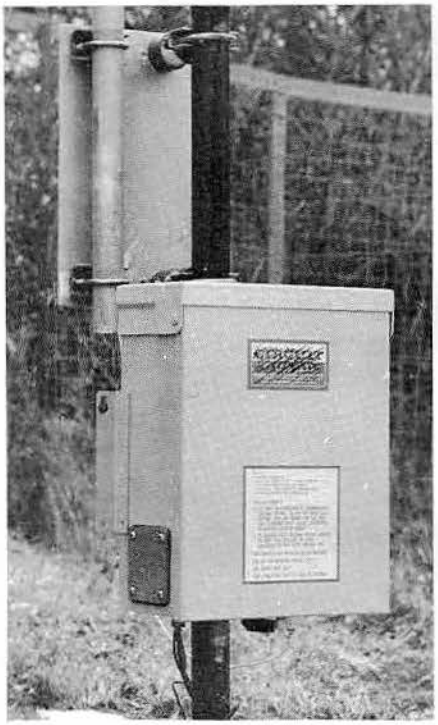

Fig. 4 — Closeup view of the base of the vertical. The aluminum tubing is affixed to a metal plate. The latter is attached to the iron support pipe by means of two surplus standoff insulators. Small aluminum plates are attached to the ends of the insulators to permit them to be fastened to the iron pipe by means of U bolts. The radial wires are connected to the bottom of the coil-housing box.

Fig. 5 — The author checks the SWR of the antenna during final adjustment of the system.

punched on the bottom surface to hold the feedthrough bushing, coaxial connector, switch and ground terminal for the radials.

W1FB designed the antenna, but he wasn't sure that an acceptable impedance match could be had on all four bands without a complex matching network. It was decided to try his idea, so the installation was completed.

Adjusting the Vertical

The author helped her OM install the antenna, then called W1FB for some assistance in tuning the system. He thought we could tune the vertical for 40 meters and make it work okay as a 3/4-wavelength vertical on 15 meters. For use on 80 meters it would be fairly short (63 feet or 19.20 m is the correct length for 3.7 MHz). With base loading it should offer adequate service out to a few hundred miles on 80 meters. Finally, it would operate as a 3/4-wavelength vertical on 10 meters.

A homemade SWR indicator was hooked in the coaxial line at the base of the vertical.[1] A small amount of transmitter power (5 W) was applied at 3725 kHz and the 80-meter switch lead was touched on the turns of the coil until minimum reflected power was indicated (Fig. 5). An SWR of 1:1 was obtained. The wire was then soldered in place on the coil. Next power was fed to the antenna on 7125 kHz, and the 40-meter switch lead was touched to the coil turns until an SWR of 1:1 was read. While using the same coil tap power was supplied to the antenna on 21.1 MHz and the SWR checked. It was approximately 3:1. By moving the coil tap just one turn we were able to get an SWR of 1.5:1 on 15 meters. A recheck on 40 meters followed. The SWR for that band was less than 2:1 — not a bad compromise! The coil was bypassed entirely for operation on 10 meters: an SWR of 2:1

[1]DeMaw, "A QRP Man's RF Power Meter," *QST*, June 1973.

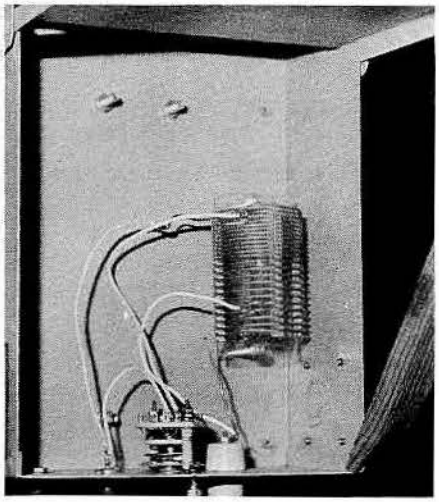

Fig. 6 — Interior view of the coil housing showing the switch, feedthrough bushing, coaxial connector, and ground post for the radials. The coil shown is a piece of Air Dux stock with a tapered pitch. It was obtained at a flea market.

was indicated at 28,000 kHz. The length of the overall antenna for operation on 28,100 kHz should be 25 feet or 7.62 m (3/4-wavelength radiator). However, the switch leads inside the coil housing add to the antenna length. If an SWR of less than 2:1 is desired, break the 10-meter switch lead and insert a 100-pF air variable capacitor. The unwanted reactance can be tuned out by this means and a low SWR will result.

Opening and closing the cover of the metal box had only a minor effect on the SWR. At last an on-the-air test of the system was possible. Fig. 6 shows the interior of the coil and switch housing.

Results

Good signal reports have been received on all bands. The first QSO on 40 meters netted an RST 599 report from North Carolina and many similar reports followed on 80, 15 and 10 meters. The author feels that a WAS award is not too far away now that this antenna is in operation.

An Alternative

There are many ways you can duplicate this design using substitute materials. For example, electrical conduit with couplers between the sections should be satisfactory in place of the aluminum tubing. The entire structure could be made from 2 x 4 inch (51 x 102-mm) lumber. If that is done, the radiator could even be a 25-foot (7.62 m) piece of no. 10 wire, supported on the side of the wood with standoff insulators.

Instead of the mounting method shown in Fig. 3, the vertical pipe could probably be inserted into a 2-foot (.61-m) length of PVC tubing, then clamped to the mounting plate. This would eliminate the need for the two standoff insulators. Better still, four or five wraps of Teflon sheeting (10 mil or 0.25 mm thickness) could be placed over the bottom end of the vertical before clamping it in place on the mounting plate. Teflon can be purchased at most plastic-supply houses.

The author hopes this idea is useful to other Novices who are trying to keep the budget within reasonable limits. This writer likes the way the antenna is working. Others should have good luck with this antenna also. Oh, by the way, the ground radials are made from various scraps of wire. The size isn't important, and they can be insulated or bare. There is quite an assortment of wire types buried in the lawn! This material was originally presented in *QST* by Marian Anderson, WB1FSB.

The Cheapie GP

Keeping an ear on 10 and 15 meters? With the trend of rising solar flux, 15 meters "opens" nearly every day — 10 meters occasionally. Don't miss these openings. Build a Cheapie GP!

Looking for an antenna to cover the 10- and 15-meter bands that won't pinch your pocketbook? Should it contain easy to obtain items and be relatively simple to construct while using ordinary hand tools? Must it be physically small and not a neighborhood eyesore? If your answer to these questions is "yup," you've turned to the right page! Detailed here is a duo-band coaxial-cable-fed, trap groundplane antenna system.

A groundplane antenna consists of a vertical quarter-wavelength radiator and an artificial metallic ground system extending radially from its base. For good results the antenna should be mounted at least one-quarter wavelength above ground. This is approximately 12 feet (3.66 m) on 15 meters. At this height and higher, only four radials for each band are necessary to provide a good ground system. If this antenna was ground mounted, many more radials would be needed to reduce earth losses to an acceptable low level. The antenna has an omnidirectional horizontal or *H*-plane pattern which means radiation from the antenna is essentially the same in all horizontal directions as shown in Fig. 7A. In Fig. 7B the approximate vertical or *E*-plane pattern of the antenna is shown for the antenna mounted one-quarter wavelength above ground. As can be seen, maximum radiation occurs at the low angles above the horizontal plane of the antenna. The antenna has an overhead null so little energy is radiated at high angles. This does not detract from the usefulness of the antenna, since DX signals seldom arrive at high angles on these bands. Instead, maximum radiation is concentrated at the *lower angles* where it will be more effective. Conversely, a horizontal dipole mounted one-quarter wavelength or less above ground will have maximum radiation straight up or nearly so. Lower-angle radiation will not occur unless the dipole is raised to a height of one-half wavelength or more above ground. If it is not possible to mount your horizontal antenna a half wavelength above ground, the vertically polarized groundplane is perhaps the logical choice over a dipole. As a general rule, the higher the groundplane can be located above power lines, gutters, house wiring and the like, the better it will perform.

A Duo-Band System

For the antenna to perform properly on two bands, it must function as a *separate* groundplane vertical on each band. This requirement is met quite simply in the case of the radials since four radials are used for each band. The 10-meter radials are 8 feet, 5 inches (2.56 m) long and the 15-meter radials are 11 feet, 7 inches (3.53 m). When the antenna is operated in the 10-meter mode, the 15-meter radials have little effect on the system. Similarly, when the antenna is used on 15 meters, the 10-meter radials do not appreciably alter the operation of the antenna. The effect of the additional radials is to change slightly the feed point resistance and the resonant frequencies of the antenna.

The vertical member of the antenna must act as a quarter-wavelength radiator on both 10 and 15 meters. To accomplish this a trap is inserted in the 15-meter vertical section. Its approximate location is a

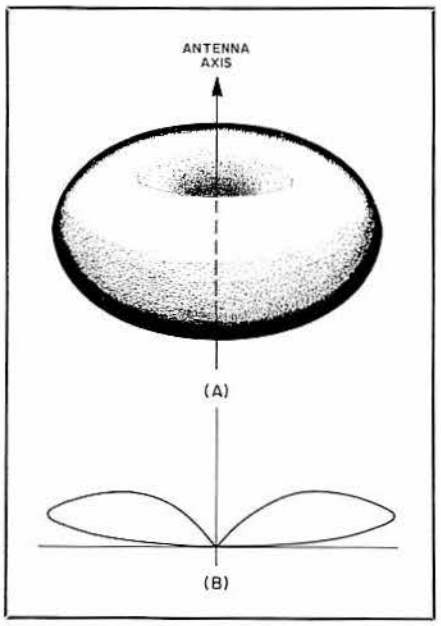

Fig. 7 — (A) Horizontal or H-plane pattern of the groundplane. (B) Approximate vertical or E-plane pattern of the antenna.

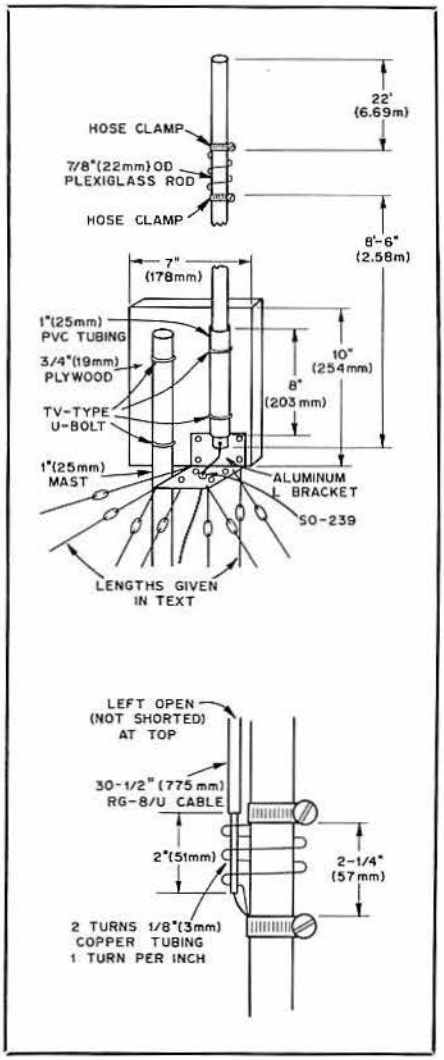

Fig. 8 — Constructional details of the duo-band antenna system.

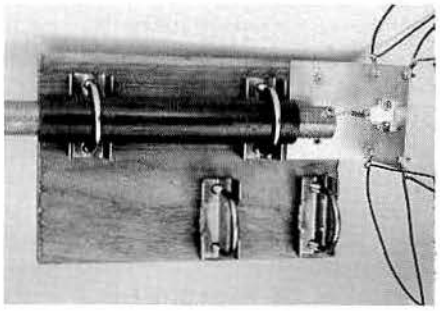

A photograph of the base assembly. The SO-239 coaxial connector and hood can be seen in the center of the aluminum L bracket. The U bolts are TV-type antenna hardware. The plywood should be coated with varnish or similar material.

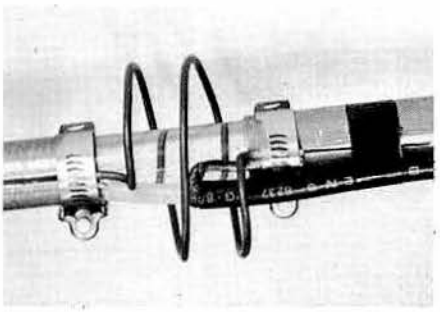

A close-up view of the trap. The leads from the coaxial-cable capacitor should be soldered directly to the pigtails of the coil. These connections should be coated with varnish after they have been secured under the hose clamps.

10-meter quarter wavelength above the base. The trap has a high impedance on 10 meters, thereby electrically divorcing the top section of the antenna when it is operated on that band. The length of the 10-meter section (section below the trap) is somewhat shorter than that of a simple 10-meter-only quarter-wavelength vertical. This is because the trap and top section of the duo-band system add top loading to the 10-meter portion of the antenna, reducing the length required for quarter-wavelength resonance. A coaxial-cable capacitor and a coil made from copper tubing form the trap which is resonant at approximately 28.150 MHz. On 15 meters the trap has a low impedance, effectively connecting together those portions of the antenna above and below the trap. The overall length of the 15-meter radiator is a bit shorter than a simple quarter-wavelength radiator would normally be for that band. This is because at 21 MHz the trap introduces inductance into the radiator — similar to the effects of a loading coil.

Construction

The vertical section of the antenna is mounted to a 3/4-inch (19-mm) thick piece of plywood board that measures 7 X 10 inches (178 mm X 254 mm). Several coats of exterior varnish or similar material will help protect the wood from inclement weather. Both the mast and the radiator are mounted to the piece of wood by means of TV U-bolt hardware. The vertical is electrically isolated from the wood with a piece of 1-inch (24-mm) diameter PVC tubing. A piece approximately 8 inches (203 mm) long is required, and it is of the schedule-80 variety. To prepare the tubing it must be slit along the entire length on one side. A hacksaw will work quite well. The PVC fits rather snugly on the aluminum tubing and will have to be "persuaded" on with the aid of a hammer. The mast is mounted directly to the wood with no insulation. An SO-239 coaxial connector and four solder lugs are mounted to an L-shaped bracket made from a piece of aluminum sheet. A short length of test probe wire, or inner conductor of RG-58/U cable, is soldered to the inner terminal of the connector. A UG-106/U connector hood is then slid over the wire and onto the coaxial connector. The hood and connector are bolted to the aluminum bracket. Two wood screws are used to secure the aluminum bracket to the plywood as shown in the drawing and photograph. The free end of the wire coming from the connector is soldered to a lug which is mounted to the bottom of the vertical radiator. Any space between the wire and where it passes through the hood is filled with GE silicone glue and seal or similar material to keep moisture out. The eight radials are soldered to the four lugs on the aluminum bracket. The two sections of the vertical member are separated by a piece of clear acrylic rod. Approximately 8 inches (203 mm) of 7/8-inch (22-mm) OD material is required. The aluminum tubing must be slit lengthwise for several inches so that the acrylic rod may be inserted. The two pieces of aluminum tubing are separated by 2-1/4 inches (57 mm).

The trap capacitor is made from RG-8/U coaxial cable and is 30.5 inches (775 mm) long. RG-8/U cable has 29.5 pF of capacitance per foot and RG-58/U has 28.5 pF per foot. RG-8/U cable is recommended over RG-58/U because of its higher breakdown-voltage characteristic. The braid should be pulled back 2-inches (51 mm) on one end of the cable, and the center conductor soldered to one end of the coil. Solder the braid to the other end of the coil. Compression-type hose clamps are placed over the capacitor/coil leads and put in position at the edges of the aluminum tubing. When tightened securely, the clamps serve a two-fold purpose — they keep the trap in contact with the vertical members and prevent the aluminum tubing from slipping off the acrylic rod. The coaxial-cable capacitor runs upward along the top section of the antenna. This is the side of the antenna to which the braid of the capacitor is connected. A cork or plastic cap should be placed in the very top of the antenna to keep moisture out.

Installation and Operation

The antenna may be mounted in position using a TV-type tripod, chimney, wall or vent mount. Alternatively, a telescoping mast or ordinary steel TV masting may be

used, in which case the radials may be used as guys for the structure.

Any length of 50-ohm cable may be used to feed the antenna. The SWR at resonance should be on the order of 1.2 to 1.5:1 on both bands. The SWR is not 1 because the feedpoint resistance is something other than 50 ohms — closer to 35 or 40 ohms. Nearby metallic objects may also have an effect on the impedance of the antenna. The antenna is resonant at approximately 21.150 MHz and 28.150 MHz.

Some amateurs place too much importance on obtaining a "no reflected power" reading on their SWR indicators. Most ham transmitters will load into lines which exhibit an SWR of up to 2:1, the exception being some of the new broadband, no-tuning transmitters. To demonstrate how little effect an SWR of 1.5 or 2:1 will have on the system, consider the following: If the antenna is fed with 100 feet (30.48 m) of RG-8/U cable and if the antenna is perfectly matched to the line (an SWR of 1), the power loss along the cable will be approximately 0.98 dB on 10 meters. If the SWR on the line is increased to 1.5:1, the additional loss on the line due to the higher SWR is less than 0.1 dB. If the SWR is increased to 2:1, the additional loss over that of the matched condition will be on the order of 0.2 dB. This amount of loss is insignificant, and for this reason a complicated matching network is not necessary. This material was originally presented in *QST* by Jay Rusgrove, W1VD.

A High-Performance, 20-, 40- and 80-Meter Vertical System

Urban dwellers with small lots take heart! Here are the details for building your own DX-effective three-band mini-vertical antenna. Cost-conscious amateurs will be happy with the low cost of this system.

In another article on vertical antennas,[1] we tried to point out some fundamental characteristics of ground-mounted verticals, namely: (1) a good image plane is necessary for efficient operation, (2) a vertical over a good image plane compares favorably with a dipole at an elevation of one-half to one wavelength, (3) a short vertical compromises little in the way of performance.

This paper describes a highly efficient, three-band vertical system for 20, 40 and 80 meters, using elements of the order of an eighth wavelength. The system consists of an 80-meter vertical in parallel with a 20/40-meter trap vertical. Actually, either the 80-meter or the 20/40-meter vertical can be constructed and used alone if one is not interested in triband operation. The input impedances of both antennas are 12-1/2 ohms and they use the same 4:1 matching transformer.[2] The antennas also use the same radial system consisting of 100 radials of no. 15 aluminum wire 50 feet (15.24 m) in length (a lesser number of radials can be used as is discussed later in the article). Because of expected lower sunspot activity and, hence. poorer propagation conditions on the higher bands, the 40- and 80-meter portions of this antenna system, in particular, should prove very effective in DX communication over the next few years.

The first part of this paper deals with the design and tune-up considerations of the 80-meter element; the second part with the 20/40-meter element and the way it is used with the 80-meter vertical forming an efficient triband system. This is followed by reports on performance. Reference is also made to other alternatives for a multiband vertical system.

80-Meter Vertical

The two considerations in designing the 80-meter element of this vertical system were: (1) a good bandwidth for a reasonable height (a height one person can handle); and (2) proper spacing between the 80 and 20/40 portions such that coupling is negligible and both can be used over the same radial system.

Prior to building the shortened vertical described in this article, two others were constructed and tested on the air. One was a 22-foot (6.71 m) vertical[3] which had a 65-kHz bandwidth. The other was a trap vertical[4] with only a 20-kHz bandwidth. Both of these antennas were used separately over the same image plane of 100 radials and were efficient radiators. Therefore, the main reason in going to a slightly longer antenna was simply *to obtain a broader bandwidth.* The eighth-wavelength vertical on 40 meters from the previous work[5] promised considerable improvement by adding only a few feet. The results are shown in Figs. 9 and 10. The total height turned out to be 29 feet (8.83 m). This resulted in a bandwidth of about 140 kHz, a little more than twice the bandwidth of the 22-footer (6.71 m).

The vertical, in Fig. 9, uses a 20-foot (6.10-m) section of thick-wall aluminum tubing. (It was used some years ago as a gin pole for erecting a beam on a 40-foot (12.2 m) tower.) An 8-foot (2.44 m) extension

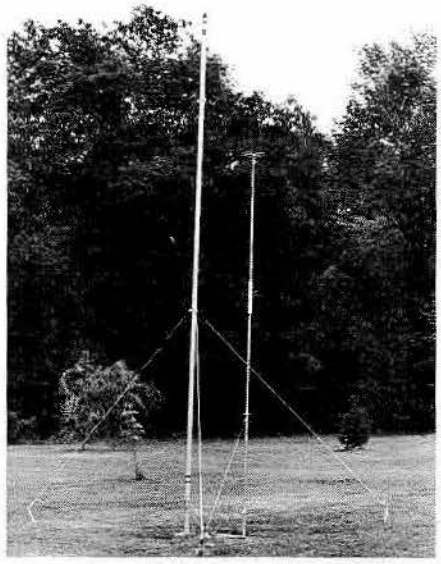

The triband vertical showing the polypropylene guys which provide an extra margin of support.

was constructed with 1-inch (25-mm) tubing bolted in place using spacers for centering. The insulator at the bottom is phenolic tubing with a canvas base.[6] It has a 1/2-inch (13-mm) thick wall, is 9 inches

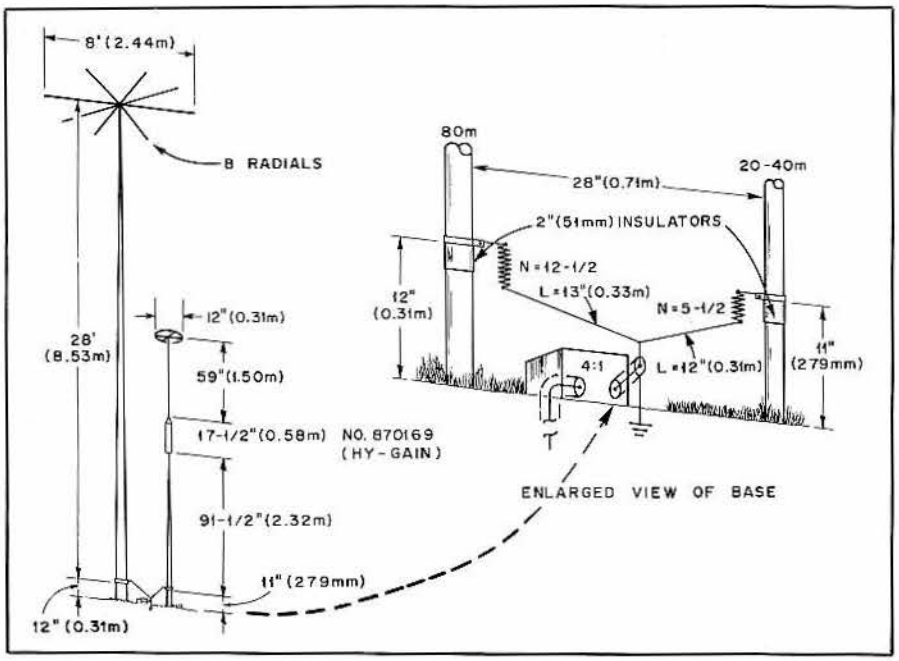

Fig. 9 — The 20-, 40- and 80-meter vertical antenna system. Tuning and construction details are given in the text.

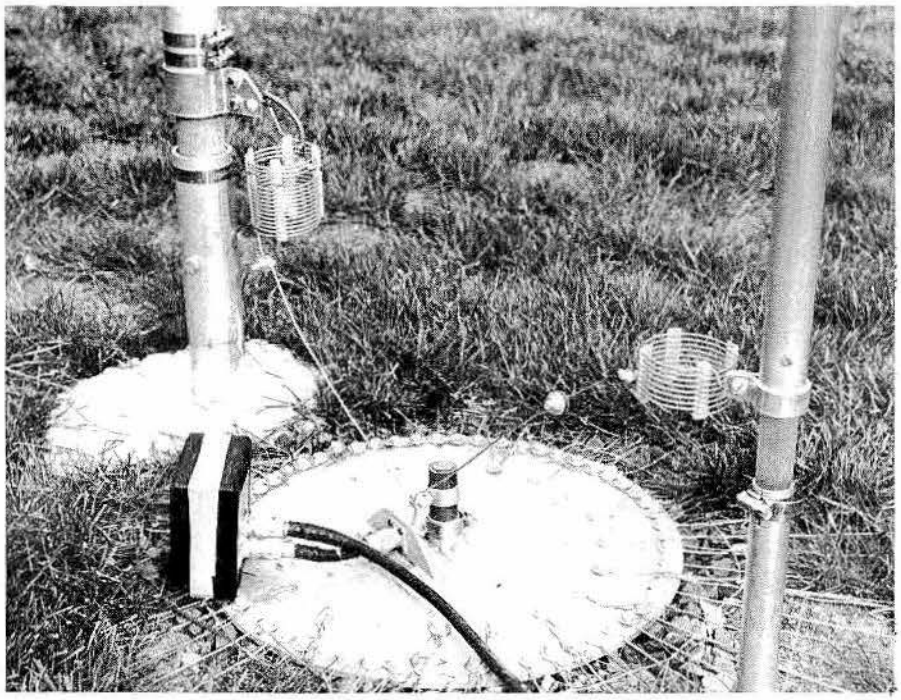

Close-up of the base of the triband vertical antenna.

(229 mm) long and has an ID of 1 inch (25-mm). The bottom aluminum tubing supporting the antenna is 3-1/2 feet (1.06 m) long with 2-1/2 feet (0.76 m) of it placed in cement. The diameter of the hole in the ground is about 1 foot (0.31 m). Even though this construction could probably be self-supporting, three simple polypropylene guys at about the 7-foot (2.13-m) level are used for extra margin of support. The radials at the top use 1/2-inch (13-mm) aluminum tubing.[7] The base loading consists of 12-1/2 turns of a B&W 3029 coil.[8] Actually, 14 turns are on the coil. A shorting stub, as shown in the close-up picture of the base of the two antennas, is used for adjustment. To place the minimum SWR near the low end of the phone band, where much of the DX is worked, 1-1/2 turns were shorted out. The final number of turns employed depends, to some extent, on the number of radials used in the image plane. A simple check is to set the shorting tap at some convenient point, like 12 or 13 turns, and plot the SWR. If the minimum value appears too high in frequency, then add about a half a turn of coil. This half turn chould change the position of the minimum SWR value by about 50 kHz. As can be seen in Fig. 10, the minimum value of SWR is practically 1:1 and occurs at 3.840 MHz. This also verifies the input impedance value of 12-1/2 ohms, as expected from the previous work on short verticals.

20/40-Meter Vertical

In extending the operation of a vertical system over other bands, many alternatives are available. A trap vertical with a 12-1/2-ohm input impedance can be connected in parallel with the 80-meter vertical. Alternatively, the trap vertical can be designed to present an impedance of 50 ohms and thus be connected to the input side of the 4:1 transformer.[9] If broadband operation is desired on only 80 and 40 meters, then one-eighth wavelength verticals on both bands can be used.[10]

For this work, a 20/40-meter trapped vertical having an input impedance of 12-1/2 ohms was used. It offered a rather simple mechanical form of parallel operation as is shown in Fig. 9 and the close-up picture. The bandwidth on 40 meters of 155 kHz appeared acceptable. This bandwidth can be extended by about 50 percent by using the 50-ohm design of a trap vertical.

In the first attempt of parallel operation, the 20/40-meter vertical was placed only 14 inches (355 mm) away from the 80-meter vertical. The coupling appeared excessive. The 80-meter vertical was detuned by approximately 50 kHz. The 20/40-meter vertical also required excessive base loading in order to present an acceptable input impedance. By doubling the spacing between the verticals to 28 inches (711 mm), the interaction between them became negligible. The final values of heights and loadings were practically the same as if the elements were operating alone.

The adjustment of the 20/40-meter vertical is somewhat more complicated than the 80-meter vertical. An impedance bridge, as described in the *ARRL Handbook,* is of considerable help. In this case, there are two degrees of freedom: (1) varying the number of turns at the base, and (2) adjusting the lengths of the vertical sections.

Basically, the tuning is as follows: The tap is set at about 5-1/2 turns and the 20-meter section adjusted to give an acceptable value of SWR, both in position in the band and in magnitude. If the impedance is too high, it can be lowered by increasing the number of turns and lowering the height of the 20-meter section for resonance. After this, the 40-meter portion is then tuned. A plot of the SWR vs. frequency can immediately give an indication of the necessary adjustment of the section above the 20-meter trap. If the minimum value appears too low in frequency, a shortening of the top section is required. In no case should large adjustments be made. A change of a few

Table 1

Some Results With Triband Vertical

Date	Station Contacted	W2FMI Signal Report	Freq.(MHz)	Input Power SSB (Peak)	Comments
3/13	K5LWL/YV6	59 + 10 dB	7	2 kW	very, very strong signal, only one signal stronger — he used a Yagi at 120 feet (36.58 m)
4/3	WB5HJY	59 + 40 dB	7	2 kW	superior to anything on band
4/4	ZF1SP	59 +	14	2 kW	very, very nice signal
4/4	WA4MUR/4	59 + 40 dB	14	2 kW	best signal on whole band
4/18	KV4HW	59 + 10 dB	7	2 kW	loudest on band
5/9	K6YIY	59	4	2 kW	K1GZL and I are only ones they hear
5/9	W9LZX	59 + 30 dB	4	2 kW	strongest (very consistent signal)
5/12	W2DU	59 +	4	2 kW	tremendous signal
5/17	VK5PB	56-7	4	2 kW	remarkably strong
5/17	W4JNY	59 + 20 dB	4	2 kW	outstanding, certainly one of best
5/22	VK5PB	59 + 10 dB	7	2 kW	really amazing
5/23	ZL3RJ	57-8	4	2 kW	one of the strongest he's heard for some time — pinned the S meter
5/27	WA2BQL	59 + 30 dB	4	200 W	very potent — Stronger than most locals — couldn't believe you were using 200 W

inches has considerable effect. If the input impedance on 40 meters appears too low, then the 20-meter section has to be lengthened. This requires that the whole procedure be repeated. In any case, the initial adjustment should be started on the highest band of the trap vertical.

Results

Short verticals have been used by the author during the past year with considerable success. Many DX contacts were made on 40 meters with antennas varying in length from 6 to 33 feet (1.83 to 10.05 m). Since an extensive ground system was used, very little difference in effectiveness was noticed between the antennas.[11] This even includes redesigned trap verticals. As was stated before, the objective of the present investigation was to design a three-band vertical system which not only yielded competitive antennas on the lower bands, but one that was capable of covering a considerable portion of 80 meters. As was seen, a separate one-eighth wavelength antenna connected in parallel with a trap vertical not only gave a bandwidth on 80 meters of 140 kHz where the SWR was less than 2:1, but was short enough to not require considerable help in erection.

During all this time of operation of short verticals on 40 meters, and as of this writing, including several months on 80 meters, very few signal reports were received which did not indicate one of the best signals on the band. Table 1 gives some of the reports and comments received. In only three specific cases on 40 meters have the short verticals been bested by other antenna systems. One is shown in Table 1 where K5LWL/YV6 reported a stronger stateside signal by an amateur using a Yagi at 120 feet (36.58 m). The other cases include a comparison with W2GO of Linden, NJ. On 40 meters, VK5PB reported 6 dB and VK2WC 10 dB in favor of W2GO's signals. He was using a two-element Yagi at 60 feet (18.28 m). The elements were 44-1/2 feet (13.56 m) in length and the boom, 20 feet (6.10 m). On 80 meters, only one other station received a stronger report on direct comparison. This was by W2HCW, when comparing my signals with VK5PB. The difference was 2 to 3 S units. His antenna was an 80-meter Yagi at 120 feet (36.58 m).

Invariably, most amateurs were surprised by the performance of these verticals. In many instances, questions were asked regarding the minimum number and length of radials required for efficient operation of ground-mounted verticals. As was noted in previous articles,[12] the answer depends to some extent on the conductivity of the soil at the respective locations. Poorer soils not only require more radials, but ones that are also considerably longer. Although more experimental work is required in this area, it appears that about 50 radials, 0.2 wavelength long, should generally give good operation. The loss in this case will be approximately 1 to 2 ohms. Doubling the number to 100 radials should reduce the loss to less than 1 ohm. It should be noted that even 1 to 2 ohms of loss are appreciable with these short antennas since their radiation resistances are only 12-1/2 ohms.

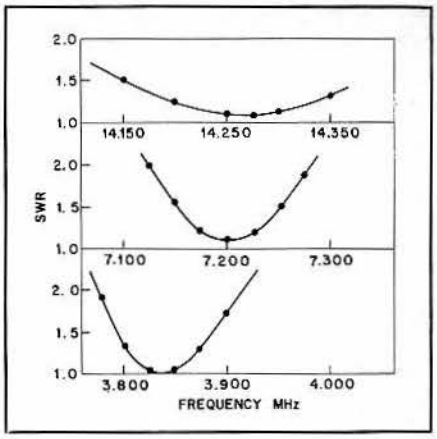

Fig. 10 — Standing wave ratio vs. frequency for the 20-, 40-, and 80-meter vertical antenna system.

Again, the author would like to acknowledge the help, encouragement, and interest shown by the many amateurs during our experimental studies on verticals. Very few antenna laboratories can boast of a greater number of willing and competent field stations. In particular, we would like to thank Al Jones, W2GO, for his considerable help in obtaining comparative reports in Australia and New Zealand. This material was originally presented in *QST* by J. Sevick, W2FMI.

References

[1]Sevick, "The W2FMI Ground-Mounted Short Vertical," *QST*, March 1973. Also appears elsewhere in this chapter.
[2]Sevick, "The W2FMI 20-Meter Vertical Beam," *QST*, June 1972.
[3]See footnote 1.
[4]Commercial unit.
[5]See footnote 1.
[6]Cadillac Plastic and Chemical Co., P. O. Box 810, Detroit, MI 48232
[7]Construction details on the top hat are also given in the reference in footnote 1.
[8]2-1/2-inch (64-mm) diameter, 6 tpi, no. 12 wire.
[9]The characterization and design of these trap verticals will be published later.
[10]See footnote 1 for details on the 40-meter vertical.
[11]See footnote 1.
[12]See footnote 1.

A Multiband Vertical Radiator

An efficient multiband radiator with no traps and no loading coils? Impossible; you can't build one without them and have it work! "Oh, yes, sure you can." I doubt it. "You wanna bet? Come on, I'll show you."

What would you say if the author told you this vertical antenna system was 89-percent efficient but had only six radials? (Efficiency is defined as the ratio of radiated power to total power delivered to the antenna.) No, it's no joke. The vertical antenna that is described here is designed to work against ground systems that are less than optimum.

By increasing the radiation resistance by about 200 ohms, we have been able to improve the effectiveness substantially of a vertical radiator with a poor ground system. The value of 200 ohms was selected as the feed-point radiation resistance because a toroid autotransformer with a 1:4 ratio will match 50-ohm coax line very nicely. An added bonus when using such an arrangement is the Faraday screen effect that reduces noise pickup from being transferred to the feed line. The noise reduction over a conventional network was determined to be about 6 dB. See Figs. 11 and 12.

The system is based on a 135-degree antenna height. The radiation resistance at the base of the structure is about 200 ohms,[1] ideal for our matching system. And at the same time the radiation pattern retains a reasonable form. The 10-meter groundplane on top of the structure acts as a top hat. On 7 MHz the phase loops cause the antenna to look like a fat radiator and between the two, top hat and phase loops, the electrical height of the antenna is raised to within the tuning range of the toriodal loading network. On 14 and 21 MHz the phase loops keep the instantaneous current on the structure in phase and eliminate high-angle lobes. When the system is switched to operate on 28 MHz, the groundplane at the top of the structure is fed through the coax line running up the lower portion of the structure.

Construction and Tuning

The photographs and the drawings show how the antenna is constructed. The system was designed so that "storebought" items could be used for the assembly, rather than fabrication of the antenna components. A list of required parts is given in Table 2.

The tuning adjustments of the system are very noncritical. Tuning can be done with an SWR indicator. The best sequence is to start with the highest frequency and work down. The 28-MHz groundplane used as a top hat can be adjusted before it is attached to the rest of the antenna. The Radio Shack 11-meter groundplane that we used comes with a hairpin or "beta" match. With a short length of 50-ohm coax for the feed line, the groundplane should be adjusted for the lowest SWR in the 10-meter band. After the groundplane has been adjusted and attached to the top of the antenna, the entire system can be raised into position for final tune-up on the lower frequencies.

At this point the SWR indicator should be inserted in the 50-ohm feed line from the transmitter, as close to the antenna matching network at the base of the structure as possible. All that remains is the adjustment of the 200-pF capacitor. The

[1] *The ARRL Antenna Book*, 13th Ed. See Fig. 2-74 and the accompanying text on page 60.

This multiband radiator, just over 36 feet (10.97 m) tall, operates on five amateur bands, 80 through 10 meters.

Table 2

Parts Required for the Multiband Vertical Radiator

3 —10-ft (3.05 m) lengths TV mast; Radio Shack 15-5066.
1 —27-MHz ground plane; Radio Shack 21-901.
3 —100-ft (30.48 m) rolls of 22-gauge hook-up wire; Radio Shack 278-1295.
1 —Amidon Balun kit (see Fig. 12).
1 —Aluminum box for tuner.
1 —28-ft (8.53 m) length of RG-8/U coax line.
4 —8-ft (2.44 m) sections of aluminum tubing (see Fig. 11).
1 —Base insulator; soft drink or (?) bottle.
1 —200-pF capacitor, air variable, surplus.
Misc. — See text and figures.

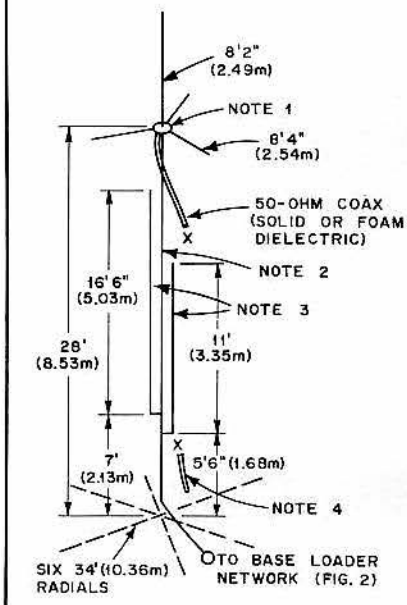

Notes

1) Radio Shack 27-MHz groundplane cut to dimensions shown. Radials are at right angle and connected to mast.
2) Three heavy-duty 10-ft (3.05-m) sections TV mast.
3) Phase loops, sections of telescoping 5/8-(16-mm) and 1/2-inch (13-mm) aluminum tubing spaced 4-1/2 inches (114 mm) from mast. See text.
4) 50-ohm coax such as RG-8/U. At upper end connect center conductor to top element, braid to ground-plane elements. Connect lower end to base loader network (Fig 12).

Fig. 11 — Details of the multiband radiating structure. See Table 2 for parts list. It is very important that a uniform spacing be maintained for the phasing loops, which may be supported at the bottom by shelf brackets. To support the upper portions of these loops, the author used homemade wooden spacers, 1/2 X 1 inch (13 X 25 mm), which were soaked in paraffin and held in place by screws passing through the loop tubing and the main radiator tubing. Homemade Plexiglas spacers may also be used.

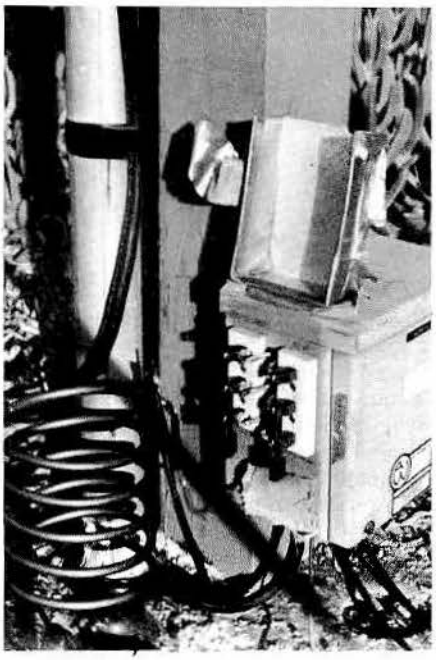

The base of the multiband antenna system. The 200-pF capacitor of the matching network is mounted inside a weatherproofed box, and the 80-meter loading coil is mounted outside. The porcelain knife switches for bandswitching are mounted outside the aluminum box under a homemade hinged cover. The structure itself is supported by a 10-foot (3.05-m) wooden post set 2 feet (0.61 m) in the ground (concrete optional).

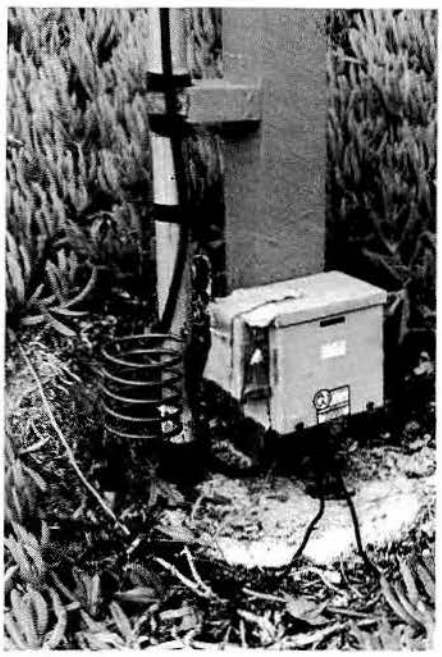

Although heavy-duty insulators were used to support the radiating mast from the post as shown here, experience has indicated that insulators are not required. The author suggests that a modified pair of chimney-mount brackets be fastened to the post with lag screws. A short length of PVC pipe or Mylar film may be placed around the mast where it is supported, if you feel it necessary to have the mast insulated from the post.

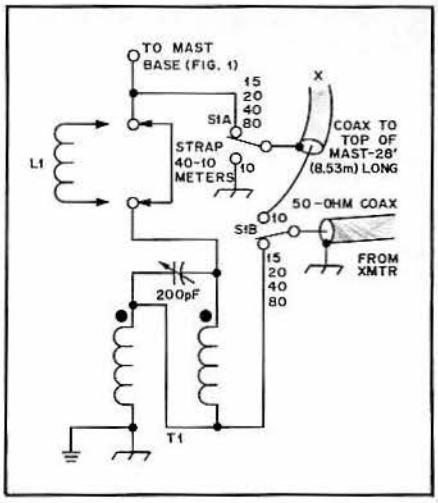

Fig. 12 — Schematic diagram of the base loading network. The connection to the mast base should be made with a short wire, no longer than one foot (0.31-m). The 200-pF capacitor should have a minimum of 1/16-inch (1.6-mm) plate spacing.

L1 — 80-meter loading coil, 0.67 μH; 4 turns of aluminum grounding wire, 3-inch (76-mm) diameter, 1 turn per inch, air core.

S1 — Dpdt, heavy-duty type. Two porcelain knife switches from the local hardware store will suffice, one for each pole.

T1 — Bifilar-wound toroidal autotransformer, 1:4 ratio; 11 turns spaced around 2-inch (51-mm) ID toroidal core: Amidon Balun Kit or equiv. (Amidon Associated, 12033 Otsego St., North Hollywood, CA 91607).

tuning will be different for each band. On 21 MHz the capacitor will be only about five percent meshed, on 14 MHz about half, and on 7 MHz nearly fully meshed. The capacitor on 3.5 MHz, along with the 3.5-MHz coil, can be adjusted to whatever section of the band you wish to work. The bandwidth will be about 400 kHz with less than 2:1 VSWR. To switch bands, all that is required is to set the double-pole, double-throw switch for the proper band and adjust the 200-pF variable capacitor.

All of the antennas constructed so far were cut to the dimensions shown in Fig. 11 and have not required any change. They have been installed in a wide variety of locations and the system design has been broad enough in tolerance to handle all of them. The writer's antenna has been in operation since 1972 and has performed exceptionally well. In the first year on the air, I managed to work 100 countries with less than 250 watts. In several experiments with just the six radials, we made comparative tests between this design and a properly matched quarter-wave vertical over the same radial system. The radiation efficiency was about 60 percent for the quarter wave vs. 89 percent for the "little monster." In the far field the signal improvement was better than 6 dB.

Now there are eight of these antennas on the air, and several more are under construction. All of the hams who have built the antenna have had comparable results to mine.

There are three hams to whom this author would like to give credit. They helped in testing and measuring the system and encouraged me to get it down on paper. They are Bob Crawford, WA6RYZ; Frank Scott, W6WOP and John Campbell, W6NVV. This material was presented originally in *QST* by A. E. Collins, K6VV.

References

The ARRL Antenna Book, ARRL, Newington, CT.
King, *The Theory of Linear Antennas*, Harvard University Press, Cambridge, MA.
Terman, *Radio Engineering*, McGraw-Hill Book Co., New York, NY.

A Triband Vertical Antenna

Keep your vertical antenna simple. Operate three bands without using traps!

The most common vertical is the quarter-wave type, which radiates well and is easily matched to a coax feed line, but has the weakness that it is a single-band antenna. Methods of adapting a vertical for multiband operation include the use of traps, loading coils and elements of different length fed in parallel. The antenna system to be described here was arrived at by treating separately the problems of designing the antenna and of designing the matching system.

The antenna design was easy. A height of 22 feet (6.71 m) is optimum for a vertical antenna for 10, 15 and 20, and several commercial verticals are of this height. It corresponds to about five-eighths wavelength on 10 meters. Greater height results in reduced low-angle radiation on 10, besides being more difficult to erect. A 22-foot (6.71-m) vertical gives better low-angle radiation than a quarter-wave vertical on all three bands and is especially good on 10 meters.

The antenna consists of 22 feet (6.71 m) of 300-ohm twin-lead, with both conductors tied together, held about an inch from a bamboo pole by means of small blocks of insulating material spaced every two feet or so along the pole and held in place with plastic electrical tape. The pole is guyed with nylon fishing line, and the antenna is operated against a groundplane of four quarter-wave radials for each band. The use of twin-lead rather than a single wire simulates a thicker conductor and reduces the impedance, making the antenna easier to match. Even so, the antenna impedances are vastly different on the three bands. The presumed values of impedance are listed in Table 3. These values are taken from published data[1] and assume a cylindrical antenna of specific radius operated against a perfect ground. The antenna is not cylindrical, and it operates against a wire groundplane, so that the impedances listed must be considered approximate only. The results obtained indicate that they are at least fairly close.

If the three antenna matching impedances are normalized to 300 ohms and plotted on a Smith chart, it can be seen that it is possible to obtain a reasonably good match to a coax line on any of the three bands by using an appropriate length of 300-ohm line as a matching section connected between the antenna and the coax line. What is not possible is to find a single length of line that will provide suitable matching on all three bands.

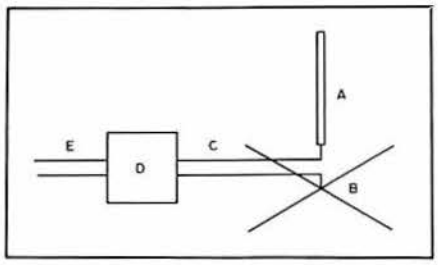

Fig. 13 — The triband vertical antenna system.

A — Vertical radiator, 22 ft (6.71 m) of 300-ohm twin-lead with conductors in parallel.
B — Four radials, each consisting of 1/4λ of wire, for each band (12 wires in all).
C — Matching section, 27.8 ft (8.47 m) of 300-ohm twin-lead.
D — Reactance unit; see Fig. 14.
E — 75-ohm coax to transmitter, any length.

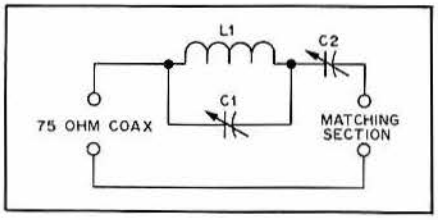

Fig. 14 — Reactance-unit circuit.

L1 — 0.86 μH; 7 turns no. 16 (or heavier), 1-inch (25-mm) dia, 1-inch (25-mm) winding length.
C1 — 30-pF air trimmer set to 23.1 pF.
C2 — 100-pF air trimmer set to 41.7 pF.

It turns out, however, that a 27.8-foot (8.47 m) section of 300-ohm line having the 0.82 velocity factor which is usual for twin-lead has interesting characteristics. Such a section of line, connected to an antenna having the impedances listed in Table 3, has the input impedances listed in Table 4. This combination of antenna and matching section is shown in Fig. 13.

It will be noted, first of all, that this combination may be used as it stands on 15 meters and fed with any usual coax. What is even more interesting, however, is that the input resistance is near 75 ohms on all three bands, though on 10 and 20 there is also considerable reactance. If a reactance unit could be made which had just the correct value of reactance to cancel out the input reactance of the matching section on all three bands, the unit could be connected in series with the matching-section input and the system fed with 75-ohm coax on all three bands.

Reactance Units

Can such a unit be made? Certainly! It's not hard at all. It consists of a simple seven-turn coil and two trimmer capacitors and is shown in Fig. 14. The trimmers are most easily adjusted with the aid of a grid-dip meter before the reactance unit is installed. C1 should be set so that L1C1 resonates at 35.85 MHz, and C2 can be subsequently adjusted by temporarily connecting it in parallel with L1C1 and varying it until the combination resonates at 21.37 MHz.

With the reactance unit adjusted as described, the antenna when first assembled showed SWRs of 2.1, 1.4, and 1.5 on 10, 15, and 20 meters respectively. Connecting the unit into the feed system apparently increased its shunt capacitance somewhat, for a small reduction in the value of C1 changed the SWR readings to 1.3, 1.5, and 1.4. These values could probably have been improved still more by further adjustment of C1 and C2, but it was not considered worth the trouble. If it is undertaken it should be borne in mind that the adjustments interact, but that C1 has its greatest effect on 10 meters and C2 on 20 meters. In any case it is not possible to obtain a perfect 1:1 match with this antenna system.

An SWR of 2, however, which can easily be bettered on all three bands, is within the loading capability of almost any transmitter and causes an *additional* loss over a perfectly matched line of less than half a dB even when the transmission line is very long. Since such a change in signal strength is undetectable, an SWR of 2 is in practice as

Table 3

Approximate impedances at base of 22-foot (6.71-m) ground-plane vertical antenna

Frequency	*Resistance*	*Reactance*
14.250 MHz	100 ohms	+200 ohms
21.375 MHz	1200 ohms	—500 ohms
28.500 MHz	60 ohms	—220 ohms

Table 4

Impedances at input end of 27.8-foot (8.47-m) matching section of 300-ohm twin-lead terminated by the impedances listed in Table 3.

Frequency	*Resistance*	*Reactance*
14.250 MHz	93 ohms	+177 ohms
21.375 MHz	63 ohms	0 ohms
28.500 MHz	75 ohms	—282 ohms

[1]Jordan, E. C., *Electromagnetic Waves, and Radiating Systems*, Figs. 13-12 and -13, New York: Prentice-Hall, Inc., 1950, pp. 482-3.

good as an SWR of 1, as far as losses are concerned.

A Few Notes

A few observations are in order. The matching section has a fairly high SWR (between 4:1 and 8:1), and it should be spaced well clear of metal objects and should not have sharp bends. TV standoffs are useful here. It is important that the same side of the matching section be connected to the coax shield and to the groundplane. If such a thing were available, 300-ohm coax would probably be preferred for the matching section, but for medium power (180 watts PEP) TV-type twin-lead for the matching section and receiving-type trimmers in the reactance unit have proved satisfactory. The parallel circuit L1C1 does not operate at its resonant frequency, and thus high circulating currents are not encountered. High power might necessitate heavier components. The reactance unit needs protection from the weather and can be built into a small plastic box and sealed with plastic electrical tape.

Although the antenna is matched at three widely separated frequencies, it is not matched at intermediate frequencies and is thus not a broad-band antenna in the usual sense. Nevertheless, it is broad enough for normal ham use. The SWR remains below 2:1 over the entire 15- and 20-meter bands, and also between 28.3 and 29.4 MHz on 10.

All SWRs mentioned in this article have been measured at the transmitter and are thus probably a little optimistic. Transmission-line losses are not known, but the line is not long (about 40 ft. [12.19 m]), and it is doubtful that the SWRs at the reactance unit are much higher than those measured at the transmitter.

This antenna is no match for a quad or a Yagi, but it has provided numerous transatlantic QSOs on all three bands. Because of its effectiveness, convenience, and the cheapness and availability of everything used in its construction, it should appeal to many hams. This material was originally presented in *QST* by Frank A. Regier, OD5CG.

A Multiband Groundplane Vertical Antenna with Tuned Feeders

Who says tuned feeders are used only with horizontal wire antennas? Go multiband with a simple vertical radiator by using a tuned-feeder system — and do it with ease!

For several years, the author has experimented with several versions of this antenna and has found them to be most satisfactory. The antenna shown in Fig. 15 provides not only outstanding performance on 10, 15 and 20 meters, but performance on 40 and 80 meters equivalent to most mobile-antenna installations. Full efficiency on these latter bands can be realized by making the vertical and radial portions proportionately longer.

The antenna system consists of the radiating element, groundplane radials, an open-wire feeder of any convenient length, a Transmatch capable of either series or parallel tuning, and an antenna SWR bridge. This combination is shown in Fig. 16.

Antenna and Radial Lengths

The author preferred to cut the antenna for resonance on one particular ham band (20 meters), but it is not necessary that the antenna be resonant on any band. Efficiency will suffer, of course, on bands where the length is significantly shorter than one-quarter wavelength. Whatever the length chosen for the antenna, the radials should be of about the same length.

Construction

Constructional details are shown in the sketch of Fig. 15. In the event the specified aluminum tubing is not available, thin-walled galvanized electrical conduit, aluminum conduit, or copper pipe may be used.

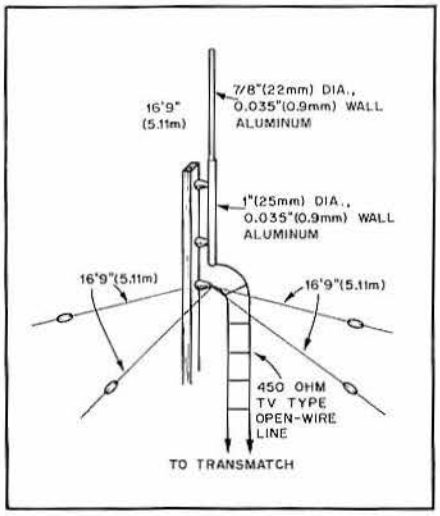

Fig. 15 — Sketch of W4VON's simple multiband antenna.

It is recommended that the vertical element not be supported by drilling holes through the tubing, as this will substantially weaken the structure. An alternative mounting arrangement is shown in Fig. 17. The insulators are porcelain standoff types with a lag-screw insert. They will be found at electrical supply houses (also at Sears), and are sometimes referred to as "saddle" type insulators. The hose clamps are stainless-steel gear type.

Adjustment

Operation of the antenna is simple. The Transmatch (a suitable one, including SWR bridge, is described in the ARRL *Handbooks)* and SWR bridge are connected, and the tuning network adjusted for

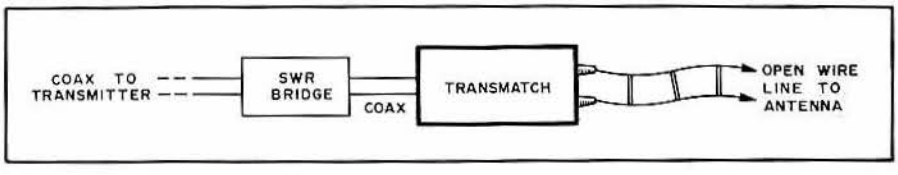

Fig. 16 — Recommended setup for coupling antenna line to low-impedance transmitter output.

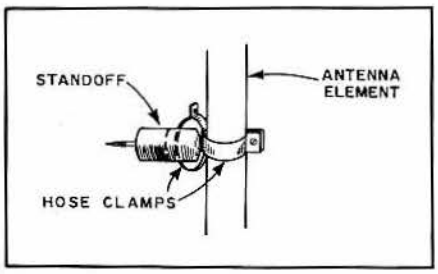

Fig. 17 — Suggested method of mounting radiator element without drilling holes in aluminum tubing.

maximum forward and minimum reflected power. Initially, it will be necessary to determine experimentally whether series or parallel tuning is required for the particular combination of band, feeder length, and antenna length selected.

The tuned-line-fed groundplane vertical antenna gives excellent performance, can be easily constructed in just a few hours even by a beginner, requires a minimum of installation space and costs less than $5, excluding the Transmatch and SWR bridge. The tuned circuit of the Transmatch provides excellent discrimination against harmonic output from the transmitter. Ease of construction and portability make this antenna an ideal one for Field Day use.

In case one wonders about the mismatch between the line and the antenna, the secret is in the use of open-wire line. The loss in such a line with an SWR of 25:1, at 10 meters, is less than the loss in RG-58/U when the latter is matched. This material was originally presented in *QST* by Arthur S. Gillespie, Jr., K4TP.

A Helically Wound Vertical Antenna for the 75-Meter Band

"Around and around she goes, and where she comes out — nobody knows." True, perhaps, with a wheel of fortune, but with a helically wound vertical the rf comes out effectively for DX and local work!

In order to have a full-size vertical antenna for the 75-meter band, the antenna would have to be around 65 feet (19.81 m) tall. That, alone, would require guying, or some other means of support which would result in a structure with no aesthetic appeal to any nonhams (who comprise almost 100 percent of the author's neighborhood). By using a helical configuration, the overall antenna height is reduced, thus eliminating the need for guying. With the helically wound antenna, more equal current and voltage distribution is accomplished (as compared with a lumped impedance from a loading coil). As a result, a better radiation pattern is produced. With this system very little reactance has to be cancelled out, eliminating the need for an overly large "top hat."[1] This antenna will easily take the full legal power limit.

Construction details for the antenna are shown in Fig. 19. The following is a list of parts used in constructing the antenna system.

1 — 20-ft (6.10-m) section of 4-inch (102-mm) OD plastic pipe (obtained at a local plumber)

130 ft. (39.62 m) no. 12 plastic-insulated

[1][Editor's Note: Some form of metal top hat should be connected to the last turn of the driven element at the high-impedance end of the radiator. Extremely high levels of rf voltage can develop at the end of the helix, sometimes causing the tip of the antenna to burn. The top hat tends to lower the Q of the antenna, thus reducing the voltage level at the far end. An aluminum pie tin mounted on a ceramic cone insulator works well in this application.]

The dark pole to the immediate left of the tower is the WAØWHE helically wound vertical antenna.

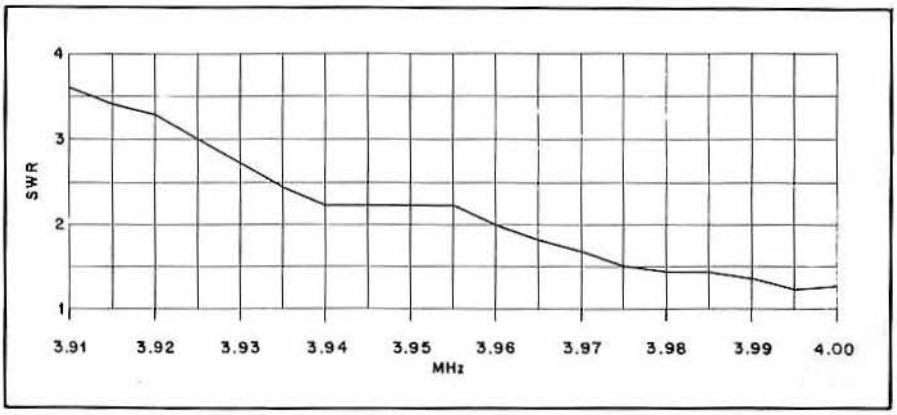

Fig. 18 — Measured SWR of the vertical antenna.

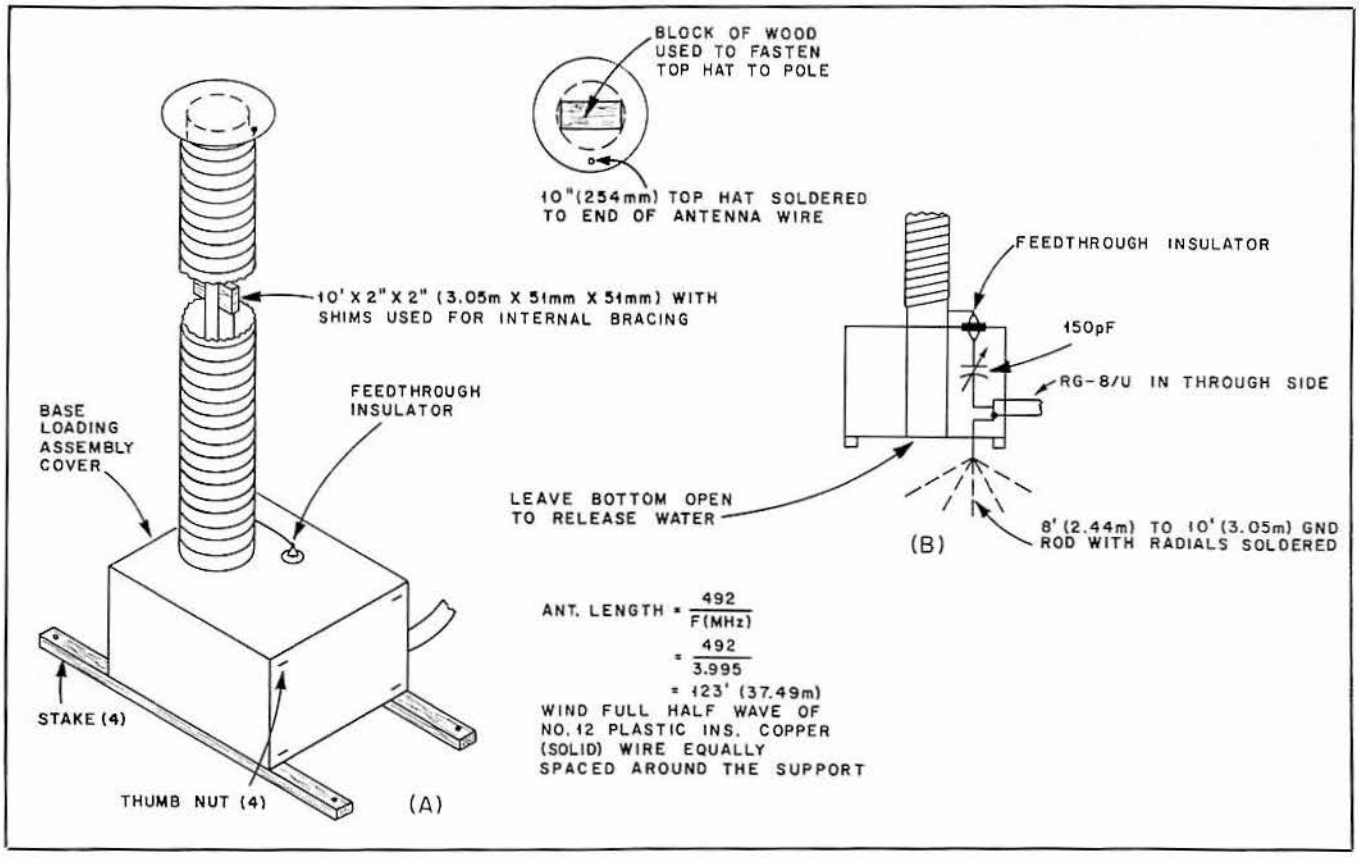

Fig. 19 — Construction details of the helically wound antenna.

solid copper wire (allow a little extra, about 2 ft. [0.61 m])

1 — 10-in. (254-mm) disk of sheet metal (top hat; stop at a sheet metal or furnace repairman — I got this free)

260 ft. (79.25 m) no. 14 solid bare copper wire (I used only four radials in this system; use as many as you have room or money for)

20 sq. ft. (1.86 sq. m) of marine plywood for base

2 — 2 × 2 10-ft. (3.05 m) sections, for internal bracing

1 — 8-ft (2.44-m) copper ground rod (for radial junction)

The cost can be reduced considerably if all materials are readily located or already owned.

Fig. 18 shows the results of SWR measurements. The SWR indicator used to make the measurements was a Midland model. The antenna was adjusted for minimum SWR at resonant frequency with the tuning capacitor at the base. The frequency for this antenna is 3995 kHz with 123 feet (37.49 m) of wire wound on the support and one 8-ft. (2.44-m) ground rod and four 65-ft. (19.81-m) radials. There are numerous configurations possible with this system including a broadcasting favorite such as phasing two or more structures. I forgot to mention . . . give the entire structure one or two coats of marine varnish to seal the turns. This material was originally presented in *QST* by Gary L. Ellingson, WAØWHE.

The Ground-Image Vertical Antenna

The name of the game with vertical antennas is the "ground system." Not just any hastily contrived radial ground will do the job right. Read these details for building an effective ground that provides positive results.

Even though a beam antenna supported at the modest height of 40 feet (12.19 m) is a compromise (a 20-meter beam should be higher to be really effective), it still can be an obstacle to good neighborly relations, at least if your neighbors don't appreciate the ecological beauty of such an installation. Moreover, even that modest sort of an installation presents quite a number of engineering problems.

This report presents the results of the first phase of an investigation to find a less conspicuous but equally effective antenna for use at a new location. The author hopes it will provide suggestions for those faced with a similar problem. At the least, it may be of some value to those with a general interest in the subject of antennas.

This first part of this section deals briefly with theoretical considerations, the second with experimental results on quarter-wavelength and five-eighths-wavelength verticals, and the third on the test equipment. It should be pointed out at the outset that the information presented here is the work of a hobby and as such cannot be exhaustive. It is hoped that others will repeat some of the experiments, extend the work, and report the effect in practice of a groundplane system above 3 MHz. To my knowledge such practical data have not been reported.

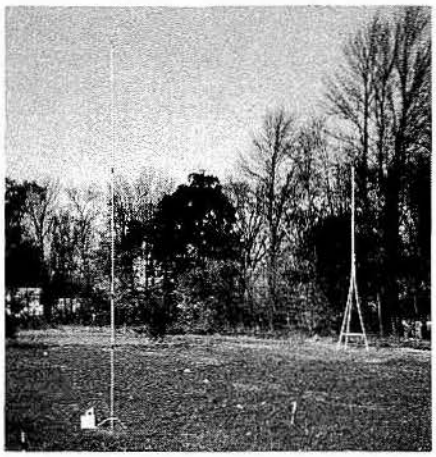

The 20-meter vertical antenna in the foreground, and the 26-foot (7.93-m) test tower.

The base of the vertical element of the antenna and the impedance bridge. Forty radials, in bundles of five are fastened to the aluminum base plate and are tied down with a ring made from copper tubing.

Theoretical Considerations

A beam antenna possesses the advantage of gain and directivity. Nevertheless, its DX capability is determined primarily by its vertical radiation pattern. A large portion of the radiated energy should be directed between 5 and 25 degrees from the horizon.[1,2] Horizontally polarized antennas yield lower angles of radiation with increase in height above the ground. This is a result of the interference pattern created by reradiation from the earth's surface. Since the earth is a somewhat conducting medium, the electric field tangential to the surface must be approximately zero. This "boundary" condition is brought about by the induced surface currents which create an electric field of opposite phase. This field then combines constructively and destructively with the initial radiation from the antenna. A model for this condition is an image antenna of opposite phase below the earth's surface as a depth equivalent to the height above the surface.[3] In order to get a lobe below 15 degrees, the antenna height must exceed a wavelength. This is greater than 60 feet (18.29 m) on 20 meters.

On the other hand, a vertical antenna, in the ideal case, possesses an image which is in phase to produce a lobe tangential to the earth's surface. Only when the antenna length is increased to a wavelength, or multiple thereof, does the tangential lobe disappear. This is true whether the antenna is on the ground or suspended in space. Therefore, a vertical beam, i.e., an array of vertical antennas coupled together with an appropriate feed system, on the surface of the earth, seemed to be the logical choice for the new installation since it would appear to meet the following objectives: The system should

1) Exhibit a minimum profile.
2) Be easy to install and tune.
3) Offer a low angle of radiation.
4) Not require a large outlay of money.

The author proceeded, therefore, to construct an array with four vertical elements. When the tests were begun, it immediately became apparent that the simple procedures the writer was using were inadequate to cope with such a complex system. The author had to start anew to develop a test procedure and to build some suitable test equipment. The logical step was to backtrack to a single vertical antenna and use it as a standard on which to develop some basic test standards. As discussed subsequently, the writer found that relatively simple equipment, e.g., a simple impedance bridge, a field-strength meter, and a test oscillator, gave this author all of the data about the system that he needed.

It is important to note that a true ground-image antenna differs substantially from a ground-plane antenna system which relies merely on a few $\lambda/4$ radials above the ground. A true ground-image system results when a sufficient number of radials are used and an image of only the vertical section is sufficient to describe it. Considerable information[4,5] is available on ground-image systems for verticals operating below 3 MHz. The results have shown that some

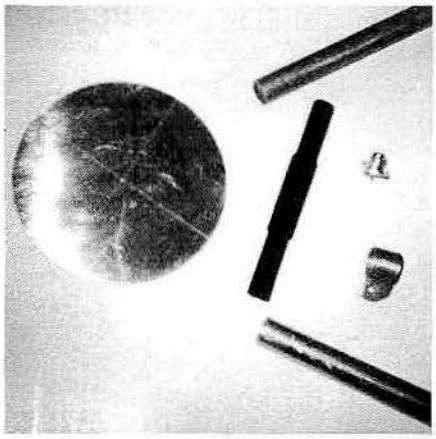

Base hardware for the antennas being tested. The insulator was made from 1-inch (25-mm) maple dowel, turned down to accept the 7/8-inch (22-mm) inside diameter of the ground and antenna tubing.

Table 5

Comparison of responses of 1/4-wavelength and 5/8-wavelength vertical antennas at low radiation angles. Data were taken by field-strength meter mounted on a wooden tower at a distance of 7.5 wavelengths at 14.25 MHz. Field strength (E) is normalized to maximum value obtained with 5/8-wavelength case.

θ	$E(\lambda/4)$	$E(5/8\lambda)$	GAIN OF 5/8-λ ANTENNA
0.1°	0	0.58	∞
0.4°	0	0.62	∞
0.75°	0.62	0.80	3.4 dB
1.1°	0.69	1.0	3.2 dB
1.5°	0.62	0.92	3.4 dB
2.25°	0.48	0.80	4.3 dB
3°	0.41	0.69	4.5 dB

The triband trap vertical antenna, which has an overall height of only 12.5 feet (3.81 m). With the system of 40 radials, performance of this antenna on 20 meters was about the same as that of the 1/4 and 5/8-wavelength vertical elements.

100 radials of $\lambda/2$ in length, buried just below the surface, provide an adequate ground system. At higher frequencies, the dielectric effect of the earth becomes important, resulting in severe discrimination of radiation or reception at very low angles.[6,7] At low angles, the waves not only suffer by absorption, but also by a change in phase which results in destructive interference. Since little specific information was

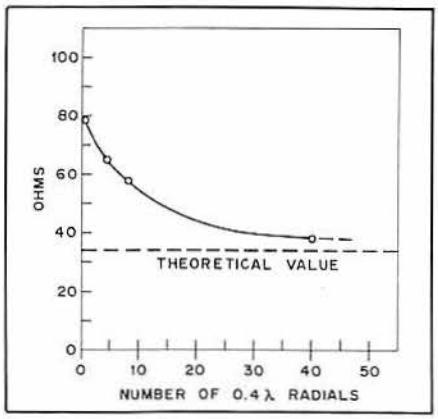

Fig. 20 — The input impedance of a 20-meter quarter-wave vertical antenna as a function of the number of radials 0.4-wavelength long. The four and eight radials consisted of bundles of five wires of no. 18 guage. The 40-radial point was obtained by fanning out the eight bundles.

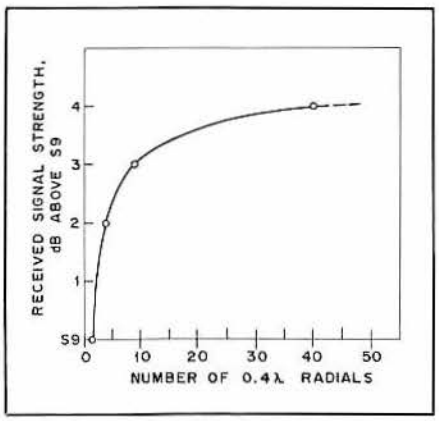

Fig. 21 — The improvement of low-angle radiation of a quarter-wavelength vertical antenna on 20 meters as a function of the number of added radials. A test oscillator was mounted on a wooden tower four wavelengths away at an elevation angle of six degrees from the base of the vertical.

available at higher frequencies, the objective of the present work was to measure the input impedance and vertical radiation pattern at low angles of a vertical antenna as a function of the number of radials, in order to determine the feasibility of a vertical-array system as a competitor to beams at high elevation. The results of the tests were most gratifying. The author found that many of the "rules of thumb" which have developed and have been perpetuated to the point where they are practically taken for granted were more myth than truth.

Experimental Results

The classical paper on radial systems, which reports experimental results at 1 and 3 MHz, indicates that a large number of radials 0.4λ long should be used.[8] This appeared to be a good starting point for a 20-meter vertical. Accordingly, to check the number of radials needed, this author used eight bundles of wires, each 25 feet (7.62 m) long, and each made up of five no. 18 copper wires. Each bundle was bolted to a

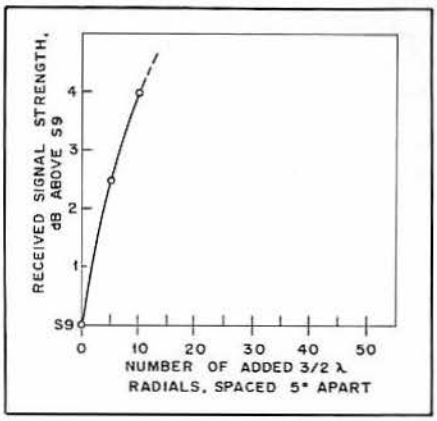

Fig. 22 — The result of interlacing 3/2-wavelength radials in a particular direction. Data were obtained by using a test oscillator on a wooden tower eight wavelengths away, at an elevation angle of 3 degrees from the base of the vertical. The results indicate the advantage of longer wires and the possibility of directional properties of a nonsymmetrical radial system.

5 × 1/4-inch (127 × 6-mm) aluminum plate as shown in the photograph. The writer was then able to use each bundle as a radial, measure the input impedance of the system, and then separate the bundles, wire by wire, to increase the number of radials in the system.

Fig. 20 shows the input impedance as a function of the number of radials used. Measurements were made with a simple impedance bridge. (Its construction is discussed later.) The antenna was resonated before each measurement was made, and the difference between the 40-radial system and the 8-radial system resulted only by fanning out the bundles of wires. This technique points out another important feature of ground systems and refutes one of the old myths: since the current carried by the radial system is equally divided among n radial elements, each radial is required to carry only 1/n of the total current. This means that relatively small diameter wire is perfectly adequate.

Moreover, it was found that at the higher frequencies it is best to keep the radials near the surface of the ground. Radials buried more than a few feet become less effective! Thus, you should not rely on the old admonition that radials should be 6 feet (1.83 m) down to be effective. This writer found that burying the wires slightly below the surface is the best way of installing the system. Mechanically the radials can be nailed down, electrically they are most effective, and esthetically they provide little interference to a healthy stand of grass.

It will be seen from Fig. 20 that the input impedance for a vertical antenna is drastically affected by the number of radials. Many radial wires are necessary to prevent an excessive loss of power and to provide a convenient input impedance. Fig. 20 also shows the theoretical impedance limit for an antenna having an effective height-to-radius ratio of 300:1.[9]

Fig. 21 shows the effect on low-angle radiation as a function of the number of radials. These data were obtained by placing a test oscillator on a wooden tower, four wavelengths away. A photograph shows the 20-meter vertical and the 26-foot wooden test tower.

The effect of using longer radials in a particular direction is shown in Fig. 22. Radials of no. 18 wire, 3/2 wavelengths long, were put down between the existing 40 radials. The spacing between the longer wires was five degrees. The considerable improvement indicates the need for longer wires and the directional properties a groundplane could give.

A 5/8-wavelength vertical was also constructed and tested. It consisted of a 40-ft. (12.19-m) telescoping aluminum pole and a loading coil of eight turns of no. 12 wire with a diameter of 2.5 inches (64 mm). The comparison in low-angle radiation at a distance of 7.5 wavelengths is presented in Table 5. A field-strength meter was mounted at different heights on the 26-foot (7.93-m) tower. The groundplane for these data consisted of the 40 0.4-λ radials plus the 11 3/2-λ ones. Measurements were taken in the direction of the added longer radials. The results show the improvement in low angle radiation offered by the 5/8-λ vertical. The input impedance of this longer antenna was found to be 76 ohms.

On-the-Air Checks

From these experiments and measurements the author decided to settle on a 1/4-λ antenna with approximately 40 radials. The installation is shown in the photograph. This writer then proceeded to make on-the-air tests to compare its effectiveness with an inverted-V antenna having its apex at 0.4 wavelength, and with a 5/8-λ vertical using the same ground system. Surprisingly, the 1/4-λ vertical seemed to perform just as well as the much taller 5/8-λ vertical. This could result from the fact that most signals arrive after several hops and the optimum lobe angle is probably as high as 15 to 20 degrees.[10] At that angle, the λ/4 antenna actually enjoys an advantage. With practically all DX contacts, the verticals had a 6- to 8-dB improvement over the inverted V! The only exceptions were at intermediate distances and for local contacts. At about 500 or 600 miles, the inverted V with its higher angle of radiation gave better results. Locally, the verticals gave far superior performance. Improvements of 10 to 15 dB were recorded. A triband trap vertical antenna was also tested on 20 meters and found to be practically the same in impedance and performance. This antenna had an overall height of only 12.5 feet (3.81 m)!

Test Equipment

A most interesting aspect of antenna measurements is that the equipment can be rather simple and in many cases constructed from items most amateurs have in their junk boxes. All that is really needed is some standard to compare with, such as a wattmeter or an S meter that is known to have reasonable accuracy. This writer has used both — the wattmeter in a Drake L-4B linear amplifier and the S meter in a R-4B receiver.

The impedance bridge shown in the photograph was patterned after the one shown in the *ARRL Handbook*. Care was taken in shielding the input and output circuits. The meter was mounted externally in order to minimize stray pickup. A calibration curve was obtained at 14.25 MHz by using many carbon resistors of known values as the load.

The field-strength meter is a simple diode detector and dc amplifier. The instrument was constructed to cover the 10-, 15- and 20-meter bands. Its meter was also mounted externally, The antenna length for the field-strength meter was determined by the strength of the available field. In addition to these pieces of test equipment, a 20-meter transistorized crystal oscillator was used for many of the tests.

Conclusion

The performance of a vertical antenna on the ground is highly dependent upon a good ground system, and, properly installed, the antenna can be a very good performer indeed for DX and local contacts. This is particularly true at the higher frequencies where the dielectric property of the earth plays a major role. Forty radials of no. 18 wire, 0.4λ long, will increase the total radiated power by about 3 dB. Radials can be thin if a sufficient number are used. The thought of using thick wires buried deeply, probably a carryover from lightning grounds, is not valid at higher frequencies. The idea of using only four buried radials, as commonly recommended, is a serious error, and if this article does nothing more than eliminate that misconception, this author will be satisfied. Since the electric field only penetrates the ground for a foot or two at the higher frequencies, the radial wires need be buried only as deep as necessary to escape children's feet and the lawn mower. Finally, these results from the single vertical antenna indicate that a vertical array could be a competitor to the more elaborate horizontal beams and warrants further investigation. This material was originally presented in *QST* by Jerry Sevick, W2FMI.

References

[1]Terman, *Radio Engineering*, McGraw-Hill, New York, 1947, p. 651.

[2]Friis, Feldman, and Sharpless, "The Determination of the Direction of Arrival of Short Radio Waves," *Proceedings of the IRE*, Vol. 22, No. 1, January 1934.

[3]Williams, "Antenna Theory and Design," *The Electrical Design of Antennae*, Vol. 2, Second Edition, Sir Isaac Pitman and Sons Ltd., London, p. 126.

[4]Brown, Lewis, and Epstein, "Ground Systems as a Factor in Antenna Efficiency," *Proceedings of the IRE*, Vol. 25, No. 6, June 1937.

[5]Wait, "Input Resistance of L. F. Unipole Aerials," *Wireless Engineer*, May 1955.

[6]Feldman, "The Optical Behavior of the Ground for Short Radio Waves," *Proceedings of the IRE*, Vol. 21, No. 6, June 1933.

[7]Jager, "Effect of the Earth's Surface on Antenna Patterns in the Short Wave Range," *Internat Elekitron Rundschau 1970*, Nr. 4.

[8]See footnote 4.

[9]King and Harrison, "The Impedance of Short, Long, and Capacitively Loaded Antennas with a Critical Discussion of the Antenna Problem," *Journal of Applied Physics*, Vol. 15, February 1944.

[10]See footnote 2.

The W2FMI Ground-Mounted Short Vertical

Just because the vertical is physically short doesn't mean it won't provide excellent results in DX work. Theory says it can be done. Here's how!

A short vertical antenna, properly designed and installed, approaches the efficiency of a full-size resonant quarter-wave antenna. Even a six-foot (1.83 m) vertical on 40 meters can produce an exceptional signal. Theory tells us that this should be possible, but the practical achievement of such a result requires an understanding of the problems of ground losses, loading, and impedance matching. This paper covers design principles which are applicable to all of our amateur bands.

Background

Earlier work by the author[1] on the radiation efficiency of a ground-mounted vertical resulted from the desire to design a simple, inexpensive, low-profile DX beam for 20 meters. This first work reviewed the theoretical considerations involved and pointed out that a good ground system is essential to achieve efficient operation of a resonant quarter-wave antenna. The second work applied these results to a 20-meter beam.[2] In the process of trying to extend the results of these investigations to the 40-, 80- and 160-meter bands, and to possible multiband operation, the need arose to understand the operation of a shortened vertical and the effects of different loading schemes on the input impedance.

The first part of this paper deals with the theoretical considerations of a short vertical antenna and the experimental procedures involved in measuring the various parameters. This is followed by experimental results which show the trade-offs involved in shortening antennas by various loading schemes. Finally, specific designs are given for the 40- and 80-meter bands.

Theoretical and Experimental Considerations

There are several old familiar axioms in Amateur Radio that are not completely understood by the amateur. The author refers specifically to the two sayings: *Make the antenna as long as possible and erect it as high as possible,* and, *A full-size beam is better than a smaller beam, and a tall vertical is always better than a short one.* The first axiom is particularly relevant to horizontal antennas, where height is most important for reliable DX operation.[3] Increasing the length tends to increase the gain in certain directions. But with the vertical antenna, taking it off the ground and feeding it at a voltage point (like the J antenna) in order to eliminate radials can result in poorer performance because of increased earth loss.[4,5] More experimental work remains to be done on this phase of vertical antennas. The second axiom noted above is generally true, but misinterpreted by many. The author refers to those important properties: power gain — important in transmitting and capture cross-section — important in receiving. (Power gain is the gain, in magnitude, compared to an isotropic radiator; cross-section is a fictitious area related to the ability of the antenna to intercept the radiated power and make it available to the receiver for detection.) As will be seen below, very little is compromised in these properties by shortening the antenna.

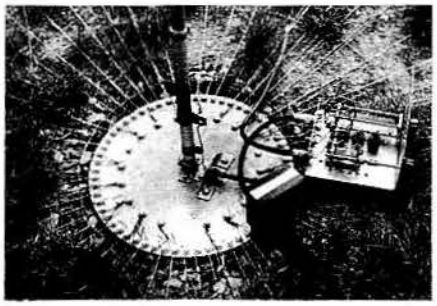

The matching network and base hardware showing 115 radials with the 6-foot (1.83-m) vertical. The pi network is covered with a plastic bag.

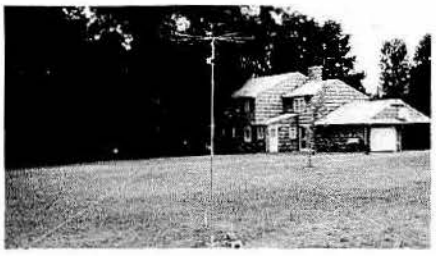

The 10-foot (3.05-m), 40-meter vertical designed for an input impedance of 12.5 ohms in order to use a 4:1 step-up bifilar transformer. The top hat has a diameter of 4 feet (1.22 m) and the coil, placed one foot (0.31 m) below, has 14 turns. Shown at the base is the transformer and impedance bridge.

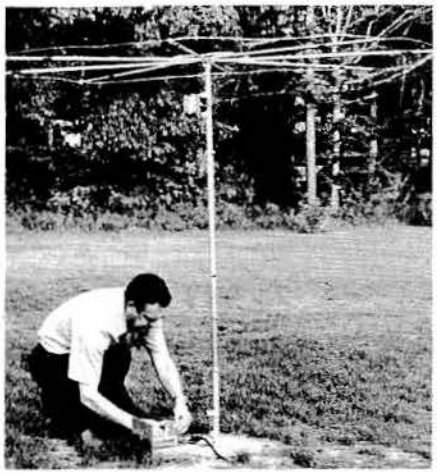

The author with the 6-foot (1.83-m), 40-meter vertical.

The short antenna has been defined as one that is small compared to a wavelength. In a more exact form, it is defined in such a manner as to simplify the mathematics in the theoretical calculations. King[6] has used the following inequality as the definition where

$$\beta_0 h = \leq 0.5$$

$$\beta_0 = \frac{2\pi}{\lambda}$$

h = half-length of a center-fed antenna or the height of a ground-mounted vertical.

λ = the wavelength

$\beta_0 h$ is actually a quantity which is used to express the height of an antenna in terms of an angle in radians. Thus, this quantity is independent of the frequency. Since 40

Table 6

Inductive Loading

	No. of Turns*	h	$R_{rad.}$
1) *Base Loading*			
a)	7	24 ft 3 in.	14.5 ohms
b)	10	18 ft 9 in.	7.5 ohms
c)	12	15 ft 7 in.	5.5 ohms
d)	14	13 ft	4 ohms
e)	18	8 ft 10 in.	2 ohms
2) *Midpoint Loading*			
	*No. of Turns**	*h*	$R_{rad.}$
a)	6	28 ft 5 in.	28.5 ohms
b)	11	24 ft 3 in.	25.2 ohms
c)	15	19 ft 8 in.	16.5 ohms
d)	18	15 ft 8 in.	12.3 ohms
e)	24	14 ft 6 in.	10.5 ohms
3) *Three-Quarter Point Loading*			
	*No. of Turns**	*h*	$R_{rad.}$
a)	10	29 ft 4 in.	32.5 ohms
b)	18	23 ft	26 ohms
c)	23	21 ft 2 in.	23.5 ohms
d)	24	19 ft 2 in.	22 ohms

*B & W 3029, 2-1/2 in. dia, 6 TPI, no. 12 wire.

1 ft = 0.3048 m

Table 7

Top Hat and Distributed Loading

1) *Top Hat Loading* (4-spoked wheel with 1/8-inch Al wire rim)

	Diameter	*h*	$R_{rad.}$
a)	1 ft	30 ft 10 in.	34 ohms
b)	2 ft	28 ft 7 in.	32.5 ohms
c)	4 ft	24 ft	30 ohms
d)	7 ft	19 ft 2 in.	23.5 ohms
e)	4 ft*	23 ft 4 in.	29.4 ohms

2) *Distributed Loading* (Helical Antenna)

	No. of Turns	*h*	$R_{rad.}$	*Top Hat at 1.5 ft Above Coil*
a)	111	12 ft	8 ohms	1 ft dia.
b)	105	12 ft	10 ohms	2 ft dia.
c)	113	7 ft	6 ohms	2 ft dia.
d)	75	7 ft	7.5 ohms	4 ft dia.

*8-spoked wheel
1 ft = 0.3048 m

Table 8

Parameters of the 40-Meter Short Vertical Designs

Total Height	$R_{rad.}$ (ohms)	*No. Turns**	*Dia. Top* (ft)	*Bandwidth*
6 ft	3.5	14	7	100 kHz
8-1/2 ft	7.5	at 6 in. below top hat		
8-1/2 ft	7.5	75 on 7 ft dowel 1-5/8 in. in dia.	4	100 kHz
10 ft	12.5	14 1 ft below top hat	4	125 kHz
15 ft 10 in.	12.5	7 at base	4	540 kHz

*Except for helical antenna, coil wire is same as shown in Table 6.
1 ft = 0.3048 m

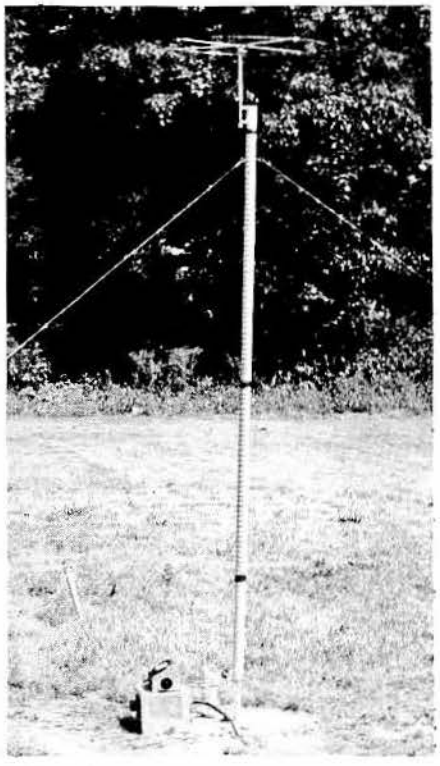

Eight-and-one-half-foot (2.59-m) helical antenna using a 2-foot (0.61-m) top hat 1-1/2 feet (0.46 m) above the 7-foot (2.13-m) helix. The 75 turns have approximately a 3-inch (76-mm) pitch below the midpoint and 1.5-inch (38-mm) pitch above. Very little difference was noted in reversing the pitches. The input impedance was 7.5 ohms.

meters was used mostly for experimental results presented in this article, the inequality above assures accurate theoretical calculations for verticals of 11 feet (3.35 m) or less.

The theoretical results show that the power gain for a *very* short antenna, even less than 1-foot (0.31-m) high on 40 meters, is 1.5.[7] This increases slowly to 1.513 for an 11-foot (3.35-m) antenna. These gains are to be compared to about 1.62 for a resonant quarter-wave vertical. It can be seen that this difference amounts to less than 0.4 dB or 0.07 S unit, based on 6 dB per S unit.

In a similar fashion, the capture cross-sections differ by relatively small amounts. For the *very* short antenna, a cross-section value is 0.119 λ^2, while for the quarter-wave vertical it is 0.13 λ^2. This is surprising to many since it is difficult to visualize a vertical of a foot or two (0.31 or 0.61 m) in height on 40 meters, having practically the same receiving ability as a 33-foot (10.06-m) quarter-wave antenna!

But the important property of a short vertical that makes its capture cross-section nearly the equivalent of a full 1/4-λ antenna is its *very small value of input resistance.* Fig 23 shows the theoretical curve and the 40-meter experimental results for the input resistance of a ground-mounted vertical as a function of height.[8] The experimental data were obtained by essentially canceling out the capacitive reactance of the vertical by an inductance at the base of the antenna and

Base of the vertical antenna with 60 radials. The aluminum disk is 15 inches (0.38 m) in diameter and 1/4 inch (6 mm) thick. Sixty tapped holes for 1/4-20 aluminum hex-head bolts form the outer ring and 20 form the inner ring. The insulator is polystyrene material with a 1-inch (25-mm) diameter. Also shown is the impedance bridge for measuring input resistance.
Originally, circular wires were used to connect all radials together. These were positioned every 2 feet (0.61 m), starting from the antenna base. Then, one at a time, they were removed, meanwhile keeping a check on the antenna radiation resistance. There was no apparent change in the radiation resistance, so it was concluded that the interconnecting rings of wire were not needed in the ground system.

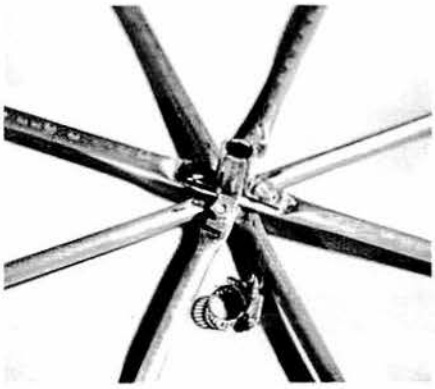

Construction details for the top hats. For diameters of 4 and 7 feet (1.22 and 2.13 m), 1/2-inch (13-mm) aluminum tubing was used. The hose clamp is of stainless steel. The rest of the hardware is all aluminum.

measuring the resistive value with an impedance bridge. Since an extensive, low-loss radial system was used, the resistance measured was actually that of the antenna itself, which is called the *radiation resistance.*

Fig. 24 shows the input resistance of a quarter-wave resonant vertical as a function of the number of radials. At the 115-radial point, the input resistance approaches the theoretical value of 35 ohms, which strongly indicates low earth loss and, hence, reliable data in short antenna measurements. The picture also shows the base hardware for 60 radials. The wire is 15-gauge aluminum. There is nothing sacred about 15 gauge. No. 22 wire, or even no. 28, would be just as good.

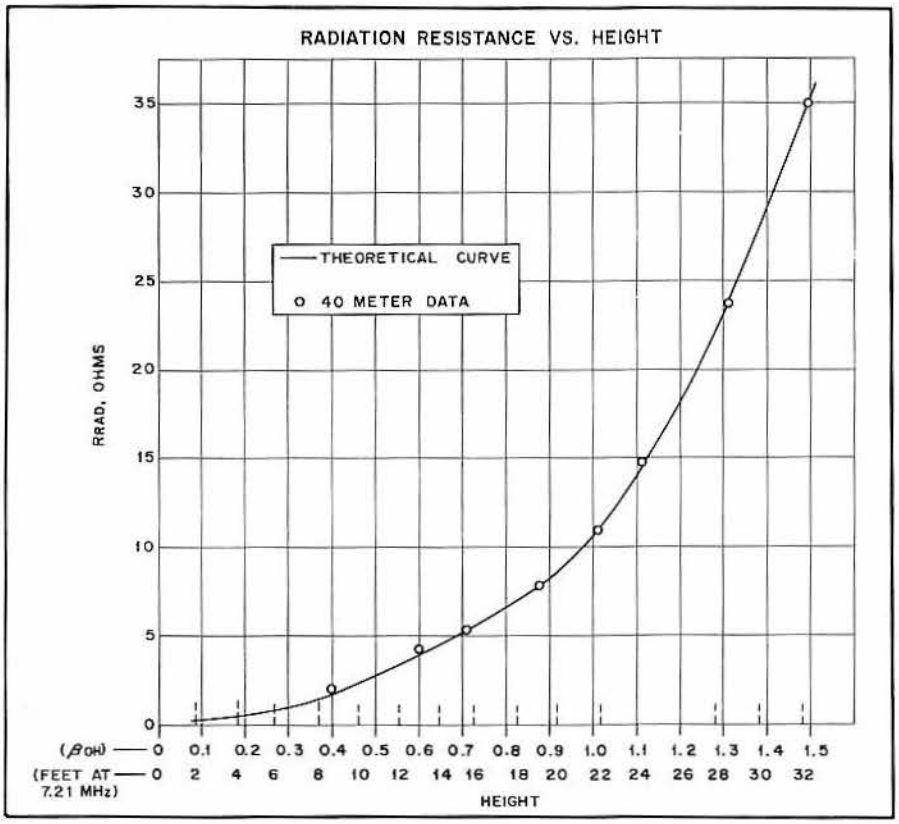

Fig. 23 — Theoretical curve and experimental results for the radiation resistance as function of height.

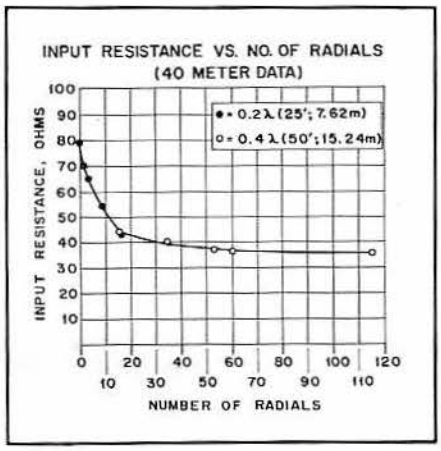

Fig. 24 — Input resistance of a quarter-wave ground-mounted resonant vertical as a function of the number of radials.

It should also be noted that very little difference was noted whether 0.2-λ or 0.4-λ radials were used. At 16 radials, the results are practically identical. In fact, this curve is also similar to the one obtained on 20 meters which was reported earlier.[9] More work remains to be done on the trade-offs in performance versus length of radials for ground-mounted verticals.[10]

Experimental Results

In designing a shortened vertical beam for 40, 80 or 160 meters, a most important consideration is the value of the input impedance of the driven element. As seen in Fig. 23, a shortened vertical using base loading has an extremely low value, particularly at one-eighth wavelength and less. This input impedance is then usually lowered in the presence of other elements in a beam array. The resulting very low value of input impedance makes it difficult to design matching networks. Therefore, an experimental investigation was undertaken to see what increases in radiation resistance could be obtained by other methods of loading, i.e., top hat, three-quarter point, midpoint, and distributed (helical antenna). The results of these experiments are shown in Fig. 25. Table 6 shows the individual points for inductive loading and Table 7 for top hat and distributive loading. Several interesting points were brought out by these experimental results. Fig. 25 shows that top-hat loading yielded the largest value of radiation resistance for a particular height. Surprisingly, the helical antenna[11] yielded a value less than midpoint loading. The three-quarter point and midpoint loading curves were not extended to lower values of height because data were very difficult to obtain below the points shown on the respective curves. The combinations of inductances and lengths below the heights shown on these two curves were probably beyond resonant conditions at the frequency used in the measurements. The other curves were extended by dashed lines indicating no difficulties were encountered in the measurements and other lengths were very possible.

Another interesting aspect of the top-hat loading curve is that a four-spoked wheel approaches to a good degree a solid disk. Doubling to eight spokes only improves the loading by about nine percent as noted in Table 7. Thus, *a few radials on the top of a vertical are very effective.*

Four radials at the base, approximating a ground system, are practically *useless* as noted in Fig. 24. Also, it can be seen from Table 7 that the reduction in length because of top-hat loading is approximately equal to twice the diameter of the disk.

On 160 meters, top hats have been made with sloping wires or struts with success.[12] Because of the sloping nature of this top hat, some cancellation of the antenna current takes place, thus reducing the radiation resistance further.

Although the curves in Fig. 25 were obtained from experiments at 7.21 MHz, these data can be applied to the other bands by proper scaling. For example, by doubling all dimensions, including the number of turns of the loading coils, the radiation resistance values would apply at a frequency of 3.6 MHz. By increasing the dimensions by only 1.85 instead of 2, the results would then apply to a frequency of 3.9 MHz. In like manner, a proper scaling factor could be used to apply these results to a portion of any of the amateur bands.

40- and 80-Meter Short-Vertical Designs

As was stated before, a most important consideration in designing short verticals is a knowledge of the input resistance and how it varies with different types of loading. The objective is to obtain a resistance value large compared to earth losses, so that efficient operation is obtained. In the author's specific case, using 115 radials, practically no earth loss was measured, and, hence, any radiation resistance above a few ohms assured good operation and an opportunity to verify the theoretical predictions for very short vertical antennas.

Since a broad-band, bifilar, 4:1 step-up transformer was available from previous work,[13] the first design was for the shortest vertical having an input resistance of 12.5 ohms. From the curves of Fig. 25, it appeared that a 16- or 17-foot (4.88- or 5.18-m) antenna with a coil of some 13 turns (extrapolated from Table 6) at 8 or 9 feet (2.44 or 2.74 m) from the base would provide the proper impedance at 40 meters. Further, it was decided that some 7 or 8 feet (2.13 or 2.44 m) of length above the coil could be replaced by an eight-spoked top hat having a diameter of 4 feet (1.22 m). The actual design that resulted, after proper tuning, is shown in the picture. The antenna had a total height of only 10 feet (3.05 m) and a 14-turn coil placed 1 foot (0.31 m) below the top hat. This height was about one foot (0.31 m) higher than first expected, but upon careful examination it was noted that the top hat also reduced the radiation

resistance, while replacing a section of the vertical portion. Therefore, the height had to be increased somewhat when considering top-loading effects. Also shown in a picture are the construction details for the top hat.

Two other shortened verticals for 40 meters were investigated. One was an 8-1/2-foot (2.59-m) helical using a 4-foot (1.22-m) top hat and 75 turns on a 1-5/8-inch (41-mm), 7-foot (2.13-m) long, wooden dowel. The input impedance was 7.5 ohms and it was matched with a standard pi network. Pictures are shown with the network. Several tests were made by doubling the winding pitch below and above the midpoint, keeping the number of turns constant, with very little difference in results.

The second antenna, also for 40 meters, using a 7-foot (2.13-m) top-hat, resulted in a matched vertical only 6 feet (1.83 m) high. It had a 14-turn coil, 6 inches (152 mm) below the top hat and an input impedance of only 3.5 ohms. Matching was accomplished with the 4:1 transformer and the pi network. A picture of the antenna and matching network is shown.

A larger 40-meter vertical antenna was also investigated. It had a 4-foot (1.22-m) top hat and 7 turns of base loading which resulted in a height of 15 feet 10 inches (4.83 m) (approximately 1/8 wavelength) and an input impedance of 12.5 ohms. The purpose of this design was to compare its low-angle radiation and bandwidth[14] with the other antennas. Table 8 shows the parameters of these various short vertical designs. Fig. 26 shows the SWR curves of three of the short antennas compared to a quarter-wave resonant vertical and Fig. 27 shows the SWR of the 6-foot (1.83 m) antenna.

As can be seen by the SWR curves, shortening an antenna generally decreases its bandwidth. Also by comparing the 8-1/2- and 6-foot (2.59 and 1.83-m) antennas top-hat loading appears to affect the SWR the least. It should also be noted that an eighth-wavelength antenna appears to have a reasonable bandwidth and would probably result in a practical beam design.[15]

And finally, the four short-vertical designs described above were compared with a resonant quarter-wavelength antenna for low-angle radiation and on the air with other amateurs signals. The low-angle radiation measurements were made at three wavelengths in distance and at heights of 1, 3, 6 and 8 feet (0.31, 0.91, 1.83, 2.44 meters). This relates to vertical angles of 0.15, 0.45, 0.90 and 1.2 degrees, respectively. All measurements were made under matched conditions and with a constant 100 watts fed into the antennas under test. In no case were there any appreciable differences noted in the field strength measurements. In fact, the 6-foot (1.83-m) antenna seemed to give slightly higher readings! These measurements certainly tend to verify the theory on the power gain predicted for short verticals. On-the-air checks were again very gratifying and exciting. Over 200 contacts with the 6-foot (1.83-m) antenna strongly indicated the efficiency and capability of a short vertical. Invariably at distances greater than 500 or 600 miles, the short verticals yielded excellent signals.

As was stated previously, all of the results obtained by measurements on 40 meters can be scaled, by the appropriate ratios of frequencies, to other bands. This was tried out on 80 meters. Since a 7-foot (2.13-m) top hat was available (instead of an 8-foot [2.44-m] one), the height turned out to be 22 feet (6.71 m) instead of 20 (6.10 m). The loading coil had 24 turns and was placed 2 feet (0.61 m) below the top hat. On-the-air results duplicated those on 40 meters. The bandwidth was 65 kHz (half of the 40-meter value) as shown in Fig. 28.

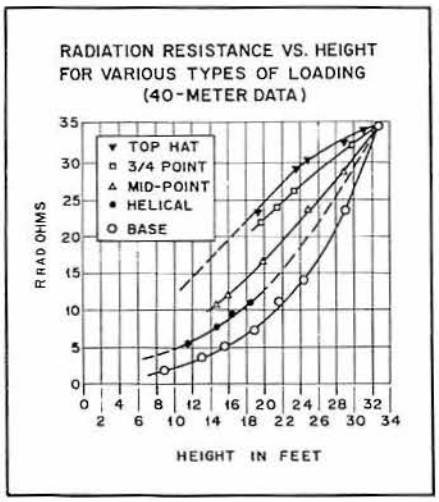

Fig. 25 — Experimental results of radiation resistance as a function of height of antenna for various types of loading (40-meter data).

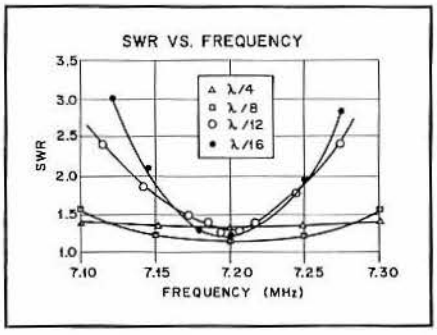

Fig. 26 — Standing wave ratio of various short verticals compared to a resonant quarter-wave antenna. The sixteenth-wavelength antenna is the 8-1/2-foot (2.59-m) helical design, the twelfth-wavelength is the 10-foot (3.05-m) antenna, and the eighth-wavelength is the 15-foot 10-inch (4.83-m) antenna. (All three are described in the text.)

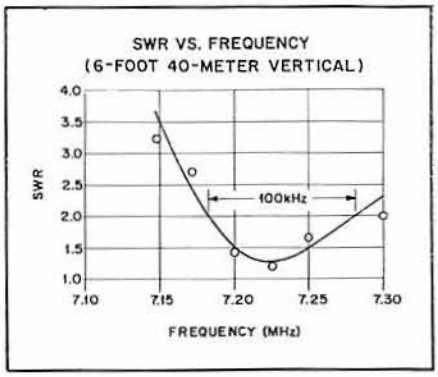

Fig. 27 — Standing wave ratio of the 6-foot (1.83-m) vertical using a 7-foot (2.13-m) top hat and 14 turns of loading 6 inches (152 mm) below the top hat.

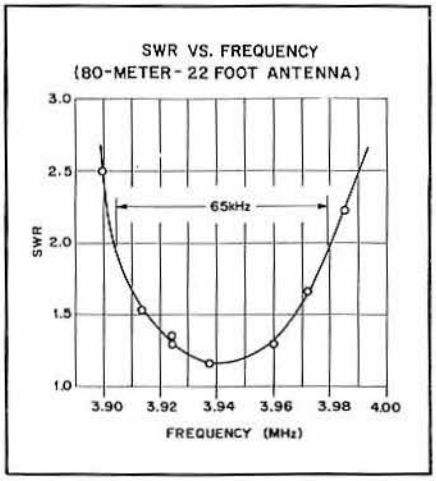

Fig. 28 — The standing wave ratio for the 22-foot (6.71-m), 80-meter vertical.

Conclusions

Several interesting results came out of this investigation which, even to one schooled in antenna theory, are difficult to believe. The author refers specifically to the ability of very short verticals to radiate and receive as well as a full-size quarter-wave antenna. The differences are practically negligible. But, as was seen, the trade-offs are in lowered input impedances and bandwidths. However, with a good image plane and a proper design, these trade-offs can be entirely acceptable.

As a result of this investigation, other problems were noted which indicate the need for further experimentation. The writer refers specifically to the trade-offs encountered when shortening the radials (to 0.1 wavelength, for example), the efficiency of ground-mounted versus elevated verticals as a function of height above ground, the characteristics of a multiband vertical over a low-loss image plane, and a shortened vertical beam using elements of the order of an eighth wavelength.

Another point should be mentioned in relation to the results reported here. Even though they were obtained on short, ground-mounted verticals, they are valid for center-fed verticals or horizontal antennas as well. The only differences are that the impedance values should be doubled and the effect of the image antenna accounted for.

The author would like to acknowledge the support of many amateurs for their fine words of encouragement and excellent reporting during on-the-air contacts. In this study, some 350 amateurs reported on comparisons between signals from these short verticals and those of other stations. This material was originally presented in *QST* by Jerry Sevick, W2FMI.

References

[1]Sevick "The Ground-Image Vertical Antenna," *QST*, July 1971. Also appears elsewhere in this chapter.

[2]Sevick, "The W2FMI 20-Meter Vertical Beam," *QST*, June 1972.

[3]See footnote 1.

[4]Miller, Poggio, Burke, Seldon, "Analysis of Wire Antennas in the Presence of a Conducting Half-Space. Part II. The Vertical Antenna in Free Space," *Canadian Journal of Physics*, Vol. 50, 1972.

[5]Feldman, "The Optical Behavior of the Ground for Short Radio Waves," *Proc. of the Inst. of Radio Engineers*, Vol. 21, no. 6, June 1933.

[6]King, *The Theory of Linear Antennas*, Harvard Univ. Press, Cambridge, MA, 1956.

[7]See reference in footnote 6, p. 497.

[8]See reference in footnote 6, p. 190.

[9]See footnote 1.

[10]Weeks, *Antenna Engineering*, McGraw-Hill Book Company, 1968, p. 48.

[11]The diameter of the helical antenna was 1-5/8 inches (41 mm). Each helical antenna had a top hat 18 inches (457 mm) above the helix in order to terminate the upper turns with sufficient capacitive reactance.

[12]See reference in footnote 10, p. 44.

[13]See footnote 2.

[14]Bandwidth is defined as the range in frequency where SWR is less than 2:1.

[15]See footnote 2.

Optimizing Vertical Antenna Performance

Do you have tower restrictions, a small yard or patio, almost no room for antennas? If so, here are some suggestions for making your signal bigger in spite of the handicaps.

Antennas never cease to be a hot topic of conversation among amateurs; the interesting articles by John Stanley, K4ERO/HC1[1] and Roger Hostenback, W5EGS,[2] on the optimum grounding of vertical antennas have led the author to communicate these thoughts on the subject. Obstacles at the author's present location (typical of many suburban dwellings) place severe limitations upon where ground wires can be placed. These obstacles are large boulders, areas of concrete, the house, vegetable and flower beds, and the neighbors' property lines. It has not been possible to lay out radials of uniform length or of uniform angular distribution. Nevertheless, the author has had successful results with vertical antennas. Although the writer must make a number of statements which are based upon fragmentary evidence and are lacking in scientific rigor, they should be useful for suggesting how others might proceed to optimize their particular situations.

The writer has three very dissimilar vertical antennas. Much of the discussion will pertain to their individual ground systems, although strictly speaking they cannot be independent; a change of the grounding conductors of one vertical is bound to affect the others. For brevity the writer shall not discuss the methods of impedance matching of the antennas as this is a topic thoroughly covered elsewhere. The author *shall* mention some problems of using dissimilar antennas in a phased array, although the results are preliminary.

The three antennas are (1) a shunt-fed crank-up tower having a three-element triband Yagi on top, the height being variable from 27 to 41 feet (8.23 to 12.50 m); (2) a 40-foot (12.19-m) insulated base-loaded antenna consisting of a 30-foot (9.14-m) pipe mast topped by a whip, located approximately 70 feet (21.34 m) south of the tower and hereafter referred to as the "south antenna"; (3) about 20 feet (6.10 m) east of the tower, a vertical antenna termed the "north antenna," which was described in an earlier *QST* article.[3] Fig. 29 shows the layout. The north antenna has been used with various heights up to 40 feet (12.19 m) but in the present experiments it is used in its "summer" configuration with a height of 25 feet (7.62 m) and with a 7/14-MHz trap located 10 feet (3.05 m) from the base. For 3.5-MHz operation additional loading is supplied at the base.

The Grounding Systems

None of the three verticals have anything approaching an optimum ground system; while the south antenna has the best on paper, it is not necessarily the best in performance. When the south antenna was first placed into operation the grounding system consisted of about 200 feet (60.96 m)

How do you ground a vertical antenna when there is no ground?

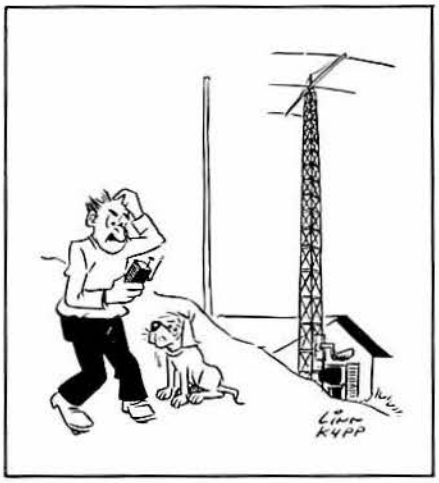

Optimizing ground-wire currents is well worth the time and effort required.

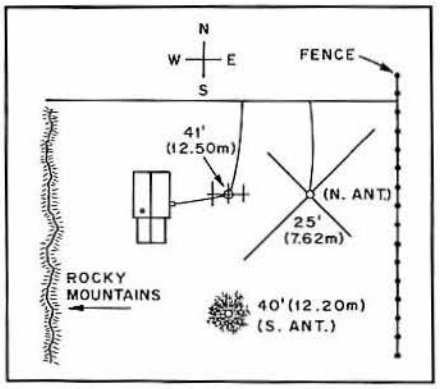

Fig. 29 — The WØJF backyard, with antenna farm.

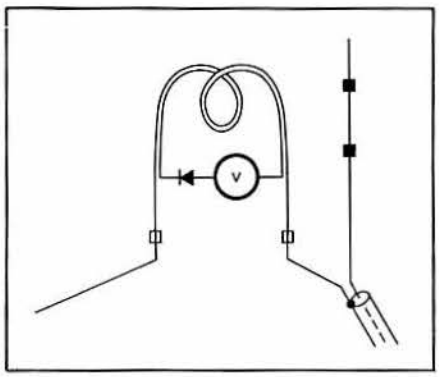

Fig. 30 — Suggested substitute for a thermocouple ammeter.

of wire distributed among a few conductors which went out more or less radially. One was about 60 feet (18.29 m) long, the others 30 feet (9.14 m) or less. On 7 MHz the performance was generally inferior to that of a horizontal half-wave dipole 30 feet (9.14 m) above ground. Later, the ground system was augmented to utilize about 1000 feet (304.80 m) of wire, and the vertical then began outperforming the dipole.

While the author foresaw Stanley's statement that possibly not all of this additional wire would be effective, it was assumed that any wires added at least would do no harm, and the writer tried to put wires in the entire immediate area of the antenna, subject to the constraints mentioned above. Several of the radials have bends to avoid obstacles. In a few cases a single wire goes out from the antenna to a junction some distance away, and then several wires fan outward from the junction. Three wires are connected at the far ends to a few square feet of chicken wire. Where the wires are in shrubbery they are above ground; otherwise they are an inch or two (25 or 51 mm) below. None of the additional wires were as long as 60 feet (18.29 m), and the lengths were generally determined by the obstacles they encountered. Haphazard as this system was, the improvement was spectacular.

While making this change in the south antenna's grounding, the author carried out two simple experiments. First, when operating at 7 MHz, a 33-foot (10.06-m) piece of wire was added, which in free space would be 1/4-λ long, but which when laid on the ground would be longer (in wavelengths). The writer connected it to the rest of the ground system through a thermocouple ammeter, and read the current while applying power. With this wire then cut in half and laid out as separate radials in opposite directions, it was found that the total current increased. Cutting these 1/8-λ pieces in half and distributing the resulting fragments as four radials in directions at 90 degrees to each other caused the total current to decrease. These observations led the author to conclude that for a given total amount of wire the most efficient layout would be radials having lengths of about 1/8 a free-space wavelength. This conclusion is consistent with Stanley's Table 1.[1]

In the other experiment, the author also used a 33-foot (10.06-m) piece of wire, but half of it was no. 34 and half no. 12 wire. With the thick end adjacent to the antenna, the current was higher than with the wire turned around so that the thin end was adjacent. The experiment showed that wire diameter is of some consequence, and it is more important to have heavy conductors close to the antenna.

The Tower and the North Antenna

Grounding of the tower is very heterogeneous; first of all, of course, the bottom of the tower is buried in the ground some 8 feet (2.44 m). There are two radials about 25 feet (7.62 m) long going in a more or less southerly direction, then a short wire going to a water faucet on the wall of the house. Finally, and probably most important, there is a wire that goes northward about 20 feet (6.10 m) and makes a junction with the middle of a 120-foot (36.58-m) east/west wire. The eastern end of this wire is located at the common corner with the property of the neighbor to the northeast and at that point is bonded to his extensive chain link fence. About 25 feet (7.62 m) west of this bond to the fence, there is a junction with a southward wire which is connected to the base of the north antenna. Otherwise, the grounding system of the north antenna, consisting of a few radial wires, is as described in the earlier *QST* article.

Some observations were made by connecting a thermocouple ammeter and a selection of capacitors and inductors in series with various conductors connected to the base of the tower. On 3.5 MHz, with the wire that goes to the fence, the author found a very strong resonance using a 300-pF capacitor. No such resonance was found with this wire of 7 MHz nor on 1.8 MHz, nor did there seem to be any resonance with any of the other wires.

No attempt has been made to bond the upper and lower sections of the tower (where they telescope) together. No such bonding seems necessary, except in the rare case of an extremely strong wind, when there is some receiver noise resulting from poor conductivity between the sections. Cranking the tower up and down seems to have little effect upon the degree of impedance mismatch.

On 3.5 MHz, using a power of about 150 watts, the author had contacts all over the world using this shunt-fed tower, usually not cranked all the way up. The south antenna has also given fairly good account of itself, but with its thousand feet (304 m) of radial wires its performance is still not quite as good as that of the tower with its meager "black magic" grounding.

On 7 MHz, the behavior of the tower is the reverse even though the impedance match is somewhat superior to that on 3.5 MHz. The performance, despite the good match, is far inferior to the south antenna or even the north antenna. Offhand, one would expect the performance, such as it is, to be better with the tower cranked down to minimum height, when it would be close to 1/4λ, but the few reports received on the air indicate better performance is obtained at maximum height. The overall performance of the tower on 7 MHz is a complete mystery.

The author has used the tower on 1.8 MHz only rarely, but has worked as far as 1000 miles, even though there is a very bad impedance mismatch on the feed line. One of the author's future projects is to cure that, since the tower may be magic on the top band, too!

What if You Don't Have a Thermocouple Ammeter?

The preceding discussion has, the author hopes, suggested that individuals may be able to optimize their ground systems by measuring the currents in individual ground wires. In this regard the writer has been fortunate in having available a number of thermocouple ammeters, instruments not commonly available in ham shacks. However, it was found easy to make a substitute which can serve to measure relative current and to detect resonances. Take a short length of twin-lead, speaker cord or similar cable, about a foot (0.305 m) long. Connect one wire of the pair in series with the circuit to be studied (the ground wire). Connect the two ends of the other wire of the pair to a semiconductor diode and a sensitive dc meter in series (Fig. 30). For convenience and for reproducibility in results, coil the cable up and secure it to a terminal board.

Using Dissimilar Antennas in a Phased Array

The author can use any two of the three verticals as a phased array by connecting the feed lines in parallel at the transmitter. In the shack the author has a switchboard that can switch additional lengths of line in series with one antenna or the other. The writer does not attempt to change the impedance match at the bases of the individual antennas, but does generally retune the transmitter as the phasing is changed. Some of the effects observed must be attributed to variations in impedance mismatches rather

than to basic changes in directivity. Nevertheless, some gain can usually be obtained by combining the verticals in one way or another.

In the use of two dissimilar antennas, two questions arise which may not apply when identical antennas are used. First, is there really an advantage in using the two of them in a phased array over using the better of the two alone? The relevance of this question may be seen by considering the extreme case where one is very much better than the other. In such a case the field strength of the poorer one is so much less that there is little difference whether it is in or out of phase with the field of the better one, and there can be little or no observable directional effect when the two are used together. Furthermore, the power supplied to the better antenna is cut in half while the other half of the power is largely wasted.

This simple argument suggests that in most cases the two antennas should be nearly equal in the field strengths they produce if they are to be effective in a phased array. However, the actual situation is sufficiently complex that exceptions may be found. For one thing, the better antenna may have "blind" directions in its pattern because of obstructions, and the poorer one may help to fill those in. Also, the impedance effects which have been mentioned before are hard to predict. The author can only suggest that one may find it worthwhile to try using two such antennas together, and may find unexpected advantages in some directions.

On 3.5 MHz the north antenna is generally much poorer than the tower. However, in some directions observers have consistently reported a small gain in using the two together over the tower alone. Incidentally, it should be mentioned that observations made on receiving are not reliable tests, partly because of impedance effects. Also, some of the noise received may be generated locally and its effect may mask the true pattern of the array. The only reliable evaluation is by transmitting to distant observers.

The second question concerning dissimilar antennas involves solving for an unknown quantity: the relative phase of the two antennas. The relative phase of the field of an antenna is *not* determined solely by the length of the transmission line connecting it to a transmitter. The impedance of the antenna usually contains a reactive component, and its presence gives rise to a phase shift. With two identical antennas these phase shifts are the same and do not affect the relative phase between the two antennas, which is determined only by the difference in feed-line lengths. With dissimilar antennas these phase shifts are generally not identical, and they may vary in different ways with shifts in frequency or with variations in the moisture content of the earth. Not unrelated was a discovery made when changing the grounding of the south antenna from 200 feet (60.96 m) of wire to 1000 (304.80 m). There was a substantial change in the phasing when it was used in an array with the tower.

The author has experimentally answered this phasing question by setting up a small probe antenna at a point equally distant from the two antennas and connecting it to a field-strength meter. The line lengths are varied until a minimum (usually quite sharp) is observed. Then it is known that the antennas are 180 degrees out of phase, and the array is a bidirectional end-fire one (W8JK). If the author adds or subtracts 1/2 λ of line from one antenna, the antennas should be in phase and a maximum should be observed. The experimental observations are in agreement with such predictions. If a length of line equal in electrical wavelengths to the spacing between the antennas is then added or subtracted from the feed line of one of them, the combination approximates a unidirectional end-fire array. The favored direction is away from the element which has the longer equivalent feed line (larger phase shift from the transmitter).

To reiterate, the results with phasing dissimilar verticals are very preliminary, and there is little that can be said about them except for the fact that at times very noticeable gains over using the better single antenna are observed.

Vertical Versus Horizontal Antennas

The author used some *horizontal* antennas and observed the differences in performance between them and the vertical antennas at a particular location. Horizontal antennas were not tried on 7 and 3.5 MHz any higher than 30 feet (9.14 m) above ground, however.

The first foothills of the Rocky Mountains rise up immediately to the west of the author's QTH, the nearest ones subtending a vertical angle of about 10 or 15 degrees. As expected, propagation to the west is usually difficult. To the east there are some power wires running north and south. The land slopes off to the north, and has a line-of-sight view for 12 miles from the base of the antenna tower.

The writer finds a tendency for horizontal antennas to be superior to the west, over the mountains, and for verticals to be superior to the east. Standard theory explains these findings as follows: Probably many of the signals coming over the mountains are scattered by the surface of the ground. Those familiar with advanced electromagnetic theory remember that according to the Fresnel equations, the reflection coefficient is greater when the wave is polarized with the electric vector parallel to the surface (i.e., horizontal). Therefore, this scattered radiation is probably horizontally polarized. On the other hand, the electric field from the vertical antenna is perpendicular to the direction of the power wires and is less disturbed by them than the field of a horizontal antenna.

Although very few firm results were presented, the author hopes he has suggested some procedures which will help those facing restrictions on grounding systems they can use. With a little persistence and ingenuity, they should be able to build effective antennas. It *is* possible to evaluate simple arrays yourself and to improve their performance according to your own communication requirements. This material was originally presented in *QST* by Yardley Beers, WØJF.

References

[1]Stanley, "Optimum Ground Systems for Vertical Antennas," *QST*, December 1976.

[2]Hoestenback, "Improving Earth-Ground Characteristics," *QST*, December 1976.

[3]Beers, "Short Antennas for the Lower Frequencies," *QST*, September 1970.

Some Plain Facts about Multiband Vertical Antennas

Does engineering jargon, page-long equations and references to the *IEEE Proceedings* have you gnawing your nails in frustration? Take heart, for these bits of knowledge about multiband vertical antennas are given in plain lingo.

During discussions with newcomers, and old-timers for that matter, it becomes apparent that there is considerable confusion as to what exactly a multiband vertical antenna is. The confusion concerns the method of feed, how much mismatch one can expect, how many radials are required, how the particular antenna is built for multiband use, plus some other points.

This article breaks the subject into simple language and provides the reader with sufficient expertise to assure him that he won't wind up with a system he really doesn't want. Before going into a discussion of the different types of multiband "verticals" we will offer some simple antenna facts.

Some Basic Theory

The term "multiband antenna" has come to mean many things to hams. With trap antennas, tapped coils, random wires, and so forth, there is plenty of reason for the confusion. Simply, a multiband antenna is one that can be used on more than one band. How we make it work on different bands is another story.

Basically, any piece of wire of *any* length can be classed as a multiband antenna. For example, a length of wire 4 feet (1.22 m) long *could* by used on *any* amateur band, from 160 meters on up. But how well the piece of wire would work is a completely different matter.

In the feed point of any antenna there is *radiation resistance*. The energy supplied to an antenna is dissipated in the form of radio waves and in heat losses in the wire and nearby insulating materials. The radiated energy is the useful part, but so far as the transmitter is concerned it represents a power consumption just as much as does the energy lost in heating the wire. In either case the dissipated power is equal to I^2R; in the case of heat losses, R is a real resistance (ohmic losses), but in the case of radiation, R is an *assumed* resistance. This fictitious resistance is the radiation resistance. This brings us to our first important point about multiband antennas.

Whenever one reduces the size (length) of an antenna physically, the radiation resistance is reduced also. As an example, assume we have a 20-meter quarter-wave antenna, which is approximately 16 feet (4.88 m) long. Let's imagine we made it out of no. 40 wire, which has a resistance of about 1 ohm per foot, (0.31 m). The radiation resistance of a resonant quarter-wave vertical operated against a perfect ground is on the order of 35 ohms. In this case, the feed-point impedance of our antenna would be roughly 35 ohms in radiation resistance plus 16 ohms in ohmic resistance. If we were to feed 51 watts into this antenna 16 watts would be dissipated as heat (lost power) and the remainder — 35 watts — would be radiated. Now, suppose we use this same antenna on 80 meters. As mentioned above, when we reduce the size of an antenna physically the radiation resistance is also reduced. On 80 meters our 16-foot (4.88-m) antenna would have a radiation resistance on the order of 1 ohm! However, we would still have the ohmic resistance of 16 ohms. It doesn't take much figuring to realize that just about all of our power would be lost as heat.

Of course we wouldn't use no. 40 wire for such an antenna. More likely the antenna would be made from aluminum tubing and the ohmic losses would be very low, but probably still more than the radiation resistance. There is an old axiom in Amateur Radio that offers some pretty good advice: Always make the antenna as long as possible and erect it as high as possible. Also, there is a joke that goes with that axiom — if such an antenna stays up, it is too small!

At this point we have only mentioned radiation and ohmic resistance in the antenna feed point. These are the two resistances that exist when the antenna is resonant. When the antenna is not resonant, there is reactance present in the feed point. Reactance is also expressed in ohms, but it isn't a real resistance in the sense that power can be dissipated therein. We won't go into a long discussion on reactance because it would take up too much space. An excellent explanation can be found in the League publication, *Understanding Amateur Radio*. Simply, reactance can be likened to a gate or door that stops or hinders the flow of current into a circuit. When an antenna is operated at some frequency other than the resonant frequency there will always be reactance present. Keep in mind that with *any* antenna, multiband or otherwise, we always have a condition on some band or frequency where the antenna is not resonant. Therefore, there will be reactance at the feedpoint.

Types of Vertical Antennas

The basic and most popular type of vertical is one that is a quarter wavelength long and is operated against ground or in a groundplane configuration. The antenna is usually made from tubing and the radials are wire. An ideal groundplane (simulated earth ground) would be a sheet of metal with

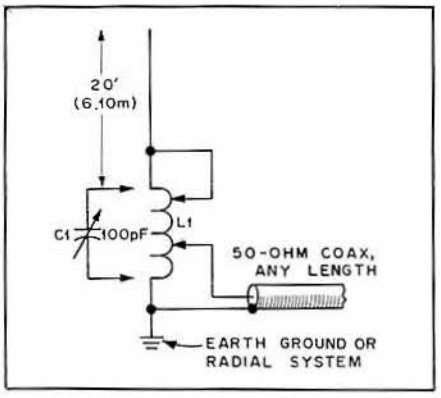

Fig. 31 — A typical multiband vertical antenna. A description of the system is given in the text.

a radius of one-quarter wavelength or more. However, this is only practical at vhf so the customary method is to use wires as the radials. Probably the number one question asked about groundplane antennas is, "how many radials are required?" The answer is simply, the more radials used, the better the antenna will perform, at least up to a certain point. This should not be construed to mean that an antenna with only two or three radials won't work. Such an antenna will work, but for *maximum* performance one should consider 40 or more radials. If the reader is interested in performance data for a few radials versus many, he should read the article in *QST* by Sevick.[1]

The feed-point impedance of quarter-wave groundplane is on the order of 35 ohms. The impedance can be raised by drooping the radials down until a 50-ohm match is obtained. Exactly how much droop is required depends on the number of radials.

The quarter-wave groundplane is essentially a single-band antenna. However, a 40-meter quarter-wave vertical can also be used on 15 meters, a happy circumstance for the Novice. In this case, a 40-meter quarter wave works out to be three quarter waves on 15 and any *odd* multiple of quarter waves will provide a relatively low-impedance feed.

Multiband Verticals

When we get into the field of multiband verticals we find that considerable confusion exists. As pointed out previously, *any* antenna can be *called* a multiband antenna, but how we get power into such an antenna is another matter.

Up until the '50s any amateur multiband antenna was a system that usually consisted of an antenna, tuned feeders, and an antenna coupler. In the early '50s more and more amateurs started to use coaxial cable for feeders, along with band-switching transmitters. The next logical step was the use of a multiband antenna system that required no adjustments and always presented a matched condition to the feed line — in other words, an antenna that had a 50-ohm feed-point impedance on every desired band and frequency within a given band. A logical development was the multiband trap antenna.

By inserting traps in an antenna it was possible to make an antenna "look" like a resonant half-wave dipole in whichever band was used; or, in the case of multiband verticals, making the vertical look like a resonant quarter-wave antenna for the desired band. However, and this is important as far as the newcomer is concerned, to our knowledge there is *no* multiband trap antenna that will provide a perfect match on all bands, *regardless* of what some antenna manufacturers may tell you. Many hams have spent countless hours trying to adjust trap antennas for that "perfect" match when actually, it is just about impossible to obtain such a condition.

Nontrap Multiband Verticals

Several antenna manufacturers sell multiband antennas that consist of a vertical piece of tubing, usually 16 to 20 feet (4.88 to 6.10 m) long. The tubing is used with a loading coil at the ground end. By making appropriate taps and adjustments on the coil the antenna can be matched (or closely matched) on any given band. This type antenna has *no* traps. This in turn means that the coil taps and adjustments *must* be altered when one changes bands. Some misguided amateurs buy these antennas expecting all they need do is put them up and the antenna will work on all bands, automatically. Let's make one point clear: such an antenna *is* a multiband antenna, but requires adjustment *at the antenna* when one changes bands.

Of course, the next question should be, "If the antenna is that simple can't I build my own?" Yes, it is a very simple multiband antenna to make and install. Two or three sections of inexpensive 10-foot (3.05-m) TV mast sections can serve as the vertical radiating element. The mast can be supported on an insulator, such as a beverage bottle, and the mast guyed with nylon line. Fig. 31 shows a diagram of the antenna system. L1 should be a coil made of bare wire, no. 12 or 14, so that it can be tapped at every turn. A convenient coil size is 2-1/2 inches (64 mm) in diameter, six turns per inch (25 mm), such as B & W 3905-1 stock. The number of turns required, assuming 80 meters as the lowest band to be used, should be about 30 turns with an antenna length of 25 feet (7.62 m).

Adjustment of the antenna requires the use of an SWR bridge. Connect the coax line across a few turns of L1 and make a trial position of the shorting tap. Measure the SWR, then try various positions of the shorting tap until the SWR reaches its lowest value. Then vary the line tap similarly. This should bring the SWR down to a low value. Small adjustments of both taps should provide an SWR close to 1. If not, try adding C1 and repeat the adjustment procedure, varying C1 each time until a match is achieved. Radials will enhance

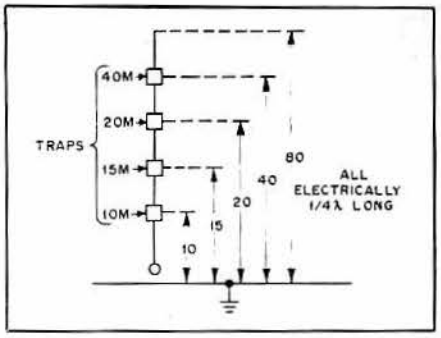

Fig. 32 — Drawing of the theoretical multiband trap vertical. In commercial practice, certain traps may be grouped together, giving the impression that only a single trap is used.

the performance of the antenna. The number of radials is up to the individual amateur.

Trap Verticals

As mentioned earlier, traps can be installed in a multiband vertical. These traps are usually parallel-tuned circuits and the objective is to make each section of the antenna work as a quarter-wave vertical or odd multiple thereof on the desired band. Fig. 32 shows an example of this type antenna.

The purpose in using this type antenna is to provide a system that always presents a matched condition for the feed line. Unfortunately, there is so much interaction between various sections of the antenna that it is impossible to come up with a *perfect* match on each band. What is an *acceptable* match is another story.

Amateurs as a whole are inclined to attach too much importance to an SWR of 1. They feel that if their SWR bridge isn't showing an absolute zero reflected power that something is horribly wrong and they won't work out. The plain fact is that using a feed line such as RG-8/U (assume a 100-foot [30.48 m] length) one could have an SWR of as much as 5:1 and have *no* appreciable loss in the system. However, there is one clinker in this thinking!

In many instances commercially made transmitters and transceivers are designed by the manufacturer to work into a 50-ohm load only. They don't allow much leeway from this figure. When there is a mismatch in the antenna system, it can become impossible to load and tune the final amplifier of the transmitter. There just isn't enough tuning range in the tank circuit of the amplifier to handle the reactance that may be present in the load. There is a way around this problem however, and that is using a Transmatch in the feed line to disguise the mismatch.[2] The Transmatch can be adjusted so that the transmitter "sees" a 50-ohm load regardless of the mismatch at the antenna.

The Harmonic Problems

Another consideration should be mentioned. As pointed out earlier, *any* antenna can be a multiband antenna. By the same

token any harmonics generated in the transmitter that reach the antenna can be radiated. It is true that a single-band antenna will reject harmonic energy, but *not* completely. In the case of a multiband trap antenna there is no rejection of some harmonics, simply because the antenna is designed to be resonant on all hf amateur bands. The solution to this problem is the use of a selective circuit installed in the feed line. A Transmatch is such a circuit and should provide adequate harmonic rejection.

Some Other Thoughts

The question is frequently asked, "Should I mount my vertical on the ground, or get the base up in the air?" Getting the antenna up in the clear is always better than having it mounted at earth level and surrounded by rain gutters, house wiring, trees, power lines and so forth. However, getting the vertical antenna up in the air also means that radials, as many as possible, should be used. The average installation (if there is such a thing) usually consists of three or four radials (or more) cut for the lowest operating frequency. Such a system should give a good performance.

Another important matter is that of the earth ground. When verticals are mounted at ground level the ground losses can be very important. Too many amateurs buy their verticals, get a 5-foot (1.52-m) long TV-type ground rod and drive it into the earth at the base of the antenna. They think this provides a good ground connection. As a matter of fact, the TV-type ground rods are practically worthless for amateur work. A *good* ground rod is the type used by the power company for home installations. This is a rod that is heavily galvanized, 5/8 inch (16 mm) in diameter, and about 10 feet (3.05 m) long. The amateur should be able to buy these rods from any wholesale electrical supply house. If possible, tie your ground connection to the water-system piping, assuming metal piping is used.

You'll hear the statement from fellow hams that verticals are poor antennas and radiate poorly in all directions. This isn't true, because a vertical *can* by a good antenna, but you have to give it a fighting chance. This material was originally presented in *QST* by Lewis McCoy, W1ICP.

References

[1]Sevick, "The Ground-Image Vertical Antenna" *QST*, July 1971. Also appears elsewhere in this chapter.

[2]A suitable Transmatch is described in the transmission-line chapter of any edition of *The Radio Amateur's Handbook*.

Shunt-Feeding Towers for Operation on the Lower Amateur Frequencies

The 160- and 80-meter DX antenna you've dreamed about may already be standing on your property — just waiting to be used as a DX vertical. Read this presentation and learn how to shunt-feed your tower on 1.8 and 3.5 MHz!

Shunt-feeding a tower used to support beam antennas for 14 MHz or higher frequencies has obvious advantages for the amateur who wants to work all lower bands. If a good ground system is installed, the result may be a very effective antenna for DX work on 80 and 160. The shorter tower installations may work very well on 40 meters, if the effective height above ground is less that 5/8 wavelength. Beyond this height the radiation angle goes higher, and the effectiveness for DX goes down.

The shunt-fed tower is at its best on 160, where a full quarter-wavelength vertical antenna is rarely possible. Almost any tower height can be used. If the beam structure provides some top loading, so much the better — but anything can be made to radiate, if it is fed properly. A self-supporting, aluminum, crank-up, tilt-over tower is used at W5RTQ with a TH6DXX tribander mounted at 70 feet (21.34 m). Measurements showed that the entire structure has about the same properties as a 125-foot (38.10-m) vertical. It thus works quite well on 160 and 80 in DX work requiring low-angle radiation. It can also be used on 40, but results are rather poor because of high radiation angle. WB5FKX, with a 37-foot (11.28-m) tower and a 21-MHz beam, finds that shunt feed on 40 enables him to work DX that he never knew existed before.

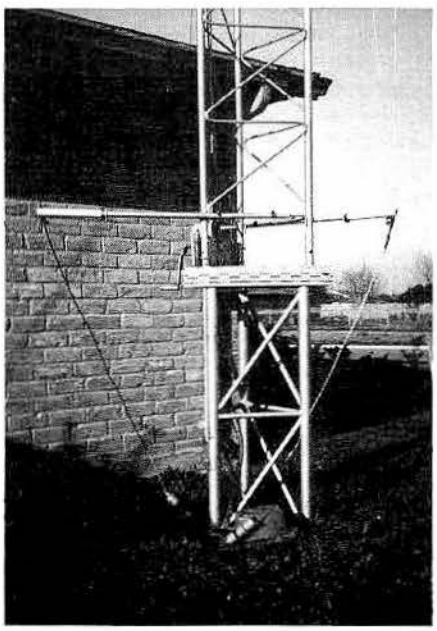

Close-up view of the base of the shunt-fed tower, showing the two bottom arms and their insulators.

Preparing the Structure

Usually some work on the tower system must be done before shunt-feeding is tried. Metallic guys should be broken up with insulators. They can be made to simulate top loading, if needed, by judicious placement of the first insulators. Don't overdo it; there is no need to "tune the radiator to resonance" in this way. If the tower is fastened to a house at a point more than about one-fourth of the height of the tower, it may be desirable to insulate the tower from the building. Plexiglas sheet, 1/4-inch (6-mm) or more thick, can be bent to any desired shape for this purpose, if it is heated in an oven and bent while hot.

All cables should be taped tightly to the tower, preferably on the inside, and run down to the ground level. It is not necessary to bond shielded cables to the tower

Table 9

Shunt-Feed Details for Several Towers Used on 160 Meters

Station	*Height of Tower* (ft)	*"Top-Hat"* (Beams)	*Average Height of Beam* (ft)	*Height of Wire-to-Tower Connection* (ft)	*Wire-to-Tower Spacing* (in.)	*Tuned Value of Gamma Capacitor*
W5RTQ	69	TH6DXX	70	68	30	150 pF
K5PFL	86	Stacked 40, 20, 15, 10 M beams	95	75	24	125 pF
K4PUZ	64	TH6DXX	66	63	8	300 pF
K8KAS	70	TH6DXX	77	68	24	225 pF
W1CER	50	QST 20-M DX Weasel	55	47	44	400 pF

1 ft = 0.3048 m
1 in. = 25.4 mm

electrically, but there should be no exceptions to the down-to-the-ground rule.

No rf problems have developed with rotators, beam traps, or even TV sets where the TV antenna is part of the radiating structure, as is the case at WB5FKX. His only precaution was use of coax on the TV antenna. It would be well to proceed with caution, as every installation could be different in this respect.

Though the effects of ground losses are less severe with the shunt-fed vertical than with the simple quarter-wave antenna, a good system of buried radials is very desirable. The ideal would be 120 radials, each 250 feet (76.20 m) long, but fewer and/or shorter ones must often suffice. You can sneak them around corners of houses, along fences or sidewalks, wherever they can be put a few inches under the surface, or even on the earth surface. Aluminum clothesline wire is used extensively at W5RTQ, and it stands up well. Neoprene-covered aluminum wire may be safer in highly acid soils. Contact with the soil is not important. Deep-driven ground rods, and connection to underground copper water pipes, are good, if usable.

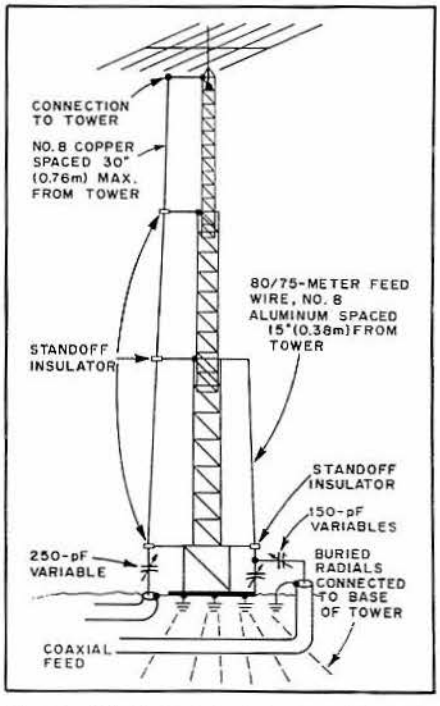

Fig. 33 — Principal details of the shunt-fed tower at W5RTQ. The 160-meter feed, left side, connects to the top of the tower through a horizontal arm of 1-inch (25-mm) diameter aluminum tubing. The other arms have stand-off insulators at their outer ends, made of 1-foot (0.31-m) lengths of plastic water pipe. The connection for 80/75, right, is made similarly, at 28 feet (8.53 m), but two variable capacitors are used, to permit adjustment of matching with large changes in frequency.

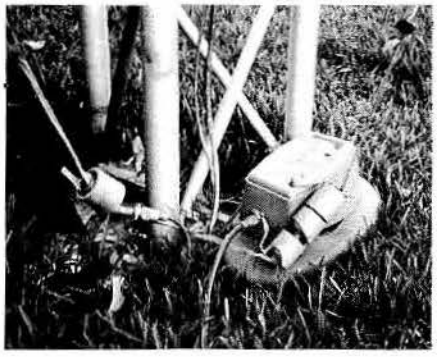

Though variable capacitors are shown in Fig. 33, they were all replaced with fixed-value units except one, which is inside a plastic box at the tower base.

Installing the Shunt Feed

Principal details of the shunt-fed tower for 80 and 160 meters are shown in Fig. 33. Rigid rod or tubing can be used for the feed portion, but heavy gauge aluminum or copper wire is easier to work with. Flexible stranded no. 8 copper wire is used for the 160-meter feed at W5RTQ, because when the tower is cranked down, the feed wire must come down with it. Connection is made at the top, 68 feet (20.73 m), through a 4-foot (1.22-m) length of aluminum tubing clamped to the top of the tower, horizontally. The wire is clamped to the tubing at the outer end, and runs down vertically through standoff insulators. These are made by fitting 12-inch (0.31-m) lengths of PVC plastic water pipe over 3-foot (0.91-m) lengths of aluminum tubing. These are clamped to the tower at 15 to 20-foot (4.57 to 6.10-m) intervals, with the bottom one about 3 feet (0.91 m) above ground. The lengths given allow for adjustment of the tower-to-wire spacing over a range of about 12 to 36 inches (0.31 to 91 m), for impedance matching.

The gamma-match capacitor for 160 is a 250-pF variable with about 1/16-inch (1.6-mm) plate spacing, which is adequate for the power levels presently authorized. The omega match used for 80 and 75 permits retuning for large excursions in frequency encountered in using both cw and phone on this band. Two capacitors are required, each about 150 pF, with plate spacing of about 3/16 inch (4.8 mm), if full power is used. They can be mounted in plastic refrigerator containers for protection against the weather. Use well-insulated knobs to avoid rf burns during the adjustment process.

Separate 50-ohm lines run underground to the station. The shield side of their connectors should be grounded to the base of the tower and to the buried radials as directly as possible.

Tuning Procedure

It is suggested that the 160-meter wire be connected to the top of a structure 75 feet (22.86 m) tall or less. Note, from Table 9, that the monster at K5PFL was fed at 75 feet (22.86 m) above ground. Mount the standoff insulators so as to have a spacing of about 24 inches (0.61 m) between wire and tower. Pull the wire taut and clamp it in place at the bottom insulator. Leave a little slack below to permit adjustment of the wire spacing, if necessary.

Adjust the series capacitor in the 160-meter line for minimum reflected power, as indicated on an SWR meter connected between the coax and the connector on the capacitor housing. Make this adjustment at a frequency near the middle of your expected operating range. If a high SWR is indicated, try moving the wire closer to the tower. Just the lower part of the wire need be moved for an indication as to whether reduced spacing is needed. If the SWR drops, move all insulators closer to the tower, and try again. If the SWR goes up, increase the spacing. There will be a practical range of about 12 to 36 inches (0.31 to .91 m). If going down to 12 inches (0.31 m) does not give a low SWR, try connecting the top a bit farther down the tower. If wide spacing does not make it, the omega match shown for 80-meter work should be tried. No adjustment of spacing is needed with the latter arrangement which may be necessary with short towers or installations having little or no top loading.

The two-capacitor arrangement is also useful for working in more than one 25-kHz segment of the 160-meter band. Tune up on

the highest frequency, say 1990 kHz, using the single capacitor, making the settings of wire spacing and connection point permanent for this frequency. To move to the lower frequency, say 1810 kHz, connect the second capacitor into the circuit and adjust it for the new frequency. Switching the second capacitor in and out then allows changing from one segment to the other, with no more than a slight retuning of the first capacitor.

The omega match is recommended for 80-meter operation, because of the wide tuning range required. It was found that the point of connection could be at 28 feet (8.53 m), using a single support at the top of the first tower section. This served as a mount for the second standoff insulator for the 160-meter feed, as well.

A 40-meter feed, not shown, was connected at about 20 feet (6.10 m) up, with about 8 inches (203 mm) spacing between wire and tower.

Substituting Fixed-Value Capacitors

Depending on the frequencies used and the matching problems in a given installation, it may be possible to put fixed-value capacitors in place of some or all of the variables shown in Fig. 33, and then switch them remotely, or by hand, when changing frequency. This was done at W5RTQ. The 160-meter gamma capacitor is now a fixed-value, 150-pF type designed for high rf current service. It does not have to be weatherproofed, and it gives a satisfactory match over the small frequency range used on this band.

Two or three similar capacitors connected in series are used in covering the cw and phone frequencies in the 80-meter band. Operation around 3800 kHz requires about 50 pF in the omega (parallel) capacitor, so the three 150-pF units are used in series. Moving to cw operation near 3500 kHz requires about 75 pF, so only two 150-pF capacitors are used in series. The only variable now in the system is the 150-pF capacitor mounted in the plastic refrigerator box at the base of the tower. It is the series or gamma capacitor in the 80-meter feed. Even this could be replaced with a fixed unit, as it has been found unnecessary to adjust it in the course of normal operation of the station, if only small changes in frequency are made in using the two modes.

Because every tower installation is likely to be different from every other one in some respects, the values and dimensions given here may be subject to change, but the general principles should hold. Proof of this was found in the May 1975 issue of *Ham Radio,*[1] wherein W4OQ describes shunt-feeding in very similar terms. He also presented estimates of the electrical height of various tower-beam combinations that prospective shunt-feed users should find of interest.

It is hoped that this information will inspire others to try shunt-feeding their towers. This method offers an effective way to fire up on the lower frequencies that is useful to many who may have wanted to work these amateur frequencies but have shied away from doing so because of limited antenna space. This material was originally presented in *QST* by Earl W. Cunningham, K6SE.

[1]True, "Shunt-Fed Vertical Antennas," *Ham Radio,* May 1975.

The Minooka Special

This 160-meter vertical antenna could be just the one for you, if you reside on property of city-lot size or are a mobile operator. You can make it from readily available, inexpensive material.

Inspiration for the design offered here resulted in part from the author's survey of antennas in use by 160-meter operators, worldwide. An extensive report was compiled, which filled a loose-leaf notebook! A boil-down of the most useful information resulted in an 11-page report which was made available to numerous amateurs. Subsequently, the writer was encouraged to submit some of the data for publication. Approximately 60 operators were polled. The following information from that inquiry should be of interest to those who are curious about "preferred" antennas for top-band use.

Question 1: "If you could put up any antenna for 160, what would it be?" *Result:* 60% favored verticals, 30% said horizontals, and 10% indicated mixed feelings. (The term "vertical" includes various configurations — 1/4, 1/2, and 5/8 wavelength, vertical arrays, and inverted Ls.)

Question 2: "Comparing antennas that an average ham could build, do you prefer verticals or horizontals for 160?" *Result:* 70% said vertical, 17% favored horizontal, 5% inverted L, 2% horizontal and vertical, 2% inverted V, and 3% had no opinion. Reasons given for the responses were, "Because of signal comparisons and past experience. A backyard-compatible vertical is more effective than a backyard-compatible horizontal."

Question 3: "Do you operate mobile on 160? If so, what is the antenna used?" *Result:* Three used base-loaded verticals, eight used center-loaded ones, and one employed a Heliwhip. Some of the operators used capacitance hats. Other questions in the survey dealt with receiving antennas, types of soil and terrain, besides requesting complete details of the present transmitting antenna.

Fig. 34 shows some of the vertical systems used when the poll began in 1969. Additional configurations used by successful 160-meter operators are illustrated in Fig. 35. It can be seen that a great deal of useful "backyard theory" is represented in the systems shown. The experience and trials of others can save countless years of experimenting with antennas (not that some of us can't use the exercise)! It is hoped that these data will be of value to future 160-meter operators.

The Minooka Special

The following is a description of an effective vertical antenna for 160 meters, designed with these objectives in mind:

1) Highly effective for 160-meter DX and local work.
2) Easy to build and adjust.
3) Very economical.
4) Fits neatly into back yard.
5) Reasonable bandwidth.
6) Good for portable and DXpedition work.
7) Can be scaled down for mobile operation.

The resultant antenna (Fig. 36) is top loaded inductively and can be built by anyone from readily available material. Only a dip meter and SWR indicator are needed for tune-up. Many versions were built and tested, ranging from 7-foot (2.13-m) mobile types to 60-foot (18.29-m) backyard

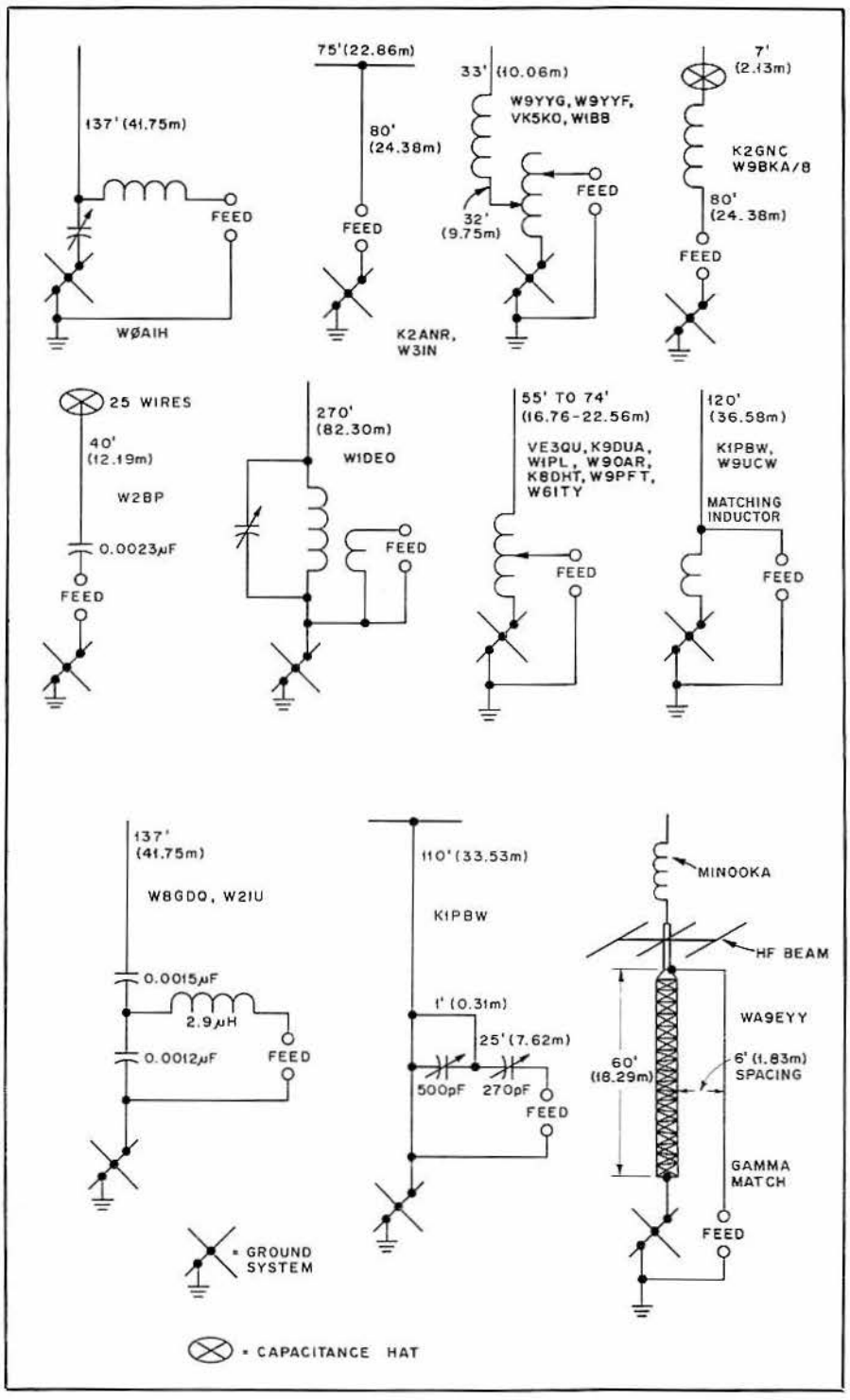

Fig. 34 — Illustrations of vertically polarized 160-meter antennas used by various operators for DX and local work. L and C values are not specified in some of the examples because the data were not furnished by the users.

Table 10

	No. 1	*No. 2*	*No. 3*	*No. 4*	*No. 5*	*No. 6*
X	5 ft (1.52 m)	8 ft (2.43 m)	4 ft (1.22 m)	4 ft (1.22 m)	19 ft (5.79 m)	3 ft 3 in. (0.99 m)
Y	2 ft (0.61 m)	15 in. (381 mm)	3 ft 6 in. (1.07 m)	4 ft (1.22 m)	11 in. (279 mm)	3 ft (0.91 m)
Z	As long as possible					
Wire Size	No. 20	No. 19	No. 18	No. 16	No. 19	No. 22

Here is a 50-foot (15.24-m) version of the Minooka Special. It is tuned remotely at K9SKX, and is used on 160 through 20 meters. Nylon or polypropylene guy lines should be used.

or DXpedition models. They have been used with good results from 20-foot (6.10-m)-wide backyards in cluttered Chicago, to vast beaches on Carribean islands, and in South America. The fixed-tuned bandwidths vary from 10 kHz for mobile versions, to 50 kHz for the larger fixed-station models (SWR 2:1 or better).

Construction

The physical layout of the antenna is centered around the use of 3/4-inch (19-mm) diameter rigid PVC water pipe. This sturdy tubing has an outside diameter of 1 inch (25 mm). The inner diameter provides an "interference fit" for 1/2-inch (13-mm) EMT conduit (thinwall). A 3/8-24 nut is driven into a 5-inch (127-mm) length of conduit, then aligned and braized into position. Next, the conduit is taper-ground and polished on the opposite end, then driven into the PVC tubing (see table of dimensions).

In the construction of mobile antennas another piece of conduit is driven into the bottom of the PVC coil form and a 3/8-24 bolt is brazed into the bottom end. The bolt will mate with standard mobile antenna mounts. For larger versions of the antenna the PVC material can be mounted in TV masting, or whatever. A standard 8-foot (2.44-m) stainless-steel whip between 3 and 8 feet (0.91 and 2.44 m) in length can be screwed into the top section. For home-installed versions of the antenna a

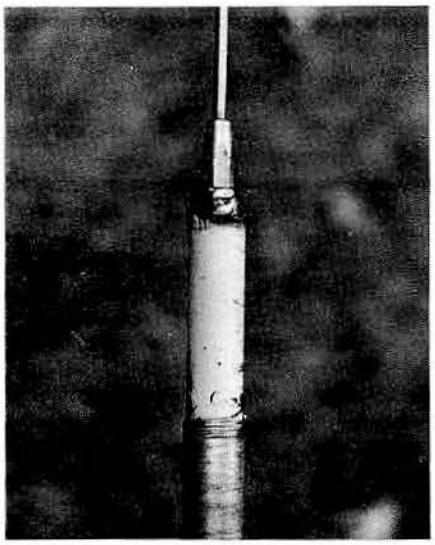

Close-up view of the top section of a coil assembly. This unit was used during mobile operation for over three years (40,000 miles or 64,374 km).

A mobile version of the Minooka Special is shown mounted on the author's car.

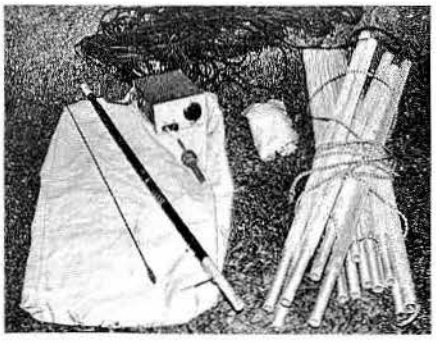

A portable version of the 160-meter vertical antenna. It was used by W9YYG and W9UCW at HKØBKX in January 1974.

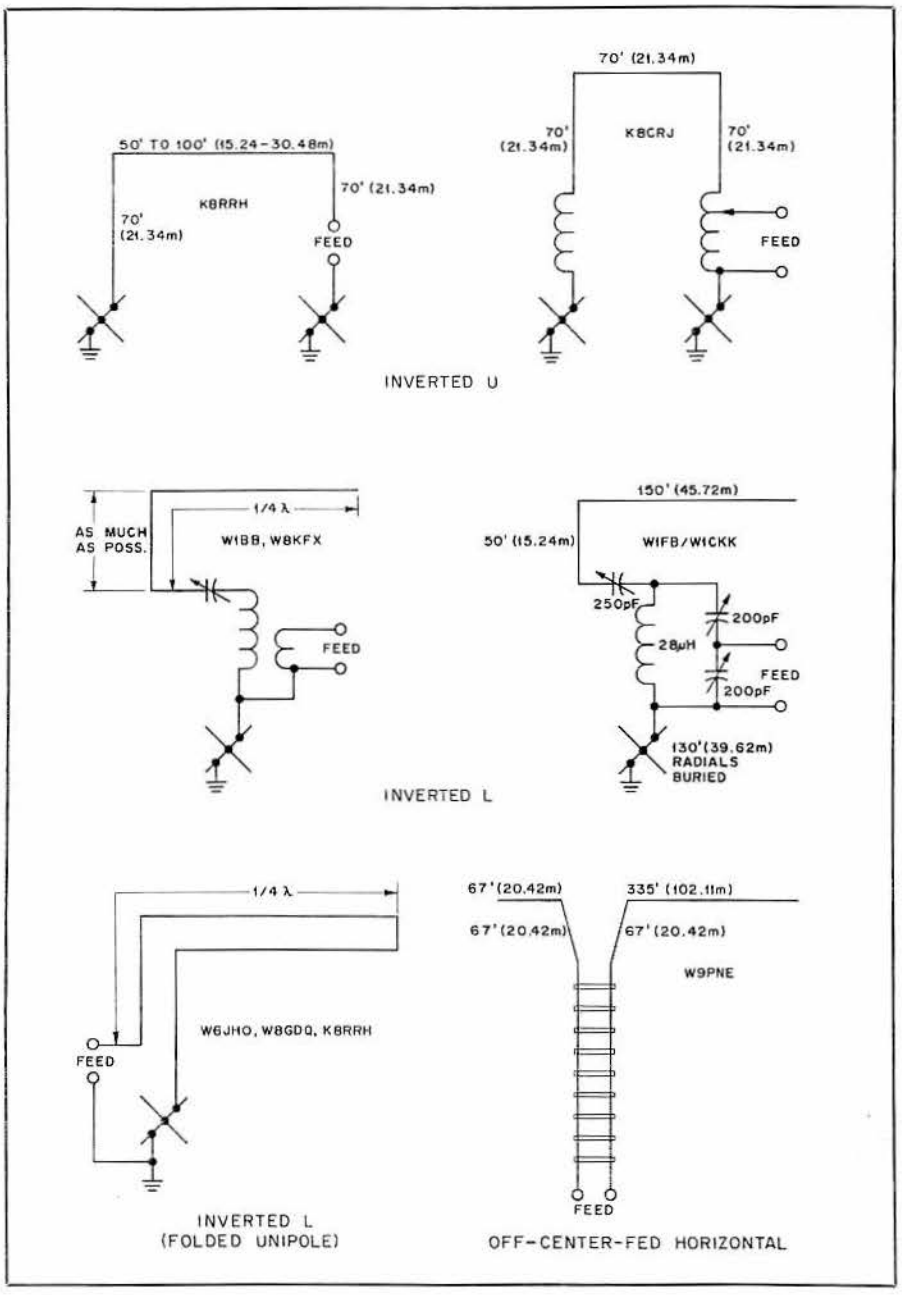

Fig. 35 — Examples of additional antennas for 160 meters which proved effective for long-haul work.

3- or 4-foot (0.91- or 22-m) piece of thin-wall tubing can be used in place of the whip. This will save on the cost of materials, and will eliminate the need to have brazing done. The coil wire should be soldered to the conduit to assure a good electrical connection.

Adjustment

Pick a set of dimensions from the table which suits your application, but add a few inches more of coil turns (all turns close wound) than are recommended. This will allow leeway for pruning the system to resonance.

To simplify adjustment it is suggested that the system be assembled first with only the coil and top section (no base section). Place the antenna where it is in the clear (on the car or fixed-station site), and where it can be tuned against the proposed ground system — car body or ground radials.

A three-turn link should be connected temporarily between the lower end of the coil and the ground system. This will permit rough tuning of the system to resonance by inserting a dipper coil into the link and adjusting the coil turns on the antenna until a dip is noted in the desired part of the band. Upon completion of the pruning the constructor can, if he wishes, cover the coil with weatherproof tape or shrink tubing. The antenna should be tuned for roughly 2000 kHz if the entire band is to be used. Adjust the resonance for 1850 kHz if only the low segment will be utilized.

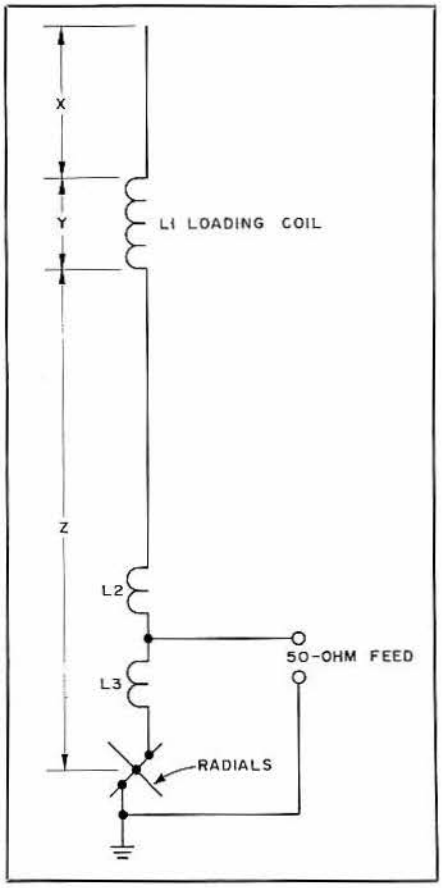

Fig. 36 — Electrical details of the Minooka Special. Table 10 gives specific information concerning dimensions X, Y and Z. L2 may vary in size from 1 to 20 turns, and L3 will contain between 5 and 10 turns, typically. L2 and L3 are made from no. 18 wire, spaced 1/8 inch (3 mm) between turns. The coil diameter is 1-1/2 inches (38 mm). Refer to text for tuning instructions.

Erect the antenna with all of its parts — coil, top and bottom section — and insert inductors L2 and L3 of Fig. 36 as shown. With L3 temporarily out of the system, adjust L2 for the lowerest value of SWR obtainable at the desired operating frequency. Then, place L3 back in the circuit and adjust it for an SWR reading of 1. Addition of the base section later on will not affect the resonant frequency of the overall system materially, provided the base section does not exceed, say, 60 feet (18.29 m).

The foregoing steps are used also in adjusting the mobile version of the antenna. However, because of the small size it is possible to adjust the antenna in completely assembled form. Only L3 of Fig. 36 is needed for mobile antennas. The main coil, L1, is adjusted for resonance, then L3 is set for lowest SWR. L3 can be mounted inside the trunk or under the bumper in a weatherproof enclosure.

For fixed-station operation it is recommended that a good ground system be employed. One should use at least 10 radials of, say, no. 18 or larger wire, 10 to 50 feet (3.05 to 15.24 m) in length. If you can manage 40 radials, 60 feet (18.29 m) in length, all the better.[1]

Concluding Comments

Three fixed-station versions of the Minooka Special have been tested and used at W9UCW. Each was compared against the regular antenna, which is a one-quarter wavelength vertical (130 feet [39.62 m] high), and operates against a radial system that contains 12,000 feet (3657.6 m) of wire. The short verticals were always inferior to the big antenna by approximately 5 dB.

Using version no. 4 from the table (4-foot [1.22-m] base section), the author worked W1s through W6s from the mobile setup. The rig was an HW-18 transceiver. Contacts were also made with VP9 and KV4 stations from the car.

While DXing from San Andres (HKØ) reports were received of signal strengths exceeding S9 plus 20 dB from Maine to Washington. Good reports were received from Europe also.

Because the loading coil acts as an rf choke at 3.5 MHz and above, several versions of the antenna have been used successfully from 160 through 20 meters with an appropriate L-network matching section installed at the base of the system.

Acknowledgements

The author wishes to express his gratitude to all who helped make this article possible, . . . particularly K9SKX, WA9EYY, and W9YYF, who assisted with the initial experiments on the Minooka Special. The participants in the antenna survey (a list too large to include here) deserve considerable thanks for their help as well. This material was originally presented in *QST* by Barry A. Boothe, W9UCW.

[1][Editor's Note: The reader should be aware that 1/4-wavelength radials (or longer ones) are recommended for best efficiency in a system of this kind. Detailed information on the subject is given in *The ARRL Antenna Book*, 13th Edition. The recommendations given by the author are no doubt based on the lack of space available in the typical urban lot, around which his design was established. See Hills, "The Grounds Beneath Us." *RSGB Bulletin*, June 1966.]

Inexpensive 5/8-Wave Vertical Antenna with Coaxial Transformer

The author's hastily constructed 5/8-wave vertical antenna (inspired by WØJF's results[1]) consists of a supporting structure made from sections of 2 ⅌ 2-inch (51 ⅌ 51-mm) lumber on which four lengths of 300-ohm TV ribbon are affixed. Each section of ribbon line is 41 feet 6 inches (12.65 m) long. A length of this line is attached to each side surface of the 2 ⅌ 2 support mast, then the ends (top and bottom) of all four line sections are connected in parallel to form a single vertical conductor. The coax-line dimensions are near those of W2JTJ,[2] and are shown in Fig. 37. The SWR varies from a flicker of reflected power at 14,000 kHz to 1.5:1 at 14,350 kHz. (The next task is to get that lowest-SWR point shifted to 14,275 kHz.) The whole thing is leaning against a tree, almost vertical, and seems to work well. This material was originally presented in *QST* by Robert J. Earl, W1DRV.

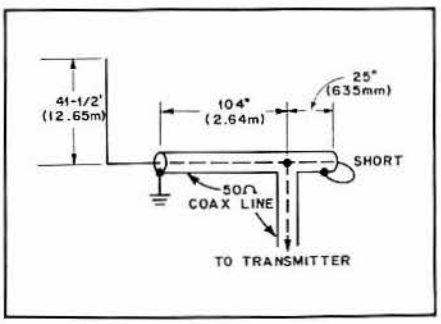

Fig. 37 — Coax-line transformer for 20-meter 5/8-wave vertical antenna.

References

[1]Beers, "Short Antennas for the Lower Frequencies," *QST*, August and September 1970.

[2]Czerwinski, "Coaxial Transformer for Voltage-Fed Antennas," *QST*, June 1961.

A Backyard 160-Meter Vertical

A 160-meter band was the favorite one at the author's QTH this winter. The same could be said for many other amateurs and the simple antenna described here may be of interest.

Some of the old-timers will tell the newcomer to 160 meters that the best antenna for local and DX work is the vertical. Since a full-size vertical would be very large, the question is finding a type that will fit into a closely packed residential area.

As a starter, the writer took an old 40-foot (12.19-m) telescoping mast and insulated it from the ground. (This can be done by setting it on top of a large soft-drink bottle, or clamping it to a wooden post.) The antenna was fed at the base with RG-58A/U 52-ohm coaxial cable. The shield was wired to a radial system and a ground rod. A hint for the radials — buy some aluminum clothesline and cut a number of slits in your yard with a flat spade. Next, push the wire into the slits and tamp the grass back together. If there are any swampy parts of the yard, these seem to make the best ground areas.

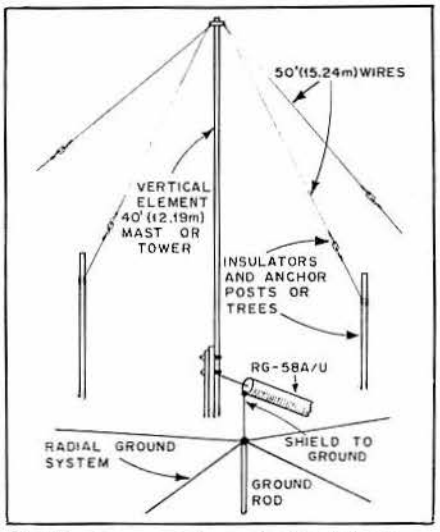

Fig. 38 — A space-saving vertical for 160 meters. While not always possible, it is desirable to have the wires for the top hat run off at right angles to the mast.

Rather than using a loading network at the base of the antenna, the author constructed a capacitive hat to load it at the top instead. The top hat was made from four 50-foot (15.24-m) pieces of wire strung out from the top of the mast in guy-wire fashion. They are connected electrically to the top, and stretched until they are as close as possible to a 90-degree angle with respect to the mast.

The system described works well with a 40-foot (12.19-m) mast, but other lengths could be used instead. However, the top hat may have to be adjusted in order to bring the system to resonance. While my vertical occupies very little space, it seems to perform as well as do many "full-size" antennas on 160 meters. This material was originally presented in *QST* by Mike Mussler, WB8JJA.

Chapter 2

Yagi Antennas

The antenna systems treated in this chapter are variations of the basic directional gain antenna devised many years ago by Yagi and Uda. Over the years the fundamental design and its variations have been referred to simply as the Yagi. How Mr. Uda was excluded from the credits remains a mystery, as he was a co-developer of the antenna under discussion.

Yagi types of antennas appeal to all manner of hf- vhf- and uhf-band operators. The primary response characteristic of the Yagi is unidirectional, discounting minor response lobes off the front, sides and rear of the antenna. The major lobe concentrates the radiated energy in a desired direction to provide gain in dB and discrimination against interference from unwanted directions.

Yagis can be used singly or in array combinations. In the latter case, each time the size of an array is doubled the system gain can be made to increase by 3 dB — assuming that the phasing, impedance matching, and aperture parameters are correct. Thus, a pair of 3-element Yagis which are "stacked" in an array to meet the foregoing criteria will exhibit 3 dB more gain than a single 3-element Yagi. To effect another 3 dB increase in gain, four 3-element Yagis would need to be placed in a given array of Yagis, and so on.

This chapter deals with the cream of the Yagi crop, so to speak, as taken from past issues of *QST*. When zoning laws and available property permit, the Yagi is preferred over the single-element vertical antennas described in chapter 1.

The 20-Meter DX Weasel

Short antennas have always captured the interest of amateurs.

The antenna presented here is a monoband version of the Bite-Size Beam for 20 and 15 meters published elsewhere in this chapter. It is designed for 20-meter operation only. Most of the parts were "lifted" from the original array.

The reader is cautioned against attempting to figure why some of the dimensions were selected. As a point of interest, they just happened that way. One new twist was added to this system — capacitance hats. The hats provided one noticeable improvement in performance which became obvious during the initial tune-up phase of the project. The hats lowered the Q of the elements and hence broadened the overall response of the system. While only conjecture, one might say that it is this broad tuning which causes the parasitic elements to perform as they do. Element tuning on the Bite-Size Beam[1] was critical. If the dimensions given here are followed carefully, the antenna should provide excellent characteristics for gain and pattern. Front-to-back measurements indicate approximately 20 dB. The front-to-side ratio was measured in excess of 25 dB. There are no objectionable side lobes. The SWR is less than 2:1 at each end of the band when the gamma capacitor and rod are set for proper operation at 14.1 MHz. There is no need to select phone or cw as the primary mode of operation.

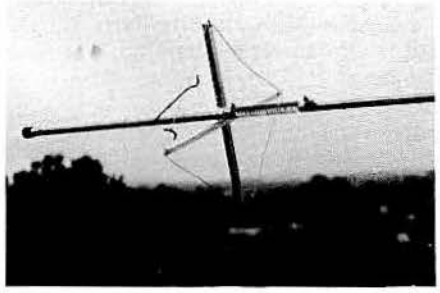

Details of the loading coil and capacitance hat on one of the elements.

Construction

The boom and all the elements are made from 1-1/4-inch (32-mm) diameter aluminum tubing available at most hardware stores. The two boom sections and the two pieces which make up the center portion of the driven element are coupled using 15-inch (0.38-m) sleeves of 1-3/8-inch (35-mm) OD aluminum tubing. Sheet-metal screws should be used to secure the sections within the coupling sleeves.

The loading coils are wound on 1-1/8-inch (29-mm) diameter Plexiglas rod. Details are shown in Fig. 1. Be sure to slit the ends of the aluminum tubing where the compression clamps are placed. The coils are made from no. 14 enameled wire. The specified number of turns are equally spaced to cover the entire 9 inches (229 mm) of Plexiglas.

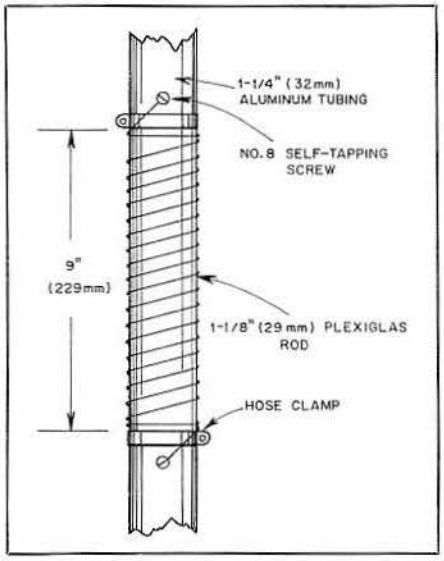

Fig. 1 — Details for joining sections of aluminum tubing and Plexiglas rod.

The capacitance hats are constructed from 3/4-inch (19-mm) angle aluminum. Two pieces 2 feet (0.61 m) in length are required for each hat. The model shown in the diagrams has the angle aluminum

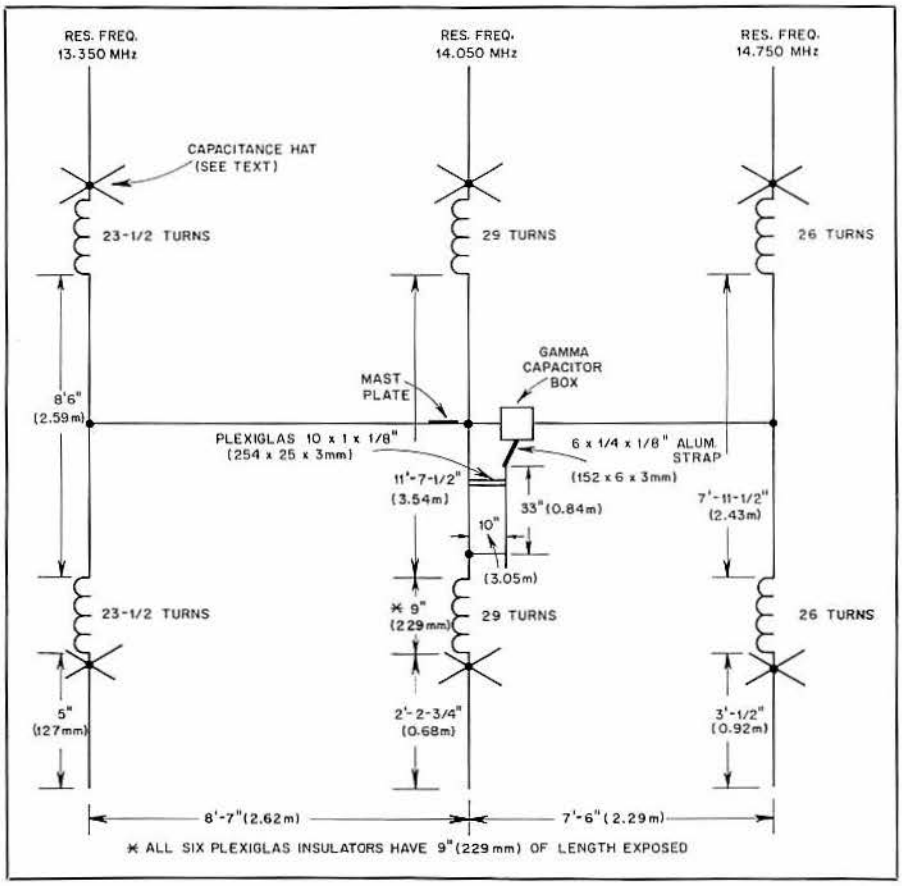

Fig. 2 — Constructional details for the 20-meter beam. The coils on each side of the element are identical. The gamma capacitor is a 140-pF variable unit manufactured by E. F. Johnson Co.

fastened to the element using aluminum strips and no. 8 sheet-metal screws, but sheet-metal screws alone can be used. Solder lugs are fastened to the ends of the angle aluminum and no. 12 or 14 wire connects the ends of the aluminum, resulting in a square loop. The wires should be soldered at each of the solder lugs.

All of the elements are secured to the boom with TV U-bolt hardware. Plated bolts are desirable to prevent rust from forming. An aluminum plate 9 inches (229 mm) square by 1/4-inch (6-mm) thick was used as the boom-to-mast plate.

A boom strut is recommended because the weight of the elements is sufficient to cause the boom to sag. A 1/8-inch (3-mm) diameter nylon line is plenty strong. A U-bolt clamp is placed on the mast several feet above the antenna and provides the attachment point for the center of the truss line. To reduce the possibility of water accumulating in the element tubing and subsequently freezing, crutch caps are placed over the ends. Rubber feet suitable for keeping furniture from scratching hardwood floors would serve the same purpose.

A piece of Plexiglas was mounted inside an aluminum Minibox to provide support and insulation for the gamma capacitor. A plastic refrigerator box would serve the purpose just as well. The capacitor housing is mounted to the boom by means of a U bolt. The gamma rod is made of 3/8-inch (10-mm) aluminum 40 inches (1.016 m) long and is connected to the gamma capacitor by a 6-inch (152-mm) length of strap aluminum.

Tune-Up and Operation

The builder is encouraged to follow the dimensions given in Fig. 2 as a starting point for the position of the gamma rod shorting strap. Connect the coaxial cable and install the antenna near or at the top of the tower. The gamma capacitor should be adjusted for minimum SWR at 14.1 MHz as indicated by an SWR meter (or power meter) connected in the feed line at the gamma capacitor box. If a perfect match cannot be obtained, a slight repositioning of the gamma short might be required.

Evaluation of performance is always a difficult task. The 20-Meter DX Weasel is mounted on top of a 50-foot (15.24-m) high tower at the QTH of W1FB. The transmitter input power for the testing period was 3 watts. Many European stations as well as a ZL have been contacted with ease. In fact, the Weasel has been responsible for cracking a few pileups on the first call!

Table 1

Complete Parts List for the Short Beam

Qty	Material
2	10-foot (3.05-m) lengths of 1-1/4-inch (32-mm) dia. aluminum tubing (one for the reflector center section, one for the reflector end sections).
3	8-foot (2.44-m) lengths of 1-1/4-inch (32-mm) dia. aluminum tubing (two lengths for the boom, one length for the director element center).
4	6-foot (1.83-m) lengths of 1-1/4-inch (32-mm) dia. aluminum tubing (two lengths for the driven element center, two lengths for the director and driven element ends).
2	15-inch (0.38-m) lengths of 1-5/8-inch (41-mm) dia. aluminum tubing.
1	40-inch (12.19-m) length of 1-3/8-inch (10-mm) dia. aluminum tubing.
4	6-foot (1.83-m) lengths of 3/4-inch (19-mm) angle aluminum.
6	12-inch (0.31-m) lengths of 1-1/8-inch (29-mm) dia. Plexiglas rod.
1	9-inch (229-mm) square, 1/4-inch (6-mm) thick aluminum plate.
8	U bolts.
12	Compression hose clamps.
8	Crutch caps.
38 ft	No. 12 enameled copper wire.
60 ft	No. 14 enameled copper wire.

Obtaining the Material

Table 1 lists all of the major parts used in the 20-meter Weasel. Most of the U-bolt hardware as well as the aluminum tubing should be available from large hardware stores. The Plexiglas rod, however, presents a bit more of a problem as indicated by mail received by the ARRL Technical Department. Many large plastic supply dealers stock the cast rod. The problem is that there are not very many large dealers! Additionally, Plexiglas is a petroleum-base product which means the cost is no doubt higher than one would expect. Those amateurs who are unable to locate aluminum hardware or Plexiglas should consult the yellow pages to see who their nearest supplier is. This material was originally presented in *QST* by Robert Myers, W1XT and Jay Rusgrove, W1VD.

[1]See page 45.

The HW-40 Micro Beam

A helically wound 2-element 40-meter Yagi.

Disconsolate pleas from apartment dwellers and other amateurs who live on property that is too small in area to permit the use of large 40-meter antennas prompted the authors to develop the antenna described here. The particular dimensions represented in this design were dictated primarily by the kind of fiberglass tubing that was immediately available. Kirk quad spreaders were obtained for use as forms on which to wind the helical elements. Longer (or shorter) elements can be used with good results. This article is intended as a guide in the design of similar antennas.

The HW-40 is scaled down to 28 percent of full size. Two elements are used, each being 18 feet (5.49 m) in length, tip-to-tip. Thus, the elements are just 2 feet (0.61 m) longer than those of a full-size 10-meter Yagi. A 16-foot (4.88-m)-long Reynolds aluminum-tubing boom (two 8-foot [2.44-m] lengths joined) provides 0.12-wavelength spacing between the driven element and reflector. The weight of the array is approximately 25 pounds, making it practical to use a TV-type antenna rotator with the system.

The HW-40 beam, just 28 percent of full-size, is light enough to require only a TV-rotator.

Design Considerations

Some may argue that helically wound antennas will tend to radiate off the ends of the elements (axial mode), and that the condition will prevent the Yagi from exhibiting normal front-to-side and front-to-back characteristics. It was established by Kraus,[1] that axial-mode radiation occurs only when a helix is one wavelength or greater in circumference. Generally, when the circumference is less than two-thirds wavelength, a nearly sinusoidal type of current distribution exists. This is effected by alternate reinforcement and cancellation of the two traveling waves which are directed oppositely. Each is of nearly identical current amplitude (I_0), hence the T_0 transmission mode results for both traveling waves on the helix. Because of the foregoing condition the helices of this antenna radiate in the *normal mode* and will exhibit linear polarization characteristics. The diameter of these helices is merely 0.0009469 wavelength, eliminating any opportunity for axial-mode radiation. Front-to-side and front-to-back checks of the beam indicate, indeed, that normal-mode radiation is occurring. A number of relative tests were performed locally at distances up to 20 miles, and the front-to-back characteristics indicate a 10-dB figure. Front-to-side checks confirm a figure of approximately 28 dB. The effect is not so pronounced when receiving high-angle incoming signals. Depending upon the time of day, distance involved, and other propagation factors, various directivity traits will be observed.

Helically wound elements were chosen in preference to lumped-inductance elements in order to obtain linear voltage and current distribution across the elements, and to make the matching technique less difficult. Even if end-loaded elements with capacitance hats were used, the 18-foot (5.49-m) dimension would make it impossible to use a gamma match of conventional design. Because of the very low value of radiation resistance of short loaded antennas, other conventional matching schemes would not lend ease to matching a 50-ohm coaxial feeder to the system.

There are certain penalties one must accept when using physically shortened antennas of this kind, and an in-depth treatment of the subject was given by Sevick in *QST*.[2] It was a fortunate circumstance in this case that the feed-point impedance of the beam turned out to be approximately 12 ohms. Therefore, a 4:1 toroidal balun was installed at the feed point to provide a near-perfect match to the 50-ohm transmission line. In addition to encountering low values of feed impedance, the bandwidth of loaded elements is greatly less than with full-size antennas. This beam was tuned for operation at a center frequency of 7050 kHz. It works well from 7025 to 7075 kHz, with an SWR no greater than 2:1. It is flat at 7050 kHz. Those wishing to duplicate this Yagi should be willing to accept this design trade-off in the interest of having an effective directional antenna. It is recommended, therefore, that it be tuned for one's favorite part of the 40-meter band. The use of a Transmatch will, however, permit excursions into portions of the band where the SWR becomes greater than 1:1.

Construction Details

The construction of the 40-meter beam is very simple and requires no special tools or hardware. Two fiberglass 15-meter quad arm spreaders are mounted on an aluminum plate with U bolts, as shown in the photograph. A wooden dowel is inserted approximately 6 inches (152 mm) in the end of each fiberglass arm to prevent the U bolts from crushing the poles. The aluminum mounting plate is equipped with U-bolt hardware for attachment to the 1-1/4-inch (32-mm) diameter boom.

A plastic refrigerator box is mounted on each element support plate and is used to house a Miniductor coil. No. 14 copper wire is used for the elements. The wire is wound directly on the fiberglass poles at a density of *40 turns per foot* (not turns per inch!) for a total of 360 evenly spaced turns. The wire is attached at each end with an automotive hose clamp of the proper size to fit the fiberglass rods. Since the fiberglass is tapered, care must be taken to keep the turns from sliding in the direction of the tips. Several pieces of plastic electrical tape were wrapped around the pole and wire at intervals of 1 foot (0.31 m). All of the element half sections are identical in terms of wire and pitch. Coil dimensions and type are given in Fig. 3.

The driven-element matching system consists of a 4:1 balun transformer and a link tightly coupled to the Miniductor. Complete details are given in Fig. 4.

Mounted at the end of each element (held in place by the hose clamp) is a short section of stiff copper wire used to allow for final tuning of the system as well as to broaden the frequency response of the antenna. Since the overall antenna is very small in relation to a full-sized array, the SWR points of 2:1 are rather close to each other, as mentioned earlier. The antenna shown in the photograph provides an SWR of less than 2:1 within about 25 kHz either side of resonance. Tuning the antenna for phone-band operation should not be difficult and the procedure outlined below should be suitable.

Tuning

The parasitic element is adjusted to be about four percent lower in frequency than

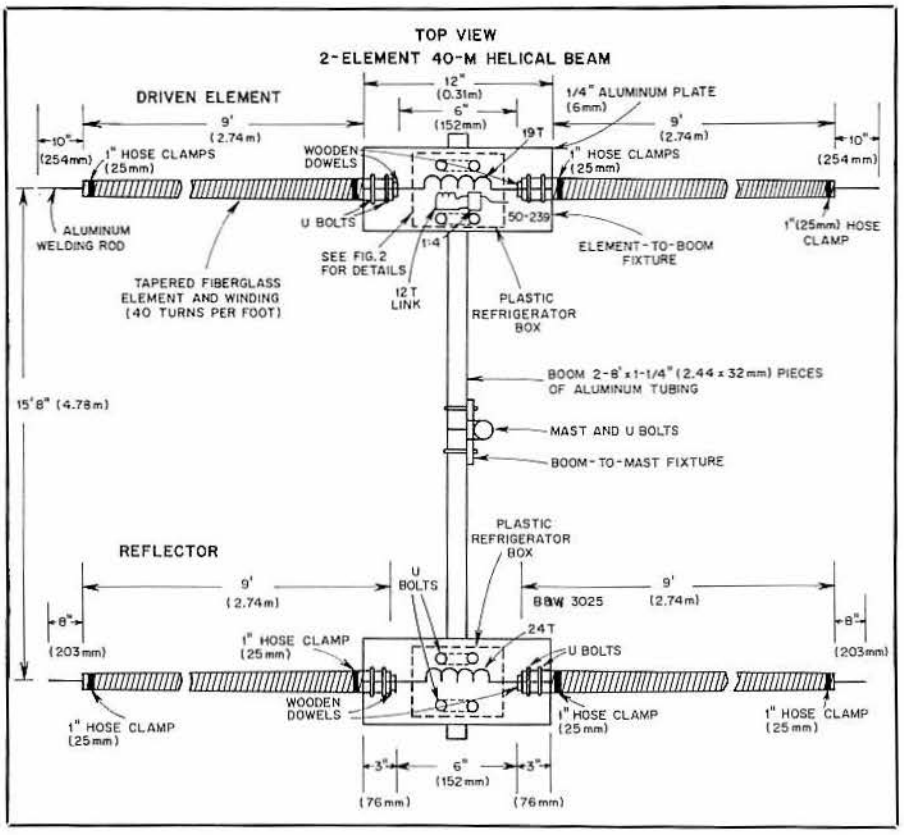

Fig. 3 — Overall dimensions for the 40-meter short beam. The boom consists of two pieces of standard 1-1/4-inch (32-mm) dia do-it-yourself aluminum tubing.

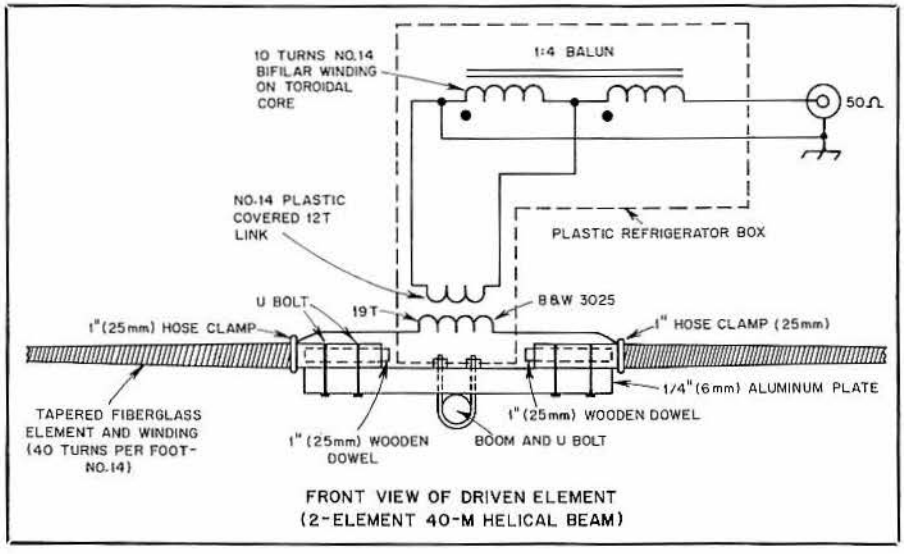

Fig. 4 — Schematic diagram of the balun assembly mounted inside the plastic utility box. The core is a single T-200-2 Amidon. The 12-turn link is wound directly over the 19-turn Miniductor.

the driven element. A grid-dip oscillator was coupled to the center loading coil and the element tips were trimmed (a quarter of an inch [6 mm] at a time!) until the GDO indicated resonance to be at 6.678 MHz. For phone-band use, the ends could be snipped for 6.840 MHz. Adjusting the driven element is simple. Place an SWR meter or power meter at the input connector and cut the end wires (or add some if necessary) to obtain a proper match between line and antenna.

Performance Characteristics

Once the initial near-ground tuning of the elements was completed, the HW-40 was carried aloft and mounted on the 40-foot (12.19-m) tower at W1FB. Final touching up of the matching and element resonances was effected after the beam was in place on the tower. It is important to realize that shortened antennas are sensitive to changes in environment because of their narrow-band characteristics. Thus, height above ground and distance from nearby objects will cause some change in resonance of the elements. The resonant frequency of the HW-40 changed some 150 kHz between tuning at several feet above ground to final tweaking atop the tower.

It should be noted that the 40-meter beam has yet to be tested at an ideal height above ground. A distance of 40 feet (12.19 m) above the earth is not much more than one-quarter wavelength at 7 MHz, though performance thus far has been better than one might expect when using a beam or dipole less than one-half wavelength above ground.

Comparisons were made between the beam and three types of wire antennas . . . an inverted V, a 3/4-wavelength end-fed wire, and a full-wave 40-meter loop (with its theoretical 2-dB gain).[3] The results have been interesting, though at times rather confusing. The confusion results from the time-of-day/propagation syndrome mentioned earlier. At no time, however, did the inverted-V or 3/4-wavelength antennas surpass the performance of the HW-40. The beam was always as good as or better than the other two radiators, regardless of band conditions or time. During contacts with European or South American DX stations, the beam was always the best antenna, usually by two S units or more. During daytime contacts out to, say, 1000 miles, the wire antennas equalled the beam at times.

When comparing the beam to the full-wave loop, results became less easy to evaluate. That is, the antennas took turns being best. Frequently, the loop outperformed the beam (in the favored direction of the loop) both on short-haul and DX contacts. At other times the beam had the edge by a couple of S units. At this time it is impossible to say which antenna would provide the best all-year, all-around service. But, it has been observed that the beam is far less subject to pickup of man-made and atmospheric noise because of its narrow-band characteristics (the loop exhibits the opposite bandwidth trait— broad). Reduction in noise during reception can be a blessing, especially when working with the weaker signals! Another beneficial effect of the narrow-band feature is that strong, near-frequency signals do not se severely affect the receiver with respect to overloading and cross modulation, as is the situation with other types of antennas. The proof of this came when trying to operate while W1AW (two blocks away from W1FB) was transmitting code practice. Until the beam was erected it was impossible to use the 40-meter band, but with the beam connected to the receiver, and with the antenna pointed away from W1AW, it became possible to operate within 10 kHz of W1AW without knowing that station was on the air! So, if

some kW operator lives down the street from you, this little beam could put you back in business.

While running approximately 80 watts output, the short beam has been extremely effective in working DX. DX stations now answer our CQs, whereas with the wire antennas (loop excepted) this seldom happened. Signal reports from DX stations average 579, with many 589 and 599 reports. During QRP operation with the beam (2 watts output), a number of DX stations have been raised and worked. The signal reports are lower of course, but RST 559 and 569 indicates that something good must be happening! One unrelated event occurred while testing the beam and loop with the QRP setup: a station in the 4th call area called CQ and was answered. He came back and said, "No QRP lids, CQ kWs only." It's unlikely that the HW-40 beam can be blamed for that, especially since we went on to work five European stations later that day with the 2-watt equipment!

Acknowledgements

The authors wish to express gratitude to those who helped construct, test and erect the 40-meter beam. Special thanks to K1JX, who "clomped" up and down the ARRL test tower and the W1FB station tower numerous times with test gear (and the beam) until the final design goals were met. Thanks also to W1NPG (SK) who labored silently while winding the helices, and subsequently endured the unbearable Connecticut heat-wave temperatures of August, while putting two coats of exterior spar varnish on the completed elements. The element dimensions and turns information were developed by K1TD to test a newly developed calculator program. This material was originally presented in *QST* by Robert Myers, W1XT and Doug DeMaw, W1FB.

References

[1]Kraus, *Antennas*, First Edition, McGraw-Hill Book Co., Chapter 7.
[2]Sevick, "The Ground-Mounted Short Vertical," *QST*, March 1973, p. 13. (See Chapter 1.)
[3]DeMaw, "The Novi-Loop," *QST*, October 1973. (See Chapter 4.)

A Bite-Size Beam for 20 and 15 Meters

Do you want to work DX from your space-restricted QTH with increased effectiveness? If the answer is yes, perhaps this two-band Yagi system is just the one for you.

There is no doubt that a hundred-foot (30.48-m) tower with stacked monobanders for 20 and 15 meters is one way to generate an effective signal in the pileups. But what are the characteristics of this big system which make it perform better than a dipole strung between two trees? First, the tall tower places the antenna up in the clear, away from most of the surrounding ground clutter. Even a relatively short tower (40-foot [12.2-m] variety) provides this advantage in many instances. The ability to point the major radiation lobe of the antenna in the correct direction is another reason the high monobanders outperform the kinky wire. But if the antenna is capable of supporting its own elements, the directional characteristics can be used to good advantage whether the beam is mounted at 100 feet (30.5 m), or at 40 feet (12.2 m). And without any question, the ability to reject interference aids substantially in the reception of weak signals.

A typical one-foot (0.31-m)-per-side triangle tower is self-supporting (when properly installed) to 40 feet in height and requires less than one square foot of property. For many amateurs, the major limiting factor is the inability to turn a monoband beam (or even a large tribander) without hitting some object like a tall tree. Hesitation on behalf of the amateur to place what might be considered by his neighbors an offensive amount of hardware in the sky near his home is another reason beams are ruled out. The 2-element-per-band, 20- and

15-meter, interlaced Yagi presented here, overcomes these problems. It is lightweight and is less than 16-feet (4.88-m) square. And it's probably no more obtrusive than a large TV antenna.

So What if It's Short!

A popular misconception among amateurs is that any element short of full size is no good in an antenna system. Reducing the size of an antenna by 50 percent does lower the efficiency by a decibel or two, but the gain capability of a parasitic array outweighs this small loss in efficiency. Mounting the antenna above the interference-generating neighborhood can greatly reduce susceptibility to man-made noise and certainly aids in the reduction of rf heating to trees, telephone poles, and buildings. It has been said that a brick wall, or dense foliage, can attenuate a signal passed through it by as much as 20 dB. Placing the antenna above these energy-absorbing objects is very desirable.

The coils are wound on Plexiglas rod. Compression clamps are used to hold the Plexiglas in position. Sheet-metal screws and solder lugs provide attachment points for the ends of the loading coils.

View of the short beam from the front yard at W1FB.

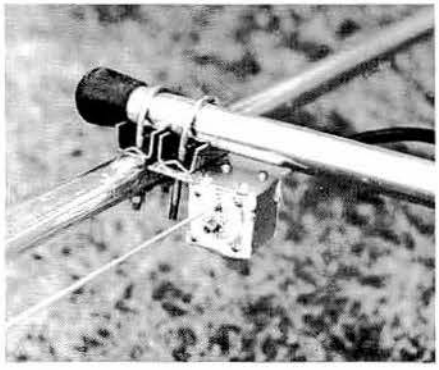

The gamma assembly is held in place by means of a small U bolt. The capacitors are mounted on etched circuit board.

It is a generally accepted fact that traps are difficult to build and adjust, as well as their being lossy. Loading coils, on the other hand, are easy to wind and require essentially no adjustment. If the wire size is large, losses are not a major factor. W2FMI lauded the merits of short antennas in an earlier article explaining that in reality, short (50 percent) elements do not materially depreciate the gain.[1] With these ideas in mind, the authors designed and built a shortened-element, but wide spaced, director array for 20 meters interlaced with a similar 15-meter reflector configuration also having optimum spacing for maximum gain. By placing the 15-meter driven element in front of the 20-meter array, the longer 20-meter elements tend to act as reflectors on 15 meters. There are no unwanted reflectors "in front" nor any directors "behind" the active array — elements which could cause pattern distortion and poor front-to-back ratio.

Construction

The dual-band beam has four elements, the longest of which is 16 feet (4.88 m). All of the elements and the boom are made from 1-1/4-inch (32-mm) diameter aluminum tubing available at most hardware stores. Element sections and boom pieces are joined together by slotting a 10-inch (254-mm) length of 1-1/4-inch (32-mm) tubing with a nibbling tool and compressing it for a snug fit inside the element and boom tubing. Coupling details are shown in Fig. 6.

The loading coils are wound on 1-1/8-inch (29-mm) diameter Plexiglas rod. The rod slips into the element tubing and is held in place with compression clamps. Be sure to slit the end of the aluminum where the compression clamps are placed. The model shown in the photographs has coils made of surplus Teflon-insulated miniature audio coaxial cable with the shield braid and inner conductor shorted together. A suitable substitute would be no. 14 enameled copper wire wound to the same dimensions as those given in Fig. 5.

All of the elements are secured to the boom with common TV U-bolt hardware. Plated bolts are desirable to prevent rust from forming. A 1/4-inch (6-mm) thick boom-to-mast plate is constructed from a few pieces of sheet aluminum cut into 10-inch (254-mm) square sheets and held together with no. 8 hardware. Several cookie tins could be used if sheet aluminum is not available. One local amateur used a plate from a large electrical box as a boom-to-mast bracket. Since it is galvanized, it is quite resistant to the harsh New England winters.

A boom strut (sometimes called a truss) is recommended because the weight of the elements is sufficient to cause the boom to sag a bit. A 1/8-inch (3-mm) diameter nylon line is plenty strong. A U-bolt clamp is

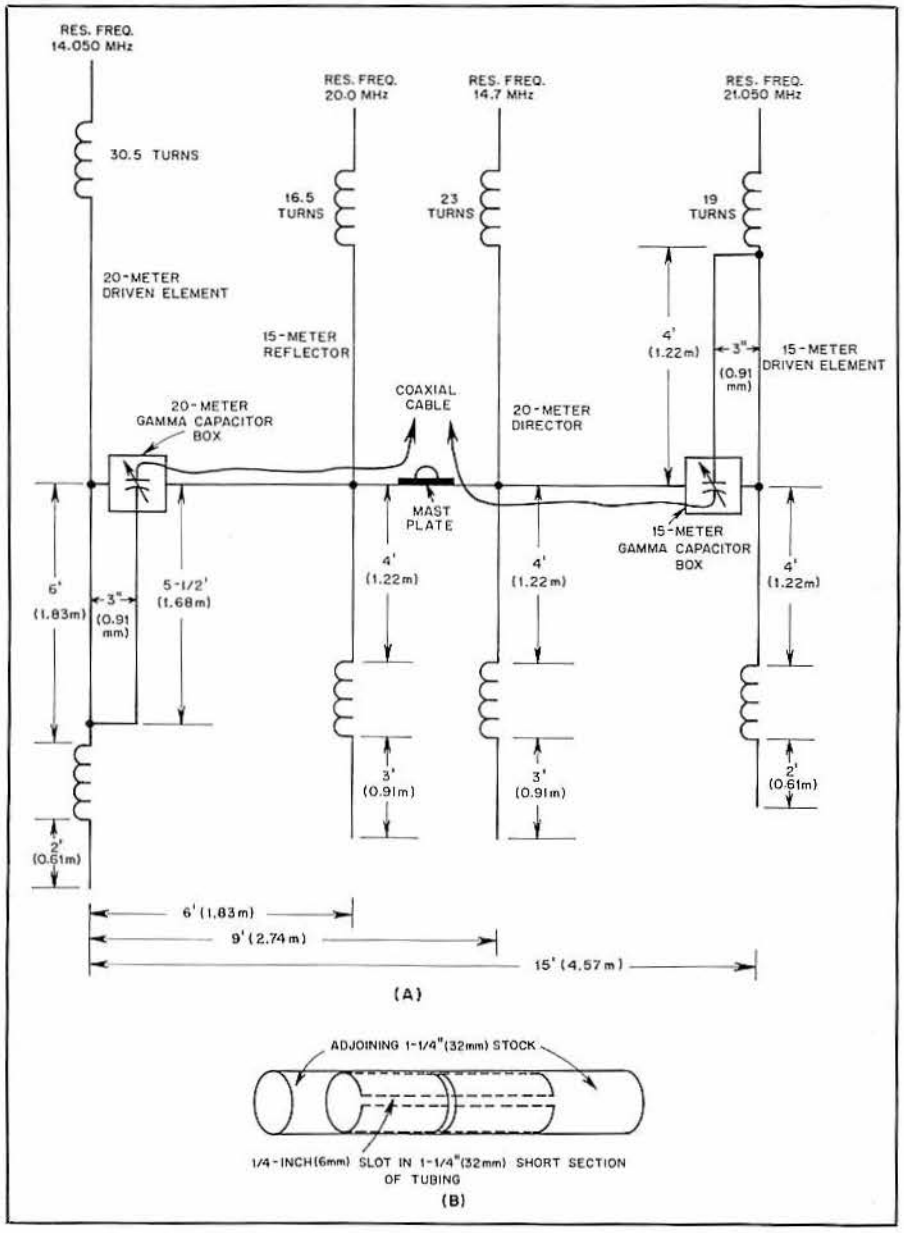

Fig. 5 — Constructional details for the 20- and 15-meter beam. The coils for each side of the element are identical. The gamma capacitors are each 140-pF variable units manufactured by E. F. Johnson Co. The capacitors are insulated from ground within the container. Since the design is one-half size for each band, the tuning is somewhat critical. The builder is encouraged to follow carefully the dimensions given in the text.

Table 2

Complete Parts List for the Short Beam

Qty	Material
9	8-foot (2.44-m) lengths of aluminum tubing, 1-1/4-in. (32 mm) dia
11	U bolts
2	Variable capacitors, 140 pF (E. F. Johnson)
4 ft	Plexiglas cast rod, 1-1/8-in. (29 mm) dia
16	Stainless steel hose clamps, 1-1/2-in. (38 mm) dia
1	Aluminum plate, 8-in. (203 mm) square
10 ft	Aluminum solid rod, 1/4-in. (6 mm) dia
2	Refrigerator boxes, 4 X 4 X 4 in. (102 X 102 X 102 mm)
25 ft	Nylon rope, 1/8-in. (3 mm) dia
16	No. 8 sheet metal screws
16	No. 8 solder lugs
8	Plastic (or rubber) end caps, 1-1/4-in. (32 mm) dia

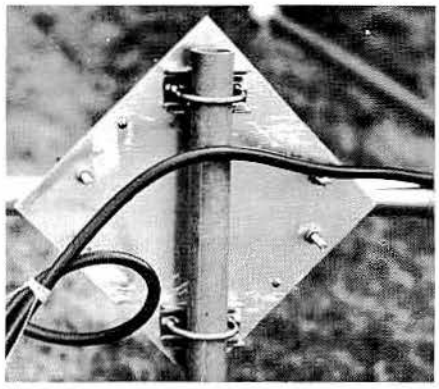

The boom-to-mast plate.

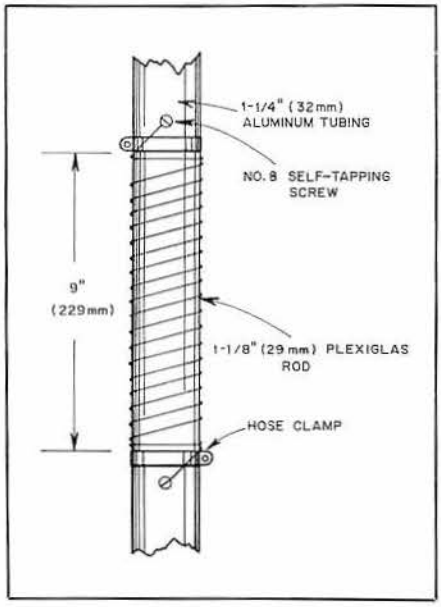

Fig. 6 — Coupling details for joining sections of aluminum tubing.

placed on the mast several feet above the antenna and provides the attachment point for the center of the truss line. To reduce the possibility of water accumulating in the element tubing and subsequently freezing (rupture may be the end result), crutch caps are placed over the element ends. Rubber feet suitable for keeping furniture from scratching hardwood floors would serve the same purpose. In fact, the rubber tips prevent the element ends from damaging surrounding objects during installation.

A heavy-duty steel mast should be used, such as a 1-inch (25-mm)-diameter galvanized water pipe. Steel TV mast is also acceptable. Any conventional TV-type antenna rotator should hold up under load conditions presented by this antenna. Nevertheless, certain precautions should be taken to assure continued trouble-free service. For instance, whenever possible, mount the rotator inside the tower and extend the mast through the tower top sleeve. This procedure relieves the rotator from having to handle lateral pressures during windy weather conditions. A thrust bearing is desirable to reduce downward forces on the rotator bearings.

Hookup and Operation

The monoband nature of the beam requires the use of two coaxial feed lines. The coaxial cable is attached to the 15-meter element (at the front of the beam) at the gamma-capacitor box. The other end of the cable is connected to a surplus 28-V dc single-pole coaxial switch.[2] The cable for the 20-meter element is connected in a similar fashion. The switch allows the use of a single feed line from the shack to a point just below the antenna where the switch is mounted. It is a simple matter to provide voltage to the switch for operation on one of the two bands. At the price of coaxial cable today, a double run of feed line represents a substantial investment and should be avoided if possible.

An etched-circuit board was mounted inside an aluminum Minibox to provide support and insulation for each of the gamma tuning capacitors. Plastic refrigerator boxes available from most department stores would serve just as well. The capacitor housing is mounted to the boom by means of U bolts.

The builder is encouraged to follow the dimensions given in Fig. 5 as a starting point for the position of the gamma rods and shorting bar. Placing the antenna near the top of the tower and then tilting it to allow the capacitors to be reached makes it possible to adjust the capacitors for minimum SWR as indicated by an SWR meter (or power meter) connected in the feed line at the relay. If the SWR cannot be reduced below some nominal figure of approximately 1.4:1, a slight repositioning of the gamma short might be required. The dimensions given are for operation at 14.050 MHz and 21.050 MHz. The SWR climbs above 2:1 about 50 kHz in either direction from the center frequency. Although tests were not conducted at more than 150 watts input to the transmitter there is no reason why the system would not operate correctly with a kilowatt of power supplied to it.

After many months of testing at the QTH of W1FB, several characteristics were noted. First, the antenna withstood several wind and ice storms common to Connecticut. Performance turned out to be what can be expected from a 2-element Yagi. Since the 20-meter portion of the antenna is a director array, the front-to-back ratio is a bit less than 10 dB. On 15 meters, where the system operates with a reflector parasitic element, the front-to-back ratio is considerably better — on the order of 15 dB.

This antenna was mounted atop a 40-foot (12.2-m) tower where previously there was connected a 20-meter sloping dipole pointed at Europe (a multielement array for 2 meters graced the top of the tower!). The number of European stations contacted increased rather dramatically with the installation of the beam. Except in pileups on rare DX stations, DX is now worked as a routine, even though W1FB is a QRP fan and typically runs less than 2 watts of output power.

No doubt the increased effectiveness of the signal was caused by several factors. The antenna certainly has gain (although at ARRL hq. we have no way of making accurate measurements) and is well above the nearby small trees. More importantly, the antenna is now far from the aluminum house siding which once was directly in the pattern of the 20-meter "sloper." Of course, the front-to-back characteristic has the tendency of making DX signals louder in relation to stateside stations and therefore makes receiving much easier.

If previously you've felt that a beam and tower were not possible at your QTH, perhaps re-evaluation of the situation is in order. This antenna, as shown in the photograph, does not appear offensive when viewed from the front yard. Yet the overall amount of property occupied (at ground level) is less than one square foot. And the turning radius is slightly over 11 feet (3.35 m)! This material was originally presented in *QST* by Robert Myers, W1XT and Clarke Greene, K1JX.

References

[1]Sevick, "The W2FMI Ground-Mounted Short Vertical," *QST*, March 1973. (See Chapter 1.)
[2]Purchased from Fair Radio Sales, Lima, OH.

Linear Loaded 20-Meter Beam

Build this novel minibeam for 20 meters . . . it works!

Full-sized antennas are fine if you have the height and room for them. But much of the advantage is usually lost with average installations. So why bother with a sad-looking monster a few feet atop the house when a trim, smaller model will do the job. This article deals with a method that eliminates the messy and expensive loading coils as well.

Having built an HW-32A transceiver, the author's 20-meter activity was restricted to the phone band. A homemade vertical antenna did a fair job in the states, but not for DX. This writer's thoughts ran to a beam and the aluminum tubing that could be obtained for full-size construction. A 2-element beam was constructed, using a gamma match and information found in the *Handbook*. The beam worked electrically, but the mechanical construction left much to be desired. It flopped in the wind like a wounded butterfly. The author tried to correct this with a wooden framework, but it was just as bad. Something with shorter elements was desired, something that was rigid and would still perform well. But all of the author's research turned up only loading coils or other methods involving a loss compromise.

The author's aluminum supply included four 12-ft (3.66-m) lengths of 7/8-inch (22-mm) diameter tubing. This would give two elements of 24 ft (7.32-m) length and a minimum of sag. The problem was how to mount them and make up the difference in physical and electrical length for a half-wave length. Loading coils were ruled out. The possibility of folding wire under the elements seemed to have merit. (Later, this was found to be called linear loading.) This dictated a split element and standoff supports for the tubing.

Two 2-ft (0.61-m) lengths of aluminum channel were obtained for the element supports (Fig. 7). each 12-ft (3.66-m) section was attached using 1-in. (25-mm) ceramic standoff insulators. A 34-in. (19-mm) birch dowel was used to stiffen and prevent crushing of the tubing where the attachment was made. Element supports were grooved and attached to a 10-ft (3-m) TV mast section using a single 5/16-in. (8-mm) U bolt.

The folded additional loading wire was no. 12 copper house wire with the insulation stripped off, and was supported by two bakelite blocks on each element section. The blocks were anchored to the tubing by small sheet metal screws. Ends of the wire sections were formed into a loop to hold their position.

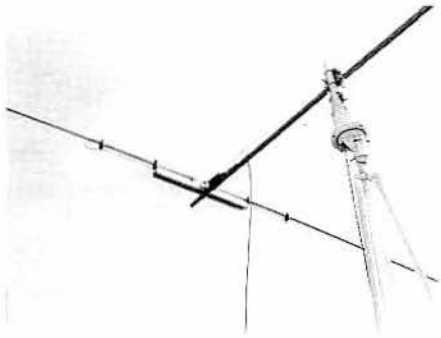

The beam atop the author's tower.

Tune-Up and Adjustments

My thinking in regard to coaxial-cable-fed dipoles is that they should use a balun or matching device of some kind. This beam, having a split driven element, seemed to call for a 1:1 balun since it was to be fed with RG-58/U (Fig. 8). Formulas found in handbooks for beam-element lengths did not seem to work for the linear-loading design, so cut-and-try was used many times. In final tests, a grid-dip meter was utilized with a calibrated receiver to determine the driven-element total length of 35 ft (10.67 m). A reflector with 10-ft (3.05-m) spacing was used.

It was found that adding a reflector of five-percent greater length lowered the frequency (with the beam near the ground) but on raising the beam to rooftop, the frequency had increased. The 10-ft spacing gave a 3:1 VSWR which was very difficult to reduce. Testing this arrangement on the air seemed to indicate more gain in the back direction than in the front. After many tests and much rebuilding of the wire lengths, the director element approach seemed to give the most encouraging results. The VSWR was down to 1.5:1 and the five-percent shorter director raised the frequency to the phone band. Spacing was reduced to 7 ft 6 in. (2.29 m).

More research brought out the possibility of inductive matching to get the VSWR

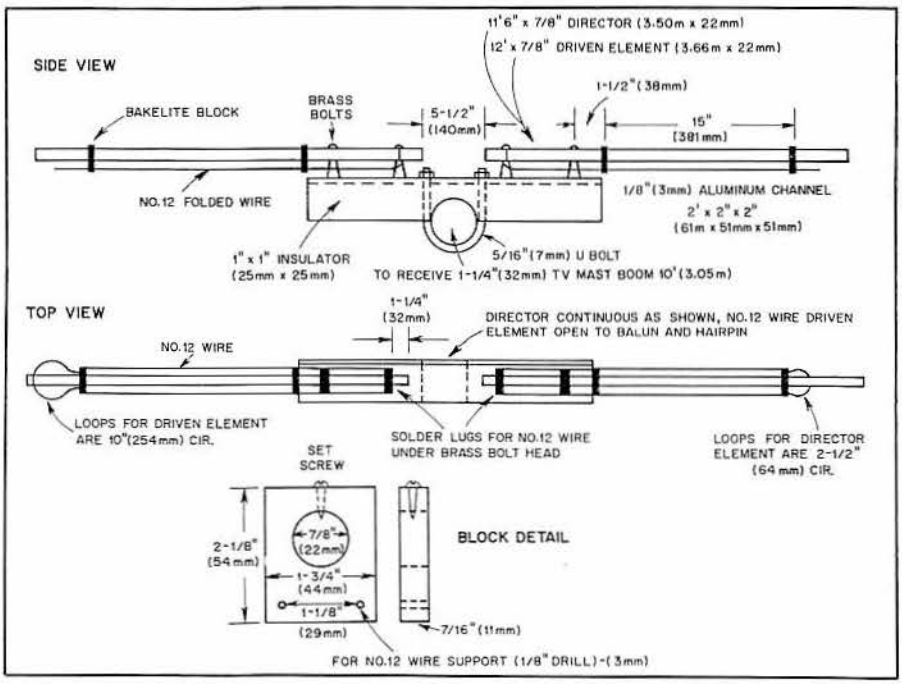

Fig. 7 — Construction details of the loaded beam.

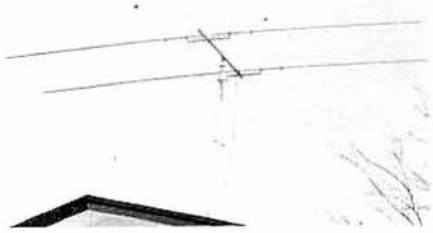

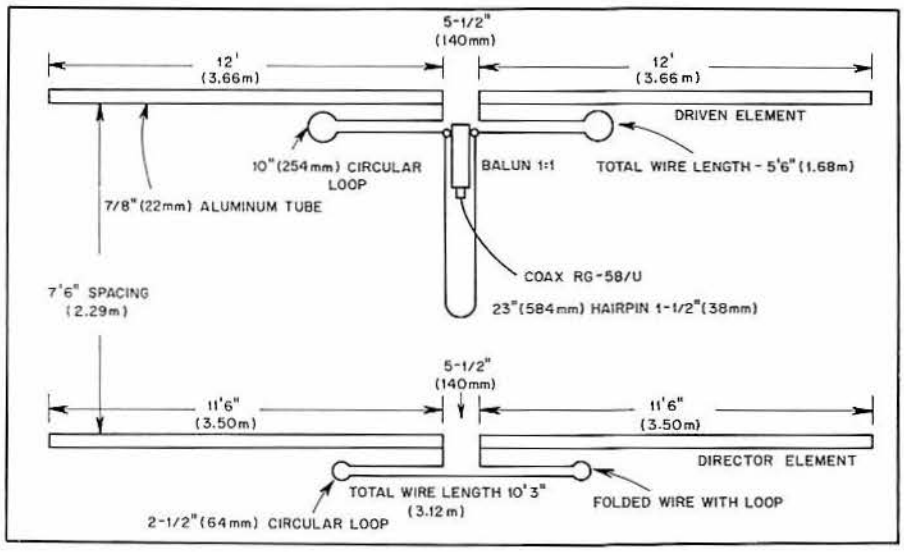

Fig. 8 — Critical electrical dimensions.

down to a more reasonable level. Many hairpin lengths and widths were tried with varying results. The final hairpin was 23-in. long by 1-1/2 in. (580 × 38 mm) wide with a slight fan shape to fit the balun connections. This reduced the VSWR at 14,200 kHz and 14,350 kHz with a flat response in between.

On-the-Air Tests

The help of other amateurs in tests for front-to back ratio was very helpful. Average reports have been 2.5 S units in the forward position over the back position. The author did not have a reference dipole for gain tests, but has heard and worked more DX than in the past 20 years. The beam is mounted on a rooftop 10-ft (3-m) steel tower 38 ft (11.6-m) above the ground. It weighs around 20 pounds and is rotated by an older-type TV rotator. This material was originally presented in *QST* by Cole Collinge, WØYNF.

The Log-Yag Array

The Yagi antenna array has been around for years and years. A relative newcomer to hams is the log-periodic dipole array (LPDA), which offers nearly constant gain over a greater bandwidth than the Yagi. Guess what happens when you cross a Yagi with an LPDA . . . .

With the decline in sunspot activity, a number of amateurs have considered monoband Yagi arrays. The first problem encountered seems to be array length, that is, overall size for a desired gain and bandwidth. The Log-Yag principle, as will be discussed shortly, has produced a system which will provide the amateur with another alternative to the long-boom Yagi, stacked Yagis, or loop-antenna systems. The L-P Yagi (Log-Yag) array is not a new system; many such arrays have been designed and developed by Oliver Swan[1] and others.[2] This article, however, will provide the basic theory of operation, design procedure, and the construction of a practical antenna.

Theory of Operation

The Log-Yag array utilizes an LPDA-driven[3] group of elements, designed to cover a desired bandwidth, in conjunction with parasitic elements to achieve higher gains and greater directivity than would be realized with either the LPDA or Yagi array alone. The Yagi array requires a long boom and wide element spacing for wide bandwidth and high gain. This is because the Q of the Yagi system increases as the number of elements is increased and/or as the spacing between adjacent elements is decreased.[4,5] An increase in the Q of the Yagi array means that the total bandwidth of that array is decreased; optimum gain, front-to-back ratio, and side lobe rejection are obtainable only over small portions of the band. Dr. I. L. Morris, using a high-speed digital computer, has completed extensive research on 4-, 8-, and 10-director Yagi-Uda arrays.[6] His work is comprehensive and is recommended reading for all technically minded amateurs. The parameters varied in his study were element length, spacing, radius and number. As can be seen in Fig. 9, the forward gain and front-to-back ratio

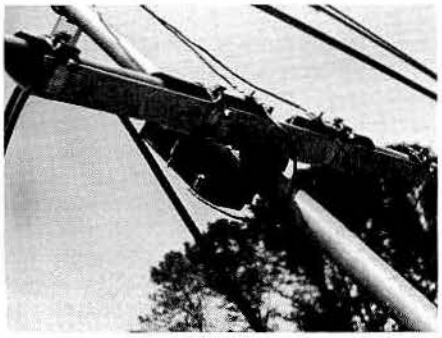

The attachment of the elements to the boom.

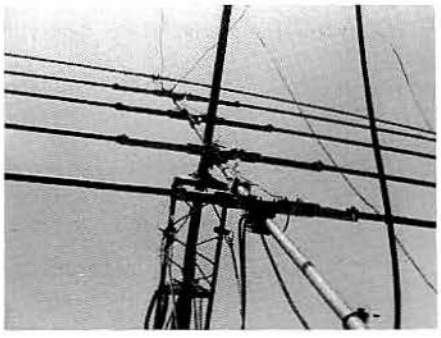

From the front to the back of the Log-Yag array. Note the truss provides lateral and vertical support.

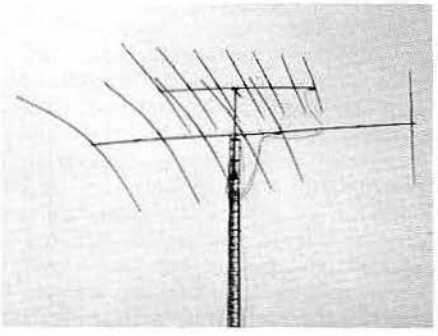

The completed Log-Yag array ready for use. The array mounted above the Log-Yag is a 7-element LPDA for 21 to 30 MHz.

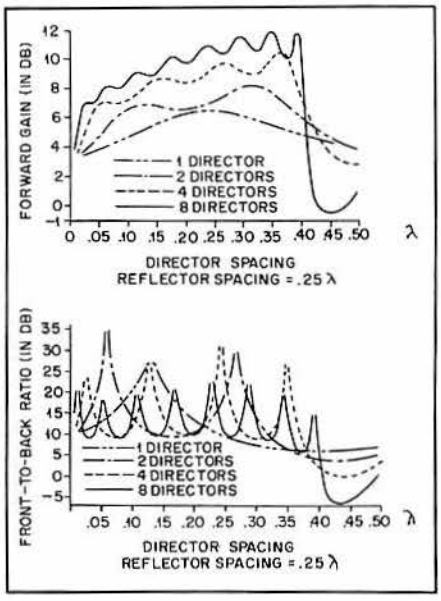

Fig. 9 — The effects of director spacing on various Yagi arrays. The change in gain and front-to-back ratio is plotted for the change in director spacing. The reflector spacing has been held constant.

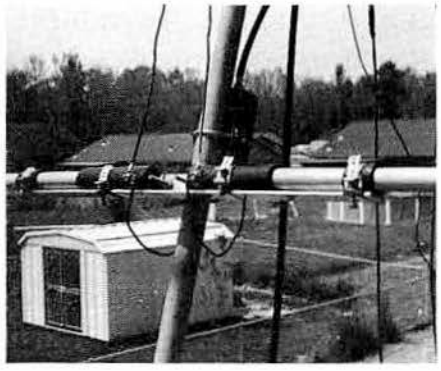

The connections between the balun and the input terminals.

deteriorate sharply as element spacings decrease. If the elements are closely spaced, then as the frequency is shifted either side of the array design frequency the electrical spacing between adjacent elements changes rapidly. This causes a higher SWR and a deterioration of forward gain and front-to-back ratio.

The Log-Yag system overcomes this difficulty by using a multiple driven element "cell" designed in accordance with the principles of the log-periodic dipole array.[7,8] Since this log cell exhibits both gain and directivity by itself, it is a more effective radiator than a simple dipole driven element. The front-to-back ratio and gain of the log cell can be improved with the addition of a parasitic reflector and director. It is not necessary for the parasitic element spacings to be large with respect to wavelength, as in the Yagi array, since the log cell is the determining factor in the array bandwidth. In fact, the element spacings within the log cell may be small with respect to a wavelength without appreciable

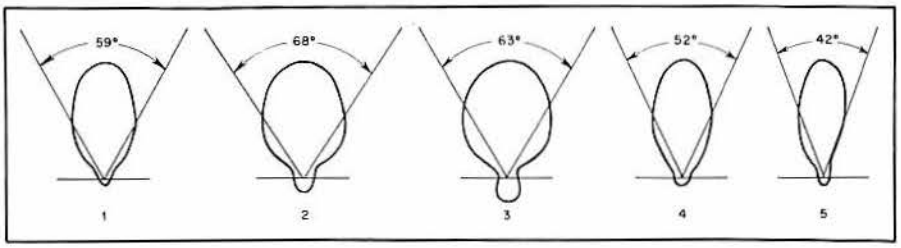

Fig. 10 — Beam patterns of 20-meter arrays.
No. 1 — 3-el. log cell, dir. @ 0.1λ, ref. @ 0.2λ.
No. 2 — 5-el. log periodic, $\sigma = 0.1$.
No. 3 — 3-el. log cell, 1st dir. @ 0.1λ, 2nd dir. @ 0.2λ.
No. 4 — 4-el. log cell, ref. @ 0.15λ.
No. 5 — 4-el. log cell, dir. @ 0.15λ, ref. @ 0.085λ (described in this article).

deterioration of the cell gain. For example, decreasing the relative spacing constant (σ) from 0.1 to 0.5 λ will decrease the gain by less than 1 dB. Hence, a further reduction in boom length. It can be seen that the Log-Yag array will exhibit high theoretical gain (11 dBd), high front-to-back ratio (30 dB), high cross polarization (front-to-side ratio —45 dB), and a wideband response utilizing boom lengths approximately one half that of a Yagi with similar characteristics.[2]

The author has built many monoband 14-MHz Log-Yag arrays in an attempt to find an optimum combination of elements, while holding the boom length to that of a full-sized, three-element monobander Yagi. Relative radiation patterns for various element combinations are found in Fig. 10. The final array design takes the form of a four-element log cell, parasitic reflector spaced at 0.085 λ_{max} and parasitic director spaced at 0.15 λ_{max} where λ_{max} is the longest free-space wavelength within the array passband. It has been found that array gain is almost unaffected with reflector spacings from 0.08 λ to 0.25 λ and the increase in boom length is not justified.[9] The function of the reflector is to improve the front-to-back ratio of the log cell while the director sharpens the forward lobe and decreases the half-power beamwidth. As the spacing between the parasitic elements and the log cell decreases, the parasitic elements must increase in length.[10]

The log cell is designed to meet upper and lower band limits with $\sigma = 0.05\lambda$. The design parameter τ is dependent on the structure bandwidth, B_s. When the log-periodic design parameters have been found, the element length and spacings can be determined. A review of the "Log-Periodic Dipole Array" is recommended though not necessary for the design of the Log-Yag array.[3,7,8]

The method of feeding the antenna is identical to that of feeding the log-periodic dipole array without the parasitic elements. As shown in Fig. 11, a balanced feeder is required for each log-cell element, and all adjacent elements are fed with a 180° phase shift by alternating connections. Since the Log-Yag array will be covering a relatively small bandwidth, the radiation resistance of the narrow-band log cell will vary from 80 to 90 ohms (tubing elements) depending on the operating bandwidth. The addition of parasitic elements lowers the log-cell radiation resistance. Hence, it is recommended that a 1-to-1 balun be connected at the log-cell input terminals and 52-ohm coaxial cable be used for the feed line. The measured radiation resistance of the 14-MHz Log-Yag installed at the author's QTH is 37 ohms, 14.0 to 14.35 MHz. It is assumed that tubing elements will be used. However, if a wire array is used then the radiation resistance R_o and antenna-feeder input impedance Z_o must be calculated so that the proper balun and coax may be used. The procedure is outlined in detail in *The ARRL Antenna Book*.[3,7]

Design Procedure

The following step-by-step design procedure may be used to design any monoband Log-Yag for any desired bandwidth.

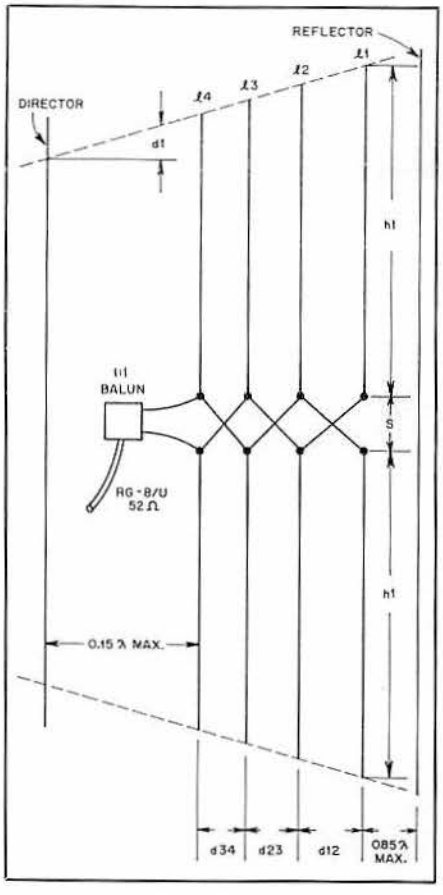

Fig. 11 — Layout of the Log-Yag array.

1) Determine the operating bandwidth, B, between f_1, lowest frequency (band edge), and f_n, highest frequency (band edge).

$$B = \frac{f_n}{f_1}$$

2) Determine the structure bandwidth (log-cell array) B_s.

$$B_s = 1.15B$$

3) Determine the design parameter τ (based on 4-element log cell, note 1).

$$\tau = \frac{1}{\sqrt[3]{B_s}}$$

Note 1. The design parameter τ is chosen for a four-element log cell since it provides the best bandpass for most amateur bands. For log cells with any number of elements

$$\tau = \frac{1}{\sqrt[(n-1)]{B_s}}$$

where n = number of elements within the log cell.

4) Determine the apex half-angle α: Since $\sigma = 0.05$ (relative spacing constant), then

$$\cot \alpha = \frac{0.2}{1-\tau}$$

5) Determine the longest free-space wavelength λ_{max}, log-cell boom length, L (ft) and longest element length within the log cell l_1 (ft).

$$\lambda_{max} = \frac{984}{f_1 MHz}$$

$$L = \left[\frac{1}{4}\left(1 - \frac{1}{B_s}\right)\cot \alpha\right]\lambda_{max}$$

and

$$l_1 = \frac{492}{f_1 MHz}$$

$$l_2 = \tau l_1$$

$$l_3 = \tau l_2$$

$$l_4 = \tau l_3$$

6) Determine the element spacing (d_{12}), distance between elements l_1 and l_2 (ft).

$$d_{12} = \frac{1}{2}\left(l_1 - l_2\right)\cot \alpha$$

and

$$d_{23} = \tau d_{12}$$

$$d_{34} = \tau d_{23}$$

7) Determine the parasitic element lengths (ft) and spacings (ft).

$$l_{REF} = \frac{509.6}{f_1 MHz}$$

$$d_{REF} = \frac{84}{f_1 MHz}$$

$$l_{DIR} = \frac{450.8}{f_1 MHz}$$

$$d_{DIR} = \frac{148}{f_1 MHz}$$

This completes the design.

The Finished Log-Yag

The proof is always to be found in the completed and operating product. The

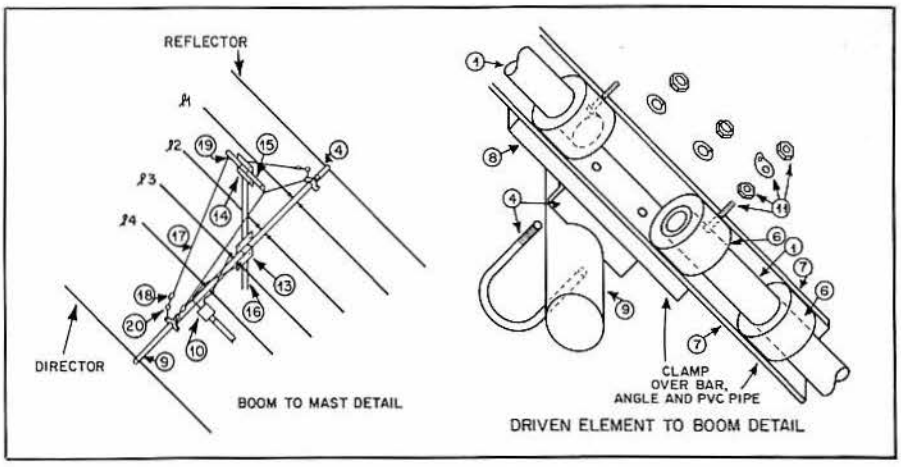

Fig. 12 — Assembly details. The numbered components refer to Table 6.

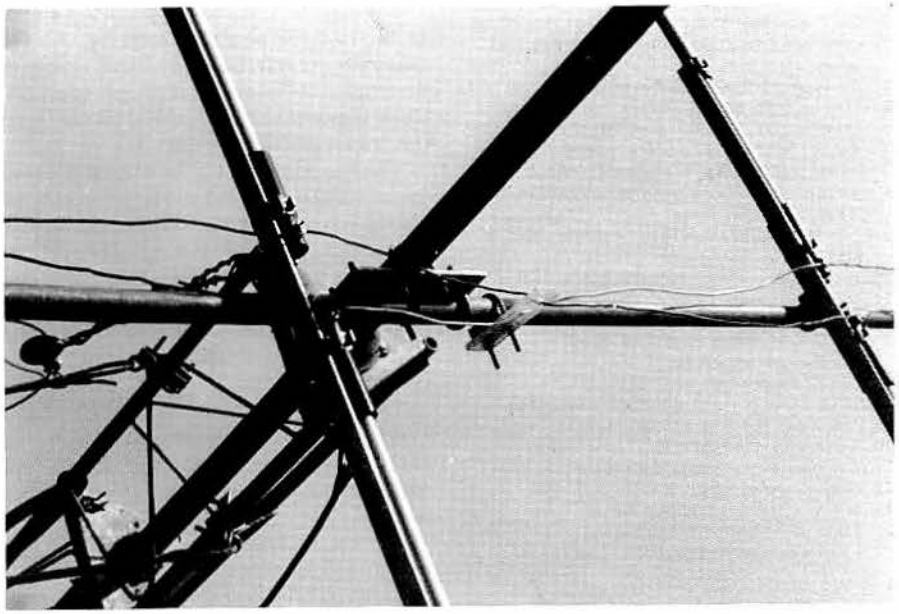

The interconnection between the elements of the log cell changes sides between each element.

Table 3

Array Characteristics

1. Frequency range	14–14.35 MHz
2. Operating bandwidth	B = 1.025
3. Design parameter	τ = 0.946657
4. Apex half angle	a = 14.92°, cot = 3.753
5. Half-power beam width	42° (14-14.35 MHz)
6. Bandwidth of structure	B_s = 1.17875
7. Free-space wavelength	λ_{max} = 70.28 ft
8. Log cell boom length	L = 10.0 ft
9. Longest log element	l_1 = 35.14 ft (a tabulation of element lengths and spacings given in Table 2)
10. Forward gain over dipole	11.5 dB (theoretical)
11. Front-to-back ratio	32 dB (theoretical)
12. Front-to-side ratio	45 dB (theoretical)
13. Input impedance	Z_O = 37 ohms
14. SWR	1.3 to 1 (14-14.35 MHz)
15. Total weight	96 pounds
16. Wind-load area	8.5 sq. ft
17. Feed-point impedance	Z_O = 37 ohms
18. Reflector length	36.4 ft @ 6.0 ft spacing
19. Director length	32.2 ft @ 10.5 ft spacing
20. Total boom length	26.5 ft

The mechanical construction of the log cell is identical to that described in *The ARRL Antenna Book*, except for the lengths and spacings.[3,7] Fig. 12 shows how the log cell is constructed as well as the addition of the parasitic elements.

1 ft = 0.30478 m

Table 4

Array Dimensions

Element	*Length Ft*	*Spacing Ft*
Reflector	36.4	6.0 (Ref. to $/_1$)
$/_1$	35.14	3.51 (d_{12})
$/_2$	33.27	3.32 (d_{23})
$/_3$	31.49	3.14 (d_{34})
$/_4$	29.81	10.57 ($/_4$ to dir.)
Director	32.2	

1 ft = 0.30478 m

Table 5

Element Material Requirements

Element	*1-in. Tubing Length (Ft)*	*Qty.*	*7/8-in. Tubing Length (Ft)*	*Qty.*	*3/4-in. Tubing Length (Ft)*	*Qty.*	*1 1/4-in. Angle Length (Ft)*	*1 X 1/4-in. Bar Length (Ft)*
Reflector	12	1	6	2	8	2	None	None
$/_1$	6	2	6	2	8	2	3	1
$/_2$	6	2	6	2	8	2	3	1
$/_3$	6	2	6	2	6	2	3	1
$/_4$	6	2	6	2	6	2	3	1
Director	12	1	6	2	6	2	None	None

1 ft = 0.30478 m

Table 6

Materials List

1. Aluminum tubing — 0.047 in. wall thickness
   1 in. — 12 ft lengths, 24 lin. ft
   1 in. — 12 ft or 6 ft lengths, 48 lin. ft
   7/8 in. — 12 ft or 6 ft lengths, 72 lin. ft
   3/4 in. — 8 ft lengths, 48 lin. ft
   3/4 in. — 6 ft lengths, 36 lin. ft
2. Stainless steel hose clamps — 2 in. max., 8 ea.
3. Stainless steel hose clamps — 1-1/4 in. max., 24 ea.
4. TV-type U bolts — 1-1/2 in., 6 ea.
5. U bolts, galv. type: 5/16 in. X 1-1/2 in., 4 ea.
6. U bolts, galv. type: 1/4 in. X 1 in., 2 ea.
7. 1 in. ID water-service polyethylene pipe 160 lb/in.^{2} test, approx. 1-3/8 in. OD, 7 lin. ft
8. 1-1/4 in. X 1-1/4 in. X 1/8 in. aluminum angle — 6 ft lengths, 12 lin. ft
9. 1 in. X 1/4 in. aluminum bar — 6 ft lengths, 6 lin. ft
10. 1-1/4 in. top rail of chain-link fence, 26.5 lin. ft
11. 1:1 toroid balun, 1 ea.
12. No. 6-32 X 1 in. stainless steel screws, 8 ea.
    No. 6-32 stainless steel nuts, 16 ea.
    No. 6 solder lugs, 8 ea.
13. No. 12 copper feed wire, 22 lin. ft
14. 12 in. X 6 in. X 1/4 in. aluminum plate, 1 ea.
15. 6 in. X 4 in. X 1/4 in. aluminum plate, 1 ea.
16. 3/4 in. galv. pipe, 3 lin. ft
17. 1 in. galv. pipe — mast, 5 lin. ft
18. Galv. guy wire, 50 lin. ft
19. 1/4 in. X 2 in. turnbuckles, 4 ea.
20. 1/4 in. X 1-1/2 in. eye bolts, 2 ea.
21. TV guy clamps and eyebolts, 2 ea.

1 in. = 25.4 mm
1 ft = 0.30478 m

author's 14-MHZ Log-Yag on-the-air performance on cw and ssb substantiates the theory. The characteristics of the array are given in Table 3.

The materials needed are given in Table 5. In the construction diagram, Fig. 12, the materials are referenced by their respective material list number. The photographs show the overall construction picture, and the drawings show the details.

The materials should be available from most hardware and electronic stores. However, some have found difficulty in obtaining aluminum tubing. This can be solved by writing to the manufacturer and asking for the name of their distributor nearest your locality. Commercial antenna manufacturers will sell their tubing, but the cost is at a premium.

This array is in operation at K4EWG and W4BBP. The results on the air are nothing short of fantastic! It will give the stacked Yagis and long-boom Yagis a run for their money.

It is the authors' hope that this antenna design will stimulate additional work and research by other amateurs. The field seems wide open, and Yag-Log combinations are endless. The optimum design is by no means achieved in this article. It does seem, however, that a log cell of more than four elements would be necessary only where the array bandwidths, B, exceed 1.03 ($B = f_n/f_1$).

The authors wish to thank George Smith, W4AEO, for his work in substantiating a consideration for log periodic gain.[8] This material was originally presented in *QST* by P. D. Rhodes, K4EWG and J. R. Painter, W4BBP.

References

[1]"The Swan Multidrive 2-Meter Antenna," *QST*, Oct. 1969.
[2]Orr, *Radio Handbook*, 18th edition, pp. 547-548.
[3]Rhodes, "The Log-Periodic Dipole Array," *QST*, November 1973.
[4]*The ARRL Antenna Book*, 13th edition, p. 151.
[5]See ref. 2 above, p. 558.
[6]King, Mack and Sandler, "Arrays of Cylindrical Dipoles," *Yagi-Uda Programme Apdx. V*, 1968, pp. 218-232,468-470.
[7]See ref. 4 above: pp. 160-164, 208-210, and Fig. 9-18.
[8]Smith, "Yes, I've Built Sixteen Log Periodic Antennas!" *73*, March 1975. See pp. 98-99.
[9]Orr, "Antennas," *CQ*, March 1975. See section headed "The KLM Antenna."
[10]See ref. 4 above, p. 204 and Fig. 9-5.

Chapter 3

Quad Antennas

A currently popular form of directional gain antenna is called the "quad." In general performance principles, it compares favorably to the Yagi beams discussed in chapter 2. The proper name for this antenna is the "cubical quad." It was developed by Clarence Moore, W9LZX, in 1942 when he was an engineer for HCJB in Quito, Ecuador. The design came as a solution to large corona discharges at the ends of existing beam-antenna elements. The problem was caused by the highly ionized air at the transmitter location, some two miles above sea level. Operation was in the commercial 25-meter band, which for the intentions of the broadcaster, required a gain type of antenna.

Moore concluded that a gain antenna with no ends was required to handle the 10-kW power without corona or flashover. Thus, the quad was born. Not only did it handle the power without difficulty, it later became a popular amateur antenna after he developed a model for use on 20 meters.

The primary limitation of quad antennas is the unwieldy nature of the "beast," especially at 40 and 20 meters, compared to a Yagi. The supporting framework is subject to extreme stress from ice and wind loading. Nonetheless, the quad has proven to be one of the most effective DX beams that an amateur can buiid at modest cost. This chapter contains data on various types of quads for a number of amateur bands. It is a compendium of the best on the subject, as published in past issues of *QST*.

Quads and Yagis: Comparisons, Patterns and Working Dimensions

Want a fresh look at the Yagi vs. quad question? This is "must" reading for the antenna-minded.

The material in the following sections will present a discussion of two time-tested antenna arrays.

In this class of arrays the Yagi (more properly the Yagi-Uda) antenna is the grandfather of them all. There are very few antennas which can compete with the electrical operation and simplicity of construction of this array. However, in the early 1940s C. C. Moore, of radio station HCJB, brought into being a parasitic array of loop elements with properties very comparable to those of the Yagi-Uda array. Since its conception this array has become very popular in Amateur Radio circles. It has come to be known as the "cubical quad" or "quad" antenna because of the common use of square loops and box-like construction.[1]

The material to follow will attempt to present an unbiased comparison of these two arrays based upon the experimental and theoretical results of many workers. This material is prefaced by a short section of introductory antenna concepts and definitions so that certain terms and notation will have more meaning when the comparisons between the quad and Yagi antennas are made. Finally, in the last section, some of the experimental patterns of modeled quad and Yagi arrays are presented. A compilation of some of the working dimensions for both types of arrays are also given. This latter material should be of interest to the builder and experimenter.

Introductory Antenna Theory and Definitions: Polarization

Inspection of the radiation field of an antenna will show it to have plane-wave character and to be made up of electric and magnetic field lines which are perpendicular to each other. Polarization of an electromagnetic wave is defined as that direction in which the electric field lines are oriented. If the electric field vector is fixed (in direction) in a plane it is said to be linearly polarized. For example, the polarization of a dipole is linear. If the plane in which this dipole lies is horizontal or parallel to some reference plane (e.g., the surface of the earth), it is called a horizontally polarized antenna. Vertical polarization would result if the dipole were placed perpendicular to the reference plane. It should be noted that if the electric vector does not stay fixed in position but rotates (its tip tracing out an ellipse), then the wave is said to be elliptically polarized. Circular polarization is a special case of elliptical polarization. Elliptical polarization will have a right- or left-hand sense, depending upon the direction of rotation of the electric vector.

Directivity and Gain of an Antenna

The degree to which a particular antenna can concentrate the antenna pattern into a beam is known as *directivity*. Mathematically, it is the ratio of the power density (in watts per square unit of measure) that would be available at an observation point to the power density one would have if the total radiated power were radiated *equally* well in *all* directions.[2] Directivity is a function of the antenna pattern alone and does not take into account antenna efficiency or losses.

The gain of an antenna can be defined in terms of directivity when antenna efficiency is taken into consideration. If K is the antenna efficiency, a number between 0 and 1, then antenna gain is given by

$$G = KD$$

where

G = antenna gain
K = antenna efficiency
D = directivity

The gain in decibels is then given by

$$\text{dB gain} = 10 \log_{10} G.$$

Please note that the above definition has

been such that it is a function of the observation point. In amateur circles gain is usually measured at that observation point where the maximum power density is observed. Further, when considering practical Yagi and quad arrays for the hf range, K is normally taken as 1. Gain measured in the above manner is normally called gain with respect to an isotropic antenna. It is interesting to note that since a half-wave dipole concentrates its pattern into certain directions, it will have some gain with respect to an isotropic antenna. This gain with respect to isotropic is found to be

$$G = 1.64$$

or, in dB,

$$G_{dB} = 2.15 \text{ dB}$$

If the vertical and horizontal half-power beam widths are known for a given antenna the following formula will give (somewhat on the generous side) the gain of the antenna with respect to an isotropic antenna

$$G = \frac{40{,}000}{\theta_H \theta_V}$$

where

θ_H = horizontal half-power beam width in degrees.

θ_V = vertical half-power beam width in degrees.

This formula assumes low-side and back-lobe levels for the antenna pattern. If the gain with respect to isotropic is known then the gain with respect to a half-wave dipole is obtained by subtracting 2.15 dB.

Antenna Aperture or Area

This concept is of most use when discussing a receiving antenna. It is a measure of the antenna's ability to gather in available radiated power at some receiving position. Antenna area and gain are *directly* related

$$G = 4\pi \frac{A}{\lambda^2}$$

where

G = antenna gain

λ = operating wavelength

A = area (based upon square units of length measurement, with the length measurement the same as that assumed for λ). It should be noted that one *cannot* have two antennas with the same gain and different areas. One hears this concept misused (in the sense of the above sentence) quite often on the amateur bands. That is to say, if you feel that one antenna has more capture area than another, then it must also have more gain.

Antenna Patterns

The pattern of an antenna may be plotted by recording the received electric field strength or power density as a function of viewing (observation) angle. The properties of most antennas used by radio amateurs (below 30 MHz) can be described by two basic patterns. Consider a pattern due to a radiating half-wave dipole, this pattern to be obtained by moving a sampling or test antenna about the dipole in the horizontal plane which contains the dipole. This pattern is called the horizontal-plane or E-plane pattern (the pattern was taken in a plane containing the electric E-lines, hence the name E-plane pattern). If the sampling antenna is placed directly in front of the horizontal dipole (and in the horizontal plane) and moved up over the top of the dipole (in a plane perpendicular to the horizontal plane), and on around until it returns to the starting position, the result is the vertical-plane or H-plane pattern (since the test antenna moved in a plane parallel to the magnetic H-lines it is called an H-plane pattern).

For Yagi and quad arrays these two patterns will give enough essential information to determine their expected radiating properties.

Comparison of Quad and Yagi Arrays

The cubical quad antenna was first introduced to the radio world in 1942 by Clarence C. Moore at HCJB to alleviate a serious corona problem occurring on a large commercial shortwave Yagi array. It is a parasitic array formed with loop elements which are approximately one wavelength in circumference.

Important to proper operation of a quad antenna are considerations of proper element sizes, spacing between elements, boom length, feed impedance and so forth. The following material presents a discussion of these considerations and a comparison of the quad and Yagi arrays.

Polarization of a Quad Antenna

The polarization of a quad antenna can be determined by considering the current distribution on the driven element. To stress the point that square, diamond, or circular loop all produce essentially the same polarization, consider the current distribution shown in Fig. 1. A little thought reveals that fact that the vertical components of current produce radiated fields that cancel each other, and the horizontal components of current produce a radiated field (broadside to the loop) with all components adding. The polarization of any of these loops is then linear and parallel to an imaginary horizontal line drawn through the current minima. Hence, if a quad loop is fed at the bottom it produces horizontal polarization, and if fed on the side it will have vertical polarization. The geometrical form of the loop, square, diamond or circular, does not mean that the (broadside) radiation has a possible combination of both horizontal and vertical polarization or circular polarization. This seems to be a common misconception in amateur circles. The linear polarization properties introduced above can be verified easily experimentally. It should be further noted that there are no noticeable differences in the radiating properties or impedance of a loop 1 wavelength in circumference whether it be of the circle, diamond or square configuration.

Angle of Radiation for a Horizontally Polarized Quad Antenna

Placement of an antenna above a conducting ground will alter its free-space radiation pattern, positioning the maximum of its main lobe at possibly a new angle with respect to a horizontal reference line. The angular position of this main lobe is called the *angle of radiation*. The angle of radiation of an antenna is a function of its height above the conducting ground and its polarization. Given the height and the polarization, the angle of radiation can be determined by using the concept of the antenna's virtual image or ray theory and reflection of the wave by the ground.

The following conclusions can now be drawn:

The angle of radiation of a *horizontally* polarized quad antenna, at a given boom height, is essentially the *same* as that of a *horizontally* polarized Yagi at the same boom height.

This must be so because the boundary conditions imposed upon the electromag-

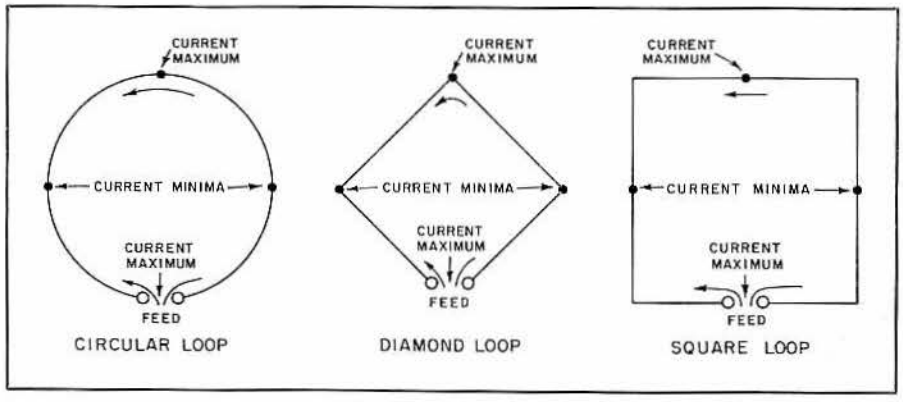

Fig. 1 — Current distribution on circular, diamond and square loops 1 wavelength in circumference.

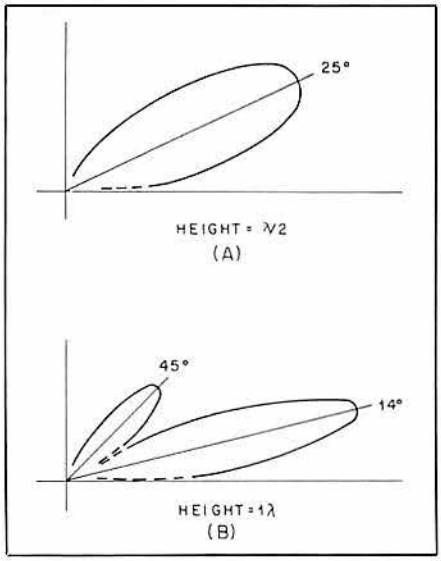

Fig. 2 — Vertical-plane radiation patterns for a horizontally polarized quad or Yagi array above perfectly conducting ground.

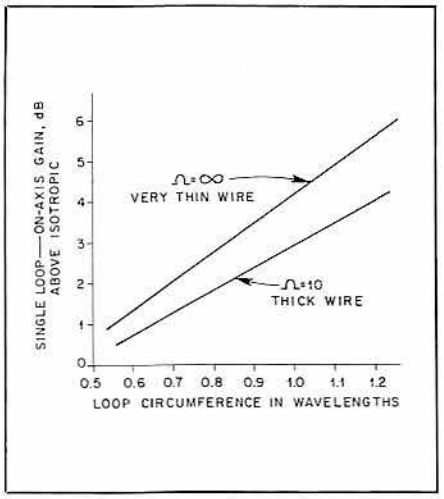

Fig. 3 — On-axis gain of a single loop as a function of loop circumference. (From "Studies of Large Circular Loop Antennas" by S. Adachi and Y. Mushiake *Sci. Rep. Ritu*, B-[Elect. Comm.] vol. 9, no. 2, Tohoku Univ., Sendai, Japan, 1957.)

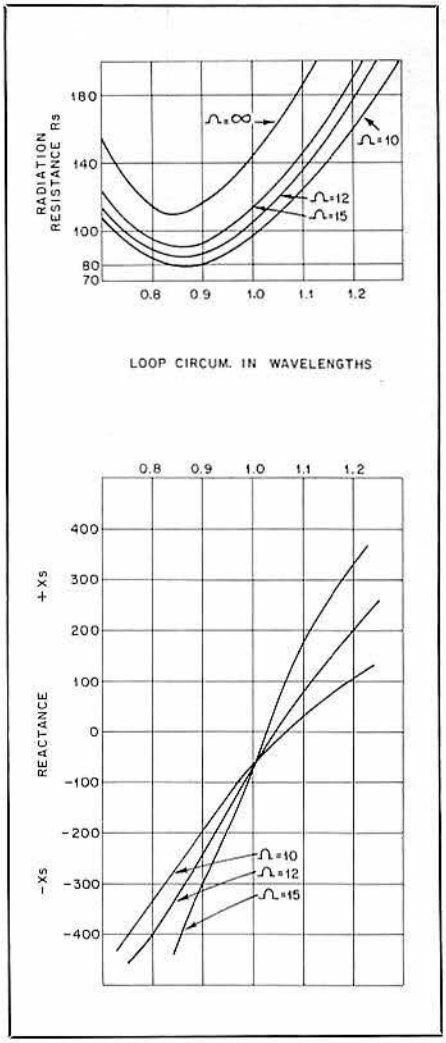

Fig. 4 — Reactance and radiation resistance of a single loop versus circumference. Note: Ω is a measure of the ratio of loop circumference to wire diameter. $\Omega = 2\ln 8a/\rho$ where a = loop radius and ρ = wire radius.

netic wave at the surface of ground are completely insensitive to the fact that the wave is produced by a quad antenna as opposed to the wave produced by a Yagi antenna.

Typical patterns of a quad *or* Yagi antenna placed at a height of 1/2 λ or 1 λ above a perfect ground are shown in Fig. 2 at A and B.

Gain Comparisons of the Quad Antenna with the Yagi Antenna

The gain of a quad array (of given boom length) seems to be somewhat higher than that of a Yagi array of the same boom length. This gain difference can be explained by considering the theoretical work of Adachi and Mushiake of Tohoku University in Japan. In 1952 and 1957 they published two papers which discussed the current distribution, impedance, and radiating properties of loops of large circumference.[3]

Fig. 3 shows the gain of a single loop as a function of wavelength and wire diameter. Fig. 4 shows the variation of reactance and radiation resistance for a single loop. Please note the dependence upon the circumference-to-wire-diameter ratio in these two figures. They showed that the broadside gain of a single loop 1λ in circumference was approximately 2 dB above that of a half-wave dipole. This result implies that a parasitic array of loop elements should have the same gain advantage when compared to a Yagi array of comparable boom length.

This gain differential for the quad array does appear and can be verified experimentally. Fig. 5 demonstrates this comparison. The points on the figure were obtained as follows: For the antenna under consideration E and H plane patterns were made. The gain was then calculated using the E and H-plane half-power beam widths of these radiation patterns and the formula discussed above. This gain and the boom length of the antenna were then used to determine a point on the graph given in Fig. 5, where gain and boom length represent the parameters under consideration. The data points for many, many antennas, both quad and Yagi, were then placed on the graph and a smooth curve representing an average for each type of antenna was then drawn.

The expected gain difference of 2 dB does indeed appear in favor of the quad antenna. This gain differential is essentially that predicted by the results of the Japanese workers cited above.

The measurements used to obtain the above gain comparisons were performed at 440 MHz. A measuring frequency of 440

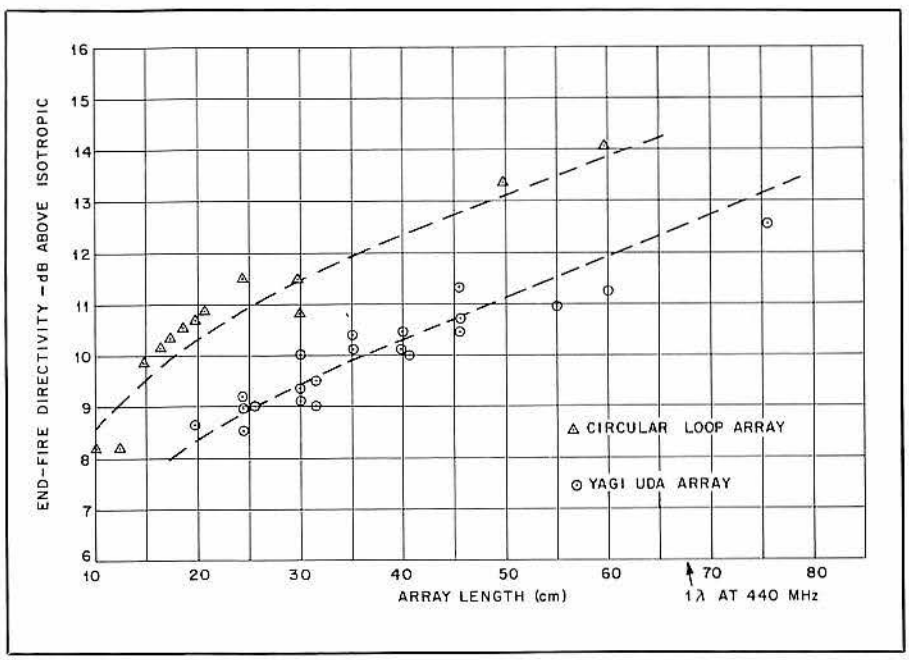

Fig. 5 — Quad and Yagi array gain as a function of boom length.

Table 1

Quad Dimensions

2-element Quad (WØHTH)
Spacing (given below)
Boom length (given below)

Band	*40 M*	*20 M*	*15 M*	*10 M*
Reflector	144 ft 11-1/2 in.	72 ft 4 in.	48 ft 8 in.	35 ft 7 in.
Driven Element	140 ft 11-1/2 in.	70 ft 2 in.	47 ft 4 in.	34 ft 7 in.
Spacing	30 ft	13 ft	10 ft	6 ft 6 in.
Boom length	30 ft	13 ft	10 ft	6 ft 6 in.
Feed method	Directly with 23 ft of RG-11, then any length RG-8 coax.	Directly with 11 ft 7 in. RG-11, then any length RG-8 coax.	Directly with 7 ft 8-1/2 in. RG-11, then any length RG-8 coax.	Directly with 5 ft 8 in. RG-11, then any length RG-8 coax.

(Note that a spider or boomless quad arrangement could be used for the 10/15/20 meter parts of the above dimensions yielding a triband antenna)

4-element Quad* (WØAIW [20 M] /WØHTH** /KØKKU/KØEZH/W6FXB)
Spacing: equal; 10 ft
Boom length: 30 ft

Band	*20 M*		*15 M*	*10 M*
	Phone	CW		
Reflector	72 ft 1-1/2 in.	72 ft 5 in.	48 ft 8 in.	35 ft 8-1/2 in.
Driven Element	70 ft 1-1/2 in.	70 ft 5 in.	47 ft 4 in.	34 ft 8-1/2 in.
Director 1	69 ft 1 in.	69 ft 1 in.	46 ft 4 in.	33 ft 7-1/4 in.
Director 2	69 ft 1 in.	69 ft 1 in.	46 ft 4 in.	33 ft 7-1/4 in.
Feed Method	Directly with 50-ohm coax.		Directly with 50-ohm coax.	Directly with 5 ft 9 in. RG-11, then any length RG-8 coax.

*Common boom used to form a triband array.
**The 2-element 40-meter quad given above is added to form a four-band quad array.

4-element Quad (WØHTH/K8DYZ*/K8YIB*/W7EPA*)
Spacing: equal; 13 ft 4 in.
Boom length: 40 ft

Band	*20 M*	*15 M*	*10 M*
Reflector	72 ft 5 in.	48 ft 4 in.	35 ft 8-1/2 in.
Driven Element	70 ft 5 in.	47 ft 0 in.	34 ft 8-1/2 in.*
Director 1	69 ft 1 in.	46 ft 1 in.	(Directors 1-3 all
Director 2	69 ft 1 in.	46 ft 1 in.	33 ft 7 in.)*
Feed method	Directly with 50-ohm coax.	Directly with 7 ft 9 in. RG-11, then any length 50-ohm coax.	Directly with 50-ohm coax.

*For the 10-meter band the driven element is placed between the 20/15 reflector and 20/15 driven element. The 10-meter reflector is placed on the same frame as the 20/15-meter reflectors and the remaining 10-meter directors are placed on the remaining 20/15-meter frames. The 10-meter portion is then a 5-element quad.

6-element Quad (WØYDM, W7UMJ)
Spacing: equal; 12 ft
Boom length: 60 ft

Band: 20 M

Reflector	72 ft 1-1/2 in.
Driven Element	70 ft 1-1/2 in.
Directors 1, 2 and 3	69 ft 1 in.
Director 4	69 ft 4 in.
Feed Method	Directly with 50-ohm coax.

1 ft = 0.3048 m

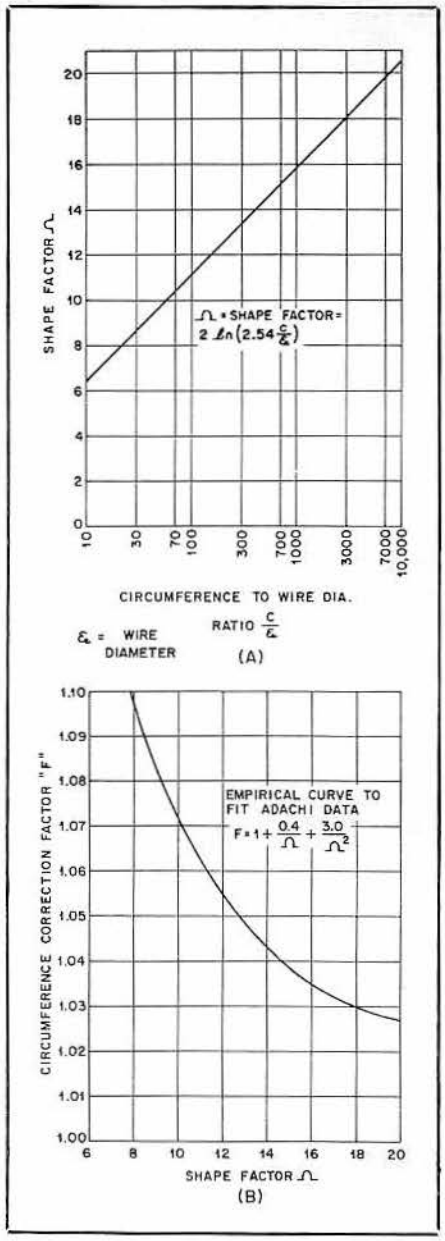

Fig. 6 A: Shape factor as a function of the loop circumference-to-wire diameter ratio. B: Loop "resonant length correction factor" versus shape factor. (Circled values obtained from S. Adachi, and Y. Mushiake, "Studies of Large Circular Loop Antennas" *Sci. Rep. Ritu*, B-[Elect. Comm.] vol. 9, no. 2, Tohoku Univ., Sept. 1957.)

MHz was chosen so that 1 cm (at this frequency) is equivalent to 1 foot of measurement at 14 MHz. Hence, to relate these results directly to the 20-meter amateur band, boom length in cm from the curve can be read as boom length in feet. For example, the gain of a quad on a 40-foot (12.19-m) boom should be slightly more than 1 dB above a quad on a 25-foot (7.62-m) boom. Comparison of the signals from these two antennas at a receiving station will not reveal much difference; however, in the DX pile-ups the longer antenna should have a slight advantage. Another interesting interpretation of these results is to note that a quad on a 30-foot (9.14-m) boom is equivalent to a Yagi on a 55-foot (16.76-m) boom. Hence the boom of a Yagi antenna must be about 1.8 times longer than the boom of a quad in order for the two gains to be comparable.

Impedance Properties and Matching

The driving-point impedance of a quad antenna depends upon the element spacing and number of elements. For 2-element quad antennas the results of Bill Orr in his *Quad Antenna* handbook can be used to determine the driving-point impedance. For multielement quads (3 or more elements)[4] the impedance will range from 40 to 60 ohms. Matching of these multielement quads is most easily done by direct feed with a 50-ohm coaxial line. A 1:1 balun can be used but experimental results show that it does not give performance any better than that obtained with direct feed. A gamma match can be used to obtain an exact match to any chosen coaxial line. For details of using a gamma match on a quad antenna see Bill Orr's *Quad Antenna* handbook.

If a single boom is used to construct a multiband quad antenna, then it is recommended that a separate feed line to each driven element be used.

Approximate Formulas for Quad Antenna Element Lengths

The multielement quad antenna gained its first real popularity following the work

of Lee Bergren, WØAIW, in the early 1960s. He published the results of his work in *QST* in 1963.[5] Many experimentalists have used his dimensions for antennas in the 20-meter amateur band and have scaled them to other bands. Based upon Bergren's work and others the following empirical formulas can be used to determine the element lengths of a quad antenna

$$\text{Circumference of driven element} = \frac{1005}{f_{MHz}} \text{ feet}$$

$$\text{Circumference of reflector element} = \frac{1030}{f_{MHz}} \text{ feet}$$

$$\text{Circumference of director elements} = \frac{975}{f_{MHz}} \text{ feet}$$

These results should only be used for quad antennas operating below 30 MHz. It is interesting to note that for quad antennas the reflector and directors are only 2-1/2 to 3 percent different in length from the driven element. This is a smaller change than that normally encountered in Yagi arrays.

The above figures should not be used for vhf or uhf quad antennas. At these higher frequencies the circumference-to-wire-diameter ratio becomes small enough that its effect upon the resonant properties of the loop must be considered. Here again, the results of Adachi and Mushiake are useful and the effects of wire size on the resonant length of the loop can be taken into account. These results are given in graphical form in Fig. 6 where, based upon the circumference-to-wire-diameter ratio, a circumference correction factor can be obtained. Once the correct size of the driven element is determined (using the results of Fig. 6) a quad antenna can be designed by making the reflector approximately 3 percent longer and the directors 3 percent shorter.

The above results can be used to obtain workable dimensions but, just as with approximate formulas for Yagi antenna element lengths, the "best" dimensions would have to be determined experimentally by tuning the array.

A Collection of Quad and Yagi Patterns and Dimensions: E and H Plane Patterns for Quad and Yagi Arrays

The previous section referred to a group of experimental tests, where a series of model antennas were constructed and the E and H plane patterns obtained.

It should be noted that these patterns have direct interpretation in light of the 20-meter band. Recall that the experiments were performed at 440 MHz, where dimensions for boom length, element size, and spacing in cm are directly equivalent to dimensions in feet for the 20-meter band. For example, the patterns for a 440-MHz, 5-element Yagi on a 55-cm boom can also be taken as the pattern for a 14-MHz, 5-element Yagi on a 55-foot boom.

Perusal of these patterns will give a

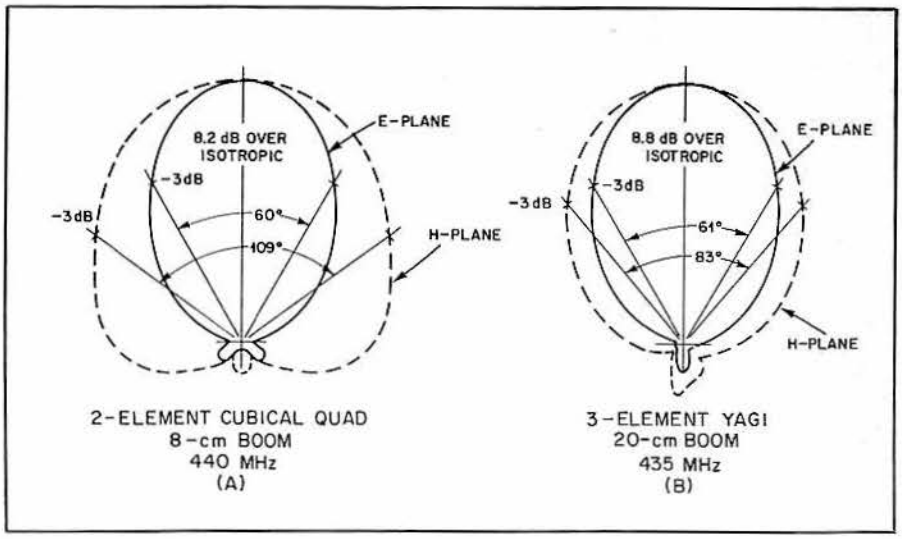

Fig. 7 — E and H plane radiation patterns for (A) 2-element quad antenna and (B) 3-element Yagi antenna.

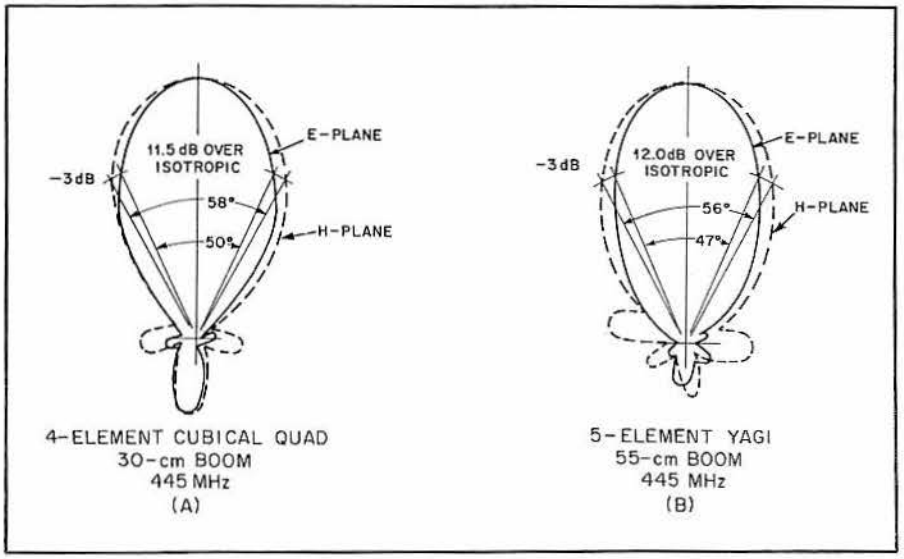

Fig. 8 — E and H plane radiation patterns for (A) 4-element quad antenna and (B) 5-element Yagi antenna.

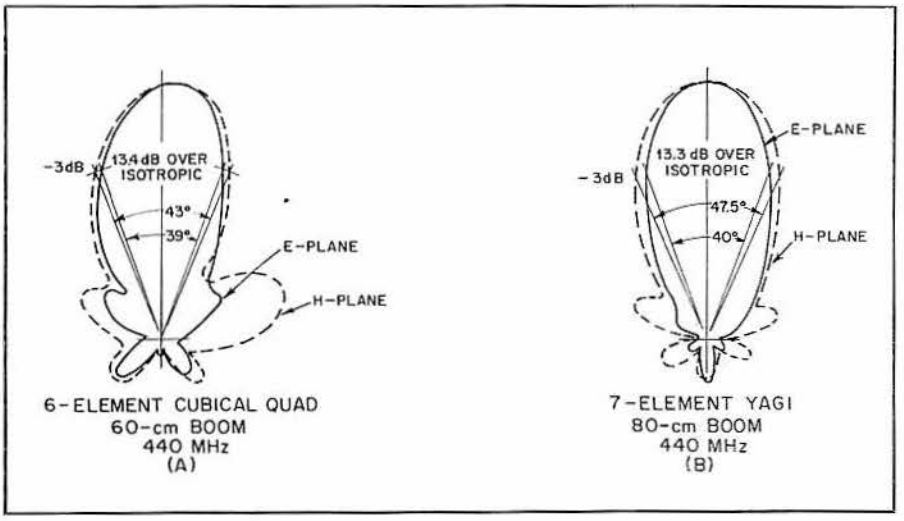

Fig. 9 — E and H plane radiation patterns for (A) 6-element quad antenna and (B) 7-element Yagi antenna.

visual means of comparing the quad and Yagi arrays. It is interesting to note the dependence of gain and pattern beam width upon array boom length. Without further comment, typical patterns for both types of antennas are given in Figs. 7 through 9.

A Tabulation of Dimensions of Working Arrays

Presented in tabular form are a few representative dimensions for both quad and Yagi antennas. These are dimensions presently in use by a number of amateurs. Most of the Yagi dimensions are due to amateurs across the country who sent their dimensions to Mr. Hal Wolff or the author to be modeled on the antenna range at the University of Denver. The quad dimensions also are those now in use by a number of amateurs in this country and abroad. It should be noted that most of these dimensions, and the resulting model antennas, provided the necessary data used in the previous section to compare the quad and Yagi. Where known, either the user(s) or the originator of a set of dimensions is indicated. The first set of dimensions is for quad antennas, the second set for Yagi antennas.

Summary

A comparison between the quad and Yagi antennas, on the basis of gain, has been given, this comparison being based upon both theoretical and experimental results. The results indicate that if both antennas have the same boom length the gain of the quad array will be about 2 dB higher than that of the Yagi. For either antenna, gain is a function of boom length and will increase approximately 2.5 dB each time the boom length is doubled. Hence, a 2-dB gain advantage is equivalent to a boom-length advantage of 1.8. In other words, for the quad and Yagi arrays to have comparable gain, the boom length of the Yagi antenna must be 1.8 times longer than that of the quad.

The size of the wire used for the loop element (relative to the loop circumference) will have an influence upon the resonance and radiating properties of the loop. The influence of this shape factor — i.e., the ratio of loop circumference to wire diameter — can be accounted for by using the referenced results of Adache and Mushiake.

In conclusion, it might be stated that one type of antenna (quad or Yagi) is not necessarily better than the other. The choice between a quad or Yagi array will depend critically upon many factors. For example, if single-band operation is of main importance and the geographical area where the antenna is to be used does not have high-wind problems, the best and simplest choice would be a long-boom Yagi antenna. If multiband operation is desired, or if wind problems were to limit the length of the boom to some nominal value, then the quad antenna would be a good choice. Likewise, the choice of available materials in your locale, and the acceptance of the appearance of the antenna by your neighbors or family, constitute other determining factors. The best approach is to survey your requirements and

Table 2

Yagi Dimensions

3-element Yagi (W6SAF)
Boom length: 24 ft
Band: 20M

	Element Length	*Spacing*
Reflector	34 ft 10-3/4 in.	R—DE: 13 ft 9-1/2 in.
Driven Element	33 ft 2-1/2 in.	DE—D: 10 ft 4-1/2 in.
Director	31 ft. 9-1/2 in.	

3-element Yagi (WØOKC)
Boom length: 26 ft
Band: 20M

	Element Length	*Spacing*
Reflector	35 ft 6 in.	R—DE: 14 ft
Driven Element	33 ft 4 in.	DE—D: 12 ft
Director	31 ft 7 in.	

3-element Yagi (WØCM, formerly WØJYW)
Boom length: 30 ft
Band: 20M

	Element Length	*Spacing*
Reflector	35 ft 4-1/2 in.	R—DE: 13 ft
Driven Element	32 ft 2-1/2 in.	DE—D: 17 ft
Director	31 ft 10 in.	
Feed Method	Folded dipole	

4-element Yagi (KØKKU)
Boom length: 30 ft
Band: 20M

	Element Length	*Spacing*
Reflector	35 ft 6 in.	(all elements equally spaced)
Driven Element	33 ft 4 in.	
Director 1	31 ft 9-1/2 in.	
Director 2	31 ft 2 in.	

4-element Yagi (W4PLL)
Boom length: 30 ft
Band: 20M

	Element Length	*Spacing*
Reflector	35 ft 4-1/2 in.	(all elements equally spaced)
Driven Element	33 ft 4-1/2 in.	
Director 1	31 ft 9-1/2 in.	
Director 2	31 ft 9-1/2 in.	

4-element Yagi (K6VIZ)
Boom length: 32 ft
Band: 20M

	Element Length	*Spacing*
Reflector	35 ft 6 in.	R—DE: 10 ft
Driven Element	32 ft 8 in.	DE—D1: 10 ft
Director 1	31 ft 8 in.	D1—D2: 12 ft
Director 2	31 ft 1 in.	

4-element Yagi (WØOKC)
Boom length: 36 ft
Band: 20M

	Element Length	*Spacing*
Reflector	35 ft 6 in.	R—DE: 14 ft
Driven Element	33 ft 4 in.	DE—D1: 10 ft 8 in.
Director 1	31 ft 8-1/2 in.	D1—D2: 11 ft 4 in.
Director 2	31 ft 1 in.	

4-element Yagi
Boom length: 40 ft
Band: 20M

	Element Length	*Spacing*
Reflector	35 ft 6 in.	R—DE: 14 ft
Driven Element	33 ft 4 in.	DE—D1: 12 ft
Director 1	31 ft 7 in.	D1—D2: 14 ft
Director 2	31 ft 0 in.	

5-element Yagi (WA6ZZK)
Boom length: 40 ft
Band: 20M

	Element Length	*Spacing*
Reflector	34 ft 10 in.	R—DE: 10 ft
Driven Element	33 ft 4 in.	DE—D1: 9 ft
Director 1	32 ft 6 in.	D1—D2: 10 ft 6 in.
Director 2	32 ft 2 in.	D2—D3: 10 ft 6 in.
Director 3	31 ft 10 in.	

5-element Yagi
Boom length: 46 ft
Band: 20M

	Element Length	*Spacing*
Reflector	35 ft 7-3/4 in.	
Driven Element	34 ft 5-3/8 in.	(All elements equally spaced at 11 ft 6 in.)
Director 1	33 ft 2 in.	
Director 2	31 ft 9-1/2 in.	
Director 3	30 ft 4-1/2 in.	

1 ft = 0.3048 m

5-element Yagi (K6EVR)
Boom length: 46 ft
Band: 20M

	Element Length	Spacing
Reflector	35ft 4in.	R—DE: 12ft
Driven Element	33ft 5in.	DE—D1: 10ft
Director 1	31ft 8in.	D1—D1: 12ft
Director 2	31ft 8in.	D2—D3: 12ft
Director 3	31ft 8in.	

5-element Yagi (W8PWH)
Boom length: 52 ft
Band: 20M

	Element Length	Spacing
Reflector	35ft 11in.	R—DE: 13ft 10in.
Driven Element	33ft 4-1/2in.	DE—D1: 10ft 5in.
Director 1	32ft 10in.	D1—D2: 13ft 10in.
Director 2	31ft 2in.	D2—D3: 13ft 10in.
Director 3	30ft 9in.	

5-element Yagi (W4EX, formerly W4DQH)
Boom length: 54 ft
Band: 20M

	Element Length	Spacing
Reflector	35ft 0in.	R—DE: 13ft 6in.
Driven Element	33ft 4in.	DE—D1: 11ft 6in.
Director 1	32ft 3in.	D1—D2: 13ft
Director 2	32ft 1in.	D2—D3: 16ft
Director 3	31ft 11in.	

5-element Yagi (W6RR, formerly W6ITA)
Boom length: 55 ft
Band: 20M

	Element Length	Spacing
Reflector	34ft 9in.	R—DE: 16ft 9in.
Driven Element	33ft 7in.	
Director 1	31ft 11in.	(All elements
Director 2	31ft 9-1/2in.	equally spaced)
Director 3	31ft 8in.	

6-element Yagi
Boom length: 46 ft
Band: 20M

	Element Length	Spacing
Reflector	35ft 5in.	
Driven Element	34ft 5-1/2in.	(All elements
Director 1	32ft 7in.	equally spaced
Director 2	32ft 3in.	at 9ft 2-3/8in.)
Director 3	31ft 4-1/2in.	
Director 4	31ft 1/2in.	

6-element Yagi (WØOKC)
Boom length: 46 ft
Band: 20M

	Element Length	Spacing
Reflector	35ft 4in.	R—DE: 10ft
Driven Element	33ft 4in.	DE—D1: 8ft
Director 1	31ft 11in.	D1—D2: 9ft
Director 2	31ft 3-1/2in.	D2—D3: 9ft 6in.
Director 3	31ft 1/2in.	D3—D4: 9ft 6in.
Director 4	30ft 11in.	

6-element Yagi (WØOKC)
Boom length: 74 ft
Band: 20M

	Element Length	Spacing
Reflector	35ft 5in.	R—DE: 16ft 6in.
Driven Element	33ft 4in.	DE—D1: 9ft 9in.
Director 1	31ft 9-1/2in.	D1—D2: 14ft
Director 2	31ft 2-1/2in.	D2—D3: 17ft 6in.
Director 3	30ft 11in.	D3—D4: 21ft
Director 4	30ft 8in.	

7-element Yagi (W6HAW)
Boom length: 80 ft
Band: 20M

	Element Length	Spacing
Reflector	35ft 5in.	R—DE: 14ft
Driven Element	33ft 4in.	DE—D1: 11ft
Director 1	31ft 8in.	D1—D2: 12ft
Director 2	31ft 4in.	D2—D3: 13ft
Director 3	30ft 8in.	D3—D4: 14ft
Director 4	30ft 8in.	D4—D5: 16ft
Director 5	30ft 8in.	

8-element Yagi (WA6EKD)
Boom length: 100 ft
Band: 20M

	Element Length	Spacing
Reflector	34ft 9in.	(All elements
Driven Element	33ft 5in.	equally spaced
Director 1	32ft 2in.	at 14ft 4in.)
Director 2	31ft 11-3/4in.	
Director 3	31ft 9-7/8in.	
Director 4	31ft 8in.	
Director 5	31ft 2in.	
Director 6	30ft 11-3/4in.	

environmental restrictions, make your choice and proceed accordingly.

Acknowledgements

It is very difficult to acknowledge systematically and completely all those who have made the quad antenna a successful communications antenna. However, surely credit must be given to C. C. Moore, the father of the quad antenna, to William Orr, who presented the first written material on the theory and construction of 2-element quads; to Lee Bergren, who showed the feasibility and advantages of using multielement quad arrays; to the Japanese workers, Adache and Mushiake, of Tohoku University, who presented a detailed analysis and experimental verification of the electromagnetic properties of loop antennas of large circumference; and finally, to all the radio amateurs, in all corners of the world, who developed constructional and design techniques and proved or disproved their validity.

The author would like also to acknowledge the help of Mr. Hal Wolff (WAØIOR) for his aid in constructing the model Yagi and quad arrays and running the patterns. These patterns were obtained by using the antenna range of the Denver Research Institute of the University of Denver.[6] Many Denver-area amateurs have entered into these quad experiments, notably Messrs. Jim Snyder (KØZCM), Butch Ford (WAØIMX), Ed Wood (KØKKU), Keith Farris (WØYDM), Warren Wheeler (WØREQ) and many others. The author gratefully acknowledges their assistance, help and encouragement. This material originally presented in *QST* by J. E. Lindsay, Jr., W7ZQ.

References

[1]For a colorful description of C. C. Moore's invention of the cubical quad antenna see the introduction of W. I. Orr's *Quad Antennas*, Radio Publications, Inc.

[2]An antenna which radiates equally well in all directions is called an isotropic radiator or isotropic antenna.

[3]Adachi and Mushiake, "Theoretical formulation for large circular loop antennas by integral equation method," *Repts. of the Research Institute of Elec. Commun.*, Tohoku University, Sendai, Japan, Sci. Rept. Ritu, B(Elec. Commun.), vol. 9, no. 1, 1957.

Idem., "Studies of large circular loop antennas," *Repts. of the Research Institute of Elec. Commun.*, Tohoku University, Sci. Rept. Ritu, B(Elec. Commun.), vol. 9, September 1952.

[4]Element spacing of 0.14λ to 0.2λ being considered.

[5]Bergren, "Multielement Quads," *QST*, May 1963.

[6]At the time these tests were performed (1962-64), the author was head of the Antenna Laboratory, Denver Research Institute, University of Denver. Mr. Hal Wolff was the research technician at this facility.

Additional References

Jasik, *Antenna Engineering Handbook*. New York: McGraw-Hill, 1961, pp. 16-25.

Lindsay, "A circular loop antenna with non-uniform current distribution," *IRE Trans. Antennas and Propagation (Communications)*, vol. AP-8, pp. 439-441, July 1960.

Lindsay, "A parasitic end-fire array of circular loop elements," *IEEE Trans. Antennas and Propagation (Communications)*, vol. AP-15, No. 5, pp. 697-698, Sept. 1967.

A Triband One-Loop Cubical Quad Element

Why not trade gain for economy and structural reliability? This three-band "DX Getter" consists of a single quad loop. It will stay aloft in high winds and won't look like an ugly monster to those who dwell nearby.

The advantages of a rotatable beam antenna are well known to all DXers. A problem arises in many situations regarding just how a reasonable compromise between antenna performance and cost, size and weight can be obtained. Because this author likes to live in peace with the XYL, the neighbors and the local council, the antenna must not be considered dangerous or an eyesore as far as appearance is concerned. In addition, the antenna must not hang over the fence of the 50- × 150-foot (15- × 46-m) block, half of which is already occupied by buildings. With these limitations firmly implanted in mind, the author added such factors as cost and difficulty of erecting and supporting a full-size, 20-meter Yagi or cubical quad. After weighing all the facts, it was felt that the only way out was to construct an economy-style, reduced-size antenna.

A single-loop, cubical-quad triband element is shown in Fig. 10. Such a cubical quad has only one-fourth the weight and wind resistance of a full-sized, three-element cubical quad of the same mechanical strength. The mechanical and installation difficulties are many times smaller; the cost of mast and rotor are also considerably reduced. Yes, the antenna is a compromise and the gain is less than that of a 3-element quad, but this antenna still puts a signal in good DX company. This quad, because of its smaller physical size, will be tolerated in many more locations than its big brother. If desired, this quad could be used as an indoor antenna strung between two opposite room walls.

Rather than going to a complicated switching arrangement to change bands, it was decided to apply what the author called the "triband-antenna principle" to this antenna. The theory behind this principle evolves around the same general ideas outlined by Pichitino in *QST*[1] several years ago. Antennas constructed along these guidelines do not operate harmonically and have only the desired resonances. The quad that was built is shortened only at the lowest operating frequency. It is full size at the middle operating frequency and much longer at the highest operating frequency. In addition, no heavy blocking tuned circuits are used near the element ends.

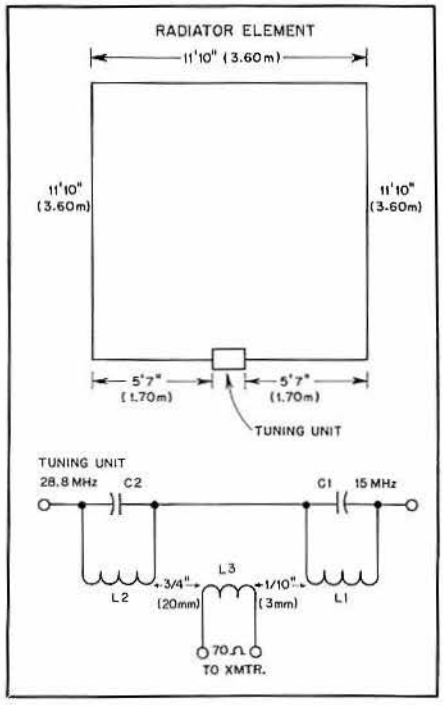

Fig. 10 — Single-loop triband cubical-quad element. Metric dimensions are shown; approximate English-unit dimensions are given in parentheses. Frequencies shown for C1L1 and C2L2 are those to which these circuits are tuned when disconnected from the loop.
C1 — 55 pF.
C2 — 49 pF.
L1 — 7 turns, No. 12, 38-mm (1-1/2-inch) diameter, space wound to 16 mm (5/8-inch) length.
L2 — 4 turns, No. 12, 38-mm (1-1/2-inch) diameter, space wound to 18 mm (11/16-inch) length.
L3 — 4 turns, No. 12, 38-mm (1-1/2-inch) diameter, space wound to 10-mm (3/8-inch) length.

With C1 giving 20-meter resonance depends mainly on the total element length and L1. Fifteen-meter resonance is controlled principally by C1 and L2. Ten-meter resonance is determined by C2 and L2. Once the antenna is constructed, it may be fine-tuned on each band by varying the constants that control the resonant frequencies. After the quad was tuned up, the author found the SWR on each band to be very satisfactory. On 20 meters, the antenna resonated at 14.15 MHz with a resulting SWR of approximately 1:1. With a 15-meter resonance at 21.3 MHz, an SWR of 1.3:1 was measured. On 10 meters, 28.6 MHz was selected as the resonant frequency. The resulting SWR at resonance on this band was 1.5:1. The phase relationship of the fields in L1 and L2 varies from band to band so that too much direct coupling between these coils should be avoided.

Although the author used copper wire to make the loop element, you may desire to use aluminum tubing. The actual constructional details are left to the builder. The materials used and the methods of supporting the antenna are limited only by your imagination. The techniques employed may be as simple or as sophisticated as you may desire. DJ2UT used short pieces of coaxial cable as capacitors and placed them inside the tubing which he used for the element. The coils and inner capacitor ends were sealed and molded in resin. Fifteen- and 10-meter resonances are obtained by shifting copper rings over the ends of L1 and L2. This can be done without affecting the sealed coils in any way.

The author concluded this antenna to be rather efficient based on observations that the tuning network does not become warm and a low SWR has been measured across each of the three bands. This writer wishes to thank OM Sommer, DJ2UT, and his co-workers for the very considerable amount of work carried out, and the many practical ideas which have made successful antennas with the triband principle possible. This material was originally presented in *QST* by Hans F. Ruckert, VK2AOU.

[1]Pichitino, "A New Principle in Two-Band Rotary-Beam Design," *QST*, October 1948.

A 2-Element, 15-Meter Quad for the Novice

Why not build this 2-element quad for 15 meters? It is easy to construct, inexpensive and in many ways quite novel.

Not being blessed with a large area for antennas, the author decided on an optimum-spaced, 2-element monoband quad. The standard formulas were used for sides and spacing, and the antenna is fed with 50-ohm cable through a quarter-wave "Q" section of 75-ohm coax cut to the standard formula. The reflector has a tuning stub.

The driven element grid-dips at 21,150 kHz and the reflector was tuned by using the grid-dip oscillator as a signal generator. The grid-dip meter was placed in a neighbor's home. Then, the back of the quad was aimed at the dip meter, and the reflector was tuned for the lowest indication on the S-meter.

One of the checks made on the antenna was with VE5XH, in Swift Current, SK. Doug gave the following information: The quad has 2 S-units gain over my 1/4-wave groundplane which was at the same height. Strength off the front was S9 and to the rear was S2, indicating a good front-to-back ratio. Because the constructional details are rather novel, the author felt that other hams might be interested in how this antenna was built.

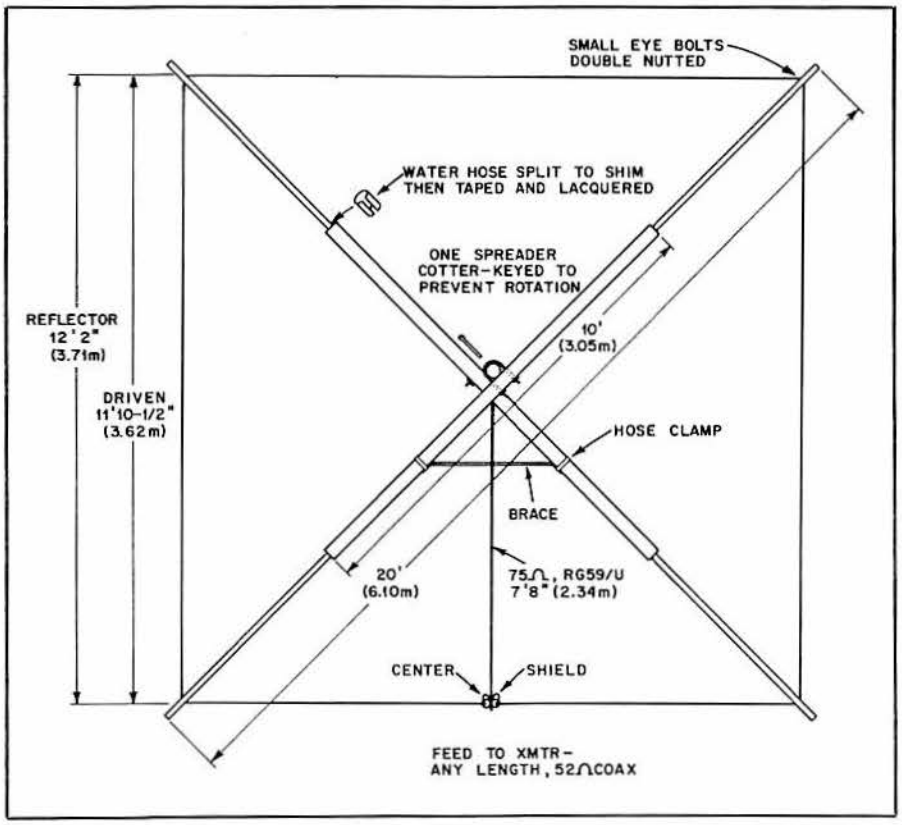

Fig. 11 — Detailed drawing of the quad. The cotter pin and cross-brace are required to prevent shifting of the spreaders. Small sections of split water hose are used for shims between the aluminum tubing and the plastic water pipe.

Construction

The author used 1-1/4-inch (32-mm) TV steel mast pipe, 10 feet (3 m) long, for the boom. Also, 10-foot lengths of TV mast sections, but aluminum, are used for the spreaders. However, 10-foot long spreaders are not long enough for a 15-meter quad; 20-foot (6.1-m) lengths are required. In order to obtain the required length, 20-foot lengths of one-inch (25 mm) diameter, ridged plastic water pipe were run completely through the 10-foot aluminum pipe sections. Pieces of rubber hose were used as shims between the aluminum pipe and the plastic pipe and these were taped where the plastic pipe emerges from the aluminum.

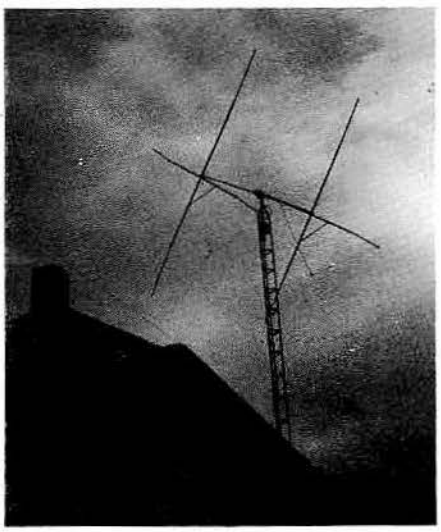

The completed quad on the tower. For tune-up, the quad was temporarily mounted on the garage roof.

The plastic water pipe comes in 20-foot lengths, 80 feet (24.4 m) being required. This pipe was purchased from a local plumbing and lighting outlet; the cost was $10 for the 80 feet. It is ridged plastic, but is not strong enough to support itself; so the aluminum mast pipe is used for the center portion of the spreaders.

The spreaders are clamped to the boom with standard U bolts, and one spreader in each element is pinned to the boom with a 5/16-inch (8 mm) cotter key. Additionally, a piece of one-inch (25 mm) conduit is used in each element as a cross-brace, to hold the correct angle between the spreaders.

The formulas and element lengths for 21,150 kHz are as follows

Driven element

$$\frac{1005}{f\,(MHz)} = 47 \text{ feet, 6 inches (14.48 m)}$$

Reflector

$$\frac{1030}{f\,(MHz)} = 48 \text{ feet, 8 inches (14.83 m)}$$

Boom spacing

$$0.2 \text{ wavelength} = 0.2 \times \frac{984}{f\,(MHz)} = 9 \text{ feet, 3 inches (2.84 m)}$$

75-ohm matching section

$$\frac{246 \times V}{f\,(MHz)} = \frac{162.4}{f\,(MHz)} = 7 \text{ feet, 8 inches (2.34 m)}$$

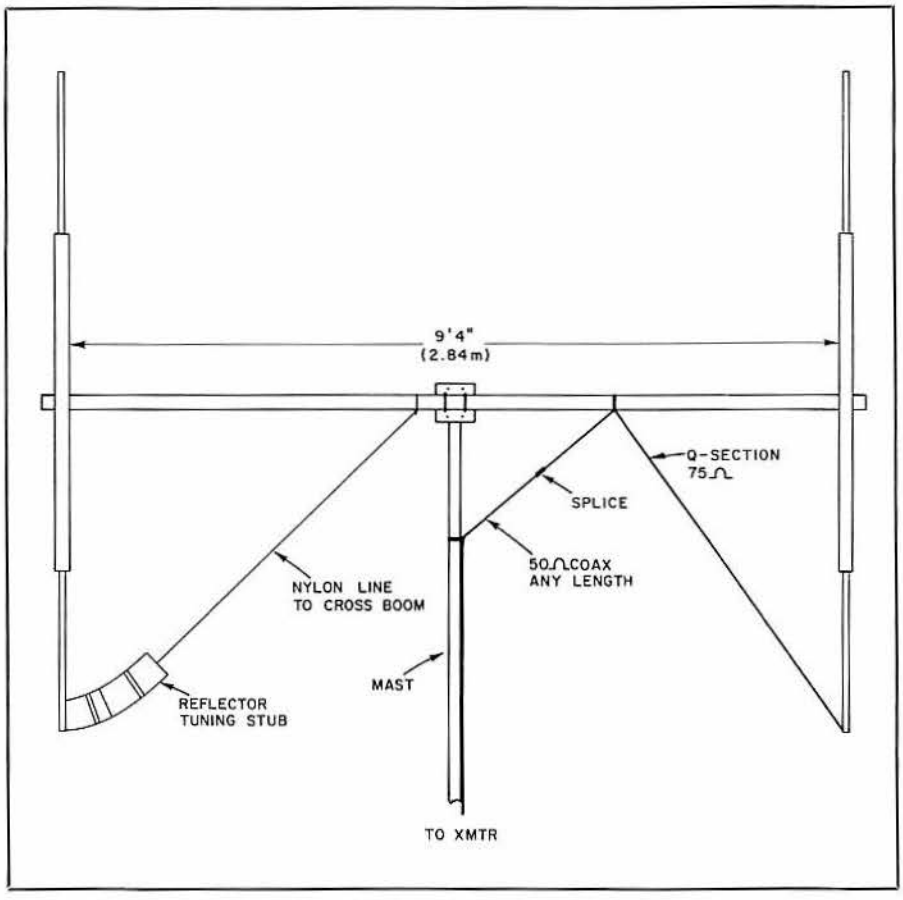

Fig. 12 — Side view, showing the mounting plate, Q matching section, and coax feed.

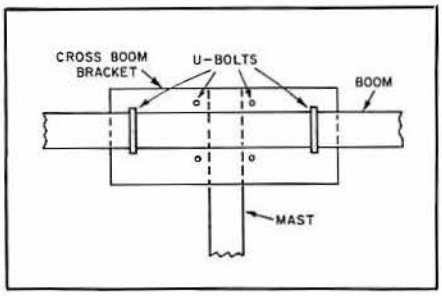

Fig. 13 — The cross-boom bracket, made from 3/8-inch (10 mm) aluminum plate. Ordinary TV U bolts are used to secure it to the boom and mast.

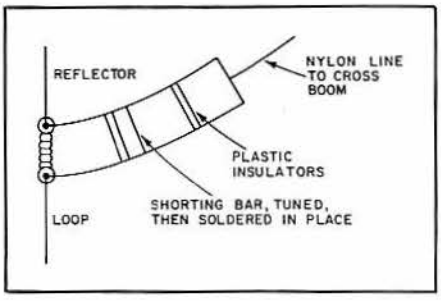

Fig. 14 — The reflector tuning stub is 36 inches (0.91 m) long. The shorting bar, a short piece of wire the same size as used in the stub was approximately 10 inches (254 mm) from the insulator when adjusted for maximum front-to-back ratio. Spacing between wires of the stub may be of the order of a few inches; this spacing is not critical since the stub length is adjusted by the shorting stub in the tune-up procedure.

The author used no. 14 soft-drawn enameled wire for loops and they were secured to the plastic pipe with double-nutted eye bolts. The reflector tuning stub was made from no. 12 copperweld wire. The total length of my stub is 36 inches (0.91 m), and after tuning, the shorting bar ended up approximately 10 inches (254 mm) from the loop.

The SWR showed almost a perfect match across the entire band. Since the quad was put up, the author has worked all continents and 35 countries on the Novice band. Stateside contacts always run S8 to S9. The total cost of the antenna was $28 at the time the system was built. This material was originally presented in *QST* by John Daebelliehn, WA9BJC.

A Practical 40-Meter Quad

One of the most perplexing problems continuously plaguing Field Day committees is how to install a good antenna system. For most clubs, finding a good location is generally the easiest job. The location must then be surveyed by the club antenna specialists. Deciding how many transmitters to use depends mostly on how many indivudual antennas can be set up for simultaneous operation as well as how many operators are available for the 24-hour stretch. Of course, an abundance of equipment is desirable.

Propagation conditions for Field Day and Sweepstakes generally favor the lower bands since they usually remain open all night. Success on the higher frequency bands (10 and 15 meters) depends primarily on catching the short-duration openings. The old trick of tying a rock to the end of a long piece of wire, tossing it into the tallest tree and loading it with a coupler just won't "cut the mustard" anymore. Gain and directivity into the dense population areas is the goal. However, the antenna must be simple to construct, easy to tune, and moderately stable against the wrath of Murphy and Mother Nature.

Our club decided to try a 2-element full-sized cubical quad for 40 meters. The immediate reaction within the more conservative ranks of our club was, "A 40-meter quad? It'll never work — the first breeze will knock it down!" With these objections in mind, we went ahead with our plans. Our location was approximately rectangular in shape, 60 feet wide, 500 feet long (18 × 152 m) and above the rest of the terrain. Of course, it just happened to be one of the highest locations in Winnebago County, IL!

The sketch illustrates the basic construction of the quad. Dimensions were estimated using the formula

$$L(\text{feet}) = \frac{248}{f(\text{MHz})}$$

where L is the length of one side of the diamond.

The parasitic element was constructed as a reflector using an extra long stub. A small relay shorts out the stub, thus converting the parasitic element from a reflector to a director (see Fig. 15).

The resonant frequency of the driven element is 7150 kHz, the middle of the band. The distance L for the driven element is 34 feet 8 inches (10.57 m). The parasitic element dimension is 5 percent smaller than the driven element. The stub is constructed so that the total circumference of the parasitic element with stub in the line is 5 percent greater than the driven element. L for the

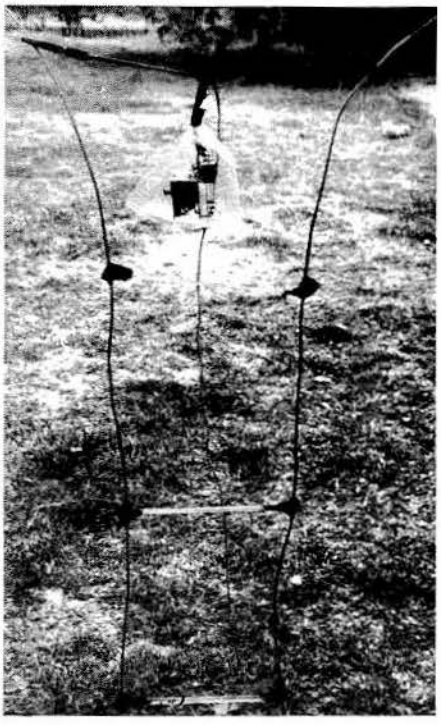

Fig. 15 — A simple relay arrangement is used to short out the stub and change the pattern of the antenna from one direction to another. A small plastic bag provides weatherproofing in the event it rains. (Doesn't it always?)

director is 33 feet (10.06 m). The stub length is 6 feet 9 inches (2.06 m). Eight-inch (203-mm) plastic spacers are placed between the two wires of the stub.

Supporting the quad is very simple. The mast is 50 feet (15.24 m) high, and guyed with nylon ropes. The boom is constructed from two telescoping sections of electrical conduit and is 18 feet (5.49 m) long. The elements are made from no. 14 stranded wire. The driven element is fed directly with RG-58/U coaxial cable. Location of the stub short is determined by the point of maximum front-to-back ratio. The boom-to-mast construction utilizes the support base from a Ham-M rotator. All it takes is a couple of U bolts and the boom-to-mast assembly is complete (see Fig. 16). The wire is strung from the end of the boom and is supported by a small piece of nylon rope and an egg insulator.

Results

Orientation for the quad was east and west. Favoring the eastern direction was the driven element/reflector combination, whereas the driven element/director combination was broadside to the western direction. A local amateur, approximately 5 miles (8 km) west of the Field Day site, assisted in tuning the quad for maximum front-to-back ratio. The end result was approximately 25 dB.

Results were a tremendous surprise! The antenna worked just as planned. The class of entry for simultaneous operation of two transmitters was used. One transmitter operated on 20 and 80 meters; the second transmitter was set up for 15 and 40 meters. Our club, W9AXD/9, scored third place in the two-transmitter class. Our biggest totals came from 40 meters — 693 contacts, over one third of our total number. For the first four hours of the contest, the antenna was aimed east. A rate of 90 contacts per hour prevailed for five solid hours. From that point on it was a steady decline after a sharp drop to about 45 contacts per hour. It was later surmised that the reason for the drop in contact rate was lack of activity and difficulty in finding stations that hadn't been worked before. The East Coast QRM was drastically reduced by changing the switch from "east" to "west." By midmorning we were surprised to find only a dozen W5 stations listed in the log. The antenna may not have been too effective in the southern direction.

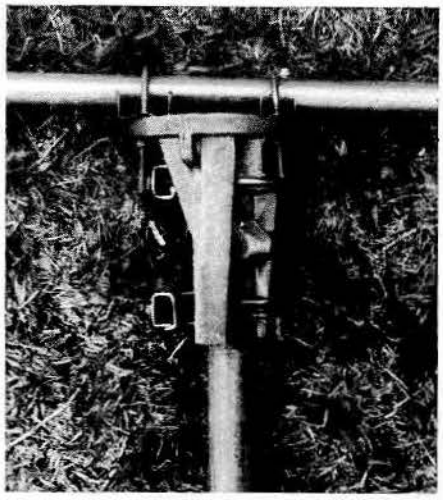

Fig. 16 — The bottom section of a CDE Ham-M rotor can be adapted to serve as a boom-to-mast bracket.

There is no reason why this arrangement could not be used for DX operating. The antenna could be positioned just underneath a beam for the higher frequency bands with the peak of the diamond supported from a boom placed through the top section of the tower.

This material was originally presented in *QST* by Peter H. Grillo, W6RTT.

Build This C-T Quad Beam for Reduced Size

This quad-beam antenna, while smaller in size than a conventional quad, performs like a veteran. The trade secret is to use capacitive tuning.

One of the main drawbacks of the quad beam is its large size compared to the Yagi beam. Previous efforts to reduce the size of the quad have utilized systems of inductive tuning. Loading coils have been used on one or two sides[1] or in the corners. Linear inductors on the vertical sides have also been used.[2] The purpose of this article is to explain a simple method of capacitive tuning to reduce the size of the quad. The C-T (capacitor-tuned) loop is diagrammed in Fig. 17.

It is well-known that the physical size of the dipole antenna can be reduced by replacing a portion of the antenna with a capacitive body and adding an inductor to restore the system to resonance. It seems less well-known that the full-wave loop antenna also may be reduced in physical size while holding the resonant frequency of the system constant by adding capacitance at the voltage loops. No inductors are needed. The capacitance may be added by any of the methods shown in Fig. 18.

The outside dimensions of the C-T loop may be anything chosen by the builder with the larger limit being the full-size, full-wave loop. The limit on the amount of size reduction effectively attainable depends both upon the electrical resistance in the circuit and upon the tendency in loop antennas for the current to become equal at all points in the circuit when the loop becomes very small in proportion to the free-space wavelength at the frequency under consideration. The geometrical shape of the loop is unimportant to basic operation provided that the capacitance is placed at or between the voltage loops. The bottom half of the chart in Fig. 21 shows the effective dimensional range of the C-T loop. The top half shows the tuning range that can

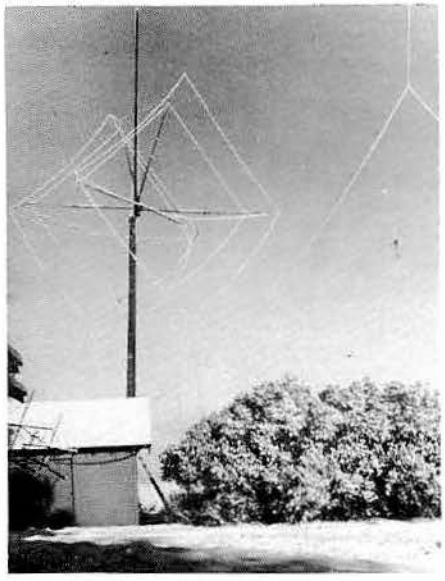

A winter snow sets the scene and accentuates the diamonds of the C-T quad-beam antenna at W7WKB.

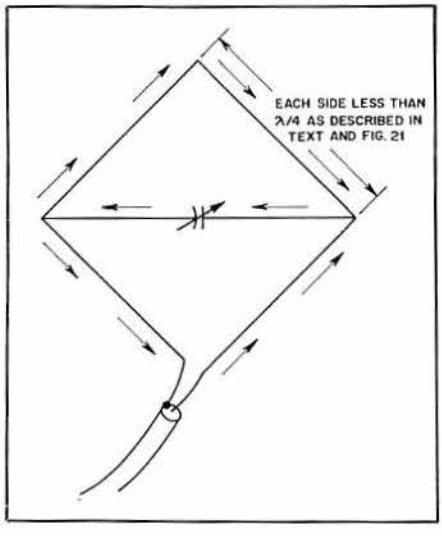

Fig. 17 — The C-T quad design with arrows indicating current flow for 1/2 cycle. The center capacitor is located at the minimum-current (highest-voltage) point in the loop. Each side is less than 1/4-wavelength long. See text and Fig. 21.

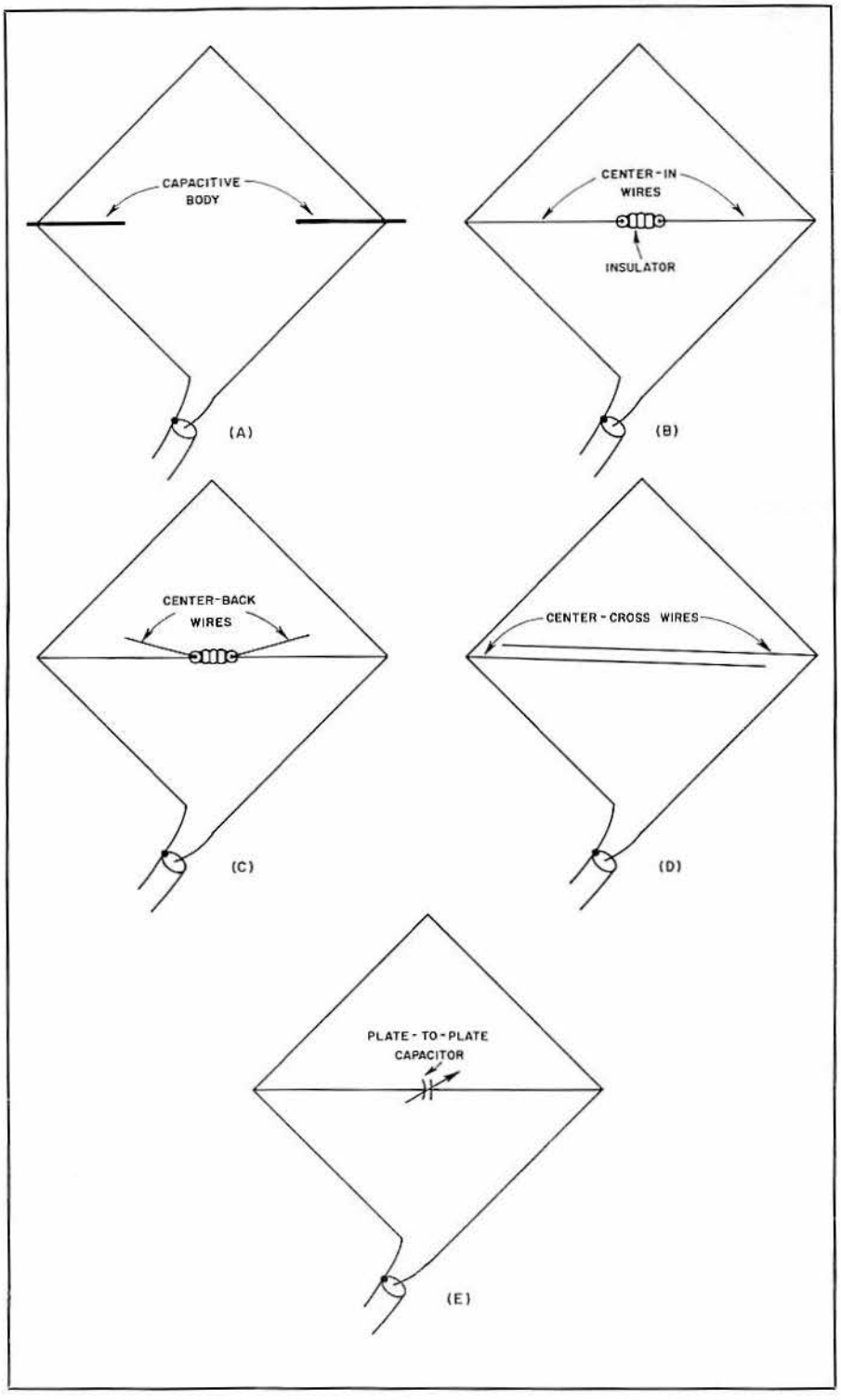

Fig. 18 — Methods of adding capacitance to the C-T loop are shown here. In Fig. 18C, if the center-back wires are placed too closely to the center-in wires, they become ineffective. A 12-inch (0.3048 m) spacing from the end of the center-back wire to the center-in wire is satisfactory. Wires running back toward the loop center may be attached to the outside ends of the center-back wires if more capacitance is needed. In Fig. 18D, the capacitance added by the center cross wires varies with both the length of wire and spacing between wires.

be expected by using various methods of adding capacitance to the diamond quad. These dimensions are intended as guidelines only.

The feedpoint resistance of the full-size, 1-wavelength loop is about 100 ohms. The feedpoint resistance of the C-T loop decreases as it is made smaller but will offer a good match to a 50-ohm coaxial line over the entire usable range as shown in the chart. A gamma match may be used if an exact match is desired.

More than one C-T loop may be used to form the C-T quad beam. A parasitic reflector was used in this installation because of the higher radiation resistance attainable while maintaining good gain. Maintaining the radiation resistance as high as possible is particularly important in small beams, both to keep efficiency high and to prevent the bandwidth from becoming too narrow.

Tuning and Mounting

The use of a grid-dip meter to attain initial band resonance is very helpful. By using a grid-dip oscillator, this beam was tuned initially with the driven element to resonate at the center of the band of interest. The reflector was then tuned to resonate at a frequency three percent lower than the driven element. Final adjustments were made using a test oscillator located about 1000 feet (300 m) away as a reference signal.

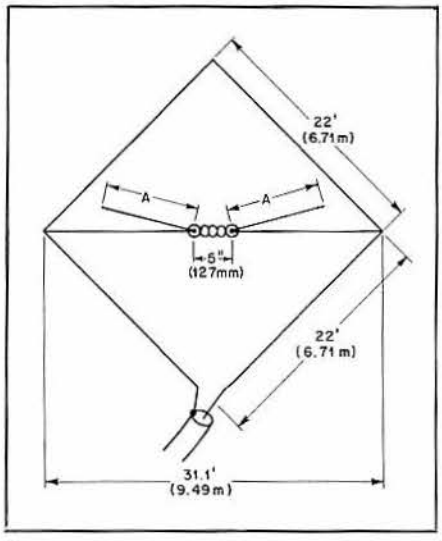

Fig. 19 — Dimensions for the 40-meter C-T quad are shown above. For the 2-element beam the spacing between the driven element and the reflector is 20 feet (6.10 m). The length of the center-back wire (dimension A) is 12 feet, 9 inches (3.89 m) for the reflector, and 9 feet, 11 inches (3.02 m) for the driven element.

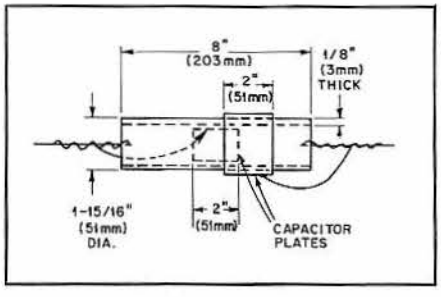

Fig. 20 — A variable capacitor is illustrated here. It can be used to tune the C-T quad. The eight-inch (203-mm) tubular portion is made from plastic water pipe. The cylindrical capacitor plates are formed from a copper sheet. One plate slides inside the eight-inch (203-mm) tube and the other over the outside of the tube. Maximum capacitance is approximately 25 pF.

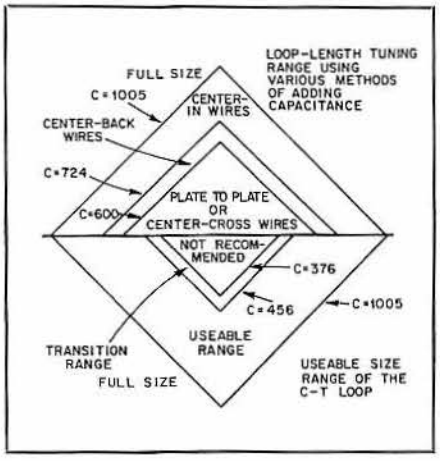

Fig. 21 — The chart shown above, providing dimensional guidelines for a single C-T loop, is based on the equation LF = C, where L is the outside dimension in feet, F is the frequency in MHz, and C is a constant chosen for the size of the C-T loop to be constructed. Use the largest size possible for the best electrical results. This is particularly true when using C-T loop elements to form a parasitic beam.
To use the chart, pick the largest C (up to C = 1005) feasible for your application. Use bottom half of the chart to see if the C-T loop will operate at the dimensional size selected. Then refer to the top half of the chart for the recommended capacitance method.

Table 3

Data for plotting SWR curve. Information in this table is used for plotting the SWR curve for the 40-meter C-T quad beam, as described in the text.

Frequency (MHz)	*SWR*
7.500	4.87
7.450	4.00
7.400	3.08
7.350	2.33
7.300	1.82
7.275	1.78
7.250	1.94
7.200	3.44
7.150	5.25
7.100	8.08

The director was tuned for lowest SWR and the reflector for best gain. If you lack a grid-dipper, initial resonance can be established by listening to your station receiver for a strong signal while making the adjustments. A dramatic increase in signal strength will be noticed at resonance. Tuning is accomplished by shortening or lengthening the capacitance wires.

The single loop or beam may be mounted either horizontally or vertically for horizontal or vertical polarization, but in either case it should be mounted as high above the ground as possible. Loop antennas operating close to ground will show a much higher feedpoint resistance than normal and will waste considerable power in ground heating effects. A rough guideline is to mount the antenna so that the bottom point is at least half the loop diameter above the ground.

The working 40-meter version of the C-T quad beam had a diamond configuration because of the greater mechanical strength and because of the longer center wire for tuning purposes. Final dimensions are shown in Fig. 19. A good quality center insulator should be used because of the high voltages present at the center.

A tubular tuning capacitor was originally installed in the driven element and worked well until the kW power level was reached. It then promptly arced over, leaving a conductive carbon deposit. A version using 2-inch (51-mm) plates as shown in Fig. 20 adequately tuned the reflector even at the kW level for some time. The capacitors, as shown, were not tried under wet conditions, but would probably be satisfactory at power levels up to 400 watts. For long-term use, the method shown in Fig. 18D is preferred over plate-to-plate capacitors because the high voltages are handled more easily.

Because some dielectric heating was noticed in this capacitor, the wire-tuned version was adopted. The wire version is recommended over the methods shown in Fig. 18D and 18E, any time the loop is large enough to be tuned by no more than one doubled-back wire (as shown in Fig. 18C). Tuning wires eliminate the capacitor with its heat loss and allow somewhat better current distribution. Less center radiation occurs because of partial canceling effects in the doubled-back wires. It would be wise initially to cut each center-back wire 12 inches (0.31 m) longer than shown to allow tuning. Pruning each center-back wire by 1 foot (304.8 m) increases the resonant frequency by roughly 100 kHz in the 40-meter version. No. 14 Copperweld wire was used throughout.

Performance

The antenna described performed up to expectations and has prompted many complimentary reports. The SWR curve information shown in Table 3 was attained using a 75-ohm coaxial feed line without any matching network. The SWR would be lower if a 50-ohm line or if a matching network were used. Forward signal strength as compared to the strength to the rear showed a maximum 30-dB difference as measured by means of the receiver S meter. Typical difference, as finally adjusted, was 12 dB.

The gain of the C-T quad over a comparable double Zepp (full wave on 40) was typically at least one S unit better when both antennas were at a height of 45 feet (13.7 m). The Zepp was better on very short skip but the C-T quad consistently was favored on longer skip. When elevated to 65 feet (19.8 m), the C-T quad gave outstanding results. At this height, two S-units improvement over a vertical antenna at distant points was noted many times.

The C-T quad may be built for any band. It should be most useful in meeting requirements for an inexpensive easily tuned wire-beam antenna where the full-size quad is unsuitable for mechanical or economic reasons. This material was orginally presented in *QST* by Roger Sparks, W7WKB.

References

[1]Pinner, "The Short Quad," *QST*, February 1964.
[2]Courtier-Dulton, "Some Notes on a 7-MHz Linear-Loaded Quad." See Chapter 4.

A Nearly Full-Size, Rotatable, 2-Element Quad for 80 Meters

We don't expect readers to rush right out and duplicate this antenna system — but this doesn't mean a lot of hams wouldn't like to!

Many hams have been thinking about new 80-meter antennas to improve their DX capabilities. On the higher amateur frequencies, antenna gain is relatively easy to acquire with a compact Yagi or quad. It is much harder in this respect on 40 meters. On 80 meters, however, the problem of securing any increase in antenna gain over a conventional dipole or groundplane is very difficult indeed, particularly where space is limited. Rhombics, Vs or multi-element collinear arrays become completely impractical on the normal urban or suburban lot. Even a phased vertical array is hard to handle on a city lot, and too often, performance is marginal because it is impossible to install an optimum ground system at such a location.

The author solved this problem at his QTH by constructing an almost full size 2-element quad for 80 meters. A unique tuning arrangement permits this antenna to be operated at any frequency within the 80-meter band with an SWR of close to 1. While certainly not adaptable to every individual's situation or pocketbook, a description of this antenna should be of interest to many amateurs. As far as it is known, this is the first and only set of beams, on one rotatable tower, covering all bands from 2 to 80 meters. By connecting the 2 quad elements in series to form a rotatable, bidirectional loop, the frequency coverage has been extended to 160 meters.

At this point, a few comments might be in order on the circumstances which led to this sizeable 80-meter antenna project. In June 1965, the writer returned to ham radio activity after a QRT of almost 30 years. During the first year of operation, the antennas of K3JH were a conventional commercial tribander for 10, 15 and 20 meters mounted on a 60-foot (18.3-m) tilt-over tower, and a trapped, inverted V for 40 and 80 meters. A bit of DX chasing soon led to the conclusion that better antennas were needed. Since the QTH is on a suburban lot about 175-feet (53.3-m) square, and heavily wooded, a "Christmas tree" array seemed the best alternative. Consequently, in the summer of 1966, with a great deal of help from Bob Scully, W2FXN, a 115-foot (35-m) rotary tower was installed along with full-size monoband beams for all bands from 2 through 40 meters.

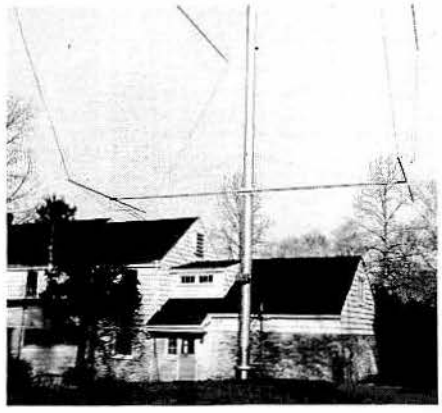

The bottom support of the quad elements is shown in this view, along with the tuning-network box, which is mounted on the mast.

This rotary steel tower is 16 inches (0.41 m) OD at the base with 1-inch (25-mm) thick walls. The tower rests in a 1/2-inch thick steel bearing-tube 15 feet (4.57 m) long and 20-inches (0.51-m) OD. The bearing tube is imbedded in a block of concrete 8 × 8 × 16 feet (2.44 × 2.44 × 4.88 m) which weighs 70 tons. The tower tapers to 5-1/2 inches (140 mm) at the top, and was designed to carry nine full-size monoband beams through 125-mph winds.

Initially, the antenna complement was as follows

2/6meters	—	Vert. groundplane at 115 feet (35 m)
6 "	—	6 el at 113 feet (34.5 m)
2 "	—	15 el at 109 feet (33.2 m)
20 "	—	5 el at 104 feet (31.7 m)
15 "	—	5 el at 96 feet (29.3 m)
10 "	—	6 el at 86 feet (26.2 m)
40 "	—	3 el at 77 feet (23.5 m)

A rotary ball-bearing ring and clamp at the 70-foot (2.13-m) level on the tower was used to support one end of an inverted L for 80 meters. This long wire, which could be used also on the higher frequencies, was fed through a Matchbox at the base.

Performance on 40 through 2 meters with this antenna system was generally excellent. The L and inverted V on 80, however, left much to be desired, especially when compared to the antenna performance on the other bands.

In attempts to improve this situation, several different 80-meter antennas were installed at various times between 1966 and the spring of 1969. Included in this effort were a top-loaded groundplane and a pair of phased verticals. None of these antennas provided sufficient improvement in DX performance on 80 to be considered satisfactory.

With the advent of the 5-Band DXCC, the question of how to do better on 80 meters again became a matter of concern. It was at this time that the concept of a quad of some sort, to be mounted on the rotary tower, began to emerge. Since 40-meter quads had been constructed previously, and were mechanically feasible, the thought at first was to build a half-size quad for 80 meters, using loading coils. Preliminary calculations indicated the possibility of achieving some gain over a dipole in addition to the obvious advantage of being able to rotate the array.

It was quickly determined that a half-size quad mounted at 57 feet (17.4 m) would fit underneath the 40-meter Yagi. Construction could be quite conventional using fiberglass X frames in each element, and a spacing of 0.15 wavelength.

Design Considerations

The proposed design was discussed with a number of amateurs including Jim Lindsay, WØHJ, Dunc Carter, W5IOU, and Claus Moeller, DL7CM, who were most helpful with advice and suggestions. A search of the literature disclosed that a number of loaded antennas of various types had been built. In most cases, however, performance had been judged empirically, and there was little in the way of specific comparative data on the performance of loaded versus unloaded configurations, or versus a reference dipole. Because of this, the decision was made to build and test a 14-MHz model of a half-size quad. This would enable a direct comparison between the performance of a miniaturized quad and other antennas. Of particular interest was a comparison with a dipole, since this was the more normal antenna used by amateurs on 80 meters.

Henry Pemberton, W3PN, who had become interested in the project, provided the X frames and supports from an old 20-meter quad, for use in the test model. Tom Consalvi, W3EOZ, provided some suitable coil stock for the test design. With this help, the 14-MHz model was quickly constructed. No trouble was experienced in pruning

the coils and resonating the loops. Except for one bad piece of insulation on one coil, which promptly burst into flame when rf power was applied to the antenna, the driven element could be fed with a full kilowatt at an SWR of 1. The SWR, however, would rise sharply when the coils, which had no protection from the weather, became wet from rain. All testing, therefore, had to be done on dry days.

Since the 80-meter version was to be mounted on the tower one-quarter wavelength above ground, the 14-MHz model was mounted for the tests at the same relative height. Standard procedures for tuning up the quad were used, and will not be detailed here. Impedance of the loaded loop was measured at 60 ohms, so it could be driven nicely with a 50-ohm line. The bandwidth was 125 kHz, measured between frequencies each side of the resonant frequency where the SWR was 3:1. This was the result expected, due to the heavy loading.

Extensive on-the-air comparisons were made between the model and various other antennas. These included a dipole at the same height above ground as the model, a 3-element tribander at 60 feet (18.3 m), two different inverted Vs at 50 feet (15.2 m) and a 5-element monoband Yagi at 104 feet (31.7 m). The regular antenna switching arrangements in the station were such that almost instantaneous comparisons could be made between the different antennas, minimizing QSB differences in the receiver. In the transmit mode, many amateurs compared signal differences between the test model and the other antennas. It is impossible to list the calls of all those who helped in this way.

After considerable testing, adjustment, readjustment, and minor configuration changes in the model, the results were found to be quite discouraging. The simple conclusion was that a loaded half-size quad had insufficient gain compared to a dipole to warrant proceeding any further with an 80-meter version.

Further Exploration

Before abandoning the 80-meter project, however, we decided to explore some practical ways to increase the size of the elements, preferably without using the normal-type quad X frames, which would be difficult if not impossible to handle when the antenna grew too large. This thinking developed the concept of using the 14-MHz boom at 104 feet (31.7 m) to support diamond-shaped elements at the top, and using a boom and spreaders rather than an X frame to hold the elements at the center. The bottom of the quad elements could be supported easily with a relatively light boom and spreaders near the base of the tower.

In order to reduce the size of the center boom and spreaders, the first model was kite-shaped with an included angle at the top of about 50 degrees. Unfortunately, the

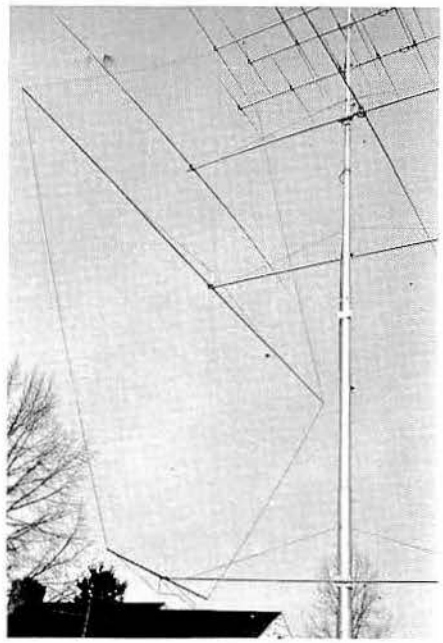

A detailed view of one of the quad elements, showing the method of supporting the loop.

results were poor, and compared to a dipole there was no gain. We concluded that this configuration was so squashed together that the antenna was acting like a dipole instead of a quad. A series of configurations was then drawn up on paper. The boom and spreader sizes were varied, but the included angle at the top of each diamond element was kept at 75 degrees or more. This helped to pin down a configuration which would be mechanically feasible, and which would be a reasonable compromise among the various considerations to be taken into account. The one selected is shown in Fig. 22.

Because these elements are almost full size at 4 MHz, making a 20-meter model quite large, it was decided to build and test a model of this configuration on 15 meters. The test procedures for this model were the same as those previously described for the 20-meter model of the half-size quad. This model showed substantial gain compared to the reference dipole at the same height. Also, the model mounted only 15 feet (4.6 m) above the ground compared favorably in performance with the tribander at 60 feet (18.3 m). The 5-element monobander at 96 feet (29.3 m) consistently provided better gain, as was to be expected. The impedance of the driven element was about 80 ohms. Bandwidth between SWR points of 3:1 was 250 kHz, or about twice what was measured on the half-size model.

Mechanical Considerations

After a lengthy test period, during which many on-the-air comparisons were made, the results were good enough to make the decision to build an 80-meter version of this antenna. Because of the size of the proposed antenna, considerable thought had to be given to the mechanical design to assure longevity comparable to the other beams which are rated for 125-mph winds. The wire in the quad elements is no. 12 stranded copperweld. All other metal in the antenna is aluminum or stainless steel. The two quad elements are suspended from the 20-meter boom at 104 feet (31.7 m). The insulators are five glazed porcelain knobs. Spacing is one-eighth wavelength, 36 feet (10.97 m). The 20-meter boom is 46 feet (14.02 m) long, and is made from 4-inch (102-mm) OD, 1/4-inch (6-mm) wall T-6 aluminum tubing at the center, and similar material tapering from 3-1/2 inches (89 -mm) to 3-inch (76-mm) OD at the ends. A 1/4-inch stainless steel cable supports the boom 18 feet (5.49 m) out from each side of the tower. Originally, the plan was to slide the quad elements down this cable from the tower. Unfortunately, the steel plates holding the Yagi elements to the boom on the other beams were found to be rusting because of poor plating. Rather than dismantle the beams, a crane was brought in so that these plates could be cleaned and painted by a man carried up in a boatswain's chair. At the same time, the elements were hung from the 20-meter beam, and the center boom and spreaders for the quad were installed with relative ease.

Dimensions

The 36-foot (10.97-m) center boom at the 57-foot (17.37-m) level of the tower is made of a single 24-foot (7.32-m) section of 3-1/2-inch (13-mm), 1/4-inch (6-mm) wall, T-6 tubing with 7-foot (2.13-m) sections of 3-inch (76-mm) OD pipe telescoped and bolted at each end. The boom is supported from the tower with a 3/16-inch (4.76-mm) stainless-steel cable. The spreaders at each end of this boom are 70 feet (21.34 m) long. Each consists of a 24-foot (7.32-m) piece of 2-1/2-inch (64-mm) OD, 1/8-inch (3-mm) wall, T-6 tubing at the center, with two short pieces of 2-1/8 × 1/8-inch (54 mm × 3-mm) tubing telescoped and bolted at each end to make up a length of 30 feet (9.14 m). To complete the spreaders, 20-foot (6.10-m) sections of 1-1/2- and 1-1/4-inch (38- and 32-mm) fiberglass poles are attached to each end of the aluminum centerpiece. Use of the fiberglass reduces weight and eliminates a one-quarter wavelength piece of metal from the middle of the quad element. A 1/8-inch (3-mm) cable and strut supports each spreader to minimize sag, which is very slight as may be noted in the photograph. A welded aluminum T structure and stainless steel clamps are used to hold the spreaders on to the ends of the boom. A stainless steel clamp and Teflon grommet is attached to the ends of each spreader to hold the element wires in place. The only function of the spreaders is to hold the two opposite sides of each quad element apart without too much fore and aft flopping around when the antenna is rotated. The length of the spreaders, wind loading, and safety factor dictates the heavy mechanical design.

The lower boom, which is 23 feet (7 m) off the ground, is made of a 24-foot (7.32-m)

section of 2-1/4 × 1/4-inch (57- × 6-mm) T-6 tubing with shorter 2- × 1/4-inch (51- × 6-mm) pieces telescoped and bolted at each end to make the total length of 36 feet (10.97 m). To maintain symmetry, 17-foot (5.18-m) spreaders are attached to each end of the lower boom. These spreaders are made of 1-1/2-inch (38-mm) fiberglass. They are attached to the boom with aluminum angles and stainless-steel clamps. A light stainless-steel cable and strut holds the lower spreaders firm against the pull of the quad-element wires, which are attached to each end of the lower spreaders with stainless-steel clamps. The wires are taped along the fiberglass almost to the center of the spreaders, and then go off at right angles to the tuning box, which is mounted on the tower 13 feet (4 m) above ground. The distance from the end of the lower boom to the tower is about 18 feet (5.5 m), and the 36 feet (11 m) of wire which connects the quad proper to the tuning box represents loading.

Tuning

Each element, including the 36 feet (10.97 m) of connecting wire just mentioned, resonates at 4050 kHz. Thus, a small amount of additional inductive loading is required to tune the antenna to resonance within the 80-meter band. This is accomplished by putting two relatively small motor-driven coils in series with each loop of the antenna. The reversible motor for each pair of coils in each loop is controlled by a two-way toggle switch mounted on the antenna control panel in the shack. In the case of the driven element, tuning is accomplished simply by applying power to the antenna and then adjusting the loading inductances by the motor-control switch to the point where the SWR is minimum, usually very close to 1. Tuning the reflector can be accomplished by turning the back of the quad toward a distant signal, and adjusting the reflector loading coils for minimum received signal. This seemed a bit cumbersome to do each time the operating frequency was changed from cw to ssb and vice-versa, so a microswitch was added to the reflector coils and motor assembly. Each revolution of the coils flicks the microswitch, which actuates a light on the control panel in the shack. By counting the blinks of the light, and referring to a chart which shows the resonant frequency of the reflector versus the number of turns of inductance in the loop, the reflector can be tuned to any desired frequency. With this tuning scheme, it is quite easy to tune the quad for best performance at any point in the 80-meter band. The bandwidth between the 3:1 SWR points is close to 200 kHz, so retuning is required only for large frequency changes within the band. Frequency flexibility otherwise is quite good.

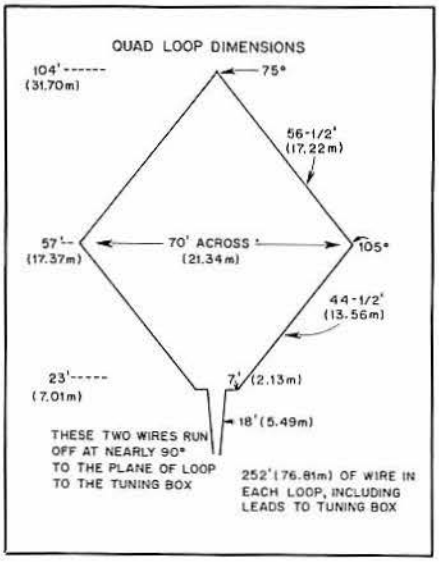

Fig. 22 — Dimensions of one of the quad loops.

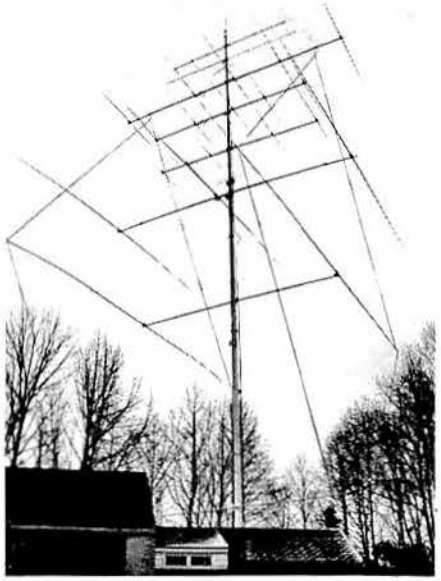

Here is the complete antenna system, 2 through 160 meters, all rotatable, directional arrays.

The impedance of the driven element measures about 75 ohms. The antenna is coupled to the transmitter through a balun and 50-ohm line. The difference between the resonant frequency of the driven element and the reflector, when the latter is tuned for maximum front-to-back ratio, is in the order of only 1-1/2 percent. This probably results from the quad being only a one-quarter wavelength above the ground. The front-to-back ratio is about 20 dB, and the front-to-side, 50 dB. All measurements have an indicated gain over a dipole in the order of 6 to 7 dB. No degradation in performance, or SWR, has been observed during heavy rain. The small loading coils are protected from the weather, of course, in their aluminum tuner box, so the problem, which was encountered with unprotected load coils in the 20-meter test model, has been eliminated.

Tests were conducted with the second element tuned as a director instead of a reflector; there was no noticeable improvement in gain, whereas the front-to-back ratio was diminished. It is felt that the best results are obtained with the reflector.

Some thought was given to driving both elements at a 135-degree phase difference to obtain a cardioid pattern. It is felt, however, that the conventional quad pattern, with deep nulls on each side, and a reasonably good front-to-back ratio, is more desireable for DX. So, nothing further has been done with such a phasing arrangement.

Results

DX results on 80 meters have improved considerably since the new antenna was put on the air. On cw, the gain seems to drop off somewhat as compared to the phone end of the band. Probably this is due to the fact that the relative size of the antenna is smaller at the cw operating frequencies. Nevertheless, reports usually are from one to several S units higher than other U.S. stations with comparable power input, and conventional antennas. In most instances during pile-ups in a recent cw contest, it took only a call or two to get through, whereas, previously, the station was usually last. It was found also that contacts could be made earlier, as the band opened. In several instances like this, it was amazing to get a response from a DX station, and then to hear other U.S. stations calling without success.

Reports from overseas on ssb are outstanding. During a recent phone contest, several dozen DX contacts were made in just a few hours — everyone on the first call.

During the day, on 80 meters, it is quite easy to work into Canada or the Carolinas with good signals at both ends of the circuit. On a dipole, very often the other station is completely unreadable, if not inaudible. This points up the fact that one notices great improvement in reception with the quad compared to a dipole, which on 80 is just as important as being able to transmit a better signal.

Once it was determined that the quad worked well on 80 meters, the possibility of operating the antenna on 160 meters was explored. Since the loops independently resonated at 4050 kHz, and there was considerable inductive loading available in the coils, it was felt that it might be possible to resonate the antenna on 1.8 MHz by putting the two loops in series. Actually, with the load coils tuned to minimum, the series-connected loops resonated at 1775 kHz because of the mutual coupling. By shortening out the coils entirely, the pair of loops were resonated at 1805 kHz. Therefore, the SWR at the low end of the 160-meter band is very low.

Domestic reports on 160 meters have been excellent. Consistent directional effects have been noted by several observers when the two-turn loop is rotated. The pattern is the typical figure eight, with deep nulls off each side of the loop. It remains to evaluate how well the antenna works on 160-meter DX.

Following completion of the antenna in September, there have been several severe

storms, with winds gusting as high as 65 mph. These velocities barely moved the wires and spreaders around. It is apparent that the heavy construction is adequate to handle the winds of much higher velocity for which the antenna was designed. Although it is probably one of the largest quads in existence, it certainly appears as though it will stay up a long time, even through rough weather.

In conclusion, this project could never have been completed successfully without the help of many domestic and overseas amateurs. Their reports, advice, and assistance will always be appreciated. Although this has been a sizeable and difficult antenna task, a great deal of satisfaction has been derived from carrying it through from concept to on-the-air operation. The simple lesson has been relearned with regard to antennas — that one cannot get something for nothing. Mini-size antennas are better than no antennas, but there is no substitute for full-size antennas if one wants full-size results. This material was originally presented in *QST* by Joe Hertzberg, N3EA.

The Folded Mini Quad

A full-wavelength loop can take a variety of forms. Despite the shape suggested here, the author claims good results.

An unusual type of full-wavelength wireloop antenna is in use here on 2 and 15 meters. The design, which the author had not seen previously, provides an antenna that occupies minimum space; the antenna is omnidirectional, vertically polarized, broadbanded and requires no ground-plane.

It evolves from a full-wavelength loop.[1] The loop, if fed on the side (x-y) as in Fig. 23A, radiates a vertically polarized signal. The radiation pattern is bidirectional, with maximum radiation broadside to the plane of the loop and with the highest field strength in the plane A-A′.

The loop can be deformed into a square, such as in the elements of a quad, and without much loss of efficiency into a rectangle (Fig. 23C). Vertical polarization, bidirectional signal pattern and maximum radiation from the plane A-A′ are retained.

A 90 degree bend at A-A′ and two further right angle bends at B-B′ and C-C′ transforms the flat loop into a cube. The circumference is still a full wavelength and each side of the cube measures 1/10 wavelength. Again, vertical polarization is retained, but the appreciable bidirectional radiation from the sides of the cube adjacent to A-A′ leads to a nearly omnidirectional radiation pattern.

My 2-meter antenna was constructed from aluminum clothesline wire; the length in feet was chosen by 1005/f MHz. It is fed with 50-ohm coaxial cable through a Pomona Electronics no. 1699 adapter and no matching device is used. The SWR is less than 1.2:1 from 144 to 146.5 MHz and climbs to 1.4:1 at 148 MHz. The radiation pattern was measured with a simple field-strength meter, using a half-wave dipole as pickup element and a 20-kΩ resistance in series with the 20-μA meter to improve linearity.[2] The front-to-back ratio is 1.8 dB with no prominent sidelobes apparent, but a rather sharp 3-dB dip is caused by the "shadow" of the feed line and hardware.

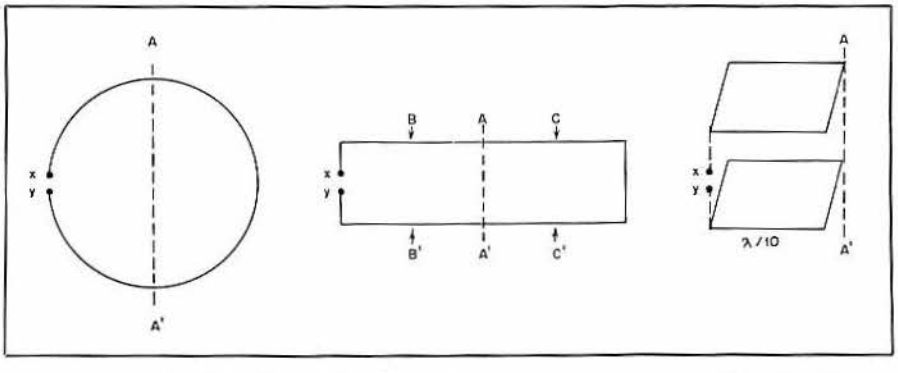

Fig. 23 — Conversion of the full-wavelength loop to the space-saving cubical configuration. The length of the wire and the vertical polarization remain but the pattern changes from bidirectional to omnidirectional. The spacing between the feed point and the adjacent side is not critical. The spacing on 2 meters is about 1-1/2 inches (38 mm), and on 15 meters is about 4 inches (102 mm).

Performance

Fed with 10 watts and used as an indoor antenna, it gives consistent communication with 2-meter fm base and mobile stations within a 10- to 15-mile radius. It performs better on receive and transmit than a 1/4-wave whip at the same location.

A 15-meter version of the antenna was then constructed and suspended in the attic with string and tacks. It is operated with 100 watts and the rig loads almost as well as the 2-meter version, but with a slightly higher SWR. The first contacts were with California and it has since given excellent performance to the West, Midwest and South as well as to South America and Europe.

The close proximity of antenna sections radiating out of phase may lower the efficiency over that of a loop, yet, in terms of space requirement, construction cost and ease of installation (no radials!) and tuning, the antenna is hard to beat. As a full-wave loop it should have a slight edge over a vertical. The author recommends further experimentation and modification, e.g., into the even more space-saving configuration of a cylinder. This material was originally presented in *QST* by Max Blumer, WA1MKP, SK.

References

[1] *The ARRL Antenna Book*, 13th ed., 1974, p. 65.
[2] *The Radio Amateur's Handbook*, 46th ed., 1969, p. 553.

A Convenient Stub-Tuning System for Quad Antennas

The cubical quad has been a popular antenna with amateurs for a number of reasons — relatively light weight, small turning radius, low cost, and good DX performance at rather low heights when compared to other antennas. The authors' experience with quads has demonstrated, however, that best possible performance requires careful parasitic-element tuning. Cutting elements according to various "established" length formulas has often yielded less than satisfactory results. While adjustments for maximum forward gain are generally uncritical, a mediocre front-to-back ratio often results unless time and care are taken to tune the parasitic elements. Factors such as spacing between elements, proximity of the antenna to ground, or influence of other objects (including the other concentric loops in a multiband array) require that the electrical length of the parasitic elements be adjusted using empirical methods if optimum performance is to be realized from the system. It was felt that if one was going to the trouble of erecting a good antenna system, it was worth seeing to it that the antenna was delivering the performance of which it was capable.

These considerations led to the development of the parasitic-element tuning system described here. While the scheme is applicable to quads in general, whether rotary or fixed, the original intended application was in a fixed two-element, full-size 40-meter quad. The descriptions here apply to this 40-meter system, but the general information allows one to follow the same scheme with a quad for any band.

A 40-Meter System

This 40-meter antenna consisted of two non-rotatable full-wave wire loops suspended from a boom which was mounted near the top of a tower. Spacing between elements was 22 feet (6.71 m). The corners of the loops were tied down to convenient anchor points by means of ropes, thereby eliminating the need for spreaders. With the elements thus fixed in place, the antenna was oriented in one general direction and could not be steered elsewhere. A driven-element and reflector combination was used.

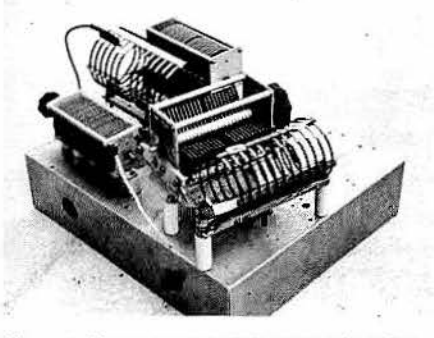

The matching network built by the authors for the modified 40-meter system. Relays, used in the switching circuitry, are not visible. The builder is left to choose a suitable network of his own to meet his operating requirements. Basic design information can be found in *The Radio Amateur's Handbook* or *The ARRL Antenna Book*.

Early experiments with the antenna demonstrated the need for careful reflector tuning. Several trips were made up the tower to alternately prune and add wire to the reflector before the antenna exhibited good performance at the frequencies of interest. But when tuned properly, the quad really performed! In many instances signals which were inaudible while using an 80-foot (24.4-m) high reference dipole were perfectly readable with the quad (at a median height of about 100 feet [30.5 m]). Reception was further enhanced by rejection of unwanted signals off the back of the quad.

Now if only the quad could be made rotatable. . . . Unfortunately, a full-size rotating system (spreaders would be needed) was out of the question. The cost, difficulties of construction and installation, and the severe effects of New England winters discouraged such ideas. The authors, being avid contesters and DXers, were willing to settle for the next best alternative — keeping the fixed quad, but electrically switching its pattern.

The solution involved a tunable stub attached to one of the elements to lengthen or shorten it electrically. With the appropriate stub switched in, the single element could be made to look like either a reflector or director and thus cause the pattern to be reversed. In order that adjustments be made quickly, easily, and from a convenient location (such as the shack or the bottom of the tower), it involved more than the conventional short stub often used with quads. Rather, the situation called for a long stub — long enough to reach the desired remote location — terminated in a variable reactance. Tuning the element, then, involved nothing more than adjustment of the value of reactance which could be provided conveniently by means of a variable capacitor.

The electrical principle is simple. One adds inductive reactance to lengthen an element electrically, or capacitive reactance to shorten it. Typically, the former arrangement is used with quads in a driven-element and reflector combination in which both elements are cut to the same physical length. A stub, shorted at the end, is attached at the center of the bottom section of the reflector. By varying the position of a shorting bar along the stub, the amount of inductive reactance presented to the element can be varied and the electrical length altered correspondingly. Because the stub is short in length, this adjustment must be made at the antenna itself, preferably near or at its final height.

Now, if the stub is cut to some different length which happens to be longer than in the above case, the parasitic element can still be made to see the proper amount of inductive reactance (if it is a reflector) provided the stub is terminated properly with some other reactance (in general, something other than a short). Varying the reactive termination is then equivalent to moving the shorting bar along the conventional stub. This is a consequence of the impedance-transforming property of transmission lines. The long stub can be treated as a transmission line. If we know its characteristic impedance, its length, and the impedance that must be seen at the parasitic-element end of the line, the Smith Chart can tell us what kind of termination is required at the opposite end.

A reflector cut to the same physical dimensions as the driven element — self-resonant at the desired operating frequency — must "see" roughly 150 ohms of inductive reactance at the terminals where the stub is attached. Although little information is available about the use of directors with quads, it is assumed initially that a director, also cut to the same length as the driven element, must see a roughly equal but opposite amount of reactance, or about 150 ohms of capacitive reactance. If one desires to make the termination at the end of the stub a variable capacitor for convenience of tuning, which was the case in the 40-meter system under consideration, the problem can be rephrased slightly: what length of line of a given characteristic impedance is required so that a variable capacitor (a 10- to 350-pF unit was used) causes the parasitic element to see the above reactances? This is easily solved with a Smith Chart. Two somewhat different systems evolved from these ideas. The second, a modification of the first, will be described last.

The design procedure for the 40-meter version went as follows: The driven and parasitic elements were cut to the same length, given by the more or less standard formula, $L = 1005/f$, where L is the length in feet, and f the frequency in MHz. This resulted in a loop circumference of 143 feet, 6 inches (43.74 m) at a frequency of 7.0 MHz. In the practical installation, the loops were triangular in shape rather than

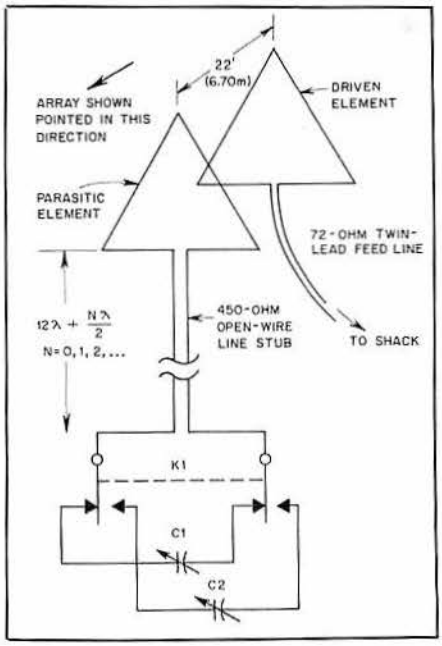

Fig. 24 — Configuration of 2-element switchable 40-meter quad. Triangular loops are shown, although square or diamond loops can be used too. Both elements are cut to the same dimensions: 143 feet, 6 inches (43.74 m) for 7.0-MHz operation. The selection of either C1 or C2 by means of K1 determines which direction the array is pointed. Switching components K1, C1 and C2, can be installed inside the shack or on the ground. The stub line is cut long enough to reach them. Feeding the driven element with 72-ohm Twin Lead results in a low SWR.

C1 — 10- to 350-pF air-variable capacitor, adjusted for director operation as described in text.

C2 — Same as C1, except adjusted for reflector operation.

K1 — Dpdt relay (Potter and Brumfield KA11DG or equivalent).

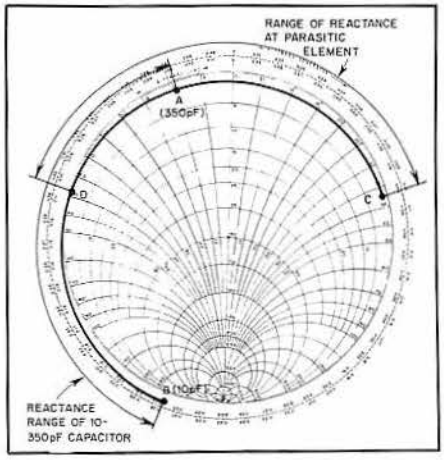

Fig. 25— Example of Smith Chart calculations required to arrive at correct stub dimensions. A 10- to 250-pF capacitor is used as the variable-reactance element which terminates the 450-ohm transmission line used for a parasitic-element stub. The chart is normalized to 450 ohms. The arc between points A and B represents the range of reactance of the capacitor as it is tuned between the extremes of its range. If the capacitor is connected to a 0.12-wavelength long stub (plus any multiple of one-half wavelength) with a 450-ohm characteristic impedance, the range of reactance represented by the arc between points C and D is presented to the parasitic element. This range is sufficient to cause a properly cut parasitic element to look like either a director or reflector. Further discussion of Smith Chart calculations can be found in the latest edition of *The ARRL Antenna Book*.

square or diamond. Shape is relatively uncritical — performance is approximately equivalent for the various geometric configurations, and ease of installation was considered more important. The triangle has the advantage of requiring only three tie-off points — one at the top where it hangs from the boom and two at the bottom — whereas the other two forms require support at four corners. Furthermore, the triangle requires less vertical height — approximately 41 feet (12.5 m) on 40 meters, assuming equal-length sides — as opposed to the diamond which needs about 50 feet (15.25 m). The square requires the least vertical height but is the most difficult to support mechanically. The resultant configuration is shown in Fig. 24.

The stub line was made from 450-ohm open-wire transmission line because of its relatively low cost in commercially made form and its low-loss characteristics. The reactance range of the 10- to 350-pF capacitor by itself at 7 MHz was then plotted on the Smith Chart as shown in Fig. 25. (Recall that $X^L = 2\pi fL$ and $X^C = 1/2\pi fC$ where X^L and X^C represent values of inductive and capacitive reactance respectively, given in ohms, L and C the corresponding values of inductance in henrys and capacitance in farads, and f, the frequency in hertz.) The low-capacitance end of the range is indicated as point B in Fig. 25 with the Smith Chart normalized to 450 ohms in this example, while the other extreme comes out at point A. If the capacitor was then connected at the end of a 0.12-wavelength section of the 450-ohm line (approximately 16 feet [4.88 m] in open-wire line), the impedance seen at the other end of the line would vary between the range of slightly greater than +j300 to -j300, represented by points C and D. This would meet the +j150 and -j150 reactive loading requirements of the parasitic element for reflector and director operation, respectively. Actually a stub length of 0.12 wavelength, plus any multiple of a half wavelength, would work too, because any half-wavelength section of transmission line merely repeats at one end the impedance that appears at the other. Thus, the distance to the desired remote location dictates the minimum required line length. Another advantage of using 450-ohm line, as opposed to a line with a lower characteristic impedance, becomes apparent when working examples on the Smith Chart — for a given capacitor tuning range, the 450-ohm line produces a greater range of reactance change at the antenna end of the line. A 300-ohm line would serve almost as well, however, providing only slightly less tuning flexibility.

The stub was terminated at a dpdt relay which was controlled from the station operating position and which was used to select one of two variable capacitors — one adjusted to provide reactance for reflector operation and the other for director operation, as shown in Fig. 24. In this manner, the pattern could be flipped around 180 degrees instantly from the shack. The driven element was fed directly with 72-ohm transmitting-type Twin-Lead. A low SWR was obtained with no special provisions made for matching.

The director and reflector tuning should be done empirically, as was stated before. Experience has shown that quads tune rather broadly for maximum forward gain. It was found that fairly large changes in the settings of the variable capacitors did not alter the gain significantly. It is best, therefore, to tune for maximum front-to-back ratio, on which the settings had considerably more effect. On-the-air signals arriving from the rear direction can be nulled by tuning the capacitors. The nulls should be fairly pronounced if the

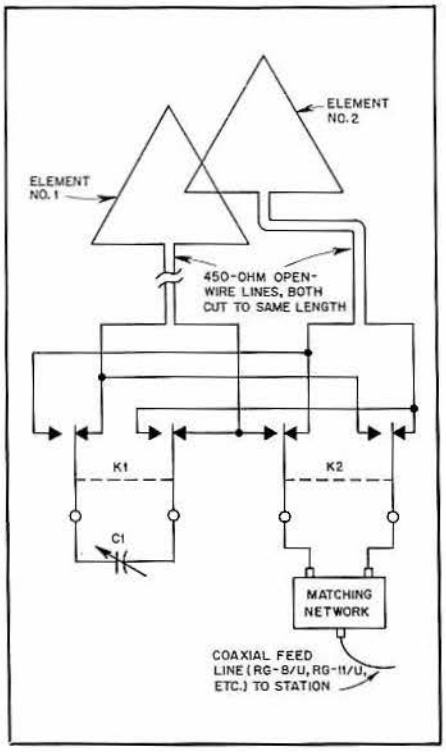

Fig. 26 — Configuration of modified 2-element switchable 40-meter quad. The lines from each element are both cut to the same length, which can be the same as the parasitic element line in Fig. 24 or other suitable length. Both elements are cut to the same dimensions as in Fig. 24. The positions of K1 and K2 determine whether an element is fed as a driven element or terminated as a reflector. The array pattern can be switched by determining which element operates as a reflector or driven element. Only one tuning capacitor is required, but a matching network is needed to match a coaxial feed line.

C1 — 10- to 250-pF air-variable capacitor, adjusted for reflector operation.

K1, K2 — Dpdt relays operated simultaneously, or both may be replaced by a single four-pole, double-throw relay (Potter and Brumfield KA11DG or equivalent).

system is set up as described here. The exact amount of attenuation of signals off the back of the antenna varies from signal to signal. It was observed that the 40-meter antenna exhibited the greatest front-to-back ratio for signals arriving from distant locations (at low radiation angles). Alternatively, field-strength measurements can be made to determine the proper settings for minimum radiation or reception off the rear of the antenna. In this fashion, one capacitor is adjusted for director operation and the other for reflector operation.

When making large excursions in operating frequency on 40 meters, it is necessary to touch up the tuning. A director tuned for operation in the low end of the cw segment is self-resonant approximately in the middle of the phone portion and provides little usable gain at those higher frequencies. Retuning is done easily, however — something which is not possible using fixed-tuned elements.

A Modified 40-Meter System

The 40-meter system described above provided very good results over a period of months, including stateside and DX contest work and casual DXing. After some thought, however, a modified system was constructed. The new configuration provided some advantages over the orginal scheme.

The same principle of operation was retained. The new system shown in Fig. 26, used only a reflector-type parasitic element, but the switching system now allowed either element to operate as the driven element or reflector. In this manner, the antenna pattern could still be reversed by choosing the appropriate element for the desired function.

Several factors prompted the change. It was found with the original system that a considerably higher front-to-back ratio could be had using a reflector rather than a director. The latter yielded no more than about 10-dB discrimination against signals received off the back of the antenna, even with careful tuning, whereas with the former the figure was approximately as high as 25 dB. Although most available literature made little mention of quad performance using a director, this observation agreed with what little published data could be found on the subject.[1] The reflector-only model also had the advantage that just one tuning adjustment was required, since one stub reflector served both elements in an identical fashion. Furthermore, because the system behaved the same no matter which direction the array was switched, the SWR did not change when switching, and the transmitter was thus always tuned properly. With the original scheme the antenna feed-point impedance changed when switched between director and reflector operation. Although the resultant SWR was not objectionable in either case (it did change, though), it was necessary to retune the transmitter after switching, or tolerate a moderate amount of mistuning.

The design procedure for the new arrangement is basically the same as before. Both elements are cut to the same length. Only the stub requirements for a reflector need be considered now in doing the Smith Chart calculations. Once the stub line length is determined, two such identical-length lines, both made from the same type of transmission line, are cut, one for each element. A four-pole, double-throw relay, or two dpdt relays operated simultaneously, are required in the hookup shown in Fig. 26, to switch the two lines between the parasitic-element termination and the main feed-line matching network.

The new system has one disadvantage, however. A matching network is required between the transmitter and driven element because of the mismatch between the main feedline, which is presumably coax, and the driven-element open-wire feed line. The original system required no special matching. This presented no problem in the 40-meter system considered here since a suitable network was easily constructed. The builder is left to choose a suitable matching network of his own as there are numerous possibilities to take care of the varied matching requirements which may arise under different situations. Depending upon one's preferences and requirements, the modified scheme may or may not prove more attractive.

Additional Remarks

A few general comments can be made at this point. Although a variable capacitor has been designated thus far as the termination for the stub, there is no reason for not using a coil or some other combination of inductance and capacitance if it will work with a stub length which happens to be convenient. The builder can choose for himself. The 10- to 350-pF capacitor described earlier had approximately 0.05-inch (1.27 mm) spacing between plates. While it is difficult to predict the voltages present in the parasitic element (and across the capacitor), no arcing between plates was observed during transmitting periods, even while running one kilowatt transmitter dc input. This suggested the plate spacing was adequate.

The lines from each element should be brought away perpendicular to the elements as much as possible, and open-wire line should be kept reasonably clear of nearby objects, especially metal ones. Also, the velocity factor of the line being used (0.95 for "ladder" line) must be remembered when computing physical lengths.

The authors erected a single diamond-shaped 80-meter quad loop with its bottom close to the ground. The antenna was tried as both a vertically and horizontally polarized radiator. For DX work, the vertically polarized version yielded unquestionably superior results in terms of greater signal strengths at long distances and the beneficial feature of rejection of unwanted high-angle radiation from stateside stations when receiving. A parasitic element to accompany the single loop was not tried. These observations suggest interesting possibilities for vertically polarized ground-mounted quads for low frequencies.

The ideas presented here are applicable to any quad antenna, but should be especially useful in designing large arrays which cannot be turned physically. The design procedure is simple in any case. The feature of continuously variable tuning eliminates the guesswork in cutting fixed-length, fixed-tuned elements. The system will serve well in any situation where, say, climbing the tower to work on the antenna is not convenient.

A fixed, switchable array is an asset to the contestant or DXer who finds it necessary to change antenna headings in a hurry. From the northeastern U.S., a single such array provides good coverage of Europe and Africa in one direction and of the western U.S. and the Pacific in the other. If two suitable supports spaced a reasonable distance apart are available, two arrays of this type, perpendicular to each other, can provide a wide range of coverage. This material was originally presented in *QST* by John E. Kaufmann, WA1CQW and Gary E. Kopec, K8RX.

[1] "Technical Topics," *Radio Communication*, February 1973, p. 101.

Some Notes on a 7-MHz, Linear-Loaded Quad

If you like to experiment with antennas, here are enough new ideas about the construction of quad antennas to keep you going.

Most amateurs who have a serious interest in working DX in the 3.5- to 28-MHz bands would like to have antennas providing them with forward gain on all of these bands. Today, a triband trap Yagi or cubical quad may be employed to achieve this objective on 14, 21 and 28 MHz. Rotary beams are, for all practical purposes, out of the question for 3.5 MHz, but it is possible to achieve some gain with a 7-MHz rotary beam without having to pay a fortune for a supporting structure.

The Hy-Gain linear-loaded 2-element Yagi or the Mosley inductively loaded beam for 7 MHz can achieve this objective. The writer, however, prefers quads to Yagis, based on his own experience. Difficulties often arise when one seeks to mount beams for several different bands on the same tower without marked loss of performance on any band. The primary problem is, of course, that a full-sized cubical quad for 7 MHz is a monstrous structure. Such antennas have been erected, but they are not suited for the average amateur with a limited budget.

The first step in building a 7-MHz quad is, therefore, to design a single 7-MHz quad loop of reasonable size which is mechanically strong enough to survive most weather conditions.

Linear Loading

As a general rule, a reduction in antenna size to two-thirds of full size can be effected without a noticeable drop in performance, providing care is taken to limit the losses introduced by the loading devices. This means that one can think in terms of a loop for 7 MHz with 24 feet (7.32 m) on a side instead of 36 feet (10.97 m) on a side. An additional factor in choosing a 24-foot-per-side length was that the longest bamboo spreaders that the writer could obtain were 18 feet (5.5 m). Attempts were made to lengthen these spreaders, but results were not satisfactory mechanically.

If a 24-foot loop is to be used, the next questions are where to put the loading and what form of loading to use. A full-sized quad loop has symmetrical current distribution. The current maxima occur in the middle of the horizontal sections, and the current minima develop in the middle of the vertical sections. The current distribution in the vertical elements is such that

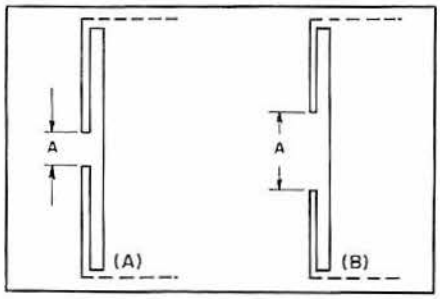

Fig. 27 — A method for linear-loading of one side of a quad element.

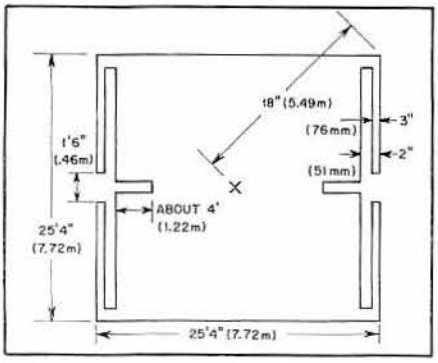

Fig. 28 — Dimensions used for the 7-MHz quad elements when the loop has been cut for resonance at the low end of the band. Depending on the height above ground and the particular portion of the band to be operated, the amount of center loading at the vertical sides may have to be varied slightly.

most vertical radiation is canceled out. It is desirable to retain this current distribution in the shortened loop. It is also desirable not to put the loading in the center of the horizontal elements, since maximum radiation occurs at the current maxima, and it does not make sense to cut out the portion of an antenna that does the most effective work. The writer, therefore, chose to put the loading in the vertical sides.

There are two popular methods of loading, stubs or coils. The writer dislikes coils for loading since, if they are wound with a heavy-gauge wire (desirable in order to avoid undue losses), they are bulky and difficult to weatherproof. The choice was therefore stub loading. It would have been possible to insert a stub at each corner of the loop, tied back to the spreaders. But, the current flowing in such stubs would be

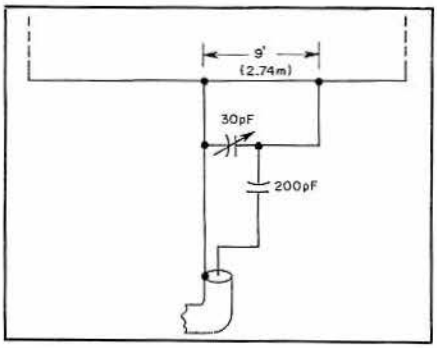

Fig. 29 — Diagram of the matching section used on the 40-meter driven element. The gamma capacitor employs a 100-pF air variable and a 100-pF high-voltage silver mica connected in parallel.

unbalanced, and radiation in unwanted directions would take place from the stubs themselves. There is also the consideration that if the same spreaders are used for 14-, 21- and 28-MHz loops, stubs at the corners of the 7-MHz loop would have to be mounted well clear of the loops for the other bands.

The original linear-loaded 7-MHz quad element was tried by the writer in a four-band quad some years ago. A single stub in the center of each vertical side was used. The loading stubs were made 14 feet (4.27 m) long and were tied on to a point near the center of the boom. Performance of this quad on 7 MHz was excellent, but the 21-MHz quad mounted on the same boom was almost useless, probably due to pickup at 21 MHz by the 7-MHz loop with subsequent reradiation. An attempt was made to find an efficient method of loading which did not involve long stubs "floating around." The next step was to try folding the wires in the vertical sections back on themselves as shown in Fig. 27A. Current distribution either side of the center part of the vertical elements is symmetrical, as desired. This change resulted in a loop that was resonant near 7 MHz, although its resonant frequency was slightly high. Shortening of the stubs slightly, as shown in Fig. 27B, was tried. This had virtually no effect on resonant frequency. This is no doubt because the increased end-loading effect of the portion A almost equalled the reduction in stub length. Short stubs (abour 4 feet [1.22 m] long) were then

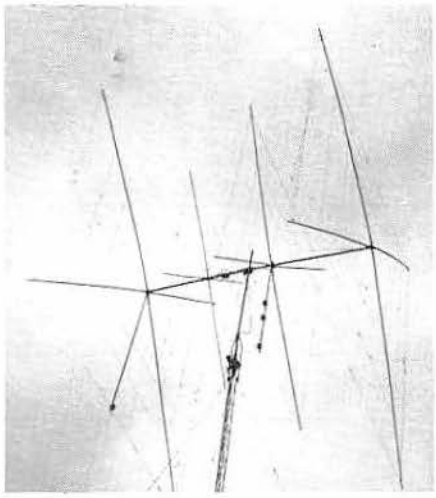

G3FPQ's compact 4-band quad has 2 elements for 7 MHz, 3 elements for 14 MHz, and 4 elements for 21 and 28 MHz. Pairs of Yagi-type directors are used in place of the usual loop director for the three higher frequency bands.

inserted at the center of the vertical sides, at right angles to the vertical sides as shown in Fig. 28, and resonance at 7 MHz was achieved.

A four-band quad for 7, 14, 21 and 28 MHz was then constructed. Much to the writer's delight, there appeared to be no noticeable interference with the pattern of the 21-MHz quad by the 7-MHZ elements. The loading effect of the stubs would be different at 21 MHz since they would include current maxima; the result is to give a loop which, while resonant at 7 MHz, does not appear to have a third-harmonic resonance in or near the 21-MHz band.

Yagi-Type Directors

The reader can probably see from the photograph that the directors for 14, 21 and 28 MHz consist of pairs of stacked Yagi-type elements level with the driven elements. There are two pairs of Yagi directors for the 10- and 15-meter elements at approximately 6-foot, 6-inch (2 m) spacing, and one pair of Yagi directors for 20 meters at approximately 13-foot (4 m) spacing. The overall length of the directors is 31 feet, 3 inches (9.52 m) on 20 meters; 20 feet, 10 inches (6.35 m) on 15 meters; and 15 feet, 2-1/2 inches (4.63 m) on 10 meters. Performance of the author's array on 10, 15, and 20 meters at the moment is little, if any, better than an ordinary 2-element quad. The writer has only recently had an opportunity to start checking out the directors to see what adjustment they need. Current indications are that they require lengthening, but there is a good deal more experimental work to be done. Anyone who wants to try this system must be prepared to do a good deal of cut and try to tune the directors, if any real increase in performance over a standard two-element quad is to be achieved.

One also has to bear in mind that when dealing with multiband quads the resonant frequency of Yagi-type directors is likely to be affected to a far greater extent by the proximity of other elements than would be the case for a quad-loop director. This is because a Yagi director is a comparatively high-Q element. From the theoretical point of view, the drawback to quad-loop directors is that the reactances involved are such that there is a comparatively low degree of mutual coupling between the quad-driven element and the quad-loop director. This, of course, reduces the efficiency of the loop as a director. This problem should not apply to the same extent with Yagi-type directors, and, in theory at least, they should prove to be more efficient than quad-loop directors. The question now is whether practice follows theory or not. This writer won't have an opportunity to conduct any detailed experiments until the summer. When deciding the original length for the Yagi directors, allowance was made for a rise in frequency of approximately 100 kHz. But, the only way to cope with the effects on the director resonant frequency of the proximity of other elements is by field-strength measurements, coupled with a good deal of cut and try. As in any multiband quad, separate feed lines should be used for each band to minimize interaction between bands.

The author's quad has been up for six months now, and final tuning remains to be done to the 7-MHz reflector loop to achieve maximum front-to-back ratio. But the results, even on a cut-and-try basis, are well worth the work that went into the array. This material was originally presented in *QST* by David. L. Courtier-Dutton, G3FPQ.

Spider Quad Mount: Simplified

There seems to be a growing interest in the spider quad. The photograph shows a version of a hub or "spider" mount. Using a 2-foot (0.61-m) length of 2-inch (51-mm) diameter steel pipe, a mount can be constructed easily. Two cuts, 10 inches (254 mm) long, are made through the diameter at each end of the pipe. This leaves 4 inches (102 mm) in the middle for the boom. The cut ends are then bent to an angle to suit the desired spacing. The unit shown in the photograph is bent to 108 degrees. The spreaders may be attached to the boom mount with hose clamps, bolts or wire.

The beauty of this design is that it can be made to any size desired. Also, it can be enlarged to a 4-element version, as shown in Fig. 30.

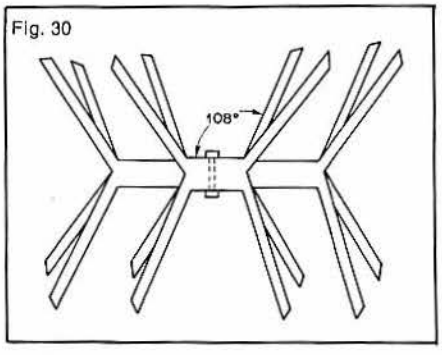

Fig. 30

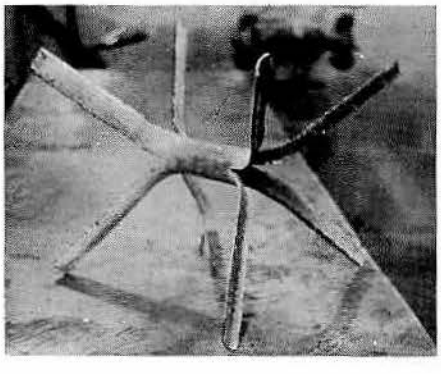

One of these spider mounts is in use at KP4DJI (constructed by KP4DIO and KP4DJI) using bamboo spreaders. The results have been excellent. This material originally presented in *QST* by Lynda B. Crowley, KP4DIP.

Two-Band Quad Matching

While experimenting with a 2-element, 2-band cubical quad antenna the problem of matching the antenna to a 50-ohm transmission line arose. The antenna is a "plain vanilla" quad built around information in W6SAI's book, *Quad Antennas*. The author's method of feeding the antenna *did not* produce fantastic front-to-back ratio or forward gain. It merely made the standing-wave ratio more acceptable to the 32S-3B used at the home QTH.

After building the 2-band quad, the author checked it with a General Radio 1606 impedance bridge and found the 10-meter antenna to be about 118 ohms and the 15-meter antenna to be about 91 ohms at resonance. This is 2.36:1 and 1.82:1, or approximately 2:1 for a 50-ohm transmission line. The feed system described here made the VSWR much nearer the desired 1:1.

The heart of the system is a ferrite-core autotransformer. The measured impedance ratio is very close to 50:107 ohms. The insertion loss is less than 0.2 dB from 15 to 30 MHz when terminated in 107 ohms. When it is terminated in 50 or 200 ohms the insertion loss is less than 0.35 dB from 15 to 30 MHz. Several transformers were built before these figures were obtained, and after a suitable design was achieved it was connected to the quad as shown in Fig. 31. You do not have to sacrifice F/B ratio for a more acceptable VSWR by detuning the reflector stubs; simply adjust the tuning stubs for maximum F/B ratio and then design the transformer for the proper impedance ratio. Also, lowering the VSWR places a larger portion of the desired band within an impedance range the average pi-section tuner will accept.

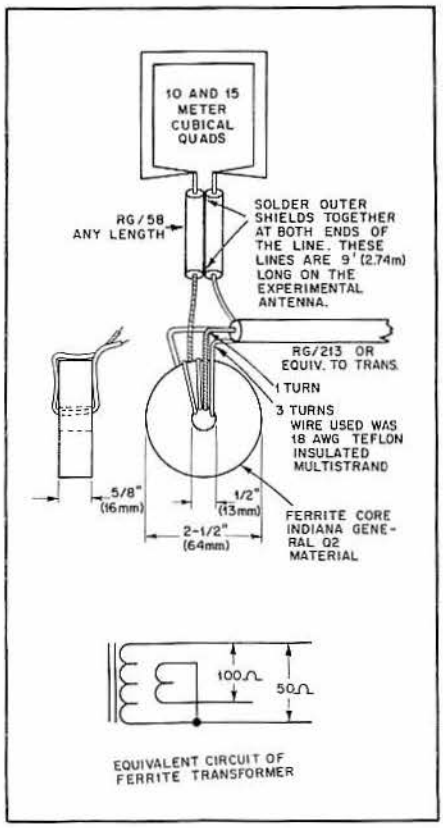

Fig. 31 — Two-band quad matching.

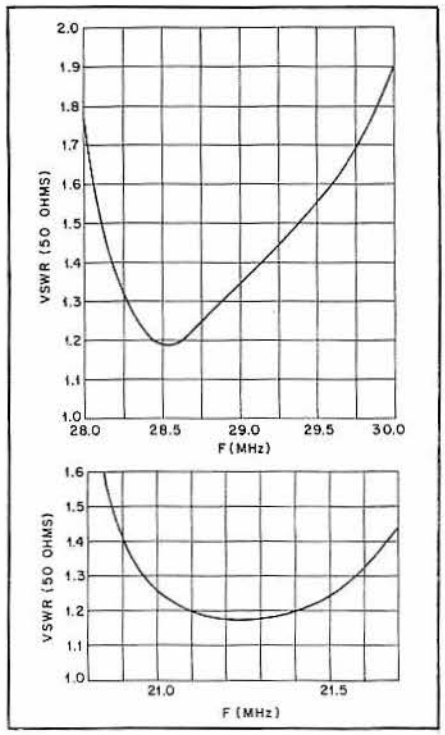

Fig. 32 — Standing-wave ratio curves taken with a laboratory-type VSWR bridge. Measurements were made at the transmitter ends of the transmission line with the antenna array mounted on a steel tower 44 feet (13.4 m) above ground.

In answer to on-the-air inquiries: Yes, performance of the antenna varies considerably from one end of the band to the other.

This antenna feed system is a broadband device, so don't forget to use a low-pass filter. This material was originally presented in *QST* by Toney L. Magnino, W5MVK.

Chapter 4

Miscellaneous Antenna Types

Here is a potpourri of useful antennas for the hf-band enthusiast. This chapter contains information on how to build and operate loop antennas, limited-space antennas and variations of the quad. Once again, the work of numerous *QST* authors has been collected for a timeless volume of useful construction details that can benefit amateurs whose operating objectives are numerous and varied.

For the most part, the antennas described in this section are simple and inexpensive to build. The performance characteristics are consistent with the operating needs of ragchewers, contesters and DX-chasers alike, assuming that the builder does not strive to have the loudest signal on the amateur bands.

Beat the Noise with a "Scoop Loop"

Operators on 160 and 80 meters fight a common foe — noise. Atmospheric QRN is compounded by the presence of man-made noise. Loop antennas for receiving may offer an economical solution to your noise problems. Here are some timely details.

If you've been tempted to massage your receiver with a 10-pound hammer because you can't copy some of the weak signals being heard by your colleagues, you may need a receiving loop! A high ambient noise level on 160 meters has stifled the author's DX work for several years, and more than once was ready to capitulate in favor of the man-made and atmospheric noises that the 75-foot (22.9-m) shunt-fed vertical responded to. "Grrrr," would be the snarl as the author listened to stations with Beverage antennas: They were handing out RST 579 signal reports to DX stations, and the author couldn't find the DX signals in the noise, let alone copy them.

Something had to be done. It was a matter of giving up on 1.8-MHz efforts toward DXCC, or putting forth a zealous attempt toward an improved signal-to-noise ratio. Some effective outdoor receiving antennas were erected (half-wavelength open loop — parallel to the ground, and a 200-foot [61-m] end-fed wire a few feet off the ground), but they did not always respond well to DX signals: It depended on band conditions. Also, there was the danger of receiver front-end damage caused by unwanted excitation of the large receiving antennas (resonant) during the transmit period. They were in close proximity to the vertical antenna, which was used for transmitting purposes. Lethargy prevented the author from installing a protective circuit at the receiver front end, and as a consequence the writer "blew" a JFET preamp and two protective diodes in the front end of the FT-301D transceiver.

Revisiting the Past

While for many years experimenting with small receiving loops for 40, 80 and 160 meters, the efforts were casual. The best of the loops was an outdoor one of the shielded variety, five feet (1.52 m) on a side, and fashioned from RG-59/U coaxial cable.[1] However, it was necessary to go out-of-doors each time to rotate it, and the author wasn't enthusiastic about investing in a rotator to use with the loop.

Recently, it seemed that some work could be done with indoor types of receiving loops. After all, loops of that kind have been around since radio was invented, and plenty of amateurs are using them effectively. After scanning available literature (Terman, Kraus, Jasik and Keen),[2] the author set about the task of building a framework for the chosen design. This time a multiturn loop would be tested (Fig. 1).

Construction

The photograph shows the general structure of the loop. In Fig. 2 are the dimensions of the wooden frame used to contain the antenna wires. There is nothing magic about the size of the antenna: Two pieces of wood that were stored in the workshop were used, each being 48 inches long, 1-1/2 inches wide and 3/8 inch thick (1.22 m × 38 mm × 10 mm).

Arbitrarily, the author decided to make L1 of Fig. 1 a five-turn winding. Holes were drilled (five) in each end of the cross-frame to accommodate the loop turns and hold them in place. Actually, there should be six holes at the bottom point of the frame to permit the final end of L1 to be secured during the threading-through process.

Five additional holes were drilled (Fig. 2) 3/4 inch (19 mm) below the holes for L1. These are used to contain L2, the one-turn output link of the antenna. L2 requires two holes at the bottom member of the frame — again to provide an anchor point for the ends of L2. Alternatively, V-shaped notches can be filed on the ends of the cross-frame. The wire for L1 can be laid in the grooves rather than threaded through the holes shown in Fig. 2. L2 should, however, be wound inside L1, through the five holes shown in the drawing.

A mounting base for the assembled antenna can be made to the builder's specifications. This writer used a piece of 3/4-inch (19 mm) plywood which has dimensions of 30 × 12 inches (0.76 m × 305 mm). A 1-inch (25 mm) diameter hole was drilled in the center of the board to accept an 18-inch (457 mm) length of 1-inch diameter dowel rod. The latter is lashed to the framework of the loop to enable the

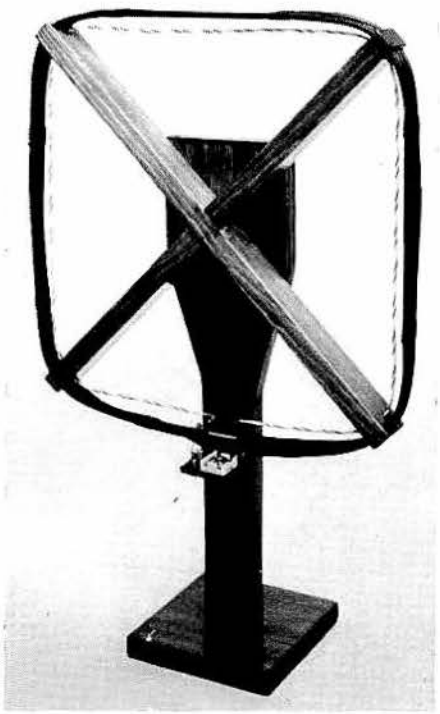

The silhouette is of an indoor version of the four-turn shielded loop described in this article. A wooden framework is used to support the main loop winding and the one-turn pickup link. The resonating capacitor is mounted on an aluminum L bracket along with a phono jack and an 860-pF disk capacitor. The latter is used between the output link and the phono jack instead of a trimmer capacitor. The framework was built by Technical Secretary Marian Anderson's OM, Bob. It has been stained and coated with clear lacquer.

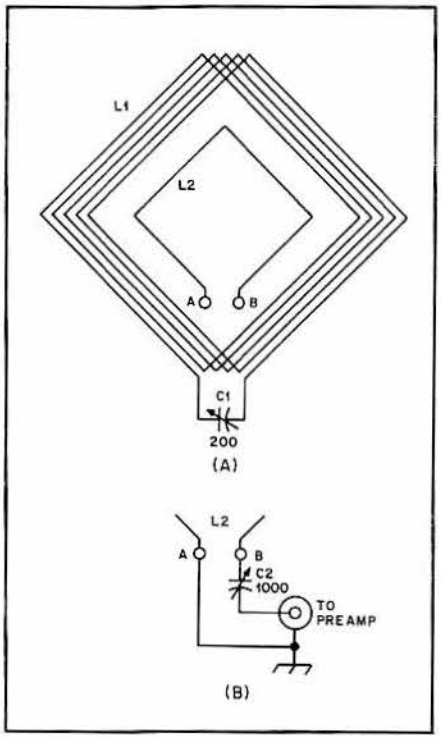

Fig. 1 — Schematic diagram of the receiving loop. C1 and C2 are mica compression trimmers. The illustration at A shows the 1-turn link inside the 5-turn one. At B is an expanded diagram of the feed point for L2.

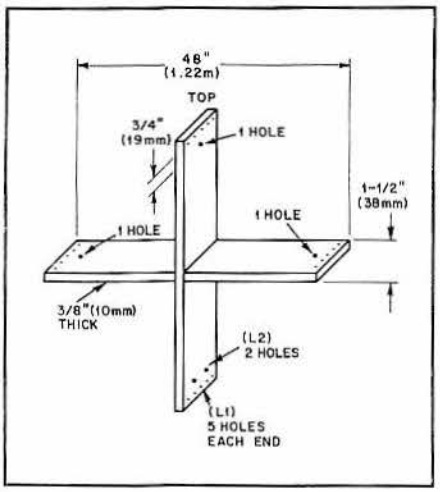

Fig. 2 — Dimensional drawing of the wooden frame which contains the Scoop Loop. Further information concerning the structure is given in the text.

operator to rotate the loop as desired. Although this is a "kluge" type of assembly, it serves its purpose adequately. A *carpenter* should be able to conceive a more practical base and support system for the antenna!

Number 22 insulated hookup wire was used for the loop turns. There is nothing critical about the wire size, but it is best to use the larger gauges. This will make the loop more rugged.

Performance

A variety of feed systems were tried before the author settled for the method illustrated in Fig. 1. Direct connection to the terminals of L1 required careful balancing to assure a uniform loop-response pattern. Unbalance causes pattern distortion, and if it's bad enough the maximum response can occur off the broad side of the loop rather than in the plane of the antenna.

Addition of a one-turn coupling loop, L2, proved to be the easiest method for assuring good balance. Bandwidth of the loop is dependent upon the Q. The latter can be controlled by the amount of capacitance used at C2: the lighter the coupling, the greater the loaded Q. Loop resonance is effected by means of C1. Since there is interaction between L1 and L2, it is necessary to readjust C1 each time C2 is tweaked. In this application it should be stressed that C2 is not used for the purpose of obtaining an SWR of 1. It is purely a *coupling* device. Hence, a 50-ohm condition does not necessarily exist at the loop output terminals.

During initial experiments the pickup loop, L2, was connected directly to the 50-ohm input port of a 40-dB broadband preamplifier which was designed by W7ZOI (Fig. 3). Without C2 in the circuit the coupling was excessive. This resulted in low Q, and the loop bandwidth was approximately 150 kHz at the 3-dB points of the response curve. After C2 was added and adjusted to provide a bandwidth of 25 kHz, the loop gain increased 10 dB. Alternatively, one might make L2 smaller and locate it closer to the center of the loop frame in order to lighten the coupling between the two windings. This could be a somewhat tedious mechanical procedure: The writer's inherent lassitude favored the addition of C2 for the purpose!

Performance Characteristics

A test range was set up for checking the null properties and relative gain of the loop. The equipment was arranged in an outdoor location, well away from power wiring and other station antennas. A crystal-controlled weak-signal source (2N2222A oscillator and 9-volt battery) was placed some 100 feet (30.48 m) from the test loop. It contained a 36-inch (0.91-m) whip antenna (vertically mounted) for radiation of the test signal. The 75-foot (22.86-m) transmitting vertical was shorted out at the feed point to prevent it from being resonant and affecting the loop antenna during the test period.

A 50-ohm Tektronix step attenuator was placed in the coaxial line between the loop and the receiver. The attenuator was used to measure accurately the changes in S-meter reading on the FT-301D transceiver which was used as a detector during the measurements.

A null depth of —21 dB was obtained with the loop. An extremely sharp null was noted. As the broad side of the loop was moved toward the signal source, the null began slowly, then fell deeply to —21 dB over the final 10 degrees of rotation. No evidence of pattern distortion was observed. The null was dead off the broad side of the antenna, and maximum response was directly off the thin side of the loop.

A comparison between the 75-foot (22.86-m) transmitting vertical (shunt-fed tower, top loaded and with buried radials) and the wire loop indicated that on groundwave signals the loop (without preamp in line) was —18 dB respective to the vertical. This suggested that in a practical installation a single JFET or dual-gate MOSFET preamp would provide unity gain with the transmitting vertical.

Using the Loop Indoors

The author's home has aluminum siding, and as is the case with all modern homes there is a network of water pipes, phone wires, TV lead-in conductors and house wiring. The author wondered how well the loop would perform within all of these unwanted signal obstacles, some of which form loops by themselves! The ham shack is at ground level inside the family room, and the loop was placed on a stand at floor level. The clutter of unwanted conductors disturbed the directivity of the loop somewhat, but the signal-pickup ability of the antenna was not impaired.

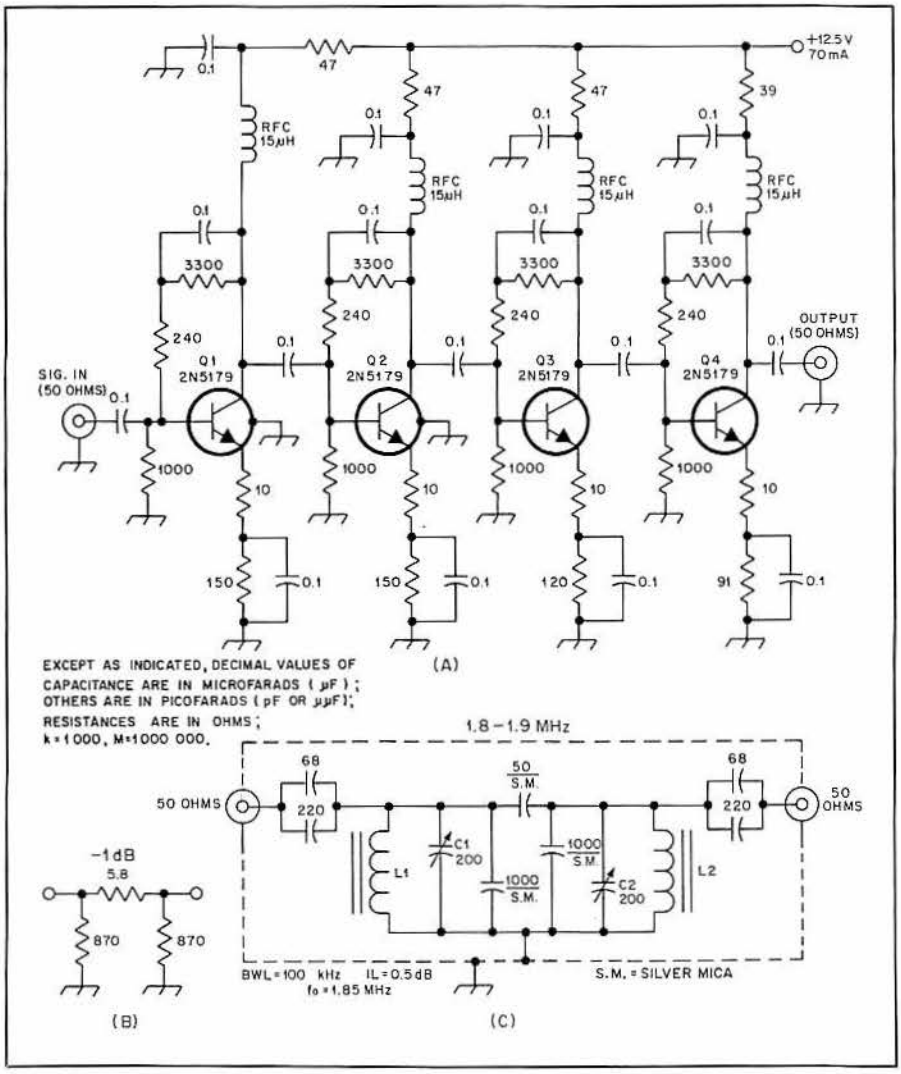

Fig. 3 — The W7ZOI broadband 40-dB preamplifier is shown at A. Capacitors are disk ceramic or chip types. Resistors are 1/4-w composition. The upper 3-dB point of the amplifier is at 65 MHz. Heavy feedback is used to stabilize gain and provide a 50-ohm characteristic. At B is a 1-dB attenuator pad which can be used between an antenna of unknown impedance and the filter at C to provide a proper load for the filter. The Butterworth band-pass filter at C is suitable for use with the preamp at A. It will help reject out-of-band signals to improve the IMD characteristics of the preamp. When the preamp is used with nonresonant receiving antennas, it will be necessary to employ the filter to protect the preamp from signals across its response range (bc band through vhf). The preamp and filter would be fine for use with Beverage antennas. C1 and C2 are mica trimmers. L1 and L2 consist of 31 turns of no. 22 enameled wire on Amidon T68-6 toroid cores (5.1 μH).

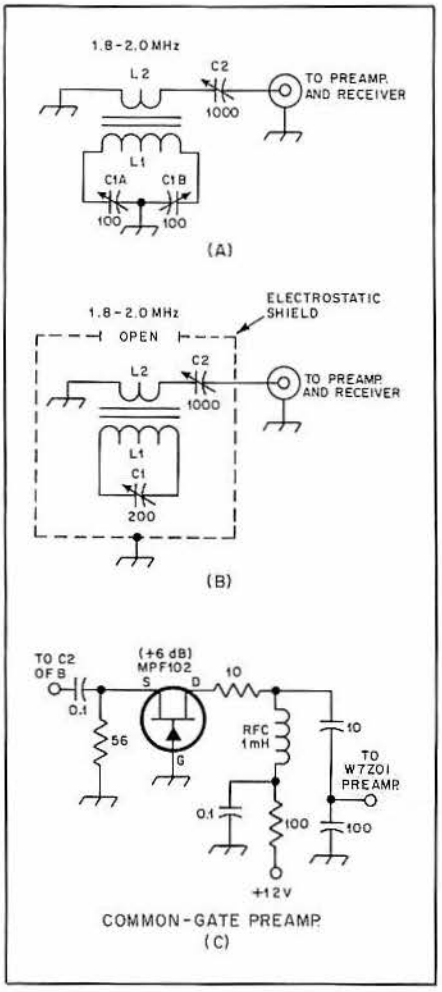

Fig. 4 — The drawing at A shows the circuit of a 7 X 5/8-inch (178 X 16-mm) ferrite-rod loop (see text). At B is the final version which employs an electrostatic shield. C1 and C2 are mica compression trimmers (see text for other details). The circuit at C was used ahead of the W7ZOI preamplifier to improve the system noise figure.

A step attenuator was inserted between the W7ZOI preamplifier and the station receiver so that unity gain could be established between the loop and the 160-meter vertical (22 dB of gain had to be gotten rid of). An antenna switch was added to the system to permit rapid comparisons between the antennas.

Extensive tests proved that the loop outperforms the vertical by a substantial margin when it comes to digging weak signals out of the noise (man-made and atmospheric). The author has copied PAØHIP, PYØZAE, G3MYI, W6RW, W6BLZ, W5AB and others perfectly Q5 on the loop (indoors) when they couldn't be found, or were unreadable on the vertical. It is only fair to say that on some occasions the vertical was the better antenna for receiving. Propagation conditions and ambient noise levels at a given time will determine which antenna can provide the best reception. Typically, the ambient noise level from the W1FB vertical is S3 on a receiver that is calibrated to indicate S9 on a 50-μV signal.[3] The same receiver shows no noise response when the loop is connected to it. However, static crashes (atmospheric noise peaks) are as loud with the loop as they are with the vertical when a storm is in the immediate area. Noise from distant storms can be discriminated against by turning the loop null toward the storm front. It appears that the major part of the author's ambient noise is man-made in nature. At times it peaks as high as S8.

When the loop is used indoors it responsds to unwanted 15.750-kHz TV spurs, and when appliances are actuated the transients kick the receiver S meter rather hard. This is because the loop is contained within loops formed by house wiring. This type of interference has not been observed while using the vertical antenna, even though it is affixed to the rear of my house. To prove that the house wiring was causing the problem with TV birdies and transients, the loop was located out-of-doors for two nights. The interference vanished!

Some Other Loop Experiments

Ferrite-rod loops have been used to advantage for many years (bc-band radios, direction-finder receivers for boats and aircraft, etc.), so it seemed worthwhile to investigate a model of that type of antenna before concluding the tests. Two versions were tried, each with a preamplifier.[4] The first consisted of a single 7 X 5/8-inch (178 X 16 mm) Amidon Assoc. ferrite rod on which was wound a 40-turn solenoidal coil of no. 22 insulated hookup wire. The loop was tuned to resonance by means of a 100-pF per section split-stator variable. A four-turn output link was wound over the center

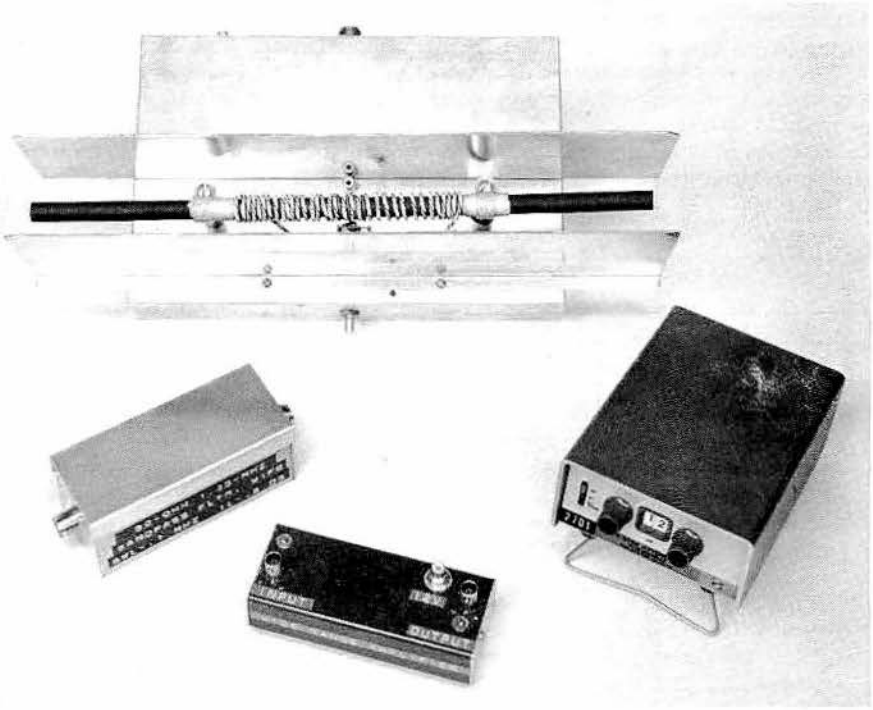

View of the ferrite-rod loop and test setup accessories. In the foreground (left) is the Butterworth band-pass filter. Below it at the center is the broadband preamplifier, and the Tektronix 2701 step attenuator is at the far right.

of the primary winding. The latter occupied approximately 3 inches (76 mm) of the center portion of the rod. A small aluminum chassis served as the foundation for the antenna, and the rod was spaced some 3 inches (76 mm) above the chassis. Performance tests showed the antenna to be less efficient than the large 5-turn wire loop. As referenced to the 75-foot (22.86-m) vertical, the ferrite loop was —38 dB. Furthermore, it was prone to the same induction effects which plagued the wire loop when both were used indoors. The rod-loop null was dismal — some 10 dB!

An improved model of the loop was built by using epoxy cement to join together a pair of 7-inch (178-mm) ferrite rods, end to end. The sensitivity (μV per meter) increases with the length of the rod, but is dependent upon the length of the coil which is wound on the rod. A multilayer coil contained at the center of the rod should be considerably better than a solenoidal coil spread over the major portion of the rod: The shorter the coil, the higher the Q of the antenna.

The author did not have Litz wire available, and was unable to build a multilayer coil, so a short solenoidal winding was placed on the center 5 inches (127 mm) of the 14 × 5/8-inch (356 × 16 mm) rod. It consisted of 32 turns of no. 12 insulated wire, spaced one wire diameter between each turn. The ferrite rods are made of Q2 material (μ = 125).

Fig. 4 shows the schematic diagram of the rod loop. A four-turn output link is wound over the center of L1. C1 is a mica compression trimmer which tunes the loop to resonance. C2 is used as a coupling capacitor to control the loop loading.

It seemed worthwhile to try shielding the loop, so a pair of aluminum L brackets were bolted to the chassis as shown in the photograph. Each bracket is 16 × 3-3/4 inches (406 × 95mm). The shields are spaced 1 inch (25 mm) either side of the loop.

The top of the U-shaped channel must be left open to prevent the shield from acting as a shorted turn. Proof of the effect can be seen by shorting across the open end of the trough (over the center of the rod) with a screwdriver. The received signal will vanish! An electrostatic shield, when used with a loop antenna, should minimize induced fields from nearby conductors and precipitation static, thereby making the system better for indoor use.

Rod-Loop Tests

The same outdoor test setup was employed for checking the performance of the rod loop. The nulls occur off the ends of the rod, and maximum response is found off the broad sides of the rod. A null of —23 dB was obtained with the loop, but efficiency was less than that obtained with the 5-turn wire loop. When compared to the 75-foot (22.86-m) vertical a reading of —31 dB was obtained, 13 dB inferior to the wire loop. The noise figure of the W7ZOI broadband preamplifier was too high for use with the new antenna, so a common-gate JFET pre-preamplifier was added between the loop output and the input to the 'ZOI unit. Ideally, a 30- or 35-dB preamplifier (two JFETs) should be used with the rod loop to assure a low noise figure and ample gain.

With the coupling set for maximum loop gain, the bandwidth (measured with an HP spectrum analyzer) is 10 kHz at the 3-dB points. The loop was measured independent of the shields and preamp for unloaded

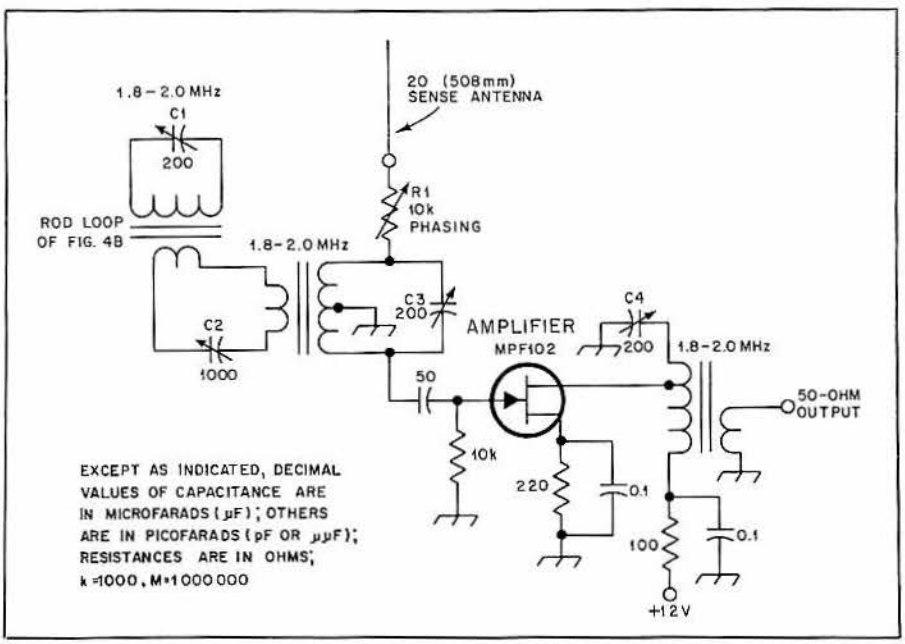

Fig. 5 — Suggested circuit for using a sense antenna with the rod loop. The sense antenna can be mounted 6 to 10 inches (152 to 254 mm) in front of the broadside of the rod loop (centered). C1, C2, C3 and R1 are adjusted alternately for the deepest null possible off the rejection side of the loop (side opposite the sense antenna). It may be necessary to experiment with the length of the sense antenna to obtain the best null in the cardioid response pattern. The tuned circuits for the JFET preamp can be wound on T-68-2 toroid cores.

Q by means of an HP Q meter. A reading of 430 was obtained.

The electrostatic shield cured the unwanted pickup of TV spurs and appliance transients during indoor use. The author would like to mention that the wire and rod loops are affected to some extent by the presence of the 75-foot (22.86-m) vertical. The latter is only 20 feet (6.10 m) away from the operating position. It tends to reradiate noise and signals. Some of that energy is picked up by the loop antennas. If an indoor loop is to be used regularly, or if it is outdoors, but within 100 feet (30.48 m) or so of the vertical, the latter should be shorted out or detuned during the receive period. An spst relay could be slaved to the regular antenna change-over relay to accomplish this.

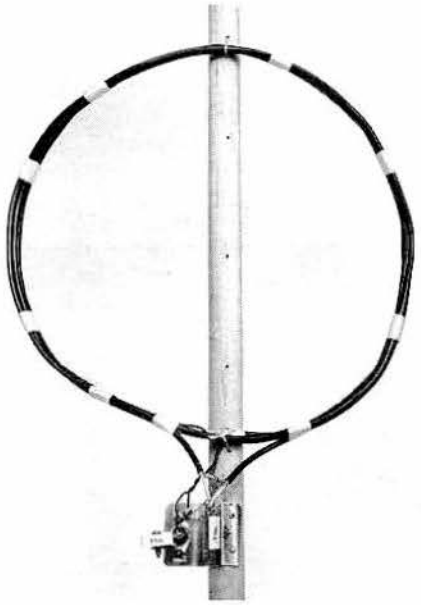

The 4-turn coax loop with electrostatic shielding. The trimmers are visible on aluminum brackets below the loop.

An improvement in performance for either type of loop could be had by adding a sense antenna and appropriate phasing circuit (Fig. 5). This would provide a cardioid pattern and result in a unidirectional response. Greater reduction of QRN and QRM would be effected through that technique. A weatherproof system of that type could be placed out-of-doors for year-round use. A TV type of rotator would be useful for changing the loop position, as desired.

The W1FB 4T-ES Loop

During a final investigation of loop types and performance characteristics, an attempt was made to devise a shielded loop small enough to be practical indoors. The primary objective was to develop a loop from ordinary materials — something that was inexpensive and easy to build. It should have efficiency comparable to that of the 5-turn wire loop described earlier in this report. A reasonable null depth and an undistorted pattern were sought also. From these criteria evolved the 4T-ES (four turn, electrostatic shield) loop shown in Fig. 6.

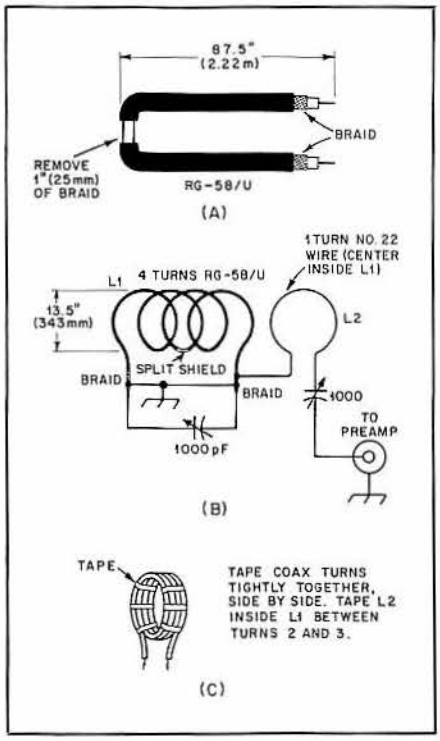

Fig. 6 — Structural details of the W1FB 4T-ES loop antenna. At A is an illustration of the total length of RG-58/U before the loop is formed. An expanded view of the loop turns and pickup link is given at B. Drawing C shows how the loop turns are taped together side by side as the antenna takes its final form.

It consists of four turns of RG-58/U cable which are formed into a circular configuration to provide a diameter of 13-1/2 inches (343 mm). There is nothing critical about the diameter, and RG-59/U coaxial cable could be used instead of the type specified. The turns are formed side by side, then taped at several points to maintain the loop form.

It is necessary to split the shield braid at the electrical midpoint of the loop. This prevents the shield from acting as a shorted turn. The principle is the same as that described for the ferrite-rod loop with its aluminum-channel shield. The braids are joined at the loop feed point and made common to one end of L2. The three grounded elements are then attached to the coaxial connector ground terminal on the loop support frame.

Loop performance was checked by using the test procedure discussed earlier. A null depth of —26 dB resulted. There was no discernible pattern warping, and the null occurred deeply over just a few degrees of rotation. The 4T-ES was 18 dB inferior to the 75-foot (22.86-m) vertical antenna when checking distant signals. The unloaded Q was measured by means of the HP Q meter. A value of 85 was obtained. Because C2 was set for light loading of the loop, a bandwidth (3-dB points) of 20 kHz was obtained when the preamplifier and receiver were connected to the antenna.

Numerous comparisons were made on DX signals from Europe and the Caribbean area during the ARRL DX Contest in March of 1977. In all instances the 4T-ES was as good as or better than the 75-foot (22.86-m) vertical. Ambient noise was considerably lower in amplitude while using the loop, even though all tests were performed with the loop indoors at ground level. There was no reduction in atmospheric noise (which was high that weekend) because the maxima of the loop favored the N.E. and S.W. directions: The storm front was S.W. of Connecticut. However, rotation of the loop caused a drop of 26 dB in the static crashes when the loop nulls were S.W. and N.E. Because of the electrostatic shielding there was minimum noise induction from the house wiring — a contrast to the performance characteristics of the unshielded 5-turn wire loop. The W7ZOI broadband preamplifier and an attenuator were used during the tests. There were some instances when the loop provided a stronger signal response than the vertical, even though the two systems were adjusted for unity gain.

The 4T-ES is suitable for use indoors,

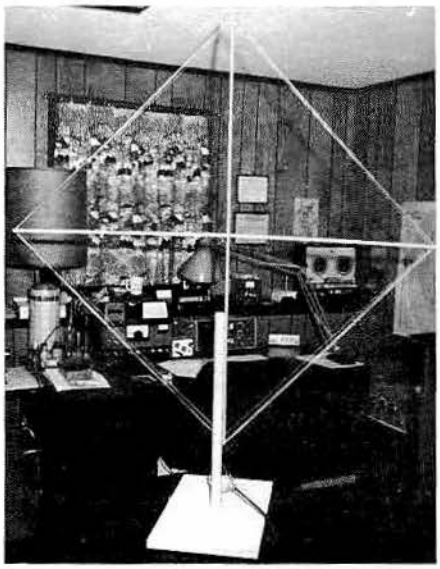

Close-up view of the 160-meter indoor receiving loop at W1FB. The antenna is resting on a piano bench, and is situated near the operating position so that it can be hand-rotated as necessary.

but it could be weatherproofed for outside installations. Epoxy cement could be used to seal the open ends of the coaxial cable of L1, and the trimmer capacitors would survive the natural elements if housed in a metal or plastic container.

In Summary

The loops that have been discussed here should be suitable for use on 40 or 80 meters if scaled accordingly. They may not show much directivity on sky-wave signals because of the "tumbling effect" at the higher frequencies. But QRM from nearby amateurs could be reduced greatly, and man-made noise sources could be rejected significantly by correct orientation of the loop.

The author has attempted to discuss some of the characteristics of small loops which are not treated in most of the references contained in amateur journals. There is plenty of latitude remaining for experimentation, and the reader is encouraged to apply his or her skills in developing better loops for amateur use. Meanwhile, why not build a small loop and scoop those weak signals out of the noise? It could mean some new countries for you on "top band" or 80 meters. This material was originally presented in *QST* by Doug DeMaw, W1FB.

References

[1]DeMaw, "A Receiving Loop for 160 Meters," *QST*, March 1974.

[2]Terman, *Electronic & Radio Engineering*, McGraw-Hill. Kraus, *Antennas*, McGraw-Hill. Jasik, *Antenna Engineering Handbook*, McGraw-Hill. Keen, *Wireless Direction Finding*, 3rd Edition, Iliffe & Sons, Ltd.

[3]DeMaw, "His Eminence — the Receiver," Parts 1 and 2, *QST*, June and July 1976. Receiver used in combination with an Autek Research QF-1 RC active audio filter.

[4]DeMaw, "Build This Quickie Preamp," *QST*, April 1977.

The Half Square Antenna

Do those 100 countries still elude you for 80-meter DXCC? In terms of dollars versus decibels, a half-square antenna may be your best bet for putting punch into your signal.

With 5-band DXCC as bait, considerable interest has arisen in DX and antennas for the lower frequency ham bands. The author's attempts to get a decent 80-meter DX antenna have gone through an evolutionary cycle with a lot of iterative tries and with steadily improving results. The half-square antenna that is the latest of these has some interesting properties and gives about as many "dBs per buck" as any this author has seen.

Before describing this configuration, it might be interesting to cover briefly the different antennas tried which didn't work as well. The writer's available options were set up by (1) a yard full of tall trees and (2) very little money to spend. The first antenna was an inverted V hung on the 75-foot (22.9-m) tower. This is really a quite good antenna — primarily because it has the high current part of the antenna at the highest support point. It provided a standard against which all succeeding antennas were checked. The next step was to add a parasitic element (director) which didn't seem to help at all. This is perhaps not so surprising with the ground so close. Viewed simply, normal parasitic coupling is dependent upon a fair proportion of the current in the driven element being coupled to the parasitic element. When they are both close to the ground, the reverse polarity of the image of the driven element starts to couple heavily to both the driven element and the parasitic element, making it practically impossible to get the desired parasitic current at any useful spacings.

This effect has been shown experimentally to be less with closed-loop type antennas such as the quad. Based on this supposition, the author next constructed a 2-element quad, supported at the corners by ropes tied off to trees. With only 75-foot (22.9-m) trees and the consequent sag, the bottom was only about 6 feet (1.83 m) off the ground. However, the quad did work, had an acceptable feedpoint impedance, and gave a few dB (about 1/2 an S unit) improvement over the inverted V on European contacts. Obviously, the only useful low-angle radiation in this antenna came from the upper half of it, the lower half serving to feed or excite the upper half. A major problem with the quad was keeping it up. It had to be very tightly stretched between trees to keep it from sagging to the ground and as a result the wire often broke.

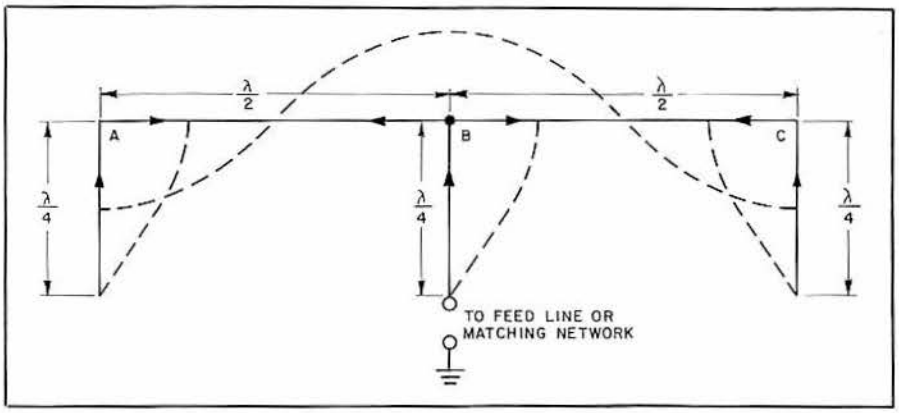

Fig. 7 — Bobtail array. The dotted lines show the approximate current distribution along the antenna and the arrows indicate the relative directions. With this array, the high-current points occur at the highest points on the antenna.

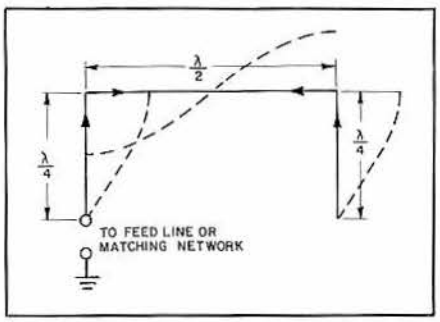

Fig. 8 — The "half-square" evolved when one leg broke off the bobtail. The input impedance of both the bobtail and half-square antenna is very high, which eliminates the need for an elaborate ground system at the feed point. Either a parallel-tuned circuit or a quarter-wave transformer can be used to match to a 50-ohm feed line.

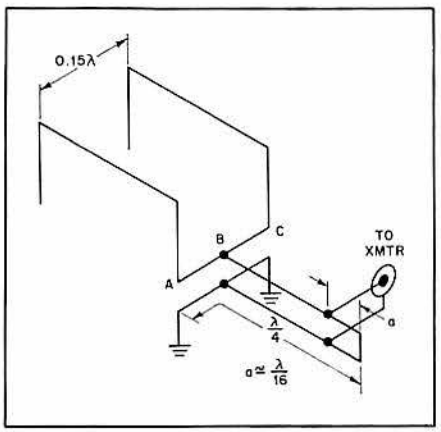

Fig. 9 — Two-element half square array gives greater gain and a very wide bandwidth.

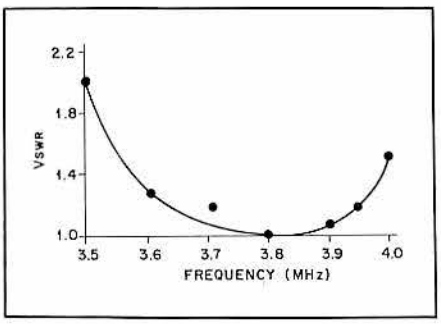

Fig. 10 — Measured SWR of the shown in Fig. 9.

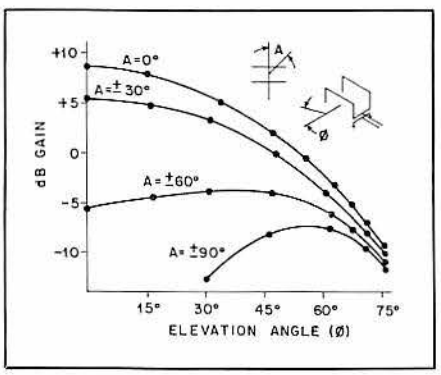

Fig. 11 — Computer-pattern plot for a 2-element half square array with 0.15-wavelength spacing between elements. The angles referred to in the drawing are shown in the inset.

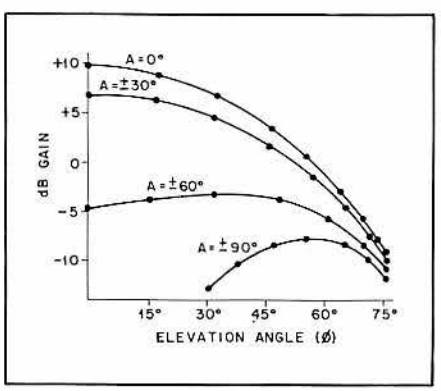

Fig. 12 — Computer-pattern plot for the of Fig. 11 with 0.25-wavelength spacing.

To try another tack which would avoid the parasitic coupling problem an 8JK array with four half-wave elements was tried, all elements being fed. With the span of this being so long and with lots of high-voltage points which had to be kept from touching the trees, the author only managed to get it to a height of about 40 feet (12.19 m). The signal-report results with this were essentially identical to the quad on the path to Europe. The horizontal beamwidth was noticeably less than the quad. It probably would have done better if the writer could have gotten it to 75 or 80 feet (22.86 or 24.38 m) in height.

The next antenna tried was the so-called bobtail which is shown in Fig. 7. This is a broadside vertical array with approximately twice the current in the center leg as the two outer legs and with current distribution in the horizontal wires which tend to cancel horizontally polarized emission.[1] A major reason for trying this was the author's frustration with trying to use the maximum available height of the trees and still be able to feed the antenna and keep the high-voltage points clear of the tree branches. The author had avoided vertical antennas before because of the difficulty in getting a good low-loss ground. Also, the trees looked like great vertically polarized rf energy eaters. The bobtail is particularly nice for tree hanging since its highest support points (A, B, and C in Fig. 7) are all at low impedance and looked as if they could be directly slung over a tree limb with no insulators. It is fed from the bottom at a high-impedance point so the ground system doesn't need to be as good as it does with low-impedance feedpoints. Also, like the inverted V, the bobtail has its maximum current at the highest support point. It can be excited from a parallel-resonant tank circuit or a quarter-wavelength stub.

The bobtail has been an outstanding performer. It's at least an S unit better than the inverted V and works great on DX paths to the Far East (JA, KG6, and VS6). The author put up two of these at right angles and found their interaction to be practically nil even though their center legs are quite close. When switching, the author ground the feed point of the one not in use.

The Half-Square Antenna

With such fine results, it was thought the ultimate "tree-hung" antenna had been discovered. However, after a particularly bad storm, it was noticed that one leg of the bobtail had broken off and yet the antenna feed impedance hadn't changed noticeably. Furthermore, the results compared with the inverted V seemed about the same as the full bobtail. Fig. 8 shows the configuration. It is a 2-element (instead of 3) vertical broadside array with the same current in both legs. It has all the advantages of the bobtail except that the radiation from the horizontal part of the antenna doesn't cancel as well in all directions and some end-fire, horizontally polarized energy does spill off. This might

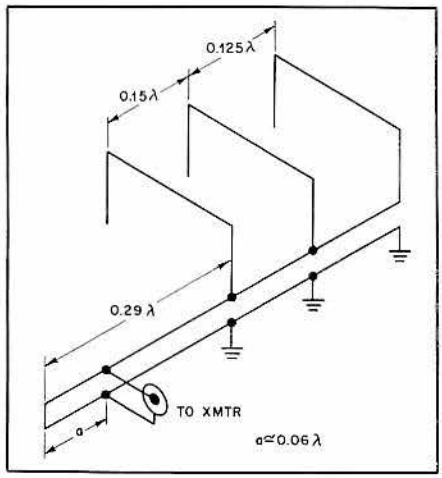

Fig. 13 — A 3-element half-square array.

be considered an advantage or a disadvantage, depending on whether you're seeking coverage or discrimination! In discussing this with Ed Watters, WA3LGX, he pointed out the kinship this antenna has with the bisquare array. It's sort of half of a bisquare laid sideways with the ground image antenna making up the other half. That, plus its obvious shape, led the author to dub it the half-square antenna.

After using a single half-square for awhile, it was decided to add another element with about 0.15-wavelength spacing. With the new element in place, a check was made to see what parasitic coupling there might be between elements. With several hundred watts fed into the driven element there was no evidence of rf on the parasitic element (using a neon bulb). This was a very gross measurement which tended to confirm what was expected. The very close proximity of the antenna to ground tends to reduce greatly parasitic coupling to a nearby element. Being puzzled why it should appear so small, the only hope was to devise a means of measuring this coupling more accurately.

Having had to tear down the 8JK antenna to get enough wire for this antenna, as a first try for feeding it, the author just used the 8JK open-wire line and stub match as it existed. The one wavelength of wire for each element was taken directly from the 8JK also. Fig. 9 shows the configuration. Unlike the 8JK, which was narrowband (centered around the middle of the band), this configuration gave the very flat SWR shown in Fig. 10 — on the first try! The SWR was not very different whether the feed-line stub was connected to point A, B, or C (Fig. 9). B gives a bidirectional characteristic while connection to A or C gives some unidirectivity. The author is still suspicious of the wide bandwidth and suspects the two elements may be different effective lengths, giving a stagger-tuned effect. If the spacing between these two were increased to a quarter wave and fed at point A or point C, it should theoretically add another couple of dB gain

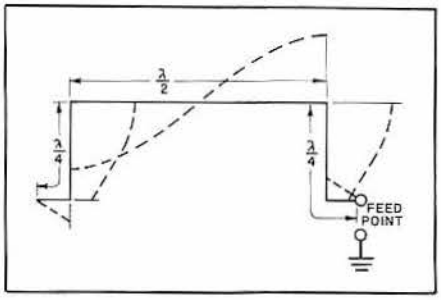

Fig. 14 — Any of the antennas mentioned can be bent as shown in order to keep the current loops at the upper corners.

and give a more significant front-to-back ratio than with the 0.15-wavelength spacing. WA3LGX plugged the dimensions and shape of this antenna into a generalized computer program he has developed for wire antennas and got the curves shown in Figs. 11 and 12. Fig. 11 defines the forward pattern for 0.15-wavelength spacing assuming a perfectly conducting earth. Fig. 12 is for quarter-wave spacing. The actual patterns will be modified at angles below 10° to 15° by the earth's resistivity[2] as is the case with any vertical antenna. The 0.15-wavelength-spaced antenna was used for some time and consistently gave better results than the bobtail on the path to Europe.

The writer took one other step beyond the 2-element array and added another element at 1/8-wavelength spacing (see Fig. 13). The extra element is fed, as are the other two, with an extension of the same open wire line. This antenna is considerably quieter (less QRN) than any of the other 80-meter antennas the writer had and has better than half an S unit advantage over the bobtail on European signals. It doesn't require any retuning to cover the whole band.

With these antennas not insulated at their support points, one might expect some effects when the tree sap rises or in wet conditions. The author hasn't been able to notice any differences from dry weather to monsoon-type rains or wet snow covering everything. The trees are slightly over 1/4-wavelength high on 80 meters. Considered as antennas or absorbers, they would look like grounded 1/4-wavelength vertical radiators. The vertical sections of the half-square antenna that run close to the trees are just the opposite. That is, at the bottom of the antenna the voltage is high and at the top, the voltage is low. This should minimize coupling to the trees, as opposed to, for example, using 1/4-wavelength grounded verticals for the antenna elements.

160-Meter Operation

Now if you look closely, you can see that the 80-meter half-square whether 1, 2 or 3 elements, should make a good antenna for 160 meters. Each element is 1/2-wavelength long on 160 meters, voltage fed on the end, and the high current part of the antenna is at the maximum height. True, a higher impedance part of the antenna touches the tree, but you can't have everything free! While not having managed to work any DX with the few watts available on 160 meters, the author can *hear* Central European ham stations quite well on this band for the first time ever at this location. Of course, a different stub or tuning arrangement is necessary for getting a low SWR on 160 meters. The writer just unshorted the stub and put a tapped coil (about 14 microhenries) in series with the coax feed line to tune it.

Construction Details

These antennas were all built with no. 14 soft-drawn copper wire. The elements are pulled over the top limbs of trees that have approximately the correct spacing and tied to nylon strings at about shoulder level. If your trees aren't a full quarter wave high, the extra wire can be stretched out parallel to the ground at each end as shown in Fig. 14. Note that you still get the maximum current point at the highest support point you have.

The best technique found for getting a line over the highest tree is to use a fisherman's casting reel (I use a Zebco 202) with an 8-pound nylon line and a 1- or 1-1/2-ounce sinker. The reel is put in the RELEASE position and a sling shot is used to shoot the sinker and line over the desired tree. This is a very accurate technique and you can easily put a line over 90-foot (27.43-m) trees. The light fishing line is used to pull over a heavier line. It's a good idea to paint the sinker a bright color since the line is almost invisible. You can waste a lot of time looking for the sinker at the end of the line.

Be sure to leave enough droop in the horizontal section of the antenna to allow for tree motion in high winds. The open-wire feed line used for the harness and stub sections is made with the same no. 14 wire spaced 3-1/2 inches (89 mm).

The avid Field Day or camping fan will notice the obvious advantages of the half-square antenna for that type of operation. It uses minimum materials, goes up very quickly, will really put out a booming signal on 80 meters, and can be taken down in just a few minutes. You can also make good use of the fishing rod in between your turns at the key. This material was originally presented in *QST* by Ben Vester, K3BC.

References

[1][Editor's Note: While complete cancellation of the horizontally polarized component occurs at a point broadside to the array, some radiation from the flat-top portion will exist at other angles. This is because of incomplete cancellation of the components from the opposite ends of the flat top.]

[2]*The ARRL Antenna Book*, 12th Edition, p. 46.

The HRH Delta-Loop Beam

Here's an antenna that should excite the interest of the amateur fraternity. The Delta-Loop beam has all the features of a quad without many of the disadvantages.

The evolution and design of the antenna shown in the photographs came about primarily because of a lack of confidence in the mechanical durability of quads. Anyone who has ever built and used quads knows how difficult it is to keep them up in icing and high wind conditions.

The author being an old-time mechanic, felt there had to be a better design for an antenna that used full-wave elements in a parasitic array, so some years ago a start was made to find that better design. One thing that nearly all readers will agree is that Mother Nature is about the best designer there is. Along these lines, just observe the growth of branches on tree limbs. You'll find that many of the smaller branches will grow up in a semivertical pattern from the limb; see Fig. 15. It takes a considerable amount of icing and wind to break such branches, indicating the soundness of the design. This same idea should apply to elements mounted on a boom.

To test the idea, an element of aluminum tubing was mounted on a boom. The element was mounted as shown in Fig. 17. The boom was then secured to the family car with the element in a vertical position. The assembly was then tested at 65- to 75-mph. Even though the element was only secured to the boom as shown in Fig. 17, there was no "set" or permanent bending. This test opened the door to several possibilities in beam design.

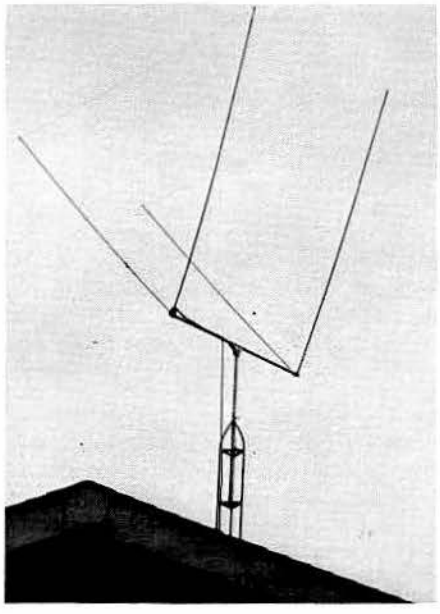

This is a 10-meter, 2-element Delta Loop that is very similar in construction to the antenna described in the article.

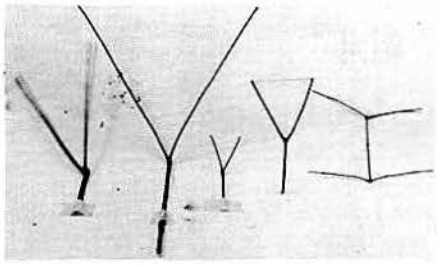

Fig. 15 — The basic idea for the Delta-Loop beam was conceived from the growth of tree limbs and branches. Here are just a few of nature's configurations that lend themselves to antenna design!

A loop aerial can take many shapes. Anyone who studies the history of the quad will find that many different configurations have been used. Why not use a triangle?[1] It should be possible to achieve a very good design using a vertical triangle. See Fig. 16. This shape appears ideal for a beam with full-wave elements, and has most of the advantages of the quad without many of the disadvantages. This led to the construction of several antennas of the type shown in the photographs, and some of these advantages become quickly apparent.

First, the entire antenna is *above* the boom. Second, the antenna is constructed primarily of aluminum tubing, which provides extra strength as compared with wire elements. Third, the antenna has Plumber's Delight type construction, meaning that the antenna is at ground potential for lightning protection, plus the fact that this type construction lends itself to gamma matching of the feed point, eliminating the need for a balun. Last, but not least, we find the antenna is very attractive in its symmetry. Of course, the important point is how well does the antenna perform?

Several 10-meter models have been tested and the unit shown in the roof-mounted position is 20-meter Delta Loop. Using a gamma match with 50-ohm coaxial feed, a 10-meter model was matched at 28.8 MHz. The antenna consisted of a driven element plus reflector with the elements spaced 6-1/2 feet (2 m) apart, or approximately 0.2 wavelength. Surprisingly, the antenna was extremely flat across the entire 10-meter band, the worst mismatch being *less* than 1.2 to 1.[2]

The author has no means of measuring gain or front-to-back ratios. However, with the spacing and element sizes the same as a quad, the gain should be the same, or at least so close the difference would be insignificant. On-the-air tests have shown the antenna to be as good as or better than quads the author has had up. Front-to-back and front-to-side reports have been outstanding, both on ground wave and skip.

Element Lengths

Many tests have been made on driven elements to determine the effect of element lengths on SWR. It was found that the flattest curve was obtained with the formula

$$\frac{1005}{f_{MHz}} \text{ (feet)}$$

for the driven element. The reflector should be about three percent longer, or

$$\frac{1030}{f_{MHz}}$$

If directors are desired it would appear that a length three percent shorter than the driven element would be adequate.

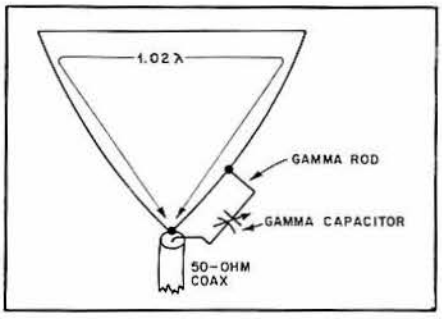

Fig. 16 — This drawing shows the driven element and feed method of the Delta Loop. Tests have shown that the overall length of the antenna is slightly longer than a wavelength (1.02λ). Each side of the antenna is approximately 1/3 wavelength long. The top, or wire section, is made slightly shorter to put tension on the vertical members.

Table 1

Bill of Materials

Tubing used is 6061 T6.
4 — 12-foot lengths of 3/4-inch OD, 0.035 wall (elements).
1 — 12-foot length 1-3/4-inch OD, 0.065 wall (boom).
8 — 3/4-inch diameter stainless steel hose clamps.
1 — 9-inch length of 3/8-inch OD by 5/16-inch ID.
1 — 9-inch length of 1/2-inch OD to slide over 3/8-inch section.
25 feet of copper wire no. 12 or 14, or equivalent in stranded wire.

Feet X 0.3048 = m.
Inches X 25.4 = mm.

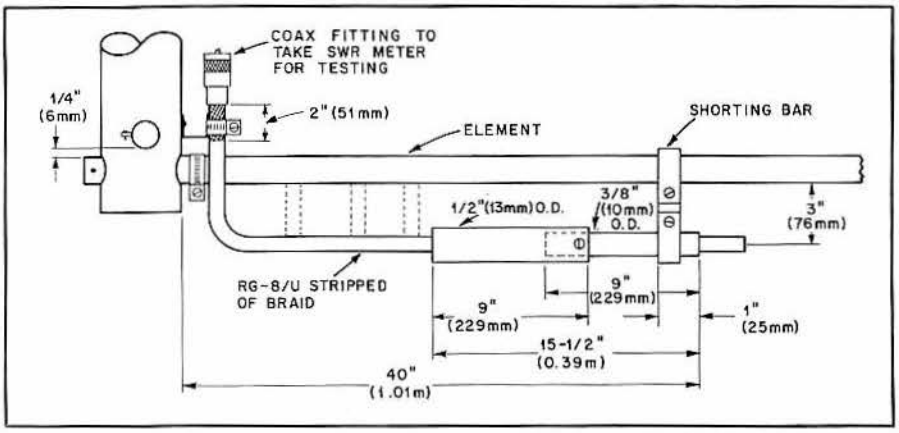

Fig. 18 — Here are the details on the gamma-matching section. As mentioned in the text, the coax fitting can be a female type SO-239, mounted on a small bracket which is mounted on the boom. Spacing insulators for spacing the gamma line from the element can be made up from pieces of Lucite or Plexiglas.

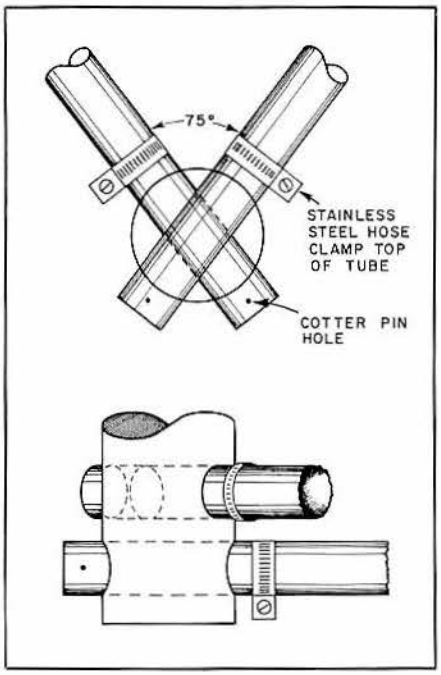

Fig. 17 — This drawing shows the method of mounting the element to the boom. A cotter pin is used on the under side of the boom and a hose clamp on the top to hold the element securely to the boom.

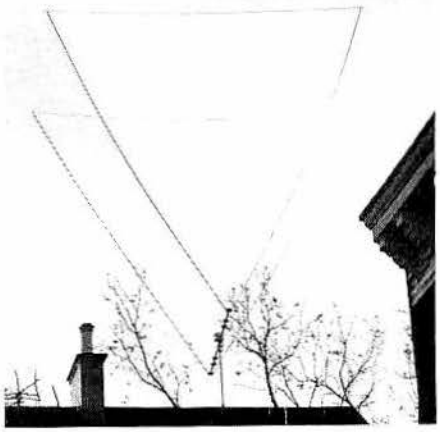

Here is our roof-mounted 20-meter Delta-Loop beam that is now undergoing a series of tests.

As to element spacing, the author has long been an advocate of wide spacing (0.17 to 0.2 wavelength) whenever possible. In the 10-meter tests 0.2 wavelength spacing was used.

For readers who are interested, complete construction information on a 10-meter model, including a list of the required tubing, follows.

Construction Notes

Fig. 17 shows the method of mounting the element tubing to the boom. The angle between the semi-vertical elements is shown as 75 degrees but this can vary a few degrees either way without any appreciable effect on the performance of the array. It is difficult to drill and line up the element support holes in the boom and come out to *exactly* 75 degrees.

There are a couple of methods of making the holes in the boom to hold the elements. One of the simplest is to use a Greenlee-type chassis punch. This makes a clean hole in the boom. Another method is to drill holes large enough to take the end of a 3/4-inch (19-mm) reamer and then ream out the holes to the necessary diameter.

One not accustomed to working with angles might find it difficult to drill holes at a 75-degree angle. A simple method is to first drill holes to take a single element. Next, make a jig from a piece of stiff cardboard or similiar material, using a protractor to get the 75-degree angle. Then insert the single element into the boom and lay the jig along the element; this will give you the correct alingment for the other element.

The elements are inserted through the boom just far enough to take a cotter pin on the underside of the boom. On the top side, a hose clamp is used to hold the element to the boom and prevent slippage. A length of copper wire can be wrapped around both elements just below the clamp to insure a good contact between the elements and the boom. Hose clamps are also used at the tops of the elements to hold the horizontal wire.

Fig. 18 shows the details of the gamma matching section. The gamma section is made up from the inner conductor of the coax, including its insulation, and two sections of telescoping aluminum tubing. The outer covering and braid is removed from a 52-inch (1.32-m) length of RG-8/U coax. In Fig. 18, a male coax fitting is shown with a short length of braid, 2 inches (51 mm) long, which is grounded to the boom via a clamp and bracket. If desired, a chassis-type coax fitting, type SO-239, could be mounted on the boom with a small metal bracket. The capacitor section is made of two lengths of tubing 3/8-inch (10 mm), and 1/2-inch (13 mm) diameter, respectively, and both 9 inches (229 mm) long. The 3/8-inch (10 mm) tubing fits over the insulation around the coax inner conductor while the 1/2-inch (13 mm) tubing slides over the 3/8-inch (10 mm) material. The larger tube is drilled and tapped to take a locking screw. Spacing of the section from the element is 3 inches (76 mm).

In adjusting the gamma, figures given in

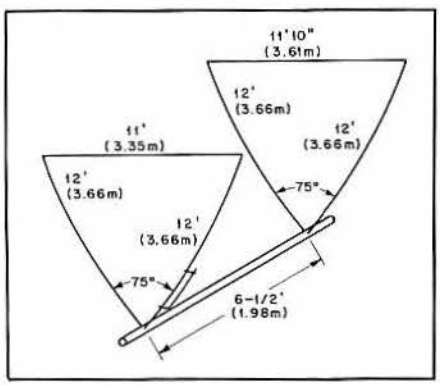

Fig. 19 — For those interested in exact figures, this sketch provides the element and boom lengths for a Delta-Loop beam for 28.8 MHz.

Fig. 19 can be used as a guide. In order to avoid matching errors, the gamma should be adjusted with the SWR bridge right at the beam. Set the shorting bar to the dimension given in the diagram and slide the 1/2-inch (13 mm) tubing over the smaller tubing, looking for a setting that gives a match. If one cannot be obtained, move the shorting bar and sliding tubing assembly a short distance, say an inch (25 mm), and then try different settings of the 1/2-inch (13 mm) tubing until you find a match. We found that the settings were not critical in getting a match. Once the beam is matched, the regular feed line to the station can be attached to the feed point. The connection should be taped to prevent moisture from getting into the fitting and coax.

As stated earlier, the antenna is extremely flat across the entire 10-meter band. The present model was designed for 28.8 MHz and matched at this frequency. The SWR at the highest point, at 29.7 MHz, was about 1.2 to 1. This dropped to 1 to 1 at about 29 MHz and stayed at 1 to 1 all the way down to 28 MHz. This feature of the antenna certainly is a help when using a transceiver designed for 50-ohm output. The beam has proved its ruggedness through winds and icing conditions. All in all, we think the Delta-Loop beam is one of the best performers we have seen. This material was originally presented in *QST* by Harry R. Habig, K8ANV.

References

[Editor's Note: A triangular loop configuration also was described in *QST* in April 1968, "Technical Correspondence" by Norman Watson, W6DL, independently of K8ANV's design. Mr. Habig has been working for some years on this design and has a patent pending.]

[Editor's Note: A 10-meter model of the Delta Loop beam tested at ARRL headquarters was matched at 28.8 MHz and an SWR curve was made using a Bird Wattmeter. The largest mismatch also was less than 1.2 to 1 MHz (at 29.7 MHz).]

The Delta-Loop Beam on 15

DX capability, low SWR and readily available construction materials are highlights of this 15-meter beam antenna. Similar to a quad, but rugged as a Yagi — those are the virtues of the Delta Loop.

Some of the features of the 15-meter beam described in this article include a very low SWR across the entire band, use of readily available materials, "Plumber's Delight" type construction — which is always an appealing feature of any beam antenna — and last but not least, excellent performance. On the last point, the antenna shown in the photographs was tested during a DX contest with a transmitter input power of 100 watts. The boom of the antenna was mounted only eight feet (2.44 m) above the ground, but in about five hours of contest operation 58 different countries were worked — and, believe it or not, the majority of the reports received were 59. Possibly conditions were above par, but even so the antenna shows it can do a real job under crowded band conditions.

As stated above, the beam uses Plumber's Delight type construction. For the newcomer's information, this type of construction has the antenna elements connected directly to the boom which in turn can be connected directly to earth ground without having any effect on the performance of the antenna. This is desirable because of the lightning protection offered by the system.

Fig. 20 is a drawing of the Delta-Loop driven element. The overall length around the driven element is slightly over one wavelength. Each side is approximately 1/3 wavelength long. The reason we say "approximately" is that the top section of the antenna is made of wire and is slightly shorter than 1/3 wavelength in order to put tension on the wire. A gamma-match feed system is used, eliminating the need for a balun.

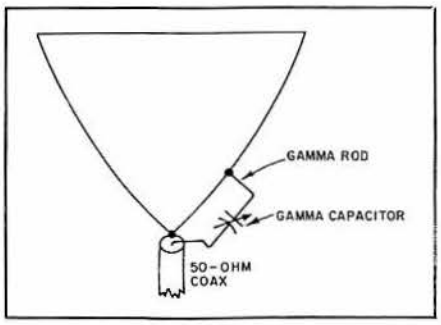

Fig. 20 — Basic configuration of the Delta-Loop driven element. Each side is approximately 1/3-wavelength long.

The formula used in figuring the driven element length is

$$\frac{1005}{f_{MHz}},$$

where f is the desired resonant frequency of the driven element. The answer will be in feet. The reflector length formula is

$$\frac{1030}{f_{MHz}}.$$

For a frequency of 21.2 MHz this figures out to a driven element 47 feet 5 inches (14.45 m) long and a reflector that is 48 feet 7 inches (14.81 m) long. Element spacing is approximately 0.2 wavelength or about 9 feet (2.74 m). Fig. 21 shows the two elements with the lengths of each segment.

Material Requirements

The beam elements were built primarily from Reynolds Do-It-Yourself aluminum tubing, which *should* be available from most hardware dealers. The reason we say "should" is because in some sections of the country hardware stores don't stock the tubing. However, most dealers will order the tubing for you. If you live in an area near or in a city of reasonable size, a look through the Yellow Pages will show any aluminum tubing dealers. The Reynolds

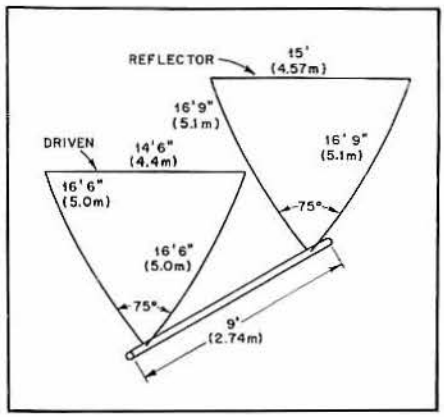

Fig. 21 — The element dimensions and the boom length. All measurements on the elements are made from where the element enters the boom; the portion of the element extending through the boom is not counted.

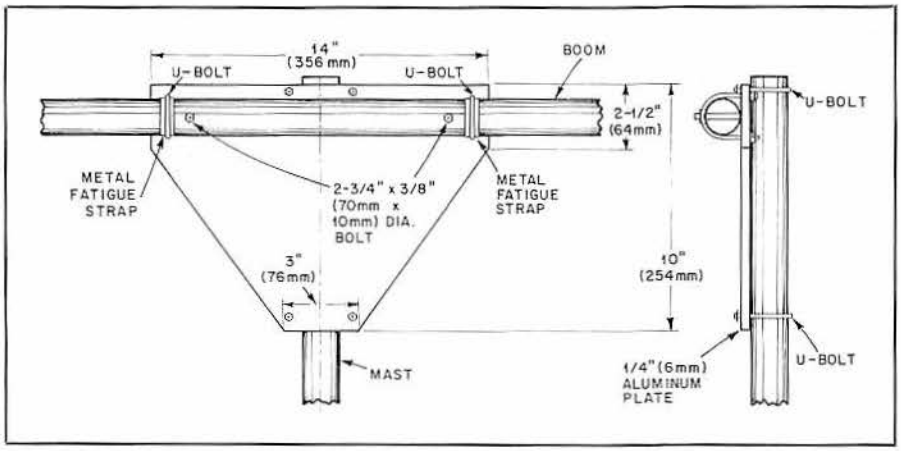

Fig. 22 — Construction details for the boom-to-mast mounting bracket. The U bolts holding the boom are 2-inch (51-mm) type. Those holding the mast will depend on the mast diameter — we used 1-1/2-inch (38-mm) U bolts for a 1-1/2-inch diameter mast.

Table 2

Shopping List

Quantity	*Length (ft)*	*Diameter (in.)*	*Reynolds no.*
4	8	1	4242
4	8	3/4	4222
2	6	7/8	4231
1	9	2	See Text.

3 feet of 3/8- or 1/2-inch diameter aluminum tubing.
12, 1-inch diameter hose clamps, stainless steel.
35 feet of no. 12 or 14 copper wire, solid or stranded.
1 variable capacitor, 100 pF maximum, 0.025 spacing or greater.
1 one-quart freezer container.
1 SO-239 Coax chassis connector.
5 1/4-inch diameter aluminum nuts and bolts, 1-1/4-inches long.

Feet X 0.3048 = m.
Inches X 25.4 = mm.

Do-It-Yourself tubing comes in 8-foot (2.44-m) lengths but most of the commercial tubing available from metal distributors comes in 12-foot (3.66-m) lengths. If you obtain the 12-foot types, be sure to specify type 6061 (61S) alloy as this material affords excellent strength for antenna elements. The boom used in this antenna was made from this alloy and is 2 inches (51 mm) in diameter with a 0.065-inch (1.65-mm) wall. Another source of aluminum or steel tubing is electrical supply houses; although this type of aluminum is a little too soft for the elements it would be suitable for a boom. Also, electrician's thin-wall steel tubing is available in various sizes, including the 2-inch diameter, for a boom. In a pinch, the boom could be made of wood, such as a length of 2 × 4. In such a case, the bottoms of the elements could be connected together with a length of wire to maintain the Plumber's Delight feature. The shopping list included here should prove of help in purchasing the parts.

Construction

The first step in building the antenna is to make up the vertical elements. The description given here is based on using the Reynolds tubing. Using a hack saw, cut the 7/8-inch (22-mm) tubing into 2-foot (0.61-m) sections. This particular type is made by Reynolds for the purpose of telescoping the 1- and 3/4-inch (25-mm and 19-mm) diameter sections together and comes in 6-foot (1.83-m) lengths. After cutting off four 2-foot (0.61 m) lengths you'll have one 4-foot (1.22-m) piece remaining. Cut this into four 1-foot (0.31-m) lengths and set these pieces aside for the time being.

Next, cut two lots, the thickness of the hacksaw blade, about 2 inches (51 mm) deep in one end of each of the 1-inch (25-mm) and 7/8-inch (22-mm) diameter lengths. Slide the 7/8-inch tubing inside the 1-inch diameter to a length of about 6 inches (152 mm) and then slip the hose clamps over the slots and tighten them. The 3/4-inch (19-mm) tubing can then be inserted into the slotted ends of the 7/8-inch (22-mm) tubing and these sections clamped with hose clamps. Two of the elements should be adjusted to the proper length for the driven element and two for the reflector, as per Fig. 21 (or whatever length you wish from the formulas). Some amateurs may prefer to cut their antennas for the cw portion of the band and others for the phone section.

The next step is to cut the 1-inch (25-mm) holes in the boom to take the ends of the 1-inch diameter elements. We used a 1-inch chassis punch to make the holes, but a 1-inch metal reamer could also be used. The aluminum is easy to cut or punch so making the holes should be no problem. What can be a problem is lining up the holes so that the 75-degree angle between the elements is obtained. We made a jig from a piece of cardboard, using a protractor. Once one set of holes for the director and reflector were made the elements were temporarily mounted in the boom. The cardboard jig was laid on the elements and the 75-degree holes were marked off and drilled.

When the holes are all drilled, the boom can be laid on the ground and the element ends inserted into the boom holes. We allowed about 1/4-inch (6-mm) extension of the base of the elements through the boom so as to allow space for cotter-pin holes. However, before drilling the cotter-pin holes, insert the four 1-foot (0.31-m) lengths of the 7/8-inch (22-mm) tubing into the elements at the boom. This will serve to give added strength to the elements at the support point. Drill each of the four ends to take the cotter pins and install the pins. Tighten down the hose clamps on the top side of the boom to secure the elements in place.

Drill the tops of the elements to take the 1/4- × 1-inch (6-mm × 25-mm) aluminum bolts. The top wires can then be installed.

The close-up view shows the gamma installation. The gamma capacitor is mounted inside a plastic freezer container which is held in place by a small metal L-shaped plate mounted on the box and the boom, using four self-tapping screws. This plate also holds an SO-239 coax chassis fitting to take the feed line. We like to install an SWR bridge directly at the beam when making SWR or matching tests to reduce matching errors, and having the fitting there simplifies the procedure. The gamma rod, made from a length of 3/8-inch (10-mm) aluminum tubing 36 inches (0.91 m) long, is flattened at one end for a length of 1-1/2 inches (38 mm). The flatted portion is bent over at right angles and drilled to take one of the 1/4- × 1-1/4-inch (6-mm × 32-mm) aluminum bolts, which is mounted through the top of the freezer box. The gamma rod is held in place by this bolt and by the shorting bar between the rod and the element. The shorting bar is made from a piece of aluminum, 1 inch (25 mm) wide and long enough to fit around the two pieces of tubing and provide a separation of 3 inches (76 mm) between the rod and the elements.

How you mount the antenna boom to the supporting mast will depend a great deal on what type of tower or supporting structure you have. The method shown in the photo is a fairly simple one, and easy to make up. Fig. 22 shows details of the construction of the mounting unit. The one shown in the photo supporting the beam was made from two pieces of 1/16-inch (2 mm) thick aluminum plate. However, we found that even with the double plate there was still too much "give" in the mounting setup, so a replacement was made from 1/4-inch (6 mm) thick aluminum. This made the mount competely steady. Either a plate of 1/4-inch aluminum or 1/8-inch (3 mm) steel should be adequate for the jobs. The 2-inch (51 mm) U bolts that hold the boom to the mounting plate were adequate, but just for added insurance, 3/8-inch (10 mm), 2-3/4-inch (70 mm) long machine bolts (two required) were installed through the boom and mounting plate for greater holding strength.

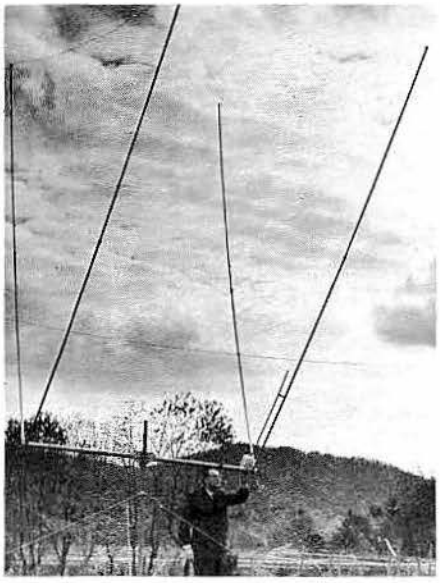

This view shows the completed antenna being matched.

During our tests, a weather front moved through the area and we had wind gusts up to 40 mph plus icing and snow loading on the antenna. The antenna and elements showed very little movement in these winds, and the entire antenna appeared very strong.

Adjustments

Adjustment of the gamma section is quite simple. Install an SWR bridge at the gamma feed point and tune up the rig on the desired frequency, Set the gamma shorting bar 24 inches (0.61 m) from the base of the gamma rod and tighten the gamma-bar nuts and bolts just enough to make electrical contact. Set the SWR bridge to read reflected power and adjust the gamma capacitor for a dip. The object is to find a setting of the capacitor and the gamma bar that gives a reading of zero in the reflected position. This may take a few tries, but you'll find the settings are not critical. If you adjust the antenna near the ground you may find it will require a new adjustment when it is up in its permanent location.

How you mount the antenna in its permanent location will depend on what you have to hold the antenna. If you use a boom mounting-plate-to-mast assembly such as already described, the U bolts holding the boom could be left slightly loose and the 3/8-inch (10-mm) bolts left out. The antenna could then be installed in an upside-down position and then rotated into place. Two men are better than one for this job, but one man *can* do the job. If a hole, say 1/2-inch (13-mm) diameter, is drilled through the boom a 1/2-inch rod could be slid through to serve as a lever to rotate the boom and antenna into an upright position and the U bolts and hardware could be then tightened down.

We think the Delta-Loop beam is an excellent antenna and offers many possibilities. Certainly the results obtained to this point prove the antenna is a real performer. Our tower is a crank-up job, making antenna testing a fairly simple project. The antenna was first matched at the 8-foot (2.44 m) level (boom height) and at the cranked-up height, about 55 feet (16.76 m) above ground. A very slight readjustment of the gamma capacitor was required at the greater height in order to get down to a 1-to-1 SWR. However, the change in SWR from the 8-foot to 55-foot (2.44- to 16.76-m) heights was very small. Also, the highest SWR was at 21,450 kHz, the top end of the band, with a mismatch no worse than 1.2 to 1. At 21,300 kHz the SWR dropped to 1 to 1 and remained at that figure all the way to the lower band edge.

The entire antenna weighs about 15 pounds (using the aluminum boom) so the antenna could be rotated with a heavy-duty TV rotator. One last note: We sprayed the cotter pins and hose clamps with a clear acrylic spray to reduce corrosion. This simple precaution should be taken in all antenna construction to prevent or reduce rusting. This material was originally presented in *QST* by Lewis G. McCoy, W1ICP.

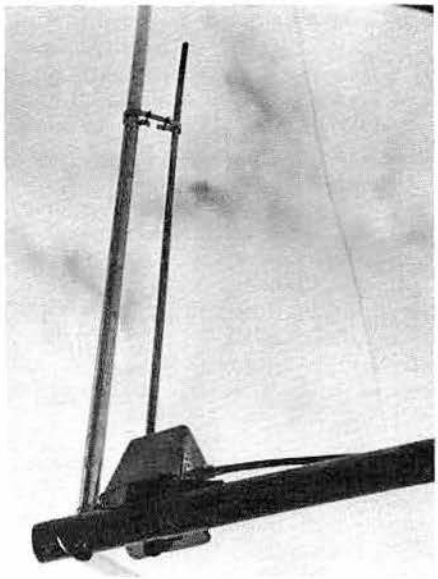

The plastic freezer box is held in place by the small metal bracket which is attached to the boom with self-tapping screws. Also on the bracket is a coax fitting to take the RG-8/U coaxial feed line. The gamma rod is mounted on top of the box and is held to the element with the shorting clamp.

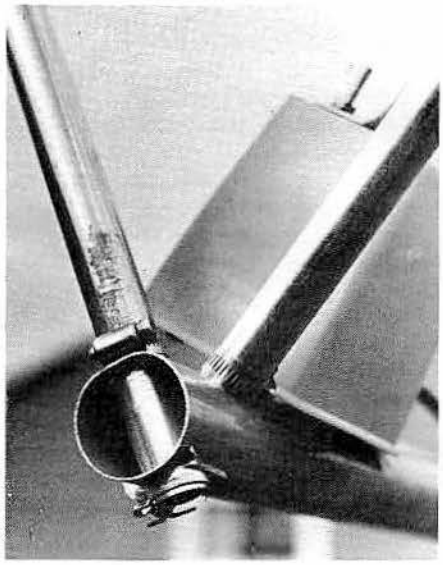

In this close-up view of the end of the boom, the mounting of the element ends are clearly shown. Cotter pins are used on the bottom end of the element and hose clamps on the top side of the boom. This secures the elements to the boom. The plastic freezer box that houses the gamma capacitor is clearly visible behind the elements.

Antennas for Travel Trailers and Campers

Pounding brass and rendering "lip service" from an RV or mobile home can be disappointing as all get-out if the antenna doesn't "play" well. Here are some tips for rig-mounted radiators that get the job done.

Who knows why so many hams like to go camping? Perhaps it's their Field Day training; perhaps it's the next logical step after mobile operation, or perhaps they just cannot leave home without their rigs. At any rate, it is nice to have your own means of communication with the outside world when you are away from home in the Maine woods, at the Grand Canyon, or even down in Mexico.

One thing all hams know is that no matter how good a transmitter you may have, you cannot get out without an antenna; and the better the antenna is, the better you get out. The antenna is usually no problem for the home station. The sky is the limit, so to speak. A 65-foot (19.81 m) crank-up tilt-over tower with a triband beam on top, and a couple of inverted Vs for 40 and 75 are not at all uncommon. But did you ever contemplate transporting such an antenna system to a state park, or some other campground, and setting it up while your XYL cooked suppper? Obviously, the mobile operator is faced with vastly different problems than those confronting the ham who stays at home, when it comes to antennas.

In 1929, the author built a 14-foot travel trailer, which was christened "Black Maria." Shortly thereafter, the writer got a ham license, and one of the first thoughts was toward a rig for the trailer. This was in the days when mobile operation was still a novelty, and the story of Black Maria was the author's first contribution to *QST*, in 1933. The rig used a pair of 33s in parallel operating from a B-battery pack.

Over the ensuing 35 years, many portable antenna designs have been tried, and much has been learned about their relative performance. The degree to which a trailer traveler is restricted in a choice of an antenna varies widely, of course, depending upon the facilities available at each stopping point. These are seldom known in advance, but to get the most out of the equipment, the trailer operator should be prepared to take maximum advantage of whatever facilities he may find on each occasion.

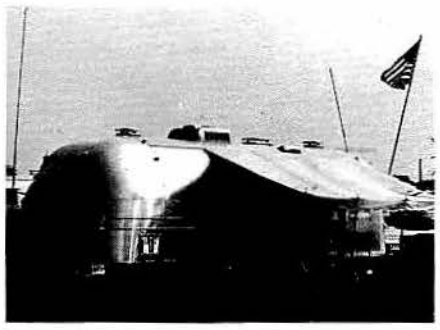

The author's 30-foot (9.14 m) Airstream trailer with the 75-meter Airstream Loop in place. The "tuning" mast is the one carrying the flag.

Dipole Antennas

Long ago, it was found that a simple dipole for 40 or 75 would far outperform the author's mobile whip, even with the dipole only a few feet above ground. While writing this, sitting in the latest Black Maria — a 30-foot Airstream job — up in Port Colburne, ON, the author was listening to the 75-meter phone band. The dipole is only 8 feet (2.44 m) above ground. When checking into the Airstream Travel Trailer Net, which meets every Sunday on 3963 kHz at 8 A.M. local time, the writer worked other trailer stations in Connecticut, New Jersey, Maryland, Pennsylvania, New York and Ohio. Several times the author switched to the mobile whip and could not be heard through the QRM. Such a dipole can be prefabricated and, when rolled up, occupies very little storage space.

When the length of the stay warrants it, and trees or other supports are available, the antenna will be even more effective when raised to a respectable height. A bow and arrow is kept on hand for shooting lines over taller trees. Incidentally, Hy-Gain makes a deluxe portable dipole consisting of two stainless-steel tapes in a double plastic housing. The tapes are calibrated in meters, and can be quickly reeled out to the proper length for use on any desired band. The unit is fitted with a coax connector, making installation very easy.

If only a single support is available, the dipole can be used in "inverted-V" fashion. A convenient way of putting up such an antenna is to use three or four 5-foot (1.52 m) lengths of 1-1/4-inch (32 mm) aluminum TV masting as a center pole, mounting it on the front of the trailer. The author has a mounting for such an arrangement clamped to the bumper, as shown in one of the photographs. The mast can be equipped with light nylon halyards for hoisting the center of the dipole. The ends of the dipole can be attached to whatever may be handy, but the higher, the better.

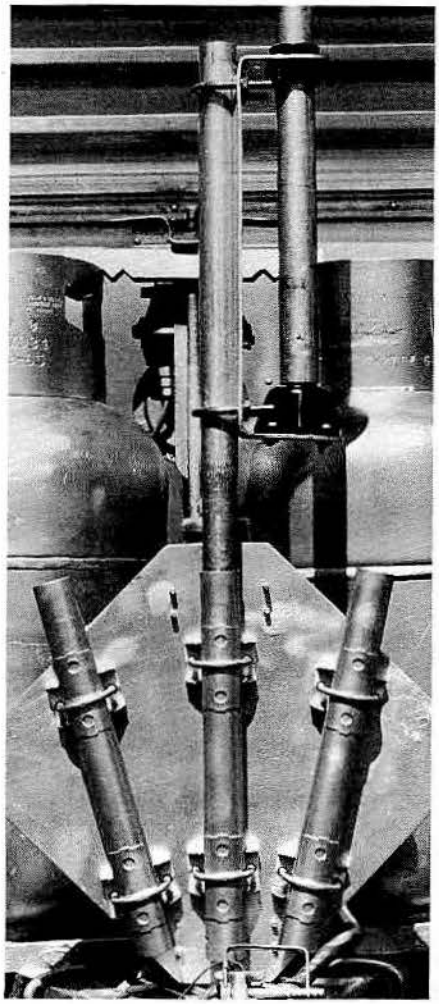

Insulated mounting at one end of the "Airstream Loop" 75-meter antenna. The "tuning" mast can be mounted directly in one of the other sockets. The tuning will vary with the spacing between masts as well as the length of the "tuning" mast. The insulated mounting can be transferred to one of the side sockets to obtain maximum spacing.

Loaded Antennas

Of course, there are many times when the surroundings, or the shortness of the stopover, make erection of a conventional dipole impractical. On these occasions, the author used one or another of several arrangements shown in the accompanying photographs and sketches. Where the

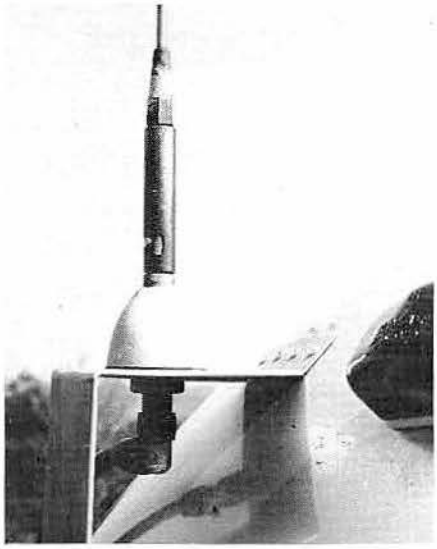

An elevated mounting for a mobile whip at a top rear corner of the trailer body. The bracket is fastened by pop rivets. This point may also be used, with the whip removed, for feeding wire dipoles.

A check with a 20-watt fluorescent lamp by W1WKZ indicates the "hot" points on the Airstream Loop 75-meter antenna system.

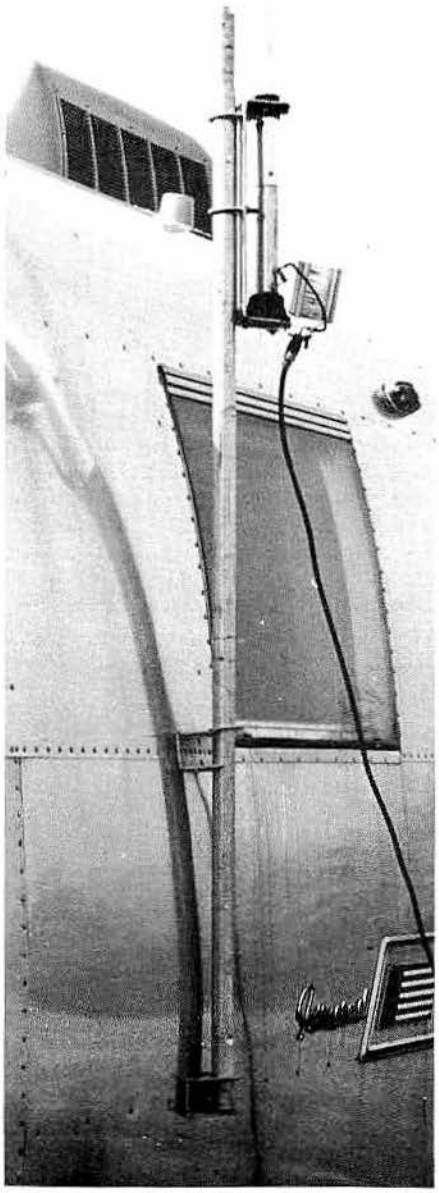

A 25-foot (7.62 m) base-loaded antenna mounted on brackets attached to the side of the trailer.

antenna system is one that requires a ground for operation, it was found that a quarter-wave wire counterpoise connected to the trailer, and strung out a few feet above ground, is usually a much better "ground" than the trailer alone, even if the trailer is actually grounded to a driven rod. The author carries two each of wires cut to lengths of 8, 16, 32 and 60 feet (2.44, 4.88, 9.75 and 18.29 m) for use as counterpoise on the 10-, 20-, 40- and 75-meter bands, respectively. One end of each wire is fitted with a large battery clip, while the other is terminated in an insulator. Trailer awning poles come in handy as counterpoise supports when nothing else is available.

"Airstream Loop" Antenna

Of particular interest is the 75-meter folded configuration shown in the sketch of Fig. 23, which is called the "Airstream Loop," although, strictly speaking, it does not function as a true loop. With the fittings that are provided, this antenna can be put up in a few minutes, and its performance seems to be about equal to that of a low dipole. It has the advantage that it is completely supported by the trailer, and requires no external supports. It is contained entirely within your own campsite. There are no wires strung out for you or your neighboring campers to trip over or be garroted by in the dark. A 30-foot (9.14-m) length of wire is strung between, and connected to, two poles made of aluminum TV mast sections. A third mast (A), of approximately the same length as the others, and connected to the trailer, is an essential part of the system. This arrangement appears to work as a folded half-wave antenna, the 30-foot (9.14-m) wire and the two poles connected to it forming one half of the antenna, while the other half is formed by the trailer body and mast (A). Probing with a fluorescent lamp shows that the end of the trailer opposite the feed point is "hot" while the feed-point end is "cold." The system can be tuned by adjustment of the length of pole A, and/or changing the spacing between A and the adjacent pole. The spacing can be changed by a selection of the pole mounting sockets shown in one of the photographs. In this manner, the resonant frequency can be changed by almost 150 kHz. For any adjustment, the transmitter can be tuned about 30 kHz either side of the resonant point before the SWR exceeds 3 to 1. Since the "hot" end of the trailer is the front end in my case, the tow car must be unhitched, and an insulating block used under the customary supporting jack.

In a similar arragement for 40 meters, mast A is omitted, and a wire approximately 21 feet (6.40 m) long is connected to the pole at the feed-point end. The open end of the wire is supported from the pole at the opposite end of the trailer by a length of nylon rope.

40-Meter Monopole

Another 40-meter antenna that has been used with considerable success is a 34-foot (10.36 m) length of 300-ohm ribbon line connected as a folded monopole, and strung up in the same manner as the antenna just described. One conductor of the ribbon is grounded to the trailer at the feed point, while the other conductor is connected to the center conductor of the coax line. The two ribbon conductors are connected together at the far end.

Matching

Standing-wave ratios up to 5 or 6 to 1 are hardly worth worrying about at 4 MHz so

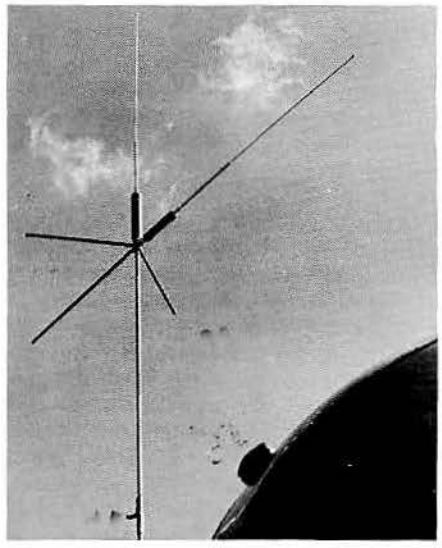

A five-band antenna system. A New-Tronics mobile antenna base section is fitted with a Waters Add-a-Band adapter. The short resonators for 10, 15 and 20 meters are Waters. The 80-meter resonator (top) is New-Tronics. A threaded stud has been added to the vacant side of the adapter to take a New-Tronics 40-meter resonator. The system is fed at the base with a single coax line.

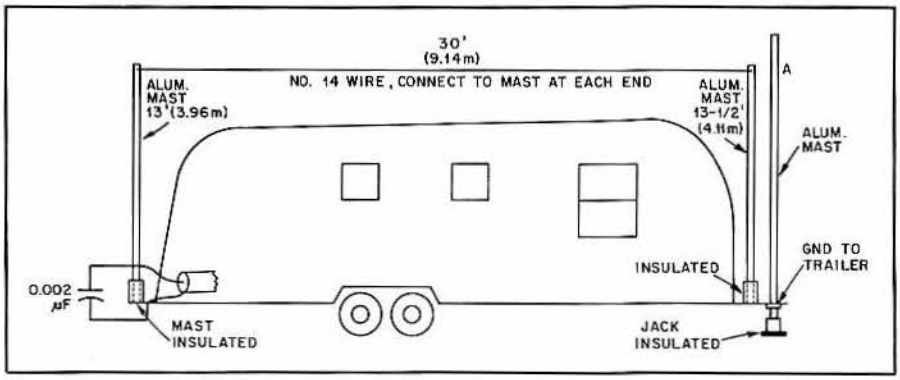

Fig. 23 — 75-meter "Airstream Loop"

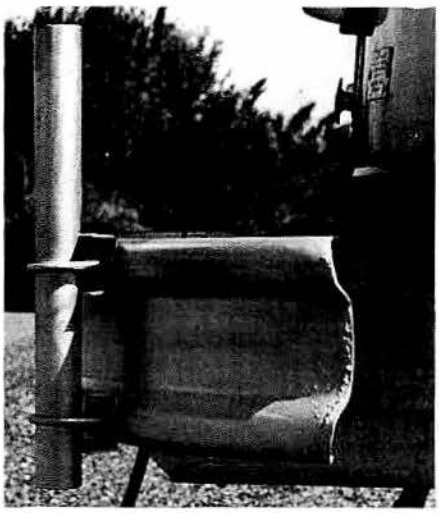

A bumper-mounted socket for TV masting.

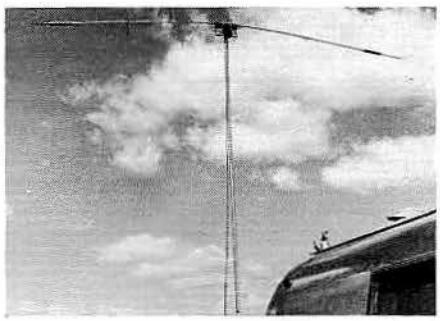

An 80-meter dipole made of two New-Tronics 75-meter mobile whip back to back. The 15-foot (4.57 m) mast is bumper-mounted. A 1-to-1 balun is mounted on the center insulating panel, which is secured to the mast with U bolts. This antenna is quite narrow-band when operated on 75 meters, making it necessary to retune the antenna for excursions of more than 30 or 40 kHz.

far as additional power loss is concerned. However, an SWR greater than 1 to 1 causes the line input impedance to vary, depending on the length of the line. The output circuits of many transmitters and transceivers are not designed to work into loads departing significantly from 50 ohms. With these units, it may not be possible to load the final stage, or components in the output stage not designed for the voltages that develop with higher-impedance loads may be damaged. Use a Monimatch, or other reflectometer, and adjust the antenna for minimum SWR. The author carries along several mica capacitors ranging in value from 50 pF to 0.002 μF with battery clips attached, which are used to shunt the line at the feed point. Start out with the lowest value, and double the capacitance in steps until you get an SWR of 1 to 1 somewhere in the band, and then adjust the antenna length for resonance at the desired frequency.[1]

To get some idea of the relative performances, a series of checks was made at 3825 kHz on several of the antennas described. A receiver with a horizontal antenna was set up at a distance of eight miles from the trailer, and S-meter readings were taken with the results shown in the accompanying tabulation. All readings were made with identical input power to the transmitter, and with the antennas adjusted for an SWR of 1 to 1.

To sum it all up:

1) Carry a complete set of mobile whips for lunch stops, or other occasions where you just do not have the time or room for anything better.

2) If at all possible, use a 1/4-wave counterpoise clipped to the trailer when using a mobile whip.

3) If you have the time or space, clip a 1/4-wave wire, instead of a whip, to your mobile antenna mount, and run it out to a bush or tree.

4) In addition to (3), clip a 1/4-wave counterpoise to the trailer, and run it in the opposite direction.

5) If you are stopping for a short time, or for the night, rig up the 5-band mobile whip with five 1/4-wave counterpoises, one of appropriate length for each band.

6) If you want to concentrate on one band, put up the 16-foot (4.88 m) mobile-whip dipole, if your space is limited.

7) If you have plenty of room, put up a 1/2-wave dipole for your favorite band.

8) If you want to work all bands, and space for dipoles is limited, then put up your trap vertical with the 75-meter resonator tuned to your favorite frequency.

9) If you are going to spend a week in a particular campground, shoot some lines over a couple of high trees with a bow and arrow, and get your dipoles up in the air as high as possible.

10) The use of balloons and kites is good, but depends completely on the wind.

11) Next best to a high dipole, put up the "Airstream Loop" antenna for 75 meters.

12) If all else fails, bring your 2-kW PEP linear and your 2.5 kW ac gas generator along. This will at least keep the other campers awake. Don't forget a low-pass filter for TVI! This material was originally presented in *QST* by Philip S. Rand, W1DBM.

[1][Editor's Note: This method is equivalent to the use of a stepdown L network. It can be used when the antenna feed-point impedance is lower than the line impedance. To obtain a match, the antenna length must be somewhat longer than a resonant length, so that the antenna shows inductive reactance at the feed point. (This reactance serves as a substitute for the reactance of the coil of a conventional L network.) For an accurate match, it is necessary to adust the antenna length and the value of the capacitor until the appropriate transformation ratio is obtained.]

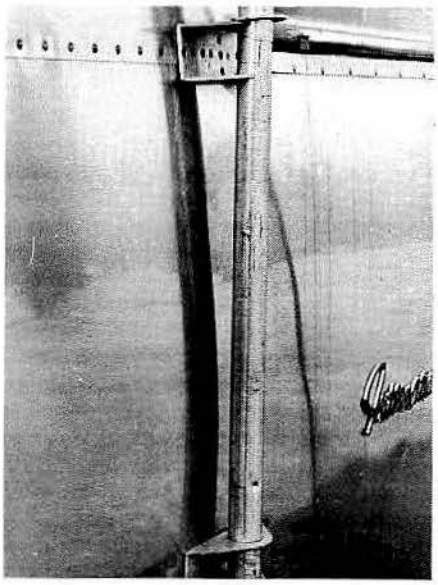

Brackets for mounting TV masting on the side of the trailer. The upper bracket is fitted with a removable U-shaped yoke bolted to the bracket. The brackets are fastened to the trailer with pop rivets.

Table 3

Hustler 75-meter mobile whip mounted vertically on top rear corner of trailer	S7
Same as above, with 60-foot counterpoise wire connected to trailer	S9
Two Hustler 75-meter mobile whips back to back as a horizontal loaded dipole	S9 + 5 dB
60-foot horizontal wire 8 feet high, using trailer as ground	S9 + 10 dB
Hustler 4BTV trap vertical with 75-meter resonator	S9 + 10 dB
120-foot dipole, 15 feet high at center	S9 + 20 dB
"Airstream Loop" antenna	S9 + 20 dB
Home-station dipole 50 feet high	S9 + 30 dB

Feet = 0.3048 = m.

The Apartment Dweller's Dilemma

Having trouble getting a signal out from "concrete city"? Nonresonant, random-length wires can provide surprising results if a Transmatch is used to make the rig happy with the load it sees.

It is apparent that many would-be amateurs living in apartment buildings believe it is impossible to get an effective signal on the air. They feel the need to have an outdoor antenna in order to make contacts. This isn't true. Of course, the apartment dweller can always go mobile, but there comes a time when the amateur wants a home station. This article treats the problem and, hopefully, will get a few more hams on the air.

Some General Considerations

There are exceptions to the following rules but, in general, they can be depended upon.

1) An outdoor antenna will work better than an indoor one.

2) An antenna inside a frame building with wood exteriors is better than the same antenna in a steel-and-concrete building.

3) The higher above ground, inside or out, the better the antenna will work.

4) The bigger (or longer) you can make an indoor antenna, the better — even if it means running the wire around corners.

5) Even a poor antenna *should* produce some contacts.

The Coupling Problem

Most transmitters are designed to work into a 50-ohm load, and contain little or no provision for adjusting the transmitter when the load is other than 50 ohms. Unfortunately, there is no random-length wire antenna that will present a 50-ohm load on all bands. What is required is a Transmatch. A Transmatch is simply an adjustable LC network that converts the unknown antenna impedance to 50 ohms. This unit, shown in Fig. 24 and the photographs, will cover the 80- through 10-meter bands and can handle 1 kW of rf power. In addition to matching the transmitter to the antenna load, the Transmatch helps reduce harmonic radiation. Many Novices get in trouble with the FCC because of 2nd-harmonic radiation from the 80-meter signal. This unit should reduce such harmonic radiation. Also, the use of a Transmatch can provide better front-end selectivity for the receiver. Some receivers are subject to severe cross modulation when operated near a broadcast station. The Transmatch should reduce this effect.

The completed Transmatch. The counter dial and knob are James Millen Mfg. Co., Inc. products. Check with G. R. Whitehouse, Amherst, NH 03031.

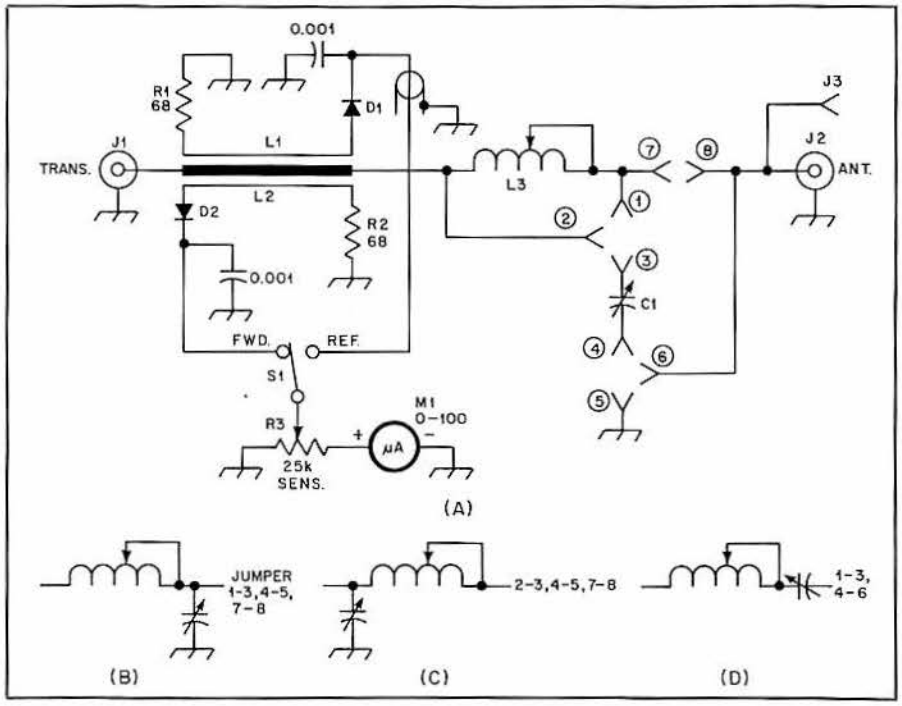

Fig. 24 — Circuit diagram of the L-network Transmatch. The eight banana jacks are E. F. Johnson type 108-900, and three dual banana plugs are required, E. F. Johnson type 108-200.
C1 — Variable capacitor, 350 pF (E. F. Johnson 154-10).
D1, D2 — 1N34A germanium diode.
J1, J2 — Chassis connector, type SO-239.
J3 — Feedthrough terminal, isolantite.
L1, L2 — See Fig. 25, part of etched circuit assembly.
L3 — Variable inductor, 28 μH (E. F. Johnson 220-203).
M1 — 100-μA meter.
R1, R2 — 68-ohm, 1/2-watt carbon or composition, *not wirewound.*
R3 — 25,000-ohm carbon control, linear taper.
S1 — Spst toggle.

Circuit Details

The unit shown in Fig. 24 is designed to be used in three configurations. They are shown at B, C and D. With one of the three hookups, it should be possible to match practically any antenna to the transmitter.

In order to get complete band coverage and avoid the complexities of band-switching, banana and jack plugs are used to change the circuit to the configuration needed. For example, if one wanted the setup shown at B, he would jumper terminals 7 and 8, 1 and 3, and 4 and 5. Using the banana plugs makes for easy changing of the circuit.

Whenever a Transmatch is used, the operator should have a way of knowing when the unit is adjusted correctly. The answer to this need is a Monimatch or other SWR indicator. If you have an SWR meter, it can be connected in the line between the transmitter and the coupler. If

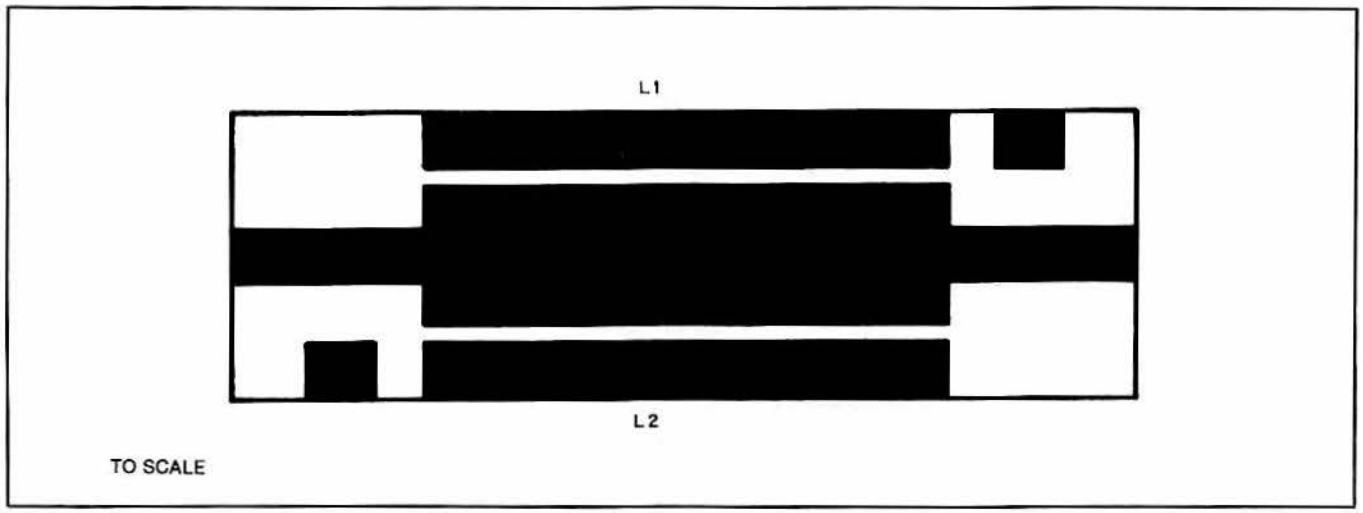

Fig. 25 — Etched circuit-board template. The foil side is shown, with etched portion shaded.

not, you can build the Monimatch[1] shown in Fig. 24, and include it in the cabinet with the Transmatch.

Construction Details

The chassis for mounting the Transmatch is made from a piece of aluminum measuring 10 × 19 inches (254 × 482 mm). The ends of the 19-inch length of aluminum are bent up to form a U-shaped chassis, the ends being 4-1/2 inches high to form a chassis 10 × 10 × 4-1/2 inches (254 × 254 × 114 mm). The back side of the U has an opening cut out, 3-1/4 inches high by 4-1/2 inches (83 × 114 mm) long. A piece of Plexiglas is mounted over this opening. The jack-plug sockets are installed directly on the plastic. Connections from the roller inductor, L3, and variable capacitor, C1, are made to the banana jacks. Be careful when drilling the holes for the jacks to insure that they will mate with the plugs. Fig. 25 shows the details for a pc-board Monimatch.

Methods for making etched circuit boards are given in detail in the construction chapter of The Radio Amateur's Handbook, so we won't treat the process here. When installing D1 and D2 on the board, be sure to use a heat sink while soldering the leads. Too much heat can ruin the diodes. Shielded leads are used from the circuit board to S1 to prevent unwanted rf pickup.

Today's equipment builder soon finds out that locating parts can be a tough problem. Fortunately, we have found a distributor who will furnish all the parts. With the exception of the chassis, the parts for the Transmatch can be purchased from Barry Electronics.[2]

Some Antenna Ideas

With this Transmatch one should be able to match any random-length antenna to his transmitter. To test the system, we strung up 25 feet (7.62 m) of wire in the ARRL lab (a steel-and-concrete building, first floor). The Transmatch provided the desired 50-ohm impedance on all bands. We didn't get any "60-over-9" reports, but we *did* make contacts.

As to your antenna installation, we suggest running the wire up to the ceiling, around the room, perhaps into the next room, making the antennas as long as possible. If the XYL objects to the wire, use an invisible antenna. Nope, we're not

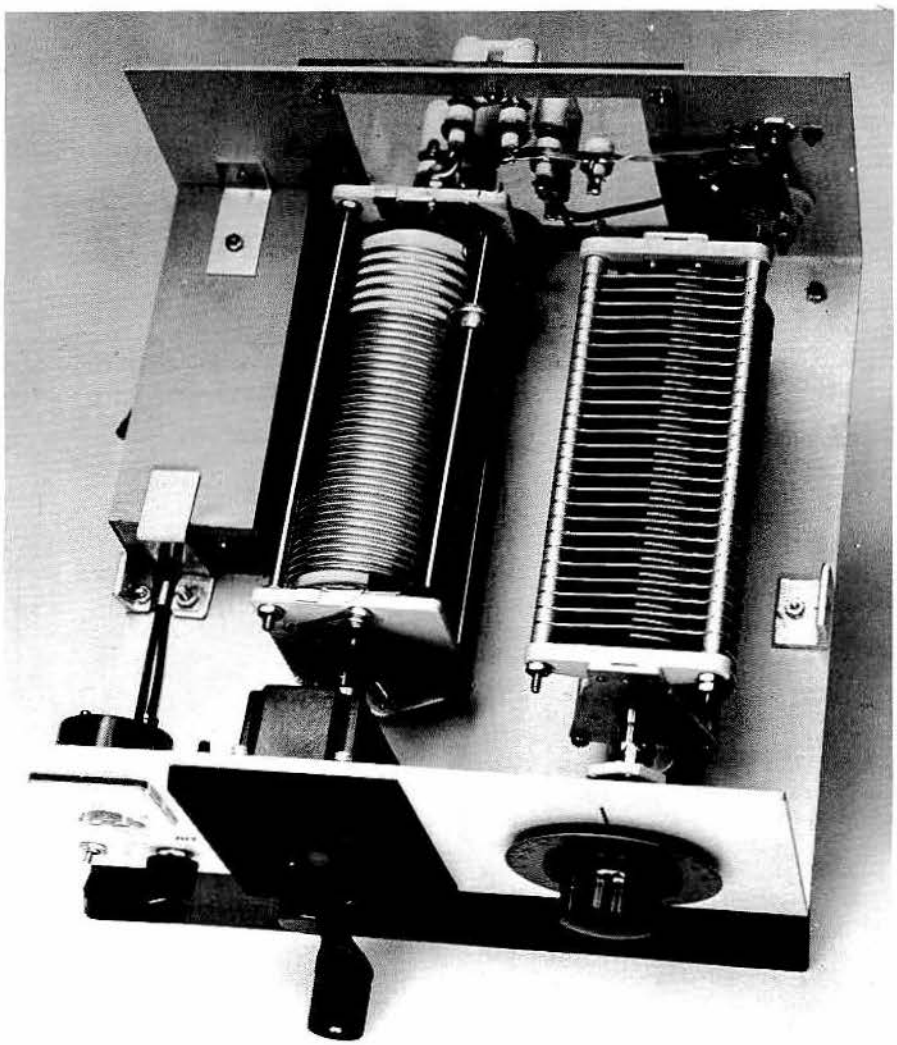

The Monimatch is at the upper left, covered by a metal enclosure. Connections from the roller inductor and the variable capacitor to the terminals on the jacks are made with thin strips of copper, although no. 12 or 14 wire can be used instead. The two antenna terminals are at the rear right. The top terminal is for use with a coax-fed antenna, if desired.

joking! You can make the antenna from no. 26 or 28 wire, which will be practically invisible. Also, you can conceal the wire behind molding. Be sure to insulate the wire if it runs near any metal. In some cases, it is impossible to get the wire outside. However, if you have a screen in one of your windows, terminate the end of the antenna at the screen. The screen *is* outside and it will help the system radiate. While it may be difficult to install, the antenna length to shoot for is approximately 120 to 130 feet (36.58 to 39.62 m) because this is a good length for multiband operation.

If you cannot put an antenna on the apartment roof, there is still a trick or two for having an outside antenna. You can drop a wire out the window and let it hang down. How long the wire should be will depend on how high up you are. You can make the wire long enough to reach nearly to the earth, but high enough to be beyond the reach of passersby. *Safety first,* always! There is no electrical law that states that a vertical must be fed at the bottom. Just connect the end of the wire to your Transmatch and tune up the system. You can use small-diameter wire. Use a lead sinker on the end of the wire and possibly imbed the sinker in a small sponge-rubber ball. (That way, you won't break your neighbor's window.)

If there is a support to which you can attach the far end of the antenna you can use the invisible-wire trick. Use rubber bands for insulators. Erect no. 26 or 28 wire. Don't be too discouraged if the wire gets broken by passing birds!

We know one ham who lived in a basement flat. He ran a wire through the wall to the bottom of a rain gutter, tuned up the system, and managed to work DXCC. (Safety first, again. The downspout should be beyond the reach of human beings!) The general idea is to use ingenuity. With a Transmatch you never can tell *what* will prove to be a useful antenna.

How to Tune Up

Using the Transmatch is not complicated. Although it takes some time to find the correct combination of settings, once determined, they can be logged for later reference. Use a short length of 50-ohm coax to connect the Transmatch to the transmitter. Attach the antenna to the Transmatch. Tune up your transmitter on the desired band, making sure that the final amplifier is resonated, but with the power output reduced. With the Monimatch in the forward-reading position, set the sensitivity control for a full-scale reading. You may have to increase the output of the transmitter to get full deflection, but be sure to keep the final amplifier tank in resonance. Switch the meter to the reflected position, and then adjust L1 and C1, until you get the lowest indication of reflected power. It should be possible to get the meter to read zero. When you have a zero reading in the reflected position, versus full scale in the forward setting, the Transmatch is correctly adjusted, and the SWR is 1. You may have to change the circuit to one of the other configurations in order to get a match, but one combination should work. Once you have the Transmatch set properly, you can then adjust the transmitter to its rated power input. One other point: It isn't always possible to get a good ground connection in an apartment. Therefore, a connection to a cold-water pipe or earth ground should be used. This material was originally presented in *QST* by Lewis G. McCoy. W1ICP.

References

[1]McCoy, "An Etched-Circuit Monimatch for Checking Your Antenna System," *QST,* October 1969. (See Chapter 5.)

[2]Barry Electronics, 512 Broadway, New York, NY 10012.

A 40-Meter DDRR Antenna

This antenna consists of a 1/4-wavelength element grounded at one end and wound into a single-turn coil, a few conductor diameters above the ground (see Fig. 26).

Shortly after the author's article on a practical DDRR Antenna appeared,[1] a number of inquiries were received regarding low-frequency versions of this antenna for operation at ground level. After a little experimenting, the author came up with this version of a 40-meter DDRR which works quite well. In early tests very fine QSOs were held with stations as far away as Phoenix, while the antenna was located inside the garage and surrounded by myriad metallic objects. When the antenna was relocated to the backyard, marked improvement was noted, even though this antenna site was marred by a sharp rise of 4 feet (1.22 m) in ground elevation, plus close proximity to house wiring and power lines. In spite of these obstacles solid contact was easily achieved with stations up and down the West Coast. Encouraged by these results, we moved the antenna to a rooftop location which put it well in the clear insofar as metallic objects above the groundplane were concerned. In this location, the DDRR really proved its worth. In spite of its low profile, a little over 1 foot (0.31 m), and its very small span, a few inches over 9 feet (2.74 m), it was more than adequate when competing with any signal on the band. The obvious conclusion from my experiments is that the 40-Meter DDRR is the apartment-dweller's dream. It is principally for that group that this article is prepared. Other interested amateurs might be those who are limited, as this author is, by too much house on too little real estate; or those who for other reasons cannot cope with high towers, masts and guy wires.

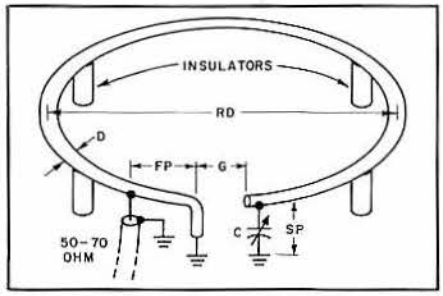

Fig. 26
RD = 0.078 λ (28°)
SP = 0.11D (2.5°)
FP = 0.25 h (See Note 1)
C = (See Note 2)
D = (See Note 3)
G = (See Table 4)

Notes: (1) Actual dimension must be found experimentally. (2) Value to resonate the antenna to the operating freq. (3) d ranges upward from 1/2" (13 mm). The larger "d" is the higher efficiency is. Use largest practical size, e.g., 1/2" (13 mm) for 10 meters, 5" (127 mm) or 6" (152 mm) for 80 or 160 meters.

Before this writer's enthusiasm sends you out to rip down your inverted V or to dismantle your beam, remember this: The DDRR, for all of its capabilities, will not supplant a full-size single-frequency antenna which is properly erected over clear terrain. What it will do is provide an

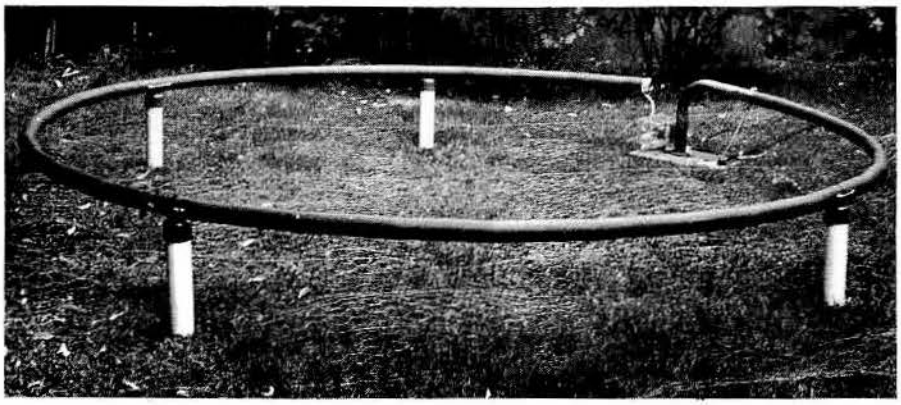

The chicken-wire groundplane is evident in the background. The base plate can be seen at lower right. Note the relative positions of the 52-ohm coaxial feed at the left end of the plate, the flange on the foot of the post, and the tuning unit at the right-hand end of the plate.

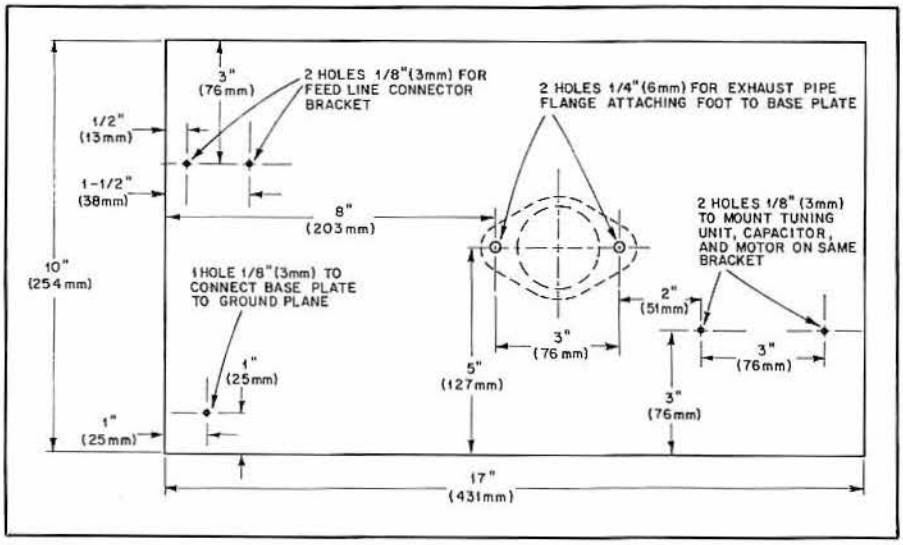

Fig. 27 — Drawing of the base plate which can be made from either steel or aluminum, as described in the text.

Table 4

Dimensions for 1/4 Wavelength DDRR Elements

Band (Meters)	*160*	*80*	*40*	*20*	*15*	*10*	*6*	*2*
Feed Point (FP)*	12"	6"	6"	2"	1.5"	3"	1"	1/2"
Gap (G)	16"	7"	5"	3"	2.5"	2"	1.5"	1"
Capacitor, pF (C)	150	100	70	35	15	15	10	5
Spacing (Height) (SP)	48"	24"	11"	6"	4 3/4"	3"	1 1/2"	1"
Tubing Diameter (D)	5"	4"	2"	1"	3/4"	3/4"	1/2"	1/4"
Ring Diameter (RD)	36'	18'	9'	4.5'	3'4"	2'4"	16 1/4"	6"

*See Fig. 26 for explanation of designations.

Feet X 0.3048 = m.

Inches X 25.4 = mm.

antenna which will enable communications of respectable quality, where heretofore it has been impossible because of inadequate space to erect a 40-meter antenna.

Some consideration should also be given to the fact that the high-Q nature of the DDRR and its resultant narrow-band characteristics serve to reduce the noise level. Boyer[2,3] reports that in the initial experiments it was found that DX stations which could copy signals from either a vertical or a DDRR could only be heard on the DDRR due to the reduction in background noise. So if you have a noisy location, it might be to your benefit to try the DDRR, regardless of what antenna you are presently using.

Constructing the 40-Meter DDRR

In this application, 2-inch (51 mm) diameter automobile exhaust pipe was used as the radiating element. The local muffler shop not only supplied the material, but also undertook to bend it to

The braided lead across the flared joint is to assure electrical continuity. The screws used are self-tapping sheet-metal screws. The top end of the insulator (2-inch [51 mm] diameter PVC pipe) is a standard PVC pipe cap; the bottom is closed off with a cap from an aerosol can (2-inch [51 mm] ID).

specifications. This was an obvious course since the material and the power bender were right at hand.

The dimensions for 40 meters are:

Ring — 9 foot (2.74 m) diameter, center to center.

Height — 12 inches (0.31 m) from ground plant to element center.

Gap — 6 inches (152 mm) from upright post center to open end of ring.

In forming the ring to these dimensions, four 10-foot (3.05 m) lengths of tubing were used. A 10-degree bend was made at 9-inch (229 mm) intervals in three of the lengths. The fourth length was similarly treated, except for the last 18 inches (0.46 m) which were bent at right angles to form the upright leg of the ring. One end of each section was flared so that the sections could be coupled together by slipping the end of one into the flare of its mate.

The required flares are easily made at the muffler shop with the aid of the forming tools. Another task which can best be completed at the shop is to weld a flange onto the end of the upright leg. This flange is to facilitate attaching the leg to the mounting plate which provides a chassis for the tuning mechanism and the coaxial-feed coupler. After bending and flaring is complete, the ring is assembled and minor adjustments made to bring it into round and to the proper dimensions. This can best be done by drawing a circle on the floor with chalk and fitting the ring inside the circle. The circle must be slightly larger than the center-to-center diameter so that the reference line can be seen easily. For example, with two-inch (51-mm) tubing the actual diameter of the reference circle must be 9 feet, 2 inches (2.79 m). When you

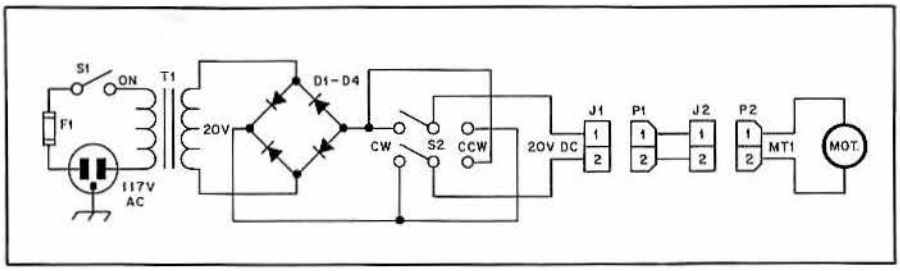

Fig. 28 — Circuit diagram of the power supply and control motor.
D1 through D4 — 1 A, 50 PRV, or equiv.
F1 — Fuse, 1 A.
J1, J2 — Two-terminal jack.
MT1 — Motor (see text).
P1, P2 — Two-terminal plug.
S1 — Spst.
S2 — Dpdt, center off.
T1 — Transformer (see text).

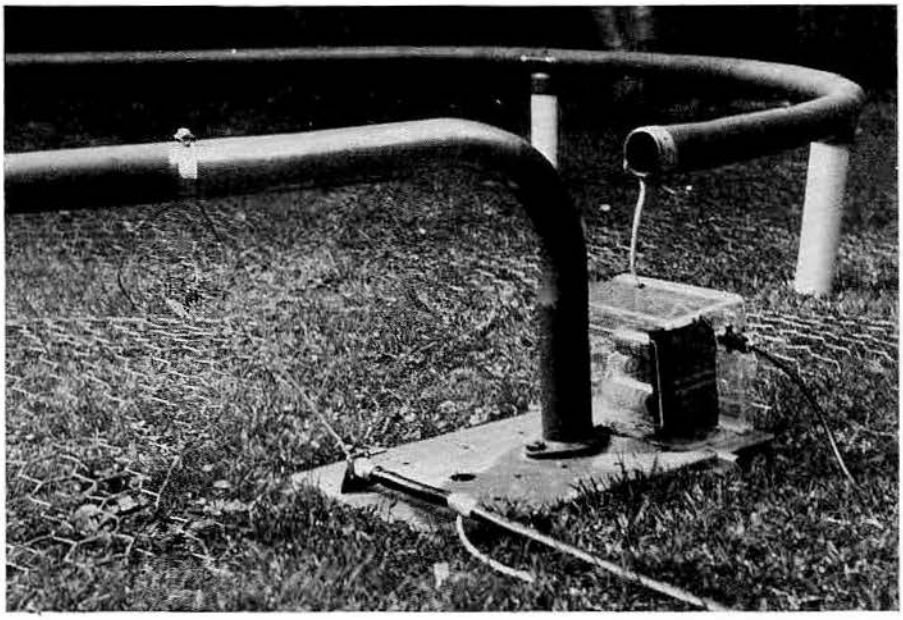

Clamps used to connect the feed line and the open end to the capacitor are standard hose clamps. The heavy black lead, center to lower right, is the 52-ohm feed line. The smaller line coming from the plastic housing is the motor control line.

have a satisfactory fit between the tubing ring and the chalk ring, drill a 1/4-inch (6-mm) hole through each of the joints to accept a 1/4-inch bolt. These bolts will clamp the sections together. Also, they can be used to attach the insulators which support the ring at a fixed height above the groundplane.

Making and Attaching the Insulators

Insulators for the antenna were made from 11-inch (279-mm) lengths of 2-inch (51-mm) PVC pipe inserted into a standard cap of the same material. The PVC caps are first drilled through the center to accept the 1/4-inch (6-mm) bolt previously installed at the joints. The caps are then slipped onto the bolts and nuts are installed and tightened to secure the caps in place. The 11-inch length of pipe, when inserted into the cap and pressed firmly until it touches bottom, results in a total insulator length of 12 inches (0.31 m). Four insulators are required: one at each of the joints and one near the open end of the ring for support. It is wise to locate this insulator as far back from the end of the ring as possible because of the increasing high rf voltage that develops as the end of the ring is approached.[4] As a final measure, the bottom ends of the insulators were sealed to prevent moisture from forming on the inside surfaces. Standard PVC caps could be used here, but we found that plastic caps from 15-ounce aerosol cans fit well.

Making the Mounting Plate

The mounting plate is required to provide good mechanical and electrical connections for the grounded leg of the radiator, the coaxial feed-line connection, and the tuning mechanism. If you are using aluminum tubing, you should use an aluminum plate, and for steel tubing, a steel plate to lessen corrosion from the contacting of dissimilar metals. Dimensions for the plate are shown in Fig. 27. The important consideration here is that good, solid mechanical and electrical connections are made between the ground side at the coaxial connector, the ring base, and the tuning capacitor.

The Tuning Unit

We found that the 9-foot (2.74 m) ring resonated easily with approximately 20 pF of capacitance between the high end of the ring and the base plate or ground. A 35-pF double-spaced variable from the junk box was pressed into service here (Cardwell NG-35-DS). Any variable which will tune the system to resonance and which will not arc under full power should be satisfactory. Remember, the rf voltage at the high impedance end of this antenna can reach 20 to 30 kV with high power, so if you are using the maximum legal limit, you would do well to consider using a vacuum variable capacitor. Since we limited our power to 500 watts PEP, the double-spaced Cardwell unit was satisfactory. To provide for full band coverage, the capacitor was coupled to a reversible, slow-speed motor which enabled the antenna to be remotely tuned from the operating position. An indicated SWR of 1.1 to 1 was easily achieved over the entire 40-meter band. The motor used was a surplus item made by Globe Industries of Dayton, OH.[5] At 20 volts dc the shaft of this motor turns at about 1 rpm which is ideal for DDRR tuning. The gears used were surplus items. If you cannot obtain gears, string and pulley drive will do almost as well, or you can mount both the motor and the capacitor in line and use direct coupling. Of course, if you operate on a fixed frequency or within a 40- to 50-kHz segment of the band, you can dispense with the motor entirely and simply tune the capacitor manually. In any case, the tuning unit must be protected from the weather. We used a plastic refigerator box to house the tuning capacitor and its drive motor.

Fig. 28 shows the electrical connection for the motor. A small train transformer or power supply for toy slot-cars will work admirably as a tuning motor power source. Standard ac zip cord was used for the connection between the control unit and the motor.

Electrical Connections and the Groundplane

The connection between the open end of the ring and the tuning capacitor is made with no. 12 wire or larger. On the end of the base plate opposite the tuning unit, and directly under the ring about 8 inches (203 mm) from the grounded post, install a bracket for a coaxial connector. The connector should be oriented so that the feed line will lead away from the ring at close to 90 degrees. Install a clamp on the ring directly above the coaxial connector. Connect a lead of no. 12 or larger wire from the coaxial connector to the clamp. This wire must have a certain amount of flexibility to accommodate the movement necessary when adjusting the match. The

matching point must be found by experimentation. It will be affected by the nature and quality of the groundplane over which the antenna is operating. The antenna will function over earth ground; however, in our location we found the electrical ground to be unpredictable. A groundplane surface of chicken wire (laid under the antenna and bonded to the base plate) provided a constant ground reference and improved performance. In a rooftop location sheet metal roofing should provide an excellent groundplane. A poor ground usually results in a matching point for the feed line far out along the circumference of the circle. In our installation a near-perfect match was obtained with the feed line connected to the ring about 12 inches (0.31 m) from the grounded post. During testing, when the antenna was set up on a concrete surface without the groundplane, a match was found when the feed line was connected nearly 7 feet (2.13 m) from the post!

As shown in photos, the compactness of the antenna is readily apparent. The groundplane is made up of three 12-foot (3.66-m) lengths of chicken wire, each 4 feet (1.22 m) wide, which are bonded along the edges at about 6-inch (152-mm) intervals. In our installation the antenna, with the groundplane, could be dismantled in about 30 minutes. If portability is not important, it is best to bond all of the joints in the tubing so that good electrical continuity is assured.

After all construction is completed, the antenna should be given a coat of primer paint to minimize rust. If it suits you, there is no reason why a final coat of enamel could not be applied.

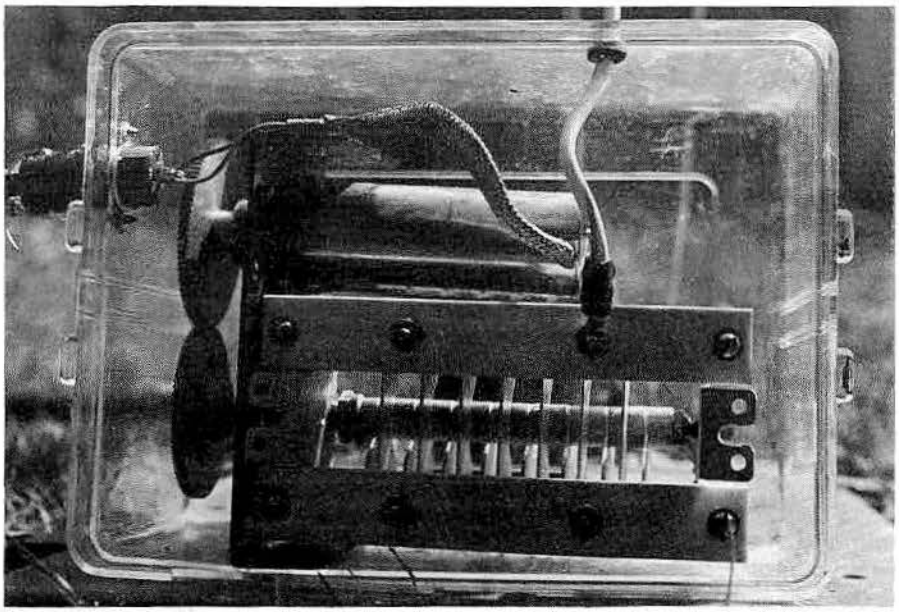

The tuning motor, above the capacitor, couples to the capacitor shaft through the gears at left. Both the motor and the capacitor are mounted on a common bracket which attaches to the base plate by two bolts through the weatherproof housing. The lead passing upward through the grommet connects the stator of the capacitor to the open end of the ring.

Tuning Procedures

Once the mechanical construction is completed, the antenna should be erected in its intended operating location. Coupling to the station may be accomplished with either 52-ohm or 72-ohm coaxial cable. Tune and load the transmitter as with any antenna. While observing an SWR meter in the line, operate the tuning motor. Indication of resonance is the noticeable decrease in indicated reflected power. At this point, note the loading of the transmitter; it will probably increase markedly as antenna resonance is approached. Retune the transmitter and move the feed-point tap on the antenna for a further reduction in indicated reflected power. There is interaction between the movement at the feed tap and the resonance point; therefore, it will be necessary to operate the tuning motor each time the tap is adjusted until the lowest SWR is achieved. Don't settle for anything less than 1.1 to 1. With a good ground and proper tuning and matching, this ratio can be achieved and maintained over the entire band. Once the proper feed point has been located, the only adjustment necessary when changing frequency is retuning the antenna to resonance by means of the motor. If the antenna is to be fixed tuned, provide an insulated shaft extension of 18 inches (457 mm) or so to the tuning-capacitor shaft for manual adjustment. This not only provides insulation from the high rf voltage but also minimizes body-capacitance effects during the tuning process.

Alternatives

A number of materials other than the steel tubing used here are well suited for the ring element. Standard E.M.T. or electrical conduit would work as well with a slight increase in weight. One advantage to be gained through the use of conduit is the elimination of the flaring operation since standard couplings would serve to connect each segment of the ring to its adjacent member. Another suitable material is copper tubing. This material is superior to either exhaust pipe or conduit in terms of its conductivity characteristics. Another advantage of copper is that it is available in continuous lengths and the joints could be omitted entirely.

The 2-inch (51 mm) dimension is by no means mandatory. Smaller diameter tubing has been used with satisfactory results.[6] In fact, DDRR antennas have been fabricated with wire elements. But, if the element diameter is reduced, the antenna tunes more *sharply*. Some experimenters may wish to go in the other direction and use a larger diameter. The author recommends the use of aluminum downspout with a diameter of about 4 inches (2 mm). This material does not lend itself to bending, however, and the ring must be configured as a regular polygon of eight or more sides. Because of the large number of joints involved, welding is about the only practical means of joining the segments. Unless you are equipped to do this work yourself, the cost of welding might be prohibitive. Anyone who undertakes to make a DDRR antenna of a large element diameter will be rewarded in terms of improved performance.

Performance

Results have been quite encouraging, and it is hoped that more and more hams will equip themselves with the DDRR in the future. The antenna has proved its worth and deserves more investigation by the amateur fraternity than it has been given in the past. No intensive efforts have been made to work DX with the antenna described here: however, a low angle of radiation is conducive to DX, and this antenna demonstrates a low radiation angle. It was found that distant areas, such as the East Coast, are more easily contacted than are stations nearby. All of the results could be attributed to peculiarities of individual stations or skip conditions, but since they are charateristics which can be anticipated with high-efficiency antennas having low radiation angle, we prefer that interpretation. Besides, where else will you find an antenna for 40 meters that is small enough to fit into a corner of the backyard and not protrude above the fence; or for that matter, which could be

mounted on the roof of an apartment building or even a ranch-type house and not be visible from the street?

Nearly everyone who listened to the description of this new antenna was enthusiastic. The author hopes to hear many hams on the air working with the DDRR in the near future. This material was originally presented in *QST* by W. E. English, W6WYQ.

Parts List

4 — 10-ft (3.05 m) lengths of 2-in. (51 mm) tubing, exhaust pipe, conduit or copper tubing.
1 — base plate 7-1/2 X 19 X 1/8 inches (191 X 482 X 3 mm), steel, aluminum, or copper to match tubing.
4 — PVC pipe caps for 2-inch (51 mm) pipe.
4 feet (1.22 m) of 2-inch PVC pipe.
2 clamps for 2-inch tubing.
4 — 1/4 X 4-inch (6 X 102 mm) bolts with nuts.
1 reversible motor with 1-rpm shaft output.
1 wide spaced variable capacitor. 5 to 35 pF (Millen 16550 or equiv.).
1 coaxial connector SO-239.
2 sets 2-connector plug and socket for motor control.
36 feet (10.97 m) of 4-foot (1.22 m) chicken wire or equivalent.
1 flange to attach tube to base plate.
2 — 1/2 X 1-inch (13 X 25 mm) bolts with nuts (flange mounting).
8 — 3-inch (76 mm) bonding strips no. 8 braided wire.
4 plugs 2-inch (51 mm) ID for insulator bases.

References

Hicks, "The DDRR Antenna: A New Approach to Compact Antenna Design," *CQ*, June 1964.
Horn, "The Half Wavelength DDRR Antenna," *CQ*, September 1967.
The Radio Amateur's Handbook, 46th ed., The American Radio Relay League.

Notes

[1]English, "A Practical DDRR Antenna," *73*, June 1970.
[2]Boyer, U.S. Patent Nos. RD 26196, RE 3,151,328 (All rights assigned to the Northrop Corporation.)
[3]Boyer, "Hula-Hoop Antennas: A Coming Trend?" *Electronics*, January 11, 1963.
[4]Editor's Note: Because of the danger of rf burns, in the event of accidental contact with the antenna, precautions should be taken to prevent random access to the completed installation.
[5]Globe C-5A-1106 (available from Lectronic Research Labs Inc., 75 Arch St., Philadelphia, PA 19106).
[6]See footnote 1.

Novi-Loop

A medium-size roll of wire, some insulators and a day of good antenna "puttin' up" weather can net you a Novi Loop. What will it do for you? Well, follow these instructions and get set to work 40-meter DX. Nuff said!

One of the sad facts of life for many beginners is the matter of poor antenna performance. Many enthusiastic Novices have fallen behind in their efforts to work DX because of bitter disappointment caused by poor performance in the antenna department. All too often it is suggested that a simple end-fed hunk of wire is ample for all-around Novice band operation, or that a dipole will suffice for most Novice operation. Sure, almost any kind of radiator that can be tuned to the operating frequency and marched to the impedance of the feed line and transmitter will enable the operator of a low-power station to make some contacts from time to time. It depends on how high the system is above ground, how free and clear it is of surrounding objects that can detune the radiator and absorb the energy radiated from it, and upon the condition of the band at a given time. It should stand as a firm rule, then, that any amateur who wants good results should erect the best antenna system he can, consistent with available space, finances and structural practicality. It is possible to advance beyond the plateau of simple dipoles and random-length wires in the quest for better performance, and without going to the expense and effort of erecting large directional beams such as the cubical quad or Yagi.

What will be described here can be applied to any of the high-frequency amateur bands. However, the example given relates to only the 40-meter Novice band. The antenna is a full-wave loop of wire, mounted through necessity at W1FB in a rectangular format, and matched with a simple quarter-wavelength coaxial transformer. It has given excellent performance in DX work and for making "solid" stateside contacts. Total cost for the antenna system (wire, matching transformer and insulators) is under $12, exclusive of the feed line used to connect the antenna to the rig.

Antenna Features

Full-wave, closed-loop antennas are broadband, low-Q devices. This is a handy feature because it permits the operator to move his transmitter frequency within a particular band without need to compensate for an increase in standing-wave ratio (SWR) which might otherwise occur if other types of antennas were used. (The higher the Q of an antenna, the narrower its bandwidth, even though an SWR of 1 can be obtained at some frequency within the band for which it is built.) The foregoing rules out the need for a Transmatch with the loop antenna, provided the feed method recommended here is applied.

Another interesting feature of this kind of antenna is the theoretical gain of approximately 2 dB it exhibits over a half-wave dipole. The angle of radiation from a properly erected full-wave loop is considered to be lower than that of a dipole when both are less than one-half wavelength above ground. This feature suggests the superiority of the loop in situations where significant height above ground is not a practical goal for the chap wishing to put up a 40-meter antenna.

A full-wavelength closed loop need not be square. It can be trapezoidal, rectangular, circular, or some distorted configuration in between those shapes. For best results, however, the builder should attempt to make the loop as square as possible. The more rectangular the shape, the greater the cancellation of energy in the system, and the less effective it will be. The effect is similar to that of a dipole whose effectiveness becomes impaired as the ends of the dipole are brought closer and closer together. The practical limit can be seen in the "inverted-V" antenna, where a 90-degree apex angle between the legs is the minimum value used. Angles that are less than 90 degrees cause serious cancellation of the rf energy.

The loop can be fed in the center of one of the vertical sides if vertical polarization is desired. For horizontal polarization it is necessary to feed either of the horizontal sides at the center. At the time of this writing there have been no data compiled to provide a comparison between the performance, vertical versus horizontal. Such an experiment could be interesting (and possibly productive) for the Novice.

Erecting the Antenna

Optimum directivity occurs at right angles to the plane of the loop, or in more

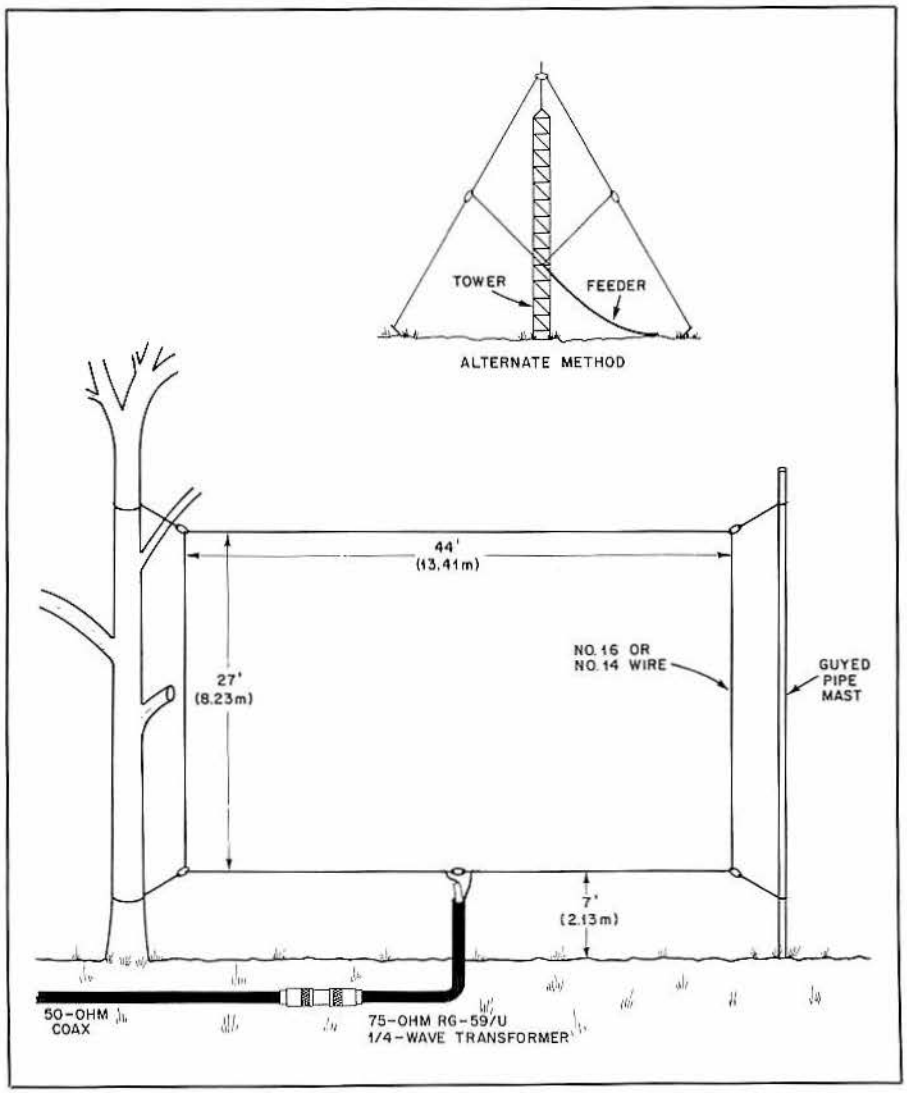

Fig. 29 — Details of the full-wave loop. The dimensions given are for operation at the low end of 40 meters (7050 kHz). The height above ground was 7 feet (2.13 m) in this instance, though improved performance should result if the builder can install the loop higher above ground without sacrificing length on the vertical sides. The inset illustrates how a single supporting structure can be used to hold the loop in a diamond-shaped configuration. Feeding the diamond at the lower tip provides radiation in the horizontal plane. Feeding the system at either side will result in vertical polarization of the radiated signal.

simple terms, broadside from the loop. Therefore, one should try to hang the system from available supports which will enable the antenna to radiate the maximum amount in some favored direction. The bidirectional pattern is maximized NE and SW at the writer's QTH. This gives good results in working Europeans and the stations "down under." Excellent signal reports have been obtained off the sides of the loop when working within the USA.

Just how the wire is erected will depend on what is available in one's yard. Trees are always handy for supporting antennas, and in many instances the house is high enough to be included in the lineup of solid objects from which to hang a radiator. If only one supporting structure is available it should be a simple matter to put up an A frame or pipe mast to use as a remaining support. (Also, tower owners see Fig. 29 inset.)

The overall length of the wire used in a loop is determined from the formula

$$\frac{1005}{f\ (MHz).}$$

Hence, for operation at 7125 kHz the overall wire length will be 141 feet (42.98 m). The matching transformer, an electrical quarter wavelength of 75-ohm coax cable, can be computed by dividing 234 by the operating frequency in MHz, then multiplying that number by the velocity factor of the cable being used. Thus, for operation at 7125 kHz

$$\frac{234}{7.125\ (MHz)} = 32.84 \text{ feet}$$

If coax with solid polyethylene insulation is used, a velocity factor of 0.66 must be employed. Foam-polyethylene coax has a velocity factor of 0.80. Assuming we are to use the solid dielectric coax, RG-59/U, the length of the matching transformer becomes 32.84 (feet) × 0.66 = 21.67 feet, or 21 feet 8 inches (6.605 m). The transformer will convert the 100-ohm feed-point impedance of the loop to 50 ohms, a convenient value for connecting the system to the transmitter. The loop described here was measured with the K1TD Macromatcher[1] and found to exhibit an impedance of 110 ohms. Some inductive reactance was indicated. By removing 1 foot (0.31 m) of wire from the overall loop the reactance dropped to zero, though the antenna loaded up fine prior to the final trimming. The feed impedance at 21 MHz was also 110 ohms, but considerable inductive reactance was observed. Most certainly one could use the antenna on 15 meters with reasonable success, despite the SWR which might be present.

Results

During two weeks of testing the loop gave an excellent account of itself. It was compared with the writer's two-element short beam for 40 meters, and the results indicated that the loop was better than the beam on some occasions. At other times the beam provided better performance, or was at least equal to the loop. The differences noted were the result of band conditions and the time of day. High-angle signals can cause misleading results when comparing antennas for hf-band use. More meaningful tests can be made on ground-wave contacts, however, and several checks made between the loop and the beam indicated that radiation at right angles to the plane of the loop compared closely with that from the front of the beam. The beam is rotatable and installed 40 feet (12.19 m) above ground.

With 150 watts dc input to the transmitter PA, and operating at the low end of 40 meters (loop was cut for 7050 kHz), the first night of operation resulted in the logging of three Russian stations, two Polish ones, two Yugoslavians, one Italian station and two English ones. The lowest report was RST 549. The highest report was RST 599. Generally speaking, the loop has outperformed the beam during most long-haul contacts. Though no effort has yet been made to work South American stations (off the side of the loop), they have been heard loud and clear, as have some VK stations via long path at approximately 2300 UTC.

It is quite likely that the Novice who chooses to erect his own Novi-Loop will have a commanding signal on 40 meters. If backyard space permits, it should be a worthwhile venture. Don't forget, the formulas and guidelines given here are applicable to the other hf Novice bands as well. This material was originally presented in *QST* by Doug DeMaw, W1FB.

[1]Hall, "The Macromatcher," *QST*, January 1972.

Chapter 5

Antenna Theory and Test Methods

In order to obtain top performance from a given style of amateur antenna, it is important to understand the basic principles of operation. Additionally, some test procedures are necessary if one is to ensure that his or her antenna is functioning at its best. This chapter contains assorted data on antenna theory, plus a number of common-sense test methods.

These reprints of popular *QST* articles were chosen for all amateurs, regardless of their technical-aptitude levels. There's something to honor in the phrase, "Learn by doing." This chapter will help to make that philosophy a reality.

Quad vs. Triband Yagi

The controversy about quads working better than Yagis, or vice versa, may never end. But, we'll bet our newest roll of RG-8/U that you'll find some interesting reading on the subject in this report.

While stationed in Japan, a sort of DX crossroads of the world, this writer had the opportunity to observe, firsthand, the excellent performance of the cubical quad in competition with the Yagi, dipoles and an assortment of other antenna systems. In pursuing this undertaking certain steps were necessary to insure than any conclusions made would be meaningful. With this in mind a play emerged.

Objectives

In the many articles written on the cubical quad, it is noteworthy that only on a few occasions have the authors been privileged to compare the quad with other types of antennas on a real-time basis, and from the same operating location. Furthermore, when such comparisons were made, the authors generally compared against some type of monoband antenna system. A casual scanning of the 10-, 15- and 20-meter phone bands would lead one to conclude that the triband Yagi enjoys a rather high position of popularity among the antennas in general use. This being the case, it appeared that a worthwhile contribution to the data already available on the Yagi and quad might be made by conducting a series of controlled comparative tests, employing the triband Yagi and the quad. The test objectives were then defined: to compare various configurations of a cubical quad antenna with a representative commercial triband Yagi; such tests to be conducted over short, medium, and long transmission paths, and to arrive at conclusions regarding the relative merits of each antenna.

Table 1

	Mod. 1	*Mod. 2*	*Mod. 3*	*Mod. 4*
Reflector Element	72'3"	70'4"	72'5"	72'5"
Driven Element	69'	70'4"	70'5"	70'5"
Director Element	—	—	—	69'1"
Spacing "A"	7'6-1/2"	8'5"	13'4"	13'
Spacing "B"	—	—	—	13'
Stub	20-30"	34-38"	—	—

Feet X 0.3048 = m.
Inches X 25.4 = mm.

Test Plan and Procedure

Every effort was made to conduct the tests in a manner which would lessen the possibility of compromising the techniques employed by either the writer or participating stations:

1) The test to be performed by establishing communications with Amateur Radio stations located throughout the world on a random and scheduled basis.

2) Amateur Radio stations volunteering to assist in this effort to be briefed on conduct of test and data desired.

3) A voice ssb transmission to be made to the participating station, identifying the first antenna used as antenna "A."

4) The voice transmission to be followed immediately by an unmodulated carrier for a period of approximately 5 seconds.

5) The antennas would be switched, and a voice transmission made identifying the antenna as "B," and the procedures above repeated.

6) Participating stations will note signal strength related to each antenna, and provide a numerical value as observed on his S meter or other indicating device. These values to be logged, and the test reinitiated with another volunteer station.

Equipment Preparation

1) Antenna heights to be as nearly identical as possible.

2) Center of antenna horizontal lobe patterns to be as nearly identical as possible when pointing the antennas toward a participating station.

3) Resonant frequency of each antenna to be matched as closely as possible.

4) Transmission lines to be matched to antennas and transmitter loading to be as nearly identical as possible with each antenna.

5) Instantaneous transfer of antennas.

6) Relative power and SWR to be monitored continuously.

7) Prior to and after each data gathering session, equipment parameters will be verified. If a significant deviation in any parameter is noted, data collected will be discarded.

Antenna performance conclusions to be based on an analysis of data derived from a minimum of 50 unmodulated-carrier observations with each antenna configuration, and supplemented with data gathered during conventional ssb QSOs.

Table 2

	Mod. 1	*Mod. 2*	*Mod. 3*	*Mod. 4*
Total Observations	50	60	60	52
Less than 2100 miles	12	2	3	3
2100 to 4800 miles	33	31	33	32
Greater than 4800 miles	5	27	24	17
Signal Difference				
More than 1 S unit better	—	—	—	—
Less than 1 S unit better	—	—	7	9
No discernible difference	1	5	51	43
Less than 1 S unit poorer	27	46	2	—
More than 1 S unit poorer	22	9	—	—

Antenna Selection

This writer had been using a four-element commercial triband Yagi (boom length 24 feet [7.32 m], and 55 feet [16.76 m] above ground) for approximately 1-1/2 years, so the properties of this antenna were fairly well established. Furthermore, in on-the-air comparisons with competitive models of triband Yagis in use by other U.S. amateurs operating from the Tokyo area, the antenna appeared representative of commercial triband antennas in general use by the amateur community. Therefore, the Yagi in use at the author's station was selected as the reference antenna.

Text material concerning quad antennas, available to the author in Japan, was reviewed. It became evident that there are almost as many variations in quad design as there are writers on the subject. After much deliberation, and many discussions with amateurs throughout the world, the decision was made to test three models of the quad (a fourth model was tested as will be noted later). Since the physical characteristics of the quad are fairly standard, only the dimensions of the elements and the spacing between them was considered. The dimensions for the three models tested were obtained from a Japanese manufacturer of cubical quads, from Orr's book, *All About Cubical Quad Antennas,*[1] and from Dr., J. E. Lindsay, Jr., WØHJ.[2]

Preliminary Testing

Several days were spent "dry running" the test plan to validate the concept, and to smooth out the operating procedures and techniques. Of particular concern was the possible time required to make a valid data-gathering observation. If data were to be reasonably accurate, the transmission path had to be stable, and the signal-strength observations must be taken on each antenna during a short period of time. The dry runs were valuable in this respect.

A problem became evident during the first day of testing. It appears that those of us who speak and understand English do not always convey the same message when using the same words. As a result it was necessary to modify the verbal format, utilizing simple sentences and placing them in a logical sequence.

It also became apparent that the test could not be conducted under all transmission-path conditions; that even under ideal conditions several observations were often necessary before a conclusive report could be compiled. It was decided to conduct the tests only on 20 meters. The operating time available to the writer favored openings on 20 meters to Europe via the long path, and to Australia, the U.S. and various islands in the Pacific. It was also decided to orient the test antennas so that the topography and obstructions seen by each antenna would be essentially the same. (Physical separation between the two antennas was in the order of one wavelength.)

Testing

Dimensions of the first quad model selected were furnished by a Japanese manufacturer of cubical-quad antennas. (see Table 1). The antenna was assembled, utilizing commercially manufactured heavy-duty hardware and fiberglass spreaders. It was tuned to a center frequency of 14,200 kHz. Testing of the first model began in November 1967 and continued for one month. The results for this period are given in Table 2.

In mid-December 1967 the first quad was replaced by a model constructed according to the formula and dimensions given in Orr's book. The results obtained with model 2 are contained in Table 2.

Construction of the third model (with wider element spacing) was carried out next. Two matching systems (Gamma and Q-section) were experimented with on this antenna. A satisfactory match could be had with either system. However, the Q-section was used for the test because it was the technique used with the previous two quad models (SWR with each antenna was never more than 1.3:1 with a difference between antennas no greater than 0.1). The results conducted with this model were most enlightening, as shown in Table 2. The model antenna was also used extensively during the first weekend of the 1968 ARRL DX Contest. Though these contacts were not used in tabulating test samplings, it is interesting to observe that openings to the U.S. (using the quad) lasted 15 to 30 minutes longer on each end of the period than with the Yagi. It is assumed that this phenomenon would also apply to each of the other quad models.

The fourth quad tested was a 3-element wide-spaced model constructed according to more dimensions furnished by WØHJ. The results of the samplings were somewhat disappointing and are given in Table 2. (Frankly, the author felt that the 3-element quad would show a substantial improvement over the Yagi in every case.) The 3-element model did appear to have a better front-to-back and front-to-side ratio than either the Yagi or the other quad models. One positive comment: The 3-element model is a monster to assemble and put up! In the author's opinion the difference in performance isn't worth the small improvement. Perhaps, on the other hand, if one accepts the 2-element model as

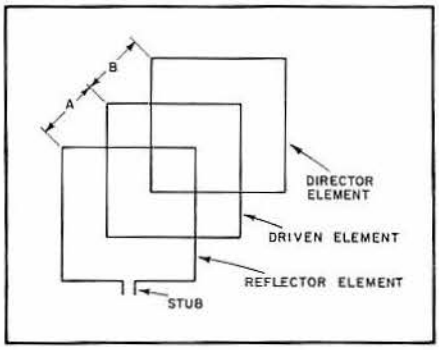

Fig. 1 — Element spacing information for Table 1.

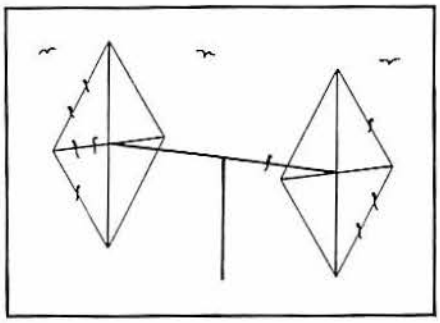

Fig. 2 — CLOSE SPACING IS FOR THE BIRDS!

the departure point between a simple mechanical structure and a major project, a 4-element model might be more worth the effort. However, this is purely conjecture on the part of the author.

Summary

The antenna tests indicate that:

1) One can expect to achieve the same or better results with a 2-element quad of proper dimensions than with a 3- or 4-element triband Yagi.

2) A wide-spaced quad will perform substantially better than a close-spaced quad.

3) Dollar for dollar, the quad appears to be a better investment than a Yagi.

Acknowledgements

The writer wishes to thank all of the amateurs who participated in the series of tests, particularly the VK gang, who night after night tolerated the request for observations. The support couldn't have been better, and on many occasions, upon completing a check with a particular station, several other stations would call to give their observations (which were taken during the same transmission test). This material was originally presented in *QST* by Col John H. Parrott, Jr., W4FRU.

References

[1]Orr, *All About Cubical-Quad Antennas*, Radio Publications, Wilton, CT 06897.

[2]Dimensions later published: Lindsay, "Quads and Yagis," *QST*, May 1968. (See chapter 3).

High Versus Low Antennas Performance Tests Using Identical Arrays

This section compares the performances of identical antennas mounted side-by-side at different heights, and produces some experimental evidence to support the practical importance of antenna height for most types of Amateur Radio communication.

"The higher the better" is the traditional rule of thumb for ham radio antennas. Few amateurs would disagree with this axiom, and most experienced antenna builders can recall how much better they got out after "raising the beam another 15 feet (4.57 m)." However, few empirical studies of the effect of antenna height on signal strength have been published in amateur circles.

This is unforunate, since several amateurs have studied the question methodically, including Dr. J. E. Lindsay, who has now published his definitive treatise on quads and Yagis[1] but not his excellent work in this area. And while both *The ARRL Antenna Book* and Orr's *Beam Antenna Handbook*[2] discuss the importance of antenna height in theoretical terms, neither reports the results of practical studies in the field.

With this in mind, the author set out to study the effect of height on signal strength at various distances, on several bands, and with various forms of propagation. Only amateur equipment was available for the study, but in other respects, the author strived to keep the methodology as rigorous as possible.

The Method

The author's approach was to erect identical antennas atop two towers of different heights and obtain comparative signal reports — with some safeguards to minimize reporting errors and to assure proper statistical treatment for the resulting data. For the main tests, one tower was 72 feet (21.95 m) high (the practical maximum for the author's residential backyard at the time of the tests), while the other stood 34 feet (10.36 m) high (about the minimum usable height for DX work, according to Orr). The two towers were placed as far apart as possible without trespassing — about 50 feet (15.24 m). With this separation, no interaction was evident on any band.

The two cubical quads used by the author to study the effects of antenna height on performance. The antenna at right is atop a 34-foot (10.36 m) tilt-over mast described by the author in June 1969 *QST*. The quad at left is on a 72-foot (21.95 m) tower.

A pair of 2-element cubical quads were selected for the 10-, 15- and 20-meter experiments. Each had an eight-foot (2.44 m) boom with all elements mounted concentrically on two sets of spreaders, and each antenna was fed with a single feed line (85 feet [25.9 m] of RG-8/U in both cases). This design obviously involves some compromises in element spacing and impedance matching, but both quads developed good SWR curves and front-to-back ratios when tuned. And, more important for our study, whatever compromises existed were essentially the same for both the high and low antennas.

It became apparent during the tests that many amateurs regard cubical quads as exceptional performers at low heights, but (unlike Yagis) not much better if raised higher. This popular impression is contrary to Lindsay's findings, which suggest that quads and Yagis respond quite comparably to changes in their height. Accepting Lindsay's conclusions, we assumed that our findings would be roughly the same if Yagis had been used for the primary experiments.

Table 3

Comparative Performance Data for High and Low Antennas

Band/path	No. reports	No. favoring high antenna	No. favoring low antenna	No. reporting no difference	Mean high-antenna advantage
20/DX	16	16	0	0	2.1 S units
20/U.S.	18	15	0	3	1.4 S units
15/DX	12	12	0	0	1.8 S units
15/U.S.	36	20	0	16	0.9 S units
15/ground-wave	12	12	0	0	2.2 S units
10/DX	8	7	0	1	1 S unit
6/ground-wave	5	5	0	0	2 S units
6/E-skip	10	2	7	1	−1.3 S units
2/ground-wave	16	16	0	0	3.3 S units

The author wanted to determine how well high and low antennas would perform not only on DX work, but on "Stateside" F-layer communications, ground-wave work, and E-skip as well. Thus, separate tabulations were kept for DX reports (i.e., those from stations more than 4000 miles away) and for reports from "Stateside" stations (i.e., F-layer reports over 1500—3000-mile paths) on each frequency band.[3] The author was careful to avoid seeking reports during anything that resembled an E-skip opening on 10, 15, and 20 meters, in the interest of studying E skip vs. antenna height separately on 6 meters.

To study the effect of height on vhf groundwave signals, the author replaced the cubical quads on the two towers with two pairs of seven-element 2-meter Yagis, each fed in phase with ratio-dipole driven elements. A move to a new home prevented the use of the same two towers for 6-meter experiments, but the author later set up two 3-element 6-meter Yagis — one atop a new 90-foot (27.43 m) tower, and the other on a 42-footer (12.8 m) — to continue the study.

On each band, the tests were conducted on ssb (except on 2 meters, where a-m was used), with an audio tone serving as a reference signal. The author switched between the high and low antennas repeatedly on each test, in an effort to counteract the effects of QSB.

This test procedure does introduce some sources of error, including the variability of hams' skills in observing the results, and the lack of receiver S-meter standardization. To cope with this kind of sampling fluctuation, the author obtained a number of reports on each band and then used t-distribution statistical methodology to evaluate the resulting data. Even with these efforts to make the study as rigorous as possible, however, the author makes no claim to finality for the results obtained. The findings on each band did prove to be statistically significant (at the 0.05 level of significance or better), but you don't "prove" things or arrive at exact parameters this way. The only claim the author makes for his results is that they suggest general trends that will probably be confirmed if this study is replicated elsewhere. There is no implication here that a 72-foot (21.95 m) high antenna produces "12-dB gain" over a 34-foot (10.36 m)-high antenna in 20-meter DX work just because the mean advantage in our tests was about two S units in this instance.

The Results

The results of these tests, summarized in the accompanying table, were interesting in several respects. With the exception of one case on 10 meters, every single DX station reported a substantially better signal from the high quad than the low one. This is thoroughly predicted in the literature, but we also found that the high quad produced a significantly stronger signal (taking the mean, or average, figure) on "Stateside" work. And on ground-wave work, the high antennas were absolutely consistent in outperforming lower ones. However, E-skip contacts proved to be another story, a point to be covered in detail later. The mean advantage of the high quad over the low quad in DX work was 2.1 S units on 20 meters, 1.8 S units on 15, and one S unit on the 10-meter band.

Since the author's linear amplifier (a commercial unit using two 3-400Zs) produces a signal gain of about two S units over the exciter alone on most S meters, it became apparent that many DX stations could not distinguish the kilowatt feeding the lower quad from the exciter "barefoot" with the higher array. The implications of this dramatic difference in signal strength for DX-contest operations are obvious: it's no wonder the "big guns" using antennas 130 feet (39.62 m) high get through the pileups quickly, with or without big linears.

On Stateside F-layer work, the pattern was less consistent, although the high array continued to hold a significant edge. While a majority of the reports still favored the high quad by one or two S units, more than a third of the stations dissented, reporting equal or virtually equal signals from the two quads. No one reported a stronger signal from the lower antenna, perhaps because of the author's effort to avoid E-ship contacts in this phase of the study. The mean advantage of the higher quad was 1.4 S units on 20-meter Stateside work, and 0.9 S unit on 15 — still a substantial advantage, but not enough to render a low antenna useless for portable work, as generations of Field Day operators can attest. In fact, the author previously described a portable quad[4] that stood only 19 feet (5.79 m) high, but nevertheless worked very well for "back-home" contacts during a long vacation. An antenna only 19 feet (5.97 m) high is clearly undesirable, but if higher antennas are not feasible, much successful hamming can still be done. (This is especially true on an occasion like Field Day, when almost everyone's antenna is low, and the few beams that are 40 [12.19 m] or more feet high seem to dominate the bands; if the competition is using a low antenna you can too!)

Ground-wave Tests

Although the plan was to study the effect of antenna height on ground-wave communication only on vhf bands, a number of stations within 100 miles volunteered reports on the hf bands. These reports were not tabulated except on 15 meters, but they consistently favored the higher array by at least two S units.

In the vhf experiments, height again proved decisive for gound-wave work. On both 2 and 6 meters, every station favored the high antenna. On two meters, the mean advantage was an amazing 3.3 S units. Surprisingly, the higher array appeared to be equally superior on contacts with San Bernardino-Riverside stations (some 30 miles from Beaumont, CA, where these tests were conducted) and on contacts into the Los Angeles basin (almost 100 miles away).[5]

After moving and acquiring the 90-foot (27.43 m) tower, the author put a single 7-element 2-meter Yagi up and took an S-meter reading on a nearby repeater with the new tower cranked down. As the tower ascended to its full height, the signal rose from S8 to 15 dB over S9 on a popular transceiver's S meter.

On 6 meters, only a few ground-wave tests were conducted, but the results were similar: Everyone favored the higher antenna substantially.

6-Meter E-Skip Tests

However, on 6-meter E skip an entirely different relationship developed: The *lower* antenna had the advantage in seven out of 10 tests during single-hop openings.[6] Only one station favored the high antenna, and the low array had a mean advantage of 1.3 S units over the high array!

Although this finding is surprising and contrary to every other test conducted, it is consistent with the one previous practical study of antenna height vs. signal strength the author could locate in ham radio literature. Working in the late 1940s, Leroy May[7] set up identical 6-meter Yagis at heights of 35 and 75 feet (10.67 and 22.8 m), and compared 350 received signals on the two arrays. He found that the low array was superior for distances below 1000 miles

while the higher array began to pull ahead at distances exceeding 1100 miles.

The author made no attempt to fully replicate May's work, but all of our 6-meter E-skip experience supports him: For contacts into many major cities from greater Los Angeles, a high antenna is a handicap! Much to his chagrin, the author has frequently seen his 90-foot (27.43 m) - high Yagi outperformed on 6-meter E skip by a beam sitting 10 feet (3.05 m) above somebody's roof on a TV mast.

Conclusions and Recommendations

It is customary when reporting a study such as this to conclude by summarizing the findings and making some recommendations. The conclusion here must be that, for every application except E-skip work, there are worthwhile advantages of having an antenna at least 70 feet (21.34 m) high. This height advantage is most pronounced on ground-wave and long-haul DX work.

The only logical recommendation we can make, then, is that all hams should own towers 70 feet (21.34 m) high. May all of the XYLs, frightened neighbors, bill collectors, and zoning-conscious city officials of the world forgive us!

Alternately, maybe we should suggest that all hams (except the author) use 35-foot (10.67 m) towers to give the author a better chance in DX contests. Or better yet, how about an antenna-height multiplier for the DX contests? Let's see, that's 1.5 if your antenna is below 75 feet (22.86 m), 2.0 if it's below 40 feet (12.19 m), and 3.0 if you bury it in the ground . . . This material was originally presented in *QST* by Wayne E. Overbeck, N6NB.

References

[1]Lindsay, "Quads and Yagis," *QST*, May 1968 (See chapter 3).

[2]Orr, William I., *Beam Antenna Handbook*, 3rd Edition.

[3]No 10-meter "Stateside" tests are reported because the muf was too low for reliable F-layer work across the U.S. when these tests were run.

[4]Overbeck, "The 20-Minute Portable Quad," *QST*, May 1967.

[5]On the hf bands, it is normally assumed that a high antenna has a greater advantage over a low antenna on long-haul DX than it does on shorter paths, but the opposite may well be true for vhf ground-wave work. This is suggested in the *ARRL VHF Manual*, (1st Edition, pages 24,25). Thus, one would expect that an increase in height would result in greater improvement in signals over the 30-mile path than over the 100-mile path.

[6]At the time of the 6-meter tests, E skip was barely "in season." The author is continuing this study during seasons of more frequent E-skip openings.

[7]May, "Some Practical Results on the Question of Antenna Height," *CQ*, April 1953.

Limited-Space Antennas and Methods Of Coupling

When short, random-length wire antennas prove disappointing, chances are the installer didn't follow a few basic rules for good performance. These tips should lead the way to better results with "randoms."

One very popular type of antenna, probably because of its simplicity, is a wire of either a predetermined or random length, fed at one end. It is common procedure among amateurs these days to refer to such an antenna as a "long wire." Actually, this term is usually incorrect because, by definition, a long-wire antenna is a wire that is several wavelengths long at the operating frequency. But no matter what you call it, the end-fed wire can be a very simple antenna to put up and use, if certain steps are taken.

Transmitter Loads

Nearly all transmitters described these days are designed to work into 50- to 70-ohm loads, with little thought given to any load that departs very far from these figures. If the load is something different than the above figure it may be impossible to get the amplifier in a transmitter to load up. In order for the final amplifier stage to operate at its best efficiency, the load (the antenna system) must be within the design range of the amplifier.

An end-fed wire may present a load of 50 to 70 ohms, but if it does it will be a case of pure luck on the part of the user — and what's more important, that load won't stay the same across a band. In other

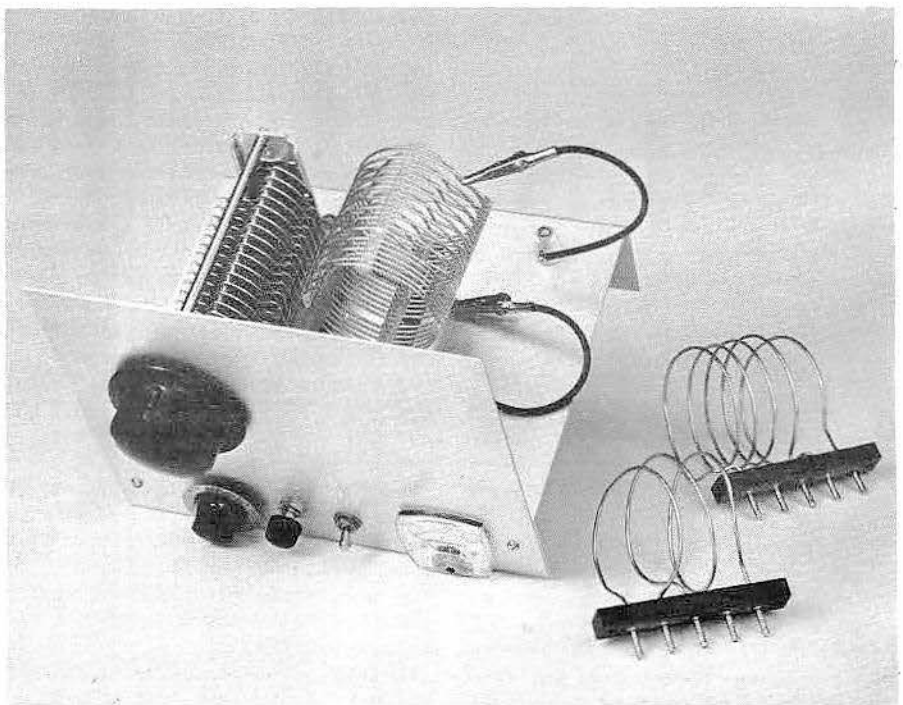

The completed transmatch with the 80/40-meter coil plugged in. At the rear is the 20-meter coil and the 10/15-meter unit is to the front. In regular operation, the antenna would be attached to the standoff insulator at the top rear of the chassis. The clip lead visible below the coil is the one attached to the jack bar.

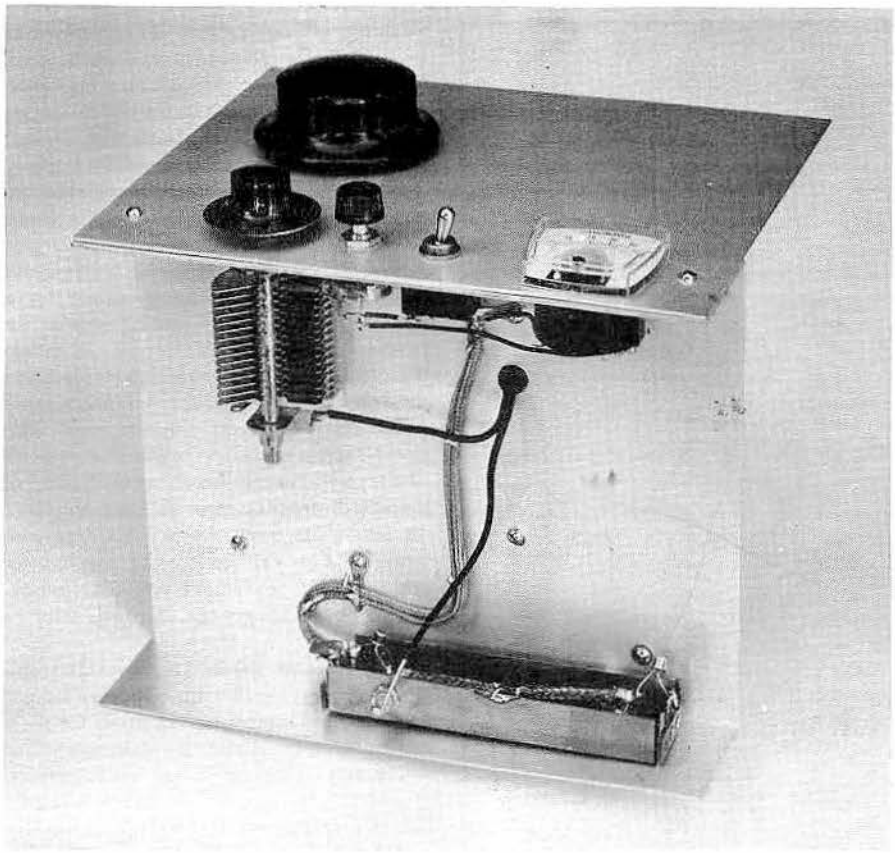

The wiring below deck. At the rear of the chassis is the Varimatcher section. C2 is at the left front of the chassis.

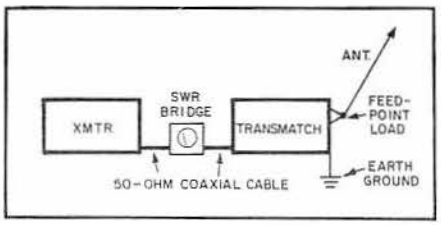

Fig. 3 — This block diagram shows the set-up for using a Transmatch. Not shown is an antenna relay which normally would be inserted in the coaxial line. If a low-pass filter is used, it should be the last item in the line before the Transmatch.

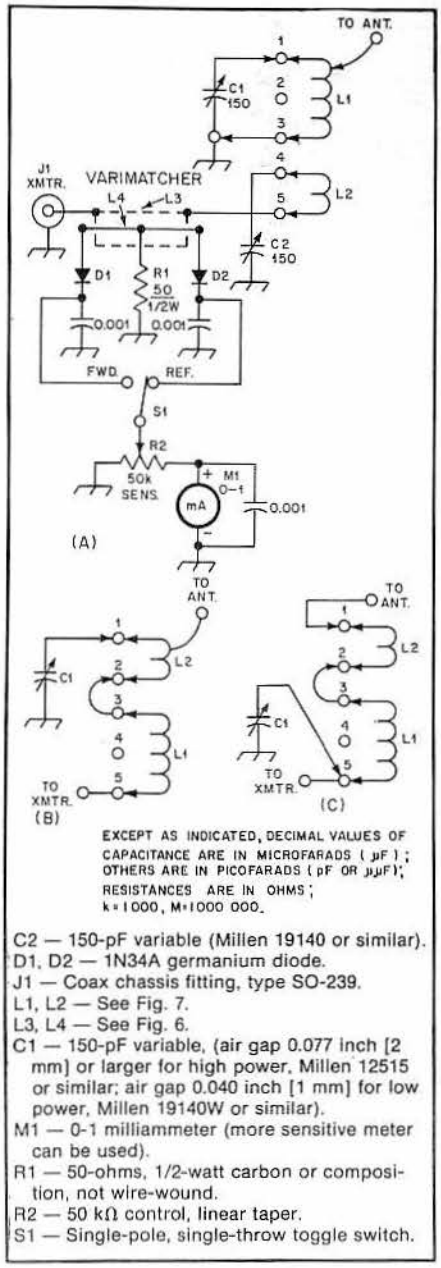

C2 — 150-pF variable (Millen 19140 or similar).
D1, D2 — 1N34A germanium diode.
J1 — Coax chassis fitting, type SO-239.
L1, L2 — See Fig. 7.
L3, L4 — See Fig. 6.
C1 — 150-pF variable, (air gap 0.077 inch [2 mm] or larger for high power, Millen 12515 or similar; air gap 0.040 inch [1 mm] for low power, Millen 19140W or similar).
M1 — 0-1 milliammeter (more sensitive meter can be used).
R1 — 50-ohms, 1/2-watt carbon or composition, not wire-wound.
R2 — 50 kΩ control, linear taper.
S1 — Single-pole, single-throw toggle switch.

Fig. 4 — Circuit diagram of the Transmatch and Varimatcher. All 0.001-μF capacitors are disk ceramic.

words, the antenna will present a 50- to 70-ohm load for only a very limited frequency range. Once we QSY the load may change to where it is no longer within the tuning range of the amplifier. Our problem boils down to having the transmitter *always* see a load of 50 to 70 ohms, regardless of the band or frequency in use. This in turn means we must make the antenna system look like a 50- to 70-ohm load, no matter which band we use it on.

The Transmatch, an Adjustable RF Transformer

Let's make one point clear about end-fed wires, or any antenna, for that matter: There is no way of predicting what the feed-point impedance (load) will be before making and installing the antenna. We can come close, but there are many factors that get into the act to determine what the impedance will be. The antenna's height, its proximity to nearby objects, its length, and the antenna's relation to earth ground are just a few of the factors. If we don't know what the feed-point impedance is, how can we make the transmitter always work into a 50-ohm load? The easiest way is to insert a Transmatch between the transmitter and the feed point. A Transmatch is simply an adjustable rf transformer that takes our unknown feed-point load and converts it to a desired load, 50 ohms in the case shown in Fig. 3.

Note in Fig. 3 that we show a random-length antenna and an earth ground connection. In this case, our unknown load exists between the end of the antenna and ground. On the transmitter side of the Transmatch we have 50-ohm coaxial cable and inserted in this cable is a 50-ohm reflectometer or SWR (standing-wave-ratio) bridge. The reflectometer is simply a measuring instrument that tells us when our Transmatch is properly adjusted to convert our unknown load to a 50-ohm load. If the Transmatch has adequate matching range, we can convert any feed-point load to 50 ohms. And this means that we can take any random length wire and make a working antenna out of it for any amateur band or frequency. There are some practical limits as to how short a wire we can use, but actually the antenna can be quite short in relation to a wavelength and still work.

Limited-Space Antennas

Many hams live in apartments or locations where it is impossible to put up an "antenna farm" or even a half-wave dipole for 80 or 40 meters. Random-length wires are sometimes the best bet in these circumstances. For hams who live under such conditions there are some general rules that can be followed for best performance. If possible, always get the antenna up on the roof. If not, get the antenna as high as possible. Make the wire as long as possible, even if it has to go around corners. Don't overlook existing antenna possibilities, such as rain gutters or roof flashing. In a moment we are going

to describe a Transmatch that can be used to couple practically any wire or metal structure to the transmitter, including rain gutters.

If it is impossible to get an outdoor antenna up (and don't overlook "invisible" antennas[1]). an indoor antenna will work, but not as well as an outdoor one. With the Transmatch to be described, you can run a wire around the ceiling molding and couple the wire to the rig, maintaining that 50-ohm load we mentioned earlier. When you hear hams talking about loading up the bed spring, don't laugh — many a ham has made contacts that way. All you need is some method of coupling the bed spring to the rig; that's what our Transmatch will do.

The Transmatch

Shown in Fig. 4 is the circuit for a Transmatch that will do the job we've been talking about. This unit will match practically any wire to our 50-ohm rigs on any band from 80 through 10 meters. Depending on which capacitor plate spacing you use for C1 the Transmatch can be used for Novice powers or up to the legal limit of 1 kW. Actually, the closer-spaced capacitor will handle 200 watts or so. The same type coil stock is used for either power level, high or low.

Also included in the Transmatch shown in Fig. 4 and the photographs is an SWR bridge. This is a necessary item in order to know when the Transmatch is correctly adjusted. If you already have a Monimatch or reflectometer, the unit described can be eliminated from the Transmatch.

With the random-wire antenna we'll be dealing with various loads, depending on the frequency and band in use. Shown in Fig. 5 are the three basic circuit configurations used with the Transmatch. The circuit can be changed to conform with type A, B, or C by reversing the plug-in coil in the jack bar or by changing the capacitor C1 from the output side of the L configuration, as in B, to the input side, as in C. The capacitor is changed by means of a clip lead connected to the stator.

Some loads may require the circuit setup of A. In this configuration, a link-coupled parallel-tuned circuit is used, the antenna being tapped onto L1.

Construction Details

The chassis used to hold the parts is 2 × 7 × 9 inches (51 mm × 178 mm × 229 mm) and the panel measures 7 × 9 inches (178 mm × 229 mm). Any chassis large enough to hold the parts can be used. C1 and the jack bar for the plug-in coils are mounted on top the chassis, and the Varimatcher reflectometer and C2 are mounted below

[1]Any wire that is no. 28 or smaller is practically impossible to see when strung up as an antenna. Many hams use "invisible" antennas to prevent a touchy landlord situation.

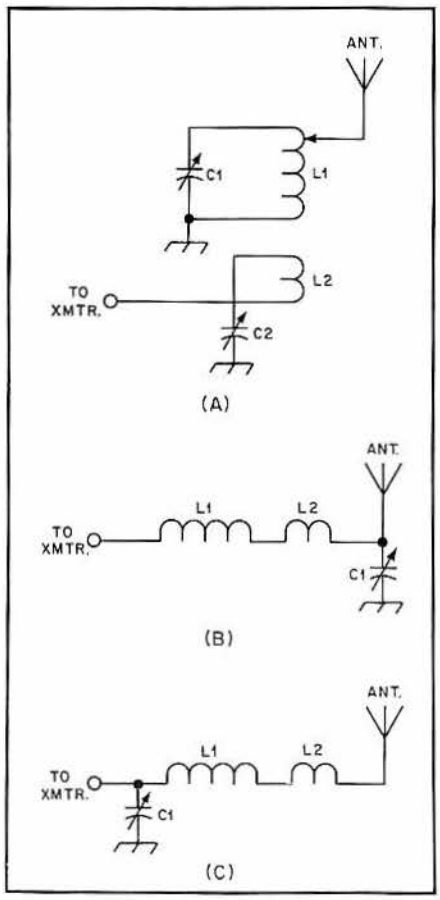

Fig. 5 — Three possible configurations with the Transmatch as described in the text. To set up types B or C the plug-in coil is reversed in the jack bar and terminal no. 3 of the jack is clipped to terminal no. 2.

the chassis top. The remaining components are mounted on the chassis front.

A 4-inch (102 mm) length of RG-58/U coaxial cable is used for the pickup and conductor sections of the SWR bridge. Details for making this section are given in Fig. 6. Study these details and the photograph of the bottom view carefully before starting construction. The black outer covering of the coax is removed, leaving the braid and inner conductor with its insulation. The outer braid will be L3 and the inner conductor L4. You'll notice that there is an open area at the center of the coax braid. This is to allow room for the connection of one end of the 50-ohm resistor to the center of the inner part of the coaxial line. Use a probe or pointed instrument to open up the area in the braid and then carefully tin the edges of the opening with solder so as to prevent any of the hair-like wires from shorting to the resistor lead or inner conductor. The ends of the braid can be wrapped with a few turns of solid wire and tinned. The wire ends will provide a support for the connection to the feed-through terminal and the inner pin of J1.

The metal trough that houses the bridge section is made from a piece of copper flashing, although tin or aluminum could be used. It is a good idea to drill the holes for J1 and the feed-through bushing before bending up the trough into a U. Also, when soldering the leads for the diodes, D1 and D2, use a heat sink between the body of diode and the point being soldered, because too much heat can ruin the diode.

Using the Transmatch

In making the antenna, shoot for a length of at least 1/4 wavelength at the lowest operating frequency. In other words, if you plan on working 80 meters as the lowest band, then the antenna should be 60 feet (18.29 m) long, at least. This doesn't mean that shorter wires won't work — they will, but not nearly as well. A lot of hams will say they can't get up a length of 60 feet! The wire doesn't *have* to run straight. You can go around corners, up and down, or what have you. The important point is to get up as much wire as possible.

By the same token, many hams think (mistakenly) that they have to have a good earth ground connection in order for their station to work. It's fine if you have one but if you don't, forget it. If you have access to a water pipe or other earth ground connection make a connection to the rig and the Transmatch, but if you can't, don't worry. The antenna will still work.

With the antenna connected and the rig on the desired frequency, feed enough power through the system to get at least a half-scale reading on the Varimatcher meter, and have the Transmatch set up as in (A). Tap the antenna onto the first turn of the coil L1 at the "hot" end, or end opposite the ground. Incidentally, always turn the rig off when making any adjust-

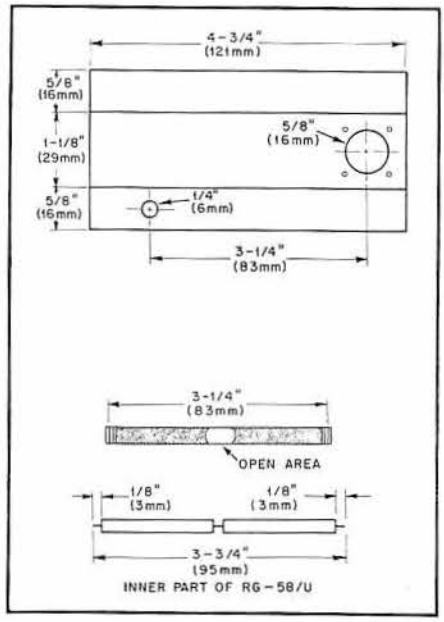

Fig. 6 — Constructional details of the Varimatcher bridge section. The braided portion of the coax is L3 and the inner portion is L4.

ments on the Transmatch. There may not be any dc voltages present but some very, very high rf voltages can be developed on the Transmatch coils and can cause a nasty rf burn.

With the antenna tapped on near the hot end of L1 switch S1 to read reflected power and adjust C1 and C2 for a dip or minimum reading. If you cannot get the reflected reading down to zero, or close to it, turn off the power and move the antenna tap closer to the ground end of the coil. You'll eventually find a tap point that will give a reading of zero in the reflected position versus full scale in the forward position of S1. If you find that the tap point on L1 is very close, say within 25 percent, to the ground end, you may want to try configuration B or C.

In eight of these configurations, start at the antenna end of the coil and, using another short clip lead, short out turns or portions of turns as you move the antenna tap towards the transmitter end of the circuit. In other words, the antenna is always on the end of the coil, but you may have some of the coil shorted out in order to get a match as indicated by M1.

Once you get a match for any given band, make a chart of the taps and so forth so you can return to the setup when you change bands.

The main reason for using configurations B and C is that if the antenna is tapped near ground on L1 in configuration A, extremely high rf voltages can develop across C1 even with Novice powers. We don't recommend playing around with "arcs" from coils but it might be wise to prove to yourself just how much voltage can be developed. With the antenna tapped near the ground end of L1, take a pencil and hold it by the wood, not at the eraser end but in the center. With the key closed and the rig loaded up to about 75 watts, touch the lead end of the pencil to the stator of C1. You'll quickly see why caution is necessary. Such an arc can make a very nasty and painful burn.

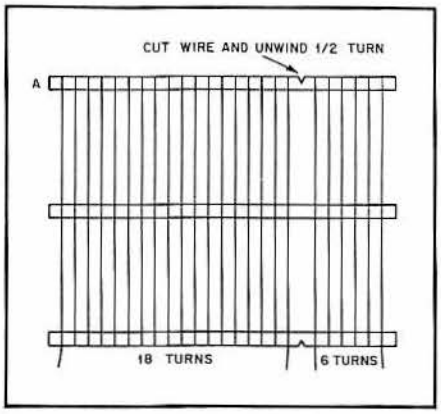

Fig. 7 — The 80/40-meter coil. To use the coil on 40 meters, short out 10 turns, counting from the "A" end of the coil. Shorting clips should be copper and the shorting leads should be insulated. Coil stock is no. 14 wire, 8 turns per inch (25 mm), 2-1/2 inches (64 mm) in diameter (Air Dux 2008T, B & W 3906-1, or Polycoils 1775).
The 20-meter coil consists of 4 turns of no. 12 solid wire, 2-1/2 inches in diameter, with the turns spaced so that L1 is 1-1/2 inches (38 mm) long. L2 is one turn of no. 12, same diameter as L1, spaced 1/2 inch (13 mm) from the end of L1.
The 15/10-meter L1 coil is 2 turns of no. 12 solid wire, 2-1/2 inches (64 mm) in diameter, turns spaced to cover 1-1/2 inches (38 mm). L2 is a single turn, same diameter as L1, spaced 1/2 inch (13 mm) from L1.
All coils are mounted on Millen type 40305 plugs and the socket (jack bar) is a Millen 41305. See G. R. Whitehouse ads in *QST*.

If you want to try using antennas that are *very* short for the frequency, such as 10 feet (3.05 m) long on 80 meters (similar to a mobile whip) certain additional steps may be required to obtain a match with the Transmatch. When you make the coil for 80 and 40 meters you'll have some coil stock left over. With very short antennas, this can be used as a "loading" coil. Connect the antenna to one end of the coil and connect the other end to the antenna terminal on the Transmatch. Then go through the tune-up procedure. You may have to use a clip lead to short out turns on the coil but you'll find a setup that will permit matching with the Transmatch. Again, avoid coming in contact with the series loading coil because very high rf voltages can develop in such a setup.

Some beginners may not be aware of it, but a fluorescent lamp or neon bulb will light up when in an rf field, if the rf voltage is high enough. If you have a fluorescent lamp (a burned-out one is OK), the lamp can be laid along the antenna wire where it leaves the Transmatch. This makes a good output indicator, showing when power is flowing in the antenna. This material was originally presented in *QST* by Lewis G. McCoy, W1ICP.

Off-Center-Loaded Dipole Antennas

So you can't manage a buried radial system on your city lot, eh? Then why not scrap those plans for a vertical antenna and try K1TD's version of a short dipole? Here are the design tips you need.

In these times when much of our amateur population lives in urban areas, the subject of shortened antennas for the lower frequency amateur bands is a very popular one. Physically short ground-mounted vertical antennas with lumped-constant loading to make them resonant can be quite efficient radiators, if a good radial system has been installed. This has certainly been evidenced in Sevick's series of *QST* articles.[1] To many amateurs, however, the "hitch" in constructing such a system is the installation of a good radial system. It must be admitted that for the "top" amateur bands, 160 and 80/75 meters, an efficient system of buried radials requires a sizable amount of real estate, even for a physically short radiator. On the average city-size lot, 50 or 75 by 120 to 150 feet (15.24 - 22.86 m by 36.58 - 45.72 m), it's almost impossible to install a highly efficient radial system for 80/75 meters, much less for 160 meters, when structures like a house and perhaps a separate garage exist. Or to some amateurs, just the thought of burying hundreds or maybe thousands of feet of wire is enough to turn off any enthusiasm for the project.

What's the alternative? A dipole type of antenna with lunped-constant loading. At modest heights, 30 or 40 feet (9.14 or 12.19 m), such an antenna will prove to be quite satisfactory if it is physically longer than about 0.2 wavelength. Shorter lengths may also be used, at reduced efficiency. Such an antenna can be fed directly with 50-ohm coaxial line, and it can be operated with no earth ground. (Of course the chassis of the transmitter and/or receiver should be grounded adequately for protection against shock hazard.)

Nearly all of us are familiar with the concept behind the use of inductive loading. A vertical antenna which is shorter than a quarter wave (or a dipole antenna which is

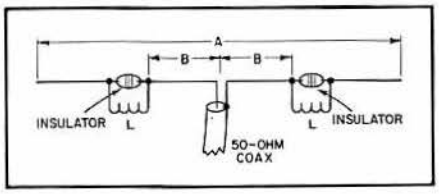

Fig. 8 — A dipole antenna lengthened electrically with off-center loading coils. For a fixed dimension A, greater efficiency will be realized with greater distance B, but as B is increased, L must be larger in value to maintain resonance.

(Eq. 1):

$$L_{\mu H} = \frac{10^6}{68\pi^2 f^2} \left\{ \frac{\left[\ln \frac{24\left(\frac{234}{f} - B\right)}{D} - 1\right] \left[\left(1 - \frac{fB}{234}\right)^2 - 1\right]}{\frac{234}{f} - B} - \frac{\left[\ln \frac{\left(24\,\frac{A}{2} - B\right)}{D} - 1\right] \left[\left(\frac{\frac{fA}{2}}{234} - fB\right)^2 - 1\right]}{\frac{A}{2} - B} \right\}$$

where

$L_{\mu H}$ = inductance required for resonance
ln = natural log
f = frequency, MHz
A = overall antenna length, feet
B = distance from center to each loading coil, feet
D = diameter of radiator, inches

shorter than a half wave) will exhibit capacitive reactance at its base (or center) feed point. To cancel such capacitive reactance, a coil having the proper inductive reactance may be connected in series with the base feed point of the vertical. The same result will be obtained through the use of two such coils for a dipole, one coil connected in series with each half. It is not necessary for the inductor to be installed at the feed point, however. In fact greater radiating efficiency results through improved current distribution if the inductor is located along the radiator some distance away from the low-impedance feed point, *viz,* in the manner of a center-loaded mobile whip antenna. Fig. 8 shows this concept extended to a dipole element, with off-center loading. The inductors resonate the antenna to the operating frequency, but do little actual radiating themselves. (This is in contrast to helically wound or continuously loaded elements, where a long thin inductor is the radiator as well as the loading element.)

In the antenna represented by Fig. 8, there are many variable factors to be considered when a practical antenna for a given frequency is being constructed. Of primary consideration from an efficiency standpoint is the overall length, shown as dimension A. Another consideration for efficiency is the distance of the coils from center, dimension B. The longer the overall length (A), up to a half wave, and the farther the loading coils are placed from the center (B), the greater is the efficiency of the antenna. However, the greater is distance B (for a fixed overall antenna size), the larger the inductors must be to maintain resonance. Theoretically, if the coils were placed at the outer ends of the dipole, they should be infinite in value to maintain resonance. Capacitive loading of the ends, either through proximity of the antenna to other objects or through the addition of capacitance hats, will reduce this requirement to a more practical value.

What Inductance Values?

As a matter of personal interest, this writer has been doing experimental work for a number of years with off-center-loaded antennas. One big drawback to such experimentation was the ever-present need for a large amount of cut-and-try work to arrive at resonance whenever a new set of dimensions was to be used. Probably the number of pruned-off turns from coil stock from such experiments, if straightened out and soldered end to end, would make up several full-sized half-wave antennas for the 160-meter band. Therefore, most of the writer's work of late in this area has been in going through paperwork exercises, looking for a way whereby at least "ball-park" values of inductance needed for a particular system could be calculated.

The equation contained in the Mobile chapter of *The ARRL Antenna Book* for determining the capacitance of a vertical antenna shorter than a quarter wavelength looked promising in early computations, and, indeed, it became the basis for the calculation procedure which finally resulted. This procedure has been found to produce results much closer than mere "ball-park" values for the necessary inductance — for wire antennas "in the clear" at moderate heights, the final inductance values found by cut-and-try pruning for lowest SWR at the desired frequency have been so close to the value from calculations that a laboratory bridge was necessary to measure the difference. The results are equally good for elements using tubing. Once the needed inductance value is determined by calculations, it is generally found sufficient to obtain coil dimensions from an ARRL L/C/F Calculator (see LaPlaca[2]) or by equation. Any significant pruning which has been found necessary could always be attributed to objects in proximity to the ends of the antenna.

The complete set of calculations is expressed in the mathematical relationship as Eq. 1, presented here primarily for mathematics buffs or those having access to electronic computers. This equation yields the inductance required, in microhenrys, for single-band resonance of a shortened antenna of a particular physical size at a given frequency, for a specific position of the loading coils from the center of the antenna. To spare the reader the task of performing some rather tedious calculations, Fig. 9 has been prepared from Eq. 1. The curves of the chart have been normalized, and may be used for any frequency of resonance. The chart is based on a half-wavelength/diameter ratio of the radiator of approximately 24,000. (This corresponds to no. 14 wire on 80 meters or no. 8 wire on 160 meters.) For "thinner" conductors, the required inductance will be somewhat greater than that determined from Fig. 9, and less inductance will be required for "thicker" conductors.

The use of the chart is as follows: At the intersection of the appropriate curve from the body for dimension A and the proper value for the coil position from the horizontal scale at the bottom of the chart, read the required inductive reactance for resonance from the scale at the left. Dimensions A and B are shown in Fig. 8, and for use with the chart are expressed as percentages. Dimension A is taken as percent length of the shortened antenna with respect to the length of a resonant half-wave dipole of the same conductor material. Dimension B is taken as the percent of coil distance from the feed point to the end of the shortened antenna. For example, resonating an antenna which is 50 percent or half the size of a half-wave dipole (one-quarter wavelength overall), with loading coils positioned midway between the feed point and each end (50 percent out), would require loading coils having an inductive reactance of approximately 950 ohms at the operating frequency. If the antenna is hung "in the clear," and if the length/diameter ratio of the conductor is near 24,000, inductance values as determined from the chart will be very close to actual values required. (Eq. 1 above takes the diameter of the radiator into account, and thus may be used for any length/diameter ratio.) For practical

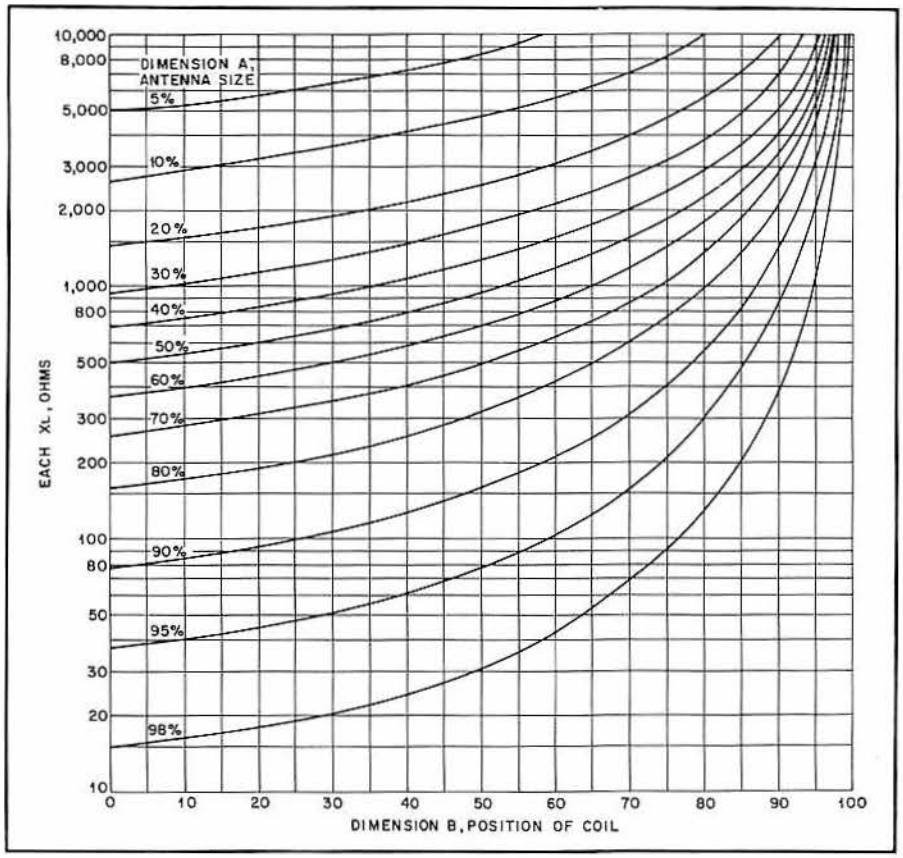

Fig. 9 — A chart for determining approximate inductance values for off-center-loaded dipoles. At the intersection of the appropriate curve from the body of the chart for dimension A and the proper value for the coil position from the horizontal scale at the bottom of the chart, read the required inductive reactance for resonance from the scale at left. See Fig. 8 regarding dimensions A and B.

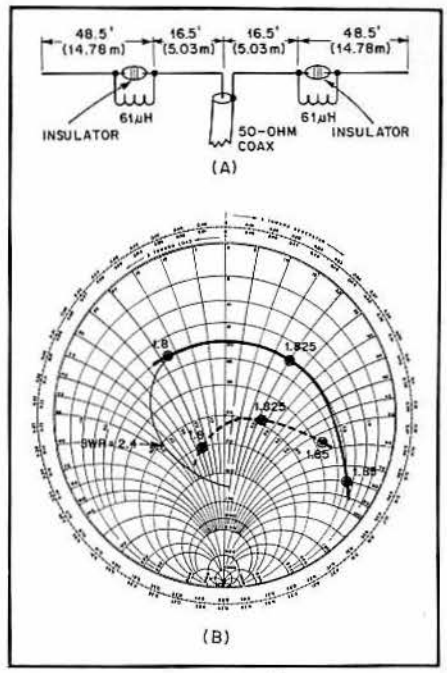

Fig. 10 — At A, an 80-meter dipole loaded for 160-meter operation. The inductors are 37 turns of coil stock having a 3-inch (76 mm) dia and 10 turns per inch (25 mm) (B & W 3035). At B, the impedance plot of this antenna installed at a height of 50 feet (15.24 m) (solid curve), and the plot of a 160-meter half-wave dipole (broken curve).

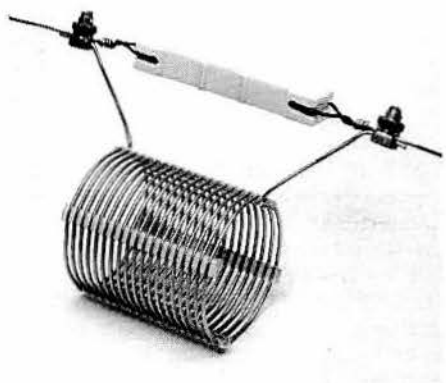

Fig. 11 — Copper electrical service connectors, sold under one trade name of Servit, provide a simple means of installing the loading coils. The antenna wire and the ends of the coil wires should be tinned to prevent corrosion. In addition, a protective coating of acrylic spray may be used at each connection.

purposes, dimension B may be taken as that distance from the center of the feed-point insulator to the inside eye of the loading-coil insulator, and dimension A as the eye-to-eye distance inside the end insulators (which are not drawn in Fig. 8).

Proximity of surrounding objects in individual installations may require some pruning of the coils, and the exact amount of final inductance required should be determined experimentally. If the antenna is hung in inverted-V style, with the ends brought near the earth, the required inductance will almost always be somewhat less than that determined from the chart or equation. A grid-dip meter, Macromatcher (see Hall and Kaufmann[3]), or SWR indicator may be used during the final adjustment procedure.

Practical Antennas

Although one might erect an inductively loaded antenna that is cut for a single amateur band, it is possible to use the antenna itself for two, three or more bands of operation, if provision is made to lower the antenna for band changes. A simple rope halyard and pulley arrangement at one of the supports will do the trick. Fig. 10A shows a three-band antenna of this nature, for 160, 80 and 20 meters. If the insulators shown are left open, with nothing bridging them, the antenna is a simple half-wave dipole cut for 14.18 MHz. (The 48.5-foot [14.78 m] lengths act merely as support wires, and have negligible effect on operation of the antenna.) If the insulators are bridged with short lengths of antenna wire, the antenna becomes a center-fed 80-meter dipole, resonant at about 3.6 MHz. For 160-meter operation the 20-meter insulators may be bridged with loading coils to resonate the antenna at 1.8 MHz, as shown in Fig. 10A. Burndy or other manufacturers' "Servit" type of electrical connectors may be used for ease in making band changes quickly, as shown in Fig. 11.

The calculation procedure for determining loading-coil values for the antenna of Fig. 10A, using the chart of Fig. 9, goes like this. If operation is desired on 1.8 MHz, the length of a full-sized half-wave dipole is found from the relationship 468/f to be 260 feet (79.25 m). The 130-foot (39.62 m) length of Fig. 10A represents 50 percent of this size, meaning that the dimension-A curve marked "50 percent" in Fig. 9 is to be used. The position of the coils is 16.5/(16.5 + 48.5) × 100, or 25 percent of the distance out from center, dimension B. From the intersection of 25 (horizontal scale at bottom) and the 50 percent curve, the required inductive reactance is read from the scale at the left of Fig. 9 to be 650 ohms. The inductance, L, is $650/2\pi f$ or 57.5 microhenrys, if no. 8 wire is to be used. For smaller diameter wire, the inductance should be somewhat larger. (Calculations from Eq. 1 for no. 12 wire indicate the required inductance is 60.99 μH.)

The radiation resistance of a shortened antenna loaded to resonance is less than that of a full-sized antenna. Further, the shortened antenna is "sharper," meaning that the change in reactance versus frequency is greater. In other words, the shortened antenna acts as a tuned circuit having a higher Q than a full-sized antenna.

To check these characteristics, the line input impedances for the antenna of Fig. 10A were measured with a laboratory bridge, and the electrical line length at the measurement frequency was then taken into account to determine the impedance at the antenna feed point. The antenna was constructed of no. 12 wire and hung at a height of 50 feet (15.24 m) as a "flat-top" radiator.

The solid curve of Fig. 10B is a plot of the feed-point impedance versus frequency for this antenna. The plot on Smith Chart coordinates is more meaningful than a simple SWR-vs.-frequency curve because the magnitudes of the resistive and reactive components are shown, as well as the sign of the reactance. (Capacitive reactance is negative, plotted to the left of the vertical center line, and inductive reactance is positive, plotted to the right.) In this presentation, a 50-ohm nonreactive impedance will appear at the exact center of the chart. The SWR in 50-ohm line for a given frequency may be determined by first noting the distance from the center of the chart to the particular impedance plot on the curve, and next measuring this same distance down the vertical center line from chart center (a drawing compass is helpful for this task), and finally dividing 50 into the value read at that point on the center line. For example, the SWR at 1.8 MHz equals 120/50 or 2.4, as indicated by the segment of the 2.4 SWR circle in Fig. 10 B. It may be seen that resonance (zero reactance) occurs at approximately 1810 kHz, where the resistance is about 22 ohms. The SWR at resonance is 2.33:1, and climbs to 3:1 at 1825 kHz. At 1850 kHz, the SWR is 10:1. Without any matching provisions the antenna is relatively sharp, as mentioned earlier. If one sets the usable bandwidth as the frequency range where the SWR is 3:1 or less, it is approximately 35 kHz, or 1.9 percent of the resonant frequency. As far as efficiency is concerned, ohmic losses are low, and the antenna is a good performer on 160 meters. Because of its horizontal polarization, it has proved to be most effective at night, and stations several hundred miles away have been worked with S 9 reports received for the 50-watt signal.

For a comparison of impedances, the broken curve of Fig. 10B is a plot of measured impedances of a full-size half-wave dipole, 260 feet (79.25 m) long overall, hung in place of the shortened antenna. From this curve it may be seen that resonance occurs at 1810 kHz, where the resistance is 59 ohms. The 3:1-SWR bandwidth for the half-wave antenna is in the order of 60 kHz, or 3.3 percent of the resonant frequency. It is interesting to note on this curve that the SWR at resonance is 1.18:1, and that it is a somewhat lower value, 1.15:1, at a frequency a few kilohertz above resonance. (Measurements were made every 5 kHz across this band, but plot points are shown only for 25-kHz increments to avoid crowding of the data.) This

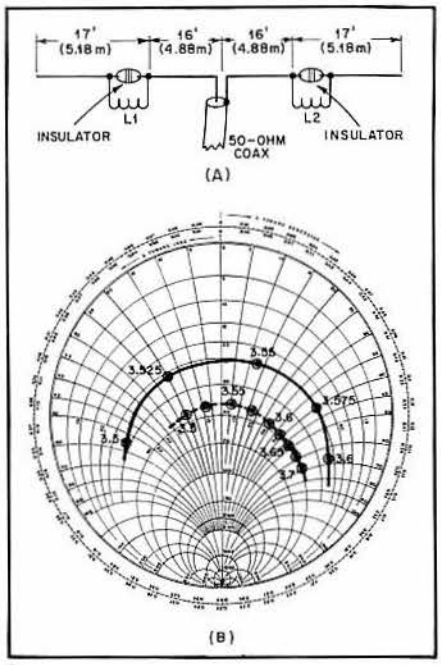

Fig. 12 — At A, a 40-meter dipole loaded for 80-meter operation. For resonance at 3.55 MHz the coils should be approximately 40 μH (27 turns of stock); 3.75 MHz, 35 μH (24 turns); 3.9 MHz, 31 μH (22 turns); and 4.0 MHz, 29 μH (21 turns). These are calculated inductance values for no. 12 antenna wire. Coil stock referenced above is 3-inch (76 mm) diameter, 10 turns per inch (25 mm) (B & W 3035). At B, the impedance plot of the 3.55-MHz version (solid curve) and of an 80-meter half-wave dipole (broken curve).

evidence refutes the oft-heard statement that the SWR-vs.-frequency curve is *always* lowest at antenna resonance. Points to remember are that the SWR in a transmission line is completely dependent upon the characteristic-impedance value of the line in use. Using a line of different impedance may shift the position of the SWR curve along the frequency axis in a simple SWR-vs.-frequency plot. This is definitely true in this case — if the 160-meter half-wave dipole were to be fed with 75-ohm line, the lowest SWR would occur at a frequency about 5 kHz *below* antenna resonance, whereas with 50-ohm line the lowest SWR is at a frequency slightly *above* resonance. The reason this happens is that the resistive component of the impedance, which consists of the radiation resistance plus any loss resistance, is not constant with frequency, even over a rather narrow frequency range. It must be acknowledged that the differences here are very slight, however, and for practical purposes the frequency of lowest SWR is (within a few kilohertz) the resonant frequency of the antenna.

Another point concerning the SWR values bears noting. The values as determined from the plots in the manner described above are quite accurate, having been determined by measurements with laboratory equipment. In contrast, measurements with simple SWR indicators usually cannot be relied upon for anywhere near the equivalent accuracy.

For example, the author owns a commercially manufactured SWR indicator of the Monimatch type (see McCoy[4]) which, under a particular set of conditions, indicates a 2.5:1 SWR in a line where laboratory measuring equipment shows the *true SWR to be 4:1.* A significant difference! Herein lies another reason why impedance plots on Smith Chart coordinates are more meaningful than a simple SWR-vs.-frequency curve — greater accuracy may generally be expected.

A Half-Size 80-Meter Antenna

Fig. 12A shows the 3-band concept described earlier as it can be applied to 80, 40 and 20 meters. Its overall length is 66 feet (20.12 m), not a difficult length to use on a small lot. This antenna was constructed for 80-meter operation with a design-center frequency of 3.55 MHz, using no. 12 antenna wire and 40-μH loading coils — 27 turns of stock having a diameter of 3 inches (76 mm) and a pitch of 10 turns per inch (25 mm) (tpi). Feed-point impedances versus 80-meter frequency for the antenna, hung at a height of 50 feet (15.24 m), are shown by the solid curve at B of Fig. 12. Actual resonance occurred at 3.54 MHz, where the resistance was about 26 ohms. The bandwidth within which the SWR is 3:1 is 60 kHz, or 1.69 percent of the resonant frequency.

Also shown in Fig. 12B, by the broken curve, are the feed-point impedances of a half-wave dipole, 132 feet (40.23 m) overall length, hung in place of the shortened antenna. Resonance occurs at 3.54 MHz, where the resistance is 43.5 ohms and the SWR is 1.15:1. The broader nature of the half-wave antenna is exhibited by the "tighter" curve which swings closer to the 50-ohm center point of the chart than the shorter, loaded antenna. The SWR at 3.5 MHz is 1.6:1, and remains below 3:1 to 3.67 MHz.

Capacitive and Inductive Loading

One would assume that a combination of capacitive and inductive loading might provide a different feed-point impedance than would inductive loading alone, because of different current distributions in the radiators. To check out this assumption, the antenna of Fig. 12A was used as a "test bed" for comparative measurements. Capacitance hats were attached at different points along the 17-foot (5.18 m) lengths of wire outside the coils, and the coils were pruned to reresonate the antenna at about the same frequency as before. The impedance measuremnts were then repeated.

Dangling End Sections

First, "hats" consisting of 18 inches (457 mm) of no. 12 wire were affixed to the antenna ends and permitted to dangle. This lowered the resonant frequency to 3435 kHz. By calculations, this was approximately the same effect as that of extending the 17-foot portions of the antenna by the same amount as the dangling lengths, so it

Table 4

Characteristics of Various Loading Techniques, 66-Foot, 80-Meter Dipole

Loading	*Approx. feed-point resistance, resonance*	*SWR at resonance*	*3:1-SWR bandwidth, % of resonant freq.*
40-μH coils only	26 ohms	1.92:1	1.69
36.5-μH coils, 18" dangling ends	26	1.90:1	1.79
36" hats outside 32.5-μH coils	23	2.15:1	1.68
30-μH coils, 36" hats at ends	25	1.98:1	2.05
None (λ/2 dipole)	43.5	1.15	Greater than 3.6

Coil positions for each loaded antenna were 16 feet from antenna center. All antennas were constructed of no. 12 wire and installed at a height of 50 feet.

Feet X 0.3048 = m.

Inches X 25.4 = mm.

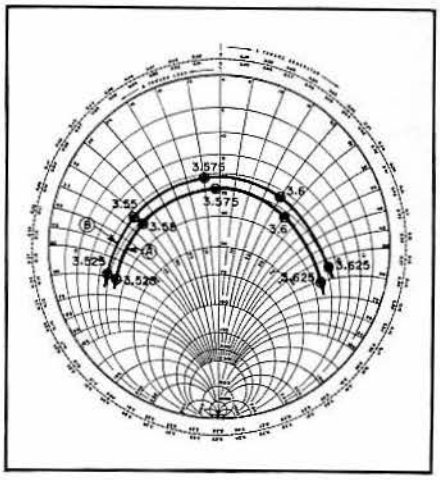

Fig. 13 — Curve A is the impedance plot of the antenna of Fig. 12A with 18-inch (457 mm) dangling end sections added and the coil trimmed to restore resonance near the original frequency. Curve B is a plot of the same antenna with X-shaped capacitance hats added at a point just outside the loading coils (dangling sections removed and coils trimmed to reestablish resonance.).

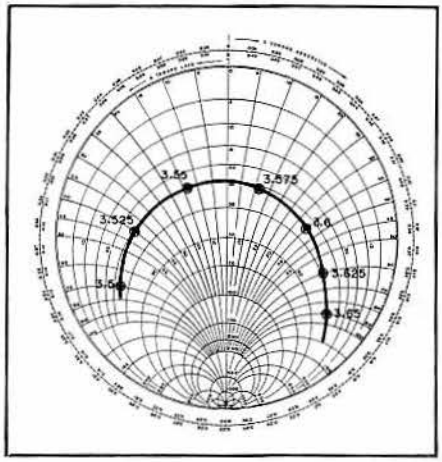

Fig. 14 — Impedance plot of a 66-foot (20.12 m) dipole using a combination of off-center inductive loading and capacitive end loading. Of all the shortened configurations tried, this arrangement offered the greatest bandwidth.

would seem to make little difference whether short sections of extra length are added inside the supporting insulators or are at the ends, suspended at right angles to the main antenna wire.

The inductors were reduced from 40 to 36.5 μH (25-turn coils replaced the original 27-turn coils), and resonance occurred at about 3575 kHz. At this frequency the resistance was 26 ohms and the SWR 1.90:1. The 3:1-SWR bandwidth, 64 kHz, is 1.79 percent of the frequency of resonance. The impedance plot for this arrangement is shown as Curve A in Fig. 13. The resistance at resonance for this antenna is identical to that with the coils alone, and the bandwidth is only 4 kHz greater, 64 kHz vs. 60. From these results, one would conclude that the main advantage offered by the "danglers" is a small saving of space over a flat-top antenna.

Capacitance Hats near Loading Coils

Next the dangling end sections were removed and a pair of capacitance hats was formed, each from two 36-inch (0.91 m) lengths of no. 12 solid wire. The two wires for a single hat were attached at their centers to the antenna wire at a point just outide one of the loading coils. The hat wires were then bent radially to form an X at right angles to the antenna wire, like four spokes of a wheel with the main antenna wire at the hub. The diameter of the X-shaped hat was thus 36 inches. The second hat was placed in a like manner just outside the second coil. Burndy connectors were used to affix the hat wires. The resonant frequency of this configuration with the original 40-μH loading coils was found to be 3290 kHz. The effect of adding the hats was about the same as that of extending the 17-foot (5.18 m) lengths to 19 feet (5.79 m).

When the inductors were replaced with 23-turn coils (32.5 μH), the antenna resonated at about 3.575 MHz, the resistance being 23 ohms. The SWR at resonance is 2.15:1, and the 3:1-SWR bandwidth for this configuration is 60 kHz, 1.68 percent of the resonant frequency. The impedance of this arrangement versus frequency is shown by Curve B of Fig. 13.

It is surprising to note that, by the standards of most amateurs, the characteristics of this antenna are not as good as those of the same length antenna with loading coils alone. The SWR at resonance for the antenna with combination capacitive and inductive loading is higher (2.15 vs. 1.92), and the 3:1-SWR bandwidths are the same, 60 kHz. Perhaps a significant factor here, though, is that the diameter of the capacitance hats used for these measurements was small, only 0.011 wavelength. Supporting much larger hats presents mechanical problems with wire antennas, however, as even these were a bit flimsy and would require reshaping after gusty weather.

Capacitance Hats at Antenna Ends

Finally, the X-shaped capacitance hats were moved to the outside ends of the antenna, just inside the end insulators. With the original 40-μH coils, resonance appeared at 3215 kHz. From calculations, it was as if the 17-foot (5.18 m) end sections were actually 21 feet (6.40 m) long. With 30-μH coils (22 turns) in place, the resonant frequency was 3560 kHz. At this frequency the resistance was 25 ohms and the SWR 1.98:1. The 3:1-SWR bandwidth is 73 kHz, or 2.05 percent of the resonant frequency. The impedance plot of this antenna is given in Fig. 14.

It is interesting to note that the position and shape of the plot for this antenna on Smith Chart coordinates is nearly identical to that for the same length antenna with loading coils only, the solid curve of Fig. 12B. For this antenna, however, the plot points for 25-kHz frequency increments appear closer together, which accounts for the increased bandwidth.

Conclusions

The measured characteristics of these various configurations of loading for the 80-meter antennas are tabulated in Table 4. Remember that the overall "flat-top" length of each antenna arrangement is 66 feet (20.12 m), and that the loading coils are always positioned 16 feet (4.88 m) each side of the center of the antenna, being pruned for resonance at approximately 3550 kHz. For comparison, information for a half-wave dipole is also included.

Of the various arrangements, capacitive end loading decidedly provides the greatest bandwidth, excepting the full-size half-wave antenna, of course. Although there are slight differences in the resistance value at resonance, all are of the same order of magnitude. These values, as well as those for the 160-meter antenna discussed earlier, tend to confirm a *broad* rule of thumb that the writer has formulated for this type of antenna: The feed-point impedance value at resonance is roughly proportional to the length of the antenna. That is, a loaded antenna which is half the size of a half-wave dipole will have approximately half the radiation resistance of the full-sized antenna.

Eq. 1 given earlier or the chart of Fig. 9 allows one to calculate loading-coil values for antennas with loading coils only. Additional capacitive loading is not taken into account. Calculating the effects of various capacitive loading arrangements appears to be difficult, and work remains to be done in this area.

Multiband Antennas with Loading Coils

All of the foregoing material has been devoted to the loading of an antenna for resonance at a single frequency. Resonated as described, the antenna is electrically a half wave in length. It will, however, operate well on higher frequencies — frequencies at which it is an odd multiple of half waves in *electrical* length . . . three half waves, five half waves, etc. Because of the lumped loading of the shortened antenna, these higher frequencies will likely not be closely related to odd-order harmonics of the fundamental frequency, as the case would be for a nonloaded radiator. (For example, it is a well-known fact that a 7-MHz half-wave dipole operates well on its third harmonic, 21 MHz.)

A loaded dipole will become an electrical 3/2-λ antenna at some frequency below that which is three times the fundamental resonant frequency. Depending upon the overall antenna length, coil value, and coil position, it is possible for an 80-meter loaded dipole to become a 3/2-λ performer on 40 meters. With such an arrangement, one would have a dual-band antenna without requiring the use of traps. The idea can be expanded upon to arrive at a loaded antenna without traps which will operate on more than two bands. This scheme offers considerable constructional simplification as compared with trap arrangements.

The multiband loading-coil concept has been recognized for better than half a century, but little use of the technique has been made by amateurs. Some years ago a very good article on the subject was published by William Lattin, W4JRW.[5] That article is recommended reading for anyone interested in more details on the concept. Supplemental information has been published by Buchanan.[6] Attempts by this writer to calculate antenna sizes and coil values for dual-band antennas have met with some success. From calculations and experiments to date, it appears that with only two loading coils (one each side of center), the antenna must always be greater than a half wave in physical length for the higher of the two frequency bands. In other words any 80/40 meter arrangement, for example, apparently would need to be longer than 66 feet (20.12 m) from tip to tip. However, much work also remains to be done in this area. This material was originally presented in *QST* by Jerry Hall, K1TD.

References

[1]Sevick, "The Ground-Image Vertical Antenna," *QST*, July 1971. (See chapter 1.) Also, "The W2FMI Ground-Mounted Short Vertical," *QST*, March 1973. (See chapter 1.) "A High Performance 20-, 40- and 80-Meter Vertical System," *QST*, December 1973. (See chapter 1.) "The Constant-Impedance Trap Vertical," *QST*, March 1974, p. 29.

[2]LaPlaca, "Using the ARRL L/C/F Calculator," *QST*, December 1973, p. 26.

[3]Hall and Kaufmann, "The Macromatcher, An Rf Impedance Bridge for Coax Lines," *QST*, January 1972, p. 14. Information also contained in *The Radio Amateur's Handbook* and *The ARRL Antenna Book*.

[4]McCoy, "Monimatch, Mark II," *QST*, February 1957, p. 38. Also, "An Etched-Circuit Monimatch For Checking Your Antenna System," *QST*, October 1969. (See chapter 4.)

[5]Lattin, "Multiband Antennas Using Loading Coils," *QST*, April 1961, p. 43.

[6]Buchanan, "An Inexpensive 40- and 80-Meter Antenna, Hints and Kinks," *QST*, September 1962, p. 62.

Efficient Short Radiators

If you're cramped for space to put up a beam antenna, you'll want to investigate these ideas as one way to shrink 'er down to usable size.

Shortened antennas have been popular with amateurs for either esthetic, space limitation or economic reasons. And most are inefficient radiators with narrow bandwidth. This section will first define some limitations and problems of conventinal short antenna designs. A design for a half-size 2-element Yagi, the performance of which is competitive with its full-size equivalent, will follow.

It has been proved that no appreciable difference exists between the directive patterns of "short" and full half-wave horizontal dipoles. Since the gain of a half-wave dipole over an isotropic radiator is determined by the dipole directive pattern and since the length of the dipole (up to λ/2) has negligible effect on its directive pattern, the length of the dipole (up to λ/2) has a negligible effect on its gain. An assumption is made that the efficiencies of both the short and half-wave dipoles are equal. The efficiency of an antenna can be expressed as

$$\text{Eff} = \frac{R_r}{R_r + R_{loss}} \qquad \text{Eq. 1}$$

where R_r = radiation resistance
R_{loss} = loss resistance of conductors, coils, etc.

The radiation resistance (R_r) of a horizontal dipole is determined by its length and height above ground. In free space, the R_r of a half-wave dipole is 73 ohms. As the length of the dipole is reduced, the R_r decreases as the square of the length. Thus, for a half-size dipole (as compared with λ/2), the R_r decreases to a value one-fourth that of the λ/2 dipole or approximately 13 ohms.

The efficiency of a half-wave dipole is very high, being on the order of 95 percent. The R_r is large and R_{loss} small by comparison. If we reduce the overall length by a factor of two, the R_r decreases by a factor of four. Input impedance at the center of the dipole is comprised of a low resistance and large capacitive reactance, so inductive loading is required in order to resonate the dipole. The inductive reactance needed to center-load the antenna will be approximately 1 kΩ (depending on conductor size used for the antenna). Assuming a coil Q of 200 and computing efficiency using Eq 1: This means that 28 percent of the transmitting power applied to the antenna is dissipated in the loading coil. The author has neglected any additional losses in the matching network which would result if the above antenna were driven by a 50-ohm source.

Let's suppose we decide to build a 2-element Yagi using shortened center-loaded elements. The driven element by itself has an R_r of 13 ohms. Adding a close-

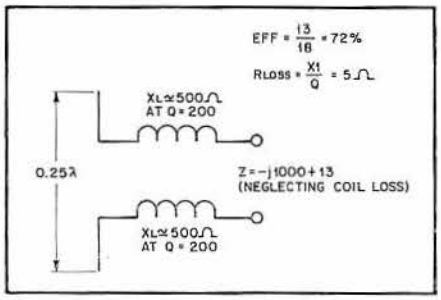

Fig. 15 — Electrical equivalent for the center-loaded dipole discussed in the text. Efficiency is 72 percent, as determined by Eq. 1.

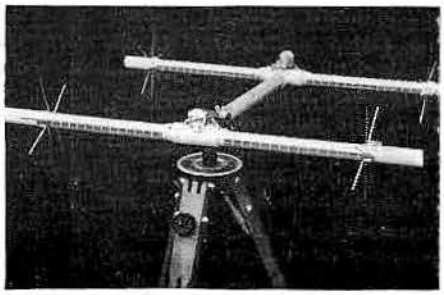

The 100-MHz "model" used by the author for testing shortened elements in a Yagi antenna design.

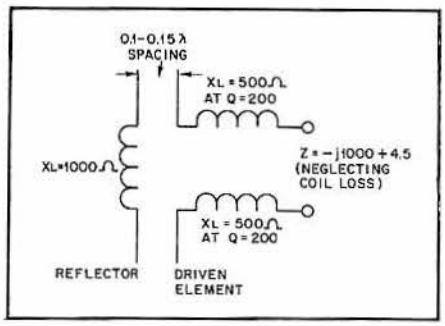

Fig. 16 — Electrical equivalent of a loaded 2-element antenna. The efficiency is 47 percent.

spaced parasitic element reduces the radiation resistance by approximately a factor of three. Thus, the driven element has an impedance composed of approximately 4.5 ohms resistive and 1 kΩ reactive. Loading both the driven and parasitic elements with the same inductors that were used for the dipole and computing efficiency

$$\text{Eff} = \frac{4.5}{4.5 + 5} = 47 \text{ percent}$$

This efficiency equates to slightly more than a 3-dB power loss in the driven element. The writer has neglected the sizable loss in the matching network since it must transform the 50-ohm source to the 9.5-ohm impedance of the antenna at resonance. In addition, the loading coil of the parasitic element will contribute approximately 1 dB of loss.

Taking into account the losses on loading coils of both the driven and parasitic elements and the loss on the driven element to feed-line matching network, we can easily account for a 5-dB power loss. Such a power loss would nullify the gain of a properly tuned Yagi, making it little better than a full-size dipole.

It should be obvious from the previous examples that the poor performance of short dipoles, and particularly Yagis, is a direct result of losses in loading inductors. If we can reduce these losses while raising the radiation resistance, the increase in efficiency will (might?) make the short dipole or Yagi competitive with its full-size counterpart.

Test Antenna

The helically wound whip antenna has always been appealing because the R_r tends to be higher than that of the base-loaded whip. This is because it is continuously loaded. In fact, using end-loading (large capacitance hats), the current distribution will be much more constant, yielding an R_r of up to four times that of a base-loaded whip. The author decided to use the helical design for a short test dipole and investigate the properties of this antenna versus that of a full-size dipole.

Conventional design for a helically wound antenna uses a form (wood, bamboo, fiberglass) wound with approximately $\lambda/2$ of no. 14 wire per $\lambda/4$ element. The writer felt that the resistive R_{loss} of this large amount of wire would be as great as that of the loading coils in the center-loaded dipole, making the helical design ineffective. As it is desirable to reduce conductor resistance, the surface area of the conductor must be substantially increased. Tubing is not mechanically suitable, and because skin depth is only on the order of 0.001 inch (0.03 mm),[1] the use of tubing is not required. Some 1/2-inch (13 mm) wide copper tape[2] was on hand and a study of its skin resistance revealed a loss per unit length of 12 percent less than that of the no. 14 wire.

A helically wound dipole was constructed (using the 1/2-inch [13 mm] wide tape) for use at 100 MHz. This frequency was chosen so that field-strength measurements could be performed using a local fm broadcast station as the signal source. A 28-inch (711 mm) length of 3/4-inch (19 mm) CPVC tubing (plastic water pipe) was wound with 38 equally spaced turns of the 1/2-inch (13 mm) wide tape. Using a grid-dip meter, resonance was measured at 104 MHz. Next, two 5-1/2-inch (140 mm) diameter six-spoke capacitance hats were attached to the ends. Resonance was again measured and found to be 84 MHz. A C-match[3] was constructed to transform the low impedance of the short dipole to 50 ohms. The C-match requires that the element be made to look inductive by lowering its resonant frequency. A variable capacitor is then shunted across the feed point and adjusted for resonance. This L/C ratio determines the impedance transformation. A 100-pF variable capacitor was shunted across the feed point of the test dipole and a 50-ohm coaxial cable was attached. Since the dipole is a balanced antenna, feed-line decoupling was necessary. The author used a quarter-wave sleeve (bazooka).

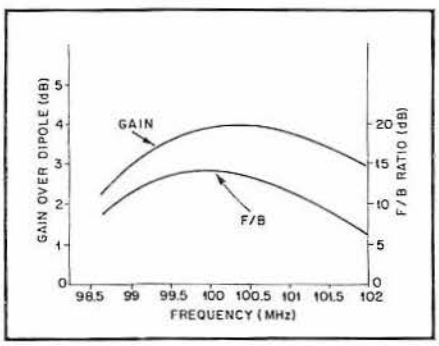

Fig. 17 — Curves depicting gain and FBR (front-to-back ratio) vs. frequency when the Yagi antenna is tuned for operation at 100 MHz.

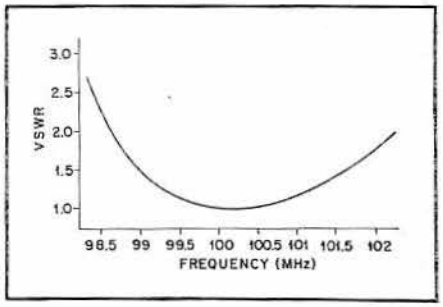

Fig. 18 — VSWR vs. frequency when the Yagi antenna is tuned for operation at 100 MHz.

Antenna Tuning

Rf power was applied to the test antenna through an SWR meter (measurements were taken in a screen room). Turns were removed, one at a time, and the shunt capacitor adjusted until a 1:1 match occurred. The capacitance hats were always installed at the tips of the element. When adjusted for a 1:1 match, the dipole consisted of 32 turns of copper tape, center fed, with 40 pF shunting the feed point and an overall element length of 21 inches (533 mm) which is 37 percent of the length of a full-size dipole. Tuning was very simple and took but 15 minutes to complete.

Measurements

The feed-point impedance was measured (with C-match disconnected) to be 20 ohms. The skin depth resistance was computed to be 0.24 ohm. Computing efficiency

$$\text{Eff} = \frac{20}{20 + 0.24} = 98 \text{ percent}$$

which is essentially the same as a full-size dipole. Bandwidth between 2:1 SWR points was measured to be greater than 6 percent of the operating frequency. Large capacity hats (for 100 MHz) and wide tape

play an equally important role in reducing the Q of the antenna sufficiently to obtain a wide bandwidth. Next, a low-level signal generator and dipole were set up 5 wavelengths away from the test antenna. Using an Empire NF-105 noise and field-strength meter, a comparison was made on field strength between the test antenna and a full-size dipole. Results indicated no apparent measurable difference between the short helically wound dipole and a full-size dipole. Field-strength measurements were then taken on the signal from a local fm broadcast station. Again, there was no apparent difference; not bad for an antenna that is less than half size. The next question to be answered was whether gain could be secured by the addition of a parasitic element.

A boom and a parasitic element were added to the shortened test dipole. Although a director might provide better gain and front-to-back ratio (FBR), the decrease in radiation resistance, to a very low value (dipole by itself equals 20 ohms) because of the close spacing, was thought to decrease efficiency and bandwidth. A parasitic reflector was constructed, similar to that of the driven element. The element was split in the center and a 100-pF capacitor installed for tuning purposes. Element spacing was adjusted to 0.15 λ. With the capacitor fully meshed, the six-spoke capacitance hats were physically positioned on the element (both equidistant from element center) so that the reflector resonated at 93 MHz. Nominal reflector tuning calls for reflector resonance approximately 5-percent lower in frequency than the driven element, or 95 MHz. With the above configuration, the author was able to adjust reflector resonance, using the variable capacitor, anywhere in the range of 93 to 96.5 MHz or 3.5 to 7 percent lower in frequency than the driven element.

Using the same field-strength measurement set up as with the dipole, the reflector was aimed at the source signal and adjusted (using the variable capacitor at element center) for minimum pickup. The driven element was then readjusted for a 1:1 SWR and the process repeated until minimum rear pickup and a 1:1 SWR occurred simultaneously. Gain and FBR measurements were made at the design frequency and at points two percent of the design frequency on either side. The results are described in Fig. 17. The bandwidth measurements are given in Fig. 18.

As can be seen from the curves in Fig. 17, a gain of 4 dBd, and a 15-dB FBR can be secured quite easily with a physically short Yagi. As with other Yagis, the gain is relatively constant over a wide frequency range. However, the FBR drops quite fast especially when trying to use the antenna below its design frequency. From curves given in Fig. 18, the bandwidth between the 2:1 VSWR points is shown to be about 3.7 percent. Translated to 20 meters this bandwidth would be 500 kHz, equal to or greater than the average 3-band trap Yagi. If indeed the design were scaled to 14 MHz, the antenna would have element lengths of slightly over 12 feet (3.66 m) and a boom length of 10 feet, 6 inches (3.20 m).

Adapting Design to Ham Bands

Since it has been shown that a physically short Yagi can provide significant gain and FBR, a few design pointers are in order. First, make the element length no shorter than physically necessary for your particular situation. Bandwidth and efficiency will improve with greater lengths. Second, the use of large capacitance hats is recommended, as this reduces the helical conductor length and thus R_{loss}. Third, use large forms of good dielectric quality (fiberglass). The larger the form diameter, the greater the length reduction for a given number of turns. Also, with large diameter forms, 1.5 inch (38 mm), the width of the conductor can be increased, thus reducing R_{loss}. Fourth, regardless of the matching network used, construction of capacitance hats, etc., *solder all* joints and *seal* with silicone rubber. *Do not rely on pressure joints.* Fifth, to secure a reasonable FBR with any Yagi using a split driven element and fed with coaxial cable, some form of balun transformer is required to keep currents from flowing on the outside of the coax braid. Sixth, the use of a grid-dip meter is the only practical method to secure resonance with a fixed physical length. Construction will require some cut and try. Proximity to surrounding objects will affect resonance, and should be avoided when tuning the array.

No doubt the author has left out items, which may prove to be a problem for the reader. This article was intended to be more thought provoking than constructional, although there should be enough information here to build your own antenna with a reasonable amount of experimental effort. My current plans call for construction of a 2-element 10-meter Yagi (for reception of OSCAR signals) with 6-foot (1.83 m) elements and a 5-foot (1.52 m) boom. The author wishes to thank Mike Povlich, WB9HGS and Russ Mills for their assistance with measurements. This material was originally presented in *QST* by Ronald J. Gorski, N9AU.

References

[1]Kuecken, *Antennas and Transmission Lines*, Howard W. Sams and Company, Indianapolis, IN, 1st Edition (1969), p. 274.

[2]Copper tape available from Minnesota Mining and Mfg. Check Yellow Pages for the address of a local distributor.

[3]Orr, *Beam Antenna Handbook*, Radio Publications Inc., Wilton, CT, 3rd Edition, p. 63.

Simple Arrays of Vertical Antenna Elements

Work DX with a vengeance! Simple arrays of vertical elements will provide good low-angle radiation. DXCC may be closer than you think if you can manage a system like this one!

Because of the excellent low-angle radiation properties of vertical antenna elements and because of the benefits to be gained by horizontal-plane directivity, it is interesting to attempt to determine "optimum" arrangments of elements to produce "beam" antenna arrays. Because of the enormous variety of configurations possible, and the great difficulty of either experimental modeling or calculating exact theoretical performance, it has not been practical in the past to arrive at valid conclusions. However, it is now quite easy to simulate such antenna arrays by computer programs, and these can produce relatively quick and precise answers to a very large number of postulated configurations. After a number of computer trial runs, "optimum" configurations can be found quite readily. Such a computer program for quarter-wave elements has been written and supplied by H. Hurwitz, WA2VBW. Using a modification of this program, the author has investigated a

Table 5

Case	Element	Current	Phase	X	Y	Beam Direction	Beam Gain	Back Radiation	Minor Lobes
1	1	1	0	0	0	0°	3 dB	-3 dB	-α
	2	1	-90	0.25	0				
2	1	1	0	0	0	0°	4.1 dB	5.7 dB	-11.5
	2	1	-120	0.25	0				
3	1	1	0	0	0	90°	1.1 dB	0 dB	0 dB
	2	1	0	0.25	0				

Table 6

I1	I2	φ1	φ2	Beam Gain	Back Radiation	Minor Lobes
1	0.8	0	-120	4.0 dB	-5.5 dB	-10.8 dB
1	1	0	-120	4.1	-5.7	-11.5
1	1.2	0	-120	4.1	-5.6	-12.5
1	1	0	-100	3.4	-3.8	-11.1
1	1	0	-120	4.1	-5.7	-11.5
1	1	0	-140	4.6	-6.6	-6.6

Table 7

Element	Current	Phase	X	Y	Beam Direction	Beam Gain	Back Radiation	Minor Lobes
1	1	0	0	0				
2	1	-120	0.25	0	0°	5.6 dB	-8.7 dB	-8.7 dB
3	1	-240	0.5	0				

Table 8

Element	Current	Phase	X	Y	Beam Direction	Beam Gain	Back Radiation	Minor Lobes
1	1	0	0	0				
2	1	0	0.25	0	90°	2.7 dB	0 dB	0 dB
3	1	0	0.5	0				

Table 9

Element	Current	Phase	X	Y	Beam Direction	Beam Gain	Back Radiation	Minor Lobes
1	0.5	0	0	0.145				
2	1	-110	0.25	0	0°	4.35 dB	-6.1 dB	-15. dB
3	0.5	0	0	0.145				

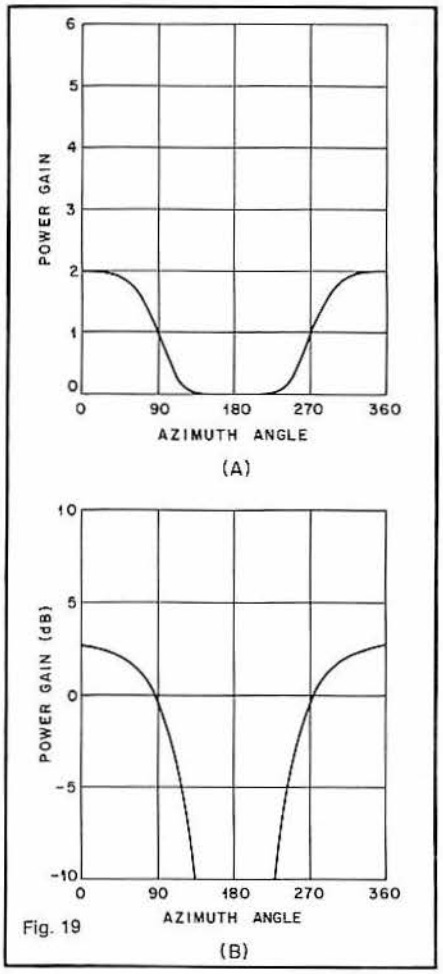

Fig. 19

large number of simple array configurations, which are potentially quite useful at the lower amateur frequencies, with the salient results given here. It is hoped that these will prove interesting to those considering construction of such arrays.

Technique for Optimizing Arrays

We must first try to define the problem and the parameters leading to an optimum design. The horizontal-plane pattern of an array of (vertical) elements depends only on the magnitudes of the individual element currents and their phases, and not on the way the currents are produced (e.g., driven or parasitic). The computer program allows one to specify the locations (x,y coordinates) of any number, n, of quarter-wave elements; also one must specify the magnitude of current and its phase in each element (usually normalized to unity current and zero phase for a given fiducial element). With these data inputs the radiation pattern is calculated and plotted out, giving the relative power gain in each azimuth angle interval, say, 5 or 10 degrees. The power gain is normalized to that power which would have been radiated at the same azimuth by a *single* vertical element using the same input electrical drive power. By using trial values of the current in all elements, in both amplitude and phase, one soon develops a feel for the behavior of the system, and can usually arrive at a "best" value for all the currents and phases. One can then try different geometrical separations of the elements and in this way arrive at the "best" spacing. Usually this best configuration is a compromise between power gain and good pattern control, e.g., front-to-back ratio, or more generally, main lobe to minor lobe (side or back) ratio.

In addition to the optimization described above it must be noted that if the array is to be used primarily to produce a "beam" in a given general direction with little emphasis on other directions, one usually finds a linear array of elements best (equivalent to an end-fire Yagi array). However, if the array is to be used for all directions, a more (circularly) symmetrical array should be considered. These points will become clear in the discussion of results.

Two-Element Array

In the case of two elements there is only one possible configuration. Consider one element at the origin of the x,y plane (coordinates 0,0) and the other element along the x axis (coordinate x,0). The parameters available are x, which we specify in units of wavelength, λ, the rf currents I1 and I2 in each element (we shall normalize one of the currents, e.g., I1, to unity) and the phases, $\phi 1$ and $\phi 2$, of the currents (we shall generally normalize the phase of the current in element 1 as zero and specify the relative phase of the current in element 2 in electrical degrees, either positive for leading currents or negative for lagging currents). It soon becomes apparent that the region of main interest is where the spacing x is in the neighborhood of 0.25, i.e. λ/4, and there the currents are nearly equal in magnitude. The reasons are that, for spacings of 0.5 or greater, other strong lobes appear in the pattern, and for grossly unequal currents relatively poor

Table 10

Element Spacing	Optimum $\phi 2$	Beam Gain	Back Radiation	Minor Lobes
0.2	-130°	4.65 dB	-6.5 dB	-18 dB
0.25	-120°	4.6	-6.5	-16
0.3	-110°	4.4	-6.2	-14
0.35	-110°	4.2	-5.8	-12

Table 11

Element	Current	Phase	X	Y	Beam Direction	Beam Gain	Back Radiation	Minor Lobes
1	1	0	0	0				
2	1	-120	0.25	0	0°	7.4 dB	-9.9 dB	-9.9 dB
3	1	-240	0.5	0				
4	1	0	0.75	0				

Table 12

Element	Current	Phase	X	Y	Beam Direction	Beam Gain	Back Radiation	Minor Lobes
1	1	0	0	0				
2	1	0	0.25	0	90°	4.2 dB	0 dB	0 dB
3	1	0	0.5	0				
4	1	0	0.75	0				

Table 13

Element	Current	Phase	X	Y	Beam Direction	Beam Gain	Back Radiation	Minor Lobes
1	1	0	0	0				
2	1	-110	0.25	0	45°	6.4 dB	-18 dB	-18 dB
3	1	-220	0.25	0.25				
4	1	-110	0	0.25				

Table 14

Element	Current	Phase	X	Y	Beam Direction	Beam Gain	Back Radiation	Minor Lobes
1	1	0	0	0				
2	1	-120	0.25	0	0°	5.1 dB	-11.5 dB	-11.5 dB
3	1	-120	0.25	0.25				
4	1	0	0	0.25				

Table 15

Square side Length (inλ)	ϕA opt.	ϕB opt.	Beam Gain	Back Radiation	Minor Lobes
0.167	-130	-260	6.6 dB	-22 dB	-22 dB
0.25	-110	-220	6.4	-18	-18
0.333	-80	-160	5.6	-18	-18

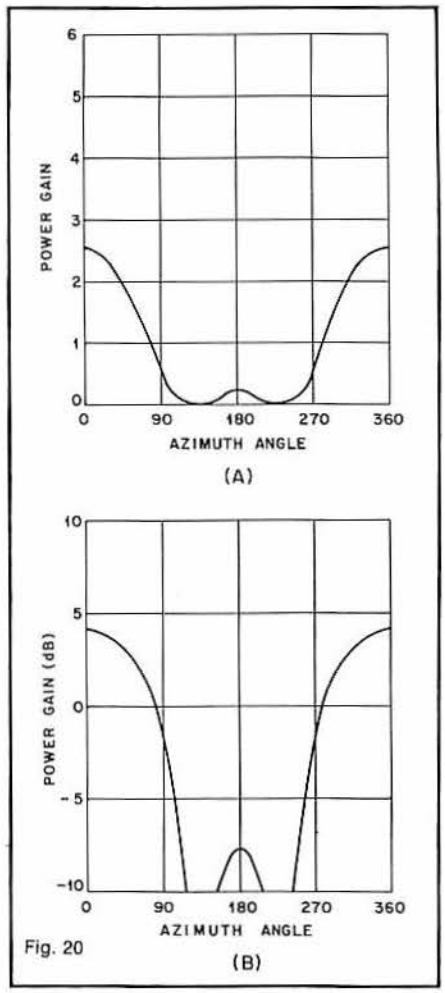

Fig. 20

peak gain and pattern discrimination result. Although the spacing x is not especially critical in the neighborhood of 0.25 (one can essentially compensate by adjustment of phase angle) we shall now examine the case where x = 0.25, and where I1 = I2 = 1. Best overall pattern discrimination (minimum back lobe) for the endfire case occurs where $\phi 1 = 0$, and $\phi 2 = 90$ degrees, and the power-gain pattern is shown in Fig. 19A.

Peak gain is 2 (or 3 dB) and occurs along the x-axis direction. Fig. 19A shows the power pattern of the array, i.e., it shows quantitatively where the radiated power goes. However, if one is looking at what an S meter would indicate, one can present exactly the same information on a vertical *logarithmic* scale as shown in Fig. 19B.

The vertical scale is shown in dB relative to the value for a single vertical radiator. This type of display is useful in judging excellence of pattern with respect to minor lobes. For all future cases discussed here, both displays will be shown.

It is possible to increase the gain of this array at the expense of some back lobe by increasing the phase lag in element 2, e.g., if $\phi 2 = -120$ degrees the peak gain, again along the x axis, is 2.59 (or 4.1 dB) and the entire pattern is shown again in Figs. 20A and B.

Note that the back lobe now shows a gain of 0.186, which is −11.5 dB relative to the forward lobe.

These two elements can be used to form either a beam along the +x axis as shown, or reversed along the −x axis (by reversing the phase $\phi 2$, i.e., making it +120 instead of −120 degrees) or if the two elements are driven in the same phase, i.e., $\phi 1 = \phi 2 = 0$, one produces a bilateral broadside beam as shown in Fig. 21.

Here the peak gain is 1.1 dB, but there is a "back" lobe of equal magnitude to the front lobe. Note that all patterns will be symmetrical around the x axis, or more generally around the line of any set of linearly-positioned elements. This example has illustrated some of the aspects of all of the results to be presented; namely, that:

a) The best element spacing will be found to be in the neighborhood of 0.25 wavelength.
b) Current ratios and phases can be adjusted to produce either a best *pattern discrimination* (minor lobe rejection) or best *main lobe gain*. It is generally not possible to get both at the same time, and a compromise must be made.

It may be useful to tabulate the salient results of each "best" case by noting the coordinates of the elements in the x,y plane, the individual drive currents, the individual phases, main beam heading in the x,y plane, main beam gain, and the

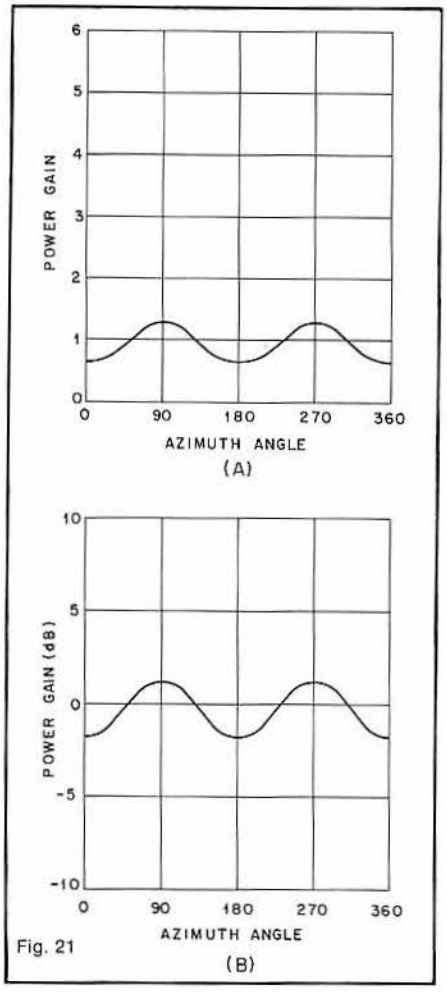

Fig. 21

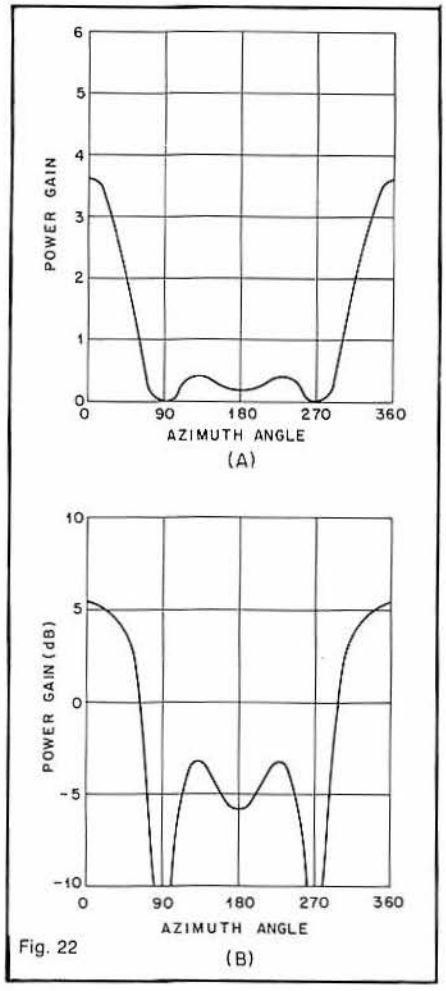

Fig. 22

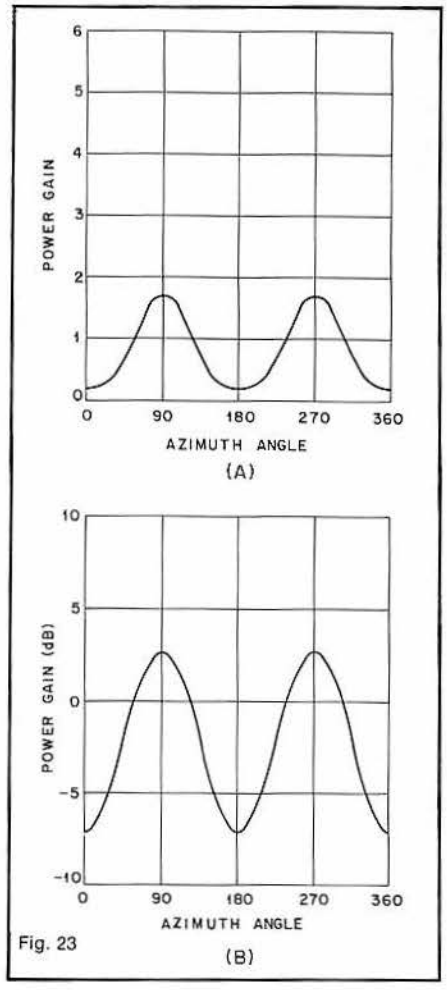

Fig. 23

largest pattern gain (such as given by either the side of the main lobe or by minor lobes) observed anywhere in the entire 180-degree sector centered just opposite in direction to the main lobe. We shall designate this quantity as "back radiation" and express it in dB relative to the main lobe gain. We shall also tabulate the largest minor lobe in this sector and label it "minor lobe," again expressed in dB relative to the main lobe. Thus for the cases just described, Table 5 is presented.

The sensitivity of these results to variations of currents and phases is not high. For example, one can summarize case 2 above with somewhat altered I2, or $\phi 2$, as shown in Table 6.

The author feels that end-fire case 2, where $\phi 2 = -120$ degrees, probably represents the "best" design with a good pattern and gain. Other more complicated cases presented below are optimized in this same way and only the "best" configuration will be shown with actual results.

Three-Element Arrays

For three elements, two different geometries suggest themselves: the linear array, best for a single preferred directional line, and an equilateral triangle configuration, the closest approach to circular symmetry. The latter, as we shall see, could be switched to give "beams" in any one of six angular positions (every 60 degrees). Let us consider first the linear array.

Linear Array — As in the 2-element linear array just discussed, the optimum arrangement seems to center around an element spacing of about 0.25 wavelength with approximately equal current drives. The optimum end-fire case is shown in Table 7; the broadside case is shown in Table 8.

The patterns for these cases are shown in Figs. 22 and 23.

Remember that for the end-fire case, which one can think of as a 3-element Yagi on its side, the rather large side lobe results because the pattern lies in a plane perpendicular to the elements. Side radiation is hard to avoid, as one cannot take advantage of the nulls off of the ends of excited elements.

Equilateral Triangular Array — For this case, the optimum situation appears to be as shown in Table 9. The behavior is very similar to the case of two elements in end-fire. See Table 5 (we have just split one of the two elements and have moved the separate pieces to the triangle corners). The pattern is shown in Fig. 24.

Reversing the phases will reverse the beam direction, and by rotating the drive currents (and phases) around the triangle, one can produce six beam directions (every 60 degrees). This is an attractive feature, but it does not come free; the maximum gain of the system is somewhat less than one obtains with the three linearly-disposed elements (which are chiefly useful in a direction along the line of the array).

The exact size of the triangular array is not critical — one must simply choose the best phase angle for the particular geometry. The "best" phase angles, $\phi 2(\phi 1 = \phi 3 = 0)$, as determined by computer runs, for different spacings (triangle side lengths expressed in terms of λ) are shown in Table 10.

Four-Element Arrays

With four elements, there are at least three configurations which are interesting to investigate. As before, the linear array with a preferred beam direction is one type, but there are two configurations which possess a measure of circular symmetry. One of these is described by three antenna elements at the corners of an equilateral triangle with the fourth element at the geometric center of the triangle. This one we shall designate as a center-filled triangle. The other type is a square array.

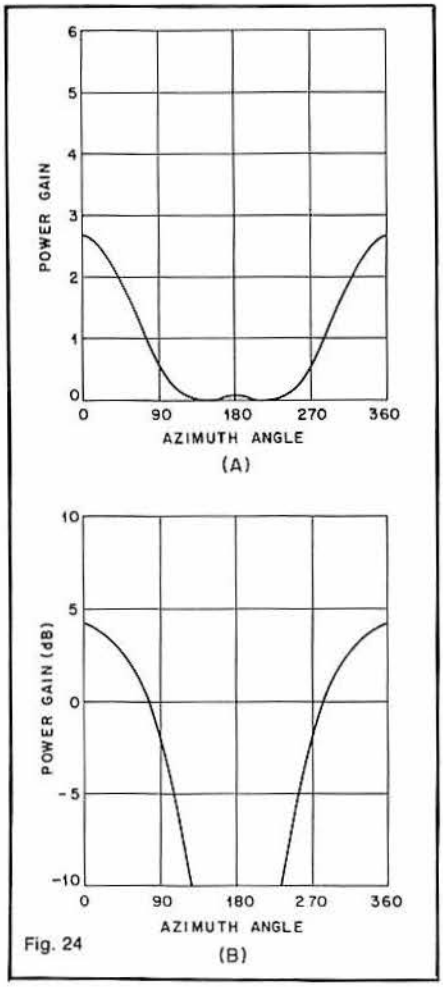

Fig. 24

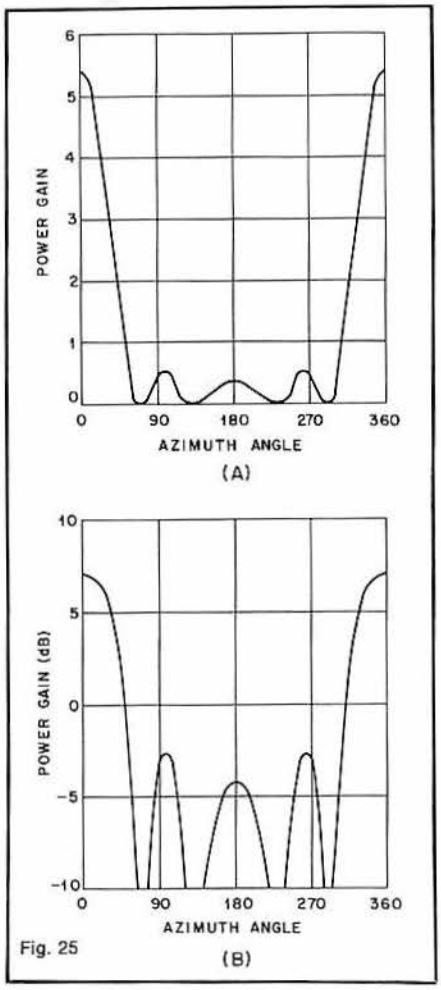

Fig. 25

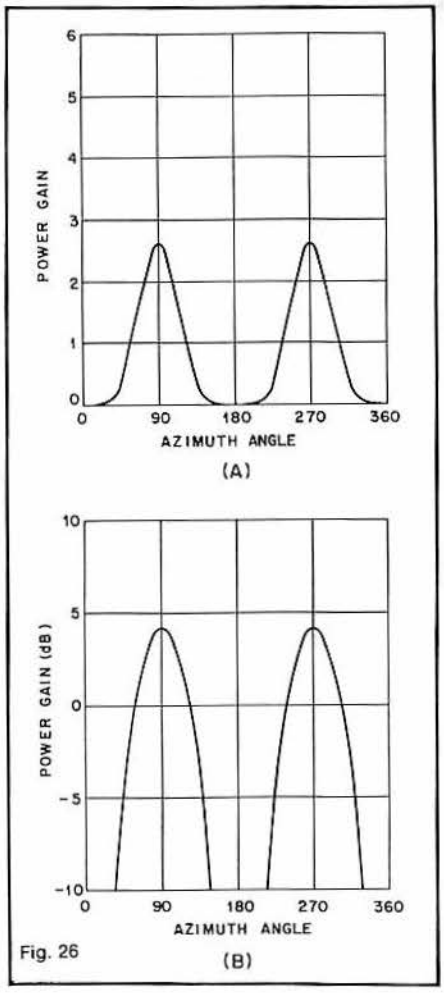

Fig. 26

Let us take these three types in order.

Four-Element Linear Array — For this case the optimum end-fire solution appears to be as shown in Table 11. The gain and major lobe shape of this configuration seems to be excellent. The broadside case is shown in Table 12. Patterns for this case are shown in Figs. 25A, B, and 26A, B.

Note that for this array there is poor coverage in some azimuthal directions (e.g., ±45 degrees) if only the two tabulated phase arrangements are used.

Center-Filled Triangle — A large number of situations were examined for this configuration, but unfortunately no combinations of spacing, currents or phases were found that looked very good. The best pattern was not particularly better than that of the three-element triangle alone, and was substantially inferior to that of the 4-element square to be discussed next.

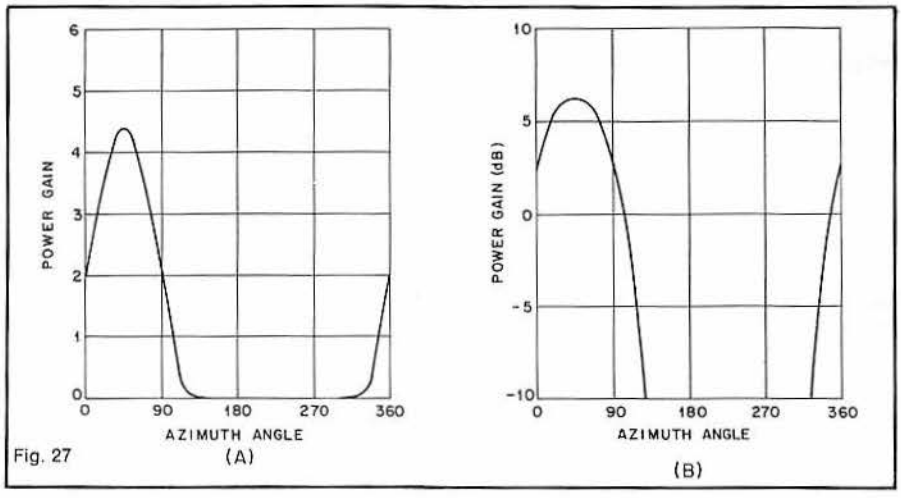

Fig. 27

Four-Element Square Array — For this case the best situation appears to be as shown in Table 13. Note that this arrangement fires diagonally and produces a respectable gain and excellent pattern. The "broadside" arrangement for the same square is shown in Table 14. The computed patterns are shown in Figs. 27 and 28.

The diagonal-fire pattern is exceptional, providing extremely low back radiation and minor lobes. The broadside pattern is not nearly as good, somewhat superior but reminiscent of the end-fire pattern obtainable with just 2 elements (see Fig. 20). In fact, the power-gain coverage at all angles (including the broadside angle) just using the switched four diagonal beams is large enough that it probably is not worthwhile using the broadside arrangement at all even to "fill" between diagonal beams.

This square array is superior to the center-filled triangle, and to all other simpler configurations (circular) in both gain and pattern discrimination. It is sufficiently good that one might ask what particular properties of the square have led to the nearly ideal performance. The

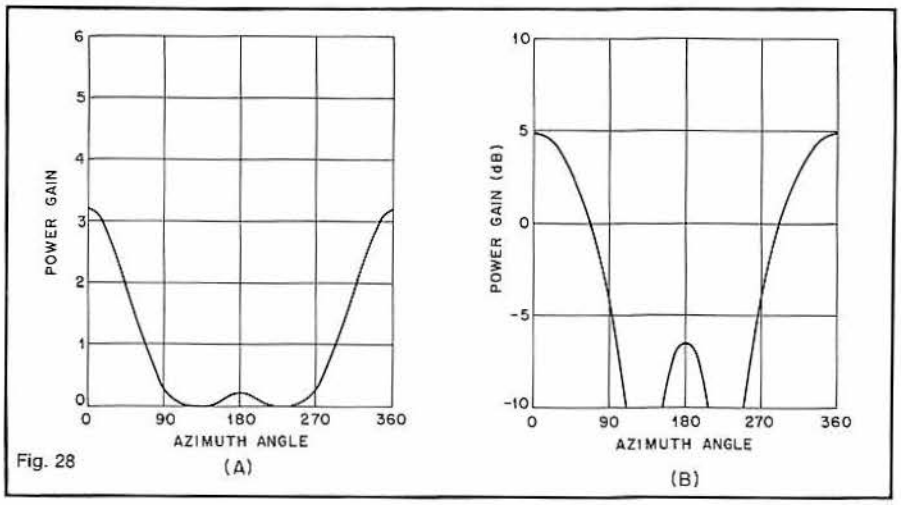

Fig. 28

author believes that there are two parameters which are noteworthy: first, the gain is respectable in diagonal fire because one can view the square along its diagonal as a three-element linear array in which the center element is split, each half being displaced to the other corners of the square. Thus the array behaves something like a 3-element (Yagi-like) linear array which is known to have a good gain. Secondly, the lobes are much smaller than the linear array due to the tendency for the phase cancellation of waves produced by the spatially-separated corner elements.

Again, as in previous examples, the actual dimensions of the square are not very critical, as long as one adjusts the phase (delay), ϕA in elements 2 and 4 and the larger phase delay, ϕB, in element 3 to the "best" value. Examples of such "best" phase values for different size squares are shown in the Table 15.

It turns out that the calculated gain figures for the smaller arrays are actually slightly larger than the gain for the larger squares, but as a practical matter this fact is probably offset by the larger (reactive) currents required for radiation. The larger currents are necessary because of the mutual coupling and phase relations between elements and the required phase relationships; in practice with the inefficiencies usually caused by ground currents when using vertical antennas, the gain differences for the various squares are probably inconsequential. The patterns for all cases are quite good, but the best pattern is obtained for the $\lambda/4$ square. Incidentally, the 0.167λ and 0.33λ square allows the possibility that a single square can be used for two amateur bands, and this has indeed become the subject of a practical antenna system.[1]

Conclusion

Computer trial runs, through a program developed by WA2VBW, have facilitated the investigation of a large number of $\lambda/4$ vertical antenna-array configurations. "Best" configurations, drive conditions, power gains and patterns have been found for the cases of two, three and four elements. Especially interesting is the case of four elements arranged in a square whose side dimension is about one-quarter wavelength.

Cases using more than 4 elements have been investigated, but the complexity, probable cost, and difficulty of installation of such configurations, reduces their utility and so they will not be reported here.

The author wishes to acknowledge the contribution of Henry Hurwitz, WA2VBW, who supplied the original computer program for this investigation. This material was originally presented in *QST* by James L. Lawson, W2PV.

References

[1]Lawson, W2PV, "75/80 Meter Vertical Antenna Square Array," *QST*, March 1971.

360-Degree Steerable Vertical Phased Arrays

Microwave power-splitting and phasing techniques were applied to the design of this 80-meter array. It has established an outstanding record for performance on long and difficult paths.

The possibility of providing effective 360-degree horizontal coverage with an array switched electrically, rather than rotated mechanically, has long intrigued many designers. Such a solution to the directional antenna problem is of particular interest to amateurs operating on the lower frequencies, where any mechanical rotation system is difficult and expensive to build. One of the authors, now W1CF, writing under his old call, W1HKK, described an 80-meter switchable phased array of four quarter-wave in-line elements more than 10 years ago.[1] The present article describes several novel array designs, using up-to-date technology, which provide greatly improved operation. Also covered are techniques used for effective power division, the beam-forming phasing system, switching, and impedance matching. Ground radials, cable and connector selection, and dc continuity testing are discussed.

One of these arrays recently constructed for 80-meter use has a single 97-degree lobe with a gain over a single vertical of approximately 7 dB at low angles. Its front-to-back ratio is 25 dB, and its front-to-side ratio is more that 12 dB, over the whole 80-meter band. It is switchable over 360 degrees in four 90-degree steps.

Computer-Modeled Arrays and Patterns

In the spring of 1975, while sitting over a cup of coffee, the three authors discussed the possibility of rebuilding the 1965 4-

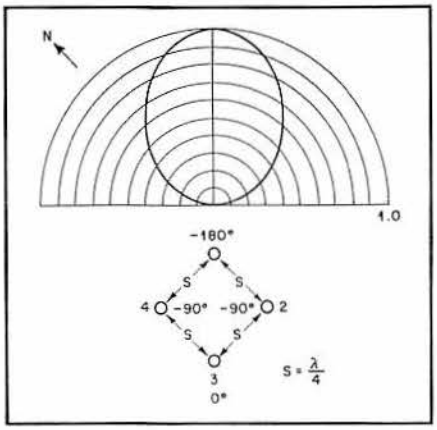

Fig. 29 — Polar plot of relative power, and planar view of the four-element diamond array showing the pattern obtained with no dc voltage on the switching relays, as in Fig. 31. Minor lobes are too far down to show on this scale.

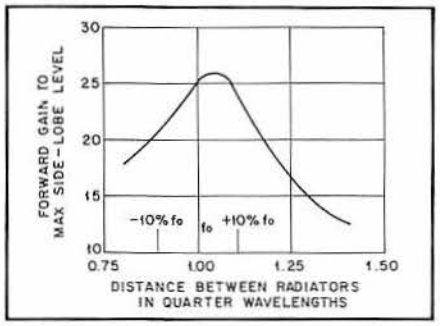

Fig. 30 — Bandwidth and side-lobe study of the four-element diamond array.

element array, using many improvements in technology that have evolved in the last 10 years. Dr. Joseph White accelerated the effort by coming up with a computer program written in Fortran IV, called ARRAY, which allows the user to plot patterns of arrays of from 2 to 99 elements in various spacings and combinations of phase and power, without ever leaving the computer terminal. Over 30 iterations using 4 elements were explored, and the computer-printed polar plots and other gain data analyzed, before we arrived at a configuration which provided good forward gain over a broad beamwidth, with no measurable unwanted lobes.

The configuration selected has four quarter-wavelength vertical elements in a square, with quarter-wave spacing between adjacent elements, as shown, with its predicted pattern, in Fig. 29. All elements are fed with equal amplitudes, the rear element at 0°, the two side elements at -90° and the lead element at -180°. The beam is transmitted along the diagonal from the rear to lead element. Gain due to horizontal beam formation alone is about 5.3 dB over a single vertical element. Front-to-back ratio is 25 dB. Front-to-side ratio is 12 dB, at 90° either side, increasing to much higher levels at 135° either side. Since most of the vertical energy is concentrated at low angles by the array, as much as 4 dB of gain additional to the predicted 5.3 dB in the horizontal plane can be achieved in theory, with perfectly conducting ground. The authors estimate that a good radial system and less-than-perfect ground yield an additional gain of 2 dB, or a total gain just over 7 dB for the system described.

The computer predicts a half-power beamwidth of 97°, so a suitable switching matrix can be used to direct the beam to four different quadrants, with only a slight loss of forward gain at the cross-over points, and virtually no deterioration of the front-to-back and front-to-side suppression. A computer study of the effect of variations in element spacing on forward-gain to maximum side-lobe level, plotted in Fig. 30, led to selection of $\lambda/4$ spacing of the corners of the square array. The 80-meter beam erected according to the computer-synthesized array design has proven to be remarkably successful. On-the-air results clearly approximate the performance anticipated by the program.

RF Power Dividers

Good power splitters are essential to the operation of phased arrays. Two-way and three-way power dividers will be discussed. Amateurs in broadcasting are well aware that tapped coils are the mainstay for power division in their industry. This reactive technique presents many problems.[2] The authors, being more versed in microwave techniques, thought it logical to scale up in wavelength the methods of power division used most successfully in the microwave region, particularly what is now known as the Wilkinson Power Divider,[3] shown in Fig. 31. Power from the transmitter is fed through a 50-ohm line of any length to a coaxial T, feeding two quarter-wavelength 70-ohm lines, W1 and W2. The two inner conductors of the 70-ohm lines are connected through a 100-ohm noninductive resistor, R1. This type of divider gives an equal power split, matches to 50-ohm loads at the two outputs, and has the unique property that any energy returning to the two outputs out of phase, due to mismatches or mutuals, is absorbed in the 100-ohm resistor.

The 90-degree phase-delay cable (DL) used in one side of each of the three power-splitting hybrids serves to assure that equal power reflections from the antennas are absorbed. Theoretically the resistors absorb none of the forward power. This technique provides approximately 30 dB of isolation from one output terminal to the other, to unwanted energy.

Reference is made in the 1965 article to difficulty in adjusting a phased array, because of element interaction due to mutual impedances between elements. The Wilkinson Power Divider, when used to feed phased arrays, reduces these problems and those resulting from imperfect match at the antenna inputs, and contributes to the realization of the predicted patterns. The "Wilkinson," is a remarkably simple and uncritical solution to the problem of power division. The 3-element vertical array described later uses a three-way "Wilkinson," shown in Fig. 33. It is constructed by splitting the 50-ohm input three ways, into three quarter-wave lengths of 93-ohm coaxial cable. The center conductors are connected together through 150-ohm noninductive resistors. An alternative approach is to return each center conductor to an ungrounded common point, through 50-ohm noninductive resistors.

Feeding, Switching and Phasing

The 4-element diamond array erected at W1CF uses three Wilkinson two-way

Terminations and switching relays at the center of W1CF array.

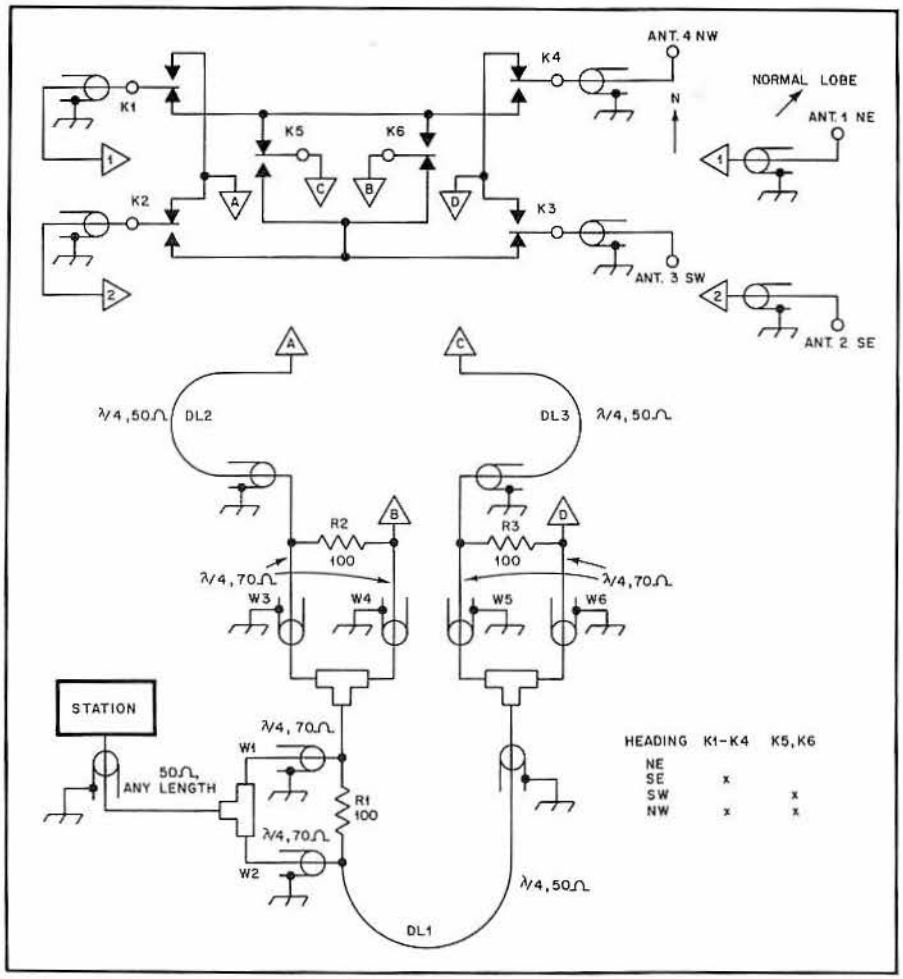

Fig. 31 — Schematic diagram of the Wilkinson Power Dividers, phasing lines, and switching relays (rf connections) for the four-element array. Dc switching commands for the four pattern headings are given at the lower right.

power dividers, as shown in Fig. 31. Phasing is accomplished with three 90-degree sections of RG-8/U cable, DL1, DL2, DL3. The four outputs are at 0°, -90°, -90° and -180° respectively in phase relationship, with power from the transmitter divided into four equal parts. Every effort was made to preserve symmetry throughout the system, in the hybrids, phase shifters, rf switching, feeds, and antenna placement, in order to have the array perform uniformly as it is switched between the four headings.

The switching can be done with six spdt coaxial relays, as in Fig. 31, or with one transfer relay and four spdt relays. With no voltage on the relay coils, the arms are in the positions shown in Fig. 31, giving northeasterly directivity (57° true, on Paris) the heading used most of the time at W1CF. The array is about 500 feet (152.40 m) from the transmitter, necessitating use of remote relays. A prospective user should consider the tradeoff between cable and relay costs. If the array is close to the station, four equal lengths of 50-ohm line can be brought into the station, and the switching done with a 4-pole, 4-position switch.

The long run of line here was dictated by the desire to take advantage of ground qualities and concealment afforded by swampland 500 feet (152.4 m) from the house. Not wanting to be electrocuted, we used 28 volts dc for operation of the switching relays. By judicious use of binary arithmetic, the switching commands require only three wires. Selection of the four beam headings is done at the operating position with a 4-wafer, 4-position switch. Relays should be selected for reliability and ease of weatherproofing. The cluster of relays and teminations shown in the photograph is at the geometrical center of the W1CF array. The connectors are protected against moisture by 3/4-inch (19 mm) heat-shrink tubing, which should extend from the bottom half inch (13 mm) of the connector 2 inches (51 mm) down the cable. In addition, wide plastic wastebaskets are used to protect these components. The expensive precautions were taken as the result of hard experience with moisture in the cables and connectors in the 1965 array.

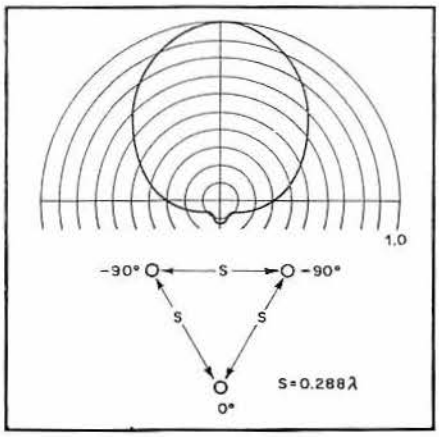

Fig. 32 — Polar plot of relative power, and planar view of the three-element triangular array.

Radiators and Radials

Relays K1 through K4 (Fig. 31) connect to their respective radiators through equal lengths of 50-ohm line, with no special attempt made for matching. The radiators are 57.5 feet (17.53 m) tall, above the base insulators. Constructional details follow the 1965 article, except as outlined below. Base insulators are 2-inch (51-mm) ID PVC pipe, 1/4 inch (6-mm) wall, 18 inches (457 mm) long, affixed to the aluminum with PVC cement and self-tapping screws. Each radiator is guyed at three levels with 3/16-inch (5-mm) galvanized cable, broken every 30 feet (9.14 m) with egg insulators.

Though 120 radials are considered to be the optimum number, only 40 per element are used here. Most are 65 feet (19.81 m) long, no. 12 galvanized wire, lying directly on the ground. This presents no hazard, as there is no foot traffic through the swamp area. The center radials are interconnected to two common busses in the central region, as recommended in reference 2. The authors feel intuitively that the square geometry of the array, in addition to providing considerable symmetry of the mutuals, allows a higher packing density for the radials, reducing ground losses.

Though the array has quarter-wavelength elements, all the feedpoints are at 50 ohms, and any type of vertical element can be used, provided an effort is made to match the inputs, and networks used for matching are *the same for all 4 elements.* Obviously, a height of 5/8 wavelength would be desirable, particularly for arrays built for higher frequencies. An indication of match would be to put rf voltmeters across the 100-ohm resistors, and tune the matching networks simultaneously for minimum voltage across the resistors. A nice thing about the λ/4 case is that the match is close enough that this step has not been necessary.

Testing

Before the array is fired up somebody should go to each element and short the input, while another person watches an ohmmeter placed across the main line at the station end. Make sure that a very low dc resistance is measured. Then, with the array in the normal position, as in Fig. 31, make sure that the resistance across the

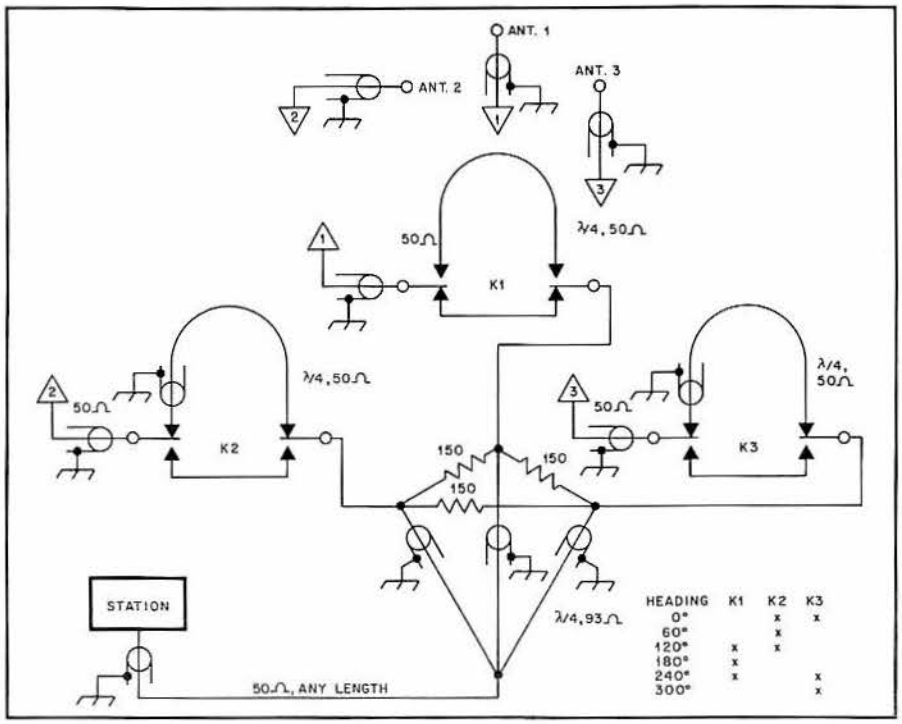

Fig. 33 — Schematic diagram of a three-element vertical array and its directivity switching and power dividing circuitry. Interconnecting leads should be as short and symmetrical as possible. The 50-ohm lines between the relays and antenna elements should be all the same length.

input is high. If it is low, check for moisture in the cables or connectors or for other leakage resistance. Silicone grease in the connectors is a good moisture preventive measure. It is recommended that these resistance checks be repeated periodically to be sure that all is well.

When the array is ready for use, go easy at first, as any reflected energy will be dissipated in the 100-ohm resistors. If they become hot, better matching is necessary, and if they blow up, perhaps higher-wattage resistors are needed. At W1CF, resistor banks were made up of 6, 20-watt, 150-ohm surplus resistors in series-parallel to give 100 ohms. These handle the dissipated power when the system is driven from a 4CX1000A amplifier, and after a month of operation there was no evidence of resistor damage. No attempt should be made to hot-switch the directivity. This was done inadvertently, and the result was the need for extensive emergency repairs — in midwinter.

Performance

In the short time that the array has been in use, all continents have been worked on 80-meter phone, including several stations in Japan and India, tough paths from New England. Gain and side and back rejection on all signals except those arriving from very high angles are just what the computer program predicted.

In receiving in the "search" mode, one hand tunes the receiver while the other operates the lobe selector switch, to see which position "listens" best. The big W1CF rotary array for 10, 15 and 20 takes 45 seconds to rotate 360°, which tends to discourage frequent directional checks. With the phased array a complete scan takes but a few seconds. The high front and side rejection eliminates most of the interference from signals in unwanted directions, and in transmitting the clean patterns help to prevent ruffled feathers.

A surprising by-product has been the reduced atmospheric noise pickup from unwanted directions. In particular, when listening toward Europe atmospheric noise coming from electrical storms in the southwest is greatly reduced, improving the signal-to-noise ratio on signals arriving from across the pond. The array is an order of magnitude better on both transmitting and receiving than any antenna previously used on 80 at W1CF. It has more than held its own with the competition, in all four quadrants. Of special interest to operators who like to use both phone and cw on 80 is the fact that the SWR is close to unity, from 3.5 to 4 MHz.

Triangle 3-Element Array

Anticipating that some amateurs may wish to use three rather than four elements, the ARRAY program was used to explore equilateral triangle configurations. Though it was not reduced to practice, a 3-element vertical array with 0.288λ spacing between adjacent radiators looks promising. The lead element is driven at 0° and the two side elements at -90°. The forward lobe is 135° wide, with a gain of close to 5.5 dB, including an estimated 1 dB contributed by vertical focusing. Front-to-back ratio is 12 dB. With suitable switching, the pattern can be aimed in six different directions, again providing 360-degree coverage. The three-way Wilkinson mentioned earlier must be used with three 90-degree sections of 50-ohm line, to provide the proper phase relationships. Several other configurations appear promising, but involve more complex switching and power-dividing circuitry.

Applications for Other Frequencies

The diamond and triangle antenna configurations may find uses at other frequencies, as was done with the 1965 design.[4] Formulas are given below for determining the line lengths and element spacings. A 2-meter phased array can be mounted on the roof of a car and wafer-switched to the desired directions. For people who like to experiment with logic and rf switching with semiconductors, circuits can be devised so that the receiver can scan periodically, and the antenna steered to the desired signal.

The authors wish to thank the many people who have contributed to the success of this project, including W1FRR, K1GXT, W1HMV, W1FXT, K1CCK, M. E. Hines, F. Howe, H. Wells, R. Rearwin, H. P. Scott, and many others. We also wish to thank Microwaves Associates, Inc., for the use of their superb computer facilities.

Formulas for length of quarter-wave (90°) phasing lines, and spacing of radiators, are given below:

Electrical λ/4, solid-dielectric coaxial line, 50 or 70 ohms (RG-8, -11, -58, -59):

$$L_{ft} = \frac{162.36}{f_{MHz}}$$

Electrical λ/4, solid-dielectric coaxial line, 93 ohms (RG-62, -71):

$$L_{ft} = \frac{206.64}{f_{MHz}}$$

300-ohm Twin-Lead — parallel three λ/4 sections to approximate 93-ohm cable (requires 1 input and 3 output 1:1 baluns):

$$L_{ft} = \frac{201.72}{f_{MHz}}$$

Radiator spacing, diamond array:

$$S_{ft} = \frac{246}{f_{MHz}} > 0.25\lambda$$

Radiator spacing, triangular array:

$$S_{ft} = \frac{283.4}{f_{MHz}} > 0.288\ \lambda$$

This material was originally presented in *QST* by Dana W. Atchley, Jr., W1CF, Harold E. Stinehelfer and Joseph F. White, Ph.D.

References

[1]Atchley, "Switchable 4-Element 80-Meter Phased Array," *QST*, March 1965.
[2]National Association of Broadcasters, *Engineering Handbook*, 6th Edition.
[3]Wilkinson, "An N-Way Hybrid Power Divider," *IRE Transactions on Microwave Theory and Techniques*, January 1960.
[4]Botts, "A Four-Element Vertical Beam for 40/15 Meters," *QST*, June 1975.

An Etched-Circuit Monimatch for Checking Your Antenna System

Why buy an expensive SWR indicator when you can build this slick little unit at home? Not only will you save money, but you'll learn something about how SWR meters operate. Try the W1ICP circuit — you'll like it!

A Novice who reads the instruction manual that comes with his transmitter and uses a 50-ohm dummy antenna can follow the tune-up procedures fairly accurately. With the dummy antenna he will find that the settings for the tuning controls will be fairly close to those specified by the manufacturer. However, when an antenna system is attached to the rig, in many instances the adjustments are far removed from any "book" setting. When this happens the Novice finds that he cannot get proper tuning of the rig, or worse yet, actually damages the equipment by trying to "force" it to work.

Nearly every transmitter these days, whether commercial or home-built, has a final amplifier stage that is designed to work into a 50-ohm load. If the load is something other than 50 ohms it may be impossible to tune the amplifier stage correctly. Of course, an important part of the problem is finding out what the load is — or, rather, how far from 50 ohms it happens to be. The piece of measuring gear described in this article is a device for doing just this. However, before describing the Monimatch and what it can do, let's take a little closer look at antenna-system loads.

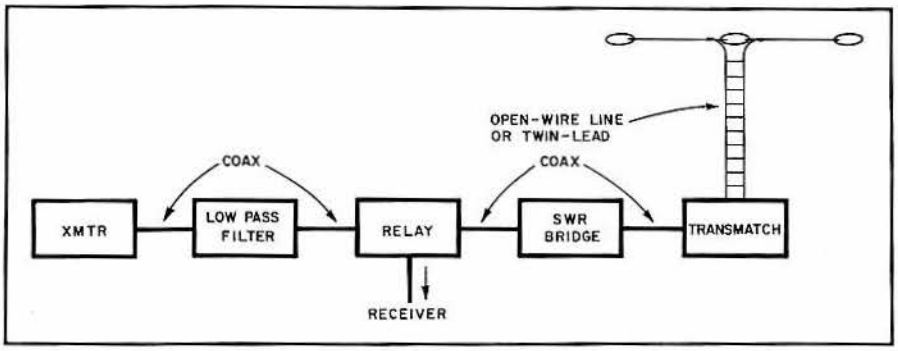

Fig. 34 — A typical setup for using a Monimatch in a multiband antenna system using a single dipole. The length of the dipole is not critical but it should be at least 1/4 wavelength overall at the lowest operating frequency for good efficiency. The feed line can be any length. The antenna relay and low-pass filter may be omitted if not needed.

The "50-Ohm" Load

The evolution of transmitter design since WW II has been influenced by several factors that have led to design that is more or less standard these days. First off, television came along right after the war and the hams quickly discovered that extremely tight shielding of a transmitter was needed to prevent undesired radiation that could cause TVI. However, when tight shielding was installed, band changing without band-switching became a real chore because there were so doggone many screws to unscrew and rescrew.

The one type of tank circuit that lent itself very well to the problem was the pi network. It was a fairly simple job to design a tightly shielded bandswitching transmitter, using the pi network, that would work into a 50-ohm load. Why 50 ohms? Simply because at this time 50-ohm coaxial cable had become a very popular type of transmission line. During the war, techniques were developed that made the manufacture of flexible coaxial cable a

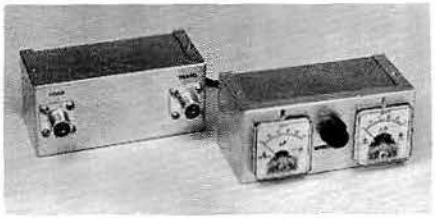

Here is the completed Monimatch with the two meters and the sensitivity control in the box at the right. The sensing unit is at the left.

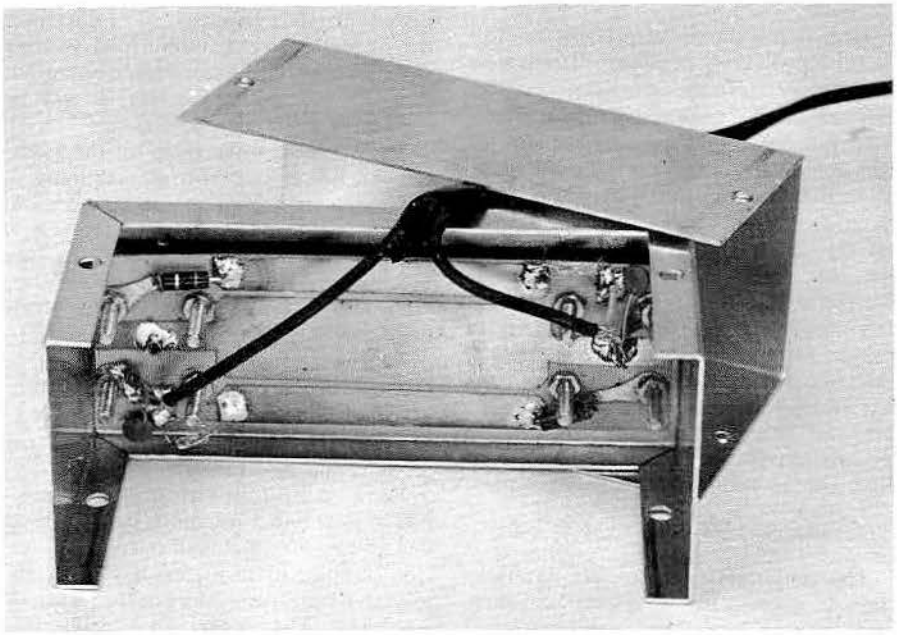

This is the sensing unit of the etched circuit Monimatch. As pointed out in the text, be sure to use a heat sink when soldering the diodes and resistors to the circuit board. The two shielded pickup leads are routed out the back of the Minibox, through a rubber grommet.

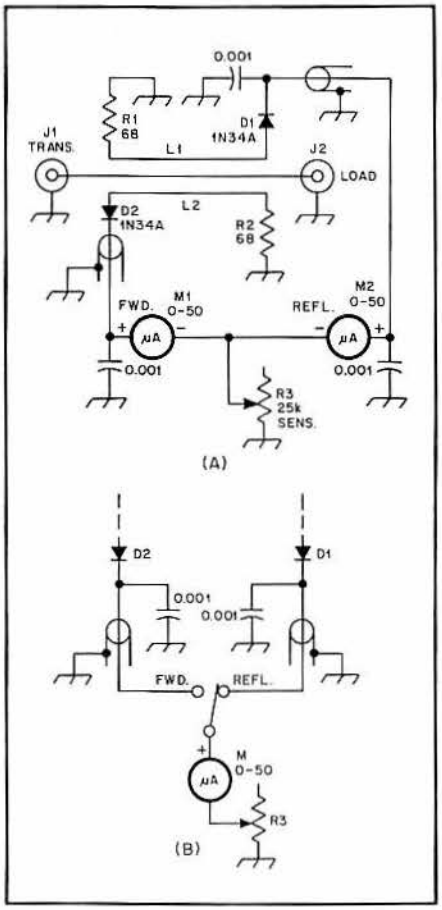

Fig. 35 — Circuit details of the etched-circuit Monimatch. The 0.001 μF capacitors are disk ceramic.
D1, D2 — 1N34A germanium diodes.
J1, J2 — Coax chassis fittings, type SO-239.
L1, L2 — See text and Fig. 36.
M1, M2 — 0-50 μA meter (Lafayette 99 H 5049).
R1, R2 — 68-ohm, 1/2-watt carbon or composition.
R3 — 25 kΩ control, linear taper.
S1 — Spdt switch.

reliable and economical process. So TVI and the availability of coax feed lines were the primary contributing factors that led to our present-day transmitter design.

If the load that is attached to the transmitter is something other than 50 ohms then the transmitter may be difficult to load, depending on a couple of other factors. While it is possible to design a pi network that will handle quite a wide variety of loads, many present day manufacturers, in order to compete in given price ranges, use a minimum number of parts in the tank circuit of the amplifier. For such rigs to operate properly the load must be between 25 and 75 ohms. This of course means that the user *must* furnish a load that will fall within this range.

Transmission Lines

The output terminal on all rigs these days is a coax fitting, which of course implies that a coaxial line must be attached to the rig. This doesn't mean that the coaxial line has to go all the way to the antenna. It could be connected to a Transmatch or a balun. What is important is that the first thing in the antenna system is the coaxial line that is attached to the rig.

Many Novices mistakenly believe that if you attach a 50-ohm coaxial cable to rig you *automatically* have a 50-ohm load. This is not true. The 50-ohm designation on the cable merely means that 50 ohms is the *characteristic impedance* of the cable. The characteristic impedance of a transmission line is determined by the size of the conductors used, the spacing of the conductors, and the dielectric material used to separate and support the conductors. The only time you would have a 50-ohm load using 50-ohm cable is when the line is terminated in its characteristic impedance. In other words, if the antenna has an impedance of 50 ohms then you will have a 50-ohm load on the rig. If the antenna has an impedance of other than 50 ohms then the load at the transmitter will be something other than 50 ohms. This in turn leads us up to a short discussion of standing-wave ratio.

SWR

If a transmission line is terminated in its characteristic impedance, all the power fed into the line from the transmitter will be delivered to the load end — in this case, the antenna. Actually, not quite all the power will reach the antenna because there is always some loss in the transmission line itself. However, what is important is that when the line is terminated in its characteristic impedance none of the power that reaches the end is reflected back toward the transmitter; all of it is used up in the antenna.

When the antenna impedance is different from the line impedance some of the power will be reflected back toward the transmitter end. Standing waves of voltages and currents will then exist on the transmission line. When this happens, the transmitter will no longer "see" a 50-ohm load. Exactly what the load will be will depend on several factors,[1] but suffice to say it will be something other than 50 ohms.

The standing-wave ratio on the transmission line is the ratio of maximum to minimum voltage or maximum to minimum current that exists along the line. If the line were matched in its characteristic impedance the voltage would be the same along the line and of course the SWR would be 1 to 1. The SWR is determined by dividing the resonant antenna impedance into the line impedance, or vice versa. For example, if the antenna impedance were 25 ohms and a 50-ohm line were used, the SWR would be 2 to 1.

For a moment, let's assume that regardless of how bad a mismatch exists, we are still able to tune and load our transmitter. The question then arises, how does the mismatch affect the losses in the transmission line? The answer to the question depends on how efficient the transmission line is.

Remember earlier we said there are always some power losses in every transmission line. If we have a mismatch at the antenna end, some of the power that reaches the end will be reflected back down the line. In traveling back, some of this power will be dissipated in the line, and the higher the SWR the higher these additional losses will be, because a higher SWR means that a greater proportion of the power will be reflected. In a transmission line that is 100 percent efficient (one that has no losses) it follows that regardless of how high an SWR exists, we wouldn't have any losses due to the SWR. Unfortunately, there "ain't no such" line, although some types of lines are much less lossy than others.

Also unfortunately, coaxial lines fall into the class that can be considered to be lossy lines. Just as an example, let's assume that you are using 100 feet (30.48 m) of RG-58/U on the Novice 15-meter band, and you are getting 50 watts out of your 75-watt Novice rig. This 50 watts is what is leaving your transmitter on the way to antenna via the 100 feet (30.48 m) of line. The loss for 100 feet (30.48 m) of RG-58/U at 21 MHz is 1.9 decibels. Translating this figure to power, we would lose about 20 of our 50 watts in the losses in the feed line, leaving only 30 watts to reach the antenna and be radiated. This is assuming the antenna impedance to be 50 ohms, the same as that of the line. If there is a mismatch the losses will be higher, as pointed out earlier. Suppose the SWR is 3 to 1, using the same setup. The *additional* loss in the system because of the SWR would be 1 dB, or a total of close to 3 dB. A 3-dB loss represents almost exactly one-half the power — that is, only 25 watts reach the antenna to be radiated. RG-8/U cable has the same characteristic impedance as RG-58/U but has less loss because it has larger conductors and more spacing between the conductors (and of course is more expensive).

The closest thing to a lossless transmission line is open-wire line. An open wire line on 21 MHz has only 0.08 dB loss per 100 feet (30.48 m). Even with a very high mismatch — for example, an SWR of 20 to 1, the additional losses are still less than 1 db!

This should not be interpreted to mean that coax is an undesirable type of line to use. For beam antennas it is difficult to beat the ease and convenience of using coax. However, for a single antenna, such as a dipole that is to be used on all bands and all frequencies, the best system is one consisting of a Transmatch and a feed line of open-wire line, such as shown in Fig. 34. With this system you can forget about line losses, SWR on the line, and mismatches between the antenna and feed line. By correctly adjusting the Transmatch, you can always give your rig a 50-ohm load regardless of what the load is on the antenna side of the Transmatch. If we use an SWR bridge in the short length of 50-ohm coaxial line that connects the rig to the

Transmatch, we can adjust the Transmatch so that the 50-ohm line shows a match, or SWR of 1 to 1, and the transmitter always sees a 50-ohm load.

The SWR bridge in the photographs and drawings is simple to build, and when installed in 50-ohm cable, will show the relative mismatch in the line, and also will indicate when you get the Transmatch properly adjusted for a match. The SWR bridge can also be used as an output indicator, which is very handy when tuning up the rig.

SWR Bridge Circuit Details

The etched-circuit Monimatch shown here is a reflectometer that samples the forward and reflected voltage in a 50-ohm line. Fig. 35 shows the circuit diagram. L1 and L2 are the pickup lines. In operation, a very small amount of power is coupled into the pickup lines and the rf voltages are rectified by D1 and D2. The rectified voltages are then fed to the two meters, M1 and M2, and the SWR then determined from the readings.

While a Monimatch is not a precise piece of measuring equipment, the SWR readings will be close enough for practical purposes. In order to determine the SWR, the forward-reading meter is set to full scale by adjusting R3, the sensitivity control, and then the reading on the "reflected" meter is noted. The formula for the SWR using this system is

$$\frac{F+R}{F-R}.$$

For example, let's assume the "reflected" reading is 5, with the "forward" reading being 10. Then 15 divided by 5 (that is, 10+5 divided by 10 − 5) would mean the SWR is 3 to 1. The closer the "reflected" reading is to zero, versus full-scale reading on "forward," the closer you come to 1 to 1, or a matched condition.

In the unit shown, two meters are used, one for the forward and the second for the reflected reading. However, if desired a single meter can be used and switched as shown in Fig. 35 at B. We used two meters in the indicator as this permits constant monitoring of what is happening in the line. The meters are inexpensive ones made in Japan.

Construction Details

Fig. 36 is a full-sized template of the etched circuit board. A *QST* article[2] went into detail showing simple methods for making etched circuits, so we won't treat the process here. In making this board, it is suggested that the board be covered with masking tape and then the pattern of Fig. 36 transferred to the tape. Using a sharp knife edge or razor blade and a straight edge, the masking tape can be carefully and accurately cut to the pattern.

After the board is etched, it can be positioned in the Minibox over the chassis connector holes and the board can then be marked at the drilling points for the mounting holes and the center conductor pins of the coax fittings. When installing the mounting screws, be sure they don't short to the center — conductor portion of the foil on the board.

There are a couple of other construction points that should be stressed. The lead lengths on R1 and R2 should be kept as short as possible. Also, be sure to use carbon or composition resistors, *not* wirewound. When mounting the resistor and diode ends to the pickup sections, L1 and L2, the connections should be at the very ends of the sections. Also, use a heat sink when soldering the leads on any of the components mounted on the board, as too much heat from the iron can ruin the component.

The Monimatch and meters are mounted in separate Miniboxes, 2-1/4×2-1/4×5 inches (57 mm × 57 mm × 127 mm). The two connectors on the Monimatch sensing unit, J1 and J2, are mounted with their center pins 3-3/4 inches (95 mm) apart, center-to-center. In order to avoid an impedance "bump" in the feed line when the bridge is inserted in the line, the circuit board should be mounted 1/4 inch (6 mm) above the base of the Minibox. Quarter-inch (6 mm) spacers can be used under the circuit board at the screws holding both the board and the coax fittings to position the board accurately.

Shielded conductors should be used for the connections from the diodes to the meter enclosure. The shields should be grounded to the chassis at both boxes. These lead lengths are not critical, and the Monimatch can be remote from the meter indicator.

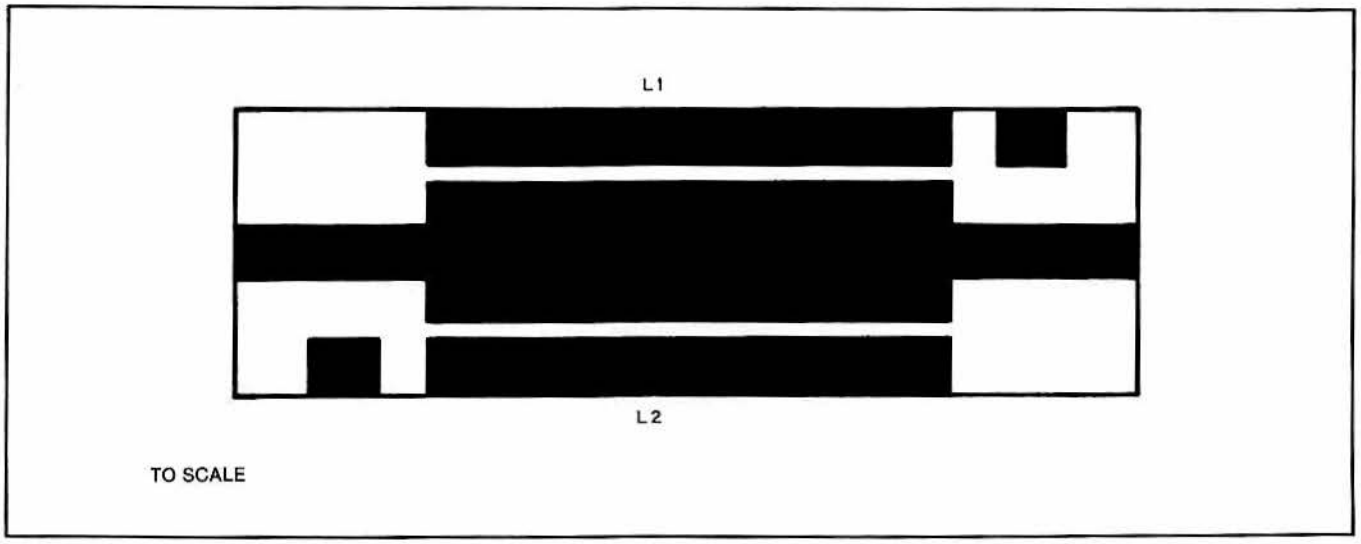

Fig. 36 — Etched circuit board template. The foil side is shown; the etched portion is shaded.

Using the Bridge

If you are using coax feed from the rig to the antenna, the bridge can be installed at any convenient spot in the line. If you are using a Transmatch, similar to the system as shown in Fig. 34, the Monimatch should be installed on the transmitter side of the Transmatch. Any relays or filters should be installed between the bridge and the transmitter, as shown.

Set R3 so that the arm of the control is at the top of the resistance — in other words, with all the resistance in series with the meter circuit. Tune up your rig in the normal fashion, and once tuned up adjust the sensitivity of the "forward" meter by moving the arm of R3 until the meter reads full scale. You can then determine the SWR by the formula mentioned earlier.

When adjusting a Transmatch, feed just enough power through the system to obtain about half-scale reading on the "forward" meter and then adjust the Transmatch controls for a match, as indicated by zero reflected power. You may have to adjust R3 as you adjust the Transmatch to keep the "forward" meter from reading more than full scale. Once you have the Transmatch adjusted for a 1-to-1 ratio as indicated by the bridge, the transmitter can be loaded up in the normal manner. We usually reduce the forward reading to about half scale, and then tune the rig for maximum output, as indicated by the meter. When doing this, you may notice that maximum output as indicated by the bridge meter occurs at some setting other than the normal transmitter plate meter "dip" reading. (Normally, the instruction manuals tell you to tune for a plate dip if the transmitter has no output meter.) However, the amplifier stage will work better if you tune for maximum output rather than the dip — keeping the plate loading within the transmitter ratings, of course.

Once you become familiar with the use of the bridge and interpreting the readings, you'll find it a very valuable device in your station. This material originally presented in *QST* by Lewis G. McCoy, W1ICP.

References

[Editors Note: It is recommended that the newcomer obtain a copy of *The ARRL Antenna Book* for more detailed information on transmission line operation than can be provided in this article.]

Schiebold, "Fast'n' Easy Printed Circuit Boards," *QST*, August 1969.

In-Line RF Power Metering

Problems are frequently encountered in designing and building reflected-power meters and SWR bridges. Examples of practical in-line rf wattmeters are given here, along with complete details for building a unit that will provide two power ranges, forward and reflected, for use from 3.5 to 30 MHz.

It is neither costly nor difficult to build an rf wattmeter. And, if the instrument is equipped with a few additional components it can be switched to read reflected power as well as forward power. With the foregoing feature the instrument can be used as an SWR meter for antenna matching and Transmatch adjustments.

Perhaps the most difficult task faced by the constructor is that of calibrating the power meter for whatever wattage range he desires to have. The least difficult method is to use a commercial wattmeter as a standard. If one is not available, the power output of the test transmitter can be computed by means of an rf ammeter in series with a 50-ohm dummy load, using the standard formula, $P = I^2R$. Or, if one is not interested in obtaining power readings the bridge can be used solely as an SWR indicator, as is done with the Monimatch-style SWR bridge.[1]

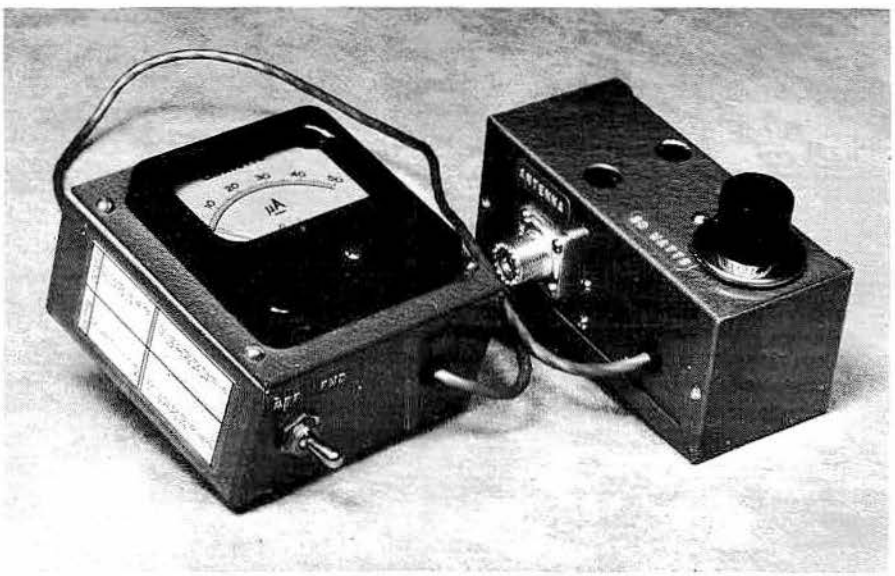

The advantage of the circuits shown here over those of Monimatch bridges is that these instruments are not frequency-sensitive. Monimatch indicators become more sensitive as the operating frequency is increased, thus making it impractical to calibrate them in watts for more than one band, or for more than one portion of a given band. The units described here are more sensitive than Monimatches are. This makes it possible to calibrate them for power levels as low as 1 watt, full scale, in any part of the hf spectrum.

All of the circuits shown in this article are similar to the basic one which was described in *QST*.[2] Some of the circuits are those of commercial power meters, and are used to illustrate variations in the basic Bruene design. The reader may wish to experiment with some of these circuits.

Design Philosophy

Referring to the circuit of Fig. 37B, the circuit used by Collins Radio Company, the transmission-line center conductor passes through the center of a toroid core and becomes the primary of T1. The multi-turn winding on the core functions as the transformer secondary. Current flowing through the line-wire primary induces a voltage in the secondary which causes a current to flow through resistors R5 and R6. The voltage drops across these resistors are equal in amplitude, but 180 degrees out of phase with respect to common or ground. They are thus, for practical purposes, respectively in and out of phase with the line current. Capacitive voltage dividers, C3C7 and C4C8, are connected across the line to obtain equal-amplitude voltages *in* phase with the line voltage, the division ratio being adjusted so that these voltages match the voltage drops across R5 and R6 in amplitude. (As the current/voltage ratio in the line depends on the load, this can be done only for a particular value of load impedance. Load

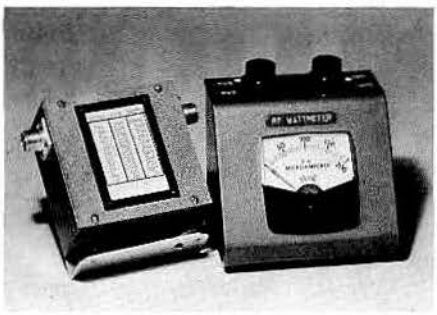

values chosen for this standardization are pure resistances that match the characteristic impedance of the transmission line with which the bridge is to be used, usually 50 or 75 ohms.) Under these conditions, the voltages rectified by D1 and D2 represent, in the one case, the vector *sum* of the voltages caused by the line current and voltage, and in the other, the vector *difference*. With respect to the resistance for which the circuit has been set up, the sum is proportional to the forward component of a traveling wave such as occurs on a transmission line, and the difference is proportional to the reflected component.

The Collins circuit uses two 8-μF capacitors, C5 and C6, to permit the meter to approach the PEP level during ssb operation. The dc voltages in the forward and reflected lines charge the capacitors to permit a near-peak reading. The discharge rate is set by the series calibrating resistors, R1 through R4, and is dependent upon which of them is switched into the metering line at a given time. The circuit of Fig. 37B uses two 43-pF capacitors, C1 and C2, to cancel the inductive reactances of R5 and R6. Such reactance may become manifest at the high end of the range for which the instrument is built. If reactance is present in that part of the circuit the meter readings may not be accurate, especially at 10 and 15 meters. The capacitors were not needed in the circuit of Fig. 38, perhaps because the resistor leads were very short when they were mounted on the etched-circuit board.

Some Design Hints

It is important that the layout of any rf bridge be as symmetrical as possible if good balance is to be had. The circuit-board layout for the instrument of Fig. 38 meets this requirement. Also, the input and output parts of the equipment should be isolated from the remainder of the circuit so that only the sampling circuits feed voltage to the bridge. A shield across the end of the box which contains the input and output jacks, and the interconnecting line between them, is necessary. If stray rf gets into the bridge circuit it will be impossible to obtain a complete zero reflected-power reading on M1 even though a 1:1 SWR exists.

Referring again to Fig. 38, resistors R1 and R2 should be selected for the best null reading when adjusting the bridge into a resistive 50- or 75-ohm load. Normally the value will be somewhere between 10 and 47 ohms. The 10-ohm value worked well with the homemade instruments shown here. It was found that half-watt resistors exhibited somewhat less inductive reactance at 30 MHz than did some 1-watt units tried. R1 and R2 should be as closely matched in resistance as possible. They need not be exactly 10 ohms, so a VTVM can be used to match them. The resistors used for the circuit of Fig. 38 were actually 10.5 ohms each, and were chosen from an assortment of "10-percenters" on hand.

Silver-mica capacitors C3 and C4 were close enough in value so that special selection was not required. There should be enough leeway in the ranges of C1 and C2 to compensate for any difference in the values of the 330-pF capacitors. Ideally, however, C3 and C4 should be matched in value.

Diodes D1 and D2 should also be matched for best results. An ohmmeter can be used to select a pair of diodes whose forward dc resistances are within a couple of ohms of being the same. Similarly, the back resistances of the diodes can be matched. The matched diodes will help to assure equal meter readings when the bridge is reversed. (The bridge should be perfectly bilateral in its performance characteristics.) Germanium diodes are used in the bridges described here, but

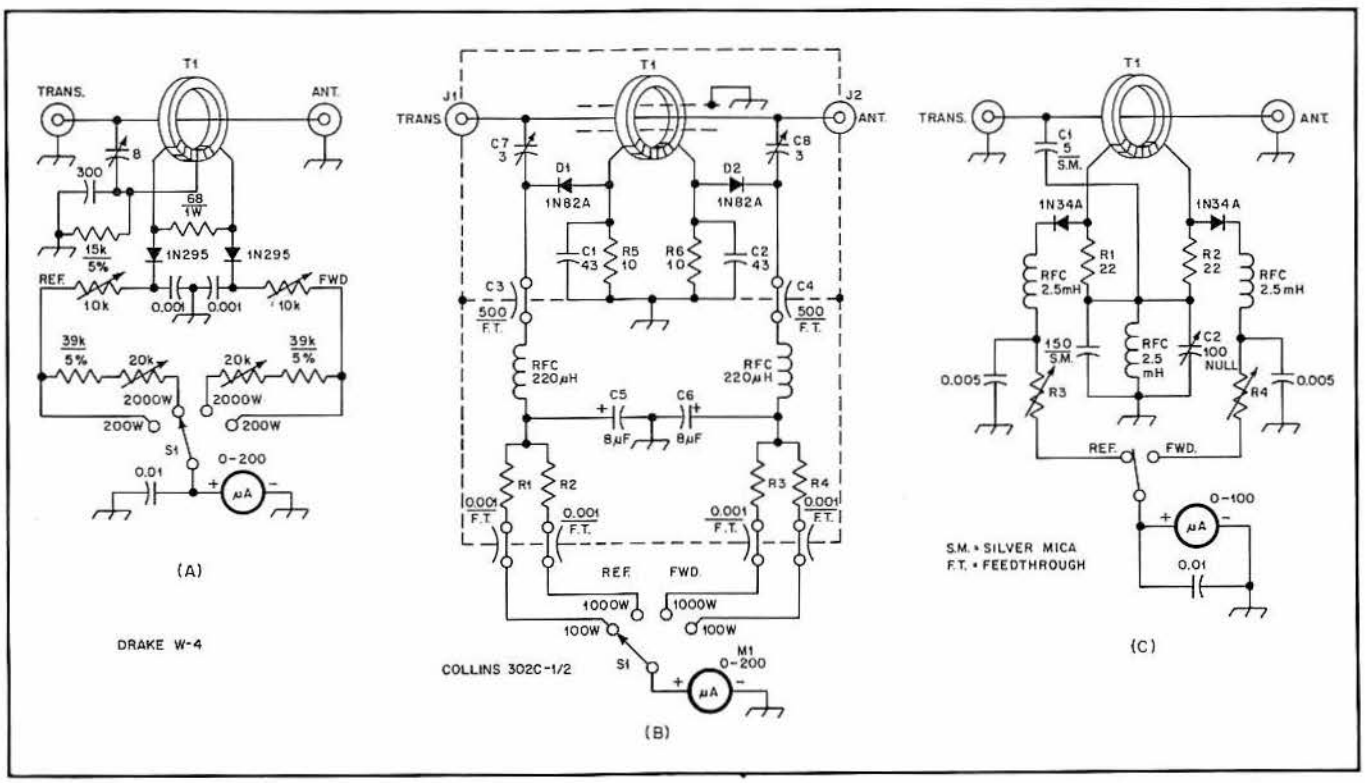

Fig. 37 — Schematic diagrams of typical in-line power meters. At A, the R. L. Drake W-4 instrument. It uses a center-tapped transformer at T1 and has but one capacitive voltage divider in the sensing circuit. The circuit at B is discussed in the text, and is used by Collins Radio Company. The capacitive voltage dividers in this circuit use two 500-pF feedthrough capacitors in place of the silver-mica capacitors specified in Fig. 38. Capacitors C5 and C6 permit a charge time that enables the meter to read near-peak power on ssb. Calibrating resistances R1 through R4 are factory selected. The circuit at C is similar to one used by Comdel in their power meter. In this circuit C1 is a fixed-value (small) capacitor, and the bridge is nulled by the larger capacitor in the divider, C2.

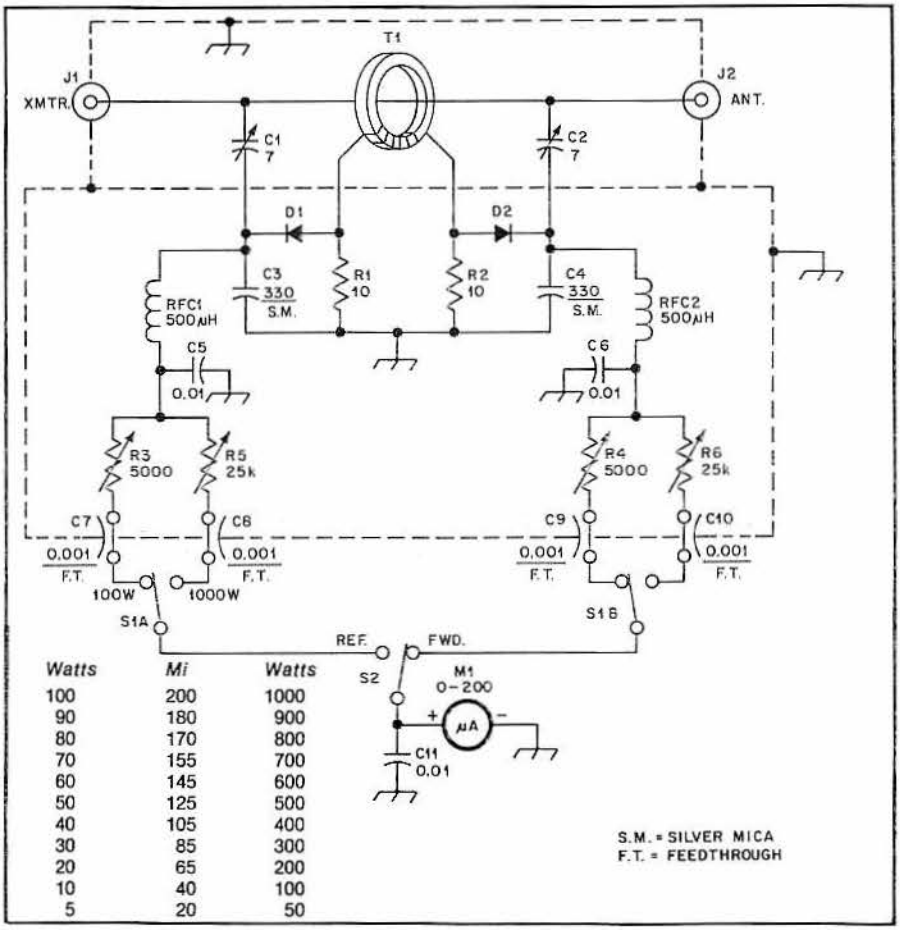

Watts	Mi	Watts
100	200	1000
90	180	900
80	170	800
70	155	700
60	145	600
50	125	500
40	105	400
30	85	300
20	65	200
10	40	100
5	20	50

Fig. 38 — Schematic diagram of a practical power wattmeter. A calibration scale for M1 is shown also. Fixed-value resistors are 1/2-watt composition. Fixed-value capacitors are disk ceramic unless otherwise noted. Decimal-value capacitances are in μF. Others are pF. Resistance is in ohms; k = 1000.

C1, C2 — 1.3- to 6.7-pF miniature trimmer (E. F. Johnson 189-502-4. Available from Newark Electronics, Chicago, IL).

C3-C11, incl. — Numbered for circuit-board identification.

D1, D2 — Small-signal germanium diode. IN34A, etc. (see text).

J1, J2 — Chassis-mount coax connector of builder's choice. Type SO-239 used here.

M1 — 0- to 200-μA meter (Triplett type 330-M used here.)

R1, R2 — Matched 10-ohm resistors (see text).

R3, R4 — 5000-ohm printed-circuit carbon control (IRC R502-B).

R5, R6 — 25,000-ohm printed-circuit carbon control (IRC R253-B).

RFC1, RFC2 — 500-μH rf choke (Millen 34300-500 or similar).

S1 — Dpdt single-section phenolic wafer switch (Mallory 3222J).

S2 — Spdt phenolic wafer switch (Centralab 1460).

T1 — Toroidal transformer; 35 turns of no. 26 enam. wire to cover entire core of Amidon T-68-2 toroid (Amidon Assoc., 12033 Otsego St., No. Hollywood, CA 91607).

silicon diodes can also be used. Silicon diodes conduct at a higher voltage than germanium diodes do — approximately 0.7 volt — and will not work too well in low-power wattmeters. Some silicon diodes were tried, but ceased to conduct at approximately 8 watts in the circuit of Fig. 38. This effect can cause misleading results when low values of reflected power are present during antenna adjustments. The SWR can appear to be zero when actually it isn't. The germanium diodes conduct at approximately 0.3 volt, making them more suitable for low-power readings.

Any meter whose full-scale reading is between 50 microamperes and 1 milliampere can be used at M1. The more sensitive the meter, the more difficult it will be to get an absolute reflected-power reading of zero. Some residual current will flow in the bridge circuit no matter how carefully the circuit is balanced, and a sensitive instrument will detect this current flow. Also, the more sensitive the meter, the larger will have to be the calibrating resistances, R3 through R6, to provide high-power readings. A 0- to 200-microampere meter represents a good compromise for power ranges between 100 and 2000 watts.

Construction

The power meter of Fig. 38 is built in two sections. The rf circuit and the calibrating resistors are housed in a 4×4×2-inch (102 × 102 × 51 mm) aluminum utility box. All components other than J1, J2, and the feedthrough capacitors, are assembled on the etched-circuit board.[3] Switches S1 and S2, and the meter, M1, are installed in a sloping-panel utility box which measures 5 × 4 inches (127 × 102 mm). Four-conductor shielded cable — the shield serving as the common lead — is used to join the two pieces. There is no reason why the entire instrument cannot be housed in one container, but it is sometimes awkward to have coaxial cables attach to a unit that occupies a prominent place in the operating position. Built as shown, the two-piece instrument permits the rf pickup head to be concealed behind the transmitter, while the control head can be mounted where it is accessible to the operator.

Toroidal transformer T1 fits into a cutout area on the circuit board. A 1-inch (25 mm) long section of RG-8/U cable — vinyl jacket and shield braid removed — provides a snug fit in the center hole of the toroid, and is used to complete the line between J1 and J2. The inner conductor of the RG-8/U section solders to the circuit board, thus holding T1 in place.

A flashing-copper shield divides T1 and its center-conductor line from the remainder of the circuit. This partition is shown in dotted lines in Fig. 38. It is mounted on the non-foil side of the circuit board and is secured at each end to solder lugs which are mounted under the retaining screws for J1 and J2.

The circuit board is held in place, at the end near T1, by means of an aluminum L bracket. The circuit-board end nearest the feedthrough capacitors is held in place by a no. 6 spade bolt. A solder lug is mounted under the no. 6 nut (outside the case) which secures the spade bolt. The lug serves as a connection point for the common lead between the rf head and the control box. Two solder lugs are mounted under the bottom two retaining screws of each coax connector. The free ends of the lugs are soldered to the copper foil of the circuit board.

A partition is visible in the foil-side view of the rf head. It can be eliminated if desired, since it did not prove necessary when the unit was tested. Similarly, an extra shield partition is shown on the top side of the board. It too can be eliminated, for it turned out to be unnecessary. The flashing-copper shield discussed earlier is the only one required for the circuit of Fig. 38.

Checkout and Tune-up

Once the instrument is wired and ready to test it should be inspected for unwanted solder bridges between the circuit-board foils. It is usually a good idea to scrape out the rosin buildup between the foils, and this can be done with the blade of a small screwdriver. A continuity check for "opens" and "shorts" should also be made before power is applied to the unit. Make certain that the diodes are installed for the correct polarity — the banded ends (cathodes) toward C1 and C2.

Connect a noninductive 50-ohm dummy load to J2. A Heath Cantenna or similar load will serve nicely for adjustment purposes. Place S2 in the FORWARD position, and set S1 for the 100- range. An rf ammeter or calibrated power meter

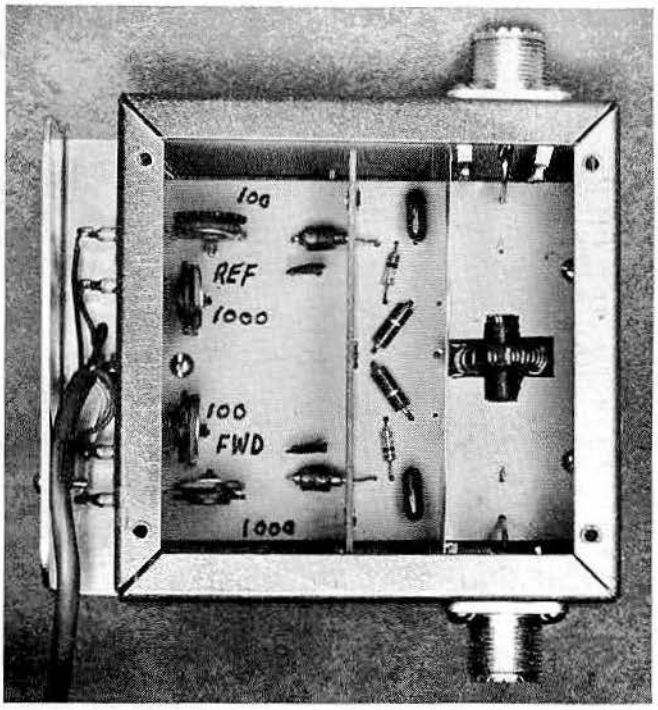

Top view of the rf head for the circuit of Fig. 38. A flashing-copper shield isolates the through-line and T1 from the rest of the circuit. The second shield (thicker) is not required and can be eliminated from the circuit. If a 2000-watt scale is desired, fixed-value resistors of approximately 22 kΩ can be connected in series with high-range printed-circuit controls. Or, the 25 kΩ controls shown here can be replaced by 50 kΩ units.

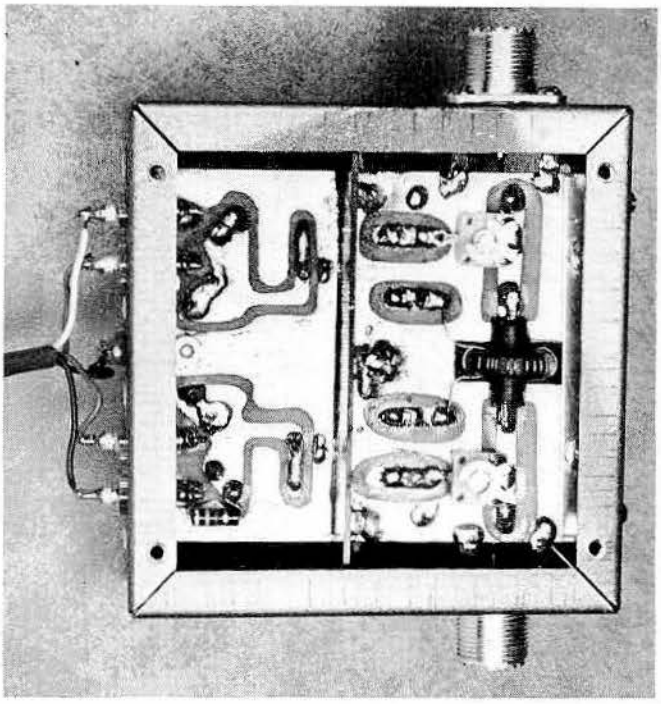

Bottom view of the rf head for the circuit of Fig. 38. The fixed-value resistor at the lower left does not belong in the circuit, but was added as a shunt for one of the calibrating controls which was too high in value — a 50 kΩ unit that was on hand. The shield partition shown here proved unnecessary and can be eliminated.

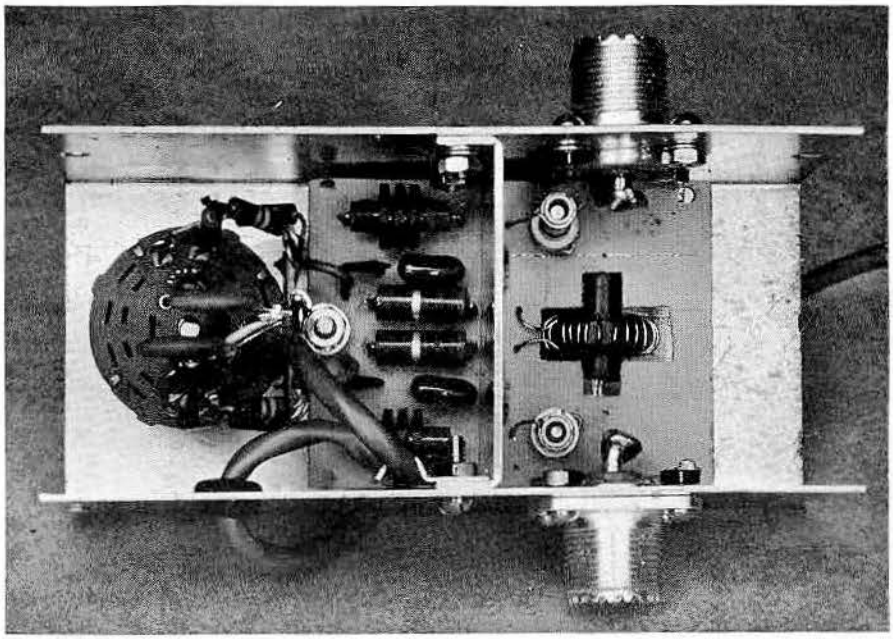

Fig. 39 — Inside view of the 5- and 50-watt power meter rf head. Component values are the same as in the circuit of Fig. 38, except for the calibrating resistances (see text). An aluminum shield isolates the through-line and toroid from the remainder of the circuit. A 50-μA meter is used in this model.

should be connected between J2 and the dummy load during the tests, providing power calibation points against which to plot the scale of M1. Apply transmitter output power to J1, gradually, until M1 begins to deflect upward. Increase transmitter power and adjust R4 so that a full-scale meter reading occurs when 100 watts is indicated on the rf ammeter or other standard in use. Next, switch S2 to REFLECTED and turn the transmitter off. Temporarily short across R3, turn the transmitter on, and gradually increase power until a meter reading is noted. With an insulated screwdriver adjust C2 for a null in the meter reading.

The next step is to reverse the coax connections to J1 and J2. Place S2 in the REFLECTED position and apply transmitter power until the meter reads full scale at 100 watts output. In this mode the REFLECTED position actually reads forward power because the bridge is reversed. Calibrating resistance R3 is set to obtain 100 watts full scale during this adjustment. Now, switch S2 to FORWARD and temporarily place a short across R4. Adjust C1 for a null reading on M1. Repeat the foregoing steps until no further improvement can be obtained. It will not be necessary to repeat the nulling adjustments on the 1000-watt range, but R5 and R6 will have to be adjusted to provide a full-scale meter reading at 1000 watts. If insufficient meter deflection is available for nulling adjustments on the 100-watt range, it may be necessary to adjust C1 and C2 at some power level higher than 100 watts. If the capacitors tune through a null, but the meter will not drop all the way to zero, chances are that some rf is leaking into the bridge circuit through stray coupling. If so, it may be necessary to experiment with the shielding of the through-line section of the rf head. If only a small residual reading is noted it will be of minor importance and can be ignored. In the circuit of Fig. 38 there remained approximately one-half a meter division when the null was reached, and this occurred only on the 1000-watt range. Since this was representative of less than 2 watts of power, it was deemed inconsequential.

With the component values given in Fig. 38 the meter readings track for both power ranges. That is, the 10-watt level on the

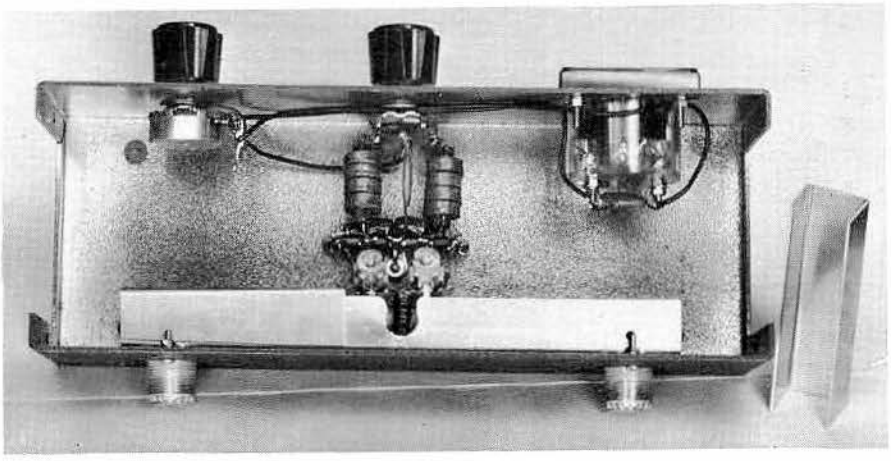

Inside view of the modified Heath HM-15 bridge. The new components are grouped at the center of the chassis on a 5-lug terminal strip. The nulling capacitors are connected between the inner line and the terminal strip. Press-fit aluminum shield covers are slipped over the trough line to aid in rf isolation. One cover is in place; the other is at the right of the photo. Improved shielding might be effected by installing an aluminum plate between the terminal strip and the two nulling capacitors.

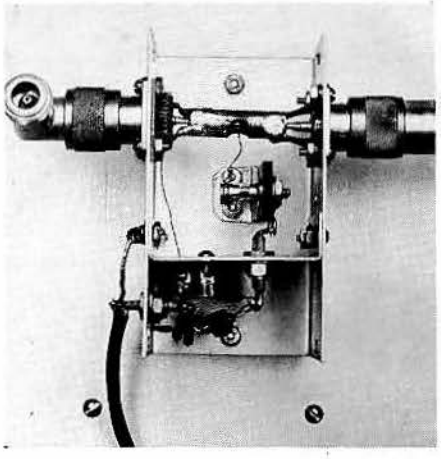

Inside view of a 2000-watt power meter built by N1RM. This bridge is patterned after the circuit of Fig. 37B. Point-to-point wiring is used throughout, thus avoiding the need for a circuit board. Two piston trimmers are used for the nulling capacitors and are mounted one above the other on a phenolic block. The two 500-pF feedthrough capacitors are part of the capacitive voltage dividers.

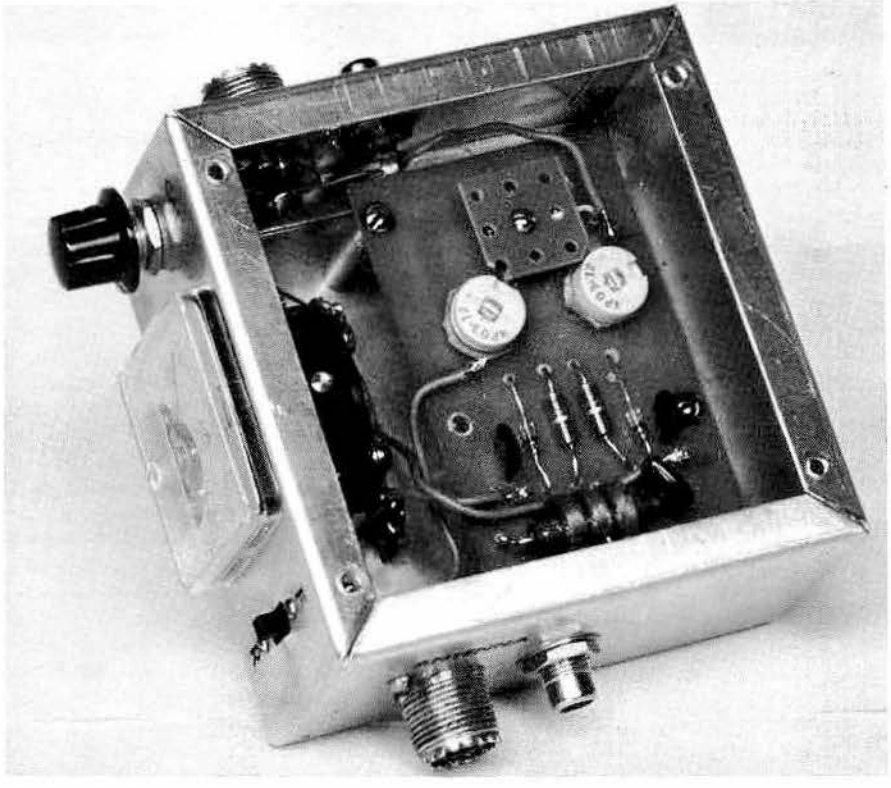

Fig. 40 — Inside view of a 3-watt power meter for QRP rigs. Its circuit is given on page 16 of June 1969 *QST*. Ceramic trimmers are used for nulling the bridge. Type SO-239 connectors are paralleled with phono jacks to add versatility. A 4 X 4 X 2 inch (102 X 102 X 51 mm) utility box houses the entire unit.

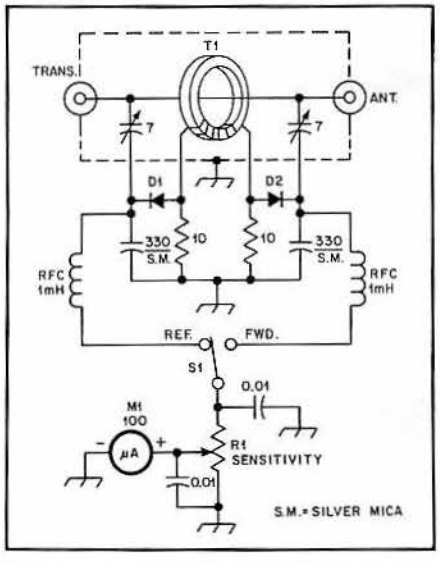

Fig. 41 — Schematic diagram of the modified Heath HM-15 SWR meter. D1, D2, M1, R1 and S1 are original components from the HM-15. T1 is the same as in Fig. 38. See text for additional details.

100-watt range, and the 100-watt point on the 1000-watt range fall at the same place on the meter scale, and so on. This no doubt results from the fact that the diodes are conducting in the most linear portion of their curve. Ordinarily, this desirable condition does not exist, making it necessary to plot separate scales for the different power ranges.

Tests indicate that the SWR caused by insertion of the power meter in the transmission line is negligible. It was checked at 28 MHz and no reflected-power could be noted on a Bird wattmeter. Similarly, the insertion loss was so low that it could not be measured with ordinary instruments.

Other Circuits

Additional circuits and photos are shown for variations in the basic design used at Fig. 38. A low-power model, having scales for 5 and 50 watts, is shown in Fig. 39. It uses fixed-value resistors for meter calibration. The required values of resistance were first determined by temporarily inserting a potentiometer in the meter line, obtaining the required full-scale reading, then substituting fixed-value resistances of the proper ohmage. The meter readings for the two power ranges do not track in this model.

A low-power meter was designed for use with the QRP transmitter described in June 1969 *QST*. It is shown in Fig. 40, and has a full-scale calibration of 3 watts. To obtain additional sensitivity, the primary of the toroidal transformer consists of a

one-turn link instead of the single wire that would normally pass through the hole in the toroid core.

Some experiments were conducted to see if a Heath HM-15 SWR bridge (a Monimatch type) could be modified to work in a Bruene circuit. The results were satisfactory, and the circuit is given in Fig. 41. No attempt was made to obtain a calibration scale for the meter. The unit is being used as a simple SWR indicator, but now has better sensitivity in the lower part of the hf spectrum — 7 watts, full scale, from 3.5 to 30 MHz. Also, the instrument is no longer "frequency-conscious" as was the case before modification. The original pickup lines were discarded, the FWD-REV panel switch was rotated 180 degrees so that the labels were correct for the new circuit, and press-fit shield covers were installed on the trough line as shown in the photo. A power scale could be plotted by setting the sensitivity control in a fixed position — possibly replacing the existing control with a screwdriver-adjust type. A new 100-μA meter could be installed to provide a better scale for calibration in watts.

It was necessary to dismantle the trough line so that the toroidal transformer could be slipped over the inner line. A few wraps of mylar tape were wound over the center of the inner line to insulate the toroid winding from the line, and to provide a snug fit to keep the toroid in place. The trough was notched out with a nibbling tool to allow clearance for the toroidal transformer. Additional shielding can be added between the line and the rest of the circuit to further assure a zero meter reading in the reflected position.

It is hoped that the experimenter will find sufficient information here to enable him to build a power meter that will satisfy his specific needs. This material was originally presented in *QST* by Doug DeMaw, W1FB.

References

[1]"Monimatch Mark II," *QST*, February 1957.
[2]Bruene, "An Inside Picture of Directional Wattmeters," *QST*, April 1959.
[3]The etched-circuit board pattern and parts layout sheet for this power meter are available from ARRL hq. Send 25 cents and an s.a.s.e. Check with Circuit Board Specialists, P. O. Box 969, Pueblo, CO 81001 for negative and circuit boards.

A Resistive Antenna Bridge — Simplified

SWR indicators are neat, but when it comes to making measurements of resonant impedances, you need a true bridge type of instrument. Measure those low antenna resistances directly with this W2FMI circuit, and do it up to 30 MHz with ease!

As shown previously,[1] a bridge using a single variable capacitor can be used to measure resonant impedances of antennas and losses in coils with reasonable accuracy. With addition of an L/C network, the bridge can also be very useful in adjusting antennas for resonance conditions. Recently it was brought to the author's attention that a bridge using a variable resistance could also perform well. This is possible because the range of antenna impedances is generally low enough to allow for low values of resistance in the arms of the bridge. Under these conditions parasitic capacitances are negligible up to 30 MHz.

Resistive bridges have the advantages of small size, readily available components, and dial calibrations which can be made practically linear. Two bridges are shown with their respective calibration curves. The first is a linear device. The second expands the lower portion of the calibration curve, 0 to 30 ohms, to measure lower values of antenna impedance and coil losses more accurately.

[1]Sevick, "Simple RF Bridges," April 1975 *QST*, page 11.

Bridge Details

The resistive bridge with a variable resistance in one arm and equal resistances in the other two is shown in the photographs, and schematically in Fig. 42A. The nonlinear bridge is similar mechanically. The small enclosures and compact layout minimize lead lengths. With the linear version the dial practically reads directly in

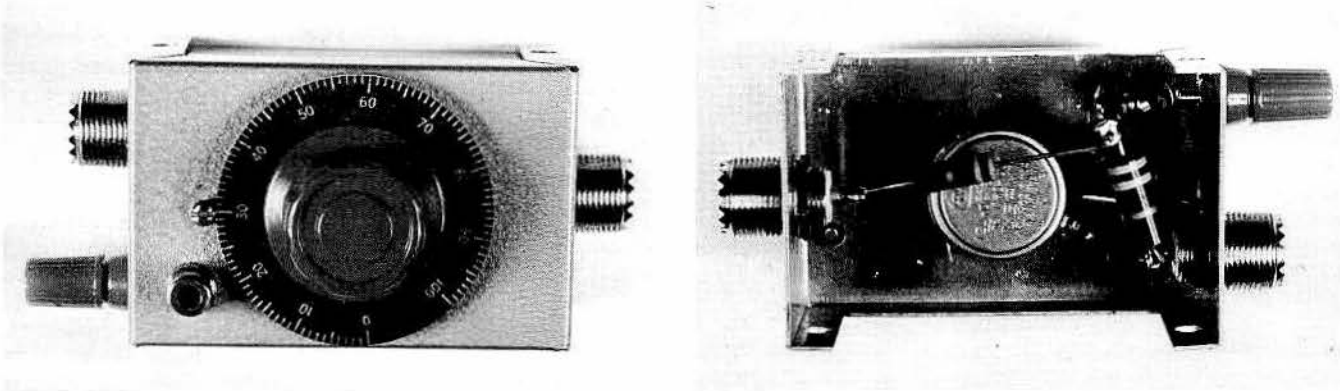

Exterior and interior view of the resistive bridge. Appearance and component arrangement are essentially the same for the two types described.

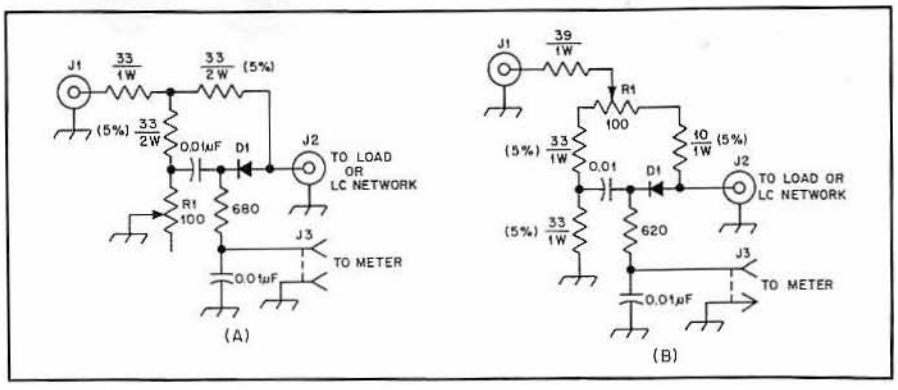

Fig. 42 — Schematic diagram and parts information for the linear (A) and nonlinear (B) resistance bridges. Resistor wattages are the minimum recommended.
D1 — Germanium diode.
J1, J2 — Coaxial connector, chassis type.
J3 — Phono jack.
R1 — 100-ohm, 2-watt linear control (Allen-Bradley, Type J).

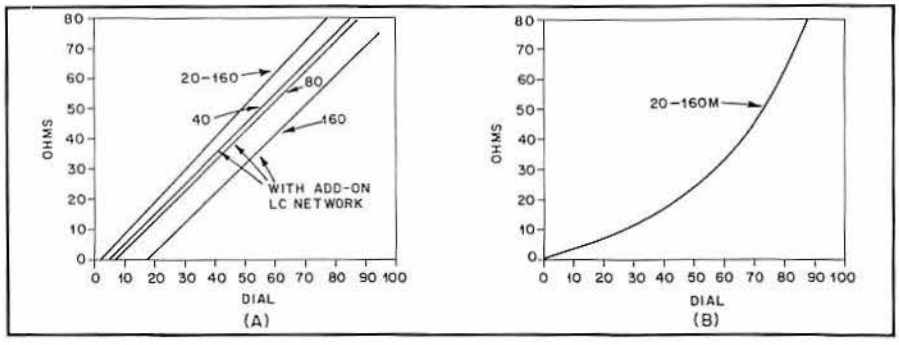

Fig. 43 — Calibration curves for the linear (A) and nonlinear (B) resistance bridges. The add-on L/C network used was described in the author's *QST* article on capacitive bridges.

ohms. In using the L/C network described in the previous article, a constant offset occurs, because of ohmic loss in the coils. This can be as high as 20 ohms, as is shown by the 160-meter curve with the L/C network, Fig. 43A.

The variable resistor used in the bridges has a parasitic (stray) capacitance of the order of 10 to 20 pF, which has little effect even at 14 MHz. Other potentiometers of similar design can probably be substituted. The calibration curves provide a good check. If the difference between the calibrations for the lowest and highest frequencies to be used is greater than an ohm or two, parasitic capacitances are probably excessive.

The nonlinear bridge uses most of the same components, but the control is connected in the differential mode, as shown in Fig. 42B. Resistance is subtracted from one arm and added to the other, tending to spread out the low end of the resistance scale for increased accuracy. In this version, the dial can be read easily to 0.5 ohm.

Results

The author has found these resistance bridges to be entirely satisfactory for measurements in the range of 1.8 to 30 MHz. Because of their greatly expanded scales, as compared with the capacitive bridges, and generally lower values of resistance in all arms of the bridge, they tend to have less marked nulls when used with very low-power signal sources. Increasing the minimum power to 20 or 30 milliwatts, when using the sensitive meter described previously, should take care of this.

In closing, the writer wishes to thank Roger A. Sykes, W1PP, for bringing the resistive bridge to the author's attention. This material was originally presented in *QST* by Jerry Sevick, W2FMI.

Why a Transmatch?

Let's cut away some of the mumbo jumbo about antennas. Here's some basic information to help the newcomer make the decision that best suits his need.

These days, nearly all transmitters have a pi-network tank circuit in the final amplifier. There are good reasons for this. With the pi tank it is possible to design a band-switching transmitter with excellent shielding (in order to prevent undesired harmonic radiation as far as TVI is concerned) and to accomplish the job with a minimum of complications. Additionally, the tank circuit easily can be set up to work into 50- or 70-ohm loads, the characteristic impedance of the popular types of coaxial feed lines. However, as we will see, this is where a "clinker" can get into the act.

When a pi network is designed to work into a 50-ohm load, the load *must* be 50 ohms in order for the transmitter to work at full efficiency. Merely connecting 50-ohm coax to the tank circuit does *not* accomplish this. For the tank to "see" a 50-ohm load, the far end of the coax — the load or antenna end — must also have the same impedance as the coax, 50 ohms. If the load is not 50 ohms the pi network will see some other value than 50 ohms. Usually, too, the tank will see reactance as well as resistance when the line is not matched. While reactance is expressed in ohms, it isn't a true resistance, and what it does is make it more difficult to put power into the line unless certain steps are taken to compensate for it.

Pi-Network Tank Circuits

In the conventional transmitter pi tank we have two controls, customarily referred to as the "tuning" and "loading" controls. The tuning control is the one that resonates the tank circuit to the desired frequency. The loading control, when adjusted properly, permits the final amplifier stage to be loaded to the desired input. To a limited extent it can also be used to compensate for the reactance in the load.

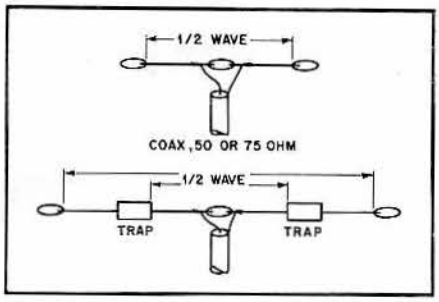

Fig. 44 — At the top is a simple half-wave dipole using coax feed. At the bottom is a drawing of a trap dipole. When a signal is fed to this antenna, for example an 80-meter one, the feed line "sees" a more-or-less resonant antenna on 80. When the transmitter is switched to 40, the traps "divorce" the 80-meter portion and the feed line sees a resonant 40-meter half-wave.

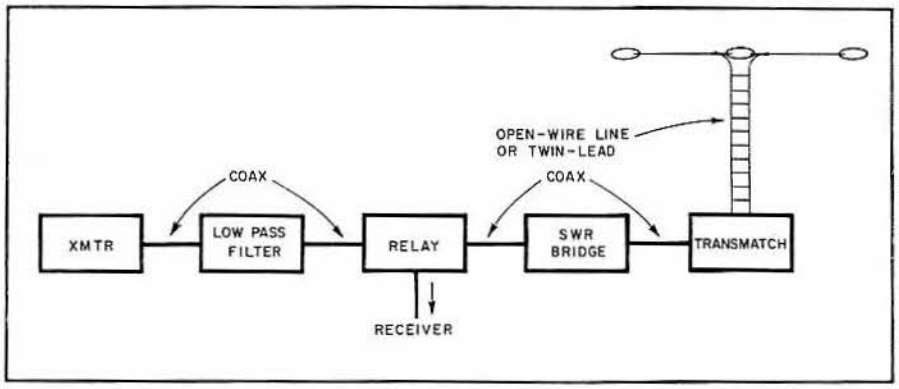

Fig. 45 — This drawing shows an ideal multiband antenna system. The units can be connected together by either 50- or 70-ohm coaxial line. The SWR bridge must match the line used. By putting the antenna relay in this section of the line, the Transmatch can be used to advantage for receiving as well as transmitting.

The clinker in this is that the reactance of many antenna-system loads may have too wide a range for the loading capacitor to handle. If you've ever been in the situation where is was impossible to load (or unload) the amplifier stage, the likely reason is that the load is too reactive to be handled by the tank circuit.

Such a condition can lead to some serious difficulties. While a correctly tuned pi network will offer good harmonic attenuation, an improperly adjusted tank may provide *no* harmonic attenuation. In fact, many Novices who receive second-harmonic violation notices for their 80-meter operation can lay the blame on poor loads and incorrectly adjusted tank circuits. This leads us to the real crux of the problem. How do we get a 50-ohm load on the various bands and frequencies desired?

Antenna Loads

As we said earlier, in order for a transmitter to see a 50-ohm load the far end of the 50-ohm coax must also see 50 ohms. The point where you feed the antenna has a certain impedance; in a half-wave dipole, for example, the impedance will be in the neighborhood of 50 ohms, depending somewhat on the dipole's height above ground. Also, at resonance there will be no reactance in the impedance. When we change frequency, the antenna is no longer resonant and reactance is introduced into the impedance. In turn, reactance is present at the transmitter end of the line. Whether or not the transmitter tank circuit can compensate for it will depend on the range of the loading capacitor.

How do we go about getting an antenna that will look like 50 ohms over a wide range of frequencies within a band — and, for that matter, on several bands? It isn't exactly easy.

For example, if we cut an 80-meter half-wave dipole for the center of the band, 3750 kHz, it is possible to obtain a fairly good match for 50-ohm coax at that frequency and approximately 50 kHz each side of 3750 kHz. However, at the band edges, 3500 and 4000 kHz, the impedance will be very reactive and the mismatch between the coax and the feed point may be as high as 10 to 1. It would be difficult, if not impossible, for our pi network to handle that type of mismatch. Actually, there is no "simple" antenna, by ham standards, that can be coax fed on 80 meters and cover the entire band with a reasonable match. The 40-, 20- and 15-meter bands are narrow enough so that the pi tank will handle a coax-fed dipole under normal circumstances. However, a coax-fed dipole is essentially a one-band system so such an antenna is not the answer if we want to work "all" bands and all frequencies with a single antenna.

Trap Antennas

One type of multiband antenna with coax feed is the trap antenna, either horizontal or vertical. The horizontal variety is essentially a dipole with traps added to divorce parts of the antenna so the coax "sees" an electrically resonant dipole on the band in use. However, the trap dipole is no "broader" than a single dipole. Fig. 44 shows such a trap dipole antenna.

There are a couple of drawbacks to trap dipoles. First, a coax-fed single-band dipole is essentially a selective circuit, in that it tends to discourage undesired harmonics from being accepted and radiated. For example, a 40-meter harmonic would have a tough time in an 80-meter coax-fed dipole because the antenna and line are badly mismatched on 40. A trap system, however, does not discriminate against such undesired signals. Also, traps introduce power loss — probably not a great deal, but nevertheless loss. But if you want to use coax line and have multiband operation, the trap dipole is an answer. On the other hand, a Novice may ask, "Is there a better multiband system, one without the trap losses and harmonic problems?" The answer is yes, but before describing it let's take a look at feed lines.

Feed Lines

Three common types of feed lines are used by amateurs: coaxial, twin-lead, and open-wire. Each has a certain amount of loss, with coax the lossiest, twin-lead next, and open-wire line the most efficient. An important point to keep in mind is that the greater the mismatch, or standing-wave ratio, on the transmission line, the greater the line loss. Also, the loss in any line increases with frequency: The loss will be least at 80 meters and will become progressively greater as we approach vhf or uhf. As an example, the loss in 100 feet (30.48 m) of RG-58/U line at 144 MHz is about 6 decibels. Translating this to power, if we had a transmitter that was putting out 100 watts only about 25 watts would reach the antenna, at the end of a 100-foot (30.48 m) line, to be radiated. The remaining 75 watts would be dissipated as heat in the line! And, most important, this figure is based on the coax being *matched* at the antenna end. The mismatch or SWR will depend entirely on the impedance of the transmission line and the impedance of the antenna. If there is a mismatch, the losses increase. On 80 meters, this same coax has a loss of less than 1 dB for 100 feet (30.48 m) of line, so we could tolerate more of a mismatch.

But don't overlook the fact that if the line and antenna are mismatched it may be impossible to make the amplifier load, even if the extra loss can be tolerated. The question that then comes to mind is if we use a low-loss line so we can tolerate a high degree of mismatch, how can we make the transmitter see a 50-ohm load? The answer to this is to use a Transmatch between the transmitter and antenna.

The Transmatch

A Transmatch is simply an adjustable rf transformer that converts an unknown load (antenna side) to a desired load (transmitter side). It consists of inductances and capacitances which can be adjusted to provide a perfect 50-ohm load for the transmitter on any band or frequency.

Let's take an example to show how a Transmatch can do the job. The impedance at the center of an 80-meter dipole is

Approximate Attenuation in Decibels/100 ft. (30.48 m)

Type	Z_0	3.5	7.0	14.0	21.0	28.0	50.	144	220	420
RG-58/U	52.5	0.68	1.0	1.5	1.9	2.2	3.1	5.7	7.2	10.4
100W. Output		8	18	28	35	38	51	72	81	92
RG-8/U	52.	0.30	0.45	0.66	0.83	0.98	1.35	2.5	3.3	4.8
RG-59/U	73	0.64	0.90	1.3	1.6	1.8	2.4	4.2	5.2	7.2
RG-11/U	75	0.38	0.55	0.80	0.98	1.15	1.55	2.8	3.8	4.9
Twin-lead	300	0.18	0.28	0.41	0.52	0.60	0.85	1.55	1.9	2.8
Open-wire	—	0.03	0.05	0.07	0.08	0.1	0.13	0.25		

This chart shows the attenuation figures in decibels for common types of feed lines. Z_0 is the nominal impedance. In the case of open-wire line, the impedance will depend on the size of the conductors and their spacing. The second line of the chart indicates the amount of power that would be lost in a 100-foot (30.48 m) run of RG-58/U when properly matched. For example, on 21 MHz, the loss per 100 feet (30.48 m) is 1.9 dB. With 100 watts output from the transmitter, 1.9 dB represents a loss of 35 watts in the line. A mismatch will increase the line loss.

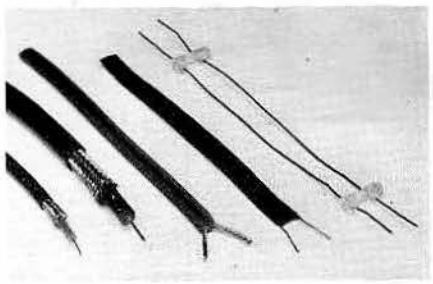

At the left are two examples of coaxial feed lines. The three lines at the right are balanced-type lines, 70-ohm, 300-ohm twin-lead, and TV open-wire line.

between 50 and 70 ohms on 80 meters. On 40 meters, the impedance at the same point on this same antenna is about 4000 ohms. If we feed this antenna with 300-ohm twin-lead the mismatch on 40 would be on the order of 13 or 14 to 1. However, bear in mind that 300-ohm line has relatively low loss, so we can probably tolerate the high SWR if the line is fairly short — less than 100 feet (30.48 m). Our only problem in making this antenna work on 40 is to take care of coupling the line to the transmitter. To do this the feed line is connected to the Transmatch and the Transmatch is then adjusted so that the transmitter sees a 50-ohm load. What we have now is an 80-meter dipole being used efficiently on 40, and our transmitter is working into the load it was designed for.

Now let's suppose that we feed this same antenna with 50-ohm coax. On 40, the mismatch would be 4000/50, or about 80 to 1! Because coax is not a low-loss line, the loss in the transmission line would be prohibitive. However, with twin-lead — or, even better, open-wire line — the loss is usually insignificant.

Also, and most important, a Transmatch adds selectivity at the output of the transmitter. It will discriminate against any undesired harmonics or spurious signals. And, if the antenna switching is set up so that the Transmatch is in the circuit on receiving, it will provide more selectivity for the receiver. In fact, a common problem for hams who live near broadcast stations is cross-modulation of 80- and 40-meter ham signals by the strong bc signal. A Transmatch will provide enough selectivity in most cases to eliminate bc cross modulation when it occurs in the receiver's front end.

Many hams are reluctant to use a Transmatch because it requires additional adjustments. However, the advantages are so great in a multiband system that any additional adjustments are more than worth the effort. With a Transmatch, the antenna doesn't have to be a half wave long to work on any band. For example, we described a complete multiband system just recently[1] using an antenna only 100 feet (30.48 m) long. Most hams can manage to get up a 60-foot (18.29-m) dipole, either horizontal or in an inverted-V configuration, and such an antenna also will work on 80 through 10. One method of putting up a multiband system is to find two supports for each end of the antenna, cut a wire long enough to run between them, put an insulator in the center of the antenna and at each end, and attach open-wire or twin-lead feeders long enough to reach the station. That's all there is to it. Bear in mind that a dipole fed this way doesn't have to be a half wave long; it can be any length, and it will work. Of course it is always a good idea to make it as long as possible and get it up as high as possible. Also, if possible, make it at least 1/4-wavelength long at its lowest operating frequency — about 60 feet (18.29 m) for 80 meters, for example.

A Few Notes

Many hams are reluctant to use open-wire line because of the problems in getting it into the shack from outdoors. One simple answer to this is to bring the line to the entrance — window sill, doorway, or whatever — and at that point attach 300-ohm twin-lead (which is insulated) and run the twin-lead in to the Transmatch. The fact that the two lines are not alike is of no concern because the load at the antenna side of the Transmatch is going to be some unknown value anyhow.

References

[1]McCoy, "A Complete Multiband Antenna System," *QST*, November 1967.

You may have read or heard that you must use coaxial lines in order to avoid TVI. Don't believe it. If you have a well-shielded transmitter and use a low-pass filter with it you won't have any harmonics coming out. Ask youself this simple question: "If there are harmonics, what difference can the kind of transmission line make?" The answer is, of course, "No difference."

One of the beauties in using a Transmatch is that the coaxial line between it and the rig can always be matched, and this matched section is where you put your low-pass filter. This eliminates any danger to the filter from excessive voltage or current caused by a mismatch.

One typical Novice question is "If my transmitter loads properly and I have no TVI problem, do I need more matching between the transmitter and antenna? I am using coax feed. What good would it do me to pay for the additional complexity of changing from band to band?" The answer to such a question depends on several factors. Is the harmonic attenuation — not TVI, but low-frequency harmonics — adequate? This could be a problem the Novice isn't aware of. As to the complexities of band changing, this will depend on how much the Novice desires to work other bands.

What we have tried to do in this article is to show the reader the problems and the recommended cure. There is nothing new about the multiband system using tuned feeders; it has been used for many years, and the interesting thing about it is that it is still the best multiband system. For further information it is recommended that the newcomer study *Understanding Amateur Radio* and *The ARRL Antenna Book* to gain a better insight as to how antennas work. This material was originally presented in *QST* by Lewis G. McCoy, W1ICP.

The Ultimate Transmatch

Most hams would like to own a Transmatch that could cover 80 through 10 meters, and work during coax-to-coax or balanced-lines conditions. Here is just such a unit. It will match the proverbial bedsprings, or any other nonresonant or resonant antenna — without plug-in coils or band switching — even on 160 meters.

Some amateurs assume that because they use coaxial feed lines they don't need a Transmatch. This can be an incorrect assumption.

The Harmonic Problem

A large number of hams have found to their sorrow that the harmonic suppression in their transmitters may leave much to be desired. The FCC issues many citations to Novices each year for second-harmonic violations.

A typical Novice station might consist of a transmitter and receiver, with direct coax feed to a trap dipole or vertical antenna. In a properly adjusted transmitter of typical design, often there is insufficient attenuation of the second-harmonic energy. This can mean that the second harmonic of the signal can reach the antenna and be radiated. What is required to eliminate or reduce the second harmonic, and higher-order harmonics, is more selectivity between the transmitter and the antenna. A Transmatch is an excellent aid in taking care of the harmonic problem.

The 50-Ohm-Load Problem

Still another reason for using a Transmatch is that nearly all manufacturers of transmitters design their rigs to work into a nonreactive, 50-ohm load. Any departure from this load impedance causes difficulty in tuning and loading the final-amplifier stage. It might be pertinent to point out that simply because a ham uses 50-ohm coax, it doesn't necessarily follow that he will have a 50-ohm load. Basically, in order to have a 50-ohm load when using 50-ohm coax, the coax must be terminated in a 50-ohm resistive impedance. In other words, the antenna impedance must be 50 ohms.

When the terminating impedance of the coaxial cable is other than 50 ohms, then the transmitter will be "looking" at some value other than 50 ohms. It is practically impossible to design a single antenna that will have an impedance of 50 ohms on all of the bands a ham might want to use. One answer to the problem is to employ a device that will "match" the unknown load to the 50-ohm impedance required by the transmitter. One such circuit or device is a Transmatch, simply an adjustable rf transformer that can match the unknown load presented by the transmitter end of the feed line to the required 50-ohm transmitter impedance.

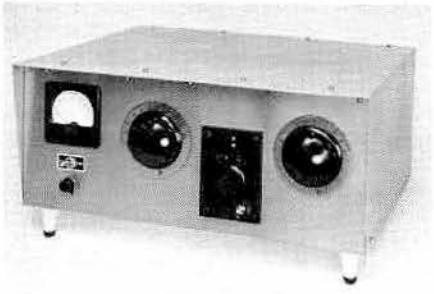

The kW version of the Ultimate Transmatch. The knobs and dial counter are standard Millen components. The front bottom of the cabinet is tilted by means of two 2-inch (51 mm) standoff insulators used as feet.

Receiver Cross-Modulation

In addition to taking care of the problems just outlined, a Transmatch can serve another very useful function at the receiver. Some receivers are susceptible to what is known as cross-modulation, or front-end overloading, by strong nearby radio stations. This is particularly true on 160 or 80 meters when a broadcast station is nearby. The bc station overloads the front end of the communications receiver, causing "birdies" and other unwanted responses across the band. A Transmatch will eliminate or greatly reduce this problem in nearly all instances.

The Ultimate Transmatch

We shall describe two Transmatches — one for the Novice power limit, and another for the legal 2-kW PEP limit. We have found that many amateurs on the verge of taking their General, or higher-class licenses, would rather invest initially in a unit that will take care of all of their future needs.

Some years ago, a Transmatch was described that was designed for use with coaxial feed lines.[1] It was called "the 50-Ohm Transmatch." This unit handles mismatches on the order of 4:1. It can transform a load of about 200 ohms, or 12 ohms, to a 50-ohm impedance. The circuit of the Transmatch described in this article, Fig. 46, is similar, but with two notable exceptions. In place of a tapped, switched inductor, a variable inductor is used. (The idea for this innovation came from Al LaPlaca, K2DDK.) The variable inductor is a coil wound on an insulated form that can be rotated so that a movable wheel shorts out and grounds the unused portion of the coil. Using the roller inductor, along with the two variable capacitors, the Transmatch provides an almost unlimited matching range, plus the feature of 80- through 10-meter coverage without band switching. With the values shown in the units, it is even possible to add one fixed capacitor to obtain 160-meter coverage.

The other exception is the use of a 1:4 (unbalanced-to-balanced) balun transformer on the output side of the Transmatch, which permits the use of balanced feed lines. This means that a Transmatch can cover 160 through 10 meters (including the MARS frequencies). It can be used to match into coaxial lines, random-length end-fed wires, or balanced feeders, and can do the job without using switches.

The two units shown in the photographs underwent extensive tests as to efficiency, power-handling capabilities, and methods of adjustment. In coax-to-coax tests, power inputs and outputs through the Transmatch were carefully measured while using Bird Thruline wattmeters and an adjustable dummy load. As carefully as could be measured, and with indicated mismatches of up to 15:1, the Transmatches showed an efficiency of over 95 percent. This small loss in efficiency more than outweighs the usefulness of the device.

Many tests were made with the high-power version to check heating of the roller inductor and the balun. Under a key-down condition, with 1200 watts indicated power through the Transmatch, the transmitter was kept on for 15-minute periods. In one test, the measured rf current through the coil was in excess of 15 amperes. The roller inductor used in the unit is rated at 5 amperes, so this was considered a fairly rugged test. The coil did get warm, but not enough to be a cause for concern. Keep in mind that in regular amateur work, 15

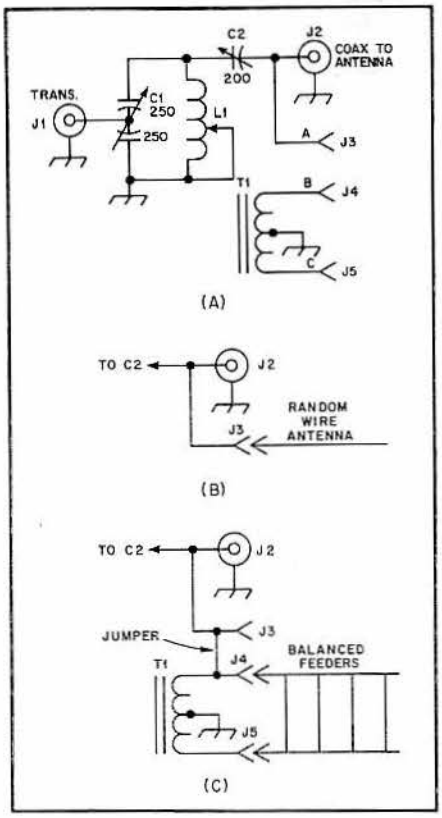

Fig. 46 — Circuit diagram of the Ultimate Transmatch.
C1 — Split-stator variable, 250 pF per section; see text. For low-power version, E. F. Johnson type 16250; or similar, for high-power version, Millen type 16250, or similar.
C2 — 200-pF variable, for low power, E. F. Johnson type 167-12 or similar, for high power, Millen type 16520 0.171-inch (0.43 cm) spacing, 16520A, 0.077-inch (2 mm) spacing, or similar.
J1, J2 — Coax chassis fitting, type SO-239.
J3, J4, J5 — Feed through insulators.
L1 — Roller inductor, see text. If 160-meter operation is desired, total inductance should be 28 μH, E. F. Johnson type 229-203; otherwise, 18 μH is adequate, E. F. Johnson type 229-202.
T1 — 1-to-4 balun; see text for details, cores are Amidon type T-200-2.

minutes would be a ridiculous figure for continuous operation.[2] In cw and ssb operation, the duty cycle would be in terms of seconds or even fractions of seconds.

The balun used for balanced operation in the high-power unit was made up from three Amidon 1-kW cores — more about that in a moment. N1RM has made extensive checks on a single-core balun. It was found that a single core would easily handle 500 watts of power during severe mismatch conditions. Failure of the core, most likely due to saturation and heating, took place at the 700-watt level. In the high-power Transmatch shown here, three cores are used. They are wrapped with glass insulating tape and then wound with Teflon covered wire. Wire insulation material can be important because of the extremely high rf voltages that may be developed with some load conditions. In many tests of long duration, using up to 1400 watts output into a dummy load, it was almost impossible to detect any heating of the balun.

Bear in mind that the balun would only be needed if balanced-line operation were desired. For coax-to-coax or random-wire feed, the balun can be omitted.

Construction Information

A look at Fig. 46, at A, will show that the circuit is a very simple one. The input line from the transmitter is connected to the rotor of C1, a split-stator capacitor. This means that the capacitor must be insulated from the chassis, using standoff pillars, and from the panel by means of an insulated shaft coupler. The same is true for C2. In the kW unit shown, we have installed a power bridge. Construction details are not given here for the bridge because such a unit was described in detail in *QST*[3]. Also, many amateurs already have a Monimatch[4] or some other type of SWR indicator. An SWR bridge or matching indicator is needed in the 50-ohm line between the rig and the Transmatch to show when the Transmatch is correctly adjusted.

Layout of the components should follow the same arrangement shown in the photographs — C1 at the input side, the roller inductor at the center, and then C2. If a balun is going to be installed, allow enough room behind the roller coil for mounting the balun. In the two units shown, the cabinets are made up from aluminum sheet stock. If desired, a commercial chassis and cabinet can be used. In the low-power Transmatch, leave at least 1/2-inch (13 mm) spacing between the edges of the capacitors and any part of the chassis and cabinet. Allow 1-inch (25 mm) spacing in the kW unit.

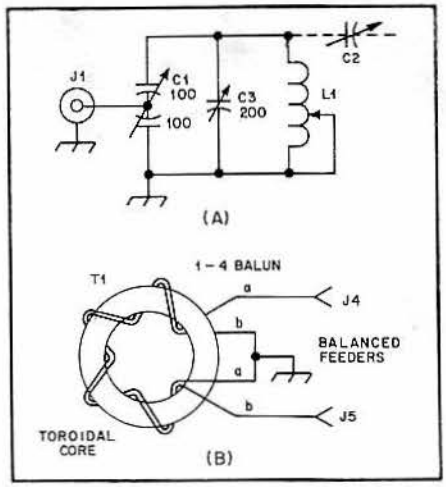

Fig. 47 — At A, details for padding a low-value variable for C1 by installing a second variable, C3, the same value as the low-power unit C2. In the case of tuning 160 meters, using an inductor of 28 μH for L1, and 250 pF per section for C1, a fixed capacitor of 100 pF can be used at C3, Centralab type 850-100N, or similar. At B, details for connecting the bifilar windings on the balun are given. The ungrounded leads a and b are connected to J3 and J4, the feedthrough insulator terminals.

Balun Details

For the low-power Transmatch, a single toroid core will more than handle the power. Incidentally, the low-power unit was tested under all conditions at about 100 watts through the Transmatch. The

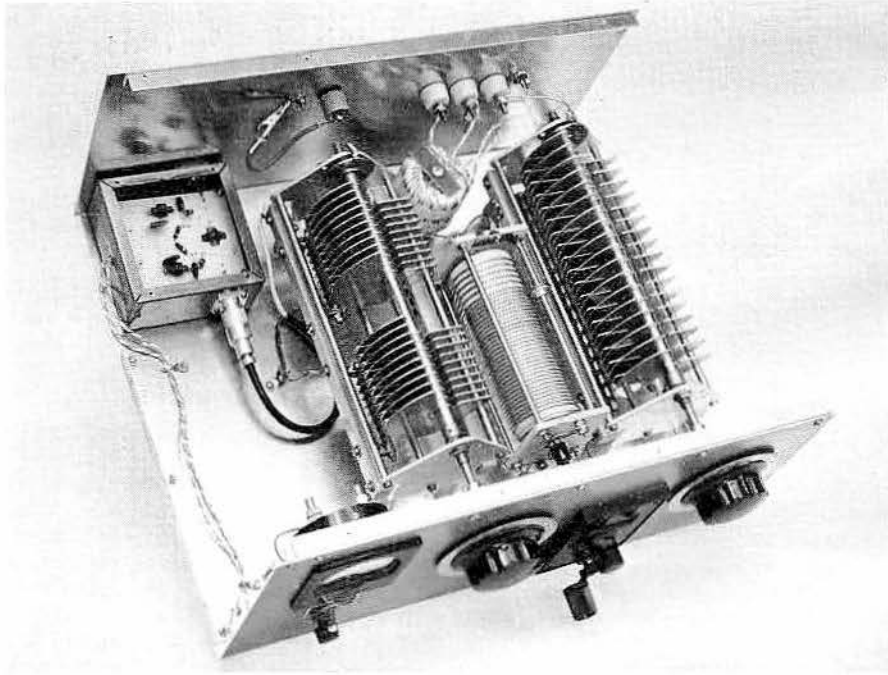

At the rear of the roller inductor is the 1:4 balun. The balun is set on top of a standoff insulator and is held in place with a piece of insulated board and a screw. The fixed capacitor mounted on the rear wall is the 160-meter unit. Both the variable capacitors and inductor are mounted on 1-inch (25 mm) high standoff insulators.

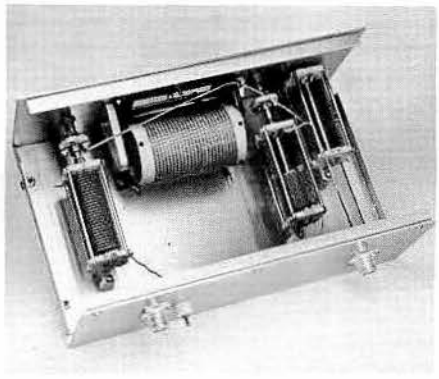

This is the low-power Transmatch. The salvaged roller inductor is mounted on the front panel, making use of the original mounting brackets.

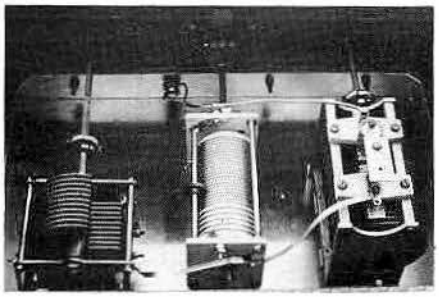

Here is an inside view of the Ultimate Transmatch as built by Al LaPlaca, K2DDK, who came up the idea of using the roller inductor. The installation on top the right-hand capacitor is the homemade 160-meter switch and fixed loading capacitor.

power-handling capabilities of the units depend primarily on the plate spacing used for C1 and C2, aside from the balun requirements mentioned earlier. At the 100-watt level, a plate spacing of 0.03 inch (0.8 mm) is adequate. A 0.045-inch (1 mm) spacing should handle 500 watts. In the kW unit shown, C1 has a 0.077-inch (2 mm) spacing. While a 0.077-inch spacing capacitor wasn't tried at C2, such plate spacing should work at the kW level.

In making the low-power balun, wind two layers of Scotch brand electrical tape around the core before putting on the wire. This will provide extra insulation, and will protect the edges of the wire to prevent the enamel from being scraped away. Fig. 47, at B, shows a sketch of the winding. The winding consists of 10 bifilar turns of no. 14 Formvar insulated wire. Connected as shown, this will provide a 1:4, unbalanced-to-balanced configuration.

Three cores are needed in the high-power balun. Each core is covered with two layers of 3-M type 27 glass-cloth insulating tape. Next, the three cores are stacked, then covered with two more layers of the tape. The winding consists of 15 bifilar turns of either no. 12 or 14 insulated wire. The insulation should have a minimum rating of 1000 volts and can be either Teflon or vinyl-nylon (or any other suitable covering with a minimum voltage rating of 1000 volts).

In making the low-power Transmatch, a roller coil from a junked 40-meter ARC-5 transmitter was salvaged and installed in the unit. Many amateurs know other hams who have old ARC-5 gear, and these units are a good source for the roller coils. However, some hams may not be able to locate used ARC-5 transmitters, so we have included some information on sources of surplus and new roller inductors. There may be surplus outlets in your area worth investigating. Look for a roller coil that has a minimum inductance of 10 μH when used with C1 having a value of 200 pF per section. Such a combination will cover a low frequency of 3500 kHz. In the unit shown, in addition to the ARC-5 roller, we used a value of 100 pF per section for C1 and padded that capacitor with another of 200 pF (single section) in order to provide the required coverage. This added capacitor is shown in Fig. 47 at A. By using this approach, it is sometimes easier to save money then when trying to locate a 200-pF-per-section variable for C1. (Incidentally, you can use a variable at C1 of more than 200 pF per section for good coverage with the roller inductance specified above.)

An even better approach to get the required capacitance for C1, because it is better to maintain the symmetry of the circuit as shown in Fig. 46 at A, would be to gang two 200-pF variables to make up your own split-stator capacitor, with the desired plate spacing. (There may be some around, but we couldn't find any manufactured split-stator with the required plate spacing and capacitance). Still another approach would be to clip fixed transmitting-type mica capacitors across each section of C1 to obtain the required capacitance for use on 160 and 80.

Finding the Parts

As most hams are finding out, it is becoming more and more difficult to buy, or find, components for construction projects. Some searching was done, and the following information is worth passing on. Barry Electronics of New York City has informed us that they will fill any order for any amateur component at the manufacturer's current amateur net price. The parts specified in Fig. 46 are currently manufactured items. Also, Fair Radio Sales in Lima, OH has some surplus roller inductors and counter dials in stock. The roller-inductor catalog number is 5950-199-6469, and the counter dial is listed as RT-45. Also, Millen components can be purchased directly from G. R. Whitehouse, Amherst, NH 03031.

Using the Transmatch

One of the first considerations in using a setup for "coax-to-coax" is exactly how much, or how high an SWR can be tolerated. As has been pointed out, this Transmatch will handle *any* mismatch on the line. Without getting into a lot of details, a few observations about coaxial lines are in order. First, the higher the SWR, the greater the losses in coaxial lines. The amount of losses depends on the line construction and the *frequency* at which the line is used — the lower the frequency, the less will be the losses. For example, RG-8/U has a loss per 100 feet (30.48 m) of line of only 0.33 -dB at 3.5 MHz with an SWR of 1 (a matched condition). At 28 MHz, this same line would have a loss of slightly less than 1 dB. However, as the SWR rises, so do the losses. With an SWR of 10:1, for example, the additional losses at 3.5 MHz would amount to about 0.6 dB, or an overall loss of about 1 dB. For the same SWR at 28 MHz, the losses would be about 2.5 dB, or a total loss of about 3.5 dB. Since a loss of 3 dB would mean half of the ouput power from the rig would be dissipated in 100 feet (30.48 m) of line, one could easily tolerate the condition at 80 meters, but the losses would be prohibitive at 28 MHz. This means that the amateur would be wise to keep the match at the antenna feed point as close to 50 ohms as possible, and thereby keep the SWR low.

With trap or multiple dipoles, the SWR should be less than 5 to 1; the Transmatch would be ideal. Keep in mind that you must provide a load for a transceiver or amplifier that is close to 50 ohms. The Transmatch will provide a means.

In a coax-to-coax system, set both C1 and C2 at maximum capacitance (plates fully meshed), then feed enough power through the Transmatch to get a full-scale forward reading on your SWR indicator. It is always important to use low power when adjusting a Transmatch. Next, switch the SWR bridge to read reflected power, then run the roller inductor slowly through its range. At some point you will notice a sharp dip in the reflected-power reading. Once this point is reached you should adjust C1 and C2, with possibly a slight adjustment of the roller coil, to get a perfect match. Power can then be increased to the desired level. You'll find that several different settings of the Transmatch may provide a perfect match. The one to shoot for is the condition that requires the most capacitance at C1 and C2 for a matched condition.

If a random-length, end-fed antenna is used, merely connect the end of the antenna to terminal J3, Fig. 46B, and go through the adjustment procedures outlined above. It is helpful to have an earth ground connection on the Transmatch. Also, if possible, use an antenna length that comes out to a quarter wavelength, or odd multiple thereof. Such an antenna will be of low impedance, and will reduce the chances of high rf voltages appearing on the Transmatch or associated equipment.

If balanced feeders are used, the feeders should be connected to terminals J4 and J5 with a short jumper connected between terminals J3 and J4. Again, the previously discussed tune-up and adjustment proce-

dures should be followed in setting up the Transmatch.

Some Other Thoughts

Some amateurs might be concerned about the amount of voltage that can be developed in a mismatched coaxial line. In a matched condition, with 1000 watts in a 50-ohm line, the rf voltage would be about 220 volts. With a standing-wave ratio or 20:1 (!), the increase in voltage would be 4-1/2 times, or approximately 990 volts. This however, is well within the rating of the RG-8/U cable.

This Transmatch should satisfy the needs of those hams who desire a multi-band unit without switches or plug-in coils. Once the settings for the controls are determined, a chart can be made up for any given istallation. Band changing is then quickly done. This material was originally presented in *QST* by Lewis G. McCoy, W1ICP.

References

[1]"The 50-Ohmer Transmatch," *QST*, July 1961.

[2][Editor's Note: However, teletype operation would be continuous (to say nothing of those long-winded a-m operators!).]

[3]"In-Line RF Power Metering," *QST*, December 1969. (See chapter 4.)

[4]*Understanding Amateur Radio*, p. 209.

Build a Baby Ultimate

Got a match? Not a classic "match," but one between the antenna and your QRP rig may be what you need. If so, this article is for you.

Nobody needs or wants a 50-pound Transmatch during a QRP junket to a favorite lake, campsite or other distant location. The entire point of QRP operation is negated when the low-power station can be held on the palm of one's hand, but the accessory gear needs to be transported by hand truck to the car, airport or whatever! Operators who prefer to use a random-length wire antenna for field work will require a matching network between the 50-ohm transmitter output and the end of the antenna, whose characteristic impedance can be anything from a few ohms to a couple of thousand. For low-power work (25 watts or less) it doesn't take a big Transmatch to do the job, and some novel ideas can be applied to make the matcher cover 80 through 10 meters without a roller inductor or messy tapped-coil switching arrangement. This article shows some tricks that can be applied to meet that goal.

The heart of the Baby Transmatch is the half-toroid variable inductor. It is the by-product of a few "skull sessions" between Andy Pfieffer, K1KLO, and the writer. Both amateurs are QRP "freaks," and finding the proper mechanical technique for building a miniature panel-operated variable inductor of reasonable inductance range was challenging and productive. The machine-shop skill and impagination of K1KLO can be realized when viewing the accompanying close-up photograph. Early efforts along this line provided a slider type of full-toroid variable inductor (rheostat style), and dismal results were had: the inductor Q was very low, approximately 5, as a result of the shorted-turn syndrome. Finally, a powdered-iron Toroid core of Q1 material, 1-inch (25 mm) diameter, with 3/16 by 3/16-inch (5mm by 5mm) walls, was sawed in half and cemented to a plastic arm. The arm was glued to the shaft of the control so that it would enable the operator to change the coil inductance by moving the semicircular toroid section in and out of the coil.

Exterior view of the Baby Ultimate. Dymo tape labels are used to identify the controls.

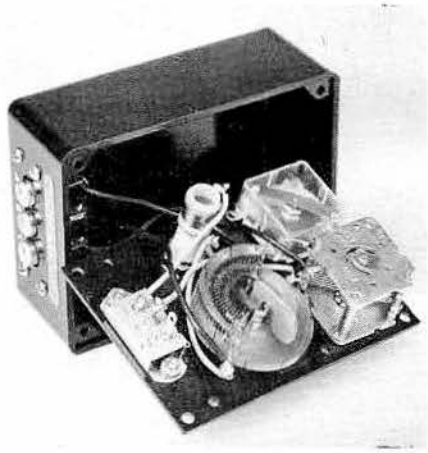

Interior view of the matcher showing the K1KLO variable inductor (lower center).

The coil in this unit was air wound, then cemented to a semicircular piece of plastic which is affixed to a plastic disk of 1-1/2-inch (38 mm) diameter. The overall coil-and-plastic assembly is glued to the 3/8-inch (10 mm) bushing and 1/4-inch (6 mm) diameter control shaft. Although all of the metal work was done from scratch on a lathe, an old volume control or rheostat bushing and shaft can be modified to perform the function required. All that's needed here is some amateur ingenuity! The tuning range of the variable inductor is 3 to 9 μH, and the unloaded Q was measured as 150 at 7.9 MHz.

It is reasonable to conclude that the K1KLO "giz," as he calls it, could be made to cover a greater inductance range by making the coil bigger in ID and cementing both halves of the toroid core together — one atop the other — to provide greater permeability overall. Ferrite material is unsuitable for this component because of the hardness of ferrite. Without special cutting tools the latter will resist all efforts to saw through it. One-half of an Amidon 1-kW balun-kit, powdered-iron toroid should be excellent for larger units of this kind.

Other Circuit Features

As is shown in Fig. 48A, S1 is used to switch an additional variable inductor (L1) in parallel with the K1KLO unit, L2. This provides a lower minimum-inductance amount for operaion on 15 and 10 meters.

Fig. 48B illustrates some variations which will extend the Transmatch range down to 80 meters. The model shown photographically was designed for 40 through 10 meters. In the second example, S2 and L3 have been added to increase the total inductance to permit 80-meter matching. Also, C1 has been changed to a

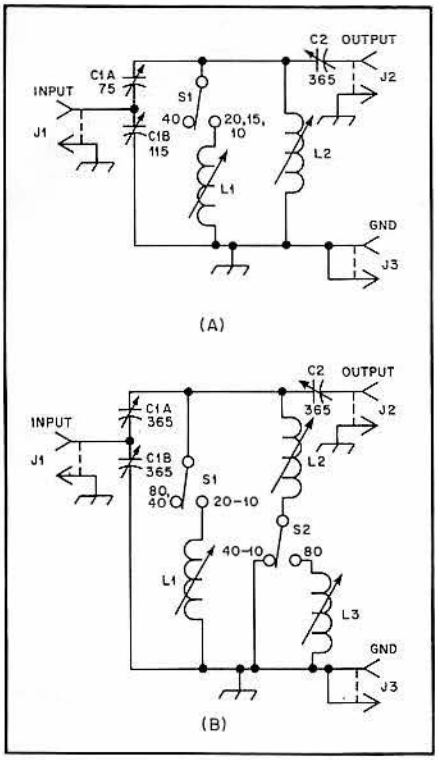

Fig. 48 — The diagram at A is for the 40- through 10-meter Transmatch. At B, a suggested circuit for coverage from 80 through 10 meters.
C1 — Dual-section air variable (Miller 2109, J. W. Miller Co., 19070 Reyes Ave., Compton, CA 90224). See text.
C2 — Calectro or Archer single-section miniature 365-pF variable.
J1-J3, incl. — Phono jack.
L1 — 3.1-to 4.8-μH slug-tuned inductor (Miller 4504 with red core).
L2 — See text. Contains 32 turns of no. 22 enam. wire, air wound, 7/16-inch (11 mm) OD.
L3 — 5.5-to 8.6-μH slug-tuned inductor (Miller 4505 with red core.)
S1, S2 — Spdt slide or toggle switch.

two-section 365-pF, bc-style variable, also for the same reason. A dual 365-pF capacitor can be used for the circuit at A, but the tuning rate will be much sharper than with the unit specified.

Three phono jacks are used for external connections. The first photograph shows a pair of clip leads which have been soldered to two phono plugs. These are used for making connections to a single-wire antenna and ground.

The slug screw of L1 protrudes from the top panel of the small plastic meter case. This feature enables the operator to have additional control of the overall inductance amount during operation on 15 or 10 meters. All internal ground connections are brought to a common point — J3, which has both of its terminals joined.

The "Ultimate" design is based on one which was popularized by W1ICP when he described in *QST* a 1-kW version of the circuit.[1] The network will match a wide range of impedances, but it should be pointed out that this circuit is not capable of providing much (if any) harmonic attenuation. Examination of the circuit will show that the network is basically a high-pass type.

Building the Transmatch

A 1-1/2 × 2-3/4 × 4-inch (38 mm × 70 mm × 102 mm) plastic meter style of case is used to house the Transmatch. The box used by the writer was made by RCA as an enclosure for a 9-volt regulated power-supply kit. Similar boxes are available at Radio Shack and other parts stores, but most have a metal cover. If the latter are used, it will be necessary for the builder to isolate the rotors of C1 and C2 from the metal plate. Adhesive-backed plastic feet are affixed to the bottom of the case. They will keep it from moving about on the operating table.

Using the Transmatch

When matching the 50-ohm transmitter to a given antenna (fed with coaxial line or single wire in nature), an SWR indicator will be necessary between the transmitter and the Transmatch.[2] C1, C2 and L2 are adjusted one at a time for the lowest reflected-power reading on the meter. There will be interaction between the controls, so it will be necessary to go over them several times to effect an SWR of 1.

Some difficulty may be encountered while working with a voltage-fed (high impedance) wire antenna. The symptom is one of hand capacitance affecting the SWR reading. In such instances the tune-and-try method will be required, moving the hands away from the box after each adjustment. For this reason the builder may wish to house the circuit in a metal box and use insulating shaft couplings on C1, C2 and L2. Of course, this will make the unit somewhat larger.

The writer used this Transmatch for two weeks in October 1975 while on a QRP sortie to Barbados (8P6EU). Maximum power used was 20 watts output, and minimum power was 2 watts ouput. The 40-, 20- and 15-meter bands were used, and all manner of antennas (end fed and coaxially fed) were employed. In all cases the SWR could be set for a 1:1 condition. Insertion loss through the Transmatch was measured at 14 MHz while delivering 20 watts to a test dummy load. The loss was approximately 0.1 dB at a matched condition. No heating of the components was noted.

One final word is in order. Always use the maximum possible amount of capacitance at C2 when adjusting the Transmatch for an SWR of 1. There can be several settings of C1, C2 and L2 which will provide a match. Best efficiency will always occur with maximum usable C at C2, and this is true of all variations of the Ultimate Transmatch.

If you're a QRP enthusiast, this matcher should be part of your setup when 50-ohm antennas aren't used. It is lightweight, small of size, and can be tucked away in the XYL's handbag when enroute, if need be! This material was originally presented in *QST* by Doug DeMaw, W1FB.

References

[1]McCoy, "The Ultimate Transmatch," *QST*, July 1970. (Included in this chapter.)
[2]DeMaw, "A QRP Man's RF Power Meter," *QST*, June 1973, p. 13.

Simple Broadband Matching Networks

This article gives complete details on constructing broadband matching transformers for ratios of 4:1, 6:1, 9:1 and 16:1.

Are you looking for a physically small DX antenna? To obtain low-angle radiation on 80 and 160 meters, many amateurs use vertical antennas. Horizontal antennas would have to be at elevations of a half-wavelength or greater to be comparable. Suitable supporting structures are beyond the reach of most amateurs at these lower-frequency bands. Quarter-wavelength verticals require some 60 feet (18.29 m) on 80 meters and 120 feet (36.58 m) on 160 meters — still very tall structures! However, short verticals over a good image plane have been shown theoretically[1] and experimentally[2] to perform practically as well as their full-size quarter-wavelength counterparts. The only problems are very low input impedances and narrower bandwidths.

This paper describes broadband matching networks which can efficiently match 50-ohm coaxial cable to verticals as short as 1/25 wavelength. Also included is information on short vertical antenna designs incorporating large top hats in order to improve bandwidth, such as a very short 40-meter vertical and a dual-band 80- and 160-meter short vertical with remote switching. In addition, loading coils using powdered-iron toroidal cores are discussed.

Connie, W2FMI's better half, is making use of the shade under Jerry's 40-meter umbrella antenna. It is hoped that Jerry warns her about touching the antenna when he is running high power!

Broadband Matching Transformers

Broadband transformers have been widely used because of their inherent bandwidth ratios (as high as 20,000:1) from a few tens of kilohertz to over a thousand megahertz. This is possible because of the transmission-line nature of the windings. The interwinding capacitance is a component of the characteristic impedance and therefore, unlike the conventional transformer, forms no resonances which seriously limit the bandwidth.[3] At low frequencies, where interwinding capacitances can be neglected, these transformers are similar in operation to the conventional transformer. The main difference (and a very important one from a power standpoint) is that the windings tend to cancel out the induced flux in the core. Thus, high-permeability ferrite cores, which are not only highly nonlinear but also suffer serious damage even at flux levels as low as 200 to 500 gauss, can be used. This greatly extends the low-frequency range of performance. Since higher permeability also permits fewer turns at the lower frequencies, high-frequency performance is also improved since the upper cutoff is determined mainly from transmission-line considerations. At the high-frequency cutoff, the effect of the core is negligible.

The applications of broadband transformers to antennas and broadband circuits have been covered by a number of authors.[4,5] This paper extends the application of these transformers to include the operation of short ground-mounted vertical antennas with impedances as low as 3 to 4 ohms. Further design considerations illustrate variable matches to vertical antennas having impedances even greater than 35 ohms.

Bifilar matching transformers for ground-mounted verticals lend themselves to unbalanced operation. That is, both input and output terminals can have a common ground connection. This eliminates the third magnetizing winding required in balanced-to-unbalanced (balun) operation. By adding third and fourth windings, as well as tapping windings at appropriate points, various combinations of broadband matching can be obtained. Fig. 49 shows a 4:1 unbalanced-to-balanced configuration. This transformer can be used with verticals of 12.5 or 200 ohms when using 50-ohm cable. No. 14 wire can be used and it will easily handle 1000 watts of power. By tapping at points 1/4, 1/2 and 3/4 of the way along the top winding, ratios of approximately 1.5:1, 2:1, and 3:1 can also be obtained. It should be noted that one of the wires was covered with vinyl electrical tape in order to prevent voltage breakdown between the windings. This was necessary when a step-up ratio was used at high power to match antennas with impedances greater than 50 ohms.

Fig. 50 shows a transformer with four windings, permitting wide-band matching ratios as high as 16:1. A picture shows a four-winding transformer with taps at 4:1, 6:1, 9:1 and 16:1. In tracing the current flow in the windings when using the 16:1 tap, one sees that the top three windings carry the same current. The bottom winding, in order to maintain the proper potentials, sustains a current three times greater. The bottom current cancels out the core flux due to the other three windings. If this transformer is used to match into low impedances, like 3 to 4 ohms, the current in the bottom winding can be as high as 15 amperes if the high side of the transformer is fed with 50-ohm cable handling a kilowatt of power. If one needs a 16:1 match like this at high power, then cascading two 4:1 transformers is recommended. In this case, the transformer at the lowest impedance side only requires each winding to handle 7.5 A. Thus even no. 14 wire would suffice in this application.

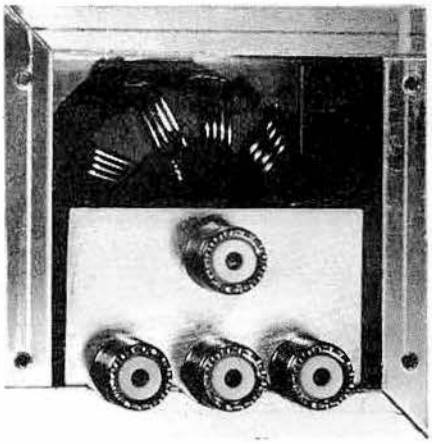

A 4-winding, wideband transformer (with front cover removed) with connections made for matching ratios of 4:1, 6:1, 9:1, and 16:1. The 6:1 ratio is the top coaxial connector and, from left to right, 16:1, 9:1, and 4:1 are the others. There are 10 (quadrifilar) turns of no. 14 enameled wire on a Q1, 2.5 inch (64 mm) ferrite core.

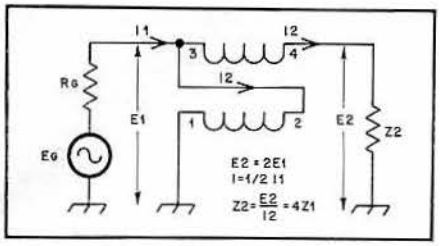

Fig. 49 — Four-to-one broadband bifilar transformer. Upper winding can be tapped at appropriate points to obtain other ratios such as 1.5:1, 2:1 and 3:1.

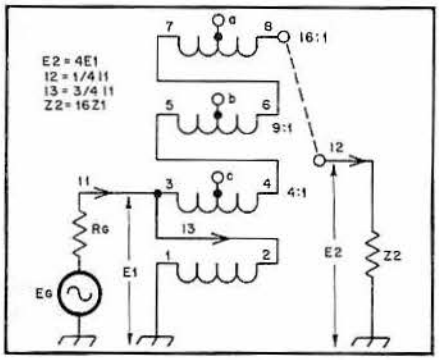

Fig. 50 — Four-winding, broadband, variable impedance transformer. Connections a, b and c can be placed at appropriate points to yield various ratios from 1.5:1 to 16:1.

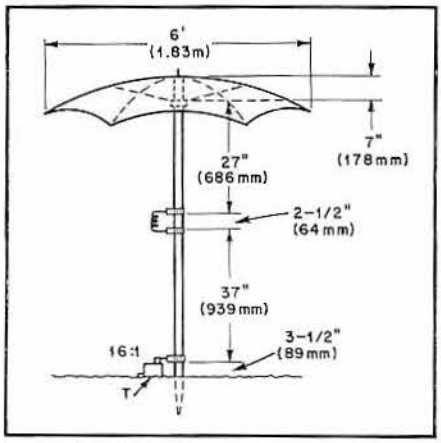

Fig. 51 — Final design and bandwidth characteristic of a short 40-meter vertical having an input impedance of 3.5 ohms and utilizing a commercial beach umbrella. This antenna established its worth as a prototype for the lower frequencies.

The popular cores used in these applications are 2.5 inch (64 mm) OD ferrites[6] of Q1 and Q2 material and powdered iron cores,[7] of 2-inch (51 mm) OD. The permeabilities of these cores, μ, are nominally 125, 40 and 10, respectively. Powdered iron cores of permeabilities 8 and 25 are also available.

In all cases these cores can be made to operate over the 10- to 160-meter bands with full power capability and very low loss. The main difference in their design is that lower permeability cores require more turns at the lower frequencies. For example, Q1 material required 10 turns to cover the 160-meter band, Q2 required 12 turns, and powdered iron (μ = 10) required 14 turns. Since the more common powdered-iron core is generally smaller in diameter and requires more turns because of lower permeability, higher ratios are sometimes difficult to obtain because of physical limitations. Although most of the author's experimentation on these transformers was done on the 40-, 80- and 160-meter bands, the results indicated that they should operate on the higher bands equally well. When working with low impedance levels, unwanted parasitic inductances come into play, particularly on 14 MHz and above. In this case lead lengths should be kept to a minimum.

All the results obtained by the author have shown that the transformers can be used to match a variety of loads and impedance ratios, they can be used over many bands, and that they exhibit negligible loss in operation. More importantly, the core materials are readily available and low in cost.

A Short Vertical Antenna Design

These transformers permit efficient matching to impedances as low as 3 to 4 ohms. This means, with some top-hat loading, antennas could be 4 to 5 feet (1.22 to 1.52 m) tall on 40, 8 to 10 feet (2.44 to 3.05 m) on 80, and 16 to 20 feet (4.88 to 6.10 m) on 160 meters. With the capability of tapping off any portion of the transformer windings, thus providing variable matching, the heights of these antennas can be increased at will depending upon the bandwidth desired.

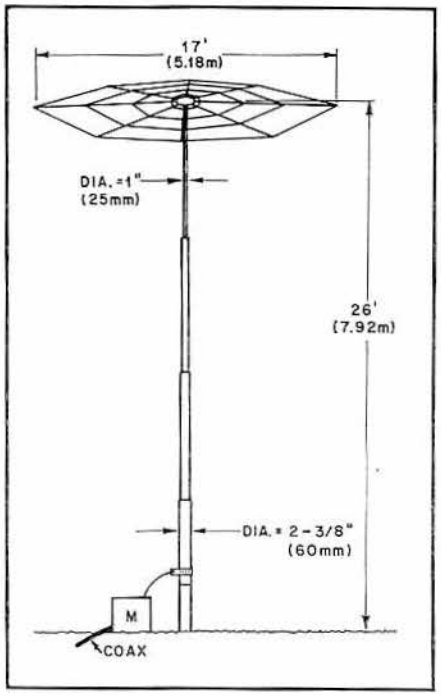

Fig. 52 — The 80- and 160-meter dual-band vertical system. The remotely switched matching network is described in the text. Not shown are three sets of polypropylene guy ropes at heights of about 9, 18 and 26 feet (2.74, 5.49 and 7.92 m).

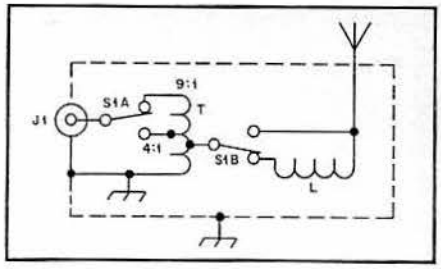

Fig. 53 — The remotely switched matching network for the 80- and 160-meter dual-band vertical antenna. The indicated switch positions are for 160-meter operation.
S1 — Dpdt antenna relay.
J1 — Coaxial connector, chassis type.
L — Load coil for 160 meters, 22-1/2 turns, no. 14 wire on 4 cores of 2-inch (51 mm) OD powdered-iron, permeability of 10 (Amidon T-200-2).
T — Broadband transformer (see text).

The first short vertical designed by the author was brought about by a trip to a local shopping center. The author saw a beach unbrella that had about the right proportions one would use in designing a short 40-meter vertical. The "antenna" was purchased (at a nominal price) and a 14-turn coil, connected across an insulated section about three feet (0.91 m) from the ground, was used to tune the vertical to resonance. The measured input impedance was 3.5 ohms and was matched easily to 50-Ω line with a 16:1 transformer. Fig. 51 shows the final design and the bandwidth characteristic. Several months of operation on 40 meters verified the outstanding capability of this short vertical antenna (with an extensive radial system) and established its worth as a prototype for the lower frequencies. A further study showed that the 6-foot (1.83 m) diameter top-section was about the equivalent of a 4-1/2-foot (1.37 m) diameter solid disk.

A Dual-Band 160- and 80-Meter System

The antenna shown in Fig. 52 is a dual-band design using a remotely switched matching network (see photograph) which not only changed a tap on a broadband transformer from 4:1 to 9:1, but also introduced a powdered-iron base-loading coil for 160-meter operation.

The circuit diagram for the remote matching network is shown in Fig. 53. The loading coil was made with four powdered-iron (μ = 10, 2-inch [51 mm] OD) cores. They were first wrapped individually with several layers of vinyl electrical tape before being combined and wrapped again. The necessary inductance was obtained with 22-1/2 turns. A slight adjustment of the loading coil and the height of the antenna was found necessary in order to put the minimum SWR at 1812 kHz. In general, a 1-foot (0.31 m) change in height of the antenna changes the 80-meter resonance by 60 kHz and the 160-meter resonance by 15 kHz. A change of 1/2 turn on the

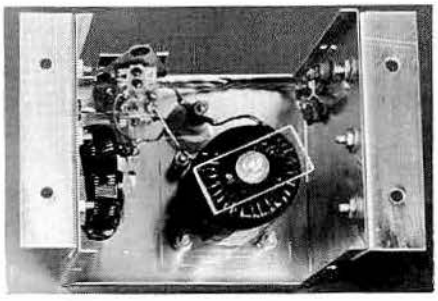

Bottom view of the matching network for the dual-band 80- and 160-meter vertical. The loading coil is on the right and the trifilar 4:1 and 9:1 matching transformer on the left. The dpdt 24-volt antenna relay switches in or out the loading coil and changes the taps on the transformer to the appropriate ratio. The enclosure is the conventional 4 X 5 X 6-inch (102 mm X 127 mm X 152 mm) aluminum Minibox.

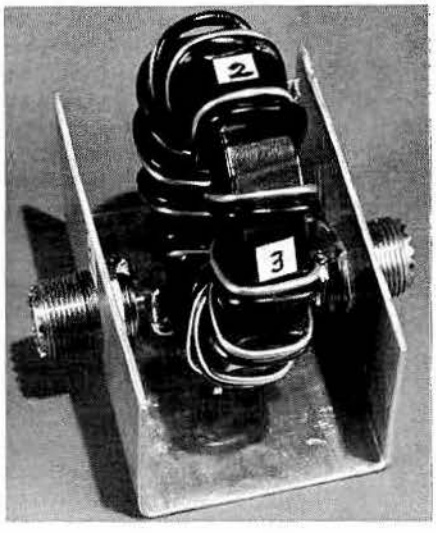

The broadband bifilar transformer shown has 12 bifilar turns, no. 14 wire, on a ferrite (Q1 material, 2.5 inch [64 mm] OD) core. Taps are also placed at 3, 6, and 9 turns, thus yielding ratios of 1.5:1, 2:1, 3:1 and 4:1. This transformer has a connection at the 1.5:1 ratio tap. Extra insulation was provided for the enameled wire in order to prevent voltage breakdown when matching into loads greater than 50 ohms.

powdered-iron core coil changes the 160-meter resonance by about 50 kHz. It should be noted that the windings had extra insulation (about one layer of vinyl tape) added on the inside part of the windings in order to prevent breakdown between them.

Low-permeability ferrite material Q2 (μ = 40, but still four times larger than the powdered iron material) was also investigated for use as a core for a 160-meter loading inductance. It was hoped that with several stacked cores of this material, the flux density would be reduced to a level where nonlinearities and permanent damage could be avoided. Two cores and about 10 turns of wire were used. The result was negative. Large changes in inductance were noted on voice peaks by the sudden large changes in the SWR. Also, small but permanent changes in the SWR were observed, indicating permanent damage. In contrast to ferrite, powdered iron maintains its linearity at high flux densities and suffers no permanent damage. As noted above, four cores of permeability 10, and 22-1/2 turns, provided the proper inductance (approx. 30 μH). The loss in this coil was about equal to the air-wound coil (33 turns, 6 tpi, no. 12 wire, 2-1/2-inch [64 mm] OD). Two stacked powdered-iron cores of permeability 25 were also investigated. This arrangement required about 17 turns, but was rejected because the loss, which was mainly in the two cores, went up to 3 ohms. This is certainly intolerable since it is of the order of magnitude of the radiation resistance of the very short vertical.

Concluding Remarks

The predominant characteristic of the short antenna is probably its very low value of radiation resistance. One must be careful of excessive ground and ohmic losses in coils and matching networks. A good image plane can eliminate the ground-loss factor. The application of a top hat eases the problem somewhat because it increases the effective length and thus the radiation resistance. The radiation resistance can be increased five-fold[8] by resorting to complete top-hat loading of a vertical. Combinations of top-hat and inductive loading can be used depending upon the radiator height and the bandwidth desired. One can also resort to a short folded unipole. With these combinations at his disposal, the designer is left with the problem of efficiently matching his transmission line to various impedance levels. The wide-band transmission-line transformer can provide the answer. It is capable of operating very efficiently over a wide range of impedances and impedance ratios.

The author would like to acknowledge the generosity of the following companies who supplied cores and information for the experiments: Indiana General Corp., Amidon Associates, and the Arnold Engineering Co.

Finally, the author would like to thank his colleague Mort Fagen, WA2EIT, for his encouragement and discussions of the antenna papers the author has written. This material was originally presented in *QST* by Jerry Sevick, W2FMI.

References

[1]King, *The Theory of Linear Antennas,* Harvard University Press, Cambridge, MA, 1956.
[2]Sevick, "The W2FMI Ground-Mounted Short Vertical," *QST,* March 1973. (See chapter 1.)
[3]Ruthroff, "Some Broad-Band Transformers," *Proc. IRE,* Vol. 47, p. 137, August 1959.
[4]Turrin, "Application of Broadband Balun Transformers," *QST,* April 1969.
[5]Krauss and Allen, "Designing Toroidal Transformers to Optimize Wideband Performance," *Electronics,* August 16, 1973.
[6]Indiana General Corp., Electronics Div., Keasby, NJ 08832.
[7]Amidon Associates, 12033 Otsego Street, North Hollywood, CA 91607; The Arnold Engineering Co., Marengo, IL.
[8]See reference 2.

An RF-Sensed Antenna Changeover Relay

Flick of the switch, sir? Not with this system — it's automatic!

One subject that can be confusing for the newcomer to Amateur Radio is that of antenna-changeover systems. Several systems have been devised over the years and most can be classified into three or four main categories. Before delving into a discussion on these systems, a brief look at the simplest method of all might be in order, that is, no antenna changeover at all. With this setup two separate antennas are used, one for the transmitter and one for the receiver. This system is impractical for the most part since duplicate antennas would be required for each band of operation. There are instances, however, when separate antennas with different directive patterns can be used to an advantage, as in the case of specialized receiving antennas. Generally speaking, most stations use the same antenna for transmit and receiver purposes, so this is more the exception than the rule.

Several antenna-changeover systems, designed to transfer a single antenna from the receiver to the transmitter, are shown in Fig. 54. At A, a manual switch is used to transfer the antenna connection. This scheme is simple and works well, but is not without several drawbacks. Good-quality, high-power rf switches are often costly and

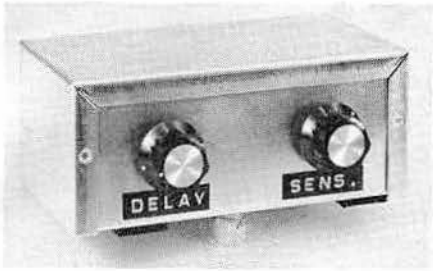

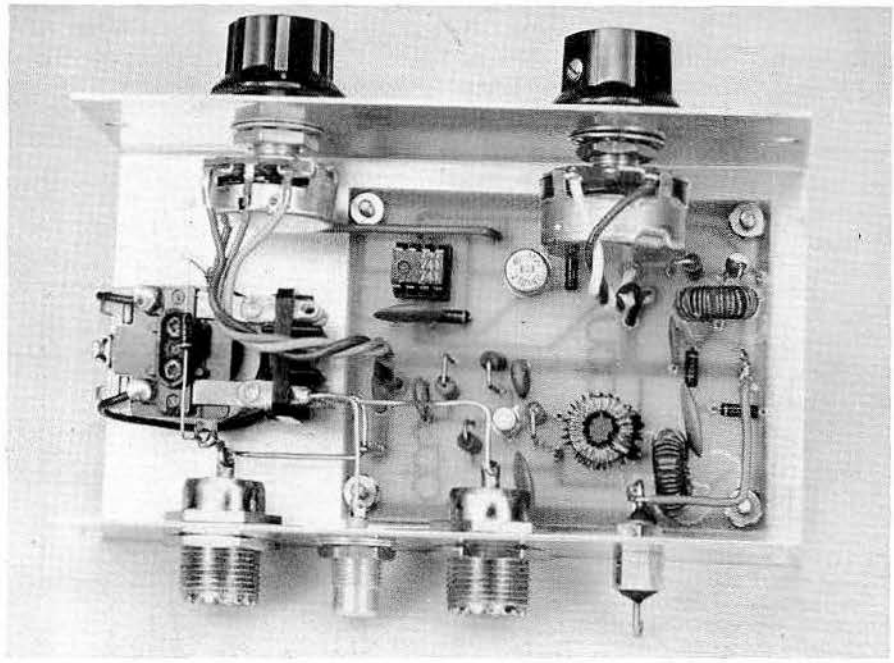

The inner layout of the antenna-changeover relay. Wiring or placement of circuit board and other components is not critical.

hard to locate and, of course, the operator is required to switch manually from receive to transmit.

One of these problems was eliminated with the advent of the coaxial relay. These relays were, in most cases, mounted external to the transmitter and receiver with connecting cables running to and from the unit, as shown in Fig. 54B. Many of these relays were rated for a kilowatt a-m signal, and maintained the 50-ohm line impedance. The voltage needed for the relay field was switched on or off with a low-powered toggle or foot switch. Alternatively, the transmit-receive switch might be located on the front panel of the transmitter with control voltage or a normally open or closed circuit available at a socket on the rear apron. Several extra sets of relay contacts were usually furnished with the relay to perform various functions, including that of muting the station receiver during transmit periods. Although this system of antenna transfer represented an improvement over the previous setup, it was still necessary for the operator to switch the antenna manually via the relay-control switch.

It's been said that laziness is the mother of invention and so it seemed natural that a more automatic system be developed. The relatively modern scheme at Fig. 54C has the transfer relay built into the transmitter. This system is quite popular and is used by most commercial manufacturers of amateur equipment that offer a separate transmitter and receiver. When the key is pressed the relay activates automatically and switches the antenna to the transmitter. A variable-length delay is usually included to hold the relay closed, thereby keeping the antenna connected to the transmitter during code characters. After the last group of code characters is sent, the relay will remain closed for a second or two — the amount of time controllable. When the relay deactivates, the antenna is reconnected to the receiver.

Unfortunately, some amateurs who build their own equipment or purchase transmitters and receivers of different manufacture, sometimes resort to switching methods A or B. These setups, of course, do not include the automatic features of system C. The circuit described here and shown in simplified form in Fig. 54D was designed with this in mind. Basically, this system detects the presence of rf at the output of the transmitter and

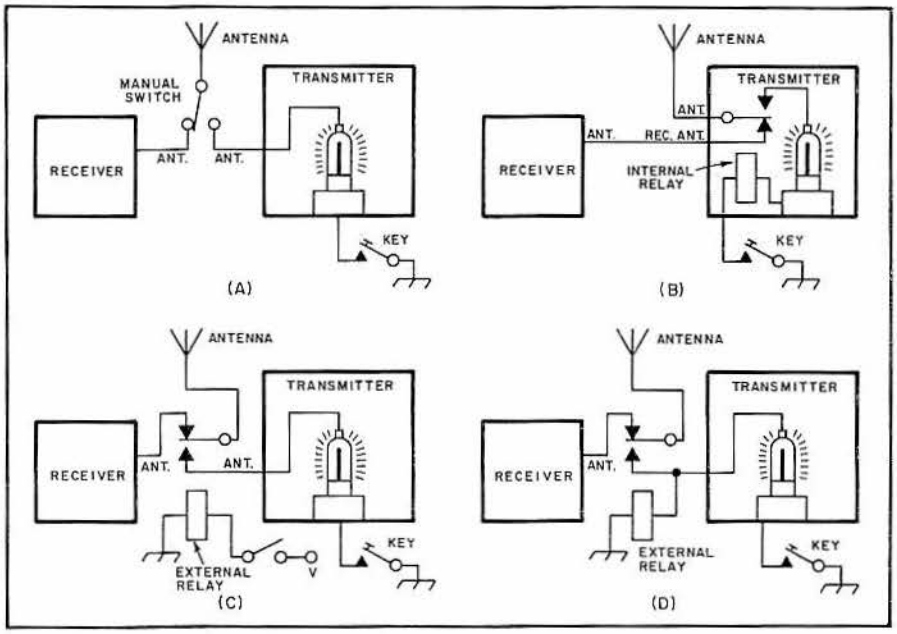

Fig. 54 — Several different antenna-changeover systems in block diagram form.

immediately breaks the antenna connection to the receiver. At the same time the antenna connection to the transmitter is made. One of the features of this system is that no modifications to either the transmitter or receiver are required.

Circuit Description

R1 of Fig. 55 serves as an rf-voltage divider to permit the circuit to be used with transmitters of various power-output amounts. Rf energy is routed through C1 to the base of broadband amplifier Q1. The amplified hf-band energy is supplied to a voltage-doubler (D1 and D2) through a broadband toroidal step-down transformer, T1. The rectified rf voltage at the output of D1 and D2 is filtered by means of RFC2, C5 and C6. This prevents unwanted rf from reaching U1 and affecting its performance.

C6, R7 and R6 comprise a timing network (variable) which governs the hold-in time of the relay, K1. The smaller the resistance amount at R6, the shorter will be the time delay.

U1 functions as an inverting amplifier. When the input dc voltage at pin 2 increases, the output dc voltage at pin 6 decreases. The output voltage causes the base of relay driver Q2 to be forward biased

negatively when it drops below approximately 1.4 volts. Diodes D5 and D6, by virtue of their combined barrier voltages (0.7 V each), establish the 1.4-V fixed bias level. Without the diodes, Q2 would conduct sufficiently to prevent the relay from dropping out during no-signal periods. D4 is used to suppress transients caused by the field coil of K1. When no rectified rf reaches U1, Q2 is cut off because of the high positive base voltage it receives from U1, and the relay contacts to the transmitter are open.

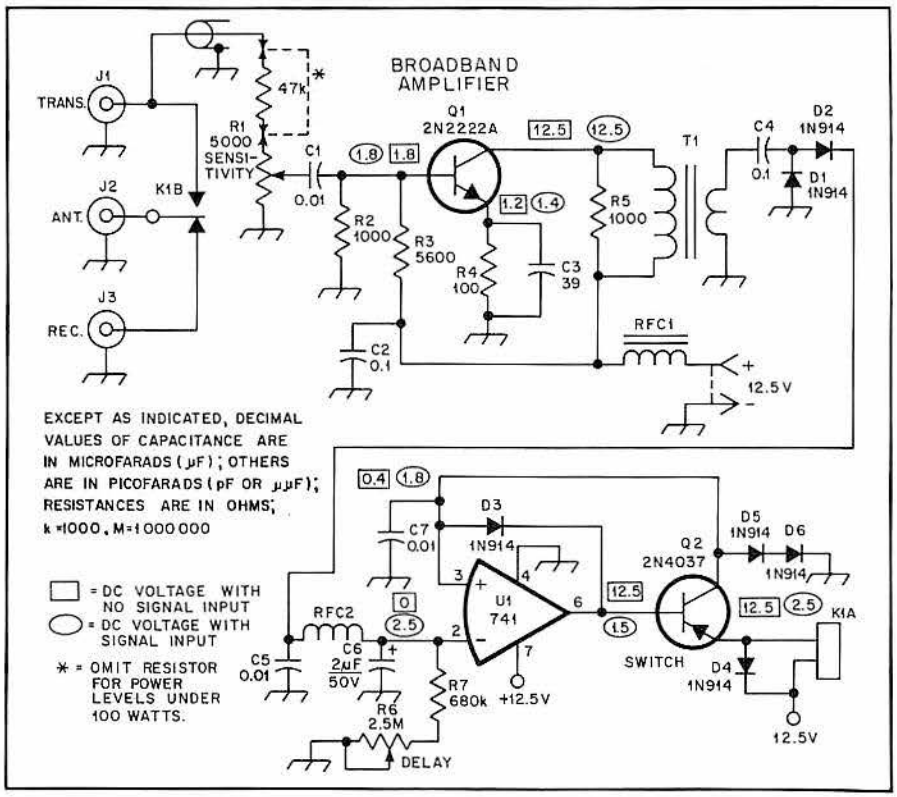

Fig. 55 — Schematic diagram of the rf-sensed antenna-changeover relay. All resistors are half-watt composition type. Capacitors are disk-ceramic unless noted otherwise. Component numbers not appearing in the parts list are for identification purposes only.

J1, J2 — Connector, SO-239.
J3 — Connector, phono-type.
K1 — Dpdt relay, 5-ampere contacts, 12-volt field.
R1 — Linear potentiometer, 5000 ohms.
R2 — Linear potentiometer, 2.5 megohms.
RFC1, RFC2 — Rf choke, 42 turns no. 28 enam. wire on an Amidon FT-50-43 core.
T1 — Broadband transformer. Primary: 25 turns no. 28 enam. wire on an Amidon FT-50-43 core; secondary: 5 turns no. 28 enam. wire wound over primary winding.
U1 — Op amp, 741.

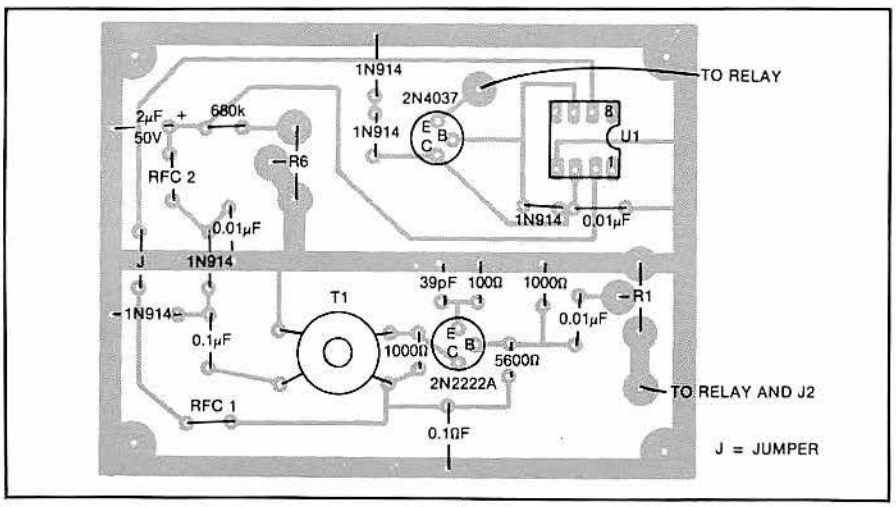

Fig. 56 — Circuit-board etching pattern for the changeover relay. The pattern is shown at actual size from the foil side of the board with gray areas representing copper. Decimal-value numbers alone represent capacitance in microfarads. Whole-number values with no units represent resistances in ohms; k = 1000. J = wire jumper. All components are mounted on the nonfoil side of the board. K indicates the cathode of a diode.

Construction

In Fig. 56 is a suggested printed-circuit board layout showing the foil pattern and parts placement. R1 and R6 may be circuit-board-mounted potentiometers if the builder desires, as the board layout was designed to accommodate such units. Potentiometers of this type are entirely suitable if the builder does not anticipate frequent changes in power levels and length of delay, as these controls must be readjusted for such changes. If the builder is interested in having access to these controls, panel-mounted potentiometers can be used at the front apron, in which case wires will have to be run from the circuit board to the controls.

Our finished model was housed in a 5 × 3 × 2-inch (127 mm × 76 mm × 51 mm) aluminum Minibox. R1 and R6 were mounted on the front panel and Kurz-Kasch knobs were placed on the control shafts to dress up the appearance of the finished product. D4 is attached directly to the relay terminals. The rear panel supports the terminals for the transmitter, antenna, receiver antenna and power supply. SO-239 connectors were used for the transmitter and antenna connections, and a phono connector was employed for the receiver antenna. Any type of connectors may be substituted to match those used in the builder's station. The power-supply lead is brought out through a feedthrough capacitor. This type of feedthrough is not necessary; a simple feedthrough insulator or wire could be used instead. In our case, the capacitor lead served as a convenient tie point during preliminary testing of the unit.

Operation

Connect the antenna, transmitter, receiver antenna lead and the power-supply connections to the appropriate terminals. Set R6, the time-delay control, to its minimum delay position (ccw) and the sensitivity control to its midrotation position. While keying the transmitter, decrease the setting of the sensitivity control to a point just above that where the transmitter no longer makes the relay energize. Once this has been set, it may be left in that position until a moderate change in power level has been made. The delay control should then be adjusted for the length of delay desired. The circuit shown has been tested from 1.8 to 30 MHz and at dc power input levels up to and including 1000 watts. This material was originally presented in *QST* by Doug DeMaw, W1FB, and Jay Rusgrove, W1VD.

Measuring Antenna Gain with Amateur Methods

Beat the cost of expensive test gear. Make your antenna measurements using this unique method! A VU meter, a handful of parts and this simple explanation are all you need.

Several excellent articles have been written about the techniques used at vhf conferences to measure antenna gains. Two such articles in particular, by Clark[1] and Knadle,[2] suggest very good antenna-range procedures. Both describe techniques which, if properly applied, will produce accurate relative antenna-gain data (in decibels) for vhf-uhf antennas.

However, these antenna range-measurement systems require equipment most amateurs lack — ratiometers, precisely calibrated attenuators, or at least specialized detectors and commercial grade audio or VSWR meters. Moreover, setting up a near-field antenna range is a tricky business in itself. One text[3] simply warns amateurs not to expect accurate antenna-gain measurements if they try it! The problem, of course, is that outdoor antenna ranges invite all sorts of error-causing reflections from various objects, not the least of them being the earth itself.

Ground reflections alone can completely invalidate the results on an otherwise good antenna range. At the 1973 West Coast VHF Conference, for instance, the author's 8-element quagi for 432 MHz[4] was measured at precisely the same gain as a well-built 15-element Yagi more than twice its size, despite the fact (established in other tests) that the bigger antenna had 2 to 3 dB more actual gain! The problem was that, even with the sophisticated measuring equipment in use, ground reflections were distorting the results. The best "gain" indication came with both antennas within a few inches of the earth, and the smaller quagi with its lower Q didn't mind the detuning effects of the earth's proximity as much as the bigger and higher Q array.

With results like that, wild claims are sometimes made for one vhf antenna or another. And the claims may be even wilder on the hf bands, where an amateur may well be told his signal is two of three S units louder than another ham's signal when the actual gain difference between the two antennas is insignificant. The ham who "won " the comparison by several S units, of course, is likely to go away thinking his antenna is 12 or 18 dB better than the other guy's, since S meters are supposed to show 6-dB signal difference per S point.

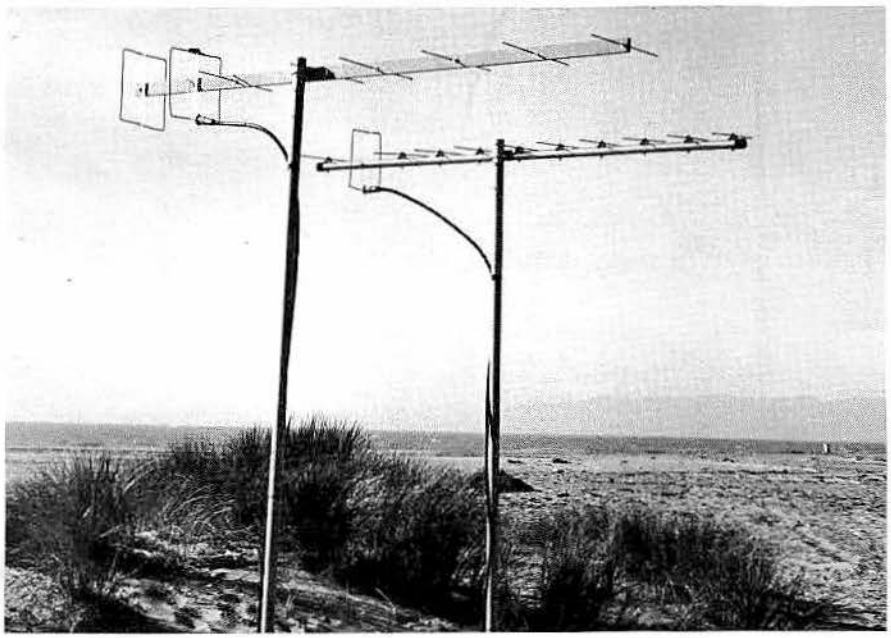

For the antenna gain-measurement technique described here, two identical masts in a clear area (here a southern California beach) are required. With the test and reference antennas at equal heights and fed with identical feed lines, the signal produced by the two antennas is compared by rapid and repeated switching. Here an 8-element quagi is tested against an 11-element Yagi that has been modified for quagi-type drive. The modified Yagi delivers 3 dB more gain than the conventional version, but 2 dB less than the quagi.

A Better Way

This article describes a more reliable and valid way to estimate antenna gain, and without expensive or hard-to-find test equipment. The technique requires only this equipment: a cooperative nearby ham with a transmitter capable of generating a few watts of steady carrier, a receiver whose agc can be turned off, an ordinary audio VU meter, and some antennas to measure.

The technique is nothing more than a more rigorous application of the test procedure radio amateurs have always used when they asked for "comparison" signal reports. It takes advantage of the fact that audio VU meters, unlike S meters, are calibrated directly and fairly accurately in decibels, with easy readout down to fractions of a dB. And with the agc turned off, most receivers will closely reproduce changes in the signal input at the antenna terminals with corresponding changes in audio output until they are badly overloaded.

This means that a nearby amateur's signal transmitted at a reasonably low power level can be used to compare the gain of various antennas by rapidly switching back and forth between them and averaging the results.

The only trick is to use a "test signal" that is coming from a point source — not a signal that is being reflected from surrounding objects. If your test antennas can "see" the signal source a few miles away and are well clear of nearby objects (and clear of the earth itself), valid results should be attainable if the procedures below are followed.

The author has spent many hours working with both local antenna ranges covering a few dozen wavelengths, and on-the-air signals from local stations. It is apparent that ground reflections and other

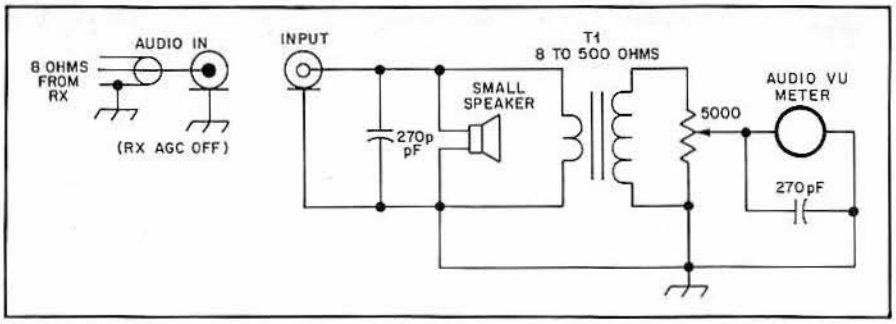

Fig. 57 — The audio VU-meter system for antenna gain measurements.

Fig. 58 — This small box houses all the test equipment required for antenna gain measurements using the technique described here. The front-panel audio VU meter is calibrated directly in decibels, with readout possible to about 0.2 dB in the most expanded part of the scale. Not visible are the meter level potentiometer (on rear), and small speaker which is mounted downward.

such error sources are less serious problems when a steady, on-the-air carrier a few miles away — and not a local signal a few dozen wavelengths away — is the signal source.

Test Procedures

Here's how the procedure works at vhf (at hf, it's a little more complicated because antennas are larger, as we'll see later):

1) Build an audio VU metering circuit like the one shown in the photo and Fig. 57. All parts should be readily available anywhere that consumer electronics parts are sold. The speaker and meter-gain control are handy to have when the receiver itself is located some distance away from the antenna test site, but they aren't absolutely essential.

2) Get a nearby amateur (perhaps one to five miles away) to generate a steady carrier into an antenna of the same polarization as your test antennas. A small beam pointed toward your test site is much better than a dipole or groundplane antenna because it is less likely to invite reflection error. A beam pointed somewhere else is worst of all!

3) Two of the antennas to be tested should be set up side by side, with identical lengths of feed line going to a coaxial relay or well-isolated switch. The two supporting poles should be high enough that the test antennas are at least two wavelengths above ground (13 feet [3.96 m] or more at 2 meters) and clear of nearby obstructions. To minimize interaction between the two antennas, the two masts should also be at least one to two wavelengths apart and standing side by side in relation to the signal source.

4) Make sure you can raise and lower your antennas and move them from side to side by at least a full wavelength or so (81 inches [2.06 m] at 2 meters) without the indicated signal varying more than about 1 dB. If you can't do that, you probably have reflection problems that will have to be solved before you can make valid readings. If this is the case, try different sites until you do achieve nonspotty reception.

5) Check the receiver agc to be sure it is off; then rapidly switch between the two antennas and record the difference in decibels. Do it several times and calculate the average figure (the mean, for statisticians).

6) Next reverse the two antennas. Put antenna no. 1 on mast no. 2 and attach it to feed line no. 2. Move antenna no. 2 over to mast no. 1 and feed line no. 1. Do not eliminate this step and expect valid results.

Now run the test again. If there are more than very slight differences from the previous test, one antenna or the other is seeing some obstruction or reflection source. Your site isn't clear enough for good results; try a different one.

Since this test procedure requires only receiving, there is no reason not to perform it somewhere other than at home — anywhere that is clear of obstructions. Use a receiver or transceiver that runs on battery power, if necessary.

7) If you have followed steps one through six, you now have an accurate indication of the relative gain of your two antennas. Now you can make one of your antennas a "reference" antenna and compare any other antennas you or

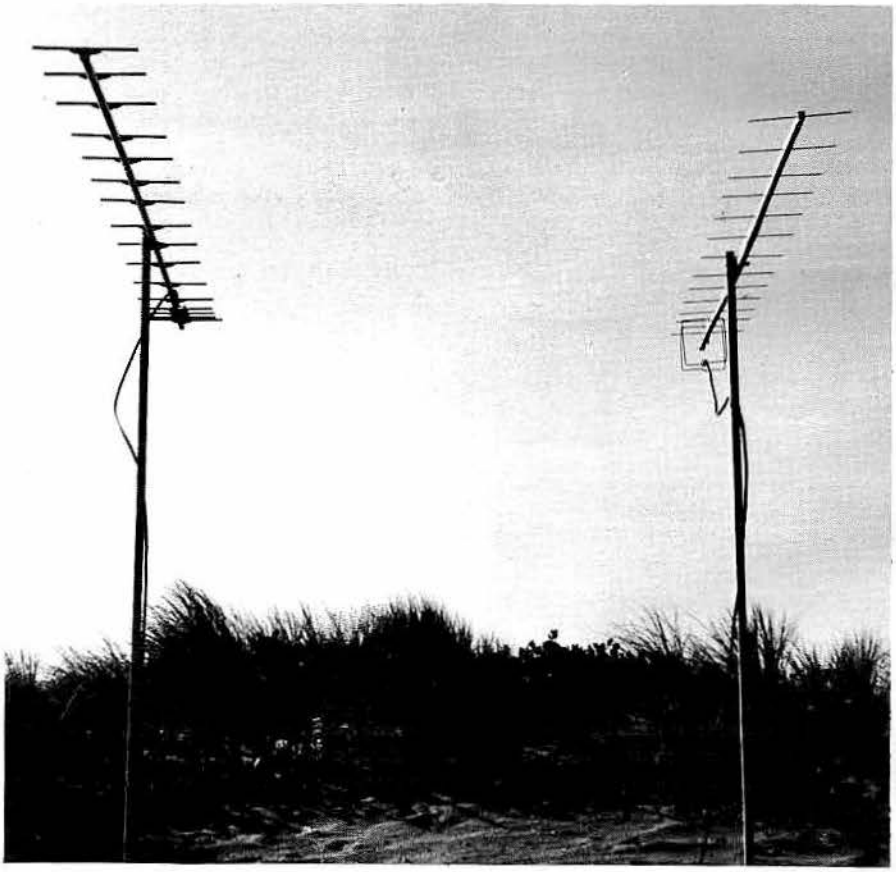

Fig. 59 — Here a 15-element long-boom quagi for 432 MHz is compared to a 16-element log-periodic Yagi, using the test procedure described in this article. The two antennas both deliver 15 dB gain over a dipole, decisively better than any other 432-MHz antenna tested here. The antennas to be tested are set up side by side and fed with identical lengths of coax. The antennas should be at least two wavelengths above ground and clear of nearby obstructions. To minimize interaction between the two antennas, the masts should also be at least one to two wavelengths apart, and standing side by side in relation to the signal source.

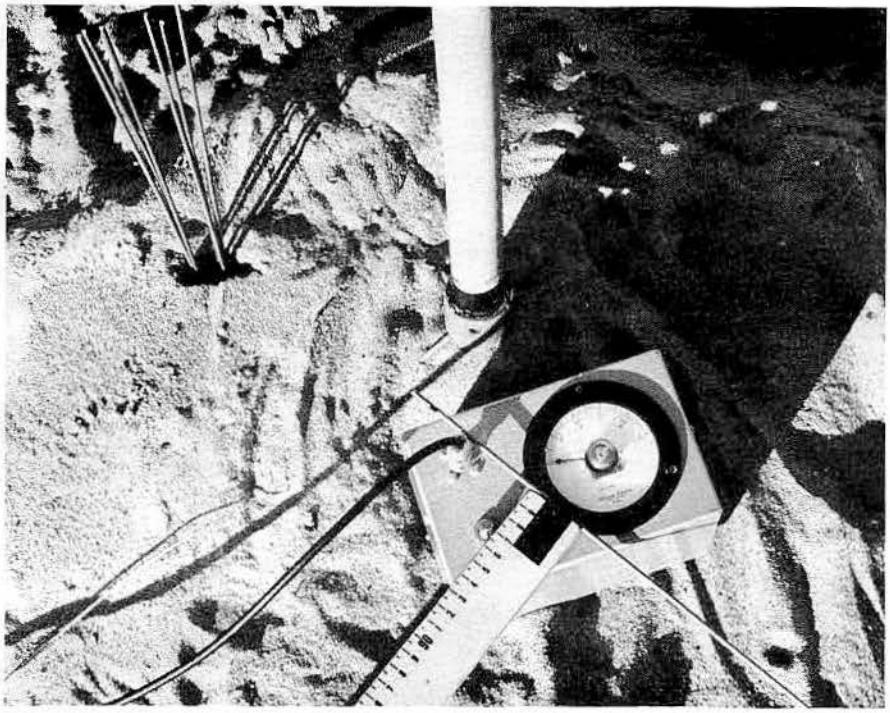

Fig. 60 — An earlier version of the metering system in Fig. 57, with assorted elements of various lengths and the yardstick used to make temporary placements on the boom.

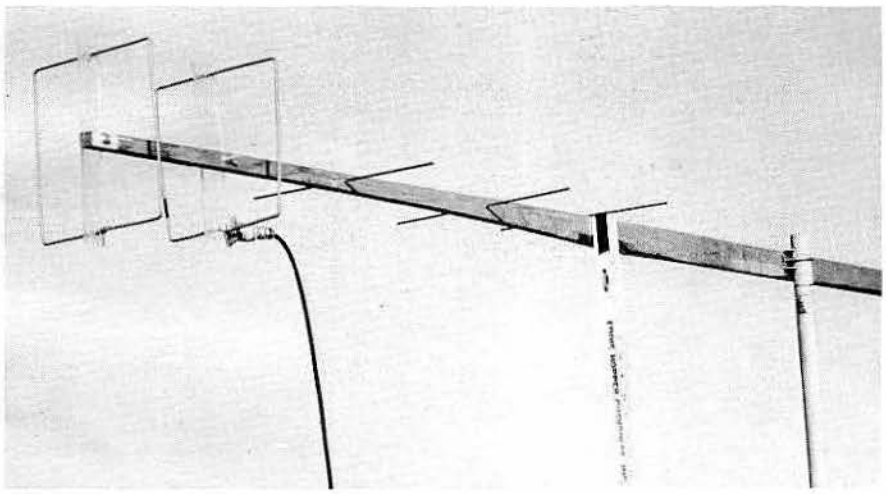

Fig. 61 — The technique used to design a new vhf or uhf antenna experimentally. The boom is shown with the first few elements already in place, and each additional element is adjusted back and forth on the boom until a point of maximum indication of the VU meter is found.

neighboring hams have against this reference.

So how do you determine how much gain your antennas have over a dipole? Some people would say, "Simple, make the reference antenna a dipole." But it may not be that easy, because dipoles are notorious for finding reflections that more directional antennas can't "see." At vhf conference gain-measurement seminars, dipoles have sometimes shown as much as 3 or 4 dB gain over a dipole!

The best reference antenna is probably a small beam of known (or approximately known) gain, assuming you don't have the National Bureau of Standards type of reference antenna that professionals use for this purpose. A 3-element Yagi or a 2-element quad built to handbook dimensions will usually deliver about 6 dB gain over a dipole at 2 meters, if the SWR is okay at the design frequency.

Thus, if you find that a particular 8-element antenna consistently produces 4.5 more dB on the VU meter than your little reference beam, you'll know you have an antenna with about 10.5 dB gain. You won't be exactly correct, but you'll be close to the right figure. Conversely, if your bigger beam doesn't show much gain over the small one, and there are no measurement errors of the sort just described, you'll know for sure that something is wrong with the big antenna.

Once you have established the integrity of your test site, you can even design your own antennas very accurately, using the audio VU-meter technique. To do that, set up your reference antenna and begin designing your new antenna by putting an empty boom on the other pole. Now start with 2 or 3 elements, get a decent SWR and try adding more elements.

As you add elements, you will be able to actually see where each new element "wants to be" on the boom, and you can see your new antenna gain over the reference antenna increase as you go along. Try all sorts of element lengths and spacings as you progress.

Antenna design professionals call this process "perturbation" and they do it with sophisticated mathematics, but you can design antennas that work just as well as theirs on your own antenna range, once you master this technique. Then, if you do go to a vhf conference with your best home-designed antennas, you'll know about how much gain they have before you enter the gain contest. And you'll never come away from such an event with an antenna that has "minus 3 dB gain!" Moreover, you'll know that your measurements, made without any of the sophisticated equipment you saw at the vhf conference, are about as accurate as anybody's. In fact, you may find your own measurements are more valid than the ones at the conference, especially if the antenna-gain figure jumps all over the place when you raise and lower it at the conference antenna range.

HF Antenna Measurements

So far, all of this has been devoted to vhf antenna-gain measurements. Many readers will say, "That's fine, but I want to measure the gain of my 5-element 20-meter beam!" Of course, an audio VU meter and a receiver without agc are a much better way than the notoriously inaccurate S meter to compare two dissimilar hf antennas. The author has seen an S meter show three or four *S units* of signal difference between two antennas that are really only 3 or 4 dB apart in gain.

However, the only accurate way to calculate the gain of an antenna is to compare it to a reference antenna at the same height and then switch the two antennas to opposite masts to validate the data. That may be impractical at hf, but perhaps not as much so as it seems at first. Most amateurs motivated enough to install a 5-element beam on a crankup tower can probably find a way to temporarily set up a smaller beam (not a dipole) on a 20-foot (6.10 m) mast above a roof. Then the two antennas at identical heights can be compared on stable, line-of-sight signals.

The results of this test can be invalidated by obstructions or even by other antennas mounted on the same tower with the test

antenna, but at least this will be more valid than a comparison against another ham's readings, when the two locations and rigs may be entirely different.

And if you can switch your test reference hf antennas to opposite masts, you can measure the actual gain of one over the other. One suggestion before you put that giant, long-boom array on the big tower: Put a little beam on the tower and an identical one on the rooftop mast and perform the audio VU-meter tests to see if the two antenna sites do seem to be identical. If they are comparable, then you can put the big antenna on the tower and find out how much gain it has, if any, over the small one on your roof when the two are at the same height.

This may seem cumbersome, and in fact it is! That's why most antenna designers do their research at vhf where antennas are so nice and small, and then scale their best designs up for the hf bands. But if you really want to know your big beam's actual gain, this is probably the easiest way to find out.

Conclusions

The antenna gain-measuring technique described in this article has repeatedly been proved to be reliable and valid. The author has used it to design new antennas that work well enough for all kinds of contest and DX work, including moonbounce. For a dedicated amateur, working DX on a home-designed antenna far surpasses the thrill of working the same DX with an antenna purchased at a store! But remember, whether you're working 20 meters or 23 centimeters, a signal source, a receiver with its agc disabled and an audio VU meter are the only pieces of equipment you need to measure antenna gain with this technique. This material was originally presented in *QST* by Wayne Overbeck, PhD, N6NB.

References

[1]Clark, "Direct Methods for Measuring Antenna Gain," *Ham Radio*, July 1969.

[2]Knadle, "UHF Antenna Ratiometry: An Outdoor Range Improvement Technique," a paper presented to IEEE Intercon session L, April 1975.

[3]Brier and Orr, *VHF Handbook for Radio Amateurs*, Radio Publications, Inc., Wilton, CT p. 225.

[4]Overbeck, "The VHF Quagi," *QST*, April 1977.

[5]Knadle, "UHF Antenna Ratiometry," *QST*, February 1976.

Understanding Antennas for the Non-Technical Ham

A Book By Jim Abercrombie, N4JA
(Jim Abercrombie *n4ja@prtcnet.com*)

Illustrations by Frank Wamsley, K4EFW

Edited by Judy Haynes, KC4NOR

Copyright July 2005. Second Edition

This is a book length web article provided by the author FREE for all hams.

Note: This is copyrighted material and is the property of Hamuniverse.com and/or the article author and is to be used only for personal non-profit educational use.

Hamuniverse.com is Powered by Ham Radio!
© 2000 - 2008 N4UJW Hamuniverse.com or article author! - All Rights Reserved.

Preface

One reason for writing this book is to educate you so you can make an informed choice concerning the best antenna for you. Another reason is to dispel the many antenna myths that circulate in the amateur community. The third reason is a desire to teach basic antenna theory to the average ham. Therefore, to achieve that goal, you should read this book from cover to cover. It was written primarily for the newcomer and the non-technical old-timer.

This book is about common medium wave and high frequency (short wave) antennas, but the theory presented here relates to antennas of any frequency. It is in a condensed form and the antenna theory is explained so most hams can understand it. Realizing many hams are mathematically challenged, only simple mathematics procedures are used. If you can add, subtract, and divide using a calculator, you will not have trouble with this book.

A few principles in here are based on conclusions drawn from the Laws of Physics. Everything else in this book can be found scattered through The *A.R.R.L. Antenna Book* and nothing in here contradicts what is written there.

Contents

1. Why All The Fuss About Antennas 1
2. How Antennas Work 3
3. Polarization Of Electromagnetic Waves 5
4. Frequency 6
5. The Ionosphere and Modes of HF Propagation 7
5.1 The Ionosphere 7
5.2 Ground-Wave Propagation 8
5.3 Direct Wave or Line of Sight Propagation 8
5.4 Propagation by Refraction 9
5.5 Skywave Propagation 9
5.6 Greyline Propagation 10
5.7 Long Path Propagation 10
5.8 160-Meter Propagation 11
5.9 80-Meter Propagation 11
5.10 40-Meter Propagation 11
5.11 30-Meter Propagation 12
5.12 20-Meter Propagation 12
5.13 17-Meter Propagation 12
5.14 15-Meter Propagation 12
5.15 12-Meter Propagation 12
5.16 10-Meter Propagation 13
6. Standing Wave Ratio 14
7. Real Antenna Systems 16
8. Half-Wave Resonant Dipole Antennas 17
8.1 The Half-Wave Flat-Top Dipole 17
8.2 Inverted-V Dipole 18
8.3 Dipole Shape Variations 20

8.4 Calculating the Length of a Half-Wave Resonant Dipole 20
8.5 The Decibel 21
9. Antenna Basics 22
9.1 Resistances and Reactance 22
9.2 Feeding Dipoles Efficiently 23
9.3 The Cause of Feed-Line Radiation 25
9.4 Baluns 26
10. Other Types of Dipoles 27
10.1 A Shortened Dipole Using Loading Coils 27
10.2 All Band Dipole 28
10.3 The Sloping Dipole 28
10.4 Half-Wave Resonant Sloping Dipole 28
10.5 The Folded Dipole 29
10.6 The Double Bazooka Dipole 30
10.7 Broad-Banded Coax-Fed Fan Dipole 31
10.8 Two-Element Collinear Dipole 31
10.9 4-Element Collinear Dipole 32
10.10 Coax-Fed Dipoles Operated on Odd Harmonic Frequencies 33
10.11 All Band Random Length Dipole 35
10.12 All Band Center-Fed Random Length Dipole 35
10.13 A 2-Band Fan Dipole 35
10.14 Trapped Dipole for 75 and 40 Meters 36
10.15 The Extended Double Zepp Dipole 37
10.16 The G5RV Dipole 37
10.17 Off-Center Fed Dipoles 39
11. End-Fed Antennas 42
11.1 End-Fed Zepp 42
11.2 End-Fed Random Length Antenna 42
12. The Half Sloper 44
13. Vertical Antennas 46
13.1 Why Verticals Are Used 46
13.2 Disadvantages of Using Quarter-Wave Verticals 47
13.3 Long and Short Verticals 48
13.4 Unscientific Observations of Verticals 49

13.5 The Inverted-L Vertical 50
13.6 Vertical Mobile Antennas 51
14. One-Wavelength Single Loop Antennas 54
14.1 The Horizontally Oriented Loop 54
14.2 The Vertically Oriented Single Loop for 40 and 80 Meters 56
15. Directional Beam Antennas 59
15.1 The Monoband Yagi 59
15.2 Trapped Multi-Band Yagis 62
15.3 The SteppIR Antenna 65
15.4 The Log-Periodic Array 65
15.5 Directional Cubical Quad and Delta Loop Antennas 66
15.6 The Quagi 72
16. Gain Versus Front-to-Back 73
17. Feed-Lines Commonly Called Transmission Lines 74
18. Antenna Safety 76
18.1 Erecting Antennas on Masts 76
18.2 Tower Safety 76

1.

Why All The Fuss About Antennas

Definition: An antenna is a piece of metal, a conductor of electricity, to which you connect the radio. It radiates your signal and receives the signals you want to hear.

Definition: An antenna system consists of the antenna, the feed-line, and any matching unit. Most antennas are made of copper or aluminum, while most mobile antennas are made of stainless steel. A feed-line consists of two conductors that carry the signal to and from the radio and to and from the antenna. A matching unit can be an antenna tuner, a series matching section, or one of several different kinds of matching circuits at the feed-point.

Does the type of antenna make much difference? Here is an example: Once in 1959 two of us were involved in testing two antennas on 15 meters. The late R. Lynn Kalmbach, W4IW, using one antenna received a 30-dB better signal report on his antenna from a station in England than we did on our antenna. (Decibel or dB will be explained later). Thirty dB means his signal appeared that he was running 1000 times more transmitter power than we were. At that time, we didnt live that far apart so we couldnt blame it on propagation. We both were running about equal power. Both antennas were at 50 feet. The comparison proved that a good antenna could make a difference. Lynn used a home-built G4 ZU mini-beam; we were using a 15-meter 2-element Mosely Mini-Beam, which had short loaded elements. Evidently, it had a lot of loss.

Another example: Today we hear people breaking in to our ragchews with signals almost level with the noise. Why is that? The reason is they are using the wrong antennas. Their signals are 20 to 30 decibels below everyone elses. They are making contacts, but just barely. The first question our group asks, “What kind of antenna are you using?” Experienced amateurs know the antenna can make all the difference. The guy with the poor signal sometimes will blame his bad signal report on band conditions or his lack of a linear amplifier. He is just sticking his head in the sand.

What we are trying to prove is next to your radio, the most important part of your station is the antenna. Many years ago, an old-timer said, “For every dollar you spend on a radio, you should spend two dollars on your antenna.” That is also true today. You can do more to improve your signal strength with antennas than you can ever do by increasing your power. Having the ability to make contacts on a particular antenna doesnt mean it works well! Any antenna will make contacts, but your signals will be stronger on some antennas than on others. In addition, some antennas hear better than others.

2.
How Antennas Work

First of all to work properly the antenna system must be matched to the transmitter. That is, all modern transmitters have an output impedance of 50 ohms. Antenna systems range in impedance of a few ohms to several thousand ohms. There are several ways to match them: pruning the length of the antenna, using an antenna tuner, matching the antenna with a length of transmission line called a matching section, or the use one of several matching systems at the antenna feed-point. Antenna matching is beyond the scope of the material found in this book and it is suggested you consult a more comprehensive antenna manual. Simple half-wave dipoles eliminate the need for a matching system because a resonant half-wave dipole has an impedance near 50-ohms.

You must understand electromagnetism to understand how antennas work. If you attach the two poles of a direct current (DC) voltage source to the two ends of a coil of wire, current will flow through the coil of wire and it will become magnetized. The magnetized coil is known as an electromagnet. Its magnetism will extend out to infinity becoming weaker with distance. Remove the voltage and the magnetic field collapses back into the coil. If an alternating current (AC) is connected to the coil, the magnetism moves out and collapses into the coil in step with the frequency of the alternating current source. The north and south poles of the electromagnet reverse on each half-cycle of the AC voltage.

If voltage and current can cause a coil to become magnetized, the reverse is true: A magnetic field can produce a voltage and a current in a coil. This is known as Faradays Principle of Magnetic Induction. A voltage will be produced at the ends of the coil of wire as you move any permanent magnet close to and parallel to the coil. The difference in this case is the magnet must be kept moving. Move the magnet in one direction, and current will flow in one direction. Reverse the direction the magnet is moving and the current will flow in the opposite direction. Moving the magnet back and forth produces alternating current. An AC generator spins a coil of wire between the two poles of a magnetic field. It doesnt matter which one is moving. The coil or the magnet can be moving. Any moving magnetic field can induce current in anther coil. It doesnt have to be a piece of metal we call a magnet. Imagine a moving magnetic field produced by AC circulating in and out of a coil. If that moving magnetic field passes through a second nearby coil, it will induce an alternating current in the second coil. A transformer uses this method to work. Transformers have a continuous iron core running from

the inside of one coil through the inside of the second coil to confine the magnetism inside the iron core. This makes the transformer nearly 100% efficient since only a little of the magnetic energy escapes.

A straight wire that has an AC current flowing through it also has a magnetic field surrounding it. But it is a weaker field than is produced by a coil. The magnetic field from the wire radiates out into space and becomes weaker with distance. The radiating magnetic field from a wire is known as “electromagnetic radiation” and a radio wave is one type of it. The wire that radiates becomes the transmitting antenna. Some distance away, a second wire in the path of these waves has current induced into it by the passing electromagnetic waves. This second wire will be the receiving antenna. The voltage in the receiving antenna is many times weaker than the voltage in the transmitting antenna. It may be as weak as one-millionth of a volt or less and still be useful. The receiving antenna feeds that voltage to the amplifiers in the receiver front-end where it is amplified many thousands or millions of times.

The dipole antenna is made of a wire broken in the center and where broken, each half of the wire connects to an insulator that divides the wire in two. Two wires from the voltage source, which is the transmitter, are connected across the insulator. On one side of the dipole, the current in the form of moving electrons flows first from the voltage source toward one end of the dipole. At the end, it reflects toward the voltage source. The same thing occurs on the other half of the wire on the other half cycle of alternating current. An antenna that is the right length for the current to reach the far end of the wire just as the polarity changes is said to be resonant. Because electricity travels at 95% the speed of light in a wire, the number of times the polarity changes in one second (frequency) determines how long the wire has to be in order to be resonant.

3. Polarization Of Electromagnetic Waves

Electromagnetic waves travel away from the wire in horizontal, vertical, slanted, or circular waves. If the antenna wire runs horizontal or parallel to the earth, the radiation will be horizontally polarized. A wire or conductor that runs at right angles to the earth produces vertical radiation. A slanted wire has components of both horizontal and vertical radiation. Crossed wires connected by proper phasing lines that shift the phase from one wire to the other wire by 90 degrees will produce circular polarization. Amateurs working orbiting satellites at VHF, UHF, and microwave frequencies use circular polarization.

When your high frequency signals are reflecting off the ionosphere, it isnt important if the other stations antenna has the opposite polarization from yours (the polarization does matter for line of sight communication). The reflected polarized waves passing through the ionosphere are slowly rotated causing fading signals (QSB). The reason the polarization of antennas is most important is that it determines the angle of radiation. Horizontally polarized antennas at ordinary heights used by hams produce mostly high angle radiation and weaker low angle radiation, but this doesnt mean there is no low angle radiation. It is there but is weaker than high angle radiation. However, you must put a horizontally polarized antenna up more than one-wavelength high to get a strong low angle radiation. One wavelength is 280 feet on 80 meters, 140 feet on 40 meters, and 70 feet on 20 meters. High angle radiation works nearby stations best and low angle radiation works distant stations (DX) best. A vertically polarized antenna produces mostly low angle radiation, with its high angle radiation being weak. For this reason, vertical antennas do not work as well as horizontal antennas do at ordinary heights for working stations less than about 500 miles away.

4.
Frequency

The number of times the polarity of an AC voltage changes per second determines its frequency. Frequency is measured in cycles per second or Hertz (Hz). A thousand cycles per second is a kilohertz (kHz). One million hertz is a Megahertz (MHz). The only difference between the 60 Hz electric power in your house and radio frequencies (RF) is the frequency, but 60 Hz electricity in a wire also produces electromagnetic radiation just like radio waves. Useful radio waves start at 30 kHz and go upward in frequency until you reach the infrared light waves. Light is the same kind of waves as RF except light is at a much higher frequency. Light waves are used like radio waves when they are confined inside fiber optic cable. Above the frequencies of light are found x-rays and gamma rays.

The radio bands: The Long Wave Band (LW) starts at 30 kHz and goes to 300 kHz. The Medium Wave Band (MW) is from 300 kHz to 3000 kHz or 3 MHz. The High Frequency Band (HF) is from 3 MHz to 30 MHz. The Very High Frequency Band (VHF) is from 30 MHz to 300 MHz. The Ultra-High Frequency Band (UHF) is from 300 MHz to 3000 MHz or 3 GHz. Above these frequencies are several microwave bands which are defined as the Super High Frequency Band (SHF).

5.
The Ionosphere and Modes of HF Propagation

In the upper air around fifty miles and higher where the air molecules are far apart, radiation from the sun strips electrons from oxygen molecules causing the molecules to become ionized forming the ionosphere. The ionized oxygen molecules and its free electrons float in space forming radio-reflecting layers. Ionization of the ionosphere varies by the time of day, seasons of the year, and the sunspot cycle. The strength of ionization also varies from day to day and hour to hour. Since the height of the ionosphere varies, the higher the ionized layer becomes, the farther the skip will be.

5.1 The Ionosphere

The part of the earths atmosphere called the ionosphere is divided into three layers. The three layers are, from lowest to highest, the D layer, the E layer, and the F layer. Each layer has a different effect on HF radio propagation.

Being at a lower altitude, the D layer molecules are squeezed closer together by gravity than those in higher layers, and the free electrons reattach to the molecules easily. The D layer requires constant radiation from the sun to maintain its ionization. Radio waves at lower frequencies such as the frequencies of the AM broadcast band cannot penetrate this layer and are absorbed. The higher frequency signals are able to pass through the D layer. The D layer disappears at night causing AM broadcast stations to reflect from the higher layers. This is why AM broadcast signals only propagate by ground wave in the daytime and they can be received from great distances at night. Like the broadcast band, the D layer absorbs signals on 160 and to a lesser extent 80 meters during the day making those bands go dead. During solar flares, the D layer becomes ionized so strongly that all high frequency radio waves are absorbed, causing a radio blackout.

E-layer propagation is not well understood. Being at a lower altitude than F layer, the E layer is responsible for summertime short skip propagation on the higher high frequency bands. The skip zone is around 1000 miles, but at times when the E-cloud covers a wide area in the summer, double hops can be seen. A double hop occurs when the signal reflects from the ionosphere, then returns to the ground, reflects from the ground back to the ionosphere where

it is reflected back to the ground. A double hop can propagate the signal 2000 miles or more. The E-layer forms mostly during the day, and it has the highest degree of ionization at noon. The E layer like the D layer disappears at night. Even so, sporadic-E propagation can and does form at night. There is a minor occurrence of sporadic E propagation during the wintertime. On rare occasions, sporadic E propagation can surprise you by occurring anytime regardless of the sunspot cycle or the season of the year.

The F layer is the highest layer and it is divided into two levels: F1 and F2. At night the F1 and F2 merge into one layer. During the day, the F1 layer doesnt play a part in radio propagation, but F2 does. It is responsible for most high-frequency long distance propagation on 20 meters and above. However, the F layer makes it possible for you to work DX on the lower bands at night. Sunspots are responsible for the ionization layers and in years with high sunspot numbers, worldwide contacts can be made easily on 10-20 meters by F2 layer propagation. In years of low sunspot numbers, working distant stations is difficult on those bands. Consequently, 10 and 15 meters will be completely dead most days and 20 meters will go dead at night. In years of low sunspot numbers DX contacts are easily made at night on 160, 80, and 40 meters. The sunspot numbers increase and decrease in 11-year average cycles.

Since the curvature of the earth averages about 16 feet every 5 miles, an object 5 miles from you on perfectly flat earth will be 16 feet below the horizon. Because light travels in straight lines, you cannot see objects beyond the horizon. Radio waves travel in straight lines, but there are ways to get them beyond the horizon. This is referred to as propagation.

5.2 Ground-Wave Propagation

Ground wave works only with vertical polarization. One side of the antenna is the metal vertical radiator and the other side of the antenna is the earth ground. The surface wave in the air travels faster than the part of the wave flowing through the ground. The surface of the earth is curved like the curved part of a racetrack. On the curved track, a car on the outside of the track has to travel faster than the car on the inside lane to stay even, and the two cars travel in a curved path. Although the wave in the air travels faster than the wave on the ground, the two parts of the wave cannot be separated. Because of this, the radio wave also travels in a curved path that follows the curvature of the earth.

The AM broadcast stations use ground wave propagation during the day and skywave propagation at night. Since radio waves at lower frequencies conduct better through the ground, an AM broadcast station on 540 kHz will be many dB stronger than a station on 1600 kHz, if both run the same power. This fact is important in understanding why ground mounted verticals do not work as well at high frequencies as they do on the broadcast band.

5.3 Direct Wave or Line of Sight Propagation

Antennas located on high structures can “look” over the horizon and “see” the receiving antennas. Because refraction is involved, direct waves travel 20% farther than light waves due to scattering of radio waves by the environment. Trees and other foliage are invisible to HF radio waves. Direct wave propagation is possible at all frequencies, but this mode of propagation is seldom used on our high frequency bands, but it is the usual propagation mode

used by repeaters and others on VHF and UHF. If you watch TV on an outside antenna or on a "rabbit ears antenna," you are receiving the signal by direct wave propagation.

5.4 Propagation by Refraction

Refraction occurs when the lower part of a wave travels slower than the top part of the wave because the wave is passing through two media. These media can be two layers of air at different temperatures or they can be air and a solid. One form of refraction is caused by a radio wave passing over a hill or ridge being bent as it passes over the obstruction. This is known as "knife edge refraction." Another form of refraction occurs when layers of air of different temperatures bend the radio waves around the horizon. This is called tropospheric ducting. This mode of propagation makes long distance contacts possible at VHF frequencies. Tropospheric ducting does occur on 10 meters and lower frequencies and is noticeable when other forms of propagation are absent. On high frequency bands, many hams mistakenly call tropospheric ducting and direct wave "ground wave."

5.5 Skywave Propagation

Skywave propagation occurs when radio waves are reflected from the ionosphere. Practically all HF communication is done by skywave. In the ionosphere, the waves are really refracted twice, and they just appear to be reflected. The reflections are frequency sensitive, meaning each ham band reflects differently from the others. Low frequencies, such as 80 meters, reflect mainly from the lower levels of the ionosphere and the reflected signal comes nearly straight back down. This causes 80 meters to propagate to points from local out to more than a few hundred miles in the daytime. At night, when the D layer and E layer are absent, signals striking the ionosphere at lower angles may propagate many thousands of miles on 80 meters. On the bands from 20 to 10 meters, high angle signals pass straight through the ionosphere and do not reflect back down to the nearby stations. The low angle signals on these higher bands reflect from the ionosphere near the horizon and return to the Earth some miles away. The in-between region cannot hear the transmitted signals nor can you hear signals coming from this region. The in-between region is called the "skip zone." Only when the ionosphere is weakly ionized do you have a skip zone on 80 meters.

Another interesting type of skywave propagation seen on the higher HF bands is called chordal hop propagation seen frequently in trans-equatorial (TE) propagation, which is propagation crossing the equator. When this occurs, signals entering the ionosphere are trapped inside the F2 layer then they are finally refracted back to earth across the equator thousands of miles away. There is no propagation between the signal entry point and the exit point. This is skip in the extreme. On many occasions, we have worked stations far away across the equator in the southern part of South America and stations in between could not be heard. We have frequently worked VQ9LA in the Chagos Archipelago located in the Indian Ocean. The path to The Chagos Archipelago is across Europe and the Middle East and finally across the equator to his location in the Indian Ocean. One time when he was working Europe and North America at the same time, we could not hear the European stations because our path to him was via chordal hop propagation. Another way of describing chordal hop propagation is to call it ionospheric ducting.

Skywave propagation sometimes produces an effect called “backscatter.” What happens is the radio waves that strike the ionosphere, instead of only reflecting father away from the transmitting station, part of the signal reflects backwards toward the transmitting station. Stations that are too close to hear each other by direct wave can communicate by the backward reflecting waves. Both stations that communicate by backscatter must point their directional beam antennas in the same direction although their direction toward each other may be at some other azimuth. Backscatter will confuse front-to-back measurements of directional beam antennas. This is because, when you turn the back of the antenna toward the station you are hearing, you may be able to hear him on backscatter from a direction opposite from him. You will be hearing him from the ionized atmospheric cloud in the opposite direction. During intense solar magnetic storms, when aurora occurs at high latitudes, stations are able to communicate by backscatter on VHF and UHF by both stations pointing their directional beams toward the aurora. This will be due north for stations in the Northern Hemisphere and due south for stations in the Southern Hemisphere. Audio from aurora backscatter will have a “wispy” sound.

5.6 Greyline Propagation

Greyline propagation occurs when the sun is low in the sky near dawn or dusk, although we have seen greyline propagation occur as early as two hours before sunset or as late as two hours after sunrise. It is often used to work stations on the other side of the world on 160 and 80 meters. For example, at certain times of the year when it is approaching sunset here in the States, the sun will have just risen in Asia or Australia and vice-versa. At that time, radio waves propagate along the semidarkness path that encircles the Earth called the greyline. Both locations must be in the greyline in order to make 2-way contacts. The tilt of the Earth makes the position of the greyline change as the seasons change. Greyline propagation occurs between any two locations for a brief period of a few weeks. Afterwards, different places fall into the greyline. For several weeks in the fall of the year, an interesting example of greyline propagation occurs in the southeastern part of the U.S. On 3915 kHz, the BBC outlet in Singapore can be heard for about an hour before sunset coming in by greyline propagation. Stations to the east hear it before we do. Stations farther to the west can hear the fading signals after it fades out here because the greyline moves as the earth rotates. For those hearing it, the signal fades in, it peaks, and it slowly fades out.

5.7 Long Path Propagation

Long path propagation occurs when signals propagate the long way around the world. It can occur on any band. It usually occurs from stations on the opposite side of the world from you. We have worked South Africa via long path by beaming northwest early in the morning on 20 meters. When this happens, we are working him long path through the nighttime side of the earth. Since at all times half the Earth has daytime and half the Earth has night, long path propagation is determined by whether the signal is propagated through the nighttime path or daylight path. Sometimes the daylight path will bring in stations by long path propagation and at other times the darkness path provides long path propagation. One night on 20 meters, we heard a station in India coming in short path and long path simultaneously, but the short path was stronger. At the same time, California was working India by long path and they could not hear him short path. They were working him through the daylight path, and he was stronger here on the East Coast via the nighttime path.

5.8 160-Meter Propagation

Each amateur band propagates signals differently. The 160-meter (1.8-2.0 MHz) band is our only MW band and it acts similar to the broadcast band. It is primarily a nighttime and wintertime band as it suffers from high summertime static (QRN). Most hams that use this band for nearby contacts use horizontal dipoles or inverted-V antennas. Some hams use vertical antennas on this band to work distant stations (DX). These DX contacts are made in the fall and wintertime at night via F layer or greyline propagation when the static levels are low. Dipoles and inverted-V antennas do not work well for DX on this band.

5.9 80-Meter Propagation

The CW part of this band is called the 80-meter (3.5 4.0 MHz) band and the voice part of the band is known as 75 meters. Like 160 meters, eighty meters suffers from the same QRN in the summertime. Working DX on this band is a popular avocation during the fall and winter. However, 80 meters is used primarily for working nets and ragchewing. Eighty meters is primarily a nighttime band. This band can vary from being open most of the day in years with low sunspot numbers to being closed during the middle of the day in years with many sunspots. Many DX contacts have been made using dipoles and inverted-V antennas, but a vertical with many ground radials will be better.

5.10 40-Meter Propagation

The 40-meter (7.0-7.3 MHz) band has propagation that can act like either 80 meters or 20 meters. It just depends on the stage of the sunspot cycle. During the years with high sunspot numbers, nearby contacts are possible all day. At night, the skip lengthens making contacts possible to those parts of the world where it is still dark. Working DX on 40 meters is a nighttime or greyline event. When the sunspots are low, 40 meters may have long skip during the day, and nearby contacts may be impossible or they may be very weak. During the time when we suffer from low sunspot numbers, many DX contacts are made during early morning, late afternoon, and at night.

If your primary interest on 40 meters is SSB, our 40-meter voice band is a broadcast band in Regions 1 and 3. Region 1 is Europe, North Asia, and Africa and Region 3 is the Pacific, Southern Asia, and Australia. The top part of 40 meters is a voice band in Region 2, which is North and South America. To work SSB on 40 meters at night, you will have to find a frequency between broadcast stations. Strong broadcast stations heard at night begin to fade out slowly as the morning sun rises and moves higher in the sky. As the suns angle declines in the afternoon, the broadcast stations begin to break through the noise becoming stronger as the sun begins to set. It is only in the middle of the day when no broadcast stations are heard on 40 meters.

Since DX stations in region 1 and most of region 3 can only transmit below 7100 kHz, working DX on 40-meter SSB is still possible. Stations in those regions will have to transmit below 7100 kHz. (Australian and New Zealand amateurs can operate up to 7200 kHz.) They call CQ and announce where they are listening in our voice band above 7150 kHz. This is what is called “working split.”

5.11 30-Meter Propagation

The 30-meter (10.1-10.15) band has such a narrow frequency that the only modes allowed here are CW and digital modes. That means no SSB. Propagation here is much like 40 and 20 meters. Unlike 20 meters, this band stays open longer at night during years with low sunspot numbers. During the daylight hours, it has much shorter skip than 20 meters. In the United States, we are allowed only 250 Watts.

5.12 20-Meter Propagation

The 20-meter (14.0-14.35 MHz) band is the best DX band because it is open for long-skip for more hours than any other band and it does not suffer from QRN as the lower bands. In years of high sunspot numbers, short-skip and long-distance DX can be worked at the same time during daylight hours. Although DX is there most of the time, most of the DX worked is at sunrise, sunset, and all night during peak sunspot years. During the years of low sunspots, it is common to work into Europe and Africa during the day and into Asia and the South Pacific during the evening hours and early at night. Low sunspot numbers cause 20 meters to go dead for east to west contacts at night an hour or so after sunset, but there is some TE propagation. During periods of moderate sunspot numbers, the propagation on this band is a blend of propagation of low and high sunspot years.

5.13 17-Meter Propagation

The 17-meter (18.067-18.167 MHz) band propagation acts much like 20 meters except it is affected more by low sunspot numbers than 20 meters. In periods of low sunspot numbers, this band does not stay open as late as 20 meters, fading out as the sun begins to set. Yet, the 17-meter band does stay open all night when the sunspot numbers are high. The propagation on this band is like a blend of 20 meters and 15 meters, but it is closer to 20 meters. Most users of this band use dipoles and other simple antennas since triband beam antennas wont work here.

5.14 15-Meter Propagation

15 meters (21.0-21.45 MHz) is a fantastic DX band during the high sunspot years. This band may be open for 24 hours, and it is common to work more than 100 countries during a contest weekend on this band. Many have worked more than 300 different countries on 15 meters. In years of low sunspot numbers, 15 meters may be completely dead for several days in a row. When it opens during those years, you may hear only the Caribbean, South America, and on rare occasions the extreme southern part of Africa via TE propagation.

5.15 12-Meter Propagation

The 12-meter (24.89-24.99 MHz) band is much like 15 meters, but it is affected more by sunspot numbers. Because this band is little used, many hours can pass without hearing any amateur signals. Occasionally you will hear South American Citizen Band “pirates” on lower

sideband. It is mostly a daytime band but openings to Asia and the South Pacific are common early at night during peak sunspot years. The reason this band is little used is that tri-band beam antennas don't cover this band.

5.16 10-Meter Propagation

The 10 meter (28.0-29.7 MHz) band that is most affected by the sunspot numbers. You may have noticed in this discussion, the higher the frequency, the more it is affected by sunspots. During peak sunspot years, 10 meters can be open some days for 24 hours. Mostly it is a daytime band. When they are at the peak, the sunspots enable you to work worldwide with power as low as 5 Watts. A 10-meter confirmed country total of over 250 is common. In the low sunspot years, the band can be closed for days. 10 meters can open for very short skip by sporadic E propagation during the summer months. Very short skip means contacts as close as 200 miles out to 1000 miles. Sporadic E propagation can suddenly occur without regard to the sunspot numbers.

6.
Standing Wave Ratio

A standing wave ratio bridge is used to measure the standing wave ratio, or SWR. SWR is an indication of how well the radiating part of an antenna is matched to its feed-line or how well the tuner is matching the antenna system. Most amateurs pay far too much attention to SWR. An SWR reading below 2:1 is acceptable, because the mismatch is so small that the feed-line loss can be ignored. If you are using a modern transceiver, its power may fold back to a lower power output above this SWR level.

When you have mismatch between the feed-line and the antenna, part of the power feeding the antenna system reflects back toward the tuner and the transmitter. The part of the power going toward the radiating part of the antenna system is called forward power. The part reflected back down the feed-line is called reflected power. The larger the mismatch the larger the reflected power will be.

If the feed-line and antenna are not matched, waves traveling toward the radiating part of the antenna system meet the waves being reflected back down the feed-line. The waves interfere with each other, and at certain points along the feed-line, the amplitudes of both waves combine. This will result in a current maximum to be found at that point; and at that point, the current will appear to be standing still. The length of feed-line and the frequency will determine where this point occurs. At another point, the forward and reflected waves interfere, and they subtract from each other. At that point, there will be a current minimum. If you could visualize this phenomenon, you would see a series of current maximums and minimums standing still along the feed-line. This is why we refer to them as standing waves. At different points along the feed-line, where you have high current, you will have low voltage, and where you have low current, you will have high voltage. At any point along the feed-line, multiplying the voltage times the current will equal the power in Watts. When the feed-line is matched to the antenna, current and voltage remain the same all along the feed-line because there is no reflected current to interfere with the forward current.

As happens with the current, the voltage will also appear to be standing still. The voltage maximums and voltage minimums will not be at the same locations as the current maximums and minimums. SWR is the ratio of the maximum voltage to the minimum voltage on the line. It is called *Voltage Standing Wave Ratio* or VSWR, but we shorten it to just SWR. There is

also a current SWR or ISWR, and it is the same value as the VSWR. For example, if the standing wave voltage maximum is 200 volts and the minimum voltage is 100 volts, the VSWR will be 2:1. If the voltage maximum and voltage minimum are equal, the SWR will be 1:1. If the voltage minimum is zero, the SWR is infinite.

In measuring SWR at the transmitter, you need to realize that feed-line losses affect the SWR readings. If the feed-line losses are high, much of the power reflecting back from the antenna will be lost, and the SWR reading on the meter will indicate it is lower than it actually is. If a feed-line is so lossy that it consumes all forward and reflected power, it will measure an SWR of 1:1.

When measuring SWR on an antenna having a small amount of reflected power, the length of the feed-line between the bridge and the antenna may affect your SWR reading. An example of this is a 70-ohm antenna being fed with 50-ohm coax. Different lengths of feed-line will give you small differences in SWR readings because at certain lengths, the mismatched feed-line starts to act like a series matching section. In the case of a 70-ohm antenna fed with 50-ohm coax, if the feed-line is a half wave long, the SWR will measure 1.4:1. At some particular length of feed-line and on one frequency, the SWR will measure 1:1 because that length of that feed-line transforms the impedance to make a match. Some hams have adjusted their feed line length to get a perfect match. This is called “tuning your antenna by tuning your feed-line.” With other feed-line lengths, you will measure something different. Suppose the impedance of the feed-line and the antenna are perfectly matched. Then there is no reflected power. You will get a 1:1 reading on the SWR-bridge with any length of feed-line.

There is a myth that reflected power is burned up as heat in the transmitter. The reflected power coming back down the feed-line sees an impedance mismatch at the transmitter or tuner and it reflects back up again. The reflected power does not get back into the transmitter. Because the reflected power reflects back and forth, the radiating part of the antenna system absorbs most of the power being reflected back up each time. All of it eventually is radiated except for the power lost in the feed-line. The losses in a real feed-line will burn up some of the power on each pass. This is why the feed-line loss increases with SWR.

Built-in tuners are found in most modern transceivers. If yours doesnt have one, then you can use an outboard tuner to give the transceiver a proper load. The place you want a 1:1 SWR is between the output of a transceiver and antenna or between the transceiver and the input of a tuner in order for the transmitter to deliver its maximum power. Because built-in tuners are in most modern transceivers, many hams use them to match antenna systems having high loss.

7.
Real Antenna Systems

In this book, we will be talking about the losses that rob an antenna of its maximum performance. The ideal antenna system will radiate 100% of your transmitter power on all bands without a tuner and in the direction you want to work. Such an antenna system does not exist. Many new hams succumb to antenna advertisements making claims that are exaggerated. No antenna will have low SWR, work all bands without a tuner, and radiate efficiently at the same time. A dummy load has a low SWR and will load up on all bands, but it will not radiate a signal. A resonant coax-fed dipole antenna will have a low SWR and will radiate efficiently on the band for which it is resonant, but it will not work well on all bands. For example, if the tuning range of your tuner has a sufficient range, you will be able to load up any antenna with it, but it will not necessarily radiate a signal efficiently. It may have high tuner and feed-line losses.

When you choose an antenna, you must decide how much loss you can accept. DXers and hams that work weak signals at VHF frequencies try to eliminate as much loss as possible. If your contacts are going to be made under good band conditions and without much interference, you can get by with high losses. In that case, coax-fed antennas used on bands where they are not resonant will allow you to make contacts. You can be greatly surprised by how little radiated power can be used to make contacts under ideal conditions. If you want to make contacts regularly under changing band conditions, you will want to eliminate as much loss as possible and use antennas with gain. Lower loss will enable you to hear weaker signals.

Nothing will take the place of resonant half-wave dipoles, not because they radiate more efficiently, but because they dont require lossy tuners and dont have high coax losses. Remember that all antenna systems have compromises.

8.
Half-Wave Resonant Dipole Antennas

Most dipoles consist of two pieces of wire of equal lengths with one of the two ends connected together through an insulator. The far ends of the wires are also connected to insulators. The two conductors of a feed-line are separated and connected across the gap at the center insulator. The antenna is held up by rope that connects the insulated ends of the antenna to two supports. It is a “balanced” antenna, because equal currents flow on both halves of the antenna. Coax is an unbalanced feed-line. (The possible effect of using an unbalanced feed-line on a balanced antenna like a dipole will be discussed later.) The dipole that is stretched between two high supports is called a flattop dipole, distinguishing it from other configurations.

8.1 The Half-Wave Flat-Top Dipole

The simplest antenna system of all is the half-wave resonant dipole fed with coax and no tuner. The only reason for using a half-wave resonant dipole antenna is to eliminate the need for a matching device such as a tuner. The feed-point impedance will be near 50 ohms at ordinary heights and they can be fed directly with 50-ohm coax from the output of todays modern radios. The two halves of a dipole are fed 180 degrees out of phase, meaning when one side is fed positively, the other side is fed negatively. That is why a feed-line has two conductors. Of course, the sides swap polarity on each half cycle.

If you could visualize the current flowing on the half-wave dipole, the current will appear to be standing still. The maximum current will be seen at the center of the wire and no current will be at the ends. This occurs because the electrons flowing out to the ends reflect back toward the center where they meet the next wave and the current is reinforced there. The minimum voltage occurs at the center and the maximum voltage occurs at the ends of the half-wave resonant dipole. If you were to measure the voltage and the current at any point on the dipole wire, the voltage times the current will equal the power in Watts.

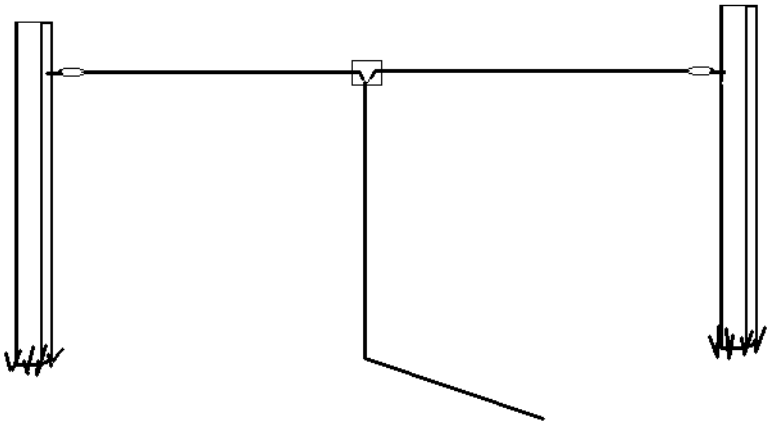

Figure 8.1: Flat Top Dipole

8.2 Inverted-V Dipole

Another configuration for the half wave resonant dipole is one having one support in the center and the ends stretched down toward the ground. The single support can be a tree, mast, or tower. The ends of a dipole have high RF voltages on them, and need to be at least 10 feet above ground for safety. This antenna is called an "inverted-V," because the shape of the dipole looks like a "V" turned upside down. Most dipoles illustrated in this book can be put up in the inverted-V configuration. This configuration works well because the current is concentrated on the middle two-thirds of the antenna at the apex. The current in an antenna is what is responsible for the radiation. The ends of the antenna have very little current in them and it doesnt matter if the ends are close to the ground. The middle of the antenna is up high where the radiation is taking place and that is the place you want the radiation to be. An inverted-V has an advantage that the horizontal space required for it is less than what is needed for a flattop dipole. The angle between the wires on an inverted-V needs to be greater than 90 degrees. The gain of an inverted -V is 0.2 dBd and it has a radiation pattern nearly omni-directional. Since it is easy to construct and works so well, the inverted-V is the most commonly used dipole. An explanation of the decibel will come later.

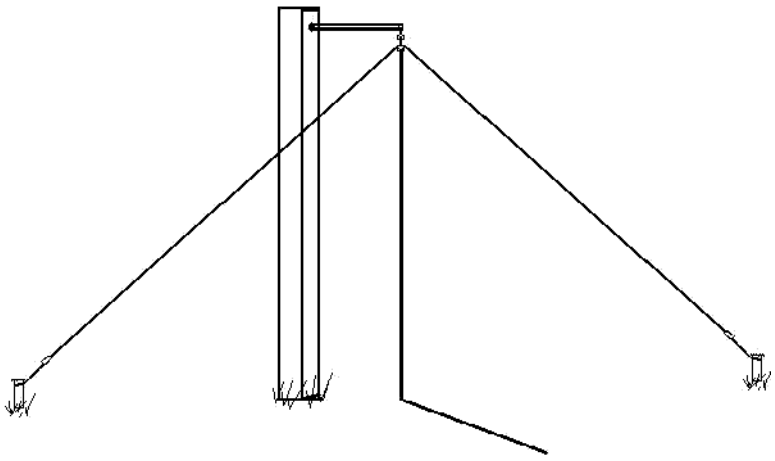

Figure 8.2: The Inverted-V Dipole

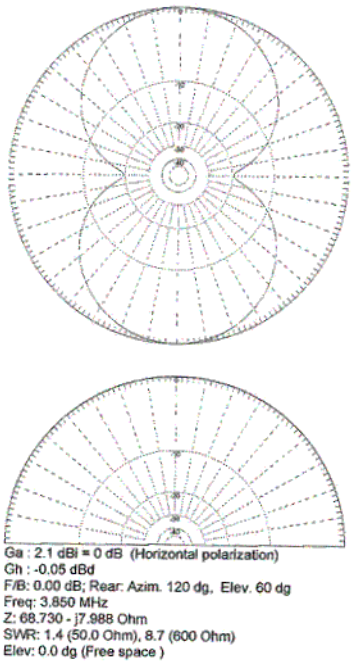

Figure 8.3: Radiation Pattern of Inverted-V for 80-Meters at 65 Feet

In *Figure 8.3: Radiation Pattern of Inverted-V for 80-Meters at 65 Feet* on page 19, the top graph shows how the radiation would appear to you, if you were situated above the dipole and you were looking down on it. The plane of the antenna runs from side to side on the top graph, and that graph demonstrates only a 5-dB null off the ends of the antenna. Therefore, it is essentially omnidirectional. The bottom graph shows how the radiation would appear if you were looking at the antenna from the end of the wire. As you can see, the pattern shows no radiation at the horizon and its maximum radiation is at about 40 degrees above the horizon, and the radiation straight up is only down 3 dB from its maximum. This antenna was modeled on 80 meters with the apex at 65 feet above ground and the ends at 35 feet.

It is a myth that a horizontal antenna orientation makes a difference on 80 meters at heights used by most amateurs. I have heard many amateurs say on 80 meters, “The reason my signal is weak to you is because you are off the end of my dipole.” The radiation pattern from a dipole is essentially non-directional until the dipole is elevated more than a half wave, that is about 125 feet on 80 meters, and it is 65 feet on 40 meters. The main reason it makes no difference regarding orientation is because propagation for signals closer than 500 miles (the distance of most 80 meter contacts) is essentially by high angle radiation nearly straight up and down. Only signals radiated and received at low angles make a difference in antenna orientation even at low heights above ground. At low heights, there are nulls about 3 to 4 dB off the dipole ends.

8.3 Dipole Shape Variations

The wire of a dipole doesnt have to be run in a straight line. A dipole does not have to be perfectly horizontal. Thats the way it is usually depicted in books and magazines, but you can bend the legs of the antenna up, down or sideways.

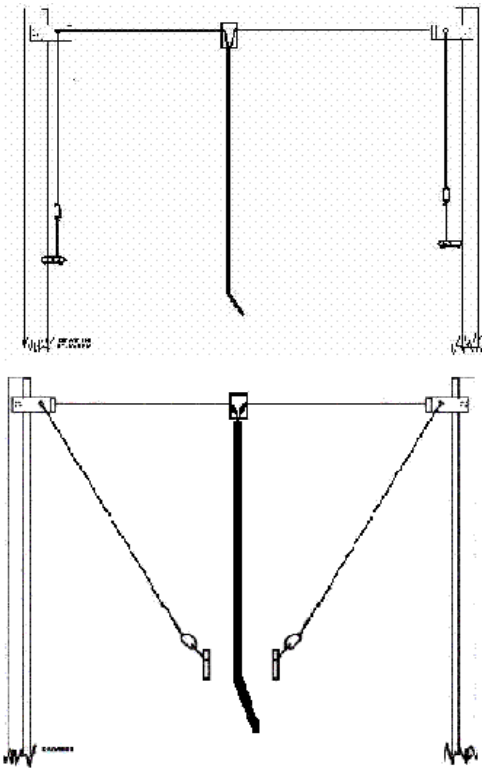

Figure 8.4: Two Dipole Shape Variations

If you make either wire one-half wavelength long and carefully prune it to resonance, you can use it without a tuner on and near its resonant frequency. Both antennas have the current part at the top where most of the radiation takes place. The vertical parts of these antennas radiate a weak vertically polarized wave. The only reason these dipoles are contorted this way is to make them full-sized and to fit in the available space. Other shapes are possible, and you can be creative at your location.

There are many more dipoles than the ones just described. We explore the other kinds of dipoles in *Section 8. Half-Wave Resonant Dipole Antennas* on page 17.

8.4 Calculating the Length of a Half-Wave Resonant Dipole

The approximate length in feet of a half-wave resonant dipole is found by dividing 468 by the frequency in MHz. The actual length of it will be determined by several factors. Using larger diameter wire will make the dipole resonate lower in frequency. Therefore, to make it resonant at the higher desired frequency,

It must be shortened. Raising a dipole higher above ground will make it resonate higher in frequency. An insulated wire will make the dipole resonate lower in frequency than a bare wire.

Using the above formula, cut the antenna a little longer than the calculations say. If the SWR is best at a lower frequency than you desire, the antenna will have to be made shorter by pulling the excess wire through the end insulators, folding the ends of the extra wire back on itself. Then wrap the ends of the overlapped wire on itself so it wont come loose. This causes the excess wire to "short" itself to the rest of the antenna. If you are using insulated wire, you will need to cut off the excess wire. The reverse is true if the antenna resonates too high in frequency. The extra wire can be let out to make it resonate on a lower frequency. This is why you originally cut the wire a little longer.

8.5 The Decibel

The decibel (dB) is a unit of measurement for comparisons of the ratio of power, current, and voltage and is the term we will use in comparing antennas in this book. At one time, antenna comparisons were made using a dipole as a standard, but today most comparisons use the isotropic radiator as a reference. An isotropic radiator is an imaginary antenna that radiates equally well in all directions. It has no gain. The terms "dBi" and "dBd" are used to label which reference is being used. In this book, we will use the dipole as a standard for the most part.

How do you derive decibels from power ratios? The formula for power ratios is dB = 10 log P1/P2. For voltage and current, the values are doubled. Formulas of this type are beyond the scope of this book. Doubling the power will produce a 3 dB stronger signal. Double the power and double it again will equal a 4 times power increase and that gives 3 dB plus 3 dB or 6 dB. Double 4 and that is a power increase of 8 and that adds 3 more dB for a total of 9 dB. Increasing the power from 1 Watt to 10 watts or increasing it 10 times will give a 10-dB increase. Multiply 10-Watts times 10 give us 100 watts, which adds another 10 dB above 1 Watt for 20 dB. Therefore, increasing the power another 10 times to 1000 Watts will produce a signal 30 dB stronger than 1 Watt.

Your receiver, if modern, will have a signal strength meter or "S Meter." That meter is calibrated in "S-Units" from one to nine and decibels over S-9. S-9 is usually calibrated using 50 microvolts (uV) from a signal generator. Each S-unit is approximately a difference of 5 or 6 dB. Therefore, a reading of S-9 is about 6 dB stronger than S-8. Therefore, from S-0 to S-9 is 54 dB. On some low cost transceivers, the S-units and dB above S-9 are only relative signal readings and actually have nothing to do with decibels.

9.
Antenna Basics

9.1 Resistances and Reactance

Two factors measurable in antenna impedance are resistance and reactance. When we refer to antenna resistance, we are referring to its radiation resistance. It is neither a resistance like the electronic component called a "resistor," nor is it the same as the resistance found in all conductors. Those types of resistances, called "loss resistances," change electrical energy into heat energy. Heat energy disappears by radiating out into its surroundings and it dissipates away to infinity. When we feed RF into the antenna, the energy put into the radiation resistance disappears from the antenna by radiation of electromagnetic waves, and that makes an antenna appear to have a resistor in it. Loss resistance robs power from the radiation resistance and lowers the efficiency of an antenna system, but the loss resistance in dipoles is very low if the feed-line loss is low. The efficiency of any antenna system is found from a ratio of radiation resistance and loss resistance. We can either calculate the loss resistance by the loss in the feed-line from published tables and by estimating the loss in tuning units. Feed-line loss and tuning unit loss can be measured, but that is beyond the scope of this book.

Antenna systems having reactance prevent the transmitter from delivering its full power and the reactance needs to be tuned out. There are two kinds of reactance: capacitive and inductive. Antennas have both. In antennas, reactance is a virtual reactance meaning the antenna acts as if there were a capacitor or an inductor in the antenna, but neither is there. You can only measure the sum of both reactances but not a value for either one. Using an antenna analyzer, you can determine whether the sum of the reactance is inductive or capacitive. Inductive reactance is a negative number and capacitive reactance is a positive number.

The reactance of an antenna forms the "J" factor in antenna impedance measurements. The "J" factor is measured in ohms and the reactance is expressed as + or "J" ohms depending on whether it is capacitive or inductive reactance. Capacitive reactance is expressed as +J ohms and inductive reactance is expressed as -J ohms. Capacitive and inductive reactance are opposite factors and one can cancel the other. An antenna having 6 ohms capacitive reactance or + J 6 ohms and an inductive reactance of J 5 ohms will result in an antenna with a reactance of 1 ohm capacitive or + J 1. Since one term is positive and the other term is negative, you subtract smaller value from the larger. The answer has the sign of the larger one. In antennas,

the reactance and resistance together determine the overall impedance of the antenna. The J factor is mentioned here only because you may see it in other books and on the extra class examination, but it will not be used further here.

A resonant antenna has equal amounts of inductive and capacitive reactance, and the sum of the reactance equals zero. As an example, when the inductive reactance equals J 5 and the capacitive reactance equals +J 5, their sum equals zero. When the sum of the total reactance of an antenna is tuned to zero, its impedance is totally resistive. The use of an antenna analyzer will tell you if the antenna is too long or too short for resonance. The simplest way to tune out antenna reactance is to change its length. The sum of the reactance of a long antenna will be inductive, and the sum of the reactance of a short antenna will be capacitive. If an antenna is short because it wont fit your property, it can be tuned to resonance by putting an inductor (coil of wire) in each leg. These coils are called “loading coils.” An equal amount of inductive reactance will cancel the excessive amount of capacitive reactance. An antenna with loading coils is described in section “X.” When an antenna is too long, the sum of its reactance will be inductive, and a variable capacitor can be inserted in each leg to tune out the inductive reactance. This is seldom done because it is easier to shorten the antenna.

A resonant antenna may still have SWR if its radiation resistance is not exactly 50 ohms. Not many resonant antennas have a radiation resistance of exactly 50 ohms, and most real antennas have a small amount of SWR. An antenna is resonant only at one frequency per band. It will also be resonant on its harmonic frequencies, where its radiation resistance will range from high to very high. Hams talk about using resonant antennas. What is meant by this is they use an antenna on its fundamental frequency close to resonance, the resistance is near 50 ohms, and the SWR without a tuner is near 1:1.

To calculate the impedance of an antenna with both resistance and reactance requires a mathematical procedure called the Pythagorean Theorem. That type of math is beyond the scope of this book. However, you should know how to use the Pythagorean Theorem to solve impedance problems on the Extra-Class test. Otherwise, you will have to memorize the answers from the question pool.

9.2 Feeding Dipoles Efficiently

For maximum power transfer from transmitter to the antenna, the antenna system must be resonant, and the resistance of the load (antenna system) has to be equal to the internal resistance of the source (transmitter). Notice we said an antenna system, not the antenna, must be resonant. As mentioned previously, an antenna system consists of the antenna, the feed-line, and any matching networks (tuners). A tuner at the input end of the feed-line can make a non-resonant antenna system resonant, and have a resistance of 50 ohms, and that matches the internal resistance of the transmitter. A tuner will not change the SWR between the tuner and the dipole part of an antenna system, and will not remove the reactance from the dipole.

When the load of an antenna system does not match the source and the impedance is high, the load will not draw power from the source and high RF voltages will be present at the output of the final transistors. In this case, high RF voltages can damage the output transistors of the transmitter. When the impedance of the load is low, too much of the power may be dissipated

across the internal resistance of the transmitter possibly destroying the output transistors. These are the two reasons why transceivers “fold back” their power when the SWR is high.

It is a myth that the dipole part of an antenna has to be resonant to be efficient. When power reaches the radiating part of the antenna system, it obeys the “The Law of Conservation of Energy.” The Law of Conservation of Energy states, “Energy can neither be created nor destroyed. Only its form can be changed.” (What is important is to get the power to the dipole itself, because in some systems power is lost in the feed-line, especially when using coax with high SWR) The miniscule amount of power in the dipole that does not radiate is changed into heat, another form of energy. Because the dipole part of an antenna system is made of conductors with low loss resistance, 99% or more of the power reaching it will radiate regardless of its length if that length is reasonable. The loss resistance of the conductors of the radiating part of most antenna system is so low it can be ignored. (Short mobile HF antennas are an exception because they may be lossy because of the very high current flowing in them.)

Not all the energy fed into an antenna system will reach the antenna itself. If the system has a tuner, part of the power is lost in the inductor of the tuner and part is lost in the feed-line. When properly tuned, tuners using T-networks lose about 10% of the power and L-network tuners lose about 5% of the power being fed to them. Notice we said properly tuned. However, improper tuning of the antenna tuner may cause you to believe the feed-line is matched, but when this happens there is a very high circulating current in the inductor causing it to get hot. This causes extremely high losses, and very little power reaches the radiating part of the antenna. In addition, so much heat is produced in the inductor that it can be damaged. We melted the plastic insulation that forms the inductor on one tuner this way. For this reason, some hams dont like tuners, preferring to use resonant antennas. Read the instructions for your tuner for proper tuning or you may wind up with a poor signal and a damaged tuner. The resistive losses in the conductors of the feed-line and the dielectric losses in the feed-line also rob power from the system. These are the reasons for you to use the best tuners and feed-lines possible.

Another loss to be considered is feed-line radiation. Any energy that radiates from the feed-line does not reach the radiating part of the antenna, and it may be absorbed by near-by objects and may not radiate in the desired direction. When coax radiates, it is called common-mode radiation. If the feed line can radiate, it can also receive signals. This can be detrimental because the coax can then pick up noise from near-by power lines, etc. Feed-line radiation will also destroy the directional pattern of a beam antenna. The causes of feed-line radiation will be described in the next section.

As we pointed out earlier, when you are using a half-wave resonant dipole fed with low-loss coax without using a tuner, almost all of the power coming out of the transmitter will radiate. On its resonant frequency, the dipole is one of the most efficient antenna systems a ham can use. However, a half-wave resonant dipole has a finite bandwidth. Why use a tuner with resonant antennas? On 160 and 80 meters the bands are wide compared to the percentage of frequency. The width of 80 meters is 500 kHz and its frequency is 3500 kHz. The width of 80 meters is 14% of the frequency. The 350 kHz of 40 meters is 5% of the frequency and most of the band can be covered without a tuner. The 350 kHz width of the 20-meter band is 350 divided by 14000 kHz, or 2.5 % of the frequency, etc. The percentage of frequency for a band will determine if a resonant dipole will work the whole band without a tuner. If you are planning to move around on 160 or 80 meter bands, it makes sense to have a tuner, because the bandwidth of resonant dipoles on those two bands is narrow. For example, the normal 2:1

SWR bandwidth of an 80-meter dipole is less than 200 kHz and the band is 500 kHz wide. However, if you have an antenna resonant for the voice portion of the band, you can still use a tuner to work the CW part of the band without inducing more than a dB of loss. Except for 40 and 10 meters, full-sized resonant dipoles on the rest of the HF bands will have enough bandwidth for them to cover the whole band.

The best place to insert a tuner is up at the antenna feed-point. However, if it is placed there, you wont be able to reach the tuners controls. Therefore, it is more practical to place it between the transceiver and the shack-end of the antenna feed-line. A piece of 50-ohm coax connects the radio to the tuner. With the tuner located in the shack, adjustments can be made. Remote automatic antenna tuners can be placed at the antennas feed-point, but the disadvantage of them is that the ones available today will not handle high power.

A coax-fed dipole and a tuner should not be used to feed an antenna on its even harmonically related bands. The even harmonics are 2, 4, 6, etc, times the fundamental resonant frequency. If an 80-meter antenna being fed with coax through a tuner is used on 40 meters, it will put out a weak signal because the SWR will be around a hundred to one. Coax has a tremendous loss with SWR this high. Only a few Watts from a hundred-Watt transmitter will reach the antenna. However, you will be able to make contacts with those few Watts. If you want to use any antenna having high SWR, ladder-line has much less loss than coax. If you feed an 80-meter dipole on 40 meters using ladder-line and a tuner, it will only be slightly less efficient than a half-wave 40-meter coax-fed resonant dipole. However, the SWR will still be high between the tuner and the antenna, but this doesnt matter since ladder-line has an insignificant loss. Since the feed-point impedance will be high, the SWR will only be about 9:1 in the ladder-line because ladder-line is a high impedance feed-line.

Extremely short antennas may not work at all because of the above mentioned reasons. To reiterate, the extremely high capacitive reactance may make it impossible for its reactance to be tuned out and reactance prevents a transmitter from delivering power to the antenna. Even if you are able to tune out the capacitive reactance, tuning it out requires an inductor and most of the power will be lost in the inductor. Do not take the statement about the Conservation of Energy to mean you can put up any piece of wire and it will radiate your entire signal.

9.3 The Cause of Feed-Line Radiation

Contrary to popular myth, SWR in a feed-line will not cause it to radiate. The cause of feed-line radiation is unequal current in the two conductors of the feed-line. What are the causes of unbalanced current in a feed-line? They are an unbalanced feed-line feeding a balanced antenna; the feed-line being brought away from and parallel to one leg of the antenna; the antenna not being fed in its center; and one leg of the antenna being close to metal objects. In coax, unbalance causes RF to travel on the outside surface of the coax shield, and the shield radiates. When everything is balanced, coax normally has current flowing on its center conductor and on the inside of its shield. The shield prevents it from radiating.

Ladder-line will also radiate when it is fed from the output of a tuner not having a balun. Baluns are discussed in the next section. Since the output of a transceivers tuner is unbalanced and feeding ladder-line directly from your transceivers tuner, the currents in the ladder-line will not be balanced. When balanced, ladder-line has equal currents with a 180-degree phase difference, which produce waves that null each other out, and no radiation takes place. Hams

mistakenly refuse to bring ladder-line into the shack because of a fear of feed-line radiation, but ladder-line does not radiate when balanced. The simple cure for feed-line radiation is to use a balun at the antenna feed-point for coax and a balun at the output of the tuner when using ladder-line.

9.4 Baluns

The word “Balun” is a contraction of “balanced to unbalanced.” It is pronounced “bal un” like “bal” in “balanced and like “un” in “unbalanced”. Many hams mistakenly pronounce an “M” at the end of the word making it “balum.” A balun transforms the unbalanced transmitter output to a balance feed-line such as ladder-line. It is also used to connect an unbalanced feed-line such as coax to a balanced dipole. In the latter case, the balun is located at the antenna feed-point and is constructed so the balun takes the place of the center insulator.

There are two kinds of baluns: voltage baluns and current baluns. They both accomplish the same thing. The difference in baluns is in the way they are wound. A voltage balun produces equal voltage with opposite polarity at its output. As its name implies, a current balun provides equal currents with opposite polarity at its output.

Running the coax through ferrite beads can make a 1 to 1 current balun. In addition, you can build a 1 to 1choke current balun by winding 8 to 10 turns of coax around a two-liter soda bottle and placing the coiled coax at the antenna feed-point. Any balun is designed to “divorce” your antenna from the feed line. It is used to prevent common mode radiation of coax, which makes the coax to be part of your antenna. You want it to be able to deliver all your power to the radiator itself. A choke balun does this perfectly, without using any ferrite beads or toroids. In most cases common mode coax radiation does not occur when a balun is not used, but it is preferable to use one to be safe.

Other baluns provide a step-up or step-down impedance transformation. A 4-to-1 balun steps up the impedance four times. It will transform a 50-ohm impedance to 200 ohms. This type of balun transformer is used at the output of tuners to increase the tuning range of a tuner 4 times. If a tuner without a balun can match 500 ohms, a 4-to-1 balun will increase the range of impedances it can match to 2000 ohms. Many hams think the 4-to-1 balun is used to match 50 ohms to 450-ohm ladder-line but it is not. It would take a 9-to-1 balun to match 50 ohms to 450 ohms, and it is not important to match the impedance to ladder-line.

A balun should always be placed at the input end of ladder-line or open wire feeders to prevent feed-line radiation. When using ladder-line a step up balun is commonly used although a 1:1 balun will work.

10 Other Types of Dipoles

10.1 A Shortened Dipole Using Loading Coils

If you are unable to put up a full-sized dipole on your property, putting loading coils into the dipole could shorten the antenna. See *Section 11.1 End-Fed Zepp*. A short antenna has capacitive reactance and the capacitive reactance can be tuned out with a coil. The overall length of the shortened antenna will be determined by the amount of inductance in the coil. Pre-tuned antennas of this type are available from at least one manufacturer. The main problem with loaded antennas is they are very narrow banded. If the loading coils are wound with small diameter wire, the coils may introduce unwanted loss into the antenna. Loading coils can also be found in shortened vertical antennas for high frequency (HF) mobile use.

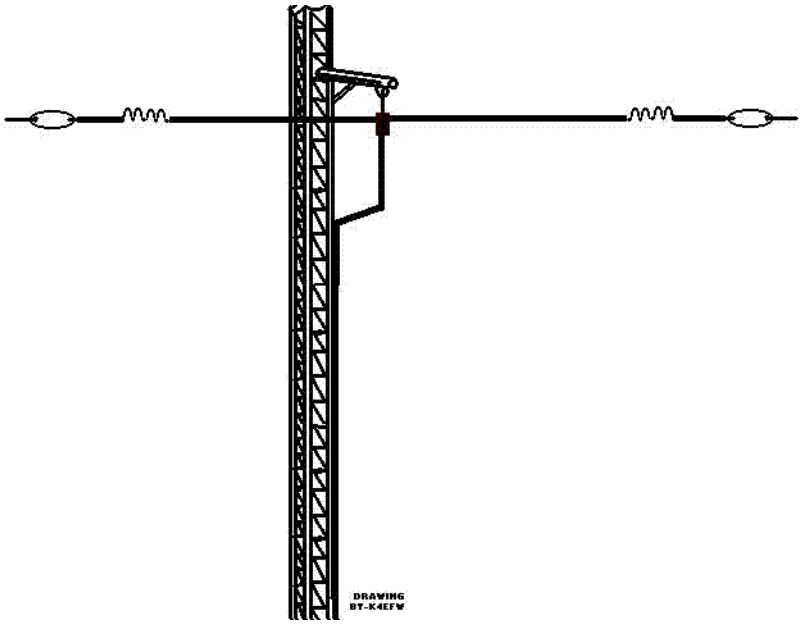

Figure 10.1: A Shortened Loaded Dipole

10.2 All Band Dipole

In *Figure 10.2: All Band Dipole*, a dipole is cut to a half wave on the lowest band you want to operate. Feeding it with ladder-line and a tuner makes it possible for you to work all the other higher bands. The only losses in this antenna system are the loss in the tuner and the very small loss in the ladder-line. This system is more than 90% efficient. As mentioned above the balun in the tuner will be used, or if your tuner doesnt have a balun, an external balun can be connected between the tuner and ladder-line with a short run of coax. Four-to-one baluns are the most commonly used ones for this arrangement.

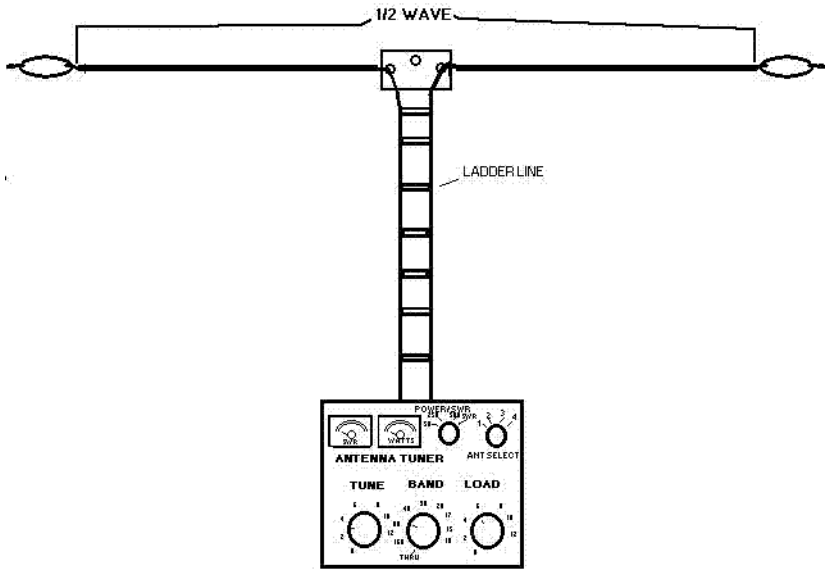

Figure 10.2: All Band Dipole

10.3 The Sloping Dipole

A lower angle of radiation can be achieved by tying one end of a half-wave dipole to a high support and the other end near the ground. It is fed with or without a balun with 50-ohm coax. The sloping dipole will show some directivity and have low angle gain in the direction of the slope. More directivity can be gained if the dipole is strung from a tower, and the tower is acting as a passive reflector. The sloping dipole is mostly a vertically polarized radiator and it works well for DX. Since the sloping dipole is fed in its center, it does not need to be grounded to the earth as a quarter-wave vertical does. Make sure the bottom end of a sloping dipole is at least 10 feet above ground because like all dipoles there is high RF voltage on its ends.

10.4 Half-Wave Resonant Sloping Dipole

In *Figure 10.2: All Band Dipole*, the field of maximum radiation is in the direction of the slope or toward the right side of the picture. The formula for the length of a sloping dipole is the same for any half-wave resonant dipole.

10.5 The Folded Dipole

The B&W Company makes a folded dipole that claims to have a good match on all bands and it does. However, on the low bands much of the power is burned up in the resistor that connects the two ends together. The power going toward the ends encounter the resistor and is consumed as heat. All that power is lost and does not radiate, and no power is reflected back to the feed point making the antenna have low SWR. On the higher bands, a large part of the power radiates before it reaches the resistor and the antenna is moderately efficient on those bands. On 80 meters the 90 foot-long dipole model will produce a signal at least 10 dB lower than that from a resonant dipole.

If you remember the single channel TV antennas used years ago, the driven element was a folded dipole. Folded dipoles are very broad-banded. That is the reason they were used for TV antennas since a TV channel is 4 MHz wide.

When constructing a folded dipole, the formula for calculating the length of it is the same as for any dipole. The folded dipole consists of two parallel conductors with the ends tied together. The conductors can be spaced from less than an inch to more than two inches apart when made from TV ribbon or ladder-line. At the ends, strip the insulation back several inches, Twist the bare wires together, solder them, and run them through insulators. The feed-point is in the center of only one of the two parallel conductors.

The feed-point impedance of a folded dipole at resonance is close to 300 ohms resistive and can be fed directly with 300-ohm TV twin-lead or a tuner with its balun. This antenna was very popular years ago when coax was expensive and 300-ohm TV twin-lead was relatively cheap. A length of 450-ohm can be substituted for the twin-lead. An alternate feed method is placing a 6:1 balun at the feed-point and then feeding it with 50-ohm coax. The folded dipole will not radiate its second harmonic, so it is not good for a multi-band tuner-fed antenna.

Another folded dipole type is the three wire folded dipole. We have seen this dipole only in books and do not know anyone who uses one. The feed-point impedance is 600 ohms resistive and is fed with home-built 600 ohm open wire feeders.

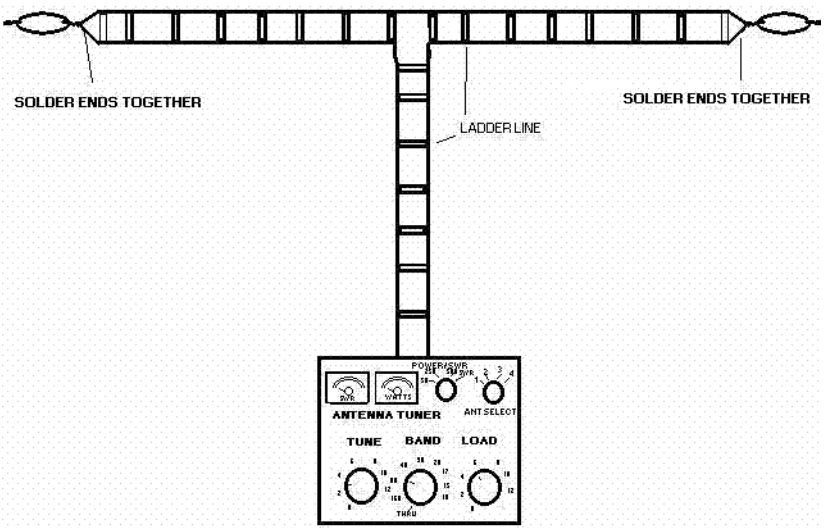

Figure 10.3: Folded Dipole

10.6 The Double Bazooka Dipole

The double bazooka is claimed by its users to be broad-banded, a quality especially interesting for those hams operating on 75/80 meters. Tests done at the A.R.R.L. have shown the double bazooka is only slightly more broad-banded than a regular dipole, probably due to the use of a large conductor (coax) for the center part of the antenna. The double bazooka will not transmit its second harmonic, and its users say it does not need a balun. Other users say it is quieter than a regular dipole.

The center of the antenna is made from RG-58 coax. To find the length of coax needed, divide 325 by the frequency in MHz. The coax forms the center part of the double bazooka and a piece of number 12 wire on each end completes the antenna. The length of each of the end wires is found by dividing 67.5 by the frequency in MHz. To increase the bandwidth some builders use shorted ladder-line in place of the number 12 wire, which makes the end pieces to be electrically larger.

The feed-point of the double bazooka is unique. At the center of the coax dipole, remove about 3 inches of the plastic covering, exposing the shield. Cut the shield in the center and separate it into two parts. Do not cut the dielectric or the center conductor. Leave the center conductor with its insulation exposed. On the feed-line strip off about 3 inches of outer insulation, separate the shield from the center conductor, and strip about 1 inches of the insulation from the center conductor. To attach the feed-line, solder the two exposed feed-line conductors to the two pieces of the separated exposed shield of the dipole center. It goes without saying: seal the feed-point to prevent water from getting in. At each of the two ends of the coax forming the center of the antenna, the coax is stripped back and the center conductor and shield are

shorted together and soldered. The end wires are soldered to the shorted coax ends, run to insulators at the end of the antenna, and the soldered joints are sealed against the weather.

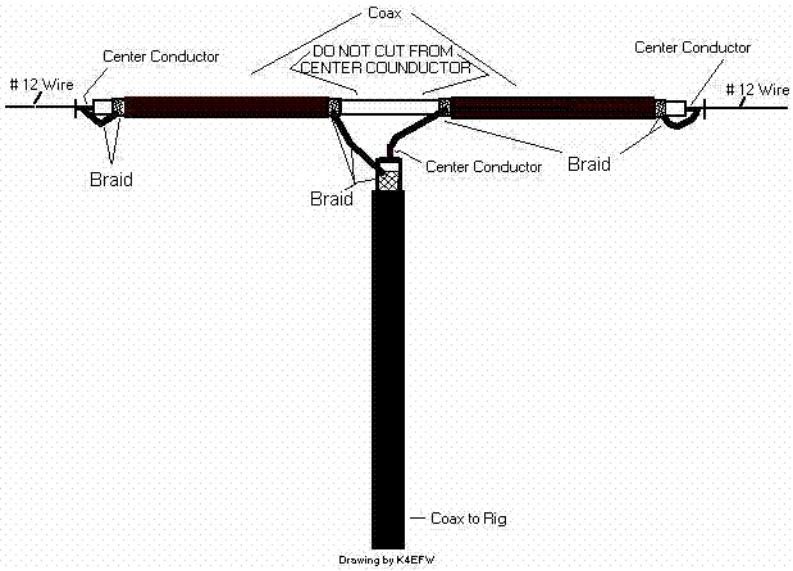

Figure 10.4: Double Bazooka Dipole

10.7 Broad-Banded Coax-Fed Fan Dipole

A broad-banded dipole for 75/80 meters can be constructed by attaching two equal length dipoles to the center feed-point and spreading the ends about 3 feet apart using PVC water pipe to separate them. The completed dipole looks like a bow tie. This makes the antenna to appear electrically to have that of a large diameter conductor. Because of this, the overall length will need to be shorter than a single wire alone. When we used the antenna, we found a length of 110 feet would cover most of the 75/80-meter band without a tuner. It is fed with 50-ohm coax. The use of a balun is optional. The antennas for most of the higher bands have enough bandwidth so they do not need broad banding.

10.8 Two-Element Collinear Dipole

The 2-element collinear dipole is an antenna that is a full-wavelength antenna having a 2-dBd gain. It can be fed with ladder-line and a tuner and used as a multiband antenna, or it can be fed with a quarter-wave-matching stub with 50-ohm coax cable to make it a single band array. In the stub matching system, a quarter wavelength of ladder-line is connected across the center insulator, and the opposite end of the ladder-line is shorted. A shorted quarter-wave piece of feed-line acts like an open circuit. Going from the shorted end of the ladder-line toward the dipole, there will be a point where a piece of 50-ohm cable will find a perfect match. The 50-ohm feed-point will have to be found empirically (trial and error).

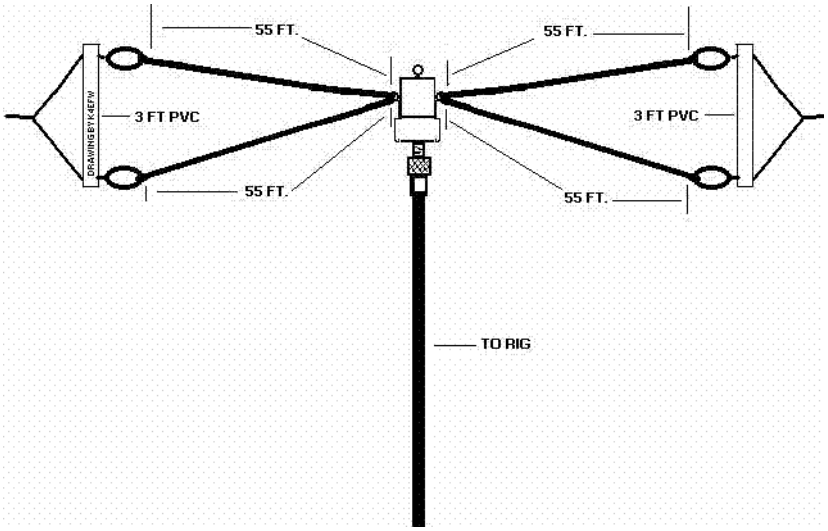

Figure 10.5: Broad-Banded Fan Dipole for 80 Meters

10.9 4-Element Collinear Dipole

The 4-element collinear dipole array consists of four half-wave segments connected end-to-end with an insulator between each two adjoining segments. The feed-point is at the center of the array. The antenna is fed with ladder-line through a tuner. A quarter wave shorted ladder-line stub hangs down vertically from the insulators between the inside and the outside half-wave segments. This stub provides a 180-degree phase shift so that all half-wave segments are fed in phase. This antenna has a 6-dBd gain and it radiates bi-directionally at an angle perpendicular or broadside to the plane of the wires.

This antenna is too long for most hams to use on 80 and 40 meters, and the stubs hanging vertically will be too close to the ground. For 20 meters, the four-element collinear array will be 97 feet long and the stubs will be 18 feet. To find the length of each half-wave segment, divide 468 by the frequency in MHz, and for the quarter-wave stubs, divide 246 by the frequency in MHz.

MFJ has begun marketing the four-element collinear monoband array. They have them for 20, 17, and 15 meters. This antenna is so easy to build that you can do it yourself. All you need is 5 insulators, antenna wire, and some ladder-line.

It will have no gain if you use it on bands for which it is not designed because the stubs are used as phasing lines. It is definitely not a multiband antenna.

It is possible to add more half-wave segments to the ends of this array to make it have 6, 8, 10, etc half wave segments. Adding more segments will add more gain and make the lobes narrower.

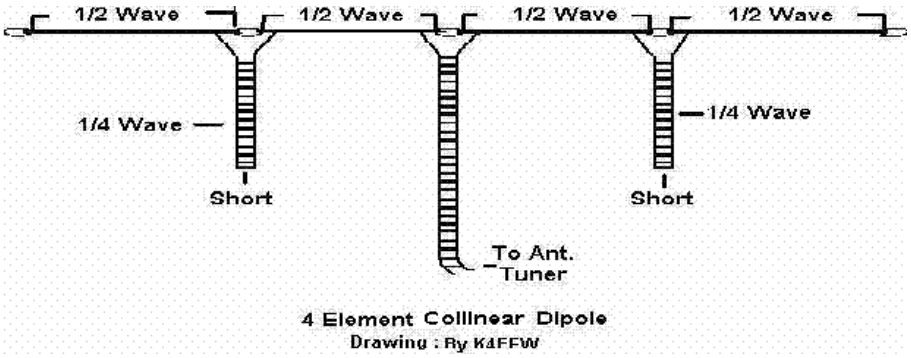

Figure 10.6: 4-Element Collinear Dipole

10.10 Coax-Fed Dipoles Operated on Odd Harmonic Frequencies

Antennas fed with 50-ohm coax can be used on other bands for which they are not cut. An 80-meter dipole will have a relatively low SWR and will be resonant at a single frequency on 10 meters and not

much power will be lost in the coax even if operated off resonance. A 40-meter dipole will work the same way on 15 meters. Using coax, a dipole will work on its fundamental frequency and on odd-harmonic frequencies and it is not necessary to use ladder-line. The fundamental frequency is the frequency for which the antenna is a half-wavelength long, and the odd harmonics are 3 times, 5 times, 7 times, etc. the fundamental resonant frequency. A frequency of 21 MHz is 3 times or the third harmonic of 7 MHz, and 28 MHz is the seventh harmonic of 4 MHz.

Antennas operated on their odd harmonics will be resonant a little higher in frequency than exact multiples of their fundamental frequencies. Since the odd harmonic antennas input impedance is higher than it is on its fundamental frequency, many amateurs use a series quarter-wave matching section of 70-ohm coax to give it a better match. The 80 meter inverted-V dipole in use here has a 2:1 SWR on 10 meters indicating it has an impedance of around 100 ohms. However, modeling the antenna for 10 meters shows the resonance to be below 28 MHz, probably because the antennas fundamental resonant frequency is 3920 instead of 4000 kHz. A quarter wave 70-ohm matching section should bring the SWR down to a much lower level.

As said earlier, if you try to use coax with a dipole on its even harmonic frequencies, the feed-point impedance will be very high, the SWR will be extremely high, and the coax will absorb most of the power. In addition, when operating a coax-fed antenna on its even harmonics, the tuner may not be able to provide a match. Operating any antenna on any of its harmonic frequencies, odd or even, will work better if it is fed with ladder-line and a tuner.

This antenna is matched by a quarter-wave 70-ohm series matching section. Three half waves will resonate higher than you would expect because the center half wave doesnt have to contend with end effects. To calculate the length of a three half-wave dipole, divide 1380.6 by the frequency in MHz. Five half waves is found by dividing 2316.6 by the frequency.

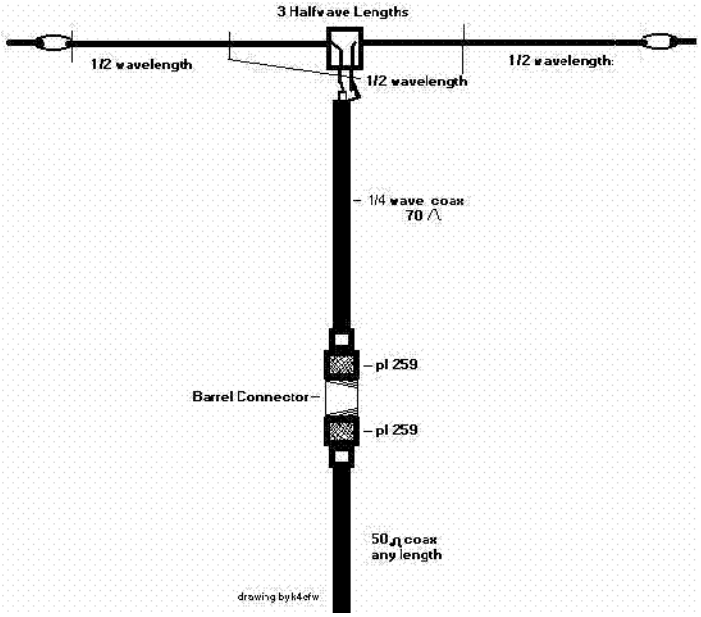

Figure 10.7: 3 Half-wave Dipole

To use a 3 half-wave antenna on 15 meters, the 70-ohm matching section needs to be 7 feet 7 inches and the antenna needs to be 64 feet long for a good match. It will be just a little long on 40 meters. When using a 40-meter dipole with a 15-meter quarter-wave matching section, it will still have acceptable SWR on 40 meters.

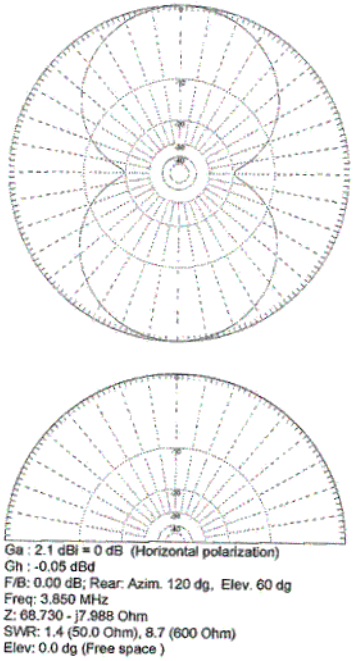

Figure 10.9: Radiation Pattern of a 15-Meter Three Half-Wave Dipole at 65 Feet

The pattern shows 6 lobes, 4 major lobes and 2 minor lobes. The vertical radiation pattern shows low angle radiation.

10.11 All Band Random Length Dipole

A random length of wire cut into two pieces can be used as a dipole, and it will radiate efficiently. It has to be at least a half-wave length on the lowest band you want to work. It looks the same as the all-band dipole and is the same, except it is not resonant on any band. The random length dipole is being described here to emphasize that the radiating part of an antenna doesnt have to be resonant. Because it will have a feed-point impedance that is unusual, it must be fed with ladder-line a tuner, and a balun. Since you are using a tuner, it can be used on multiple bands. If you make it very long, it can have gain over a dipole. For example, if it is four wavelengths long, it will have 3-dBd gain. As you move to higher bands, the electrical wavelength of the antenna increases, and each higher band will have more gain.

A half-wave antenna radiates perpendicularly to the plane of the wire. As you move to higher bands, this antenna begins to show some gain, and instead of two lobes of radiation, the two lobes split into four lobes and the pattern resembles a 4-leaf clover. As you make the antenna longer, the four lobes move nearer the to the ends, the gain increases, and there are minor lobes of radiation between the major lobes. These minor lobes make it possible to work in all directions. The longer the wire, the closer the antennas major lobes radiate bi-directionally toward its ends

10.12 All Band Center-Fed Random Length Dipole

The problem with using a random length of wire for this antenna is you may find that because of limitations of your tuner, you may not be able to tune a particular length of antenna on some bands. Certain lengths will tune all bands and one of those lengths is 135 feet. That particular length will be nearly resonant on all bands of 80-10 meters. Resonance only makes it easier to tune, but it has no effect on efficiency. A length of 260 feet will tune from 160-10 meters. Lengths of 260 and 135 feet have been used here successfully. Some hams use random lengths of wire without problems. Then some hams have had problems with other random lengths. The ones having the problems solved the tuner problems by changing the length of the dipole wire. If you plan to put up this antenna using a random length of wire, you will need to experiment with various lengths until you find a combination that works.

Tests were performed here using two towers of equal height and spaced 100 feet apart. On one tower, was an 80-meter inverted-V 120 feet long fed directly with coax, and running parallel to it on the other tower was a 135-foot long inverted-V fed with ladder-line and a tuner. At the resonant point of the coax-fed dipole and having tuned the ladder-line fed antenna, it was possible to switch antennas instantly and many hams were asked to look at their “S-meters” while the antennas were switched. All hams that participated in the test said the signals from both antennas were equal. The signals were measured on analog S-meters, not on segmented LCD meters found on most of todays transceivers.

10.13 A 2-Band Fan Dipole

A 2-band dipole can be constructed by connecting together the feed point two dipoles for even harmonically related bands. It is fed with 50-ohm coax with or without a balun. The best example of this is 80 and 40-meter dipoles connected together. Both dipoles are cut for

half-wave resonance on each of the two bands. They are fed together and the ends of the wires are spread apart. If the ends are close together, there will be interaction between the dipoles. In such an antenna system, both dipoles must be carefully pruned for lowest SWR one band at a time. The lower band will be tuned first since the shorter dipole will not interact with the longer one. Each dipole has a low antenna resistance on the band for which it is resonant. RF energy follows the path of least resistance, and it automatically selects which dipole will receive power. The remaining antenna will have a high impedance. High impedance will block RF. Such an antenna will have a narrower bandwidth than a single band dipole, but close to the resonant frequency of each dipole, a tuner will not be needed. To connect many dipoles for multiple bands is possible, but it is not recommended because multiple wires are prone to interact and it will be impossible to achieve a low SWR on some bands. However, on the two band model, the 40-meter dipole will resonate close to 15 meters, the 80-meter dipole will resonate close to 10 meters, and working four bands with this set-up is possible. Some hams are using this antenna successfully with a tuner on all bands, although the signal on 20 meters suffers somewhat because of high SWR.

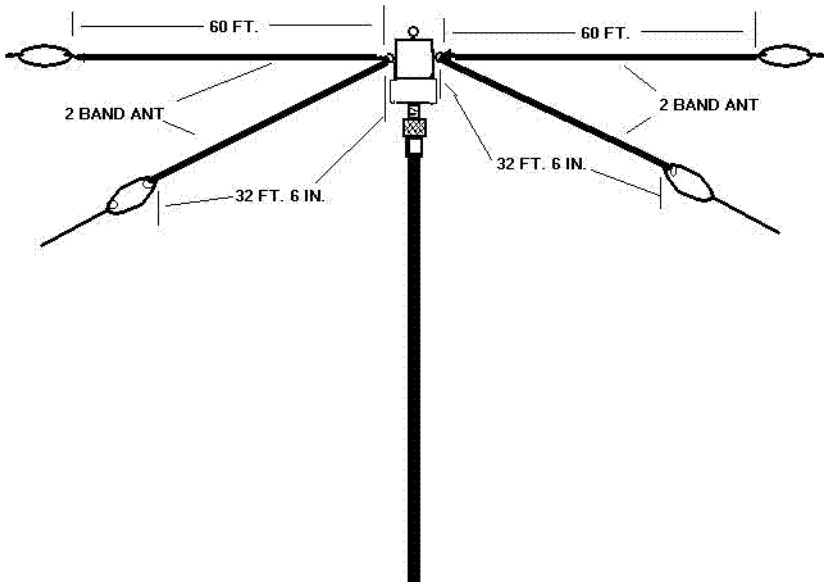

Figure 10.10: Two-Band Fan Dipole for 40 and 75 Meters

10.14 Trapped Dipole for 75 and 40 Meters

A trap is constructed from a capacitor and an inductor connected in parallel. It acts as an open switch on the frequency for which it is resonant. A trap is placed on each side of the dipole. For a 75 and 40 meter trapped dipole, the traps must be resonant on 40 meters, and each trap should be placed a quarter wave from the center insulator. The center section between the traps is electrically isolated from the ends of the dipole by the traps on 40 meters, and the center section of the antenna becomes a full-sized half wave resonant dipole for that band. This antenna is fed with 50-ohm coax and an optional balun. Wires connected to the outside of the traps are run to the end insulators and are tuned so the entire antenna resonates on 75 meters. The 75 and 40 meter trapped dipole will be shorter than a 75-meter dipole because the inductor in the 40-meter trap acts as a loading coil on 75 meters. In addition, the ends of the antenna can

be tuned to operate on the 80-meter CW band instead of the 75-meter voice band. Several sets of traps can be inserted at the correct points in the dipole to make a multi-band dipole. Multi-band trapped dipoles are being sold, but in many cases they will require the use of a tuner. If a good match is found at a frequency on some bands, the bandwidth without a tuner will be very narrowThe antenna is only 108 feet long instead of 120 feet because of the

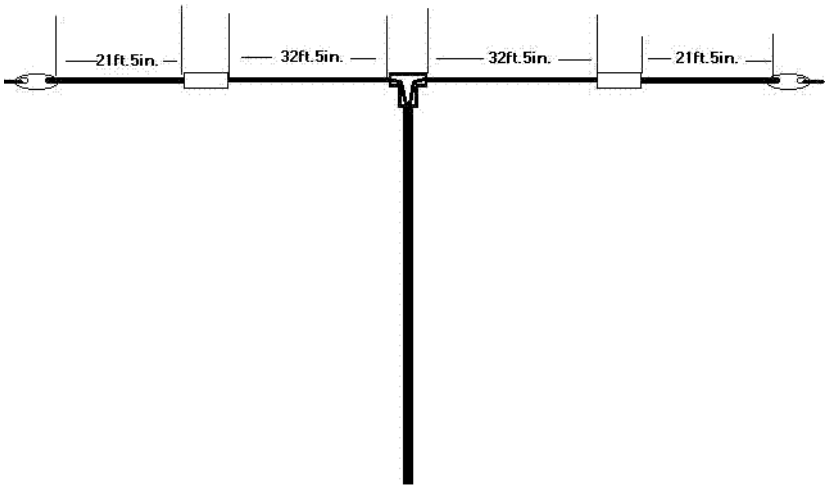

Figure 10.11: Trapped 75- and 40-Meter Dipole

loading effect of the traps on 75 meters. These dimensions are for antennas using the traps made by W2AU. If you use other brands of traps, the length of the end wires will have to be adjusted. What you do in that case is make the wire long, measure its resonant frequency on 75 meters, and prune the ends to resonance at your favorite frequency.

10.15 The Extended Double Zepp Dipole

An extended double zepp is a long dipole with 3-dBd gain. It is the longest dipole antenna, which will radiate at right angles to the plane of the antenna. To find the overall length of an extended double zepp, divide 1197 by the frequency in MHz. Each leg of the antenna is 0.64 wavelength long and the total length is 1.28 wavelengths. An extended double zepp for 75-meters at 3.8 MHz is 315 feet. Not many amateurs have space for that antenna. The extended double zepp is mostly fed with ladder-line. Another method of matching an extended double zepp is to use tuned lengths of 450-ohm ladder-line as a series matching transformer connected between the 50-ohm coax and the dipole. The length of the matching section of 450-ohm ladder-line can be found by dividing 135 by the frequency in MHz.

10.16 The G5RV Dipole

An interesting antenna you can buy that will work somewhat on all high-frequency bands is the so-called G5RV antenna. It is named after the call letters of Louis Varney (SK) who designed it. It is a 102-foot long or three half-wavelength dipole antenna on 20 meters (14.150 MHz), and can be used with a tuner on other bands as well. In his original design, Varney calculated the length to be 102.57 feet, but chose to make it an even 102 feet since a tuner was going to be used with it anyway. It was originally fed through a 34-foot 500-ohm homebrew

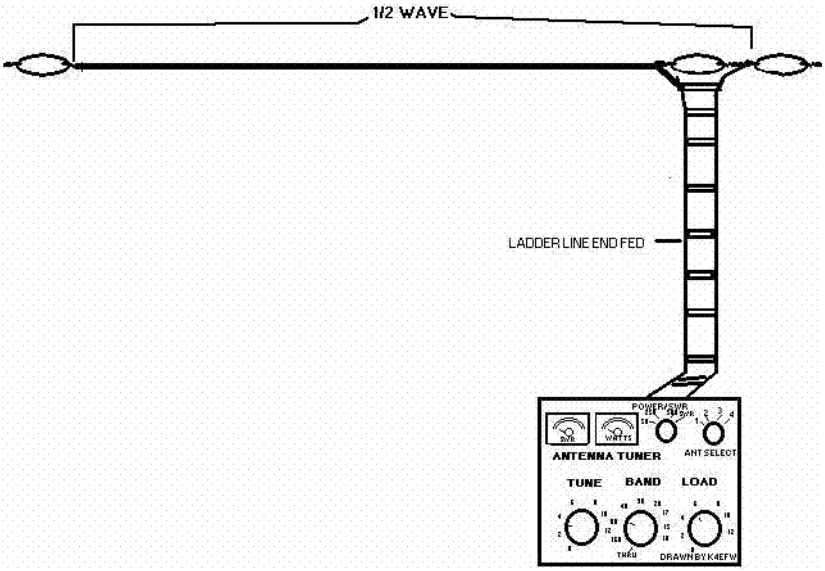

Figure 10.12: Extended Double Zepp Dipole

open wire matching section from a 70-ohm coax or parallel conductor feed-line. The 34-foot open wire line is a half wavelength on 20 meters and at the end of a half-wave feed-line, you will see the antennas impedance repeated regardless of the feed-line impedance. The ladder-line helps partly to match the antenna on the other bands.

The G5RV antenna is around 20 feet short of being a half-wave on 80 meters, and on bands on 20 meters and up, it has theoretical gain. We believe that gain is negated by losses in the coax of the feed system, except for 20 meters. At the frequency of the best match, commercially made models of the G5RV are said to have a 1.8:1 SWR on 80 meters. Where the coax joins the open wire, Varney recommended using a choke made of 8 to 10 turns of coax. He advised against using a balun, because, as he says SWR of 2:1 or higher may cause the balun to heat and possibly burn out. The SWR will be moderately high or high on bands other than 20 meters. Varney recommends using the lowest loss coax available and as short a run as practical because of feed-line losses caused by high SWR. This recommendation is very important today, as it was when Varney designed it. Some G5RV antennas put out decent signals and some others have relatively weak signals. Without further investigating, the only way to explain this is that some are using lossy coax and baluns while others are not, and the height above ground may play a part in how well it works.

The G5RV antennas being made today use small diameter 50-ohm coax, 450-ohm ladder-line, and a balun between the ladder-line and the coax, contrary to Varneys suggestions. There are several variations of the G5RV antenna being sold today because many believe they can improve the original design. If you use a G5RV antenna, a tuner will be required.

The G5RV shown in *Figure 10.13: G5RV Dipole* on page 39 is close to the original version of the antenna. This one pictured below is from an old article that K4EFW found somewhere. It is like the one he used. As you can see, it uses 300-ohm TV ribbon. The length of the parallel TV ribbon is 36 feet, but modern designs of this antenna use 34 feet of 450-ohm ladder-line. All these variations work equally well when they are used with a tuner. It is shown in the inverted-V configuration but it could be put up in the flattop configuration as is, with no modification.

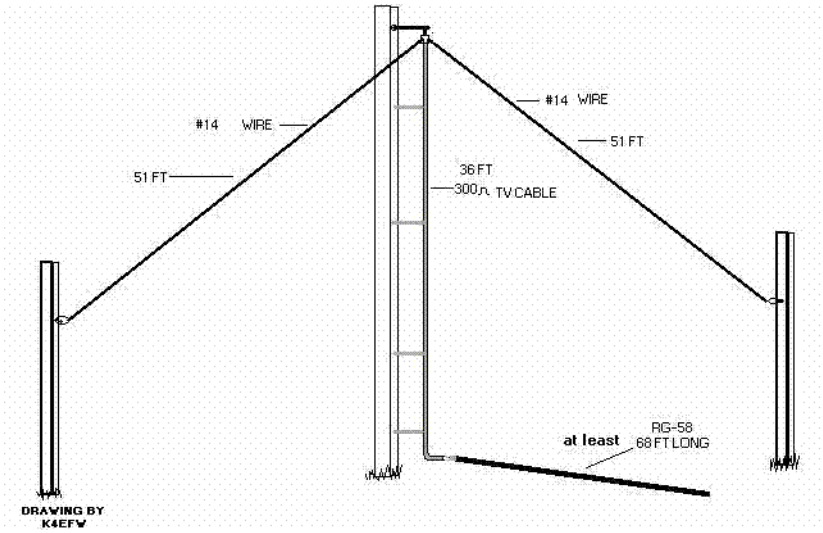

Figure 10.13: G5RV Dipole

Jeff, AI8H, in Oxford, Georgia, had a pair of G5RV dipoles oriented in different directions. Recently he put up a 75-meter half-wave inverted-V. Being able to switch antennas, he ran A-B tests on 3902 kHz and the inverted-V was 10 dB stronger than the first G5RV and 15 dB stronger than the other one. Now if we are saying the stronger signal is 40 dB over S-9 and the weaker signal is 25-30 dB over S-9, no one will notice the difference. Only under marginal band conditions will the difference be important. In addition, the G5RV antenna will work better on the other bands.

10.17 Off-Center Fed Dipoles

A long dipole consisting of multiples of equal half-wave segments is normally fed in the center using ladder-line. Dipoles do not necessarily have to be fed in the center. They can be fed in the center of any one of these half-wave segments, even fed off-center. A fair match will occur if coax is used.

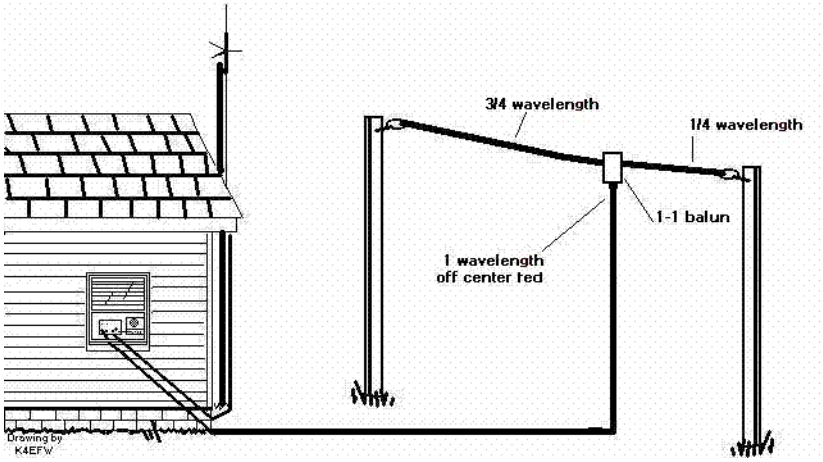

Figure 10.14: One Wavelength Off-Center Fed Dipole

The dipole shown in *Figure 10.14: One Wavelength Off-Center Fed Dipole* on page 39 is a one-wavelength dipole. It is nothing but two half waves end to end. It is being fed in the center of one half-wave segment or a quarter wave from one end. It is possible to make it any number of half waves, and if it is fed a quarter wave from one end, it will have a fair match. The way it is shown above is an example of how to feed an antenna with even multiples of a half wave using coax. A 2:1 or 4:1 balun will improve the match on longer versions.

The windom antenna is another example of an off-center fed antenna. The original windom was fed off center with a single wire. The other side of the transmitter was connected to ground. The feed-point impedance at the transmitter was reported to be 500 ohms on all bands. The antenna was designed by William L. Everett and J.F Byrne at Ohio State University. W8GZ, whose last name was Windom, described the antenna in the September 1929 issue of *QST.*

A lot of research concerning the modern variations of the Windom antennas has been done, including the ones described by Fritzel, K4ABT, W4RNL, The Carolina Windom, and ON4BAA. The main differences in these variations are the slight differences in the position of the feed-point and the impedance of the baluns used for matching. The Windoms are sensitive to the height over ground, meaning the height above ground affects the SWR. The offset position of the feed-point will also determine the feed-point impedance. The one sold by K4ABT is a variation of the Fritzel antenna, and the one sold by Radio Works, The Carolina Windom, (shown in *Figure 10.15: Windom Dipole* on page 41) claims it has a vertical radiator.

There are two variations of Windoms, both claiming they have vertical radiators, The Carolina Windom and the one previously marketed by W4COX have two pieces of transmission line in series. The upper piece is connected to the dipole, and the lower piece is connected to the transmitter. The feed-point of the dipole is placed off center. In The Carolina Windom being marketed today, the upper transmission line is coax. The one made by W4COX had the upper piece made from ladder-line, but in either case, the principle is the same. The two pieces are connected together through a line isolator, a type of balun. The line isolator keeps the lower piece of transmission line from radiating. Because the antenna is fed off-center, the marketers of The Carolina Windom claims it causes an unbalance of current in the upper piece of transmission line. This is doubtful because there is a balun at the feed-point, which should prevent the feed-line attached there from radiating. The main difference between The Carolina Windom and the one sold by W4COX is that a 4:1 transformer is between the coax and the ladder-line, and a 1:1 line isolator is between the upper and lower coax cables. Both variations of this antenna show low SWR on several bands, but a tuner is used to match it.

Another unique variation of the Windom dipole is the Fritzel antenna, named after its inventor and manufacturer, Dr. Fritz Spillenger (SK), a German ham, call sign DJ2KY. Alpha Delta is now selling an almost exact duplicate of the original Fritzel antenna. Alpha Delta calls it an OCF antenna and it is made by Buckmaster Antennas. There are two models of the Alpha Delta antenna: one for low power and one for high power, the power rating of the balun being the limiting factor. The Fritzels short side is 0.18 wavelength long and its long side is 0.32 wavelength long. It is fed with coax and a 6:1 balun. Theoretically, the feed point impedance is 300 ohms, and the balun provides a 50 to 300 ohm impedance transformation. Modeling the antenna on its lowest resonant frequency at 35 feet, it shows about 120 ohms impedance. The original Fritzel antenna being used by K4LMS reportedly will work all bands with a tuner, but it will work 40, 20, 17, 12, and 10 meters without a tuner with an acceptable SWR. The

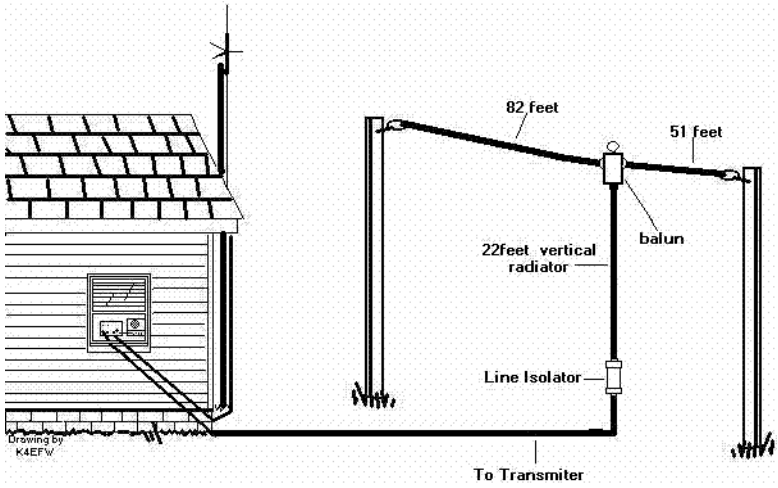

Figure 10.15: Windom Dipole

Windom being sold by K4ABT uses a 4:1 balun and the feed-point is at a slightly different location. That one is shown in *Figure 10.16: Windom Dipole (Fritzel Type)*.

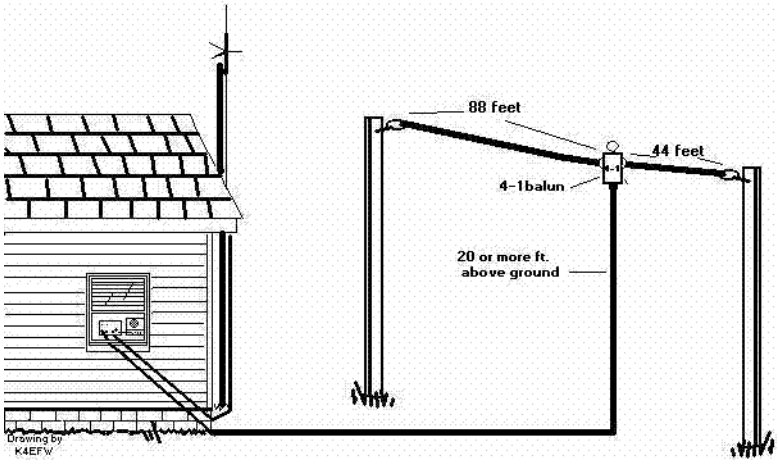

Figure 10.16: Windom Dipole (Fritzel Type)

The difference between the Windom antenna sold by K4ABT and the original Fritzel is the difference in the offset of the feed-point. Since the K4ABTversion uses a 4:1 balun, it appears his is fed at the 200-ohm point, and the original Fritzel is fed at the 300-ohm point. On any resonant dipole, the lowest feed-point impedance is found at the center. As you place the feed-point offset toward either end, the impedance gets higher. The highest feed-point impedance occurs at the end of the dipole.

11. End-Fed Antennas

11.1 End-Fed Zepp

A half-wave resonant antenna can be fed from its end. When fed this way, it is also known as an end-fed zepp. An end-fed zepp will work on its fundamental frequency and on odd and even harmonic frequencies. The name “Zepp” goes back to the days of dirigibles or Zeppelins, which used trailing wire antennas that had to be fed at one end. The end of a half-wave antenna has very high impedance, and an antenna fed this way is said to be voltage fed. Feeding a half-wave resonant dipole in the center means it is current fed. The normal way of feeding the end-fed antenna is with ladder-line. One side of the ladder-line is connected to one end of the antenna and the other side of the ladder-line is connected to nothing. To secure the unconnected side of the ladder-line, it is connected to a short wire running between two insulators. Since the antenna is connected at its high impedance point, no current flows into an antenna, but there will be a large current in the center of this antenna. No current flows from the open side of the feed-line because it is at a zero current point. (See *Figure 11.1: End-Fed Zepp* on page 43.)

The end-fed zepp can be matched by cutting the ladder-line to a quarter wavelength with the bottom end of the ladder-line shorted. A certain distance above the short is a 50-ohm feet-point and it can be fed directly with coax. MFJ is marketing antennas of this type made for single bands, and they are selling the parts separately so you can build your own. You will have to find the 50-ohm point by trial and error. This method of feed makes it a single band antenna.

11.2 End-Fed Random Length Antenna

Figure 11.2: End-Fed Random length or Long Wire Antenna on page 43 shows another end-fed antenna made from a random length of wire connected to the back of the tuner. The wire then exits the shack and goes to a high support where it then runs horizontally to another high support. The tuners groundside must be connected to a good RF ground, since a poor ground causes high losses. This antenna is commonly called a “long wire.” Since the end of the antenna comes in the shack, you will be exposed to high levels of RF. In addition, this type of installation may cause RF to be picked up in the microphone, noted by distortion. The

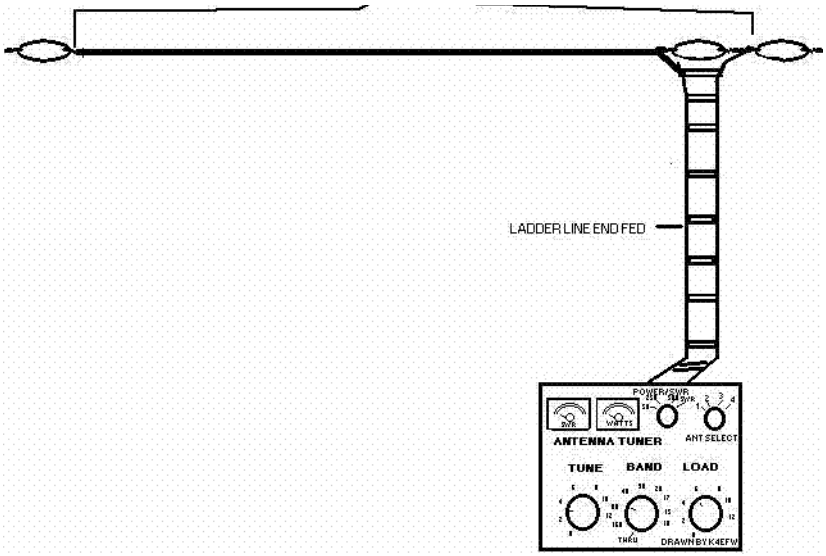

Figure 11.1: End-Fed Zepp

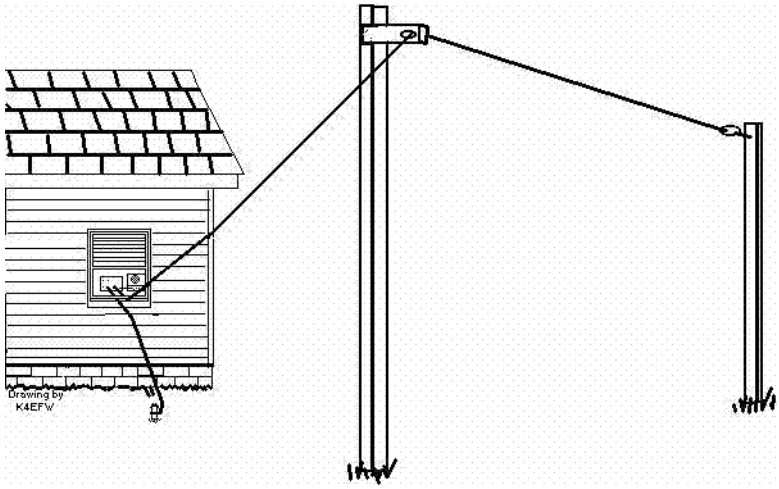

Figure 11.2: End-Fed Random length or Long Wire Antenna

feed-point of the long wire being connected directly at the output of the tuner can have an impedance of a few ohms to a thousand ohms depending on the antennas length. If the wire is cut to a multiple of a half wave at the lowest frequency, the system will be efficient since it is fed at a voltage point and very little current flows into the ground. This antenna is really a variation of an inverted-L fed directly without a feed-line from the tuner.

12.
The Half Sloper

The half sloper shown in *Figure 12.1: Half-Sloper Antenna* on page 45 is an antenna that is hard to categorize, since it is not a sloping dipole and it is not a vertical. The half sloper is half of a sloping dipole. To make one of these antennas, cut a quarter-wave radiator by dividing 234 by the frequency in MHz and tie an insulator to both ends. One insulator is tied near the top of a tower and the radiator wire is run down toward the ground. Coax is split into its center conductor and shield, and it connects across the insulator at the tower. The center conductor of the coax is tied to the quarter wave radiator and the shield is grounded to the tower. This means the tower is acting as the missing half of the dipole. It is a difficult antenna to get a good match because the height above ground of the feed-point and the angle of the slope affect the impedance. Some users of this antenna say to mount the feed-point at 45 feet up on the tower and have a beam antenna on the tower above the feed-point to use as a counterpoise. Other users say you must find the 50-ohm point on the tower, which is a tedious task. It has also been said, “Some installations work super, while others do not work well at all.” The half-sloper is used almost exclusively on 80 and 160 meters. The Alpha-Delta half sloper was tried here and its performance was disappointing. The signal from it was down a least 10 dB below a dipole and the SWR wasnt low enough. The half sloper is mostly vertically polarized and it is directional toward the slope.

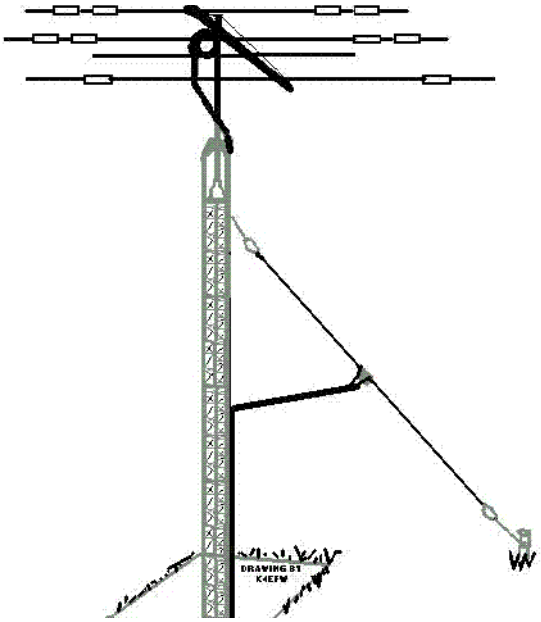

Figure 12.1: Half-Sloper Antenna

13.
Vertical Antennas

13.1 Why Verticals Are Used

Vertical antennas have the radiator mounted at right angles to the earth. The vertical is used whenever you desire to radiate your signals in all directions at a low angle. Low angle radiation is needed to work DX effectively. Radio waves traveling to the ionosphere where they are reflected need to hit the ionosphere at a point near the horizon in order to reflect farther around the curvature of the earth. In order to get a dipole to radiate a strong signal at low angles, it has to be more than a wavelength above ground. A low dipole is not particularly a good DX antenna for 80 and 160 meters. However, the average dipole at modest heights will outperform any ground-mounted vertical having a poor ground system. Vertical antennas work very well at low frequencies such as the broadcast band, but the ground losses increase as we move higher and higher in frequency (Refer to *Section 5.2 Ground-Wave Propagation* concerning ground-wave propagation). It is very difficult to get a good ground for a ground-mounted vertical unless you live next to salt water. Vertical antennas, because they are unbalanced antennas, do not need baluns. They are normally fed with coax.

If a ground mounted, quarter-wave vertical is all you can put up at your location (QTH), then use it. However, it will be a mistake to put up this antenna if you are not be able to have a ground radial system and are able to put up a dipole. Most ground mounted quarter-wave verticals manufactured today are trapped in order to work multiple bands.

The ground-mounted vertical also needs to be put out in the clear away from RF absorbing objects. These facts do not apply to half-wave verticals, which are in themselves different animals, nor do they apply to high quarter-wave verticals using elevated radials.

The approximate length of a full-sized resonant quarter wave vertical can be found by dividing 234 by the frequency in MHz. Note: 234 is half of 468, the number we used to calculate the length of a half-wave antenna. The actual length for resonance may be a little different from what you calculate, because of the diameter of the vertical element. Trapped verticals are physically short of a quarter wave in length because the traps load them. The vertical is fed at one end at the bottom where it is insulated from the ground. The center conductor of the coax connects to the vertical element and the shield is connected to the ground system.

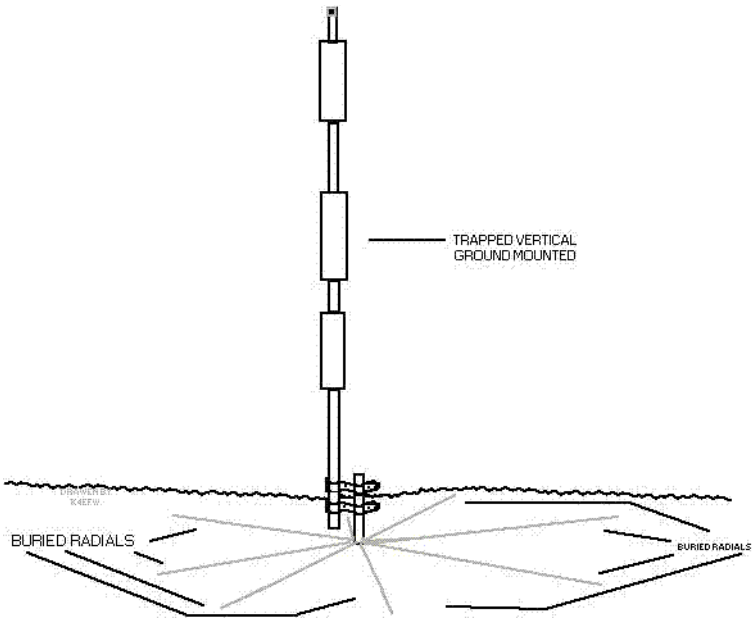

Figure 13.1: Ground Mounted Trapped Vertical

13.2 Disadvantages of Using Quarter-Wave Verticals

The most obvious disadvantage of using any vertical antenna is on 80 meters it has less than optimum high-angle radiation needed to work stations within a few hundred miles. Ground-mounted quarter-wave verticals use a ground system for the other half of the antenna and the ground system losses can be very high. The ground wave signal should eventually radiate in space at angles at the horizon, but since there are very high losses in the ground wave at amateur frequencies, a ground-mounted vertical has almost no signal down near the horizon. At angles below 10 degrees, the signal will be greatly attenuated.

A ground-mounted quarter-wave vertical with an ideal ground should have an impedance of 35 ohms resistive. If you were to measure its impedance, and it measures 60 ohms resistive on an antenna analyzer, it means it has a loss resistance of 25 ohms. Moreover, that loss resistance is mostly in the ground system. Under these conditions, only 58 percent of the power will radiate as RF, although you will have a 1.3:1 SWR. 42 percent of the power will be turned into heat by the loss resistance. With the feed-point being at ground level, some more loss comes from the radiated wave being absorbed by power lines, trees, and buildings with its associated wiring. That loss does not show up in antenna analyzer measurements.

The best ground system for a ground-mounted vertical is 120 wires, called “radials,“ radiating from the feed-point like the spokes of a wheel. These radials need to be a quarter wave long. At the feed-point, the radials are bonded together and are fed from the shield side of a coax cable. Not many amateurs have the resources to build such a ground system. Many short radials will be more effective than a few long ones. When using a ground mounted vertical, many hams drive an 8-ft. ground rod into the earth for their ground system. The ground losses are very high in that case. Using a ground rod for the ground system of a vertical antenna confirms the old adage: “Verticals radiate poorly in all directions.”

To eliminate ground losses, you can use an elevated quarter-wave vertical with an elevated ground system called a “ground plane.” The ground plane vertical, as it is called, needs to be mounted high enough to prevent the return path from coming back through the earth ground. Ground plane verticals need to be mounted above nearby objects that absorb RF. They will be nearly 100% efficient if they are high enough. The ground plane consists of two or more radials, but most ground planes have three or four. The ground plane radials do not have to be resonant, but should be at least a quarter wave long. An elevated ground-plane vertical will be more effective for working DX than a dipole.

13.3 Long and Short Verticals

Verticals can be less than a quarter wave in length. They can be loaded by coils or linear loading sections or a short vertical can be fed directly with a tuning unit at the feed-point. The loss resistance in a short vertical may be appreciable. Since the radiation resistance is very low at the feed-point of a short vertical, the current at the feed-point will be very high. The more current that flows into loss resistance, the higher the loss will be. Any coils used in the tuning unit and for loading should be made of as heavy a conductor as possible, since these can cause appreciable loss when the current is high. This is also true for the ground system. The loss described here is called “I squared R loss”, which means the loss in watts is found by multiplying the current times itself and then multiplying that answer by the loss resistance. That means if the current into a lossy antenna system is doubled, the power lost in watts is increased four times. Making a vertical very short and tuning it to resonance with an inductor will also result in an antenna with a very narrow bandwidth.

A more subtle loss of energy in very short vertical antennas is coronal discharge from the tip end of the vertical. Corona occurs when the voltage is very high at the end and electrons flow out into the air. This can be visible at night if the transmitter power is high and you are at a high altitude. Power is lost from the antenna when corona is produced because corona is a form of light and light is another form of energy.

In 1973 while we were working for radio station WWNC in Asheville, North Carolina, a trapped vertical for 10 through 80 meters was erected. The length of the antenna was only about 25 feet. A loading coil near the top made it resonant on 75 meters. The ground system was the metal body of a 75-foot long mobile home. Fair reports were received from this set-up. The reports were not bad because of our having a good ground. One night, while working 75 meter SSB, one of the neighbors came over and said, “You’re tearing up my TV.” Checking all of the inside connections proved they were tight. Our wife keyed up the transmitter while we made a trip to the antenna to check the connection there. Before arriving there, looking up, we saw blue fire coming off the end of the vertical. The corona was responsible for the television interference (TVI). It was visible because Asheville is at a relatively high altitude and the transmitter was running 700 watts. An inverted-V was put up, the TVI disappeared, and better signal reports were received.

You can realize up to a 1.5 dBd gain from a vertical antenna by making it longer than a quarter wave, but there is a limit to how long to make it and still get low angle radiation. That limit is 5/8th-wave. To find the length of a 5/8th-wave vertical, divide 585 by the frequency in MHz. For example, to calculate the length of a 5/8th-wave vertical for 20 meters (14.000 MHz) divide 585 by 14.0. It equals 41.786 feet or approximately 41 feet 9.5 inches. A tuning unit will be needed at the feed-point of this antenna, as the impedance of a 5/8th-wave antenna is

low and high current will flow into it. A tuning unit will usually have enough bandwidth to cover the entire band on each band of 20 meters and higher. A tuning unit is also called a matching network. It is similar to an antenna tuner, but has fixed inductors and capacitors. Tuning units for 80-and 160-meter verticals will cover only a portion of the bands. Outside the bandwidth limits of the tuning unit, you can use the tuner at the transmitter end. Radials or ground planes are needed for a 5/8th-wave vertical and they need to be a quarter wave long.

The impedance of a half-wave antenna is high if fed at its end. An end-fed half-wave vertical will have a small amount of gain over a quarter-wave vertical. This antenna does not have the ground losses a quarter-wave vertical has because it is fed at a high impedance point and the current flowing into the ground is negligible. Commercially made resonant half-wave trapped verticals now on the market are end fed at the bottom. A built-in matching network is found at the base, and several very short radials are mounted below the feed-point to de-couple RF from the feed-line. These antennas should be mounted as high as possible away from RF absorbing objects. Because the ground losses are lower, the half-wave vertical will outperform a quarter-wave vertical by several dB and in many cases many dB.

13.4 Unscientific Observations of Verticals

At our home, an old Hy-Gain trapped quarter-wave vertical for 40-10 meters was erected in 1961. It was mounted on the roof and had two quarter-wave radials for each band. It worked, but it was never compared to another antenna. It gave the impression it was a mediocre antenna. Other antennas replaced it.

One time in 1964, a grounded 60-ft tower was shunt fed as a vertical on 75 meters. Without having any radials, the transmitted signal was 10 dB weaker on this vertical 650 miles away in New York than on the inverted-V.

In 1969, a 4-band trapped vertical was put up on the top of a 60-ft tower. A 15-meter 4-element yagi under it was used for the ground plane. It was probably the best vertical installation we ever tried. It was good because it was high and in the clear and the 15-meter yagi made a good ground plane.

While we are on 80 meters, a ham 200 miles away frequently joins in the roundtable. He uses a trapped quarter wave vertical with a chain link fence as the ground. Several of the others are also 200 miles away run the same power. His signal is 10 to 20 dB below everyone elses on the frequency. It is good there are no interfering signals or noise or he will not be copied.

Another ham uses a Hy-Gain Hy Tower vertical with 3 ground rods as the ground system. According to our S-meter, his signal is 40 dB down below those of the other guys.

Charlie, AD5TH, works 40 meters using a Hustler 5-BTV vertical ground mounted with 72 quarter-wave radials. He has an outstanding signal for a ground-mounted vertical. His installation is out in the clear away from RF absorbing objects. He says, because of antenna restrictions at his location, it is the only antenna he can put up.

Another ham friend, N2HGL, has both a dipole and a half-wave trapped vertical on 40 meters. At a location 160 miles away, he is 10 dB stronger on the dipole, but he is equal in strength on both antennas in Indiana 600 miles away. This comparison shows the superiority of the half

wave vertical over the quarter-wave one because his signal with the half-wave vertical was equal to his signal from the dipole. If he were using a quarter wave vertical, we would expect his signal would be better on the dipole in Indiana. It also demonstrates the superiority of a dipole over a vertical for working short distances.

Bill, W4ZQL, runs a ground-mounted SteppIR vertical. He lives beside a salt-water river in Florida that he uses for a ground. He puts out a very good signal on 40 meters. No ground losses!

13.5 The Inverted-L Vertical

The inverted-L antenna is a wire vertical antenna with part of the top end bent horizontally. It resembles an “L” turned upside down. The inverted-L is used to reduce the height required by a vertical and still keep the antenna resonant and full sized. It is fed at the end at ground level the same way a ground mounted vertical is fed, and all the losses we described for a ground-mounted vertical apply here. Some current flows in the horizontal part of the inverted-L and for that reason, it has both strong vertical and weaker horizontal polarization. If you make it a half-wave antenna, you wont need a good ground because negligible current flows into the ground. A half-wave inverted-L antenna needs to be fed with 50-ohm coax and a tuning unit.

An inverted L for 160 meters is usually made of wire one-quarter wavelength long or about 127 feet. It runs vertically from near ground level to the top of a support, perhaps 60 or 70 feet. Then the end runs horizontally and is tied to a nearby support. The antenna is coax fed at ground level between the vertical section and ground system across some type of insulator. A matching network at the feed-poimt will be required to match it if the impedance is not equal to 50 ohms.

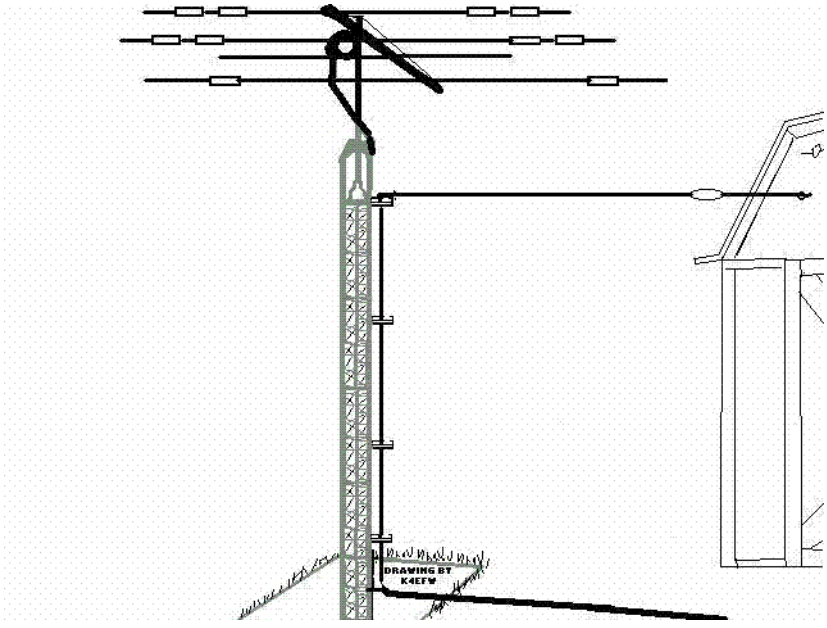

Figure 13.2: Inverted-L

The picture shows an inverted-L running up the side of a tower. The feed-point is at ground level with the center conductor of the coax attached to the bottom end of the wire. The coax shield connects to a ground system of radials. The total length of wire used in this antenna is half of what is needed for a dipole since the other half of the antenna is the radial ground system. The inverted-L is used mostly on 160 meters, but some have built them for 80 meters. The inverted-L antenna can also be cut for a half-wave to reduce ground losses.

13.6 Vertical Mobile Antennas

We have heard many good signals from mobiles, many being stronger than those from hams using ground mounted quarter-wave verticals. The mobile antenna, being so short, has a large capacitive reactance. A coil is inserted in the antenna to provide an equal amount of inductive reactance to make it resonant. As we said in the paragraph on short verticals, a coil of this type, carrying a large amount of antenna current, causes some loss resistance in the system. To reduce losses in the coil, wind it with a conductor as large as practical. (Thats exactly what some mobile antenna manufacturers have done.) The sources of loss in mobile antennas are in the coil losses, losses in the conductors making up the radiating part of the antenna, corona discharge, and the ground loss from the vehicle on which its mounted. However, because of the large amount of metal in the body of the vehicle, the ground losses are not as high as the losses from ordinary ground mounted verticals. Matching transformers are now available that step down the impedance of 50-ohm coax to the very low impedance of the loaded vertical. Good advice is to use the transformers rather than to rely on the internal tuner of the transceiver.

Some low priced single-band mobile antennas are constructed by using a polymer shaft and a small gauge wire encapsulated in polymer material running beside the shaft. The loading coil made of the same wire is also encapsulated in the polymer. The small wire, because of its size and because it carries a large RF current, will lose a lot of power by becoming hot. This type of mobile antenna is rated for 200 watts. If the wire didnt get hot, there would be no power limit.

All mobile antennas have corona loss and for such, there is no remedy. Most amateurs, because they cant see it, dont believe its there. Corona will not be visible unless you run high power and it is dark.

Ground losses from the vehicles body diminish with increasing vehicle size. This is why 18-wheeler hams have such big mobile signals. To diminish the ground losses on any mobile installation, you should use as large as a conductor as possible to bond the coax shield to the vehicle body. All metal parts of the vehicles body, fame, and drive system need to be bonded together with heavy ground straps. To make the mobile antenna system more efficient, use an antenna with an adjustable inductor and use as long a “stinger” as practical above the coil. You will increase the radiation resistance by using a longer stinger, and then the loss will be less because you will require less coil inductance. The ratio of radiation resistance to loss resistance becomes larger by raising the radiation resistance and reducing the loss resistance. As we said earlier, the efficiency of any antenna system is found from the ratio of radiation resistance to total resistance, or radiation resistance divided by total resistance times 100%. The total resistance is equal to all the loss resistances plus the radiation resistance.

The latest development in HF mobile antennas is motor driven variable inductors. These antennas are known as “screwdriver antennas.” The name refers to the electric screwdriver

motors used to vary the inductance. A control cable is run from the motor to a switch at the operators position so it can be tuned from the operators seat in the front of the vehicle. Because a mobile antenna has a very narrow bandwidth, you will have to tune it often as you move frequency (QSY). It hasnt been many years since we had to get out of the vehicle to make inductor changes or make changes in the length of the stinger when the frequency was changed.

Mobile antennas for 20 through 10 meters do not require the care in installation that is needed for 160, 80, and 40 meters because the length of a mobile antenna becomes closer to a quarter wave as you move to higher bands. The radiation resistance increases on each higher band. While moving to higher bands, less inductance is needed to tune the antenna, and that lowers the loss resistance. A 96-inch mobile whip is just a couple of inches short of being a quarter wavelength on 10 meters and a loading coil is not needed there. The band that has the least mobile antenna efficiency is 160 meters. If you reach a radiation efficiency of 2% on 160 meters on your mobile installation, you will be doing well.

Below is some information concerning mobile antennas, which was received in an email. There was a 75-meter mobile “shoot-out” in California. (A shoot-out is an event where a group of hams gets together and compares signals radiated from various antennas.) Supposedly, equal power was applied to each antenna under test. Apparently, some type of field strength meter was used. A screwdriver antenna and a bug catcher, both with top hats, were used as the standard by which other antennas were compared because they put out equal signals. The other antennas are measured in how many dB they were below the standard. Here are the results of that test, and because it is hearsay, the accuracy of these figures is not guaranteed, but they do compare to what we have observed.

Table 13.1: Antenna Shoot Out Results

Screwdriver/bug catcher with top hats	0 dB reference
Screwdriver/bugcatcher without top hats	-3dB -50%
Hustler	-7 dB -80%
Outbacker	-9 dB -88%
Hamstick	-12 dB -94%
Whip with autotuner	-14 dB -96%.

The efficiency of the best 75-meter mobile antenna is from 5% to 10%. In using the best mobile antenna on 75 meters, a 100-Watt mobile rig will radiate 10 Watts at most. This means that a Hamstick being fed with 100 Watts will radiate only 0.6 watts, which is 6% of 10 Watts. Ninety-nine and four tenths Watts will be converted to heat. The person sending this information said it was published on the Internet in some news group. Again with good band conditions, it is amazing how little signal can be used to communicate.

The things that increase the efficiency of mobile antennas are:

- Place the loading coil about half way from the feed-point to the antenna tip. Efficiency decreases if you put the coil above or below this point
- Mount the antenna as high up on the vehicle as possible. This reduces the ground losses because it reduces the capacitance of the antenna to ground
- Use a loading coil with a Q as high as possible. See the ARRL Handbook for a discussion of coil Q
- Make the antenna as long as possible. Note: long antennas are prone to strike tree limbs and bridge overpasses
- Increase the size of the mast between the loading coil and feed-point
- Put a capacity hat above the loading coil. The capacity hat reduces the number of coil turns needed to resonate the antenna
- Make the coil with as large a diameter wire possible. This decreases the coil loss, which is a large part of the total loss of a mobile antenna.

Any changes made in the antenna system that raises the radiation resistance will increase the efficiency

14.
One-Wavelength Single Loop Antennas

14.1 The Horizontally Oriented Loop

To calculate the length in feet of any one-wavelength loop, divide 1005 by the frequency in MHz. Horizontally oriented one-wavelength loop antennas have become very popular on 160, 80, and 40 meters and it is one type of NVIS antenna. (NVIS stands for “near vertical incidence skywave” because of its high angle radiation pattern.) It is claimed by its users that the loop antenna is quieter than other antennas. This is because it doesnt pick up the noise from power lines, thunderstorms, etc., coming in at low angles. These antennas radiate on their fundamental frequencies with a broad pattern straight up to put a strong signal for nearby contacts. Recently published articles on this type of antenna have called them “cloud warmers.” There are other types of antennas called NVIS antennas other than loops. They are dipoles at low heights or dipoles with parasitic reflectors placed under them to cause the signal to radiate mostly straight up. The NVIS antennas have an advantage in working nearby stations because you dont get the static noise and interference from far distances. They are definitely not DX antennas. An article on NVIS antennas appears in the December 2005 QST.

On their fundamental frequencies, horizontally oriented loops take up half the horizontal distance as a half wave antenna for that band. Loops are two-dimensional antennas having depth as well as breadth. There are two loop configurations: The square loop and the triangle loop. Some hams have pulled the loops out in irregular shapes to fit where the supports are located. The only advantage in using a rectangular loop instead of a square loop is to take up less horizontal space. This is true because the gain of a rectangular loop is diminished below a square loop. The area enclosed by the perimeter of the loop determines the gain of a loop. A circular loop has the most enclosed area, but it requires an infinite number of supports. The gain of a loop comes from the loop having two maximum current points separated by a distance of one-quarter wavelength. From here on we will call a horizontally oriented loop a horizontal loop.

We also modeled the gain of the horizontal loop for the 80-meter band over real ground. The maximum gain occurs with the loop at 7 meters or about 25 feet above ground. Mind you, this gain is straight up from the loop. At that height, its gain is about 9.25 dBi and that equates to about 7 dBd in free space. The gain of the loop diminishes slightly as the antenna is raised.

The feed-point radiation resistance at 7 meters height is 35 ohms resistive and 0.0 ohms reactance and you do not need a matching section of 70-ohm coax. At a height of 10 meters or about 33 feet, the radiation resistance rises to 63.5 ohms. There the SWR will be 1.27:1, if it is fed directly with 50-ohm coax. At 15 meters or about 50 feet, the radiation resistance rises to 118 ohms and a 70-ohm matching section will be in order. The gain drops to a little less than 7 dBi at that height. These figures may or may not be applicable to your QTH, because your soil conductivity may be different from the soil we used to model it. As you can see from the above numbers, the feed-point resistance rises as the loop is raised.

The horizontal loops also are used on their harmonic frequencies. The loop with more gain and a superior pattern is a two-wavelength loop. An 80-meter loop is a two-wavelength loop on 40 meters. The two-wavelength loop has a lower angle of radiation, but is a very large antenna for 80 meters. At 3800 kHz it has a perimeter of about 530 feet. A two-wavelength loop is not an NVIS antenna. Using coax with a tuner is not an ideal way for working a loop on its harmonic frequencies. This is because of the high SWR in the coax on some bands will cause high loss. For example, an 80-meter loop fed on 40 meters will have an SWR of 8:1 and the SWR on 20 meters will be 49.5:1. There will be some hams who will say they get satisfactory results this way, however theory suggests they will have a stronger signal if they use a ladder-line because ladder-line has less loss. Feeding a loop antenna with ladder-line makes more sense when working a loop on harmonic frequencies.

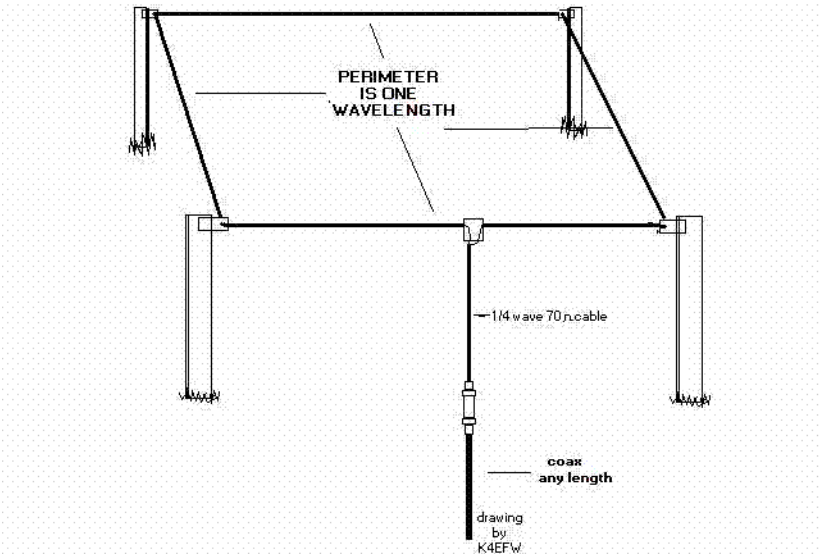

Figure 14.1: One Wavelength Horizontal Loop

To realize maximum gain, make the square and triangle have equal sides. When the sides are equal, the loop has maximum enclosed area for whatever configuration you use. Other shapes will work, but the gain will suffer.

To support a square loop, you will need four supports, one for each corner. We hope you will have trees or masts in the right places. A triangular loop will need three supports. Once you have cut the single piece of wire to the right length, run the wire through as many insulators as you have corners. At each corner of the loop, put an insulator and tie the corner to a support with a rope from the insulator. To make the feed-point, connect both ends of the loop to an insulator. Strip the insulation from the outer part of the coax. Separate the shield from the

center conductor. The ends of the coax are connected to the ends of the loop across the insulator. Most hams do not feed loops with a balun at the feed-point.

14.2 The Vertically Oriented Single Loop for 40 and 80 Meters

Vertically oriented loops radiate broadside to the plane of the loop. A horizontally polarized vertically oriented loop has both vertical and horizontal wires. From here on out, we will refer to a vertically oriented loop as just a vertical loop. When using this term, we are not referring to its polarization. If the feed-point is on one of the horizontal wires, the loop radiates horizontally polarized waves. The vertical wires radiate weaker vertically polarized waves. If the feed-point is on one of the vertical wires, vertically polarized waves will be radiated. The radiation from a one-wavelength vertical loop has both high-angle and low-angle radiation. It is a good antenna for both nearby stations and for DX contacts. It is better than a dipole for DX because the vertical loop puts out a stronger low angle signal than a dipole does.

The gain of a vertical delta loop is 4.55 dBi or about 2.4 dBd. Its feed-point impedance is about 120.5 ohms. The square vertical loop has 5-dBi gain and about 2.85 dBd and the feed-point resistance is 143 ohms. They both need to be fed with a series quarter-wave matching section of 70-ohm coax.

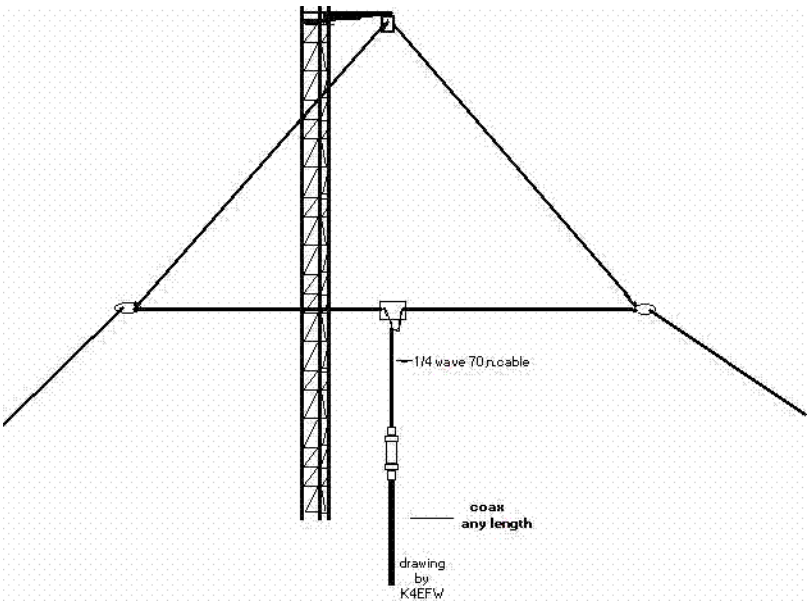

Figure 14.2: One Wavelength Horizontal LoopSingle-Element Vertical Delta Loop

Square vertical loops need two supports. The square vertical loop needs less vertical space than the delta loop. The vertical space needed for a square vertical loop for 80 meters is 92 feet. For 40 meters the vertical space is half that. It is rare to find someone using the square vertical loop these days. The vertical delta loop is more common because it needs only one high support. The apex of a delta loop for 3500 kHz needs to be 102 feet high and on 40 meters, it needs to be 62 feet. This assumes the bottom horizontal wire will be 20 feet off the ground. In order to make a vertical loop fit on a shorter support, the sides of the loop can be

reduced in length while making the horizontal wires longer. This will put the two maximum current points closer together, which has the effect of reducing the gain.

Like the horizontal loop, the formulas for finding the length in feet of these loops are the same: 1005 divided by frequency in MHz. In addition, because the feed-point resistance is nearly the same as horizontal loops, quarter-wave matching sections and other methods can be used to feed the vertical loops. The vertical loop is not as sensitive to height as the horizontal loop. Both vertical square loops and vertical delta loops can be operated on harmonically related bands. (See *Figure 14.4: Radiation Pattern of a 30-meter Delta Loop on 15 Meters* on page 58).

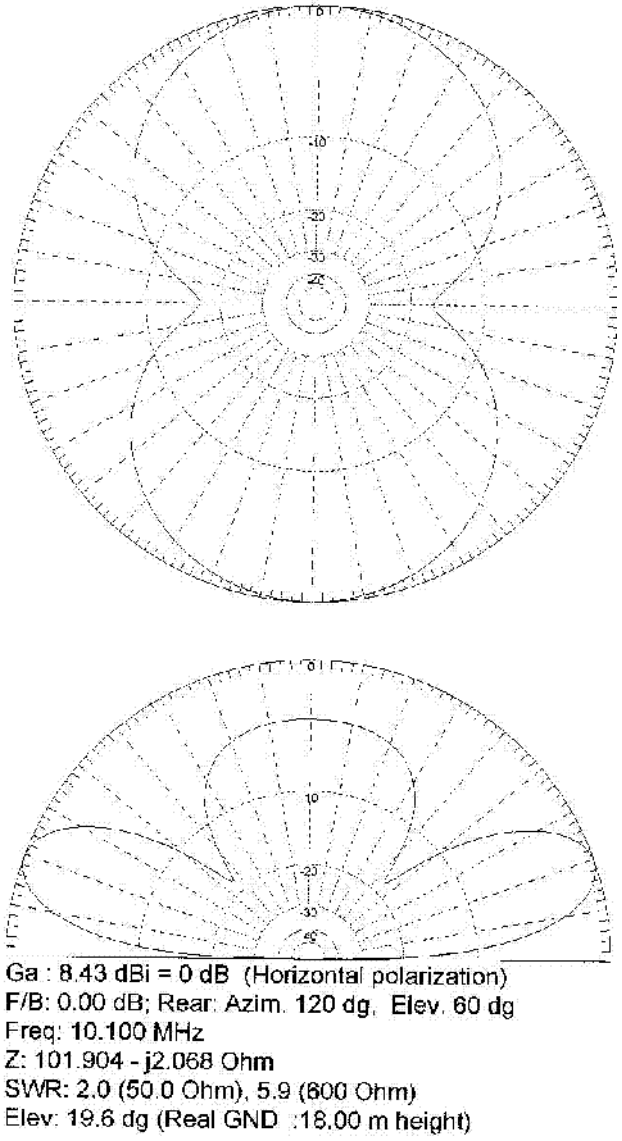

Figure 14.3: Radiation Pattern of a 30-Meter Delta Loop on 30 Meters

The Bottom Wire is at 18 Meters above Ground.

The horizontal pattern shown above demonstrates that the 30-meter delta loop has a bi-lobal pattern broadside to the plane of the loop. The vertical pattern below the horizontal pattern shows both high angle and low angle radiation. The angle of maximum radiation is at 35 degrees above the horizon. The angle of radiation straight up is only down about 1.5 dB. This is pattern demonstrates the vertical delta loop is good for both nearby stations as well as DX.

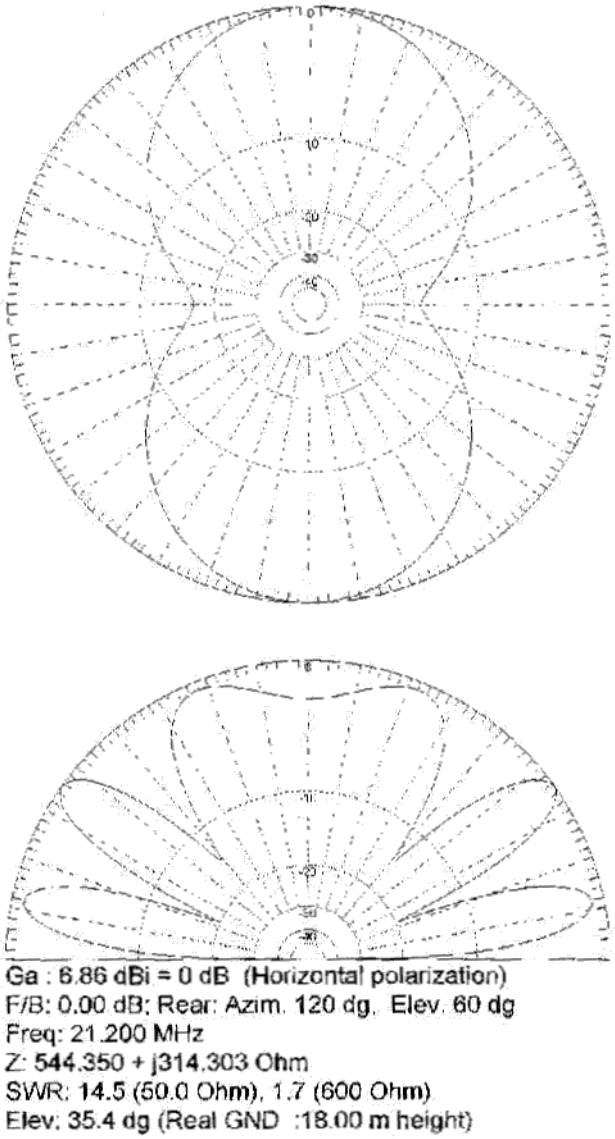

Figure 14.4: Radiation Pattern of a 30-meter Delta Loop on 15 Meters

15. Directional Beam Antennas

15.1 The Monoband Yagi

Between 1926 to 1929, Shintaro Uda and Hidetsugu Yagi developed a beam antenna that had sharp directivity and high gain. Later, work was done primarily by Mr. Yagi and yagi was the name given to the antenna until finally recognition was given to Mr. Uda. Its proper name is the Yagi-Uda Array. Most hams call it a beam.

A monoband yagi is the name given to a yagi for a single band. The performance of any commercially made monoband yagi is touted to have its dimensions tuned for maximum performance. As you will see later, this is not always the case. Monoband yagis being sold today are much improved over older designs because of computer modeling programs available.

The yagi is made of two or more aluminum elements mounted on and perpendicular to a boom. Hams use antenna rotors to turn the antenna in the direction of the station they want to work. However, there are wire beams, fixed in one direction, mainly on 80 meters, suspended between trees or other supports. Most high frequency beam antennas used by hams are in the horizontally polarized configuration, which means the elements are parallel to the ground. CB beam antennas and some 2-meter beams are vertically polarized with the elements at right angles to the ground (See *Section 3. Polarization Of Electromagnetic Waves* on page 5).

A 2-element yagi has a gain around 3 to 4 dBd. A two-element yagi will have a driven element with either a reflector or a director. The driven element is the only element receiving power directly from the transmitter. The reflector and directors are called parasitic elements because they receive power from the driven element by inductive coupling.

The 3-element yagi will have a gain of approximately 5 to 7 dBd or 7 to 9 dBi depending on its boom length. A three-element yagi has one reflector, one driven element, and one director. Because the yagi has a low radiation resistance, a matching system is located at the driven element feed-point. The ratio of the radiation off the front compared to the radiation off the back is called front-to-back ratio. Front-to-back ratio and forward gain are factors to be

considered in choosing a yagi design. Both measurements are given in dB. All yagis have a good front-to-side ratio, with the signal off the side being 50 dB below the front.

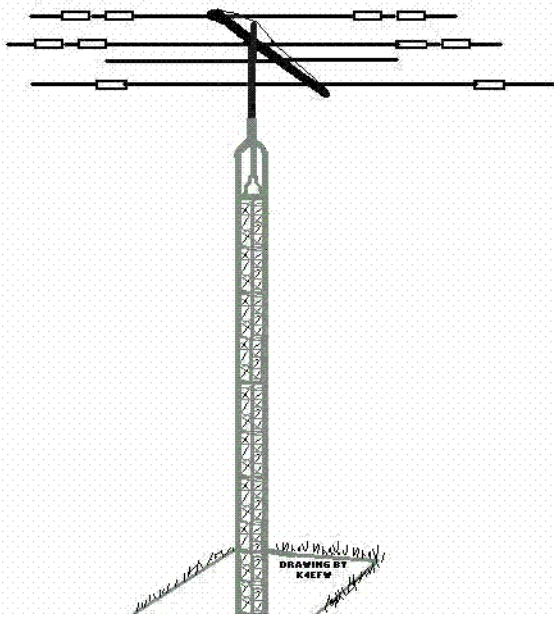

Figure 15.1: 3-Element Yagi

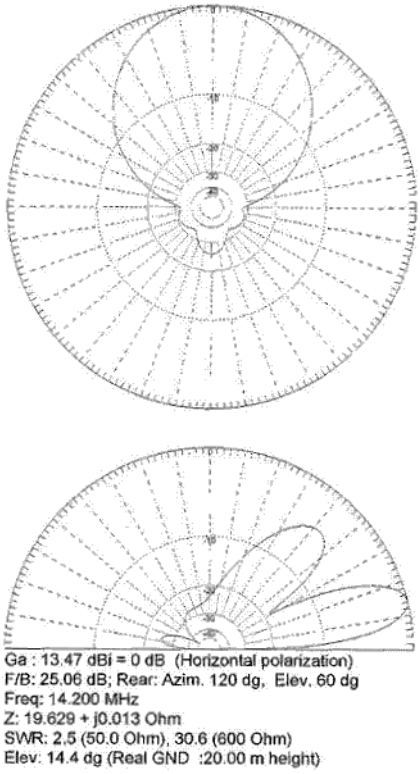

Figure 15.2: 3-Element Yagi Radiation Pattern

The reflector of a yagi is about 5% longer than the driven element. The reflector, being longer, will have inductive reactance. The inductive reactance shifts the phase of the re-radiated wave, which radiates and combines with the driven elements wave and reinforces it in the direction away from the reflector toward the driven element. A director is about 5% shorter than the driven element. The director, being shorter, has capacitive reactance, and this changes the phase of the reradiated wave to reinforce the wave away from the driven element opposite the reflector.

The gain of a yagi is derived from radiation being concentrated in one direction at the expense of the other directions. One hundred watts fed into a yagi with a gain of 6 dBd will have an apparent power of 400 Watts in the main lobe. Because one hundred watts put into a yagi radiates only one hundred Watts, and because that one hundred Watts of power is concentrated in the main lobe, it is equal to the power from a dipole being fed with 400 Watts. This is referred to as effective radiated power or ERP, but a yagi is not any more efficient than other antennas. Because of the Principal of Reciprocity, an antenna having a 6 dBd gain on transmitting will also have a 6 dBd gain on receiving.

Adding more directors and increasing the boom length will increase the gain of a yagi.

The front-to-back ratio ranges from 18 dB for a 2-element yagi to over 25 dB for a multi-element yagi, provided the parasitic elements are carefully tuned. The gain of a yagi is generally proportional to the boom length and not necessarily the number of elements. Doubling the boom length, while keeping the proper number of elements for that boom length, will add about three more dB of gain.

Tuning the yagi for maximum gain makes the bandwidth very narrow, and it will have a poor front-to-back ratio. For these reasons, we dont recommend tuning a yagi for maximum gain, because you will only increase the gain by a fraction of a dB at the expense of front-to-back and feed-point impedance. Tuning the yagi for maximum front-to-back will help eliminate interference coming from the rear of the antenna. The building of any yagi involves compromise spacing and element tuning.

As you make the yagi larger by adding directors, the main radiation lobe becomes narrower increasing the gain and ERP. The gain of a yagi with four elements is about 7 to 8 dBd. You used to see 3 or 4 element yagis advertised claiming a gain of more than 10 dB, but they never said if that gain was referenced to an isotropic or a dipole. That gain also involves the gain derived from signals reflected from the ground adding to the direct wave. A more realistic gain figure is the “free space gain.” Some companies, who sell monoband yagis, inflate their gain figures. Beware! Increased spacing of the elements will increase the gain of a yagi up to a point. Increasing the spacing past that point will reduce the gain. The spacing of a reflector or director needs to be in a range of 0.1 to 0.3 wavelengths. With a 3-element yagi maximum gain occurs with both parasitic elements spaced at about a quarter wavelength. Second and third directors can have wider spacing.

Most hams do not build yagis but buy them from the many companies who sell them. Ham catalogs are full of pre-cut and tuned yagis that come in boxes ready to be assembled in the back yard. Many of these are very good. However, there is a lot of satisfaction to be gained from building your own.

In 1971, we purchased, a 15-meter monobander being sold by a reputable company. Its performance was disappointing. It had only a 10-dB front-to-back ratio. That design is no longer being sold. After reading some books, we readjusted the antenna elements to some new dimensions and it performed much better. This was the beginning of our yagi building.

During the last nearly 50 years, we built many yagis. During the period of 1979 until 1986, many multi-element yagis were constructed, gain measured, formulas derived for spacing and element length, and the radiation patterns plotted on graphs. In 1986, a computer program titled *Yagi* by Dean Straw, N6BV, was bought. From that point on, that program was used to design and set the element lengths to their proper values. Not much difference in performance of the new designs was seen over what was previously used, but tuning parasitic elements and running back and forth to the field strength meter was eliminated. There are many better computer programs available today for designing yagis and other antennas.

The largest yagis we built were a 4 element 20-meter yagi on a 38-foot boom, a 5 element 15 meter one on a 27-foot boom, and a 5 element 10 meter beam on a 24-foot boom. These are modest designs compared to some of the big antennas used by contest stations. All these yagis were stacked one above the other on a 20-foot mast coming out of the top of the tower. The 20 meter one was on the bottom, next came the 15-meter, and the 10-meter yagi was on top. This method of stacking yagis for different bands one above the other makes what is called a "Christmas tree array." These antennas worked well. Since retiring and moving back home, we use pre-tuned directional antennas because of the lack of a good place for an antenna range. Climbing is not now an option because of age and infirmity.

If you make the reflector 5% longer than the driven element and the director 5% shorter than the driven element, you will be pretty much in the ballpark. The beautiful part about a yagi is it will work reasonably well with the element lengths only in the ballpark. By carefully tuning, you will get a fraction of a dB more gain or a few more dB front-to-back, because the spacing and diameter of parasitic elements affect the length required for those elements. A yagi can be tuned for maximum forward gain, maximum front-to-back ratio, or best impedance, but you can achieve only one of these conditions at a time. Element tuning, at best, is a compromise.

Most hams who are yagi builders do not tune their antennas at all, but use published dimensions for building them. Yagi builders who do tune, tune for either gain or front-to-back and then match the driven element with a gamma match, hairpin match, a series-resonant coax matching section, or a step down balun. The feed-point of a properly tuned yagi is close to 25 ohms.

Formulas for calculating yagi element lengths will not be given in this book. Because yagi elements are made from telescoping aluminum tubing, the elements will be tapered. The diameter of the elements and the taper determine the lengths required for tuning of the elements. A tapered element will resonate higher in frequency than one not tapered. The formula to calculate the length of the tapered elements is complicated, but there are computer programs to do that.

15.2 Trapped Multi-Band Yagis

Some yagis have traps in the elements to make them into a multi-band beam. Many of these commercially made antennas are available at ham radio stores or directly from the

manufacturers. In a 3-element, 3-band design, the spacing on the booms is a compromise. A 3-band beam is known as a "tribander." The spacing is close on 20 meters, optimum on 15 meters, and wide on 10 meters. You cannot tune the trapped elements for maximum performance on three bands simultaneously and have a good match on all those bands. Since a good match is important to most hams, gain and front-to-back ratio are sacrificed for a good match on triband beams

The inductors in the traps load the elements in triband beams. Therefore, the elements are shorter than the elements of a 20-meter monobander. Regardless of the compromised design, a triband-trapped beam is much better for working DX than a dipole. Many hams have achieved working over 300 entities with tribanders having short booms.

The radiation pattern from a yagi is at a lower angle than a dipole. This gives the impression a yagi has much more gain than it does. A dipole has unity gain, but that gain will be at a higher angle. The dipole puts out a weaker signal at the low angles needed to work DX, and a yagi puts a strong signal at low angles. In comparing a dipole to a yagi, the yagi may only have a 4 dBd gain in its major lobe. The gain of the yagi at a low angle may be 10 dB or so better than a dipole at that same lower angle. The gain of any antenna is always measured in its major lobe, irrespective of where the angle ar which the maximum radiation lobe occurs.

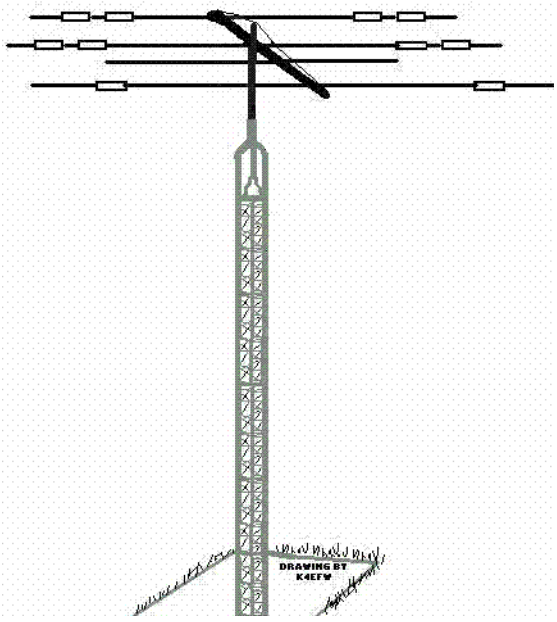

Figure 15.3: Trapped 3-Element Yagi

Figure 15.3: Trapped 3-Element Yagi shows two sets of traps in two of the elements and one set in the rear element. The front element is the director with traps for 10, 15, and 20 meters (it takes two sets of traps to make the elements work three bands). Directly behind it is the driven element with traps also for 10, 15, and 20 meters. The rear element is trapped for 15 and 20 meters (a single set of traps makes it work two bands). The entire lengths of the three longest elements are resonant on 20 meters. The short element is a reflector for 10 meters. Only the part of the antenna between the 10-meter reflector and the front director is used on 10 meters. The maximum signal is radiated in a direction coming out of the page toward you. Mosely

builds trapped antennas that have two traps in one enclosure and you can not determine the bands from the traps as you can on Hy-Gain and Cushcraft beams.

Some triband beam models as the one above are built with longer booms so they would have more gain on 20 meters, a good match on all bands, and optimum 3-band performance. They achieve this by interlacing extra monoband reflectors and directors on the boom placed between the 20-meter elements as is done with the antenna in *Figure 15.3: Trapped 3-Element Yagi* on page 63. The extra elements have no effect on 20 meters or any band for which they are not resonant. Some amateurs mistakenly think the extra elements work on all bands, but they dont. The Cushcraft A-4 shown is not a beam with four working elements on any band. The old Hy-Gain TH6DXX and Mosley Classic 36 had six elements on the boom. They both had three trapped elements and three monoband elements. They had three working elements on 20 meters, three on 15 meters, and four elements on 10 meters. The trapped reflector worked on 15 and 20-meters. The trapped driven element worked on all three bands. The trapped director worked on 10 and 20 meters. On the boom was a resonant reflector for 10 meters and one each resonant directors for 10 and 15-meters. When using one of them, we have often heard amateurs saying they were using a six-element beam. This gave the other station the mistaken idea they were working someone with an antenna with six working elements. Other beam antennas interlace additional elements of different lengths to make the tribander into a 5-bander covering 20, 17, 15, 12, and 10 meters. Hy-Gain makes a 5-band yagi for 20 through 10 meters that has 11 trapped and monoband elements. It is the Hy-Gain TH-11. Mosely makes a 6-bander that includes two elements for 40 meters. It is the Pro-67.

In order to achieve better SWR curves over a wide bandwidth, some triband yagis have two driven elements spaced 3 to 5 feet apart. The front driven element is shorter than the rear driven element. Both driven elements are trapped. This double driven element scheme is called a log-cell. A log cell, by itself, has a small gain and may slightly increase the overall gain of the tribander. The KLM KT-34 and the HY-Gain TH-7 are examples of this kind of antenna.

Is a monobander better than a tribander? We dont know if our tests can be duplicated and no one else has ever said he has actually compared the two antennas. It is “common knowledge” that traps have loss. Therefore, the ham fraternity believes a monobander has to be better. From the tests we performed here, we believe it is a myth a monobander is significantly better than a tribander having an equal boom-length. We believe the traps do not have enough loss to make enough difference to matter. However, monobanders having very long booms and many directors will outperform any tribander.

Having two towers, both having the same height and being 100 feet apart, made it possible for us to do the experiment described here. The result is useful information because it was made in a real world situation that would be comparable to the average hams location. Both antenna element lengths were set to Hy- Gain specifications. The constants were terrain, antenna height, antenna boom length, frequency, coax length, and power level. The only variable in the tests was the two antennas being tested. The test was performed to see how much loss antenna traps have. Had there been more than one variable, the tests would not have been valid, because in any scientific experiment, the test is valid only when one variable is being tested. In addition, more than one test has to be made in order to average out the collected data errors. In this case, many tests were made.

On one tower was a 20-meter four-element Hy-Gain 204-BA monobander with a boom-length of 26 feet. This antenna is arguably not one of the best monobanders made, but it is what we had and it was about the same size as our tribander. On the other tower was a trapped 6-element Hy-Gain TH-6 DXX tribander having a 24-foot boom. The entire tribander boom-length was used on 20 meters, so both boom-lengths were comparable.

The transmitted signal strength of the two antennas was compared on 20-meters. This test involved many DX stations and one local amateur 5 miles away. With both antennas pointing toward the receiving station, a carrier power of 10 watts was fed from the transmitter, and held constant while the antennas were "hot" switched several times. (The power level was unimportant as long as it was held constant on both antennas). None of the many DX stations involved in this test could see any difference in either antenna, and, yes, their analog meters could discern a difference of one dB. These tests by themselves were not conclusive because of the possibility of fading signals (QSB). A second series of tests was performed with a local ham when 20 meters was dead. Testing with him was done to eliminate QSB from spoiling the results. He could also measure no difference on his S-meter. He could also see a one-dB difference on his analog S-meter. As a third series of tests, the antennas were switched while we looked at the signals on the S-meter from distant stations and the local station. No differences in received signals were noted. Maybe the difference was a monobander has only a few tenths of a dB less loss, such a small amount of difference no one was able to see it on receiver S-meters. Certainly, the difference in the two antennas was less than one dB.

Conclusion: The Hy Gain TH6DXX and the 204-BA antennas perform equally well on 20 meters at a height of 56 feet.

15.3 The SteppIR Antenna

The latest developments in yagi designs are found in the ones being sold by SteppIR Antennas. There are two, three, and four element versions. All these versions are frequency agile and cover continuously from 13.5 to 54 MHz. The MonstIR adds three very long elements for 6.9 to 13.5 MHz. The elements are made of fiberglass tubes with beryllium-copper ribbons inside. Each element has stepping motors to wind and unwind the copper ribbons to change their lengths inside the tubes. A multi-wire control cable connecting the control box to the stepping motors accomplishes this. The proper element lengths for all frequencies in its range have been calculated by a computer and stored in the control boxs computer. As you move from frequency to frequency, the control box in the shack readjusts each element length. Thus, the antenna is configured into a properly tuned monobander for any frequency in its range. These antennas are expensive, but the hams who own them say they are worth the money.

15.4 The Log-Periodic Array

Another beam antenna that looks like a yagi is the log-periodic antenna. It is configured using many elements with each element being shorter than the one behind it. This means the longest element is at the rear of the array and the shortest element is at the front. All elements are divided in the center and insulated from the boom, and all elements are driven. On both sides of the insulator at the center of each element, wires run from the front element of the array to the rear element. Each wire criss-crosses the other ones but they do not touch. That makes a 180-degree phase reversal from one element to the next one behind it. The feed-point is across

the insulator at the shortest element. The feed-point impedance is about 200 ohms and a 4:1 balun is used to feed it.

The advantage of the log-periodic antenna is, it that it is very broad banded and it can cover all frequencies with an SWR below 2:1in its design frequency range. The disadvantage is the gain of a log-periodic antenna is lower than a yagi with an equal boom length. There are designs being sold today that cover continuously from 14 to 30 MHz. In Fort Gordon, Georgia, there used to be a monster log-periodic at the MARS station that covered from 2 to 30 MHz. The boom length was 120 feet and the antenna was rotatable.

15.5 Directional Cubical Quad and Delta Loop Antennas

We built a number of quads at various times and with them on the test stand and with the bottom wire a foot or so above the ground, worked many DX stations. When we built yagis and they were on the same test stand nine feet above the ground, we could hardly get a signal out of the back yard. Since the vertical beam-width of a quad is narrower than a yagi and the radiation angle is lower, the quad will work better at low heights. Because of its lower angle radiation, many quad users claim a quad “opens and closes” the band.

The two-element cubical quad is a square-or diamond-shaped loop antenna that has a second loop acting as a parasitic element. The quad configuration has all loops in the vertically oriented plane as *Figure 15.3: Trapped 3-Element Yagi* on page 63 demonstrates. Feeding it in one of the horizontal wires results in horizontal polarization, and feeding it in one of the vertical wires makes it vertically polarized. Every two-element quad being sold today uses a reflector for the parasitic element, although it is possible for it to have a director. The theory of operation is the same as that of a yagi.

Some quad builders believe a diamond-shaped quad has more gain than a square-shaped one. Their logic is that since the maximum current points of both wires are spaced farther apart than with a square quad, the increased spacing of the current points should produce higher gain. To find out if this was true, we built both a diamond-shaped and a square-shaped quad for two meters. Using a commercial field-strength meter connected to a receiving antenna, we fed equal amounts of power to both antennas and measured the radiated field in each ones major lobe. Field strength measurements were made a few wavelengths away and many wavelengths away from the quads. No difference in the radiated field of either could be found.

According to Bill Orr in his book about cubical quads, a two-element cubical quad is equal to a pair of 2-element beams; one is stacked over the other a quarter-wavelength. The ends of the beams bottom driven element are bent up and the top element has its ends bent down where the ends of the top and bottom elements are joined together on the side. When they are joined, this forms the square we call a quad. The bottom element is then feeding the top element from its ends. The parasitic elements have the same configuration except the wire loop has the ends bonded together to form a continuous square.

There are multi-element quad designs that use one or more parasitic directors in addition to the reflector. Adding a director will lower the feed point impedance. The wire of the reflector is about 3% longer than the driven element, and each director has about 3% less wire than the driven element. Adding directors to a two-element quad makes the horizontal beam width narrower, producing more gain.

Another quad design "the delta loop" uses triangular-shaped driven elements. One or more triangular-shaped parasitic elements make the antenna complete. Theoretically, the delta loop antenna will have slightly less gain than the cubical quad, because there is less enclosed area in the triangular loop. We believe that there are no instruments available to hams to be able to measure the difference.

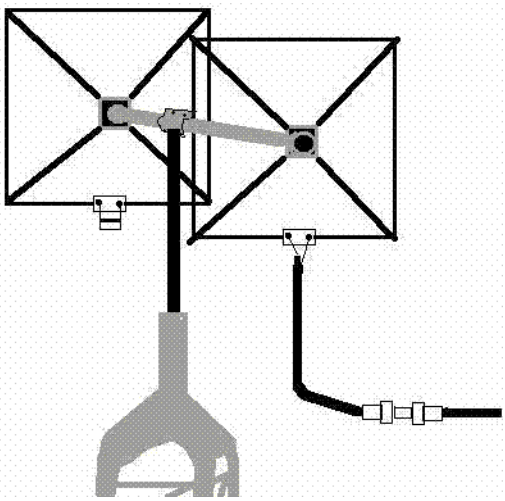

Figure 15.4: Single Band Cubical Quad

Most cubical quad and delta loop antennas that can be rotated are used on 20 meters and higher. A few ambitious hams have built rotatable quads for 40 meters. Others have made 80-meter quads, supported between trees, fixed in one direction.

In order to make the quad smaller, adding loading coils or linear loading sections in its wires has been suggested, but that will defeat the purpose of using a quad. Because the quads gain is produced by the enclosed area inside the loop, reducing the enclosed area will result in less gain.

The wires for quads for 20 through 10 meters are strung around the perimeter of an "X shaped frame made of fiberglass poles or bamboo. Each element has its own X-shaped frame. A smaller X-shaped metal structure, called a "spider," attaches the poles to the boom. The poles are referred to as "spreaders." The four spreaders attached to the spider form the "X." The "X" can be rotated 45 degrees on the boom to form a diamond-shaped quad instead of a square quad. A few have tried with limited success to make the spreaders out of PVC or aluminum.

A wire is attached near the ends of the spreaders to form a loop around them. The two ends of the wire are connected to an insulator to attach the feed-line as is done on a dipole. The quad loop has a theoretical feed-point impedance of 100 ohms. To match it, you can use a quarter-wave matching section of 70-ohm coax, a gamma-match, or a 2:1 balun. More on this is in another paragraph. The delta loop is made much the same way, but it requires only three spreaders to form an equilateral triangular loop. It is matched the same way since the feed-point impedance is about the same.

The reflector and director are formed the same way as the driven element except the two ends are shorted together to form a continuous loop. In order to get maximum performance from a

quad you need to tune the reflector for either maximum gain or best front-to-back ratio. For tuning purposes, the wire of the reflector is cut a little shorter than calculated and the ends of the loop are connected to an insulator. A shorted stub, consisting of two parallel wires, is connected to the loop ends and hangs down from the insulator. Another wire is shorted across the two parallel stub wires. The shorting wire is moved up and down the stub to tune the reflector. The stub is a means of adjusting the total length of the reflector. See *Figure 15.4: Single Band Cubical Quad* on page 67. A field strength meter is needed to do this and you need a large area and two people. The field strength meter needs to be placed several wavelengths away from the antenna. Low power is fed into the antenna while it is tuned. One person tunes the reflector while the other person reads the field strength meter. Tuning the reflector involves tuning the stub for minimum signal off the back. Once the shorting wire has found its proper position, it is soldered in place. Quads made by the formulas work satisfactorily without tuning. Tuning for maximum front-to-back ratio instead of maximum gain will do more for the performance of the quad.

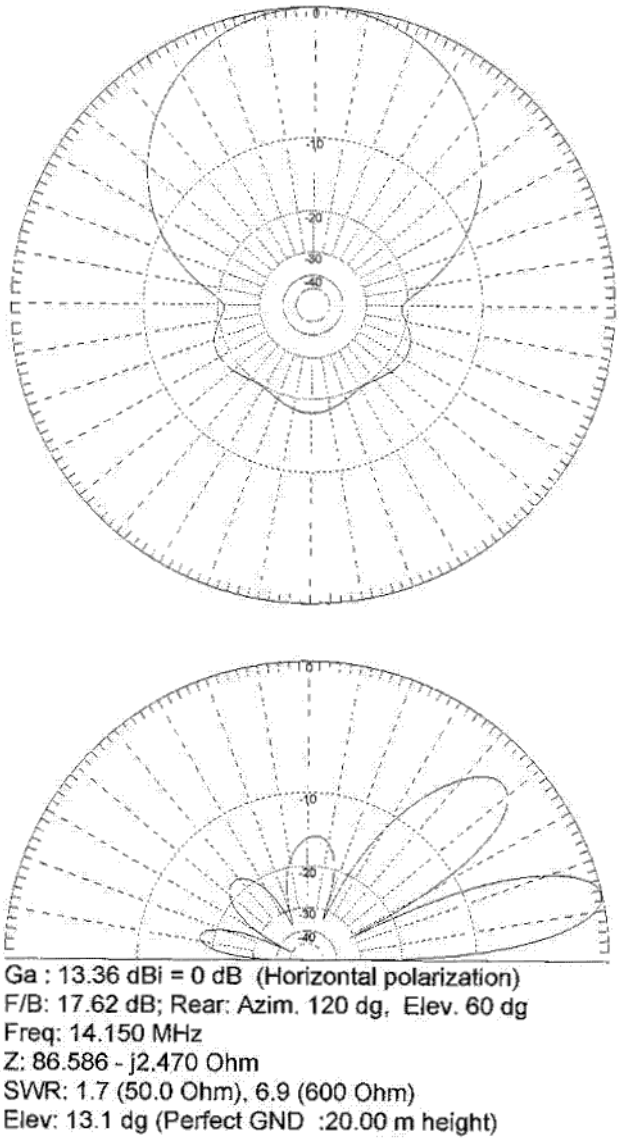

Figure 15.5: Radiation Pattern of a Two Element Cubical Quad at 65 Feet

Some believe you cannot stack another antenna above a quad. They assume that because the quad has both vertical parts of the loop, a metal vertical mast will couple to the vertical part and detune the quad. We believe a vertical mast will have to be resonant at the operating frequency to detune a quad. Using MMANA, the quad was modeled with a metal vertical mast going through the plane of the quad. The only difference observed was that the resonant frequency was changed by a couple of kHz. The gain and front-to-back remained the same.

The gain of a two-element quad is nearly the same as an average 3-element yagi. The best part of the gain of a quad is the vertical beam width, or H-plane of the major lobe logically should be narrower due to it being equal to two stacked beams. For this reason, the 2-element quad has a lower angle of radiation. A horizontally polarized quad should have a slight advantage over a yagi. A lower angle is better for working DX. While operating using both quads and yagis, we have noticed that the horizontal beam width or E-plane of a quads pattern is wider than a 3-element yagi. We believe the horizontal beam-width of the quad is the same as a two-element yagi. This is why the 2-element quad is not as directional as a 3-element yagi.

Modeling our 2-element quad in free space on 20 meters, we found its gain to be 5.49 dBd. The boom-length of the quad is 8 feet. A three-element yagi with a boom-length of 16 feet will have 6.4-dBd free- space gain on 20 meters. The free-space gain of a 20-meter optimum spaced monoband yagi on a 25-foot boom will only have slightly more gain.

The compromise spacing for a 2-element multi-band quad for 20 through 10 meters is 8 feet. This spacing is 0.115 wavelength on 20 meters, 0.175 wavelengths on 15 meters, and 0.23 wavelengths on 10 meters. These spacings are within acceptable limits. For a single-band 20-meter quad, space the elements 12 feet apart. If you want to build a 12 and 17-meter dual band quad, the spacing will be 8 feet, the same as it should be for 15 meters. Eight feet is also a satisfactory spacing for a 10-meter quad, but it can be as close as four feet.

With smaller perimeter requirements, loops for the higher bands can be strung inside and parallel to the lower band loops to make a multi-band quad. It is easier to make a multi-band quad than a multi-band yagi. Quad kits for triband and 5-band quads are available. These kits cost less than a multi-band beam.

In the construction of most quads, an insulator is put in the bottom horizontal part of the wire on the driven element so it can be fed like a dipole. A 2-to-1-balun transformer will match the feed-point to 50-ohms, then you can tie all the feed-points of a multi-band quad together. The Lightning Bolt Antennas 32MCQ/WB quad feeds five loops this way and the SWR is 1.4:1 or less on all five bands. The person manufacturing the Lightning Bolt quad went out of business on December 12, 2005.

With other more complicated schemes, each quad loop is fed separately, and each loop uses a 70-ohm odd multiple of a quarter-wave series matching section placed between the 50-ohm coax and the feed-point. Used this way, the quarter-wave matching section will match 50 ohms to 100 ohms. A remote antenna switch will have to be mounted close to the feed-point to select the desired loop. Other builders use a separate gamma-match on each driven element to get a perfect match to a 50-ohm coax but this method would also require a remote antenna switch. Without the switch, several pieces of coax, one for each band, would have to be run into the shack.

If you are going to build a monoband quad, you need to use the following formulas to cut the wire loops to these approximate lengths:

- For the driven element, you divide 1005 by the frequency in MHz.
- For the reflector, you divide 1030 by the frequency in MHz.
- For the director, you divide 968 by the frequency in MHz.
- Make any additional directors the same length as the first one

These formulas were derived experimentally from tests run here. The exact measurements will be determined by the element spacing, but the lengths cut by these formulas will be very close for any reasonable spacing.

After giving you the advantages of a quad, here are the disadvantages: The two-element quad for 20 meters is large vertically and horizontally. When the 20-meter quad is on the ground, the boom is 8 feet high and most people arent tall enough to maneuver it by holding the boom. Some quads, which are made from lightweight materials, are flimsy, and they will suffer during wind and ice storms. The best-constructed quads have their spreaders made of heavy fiberglass. Those quads, although they are heavier, stand up well under adverse weather conditions. The Lightning Bolt quad used here has stood up very well during three ice storms in the past two winters.

Here is some information we discovered after originally writing this book. The MMANA antenna-modeling program does not perform very well when modeling a quad. On 20 meters, the modeling program says the front-to-back ratio of our quad is at a maximum at 14525 kHz, but actually, it occurs at 14050 kHz. The measurements of actual front-to-back were made using a field strength meter. We reduced the power levels off the front to give the same field strength reading we got off the back. The front-to-back ratio in dB was calculated from the two power levels. What was interesting was the maximum front-to-back ratio occurs at a single discrete frequency and the front-to back deteriorates somewhat on either side of that frequency. While looking at the radiated field off the front, the field strength does not vary one dB across the whole band. Maximum gain and maximum front-to-back was very close to the same frequency. Not having tested them in this way, we believe yagi beams perform the same way regarding front-to-back ratio and gain. In working stations, the gain is the important parameter. Front to-back ratio is important in reducing interfering signals from behind the antenna. We decided to tune our quad for maximum front-to-back rather than for maximum gain. The next step is to lower the quad and carefully tune the reflector for each band. After running tests to determine the frequency where maximum front-to-back occurs, we found the maximum measured front-to-back ratio was 22 to 23 dB.

Good news! After writing the above paragraph, we lowered the multi-band quad and reduced the reflector element lengths on the two-element Lightning-Bolt Quad. The original reflector lengths were too long according to the field strength readings we made. The formulas that were originally used to cut the reflector lengths were anywhere from 1029 to 1036 divided by the frequency in MHz. We derived from field-strength measurements that the maximum front-to-back ratio occurred when the reflector length was cut by dividing 1022 by the frequency in MHz. While searching the Internet, we discovered EI7BA in Ireland used 1019 divided by the frequency on his multi-band quad. We decided to use his formula and we could lengthen the reflector by adjusting the stubs if necessary. After cutting the reflectors to the new dimensions, we made new field strength readings. The front-to-back ratio occurred near the

frequency of our calculations. In addition, the frequency of maximum field strength from the front also occurred inside each band. As an example, today we were listening to GD4PTV on the Isle of Man on 17 meters. On the front of the quad, he was S7. With the quad 180 degrees from him, he was inaudible. We also found that other stations were down by at least six S-units off the back. Originally, stations off the back of the quad were down only two S-units.

Several months later it was discovered that a multi-band quad tunes differently from a single-band quad because the interlaced elements react to detune each other. That may be the reason we found the reflectors of a multi-band quad needed to be different lengths than the 1030/frequency formula.

Here are some words of wisdom about using a field-strength meter in trying to tune a quad:

Tuning the quad reflector stubs can give you misleading data. If you look only for the minimum signal from the back of the quad, that may not be the point of best front-to-back because you may have detuned the quad so that the signal from the front may have also deteriorated.

Using a field strength meter, keep the receiving antenna as short as possible to prevent the receiving antenna from being nearly resonant. Certain receiving antenna lengths seem to be frequency sensitive, that is, as you change frequency toward the receiving antennas resonant point, the field strength meter will give a false higher reading. The only problem with using a very short receiving antenna is the meter may not have enough sensitivity to make measurements from the back of the antenna.

It will be impossible to achieve a high front-to-back ratio on certain bands on a multiband-quad because the reflector wires for adjacent bands affect the tuning by interacting with each other. When the Lightning Bolt Quad was designed, we are not certain which parameter was used in its design (gain, SWR, or front-to-back). From the field strength readings made with that design, it was impossible to draw any conclusions. If you are going to build a quad, what we said about designing a yagi is also is true for the quad: you can tune for best gain, best front-to-back, or best impedance match. You cannot tune for more than one of these parameters at a time. To tune a quad for maximum gain is relatively easy using a short antenna on the field-strength meter.

While we were trying to measure the frequency of the highest forward gain on 17 meters, we found the maximum field strength occurred at the high end of the band on one receiving antenna. Subsequently, it was strongest on the low end of the band on another receiving antenna having a different length. No changes had been made to the dimensions of the quad in either case. Trying to move the frequency of the maximum field to the middle of the band, we adjusted the length of the reflector stubs and it made no difference to the frequency where the maximum field occurred. What caused the error was we were trying to measure the field strength 100 feet in front of the quad. The long receiving antenna connected to the field strength meter was acting like a parasitic element and was not accurately measuring the signal being radiated from the quad.

15.6 The Quagi

A variation of the quad and the yagi is a marriage of the quad and the yagi called the quagi. The quagi has a quad driven element, quad reflector, and yagi directors. Hams who have built the quagi report the yagi directors work better than quad directors, but we have never compared the two types of directors.

At one time we converted a 2-meter yagi to a quagi and compared the field strength readings from both configurations. By changing the driven element and reflector to quad loops, we measured a signal increase of 1.8 dB. We also experimented to see what effect the quad reflector had on the signal. While using the quad driven element we changed the reflector back to a yagi reflector. What was surprising to us was the configuration of the reflector had no affect on the radiated signal. Only by changing the driven element from a yagi element to a quad element made any change in the field strength. All these field strength readings were made using a commercially manufactured field strength meter. To insure our readings were valid, the power being fed to the antenna was measured and kept constant.

16.
Gain Versus Front-to-Back

As we have said before the front-to-back ratio of a multi-band cubical quad can be maximized by careful tuning to achieve about 18 to 20 decibels front-to-back ratio. A properly designed yagi can achieve a front-to back ratio of better than thirty decibels. A two-element quad has about the same gain as a three-element yagi. You can tune a yagi or quad to either maximum front-to-back or maximum gain. You can also tune them to compromise settings somewhere in between. The question arises as to which maximum should either antenna be tuned? It is our opinion that either antenna should be tuned for maximum front-to-back ratio. In that case the maximum gain will be deteriorated by only a fraction of a decibel Let us explain why we reached that conclusion with an example.

Today we were on 17 meters to work VP8TD on Pitcairn Island in the South Pacific Ocean. He is a visitor to the island and will be there for about two more months as of this writing. A resident of the island, VP6TC, Tom Christian hasnt been heard from in months. I suspect he is getting elderly and doesnt get on much anymore. Anyway VP6TD had an enormous pileup going. We were using a three-element SteppIR yagi up sixty-five feet on our tower. Also, the amplifier puts out about 1490 watts on 17 meters. We make up for a lack of antenna forward gain with the amplifier. We worked him with one call through the pileup. The SteppIR replaced the two-element Lightning Bolt Quad about 10 months ago. When VP6TD answered us I could hear him over the pileup. From the rear of the antenna were several very loud Italian hams calling him, one of which continued to call even when VP6TD answered someone. The Italians were 180 degrees from the front of our antenna, or directly off the back of where we were beaming. Because of the superior front-to-back of the yagi, I could hear the Pitcairn Island station over the Italians. Had we been using the quad, the Italians would have been at least 10 dB louder and we could have found it impossible to make the contact.

Today, we were in contact with N4XPZ, Joe, on 75 meters while several more hams were talking about the VP6TD on 17 meters last evening. Joe said he tried to work the VP6TD station using a single wire antenna. He complained he could not copy the VP6 because of the Italians who continued to call even when the VP6 answered someone. That illustrated the point we are making in this section. The old adage is true: “You can’t work ‘em if you can’t hear ‘em!”

17.
Feed-Lines Commonly Called Transmission Lines

Always use the best feed-line you can afford. Resist the urge to be penny wise and pound-foolish. This is particularly true of coax. Better (less lossy) coax will cost more. This cable is carrying your precious RF signal to and from your antenna.

The most common feed lines used by amateurs are 50-ohm coaxial cables. There are many types of 50-ohm coax such as RG-174, RG-58, RG8-X, RG-8, RG-213, RG-8 foam, and 9913. In this book we will only discuss these types. A suffix letter such as an “A” or “U” may be attached to the “RG” numbers such as RG-8U or RG-58A. All these cables have a center conductor surrounded by a plastic insulating material, called the dielectric, and a copper braided shield covering it. There is a plastic covering on the outside of the shield to protect the conductors from water. The center conductor and the shield carry RF currents.

These are the common 50-ohm cables:

- RG-174 has a very small diameter, 0.101 inches. This cable is used to carry small amounts of RF between circuits in equipment. RG-174 has the highest loss and the least power handling capability of any coax. It is useless as an antenna feed-line because of its loss and low power handling ability.
- RG-58 is larger coax having a diameter of 0.195 inches. It can handle low power and can be used on the lower bands to feed antennas a one hundred feet or so away. It is not recommended to use RG-58 on 10 meters because it has a loss of 3dB per hundred feet on that band and half your power will be lost in the coax.
- The next larger cable is RG-8X, sometimes referred to as mini-8. Its diameter is 0.242 inches. The dielectric surrounding the center conductor is foam rather than the solid dielectric used in the most coax. Making cables with foam insulation can reduce the loss. Some hams are successfully feeding a kilowatt of power into RG8-X on the lower bands. You will lose 2 dB of power by using one hundred feet of RG-8X on 10 meters. On 80-meters the loss of this cable is negligible.

You will want to use RG-8 or RG-213 if you are planning to use a kilowatt or more of power from 160 to 10 meters or for short runs on VHF and UHF. RG-213 is RG-8 made to military

standards. Both have diameters of 0.405 inches. This cable has lower loss and can handle higher power because it has larger conductors and a larger diameter dielectric. RG-8 can handle 4000 watts peak envelope power on the broadcast band. RG-8 has only about 1dB loss on 10 meters per 100 feet. The loss becomes greater and the power handling rating of any coax decreases as the frequency of RF is increased.

There is a lower-loss version of RG-8. It is called RG-8 foam. Beldens number for this product is 8214. Because of the dielectric being foam, a larger center conductor has to be used to keep the impedance 50 ohms. The loss resistance of the larger conductor is less than the smaller conductor used in regular RG-8. In addition, the foam having many air pockets has less dielectric losses. Other manufacturers also make RG-8 foam. One hundred feet of RG-8 foam has a loss of 0.9 dB on 10 meters. Many amateurs will not use RG-8 foam because they mistakenly believe the foam will soak up water. Cut off a piece of this foam material and put it into a container of water. It will continue to float ad infinitum, because it doesnt soak up water. Most of the water seen in coax gets between the dielectric and the plastic outer covering and within the braid shield. Water has also gotten into the strands of the center conductor. Water will get into any coax if the ends are not properly sealed.

Solid conductors have less loss at radio frequencies compared to stranded conductors. Braid has more loss than a solid conductor used for the coax shield. A much lower loss coax, especially for higher frequencies, is available. The Belden 9913 is this product. This coax has a solid center conductor and the shield consists of a coating of aluminum foil covered with braid. The aluminum foil is a solid conductor. The braid over the foil is used to make a good solder connection because you cant solder aluminum. The mostly air dielectric material used in this product requires the center conductor to be larger to make the impedance 50 ohms. Air dielectric also has less dielectric loss than solid. There are a few manufacturers making 9913 look-alike products. One hundred feet of 9913 will have a loss of about 0.66 dB on 10 meters. There is a coax that looks like 9913 but has a stranded center conductor to make it flexible. It has a little more loss. If you are going to use 9913 on an antenna that rotates, flexing the cable as the antenna turns will cause the center conductor to break. Run the 9913 to the top of the mast, and using a barrel connector, connect the 9913 to a short run of RG-8. Run the RG-8 across the rotor to the antenna.

Coax cables of other impedances are available such as 70-ohm cable. RG-59 and RG-11 are common 70 ohm cable. Hams, except to make quarter wave matching sections, do not use these cables much anymore. There are many other types of cable other than the ones described here.

Open wire feeders, ladder-line, or window-line have much lower loss than coax. The three types are essentially the same except for the method of insulating the two wires from each other. When making open wire feed-line, you should use solid conductors, as large a conductor as possible, and as little dielectric as possible. These factors make open wire have less loss. There is so-called ladder-line for sale, which is really window line, which is made with 16 gauge solid conductors. The solid conductors make for low loss. There is another grade of the same feed-line that has 14 gauge-stranded conductors.

18.
Antenna Safety

18.1 Erecting Antennas on Masts

Erecting antennas pose some danger especially if they encounter power lines. Never erect an antenna near a power line. Make sure to leave enough clearance so if the antenna supporting structures fall they will clear the power lines. There are many cases of metal masts being raised accidentally encountering power lines, electrocuting the person or persons raising the masts. To raise a mast can expose you to a large force called leverage, which appears to increase the weight of the mast. Exerting oneself to raise a heavy mast can result in painful muscle and back injuries. Never try to raise a mast without sufficient help.

18.2 Tower Safety

A tower is a wonderful device for supporting wire and beam antennas, but a person who has never put up one should seek advice of people who have experience in erecting towers. The obvious danger is falling off the tower. It should never be climbed without a climbing belt. Most people falling off a tower do so because of some kind of equipment failure or the tower collapses because of overload.

In erecting a tower, a gin pole strong enough to support the weight of the tower section being raised should be used. Do not use improvised gin poles, as the strength of them may not support the weight of the tower section and the force from the other end of the rope being pulled by the ground crew. To hold a 50-pound tower section stationary requires a hundred pounds of force, which is the weight of the tower section and 50 pounds of force of the ground crew. The ground crew must exert more than 50 pounds of force to cause the section to be raised. There would be no greater tragedy than the gin pole breaking dropping the tower section on the ground crew. Then there is the possibility of the person on the tower being knocked loose by the falling, broken gin pole.

Another problem can arise if under-sized guy cables and clamps are used to support the tower. We have seen tower failure when guy cables broke in a windstorm, or an insufficient number of clamps holding the guy cable allowed the cable to pull through the clamps. Professional

tower people do not use cable clamps. They use “preformed tie-wraps” that grip the guy cables tighter as the force in the guy cables increases. Preformed tie-wraps are available from Texas Towers. Never tie the ground end of a guy cable to a tree. A tree swaying in a heavy windstorm can put enough force on the cable to cause it to break or to pull the tower over. Screw-in anchors available from mobile home suppliers make adequate anchors. Do not anchor a guy cable where a tree can fall across the guy cable. This could break the guy cable and cause the tower to fall. Never place a tower near a house, where if it falls, it could hit the house. Remember *Safety First!*

These lengths are for coax having a solid dielectric with a velocity factor of 0.66 and foam dielectric with a velocity factor of 0.78. , You can use odd multiples like 3, 5, 7, etc. of the lengths below if those lengths are too short for your installation

Table 18.1: Quarter Wave Matching Sections of 70-ohm Coax

		Foam dielectric cable
160 meters	85ft 6in	106ft 4in
80 Meters	43ft 4in	51ft 9 in
40 Meters	22ft 6in	27ft 6 in
30 Meters	16ft 0in	19ft 6 in
20 Meters	11ft 5in	13ft 10 in
17 Meters	8ft 11 in	10ft 9 in
15 Meters	7ft 7 in	8ft 4 in
12 Meters	6ft 6in	8 ft 0in
10 Meters	5ft 8 3/8 in	6ft 11 in

Questions? Email Jim Abercrombie *n4ja@prtcnet.com*.

Hamuniverse.com is Powered by Ham Radio!
© 2000 - 2008 N4UJW Hamuniverse.com or article author! - All Rights Reserved.

$14

More Wire Antenna Classics

Volume 2

More of the best articles from ARRL publications

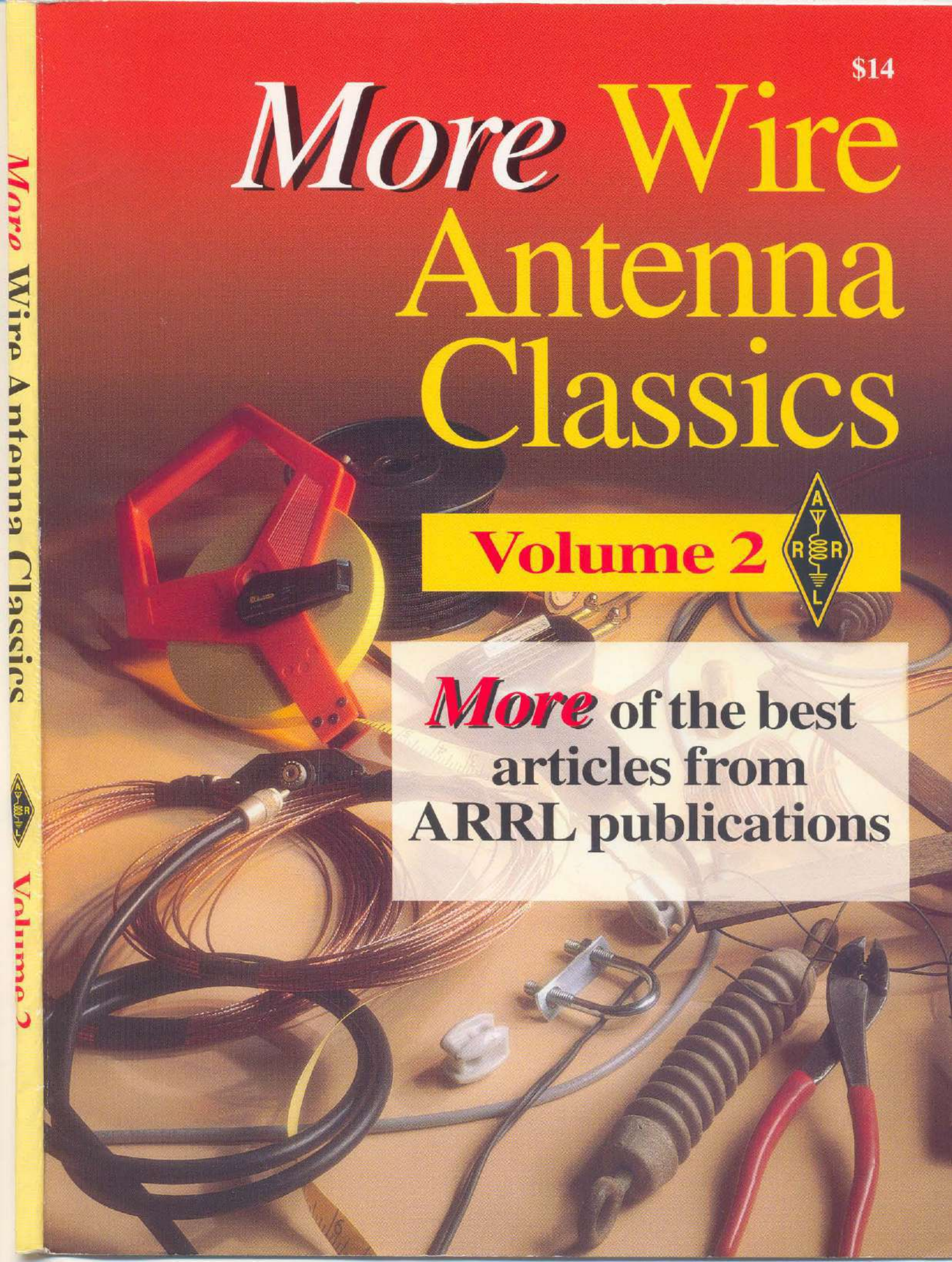

More Wire Antenna Classics Volume 2

More Wire Antenna Classics

Volume 2

Compiled by Chuck Hutchinson, K8CH

Production:
Paul Lappen

Cover Design:
Sue Fagan

Published by:

ARRL *The national association for AMATEUR RADIO*

225 Main Street
Newington, CT 06111-1494

Contents

1 Dipoles

2 Off-Center-Fed Dipoles

3 Multiband Antennas

4 Loop Antennas

5 Collinear Antennas

6 Wire Beams

7 Vertically Polarized

8 Receiving Antennas

9 Miscellanea

CHAPTER ONE

DIPOLES

1-1 **An Inverted V for Field Day**
From June 1968 *QST*

1-4 **E-Z-Up Antenna for 75 and 40**
From October 1961 *QST*

1-6 **A Zip-Cord Special Antenna**
From May 1972 *QST* (Hints & Kinks)

1-7 **Zip-Cord Special Antennas–Do They Work?**
From March 1979 *QST*

1-9 **Piggyback Antenna for the Ten-Meter Band**
From April 1973 *QST* (Hints & Kinks)

1-10 **RFD-1 and RFD-2: Resonant Feed Line Dipoles**
From August 1991 *QST*

1-14 **Off-Center-Loaded Dipole Antennas**
From September 1974 *QST*

1-20 **A Simple Broadband Dipole for 80 Meters**
From September 1993 *QST*

1-25 **Once More With the 80-Meter Broadband Dipole**
From June 1985 *QST* (Technical Correspondence)

1-26 **Fat Dipoles**
From *The ARRL Antenna Compendium, Vol 2*

By Frank Gue, VE3DPC, ex-VE6BH

From *QST*, June 1968

An 80-Meter Inverted V for Field Day

It's that time of year again when portable operation is a delight. Here is a full-sized low-frequency antenna that you can put up in the field or at home without any help.

A Field Day antenna for 80 meters should be light, portable, inexpensive, capable of easy erection without any special equipment, and it should not contain any fragile parts.

Of course, the antenna must perform adequately.

The popular inverted V suggests itself as an answer to these requirements. It can be constructed so that it guys itself, minimizing the inevitable exasperating tangle of rope and wire, and it requires only one mast. Like all dipoles the inverted V can be fed at the center with low impedance line, and elements for several bands can be connected in parallel at the feed point of the antenna.

The inverted V shown in the photographs and sketches is simple, easily managed (20 minutes to erect, 10 minutes to dismantle), and costs under $15 for all components. Not only is it a convenient antenna for portable operation, but it can serve as a fine permanent antenna for the home station as well. In fact, that's what has happened to the inverted V pictured; it's been in use in the back yard of VE3DPC ever since Field Day, 1967.

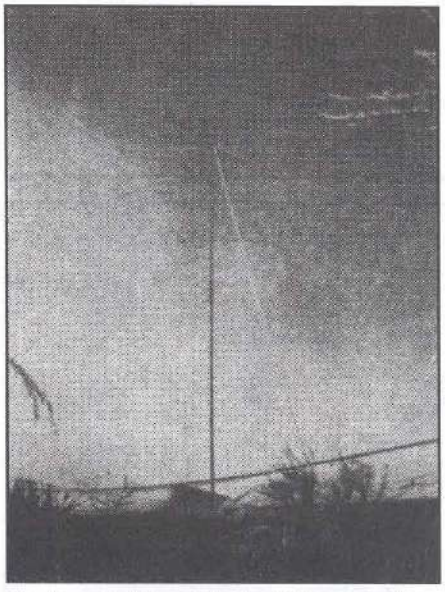

The inverted V as it looked this past winter in the author's backyard.

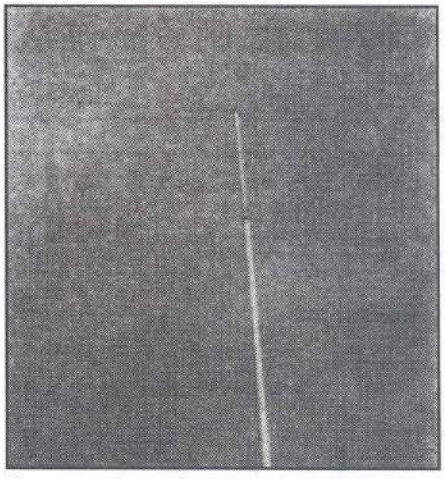

Upper portion of the 80-meter inverted V as it appeared at the Field Day site.

Assembly

As shown in Figure 1, the antenna support consists of three 10-foot sections of 1¼-inch TV mast. One end of each of the two lower sections is swaged, permitting all three sections to be force-fitted together. Hooks of music wire were installed in the top section, so that the element wire and feed line could be easily coiled for storage.

The center insulator (Figure 2) is made of maple; however, if this wood cannot be found, birch or fir can be used instead.

Figure 2 shows how the center insulator was drilled and Figure 3 shows how the feed line and antenna element were attached. Dimensions are obviously not critical, and the sketches are intended to show in a general way how the insulator was made, not to give precise detail. Just be careful where you drive the screws!

Softwood (pine) was picked for the end insulators (Figure 4) because it is adequate for the application and easier to work with than maple. Fragile ceramics should not be used in place of the wood insulators.

The 80-meter element (Figures 3 and 5) is made from small-gauge, Teflon-insulated, stranded Copperweld that was bought at a surplus outfit. This wire is worth looking for; it's tough, durable, light, and easy to handle. If operation on both 80 and 40 is desired, the builder can connect a 40 meter element to points A and B in Figure 3.[1]

The feed line can be 50-ohm coax, 72-ohm coax or 72-ohm Twin-Lead. I chose the latter because it is low cost, lightweight, very flexible, easy to store, and because it lends itself to such outrageous techniques as being tied in knots; however, since most transmitters have coax output, either a balun or an antenna coupler must be used between the feed line and the transmitter to maintain balance.[2] If elements for more than one band are to be used, the antenna coupler is preferred because it will reject harmonics of the transmitting frequency that might fall in the range of one or more of the paralleled antennas.

Raising and Lowering

Transporting the antenna to and from the Field Day site is easy. Tape the three mast sections together, wrap them with cloth to protect the car's finish, and tie the works between one of the door handles and the rear bumper. If the antenna extends past the back of the car, don't forget to tie a red flag on the end of the bundle to alert other drivers.

Upon arrival at the Field Day site, unpack the antenna and join the TV masts together. The three-section support is light enough to be "walked up" by one man, if the wind is under 10 miles per hour; however, prior to the antenna raising, you must put stakes into the ground, determine the

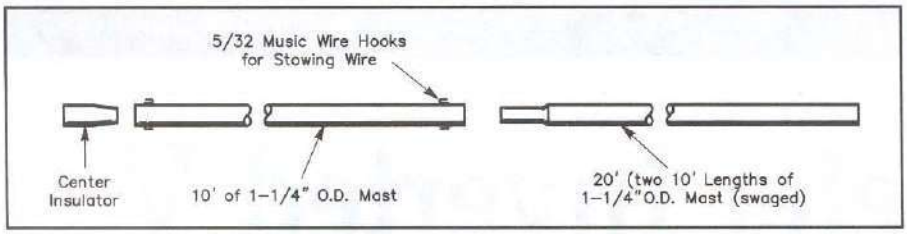

Figure 1—The makings of the inverted-V center support.

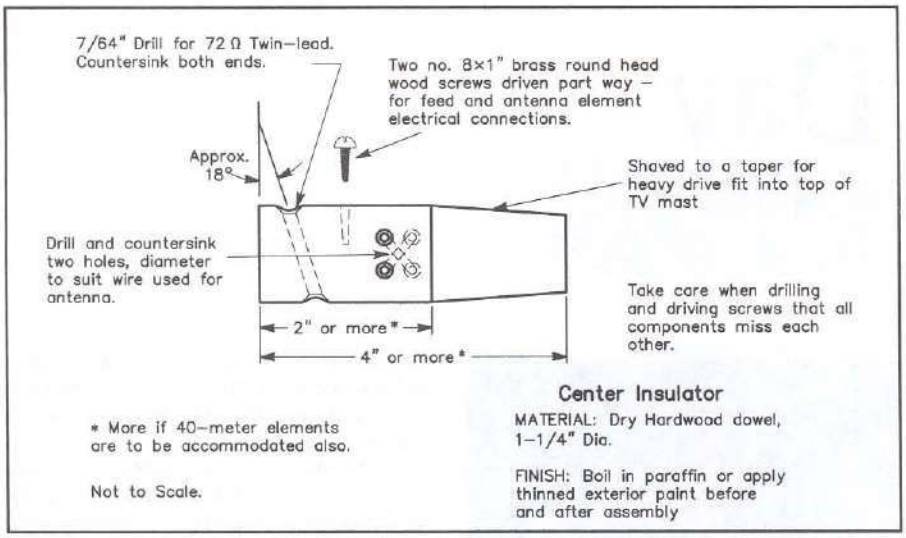

Figure 2—An X-ray view of the center insulator.

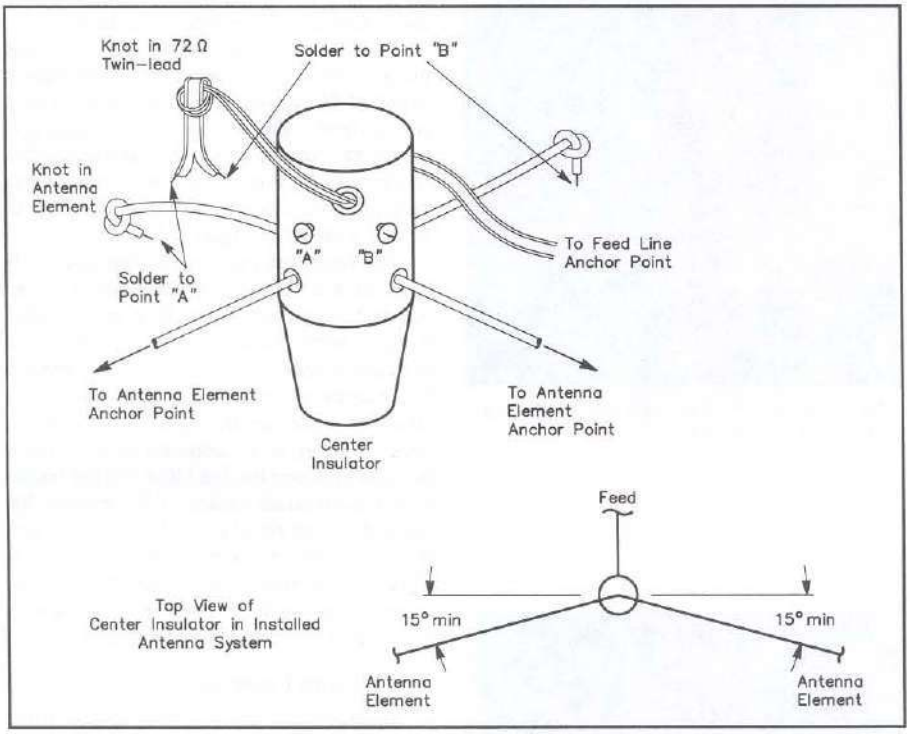

Figure 3—Details of how the feed line and element wires should be attached to the center insulator, and a top view of the installed insulator.

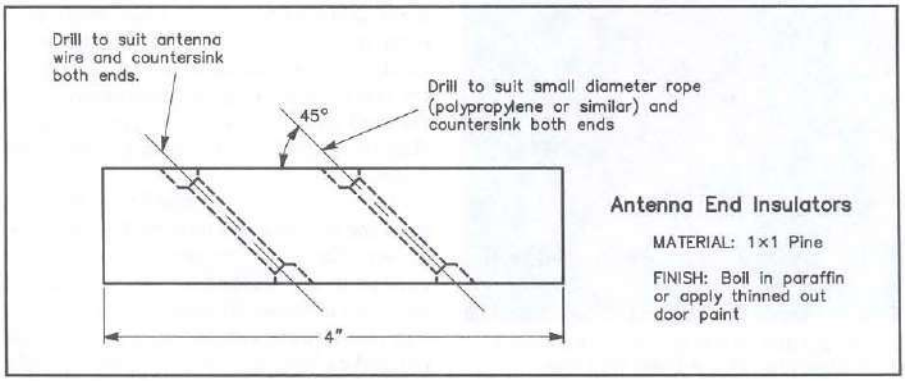

Figure 4—A sketch of one of the wooden end insulators. Two insulators are required for each dipole used.

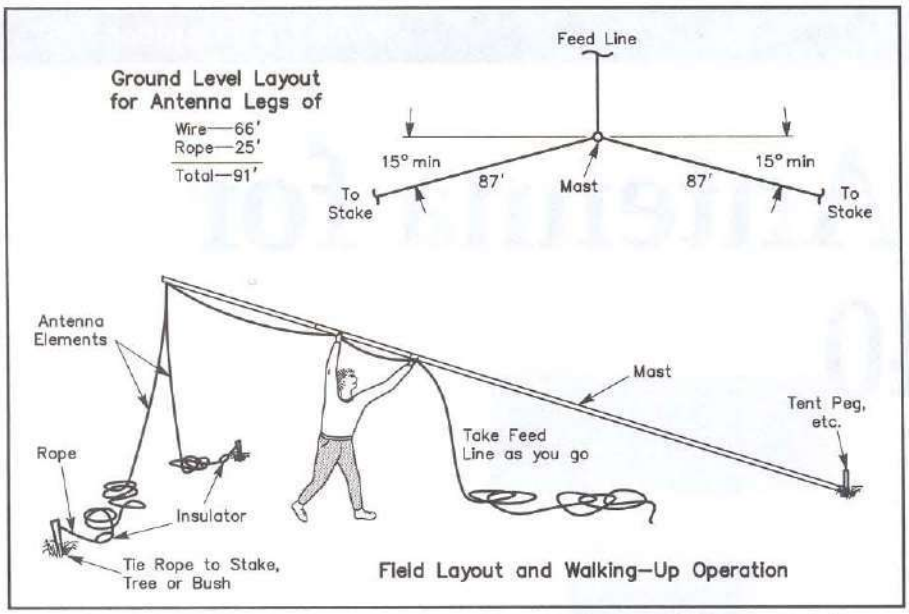

Figure 5—By using the dimensions and layout shown in the upper right corner of the sketch—so that ground stakes could be installed and proper length guys attached between them and the mast—the author was able to raise his 80-meter inverted V without any help. For other element lengths than shown, one man can easily put up the antenna by using simple geometry to determine the amount of rope required and the locations of the stakes.

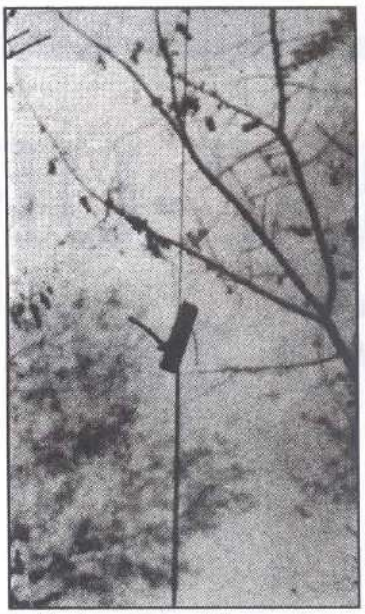

A sideview of one of the wooden end insulators.

exact length the guys will be when the antenna is in its operating position, and attach the guys to the stakes (Figure 5).

If help is available, it won't be necessary to install stakes or measure guys prior to putting up the antenna. Have the helpers pay out each half of the antenna element and keep slack out of the wire as the mast goes up. Station the men about 45 degrees off the line of the mast as it lies on the ground, and then, once the mast is up, have the helpers walk around to the final positions shown in Figure 5. The last few degrees of "walking up" is where your control is poorest.

With the rear guy (feed line) in your hand, move quickly and smoothly past top dead center and promptly and firmly apply back tension on the antenna element. Once the feed line is snubbed, you can easily correct the mast for lean by lifting the base and putting it where it suits you. If you are fortunate enough to have three helpers, there is no problem at all. Give the third man the feed line, station him as far away as possible from the mast and antenna element, and have him take up the slack as the mast goes up.

Base support can be little or nothing. The mast, which is now permanently erected in my back yard, rests directly on the grass. It was moved a couple of inches during each mowing operation, and no apparent harm came to the lawn.

Lowering the antenna is brutal but quick. Release the back guy (feed line) and let the whole system fall. If the ground is reasonably flat, this will be OK. But if the ground is very rough, the pipe may take a set as it strikes the ground. Under such conditions, it would be better to use helpers to reverse the erecting procedure.

The antenna has been left up for a period of several months, during which there have been many autumn storms and a severe ice storm. It has shown no signs of distress, and it has performed normally when wet or loaded with ice. The small size of the inverted V's parts has led to little wind and ice loading and is probably the main reason for the antenna's durability.

[1]Although dimensions for an 80-meter inverted V are given in Figure 5, these aren't necessarily the optimum dimensions for every installation: there are too many variables involved. If the antenna is not to be used with a transmatch and open-wire line, it is best to experimentally determine the length of the inverted V. This can be done by starting with an overall length equal to about 525 divided by the frequency in megahertz. The ends of the inverted V should then be trimmed until the SWR is minimum at the operating frequency. A simpler method is described in footnote 2.

[2]An easier arrangement, especially for multiband operation, can be achieved by using a transmatch and either 300-ohm Twin-Lead or 450-ohm Ladder-Line. Only one dipole—about 100 feet long (length not critical)—is all that is necessary to cover all the amateur bands between 3.5 and 30 MHz.

By John C. Allred, W5LST

From *QST*, October 1961

E-Z-UP Antenna for 75 and 40

Full-size dipoles for the 75- and 40-meter bands occupy more space than is conveniently available on the 75 by 113-foot lot at W5LST. The increasing popularity of the "drooping," or inverted-vee, dipole antenna among amateurs led us to investigate it for our somewhat crowded conditions. Based on the electrical design of Glanzer,[1] this system has performed meritoriously at W5LST. Requiring only one support, it was surprisingly easy to erect, gives a satisfactory s.w.r. over the phone bands and, importantly, the cost was less than thirty dollars complete. A plan-view sketch is shown in Figure 1.

The Mast

The mast is a telescoping Channel-master, capable of 50-foot height, but extended only to 35 feet. Extending the upper sections to less than their full lengths gives rigidity to the mast, and has apparently eliminated the need for guys on each section, as recommended by the manufacturer. To date this mast has withstood gusts of 50 miles per hour without a shudder; it is yet to be tested in a real gale, however.

As shown in Figure 2, a 9-foot length of 3-inch pipe is cast in concrete with 6 feet of its length extending above ground. Three pairs of clamps, such as those used on chain-link fence, secure the mast to the upright standard. During erection, these clamps are loosened and all three lie at the base of the standard, so that the mast need only be lifted about 6 inches to be put in place. When the mast is in place, the clamps are raised and tightened.

[1] Glanzer, "The Inverted V-Shaped Dipole," *QST*, August, 1960.

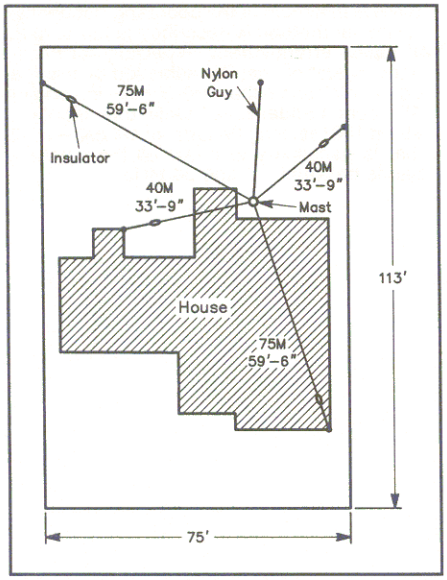

Figure 1—W5LST's layout for effective 40- and 80-meter antennas on a small lot. The two "drooping" dipoles are fed in parallel with a single coax line. Nylon-line extensions are used to reach convenient anchorages.

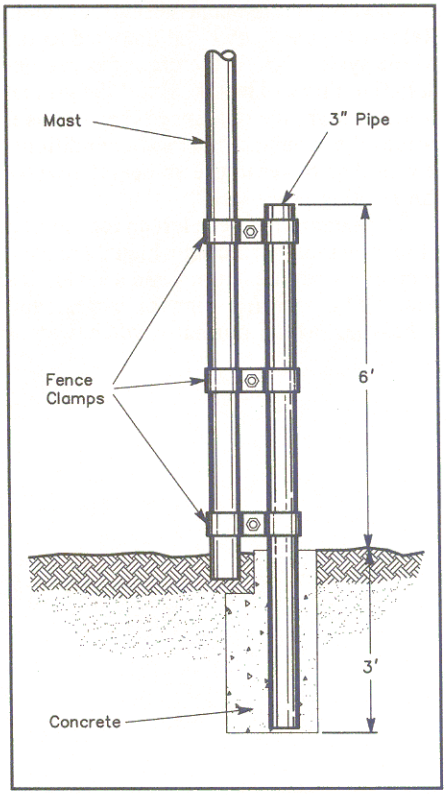

Figure 2—The mounting for the antenna mast. The 9-foot pipe is guyed temporarily while the concrete is poured.

Rigging

Except for the antenna conductors, all rigging is of nylon line of 500-pound test. A halyard is reeved through a pulley of suitable size which is wired securely to the top of the mast. The two ends of the halyard are made fast to a harness snap which, in turn, supports the center of the antennas. Provision of this halyard has proved to be a great convenience in permitting inspection of the antenna connections and the adjustment of tension in the wires without the necessity for lowering the mast.

Nylon line has a tendency to ravel at its ends but this problem is easily solved. Most fastenings were made with two halfhitches, followed by sewing the end of the line to itself with thread, as shown in Figure 3A, and doping with one of the quick-drying model-airplane cements.

Some weeks after the initial installation, it became apparent that some additional stabilization of the mast against occasional strong northerly winds would be desirable. Accordingly a nylon line was run from the harness snap at the top of the mast to a convenient anchor in the back yard, which happened to be the top of the children's swing set. Experience seems to show that the antenna wires, together with the additional nylon line, stabilize the mast against aerodynamically-excited vibration, without any appreciable strain on the antennas.

The Antennas

As shown in Figure 3, the two antennas are connected in parallel at the top of the mast. The lower ends are connected to convenient tie points so that the two legs of a given antenna are more or less in a straight line. To our great surprise, very little effect is produced by moving the ends of the an-

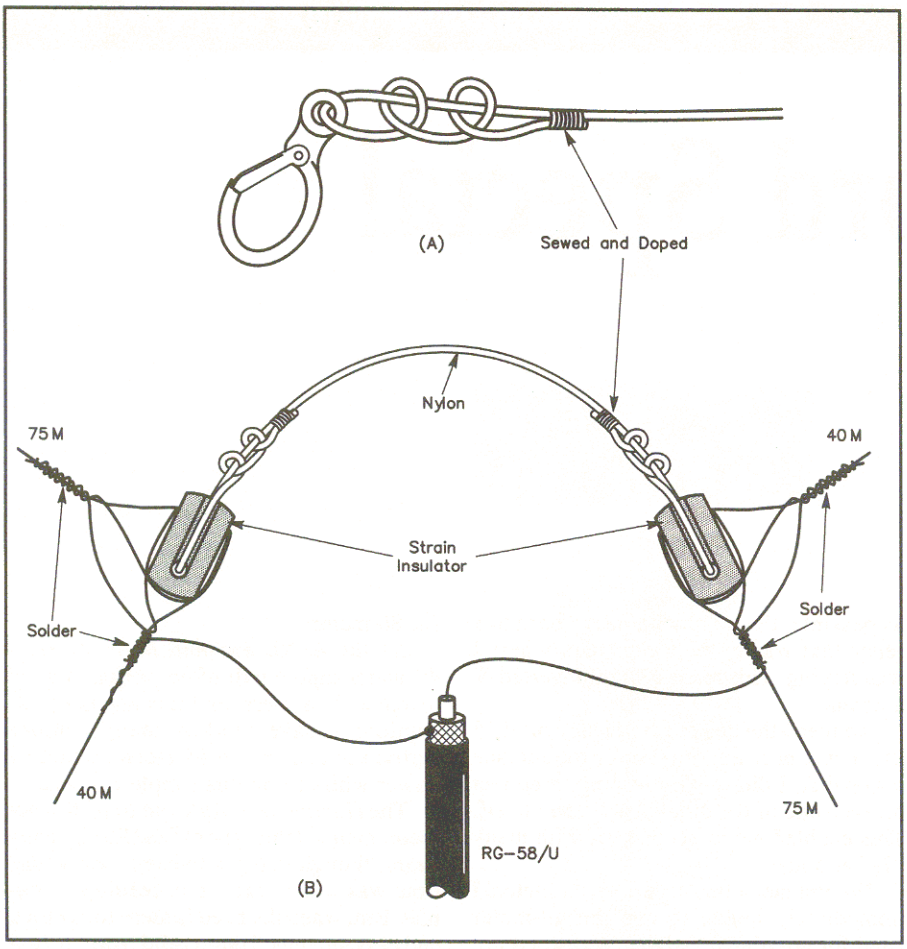

Figure 3—The halyard and feeder arrangement. The coaxial cable is sealed securely with polyethylene tape after the connections are made. The harness snap of A at the end of the hoisting halyard engages the bridle between the two insulators in B.

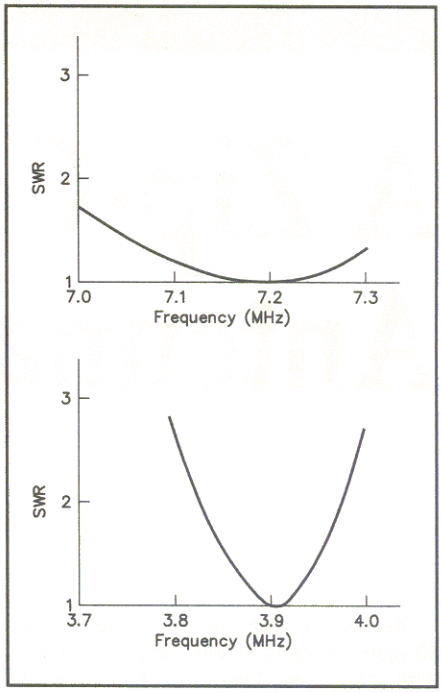

Figure 4—SWR curves as indicated by a "Monimatch"-type SWR indicator.

tennas either horizontally or vertically. There is apparently negligible electrical interaction between them as indicated by the s.w.r. bridge.

Pruning of the antennas is, as always, desirable. In our case, the optimum lengths of each leg turned out to be 33 feet 9 inches for 40 meters and 59 feet 6 inches for 75 meters. Figure 4 shows the performance of the antennas on 40 and 75 as measured by a Heath s.w.r. bridge. Although the antennas tune sharply, they are usable over the entire phone band in each case, and it would be difficult to imagine a better performer on the lower-frequency bands than this simple antenna system.

A Zip-Cord Special Antenna

Recently I found myself in need of an 80-meter antenna to help me keep in touch with some of my friends back home while operating portable in Arizona. The antenna and feed line were not readily available, but I remembered that one of my friends had recommended zipcord as a substitute feed line for a dipole, provided low power was used. Going one step further, I felt the entire antenna could be made of this low-priced material. I purchased 80 feet of zip cord at a local hardware store (at 4 cents a foot) and peeled it apart for 60 feet. This gave me the required 120 feet for a dipole, plus a 20-foot feed line which was taped to prevent further splitting. The feeder was fastened to a 2×4 which was used as a center support. The ends were extended as far as possible, then tied with heavy cord to a fence that was in the trailer park where I was staying. This made a slight inverted-V antenna.

To reach the desired frequency of 3935 kHz it was necessary to shorten the antenna somewhat. I did this by folding three feet on each end of the dipole back upon itself. This enabled me to keep skeds with many "7s" at home.

Having met with success on 80-meters I immediately began to eye the 40-meter band for possible use. I then measured out 32 feet from the center and cut the wire there, then tied a knot in the two pieces, leaving a couple of inches of bare wire dangling. Now for forty meters, I merely disconnect the wires and reconnect them for 80 meters.

As the *ARRL Antenna Book* states, a 40-meter dipole will often present a good match at 15-meters, and this one is no exception; I have worked many stations across the country on 15 meters with low power while using this simple antenna.

The *Handbook* or *Antenna Book* has not recommended this type of feed line in many years, though using a twisted pair at one time was usual practice in feeding a doublet. But, when the need is there for a quick and easy antenna, I don't think you can find an easier one as long as you remember to use low-power transmitters (100 watts or less) and trim the wire for a low value of SWR. — *Frank S. Wise, W7QYC*

By Jerry Hall, K1TD

From *QST*, March 1979

Zip-Cord Antennas– Do They Work?

Basic Amateur Radio: Parallel power cord is readily available and is easy to work with. How efficient is it when used at radio frequencies? Well, that depends.

Zip cord is readily available at hardware and department stores, and it's not expensive. The nickname, zip cord, refers to that parallel-wire electrical cord with brown or white insulation used for lamps and many small appliances. The current price is about 6 cents a foot in hundred-foot rolls in most parts of the U.S. The conductors are usually no. 18 stranded copper wire, although larger sizes may also be found. Zip cord is light in weight and easy to work with.

For these reasons, zip cord is frequently used as both the transmission line and the radiator section for an emergency dipole antenna system. The radiator section is obtained simply by "unzipping" or pulling the two conductors apart for the length needed to establish resonance for the operating frequency band. The initial dipole length can be determined from the equation $\ell = 468/f$, where ℓ is the length in feet and f is the frequency in megahertz. (It would be necessary to unzip only half the length found from the formula, since each of the two wires becomes half of the dipole.) The insulation left on the wire will have some loading effect, so a bit of length trimming may be needed for exact resonance at the desired frequency.

For installation, many amateurs like to use the electrician's knot shown in Figure 1 at the dipole feed point to keep the transmission-line part of the system from unzipping itself under the tension of dipole suspension. This way, if zip cord of sufficient length for both the radiator and the feed line is obtained, a solder-free installation can be made right down to the input end of the line. Granny knots (or any other variety) can be used at the ends with cotton cord to suspend the system. You end up with a lightweight low-cost antenna system that can serve for portable or emergency use.

But just how efficient is a zip-cord antenna system? Since it is easy to locate the materials and simple to install, how about using such for a more permanent installation? Upon casual examination, zip cord looks about like high-quality 72-ohm balanced feed line. Does it work as well? Ask several amateurs these questions and you're likely to get answers ranging all the way from, "Yes, it's a very good antenna system!" to "Don't waste your time and money – it's not worth it!" Myths and hearsay seem to prevail, with little factual data. The intent of this article is to rectify that situation.

Zip Cord as a Transmission Line

In order to determine the electrical characteristics of zip cord as a radiofrequency transmission line, we purchased a 100-foot roll and subjected it to tests in the ARRL laboratory with an rf impedance bridge. Zip cord is properly called parallel power cord. The variety purchased was manufactured for GC Electronics, Rockford, IL, being 18-gauge, brown, plastic-insulated type SPT-1, GC cat. no. 14-118-2G42. Undoubtedly, minor variations in the electrical characteristics will occur among similar cords from different manufacturers, but the results presented here are probably typical.

As the first step, we checked the physical length of the wire. GC generously provided nearly 4 feet over the specified 100-ft length, and the extra length was promptly lopped off.

We wanted to avoid measurement errors that might arise from coiling the wire on the supply spool (inductance between turns) or laying it out on the vinyl-tiled cement-slab floor (capacitance to a large surface), so the second step was to suspend the wire in a long hallway, about a foot or so below the false ceiling. Cotton twine was used for the supporting material. Undaunted by snide comments from fellow staff members about cheating the telephone company out of installation work and facetious suggestions

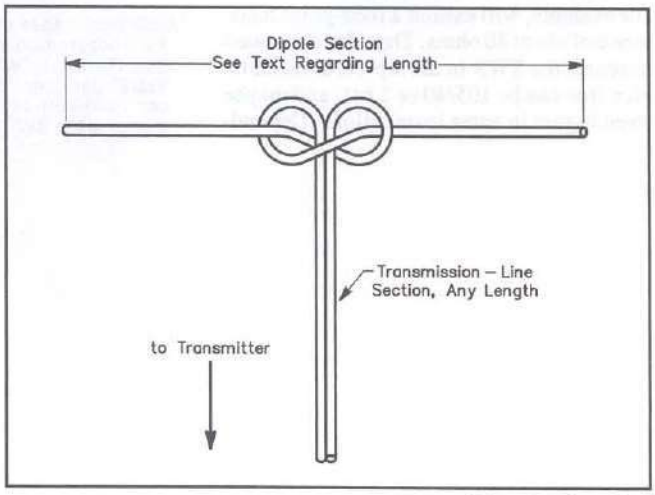

Figure 1—This electrician's knot, often used inside lamp bases and appliances in lieu of a plastic grip, can also serve to prevent the transmission-line section of a zip-cord antenna from unzipping itself under the tension of dipole suspension. To tie the knot, first use the right-hand conductor to form a loop, passing the wire behind the unseparated zip cord and off to the left. Then pass the left-hand wire of the pair behind the wire extending off to the left, in front of the unseparated pair, and thread it through the loop already formed. Adjust the knot for symmetry while pulling on the two dipole wires.

that we use two paper cups and a string for our intercom, we continued with preparation for the tests.

With a General Radio 1606A rf impedance-measuring bridge, we made measurements at the input end of the line on 10, 15 and 29 MHz, while the far end of the line was terminated first in a short and then in an open circuit. We did notice during measurements that our readings changed somewhat as people walked in the hallway, especially during the 29-MHz tests. After a seemingly endless period of shooing away would-be helpers who disrupted measurements by grabbing the line, hanging objects on it, and so forth, we finally arrived at a set of readings considered to be satisfactory for our purposes. From there, a bit of work with an electronic calculator and a Smith Chart told us what we wanted to know — the electrical characteristics at radio frequencies.

The results? Well, as the saying goes, I have some good news and some bad news.

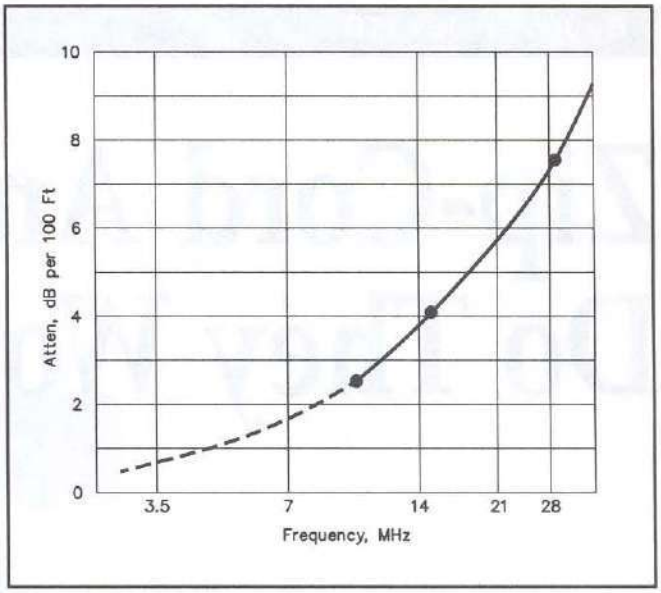

Figure 2—Attenuation of zip cord in decibels per hundred feet when used as a transmission line at radio frequencies. Measurements were made only at the three frequencies where plot points are shown, but the curve has been extrapolated to cover all high-frequency amateur bands.

First, the Good News

If ever you need a balanced 105-ohm transmission line, then zip cord is the stuff for you! Its characteristic impedance was determined to be 107 ohms at 10 MHz, dropping in value to 105 ohms at 15 MHz and to a slightly lower value at 29 MHz. The nominal value is 105 ohms at hf. The velocity factor of the line was determined to be 69.5 percent.

This reported change in impedance with frequency may raise a few eyebrows, but it is a fact that most lines do not exhibit a constant characteristic impedance across a range of frequencies. However, this writer has not previously encountered any line which was not "flat" between 3 and about 50 MHz. Zip cord may be exceptional from this standpoint, especially considering that the insulating material was not chosen for its qualities at rf.

And Now the Bad News

Who needs a 105-ohm line, especially to feed a dipole? Most of us know that a dipole in free space exhibits a feed-point resistance of 73 ohms, and at heights above ground of less than 1/4 wavelength the resistance is even lower. An 80-meter dipole at 35 feet, for example, will exhibit a feed-point resistance of about 40 ohms. Thus, for a resonant antenna, the SWR in the zip-cord transmission line can be 105/40 or 2.6:1, and maybe even higher in some installations. Depending on the type of transmitter in use, the rig may not like working into the load presented by the zip-cord antenna system.

But the really bad news is still to come—line loss! Figure 2 is a plot of line attenuation in decibels per hundred feet of line versus frequency. Chart values are based on the assumption that the line is perfectly matched (sees a 105-ohm load as its terminating impedance). For lengths other than 100 feet, multiply the figure by the actual length in feet and then divide by 100.

In a feed-line, losses up to about one decibel or so can be tolerated, because at the receiver a 1-dB difference in signal strength is just barely detectable. But for losses above about 1-dB, beware. Remember that if the total losses are 3 dB, half of your power will be used up just to heat the transmission line.[1]

Based on this information, we can see that a hundred feet or so of zip-cord transmission line on 80 meters might be acceptable, as might 50 feet on 40 meters. But for longer lengths and higher frequencies, look out! The losses become appreciable.

[1]Additional losses over those charted in Figure 2 will occur when standing waves are present. See Gibilisco, "What Does Your SWR Cost You?" January 1979 *QST*. Trouble is, you can't use a 50- or 75-ohm SWR instrument to measure the SWR in zip-cord line accurately.

What About Zip Cord Wire as the Radiator?

For years, amateurs have been using ordinary copper house wire as the radiator section of an antenna, erecting it without bothering to strip the plastic insulation. Other than the loading effects of the insulation mentioned earlier, no noticeable change in performance has been noted with the insulation present. And the insulation does offer a measure of protection against the weather. These same statements can be applied to single conductors of zip cord.

The situation in a radiating wire covered with insulation is not quite the same as in two parallel conductors, where there may be a leaky dielectric path between the two conductors. In the parallel line, it is this current leakage which contributes to line losses. The current flowing through the insulation on a single radiating wire is quite small by comparison, and so as a radiator the efficiency is high.

Now back to the original question: How efficient *is* a zip-cord antenna system? Well, that *does* depend, on the length of the wire used for the feed-line section and on the frequency. In a pinch on 160, 80, 40 and perhaps 20 meters, communications can certainly be established with this kind of antenna. For higher frequencies, especially with long line lengths for the feeder, you're on your own.

Piggyback Antenna For The Ten-Meter Band

Most amateurs from Novices on up use dipole antennas for the eighty- and forty-meter bands. In many cases, these two antennas were all the Novice needed since the fifteen-meter band could also be covered with the forty-meter dipole.

However, with the advent of the new ten-meter subband for Novices, a simple and inexpensive method of getting the needed coverage is to use a "piggyback" antenna. It can be easily added to an existing dipole, eliminating the need for additional supports or feed lines. Also, it will have no effect on either an eighty- or forty-meter dipole.

Of course, performance will not be as good as that obtained with a beam, but it should not be sold short either. A KH6 was worked during a recent contest with a power output of 1.8 watts. — *Robert M. May, II, WA4DEG*

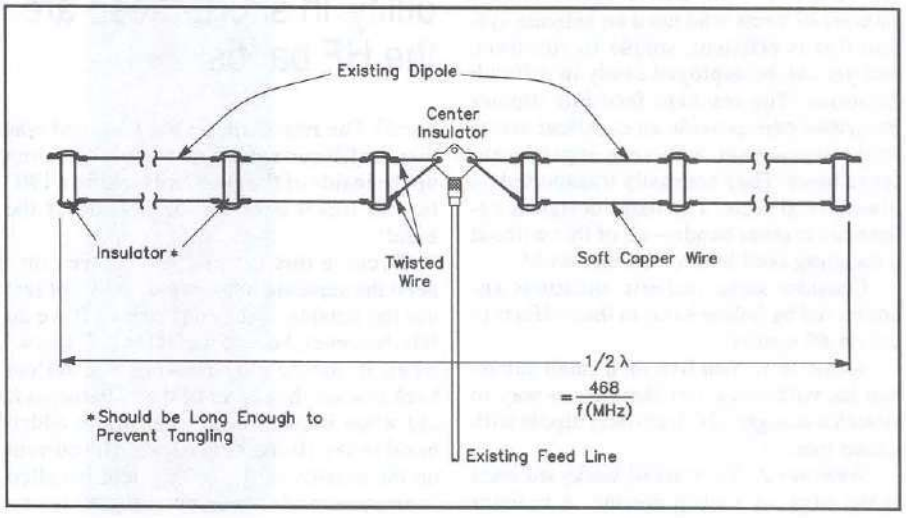

By James E. Taylor, W2OZH

From *QST*, August 1991

RFD-1 and RFD-2: Resonant Feed-Line Dipoles

This unique design offers simplicity and general utility. In short, these are "reel" great antennas for the HF bands.

During several decades of operation on the 80-meter band, I have encountered a number of hams who need an antenna system that is efficient, simple to construct, and yet can be deployed easily in difficult locations. The resonant feed-line dipoles described here provide an excellent match to the transceiver without a separate antenna tuner. They are easily transported on plastic cord reels. The basic design is extensible to other bands—all of this without a dangling feed line to contend with!

Consider some realistic situations encountered by fellow hams in their efforts to get on 80 meters:

Scenario 1: You live on a small suburban lot with trees, but there is no way to stretch a straight 120-foot-long dipole with a feed line.

Scenario 2: Your small backyard ends at the edge of a steep decline. A radiator wire could be snaked through the trees, but running a separate feed line is out of the question.

Scenario 3: You live in a high-rise building and could secretly stretch a wire upward or downward, but there is no way to install a feed line.

Scenario 4: You're going on vacation to the mountains and you know that your cottage is nestled among hundred-foot-high pines You can take along a bow and arrow and cord, but then what would you do?

In response to these problems, I began to search for a universal solution under the following ground rules. (1) No separate antenna tuner would be required, (2) the antenna could be deployed with no more difficulty than stringing up a length of coax and (3) the antenna could be easily stored and unwound from a cord reel without a tangle of cable and wire.

Several years ago I used a 10-meter vertical linear coaxial sleeve antenna, as shown in Figure 1. A vertical dipole is constructed from a quarter-wave whip and a quarter wavelength of shielding braid. Its feed line passes through the braid, yielding a simplified geometry. Although this concept could be adapted to 80 meters, who wants to deal with 60 feet of shielding braid? The important lesson I learned was that the RF current has no trouble traveling up the inside of the coax and making a 180° turn to travel back on the outside of the braid!

Because this is true, perhaps we don't need the separate outer braid. Why not just use the outside of the coax itself? If we do this, however, how do we let the RF "know" when it should stop flowing and reflect back toward the center of the radiator, as it did when it came to the end of the added braid in the 10-meter vertical? The current on the outside of the coax shield is called "common-mode" current—there is no counteracting equal and opposite current as there is inside the coax. One design approach utilizes the primary function of a balun transformer: to place in unbalanced reactance in the path of this common-mode current without affecting the desired balanced transmission line currents. The development of this concept is discussed in the Appendix.

The common-mode current on the coax shield is transformed by a quarter-wavelength stub to maximum near the transceiver. It was not surprising to note experimentally that a coil of a few turns placed at the fed end of the dipole decreases the resonant frequency of the system substantially (because of the added inductive reactance). However, an unexpected dividend of this is that, at the resonant frequency, an almost perfect impedance match to the 50-ohm source is realized! Now we have the design for our simplified antenna system! We can increase the resonant frequency by moving the coil along the cable away from the current maximum while retaining the perfect match. And at the same time we can decrease the common-mode current on this part of the line, because of the coil's inductive reactance. For the values chosen, the coil is near self-resonance from the distributed capacitance of the coil windings. The equivalent parallel-resonant circuit serves to increase the reactance at this point in the antenna, which assures a reflection when the RF reaches this virtual end of the dipole. To my knowledge, this configuration and method of resonating is unique and novel, and I refer to it as a T choke.

Constructon, Installation and Adjustment

The simple arrangement of the resonant coaxial linear dipole is shown in Figure 2.The dimensions and test results are for a nominal

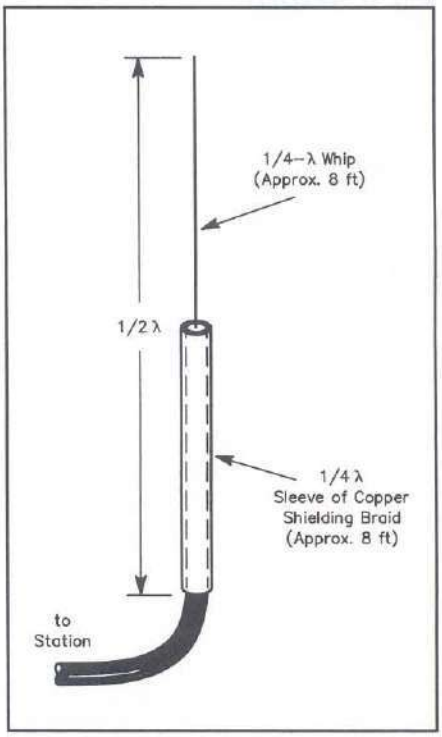

Figure 1—A vertical linear coaxial sleeve antenna for 10 meters.

frequency of 3.95 MHz. To dramatize the simplicity of the antenna, I list all required parts in Table 1.

The coaxial cable connector is assembled at the input end of the coax for connecting to the transceiver. The center conductor of the far end of the cable is connected to the antenna wire to form a hook and eye, and is securely soldered. This junction is potted in the center of a short length of PVC pipe to form a robust center insulator assembly. At the outset, 13 turns of cable can be wound on the cord reel at a point approximately 59 feet plus 25 inches from the center of the dipole. The 13 turns can then be taped in place on the reel with duct tape or equivalent. The remaining coax and wire can now be wound on the reel for ease of transporting. To avoid kinks when unwinding, secure the end of the wire and rotate the reel, keeping the wire and coax taut.

Ground losses are a great enemy of an HF antenna, especially at the lower frequencies, so place the dipole for 80 meters as far above the ground as possible! After installation, check the resonant frequency with a noise bridge or an SWR meter. If these construction details are followed, the resonant frequency should be approximately 3.95 MHz. If the resonance indication is indefinite or if the resistance is not close to 50 ohms, adjust the self-resonance of the coil by moving the turns slightly on the reel. This alters the inter-turn capacitance, permitting adjustment of the reflection of RF at the end of the dipole. During this adjustment, remember that the greatest effect is between the input and output turns, where the voltage difference is greatest. If you want to lower the resonant frequency of the antenna, remove the tape and rotate the reel to increase the 25-inch distance, thereby increasing the length of the dipole. This is done in a manner to retain the 13-turn coil—you are winding and unwinding equal lengths of cable. When the desired resonant frequency is attained, you are ready to operate! This is a broadband antenna, and not much adjustment is required.

The 13 turns is mentioned only as a nominal coil size. I have used both 11-turn and 13-turn coils. Self-resonance can be adjusted as mentioned earlier. As the number of turns is increased, the initial 25-inch distance will be decreased. For example, in my test installation a change from 11 turns to 13 turns altered this distance required for resonance from 68 inches to 25 inches. A greater impedance at this point serves to improve the isolation of the dipole from ground.

The RFD-2 for Two-Band Operation

The preceding construction information is for an antenna dedicated to a single amateur band, the RFD-1. With a slightly different configuration, referred to as the RFD-2, the RFD-1 design can be extended to cover the 40-meter band without severing the coaxial cable. Conversion from 80 to 40 meters and back requires only a few minutes. The RFD-2 design allows you to change operation to 40 meters for a few days without permanently altering the 80-meter lengths. In other words, the total dimensions of the 80-meter coaxial feedline dipole are retained but operation is adapted to 40 meters. Tbis is done simply by winding coaxial cable on reels. This is readily achieved by altering the winding of the coax on the original reel and then adding a second coil near the far end of the dipole. Once the values have been established, this band change is accomplished simply.

The RFD-2, as it has evolved at W2OZH, is shown in Figure 3. Total dimensions are given in Figure 3A. The length of the feed line has been increased from that of the RFD-1 to 143 feet to make allowance for the cable used in the 13-turn coil. This assures an isolating stub which is approximately 1/4 λ on 80 meters, and at the same time permits a stub length that is close to 1/4 λ on 40 meters, thereby achieving the desired high impedance for isolation on both bands. Also, the no. 12 terminating antenna wire has been replaced by a length of coaxial cable—the outer jacket provides insulation so the coax can now be coiled to provide the desired dipole length on 40 meters.

As pointed out earlier, a self-resonant coil is used to assure a high coefficient of reflection at the fed end of the 80-meter dipole. For other bands it is necessary to calculate the approximate number of turns required to approach self-resonance. A suitable winding for 80 meters was determined to be 13 turns on a 6-inch diameter reel, so the numbers for other bands can be obtained by a simple scaling calculation. Details are given in the Appendix. For guidance in adapting the design for the other HF bands, the approximate number of turns for the terminating coils is shown in Table 2.

For wavelengths shorter than 40 meters it may be desirable to use a radiating section longer then 1/2 λ. The length either side of center can be any odd number of quarter wavelengths. For example, on 20 meters the radiator could be 3/2 λ (three

Table 1
RFD-1 Parts List

- 1–118-foot length RG-8X (minifoam) coaxial cable
- 1–59-foot length no. 12 stranded or Copperweld wire
- 1–PL-259 male coaxial cable connector
- 1–10-inch-diameter cord reel (Doscocil model no. 32500 or equiv.)
- 1–3-inch length of 1/2-inch OD PVC pipe (for center insulator)
- 1–Epoxy potting compound (sufficient to fill pipe)

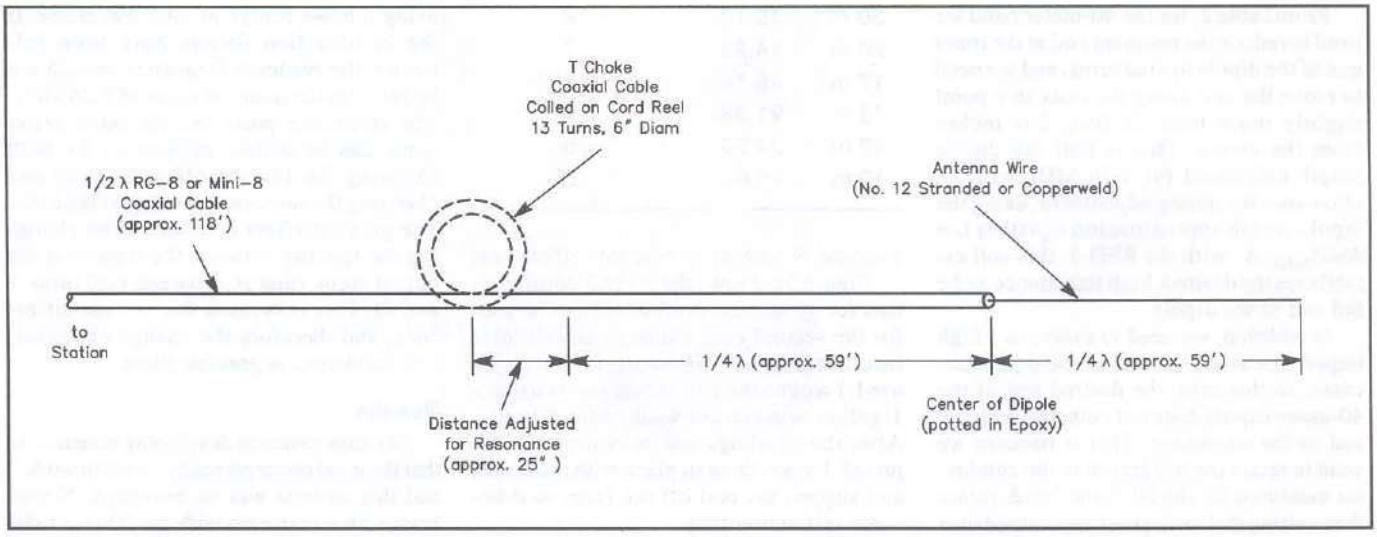

Figure 2—The RFD-1 (resonant feed-line dipole) antenna for 80 meters.

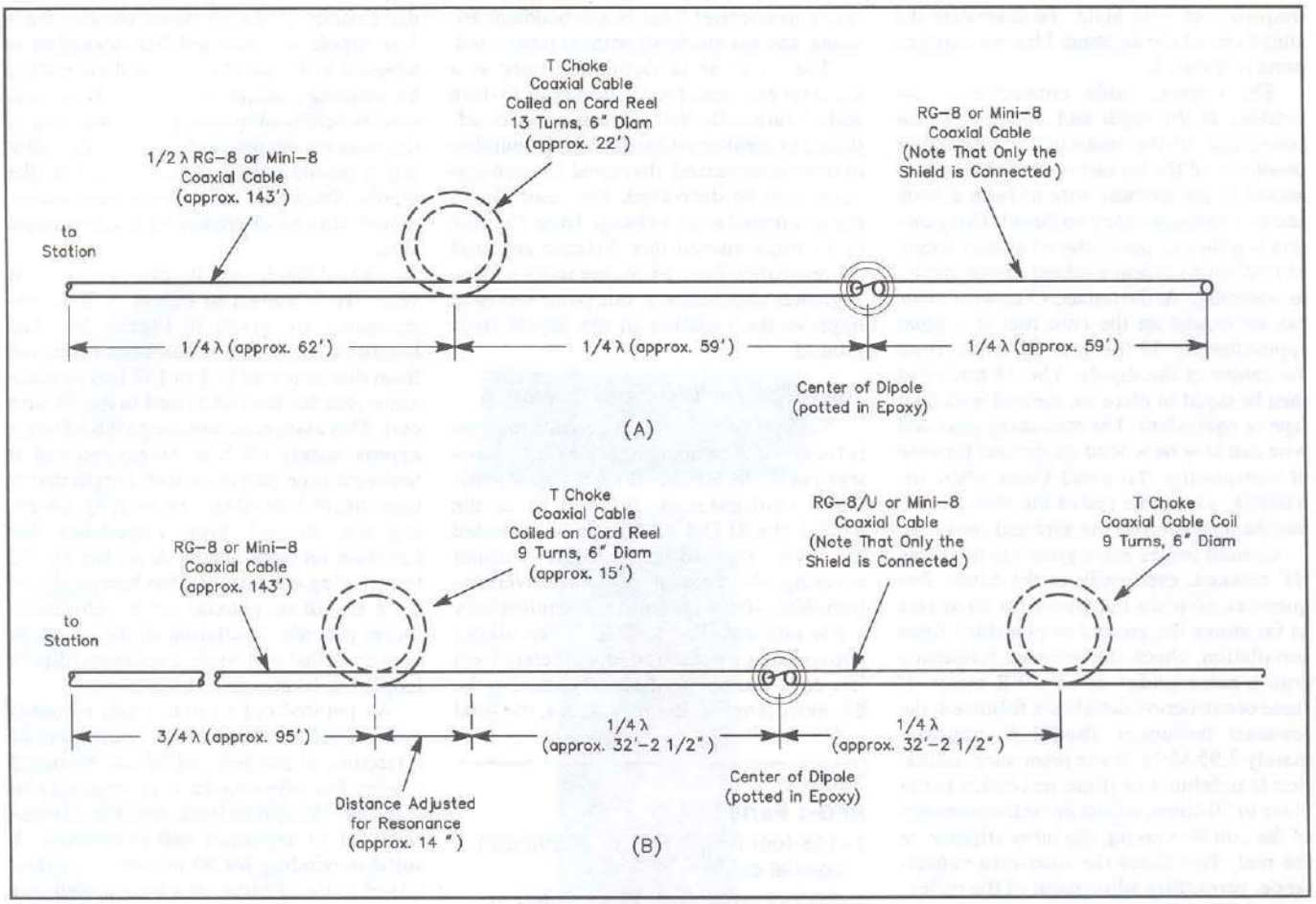

Figure 3—The RFD-2 antenna can be configured for either of two bands. Shown at A is the setup for 80 meters, and at B for 40 meters.

quarter waves either side of center). Depending upon the antenna orientation, the additional radiation lobes may be advantageous. Also, the unused conductor lengths at the ends are less apt to cause trouble because of parasitic excitation from the main radiator.

Arrangement and Construction

FromTable 2, for the 40-meter band we need to reduce the resonant coil at the input end of the dipole to nine turns, and we need to move the coil along the coax to a point slightly more than 32 feet, 2¾ inches from the center. This is half the dipole length calculated for 7.26 MHz with an allowance for tuning adjustment, using the dipole-length approximation equation $L = 468/f_{MHz}$. As with the RFD-1, this coil establishes the desired, high impedance at the fed end of the dipole.

In addition, we need to establish a high impedance at the far end of the dipole because, in this case, the desired end of the 40-meter dipole does not coincide with the end of the conductor. This is because we want to retain the full length of the conductor measured for the 80-meter band, rather than cutting it. The desired high impedance reflecting termination is achieved by use of a second, 9-turn, self-resonant coil of coax.

Table 2
Scaling of RFD-1 to Other Bands

Band	*Frequency*	*Turns*
160 m	1.90	19
80 m	3.95	13
40 m	7.26	9
30 m	10.12	8
20 m	14.29	7
17 m	18.14	6
15 m	21.38	6
12 m	24.96	5
10 m	28.65	5

Figure 3B shows the RFD-2 configuration for 40 meters. A cord reel can be used for the second coil, although any suitable insulating 6-inch diameter form can be used. I wound the coil in two layers using a 1-gallon windshield-washer-fluid bottle. After the windings had been properly adjusted, I taped them in place with duct tape, and slipped the coil off the form so it became self-supporting.

As with the RFD-1, it is desirable to place the antenna as high above ground as possible to reduce ground losses and to help achieve low-angle radiation, if that is desired. The dipole does not have to be installed in a straight line, and if you can gain appreciably greater height by bending it, this may be a desirable compromise.

After the antenna with its two coils is erected, measure the resonant frequency using a noise bridge or an SWR meter. If the construction details have been followed, the resonant frequency should not be far from the nominal value of 7.26 MHz. The resonance point and the input resistance can be shifted moderately by both changing the 14-inch offset distance and changing the inter-turn spacing of the coils. The greatest effect is produced by changing the spacing between the input and the output turns (that is, between coil turns 1 and 9). This is because the voltage difference, and therefore the change in capacitive influence, is greatest there.

Results

My experience in developing antennas is that the good concepts really "want to work," and this antenna was no exception. Noise-bridge measurements with the RFD-1 indicated an input resistance at resonance of

49 ohms, and from a practical standpoint the SWR is 1:1. An H-field antenna probe was used to evaluate the power radiated at the center of the dipole compared with that at the current loop near the feed-point. The current ratio was 5.5 to 1, which corresponds to a power ratio of 30 to 1, or 15 decibels. This indicates that the coil is very effective in attenuating the common-mode current flowing back toward the feed point.

For the RFD-2 with the 40-meter dimensions shown in Figure 3B, the initial resonance point was within the 40-meter phone band and the SWR was essentially 1:1. Slight adjustment brought the resonant frequency up to the desired value, and the input resistance was very close to 50 ohms. A salient characteristic of the RFD antennas is the ease with which an impedance match is attained. It appears always to be easy to get a reflected power indication of zero. This is probably because the common-mode current on the shield of the coax is indistinguishable from the desired radiating current—in other words, the common mode is used rather than avoided.

Appendix

When the separate outer braid of the antenna shown in Figure 1 is removed, there must be some way to let the RF "know" when it should stop flowing on the shield of the coax and reflect back toward the center of the radiator. A balun box that I made up for another purpose is one approach: 30 turns of bifilar winding on an Amidon T-200-2 iron-powder toroidal core. The turns formula for such a balun transformer is

$$T=\sqrt{\frac{\text{desired L}(\mu H)}{A_L}}$$

where

T = no. of turns

A_L = inductance index (microhenries per 100 turns)

From this, the inductive reactance for unbalanced current is

$$X_L=2\pi fL=\frac{2\pi fT^2A_L}{10^4}$$

At a frequency of 4 MHz, this 30-turn coil has an unbalanced reactance of only 270 ohms. We would need about ten of these in series to support the RF field at the end of a dipole antenna!

An alternative method involves placing a toroidal isolation transformer in the coaxial line at the fed end of the linear dipole. I actually wound such a transformer on two stacked T-200-2 cores, to provide a 1-kW power capability. This configuration worked, after a fashion, but the impedance match was less than desired, probably because of excessive capacitance between secondary and primary windings. However, before I took steps to control this, a simpler approach came to mind.

We need to isolate the transceiver from the fed end of the dipole, so why not cut the coaxial feed line to be a quarter wavelength long? (This length is measured in free-space, not in the line.) This serves to tranform the high impedance of the fed end of the dipole to the low impedance at the grounded transceiver. Any unused portion of this approximate 60-foot length of coax can be wound in a coil and used for further isolation and, as it turns out, for tuning the system to resonance.

Scaling for a Second Band

For coverage of a second band, we would like to have the same inductive reactance that we had for the 80-meter coil.

From handbooks, the inductance of a coil of assumed dimensions is

$$L = AN^2$$

where

A = a constant determined by the coil geometry

N = number of turns

Thus, we have for the reactance

$$X_L = 2\pi fL = 2\pi fAN^2$$

For equal reactances we can calculate N_2, the new number of turns, at frequency f_2, from N_1, the known number of turns at frequency f_1, by the equation

$$N_2=N_1\sqrt{\frac{f_1}{f_2}}$$

By Jerry Hall, K1PLP

From *QST*, September 1974

Off-Center-Loaded Dipole Antennas

In these times when much of our amateur population lives in urban areas, the subject of shortened antennas for the lower frequency amateur bands is a very popular one. Physically short ground-mounted vertical antennas with lumped-constant loading to make them resonant can be quite efficient radiators, if a good radial system has been installed. This has certainly been evidenced in Sevick's series of recent *QST* articles.[1] To many amateurs, however, the "hitch" in constructing such a system is the installation of a *good* radial system. It must be admitted that for the "top" amateur bands, 160 and 80/75 meters, an efficient system of buried radials requires a sizable amount of real estate, even for a physically short radiator. On the average city-size lot, 50 or 75 by 120 to 150 feet, it's almost impossible to install a highly efficient radial system for 80/75 meters, much less for 160 meters, when structures like a house and perhaps a separate garage exist. Or to some amateurs, just the thought of burying hundreds or maybe thousands of feet of wire is enough to turn off any enthusiasm for the project. What's the alternative? A dipole type of antenna with lumped constant loading. At modest heights, 30 or 40 feet, such an antenna will prove to be quite satisfactory if it is physically longer than about 0.2 wavelength. Shorter lengths may also be used, at reduced efficiency. Such an antenna can be fed directly with 50-Ω coaxial line, and it can be operated with no earth ground. (Of course the chassis of the transmitter and/or receiver should be grounded adequately for protection against shock hazard.)

Nearly all of us are familiar with the concept behind the use of inductive loading. A vertical antenna which is shorter than a quarter wave (or a dipole antenna which is shorter than a half wave) will exhibit capacitive reactance at its base (or center) feed point. To cancel such capacitive reactance, a coil having the proper inductive reactance may be connected in series with the base feed point of the vertical. The same result will be obtained through the use of two such coils for a dipole, one coil connected in series with each half. It is not necessary for the inductor to be installed at the feed point, however. In fact, greater radiating efficiency results through improved current distribution if the inductor is located along the radiator some distance away from the low-impedance feed point, *viz*, in the manner of a center-loaded mobile whip antenna. Figure 1 shows this concept extended to a dipole element, with off-center loading. The inductors resonate the antenna to the operating frequency, but do little actual radiating themselves. (This is in contrast to helically wound or continuously loaded elements, where a long thin inductor is the radiator as well as the loading element.)

In the antenna represented by Figure 1, there are many variable factors to be considered when a practical antenna for a given frequency is being constructed. Of primary consideration from an efficiency standpoint is the overall length, shown as dimension A. Another consideration for efficiency is the distance of the coils from center, dimension B. The longer the overall length (A), up to a half wave, and the farther the loading coils are placed from the center (B), the greater is the efficiency of the antenna. However, the greater is distance B (for a fixed overall antenna size), the larger the inductors must be to maintain resonance. Theoretically, if the coils were placed at the outer ends of the dipole, they should be infinite in value to maintain resonance. Capacitive loading of the ends, either through proximity of the antenna to other objects or through the addition of capacitance hats, will reduce this requirement to a more practical value.

What Inductance Values?

As a matter of personal interest, this writer has been doing experimental work for a number of years with off-center-loaded antennas. One big drawback to such experimentation was the ever-present need for a large amount of cut-and-try work to arrive at resonance whenever a new set of dimensions was to be used. Probably the number of pruned-off turns from coil stock from such experiments, if straightened out and soldered end to end, would make up several full-sized half-wave antennas for the 160-meter band. Therefore, most of the writer's work of late in this area has been in going through paperwork exercises, looking for a way whereby at least "ball-park" values of inductance needed for a particular system could be calculated.

The equation contained in the Mobile chapter of *The ARRL Antenna Book* for determining the capacitance of a vertical antenna shorter than a quarter wavelength looked promising in early computations,

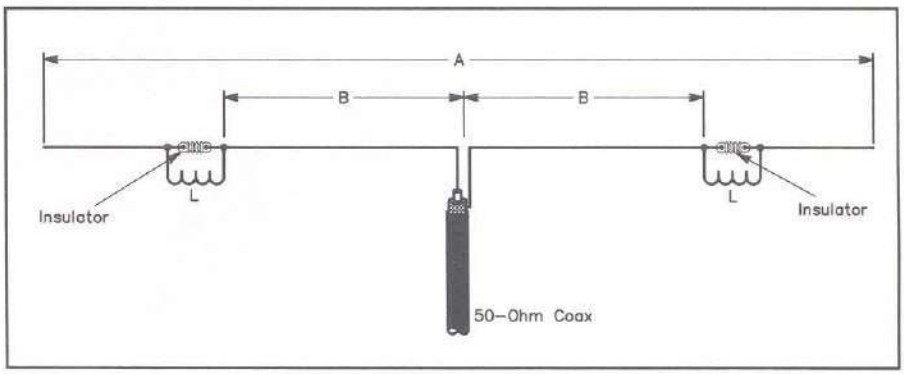

Figure 1—A dipole antenna lengthened electrically with off-center loading coils. For a fixed dimension A, greater efficiency will be realized with greater distance B, but as B is increased, L must be larger in value to maintain resonance.

and, indeed, it became the basis for the calculation procedure which finally resulted.

This procedure has been found to produce results much closer than mere "ball-park" values for the necessary inductance – for wire antennas "in the clear" at moderate heights, the final inductance values found by cut-and-try pruning for lowest SWR at the desired frequency have been so close to the value from calculations that a laboratory bridge was necessary to measure the difference. The results are equally good for elements using tubing. Once the needed inductance value is determined by calculations, it is generally found sufficient to obtain coil dimensions from an ARRL L/C/F Calculator (see LaPlaca*) or by equation. Any significant pruning which has been found necessary could always be attributed to objects in proximity to the ends of the antenna.

The complete set of calculations is expressed in the mathematical relationship below as Eq. 1, presented here primarily for mathematics buffs or those having access to electronic computers.

This equation yields the inductance required, in microhenrys, for single-band resonance of a shortened antenna of a particular physical size at a given frequency, for a specific position of the loading coils from the center of the antenna. To spare the reader the task of performing some rather tedious calculations, Figure 2 has been prepared from Eq. 1. The curves of the chart have been normalized, and may be used for any frequency of resonance. The chart is based on a halfwavelength/diameter ratio of the radiator of approximately 24,000. (This corresponds to No. 14 wire on 80 meters or No. 8 wire on 160 meters.) For "thinner" conductors, the required inductance will be somewhat greater than that determined from Figure 2, and less inductance will be required for "thicker" conductors.

The use of the chart is as follows: At the intersection of the appropriate curve from the body for dimension A and the proper value for the coil position from the horizontal scale at the bottom of the chart, read the required inductive reactance for resonance from the scale at the left. Dimensions A and B are shown in Figure 1, and for use with the chart are expressed as percentages. Dimension A is taken as percent length of the shortened antenna with respect to the length of a resonant half-wave dipole of the same conductor material. Dimension B is taken as the percent of coil distance from the feed point to the end of the shortened antenna. For example, resonating an antenna which is 50% or half the size of a half-wave dipole (one-quarter wavelength overall), with loading coils positioned midway between the feed point and each end (50% out), would require loading coils having an inductive reactance of approximately 950 ohms at the operating frequency. If the antenna is hung "in the clear," and if the length/diameter ratio of the conductor is near 24,000, inductance values as determined from the chart will be very close to actual values required. (Eq. 1 above takes the diameter of the radiator into account, and thus may be used for any length/diameter ratio.) For practical purposes, dimension B may be taken as that distance from the center of the feed-point insulator to the inside eye of the loading-coil insulator, and dimension A as the eye-to-eye distance inside the end insulators (which are not drawn in Figure 1).

Proximity of surrounding objects in individual installations may require some pruning of the coils, and the exact amount of final inductance required should be determined experimentally. If the antenna is hung in inverted-V style, with the ends brought near the earth, the required inductance will almost always be somewhat less than that determined from the chart or equation. A grid-dip meter, Macromatcher, (see Hall and Kaufmann*) or SWR indicator may be used, during the final adjustment procedure.

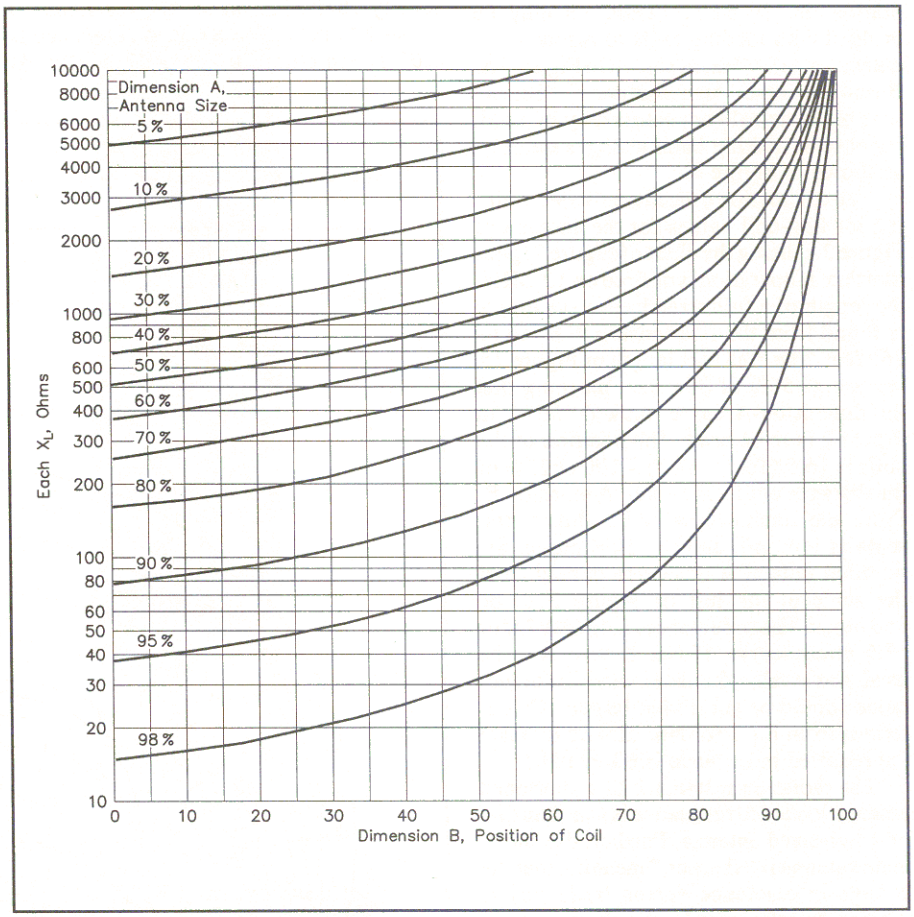

Figure 2—Chart for determining approximate inductance values for off-center-loaded dipoles. At the intersection of the appropriate curve from the body of the chart for dimension A and the proper value for the coil position from the horizontal scale at the bottom of the chart, read the required inductive reactance for resonance from the scale at left. See Figure 1 regarding dimensions A and B.

(Eq. 1):

$$L_{\mu H} = \frac{10^6}{68\pi^2 f^2}\left\{\frac{\left[ln\frac{24\left(\frac{234}{f}-B\right)}{D}-1\right]\left[\left(1-\frac{fB}{234}\right)^2-1\right]}{\frac{234}{f}-B} - \frac{\left[ln\frac{24\left(\frac{A}{2}-B\right)}{D}-1\right]\left[\left(\frac{fA}{2}-fB\right)^2-1\right]}{\frac{A}{2}-B}\right\}$$

where
$L_{\mu H}$ = inductance required for resonance
ln = natural log
f = frequency, megahertz
A = overall antenna length, feet
B = distance from center to each loading coil, feet
D = diameter of radiator, inches

Practical Antennas

Although one might erect an inductively loaded antenna that is cut for a single amateur band, it is possible to use the antenna itself for two, three, or more bands of operation, if provision is made to lower the antenna for band changes. A simple rope halyard and pulley arrangement at one of the supports will do the trick. Figure 3A shows a 3-band antenna of this nature, for 160, 80, and 20 meters. If the insulators shown are left open, with nothing bridging them, the antenna is a simple half-wave dipole cut for 14.18 MHz. (The 48.5-foot lengths act merely as support wires, and have negligible effect on operation of the antenna.) If the insulators are bridged with short lengths of antenna wire, the antenna becomes a center-fed 80-meter dipole, resonant at about 3.6 MHz. For 160-m operation the 20-meter insulators may be bridged with loading coils to resonate the antenna at 1.8 MHz, as shown in Figure 3A. Burndy or other manufacturers' "Servit" type of electrical connectors may be used, for ease in making band changes quickly, as shown in Figure 4.

The calculation procedure for determining loading-coil values for the antenna of Figure 3A, using the chart of Figure 2, goes like this. If operation is desired on 1.8 MHz, the length of a full-sized half-wave dipole is found from the relationship $468/f$ to be 260 feet. The 130-foot length of Figure 3A represents 50% of this size, meaning that the dimension-A curve marked "50%" in Figure 2 is to be used. The position of the coils is $16.5/(16.5 + 48.5) \times 100$ or 25% of the distance out from center, dimension B. From the intersection of 25 (horizontal scale at bottom), and the 50% curve, the required inductive reactance is read from the scale at the left of Figure 2 to be 650 ohms. The inductance, L, is $650/2\pi f$ or 57.5 microhenrys, if No. 8 wire is to be used. For smaller diameter wire, the inductance should be somewhat larger. (Calculations from Eq. 1 for No. 12 wire indicate the required inductance is 60.99 µH.)

The radiation resistance of a shortened antenna loaded to resonance is less than that of a full-sized antenna. Further, the shortened antenna is "sharper," meaning that the change in reactance versus frequency is greater. In other words, the shortened antenna acts as a tuned circuit having a higher Q than a full-sized antenna. To check these characteristics, the line input impedances for the antenna of Figure 3A were measured with a laboratory bridge, and the electrical line length at the measurement frequency was then taken into account to determine the impedance at the antenna feed point. The antenna was constructed of No. 12 wire and hung at a height of 50 feet as a "flat-top" radiator.

The solid curve of Figure 3B is a plot of the feed-point impedance versus frequency for this antenna. The plot on Smith Chart coordinates is more meaningful than a simple SWR-vs.-frequency curve because the magnitudes of the resistive and reactive components are shown, as well as the sign of the reactance. (Capacitive reactance is negative, plotted to the left of the vertical center line, and inductive reactance is positive, plotted to the right.) In this presentation, a 50-ohm nonreactive impedance will appear at the exact center of the chart. The SWR in 50-ohm line for a given frequency may be determined by first noting the distance from the center of the chart to the particular impedance plot on the curve, and next measuring this same distance down the vertical center line from chart center (a drawing compass is helpful for this task), and finally dividing 50 into the value read at that point on the center line. For example, the SWR at 1.8 MHz equals 120/50 or 2.4, as indicated by the segment of the 2.4 SWR circle in Figure 3B. It may be seen that resonance (zero reactance) occurs at approximately 1810 kHz, where the resistance is about 22 ohms. The SWR at resonance is 2.33:1, and climbs to 3:1 at 1825 kHz. At 1850 kHz, the SWR is 10:1. Without any matching provisions the antenna is relatively sharp, as mentioned earlier. If one sets the usable bandwidth as the frequency range where the SWR is 3:1 or less, it is approximately 35 kHz, or 1.9% of the resonant frequency. As far as efficiency is concerned, ohmic losses are low, and the antenna is a good performer on 160 meters. Because of its horizontal polarization, it has proved to be most effective at night, and stations several hundred miles away have been worked with S-9 reports received for the 50-watt signal.

For a comparison of impedances, the broken curve of Figure 3B is a plot of measured impedances of a full-size half-wave dipole, 260 feet long overall, hung in place of the shortened antenna. From this curve it may be seen that resonance occurs at 1810 kHz, where the resistance is 59 ohms. The 3:1-SWR bandwidth for the half-wave antenna is in the order of 60 kHz, or 3.3% of the reso-

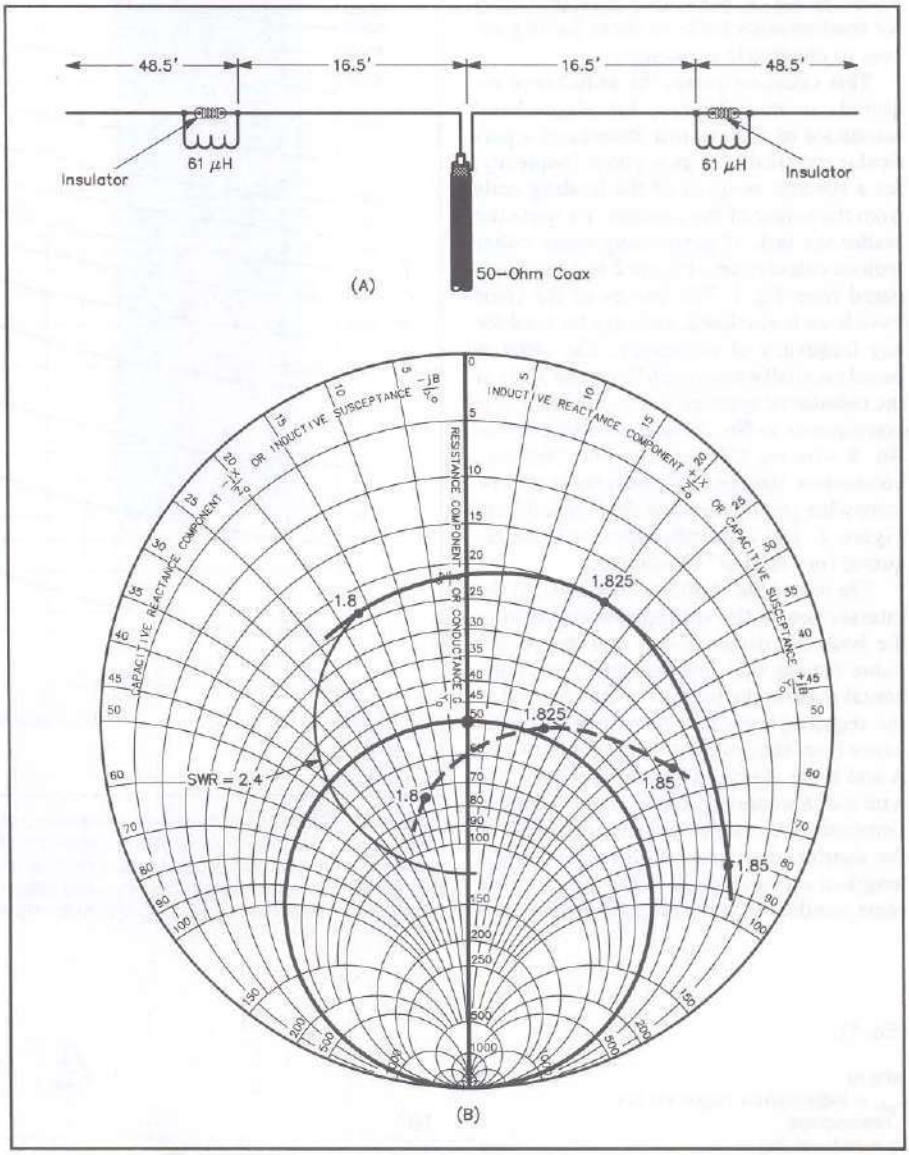

Figure 3—At A, an 80-meter dipole loaded for 160-meter operation. The inductors are 37 turns of coil stock having a 3-inch diameter and 10 turns per inch (B&W 3035). At B, the impedance plot of this antenna installed at a height of 50 feet (solid curve), and the plot of a 160-m half-wave dipole (broken curve).

nant frequency. It is interesting to note on this curve that the SWR at resonance is 1.18:1, and that it is a somewhat lower value, 1.15:1, at a frequency a few kilohertz above resonance. (Measurements were made every 5 kHz across this band, but plot points are shown only for 25-kHz increments to avoid crowding of the data.) This evidence refutes the oft-heard statement that the SWR-vs.-frequency curve is *always* lowest at antenna resonance. Points to remember are that the SWR in a transmission line is completely dependent upon the characteristic-impedance value of the line in use. Using a line of different impedance may shift the position of the SWR curve along the frequency axis in a simple SWR-vs.-frequency plot. This is definitely true in this case — if the 160-meter half-wave dipole were to be fed with 75-ohm line, the lowest SWR would occur at a frequency about 5 kHz *below* antenna resonance, whereas with 50-ohm line the lowest SWR is at a frequency slightly *above* resonance. The reason this happens is that the resistive component of the impedance, which consists of the radiation resistance plus any loss resistance, is not constant with frequency, even over a rather narrow frequency range. It must be acknowledged that the differences here are very slight, however, and for practical purposes the frequency of lowest SWR is (within a few kilohertz) the resonant frequency of the antenna.

Another point concerning the SWR values bears noting. The values as determined from the plots in the manner described above are quite accurate, having been determined by measurements with laboratory equipment. In contrast, measurements with simple SWR indicators usually cannot be relied upon for anywhere near the equivalent accuracy.

For example, the author owns a commercially manufactured SWR indicator of the Monimatch type (see McCoy*) which, under a particular set of conditions, indicates a 2.5:1 SWR in a line where laboratory measuring equipment shows the *true SWR to be 4:1.* A significant difference! Herein lies another reason why impedance plots on Smith Chart coordinates are more meaningful than a simple SWR-vs.-frequency curve — greater accuracy may generally be expected.

A Half-Size 80-Meter Antenna

Figure 5A shows the 3-band concept described earlier as it can be applied to 80, 40, and 20 meters. Its overall length is 66 feet, not a difficult length to use on a small lot. This antenna was constructed for 80-m operation with a design-center frequency of 3.55 MHz, using No.12 antenna wire and 40-μH loading coils—27 turns of stock having a diameter of 3 inches and a pitch of 10 turns per inch (tpi). Feed-point impedances versus 80-m frequency for the antenna, hung at a height of 50 feet, are shown by the solid curve at B of Figure 5. Actual resonance occurred at 3.54 MHz, where the resistance was about 26 ohms. The bandwidth within which the SWR is 3:1 is

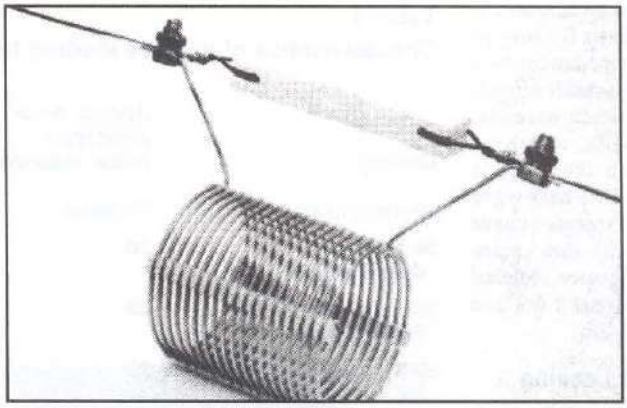

Figure 4—Copper electrical service connectors, sold under one trade name of Servit, provide a simple means of installing the loading coils. The antenna wire and the ends of the coil wires should be tinned to prevent corrosion. In addition, a protective coating of acrylic spray may be used at each connection.

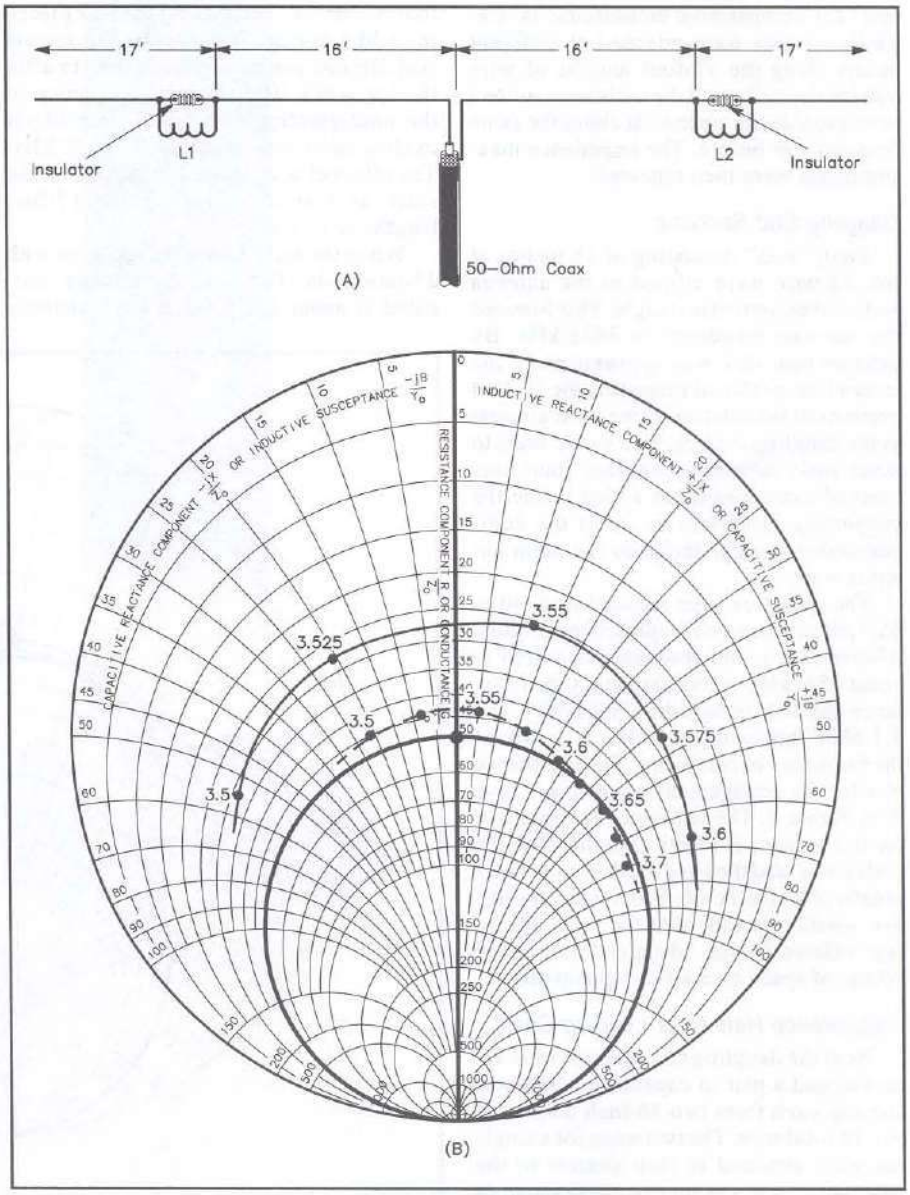

Figure 5—At A, a 40-meter dipole loaded for 80-meter operation. For resonance at 3.55 MHz the coils should be approximately 40 μH (27 turns of stock); 3.75 MHz, 35 μH (24 turns); 3.9 MHz, 31 μH (22 turns); and 4.0 MHz, 29 μH (21 turns). These are circulated inductance values for No. 12 antenna wire. Coil stock referenced above is 3-inch diameter, 10 turns per inch (B&W 3035). At B, the impedance plot of the 3.55-MHz version (solid curve) and of an 80-m half-wave dipole (broken curve).

60 kHz, or 1.69% of the resonant frequency.

Also shown in Figure 5B, by the broken curve, are the feed-point impedances of a half-wave dipole, 132 feet overall length, hung in place of the shortened antenna. Resonance occurs at 3.54 MHz, where the resistance is 43.5 ohms and the SWR is 1.15:1. The broader nature of the half-wave antenna is exhibited by the "tighter" curve which swings closer to the 50-ohm center point of the chart than the shorter, loaded antenna. The SWR at 3.5 MHz is 1.6:1 and remains below 3:1 to 3.67 MHz.

Table 1
Characteristics of various loading techniques, 66-foot 80-m dipole.

Loading	*Approx. feed-point resistance, resonance*	*SWR at resonance*	*3:1-SWR bandwidth, % of resonant freq.*
40-μH coils only	26 ohms	1.92:1	1.69
36.5-μH coils, 18″ dangling ends	26	1.90:1	1.79
36″ hats outside 32.5-μH coils	23	2.15:1	1.68
30-μH coils, 36″ hats at ends	25	1.98:1	2.05
None (λ/2 dipole)	43.5	1.15	Greater than 3.6

Coil positions for each loaded antenna were 16 feet from antenna center. All antennas were constructed of No. 12 wire and installed at a height of 50 feet.

Capacitive and Inductive Loading

One would assume that a combination of capacitive and inductive loading might provide a different feed-point impedance than would inductive loading alone, because of different current distributions in the radiators. To check out this assumption, the antenna of Figure 5A was used as a "test bed" for comparative measurements. Capacitance hats were attached at different points along the 17-foot lengths of wire outside the coils, and the coils were pruned to reresonate the antenna at about the same frequency as before. The impedance measurements were then repeated.

Dangling End Sections:

First, "hats" consisting of 18 inches of No. 12 wire were affixed to the antenna ends and permitted to dangle. This lowered the resonant frequency to 3435 kHz. By calculations, this was approximately the same effect as that of extending the 17-foot portions of the antenna by the same amount as the dangling lengths, so it would seem to make little difference whether short sections of extra length are added inside the supporting insulators or are at the ends, suspended at right angles to the main antenna wire.

The inductors were reduced from 40 to 36.5 μH (25-turn coils replaced the original 27-turn coils), and resonance occurred at about 3575 kHz. At this frequency the resistance was 26 ohms and the SWR 1.90:1. The 3:1-SWR bandwidth, 64 kHz, is 1.79% of the frequency of resonance. The impedance plot for this arrangement is shown as Curve A in Figure 6. The resistance at resonance for this antenna is identical to that with the coils alone, and the bandwidth is only 4 kHz greater, 64 kHz vs. 60. From these results, one would conclude that the main advantage offered by the "danglers" is a small saving of space over a flat-top antenna.

Capacitance Hats Near Loading Coils:

Next the dangling end sections were removed and a pair of capacitance hats was formed, each from two 36-inch lengths of No. 12 solid wire. The two wires for a single hat were attached at their centers to the antenna wire at a point just outside one of the loading coils. The hat wires were then bent radially to form an X at right angles to the antenna wire, like four spokes of a wheel with the main antenna wire at the hub. The diameter of the X-shaped hat was thus 36 inches. The second hat was placed in a like manner just outside the second coil. Burndy connectors were used to affix the hat wires. The resonant frequency of this configuration with the original 40-μH loading coils was found to be 3290 kHz. The effect of adding the hats was about the same as that of extending the 17-foot lengths to 19 feet.

When the inductors were replaced with 23-turn coils (32.5 μH), the antenna resonated at about 3.575 MHz, the resistance being 23 ohms. The SWR at resonance is 2.15:1, and the 3:1-SWR bandwidth for this configuration is 60 kHz, 1.68% of the resonant frequency. The impedance of this arrangement versus frequency is shown by Curve B of Figure 6.

It is surprising to note that, by the standards of most amateurs, the characteristics of this antenna are not as good as those of the same length antenna with loading coils alone. The SWR at resonance for the antenna with combination capacitive and in-

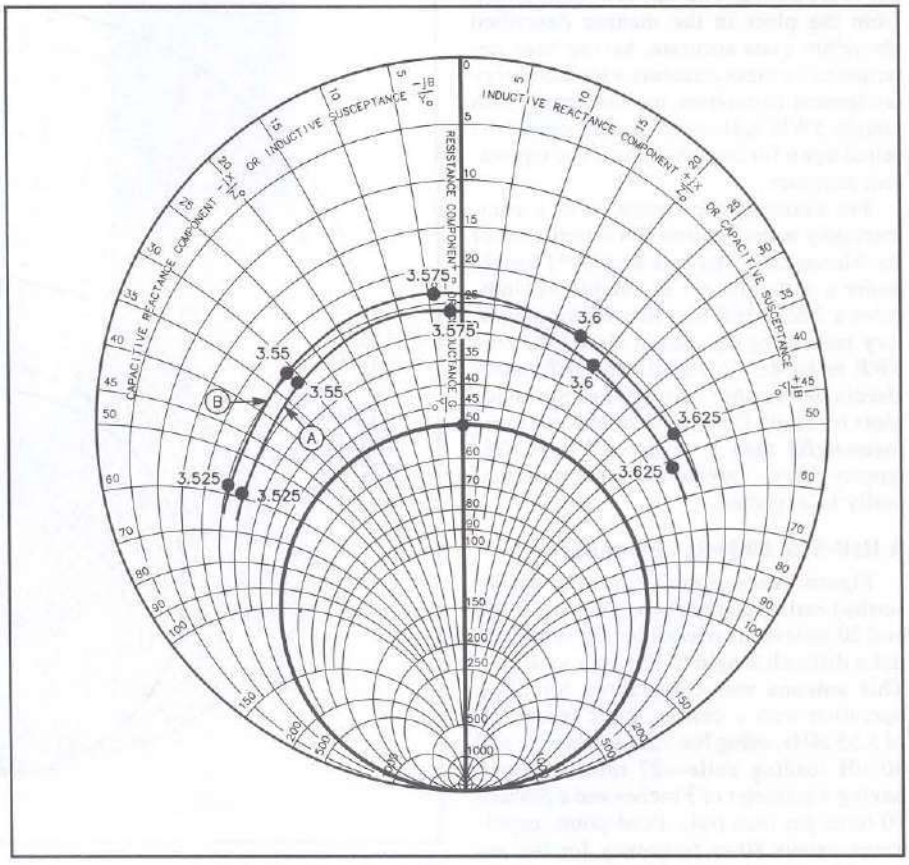

Figure 6—Curve A is the impedance plot of the antenna of Figure 5A with 1.5-foot dangling end sections added and the coil trimmed to restore resonance near the original frequency. Curve B is a plot of the same antenna with X-shaped capacitance hats added at a point just outside the loading coils (dangling sections removed and coils trimmed to reestablish resonance).

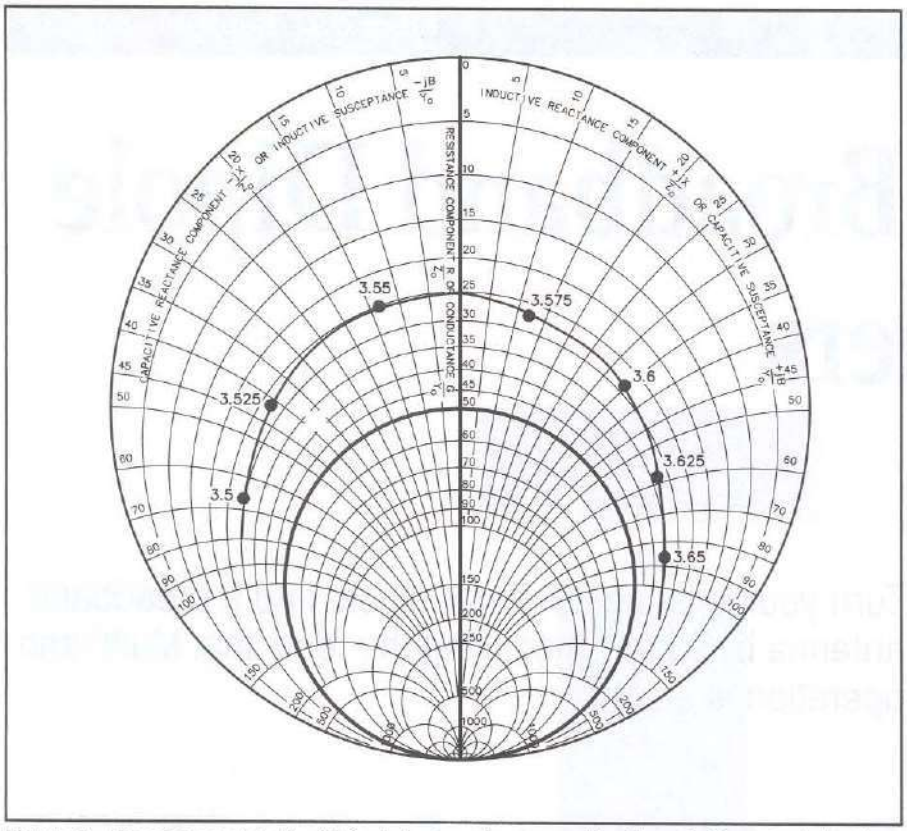

Figure 7—Impedance plot of a 66-foot dipole using a combination of off-center inductive loading and capacitive end loading. Of all the shortened configurations tried, this arrangement offered the greatest bandwidth.

ductive loading is higher (2.15 vs. 1.92), and the 3:1-SWR bandwidths are the same, 60 kHz. Perhaps a significant factor here, though, is that the diameter of the capacitance hats used for these measurements was small, only .011 wavelength. Supporting much larger hats presents mechanical problems with wire antennas, however, as even these were a bit flimsy and would require reshaping after gusty weather.

Capacitance Hats at Antenna Ends:

Finally, the X-shaped capacitance hats were moved to the outside ends of the antenna, just inside the end insulators. With the original 40-μH coils, resonance appeared at 3215 kHz. From calculations, it was as if the 17-foot end sections were actually 21 feet long. With 30-μH coils (22 turns) in place, the resonant frequency was 3560 kHz. At this frequency the resistance was 25 ohms and the SWR 1.98:1. The 3:1-SWR bandwidth is 73 kHz, or 2.05% of the resonant frequency. The impedance plot of this antenna is given in Figure 7.

It is interesting to note that the position and shape of the plot for this antenna on Smith Chart coordinates is nearly identical to that for the same length antenna with loading coils only, the solid curve of Figure 5B. For this antenna, however, the plot points for 25-kHz frequency increments appear closer together, which accounts for the increased bandwidth.

Conclusions:

The measured characteristics of these various configurations of loading for the 80-meter antennas are tabulated in Table 1. Remember that the overall "flat-top" length of each antenna arrangement, is 66 feet, and that the loading coils are always positioned 16 feet each side of the center of the antenna, being pruned for resonance at approximately 3550 kHz. For comparison, information for a half-wave dipole is also included.

Of the various arrangements, capacitive end loading decidedly provides the greatest bandwidth, excepting the full-size half-wave antenna, of course. Although there are slight differences in the resistance value at resonance, all are of the same order of magnitude. These values, as well as those for the 160-m antenna discussed earlier, tend to confirm a *broad* rule of thumb that the writer has formulated for this type of antenna: The feedpoint impedance value at resonance is roughly proportional to the length of the antenna. That is, a loaded antenna which is half the size of a half-wave dipole will have approximately half the radiation resistance of the full-sized antenna.

Eq. 1 given earlier or the chart of Figure 2 allows one to calculate loading-coil values for antennas with loading coils only. Additional capacitive loading is not taken into account. Calculating the effects of various capacitive loading arrangements appears to be difficult, and work remains to be done in this area.

Multiband Antennas with Loading Coils

All of the foregoing material has been devoted to the loading of an antenna for resonance at a single frequency. Resonated as described, the antenna is electrically a half wave in length. It will, however, operate well on higher frequencies — frequencies at which it is an odd multiple of half waves, in *electrical* length . . . three half waves, five half waves, etc. Because of the lumped loading of the shortened antenna, these higher frequencies will likely not be closely related to odd-order harmonics of the fundamental frequency, as the case would be for a nonloaded radiator. (For example, it is a well-known fact that a 7-MHz half-wave dipole operates well on its third harmonic, 21 MHz.)

A loaded dipole will become an electrical 3/2-λ antenna at some frequency *below* that which is three times the fundamental resonant frequency. Depending upon the overall antenna length, coil value, and coil position, it is possible for an 80-meter loaded dipole to become a 3/2-λ performer on 40 meters. With such an arrangement, one would have a dual-band antenna without requiring the use of traps. The idea can be expanded upon to arrive at a loaded antenna without traps which will operate on more than two bands. This scheme offers considerable constructional simplification as compared with trap arrangements.

The multiband loading-coil concept has been recognized for better than half a century, but little use of the technique has been made by amateurs. Some years ago a very good article on the subject a was published by William Lattin, W4JRW.* That article is recommended reading for anyone interested in more details on the concept. Supplemental information has been published by Buchanan.* Attempts by this writer to calculate antenna sizes and coil values for dual-band antennas have met with some success. From calculations and experiments to date, it appears that with only two loading coils (one each side of center), the antenna must always be greater than a half wave in physical length for the higher of the two frequency bands. In other words: any 80/40 meter arrangement, for example, apparently would need to be longer than 66 feet from tip to tip. However, much work also remains to be done in this area.

References

Buchanan, "An Inexpensive 40- and 80-Meter Antenna," Hints and Kinks, *QST*, September, 1962, p. 62.

Hall and Kaufmann, "The Macromatcher, An RF Impedance Bridge for Coax Lines," *QST*, January, 1972, p. 14. Information also contained in the 50th and subsequent editions of *The Radio Amateur's Handbook*, and the 13th edition of *The ARRL Antenna Book*.

LaPlaca, "Using the ARRL L/C/F Calculator," *QST*, December, 1973, p.26.

Lattin, "Multiband Antennas Using Loading Coils," *QST*, April, 1961, p.43.

McCoy, "Monimatch, Mark II," *QST*, February, 1957, p. 38. Also, "An Etched-Circuit Monimatch For Checking Your Antenna System," *QST*, October, 1969, p.29.

Sevick, "The Ground-Image Vertical Antenna," *QST*, July, 1971, p. 16. Also, "The W2FMI Ground-Mounted Short Vertical," *QST*, March, 1973; "A High Performance 20- 40- and 80-Meter Vertical System," *QST*, December, 1973, p. 30; and "The Constant-Impedance Trap Vertical," *QST*, March,1974,p.29.

By Frank Witt, AI1H

From *QST*, September 1993

A Simple Broadband Dipole for 80 Meters

Turn your existing 80-meter dipole into a broadband antenna by simply modifying the feed line. Multiband operation is an option.

A conventional coax-fed, half-wave dipole doesn't provide a low SWR over the entire 80-meter band—an inconvenience for those of us who like to operate phone and CW on that band. Several approaches to overcoming this limitation, short of an antenna tuner in the station, have been described.[1,2] The antenna system described here is simpler than any of its predecessors and has the following features:

- A 2:1 SWR or better is achieved over all or most of the 80-meter band.
- Antenna length and appearance are the same as those of a conventional half-wave dipole. Consequently, it's lightweight and has small wind and ice loading.
- The antenna configuration permits multiband operation with a single feed line.
- The losses due to broadband matching are acceptable.
- The cost is about the same as a conventional half-wave dipole.

All the SWR data given in this article were measured at the transmitter end of the feed line. The reference impedance is 50 Ω, since most equipment is designed for this impedance. The term *antenna system* as used throughout this article includes not only the radiating wire, but also the feed line, balun (if used), any lightning-protection measures, antenna tuner and so forth.

The dipole antenna itself is not broadband; the system uses a broadband *match*. The key broadbanding element of this antenna system is the *transmission-line resonator*: Part of the transmission line compensates for the reactance presented by the dipole away from its resonant frequency. This part of the line is a multiple of an electrical half wavelength. Another part of the line presents an appropriate source impedance to the transmission-line resonator (TLR).

First I'll describe a version of the broadband antenna system, along with some practical results. Then I'll cover the important matter of antenna-system loss. Following that are some variations to suit specific requirements, and a method for using the antenna for several bands. I'll also compare transmission-line-resonator broadbanding to other broadbanding methods.

The 80-Meter Broadband Antenna System

Figure 1 shows the simple broadband antenna system as used at my station. The antenna proper is a center-fed half-wavelength dipole. The transmission line is segmented into one electrical wavelength of 50-Ω coax and an electrical quarter wavelength of 75-Ω coax. The calculated and actual lengths are shown in Table 1. Lengths were calculated using the formulas given later in this article, using a center frequency (F_0) of 3.75 MHz and VF (velocity factor) of 0.66. The actual lengths resulted after I performed the tuning procedure described later. Manufacturing variations from the published cable velocity factors, and some stretching of the coax, contributed to the differences between actual and measured values. (The actual lengths were measured on untensioned cable.) The antenna is installed as an inverted V with a 140° included angle and an apex height of 60 feet. The wire size is #14, but is not critical.

Table 1
Calculated and Actual Lengths of the Broadband Dipole Antenna at AI1H

	Calculated	*Actual*
1/4-λ Coax	43.3 feet	43.3 feet
1-λ Coax	173.1 feet	170.5 feet*
Dipole	124.5 feet	122.7 feet

*Includes 11 inches for balun.

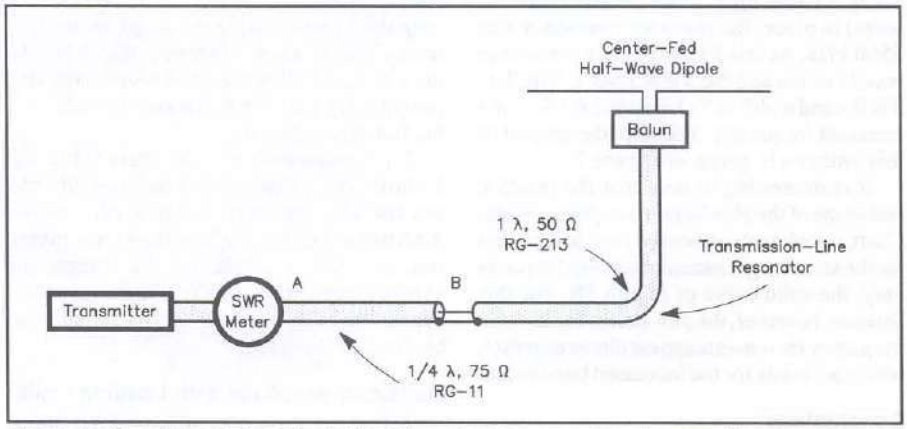

Figure 1—One form of the simple broadband antenna system. It resembles a conventional dipole except for the 1/4-wavelength, 75-Ω segment. Points A and B are discussed in the text.

This system's SWR (at the transmitter) as a function of frequency is shown in Figure 2. For comparison, the SWR for the same dipole fed with about 5/4 wavelengths (214 feet) of RG-213 coax is also shown. (This is the same total length as the RG-213 and RG-11 segments used in the broadband system.) The broadband system's 2:1 SWR bandwidth is 2.2 times that of the conventional system—and the *only* difference is the feedline configuration!

The radiating properties of the broadband antenna over the 80-meter band are essentially identical to those of a dipole cut for any specific frequency in the band. Also, since the antenna system is designed for a 50-Ω transmitter, the feed-line length may be extended by adding the required length of 50-Ω coax between the transmitter and the quarter-wave segment (point A in Figure 1).

A 1:1 current balun should be installed at the antenna's feed point. I use the balun on general principles. Often, it provides no visible difference in operation, but the balun does minimize feed-line radiation. You can determine whether your antenna needs a balun by measuring the SWR versus frequency with and without a balun installed. If the balun is not needed, the two sets of data will be identical.

Antenna-System Losses

It's important to know the losses in any antenna system. This is especially true for broadband antennas, because loss alone can broadband an antenna system. As the next section shows, the configurations presented in this article do not yield a significant loss penalty. Although other loss contributors exist in antenna systems, we will focus on the primary ones: *feed-line loss* and *mismatch loss*. Other losses, such as ohmic loss in the antenna wire, are the same for both the conventional and broadband systems described here.

Feed-line loss is the easiest to understand. It is unavoidable, and is lowest when the feed line is *flat* (when the line SWR is close to 1:1). At HF, feed-line loss results primarily from ohmic losses in the copper conductors.

Mismatch loss occurs when the impedance seen by the transmitter is not the complex conjugate of the transmitter's impedance (when the line SWR at the transmitter is not 1:1). For a 50-Ω transmitter, the mismatch loss is 0 dB when the load impedance is 50 Ω. When the load impedance is not 50 Ω, the mismatch loss can be made to be 0 dB if a transmitter with a tunable output stage (such as a conventional tube-type linear amplifier) is tuned for a conjugate match. An antenna tuner can also provide this match. In this case, however, the antenna-tuner loss (perhaps as much as 1 dB) replaces the mismatch loss in the total-loss equation. That subject isn't discussed here.

If you don't use an antenna tuner and the transmitter has a fixed-tuned 50-Ω output, loads that present the transmitter with an SWR under 2:1 are highly desirable. The impact of high SWR on mismatch loss will become clear in the next section.

Loss must be kept in perspective. All of the broadband antenna systems described here have a worst-case total loss of less than 3 dB—not enough to notice in many 80-meter QSOs. (If the loss is 3 dB, half of the transmitter's output power is radiated and half is lost elsewhere.) The main effect of loss is stress on system components: that on the transmitter due to the mismatched load, and that on the transmission line due to heating.

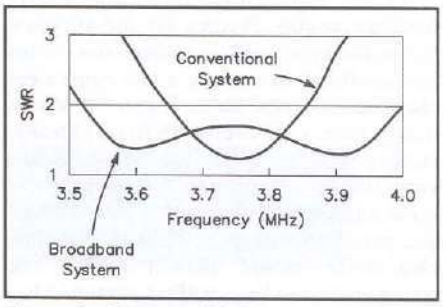

Figure 2—Measured SWR versus frequency for the broadband and conventional antenna systems.

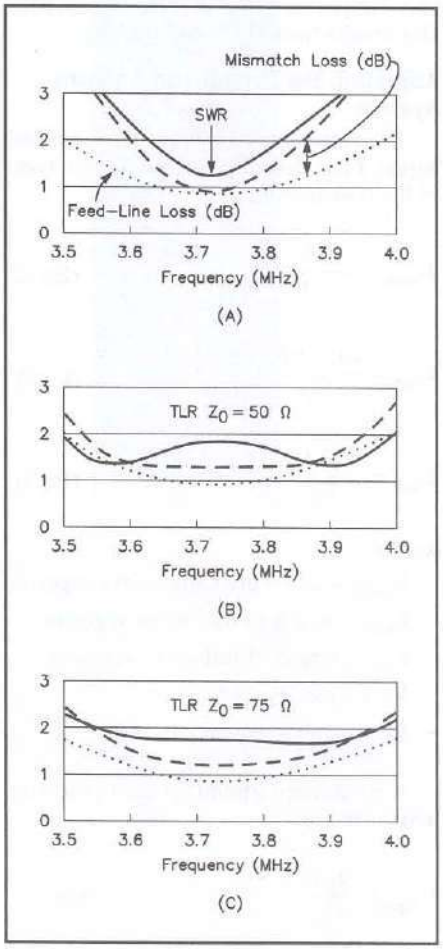

Figure 3—Antenna-system configurations for long feed-line runs. The solid lines are SWR; the dotted lines are feed-line loss; and the dashed lines are feed-line loss plus mismatch loss. At A, a conventional system using an RG-213 feed line; at B, the feed line is a 1/4-λ section of RG-11 (75 Ω) followed by 1 λ of RG-213; and at C, a 1/4-λ segment of RG-11 is followed by 1 λ of RG-11 (one 5/4-λ piece of RG-11). The total feed-line length in each case is 216.4 feet.

Variations

The broadband antenna system described above is well-suited for the installation at my station, where the distance between the shack and the antenna is rela-

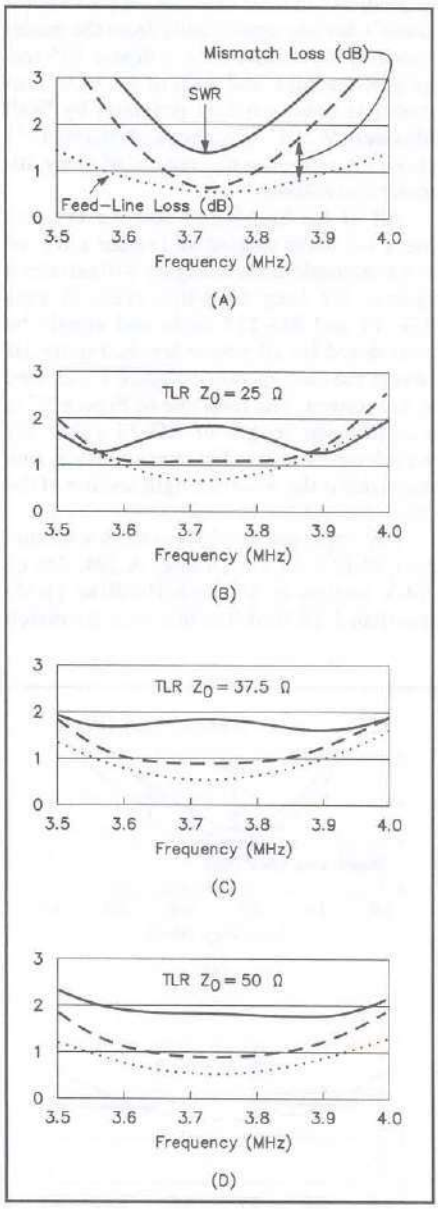

Figure 4—Antenna systems for high power and shorter feed-line runs. The solid lines show SWR; the dotted lines represent feedline loss; and the dashed lines show feed-line loss plus mismatch loss. At A, the feed line is RG-213; at B, it's a 1/4-λ section of RG-11 followed by two paralleled 1/2-λ lengths of RG-213; at C, a 1/4-λ segment of RG-11 is followed by two paralleled 1/2-λ lengths of RG- 11, and at D, 1/4-λ of RG-11 is followed by 1/2-λ of RG-213. The total feed-line length in each case is 129.8 feet.

tively long (more than 200 feet) and because I use a 1-kW amplifier. Other feedline combinations are better suited to other installations. Some of these are shown in Figures 3 through 5, along with calculated SWR and loss data. From this information, you can select an appropriate feed-line combination for your needs.

The figures also show the characteristics of conventional dipole antenna systems. If you compare them, you'll see that the transmission-line resonator provides broadbanding without a significant loss penalty. I haven't tried all these combinations, but based on my experience, they should perform as predicted in most situations if the radiator doesn't deviate significantly from the model I used in my calculations: a dipole 125 feet long, 40 feet high, and made of #14 wire. This model is based on data provided by Walt Maxwell, W2DU, in his book, *Reflections*.[3] I chose his data since it is typical of many 80-meter installations.

All of the broadband antenna systems use a 1/4-wave section and either a 1/2- or 1-wavelength section. Figure 3 illustrates a system for long feed-line runs. It uses RG- 11 and RG-213 cable and should be considered for all power levels. Figure 3B covers the case shown in Figure 1 and used at my station. The feed line of Figure 3C is a continuous length of RG-11 cable 5/4 wavelengths long. The transmission-line resonator is the 1-wavelength section of the cable nearest the antenna.

This approach would also work with surplus 75-Ω CATV Hardline. A 3/4, 5/4 or 7/4-λ section of 1/2-inch Hardline yields less than 2 dB feed-line loss plus mismatch loss over the entire band, and less than 1 dB total loss over any 300 kHz of the band. This configuration is particularly attractive to contesters and DXers, because even a fairly long line7/4 λ is 372 feet of 1/2-inch CATV Hardline—gives low loss and a very good match over, say, the 3.5- to 3.8-MHz range.

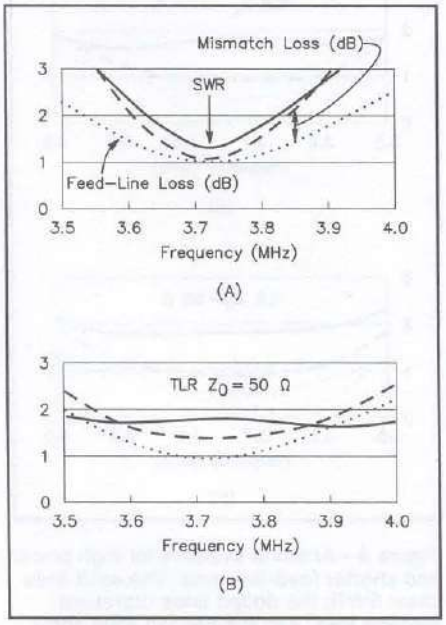

Figure 5—Antenna systems for low power and shorter feed-line runs. The solid lines show SWR; the dotted lines represent feedline loss; and the dashed lines show feed-line loss plus mismatch loss. At A, the feed line is RG-58; at B, it's a 1/4-λ section of RG-59 followed by 1/2 λ of RG-58. The total feedline length in each case is 129.8 feet.

Three broadband antenna systems are shown in Figure 4. All of these are candidates for applications requiring shorter feedline lengths. Figures 4B and 4C show the performance realized when coax cables are paralleled to achieve a low equivalent characteristic impedance. Figure 3B, which results from a 1-wavelength RG-213 transmission-line resonator, and Figure 4B, are very similar. The latter system uses the same amount of cable, but it's cut in half and parallel-connected. This will become clear in the sidebar, "How It Works." The configuration in Figure 4D is attractive because of its simplicity.

Lower-power applications without long feed-line runs can use RG-58 and RG-59 coax. Figure 5B shows how excellent broadbanding is achieved with a remarkably simple feed line. Again, no loss penalty results from the broadbanding.

Adjusting the Broadband Antenna System

The antenna system is easy to build and adjust. First calculate the lengths (in feet) of the transmission-line segments:

$$L_{quarter} = \frac{245.9\,VF}{F_0} \qquad \text{(Eq 1)}$$

$$L_{half} = \frac{491.8\,VF}{F_0} \qquad \text{(Eq 2)}$$

$$L_{full} = \frac{983.6\,VF}{F_0} \qquad \text{(Eq 3)}$$

where

$L_{quarter}$=length of quarter-wave segment

L_{half} = length of half-wave segment

L_{full} = length of full-wave segment

VF = velocity factor

F_0 = center frequency in MHz

A good starting point for the dipole wire length (in feet) is:

$$L_{dipole} = \frac{467}{F_0} \qquad \text{(Eq 4)}$$

For the 80-meter application, I suggest using an F_0 of 3.75 MHz. It's a good idea to cut the wires so that the overall length is 4 feet longer than necessary, in case you need to lengthen the wire during tuning. Pass 2 feet of the extra wire through each end insulator and wrap it back around the antenna wire.

To tune the antenna system, you'll change only the dipole and transmission-line-resonator lengths. The best approach is to build the antenna system as I have outlined here and to measure the SWR at the transmitter end of the system. Any tilt or frequency offset in the SWR characteristic can be removed by increasing or decreasing the dipole or transmission-line resonator length. Start by changing the length of the dipole. To improve the SWR at the high end of the band, the dipole must be shortened; to improve the SWR at the low end of the band, the dipole must be lengthened. Progressively add or subtract 6 inches from both legs of the dipole until the SWR curve is symmetrical about the center frequency.

Frequency offset may be required to center the SWR characteristic in the 80-meter band. You can move the entire curve along the frequency axis without causing asymmetry by changing both the dipole and transmission-line resonator lengths using the following equation:

$$L_{New} = L_{Old}\left(\frac{3750 - \Delta F}{3750}\right) \qquad \text{(Eq 5)}$$

ΔF is the required frequency offset in kilohertz. Shortening the dipole and resonator moves the curve center up in frequency, and lengthening them moves the center down. The length of the quarter-wave segment need not be changed, since the SWR characteristic is not very sensitive to its length.

Lightning Protection

Every antenna system should be designed to minimize the likelihood of a lightning strike. One part of this is keeping all parts of the antenna proper at ground potential. The grounding should be done *outside the shack*, by means of a good ground rod.

I recommend that you install a coaxial lightning protector, which bleeds any static charge from the center conductor, at point B of Figure 1. The protector (and therefore the feed-line shield) should be connected to a high-quality ground rod (the kind electricians use) driven 8 feet into the ground.

Conversion of Existing 80-Meter Dipoles

A study of the cases shown in Figures 3B, 4D and 5B suggests that it's possible to easily convert many existing 80-meter half-wave dipole antennas. Because the most popular way to feed an 80-meter dipole is with a 50-Ω coaxial feed line, the conversion to a broadband antenna system is straightforward. First trim the dipole for resonance at about 3.75 MHz. Then cut the 50-Ω feed line at a multiple of an electrical half-wavelength (at 3.75 MHz) from the antenna. Calculate this length using Eq 2 or Eq 3. Add the 75-Ω quarter-wave section, then complete the run to the shack (if necessary) with 50-Ω coax. Then use the tuning procedure described earlier to optimize the system.

Multiband Operation

Most broadband 80-meter antenna systems are usable only on the 80-meter band, because the broadbanding elements do not allow efficient power transfer on other bands. This is not true with the approach described here, since the structure consists only of a center-fed dipole and a transmission line. Moreover, the transmission-line segments are close to multiples of an electrical half-wavelength near 40 meters and other bands. This opens the possibility for paralleling other half-wave dipoles with the 80-meter dipole and sharing the feed line.

To minimize their interaction, the various dipoles should be spaced from each other away from the feed point. Of course, some interaction will occur and you must tune the multiband system to meet your requirements. I recommend first tuning the 80-meter broadband system and then the next-highest-frequency dipole, and so forth. Only the 80-meter antenna will be broadband, but such broadbanding is not required on the other bands. Figure 6 shows the result of adding a 40-meter dipole to the Figure 1 antenna. Each dipole leg is 34.4 feet long. Note that the SWR on 80 meters changes very little compared to Figure 2. No change was made to the 80-meter dipole or the transmission line.

The multiple-dipole approach described above achieves resonance on several bands and eliminates the need for an antenna tuner on those bands. Of course, if you use an antenna tuner, operation on all HF bands should be possible, but this arrangement is usually not as effective as the multiple-resonance antenna system described here because the feed-line loss is much higher.

Comparison with the Coaxial-Resonator Match

How does the simple broadband dipole described here stack up against other approaches for achieving a good match over the entire 80-meter band? The coaxial resonator match broadband dipole[4,5] represents one of the more efficient designs published to date. It achieves broadband matching at the antenna by the integration of 1/4 wavelength of coaxial cable as a part of the antenna.

Since the coaxial-resonator match achieves a good match at the antenna, the SWR on the feed line is low and the feedline loss is about the same as its matched loss. However, the coaxial cable in the match itself increases the system loss. The net result is that the total loss is about the same with the coaxial-resonator match, but the SWR at the transmitter is lower, never exceeding about 1.6:1 between 3.5 and 4 MHz. Once the SWR is less than 2:1, however, a lower SWR has little value unless you're using a transmitter that significantly reduces power at such SWRs.

Note that the approach described in this article uses a thin wire for the antenna. Most other broadbanding approaches use additional wires or radiators made partly from coaxial cable and are vulnerable to damage from wind and ice loading. Their additional weight and complexity are also limitations.

From the above comparison, the simple broadband antenna system has, by its very simplicity, an edge over the coaxial resonator match, at least in applications where the simpler approach is feasible. Because of the limitations of available coaxial cables, the opportunity for a satisfactory design is constrained. On the other hand, the coaxial resonator match has more adjustment parameters, is useful over a much broader range of applications and yields the lowest SWR over the band.

How It Works

A fundamental way of achieving a broadband match to a resonant dipole antenna involves a parallel-tuned LC network and an appropriate source resistance. In an *RF Design* article,* I described the method for designing such networks, even with lossy resonators. The top of Figure A shows the equivalent circuits of the antenna and matching network. The bottom of Figure A illustrates the corresponding elements in the antenna system.

The role of the resonator is played by the transmission-line segment nearest the antenna. It must be a multiple of an electrical half-wavelength. The quarter-wavelength "Q"-section, made from 75-Ω coax, transforms the 50-Ω transmitter reactance to 112.5 Ω ($75^2/50=112.5$). I won't go into the design details here; they're the subject of another article, "Broadband Matching Using the Transmission-Line Resonator," in preparation for *The ARRL Antenna Compendium, Volume 4.*

For the structure of Figure A to yield a broadband match, the characteristic impedance of the transmission-line resonator and the transmitter resistance must be within a range of values. Fortunately, commonly used transmission lines, which are available in 50- and 75-Ω characteristic impedances, work well in this application. The broadband systems of Figures 3 through 5 show the usefulness of this approach.

Figure B makes another significant point. For this application, the network parameters of a one-wavelength transmission-line resonator (top) are similar to those of a half-wavelength resonator (bottom) with half the characteristic impedance of the upper resonator. Parallel-connecting two identical cables is a convenient way of achieving lower characteristic impedances. This explains the similarity of Figures 3B and 4B and the similarity of Figures 3C and 4C.—*AI1H*

*F. Witt, "Optimum Lossy Broadband Matching Networks for Resonant Antennas," *RF Design*, Apr 1990, pp 44-51 and Jul 1990, p 10.

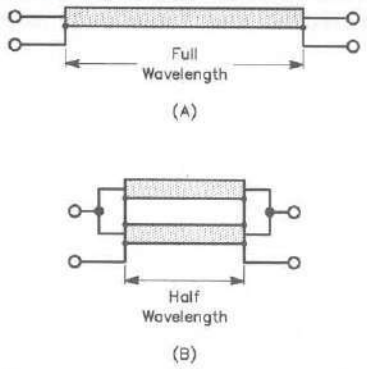

Figure A–Lossy broadband-matching-network equivalent circuit (top), and corresponding simple broadband antenna system elements (bottom).

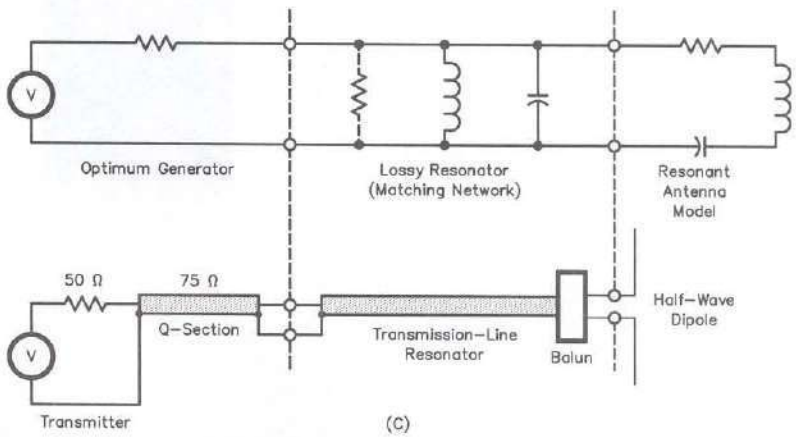

Figure B–These two transmission-line resonators behave essentially the same in this application. The characteristic impedance of each cable segment is the same, making the characteristic impedance of the lower resonator half that of the upper one.

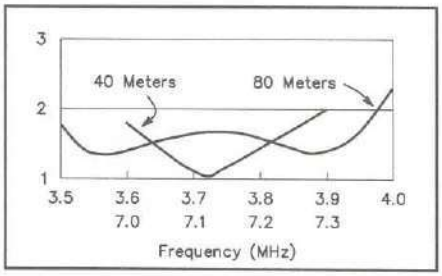

Figure 6—Measured SWR for the 80- and 40-meter multiband antenna system.

Summary

The simple broadbanding technique I've described here capitalizes on the common availability of coaxial cables that fit the application. It overcomes the narrow bandwidth limitations of a conventional 80-meter, half-wave dipole without significant disadvantages. Even parallel dipoles for other bands may be fed with the same feed line.

The limitation of available coaxial cable parameters can be overcome by using the transmission-line resonator as a resonant transformer. Applying this technique is described in an upcoming *ARRL Antenna Compendium* article, "Broadband Matching Using the Transmission-Line Resonator."

This work has benefited from the support and encouragement of my wife, Barbara, N1DIS. Also, I must credit Andrew Griffith, W4ULD, for helping to turn my attention to the approach described here. After reading my *QST* article on match bandwidth of resonant antenna systems,[6] Andy noted that antenna systems should be viewed from their match to a 50-Ω transmitter, even if the feed line does not have a 50-Ω characteristic impedance. He showed examples of the narrowing of match bandwidth to make his point. In my response, published with Andy's letter in *QST*,[7] I pointed out that match bandwidth of an antenna system may actually be *increased* by selecting the right cable length and characteristic impedance. As an example, I showed in Figure 3 of that correspondence the large match bandwidth of a dipole fed with a 5/4-wavelength, 75-Ω RG-11 cable. Note that this is the same case shown in Figure 3C of this article. Thank you, Andy!

Notes

[1]G. Hall, ed, *The ARRL Antenna Book*, 16th ed (Newington: ARRL, 1991), pp 9-1 through 9-12.

[2]M.W. Maxwell, *Reflections: Transmission Lines and Antennas* (Newington: ARRL, 1990), pp 18-1 through 18-6.

[3]See Note 2, p 15-19. I frequency-scaled Walt's data, which is equivalent to changing the wire length. This antenna has a Q of 13 and a resonant resistance of 65-Ω. I took into account the fact that the antenna's radiation resistance increases with frequency.

[4]F. Witt, "The Coaxial Resonator Match and the Broadband Dipole," *QST*, Apr 1989, pp 22-27.

[5]F. Witt, "The Coaxial Resonator Match," *The ARRL Antenna Compendium, Volume 2* (Newington: ARRL, 1989), pp 110-118.

[6]F. Witt, "Match Bandwidth of Resonant Antenna Systems," *QST*, Oct 1991, pp 21-25.

[7]A. Griffith and F. Witt, "Match Bandwidth Revisited," *QST*, Technical Correspondence, Jun 1992, pp 71-72.

Once More With the 80-Meter Broadband Dipole

With reference to earlier items by K1TD and W7ZOI in *QST*, it *is* possible to design a simple, adjustment-free matching network that will make an 80-meter dipole have a reasonable SWR across the band.[1,2] When using Hayward's RLC model of the dipole, a simple parallel-tuned circuit across the antenna feed point gives less than 2:1 SWR across all but the bottom 10- to 20-kHz of the band, as shown in Figure 1.

This method *does* require a source impedance of 140 ohms, so a broadband matching transformer will be needed at the input. I see no reason why you couldn't just tap the input down on L1 and use L1 as an autotransformer to accomplish the impedance matching function. In fact, although I have not tried it, it may be possible to include the balanced-to-unbalanced transformation in the same coil, as shown in Figure 2. To tune this network, use a dip meter with no antenna connected. Then install the network on the antenna and adjust the input tap for the best compromise SWR across the band.

By choosing a lower characteristic impedance, you can get much better SWR over a narrower bandwidth (Figure 1). Retune both the antenna and the network to center the response on either the phone or CW portion of the band.

You can get better SWR in both the fullband and narrow-band case by adding a series-tuned circuit to the input (Figure 3). The improvement is marginal, however, and complicates the impedance step-up arrangement, so it is probably not worth the effort. It would be better to take Hayward's suggestion and make the antenna itself inherently more broadband. One method is to "fatten" the elements by using a wire cage arrangement or similar. Of course this would change the values of Zo, L1 and C1.

The original graphs for Figures 1 and 3 were drawn with an HP-87. I would be happy to send a copy of the rogram to anyone who sends me an s.a.s.e.—*Alan Bloom, N1AL*

[1] J. Hall, "The Search for a Simple, Broadband: 80-Meter Dipole," *QST*, April 1983, p. 22.
[2] W. Hayward, "Limitations to Broadband Impedance Matching," Technical Correspondence, *QST*, July 1984, p. 45.

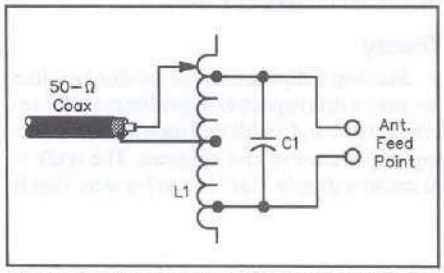

Figure 2—Proposed method of feeding a balanced antenna with unbalanced line. The shielded conductor of the coax line must be connected at the exact center of the coil, which is an electrically neutral point in the antenna system.

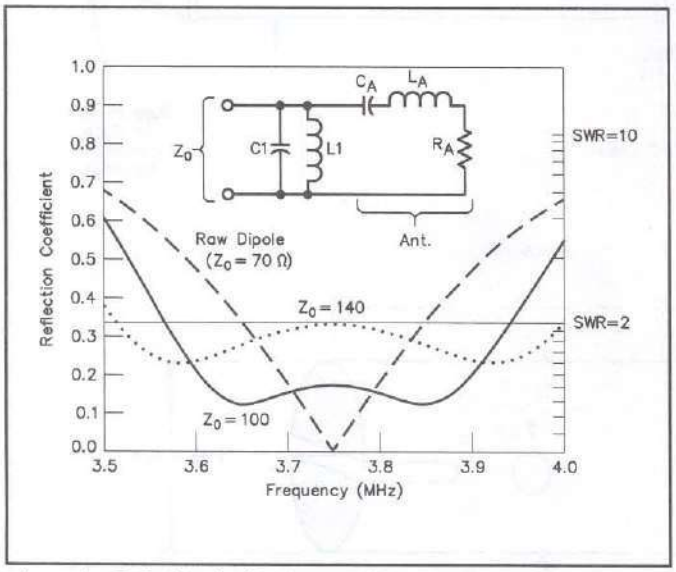

Figure 1—Calculated reflection coefficient and standing-wave ratio vs. frequency for a single-wire dipole and dipoles with lumped constants (C1 and L1) at the feed point.

For the curve where Zo is 140 ohms:
C1 = 2000 pF
L1 = 0.9006 μH

For the curve where Zo is 100 ohms:
C1 = 3500 pF
L1 = 0.5146 μH.

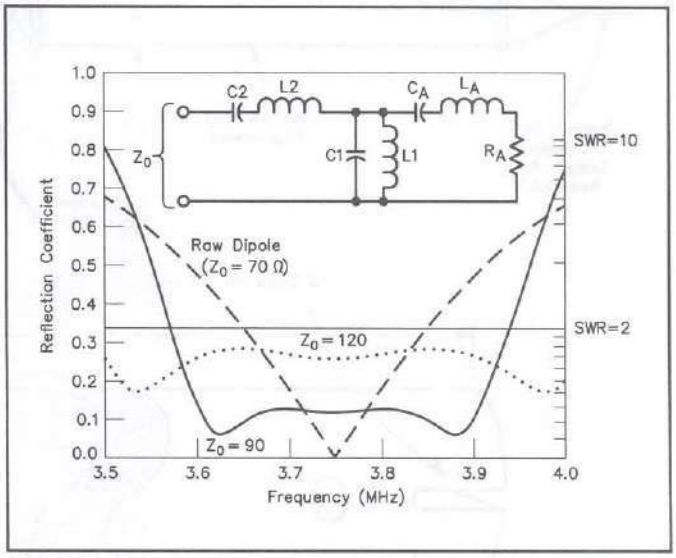

Figure 3—Calculated reflection coefficient and standing-wave ratio vs. frequency for an antenna with shunt and series lumped constants at the feed point (C1-L1 and C2-L2, respectively).

For the curve where Zo equals 120 ohms:
C1–3500 pF
C2–60 pF
L1–0.5146μH
L2–30.0211 μH

For the curve where Zo equals 90 ohms:
C1–7000 pF
C2–60 pF
L1–0.2573 μH
L2–30.0211 μH

Fat Dipoles

Antennas without problems make radio communications enjoyable. I design overseas radio stations for a living, so I'd rather not have to fight my own ham station when just relaxing and rag chewing. Fat dipoles do the things I want. They match the coax line well over a wide band, and they launch the signal remarkably well.

Theory

Making a dipole conductor thicker than normal with respect to wavelength will increase the bandwidth and modify the working impedance of the antenna. The trick is to make a dipole "fat" in such a way that it may be easily constructed from cheap materials, be highly efficient and at the same time arrange things so that it will match the transmission line from the lower band edge to the upper band edge.

I started with the assumption that my band of interest would be the 80/75-meter band. From end to end, this requires a 13% bandwidth to the 2:1 SWR points for my broadband-solid-state final. I also assumed that this antenna was going to be at a nominal height of 30 feet or 0.11 wavelength above ground. The calculations indicated that a dipole built of four quarter-wavelength no. 14 wires (0.064 inch) with a spacing of 0.0114 wavelength would produce the necessary results. The correct length would have to be 0.45 wavelength to match a 50-ohm line.

Length = 442.5/f feet
Width = 11.25/f feet
Height = 112.5/f feet
where f = center frequency in MHz

Construction

Very few problems will be encountered in building this simple fat dipole if you follow the drawing (Figure 1). First you will need five good insulators. I prefer egg type

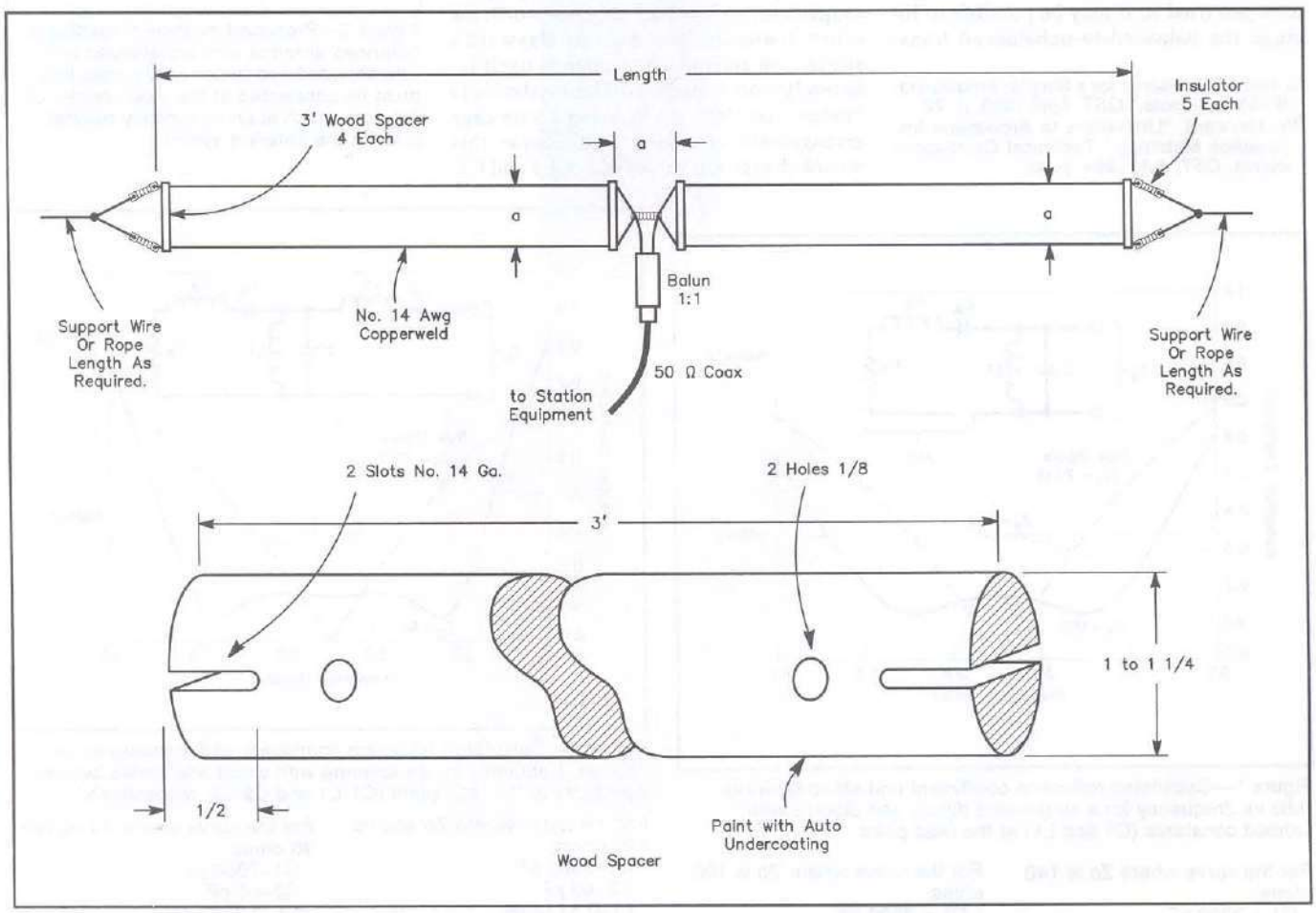

Figure 1—The fat dipole with construction details of the spreaders. See Table 1 for the length and spreader dimensions (A).

insulators but there is no critical problem here. One insulator is for the center of the dipole and the others are for the four ends. You will need four 3-foot-long broom sticks or 1-inch wood or plastic rods with good weatherproofing. I painted mine with auto undercoating but outdoor paint or varnish should also work. Copperweld wire is very desirable because it won't stretch and change the tuning of your antenna. This type of wire is available through advertisements in *QST*. The same source may also be able to supply the essential wide-band balun transformer and coax. Either the RG-58 or RG-8 types of coax cable are satisfactory but the latter requires more support because of its greater weight.

Measure your wire carefully and leave enough extra so that the insulators can be attached. The final length will need to be the calculated value, from insulator wire end to insulator wire end. After building the four-wire section, attach dowel rods as shown to act as spreaders. Fasten each rod in place with pieces of wire threaded through the holes and then wrapped around the antenna wire. Wrap these spreader wires tight enough so that the rods will not slip out of place. Snip off projecting wire ends wherever they occur to prevent RF corona power loss. Then, using either wire or rope, make a bridle to hold the ends of the antenna.

Table 1
Dimensions and Bandwidths on Various Bands

Frequency, MHz	*Length, ft*	*Spacing (A), ft*	*Bandwidth, MHz*
1.9	233	5.9	0.252
3.75	118	3	0.5
7.15	62	1.6	0.951
14.175	31.2	0.8	1.885
21.225	20.85	0.53	2.823
28.860	15.34	0.39	3.837

Last, solder the balanced end of the balun transformer to the dipole. Each wire from the balun should go to the pair of wires on the same side of the dipole. The solder job should be of the best quality and permanent because it is hard to repair later. The coax needs to be connected to the unbalanced side of the balun. If you use large-diameter coax (3/8 inch) then think about ways to support the weight. Perhaps a piece of nylon rope from the dipole center insulator to the coax will help take the load, but I'll leave the details of the problem up to you. After this final construction step, haul the antenna up in the trees, using care that no twists are allowed.

Operation

For once I had a 75-meter antenna that worked better than predicted. The SWR was 1.6:1 or better from 3.5 to 4.0 MHz. Better yet, reports received were excellent with my old 100-watt solid-state transceiver. Moving up and down the band gave no loading problems from the broadband final. The fat dipole is just what I needed for a good, relaxing rag chew after a hard day with the 500-kW rig at the office.

CHAPTER TWO

OFF-CENTER-FED-DIPOLES

2-1 **The Off-Center-Fed Dipole Revisited: A Broadband, Multiband Antenna**
From August 1990 *QST*

2-9 **Improved Feed for the Off-Center-Fed Dipole**
From May 1996 *QST* (Technical Correspondence)

2-11 **Off-Center-Fed Dipole Comments, Part 2**
From October 1996 *QST* (Technical Correspondence)

2-13 **Off-Center-Fed Dipole Comments, Part 3**
From October 1996 *QST* (Technical Correspondence)

2-14 **Choke the OCFD**
From September 1997 *QST* (Technical Correspondence)

By John Belrose, VE2CV and Peter Bouliane, VE3KLO From *QST*, August 1990

The Off-Center-Fed Dipole Revisited: A Broadband, Multiband Antenna

The search for a simple broadband, multiband antenna with acceptable SWR over the entire 80/75meter band continued with the publication of the article by Witt, AI1H, in April 1989 *QST*. This inspired author Belrose, VE2CV, to reopen his files on the "Windom antenna," or, more properly, the off-center-fed dipole. Particularly since the opening of the 10, 18 and 24-MHz bands, this time-honored, somewhat controversial antenna is attracting a revival in interest and usage because of its multiband characteristics. Thus, the off-center-fed dipole deserves an update. Certainly, most North American radio amateurs have not heard about the German version of this antenna.

Even though it is one of the simplest antennas, the drooping dipole (a dipole with drooping ends, popularly referred to as an inverted V) is effective on 80 meters. For good DX performance, the apex of an 80-meter drooping-dipole antenna should be as high as possible above ground (at least 15 meters [50 feet]), because the antenna's vertical radiation angle decreases with height above ground. The arms of an 80-meter drooping dipole should not be too close to the ground (say, greater than 3 m [10 ft]). The input impedance ($R_a \pm jX_a$) of a drooping dipole depends on the operating frequency, the length of the dipole, the angle between its arms, the dipole's height above ground, and–particularly the resistive component–on the conductivity of the earth beneath the antenna. The included angle between the arms of an 80-meter drooping dipole should be about 127°, since, in this configuration, the antenna's pattern is dipole-like, and its input impedance is about 50 Ω for antenna heights typically employed by radio amateurs. The principal disadvantage of such an antenna is that its SWR bandwidth–less than 200 kHz–is too narrow to cover the 80/75-meter band.

The broadband performance of an antenna can be improved through the use of a matching network at the feed point. This network can comprise discrete components (see Hall,[1] Hayward,[2] Bloom,[3] Hately,[4] and Li, et al[5]); or transmission-line stubs (Snyder,[6] Hansen,[7] and Witt,[8]). Authors Li, et al give a microcomputer program for the design of LCR networks for broadband matching.

Another way to improve broadband performance is to use two dipoles fed in parallel: one dimensioned for the middle of the lower half of the band, and the other for the middle of the upper half of the band. The drooping-dipole configuration is ideal for this arrangement, since the ends of the two dipoles can be fanned (for angular separation) in either the vertical or horizontal plane. An alternative is to use an off-center-fed dipole, which, in addition to broadbandedness, has multiband performance characteristics. This article is concerned with such an antenna.

The "Windom Antenna" and Single-Wire Feed

The original Windom antenna (devised in 1928-29), named after Loren Windom, W8GZ, the amateur who wrote a comprehensive article about it,[9] employed single wire feed at a point of 1/6 to somewhat over 1/7 of the antenna length from the center (see Figure 1A). Windom reported on a detailed experimental study by colleagues John Byrne, W8DKZ, Edward Brooke, W2QZ, Jack Ryder, W8DKJ, and Prof W. L. Everitt of the Ohio State University Dept of Electrical Engineering. They found that if ammeters were placed on the antenna, with the single-wire feeder at the position just described, the current distribution on the dipole was sinusoidal and symmetrical, with no discontinuity in the vicinity of the feed point, and no standing wave on the feeder. Clearly, the feeder was terminated in its characteristic impedance.

This article did not discuss pattern, and it was many years before the computational tools for predicting pattern were available. Parfitt and Griffin[10] have recently analyzed the single-wire-fed dipole (the Windom antenna), and their results show, as anticipated, that radiation from the feed wire does

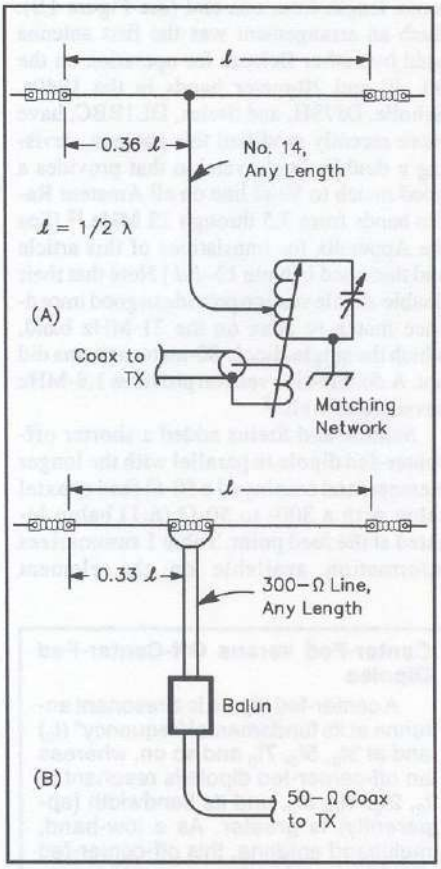

Figure 1—Two versions of the off-center-fed dipole. At A, the original "Windom antenna"–actually a Hertz (1/2 λ) element excited via a single-wire feeder; at B, a dipole off-center-fed via balanced line. The single-wire-fed version dates from the late 1920s; the balanced-line-fed version (sans balun) dates from the 1940s, and the balanced-line-and-balun version appeared in ARRL publications beginning in the late 1950s.

modify the antenna pattern, primarily at low elevation angles with the horizon. The feed line for their modeled antenna was vertical.[11] The pattern was basically dipole-like, with a squint away from the broadside. Current on a wire, whether uniform (a traveling wave) or sinusoidal (a standing wave) leads to radiation, unless the radiation that results from this feedwire current is canceled by an equal amplitude, out-of-phase current on an adjacent parallel wire (as in a balanced transmission line). For the Windom antenna, feeder radiation could be significant, depending on the arrangement and the length of the transmission line.

The Windom antenna was widely used during the 1930s and into the 1940s. For example, in author Belrose's experience, the British Columbia Forest Service were using the single-wire, off-center-fed dipole in the mid-1940s. It was a simple antenna that was easy to tune and match with the π network employed in the output circuit of their transmitter.

The Off-Center-Fed Dipole and Balanced Transmission Line

A later version (1940s) of an off-center fed dipole (*mis*called Windom) employed 300-Ω ribbon feed at a point 1/3 of the antenna length from one end (see Figure 1B). Such an arrangement was the first antenna used by author Belrose for operation on the 80, 40 and 20-meter bands in the 1940s. Scholle, DJ7SH, and Steins, DL1BBC, have more recently modified this antenna, devising a double-dipole version that provides a good match to 50-Ω line on all Amateur Radio bands from 3.5 through 28 MHz.[12] [See the Appendix for translations of this article and that cited in Note 13–*Ed.*] Note that their double-dipole version provides a good impedance match to coax on the 21-MHz band, which the single-dipole 80-meter antenna did not. A double-size version provides 1.8-MHz coverage as well.[13]

Scholle and Steins added a shorter off-center-fed dipole in parallel with the longer element, and employed a 50-Ω feed coaxial cable with a 300- to 50-Ω (6:1) balun located at the feed point. Table 1 summarizes information available on the element lengths for single and double off-center-fed dipoles. Since the dipole must be resonant on harmonic frequencies, its length must be somewhat longer than optimum for the 75-meter band, as noted by Scholle and Steins. It is apparent from their SWR curves that the resonant frequency of their antenna is less than 3.5 MHz.

In the arrangement employed by Scholle and Steins, the longer elements were horizontal and the shorter elements sloped (the included angle between the arms of which was Λ≈100°). The authors' version was a drooping-dipole configuration (Λ≈127°) with the angle between the arms of the two dipoles approximately 45°. This antenna was fed with two 15-meter (50-foot) lengths of RG-62A (foam dielectric) coaxial cable configured as a balanced transmission line.[14]

We fabricated a *single* off-center-fed dipole (dimensionally identical with the longer element of the Scholle and Steins "double dipole") and used it as a Field Day antenna (in 1985) for 75/80 in. The stimulus for this, and for carrying out a detailed study, was a search for a simple all-band antenna conducted for the Canadian National Institute for the Blind.[15] We experimented with 4:1 and 6:1 baluns, primarily because 4:1 baluns are easier to come by (more on baluns later). The antenna was operated in a drooping-dipole configuration (Λ≈127°), with the apex (which, in our case, was the feed point) at about 12 meters (40 feet). (In retrospect, we should have positioned the center of the antenna at apex height, since in this configuration the current maximum on the antenna [for 80-meter operation] would be at maximum height.) Extensive impedance and SWR measurements were made. To facilitate this, we employed a low-loss (foam-dielectric) coaxial feeder consisting of a 32.3-meter (106-foot) length of Belden 8214 (velocity factor, 0.8.) This feeder was 1/2 λ long at 3.5 MHz, 1 λ at 7 MHz, and so on. High-quality commercial baluns (made by Antenna Engineering, Australia[16]) were used between the feed line and the antenna.

Figure 2 shows our SWR measurements for the 80/75-meter band. With the 6:1 balun in line, the 2:1 SWR bandwidth was 3.47 to 3.93 MHz—broadbanded, indeed. The SWR was even lower on 40 and 20 meters, and less than 2:1 for the lower half of the 10-meter band; see Figure 3. Clearly, these bandwidths are not in accord with simple

Table 1

Summary of Element Lengths for Published Off-Center-Fed-Dipole Designs

Figure 1B Version	13.5 m (44.29 ft)	27.94 m (91.67 ft)
cq-DL double-dipole version	13.8 m (45.28 ft) 4.69 m (15.39 ft)	27.7 m (90.88 ft) 9.38 m (30.77 ft)
cq-DL double-sized, double-dipole version	25.88 m (84.91 ft) 4.69 m (15.39 ft)	51.77 m (169.85 ft) 9.38 m (30.77 ft)
Author's double-dipole version, (balanced coaxial-line feed, Figure 4)	23.3 m (76.44 ft) 6.78 m (22.24 ft)	48.2 m (158.13 ft) 13.58 m (44.55 ft)

Center-Fed versus Off-Center-Fed Dipoles

A center-fed dipole is a resonant antenna at its fundamental frequency* (f_0) and at $3f_0$, $5f_0$, $7f_0$ and so on, whereas an off-center-fed dipole is resonant at f_0, $2f_0$, $4f_0$, $8f_0$, and its bandwidth (apparently) is greater. As a low-band, multiband antenna, this off-center-fed dipole has advantages over the center-fed dipole, but a disadvantage (or advantage, depending on the antenna configuration and one's point of view) is that feeder radiation can contribute to the antenna's resultant radiation pattern. The use of a current balun minimizes feeder radiation.—*VE2CV and VE3KLO*

*The frequency at which it is 1/2 λ long.

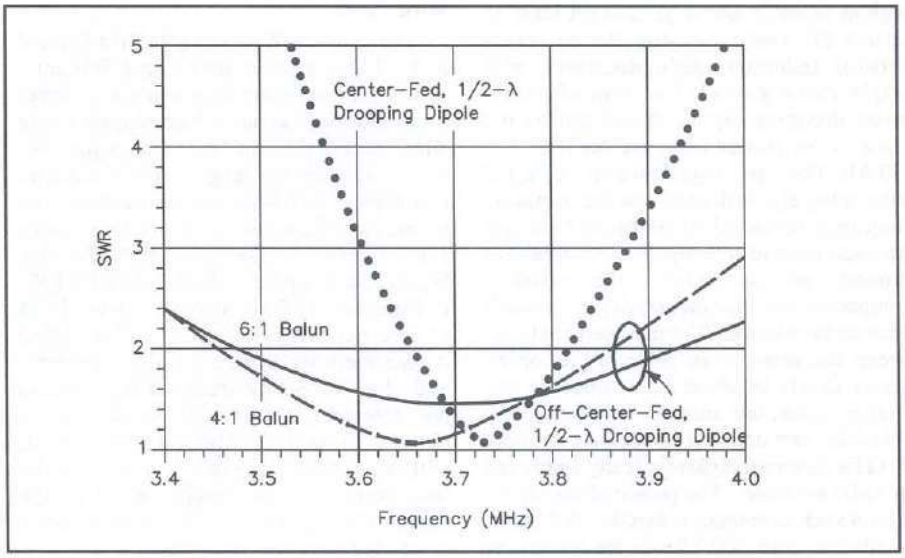

Figure 2—SWR vs frequency for a single off-center-fed dipole employing different baluns (4:1 and 6:1) at the feed point, compared with a center-fed 1/2-λ dipole. Both antennas were operated in a drooping-dipole configuration.

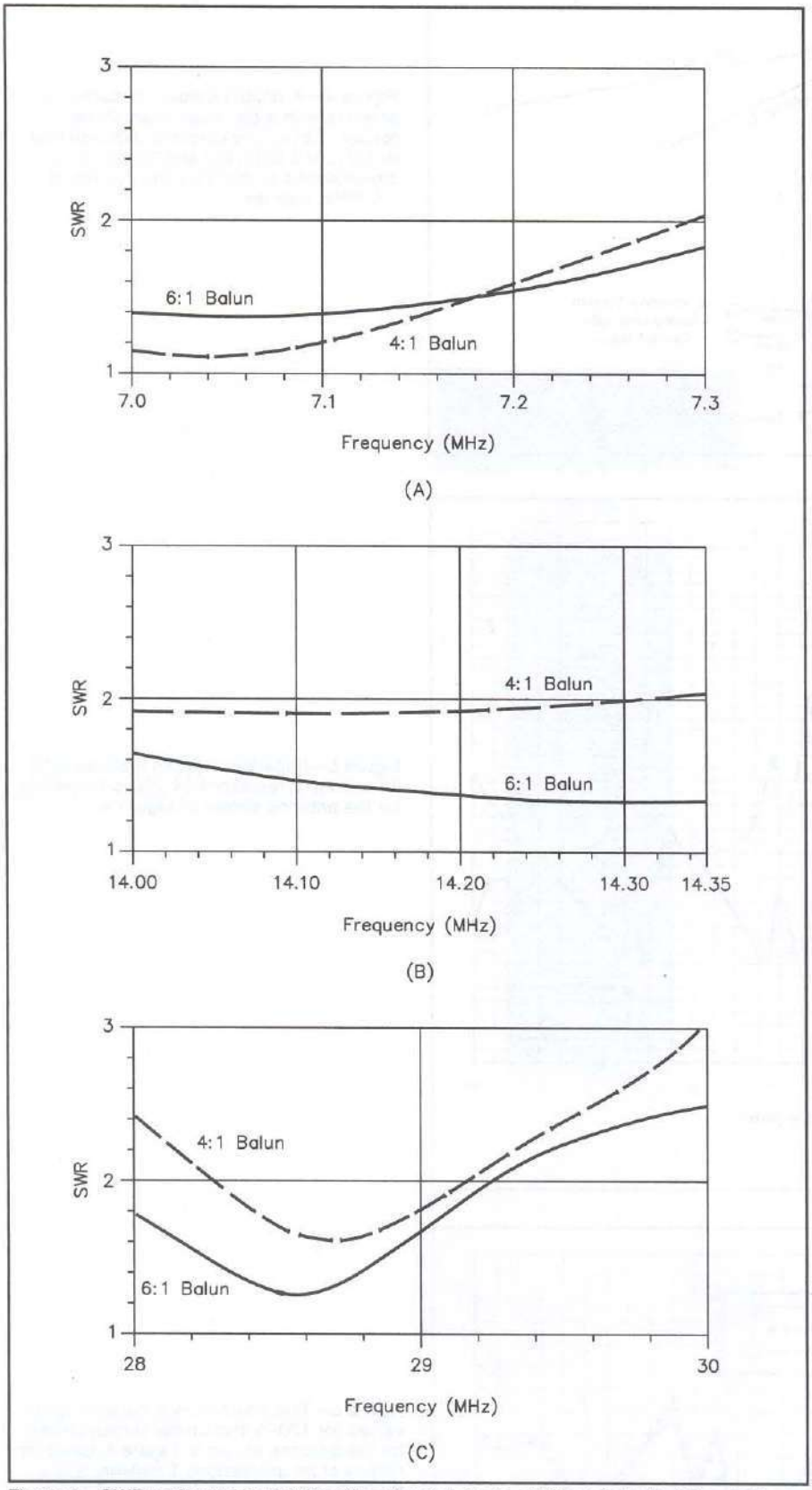

Figure 3—SWR vs frequency for the off-center-fed dipole of Figure 2 at 40, 20 and 10 meters.

theory.[17] Fifteen-meter data are not shown because this single off-center-fed dipole was not resonant on the 15-meter band.

The 4:1 balun provided somewhat sharper resonances and lower SWR at resonance in the 80/75- and 40-meter bands, but a low SWR was not obtainable in the 20-meter band. The measured impedance at resonance in the 80/75-meter band with this balun was exactly 50 Ω; hence the antenna's effective feed-point impedance was 200 Ω. This explains why the minimum SWR with the 6:1 balun was 1.5:1; the 6:1 balun, however, seems to be a better compromise if operation on other bands is wanted.

As noted, we employed high-quality commercial baluns (from the AEA Model 250 series). Radio amateurs have several alternatives in this connection; these include using a 4:1 balun and 75-Ω coax; or purchasing or winding your own 6:1 balun (see Orr, W6SAI[18]),and using 50-Ω coax.

Aside from impedance matching, however, there are other factors to consider in feeding an off-center-fed dipole and selecting a balun for this service. Next, we address some of these aspects.

Balun and Feeder Considerations

In the autumn of 1989, we decided to have another look at off-center-fed dipoles. Because of the multiple-resonant-frequency response of the double off-center-fed dipole, we decided to explore the potential of this antenna system for broadband frequency coverage. If used with a suitable antenna-system tuning unit (ASTU), a double off-center-fed-dipole system could perhaps be used on any frequency from 1.8 to 30 MHz. Since conventional baluns do not perform satisfactorily into reactive loads, we decided to eliminate the balun, at least insofar as the antenna and its feeder were concerned. We fed our antenna with a balanced 190-Ω transmission line consisting of two 15-meter (50-foot) lengths of RG-62A (foam-dielectric) coaxial cable as shown in Figure 4 and described in the work cited in Note 15. Teflon-dielectric cable would have been preferable because of Teflon's superior insulating characteristics but 95-Ω, Teflon-dielectric coax is unavailable.

We started out with a single dipole element dimensioned to 1/2 λ at 2 MHz. This antenna exhibited an antiresonant response (very high input impedance, measured at the transmitter end of the transmission line) at 7.6 MHz. Next, we installed the shorter dipole and dimensioned it to *minimize* the system's impedance at 7.6 MHz. Figure 5 shows the system's impedance v frequency. Except for a narrow band of frequencies near 6 MHz, the input resistance fell in the range of 20 to 400 Ω; and the input reactance fell in the range $+j100$ to $-j200$ Ω. This double off-center-fed dipole system is rather easily tuned and matched, since its reactance is low.

Figure 6 graphs antenna currents for a transmitter output power of 100 W. The antenna system was tuned using an unbalanced T network, with a ferrite-bead current balun of the type described by Maxwell[19] between the ASTU and the antenna. A balanced T network patterned after that described by Belrose was initially used since this is the type of ASTU that, in principle, should be used to tune and match a balanced antenna system. Unfortunately, however, this tuner employed a standard toroidal-core balun—a *voltage* balun, which applies almost-equal *voltages* to the wires of a balanced feeder. Even though the balun was on the "tuned side" of the ASTU—a practice we recommend—and the ASTU it-

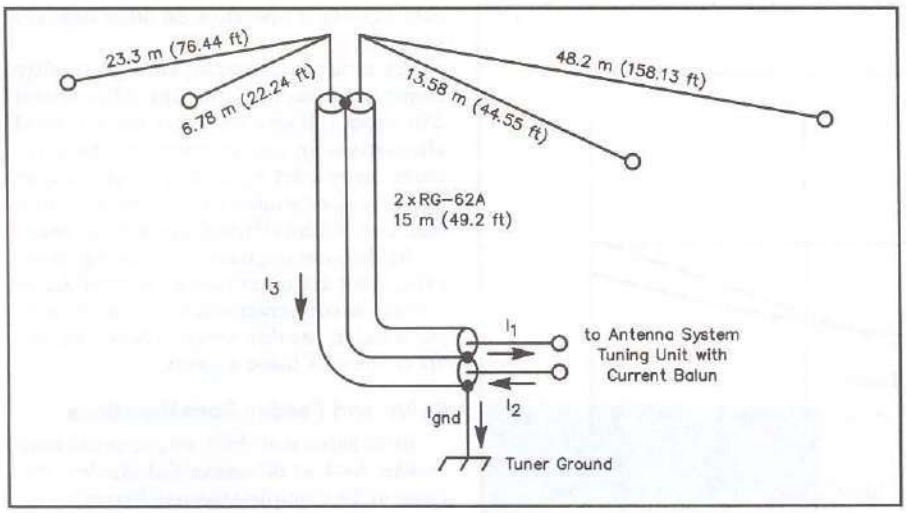

Figure 4—A double-dipole, off-center-fed antenna with a balanced coaxial-line feeder. The longer dipole is dimensioned to 1/2 λ at 2 MHz; the shorter dipole is dimensioned to minimize the system at 7.6 MHz. See text.

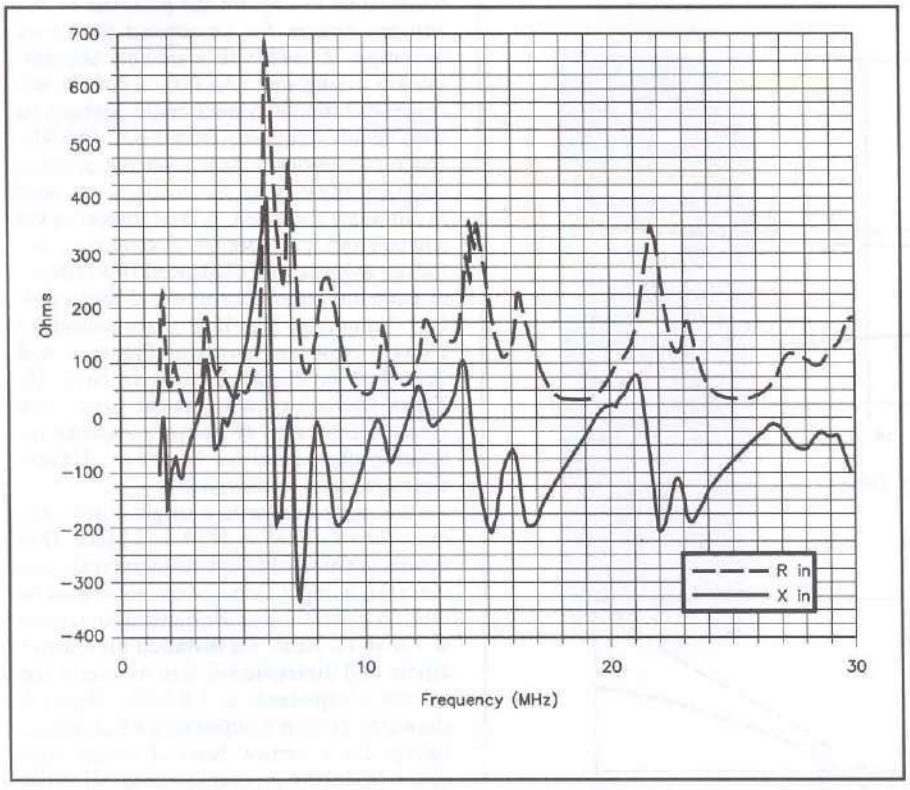

Figure 5—Impedance (input resistance [R in] and input reactance [X in]) vs frequency for the antenna shown in Figure 4.

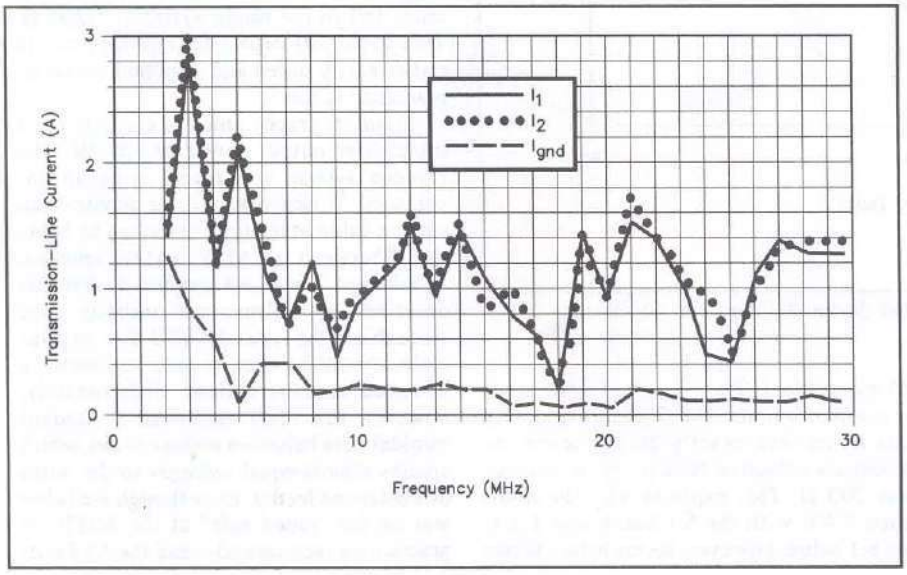

Figure 6—Transmission-line currents (peak values for 100-W transmitter output power) for the antenna shown in Figure 4, tuned by means of an unbalanced T network and a ferrite-bead-choke (W2DU) current balun.

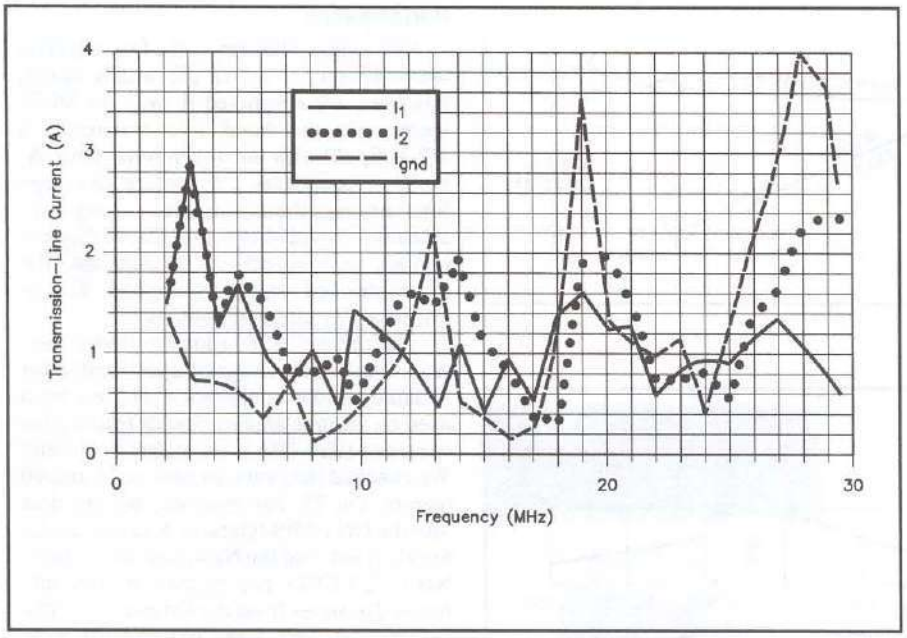

Figure 7—Transmission-line currents (peak values for 100-W transmitter output power) for the Figure 4 antenna, tuned by VE2CV's balanced tuner, which employed a voltage balun.

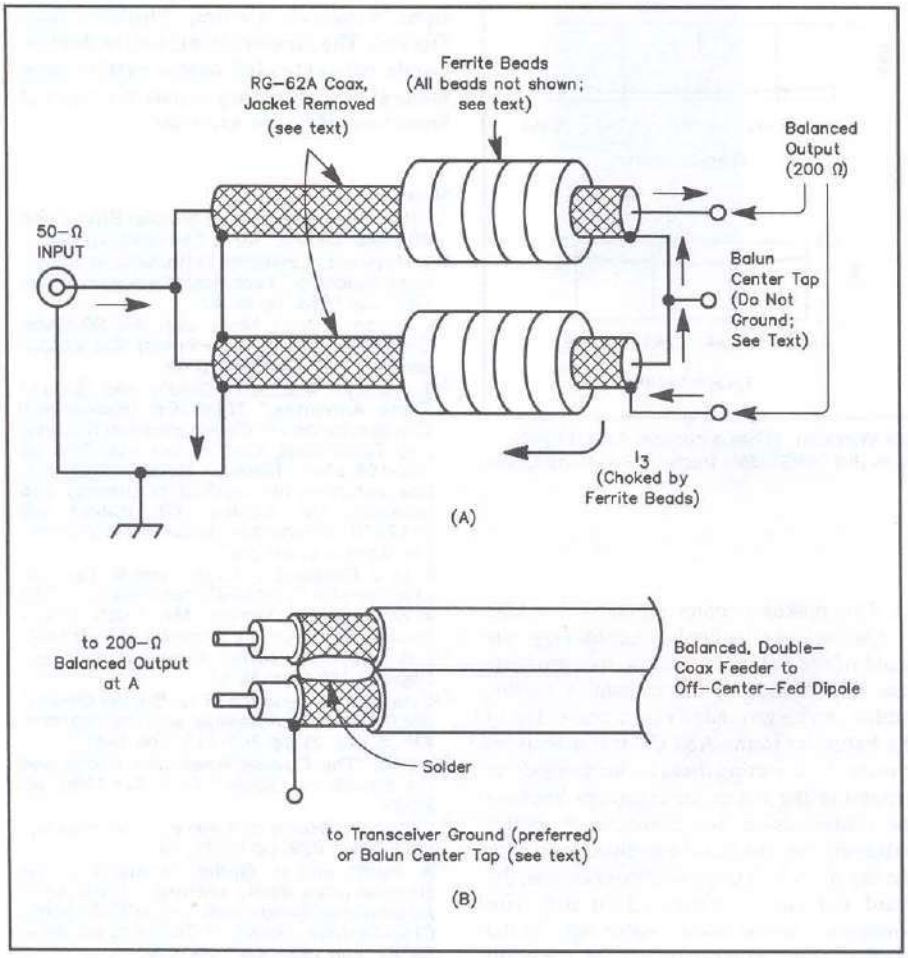

Figure 8—At A, a 4:1, ferrite-bead current balun; at B, connections to the balun end of the dual-coax-balanced feed line.

self was balanced, we found that the transmission-line currents (I_1 and I_2 in Figure 4) differed greatly in amplitude at some frequencies. The difference may surprise you; it did us (see Figure 7).

For an antenna that is asymmetrical with respect to its feeder–such as an off-center-fed dipole–a *current* balun must be used, since this type of balun forces almost equal *currents* into each conductor of the balanced line. This is necessary if transmission-line radiation is to be minimized. If these currents are exactly equal, there will be no difference in current flowing in the ground lead (I_{gnd}), which connects the braids of the coax to the tuner ground. Any current on this lead is then due to radiation-coupled current (I_3) induced on the *outside* surface of the coaxial shield. Clearly, we want this current to be small (to minimize radiation from the transmission line), and indeed it *is* small except at frequencies below 3 MHz (see Figure 6). (Our antenna was suspended from a bracket at the 12-meter [40-foot] level on a 21-meter [70-foot] aluminum-lattice mast. In the final analysis, reradiation by this mast should be considered because current may have been induced on the mast surface.)

Off-Center-Fed Dipoles for the Amateur Radio Experimenter

The off-center-fed dipole used by author Belrose in the 1940s was fed with 300-Ω twin lead via a balanced ASTU that was link coupled to a balanced (push-pull) power amplifier. There was no concern about balun losses and what type of balun to use because the system contained no balun. [20]

The authors' double-dipole, off-center-fed antenna employed a balanced coaxial feed line. This antenna was attractive for the authors because it could be used throughout the HF range if fed via a suitable matching network. If you decide to fabricate and try an off-center-fed dipole system, we suggested that you dimension it in accord with the Scholle and Steins versions, which are optimized for the amateur bands. Furthermore, we suggest that you feed such an antenna with a balanced transmission line. We have used dual RG-62A cables to make a balanced 190-Ω line, but one could use paralleled RG-63 (125-Ω) coaxial cable, which would make a balanced transmission line more in accord (Z_o ≈250 Ω) with the traditional 300-Ω-twin-lead feeder. In such a system, the balun, and the ASTU (if required), can be in the shack to allow experimentation in achieving balanced current feed and reducing losses in the balun. Whatever method you use, feed your off-center-fed antenna via a current balun.

A shield-choke current balun can be constructed by slipping ferrite beads (–43 or –73 material) over a length of coaxial cable. (Depending on the beads obtainable and the diameter of the cable you use, you may need to remove the cable's outer jacket and install the beads directly around the

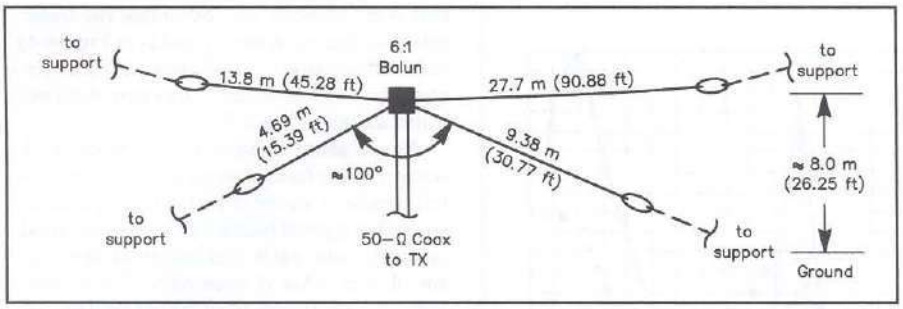

Figure A—Double Windom.

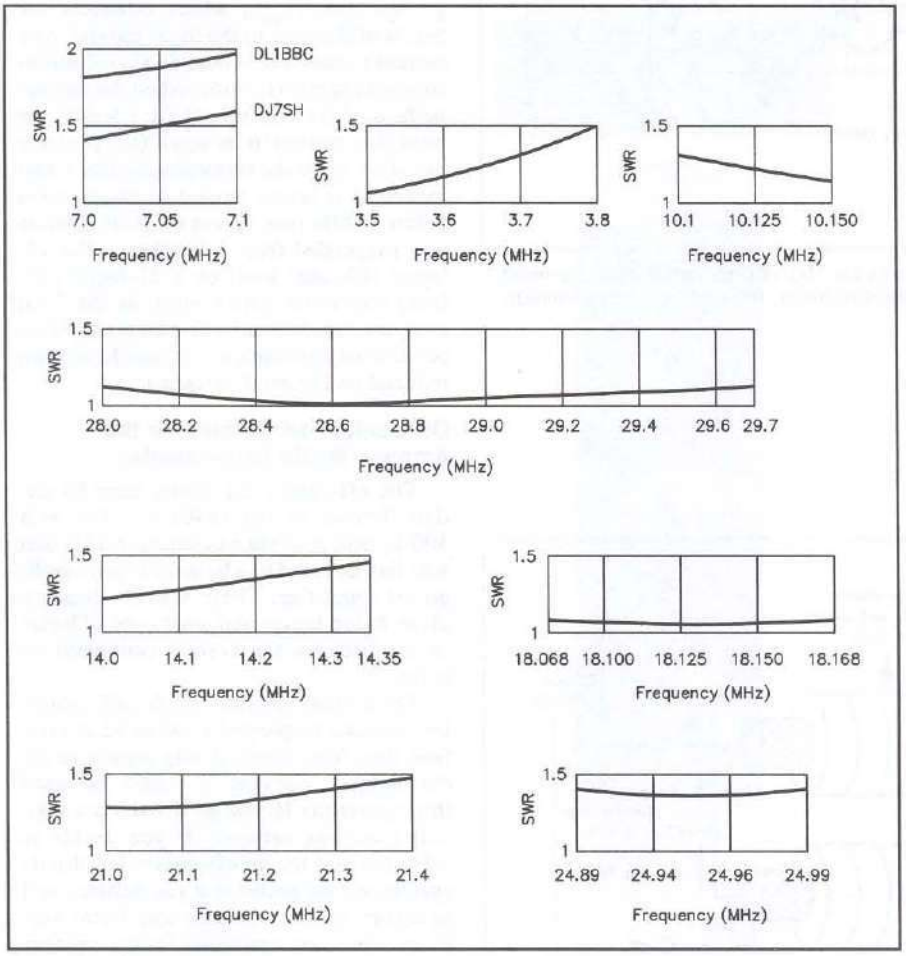

Figure B—SWR curves for the eight-band double Windom. [These curves do not cover all US amateur frequencies because allocations in the FRG differ from those in the US—*Ed.*]

shield.) As described in the work cited at Note 19, Walt Maxwell, W2DU, used 50 beads of no. 73 ferrite (Amidon no. FB-73-2401, Palomar FB-24-73 or equiv) on a piece of Teflon-dielectric cable to make a practical, low-loss, 1.8-to-30-MHz balun about 12 inches long.[21] Such a balun, however, is a 1:1 transformer—not very useful for the present application, where impedance transformation is also required. A 4:1 balun of similar type (see Note 20) can be constructed by using two equal lengths of RG-62 (95-Ω) coaxial cable, each fitted with ferrite beads. The inputs to these two coaxial-cable baluns are connected in parallel, and the outputs in series (see Figure 8). This makes a center-tapped 4:1 balun.

Our antenna feeder has a center tap: the braid of the balanced coaxial transmission line. The braids of the transmission-line cables can be grounded to the center tap of the balun, or to the ASTU (or transceiver) ground. Connecting them to the transceiver ground is the better arrangement because the transmission-line currents are better balanced, and the braid current is less. (For the braid-to-ASTU-ground connection, the braid current is measured in the wire connection to the balun center tap; in the braid-to-transceiver-ground case, the braid current is measured in the connection to the equipment ground.)

Performance

Our single-element Field Day antenna worked well for us; as previously noted, however, we employed it only on 80/75 meters. On this band, it is essentially a 1/2-λ dipole with unconventional feed. At higher frequencies, the pattern develops lobes because the dipole acts as a long-wire antenna. Provided that this directivity coincides with directions of interest, the off-center-fed dipole is a good, simple broadband/multiband antenna.

The authors' 1989 (double-dipole) version, while not designed specifically for Amateur Radio communication, has been used on various amateur bands (during the winter of 1989-90). It works, but how well? We checked into various nets on 75 and 40 meters. On 75, for instance, we checked into the ONTARS (Ontario Amateur Radio Service) net, and the Newfoundland Phone Net (1730 EST), two regions at quite different distances from the Ottawa area. The reports received were comparable with those given to other stations by net control. On the 160-meter band, we found that we could work stations we could hear, provided that they were running comparable power (100 W) and their local noise levels were reasonable. We have not yet determined the antenna's gain and pattern.

Acknowledgment

The authors work at the Communications Research Centre, Shirleys Bay, Ontario. The measurements for the double-dipole off-center-fed dipole system were made at the Laboratory as part of a study of broadband HF wire antennas.

Notes

[1]J. Hall, "The Search for a Simple, Broadband 80-Meter Dipole," *QST*, Apr 1983, pp 22-27.

[2]W. Hayward, "Limitation to Broadband Impedance Matching," Technical Correspondence, *QST*, Jul 1984, pp 45-47.

[3]A. Bloom, "Once More with the 80-Meter Broadband Dipole," Technical Correspondence, *QST*, Jun 1985, p 42.

[4]M. Hately, "Multiband Dipole and Ground Plane Antennas," *Third IEE International Conference on HF Communication Systems and Techniques*, Conf Series Pub 245, pp 102-106,1985. Maurice Hately, GM3HAT, has patented his method of feeding and matching HF dipoles (UK Patent GB 2112579), and he manufactures and markets his "dipoles of delight."

[5]S. Li, J. Rockwell, J. Logan, and D. Tan, *Microcomputer Tools for Communications* (610 Washington St, Dedham, MA 02026: Artech House, 1983), Ch 14: Broadband Matching.

[6]R. Snyder, "The Snyder Antenna," *rf design*, Sep/Oct 1984, pp 49-51.

[7]R. Hansen, "Evaluation of the Snyder Dipole," *IEEE Trans on Antennas and Propagation*, AP-35 (No. 2), pp 207-210, Feb 1987.

[8]F. Witt, "The Coaxial Resonator Match and the Broadband Dipole," *QST*, Apr 1989, pp 22-27.

[9]L. Windom, "Notes on Ethereal Adornments," *QST*, Sep 1929, pp 19-22, 84.

[10]A. Parfitt and D. Griffin, "Analysis of the singlewire-fed dipole antenna," *IEEE AP-S International Symposium, Vol III* (IEEE cat no. CH2654-2/89, Library of Congress no. 89—84327, Jun 1989, pp 1344-1347.

[11]Such an arrangement is an extreme case because the feeder is perpendicular to the

ground—a configuration probably atypical of singlewire feed in Amateur Radio installations, and one that affords practically zero cancellation between feeder and ground currents. At the other extreme, one of the amateur systems described in Windom's "Notes on Ethereal Adornments" (see Note 9) employed a *1200-foot-long* (365.8-m) feed wire that likely more nearly approached parallelism with the ground. Clearly, "modeling a Windom" is a fuzzy procedure.–*Ed.*

[12]H. Scholle and R. Steins, "Eine Doppel-Windom Antenne für Acht Bänder," *cq-DL*, Sep 1983, p 427.

[13]H. Scholle, "Eine Doppel-Windom Antenne für Neun Bänder," *cq-DL*, Jul 1984, pp 332-333.

[14]J. Belrose, "Tuning and Constructing Balanced Lines," Technical Correspondence, *QST*, May 1981, p 43.

[15]J. Swail, VE3KF, and W. Loucks, VE3AR, private communications, Apr 1985.

[16]Antenna Engineering, Australia Pty Ltd, PO Box 191, Croydon, Victoria 3136, Australia.

[17]W. Wrigley, "Impedance Characteristics of Harmonic Antennas," *QST*, Feb 1954, pp 10-14.

[18]W. Orr, Ham Radio Techniques, *ham radio*, Jan 1983, pp 68-69.

[19]M. Maxwell, "Some Aspects of the Balun Problem," *QST*, Mar 1983, pp 38-40.

[20]J. Belrose, "The Balun Saga Continued," *QST*, in preparation.

[21]As a less-costly alternative, 10≈1-inch-long mix-77 beads—with an inner diameter to pass the coax used—*may* serve as a substitute. (The authors do not have experience with beads of this material, however.) Consult your ferrite-bead supplier on the availability of beads of this type.–*Ed.*

APPENDIX

A Double Windom Antenna for Eight or Nine Bands

This work, which originally appeared as two articles in *cq-DL*, was translated from the German by Dr. George Elliott Tucker, WA5NVI.

Part 1: A Double Windom Antenna for Eight Bands

By Hubert Scholle, DJ7SH, and Rolf Steins, DL1BBC

The asymmetrical dipole antenna developed and described by Windom (W8GZ) in 1929 has been used by many amateurs for many years as the FD4. This has also been the case in Germany.

We discovered in an older periodical (*QRV*) the explanation by F. Spillner (DJ2KY) that this antenna, with the addition of a small one-band Windom for 15 m, can be used as a five-band Windom. After the installation of the additional elements, this antenna worked very well for two years at DL1BBC.

With the opening of new bands (10, 18 and 24 MHz), the thought occurred to try out a new extension of the FD4 to eight bands (3.5 to 29.7 MHz).

What worked for 21 MHz must also be possible for 10 MHz.

So we took off the 21-MHz extension to my antenna and hung two elements of 4.69 and 9.38 m (15.39 and 30.77 ft), respectively, on the FD4 and stretched these downwards from insulators as an inverted V (Figure A).

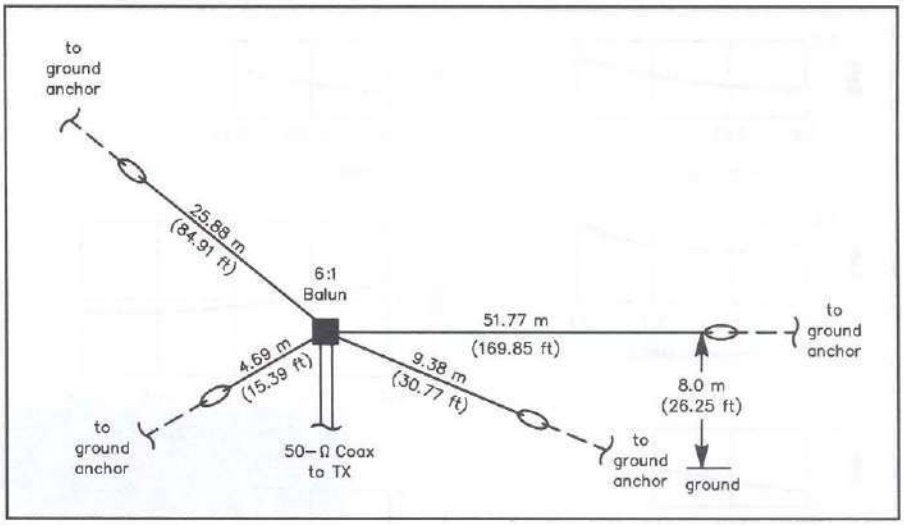

Figure C—A double Windom antenna for nine bands.

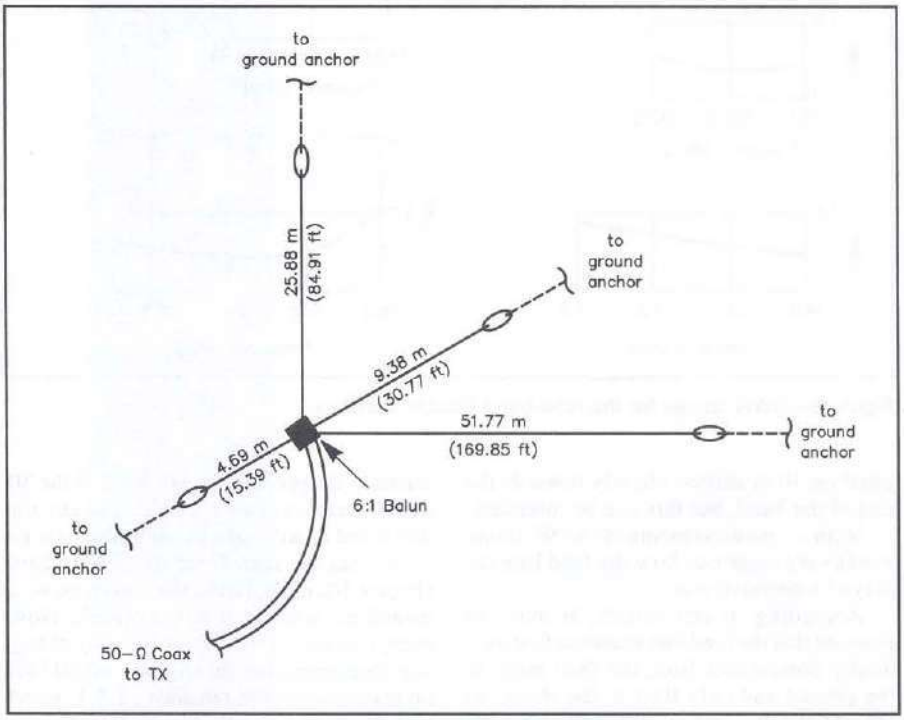

Figure D—Top view of the nine-band double Windom. [The elements are positioned to reduce coupling between the antenna's two off-center-fed dipoles.—*Ed.*]

To calculate the length we used the formula:

$$L/2 = 142.5 \div f \qquad \text{(Eq A)}$$

Whatever would work for 30 m should also work on 15 m.

As suspected, it worked.

As a by-product, it turned out in the measurements that this double Windom resonated just as well on 18 MHz and 24 MHz. So our eight-band Windom came into being with really simple means.

Construction

Thanks to our neighbors, we were able to extend the basic antenna (FD4) to its full length.

At DL1BBC it was installed about 6.9 m (22.63 ft) above the ground, rising to about 8 m (26.25 ft) at each support point. At DJ7SH it hung about 5 m (16.4 ft) above the ground and partly ran over a garage roof. Both extension legs were stretched downwards as an inverted V with an angle of about 100°. Changing this angle allows the whole antenna to be easily tuned during final adjustments.

After construction, the first measurements showed that because of the length of the 30-m elements, the 80, 40 and 20-m bands each had a resonance point that was shifted towards the low end of the band. This effect was eliminated by lengthening slightly the 30-m section, so the resonance points fell more in the middle of the bands.

With this adjustment, the resonance

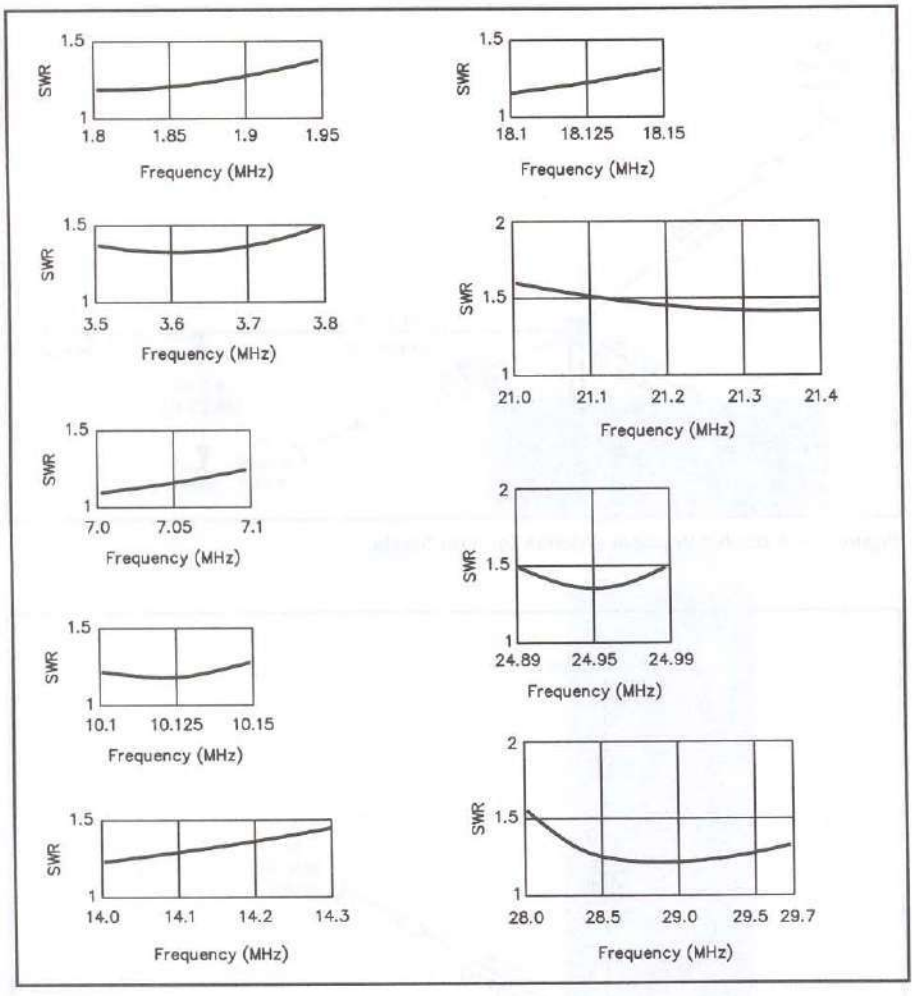

Figure E—SWR curves for the nine-band Double Windom.

point on 30 m shifted slightly towards the end of the band, but this can be tolerated.

With all measurements of the Windom, it was very clear that how the feed line ran played a decisive role.

According to our results, it must be stressed that the feed line must run first vertically downwards from the feed point to the ground and only then to the shack, as otherwise the entire antenna may be detuned. This is especially the case when the height of the antenna is under 10 m (32.8 ft). The 50-ohm-coax feed at DL1BBC was pulled through an old garden hose and then buried under the lawn.

The lower antenna height at DJ7SH had the result that, with the first construction attempt, the precalculated length of the 30-m elements was exactly right. The antenna delivered on all eight bands at the first go.

As can be seen from the SWR charts (Figure B), at DL1BBC the match on 40 m turned out somewhat less favorable. However, this was immediately fixed by changing the antenna height slightly. At DJ7SH, no resonance curve ran above 1.5:1, which was the goal since neither station uses an antenna tuner.

Performance

First contacts were made with both antennas. These showed that the antennas had a good degree of performance for a long wire. Especially the downwards sloping extension elements have a clear advantage over the horizontal basic antenna for DX.

With the first try on 30 m, many contacts were made with the US (East and West coasts), with signal reports between S6 and S7 while running 100 W.

At present, we cannot make a concrete statement about contacts within Europe.

This article makes no scientific claims, but intends to stimulate the long-wire enthusiast, and especially the friends of CW.

Part 2: Adding Another Band

Because the response was unexpectedly great to the publication of the above in *cq-DL*, we went to work again on an extension, as it was worthwhile to add 160 m.

With a half wavelength at 1.835 MHz, we calculated the basic length of the antenna to be 77.65 m (254.75 ft). We tapped the antenna at 25.88 m (84.9 ft) from one end and fed it with 50-ohm coax through a 6:1 balun. The basic antenna of this length was installed horizontally as a reclining L at DL1BBC. The additional elements, with lengths of 4.69 and 9.38 m (15.39 and 30.77 ft), were attached at the balun. This additional Windom for 10 and 21 MHz was again stretched downwards as an inverted V with an angle of about 100°. Here the additional Windom was mounted so that its elements were not extended in the same direction as those of the reclining L, which gave sufficient decoupling (Figures C and D).

For the feed, the Fritzel company made available for testing a new 6:1 balun, series 83, which can also handle high power. The SWR charts (Figure E) were obtained with the wire lengths given in the preceding paragraph. In case builders experience slight resonance shifts, these can be balanced out by lengthening or shortening the additional Windom.

Performance

First contacts were made with the antenna installed at DL1BBC. Here it was once again shown that the antenna has a good degree of performance for a long wire, especially for 1.8 and 3.6 MHz within Europe. The additional Windom again had the degree of performance described in the first part of this article.

The authors welcome questions and exchange of information. (When writing, please include return postage.)

Improved Feed for the Off-Center-Fed Dipole

By Richard A. Formato, K1POO

Theoretical data suggest that the commonly used feedpoint for the off-center-fed dipole (OCFD) may not be the best. The OCFD is an attractive multiband antenna because it's simple, inexpensive and requires no antenna tuner. Improving its performance simply by moving the feedpoint makes the antenna even more attractive. This note illustrates how the feedpoint influences antenna performance by analyzing computer-modeled SWR data for three different feedpoint locations.

The OCFD (shown schematically in Figure 1), consists of a single wire radiator of length L, fed off center a distance D from one end. The usual implementation uses a "1/3 feed," that is, the RF source is located one-third of the way from the end, so that D ≈ L/3. Why the feedpoint should be located there is not exactly clear. The ninth edition of *The ARRL Antenna Book*,[1] for example, observes that there is not much theoretical justification for this choice. Nevertheless, the 1/3-feed is accepted practice for building an OCFD.

Design details for a 1/3-feed three-band OCFD (80, 40 and 20 meters) appear in the 17th edition of *The ARRL Antenna Book*.[2] A 4:1 current balun at the feedpoint matches this antenna to any length of 50-Ω coax. More recently, Bill Wright, GØFAH, described a four-band, 1/3-feed OCFD (40, 20, 15 and 10 meters) fed with 300-Ω ladder line.[3] Matching 50-Ω coax requires a 4:1 balun on 40, 20 and 10 meters, and a 1:1 balun on 15 meters. Four-band operation, therefore, requires switching baluns. Another minor limitation is that the ladder-line length can be only an odd multiple of the wavelength at 21 MHz because the line is used as an impedance transformer. A simpler approach to achieving four-band operation is to feed the OCFD at a different point along its length.

I computer-modeled a 21.03-meter (69-foot) long, 0.2053-cm-diameter (#12 AWG) OCFD in free space. The dimensions are the same as those in the GØFAH design. Free-space results are a good approximation for antennas high enough above the ground (typically a significant fraction of a wavelength). The band-center SWR was computed on 40, 20, 15 and 10 meters at the antenna-input terminals for a feed system impedance of 200 Ω. The theoretical values of input resistance and reactance were used to calculate SWR (the antenna was not assumed to be tuned). Because the feedpoint impedance is 200 Ω, a 4:1 balun is required to feed the antenna with 50-Ω coaxial cable. The results for three different feedpoints appear in Table 1.

For the conventional 1/3-feed (D = 6.98 m), the 40 and 10-meter SWR values are slightly over 2, while the 20-meter SWR is about 1.75. In marked contrast, the 15-meter SWR is off the scale (the actual value > 20). It is this behavior that makes a special feed system necessary on 15 meters, a complication that can be avoided by moving the feedpoint.

When the OCFD feed is located 8.65 meters from one end, the 40, 20, and 10-meter SWRs are somewhat higher than they are with the 1/3 feed, but the 15-meter SWR is very low (≈ 1.2). Moving the feedpoint 1.67 meters closer to the antenna's center of the antenna results in a much better average SWR. And, more importantly, special matching is not required to achieve SWR ≤ 2.5 at the antenna terminals on all bands. Balun and coaxial cable losses, which are inevitable, reduce the SWR at the coax input to even lower levels. For most installations, it is probably reasonable to expect SWR at the transmitter to be less than 2 on all bands.

With the feedpoint located 3.65 meters from one end, the SWR on 40, 20 and 15 meters is excellent. The 40-meter SWR is only slightly above 2, and the 20 and 15-meter SWRs are below 2. The highest SWR occurs on 10 meters, where it's approximately 2.4. Because the SWR is reduced by feed-system losses, it will be less than 2.4 at the coax input. And, because balun and cable losses increase with frequency, the SWR reduction will be greatest on 10 meters where it is needed most. Feeding the antenna 3.65 meters from one end may well provide the best overall four-band performance.

In a specific implementation, the OCFD, like any antenna, must be tweaked for optimum SWR. This is accomplished by adjusting the feedpoint location. Other antennas, nearby metallic objects, and the earth are typical factors that influence antenna performance. Since these factors are not included in the computer model, they must be dealt with empirically by adjusting the antenna on-site. The data presented here provide a starting point for experimenting with different feedpoints. Depending on the total antenna length L, height above ground, earth electrical parameters, and feed system Z_0, it should be possible to operate a single OCFD on four or more bands without an antenna tuner or special feed arrange-

[1] *The ARRL Antenna Book*, 9th Edition (Newington: ARRL, 1960), pp 191 to 192.

Table 1

SWR Versus Feedpoint Placement (see Figure 1)

Feedpoint Distance D (m)	SWR
40 Meters	
8.65	2.5
6.98	2.1
3.65	2.0
20 Meters	
8.65	2.0
6.98	1.7
3.65	1.7
15 Meters	
8.65	1.2
6.98	21.3
3.65	1.9
10 Meters	
8.65	2.2
6.98	2.2
3.65	2.4

[2] R. Dean Straw, N6BV, Editor, *The ARRL Antenna Book*, 17th Edition (Newington: ARRL, 1994), pp 7-20 to 7-21.

[3] Bill Wright, GØFAH, "Four Bands, Off Center," *QST*, Feb 1996, p 65.

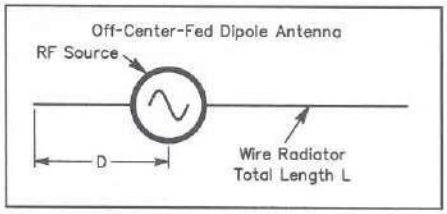

Figure 1—The basic off-center-fed dipole (OCFD).

ment. It's apparent that the OCFD's SWR varies dramatically as the feedpoint is moved, and that the commonly used 1/3-feed is not necessarily the best. Other feedpoints may therefore produce a better antenna.

Dean Straw, N6BV, Senior Assistant Technical Editor, comments:

I've modeled what Richard describes and find that he's basically correct in his assertions. However, I would add a couple of caveats:

- The SWR across an individual band will vary. For example, the 40-meter SWR will rise above the level he describes at the ends of the band, because it is a rather large band, percentage-wise. This antenna is no different from an ordinary center-fed 40-meter dipole in that sense.
- The azimuth patterns for this OCFD will not be symmetrical, as is the case for any such off-center-fed antenna. This is nothing new, but should still be mentioned, particularly for those hopeful folks who want a "one-thing-to-all-people" antenna.
- The ham who tries this approach on 30, 17 or 24 meters may burn out the 200:50-Ω balun transformer. The SWR is very high indeed on those bands.

Off-Center-Fed Dipole Comments, Part 2

By Richard A. Formato, K1POO

In an earlier correspondence,[1] I suggested that the conventional "1/3-feed" used for the off-center-fed dipole (OCFD) is not the best choice. This letter provides additional information, and responds to comments made by Dean Straw, N6BV, at the end of that correspondence. Before addressing the comments, it is important to examine in more detail the SWR data which are the basis of my earlier letter. Figure 1 plots computer-modeled free-space SWR for the prototype 21.03-meter long, 0.0253-cm-diameter OCFD. SWR for a 200-Ω feed system impedance was calculated at the antenna-input terminals every 50 kHz for source frequencies from 5 to 30 MHz. Three feed-point locations were modeled, 3.65, 6.98 (1/3 feed), and 8.65 meters from the end of the antenna; the curves are labeled accordingly.

The most important features of the SWR curves are the locations of minima and maxima, and the corresponding SWR.

[1]Richard A. Formato, K1POO, "Improved Feed for the Off-Center-Fed Dipole," *QST*, May 1996, page 76.

Table 1
SWR Minima

3.65 m		6.98 m (1/3-feed)		8.65 m			
Freq (MHz)	SWR	Freq (MHz)	SWR	Freq (MHz)	SWR	Band (Meters)	Fc
6.95	1.27	7.05	2.03	7.05	2.49	40	7.15
14.15	1.70	14.05	1.62	14.00	1.61	20	14.20
21.20	1.91	———	———	21.15	1.14	15	21.20
28.25	1.18	28.30	1.30	28.25	1.41	10	28.85

Table 1 lists minimum SWRs and the frequencies of the minima for the three feed points. For reference, the right-hand columns list the corresponding amateur band and its approximate center frequency.

The main point of my previous correspondence was that the 3.65 and 8.65-meter feeds *might* permit four-band operation without a matching network, because these feed points each result in *four* SWR minima between 5 and 30 MHz (see Figure 1). By contrast, the 6.98-meter SWR curve has only *three* minima in that range. The 1/3-feed antenna cannot possibly operate on more than three bands without some sort of matching, which is why the GØFAH design[2] requires two baluns and a specific transmission line length for 15 meters.

How feasible four-band operation is depends only on where the minimum SWRs occur relative to the ham bands, and how low the SWR is across the bands. Table 1 shows that the prototype OCFD has SWR minima very close to the 40, 20, 15 and 10-meter bands. With some on-site tweaking,

[2]Bill Wright, GØFAH, "Four Bands, Off Center," *QST*, Feb 1996, page 65.

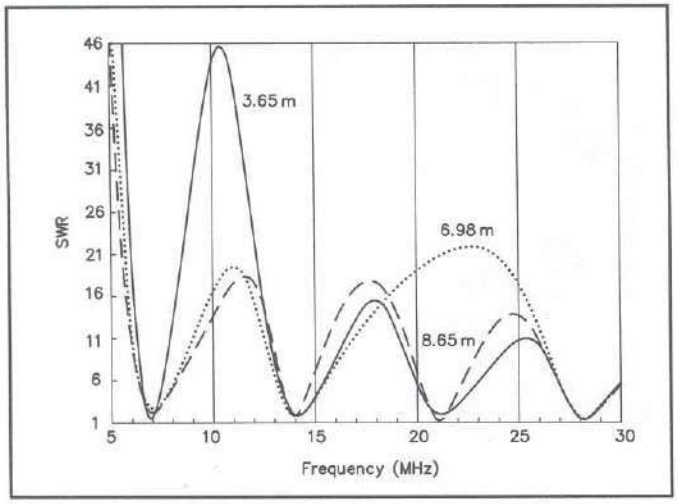

Figure 1—A plot of computer-modeled free-space SWR for the prototype 21.03-meter long, 0.0253-cm-diameter OCFD. SWR for a 200-Ω feed system impedance was calculated at the antenna-input terminals every 50 kHz for source frequencies from 5 to 30 MHz.

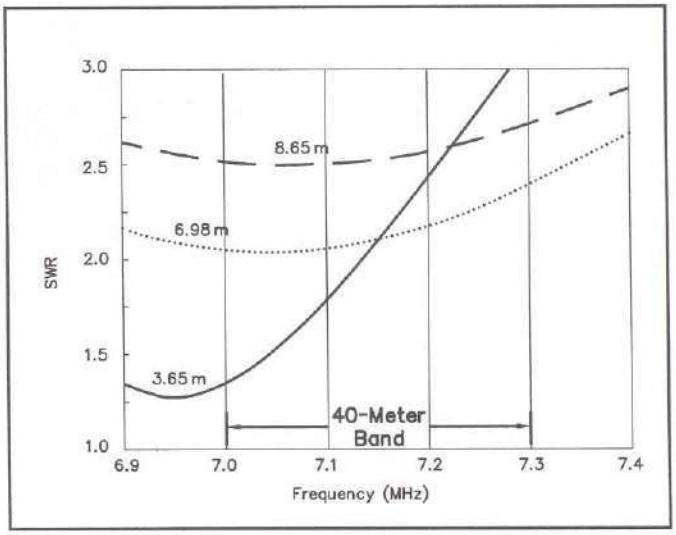

Figure 2—A plot of the prototype OCFD's SWR from 100 kHz below to 100 kHz above the 40-meter band in 5-kHz steps.

it is reasonable to expect that this antenna, fed either 3.65 or 8.65 meters from the end, could provide good SWR across all four amateur bands without a matching network.

The prototype OCFD dimensions were chosen because they correspond to the GØFAH design, thus permitting direct comparison with that antenna, not because they are optimized in any way. In fact, the prototype dimensions are *not* optimum for a four-band OCFD. In free space, the frequencies at which SWR minima occur, and the depth of the minima, are determined by three parameters: radiating-element length and diameter, and feed-point location. Changing any one of these changes both the frequencies of the SWR minima and the minimum SWR values.

Optimizing a four-band, free-space OCFD comes down to determining a set of antenna parameters that produces an acceptably low SWR (typically less than 2) across the 40, 20, 15, and 10-meter bands. Although I have not determined optimum parameter values, the very good predicted performance of the prototype antenna suggests that still better performance is almost certainly achievable. The purpose of my first letter was to encourage experimentation with OCFD designs, which would hopefully advance the state of the art by producing near-optimum designs.

Turning next to the comments at the end of my first correspondence, they are addressed as follows:

SWR Variation Across a Band

In terms of SWR behavior, the OCFD is much different from an ordinary center-fed dipole (CFD). The CFD is intentionally cut (tuned) to place minimum SWR within the band, which is why SWR increases toward the ends of the band (moving away from the minimum). An OCFD may or may not exhibit this behavior, depending on where its SWR minima occur. To illustrate, Figure 2 plots the prototype OCFD's SWR from 100 kHz below to 100 kHz above the 40-meter band in 5-kHz steps. The SWR does *not* increase toward each end of the band. If the SWR minimum is either outside or at one end of the band, as it is in Figure 2, the SWR will increase in one direction (up or down band), but decrease in the other, quite unlike an ordinary CFD. The OCFD's SWR will increase at both band edges *only* when its SWR minimum is inside the band, which generally is not the case.

Azimuth Pattern

The OCFD does indeed have an asymmetrical azimuth pattern, because the radiating element is not symmetrical about the feed point. But feeding the OCFD 8.65 meters from the end provides a *higher* degree of symmetry than the conventional $^1/_3$-feed. Locating the feed 8.65 meters from one end should result in a more symmetrical azimuth pattern than the conventional feed, not less. Of course, feeding the OCFD 3.65 meters from the end increases its asymmetry compared to the $^1/_3$-feed, so that the pattern for this implementation would be expected to be less symmetrical. Even so, pattern asymmetry is not necessarily undesirable. Many operators may want to take advantage of the OCFD's pattern by orienting the antenna to radiate in a preferred direction. This consideration applies to any antenna, even to the single-band CFD, which is an extremely poor radiator in the direction of the antenna axis at low to moderate take-off angles.

Operating the OCFD Out-of-Band

Regardless of where the feed is placed, or how it is implemented, certainly no attempt should be made to operate a 40, 20, 15, 10-meter OCFD on any other band. High SWR conditions may very well result in balun damage.

The data presented here provide additional insight into the advantages of feeding the OCFD at points other than $^1/_3$ of its length from the end. With computer-models for wire antennas widely available, it should be possible to optimize the OCFD in free space and over typical ground so that multiband operation is achievable without a matching network.

Off-Center-Fed Dipole Comments, Part 3

By Roy O. Hill, Jr, W4PID

QST's May 1996 Technical Correspondence column article "Improved Feed for The Off-Center-Fed Dipole" contained a statement that surprised me: "Why the feed point should be located [1/3 of the way from the end] is not exactly clear. The ninth edition of *The ARRL Antenna Book*, for example, observed that there is not much theoretical justification for this choice." It seems to me that there is plenty of theoretical justification. I am not an electrical engineer, and I am going to keep this simple. I won't say anything about computer simulations, ground effects, reactance, unbalanced feed-line currents, or adding 15-meter coverage; and I will use the *lowest* frequencies on the 80, 40, and 20-meter bands with full awareness that the frequencies actually used will be higher than that.

Thirty or 40 years ago, it was more or less generally accepted that the impedance of a half-wave antenna was about 4 kΩ at the ends, about 72 Ω at the center, and that the impedance along the antenna could be accurately represented by a straight line on semi-log graph paper. Using these premises, I plotted the impedance along a half-wave 3.5-MHz antenna on the graph of Figure 3. Then I added 7.0 MHz and 14.0 MHz plots for the same antenna.

All three lines cross at two points at about the 280-Ω impedance mark. These two points are 1/3 of the way (within 0.1 percentage point as I measure it) from the ends of the antenna. The antenna can be fed with 300-Ω line at either of the triple-crossing points and it will work on all three frequencies. You could miss the exact crossing point (or change the frequency) somewhat and still have an impedance between 150 and 600 Ω, which would present an SWR less than 2[4]—an allowable value for most transmitters. All this was pretty widely known in the 1950s. What happened to it? Was all the old low-tech knowledge thrown out when the modern high-tech stuff came along?

[4]This is only accurate if the impedance is purely resistive. With reactive impedances, it is entirely possible to have an SWR higher than 2.—*Zack Lau, KH6CP*

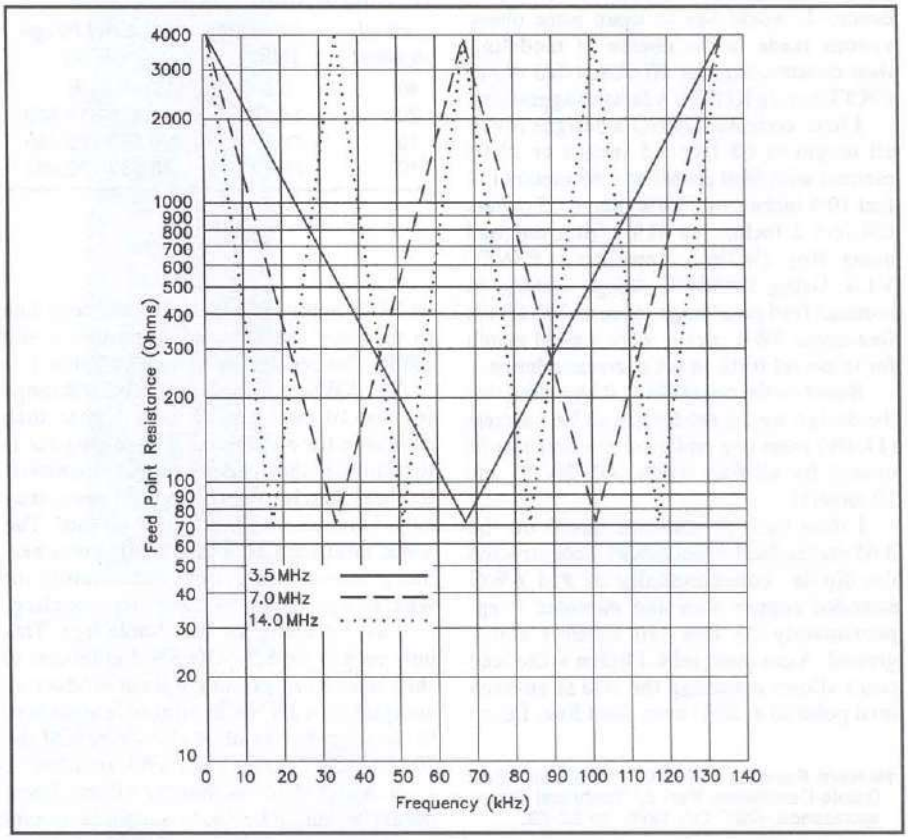

Figure 3—Impedance plot of an OCFD for 3.5, 7 and 14 MHz as a function of distance (in feet) from either end.

Also, the article mentioned that the "1/3-feed" antenna requires no antenna tuner. That is true, of course, for loading the antenna, but back in the days I've been talking about, the ARRL was stressing that you should *not* use a multiband antenna without an antenna tuner because of the danger of harmonic radiation. Do we not worry about harmonic radiation any more?

A little over 30 years ago, using as a guide a graph like the one shown in Figure 3, but using frequencies more like those on which I would be operating, I put up an antenna fed with 300-Ω ribbon 80 feet from one end and 44 feet from the other. I have used this antenna ever since. I do use an antenna tuner with it. The system works fine and causes no RFI or TVI. I used similar antennas for about 12 years before that, at other locations.

I just couldn't pass up that "not much theoretical justification" quoted from an ARRL publication without comment. The 1/3 feed has, not only plenty of theoretical justification, but plenty of practical justification—from use.

Choke the OCFD

By Dale Gaudier MØAOP/K4DG

After reading with interest Richard (K1POO) Formato's technical correspondence,[3] I would like to share some observations made in the course of modeling, then constructing, an off-center-fed dipole (OCFD) using K1POO's design suggestions.

I first modeled K1POO's designs (overall length of 68 feet 5.5 inches or 21.03 meters) with feed points at 3.65 meters (11 feet 10.5 inches, or 17.4%) and 8.65 meters (28 feet 2 inches, or 41%) from one end using Roy (W7EL) Lewallen's *EZNEC* V1.0. Using K1POO's design criteria (a nominal feed point impedance of 200 Ω) the free-space SWR curves were a good match for those set forth in his correspondence.

Based on the model data, it appeared that the design with a feed point at 3.65 meters (17.4%) from one end gave the best results overall for all four bands (40, 20, 15 and 10 meters).

I then built an antenna based on the 3.65-meter-feed-point model. I constructed the dipole conventionally of #14 AWG stranded copper wire and mounted it approximately 33 feet (10 meters) above ground. A commercial 4:1 balun at the feed point allows matching the 200 Ω antenna feed point to a 50 Ω coax feed line. I used an SWR analyzer attached to the feed line to measure the antenna's resonance and SWR. The results are shown in Table 1.

Table 1
Results without the RF Choke

Band (meters)	Minimum (MHz)	2:1 SWR Range (MHz)
40	~8.5	(SWR >>3)
20	14.17	13.250 - 15.500
15	21.58	20.420 - 22.350
10	29.69	28.550 - 30.480

The SWR minimum and 2:1 SWR range for the 10 meter band were higher than desirable for an antenna whose purpose is to minimize the need for a tuner. However, the real puzzle was the lack of resonance anywhere near the 40 meter band! The SWR minimum around 8.5 MHz was neither pronounced nor deep, and certainly not what was predicted by computer modeling.

I tried pruning the two dipole legs. This only caused the 8.5-MHz SWR minimum to shift somewhat. Pruning did not produce an acceptable (< 2:1 SWR) minimum anywhere in the 40 meter band; it also decreased the 20, 15 and 10-meter band SWR minima.

It occurred to me that the effects I was observing might be due to unequal currents flowing at the feed point (possibly due to the asymmetrical design of the OCFD). I made a simple RF choke by coiling several turns of the RG-8X feed line close to the feed point and balun. After some initial adjustments of the choke diameter and number of turns, I had my 40-meter resonance! (See Table 2.) The coil is 5½ turns of RG-8X with an inside diameter of 9½ inches (24 cm). Note that the 40-meter band minimum and 2:1 SWR range can be raised by removing part of a turn from the RF choke.

Table 2
Results with the RF Choke

Band (meters)	Minimum (MHz)	SWR Minima	2:1 SWR Range (MHz)
40	7.00	1.1	6.850 - 7.220
20	14.10	1.2	13.520 - 14.420
15	21.22	1.1	20.420 - 22.340
10	28.34	1.4	27.460 - 29.050

As is apparent, the OCFD design of K1POO is surprisingly broadband, and with a little adjustment, will cover virtually all of the 40, 20, 15 and 10-meter bands with an SWR of 2:1 or less. However, an RF choke appears to be necessary for this design to work on its fundamental frequency.

[3]Richard Formato, K1POO, "Off-Center-Fed Dipole Comments, Part 2," Technical Correspondence, *QST*, Oct 1996, pp 72-73.

CHAPTER THREE
MULTIBAND ANTENNAS

3-1 **A Trap Collinear Antenna**
From August 1963 *QST*

3-3 **Antenna Traps of Spiral Delay Line**
From November 1972 *QST*

3-6 **Build a Space-Efficient Dipole Antenna for 40, 80 and 160 Meters**
From July 1992 *QST*

3-8 **Trap Construction Information for Al (W8NX) Buxton's July 1992 Dipole**
From September 1992 *QST* (Technical Correspondence)

3-9 **Two New Multiband Trap Dipoles**
From August 1994 *QST*

3-13 **A Center-Fed "Zepp" for 80 and 40**
From May 1966 *QST*

3-16 **All-Band Antenna**
From March 1967 *QST* (Technical Correspondence)

3-17 **Multiband Antennas Using Decoupling Stubs**
From December 1960 *QST*

3-20 **"All-Band" Antenna**
From December 1954 *QST* (Hints & Kinks)

3-21 **Three-Band Matching System for a Forty-Meter Doublet**
From January 1975 *QST* (Hints & Kinks)

3-22 **A "Z" Antenna for the 10-160 Meter Bands**
From December 1979 *QST* (Technical Correspondence)

3-23 **Compact Multiband Antenna Without Traps**
From November 1981 *QST*

3-25 **Five Bands, No Tuner**
From June 1995 *QST*

3-26 **The NRY: A Simple, Effective Wire Antenna for 80 through 10 Meters**
From March 1993 *QST*

By Wesley M. Bell, W7QB

From *QST*, August 1963

A Trap Collinear Antenna

Simple 3-Band Radiator with In-Phase Elements

This antenna covers the 15, 20, and 80-meter bands. On the two higher frequency bands the antenna operates with two extended half waves in phase thereby realizing some gain over the dipole operation of a conventional trap antenna.

As your *ARRL Handbook* tells you, broadside gain over a dipole approximately equivalent to doubling transmitting power may be obtained by using a center-fed antenna about 1¼ wavelengths long (extended double Zepp). Advantage of this is taken in the three-band trap antenna shown in Figure 1. The basic antenna is a dipole for 80 meters. The traps isolate sections of approximately 1¼ wavelengths for 20 and 15 meters. Since the center of a 1¼ wavelength wire is not at a current loop, wire is added in the form of a short open-wire feeder to make the total length about 1½ wavelengths, thereby bringing a current loop at the point where the system is fed by coax line. A balun is used to couple the unbalanced line to the balanced antenna system.

Trap Construction

The coil and capacitor specifications given under Figure 1 should be adequate for transmitters running at 100 watts input or less. For higher power, the inductance and capacitance values should be the same, but coils should be wound with heavier conductor, and capacitors should be of the transmitting type, such as the Centralab 850SL type. I made my own coils by wrapping a 2¼-inch form with waxed paper and winding the turns with double strands of No. 18 wire, unwinding one strand and cementing the remaining turns with strips of model-airplane glue. When the glue was dry, the completed coil was slipped off the form. At least one full extra turn should be wound to allow for pruning.

As shown in Figure 2, the capacitor is placed inside the coil, and the terminals of both capacitor and coil soldered to the heads of brass machine screws. These screws serve to hold the assembly central in a plastic waterproof container as shown in Figure 3. The container is the 1-pint size commonly found filled with chip dip, ice cream, potato salad, oysters and whatnot in grocery stores. The screws are fastened in the top cover and bottom of the container with nuts. The container is suspended from an insulator at the appropriate point in the antenna by short lengths of wire dropped from the insulator to the mounting screws where they are secured by a second set of nuts.

After mounting the traps in the containers, they should be resonated to the designated frequencies by carefully pruning the coils while checking with a grid-dip meter. The strain insulator with its wire wraps must be included, as shown in Figure 3, since the insulator capacitance is in parallel with the trap capacitor. (See *ARRL Handbook*.) As resonance is approached, final adjustment can be made by forming what is left of the last turn into a hairpin, and bend-

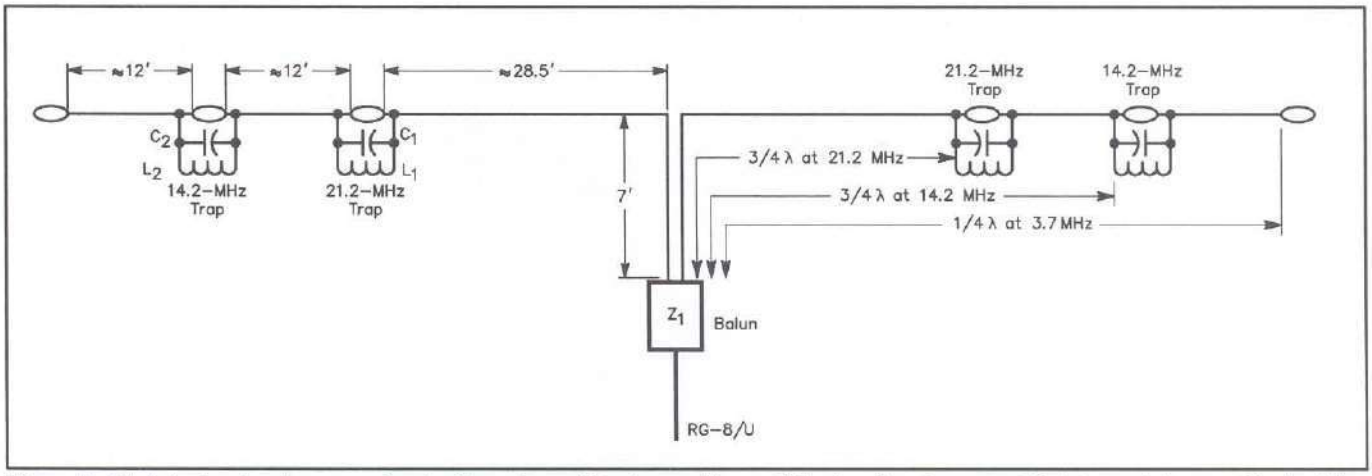

Figure 1—Sketch showing the approximate dimensions of the trap collinear. Wire lengths shown on left side are in terms of feet, while the approximate wavelength equivalents (electrical length) are shown on the right side. Frequencies and approximate wire lengths are for the centers of the three bands as a compromise for full-band coverage. It may be desirable to increase frequency for phone-only operation or lower frequency for c.w.-only operation.

C1, C2—25-pf. 6000-volt disk ceramic. See text.
L_1—Approx. 2 µH–4¾ turns No. 18, 2¼-inches diam., ⅜ inch long, or 5 turns No. 18, 2-inch diam., 16 tpi. See text.
L_2—Approx. 5 µH.—8 turns No. 18, 2¼-inch dia., ⅝ inch long, or 9 turns No. 18, 2-inch diam. 16 tpi. See text.
Z_1—1 to 1 balun.

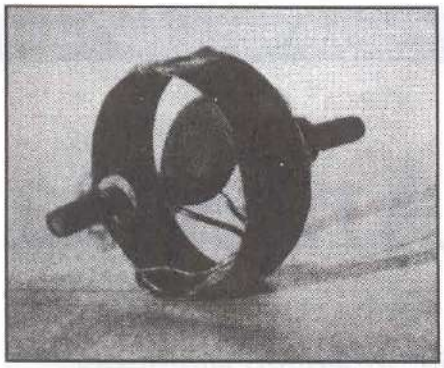

Figure 2—Trap components ready to be mounted in weather-proof container.

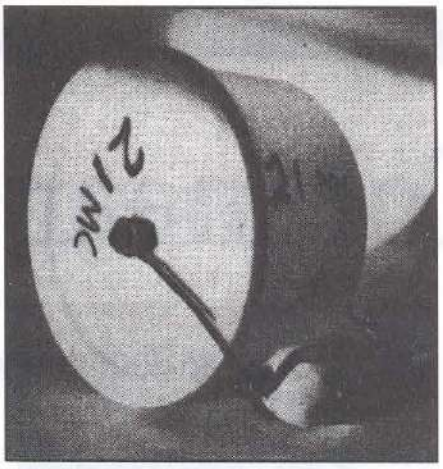

Figure 3—The completed 21-MHz trap and its supporting insulator ready for checking with a grid-dip oscillator.

ing or twisting the hairpin to alter its inductive relationship to the main part of the coil.

Antenna Adjustment

Antenna resonance can be checked by shorting the ends of the 7-ft. open-wire line and coupling to a grid-dip meter. Initially, the wire lengths should be made a foot or so longer than the lengths shown in Figure 1. Start out with the 21-MHz sections only, anchoring the outer end of each wire section to one side of a 21-MHz trap insulator and connecting it to one side of the trap. An additional insulator should be attached temporarily between the other side of the trap insulator and the antenna-supporting rope. Then gradually shorten the wire until the grid-dip meter shows the desired resonant frequency.

Then add the second sections and traps and adjust similarly for the desired frequency in the 14-MHz band. The end sections of wire are then added and adjusted to show resonance at he desired frequency in the 3.5-MHz band.

In making the antenna adjustments, do not adjust the traps after they have once been set with the g.d.o.; change only the lengths of the wire sections. Devote plenty of time and patience to the adjustments. The job just can't be done correctly in a few minutes.

I use a center supporting pole, and the balun is enclosed in a weather-proof box mounted at the top of the pole.

Results with this antenna have been good. Using it in " inverted-vee" fashion, with one pole at the center and the ends attached to bushes, fences, clotheslines, or whatever else might be handy, I changed directions by simply walking the ends around to different positions. Without half trying, I worked 44 countries with a DX-60. I'm moving to the country soon where I plan to put up several of these antennas. 1 hope to add reflectors too. (Well, a guy can dream, can't he?)

By William J. Lattin, W4JRW

From *QST*, November 1972

Antenna Traps of Spiral Delay Line

Most "traps" used in amateur radio multiband antennas are made of lumped inductance and capacitance in parallel. These consist of inductors made of coil stock of No. 12 or No. 14 wire and ceramic capacitors having voltage ratings up to 15,000 volts dc, which are relatively expensive. Vacuum capacitors would be the best, of course, but are also rather expensive.

Another type of trap has a capacitor made of two pieces of aluminum tubing arranged with a small-diameter tube inside a larger tube. Some have polystyrene dielectric, others air dielectric. The *ARRL Handbook* has a very complete description of these types.

Quarter-wave stubs of transmission line can be used for isolating sections of an antenna.[1] Loading coils can be used to modify the harmonic responses of a doublet to the second, third, fifth, seventh, and so on, to obtain a multiband antenna.[2] However, the use of loading coils is quite complicated if more than two bands of frequencies are desired. Traps tuned to the desired resonant frequencies make it much easier to adjust the lengths of the antenna sections, and also to obtain closer spacing between bands than can be obtained with loading coils.

Since quarter-wave sections of transmission line can be used as decoupling stubs for isolation of sections of an antenna, the idea occurred that perhaps quarter-wave sections of spiral delay line (SDL) might be used to make a very simple trap, without lumped capacitance. Spiral delay line is coaxial line with a helical inner conductor.

Construction of SDL Traps

Figure 1 shows the coil which is the helical inner conductor of the spiral delay line, along with the polystyrene tubing and end pieces for the coil, and the aluminum tube. The completed assembly is shown in the title photograph and Figure 2.

For a 28.5-MHz trap, a coil of No. 12 magnet wire was wound on a 1/2-inch rod, 37 turns, close wound. The coil was removed from the 1/2-inch rod and it sprang out to about 3/4-inch OD. The coil was 3 1/4 inches long. Enough wire was used to allow end wires straightened out to be 2 inches long on each end of the coil. Two pieces of 3/4-inch OD polystyrene rod cut 1/2-inch thick were drilled in the center to fit over the No. 12 wire ends and one was slipped over each end of the coil. This coil was placed inside a piece of 1-inch OD × 3/4-inch ID polystyrene tube 4 1/4-inches long, and a piece of 1 1/8-inch OD × 1-inch × 4 1/4-inch long aluminum tube slipped over this. The assembly was held together with No. 6-32 × 5/16-inch screws in holes drilled and tapped just far enough into the polystyrene end pieces to hold the screws in place. The short for this quarter-wave section of spiral delay line was made with a solder lug under one screw with a wire soldered between it and one end of the coil, as shown in the photographs.

The curve in the graph, Figure 3, shows the number of turns of No. 12 wire required for quarter-wave sections of the above construction. A close-wound coil of No. 12 magnet wire has approximately 12 turns per inch. The length of the assembly for a particular frequency can be determined approximately by dividing the number of turns on the coil by 12 to get the length in inches.

The traps were adjusted to frequency through the use of a grid-dip meter (checked on a receiver for accuracy of each frequency). The coil can be changed quite easily to the desired frequency by trimming turns if an extra turn or two is put on for this purpose. The coil can also be wound with spacing between turns and compressed or expanded to get the trap exactly on frequency.

After the assembly is completed and tuned to frequency, the coil can be sealed in the polystyrene tube with polystyrene ce-

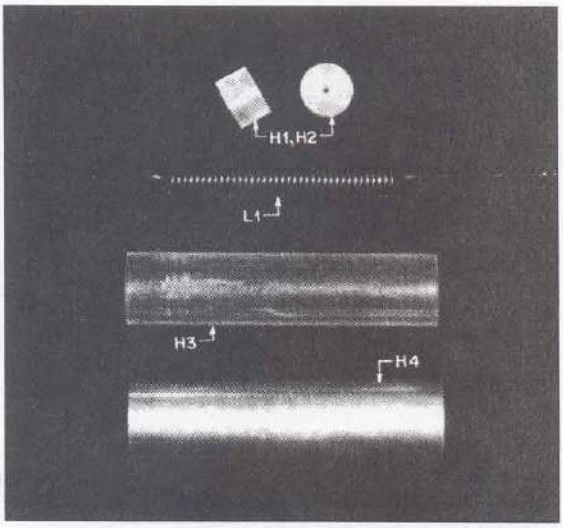

Figure 1 — The parts used in the make-up of a W4JRW SDL trap.
H1, H2 — End pieces of 1/2-inch length of 3/4-inch OD Polystyrene rod with center hole for No. 12 wire.
H3 —1-inch OD × 3/4-inch ID polystyrene tube, length one inch greater than that of coil turns of L1
H4 —1 1/8-inch OD × 1-inch ID aluminum tube, length equal to that of H3.
L1— Close-wound coil of No. 12 enam. or magnet wire, 3/4-inch OD to fit inside H3. See Figure 3 and text for turns information.

[1]Lattin, "Multiband Antennas Using Decoupling Stubs," *QST*, December, 1960, p. 23.
[2]Lattin, "Multiband Antennas Using Loading Coils," *QST*, April, 1961, p. 43.

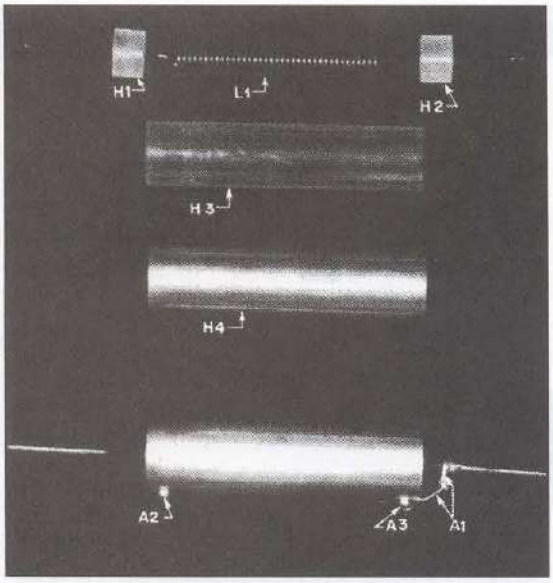

Figure 2—Assembly of the SDL traps. See Figure 1 and text for identification of parts not listed below.
A1—Solder lug and short length of wire assembled and soldered to short one end of H4 to one end of L1.
A2, A3—See text. The screw at A2 must not contact the wire of L1.

ment or coil dope. An inert gas could be sealed inside quite easily, but there seems to be no particular advantage to this.

Trap Ratings and Performance

The thickness of the polystyrene tube used was 1/8 or 0.125 inch. The average voltage rating for polystyrene is given in various handbooks as 500 volts per mil (.001 inch). This would be 62,500 volts for the thickness of 1/8 inch. The maximum power rating of these traps has not been determined. They have been used with a 2-kW PEP ssb transmitter without any failures from either voltage breakdown or heating. Larger wire, polystyrene tubing, and aluminum tubing can be used, of course, but the curve of Figure 3 will be different. Formulas for characteristics of spiral delay lines can be found in radio handbooks and textbooks in which this type of line is described.

The resonant impedance of the traps was measured and found to be approximately 100,000 ohms. For comparison, a trap made of No. 12 wire and a ceramic capacitor gave about the same resonant impedance. Several lumped-constant 15-meter traps borrowed from triband beams were measured and values from 16,000 to 28,000 ohms were found!

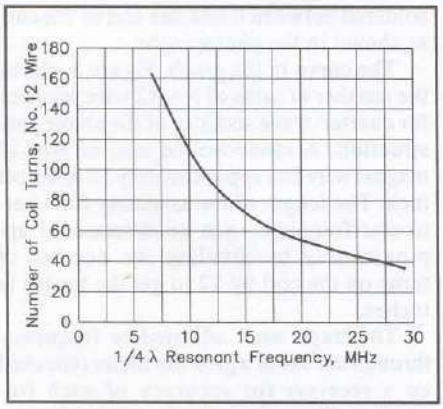

Figure 3—Resonant frequency of spiral-delay-line trap versus number of turns in coil.

The SDL traps can be used in beam antennas, of course, with suitable mechanical modifications to fit the aluminum tube used in the beam. Spiral delay line can be used for other purposes, such as matching transformers, phasing, and any place where coax line is used but short dimensions are needed. The Zo (characteristic impedance) is a function of wire size, diameter, and spacing of the helical coil, dimensions of the insulator and external aluminum tube. Measurement with an rf bridge indicated a Zo of about 250 ohms for the construction used in these traps.

Figures 4 and 5 give the dimensions of two doublet antennas experimented with here. The antenna of Figure 4 has two 7.2-MHz traps and resonates at 3.9 and 7.2 MHz. The antenna of Figure 5 has eight traps, two each for 10 meters, 15 meters, 20 meters, and 40 meters. Resonances are at 3.9, 7.2, 14.3, 21.3, and 28.6 MHz. The flat-top portions were made of No. 12 solid copper wire. The feeder used was RG-8/U. No balun was used in our experiments. It was found that if a trap was not tuned exactly to frequency, it could still be used by changing the wire lengths in the antenna adjacent to the trap to get the desired antenna resonance. An antenna shortened and using traps is sharper in resonance than a full-length doublet. This is generally very well known, but perhaps bears repetition.

SWR curves are also shown in Figures 4 and 5 for these two antennas. During measurements, the antennas were supported in the center about 30 feet high and were 20 feet high at the ends. Measurements were made at the transmitter with 100 feet of RG-8/U coax between the transmitter and the antenna.

It is advisable to support doublet antennas at the center as well as at the ends, with strain relief at the ends – a simple arrangement of a screw eye, plastic rope, and a sash weight or a brick will do.[3] Since RG-8/U coax is fairly heavy, the center support is helpful to reduce the strain on the antenna. The breaking load of No. 12 copper wire is given in handbooks as 197.5 pounds for soft or annealed wire and 261.6 pounds for medium hard-drawn wire. In a high wind any type of support such as trees, towers, push-up masts, and so on, may move a few inches, putting thousands of pounds of tension on a wire stretched between them. Is there any ham who hasn't broken a wire antenna stretched between two trees when no strain reliefs were used?

One spiral-delay-line trap was tested with a hoist and concrete blocks for weight and didn't break at 200 pounds. As the No. 12 wire used in the antenna was softer than

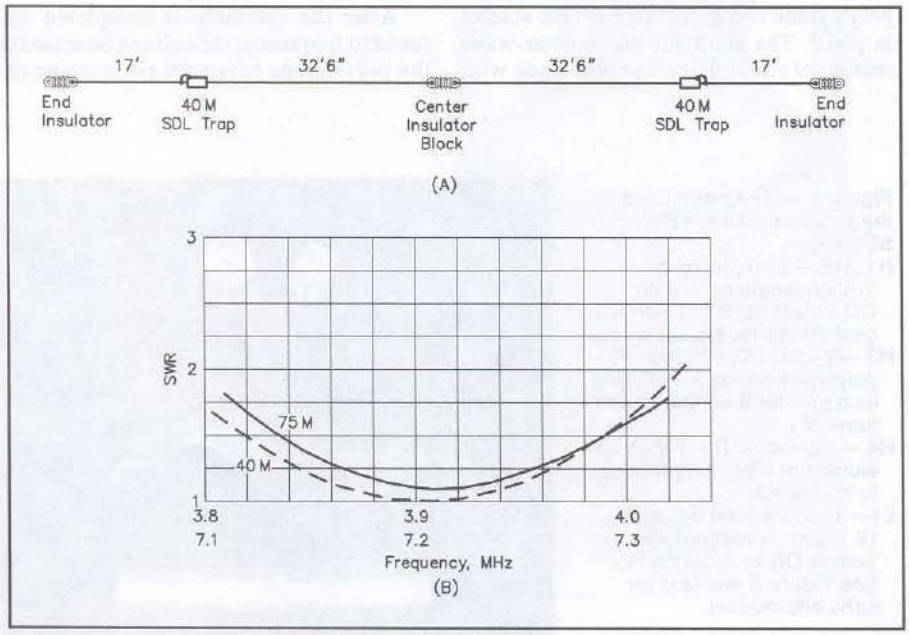

Figure 4—At A, dimensions for a 2-band spiral-delay-line antenna, resonant at 3.9 and 7.2 MHz (not drawn to scale). At B, the measured SWR values with this antenna.

[3] [EDITOR'S NOTE: To reduce wear and eventual breaking of the plastic-rope halyard, a pulley should also be used; large-diameter types sold in hardware stores as clothesline pulleys are economical and quite satisfactory.]

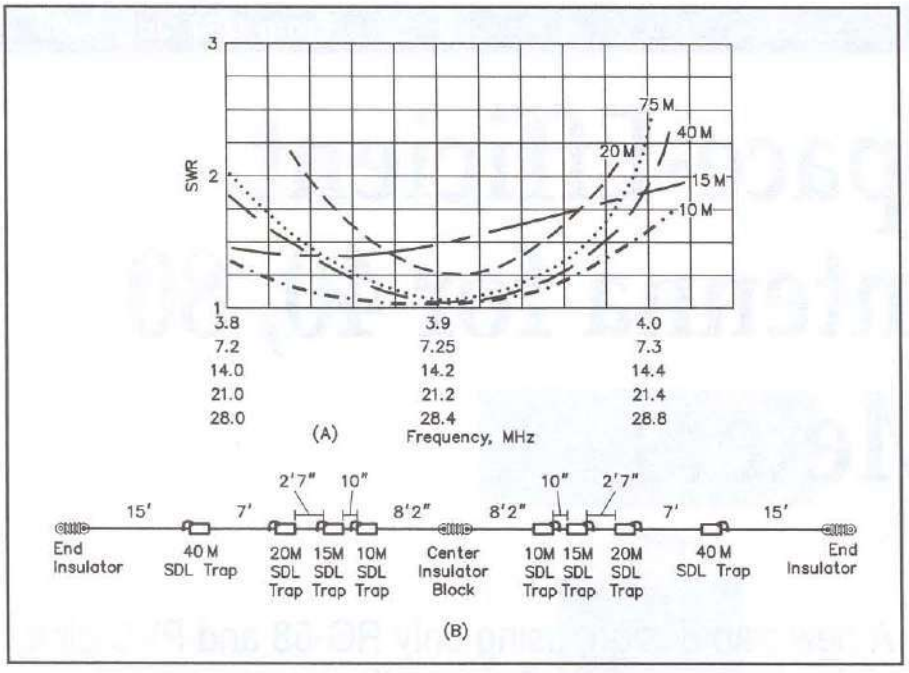

Figure 5—At A, the measured SWR values for a 5-band SDL antenna and at B the dimensions for this antenna.

the No. 12 magnet wires in the SDL traps, it appeared that the antenna wire would probably stretch before the wire in the traps. We have had the antenna up for almost two years, supported by three large trees, with strain reliefs at the ends. The antenna was not damaged at all by an 85-mph wind during a storm which bent the top section of our guyed crank-up tower into an inverted U shape with the triband beam hanging down. We did have one ice storm, but it wasn't severe enough to lift the strain-relief weights at the ends of the antenna.

If one desires, he can make the traps stronger by using two screws 180 degrees apart at each end, or even three screws at 120-degree spacing. Also the ends could be made of copper-weld wire soldered to the inner coil. The materials are not difficult to obtain. Most cities now have plastic supply distributors, and also aluminum tubing suppliers. The magnet wire can be obtained at a motor repair shop or from an electrical supply distributor.

By A. C. Buxton, W8NX

From *QST*, July 1992

Build a Space-Efficient Dipole Antenna for 40, 80 and 160 Meters

A new trap design, using only RG-58 and PVC pipe, yields better space efficiency than conventional coaxial traps.

These days more than ever before, many hams who want to work the low bands need an effective antenna that fits on a small lot. I'll show you how to build a shortened dipole for 160, 80 and 40 meters using improved coaxial-cable traps that I call Super Traps. The antenna, which covers the three ham bands below 7.3 MHz, is about the same length as a fullsize 80-meter dipole. If you install the antenna as an inverted V with a 90° included angle, the baseline length is 88 feet. The antenna uses traps that are easily constructed, rugged and weatherproof. They use no exposed capacitors or inductors.

You can feed the antenna directly with balanced 75-Ω line or via a 1:1 balun with either 50- or 75-Ω coaxial cable. Feed-line length is not critical. The antenna resonates at 1.865, 3.825 and 7.225 MHz. I installed such an antenna on my lot as an inverted V, with the apex 38 feet high and the ends at about 15 feet.

As part of this project, I developed a BASIC-language computer program[1] for trap design; a listing is available from the ARRL.[2] You can use this program to design these traps for frequencies of your choice, but you don't need a computer to make the antenna described here.

Figure 1 shows the antenna layout. The antenna is made of #14 stranded wire and two pairs of coaxial traps. Construction is conventional in most respects, except for the high inductance-to-capacitance (L/C) ratio that results from the unique trap construction. Two recent *QST* articles give tips on dipole construction and feeding.[3,4]

The traps use two-layer windings of the core (dielectric and center conductor) of RG-58 coaxial cable. Coaxial cable with flexible, rugged stranded-wire center conductors is preferable to that with a more brittle solid-wire center conductor. Figure 2 shows the traps. The 3.8-MHz trap is shown with the weatherproofing cover of electrical tape removed to show the construction details.

Precautions and Trap Specifications

With this trap-winding configuration, there are two thicknesses of core dielectric material between adjacent turns, which doubles the breakdown voltage of the traps. The transformer action of the two windings gives a second doubling of the trap-voltage rating. Thus, the trap voltage rating is 5.6 kV (four times RG-58's 1.4-kV rating). Conventional coaxial-cable traps made of RG-58 have a rating of 2.8 kV.

The 7-MHz traps have 33 µH of inductance and 15 pF of capacitance, and the 3.8-MHz traps have 74 µH of inductance and 24 pF of capacitance. The trap Qs are over 170 at their design frequencies, as measured on a Boonton Q meter.

These traps are suitable for operation at the 1-kW power level. When making the traps, *do not* use RG-8X or any other foam-dielectric cable. Winding such cables on small-diameter forms causes the center conductor to migrate through the dielectric toward the inside, decreasing the breakdown rating and compromising trap performance. The core diameter also differs from that of RG-58.

Construction

Although these traps are similar in many ways to other coaxial-cable traps, the shield winding of the common coax-cable trap has been replaced by an outer winding that fits snugly into the grooves formed by the inner layer. Capacitance is reduced to 7.1 pF per

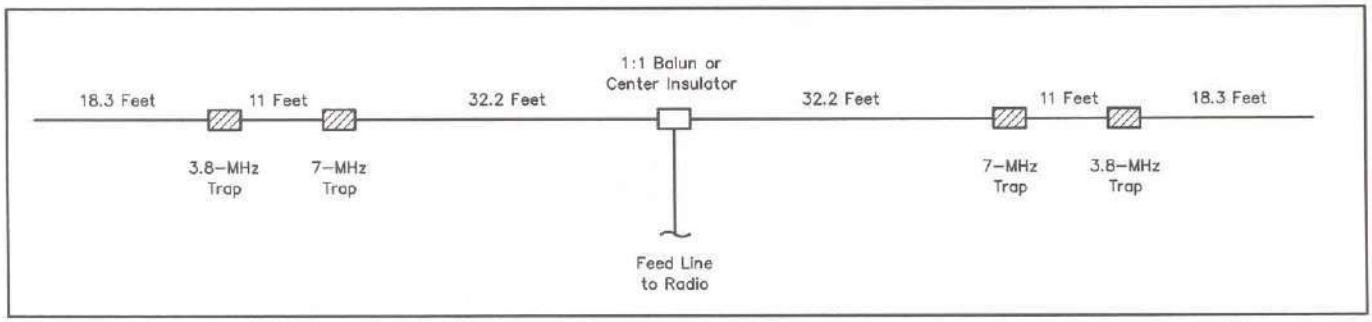

Figure 1—The shortened dipole resonates in the SSB portions of the 40, 80 and 160-meter bands. The antenna is 124 feet long.

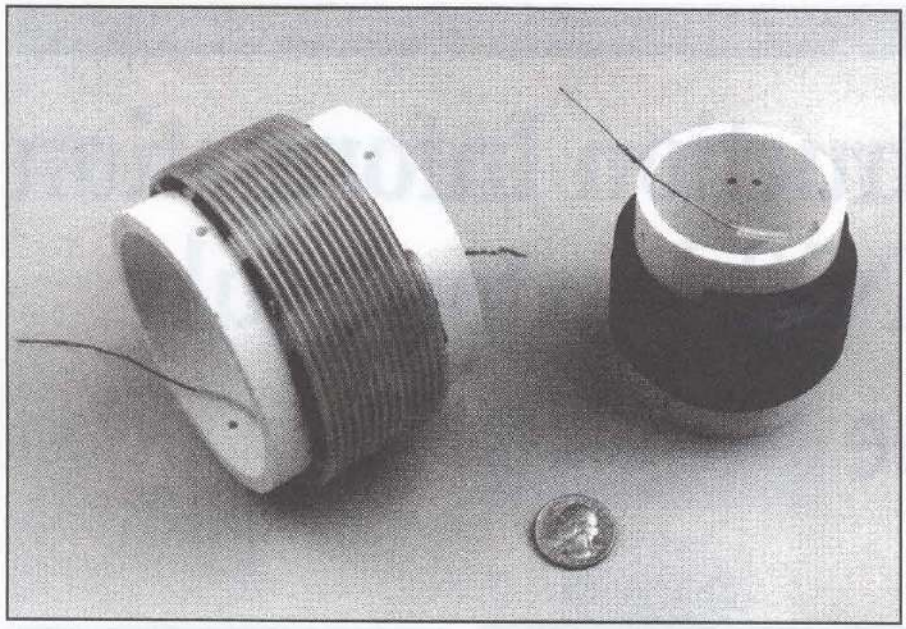

Figure 2—The improved coaxial-cable traps use two layered windings to provide an unusually high inductance-to-capacitance ratio, higher Q, and twice the breakdown voltage of single-layer traps. The 3.8-MHz trap is shown without its protective electrical-tape wrap to show the details of trap construction. This construction method makes for simple, lightweight, rugged and weatherproof traps.

foot, compared to 28.5 pF per foot with conventional coax traps made from RG-58. Trap reactance can be up to four times greater than that provided by conventional coax-cable traps.

The coil forms are cut from PVC pipe available at plumbing-supply stores. The 7-MHz trap form is made from 2-inch-ID pipe with an outer diameter of 2.375 inches. The 3.8-MHz trap form is made from 3-inch pipe with an outer diameter of 3.5 inches. The 7-MHz trap uses a 12.3-turn inner winding and an 11.4-turn outer winding. The 3.8-MHz trap uses a 14.3-turn inner winding and a 13.4-turn outer winding. All turns are closewound. The inner-trap frequency is 7.17 MHz and the outer-trap frequency is 3.85 MHz.

If you are unable to get PVC forms of exactly the same diameters as those called for here, compensate for the effect of form-size differences by taking advantage of the fact that the number of turns varies inversely with the form diameter. Thus, if the form diameter you use is, say, 5% larger than mine, reduce the number of turns by 5%. If necessary, add or remove fractions of a turn at the end of the outer winding. If you have a computer, you can use the BASIC programs[5] to calculate the exact number of turns for other form diameters. Stay as close as you can to the prescribed diameters because too much deviation changes the loading effect of the traps. A small change in trap loading may require a change in the lengths of the tip segments beyond the traps.

Use a #30 (0.128-inch diameter) drill for the feed-through holes in the PVC coil forms. The start and end holes of the 7-MHz traps are spaced 1.44 inches center to center, measured parallel to the trap center line. The holes in the 3.8-MHz traps are 1.66 inches apart. Wind the traps with a single length of coax core. The unspliced lengths are 17.55 feet for the 7-MHz traps and 28.45 feet for the 3.8-MHz traps. These lengths include the trap pigtails and a few inches for fine tuning.

Strip the jacket from the coax. This is easily done using a wood vise with wide jaws to hold the cable while cutting the jacket longitudinally with a sharp knife or razor. The coax outer conductor (braid) is best removed by pushing (not pulling) it off.

Use electrical tape to keep the turns of the inner-layer winding closely spaced during the winding process. This counteracts the tendency of the tension in the outer-layer winding to spread the inner–layer turns. Stick the tape strips directly to the coil form before winding and then tightly loop them over and around the inner layer before winding the outer layer. Use six or more tape strips for each trap.

If possible, check the resonant frequencies of your traps with a dip meter. Try to maintain an accuracy of 50 kHz or better.

For low-noise reception, erect the antenna as close to horizontal as possible. If you let the ends of the antenna droop toward the ground, as I have done with my inverted-V installation, you may have to accept a somewhat higher noise level in the interest of structural simplicity and reduced baseline length. Some feel that the inverted V configuration is better for DXing than a horizontal dipole at the same height. For an inverted V with a 90° included angle (legs that slope downward at 45°), you'll need a minimum apex height of about 55 feet and a baseline length of 88 feet. Get the apex as high as you can and keep the ends at least 10 feet above the ground for safety.

Configuration and Performance Trade-Offs

You seldom get something for nothing. This antenna proves no exception to that rule. As with all trap dipoles, this one has less-than-ideal bandwidth due to the loading effect of the traps. This is the price paid for multiband coverage and physical shortening. This antenna covers 65 kHz of 160 meters, 75 kHz of 80 meters and the entire 40-meter band with SWRs under 2:1. The bandwidth limitations on 160 and 80 meters can be largely offset with an antenna tuner.

It is also important to recognize that the traps are used in low-current portions of the antenna, minimizing I^2R trap losses. A relatively high radiation resistance is therefore also retained.

Good luck with your low-band antennas!

Notes

[1]I wrote the program in GWBASIC 3.2. It uses generic BASIC commands and can be easily converted for use with computers other than IBM PCs and compatibles.

[2]For a copy of the BASIC program, send a business-size SASE to the ARRL Technical Department Secretary, 225 Main St, Newington, CT 06111-1494. Request the July 1992 *QST* BUXTON BASIC PROGRAM listing.

[3]J. Healy, "Antenna Here is a Dipole," *QST*, Jun 1991, pp 23-26.

[4]J. Healy, "Feeding Dipole Antennas," *QST*, Jul 1991, pp 22-24.

[5]See note 2.

Trap Construction Information for Al (W8NX) Buxton's July 1992 Dipole

Several readers have written asking for clearer instructions on how to build the antenna traps described by A. C. Buxton, W8NX, in his July 1992 *QST* article, "Build a Space-Efficient Dipole Antenna for 40, 80 and 160 Meters." For those of you who didn't write, but aren't sure how to build the traps, here's what you need to know.

The trap-winding technique is deceptively simple. Each trap is simply comprised of one winding atop another, wound in the same direction. First, drill four holes in the form for wire entry and exit, as described in July *QST*. Starting from inside the form, pass the wire through the hole labeled "1" in Figures 1 and 2. Wind a layer of the inner conductor on the form. Then, run the wire end down through a second hole into the form (just below the one labeled "EXIT" in Figure 2) and, inside the form, bring the wire back to a point adjacent to where the first winding started. Bring the wire up through the hole marked "2" and wind another layer on top of the first, in the same direction as the first winding. Pass the wire down through the hole labeled "EXIT" and you're done. The tape you see in the photos, described in the article, helps hold the bottom winding's turns together and the top winding in place as you're assembling the trap.

The wires passing through holes in the form are strain-relieved, but use the two mounting holes you drilled in the form to support the trap, just to be on the safe side.
–Rus Healy, NJ2L

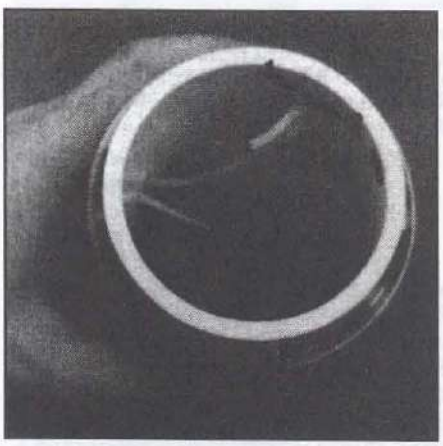

Figure 1—An inside view of a W8NX two-layer trap shows how the windings enter and exit the form. Two holes at each end of the form pass the windings into and out of the form.

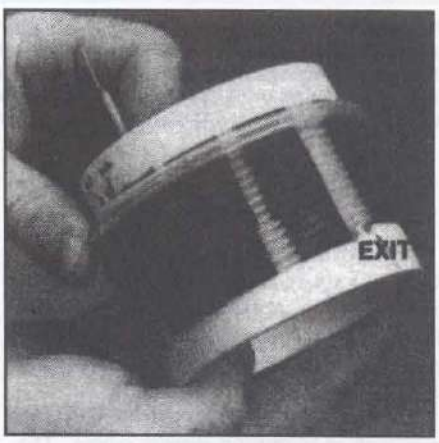

Figure 2—An outside view of a partially assembled W8NX trap. The bottom winding starts at hole "1" and reenters the form just below the "EXIT" hole. The wire then comes back through the inside of the form to hole "T," and is used to make a second winding atop the first. It reenters the form at the "EXIT" hole.

By Al Buxton, W8NX

From *QST*, August 1994

Two New Multiband Trap Dipoles

W8NX details a new coax trap design used in two multiband antennas; one covering 80, 40, 20, 15 and 10 meters, and the other covering 80, 40, 17 and 12 meters.

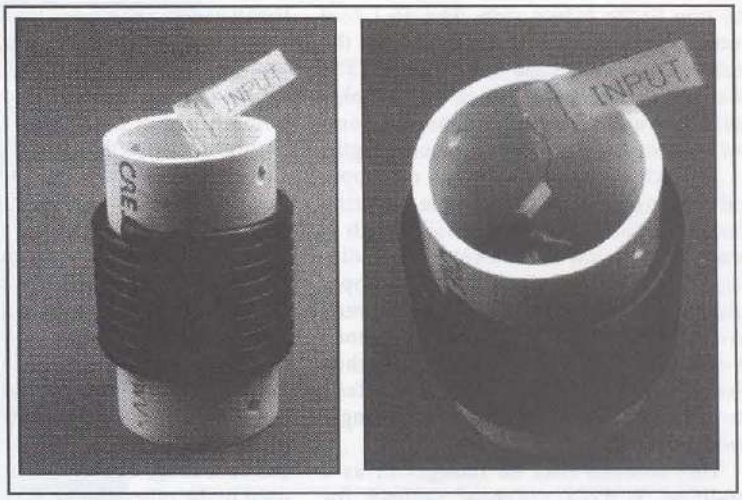

Over the last 60 or 70 years, amateurs have used many kinds of multiband antennas to cover the traditional HF bands. The availability of the 30, 17 and 12-meter bands has expanded our need for multiband antenna coverage. A fortunate few have the space and resources for multiband antennas like rhombics or long Vs, but many hams have employed inverted-L long wires or parallel dipoles. Old-timers will recall the offcenter-fed *Windom* of the '30s–the first version using a single-wire transmission line, and the later design using two-wire feed line. Over the years, random-length dipoles with open-wire feeders and associated tuners have been used successfully as multiband antennas. The G5RV multiband antenna is a specialized example of this approach.[1]

The *log periodic array* represents a kind of brute-force approach to the goal of achieving coverage of multiple HF ham bands. It seems inefficient because of the large gaps between our relatively narrow amateur HF bands.

Over the last few decades, two factors have affected the development of multiband antennas—the popularity of low-impedance (usually 50-Ω) coaxial feed lines, and the appearance of untuned, 50-Ω solid-state amplifiers. The impedance of an antenna is relatively low only at its fundamental frequency and at odd-order harmonics. Although antenna tuners are often necessary to resonate an antenna system, the quest for expanded multiband coverage with simple antennas continues.

At the end of the 1930s, a different technological approach appeared in the form of resonant traps in antennas. The *Mims Signal Squirter* is the grandfather of modern day tribanders.[2] This article discusses in detail an innovative trap design employed in two multiband dipoles.

One W8NX Trap Design—Two Multiband Dipoles

Two different antennas are described here. The first covers 80, 40, 20, 15 and 10 meters, and the second covers 80, 40, 17 and 12 meters. Each uses the same type of W8NX trap—connected for different modes of operation—and a pair of short capacitive stubs to enhance coverage. The new W8NX coaxial-cable traps have two different modes: a high- and a low-impedance mode. The inner-conductor windings and shield windings of the traps are connected in series in the conventional manner for both modes. However, either the low- or high-impedance point can be used as the trap's output terminal. For low-impedance trap operation, only the center conductor turns of the trap windings are used. For high-impedance operation, all turns are used, in the conventional manner for a trap. The short stubs on each antenna are strategically sized and located to permit more flexibility in adjusting the resonant frequencies of the antenna.

Figure 1 shows the configuration of the 80, 40, 20, 15 and 10-meter antenna. The radiating elements are made of #14 stranded copper wire. The element lengths are the wire span lengths in feet. These lengths do not include the lengths of the pigtails at the balun, traps and insulators. The 32.3-foot-long inner 40-meter segments are measured from the eyelet of the input balun to the tension relief hole in the trap coil form. The 4.9-foot segment length is measured from the tension relief hole in

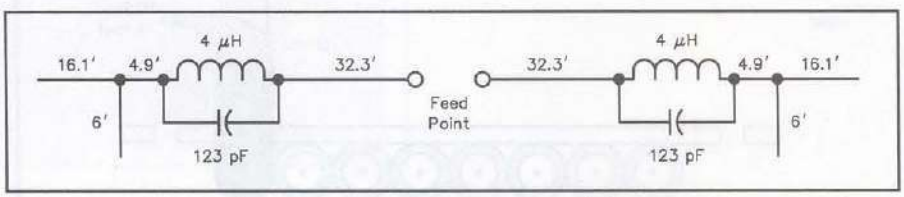

Figure 1—A W8NX multiband dipole for 80, 40, 20, 15 and 10 meters. The values shown (123 pF and 4 μH) for the coaxial-cable traps are for parallel resonance at 7.15 MHz. The low-impedance output of each trap is used for this antenna.

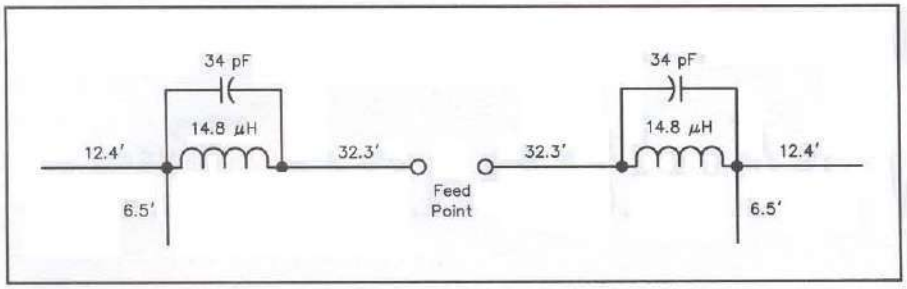

Figure 2—A W8NX multiband dipole for 80, 40, 17 and 12 meters. For this antenna, the high-impedance output is used on each trap. The resonant frequency of the traps is 7.15 MHz.

the trap to the 6-foot stub. The 16.1-foot outer-segment span is measured from the stub to the eyelet of the end insulator. The coaxial-cable traps are wound on PVC pipe coil forms and use the low-impedance output connection. The stubs are 6-foot lengths of 1/8-inch stiffened aluminum or copper rod hanging perpendicular to the radiating elements. The first inch of their length is bent 90° to permit attachment to the radiating elements by large-diameter copper crimp connectors. Ordinary #14 wire may be used for the stubs, but it has a tendency to curl up and may tangle unless weighed down at the end. I recommend that you feed the antenna with 75-Ω coax cable using a good 1:1 balun.

This antenna may be thought of as a modified W3DZZ antenna[3] (shown for many years in various ARRL publications) with the addition of capacitive stubs. The length and location of the stub give the antenna designer two extra degrees of freedom to place the resonant frequencies within the amateur bands. This additional flexibility is particularly helpful to bring the 15 and 10-meter resonant frequencies to more desirable locations in these bands. The actual 10-meter resonant frequency of the W3DZZ antenna is somewhat above 30 MHz, pretty remote from the more desirable low frequency end of 10 meters.

Figure 2 shows the configuration of the 80, 40, 17 and 12-meter antenna. Notice that the capacitive stubs are attached immediately outboard after the traps and are 6.5 feet long, 0.5 foot longer than those used in the other antenna. The traps are the same as those of the other antenna, but are connected for the high-impedance output mode. Since only four bands are covered by this antenna, it is easier to fine tune it to precisely the desired frequency on all bands. The 12.4-foot tips can be pruned to a particular 17-meter frequency with little effect on the 12-meter frequency. The stub lengths can be pruned to a particular 12-meter frequency with little effect on the 17-meter frequency. Both such pruning adjustments slightly alter the 80-meter resonant frequency. However, the bandwidths of the antennas are so broad on 17 and 12 meters that little need for such pruning exists. The 40-meter frequency is nearly independent of adjustments to the capacitive stubs and outer radiating tip elements. Like the first antennas, this dipole is fed with a 75-Ω balun and feed line.

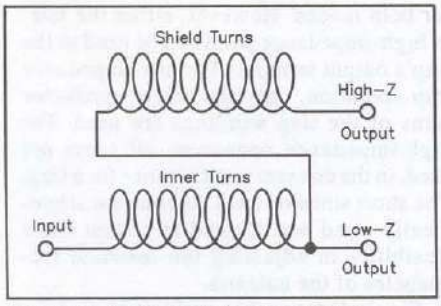

Figure 3—Schematic for the W8NX coaxial-cable trap. RG-59 is wound on a 2⅜-inch OD PVC pipe.

Figure 3 shows the schematic diagram of the traps. It explains the difference between the low and high-impedance modes of the traps. Notice that the high-impedance terminal is the output configuration used in most conventional trap applications. The low-impedance connection is made across only the inner conductor turns, corresponding to one-half of the total turns of the trap. This mode steps the trap's impedance down to approximately one-fourth of that of the high-impedance level. This is what allows a single trap design to be used for two different multiband antennas.

Figure 4 is a drawing of a cross-section of the coax trap shown through the long axis of the trap. Notice that the traps are conventional coaxial-cable traps, except for the added low-impedance output terminal. The traps are 8¾ close-spaced turns of RG-59 (Belden 8241) on a 2⅜-inch-OD PVC pipe (schedule 40 pipe with a 2-inch ID) coil form. The forms are 4⅛ inches long. Trap resonant frequency is very sensitive to the outer diameter of the coil form, so check it carefully. Unfortunately, not all PVC pipe is made with the same wall thickness. The trap frequencies should be checked with a dip meter and general coverage receiver and adjusted to within 50 kHz of the 7150 kHz resonant frequency before installation. One inch is left over at each end of the coil forms to allow for the coax feed-through holes and holes for tension-relief attachment of the antenna radiating elements to the traps. Be sure to seal the ends of the trap coax cable with RTV sealant to prevent moisture from entering the coaxial cable.

Also, be sure that you connect the 32.3-foot wire element at the start of the inner conductor winding of the trap. This avoids detuning the antenna by the stray capacitance of the coaxial-cable shield. The trap output terminal (which has the shield stray capacitance) should be at the outboard side of the trap. Reversing the input and output terminals of the trap will lower the 40-meter frequency by approximately 50 kHz, but there will be negligible effect on the other bands.

The title-page photos show a coaxial-cable trap. Details of the trap installation are shown in Figure 5. This drawing applies specifically to the 80, 40, 20, 15 and 10-meter antenna, which uses the low-impedance trap connections. Notice the lengths of the trap pigtails: 3 to 4 inches at each terminal of the trap. If you use a different arrangement, you must modify the span lengths accordingly. All connections can be made using crimp connectors rather than by soldering. Access to the trap's interior is attained more easily with a crimping tool than with a soldering iron.

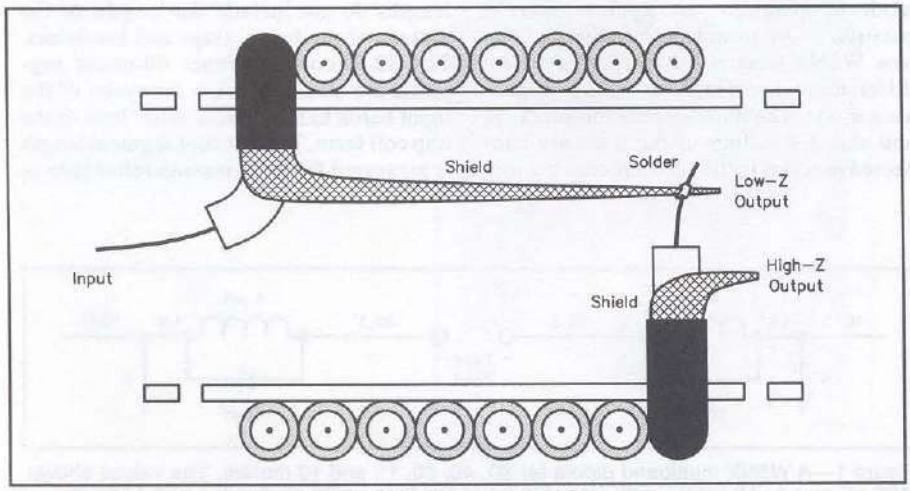

Figure 4—Construction details of the W8NX coaxial-cable trap.

Antenna Patterns

The performance of both antennas has

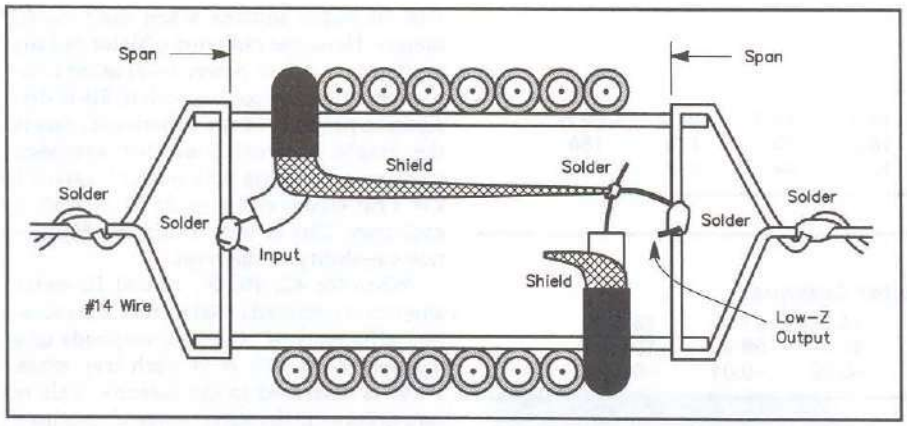

Figure 5—Additional construction details for the W8NX coaxial-cable trap.

been very satisfactory. I am currently using the 80,40, 17 and 12-meter version because it covers 17 and 12 meters. (I have a tribander for 20, 15 and 10 meters.) The radiation pattern on 17 meters is that of 3/2-wave dipole. On 12 meters, the pattern is that of a 5/2-wave dipole. At my location in Akron, Ohio, the antenna runs essentially east and west. It is installed as an inverted V, 40 feet high at the center, with a 120° included angle between the legs. Since the stubs are very short, they radiate little power and make only minor contributions to the radiation patterns. The pattern has four major lobes on 17 meters, with maxima to the northeast, southeast, southwest, and northwest. These provide low-angle radiation into Europe, Africa, South Pacific, Japan and Alaska. A narrow pair of minor broadside lobes provides north and south coverage into Central America, South America and the polar regions.

There are four major lobes on 12 meters, giving nearly end-fire radiation and good low-angle east and west coverage. There are also three pairs of very narrow, nearly broadside, minor lobes on 12 meters, down about 6 dB from the major end-fire lobes. On 80 and 40 meters, the antenna has the usual figure-8 patterns of a half-wavelength dipole. I have some pattern distortion and input impedance effects from aluminum siding on my house. Nevertheless, DX is easily workable on either of these antennas using a 100-W transceiver, when the high-frequency bands are open.

Both antennas function as electrical half-wave dipoles on 80 and 40 meters with a low SWR. They both function as odd harmonic current-fed dipoles on their other operating frequencies, with higher, but still acceptable, SWR. The presence of the stubs can either raise or lower the input impedance of the antenna from those of the usual third and fifth harmonic dipoles. Again, I recommend that 75-Ω, rather than 50-Ω, feed line be used because of the generally higher input impedances at the harmonic operating frequencies of the antennas.

The SWR curves of both antennas were carefully measured. A 75 to 50-Ω transformer from Palomar Engineers was inserted at the junction of the 75-Ω coax feed line and my 50-Ω SWR bridge. The transformer prevents an impedance discontinuity, with attendant additional undesired line reflections appearing at the 75 to 50-Ω junction. The transformer is required for accurate SWR measurement if a 50-Ω SWR bridge is used with a 75-Ω line. No harm is done to any equipment, however, if the transformer is omitted. Most 50-Ω rigs operate satisfactorily with a 75-Ω line, although this requires different tuning and load settings in the final output stage of the rig or antenna tuner. I use the 75 to 50-Ω transformer only when making SWR measurements and at low power levels. The transformer is rated for 100 W, and when I run my 1-kW PEP linear amplifier the transformer is taken out of the line. (I hope my absent-mindedness doesn't catch up with me some day!)

Figure 6 gives the SWR curves of the 80, 40, 20, 15 and 10-meter antenna. Minimum SWR is nearly 1: 1 on 80 meters, 1.5:1 on 40 meters, 1.6:1 on 20 meters, and 1.5:1 on 10 meters. The minimum SWR is slightly below 3:1 on 15 meters. On 15 meters, the stub capacitive reactance combines with the inductive reactance of the outer segment of the antenna to produce a resonant rise that raises the antenna input resistance to about 220 Ω, higher than that of the usual 3/2-wavelength dipole. An antenna tuner may be required on this band to keep a solid-state final output stage happy under these load conditions.

Figure 7 shows the SWR curves of the 80, 40, 17 and 12-meter antenna. Notice the excellent 80-meter performance with a

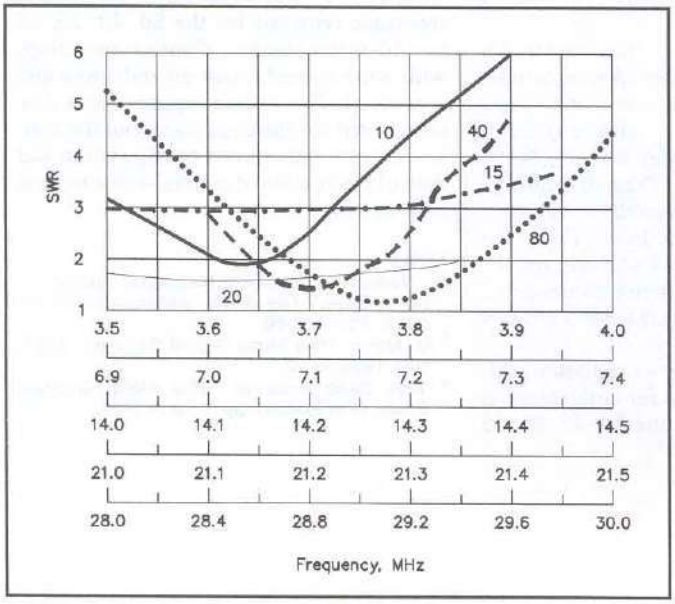

Figure 6—Measured SWR curves for an 80, 40, 20, 15 and 10-meter antenna, installed as an inverted-v with 40-ft apex and 120° included angle between legs.

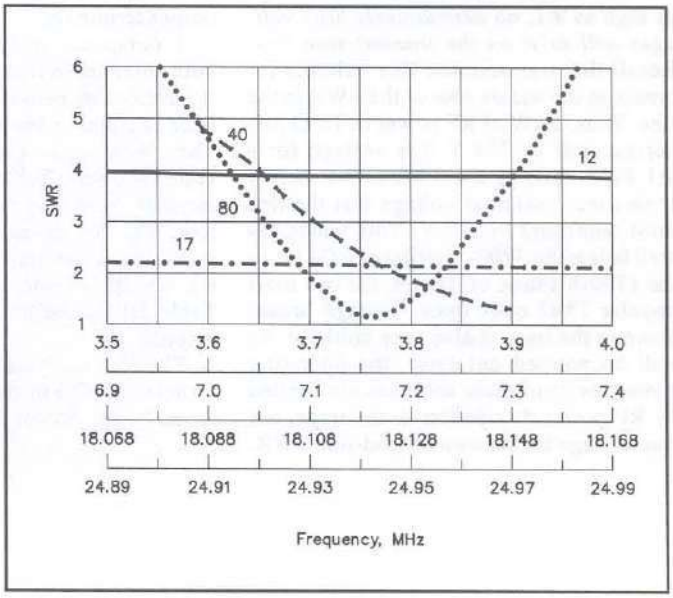

Figure 7—Measured SWR curves for an 80, 40, 17 and 12-meter antenna, installed as an inverted-v with 40-ft apex and 120° included angle between legs.

Table 1
Trap Q

Frequency (MHz)	3.8	7.15	14.18	18.1	21.3	24.9	28.6
High Z out (Ω)	101	124	139	165	73	179	186
Low Z out (Ω)	83	103	125	137	44	149	155

Table 2A
Trap Loss Analysis: 80, 40, 20,15, 10-Meter Antenna

Frequency (MHz)	3.8	7.15	14.18	21.3	28.6
Radiation Efficiency (%)	96.4	70.8	99.4	99.9	100.0
Trap losses (dB)	–0.16	–1.5	–0.02	–0.01	–0.003

Table 2B
Trap Loss Analysis: 80, 40, 17, 12-Meter Antenna

Frequency (MHz)	3.8	7.15	18.1	24.9
Radiation Efficiency (%)	89.5	90.5	99.3	99.8
Trap losses (dB)	–0.5	–0.4	–0.03	–0.006

nearly unity minimum SWR in the middle of the band. The performance approaches that of a full-size 80-meter wire dipole. The short stubs and the very low inductance traps shorten the antenna somewhat on 80 meters. Also, observe the good 17-meter performance, with the SWR being only a little above 2:1 across the band.

But notice the 12-meter SWR curve of this antenna, which shows 4:1 SWR across the band. The antenna input resistance approaches 300 Ω on this band because the capacitive reactance of the stubs combines with the inductive reactance of the outer antenna segments to give resonant rises in impedance. These are reflected back to the input terminals. These stub-induced resonant impedance rises are similar to those on the other antenna on 15 meters, but are even more pronounced.

Too much concern must not be given to SWR on the feed line. Even if the SWR is as high as 9:1, *no destructively high voltages will exist on the transmission line.* Recall that transmission-line voltages increase as the square root of the SWR in the line. Thus, 1 kW of RF power in 75-Ω line corresponds to 274 V line voltage for a 1:1 SWR. Raising the SWR to 9:1 merely triples the maximum voltage that the line must withstand to 822 V. This voltage is well below the 3700-V rating of RG- 11, or the 1700-V rating of RG-59, the two most popular 75-Ω coax lines. Voltage breakdown in the traps is also very unlikely. As will be pointed out later, the operating power levels of these antennas are limited by RF power dissipation in the traps, not trap voltage breakdown or feed-line SWR.

Trap Losses and Power Rating

Table 1 presents the results of trap Q measurements and extrapolation by a two-frequency method to higher frequencies above resonance. I employed an old, but recently calibrated, Boonton Q meter for the measurements. Extrapolation to higher frequency bands assumes that trap resistance losses rise with skin effect according to the square root of frequency, and that trap dielectric losses rise directly with frequency. Systematic measurement errors are not increased by frequency extrapolation. However, random measurement errors increase in magnitude with upward frequency extrapolation. Results are believed to be accurate within 4% on 80 and 40 meters, but only within 10 to 15% at 10 meters. Trap Q is shown at both the high- and low-impedance trap terminals. The Q at the low-impedance output terminals is 15 to 20% lower than the Q at the high-impedance output terminals.

I computer-analyzed trap losses for both antennas in free space. Antenna-input resistances at resonance were first calculated, assuming lossless, infinite-Q traps. They were again calculated using the Q values shown in Table 1. The radiation efficiencies were also converted into equivalent trap losses in decibels. Table 2A summarizes the trap loss analysis for the 80, 40, 20, 15 and 10-meter antenna and Table 2B for the 80, 40, 17 and 12-meter antenna.

The loss analysis shows radiation efficiencies of 90% or more for both antennas on all bands except for the 80, 40, 20, 15 and 10-meter antenna when used on 40 meters. Here, the radiation efficiency falls to 70.8%. A 1-kW power level at 90% radiation efficiency corresponds to 50-W dissipation per trap. In my experience, this is the trap's survival limit for extended key-down operation. SSB power levels of 1 kW PEP would dissipate 25 W or less in each trap. This is well within the dissipation capability of the traps.

When the 80, 40, 20, 15 and 10-meter antenna is operated on 40 meters, the radiation efficiency of 70.8% corresponds to a dissipation of 146 W in each trap when 1 kW is delivered to the antenna. This is sure to burn out the traps—even if sustained for only a short time. Thus, the power should be limited to less than 300 W when this antenna is operated on 40 meters under prolonged key-down conditions. A 50% CW duty cycle would correspond to a 600-W power limit for normal 40-meter CW operation. Likewise, a 50% duty cycle for 40-meter SSB corresponds to a 600-W PEP power limit for the antenna.

I know of no analysis where the burnout wattage rating of traps has been rigorously determined. Operating experience seems to be the best way to determine trap burn-out ratings. In my own experience with these antennas, I've had no traps burn out, even though I operated the 80, 40, 20, 15 and 10-meter antenna on the critical 40-meter band using my AL-80A linear amplifier at the 600-W PEP output level. I have, however, made no continuous, keydown, CW operating tests at full power purposely trying to destroy the traps!

Summary

Some hams may suggest using a different type of coaxial cable for the traps. The dc resistance of 40.7 Ω per 1000 feet of RG-59 coax seems rather high. However, I've found no coax other than RG-59 that has the necessary inductance-to-capacitance ratio to create the trap characteristic reactance required for the 80, 40, 20, 15 and 10-meter antenna. Conventional traps with wide-spaced, open-air inductors and appropriate fixed-value capacitors could be substituted for the coax traps, but the convenience, weatherproof configuration and ease of fabrication of coaxial-cable traps is hard to beat.

Notes

[1] L. Varney, "The G5RV Multiband Antenna... Up-to-Date," *The ARRL Antenna Compendium, Vol. 1*, p 86.
[2] M. Mims, "The Mims Signal Squirter," *QST*, Dec 1939, p 12.
[3] "Five Band Antenna," *The ARRL Antenna Book*, 16th Edition, pp 7-10 to 7-11.

By William C. Gann, W4NML

From *QST*, May 1966

A Center-Fed "Zepp" for 80 and 40

Fast QSY for the Phone-C.W. Operator

The center-fed "Zepp" antenna is reviewed by W4NML, showing how complete coverage of a single band is made easy by using old concepts. Although the author shows how to use the Zepp on 80 and 40, only, the system can be used from 80 through 10 meters by employing an all-band transmatch.

Multiband antennas fed with resonant feeders were very popular in the pre-coax cable days. This article is presented to review a good, but seemingly forgotten system. This antenna should be of interest to traffic and contest operators, and to the casual operator who likes to use both the c.w. and phone portions of the 80- and 40-meter bands.

Our section s.s.b. net meets on 3965 kHz and the c.w. net meets on 3575 kHz. Many schemes were tried to make one antenna usable on both ends of the band so that a low s.w.r. could be maintained while securing efficient operation at the different frequencies. None of the antennas tried would permit an excursion of more than 300 kHz without a serious s.w.r. problem between the transmitter and the line. Getting from 80 to 40 meters with such an antenna was even more perplexing. The writer's dilemma was finally solved by the installation of the old reliable center-fed Zepp antenna.

Choosing the Dimensions

In order to use the antenna on 40, 75, and 80 meters, tuned feeders are required[1]. So that the feeders can be matched to the transmitter, a transmatch is used at the "shack" end of the line. Parallel tuning is used to minimize the complexity of the transmatch. This requires that the transmission line presents a high impedance to the transmatch on both bands.

The charts in the handbooks did not give a set of Zepp antenna dimensions that were suitable for the author's installation. Because of the existing tower, which would permit the antenna to be supported at the 50-foot level, and because the ham shack was adjacent to the tower, the prescribed feeder lengths were not practical. A graph was plotted to show the frequency extremes to which the antenna would be tuned, showing the minimum and maximum impedance points across the bands. It was determined that the combined length of one leg of the feed line and one section of the dipole would be 114 feet.[2] A length of 53 feet was used for the feed line and each leg of the driven element was cut to 61 feet.

To broaden the antenna's response, the driven element's effective area was made larger by paralleling two lengths of No. 12 copper wire as shown in Figures 1 and 2. With this arrangement, the Q of the antenna is lower, permitting the operator to QSY approximately 200 kHz without readjusting the transmatch.

Construction Notes

The driven element and the feed line are made from No. 12 copper wire. The 4-inch wide ceramic spreaders used to hold the feeder wires apart are made by the E. F. Johnson Co. Light-weight poly spacers are used to spread the driven-element wires and are sold as TV "clothespins" by the Telco Co. (Figure 2). All of the spreaders are attached to the No. 12 wire by short pieces of No. 18 copper wire. The distance between the spreaders is 4 feet for both the driven element and the feed line.

Sections of 1 × 4-inch lumber are used to hold the feeders away from the steel tower (Figure 3). Each piece is 24 inches long, notched at one end, and is fastened to the tower with U-bolts. Porcelain telephone-type insulators are attached to the feed-line end of each board, offering low-loss anchor

[1] Center-fed Antennas, *A.R.R.L. Antenna Book*, Chapter 6.

[2] This length is generally 145 feet for operation in the 3.5- to 30-MHz range when the antenna is mounted horizontally (no droop), away from steel towers, and with a singlewire driven element.–*Editor*

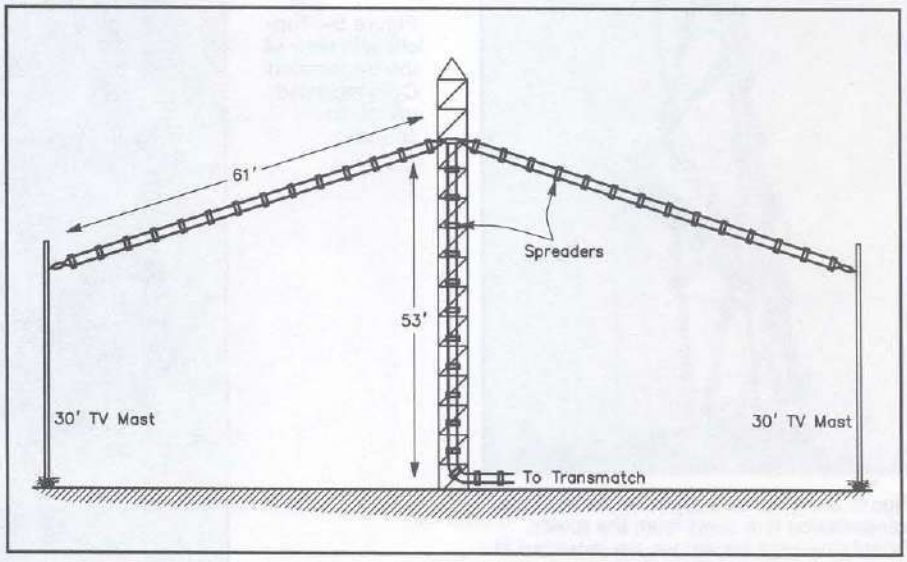

Figure 1—Layout of the 2-band Zepp antenna. Dimensions for each part of the antenna are shown. Feed point is anchored to one of the wooden support arms (See Figure 3).

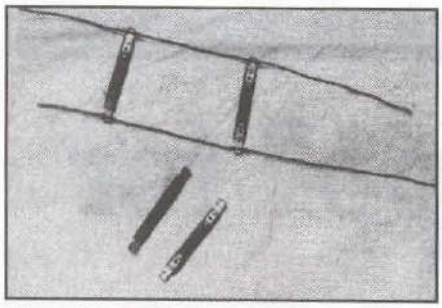

Figure 2—Details showing how the driven element spreaders are attached to the No. 12 wire. No. 18 copper wire is wrapped above and below each spreader to hold it in place.

points for the transmission line. The uppermost support arm, at the 50-foot level, is used as a mount for the center of the driven element.

The far ends of the antenna are supported by 30-foot TV masts. A pulley and halyard arrangement is used for raising and lowering the ends of the antenna. Because the end supports are not as high as the feed point of the antenna, the dipole has a slight droop, but this does not seem to impair the performance.

The transmission line is brought into the operating position by means of feed-through insulators, mounted on a plywood strip which fits under a partially raised window. Insulated No. 12 house wire is used between the feed-through insulators and the transmatch.

Transmatch

Ideas for the author's tuner (Figure 4) were taken from the excellent transmatch

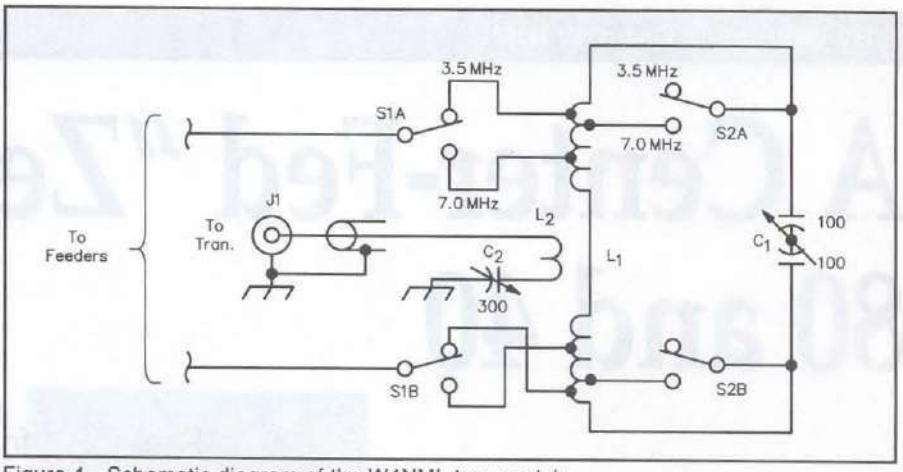

Figure 4—Schematic diagram of the W4NML transmatch.

C_1—100 pf. per section transmitting variable. (Split stator type with 0.175-inch spacing between plates.)
C_2—300-pf. variable capacitor(0.078 spacing or greater).
J_1—SO-239 coax connector.
L_1—56 turns, 3-inch diam., 8 turns per inch coil. S_1 taps are 9 turns from ends of coil for 80 meters, and are 22 turns from ends of coil for 40 meters. S_2 taps are 5 turns from ends of coil for 80 meters and 17 turns from ends of coil for 40 meters. (Air Dux 2408T or Polycoils 1779 usable.)
L_2—8 turns of Air Dux 2408T (center portion of L_1).
S_1, S_2—Ceramic rotary, 2 poles, 2 positions, 2 sections.

article by McCoy.[3] Band changing is made possible by a large ceramic switch (origin unknown) which was obtained at a hamfest. An identical switch is used for selecting the taps for the feed line (Figure 5). Coil L_1 contains 56 turns of No. 14 wire, is 3 inches in diameter, and has 8 turns-per-inch (Air Dux 2408T). A stationary link, L_2, at the center of L_1, contains 8 turns of No. 14 wire and is a part of the Air Dux coil from which L_1 is made. The link is tuned with a 300-pf. variable capacitor. The author did not have a unit of the correct type, so two 150-pf. capacitors were parallel-connected (mounted under the chassis). Capacitor C_1 is a 100-pf-.per-section variable

[3] *QST*, July 1965.

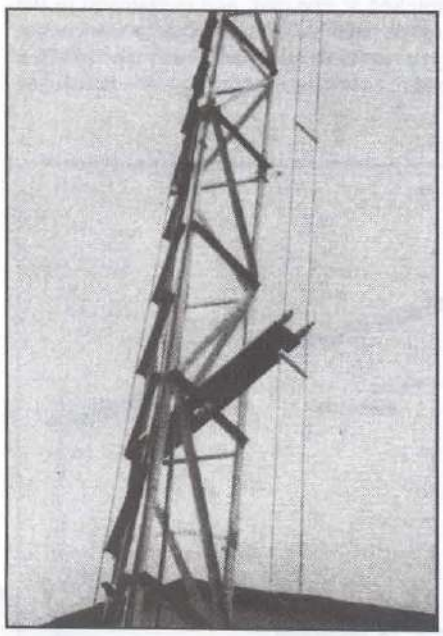

Figure 3—Wooden support arms hold the transmission line away from the tower. Telephone-type insulators are mounted at the end of each board to make the feed line secure.

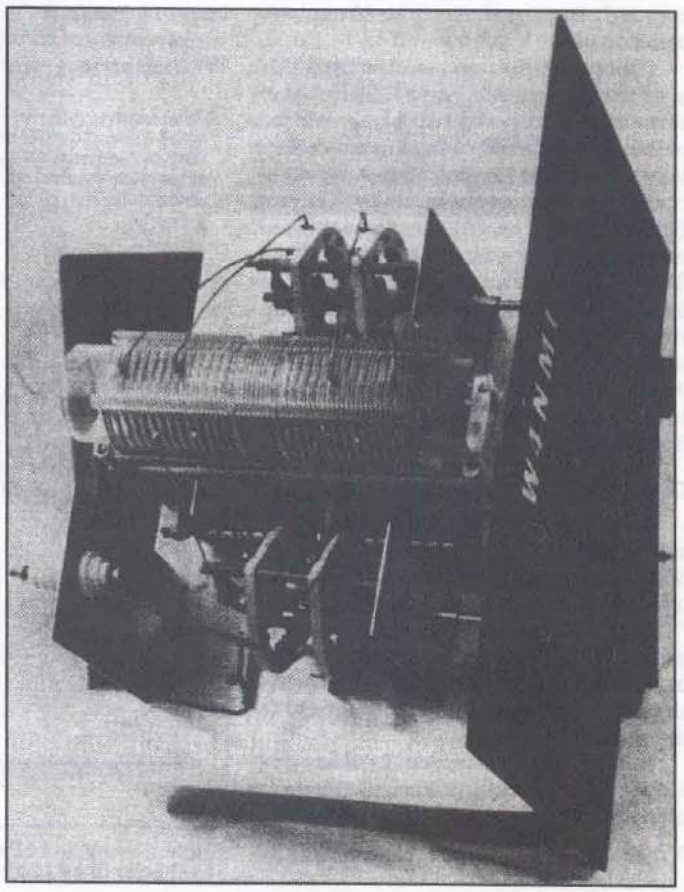

Figure 5—Top-chassis view of the transmatch. C_2 is mounted under the chassis.

with wide spacing. To give L_1 some rigidity, it is mounted on a plexiglass tube which is supported by the frame of C_1 with standoff insulators.

Results

While using clip leads, the correct tap points for the feeders were found by operating the transmitter through a Collins wattmeter and tuning C_1 and C_2 for zero reflected power. The transmatch permitted the transmitter to "see" 50 ohms in any part of either band. After establishing the correct tap points for the feed line, permanent connections were made between L_1 and the switches.

Next, the tuner was used with the 30L-1 amplifier at an output level of 700 watts. After a 30-minute QSO, no evidence of coil heating could be detected.

When compared to other antenna systems used by the author, the new skywire showed improved performance. It was believed that some sacrifice in efficiency would result from changing to the new antenna. Happily, it was found that we could have our cake and eat it too! Extended use indicated that the performance was, indeed, better than with previous antennas used.

I wish to thank three friends for their help in making this article possible: K4WWN for his tower climbing and photography work, K4ADK for building the transmatch cabinet, and Roy LeCrone for additional darkroom and photographic assistance.

Although this antenna system is an old standard, it may be the answer to your QSY problems. The cost is nominal and the results are most rewarding.

All-Band Antenna

With reference to the article on a Center-fed Zepp for 80 and 40 in May 1966 *QST*:

I set out to accomplish several things with an antenna to be installed on a California lot which runs east-west:

1) One pole.
2) No guys.
3) Good for short skip up and down the West Coast on 80, 75 and 40 meters.
4) Throw lobes across populated DX areas on 20 and 15 meters with a fairly low radiation angle.
5) Allow some onmidirectional DX on 40 meters.
6) Keep away from anything with critical antenna length or critical tuning.
7) Minimum cost.

Figure 1 shows the arrangement I ended up with. Results have been exceptional for a simple system of low height.

I use No. 14 wire for the antenna. The feeders are also No. 14. The center is mounted on an unguyed wooden pole about 34 feet high. Each section of the antenna is 65 feet long and the ends are only 14 feet high. Thirty-foot feeders are used with series tuning on 80 and 40 and parallel tuning on 20, 15 and 10 meters. Loading from 3.5 to 30 MHz is excellent and not at all critical in tuning. The fact that the feeders are less than 1/8 wave on 80 allows reactance to be tuned out in the feeder-tuning arrangement on that band. The antenna is a bit long for the high end of 75 meters, but tuning there is good (this length was picked because of the slightly longer physical length required on the upper bands for end effect).

I have the antenna itself running east-west, giving some directivity north-south for QSOs with short skip up and down the west coast on 80 and 40 meters (it was found in an earlier antenna . . . vertical . . . that a vertical was not satisfactory for high-radiation-angle short-skip operation). On 20 and 15 the lobes tend to cut across major population DX areas. The tilt of the wire, which lowers the vertical radiation angle plus apparently some lobe addition, seems to give better results in the desired DX directions on 20 and 15 meters than 33-feet-high half-wave horizontal antennas oriented in the correct directions. Quite a bit of omnidirectional DX has been worked on 40 meters, undoubtedly because of the antenna tilt. DX operation on 15-meter c.w. has been really exceptional. Quite often I hook a DX station through the pileup when local beam stations miss (power output is about 150 watts). Since 10 has opened up I have used the antenna quite a bit on that band with very good results for both North American and DX contacts.

As a result of playing around on 160 meters with the bottom of the feeders connected together and working the antenna as a "T" against ground, I decided to see what happened when it was operated as a top-loaded vertical on 80 and 40 meters. The feeders were tied together and the antenna worked against a ground consisting of two 8-foot rods in water-soaked earth. On 80 this places the maximum-current point directly at the top of the vertical section (1/8 wave long) and on 40 gives the effect of a 1/4-wave vertical with maximum current at the bottom. This arrangement gave much better results than the Zepp where low-angle radiation was required, and less effective results than the Zepp where medium- and high-angle radiation was required. An exception is directly off the ends on 80 meters, where the vertical and Zepp seem to give the same results. The Zepp arrangement is therefore now used for short and medium skip on 80 and 40 and the vertical arrangement for long skip or DX. In receiving, the signal-to-noise ratio decreases greatly with the vertical arrangement (vs horizontal), thus somewhat offsetting the overall advantage of the vertical for DX operation. If this condition is extreme, I use the Zepp for receiving and the vertical for transmitting, for DX operation. It appears that the vertical transmitter and horizontal receiver is by far the best DX arrangement for metropolitan areas, but most likely the vertical for both would be best for rural areas where the QRN is lower. – *Dave Hardacker, W6PIZ*

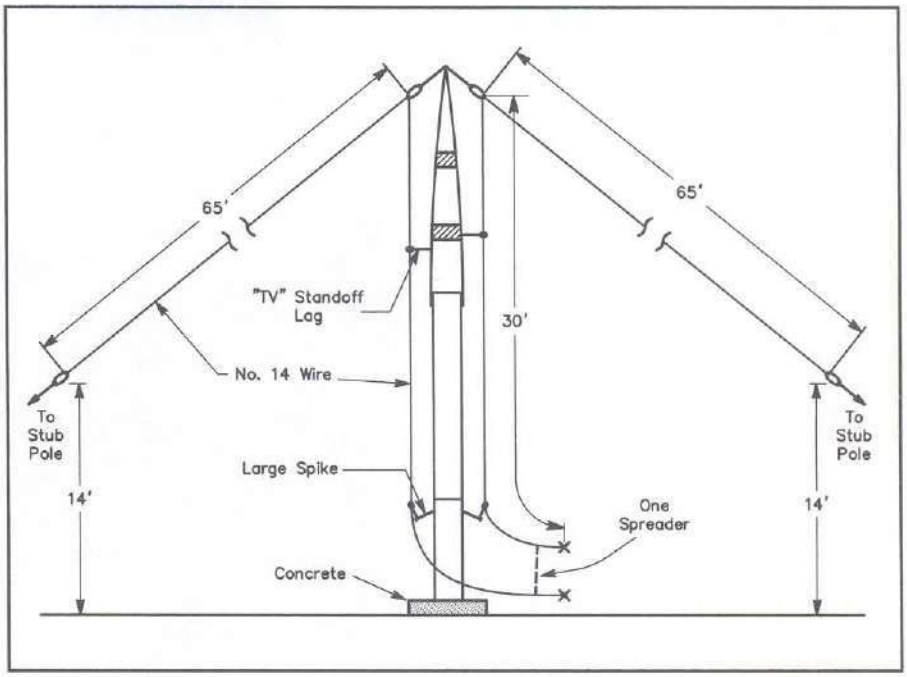

Figure 1–The W6PIZ all-band antenna. Power is applied through a series- or parallel-tuned link-coupled matching circuit at X-X for operation on 3.5 through 30 MHz (see text). For 2 MHz, and also for certain types of work on 3.5 and 7 MHz, points X-X can be connected together and the antenna worked against ground.

By William J. Lattin, W4JRW From *QST*, December 1960

Multiband Antennas Using Decoupling Stubs

Substituting Transmission Line Sections for Lumped-Constant Traps

Since W4JRW obtained a patent on this multi-frequency antenna system nearly ten years ago we can't call it "new," but at least it should be welcome news to those seeking a simple way to get good radiation on several bands, Shorted 1/4-wavelength stubs provide r.f. insulation and also serve as part of the antenna.

Since amateurs usually desire to operate on more than one band, several methods have been devised to use a single antenna on several bands. The earliest arrangements employed various combinations of feeder lengths, antenna lengths, and series or parallel tuning of the coupling circuit. Later on, the use of parallel-tuned "traps" with lumped constants which act as insulators at a particular frequency was invented.[1] A practical arrangement of this system for amateur use was developed[2] and is in rather wide use.

It is well known that the parallel-tuned circuit and quarter-wavelength shorted stub of Figure 1 are very similar electrically. Both configurations show a high impedance across points A and B. However, if a stub is connected to an antenna in this manner it does not act as an insulator but rather as a phase changer. The collinear antenna uses such stubs to operate a series of halfwave sections in phase.

There is a different connection possible for the stub, that is from A to C, which will result in insulator action or decoupling in an antenna.[3] For instance, shorted stubs a quarter wavelength long at 28 MHz can be attached to the ends of a 28 MHz dipole as in Figure 2. The 28 MHz dipole is effectively isolated or decoupled from the balance of the antenna which can be made long enough to resonate at 14, 7 or 3.5 MHz. If another pair of stubs is added for 14 MHz,

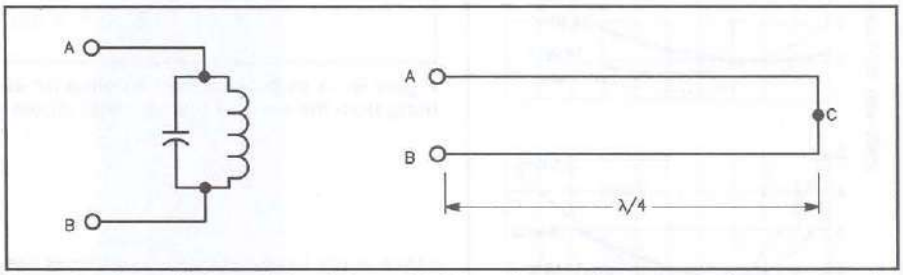

Figure 1—A parallel-tuned circuit has a high impedance at its resonant frequency, and so does a 1/4-wavelength shorted transmission line.

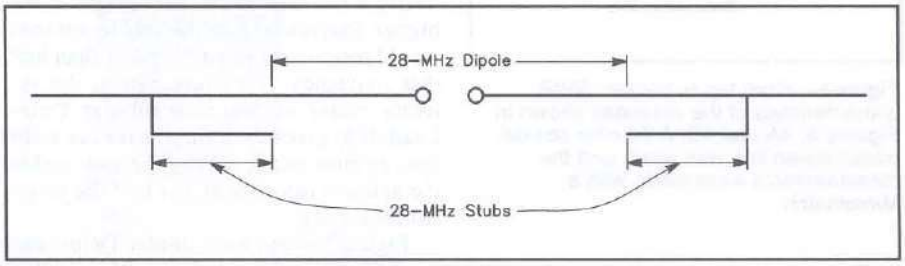

Figure 2—A two-band antenna for 28 MHz and some lower frequency. The center portion is an ordinary 10-meter dipole. The shorted stubs are 1/4 wavelength long at 28 MHz and look like an open circuit at that frequency when connected to the dipole as shown. Extensions on the ends of the stubs can be used to resonate the antenna at any frequency less than half of 28 MHz.

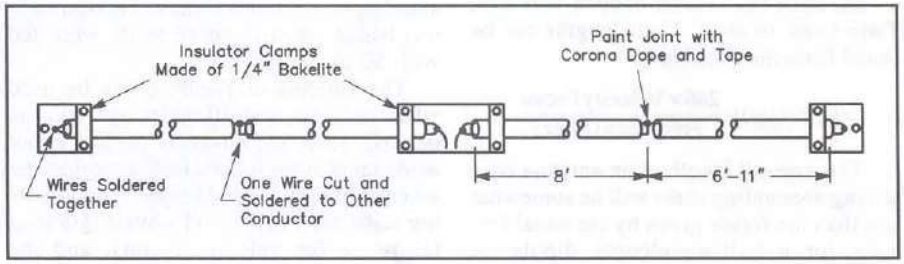

Figure 3—Construction and dimensions of an antenna for 10 and 20 meters using 300-ohm tubular Twin-Lead for both the dipole and stubs. Either a 50- or 75-ohm transmission line can be connected at the center of the dipole.

[1] Morgan, "A Multifrequency Tuned Antenna System," *Electronics*, August, 1940.
[2] Buchanan, "The Multimatch Antenna System," *QST*, March, 1955.
[3] Lattin, Patent No. 2,535,298.

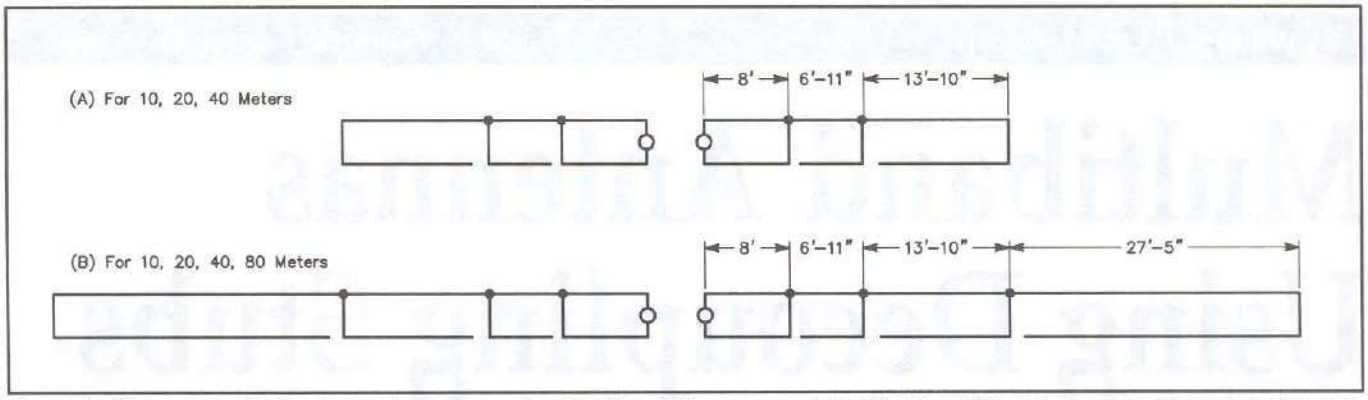

Figure 4—Dimensions of stub-decoupled antennas for 10, 20 and 40 meters and 10, 20, 40 and 80 meters made of tubular Twin-Lead. Either antenna can also be used on 15 meters where the 40-meter section is 3/4 wavelength long.

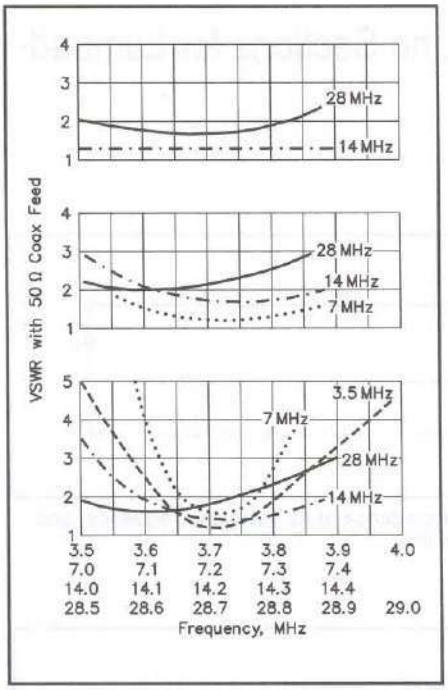

Figure 5—From top to bottom, SWR characteristics of the antennas shown in Figures 3, 4A and 4B. A 50-ohm coaxial transmission line was used, and the measurements were made with a Micromatch.

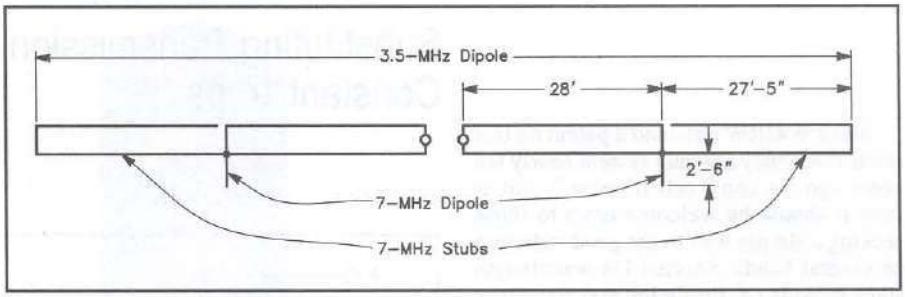

Figure 6—A stub-decoupled antenna for 40 and 80 meters. In this case wires must be hung from the ends of the 40-meter dipole to resonate the antenna in that band.

there will be isolation at both 28 and 14 MHz, and a 10-20-40-meter or 10-20-80-meter antenna can be made.

The stubs can be made of open-wire line, Twin-Lead, or coax. Their lengths can be found from the formula

$$\text{Length (feet)} = \frac{246 \times \text{Velocity Factor}}{\text{Frequency (MHz)}}$$

The over-all length of an antenna containing decoupling stubs will be somewhat less than the figure given by the usual formula for a half-wavelength dipole — *Length* (feet) = 468/*Frequency* (MHz). For instance, an antenna for 10 and 20 meters must be 29 feet, 10 inches long for resonance at the lower frequency, whereas the formula gives a length of 33 feet.

If open line with a velocity factor of nearly unity is used for the stubs, the over-all length of a two-band antenna would be nearly a full free-space wavelength at the higher frequency and the whole antenna would resonate at something *less* than half that frequency. Very fortunately, the velocity factor of 300-ohm tubular Twin-Lead (0.8) gives such lengths for the stubs that, in most cases, adding the stub makes the antenna resonate at just half the original frequency.

Figure 3 shows how tubular Twin-Lead can be used for the antenna itself as well as the stubs and includes dimensions for 10- and 20-meter operation. The foam-filled type of Twin-Lead is recommended to keep out moisture. Lengths for three- and four-band antennas using the same construction are given in Figure 4. Figure 5 indicates the standing-wave ratios observed across various bands when these antennas were fed with 50-ohm coax.

The antenna of Figure 6 can be used when only 40- and 80-meter operation is desired. Since the 40-meter portion is not made up of stubs it must be longer than the antenna of Figure 4A. However, the isolating stubs must still be 1/4 wavelength long (allowing for velocity factor), and the whole antenna would resonate at a frequency below 3.5 MHz if the stubs were simply added to the ends of the 7-MHz dipole. To get around this, the dipole is shortened until the whole antenna tunes to 80 meters. Then resonance at 40 meters is restored by adding extra lengths of wire at the stub junctions. These wires are short and can just hang down from the antenna as shown.

Any of the antennas which will operate on 40 meters can be used on 15 meters as the 40-meter stubs will be approximately 3/4 wavelength long and will provide decoupling. The result is equivalent to operating a 7-MHz dipole at three times its resonant frequency, and we have found the s.w.r. is usually not lower than 3 to 6 when using 40-meter antennas of any type on 15 meters[4].

The power rating of the antenna will depend on the insulation at the stub junctions. These junctions can be painted with corona dope and covered with vinyl tape. It has been our experience over several years that the insulation will not break down with a kilowatt-input transmitter, 100 percent modulated, except when wet or very damp. In this case, the input should be reduced to

[4] Theoretically, a center-fed antenna working on its third harmonic shouldn't be more than about 50 percent higher in resistance than on the fundamental. One would expect an s.w.r. on the order of 2 to 1 rather than such high figures. – Ed.

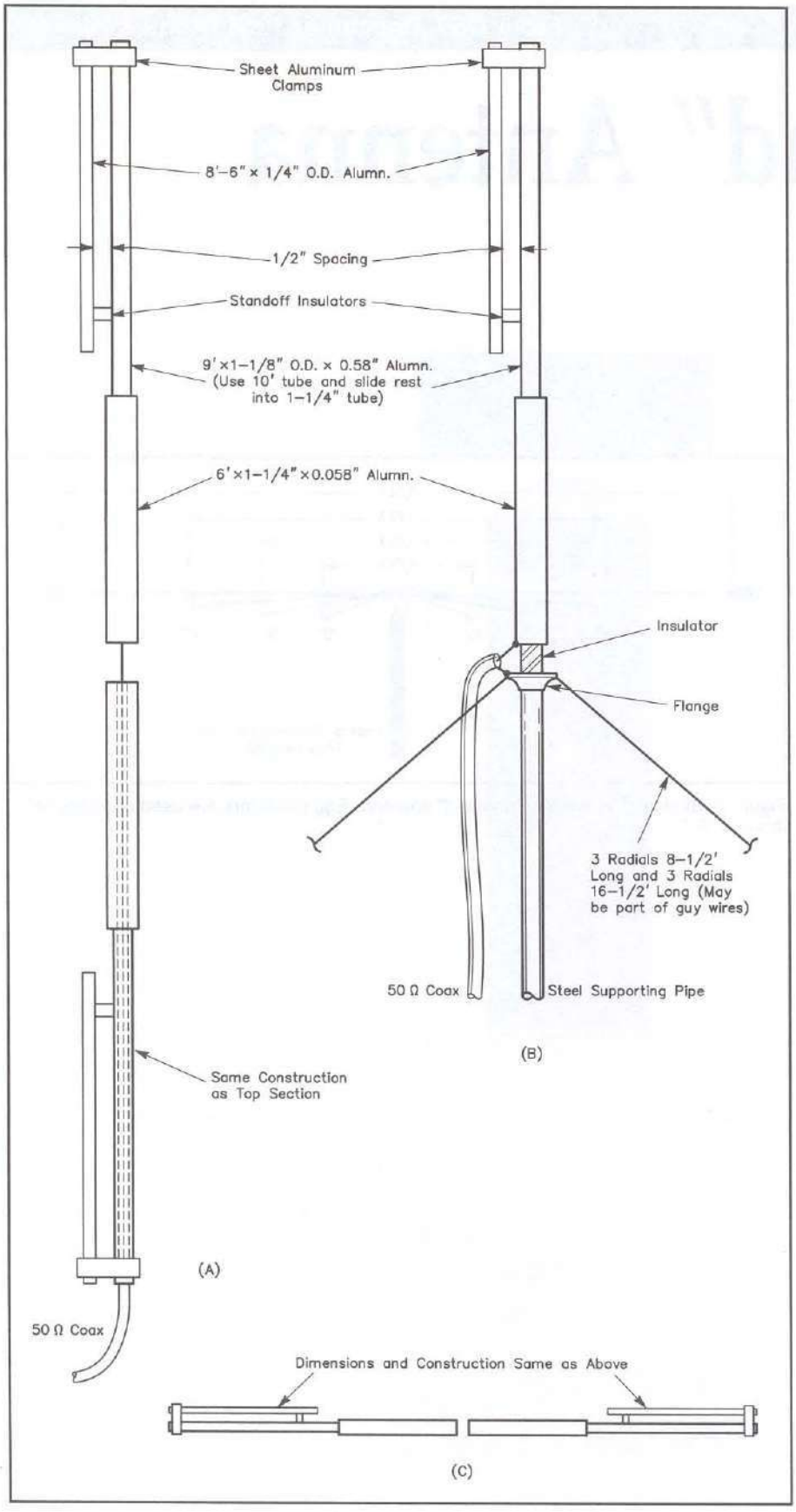

Figure 7—Dimensions and suggested construction for coaxial, ground-plane and tubing dipole antennas for 10 and 20 meters. The arrangement in A might be mounted with standoff insulators attached to the 1¼-inch sections near the center of the antenna. The dipole in C could be closed at the center and fed with a gamma or "T"-matching system. Similarly-constructed parasitic elements could be added to make a multiband beam.

perhaps 500 watts unless special precautions have been taken to seal up the junctions at the open ends of the stub. Of course, on the lowest band for which the antenna is designed the stubs do not have voltage across them and will not be subject to breakdown or flashover. The high voltage across the open end of a stub occurs only at the resonant frequency of that stub.

Figure 7 shows the construction of several 10 and 20-meter antennas which have been built and the dimensions required for resonance in these bands. The spacing between the rods forming the shorted stubs is not critical—the same lengths were obtained with 1-inch instead of 1/2-inch spacing. Insulators should be made of low-loss material. Reflectors and directors for a multiband beam could be made up the same way.

"All-Band" Antenna

Figure 1 is a sketch of an "all-band" antenna system that I have been using with success for some time. The idea is not a new one, having appeared in *QST* at least 10 years ago. However, I feel that there are many newcomers since that time who would be interested in a simple system that can be fed with a single 70-ohm transmission line.

The arrangement consists of dipoles, cut for each band and connected in parallel at the center. Although I have not checked standing-wave ratios, the results seem to indicate that it gets out as well as a bunch of individually-fed doublets. If you haven't tried it, you're in for some surprises.– *R. L. Cope, W8MOK*

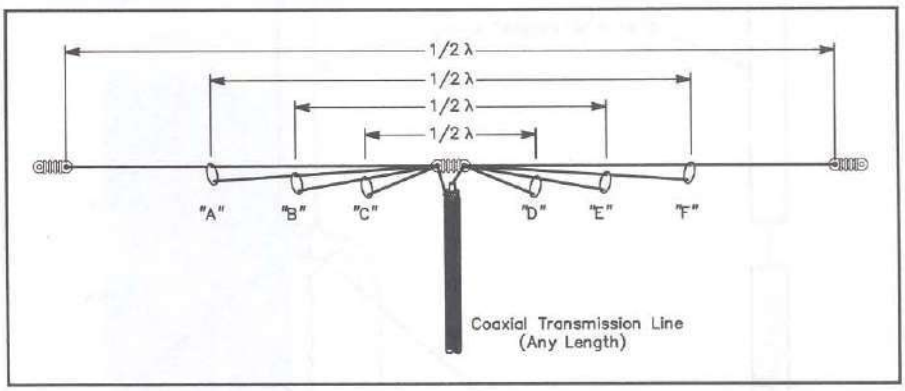

Figure 1–Sketch of W8MOK's "all-band" antenna. Egg insulators are used at points "A" through "F."

Three-Band Matching System for a Forty-Meter Doublet

A common method for energizing a half-wave antenna is to feed it at the center with parallel-conductor TV lead-in, or Twin-Lead as it is usually called, and to use an open stub for matching the 50- to 70-Ω antenna resistance to the 300-Ω impedance of the line. However, this technique, as described in the latest edition of *The ARRL Antenna Book*, generally gives proper matching on only one band.

After a number of trial-and-error calculations on a Smith Chart, along with lots of cut-and-try experimenting, I devised a three-stub matching scheme so that I could operate my 40-meter doublet on 40, 20 and 15 meters. Figure 1 illustrates this method and gives the lengths of the stubs and their positions along the feed line. The dimensions shown are for standard Twin-Lead, with a velocity factor of 0.82. All of the stubs are open at the ends and are made from the same type of line as the feed line. Note that the two lower stubs are connected at the same point on the feed fine.

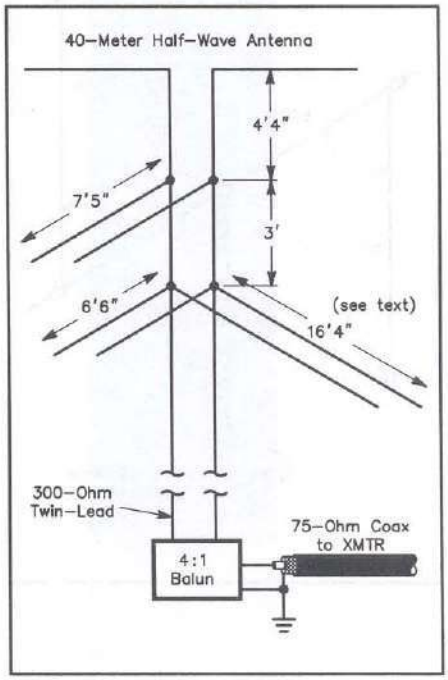

The length of the longest stub is fairly critical. It should first be cut to 17 feet and then trimmed no more than two inches at a time, until the SWR is minimum in the center or the desired portion of the 20-meter band. The feed fine can then be matched with a 4:1 broad-band balun to a 75-Ω coaxial cable from the transmitter. With my antenna, the described matching system gives an SWR of less than 2.5 to 1 over all of the three bands, with minimum values of 1.3 to 1 on 40 and 15 meters, and 1.7 to 1 on 20 meters. As with any multiband antenna, one must guard against harmonic radiation. – *Frank Stuart, K7UUC*

A "Z" Antenna For the 10-160 Meter Bands

One of my interests in ham radio is designing and constructing antennas for both general amateur use and for the Army MARS system. For the amateur who has limited space, I have designed a "Z" antenna that covers the bands from 10 through 160 meters. It is easily constructed from wire. Spreaders for the transmission line are fabricated from Lucite strips or Plexiglas rods. (Refer to the yellow pages of telephone directories for the names of dealers who handle Plexiglas or the equivalent.) For two no. 14 wires, a 2-inch (51-mm) spacing is adequate.

Although a height of 100 feet (30 meters) is indeed desirable for this antenna, hams who settle for elevations between 30 and 50 feet (9 and 15 meters) will still obtain good results. The angles α between the wire segments will depend on individual situations such as the placement of trees or other supports. Generally, the wider the angle, the better the performance.

W1NH, the New Hampshire SCM, who is really into antennas, says my design is "FB." My evaluation of the antenna is that the"aerial" is great.–*John N. MacInnes III, WB1FPD*

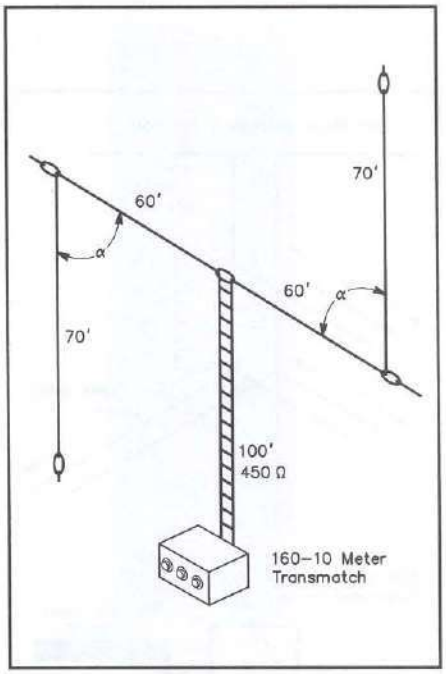

A 10- to 160-meter horizontal Z antenna. Inexpensive no. 14 copper-clad (electric fence) wire may be used. For complete information on open-wire transmission lines, see *The ARRL Antenna Book*, any recent edition.

By Taft Nicholson, W5ANB/AAR6AG
From *QST*, November 1981

Compact Multiband Antenna Without Traps

Looking for an inexpensive, easy-to-build, portable antenna to use with your tube-type transmitter? This first cousin of the G5RV may be the aerial of your dreams.

Do you need an antenna for portable operation? I do! My preference is for making things as simple as possible. I don't like traps and matching units. The antenna shown in Figure 1 has no traps, needs no matching unit for the 10-, 20- and 40-meter bands (when used with vacuum-tube PAs), is lightweight and installs easily. What more could you ask for?

Construction

Construction is simple. Cut two lengths of stranded copper wire (such as Radio Shack 278-1292) to 44 feet, 2 inches each (m = ft × 0.3048). Attach 36 feet, 8 inches of 300-ohm twin lead as shown in Figure 1. Coaxial cable attaches to the other end of the twin lead at the points marked A and B in the diagram. I wound 7 feet, 2 inches of RG-58/U coaxial cable into an rf choke to minimize problems with rf flowing on the outside of the coaxial cable. This length of cable in the choke evolved from an attempt to match the antenna to the transmitter for operation on 15 meters.

Alternatively, you could use open-wire feeders in place of the twin lead. If you choose that method, you will need to make the section 42 feet, 6 inches long. Or you could attach the twin lead or openwire conductors to a matching unit. When using a matching unit, there is no particular merit in the lengths given in the diagram.

SWR

The SWR of the antenna is less than 3:1 on 10, 20 and 40 meters. I have no difficulty loading transmitters with tube-type PAs (e.g., Galaxy V, Swan 350 or Drake T4X). This antenna will work with some transmitters on 15 meters, but tuning is quite critical.

However, 80-meter operation is a problem. I have not been able to obtain full output power with these transmitters on frequencies below 3.750 MHz. The SWR measures between 5:1 and 8:1 for the lower part of the band. I constructed a loading coil to go between the choke and the twin lead (Figure 2). The coil consists of 44 inches of twin lead wound on a 7/8-inch diameter form (my left thumb). Once the coil was wound, I removed it from my thumb and used electrical tape to secure it. For 80-meter operation, attach ends C and D to the choke and ends E and F to the twin lead. Remove the coil for operation on the other bands. Banana plugs and sockets can be used to facilitate the insertion and removal of the coil.

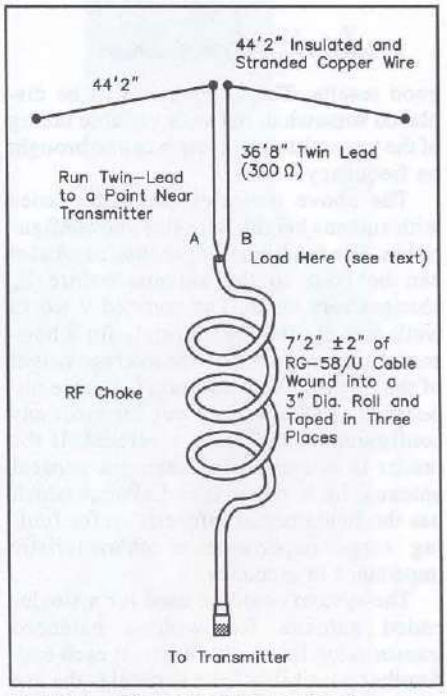

Figure 1—Diagram of the compact multiband antenna. For 80-meter operation the loading coil is inserted at points A and B. Banana plugs and jacks may be added here to facilitate insertion and removal of the loading coil.

Installation

The antenna should be as high as practical. I've had satisfactory results with the center of the antenna only 25 feet above ground, with the ends tied to fences or other convenient supports. Telescoping TV mast sections make a good support if nothing else is available. The legs of the antenna serve as two of the guy wires. One or two additional guy supports should be added (nonconducting material such as nylon rope is best).

This compact multiband antenna works satisfactorily on all bands from 20 through 80, and 10, meters. It has no traps and requires no matching unit when used with tube-type equipment. I have used it for portable operation in and out of the country. It is easy to pack, carry and erect. Perhaps you might want to try one. I think you'll like it! A brief discussion of the theory of operation follows in the appendix.

[Editor's Note: A description of the G5RV appears in the RSGB *Radio Communications Handbook*. Gray described it in the June issue of *Ham Radio Horizons*. A similar design was depicted in the Collins Radio manuals of the 1930s.]

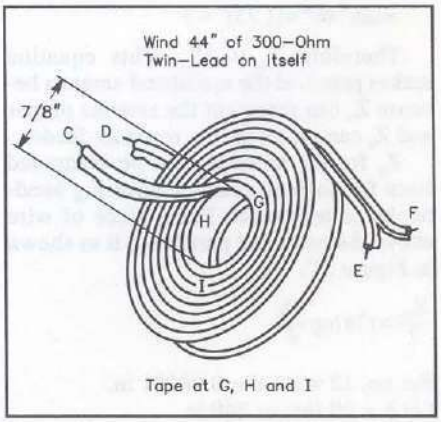

Figure 2—Loading coil for 3500-3750 kHz operation. Points E and F on the coil are connected to the coaxial cable. Points C and D are connected to the twin lead.

Appendix

This multiband antenna evolves from two connected transmission lines with critical length and ratios of surge impedances. The system is self-resonant at a fundamental frequency and at most of the even harmonics and several of the odd harmonics. The first five are 2nd, 4th, 5th, 7th and 8th.

Consider the transmission lines in Figure 3.

The two lines are of equal length, "ℓ" and different surge impedances, Z_o and Z_s.

Looking into the lines:

$$X_o = \frac{Z_o}{\tan(2\pi\ell/\lambda)} \text{ and } X_s = Z_s \tan(2\pi\ell/\lambda)$$

where

λ = wavelength

X_o = reactance looking into open line

X_s = reactance looking into shorted line

From the theory of resonant circuits, we know if we connect the lines the system will be resonant at all frequencies where $\overline{X}_o = \overline{X}_s$ provided the two reactances are of equal value and opposite signs. The open and shorted line provide this condition except at some harmonics.

Joining the lines as depicted in Figure 4 we find that

$$\frac{Z_o}{\tan(2\pi\ell/\lambda)} = Z_s \tan(2\pi\ell/\lambda)$$

$$\frac{Z_o}{Z_s} = \tan^2(2\pi\ell/\lambda) = \tan^2(360°\,\ell/\lambda)$$

If the angle $2\pi\ell/\lambda$ is made 60°, then the amplitude of the tangent at 120° or second harmonic will be the same. This will be true for 240° (4th harmonic) and 300° (5th harmonic). Similarly, these harmonic responses will continue at discrete angles above 360°, e.g., 7th, 8th, 10th, 11th, 13th, 14th and so on. The signs of the tangents wash out when squared.

The angle $2\pi\ell/\lambda$ becomes 60° by making $\ell = \lambda/6$ (1/6 of a wavelength) at the fundamental frequency.

$$\frac{Z_o}{Z_s} = \tan^2(360° \times 1/6)$$

$$= \tan^2 60° = (1.73)^2 = 3$$

Therefore $Z_o = 3Z_s$. This equation makes practical the multiband antenna because Z_o can represent the antenna proper and Z_s can represent the resonant feeder.

Z_o for the antenna may be computed from formulas in radio engineering handbooks or textbooks. For a piece of wire above the earth and parallel to it as shown in Figure 5C.

$$\frac{Z_o}{2} = 138 \log \frac{4h}{d}$$

For no. 12 wire, d = 0.08081 in.
Let h = 20 feet or 240 in.

$$\frac{Z_o}{2} = 138 \times \log\left(\frac{960}{0.08081}\right)$$

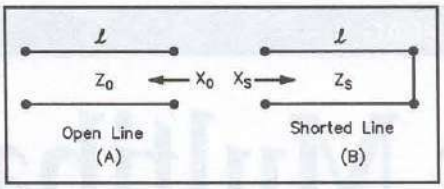

Figure 3—Two identical lengths of transmission line. Looking into the lines, the opposite ends are open and shorted at A and B, respectively.

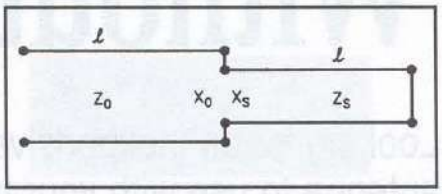

Figure 4—The two transmission lines from Figure 3 are joined to form one line.

138 log (11879) = 562 ohms

This value is not critical. One can use 300-ohm twin lead or 400-ohm open line with

If the wire size had been no. 18,

$$\frac{Z_o}{2} = 605 \text{ ohms}$$

If we use no. 12 wire, then we would have 562 ohms on one side and + 562 ohms on the other side.

$$Z_o = \frac{Z}{2} + \frac{Z}{2} = 1124 \text{ ohms}$$

From the formula $\frac{Z_o}{Z_s} = 3$

$$Z_s = \frac{Z_o}{3} = \frac{1124}{3} = 374.6 \text{ inches}$$

good results. The harmonics will be displaced somewhat, but with variable tuning of the transmitter the system can be brought on frequency.

The above indicates that $Z_o/2$ varies with antenna height, wire size and configuration. The function is logarithmic and a lot can be done to the antenna before Z_o changes very much. The inverted V works well; just use the $Z_o/2$ formula for a horizontal wire and let h be the average height of the inverted V. A formula for surge impedance can be worked out for most any configuration, including a vertical. If the reader is interested in feeding a vertical antenna, he is referred to LaPort,[1] which has the fundamental information for finding surge impedance or characteristic impedance of antennas.

The system could be used for a single-ended antenna fed with a balanced transmission line with a balun at each end. Another possibility for a vertical is the use of a two-wire, grounded, open transmission line, as discussed in LaPort's book.[2] The ground system would be critical.

When experimenting with these multiband lines, it is convenient to have some

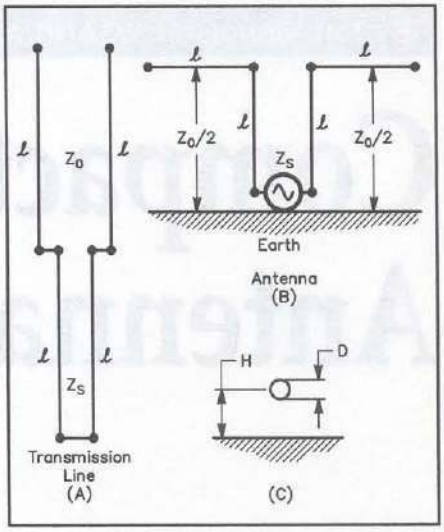

Figure 5—At A and B, the open portion of the transmission line evolves into the flat-top portion of the antenna. At C, diagram illustrating the formula for calculating Z_o for the antenna.

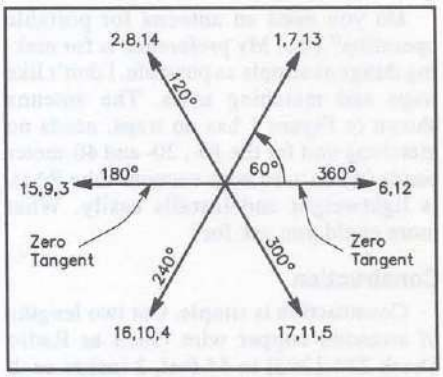

Figure 6—Angular position chart useful for determining "stock numbers" to apply to the chart.

"stock" numbers to apply to the lines (see Figure 6). One-sixth of a wavelength is one-third of a half wavelength. A convenient length for a half wave on 80 meters is 135 feet. One-third of that is 45 feet or $\lambda/6$ for 80 meters. One-sixth of a wavelength on 40 meters is 22-1/2 feet. When you are designing an antenna, these lengths need to be multiplied by the propagation constant of the line. After construction and testing, the dimensions can be pruned for end effect, etc.

When operated as a transmission line, the system as described may have application in end-feeding half-wave antennas, especially two half waves in phase. The system transforms a high impedance to a low impedance as a quarter-wave line will; however, it will do this at several even harmonics, in contrast to the quarter-wave line that is only responsive to odd quarter wavelengths.

The author wishes to thank Walt Maxwell, W2DU, for his detailed analysis of the theory section of this article.

Notes

[1]E. LaPort, *Radio Antenna Engineering* (New York: McGraw-Hill Book Co., 1952).

[2]See note 1.

By Bill Wright, G0FAH

From *QST*, June 1995

Five Bands, No Tuner

Enjoy some of the advantages of a multiband, ladder-line-fed antenna without an antenna tuner.

Reading "The Doctor is IN" (*QST*, January 1995) reminded me that the search continues for a simple backyard antenna. A wire *dipole* antenna fed at the center with 450-Ω ladder line is a good choice. The ladder line keeps your losses low—even at moderately high SWRs. All you need is an antenna tuner and you're in business. No coils or traps necessary.

But can you do away with the tuner and still keep the ladder line? That would certainly make life simpler. To achieve this, your transceiver needs to "see" an impedance that looks reasonably close to 50 Ω on as many bands as possible. Without an antenna tuner acting as the middleman between the 450-Ω ladder line and your 50-Ω radio, this could be a problem.

Table 1
Calculated SWRs for a 94-foot Dipole Fed with 41 Feet of 450-Ω Ladder Line

Note: Although the antenna is cut for the CW portions of the band, expect similar results at other frequencies.

Frequency	*SWR*
3.56	7.6:1
7.1	2.4:1
14.2	1.5:1
18.1	2:1
24.9	1.5:1
29	2.4:1

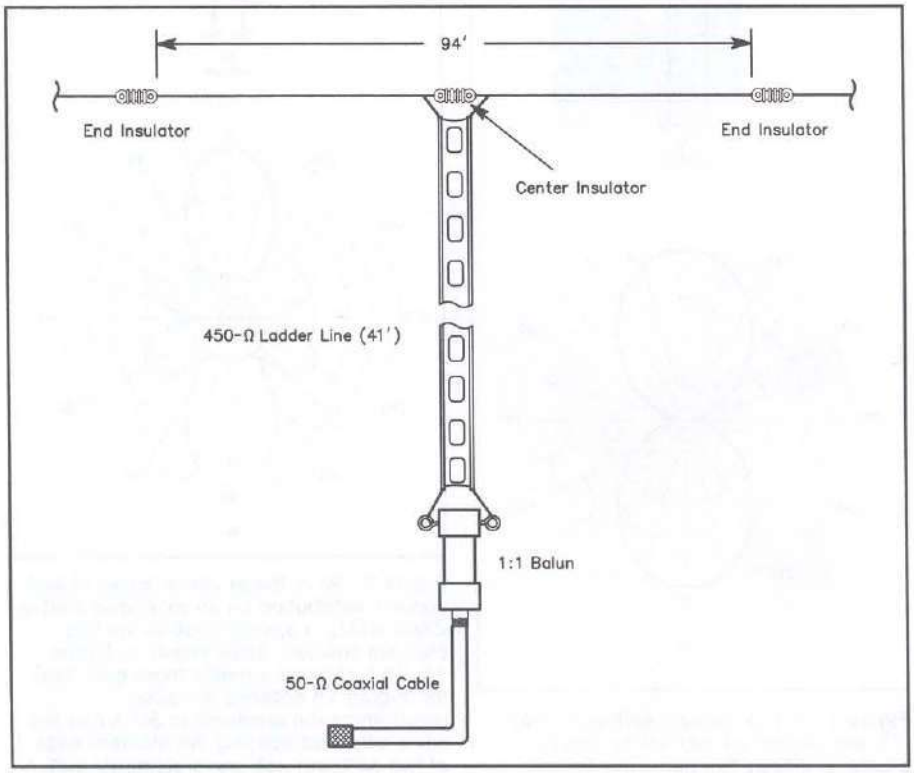

Figure 1—The wire dipole antenna is 94 feet in length. If you don't have 94 feet of open space, don't hesitate to droop the ends of the dipole to make it fit. Feed the antenna with 41 feet of 450-Ω ladder line that is connected to a 1:1 balun. From the balun to your radio, use 50-Ω coax.

Can It Be Done?

A few years ago I attempted to design an antenna that would work on several HF bands from 80 to 10 meters. Full details were published in the spring 1992 edition of *SPRAT*, the journal of the G-QRP club.

My inspiration was the venerable G5RV. I took a 94-foot-long dipole and fed it with ladder line (see Figure 1). By cutting the ladder line to a specific length and using a 1:1 balun to make the transition to coaxial cable, I found that I could get close to 50-Ω (and thus achieve reasonably low SWRs) on at least five bands: 40, 20, 17, 12 and 10 meters (see Table 1).

The on-air results were better than I expected. My radio was happy and I didn't need to meddle constantly with an antenna tuner.

Of course, you'll need an antenna tuner to work the bands where the SWR exceeds 3:1.

A simple tuner will do the job, though. Because you're using *unbalanced* coax ahead of the balun, you won't need one of the more expensive tuners designed for *balanced* feed lines.

For best results, put your antenna as high as possible. If the ends must bend downward to accommodate the size of your lot, don't worry. Run the ladder line to your balun and take your coax from there to your radio. Keep the coax portion as short as possible.

Conclusion

By eliminating the antenna tuner completely, you lose the flexibility of loading your ladder-line-fed antenna on virtually any band. In return, however, you gain the convenience of operating on several bands without making tuner adjustments each time you change frequency. Your losses are held to a minimum, which means that most of the power your radio generates is radiated by your antenna. Not a bad compromise! Of course, the results I achieved will vary when used at other locations. Still, it's a simple, fun project in the experimental spirit of Amateur Radio.

By Rick Olsen, N6NR

From *QST*, March 1993

The NRY: A Simple, Effective Wire Antenna for 80 through 10 Meters

Known as a *broadside collinear curtain array*, this antenna is simple to build, rakes in DX signals and has gain over a dipole on all the bands it covers!

Hams' thoughts ultimately turn to antennas. So it was with me a while ago. I had just moved to the emerald beauty of the Pacific Northwest and began pondering the 160-foot-tall Douglas firs in my backyard. I had considered putting up a crank-up tower, but decided that neighbors, architectural committees and crank-ups don't mix. Then I thought about topping a tree. Nope–I moved here because I love these trees.

I started sniffing around for alternatives. I obtained a copy of fellow ARRL Technical Advisor Roy (W7EL) Lewallen's antenna modeling program, *ELNEC*, along with a copy of *The ARRL Antenna Book*, and began to incubate the seeds of what would become my most enjoyable antenna project since I built a four-element quad back in 1974.

Hanging ropes from big trees is not a new idea.[1,2] I began by pacing off the distances between the monsters in my yard so I would know how much space I had to work with and how I could optimally direct my signal to places like Europe, Africa and the Caribbean.

Next came the selection of a configuration. Because the trees are approximately 120 feet apart, my first choice was a multielement collinear array. But a good friend, Terry Conboy, N6RY (in *NRY*, I'm the *NR* and he's the *RY*), suggested stacking a pair of *extended double Zepps*. I filed his suggestion away in my memory for the time being. I started my analysis.

The ARRL Antenna Book, on page 8-32, describes the basic function of the collinear array. In sum, it concentrates energy perpendicular to the wire, hence the term *broadside array*. This antenna's physical layout and pattern are shown in Figure 1. Such an antenna's gain can be increased by varying the end-to-end spacing of the elements.[3]

Chapter 8 goes on to explain three- and four-element arrays. Disappointment set in when I sized a four-element in-line array for 20 meters: It wouldn't fit between the trees! What *would* fit, however, was a "two-over-two." In fact, depending on the vertical separation, this array might even have some gain over the four-element collinear arrangement.[4]

My choice was made. I wanted to maximize performance on 20 meters and take what I could get on the other bands. I chose two 1-λ, center-fed wires vertically spaced 5/8 λ apart. According to *ELNEC*, with the array 100 feet high at the top and modeled

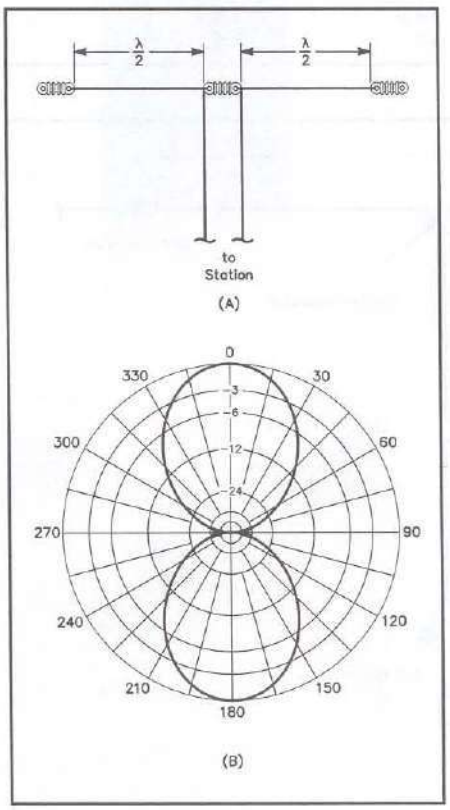

Figure 1—A two-element collinear array (A), also known as *two half-waves in phase*, is merely two half-wave wire elements placed end to end. This antenna has about 1.5 dB gain over a dipole in the same surroundings, and B shows its free-space pattern.

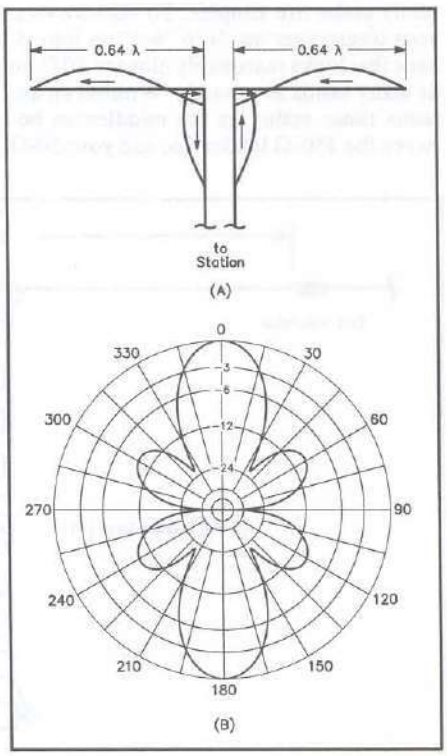

Figure 2—At A, the physical layout of and current distribution on an *extended double Zepp* (EDZ), a special case of the two-element collinear array shown in Figure 1A. This antenna exhibits more gain than the Figure 1A antenna because lengthening the elements to 5/8 λ has the same effect as spacing the element ends of two collinear half-wave elements 0.28 λ apart. (See Note 3.) At B, the antenna's azimuth-plane pattern in free space. This antenna has about 3 dB gain over a dipole in the same surroundings.

over lossy ground, this antenna's gain is approximately 12 dBi.[5] Not bad! The only problem is that this antenna's 20-meter feedpoint impedance is very high.

Reenter N6RY and the extended double Zepp. Take a look at Figure 2A. The extended double Zepp is simply a 1.25-λ, center-fed wire (two end-to-end 5/8-λ elements). There's a hidden message here! Have you found it?

Well, at first, I didn't either. Terry explained to me that the extended double Zepp (EDZ) is essentially two half-wave collinear elements spaced just over 1/4 λ apart. The extended double Zepp's added gain over two half waves in phase comes *not* from the extra 0.28 λ of wire between them, but from the *increased end-to-end spacing of the outermost pair of halfwave elements.* (Radiation from the inner 0.28-λ actually works *against* that from the outer halfwaves, but the gain increase from the new element spacing more than overcomes this disadvantage.) Figures 1B and 2B are similar. The EDZ has broader lobes and useful smaller lobes, both of which are attractive for a fixed array.

Sure enough, it was right in front of me all the time in the *Antenna Book* (page 8-34, fifth paragraph). In fact, the *whole darned array* was right in front of me in Chapter 8! I just needed some help piecing it all together. I modeled this array every way I could imagine, looking for the best possible performance. My wife didn't see me in the evenings for two weeks! Figure 3 shows the final configuration.

Figures 4, 5 and 6 show some of the results of my modeling. I used a design frequency of 14.2 MHz, a height of 100 feet above ground (for the top wire), elements made of #14 copper wire, and ground coefficients typical of the Pacific Northwest. All the elements in this array are fed in phase, as described in a bit.

As the figures show, the antenna's gain and patterns are impressive. On the 80- and 40-meter bands, the antenna has remarkably dipole-like patterns and gains and seems to work at least as well as a dipole in the same height range. On the higher bands, it works *much* better than a dipole. Its predicted gains in my installation are 9, 11 and 14 dBi at 7, 10.1 and 14 MHz, respectively. At 18.1 MHz (Figure 6) and above, the array begins to take on long-wire properties. It has several major lobes in directions closer to the wire axis, which the lower-frequency patterns don't provide.

To help you evaluate the NRY's patterns, Figures 4-6 superimpose the patterns of halfwave dipoles cut for 10.1, 14 and 18.1 MHz, respectively, on the NRY's patterns. These comparisons assume that the dipole is the same height as the NRY's feed point (halfway between the elements, or about 22 feet lower than the top wire), and over the same ground.

You may wonder about this antenna's effectiveness as a function of height. According to the *Antenna Book*, arrays like this have the best gain when the lower element is at least 1/2 λ above the ground (33 feet at 14 MHz). And, of course, as with all horizontally polarized antennas, this array's radiation angle decreases as you raise the antenna, which makes for better DX performance. The bottom line is that for DX work, you don't have to get the array up 100 feet for it to work well—you just need to put it up as high as you can. For closer-in coverage, it will work well at lower heights.

Another advantage of this array is that its feed-point impedances are manageable. To maintain my goal of broadband use, I decided to feed the antenna as shown in Figure 3. This is the "lazy-H" configuration described starting on page 8-37 of *The ARRL Antenna Book*. The attractiveness of this configuration is that it doesn't rely on specific phasing-line lengths to work properly. To the extent made possible by the different mutual impedances between each element and the ground, the phase relationship between elements remains constant regardless of frequency.

Final Dimensions

The antenna's physical dimensions (86 feet, 10 inches long and 43 feet, 5 inches high, not counting insulators) are easy to remember because the height is half the length. Because the antenna is basically 1.25 (5/4) λ long, center-fed and vertically spaced 5/8 λ apart, you can easily scale it to whatever band you like. For instance, to scale it to 10 meters, divide all the dimensions by two (28 MHz/14 MHz = 2).

Construction

Now for the really fun stuff: putting this thing up in the air! Building the antenna is a breeze. It took me all of about an hour to cut and solder the wires and attach the tethers. The harder part was preparing the trees.

If you have a friend like Bernie Olshausen, N6RUX, you have it made. He's a crack shot with a slingshot, similar to that described by Wade Calvert, WA9EZY, in *QST* a couple of years back.[6]

Once Bernie landed the fishing lines over the right tree limbs, the next job was to pull up some lightweight twine (we used seiner twine—the stuff fish nets are made of) with the fishing line. This is important; rope sometimes snags as it goes over limbs, and you don't want to try to pull it over with 6-pound-test fishing line! With the twine, we pulled up some 800-pound-test nylon rope with a pulley on one end, using another piece of nylon rope through the pulley to act as a catenary for the array.

It's important to use a strong, weather-resistant catenary rope to hang the array, because the antenna loses its desirable properties quickly when it takes on the shape of a V. You can expect a 2-dB gain

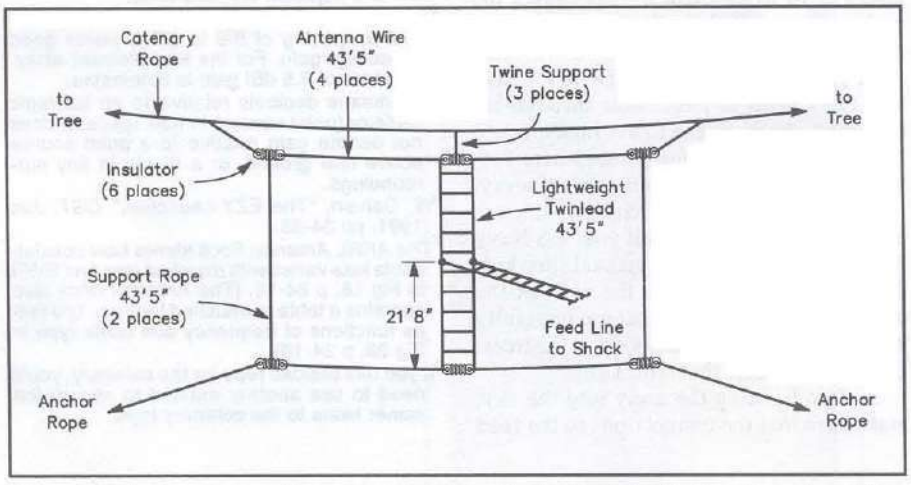

Figure 3—The broadside collinear curtain array—the NRY—in its final configuration. This antenna is cut for 20 meters, but works well on all the HF ham bands. The array hangs from a catenary rope via three short lengths of twine. The lower end insulators are supported by ropes to those of the top wire, and the center insulators are joined by the phasing line, which is 43 feet, 5 inches of parallel-wire feed line. The feeder to the radio is made of the same type of line connected at the halfway point on the phasing line.

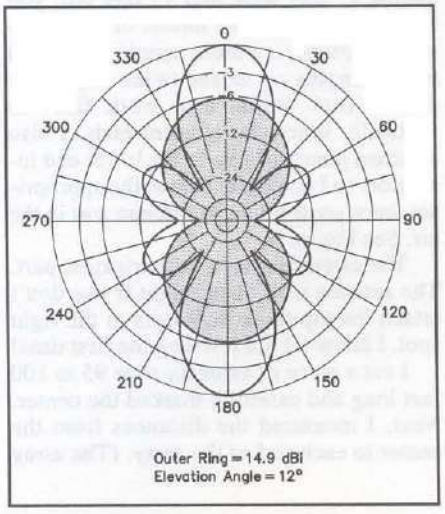

Figure 4—The NRY's 14-MHz azimuth-plane pattern with the bottom wire at 56.5 feet and top wire at 100 feet. For comparison, the shaded part shows the pattern of a half-wavelength, 14-MHz dipole at 78 feet (the same height as the NRY's feed point).

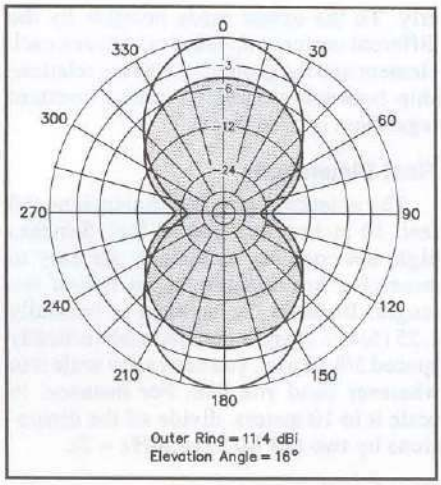

Figure 5—The NRY's 10.1-MHz azimuth-plane pattern with the bottom wire at 56.5 feet and top wire at 100 feet. For comparison, the shaded part shows the pattern of a half-wavelength, 10.1-MHz dipole at 78 feet (the same height as the NRY's feed point).

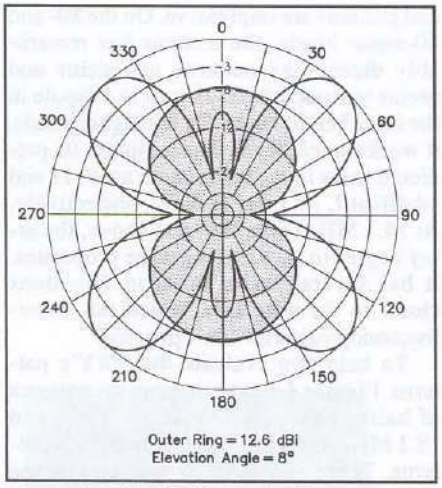

Figure 6—The NRY's 18.1-MHz azimuth-plane pattern with the bottom wire at 56.5 feet and top wire at 100 feet. For comparison, the shaded part shows the pattern of a half-wavelength, 18.1-MHz dipole at 78 feet (the same height as the NRY's feed point).

decrease at 20 meters with a 20° variance from the flat-top configuration. The rope, therefore, must be strong enough to minimize droop and maintain integrity in the sun and wind. We'll get back to the rope in a minute.

For the phasing harness I used low-loss, 300-Ω twinlead. Any parallel-wire feeder should work fine. Don't use coaxial cable in the feed system. It's too heavy, unbalances the array and has very high loss when operated at a high mismatch.[7]

To assemble the feed system, I used porcelain insulators and equal lengths of 300-Ω line. I then cut the #14 antenna wire to the proper length and soldered it to the feed system in a standard dipole configuration.

Next came the tethers. For an antenna almost 87 feet wide and 43 feet tall, you need to provide some means of maintaining the proper element spacings. I used equal lengths of seiner twine (nylon or dacron rope would also work fine) to vertically space the element ends. I also attached plenty of line to the lower end insulators so I could tie them to the appropriate fence posts once the antenna was in the air. See Figure 3.

The catenary rope is the trickiest part. The antenna won't hang right if you don't attach the top three insulators in the right spot. I know—I did it wrong the first time!

I cut a piece of catenary rope 95 to 100 feet long and carefully marked the center. Next, I measured the distances from the center to each end of the array. (The array itself is a handy measuring line.) Then I added about 10 more inches and marked the line. I'll tell you why in a minute.

Then I cut three pieces of twine, each about 24 inches long. At the center of the catenary rope, I carefully opened the rope weave and passed about 6 inches of twine through it, then let the catenary rope retake its natural shape. Wrapping the twine around the rope several times on either side of the joint relieved the tension placed on the rope introduced by passing the twine through it.[8] I then tied the other end of the twine to the top center insulator so that the spacing between the rope and the insulator is 12 inches.

After doing that, I attached the twine at the end marks on the catenary rope in the same manner. The distance to the end insulators is 18 to 20 inches. This causes the ends to hang off the rope at an angle and provides strain relief.

If you use a braided rope (with a weave you can't open to pass twine through it), one good alternative is to use insulators in the catenary rope (at the points where I attached the twine) as tie points for the array.

Now you're ready to haul the antenna up on the lanyards. Consult your US Navy *Marlinspike Seamanship* manual (just kidding, of course) and join the ends of the catenary to the lanyards that are hopefully by now through the pulleys, up in the trees. Use a strong knot that won't slip.

Before hoisting the array into the sky, *make sure* that the connections to the feed harness at the top and bottom are the same (ie, that the left elements both attach to the same wire in the twinlead). This thing does not work right if the top and bottom are fed 180° out of phase!

Now you're ready to haul it up and connect the feed line to the antenna tuner. Check to make sure that the symmetry and top-to-bottom wire spacings are within reasonable limits, then tie the bottom tethers off so that the bottom wire is as flat as you can make it.

You're Done!

This is quite an effective antenna. I've installed two of them: One is boresighted on the Middle East and works like gangbusters into Europe as well; the other favors the Caribbean and most of the US. In the first three months after putting them up, I worked 105 countries on CW, including some rare ones, with a 100-watt transceiver. I'm surprised at how easily I can bust pile-ups—especially on 30 and 20 meters.

I hope you have an opportunity to try this array on for size. Don't limit yourself to just the backyard, either: It's a great Field Day antenna, to say the least. It also comes in handy for emergency work where you need a gain antenna.

You don't have to be a rocket scientist to design effective antennas! Your old friend *The ARRL Antenna Book*, and other ARRL publications, like Walt (W2DU) Maxwell's *Reflections*, the *Handbook*, the *Antenna Compendium* series and Wilfred Caron's *Antenna Impedance Matching*, are serious reference guides and sources of numerous ideas. It doesn't hurt to have your favorite antenna-modeling software loaded on your PC, either!

Notes

[1]D. Brede, "The Care and Feeding of an Amateur's Favorite Antenna Support—the Tree," *QST*, Sep 1989, pp 26-28, 40.

[2]J. Hall, ed, *The ARRL Antenna Book*, Chapter 22 and pp 4-3 and 15-3.

[3]*The ARRL Antenna Book*, Fig 8-38, p 8-32, illustrates how gain varies with the spacing of the two adjacent element ends.

[4]The *Antenna Book*'s Fig 8-45, p 8-35, suggests that a spacing of 5/8 to 2/3 λ yields good broadside gain. For the four-element array, upwards of 8.5 dBi gain is obtainable.

[5]dBi means decibels relative to an *isotropic radiator* (point source) in free space. It *does not* denote gain relative to a point source above real ground, or a dipole in any surroundings.

[6]W. Calvert, "The EZY-Launcher," *QST*, Jun 1991, pp 34-35.

[7]*The ARRL Antenna Book* shows how coaxial-cable loss varies with matched loss and SWR in Fig 18, p 24-18. (The *Antenna Book* also contains a table of matched loss per 100 feet as functions of frequency and cable type in Fig 26, p 24-18).

[8]If you use braided rope for the catenary, you'll need to use another method to secure the seiner twine to the catenary rope.

CHAPTER FOUR

LOOP ANTENNAS

4-1 **Dual Full-Wave Loop Antennas**
From March 1982 *QST*

4-2 **A Gain Antenna for 28 MHz**
From July 1994 *QST*

4-3 **10-Meter "Lazy Quad"**
From July 1968 *QST* (Technical Correspondence)

4-4 **The Full-Wave Delta Loop at Low Height**
From October 1984 *QST*

4-7 **A Triband 75/40/30-Meter Delta Loop**
From *The ARRL Antenna Compendium Vol 5*

4-9 **A Two-Band Loop for 30 and 40 Meters**
From March 1989 *QST* (Hints & Kinks)

4-10 **Feeding an 80-Meter Delta Loop at 160 Meters**
From April 1990 *QST* (Hints & Kinks)

By John Griggs, W6KW

From *QST*, March 1982

Dual Full-Wave Loop Antenna

Achieving gain from an antenna at 7 and 3.5 MHz normally requires a rather large piece of real estate, a high tower or both. To obtain significantly improved performance over a dipole at these frequencies, and to do it inside an average city lot, is a goal worth pursuing! With this in mind I decided to replace my inverted-V dipoles on 7 and 3.5 MHz with a dual full-wave loop antenna, one inside the other.

I had noticed the strong signals on 7 MHz from Pat Kearins, W7UI (now a silent key), and from Carl Winter, W6OAW, on 3.9 MHz, and was interested to find that both were using full-wave loops. Both signals would pin my S-meter and my QTH is well over 200 miles from either station. The antenna at W7UI was a loop suspended by a very high supporting structure. This loop resembled a square, with one corner facing up, one facing the ground, and the other two corners pulled outward by guy wires.

My attention was attracted to a horizontal loop antenna used by another ham on 3.9 MHz that produced extremely strong signals. It was a square loop, 65 feet on a side, with each leg parallel to the ground but only 14 feet high. Fed by a tuned line, it functioned well, but it was most effective for relatively short ranges, up to 200 miles or so.

Of more interest to me, however, was the 75-meter rectangular loop used at W6OAW. I learned that this was a dual antenna, i.e., a full-wave rectangular loop for 3.9 MHz suspended about 40 feet above ground, with another full-wave loop for 7 MHz inside the first, in the same plane. The 3.9-MHz loop is a closed circuit, whereas the 7-MHz loop is an open circuit. This permits operation on 10, 15 and 20 meters as well as 40 meters when used with open-wire feed line and a matching network. The outer loop is fed with coaxial cable.

Design Planning

In considering loop antennas for my lot, which is 75 feet wide by 125 feet deep, I found that I could use two 40-foot high pipe masts, 130 feet apart along a diagonal across my lot. I duplicated the W6OAW arrangement, except that I hung the antenna vertically and made both loops closed-circuit designs. I could use them only on the bands for which they were cut, 7.2 MHz and 3.8 MHz. Each is fed with a quarter-wave matching section of RG-59/U, which provides a 50-ohm match for the RG-8/U cables leading in to my operating position.

Construction

See Fig. 1 for construction details and dimensions. Matching the 104-ohm antenna impedance to the 50-ohm line impedance requires a quarter-wave coaxial line having a characteristic impedance of 72 ohms. The formula for a $^1/_4$-wave section is:

$$\frac{246}{f\,(\mathrm{MHz})} = \ell\,(\mathrm{ft}) \qquad \text{(Eq. 1)}$$

This result must be multiplied by the velocity-factor of the coaxial cable, 0.66 for RG-59/U 73-ohm cable. The quarterwave section was determined to be 42.7 feet for 3.8 MHz and 22.6 feet for 7.2 MHz. These connect to RG-8/U cables for a 50-ohm match to the transceiver.

The top section of the 3.8-MHz loop is fed at the center because of the length of the quarter-wave line, but the shorter matching section for the 7.2-MHz loop allows me to feed the bottom portion of that antenna.

The inner loop is supported from the corners of the outer loop by means of nylon rope and suitable insulators. It is best to use lightweight, high-quality insulators and wire no larger than no. 14 to reduce the weight of the array. Pulleys (and rope) will be required at the tops of the 40-foot poles and also at the 18-foot level. The fact that the bottom horizontal section of the antenna narrowly misses the top of my house roof seems to have no deleterious effect on its operation.

Measure the antenna sections carefully, and cut them to length. Pay particular attention to locate the feed point at the exact center of the horizontal wire sections. This provides horizontal polarization. Feeding the loop at the center of either vertical section will provide vertical polarization.

Tuning

If trimming is needed to resonate the antenna to your favorite operating frequency, cut or add equal length pieces at each vertical section. Do not shorten the sides to the point at which the top and bottom sections are less than 0.1 wavelength apart. Careful pruning of the horizontal sections would be required if such a problem develops.

Information given to me by those using this antenna seems to confirm my results. A typical comment is "Boy are you ever loud!" A gain of 1.8 dB over a dipole is claimed for this type of antenna. The principal difference appears to be a lower angle of radiation. While it is possible to work stations off the ends of the antenna, maximum radiation occurs broadside to the element. What I like about the antenna is the ability to hear weak stations. It is outstanding in this regard.

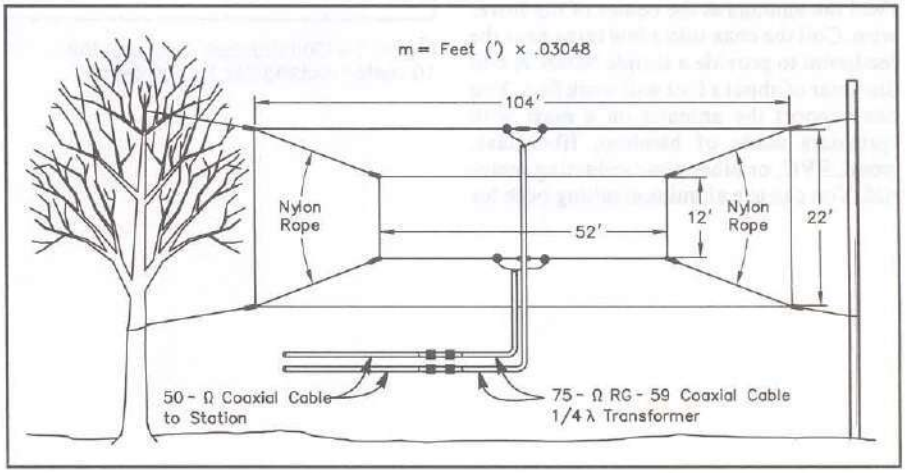

Fig 1—Dimensions for the dual full-wave loop antenna. Input impedance is on the order of 104 ohms. A quarter-wave matching section of RG-59/U is used to provide a match to 50 ohms.

By Brian Beezley, K6STI

From *QST*, July 1994

A Gain Antenna for 28 MHz

Give your 10-meter signal a boost with this simple antenna.

Although in coming years the 10-meter band won't provide the excitement it did at the peak of sunspot cycle 22, DX openings will still occur, especially during spring and fall. And who knows? With the large number of 10-meter operators and wide availability of inexpensive, single-band radios, the band may be the hangout for local ragchews that it was before the advent of 2-meter FM.

I'd like to present a simple antenna for 10 meters that provides gain over a dipole or inverted V. Similar designs have been published before, but because I never hear them on the air, I think they must not be fully appreciated. The antenna is a resonant, rectangular loop with a particular shape. It provides 2.1 dB gain over a dipole at low radiation angles when mounted well above ground. This represents a power increase of 62%. The antenna is simple to feed–no matching network is necessary. When fed with 50-Ω coax, SWR is close to 1:1 at the design frequency. SWR is less than 2:1 from 28.0 to 28.8 MHz for an antenna resonant at 28.4 MHz.

The antenna is made from #12 wire (see Figure 1). For horizontal polarization at 28.4 MHz, the loop is 73 inches wide and 146 inches high (just larger than 6×12 feet). Feed the antenna at the center of the lower wire. Coil the coax into a few turns near the feedpoint to provide a simple balun. A coil diameter of about a foot will work fine. You can support the antenna on a mast with spreaders made of bamboo, fiberglass, wood, PVC, or other nonconducting material. You can use aluminum tubing both for support and conductors, but you'll have to readjust antenna dimensions for resonance.

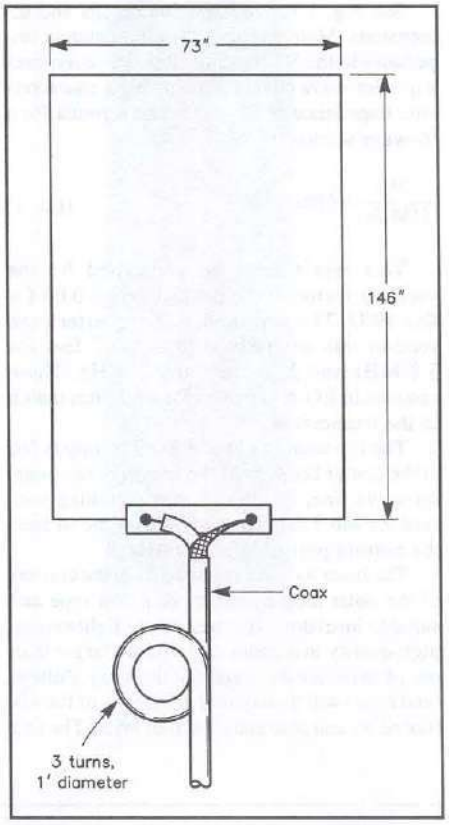

Figure 1—Construction details of the 10-meter rectangular loop antenna.

This rectangular loop has two advantages over a resonant square loop. First, a square loop has just 1.1 dB gain over a dipole. This is a power increase of only 29%. Second, the input impedance of a square loop is about 125 Ω. You must use a matching network to feed a square loop with 50-Ω coax. The rectangular loop achieves gain by compressing its radiation pattern in the elevation plane. The azimuth pattern is slightly wider than that of a dipole (it's about the same as that of an inverted V). A broad pattern is an advantage for a general-purpose, fixed antenna. The rectangular loop provides bidirectional gain over a broad azimuth region.

You should mount the loop as high as possible. To provide 1.7 dB gain at low angles over an inverted V, the top wire must be at least 30 feet high. The loop will work at lower heights, but its gain advantage disappears. For example, at 20 feet the loop provides the same gain at low angles as an inverted V.

A small, 3-element Yagi can provide 6 dB gain over a dipole and great rejection of signals to the rear. If you can install a beam and rotor, you'll find it much more effective than a loop. But for a simple, cheap, gain antenna that can be thrown together quickly, the rectangular loop is hard to beat.

Note: I used the AO 6.0 Antenna Optimizer program to automatically optimize the dimensions of a rectangular loop for maximum forward gain and unity SWR. I used NEC/Wires 1.5 to verify the design with the Numerical Electromagnetics Code.

10-Meter "Lazy Quad"

Among your readers that like to tinker with antennas there may be some that would like to try the antenna shown in Figure 1. The basic idea came from a station using a somewhat similar configuration on 15 meters, and I make no claim of originating the idea. However, I have never heard of anyone using the antenna on 10 meters. Since it is currently nameless, and has features similar to both a Lazy H and a quad, perhaps it should be known as a "Lazy Quad."

The major advantages of the antenna are: (1) extreme simplicity, (2) feasibility of installation on a light unguyed pole, (3) small horizontal space requirements (as compared to a horizontal dipole), (4) low QRN in receiving (as compared to a vertical dipole), (5) ability to withstand high wind loads and (6) broadband operation.

When looking at loop 1 we see a horizontally-polarized full-wave loop radiating broadside, with maximum currents along the top and bottom horizontal wires H_1 and H_2. When looking at loop 2 we see a similar horizontally-polarized loop with maxiinum current on wires H_2 and H_3. When looking at wires H_1 and H_3 we notice two in-phase horizontal wires spaced a half wave, both carrying maximum current. Minimum currents appear on the vertical portions of the loops where the tuning stubs are inserted.

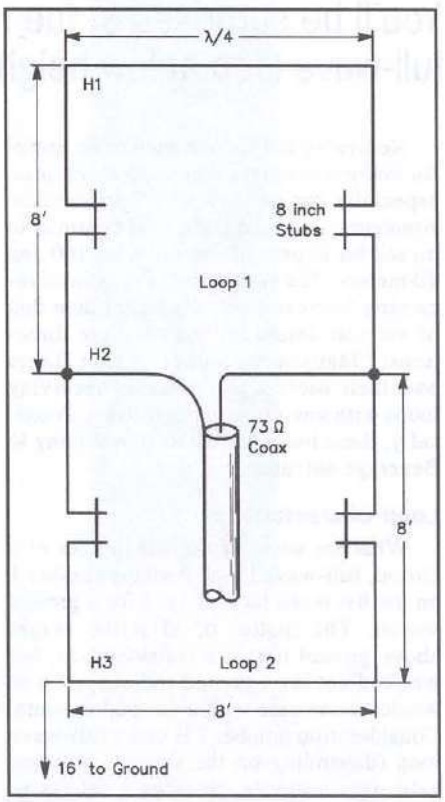

Figure 1—W6PIZ's "Lazy Quad" for 10 meters. The loops are No. 14 wire, with the horizontal sections mounted an 8-foot lengths of 1×2 wood. The adjustable stubs are of the same type wire and are self-supporting since the length is only 6 inches. The antenna at W6PIZ is mounted on an unguyed wooden pole 32 feet high.

I operate mostly on 10-meter c.w. and have the antenna peaked at 28,050 MHz. In my specific case the length of each stub is 6 inches for this frequency. Loading is almost constant from 28 to 30 MHz.

The coax feed line is run straight down the pole (wood) to the ground, and there is little antenna effect on the feeder.

Results have been consistently better than had been obtained with vertical or horizontal dipoles previously installed at the same effective height at the same location. Indications are that it outperforms some beams of the same approximate height, perhaps because of the broad vertical pattern (which allows longer QSOs under critical skip conditions), as compared to the beams.

Perhaps some of your readers might be urged to try this basic idea with a reflector of the same basic configuration as the driven element. It would appear that the Double Lazy Quad would be anything but lazy in operation. — *Dave Hardacker, W6PIZ*

By Doug DeMaw, W1FB and Lee Aurick, W1SE From *QST*, October 1984

The Full-Wave Delta Loop at Low Height

You'll be surprised at the results you'll get from a full-wave loop at low heights.

Property size and antenna-support height are ever-present concerns of the urban amateur. Many good antennas are untried because the radio amateur is unable to imagine how a large wire antenna could be squeezed onto a small lot. Certainly, this is typical in the case of full-wave loop antennas. But there is no rule that dictates using a symmetrical loop. It can be distorted rather severely without spoiling the performance. The same philosophy is appropriate with regard to height above ground and the plane in which the antenna is erected. In most instances, a less-than-optimum full-wave loop will outperform a dipole or inverted V antenna that is close to the ground in terms of wavelength. It is possible that such a loop will give comparable or better performance than a vertical antenna that is less than 90 degrees (with respect to ground), or one with a substandard ground screen.

We want to discuss the Practical considerations of loops that can be supported from low supports on small pieces of property. The results we have obtained are noteworthy with respect to all-around "solid" communications within and outside the USA. Perhaps you will be inspired to unroll some wire and try a loop at your QTH.

Some Loop History

Loops were used first as receiving antennas. While single- and multiturn small loops worked well for receiving, they were not satisfactory for transmitting: They were inefficient in terms of gain, and the feed impedance was generally a fraction of an ohm, making them difficult to match. The losses were significant. But, it was possible to use a compact loop (less than 0.5 wavelength) for receiving in place of a fullsize version that could require thousands of feet of conductor. One of us owned a portable broadcast-band receiver in the 1930s. The loop antenna was stored in the lid of the cabinet, and needed to be mounted atop the radio during reception periods! The radio was heavy: it weighed 91 pounds, including the various dry batteries.

Receiving loops continued to be useful for many years in the commercial services, especially for LF and VLF applications. Amateurs also used them (and continue to do so) for improved reception on 160 and 80 meters. The signal-to-noise ratio of receiving loops is markedly better than that of vertical antennas, and they are directional.[1] Many successful 160-meter DXers owe their success to the use of receiving loops with low-noise preamplifiers. Practically, these loops are the next best thing to Beverage antennas.[2]

Loop Characteristics

What are some of the advantages of a closed, full-wave loop? Perhaps number 1 on the list is the lack of need for a ground screen. The matter of effective height above ground is still a consideration, but we need not lay a ground-radial system as would be the case with a vertical antenna. Consideration number 2 is that a full-wave loop (depending on the shape) has some gain over a dipole. Number 3 relates to noise factor. A closed loop is a much "quieter" receiving antenna than are most vertical and some horizontal antennas.

To illustrate this point, the 160-meter antenna at W1FB is a $^3/_8$-wavelength inverted-L with twenty $^3/_8$-wave radials. Since this is essentially a vertically polarized antenna, it is noisy (man-made and atmospheric noise). There are times when an S9 signal is unreadable because of the ambient noise being S9 or greater in strength. Upon switching to the 75-meter Delta loop, the same signal will rise above the noise by 1 or 2 S units, while the noise and signal will drop well below S9. For example, the received signal may drop to S6 on the loop, but the noise will decline to S4.

Feed-point selection will permit the choice of vertical or horizontal polarization. Various angles of radiation will result from assorted feed-point selections. The system is rather flexible when we want to maximize close-in or faraway communications (high angle versus low angle). Figure 1 illustrates various configurations that can be used. The arrangement at C is used at W1SE, and the shape at D is being applied

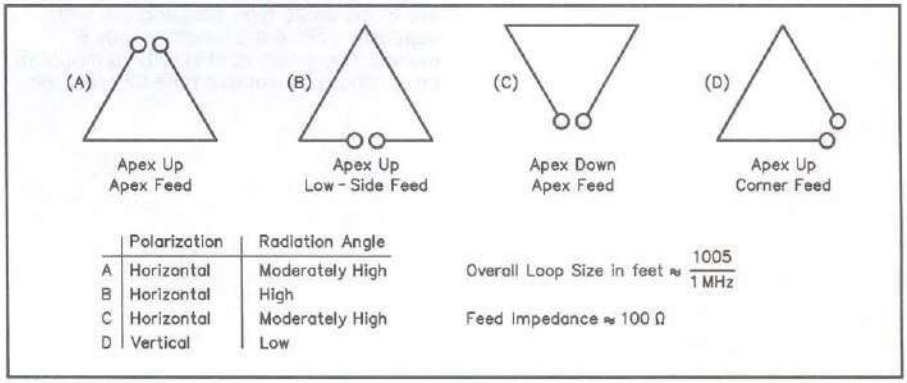

Figure 1—Various configurations for a full-wave Delta loop. Radiation angles and polarization are affected by the feed-point placement and location of the apex.

at W1FB. Both antennas are cut for 80-meter operation. The bandwidth at resonance is on par with that of a dipole. A Transmatch is used for matching the system to the transmitter in those parts of the band (75 and 80 meters) where the SWR is too high to deal with.

Our loops are not deployed in a vertical plane, owing to the lack of tower height. A 60-foot tower and 50-foot tree support the W1SE antenna. A single 50-foot tower is used at W1FB. Both loops are tilted away from the supports at roughly 45 degrees (Figure 2). This shows the present W1FB system. The loop is broadside northeast and southwest for maximum radiation in those directions at 80 meters. More on this later.

When these low-to-the-ground experiments began in the summer of 1983, we were joined by Bill Martinek, W8JUY, near Traverse City, Michigan. Bill experimented with various loop configurations so that he and W1FB could make signal comparisons locally and afar. He finally adopted the W1SE format with the apex down (Figure 1C, with the flat top strung between two 50-foot trees). In order to keep the loop completely vertical (not sloping), he chose a triangle that was not equilateral. The upper side of his triangle is substantially longer than the two downward sides. His signal on 75 meters is consistently 10 to 20 dB stronger than with his inverted V. The point of this discussion is that you need not use an equilateral triangle if it will not fit on your property. Erect whatever you can, then give it a try!

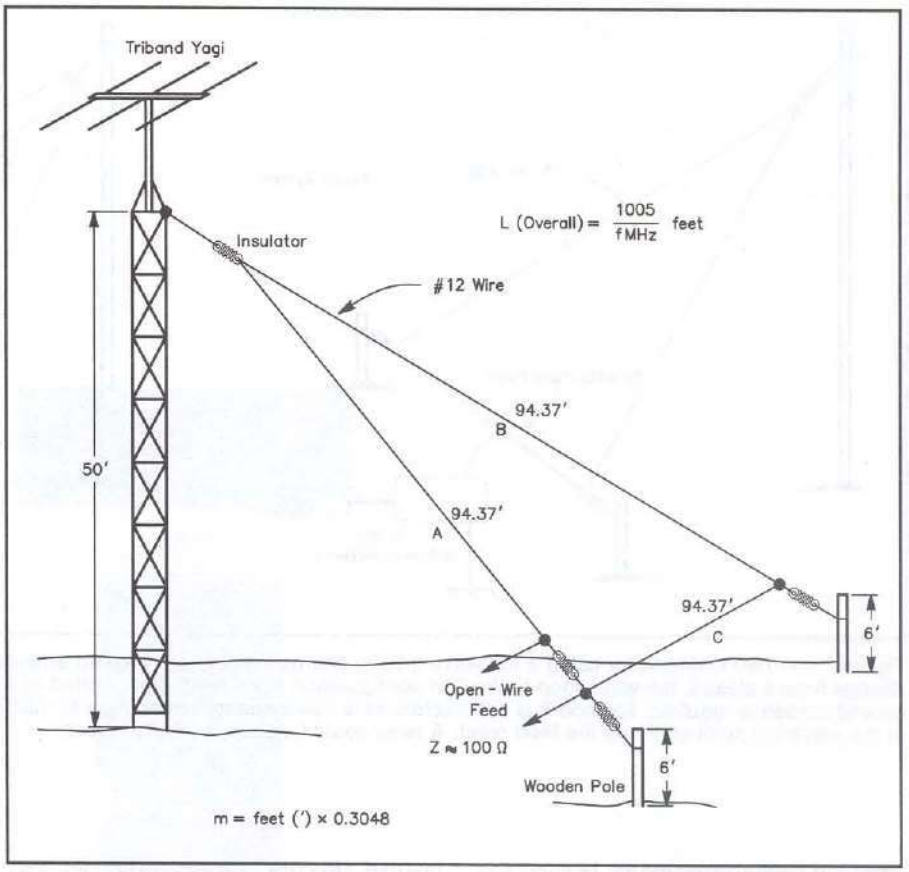

Figure 2—A tilted Delta loop for 80 meters is used at W1FB. The tower height is only 50 feet. Homemade open-wire line is used as the feeder to permit multiband use with vertical polarization and a low radiation angle.

Feed Methods

A Q section is used for feeding the W1SE loop. A Q section is a quarter-wavelength line with an impedance that is somewhere between the antenna feed impedance and that of the feed line. Calculation is a simple matter:

$$Z \text{ (Q section)} = \sqrt{Z1\ Z2} \text{ ohms} \qquad \text{(Eq. 1)}$$

where Z1 is the antenna impedance, and Z2 is the feeder impedance in ohms. In this case, assuming approximately 100 ohms for the antenna. feed impedance, we would have $\sqrt{100 \times 50} = 70.7$ ohms for the Q-section impedance. This represents a close match to 52-ohm coaxial cable. The Q-section length (made from RG-59/U) can be determined from L(feet) = 246 V/f(MHz), where V is the velocity factor of the coaxial line for the matching section. (The length should be verified using a dip meter.) For operation at the W1SE-chosen frequency of 3.825 MHz, the calculation calls for a Q section of 42 feet 5 inches (Figure 3).

Open-wire feed is used at W1FB (Fig 6B) to permit multiband operation through 10 meters. Unfortunately, a short run of RG-8/U was needed to bring the feed line to the ham station–under the driveway. The coaxial cable was buried in the ground for this reason. A homemade 4:1 toroidal balun transformer (two stacked T200-2 Amidon

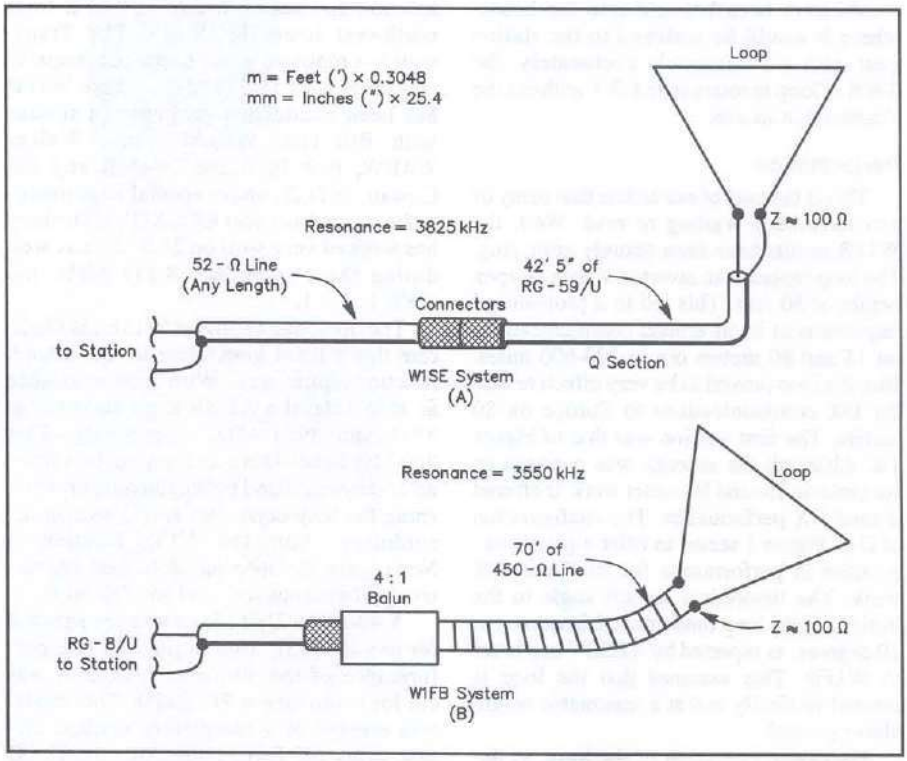

Figure 3—At A is the feed method used at W1SE. A coaxial Q section closely matches the 100-ohm feed impedance to a 52-ohm coaxial line. Illustration B shows the W1FB feed arrangement. Open-wire line, a balun transformer and a short length of RG-8/U cable permit multiband use with a Transmatch. Ideally, the open-wire line would continue all the way to the Transmatch, and the balun transformer would be located at the Transmatch.

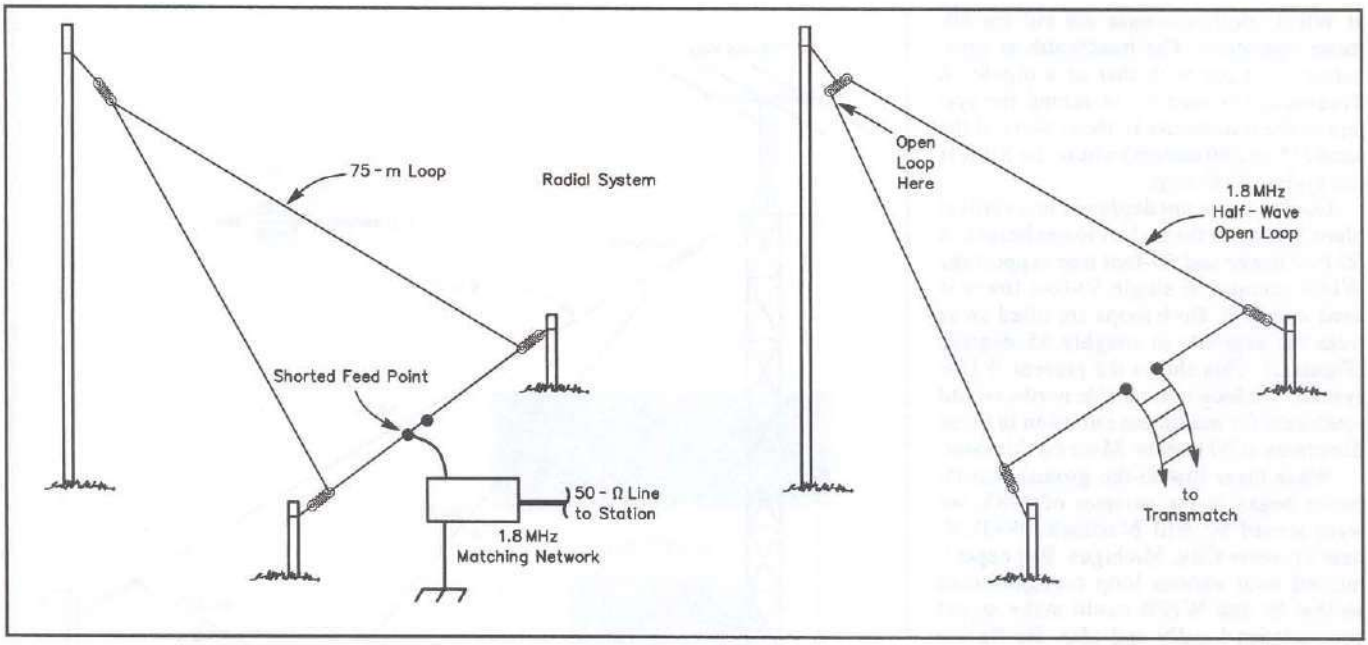

Figure 4 — Two methods for using a full-wave loop at half frequency. A switching arrangement could be applied at the feed point to change from a closed, full-wave loop to the first configuration seen here. The method at A performs as a 1/4-wavelength radiator, but a ground screen is required. Method B is satisfactory as a 1/2-wavelength open loop for half-frequency use. It requires opening the loop at the electrical point opposite the feed point. A relay could be used for this purpose.

cores and Teflon-insulated no. 14 wire) was enclosed in a weatherproof box and mounted on one of the support poles for the 450-ohm open-wire line. The RG-8/U was run underground from that location (about 25 feet). Ideally, the openwire line would have been brought into the house, where it would be matched to the station gear with a Transmatch. Fortunately, the SWR at loop resonance is 1.3:1 without the Transmatch in use.

Performance

This is the part of our article that many of you have been waiting to read. Well, the W1FB results have been entirely gratifying. The loop replaced an inverted V with an apex height of 50 feet. This led to a pronounced improvement in all-around communications on 75 and 80 meters out to 500-600 miles. But, the loop proved to be very effective also for DX communications to Europe on 80 meters. The first version was that of Figure 1B. Although the antenna was outstanding for close-in 75- and 80-meter work, it offered dismal DX performance. The configuration at D of Figure 1 seems to offer a good compromise in performance for local and DX work. The theoretical launch angle to the horizon at the loop fundamental frequency is 10 degrees, as reported by VE2CV in a letter to W1FB. This assumes that the loop is erected vertically and at a reasonable height above ground.

Harmonic operation of the loop, as depicted in Figure 1D, is superb. At times it outperforms the trap tribander atop the tower during DX operation to Europe and Africa. The loop shows an average 6-dB signal increase on 20 and 15 meters in the favored direction, owing to the gain and lower radiation angle of the loop. Radiation at the harmonics is in the plane of the loop rather than broadside to it. This makes it ideal for contacts into Africa. It is perhaps the most effective 40-meter DX antenna that has been used at W1FB from northwest lower Michigan. The Transmatch is required on all harmonic frequencies other than 18.111 MHz, where W1FB has been conducting propagation studies with Bill Orr, W6SAI, Prose Walker W4BW, Bob Haviland, W4MB and Stu Cowan, W2LX, under special experimental/research licenses (KM2XQV). The loop has worked very well on 24.9 MHz as well during these tests. At 18.111 MHz, the SWR is 1.4:1.

The operating results at W1SE also indicate that a tilted loop, close to the ground, functions quite well. With loop resonance at 3825 kHz, the 2:1 SWR points occur at 3734 and 3934 kHz, respectively. This 200-kHz bandwidth spectrum can be shifted up or down the band by lengthening or shortening the loop conductor and Q section accordingly. From the W1SE location in Newington, the loop has delivered impressive performance for local and DX work.

A 40-meter Delta loop was constructed for use at W1SE after noting the fine performance of the 80-meter system. It was cut for resonance at 7016 kHz. This model was erected in a completely vertical format, using 143 feet 3 inches of wire. The Q section is 23 feet 2 inches long. The apex (feed point) is 4 feet above ground. The SWR on 40 meters is less than 2:1 across all of the band. The 80- and 40-meter W1SE loops showed resonance slightly apart from the design frequency, perhaps because of the proximity of the antennas to ground. Resonance on 40 meters was checked as 7050 kHz. Both loops are performing better for local and DX contacts than any of the many antenna types tested at W1SE. We would be even more impressed if we could elevate our Delta loops so the lower portions were a half wavelength or greater above ground.

In Conclusion

There is no rule that dictates the shape of a full-wave loop. The triangular format is convenient for mounting the radiator. If the apex is at the top, only one high support structure is needed. You may have one or more tall trees that can be used as supports. Circular, square or rectangular shapes have been used by many amateurs and the results were good. Certainly, a loop is an impressive receiving antenna, in terms of noise reduction. In some urban locations, that may be more important than transmitting a "death-ray" signal! There is something to be said about the age-old expression, "If you can't hear 'em, You can't work 'em."

An 80-meter Delta loop can be used on 160 meters by adopting one of two simple methods (Figure 4). A closed loop does not, however, offer good results when the overall length is a half wavelength. Either of the techniques in Figure 4 will work, but the method at A requires a ground radial system for best results.

Notes

[1]D. DeMaw, "Beat the Noise with a Scoop Loop," *QST*, July 1977, and "Maverick Trackdown," *QST*, July 1979.

[2]H. H. Beverage and D. DeMaw, "The Classic Beverage, Revisited," *QST*, Jan. 1982.

By David J. Crockett, WB4DFW From *The ARRL Antenna Compendium Volume 5*

A Triband 75/40/30-Meter Delta Loop

WB4DFW wanted to use his Delta Loop on other bands besides 75 meters, so he installed some coaxial traps. He also reveals an effective technique to prevent breakage when support trees sway in the wind.

I've been using horizontally mounted, coax-fed Delta Loop antennas on 75 meters for many years. I've found them to be superior to dipoles—they are generally quieter on reception (perhaps because they are dc-grounded), exhibit broader bandwidth (typically less than 2:1 SWR over more than 200 kHz using a coaxial matching section), and are often more easily adaptable to available tree supports. They also don't fall down very often when installed correctly!

Outside of using an antenna tuner, a 265-foot-long 75-meter loop doesn't lend itself to working other bands–and I don't have a tuner. So while listening to a virtually dead 75-meter phone band one day and wishing I had a way to hit 30 meters for a long-overdue dose of CW, I had a brainstorm. Why not use traps? I'd homebrewed coaxial traps based on Sommer's article[1] several times in the past, and I knew they were easy to make and adjust.

The Traps

A quick examination of the latest incarnation of my 75-meter loop found it to be a reasonably equilateral triangle (a little over 85 feet per leg). I calculated that a 30-meter dipole should be something over 46 feet in total length (465/frequency in MHz). It appeared to be a simple enough matter to station some homebrewed coaxial traps 23 feet on each side of the feedpoint. A little more calculating found that it might even be practical to put in a pair of 40-meter traps as well.

Sommer gives a useful set of nomographs for computing trap dimensions on PVC pipe forms, using either RG-58 or RG-174 coax (the former capable of handling a kW with few problems). I opted for the larger cable. The 30-meter traps each require 46.8 inches of coax on a 1.62-inch OD section of PVC (6.75 turns). The 40-meter versions each use 61 inches of coax on a 2.25-inch OD PVC section (6.0 turns). Both PVC sections can be any convenient length. I used four-inch long pieces.

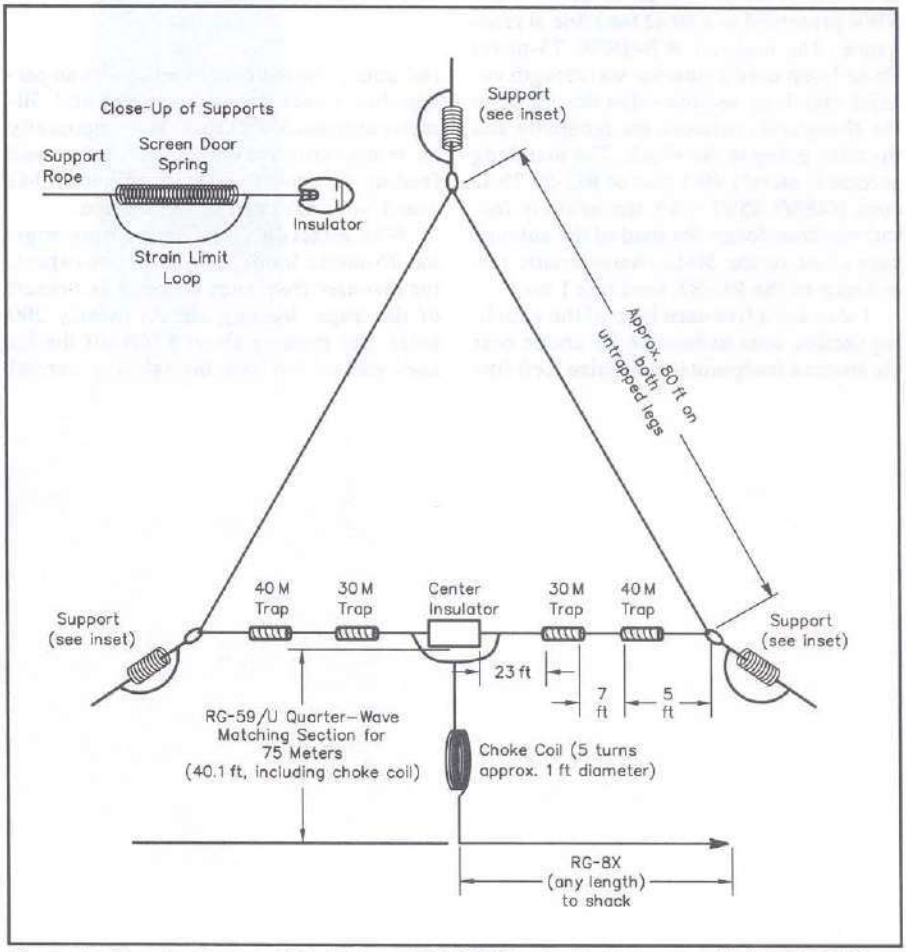

Figure 1—Overhead view of the Triband 75/40/30-meter Delta Loop, which WB4DFW mounted 40 feet off the ground. The traps were constructed with RG-58 coax. See text for winding details.

I wound the 30-meter traps in less than an hour and inserted them in the loop antenna 23 feet either side of the feedpoint. A quick SWR check found them resonant well below the bottom of the 30-meter band, but spacing the turns slightly apart and securing them with electrical tape raised the resonance easily enough, with the SWR bottoming out at 1.2:1 at 10.125 MHz.

The 40-meter traps went together with similar ease. Placement in the existing antenna was a little more challenging than with the first set of traps. The loading caused by the 30-meter traps made determining the physical location for the 40-meter traps uncertain. Grebenkemper notes that traps in a half-wave antenna tend to "pull" an antenna toward resonance,[2] even if they are not placed at exactly the optimum location. So, I simply took the formula length for 40-meter resonance, generously subtracted the physical length of the coax in each of the 30-meter traps and installed the 40-meter traps accordingly.

The approach was unscientific, but SWR was 1.3:1 at 7.1 MHz on the first try. Dumb luck, I guess, and I opted to make no further adjustments. The final antenna layout is shown in Figure 1, and a close-up photo of a trap is shown in Figure 2.

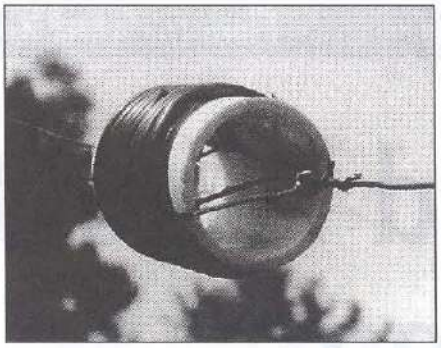

Figure 2—Close-up photo of one of the 40-meter traps. The ends of the coax cable used in each trap have been sealed against moisture with silicone caulking. See text for construction details.

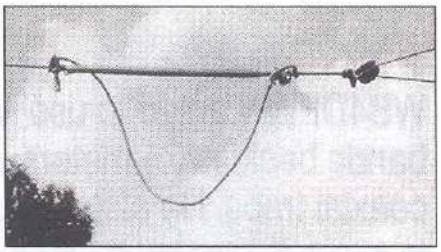

Figure 3—Photo of one of the support system springs, with rope used to limit total stretch. The rope is twice the length of the unstretched spring.

The Matching Section

The ARRL Handbook notes that the typical impedance of a full-wave loop antenna is on the order of 100 Ω, or about a 2:1 SWR presented to a 50-Ω feed line at resonance. The original WB4DFW 75-meter Delta Loop used a quarter-wavelength coaxial matching section (also described in the *Handbook*) between the feedpoint and the coax going to the shack. The matching section is merely 40.1 feet of RG-59 75-Ω coax [(465/3.85)/2 ×.66, the velocity factor] and transforms the load of the antenna very close to the 50-Ω characteristic impedance of the RG-8X feed line I use.

I also use a five-turn loop of the matching section coax to form an RF choke near the antenna feedpoint to minimize feed-line radiation. The matching section has no perceptible effect on the new 40 and 30-meter antenna SWRs (checked empirically by temporarily removing the section and feeding the antenna directly with the 50-Ω coax), so it has been left in service.

What effect did all this have on my original 75-meter loop? As one might expect, the resonant frequency dropped as a result of the traps' loading effects (nearly 200 kHz). But pruning about 8 feet off the far apex end of the loop brought my normal 1.2:1 resonant SWR back to my regular 3.842-MHz stomping grounds.

Keeping It Up in the Air

Here in South Carolina, pines are a great source of antenna support but their swaying during summertime thundershowers can wreak havoc on long, unprotected wire antennas. Over the years, I've found a simple shock-absorber system using a run-of-the-mill screen-door spring placed between a support rope and each antenna insulator can save a lot of grief. See Figure 3 for a closer look at the details.

A special aspect of my system is the employment of a "strain limit rope" in parallel with each spring. This piece of rope, approximately twice the length of the unstretched spring, keeps swaying pines from overly taxing the spring and gives a nice visual reference for gauging how much tension the antenna is operating under. It also provides a fail-safe for the inevitable corrosion-caused failure of the spring after several years aloft. It makes a fine bird perch, too.

So, How Does It Play?

Performance on all three bands has been most satisfactory. The 2:1 SWR bandwidth of the 30-meter section far exceeds the band edges. Similar 40-meter bandwidth is about 100 kHz (noticeably narrower than dipoles I've used, and I suspect partially attributable to my guesswork on the 40-meter trap placement). The 75-meter bandwidth is now approximately 150 kHz (slightly narrower than before the traps were installed). Signal reports both ways on all three bands are comparable to any other non-directional HF antennas I've used.

Notes and References

[1]Robert C. Sommer, "Optimizing Coaxial Cable Traps," *QST*, Dec 1984, pp 38-42.

[2]John Grebenkemper, "Multiband Trap and Parallel HF Dipoles-A Comparison," *QST*, May 1985, pp 29-30.

A Two-Band Loop for 30 and 40 Meters

After trying to find a way to place a 30-m delta loop inside an existing 40-m loop, I remembered an article in *All About Cubical Quad Antennas*[1] describing a 1½-λ, or "Mini X-Q," loop. The gain of this antenna was said to be about 1 dB more than a 1-λ loop. I installed a large, ceramic SPST knife switch in the center of the delta-loop's bottom leg (see Fig 11). With this switch open, the full-wave, 40-m loop becomes a 1½-λ, 30-m loop! The resonant frequency of this arrangement was 10.5 MHz. By adding 18-inch wires to the loop at both sides of the switch, I obtained resonance at 10.125 MHz.

Since the bottom of the loop is only 12 ft above ground, it's a simple matter to reach the band switch from ground level. (Caution: High RF voltage appears at the switch when the antenna is used for transmitting on 30 m.) Incidentally, the loop also works well on 15 m (SWR under 2:1 across the band) when set for 40 m, and I have used the 30-m configuration successfully on 80 m with the help of an antenna tuner.—*James Brenner, NT4B*

[1]W Orr and S. Cowan, *All About Cubical Quad Antennas* (Wilton, CT: Radio Publications, 1970).

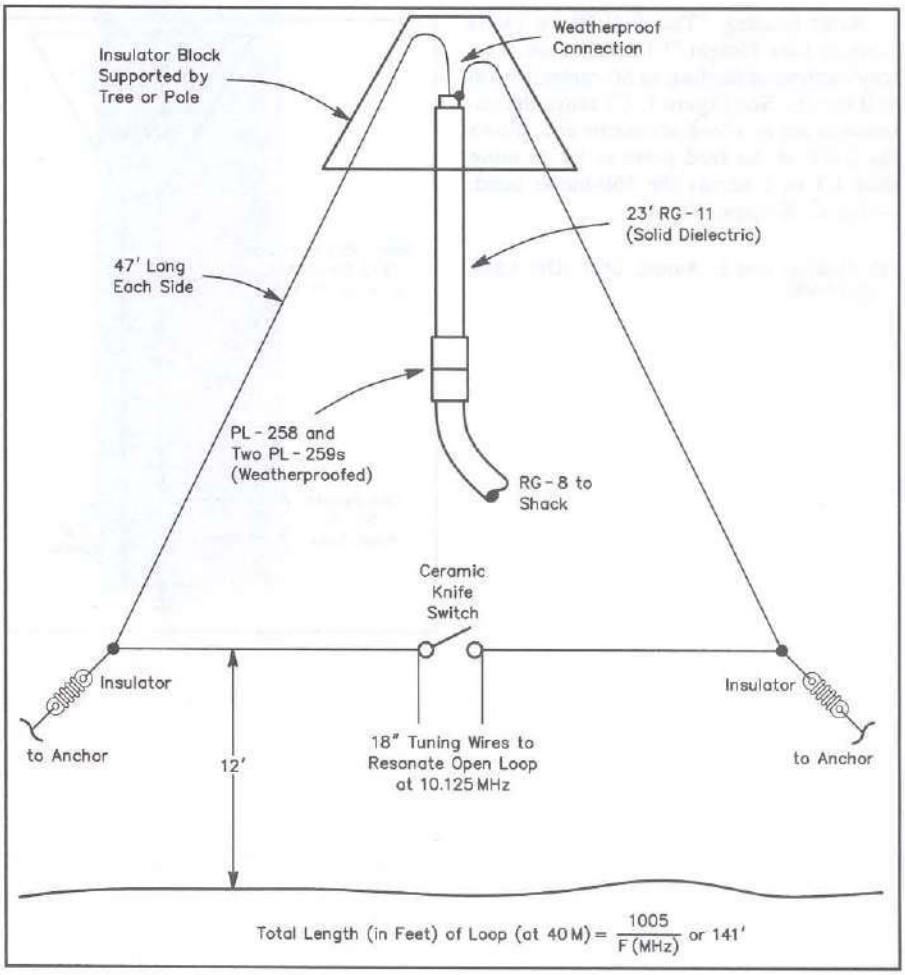

Fig 11—Jim Brenner's 30- and 40-meter loop. Note the 18-inch tuning wires used to lower the antenna's 30-m resonance from 10.5 to 10.125 MHz. The antenna is top-fed via a ¼-λ 40-m matching section. See text.

Feeding an 80-Meter Delta Loop at 160 Meters

After reading "The Full-Wave Delta Loop at Low Height,"[1] I found a satisfactory method of feeding an 80-meter loop at 160 meters. See Figure 1. C1 tunes the antenna to act as a $^3/_4$-λ resonator and allows the SWR at the feed point to be no more than 1.1 to 1 across the 160-meter band. —*Roy C. Koeppe, K6XK*

[1]D. DeMaw and L. Aurick, *QST* (Oct 1984, pp 24-25).

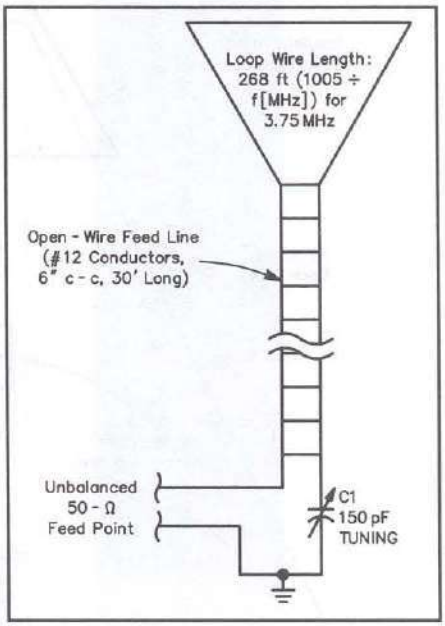

Figure 1—Roy Koeppe enjoys satisfactory 160-meter operation with an 80-meter delta loop by feeding the loop as shown here. On 80 through 10 meters, Roy takes C1 out of the circuit and feeds the loop via its open-wire feed line and a balanced tuner.

CHAPTER FIVE

COLLINEAR ANTENNAS

5-1 **The Extended Double-Zepp Antenna**
From June 1938 *QST*

5-7 **Try an Extended Double-Zepp Antenna**
From February 1992 *QST* (Hints & Kinks)

5-8 **Notes on Wire-Antenna Construction**
From March 1992 *QST* (Hints & Kinks)

5-10 **Collinear Arrays**
From *The ARRL Antenna Book* 18th edition

By Hugo Romander, W2NB

From *QST*, June 1938

The Extended Double-Zepp Antenna

Simple Antenna Structures Having Improved Gain and Horizontal Diversity

The questions of antenna directivity and antenna "gain" are becoming increasingly popular in discussions on antenna systems among amateurs, and it would therefore seem proper to preface an article dealing with directive antenna arrays with a warning, or perhaps a reminder, that one cannot have high gain and radiate in all directions at the same time. To most amateurs this is an obvious fact, but it may not be as well known that this principle is almost equally important in the *vertical* plane. Those of us fortunate enough to have available large open spaces in which to hang wires will find long-wire antennas, such as the "V" and the horizontal diamond, the easiest way to obtain high gain, but the radiation from such antennas is restricted in the vertical plane fully as much as in the horizontal plane. The result may well be that in the very direction such an antenna is supposed to work best, a simple horizontal doublet will put in a far better signal at certain distances.

It would seem, therefore, that the most practical antenna for a variety of distances is one with a fairly wide radiation pattern in the vertical plane.[1] The "stacking" of elements or the use of long wires is not recommended for distances under 1000 miles, except for the very short distances normally reached by the ground wave. The most universal high-gain antenna must restrict its radiation in the horizontal plane only and its height above ground must also be considered to obtain the best compromise in the vertical plane. It is the purpose of this article to discuss the merits of a simple antenna array which combines these desirable features.

THE DOUBLET

Let us discuss, first, the simple doublet, since this antenna will serve admirably as our basis of reference or comparison. To be more specific, consider this doublet as suspended horizontally and fed at one end in the time-honored fashion of the Zepp feeder, as in Figure 1A. Ignoring, for the moment, the fact that the open-ended feeder wire will be at somewhat higher potential than the other feeder wire and will therefore radiate, the horizontal radiation pattern about this doublet, if you're lucky, will be about as shown on Figure 2. Of course, it is assumed the antenna is sufficiently remote from power-line wires and house plumbing to be unaffected by such linear conductors, since our problem is complicated enough without having to consider the mutual impedance between our doublet and the neighbor's b.c.l. antenna!

This pattern of the horizontal doublet is, no doubt, familiar to most amateurs. Less familiar, perhaps, is the vertical radiation pattern (in the direction of maximum horizontal radiation) as shown in Figure 3. Here it is assumed that the height of the doublet above ground is one-half wavelength and that the earth has perfect conductivity. Fortunately, even the relatively low-conductivity soil and sand on Long Island reflects a high percentage of the horizontally polarized waves radiated at angles less than 50° to the earth's surface. Such reflected

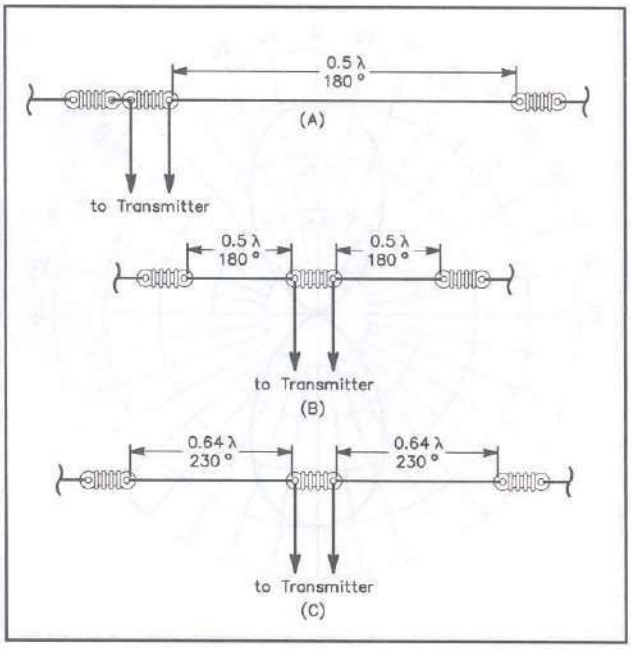

Figure 1—Basic Antenna Configurations (A) The half-wave Zepp; (B) Double Zepp or "two half-waves in phase"; (C) Extended double-Zepp.

[1] Although this viewpoint appears to be opposed to that expressed in the article "Simple Directional Arrays Using Half-Wave Elements," by N. C. Stavrou, in May, 1938 *QST* there is no actual conflict. As the present author points out, ihe broad vertical characteristic is to be preferred when the antenna is to give optimum results over short as well as long distances; the former article was concerned with long-distance transmissions, where the lowest possible angle gives best results under nearly all conditions. The type of work to be carried on naturally will be a determining factor. In any event, the simpler structures are not likely to be too sharp in either plane for satisfactory general work. —EDITOR

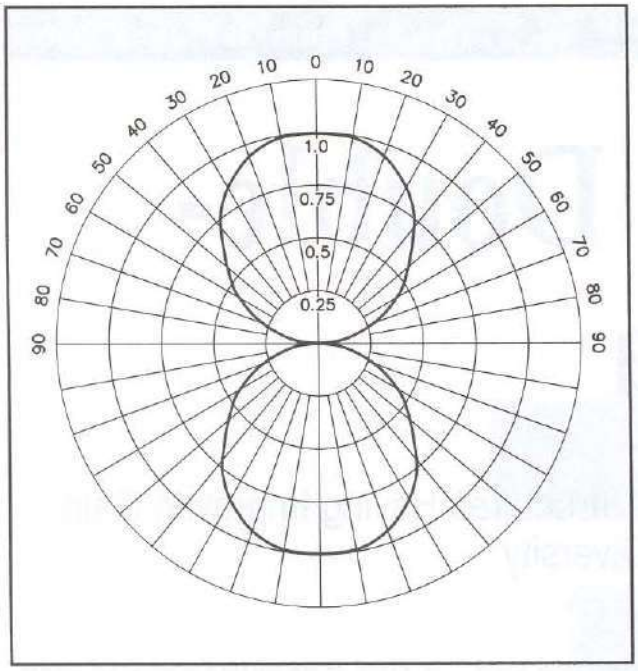

Figure 2—Horizontal pattern (relative field strength) of a doublet half-wave antenna.

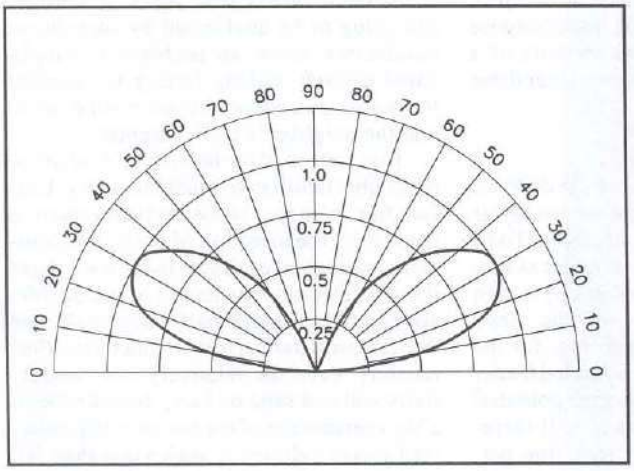

Figure 3—Vertical-plane pattern for a horizontal antenna, ½-wave above perfect earth in direction of maximum radiation.

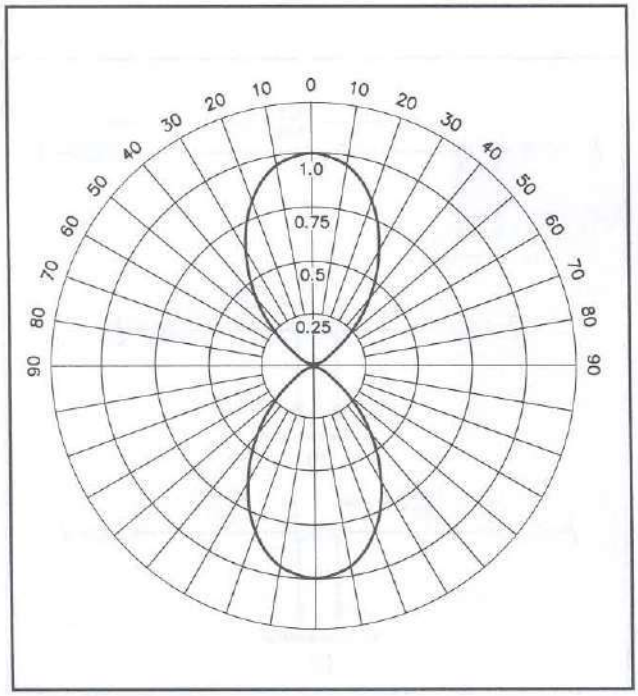

Figure 4—Horizontal pattern of a double-Zepp or two half-waves in phase.

waves, combining with the direct radiation from the antenna within the range of vertical angles in which we are most interested, are responsible for a maximum gain of nearly 6 db over the same doublet in "free space"; that is, without the presence of the earth.

This gift of 6 db must not be taken too much for granted, however. Consider the fact that most amateur communications at high frequencies utilize vertical angles ranging from 10 degrees to 50 degrees. That 6 db must, therefore, come from radiations reflected from the earth's surface quite some distance from the doublet, and in the desired direction of transmission. If the ground slopes sharply upward, or houses or wires are in this area, it becomes questionable, indeed, whether any great portion of the available 6 db is realized. This is especially true for the lower angles of radiation, but usually nothing can be done about this situation, so let us see if we can make up for our ground reflection losses by increasing the horizontal directivity.

THE DOUBLE-ZEPP

By the simple expedient of attaching another doublet to the open-ended terminal of the Zepp feeder, as in Figure 1B, and hanging this doublet parallel and coaxial with the original doublet, an appreciable gain may be obtained. The horizontal radiation pattern will be as shown in Figure 4. The gain should measure about 1.9 db, corresponding to a 55 per cent increase in power. This antenna is widely used among amateurs and is popularly known as the "double-Zepp" antenna, or "two half-waves in phase." A fair amount of gain and a reduction in interfering signals from end-wise directions is easily realized, but the gain is rather disappointing, since it would seem one is entitled to 100 per cent gain in power when doubling the number of radiating members.

The reason why only 1.9 db is realized with the double-Zepp is made clear only after a mathematical study of the situation. Briefly, the close proximity of the two doublets causes a mutual coupling between them, and this coupling (mutual impedance) has an adverse effect on the radiation resistance insofar as gain in the broadside direction is concerned. Obviously, the thing to do is to move the doublets further apart, but this complicates the method of feed. A much simpler way of obtaining increased gain was evolved by Mr. A. A. Alford, of Mackay Radio and Telegraph Company, from the principles discussed in Mr. G. H. Brown's article on broadcast antennas in the Proceedings of the I.R.E. for January, 1936. Mr. Alford presented this idea in a paper delivered at an I.R.E. meeting in Washington.

EXTENDED DOUBLE ZEPP

The gain of the double-Zepp may be increased from 1.9 to 3.0 db by the simple expedient of increasing the length of each doublet until its electrical length is 0.64

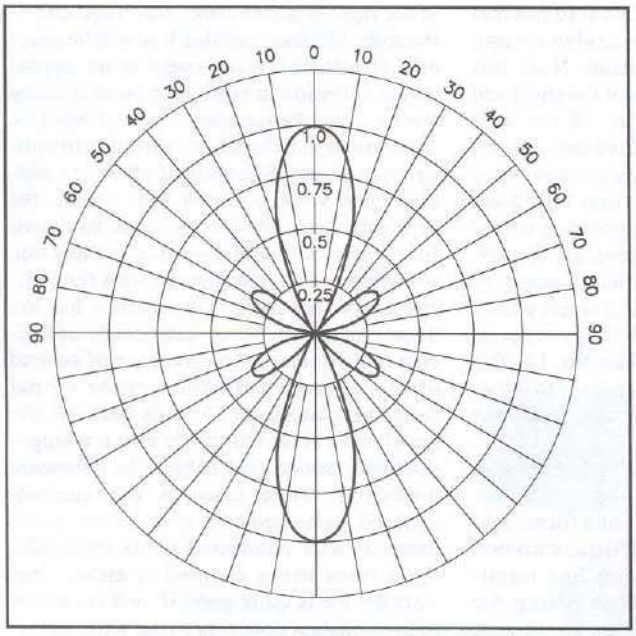

Figure 5—Horizontal pattern of double 230-degree Zepp

wavelength instead of 0.5 wavelength. In electrical degrees the double-Zepp consists of two 180-degree elements; the *extended* double-Zepp for maximum gain should consist of two 230-degree elements. See Figure 1C. In this way the power gain may be increased from 55 per cent to 100 per cent. The gain decreases rapidly for extensions beyond 230 degrees, and therefore, when operating over a band of frequencies, each of the two elements should not exceed 240 degrees for the highest frequency. The horizontal pattern for the double 230-degree Zepp is shown in Figure 5. The vertical pattern in a plane perpendicular to the antenna will be the same as for the simple doublet.

ANTENNA IMPEDANCE

The impedance of this antenna at the termination of the transmission line is of interest, since it has an important bearing on the standing-wave ratio of current or voltage in the line, and it will be compared with that of the ordinary double-Zepp. The double 180-degree antenna presents an impedance of approximately 4400 ohms of almost pure resistance as a termination for the transmission line. This value will be slightly affected by the size of wire used in the antenna and, to a moderate extent, by the height above ground or the influence of nearby conductors, and so the "free space" value is given for No. 14 wire. With this antenna and a 600-ohm surge-impedance line the ratio of maximum to minimum current along the line will be 4400 divided by 600, or 7.3. Incidentally, the terminating resistance of the simple Zepp-fed doublet is about 12,000 ohms, resulting in a standing wave ratio of 20 on our 600-ohm line. For calculation of the surge impedance of the line the reader is referred to *The Radio Amateur's Handbook*.

The impedance at the center of the double 230-degree antenna is not a pure resistance, and hence its effect upon the transmission line be such that maxima or minima of voltage and current along the line will not be odd multiples of a quarter wave from the antenna, as with the ordinary Zepp or double-Zepp antennas. As might be expected, the current or voltage maxima will be shifted towards the antenna, since the two doublets are longer than normal, and this shift is approximately 0.13 times the wavelength. At any rate, the antenna impedance is such that the equivalent pure resistance at any voltage maximum will be about 6000 ohms; that is, the standing-wave ratio will be 10 on a 600-ohm line.

Knowing the standing-wave ratio, it becomes an easy matter to calculate the input resistance to the transmission line if it was cut, let us say, at any current maximum. Thus, for the simple Zepp-fed doublet, this resistance would be 600 divided by 20, or 30 ohms. For the ordinary double-Zepp antenna this resistance would be 600 divided by 7.3, or 92 ohms. For the double 230 degree antenna this resistance would be 600 divided by 10, or 60 ohms. Those who do not use correcting stubs or other methods to obtain a "flat" line (standing wave ratio of 1), but who cut their transmission lines at the maximum current point after the manner of the "tuned feeder," will find these figures useful in calculating the power output of their transniitters.

FEED LINES

However, the use of flat lines, in amateur circles usually referred to as untuned lines, is becoming increasingly popular as their merits are more generally known, and the figures given are essential in calculating the length and position, for example, of a correcting stub, the latter being one of the simplest devices for reducing the standing-wave ratio to unity. A discussion of the use of the correcting stub may be found on page 307 of the *Handbook* (15th edition) where a table indicates the lengths and positions of the stub for various standing-wave ratios. The shorted stub or "loop" will generally be most practical, and some idea of dimensions may be obtained from the fact that when using the double 230-degree Zepp on 14,200 kHz the stub should be 3.5 feet long; that is, it should be composed of the same kind of wire as is used in the transmission line, this wire being 7 feet long and bent to form a U-shaped rectangle with a width equal to the transmission line. At the frequency mentioned, where each extended doublet is 43 feet long, the correct location for the stub will be about 8 feet from the antenna.

Ordinarily the best place to introduce power into an antenna is at a point symmetrically located with respect to the opposite ends of the system. This will not always be practical, because of space limitations, and hence it may become necessary to feed the extended double-Zepp antenna at one end in true Zepp fashion. Some sacrifice in gain will result, due, for the most part, to unequal distribution of current between the two doublets and to radiation from the feeder because it has an unbalanced load. Physical dimensions of feeder, extended doublets, and phasing stub are shown in Figure 6. Note that the phasing-stub length is shorter than a quarter wavelength, but by an amount not exactly

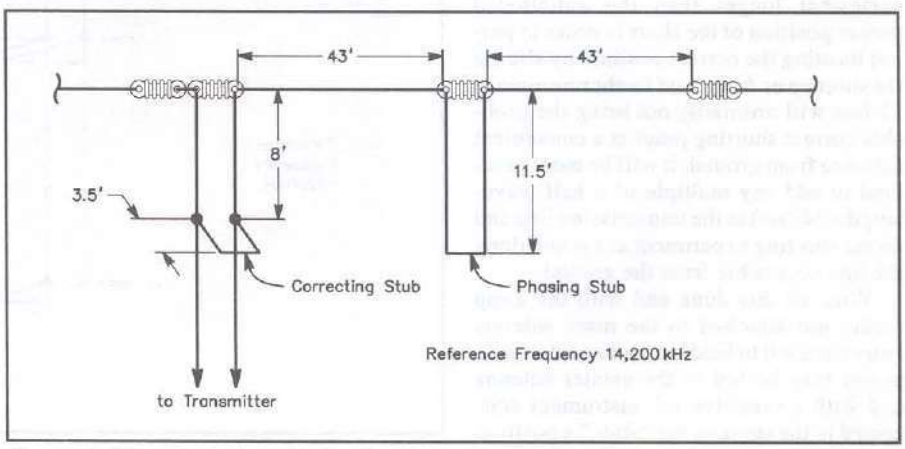

Figure 6—End-fed double 230-degree Zepp with 600-ohm non-resonant transmission line.

equal to the extension of each doublet beyond a half wavelength. This discrepancy is due to interaction between the doublet wires and the wires of the phasing stub. Again a reference frequency is given to simplify calculation of lengths at other frequencies by inverse proportion. The figures given should be regarded as approximations, and tests made individually to determine dimensions and positions of important elements.

ANTENNA ADJUSTMENTS

One of the most effective methods of adjusting an antenna system is to use the transmitter to excite, at the desired frequency, another antenna stretched out, perhaps temporarily, at least 8 or 10 feet from the ground. This "exciter" antenna should preferably be at least one-half wavelength away from the antenna to be adjusted. If the two are parallel to each other, so much the better. Using the end-fed extended double-Zepp antenna as an example, the first consideration is the length of each doublet, and this brings up the problem of "end-effect." We have approximately solved this by cutting our doublets 5 per cent short of the theoretical length. Actually the end effect, which normally exists only at the ends of the antenna, depends on the wire size and the size of the insulator fitting (if metal caps are used), as well as the frequency. Moreover, the end-effect does not vary quite as rapidly as a direct function of the wavelength, so that if an end-effect of 1 foot is correct at 14,200 kHz, it is more nearly 1.5 feet than 2 feet at 7100 kHz.

The theoretical "uncorrected" length of each half of an extended double-Zepp antenna at 14,200 kHz is 44.3 feet. The end-effect may be no more than 1 foot, but since it is better that the antenna be a little too short than too long, let's make the correction 1.3 feet, so that each half will be exactly 43 feet long. At the center insulator which separates the two halves a "stub" must be connected, if the system is to be end-fed. Now, this stub will, take the form of a transmission line shorted at the end opposite from the antenna, and for the frequency under consideration its shortest length will be about 12 feet. Since it is our intention to make this transmission line somewhat longer than the anticipated proper position of the short in order to permit locating the correct position by sliding the short up or down, and furthermore since 12 feet will ordinarily not bring the probable correct shorting point at a convenient distance from ground, it will be more practical to add any multiple of a half wavelength (34 feet) to the transmission line and do the shorting experiment at a point along the line accessible from the ground.

With all this done and with the Zepp feeder *not* attached to the main antenna (why not use it to feed the exciter antenna?), power may be fed to the exciter antenna and with a sensitive r.f. instrument connected in the short on the "stub," a position of the short may easily be found where maximum current flows. This assumes that the main antenna has been hauled up into its normal operating position. Note this maximum-current position of the short and measure in exact multiples of one-half wavelength from this point towards the antenna, thus arriving at the nearest point to the antenna at which a short may be placed. This will give the shortest possible center stub. Of course, it is not necessary that the center stub be made that short, since very little loss will be incurred if it is left a half-wave or even a wavelength longer–that is, if the wire is not smaller than No. 14. The Zepp feeders may now be attached to either end of the antenna, as it is now ready for operation.

The method of adjusting the center stub just outlined is also useful where it is desired to feed any of the antenna forms discussed above with an untuned transmission line—that is, a transmission line terminated by its surge impedance. Using the example cited in the previous paragraph, let us assume the point of maximum current through the short has been found and, after soldering a piece of wire across the line at this point, the extra length of transmission line is chopped off. The two-wire line from the transmitter may now be tapped in above this shorted end of the stub, and it is only a question of position of the feeder tap from the shorted end to terminate the line properly. See Figure 7. This point will be approximately 3.3 feet from the short for a 600-ohm transmission line. Of course, when all this is done, we will have the same transmission line with correcting stub discussed earlier in this article.

LINE-CURRENT MEASURING DEVICES

The same principle holds true for the double Zepp and for center feeding the simple doublet, the only ambiguous point being that of knowing when the transmission line from the transinitter is connected at the right distance from the closed end of the stub. The transmission line will be properly terminated when there is no appreciable variation in voltage or current along the line, and hence some method must be used which will detect any variation in voltage or current. Simplest of all is the old-fashioned wood-covered lead pencil, for with this device bright arcs may be drawn from either wire and the voltage at any one point judged by comparison with the voltage at another point. This method has the disadvantage of being both crude and liable to error due to the presence of second or higher-order harmonics in the output from the transmitter. A little better is the small neon bulb, but this is also a voltage-operated device and subject to harmonic distortion. Then there is the current-squared galvanometer with a few small turns of wire connected to its terminals, these turns being coupled to either line. This device is quite good if one is careful to use constant coupling to the wire, but its disadvantages are that coupling between the meter and line is both inductive and capacitive, causing the meter to read differently according to how it is held up to the line, and that the meter will also be influenced by harmonics.

The most satisfactory device seems to be a sensitive galvanometer in a miniature tuned circuit coupled to the line. Such a device combines sensitivity with freedom from harmonic distortion, but the effects of capacity are still there to some extent. The tuned circuit should therefore be carried along the line with its position relative to the plane of the two wires maintained constant. See Figure 8. Checking along one of the two wires only is usually sufficient, but if one suspects an unbalance exists, the other line should also be checked. If the antenna system is reasonably symmetrical, unbalanced currents will most likely be due to improper coupling to the transmitter, but that is another story. At any rate, if a cur-

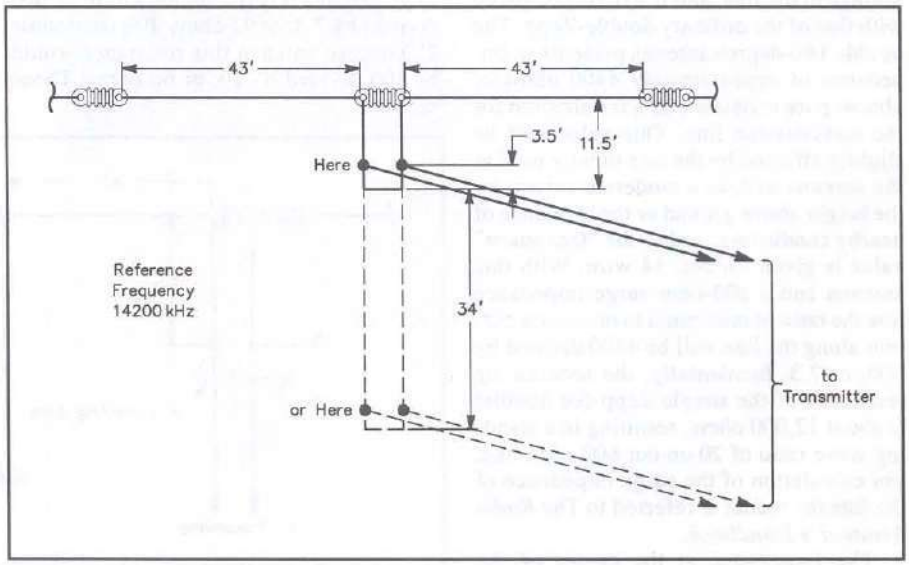

Figure 7—Center-fed double 230-degree Zepp with 600-ohm transmission line.

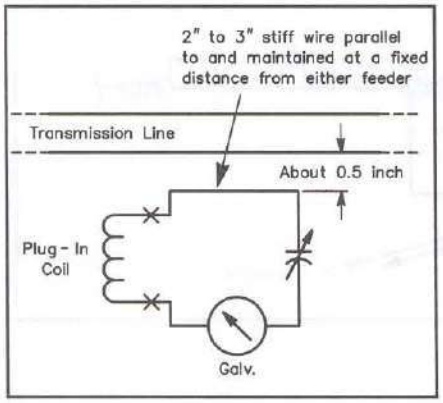

Figure 8—Portable line-current indicator.

rent maximum (voltage minimum) appears at the junction of transmission line and stub, the connection to the stub is too near the shorted end, and if the current is a minimum the opposite, of course, will be true. If the current maximum or minimum (assuming standing waves actually exist) does not occur near the stub, there has been a slip-up somewhere in the procedure, for this will be evidence that the stub itself did not tune the antenna to resonance.

PARASITIC ELEMENTS

The use of spreaders several feet in length to support each end of a "flat-top" antenna composed of two wires is again becoming popular, and for a good reason. Gains of around 5.5. db for a bi-directional array and around 7 db for a unidirectional array are thus made possible. One of the most promising arrangements is that of two double-230-degree antennas supported parallel to each other only 0.2 wavelength apart, as illustrated in Figure 9. Antenna A is excited by the transmitter using the same technique as when exciting a single double-230-degree antenna. Antenna B may be tuned by proper positioning of a short on its stub to become either a director or a reflector. In fact, this stub might be extended by multiples of a half wavelength to enter the operating room where, by means of a single switch the shorting position may be changed from that corresponding to a director to the position corresponding to a reflector, thus reversing the directivity of the antenna system. Information as to the gain of such an antenna system when one antenna is used as a director is not available, but when it is used as a reflector and adjusted to give a *minimum* signal to the rear, the signal forward will be 7 db better than a simple doublet, and the signal backwards will be 7 db less than from a doublet, resulting in a front-to-back ratio of 14 db. Adjustment of the reflector shorting bar should be on the basis of minimum backward signal from the antenna, or minimum signal received from a station in that direction when using the antenna system for reception, since this adjustment can be made more accurately than one resulting in maximum front signal. This will minimize QRM for both transmitting and receiving. The same principles hold true when adjusting the auxiliary antenna for use as a director.

If adjustments of the auxiliary antenna are to be made when transmitting and an ammeter is temporarily inserted in the shorting bar, minimum backwards signal will occur for the reflector when the short is moved slightly further from the antenna than that position corresponding to maximum current through the short. For the director, optimum conditions will be obtained when the short is slightly closer to the antenna than the maximum shorting current position. From this it can be seen that the proper adjustment of the auxiliary antenna is quite critical and certainly very important. Since field strength instruments are not generally available, a receiver fitted with a signal strength indicator of some sort located within a few miles of the antenna and in the desired direction should prove to be the next best thing. Connecting your own receiver to the antenna, with the other fellow transmitting, is perhaps even more practical in search for that minimum-signal adjustment.

The presence of the auxiliary antenna only 0.2 wavelength away from the driven antenna and adjusted properly for maximum forward or backward radiation will obviously affect the radiation resistance and impedance of the driven antenna. As a result, if the auxiliary antenna is left open-circuited and the stub on the driven antenna is adjusted in accordance with the method previously given, this adjustment will not be correct when the auxiliary antenna is, in turn, properly tuned. Moreover, the impedance of the driven antenna will differ slightly according to whether the auxiliary antenna is tuned as a director or as a reflector. If quick change from reflector to director is contemplated, some sort of compromise is indicated in the adjustment of the stub on the driven antenna. From a practical standpoint, however, the adjustment of the auxiliary antenna should be made first, be it reflector or director, with the driven antenna excited by the two-wire transmission line without a correcting stub. This may require temporary adjustment of the transmission-line length, either physically or by means of series coils or condensers, to bring a low-impedance point at the coupling coil to the transmitter in order to load the latter satisfactorily. In fact, if the line length from antenna to transmitter is not more than a wavelength or so, the reduction in line losses resulting from the use of a correcting stub is hardly worth the trouble of installing it. The point is, if a "flat" line is desired, adjustments of the stub at the driven antenna should not be made until after the auxiliary antenna has been tuned to give the desired radiation pattern.

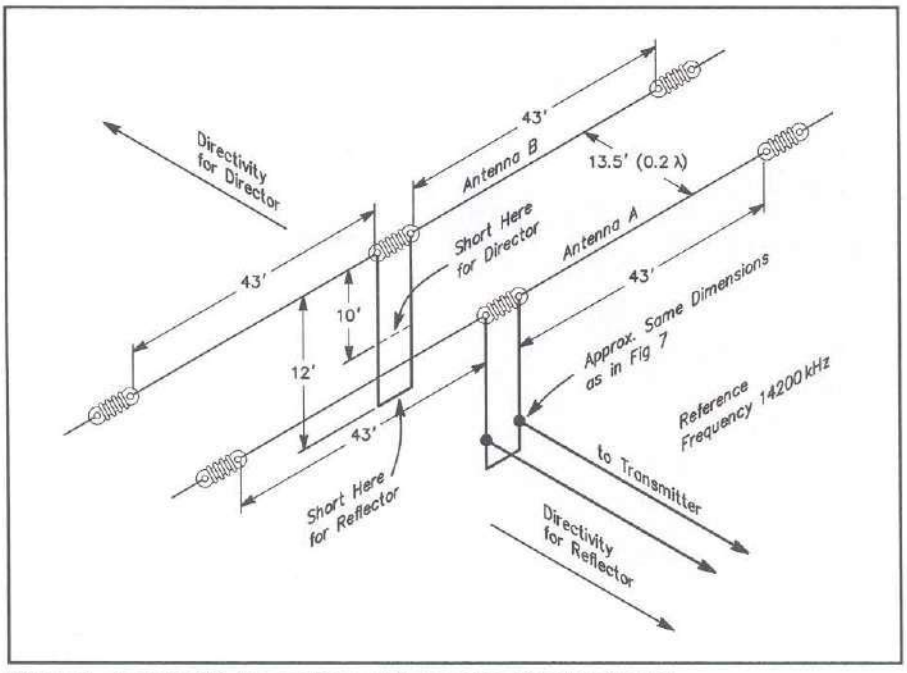

Figure 9—Double 230-degree Zepp with parasitic reflector-director.

LARGER COLINEAR ARRAYS

Now let us suppose our backyard is big enough to hang up more than two doublets end to end. An interesting possibility would be a four-element array of 230-degree elements. But here the principles of the extended double-Zepp must be carefully considered in designing the length of each element and the length of the phasing stub separating them. The actual arrangement will be as shown in Figure 10. Both degrees and dimensional designations are used to indicate the electrical and physical length of each element. The length of the stubs indicated is approximate only and must be adjusted for best results. The lengths of the various antenna elements as shown, however, may be assumed correct. The transmission line can be tapped on to any of the stubs, but connection to the center one will give the greatest gain.

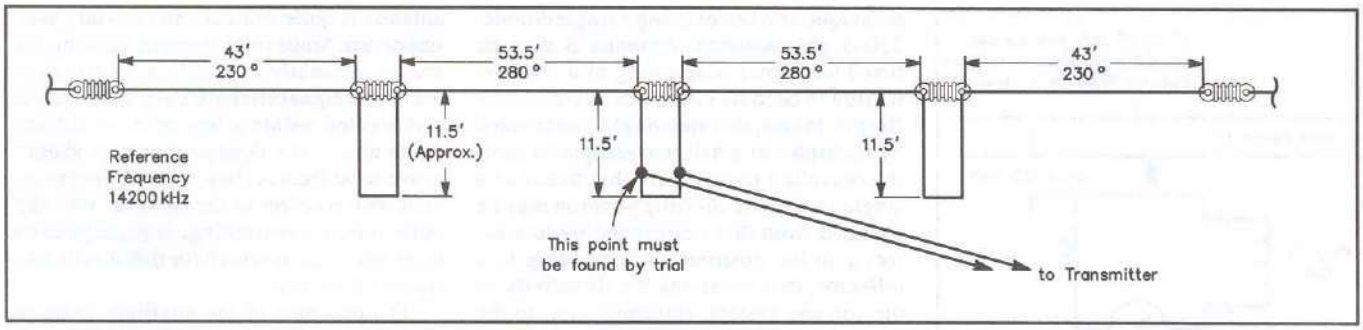

Figure 10—Four-element array with 230-degree elements.

The principle of the design shown for four elements is to provide the same separation in space between each doublet center as is provided between the two doublet centers in the double-230-degree antenna. Each phasing stub will, of course, be considerably shorter than a quarter wavelength, and when adjusting their length to tune the whole antenna to resonance, all three stubs must be made the same length; that is, if one is shortened two inches, the other two must also be shortened by two inches, assuming they were all the same length to start with.

This may prove to be an awkward and tedious method of adjustment, but the procedure may be simplified by adjusting the length of the center stub only as a first approximation. The use of an "exciter" antenna temporarily rigged nearby is assumed. If it is found the center stub must be shorter than the other two stubs by 3 feet, for instance, in order to obtain maximum current through its shorting bar, the other two stubs should be shortened by 1 foot and a new position found for maximum current through the center stub. This new position should correspond closely to equal length for all three stubs. This procedure of tuning the four-element array should be followed even though a stub at the center will not be used, finally, its place being taken by the transmission line itself. Such a connection will result in standing waves along the line and it will have to be "tuned" to permit easy coupling to the transmitter or receiver.

The horizontal pattern of the four-element array just described will have two major lobes at right angles to the antenna and several minor lobes of small amplitude. The gain in actual practice has proved to be greater than anticipated, and probably is more than 7 db. The major lobes will be much narrower than for the double-230-degree antenna, thus requiring more careful "aim" in erecting the array, or provisions for swinging it about. It is assumed this array, as well as the others described, is hung horizontally. It may be hung vertically, of course, but the possible restrictions due to sharp directivity in the vertical plane should then be considered. In general, the horizontally polarized antenna will prove most practical, chiefly because the ground reflection usually encountered with vertically polarized radiations is inferior, and because high masts are not often available.

The adjustment of the antennas described in this article may seem a bit involved as compared with the simple doublet or the double-Zepp antenna, but the extra gain thus made available should make their use worthwhile. For that matter, the double-230-degree antenna need not be tuned at all, its construction being made in accordance with the dimensions given and the transmission line tuned to fit the transmitter. In this respect the simplest of all directive antennas, size and gain also taken into consideration, is the extended double-Zepp.

Try an Extended Double-Zepp Antenna

Although the extended double Zepp (EDZ) antenna (Figure 1) has been in just every antenna handbook since the year one, hams seldom use it. Its overall length is 1.28 wavelengths (1.28 λ), and it's bi-directional broadside. Fed with open-wire line and a balanced antenna tuner, an EDZ also makes a fine multiband antenna. Let's look at an extended double Zepp for 17 meters. We can calculate the overall length of its two wire elements with the formula

$$\frac{984}{f(\text{MHz})} \times 1.28 = \text{length in feet} \qquad \text{(Eq 1)}$$

Using this formula, an 18.15-MHz EDZ works out to be 69.4 feet long. At this frequency, the EDZ exhibits, 3 dBd gain [*AB* page 8-34][1] in a figure-8 pattern with two major and four minor lobes. It still performs usefully, when operated on several bands lower in frequency than 17, however. At 20 meters, a 17-meter EDZ acts as two slightly long half waves in phase, exhibiting between 1.6 and 2 dBd gain [*AB* page 8-32]. At 40 meters, it's a slightly long ½-λ dipole [*AB* page 2-16,2-17,3-11 and 3-12]. All of these modes are directional broadside if the EDZ is positioned at least ½-λ high at 40 meters [*AB* pages 3-8 and 3-9]. At 15 meters, it exhibits a four-leaved-clover pattern, with minor lobes broadside; at 10 and 12 meters, it's close to two full waves in phase and produces a pattern similar to that at 15 meters. It can even be used as a short 75-meter dipole–not bad for a 70-foot piece of wire.

Scaled for 28.7 MHz–43 feet, 10 inches long—the extended double Zepp gives a 3-dBd-gain, figure-8 pattern at 10 meters and a similar pattern with a bit less gain at 12 meters. It acts as two halfwaves in phase at 15 meters, with about 1.6 dBd gain and a figure-8-pattern. At 17 and 20 meters, it's somewhat long for a half-wave dipole; a tuner can make it work at 40. On all of these bands, assuming that it's at least ½ λ high at its lowest band of operation, the 10-meter EDZ is directional broadside.

There's nothing magic about the extended double Zepp. It's a tried-and-true dipole that offers useful gain at its design frequency and good multiband performance. *–Bob Baird, W7CSD*

[1]This and the other AB references in this item refer to pages in G. Hall, ed, *The ARRL Antenna Book*, 16th ed (Newington: ARRL, 1991).

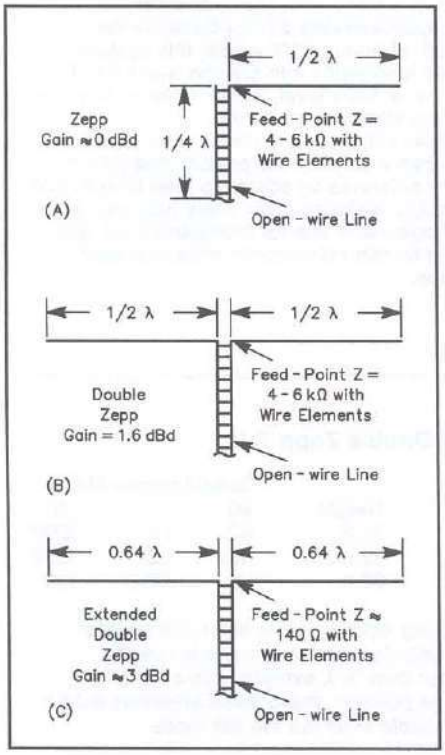

Figure 1—Evolution of the extended double Zepp antenna. At A, the classic Zepp—a ½-λ wire end-fed via an open-wire feeder operated with one of its two wires unterminated. (Antenna lore tells us that this feed method received its name from its use in zeppelin radio installations.) Commonly, Zepp systems use a feeder length of ¼ λ (or an odd multiple thereof) to transform the antenna's high feed-point impedance to a low impedance at the feeder terminals. Assuming efficient feed, this system exhibits 0 dBd gain—that is, *no gain* relative to a half-wave dipole cut for the same frequency and erected in the same position.

B shows a double Zepp, also known as *two half waves in phase* or (incorrectly) a center-fed Zepp. This is a form of collinear antenna because each ½-λ wire acts as an element, and because both elements lie along one line. It's also a *dipole*—a *full-wave* dipole that exhibits about 1.6 dB gain relative to a half-wave dipole in the same position. As with the Zepp, feeders cut to an odd multiple of ¼ λ make for least hassle feed with the double Zepp, but a good balanced antenna tuner should be able to handle whatever impedance appears at the feed-line input terminals.

A double Zepp becomes an *extended* double Zepp when you make its wires 0.64 λ long instead of 0.5 λ. Its gain increases, too—to about 3 dB relative to a half-wave dipole in the same position and cut for the same frequency.

The rough feed-point impedances shown here are for wire elements (fatter elements, such as those made of aluminum tubing, will lower these values somewhat) and convey only the resistive portion of the antennas' impedance. For more on the extended double Zepp antenna, see *The ARRL Antenna Book* and J. Reh, "An Extended Double Zepp Antenna for 17 Meters," *QST*, December 1987, pp 25-27.

Notes on Wire-Antenna Construction

Robert J. Zavrel, W7SX, seconds last month's extended-double-Zepp hint as he reports on how he keeps three EDZs high in trees for world-encompassing coverage (Figure 1) at 80, 40 and 20 meters—*Ed.*

What is a terminal DX hound to do when he suddenly moves to a rural area and has access to the stuff dreams are made of: several 100-foot-plus ponderosa pine trees atop a gentle rise in a reasonably clear area, only 500 feet from his house? The answer: *Wire antenna arrays!* A few months spent confronting the practical problems of installing three extended-double-Zepp antennas in these trees has yielded some solutions that I'd like to share.

Counterweights. Although my pines are wonderful supports for wire antennas, they have a few minor disadvantages. Among these is the fact that they sway in the wind. Because too much tension can snap antenna wires and supporting cords in strong winds, a wire-antenna engineer must compensate for variable tension in a horizontal wire antenna strung between two of these majestic plants. The textbook solution to this problem involves installing pulleys where the wires meet the trees. Ropes attached to the wire-end insulators pass over the pulleys and connect to counterweights hanging near the ground. Installed with antenna-to-counterweight lines of sufficient length, such a system also allows the antenna to be raised and lowered without further climbing.

My system includes three extended double Zepps, each fed with 450-Ω, low-loss TV twinlead. Including its supporting lines, each EDZ spans 165 feet. Counterweighting the ends of these antennas serves two purposes: It keeps tree movement from snapping them, and it keeps their wires reasonably horizontal. But how much weight is required, and what should the weights consist of? Charts exist for computing tension necessary to keep a singlewire span taut, but the presence of a twinlead feeder at the span's center renders such charts useless.

Enter experimentation! I strung the extended double Zepp, minus feed line and plus pulleys, between the two trees at about 15 feet above ground. Next, I weighed the feed line. Then I located an object of simi-

Figure 1—Proving the multiband effectiveness of the extended-double-Zepp antenna, "The W7SX Wire Farm" consists of three center-fed wires supported by three ponderosa pines that form a nearly equilateral triangle atop a small rise. (Total cost for the system, including all hardware, wire, feeders, control lines and $150 fee for the tree climber, approximately $700.) Because the ground slopes to the south at about a 10° angle, this system works best for VK, ZL and long paths into Europe and Asia. To the north, the horizon is essentially level. Table 1 shows how the antennas function on the system's three bands.

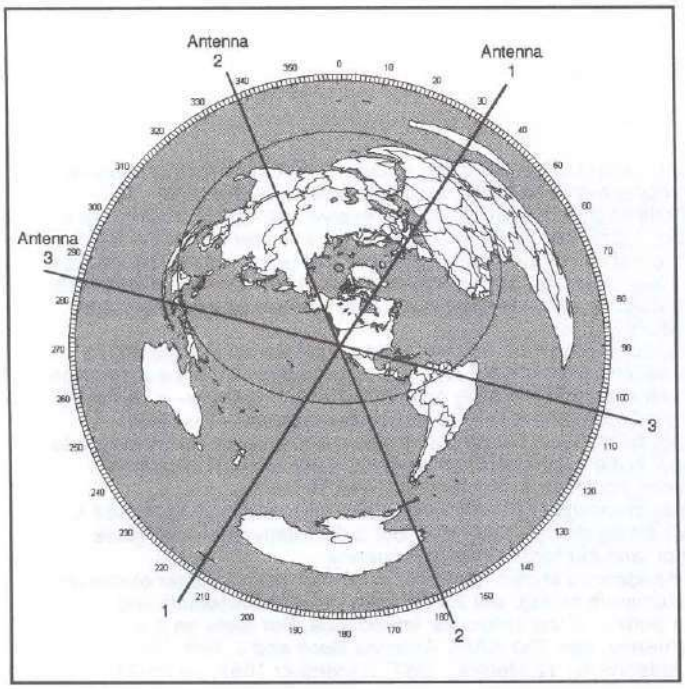

You're not a second-class citizen just because your best antenna is a dipole. You can easily set the pattern and gain of center-fed horizontal wire antennas by adjusting their length. Get the wires as high as possible, keeping them away from nearby objects, use a tuner and open-wire line for multiband feed, and have a blast! Surrounding terrain may greatly influence your antenna's DX performance.

Table 1
The W7SX Extended Double Zepp Trio

			Band/Antenna Mode		
	Length	*Height*	*80*	*40*	*20*
Antenna 1	82 ft	98 ft	SD	LD	EDZ
Antenna 2	82 ft	98 ft	SD	LD	EDZ
Antenna 3	164 ft	82 ft	LD	EDZ	LW

SD = short dipole; LD = long dipole; EDZ = extended double Zepp, LW = long wire (dipole legs 1 λ or more in length). Because a dipole longer than ½ λ exhibits gain over a half-wave dipole in the same position, these three antennas exhibit gain over a half-wave dipole in all but the SD mode.

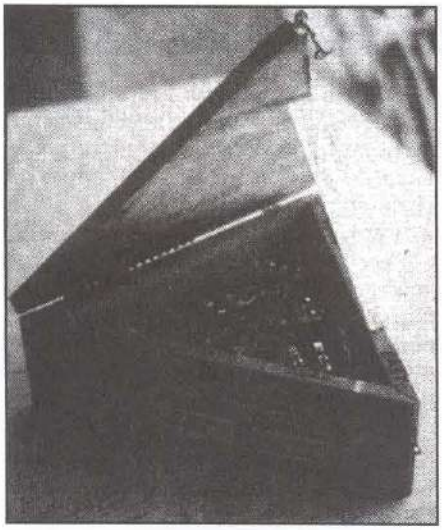

Figure 2—Bob Zavrel uses a triangular relay box to switch feeders between antennas mounted in a triangular pattern; a square box in this situation twists feeders, en-couraging antenna sway to break feeder wires. *(W7SX photo)*

lar weight, put it in a plastic bag, tied the bag at the antenna feed point, and experimented with various weights. Two 15-lb weights kept the antenna wire horizontal without overtension.

Next, I needed to construct multiple

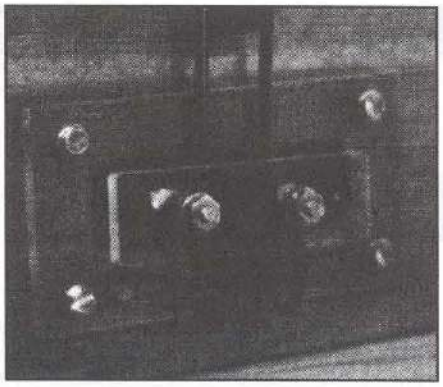

Figure 3—A combination feedthrough insulator/strain relief made of fasteners and two plexiglass plates.

15-lb weights at minimum cost—weights that had to be long and narrow to avoid collisions with the supporting trees and other nearby objects. I decided that slumpblock bricks inside a 2 × 4 wood frame would be satisfactory. (Slump blocks are long, narrow and about 12 lbs each; some are just as wide as a standard 2 × 4.) Including bricks, wood and nails, each weight cost me about $1.50, so the price was right—and 2 × 4s can be easily drilled for attaching ropes.

The relay box. A square relay box centered between three antennas twists the antennas' open-wire feeders at the feed points. I solved this problem for a triangular, relay-switched vertical array[1] and my three-EDZ system by building triangular relay boxes (Figure 2). (Use redwood, cedar or cypress and weatherproof the box with sealant.[2]) Plexiglass plates and screws insulate the feeder wires from the box, continue the feeders to the relays and provide strain relief (Fiureg 3).

Results with the system. Using a 600-W amplifier, I often get through pileups first on long path. Short path to Europe is more difficult because the ground slopes slightly upward in that direction. My blissful encounters with nature's gift to the RF enthusiast continue!–*W7SX*

[1]See Volume 3 of *The ARRL Antenna Compendium.*

[2]In my work with wire antennas, I discovered a reference on wood that may be of interest to amateurs: *Wood Handbook: Wood as an Engineering Material* (Washington, DC: US Department of Agriculture, rev 1987), 466 pages (for sale by the Superintendent of Documents, US Government Printing Office, Washington, DC 20402).This text describes, among many mechanical and structural considerations, electrical qualities of wood that come into play when wood supports are used in RF fields.

Collinear Arrays

Collinear arrays are always operated with the elements in phase. (If alternate elements in such an array are out of phase, the system simply becomes a harmonic type of antenna.) A collinear array is a broadside radiator, the direction of maximum radiation being at right angles to the line of the antenna.

Power Gain

Because of the nature of the mutual impedance between collinear elements, the feed point resistance is increased as shown earlier in this chapter (Figure 9). For this reason the power gain does not increase in direct proportion to the number of elements. The gain with two elements, as the spacing between them is varied, is shown by Figure 38. Although the gain is greatest when the end-to-end spacing is in the region of 0.4 to 0.6 λ, the use of spacings of this order is inconvenient constructionally and introduces problems in feeding the two elements. As a result, collinear elements are almost always operated with their ends quite close together–in wire antennas, usually with just a strain insulator between.

With very small spacing between the ends of adjacent elements the theoretical power gain of collinear arrays is approximately as follows:

2 collinear elements—1.6 dB
3 collinear elements—3.1 dB
4 collinear elements—4.2 dB

More than four elements are rarely used.

Directivity

The directivity of a collinear array, in a plane containing the axis of the array, increases with its length. Small secondary lobes appear in the pattern when more than two elements are used, but the amplitudes of these lobes are low enough so that they are not important. In a plane at right angles to the array the directive diagram is a circle, no matter what the number of elements. Collinear operation, therefore, affects only E-plane directivity, the plane containing the antenna. At right angles to the wire the pattern is the same as that of the individual 1/2-λ elements of which it is composed.

When a collinear array is mounted with the elements vertical, the antenna radiates equally well in all geographical directions. An array of such "stacked" collinear elements tends to confine the radiation to low vertical angles.

If a collinear array is mounted horizontally, the directive pattern in the vertical plane at right angles to the array is the same as the vertical pattern of a simple ½-λ antenna at the same height (Chapter 2).

TWO-ELEMENT ARRAY

The simplest and most popular collinear array is one using two elements, as shown in Figure 39. This system is commonly known as "two half-waves in phase." The manner in which the desired current distribution is obtained is described in Chapter 26. The directive pattern in a plane containing the wire axis is shown in Figure 40.

Depending on the conductor size, height, and similar factors, the impedance at the feed point can be expected to be in the range from about 4 to 6 kΩ, for wire antennas. If the elements are made of tubing having a low λ/dia (wavelength to diameter) ratio, values as low as 1 kΩ are representative. The system can be fed through an open-wire tuned line with negligible loss for ordinary line lengths, or a matching section may be used if desired.

THREE- AND FOUR-ELEMENT ARRAYS

When more than two collinear elements are used it is necessary to connect "phasing" stubs between adjacent elements in order to bring the currents in all elements in phase. It will be recalled from Chapter 2 that in a long wire the direction of current flow reverses in each ½-λ section. Consequently, collinear elements cannot simply

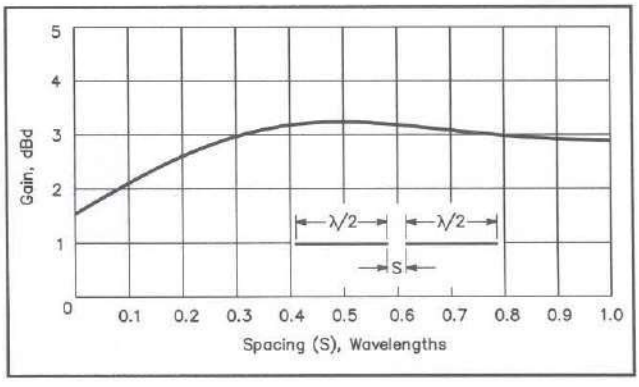

Figure 38—Gain of two collinear ½-λ elements as a function of spacing between the adjacent ends.

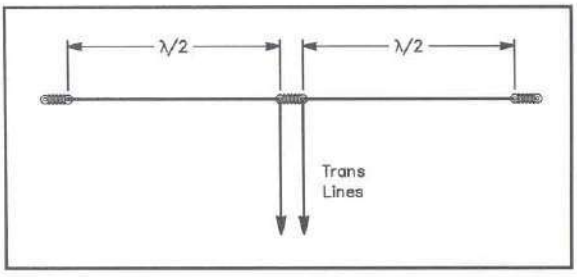

Figure 39—A two-element collinear array (two half-waves in phase). The transmission line shown would operate as a tuned line. A matching section can be substituted and a nonresonant line used if desired.

be connected end to end; there must be some means for making the current now in the same direction in all elements. In Figure 41A the direction of current flow is correct in the two left-hand elements because the transmission line is connected between them. The phasing stub between the second and third elements makes the instantaneous current direction correct in the third element. This stub may be looked upon simply as the alternate $^1/_2$-λ section of a long-wire antenna folded back on itself to cancel its radiation. In Figure 41A the part to the right of the transmission line has a total length of three half wavelengths, the center half wave being folded back to form a $^1/_4$ λ phase-reversing stub. No data are available on the impedance at the feed point in this arrangement, but various considerations indicate that it should be over 1 kΩ.

An alternative method of feeding three collinear elements is shown in Figure 41B. In this case power is applied at the center of the middle element and phase-reversing

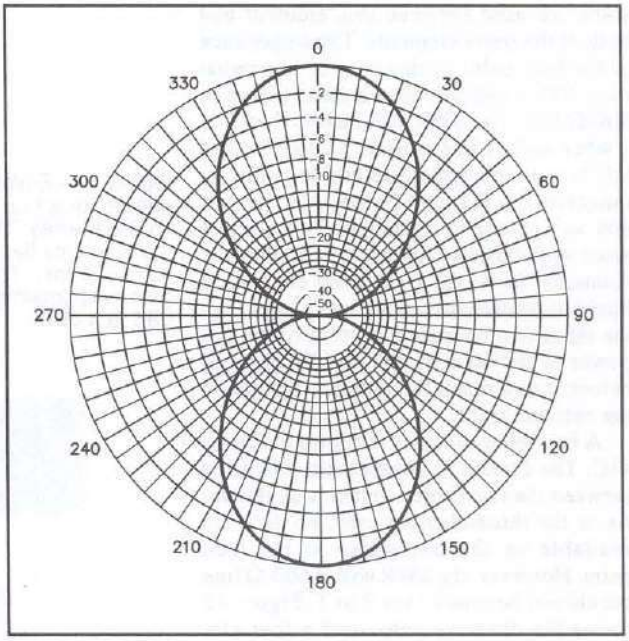

Figure 40—Free-space E-plane directive diagram for the two-element collinear array of Fig 39. The axis of the elements lies along the 90°-270° line. This is the horizontal pattern at low wave angles when the array is horizontal. The array gain is approximately 1.6 dBd (3.8 dBi).

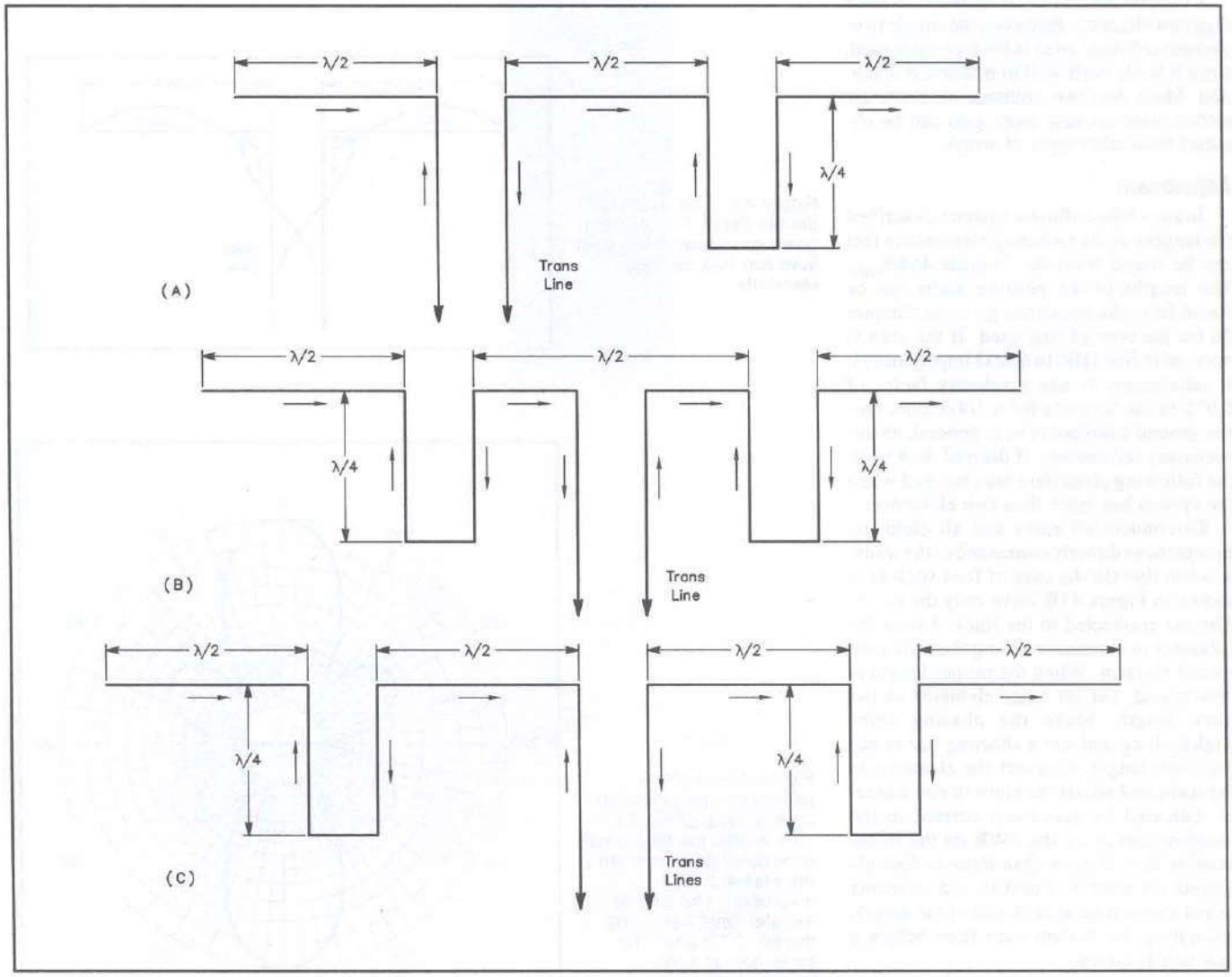

Figure 41—Three and four-element collinear arrays. Alternative methods of feeding a three-element array are shown at A and B. These drawings also show the current distribution on the antenna elements and phasing stubs. A matched transmission line can be substituted for the tuned line by using a suitable matching section.

stubs are used between this element and both of the outer elements. The impedance at the feed point in this case is somewhat over 300 Ω and provides a close match to 300-Ω line. The SWR will be less than 2 to 1 when 600-Ω line is used. Center feed of this type is somewhat preferable to the arrangement in Figure 41A because the system as a whole is balanced. This assures more uniform power distribution among the elements. In A, the right-hand element is likely to receive somewhat less power than the other two because a portion of the fed power is radiated by the middle element before it can reach the element located at the extreme right.

A four-element array is shown in Figure 41C. The system is symmetrical when fed between the two center elements as shown. As in the three-element case, no data are available on the impedance at the feed point. However, the SWR with a 600-Ω line should not be much over 2 to 1. Figure 42 shows the directive pattern of a four-element array. The sharpness of the three-element pattern is intermediate between Figures 40 and 42, with four small minor lobes at 30° off the array axis.

Collinear arrays can be extended to more than four elements. However, the simple two-element collinear array is the type most used, since it lends itself well to multiband operation. More than two collinear elements are seldom used because more gain can be obtained from other types of arrays.

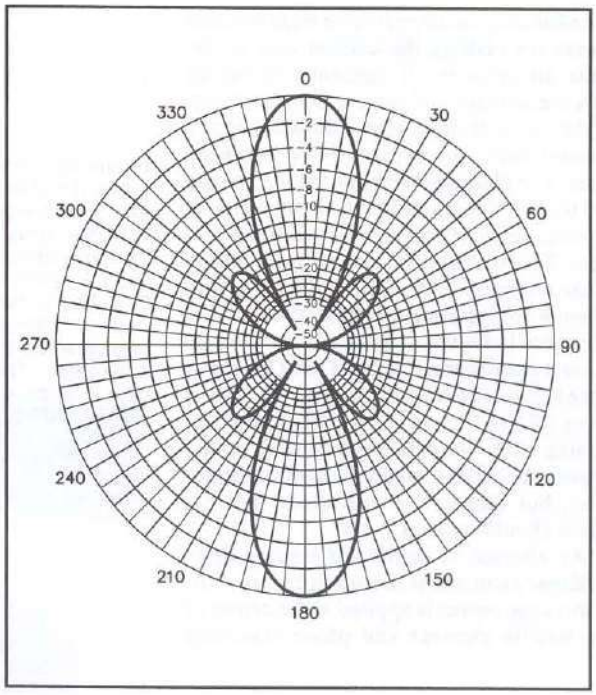

Figure 42—E-plane pattern for a four-element collinear array. The axis of the elements lies along the 90°-270° line. The array gain is approximately 4.2 dBd (6.4 dBi).

Adjustment

In any of the collinear systems described the lengths of the radiating elements in feet can be found from the formula $468/f_{MHz}$. The lengths of the phasing stubs can be found from the equations given in Chapter 26 for the type of line used. If the stub is open-wire line (500 to 600 Ω impedance) it is satisfactory to use a velocity factor of 0.975 in the formula for a 1/4-λ line. On-the-ground adjustment is, in general, an unnecessary refinement. If desired, however, the following procedure may be used when the system has more than two elements.

Disconnect all stubs and all elements except those directly connected to the transmission line (in the case of feed such as is shown in Figure 41B leave only the center element connected to the line). Adjust the elements to resonance, using the still-connected element. When the proper length is determined, cut all other elements to the same length. Make the phasing stubs slightly long and use a shorting bar to adjust their length. Connect the elements to the stubs and adjust the stubs to resonance, as indicated by maximum current in the shorting bars or by the SWR on the transmission line. If more than three or four elements are used it is best to add elements two at a time (one at each end of the array), resonating the system each time before a new pair is added.

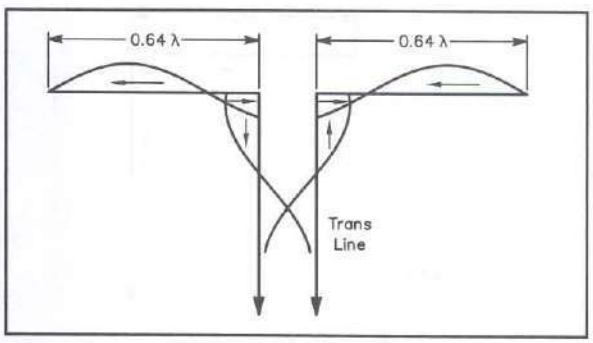

Figure 43—The extended double Zepp. This system gives somewhat more gain than two ½-λ collinear elements.

THE EXTENDED DOUBLE ZEPP

An expedient that may be adopted to

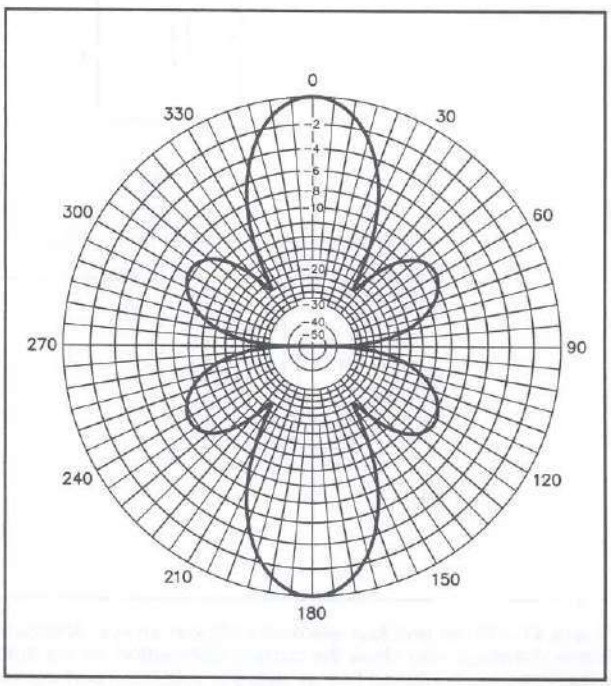

Figure 44—E-plane pattern for the extended double Zepp of Fig 43. This is also the horizontal directional pattern when the elements are horizontal. The axis of the elements lies along the 90°-270° line. The array gain is approximately 3 dBd.

obtain the higher gain that goes with wider spacing in a simple system of two collinear elements is to make the elements somewhat longer than $^1/_2$ λ. As shown in Figure 43, this increases the spacing between the two in-phase $^1/_2$-λ sections at the ends of the wires The section in the center carries a current of opposite phase but if this section is short the current will be small; it represents only the outer ends of a $^1/_2$-λ antenna section. Because of the small current and short length, the radiation from the center is small. The optimum length for each element is 0.64 λ. At greater lengths the system tends to act as a long-wire antenna, and the gain decreases.

This system is known as the "extended double Zepp." The gain over a $^1/_2$-λ dipole is approximately 3 dB, as compared with approximately 1.6 dB for two collinear $^1/_2$-λ dipoles. The directional pattern in the plane containing the axis of the antenna is shown in Figure 44. As in the case of all other collinear arrays, the free-space pattern in the plane at right angles to the antenna elements is the same as that of a $^1/_2$-λ antenna—circular.

CHAPTER SIX

WIRE BEAMS

6-1 **The K6NA 80-Meter Wire Beam**
From *The ARRL Antenna Compendium Volume 5*

6-10 **Construct a Wire Log-Periodic Dipole Array for 80 or 40 Meters**
From August 1986 *QST*

6-14 **Input Impedance of LPDA Antennas**
From October 1986 *QST* (Technical Correspondence)

6-15 **The WA1AKR 40- and 75-Meter Slopers**
From August 1980 *QST* (Technical Correspondence)

6-16 **Inexpensive 30-Meter Beam Antenna**
From June 1983 *QST* (Hints & Kinks)

6-17 **Try the "FD Special" Antenna**
From June 1984 *QST*

6-21 **Build a 4X Array for 160 Meters**
From February 1985 *QST*

6-25 **The 'BRD Zapper: A Quick, Cheap and Easy "ZL Special" Antenna**
From June 1990 *QST*

6-27 **Combination Driven Arrays**
From *The ARRL Antenna Book* 18th edition

The K6NA 80-Meter Wire Beam

Ever get crunched in a DX pileup on 80/75 meters by K6NA? Lots of folks have! K6NA reveals the secrets behind his two-element "killer" Yagi.

This article describes a practical design for a two-element, horizontal wire Yagi for the 75/80-meter band using just two support towers. Designed with DXing and contesting in mind, this radiator-and-reflector combination features moderate gain and good front-to-back ratio, combined with instant beam reversal and band-segment (mode) switching. It uses tuned feeders and a balanced-output antenna tuner at the operating position for matching at the transmitter. Remote relays at ground level handle reversal and parasitic-tuning requirements, taking advantage of the convenient properties of half-wave transmission lines.

I designed this antenna empirically, before PC-modeling programs were readily available. I've confirmed that it really works, through years of successful 80-meter operation. Later, I verified this with computer modeling. Figure 1 shows the general layout of my system.

Background

At my former location I had two towers, 70 and 100-feet high, fairly close together on a half-acre of property. There was an assortment of quads and Yagis for 10-40 meters,[1] but as is often the case with all-band DXers, the 80-meter antenna was an afterthought. Through the years I experimented with many types, looking for the "silver bullet" antenna for 80 that would finally make this challenging band a pleasure to operate.

Each season numerous magazine articles and endless discussions by experts extolled the virtues of this or that magic 80-meter DX antenna. I even tried some of them: a diamond quad loop, a delta loop (bottom-fed or corner-fed), a pair of parasitic deltas, phased quarter-wave slopers (tilted ground planes), a $\lambda/4$ vertical with lots of radials. I always came back to a basic truth: with the tower heights available, and faced with the reality of rough, rocky, lossy earth, my 95 foot high inverted-V dipole was usually as good as–or better than—any of the "trick" antennas I had spent hundreds of hours building. As a bonus, usually the dipole was quieter on receive.

Even Jim Lawson, W2PV, in an early *QST* article about broadbanding an 80-meter antenna, mentioned almost in passing that his high (110-foot) inverted-V was superior to his four-element phased vertical array, at least on transmit.[2] What I observed about 80-meter DXing in the 1970s was that most attempts using vertically polarized systems to achieve low-angle radiation were not satisfactory. This was due to excessive ground losses (both near-field return-current losses and far-field reflective losses); in addition, verticals were generally noisy on receive.

Neither vertically polarized antennas nor relatively low horizontal antennas were really getting thejob done. I resolved to construct my next station thinking about the 80-meter band from the start."High and horizontal" would be the goal.

Design Criteria

My new station would have two main towers, each 140 feet high. Because I had all-band contesting in mind, there would be numerous other antennas on the towers. I wanted to put a three-element 40-meter beam on top of one tower and a large 20-meter Yagi on the top of the other. Though it likely would be an excellent performer, a rotating beam of some type for 80 meters was ruled out because I did not want to dedicate the top of one tower to it. Also, there was the near-certainty of difficult maintenance problems with such a gigantic antenna. Instead, I settled on a design for a fixed-wire beam. These would be the main criteria for reliable, day-to-day operation:

- Oriented properly for best results in both DX and domestic contests
- Moderate gain, with a wide lobe for good azimuth coverage
- Instant beam reversal with a decent front to-back ratio
- Near-instant band-segment (phone or CW mode) switching, especially for casual, daily DXing
- Easy, low-loss matching anywhere in the band
- Horizontally polarized to minimize both ground-reflection losses and noise on receive
- High enough to produce reasonably low angle radiation
- Reliable and easy to maintain without disrupting other antennas on the towers.

Design Discussion

Some discussion of these interrelated design criteria will aid in understanding the trade-offs and choices I made while planning this antenna. For example, from San Diego the typical short path to Europe on 80 meters *is not* the expected true Great-Circle path of about 25°. Rather, the short path toward Europe is almost always a "bent" or skewed path, where signals pass to the south or southeast of the highly absorptive auroral oval, propagating by means of a scatter mode that uses ionized patches over the central Atlantic Ocean. Consequently, our pseudo short-path heading toward Europe is commonly 50° to 90° in azimuth. Occasionally, European signals on 80 meters arrive in California from the southeasterly direction. Rarely, around the time of the Equinox, they may even arrive by scatter path from straight south, as reported by some rotary beam users in California.

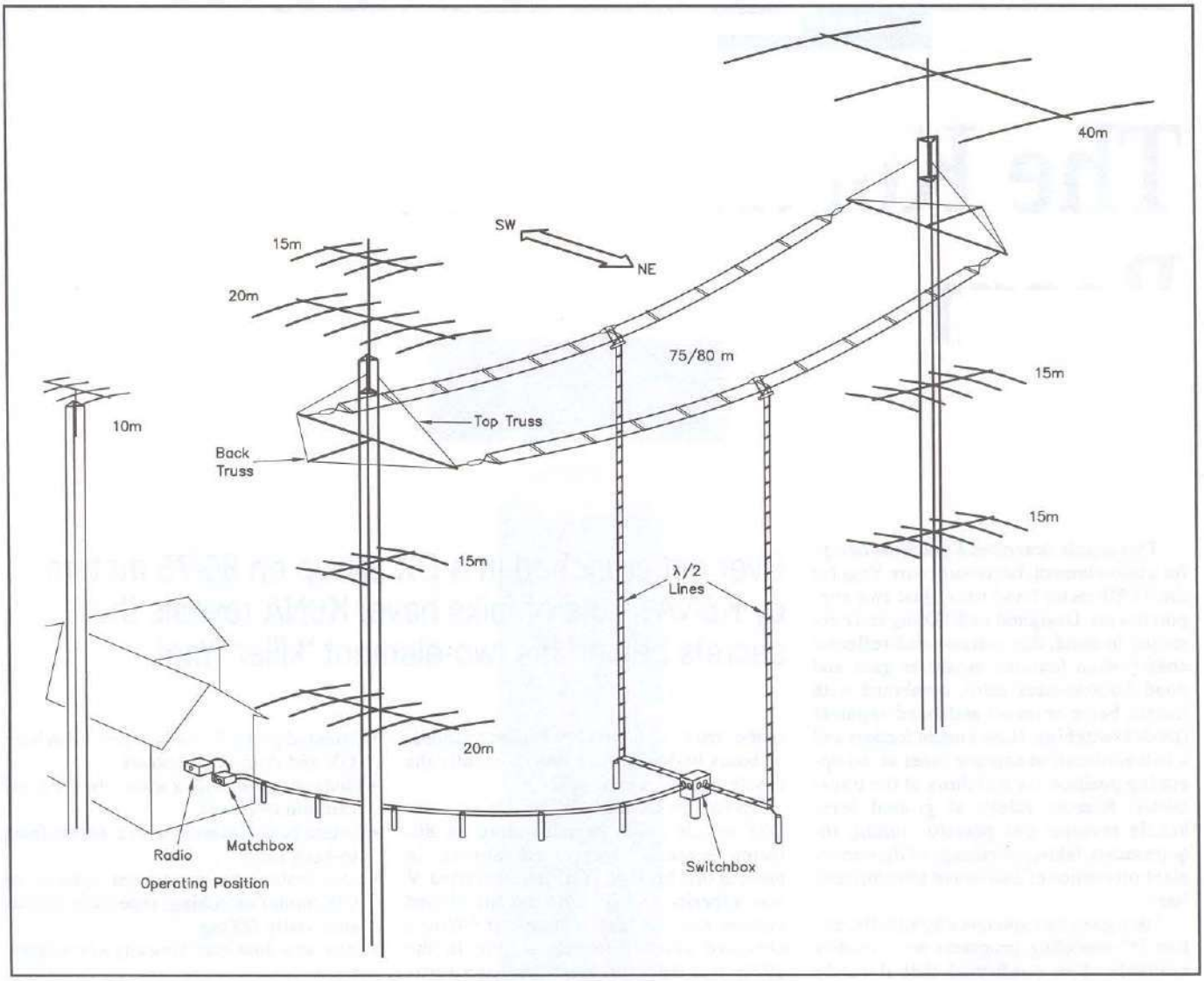

Figure 1—The antenna farm at K6NA, showing the 80-meter wire beam installed on the pair of 140-foot towers, using 35-foot long crossarms made of aluminum tubing and fiberglass. The rearward truss and upper truss wires make each crossarm rigid. For clarity, the tower guy wires are not shown.

I decided to orient the two support towers so that the reversible wire beam, slung between the towers on a pair of horizontal crossarms, would point at 60°/240°. This would provide good coverage across the USA and into Europe (both short and long path), Africa, the Caribbean and South Pacific areas, which together make up about 85% of my annual QSOs on 80 meters.

I could build a simple two-element parasitic design, using λ/2 elements on a reasonable boomlength of about 35 feet, or λ/8.[3] Figure 2B shows that such a design has a half-power azimuth beamwidth of about 74° in the azimuth plane. I was willing to accept the slightly lower gain and front-to-back ratio compared to a three-element design (which would be more difficult mechanically), or a two-wire phased array using double-extended Zepp elements. The Zepp would require the towers to be placed about 350 feet apart. Either of these antennas conceivably would provide more gain, but at the price of reduced azimuthal coverage. A reversible, all-driven array has the additional disadvantage that its phasing and matching networks become overly complicated to make it work properly at both ends of the band.

To achieve the twin requirements of easy mode-switching and beam reversal, I decided to construct a symmetrical, two-element Yagi beam. The elements are identical dipoles, self-resonant near 3.675 MHz. This frequency is about 3% to 4% lower than the phone operating area around 3.800 MHz, meaning that each element could be used as a reflector in the phone band with no additional loading. Each dipole is fed with λ/2 of open-wire line. These lines come together in a relay box at ground level. Power is applied to one or the other driven element, and a short is applied across the base of the remaining feeder to force the remaining element to act as a parasitic reflector.

To operate near 3.5 MHz, the reflector simply is retuned to about 3.4 MHz, using an inductor in place of the direct short in the relay box. Supplying RF to the relay box is accomplished using low-loss, open-wire feeders. A balanced-output tuner in the shack is simply touched up to move between phone and CW subbands, and to accommodate the change in SWR. There is no requirement for an exact match at the line input to the driven element because of the low-loss transmission lines.

With the crossarm supports mounted at 130 ft, the dipoles are about λ/2 high and thus produce fairly low-angle radiation. A horizontally polarized antenna is less responsive to man-made noise sources, which have a large vertical component. The height allows λ/2 lines to reach down to the switchbox near ground level. All switching relays are in this weatherproof box, so the system is reliable and easy to maintain. No inaccessible relays or matching networks are up at the elements, where failures might occur.

Construction

No doubt, the 80-meter wire beam can be built and integrated into many existing

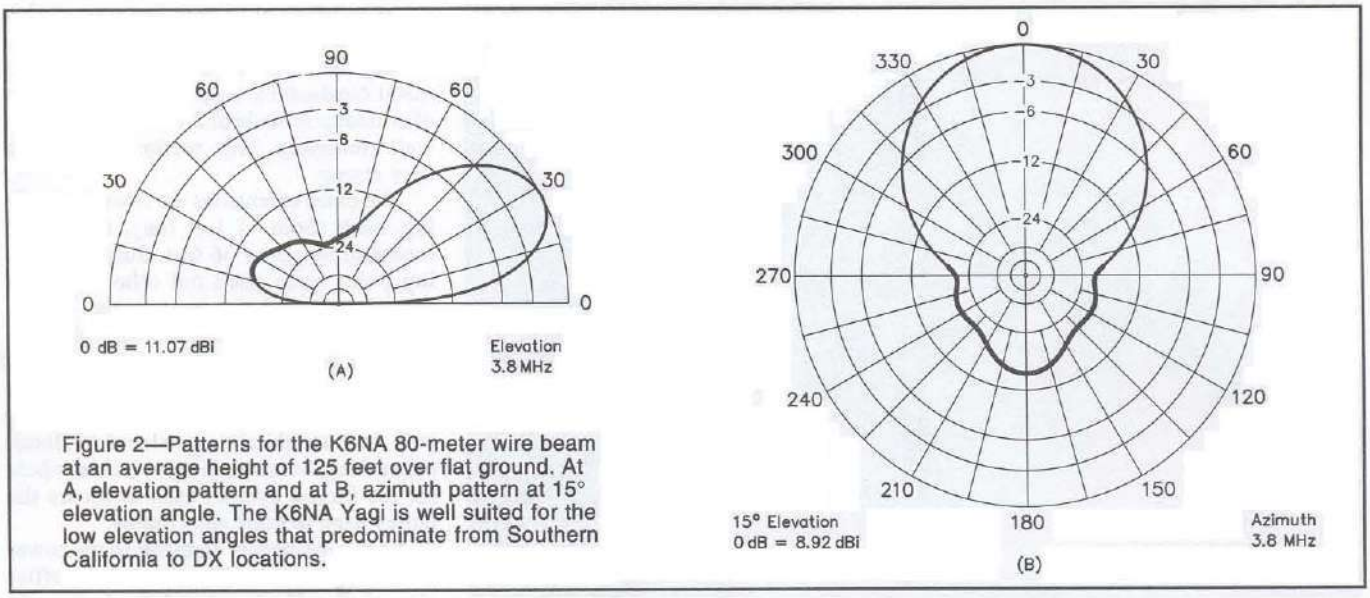

Figure 2—Patterns for the K6NA 80-meter wire beam at an average height of 125 feet over flat ground. At A, elevation pattern and at B, azimuth pattern at 15° elevation angle. The K6NA Yagi is well suited for the low elevation angles that predominate from Southern California to DX locations.

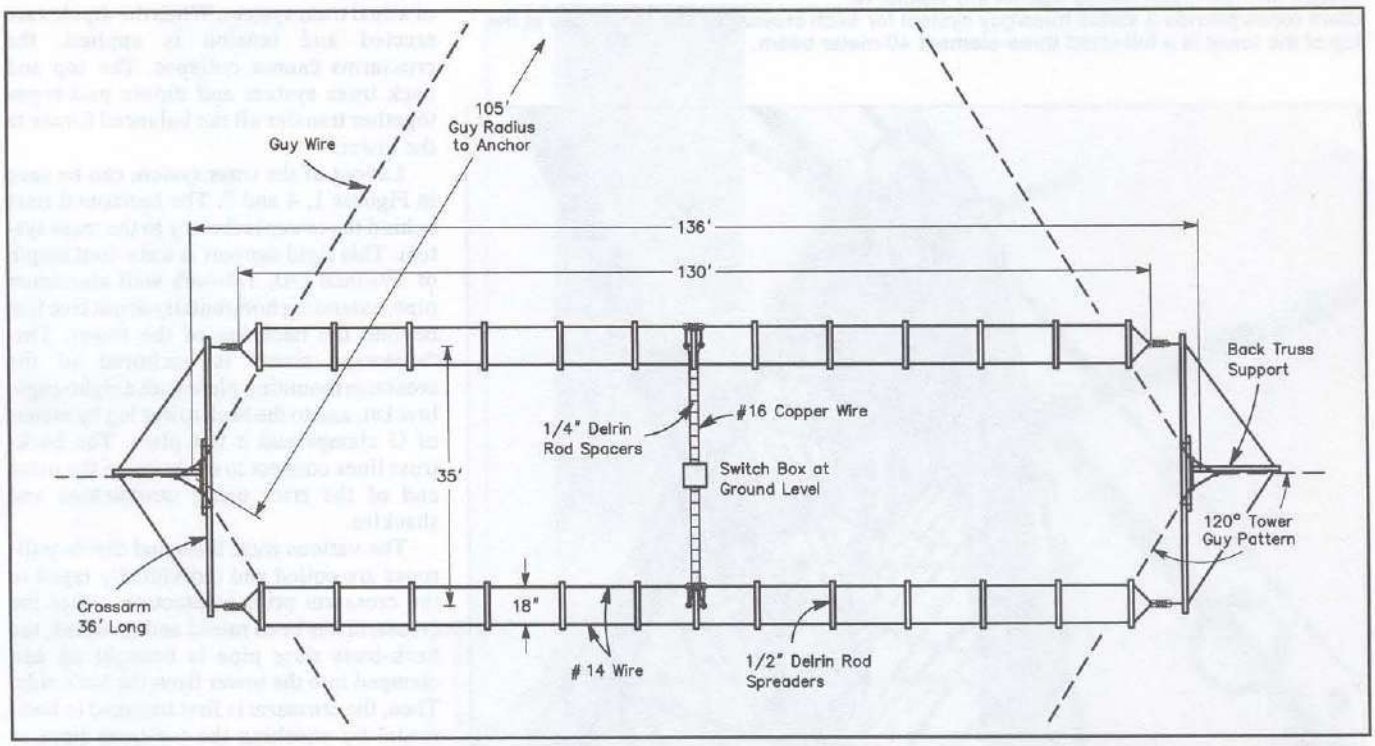

Figure 3—Top view of the 80-meter wire beam mounted on the towers, with details of the crossarms and rearward truss system that prevents the tensioned antenna wires from bending the crossarms inward. The tower-guy placement geometry provides several advantages for antenna-farm management! See text.

multi-tower systems. I had the luxury of planning the tower and guy arrangement well in advance of building the antenna. This helped make erection and maintenance simpler. Such planning contributes to convenient erection of other antennas too!

Figure 3 shows the recommended two-tower layout that has served very well for this and other projects. Through symmetry of guy-anchor placement, any forces due to loading by wire antennas or temporary trams are balanced out. Note that each tower has an opposing, backward-facing guy exactly in line with its counterpart and parallel with the centerline of the towers.

When the 36-foot crossarm is mounted about 10 feet below the top of the tower and the topmost guy bracket, the ends extend out beyond and above the sloping, upper guys. This arrangement keeps the dipoles in the clear, allowing them to be raised and lowered using ropes and pulleys with minimal guy-wire interference, without having to remove or move the crossarms.

This tower/guy layout also presents two parallel tower faces on which to mount the booms and to correctly orient the wire antenna. Non-parallel tower faces can work, but the mounting brackets would be more complex and some advantages of symmetry would be lost. For safety, significant sideloads should be distributed across *at least two* tower legs. In addition, guys passing through the central area between the towers would complicate the raising and lowering of the wire antennas, so this should be avoided if possible.

Another advantage of the layout in Figure 3 concerns the overall use and maintenance of other antennas in the system. Note that the 140-foot towers are 136 feet apart, and the guy radius (distance from tower to each of its guy anchors) is 105 feet. These facts, together with the generally uncluttered work area between the towers, make

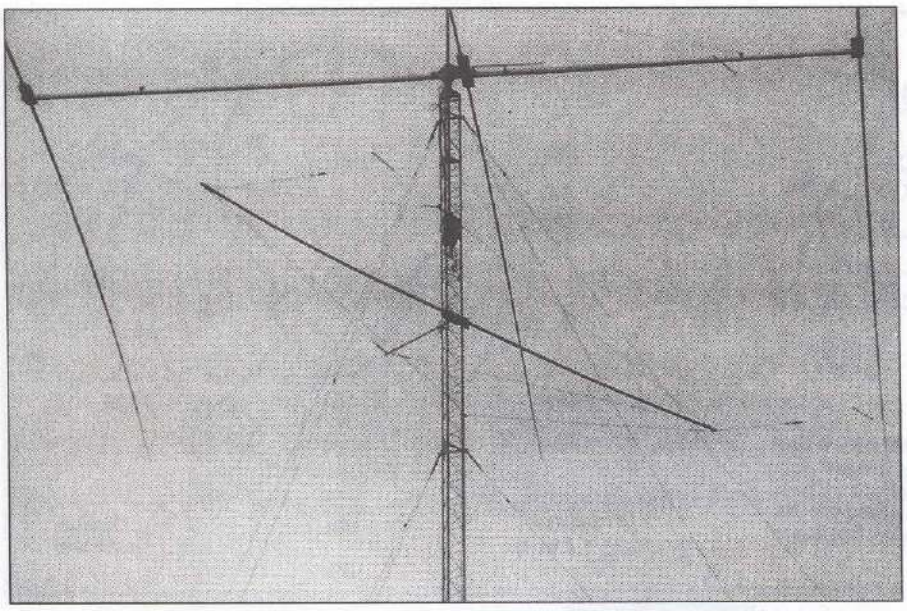

Figure 4—Photo of one of the crossarms (booms) mounted on the tower. The truss system and 80-meter folded dipoles are visible. Note that the truss, dipoles and pull-down ropes provide a stable truss/guy system for each crossarm. The large Yagi at the top of the tower is a full-sized three-element 40-meter beam.

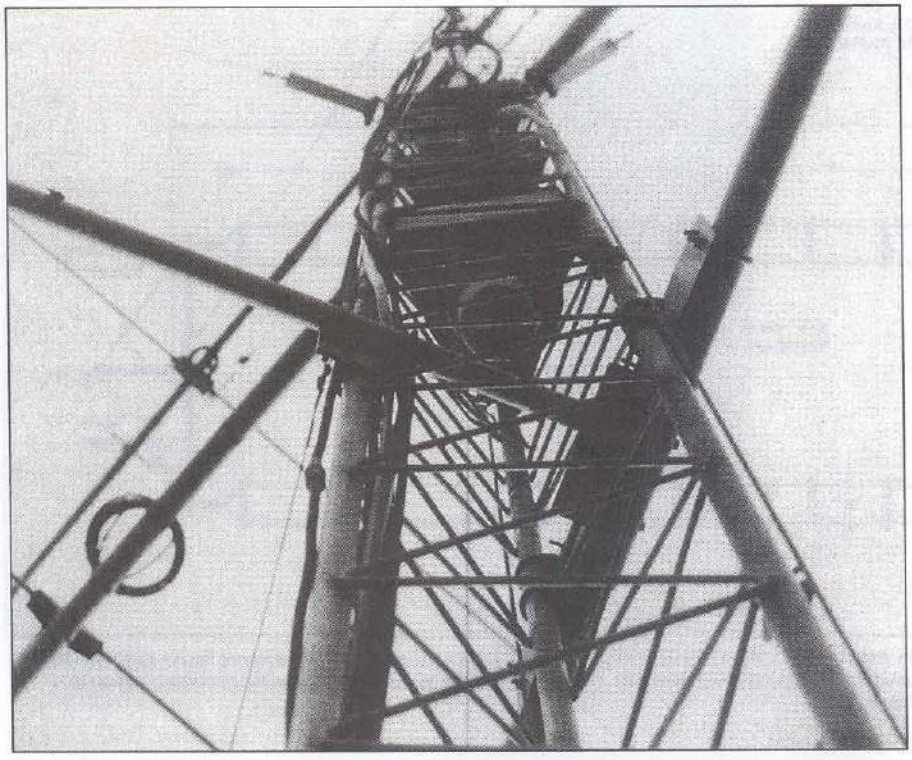

Figure 5—Photo showing mounting method for installing the 80-meter crossarm and associated horizontal back-truss pipe. The horizontal riser prevents the crossarm from collapsing when the side load (antenna tension) is applied. Note how a plate with U-bolts is used to secure the back-truss pipe to one of the tower legs, while the other end is secured with an L-shaped bracket and U-bolts to the mounting plate for the crossarm.

it convenient to run a temporary tram wire anchored at the base of one tower to the top (or anywhere along the length) of the other tower. The tram can be used to raise the 80-meter crossarms themselves, or to move other HF Yagis. If an upper-mast-mounted beam is to be erected, the 80-meter wires first can be lowered easily to the ground. If the tram has to reach only to the area of a side-mounted beam, the wire antenna may stay in place above it. I can detach the 80-meter feeders from the feed-through insulators at the switchbox, and pull them away from the vicinity of the tram wire, if necessary.

Crossarms and Trusses

I made each crossarm (boom) using aluminum and fiberglass. In order to eliminate the possibility of "boom resonance" that might interfere with nearby HF Yagis and to keep the 80-meter wire ends away from metal conductors, only the middle 14 feet of crossarm is made of 2-inch OD, 1/4-inch wall aluminum. This section is stiff and very strong.

The outer extensions are fiberglass tubing, each about 11 feet long, for a total crossarm length of 36 feet. Surplus vaulting poles were used but other types of fiberglass would also be suitable. The fiberglass should be wrapped with high-quality black tape (such as Scotch 33 or 88) to prevent decomposition due to ultraviolet radiation. At the end of each fiberglass pole, I mounted a six-inch sleeve of aluminum tubing, before drilling a clearance hole for the forged eyebolt used to secure the pulley used to hoist each dipole.

Each crossarm is clamped to the tower face using an aluminum plate and muffler clamps. See Figures 4 and Fig 5. Once in place, the crossarm is made rigid by means of a dual truss system. When the dipoles are erected and tension is applied, the crossarms cannot collapse. The top and back truss system and dipole pull-ropes together transfer all the balanced forces to the tower.

Layout of the truss system can be seen in Figures 1, 4 and 5. The horizontal riser behind the tower is the key to the truss system. This rigid support is a six-foot length of 1½-inch OD, 1/4-inch wall aluminum pipe, extending horizontally about five feet beyond the back leg of the tower. This "sideways riser" is anchored to the crossarm mounting plate with a right-angle bracket, and to the back tower leg by means of U clamps and a flat plate. The back-truss lines connect to eyebolts on the outer end of the riser using turnbuckles and shackles.

The various truss lines and dipole pull-ropes are coiled and individually taped to the crossarm prior to erection. After the crossarm has been raised and installed, the back-truss riser pipe is brought up and clamped into the tower from the back side. Then, the crossarm is first trimmed to horizontal by attaching the top-truss lines to the tower legs and adjusting the turnbuckles until the crossarm looks good, much like a Yagi boom truss is adjusted. Then the backtruss lines are untaped from the crossarm, one at a time, and connected to the far end of the horizontal back-truss pipe. This is an interesting maneuver, which should be accomplished only by an experienced climber/rigger! The turnbuckles are adjusted initially for moderate tension. Properly adjusted, the result is a crossarm that doesn't sag downward or fold inward when antenna tension is applied.

After the truss system has been rigged, the installer untapes one of the coiled-up dipole pull-ropes, which has been pre-rigged to extend along the arm to the outer crossarm pulley and back again to the vicinity of the tower. By attaching either a weight or tag line to the thimble, the di-

pole-end of the rope is released to hang vertically from the pulley. The rigger then pays out the coiled rope until a ground man can reach the thimble end to attach the dipole insulator. The pull-ropes ultimately are brought to the tower legs through pulleys and thence brought down to ground level. The angle of the pull-ropes completes what is essentially a four-point guy on each end of the crossarm (antenna tension, back-truss, up-truss, and angled pull-down rope). This configuration presents a stable structure when the dipoles are raised and tension applied.

I must emphasize that all subassemblies should first be fabricated and fitted to the tower at ground level. Make sure that all plates, clamps and hardware mate to the tower, referenced to diagonal braces, welds, or leg bolts. Premark the tower legs up at the target location ahead of time to preclude surprises on the tower!

Construction of the Dipoles

Two-wire folded dipoles were selected to help bring the feedpoint impedance up closer to the characteristic impedance of the feeders and to improve bandwidth. This helps minimize tuner adjustments when moving within a subband, but there is no need to go overboard trying to effect a perfect match at the load.

Each folded dipole is built with #14 stranded, non-stretch copper wire. The two parallel wires are held apart by seven horizontal spreaders located about every 20 feet along the wire length. These spreaders of black Delrin are 1/2-inch diameter rod, 18 inches long (See Figure 6). They are held in position by tie wires, as are the ribbed end insulators. I used an unbroken length (about 260 feet) of wire for each two-wire dipole, making the free ends come together at the center-feed insulator. The free ends of the wires and feeders are tied to the center insulator for strain-relief, and then the loose ends are soldered. This technique prevents breakage, because soldered connections (which are weaker due to wire heating) are not under strain, or flexing. After each dipole is assembled on flat ground, it should be stretched temporarily at low level between the towers in order to check the symmetry and mechanical behavior. When adjustments are complete, the feeder can be soldered to the antenna.

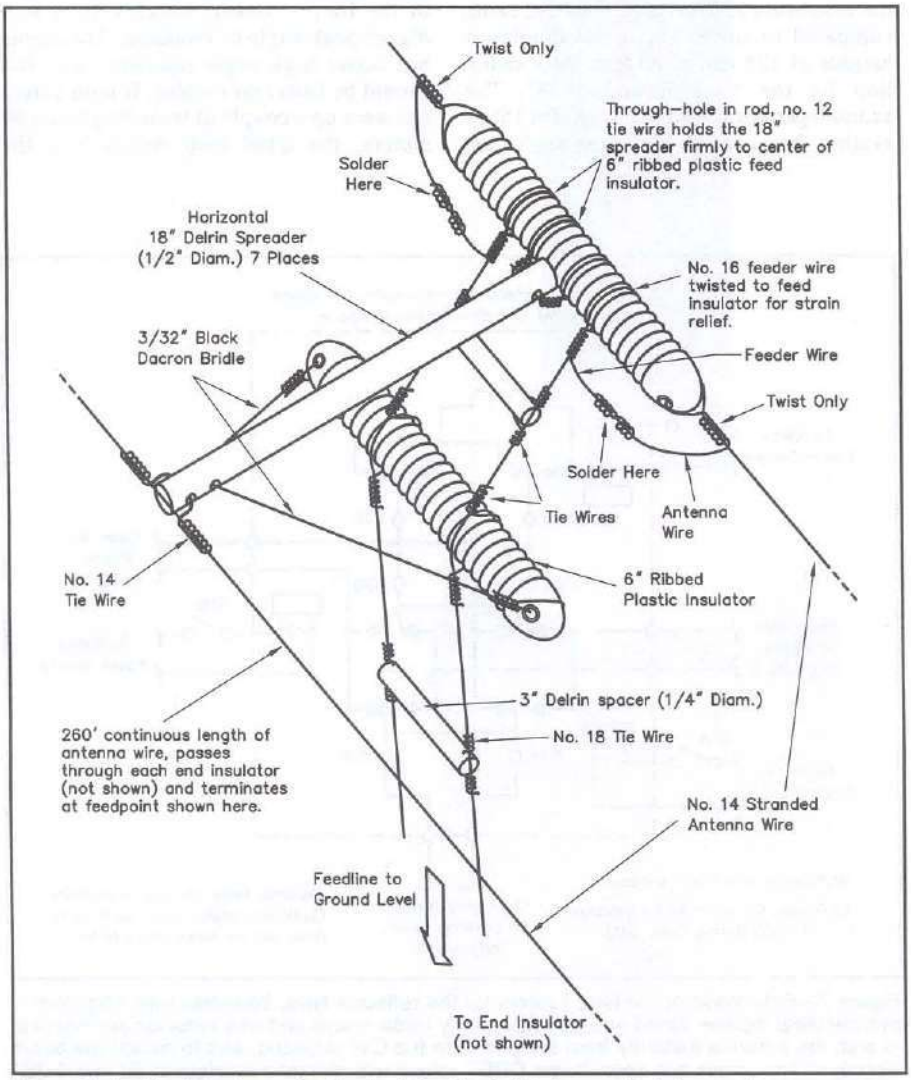

Figure 6—Folded-dipole center feedpoint with stabilizing cradle. The cradle encourages stability in the large, two-wire dipoles, preventing twist. See text.

There is little point in making any sort of analyzer measurements at five feet off the ground because the results will be misleading. When the dipole is installed in the clear at a half-wavelength in height, it will perform as predicted. However, just to be sure, I grid-dipped one dipole at its final height through the half-wave line. I had first built the $\lambda/2$ transmission line and had checked for resonance near 3.650 MHz with a grid-dip meter. When the first dipole and its feeder are on frequency, the second dipole and feeder was cloned and the array was erected. The dipoles at K6NA are about 130 feet long.

Feed Line Construction

Each feed line was constructed using old techniques but modern materials. Minimum weight is very important. The lines were made about 130 feet long, using #16, prestretched solid copper wire. Spacers are 1/4-inch Delrin rods, three inches long and spaced every four feet along the feeder. Spacers were notched and drilled, and held in position using #18 copper tie wires through the holes. The result is a very lightweight, low-loss feeder with a characteristic impedance of about 575 Ω.[4] To minimize sag in the dipole, avoid using heavy ceramic spacers.

A good technique for constructing the long, open-wire feeder is to stretch two wires tightly between the towers about four feet above the ground. Space the wires three inches apart in a plane parallel to the earth. Precut all the tie wires and make a simple, four-foot long, interval-measuring rod from a piece of wood or tubing. With all the spacers, tie wires, rod and long-nose pliers in a tool bag, the installer begins at one end, moving easily along the line, installing spacers at the correct intervals. The feeder wires sit in the notched ends, while the tie wires pass through the holes and are twisted in place over the feeder wires. When complete, the suspended line is in a good position for checking resonance with a grid-dip meter, assuming the line is insulated from the towers. The final length of each feeder described here is about 128 feet and each weighs less than three pounds.

Some additional comments about feedpoint construction will be helpful to those planning assembly of such a large, wide-spaced folded dipole and associated feeder. Initially, the dipole was built with upper and lower wires, as depicted in most antenna books. An 18-inch Delrin rod connected the lower feed insulator to the upper wire in order to distribute the weight of the feeder onto both wires and to maintain correct spacing. This worked, but with unforeseen side effects. When the dipole was raised under tension, the result was a half-twist in the parallel wires about halfway back toward the end insulator. This twist was not due to "live" or "kinky" wire! The twist was due to a catenary sort of effect.

The solution to the twist problem is to avoid the upper wire/lower wire configuration, and allow all the spreaders (including

the center spreader) to lay over into the horizontal plane. To encourage this, a simple cradle was constructed to distribute the weight of the feeder at the center of the two antenna wires. This forces the wires (and all the other balanced spacers) to form a plane parallel to the earth. Fig 6 shows the centering cradle below the Delrin rod. The feeder passes over the cradle insulator (tie wires take the load) and continues up to the feedpoint. Small Dacron lines tie the cradle insulator to the other end of the rod, keeping the load centered. These large folded dipoles have been well behaved, even in high winds.

Remote Switching

A plywood "doghouse" was constructed under the antenna center, and mounted about four feet above ground for convenience. Fig 7 is a schematic of the switching network housed in the box. Two DPDT relays control the direction of the beam pattern. The main feeder connects through K1 and K2 to one dipole, while the other dipole becomes a phone-band reflector due to the short across K3. In the shack, switch S1 activates K1/K2 for reversal. S2 is a phone/CW selector switch that allows K3 to retune the reflector element to about 3.4 MHz by means of an inductor. Relays are large, ceramic-base open-frame types.

The center-loading inductor for a CW reflector is best chosen experimentally. A coil is connected across K3, S2 is set for CW, and the tuner in the shack is adjusted for a match low in the CW band. From the tuner, a coax cable is routed temporarily back to the switchbox. At the box, the temporary coax feeds a receiver, which is used to monitor signals arriving off the back of the antenna around 3.515 MHz. A variable tap is moved along the coil until the best front-to-back ratio is obtained. After a period of testing, the tap can be soldered. With the dipoles self-resonant around 3.650 MHz, a CW reflector coil of about 17 µH was required. This consisted of a 2-inch OD coil, $2^3/_4$-inches long, on which were wound about 25 turns of #16 wire.

Operation and Maintenance

The 80-meter wire beam performs as expected. Typical F/B is 11 to 14 dB on both phone and CW modes. For high-band operators accustomed to quiet bands with low atmospherics, this level of F/B may not seem like much. However, on a consistently noisy band like 80 meters, this kind of rejection on receive is very important. The high wire beam makes it possible to work long-path Europeans (southwest heading, before sunrise in San Diego) on a regular basis in the winter months, due to effective rejection of storm noise over North America. The antenna performance is roughly comparable to that of a nearby, two-element rotary beam (195 feet high) at N6ND—we hear and work many of the same weak stations during DX sessions. In domestic contests, reports from the East Coast are excellent on both modes.

The wire beam has been very reliable for over 10 years. The first version of the antenna used #16 solid-copper wire for the elements, and there was a broken wire or two after perhaps six years. The antenna was rebuilt in 1992 with #14 stranded wire and has been perfect since then. The original dipole pull-ropes of black, 1/4-inch polypropylene lasted about seven years before they were replaced. Black Dacron, readily available from several *QST* advertisers, would be an excellent replacement for the pull-ropes, but it is more expensive than polypropylene. Do not use any color except black, and do not use polyethylene lines for permanent antenna supports.

Antenna Comparisons and Modeling

Recently, I wanted to investigate this 80-meter wire beam using computer modeling. By comparing the predicted performance of this antenna with that of several other common types of 80-meter DX antennas, the relative merits of each can be described briefly. Example antennas were modeled over average earth, with a dielectric constant of 13 and a ground conductivity of 5 mS/m. Gain figures listed are referenced to an isotropic antenna in free space.

Fig 8A shows the elevation pattern of the wire beam 125 feet high over real earth, compared to single horizontal dipoles at heights of 125 and at 70 feet. Peak radiation for the Yagi occurs at 28°. The azimuth pattern shown in Fig 8B is at 15° elevation, because low elevation angles are required for success on most DX paths from Southern California. For example, the W6 short path to Europe supports signals between 8° and 18° elevation, essentially 100% of the time.[5] The Yagi has about 5 dB of gain over the high dipole.

Note that a single high dipole is an excellent DX performer, and likely will beat any sort of beam antenna on a 70 to 80-foot tower. In addition, a high dipole has better rejection of local (high-angle) signals, so it will be a superior DX receiving antenna. Inspection of Figure 8A indicates that the high wire beam probably will outperform a 70-foot high dipole by nearly 10 dB at low elevation angles.

Some people might say: "With 140-foot towers, you should be using quad loops!" Not so fast. Figure 9A shows that with the top of a diamond-like, full-wave loop at 135 feet, the λ/2 dipole at 125 feet is superior by at least 1 dB at all angles lower than 40°, in spite of the small stacking gain expected from the loop. The expected gain from the bigger loop cannot be realized fully because the upper and lower wires are at drastically different heights (in terms of fractional wavelengths) relative to each other and the earth. This prevents proper phase addition. Further, the average height of the loop is lower, which results in a higher peak angle of radiation. The dipole has better high-angle rejection, too, and should be better on receive. If both antennas were up a couple of wavelengths on 80 meters, the quad loop would beat the

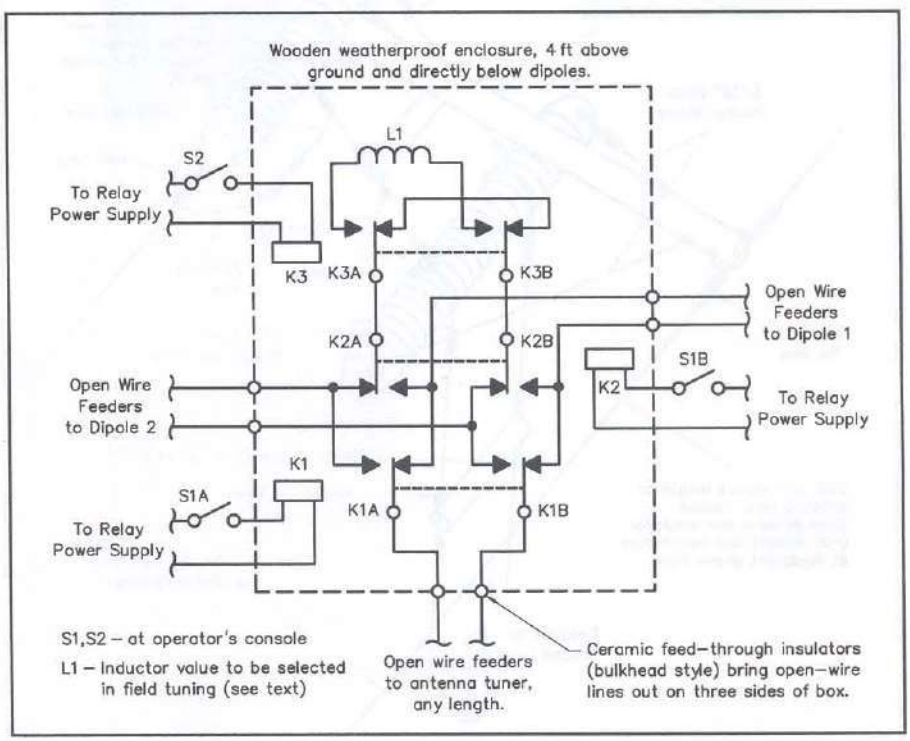

Figure 7—Schematic of the feed system for the reflector-type, 80-meter wire Yagi. With two identical dipoles tuned at 3.650 MHz, only three relays and one inductor are needed to shift the antenna instantly from the phone to the CW subband, and to switch the beam direction. The relays are open-frame DPDT relays with ceramic insulation. S1 is a DPST switch used to reverse the beam direction by activating K1 and K2. S2 activates K3 to tune the parasitic element as a CW reflector.

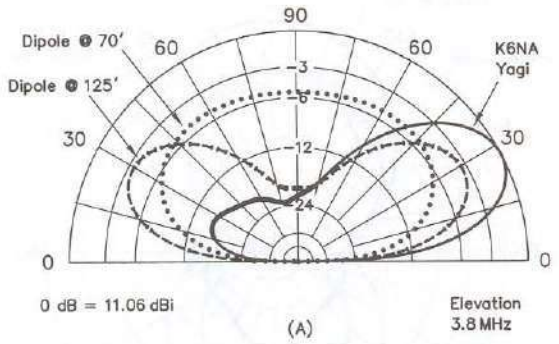

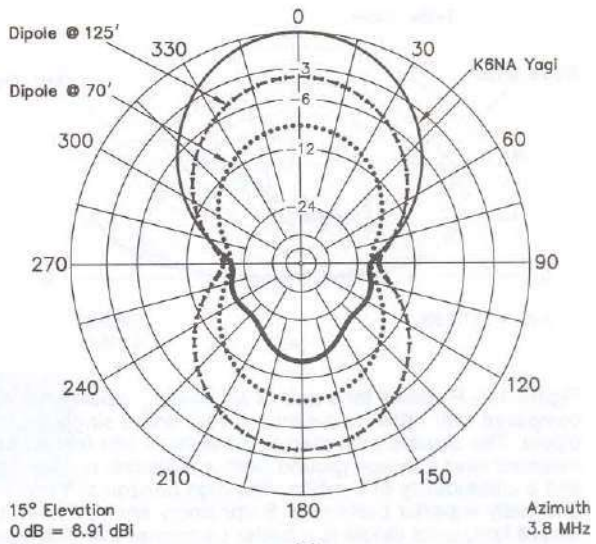

Figure 8—Comparison of patterns for K6NA two-element Yagi at 125 feet with two dipoles, at 125 and at 70 feet heights. At A, elevation pattern comparisons and at B, azimuth pattern comparisons.

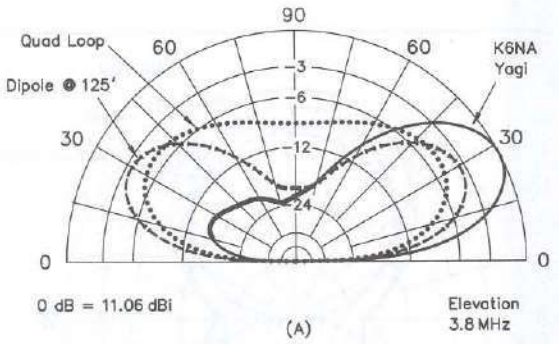

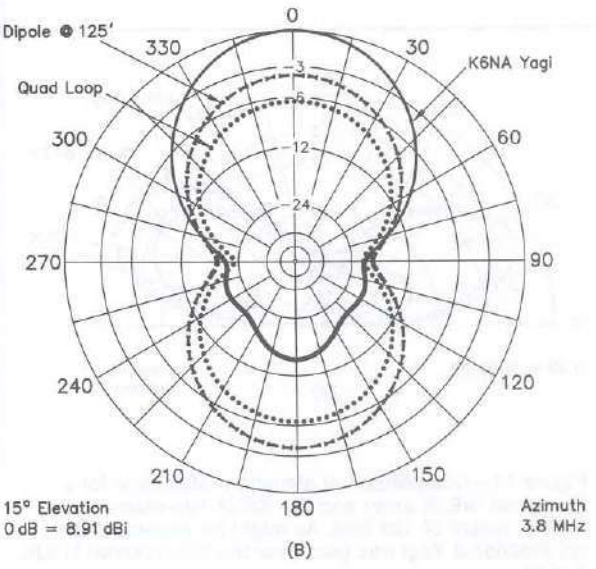

Figure 9—Comparison of elevation responses for full-wave diamond-shaped loop, K6NA two-element Yagi and a single horizontal dipole. The Yagi and dipole are at a height of 125 feet and the loop's apex is at 135 feet.

dipole...but who has a 550-foot tower?

How about a pair of half-wave slopers (that is, tilted vertical dipoles) tied from the tops of the 140-foot towers one λ/2 apart, and fed in phase for broadside gain? See Figure 10A. All the antenna books show the phased-sloper array to be a 4 dB gain, low-angle monster. The author had this exact antenna up for a few months in 1980. It performed fairly well, but was very responsive to powerline noise. For comparison, a single horizontal dipole was hung between the towers a few feet above the top ends of the slopers. With this single dipole, my local noise level dropped by 8 to 10 dB, and stations in New Zealand reported a consistent transmit advantage over the sloper array. This was a real eye-opener. As seen in Fig 10A, the high wire beam *buries* the phased slopers by 7 dB at the peak angle of 28°, and by 5 dB at 15° elevation!

The famous W8JK is a bi-directional, all-driven wire beam made from two dipoles fed 180° out of phase. At 125 feet in the air, this antenna has excellent rejection of high-angle signals, and is only slightly down from the peak gain of the Yagi configuration. See Figure 11A. It requires no relay box. For DXing, it is inferior to the Yagi because there is no way to reject signals (noise) off the back. Years ago, the author fed the two new folded dipoles as a W8JK for a few months prior to building the switchbox. It performed much like the patterns show, but once the switchbox was available to configure the array as a Yagi with good F/B ratio, the W8JK configuration was abandoned. However, a W8JK antenna 100-feet high in Kansas City would be an outstanding Sweepstakes antenna.

Figure 12 compares the horizontal wire beam to a similar antenna with inverted-V elements with a 90° included angle. The V-style gain is down a bit and the pattern is not as clean. But if you have a single tall tower and install this antenna (only one crossarm is required), you will be in the 95th percentile of effective 80-meter DXing antennas.

In Figure 13 the K6NA Yagi is compared to a quarter-wave vertical mounted over average ground. Since there are less losses due to ground reflection characteristics, horizontal polarization allows the Yagi to outperform substantially the verti-

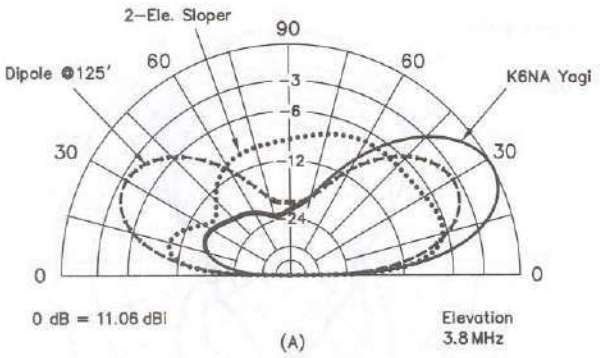

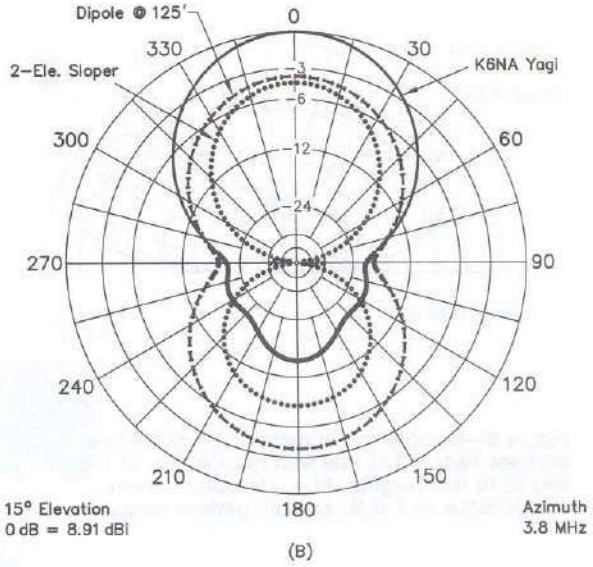

Figure 10—Patterns for a pair of λ/2 sloping dipoles fed in phase, compared with K6NA two-element Yagi and a single horizontal dipole. The slopers both start at a height of 140 feet and are mounted over average ground, with a dielectric constant of 13 and a conductivity of 5 mS/m. The high horizontal Yagi is a decidedly superior performer. Surprisingly enough, even the simple horizontal dipole is a better performer than the phased-sloper system. This is mainly due to far-field losses experienced by the mainly vertically polarized sloper system.

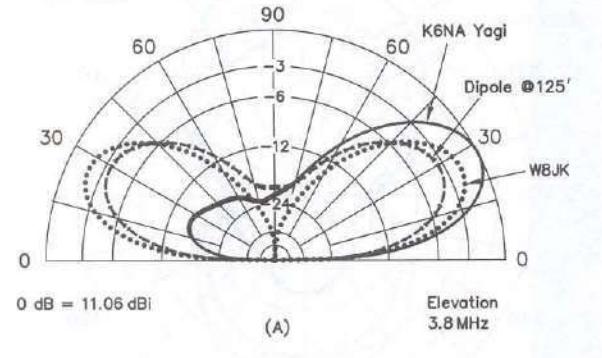

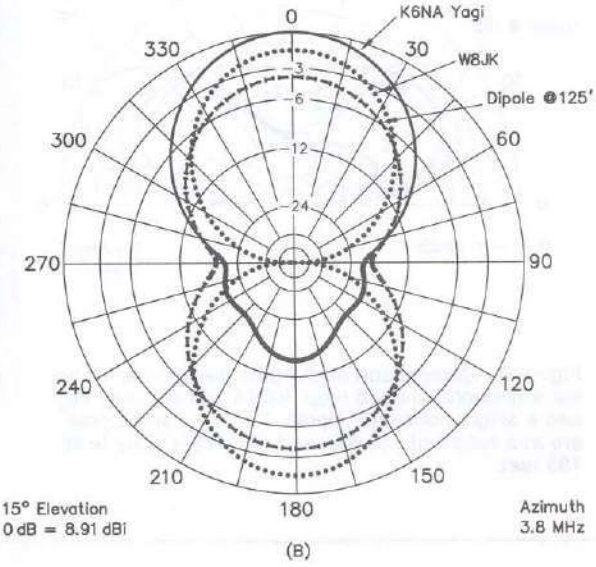

Figure 11—Comparison of elevation responses for a horizontal W8JK array and the K6NA two-element Yagi, both at height of 125 feet. As might be expected, the unidirectional Yagi has gain over the bidirectional W8JK design.

cal at all angles of interest, even down to 10°. In most locations, the vertical will be noisy on receive. *An extensive local ground screen (or elevated radials) will not make any significant change in the pattern relationship depicted here.* Only by installing the vertical in, say, a saltwater marsh extending perhaps 100 λ would its low-angle performance be improved substantially.[6]

The "Four-Square" has become popular in recent years. Figure 13 also shows the beautiful pattern of this array, along with that of the two-element beam and a single vertical. In a quiet location this vertical system with a switching matrix makes a terrific receiving antenna, allowing full azimuth coverage in four directions. However, the horizontal wire Yagi still has superior gain at all elevation angles of interest—note the 4 dB advantage at 15°—and the Yagi likely will be quieter on receive in all but the most remote locations. The remarks in the paragraph above about attempts to improve the lowangle performance of the λ/4 vertical also apply to the Four-Square array.

Conclusions

Someone once said: "All antennas work... some more so." The sometimes-large differences seen during model comparisons can be misleading, as we know from our day-to-day operating. Propagation, pileup dynamics, and operator skills (one skill is picking a quiet location ...) are important factors that determine 80-meter DXing success. Virtually every antenna discussed in the comparison section of this report is a "good" antenna. The author's first 180 countries on 80 meters were worked with an inverted-V dipole at 70 feet.

If *tall* supports are available, a horizontally polarized, gain antenna will certainly provide a statistical increase in performance over the others. In lieu of really tall

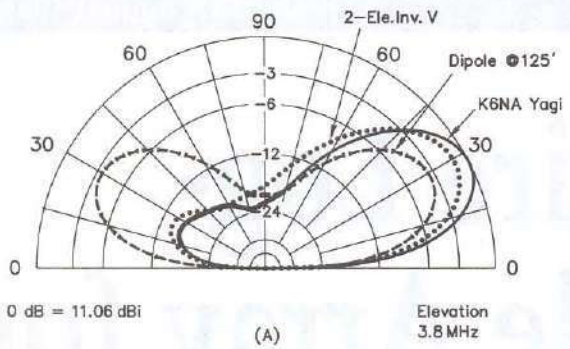

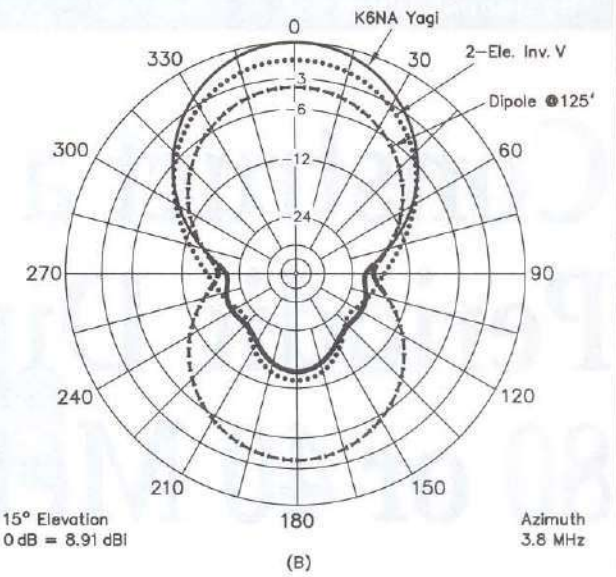

Figure 12—Comparison of the horizontal K6NA wire beam to a similar antenna using inverted-V dipole elements with a 90° included angle. The inverted-V configuration loses gain and directivity compared to the fully horizontal dipole Yagi, but the loss is only about 1 dB. The inverted-V style may be quite practical for those with a single, high tower.

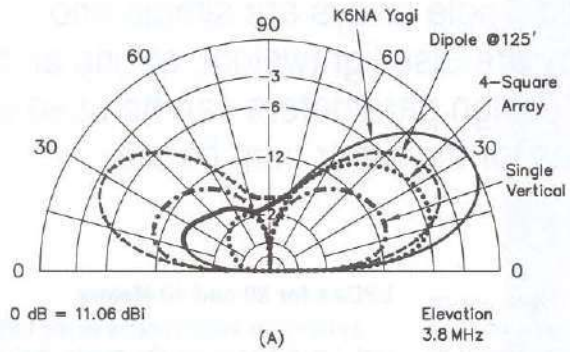

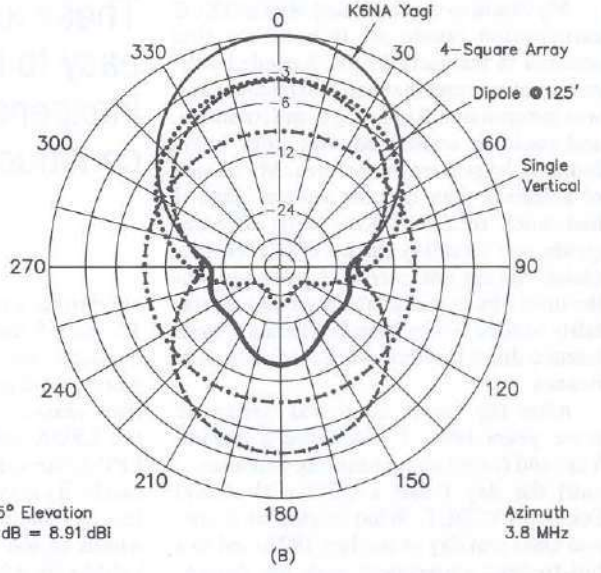

Figure 13—Comparison of K6NA Yagi to both a single ground-mounted λ/4 vertical on average ground (with a dielectric constant of 13 and a conductivity of 5 mS/m), and a "Four Square" phased vertical array. Each vertical is assumed to have 120 radials, an "optimal" ground system. Again, far-field ground losses are detrimental to verticals over poor ground.

towers, a well-installed vertical system can be an excellent antenna, especially in a quiet receiving location. As the computer models show, height above ground is the most significant variable when designing a lowband station using horizontally polarized antennas. [Hills help too!–*Ed.*]

It is hoped that some of the construction techniques for the crossarms, wire antennas, and feed lines described in this report will stimulate others to build even better horizontal arrays. You will enjoy special satisfaction using homemade open-wire lines, and a 40-year old Johnson Matchbox tuner makes a nice addition to your modern shack.

The author would like to thank H. Shepherd, W6US, for his valuable advice regarding wire antennas and open-wire feeder construction; R. Craig, N6ND, for mechanical suggestions; E. Andress, W6KUT, for manuscript review; and N6ND and J. McCook, W6YA, for modeling assistance.

Notes and References

[1]Wayne Overbeck, N6NB, "Quads vs. Yagis Revisited," *Ham Radio*, May 1979, p 12.
[2]James L. Lawson, W2PV, "160/80/75-Meter Broad-Band Inverted-V Antenna," *QST*, Nov 1970, p 17.
[3]James L. Lawson, W2PV, *Yagi Antenna Design*, W. Myers, K1GQ, editor (Newington: ARRL, 1986), p 2-2.
[4]Doug DeMaw, W1FB, editor, *ARRL Electronics Data Book* (Newington: ARRL, 1976), p 82.
[5]Frank Witt, AI1H, "Optimizing the 80-Meter Dipole," *The ARRL Antenna Compendium, Vol 4* (Newington: ARRL, 1995), p 39.
[6]Charles J. Michaels, W7XC, "Some Reflections on Vertical Antennas," *QST*, Jul 1987, p 18.

By John J. Uhl, KV5E

From *QST*, August 1986

Construct a Wire Log-Periodic Dipole Array for 80 or 40 Meters

These log-periodic dipole arrays are simple and easy to build. They are also lightweight, strong and inexpensive. The design parameters can be used to construct antennas for the other ham bands.

My desire to work DX and obtain DXCC certification caused me to build my first antenna in the early 1960s. I needed a directional antenna that had reasonable gain, was inexpensive, lightweight and rotatable, and could be assembled with stock items found in large hardware stores. My choice of antennas then was the cubical quad. I had much success DXing with different quads, and I quickly earned DXCC certification. Quads are excellent antennas, but the ones I built lacked the mechanical stability needed in southern Louisiana. I soon learned this when they were ruined by hurricanes.

After my fourth quad was destroyed some years later, I purchased a triband Yagi and forgot about building antennas ... until the day I had a QSO with Ansyl Eckols, YV5DLT. What started as a normal QSO that day in the late 1970s led to a full-fledged experiment with the design, construction, erection and use of log-periodic dipole arrays made of wire. At that time, YV5DLT was using a triband log-periodic dipole array (LPDA) for 20, 15 and 10 meters. What immediately piqued my interest was that his beam was made of wire, and that his signal had outstanding quality and strength.

During the QSO, I asked Ansyl for construction details of his antenna. His response was generous. He mailed me diagrams, schematics and photographs of the LPDA that he had named Telerana. (He subsequently published his design in *QST*.[1]) After reading and studying all of his data, I was convinced that his design had the mechanical stability to withstand hurricanes, and I began plans in my mind to build a copy of Telerana.

I began a search of the literature, reading all of the LPDA articles that I could find.[2-8] By the time I gathered and read several references, three years had passed. Sunspot activity had diminished and band conditions weren't as good. Openings on 10 and 15 meters were few and of short duration, and future conditions would be worse. I did not duplicate the Telerana for these reasons, but decided instead to apply the LPDA theory to the design of wire LPDAs for use on the 160, 80 and 40-meter bands. By making some preliminary calculations I found that an LPDA for 160 meters would be too large to fit my lot size, but LPDAs for 80 and 40 would fit. However, it would not be possible for me to rotate these LPDAs.

LPDAs for 80 and 40 Meters

I placed the same criteria on the LPDAs that I had placed on the quads–that they have reasonable gain, be inexpensive and lightweight, and that they could be assembled with stock items found in large hardware stores. This article is written to detail the design, construction, erection and use of wire LPDAs for the lower frequency bands. Figure 1 shows one method of installation. You can use the information presented here as a guide and point of reference for building similar LPDAs.

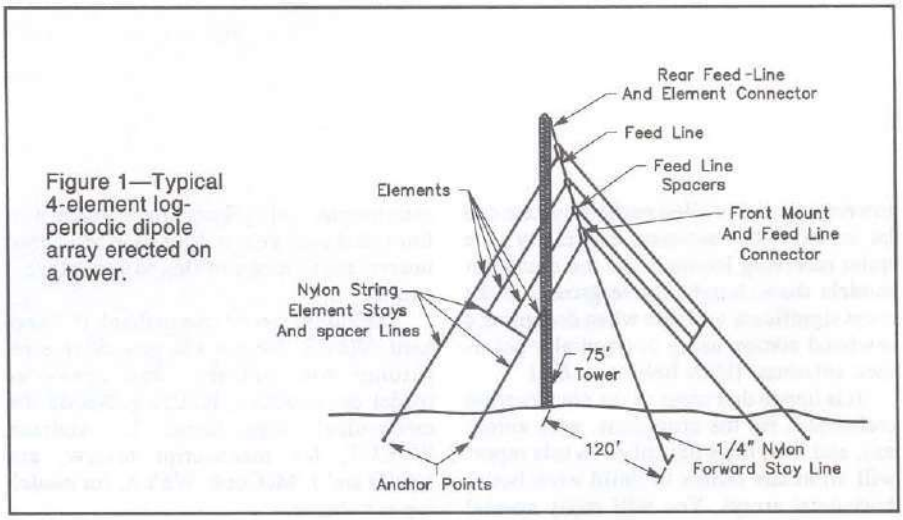

Figure 1—Typical 4-element log-periodic dipole array erected on a tower.

If space is available, the antennas can be "rotated" or repositioned in azimuth after they are completed. A 75-ft tower and a clear turning radius of 120 ft around the base of the tower are needed. The task is simplified if only three anchor points are used, instead of the five shown in Figure 1. Omit the two anchor points on the forward element, and extend the two nylon strings used for element stays all the way to the forward stay line.

For the design procedure, refer to *The ARRL Antenna Book*.[9] By using the formulas given there and other data in the text, all of the dimensions can be obtained and the LPDAs will take shape on paper. The design results are summarized in the concluding section of this article. The next step is to fabricate the fittings; see Figure 2 for details. Cut the wire elements and feed lines to the proper sizes and mark them for identification. After the wires are cut and placed aside, it will be difficult to remember which is which unless they are marked. When you have finished fabricating the connectors and cutting all of the wires, the antenna can be assembled. Use your ingenuity when building one of these antennas; it isn't necessary to duplicate my LPDAs exactly.

The elements are made of standard no. 14 stranded copper wire. The two parallel feed lines are made of no. 12 solid copper-coated steel wire, such as Copperweld. This will not stretch when placed under tension. The front and rear connectors are cut from 1/2-in-thick Lexan sheeting, and the feed-line spacers from 1/4-in Plexiglas sheeting.

Study the plans carefully and be familiar with the way the wire elements are connected to the two feed lines, through the front, rear and spacer connectors. Details are sketched in Figure 4. Connections made this way prevent the wire from breaking. All of the rope, string and connectors must be made of materials that can withstand the effects of tension and weathering. Use nylon rope and strings, the type that yachtsmen use. Figure 1 shows the front stay rope coming down to ground level at a point 120 ft from the base of a 75-ft tower. It may not be possible to do this in all cases. In my installation I put a pulley 40 ft up in a tree and ran the front stay rope through the pulley and down to ground level at the base of the tree. The front stay rope will have to be tightened with a block and tackle at ground level.

Putting an LPDA together is not difficult if it is assembled in an orderly manner. It is easier to connect the elements to the feeder lines when the feed-line assembly is stretched between two points. Use the tower and a block and tackle. Attaching the rear connector to the tower and assembling the LPDA at the base of the tower makes raising the antenna into place a much simpler task. Tie the rear connector securely to the base of the tower and attach the two feeder lines to it. Then thread the two feed-line spacers onto the feed line. The spacers will be loose at this time, but will be positioned properly when the elements are connected. Now connect the front connector to the feed lines. A word of caution: Measure accurately and carefully! Double-check all measurements before you make permanent connections.

Connect the elements to the feeder lines through their respective plastic connectors, beginning with element 1, then element 2, and so on. Keep all of the element wires securely coiled. If they unravel, you will have a tangled mess of kinked wire. Check that the element-to-feeder connections have been made properly. (See Figure 4.) Once you have completed all of the element connections, attach the 4:1 balun to the underside of the front connector. Connect the feeder lines and the coaxial cable to the balun.

You will need a separate piece of rope and a pulley to raise the completed LPDA into position. First secure the eight element ends with nylon string, referring to Figures 1 and 3. The string must be long enough to reach the tie-down points. Connect the front stay rope to the front connector, and the completed LPDA is now ready to be raised into position. While raising the antenna, uncoil the element wires to prevent their getting away and balling up into a mess. Use care! Raise the rear connector to the proper height and attach it securely to the tower, then pull the front stay rope tight and secure it. Move the elements so that they form a 60-degree angle with the feed lines, in the direction of the front, and space them properly relative to one another. By adjusting the end positions of the elements as you walk back and forth, you will be able to align all the elements properly. Now it is time to hook your rig to the system and make some QSOs.

Performance

The reports I received using the LPDAs were compared with an inverted-V dipole. All of the antennas are fixed; the LPDAs radiate to the northeast and the dipole to the northeast and southwest. The apex of the

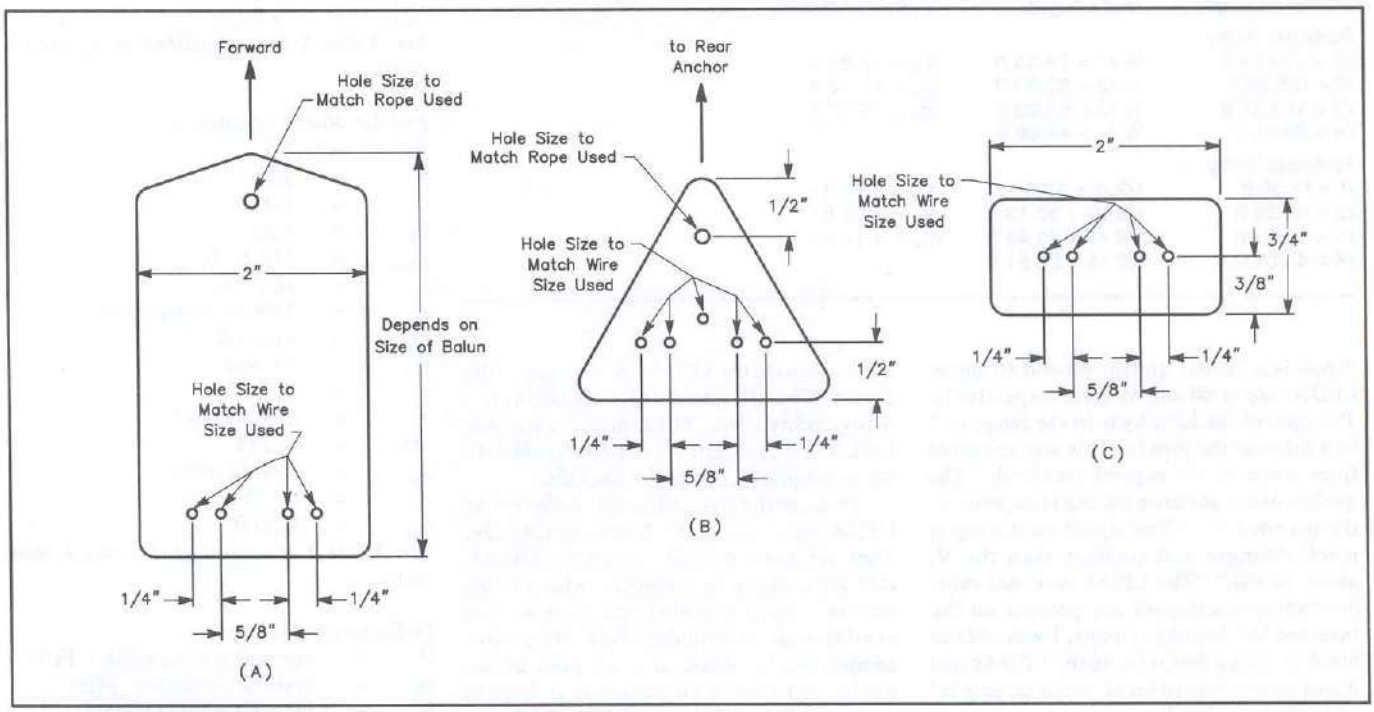

Figure 2—Pieces to be fabricated for the LPDA. At A, the forward connector, made from 1/2-inch Lexan. At B, the rear connector, also made from 1/2-inch Lexan. At C is the pattern for the feed-line spacers, made from 1/4-inch Plexiglas. Two of these spacers are required.

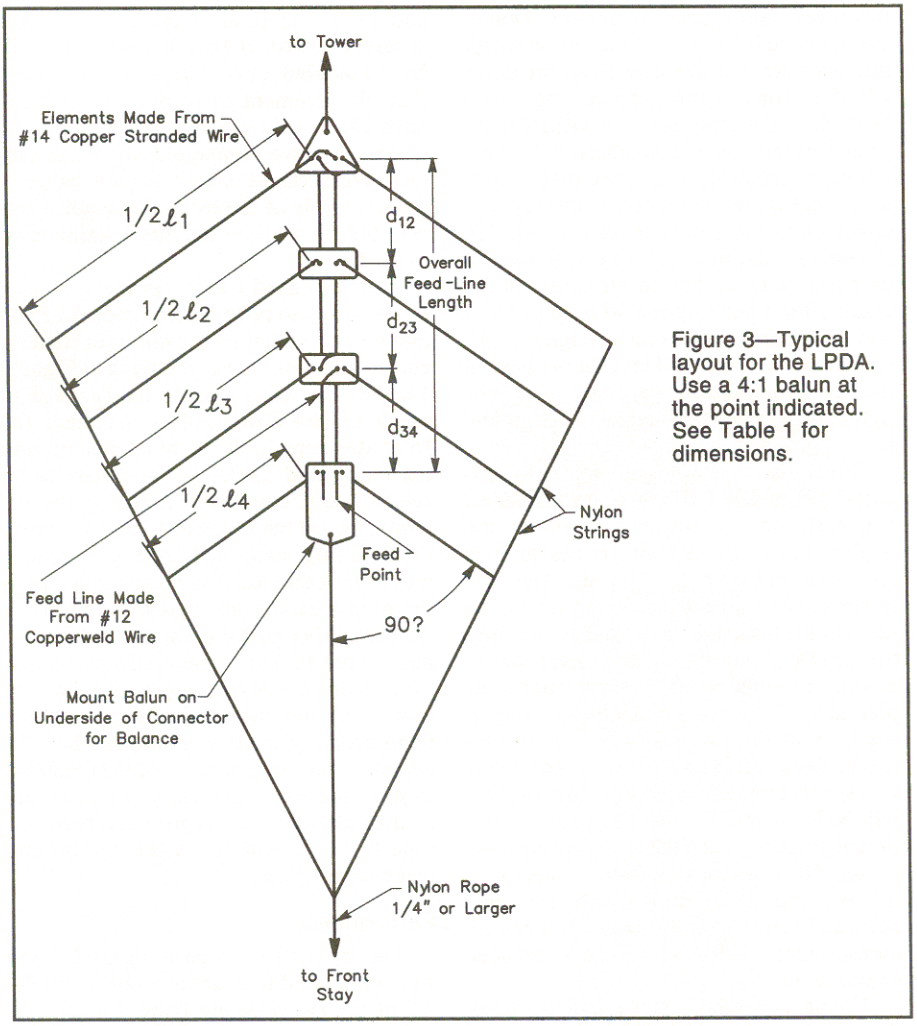

Figure 3—Typical layout for the LPDA. Use a 4:1 balun at the point indicated. See Table 1 for dimensions.

Table 1
Calculated Array Dimensions

Element Length	*Half Length*	*Element Spacing*
80-Meter Array		
ℓ1 = 149.09 ft	1/2 ℓ1 = 74.55 ft	d_{12} = 17.89 ft
ℓ2= 125.98 ft	1/2 ℓ2 = 62.99 ft	d_{23} = 15.12 ft
ℓ3 = 106.45 ft	1/2 ℓ3 = 53.23 ft	d_{34} = 12.77 ft
ℓ4 = 89.95 ft	1/2 ℓ4 = 44.98 ft	
40-Meter Array		
ℓl = 71.30 ft	1/2 ℓl = 35.65 ft	d_{12} = 8.56 ft
ℓ2 = 60.25 ft	1/2 ℓ2 = 30.13 ft	d_{23} = 7.23 ft
ℓ3 = 50.91 ft	1/2 ℓ3 = 25.46 ft	d_{34} = 6.11 ft
ℓ4 = 43.02 ft	1/2 ℓ4 = 21.51 ft	

dipole is at 70 feet, and the 40-and 80-meter LPDAs are at 60 and 50 feet, respectively. The gain of the LPDAs is in the range of 7 to 9 dB over the dipole. This was apparent from some of the reports received: "The quality of the audio on the log is superior to the inverted V." "The signal on the log is much stronger and steadier than the V, about 10 dB." "The LPDA does not fade, but fading conditions are present on the inverted V." During pileups, I was able to break in with a few tries on the LPDAs, yet it was impossible to break in the same pileups using the dipole.

During the CQ WW DX Contest I was able to break into some *big* pileups after a few calls with the LPDAs. Switching to the dipole, I found it impossible to break in after many, many calls. Then, after I switched back to the LPDA, it was easy to break into the same pileup and make the QSO.

Think of the possibilities that these wire LPDA systems offer hams worldwide. They are easy to design and to construct, real advantages in countries where commercially built antennas and parts are not available at reasonable cost. The wire needed can be obtained in all parts of the world, and cost of construction is low! If damaged, the LPDAs can be repaired easily with pliers and solder. For those who travel on DXpeditions where space and weight are large considerations, LPDAs are lightweight but sturdy, and they perform well. They'll even withstand a hurricane!

Calculations for Log-Periodic Dipole Arrays

Design constants and the results of design procedures follow. (Terms are defined at the end of this section.)

τ = 0.845
σ = 0.06
σ_{opt} = 0.152
cot α = 1.548
α = 32.86°
Gain = 7.5 dBi (5.35 dBd). [By sloping the elements forward, the gain may be increased 3 to 5 dB over this figure. *–Ed.*]
σ' = 0.065
B_{ar} = 1.39; see note 10.
R_0 = 70

Fed with 50-ohm coaxial cable and a 4:1 balun

For the 80-meter antenna,
fn = 4.1
f1 = 3.3
B = 1.24
B_S = 1.72
λ_{max} = 298.18 ft
L = 48.42 ft
N = 4.23 (rounded to 4)
ℓ1 = 149.09 ft
R_0 = 70 ohms
h = 62.4
a = 2.667×10^{-3}
h/a = 23400
Z_{av} = 937.26 ohms
Z_0 = 80.72 ohms
d_{12} = 17.89 ft
See Table 1 for calculated array dimensions.

For the 40-meter antenna,
fn = 7.5
fl = 6.9
B = 1.09
B_s = 1.51
λ_{max} = 142.61 ft
L = 18.57 ft
N = 3.44 (rounded to 4)
ℓ1 = 71.30 ft
R_0 = 70 ohms
h = 32.727
a = 2.667×10^{-3}
h/a = 12273
Z_{av} = 859.82 ohms
Z_0 = 81.76 ohms
d_{12} = 8.56 ft
See Table 1 for calculated array dimensions.

Definitions of Terms
B = operating bandwidth = fn/f1
fn = highest frequency, MHz
fl = lowest frequency, MHz
τ = design constant
σ = relative spacing constant

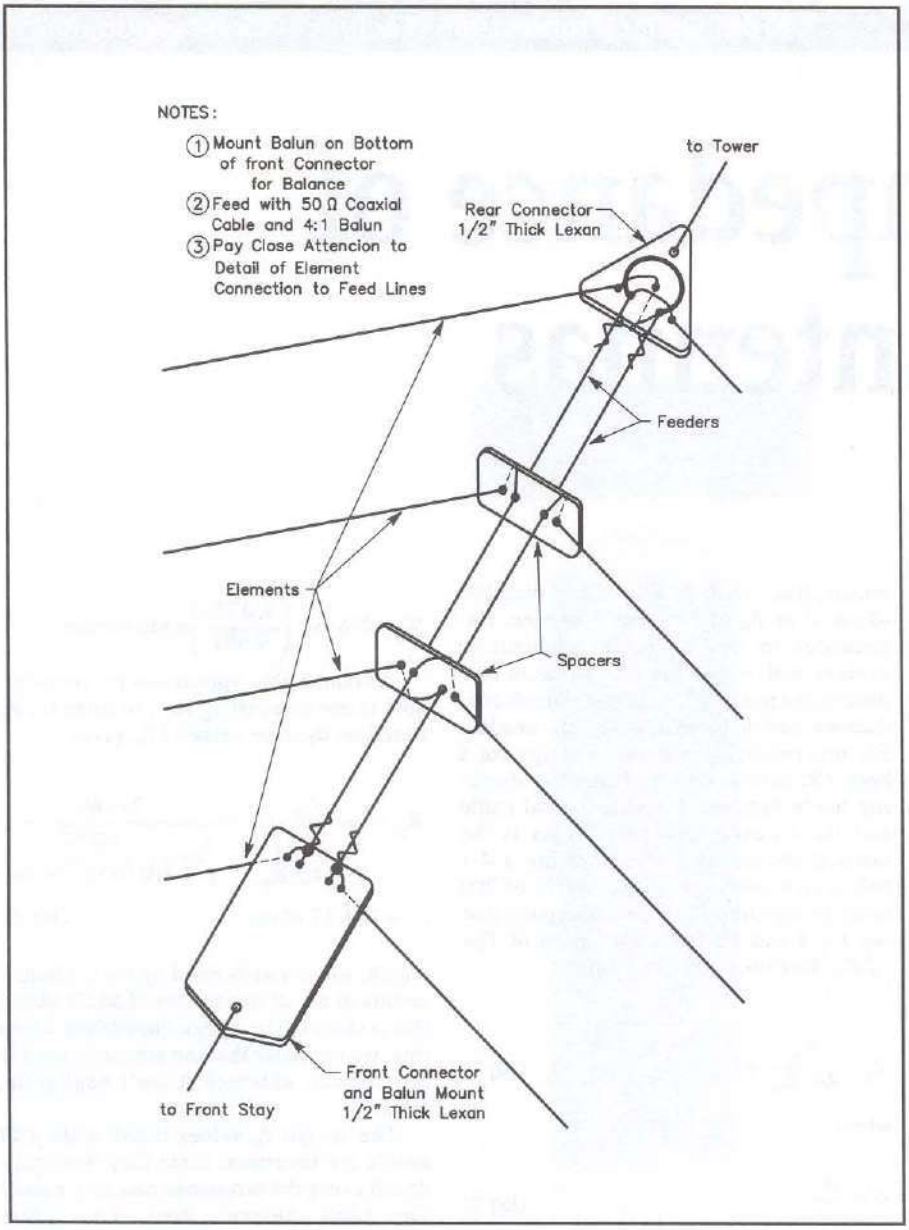

Figure 4—Details of electrical and mechanical connections of the elements to the feed line. Knots in the nylon stay lines are not shown.

σ_{opt} = value of σ for optimum gain
σ' = mean spacing factor
α = apex half-angle
B_{ar} = bandwidth of the active group. See note 10.
B_s = structure (array) bandwidth
L = boom length for N elements
N = number of elements
$\ell 1$ = longest element = 492/f1
λ_{max} = longest free-space wavelength = 984/f1
Z_0 = characteristic impedance of feeder
R_0 = mean radiation resistance level of required input impedance of active region
Z_{av} = average characteristic impedance of a dipole

$$= 120\left(\ln\frac{h}{a} - 2.25\right)$$

h = element half length
a = radius of element
ℓ = length of elements
d = spacing between elements

Notes

[1]A. Eckols, "The Telerana—A Broadband 13- to 30-MHz Directional Antenna," *QST*, Jul 1981, pp 24-27.
[2]C. T. Milner, "Log Periodic Antennas," *QST*, Nov 1959, p 11.
[3]D. E. Isbell, "Log-Periodic Dipole Arrays," *IRE Transactions on Antennas and Propagation*, Vol AP-8, No. 3, May 1960, pp 260-267.
[4]P. D. Rhodes, "The Log-Periodic Dipole Array," *QST*, Nov 1973, pp. 19-22.
[5]*The GIANT Book of Amateur Radio Antennas* (Blue Ridge Summit, PA: Tab Books, 1979), pp 55-85.
[6]C. A. Balanis, *Antenna Theory, Analysis and Design* (New York: Harper and Row, 1982), pp 427-439.
[7]G. L. Hall, ed., *The ARRL Antenna Book* (Newington, CT: The American Radio Relay League, Inc, 1982), pp 6-24 to 6-26, 9-12 to 9-14.
[8]D. A. Mack, "A Second-Generation Spiderweb Antenna," *The ARRL Antenna Compendium Vol 1* (Newington, CT: The American Radio Relay League, Inc, 1985), pp 55-59.
[9]See note 7.
[10]See Ref 6, p 435. B_{ar} is found from the following equation:

$$B_{ar} = 1.1 + 7.7(1 - \tau)^2 \cot \alpha$$

From *QST*, October 1986 (Technical Correspondence)

Input Impedance of LPDA Antennas

The log-periodic dipole array (LPDA) has intriguing possibilities, some of which have been explored by Uhl.[1] Unfortunately, some misleading information in *The ARRL Antenna Book* has kept the subject from being more accessible to the amateur.[2] The design procedure called out by *The Antenna Book* and by Rhodes refers to graphs of R_0, the mean antenna input resistance, versus the log-periodic design parameters τ and α.[3] It would appear that R_0 is dependent solely on these parameters; such is not the case. As shown by Eq 2 and 4, R_0 is dependent on τ, σ, Z_{av} and Z_0. This relationship is demonstrated by Carrel.[4] The graphs in question are from the seminal experimental study of the LPDA by Isbell, and are used to demonstrate the effect on R_0 of changing τ and σ; Z_{av} and Z_0 were constant.[5] Since τ and σ are usually chosen to provide the desired antenna geometry and directivity (gain), R_0 should be controlled by either Z_{av} or Z_0. Z_{av} is usually constrained by mechanical considerations, which leaves Z_0 as the easiest parameter to adjust for desired R_0.

The erroneous procedure determines R_0 from a graph. The correct procedure is to calculate the necessary Z_0 based on the *desired* R_0. For most practical LPDA antennas, this results in a Z_0 of less than 100 ohms, if an R_0 of 50 ohms is chosen. Impedances in this range are difficult to achieve with open-wire line, the kind normally used in an LPDA, because thick conductors and/or close spacing are needed. For this reason, it is usual to design for a higher R_0 and use an impedance-transforming balun between 50-ohm coaxial cable and the antenna feed point. This is the method chosen by Uhl. Assuming a 4:1 balun, an antenna-input impedance of 200 ohms is required. Z_0 is then calculated (using Eq 9 and 11 from page 6-25 of *The ARRL Antenna Book*) as follows:

$$Z_0 = \frac{R_0^2}{8\sigma' Z_{av}} + R_0\sqrt{\left(\frac{R_0}{8\sigma' Z_{av}}\right)^2 + 1} \quad \text{(Eq 1)}$$

where

$$\sigma' = \frac{\sigma}{\sqrt{\tau}} \quad \text{(Eq 2)}$$

$$Z_0 = \frac{200^2}{8(0.065)\ (937.26)} + 200\sqrt{\left(\frac{200}{8(0.065)\ (937.26)}\right)^2 + 1}$$

$$= 298.26 \text{ ohms}$$

The actual impedance of the feed line used by Uhl can be computed from the formula on p 3-16 of *The ARRL Antenna Book*:

$$Z_0 = 276 \log\left(\frac{2S}{d}\right) \quad \text{(Eq 3)}$$

where S is the spacing between conductors, 0.75 inch, and d is the conductor diameter, 0.081 inch for no. 12 AWG wire. Therefore:

$$Z_0 = 276 \log\left(\frac{2(0.75)}{0.081}\right) = 349.86 \text{ ohms}$$

Although this appears to be considerably in error, recasting Eq 1 to solve for R_0 based on the true value of Z_0 gives:

$$R_0 = \frac{Z_0}{\sqrt{1 + \frac{Z_0}{4\sigma' Z_{av}}}} = \frac{349.86}{\sqrt{1 + \frac{349.86}{4(0.065)(937.26)}}}$$

$$= 224.17 \text{ ohms} \quad \text{(Eq 4)}$$

which, when transformed by the 4:1 balun, results in a load impedance of 56.04 ohms; this is close to the design impedance. From this, we can infer that the actual Z_0 used is not critical, although it isn't negligible, either.

The design Z_0 values listed in the Uhl article are incorrect, since they were produced using the erroneous procedure from *The ARRL Antenna Book*. The values should be 298.26 and 308.56 ohms for the 80- and 40-meter antennas, respectively. In addition, R_0 could be made closer to the design value of 200 ohms by using a different feeder spacing to change the feeder impedance. From Eq 2:

$$S = \left(\frac{d}{2}\right)10^{(Z_0/276)} = \left(\frac{0.081}{2}\right)10^{(298.26/276)}$$

$$= 0.488 \text{ inch}$$

Rounding this value to 0.5 inch results in a Z_0 of 301.26 ohms and an R_0 of 201.46 ohms for 80 meters and 196.62 ohms for 40 meters. These translate to load impedance of 50.37 and 49.15 ohms, respectively.—*Jon Bloom, KE3Z*

[1] J.J. Uhl, "Construct a Wire Log-Periodic Dipole Array for 80 or 40 Meters," *QST*, Aug 1986, p 21.

[2] G.L. Hall, ed., *The ARRL Antenna Book* (Newington: ARRL, 1982), pp 6-24 to 6-26.

[3] P.D. Rhodes, "The Log-Periodic Dipole Array," *QST*, Nov 1973, pp 16-22.

[4] R.L. Carrel, "The Design of Log-Periodic Dipole Antennas," *1961 IRE International Convention Record, Part 1, Antennas and Propagation*, pp 61-75; also PhD thesis, University of Illinois, Urbana, 1961.

[5] D. E. Isbell, "Log-Periodic Dipole Arrays," *IRE Transactions on Antennas and Propagation*, Vol AP-8, No. 3, May 1960, pp 260-267.

The WA1AKR 40- and 75-Meter Slopers

Several amateurs have suggested that I submit a description of my sloper antenna system for publication in "Hints and Kinks." Other amateurs may be interested in this adaptation of the 8JK beam. Construction information is shown for both the 75- and 40-meter bands.

As shown in the accompanying diagram, the array has two half-wave sloping elements joined by a 1/8-wave, 300-ohm phasing line. Transposing the phasing line should bring the element currents into phase. I find the antenna is broadbanded. There appears to be no need for a Transmatch.

If one desires to suspend an additional sloper from the tower for a directional change, installation of remote switching at the top of the tower will permit the use of a single transmission line. Otherwise, separate transmission lines will be required.

Ends of the antenna are suspended by ropes with the tops placed roughly 1 foot away from the tower. An angle of 45 degrees between the antenna and ground should be maintained. Do not use an angle greater than 50 degrees. Resonance with the dimensions shown should occur near 3.8 MHz for the 75-meter sloper and 7.150 for the 40-meter antenna.

How well do my antennas work? I have contacted stations "across the pond" while competing with the big boys who sport three and four-element beams. I have also experienced little difficulty in working VKs and ZLs. – *Carl Bissonnette, WA1AKR*

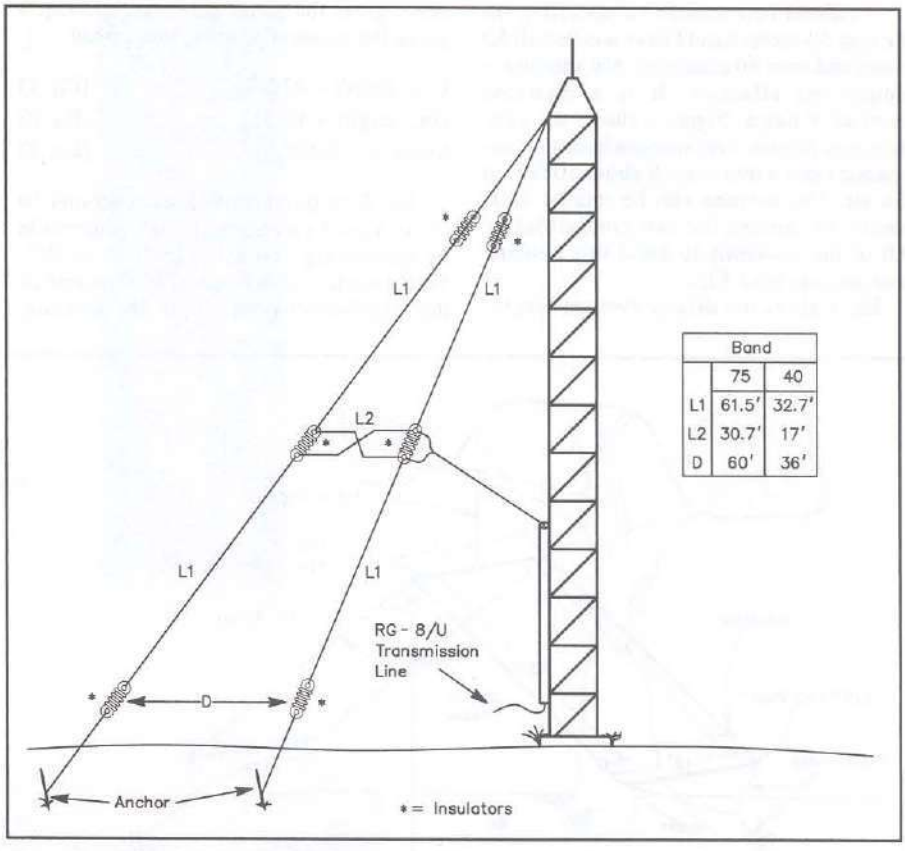

	Band	
	75	40
L1	61.5′	32.7′
L2	30.7′	17′
D	60′	36′

When Carl Bissonnette, WA1AKR, chases DX he uses a sloper like the one illustrated. Carl's arrangement is fashioned after the famous 8JK beam. The feed system resembles that of the ZL Special.

Inexpensive 30-Meter Beam Antenna

In about two months of operating on the new 30-meter band I have worked all 50 states and over 50 countries. My antenna is simple but effective. It is a rotatable inverted V beam. Figure 1 shows the construction details. The antenna boom is suspended from a tree branch about 50 feet in the air. The antenna can be rotated 360° simply by moving the two ground stakes. All of the materials to build this antenna cost me less than $25.

Eq. 1 gives the driven element length, Eq. 2 gives the director length, and Eq. 3 gives the element spacing that I used.

$$\text{D.E. length} = 476/f_{MHz} \quad \text{(Eq. 1)}$$

$$\text{Dir. length} = 450/f_{MHz} \quad \text{(Eq. 2)}$$

$$\text{Spacing} = 120/f_{MHz} \quad \text{(Eq. 3)}$$

The feed-point impedance is around 30 ohms. I used a matching transformer made by connecting two 1/4-λ sections of RG-59/U coaxial cable in parallel. One end of the transformer connects to the antenna, and the other end goes to 50-ohm cable to the shack. Figure 1B shows how this is wired. Perhaps the easiest method to join the two pieces of 75-ohm cable is to use coaxial T connectors. You should use a balun at the antenna feed point to prevent rf from flowing on the outside of the shield braid.

I also built an antenna of this type for 40 meters, and it works great. I guess the key word is rotatable! — *Jon Ferrara, N9DWR, Chattanooga, Tennessee*

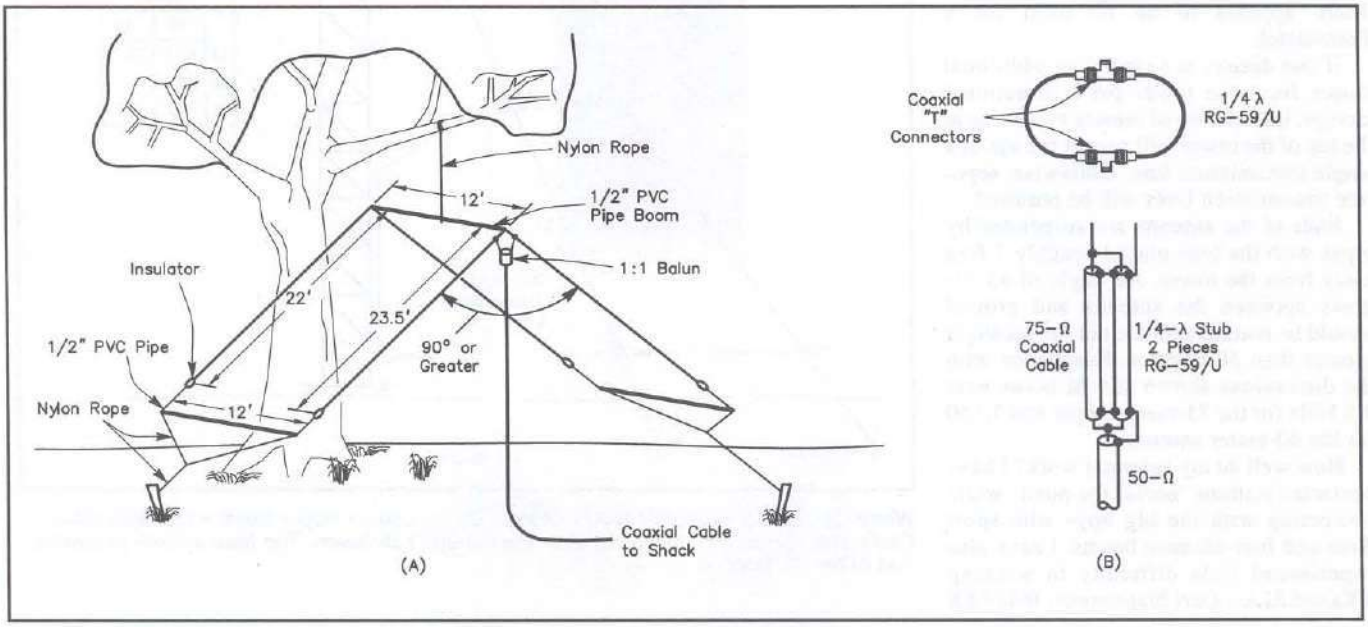

Figure 1—Construction details for a 30-meter inverted V beam are given at A. A coaxial-cable impedance-matching transformer is shown at B.

By Roy W. Lewallen, W7EL

From *QST*, June 1984

Try the "FD Special" Antenna

Looking for an antenna that's simple, inexpensive, lightweight and easy to install? Here's one that fits the description.

While the Field Day "juices" were flowing last year, my Field Day partners and I decided to become more competitive without compromising our general philosophy: Use all homemade gear, pack it in to the site, and don't let operating interfere with watching the scenery. Since most of our gear already ran the accepted QRP power limit of 10-W dc input and had been designed to provide high output efficiency, the antenna seemed like the reasonable point of attack (our high quality superheterodyne receivers have not been the limiting item). The constraints dictated that an antenna be lightweight, portable and easy to put up. It should also have substantial gain.

Because of our West Coast location, the front-to-back ratio was not a concern. But having a reasonably wide lobe toward the East was. We desired a low SWR because of the relatively high loss of our RG-58/U and/or RG-174/U feed line. We were interested only in the CW portion of the band, but this antenna works well over all of the band. It seemed that 20 meters would be our main "money-maker," so we designed the antenna for that band. It can be scaled for other bands, too.

The Research

Although a number of antenna types might have done the job, I settled quickly on a horizontal, close-spaced, driven array. Experience has shown that driven arrays are generally more tolerant of imperfect construction and erection than are parasitic arrays. Experience and much measurement have convinced me that horizontal arrays outperform vertical ones in the high-frequency bands, except perhaps from an exceptional location. In addition, we didn't want the nuisance of establishing a decent ground system — which most vertical arrays require.

The theoretical gain and front-to-back ratio of 2-element arrays with 1/8-wavelength spacing between the elements are shown in Figures 1 and 2. Note the lower curve of Figure 1. It shows the effect of losses on the gain (losses don't affect the front-to-back ratio, and change only the scaling of the pattern). Figure 3 shows the patterns of arrays with 135, 160 and 180-degree relative spacing. All are drawn to the same scale. The 1/8-wavelength spaced, 135-degree-fed array is frequently called the "ZL Special."[1] The close-spaced, 180-degree-fed array is known as an "8JK."[2] From 135 to 160 degrees, phasing was chosen because of the combination of relatively high insensitivity to loss, reasonable gain and wide forward lobes. Note that the gain stays about the same in this range, ensuring good performance if the phasing isn't exactly as predicted. Actually, it's much easier to generate and maintain precise 180-degree phasing than the angles I've chosen — particularly over a wide frequency range.

There's one major flaw (usually fatal) in a simple analysis like the one presented here: It assumes that equal-magnitude currents are flowing in the elements. This is not easy to realize, for even in arrays with elements spaced 1/2 wavelength or greater, mutual coupling has a profound effect on element impedances. This changes them dramatically and unequally, as a rule. This

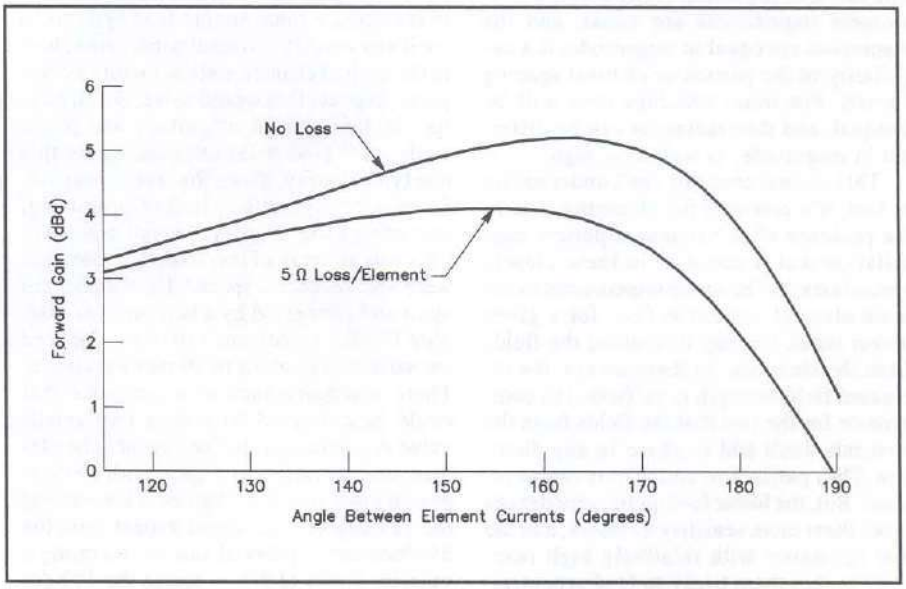

Figure 1—Curves that show gain versus phase angle for two-element arrays with 1/8-wavelength spacing.

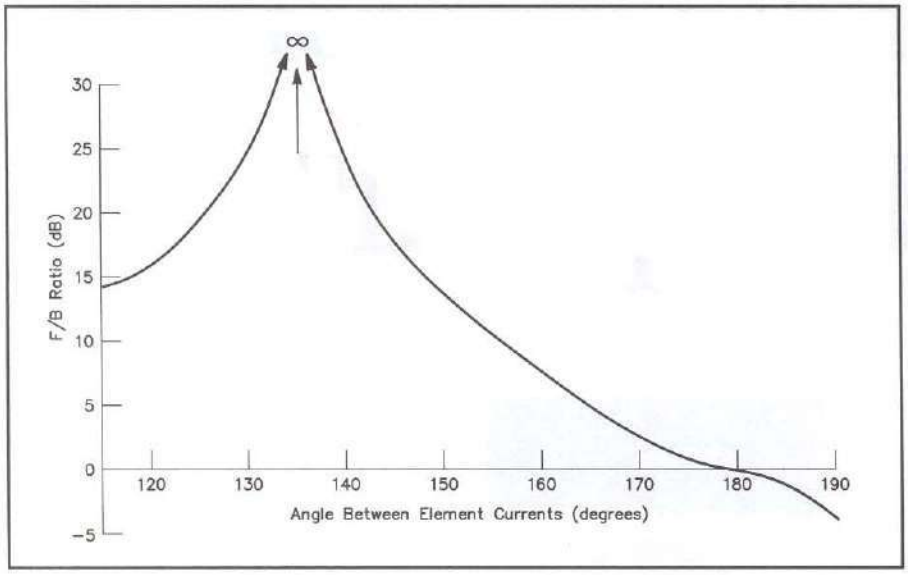

Figure 2—Theoretical F/B ratio for a two-element array with 1/8-wavelength spacing.

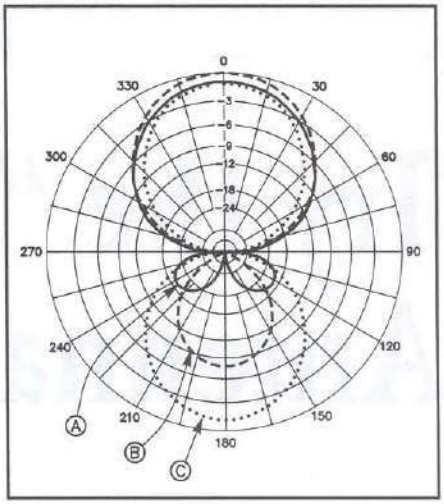

Figure 3—Dipole array patterns for 135, 160 and 180-degree relative phasing at λ/8 spacing. Curves A, B and C, respectively, represent these conditions. Add 5 dB for dBd. These curves are based on the array being fed with equal currents.

impedance change is a function of not only "mutual impedance," but also the relative magnitudes and phases of the currents flowing in the elements. In an array as closely spaced as these, coupling is so intimate that it could be argued that the term "driven array" is a misnomer. For example, the feed-point impedances of the elements in a 1/8-wavelength-spaced array, assuming equal currents can be made to flow, are

Phase Angle Between Currents (Degrees)	*Loading Element (Ohms)*	*Lagging Element (Ohms)*
135	28 – j46	28 + j46
160	13 – j22	13 + j22
180	9 + j0	9 + j0

This shows quite a change from the 74 + j0 ohms value that each element exhibits when it is not coupled to another element. The fact that the resistive parts of the two-element impedances are equal, and the reactances are equal in magnitude, is a peculiarity of the particular element spacing chosen. For other spacings they will be unequal, and the reactances can be different in magnitude, as well as in sign.

This mutual coupling isn't undesirable; in fact, it's essential for obtaining gain in the presence of rather severe pattern cancellation that is common in these closely spaced arrays. The lower impedances cause more element current to flow for a given power input, thereby increasing the fields from the elements. In these arrays, the increased field strength is sufficient to compensate for the fact that the fields from the elements don't add in phase in any direction. They partially or completely cancel instead. But, the lower feed-point impedances make them more sensitive to losses, and the low resistance with relatively high reactance makes them tricky to feed properly.

Why do these different and reactive feed impedances make feeding the arrays so difficult? The first problem is that, with few exceptions, the magnitude of current out of a line not terminated in its characteristic impedance won't be equal to the current into the line. In classic "If you can't fix it, feature it!" fashion, this impedance-transforming property is put to good use in the form of the 1/4-wavelength Q section.[3] The second (and almost always overlooked) difficulty is that, again with only a few exceptions, the phase delay of current in an imperfectly terminated transmission line doesn't equal the electrical length of the line. This effect isn't minor: The phasing of a casually designed array can easily be off by tens of degrees. In one design I investigated, an 80-degree line produced 139 degrees of phase shift.

The Solution

There are a number of approaches toward correct feeding of an array. My choice was to investigate some simple feed systems to see if any would yield results that came close to the desired characteristics. I wrote a computer program that would solve, iteratively, for element-current magnitude and phase angle, plus feed-point impedances for this one type of array, given the array specifics. Several configurations looked promising, and one of the simplest proved adequate. This was an array of two folded dipoles that were self-resonant, spaced 1/8 wavelength apart and connected by a taut piece of 300-ohm TV ribbon with one half twist. The feed impedance was close to 50 ohms resistive. There was some inductive reactance that could be corrected by adding two small-value capacitors at the feed point. The element current ratio was 1.13:1, with element phasing that was 154 degrees. This was not the 124 degrees one might expect from the 56 electrical degrees of line — assuming a velocity factor of 0.8 — minus the 180 degrees caused by the half twist.

It was this array that we used for Field Day, with very good results (see section on performance). However, when the array was reconstructed at the home QTH, a dramatic rise in SWR was noticed when operating the antenna at other than the low end of the band. Computer analysis showed that, above the design frequency, the phase angle increased. This caused a substantial lowering of the element feedpoint impedance, plus narrowing of the forward lobe. The analysis also showed the antenna to be well-behaved *below* the design frequency. Consequently, a similar array was designed (figuratively speaking) for 14.5 MHz. It gave good results over the 20-meter band.

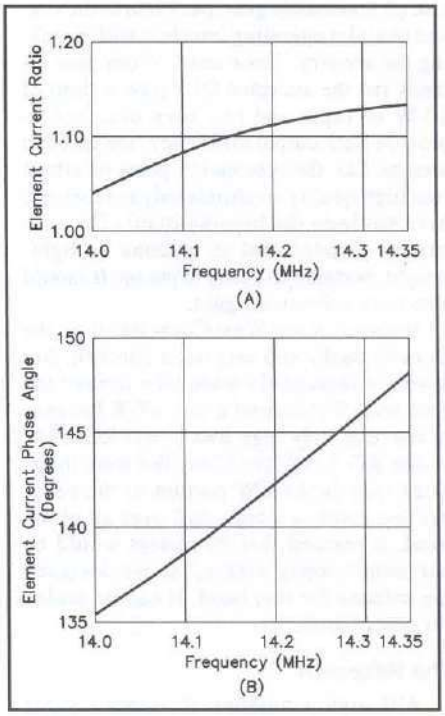

Figure 4—Element current ratio (A) and phase angle (B) as a function of frequency.

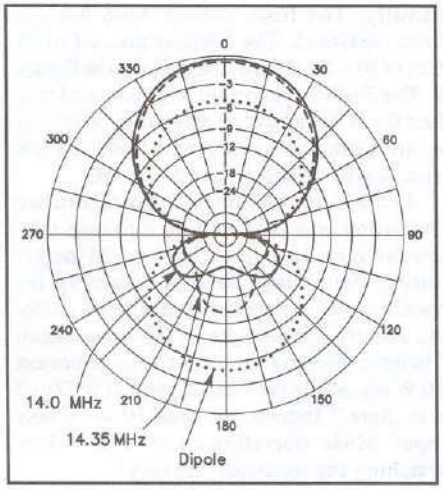

Figure 5—Calculated antenna patterns for the high and low ends of the 20-meter band. Add 5 dB for dBd.

Element phasing varies from 135 degrees at 14.0 MHz to 148 degrees at 14.35 MHz, with current ratios from 1.04 to 1.13:1 (see Figure 4). The gain can be calculated as fairly constant from 4.5 to 4.6 dBd across the band. Again, the array feed-point impedance can be corrected easily to provide a low SWR. The calculated patterns for the antenna at the top and bottom ends of the 20-meter band are shown in Figure 5. These take into account the changes in element phasing, spacing, current magnitude and element self-impedance with frequency.

Construction

The antenna is made from quality 300-ohm TV line to the dimensions given in Figure 6. Sketches of the insulators are provided in Figure 7. They are made from scrap pieces of epoxy-glass PC-board material. This results in ruggedness and minimum weight. The spreaders are readily available 10-foot lengths of "1 inch" ($1^5/_{16}$ in OD)[4] schedule 40 PVC pipe. The capacitors are used only to provide a good match to 50-ohm feed line: They don't otherwise affect the performance of the array. Small 500-V mica or monolithic ceramic units may be used for power levels up to a few hundred watts, since they are at a relatively low-voltage part of the system. Open-ended stubs could probably be substituted for the capacitors, if desired. I recommend that a balun transformer be used with this antenna. Attempts to measure the impedance of one element of this array resulted in a unique experience — the first substantial evidence of the need to use a balun transformer. The antenna-bridge readings varied greatly as the measuring equipment was moved, or as I placed my hand around the feed line. This ceased when I added a balun transformer. The phenomenon is explained by Maxwell in a recent paper.[5] Nearly any style of balun transformer will prevent the unwanted flow of current on the coaxial cable outer conductor. I use a choke type of balun transformer. It consists of 10 turns of small-diameter coaxial cable

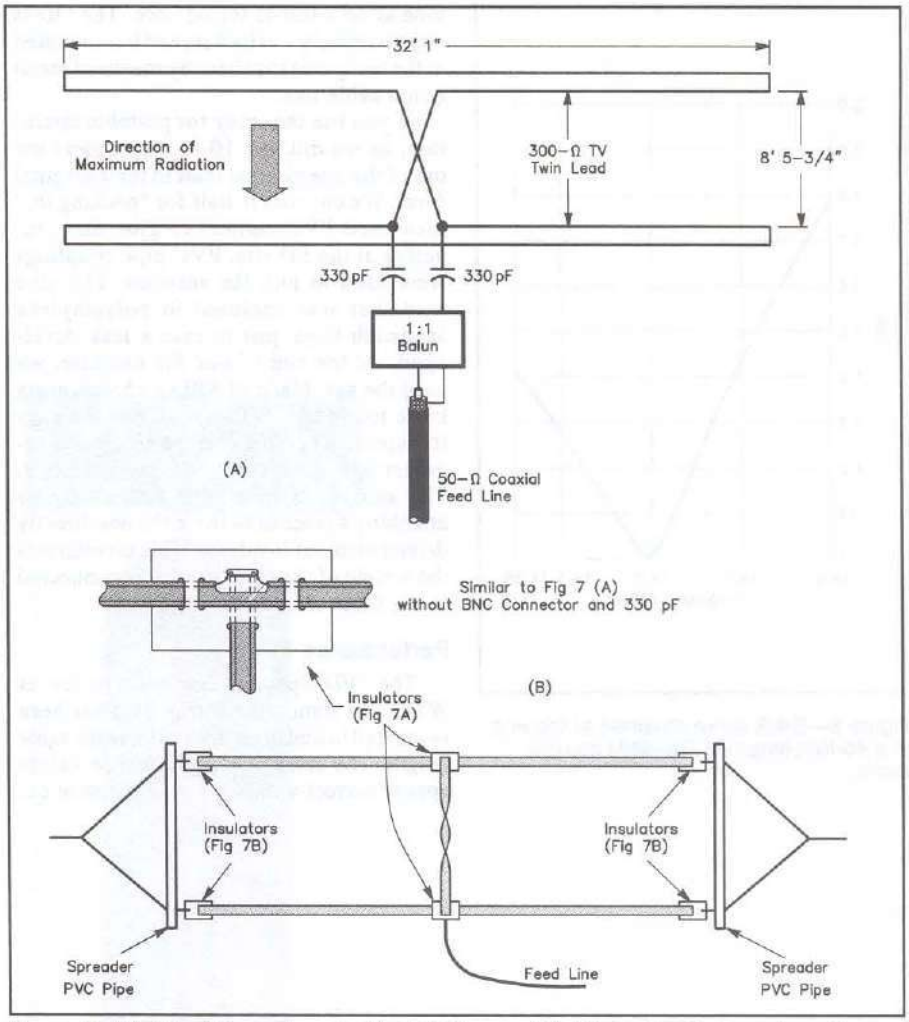

Figure 6—Electrical dimensions for the W7EL array (A). Illustration B shows how the antenna is assembled on spreaders of PVC pipe.

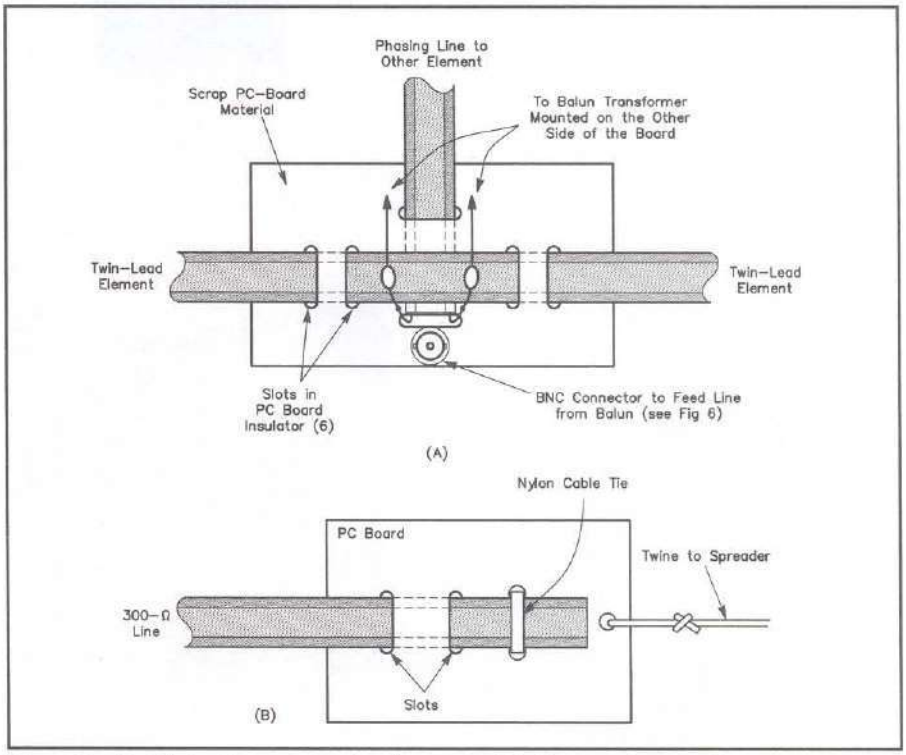

Figure 7—Details for the antenna insulators used in the two-element 20-meter array. The drawing at A shows how the TV ribbon is affixed to the feed-point/phasing-line insulating block. The example at B provides details for the end insulators.

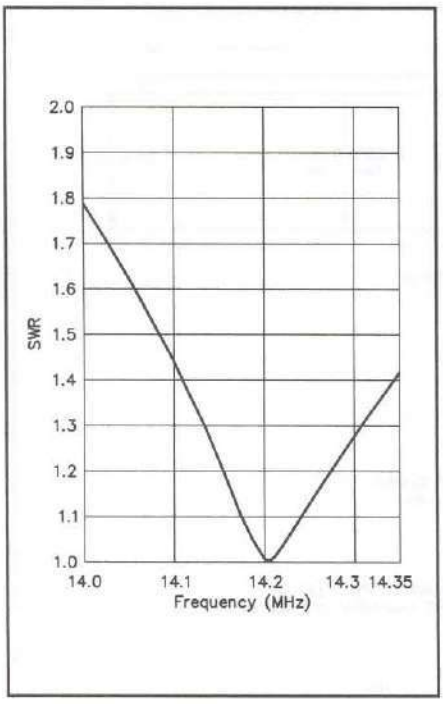

Figure 8—SWR curve obtained at the end of a 45-foot length of RG-58/U coaxial cable.

wound on a ferrite toroid core. The OD is approximately 1¼ inches, and it is mounted at the feedpoint insulator by means of small nylon cable ties.

If you use the array for portable operation, as we did, the 10-foot spreaders are out of the question, at least in their original form. We cut ours in half for "packing in," then used PVC cement to glue them together at the FD site. PVC pipe couplings were used to join the sections. The glue container was enclosed in polyethylene sandwich bags, just in case a leak developed. At the end of our FD exercise, we used the saw blade of KØED's Swiss army knife to cut the PVC pipes again for easy transport. The spreaders were glued together again for use at the home station. The antenna is held horizontal easily by attaching a piece of twine to the nondirectly driven element insulator. This counteracts the weight of the feed line that is connected to the other element.

Performance

The "FD Special" has been in use at W7EL for some time. Array gain has been compared to that of an inverted V at the same height. The calculated performance values appear correct within the measurement capability. The front-to-back ratio has not been measured. The SWR at the end of 45 feet of RG-58/U feed line is shown in Figure 8. The SWR is important only when a lossy line feeds the array, or when it is driven by an intolerant transmitter (with built-in SWR shut down), which is now the norm.

Perhaps the most revealing performance indication was provided by a person who encountered us several times on 20 meters during Field Day. He was operating for another, very competitive local club. After the exercise he remarked, "The only reason I believe you guys were running an honest 10 W is that I know Wes Hayward (W7ZOI) was there." Indeed, we used 10 W or less input while operating—and 0 W while watching the mountain scenery!

Notes

[1]My apologies to the first person who described or named this antenna. I don't know its history. (See L.A. Moxon, "Two-Element Driven Arrays," *QST*, July 1952, p 28.)

[2]Named after W8JK, Dr. John Kraus, "Antenna Arrays with Closely-Spaced Elements," *Proc. IRE*, Feb. 1940.

[3]G. Hall, ed., *The ARRL Antenna Book* (Newington: ARRL, 1982).

[4]mm = in x 25.4; m = ft x 0.0348.

[5]W. Maxwell, "Some Aspects of the Balun Problem," *QST*, March 1983.

By Riki Kline, 4X4NJ

From *QST*, February 1985

Build a 4X Array for 160 Meters

Low-angle radiation and electrical rotation of directivity are the features of this vertically polarized top-band antenna. If you are interested in 160-meter DX, this system could be your secret weapon.

Is your lament a common one — no room for an effective DX antenna on 160 meters? This complaint is voiced frequently by amateurs who live in urban areas, or who are programmed toward horizontal wire antennas. But, a number of successful top-band operators have adopted the philosophy, "If you can't go out, go up!" It is no secret that a physically short vertical antenna is generally more effective than a horizontal antenna that is close to the ground electrically, at least for DX work.

My 4X array is electrically rotatable. It is compact and is effective as a low-angle radiator. Let's examine how my antenna evolved from some basic designs. I will also cover the practical details of construction and system performance.

The Tilted Ground-Plane Look

The tilted ground plane is almost identical to the usual vertical. The physical format of this antenna resembles a four-conductor ground plane. The major difference is that the radiating elements tilt up toward the supporting structure. The 4X array contains four sloping ground planes. Each of the slope wires is 100 feet long.[1] They are supported at the high end by an 80-foot tower. A four-element, 20-meter Yagi antenna is atop the tower.

Each of the sloping wires is fed separately near ground by means of a tapped-coil matching device (Figure 1) that is returned to radial wires and ground rods. In effect, each radiator is a ground-plane vertical antenna that is slightly less than 0.25 wavelength. The matching inductor provides resonance and effects an impedance match to the coaxial feed line.

I believe that the metal tower and 20-meter antenna may possibly be functioning as a reflector because the Yagi antenna and tower combined with ground wires are resonant slightly below 1.8 MHz.

Two Tilted Ground-Plane Verticals in Phase

I had excellent results with one sloping vertical. Next, I installed a second system in the opposite direction. Switching between the two antennas (north-south sloping radiators) showed considerable front-to-back ratio (a relative reading of 15-20 dB). Subsequently, I connected the two antennas in phase. This gave a bidirectional pattern, east and west. Although I did not gather extensive data on the performance, I observed a 6-dB signal improvement with stations about 700 miles to the

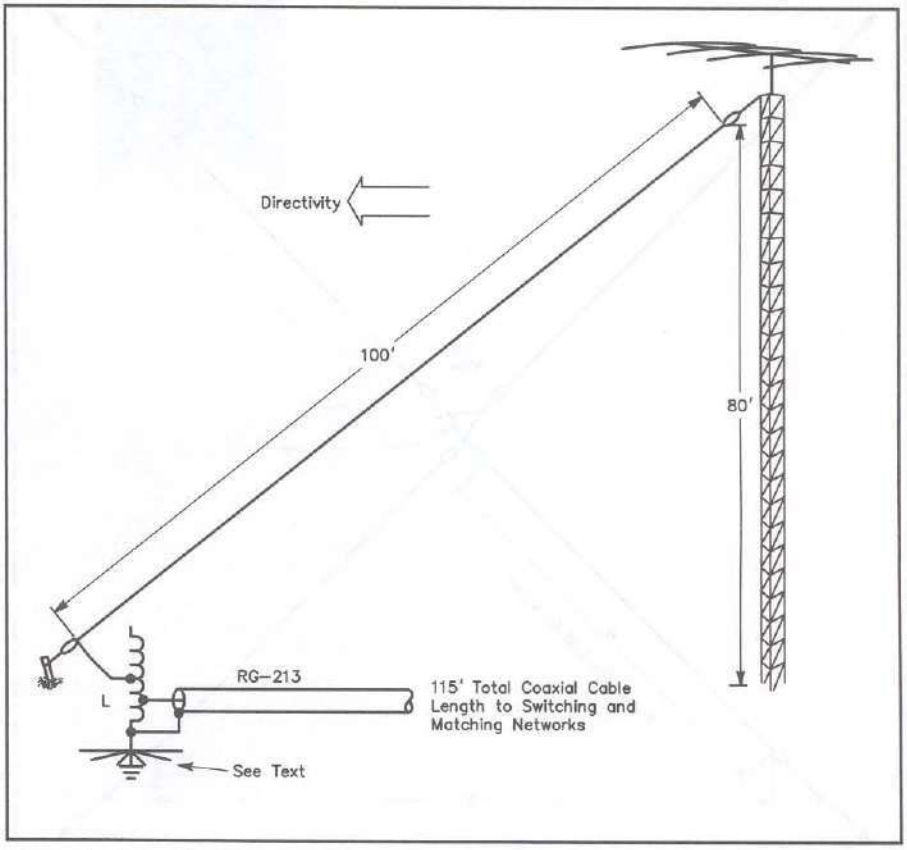

Figure 1—Basic tilted ground-plane vertical. L has 25 turns of heavy conductor (see text); length is 5½ inches, and diameter is 3 inches. Radiator is tapped 15½ turns above ground.

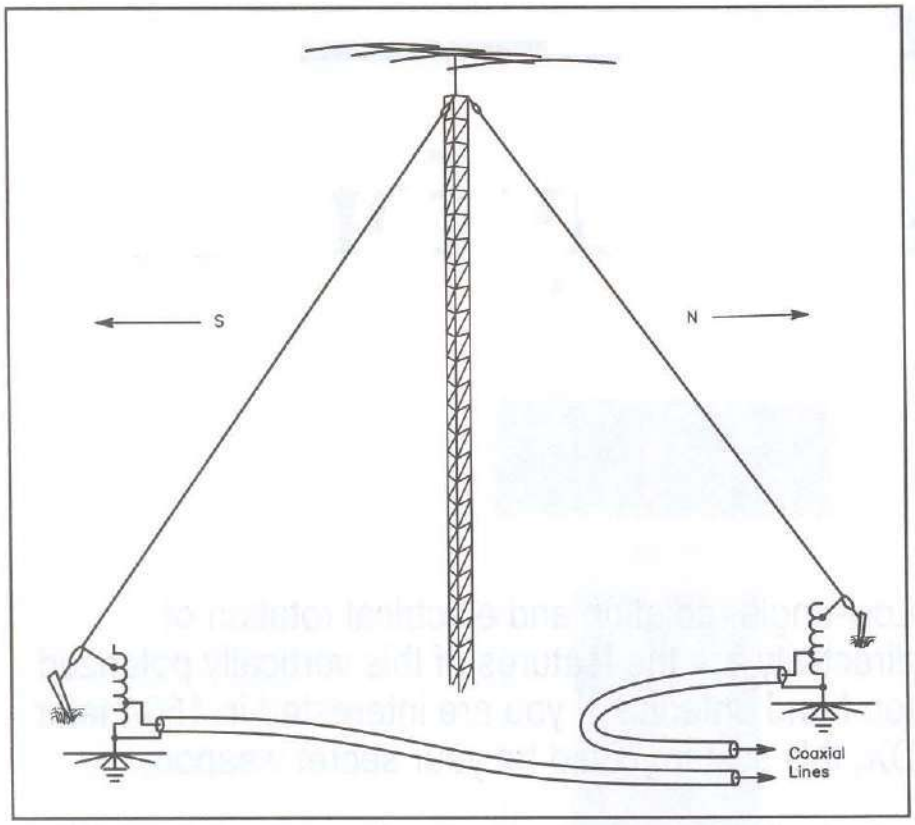

Figure 2—Two tilted ground-plane antennas that can be fed separately or in phase. The feed method is shown in Figure 1, with the method of Figure 7 used for feeding the antennas in phase.

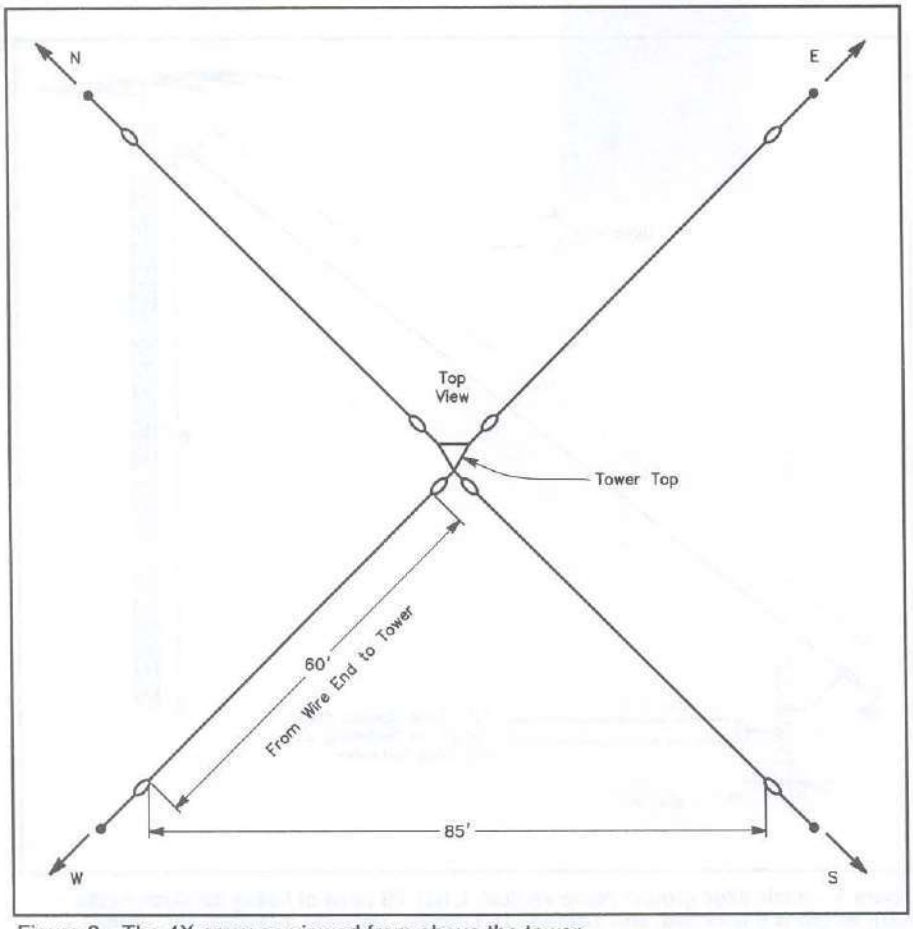

Figure 3—The 4X array as viewed from above the tower.

east. Some of you may want to explore the possibilities further. Figure 2 shows the details of the two-element phased system.

The 4X Configuration

Two more tilted ground-plane verticals were added, thereby providing east-west sloping radiators (Figure 3). A switching and phasing arrangement was added to my 4X array. It allows me to feed any of the slope wires separately, adjacent pairs in phase, or all four wires in phase. When using adjacent pairs in phase, maximum radiation is along a line that bisects the angle between the two antennas (NE, SE, SW or NW directions). When I feed all four wires in phase I note that the radiation is essentially omnidirectional. All of the unfed radiators are resonated to serve as reflectors. This concept is described in *The ARRL Antenna Book*.[2] My switching network is shown in Figure 4.

Phasing Networks

Most phasing methods call for long lengths of non-50-ohm coaxial cable.[3] I found this economically prohibitive. This negative factor inspired the approach I am using.

Each of my radiators is fed by means of 115 feet of RG-213 coaxial cable (formerly RG-8A/U 50-ohm line). The coil at the base of each wire is adjusted for the same resonance and SWR as the remaining three coils. The verticals to be fed in phase have their transmission lines connected in parallel through a suitable network for changing the reflected impedance back to 50 ohms. My networks are shown in Figures 7 and 8.

Tapped-Coil Matching

By using inductance and no intentional parallel capacitance for my matching coils, I am able to obtain greater effective antenna bandwidth because of reduced Q. Stray capacitance and antenna capacitance to the tower and ground are present, however. All electrical connections are soldered. A simple rain cover is used over each coil to protect it from moisture and dirt. The absence of switches, variable capacitors and rotary inductors enables construction of a highly reliable matching system without the need for weatherproof boxes.

This system is relatively easy to tune to obtain nearly identical performance from each antenna branch. This becomes a necessity when using "brute-force" parallel feed in the phased-pair and omnidirectional modes. Otherwise, the power distribution and phasing would be disturbed. This would distort the radiation pattern. Large-diameter, heavy-conductor, air-wound coils are best for this job. Two of my coils are made from silver-plated 1/4-inch-diameter copper tubing. The two remaining coils are made from large, flat conductor material of the kind found in some rotary inductors.

I used a dip meter to adjust the coils for resonance (coaxial cables disconnected). My coaxial cables were tapped initially one

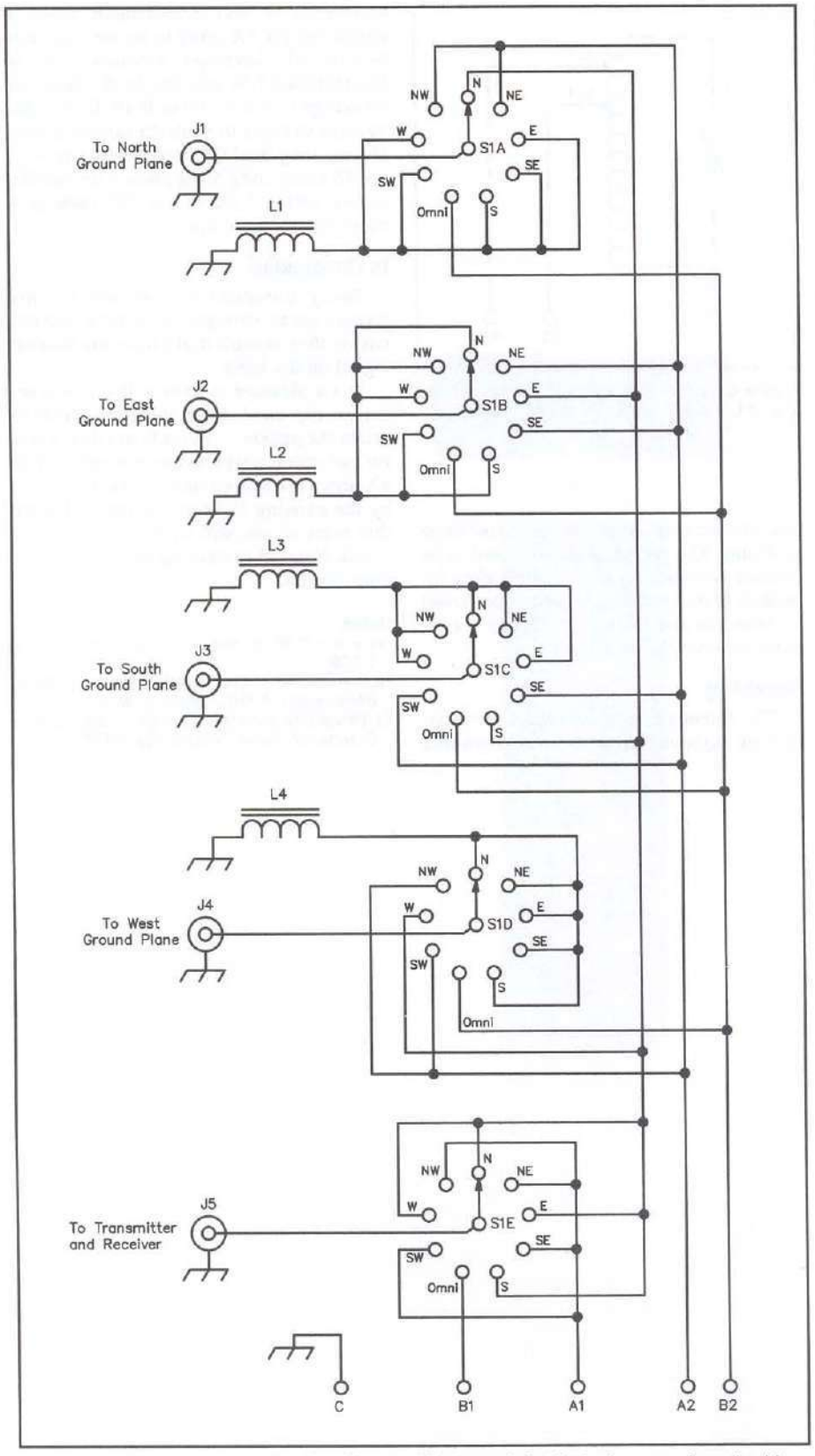

Figure 4—Switching system for the 4X array. L1 through L4, inclusive, are described in the text. A1, A2 and C are connected to the matching circuit shown in Figure 7. B1, B2 and C are connected to the matching circuit shown in Figure 8. S1 is a heavy-duty ceramic rotary switch, five poles, nine positions. J1-J5, inclusive, are coaxial connectors of the builder's choice.

Direction	SWR vs. Frequency				
	1800 kHz	1825 kHz	1850 kHz	1875 kHz	1900 kHz
N	1.4	1.0	1.2	1.8	2.6
NE	1.5	1.1	1.0	1.1	1.2
E	2.2	1.1	1.1	1.4	1.9
SE	1.2	1.0	1.0	1.0	1.1
S	1.4	1.0	1.1	1.4	2.3
SW	1.5	1.1	1.0	1.0	1.1
W	1.4	1.1	1.0	1.2	1.6
NW	1.2	1.0	1.0	1.0	1.2
Omni	1.4	1.1	1.0	1.0	1.0

Figure 5—Chart that shows SWR versus frequency in kilohertz.

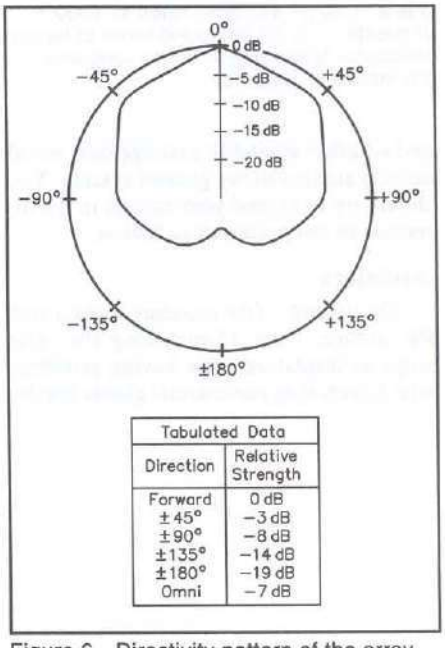

Tabulated Data	
Direction	Relative Strength
Forward	0 dB
±45°	−3 dB
±90°	−8 dB
±135°	−14 dB
±180°	−19 dB
Omni	−7 dB

Figure 6—Directivity pattern of the array. The pattern is a composite average of measurements made while receiving 10 different stations. There is no apparent difference between the two directive modes—single radiator or phased pair.

third of the way up from the ground ends of the coils. Final tap placement is made while feeding power to the antenna and observing an SWR meter. Alligator clips make this an easy matter to accomplish. When the SWR bottoms out at the same frequency for all four radiators, remove the alligator clips and solder the coil taps in place. Some interaction between the four antennas will occur, so make certain that all of the taps are where they belong before soldering them.

Reflector Tuning

The radiators not being fed are used as reflectors. This is done by switching small inductors in parallel with the ends of the coaxial feed lines. My inductors contain three or four turns of no. 16 wire wound around the center part of a 3/8-inch-diameter ferrite rod from a built-in AM broadcast receiver antenna. The coils are adjusted to give a resonance that is four percent lower than the resonant frequency of the radiators.

Ground Conditions

The efficiency and performance of the antenna depends on the quality of the ground system. Note 3 provides a good reference for ground systems, and a bibliography. Each of my radiators is worked against a counterpoise that contains two or three 1/4-wavelength wires, bent to fit in the boundaries of my property. In addition, I use a 10-foot rod in the ground. Water pipes

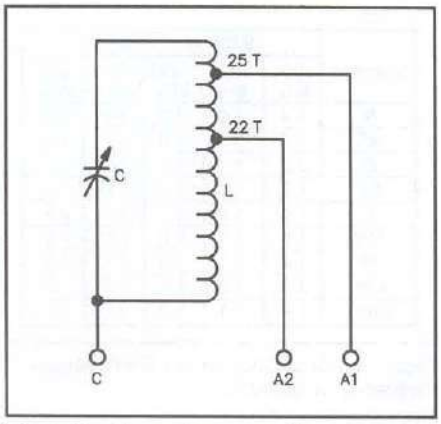

Figure 7—Phased-pair matching network. C is a 1000-pF variable, rated at 1000 V or greater. L is 30 airwound turns of heavy conductor (see text), 7 inches long and 3½ inches in diameter.

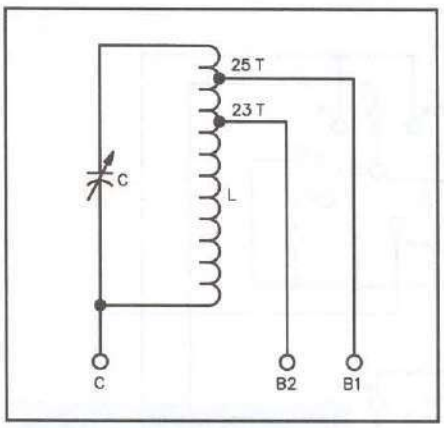

Figure 8—Network for omnidirectional use. C and L are the same as for Figure 7.

and all other available underground metal objects are tied to my ground system. You should try to extend your radials in the direction of the preferred radiation.

Insulators

The top ends of the radiators contain high RF voltage. I use 15-inch-long Plexiglas strips as insulators, after having problems with 8-inch-long commercial plastic insulators. Moisture and air pollutants caused these problems. The present insulators need to be cleaned periodically. High-quality glass insulators of the type used aboard ships should be excellent and, with luck, should not require periodic cleaning.

Receiving

The antenna directivity enhances reception by rejecting signals from unwanted directions. I was encouraged when I compared my 4X array to an 800-foot unterminated Beverage antenna that is bidirectional NW and SE. In the past, the Beverage wire showed an 8-10 dB S/N advantage over the tilted north vertical alone. During long-haul QSOs to North America, the 4X array, used in the phased-pair mode, comes within 3 dB of the S/N ratio provided by the Beverage.

In Conclusion

Many European stations tell me my signals are as strong as local ones. On occasion they remark that I have the loudest signal on the band.

It's a pleasure to have a directional array on top band. I simply turn a knob to rotate the pattern — much faster than a motor can rotate a typical beam antenna! The 4X array is compact and can be supported by the existing HF-antenna tower. I hope that some of you will try this antenna, and I look forward to hearing from you about your results.

Notes

[1]m = ft × 0.3048; mm = in × 25.4; km = mi × 1.609.

[2]G. Hall, ed., *The ARRL Antenna Book* (Newington: ARRL, 1984), p. 8-12.

[3]J. Devoldere, *80-Meter DXing* (Greenville, NH: Communications Technology, 1978).

By Rod Newkirk, W9BRD

From *QST*, June 1990

The 'BRD Zapper: A Quick, Cheap and Easy "ZL Special" Antenna

Here's a multipurpose directional wire antenna that has its origins in Kraus, Windom and Newkirk *(who?–Ed.)*.

Working Europe from Chicago with low power on 21 MHz, using an indoor, bent-ends W8JK bidirectional wire beam (Figure 1)[1], is fairly straightforward fun. Voltage feed via a λ/4 stub, gamma-matched to coax, is hard to beat for spartan simplicity. No worry about balancing element currents, no nit-picking with element lengths. Just make the whole system symmetrical and dip it to your favorite frequency by adjusting the stub-shorting point.[2] The 8JK has a similar pattern and good gain all the way from the fundamental to the second harmonic, so it's really a multiband antenna. You can roll the whole thing up in three minutes when it's not in use.

One problem: The bidirectional characteristics of the 8JK cause my ears to be flattened regularly by undesired signals from the direction opposite Europe. Unless you're in the geographical center of a three-way QSO, the unused lobe of this antenna can be a nuisance. Question: Is it feasible to convert easy 180° bidirectionality to tricky 135° *uni*directionality without resorting to clumsy center-feeding, multi-wire-dipole elements, balanced-gammas, etc?[3]

Yes—because there's a *uni*directional ZL Special lurking in our little 8JK. The principal difference between the W8JK and the ZL Special lies in the phasing: In the 8JK, the elements are fed 180° out of phase; in the ZL Special, they're driven 135° out of phase. Therefore, instead of feeding the antenna near the stub's shorting point, we'll need to feed it λ/16 from the stub's shorted end. That's where the feed path to one element is λ/8 (45°) longer or shorter than the other, which, after the stub's 180° phase reversal, produces the 135° phase shift that were looking for between the elements.

You can find the proper feed point on the stub by "sniffing" signals of known origin along *one side* of the stub with the insulated center conductor of some coax hooked to a receiver. (Start looking for this point by measuring λ/16 up from the bottom of the stub.) It's refreshing to hear Europeans rolling in while most of the murderous rearward signals now barely budge the S meter! Directivity is reversed at the opposite stub point (Figure 2).

So he's in there all right, that ZL Special, but coaxing the wily rascal out for an honest day's work is a challenge. The ZL

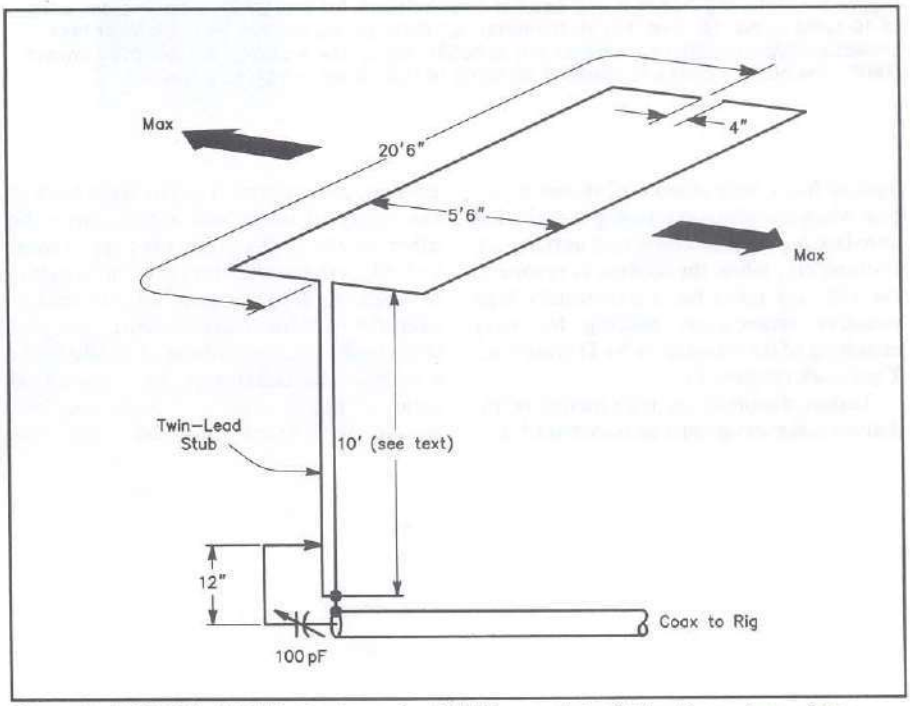

Figure 1—W9BRD's W8JK wire beam for 21 MHz, made to fit the dimensions of the townhouse bedroom that it occupies. Its dimensions aren't critical, although the element lengths should be close to λ/2 (total, each), the stub should be λ/4 or odd multiples, and the element spacing should be close to λ/8. At the bottom of the stub, connect both stub wires and the coax braid together, after resonating the system as outlined in Note 2. The 12-inch tap distance and 100-pF variable capacitor constitute a gamma match that brings the stub impedance to 50 Ω.

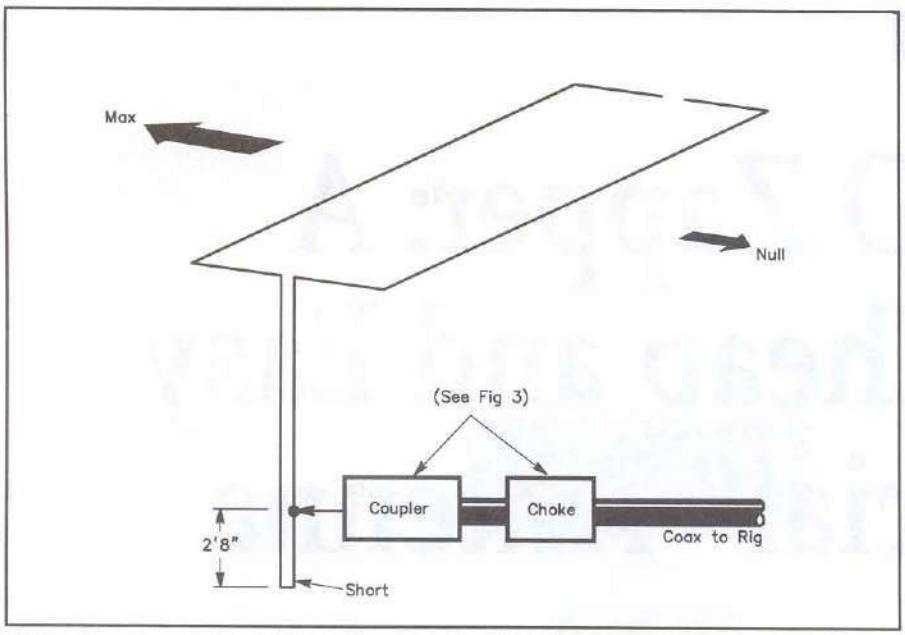

Figure 2—The antenna of Figure 1 configured for unidirectional operation with 135° element phasing. Resonate the system as described in Note 2 and connect the coupler via a very short wire to one leg of the stub about λ/16 above the stub-shorting point. The coaxial choke is needed to eliminate feed-line radiation, which can ruin the rearward null that this system provides.

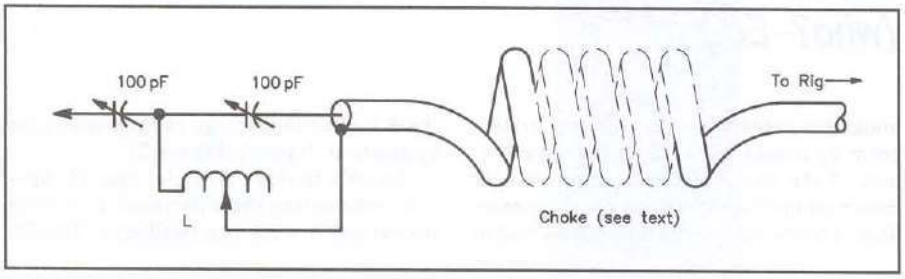

Figure 3—Matching-network and coaxial-choke details for the 'BRD Zapper. L consists of 10 turns of no. 16 wire, 1½ in. diameter, air core, space wound. For 100 W or less, broadcast-type variable capacitors are suitable. Adjust the inductor-tap point for lowest SWR. The coaxial choke is made of 30 turns of RG-58 wound on a ferrite rod.

Special has a very sharp null in one direction when the element phasing is right, but unbalancing the stub could cost us that null. Fortunately, when the system is resonant, the 135° tap point has a moderately high resistive impedance, making for easy matching of the antenna to 50-Ω coax via a T network (Figure 3).

Pattern distortion through incidental radiation and pickup must be minimized. Excessive leakage would put us right back at the mercy of those loud signals from the other direction. Therefore, the coupler must be built in the most compact form possible, mounted right at the stub, and isolated to keep the feed line from distorting the pattern. Such isolation is done at W9BRD via a home-brew coaxial choke made of 30 turns of the antenna's RG-58 feed line wound on a ferrite rod just before the matching network.

Because feeder radiation could upset the stub balance—and thus spoil the antenna's rearward null—the single-wire run from the matching network to the antenna had better be no more than an inch or two. Here, I'm borrowing on the single-wire-feed theme by Windom. Any circuitry above the choke will be hot with RF, so a bulky meters-bells-and-whistles matching unit will not do. It's best to use a compact, barebones, dedicated network. Run the stub all the way down from the flat top if possible. Incidentally, the tap point on the stub corresponding to the best rearward null is higher on the stub for element spacings wider than λ/8. System Q is also lower with wider spacings, but gain is maximum at λ/8.

As for the stub itself, TV twin lead is okay indoors, but close-spaced, end-fire elements mean high voltages and currents. If the stub is to be longer than a quarter wavelength (odd multiples only) or outside in the weather, low-loss, open-wire line is a must. You can run the stub of an outdoor version directly into the shack for handy directivity reversal.

Though we've been talking horizontal, this setup should be equally interesting as a vertical. By the way, when the elements are placed horizontally, one above the other, 135° phasing accentuates radiation and reception at high angles. Neat for local traffic nets, Sweepstakes and Field Day!

Notes

[1]Dr John D. Kraus, W8JK, first described this antenna in *QST* in "Directional Antennas with Closely Spaced Elements," *QST*, Jan 1938, pp 21-23, 37. Kraus also discussed this antenna in three articles in *Radio* magazine in 1937 and 1939, and in *Proceedings of the IRE*, Feb 1940.

[2]The easiest way to do this is with a dip meter. Jab a straight pin into each leg of the stub near the bottom, short the pins together and couple the dip meter into the system by bringing the dip motor close to the shorted pins. Locate resonance using the dip meter and measure the dip-meter frequency on your receiver. Move the pins up or down the stub and repeat the process until the antenna is resonant at or near your frequency of interest. When you've done this, cut the stub, strip and solder a short in the wires where the pins were located at resonance.

[3]Of course, this antenna can be center fed in either its bidirectional or unidirectional modes. Such flat tops are described in J. Hall, Ed., *The ARRL Antenna Book*, 15th ed, (Newington: ARRL, 1988), Chapter 8, and J. Devoldere, *LowBand DXing* (Newington: ARRL, 1987), pp 2-101 through 2-102.

Combination Driven Arrays

Broadside, end-fire and collinear elements can readily be combined to increase gain and directivity, and this is in fact usually done when more than two elements are used in an array. Combinations of this type give more gain, in a given amount of space, than plain arrays of the types just described. The combinations that can be worked out are almost endless, but in this section are described only a few of the simpler types.

The accurate calculation of the power gain of a multi-element array requires a knowledge of the mutual impedances between all elements, as discussed in earlier sections. For approximate purposes it is sufficient to assume that each set (collinear, broadside, end-fire) will have the gains as given earlier, and then simply add up the gains for the combination. This neglects the effects of cross-coupling between sets of elements. However, the array configurations are such that the mutual impedances from cross-coupling should be relatively small, particularly when the spacings are 1/4 λ or more, so the estimated gain should be reasonably close to the actual gain.

FOUR-ELEMENT END-FIRE AND COLLINEAR ARRAY

The array shown in Figure 1 combines collinear in-phase elements with parallel out-of-phase elements to give both broadside and end-fire directivity. It is popularly known as a "two-section W8JK" or "two-section flat-top beam." The approximate gain calculated as described above is 6.2 dB with 1/8-λ spacing and 5.7 dB with 1/4-λ spacing. Directive patterns are given in Figures 2 and 3.

The impedance between elements at the point where the phasing line is connected is of the order of several thousand ohms. The SWR with an unmatched line consequently is quite high, and this system should be constructed with open-wire line (500 or 600 Ω) if the line is to be resonant. With 1/4-λ element spacing the SWR on a 600-Ω line is estimated to be in the vicinity of 3 or 4 to 1.

To use a matched line, a closed stub 3/16 λ long can be connected at the transmission-line junction shown in Figure 1, and the transmission line itself can then be tapped on this matching section at the point resulting in the lowest line SWR. This point can be determined by trial.

This type of antenna can be operated on two bands having a frequency ratio of 2 to 1, if a resonant feed line is used. For example, if designed for 28 MHz with 1/4-λ spacing between elements it can be operated on 14 MHz as a simple end-fire array having 1/8-λ spacing.

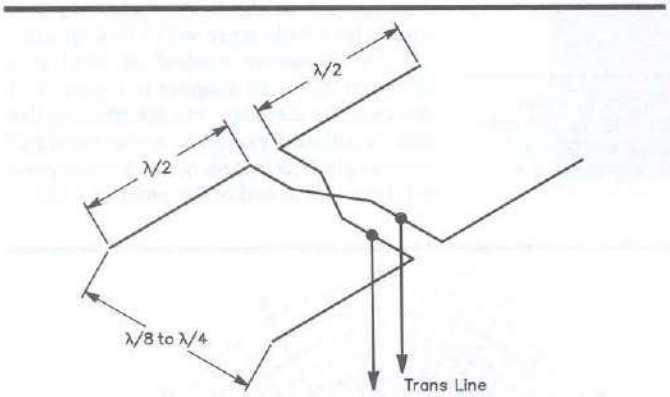

Figure 1—A four-element array combining collinear broadside elements and parallel end-fire elements, popularly known as the W8JK array.

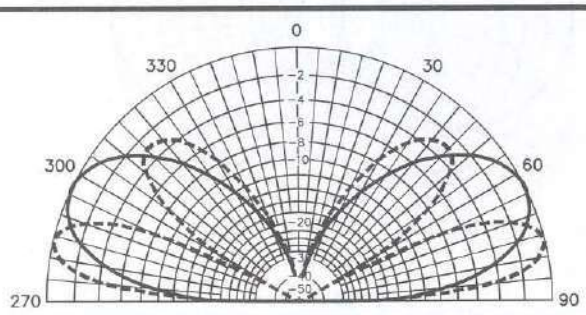

Figure 2—E-plane pattern for the antenna shown in Figure 1. The elements are parallel to the 90°-270° line in this diagram. Less than a 1° change in half-power beamwidth results when the spacing is changed from 1/8 to 1/4 λ.

Figure 3—Vertical pattern for the four-element antenna of Figure 1 when mounted horizontally. Solid curve, height 1/2 λ; broken curve, height 1 λ above a perfect conductor. Figure 2 gives the horizontal pattern.

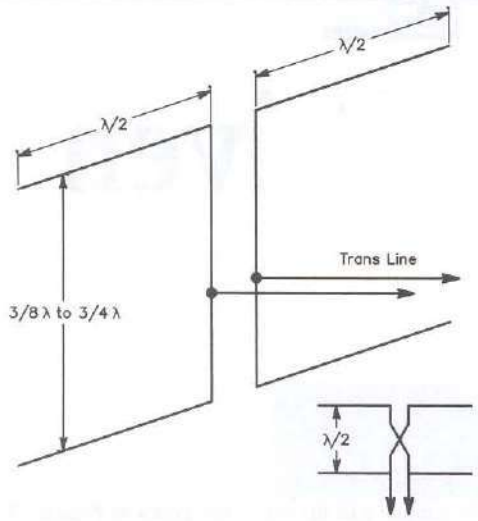

Figure 4—Four-element broadside array ("lazy H") using collinear and parallel elements.

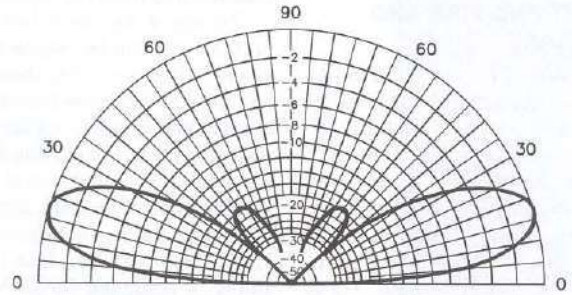

Figure 6—Vertical pattern of the four-element broadside antenna of Figure 3, when mounted with the elements horizontal and the lower set ½ λ above a perfect conductor. "Stacked" arrays of this type give best results when the lowest elements are at least ½ λ high. The gain is reduced and the wave angle raised if the lowest elements are close to ground.

FOUR-ELEMENT BROADSIDE ARRAY

The four-element array shown in Figure 4 is commonly known as the "lazy H." It consists of a set of two collinear elements and a set of two parallel elements, all operated in phase to give broadside directivity. The gain and directivity will depend on the spacing, as in the case of a simple parallel-element broadside array. The spacing may be chosen between the limits shown on the drawing, but spacings below 3/8 λ are not worthwhile because the gain is small. Estimated gains are as follows

3/8-λ spacing—4.4 dB
1/2-λ spacing—5.9 dB
5/8-λ spacing—6.7 dB
3/4-λ spacing—6.6 dB

Half-wave spacing is generally used. Directive patterns for this spacing are given in Figures 5 and 6.

With 1/2-λ spacing between parallel elements, the impedance at the junction of the phasing line and transmission line is resistive and is in the vicinity of 100 Ω. With larger or smaller spacing the impedance at this junction will be reactive as well as resistive. Matching stubs are recommended in cases where a nonresonant line is to be used. They may be calculated and adjusted as described in Chapter 26.

The system shown in Figure 3 may be used on two bands having a 2-to-1 frequency relationship. It should be designed for the higher of the two frequencies, using 3/4-λ spacing between parallel elements. It will then operate on the lower frequency as a simple broadside array with 3/8-λ spacing.

An alternative method of feeding is shown in the small diagram in Figure 3. In this case the elements and the phasing line must be adjusted exactly to an electrical half wavelength. The impedance at the feed point will be resistive and of the order of 2 kΩ.

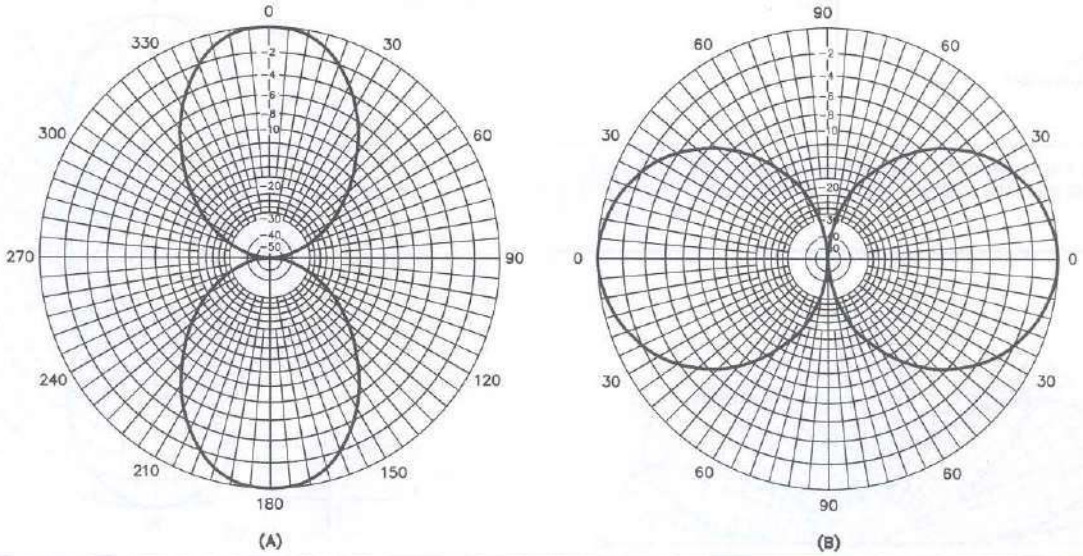

Figure 5—Free-space directive diagrams of the four-element antenna shown in Figure 4. At A is the E-plane pattern, the horizontal directive pattern at low wave angles when the antenna is mounted with the elements horizontal. The axis of the elements lies along the 90°-270° line. At B is the free-space H-plane pattern, viewed as if one set of elements is above the other from the ends of the elements.

CHAPTER SEVEN

VERTICALLY POLARIZED

7-1 **More on "Half Slopers" and Half-Sloper Variation for 160 Meters**
From December 1979 *QST* (Technical Correspondence)

7-3 **A Two-Band Half-Sloper Antenna**
From June 1980 *QST*

7-7 **The KI6O 160-Meter Linear-Loaded Sloper**
From April 1986 *QST*

7-8 **The Super Sloper**
From December 1995 *QST*

7-12 **The Inverted L Revisited**
From January 1983 *QST*

7-14 **160-Meter Antennas**
From July 1991 *QST* (Technical Correspondence)

7-16 **A Truly Broadband Antenna for 80/75 Meters**
From April 1986 *QST*

7-19 **Improved Broadband Antenna Efficiency**
From August 1987 *QST* (Technical Correspondence)

7-20 **Simple, Effective, Elevated Ground-Plane Antennas**
From June 1994 *QST*

More on "Half Slopers"

The July 1979 *QST* article on quarter-wave slopers has prompted me to write you on the subject. I have had considerable experience using them on 160 and 80, and I have tried them on 40.

The first one I know who used this type antenna was W3AU. His success with the system on 160 caused him to recommend it to W7RM and me. The original configuration used more than one sloping element fed in parallel against the tower. It resembled a top-loaded vertical with a simulated ground system. All my results have supported the view that this is an omnidirectional, vertically polarized radiating system, even when only one sloping element is used.

All the antennas of this type I have tried have been at my father's station, W6UA, and have been on a single tower. The tower is 82 feet (25 m) high, approximately 1½ feet (0.45 m) in uniform triangular cross section, and has a single set of guys at the 70-foot (21.3-m) level. The guys are broken with insulators at about 20-foot intervals, and the top section of each guy is electrically connected to the tower. The base has whatever insulation the concrete provides and there are 10-, 15- and 20-meter Yagis on top of the tower. (This is an AB105 tower, the same as is used by W3AU and W7RM.)

The first antenna of the type in question was tried on 80 meters. It was attached at the 60-ft level, so that top-loading effects of the guys, as well as the rotaries, were probably effective. The attached wire came off at 30° to vertical and was trimmed for minimum VSWR. The resultant length was within 2 feet of the formula length, and the antenna then had a VSWR less than 1.5 from 3.5 to 4.0 MHz. It worked well on transmit but was extremely noisy on receive. The original wire sloped east, so I put up an identical system, attached to the same tower level, sloping west. Electrical characteristics were nearly identical, and no directivity difference between the two could be detected either on transmit or receive.

This is logical considering how little of the antenna current in the sloping wire has any horizontal component, other antenna systems used on 80 at W6UA have been dipoles, inverted Vs, and a delta loop. The quarter-wave sloper is better than any of the others for transmitting, but it is poor on receiving. I have taken down all but the two slopers. They are used for transmitting and receiving, with frequent use of a 40-meter collinear antenna on receiving weak signals.

I also tried this system on 40, with a wire attached to the tower at 30 feet, coming off at 30°. Perhaps because there was so much tower electrically above the attachment point – at least half a wavelength – this one was much harder to tune. The wire length, which was very critical, was some feet shorter than expected, and the VSWR behavior across the band less benign. Not much time was spent on this particular antenna because it seemed no better than a λ/2 vertical. Both worked well, but neither was the equal of the collinear types available.

The most recent quarter-wave sloper system I have used has been on 160 meters. My first attempt was a single sloping element from the 75-foot level. This places whatever contribution there is from the top guy sections below the point of attachment. I couldn't get this antenna to match by altering the length of the sloping wire, even while making rather severe adjustments. There did seem to be some promise for the system, so the next season I used two sloping elements of about the "correct" length and fed the arrangement with a matching network at the bottom of the tower, with 300-ohm twin-lead going up the tower (Figure 1). This was the best antenna I have used on 160 at W6UA. Previously I had used an inverted V, a center-fed 80-meter dipole at 90 feet and a λ/2 inverted L. Since the wires must come off the tower at about 45-50° to vertical, the rationale of using two wires instead of one was to attempt to cancel the horizontal current component. As a matter of curiosity I tried adding a third wire and could find no change in setting of the matching components or in the

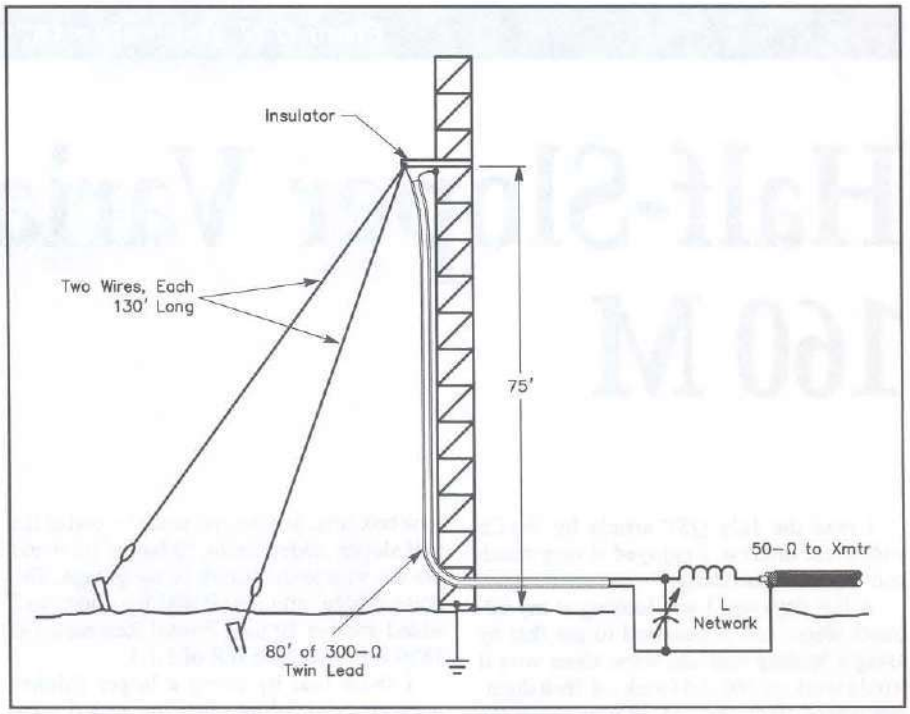

Figure 1—Illustration of the arrangement used at W6UM for a 160-meter half sloper.

overall effectiveness. Using some rough estimates of component values required for matching, length of feed line, etc., I calculate the feed impedance of the antenna itself to be approximately 100–*j*300 ohms.

My estimate of how well this antenna performs must be tempered by the realization that conditions during the past two years have been much worse than the period before. During the 160-meter contests, openings to W1, W2 and W3 have been marginal. I have worked nothing with this antenna I hadn't worked before, but the impression remains that the antenna is better than those used earlier. It has done a consistent job into the Caribbean, SA, Pacific and Japan, as well as across the USA. Receiving remains a problem because of the noise. I have taken down the 160-meter version of this antenna. If I put it up again I will definitely install some auxiliary receiving antennas.

The net result seems to be that this is an effective antenna. Getting a good match directly into coax appears easier if the sloping wire is more nearly vertical and if there is not too much loading above the attachment point. The system should be more efficient, up to a point, as there is more vertical structure above the feed point. There is no compelling reason to insist upon using a resonant configuration. The next attempt I make on 160 might well be with the existing 80-meter system, fed at 60 feet and with 80-meter sloping elements, but using a transmission line and matching network at the bottom of the tower as before.

Given that the antenna does work, the areas I feel need further investigation are better characterization and description of it for different parameters, e.g., measurement of the feed impedance as a function of frequency for different sloper attachment points, lengths, angles and conditions of top loading. I would also like to see the current flow on all of the structure mapped via a probe. If some of the results are forthcoming I hope to see them in an early issue of *QST*. — *Charles Weir Jr., W6UM*

From *QST*, December 1979 (Technical Correspondence)

Half-Sloper Variation For 160 M

I read the July *QST* article by W1CF with great interest. I enjoyed it very much and learned something.

A few days ago I was looking at my 80-meter sloper and it occurred to me that by using a loading coil and some more wire it would work on 160. So I took a 4-inch diameter coil of 10 turns of no. 10 wire out of the junk box, attached the coil to the far end of the half sloper, added about 30 feet of wire and ran the wire to the corner of my garage. The noise bridge indicated it was too short, so I added another 10 feet. Presto! Resonance at 1830 kHz with an SWR of 1.1:1.

I think that by using a larger (higher inductance) loading coil, the added wire could be shortened considerably without seriously affecting the 2-to-1 SWR points on the curve.

I have not made too many contacts on 160 yet, as there is very little activity this early in the season around here. I have had several contacts though, always getting at least as good a report as I have given. —*Philip True, W7AQB.*

By Gary E. Myers, K9CZB

From *QST*, June 1980

A Two-Band Half-Sloper Antenna

When an off-the-wall empirical design like this works well, suspicion and skepticism are warranted. Maybe you'll agree that this sloper idea is an exception!

The popularity of the half-sloper antenna seems to be increasing, as evidenced by recent articles in *QST*.[1,2,3] This type of antenna has some worthwhile advantages, particularly for the lower frequency operator – low-angle radiation for antennas of modest height, compactness and simplicity of construction. On the minus side, narrow bandwidths and difficulties in resonating the system have been reported.[3]

The antenna system to be described here evolved from a simple-minded attempt to design a two-band half sloper for 80- and 40-meter operation. A trap-type of antenna was selected as the design basis because of previous experience with trap antennas and because the inductive loading of the trap on the lower-frequency band allows a somewhat shorter overall length. The same inductive loading, however, was also expected to increase the antenna Q and thereby further decrease the bandwidth. For this reason I was prepared to experiment.

It is well that I was so prepared because the final form of the antenna bears little resemblance to the initial concept. But most interesting — and exciting — is the impressive bandwidth on 80 meters.

The Design

A diagram of the two-band half-sloper antenna system is shown in Figure 1. It can be seen that there is no obvious quarterwave dimension in the entire system. In fact, the radiator itself is a nonresonant device.

Initial attempts to prune the wires to resonance resulted only in a mound of wire clippings and one frustrated amateur. After many hours of cut-and-try experimentation, accompanied by a growing, gut-level appreciation for what apparently was happening, the magic combination of wire lengths and trap component values was found. Impedances of 40 $-j80$ ohms at 7.2 MHz and 60 $-j40$ ohms at 3.6 MHz were measured with a noise bridge. It was then a simple matter to cancel out these capacitive reactances with an inductor.

For convenience, the inductor was placed in the transmission line, rather than at the feed point – final "tweaking" of the system is more easily performed on the ground than at 40 feet (12.2 m) in the air. A Smith Chart exercise shows that the SWR on the transmission line between the feed point and inductor L is 5:1 at 7.2 MHz and 2:1 at 3.6 MHz. When RG-8/U is used, the additional loss incurred because of these SWRs is less than 0.5 dB at 7.2 MHz and is almost nonexistent at 3.6 MHz.

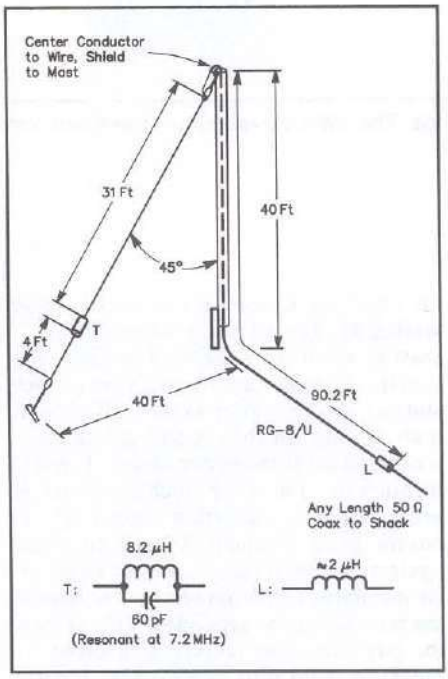

Figure 1—The two-band half sloper. To shield the transmission line from the antenna field, the line is routed up the inside of the support mast, which is grounded. Inductor L is needed to resonate the system.

Performance

This antenna performs very well. Operation at K9CZB is primarily 80-meter cw, with some 40-meter ssb. Power output is nominally 100 watts. Signal reports on 80 have been uniformly good, with comments such as U R LOUDEST 9 ON BAND AND VY FB SIG, VY STRONG. Voice operation on 40 has also resulted in good signal reports, although the praise has not been so lavish. This is my only 80/40-meter antenna, so direct comparisons were not possible. However, it appears to greatly outperform two previous antennas, a 160-foot end-fed wire and a trap dipole, both strung 30 feet above ground. All in all, it is about what I expected from a half sloper.

This kind of performance is nice, but nothing to write an article about, since that has already been done. The real performance story about this antenna can be summed up in one word: bandwidth. A glance at the SWR curves in Figure 2 will open the eyes of any 80-meter operator. As far as I know, this is unheard-of bandwidth for such a simple and compact antenna. It is a real treat to QSY 400 kHz And see the SWR meter needle barely move. This isn't a low-Q antenna —it's a *no*-Q antenna! The bandwidth on 40 is far less impressive and is, in fact, similar to what has been reported previously for half slopers.

Construction

During experiments with prototypes of this antenna, I noticed some sensitivity to feed-line placement and length. Therefore,

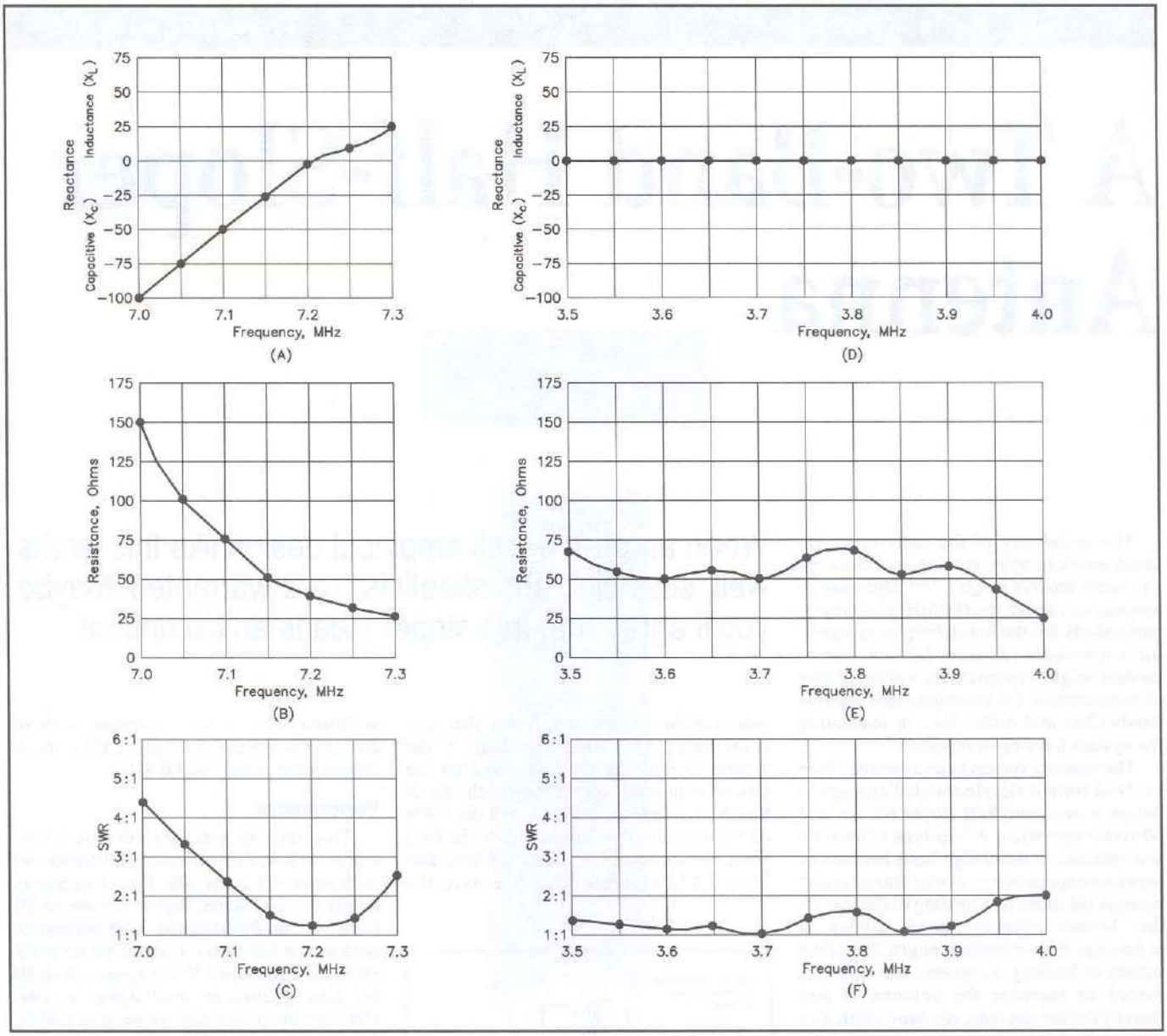

Figure 2—Loading characteristics of the antenna. The SWR curves were determined from a Smith Chart. Impedance values were measured with a noise bridge.

in later versions I ran the feed line up the *inside* of the support mast to shield it from the antenna field. This precaution seems to be effective, for no such sensitivity has been observed since. (I can't help but wonder if this might improve the behavior of any cantankerous half sloper.) If a nonmetallic support is used, or if there is no possibility of placing the feed line inside the support, double-shielded coaxial cable should serve equally well, provided the outer braid is connected to the inner braid at the top of the tower and a ground is connected to the outer braid at the bottom of the tower.

I used standard 10-foot TV mast sections for my support, simply because they were on hand. This results in a very flimsy and flexible mast in a 40-foot length, though. The first 20 feet must be doubled up with long U-bolts if the mast is to be walked up. The price of six sections of TV mast is about the same as a 36-foot telescoping push-up mast, but the latter is much sturdier and far easier to erect. If support materials are not already on hand, the telescoping mast is the better choice. I should mention that I took the trouble to bond all sections of mast together electrically to ensure good conductivity and to guard against TVI from rectification at joints after inevitable corrosion sets in. The base of the mast should be grounded. Effects from the guy wires can largely be avoided by breaking them into nonresonant lengths with strain insulators placed at the mast and every 19 feet thereafter.

The inductance and capacitance values shown in Figure 1 must be used for the trap. Construction techniques for the trap are covered in *The ARRL Antenna Book*.[4] A novel and inexpensive method of trap construction has been described by WB9OQM.[5] I built my trap using the method shown in Figure 3. Traps made in this fashion are much stronger than they appear. I've never had one break, even in high winds that caused property damage. In this antenna, however, the radiator also serves as one of the top guys. For that reason the trap was reinforced. Two 3/16-inch thick pieces of plastic were used with three layers of glass cloth and epoxy sandwiched between them. A rotary wire brush serves well to rough up the inner surfaces of the plastic to ensure good adhesion. However, one may use coarse sandpaper for that purpose. Glass cloth and epoxy are sold as a repair kit in many hardware stores.

Before the antenna wires are connected,

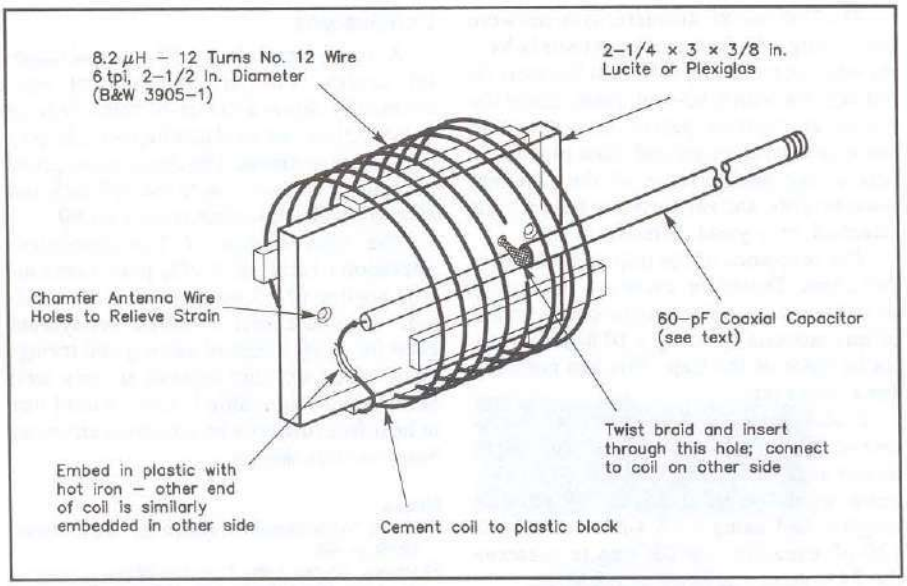

Figure 3—A simple, sturdy trap. The coaxial capacitor should be taped to the antenna wire after installation. It is not necessary to enclose the trap.

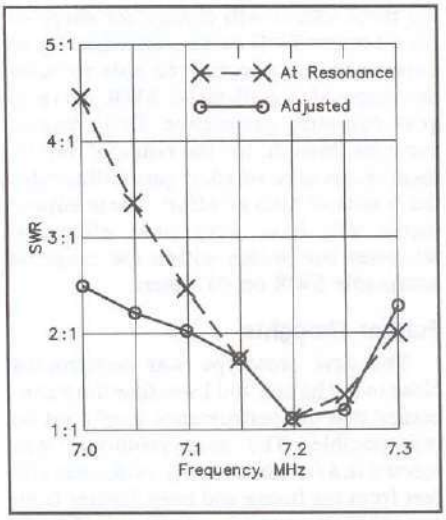

Figure 4—SWR curve for 40 meters, showing the effect of tapping L and adjusting feed-line length between L and the transmitter to obtain the best SWR curve. Such adjustments have little effect on 80-meter characteristics.

the trap must be tuned to resonance. A dip meter or noise bridge can be used to measure the resonant frequency. Start with about 30 inches of RG-8/U for the coaxial capacitor. After connecting it to the coil, as shown, 26 or 27 inches of braid will remain. At this point, the resonant frequency should be below 7.0 MHz. Trim the braid at the far end, a little at a time, snipping off the center conductor as you go. Recheck the resonant frequency each time. As 7.2 MHz is approached, continue trimming the braid, but stop cutting the center conductor. To increase the leakage path, the polyethylene dielectric should extend beyond the braid 1/8 to 3/16 inch (3.2 to 4.8 mm) when the trap is resonated at 7.2 MHz. Very close to 24 inches of braid should remain at completion. Tightly tape this end with several layers of plastic electrical tape.

The component values for this trap are exactly the same as those used in the W3DZZ trap dipole,[4] so there are several commercially made traps that may be suitable for this antenna. Traps made for a five-band, two-trap dipole, 108 feet long should have the proper values of capacitance and inductance.

In any antenna system, the radiator feed point impedance repeats itself every half wavelength along the transmission line. Inductor L must be inserted in the transmission line at a half-wave point in order to exactly cancel the capacitive reactance of this antenna system. It is, of course, advantageous to place L as close to the feed point as possible in order to minimize losses. A half wavelength at the lower frequency is as close as you can get without going to the feed point itself. The 90.2-foot length of RG-8/U shown in Figure 1 is an electrical half wavelength at 3.6 MHz for solid polyethylene dielectric coaxial cable *only*. If cable having a velocity factor other than 0.66 (e.g., foam-dielectric coaxial cable) is used, this length will have to be recalculated from the equation

ℓ = 492 V/3.6 feet
(Feet × 0.305 = m)

In this equation, V is the velocity factor of the cable to be used. Only RG-8/U or a similar type such as RG-213/U should be employed for this section of the transmission line in order to keep the losses low. If you don't mind a dB or so of loss on 40 meters, RG-58/U is acceptable. The loss on 80 meters will be negligible in any case.

The value of inductor L should be 1.75 μH, but I recommend that a coil having about 3-μH inductance be used to allow some latitude for final tune-up of the system. I mounted 12 turns of a no. 3018 Miniductor (1¼ inch in diameter, 8 turns per inch) in a small Minibox with SO-239 coaxial connectors placed at each end. After tapping the coil for the best SWR curve on 40 meters, the entire assembly was sealed and waterproofed with bathtub caulk.

Tune-up

As seems to be characteristic of half slopers, this antenna can be very touchy to tune up. If the length of transmission line between the radiator and L is not an exact integral multiple of a half wavelength at 3.6 MHz, tune-up can be a real "can of worms." Since the oft-quoted value of 0.66 for the velocity factor of standard RG-8/U is only a nominal value and can vary appreciably from brand to brand (in cheap cable from lot to lot), this length should be determined with a noise bridge.

If a noise bridge is not available, the following procedure may be tried. Cut this section of cable about 6 feet shorter than the calculated length. Prepare a section of RG-58/U, 12 feet long, with solderless connectors on each end. Connect it to both the shortened feed line, using a PL-258 double female connector, and to L. Tap L to obtain the best combination of SWRs at 3.6 and 7.2 MHz. Record the SWR figures and tap position.

Now shorten the RG-58/U by 6 inches and repeat — and repeat — until you are certain you have passed through the point where the SWR values simultaneously bottom out at both frequencies. Prepare a length of RG-58/U (from the same lot) exactly as long as the best experimental length, using permanent coaxial connectors. Seal and waterproof all connections. RG-58/U is recommended for relative ease of pruning. If you don't mind unsoldering a PL-259 each time, RG-8 could be used. However, the additional loss from such a short section of RG-58/U will be infinitesimal at these frequencies.

This procedure is obviously tedious, but it is necessary to obtain good performance on 40 if a noise bridge is not available.[6] In fact, some adjustment of this section of transmission line may be necessary even if a noise bridge is used to measure the electrical length to obtain optimum two-band performance. The exact half wavelength should always be used as a starting point, in any case.

Strangely enough, the above procedures are necessary only to optimize 40-meter performance. My experience has been that merely cutting the half-wavelength section of transmission line to the calculated length, then tapping L to obtain the best SWR at 3.6 MHz, is sufficient to obtain a ratio of 2:1 or less over the entire 80/75-meter band. So tune for 40, and 80 should take care of itself.

Once the antenna system has been resonated, it may pay to experiment with the value of L and the length of transmission line between L and the transmitter. Chang-

ing these values will change the shape of the 40-meter SWR curve somewhat. By so experimenting, you may be able to tailor the shape of the 40-meter SWR curve to your operating preference. Don't expect miracles, though, for the range of adjustment seems to be small. Figure 4 illustrates the results of such an effort. These adjustments will have very little effect on 80-meter bandwidth within the range of acceptable SWR on 40 meters.

Further Thoughts

The first prototype was constructed close to my house, and I was therefore concerned that the performance might not be reproducible. The next prototype was erected in a far corner of my yard, over 100 feet from the house and even further from any other structures or conductors. The final version was similarly located. Except for final tune-up parameters, all three behaved almost identically, even though a number of physical changes was made each time. As a final test of the soundness of the design, I built scaled versions for 40/20 and 20/10 meters. They exhibited very similar characteristics, although all parameters of the system seem to become very critical as the design frequency is increased.

The first two 80/40-meter systems were built using a 30-foot mast, yet their behavior was not markedly different from the final version with a 40-foot mast. Since the mast is an electrical part of the system, and since proximity to ground must play some role in the performance of the antenna, other heights, and supports that have beams attached, may yield different results.

The reactance of the trap at 3.6 MHz is 245 ohms. Therefore, there is a possibility of constructing an 80-meter-only version of this antenna by using a 10.8-µH inductor in place of the trap. This has not been tried, however.

Scaling up to 160/80 meters is an attractive possibility. Conceivably, a mast height as low as 50 feet could be used. A starting point would be the doubling of all wire lengths, and using a 16.4-µH coil with a 120-pF capacitor for the trap to preserve the 245-ohms reactance at 1.8 MHz.

There also seems to be a possibility that a slight increase in trap capacitor value, to resonate the tap at 7.1 or 7.15 MHz, might allow better coverage of 40 cw, but probably at the expense of the phone portion of the band. Such a change might have little effect on 80-meter bandwidth, but another round of cut-and-try could prove necessary.

Conclusions

At this point, this is still an experimental design. Further development may eventually allow a cut-to-formula type of construction, but until that happens, be prepared to experiment. The dimensions given in Figure 1 will put you in the ball park and should yield immediate results on 80.

The convenience of Transmatchless operation overall of 80/75, plus a reasonable portion of 40, coupled with an excellent radiated signal, is ample repayment even for many hours of cutting and trying. Once tuned up, this antenna is very well behaved and enjoyable to use. I would like to hear from others who construct antennas based on this design.

Notes

[1]Hopps, "A 75-Meter DX Antenna," *QST*, March 1979, p. 44.
[2]Atchley, "Putting the Quarter-Wave Sloper to Work on 160," *QST*, July 1979, p. 19.
[3]DeMaw, "Additional Notes on the Half Sloper," *QST*, July 1979, p. 20.
[4]*The ARRL Antenna Book*, 13th edition, 1974.
[5]Mathison, "Inexpensive Traps for Wire Antennas," *QST*, February 1977.
[6][Editor's Note: A third alternative is to use a dip meter to determine an exact half wavelength of line. See Downs, "Measuring Transmission-Line Velocity Factor," *QST*, June 1979.)

By Deane J. Yungling, KI6O

From *QST*, April 1986

The KI6O 160-Meter Linear-Loaded Sloper

No room for a top-band antenna? Try this one on for size!

After having good success using my linear-loaded, inverted-L antenna over the winter 1984-85 160-meter season, I decided to try linear loading on a different type of 160-meter wire antenna.[1] I have had considerable success with a quarter-wave sloper on 80 meters, but my city-sized lot isn't deep enough to accommodate a full-sized sloper for the 160-meter band. About 120 feet would be required for the sloper to be 10 feet off the ground at the low end; I have about half that distance to work with. Linear loading solved the problem.

This antenna provides an effective bandwidth of about 70 kHz with an SWR of 2:1 or less. At the design frequency of 1.840 MHz, SWR is 1.1:1 with 50-ohm feed line and no matching network or tuner.

Although the individual dimensions are not critical, the sloping wire and the ladder line must resonate at the desired frequency. If the sloping wire is less than 65 feet long, the ladder must be longer, and vice versa, If you use a different length for the sloping wire, you will need to experiment a bit to see how much to add or remove from the ladder length.

Construction

My sloper is hooked onto the tower at about the 55-ft level using a strain insulator (see Figure 1). The coaxial-cable feed fine is securely taped to one tower leg, and the shield is connected to the tower leg with a radiator hose clamp. The tower is grounded at the base with several ground rods. The center conductor of the coaxial cable is soldered to the sloper at the strain insulator and is taped for weather protection where the center conductor and shield separate.

The ladder portion of the antenna is made with the same type of wire as the sloping portion. The ladder spacers are made of 3/8-inch hardwood dowels that have small holes drilled 1 inch from each end to hold the wires. The dowels should be soaked or sprayed with a wood preservative, prior to assembly, for weather protection. Plastic spreaders could also be used, if desired. The wires are firmly tied to the dowels with waxed lacing twine or similar material where the wires pass through the holes. The dowel spacing can be adjusted, with some difficulty, after the dowels are tied.

One end of the ladder is tied to the tower with heavy monofilament fishing line, with the other end tied to a tree or whatever else is handy. The tie-off lines are fanned vertically to keep the ladder from twisting and should be tensioned enough to eliminate any sagging in the ladder. Monofilament fishing fine provides some cushioning if the supporting tree sways or if the wind is strong.

Adjustment

Initially, the ladder should be a few feet longer than shown, to allow for adjustment. The resonant frequency should be checked, and a few inches removed at a time from the tower end of the ladder until the desired frequency is achieved. At this point, the wires should be soldered together and then taped to the end dowel. It appears that there must be an BF beam, or something similar, on the tower for any quarter-wave sloper to work properly. This sloper is no different in this respect. Finally, the antenna, particularly the sloping section, should be kept as far as possible from surrounding guy wires and other objects.

This antenna requires no ground system, balun or matching network over its operational bandwidth. The linear-loaded sloper is simple to construct and easy to adjust, and its performance is superior to my linear-loaded, inverted L.

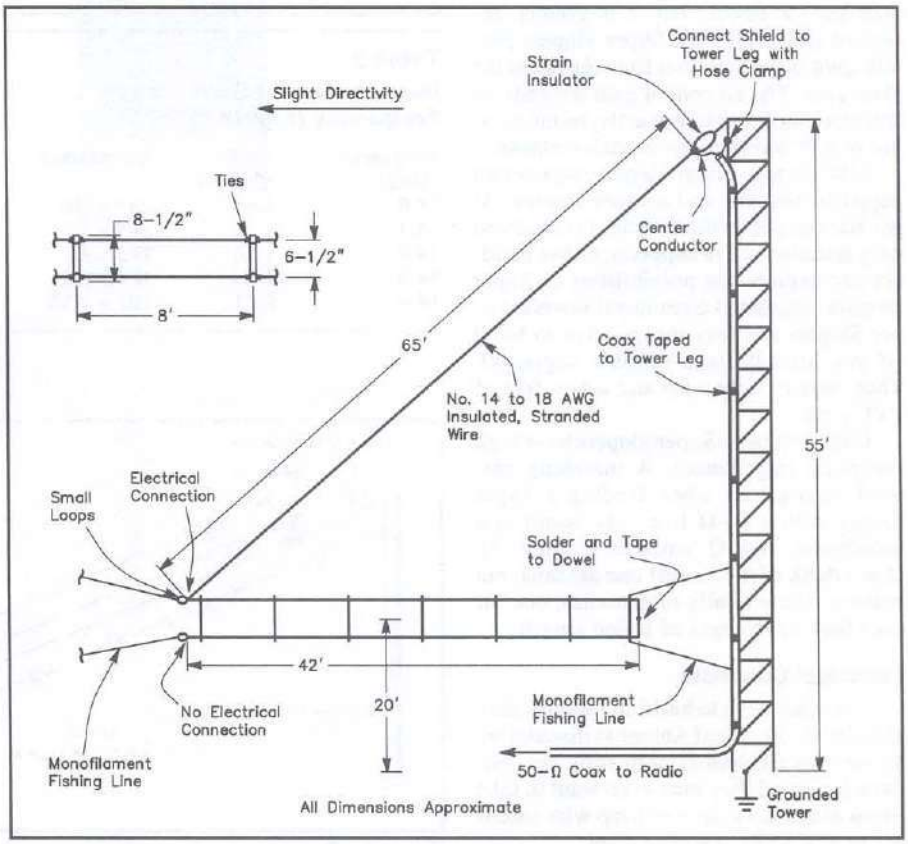

Figure 1—Construction details for the KI6O 160-meter linear-loaded sloper.

[1] D.J. Yungling, "The KI6O Top-Linear-Loaded 160 Meter Inverted 'L' Antenna," *CQ*, Apr 1985, pp 38-39.

By Roger Sparks, W7WKB

From *QST*, December 1995

The Super Sloper

Dramatically improve the front-to-back of a sloper.

You can imagine my surprise when *ELNEC*[1] revealed that a parasitic element can be combined with a long wire to form a whole family of directional antennas. There on my screen, I was looking at useful combinations not found in that bible of antennas, *The ARRL Antenna Book*. I had been exploring combinations of full-wave parasitic elements with wire arrays. How far off center can I slide a parasitic element, I wondered? "A lot," was the answer coming from *ELNEC* [and confirmed by *EZNEC—Ed.*]. As I offset a closely spaced (0.015 to 0.046 λ) parasitic element by 1/8 to 5/8 λ, a whole family of antennas appeared (see Figure 1).

I call the configuration a Super Sloper because the pattern resembles that of the well-known sloper, but it is greatly enhanced (see Figure 2). Super Slopers provide gain in the direction from the tall to the short pole. The amount of gain depends on antenna length, or more exactly, on the number of half wavelengths in each element.

Like slopers, Super Slopers require two supports, one tall and another shorter. At my station, and in this article, I considered only nonconductive supports. Other builders can explore the possibilities of Super Slopers suspended from metal towers. Super Slopers are very inexpensive to build (if you already have suitable supports). They require only wire and a few feet of PVC pipe.

Unlike slopers, Super Slopers have high feedpoint impedances. A matching network is required when feeding a Super Sloper with a 50-Ω line. The result is a broadband, low-Q antenna (Figure 3). Don't think of this as just one antenna, but rather a whole family of antennas, one for each half wavelength of added length.

Technical Concepts

If you just want to build an antenna, skip ahead to the Practical Antennas discussion. Those with a technical inclination can continue here, and they may even want to take a look at the discussion of long-wire antennas in *The ARRL Antenna Book*.

An antenna is called a long wire if it is one wavelength or longer. The radiation pattern can be described as the surfaces of two opposed cones that are coaxial with the wire and have their apexes meeting at the feed-point. The apex angle becomes smaller and the lobes grow stronger as antenna length increases. An azimuth plot of radiation pattern for single long-wire antennas over ground shows four principal lobes at low radiation angles. There are two principal lobes, *in one direction*, when the antenna is terminated in a matched, resistive load.

ELNEC shows that a parasitic element added to a single long-wire antenna creates a *unidirectional* radiation pattern similar to that created by a resistive termination. Energy eliminated from the back goes into useful forward gain. The parasitic element can be tuned as either a director or a reflector.[2]

Experience with Yagis (and many other applications of parasitic elements) led me to believe that all parasitic elements must be nearly a half wavelength long and located within the span of the driven element. That concept is completely *incorrect*. Parasitic elements can be *any* resonant length and offset from the driven element, as long as there is adequate coupling between the elements.

Here's how Super Slopers produce front-to-back ratio (F/B) and gain. The best

Table 1
Spacing and Phase Angle for Various Antenna Lengths

At the spacings listed, the current in the resonant parasitic element is equal to driven-element current ±10%. (Derived from *ELNEC*, under free-space conditions, 0.25-λ offset, at 7.1 MHz.)

Antenna Length (λ)	*Spacing (λ)*	*Phase Angle (degrees)*
0.5	0.046	−156
1.0	0.030	−147
1.5	0.023	−144
2.0	0.018	−142
2.5	0.015	−142
3.0	0.015	−144

Table 2
Impedance and SWR versus Frequency (Figure 5)

Frequency (MHz)	*SWR (200-Ω)*	*Impedance*
14.0	1.54	293 + *j*48
14.1	1.25	248 + *j*13
14.2	1.16	172 + *j*0
14.3	1.75	127 + *j*54
14.4	2.61	107 + *j*113

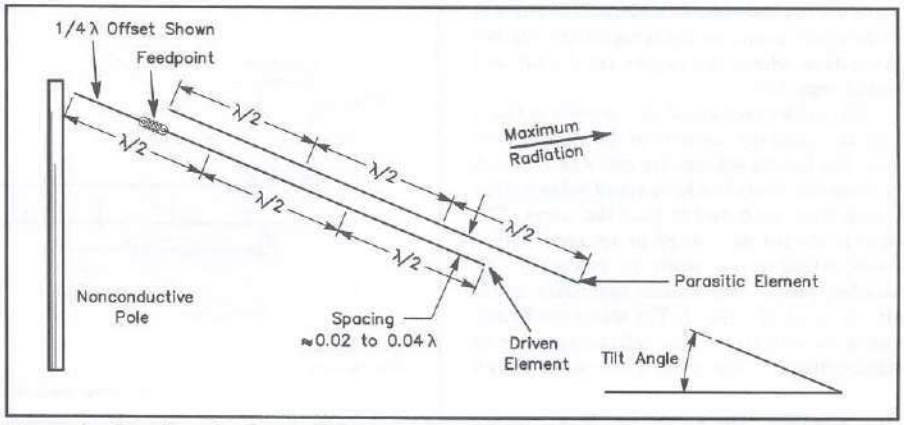

Figure 1—Drawing of a Super-Sloper antenna showing nomenclature. This is a 3-λ/2 model. See Figure 7 for construction details.

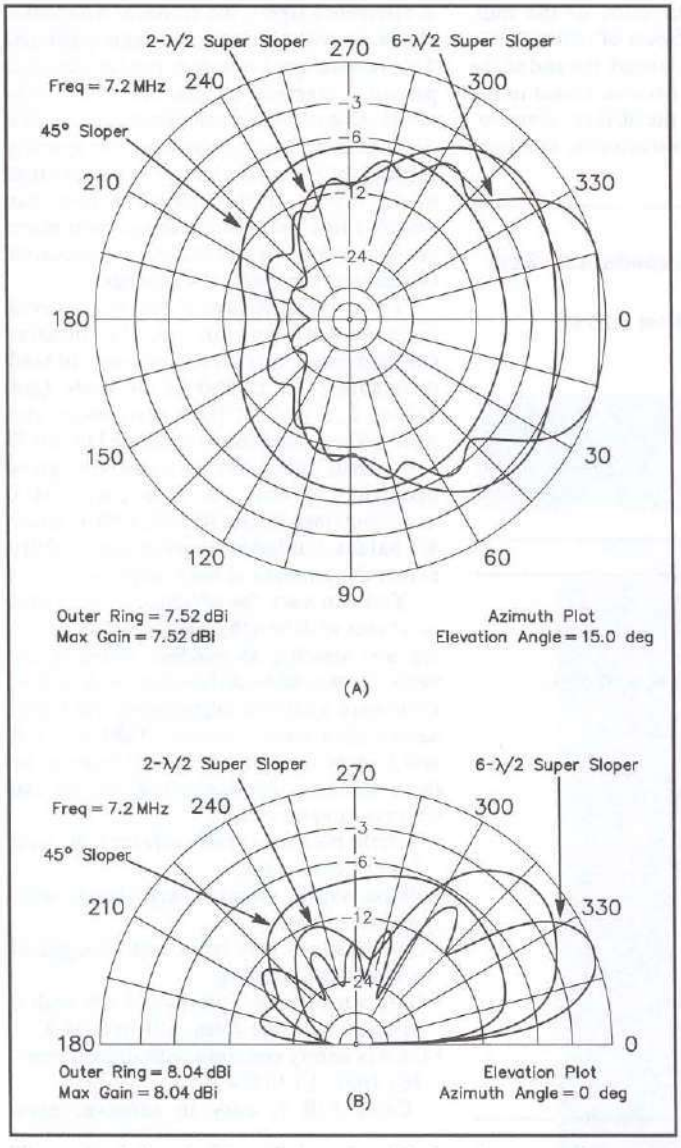

Figure 2—Azimuth (A) and elevation (B) plots for a 45° sloper, 2-λ/2 (0.25-λ offset, spaced 0.04 λ, low end 0.119 λ above ground) and 6λ/2 (0.25-λ offset, spaced 0.015 λ, low end at 0.066 λ above ground) Super Slopers. The high end of each is λ/2 high.

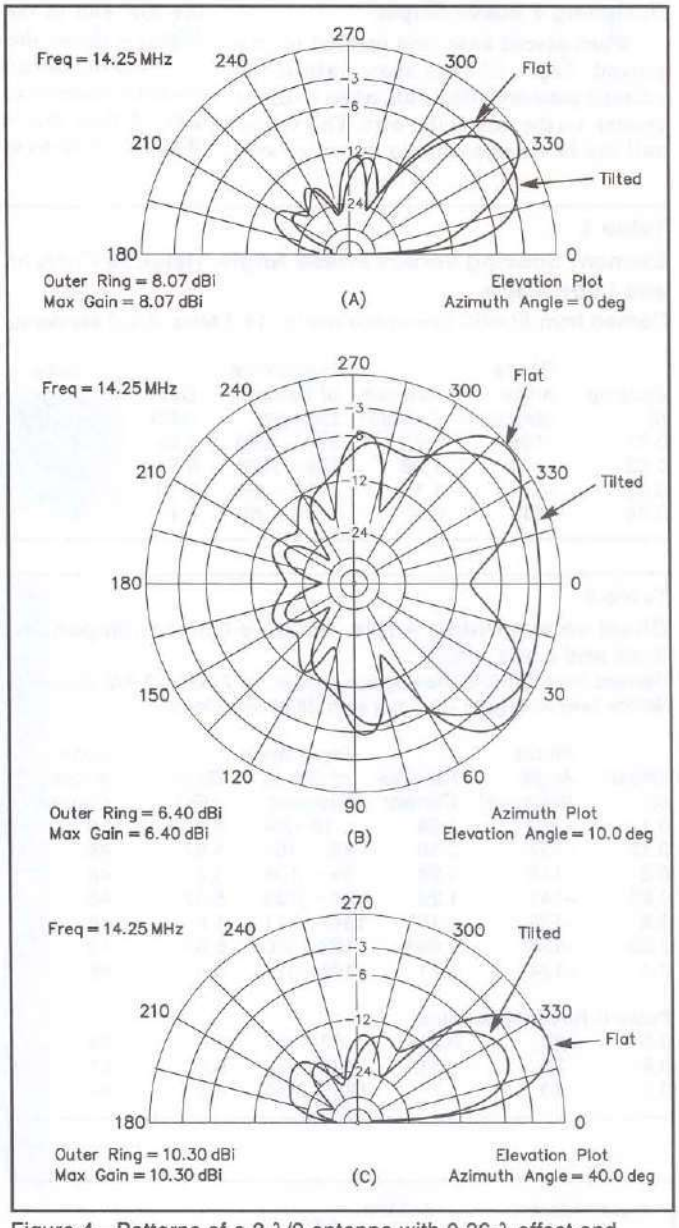

Figure 4—Patterns of a 3-λ/2 antenna with 0.36-λ offset and spaced 0.04-λ oriented flat at ½ λ vs sloping from ½ λ to 0.045 λ. A shows the elevation patterns at 0°; B shows the azimuth patterns; C shows elevation plots at azimuth=40°.

F/B results from a 180° phase shift between the currents in the driven and parasitic wires, as seen from a distant location where a pattern null is desired. A phase difference of 180° means that the signals completely cancel each other, if each element delivers equal signal strength. A phase shift of 90° is possible with a 1/4-λ offset, and the remaining 90° phase shift can come from the tuning (length) of the parasitic element. If the fields cancel in one direction, they will reinforce in some other direction, to produce gain.

By increasing the phase angle of the current in the parasitic element, the angle of maximum cancellation can be moved. This is particularly useful in Super Slopers because the principal lobes of long wires lie at some small angle to the direction of the wire. From Table 1, notice that the current in a resonant parasitic element has about –144° to –156° phasing, which is about right for correct reverse-lobe canceling.

If we want each element to deliver equal signal strengths to a distant location, nearly equal currents must flow in both the driven and parasitic elements: The coupling between elements must be very close. Table 1 suggests the approximate spacings for currents to be equal within ±10%. (The antenna also has gain at closer spacings because gain is affected less by unequal currents than is F/B.)

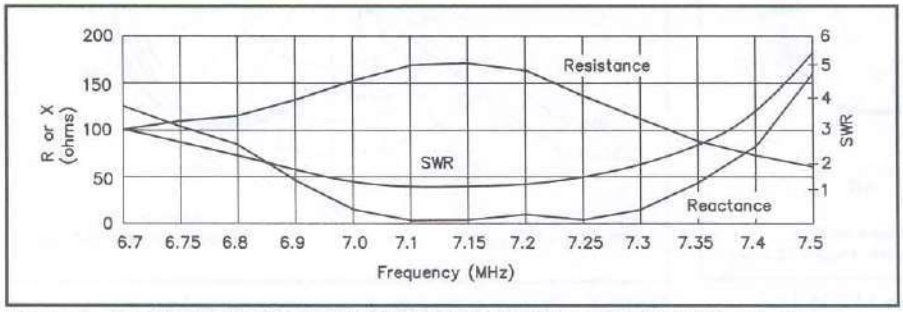

Figure 3—A plot of impedance and SWR versus frequency for the 2-λ/2 antenna described in Table 6, placed as described in Figure 6. The data source is *NEC/WIRES 1.5* (see Note 3).

Designing a Super Sloper

When placed near (and parallel to) the ground, Super Slopers show twin-lobed azimuth patterns with a null, often 10 dB or greater, on the axis of the wire. This center null can be filled by tilting the wire, with the low end in the direction of the null. Figure 4 shows the effects of tilting.

When the antenna is tilted, the end of the parasitic element can become closer to the ground than that of the driven element. When considered as two separate antennas at different heights, the driven and parasitic elements will not have the same patterns. This reduces performance, but locating the parasitic element so that its end height equals that of the driven element can solve the problem. That is, increase the spacing to place the parasitic element end above that of the driven element. Models give this design 1 to 2-dB gain advantage over more closely spaced antennas, but construction is a greater mechanical challenge.

The driven element is fed at a current antinode, 1/4 λ from an end. The antennas can be made to exhibit a wide range of feed resistances: 20 to 300 Ω, or more (see Tables 2, 3 and 4). High resistances and wide offsets combine to produce low SWR and useful gain over an unusually great bandwidth (Table 2). I've used 1/4-λ matching lines (using RG-62, a 93-Ω line), 4:1 baluns and ladder lines to successfully match the antenna at high impedances.

You can vary the antenna length (gain increases with length), height, offset, phasing and spacing as needed. These many variables would be difficult to work with if each were a critical adjustment, but fortunately, they are not critical. Tables 1, 3, 4 and 5 show the tolerant design features of these antennas. From these tables, we can observe several trends:

- Current balance greatly affects F/B, with less effect on gain.
- Phase angles change very slowly with antenna length.
- Gain changes very little with changes of current and phasing.
- Gain varies by a little over 1 dB with a spacing increase from 0.01 to 0.04 λ.
- Gain is nearly constant with offsets moving from 0.1 to 0.4 λ.

Good F/B is easy to achieve, even

Table 3

Element Spacing versus Phase Angle, Relative Current, Impedance, Gain and Lobe Angle

Derived from *ELNEC* free-space model, 14.2 MHz, 2-λ/2 elements, offset 0.25 λ

Spacing (l)	Phase Angle (degrees)	Relative Current	Impedance of Driven Element	Gain (dBi)	Lobe Angle (degrees)
0.01	–136	1.62	205 – *j*230	4.98	48
0.02	–141	1.29	128 – *j*138	5.54	48
0.03	–144	1.11	103 – *j*94	5.78	48
0.04	–149	0.97	80 – *j*59	6.1	48

Table 4

Offset versus Phase Angle, Relative Current, Impedance, Gain and Lobe Angle

Derived from *ELNEC*, free-space model, 14.2 MHz, 2-λ/2 elements, spaced 0.02 λ. Notice how little gain changes with different offsets.

Offset (λ)	Phase Angle (degrees)	Relative Current	Impedance of Driven Element	Gain (dBi)	Lobe Angle (degrees)
0.1	–167	1.08	19 –*j*54	5.7	48
0.15	–157	1.18	48 – *j*101	5.67	48
0.2	–148	1.26	89 – *j*135	5.6	48
0.25	–141	1.29	128 – *j*138	5.57	48
0.3	–139	1.16	134 – *j*111	5.6	48
0.35	–138	0.963	123 – *j*70	5.58	48
0.4	–134	0.71	108 – *j*14	5.4	48
Pattern Reversal Begins					
0.5	–26	0.25	83 + *j*46	3.0	54
0.6	39	1.31	126 – *j*57	5.2	61
0.7	43	1.71	192 – *j*180	4.0	64

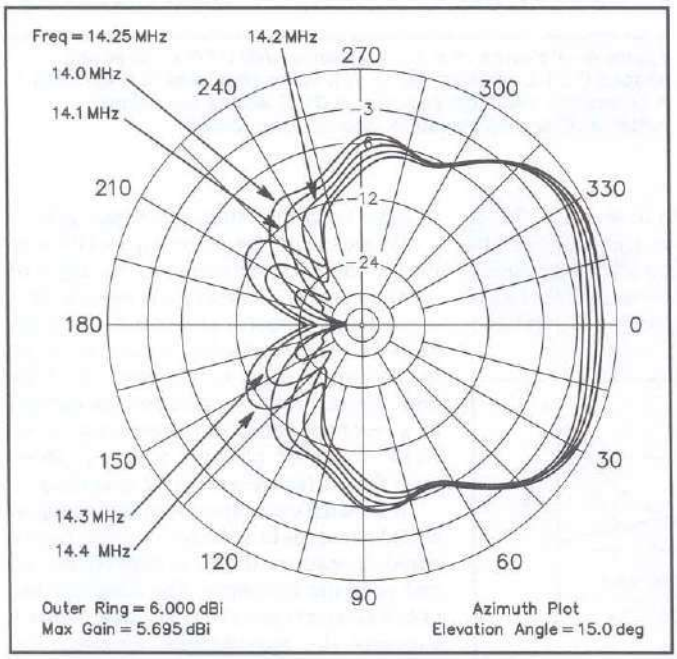

Figure 5—A radiation pattern over a range from 14.0 to 14.4 MHz. The pattern is that of a 3-λ/2 antenna with 0.36 λ offset, with the ends at ½ λ and 0.045 λ. See Table 2 for the SWR tabulation.

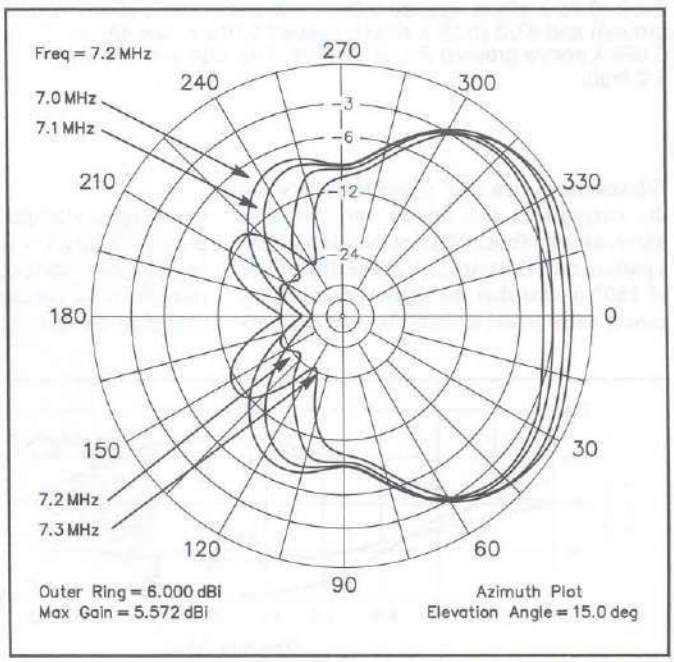

Figure 6—Pattern plots over a frequency range from 7.0 to 7.3 MHz. The antenna is 2-λ/2, with 0.25-λ offset and 0.04-λ spacing. The driven element is 1.02-λ long; the director is 0.98-λ long. See Figure 3 for an SWR curve.

though the antenna is designed for best gain or easy construction. Improved F/B ratios and reverse-oriented patterns are possible from designs optimized at specific frequencies. Computer modeling is the best way to optimize reverse patterns. Figures 5 and 6 show some possible patterns and how the patterns vary with frequency. Table 2 and Figure 3 show predicted SWR.

Practical Antennas

Table 6 describes Super Slopers constructed at my station (refer to Figure 1 for nomenclature). The principal difference between the two 3-λ/2, 20-meter antennas in Table 6 is the increased offset from 17½ feet to 22 feet. This changes the phasing, resulting in a slightly improved F/B ratio and slightly improved gain. The trade-off is a narrower pattern and a longer antenna.

A 60-foot mast supported the 3-λ/2 and 2-λ/2 20-meter versions. They were mounted back-to-back and tilted to fill the center null. Another 3-λ/2, 20-meter unit was mounted from a 38-foot mast. The 40-meter version sloped from 60 feet down to 6 feet. All antennas performed as predicted. Additional height at either end definitely increases low-angle radiation, but it reduces high-angle radiation.

Figure 7 shows how I assembled and spread the wires. The departure from straight lines (as depicted in Figure 1) has no practical effect on the antenna. Be sure to place the director over the driven element when erecting the antenna. A director placed at the side will skew the pattern, favoring the side of the director. Keep the Super-Sloper support lines tight to minimize sagging. Severe sagging leads to improper phasing and degraded results. I put a support under my 40-meter Super Sloper at midspan, but I just pull the 20-meter antenna support lines tight. The two elements have a tendency to twist and wrap together in the wind. You can prevent this by using two support ropes at the low end or by using spacers as on transmission lines. Both methods work well. Super Sloper performance suffers from excessive ground losses when the low end is at ground level. I strive for an antenna slope (tilt angle) of 10° to 20° and a minimum height of 6 feet. Higher is better.

A 200-Ω feedpoint impedance is easily transformed to 50 Ω with a 4:1 balun. Ladder line and a tuner are another option. Refer to *The ARRL Antenna Book* for other methods of transforming high feed impedances to values acceptable for modern transceivers. Do not feed the Super Sloper directly with coax unless the coax is part of an impedance-matching section.

Results and Conclusions

I've built and used six Super Slopers very successfully. The F/B is often dramatic. A difference of six S units is not uncommon when switching between two antennas built to favor opposite directions.

This family of antennas has not yet been well researched and studied. Use an antenna modeling program before building designs that are substantially different (eg, longer or made from tubing) from those described in Table 6.

Table 5
Parasitic Element Length versus Phase Angle, Relative Current, Gain and Lobe Angle

Derived from *ELNEC*, under free-space conditions with 14.2 MHz, 2-λ/2 elements, spaced 0.02 λ apart.

Percent Short (λ)	*Phase Angle (degrees)*	*Relative Current*	*Gain (dBi)*	*Lobe Angle (degrees)*
0	–140	1.30	5.54	48
1	–125	1.47	5.33	49
2	–107	1.53	5.02	51
3	–89	1.43	4.70	52
4	–75	1.23	4.44	53
5	–65	1.05	4.19	53

Table 6
Working Antenna Dimensions

Use a 4:1 step-down transformation to match 50-Ω line.

Antenna Number	*1*	*2*	*3*	*4*	*5*	*6*
Band	40 m	20 m	20 m	20 m	15 m	10m
Length*	2	3	3	2	2	2
Driven (ft)	139.3	106.5	105.6	70	46	34.5
Director (ft)	134.3	104.0	102.2	68	45	32.8
Offset (ft)†‡	34.3	17.5	22	17.5	11.5	8.6
Spacing (ft)	6	1.5	1.5	1.5	1.0	1.0
Feedpoint (ft)‡	34.3	17.5	17.25	17.5	11.5	8.6

*Length expressed as a multiple of λ/2.
†Offset is λ/4, except for antenna 3, where the offset is 0.31 λ.
‡Feedpoint and offset are both measured from the high end of the driven element.

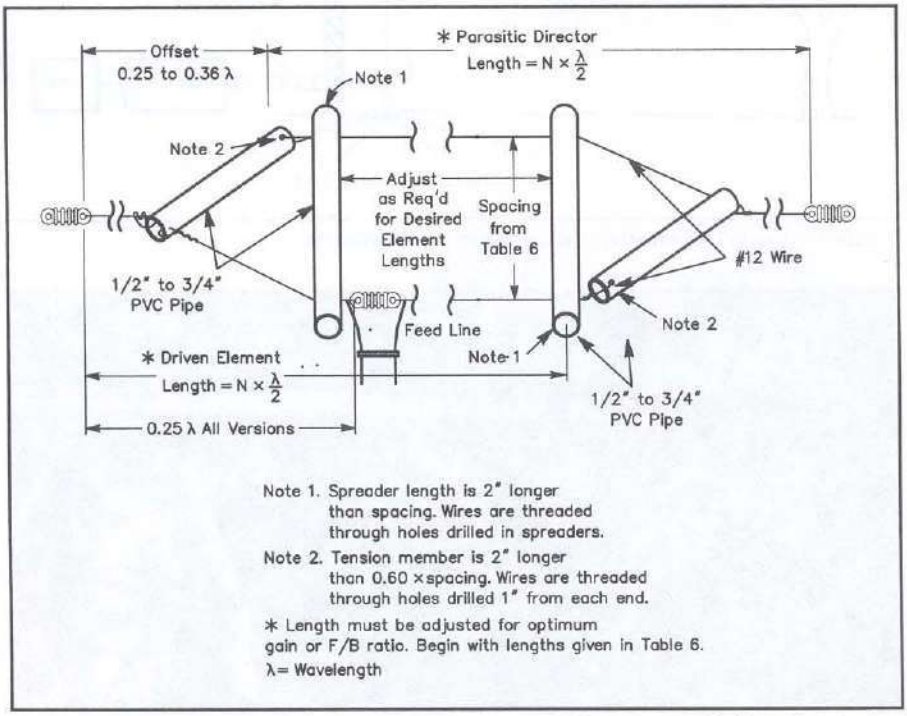

Figure 7—A method of constructing the long-wire parasitic antenna. Additional center spacers reduce the tendency of the wires to twist in the wind.

Notes

[1] *ELNEC*, and its successor *EZNEC*, are computer antenna modeling programs available from Roy Lewallen, W7EL. The description files for the antenna plots shown in this article are available as a self-extracting archive file named SUPSLOPE.EXE. This file can be found on the Internet (FTP to OAK.OAKLAND.EDU, directory pub/hamradio/arrl/qst-binaries).

[2] Parasitic elements offset more than 1/2 λ from the driven element, become reflectors.

[3] *NECIWIRES 1.5* is a computer antenna modeling program available from Brian Beezley, K6STI.

By John F. Lindholm, W1XX

From *QST*, January 1983

The Inverted L Revisited

City dwellers, don't despair. Here is a *good* 160-meter antenna that should fit on your lot!

I'll never know what inspired me to make a few contacts in the ARRL 160Meter Contest. My antenna was made by tying together the open-wire feeders of my 80-meter dipole. The performance was not fantastic, but it was the first step in getting me "hooked" on the "gentlemen's band." Working three dozen European stations from a friend's house got my interest up. My friend has a good 160-meter antenna system – and *lots* of property to fit it on!

Returning to my 60 × 150-foot lot made me feel depressed.[1] I suffered all winter while listening to the others working VKs, ZLs and even JAs at daybreak. What could I do to improve *my* signal?

Many hours the following summer were spent trying to figure out how to cram a 160-meter antenna within the confines of my small lot. Space restrictions dictated that my wire be no longer than a standard 80-meter dipole. I began to consider alternative antennas.

Shunt feeding my 50-foot tower was investigated but dismissed for various reasons. This arrangement would require disconnecting the shunt feed when cranking down the tower, and all guy wires would have to be broken up into nonresonant lengths with insulators. Additionally, my cables would have to be rerouted to ground level. I then considered a full-length dipole originating in a neighbor's yard three houses to the east, crossing my property and finally terminating in the yard two houses to the west! This idea was rejected. The legal negotiation fees would have run into six figures! After much head scratching, I settled on the inverted L, an antenna made popular by the grand master of 160-meters, Stew Perry, W1BB. I credit Stew for coming to my rescue!

The Inverted L

The inverted L was selected because it requires no more space than an 80-meter dipole and I could utilize my 50-foot crank-up tower for attachment. The vertical part is 50 feet long, and the horizontal part measures 130 feet, for an overall length of 180 feet (Figure 1). This makes the antenna approximately 3/8 λ, with the horizontal part providing top-loading. W1BB advises making the vertical section as long as possible (depending on tower height), and that an overall length of 160 to 180 feet works well.

Construction

With a bow and arrow, I successfully attached the far horizontal end of the antenna to the top of a 60-foot fir tree. From there, I ran the wire back to the top of the tower, where I bracketed a 30-inch-long two-by-four with an insulator screwed in the end (Figure 2). No. 14 Copperweld wire is used for the horizontal section, and no. 10 copper wire is used for the vertical section, which is spaced about 2 feet from the tower. These two wires are soldered to-

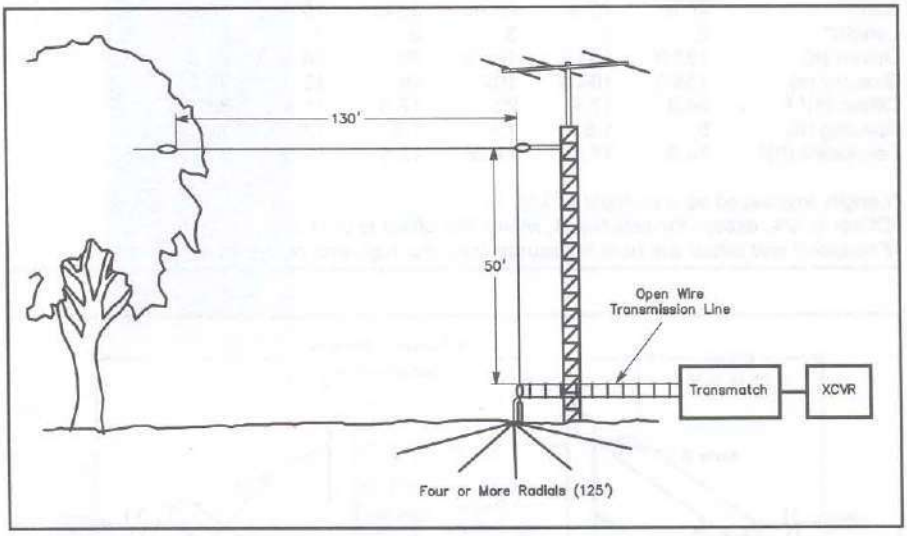

Figure 1—The W1XX inverted L is arranged in this manner.

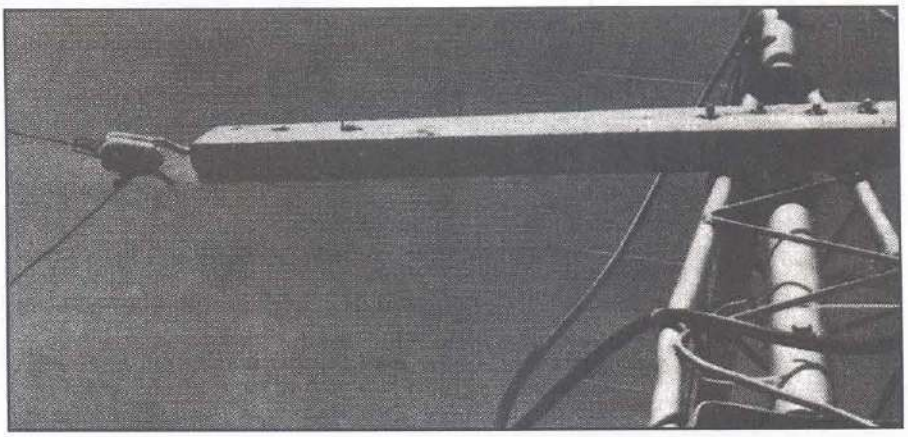

Figure 2—Detail of how the antenna is mounted to the top of the tower. TV-mast clamps are used to secure the wooden insulator.

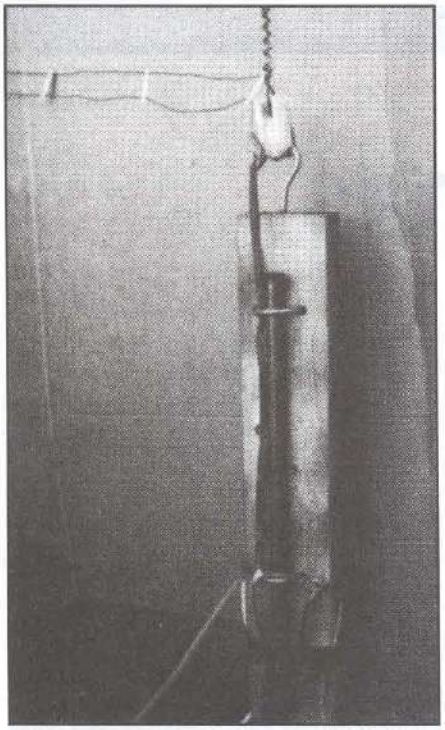

Figure 3—A ground rod at the tower base serves as a physical support for the insulator, and as an rf ground. Radial wires are connected to the rod by means of a ground bus, as described in the text.

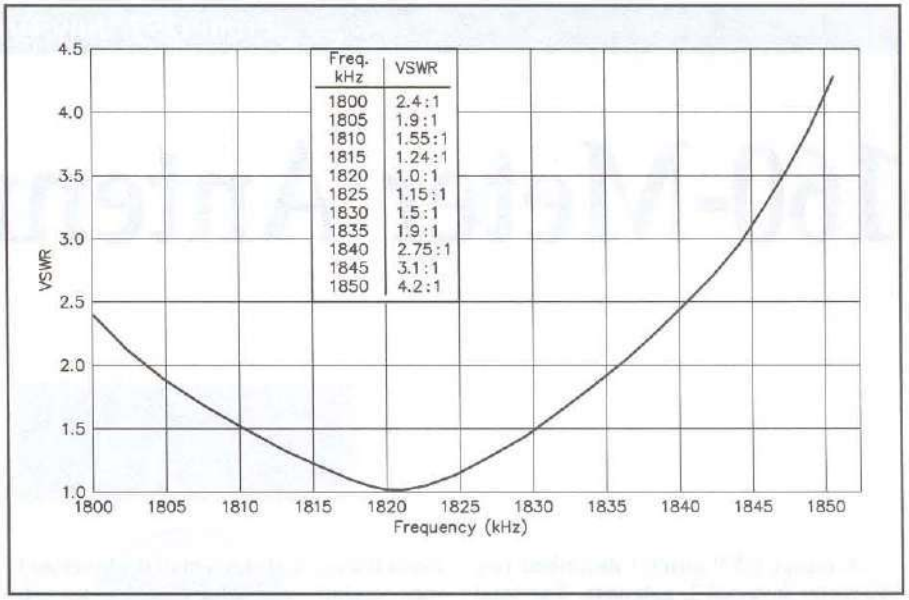

Figure 4—SWR curve for the inverted L, with the Transmatch adjusted for an SWR of 1 at 1820 kHz.

gether at the insulator.

A plumb line was used to locate a point on the ground directly below the 90° bend in the "L." At this point, a 10-foot copper-clad ground rod was pounded into the earth, leaving 18 inches sticking out. A two-by-four is clamped to the ground rod by means of TV-mast U bolts. The lower end of the vertical wire is attached to an insulator that is screwed into the top of the wooden block (Figure 3). Next, I stripped some coaxial cable (RG-8/U) of its outer braid and used this to make a ground bus around the antenna base. One side of the open-wire transmission line is soldered to the base of the vertical antenna element, and the other side to the bus, which is attached to the ground rod with a clamp. This bus also serves as a connection point for the radials. So far, less than an afternoon of work had been invested.

Radials — the More the Better

The next day, my objective was to install radial wires, which are necessary because the inverted L is essentially a top-loaded vertical radiator. Previous meditation convinced me that several radials would fit on my lot. I'd *make* them fit! All radials were cut to 1/4 λ (125 feet), using scrap wire. About 300 feet of surplus telephone ground wire provided a good start. Stripping some old coaxial cable with a single-edged razor blade produced two radials from one length of wire (outer and center conductors). My technique for radial installation consisted of creasing the earth with a spade and shoving the wire in; afterwards the turf was pressed back into place with my heel.

With space a problem, it may be impossible to place all your radials in a straight line; don't worry, because it is not necessary. My installation followed a zigzag path to avoid fixtures like the house and driveway. W1BB advises putting some radials under the horizontal part of the antenna. Unfortunately, the location of my garage prevented this. Initially, only four radials were planted, but more were added later. As with all vertical antennas, the more radials you can put in the ground, the better the performance!

Matching System

Voltage-fed antennas approximately $^1/_2$-λ long, such as the inverted L, will have a fairly high feed-point impedance. They will also exhibit inductive or capacitive reactance, depending on whether the antenna is slightly longer or shorter than $^1/_2$ λ. Since the inverted L does not have a 50-ohm impedance, a matching system is needed. To make tuning adjustments easier, I opted for locating the Transmatch *in* the shack, using open-wire line to the antenna. Being able to adjust the antenna match conveniently is recommended, since the SWR climbs rapidly as you shift frequency. For example, adjusting the Transmatch for a 1:1 SWR at 1820 kHz produces an SWR of 2.4:1 at 1800 kHz (see Figure 4). With the Transmatch located in the shack, you can easily adjust for a 1:1 SWR no matter where you operate in the band. My Transmatch consists of a plug-in, link coupled coil and variable capacitors – all scrounged at flea markets. Any of the configurations found in the *ARRL Antenna Book*[2] should work well.

Performance

Does the antenna work? Having no comparison antenna, my conclusions are subjective. But I've been on the air enough to know when, as they say, "it plays." With only four radials in place, my first night of operation yielded plenty of U.S. contacts, plus a Caribbean DXpedition on the first call. Subsequently, many European stations have been worked from my northeast location with good signal reports. Contest activity has yielded some respectable scores, including many QSOs with the Caribbean, and South and Central America — even Antarctica!

By adjusting my Transmatch, I made limited tests with the L on 75-meter ssb. Comparisons were made to a 75-meter dipole at 50 feet. For signals close in, the L was down by some 3 to 5 dB, but equal or superior to the dipole for signals from eastern Europe. Apparently, the 160-meter inverted L also provides a low angle of radiation on this band too. On bands higher than 75 meters, the radiation angle will be tilted *upwards*, rendering the antenna inefficient for DX work. This phenomenon is explained in *The ARRL Antenna Book*.[3]

Giving up the 160-meter band for lack of sufficient real estate is unwarranted. With the inverted L, you can work Top Band from your urban lot. Installation is a breeze, and the performance is admirable. *Now* what's your excuse for missing out on the excitement of 160 meters?

Notes

[1] m = ft × 0.3048.

[2] *The ARRL Antenna Book*, 14th ed. (Newington: ARRL, Inc., 1982), pp. 4-1 through 4-8.

[3] *Ibid.*, pp. 2-23 through 2-24.

160-Meter Antennas

A recent QST article[1] described two 160-meter inverted-L antennas. The total length of one of the antennas (the vertical element and the horizontal arm) is approximately 1/4 λ; the other antenna is 1/2 λ long. The current-driven 1/4-λ antenna requires a fairly extensive ground screen to realize good radiation efficiency. On the other hand, the voltage-driven 1/2-λ antenna requires only a ground stake-or no ground at all. Here's some additional information to aid you in selecting between these alternatives.

Because the current distribution of these two antennas is quite different, the radiation characteristics are also different. That explains why some signals are ". . . very loud or very weak," depending on station distance, propagation conditions and which antenna is being used.

In the captions for the figures illustrating the two antennas, it's stated that the support poles could be metal or wood. Because the vertical element of the inverted L runs parallel—and rather close to—the support pole, one may wonder whether, if the pole is metal, this proximity will influence antenna performance.

The three antenna types I'll discuss are illustrated in Figure 1; they are (A) the 1/4-λ inverted L; (B) the 1/2-λ inverted L; and (C) the T antenna. Figures 2 and 3 show the calculated[2] radiation patterns for the two inverted-L antennas, assuming average ground (σ = 3 mS/m, ε = 13). The support poles are trees (or other wooden supports) 50 feet tall. Note that the horizontal arm of the antenna is close to the ground, in terms of wavelength (0.1 λ), and that, in this case, *ELNEC* overestimates the gain of horizontally polarized antennas at a height of 0.1 λ by about 3 dB.[3]

The reason the patterns are so different is because the vertical antenna element carries a heavy current when the antenna length is 1/4 λ, whereas the vertical antenna element carries only a small current when the antenna length is 1/2 λ. Hence, there is a great difference between the vertically and horizontally polarized components of the radiation field for these two inverted Ls. The former antenna has a monopole-like pattern, whereas the latter antenna has a dipole-like pattern.

The lengths given in Figure 1 are those for resonance at 1.9 MHz. DeMaw's dimensions give wire lengths that are a bit too short for resonance (according to *ELNEC*). (In practice, one would trim the antenna length for resonance.)

If you want to work DX, it is advantageous to deploy an antenna that has a deep overhead null in its radiation pattern. This minimizes high-angle sky-wave signals, noise and interference, and improves the signal-to-noise ratio of distant weak signals. The T antenna exhibits this feature. Figure 1C provides dimensions for a T antenna with a resonant frequency of 1.9 MHz; the radiation patterns are given in Figure 4. This antenna's radiation field is almost entirely vertically polarized.

For these plots, the antenna was in the X-Z plane (Z is the vertical axis and 0° azimuth is in the + X direction). The 0° azimuth for the inverted Ls is the direction that the horizontal arm points (away from the feed). There is a slight azimuthal pattern asymmetry for these antennas because the antenna structure is not symmetrical

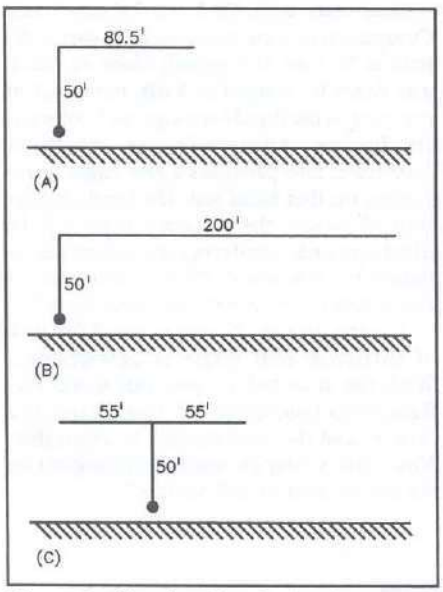

Figure 1—Sketches for simple wire antennas for 160 meters (1.9 MHz); A, 1/4-λ inverted L; B, 1/2-λ inverted L; and C, 1/4-λ T antenna.

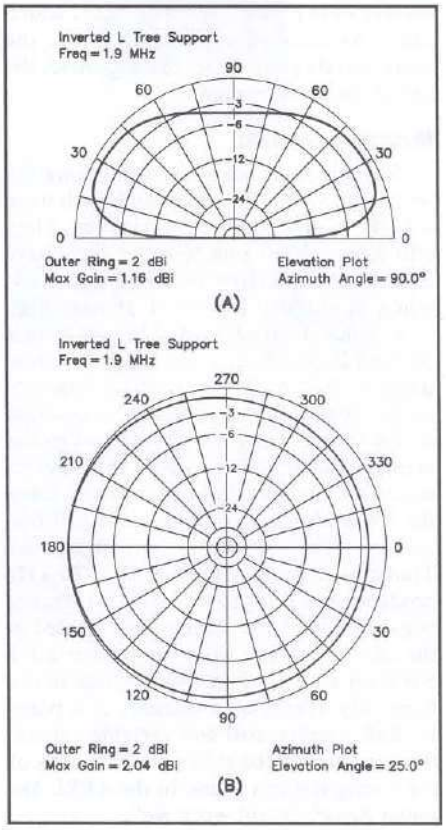

Figure 2—Radiation patterns for Figure 1A's antenna over average ground. The radiated field is dominantly vertically polarized—a monopole-like pattern. The absence of an overhead null in the vertical-plane pattern (compare Figure 2A with Figure 4A) is due to the horizontally polarized component of the field radiated by current on the antenna's horizontal arm.

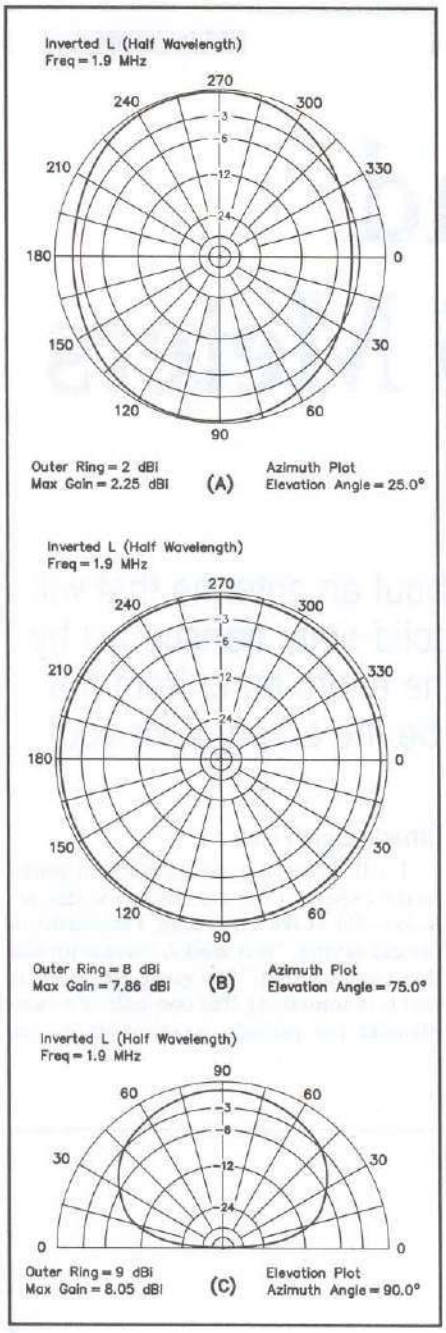

Figure 3—Radiation patterns for Figure 1B's antenna over average ground. The radiated field is dominantly horizontally polarized in the plane broadside to the antenna, and vertically polarized in the plane of the antenna—a dipole-like pattern. Hence the almost circular pattern at the high elevation angle, 75° (B), and the broadside directivity at the lower elevation angle, 25° (A).

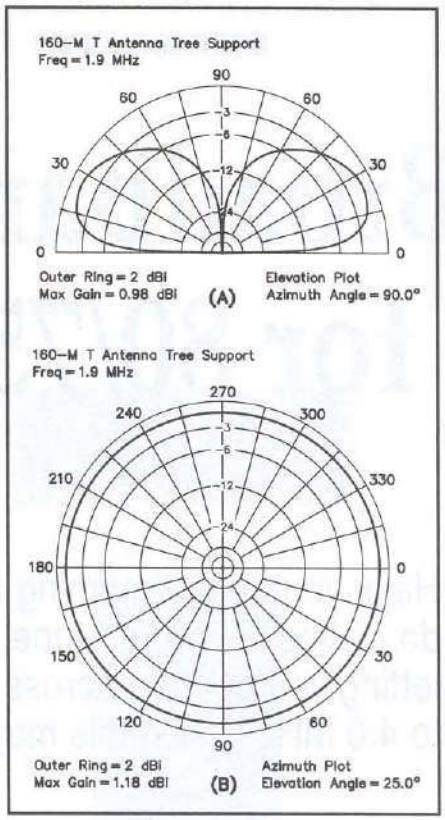

Figure 4—Radiation patterns for Figure 1C's antenna over average ground. The radiated field is almost entirely vertically polarized. The horizontally polarized component of the field radiated by current on one horizontal arm of the T is canceled by that radiated by the other arm.

with respect to the feed.

The effect of a well-grounded metal support tower was also studied. Surprisingly (to me), the effect is rather small, particularly for the 1/4 λ inverted L and 1/4 λ T antennas. The effect on the impedance of the 1/2-λ inverted L looked at first to be significant, but this is only because a small change in the resonant frequency of the antenna (the metal tower couples reactance into the antenna system and so changes the system's resonant frequency) results in a significant impedance change at frequencies near the anti-resonant frequency. Only a slight retuning of the matching circuit is necessary; the radiation patterns are affected relatively little. A 6½-foot nonconductive rope connecting the top ends of the horizontal arm to the support towers is assumed. For 50-foot support poles, it matters little (for 160-meter antennas) whether the poles are metal or wood.

But this is not the case if the support tower is also the mount for a 20-meter Yagi, because the tower and Yagi are much more nearly resonant than the tower alone. In this case, the tower carries a heavy current (0.8 A compared with the 1-A base current in the 1/4-λ inverted L). Because the phase of the tower current is +145° with respect to the phase of the current on the vertical element of the inverted L, the antenna's vertically polarized field is almost canceled. Also, the inverted L is no longer resonant: In fact, it is far from resonant; its impedance is 1547 $-j2635$ Ω, compared with the inverted L's impedance of 14 Ω with tree support.–*John S. Belrose, VE2CV*

Notes

[1]D. DeMaw, "The 160-Meter Antenna Dilemma," *QST*, Nov 1990, pp 30-32.

[2]*ELNEC* was used for all calculations. This program is available from Roy Lewallen, W7EL.

[3]*ELNEC* is a version of *MININEC*. *MININEC* assumes that the antenna is over a perfect earth for the purpose of calculating the antenna's impedance and the current distribution. The result of this approximation is that for horizontally polarized antennas, *MININEC* overestimates the gain of the antenna by an amount that increases as the height of the dipole decreases below a height of about 0.2 λ. The effect of real ground on the shape of the radiation pattern is correctly predicted, however, since for the calculation of the far-field pattern the program employs Fresnel reflection coefficients for the specified earth type.

By Brian L. Wermager, KØEOU

From *QST*, April 1986

A Truly Broadband Antenna for 80/75 Meters

Have you been dreaming about an antenna that will do justice to your no-tune, solid-state transceiver by letting you operate across the entire band from 3.5 to 4.0 MHz? Then this may be the antenna for you!

With declining sunspots and poor conditions on the higher HF bands, 80 meters has suddenly become very popular. But, unfortunately, many hams are not able to use this band to its full potential. It offers every kind of ham activity from CW to phone, from nets and ragchewing to great DXing, but many hams are too limited by the frequency range of their antennas to enjoy this band completely.

Antenna-matching networks are one answer, but they spoil the advantage of the no-tune feature of modern transceivers. Matching networks also are often less effective than many hams think; they introduce losses. The losses can be significant at some settings which provide a match. With these things in mind, I decided to try some ideas that might give me a more broadbanded antenna. The prime requirement was that it be fed with common 50-ohm coaxial cable, with no traps, coils or capacitors.

First, I tried a quarter-wave sloper. This antenna worked very well, with a bandwidth of 300 kHz between the 2:1 SWR points. It still, however, limited me from operating CW DX at the bottom of the band and the phone nets at the top of the band. There had to be a better antenna.

Antennas can be broadbanded by using large-diameter elements. With this in mind, I began experimenting with two-wire slopers, attached to a common feed point, but with the wire ends fanned out from each other. (See Figure 1.) This seemed to help, but not as much as I had hoped. It did, however, shorten the length required for the sloper. For those with a short tower, this idea could make an 80 or 160-meter sloper possible when a single-wire sloper would be too long.

The Fickle Finger of Fate Strikes!

While I was trying one of these two-wire antennas at a low height on my tower, the SWR was less than 2:1 from 3.5 to 4.0 MHz! After several attempts to get it to work the same way at the top of the tower, I discovered that these results could be attained only when my old quarter-wave sloper was at the top of the tower *and grounded* to the tower. (See Figure 2.) The two antenna elements were obviously interacting with each other, broadening the bandwidth tremendously. Further pruning of the lengths of both the sloper and the two-wire element resulted in the amazing SWR curves shown in Figure 3.

What's Going On?

I will leave the question of *why* it works to the experts. (See the sidebar to this article.—Ed.) Like a true ham, I subscribe to the old saying, "If it works, leave it up and don't mess with it." My guess, however, is that it is something like one-half of a two-element log periodic seeking its mirror

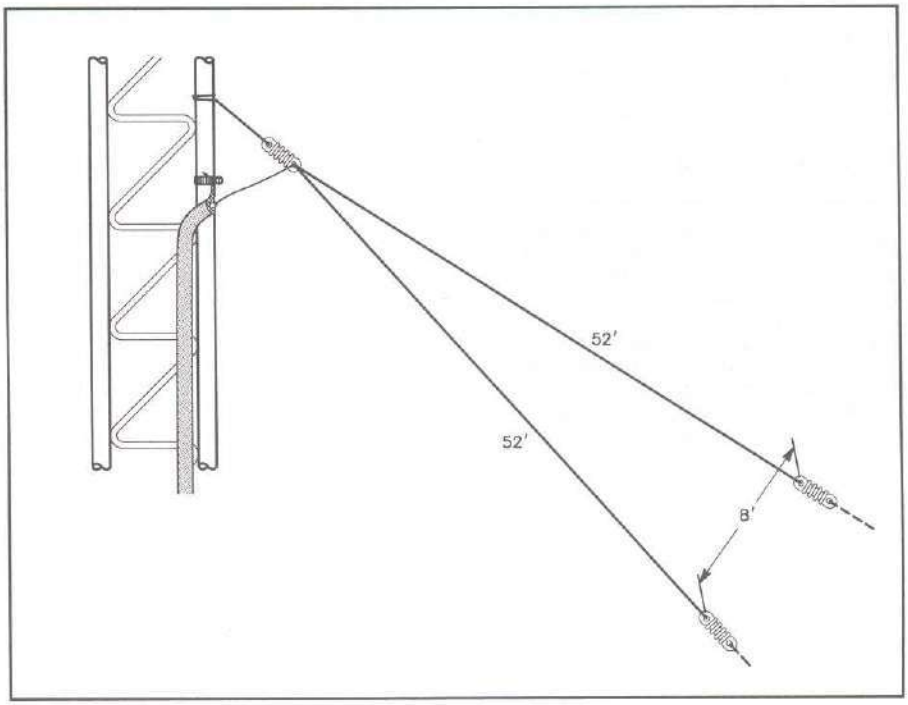

Figure 1—Arrangement of the original KØEOU experiment. The coaxial cable shield is connected to the tower, with both wires of the two-wire element connected to the center conductor. The wires are spread approximately 8 feet at the ends and are each approximately 52 feet long.

The MININEC Analysis of the KØEOU Three-Element Half Sloper

The Mini-Numerical Electronics Code (MININEC) analyzes thin-wire antennas, solving an integral equation representation of the electric fields using a method-of-moments technique. MININEC solves for the currents, impedance and patterns for antennas composed of wires in arbitrary orientations in free space and over perfectly conducting ground.

The impedance at the feed point calculates to be 79.4 + *j*1859.8 ohms. This assumes a perfect ground beneath the structure and simply a 3-foot extension of the tower above the connection of the upper wire. In practice, the impedance will be affected by both the ground conductivity and the top-loading effect of a beam antenna atop the tower.

A fair amount of current flows in the top section above the upper wire connection point. Top loading will affect the phase of this current, which will be reflected as a change in impedance at the feed point. In other words, the calculated data is not absolute. Use it as an approximation only.

A relatively high current flows at the base of the tower to ground—more than in any other part of the system. This indicates that a good earth connection, and even a radial system, would offer highest efficiency.

The antenna patterns, Figures A, B and C, are also approximations. Polarization is predominantly vertical–at low angles it may be considered to be almost completely vertical. Broadside to the direction of the wires, the polarization becomes horizontal at high radiation angles, ie, above 75 degrees. At 60-degrees elevation, the vertical component is almost 16 dB greater than the horizontal. The vertical component increases significantly at lower elevation angles, being in excess of 30 dB above the horizontal component at a 5-degree elevation. These figures all apply in a direction broadside to the wires. In the direction of the wires, both "front" and "back," the radiation is entirely vertically polarized.–*Gerald L. Hall, K1TD*

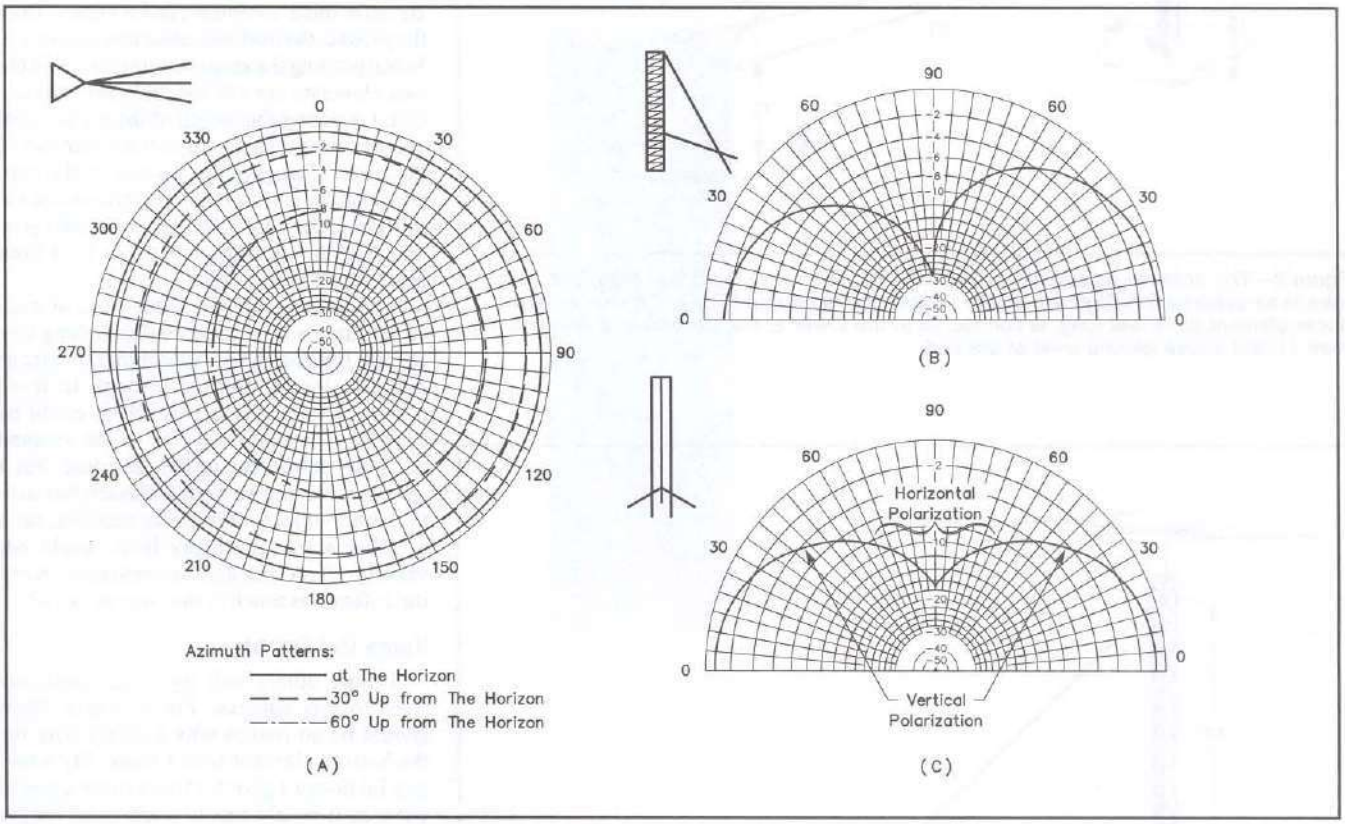

Figure A–Antenna azimuth radiation pattern for the KØEOU three-element half sloper antenna. Values are in dBi. Add 6.0 dB to the values shown.
Figure B—Antenna elevation radiation pattern, in the direction of the wires, for the KØEOU antenna. Values are in dBi. Add 6.0 dB to the values shown.
Figure C—Antenna elevation radiation pattern, in a direction broadside to the wires, for the KØEOU antenna. Values are in dBi. Add 6.0 dB to the values shown.

image in the grounded tower. The top element is tuned for the lower portion of the band and the two-wire element for the upper portion. In fact, there is a little SWR "bump" in the middle of the band that seems to give further evidence of this.

How Well Does It Work?

Although I have no way of scientifically plotting the antenna pattern, it does seem to be vertically polarized. Good DX performance from the antenna seems to verify this. Because many contacts have been made in all directions, the antenna probably has a fairly omnidirectional pattern. On-the-air comparisons with a quarter-wave sloper across town show that the antenna performs at least as well as the sloper. It also seems to have a little less noise on receive than the sloper.

Getting One Up for Yourself

If you have a tower over 40 feet high, you should be in business. The element dimensions will vary according to the height of your tower. My friend Kelly Davis, KD7XY, constructed one of these antennas on his 50-foot tower so we could see how the dimensions would change.

Measurements of his antenna are shown in Figure 4.

It is interesting to note that the height of the feed point on the tower does not appear to be critical at all. The angle of the wires in the two-wire element does not seem to be critical either. The sloper element, however, should come down *between* the two wires of the lower element. The sloper angle is about 45 degrees. As you attempt to get the

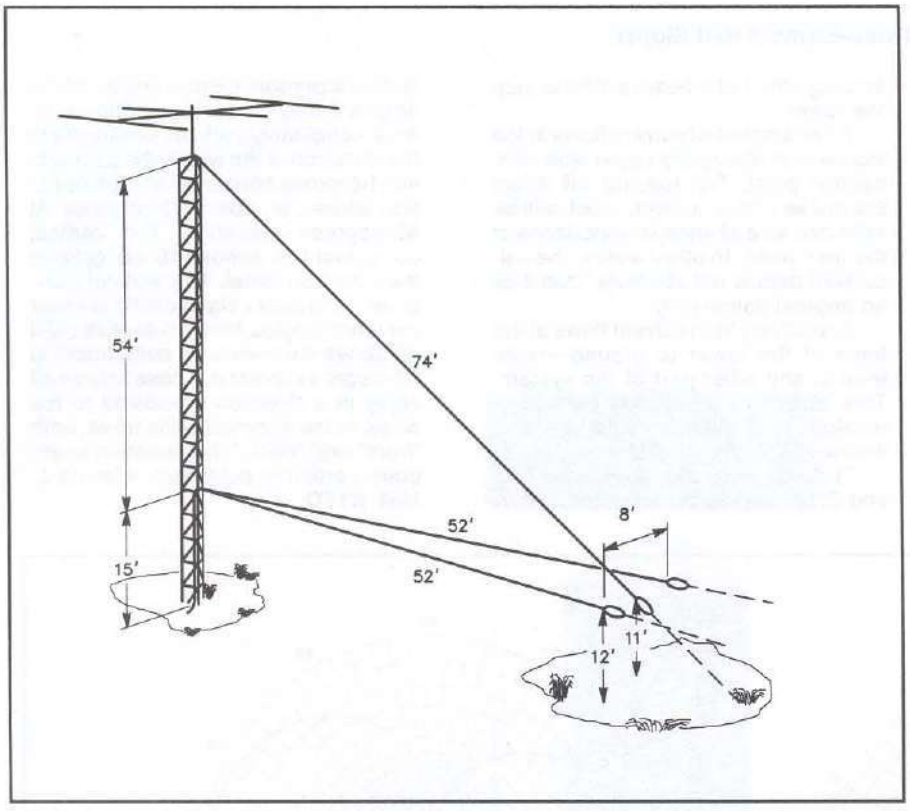

Figure 2—The antenna as constructed at KØEOU. The tower is 70 feet high. The feed point is as described in Figure 1 and is 15 feet above ground level on the tower. The sloper element is 74 feet long, is connected to the tower at the top end and slopes to a point 11 feet above ground level at the end.

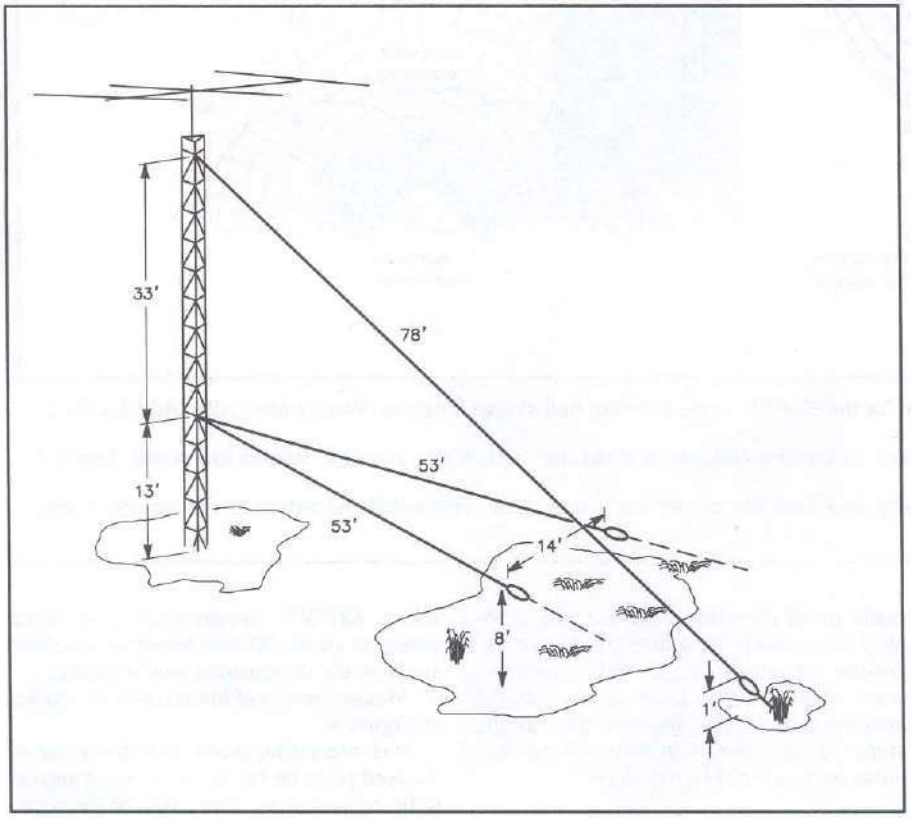

Figure 4—The antenna installation at KD7XY. The tower is 50 feet high. The sloper element is attached at 46 feet, is 78 feet long, and is only 1 foot above ground level at the end. The two-wire element is 53 feet long and is attached to the tower at 13 feet above ground level. Like KØEOU's antenna, it is virtually "flat" across the band; highest measured SWR is 1.4:1.

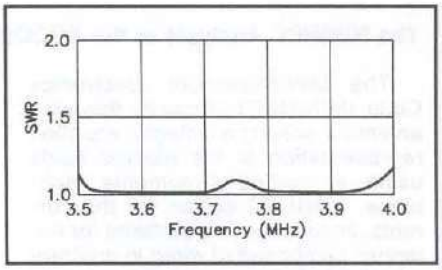

Figure 3—SWR measurements for the antenna at KØEOU. The highest SWR measurement between 3.5 and 4.0 MHz is 1.2:1.

lowest possible SWR from the antenna, remember that the angle of the sloper to the tower and its distance from the ground at the end will have an effect on the bandwidth. Because these antennas can be pruned from the ground, the trial-and-error method is easy. When pruning the antenna, remember that the two elements are cut for different frequencies. Changing the length of the top element changes the performance at the lower part of the band. Changing the lengths of the two-wire elements changes the performance at the top part of the band. Don't give up until your antenna SWR is, at the very most, 1.5:1 from band edge to band edge.

Use good insulators at the ends of each of the three wires. I used nylon fishing line at first, but one foggy, wet night the wire in the top element burned through in three places. It surprised me that there could be such high currents in a part of the antenna not even connected to the feed line, but I should have known better. Remember also that other objects around the antenna, such as other antennas or guy lines, could adversely affect antenna performance. Keep the antenna as much in the clear as possible.

Some Untried Ideas

I hope others will try some modifications to this antenna. For example, there should be no reason why a single wire for the bottom element won't work. My small city lot doesn't give me room to try a single wire, as it would surely need to be longer than the two-wire element. I would also like to see someone try cutting the top element for the high end of the band, and the bottom element for the low end. This could shorten the sloper element for someone with a shorter tower and may even give the antenna some gain in the direction of the two-wire element. It might also be possible to construct an antenna for another band inside of this one (40 meters, for example). The same feed point could be used, but with another sloper element for the second band. Another possibility is to construct the antenna with two dipoles. It is my guess (and only a guess), that it is the merging of the ends of the elements that causes the 50-ohm impedance of the antenna.

Winter gives us the best conditions on the 80/75-meter band. You can be ready to use the whole band with this simple-to-construct and very broadband antenna.

Improved Broadband Antenna Efficiency

When Brian Wermager's article. "A Truly Broadband Antenna for 80/75 Meters," arrived at HQ, I wanted to see if the antenna worked as well as claimed before publishing the information in *QST*.[1] I stopped tuning the antenna when the SWR was less than 1.6 across the entire band.

For working DX the antenna seemed to work as well as, or better than, a dipole at 50 feet. Casual contacts were not difficult to make, but in contests, it was a different matter. The results were satisfactory, but could "satisfactory" be changed to "outstanding"?

The key to improving the efficiency of this antenna is found in the sidebar accompanying the article. The MiniNumerical Electronics Code (MININEC) computer analysis done by Gerald Hall, K1TD, shows that: "A relatively high current flows at the base of the tower to ground—more than in any other part of the system. This indicates that a good earth connection, and even a radial system, would offer highest efficiency."

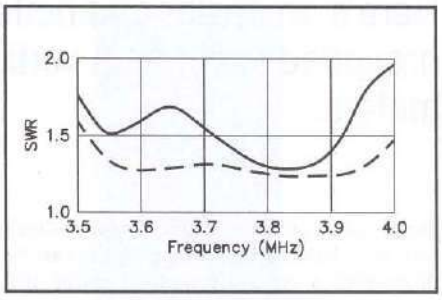

Figure 1–Graph showing SWR vs frequency for the KØEOU 80/75-meter antenna. The lower curve depicts results before adding ground radials; the upper curve was plotted after adding radials and retuning the antenna.

A system of radial wires improves antenna efficiency by cutting ground resistance losses. The decreased resistance in ground losses will also narrow the antenna bandwidth. The question now becomes: Is the narrowing of the bandwidth too much? I decided to investigate that question next.

With help from my brother-in-law, I installed 42 radials around, and bonded to, the tower base. As expected, SWR increased across the entire band. After I retuned the antenna, the SWR was below 2:1 across the entire band (see Figure 1). As for results, DX stations are typically 2 to 6 S units stronger on the KØEOU antenna than on the dipole at 50 feet. Contest QSOs are now a reality. I am not the loudest East Coast station on the band, but I am very pleased with the performance of the broadband antenna. (The dipole has been removed and stored!)—*Chuck Hutchinson, K8CH*

[1] B. Wermager. "A Truly Broadband Antenna for 80/75 Meters," *QST*, Apr 1988, pp 23-25.

By Thomas Russell, N4KG

From *QST*, June 1994

Simple, Effective, Elevated Ground-Plane Antennas

Here's an easier and better way to use your grounded tower as a vertical antenna on 160 or 80 meters.

This article describes a simple and effective means of using a grounded tower, with or without top-mounted antennas, as an elevated ground-plane antenna for 80 and 160 meters.

Grounded towers have been used as shunt-fed verticals on the low-frequency amateur bands for many years. Generally. they required a gamma- or omega-type matching network and an extensive radial system for efficient operation. Recent computer studies reveal that simple elevated radial systems consisting of only four wires can produce results equivalent to 120 buried radials. Typically, these antennas are modeled as isolated monopoles. Presumably, grounded towers could be used with an appropriate shunt-fed matching network.

I've found an even easier method!

From Sloper to Vertical

Recall the quarter-wave length sloper, also known as the half-sloper. It consists of an isolated quarter wavelength of wire, sloping from an elevated feedpoint on a grounded tower. Best results were usually obtained when the feedpoint was somewhere below a top-mounted Yagi antenna. You feed a sloper by attaching the center conductor of a coaxial cable to the wire and the braid of the cable to the tower leg. Now, imagine four (or more) slopers, but instead of feeding each individually, connect them together to the center conductor of a single feed line. *Voila*! Instant elevated ground plane.

Now, all you need to do is determine how to tune the antenna to resonance. With no antennas on the top of the tower, the tower can be thought of as a fat conductor and should be approximately 4% shorter than a quarter wavelength in free space. Calculate this length and attach four insulated quarter-wavelength radials at this distance from the top of the tower. For 80 meters, a feedpoint 65 feet below the top of an unloaded tower is called for, The tower guys must be broken up with insulators for all such installations. For 160 meters, 130 feet of tower above the feedpoint is needed.

That's a lot of tower to dedicate to a single-band antenna, especially for someone with limited real estate. What can be done with a typical grounded-tower-and Yagi installation?

A top-mounted Yagi acts as a large capacitance hat, top loading the tower. Fortunately, top loading is the most efficient means of loading a vertical antenna. The amount of loading can be approximated by using an empirical formula developed by John Devoldere, ON4UN.[1]

Devoldere found that the electrical height of a top-loaded tower can be approximated by:

$$L = 0.38F(H + \sqrt{2S - H/500}) \qquad \text{(Eq 1)}$$

where

L is the approximate electrical length in degrees

F is the frequency in MHz

H is the height of the tower under the Yagi in feet

S is the area of the Yugi in square feet

To check Eq 1, consider the case of no antenna on top, where S = 0. Then L = $0.38 \times 3.6 \times 65 = 88.9°$, which is very close to the desired 90° quarter wavelength.

The effective loading of a Yagi is the portion of the equation under the radical. The examples in Table 1 should give us an idea of how much top loading might be expected from typical amateur antennas. The term H/500 is ignored as insignificant compared with 2S.

The values listed in the Equivalent Loading column of Table 1 tell us the approximate vertical height replaced by the antennas listed in a top-loaded vertical antenna. To arrive at the remaining amount of tower needed for resonance, subtract these numbers from the nonloaded tower height needed for resonance. Note that for all but the 10-meter antennas, the equivalent loading equals or exceeds a quarter wavelength on 40 meters. For typical HF Yagis, this method is best used only on 80 and 160 meters.

[1] J. Devoldere, *Antennas and Techniques for Low Band DXIng* (Newington: ARRL, 1994).

Table 1
Effective Loading of Common Yagi Antennas

Antenna	*Boom Length (feet)*	*S (area, ft²)*	*Equivalent Loading (feet)*
3L 20	24	768	39
51 15	26	624	35
4L 15	20	480	31
31 15	16	384	28
5L 10	24	384	28
4L 10	18	288	24
3L 10	12	192	20
TH7	24	—	40 (estimated)
TH3	14	—	27 (estimated)

Construction Examples

Consider this example: A TH7 Yagi mounted on a 40-foot tower. The TH7 has approximately the same overall dimensions as a full-sized 3-element 20-meter beam, but has more interlaced elements. I estimate its equivalent loading to be 40 feet. At 3.6 MHz, 65 feet of tower is needed without loading. Subtracting 40 feet of equivalent loading, the feedpoint should be 25 feet below the TH7 antenna.

I ran 10 quarter-wavelength (65-foot) radials from a nylon rope tied between tower legs at the 15-foot level, to various

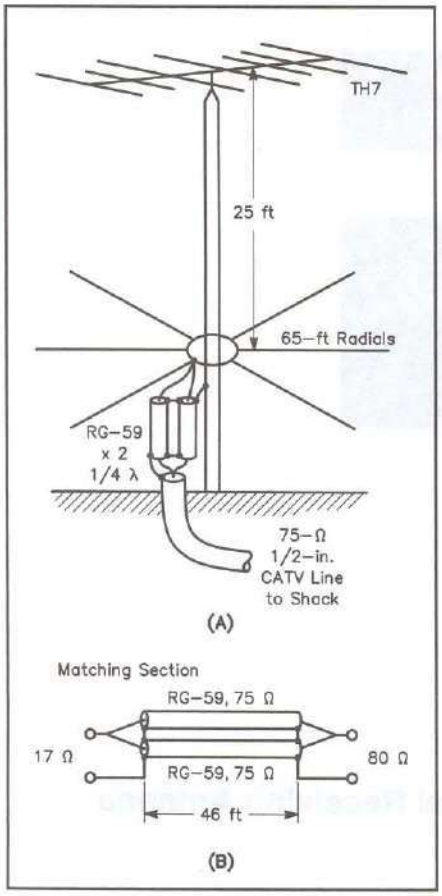

Figure 1—At A, an 80-meter top-loaded, reverse-fed elevated ground plane, using a 40-foot tower carrying a TH7 triband Yagi antenna. At B, dimensions of the 3.6 MHz matching network, made from RG-59.

supports 10 feet high. I tied nylon cord to the insulated, stranded, 18-gauge wire, without using insulators. The radials are all connected together and to the center of an exact half wavelength (at 3.6 MHz) of RG-213 coax, which will repeat the antenna feed impedance at the other end. Figure 1 is a drawing of the installation. I used a Hewlett-Packard low-frequency impedance analyzer to measure the input impedance across the 80-meter band.

An exact resonance (zero reactance) was seen at 3.6 MHz just as predicted. The radiation resistance was found to be 17 Ω. The next question is how to feed and match the antenna.

My approach to 80-meter antennas is to tune them to the low end of the band, use a low-loss transmission line, and switch an antenna tuner in line for operation in the higher portions of the band. With a 50-Ω line, the 17-Ω radiation resistance represents a 3:1 SWR, meaning that an antenna tuner should be in-line for all frequencies. For short runs, it would be permissible to use RG-8 or RG-213 directly to the tuner. Since I have a plentiful supply of low-loss 75-Ω CATV rigid coax, I took another approach.

I made a quarter-wave (70 feet × 0.66 velocity factor = 46 foot) 37-Ω matching line by paralleling two pieces of RG-59 and connecting them between the feedpoint and a run of the rigid coax to the transmitter. The magic of quarter-wave matching transformers is that the input impedance (R_i) and output impedance (R_o) are related by

$$Z_o^2 = R_i \times R_o \qquad \text{(Eq 2)}$$

For R_i = 17 Ω and Z_o = 37 Ω, R_o = 80 Ω, an almost perfect match for the 75-Ω CATV coax. The resulting 1.6:1 SWR at the transmitter is good enough for CW operation without a tuner.

The Proof is In the Log

How effective is this antenna? Well, I used to install a 60-foot aluminum tower and 100 radials, 100 feet long in a clear one-acre field every winter, and remove it every spring for mowing. The top-loaded reverse-fed elevated ground-plane antenna has replaced that antenna with no regrets. My only other 80-meter antenna is a dipole at 110 feet broadside to Europe and the South Pacific,

I use the elevated ground plane for South Africa, South America. the Caribbean, parts of the Pacific and Asia, both long and short path. With it I have worked everything I can hear, with 1200 W output, including HL (rare in Alabama); HS; UA9; UAØ; UI; UJ; UL; most of the VK9s; XV; ZS1; ZS8MI; ZS9; 3Y5X; 8Q; 9M2; and 9V1. While running 5 W output. I have even worked two JAs with this antenna. which may say more for its effectiveness than anything else.

Will It Work on 160 Meters?

You bet it will, but it takes another tower. For the 160-meter band, a resonant quarter-wavelength requires 130 feet of tower above the radials. That's a pretty tall order. Subtracting 40 feet of top loading for a 3-element 20-meter or TH7 antenna brings us to a more reasonable 90 feet above the radials. Additional top loading in the form of more antennas will reduce that even more.

Recently, a friend moved to the country, and he needed a 160-meter antenna in a hurry for an upcoming contest. He had

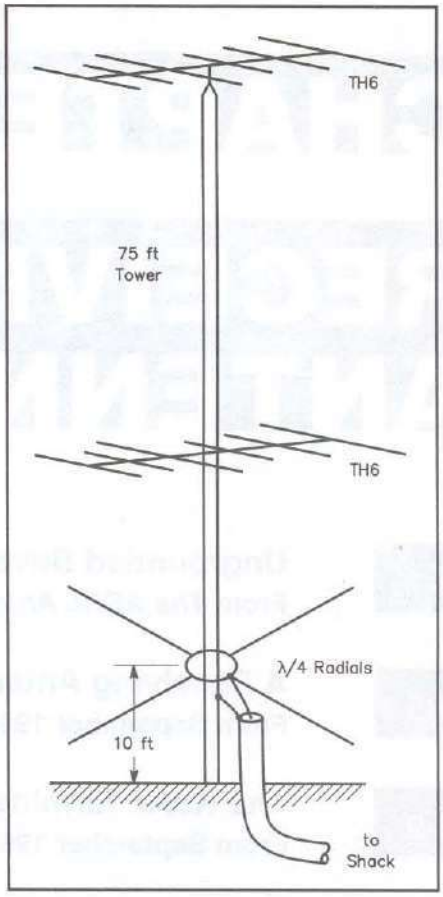

Figure 2—A 160-meter antenna using a 75-foot tower carrying stacked triband Yagis.

stacked TH6s on a 75-foot tower. I suggested he try four elevated radials at 10 feet above ground, with a tuner if necessary. He connected four radials about 120 feet long and a piece of RG-58. The SWR measured under 2:1 and he worked everything he heard in the contest. Figure 2 is a drawing of this installation.

Another friend had a 120-foot tower with no antennas on it. He ran four elevated radials at 10 foet and obtained an SWR below 1.5:1 with a 50-Ω feed line. During the contest, he even beat out some big guns.

Elevated ground-plane antennas work! This simple, reverse-feed system makes it possible to feed grounded towers easily and efficiently.

References

A. Christman, "Elevated Vertical Antenna Systems," *QST*, Aug 1988, pp 35-42 (Feedback, *QST*, Oct 88, p 44).

A. Christman, "More on Elevated Radials," *QST*, Mar 1993, p 72 (Technical Correspondence).

CHAPTER EIGHT

RECEIVING ANTENNAS

8-1 **Ungrounded Beverage Antennas**
From *The ARRL Antenna Compendium Volume 4*

8-5 **A Receiving Antenna that Rejects Local Noise**
From September 1995 *QST*

8-9 **The K9AY Terminal Loop–A Compact, Directional Receiving Antenna**
From September 1997 *QST*

8-13 **Hum Problems When Switching the K9AY Loops**
From May 1998 *QST* (Technical Correspondence)

By Brian Beezley, K6STI
From *The ARRL Antenna Compendium Volume 4*

Ungrounded Beverage Antennas

So you've heard how Beverages can help you hear better on the lower bands, but you're still not convinced they're worth the bother. K6STI analyzes the Beverage, especially an easy-to-construct "ungrounded" version.

Beverages are amazing receiving antennas. A good Beverage can turn a signal barely audible on your transmit antenna into solid, Q5 copy. A Beverage antenna (named after 1920s inventor H. H. Beverage) is a long, low wire used for receiving. They're most popular on the 160, 80, and 40-meter bands. Although occasionally pressed into service, Beverages are much too lossy for regular use as transmitting antennas.

Conventional Beverages are fed against ground. Although very long wires may develop a few dB of front-to-back ratio, unterminated Beverages are essentially bidirectional. Terminating a Beverage through a resistance to ground at the far end creates a highly unidirectional pattern. Beverages typically are 1 to 15 feet high and 1 to 4 wavelengths long.

Beverages are broadband, traveling-wave antennas. Power traveling toward the feedpoint is absorbed by the receiver, while that traveling in the opposite direction is absorbed by the termination resistance. Standing waves can't develop. Because waves traveling toward the feedpoint accumulate substantially in phase, while those arriving from other directions tend to cancel, the azimuth pattern of a long Beverage is highly directive. Beverages are nonresonant antennas and can be used over a wide frequency range.

A very useful Beverage variation uses two parallel wires, with one grounded at the far end. Waves traveling toward the far end reflect and return to the feedpoint differentially as transmission-line currents. With suitable termination and switching circuitry at the feedpoint, you can receive signals from either direction. A two-wire Beverage thus can replace two single-wire antennas.

For simplicity, I'll consider just single-wire Beverages here.

Eliminating Ground Connections

Beverages normally connect to ground at the feedpoint and far end. See Figure 1A. However, obtaining a good, reliable ground can be difficult. A short ground rod may exhibit thousands of ohms resistance to ground when installed in dry soil or when corroded. Since Beverages require a termination resistance of just several hundred ohms, a poor far-end ground can grossly misterminate an antenna and destroy its pattern. A poor feedpoint ground can reduce signal levels and encourage coax-shield pickup. You can use multiple ground rods, a ground screen, or a ground-radial system to lower ground resistance, but this greatly increases the work required to install a Beverage.

A ground connection isn't essential for Beverage operation. You can place the termination resistance about one-quarter wavelength from the far end of the wire. Since the impedance of a quarter-wave wire is low and resistive, the remainder of the wire just sees the termination resistor in series with a low resistance. Similarly, you can feed a Beverage about one-quarter wavelength from the near end. Both ends of the wire are left unconnected. See Figure 1B.

Ungrounded Beverages are simple to install and have stable properties. Their radiation patterns often are superior to those of their grounded counterparts because they don't suffer unwanted response from vertical wires. (This response can be reduced by lowering wire height. One way to do this is to slant the feed and termination wires over a long distance.)

The only real disadvantage of ungrounded Beverages is that they're frequency-dependent. For example, the low-impedance, quarter-wave wire sections become high-impedance, half-wave sections at twice the design frequency. I'll show you how to multiband an ungrounded Beverage later.

Antenna Modeling

While you can use a *MININEC*-based antenna-analysis program to model Beverage antennas, you'll have to settle for approximate results at best. The *MININEC* algorithm uses perfect-conductivity ground during current calculations. It takes lossy ground into account only later when calculating radiation patterns. Because Beverages are so close to ground, their current distribution is strongly affected by ground characteristics. *NEC*'s Sommerfeld-Norton ground model takes ground dielectric constant and conductivity into account when calculating wire currents. This lets you accurately analyze antennas in close proximity to earth. I used the *NEC/Wires 1.0* program to obtain all results presented here. I modeled antennas over average-quality earth (dielectric constant= 13, conductivity = 5 mS/m).

Wire Height

Figures 2A and 2B shows the azimuth and elevation patterns for a 1000-foot long, 10-foot high, ungrounded Beverage on 160 meters. The antenna uses # 18 wire and a 650-Ω termination resistance. It's fed and terminated 120 feet from each end. The remarkable pattern is better than that of many HF Yagis.

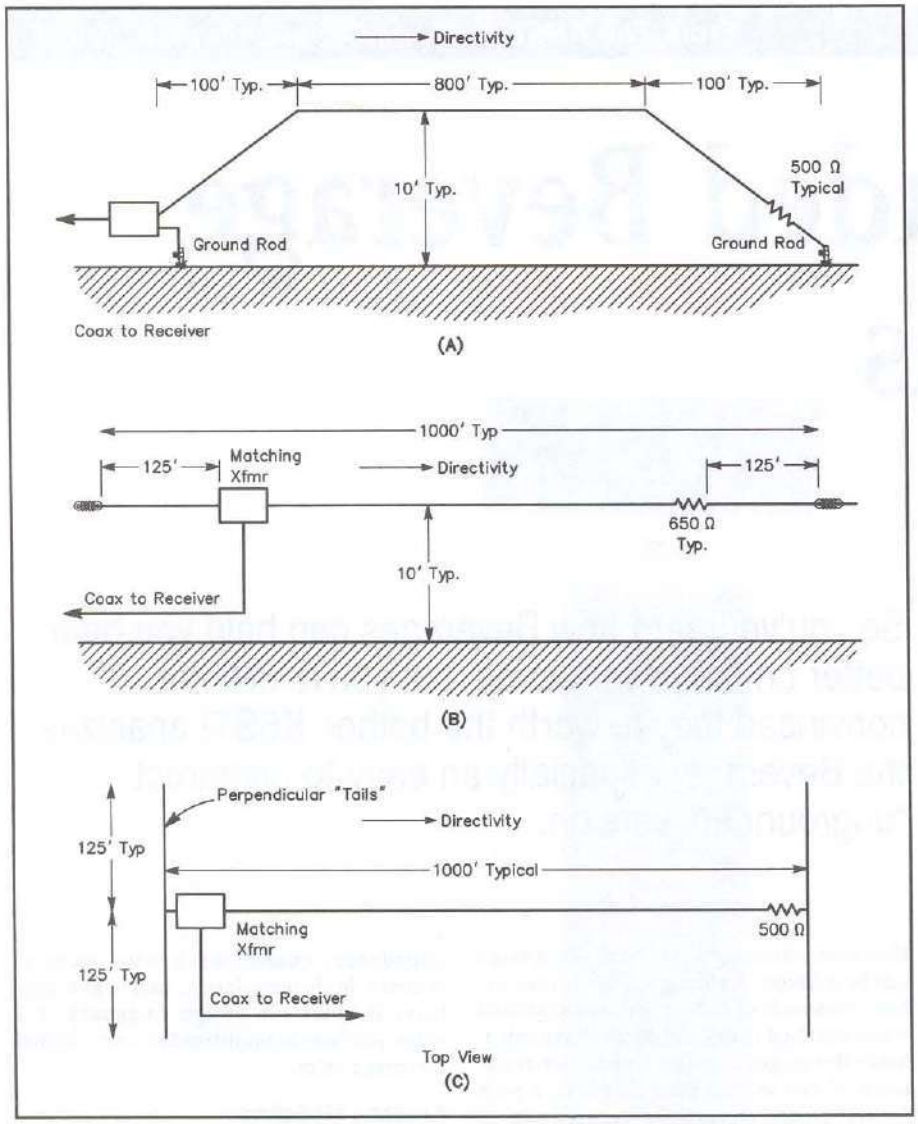

Figure 1—Single-wire Beverage antenna feeding and termination configurations. At A, conventional method is shown using slanted-wire terminations. At B, ungrounded Beverage is shown with matching transformer and terminating resistor inserted λ/4 in from either end of wire. At C, ungrounded Beverage using full span of wire by employing perpendicular "tails" at both ends. The tails function as elevated counterpoise radials at 160 meters.

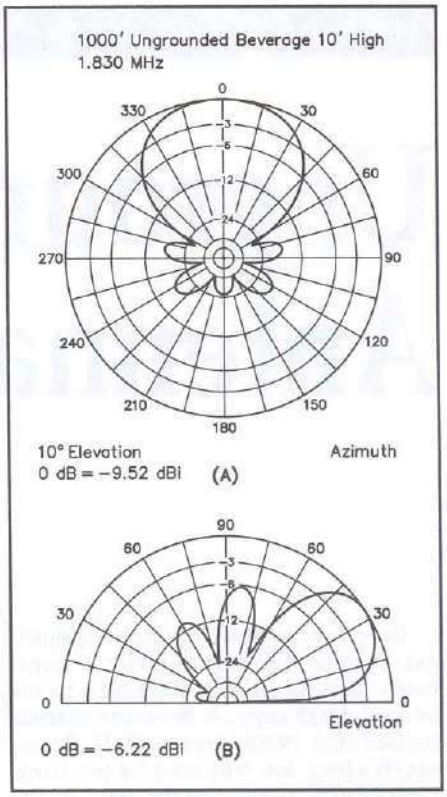

Figure 2—Azimuth and elevation patterns at 1.83 MHz for 1000-foot long ungrounded Beverage mounted 10 feet off flat ground with average conductivity and dielectric constant. The worst-case rearward lobes are better than 18 dB down compared to peak response. Note that the gain is only –9.52 dBi at 10° elevation, peaking at –6.22 dBi at about 30° elevation. If the transmission line to the receiver is very long, a preamplifier may be needed.

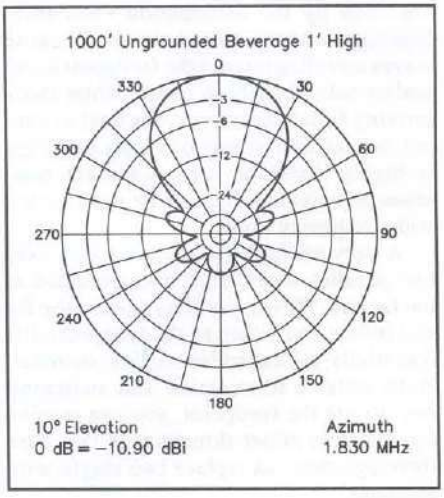

Figure 3—Azimuth response for 10° elevation angle at 1.83 MHz for 1000-foot long ungrounded Beverage mounted only 1 foot off flat ground. Compared to the higher antenna in Figure 2, this low Beverage has about 1 dB less gain, but the worst-case backlobes are suppressed even better.

Figure 3 shows the azimuth pattern of a similar Beverage 1 foot above ground. The termination resistance for this antenna is 750 Ω and it's fed and terminated 125 feet from the wire ends. The pattern is even sharper than that of Figure 2. Output is about 1 dB lower.

If you're tempted as I was to just lay a Beverage on the ground, take a close look at Figure 4. This is the Beverage of Figure 3 but just 1 inch off ground (*NEC* provides accurate results for wire heights down to within several wire radii of ground). While still useful, the pattern has degraded considerably. Signal output is quite a bit lower. (Nevertheless, some users report excellent results from on-the-ground Beverages. Don't hesitate to try one if it's your only option.)

In the West you can just lay an ungrounded Beverage in the chaparral a few feet off ground. In the East you can unroll one on top of a foot or two of snow (snow has very low dielectric constant and conductivity and should be transparent to RF at low frequencies). Beverages like these are very easy to install (no support poles or ground rods). You can roll one out just before a contest.

Occasionally a Beverage may have to clear a height-sensitive area. Figure 5 shows what can happen when wire height varies. The first 200 feet of this antenna is 3 feet high (chaparral height). Next, a 50-foot section slopes from 3 to 15 feet. This is followed by a 200-foot span 15 feet high, a 50-foot downslope, and finally the remainder of the wire at 3 feet. This model is similar to a Beverage used by K6TQ which must clear an agricultural area with produce trucks. While the rear part of the pattern is relatively unaffected, the height variation causes a large sidelobe bulge. It doesn't matter much if your Beverage is

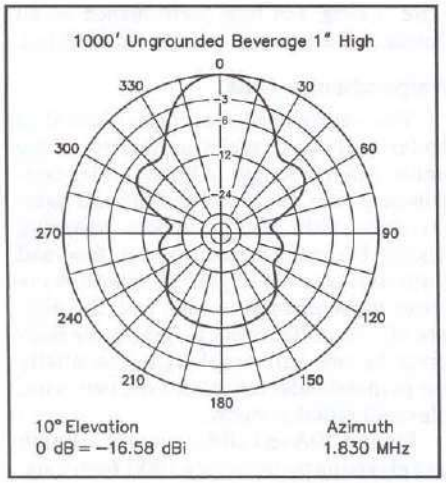

Figure 4—Azimuth response for same antenna as in Figure 3, except that the height is now only 1 inch off ground. The rearward pattern suffers and the gain fails about 5.4 dB compared to the Beverages in Figures 2 and 3.

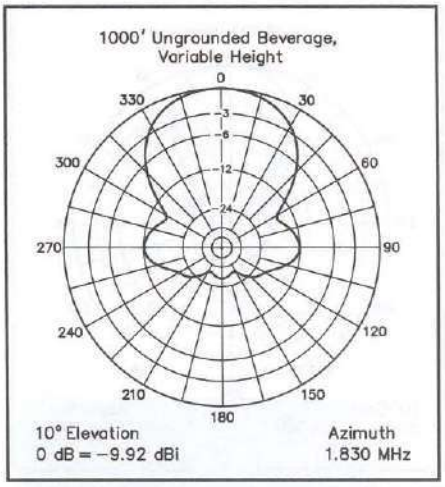

Figure 5—Azimuth response at 1.83 MHz for 1000-foot long, variable height ungrounded Beverage. The sidelobes at 90° and 270° are larger than the antenna in Figure 2, but the pattern and gain are still quite acceptable.

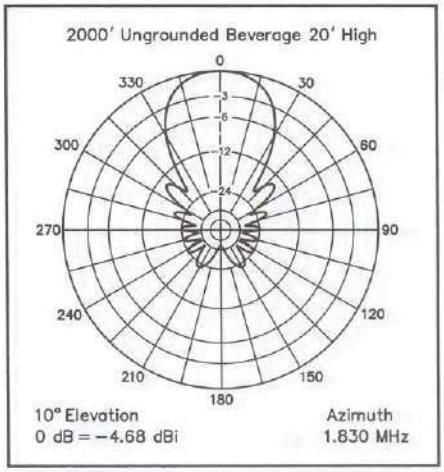

Figure 6—Azimuth response at 1.83 MHz for 2000-foot long ungrounded Beverage mounted 10 feet over flat ground. The gain is almost 5 dB higher than that of Figure 2, and the backlobes are all suppressed in excess of 23 dB. This is a great 160-meter receiving antenna, but must be oriented carefully at desired receiving bearing because of narrow frontal lobe.

high or low, but try to keep the height as constant as possible.

Wire Length

Figure 6 shows the azimuth pattern of a 2000-foot ungrounded Beverage. The termination resistance is 550 Ω. The pattern of a very long Beverage like this may be too narrow for complete coverage of a general direction.

Figure 7 shows the pattern of a 500-foot ungrounded Beverage. The termination resistance is 1100 Ω. While much broader than the patterns of longer antennas, it's still quite directive and can provide a substantial receive improvement.

Feeding Ungrounded Beverages

Conventional Beverages usually are fed with an autotransformer having a 3:1 turns ratio. This matches a 450-Ω impedance to 50 Ω. Ungrounded Beverages typically have an input resistance of 500 to 1000 Ω (roughly equal to the termination resistance) and an input reactance of up to 100 Ω. An exact impedance match isn't important; a better match just delivers a higher signal. Although usually not required to improve signal-to-noise ratio, a receive preamplifier can equalize Beverage and transmit-antenna signals for easier direct comparisons.

Both grounded and ungrounded Beverages can be sensitive to unwanted coupling at the feedpoint. If you connect coax through an autotransformer to a Beverage, the outside of the coax shield can become part of the antenna system if it exhibits an impedance similar to or less than whatever connects to it. It's the same thing that can happen with a coax-fed dipole. To prevent this, use a matching transformer with separate primary and secondary windings and low interwinding capacitance. This will isolate the outside of the coax shield from the antenna. Alternatively, you can use an autotransformer followed by a current-type balun. (Because the feed tail of an ungrounded Beverage is likely to provide a lower-impedance termination than a typical ground rod, these Beverages should be less sensitive to coax-shield pickup.)

Terminating Ungrounded Beverages

Optimal termination resistance depends on wire length, height, diameter, and ground constants. The termination resistance normally just affects the rear part of the pattern. It's easy to find the optimal value by modeling the exact geometry of your antenna with *NEC*. If you use long spans of wire with considerable sag, model the sag using multiple wires.

You can determine optimal termination resistance experimentally using a signal source to the rear of the antenna. Simply adjust the termination resistance for minimum signal.

(Actually, minimum response directly to the rear isn't quite optimal for most designs. This condition usually causes the pattern to degrade slightly over a broad region elsewhere. Nevertheless, adjusting for minimum response is close enough for all but the most fanatical Beverage enthusiast.)

Multibanding Ungrounded Beverages

If you provide a termination resistance one-quarter wavelength from the far end for each band of interest, you can use a Beverage on several bands. At the near end use a separate quarter-wave tail for each band and connect them in parallel at the feedpoint.

Figure 8 and Figure 9 show 160-meter and 80-meter patterns of a 1000-foot-long, 10-foot-high, dualband Beverage. This antenna uses a 700-Ω resistor 63 feet from the far end and a 350-Ω resistor 125 feet out. The two termination resistances provide near-optimum performance on 160. The backlobe of the 80-meter pattern is suboptimal but the sidelobes are still well down. I didn't experiment much with termination-resistance values or positions. I'll bet both can be improved.

Another alternative is to use a single termination resistance with multiple quarter-wave tails. The resistor value will be optimal on just one band since antenna length isn't constant in wavelengths. But the value won't be far off on any band if the

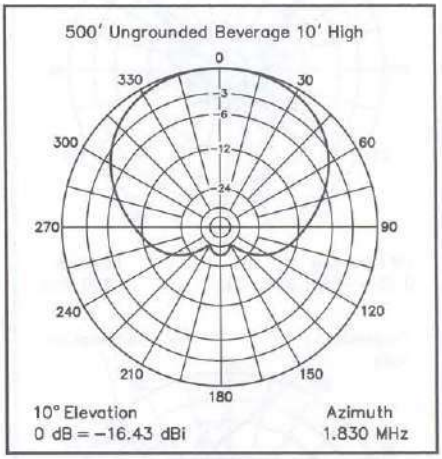

Figure 7—Azimuth response at 1.83 MHz for 500-foot long ungrounded Beverage mounted 10 feet over average ground. The gain is almost 7 dB less than Figure 2 at 10° elevation. The side lobes are large, even though the rear lobes are well suppressed.

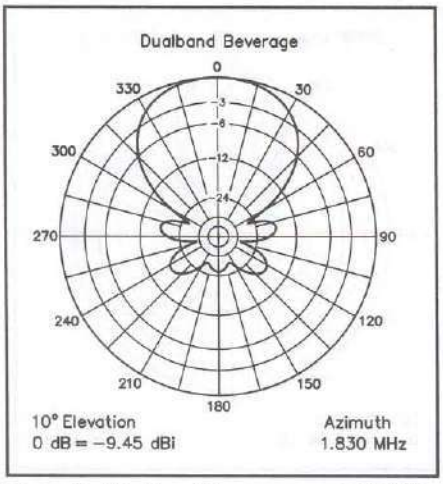

Figure 8—Dualband Beverage on 1.83 MHz, using a 700-Ω resistor 63 feet from the far end, and a 350-Ω resistor 125 feet out.

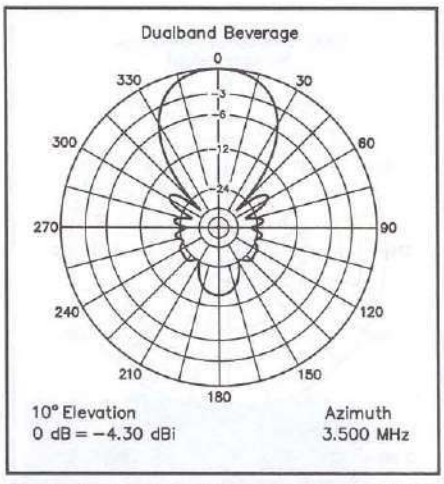

Figure 9—Dualband Beverage on 3.5 MHz, using same terminations as in Figure 7. The termination is not optimal for this band, but still yields desirable directivity.

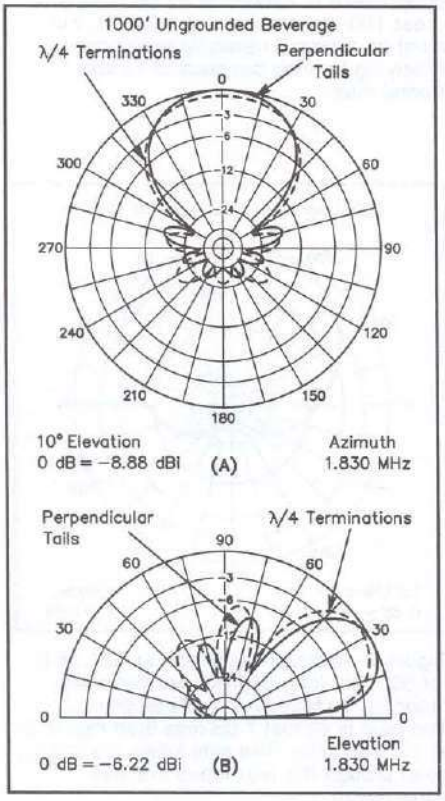

Figure 10—Ungrounded Beverage, 1000 feet long with two λ/4 perpen-dicular termination "tails." Pattern from ungrounded Beverage in Figure 2 is overlaid for comparison. At A, the azimuthal patterns at 10° elevation are shown; at B, the elevation patterns are shown.

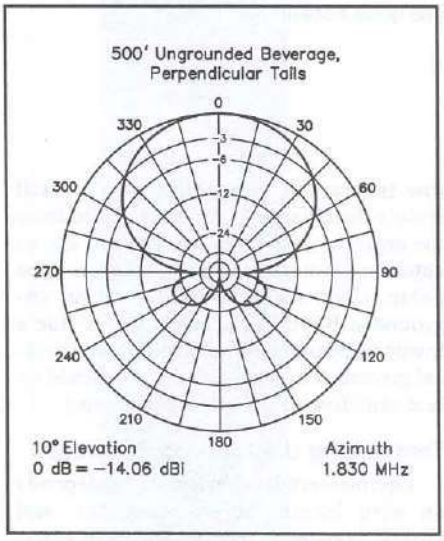

Figure 11—Azimuthal pattern for ungrounded Beverage, 500 feet long with two λ/4 perpendicular termination tails.

wire is long. For best performance on all bands, use a separate resistor for each tail.

Perpendicular Tails

The ungrounded Beverages described so far really don't make optimal use of the entire antenna length. Although they contribute power, the near- and far-end quarter-wave tails don't support traveling waves. If space permits you can feed and terminate against a pair of quarterwave wires perpendicular to each end. See Figure 1C. This effectively lengthens the Beverage by one-half wavelength. Essentially the perpendicular tails form two, two-wire, elevated radial systems.

Figures 10A and 10B shows the azimuth and elevation patterns for a 1000-foot-long, 10-foot-high Beverage with perpendicular tails, with the patterns from Figure 2 overlaid for comparison. This antenna uses a 500-Ω termination. The pattern is somewhat narrower than that of Figure 2 and the backlobes are even smaller. The elevation plot shows that overhead response is about 10 dB less with perpendicular tails and that the forward lobe cants at a lower angle.

Since the quarter-wave tails of a 500-foot Beverage comprise half its length, you might expect a more dramatic improvement for perpendicular tails on this antenna. Figure 11 shows the pattern of a 500-foot-long, 10-foot-high Beverage with perpendicular tails. This antenna also uses a 500-Ω termination. Side response is down quite a bit from Figure 7 and forward response is 2 dB greater.

While they provide better performance, designs with perpendicular tails are more complex and occupy additional space. You can make better use of the additional space by phasing two Beverages with in-line tails to obtain a much better azimuth pattern . . . but that's another story.

By Brian Beezley, K6STI

From *QST*, September 1995

A Receiving Antenna that Rejects Local Noise

Simplicity and performance combine to give birth to a compact antenna you'll want to have!

Noise can make a ham's life miserable on any amateur band. As we approach the minimum of the sunspot cycle, many hams are discovering that noise can be particularly frustrating on the low bands. In summer, static crashes caused by thunderstorm lightning can totally mask weak signals on the 160, 80, and 40-meter bands. During other seasons, power-line noise, noise from household appliances, and incidental radiation from home electronic products often limits reception.

A recent *QST* article by Floyd Koontz, WA2WVL,[1] describes a small receiving antenna for the low bands that provides a cardioid directional pattern. This pattern can reduce noise and QRM from the rear. As I marveled at the elegance and simplicity of Floyd's design, I realized that the antenna did have one shortcoming: Because it is vertically polarized, the antenna responds strongly to local noise propagated by ground waves. I wondered whether it was possible to devise a receiving antenna to better reject local noise.

The Ground Wave

Most hams who operate HF are familiar with the sky wave (or space wave) that's responsible for long-distance ionospheric propagation. See Figure 1A. The space wave has two components: The *direct wave* propagates along a straight line from the transmit antenna toward the ionosphere. The *ground-reflected wave* bounces off the earth's surface and heads in the same direction.

The space wave also exists for local propagation, as shown in Figure 1B. The direct wave travels in a straight line between the transmit and receive antennas, while the ground-reflected wave takes a midpoint bounce. But when the antennas are close to ground, the direct and reflected waves nearly cancel, leaving a very small residual space wave. When the antennas are right at the earth's surface, the waves cancel completely. So what makes local communication possible? Answer: A third wave, called the *surface wave*, that exists for antennas close to ground. This wave diminishes in intensity as you increase antenna height. The surface wave exists *only near the surface of the earth*. The combination of the direct wave, the ground-reflected wave, and the surface wave is called the *ground wave*.[2]

Surface-wave intensity varies with frequency and ground conductivity. It's stronger at low frequencies and for highly conductive ground. But the most important property of the surface wave is its polarization sensitivity. The surface wave is much weaker for horizontal fields. For example, on 80 meters the broadside ground-wave response of a short piece of wire is about 34 dB lower when oriented horizontally. The difference is about 42 dB at 160 meters.[3]

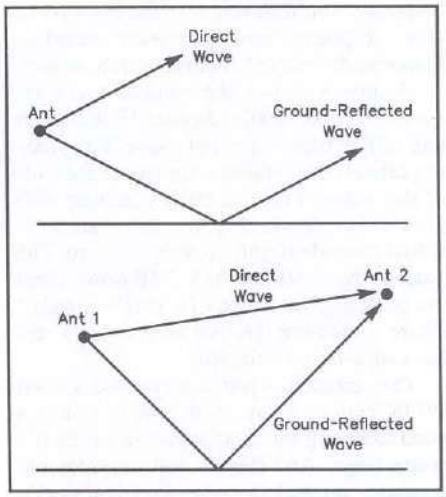

Figure 1—At A, the direct and ground-reflected components of the space wave for ionospheric propagation. At B, the space-wave components for local propagation.

The surface wave makes local AM radio broadcasting possible. Because of the poor propagation of horizontally polarized ground-wave signals, AM broadcasters universally use vertical polarization. The same phenomenon causes vertical antennas to pick up much more local noise than horizontal antennas do. Even if a noise source has a stronger horizontal component, by the time the field reaches the receive antenna, the vertical component almost always dominates.

These facts suggest that the first requirement of a receiving antenna with low response to local noise is insensitivity to vertically polarized radiation, the dominant component of the ground wave. Surprisingly, simply avoiding the use of vertical wires isn't enough. An antenna composed only of horizontal wires can still respond to vertical fields.

A Low Dipole

Figure 2 shows the ground-wave response of an 80-meter dipole 10 feet high. An easy-to-install, inconspicuous dipole like this is sometimes used for receiving when the transmit antenna is vertically polarized. The pattern shows the electric field strength 10 meters above ground at a distance of 1000 meters for an input power of 1 kW (the dipole exhibits the same pattern on receive). This geometry might be representative of that for a noisy power pole. Although the pattern may look similar to that of a free-space dipole, I think

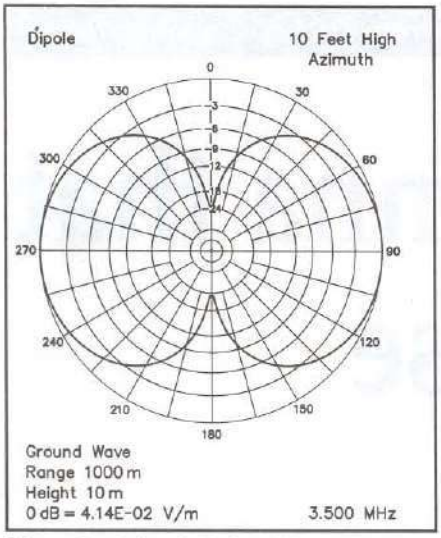

Figure 2—Azimuthal plot of the ground-wave response of a 10-foot-high 80-meter dipole. The input power to the antenna is 1 kW. The peak electric field is shown.

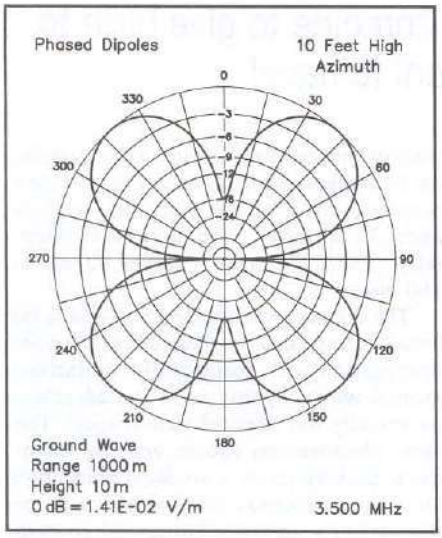

Figure 3—Azimuthal plot of the ground-wave response of two parallel dipoles 10 feet apart, 10 feet high and fed out of phase. The input power to the antenna is 1 kW. The peak electric field is shown.

you'll be surprised to know that the wire is oriented broadside to the pattern null. A low dipole actually responds to ground-wave fields best off its ends!

Here's an explanation for this peculiar behavior: The dipole has no response to the vertical component of a broadside ground wave because the electric field is perpendicular to the wire. The antenna responds only to the weak horizontal component. The vertical component also is perpendicular to the mirror image of the antenna formed by the ground-reflected wave. But away from broadside, the dipole, its image, or both, have a nonvanishing projection in the vertical plane. This enables the dipole to respond to the vertical component of a ground wave. In addition, lossy earth causes the surface wave to develop a radial component in the direction of propagation. Away from broadside, the radial component also projects onto the wire and induces current. The vertical and radial components induce maximum current when the surface wave arrives in line with the wire.

When compared to a quarter-wave vertical with four radials elevated 10 feet above ground, the low dipole has a 12.5 dB lower ground-wave response in its most sensitive direction in line with the wire. For sky-wave signals arriving at 20° elevation from their weakest direction (also off the ends), the dipole has 10 dB lower response than the vertical. Therefore, the low dipole has a signal-to-noise ratio advantage of 2.5 dB for signals and noise arriving from their worst-possible directions. In the most favorable directions broadside to the wire, the S/N advantage peaks sharply at 26.1 dB.

Raising the dipole broadens the broadside S/N peak and improves S/N off the ends. For example, for signals arriving at 20° elevation, a dipole at 50 feet has an S/N advantage over the reference vertical of 6.3 dB in line with the wire and 25.6 dB broadside. If you have just a single noise source and you can rotate a high dipole, you should be able to come within a few decibels of the latter figure most of the time. But when multiple noise sources in different directions arise (typical for power-line noise in times of low humidity), rotating the antenna won't help much. The S/N advantage of the high dipole then is likely to be near the worst-case figure.

These numbers illustrate the advantage of horizontal receiving antennas and substantiate the notion long held by amateurs that "verticals are noisy." But you can reduce ground-wave noise much more effectively if you don't rely on a simple horizontal wire.

Canceling Ground-Wave Components

Although a horizontal wire responds only weakly to a broadside ground wave, its response is substantial off the ends. If you could somehow eliminate the end response, you'd be left with the low broadside response and whatever residual response developed at intermediate angles.

Figure 3 shows the ground-wave response of two parallel dipoles 10 feet apart and 10 feet high fed out of phase. The phasing cancels everything arriving off the ends of the wires. The end nulls combine with the low broadside response to create a residual cloverleaf ground-wave pattern. The peak of the cloverleaf is 9.3 dB down from the peak end-response of a single dipole.[4] (Wire losses are ignored here to illustrate the cancellation principle.)

This antenna is just a very-close-spaced W8JK endfire array. Although it makes a good receiving antenna for the low bands, it's pretty large. And there's still considerable ground-wave pickup in the cloverleaf peaks. If the wires somehow could remain parallel for all directions, it might be possible to achieve complete cancellation of the vertical and radial components of the ground wave.

In some sense, the sides of a circular loop are parallel everywhere. Current amplitude and phase vary little in small loops of regular shape. Therefore, the currents in opposite sides of such loops are nearly equal and out of phase. Unlike a W8JK array, a small horizontal loop does not have a null anywhere along the ground. But its ground-wave response is uniformly low in all directions because the antenna responds only to the weak horizontal component. Everything else cancels out (or nearly so).

A small loop usually is defined as one with a total conductor length of less than 0.1 λ. But unless you use large-diameter conductors to minimize RF resistance, loops this small are inefficient. A preamplifier may be needed to overcome receiver noise. You can increase the output of a loop by increasing its size, but the larger you make it, the less constant the current becomes. This reduces groundwave cancellation.

The antenna of Figure 4 overcomes this difficulty by using two feedpoints, each on opposite sides of the loop to force current balance. One of the phasing lines is twisted to maintain proper phase.[5] This loop can be made quite large and still exhibit very low response to ground-wave noise.

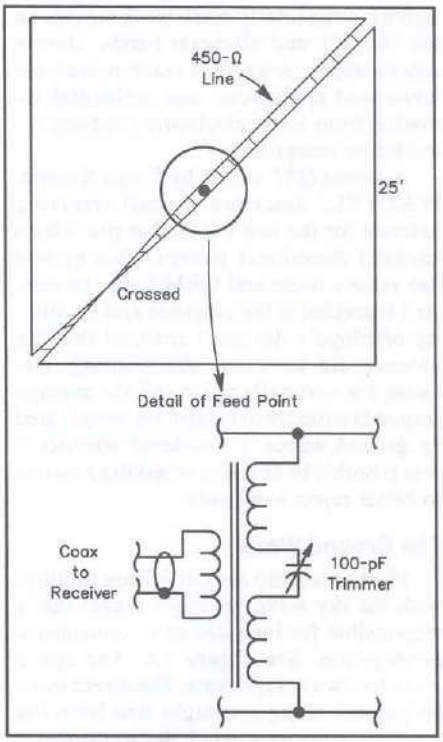

Figure 4—Basic diagram of the 80-meter low-noise loop antenna showing detail of the feedpoint arrangement. The antenna measures 25 feet on a side, is 10 feet high, and made of #14 wire. It's fed at opposite corners with phasing lines made of #14 wire spaced 1.5 inches. A small ferrite transformer at the junction of the phasing lines matches the antenna to 50 Ω coaxial feed line and also functions as a balun. The trimmer capacitor (a capacitance of about 40 pF is required) in series with the antenna-side winding resonates the loop at 3.5 MHz.

A Practical Design

The 80-meter loop of Figure 4 has a perimeter of 0.36 λ. It's 25 feet on a side, 10 feet high, and made of #14 wire. It's fed at opposite corners with phasing lines made of #14 wire spaced 1.5 inches. A small ferrite transformer at the junction of the phasing lines matches the antenna to 50 Ω and also functions as a balun. A trimmer capacitor (about 40 pF is needed) in series with the antenna-side winding resonates the loop at 3.5 MHz.

The ground-wave response of this particular loop is shown in Figure 5 and its sky-wave response in Figure 6. For signals arriving at 20°elevation, the worst-case skywave response is 20.5 dB below that of the reference vertical. This signal level is quite usable on 80 meters without a preamp. Because the loop reduces ground wave noise at least 45.1dB, S/N improvement is 24.6 dB for the worst-case combination of signal and noise directions. if you use a preamp and adjust for equal signal levels, ground-wave noise will be four S units lower on the loop *no matter what direction it comes from!* For signals arriving at higher angles, S/N enhancement approaches 30 dB.

Both the ground-wave noise pattern and sky-wave signal pattern are very uniform in azimuth. The antenna is essentially omnidirectional with an overhead null, just like a vertical. An overhead null is useful for reducing near-vertical-incidence skywave signals from nearby stations. (The loop rejects their ground-wave signals along with local noise.)

Although the S/N performance of this loop is not particularly sensitive to height, you can increase output level substantially by raising the antenna well above ground. For example, if you raise the loop to 50 feet, the output increases 15.2 dB for signals arriving at 20° elevation. At this height, the output level is only 5.3 dB below that of the reference vertical. You'll never need a preamp with a loop this high. The S/N advantage drops 0.1 dB. At a height of 20 feet, output increases 7.2 dB and S/N drops 0.6 dB.

You can shrink the loop to 10 feet on a side. The S/N advantage increases 0.5 dB, but the signal level drops 6.5 dB. You can raise the signal level 3.4 dB by doubling the loop side lengths to 50 feet, but the S/N advantage then drops 7.9 dB. You can thus trade-off loop size, S/N enhancement, and signal level. If you use smaller wire, output drops. For example, it's 1.7 dB lower for #22 wire.

Although this loop is a narrowband device and must be carefully resonated, the resonance is much broader than that of a typical small loop. You can get away with a single capacitor setting for both 3.5 and 3.8 MHz if you're willing to accept somewhat lower signal levels. The capacitor setting does not affect the patterns or skywave-to-ground-wave ratio—it simply alters output level.

The input resistance at the junction of the phasing lines varies over a wide range with loop size, height, and phasing-line characteristic impedance. The input resistance is about 40 Ω for the loop of Figure 4 at a height of 10 feet. A transformer using a type-77 ferrite core (such as an FT-82-77, FT-114-77 or FB-77-1024) with 9 turns of any size enameled wire on the coax side and 8 wire turns on the antenna side provides a good match to 50-Ω coax.[6] The input resistance drops to about 20 Ω when the loop is raised to 20 feet and to about 15 Ω at 50 feet. Use 13 turns of wire on the coax side for 20 feet and 15 for 50 feet.

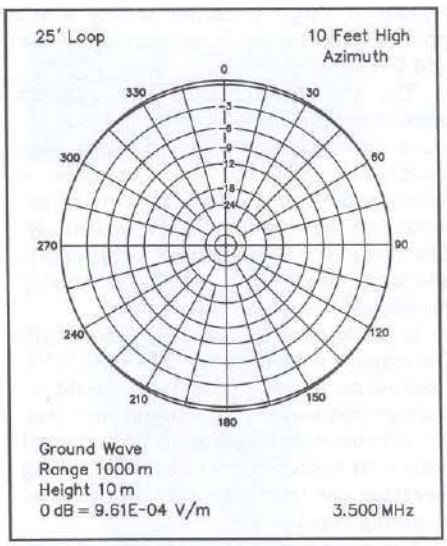

Figure 5—Azimuthal plot of the ground-wave component of a 25-foot-square, 80-meter loop at a height of 10 feet. The input power to the antenna is 1 kW. The peak electric field is shown.

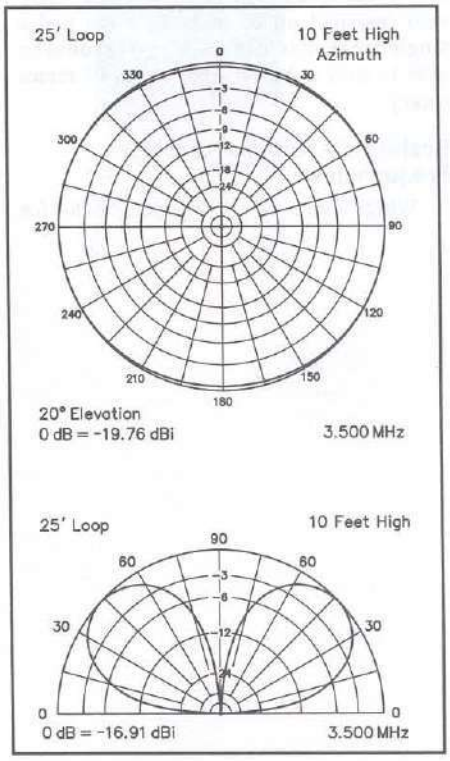

Figure 6—The sky-wave responses of the 10-foot-high, 25-foot-square, 80-meter loop. At A, the azimuthal plot; at B, the elevation plot.

Although the optimum transformer turns ratio varies with antenna height, little output is sacrificed if you use a fixed ratio.

For example, output is only 1 dB less than optimal when a loop designed for 10 feet is used at 50 feet. If you're determined to obtain the best possible match, use 16 turns of wire on the coax side and tap the winding for lowest SWR (alternatively, a switch can be used to select any of two or more taps). Use the lowest possible power when measuring SWR. It's easy to puncture the dielectric of a small trimmer capacitor with a momentary blast.

The antenna's resonant frequency shifts when the phasing lines get wet. If you use true open-wire line with plastic spacers, the frequency shift will be less than 100 kHz. But if you use 450-Ω line with segmented polyethylene dielectric, the resonant frequency decreases more than 200 kHz when the line becomes thoroughly damp. Although this won't affect signal-to-noise ratio, output drops in the desired frequency range. You may be tempted to try phasing lines of 300-Ω twinlead routed inside PVC tubing to avoid moisture effects, but line impedances this low work only for smaller loops.

This antenna should be constructed as symmetrically as possible to maximize cancellation of the vertical and radial components of the ground wave. Make the loop perfectly square and accurately align it in the horizontal plane. Cut the phasing lines to the same length. Although these loops perform well near houses, fences, and towers, try to install the antenna as far from other conductors as possible to maximize current balance. Use the shortest possible leads to interconnect the matching components. Although it's probably unnecessary, I like to split the antenna-side transformer winding and put the tuning capacitor in the center to promote equal currents in the phasing-line conductors.

To minimize the number of supports, a loop about 17 feet on a side can be constructed using a 20-meter quad spreader. You can mount the spreader well up on a tower to increase output. Alternatively, you may be able to eliminate supports altogether by stringing a loop in your attic or garage. However, the current balance of indoor loops may be degraded by electrical wiring, plumbing, heating ducts, or other nearby conductors.

On-the-Air Performance

Ed Andress, W6KUT, located in the San Diego suburb of Poway, constructed a loop 21 feet on a side and 10 feet high. Ed's location is subjected to strong, chronic power-line noise. On 80 meters, Ed uses a pair of phased quarter-wave verticals for transmitting. We used the verticals as a reference when evaluating the loop. A 20-dB preamp was available. With the preamp, signals near loop resonance were about equal to those from the verticals.

The loop performed as expected. It

dramatically enhanced the signal-to-noise ratio of most sky-wave signals. Sometimes the verticals did better during a momentary change in propagation; occasionally a particular noise arose that the loop didn't attenuate much. But overall, the loop was far superior. It made little difference on strong signals. It made listening to moderately strong signals much more pleasant. It let us copy weak signals that were buried in the noise and unreadable on the verticals.

During times of no detectable powerline noise, we often noticed a curious effect: The loop still enhanced signal-to-noise ratio by one or two S units, making copy of moderately weak signals more pleasant. On these occasions, we were unable to hear the telltale, raspy buzz of power-line noise (or any other noise signature) when we listened with the transceiver's AM detector. Unless noise happens to arrive at low angles and signals at high, there's no reason for the loop to enhance skywave S/N. We believe that the unidentified noise is local and propagates by the ground wave. We speculate that it may be the sum of hundreds of weak man-made noise sources in the densely populated suburb. (The superposition of a large number of noise sources tends to be characterless even when the individual sources aren't.)

Total Ground-Wave Cancellation

If you stack two of these loops vertically and bring both feed lines into the shack, you can form a deep null on the horizon for all azimuth angles by combining the signals with a fixed amplitude and phase offset. Except for azimuth-response irregularities caused by nearby conductors and small elevation-angle differences due to range, this system will cancel all ground-wave components. This noise canceler was to have been the original subject of this article. However, a single component loop worked so well in practice that I decided total ground-wave cancellation was overkill.

Comparison with Other Antennas

A conventional, single-feedpoint, small loop about two feet on a side—oriented horizontally—yields roughly the same S/N enhancement as the loop of Figure 4. However, output will be down about 46 dB from the reference vertical. You'll need a low-noise preamp with a loop this small unless your receiver has a very low noise figure. Still, even with a preamp, a conventional small loop makes an attractive, low-profile alternative. You must construct a low-output antenna like this carefully to avoid stray pickup. A single capacitor setting won't provide good output levels on both phone and CW.

The WA2WVL cardioid antenna attenuates thunderstorm static and ground-wave noise to the rear. If you're seldom troubled by omnidirectional local noise, it should make a more effective receiving antenna than the loop described in this article. The cardioid also requires fewer supports and less space. As a bonus, it's inherently broadband.

If you have room for a two-wavelength Beverage, it will outperform the WA2WVL cardioid on sky-wave noise and should reduce ground-wave noise arriving more than 45° off boresight by at least 15 dB. If local noise near boresight isn't a problem, a long Beverage can tremendously improve your receiving capability.

The easiest way to improve reception on 80 or 160 meters is to use the most sensitive horizontal antenna available at your antenna switch. Many hams with 80-meter verticals find that switching to a 40-meter dipole or beam improves copy of weak signals even though the antenna is nowhere near resonant on 80 meters. When just a single noise source is active, you should be able to null it by broadsiding a 40-meter rotary.

Scaling the Antenna to Other Frequencies

While I've used the 80-meter band for illustration in this article, it's easy to scale the design to other frequencies. Simply multiply lengths, heights, transformer turns and capacitor values by the number you get when you divide 3.5 by the target frequency in MHz.

That said, I don't recommend this antenna for use above 40 meters. If you're using a vertical antenna on the upper HF bands, do yourself a favor and replace it with the highest horizontally polarized antenna you can manage. Not only will your receive noise decrease, your transmit signal almost certainly will improve due to higher ground-reflection gain.[7] (Exception: If your vertical radiates over saltwater, keep it!) If you're already using a horizontal wire on upper HF, I think your next antenna project should be a rotary beam rather than a receiving loop.

Notes

[1] Floyd Koontz, WA2WVL, "Is this Ewe for You?" *QST*, Feb 1995, pp 31-33.

[2] Frederick Terman, *Radio Engineers' Handbook*, 1st ed (New York: McGraw-Hill, 1943), pp 674-709.

[3] *MININEC*-based antenna-analysis programs do not compute the surface wave, nor can they accurately model antennas close to ground. I used *NEC/Wires 2.0* with its surface-wave and Sommerfeld-Norton ground options for all antenna models in this article. All models assumed average ground characteristics (dielectric constant 13, conductivity 5 mS/m).

[4] A small cloverleaf peak requires very close wire spacing. For example, the peak is down only 5.4 dB for a spacing of 50 feet.

[5] The feed arrangement is like that of an Alford Loop. In fact, the low-noise receiving antenna really is just a variant of the VHF/UHF loop devised by Andrew Alford for a different purpose in 1940. See Terman, pp 814-815.

[6] Don't be tempted to eliminate the transformer and connect 50-Ω coax directly to a loop. The transformer functions as a current balun. It keeps noise current induced on the coax shield from entering the receiver. Just a little pickup by the shield can pollute the low-noise output of a loop.

[7] For example, on 20 meters, a horizontal dipole only 35 feet high has 3 to 6 dB broadside gain over a vertical dipole at low angles over average ground.

By Gary Breed, K9AY
From *QST*, September 1997

The K9AY Terminated Loop—A Compact, Directional Receiving Antenna

Wish you had enough room for an effective low-band receiving antenna? You do! This four-direction system fits in a 30-foot circle!

Low-band operators are always looking for ways to improve their hearing. As a low-band fan, I was impressed with the EWE antenna developed by Floyd Koontz, WA2WVL.[1,2] Koontz shows us how to build a compact, directional antenna—a design that quickly became very popular. But when I sat down at the computer to figure out the best way to install my own EWEs, a surprising new design emerged from my modeling experiments.

Ladies and Gentlemen...

Allow me to introduce you to the *terminated loop*, a concept that further shrinks the space required for a good receiving antenna *without sacrificing performance*! Figure 1 compares the real estate requirements of my four-direction loop system to that of an equivalent EWE array. The new system is not only smaller, it's easier to install, needing only one support instead of five.

The terminated loop (see Figure 2) is physically and electrically quite simple. It consists of a wire loop of any convenient shape (diamond, delta, etc), hung from a single support and with a ground rod at the bottom. A 9:1 impedance-matching transformer connects from one end of the loop to ground; a terminating resistor connects the other end of the loop to ground. This antenna is directional, favoring signals arriving from the feed point end, rejecting by several S units any signals arriving from the end connected to the terminating resistor, R_{TERM}.

Here's the real news: A very small terminated loop maintains its directional pattern. As the loop's size gets smaller, however, the desired signal strength is also reduced. The antenna described here is small enough to fit into a corner of almost *any* backyard. The loop could be made smaller, but I wanted to collect enough signal energy so that

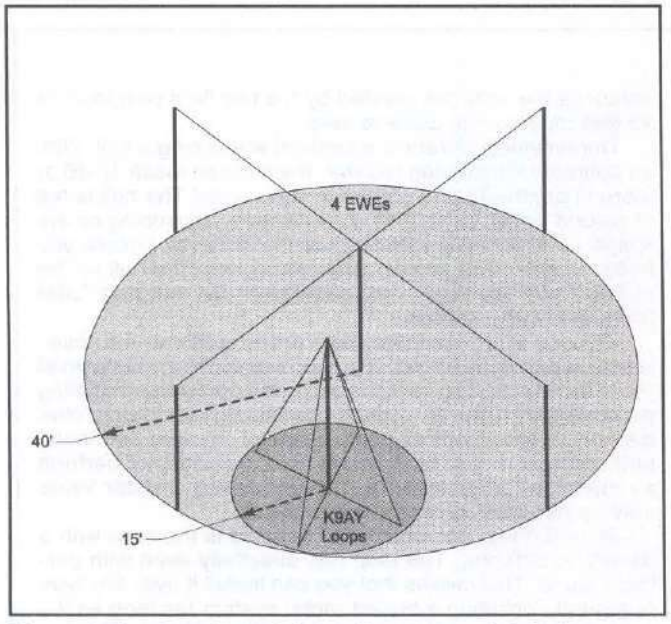

Figure 1—A comparison of the real estate needed for four EWEs and the K9AY Loop system shows that the loops need only 1/7 the area of the EWEs, yet they provide the same directional patterns.

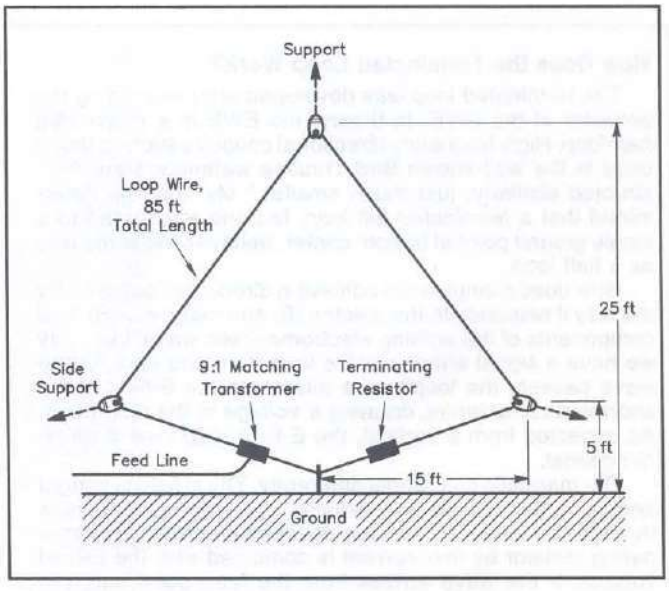

Figure 2—The basic design of a single loop in an easy-to-construct quasi-delta loop configuration. Exchanging the feed point and termination reverses the pattern. A four-direction system uses two of these loops installed at right angles to one another (as shown in Figure 1) and a relay controlled switching system.

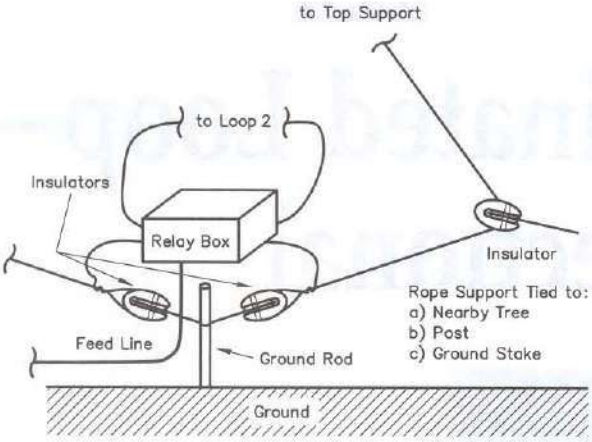

Figure 3—Construction details of a terminated loop, showing the base connections and corner supports of one of the loops. The relay box also houses the 9:1 matching transformer.

Figure 4—A photo of the central connection point at the base of a two-loop system, as installed at K9AY.

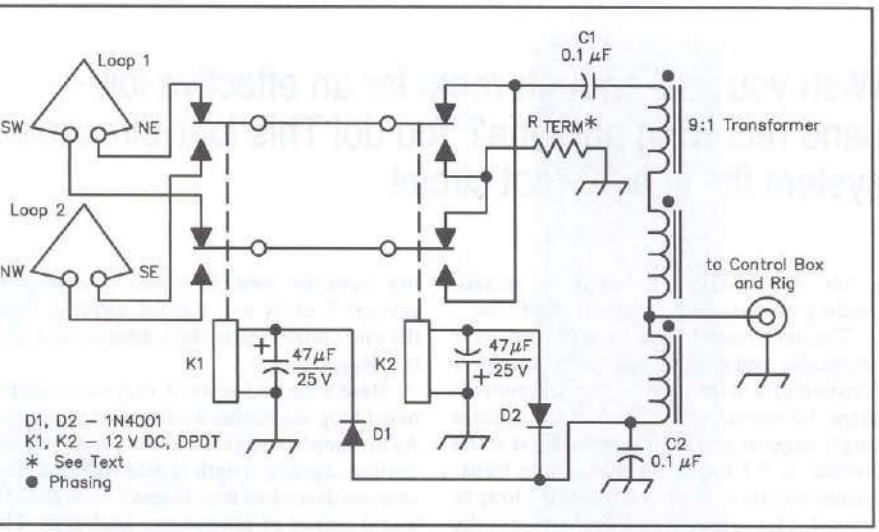

Figure 5—Schematic of the relay box located at the base of the system. The relays switch between the two loops, reversing the feed point and termination connections.

even a modest preamp (such as those included in most HF rigs) can be used. More information on the antenna's operation can be found in the sidebars "How Does the Terminated Loop Work?" and "Summary of Characteristics."

To cover all directions, two loops using the same support are oriented at right angles to each other. Each loop provides reception from two directions when the feed point and termination are reversed, for a total of four separate patterns. Here are all the details you need to build the K9AY Loop antenna system, including a relay-controlled pattern-switching system that uses the coaxial feed line to carry the switching system control voltage.

How Does the Terminated Loop Work?

The terminated loop was developed after examining the behavior of the EWE. In theory, the EWE is a *terminated half-loop*. High-frequency directional couplers such as those used in the well-known Bird Thruline wattmeters are constructed similarly, just much smaller.* My analysis determined that a *terminated full loop,* fed and terminated to a single ground point at bottom center, behaves the same way as a half loop.

How does a single loop achieve a directional pattern? By the way it responds to the electric (E) and magnetic (H) field components of the arriving electromagnetic wave. Let's say we have a signal arriving at the loop from one end. As the wave passes, the loop's wire intercepts the E-field like a short vertical antenna, creating a *voltage* at the feed point. As expected from a vertical, the E-field response is omnidirectional.

The magnetic field works differently. The H field is at right angles to the E field and induces a *current* as it passes through the loop. The voltage developed across the terminating resistor by that current is combined with the E-field voltage. If the wave arrives from the feed point end, the voltages add in phase. If the wave arrives from the opposite direction, the voltage is 180° out of phase with (and subtracted from) the E-field voltage. To maximize the front-to-back ratio, the terminating resistor must have a value that balances the voltages created by the two field components so that their sum is close to zero.

The resulting pattern is a cardioid with a single null. With an optimum terminating resistor, the null can reach 40 dB or more in depth—that's more than six S units! The null is not at ground level, but at 20 to 55° elevation, depending on the shape of the loop and local ground conditions. Unless you build a short, wide loop or a tall, skinny loop, the null will be at 30 to 40° elevation, very convenient for reducing QRM from in-country stations.

Ground is an essential part of the antenna—its resistance is part of the circuit. If ground conductivity is known at your location, it can be included in the computer modeling parameters. However, ground conditions can change over a short distance and vary with seasonal changes and moisture content. If you find that the antenna does not perform as modeled, adjustment of the terminating resistor value may be needed, as noted in the article.

Ground does not need to be lossy, as is the case with a Beverage antenna. The loop has directivity even with perfect ground. This means that you can install it over *any* type of ground, including a buried radial system (as long as it's not too close to another structure).—*Gary Breed, K9AY*

**Instruction Book*, Model 43 Wattmeter, Bird Electronic Corp, Solon, OH.

Let's Build It!

First, gather the following materials to construct the loops:

- Two lengths of **wire** about 85 feet each. Although almost any wire size will do, #14 copper is probably the best for a long-lasting installation.
- Ten simple **insulators**—anything from old toothbrush handles to fancy porcelain insulators will do.
- A three or four-foot length of **copper pipe**—the ground rod doesn't need to be driven deeply—a depth of three to four feet is sufficient. Because copper-plated steel rods eventually rust, I prefer to use 1/2 or 3/4-inch-diameter copper water pipe.
- One **support** 25 feet above ground—my antenna hangs from a limb of a Georgia Pine, but anything that gets the top of the loops up about 25 feet will work. The wooden **A** frame support described in *The ARRL Handbook* and *Antenna Book* is an excellent choice. A metal mast can be used, but make it only as long as necessary and insulate it from ground. Large metal objects affect the antenna's performance, so install it in the clear.
- You'll also need some **rope**—nothing fancy, just something strong enough to keep things in place.

Now, grab your tools and head for the backyard. Attach the midpoint of each wire length to an insulator that will be positioned at the top of the loop. The two loops must not touch each other, so leave some room between their insulators. I separated my insulators with about a foot of rope.

Aligned directly under the tops of the loops, drive a ground rod, leaving a foot or so above ground as an attachment point. Using short ropes or wires, connect four insulators a few inches away from this post to receive the lower ends of the loops. Leave a foot of wire for a pigtail after twisting the ends of the loop wires around the insulators. Figure 3 sketches the important installation details, and the photo of Figure 4 shows how my system is installed.

The lower corners of the loops are supported by insulators and ropes tied off to nearby trees, fence posts, or stakes driven into the ground. Pull out the corners with enough tension to maintain the loop shapes. At this point, the major mechanical work is finished and you should have something resembling an eggbeater, as shown in Figure 1.

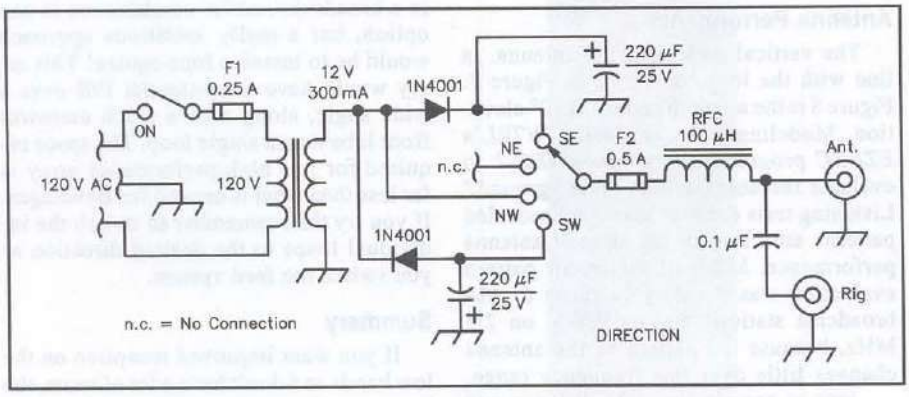

Figure 6—Schematic of the control box located in the shack. The control voltage to operate the relays is delivered via the coaxial line.

Summary of Characteristics

When choosing a specific configuration or location for your K9AY Loop system, consider this list of characteristics:

- Like all antennas, this one can be affected by nearby metallic objects or structures. Do your best to keep the antenna in the clear, away from your tower, house and power lines.
- Noise reduction in this antenna is achieved mainly by the directional pattern, although being grounded offers some reduction of wind, rain and snow static. Compared to the typical omnidirectional vertical or low inverted **V**, the reduction in overall noise and interference can be dramatic.
- The maximum circumference of the loop is a little over 1/4 λ at the highest frequency of operation. If the loop is larger, the E and H-field responses of the antenna can no longer be balanced. Smaller loops (or same-size loops at lower frequencies) retain the directional pattern, which makes this an excellent antenna for AM broadcast reception. Unfortunately, the received signal voltage is proportional to the area enclosed by the loop, so sensitivity decreases rapidly as the antenna becomes smaller. Unless you have a very good preamp, keep the loop sizes near the maximum.
- The T-Loop is not just a low-frequency antenna! It can be used at high frequencies for shortwave listening, or to provide improved reception over an omnidirectional antenna such as a vertical. Just scale the size to the desired frequency using the guidelines presented in the accompanying article.—*Gary Breed, K9AY*

The Relay Box and Controller

Figure 5 shows the relay circuit used to switch the feed and termination points of the loop wires. House the components in a weatherproof box having external connection points for the four ends of the loops, a coax connector for the feed line and a ground-wire attachment.

K1 is a DPDT relay that switches between the two loops. K2, another DPDT relay, swaps the connections of the terminating resistor and matching transformer, thereby reversing the pattern. Relay power is supplied via the coaxial feed line. C1 keeps the control voltage from reaching the antenna, and C2 provides an RF ground for the transformer.

Most builders will likely choose to orient the loops for northeast/southwest and northwest/southeast directions. The relay box has four switching modes, one for each direction: 1) northeast, when *neither* relay is energized; 2) southeast, when K1 *only* is energized; 3) southwest, when K2 *only* is energized and 4) northwest, when *both* relays are energized. Switching is accomplished using a single power connection through steering diodes D1 and D2. D1 allows K1 to operate when +12 V is applied, while D2 blocks the voltage from reaching K2. When −12 V is applied, K2 operates, but not K1. When 12 V ac is applied, the diodes rectify it to operate *both* relays.

The matching transformer is a 9:1 impedance, 3:1 turns ratio type that should be familiar to many readers. Five trifilar turns of ordinary hookup wire are wound on a 3/4-inch-diameter (0.825 inch) 43 material toroid. The terminating resistor (R_{TERM}) value will be between 390 to 560 Ω, depending on your band preference. With average ground conductivity, a value of 390 Ω provides the optimum F/B at 160 meters, while 560 Ω optimizes the loops for 80 meters. A value of 470 Ω splits the difference for "pretty good" performance on both bands. I chose to optimize the antenna for 160 meter operation, so used a 390 Ω resistor. Use an R_{TERM} power rating of at least 1 W in case some transmitter power ends up being coupled to the loops. I use a 2-W carbon resistor, but two parallel 1/2-W or four 1/4-W units of appropriate ohmic value can also be substituted.

Figure 6 is a diagram of the control box that is located in the shack. One 12 V ac transformer provides the ac relay power and feeds two half-wave rectifiers and filter capacitors to generate ±12 V. One SP4T switch selects the proper voltage to apply to the coax. The RF choke and 0.1 µF capacitor keep the RF and control voltage separated at the shack end.

Once the control unit and relay box are built and operating properly, mount the relay box at the ground rod and connect the four ends of the loops to their proper terminals. A length of 50 Ω coax carries the signal and power between the antenna and the switch box in the shack. I highly recommend keep-

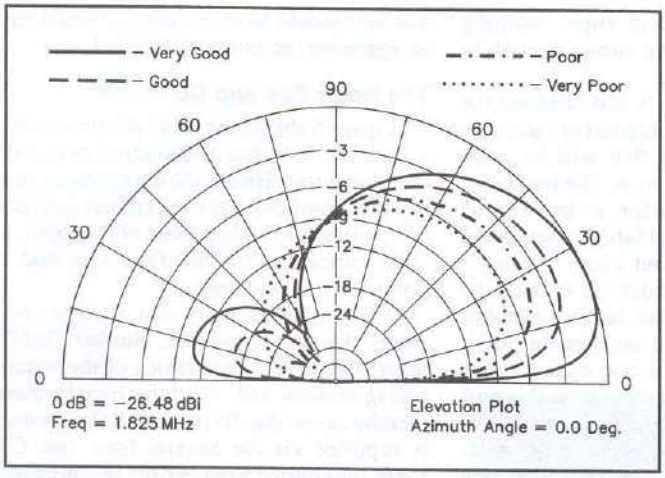

Figure 7—Vertical radiation pattern of the loops along the plane of the loop.

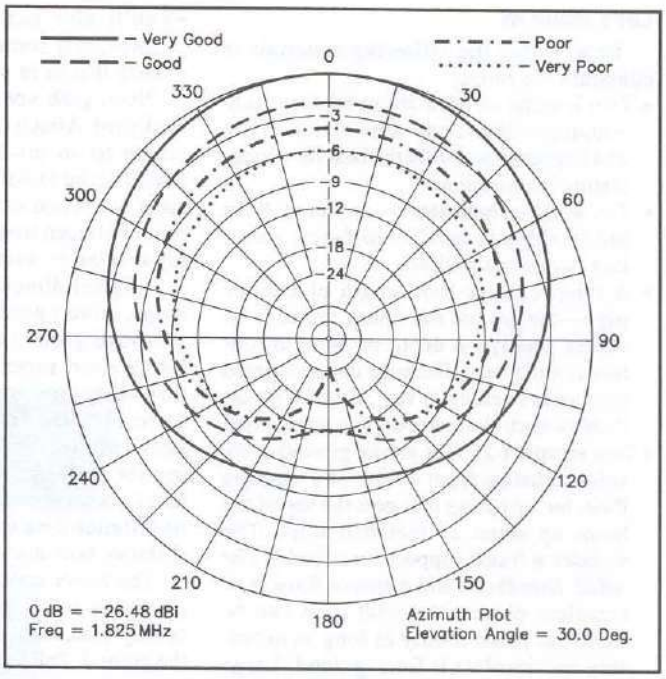

Figure 8—Horizontal radiation pattern of the loops at 30° elevation.

ing the coax on the ground (buried is better) to minimize pickup of noise or energy coupled from your transmit antenna. A receiving preamplifier is almost certainly needed, either your rig's internal preamp or an external preamp.

Evaluation and Adjustment

Next, verify that the antenna is working correctly. Some listening is probably what you'll do first, but fading makes it almost impossible to determine the antenna's actual performance. At best, you will be able to confirm that the antenna has reasonable directivity.

More accurate listening tests can be performed several ways. The best way is to enlist the aid of a nearby ham whose station is very close to being in line with one of the two loops. If such help is not available, the next-best option is to identify a local AM radio station high in the band (1400-1600 kHz) and use that as your test signal. Switch the loops to their various directions. If the test station is directly in line with one loop, you should see a front-to-back (F/B) ratio of about 2 to 3 S units as the antenna is switched toward and away from the station. You won't see a *huge* F/B because the deepest null is up at 30 to 40°.

Local ground conductivity can affect performance. You might not get an optimum pattern at your particular location with the "normal-value" terminating resistor. If you aren't getting the expected performance, substitute a 1 kΩ potentiometer for the terminating resistor and adjust it for best F/B while listening to your test station. Then, measure the pot's resistance and install a fixed-value resistor of the same value.

Antenna Performance

The vertical pattern of the antenna, in line with the loop, is shown in Figure 7. Figure 8 is the azimuth pattern at 30° elevation. Modeling was done using W7EL's *EZNEC* program,[3] which uses *NEC-2* to evaluate the antenna over "real" ground.[4] Listening tests confirm that these modeled patterns are close to the as-built antenna performance. Much of the on-air pattern evaluation was done by listening to AM broadcast stations and to WWV on 2.5 MHz, because the pattern of the antenna changes little over this frequency range. Stations at exactly the right distance and directions have verified the deep null off the back. For example, New York City area radio stations are exactly in line with my northeast/southwest loop, and show 40 dB F/B ratio when the arrival angle is just right!

The front of the pattern is quite broad, with maybe one S unit F/S. The advantage of this antenna is its rearward null, which reduces local noise and distant QRM. I installed my system just 2½ weeks before the 1996 ARRL 160 Meter Contest, so it got a thorough evaluation in a short time. During the contest, changing the pattern direction often made the difference between Q5 copy and a busted contact. For example, pointing southeast to hear Caribbean stations reduced stateside QRM by 2 or 3 S units, enough to easily hear the DX through unruly pileups.

Higher-Performance Ideas

The compact size of the K9AY Loop makes it easy to build more than one for a multielement array. Installing two of them in a broadside/endfire combination is one option, but a really ambitious approach would be to install a four-square! This array would have a substantial F/B over a wide angle, along with a much narrower front lobe than a single loop. The space required for this high-performance array is far less than what is needed for Beverages. If you try this, remember to switch the individual loops to the desired direction as you switch the feed system.

Summary

If you want improved reception on the low bands and don't have a lot of room, the terminated loop is an excellent choice. It is small, easy to build and its directional pattern makes DX much easier to hear.

Notes

[1]Floyd Koontz, WA2WVL, "Is This Ewe for You?" *QST*, Feb 1995, pp 31-33.

[2]Floyd Koontz, WA2WVL, "More EWEs for You," *QST*, Jan 1996, pp 32-34

[3]*EZNEC* 1.0 by Roy Lewallen, W7EL, PO Box 6658, Beaverton, OR 97007; tel: 503-646-2885, fax: 503-671-9046.

[4]The modeling accuracy of antennas with a direct connection to ground is somewhat uncertain, even with the power of *NEC-2*. The high accuracy ground characterization of the Sommerfield method gives answers that vary with the number of segments chosen for each wire. The *MININEC*-type ground model gives more consistent results, but on-air tests show that the deepest null is obtained with a lower value terminating resistor than this model indicates. The plots presented here are the "best fit" between modeled and observed performance.

Photos by the author.

Hum Problems When Switching the K9AY Loops

By Gary Breed, K9AY

I am pleased to report that many hams have successfully built the receiving antenna described in the September 1997 issue of *QST*.[1] I had some concern that variations in local ground conditions and nearby structures could reduce the antenna's performance, but the performance I obtained seems to be readily duplicated.

[1]Gary Breed, K9AY, "The K9AY Terminated Loop—A Compact, Directional Receiving Antenna," *QST*, Sep 1997, pp 43-46.

There is one problem that needs to be addressed. When the loops are switched to the northwest direction, an ac voltage is sent down the coax to the relay box. A few hams have reported hum or distortion when the antenna is switched in this direction. Two explanations are possible: a ground loop due to widely separated antenna and station grounds, or modulation of the core of the matching transformer. The presence of hum was not evident in my prototype, but to avoid either cause of the problem, I recommend using a *separate* three-conductor control wire to operate the relays. The power is solely 12 V dc, and no current flows through the transformer. The modifications are shown in the accompanying figures, which can replace Figures 5 and 6 in the original article.

Secondary benefits of this arrangement include the option of using an existing 12 V power supply to provide the operating voltage, and the ability to use an additional conductor to carry power to an antenna-mounted preamplifier.

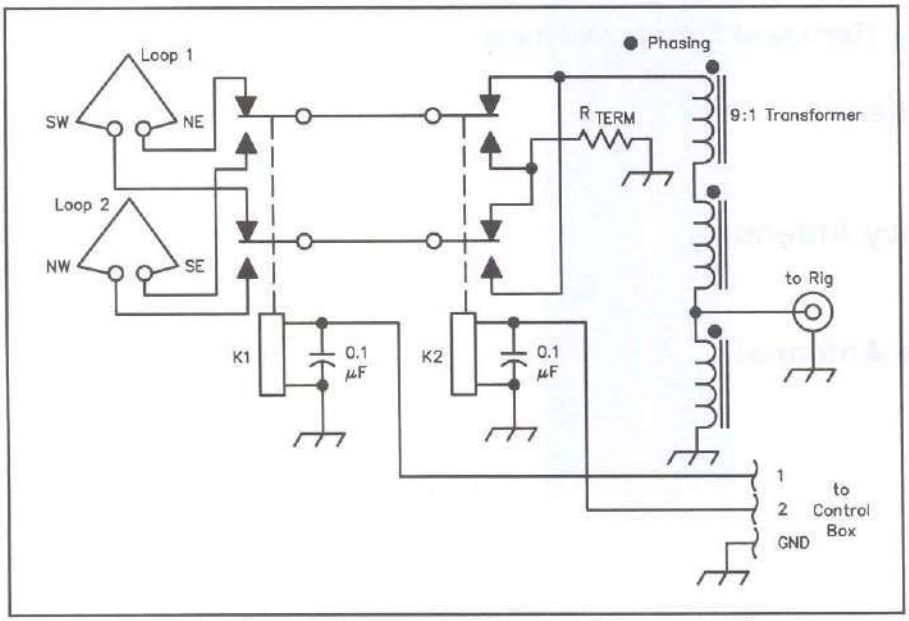

Figure 1—A revision of the schematic shown in Figure 5 of the September 1997 *QST* article.

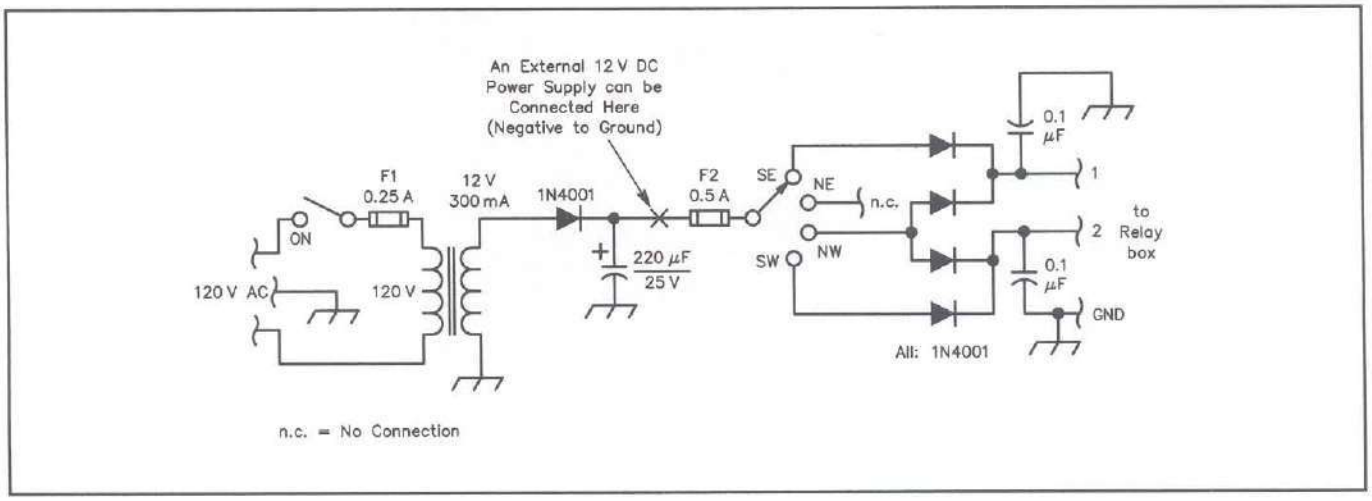

Figure 2—Changes to Figure 6 of the original article.

CHAPTER NINE

MISCELLANEA

9-1 **A Skyhook for the '90s**
From May 1997 *QST*

9-4 **Balloon Skyhooks**
From August 1997 *QST* (Technical Correspondence)

9-5 **The Clothesline Antenna**
From July 1998 *QST*

9-8 **A Variable-Frequency Antenna**
From July 1949 *QST*

9-12 **Honey, I Shrunk the Antenna!**
From July 1993 *QST*

By Don Daso, K4ZA

From *QST*, May 1997

A Skyhook for the '90s

Is your group looking to put up a BIG vertical antenna for Field Day? The crew at N4ZC started their own air corps. Their full-size 160-meter quarter-wavelength vertical is *not* supported by hot air!

PHOTO BY DON DASO, K4ZA

Inspiration, on a grand scale. What if we had one of *these* to play with?

Some History, as Introduction

By 1936, the Zeppelin company was without rival in the design, construction and operation of rigid airships. Flying successfully around the world, providing regular passenger service between Germany and South America, the *Graf Zeppelin* airship was nonetheless unsuited for the hardship of crossing the North Atlantic. The *Hindenburg* was designed and built for this route. This huge airship was one of the largest flying machines the world has ever known. Her crash and destruction at Lakehurst on May 6, 1937, ended the era of passenger transport by airship.[1]

Later, growing up on a farm near Akron, I sometimes saw the Goodyear airships passing silently overhead. Twenty-odd

PHOTO BY SCOTT DOUGLASS, K2SD

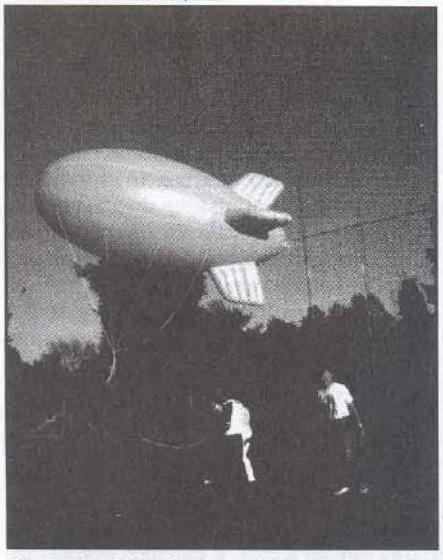

Figure 1—K4ZA fastens the antenna and tether to the miniature blimp prior to launch.

[1]The terms concerning lighter-than-air (LTA) craft are often misapplied. *Webster's Ninth Collegiate Dictionary* indicates that *dirigible*, *airship* and *blimp* all denote an LTA with *steering and propulsion* capabilities. Hence, the terms do not strictly apply to the kytoon, which has neither steering nor propusion systems. Nonetheless, *blimp* is so commonly used by manufacturers, sellers and users to describe the kytoon that we continue that usage here, as well. —*Ed.*

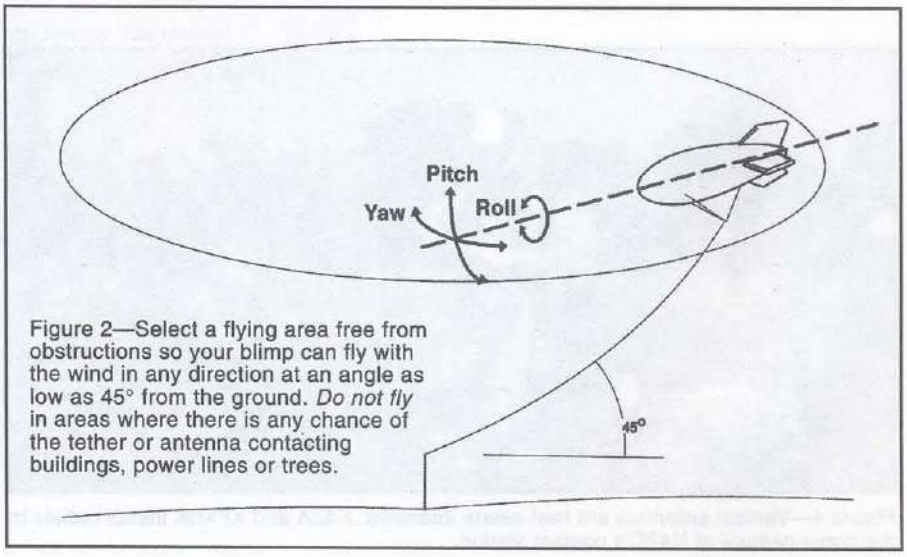

Figure 2—Select a flying area free from obstructions so your blimp can fly with the wind in any direction at an angle as low as 45° from the ground. *Do not fly* in areas where there is any chance of the tether or antenna contacting buildings, power lines or trees.

PHOTO BY DON DASO, K4ZA

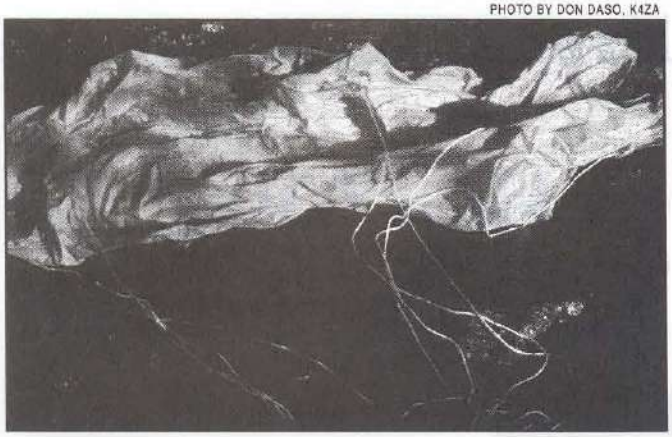

Figure 3—Here's our miniature version of the real thing—fresh out of the box and ready for inflation.

years after the *Hindenburg* disaster, I began to experiment with balloons myself—originally using surplus weather balloons to support wires, and more recently, with small blimps holding contest antennas. Many hams have considered using balloons or kites for antenna supports. Indeed, they come closer than anything else to that "skyhook" we all jokingly refer to on occasion. Yet, each one has limitations.

The Kytoon

Balloon-supported antennas tend to lose altitude in the wind, however slight. Kites cannot fly without wind. Satisfactory service from either support requires a limited range of wind and weather conditions—something that's not too common. Combining features from each—the balloon and kite—solves several of these limitations. Indeed, the Kytoon is a small, inflatable blimp-shaped balloon with kite-like surfaces that cause it to fly into the wind. An early Kytoon—with a rigid skeleton—is registered with the US Patent Office and enjoyed some success as a skyhook. (See Bibliography for further information.)

Today, the early Kytoon's bladder-and-frame construction has been replaced by completely inflatable balloons, made from 2 to 3-mil polyurethane film (see Figure 1). Brilliant skin colors are common because these miniature blimps are intended for advertising purposes. These small blimps are available from various sources, with prices varying according to size—typically from 10 to 30 feet long and starting at $300. [Beware: Many suppliers specialize in advertising Kytoons and sell them for twice the price of those sold for scientific uses.—*Ed.*]

The plastics used in their construction have been specially formulated for high elasticity, helium retention and paint application. Helium (a safe, inert gas) is available from party suppliers or welding supply companies. One tank will easily support an antenna for the typical contest weekend. If you have some room, but maybe not the resources to put up a full-sized radiator, consider a tethered Kytoon. As a modern antenna support, these miniature blimps are the skyhook of the '90s.

Tethered Flight

Most hams considering these small blimps as antenna supports concentrate on their antennas. This natural inclination can create problems. Most hams have little knowledge or experience with the basic principles of LTA flight, knots and rigging rules, with FAA regulations, with weather and especially with how these all relate to tethered flight. It's a complex process and serious business to lift an antenna aloft with a small balloon or blimp.

These blimps consist of a closed envelope of gas—usually helium—that is lighter than the atmosphere. Gas balloons can only descend by losing lift (that is, by venting gas) or when some force overcomes their lift (retrieval by tether or powered flight). As a gas balloon rises, it will reach an equilibrium altitude, where it will remain until the lift-to-weight ratio changes. These principles—which are mostly associated with larger, cargo-carrying blimps—are important, especially because our balloon will be tethered. As with any tower or antenna project, use common sense and make safety your highest priority!

Because space is three-dimensional, any "skyhook" can turn in the air—rotating in three axes: a longitudinal roll, a lateral yaw and a vertical pitch. The shape of these blimps allows them to "fly" in the wind, countering these motions, and the tether allows the blimp to move easily enough within those three axes. Generally, you will experience something like Figure 2.

A 10 to 12-foot blimp is sufficient for most antennas suitable for low-band use. Most blimp applications will be for 160 meters, because the sheer size of effective antennas for this band makes them difficult (and costly) to erect. A 10 to 12-foot-long blimp of 3 to 4 feet in diameter holds about 70 cubic feet of helium and is capable of lifting two pounds. This is sufficient for an effective $\lambda/4$ wire vertical for 160 meters.

Setup, Antenna and Ground

You'll need a working area on the ground to inflate your blimp. A 20×20-foot area should suffice. It's important to protect the thin skin of the balloon. I usually lay the balloon out on a tarp to prevent any stubs or twigs from poking the plastic skin (see Figure 3). While the plastic seems sturdy and elastic, I'm always careful and treat the balloon gently. I hold the helium tank upright, and I usually lash it securely to a two-wheeled dolly, so I can move it to the field easily. Follow the manufacturer's inflation directions carefully (each will be slightly different).

Inflation temperature is important: If possible, inflate the balloon at the same temperature it will experience in flight. Helium comes out of the tank cold. With rising temperatures, it expands quickly inside the balloon. Sunlight and warm air cause further expansion. (In very hot weather, a balloon loses some of its lifting power, but this is usually not a problem.) Do not overinflate the balloon. Finger pressure will barely dent the surface of a properly inflated polyurethane blimp. Pay special attention while closing the neck of the blimp. With many blimps, you can simply fold the neck back on itself several times and then fasten it in place with heavy rub-

PHOTO BY SCOTT DOUGLASS, K2SD

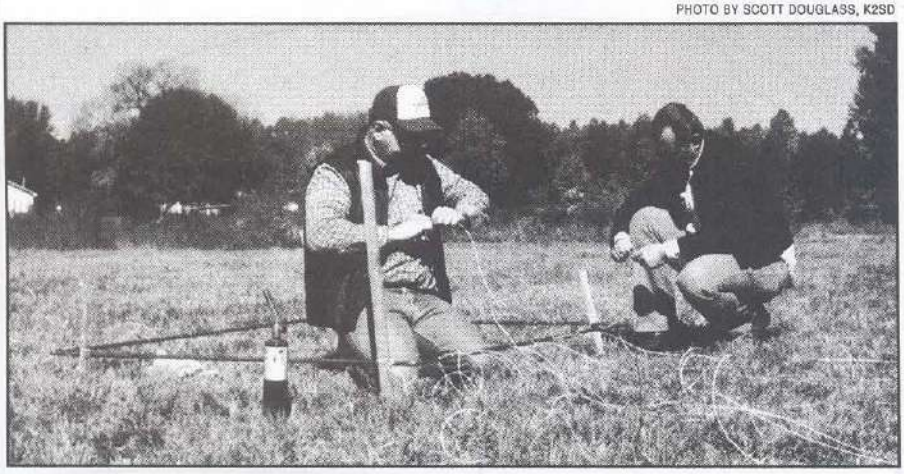

Figure 4—Vertical antennas are real-estate intensive. K4ZA and KF4HK install radials in the horse pasture at N4ZC's contest station.

PHOTO BY SCOTT DOUGLASS, K2SD

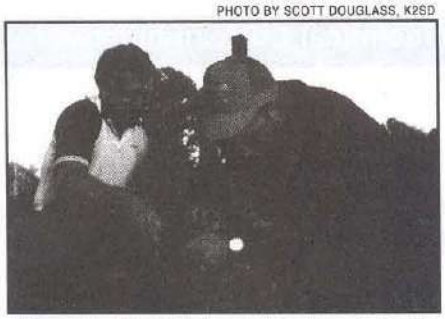

Figure 5—WA4UNZ and K4ZA work inside the large copper ground ring installing the feed system.

ber bands (folding them, if necessary) to provide a tight, leak-free fit. Refills are much easier when rubber bands, rather than knotted rope, seal the balloon.

Use a quality ball-bearing swivel between the end of the tether and the balloon's attachment line. This allows the blimp to easily turn into the wind. Fishing line works well as a tether; so do some kite lines and other synthetic ropes. I've used 100-pound fishing line and 1/8-inch nylon rope.

Stranded wire is a lightweight antenna conductor. Aluminum welding wire is light and strong enough to use. (I use phosphor-bronze wire that was originally intended for use with the "Gibson Girl" rescue unit's kite- or balloon-supported antenna. It comes on a small reel. The irony, weight and low cost appeal to me.) To save time, measure and mark the antenna length before construction begins. I have found no instances where the addition of a tether created a problem, in launch, retrieval or during flight. The antenna has never broken; and our balloon has never broken free. Obviously, it's simple insurance, and you don't want your antenna wire touching power lines or other hazards, which might happen with a runaway blimp.

The original installations at N4ZC were all within a working pasture (see Figure 4). On-ground radials were easier to install than elevated radials, albeit more labor-intensive (easier because they need no supports, labor-intensive because it requires more radials—4 versus 60). A large diameter ring of copper water pipe served as the radial connection point and made soldering easier. The ring also created a work space to stand in during set up and launch (see Figure 5). (Future installations will use a high, central wooden post, with attachment points for the antenna, tether and four elevated radials.) Our installation is over 150 feet from the nearest tower (the 20-meter array). RG-213 runs from the feed point to the base of that tower, where it connects to Hardline running to the shack.

Hints

Always wear gloves when launching and retrieving the blimp. Let the blimp rise slowly; retrieve it slowly. The lift can be terrific, and the antenna wire and tether can easily cut your hands. Always have helpers coil up the antenna and tether on spools as you walk the balloon down. (I recommend reeling in the blimp during daylight hours. It's a tempting target, and we hear gunshots in the woods all the time at N4ZC's somewhat country location. Make certain winds cannot push the blimp into nearby objects, even when it's near the ground.)

FAA regulations for flying tethered balloons—those under five pounds in weight—are clear: No person may operate a kite or balloon in a manner that creates a hazard to persons, property or other aircraft.

Avoid all dangerous situations: operation near airports, in wet or stormy weather, near electric power lines, over public streets or areas congested with people or at extreme heights (which is probably the first thing a ham will think of). Use common sense and play it safe. Using less than the legal limit with a single 1/4 vertical supported by a 10-foot blimp, I've been able to work any station heard on 160 meters.

Sources

Here are names and contact information for two suppliers of these inflatable blimps:

Toy-Tex Novelty Company, 7315 N Linder, Skokie IL 60077.

The Blimp Works, 156 Barnes Airship Dr, Statesville NC 28677.

Annotated Bibliography

There's a wide variety of applicable information and material available, but not much has appeared in Amateur Radio publications. This is new territory, in many ways, that's worthy of further experimentation. I recommend the following books and articles for further reference and study—before buying, building and flying:

R. Carleton Greene, W8PWU, "More On Balloon Supported Antennas," *QST*, Nov 1940, pp 38, 39 and 82. One of the earliest articles on using meteorological balloons as antenna supports, complete with lifting charts.

David T. Ferrier, W1LLX and William G. Baird, W9RCQ, "A New Kind of Skyhook," *QST*, Oct 1946, pp 24-25. The original use, as best I can determine, of the Kytoon as an antenna support. Although focused on emergency or Field Day use, the final line of the article presents this challenge: "Perhaps long-wire vertical antennas can now be exploited with outstanding results."

Stan Gibilisco, W1GV, "Balloons as Antenna Supports," *The ARRL Antenna Compendium*, Volume 2, (Newington: ARRL, 1989). A brief overview of the topic, with good descriptions and several safety tips.

Maxwell Eden, *Kiteworks*, (New York: Sterling Publishing Company, 1989). An excellent book about kites of all kinds—including building and flying them. It's filled with tips and techniques.

Will Hayes, *The Complete Ballooning Book*, (Mountain View, California: World Publications, 1977). Although focused on large hot-air balloons, the history, basics of flight and safety chapters are well worth your time. It also includes the FAA regulations.

John Belrose, VE2CV, "A Kite-Supported 160- (or 80-) Meter Antenna," *QST*, Mar 1981, pp 40-42. A unique application of the Parafoil—a special type of kite. Interesting tips and techniques applicable to blimp-supported antennas.

"160-Contest Results," *QST*, Jun 1976, pp 71-74. Pictures and text from W8LT, the Ohio State University Amateur Radio Club, using an original Kytoon to support a vertical antenna.

Balloon Skyhooks

By Jack M. Hughes, WB6SOI

I appreciated and enjoyed "A Skyhook for the '90s."[1] The company I work for, TCOM, L.P., has been doing this sort of thing commercially since 1981, but on a much larger scale. Since 1972, TCOM, L.P. has been an authority on and builder of aerostats.[2] We manufacture and market an aerostat system called the Tethered Aerostat Antenna Platform (TAAP).

VLF and LF transmitters and receivers are used by the military and governments worldwide for high-reliability communication of strategic information. A typical antenna system for VLF/LF communication is a complex array of wires suspended on insulated towers that take months to erect and place into operation. A unique scheme for the rapid deployment of a complete VLF/LF (up to 100 kW) communications system uses the TAAP.

An aerostat is employed to elevate an encapsulated vertical antenna/tether to a height approaching one quarter wavelength for the frequency in use. At VLF, this technique enables the system to operate with a high antenna-radiation efficiency unobtainable by other land or sea-based antennas.

The radiated-power efficiency is further enhanced by the installation of a simple groundplane consisting of eight radial wires emanating from beneath the mooring-system trailer. The radial ends are secured by ground rods and copper wire. The entire system—antenna/tether, aerostat, mooring system, transmitter and equipment shelter—is designed to be transportable by land, air or sea and to be rapidly erected at a selected site.

The aerostat is a helium-filled, aerodynamically stable tethered balloon typically 32 meters long. Its antenna/tether is composed of Kevlar with optional fiber optics and two concentric outer sheaths of aluminum braid. The Kevlar construction provides up to five times the strength of a similar-weight steel cable. A fiber-optic core provides for secure communication between the ground and the aerostat, and the double-aluminum sheaths act as the radiating elements—as well as a path for the 400 Hz electrical power to the aerostat.

The aerostat is launched and retrieved at a rate of 200 feet per minute and it does not vent helium. In addition to the helium chamber, it uses an air-filled ballonet system that expands and contracts depending on the outside air pressure to keep the aerostat rigid at all times. It can operate in winds of up to 50 knots and will survive in winds of greater than 70 knots. The system is designed to fly continuously for up to 21 days before replenishing it with helium.

I commend author Don Daso for his creativity and resourcefulness. He seems to have just as much of a thrill as we do in handling LTA vehicles.

[1] Don Daso, K4ZA, "A Skyhook for the '90s," *QST*, May 1997, pp 31-33.

[2] Aerostats are essentially helium-filled, aerodynamically shaped balloons that are tethered to ground. They're not cheap—a 15-meter-long Aerostat system costs about $175,000.

By Robert Victor, VA2ERY
From QST, July 1998

The Clothesline Antenna

Dry your laundry or work DX. Could this be the first dual-purpose antenna?

Every once in a while, you run across an idea that seems so simple, so obvious, you can't believe it hasn't been done before. Surely (you say to yourself), you're not the first person in the universe to have thought of this...

That's the case with the Clothesline antenna and me. While mulling over a variety of ideas for an antenna suited to my apartment, I started drawing some graphs of sine waves at various frequencies. One thing led to another and I wound up with a terrific solution for my antenna needs—and it was one that I haven't found any references to anywhere. As far as I'm concerned, *I've* invented the Clothesline. Still, I'm not going to be surprised if someone shows me that it's been done before!

But even if this antenna design has been around since hydrogen, it may still be new to you. And even if you have seen something similar to the Clothesline, this design may be worth a second look. For hams in a variety of situations, this could be just what the doctor ordered to cure your DX dilemma.

What It Is ... And Isn't

I will tell you what the Clothesline is, but first I'll tell you what it is not. The Clothesline isn't some dubious trick for loading up an actual clothesline with 12 cubits of RG-213 looped four turns to the foot around your washing machine. This is an antenna, it works all the HF bands, and it gets great results. It doesn't need a tuner because it's dead-on resonant on the 160, 80, 40, 20, 15 and 10 meter bands. A tiny tweak will bring in 12 and 17 meters, too.

It's remarkably easy to build. There are no traps, no stubs, no loading coils, no variable or fixed capacitors, no screws, no clamps, and you don't have to drill anything. This antenna is so simple to put up, it hurts. The Clothesline consists of little more than a piece of wire, a center insulator, some feed line, and a couple of $2 hardware-store fittings.

Too good to be true, you say? What's the catch, you ask?

Well, you *do* have to adjust this antenna for most band changes. But before you get too excited by the word "adjust," I'm not talking about unwrapping yards of black tape to get at a loading coil, or tweaking the bare shaft (whoops, hot side—sorry!) of a 50-year-old fleamarket variable capacitor. No, the Clothesline makes band changes a piece of cake. When you see how easy it is, you're going to chuckle!

The Concept

The easiest way to explain how the Clothesline works is to lead you through the simple reasoning I used to come up with the thing. I started with a drawing like the one in Figure 1. It shows a simple dipole for 80 meters. It's 132 feet long and fed in the middle with coax. Next I drew the graph of the voltage distribution along the antenna (at its fundamental resonant frequency). Note the voltage is at a maximum (with reference to ground) at the antenna ends. That's important for any dipole radiator. The ends of the antenna have to correspond to the high voltage points of the curve.

I already knew that the curve the voltage wave describes is a quarter of a full cycle—a quarter wavelength—on each half of the antenna. And that the distance between the two places where the voltage is highest, or in other words, from one end of the antenna to the other, is $^1/_4$ plus $^1/_4$—a half wavelength. That's why they call it a half-wave dipole.

I also understood why the feed point is in the middle. It's located precisely where the voltage curve is lowest with respect to ground. To me, an antenna is just like a transformer—it transforms the low impedance coming out of the coax up to the impedance needed to couple to the cosmos. Come in low, go out high. So much for the plain dipole.

THAT LAST PAIR OF LONG JOHNS YOU REELED OUT MOVED MY FEEDPOINT

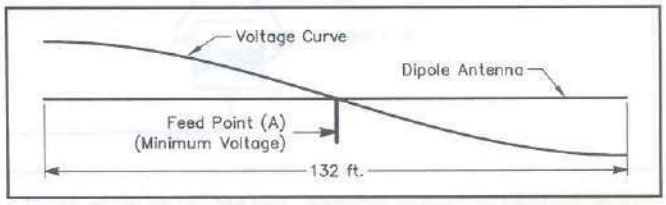

Figure 1—The voltage distribution along an 80-meter dipole antenna. Note that the voltage is at maximum (with respect to ground) at the ends of the antenna.

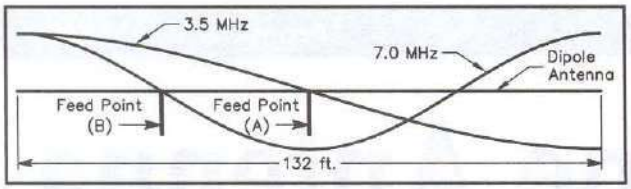

Figure 2—Take the 80-meter dipole shown in Figure 6 and overlay the voltage distribution for a 7-MHz signal. Note how the 7-MHz feed point (B) has shifted to the left of the 3.5-MHz feed point (A).

I then dropped a 7-MHz voltage curve over the original 3.5 MHz length (see Figure 2). Because the new frequency is a whole multiple of our original frequency (3.5 MHz × 2 = 7 MHz), there is still a whole number of half wavelengths from one end to the other, so the voltage peaks are still at the ends. This means this same length of wire will resonate at 7 MHz, which means it will radiate perfectly well at this frequency too.

But I noticed right away that something had changed from our earlier situation—the point where the voltage minimum crossed ground was no longer in the middle. There were now two such points, neither of them anywhere near the middle. So the antenna was resonant—the voltage peaks were at the ends—but my original feed point was now useless! Alright, I reasoned. If I shift the feed line to the new minimum I'll have the perfect setup—high voltage at the ends, low voltage at the feed point. Look out DX, here I come!

I thought about how far I'd moved the feed point. Looking at the curve, you can see that from (A) to (B) is a quarter wavelength at the new frequency, right? We doubled the frequency, which means we cut the old wavelength in half. So what used to be a quarter wave at the old frequency—from the middle to one end—will be twice that, or one-half wavelength, at the new frequency. And I wanted to get the feed point over to the new location at point (B), so I move it half that half—a quarter wavelength—over to the new minimum at (B).

I also realized that I'd added a quarter wave to the right half of the antenna, making the right-hand side $^1/_2$ plus $^1/_4$ wavelengths, or a total of $^3/_4$ wavelengths long. Since $^3/_4$ on the right plus $^1/_4$ on the left equals 1, I now had a full-wavelength antenna with some gain compared to a dipole, fed one-quarter wavelength from one end.

I kept going. I doubled the frequency again, and the same thing happened. The voltage peaks would stay at the ends, but I'd see the feed point moving further to the left by one-quarter wavelength at the new frequency for each time I doubled frequency.

I tried it for other multiples—by 3, 5, 6, 7 and so on. Just as I expected, I always wound up with some whole number of half waves, and voltage peaks at the ends. All I ever had to do was to move the feed point to the new quarter-wave point of the antenna. And for that matter, for any band other than 80, I had a choice of feed points. Each higher-band antenna had more than one voltage minimum point in its length, and I could feed at any one!

Now I drew a bunch of these curves like the ones shown in Figure 2 for 80, 40, 20, 15 and 10 meters. I dropped reference lines down from each voltage minimum to show where the feed points would lie along this single piece of wire, depending on the frequency. Because there are multiple feed points for each of the higher bands, I could see that any time I want to change frequency, I would just shift to the closest feed point for the next frequency, and away we go!

But so what? How was I going to make a simple antenna with all these feed points? For that matter, what was simple about an antenna with all these feed points anyway? The answer was, "nothing." What about a *single* feed point that somehow travels or slides along the antenna to anywhere I want it to go? Could I make that happen? I was looking out the window at my 40-meter folded dipole when I came up with the answer.

Other than the fact that it's fed with 300-Ω line rather than coax, the folded dipole is almost identical to the standard dipole. It resonates over the same lengths at the same frequencies, so my marvelous (but yet to be invented) multi-band, sliding feed-point antenna would be just as comfortable with a folded dipole 132 feet long as it would be with a plain dipole. But what about the sliding feed point?

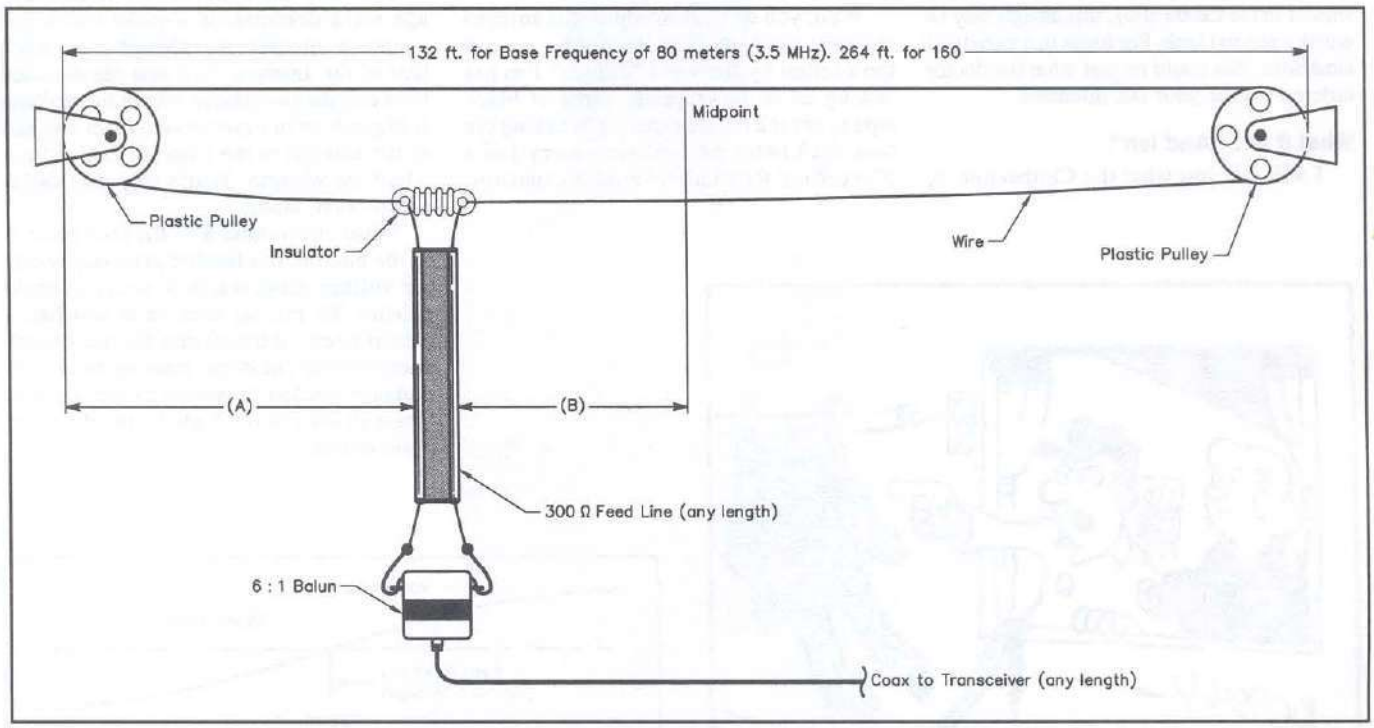

Figure 3—The Clothesline antenna. Just set (A) or (B) to equal a quarter wavelength at your operating frequency. As long as it is a multiple of your base frequency (most HF ham bands are), your antenna is tuned. You can measure out your favorite bands, peak them by observing the SWR, and put color marks or tags on the bottom wire. Roll up to the mark and you're ready to couple to the cosmos!

What would happen with my folded dipole if I just grabbed the feed line and tried to slide it along toward one end? It hit me: If the endpoints were run over pulleys the feed point would effectively slide! It would just run along the bottom of the antenna to anywhere you cared to put it. As far as the electrical nature of the antenna is concerned, absolutely nothing has changed—except the position of the feed point! And there it was—the birth of the multi-band, sliding feed-point antenna, otherwise known as the Clothesline! See Figure 3.

But wait a minute, I thought. It's a clothesline. It can't possibly work. It's too simple!

Yet no amount of poking about on paper could find fault with it. Still very skeptical, I strung up a miniature version (for 10 and 20 meters) running down my hallway. It worked! It loaded like a breeze, with the feed about 8 feet from the end on 10 meters and about 16 feet from the end on 20 meters, just where those graphs said it should. I bought some decent wire, a couple of plastic pulleys, 75 feet of 300-Ω twin lead, and threw one up on the roof to cover 40 through 10 (66 feet is all the horizontal space I have up there). Within a couple of days I had racked up dozens of DX contacts on every band. Most remarkable was the apparent gain on the higher bands. I consistently surprised other stations (and myself) with my signal strength, usually trading equal signal reports and getting lush praise from guys running far greater power and fancier antennas. My 100 W and a Clothesline are reaching the world!

How to Build and Use the Clothesline

Measure out enough wire for twice the lowest frequency. If this happens to be 80 meters, you'll need 2 × 132 feet (plus a bit for trimming). String it up like a clothesline, using nylon or rope leaders to attach the plastic pulleys to their supports. Just make sure that all the wire is used, so that the antenna is full-length. You can use long leaders if you want to hang one end off a distant support. Run each end of the wire through the pulleys top-to-bottom, attach the two ends to a center insulator and hook up your feed line. That's it!

If you're building a version for 80 or 160 meters, you'll want to install a third little pulley to ride along the top run, attached by a short piece of cord to the center insulator, to help keep the top and bottom runs of the antenna roughly parallel. Build it for 40 as the lowest frequency and you won't even need this little extra.

There is a full set of feed points between the middle of the antenna and half-way out to either end, so if you want to keep the feed line short, you can cut it to provide just enough slack to move within this range. Alternatively, because different feed points for the same frequency can affect the gain pattern, you may want the flexibility of having a choice of feed points for each frequency, and decide to leave more line slack. Losses in twin lead are so much lower than in regular coax, you can use all you want (within reason). Do be careful to stand it off from any metal it encounters on the way into the shack.

Inside, the simplest way to match the twin lead to your rig is with a balun. I use a 6:1 balun to get the impedance down to the 50 Ω my radio likes. A 4:1 balun works fine too, though the 6:1 usually presents a better match. Both baluns are sold by a number of *QST* advertisers. Ditto for the 300-Ω twin lead.

Speaking of the shack, if yours is on an upper level at your home, consider setting the Clothesline up with one end near a shack window. You'll be able to reach out, retune (that is, haul in the line), then go back to your rig to check your SWR meter.

If you don't have this luxury, don't sweat it. I calibrated my Clothesline by setting my rig on tune-up power for each band, and going up to the roof of my apartment building to peak the antenna with a field-strength meter. I confirmed each setting by checking the SWR back in the shack. On every band I tuned for, it was well below 1.5:1. As I found each feed-point setting, I marked them with various colored indelible markers for each band. Now when I want to change bands, I just go up to the apartment roof, run the Clothesline out to the right color, and I'm tuned! It takes seconds.

I can imagine other settings where you'd run the Clothesline right outside a window, out to some convenient support. Or vertical, up or down the side of a building, a tree, or a flagpole (tie a flag to it, if you like). If you're camped out in suburbia with difficult, anti-antenna neighbors, a detachable feed line using alligator clips makes it the perfect disguised antenna. Who's going to suspect a clothesline? You could even use it during the day to... wait for it... *dry clothes!* You could even make it out of your standard, garden-variety hardware-store clothesline kit—plastic pulleys, vinyl-covered wire, the works. This makes the Clothesline the only ham antenna kit I know of that you can buy complete (minus the feed line) from your local hardware store. (In a perfect world, your local hardware store would stock twin lead.) Yes, I know I said at the beginning that this wasn't a trick for loading up a real clothesline and I've been true to my word. This is an antenna that happens to *look* like a clothesline.

I mentioned covering 17 and 12 meters. If you cut the original length to resonate just a little up from the bottom of 80, at 3.615 MHz, the fifth harmonic is smack dab on 17 meters. Cut it to 3.55 MHz and harmonic number seven is on 12 meters. In fact, these are such minor variations that you can surely find a convenient center frequency on 80 that'll put you right where you want to be on all bands. Though you don't need it, a tuner (either in or out-board) can get you right down to zero reflected power. Remember, feeding with twin lead or other balanced lines keeps your losses way down, so a little elevated SWR at the band edges is no big deal.

I'm now thinking about some kind of motor drive that'll permit me to tune up from inside the shack. My first reaction to this idea was, if I'm going to get into motor drives and the like, is that any simpler than a beam? I now think the answer is "yes." The drive would be simpler, in that I wouldn't need any position feedback—all I need to do is watch my reflected power meter to know when I've hit resonance. It doesn't need a whole lot of travel because a full range of feed points is available over just a quarter-length of the antenna. As well, few beams are all-band. And since the antenna you can put up is always simpler than the antenna you can't, for those of us in apartment settings where a beam or other, more complex antenna systems are out of the question, a motorized Clothesline might well be worth the effort. I've got a sneaking suspicion that, somewhere out there, there's a cheap, off-the-shelf drive unit with "Clothesline" written all over it!

By Ralph O. Williams, W8AJC

From *QST*, July 1949

A Variable-Frequency Antenna

One to Ten Meters with a Single Antenna System

Multiband transmitters and band-switching receivers make it easy for us to jump from band to band, but the antenna has not kept pace. Many of us are prevented from operating on several bands by the thoughts of the multiplicity of antennas demanded by the conventional approach to multiband work. Here, to go with the VFO, is the VFA — tunable to resonance from the operating position. It covers 11, 10, 6 and 2, and all the television and f.m. bands in between, with the optimum performance all along the line. Ideas for the lower frequencies are included, too.

It has been the writer's lifelong ambition as a radio amateur to have a universal antenna; one that would not only work on several bands, but also tune within a band, providing optimum operating conditions on any frequency. The memory of endless trips to the rooftop or out to the mast to lower the antenna and cut off or splice on a few inches of wire to hit a special spot in the band is still fresh in mind. The old Zepp was pretty good but it required spaced feeders and tuning at the transmitter end. The half-wave aerial split in the center for a 72-ohm transmission line required no tuning at the station end but necessitated a different antenna for every band. Often the resonant frequency of these antennas varied widely from the values indicated by the formulae because of conditions not always apparent, and under some circumstances it was difficult to get adequate loading over an entire band. As the years passed matching systems were introduced, and they, too, are usually one-band devices. With all their disadvantages the antenna systems were not too bad back in the days of crystal control, but now we have VFO and often operate anywhere within the band. It goes without saying that what we need to go with VFO is a good VFA!

The group, other than amateur, most in need of a VFA, is that vast population trying to receive the various television and f.m. channels on a single antenna. A good half-wave dipole will outperform most of the existing elaborate receiving antennas providing, of course, it is possible to adjust the antenna accurately for each channel.

For years I have been giving thought to ways and means of feeding out and retrieving wire to make an adjustable center-fed half-wave antenna. The increased use of the VFO and the advent of television and f.m. broadcasting have made such an antenna practically a necessity. The folded dipole makes it a possibility, with rigging less complicated than the dial drives on some broadcast receivers! It is the purpose of this discussion to describe a remotely-controlled center-fed antenna capable of continuous adjustment from band to band and within the bands, using an untuned transmission line.

The Folded Dipole as a VFA

The folded dipole lends itself admirably to rigging with cords and pulleys so that the length of the flat top may be varied simply by pulling down on the feeders (see Figure 1). If the spacing between the center pulleys is adjusted so that the characteristic impedance of the two parallel conductors is 300 ohms the feeders will match 300 ohm ribbon regardless of their length and the length of the antenna. In this way, we have a tuned antenna with a flat line for any frequency, accomplished without resorting to sliding contacts at any point in the system. Figure 2 shows a practical hand-operated rigging that will enable the experimenter to make a set-up and observe its characteristics. Antennas of this type may be made large or small but it is suggested

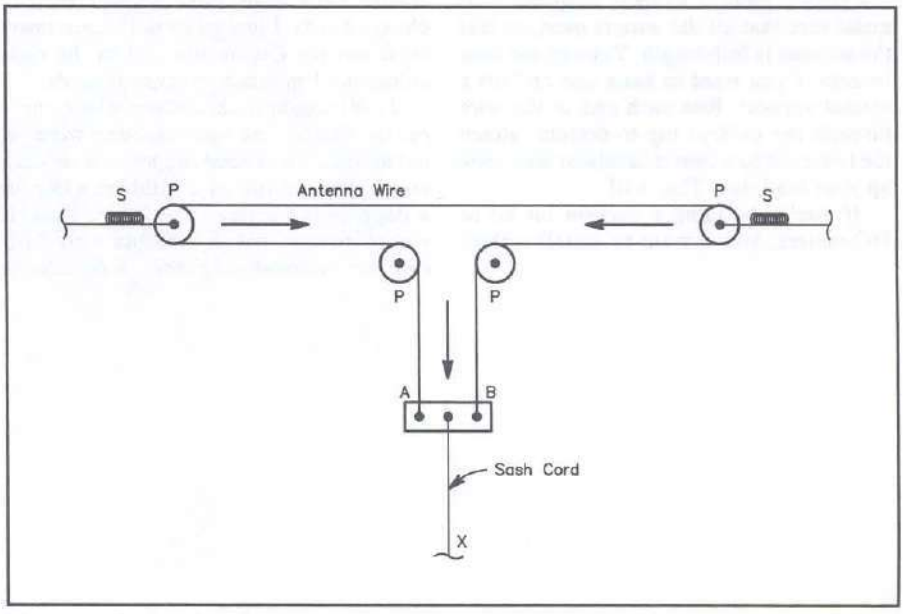

Figure 1—Basic principle of the adjustable folded dipole. Dipole and feeder section are made of one piece of flexible wire. Antenna length is changed by pulling down on the feeder at point X. Spacing of the pulleys at the center is such that the characteristic impedance of the feeder section is 300 ohms. Twin-Lead is connected at points A and B.

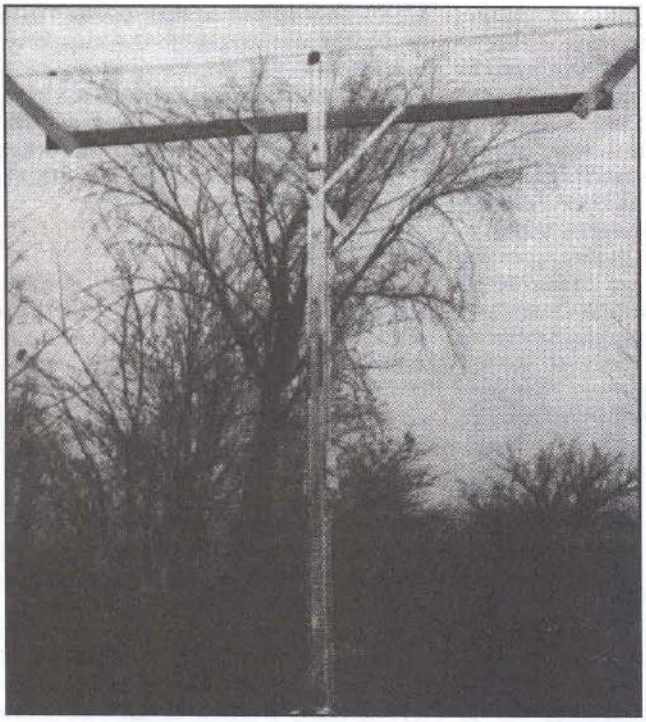

Practical working model of the folded-dipole VFA of Figure 3 used at W8AJC. The system is operated by the servo motor at the base of the mast, and is controllable from the operating position.

that the beginner make up small models for 2 and 6 meters, or simply for the f.m. and television bands, to prove the merit of the antenna.

The photograph and Figure 3 show the details of an experimental working model, made long enough to tune to 10 meters, but designed so it could be pulled down to a flat-top length of only a few inches. The tuning was fairly sharp and the results over conventional antennas for the reception of f.m. broadcasting were gratifying. A considerable improvement was noticed even within the 88-108 MHz f.m. band when the receiver was tuned to different stations and the antenna adjusted for maximum response. It was a real thrill to couple the feeders to the 10-meter transmitter and watch the plate milliammeter go up as the antenna came into resonance, and then pass through, and return for maximum; then without changing antennas, to switch on the f.m. broadcast receiver, run the antenna down to about four and a half feet to pick up a Detroit station. It was interesting to observe the effects on the received signal strength as the antenna was shortened from resonance at 10 meters to the proper length for the f.m. band, with the receiver tuned to a station on 98.5 MHz. Reception was possible with the long antenna and became good as the flat top hit fourteen feet (three half waves), falling off to a very sharp null at 121.5 inches (critical), after which it returned to full signal strength at 56.25 inches, approximately a half wave for the received signal. This ability to tune to an extremely critical null might find application in the elimination of an undesired, strong nearby signal under certain receiving conditions.

The uses to which a continuously-variable antenna may be put are limited only by the operator's imagination. Once the mechanical details have been worked out they may be used singly or in multiple, as antennas or reflectors, driven by common or separate servo motors and in various phase relations. Such antennas may be used for transmitting or receiving, or for special applications such as field operations covering a wide band of frequencies, signal-strength measurements, target transmitters for lining up rotary beams, and antenna studies. Their greatest commercial application will no doubt be in the f.m. and television fields where simplified versions, adjustable from the receiver, should find wide acceptance.

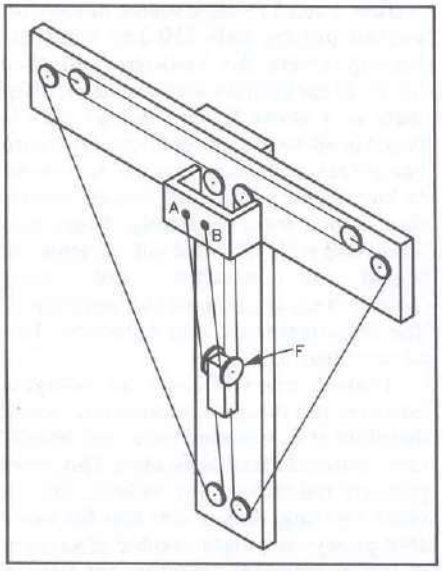

Figure 2—Hand-operated version of the variable-frequency antenna mounted on a wooden frame. To minimize mounting space, the feeders are folded back over ratio pulleys, F. The 300-ohm line connects at A and B. With this arrangement the vertical movement of pulley F is equal to the end movement of the antenna pulleys. The supporting fishline or sash cord must be taut.

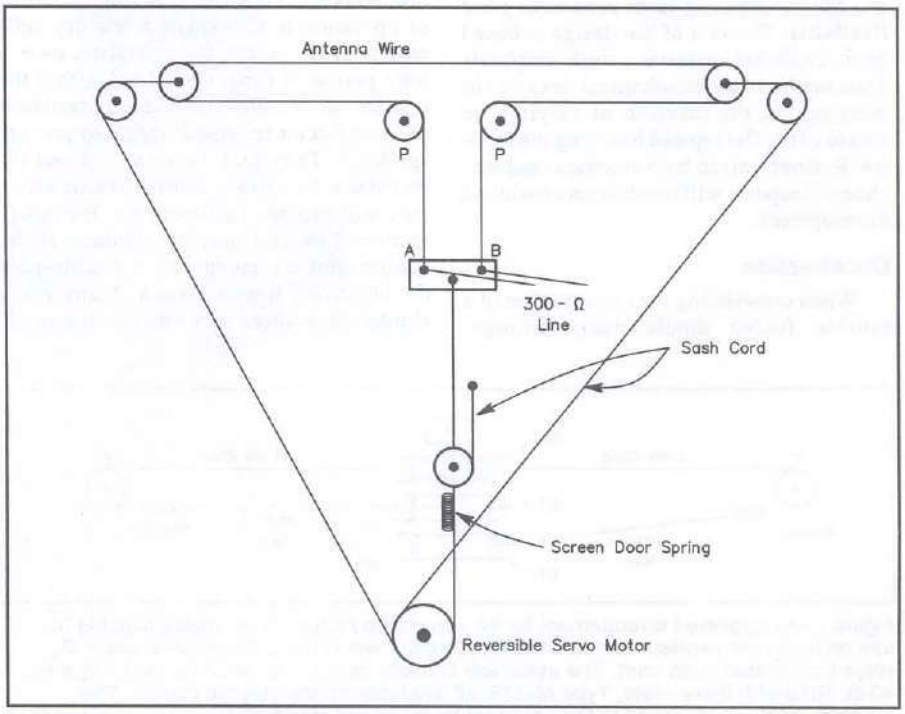

Figure 3—Diagram of the remotely-controlled antenna shown in the photograph. This system is now in use at W8AJC for 28 MHz and up. It may be reduced to a flat top of a few inches.

Other Types of Adjustable Antennas

Although the folded doublet lends itself most easily to continuous adjustment it might also be desirable to have a variable center-fed half-wave antenna suitable for use with coaxial or other low-impedance feeders. This may be done by the use of pulleys, insulators and wire, but requires a sliding contact at the center where the wind-up drums are located, and unless operated frequently it is subject to all the ills of exposed slip rings. This type of antenna is shown in Figure 4 and although at present, untried at W8AJC, it may prove worth-while on the lower frequencies, filling the long-felt need for a tunable 80-meter antenna that will work on 40 and 20 also!

Folded-Dipole Design

Useful information relative to the design of folded dipoles may be found in the ARRL *Handbook* for 1948, War Department *TM11-466*, RCA's little book *A Practical Analysis of U.H.F.* and in a paper by W. Van B. Roberts appearing in the *RCA Review* for June, 1947, page 289. The article by Roberts, in which he tells of the work done by his group at Princeton during the war under Government contract for the study of the folded dipole, is very helpful in providing the reader with a mechanism for analysis of the antenna. The literature indicates that spacing of the conductors composing the flat top should be close, in the order of 1/100 wavelength. Since our antenna is to have flexible conductors it is desirable to work with a type of wire that has a large diameter for low r.f. resistance, and at the same time has a high degree of flexibility. Such a conductor may be composed of insulated wire with a braided copper shield, the shield acting as the antenna and thus combining large area with good flexibility. The rest of the design is based upon available materials, with emphasis upon methods and mechanical devices for carrying out the function of varying the length of the flat top and handling the feeders. Refinements in both electrical and mechanical aspects will result from continued development.

Construction

When considering the construction of a tunable folded dipole many arrangements using springs or cords and pulleys will come to mind and it is up to the individual to select the method best suited to his particular use. In the beginning I tried a variety of springs, shock cords and weights to hold out the ends of the flexible antenna wire, but each of these methods had its own drawbacks and they all had the disadvantage of having to pull against a spring to shorten the antenna and depend upon the spring to pull it back out again. Metal springs come into resonance at certain frequencies. I tried metal-spring sash supports which would extend about 40 inches but they came into resonance in their extended positions and were not very smooth in operation.

It was finally decided to use cords and pulleys so arranged as to be in mechanical equilibrium and use the servo motor or other means only for the purpose of adjustment. This required less power in the servo and while it calls for more pulleys the result was smoother adjustment. I have found it convenient to support the antenna from the ends by means of insulated pulleys on a wood or other nonconducting structure. If the dipole is to be operated in a horizontal position there is no objection to using a vertical metal support pipe, but horizontal metal rods or pipes should not be used. For long antennas a center support must be provided for the feeder pulleys and the wind-up mechanism. The ends may be supported by poles, trees or buildings.

Servo Motors

The servo motor shown in the photograph is from a surplus Azon bomb tail assembly. It has plenty of power and may be reversed at will. It requires a 4-wire cable to the battery or other d.c. source. The current consumed is small and since the time of operation is also small a few dry cells will provide power for operation over a long period of time. Contained within the unit are two selenium rectifiers placed there to short circuit reverse currents to prevent sparking. They may be removed and inserted in a 30-volt a.c. line to the unit where they will provide sufficient d.c. for its operation. Reversal may be obtained at the station end by means of a double-pole double-throw toggle switch. Many other similar slow-speed servo motors are available on the surplus market, most of them reversible, and varying in size and power requirements. In some cases where d.c. is not available advantage may be taken of the gear train by connecting a universal coupling to the motor end and driving with a reversible universal fan or vacuum-cleaner motor operated from 115 volts a.c.

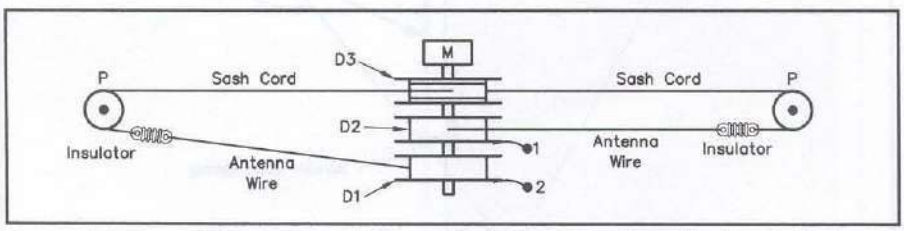

Figure 4–A suggested arrangement for an adjustable motor-driven dipole suitable for use on the lower amateur bands. Reels D_1 and D_2 reel in the antenna wire, while D_3 plays out braided sash cord. The assembly is made from a Signal Corps reel, Type RL-42-B, fitted with three reels, Type M-235, all available on the surplus market. The antenna reels are fastened to the cord reel by means of stand-off bushings secured to the center insulation. Brushes 1 and 2 connect to a 72-ohm line running to the transmitter. Success of this system depends upon maintenance of good contact at the brushes.

Sources of Materials

Antenna wire should be light, durable, flexible, of large diameter and a good conductor. For ease of adjustment it should pull around a one-inch pulley readily. Superflexible stranded copper wire of large diameter would be quite heavy whereas an insulated stranded wire, if size 20 or so and covered by a braided tinned-copper shield, would be light in weight, adequately flexible and of sufficient diameter. Belden No. 8885 shielded grid wire having an o.d. of 0. 1 inch has been found satisfactory. Too-stiff wire will make the system unwieldy.

Pulleys must be free-running for smooth operation and have as little friction as possible. A number of different kinds of pulleys normally available at hardware stores were tried and all had mechanical imperfections. Usually, though they seemed free-running when tried at the store, they turned out to have prohibitive friction when loaded and in the system. Since the number of pulleys required is fairly large and the accumulated friction may be excessive, ball-bearing pulleys are recommended. The first ones used here were homemade and turned out of fiber and used small ball bearings in the center. The ball bearings had 1/4-inch holes and a 5/8-inch o.d. and were obtained from disassembly of surplus gear trains, bomb sights, computers and other equipment so plentiful on the surplus market. Later I found a source of one-inch aircraft pulleys (AN-210-1A) with ball-bearing centers. Air Associates sells them for $1.25 each but the surplus market offers them at a lower figure. Pulleys may be found in all sorts of surplus aircraft control equipment and sometimes it is cheaper to buy a unit containing several pulleys than to buy them separately. Homemade hardwood pulleys turned out of maple and boiled in paraffin and using 1/4-inch brass axles should be satisfactory. The important thing is to have good low-friction bearings.

Twisted rope will cause the pulleys to turn over and twist and short out the aerial; therefore it is recommended that braided sash cord or clothesline be used. This, when properly fed through the pulleys, will not cause twisting. A nice size that fits available pulleys is a light braidcd clothesline 1/8-inch in diameter. Of course any flexible insulating line may be used such as dial cable, fishline or upholsterer's twine. Spring loading to prevent slipping because of stretching is advisable in some cases.

Limit Switches: If the antenna is not visible from the operating point Micro-Switches may be so placed that when the end of travel of the antenna is reached the

circuit will be opened and the motor will stop, it being possible then to reverse it and run it to the other limit where another switch will furnish protection from overtravel. The switches should not be connected in the common lead to the motor but in the circuit controlling that direction only. (Switches and associated wiring must be placed so as not to interfere with the electrical operation of the antenna.)

Conclusion

The examples shown are but a few of many possible ways of setting up remotely-controlled variable-frequency antenna systems. It is hoped that this article will serve as a basis for further development of adjustable antennae for amateur and commercial use.

By Rod Newkirk, W9BRD

From *QST*, July 1993

Honey, I Shrunk the Antenna!

Think small! Communicate with multiconductor miniature loop antennas.

Great energy and ingenuity go into efforts to boost the effectiveness of compact transmitting antennas—*compact* meaning configurations with circumferences of 1/8 wavelength or less. By this definition, a 40-meter design could be a square with 4-foot sides. In the following discussion, I depart slightly from the square. I prefer 3 1/2 feet high by 4 1/2 feet wide, suspended in the vertical plane, for convenience in my antenna's location.

The traditional small-loop approach is to insert capacitance in series with a one-turn loop, tune it to the desired frequency, and then attempt to feed power to it as efficiently as possible–no simple matter. The antenna's Q is astronomical, current and voltage are monstrous, bandwidth is razor sharp, and its radiation resistance is ridiculously low. This lossy situation can be improved by reducing the resistance of the loop material through the use of piping, foil, etc, but the resulting plumbers' nightmares are hardly worth the pains.

A more promising avenue toward practical, simple compact antennas would appear to be in the direction of varied configuration. The goal is to "cool" the system with better power distribution, and at the same time simplify the feed. For example, vast improvement in the key parameters is possible by application of the venerable "folded dipole" technique. This can be done by adding one more turn, tuned identically, connecting the two turns *in series*, and re-resonating the antenna. Now, looking into one of the twin current nodes, the input impedance will have roughly quadrupled. The one-turn loop's skimpy 5 or 6 Ω rises to approximately 25 Ω. Adding yet another such turn doubles this to about 50 Ω–a convenient match to common coax. See Figure 1. As with the folded dipole, more than four turns are unprofitable; diminishing returns raise the input impedance. little faster than ohmic resistance. Note that the tuning capacitances, each about 40 pF, must be kept nearly equal for overall system balance.

Construction techniques, conductor material, insulation and components now become less critical because voltage peaks and current nodes are distributed throughout the system. I use ordinary zip cord, two lengths entwined, giving four available turns.[1] For proper continuity, the four wires on each side of the loop are clearly tagged at alligator-clip connectors, top and bottom centers. For 7 MHz, one turn is left open (at top *and* bottom), but will become useful on the lower bands as discussed later. A more classy construction might feature braided hook-up wire of contrasting colors. Small cardboard spreaders at the clips keep adjacent capacitors separated.

Midget receiver-type capacitors are adequate for CW power output up to 100 watts. One of these should be conveniently variable, preferably a double-gang or splitstator type, for tweaking the system to the desired center frequency as indicated by a 1: 1 SWR. At 7 MHz, each capacitance is about 40 pF in my antenna, so the old war surplus Hammarlund APC midgets do nicely. Bandwidth can approach that of a normal linear dipole if a slightly higher center frequency SWR is accepted by stagger-tuning.

Excellent 40-meter results indicated that the same loop, dimensions unchanged, could have a shot at 80 meters. At 3.5 MHz, it becomes truly a miniloop, only 1/16 wavelength in circumference. Adding the fourth turn (Figure 2) raises the feed impedance at a slightly higher rate than ohmic resistance, so I included it. Armed with a bargain bag

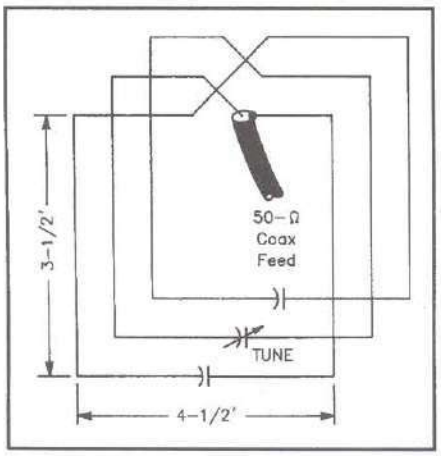

Figure 1—The three-turn loop antenna for 40 meters. Each capacitor is about 40 pF to resonate and match the antenna to a 50-Ω feed line.

Increasing Multiturn Loop Efficiency

Lots of hams use small loops in situations where they can't erect a larger antenna. Making contacts with these antennas largely depends on high radiation efficiency. Here are some things you can do to increase efficiency and effectiveness of such antennas:

- Use large-diameter copper wire. Keep the copper surface clean. Tin-plated wire is noticeably worse than copper in this application because of skin effect–most of the RF travels in the tin, which is far lossier than copper at RF.
- Use low-loss capacitors. The key here is minimizing dielectric loss, which is most favorable in vacuum- and air-dielectric capacitors. You can also parallel several capacitors to decrease losses.

Increasing the wire size used in these loops raises the antenna Q, narrowing the bandwidth and increasing the voltages and currents present. For this reason, you may have to use higher-quality capacitors than those used in the experimental versions if you increase the wire size.

Remember that high voltages can exist on a multiturn loop antenna's wires at power levels of a few tens of watts or more. Thus, it's best to keep the antenna well away from other objects.—*Roy Lewallen, W7EL*

The Ingredient Called *Belief*

Even though my busy family life keeps hamming time rare, the time I spend hamming has to be spent *right*. The idea isn't just to get on the air and contact anyone anywhere—that's too *easy*. The idea is to do something a hair off-the-wall and see if anyone shares the same orbit. So I'm one of those guys who calls CQ QRP for ten minutes at 10149.5 kHz even as game clogs the band's low end—someone who looks for (and *expects*) ragchews on 3560 at noon. And so I naturally was the guy to call a 5-watt, 3 × 2 × 1 CQ at 7138 kHz at around 10 PM one night last fall when the broadcasters had long since muscled straight-thinking NovTechs off to safer terrain. And so I naturally was *of course* immediately answered by W9BRD.

It figures. We've worked on schedule many times before, but he and I—he's the father; I'm the son—have never had to prearrange each new "first contact" after changes of station setup or locale. *Chance* is too facile a word for this, but then I haven't looked too hard for a better word, either. I don't need to; we just do our individual quirky things and click.

This time, we *both* had new setups: I'd just relocated the armful of gear constituting my "shack" to the bedroom and was talking to a low dipole through 100+ feet of mongrel coax; *he* was trying out an indoor, largely below-ground loop antenna—one of the versions shrunken in this article—with just a few tens of watts, tunneling past those steamroller broadcast signals as soundly as any medium-scale ham signal from Chicago.

Enjoying the magic of yet another first contact, I hardly gave his setup a second thought. But you may wonder if such antennas really work. Gooch's Paradox explains it thus: "RF gotta go *somewhere*." Seeking to soothe the linearless, towerless masses who toil with "*only* 100 watts," Newkirk's Tiresome Chant puts it, "Successful MF/HF radio communication may proceed at astoundingly low received-signal strengths." Reduced to generic essentials, it's this: The most important single factor in success with *whatever* you use is overcoming your own disbelief.—*David Newkirk, WJ1Z*

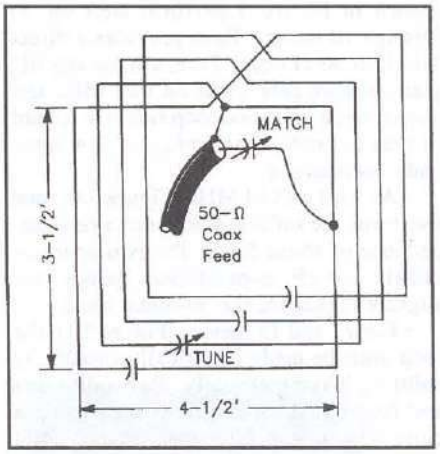

Figure 2—Extending the Fig 1 concept to 80 and 160 meters requires adding another turn to the antenna and increasing the capacitances. See the text for capacitor values.

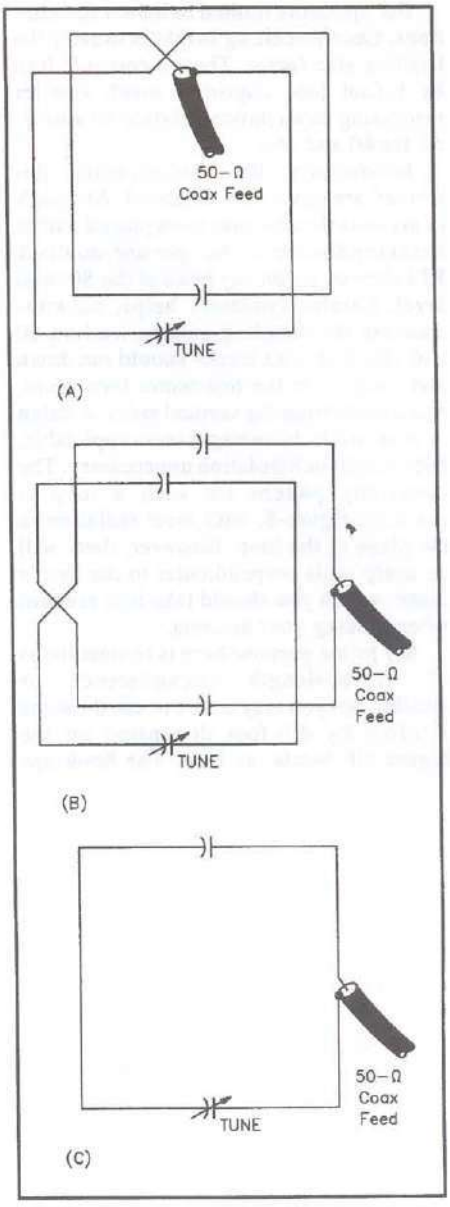

Figure 3—At A, the 30/20-meter loop; at B, the 15/17-meter version, and at C, the 10-meter variant.

of small 1-kV ceramic capacitors, I reached 3.6-MHz resonance with a value of 100 pF for each of the four capacitances. One capacitor was then replaced with an old broadcast-style, two-gang 300-300-pF variable for tweaking. I measured the feed impedance, at the center of one of the four turns, at about 18 Ω–well within the range of simple gamma matching. So another junk-box broadcast variable, three 350-pF gangs paralleled, was suspended at the loop's top center. Only about 650 pF was needed for a 1:1 match to coax after a 30-inch gamma lead was dangled to a tap at the center of one side of the feed turn. Then the system was tweakable over the entire 80-meter CW range. The remaining ceramic capacitors get slightly warm at 80 watts, which indicates significant power loss. These capacitors should be replaced with low-loss units for best performance, but I left them alone for my experiments. I easily contacted the East Coast and as far west as Arizona in the following few nights on the air.

My next inclination, as you may surmise, was to try the little gem on 160 meters. A four-foot-square transmitting loop for 1.8 MHz? I wasn't overly optimistic. Years of tinkering at W9BRD had failed to produce a decent indoor compact antenna, even of much larger size, for top-band work. But I dug into my bag of ceramics and gave it a go. The four-turn loop, now only $^1/_{32}$ wavelength in circumference, resonated at about 1.8 MHz with four 350-pF capacitors. One of these was replaced with an old broadcast-type 500-pF variable for tweaking the center frequency between 1.8 and 1.85 MHz. I double- and triple-checked the measured feed impedance—16 Ω. Now I knew it would work. The gamma-match SWR dipped to 1:1 at about 800 pF using the same lead, tap and broadcast capacitor as on 80 meters. Immediate solid 40-watt CW QSOs with WN9W, KC4WWV, WKØB and W4VZB were most gratifying.

Variations and the Higher Bands

If such a $^1/_{16}$-wavelength loop can function at 80 meters, the same should be true at 20 meters. So I wound a 1-foot-square, three-turn model on a cardboard box, hung it on a wooden bulkhead, and resonated it to 14.050 MHz with three 50-pF ceramic capacitors. This time, instead of the usual fudging capacitor, I spaced the turns $1^1/_2$ inches apart. Center-frequency tweaking thus could be done by uniformly edging the turns away from or toward each other. This spacing approach works fine for box-wound loops, but for the lower bands, I prefer closewound zip cord. Input impedance turned out to be about 11 Ω—I should have used a fourth turn—and gamma coupling worked okay, as on 80 and 160. The 1:1 feed-line dip occurred with a 120-pF series capacitor, with a gamma lead of 13 inches. In my installation, this antenna is no low-angle DX radiator, to be sure, but I've received S9 reports during many stateside QSOs. Anyone for a 3-inch-square 2-meter version?

Antennas smaller than necessary are interesting stunts that help prove a design. However, for the lowest HF bands I recommend the largest practicable circumference.

For operators limited to indoor installations, floor-to-ceiling height is usually the limiting size factor. Thus, a cooler 7-foot by 9-foot job, requiring much smaller resonating capacitances, should be a natural for 80 and 160.

Incidentally, the configurations described are quite well balanced. Although in my tests the antennas were placed within tweaking distance of the operator, no shack RFI showed up on any band at the 80-watt level. Careful symmetry helps, notwithstanding the dangling gamma lead on 80 and 160. The coax feeder should run down and away from the top-center feed point, equidistant from the vertical sides. A balun or coaxial RF choke might seem applicable, but I found such isolation unnecessary. The directivity pattern for such a loop is the usual figure-8, with most radiation in the plane of the loop. However, there will be sharp nulls perpendicular to the loop's plane, which you should take into account when placing your antenna.

My prime purpose here is to treat loops of 1/8-wavelength circumference or smaller, but you may desire to use the same 3 1/2-foot by 4 1/2 foot dimension on the higher HF bands, as I do. The hook-ups shown in Figure 3 perform well on 30 through 10 meters. Each provides a direct match to 50-Ω coax. True, almost any old piece of wire gets QSOs on 10.1 MHz and above, but a balanced loop radiator is hard to beat for indoor hamming. A few hints and observations:

- At 10. 1 and 14 MHz (Figure 3A), just two turns are sufficient to reach a feed impedance of about 50 Ω. The two approximately 20-pF capacitance values are slightly higher for the 30-meter band.
- For 17 and 15 meters (Figure 3B), the loop must be made electrically smaller by splitting it symmetrically. Two split turns and four equal capacitances then bring a close 50-Ω match. Note that the feed point is moved to the center of one of the four vertical sides. Capacitances are in the 15-pF range.
- On 12 and 10 meters (Figure 3C), one split turn will suffice for a near-50-Ω match, with two capacitors of about 12 pF. Here, splitstator midgets can ease adjustment by minimizing hand capacitance, but it's a fancy junk box that includes them. The old APC midgets, whose rotors have little more mass than their stators, will maintain enough system balance.

Cautions and Conclusions

Like any indoor antenna, the loops I describe here generate substantial electromagnetic fields in operation. Thus, they have considerable potential to generate RFI. For this reason and to prudently avoid placing yourself or others in large RF fields, you should keep all antennas as far from consumer electronic devices and people as possible, and use the least RF power necessary to conduct the desired communications. The current editions of *The ARRL Handbook* and *The ARRL Antenna Book* cover this subject in more detail.[2]

A final comment: For overall results with compact antennas, like almost any skyhook, the higher above ground the better. In my case, radiation and reception strongly favor higher skywave propagation angles. All antenna configurations I describe here were tested and operated in a cellar ham shack, where half of the system is below ground level!

Notes

[1]See the sidebar, "Increasing Multiturn Loop Efficiency," for some ideas on optimizing such an antenna's performance.

[2]See Chapter 9 of the *Handbook* and Chapter 1 of the *Antenna Book*.

Radio and Electronics Cookbook

Edited by
Dr George Brown, CEng, FIEE, M5ACN

OXFORD AUCKLAND BOSTON JOHANNESBURG MELBOURNE NEW DELHI

Contents

Preface ix

1. A medium-wave receiver 1
2. An audio-frequency amplifier 4
3. A medium-wave receiver using a ferrite-rod aerial 9
4. A simple electronic organ 12
5. Experiments with the NE555 timer 17
6. A simple metronome 21
7. What is a resistor? 24
8. Waves – Part 1 27
9. A beat-frequency oscillator 31
10. What is a capacitor? 34
11. Waves – Part 2 38
12. An LED flasher 41
13. Waves – Part 3 44
14. Choosing a switch 46
15. An aerial tuning unit for a receiver 49
16. A simple 2 m receiver preamplifier 52
17. Receiving aerials for amateur radio 54
18. The Colt 80 m receiver – Part 1 58
19. A crystal radio receiver 62
20. The varactor (or varicap) diode 64
21. A portable radio for medium waves 65
22. The Colt 80 m receiver – Part 2 70

23.	A simple transistor tester	73
24.	An introduction to transmitters	77
25.	The Colt 80 m receiver – Part 3	81
26.	A two-way Morse practice system	88
27.	The Colt 80 m receiver – Part 4	91
28.	A simple crystal set	95
29.	A crystal calibrator	100
30.	A simple short-wave receiver – Part 1	104
31.	A fruit-powered medium-wave radio	106
32.	A capacitance bridge	109
33.	A simple short-wave receiver – Part 2	113
34.	A basic continuity tester	117
35.	A charger for NiCad batteries	119
36.	An 80 metre crystal-controlled CW transmitter	123
37.	A solar-powered MW radio	129
38.	A receiver for the 7 MHz amateur band	133
39.	Diodes for protection	137
40.	An RF signal probe	140
41.	An RF changeover circuit	142
42.	A low-light indicator	146
43.	A J-pole aerial for 50 MHz	149
44.	Measuring light intensity – the photometer	153
45.	A 70 cm Quad loop aerial	156
46.	A UHF field strength meter	160
47.	Christmas tree LEDs	162
48.	An audio signal injector	166
49.	Standing waves	168
50.	A standing-wave indicator for HF	170
51.	A moisture meter	174
52.	Simple aerials	177
53.	A breadboard 80 cm CW transmitter	182

54. A 7-element low-pass filter for transmitters 186
55. Radio-frequency mixing explained 189
56. A voltage monitor for a 12 V power supply 192
57. A 1750 Hz toneburst for repeater access 196
58. A circuit for flashing LEDs 201
59. Digital logic circuits 205
60. A resistive SWR indicator 210
61. An audio filter for CW 213
62. An electronic die 215
63. The absorption wavemeter 222
64. An HF absorption wavemeter 224
65. A vertical aerial for 70 cm 228
66. A UHF corner reflector aerial 230
67. A switched dummy load 234
68. A simple Morse oscillator 238
69. A bipolar transistor tester 240
70. The 'Yearling' 20 m receiver 245
71. Adding the 80 metre band to the Yearling receiver 251
72. How the Yearling works 255
73. A field strength meter 258
74. Preselector for a short-wave receiver 261
75. An audible continuity tester 265
76. An experimental 70 cm rhombic aerial 268
77. Water level alarm 272
78. A delta loop for 20 metres 275
79. A simple desk microphone 279
80. Morse oscillator 284
81. A simple 6 m beam 287
82. An integrated circuit amplifier 291
83. A novice ATU 293
84. CW QRP transmitter for 80 metres 297

85. An audio booster for your hand-held 303
86. A grid dip oscillator 306
87. A CW transmitter for 160 to 20 metres 312
88. Matching the end-fed random-wire aerial 315

Preface

Although we are surrounded by sophisticated computerised gadgets these days, there is still a fascination in putting together a few resistors, capacitors and the odd transistor to make a simple electronic circuit. It is really surprising how a handful of components can perform a useful function, and the satisfaction of having built it yourself is incalcuable.

This book aims to provide a wide variety of radio and electronic projects, from something that will take a few minutes to a more ambitious weekend's worth. Various construction techniques are described, the simplest requiring no more than a small screwdriver, the most complex involving printed circuit boards.

Originally published by the Radio Society of Great Britain, the projects were all chosen to be useful and straightforward, with the emphasis on practicality. In most cases the workings of the circuit are described, and the projects are backed up by small tutorials on the components and concepts employed. In the 21st century it may seem strange that few of the published circuits use integrated circuits (chips). This is intentional as it is much easier to understand how the circuit works when using discrete components.

Anyone buying the *Radio and Electronics Cookbook* will find that it will lead to hours of enjoyment, some very useful and entertaining gadgets, and increased knowledge of how and why electronics circuits work, and a great sense of satisfaction. Beware, electronic construction is addictive!

WARNING: This book contains construction details of transmitters. It is illegal to operate a transmitter without the appropriate licence. Information on how to obtain an Amateur Radio Licence can be obtained from the Radiocommunications Agency, tel. 020 7211 0160.

1 A medium-wave receiver

Introduction

Let us start off with something that is really quite simple and yet is capable of producing a sense of real satisfaction when complete – a real medium-wave (MW) radio receiver! It proves that receivers *can* be simple and, at the same time, be useful and enjoyable to make. To minimise the confusion to absolute beginners, *no* circuit diagram is given, only the constructional details. The circuits will come later, when you have become accustomed to the building process. In the true amateur spirit of ingenuity and inventiveness, the circuit is built on a terminal strip, the coil is wound on a toilet roll tube (as amateur MW coils have been for 100 years!), and the receiver is mounted on a piece of wood.

Putting it together

Start by mounting the components on the terminal strip as shown in **Figure 1**, carefully checking the position and value of each one. The three capacitors are all the same, and so present no problem. They (and the resistors) may be connected either way round, unlike the two semi-conductors (see later). The resistors are coded by means of coloured bands. You can refer to Chapter 7 if you have difficulty remembering the colours and their values.

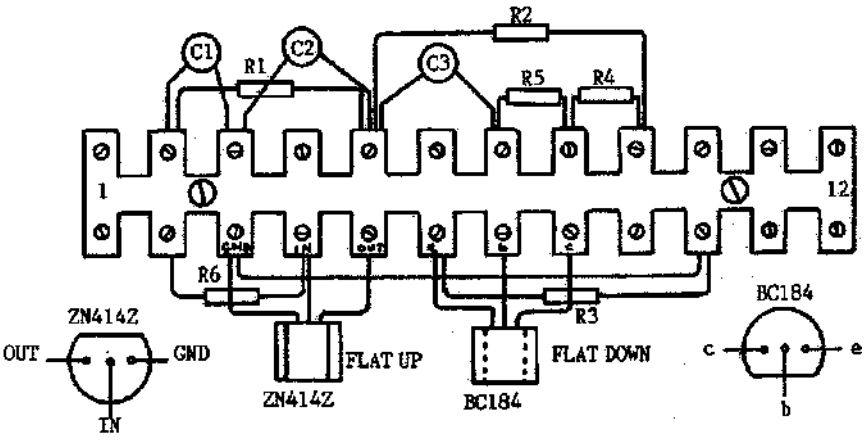

Figure 1 Terminal strip – position of components

1. Brown, Black, Yellow	100 000 ohms	(R1, R5, R6)
2. Green, Blue, Brown	560 ohms	(R2)
3. Red, Violet, Brown	270 ohms	(R3)
4. Brown, Black, Orange	10 000 ohms	(R4)

The integrated circuit (the ZN414Z) and the transistor (the BC184) *must* be connected correctly. Check Figure 1 carefully before fitting each device.

Now wind the coil. Most tubes are about 42 mm diameter and 110 mm long. Don't worry if your tube is slightly different; it shouldn't matter. Make two holes, about 3 mm apart, about 40 mm from one end, as shown in **Figure 2**. Loop your enamelled wire into one hole and out of the other, and draw about 100 mm through; loop this 100 mm through again, thus anchoring the wire firmly. Now wind on 80 turns, keeping the wire tight and the turns close together but not overlapping. After your 80th turn, make another two holes and anchor the wire in the same way as before. Again, leave about 100 mm free after anchoring. Using another piece of enamelled wire (with 100 mm ends as before), loop one end through the same two holes which contain the end anchor of the last winding, wind two turns and anchor the end of this short winding using another pair of holes. Figure 2 shows the layout.

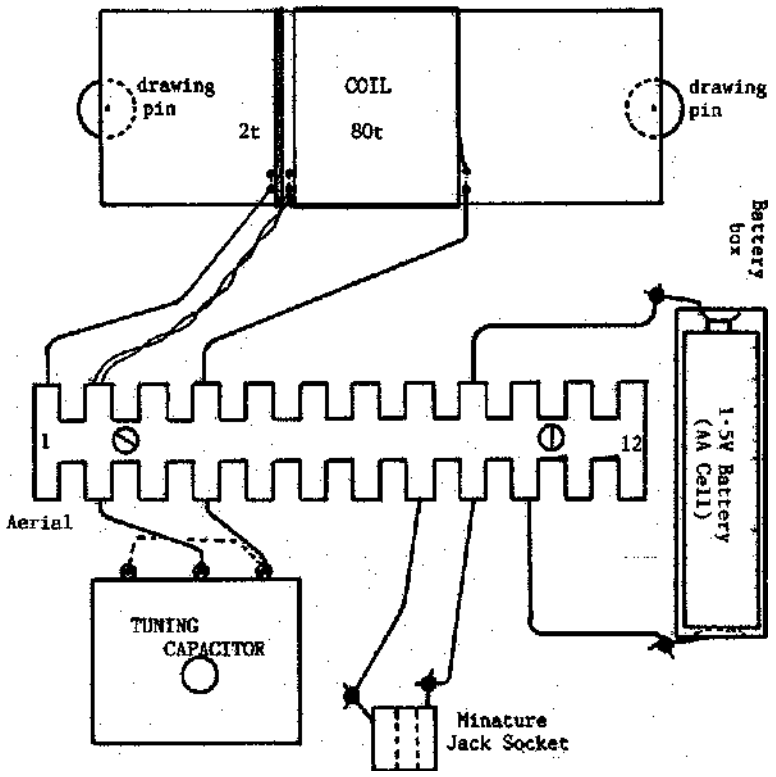

Figure 2 The layout of the parts on the wooden base

With some glass paper, remove the enamel from the ends of both pieces of wire which go through the same holes (i.e. the bottom of the large coil and the top of the small coil), then twist these bare ends together. Remove the enamel from the remaining ends of the coil. The coil is now finished!

The baseboard can be any piece of wood about 150 mm square. Fix the coil near the back edge using drawing pins and connect the wires from the coils to the terminal strip as shown in Figure 2. Using short pieces of PVC-insulated wire (and with assistance if you have never soldered before), solder one piece across the two outer tags of the variable capacitor, shown by the dotted line in Figure 2, and then two longer pieces to the centre tag and one outside tag. Connect these to the terminal strip. Then solder two more insulated wires on to the jack socket (into which you will plug your crystal earpiece), the other ends going to the terminal strip. The last two wires (one must be red) need to be soldered on to the battery box, their other ends going to the terminal strip also. Make sure the red wire goes to the *positive* terminal on the battery, and is connected to terminal 9. The other connection to the battery goes to terminal 10.

Attach the terminal strip to the baseboard with small screws or double-sided sticky tape. The other parts can be mounted the same way.

Listening is done ideally with the recommended crystal earpiece. Don't be tempted to use your Walkman earpieces; they are not the same and will not perform anything like as well. The receiver should work without an extra aerial, but one can be attached to terminal 1 if necessary. A long piece of wire mounted as high as possible is ideal. The *Audio-frequency Amplifier* project will enable you to use a loudspeaker with your receiver, using the signal from the jack socket. No circuit modifications will be needed!

Parts list

Resistors: all 0.25 watt, 5% tolerance

R1, R5, R6	10 kilohms (kΩ)
R2	560 ohms
R3	270 ohms
R4	10 kilohms (kΩ)

Capacitors

C1, C2, C3	100 nanofarads (nF)
	500 picofarads (pF)

Semiconductors

ZN414Z, BC184

Additional items
- 12-way 2 A terminal strip
- 22 metres of 28 SWG enamelled copper wire
- A few short pieces of coloured PVC-insulated wire
- Crystal earpiece
- 3.5 mm jack socket
- 1.5 V AA-size battery and box
- Toilet roll tube
- Double-sided sticky tape or selection of screws

Tools required

Small screwdriver, soldering iron.

2 An audio-frequency amplifier

Introduction

This simple amplifier can be built by anyone who is able to solder reasonably well. It doesn't require any setting up and, provided our instructions are followed exactly, will work very well. The circuit diagram is included for the benefit of our more advanced readers, but it is not needed in the construction process. Please practise your soldering before you start, and don't use a printed circuit board (PCB) until you are confident that your soldering is up to scratch.

The amplifier can be used with other projects; it will provide plenty of sound from the MW Radio or from the Morse Sounder projects. It will usually be built into other pieces of equipment, so a box is not supplied with the kit. There is no reason why it shouldn't be put into a box and used as a general-purpose amplifier to help test other projects.

The components

Before you start, you should check that you have *all* the components to hand. A list and some helpful hints are given below.

1. PCB. The plain side is the *component side* and the soldered side is the *track side*. **Figure 1** shows the track side full size. Make the PCB from the pattern given in Figure 1. Otherwise, build the circuit on a matrix board.
2. Three resistors. Locate the gold or silver band around the resistor, and turn the resistor until this band is to the right. There are three coloured bands at the left-hand end of the resistor. Find the resistor whose colours are YELLOW, VIOLET, RED, and look at the resistor colour code chart which you will find in Chapter 7. From this, you will see that YELLOW indicates the value 4, VIOLET the value 7, and RED the value 2. The first two colours represent real numbers, and the last value is the number of zeros (noughts) which go *after* the two numbers. So, the value is 47 with two zeros, i.e. 4700 ohms. In this way, the resistor coloured BROWN, GREY, BROWN has a value of 180 ohms, and the last one, BROWN, RED, GREEN, has a value of 1 200 000 ohms. The ohm (often written as the Greek letter omega (Ω)) is the unit of resistance. If you do not yet feel confident in identifying resistors by their colours, use the Resistor Colour Codes given in Chapter 7.
3. Four capacitors. The two small 'beads' are tantalum capacitors and will be marked 4.7 μF or 4μ7, with a '+' above one lead. A tubular capacitor with wires coming from each end should be marked 220 μF, with one end marked '+' or '–'. This is called an *axial* capacitor because the wires lie on the axis of the cylinder. This is in contrast to the final capacitor, where both wires emerge from the same end. This is a *radial* capacitor, and will be marked 47 μF. Again, one lead will be marked '+' or '–'. Capacitors marked like this are said to be *polarised*, and it is vital that these are placed on the PCB the right way round, so take notice of those signs!
4. Two diodes. These are tiny glass cylinders with a band around one end, and may be marked 1N4148; this is their type number. Like polarised capacitors, they *must* be put on the PCB the correct way round!

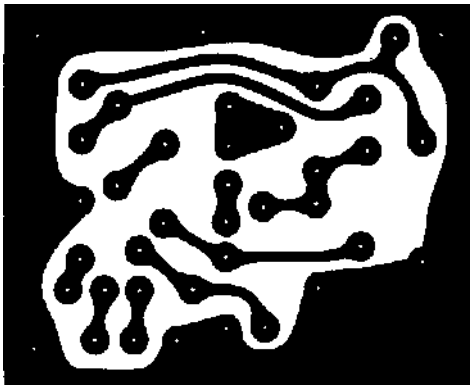

Figure 1 The toil pattern of the PCB – looking from the track side

5. Three transistors. One should be a BC548 (or a BC182), the other two should be BC558 (or BC212).
6. One volume control with internal switch.
7. One loudspeaker. This is quite fragile – don't let anything press against the cone.
8. One PP3 battery clip with red and black leads.

Putting it together

Lay the PCB on a flat, clean surface with the track side downwards. It is always useful to compare the layout with the circuit diagram, given here in **Figure 3**. Although you can't see it, the D-i-Y Radio sign should be at the top. Compare the hole positions with those shown in **Figure 2**. Bend the resistor wires at right angles to their bodies so that they fit cleanly into the holes in the PCB. Push each resistor towards the board so that it lies flat on the board. Then supporting each one, turn the board over and splay out the wires *just* enough to prevent the resistor falling out. Then, solder each wire to its pad on the PCB, and cut off the excess wire. When you have more confidence, you can cut of the excess wire *before* soldering; it often makes a tidier joint.

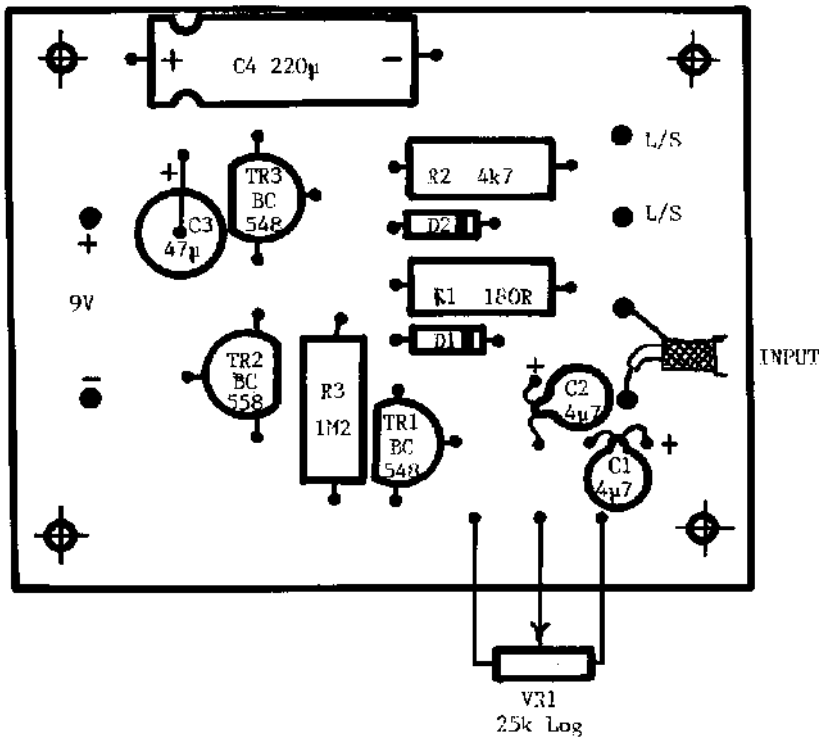

Figure 2 Positions of the components on the printed circuit board (PCB)

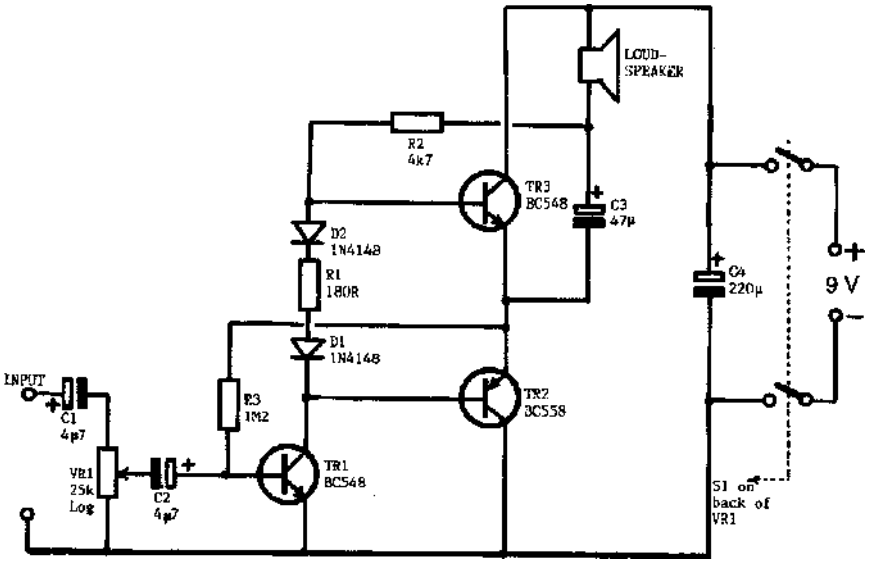

Figure 3 The amplifier's circuit diagram

Now fit the four capacitors. Each must be connected the right way round, so look at each component, match it up with the diagram of Figure 2, bend its wires carefully and repeat the soldering process you performed with the resistors, making sure that the components are close to the board and not up on stilts! Fit the two diodes the correct way round, and solder then as quickly as you can – they don't like to be fried!

Mount the transistors about 5 mm above the PCB. Make sure the correct transistors are in the correct places, and that the flats on the bodies match up with those shown in Figure 2.

Mount the volume control so that the spindle comes out from the front of the board. Use a piece of red insulated wire to the pad marked + on the PCB, and a black piece to the pad marked –, and solder these to the tags on the back of the control, as shown in **Figure 4**. Connect the two leads from the battery clip to the other tags on the switch; Figure 4 will help you. Finally, use two pieces of insulated wire about 100 mm long, twisted together, to connect the loudspeaker to the PCB.

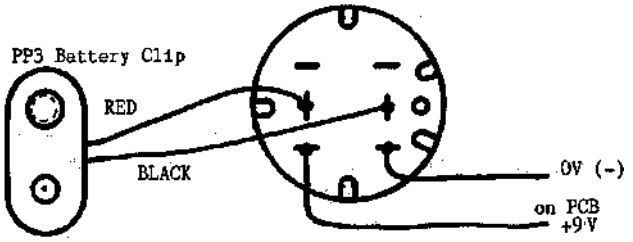

Figure 4 Connections to switch on back of VR1

Box clever!

If you wish to put the amplifier into a box, there is no problem; almost any box that is big enough will do. All that is needed is one hole big enough to accept the bush of the volume control; the PCB will be supported by the volume control. The prototype was not fitted into a box, but mounted on an odd piece of aluminium, bent into an L-shape and screwed on to a wooden base. The loudspeaker was mounted on the aluminium panel by two small pieces of aluminium with 3 mm holes drilled in them, which acted as clips around the edge of the speaker. Drill a few holes in the panel in the position of the speaker to let the sound get out!

Your input signal can be connected to the amplifier with two short pieces of wire, but if the connection needs to be long, use screened cable, with the braid connected as shown in Figure 2.

If you decide to use a different loudspeaker, make sure that its impedance (the resistance value marked on the back of the magnet) is at least 35 ohms. Anything lower may damage TR2 and TR3, and will certainly run down your battery very quickly. You will be surprised at the uses you can find for this little amplifier!

Parts list

Resistors: all 0.25 watt, 5% tolerance

R1	180 ohms (Ω)
R2	4.7 kilohms (kΩ)
R3	1.2 megohms (MΩ)
VR1	25 kilohms (kΩ) log with DPST switch

Capacitors: all rated at 25 V minimum

C1, C2	4.7 microfarads (μF)
C3	47 microfarads (μF)
C4	220 microfarads (μF)

Semiconductors

TR1, TR3	BC548 npn
TR2	BC558 pnp
D1, D2	1N4148

Additional items

- PCB
- Speaker >35 ohms
- PP3 battery clip and battery

3 A medium-wave receiver using a ferrite-rod aerial

Introduction

This design came from the Norfolk Amateur Radio Club, and enables you to build a simple Amplitude Modulation (AM) receiver for frequencies between 600 kHz and 1600 kHz. It should take you around 2 hours to build, and can be used with Walkman-type earpieces. **Figure 1** shows the circuit diagram.

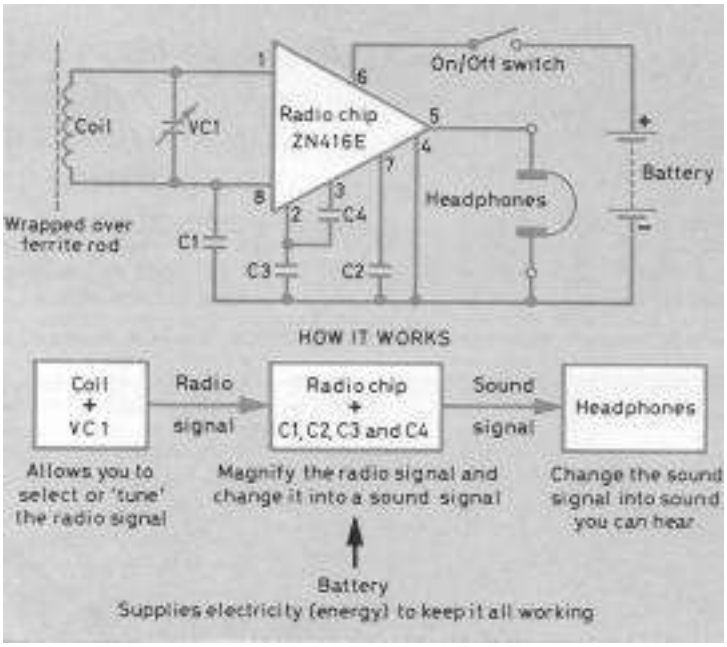

Figure 1 Circuit and block diagrams of the radio

Description

The whole circuit is built on a 50 mm by 50 mm printed circuit board (PCB) designed to fit on the inside of the lid of a plastic box, and is stuck there using sticky pads, the shaft of the variable capacitor going through a hole in

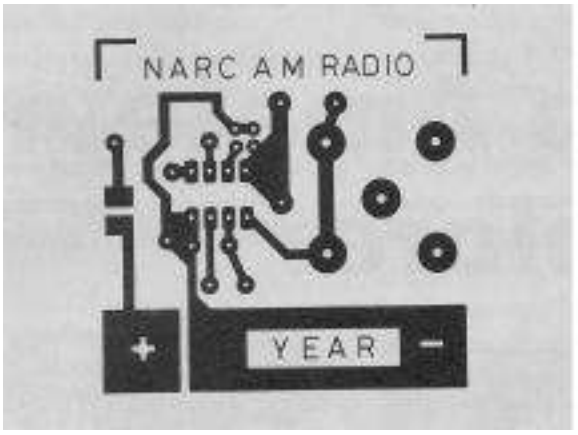

Figure 2a The PCB, solder side

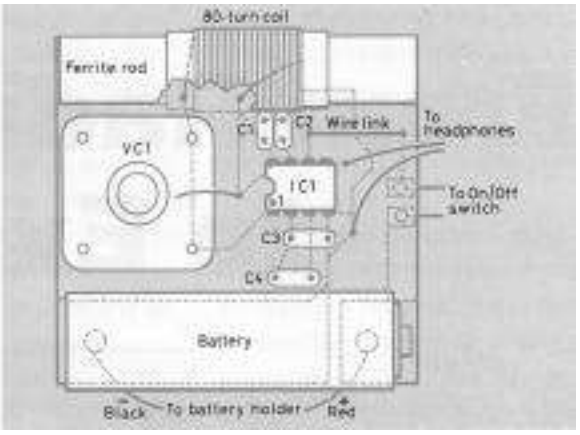

Figure 2b The PCB, component side

the lid. Only two pairs of leads are soldered to the board – one pair goes to the 1.5 V battery in its holder, and the other to the earphone socket. **Figures 2a** and **2b** show the printed circuit and the component layout double size for clarity. You are not obliged to build the circuit on a PCB.

Building it

1. **Check and identify components.** Tick the parts list.
2. **Carefully unwind the wire.** Use paper to make an insulating tube (called a 'former') around the centre of the ferrite rod and secure it with Sellotape. Now, close-wind *all* the wire (leave no gaps between adjacent turns) around the paper former. Secure the winding with more Sellotape, leaving 50 mm of wire free at each end for connection to the circuit. See **Figure 3a**.
3. **Solder in VC1.**
4. **Solder in the integrated circuit holder.** There is a notch in one end of the holder; this should face VC1. Solder also the wire link and the capacitors. Be careful to avoid solder 'bridges' between adjacent tracks on the PCB.
5. **Solder the battery leads.** These must be connected properly – the red battery lead to the + (positive) area and the black lead to the – (negative) area.
6. **Strip bare 1 cm of insulation from the ends of two wires.** Solder them between the PCB and the headphone socket (see **Figure 3b**). Use the end tabs on the socket. Using another pair of insulated wires connect the ON/OFF switch to the PCB tabs shown in Figure 2b.

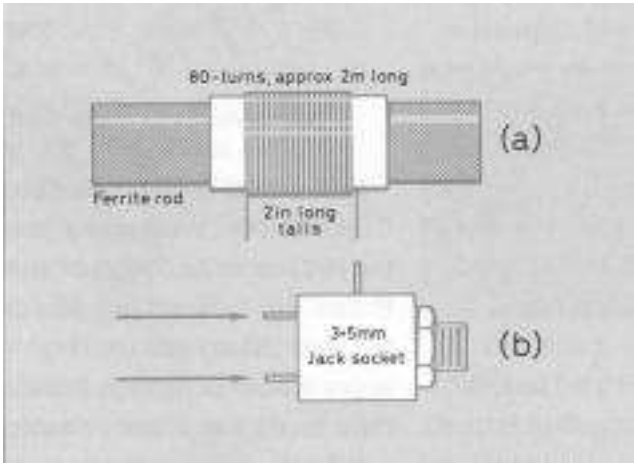

Figure 3 Details of coil and headphone socket

7. **Fix the elastic band**. This goes through the holes at the top of the PCB, with the ferrite rod being slipped through the two end loops. (Note: although the coating on the copper wire is designed to melt away during soldering, it is quite common for difficulty to be experienced in obtaining a good soldered joint; to be on the safe side, remove the coating *before* soldering (with a small piece of sandpaper).) Carefully place the wire ends of the coil through the PCB just above VC1, and solder on the track side.
8. **Fit IC1 into its holder**. This should be done carefully, making sure that *all* the pins are located above their respective clips *before* applying any pressure! Make sure also that the notch on the IC (as shown in Figure 2b) matches the notch in the holder, and faces VC1.
9. **Put battery in its holder**. Listen for some noise in the headphones as VC1 is rotated. Make sure the headphone plug is fully inserted into its socket.
10. **Fix the working board to the lid**. Use the sticky pads and apply *gentle* pressure. Fit the tuning knob, the ON/OFF switch and the earphone socket.
11. **Test again**. If all is still working, fit the lid screws and admire your completed radio!

Parts list

Capacitors

C1, C2	0.01 microfarad (μF)
C3, C4	0.1 microfarad (μF)
VC1	500 picofarads (pF)

Semiconductor

IC1	ZN416E

Additional items

- Plastic box (recommended size 76 × 64 × 50 mm internal)
- 8-pin DIL socket for IC1
- Printed circuit board
- Tuning knob for VC1
- Wire link for PCB
- 2 m of 30 SWG copper wire, self-fluxing
- Piece of paper 25 × 50 mm, to make the coil former
- Ferrite rod 70 mm long by 10 mm diameter, approximately
- Battery, AA size 1.5 V, with holder and attached wires
- Miniature earphone socket (3.5 mm stereo jack)
- ON/OFF switch (push-button SPST latched or slide switch)
- 4 off 100 mm insulated connecting wires, for jack socket and ON/OFF switch
- Pair Walkman-type earphones
- Elastic band, to attach ferrite rod to PCB
- 4 off sticky pads for securing PCB to box lid

Kits

Ready-made PCBs may be available from Alan J. Wright, G0KRU, Hewett School, Cecil Road, Norwich NR1 2PL.

4 A simple electronic organ

Introduction

This project has nothing to do with radio but, let's admit it, *any* electronics project is good experience! Why not build this little organ – it will keep the children amused at least! It uses the popular NE555 integrated circuit, which contains a circuit which will periodically switch the voltage on the output pin between the supply voltage and zero. Just how frequently this switching occurs depends upon the components external to the integrated circuit. If this switching occurs several hundred or thousand times a second, the change in voltage produced will generate a musical note when connected to a small loudspeaker. The circuit is shown in **Figure 1**.

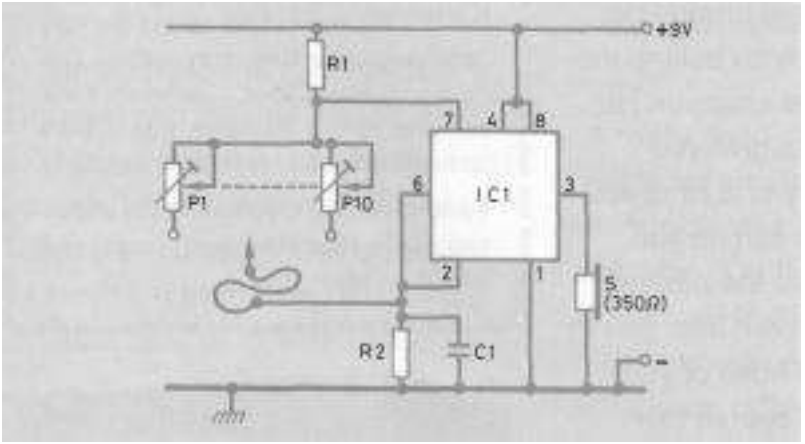

Figure 1 Circuit diagram

Putting it together

(a) Using a PCB. The job is very simple. The placement of components on the unsoldered side of the board is shown in **Figure 2** and the design on the copper track is illustrated in **Figure 3**. Put each component, in turn, on the board, making sure that it lies flat on the board with its tags or wires going cleanly through the holes provided for it; then, solder the wires to the board, cropping them before or after the soldering,

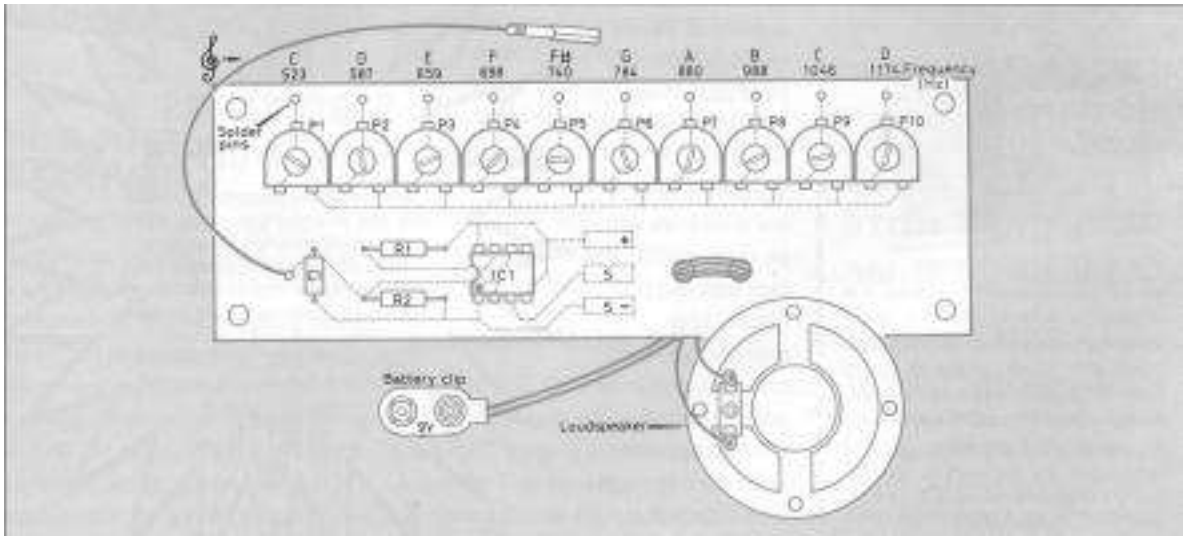

Figure 2 Position of components on the printed circuit board (PCB)

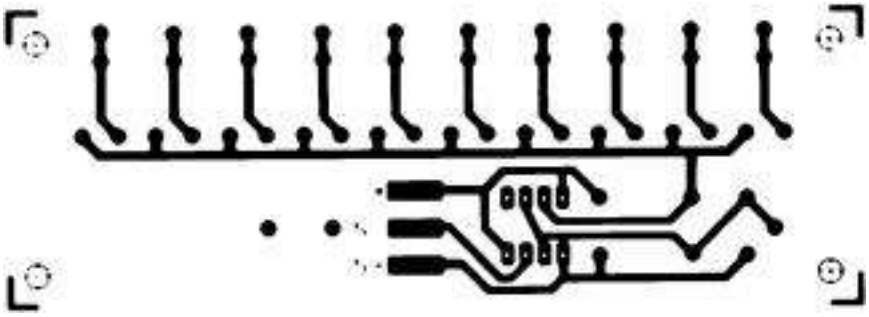

Figure 3 The connections

depending on your preference. If you choose to use a holder for your integrated circuit (highly recommended if your soldering is less than perfect), make sure that the end with a notch in it faces R1 and R2, as shown in Figure 2. Solder the two leads to the speaker to the tabs marked S (either way round), having looped them through the two holes to the right of the tabs in Figure 2. Looping them through the holes acts as a strain relief, ensuring that the soldered joints are not subjected to pulling and bending as you move the wires about. Do the same with the battery leads, the red lead going to the + tab and the negative lead to the – tab (which also has one speaker lead already attached to it). **Figure 4** shows this in detail. Treat the loudspeaker with care – the cone is quite fragile and must not be touched.

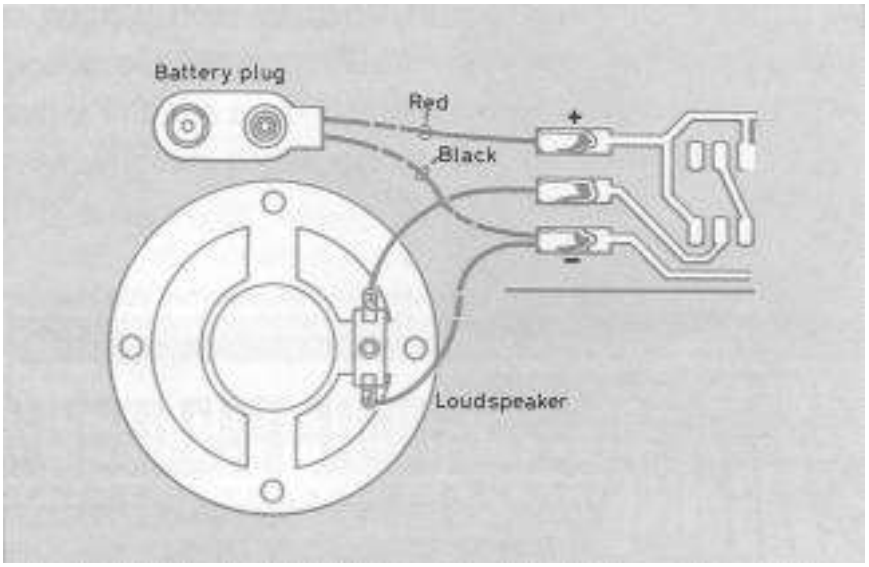

Figure 4 Battery plug and loudspeaker connections

(b) Without a PCB. This is more difficult, and you may need to enlist some help. Using some matrix board (such as Veroboard) is probably the best way of replacing the PCB. You could arrange your circuit in exactly the same way as in the PCB in Figure 3, using wires to replace the copper track.

A simple 'keyboard'

The keyboard is a row of solder pins along the rear edge of the PCB, one for each note covering the range shown in Figure 2. A flying lead with a small spade on it is provided to touch any of the pins in turn, producing any one of ten different notes.

Testing

Check first that each component is in the correct place. When inserting the NE555 chip, first make sure that the end carrying the notch lies over the end of the holder with the notch; then, make sure each pin of the chip lies directly above the hole into which it fits, before pressing *gently* to insert the chip into the socket. Make sure the battery connections are correct, and insert the battery into the clip. Nothing should happen, except for a click from the loudspeaker; touching the spade on any of the pins should produce a coarse note from the speaker. If nothing happens, check everything again; don't *assume* that wires go where you think they go!

After you get the first note, all the others should work, too, but they will sound off-tune at first. The organ needs tuning up by adjusting the 10 preset variable resistors P1 to P10. The approximate frequency to which each note should be tuned is given in Figure 2; if you can beg, borrow or steal a frequency counter, setting up is easy. If you have a piano, the organ can be tuned by comparison of the notes with those on the piano. The frequencies are given in Hertz (abbreviation Hz), and represent the number of times the IC switches on and off every second. If the sound coming from the loudspeaker is too loud or very distorted, then try putting an 330 Ω resistor (colour code orange, orange, brown) in series with the loudspeaker. This is done by taking the resistor and cutting its leads to about 5 mm; then, disconnect one speaker lead from the tab on the PCB (it doesn't matter which). Solder one end of the resistor to the vacated speaker tab, and the free speaker lead to the other end of the resistor. This will limit the volume of sound from the speaker, and lengthen the life of your battery. If it is still too loud, try a resistor of a larger value, or use a smaller resistor to make it louder.

Parts list

Resistors: all 0.25 watt, 5% tolerance

R1	2.7 kilohms (kΩ)
R2	1 Megohm (MΩ)
P1–P5	Preset resistor 100 kilohms (kΩ)
P6, P7	Preset resistor 50 kilohms (kΩ)
P8	Preset resistor 25 kilohms (kΩ)
P9, P10	Preset resistor 10 kilohms (kΩ)

Capacitor

C1	100 nanofarads (nF) or 0.1 microfarad (μF)

Integrated circuit

IC1	NE555 timer chip

Additional items

S	Loudspeaker >60 ohms (Maplin)
	1 off battery clip (for PP3 battery)
	1 off spade terminal
	12 off solder pins 'Veropins'
	3 off 10 cm lengths of 'hook-up' wire

(This article is based on projects originally designed by Radio Scouting, Netherlands.)

5 Experiments with the NE555 timer

Introduction

Several of the projects in this book use the NE555 timer, an integrated circuit which is at the heart of many circuits whose processes are determined by time intervals. **Figure 1** shows the circuit diagram of an audio oscillator using the 555. The timing voltages (governing the frequency of oscillation) are produced by R1, R2 and C2; a voltage appears at pin 3 which 'switches' at this frequency between zero and a voltage close to the supply voltage, which in this case can be anywhere between 6 V and 14 V. The output current, when applied through R3 to a small loudspeaker, produces an audible tone, provided that there is a DC path between the two test leads.

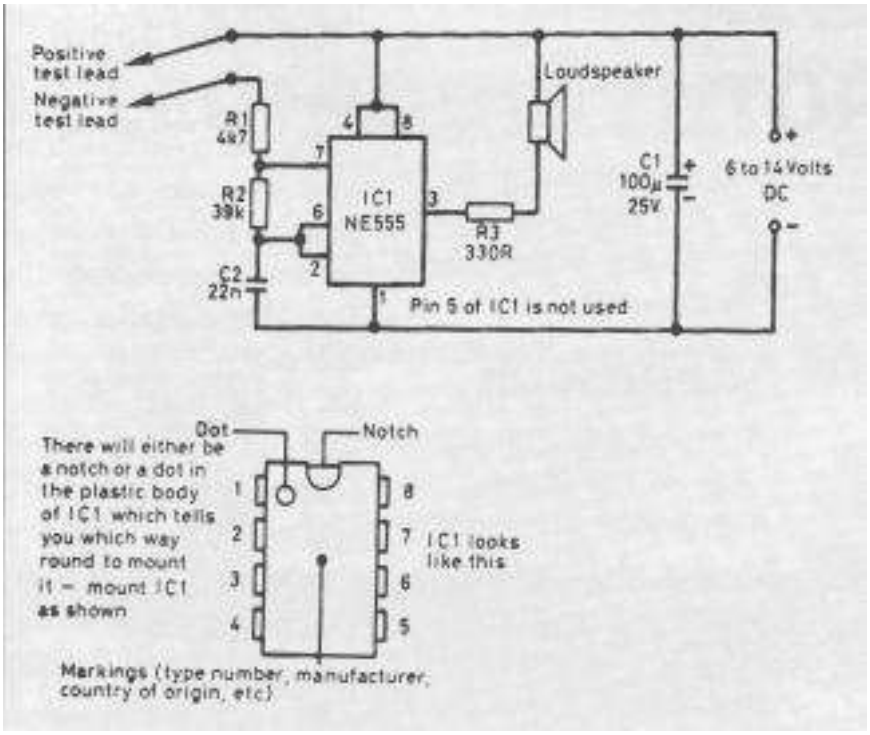

Figure 1 The circuit diagram

Construction

The simplest way to mount the components is on a piece of matrix board (Veroboard), available from any of the good suppliers. The prototype of this circuit used the type of board with copper strips along the underside; these strips are used like the copper tracks on a PCB, to join components together. Firstly, cut the four strips between the positions of the pins of the IC socket, as shown in **Figure 2**. You can buy a tool for this purpose, but a small twist drill (about 3 mm diameter) is just as good. Turn it between your fingers – if you use a drill you will end up with holes right through the board! Then solder in the IC socket (with the notch in the position shown), followed by the four links made with single-conductor insulated wire. Put in each component as shown, ensuring that C1 (an *electrolytic* or *polarised* capacitor) is connected correctly. When all the components have been soldered in, take the *555* chip and lay it on its socket, with its own notch lying above that of the holder. Then, making sure that each pin lies *directly* above its corresponding socket, press down *gently* on the chip, with the board supported on a flat surface.

Testing

Connect the circuit to a battery or small power supply, ensuring that the positive and negative leads are the right way round. Always use red and black leads here, then you are less likely to get it wrong! Switch on. Nothing

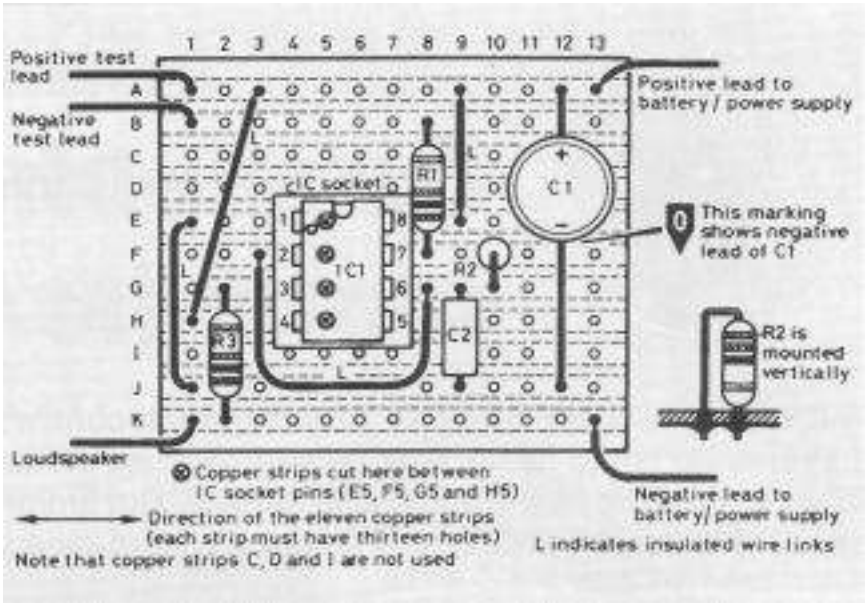

Figure 2 Veroboard layout. If you can read a circuit diagram, the project can be built using other methods

should happen until you short together the two test leads, when there should be a note from the loudspeaker. If this doesn't happen, switch off, disconnect the circuit and check your wiring and soldering. Is it exactly like Figure 2? Are the soldered joints round and shiny? If any are dull, then 'sweat' them briefly with a hot soldering iron until the solder runs, remove the iron, and check that they are as shiny as the rest. Check that there are no solder 'bridges' between adjacent tracks by holding your board up to a strong light. Then, reconnect, switch on and touch the test leads together. All should now work!

Uses of your circuit

1. As a Morse practice oscillator. Simply connect the two test leads to your key and, each time the key is pressed, you should hear a note from the speaker. The frequency of the note may be altered by putting a resistor in series with the key. To do this, remove one test lead from the key and select a resistor; connect one end of the resistor to the free test lead and the other to the empty terminal on your key. Selecting the value of resistor that you need will be a useful experiment in itself.
2. As a continuity tester. You can check fuses and lamp bulbs by connecting them across your test leads. If the speaker remains silent, the fuse or bulb has blown.
3. To indicate changes of resistance. Hold the ends of the test leads in each hand; you should hear a low note, because of the high resistance of your body. Squeeze the ends harder, and the frequency of the note should rise, because you are now making better contact. Repeat this with damp hands and the frequencies will be higher still.
4. As a thermometer. Connect the test leads to a thermistor (a device whose resistance changes with temperature) and warm it with a hair-dryer, or even in your hands, and you will hear the pitch changing with the temperature of the thermistor. A suitable 'bead' thermistor is available from Maplin (order code FX21).
5. As a diode tester. Use any diode, and connect the negative test lead to the end of the diode marked with the ring. This is the cathode of the diode. The other end, the anode, should be connected to the positive test lead, and a note should be heard from the speaker. This does not necessarily mean that the diode is working – yet. Reverse the connections and *nothing* should be heard. If this is the case, the diode *is* working.
6. As a light meter. Use a photoconductive cell (a device whose resistance changes with light intensity) connected between the test leads. A note should be heard. Shading the device with your hand will increase its resistance and the note should decrease in frequency. A suitable device is the ORP12 cell from Maplin (order code HB10).

There are many more applications. **Do not connect the test leads to other circuits that are switched on**. Your circuit, or the circuit you are connecting

it to could be damaged. Think of a *passive* device or circuit (i.e. one *not* requiring a power supply or battery) where changes of resistance occur, and you have found another application!

Parts list

Resistors: all 0.25 watt carbon film types

R1	4.7 kilohms (kΩ) – yellow, violet, red
R2	39 kilohms (kΩ) – orange, white, orange
R3	330 ohms (Ω) – orange, orange, brown

Capacitors

C1	100 microfarads (μF) 25 V radial electrolytic
C2	22 nanofarads (nF) or 0.022 microfarad (μF) polyester type with 10 mm lead spacing

Integrated circuit

IC1	NE555

Additional items

- Miniature loudspeaker (preferably 35, 40 or 80 ohm)
- 8-pin DIL socket for IC1
- 0.1 inch Veroboard ('stripboard'), size 11 strips by 13 holes
- PVC-covered stranded wire for test leads, loudspeaker and battery connections
- PVC-covered solid wire for links on the board
- A power source of between 6 V and 14 V, such as a 9 V battery (PP3)

Component sources

Cirkit
Tandy – many high street shops

6 A simple metronome

Introduction

A metronome is a device used by musicians to indicate the tempo of a piece of music. Until electronics came on the scene, this 'beating of time' was achieved in much the same way as a clock keeps time, i.e. with a pendulum device, the clicking of the escapement indicating the beats of the music.

Those of you who have already built the Morse Key and Buzzer from the designs in this book, will recognise the circuit of this metronome – it is exactly the same as was used to produce the note of the buzzer. This circuit is shown in **Figure 1**.

The circuit

Three components determine the speed at which the circuit oscillates – the speaker (LS), the resistors (VR1 + R1) and the capacitor (C1). VR1 is a variable resistor, so that the speed at which the oscillator operates can be varied. Compared with the component values of the Morse Buzzer (which operated at around 800 Hz), these components now give an oscillation frequency of around 1.25 Hz, which is far too low to be heard as a note. What we *do* hear, however, is a series of clicks, as the voltage across the speaker changes quickly from 0 to 9 V and back again.

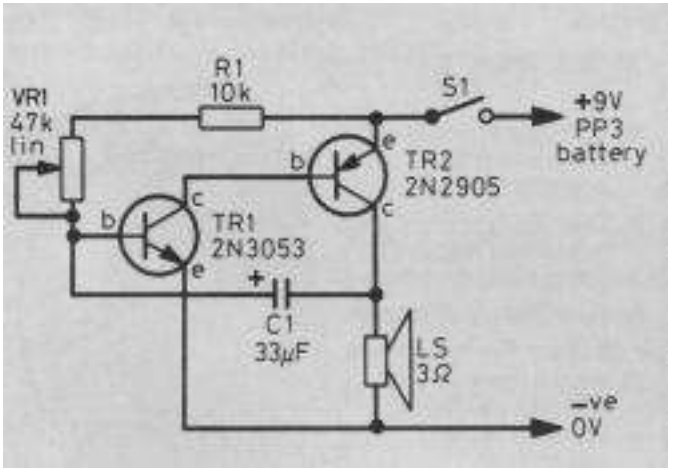

Figure 1 The metronome circuit is rather like the Morse oscillator

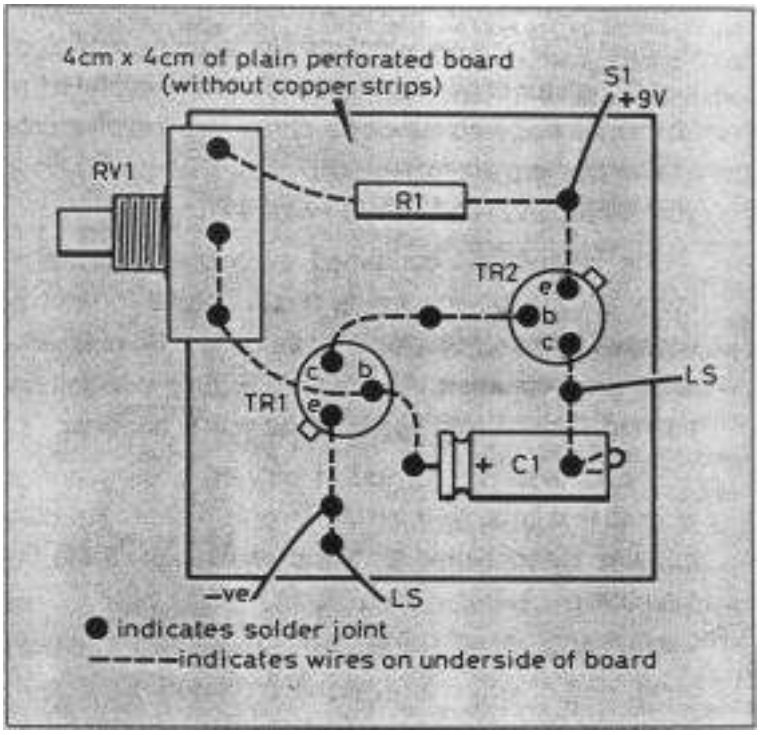

Figure 2 The component wires are pushed through holes in the circuit board and joined together underneath

Variation of speed could be achieved by varying resistance or capacitance. However, as you may already know, variable capacitors have values in the picofarad range, not the tens of microfarads used here, so it is very simple to employ a variable resistor (potentiometer) to control the oscillator. You could use a multi-way switch to switch in one of several capacitors, as well as having the variable resistor, but this was found to be an unnecessary complication. This design operates between about 100 clicks per minute and 200 clicks per minute.

Making the prototype

A single piece of plain matrix board (no copper strips) measuring about 40 × 40 mm is sufficient to hold all the components except the potentiometer and switch (see later). The case can be plastic or aluminium, and one measuring 65 × 100 × 50 mm is about right. Make sure there are holes in the case beside the speaker cone to let the sound out, and larger holes for the potentiometer and switch. If a potentiometer is used with a combined ON/OFF switch, then the extra hole for the switch is not necessary! It is advisable to construct the circuit *before* putting it in the

box, so that it can be tested to ensure that everything is working. If it is, then you can exercise your ingenuity in mounting the speaker, battery and board inside the box. A final test can be made before starting the calibration process.

Calibration

There is no 'easy' way to do this. The frequencies involved are too low to be measured with the average frequency counter, so you will need to resort to using a stopwatch and counting the number of clicks per minute.

Parts list

Resistors: 0.25 watt, 5% tolerance

R1	10 kilohms (kΩ)	
VR1	47 kilohms (kΩ) linear potentiometer	

Capacitor

C1	33 microfarads (μF) electrolytic	

Transistors

TR1	2N3053	npn
TR2	2N2905	pnp

Additional items

S1	SPST	ON/OFF switch
LS	3 ohms (Ω)	loudspeaker
	Knob with pointer for VR1	
	PP3 battery and connector	
	Aluminium case, 65 × 100 × 50 mm	
	Matrix board (plain), 40 × 40 mm	

7 What is a resistor?

Introduction

Materials that carry electricity easily are called **conductors**. They include all metals and salt water, for example. We use wire as a conductor, and the ease with which it passes an electric current depends upon the material, its thickness and its length. Silver (symbol Ag), gold (Au), copper (Cu) and aluminium (Al) are the best metallic conductors. Most wires are made of copper, although the best conductor, weight for weight, is aluminium.

Materials that *don't* carry current (or, at least, do so very badly) are called **insulators**, and they include dry wood, rubber, plastic and glass among their number. Wires are often coated with a layer of insulator to prevent adjacent wires touching and causing an accident.

Resistors

If there wasn't such a thing as resistance, the subject of electronics wouldn't exist; only infinite currents would flow and voltages wouldn't exist either! We need to reduce the flow of current if we are to make current do something useful for us. Components that resist the flow of current are called **resistors**, and they are said to have a **resistance** which is measured in ohms (Ω), named after Georg Ohm, who formulated the law (also named after him) by which the voltage and current through a conductor are related. His law gave rise to the formula *everyone* remembers:

$$I = \frac{V}{R},$$

where I is the current flowing, measured in amps,
V is the voltage across the conductor, and
R is the resistance of the conductor, measured in ohms.

From this equation, you can see that, for a constant value of voltage, V, if the resistance goes up, the current will go down, and vice versa. The circuit symbols for resistors are shown in **Figure 1**. You will find the upper symbol in older magazines; it is still preferred by many engineers. The lower symbol is the prevalent standard symbol.

Resistors are made in several ways, the cheapest using carbon; another type is usually made from a ceramic cylinder (used only as a support) on which

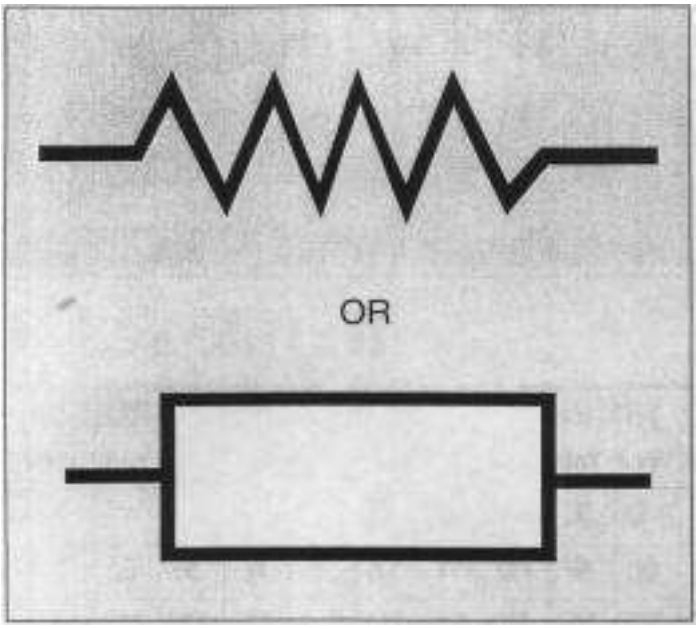

Figure 1 Circuit symbols for resistors

is placed a very thin film of metal – the thinner the film, the greater the resistance. All resistors are coated with a thin film of insulation, for the same reason we discussed earlier.

The colour code

Each resistor has coloured bands on it which enable us to see what value of resistance it has. There are normally three (but sometimes four) at one end, and a single one at the other (see **Figure 2**). The colours indicate figures, according to the list below.

Colour	*Value*	*Colour*	*Value*
Black	0	Green	5
Brown	1	Blue	6
Red	2	Violet	7
Orange	3	Grey	8
Yellow	4	White	9

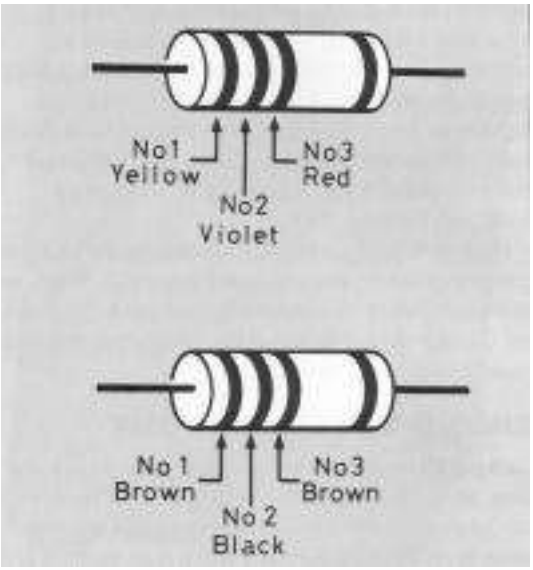

Figure 2 Some examples of resistor colour codes; top 4700 Ω (4.7 kΩ) and bottom 100 Ω

Using the colour codes is easy, once you see the logic behind it. Hold the resistor so that the single band is towards the right. The three colours on the left are read in the normal order from left to right. The first two bands *always* indicate numbers; the third band gives the number of zeros to add to the right of these two numbers. So, looking at the top resistor in Figure 2, yellow, violet, red means 4, 7, and two zeros, giving 4700 ohms! Looking at the lower resistor, brown, black, brown means 1, 0, and one zero, giving 100 ohms.

Remembering the order of the colours may be difficult at first. The colours from red to violet are the colours of the rainbow, in order, so if you know those, you're almost there! Around those colours are black and brown below the red, and grey and white above the violet, which you can imagine as getting brighter from black to white (well, almost!). It won't be long before you don't need to remember them at all.

The isolated band on the right-hand side is not part of the resistor's value; it indicates its *tolerance*, i.e. how close it might be to the indicated value. A brown band indicates ±1%, a red band ±2%, a gold band ±5% and a silver band ±10%. For example, a resistor marked as being 100 ohms with a ±5% tolerance will have an *actual* value somewhere between 95 ohms and 105 ohms.

8 Waves – Part 1

Introduction

Waves are responsible for most of the processes in life where energy is transferred from one place to another. Heat and light energy from the sun, for example, come to us as *electromagnetic waves*. Sound travels through the air as a wave; it is not the same sort of wave as light or heat, but it obeys many of the same properties. Damage is caused to coastal margins by the waves of the sea – again, another type of wave, but still obeying many of the same properties. Radio waves are of the same type as heat and light waves, as are gamma rays, X-rays, ultra-violet waves and infra-red waves. So, once we begin to understand what radio waves do, we are also learning about a huge chunk of physics at the same time! All these waves are part of the *electromagnetic spectrum*. The word 'spectrum' simply means a 'range', so what we have is a range of electromagnetic waves – that's all!

Sensing things

Light waves are invisible, but our eyes can detect the *effect* they have on different materials because the waves produce an effect on the retina of the human eye which the brain can interpret. We cannot see heat waves either, but we can feel the *effect* they have on our skin. Gamma rays and X-rays are also invisible, but their detrimental *effects* on human tissue are well known. It is not surprising, then, that we cannot see radio waves. We cannot sense them, either, until we produce a device upon which they have an *effect*. That device is a **radio receiver**; it is able to process certain characteristics of radio waves, and make these characteristics audible by generating sound waves from the loudspeaker or headphones. Other characteristics of the same waves may be turned into light as a TV picture on a cathode-ray tube, or as a fax image on a sheet of paper.

Visible waves

Let's start our description with some waves that we can actually see! When a small stone is thrown into a pond, we see circular water waves *radiating* from the point where the stone fell into the water, as **Figure 1** shows. (Notice that we use the word *radiating*, even with water waves; it is not a radio term, but one which describes any motion where the *radius* of a circle is increasing. In this case, it is the radius of the circular waves which is

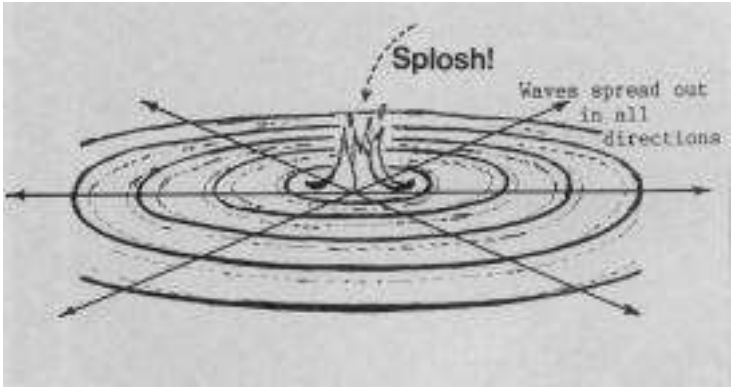

Figure 1 The waves move out from the point where the stone landed

increasing.) If you were to watch the water waves down at the water level, perpendicular to the direction in which they are travelling, you would see something like the illustration in **Figure 2**.

The horizontal line represents the water level before the wave started, and the vertical line represents the direction in which the water is displaced at any instant.

All waves are described in the same way

'Freezing' the motion of the water in this way allows us to define two very important characteristics of a wave, characteristics which we talk about every day – *wavelength* and *amplitude*. The wavelength of a wave is simply the distance (measured in metres) from any point on one wave to the same point on the adjacent wave. Look at the diagram and you will see what is meant by 'the same point on the adjacent wave'. The amplitude of a wave

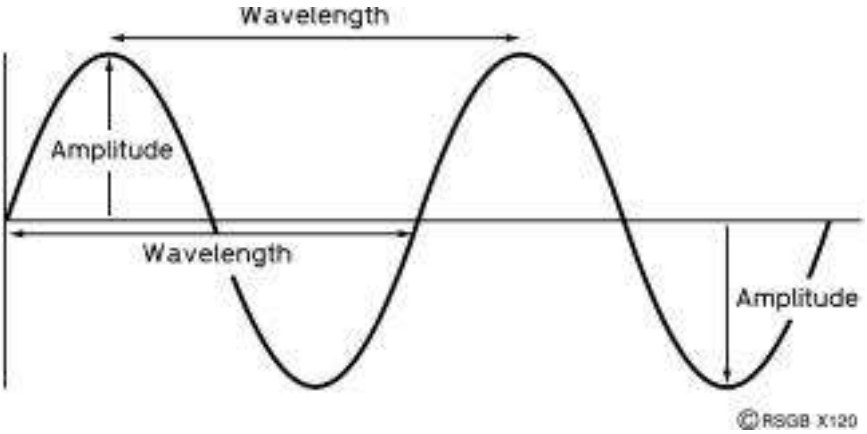

Figure 2 A water wave, viewed in cross-section

is always measured from the centre (undisturbed) position of a wave to the peak (or the trough) of the wave. Both these positions are shown, the arrow indicating that the measurement is taken *from* the centre *to* the peak or trough. The amplitude of a wave is defined as the maximum displacement of the wave from the centre position – the direction (up or down) of that displacement does not matter. Waves of greater amplitude carry more energy with them.

If we now 'unfreeze' the wave, we will see it travel from left to right (or right to left, depending on where we are looking). The speed at which it moves is called its *velocity*, and is measured in metres per second.

Another useful word is *propagate*; it means *travel*. We talk about radio waves propagating from a transmitter to a receiver. This velocity of propagation (for electromagnetic waves) is very fast indeed – they will cover 300 million metres in one second. This is virtually incomprehensible, so think of a radio wave travelling around the earth – it can travel 7½ times round the earth in one second! We use the symbol c for the velocity of radio waves (which is the same as the velocity of light, of course – all electromagnetic waves travel at this speed through air and space).

The last thing we need to know about the wave is its *frequency*. Imagine a cork floating on the water in the path of the wave; it will bob up and down. If we were able to count the number of times it went through its highest position in one second, then that number would be its frequency. Any periodic motion like this is said to go through one *cycle* each time one complete wave passes a point (in this case, our cork). We are thus counting the number of cycles per second of the cork's motion. The unit of frequency is thus 'cycles per second'; this unit is now named after Hertz, a radio pioneer, and is abbreviated to Hz.

Our description of the wave is now quite simple – we need only four quantities:

(a) **Frequency** symbol f – unit, hertz (Hz)
(b) **Wavelength** symbol λ (Greek letter lambda, pronounced 'lamb-da') – unit, metre (m)
(c) **Amplitude** symbol a – unit depends on application
(d) **Velocity** symbol c – unit, metres per second (m/s or ms^{-1})

The basic formula

Whatever may happen to a wave while it travels through different media (vacuum, air, brick, wood, etc.), one thing and **only** one thing remains constant – its frequency. Its wavelength, amplitude *and* velocity may change, but its frequency never does. Three of the four characteristics already identified are connected by the simple relationship

$$c = f \times \lambda.$$

Remember that *c* is constant if the wave travels in air or in a vacuum. This means that waves having higher frequencies (*f* large) must have smaller wavelengths (λ small) and vice versa. You can imagine frequency and wavelengths being on opposite ends of a see-saw!

Divisions of units

Because the frequencies of radio waves are so high (despite them having the lowest frequencies in the electromagnetic spectrum!) we have a problem with writing them down. Do you write in your log book that you have just heard a station on 14 100 000 Hz? Of course not, you write it as 14.1 MHz, knowing that the prefix mega (M) means 'one million'. The prefixes which you need to know (when applied to frequency) are:

kHz	kilohertz	meaning	1000 Hz
MHz	megahertz	meaning	1 000 000 Hz
GHz	gigahertz	meaning	1 000 000 000 Hz.

Notice that the 'k' in kilohertz is a lower case letter. It is **incorrect** to write it as an upper case letter. 'K' is a computer-related prefix meaning **not** 1 000 but 1 024!

When we come on to discuss heat and light waves, we will use wavelengths rather than frequencies, because of the see-saw effect – as the frequencies get larger and larger, the wavelengths get smaller, and hence are numbers which are more manageable, both to talk about and to write down!

Bands

Gamma rays, X-rays, ultra-violet waves, light waves, infra-red waves are all part of the electromagnetic spectrum, but we divide them up because they have different properties. This is why we divide up our radio frequencies into different bands. The radio waves of top-band signals (around 2 MHz) have completely different properties compared with those in the 20 metre band, so we are dividing up the *radio spectrum* in the same way – by property.

9 A beat-frequency oscillator

Introduction

Many readers will know that, although they have a short-wave radio which covers at least one of the amateur bands (e.g. 7 MHz or 14 MHz), they are unable to listen to SSB or Morse signals. This is because the receiver lacks a Beat-Frequency Oscillator (BFO). We need the 'carrier' frequency of a BFO to replace the carrier that has been removed from the signal at the transmitter. When listening to Morse signals, the BFO signal 'beats' with the incoming signal to produce a note in the loudspeaker. If you are a musician, you will be familiar with the method of using 'beats' to tune one musical instrument from another; in the BFO, the beat frequency produced is the tone signal you hear.

In the more complex amateur radio receiver, a BFO is incorporated as part of the whole system. In our model, it is an external circuit that sits alongside your radio. The circuit diagram is shown in **Figure 1**.

Construction

Built on a small piece of matrix board about 80 × 50 mm, the circuit can be fitted inside a small plastic box. For once, we *don't* want to screen the circuit to prevent it interfering with other equipment; we *want* it to interact

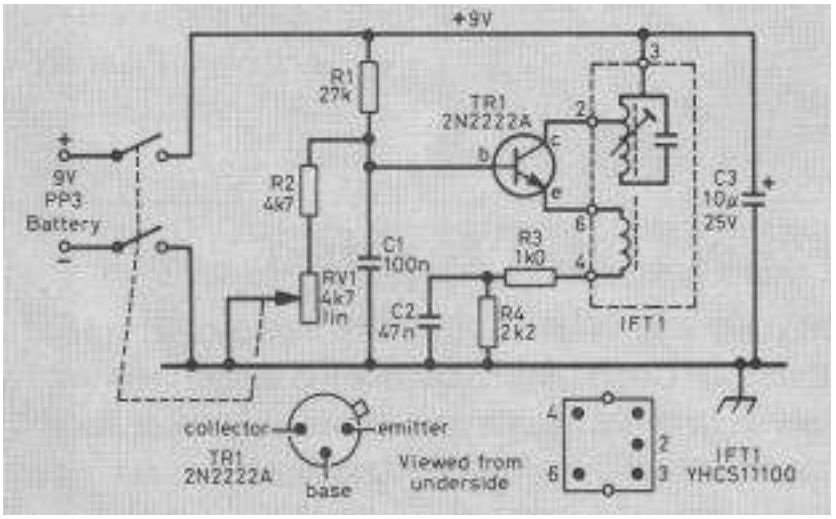

Figure 1 Circuit diagram of the BFO

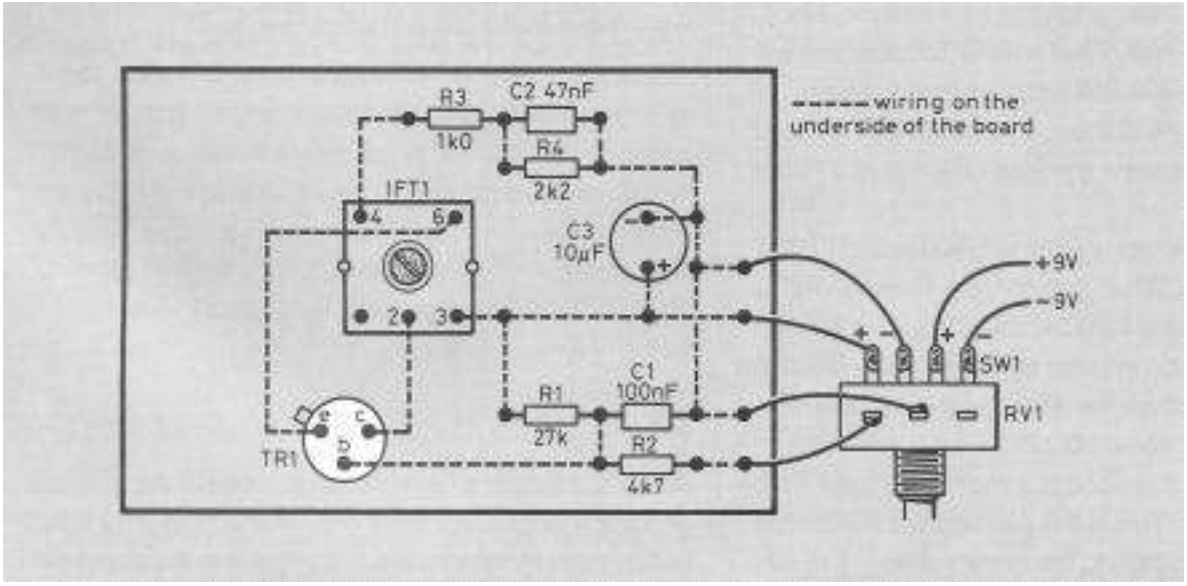

Figure 2 Matrix board layout shown from the component side. Adjust IFT1 carefully for the best results

with our receiver! This is why we use a plastic box. Maplin Electronic Components supply a suitable box, complete with the matrix board to fit inside (order code YU46).

Look at **Figure 2** carefully before you start to build the circuit, so that you can position the components correctly. Firstly, inspect the intermediate frequency (IF) transformer, IFT1, and remove its metal screening can very carefully. Again, this is to allow some signal to escape from our circuit and enter our radio. Having done this, solder the components, using the matrix board as a support. Underneath the board, the components are linked by single-conductor, insulated wire. Take particular care with the polarity of the electrolytic capacitor, C3, and the connections to the transistor, TR1 (see Figure 1).

The variable resistor, VR1, has a switch mounted behind the control itself, and the insulated leads to it from the battery should be about 10 cm long. Connect these before fitting VR1 into the case, so that the BFO can be calibrated (adjusted) correctly.

Calibration

After a final check that all the components have been fitted and soldered correctly, connect the battery, switch on, and hold the transistor between your fingers, to check that it is not getting hot. Place the circuit close to your

receiver, and set RV1 to mid-position. Tune your receiver to find an amateur SSB transmission; the frequencies listed below will help you in knowing where to look. It may sound very strange, but don't worry. *Slowly* turn the core of IFT1 with a small, non-metallic screwdriver or with the correct 'trimming tool'. The core into which the blade fits is very fragile, so attempt this process with care. When the speech sounds as natural as you can get it, leave the core at this position, and use RV1 to make the speech sound natural.

Using the BFO

For best results, you may have to move the BFO nearer or further away from your radio. At the lower end of most bands (for instance just above 7.000 MHz or 14.000 MHz) you should be able to resolve Morse code (CW) signals. If you find that the BFO signal is a little weak, solder a 15 cm length of insulated wire to pin 2 of IFT1, and place it alongside your radio. This should improve signal intelligibility. When you are happy with the performance, switch off, drill a 10.5 mm hole in the box and fit RV1, followed by the matrix board assembly. Screw the base to the box, fit the knob, and the BFO is complete!

Where to listen

Band	**Frequencies (MHz)**
15 m	21.000–21.450
17 m	18.068–18.168
20 m	14.000–14.350
30 m	10.100–10.150
40 m	7.000–7.100
80 m	3.500–3.800

Parts list

Resistors: all 0.25 watt, 5% tolerance

R1	27 kilohms (kΩ)
R2	4.7 kilohms (kΩ)
R3	1 kilohm (kΩ)
R4	2.2 kilohms (kΩ)
VR1	4.7 kilohms (kΩ), linear, with DPST switch

Capacitors

C1	100 nanofarads (nF) or 0.1 microfarad (μF), ceramic
C2	47 nanofarads (nF) or 0.047 microfarad (μF), ceramic
C3	10 microfarads (μF), 25 V radial, electrolytic

Additional items	
TR1	2N2222A npn
IFT1	Toko type YHCS11100
Box	plastic, approximate size 100 × 70 × 45 mm
Board	matrix, to fit inside the box
Connector	for PP3 battery
Knob	for RV1

10 What is a capacitor?

Introduction

A capacitor is a device that stores energy in the form of electricity. Much less energy than a battery, and for a shorter time, however. The simplest form of capacitor takes the form of two flat metal sheets separated by air; connections are made to each plate, as **Figure 1** shows. If you imagine a pair of these plates, 30 cm square and separated from each other in air by 1 mm, the capacitance of this device would be almost exactly 80 picofarads (pF), i.e. 80 million-millionths of the unit of capacitance, the farad. Now this is quite a small value, you will agree, and it comes about because the farad is such a large unit. Nevertheless, as you will probably know, we may have capacitors of value 10 000 microfarads (μF) in our radio equipment, and they can be smaller than your little finger, so they are obviously not made the same way!

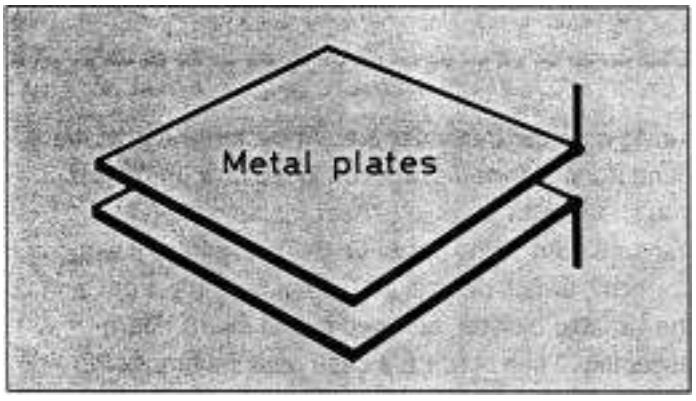

Figure 1

Large and small

We cannot go into the manufacture of capacitors here – after all, we are users of the devices, not the designers! First of all, beware of incorrect statements; the words 'capacitor' and 'capacitance' are *not* the same. For example, a large capacitor would be a description of one the size of a toilet roll. It need not have as large a capacitance as one the size of your little finger. A 'large capacitor' is one which is physically *big*, a 'large capacitance' refers to a capacitor which can store a larger amount of energy when a certain voltage is applied between its plates. The capacitors in a mains power supply are usually big **and** have large capacitances. High-power RF amplifiers may have large capacitors with small capacitances!

Electrolytics . . .

Electrolytic capacitors usually have capacitances of 1 μF or above. They differ from other capacitors in that they **must** be connected the right way round (i.e. they have positive and negative connections, just like a battery). They may explode if the connections are reversed!

. . . and the others

Other capacitors may be connected either way round, despite their names. We have *polystyrene*, *ceramic*, *silver-mica* and *tantalum*. Each has its own advantages and disadvantages, and the parts list for a project will always tell you which type is best.

Storing energy

If you were to connect a large capacitance across a 12 V power supply, nothing would appear to happen. Removing the capacitor from the supply and connecting it to a voltmeter would show that the capacitor has 12 V between its ends. This shows that, while the capacitor was connected to the supply, energy flowed from the supply into the capacitor. We say that the capacitor was *charged up* by the supply. If you are using an *analogue* voltmeter (i.e. one with a meter and pointer), you will notice that the indicated voltage slowly drops until, eventually, there is no voltage across the capacitor. This is because the capacitor has *discharged* its energy into the voltmeter. If you had used a smaller capacitance, the same would happen, except that the voltage would drop to zero more quickly – the capacitor stores a smaller amount of energy because its capacitance is smaller. Capacitors behave like other things in life – a small car can move more quickly than a large bus – a small piccolo emits a

higher note than a flute – the voltages in a circuit containing a small capacitance will change more quickly than those in a circuit with large capacitance.

Varying the capacitance

Some capacitors are capable of having their capacitance changed manually; these are called *variable capacitors*. They work like the basic capacitor of Figure 1. Imagine moving the top plate of the pair a little to one side; the capacitance is determined, not just by the size of the two plates, but by their *area of overlap*. As this decreases, so does the capacitance. Such devices are limited in their capacitance, about 500 pF being the maximum value.

AC and DC

Because the plates of a capacitor do not touch each other, a direct current (DC) cannot pass between them. However, an alternating voltage on one plate can induce an identical alternating voltage on the opposite plate, and thus a capacitor appears to pass an alternating signal, even though currents as such, do not pass between the plates. This property of passing AC and not DC is very important, and a capacitor used in this way is called a *DC blocking capacitor* or, simply, a *blocking capacitor.* A blocking capacitor can be used at the same time, to couple a signal from one circuit to the next; here it would be known as a *coupling capacitor. Decoupling capacitors* are to be found where the capacitor is employed to remove an AC signal while retaining a DC component.

Finally. . .

Unlike resistors, the manufacture of capacitors renders them susceptible to excess voltage, so if you find a capacitor labelled 10 μF 16 V, it means that operating it above 16 V may fatally damage the device (and the circuit around it). This voltage is called the *working voltage* of the capacitor; on some electrolytics, you may find it expressed as *volts working* (i.e. 8 μF 450 V WKG).

Many smaller capacitors have their properties marked on them in a colour code, like resistors. **Figure 2** shows these codes, and their meaning, and the table below summarises the values of the colours.

Table 1

Colour	*Value*	*Voltage (tantalum capacitor)*	*Voltage (polyester capacitor)*
Black	0	10	–
Brown	1	–	100
Red	2	–	250
Orange	3	–	–
Yellow	4	6.3	400
Green	5	16	–
Blue	6	20	–
Violet	7	–	–
Grey	8	25	–
White	9	3	–

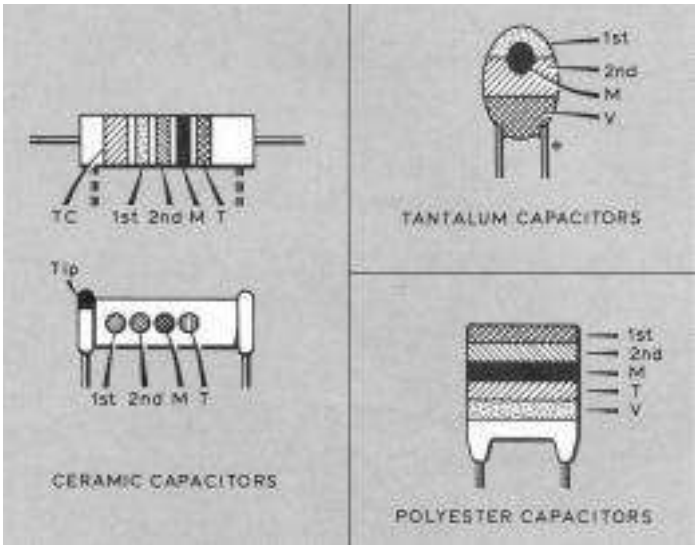

Figure 2 Some capacitors have coloured bands or stripes, rather like resistors. The colour code, which is the same as the resistor code, is shown in Table 1. The band shown on the chart as '1st' is the first number of the capacitor's value in pico-Farads, '2nd' is the second number and 'M' is the Multiplier or number of noughts. For example, a capacitor reads from the top: Brown, Black, Yellow, Black, Red. Its value is One, then Nought, then Four more noughts = 100 000 pF (also referred to as 0.1 μF or 100 nF). Its tolerance (Black) is 20% and the working voltage (Red) is 250 V. The 'V' means the maximum working voltage. The band marked 'T' shows the tolerance, just like resistors, and the one marked 'TC' is only used on special capacitors designed to change their value with temperature

11 Waves – Part 2

Introduction

We left Part 1 with the concept that radio waves are divided up into bands which have different properties. Not *all* the properties are different, though. We need to discuss several wave properties, so we will start with what happens to waves as they propagate over long distances.

Getting weaker

Imagine a torch battery connected to a bulb by wires about 1 metre long. The bulb lights normally. If we now take the bulb 100 metres away from the battery and wire it up, we would expect the bulb to be somewhat dimmer, which is exactly what would happen. It happens because of the resistance of the wires – the wires do not form a perfect conductor. A similar situation occurs with radio waves.

All waves suffer from *attenuation* – they get weaker the further they travel. In cases of extreme attenuation, we need to apply some *amplification* before the attenuated wave can be used in a receiver.

Carrying information

When we speak over the telephone, the range of frequencies in our voices extends from very low frequencies up to about 15 or 20 kHz. In audio terms, this is quite a large *bandwidth* (meaning a wide band of frequencies). For communications purposes, however, most of this bandwidth is not needed, and in the telephone system (and in our transceivers), this is cut down so that it extends from about 200 Hz to 3 kHz, a reduction in bandwidth from 20 kHz to about 3 kHz. A bandwidth of 3 kHz has been found to be sufficient to convey speech intelligibly which, after all, is just what we need!

The radio waves coming from an amateur transmitter convey our speech signals over long distances. By themselves, the speech signals do not travel very far, so they have to be combined with a radio signal that *will* travel long distances. This extra signal is called the *carrier wave* (or just the *carrier*), because its job is to *carry* the speech signals along with it! The process of combining the speech (or Morse code) with the carrier is called *modulation*.

Wider and wider

Sending Morse code is achieved simply by switching (or *keying*) the carrier on and off. The bandwidth of the transmitted signal is only about 100 Hz. Speech, with its reduced bandwidth of 3 kHz, will produce a *single-sideband* (SSB) transmitted signal with a bandwidth of 3 kHz. If the same speech signal were used to produce an *amplitude-modulated* (AM) signal from the transmitter, it would have a bandwidth of about 6 kHz. Perhaps you can now understand why the bandwidths needed to produce hi-fi broadcasts need to be so large. TV signals need bandwidths running into tens of megahertz!

Waves need aerials

Radio waves are produced whenever changing currents flow through a wire, and when that wire is made in such a way as to maximise the *radiation* from the wire, it is called an *aerial* or *antenna*. The same piece of wire will receive radiation from other aerials; an aerial will transmit and receive. This is an important property of the aerial: when a current flows through it, electromagnetic waves are launched into the air; when electromagnetic waves in the air encounter the aerial, currents are produced in it.

From the simplest transmitting aerial, waves travel in all directions, like the waves on the pond that we considered in Part 1. They will travel a long way through air and space before they become too week to be received. They won't travel very far into the earth, however! The earth will *reflect* some of the wave and will *absorb* the rest. That portion of the wave which is reflected will again travel through air and space until it is totally attenuated.

Look at **Figure 1**; A represents a radio transmitter, with B1, B2 and B3 being receiving stations. The two arrows pointing 'downwards' from A represent two of the waves from A which just graze the earth's surface. Waves above

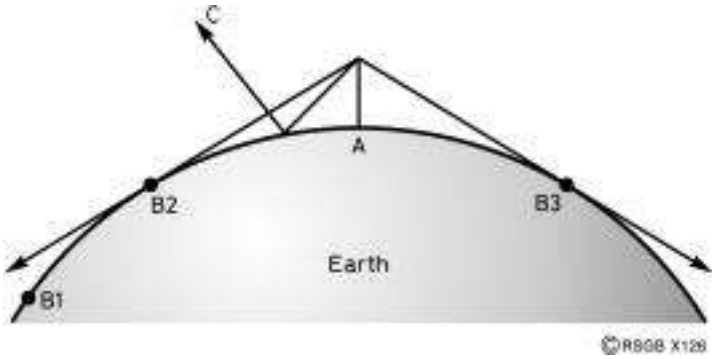

Figure 1 Stations between B2 and B3 receive the *ground wave*

these will travel on into space; waves below them will either be absorbed and reflected by the earth or received by aerials. B1 will not receive any signals from A, because it is below A's horizon. B2 and B3 can receive A's signals because they are *just* on A's horizon. Any stations between B2 and B3 will also receive A's signals, which are known as *ground-wave signals*. The wave at C represents one which is reflected by the ground and travels into space.

This description begs the question of how signals are received from stations well beyond the ground-wave range.

Mirrors in space

Suppose that there was something, out in space, that would reflect radio waves. Waves from A that travel out into space could be reflected off it and return to earth, enabling stations such as B1 to receive A's signals. The situation just described is illustrated in **Figure 2**.

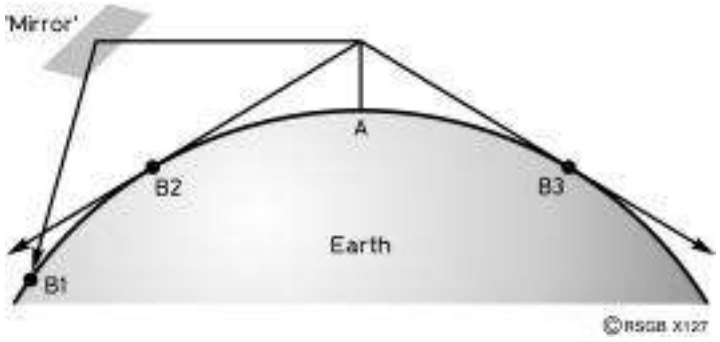

Figure 2 Reception of A's signals at B1 using the *sky wave*

Just such a mirror in the sky really *does* exist. It is not man-made, of course! The earth is surrounded by the atmosphere, a mixture of many gases, such as nitrogen and oxygen. The energy contained in the radiation from the sun is more than sufficient to *ionise* these gases, thus making them into electrical conductors. When a gas is ionised, some of its electrons are physically stripped out of the atoms and are free to move about, just as the electrons of a metal do in a wire. Consequently, we can regard this part of the atmosphere (the part illuminated by the sun) as acting like a sheet of metal, which *reflects* radio signals! It is not a perfect reflector, but is sufficient to produce long-range (DX) radio propagation via the *sky wave* under the right conditions. (A more down-to-earth example of ionised gases conducting electricity can be found in the fluorescent tube and the neon sign – many gases glow when they are continuously ionised.)

This conducting region at the extremity of the atmosphere is called the *ionosphere*, and it exists in layers between 60 km and 700 km above the earth's surface. When the ionosphere is sufficiently ionised, it glows; this is the natural phenomenon known as the *aurora borealis*, or the *northern lights*.

The property of the ionosphere that enables radio waves to be reflected does not act in a uniform way; it is very selective about which waves it reflects, and which waves go straight through it and into outer space. In general, it reflects only those waves with frequencies below about 30 MHz – the HF bands!

In Part 3 we will look at families of waves.

12 An LED flasher

Introduction

The LM3909 is an integrated circuit (IC) which will flash a light-emitting diode (LED). Using only two extra components and a battery, the circuit is cheap and has a very low current drain from a 1.5 V cell. The circuit can be used as a novelty flasher, an indicator for a dummy alarm bell box, or it could be attached to a torch so that it could be found easily in the dark! The simple circuit is shown in **Figure 1**.

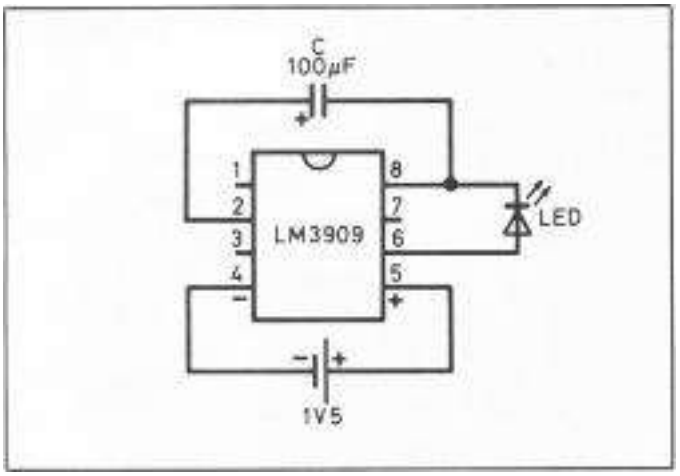

Figure 1 Circuit diagram of the LED Flasher. Pins 1, 3 and 7 of the IC are not used

Assembly

The circuit can be built on a small piece of Veroboard (the piece shown in **Figure 2** measures 15 holes by 10 strips). Using such a board, follow these instructions.

1. Depending on how far away you want the LED from the circuit board, solder a length of insulated wire to each lead of the LED. Use different colours of insulation – say, red and black, connecting the *red* lead to the *anode* (a) lead (the longer one) of the LED, and the black one to the *cathode* (k). Figure 2 shows these leads.
2. Cut the copper tracks as shown in Figure 2, using a 3 mm (⅛ inch) diameter drill, rotated between thumb and forefinger, or use the proper tool. Make *absolutely* sure that the tracks are completely broken!
3. Fit the IC holder in the correct position, using the cut tracks as guides, and make sure the small notch is facing towards the top of the board. Solder the pins to the copper tracks.
4. Mount the capacitor, positive end to the left, so that the positive lead is soldered to track F, which connects it to pin 2 of the IC; the negative lead is soldered to the right-hand side of track E, this being connected to pin 8 of the IC.
5. Solder on the battery leads, positive to the right, and the extended LED leads, positive downwards.

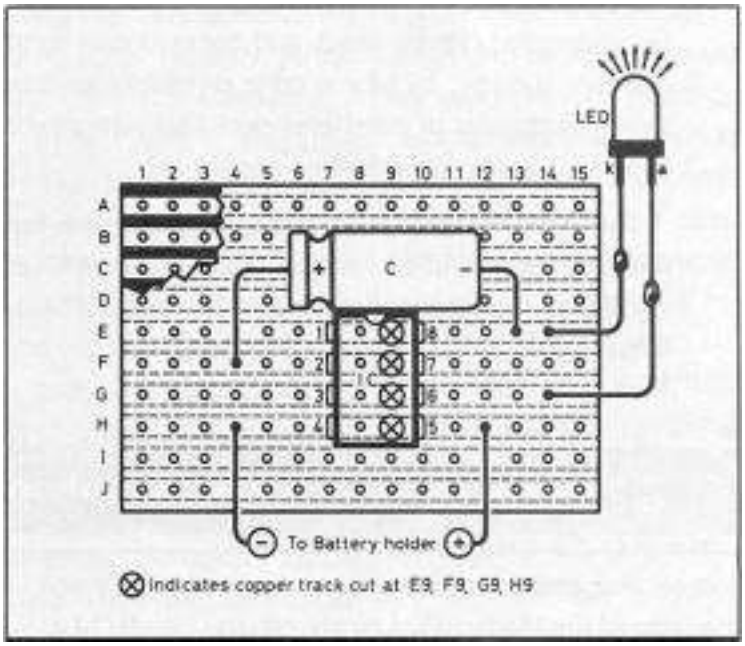

Figure 2 Board layout viewed from the component side. The tracks are cut under the board where shown

6. Check the circuit, and hold up the board to a bright light and look carefully for solder bridges between the tracks and pieces of copper swarf which may have escaped your inspection in 2 above! Remove whatever you find.
7. When all seems well, put the IC into the socket, ensuring that the notch or dot on the upper surface of the IC lines up with the notch on the holder. Line up each pin on the IC with the hole below it before pressing *gently* on the IC with the board supported on a firm surface.
8. Connect the battery; the LED should start to flash. The circuit is complete and working!

If you prefer, the whole circuit (battery included) can be mounted in a small plastic box, with the LED mounted on a clip and protruding through the panel. There are many other possibilities, and it is up to you to find an application for your own use.

Parts list

		Maplin code
LM3909	Integrated circuit	WQ39N
IC socket	8-pin DIL	BL17T
LED	5 mm diameter	WL27E
100 microfarad (μF)	Electrolytic capacitor (10 V)	FB48C
Battery holder	For AA-size cell	YR59P
Battery	1.5 V AA cell	

Small piece of Veroboard (15 holes by 10 strips)
Small plastic box (if required)
LED clip (if required)
Two lengths of coloured, insulated wire for LED (as required)

Availability

All parts can be obtained from Maplin Electronics Ltd.

13 Waves – Part 3

Introduction

When we talk about the spectrum being divided up into bands, this is just for our convenience; there are no natural divisions although, as we have seen, some of the properties of different bands really *are* different! Let's look at **Figure 1**, and see how the frequencies are divided up.

The divisions

- **Very low frequencies** (VLF) cover the range from a few kilohertz up to 30 kHz. Very long-range communication is possible, but at *very* small bandwidths. It is used for special purposes.
- **Long waves** (LW) are used for medium-distance commercial broadcasting and have frequencies from 30 kHz to 300 kHz.
- **Medium waves** (MW) are used for commercial broadcasting, and use frequencies from 300 kHz to about 1.5 MHz (1500 kHz). Typical range is about 200 km.
- **Short waves** (SW) encompass both the low-frequency (LF) and high-frequency (HF) amateur radio bands. There are nine narrow amateur bands in the SW spectrum between 1.8 MHz and 30 MHz. Some of these bands give round-the-world communication.
- **Very high frequencies** (VHF) span the range between 30 MHz and 300 MHz. Relatively short-range communication is possible. They were once used for broadcast TV before it moved to UHF. There are now three

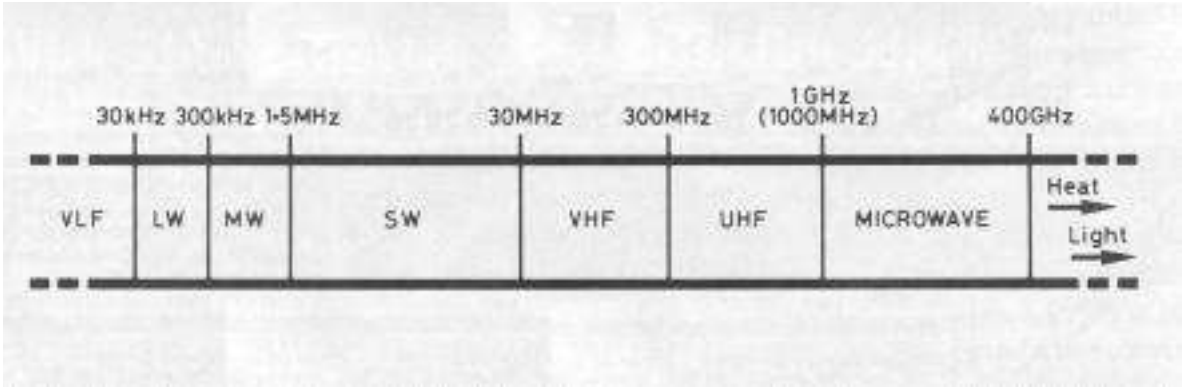

Figure 1 Diagram of radio frequency spectrum

amateur bands here – 6 m, 4 m, and 2 m. Repeaters are used to extend the usable range of mobile stations. VHF waves are not usually reflected by the ionosphere, but when they are, ranges of several thousand kilometres are possible. Weather affects these waves on a regular basis, however. In addition to amateur users, the VHF part of the spectrum is also used by the police, the fire and ambulance services, weather satellites, and many others,

- **Ultra-high frequencies**, sometimes called *centimetre waves*, cover the range from 300 MHz to 1000 MHz (or 1 GHz). The only amateur band in this range is the 70 cm band, and we share it with radar, TV and cellular telephone users as well.
- **Microwaves** begin at 1 GHz and extend to about 400 GHz. They are *never* reflected by the ionosphere, are partially attenuated by buildings, and are reflected from aircraft and cars. Microwave absorption in the atmosphere is quite significant, and rain and fog can attenuate microwaves quite heavily.
- **Heat, light** . . . Above 400 GHz we run into the infra-red bands and on into the visible light and ultra-violet bands. We generally take 400 GHz as being the limit of what we class as radio waves.

Bandwidth again

Complex signals need more bandwidth than simple signals. Even if it were possible, we would not be able to transmit a single television channel in the whole of the MW broadcast band! When TV used part of the VHF band, only five channels were possible in the range from 45 MHz to 68 MHz. By moving TV to the UHF band, we now have 47 channels between 470 MHz and 855 MHz!

It's your choice!

The number of permutations you have amongst all the modes and all the bands is enormous! Only you can decide what you are interested in and what you want to learn about. That is the attraction of amateur radio!

14 Choosing a switch

Simple, but be careful!

A switch is the simplest electronic component, but care is needed in choosing the correct one for the job. Here is a list of the main characteristics of a switch, which will help you to select what you want.

1. **Rating**. This gives the maximum voltage and current that a switch can handle. For example, a 250 V 1.5 A switch will switch mains voltage at a current not exceeding 1.5 A. If the current is greater than 1.5 A, the switch may get hot and fail. If the voltage is too great, the switch may arc each time it is switched off, thus wearing away the contacts.
2. **Number of poles**. A single switch can control many circuits; the number of poles tells you *how many* different circuits it can handle. See **Figure 1**.
3. **Number of throws**. This tells you the number of positions each pole can have. This is best illustrated in Figure 1. The simplest ON/OFF switch is a Single-Pole, Single-Throw (SPST) switch. A Single-Pole,

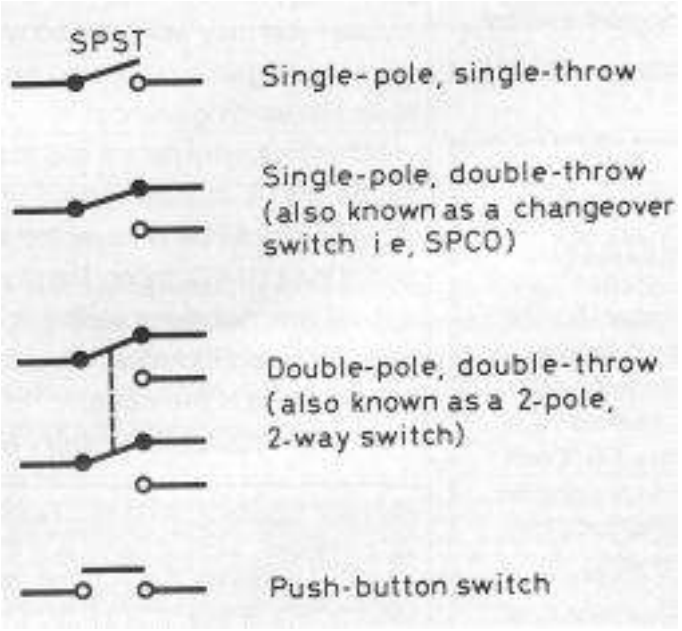

Figure 1 Some circuit symbols for different types of switch

Double-Throw (SPDT) switch may also be used as an ON/OFF switch, but is used mainly to change between two parts of a circuit, and is commonly known as a Single-Pole Change-Over (SPCO) switch. Two or more SPCO switches can be operated at once; Figure 1 shows an example. The two switches are said to be *ganged*. See also 'Types of switch' below.

4. **Number of ways**. When a switch has more than one throw, we tend to use the word 'ways' instead. This means that if a switch has one pole and six throws, we would normally call it a '1-pole 6-way' switch. Such switches tend to be rotary switches, as are described below.

Types of switch

(a) **Push-button**. These are found on calculators, telephones, electronic games and most equipment with a digital display.

(b) **Rotary**. These are switches controlled by a knob, and are turned instead of moved up and down. **Figure 2** shows the rear of such a switch and its circuit symbol. The commoner types of rotary switch are: 1-pole, 12-way; 2-pole, 6-way; 3-pole, 4-way; 4-pole, 3-way; 6-pole, 2-way. All these switches have 12 click positions, as you may have guessed, but each one comes with an adjustable end-stop so that you can set the correct number of ways according to the contacts on the switch.

(c) **Slide**. This switch is common on the cheaper types of radio, mainly as an ON/OFF or band-changing switch. They are not very rugged, but are small and cheap to produce. Very small types are manufactured for use on PCBs.

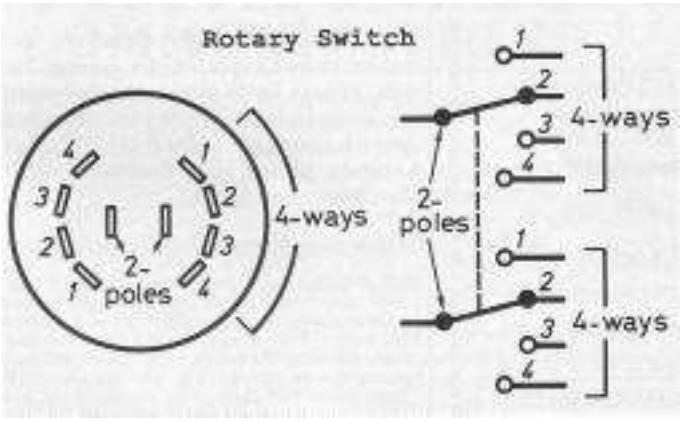

Figure 2 The rotary switch can select several different circuits at once

(d) **Toggle**. Available as two-way types or three-way, with a centre-off position. Can be manufactured to handle very high currents.

(e) **Micro-switch**. These are devices which are usually operated indirectly, such as when the cover is removed from a high-voltage power supply, or when the door of a fridge is opened. The 'micro' part of the name doesn't refer to the size of the switch, but to the *small* movement that is required to activate it.

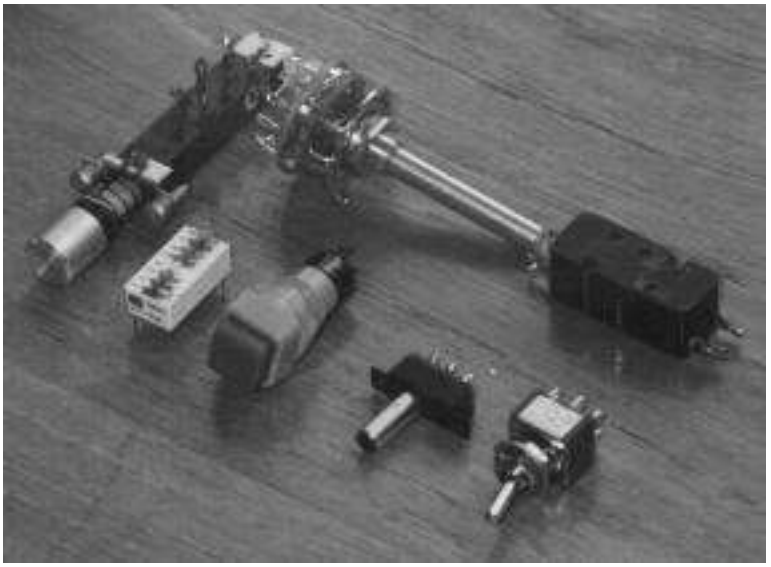

15 An aerial tuning unit for a receiver

Introduction

Any length of wire will act as an antenna (or aerial) but, to get the best results from a transceiver or receiver, an aerial tuning unit (ATU) is required. This matches the *impedance* of your aerial to the impedance at the aerial socket of your radio. Impedance is like resistance, and is measured in ohms, but it is used for alternating currents, and hence is common in audio and RF engineering. Most receivers have an impedance at the aerial socket of about 50 ohms (Ω); aerial impedance, on the other hand, can be anywhere between 20 Ω to over 1000 Ω, depending on its length and its height above ground.

Fortunately, you don't *need* to be able to calculate your aerial's impedance; all you need is a device that will perform the matching operation for aerials with a large range of impedances, and this is exactly what is described here! The subject of *matching* is a complex one, but all you need to know is that most signals will become clearer, and that there will be less noise and interference. Stations will become louder, so you will probably be able to reduce the setting of your RF gain control (always a good thing to do).

This design of ATU covers all amateur and broadcast bands from 10 m (28 MHz) to 80 m (3.5 MHz), and is very easy to build. The circuit is shown in **Figure 1**.

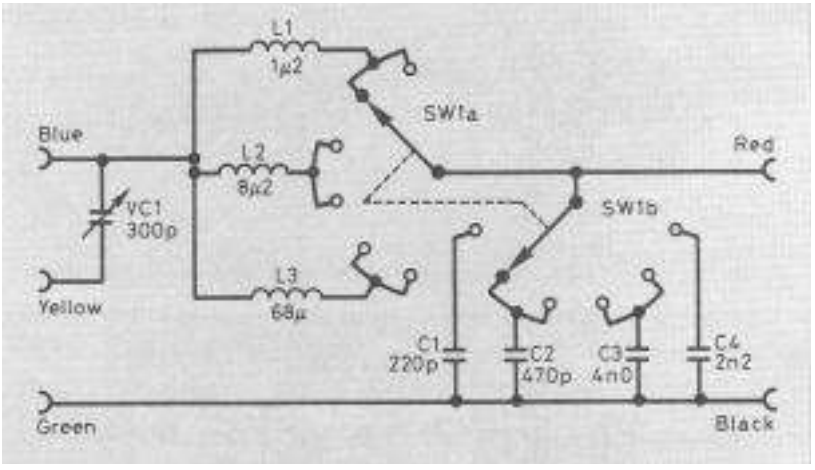

Figure 1 Circuit diagram of the Antenna Tuning Unit, showing the use of a 2-pole, 6-way rotary switch to select inductors (L) and capacitors (C)

Construction

1. Firstly, you will need a simple plastic case in which to house the ATU. The size should be approximately 85 × 145 × 50 mm.
2. Start by drilling two 10.5 mm holes in the front of the case; these are for the 6-way switch and the tuning capacitor.
3. Drill three 8 mm diameter holes in the left-hand side of the box, for the three sockets, coloured blue, yellow and green.
4. On the right-hand side of the box, drill two 8 mm diameter holes for the red and black sockets.
5. Now, fit the 6-way switch (SW1), the tuning capacitor (VC1), and all the sockets to the case. Check that the vanes of the capacitor rotate smoothly when the shaft is turned.
6. Wire up the inductors (coils). Figure 1 and the wiring diagram of **Figure 2**, will help with this. As you can see, each one side of each coil is connected to two switch connections, the other end going to VC1.
7. Solder in the fixed capacitors. One end of each goes directly to the ground socket (black), and the other end goes to the switch.
8. Solder a wire between the green and black sockets. The output from the ATU comes from the red socket, and this is connected to the two tags in the centre of the switch, as Figure. 2 shows clearly.
9. Finally, connect the blue and yellow sockets to the tuning capacitor, and the ATU construction is complete.

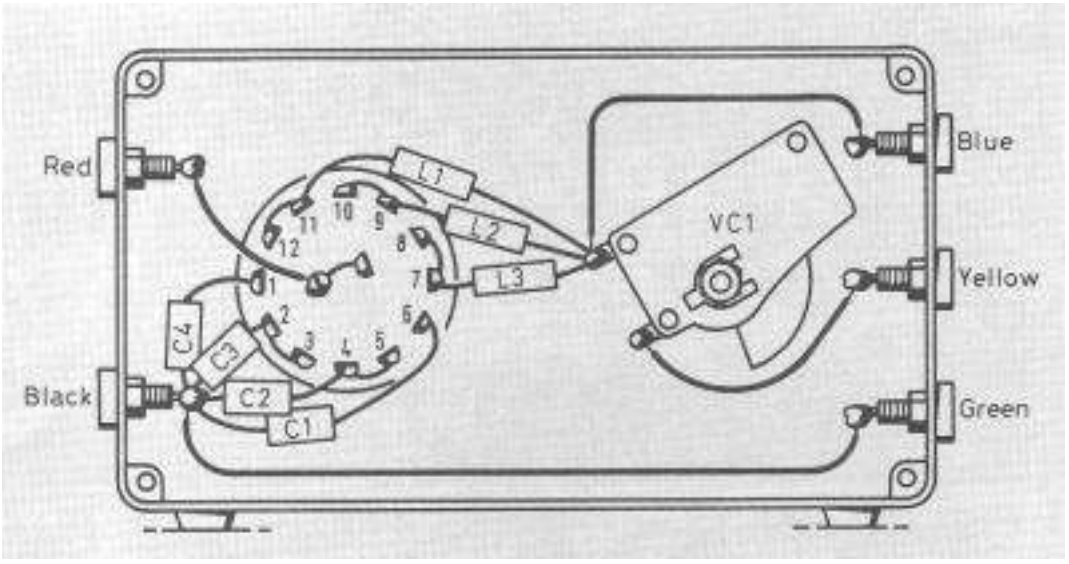

Figure 2 The internal view of the case shows the main tuning capacitor, VC1. This is a solid dielectric type, which has adjustable brass plates

In practice . . .

Figures 3 and **4** show two different ways of connecting your aerial to your ATU. In each case you will need to select each switch position in turn, and rotate the tuning capacitor through its full range while listening to a station. You should find that one switch position enables VC1 to produce a peak in the signal strength in the loudspeaker. At this point, your aerial and receiver are said to be *matched*. Stations in the same band will probably peak with VC1 at the same setting of SW1, but different bands will almost certainly require different positions of SW1.

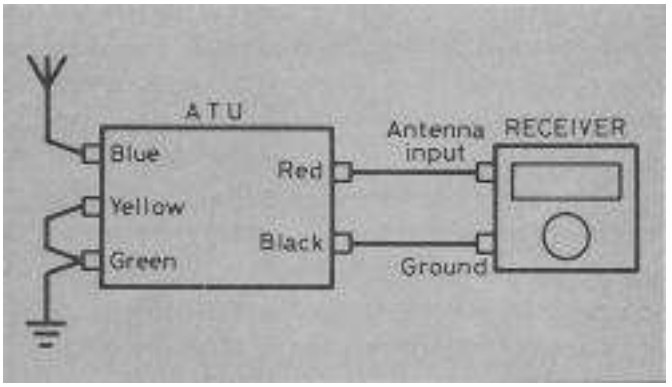

Figure 3 You may find that parallel tuning gives best results with your antenna

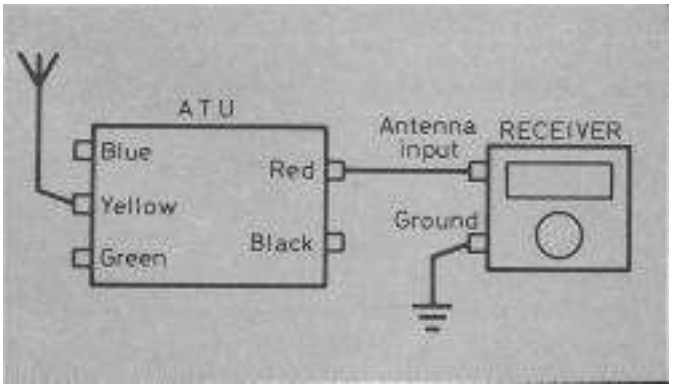

Figure 4 In other cases, series tuning could be the most effective arrangement

Parts list

Capacitors (all rated at 16 V or more)
- C1 220 picofarads (pF) polystyrene
- C2 470 picofarads (pF) polystyrene
- C3 1000 picofarads (pF) or 1 nanofarad (nF) polystyrene
- C4 2200 picofarads (pF) or 2.2 nanofarads (nF) polystyrene

Inductors
- L1 1.2 microhenries (μH)
- L2 8.2 microhenries (μH)
- L3 68 microhenries (μH)

Switch
- SW1 2-pole 6-way rotary

Sockets
- 4 mm type, one each of red, black, yellow, blue, green

Additional items
- Plastic or metal case, e.g. Maplin type YU54
- Two large knobs for SW1 and VC1

16 A simple 2 m receiver preamplifier

Introduction

Designed specifically to complement the modified air-band portable (also described in this series), this can be used with some success on many receivers suffering from 'deafness' on VHF.

The circuit

An RF preamplifier is a device which improves the input signal to an existing receiver, enabling it to work more effectively. Because of the noise which is added to the signal by the preamplifier, *very* weak signals may not be usefully enhanced, but stronger signals will be improved considerably.

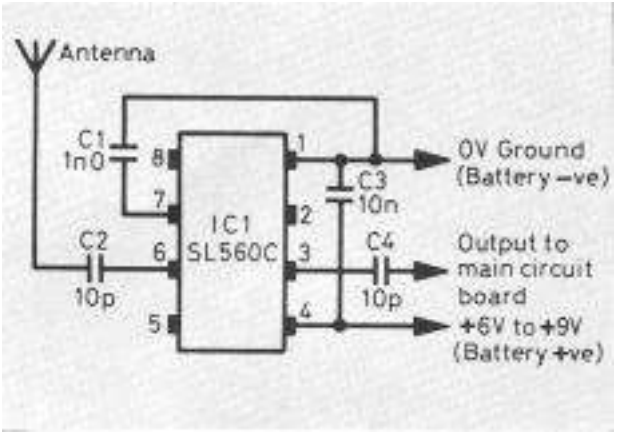

Figure 1 The integrated circuit is mounted upside down. Make sure you identify pin 1 which has a small dot next to it

This little circuit (shown in **Figure 1**) uses a GEC/Plessey integrated circuit type SL560C. With the addition of four capacitors, it is used between your aerial and the aerial input of the radio's PCB.

Putting it together

1. Use a small piece of prototype (matrix) board about 25 mm square. Use an 8-pin DIL socket for the integrated circuit (don't risk soldering the chip – it is seldom a risk worth taking). Figure 1 shows the connections to the socket, *looking from underneath*.
2. Make special note of the pin numbers, so that you know how to put the chip into the socket when you have finished. The positive and negative connections to the circuit are taken from the main PCB *after* the ON/OFF switch – so that the switch operates the preamplifier, too.
3. Unsolder the lead to the radio's telescopic aerial and connect it to the free end of C4, as shown. Then solder a short lead between the telescopic aerial and C2.
4. Sometimes it is possible to cajole your little preamplifier into the radio's plastic case, provided there is room and that you make sure that none of the soldered joints on your little board touch any of the metal inside the case when you replace the back and screw it on again.
5. If there is not enough room inside, then put the preamplifier into its own box, with battery and switch, and its own aerial. Keep the lead from the preamplifier to the aerial connection of the radio as short as possible – perhaps using screened cable.

Because your preamplifier is untuned, you will find not only that it helps with reception on 2 metres, but also that reception on the FM broadcast band is improved!

Parts list

Integrated circuit

IC1	GEC/Plessey SL560C

Capacitors

C1	1 nanofarad (nF) ceramic
C2, C4	10 picofarads (pF) ceramic
C3	10 nanofarads (nF) ceramic

Additional item

Prototype broad approx. 25 × 25 mm

17 Receiving aerials for amateur radio

Introduction

For any radio receiver to work well, it must have some form of antenna, or aerial. In almost all domestic transistor radios, the aerial is built into the set, either as a ferrite rod (which looks like a rod of dark grey metal) on which are wound coils of wire, or as a chromium-plated telescopic metal rod. Some radios have both forms of aerial, using the ferrite rod aerial for long waves (LW) and medium waves (MW) and the metal rod for very high-frequency (VHF) stations using frequency modulation.

There's broadcast reception . . .

No aerial is perfect, and these two types are *far* from perfect! As in most mass-produced equipment, *they serve their purpose*, which is not critical, and they allow the radio to be carried around easily, because they are not

big and bulky. The broadcast stations are very powerful, usually quite close, and the circuits in the radio are quite sensitive, so the need for large aerials disappears.

. . . and there's amateur DX

Here we have an application which, in comparison with the broadcast situation, couldn't be much more different. The stations do not use much power, they may be half the world away, and the requirement for good aerials and very sensitive receivers is paramount. The aerials must be large and they must be as high as possible, away from buildings and trees, which cause reduction in signal strength, and away from man-made sources of interference.

You may not have thought about this but, in general, the larger an aerial becomes, the longer the cable (or 'feeder') must be in order to reach your shack and the receiver inside it. Cables reduce the received signal, so what your aerial gains by being large, the feeder (if you're not careful) will lose!

A simple aerial . . .

We now know that a 'good' aerial is essential. But what is a 'good' aerial? It depends on your purse, your property and your enthusiasm! One of the simplest (and, incidentally, one which is *not* subject to the cable loss problem discussed above) is the **Long Wire**, shown in **Figure 1**. This is, quite literally, a long piece of wire going from a chimney stack to a tree or pole

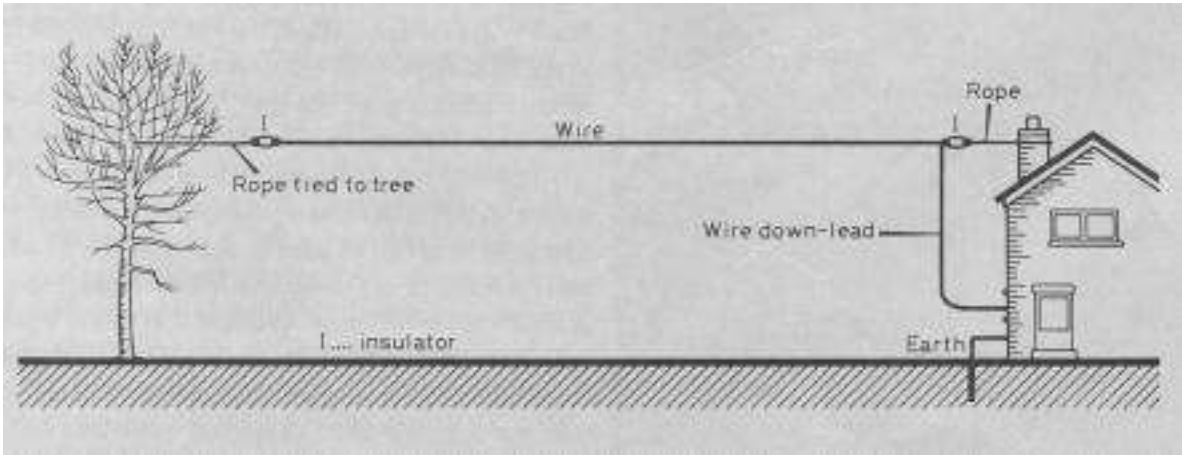

Figure 1 A tree at the bottom of the garden can provide a useful antenna support. Insulators can usually be obtained from Tandy stores or TV aerial suppliers

at the end of the garden. The longer it is, the better. Notice that the wire itself is *not* used to loop around the tree or chimney. Rope is used for both, and is secured to the end of the wire using an insulator of the 'dog bone' or 'egg' variety, to be found in profusion at rallies.

The wire is brought into the house through a window into the shack where the receiver is situated. The long wire aerial is best used with an aerial tuning unit (ATU), which is also described in this book. One of the advantages of the long wire is that it can be used on several frequency bands.

. . . and more complicated ones

Next up the ladder of complexity is the **dipole** (meaning two poles, or two elements). One form of dipole for lower frequencies would take the same basic form as the long wire, except that the feed to the receiver is taken, not from the end, but from the centre. The wire is essentially cut into two halves, and the two ends at the centre are connected to one end of a coaxial cable, which is then taken to the receiver. A smaller form of this is shown in **Figure 2**, which is conveniently mounted in a house loft. Aerials should always be mounted outside for best results, but will work when mounted inside, and the loft space is the logical situation.

The total length of the dipole should ideally be one-half of the wavelength of operation – hence the term 'half-wave dipole'. For example, a dipole for use on 20 m should be about 10 m long. Dipoles are thus 'single-band' aerials. They can be modified for use on several bands, and then become known as 'trapped dipoles', having coils and capacitors at certain points along their lengths.

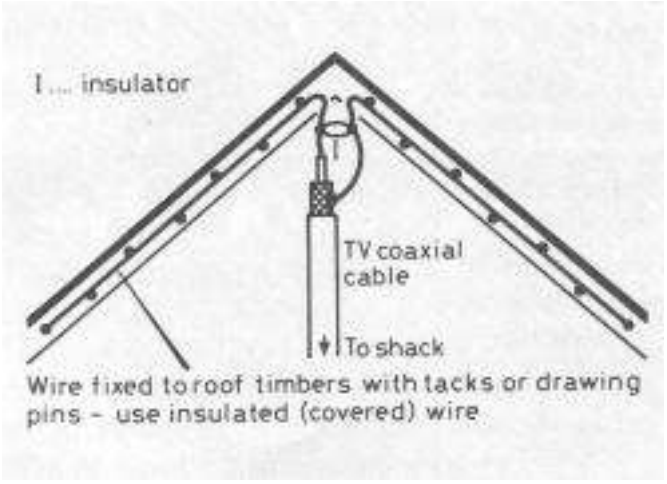

Figure 2 An indoor antenna should be mounted as high as possible

Indoor aerials

For flat- or apartment-dwellers, an indoor aerial is often the only solution, in which case the dipole of Figure 2 may be of great use. Other popular types include the **loop aerial**, of which several types are shown in **Figure 3**. The shape of the loop is of secondary importance, but it should be as large as possible.

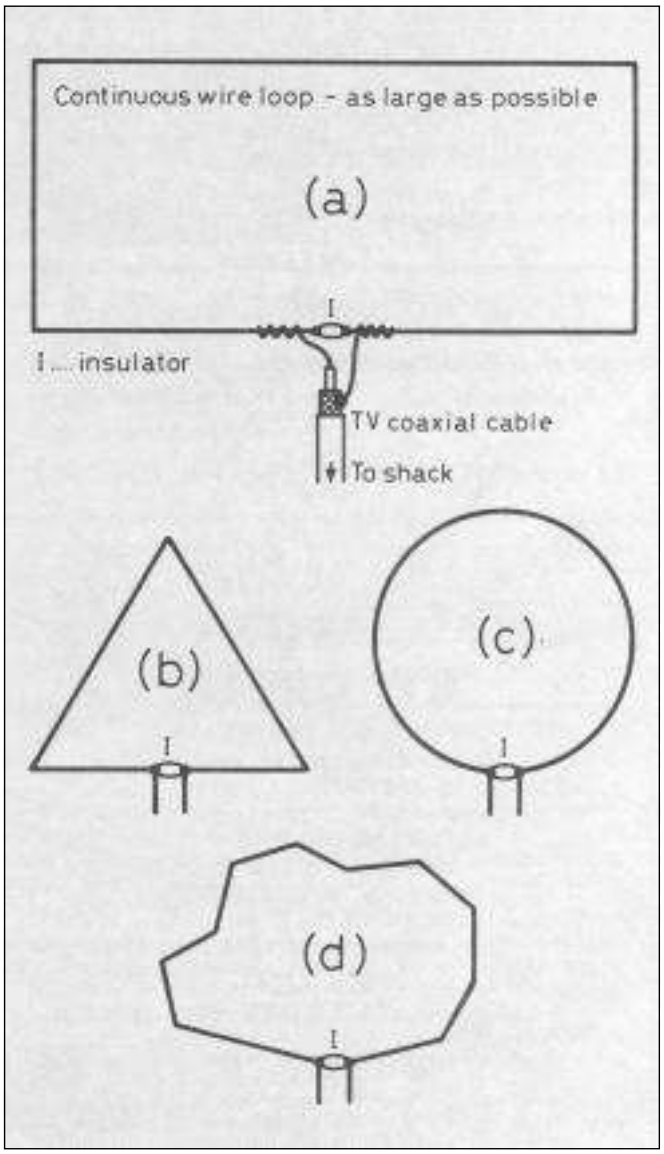

Figure 3 Try different shapes of loop antenna to see which works best

Ingenuity is called for when considering indoor aerials. A dipole can be mounted along a picture rail or pelmet. A vertical loop of aluminium foil can be stuck to an inside wall and covered with wallpaper! The designs are limited only by your imagination, and will give you hours of listening pleasure

Outdoor aerials

If you want to venture beyond the simple long-wire discussed earlier, then the erection of outdoor aerials can be a bit tricky; they can be more than a one-man job, and can involve seeking planning permission. Get some help advice from someone who has done it before – what about your local radio club? Plenty of designs for aerials appear in *RadCom*, so you should never be short of ideas!

18 The Colt 80 m receiver – Part 1

Introduction

This is the first of four parts detailing the design and construction of a simple radio capable of good reception of amateur radio signals on the 80 metre band. If you can solder and have some basic hand tools, at the end of Part 4 you will have a working receiver, in which you can take pride, and start some serious listening on 80 m! For testing, all you will need is another receiver and a multimeter.

Description

The radio will be built in three modules, or stages, as illustrated in **Figure 1**. Each of these is built on a printed-circuit board (PCB) or matrix board and can be tested in its own right. The case will need some holes drilled, and care will be needed to mount the PCBs in the case.

Get to it!

Surprisingly enough, when you are building a radio section by section (which is *always* the best way), it is easiest to start at the output and work

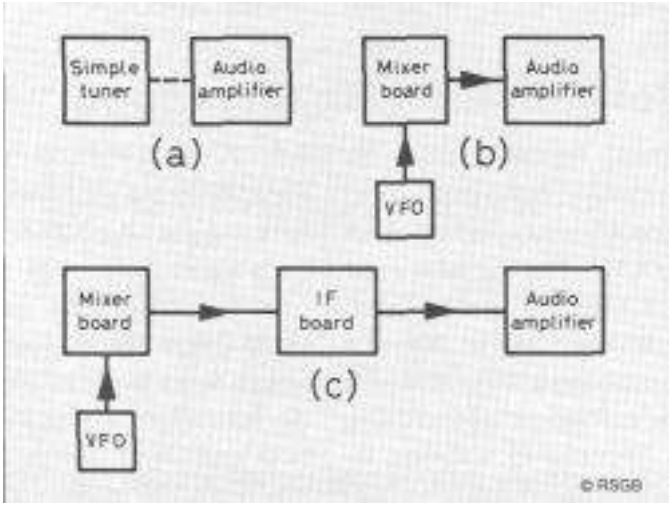

Figure 1 Build your Colt and watch it grow. A simple crystal set (a) becomes a direct conversion receiver (b) and finally an 80 metre amateur band superhet (c)

towards the input, and you can test what you have done stage by stage. You will see what this means as you progress with your construction.

Every receiver needs some audio frequency (AF) amplification to make the sound signals big enough for you to hear. The circuit for the AF amplifier is shown in **Figure 2**. It uses the TDA7052 integrated circuit (IC) plus a handful of extra components. R1 in conjunction with C2 and C3 *decouple* the battery supply, preventing any audio signals getting through to it and affecting other parts of the radio, when they are connected. C1 acts to prevent high frequencies (above the 3 kHz bandwidth) going into the amplifier input. A volume control, VR1, is connected across the amplifier input, so that the amplifier can accept signal inputs over a wide range. **Figure 3c** shows the connections, which are made with screened cable. The

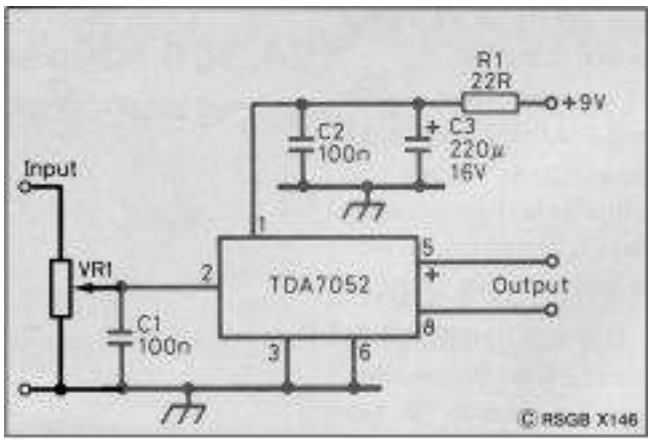

Figure 2 The Philips TDA7052 integrated circuit (IC) used in the audio amplifier needs very few extra components. It has a signal voltage gain of 100 times and the output is suitable for a loudspeaker or headphones

centre conductor of the left lead goes to the point marked 'input' in Figure 2, the braid being connected to the amplifier earth (0 V) tag. The right lead to VR1 goes to whatever signal source you have for testing – see later. VR1 is *not* mounted on the PCB.

The circuit is constructed on a small PCB or matrix board. Make sure that the electrolytic capacitor, C3, is soldered into the board the correct way – its positive and negative connections are shown in **Figure 3b** for reference. If you are **at all** concerned about soldering the IC into the board, enlist some help, *or*, obtain an 8-pin DIL socket, which you can solder in and then carefully insert the chip into the socket, making sure that is the correct way round. The markings on the chip are shown in **Figure 3a**.

The output leads from the amplifier go to a plastic 6.3 mm (¼ inch) mono jack socket, so that *neither* output lead is connected to the metal case. The amplifier will drive a pair of headphones or a small 8 Ω loudspeaker.

The battery leads must be the right way round also; the battery itself can be a PP3 or PP9, or you can use a small DC power supply.

Testing

First, check that all the components are in the right places, that your soldering is good, and that you have headphones or a loudspeaker connected. Set VR1 about halfway along its travel. Connect the battery.

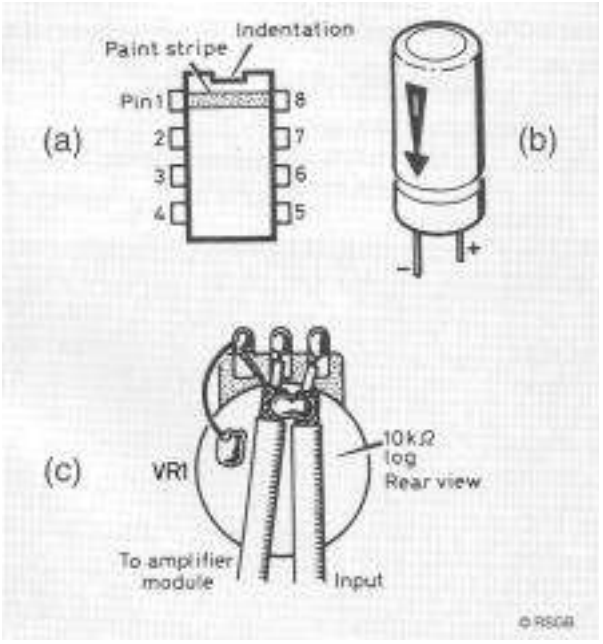

Figure 3 It is important to check the component connections carefully. The diagram shows (a) top view of the IC, (b) electrolytic capacitor and (c) volume control (VR1) connected across the input of the amplifier

A slight hissing noise should be heard; touching the input lead to the amplifier (the centre of the three connections on VR1) should produce a loud buzz. Touching the shaft at the same time will make the buzz quieter. This is the quickest way of confirming that your amplifier *seems* to be working. The only real test is to give it something meaningful to amplify! See the design of our *Crystal Radio Receiver* for full details.

Parts list

Resistors: all 0.25 watt, 5% tolerance

R1	22 ohms (Ω)
VR1	10 kilohms (kΩ) log

Capacitors

C1, C2	0.1 microfarad (μF)
C3	220 microfarads (μF) electrolytic 16 V

Integrated circuit

IC1	TDA7052 audio amplifier

Additional item

PCB	(see below)

Component suppliers:
Maplin

The next part . . .

The metal case will be marked out ready to receive the completed modules.

19 A crystal radio receiver

Introduction

Here's a quick project to fill in a winter's evening! It was originally designed as a piece of test gear for the *Colt* receiver, but can be successfully used by anyone as a first radio project. Another use for it would be as test gear for any audio amplifier project requiring an audio input for test purposes; this is ideal, as it does not require any power supply!

Details

The initial rough-and-ready test for the audio amplifier of the *Colt* receiver will have whetted your appetite; you will want to prove more conclusively that your amplifier works, and in a way that others in the household will appreciate. Buzzing noises are not convincing in this respect! You are going to put together a simple crystal set – the simplest type of radio that there is – and use it as a signal injector for your amplifier. In this way, you build a real medium-wave (MW) receiver which drives a loudspeaker, as an intermediate product of the construction of an 80 metre amateur band receiver!

The circuit diagram is shown in **Figure 1**. It has a 60-turn coil mounted on a small piece of paper or card wrapped round a ferrite rod. The coil has a connection made to its centre-tap (the middle turn of the coil). The tuning capacitor, VC1, is the most expensive part of the circuit but don't worry, it will be used in the final design of the receiver also! Connect the diode, D1, from the centre-tap to the input to the potentiometer of the amplifier circuit of the *Colt*. Be careful to connect the aerial to the *vanes* of VC1, and not to its *frame*, or you will experience some strange effects when you are tuning. If your amplifier is working correctly, you should be able to receive local stations on medium-waves quite well.

If you think the crystal set will be of use to you in the future as a signal injector, all you will need will be another variable capacitor! If you do not intend to use the amplifier, a small crystal earpiece will allow you to listen. Walkman-type headphones will *not* work!

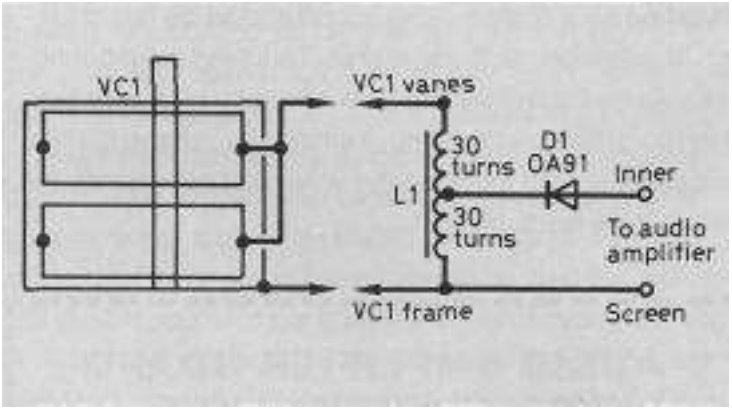

Figure 1 Both sets of moving vanes are joined as shown. L1 is wound on a ferrite rod with 32 SWG wire and centre-tapped. A single winding (no tap) can be used, joining D1 to the top of the winding

Parts list

Variable capacitor

VC1	125 + 125 picofarads (pF) twin-gang

Ferrite rod

About 100 mm to 140 mm long

Diode

D1	OA91 germanium diode

Additional items

Wire	2 m of enamelled copper wire, between 23 SWG and 32 SWG
Earpiece	High-impedance crystal type (only needed if you are not using the amplifier)

20 The varactor (or varicap) diode

Introduction

Many of the circuits for receivers and transmitters presented in this series rely upon the variable capacitor as a means of tuning. Another method of varying capacitance (without any moving parts) is provided by the *varactor diode*, sometimes called a varicap diode. This is a component which changes its capacitance as the voltage across it is varied.

The details

Figure 1 shows how a varactor diode might be connected to demonstrate its operation. Its symbol is that of an ordinary diode, with a capacitor symbol next to it. A variable voltage is applied across it in such a way that the diode is *reverse-biased*. This means that virtually no current passes through it – the positive voltage is applied to the cathode. Varactors are cheaper than variable capacitors, and they are tiny in comparison, very suitable for today's miniature circuits. If A and B were connected across the tuning coil in a simple receiver (with a series capacitor to block the DC from the battery reaching the coil), the tuning operation would be accomplished by turning the knob on the 10 kilohm potentiometer.

Varactors are available with different values, from less than 20 picofarad (pF) for VHF applications to 500 pF for medium-wave radios. They are

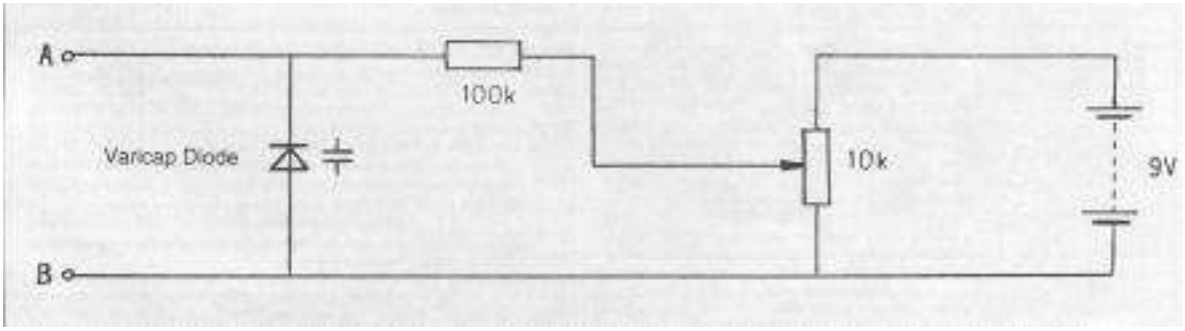

Figure 1 The capacitance of the varicap diode (between A and B) increases as the voltage is reduced, using the variable resistor

tuned usually by voltages between 2 V and 9 V. For a real application of varactors, you should consult the circuit diagram of the *Yearling* 20 metre receiver, elsewhere in this book.

In some circuit designs, several circuits are all tuned to the same frequency in order to improve the overall *selectivity* (the ability of the circuit to reject signals very close in frequency to the wanted signal). Special dual- and triple-varactors are available for circuits like this. Having been made at the same time from the same materials makes their individual characteristics virtually identical. Like all other diodes, they must be correctly wired into the circuit – their *polarity* is important.

Changes in temperature will cause the capacitance to change which, if it were part of an oscillator circuit, would cause the oscillator to drift – you would have to keep retuning the radio! This can be corrected by using a special integrated circuit called a *phase-locked loop* (PLL). Modern TV sets and satellite receivers use varactors and PLLs in this way.

Some useful varactor types

Type No.	*Tuning range*		*Description*
	pF/V	*pF/V*	
BB204B	42/2.0	15/12	Dual VHF
BB212	560/0.5	22/8	AM tuning
KV1235	450/2.0	30/8.5	Triple AM
KV1236	450/2.0	30/8.5	Dual AM
MV1404	120/2.0	9/10.0	HF tuning

21 A portable radio for medium waves

Introduction

The ZN415E integrated circuit (IC) can be used to make a very efficient AM portable MW broadcast radio with a built-in loudspeaker. Here's how!

The circuit

Figure 1 shows the circuit diagram of the portable radio. It's not as complicated as it may appear, especially after you have got started. L1 is a coil of wire mounted on a ferrite rod, acting as an aerial; VC1 is a variable capacitor which works, with L1, to tune in different stations. IC1 contains circuits of its own which boost the selected signal and it includes a *detector* which extracts the audio signal from the incoming RF signal. Earphones could be connected to the output of IC1 (between pins 4 and 5), but the output would not be powerful enough to drive a loudspeaker.

More sound

This is where IC2, an LM386 comes in. This is a small audio *power* amplifier which produces audio signals with enough power to drive a small

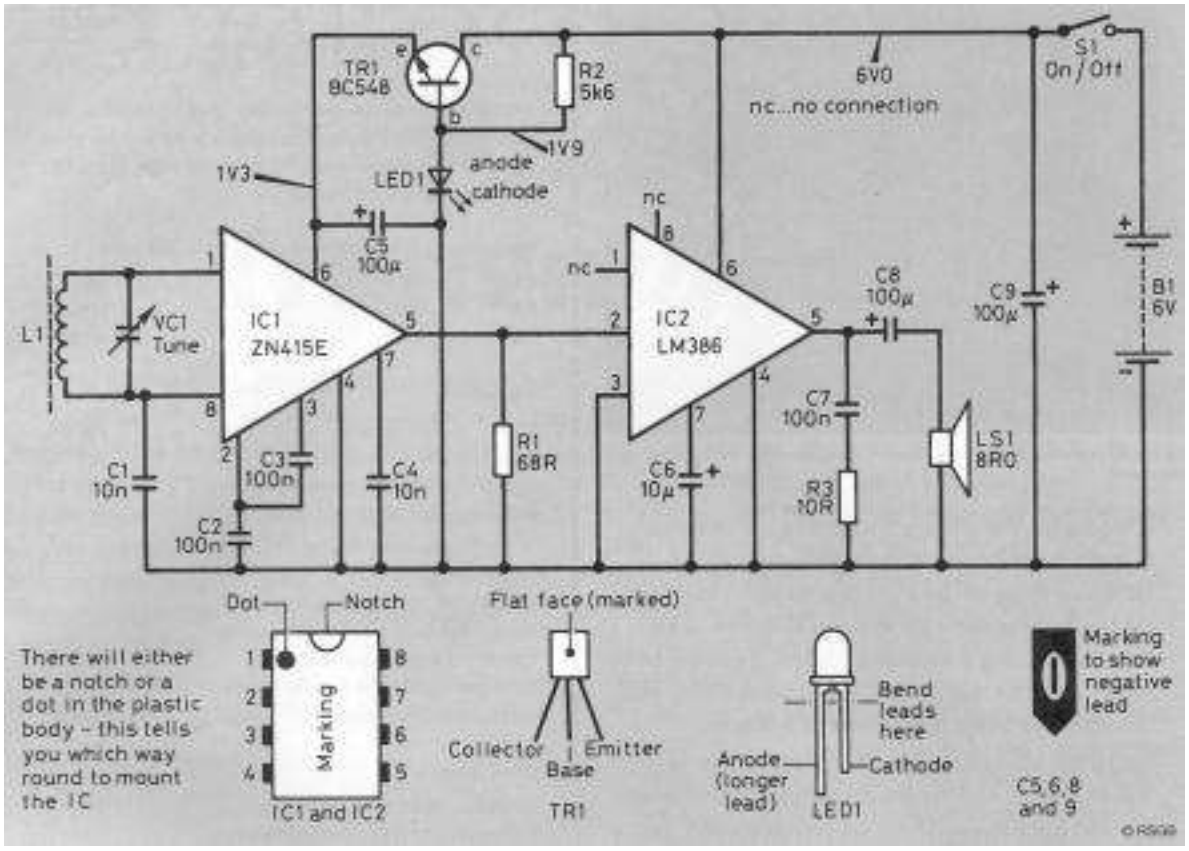

Figure 1 The circuit diagram of our easy-to-build portable radio. Take care to mount the ICs and LED the correct way round

loudspeaker, LS1. The radio uses a 6 volt battery, which is made by connecting four 1.5 volt AA cells in series (4 × 1.5 V = 6 V) using a battery holder designed for this purpose. Although a 6 V supply is ideal for IC2, it is far too great for IC1, which needs only about 1.3 V. This lower voltage is provided from the 6 V supply by TR1 (an npn transistor), R2 and LED1 (a light-emitting diode). When current passes through an LED (see the description of the LED in this series) a reasonably constant voltage of 1.9 V appears between the anode and the cathode. Because of the voltage (0.6 V) that *always* exists between the base and emitter of a working transistor, the voltage on the emitter is about 1.9 V – 0.6 V = 1.3 V, and this is used as the power supply for IC1.

To keep the radio as simple as possible, no volume control has been fitted. Instead, you can use the directional properties of the ferrite rod aerial (see the information on ferrites in this book) to reduce the volume by rotating the set about a vertical axis using the handle provided.

Putting it all together

1. Start by covering the ferrite rod with Sellotape, or alternatively wrap a piece of paper tightly around it, and secure it with Sellotape. Then, with at least 2 metres of 24 SWG enamelled copper wire, wind 75 turns tightly around the rod. To be safe, leave about 50 mm of wire at the ends of the coil, then wrap the whole coil with Sellotape to hold the turns in place, leaving only the ends free. Then, using a small piece of sandpaper, remove the enamel from the last centimetre of each end of the coil.
2. Most of the components are mounted on a piece of Veroboard (the type with parallel copper strips on one side). The piece used on the prototype measured 32 holes by 10 strips, as **Figure 2** shows. Before you start fitting components, cut the copper strips as shown. It is easier to do it now than when the board is littered with components! The strips may be cut with a 3 mm (⅛ inch) twist drill rotated between thumb and forefinger. Resist the temptation to use a hand drill – the idea is just to cut the copper, **not** to drill right through the board!
3. Solder the IC sockets and the other components on the board as shown in Figure 2. Make sure that the IC sockets are fitted with their notches towards the *top* of the board, as viewed in Figure 2. Do not insert the chips yet. Always keep the wires left over from cropping resistors and capacitors, they will come in handy at times like this: make the wire links that are clearly shown in Figure 2. Connect the electrolytic capacitors (C5, C6, C8 and C9), the transistor and the LED the correct way round; then check it again when you have done it!
4. Finally, solder lengths of stranded insulated wire to act as 'flying leads' for future connection to L1, VC1, LS1, S1 and the battery connector.
5. Apart from the battery holder, everything is mounted on the case *lid*. This makes assembly and testing much easier, and eases fault-finding if

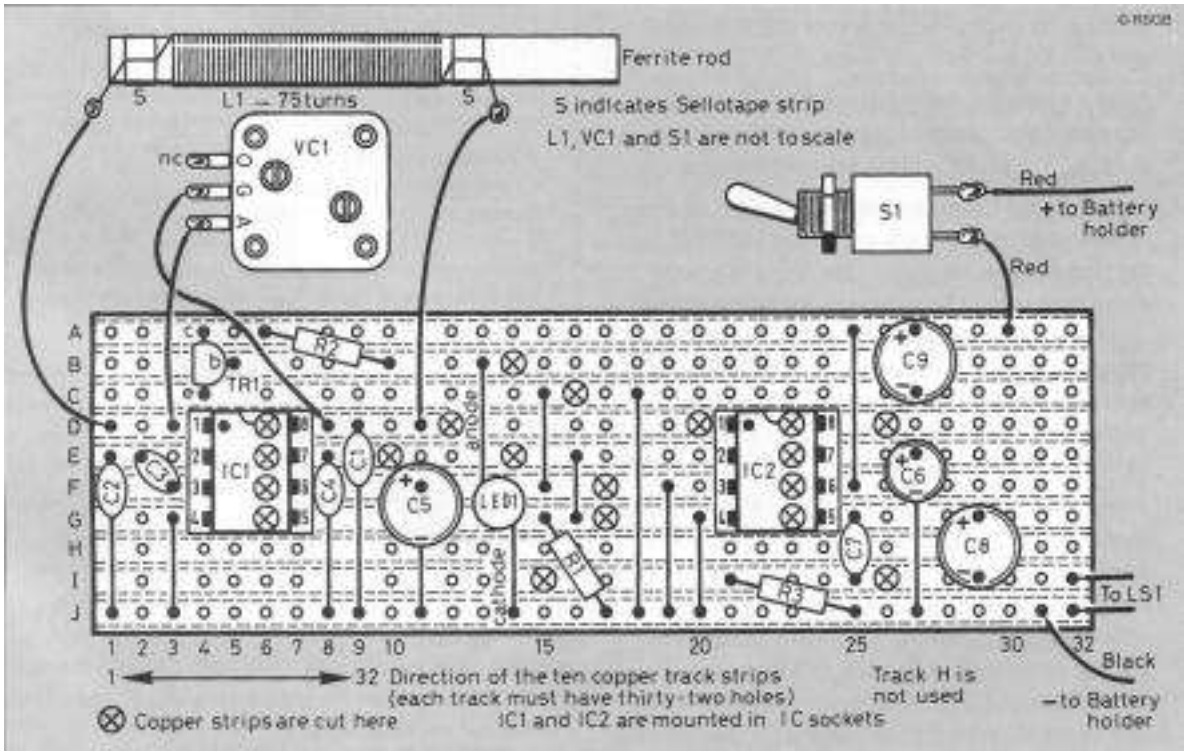

Figure 2 Veroboard layout for the Portable Radio. Make sure that all the wire links are included

the need arises! At the speaker position, make one large hole or a series of small holes to let the sound out. The ferrite rod may be stuck to the lid, as may the loudspeaker. Drill holes of the correct size to fit the particular types of variable capacitor (VC1) and switch (S1) that you are using. The Veroboard may be held in position by Blu-Tack or double-sided sticky tape.

6. Before inserting IC1 and IC2, connect the battery and switch S1 on. The LED should glow dimly (you may have to shield it with your hand in order to see it). If you have a test meter, check that there is about 1.3 V between pins 6 and 4 of IC1. If the reading is around 6 V or there is no glow, you may have connected the LED the wrong way round! When everything seems normal, switch off and disconnect the battery. Insert IC1 and IC2, making sure that the pins are straight and lie immediately above their corresponding holes in the sockets, and that the notches line up with the notches in the holders. Then push *gently* downwards on each IC in turn until the chip is firmly seated in its socket.
7. Switch on! By rotating the tuning capacitor, VC1, you should now be able to tune in many stations, rotating the radio to give you some volume control.

Final touches . . .

The handle was made with part of an old leather belt, secured to the case with 'number plate' nuts and bolts from Halfords. The loudspeaker grille is the lid from a *pot-pourri* container, and some extra holes were drilled in the back to improve the sound. See what you can find to finish off your radio!

Parts list

Maplin order codes are given for most of the parts, but you should get used to using the 'beg, borrow or steal' technique, or to use your ever-expanding junk box.

		Maplin code
Resistors: all 0.25 watt, 5% tolerance		
R1	68 ohms (Ω)	M68R
R2	5.6 kilohms (kΩ)	M5K6
R3	10 ohms (Ω)	M10R
Capacitors		
C1, C4	10 nanofarads (nF) or 0.01 microfarad (μF) ceramic	BX00A
C2, C3, C7	100 nanofarads (nF) or 0.1 microfarad (μF) ceramic	YR75S
C5, C8, C9	100 microfarads (μF) electrolytic, at least 10 V	FF10L
C6	10 microfarads (μF) electrolytic, at least 25 V	FF04E
Semiconductors		
IC1	ZN415E radio chip	
IC2	LM386 audio power amplifier	UJ37S
LED1	3 mm green LED	WL33L
TR1	BC548 npn transistor	QB73Q
Additional items		
LS1	Miniature 8 ohm loudspeaker	WB08J
S1	Miniature SPST toggle switch	FH97F
Ferrite rod	Length approx. 100 mm	YG20W
	24 SWG enamelled copper wire	BL28F

Additional items (*continued*)		
VC1	Tuning capacitor 140 to 300 picofarads (pF)	FT78K
	Tuning knob	FK41U
	8-pin DIL IC sockets (two required)	BL17T
	4 × AA-size battery holder (long)	HF94C
	PP3-type clip for battery holder	HF28F
	Plastic box approx. 158 × 95 × 54 mm	LH51F
	0.1 inch Veroboard, min. size 32 holes × 10 strips	JP46A

Plus
- Stranded insulated conductor for flying leads
- Multicore solder
- Materials for handle and speaker grille
- Double-sided sticky tape or Blu-Tack
- Sellotape
- Glue
- Four AA-size 1.5 V batteries

22 The Colt 80 m receiver – Part 2

Introduction

In Part 1 we constructed the audio amplifier module for the system and tested it in a very simple way. If you did what was suggested and built the simple Crystal Set to use as a signal source, you will know just how well the amplifier works.

The case

Metal cases for the project are available from Maplin, telephone 01702 554 161 (code XB67). From the photograph on p. 72 you can see the way the components are mounted. The audio amplifier is seen at the top right of the base, to the right of the tuning capacitor VC1. The next in this series will deal with the variable-frequency oscillator (VFO) and VC1. The current part deals with preparing the case to receive the components.

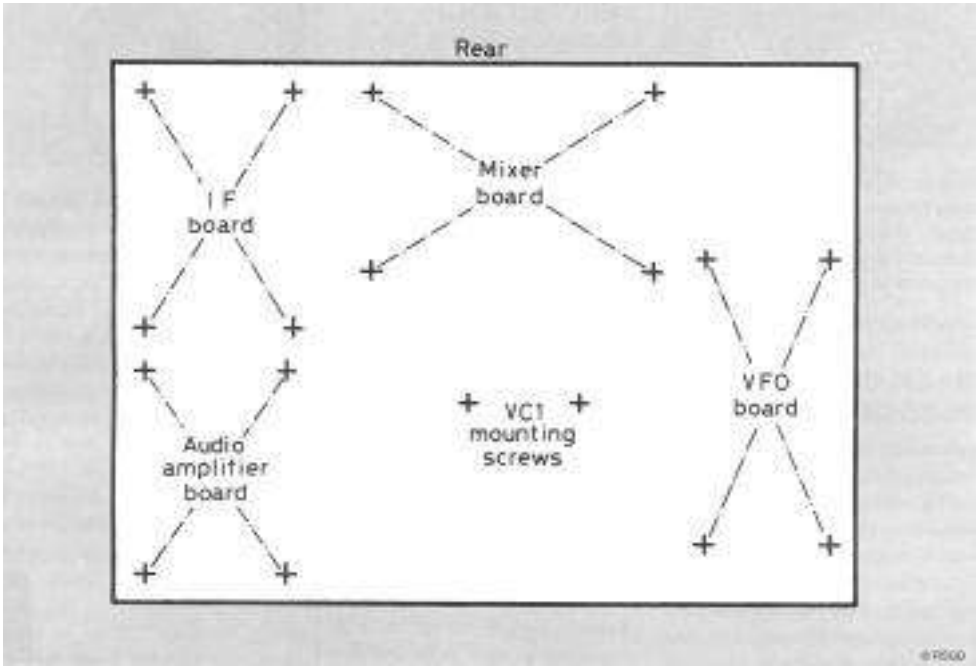

Figure 1 Fixing holes for each module are best measured from each printed circuit board or matrix board

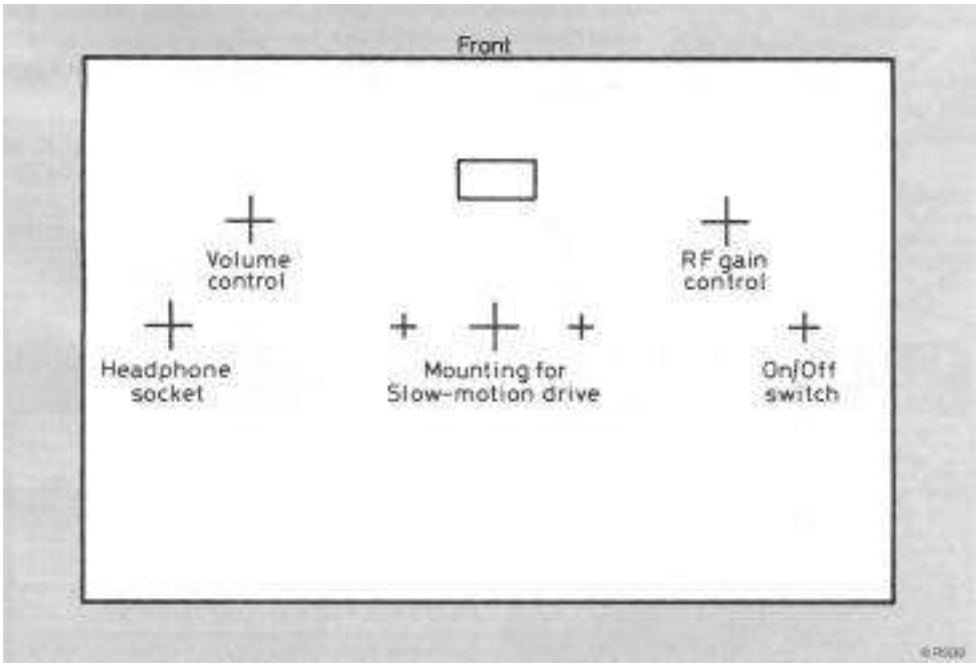

Figure 2 Position the slow motion drive to allow viewing of the tuning dial

Figures 1 and **2** show the markings for preparing the front panel and base. All the circuit boards and the tuning capacitor are mounted on the base using 10 mm stand-off pillars with 6BA bolts. The board locations are shown in Figure 1. The front panel control positions are shown in Figure 2, together with the small rectangular hole for viewing the tuning dial.

The best way to mark out the holes for the boards is to lie the boards flat on the base (before you've started soldering the components in) and marking the base through the holes in the boards. This minimises the scope for errors!

A *reduction drive* is used between the tuning knob and the capacitor shaft. This is simply a gear mechanism that slows down the capacitor shaft by a factor of six compared with the tuning knob, and makes tuning very much easier. The recommended variable capacitor also has a pulley wheel mounted on the shaft. Glued to this wheel will be a scale marked with frequency and is visible through the rectangular hole in the front panel.

The next part . . .

The variable-frequency oscillator and mixer will be added to the project.

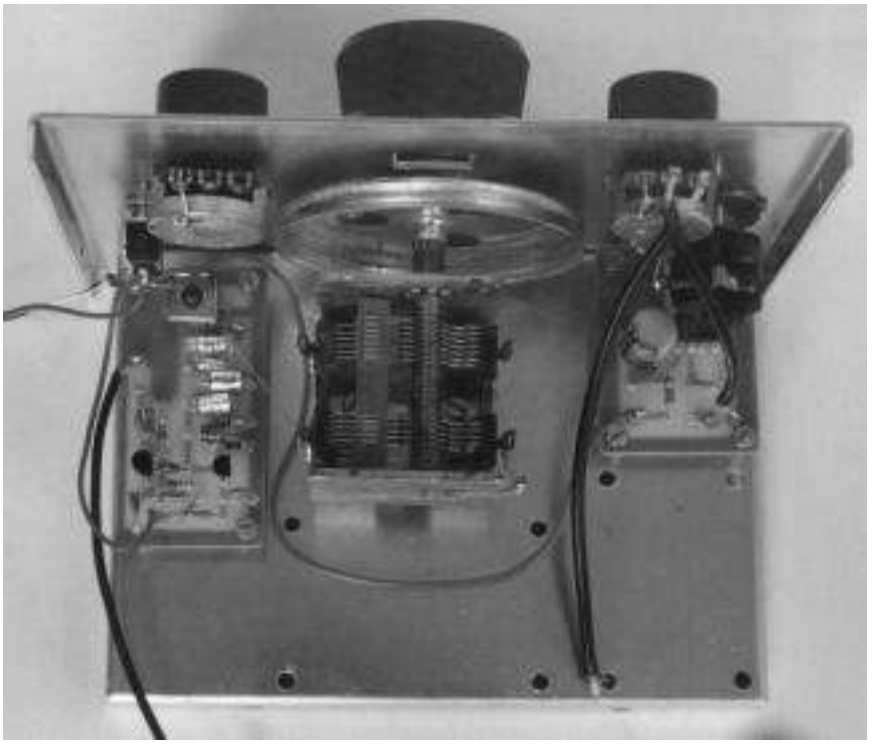

23 A simple transistor tester

Introduction

Although transistors aren't used as much as they were before integrated circuits came along, a transistor tester is still a useful piece of test equipment to have around the shack. This design is about the simplest possible and will produce an indication of whether a transistor is giving any current gain; this does not necessarily mean that the transistor is perfect but that it is working to a certain extent. This tester will **not** test field-effect transistors (FETs). If you buy a bag of transistors at a rally, this tester is useful for giving a yes/no indication of which ones go straight in the bin and which are kept for further use.

How it works

Figure 1 shows the simple wiring circuit. In order to explain the working of the circuit, a circuit diagram is shown in **Figure 2**, with the npn transistor, TR1, under test shown as part of the circuit. The pnp/npn selector switch, SW1, is omitted for clarity.

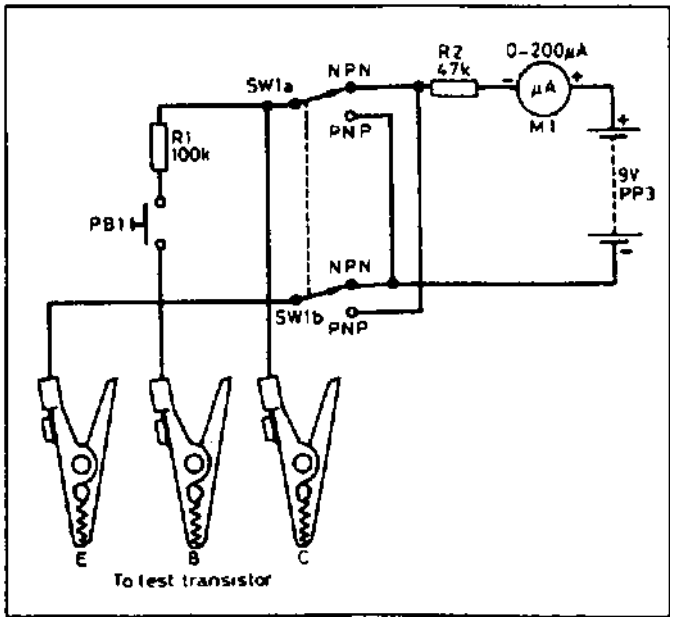

Figure 1 Circuit diagram of the transister tester

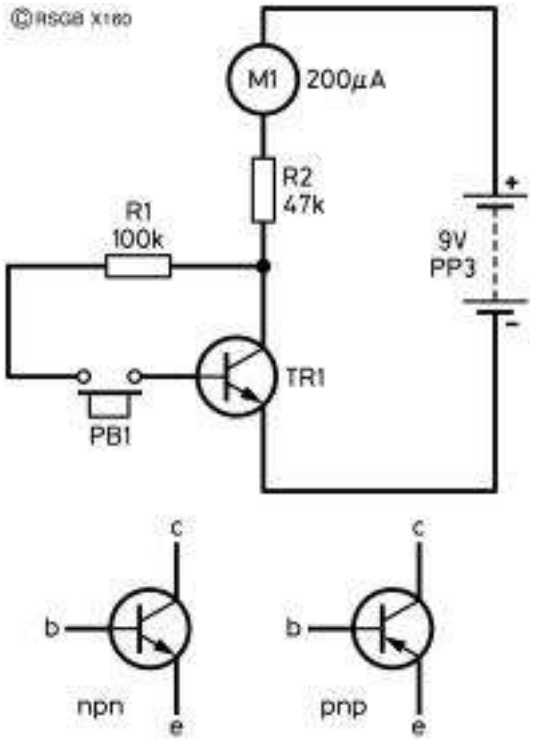

Figure 2 Testing an npn transistor

Any current that flows through the transistor, TR1, must flow from the battery, through the meter, M1, and through the protective resistor, R2. R2 prevents excessive current flowing through the meter and damaging it. Even if there is a short-circuit between emitter and collector, the maximum current that will flow is given by the simple equation

$$I = \frac{V}{R},$$

where I is the current flowing in amps,
V is the battery voltage, and
R is the total circuit resistance in ohms.

Putting in the correct values, gives

$$I = \frac{9}{47\,000} = 0.000191 \text{ A, or } 191 \text{ microamps } (\mu\text{A}).$$

The resistance of the meter, M1, will cut this down a little more, but it is within the indicating range (200 μA) of the meter.

As shown, with the push-button switch, PB1, *open*, a good transistor will not draw any current from the battery, and M1 will thus remain at zero. When PB1 is *pressed*, a *very small* current is injected into the base of the transistor. If the transistor is working, it will produce a much larger current between the collector and emitter, and this current will also flow through M1 and R2, giving a significant reading on M1, showing that all appears to be well. If an appreciable current flows when PB1 is *open*, then your transistor is suspect.

Don't be put off by the apparently complicated switch, SW1. It is there to allow the other type of transistor, the pnp type, to be tested. All it does is reverse the battery connections, so that the emitter goes to the *negative* battery terminal for testing an npn transistor, and to the positive terminal for a pnp type!

Most transistors in common use are of the npn type, which is why Figure 2 shows the testing of an npn type. The connections to the different transistor *encapsulations* (shapes) are given in any good component catalogue. Avoid the trial-and-error method to discover the connections to a transistor. This is unscientific, and can be very frustrating, particularly if the transistor is faulty in the first place!

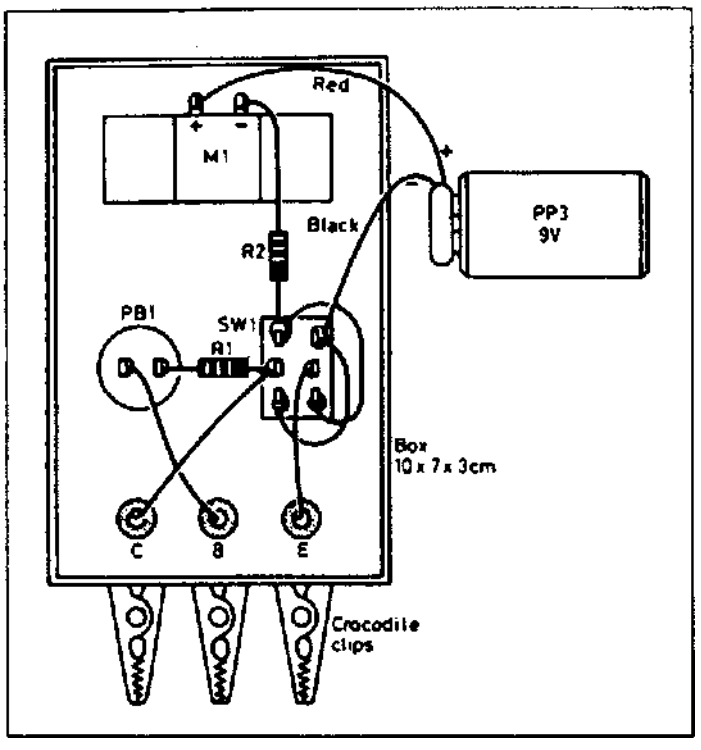

Figure 3 This shows how to wire up the tester

Construction

The unit can be built into a small plastic box, the components being soldered directly to the fixed terminals of the meter and the two switches; no circuit board is necessary! Use different colours of wire for the three test leads, and make sure you know which is which! Check the connections against the wiring diagram of **Figure 3**. When you are confident that all is correct, connect the battery and make sure there is no reading on the meter when nothing is connected to the crocodile clips!

Find any transistor for which you know the connections and the type (npn or pnp). Set the npn/pnp switch accordingly. Connect the three clips, making sure that they do not touch each other. A small reading on the meter at this stage means the transistor is suspect; a large reading means it is not working and should be thrown away! Press PB1 and watch the meter; a reading greater than half of full-scale indicates a good transistor. If it is less than half, you may have a transistor with 'low gain'; it may be usable for non-critical applications, but if you are in any doubt – throw it away!

Parts list

Resistors: all 0.25 watt, 5% tolerance

R1	100 kilohms (kΩ)
R2	47 kilohms (kΩ)

Additional items

PB1	Push-button switch
SW1	DPDT (double-pole double-throw) switch
M1	Micro-ammeter – *not* less than 200 μA full-scale deflection
	Crocodile clips (3 needed)
	PP3 battery and connector
	Plastic box about 10 × 7 × 3 cm

Common types of transistor

BC108, BC109, 2N2369A

These are small-signal npn types, used in audio amplifiers. They are in metal cases (called TO18) and have a tab next to the emitter lead. Common types have a B or C suffix (e.g. BC109C). The C suffix indicates a higher current gain than those with a B suffix. The 2N2369A is specially designed for radio use at high frequencies.

2N3703, BC212L, BCY71
These are pnp transistors, and so must be used with the collector and base *negative* with respect to the emitter. These three types are used in small amplifiers and audio oscillators. The first two have plastic encapsulations (TO92), while the BCY71 has a metal case (TO18).

BFY50, BFY51, BFY52
For slightly higher powers, these are ideal. They have been used in novice transmitters up to 600 milliwatts (mW). The TO5 case is a scaled-up version of the TO18 case. They are all npn types.

2N3055, 2N3773, TIP35C
These are high-power transistors in bigger encapsulations. The thick metal TO3 case of the 2N3055 and 2N3773 is designed to bolt to a heat sink, a large piece of metal which conducts the heat into the air more rapidly than the transistor itself can. The TIP35C is made of plastic but has a thick metal tab by which it, too, can be bolted to a heat sink.

24 An introduction to transmitters

Introduction

We usually think of a transmitter as being a 'black box'. However, that is the form a transmitter takes for our use on the amateur bands. Many electrical circuits are transmitters, even though transmitting may not be their primary function!

Anything that emits electromagnetic energy at *any* frequency is a transmitter, from radio at the low-frequency end of the spectrum, to gamma rays at the high-frequency end. We all know that a magnet will attract certain metals and that a comb rubbed on your coat sleeve will pick up small pieces of paper. The former is an example of the effect of a magnetic field, the latter of an electric field. Electromagnetic fields are combinations of both types of field, and are produced whenever an electromagnetic wave is transmitted.

What frequency?

Many everyday objects have a natural frequency of oscillation. This is called their *resonant frequency*. A wine glass will ring when struck gently; an

empty wine bottle will sound if you blow across the top; a guitar string will vibrate when plucked. These are all examples of resonance, and the resonant frequencies will **not** change unless the objects themselves are changed physically in some way. These are resonances in *sound*; we are primarily interested in electrical resonances.

The basic electrical resonant circuit is the combination of an inductor (coil) and a capacitor, as shown in **Figure 1**.

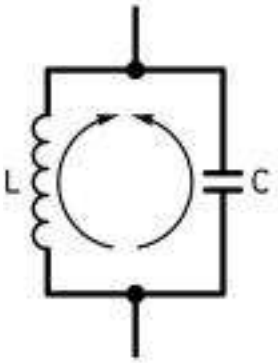

©RSGB X162

Figure 1 The basic electrical resonator. The energy in the circuit alternates between the inductor and the capacitor

A pulse of energy applied to this *tuned circuit* will make it *ring* (oscillate) at its resonant frequency. The energy in the circuit transfers between the inductor and the capacitor every cycle of the oscillation. Just like the wine glass, its oscillation dies away because it is losing some energy to its surroundings – it is transmitting! The frequency of the resonance depends on the values of *L* and *C*.

Keeping it going

If we want to keep the circuit oscillating, rather than having it die away, we must supply the circuit with just enough energy to replace the energy lost both by radiation and by losses in the circuit itself. Because of this, you will find in all oscillator circuits, a transistor, valve or FET working with the tuned circuit to provide this extra energy.

As it stands, of course, even with its transistor, our oscillator will not radiate very far. Connecting an aerial to it, and a Morse key to interrupt the power supply, it would become a very low-power CW transmitter. Add a couple more transistors to form a radio-frequency (RF) amplifier, and you have the basis of a simple low-power (QRP) transmitter.

Resonant circuits can also be made using quartz crystals; these work at the crystal frequency only, and this is marked on the crystal case.

A tiny spark transmitter

This is a simple piece of test gear that will increase your knowledge and understanding of resonance. You can use it to estimate the resonant frequency of most of the inductor/capacitor (LC) tuned circuits that you build. The circuit is shown in **Figure 2**. It operates around a relay. Any relay that operates from a 6 V to 9 V source and has contacts which are normally closed (i.e. closed when the battery is not connected). Fit the relay, a toggle switch and the battery in a metal box, and connected up as shown in the diagram. Some foam rubber inside the box may help to reduce the escaping noise of the relay. A small hole in the side of the box enables the 2-turn loop to emerge. This should be about 40 mm diameter, made with insulated wire. Switch on; there should be a loud buzzing noise from the relay. If not, you have probably chosen the wrong contacts on the relay!

When it is working, bring the loop close to the aerial of a radio – it should produce a loud noise from the speaker!

How it works

When you switch on, current flows through the relay contacts and through the relay coil. The relay operates and opens the contacts, causing the relay to 'drop out'. When it does, the circuit is completed again and the contacts are opened, and the cycle repeats. Each time the relay contacts open, there is a small spark between them, causing very rapid current surges through the wire loop. This makes the loop transmit RF energy, very briefly. In the early days of radio, this type of circuit was known as a *spark transmitter.*

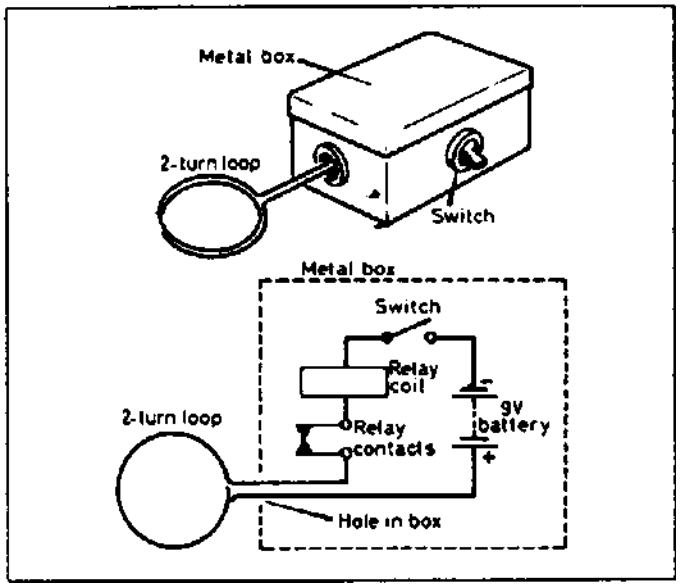

Figure 2 The current path is interrupted when relay is energised as shown above

Make a tuned circuit

Use a discarded toilet-roll centre, and wind about 10 turns of enamelled copper wire round it, keeping each turn close to the next. Scrape off the enamel for about 1 cm at each end, and solder a 100 picofarad (pF) capacitor (or a variable capacitor of about the same value) between the ends. The resonant frequency should be about 10 MHz. If you have used fewer turns or a smaller capacitor, the frequency will be higher.

Measuring the resonant frequency

Set up the buzzer as shown in **Figure 3**, with the loop around one end of your coil. Then make a similar loop, solder it to the end of a piece of coaxial cable going to the aerial socket of a calibrated receiver. Set the buzzer going, tune the receiver around 10 MHz, and search for the maximum noise level from the speaker. When you have found it, move the two loops as far away as possible from the main coil. This is called reducing the *coupling* between the coils, and it may result in a slightly different, but more accurate, resonant frequency.

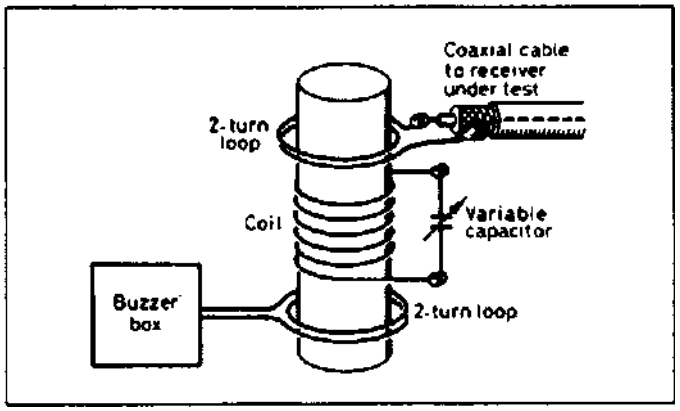

Figure 3 Experiment with the spacing between the loop and the tuned circuit

Parts list

Any small relay which operates between 6 V and 9 V
Metal box – do not use a plastic box!
9 volt battery and connector
On/off (SPST) toggle switch
Plastic foam, as required

25 The Colt 80 m receiver – Part 3

Introduction

In Part 2 we marked out the case ready for installation of the modules when they are completed. In this part, the building of the variable-frequency oscillator (VFO) and mixer will be described. This will produce a type of receiver known as *direct-conversion*, because it converts the radio-frequency (RF) signal directly into an audio-frequency (AF) signal which we can hear in a loudspeaker after amplification. A block diagram of the system is shown in **Figure 1**. The modifications needed to make a full superheterodyne receiver will be left until later.

The direct-conversion receiver covers the 80 metre amateur band and will receive both Morse (CW) and speech (SSB) signals. The audio amplifier was covered in Part 1, so your *Colt* is rapidly taking shape! By the time your construction has reached the end of this part, you will have a receiver ready to use, even if the project is not yet complete!

The direct conversion process

Like most things in radio, the principles of direct conversion are not difficult. From the aerial, the signal we want to hear is selected by the *tuned filter*, which rejects the signals we don't want. The signal then enters the

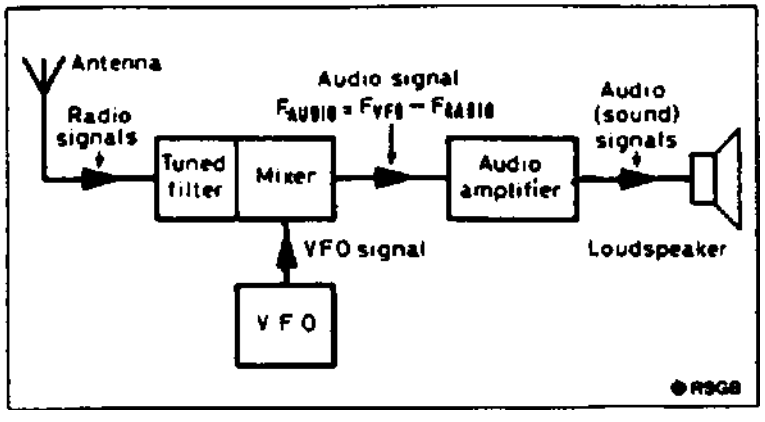

Figure 1 Stages of direct-conversion receiver

mixer, along with the signal from the *VFO*. The VFO produces a sine wave whose frequency can be varied across the whole of the 80 metre amateur band (3.5–3.8 MHz), by turning the knob on the tuning capacitor, VC1. The mixer produces, at its output, *two* signals; one signal is at the frequency of the **sum** of the signal and VFO frequencies, the other is at the **difference** of the two frequencies. It is the latter that we want. Let's look at the numbers involved. If the signal is at 3650 kHz and the VFO is at 3651 kHz, then the sum frequency is 7301 kHz, and the difference frequency is 1 kHz. If we feed the output of the mixer into our audio amplifier, the 7301 kHz signal is automatically removed (it is far too high to be considered an audio signal!) and the resulting 1 kHz signal is amplified and fed to the speaker, producing a note which we can hear!

Building the VFO

Figure 2 shows the circuit of the VFO. It is a tried and tested circuit, and should work first time. It uses a *field-effect transistor* (FET) for TR1, the oscillator itself. RFC is a *radio-frequency choke*, a coil of wire which will pass a direct current (DC) but which will prevent radio-frequency (RF) signals getting through.

All VFOs have a tuned circuit which, in this case, is formed by the coil L1 and the capacitors C1 and VC1. The frequency will also be affected to some extent by C2, C3, C4 and C5. Transistor TR2 is an *emitter follower*, a stage which gives no voltage gain but provides a good *buffer* stage, isolating the VFO from the effects of the stages that follow it. When building a VFO, the

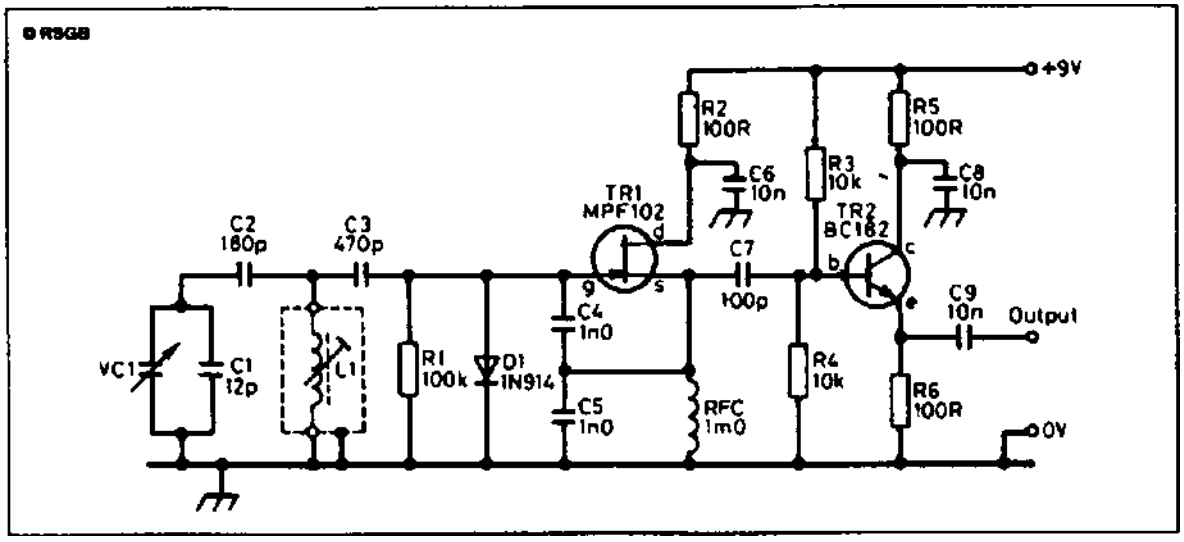

Figure 2 The variable-frequency oscillator uses a field-effect transistor (FET)

parts must be securely mounted. If components move, so does the frequency! At worst, the oscillation will become unstable and the VFO will be useless. Keep the component leads as short as possible – this improves their mechanical stability as well as their electrical stability!

Mount the parts on the printed-circuit board (PCB) or matrix board and, when completed, the VFO should look like the one shown on the left in the photograph on p. 72. Make sure that TR1, TR2 and D1 are the right way round.

On completion, check the component positions then mount it in the case as shown in the photograph, to the left of the tuning capacitor when viewed from the rear. The VFO coil, L1, will need some adjustment, but that will have to wait until the mixer is built. Connections to the other boards are made with screened cable.

The mixer board

So far, we have an audio-frequency (AF) amplifier and a VFO; the addition of a mixer board gives us a complete direct-conversion receiver for 80 m. The mixer circuit diagram is shown in **Figure 3**. Let's follow the signal path.

- From the aerial, the RF signal goes to the gain control potentiometer, RV1. This reduces very strong signals, to prevent them overloading the mixer.
- To select the required band of signals, a *bandpass* filter is made up of RF transformers T1 and T2; these are tuned by C1 and C3, and are coupled together by C2.

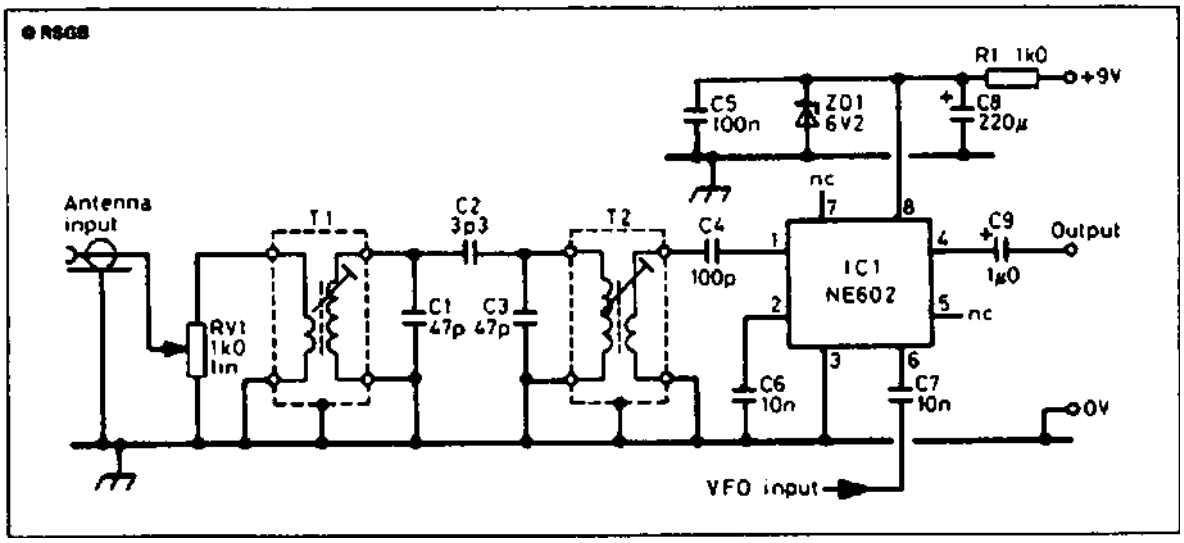

Figure 3 The mixer board has a bandpass filter and stabilised supply

- After the filter, the signal is coupled into the integrated circuit (IC) mixer type NE602, by the capacitor C4. Capacitors C5 and C8 *decouple* the supply line, to prevent unwanted signals on the supply from disturbing the VFO operation. The use of the term *decouple* is exactly the opposite of *couple*; when two circuits are *coupled* together, the signal passes from one to the other; when two circuits are *decoupled*, signals **cannot** pass from one to the other.
- The NE602 works with a 6 V supply; it is produced here from the 9 V supply by the *Zener diode* ZD1 and the resistor R1. ZD1 operates at 6.2 V, and gives a steady output for the mixer. The audio output from the mixer appears at pin 4 or IC1. This is taken to the audio amplifier board via C9 and the volume control (see Part 1).

Care must still be taken to insert some components the right way round. These are the electrolytic capacitors, C8 and C9, the Zener diode, ZD1, and the integrated circuit, IC1. Check all component positions and make sure all your soldered joints are bright and shiny.

Putting it together

The interboard wiring, shown in **Figure 4**, uses screened cable; ideally, this should be thin coaxial cable, but screened microphone cable is suitable. The diagram shows how the two controls, the RF Gain and Volume, are connected to the boards. The leads marked '+9 V' are all connected to the battery supply via a miniature on/off toggle switch. Double check all connections before connecting the battery.

Setting the VFO

Very little adjustment is needed to get the receiver going. Firstly, the VFO must be adjusted to cover the required band, in this case 3.5–3.8 MHz.

If you have a frequency counter, connect it to the output of the VFO. If you haven't, read this part anyway so you understand the process, then another means of setting the VFO will be given especially for you! Rotate VC1 until the vanes are fully meshed. Very carefully, adjust the core of the VFO coil (L1) with a plastic trimming tool so that the frequency approaches and settles at 3.500 MHz. When you rotate VC1, the frequency should increase to **at least** 3.800 MHz at the far end of its travel.

In the absence of a frequency counter, borrow a communications receiver, set it for SSB reception (USB or LSB) on exactly 3.500 MHz. Set VC1 with the vanes fully meshed and turn the core of L1 in both directions until you hear a whistle in the communications receiver. Rotate the core so that the whistle reduces in frequency. It will eventually fade out at around 200 Hz;

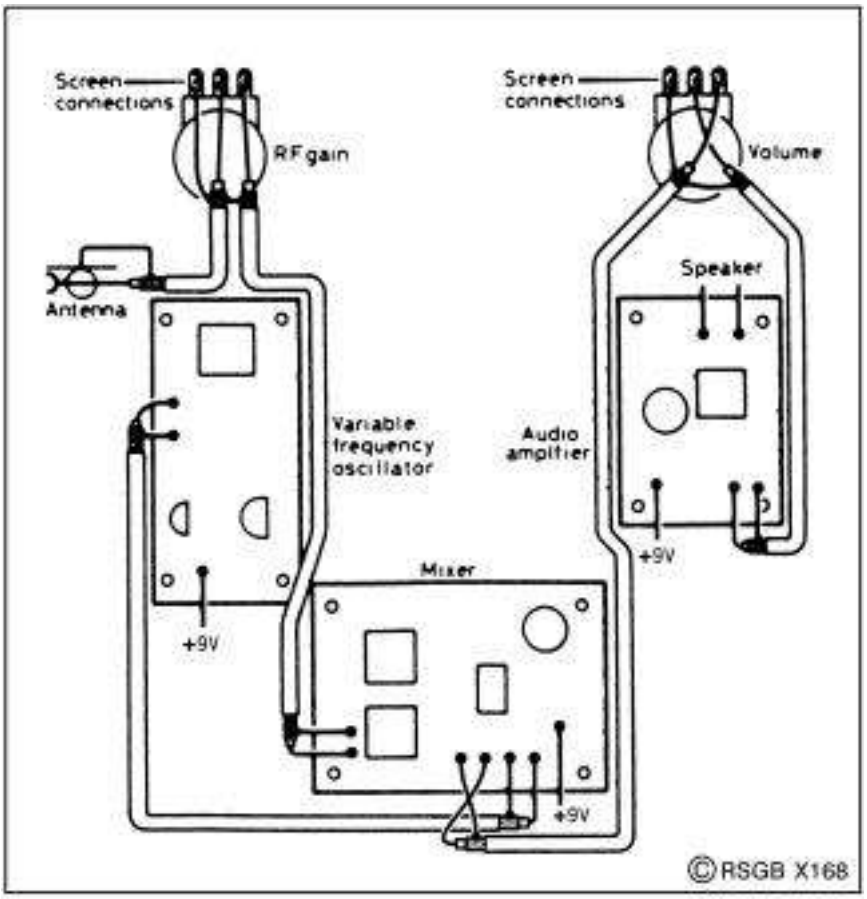

Figure 4 Make sure that interconnections between the boards are correct, including cable screens

turn the core a little further and then leave it at that position. Rotate VC1 right to the other end of its travel, and search for the whistle with the tuning knob of the communications receiver. Check that the VFO frequency is at least 3.800 MHz.

Then, whichever method you are using for frequency measurement, mark the dial with frequency steps of 50 kHz. Setting and calibration are finished!

Setting the mixer

Again, there are various ways of doing this. If you have a signal generator, inject a signal at a frequency within the 80 m band, and adjust the cores of T1 and T2 sequentially for maximum output.

If you haven't a signal generator, connect an aerial to the mixer input, set the RF Gain to maximum (fully clockwise), and find a consistent signal. Adjust the volume control to a comfortable level. Rotating the core of T2 with your trimming tool, maximise the output. Then do the same with T1, although this will have much less effect. Find another station, and check that the positions of the cores aren't too different for a maximum signal.

You may find that your receiver benefits from the insertion of an aerial tuning unit (ATU) between the aerial and the input, to compensate for the impedance of your aerial not being 50 Ω. A design for such an ATU is presented in another part of this series. If the signals are still weak, connect the ATU to the junction of C1 and C2 via a 100 pF capacitor.

Try listening!

Remember that 80 m is a variable band. During daylight hours, your will hear Morse signals at the lower end of the band, and some British and closer continental stations between 3.7 and 3.8 MHz. In the evenings, stations up to 1000 miles away should be heard. Look for Novices around 3.7 MHz!

Parts list – VFO board

Resistors: all 0.25 watt, 5% tolerance		
R1	100 kilohms (kΩ)	
R2, R5, R6	100 ohms (Ω)	
R3, R4	10 kilohms (kΩ)	
RV1	1 kilohm (kΩ) linear	
Capacitors		
C1	12 picofarads (pF) polystyrene	
C2	100 picofarads (pF) polystyrene	
C3	470 picofarads (pF) polystyrene	
C4, C5	1 nanofarad (nF) polystyrene	
C6, C8, C9	10 nanofarads (nF) polystyrene	
C7	100 picofarads (pF) min. ceramic	
VC1	140 + 140 picofarads (pF) variable	
Semiconductors		
TR1	MPF102	FET
TR2	BC182	npn
D1	1N914	silicon
Inductors		
L1	Toko KANK3334	
RFC	1 mH	RF choke

Parts list – mixer board

Resistors: 0.25 watt, 5% tolerance

R1	1 kilohm (kΩ)
VR1	1 kilohm (kΩ) potentiometer (linear)

Capacitors

C1, C3	47 picofarads (pF) min. ceramic
C2	3.3 picofarads (pF) min. ceramic
C4	100 picofarads (pF) min. ceramic
C5	100 nanofarads (nF) min. ceramic
C6, C7	10 nanofarads (nF) min. ceramic
C8	220 microfarads (μF) electrolytic 16 V
C9	1 microfarad (μF) electrolytic 16 V

Integrated circuit

IC1	Philips NE602 or NE602A

Additional items

T1/T2	Toko KANK3333
	On/off switch
	Miniature toggle switch

The next part . . .

The IF amplifier and the Beat-Frequency Oscillator will be added to convert the *Colt* into a superheterodyne receiver.

26 A two-way Morse practice system

Introduction

It is said that the pleasure of sending and receiving Morse code more than compensates for the learning effort needed. Transmitters for Morse code can be much simpler than those needed for any of the speech modes.

Many people choose to learn sending and receiving on their own. It can be much more fun if you have someone to learn with you, and it is for this reason that the following project arose. It comprises just one small circuit, and you build an identical circuit for each of the people who want to learn with you. All the individual circuits are connected with their output leads in *parallel*, as the two-way circuit of **Figure 1** shows.

A simple circuit

This diagram shows two identical circuits, as would be used if two people wanted to learn together. The circuit centres around our old friend the NE555 integrated circuit (IC). As it is connected here, it works as an *astable multivibrator*, a daunting name for what is essentially an oscillator. Each circuit is self-contained, having its own battery, Morse key, sounder and

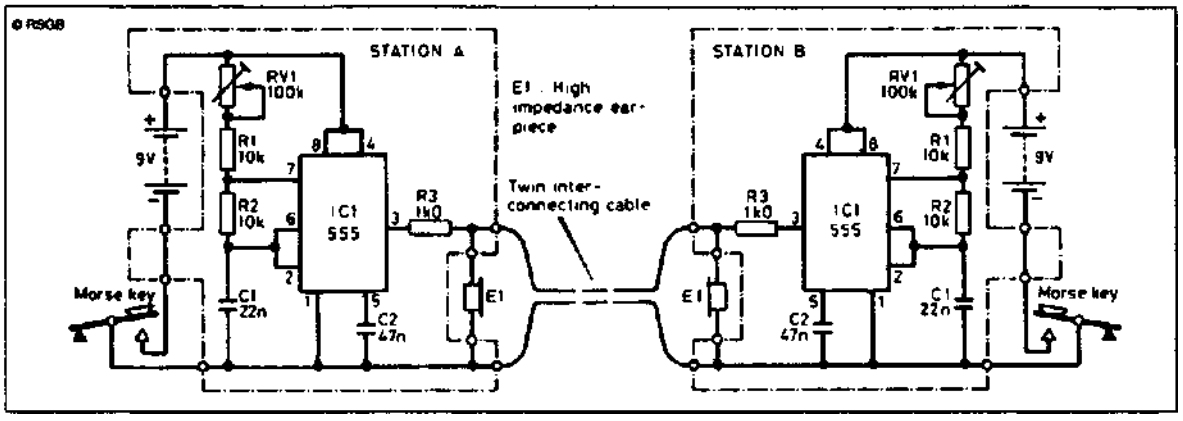

Figure 1 The circuit diagram shows two stations, but you could connect several more if needed

plastic box. The Morse key makes and breaks the power supply to the circuit, thus turning on and off the note emitted by the earpiece. The frequency of the note is controlled by the variable resistor RV1, resistors R1 and R2, and the capacitor C1. The range given by RV1 is approximately from 500 Hz to 2200 Hz.

R3 protects the output of the IC against accidental shorting either to the 0 V or to the 9 V supply rails. For best results, a crystal earpiece or high-impedance headphones should be used. You could try Walkman-type headphones, but the volume may be too low for you.

The units may be interconnected with thin twin cable (the sort used for wiring doorbells) and can be comfortably separated by 25 m, more than enough to communicate between rooms, or even with a neighbour!

In use

When an operator presses his key, the note is heard by himself and by everyone else who is connected. If more than one key is pressed at the same time, two or more notes are heard by everyone! It helps if each person adjusts his own potentiometer, RV1, to give a note which is different from the others. When one operator stops sending, the other can start immediately, without pausing to change from transmit to receive. In practice, this technique is known as *full break-in*.

The current drawn by the circuit is only 10 milli-amps (mA) when the key is down, meaning that the life of a typical PP3 battery will be virtually its shelf-life! No switch is needed, because the key acts as the switch. The current drain will be even less if the NE555 is replaced by an ICM7555 IC. It has exactly the same pin connections as the NE555, so no circuit modifications are needed.

The circuit board

The circuit is constructed easily on a small piece of Veroboard of the copper-strip type. **Figure 2** shows the layout of the prototype, the board measuring 18 holes by 10 strips. **Be aware that there is no row 'I' when you are transferring mental images of where the parts are to real positions on the board!** Break the copper tracks where shown with a 3 mm (⅛ inch) twist drill, rotated carefully between thumb and forefinger. Hold the board up to a bright light to make sure that the tracks are completely broken and that there are no fragments of copper swarf shorting adjacent tracks. Then, solder in the wire links shown in Figure 2, followed by the resistors, RV1, and the capacitors, C1 and C2. Solder the battery connector leads to tracks A and G, G being positive. Use insulated wire to connect from the board to the jack sockets used as connectors for the key and the earphones. If you use

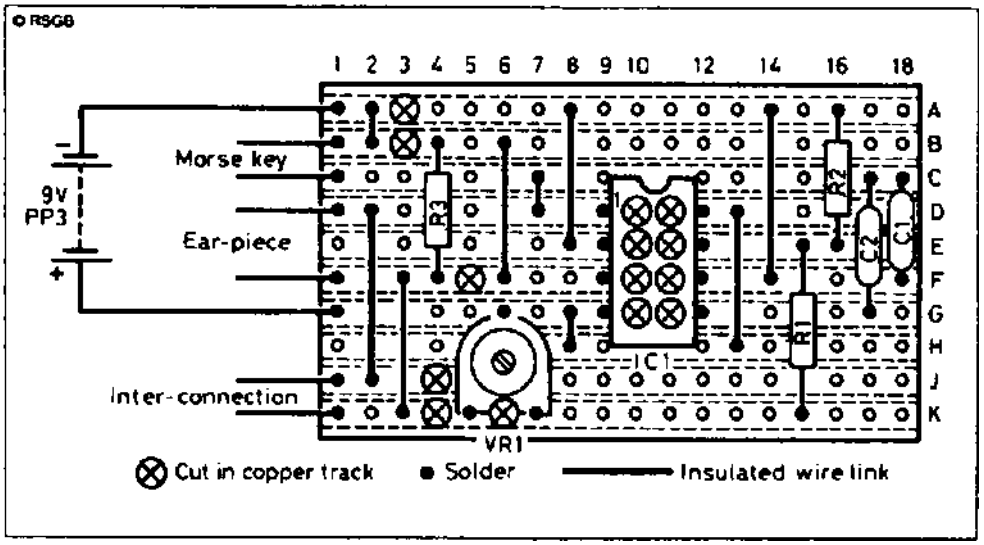

Figure 2 The Morse Duet is an easy project to build on stripboard (Veroboard)

different sized jack sockets (i.e. 2.5 mm and 3.5 mm) you won't plug the earphones into the key socket! A two-screw terminal strip is useful to connect the cable runs between operators.

The key

The circuit is designed to be used with a *straight key* (one that moves up and down). It is a requirement of the UK Morse test that a straight key is used, so it is very sensible to learn sending with a straight key before you try anything more complex! You will find many to choose from at rallies.

Parts list

For each board, you will need:		**Maplin order codes**
Resistors: all 0.25 watt, 5% tolerance		
R1, R2	10 kilohms (kΩ)	M10K
R3	1 kilohm (kΩ)	M1K0
RV1	100 kilohm (kΩ) min. preset (horizontal mounting)	UH06G
Capacitors		
C1	22 nanofarads (nF) ceramic, 25 V	WX78K
C2	47 nanofarads (nF) ceramic, 25 V	RA47B

Integrated circuit	
IC1 NE555	QH66W
Additional items	
8-pin DIL socket	BL17T
Jack plug and socket 2.5 mm	HF76H, HF78K
Jack plug and socket 3.5 mm	HF80B, HF82D
Battery type PP3	
Battery connector	HF28F
Plastic box with lid 114 × 76 × 38 mm	LH14Q
Veroboard 0.1 inch with copper strips	
18 holes × 10 strips	JP46A
Terminal strip (two section)	FE78K
Crystal earpiece	LB25C
Morse key	

27 The Colt 80 m receiver – Part 4

Introduction

In Parts 1 to 3 of this series, the design of an 80 metre direct-conversion receiver has been described. In this final part, we are going to change the circuit to operate as a superheterodyne receiver, or *superhet*. Most radio receivers are superhets, and they change the incoming signal to another frequency, known as the *intermediate frequency*, or IF, before producing an audio signal. The use of a superhet in a good receiver is mandated by the requirements for good *sensitivity* and *selectivity*.

Sensitivity and selectivity

Figure 1 shows the block diagram of the receiver. If you look closely, you will see that it is two similar circuits, one after the other. The incoming

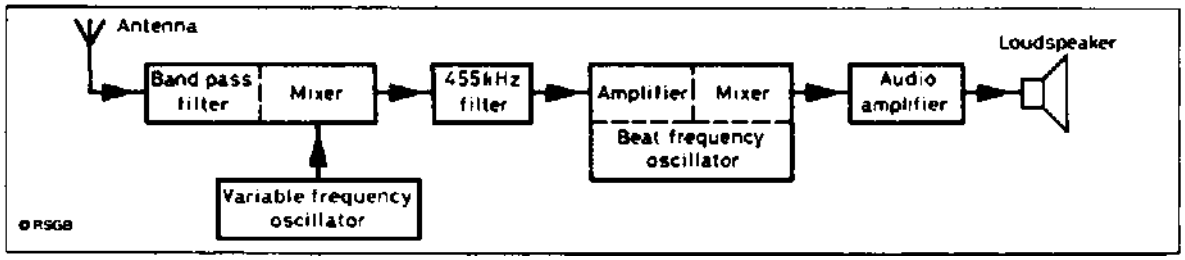

Figure 1 This is how the different stages of the Colt go together to make a superhet receiver

signal is filtered and fed to a mixer where it is combined (mixed) with the signal from the variable-frequency oscillator (VFO). This oscillator operates at a frequency which is 455 kHz higher than the incoming signal from the aerial, and the mixer output is therefore at a frequency of 455 kHz. If you are not sure about this, please refer to the section 'The direct conversion process' in Part 3 of this project. This new frequency is called the *intermediate frequency*, or IF. This frequency doesn't change; the tuning is accomplished by the VFO, and the mixer output is *always* at 455 kHz. The extraction of the audio signal from the IF signal is identical with the direct conversion process which is used in your existing receiver.

This may seem a long-winded way of doing things, but it has its advantages. A receiver must have a good *sensitivity*, or gain, so that it can receive very weak signals. In very general terms, it is easier to handle low-frequency signals than it is to handle high-frequency signals. We are changing our signal frequency from around 3.6 MHz down to 0.455 MHz (455 kHz), which is much lower and can be filtered and amplified relatively easily. A second advantage is that it is easier to provide gain at a fixed frequency than at a variable frequency. Remember that the IF is fixed, and providing gain is, again, relatively simple.

Our receiver also needs good *selectivity*, the ability to separate (or select) one station from another very close to it in frequency. This requirement is significantly simplified by the fact that the IF is fixed, and a good filter in the IF circuits can do wonders for the rejection of adjacent-frequency stations! Several stages of IF amplification and filtering are possible in more adventurous designs.

The filtered signal at 455 kHz passes to another mixer which has an associated oscillator, usually called a *beat frequency oscillator* (BFO). When receiving CW (Morse) signals, the BFO is usually tuned about 1 kHz above or below the IF (i.e. at 454 or 456 kHz) to produce a 1 kHz beat note as the audio signal. This signal is then amplified and fed to a loudspeaker or headphones.

The circuit

Figure 2 shows the circuit of the IF section shown in the photograph on p. 94; this section is added to the existing circuit to make it a superhet. The existing mixer board (described in Part 3) is used as the first mixer. Between it and the audio amplifier is connected the new IF board.

The signal output from the first mixer (at 455 kHz IF) is fed into a *crystal filter*, the most expensive part in the whole receiver. It provides the selectivity which makes the Colt such a good receiver. Another NE602 mixer/oscillator chip follows the filter. The oscillator section is controlled by the tuned circuit in T1, the frequency of which can be altered by rotating the core inside the coil. Once set, it remains fixed.

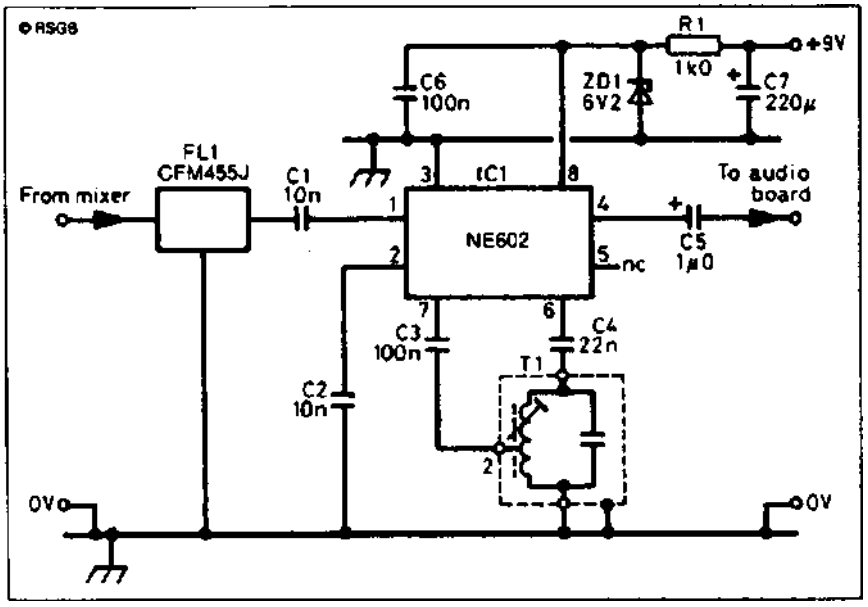

Figure 2 The IF board is connected between the mixer and audio amplifier

At this stage you should have built the first mixer and the audio amplifier, and proved that they *both* work by using the circuit as a direct-conversion receiver. When you have finished constructing and checking the IF board, you will need to add it to your existing circuits.

Adjusting and testing

There are three pairs of connections to the IF board – the 9 V supply leads, the input leads and the output leads. The IF board should be mounted on the metal baseplate, along with the other boards. **In making the following connections, make absolutely sure that the braid of each piece of coaxial**

cable is soldered to the correct connection on each board. The same applies to the polarity of the 9 V leads. Disconnect the screened lead which presently goes from the first mixer board to the AF amplifier at the amplifier end. Connect it instead to the *input* of the IF board. Connect a new piece of screened cable from the IF output to the vacated AF input. Now connect the 9 V supply leads to the same points as the supply leads from the other boards. Check these newly made connections.

You should have confidence at this point that things should be right. After all, you *have* tested the direct-conversion process and you *know* it works. All that you are now testing is the IF board. This is the attraction of building a receiver in modules, working from the speaker backwards, and testing as you go!

The VFO and BFO need to be correctly adjusted. Mesh the vanes of the tuning capacitor and, using the same frequency measurement method as you did originally, set the VFO frequency to 3.955 MHz (which is 3.500 MHz + 0.455 MHz, if you hadn't guessed!). The BFO can be set using a frequency counter, but it is just as good to set it by listening to SSB or CW signals. A high-pitched hissing sound should be heard in the speaker. As you rotate the core, the pitch should reduce, go through a minimum, then increase again. Set the core at the minimum pitch position. You may want to readjust the two cores a little as your listening skills improve but, once you are happy, they will never need to be altered again!

In conclusion . . .

You should now have built a superhet receiver capable of excellent results. It uses the same type of circuit as that found in far more advanced receivers.

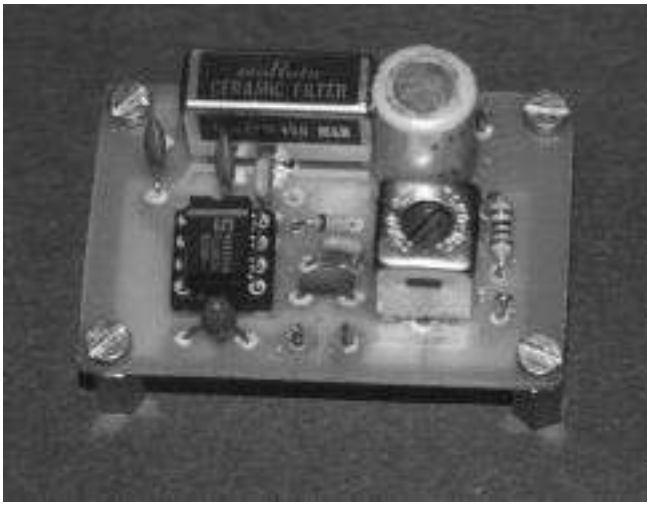

The superhet is far more sensitive than the direct-conversion type, and can weed out those elusive DX stations. You may have found that a station will appear at two places on the dial of the direct-conversion receiver; you will have no such problem with the superhet.

Parts list

Resistor		
	R1	1 kilohm (kΩ), 0.25 watt, 5% tolerance
Capacitors		
	C1, C2	10 nanofarads (nF) min. ceramic
	C3, C6	100 nanofarads (nF) min. ceramic
	C4	22 nanofarads (nF) min. ceramic
	C5	1 microfarad (μF) 16 V electrolytic
	C7	220 microfarad (μF) 16 V electrolytic
Integrated circuit		
	IC1	NE602
Additional items		
	ZD1	Zener, 6.2 V 0.5 watt
	FL1	Crystal filter, Murata CFM455J
	T1	Tuned inductor, Toko YHCS11100AC

28 A simple crystal set

Introduction

There are many designs of crystal set – they are all 'simple', and even the most seasoned radio amateur will build one of these every so often because it is something that never ceases to amaze! Although using modern components, the design is a period piece!

Design and construction

The circuit diagram of **Figure 1** shows the simplicity of the circuit. The prototype was constructed on a wooden baseboard with an aluminium front panel, although this could be made of wood if you prefer.

Winding the coil always causes the most groans but when finished, gives the most satisfaction. The construction of the coil is detailed in **Figure 2**. A discarded toilet roll centre is an ideal *former* on which to wind the coil. The coil will take up about 7 cm of the length of the tube, so assuming the tube is about 11 cm long, the ends of the coil will be about 2 cm in from each end of the tube.

The aerial coil, the *primary winding* of this radio-frequency (RF) transformer, is made from about 30 turns of 26 SWG enamelled copper wire, wound on the matchstick ribs. These ribs should be about 2 cm long, and are glued on **top** of the end of the secondary coil *after* the secondary coil has been wound. The *secondary winding* has 140 turns with *taps* every 10 turns for 70 turns. This coil covers most of the length of the cardboard tube. To make your coil-winding easier, here are some tips for completing the coil and still having some hair left at the end!

- Support the reel of wire on a dowel rod or pencil, clamped in a vice or held rigid in a vertical position by some other means. Don't leave it to trail around on the floor.
- Have a small piece of sandpaper handy to remove the enamel from the copper wire, starting with the end coming from the reel. Remove about 1 cm only, until the shiny copper is visible all round the end of the wire.

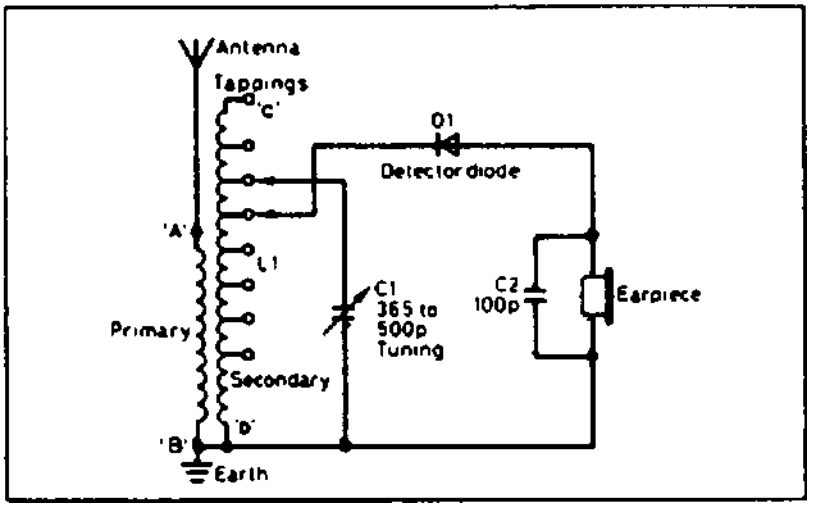

Figure 1 Circuit diagram of the crystal set

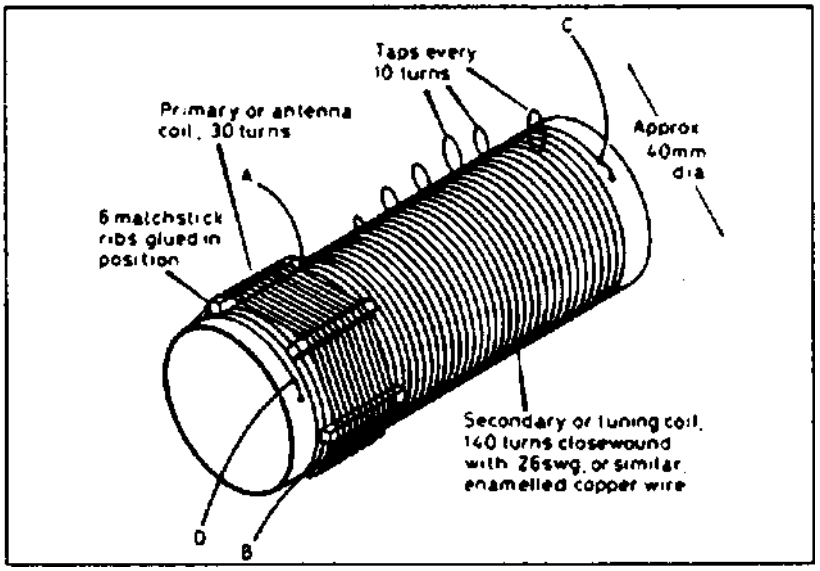

Figure 2 The coil is mounted on a cardboard tube as shown. Exact size is not too important. Try different taps for best results

- This part is the most difficult of all. Seasoned coil winders may have their own favourite ways of doing this, but for first-timers, play it safe and do it this way! Have a second bobbin (or a piece of stout card) ready, on which you will need to wind the wire loosely while you prepare the taps. Then, starting from the free end of the wire, measure 125 cm and, at this point, remove about 2 cm of the enamel with the sandpaper. Bend the wire firmly back on itself in the middle of the bared area, and *tin* (cover with solder) the exposed copper. This is your first tap. Then repeat this six more times at 125 cm intervals, thus giving you seven taps; wrap the wire as you go, on to the second bobbin or piece of card. After the seven taps, you are half-way down your coil so, to begin winding it in earnest, wind the wire carefully from the second bobbin or card **back** on to the original reel of wire.
- Looking at Figure 2, make two small holes about 3 mm apart, about 2 cm down from the top of the tube, where wire C will be entering. Poke the end of the wire into one hole, then bring it out again through the other; leave about 10 cm of wire on the free end. Loop this wire in and out once more, thus anchoring the wire firmly.
- Then, begin winding; keep the wire tight and make adjacent turns touch neatly. As you pass each tap, make sure it sticks outwards while avoiding flexing the wire too much; the wire is inherently weak at each tap.
- When you reach the last 10 cm of wire, stop. Put two more holes, like the first, beside your stopping point, and anchor the end, D, of the coil in the same way as you did with end C. The secondary winding is complete. Take a break *after* you have completed the next step!

- Prepare the six matchsticks for supporting the primary coil and glue these every 60 degrees around the end of the coil at D. Remove the enamel from the free end of the new copper wire on your reel and, using your favourite quick-drying cement, put a drop over the wire on one of the matchsticks, leaving 10 cm free as before. If you are using 26 SWG enamelled copper wire, its diameter is 0.46 mm, so 30 turns should occupy 14–15 mm of the 20 mm matchstick length. This will allow you to position the glued point such that the coil will be roughly in the centre of the matchsticks. When the glue has set, wind the 30 turns and anchor this end of the coil in the same way. Then remove the enamel at the end of the 10 cm lead.

Assembly

The coil former can be screwed to the baseboard at each end, *before* the front panel is screwed to the baseboard! As the photograph on the next page shows, the tuning capacitor is mounted in the centre of the front panel. Five solder tags (or drawing pins as a last resort) should be screwed into the baseboard. The two to the left of the photograph are the connections to the earphones, the two along the rear edge have the diode, D1, soldered to them. One end of the diode (and, for once, you can connect the diode either way round!) is connected to one earphone tag. The other end has a flying lead of about 10 cm attached to it and terminated in a crocodile clip which is used to connect to one of the taps on the coil. The fifth tag secures the end, A, of the primary coil, to which you will attach the aerial. The earth tag on the tuning capacitor, C1, serves as an anchor point for the ground connections to B and D and to the other earphone tag.

Use

The longest piece of wire you have available to use as an aerial should be connected to the aerial tag just mentioned. If you can connect the earth tag of the tuning capacitor to a good electrical earth, this will help also. You should be able to hear something as you turn the tuning knob. Try adjusting the tapping connections on the coil – change only one at a time, or you will never find the optimum positions. You now have a fully operational crystal set!

Simple it may be, but this circuit illustrates some important principles which are used even in the most expensive receivers. Firstly, the coil, L1, and the capacitor, C1, form a *tuned circuit* which *resonates* at the frequency of the station you have tuned in. This *selects* the signal you want to hear. The *modulation* on this signal is removed by the *detector*, D1, and fed to the earphones, which act as *transducers*, turning the electrical energy into sound energy which you can hear. It doesn't need a battery or other power supply either!

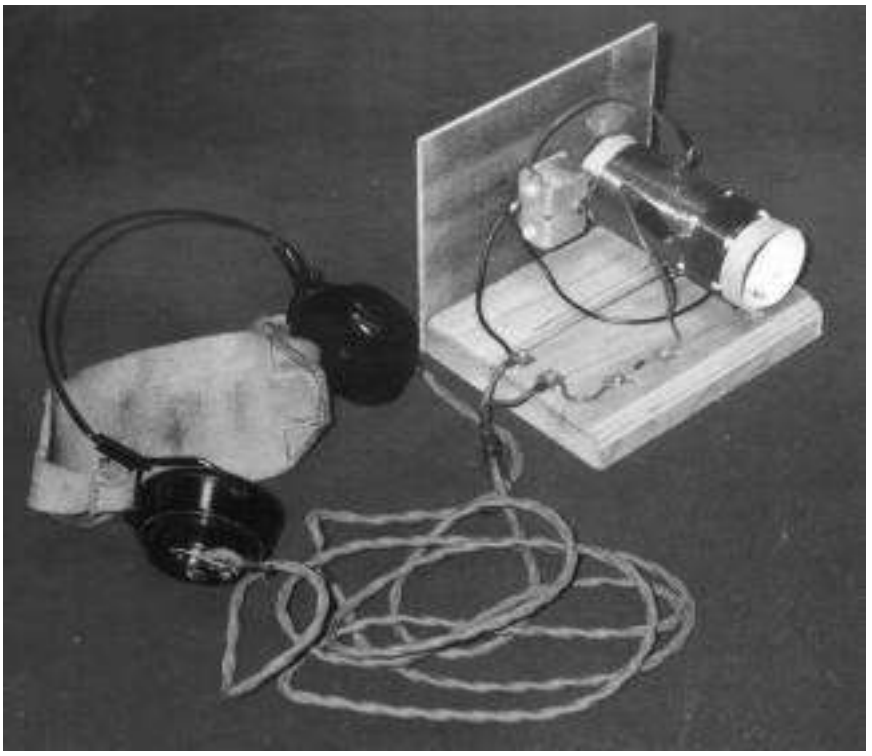

Parts list

Capacitors

C1	Variable capacitor of between 200 and 500 picofarads (pF) maximum
C2	100 picofarads (pF) min. ceramic

Additional items

D1	Germanium, type OA47 or OA90
	High impedance crystal earphone (not Walkman type)
	Tuning knob
	Wooden base, approx. 110 mm square
	Aluminium (or wood) front panel, approx. 80 × 100 mm
	Cardboard tube (toilet roll centre), about 110 mm long, 40 mm diameter
	Reel of 26 SWG enamelled copper wire for both windings of L1

29 A crystal calibrator

Introduction

A crystal calibrator is a device that produces oscillations of a precise frequency which are rich in *harmonics*. A harmonic is an integer multiple of the fundamental frequency; for example, if our fundamental frequency was 100 kHz (as it is in this circuit), there would be harmonics of this frequency at 200 kHz, 300 kHz, 400 kHz, and so on. These harmonics can be used, when picked up by any receiver, to calibrate that receiver, as the harmonics are quite accurate in frequency (see later for an assessment of accuracy). However, a gap of 100 kHz between harmonics is rather wide for most purposes, so we reduce this frequency to 25 kHz, so that the harmonics are then 25 kHz apart, thus producing a much more useful set of *marker points*. A calibrator such as this is often called a *crystal marker*, producing these marker points from 25 kHz to beyond 30 MHz.

The circuit

The circuit diagram is shown in **Figure 1**. The circuit around TR1 is the fundamental oscillator, and its frequency is controlled by the quartz crystal, X1. Even crystal oscillators are not 100% accurate, and the small trimmer capacitor, TC1, is able to 'pull' the frequency to one which is nearer the

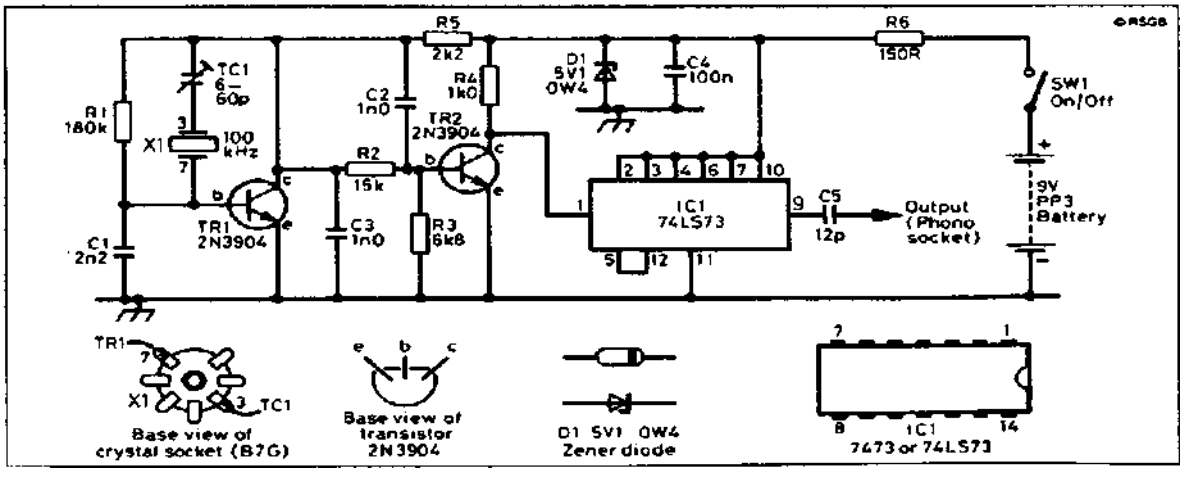

Figure 1 Circuit diagram of the calibrator which uses easily obtainable components

correct one. TR2 is a *buffer* stage, which isolates the oscillator from the rest of the circuit. It acts as a switch, and applies a good signal (switching between 0 and 5 V) to the input of IC1.

IC1 is an integrated circuit which can be connected to do several things. It is connected here to divide the incoming frequency by a factor of 4, producing on pin 9 an output frequency of 25 kHz.

The combination of R6, C4 and D1 produces a supply of 5 V for IC1; it would be damaged if the battery voltage were applied to it. You will no doubt be ready to assemble the circuit, so here is some information for you.

Construction

If possible, always build a circuit in individual stages, which you can test as you go along. It is not always easy in small projects like this, but even the crystal calibrator can be split into two for construction and testing.

It is an ideal project for assembly on Veroboard of the copper-strip type; the prototype layout is shown in **Figure 2**, on a board measuring 11 holes by 24 strips. First of all, remove the copper strip at the locations shown, using a 3 mm drill rotated between the fingers. Hold the board up to the light to ensure that there are no pieces of copper swarf bridging adjacent strips, and that the copper is completely removed where it should be! Assemble the circuit from left to right, but do not wire up anything around IC1. Be aware that the diagram shows the board *from the component side*. Although you

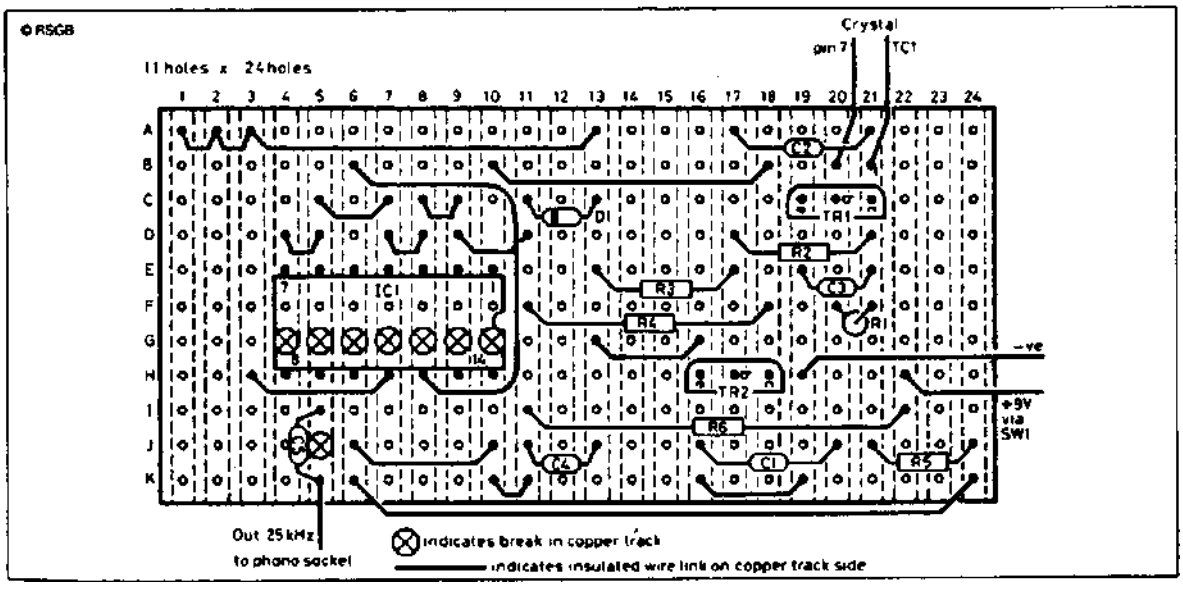

Figure 2 Stripboard, such as Veroboard, should be cut as shown to approx. 62 × 28 mm

can use virtually any kind of crystal, you will need to mount it firmly. If you use a small one, it can be soldered directly in position on the board. With one in a valve envelope, you will need a B7G valveholder. Be prepared to mount the circuit in a **metal** container; the prototype used an (empty) tin of tuna! The valveholder mounts well on any metal case.

Disconnect the aerial of your receiver, and replace it with about 30 cm of wire laid near your oscillator circuit. Connect the battery and switch on. Tune the receiver around until you can hear a whistle on SSB. Rotate the tuning knob to reduce the frequency of the whistle and, as the whistle becomes too low to hear, you have reached one of the calibration markers, and your frequency will be an integer multiple of 100 kHz. If you are already using a calibrated receiver, you will be able to verify this. Going up or down in frequency should locate another marker 100 kHz away, and so on right through the receiver's tuning range. If the signals coming from the circuit are very weak, switch off the calibrator and connect another 30 cm piece of insulated wire to the collector of TR2, and lay it close to (but *not* touching) the wire from the aerial connector. Switch on an try again; you should not now have a problem! If you have access to a multimeter, check that the voltage at the collector of TR1 is very close to 5 V. If it is close to 9 V, you have connected the diode, D1, the wrong way round!

Having verified that the oscillator is working, you can now wire up the integrated circuit socket, being careful to put the notched end of the socket pointing towards R4, the collector resistor for TR2.

Check your connections around IC1, and when you are satisfied that they are correct, line up IC1 with its socket, making sure that the notched ends are together, and press down *gently* to insert the IC into its socket. Insert the 30 cm piece of insulated wire into the output socket, connect the battery and switch on. You should still hear whistles in your receiver, but now they should be 25 kHz apart, rather than 100 kHz apart.

All that now remains to be done is to mount the circuit rigidly inside whatever casing your have chosen. Make sure that none of the connections under the board touch the metal case, and secure the valveholder, on/off switch and output connector to the case. You now have a completed crystal calibrator.

Calibration

The simplest way to calibrate your circuit is with a frequency counter. Most clubs will have one of these and, if not, will know someone who has! Connect it to the collector of TR2, where the frequency should be 100 kHz. Do *not* connect it to any part of the circuit around TR1, or you may alter the frequency you are trying to measure! If the frequency is not exactly 100.000 kHz, rotate TC1 until it is (or is as close as you can get it). Now your calibrator is as accurate as the counter with which you have calibrated it.

Accuracy

Despite your best efforts at calibration, by whatever means, your crystal will *never* have a constant frequency. Such a thing is a scientific impossibility. It is usual to express the accuracy of a crystal in parts-per-million (ppm), and it is governed by many things, principally its temperature. You will be *very* fortunate if your circuit maintains an accuracy better than about ±10 ppm. Expressed in figures, it means that the true frequency can be anywhere between 99.999 kHz and 100.001 kHz, i.e. within 1 Hz of the correct frequency.

Although this may seem more than adequate, it is as well to remember that the accuracy degrades as the frequency increases. At 1 MHz the error will be ±10 Hz and at 10 MHz it will be ±100 Hz. At 30 MHz it will be 300 Hz. Even so, this should be acceptable for most non-critical applications.

Parts list

		Maplin code
Resistors: all 0.25 watt, 5% tolerance		
R1	180 kilohms (kΩ)	M180K
R2	15 kilohms (kΩ)	M15K
R3	6.8 kilohms (kΩ)	M6K8
R4	1 kilohm (kΩ)	M1K0
R5	2 kilohms (kΩ)	M2K0
R6	150 ohms (Ω)	M150R
Capacitors		
C1, C2, C3	1 nanofarad (nF) or 1000 picofarads (pF)	WX68Y
C4	100 nanofarads or 0.1 microfarad (μF)	YR75S
C5	12 picofarads (pF)	WX45Y
TC1	60 picofarads (pF) trimmer	WL72P
Semiconductors		
TR1, TR2	2N3904 npn	QR28F
IC1	7473 or 74LS73N dual JK flipflop	YF30H
D1	5.1V 500 mW Zener	QH07H
Additional items		
100 kHz crystal		
B7G valveholder (found at most rallies)		
14-pin DIL IC socket		BL18U
Phono socket		YW06G
PP3 battery connector		HF28F
PP3 battery		
On/off switch		FH00A
Veroboard		JP47B
Metal case as required		

30 A simple short-wave receiver – Part 1

Introduction

No apologies for yet another design of short-wave radio. This is the beauty of our hobby – there is always something new to try. Not all circuits operate in the same way; not all circuits work equally well; sometimes a simple design suits the operator better than a complicated design. So here is another one for your consideration; it's a good project for a novice, *and* a good one-evening project for someone more experienced.

A basic description

Figure 1 gives the block diagram of the receiver, which employs a *regenerative detector*, one of the earliest techniques by which excellent *selectivity* (the ability to separate two stations very close in frequency) could be combined with good *sensitivity* (the ability to pick up very weak stations) using a very simple circuit. The receiver falls into the category known as *tuned radio frequency* (TRF), meaning that the whole circuit (prior to the extraction of the modulation from the carrier) operates at the incoming radio frequency. In other words, it is *not* a superhet.

As you can see, the regenerative detector has what is called a *feedback loop*, which feeds a small amount of the output signal back to the input. You have heard the effects of feedback with a public address system, when the microphone gain is too great – everything becomes very loud and then bursts into a deafening squeal! This is exactly what the feedback does here, except that it is carefully controlled, thus providing both gain and selectivity. The resulting audio is then amplified for use with headphones.

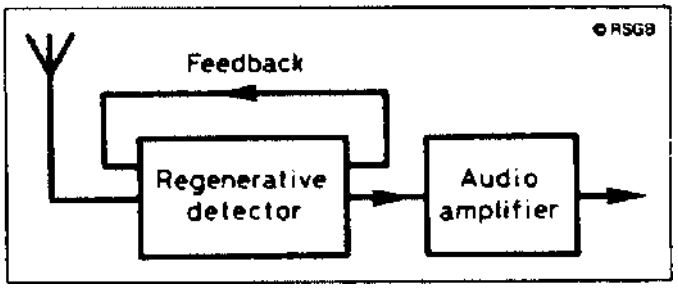

Figure 1 Just two simple stages make up the circuit

The circuit

The circuit of **Figure 2** shows the complete system. TR1 is an untuned *field-effect transistor* (FET) stage, and is used to match the aerial to the next stage. Occasionally, a regenerative detector produces unwanted signals, and TR1 also prevents them from reaching the aerial and being transmitted! The smaller of the two windings on T1 (the *primary* winding) will match a low-impedance aerial, the capacitor input matching a high-impedance aerial.

Ignore TR2 for the moment – the next stage in the signal path is TR3, the detector, using another FET. The tuned circuit is formed by T2, VC1 and VC2 (remember TR1 is untuned). The primary winding on T2 taking the output from TR1. The reason for having two variable tuning capacitors, one large, the other small, is that the large capacitor is the main tuning capacitor, while the small one is used as a *bandspread* control (for very fine tuning). The tuned signals are then detected (converted to audio frequencies) by TR3.

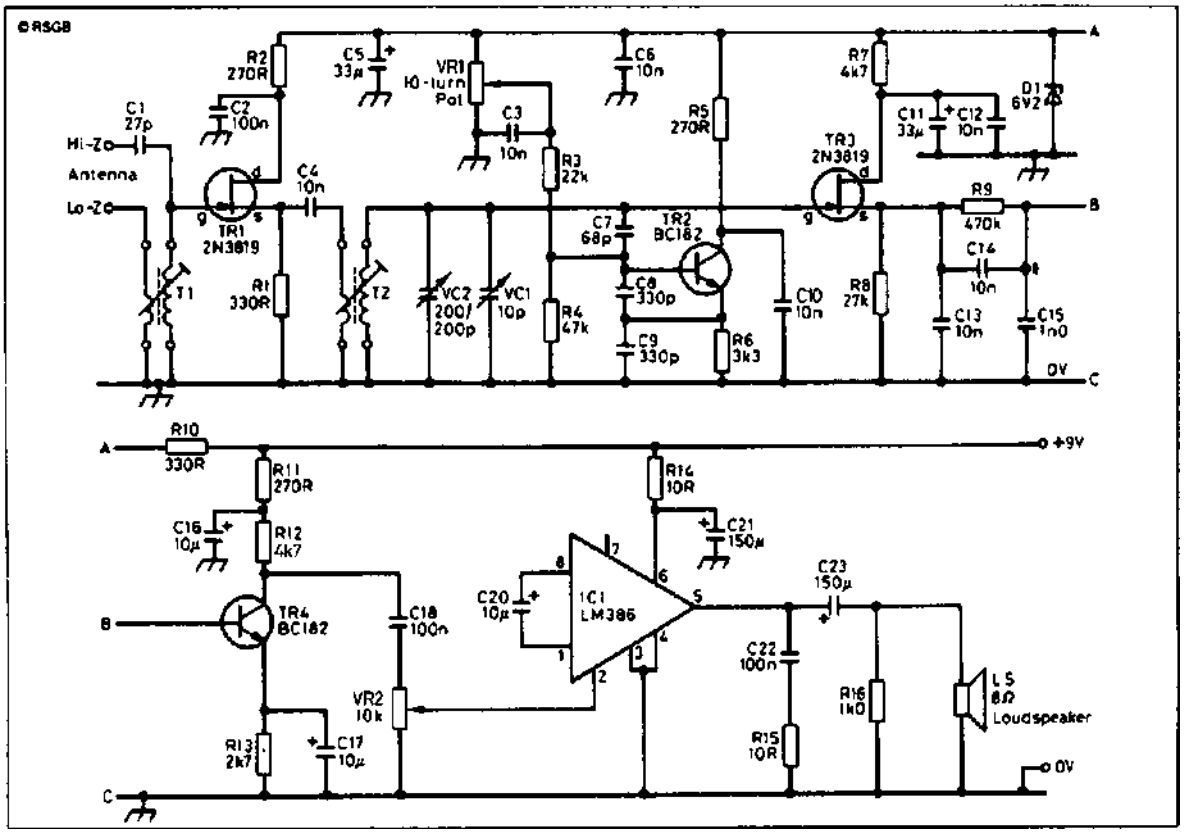

Figure 2 The circuit diagram showing the 10-turn potentiometer VR1. This is the regeneration control for the circuit

TR2 is a *Q-multiplier* stage. It is a Colpitts-type oscillator which uses C8 and C9 to give feedback and produce the oscillation. C7 couples the tuned circuit (and the input to TR3) to TR2. The tuned circuit thus controls the frequency of oscillation of TR2 and the signal passed on to TR3.

The secret of the ease of operation of this receiver is VR2, a 10-turn potentiometer (or *helipot*). The resistance wire is wound in the form of a helix, giving a much greater wire length than in a normal potentiometer, and the shaft must be turned ten times to cover the whole length. Helipots are very useful when very fine adjustments have to be made. Here, VR2 sets the regeneration (or *reaction*) level, depending on the type of signal you are receiving, as will be discussed in Part 2.

TR4 provides the first stage of audio amplification and, after the volume control, VR2, the audio amplifier integrated circuit, IC1, will drive a small loudspeaker or headphones.

In Part 2, the construction will be discussed, together with the choice of aerial, the parts list, and advice on using the receiver.

31 A fruit-powered medium-wave radio

Introduction

This is a one-evening project that will result in a working medium-wave (MW) radio, and will also teach you a little about the way electricity can be generated from the right metals and a little (safe) acid. All you need are three lemons or other citrus fruit, three pieces of copper and three pieces of zinc (or galvanised metal) for your power supply.

Construction

Figure 1 shows the circuit and **Figure 2** its layout on a simple 'plug-in' prototype board. The six pieces of metal are connected as shown, to wire the three lemons in series; use ordinary wire between each lemon and the next. If you have a meter to measure the total voltage, it should be about 1.8 V. Use a standard ferrite rod, and wind on it about 40 turns of single-conductor PVC-insulated wire.

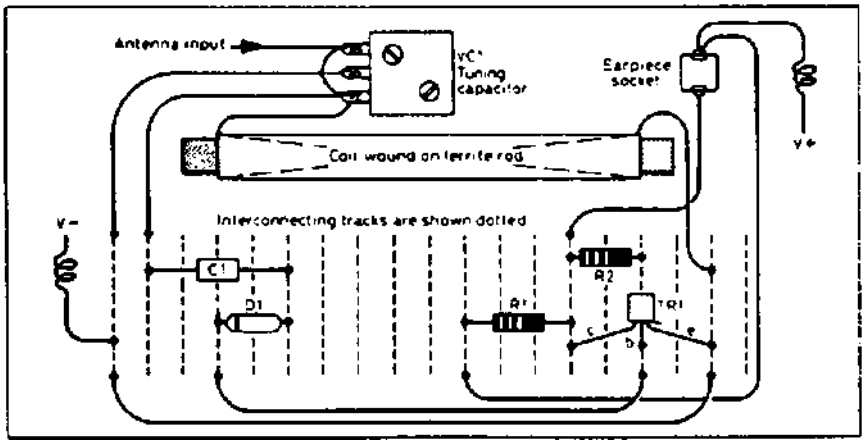

Figure 1 Most parts are plugged into the board as shown – soldering is not required

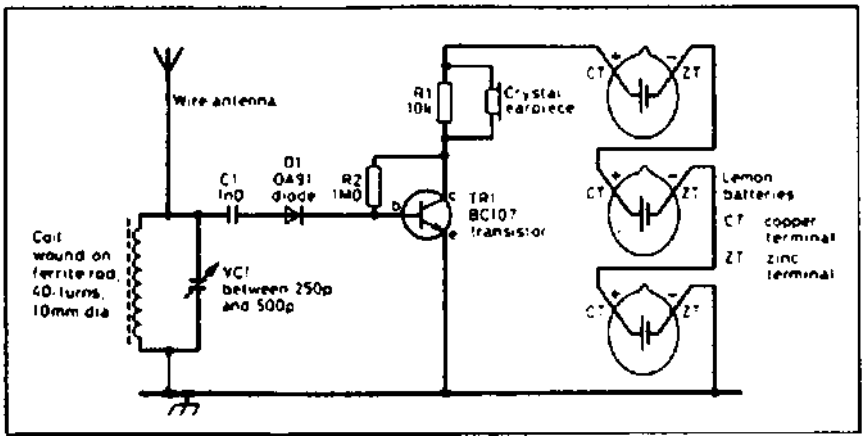

Figure 2 Three lemons power the radio, which gives good results for such a simple circuit

Wire up the circuit on the board as illustrated in Figure 2. Soldering is not required with this type of board – just plug in the components and the wires. Only one transistor is needed. The tuning capacitor, VC1, selects the station you want to hear, and D1 helps to remove the carrier from the RF signal. The resulting audio signal is fed to TR1, a small transistor audio amplifier, which makes the signal big enough to drive a crystal earpiece comfortably. Walkman-type earphones will not work, so invest in a crystal earpiece which you can use in several other projects, too! If you use a smaller capacitor than that specified for VC1, you will need more turns on the aerial coil.

Tests on the prototype indicated that the radio will run for about a week on three lemons!

Parts list

Resistors: all 0.25 watt, 5% tolerance

R1	1 megohm (MΩ)
R2	10 kilohm (kΩ)

Capacitors

C1	1 nanofarad (nF) min. ceramic
VC1	250–500 picofarad (pF) variable

Semiconductors

TR1	BC107 npn (or BC108, BC109C)
D1	OA90, OA91 germanium (not silicon)

Coil

L1	2 metres of single-conductor insulated wire on a standard ferrite rod

Additional items

Plug-in prototype board, e.g. Maplin YR84F
Wire aerial at least 3 m long
Crystal earpiece
Three juicy fruits

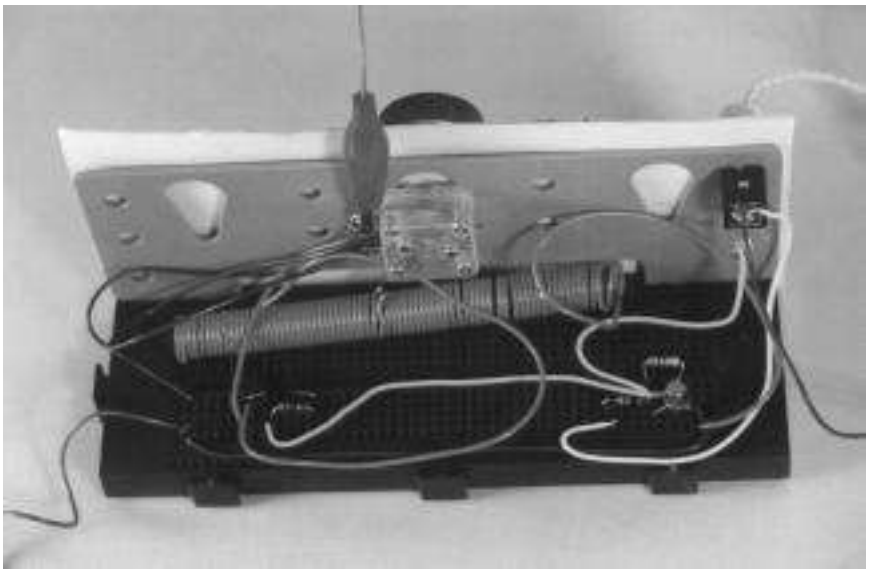

32 A capacitance bridge

Introduction

It is always valuable to have a means of measuring capacitors amongst your test gear. Universal LCR bridges (i.e. systems that can measure inductance, capacitance and resistance) can be found at most rallies, and you can work your way up to owning one of these. In the meantime, a piece of home-made equipment gives you experience as well as resulting in a useful measuring instrument.

The circuit described here is called a *capacitance bridge*, because it balances the effects of one resistor/capacitor pair against another; if one capacitor has an unknown value, then the other can be calculated. The basic bridge circuit is shown in **Figure 1**. To avoid having calculations to perform, this instrument will be calibrated by using capacitors of known values. The bridge is a useful way of performing measurements, because a knob is turned until there is a null in the signal from an earpiece or loudspeaker. The ear is very precise in being able to perceive nulls, which makes the bridge easy to use and reasonably accurate. At the null, the bridge is said to be *balanced*.

How does it work?

Figure 2 is the circuit diagram for this capacitance bridge. Transistors TR1 and TR2 form an oscillator. This is the audio oscillator shown in Figure 1, and produces an alternating voltage which is fed to the bridge. RV1 (in the collector lead of TR2) replaces both R1 and R2 in Figure 1 – that part of

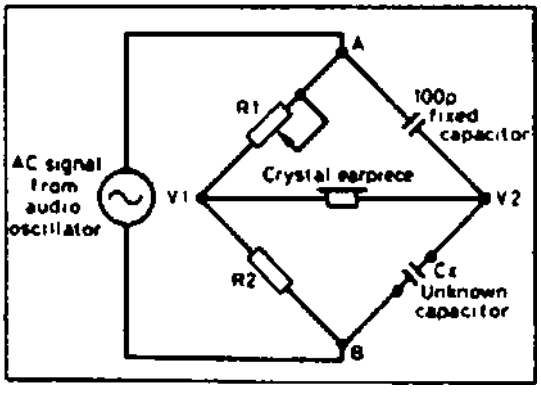

Figure 1 Simplified circuit of a capacitance bridge. R1 is adjusted for minimum sound

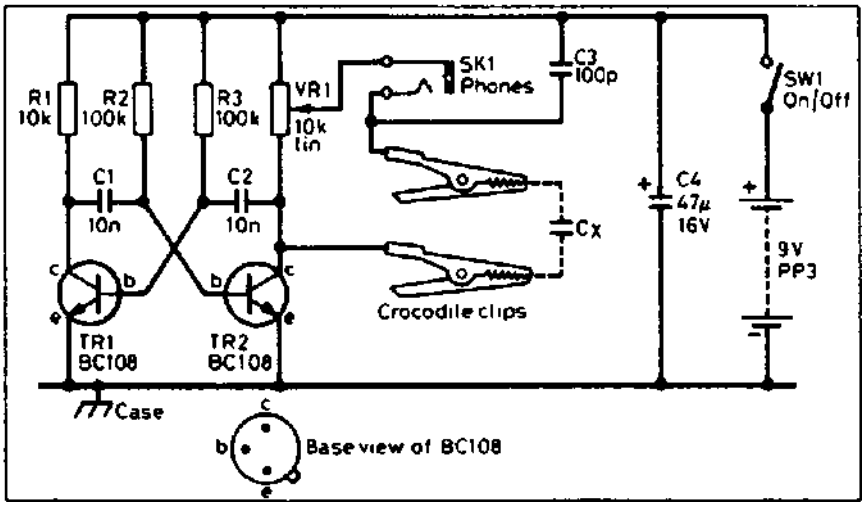

Figure 2 Transistors TR1 and TR2 give an audio signal which is adjusted by variable resistor RV1

RV1 *above* the wiper represents R1, while that part *below* the wiper represents R2. The voltage on one side of the earpiece is determined by the ratio of these values, and is adjusted by rotating RV1. The voltage on the other side of the earpiece is determined by the ratio of C3 to Cx, where Cx is the unknown-valued capacitor. When these two voltages are the same, the bridge is balanced and there is no current through the earpiece.

Figure 3 shows the layout of the components on the matrix board of the prototype. It measures 10 holes by 14 holes, and is of the plain type, i.e. no copper strips. All earth connections are taken to a single solder tag. When

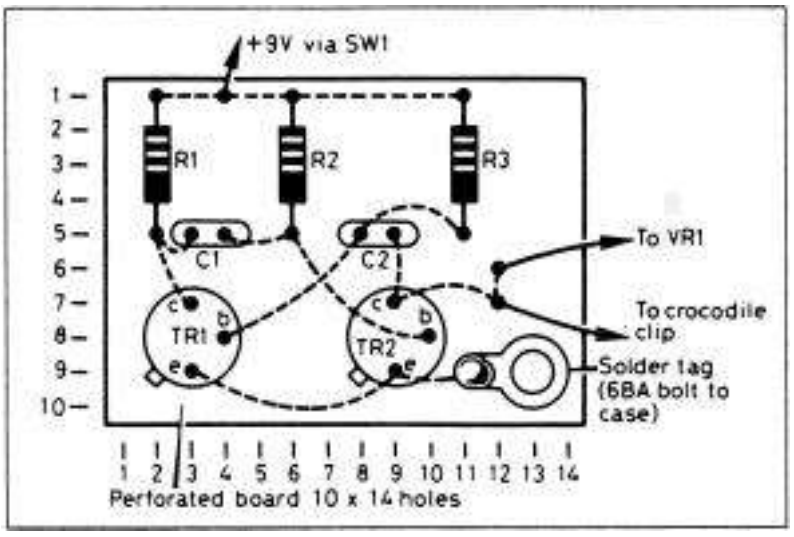

Figure 3 Components are soldered together on a small prototype board

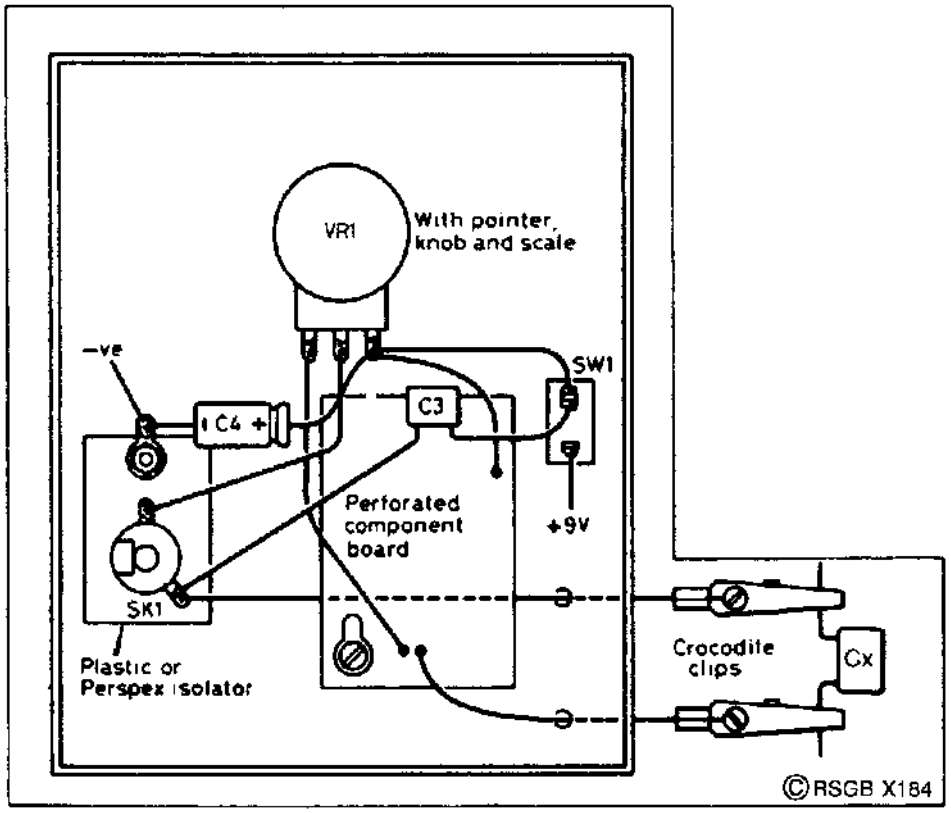

Figure 4 Layout of the parts inside an aluminium box. The earpiece socket is insulated from the case

mounting the board inside a metal box, a long screw is used with extra nuts, to earth the board to the case while providing a stand-off, thus preventing any unwanted short-circuits between the board connections and the case. Be aware that a *crystal* earpiece must be used; low-impedance headphones of the Walkman type are not satisfactory. Solder two flying leads as shown in **Figure 4**, about 15 cm long, terminated in small crocodile clips for attaching to the unknown capacitor.

Calibration

After checking the circuit carefully, attach the battery and switch on; a buzzing noise should be heard in the earpiece. This is the first sign that everything should be OK. If there is no buzz, switch off and recheck the connections.

You will now need a range of close-tolerance (1%) silver-mica capacitors covering the range 10 to 1000 picofarads (pF). Arrange the capacitors in ascending order and connect them to your bridge in sequence. After having prepared a neat piece of card or paper mounted behind the knob on the front panel, mark the dial at the positions of the nulls for all the capacitors. You have now calibrated your capacitance bridge. If you are more likely to want to measure larger capacitors, replace C3 by a 1 nanofarad (nF) capacitor, and the bridge will measure up to 10 nF approximately.

Parts list

Resistors: all 0.25 watt, 5% tolerance

R1	10 kilohms (kΩ)
R2, R3	100 kilohms (kΩ)
RV1	10 kilohms (kΩ) linear

Capacitors

C1, C2	10 nanofarads (nF) ceramic
C3	100 picofarads (pF) silver mica or polystyrene
C4	47 microfarads (μF) 16 V electrolytic

Semiconductors

TR1, TR2	BC108 npn

Additional items

SW1	SPST on/off switch
	Battery connector, PP3 type
	Earpiece, crystal type
SK1	3.5 mm jack socket for earpiece
	Battery, 9 V PP3
	Matrix board, approx. 10 holes by 14 holes
	Aluminium case, approx. 10 × 8 × 5 cm

33 A simple short-wave receiver – Part 2

Introduction

In Part 1, the design of this receiver was discussed in some detail. Now we are going to put it all together and see how it works. The receiver is laid out on a printed-circuit board (PCB) or on a matrix board.

Construction

The layout of the components is shown in **Figure 1**. Identify each part separately, insert it into the holes in the board and solder carefully. Long leads may be cropped before or after soldering, depending on your skill and preference. All electrolytic capacitors, T1, T2 and IC1, must be connected correctly. The front-panel controls are connected to the PCB terminals shown in Figure 1.

The layout of the controls and the placing of the board inside the case are matters of personal preference. The size of the prototype front panel is shown in **Figure 2**. The prototype had a slow-motion drive fitted to VC2, the main tuning capacitor. This required the capacitor to be fitted on its own small panel. The bandspread control does not need any form of

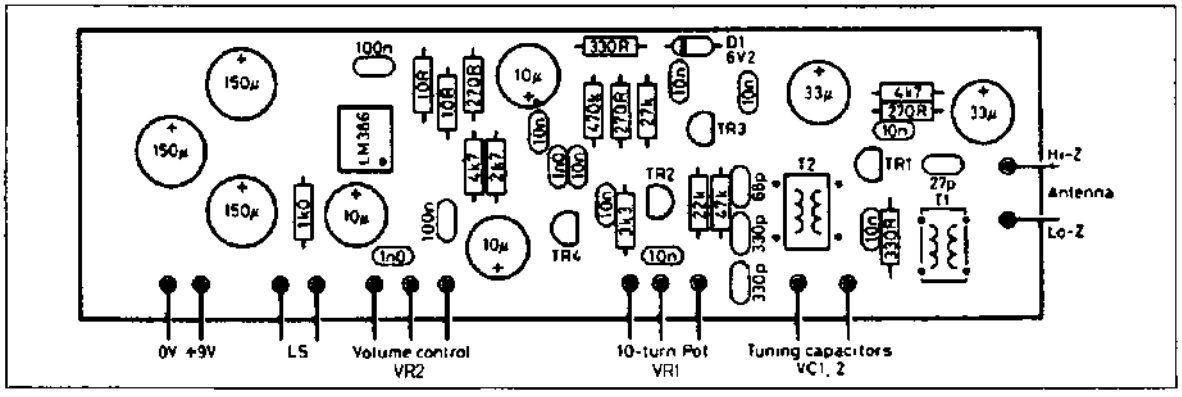

Figure 1 Layout of the receiver circuit board

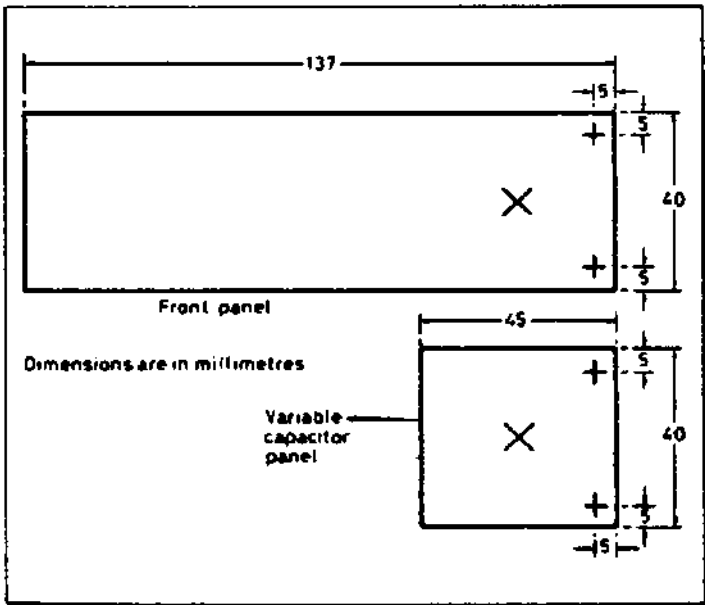

Figure 2 The case can be metal or made from PCB material

slow-motion drive. A tuning dial may be fitted behind the tuning knob on VC2 if required. The volume control, VR2, has its own on/off switch for the battery, which can be mounted behind the back panel, on which are mounted the aerial input sockets and the headphone/speaker socket. Check your soldering carefully, together with all the wiring between the board, the potentiometers and variable capacitors. When you are confident that everything is perfect, connect the battery and switch on.

The first tests

If you have a good aerial and are using an aerial tuning unit (ATU), use the low-impedance input. Excellent results are possible, though, with about 3 metres of wire connected to the high-impedance input. Set the volume control to give a gentle hiss in the headphones or speaker. Advance the reaction control to give a definite hiss. As you tune in an AM station, the hiss will change to a whistle; back off the reaction until the oscillation *just* stops. The receiver is now correctly set for AM reception.

On the amateur bands, the stations will be SSB or CW, and the reaction needs to be set *just above* the oscillation point, and will need slight adjustment from time to time for different qualities of signal. Juggling with the volume, reaction and tuning is part of the pleasure of using regenerative receivers!

In action

Practice is needed for best results. The regenerative receiver is renowned for its versatility in being able to be set up *exactly* for all types and strengths of signal. The basic receiver tunes from 6.5 MHz to 11 MHz approximately; this includes two amateur bands at 7.0 MHz and 10.1 MHz and two broadcast bands.

Parts list

Resistors: all 0.25 watt, 5% tolerance

R1, R10	330 ohms (Ω)
R2, R5, R11	270 ohms (Ω)
R3	22 kilohms (kΩ)
R4	47 kilohms (kΩ)
R6	3.3 kilohms (kΩ)
R7, R12	4.7 kilohms (kΩ)
R8	27 kilohms (kΩ)
R9	470 kilohms (kΩ)
R13	2.7 kilohms (kΩ)
R14, R15	10 ohms (Ω)
R16	1 kilohm (kΩ)
VR1	10 kilohm (kΩ) linear 10-turn potentiometer
VR2	10 kilohm (kΩ) log potentiometer

Capacitors

C1	27 picofarads (pF)
C2, C18, C22	100 nanofarads (nF)
C3, C4, C6, C10, C13, C14	10 nanofarads (nF)
C5, C11	33 microfarads (μF) 16 V electrolytic
C7	68 picofarads (pF)
C8, C9	330 picofarads (pF)
C15	1 nanofarad (nF)
C16, C17, C20	10 microfarads (μF) 16 V electrolytic
C21, C23	150 microfarads (μF) 16 V electrolytic
VC1	10 picofarads (pF) variable
VC2	200 picofarads (pF) variable

Semiconductors

TR1, TR3	2N3819
TR2, TR4	BC182
IC1	LM386
D1	6.2 V 0.5 W Zener

Inductors

T1	3 turns primary, 15 turns secondary, wound on 2-hole ferrite bead, with 28 SWG wire
T2	2 turns primary, 17 turns secondary, wound on a T68-2 toroidal former, with 28 SWG wire

Additional items

- Printed-circuit board
- Battery connector
- PP3 battery
- 8-pin DIL socket
- 8 ohm speaker or headphones (Walkman type)
- Case to suit

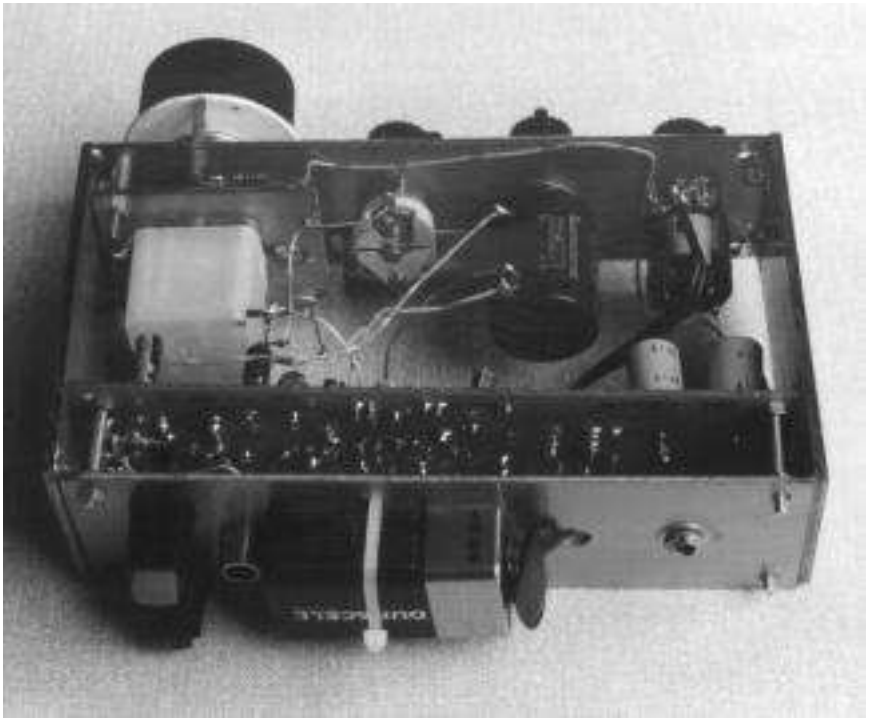

34 A basic continuity tester

Introduction

This little device can be built on a plug-in breadboard, and is ideal for testing fuses and cables, as well as doubling as a signal source for testing amplifiers, etc. It can even be used for testing npn transistors by replacing either of the transistors in the circuit, and seeing if the circuit still works!

Simple and quick to build

Using a plug-in breadboard, this circuit is so simple it could almost be built when you need it, and then dismantled again! If you want the circuit to make a different sound, the components to change are R2, R3, C1 and C2. Always make sure that R2 = R3 and C1 = C2, or the sound may be excessively 'edgy' and lacking in volume.

Basically, the circuit is an oscillator which drives a little loudspeaker directly. The fuse or cable you are testing is connected between the crocodile clips. If there is a current path between the two clips, the current also flows through the circuit, thus operating the oscillator and producing a sound from the loudspeaker.

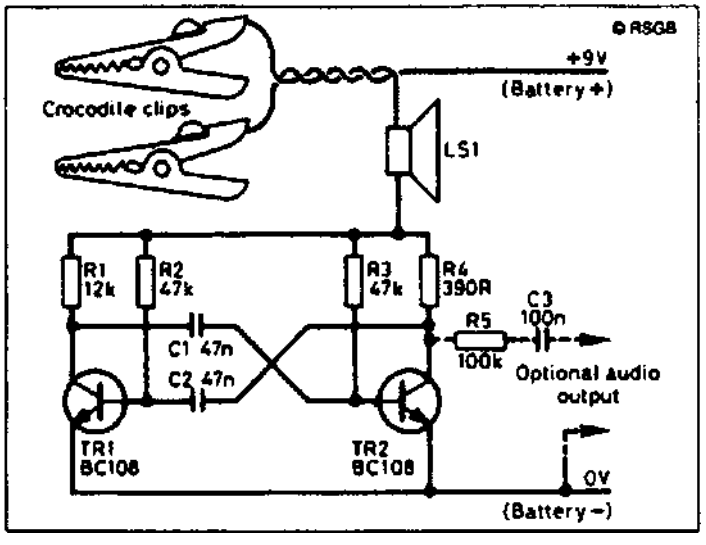

Figure 1 The circuit diagram of the continuity tester

If you want to use the circuit to produce a signal to test an amplifier, for instance, connect the croc clip which comes directly from the battery to the junction of R1, R2, R3 and R4. This supplies current to the circuit while, at the same time, bypassing the loudspeaker. Use the two components R5 and C3 between the oscillator and your amplifier. The loudspeaker is bypassed because you will want to listen to the output from your amplifier, *not* from the oscillator!

Remember, NEVER test any equipment which is still connected to the mains electricity supply. Avoid testing anything which is switched on and has its own power supply. You may damage both your tester ***and*** the circuit you are 'testing'!

Parts list

Resistors: all 0.25 watt, 5% tolerance

R1	12 kilohms (kΩ)
R2, R3	47 kilohms (kΩ)
R4	390 ohms (Ω)
R5	100 kilohms (kΩ) optional

Capacitors

C1, C2	47 nanofarads (nF) ceramic
C3	100 nanofarads (nF), 0.1 microfarads (μF) ceramic optional

Semiconductors

TR1, TR2	BC108 npn

Additional items

LS1	Loudspeaker (8 Ω)
	2 crocodile clips
	Prototype circuit board
	PP3 battery connector
	PP3 battery

35 A charger for NiCad batteries

Introduction

The cost of replacing dry batteries can be alleviated to a great extent by the use of rechargeable batteries such as those containing nickel and cadmium (called *NiCads*). They are more expensive than the batteries they replace, but they can be charged hundreds of times and thus prove cheaper in the long run.

NiCads produce only 1.2 V per cell, compared with the 1.5 V of ordinary cells, so before you rush out and buy lots of these, please make sure that the equipment on which you plan to use them will work on the reduced voltage! For example, if you are using four cells to give you a 6 V supply, NiCads will give you only 4.8 V, which is quite a reduction. Using six cells to replace a 9 V battery will give you only 7.2 V. Not all equipment is happy with these reductions!

However, we all use them when we can, and they save substantial amounts of money. Here is the circuit of a charger to keep them in prime condition.

Charging NiCads – the ampère-hour

NiCads require charging at constant current, which means that connecting one across a normal power supply (constant *voltage*) is useless and can destroy it. They need pampering to the extent of needing a long charge (around 16 hours) at a rate dependent upon the *capacity* of the battery. By the capacity of a battery, we mean how much energy it can store. You will probably know that energy is measured in joules. For the purposes of storing energy in batteries, the joule is *not* the ideal unit, so we use one that is! This unit is the ampère-hour (Ah), and must be interpreted with some realism. For example, if the battery is rated at 2 Ah, it will deliver a current of 0.5 amp for 4 hours, or 0.25 amp for 8 hours. Provided the current is not too high, the product of the current (in amps) and the time for which it will flow (in hours) before the battery is flat will always be around 2 Ah. A workable 'rule of thumb' for calculating the charging current is that its value should be around one-tenth of the numerical value of the capacity; so, for our 2 Ah battery, a charging current of around 200 mA (2 ÷ 10 = 0.2 A or 200 mA) would be used.

Constant voltage to constant current

Many integrated circuit (IC) chips are available for use as voltage regulators, i.e. they supply a constant voltage. Most of these can be persuaded to become constant current supplies with one external resistor!

The voltage regulator IC usually has only three connections – 'input', 'output' and 'common'. It is designed (in the case of the LM7805) to produce a constant 5 V output between the 'output' and the 'common' connections, at currents of up to 1 A. If a resistor is connected between these, the IC will maintain 5 V across it. If you look at **Figure 1**, you will see the circuit performing this conversion.

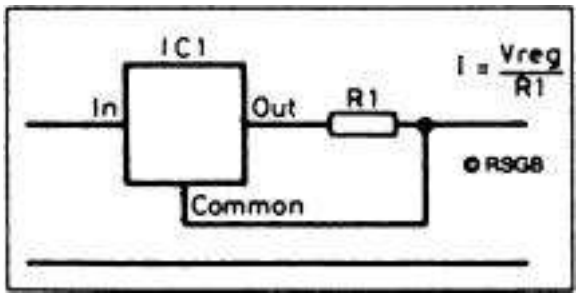

Figure 1 Voltage regulator arranged to produce a constant current

For the previous example, we derived a charging current of 200 mA, so we now need to calculate the value of resistor that will produce this current. Using the equation which is derived from Ohm's law:

$$I = \frac{V}{R}, \text{ from which } R = \frac{V}{I},$$

where R = R1, the resistance in ohms that we are calculating,
V is the voltage across R1 (5 V), and
I is the current flowing (200 mA).

So,

$$\text{R1} = \frac{5}{0.2} = 25\,\Omega.$$

25 ohms is not a 'common' or 'preferred' resistor value, so we must choose the next *largest* value, which is 27 Ω. This reduces the current, but only slightly – it is now 185 mA. When calculating resistor values in power supply circuits, we must *always* check the power that they dissipate and make sure we specify and fit a suitable resistor.

Power (in watts) is the product of the voltage across and the current through a device, so in this case it is given by:

$$\text{Power} = V \times I = 5 \times 0.185 = 0.925\,\text{W}.$$

Rather than use a 1 watt resistor operating very near its limit, it is safer to use a 2 watt resistor operating well within its limits.

Looking again at Figure 1, we now have a constant-current source producing 185 mA, when R1 is a 27 Ω, 2 W resistor. For use with NiCads requiring charging currents other than 200 mA, you will need to repeat the two equations above, using a new value for *I*.

The full circuit and its assembly

This is shown in **Figure 2**, and can be broken down into two parts. The first is the AC to DC conversion produced by the mains transformer, T1, the bridge rectifier, BR1, and the smoothing capacitor, C1. The second is the constant-current section already discussed.

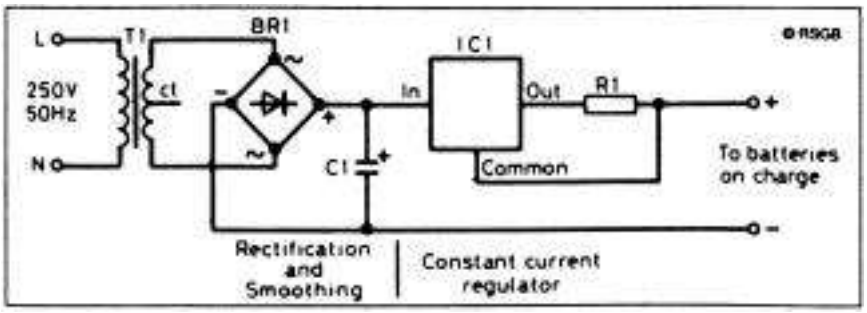

Figure 2 The complete circuit including mains components

The prototype was assembled on matrix board measuring 18 holes by 12 strips, although, as **Figure 3** shows, this is much larger than is strictly necessary. No strip cutting is needed, but make sure that IC1 and C1 are inserted correctly.

Warning! Before you attempt to wire up the transformer and the bridge rectifier, be aware that you will eventually be connecting the circuit to the mains supply, so there are three possibilities for you: (1) get a qualified friend to supervise your completion and testing of the circuit; (2) get your qualified friend to complete and test the circuit for you; (3) replace the transformer and bridge rectifier with a mains adapter.

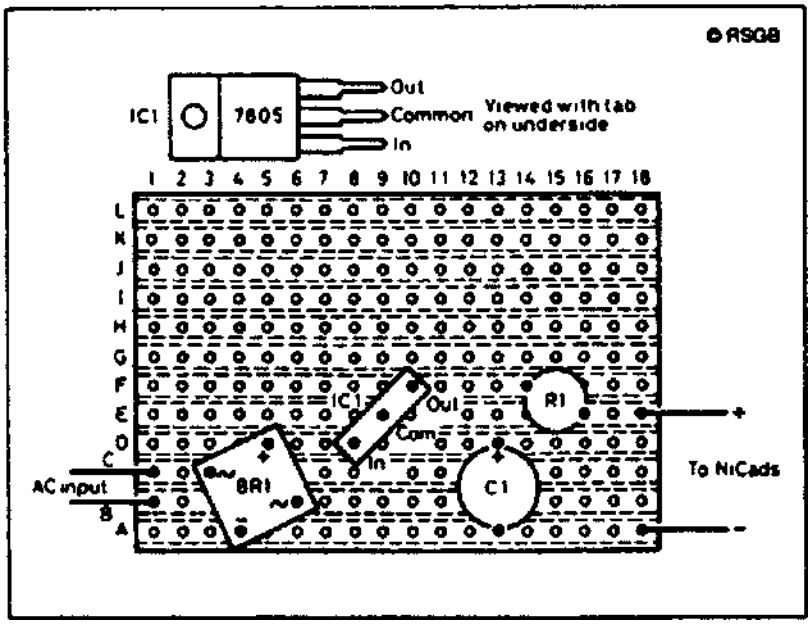

Figure 3 The charger can be built on Veroboard

If you decide to use the mains adapter, its output is connected directly across C1, because T1 and BR1 are now no longer needed. Make sure the polarity (positive and negative) is correct and that the adapter output is set to 12 V.

A quick test

If you have built the mains version, make sure all connections are correct, and that there are no soldered joints which will touch other parts of the circuit. The box must be securely closed before tests begin. The RSGB cannot be held responsible for damage to equipment or batteries! The version using the mains adapter need not be closed during tests.

Switch on. With nothing connected to the output, the unit should run cold. If this is not the case, switch off and recheck your circuit. If all is well, switch on again and connect a DC multimeter (on the current range) across the output. It should indicate only a slight difference from the calculated value of 185 mA. You can now charge your NiCads!

Other charging currents can be set by having different values for R1, perhaps selectable by a rotary switch. Remember to make sure that the values of both resistance *and* power dissipation are correct, and don't exceed the 250 mA rating of the transformer (or the 1 amp rating of the IC if you are using a bigger transformer).

Parts list

		Maplin code
Resistor		
R1	As required – see text	
Capacitor		
C1	1000 microfarads (μF) 35 V electrolytic	FF18U
Semiconductors		
IC1	LM7805 5 V, 1 A regulator	CR14Q
BR1	W005 50 V, 1 A full-wave rectifier	QL37S
Transformer		
T1	9–0–9 V, 250 mA sub-min. transformer	YN15R
Additional items		
Case		FG41U
Veroboard, 18 holes by 12 strips		
Plug to suit NiCads		
Double-sided sticky tape as required		
Insulated wire for battery connections		

36 An 80 metre crystal-controlled CW transmitter

Introduction

A simple transmitter is ideally suited to anyone venturing into our marvellous hobby for the first time. If you are put off by the complexities and prices of the 'black boxes' then this is the transmitter you've been looking for!

The circuit

The complete circuit is shown in **Figure 1**. It is a single-transistor crystal oscillator which is *keyed* (switched on and off) by the Morse key in the +12 V supply rail. The circuit first appeared in *QST* (the American equivalent of *RadCom*) in 1982, and has since appeared in a modified form in the *ARRL Handbook*. The circuit can produce about 2 watts on 80 m, and can be constructed on a piece of plain matrix board; the prototype board measured 7 cm by 3 cm, and its layout is shown in **Figure 2**.

Note that a bare copper wire runs along the bottom edge of the board to act as an earth wire for the relevant components. The only 'difficult' part of the construction is the winding and wiring of T1. The main winding is 38 turns of 26 SWG enamelled copper wire, and there are two link windings of four turns each. Make sure that all windings are wound the correct way round the toroid – Figure 1 shows this and should be studied carefully. If the windings do not have the correct *sense* (i.e. a clockwise coil has been wound anticlockwise, or vice versa), or have been connected incorrectly to the rest of the circuit, the oscillator will not work!

When putting components on the board, wire in the crystal socket *without the crystal in it*. Crystals do not like to be subjected to the horrors of a soldering iron, so keep your crystal to one side during the construction process!

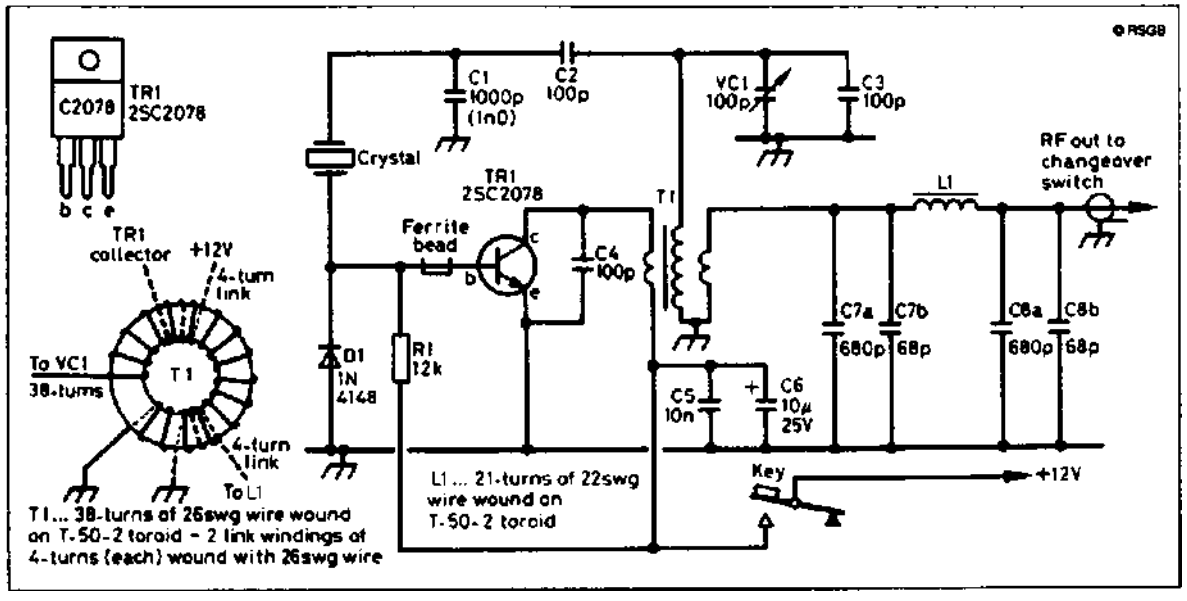

Figure 1 The simplest form of transmitter is a keyed crystal oscillator. Note that L1, C7 and C8 make up a *low-pass filter* which reduces unwanted *harmonics* (outputs at the transmitter frequency multiplied by 2, 3, 4, etc.)

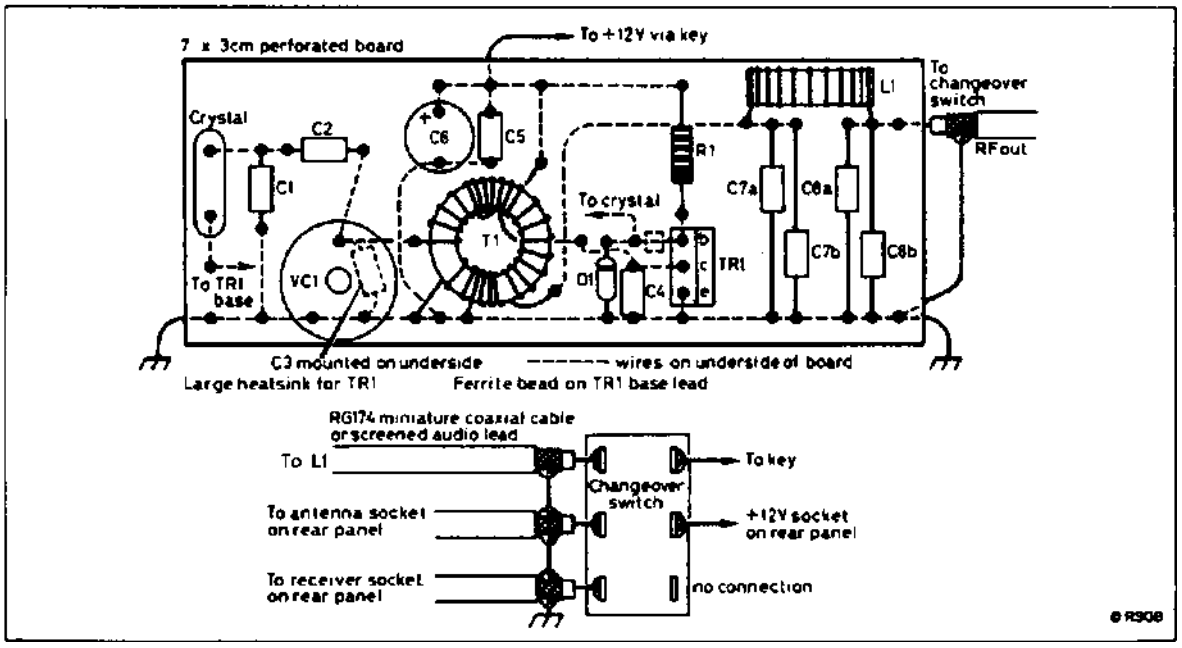

Figure 2 Component layout is straightforward on a 'matrix board' (it has holes but no copper strips). The dotted lines are the connecting wires. The lower part shows the connections for the transmit/receive switch

The output filter, which comprises C7, C8 and L1, is a *low-pass* filter, which helps reduce any *harmonics* present in your signal. Harmonics are integral multiples of your transmitter frequency, so if you are transmitting on a frequency, *f*, harmonics will be present at frequencies 2*f*, 3*f*, 4*f*, . . . and so on. L2 is another inductance using 22 SWG enamelled copper on a ferrite toroid. The changeover switch is external to the transmitter board, and is used to switch your aerial between the transmitter and the receiver; its wiring is shown in Figure 2.

Use a dummy load

A dummy load enables you to test your circuit without actually transmitting a signal. If you haven't such a thing already, it is easy to construct one to use with this transmitter. Don't use it for transmitters of more than 2 watts output, though. Use two 100 ohm, 1 watt resistors, connected in parallel across the end of a short piece of coaxial cable, terminated in a BNC, PL259 or N-type free plug, as shown in **Figure 3**. Plug this into the aerial socket on your transmitter, plug in your crystal and connect the transmitter to a 12 V supply. Have another receiver switched on and tuned to the crystal frequency. Although the radiation from your dummy load is minimal, it will

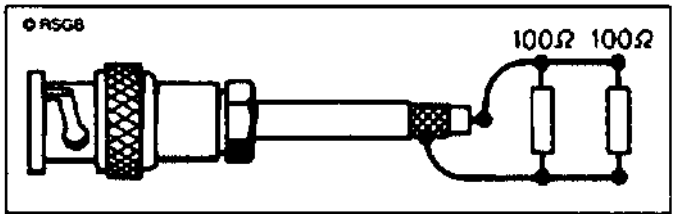

Figure 3 A simple 2 W dummy load can be made from two 100 Ω (ohm) resistors in parallel. The plug should match the socket on your transmitter

be enough to be picked up by a receiver in the same room. Send dashes with the Morse key, and adjust VC1 until the received note is *clean*. It should not sound rough, or have a *chirp* (change its frequency during a dash or dot). Avoid tuning for maximum power; this is seldom the correct setting!

You will need to put your completed transmitter in a metal box, using sockets for the power supply, aerial, receiver and Morse key. The sockets can be chosen to match your existing equipment.

Figures 4–7 are taken from the RSGB book *Practical Antennas for Novices*, and may give you some ideas on the type of aerial to be used with your transmitter.

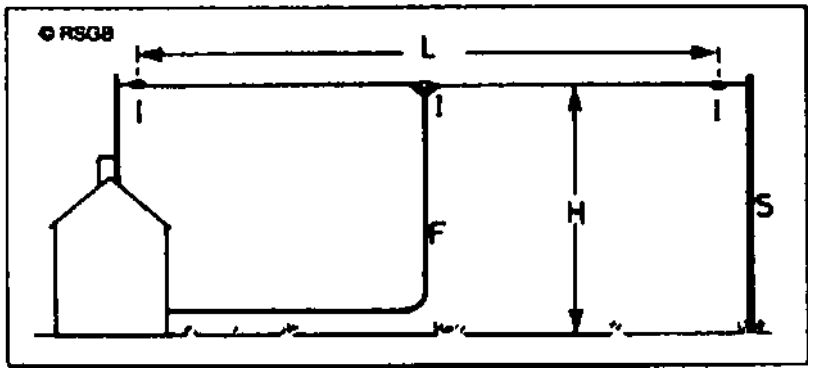

Figure 4 A simple dipole can be very effective. For the 3.5 MHz band, length L is 40 metres and height H should be as large as possible. The far support S can be a tree, pole or building. Insulators I may be home made from strong plastic and the feeder F should be 50 Ω (ohm) coax cable

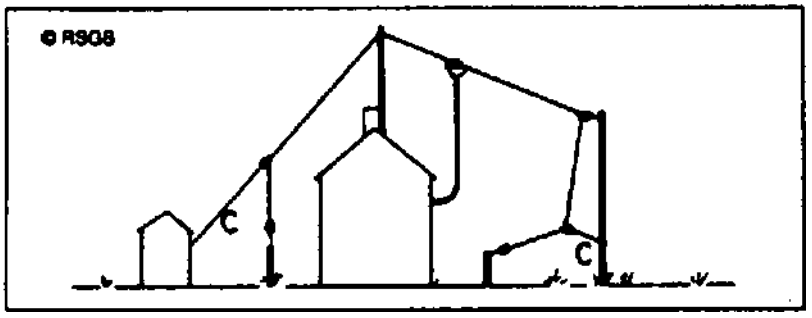

Figure 5 Your signal is radiated mostly from the centre of the dipole so the ends can droop or even be bent but the length may need shortening by a few centimetres because the ground and the bends will detune the dipole. Cords C are best made from strong plastic rope from a sailing or camping shop

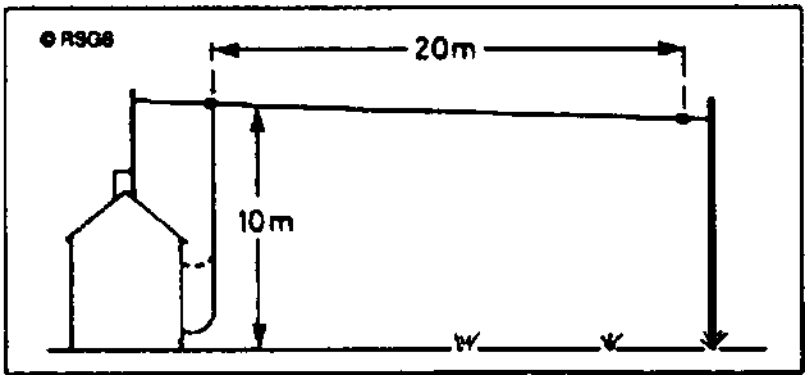

Figure 6 An 'inverted-L' takes up less space than a dipole and doesn't need coax cable. Like the dipole, the end can droop or be bent to save space as in this case most of the radiation comes from the area around the top of the vertical part

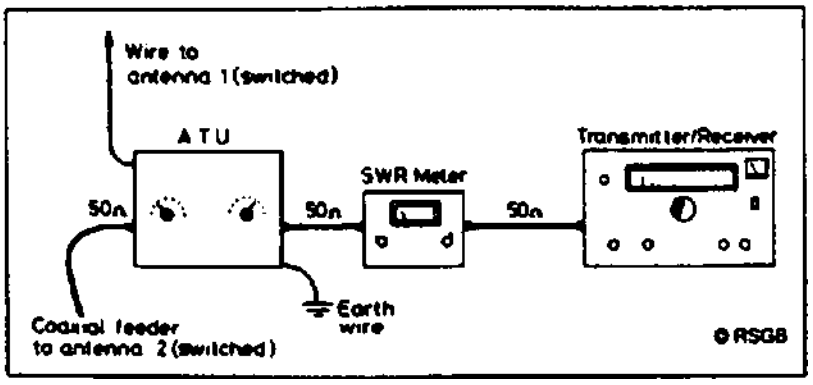

Figure 7 Almost any length of wire more than 10 m or so long will work (though it will work better the longer and higher it is) but an Aerial System Tuning Unit (ASTU or ATU) will be needed

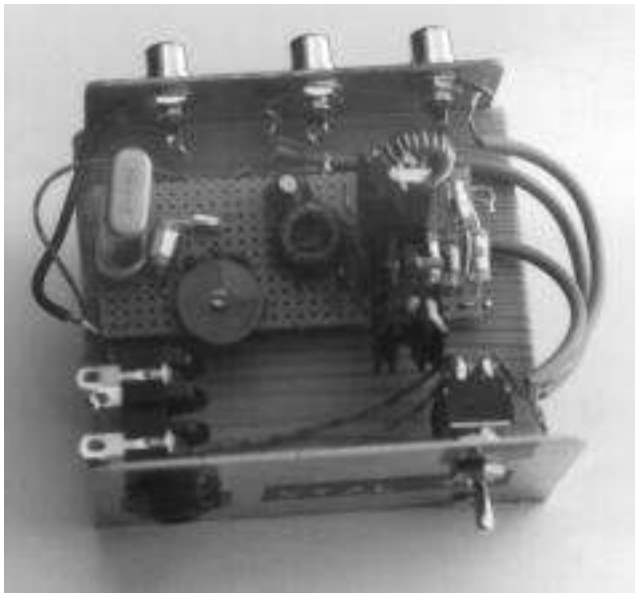

Parts list

Resistor

R1	12 kilohms (kΩ), 0.25 watt, 5% tolerance

Capacitors

C1	1000 picofarads (pF) polystyrene
C2	100 picofarads (pF) polystyrene
C7a, C8a	680 picofarads (pF) polystyrene
C7b, C8b	68 picofarads (pF) polystyrene
C3, C4	100 picofarads (pF) ceramic
C5	10 nanofarads (nF) polyester
C6	10 microfarads (μF) electrolytic 25 V
VC1	100 picofarads (pF) trimmer

Semiconductors

D1	1N4148
TR1	2SC2078 (see sources list)

Inductors

T1	38 turns 26 SWG enamelled copper on T–50–2 toroid, with two link windings of four turns
L1	21 turns 22 SWG enamelled copper on T–50–2 toroid

Additional items

- Ferrite bead
- Crystal (e.g. 3.579 MHz) and holder
- Metal box
- Socket for Morse key.
  This must be totally isolated from the metal of the box, as *both* connections can be at +12 V.
- Sockets for 12 V supply, aerial and receiver
- Switch – DPDT
- Heat sink for TR1
- RG174 miniature coaxial cable for signal leads (see Figure 2)

Component sources

Special components

2SC2078	Cricklewood Electronics Ltd, 40 Cricklewood Broadway, London, NW2 3ET.

37 A solar-powered MW radio

Introduction

What could be more ecologically friendly than a radio powered by the sun's energy? This design is quite standard, and if you have built any of the other medium-wave radios in this series, then this one should present few problems.

The solar panel

The solar panel is to the solar cell as the battery is to the cell; in other words a solar panel is several solar cells connected in series. The solar panel quoted for this radio will generate about 9 V at a current of around 30 mA on a sunny day. The circuit will operate on a supply of around 2 V, so bright sunshine is *not* necessary for satisfactory operation. The volume will be less, of course.

The circuit

The radio uses the ZN415E integrated circuit (IC), connected as shown in **Figure 1**, the complete circuit diagram. The signal is tuned in by the combination of L1 and VC1. L1 is made by winding about 35 turns of 24 SWG enamelled copper wire on a ferrite rod. A standard ferrite rod of 10 cm length and 1 cm diameter is used.

Signals selected by the tuned circuit are passed to IC1, which amplifies the signals and removes the audio component, which is then amplified further by IC2 for driving a small loudspeaker. The removal of the audio component is the process we call *detection*. In addition to this, IC1 provides *automatic gain control* (AGC), which helps to keep the audio signal constant, even when the incoming RF signal may vary due to fading.

The prototype board

Veroboard (also known as matrix board or stripboard) is ideal for the construction of the radio. The layout is shown in **Figure 2**. The board size is 11 strips by 30 holes (**please note that there is no row 'I', so take care with your counting!**). Using a 3 mm (⅛ inch) twist drill rotated between

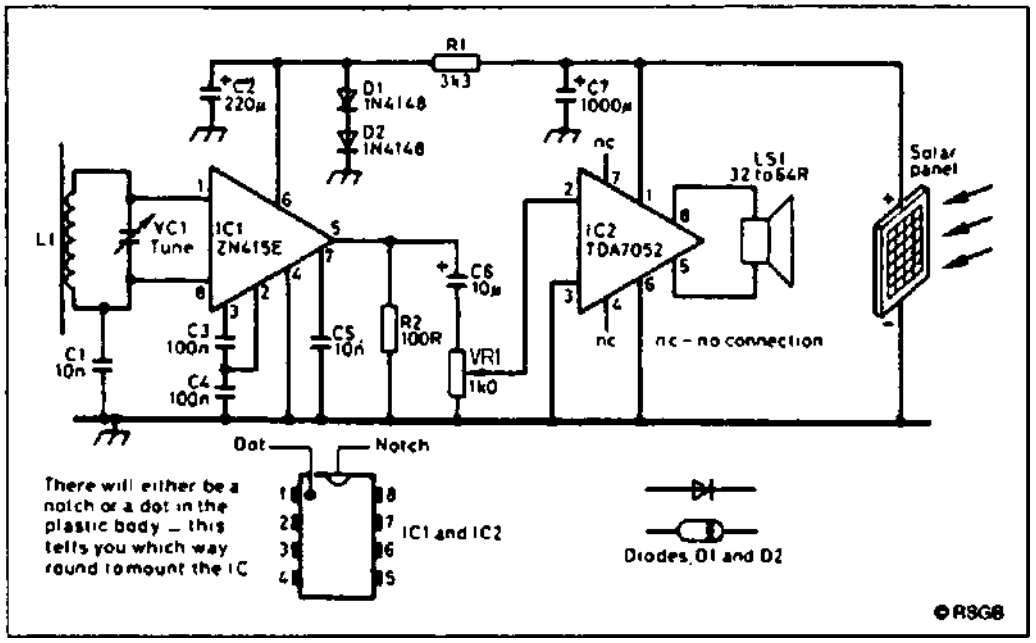

Figure 1 The radio uses just two integrated circuits (chips) and operates at any voltage from 2 to 9 V

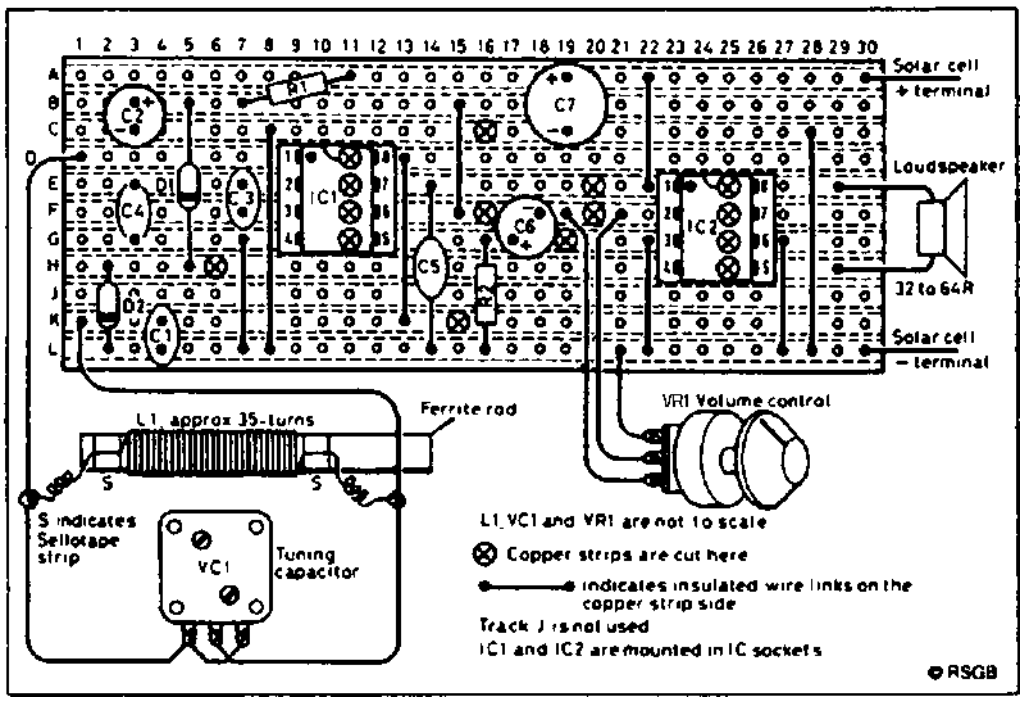

Figure 2 Follow the layout carefully, making sure that all connections are neatly soldered

your thumb and forefinger, break the strips at the points marked with a cross inside a circle. Hold the board up to the light to ensure that the tracks *have* been broken and that there is no copper swarf shorting tracks together.

Firstly, solder in the 8-pin DIL sockets for the ICs, making sure that the notches in the sockets are facing upwards, as shown on the diagram. Then, solder in the wire links, resistors, capacitors and diodes, making sure that the electrolytic capacitors (C2, C6 and C7) and the diodes (D1 and D2) are connected the correct way round. Use different colours of wire for the connections to the volume control, VR1, to avoid incorrect connections. Note the wiring of the tuning capacitor (VC1) shown in Figure 2; a two-section type is used, and both sections are wired in parallel to give twice the capacitance of a single section.

There is no on/off switch – just turn the volume down when you are finished using the set! The solar panel can be mounted parallel to the top of the case, or angled to receive the maximum energy from the sun, as shown in the photograph. You could have a battery available as a standby source to use the radio after dark; any battery of between 6 V and 9 V will do. Wire it with a simple changeover switch, so you can switch between solar and battery power. Ask a friend for help with this if you are not sure how to do it.

You may need to adjust the number of turns on L1 to get the best results, but it should be possible to receive at least five stations at good volume with your sun-powered radio!

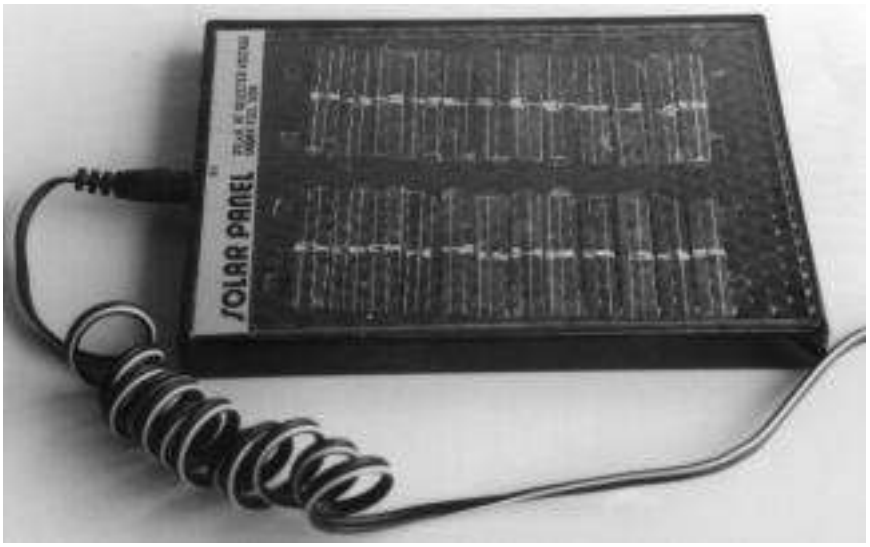

Parts list

		Maplin code
Resistors: 0.25 watts, 5% tolerance		
R1	3.3 kilohms (kΩ)	M3K3
R2	100 ohms (Ω)	M100R
VR1	1 kilohm (kΩ) log	FW21X
Capacitors		
C1, C5	10 nanofarads (nF) ceramic	BX00A
C2	220 microfarads (μF) electrolytic (10 V)	FB60Q
C3, C4	100 nanofarads ceramic	YR75S
C6	10 microfarads (μF) electrolytic (10 V)	FB22Y
C7	1000 microfarads (μF) electrolytic (10 V)	FB81C
VC1	140–300 picofarads (pF)	FT78K
Semiconductors		
IC1	ZN415E (or ZN416E)	UR70M
IC2	TDA7052	UK79L
D1, D2	1N4148	QL80B
Solar panel	9 V at 50 mA	RK23A
Additional items		
LS1	32–64 ohm miniature loudspeaker	YT28F
	Ferrite rod	YG20W
	24 SWG enamelled copper wire	BL28F
	Plastic box, approx. 220 × 140 × 70 mm	YN39N
	Veroboard, cut to size	JP47B
	8-pin DIL sockets, 2 required	BL17T
	Knobs, 2 required	FD67X
	Material for speaker grille	
	Connecting wire	

38 A receiver for the 7 MHz amateur band

Introduction

Listening on the 40 metre band (from 7.0 to 7.1 MHz) can be very rewarding – it is a popular haunt for HF Special Event stations, and at night there are signals to be heard from all over Europe. This receiver is designed purely for the 40 m band, and is ideal for those who have built the simpler receivers and are looking for something a little more challenging. The more experienced constructor may prefer to build this on prototype board.

The circuit and its construction

Figure 1 shows the circuit diagram. The receiver will work well with headphones or loudspeaker. Walkman-type headphones and speakers are ideal for use here.

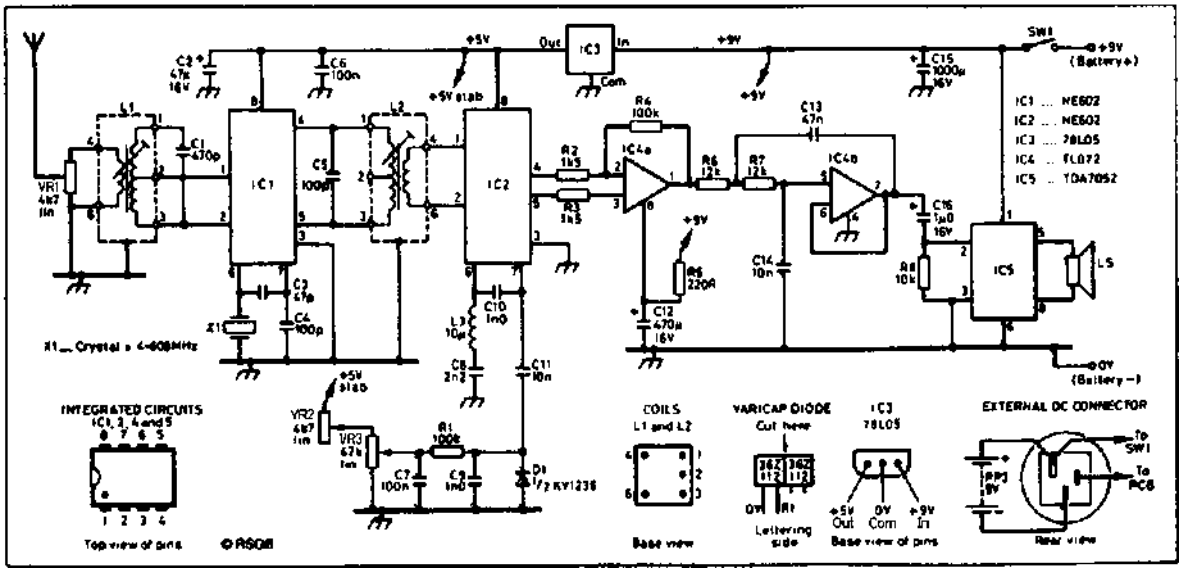

Figure 1 The receiver gives good performance on the 7 MHz amateur band as well as being simple to construct and align

Signals arriving at the aerial are coupled into IC1 via gain control VR1, which also functions as the on/off switch. Tuning is provided by varying the voltage on the *varactor diode* (or varicap), D1. VR3 is the main tuning control, and VR2 is the *bandspread* (fine tuning) control. The varactor diode is supplied as a dual device, which must be cut down the middle *carefully* with a sharp knife; with the lettering upwards, the ground lead (0 V) is on the left-hand side, as Figure 1 illustrates.

Solder in the IC sockets first, followed by the coils. After this come the links, resistors, capacitors and varactor diode. Ensure that IC3, the voltage regulator, is wired correctly, and check the polarity of the electrolytics. The crystal, X1, is very fragile, so take extra care with it. The wiring of the three controls is shown in **Figure 2**.

Before putting the ICs in their sockets, connect up the battery and check the following voltages with the negative voltmeter lead connected to the negative terminal of the battery:

Pin 8	IC1	5 V
Pin 8	IC2	5 V
Pin 8	IC4	9 V
Pin 1	IC5	9 V

When all these have been found to be correct, switch off and put the ICs carefully into their sockets. Use wire of different-coloured insulation to wire up the front-panel controls.

The case can be a small plastic box of size 22 cm by 15 cm by 8 cm, with three 10.5 mm holes drilled in the front and two 8 mm holes in the side for the aerial and earth connections. On one side are a 6 mm hole for the speaker socket and an 11 mm hole for the optional external power supply.

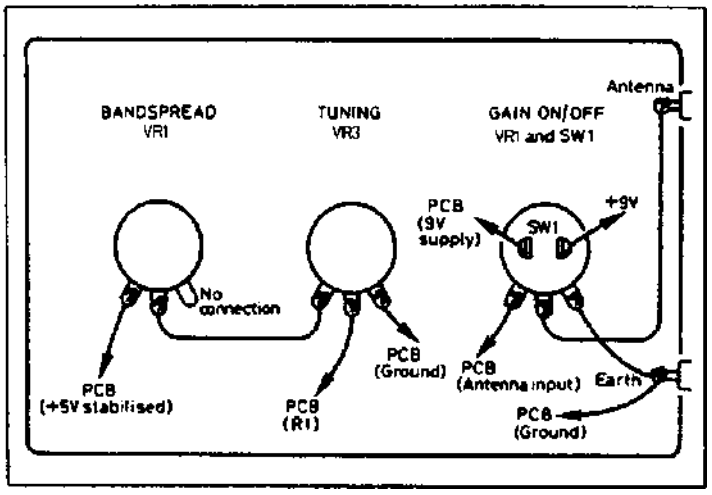

Figure 2 Rear view of the variable resistors. Check the connections carefully to make sure the wires are fitted correctly

Testing and tuning

The aerial for the receiver should be between 30 and 70 feet of wire, mounted as high as you can make it, away from trees and buildings if possible. Connect the battery and switch on. Adjust L1 and L2 for the best results. Tune slowly with VR3; you should find CW stations at the lower end of the band (anticlockwise) and SSB stations at the upper end (clockwise). You may find that it is easiest to make these adjustments *before* mounting the board in the case with double-sided sticky tape or pads. If you are planning to use an external DC supply, make sure it is a safety approved stabilised 9 V type, and **disconnect the battery before you use such a supply!**

If you suspect that the tuning doesn't quite cover the lower CW end of the band, try increasing C9 to 1200 pF. If it is the upper SSB end which is missing, decrease C9 to 820 pF.

It is always advisable to use an aerial tuning unit (ATU) between your aerial and the receiver. A suitable design of ATU is included as a project in this book.

Parts list

Resistors: all 0.25 watt, 5% tolerance

R1, R4	100 kilohms (kΩ)
R2, R3	1.5 kilohms (kΩ)
R5	220 ohms (Ω)
R6, R7	12 kilohms (kΩ)
R8	10 kilohms (kΩ)
VR1	4.7 kilohms (kΩ) linear, with SPST switch
VR2	4.7 kilohms (kΩ) linear
VR3	47 kilohms (kΩ) linear

Capacitors: all rated 16 V or more

C1	470 picofarads (pF) polystyrene 5%
C2	47 microfarads (μF) electrolytic
C3	47 picofarads (pF) polystyrene 5%
C4, C5	100 picofarads (pF) polystyrene 5%
C6, C7	100 nanofarads (nF) ceramic
C8	2.2 nanofarads (nF) polystyrene 5%
C9, C10	1 nanofarad (nF) polystyrene 5%
C11, C14	10 nanofarads (nF) ceramic
C12	470 microfarads (μF) electrolytic
C13	47 nanofarads (nF) ceramic
C15	1000 microfarads (μF) electrolytic
C16	1 microfarad (μF) electrolytic

Inductors

L1	Toko KANK3335R
L2	Toko KANK3333R
L3	10 μH 5%, e.g. Toko 283AS–100

Semiconductors

IC1, IC2	NE602 or NE602A
IC3	78L05 5 V, 100 mA
IC4	TL072
IC5	TDA7052

Additional items

D1	Toko KV1236 cut into two sections (one half used)
X1	4.608 MHz (available from Cirkit)
	3 × silver knobs, one with pointer
	Plastic case approx. 22 × 15 × 8 cm
	Speaker 8–32 Ω, or headphones
	4 × 8-pin DIL sockets for IC1, IC2, IC4, IC5
	2 × 4 mm sockets (red and black) for aerial and earth
	3.5 mm chassis-mounting jack socket for speaker
	DC power socket for external supply (if required)
	Prototype board

Kits

A complete kit is available from JAB Electronic Components.

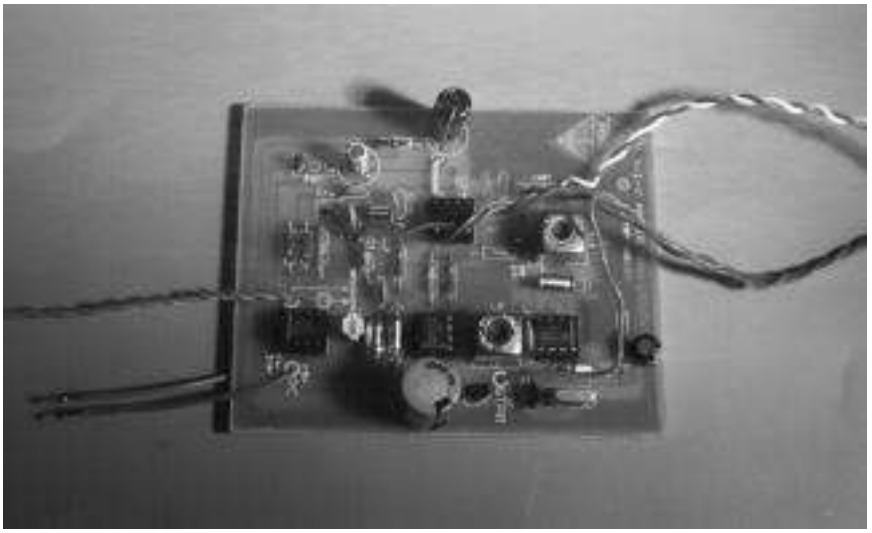

39 Diodes for protection

Introduction

Many semiconductor devices can be destroyed in an instant if their supply is reversed. With the use of batteries as power sources, it is quite common for the battery to be connected 'the wrong way round', and the scope for damaging equipment is significant and very real. Diodes can protect equipment in several ways, and you may do worse than to consider one of these approaches to protect your next expensive project.

Choose wisely!

All the diode circuits given here are so simple as to invite calamity. The circuits are not foolproof but, with a little care, will work first time. Remember that a semiconductor diode has a forward voltage drop of between 0.5 V and 0.7 V, depending on its type and the current flowing. This will be mentioned later.

The first thing you need to do is to insert a good multimeter *in series* with the circuit you want to protect; set the range to Amps DC, and switch on. Check that the circuit works properly. Then, decrease the current range on the meter until a good reading is indicated. Make a note of this current, as it is the normal running current of your circuit.

To choose a diode, you must consult the catalogues or data sheets and find one where the quoted *maximum forward current* exceeds the current you have measured; preferably it should be at least twice your measured current. Secondly, the diode will have a *peak inverse voltage* (PIV); this is the maximum voltage it can withstand when the cathode is made positive with respect to the anode, i.e when it is *reverse-biased* and not conducting. This voltage must be greater than your battery voltage, again by a factor of about 2. Except in the case of the bridge rectifier (see later), these criteria will enable the selection of a suitable diode to be made easily.

The series diode

The simplest and most obvious way to protect equipment is to insert a diode in the positive supply lead, as shown in **Figure 1**, with the diode passing current *only* when the supply is of the correct polarity. Because of the 0.6 V that exists across the diode, your equipment will normally operate on a

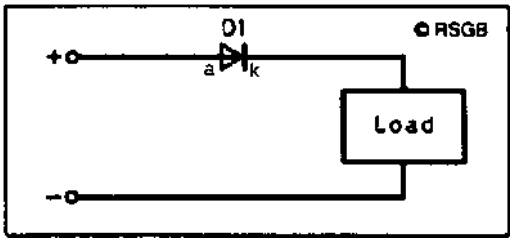

Figure 1 Series diode protection

slightly lower voltage. If you imagine reversing the supply to this circuit, you will see that the negative terminal of the battery is connected to the anode of the diode; the diode becomes reverse-biased and will not conduct any current, thus protecting the load. Your equipment will not operate when the battery connections are reversed.

The parallel diode

The circuit of **Figure 2** overcomes this voltage drop. It places the diode in parallel with the load (your equipment) but in a normally reverse-biased condition so that it draws no current when the battery is correctly connected. Reverse the battery connections, however, and a very large current will flow through the diode, thus blowing the fuse! For this technique to work successfully, the current drawn by the diode when the battery connections are reversed *must* be much greater than the maximum current drawn by the equipment, in order to blow the fuse. This is usually not a problem, however.

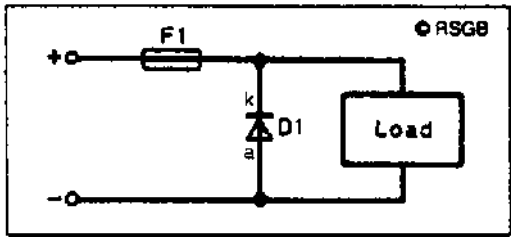

Figure 2 Parallel diode and fuse

The diode bridge

For sheer elegance, the circuit of **Figure 3** takes the biscuit! It uses four diodes connected in the form known as a *bridge rectifier*. Such rectifiers exist, and do not have to be made up from four discrete diodes.

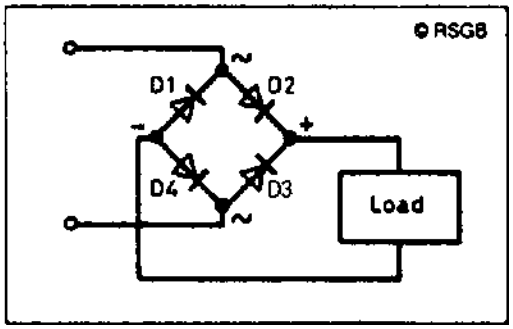

Figure 3 The diode bridge

Follow the current round the circuit from the supply, assuming initially that the top wire is positive and the bottom wire negative. It flows from the positive supply

(a) through D2
(b) through the load (top to bottom)
(c) through D4

and back to the negative of the supply.

Now assume that the bottom supply lead is positive and the top lead negative. The current flows from the positive supply

(a) through D3
(b) through the load (top to bottom)
(c) through D1

and back to the negative of the supply.

So, whichever way round the battery is connected, the current will *always* flow the same way through your equipment!

The circuit does have a drawback, however. Whichever way round the battery is connected, there are always **two** diodes conducting the current at any time. In the first case it is D2 and D4; in the second case, D1 and D3. This means that there is a total voltage drop of about 1.2 V. If your equipment can tolerate that reduction in voltage, then you will not have a problem.

Decoupling

Whenever the supply rail to a piece of equipment, or even to an individual stage of a circuit, is broken for the insertion of a device that will drop voltage, strange things can happen. This is because the supply for any circuit is assumed to have a low resistance to DC and a low *impedance* to AC. (Impedance is the AC equivalent of DC resistance.) These two are not the same, and the insertion of a diode or diodes is certain to make a big

difference to them both. To overcome any irregularities in the operation of the circuit you are protecting in any of the ways described previously, the protected supply needs to be *decoupled* with a capacitor.

If the circuit handles audio frequencies only, placing an electrolytic capacitor directly across the load in all three circuits should solve the problem. The parallel circuit of Figure 2 is less at risk than the other circuits. The size of the capacitor will be determined by the current taken by the circuit, and may need to be chosen within the range 100 μF to 10 000 μF, with a working voltage greater than the supply voltage.

If the circuit is mainly handling RF currents, placing a capacitor of 0.01μF across the load should prevent any problems. A second capacitor, also across the load, of between 10 μF and 100 μF may be needed. Again, the parallel circuit of Figure 2 is less at risk than the other two.

Don't be afraid to experiment, but confine your experimenting (at first) to small equipment and low currents, until you get a 'feel' for the technique.

40 An RF signal probe

Introduction

A radio-frequency (RF) diode probe is a simple device which, when used with a conventional multimeter, enables the measurement of RF voltages in a circuit. When constructed, this will be one of the most useful pieces of test equipment for the experimenter who revels in the construction of transmitters and receivers.

The circuit

Figure 1 shows the simple circuit diagram. It is *almost* the same as a common diode rectifier circuit, but with a simple change to make it more sensitive. The circuit is known as a *voltage-doubler*, and is often found in high-voltage supplies, with beefier capacitors and diodes, of course! Because we are dealing with high frequencies and smaller voltages, the diodes and capacitors can be physically very small. The diode circuit of D1 and D2 *rectifies* or *detects* the RF from the probe, and any remaining AC is removed (short-circuited to ground) by C2. This produces, at the output, a constant voltage proportional to the peak-to-peak RF voltage present at the input; the output voltage is fed to an ordinary multimeter (on a voltage range).

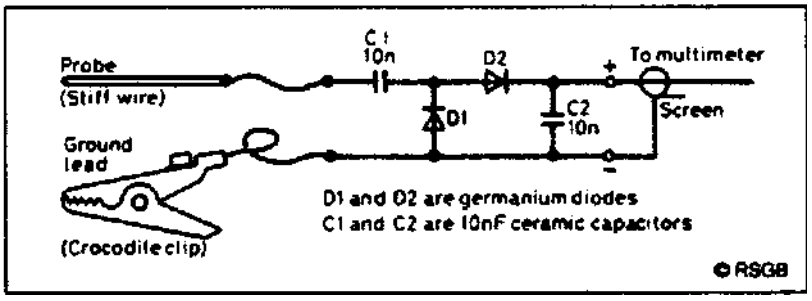

Figure 1 The diode probe can be made from four electronic components

Construction

Although the circuit layout is not critical, a description of the prototype is given here for your information. **Figure 2** has the details. The components are soldered to square pieces of copper-clad printed-circuit board (PCB) glued to a larger piece of PCB. The larger piece serves as a ground connection. Use a stiff copper wire as the probe, and an insulated flexible wire with a crocodile clip to connect the probe to the ground of the circuit under test.

Cut a piece of plain PCB, 30 mm by 45 mm and another of 15 mm by 45 mm. Cut the smaller piece into three measuring about 15 mm square. Stick the three small pieces to the larger piece, ensuring that there are small gaps between each, as Figure 2 shows. Solder the components in place. The connection to the multimeter should be thin coaxial cable or screened microphone cable. If you use unscreened cable, there may be RF pickup here which can lead to false readings.

Simple to use

Using the probe is simple. Connect it to the multimeter and set the meter to around 10 V DC – you may need to reduce this, depending upon the magnitude of the RF voltage you are trying to measure. Hold the probe by

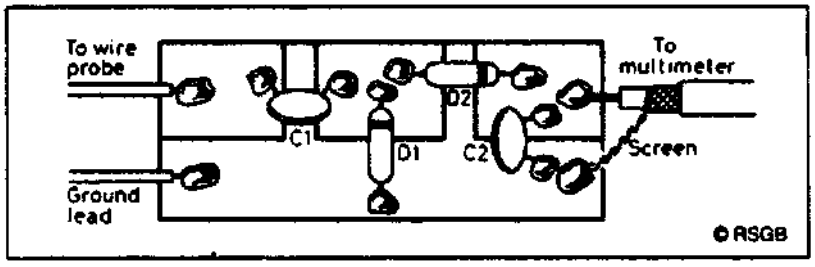

Figure 2 The components are mounted on a copper-clad PCB

its base, being careful *not* to touch any of the components. Connect the croc clip to a ground point on the circuit and touch the probe on the circuit point to be tested. If an RF signal is present, there should be a reading on the multimeter. That's all there is to it!

Parts list

Capacitors
- C1, C2 — 10 nanofarads (nF), or 0.01 microfarad (μF) ceramic

Semiconductors
- D1, D2 — Any *germanium* signal diode, e.g. OA91 or AA119

Additional items
- Stiff copper wire
- Insulated flexible wire
- Copper-clad PCB
- Crocodile clip
- Coaxial or screened cable

Source

All components are available from Maplin.

41 An RF changeover circuit

Introduction

The simplest entry route to operating an HF station is to buy or build a receiver, and to add a simple CW (Morse) transmitter. In theory, this sounds so simple, yet in practice there is one significant hurdle to be overcome. How can they both share the same aerial? A manually operated changeover switch is the obvious solution, but it takes time to perform the switching operation, by which time someone else has squeezed in before you and contacted the DX station! This small circuit accomplishes the changeover automatically, as soon as the transmitter is keyed.

How it's done

The circuit is shown in **Figure 1**, and uses the signal from the transmitter to operate a relay. A relay is a switch which is operated electrically in the following way. A coil of wire with an iron core is used as an electromagnet. When current flows through the coil, it produces a magnetic field which, in turn, is used to pull a set of switch contacts. These contacts will be used to switch the aerial from transmitter to receiver and vice versa. The relay used here has a double-pole changeover (or DPDT, or DPCO) switch. If you are confused by the different types of switch, look at the basic descriptions elsewhere in this book. The *pole* of a switch is the part that doesn't move; in Figure 1, one pole is connected to L1 and the other to the aerial output. In a circuit diagram, the switch contacts are always shown in their *normal* state, i.e. when *no* current flows in the relay coil. The changeover switch is normally in the receive position, so we say the receive switch is *normally closed*, and the transmit switch is *normally open*. We choose to have the circuit in the receive position normally, because everyone spends a lot more time receiving than transmitting. The relay is energised only when you are transmitting.

There are three RF sockets – one for the transmitter, one for the aerial, and one for the receiver. When the transmitter is not in use, there is a direct connection (via the Rx normally closed contacts of the relay) between the aerial and the receiver. The transmitter (which is not keyed at this time) is connected to a 50 ohm dummy load, R1.

When the transmitter is activated by pressing the Morse key, an RF signal appears at the transmitter socket. The wire carrying the signal to the relay

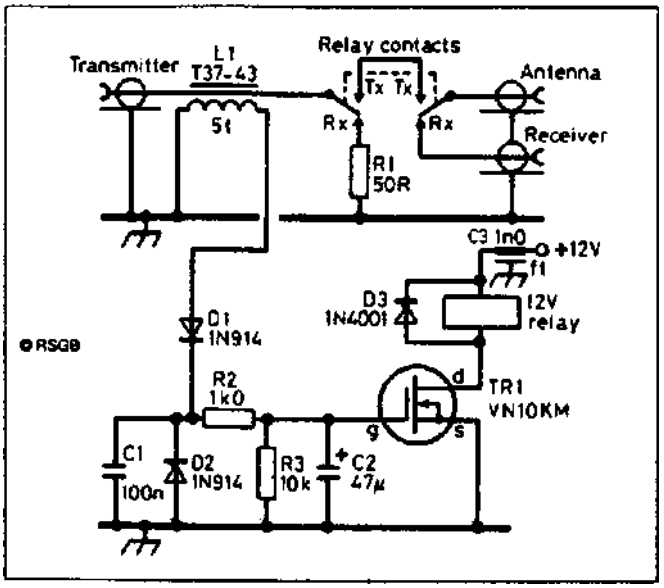

Figure 1 RF activated relay

Tx contacts passes through a toroid (a ferrite coil former, looking like a black Polo mint), which has a five-turn coil wrapped around it. This five-turn coil picks up the signal, which is then detected by D1 and D2, and converted to a steady voltage. C1 removes any remaining RF and C2 provides *hang*. Without it, the circuit would detect the gaps between every dot and dash being sent, and switch the aerial over very rapidly and very frequently! This is *not* what we want. We need the relay to remain in the transmit condition at normal Morse keying speeds, and then return to receive when the sending is complete. The combination of C2 and R3 achieves this.

The voltage appearing across C2 is fed to a VMOS field-effect transistor (FET), TR1, which acts as an electronic switch. When a voltage appears across C2, the FET switches on and passes a current through the relay coil, changing the contacts from receive to transmit. The diode, D3, across the relay winding protects the FET from being damaged by the large reverse-voltage spike which occurs across the coil when the FET switches off.

Construction

This is very simple – a circuit board is not required. The prototype was built into an old 50 g tobacco tin. All ground leads are soldered directly to the tin, thus supporting the components automatically. Phono sockets were used for the aerial, receiver and transmitter; you could use whatever connectors matched the rest of your station. The 12 V supply is fed through the tin using a 1000 pF feed-through capacitor, C3.

The 'dummy load', R1, must be able to withstand the RF output power of the transmitter. For novice use, 4 watts is adequate. Two suggestions for making up R2 from standard resistors are shown in **Figure 2**. Six 330 ohm, 1 watt resistors in parallel have a combined resistance of 330/6 = 55 Ω at 6 W. Two 100 ohm, 2 watt resistors in parallel have a combined resistance of 100/2 = 50 Ω at 4 W.

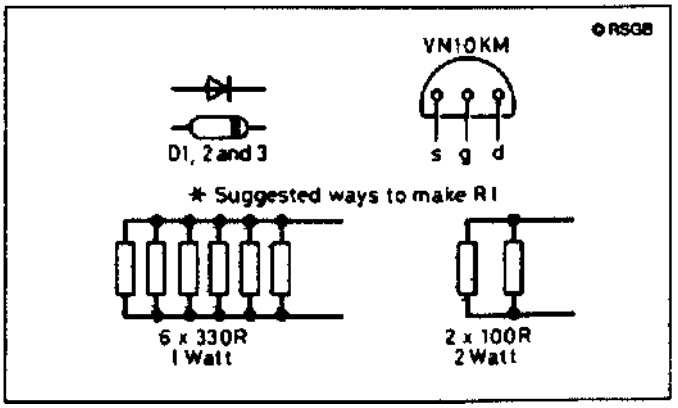

Figure 2 Component details

Make sure all the contacts to the relay are correct; also ensure that TR1, C2, D1, D2 and D3 are correctly wired.

Winding the toroid, L1, is very simple. It is made from PVC-insulated hook-up wire. Each time the wire passes through the centre of the toroid counts as one turn. The wire from the transmit socket to the relay simply passes through the centre! Use thin 50 Ω coax for the leads to the three sockets.

What happens to the receiver?

On transmit, the receiver is not connected to the aerial, but is only the separation of the switch contacts (about 0.5 mm!) away from the transmit lead. The receiver *will* pick up the transmitted signal, and there is a possibility that this signal will be enough to damage the receiver's sensitive input circuits. This can be prevented with the simple addition shown in **Figure 3**. Two diodes are connected back to back across the receiver socket. These act as a *limiter*, reducing the amount of signal that can enter the receiver. Solder these directly between the receiver socket and the tin.

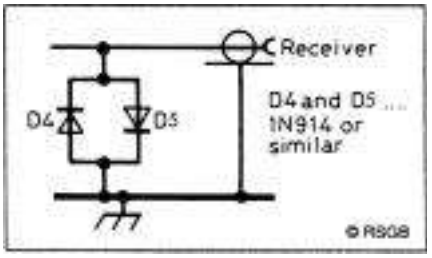

Figure 3 Receiver input protection

Warning

The wiring **must** be thoroughly checked. If the relay switch connections are wrong, there is a **great probability** that the full RF power will be applied to your receiver! You can check these connections as follows. With the 12 V supply connected, check that the relay energises (clicking sound heard) when the FET drain (d) is shorted to earth. Check the aerial and receiver connections with an ohmmeter or continuity tester. Disconnect the 12 V supply, and check that there is continuity between the centre pins of the aerial and receiver sockets. Reconnect the 12 V supply, short the FET drain to earth again (this will not damage the FET) and check that there is continuity between the centre pins of the aerial and transmitter sockets. If these tests show correct operation, disconnect the drain shorting wire (*most* important!) and your aerial auto-changeover is ready for use! Avoid using the device without the lid fitted.

Parts list

Resistors: 0.25 watt, 5% tolerance, unless otherwise stated

R1	50 ohms (Ω) – see text and Figure 2
R2	1 kilohm (kΩ)
R3	10 kilohms (kΩ)

Capacitors

C1	100 nanofarads (nF), 0.1 microfarad (μF)
C2	47 microfarads (μF) 15 V electrolytic
C3	1000 picofarads (pF) feedthrough

Semiconductors

D1, D2, D4, D5	1N914
D3	1N4001
TR1	VN10KM

Additional items

L1	T37–43 toroid
	Relay 12 V DPDT (DPCO) relay
	Three sockets to suit (phono, SO239, etc.)
	Thin coax cable and hook-up wire

42 A low-light indicator

Introduction

This is a simple one-evening project that can be built for the pure fun of it, or to use as the basis of a more complex project to switch your shack lights on when it gets dark! In its prototype form, it simply flashes an LED when the ambient light level drops to a preset point.

Operation

The heart of the circuit shown in **Figure 1** is a *photo-conductive cell*, also called a *light-dependent resistor* (LDR), a device whose resistance changes according to the amount of light falling on it. In bright light, the resistance is low (about 1 kΩ), whereas in the dark, its resistance is very high (up to 10 MΩ). The cell is made from a semiconducting material known as cadmium sulphide (CdS), and is enclosed in a small plastic container. The semiconductor is laid on a flat insulating surface in the form of a small flat ribbon. The ribbon construction gives a good area of surface for a given

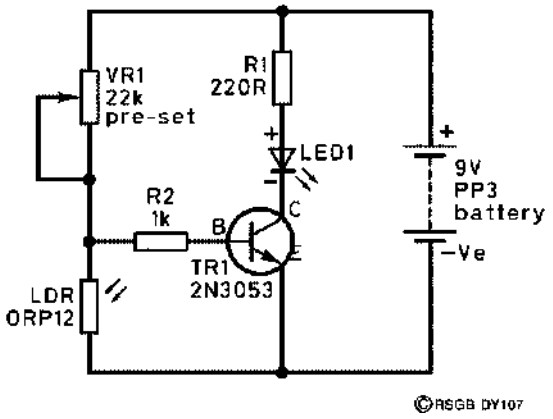

Figure 1 Circuit diagram

length of ribbon, and the length of the ribbon is maximised by laying it out in a zig-zag pattern, as can be seen diagrammatically in **Figure 2**. In the dark, CdS is an insulator; when light falls on it, electrons are released inside the CdS, making it conduct. The more light there is, the more electrons there are, and the resistance falls.

In this circuit, the LDR is connected across the 9 V supply in series with a variable resistor, VR1. In this arrangement, the voltage that exists across the LDR will be determined by the light level. As the light intensity increases, the resistance of the LDR falls, dropping a smaller voltage across it. The

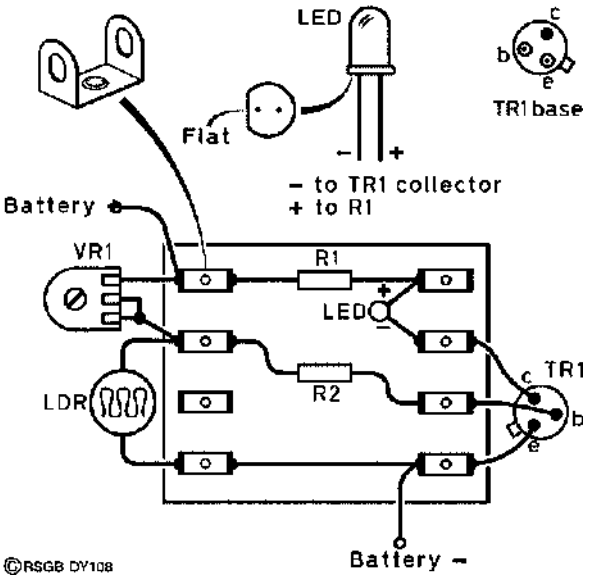

Figure 2 Component layout on tagstrip

reverse happens when the light intensity falls – the voltage across the LDR increases. This voltage is used to drive an npn transistor, TR1, connected as an electronic switch. As the voltage on the base (B) rises, it will reach a point where TR1 will suddenly start to pass current, just as an ordinary switch does when pressed. The current flowing through TR1 also flows through a flashing light-emitting diode (LED), D1 and its series resistor, R1. D1 can be a steadily glowing type, if preferred. If you want to make the circuit switch the LED on at a different ambient light level, adjust VR1.

Construction

The prototype was made on an eight-tag tagboard (Figure 2). The resistors R1 and R2 can be laid on the tagboard for soldering, the rest of the components lying above or to the side of the board. Check the circuit after you have soldered everything on, then connect the battery. The LED should flash if you put your hand over the LDR, and VR1 can be adjusted to vary the point at which the LED lights. The project can be housed in a small plastic box with holes provided for the LDR and LED and an on/off switch if you want one.

Parts list

Resistors: all 0.25 ohm, 5% tolerance

R1	220 ohms (Ω)
R2	1 kilohm (kΩ)
VR1	22 kilohms (kΩ) linear pre-set

Semiconductors

LDR	ORP12
TR1	2N3053 npn
LED1	Flashing LED

Additional items

- Plastic box
- Tagboard with 8 tags
- PP3 battery connector

43 A J-pole aerial for 50 MHz

Introduction

For FM communication (i.e. voice and data) on the VHF bands, a vertical aerial is used to give all-round (non-directional) coverage. This is a half-wave aerial which can be fed at the end, thus removing the principal problem with the conventional vertical centre-fed half-wave dipole, which is that the feeder should leave the dipole at right angles. This is no problem when the dipole is horizontal, but can be difficult for the vertical dipole.

Basic facts

A feeder must be connected to an aerial at a point where the *impedance* (AC 'resistance') of the aerial closely matches that of the feeder. The difference between the two impedances gives rise to the voltage standing-wave ratio (VSWR), which is unity only when the two impedances are the same. With 50 Ω feeders, the feed point of a half-wave aerial is at the centre, where the aerial impedance is around the same value. At the end of a half-wave aerial, the impedance is high, so it is *not* a suitable point to connect a 50 Ω feeder.

Connection at this point can be effected using an RF transformer. RF transformers act in the same way as ordinary transformers, except that they are much smaller, and usually comprise wires of particular lengths adjacent to each other. **Figure 1** is a good starting point. It shows the aerial in its diagrammatic form. Notice that the aerial is in the form of an elongated letter 'J'; this shape gives rise to its nickname – the *J-pole*. The quarter-wave RF transformer is the lower 'U' section below the half-wave element. At the bottom of the U section, the impedance is zero (this may become clearer later) and at the top of the U section it is high, thus matching the aerial impedance. The coaxial feeder cable is connected part-way up the U section, where the impedance is around 50 Ω.

The practicalities

Figure 2 shows the aerial as constructed. As it is about 4.5 metres high, it may be too high for the average house loft, but is ideal for mounting outside, supported by a non-metallic pole or hung from a tree branch. The upper half-wave section is made from 1.5 mm insulated copper wire, as used in domestic mains wiring. The quarter-wave transformer below the half-wave section is made from 300 Ω balanced line ('ribbon cable'). The

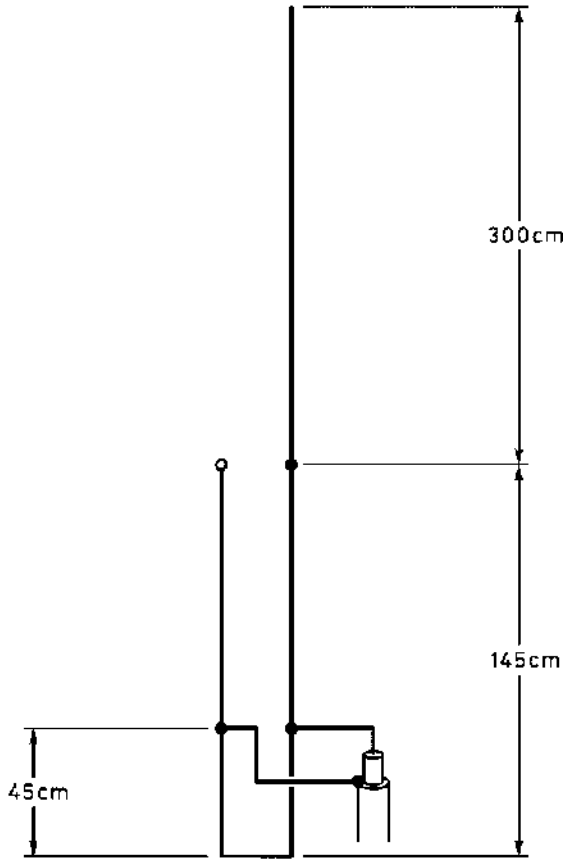

Figure 1 Overall dimensions of the 6 metre J-antenna

wires at the bottom of the transformer section are stripped of their insulation, twisted and soldered. At the upper end, only one wire of the balanced line is soldered to the bottom of the half-wave section. The other wire of the pair is not connected and is left insulated.

At the feed point of the transformer, the insulation needs to be carefully stripped from the balanced line. You will need a standing-wave meter (VSWR meter) in the coaxial line between your transmitter and the aerial, and you will need to adjust the position of the feed point. 45 cm from the bottom was the best point on the prototype, but this position is dependent upon the immediate surroundings of the aerial, and *must* be done when the aerial is in its final operating position. **Warning: *Never* make adjustments to the feed point when the transmitter is on. Make a VSWR measurement, switch off, move the feed point, switch on again, make another measurement, and so on.** You will need to aim for the lowest VSWR you can – certainly better than 2:1. Having found the best position, wrap all the exposed wires with self-amalgamating tape, to seal them against the ingress of moisture.

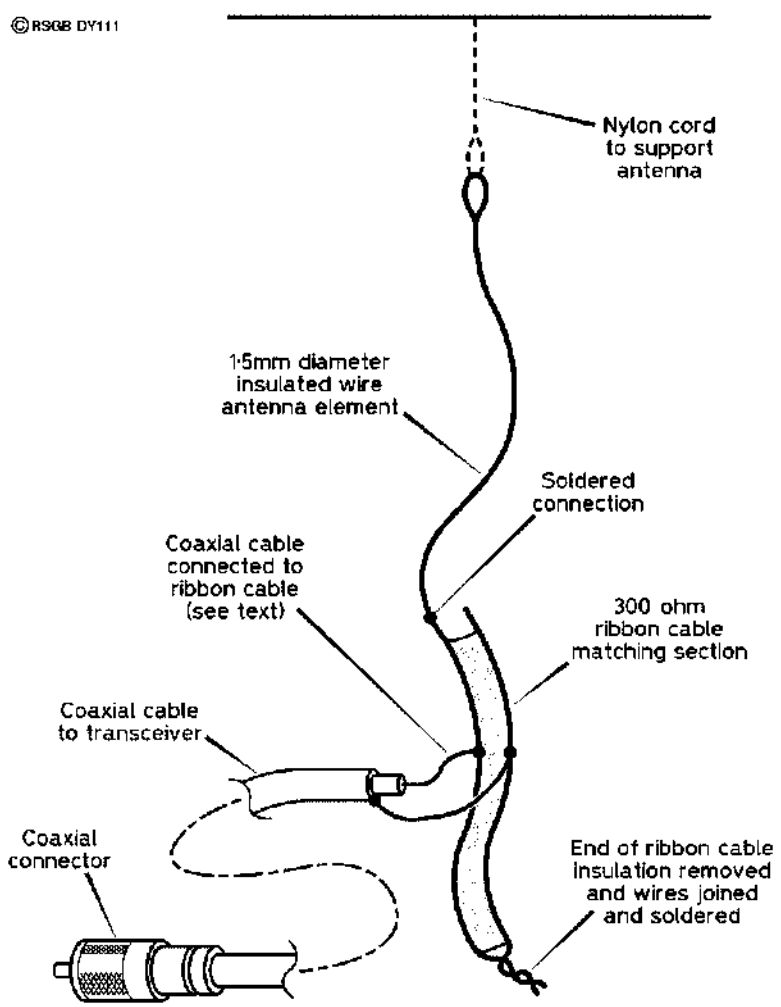

Figure 2 Construction details

How it performs

Figure 3 shows a computer prediction of how the J-pole radiates. It is called a *polar diagram*, and shows the distribution of your transmitted power when viewed 'from the end of your garden'. Most of your signal is sent at a fairly small angle to the horizontal; very little signal goes upwards, which is a good thing, of course. This also shows why the J-pole (or any other vertical aerial) should not be called 'omnidirectional', which means it radiates in all directions. It is omnidirectional *only* in the horizontal plane.

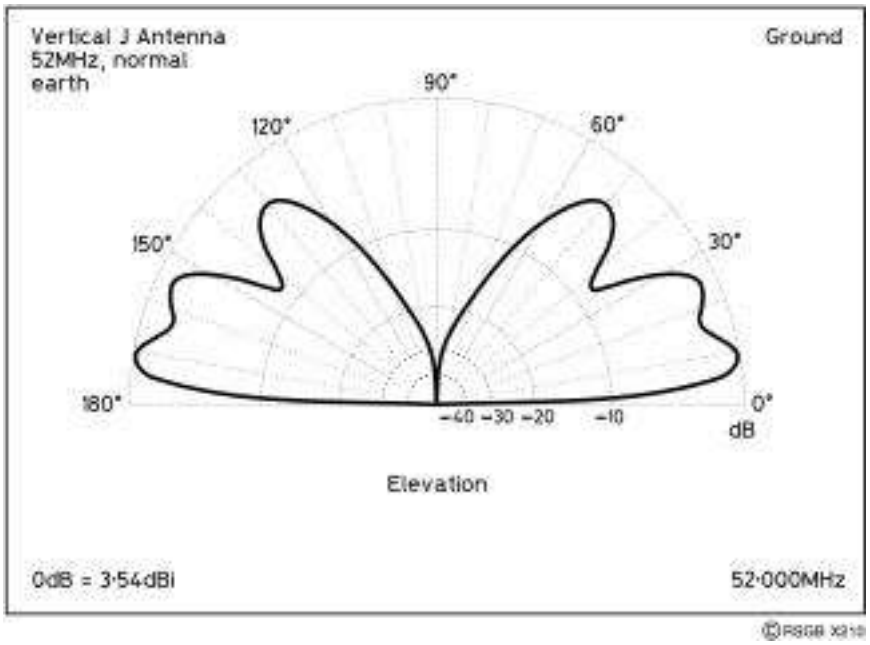

Figure 3 This polar diagram computed for the J-pole

Safety

Where you mount your aerial is a matter of personal preference and the restrictions of height and space, but the following safety rules *must* be applied.

1. Never fix an aerial where it may come into contact with power lines or telephone lines.
2. When climbing a ladder to put up an aerial outside, make sure the ladder is safe and that it is secured.
3. Don't do this alone. Preferably have someone with you. If this is not possible, make sure someone knows where you are.

Parts list

3.00 metres	1.5 mm insulated copper wire
1.50 metres	300 ohm balanced line
As required	50 ohm coaxial cable
As required	Self-amalgamating tape

44 Measuring light intensity – the photometer

Introduction

Before the days of automatic 'point-and-shoot' cameras, a photographer would use a light meter or *photometer* to measure the light level, then manually convert this reading into shutter speed and lens aperture settings to ensure a correctly exposed negative. Modern cameras have quite sophisticated photometers, which control the shutter speed and iris settings automatically.

A short explanation

A simple photometer circuit is shown in **Figure 1**, and is based on a device called a *light-dependent resistor*, or LDR. As its name tells us, its resistance depends upon the amount of light falling on it. In bright light, the resistance is relatively low (about 1 kΩ), whereas in the dark, its resistance is very high (up to 10 MΩ). The cell is made from a semiconducting substance known as cadmium sulphide (CdS), and is enclosed in a small plastic container. The semiconductor is laid on a flat insulating surface in the form of a small flat ribbon. The ribbon construction gives a good area of surface for a given length of ribbon, and the length of the ribbon is maximised by laying it out in a zig-zag pattern. In the dark, CdS is an insulator; when light falls on it, electrons are released inside the CdS, making it conduct. The more light there is, the more electrons there are, and the resistance falls.

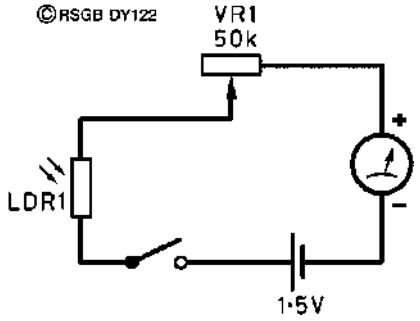

Figure 1 Circuit diagram of photometer

The photometer circuit

The circuit is simply a series connection of four things – the battery, the LDR, a variable resistor and a meter. A switch is also provided. The combination of the LDR resistance and that of VR1 determines the current flowing, which is indicated on the meter. Altering the resistance of VR1 sets the *sensitivity* of the photometer – you may want full-scale deflection of the meter needle for a bright light, or for a dim light.

It is simple to make, and a plug-in type matrix board is ideal to test the circuit, so that you can decide if you want to make a permanent version. Connect all the components in series; the only change you may want to make is the connection to VR1. If you find that the sensitivity control seems to work 'backwards', simply unsolder the wire from the end tag of VR1 and solder it to the opposite end tag. Problem solved!

In use

As soon as you connect up the battery, you will probably have a meter reading because of the daylight falling on the LDR. Shading it with your hand should reduce the reading. If the meter needle is hard over against the end-stop, turn VR1 until it indicates about half-scale. The LDR is very sensitive, and will read zero only in a dark room. If you put on a torch to see what the meter reading is, the LDR will detect the torch light, and will give a reading!

Here is a simple project where you can use the photometer in an experiment which has an analogy in radio. Draw a circle on a large (A3 or bigger) sheet of paper and divide it up into 30-degree sectors, as shown in **Figure 2**. Draw a series of smaller circles which divide the maximum radius into five. Look at the figure if you're not sure about this. Bring the LDR away from the circuit by using two long, flexible wires. The experiment must be performed in a darkened room (preferably in total darkness). Prepare a table with two columns, the left-hand one headed 'Angle (degrees)' and the right-hand one 'Meter reading'. Fill in the left-hand column 0, 30, 60 . . . and so on up to 360°.

Place the torch in the position shown, with its lens at the centre of the circle and pointing along the 0° line; switch it on. Place the LDR facing the torch and adjust VR1 until you have full-scale deflection of the meter needle. Suppose the meter indicates 10 units at this point. Enter this into your table in the 0° row. Keeping the torch the same distance from the circle centre, and pointing at it, move the LDR round all 30° positions and record the meter readings. Switch off the torch and take the sheet of paper and your tabulated results into daylight!

Lay the large sheet of paper on a table with your results beside it; then, at each 30° interval, plot the point along the radius corresponding to the meter

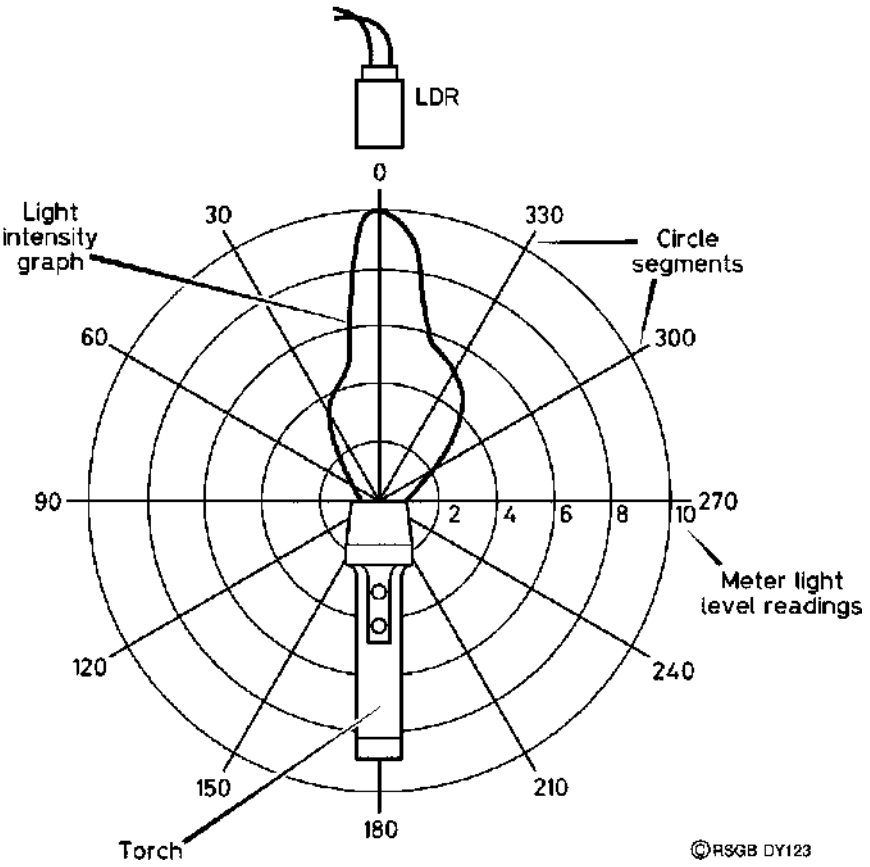

Figure 2 Torch light intensity pattern plotted at RSGB HQ

reading. Then, join up all the points and you have what is called a *polar diagram* of light intensity. The use of the word 'polar' implies that the readings have been taken in a circle and plotted that way.

Light waves and radio waves are both examples of *electromagnetic radiation*. The torch is designed to 'beam' its radiation in a particular direction, just like an aerial does. Hence the use of the word 'beam' for a directional aerial. If a similar polar diagram is drawn for a Yagi-type aerial, it will show the same general characteristics as does Figure 2, namely a main direction (or 'lobe') where most of the energy is concentrated, with evidence of *sidelobes*, indicated by 'lumps' on the otherwise smooth main lobe.

Also in this book you will find a project for the construction of a UHF field-strength meter, which you could use to carry out a measurement of the polar diagram of a UHF aerial.

Parts list

Resistor
VR1 50 kilohms (kΩ) linear

Semiconductor
LDR1 ORP12

Additional items
Meter, 50 or 100 μA
Battery clip for single AA cell
AA cell

45 A 70 cm Quad loop aerial

Introduction

This is a description of how to make an aerial for the 70 cm band which has gain compared with the 'rubber duck' or the dipole aerial. It can easily be dismantled and reassembled, making it ideal for contest use.

The principles

Most aerials which comprise several similar *elements* arranged along a *boom* are variations of the design originated by Yagi and Uda, and which takes the name (for historical reasons) of the former, and is know as the Yagi array. Let us suppose we have a Yagi aerial beaming left to right in front of us. The elements get progressively shorter from the left (look at almost any TV aerial to see this). All the elements on a Yagi aerial are classified as follows:

- The *reflector* – the leftmost element as we look at the array. It is the longest. Next to it is:
- The *driven element* – this is the element connected to the feeder, which in turn runs down to the transceiver. It is slightly shorter than the reflector.
- All the elements beyond the driven element are called *parasitic elements*, or *directors*. They are shorter than the driven element and usually get progressively shorter as we progress to the right along the boom. The directors are mainly responsible for the *directivity* (or *beamwidth*) of the array.

The progression from a simple dipole (a driven element in isolation) to a Yagi array is simple, but is nevertheless important. To make an aerial of two elements, a reflector (*not* a director) is added to the driven element. For three or more elements, directors are added to the two-element design. Adding more and more directors soon becomes impractical, the reduction in beamwidth (such as it is) does not warrant the extra expense, weight and wind resistance that is incurred.

Instead of using linear (straight) elements, as in the generic Yagi, this design uses loops. Designs using squares of wire instead of loops are known as *Quad* aerials, and HF designs require large X-shape frames to support the large squares of wire. At 70 cm, however, the use of wire loops is easier, and they are self-supporting.

Construction

This is quite simple. Any type of material (metal, plastic, wood) can be used for the *boom* (the support for the elements) and for the mast. The elements are made from 14 SWG enamelled copper wire. 16 SWG hard-drawn aerial wire, which is not enamelled, has also been used with success. Thinner wire might result in a rather 'floppy' aerial! The separate parts of the aerial are held together with *jubilee clips* (hose clips).

The driven element is secured to the boom with a jubilee clip and a three-connector plastic connector block as shown in detail in **Figure 1**, and in the photograph. Cut the wire for the driven element 70 mm longer than the 700 mm indicated in Figure 1. Then, using sandpaper, remove the enamel from one end to a distance of 20 mm, and from the other to a distance of 50 mm. After forming the loop of the driven element, bend both stripped ends through 90°, and insert them into the first to holes of the plastic connector block (Figure 1). Do not tighten the screws yet. Push both ends into the block as far as they will go, then bend the 50 mm end back on itself and pull the ends back through the connector block so that the end you have just bent goes into the third hole in the block. Now tighten the screws in the block and in the jubilee clip.

Each director and the reflector should be made 40 mm longer than the circumferences shown in Figure 1. Strip the enamel, as before, from the last 20 mm at each end. Form the wire into the loop, slip the ends under the jubilee clip (Figure 1) and tighten it. You may find that it helps to solder the stripped ends together before securing the jubilee clip.

The boom is fixed to the mast using jubilee clips and wire, as shown in Figure 1. Solder the feeder cable to the driven element, with the braid soldered to the end of the driven element which is connected to the boom (this applies to metal booms; with plastic or wooden designs, the feeder connections are not critical).

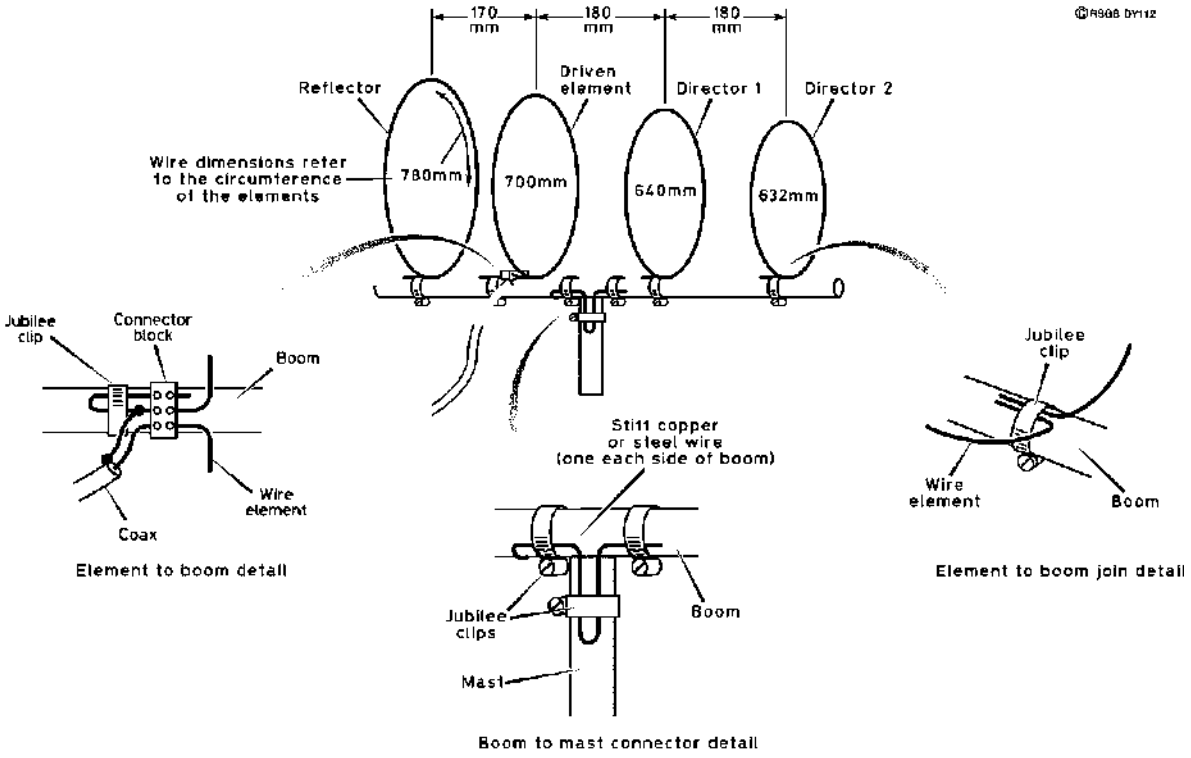

Figure 1 70 cm 4 element quad construction, with detail of how hose clamps are used in the construction

You will need a plug on the shack end of your feeder to suit the transceiver, aerial tuning unit (ATU) or the standing-wave meter (SWM) you are using. Always connect these in the order: transceiver – SWM – ATU – aerial.

Testing

Always test aerials outside and away from buildings (if possible!). This avoids getting misleading results.

Use a rubber duck, or whatever aerial you usually use, and tune around to find a repeater or beacon signal which is consistent. Note the reading on the S-meter. Then, connect your new Quad loop. Rotate it to give the strongest S-meter reading (don't forget it is directional). Verify that the meter reading varies as you rotate it. How does the S-meter reading compare with the original reading? Much depends on the siting of your original aerial; if you are comparing your Quad loop at ground level with a vertical on the chimney, you wouldn't expect your new aerial, even with its gain, to outperform a vertical which is well elevated!

Now a test on transmit is called for. The use of an SWR meter is essential here. Find a clear frequency and check that it *really is clear* before announcing your presence and carrying out the test. A reading of 1:1 is excellent, but any value less than about 1.8:1 would be acceptable. You can measure the directivity of your aerial using the field strength meter, also described in this series.

Materials

4 metres of 14 SWG enamelled copper wire
Material for boom and mast
15 amp connector block
7 Jubilee clips

The enamelled copper wire is available from AA&A Ltd, Sycamore House, Northwood, Wem, Shropshire SY4 5NN. Everything else is available from most hardware stores.

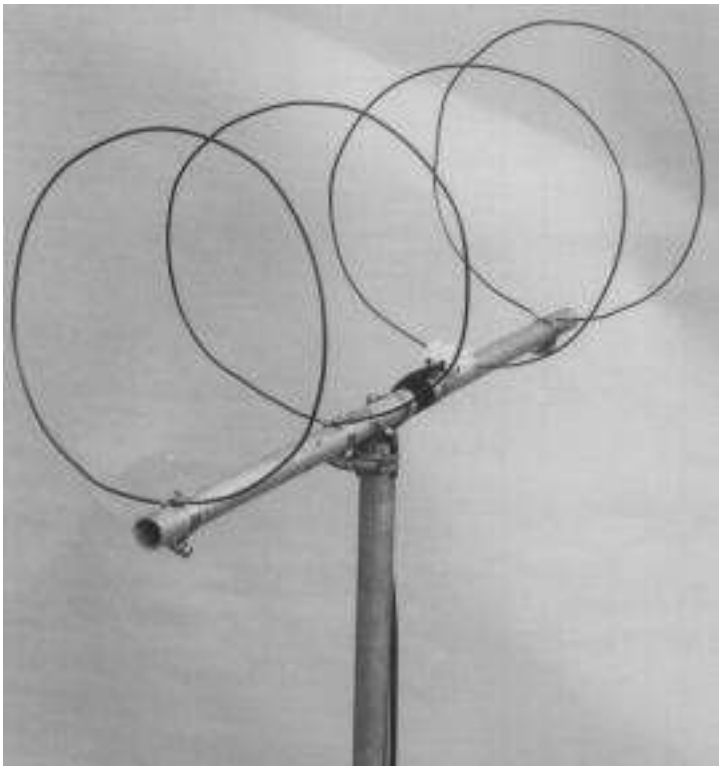

46 A UHF field strength meter

Introduction

It is always interesting, and often useful, to know just *where* the radiation is going from your aerial. How much of your radiated energy is going in the general direction of the station you are in contact with, and how much is being effectively wasted? Some of these questions can be answered with the use of a *field strength meter*. A field strength meter is simply a receiver, stripped down to its bare essentials, such that it responds only to the magnitude of the carrier. The use of a field strength meter assumes that the aerial under test is radiating a continuous carrier. Don't forget to find a clear frequency and identify your transmissions at least every quarter-hour, in order to comply with the terms of your licence.

Description

Two types of field strength meter are shown in **Figure 1**. You will recognise both circuits (Figure 1b particularly) as being types of 'crystal set' with a meter replacing the headphones. Figure 1a is a broad-band HF design (there is no tuning provision) and Figure 1b is tuned in the same way as the crystal set; with a loop of wire as an aerial, it will perform well in the VHF/UHF range.

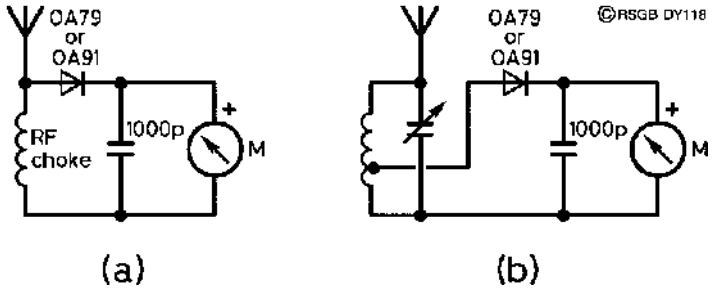

Figure 1 Construction of the UHF field strength meter

A tuned field strength meter also doubles as an *absorption wavemeter* if it is well calibrated. Such devices are useful for detecting transmitter harmonics also. This design is intended for use in the UHF band, so it will have to be sensitive around 432 MHz.

Construction

The field strength meter comprises a loop of wire, 600 mm long, which acts both as aerial and as the tuning inductance, a diode, a capacitor, a connector block, a meter and a length of twin wire. All the components, with the exception of the meter, are fixed to a pole with a jubilee clip, as shown in **Figure 2**. The meter should have a sensitivity of between 50 μA and 100 μA, or a multimeter can be used. The multimeter is more flexible, as you can select different current ranges, giving you a range of sensitivities.

Using the field strength meter

Connect your meter to the ends of the twin wire from the pole. Place a hand-held transceiver about 2 metres away, and press Transmit. If there is no meter reading switch off the transmitter and check the wiring. If the needle attempts to go negative, simply reverse the wires to the meter. If the reading is too high, either move the transmitter further away, or increase the current range on the multimeter. Try changing the orientation of the transmitter aerial, and note how the signal varies.

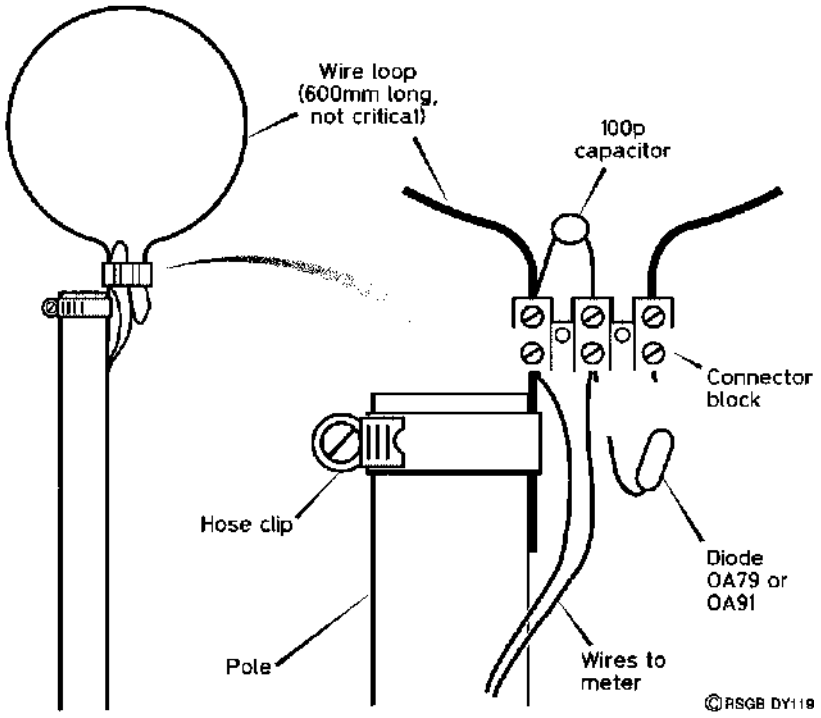

Figure 2 Assembly of the field strength meter

To measure the *polar diagram* (a graph of the signal strength against the angle between the aerial boom and the field strength meter, plotted on polar axes) of a beam aerial, mount the loop as far away from the aerial as you can, preferably at the same height, and rotate the aerial, say 15 degrees at a time, and record the signal strength, until the aerial has been turned through 360 degrees. If you need help plotting the graph, enlist the help of a friend who has done it before, or one who knows about polar graphs! If you have already built the Photometer project, you will have measured and plotted the polar diagram of the light intensity from a torch. Now you will see the great similarity!

Parts list

Capacitor	100 picofarads (pF)
Diode	Germanium, OA79 or OA91
Connector block	10 A, 3-way
Wire	600 mm of 16 SWG enamelled copper
	Length of twin cable for meter connection
Clip	Jubilee (hose) clip

47 Christmas tree LEDs

Introduction

A novelty ideal for the festive season, this circuit causes one LED at a time to light up around a small cardboard Christmas tree.

Warning

This circuit uses members of the integrated circuit family known as CMOS (complementary metal-oxide semiconductor). These use very little current and can be completed destroyed if they come into contact with the magnitudes of static electricity that most of us carry about when we walk on carpets and wear rubber shoes. You will never know if this wanton destruction has happened – all you will discover is that your circuit doesn't work and that you have tested *everything*. To avoid this problem do the following things:

1. **Before you open the little packet in which each IC is supplied, touch something which you *know* to be earthed – the metalwork of any equipment which is mains-earthed, for example. Then open the packet.**
2. **Let the IC fall gently on the bench – don't pick it out with your fingers. Touch your earthed metalwork again. Pick up the IC and insert it gently into its holder.**
3. **Repeat the process with the second IC.**

The circuit is safe from destruction while it is connected to the battery. However, when the battery is removed, the same care should be exercised with its handling, because there are no supply decoupling capacitors across each IC.

Description

Figure 1 shows the layout, and how the wires are connected from the circuit board to the LEDs around the tree. The circuit, shown in **Figure 2**, is quite complicated, so you need to be confident in your logical approach to circuit-building before you attempt this one! It uses two common integrated circuits (ICs). IC1 is simply an oscillator which provides timing pulses for IC2, which 'counts' up to a maximum of 10. The outputs of the counter are indicated by light-emitting diodes (LEDs); red, orange, yellow and green are common colours which you can use.

The circuit is built on a single piece of Veroboard measuring 29 holes by 12 strips. **Be aware that there is no strip labelled 'I', so don't make mistakes in your counting!**

First of all, cut the tracks in the positions shown in Figure 1 using a 3 mm (⅛ inch) twist drill rotated between thumb and forefinger. Then, solder in the IC sockets, the notches facing row M. Wire up and solder in the links and then the Veropins for the connections to the LEDs and battery. Having done this, the resistors and the capacitor should be fitted. When wiring the LEDs, each cathode (the lead adjacent to the 'flat' on the LED encapsulation) is connected to R4, and the anodes go to separate pins on IC2.

Testing

Hold up your circuit board to the light and check carefully for solder bridges between adjacent tracks. Then check again that the wiring is correct. Place the ICs in their holders, with the notched ends lining up with those on the holders. Connect the battery, and the LEDs should illuminate in sequence.

If you have no success, you are now wishing you had checked the circuit more carefully! Learn something from your mistake and it will not have

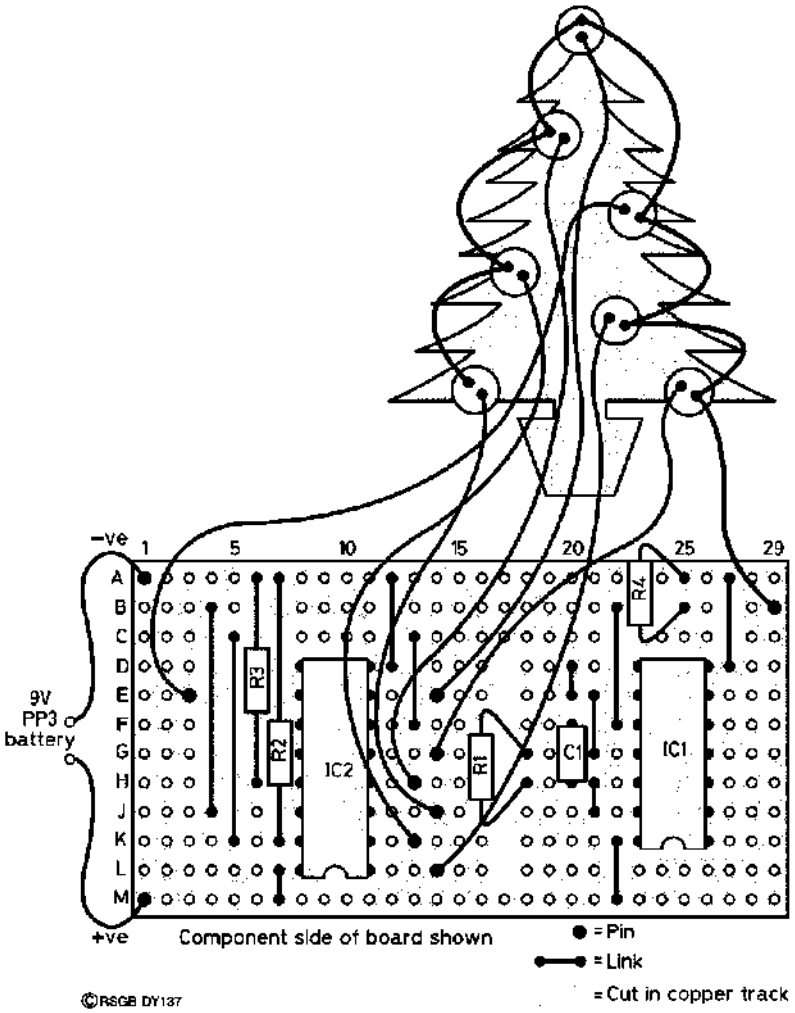

Figure 1 Christmas tree, component layout

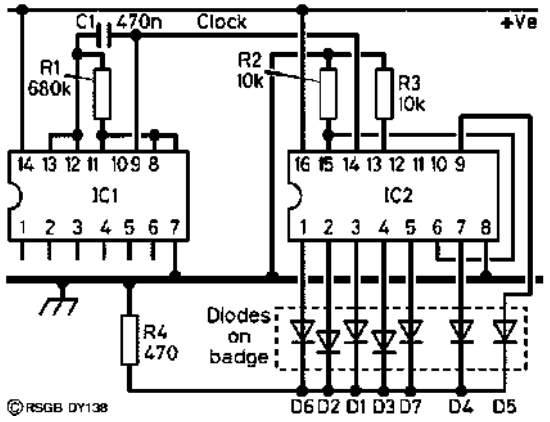

Figure 2 Christmas tree, circuit diagram

been in vain! The first thing to check is that the LEDs are the correct way round. If that is OK, then check the positions where the tracks are broken (intentionally!). After that, are the wire links in the right places – had you forgotten there is no row 'I'? Check *all* the wiring, then check *again* for solder bridges, and switch on again. One of these tests should have revealed a fault. If it *still* refuses to work, perhaps one (or both) of your ICs were damaged by static electricity, despite your precautions – or did you choose to ignore them?

Parts list

Resistors: all 0.25 watt, 5% tolerance

R1	680 kilohms (kΩ)
R2, R3	10 kilohms (kΩ)
R4	470 ohms (Ω)

Capacitor

C1	0.47 microfarad (μF) min. metallised polyester film

Semiconductors

IC1	4011
IC2	4017

Additional Items

D1–D7	5 mm LEDs in choice of colours
	14-pin DIL socket for IC1
	16-pin DIL socket for IC2
	PP3 battery clip and battery
	Veroboard, Veropins
	Insulated wire for links

48 An audio signal injector

Introduction

An audio signal injector is a device used to test audio frequency circuits. It is simply an oscillator running at a frequency in the audio range, so that when its output is fed to the input of an amplifier, it will produce a sound in the loudspeaker if the amplifier is working. The oscillation is so rich in harmonics that the signal can also be heard (sounding rather different) when injected into an RF circuit.

The design

The circuit is shown in **Figure 1**, and is a basic *astable multivibrator*, a free-running oscillator producing a roughly rectangular-wave output. The two transistors, TR1 and TR2, operating as switches, switch on and off alternately at a frequency around 500 Hz. The prototype was constructed on plain matrix board (no copper strips), as illustrated in **Figure 2**.

Both transistors are type BC108, which are only a few pence each new, and can be found at almost any rally. You can add an on/off switch, or simply disconnect the battery when you are finished using it. To make the unit in one piece, the battery can be taped to the board, as the diagram shows.

The probe itself is made from a short piece of stiff insulated wire, soldered to a tag on the board; an earth lead is also soldered to the board, and terminated in a crocodile clip to attach to the ground lead of the equipment under test.

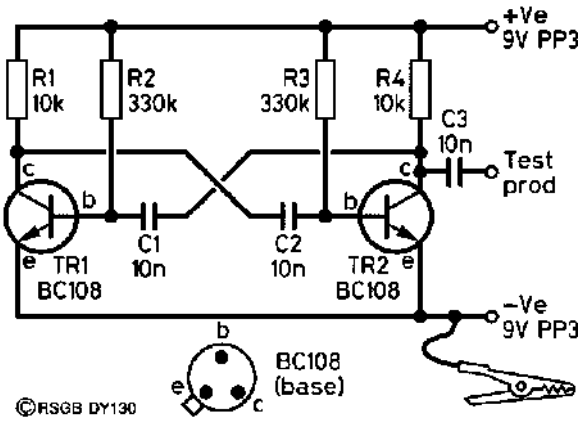

Figure 1 Circuit diagram of the signal injector

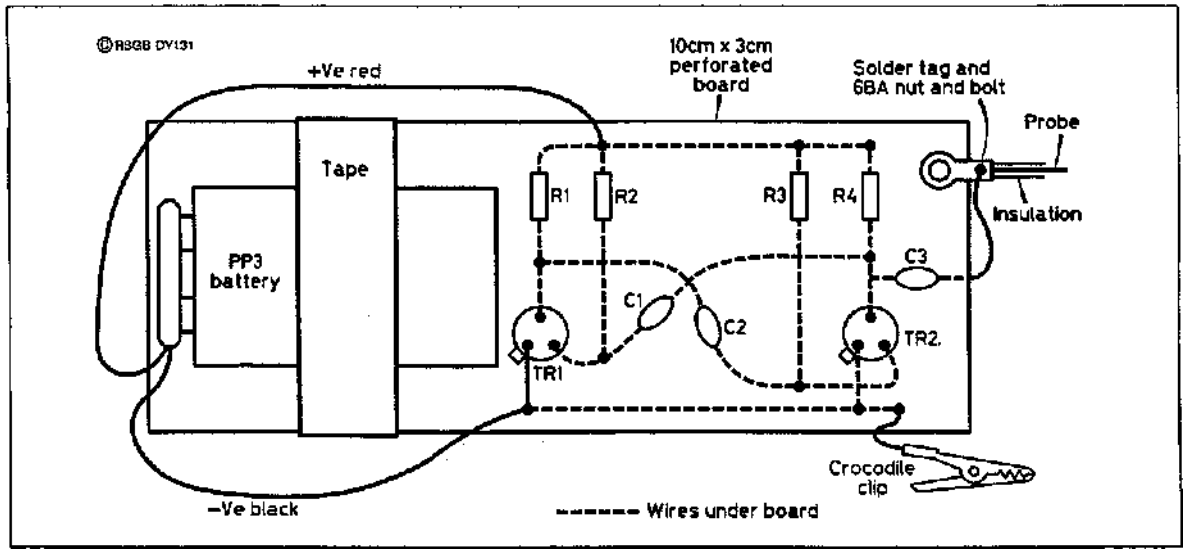

Figure 2 Component layout of the signal injector

Using it

After checking the wiring of the circuit, connect the battery. Find a transistor radio that is known to work. Carefully remove the case, switch on and apply the probe to the centre tag of the volume control. A *very* loud buzz should be heard from the speaker, indicating that the audio circuits of the radio are working. Using the injector to fault-find equipment you have made yourself is rather more instructive and rewarding, because you *know* where to inject the signal, and you should *know* what to expect when you do.

Warning

Do *not* work on any equipment connected to the AC mains. Work only on battery-powered circuits, for your own safety.

Parts list

Resistors: all 0.25 watt, 5% tolerance

R1, R4	10 kilohms (kΩ)
R2, R3	330 kilohms (kΩ)

Capacitors

C1, C2, C3	10 nanofarads (nF) or 0.01 microfarad (μF) ceramic

Semiconductors
TR1, TR2 BC108

Additional items
PP3 battery and connector
Matrix board 10 cm by 3 cm
6BA solder tags
Thick insulated wire for probe
Crocodile clip

49 Standing waves

Introduction

Everyone has, or *should* have, a standing-wave ratio (SWR) meter as part of his/her array of test gear. Most people know how to use it, but what does it really do?

Before attempting to answer that question, we need to look at some aerial fundamentals. An aerial is a *transducer*, the word meaning 'to lead across'. We use it whenever one form of energy is converted into another form. A bulb is a transducer; it converts electrical energy in the filament to radiated heat and light energy. **Figure 1** shows the situation.

An aerial, or antenna, is also a transducer; it converts radio-frequency (RF) energy in the feeder (or *transmission line*, to give it its proper name) into radiated electromagnetic energy, in the manner shown in **Figure 2**. The aerial has resistance, just like the bulb filament, and if the filament had zero resistance, there would be no radiated energy. In the same way, if the aerial had no resistance, there would be no radiation from it.

Transmission lines should convey RF energy from transmitter to aerial with the minimum power loss. A common form of transmission line is the *coaxial*

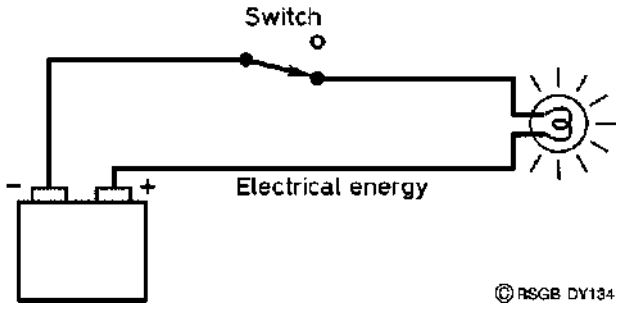

Figure 1 The light bulb converts electrical energy to electromagnetic light energy

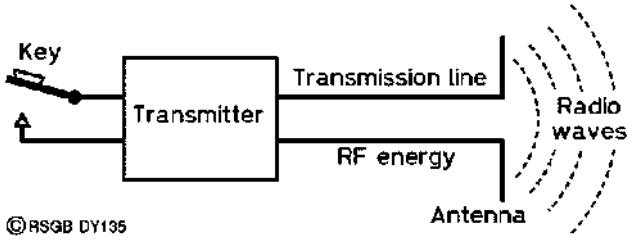

Figure 2 The antenna converts RF current to electromagnetic radio waves

cable. As you might expect, any feeder cable has a DC resistance caused by the resistance of the copper wire from which it is made. It also has an AC resistance, caused by the capacitance between the centre conductor and the braid, and by the inductance of the cable itself. This means that the feeder has an *impedance*, which is constant for the particular type of cable. This is what we call the *characteristic impedance* and, for the cables used in most amateur radio applications, it is 50 Ω.

If this impedance can be made the same as that of the aerial (it is already the same as the impedance of the transmitter output), then the transfer of energy will occur with minimum loss. If the aerial and cable impedances are *not* the same, then there is a *mismatch*, which causes some of the RF energy to be reflected back towards the transmitter. We now have a situation where RF energy is flowing along the cable from the transmitter to the aerial (the *forward* wave) and, at the same time, flowing from the aerial to the transmitter (the *reflected* wave). The two waves interact along the cable and form a stationary pattern of voltage and current. The pattern is known as a *standing wave*, and can be visualised from the waveforms in **Figure 3**. The ratio of the maximum voltage to the minimum voltage on a given wave defines the *voltage standing-wave ratio* (VSWR), or just *standing-wave ratio* (SWR) for short.

The SWR meter is easy to use. It is positioned in the feeder between the transmitter and the aerial tuning unit (ATU) if there is one, or between the transmitter at the aerial otherwise. Most meters have a single meter and a four-position switch. The transmitter is first keyed and, with the switch in

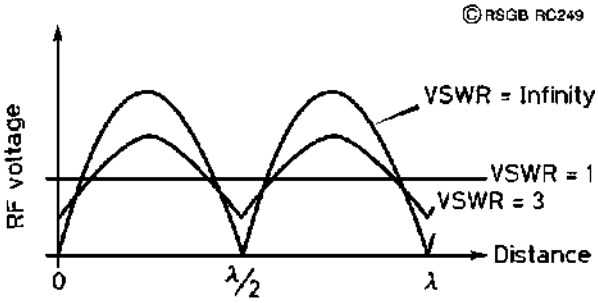

Figure 3 Standing waves on a transmission line

the 'calibrate' position, the sensitivity control is adjusted to give full-scale deflection on the meter. The switch is then changed to 'forward' to read the forward power, to 'reflected' to read the reflected power, and to 'SWR' to read the value of the standing-wave ratio. When there is no reflection (see Figure 3), the meter should read 1:1 or, simply, 1.

Most SWR meters remain in the feeder line while the transmitter is operating, so the condition of the aerial and feeder can be constantly monitored. Problems with the aerial (such as water entering the feeder at its junction with the driven element) are immediately shown up. Without the use of the SWR meter, the situation would slowly deteriorate over several months and you would be left wondering why so few stations were answering your calls!

50 A standing-wave indicator for HF

Introduction

The standing-wave ratio (SWR) meter shows how well the aerial system, including the feeder, is *matched* to the output of the transmitter. This design does not *measure* SWR, but it gives an indication of when the SWR is minimum for a given system of aerial and feeder. The design is usable on the HF bands from 1.8 to 28 MHz, and can be used at 50 MHz with reduced sensitivity.

How it works

There are two types of wave in any feeder: the *forward* wave, which travels from the transmitter to the aerial; the *reflected* wave, which travels back to the transmitter from the aerial. The presence of a reflected wave is evidence that some of your transmitted power is not being radiated, but is being returned to the transmitter to be lost as excess heat. When aerial and feeder are perfectly matched, there is *no* reflected wave, and all the power from the transmitter is radiated.

Referring to the circuit of **Figure 1**, a tiny fraction of the signal is removed by the transformer, T1, and by the capacitors, VC1 and C1. It is then detected by the germanium diodes, D1 and D2, and any residual RF removed by the capacitors, C2 and C3. The currents through the diode and meter (depending on the position of switch, S1) represent the forward and reflected signals. VR1 acts as a sensitivity control for the meter.

It pays to shop around for a suitable meter. Surplus types from tape recorders and hi-fi equipment are usually ideal for this purpose. A new one would cost several pounds. The more sensitive the meter, the more sensitive your indicator will be. Meter sensitivity is given by the current required to give full-scale deflection (FSD) of the pointer. One with an FSD of between 50 and 200 micro-amps (μA) is suitable for this circuit. The higher the FSD, the less sensitive the circuit.

Construction

The meter circuit and the sampling transformer (see **Figure 2**) are built and mounted on Veroboard of the copper-strip variety. It simplifies construction

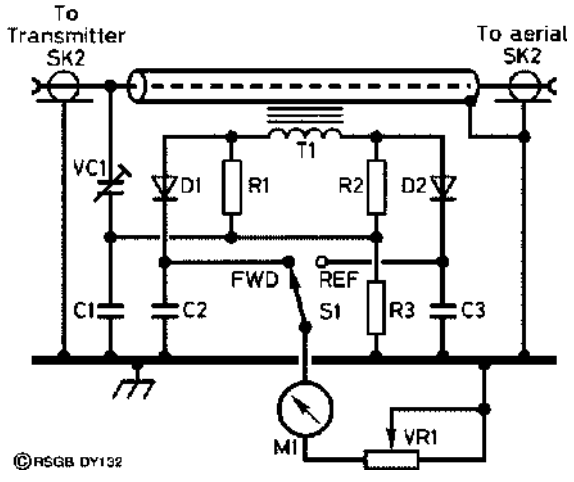

Figure 1 Circuit diagram of the SWR meter

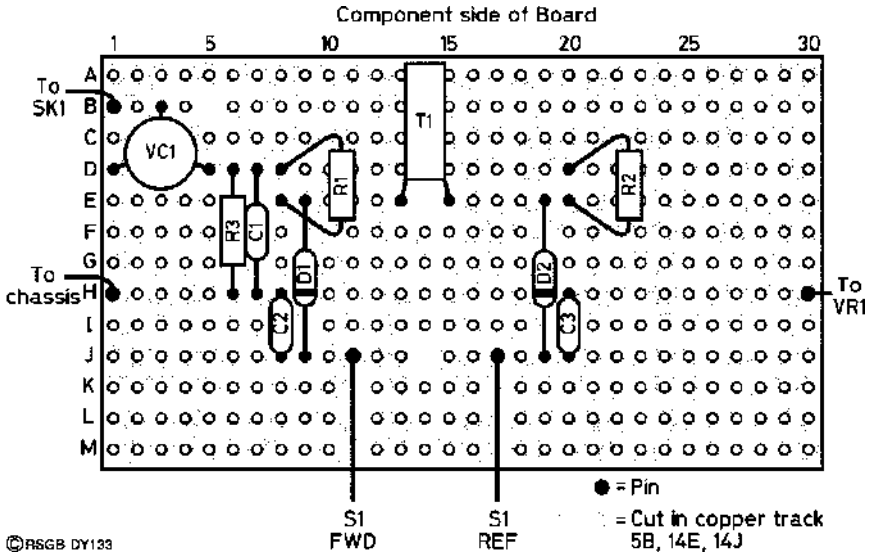

Figure 2 Component layout of the SWR meter

but reduces the operational range of the meter to below 30 MHz because of the capacitive coupling between strips. The board has 13 strips by 30 holes, although you can reduce this if you have a smaller case.

Firstly, cut the tracks at the three points shown. Then insert and solder Veropins for connections to the external components, the switch, variable resistor and the meter. Solder in the components starting with the resistors and followed by the capacitors and the diodes, ensuring that the diodes are inserted correctly.

Now you have to wind the transformer, T1, on a small toroidal ferrite core. Wind the secondary with 15 turns of 36 SWG enamelled copper wire, spaced evenly over about two-thirds of the former. The turns should not overlap, and considerable care must be taken; the wire is very thin, will kink easily and will break if you apply too much tension. The 'primary' is an 8 cm length of 50 Ω coaxial cable which passes through the toroid on its way between the input and output connectors. The braid of the cable is connected to the case at only *one* of the connectors (see Figure 1); this prevents the screen and the metal case between the two sockets forming a single, shorted turn.

The ends of the secondary winding must be carefully stripped of their enamel with sandpaper, before attaching the toroid to the board with cotton or nylon fishing line. On no account must wire be used for this!

Solder the secondary connections of T1 to the board and thread through the coaxial cable ready for soldering to the connectors.

The case used was an aluminium box (Maplin LF02C), but any suitable metal box could be used. Aluminium is preferable, as it is easily drilled with simple tools. Use standoff insulators to mount the board in the case. Once this has been done, the leads from the board to the chassis-mounted components can be soldered. So can the coaxial cable passing through the toroid. Make the lead from the input socket to VC1 as short as possible.

Setting up

You will need a 50 Ω dummy load and a transmitter to set up your indicator. Connect the transmitter to SK1 and the dummy load to SK2. Set the toggle switch, S1, to *forward* and the sensitivity control, VR1, to mid-travel. Switch on the transmitter, and set VR1 for maximum meter deflection. Switch to *reflected* and adjust VC1 until the reading is minimum (ideally zero). This completes the setting up!

Using the indicator

For setting up an aerial, connect your circuit between the transmitter and the cable leading to the aerial. With S1 in the *forward* position, key the transmitter and adjust VR1 for maximum reading on the meter. Switch to *reflected*, and then adjust your ATU to give minimum reflected power. If your adjustments are to be made to the aerial itself, to give minimum reflected power, you must make a note of the reflected reading, switch off the transmitter, make a change to the aerial, key the transmitter, and note whether the reflected power is greater or less than before. Then, make more changes to the aerial. **Never adjust your aerial with the transmitter on.** Make your adjustments on an unused frequency, and do it as quickly as possible, thus avoiding (or minimising) interference to other stations.

Parts list

Resistors: all 0.25 watt, carbon 5% tolerance
(or Maplin 0.6 watt metal film)

R1, R2	27 ohms (Ω)
R3	2.2 kilohms (kΩ)
VR1	10 kilohms (kΩ) linear

Capacitors

C1	220 picofarad (pF) disc ceramic 50 VDC
C2, C3	0.1 microfarad (μF) disc ceramic 50 VDC
VC1	20 picofarad (pF) trimmer

Semiconductors	
D1, D2	OA91 germanium
Additional items	
S1	Single-pole changeover (SPDT or SPCO)
SK1, SK2	Coaxial sockets to suit station standards
	Veroboard – 13 strips by 30 holes
	Veropins (7 off)
	Amidon FT 50–43 ferrite toroid
	Meter, less than 200 μA FSD
	36 SWG enamelled copper wire
	Short length of UR43 or RG58 coaxial cable
	Insulated stranded wire
	Aluminium box
	Standoff insulators for mounting the board
	Knob for the sensitivity control

51 A moisture meter

Introduction

Dry rot (*Merulius Lacrymans*) can strike havoc in buildings, causing the timbers to decay and crumble to dust – hence the term *dry rot*. Wood is attacked only if its moisture content rises above 20%.

Construction

The circuit of the moisture meter is shown in **Figure 1**. The two probes touch the wood, and the current that flows between them depends on the moisture content of the wood. If the moisture is sufficiently high, the current, after amplification, will be enough to light the LED.

The meter can be made on a piece of plain matrix board (no copper strips), as **Figure 2** shows. The board is big enough (10 cm by 2.5 cm) to accommodate the PP3 battery, taped on. No case is needed, unless you want

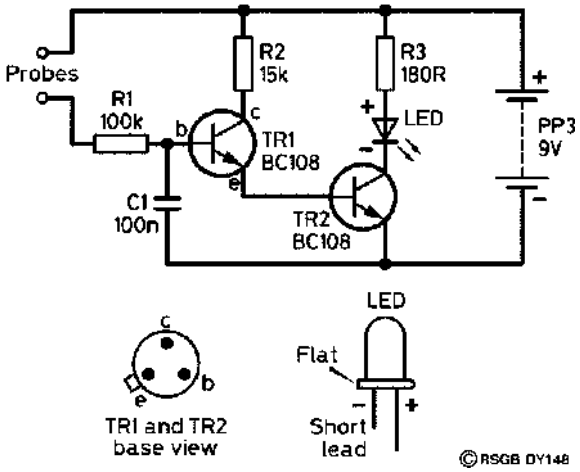

Figure 1 Circuit diagram of a moisture meter

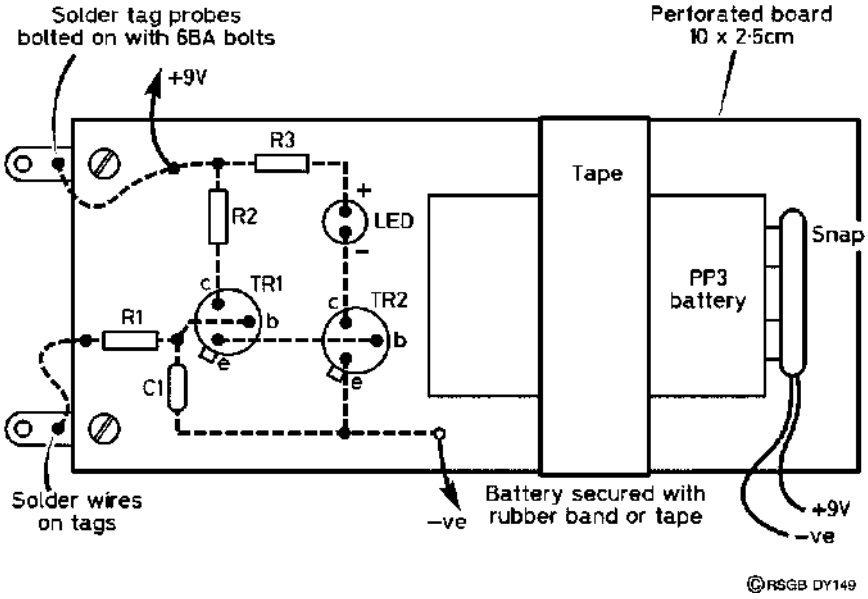

Figure 2 Moisture meter, component layout

to leave the meter in a damp location for a protracted period! Make sure that the transistors and LED are mounted correctly. In Figure 2, the connections as shown to TR1 and TR2 are illustrated as if the transistors were transparent. An on/off switch is not really necessary, as only a very small current flows when the probes do not touch anything. Use solder tags, screwed to the board, to act as probes.

After the assembly is completed, check your circuit one final time, and then connect the battery. Nothing should happen at first. If you lick your forefinger and hold it across the probes, the LED should light.

Using it

The prototype was compared with a commercial moisture meter, and the LED lit when the moisture was around 20%. This was quite fortuitous, as the point at which the LED lights depends both on the separation of the probes and on the gain of the two transistors.

In addition to searching for dry rot, the instrument may be used to monitor the moisture in the soil of household plants. In this case, probes made of 16 SWG copper (*not* enamelled) should be soldered on to the two tags, and should penetrate the soil to a depth of several centimetres, and R1 may require adjusting so that the LED extinguishes if the soil is too dry, and lights if the soil is sufficiently moist. If you wanted to leave the meter with the probes in the soil, an on/off switch *would* be necessary.

Parts list

Resistors: all 0.25 watt, 5% tolerance

R1	100 kilohms (kΩ)
R2	15 kilohms (kΩ)
R3	180 ohms (Ω)

Capacitor

C1	0.1 microfarad (μF) polyester

Semiconductors

TR1, TR2	BC108
LED	Any shape or colour will do

Additional items

- PP3 battery and connector
- Solder tags (2 off) for probes
- Matrix board 10 cm by 2.5 cm

52 Simple aerials

Introduction

The performance of *any* receiver or transceiver, no matter how expensive it is, is limited by the aerial that feeds it. Two of the most frequently asked questions are:

- Which is the best sort of aerial to use?
- Where is the best place to locate an amateur radio aerial?

To answer these questions, you must ask yourself what sort of operation you want to do. Are you interested in local, chatty contacts on the lower bands or VHF, or are you more disposed towards long-distance (DX) contacts, and on what band?

A house with a moderately sized garden is assumed in the diagrams here, to illustrate the configurations of some simple aerials. You would not need all these aerials festooned around your house, because one or two would be sufficient for your needs. The problems incurred by properties with more restricted space will be covered later.

VHF aerials

For VHF operation, the aerial should be mounted as high as possible, either on a mast or on a chimney. For all-round coverage on FM and the local repeaters, a vertical colinear is a good choice. For SSB and CW DX operation, a horizontal rotatable beam is needed. If satellite working is envisaged, you will need to contemplate mounting an elevator on top of your rotator, so that your beam can point in *any* direction, including vertically upwards! An advantage of satellite working is that the aerials do not *necessarily* have to be up in the air, provided you have a relatively uncluttered site. Your rotator and elevator can be at ground level, which is good!

If the VHF aerial is mounted on the chimney, use a double mounting bracket, particularly if you have a beam and rotator. Keep the TV, broadcast FM and amateur aerials as far apart as possible, and keeping the feeders separated is also a good plan.

The dipole aerial

One of the simplest types of aerial for single-band operation is the half-wave dipole. (The name ‘dipole’ simply means ‘two poles’ or ‘two elements’, and

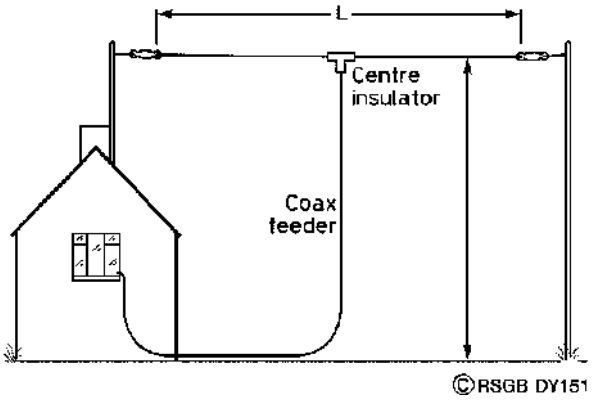

Figure 1 Layout for a dipole aerial

in this case the total length of the dipole is approximately half a wavelength at the operating frequency.) It is usually fed in the centre by coaxial cable as shown in **Figure 1**. The length of the dipole for the lowest frequency in each band is shown in **Table 1**. Normally, the length of the aerial will be 'trimmed' to be tuned to the centre frequency of the part of the band in which you will operate. This is done using the data in the right-hand column of Table 1. As an example, suppose you wanted your aerial to be resonant at 3.7 MHz. The table gives an overall dipole length of 42.86 m for 3.5 MHz. To resonate the aerial 200 kHz *higher*, then this length must be shortened by 2 × 0.595 m = 1.190 m. Your dipole would thus be 41.67 m long. Remember to allow extra wire for fixing the dipole ends to the insulators.

Table 1 Dipole lengths for lowest frequency of each band and the length to be trimmed from each to raise the resonant frequency by 100 kHz

Band (MHz)	*Dipole length (m)*	*Trim each end (mm/10 kHz)*
1.8	83.33	2190
3.5	42.86	595
7	21.43	150
10	14.85	70
14	10.71	35
18	8.33	20
21	7.14	15
24	6.03	12
28	5.36	10
50	3.00	6

On the lower-frequency bands, the lengths become rather large. In this case, you can 'bend' your dipole, as illustrated in **Figure 2**. The length of wire required to give an acceptable value of SWR (less than 2:1 on transmit) may need to be different from the calculated value, so be prepared to experiment!

Dipoles are single-band aerials, although they will often work acceptably on the third harmonic of their design frequency: a 7 MHz dipole often operates reasonably well on 21 MHz. It is possible to operate several dipoles in parallel, as **Figure 3** shows. Interaction between the elements can occur if the spacing between them is less than about 10 cm. A multi-band dipole, as shown in Figure 3, has the elements separated with plastic spacers, and drooping ends to produce maximum spacing between the elements' ends.

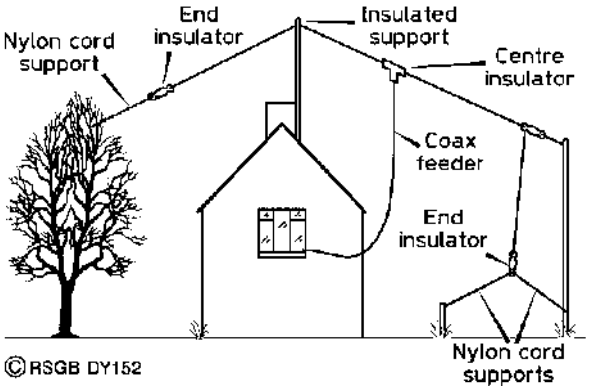

Figure 2 Possible layout for a dipole aerial in a confined space

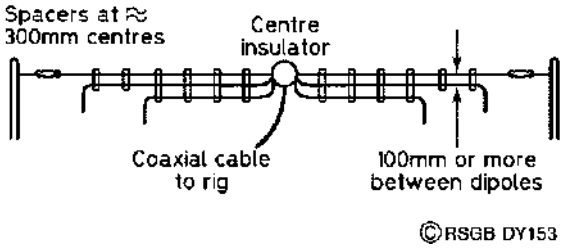

Figure 3 Multi-band dipole aerial

The long-wire aerial

This aerial is simple, cheap, easy to erect, and suits most houses and gardens, as **Figure 4** shows. Using an aerial tuning unit (ATU), an end-fed long wire can function on several bands when used with a set of radials or a counterpoise. **Figure 5** illustrates the setup. The length of the aerial will determine the bands which will be covered.

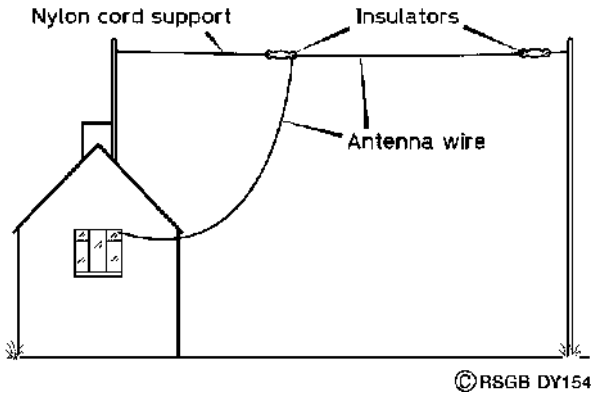

Figure 4 Long-wire or inverted-L aerial

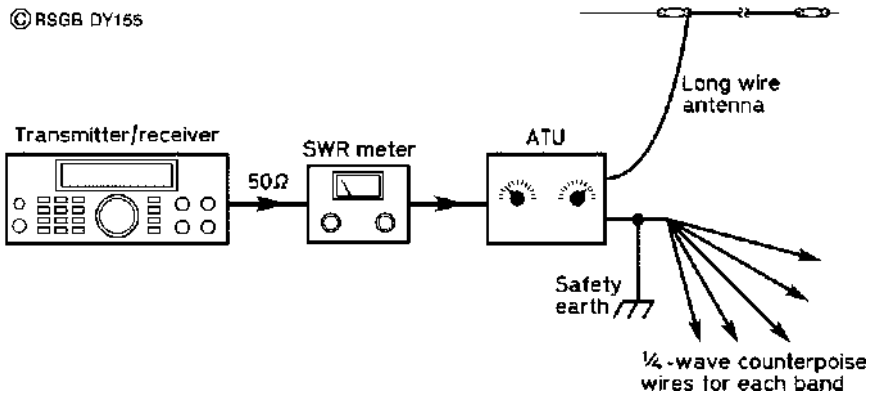

Figure 5 How to connect a radio to a long-wire aerial

A wire length of 10.5 m will work on the 40, 30, 17, 15 and 12 m bands.

A wire length of 15.5 m will work (with an ATU) on the 80, 40, 20 and 12 m bands and possibly (depending on your ATU) on the 17 and 15 m bands.

A wire length of 26.5 m will operate on all bands, but may be difficult to load on 10 m.

The wire lengths given here may need some adjustment because of the geometry of your particular house and garden. For receive-only purposes, the lengths are far less critical.

In general, you cannot get a good radio-frequency (RF) earth from a first-floor (or higher) shack. Unless a good RF earth exists within a small fraction of a wavelength of the transceiver, an *artificial ground* comprising a single $\frac{\lambda}{4}$ radial or counterpoise will be needed. You will need one counterpoise for each band you intend to use, and the wire can be concealed around the skirting-board of the shack, or under the carpet. Make sure that the free end

Table 2 Lengths of elements for vertical antennas, radials for verticals and counter-poises for end-fed long wire antennas

Band (MHz)	*Element length (m)*
1.8	39.66
3.5	20.40
7	10.20
10	7.14
14	5.1
18	3.96
21	3.4
24	2.95
28	2.55

of each counterpoise is well insulated; this point can carry a *very high voltage* when you transmit; anyone coming into contact with this can suffer very severe RF burns. Counterpoise lengths can be read from **Table 2**.

The vertical aerial

The single-band vertical aerial is sometimes used by DX operators because it has a low angle of radiation, which favours long-distance propagation. However, it must be sited clear of obstructions and must have a *good* counterpoise or radial system. Illustrations of the vertical aerial are shown, and the lengths of the vertical and radial sections are given in Table 2. The centre of the coaxial feeder is connected to the vertical section, and the braid to the counterpoise or radial system, which is made up of four or more wires buried just below the surface and joined together near the base of the aerial.

Cable entry to the house

Bringing coaxial cable into the house by an open window must be regarded as a temporary measure. Wooden window frames can be drilled, one hole for each feeder. Make the holes slope downwards from inside to out to prevent rain entering, and treat these with wood preservative. Leads from long-wire and inverted-L aerials should be kept separate from other cables.

Alternatively, a plastic pipe large enough to take all your feeders could be fitted into the brickwork (again, sloping downwards towards the outside). You may want to let a friendly builder do this for you.

53 A breadboard 80 m CW transmitter

Introduction

In the early days of radio, many circuits were built on a wooden baseboard, the parts being screwed down on the board. This was called breadboard construction, because it was a breadboard that was frequently commandeered for the process! Wives have always been generous in this respect, it appears!

This circuit was originally designed by GM3OXX, and became known as the *Oner*, because it was built on a circuit board one inch square! The circuit appeared in the G QRP Club journal *Sprat* and, since that time, many hundreds of *Oner* circuits have been built and used on the air. It is a well-proven circuit.

The transmitter has no tuned circuits in the power amplifier (PA) and thus has a rather high *harmonic* content. It **must** be used with the ***low-pass filter*** described elsewhere in this book. Without the low-pass filter, interference will be caused to other stations.

Simple aerial changeover switching is provided, which allows this circuit to be used with any of the 80 m receivers, such as the *Colt*, described in this book. It can also be used with any kit or commercial receiver for the 80 metre band.

The circuit

The transmitter circuit is shown in **Figure 1**. TR1 is a crystal oscillator, the frequency of which is controlled by crystal X1. A small trimmer capacitor, TC1, is added to allow the frequency of X1 to be varied by a small amount. If adjustment of this trimmer is made possible from the front panel, it is useful to adjust the transmit frequency to avoid other stations already on the crystal frequency. The collector load resistor, R2, of the oscillator transistor, TR1, determines the power output; a value of 3.3 kΩ seems to work well in producing an output of 3 watts.

TR1 is directly coupled to TR3, a VMOS transistor (a type of field-effect transistor (FET)). This acts as the power amplifier (PA) stage. TR3 should

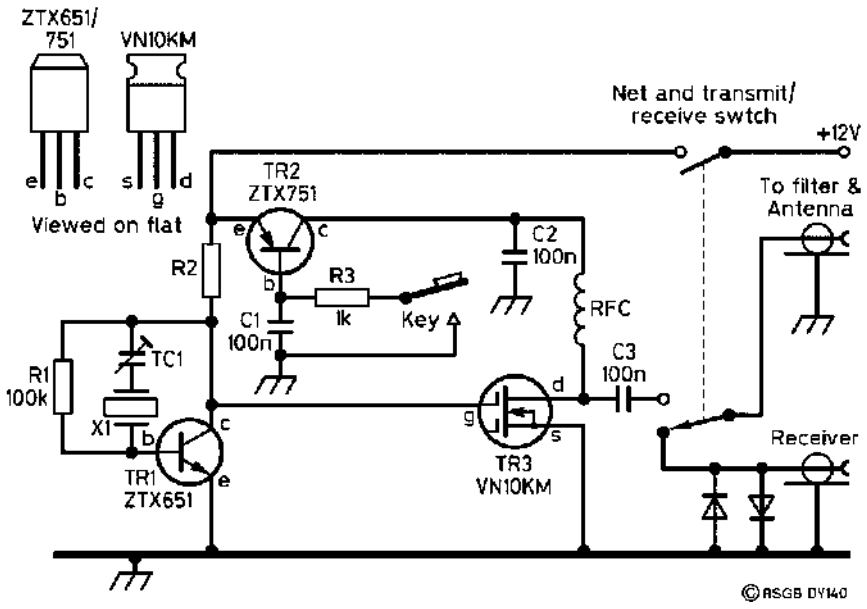

Figure 1 Circuit diagram of the breadboard transmitter

give about 3 W output, which is then coupled to the output by C3. The radio-frequency choke (RFC) providing the drain load of TR3 is simply a few turns of wire on a ferrite bead.

TR2 is an interesting addition to the circuit. It is used as a switch to 'key' the PA, TR3. The transmitter *could* be built without TR2, just placing the Morse key between the top of the RFC and the 12 volt supply. Adding TR2 is helpful, because it means that one side of the Morse key can be grounded (always a good thing), and some degree of *shaping* of the output RF waveform is provided by R3 and C1. This makes the transmission sound a little better and reduces the possibility of spurious frequencies being generated and transmitted. TR2 is a pnp transistor; note that it is the *emitter* of this transistor which is connected to the positive side of the supply.

Some form of changeover switching is needed for the aerial. A double-pole changeover toggle switch can be used. See the chapter on switches, later on in this book. One pole is used to switch the aerial between transmitter and receiver; the other pole is connected in the 12 volt supply line, and is labelled RECEIVE/TRANSMIT – NETTING. Its use will be described later. In this simple circuit, the PA cannot work when the key is open, because the key breaks its supply (via the RFC). When the key closes, TR2 switches on and applies the 12 volt supply to the top of the RFC. C2 is a *decoupling* capacitor, which prevents any residual RF signals at the top of the RFC reaching TR2.

Building

The prototype was put together as follows. Take a piece of plain printed-circuit board (PCB) measuring 5 cm by 4 cm. Then, with a *new*, *sharp blade* in a junior hacksaw, draw the blade horizontally across the surface of the copper in order to make a pattern of 6 squares along the 5 cm side and 5 squares along the 4 cm side. No more pressure should be applied than is necessary to cut through the copper! All the parts will be soldered on these pads in a form of surface-mount construction. To do this, each active pad (i.e. one that is going to have a component soldered to it) needs to be *tinned*. This means coating the pad's surface with solder, and is carried out as follows. Place the hot tip of the soldering iron on to the pad, and hold it there for a second or so. Then, with the tip still in place, touch the end of your reel of solder *on the pad*, not the tip of the iron. The solder should flow evenly all over the pad, and you can remove the iron. The solder should solidify in a rounded, shiny blob! This provides a good surface for making soldered joints.

To join component leads to the pads, cut each lead about 1 cm long, and then bend the last 2 mm at right angles to the rest of the lead. As you did before, tin the 2 mm length of each lead. Place the tinned portion on to the pad, and place the tip of your iron *on the pad*, close to the lead. The solder on the pad and on the lead will melt and run together; remove the iron and *hold the component still* until the solder solidifies. When the joint has cooled, give the lead a gentle tug to make sure you have a good joint (a good *mechanical* joint is usually a good *electrical* joint, too!). Each transistor straddles three pads, so the centre lead will need to be shorter than the other two. Take care here to get the lead lengths right – if you do, you will be surprised how much more firmly the transistor is held than if you just botched the lead lengths by bending them to fit! Make sure the connections to the transistors are correct.

Winding the RFC is quite simple. Seven (or more) turns of thin (32 SWG) enamelled copper wire are threaded through a small ferrite bead. This requires care, because the bead is small and the wire is thin. Trim the ends to within about 1 cm of the bead, remove the enamel carefully with sandpaper and tin the bare ends, prior to soldering the choke to the board.

After completion of the wiring, check the circuit against Figure 1. Breadboarding a circuit like this has its advantages, but it can have disadvantages, too. One of these disadvantages is that it can make circuit checking difficult. For a simple circuit like this, it is not too bad! Check that no solder has run between the pads. Plug in your crystal for the 80 m band, and connect up the 12 V power supply. Do not connect the Morse key yet and do not switch on the power.

Testing and operating

Clear your workbench of all metallic objects, slivers of copper, bits of wire, etc., switch on your power supply. With an external receiver, listen on and

around your crystal's frequency for a signal. Remember that the oscillator runs all the time and, because you haven't yet connected the Morse key, your receiver is close enough to pick up the signal from the oscillator. This confirms that your oscillator is running. Switch off.

Connect the station aerial to the transmitter's aerial socket, and the receiver to the transmitter's receiver socket. Connect the Morse key, put the Receive/Transmit–Netting switch in the receive position and switch on. You should be able to hear stations in the normal way. Now put the switch in the Transmit–Netting position. Signals in the receiver should almost disappear, as the circuit has disconnected the receiver's aerial.

Tune the receiver until you can hear your own crystal oscillator signal. This is known as *netting*, tuning your receiver and transmitter to the same frequency. Pressing the key will now transmit your signals when the switch is in the Transmit–Netting position; switch back to the receive position to listen for stations answering your call. As soon as you are happy that your circuit is functioning properly, **you must build the low-pass filter circuit** before using the transmitter regularly.

Parts list

Resistors: all 0.25 watt, 5% tolerance

R1	100 kilohms (kΩ)
R2	See text
R3	1 kilohm (kΩ)

Capacitors

C1, C2, C3	100 nanofarads (nF), or 0.1 microfarad (μF)
TC1	3–60 picofarads (pF) trimmer

Semiconductors

TR1	ZTX651
TR2	ZTX751
TR3	VN10KM

Additional items

RFC	7 turns of 32 SWG enamelled copper on a ferrite bead
Switch	Double-pole changeover (DPDT or DPCO) toggle
Crystal	For 80 m band
Crystal holder	HC25 type
Sockets	According to station fittings

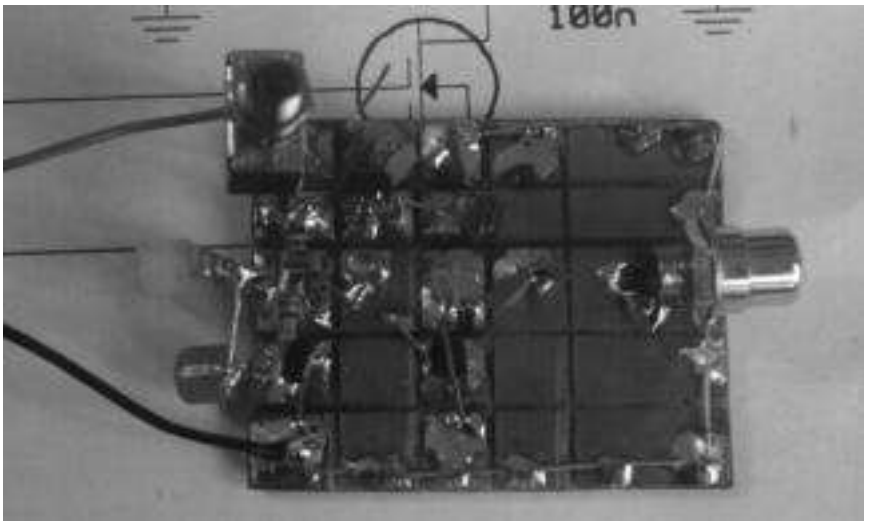

54 A 7-element low-pass filter for transmitters

Introduction

The simpler the transmitter, the more likely it is to radiate *harmonics* of its fundamental frequency. Harmonics are integral multiples of the frequency on which the transmitter is *designed* to operate. If you think you are transmitting on a frequency, *f*, for instance, you will also be radiating the harmonics of *2f*, *3f*, *4f*, . . . and so on. This results in your signals being heard on *several frequencies*, spread over a very wide frequency range. You are also contravening the terms of your licence. To avoid this, it is always advisable to use a *low-pass* filter between your transmitter and aerial. This is a filter which will *pass* your signal frequency, *f*, and all frequencies *below* it, but will *not pass* (attenuate) frequencies above *f* to any significant extent. The value of *f* is known as the *cutoff frequency* of the filter.

A design of 7-element low-pass filter

A 7-element low-pass filter (LPF) is so called because it has seven components, as the circuit diagram of **Figure 1** shows. Filters containing any odd number of elements are possible: a 3-element filter would

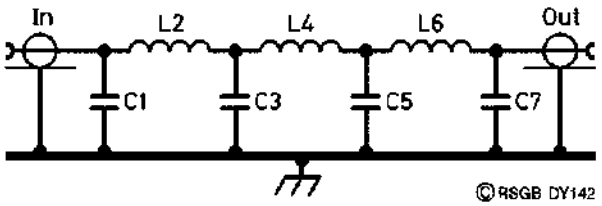

Figure 1 Circuit diagram of filter

comprise C1, L2 and C3 only, and is sometimes called a pi-network because the element disposition resembles the Greek letter pi (π); a 5-element filter would comprise C1, L2, C3, L4 and C5 only, and so on. In general, the more elements the filter has, the more effectively it attenuates signals above *f*.

The circuit of Figure 1 is designed to have an input and an output impedance of 50 Ω, which means that it can be placed in the aerial feed of any common transmitter. Filter design is a very complex business, and is best left to the experts. One such expert is W3NQN, who produced a number of computer designs of LPF using commonly available (*preferred value*) capacitors, and aimed specifically for use on amateur frequencies. The results of this work are condensed into **Table 1**. The inductors are wound on standard toroidal cores, and their details are included in the table.

Table 1 Filter component values for each brand

Band metres	*C1,7 pF*	*C3,5 pF*	*L2,6 turns*	*L4 turns*	*Core type*	*Wire SWG*
80	470	1200	25	27	T37-2	28
40	270	680	19	21	T37-2	26
30	270	560	19	20	T37-6	26
20	180	390	16	17	T37-6	24
15	82	220	12	14	T37-6	24
10	56	150	10	11	T37-6	22

Making the filter

The filter was made originally as an adjunct to the *Breadboard 80 m CW transmitter*, which you will also find in this book. It uses the same constructional technique, based on a single piece of plain, copper-clad

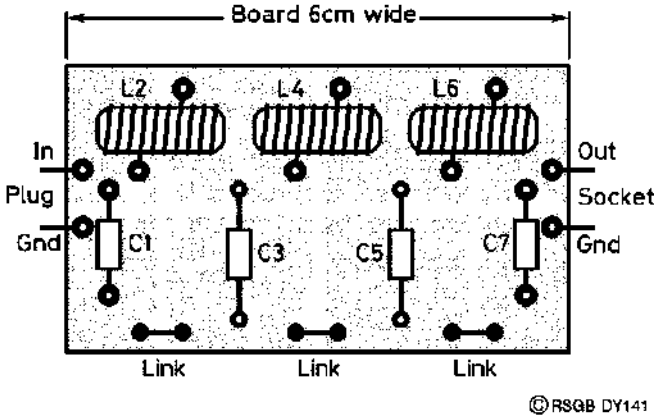

Figure 2 Layout and construction of filter

PCB, with 'pads' created by using a sharp blade in a junior hacksaw. The cuts in the copper are shown in the layout diagram of **Figure 2**. There are two ways of mounting the components: the first way is to drill small holes in each pad, as shown in Figure 2, and mount the components through the holes in the normal PCB manner; the second way is to solder the components directly to the pads, in the way that was described for the *Breadboard transmitter*.

Winding the inductors is quite simple. All you need to remember is that each time the wire passes through the core counts as one turn. Cut off the spare wire at each end of each coil to about 1 cm, scrape off the enamel with sandpaper, and tin the exposed copper. See the transmitter description if you are unsure of how to do this. Note the wire links between each of the lower pads, forming a solid 'ground' for the elements. The prototype had a plug and socket on the ends, to match the transmitter and aerial terminations.

The type of capacitor used in the design is not critical; the polystyrene type works well.

55 Radio-frequency mixing explained

Introduction

Mixers find widespread use in electronic circuitry. Many of the projects in this book, together with every TV set and radio in the home, contain mixer circuits – a good indication of their usefulness.

Confused?

Audio mixers (as used in recording studios and radio broadcast stations) are used to **add** or 'balance' the signals from various sources such as microphones, CD players, etc. These have nothing whatsoever to do with radio-frequency (RF) mixers, and should never be confused with them.

RF mixers and beat frequencies

Instead of **adding** signals (as in the audio mixer), the RF mixer **multiples them together.** As you might expect, this has an entirely different effect. The two signals entering the mixer *beat* or *heterodyne* with each other to produce *signals on other frequencies*. One example of this occurs in sound, when two musical notes of almost the same frequency are heard together. Instead of hearing two separate notes, the listener hears one note whose *intensity* (*loudness*) appears to increase and decrease. This intensity variation is called a *beat*, and its frequency is equal to the difference in the frequencies of the two original notes. The technique is used by musicians to tune their instruments. If one note is known to be a correct frequency, the other can be tuned to it by making the beat frequency as close to zero as is possible.

Multiplying together

The process of mixing presupposes that we have a device which will automatically multiply two signals together. Fortunately, this is easy; so easy, in fact, that it often occurs when we do not want it! Multiplying is achieved by any device which is *non-linear*; this means a device whose output is not a constant factor larger than its input, something that can be achieved by many electronic devices and circuits.

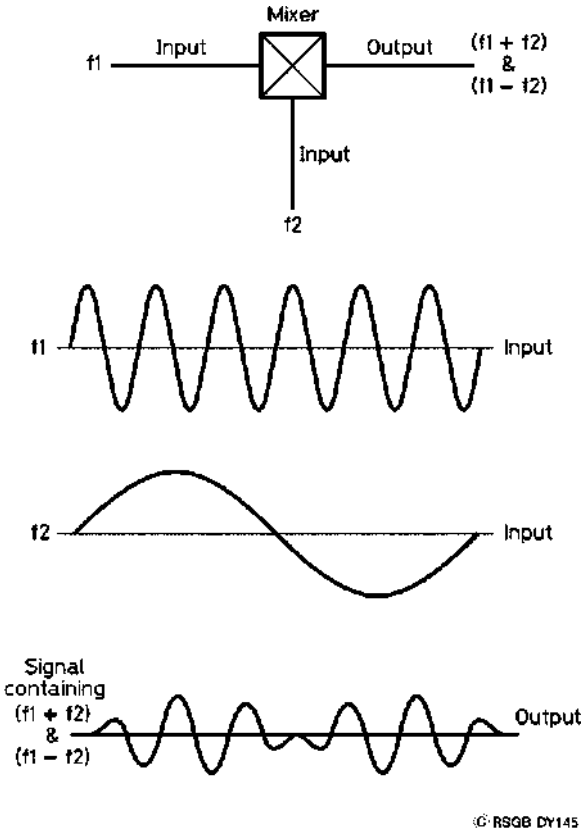

Figure 1 The effect of multiplying (or mixing) two signals together

Let us look now at what a mixer does in concrete terms. Suppose two signals, of frequencies *f*1 and *f*2 go into our mixer. These signals are shown in **Figure 1**. Putting numbers in, to make the situation clearer, suppose *f*1 is 1.000 MHz and *f*2 is 160 kHz. The beat frequency is the *difference* of these: 1.000 MHz – 0.160 MHz = 0.840 MHz, or 840 kHz. A mixer *also* produces an output at the *sum* of these frequencies; in this case the new frequency would be 1.000 MHz + 0.160 MHz = 1.160 MHz.

Suppose you fed the output of your mixer, operating with these input frequencies, into a receiver and tuned around to find what frequencies were present. You would find two signals, one at 840 kHz and one at 1.160 MHz, showing that the two 'new' frequencies were very real!

In addition to drawing out the waveform of the resultant signal, as in Figure 1, we can draw the inputs and outputs on a frequency axis, to form a *spectrum* of the signal components. This is done in **Figure 2**. The top two diagrams show the input signals at *f*1 and *f*2. The bottom diagram shows the output signals in relation to the input signals. Depending on the type of mixer used, one or both of the input signals would be removed.

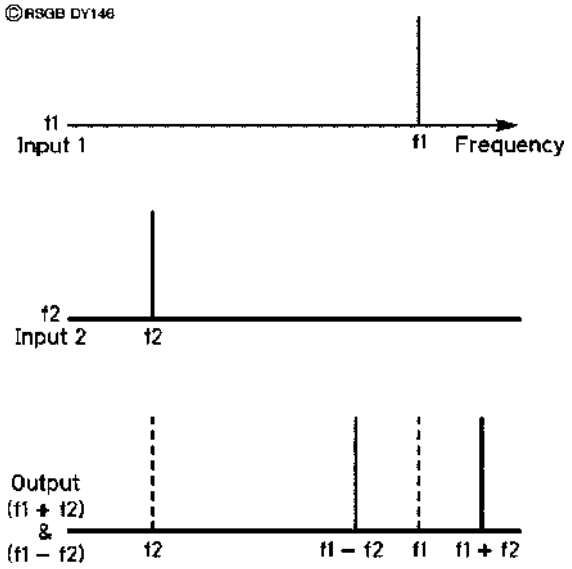

Figure 2 The result of multiplying or mixing two signals together as seen on a spectrum analyser

A mixer in every radio

Basically, a mixer is used to change a signal from one frequency to another, something it does without altering the characteristics of the incoming signal. If the incoming signal is amplitude modulated (AM), then the frequency-changed signal would be AM also. The same applies to FM, SSB, CW, and all other modulation forms you can think of. This explains why mixers are often called *frequency changers*.

Frequency changing is the key process in the type of radio known as a *superheterodyne* (or *superhet*). By mixing the incoming signal with a variable-frequency *local oscillator* as **Figure 3**, shows, the signal can be converted to the fixed frequency of a filter and amplifier. This is useful

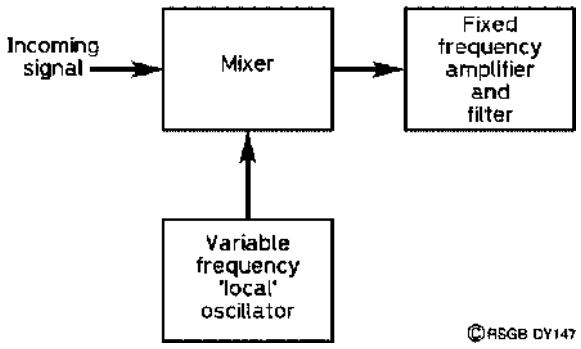

Figure 3 The basic idea of a superhet receiver

because it is easier to make a very high-quality filter and amplifier at a single fixed frequency, than at a variable frequency.

All TV receivers and virtually all radio receivers (and transmitters) use mixers. Both the *Yearling* and *Colt* receivers (see the relevant projects) are superhets, and use mixers.

56 A voltage monitor for a 12 V power supply

Introduction

If for any reason, the stabilisation of your main 12 volt power supply unit (PSU) breaks down, it is possible that a voltage much higher then the nominal 13.8 V will be applied to your precious equipment. If you would like to know the instant that this occurred, and hence be able to switch things off before it was too late, then this circuit is what you need. It will give audible *and* visual indications if the voltage rises above 14.4 V, and a visual indication only if the voltage is reduced.

The circuit

The circuit uses three ICs and is shown in **Figure 1**. The circuit is powered by the PSU whose output is being monitored, and the circuit's immunity to supply line variations is secured by the 6 volt regulator, IC1. The heart of the circuit is IC2, an LM3914; it is a *bargraph driver*, which operates ten LEDs in a display resembling a thermometer – the string of lit LEDs increases in length as the voltage on pin 5 increases.

The input voltage range on pin 5 is 1.2 V maximum, making each LED correspond to one-tenth of this, which is 0.12 V, the *step size*. R1 and R2 act as a voltage divider, so that voltages of up to the maximum of 14.4 V may be applied to R1 without exceeding 1.2 V at pin 5. R3 sets the brightness of the LEDs and R4 determines the step size.

IC3 is an *opto-isolator*, a device containing an LED and a phototransistor in one package. This enables the piezoelectric sounder to operate without affecting the operation of the bargraph driver. The input to IC3 is provided by the voltage on D8, so that if any of the LEDs at or above D8 are lit, the

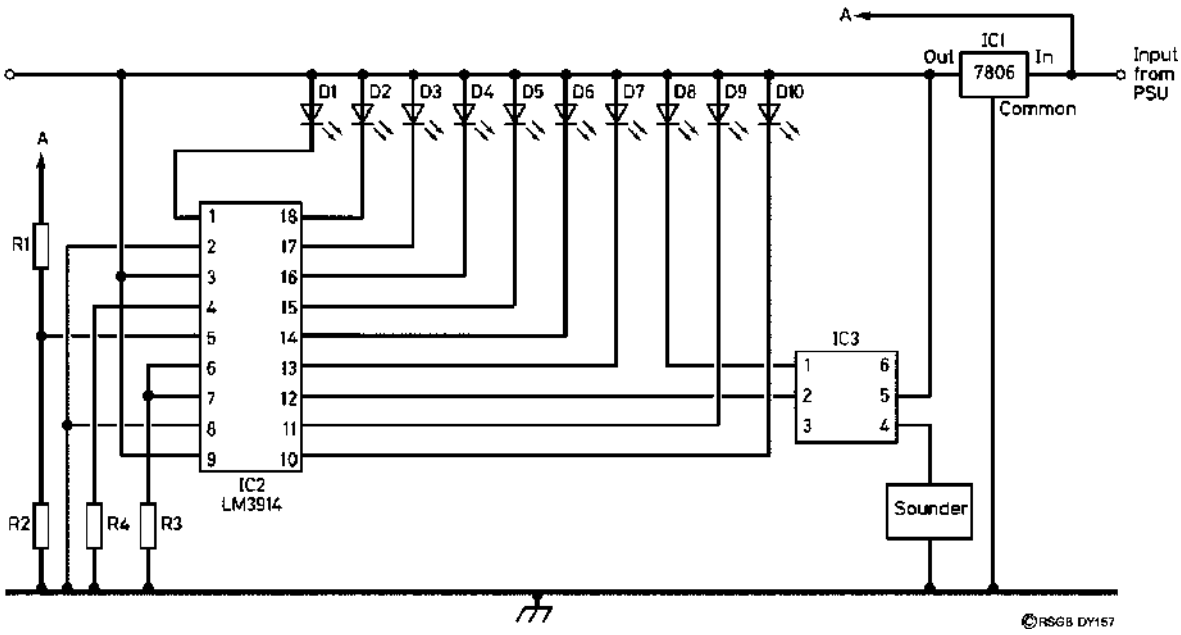

Figure 1 PSU monitor, circuit diagram

sounder will operate, indicating overvoltage. Despite the fact that some of your other equipment might be damaged by this overvoltage, the monitor circuit itself is unaffected.

Construction

The prototype was built on two pieces of Veroboard of the copper-strip variety. The main (circuit) board measured 15 strips by 25 holes, and the display (LED) board measured 4 strips by 30 holes. Track cuts are necessary in each board. The correct places are shown for the main board in **Figure 2**, but there is sufficient flexibility in the layout of the display board for a prescriptive layout not to be needed. All the anodes of the LEDs are connected to the same strip, which makes things comparatively simple!

For the main board, insert the Veropins and the wire links first, and solder them to the copper strips. Then fit the IC holders and the resistors. Fit the IC holders with their notches towards the top of the board. When fitting the voltage regulator, IC1, note than the centre lead (the 'common' lead in Figure 1) does *not* go to position A3; the track should be cut at A3, and the common lead soldered at B3. This is indicated in Figure 2.

Wire up the LED board with its ten LEDs and 11 connecting wires, each about 10 cm long. This length depends on how far away from the main

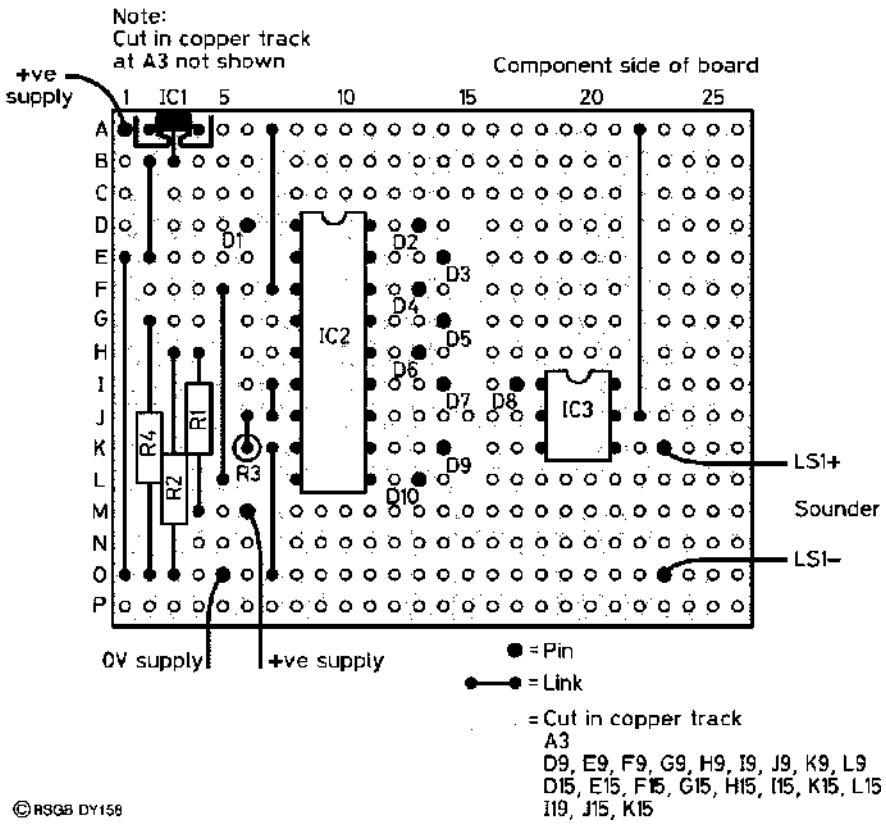

Figure 2 PSU monitor, PCB layout

board you are planning to mount the display. The LEDs should have different colours: three orange, four green and three red, to indicate 'low', 'medium' and 'high' voltage.

Now solder the other ends of these leads to the Veropins on the main board, making sure that the order is correct. Finally, connect the piezoelectric sounder to the main board; the polarity is important, so make sure the red lead goes to pin 4 of IC3 and the black lead to the ground rail. If you were careful to fit the IC holders with their notches in the correct positions, match these up with the notches on the ICs before pushing home the ICs *gently*. Check your circuit for solder bridges and unwanted pieces of copper swarf before screwing the small heat sink to the voltage regulator, IC1.

Testing

(a) **With a variable-voltage PSU**. Set the PSU for 10 V, connect the circuit and switch on. Increase the voltage slowly, and check that each LED lights up after the one before it. As the voltage exceeds about 14.4 V, the

first red LED should light and the sounder should operate. If an LED does not illuminate, you should immediately suspect either a dry joint or an incorrect LED polarity. The voltage at which the first red LED lights can be adjusted by varying R1; increase R1 if the LED comes on too early; decrease R1 if the LED comes on too late.

(b) **Without a variable-voltage PSU**. For your 'variable supply', you can use several AA-type 1.5 V cells (or 1.2 V NiCad cells) in series. The voltages produced by a range of cells is shown in **Table 1** – because of the lower voltage of NiCad cells, more of them are needed to produce a given voltage.

Once the operation of the circuit has been checked, it can be fitted into a plastic or metal box. Only two connections are needed for the PSU. You may want to drill some holes in the case to increase the apparent loudness of the sounder.

Table 1 Test voltages available from batteries in series

No. of batteries	*Voltage, nicads*	*Voltage, dry cells*
7	8.4	10.5
8	9.6	12
9	10.8	13.5
10	12	15
11	13.2	–
12	14.4	–
13	15.6	–

Parts list

Resistors: all 0.25 watt, 5% tolerance

R1	11 kilohms (kΩ) – see text
R2	1 kilohm (kΩ)
R3	1.2 kilohms (kΩ)
R4	18 kilohms (kΩ)

Semiconductors

IC1	L7806
IC2	LM3914
IC3	Opto-isolator – Maplin code WL35Q
D1–D3	3 mm LED, orange
D4–D7	3 mm LED, green
D8–D10	3 mm LED, red

Additional items

LS1	Piezoelectric sounder, wire leads
	6-pin DIL socket for IC3
	18-pin DIL socket for IC2
	Veroboard – two pieces for main and display boards, see text for sizes
	Veropins
	Heat sink for IC1
	Single-core insulated wire for links
	Insulated stranded wire for interconnecting the boards
	Case as required

57 A 1750 Hz toneburst for repeater access

Introduction

Repeaters across the UK and much of Europe need an access tone to switch the transmitter from standby ready for use. Commonly, this is a 1750 Hz tone of duration no greater than half a second. Although many UK repeaters may now be accessed using the *continuous tone-coded squelch system* (CTCSS – see the *RSGB Yearbook*), you may wish to access a repeater whose CTCSS frequency you don't know; in this case, using the universal 1750 Hz tone will gain you access. Commercial transceivers are usually fitted with an automatic toneburst, but if you are using a home-made design, then you may want to incorporate this little circuit.

Warning

This circuit uses a member of the integrated circuit family known as CMOS (complementary metal-oxide semiconductor). These use very little current

and can be completed destroyed if they come into contact with the magnitudes of static electricity that most of us carry about when we walk on carpets and wear rubber shoes. You will never know if this wanton destruction has happened – all you will discover is that your circuit doesn't work and that you have tested *everything*. To avoid this problem do the following things:

1. **Before you open the little packet in which the IC is supplied, touch something which you *know* to be earthed – the metalwork of any equipment which is mains earthed, for example. Then open the packet.**
2. **Let the IC fall gently on the bench – don't pick it out with your fingers. Touch your earthed metalwork again. Pick up the IC and insert it gently into its holder.**

The circuit is safe from destruction while it is connected to the battery.

Circuit description

The circuit is shown in **Figure 1**. The tone is generated by an integrated circuit oscillator (IC1), whose frequency is controlled by a *ceramic resonator*, XL1. Its frequency is very high, and is divided down to the 1750 Hz needed by the same chip. The ceramic resonator is designed to operate at 455 kHz, the intermediate frequency of many receivers. Because all divider circuits use powers of 2, we need the oscillator to run at 448 kHz so that when it is divided by 256 ($256 = 2^8$), we end up with 1750 Hz. Try it on your calculator:

$$\frac{448\ 000}{256} = 1750.$$

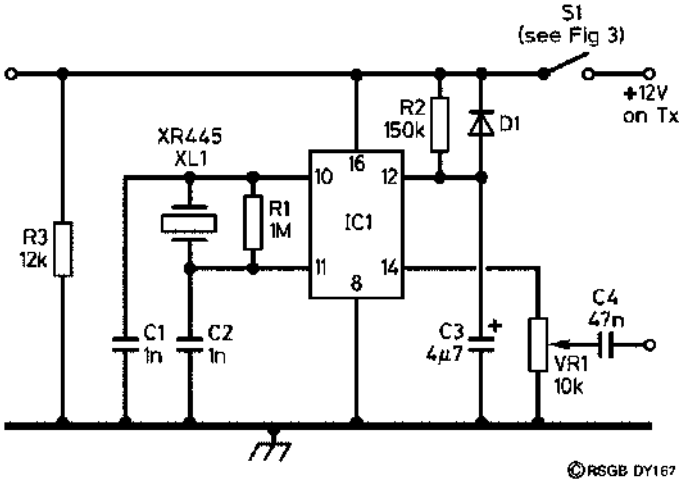

Figure 1 Toneburst module, circuit diagram

We use C1, C2 and R1 to *pull* the frequency of the oscillator away from 455 kHz to 448 kHz. The divider chain has eight *counters* in it, and each counter divides the frequency of the signal it sees by two, giving the final division of 256.

This counting process can be stopped at any time by taking the voltage on the *reset* pin (pin 12) up to the supply voltage. When the circuit is switched on by closing S1, pin 12 is at 0 V because C3 is discharged. The oscillator runs, producing the output frequency of 1750 Hz. As time progresses, C3 charges up through R2 and the voltage on pin 12 rises. When this has risen sufficiently, and in a time determined by the values of C3 and R2, the counter resets and stays in the reset state; no division takes place and there is no output. The duration of the toneburst is thus governed by C3 and R2.

When S1 is opened, the circuit is switched off, and C3 is discharged through D1 and R3, ready for the next toneburst. If you have used a repeater, you will know that a toneburst is needed **only** to activate a repeater in the standby condition; it is not needed once a contact has been established.

VR1 adjusts the amplitude of the tone fed to the microphone, and C4 prevents any voltage that may be present on your microphone connector from damaging the integrated circuit.

Construction

The prototype circuit was built on Veroboard of the copper-strip variety, measuring 20 holes by 14 strips. The layout is shown in **Figure 2**. Make the track cuts first, and check that there are no slivers of copper wedged between adjacent tracks. Then, solder in the IC socket (with the notched end

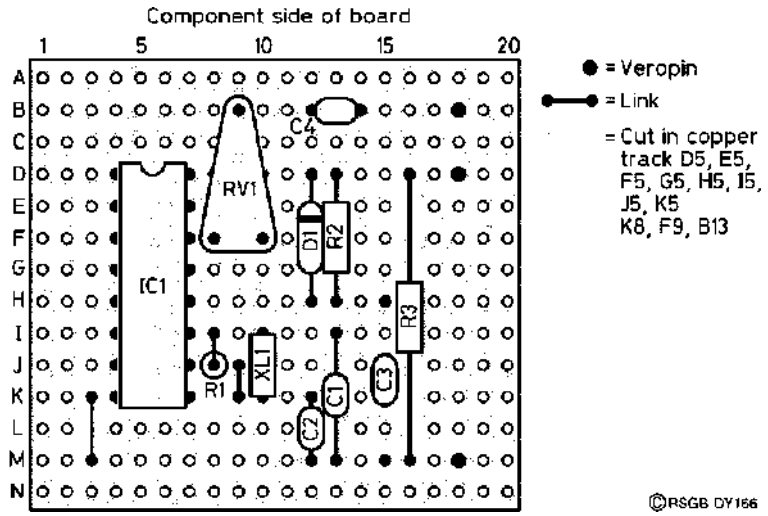

Figure 2 Veroboard component layout

facing towards track A), the wire links and the three Veropins. Having done this, solder in the resistors, capacitors and diode, making sure that D1 and C3 are the right way round! Using your best soldering technique, solder in the ceramic resonator quickly, to prevent heat damage. Recheck your circuit, check for solder splashes and bridges, and then gently insert IC1 into its socket, matching up its notch with that of the socket.

Testing

Set VR1 to half-way and connect a crystal earpiece to the output; apply power to the circuit. You should hear the tone, lasting for about half a second. If there is no tone, disconnect your circuit from the power supply, and check for dry joints in the vicinity of pin 12. Is the diode, D1, the correct way round? Is C3 the correct way round? Did you choose to ignore the CMOS safety precautions given earlier?

Once the circuit is working, you need to decide how you are going to connect it to your transmitter. Two options are shown in **Figure 3**. If you have access to a point in your transmitter circuit that has between 9 V and 12 V positive on it during transmit, you can use this to power your circuit. As the toneburst is needed only for repeaters, the switch, S1, disconnects it when not needed, as shown in Figure 3a. If you want the circuit to be self-powered, then a 9 volt PP3 battery may be used; Figure 3b shows this configuration.

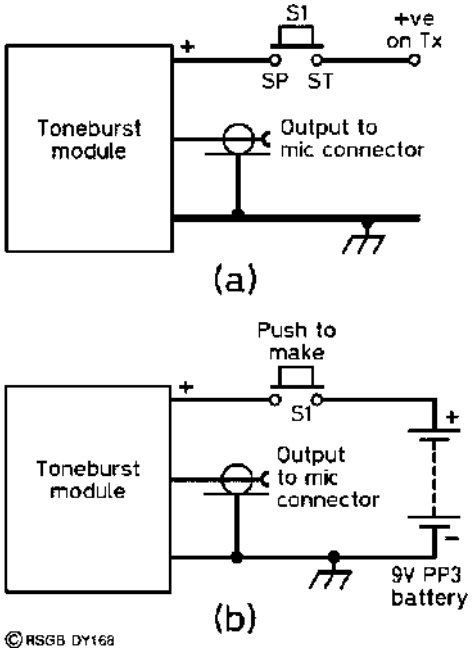

Figure 3 Toneburst module: two alternative switching arrangements

The output from the circuit board is fed directly into the microphone socket, in parallel with the microphone itself; use thin coaxial or screened cable for this lead, or you may induce hum into the microphone circuit and suffer from RF breakthrough into the audio circuits. To adjust the setting of VR1, start with it at the zero output position and connect a dummy load to your transmitter. Slowly, increase the output while monitoring your transmitted signal on another nearby receiver. Make sure you do **not** increase the output so far that the signal sounds distorted. If you would prefer that the tone was on continuously while you made this adjustment, simply connect a wire across C3 remembering, of course, to remove it as soon as you have completed the test!

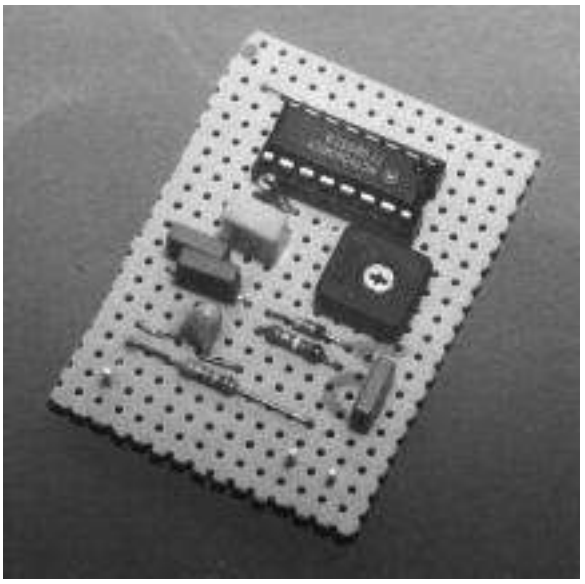

Parts list

Resistors: all 0.25 watt, 10% tolerance (or better)

R1	1 megohm (MΩ)
R2	150 kilohms (kΩ)
R3	12 kilohms (kΩ)
VR1	10 kilohms (kΩ) horizontal preset

Capacitors: all 16 V WKG or higher

C1, C2	1 nanofarad (nF) disc ceramic
C3	4.7 microfarad (μF) tantalum bead
C4	47 nanofarads (nF) disc ceramic

Semiconductors
IC1 4060
D1 1N4148

Additional items
XL1 XR455
Veroboard (see text for size)
Veropins (3)
S1 Switch (momentary action push-to-make SPST)
16-pin DIL socket for IC1
Single-core insulated wire for links
Coaxial or screened cable for microphone connection

58 A circuit for flashing LEDs

Introduction

There are many occasions when one's attention needs drawing to the fact that something important has happened. A single red light coming on is seldom sufficient to attract attention, particularly if it is surrounded by other lights and indicators. The eye is known to be very sensitive to *changes* in its peripheral vision; such changes can be brought about by movement or by differences in light level – a flashing light, for example. So, a circuit that flashes a single LED or a pair of LEDs finds plenty of uses in the amateur station.

Warning

This circuit uses a member of the integrated circuit family known as CMOS (complementary metal-oxide semiconductor). These use very little current and can be completed destroyed if they come into contact with the magnitudes of static electricity that most of us carry about when we walk on carpets and wear rubber shoes. You will never know if this wanton

destruction has happened – all you will discover is that your circuit doesn't work and that you have tested *everything*. To avoid this problem do the following things:

1. **Before you open the little packet in which the IC is supplied, touch something which you *know* to be earthed – the metalwork of any equipment which is mains earthed, for example. Then open the packet.**
2. **Let the IC fall gently on the bench – don't pick it out with your fingers. Touch your earthed metalwork again. Pick up the IC and insert it gently into its holder.**

The circuit is safe from destruction while it is connected to the battery. However, when the battery is removed, the same care should be exercised with its handling, because there is no supply decoupling capacitor across the IC.

Basic description

LEDs can be made to flash (switch on and off) by driving them from sources that switch on and off. Such a source is an *astable multivibrator*. If you have built or read about *A basic continuity tester*, elsewhere in this book, you will have come across such a beast before. That circuit used an astable multivibrator made from two transistors. This new circuit achieves the same behaviour from a single integrated circuit, the CMOS 4011. To give it its full description, the 4011 is a *quad 2-input NAND gate*. Quite a mouthful, but all it means is that inside the chip are four NAND gates, each with two inputs.

A NAND gate needs a positive voltage (known as a *logic 1*) on *both* inputs in order to produce zero volts (known as *logic 0*) at the output. Two NAND gates can be connected, as are A and B in **Figure 1**, to make our astable multivibrator. The combination of A and B has been described as the most perverse circuit in electronics; as soon as the output goes to logic 1, the circuit decides that it would prefer to have a logic 0 there, and switches over. With logic 0 at the output, the circuit now prefers to have logic 1 there, and so it goes on! We are going to use this continuous switching backwards and forwards to flash two LEDs. The rate at which A and B 'change their minds' is the frequency at which our LEDs will flash, and is controlled by the charging and discharging times of C1 through R2 and C2 through R1. As the values of R1 and R2 are the same, and those of C1 and C2 are the same, the ON and OFF states of the circuit are the same.

Gates C and D do not contribute to the flashing action; they act as *buffers* to isolate the LEDs from the multivibrator circuit itself. You will find in electronics that an oscillator is seldom used to drive another device *directly*; there is usually a buffer between it and the stage it drives.

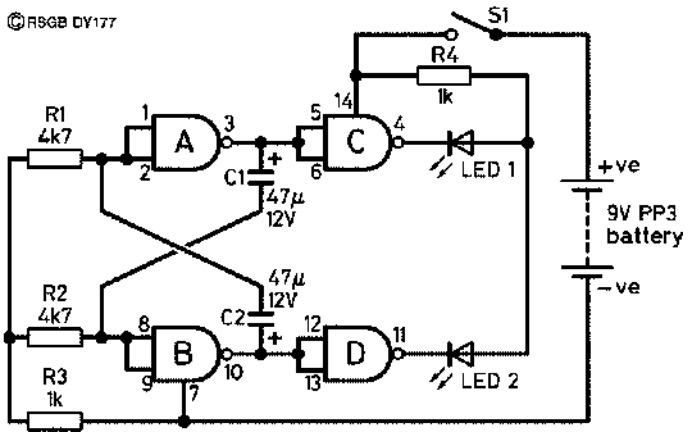

Figure 1 Flashing LEDs, circuit diagram

A characteristic of all multivibrators, astable or not, is that they have two outputs. In this case, those outputs are at pins 3 and 10, which are then buffered and appear at pins 4 and 11, respectively. When one output is at logic 1, the other is at logic 0, and vice versa. This means that LED1 is off when LED2 is on, and LED1 is on when LED2 is off, the two states switching backwards and forwards at the frequency of the oscillator.

Construction

Read the warning at the beginning of this article again. It is not intended to scare you off from building this, but is a genuine piece of advice which can save you time and irritation when all your labours result in a circuit that doesn't work! That extra bit of care can make all the difference!

Veroboard (the copper strip type) is used for the layout, shown in **Figure 2**. It measures 20 holes by 12 strips. **Be aware that there is no row 'I' in the layout, so don't miscount when you are placing components on the board!**

Firstly, cut the tracks using a 3 mm (⅛ inch) twist drill held between thumb and forefinger; check that there are no slivers of copper bridging any of the tracks, and that the tracks have been completely cut by the drill. Solder in the components carefully. Leave the IC in its carrier for the time being, and solder in the IC socket, with the notched end facing row A. On completion, check the circuit carefully. If you are happy that it is correct, follow the instructions given earlier and fit IC1 into its socket, matching up the two notches. Connect the battery and switch on. The two LEDs should flash on and off alternately. If only one LED flashes, you have probably connected the other one the wrong way round. Switch off, check and correct if necessary. If neither LED flashes, you must have a significant error in your circuit, which will need checking *again*! Or did you choose to ignore the handling precautions for the CMOS chip?

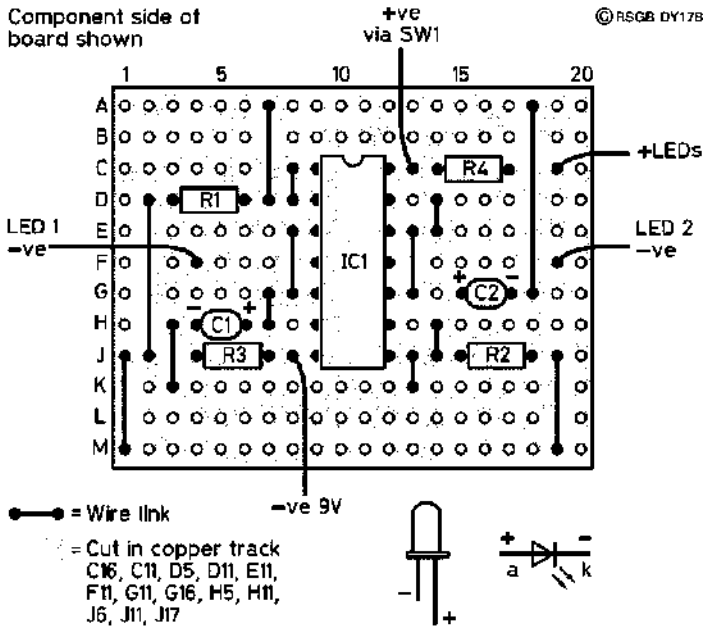

Figure 2 Flashing LEDs, component layout

The board can be mounted near to the point where you want your flashing LEDs to be seen, although long leads to the LEDs are acceptable. The LEDs can be different colours – it's all up to you now!

Parts list

Resistors: all 0.25 watt, 10% tolerance or better

R1, R2	4700 ohms (Ω)
R3, R4	1 kilohm (kΩ)

Capacitors

C1, C2	47 microfarads (μF) 12 V WKG

Semiconductors

IC1	4011

Additional items

LED1, LED2	Any size of LED, any colour
S1	SPST on/off
	Plastic box if needed, 8.5 by 5 by 2.5 cm

Source

Components are available from Maplin.

59 Digital logic circuits

Introduction

Logic circuits form the backbone of even the most advanced computer, yet their basic operation can be demonstrated by a couple of switches, a battery and a bulb.

Logic using switches

Everyone reading this article will look at **Figure 1** and know immediately how it works and be able to write down something like 'When switch A and switch B are closed, the light will come on'. Without knowing it, you have written down a logic statement involving the so-called **AND** operation; the light comes on only when switches A **AND** B are ON. Below the circuit in Figure 1, is a table showing the only possible positions of the two switches and the state of the bulb for each position. This is called a *truth table*, and is frequently used in logic analysis.

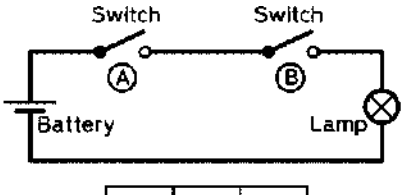

A	B	Lamp
Off	Off	Off
On	Off	Off
Off	On	Off
On	On	On

©RSGB DY182

Figure 1 Switches and lamp AND gate

Figure 2 shows a different circuit. Here, the two switches are in parallel rather than in series, as was the case in Figure 1. Again, if you analyse the circuit in words, you would say that the light will be on when switch A **OR** switch B is ON. This is an example of the **OR** operation, and its truth table is shown in Figure 2. The statement above is not complete, however; can you see why? The truth table will show you. The light comes on if A is ON, **OR** if B is ON, ***OR*** if A **AND** B are both ON. That third condition is easy to miss, but don't worry about it!

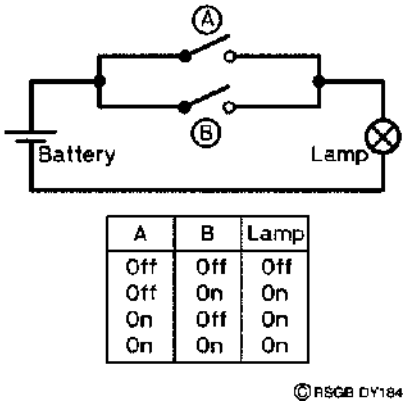

Figure 2 Switches and lamp OR gate

Believe it or not, some very complicated logic is possible (in theory) using switches and lights, but it is highly impractical and would be very slow. This is where electronic logic circuits come in.

Switches with no moving parts

You may have come across projects in this book where a statement is made such as '. . . the transistor is being used as a switch . . .'. Transistors *can* be used as switches, as were thermionic valves in the world's first programmable computer *Colossus*, at Bletchley Park. However, technology has moved on from valves, through transistors to *logic gates*, combinations of electronic switches designed specifically to perform logic functions.

These act on voltage levels as their inputs and produce changes in voltage levels as their outputs. A positive voltage is called *logic 1*, and corresponds to a switch being ON in our previous descriptions; a zero voltage is called *logic 0*, and corresponds to a switch being OFF. The output from a logic gate (normally labelled Q) is also logic 1 or logic 0, corresponding to our light being ON or OFF, respectively, in our switch analogy.

Many logic devices operate from a stabilised 5 V supply, and this determines the *ideal* voltages corresponding to the two logic states:

logic 0 ≡ 0 V,

logic 1 ≡ 5 V.

The world isn't an ideal place, so the *real* voltage ranges used by the logic gates are:

logic 0 ≡ 0.0 to 0.4 V,

logic 1 ≡ 3.0 to 5.0 V.

The **AND** circuit of Figure 1 is now called an **AND gate**, and requires logic 1 inputs on A **AND** B to produce a logic 1 at the output. **Figure 3** shows this. The truth table is identical with that of Figure 1 – logic 1 replaces ON and logic 0 replaces OFF. Now compare Figure 2 with **Figure 4** – circuits and truth tables for the **OR** function. Again, we have exact similarity.

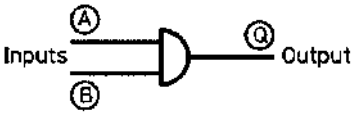

Inputs		Output
A	B	Q
0	0	0
0	1	0
1	0	0
1	1	1

©RSGB DY183

Figure 3 Electronic AND gate

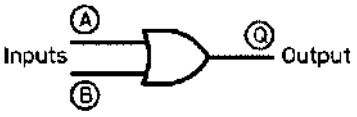

Inputs		Output
A	B	Q
0	0	0
0	1	1
1	0	1
1	1	1

©RSGB DY190

Figure 4 Electronic OR gate

There is another very common logic gate, which performs the **NOT** function. It is easy to understand. Just ask yourself the question 'What is **NOT** logic 0?', and the answer is obviously 'logic 1'. Similarly, logic 0 is **NOT** logic 1. A **NOT** gate simply changes the logic state of the input; it is also known (because of this behaviour) as an *inverter*. Its symbol and truth table can be found in **Fig 5**. Note the little circle on the output of the gate in Figure 5. In logic circuits, this symbol always implies inversion, or the presence of a **NOT** gate. Keep an eye open for it!

So far, the logic functions we have discussed have all been words which we use in everyday language, which has made the electronic interpretation of them relatively easy. Now we must introduce a function for which there is *no* analogy in normal speech – the **NAND** function. This means a

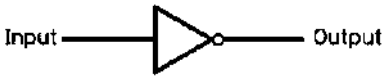

Input	Output
1	0
0	1

©RSGB DY185

Figure 5 Electronic NOT gate

combination of an **AND** gate and a **NOT** gate, and the sharp-eyed reader will have spotted the little circle added on to the normal **AND** gate symbol in **Figure 6**!

To make things easier to understand, the truth table in Figure 6 has four columns, not three as in previous tables. The third column is the standard **AND** output – compare it with the third column in Figure 3. That is the output from the **AND** gate *before* it encounters the little circle that inverts it, so the final output from the **NAND** gate is the output of the **AND** gate, inverted! The third and fourth columns are the inverse of each other.

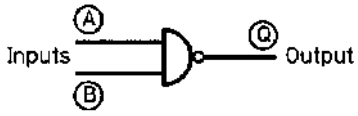

Inputs		and	Output
A	B		Q
0	0	0	1
0	1	0	1
1	0	0	1
1	1	1	0

©RSGB DY186

Figure 6 Electronic NAND gate

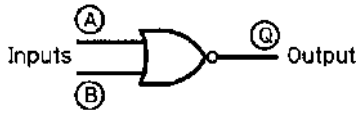

Inputs		or	Output
A	B		Q
0	0	0	1
0	1	1	0
1	0	1	0
1	1	1	0

©RSGB DY187

Figure 7 Electronic NOR gate

We can add the inverting operation to the output of an **OR** gate also, producing a **NOR** gate! The symbol and its truth table are shown in **Figure 7**. Again, notice that the final output is that of the ordinary **OR** gate, inverted!

These new functions of **NAND** and **NOR** are used more than the **AND** and **OR** functions because it makes other circuits easier to design using combinations of these gates.

A taste of Boolean algebra

The design of circuits using combinations of logic gates usually begins with a little mathematics, where the functions to be implemented are analysed. The mathematics used is surprisingly simple, and is a slightly changed version of ordinary algebra called *Boolean algebra*, which allows manipulation of logic functions to be made. Normal algebra has operations in it such as addition, subtraction and multiplication and division. The mathematician Boole found that the logical **AND** operation could be handled by the algebraic operation of *multiplication* (symbols $\times$ or $\bullet$), and the **OR** operation by the algebraic operation of *addition* (symbol +). The **NOT** operation involved a new symbol, that of a bar over the input being inverted, such as $\overline{A}$.

So, our five basic logic operators can now be written in a mathematical form:

AND	$Q = A \times B$
OR	$Q = A + B$
NOT	$Q = \overline{A}$
NAND	$Q = \overline{A \times B}$
NOR	$Q = \overline{A + B}$.

Using logic operations in a mathematical form enables the most complex logic to be designed, simplified and converted into circuit diagram form in a very efficient and rapid way. There are more logic operators than the five we have considered here but, in general, they can all be broken down into combinations of these gates alone!

60 A resistive SWR indicator

Introduction

When a transmitter produces some output power, we want to make sure that as much as possible of this power is radiated by the aerial. This often requires the use of an *aerial tuning unit* (ATU), which matches the aerial impedance to that of the transmitter.

How do you know when this matching has been achieved? The most usual way is to use a *standing-wave ratio* (SWR) indicator. If the impedance of the aerial does not match that of the transmitter output, some of your transmitter power (also known as the *forward* power) is reflected back along the aerial feeder and back into the transmitter, where it causes excess heating. The forward and reflected waves interact along the feeder to produce a wave whose position remains constant, and which is therefore called a *standing wave* or a *stationary wave*. An SWR meter simply indicates forward power and reflected power, and adjustments are made to your ATU until the reflected power is as small as possible (ideally zero, of course). If there is no reflected power then, by a process of elimination, all your forward power is reaching the aerial!

Sampling the RF

Whatever type of SWR indicator you use, it must use some sort of sampling circuit to pick up the forward and reflected waves. The project *A standing-wave indicator for HF*, elsewhere in this book, uses a toroidal transformer to separate the readings for the forward and reverse waves. This design differs in that it measures the voltages across resistors through which the RF current is passing. Its advantages are:

(a) it uses cheap parts – four resistors, two capacitors and a diode, together with a rotary switch, a surplus meter, a preset potentiometer and two sockets;
(b) within this SWR indicator, there is always a resistive path for the RF current from the transmitter, formed by R1, R2 and R3; this can prevent damage to simpler home-made transmitters, which may be damaged during adjustment of the ATU when using more conventional SWR indicators.

The only disadvantage of this form of indicator is that it must be switched out of circuit once the ATU has been adjusted for a particular band.

Construction

The SWR indicator is very simple to build, as most of the components can be mounted on the back of the 3-way rotary switch. This is shown in **Figure 1**. The switch is a 4-pole, 3-way rotary type, of which only two poles are used.

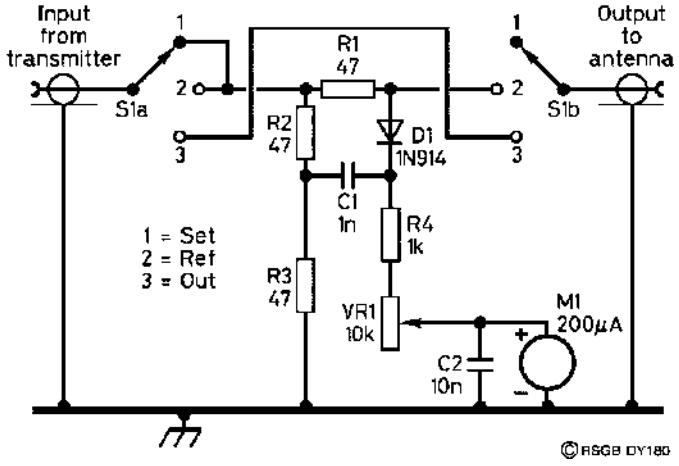

Figure 1 Resistive SWR meter, circuit diagram

Because the other switch contacts are not being used, they can be employed as support tags for other components. The ground wires are all soldered on to the metal frame of the switch. If your switch frame is of all-plastic construction, then a 12 SWG copper wire run around the switch will make a good earth connection to the metal case for the leads shown in Figure 1. The preset potentiometer used to control the sensitivity of the circuit can be mounted directly on the meter tag.

Resistors R1, R2 and R3 handle the RF power during the tuning-up process. If you have them, use 1 watt resistors; otherwise, you can use two 100 ohm half-watt resistors in parallel for each of R1, R2 and R3. The meter, M1, can be any DC type of sensitivity around 200 µA.

In use

First, find a clear frequency, and without the indicator in circuit, check that the frequency really *is* clear by asking and identifying yourself. If it is,

connect the indicator between the transmitter and the ATU which, in turn, is connected to your aerial. Turn SW1 to the SET position and key the transmitter. Adjust VR1 until the meter reads full scale. Switch off the transmitter. Turn SW1 to the REF position and key the transmitter again. Adjust the ATU until the lowest reading is obtained on the meter. Switch off the transmitter. For the chosen frequency, you have adjusted your ATU for minimum reflected power and hence the lowest SWR. You will need to repeat the process when you change bands, and possibly when you change frequency within the same band. Switching SW1 to the OUT position, you are ready to transmit. You may have noticed that it is good practice to switch the transmitter off when operating SW1. Get into that habit!

Parts list

Resistors	
R1, R2, R3	47 ohm (Ω) 1 watt (or 2 × 100 Ω, ½ watt, see text)
R4	1 kilohm (kΩ) 0.25-watt
VR1	10 kilohms (kΩ) preset
Capacitors	
C1	1 nanofarad (nF)
C2	10 nanofarads (nF)
Semiconductors	
D1	1N914 or similar
Additional items	
SW1	4-pole 3-way rotary switch, of which only 2 poles are used
M1	200 μA DC
	Case

61 An audio filter for CW

Introduction

This is a simple passive circuit (it has no power supply) that adds some audio selectivity for Morse code reception and also includes a very simple noise limiter that gives a visual indication of when noise spikes are being removed!

The circuit

Figure 1 shows the complete circuit. The tuned circuit of C1 and L1 resonates very close to 800 Hz, so initially you will have to tune a signal in carefully until it sounds loudest – you will soon be able to do this without thinking. The two LEDs connected back to back across the signal path act as a noise limiter, reducing the amplitudes of static crashes and noise from car ignition systems, etc. The LEDs blink when they conduct – this is not necessary to the operation of the circuit, but adds a little colour to your listening! The noise limiter *does* make listening more comfortable, though.

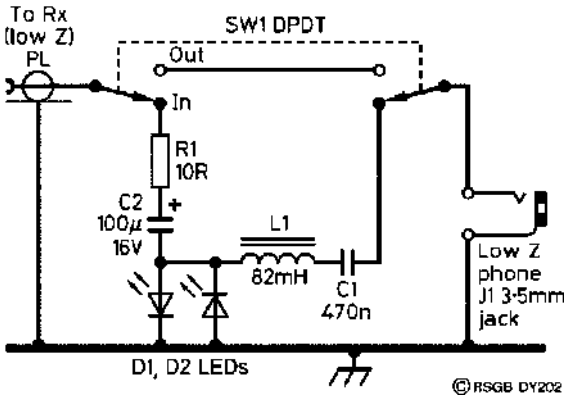

Figure 1 CW filter, circuit diagram

Construction

The circuit layout is shown in **Figure 2**. Point-to-point wiring is used, with a small tag-strip being the only item used for the extra support of C2 and R1. The LEDs and SW1 support the other components. An aluminium box (**Figure 3**) is used to make the circuit tidy and usable.

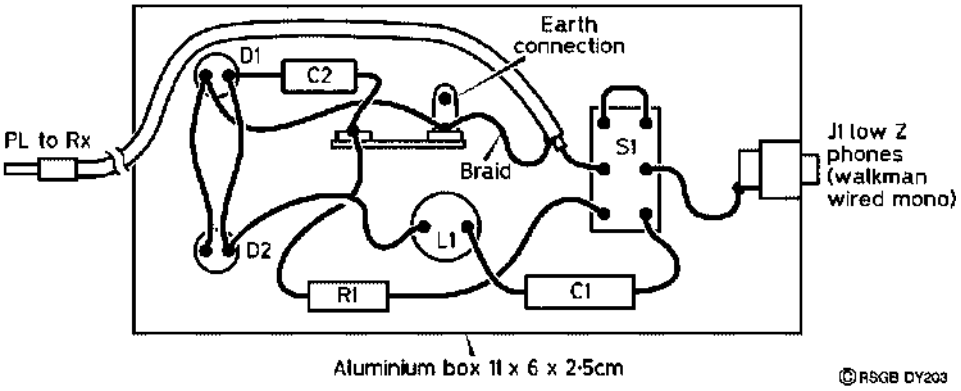

Figure 2 CW filter, component layout

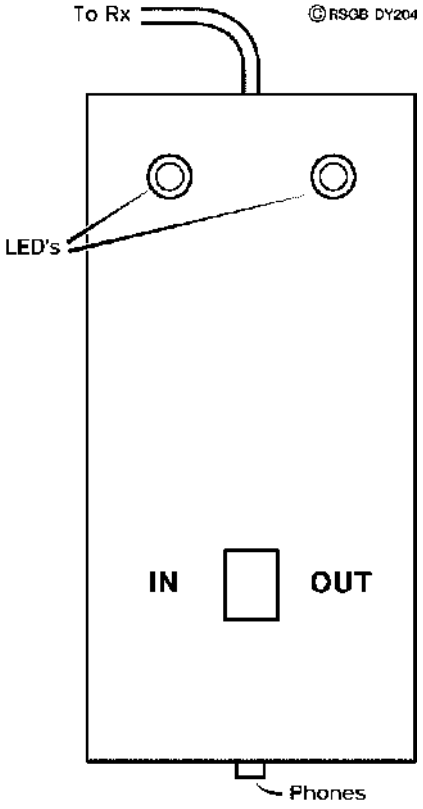

Figure 3 CW filter, front panel

You must use low-impedance headphones for the circuit to perform properly. Plug the completed unit into the headphone socket of your receiver and adjust the volume so that the LEDs are just *not* blinking on normal audio. The unit should be switched out of circuit for speech listening; this is the purpose of the toggle switch, SW1.

Parts list

Resistor
- R1 — 10 ohms (Ω), 0.25 watt, 10% tolerance

Capacitors
- C1 — 470 nanofarads (nF)
- C2 — 100 microfarads (μF) electrolytic, 16 V WKG

Inductor
- L1 — 82 millihenries (mH)

Semiconductors
- D1, D2 — LEDs

Additional items
- SW1 — DPDT
- J1 — 3.5 mm jack socket
- PL — Jack plug to suit receiver
- Aluminium box, approx. 11 by 6 by 2.5 cm

Source

Components are available from Maplin.

62 An electronic die

Introduction

Throwing a die is a venerable way of generating a 'random' number between 1 and 6. A die is easy to lose, so here is an electronic die-throwing circuit which brings the technique up to date and serves as another application of logic circuits. If you need a reminder of the basics of logic, refer to *Digital logic circuits*.

Warning

This circuit uses members of the integrated circuit family known as CMOS (complementary metal-oxide semiconductor). These use very little current and can be completed destroyed if they come into contact with the

magnitudes of static electricity that most of us carry about when we walk on carpets and wear rubber shoes. You will never know if this wanton destruction has happened – all you will discover is that your circuit doesn't work and that you have tested *everything*. To avoid this problem do the following things:

1. **Before you open the little packet in which the IC is supplied, touch something which you *know* to be earthed – the metalwork of any equipment which is mains-earthed, for example. Then open the packet.**
2. **Let the IC fall gently on the bench – don't pick it out with your fingers. Touch your earthed metalwork again. Pick up the IC and insert it gently into its holder.**

The circuit is safe from damage while it is connected to the battery.

Description

The circuit is shown in **Figure 1**. IC1a and IC1b form an *astable multivibrator*, similar to that used in 'An LED Flasher' also in this book. It runs constantly, and its output is fed to IC2 via a single NAND gate, IC1c. The other input of IC1c is held at 0 V by R3 and C3. Whenever one input of a NAND gate is logic 0 (or 0 V), there can be *no output* from the gate, irrespective of what is happening at other inputs. So, despite the fact that the oscillator (or *clock*) is running all the time, its square-wave output never

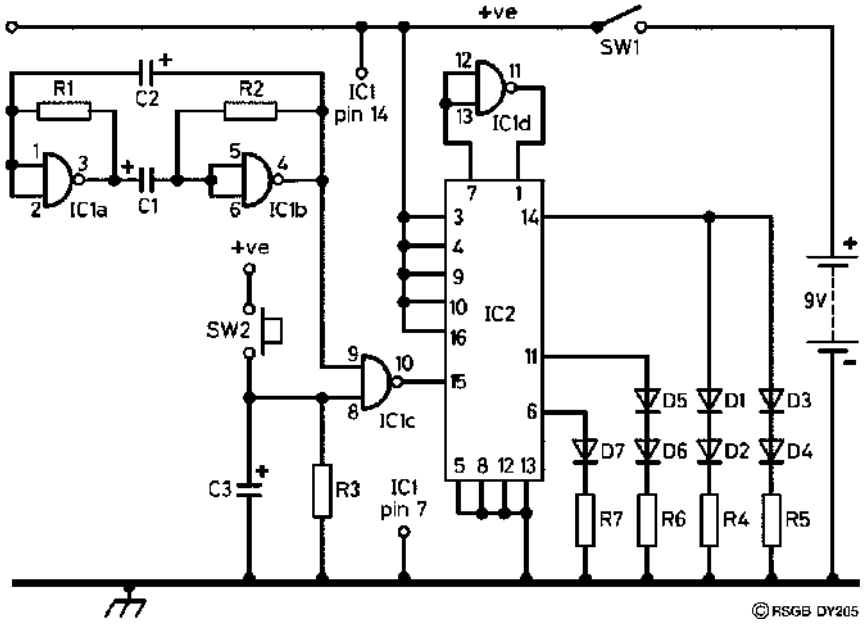

Figure 1 Electronic dice, circuit diagram

reaches IC2 until the 'other' input of IC1c is brought away from logic 0. This happens when SW2 is pressed. Pressing SW2 momentarily, as is normally done, charges up C3 to 9 V, putting a logic 1 on the second input of IC1c and allowing the clock signal through to IC2. As the switch is released, C3 begins to discharge through R3, gradually lowering the voltage on pin 8 of IC1c. As this voltage crosses 4.5 V (half the supply voltage), IC1c then treats this input as logic 0, which cuts off the clock signal from IC2 again. Thus, when SW2 is momentarily pressed, the clock signal is fed to IC2 for a short interval of time, before being blocked again.

IC2 is a binary counter, and the outputs that concern us are from pins 14, 11 and 6. Pin 14 is the *most significant bit* and pin 6 the *least significant bit*. See the panel for an explanation of what happens here.

To understand these outputs, you should be able to count in binary, using three bits. At the start of the counting process, all the bits have zero values, i.e. 000. The left-most bit is called the *most significant bit*, and the right-most bit is called the *least significant bit*. (When we write numbers normally, a number 1 in the left-hand position represents one hundred, 1 in the middle column represents ten, while the number 1 in the right-hand position means one. One hundred is a more significant number than one, hence the nomenclature.)

The three bits of our binary number have values, from left to right, of 4 ($=2^2$), 2 ($=2^1$) and 1 ($=2^0$). This means that a number 1 in the left-hand column signifies the normal number four, in the middle column it would represent two, and in the right-hand column, it would represent one. This should help you understand the patterns of bits which emerge as the clock waveform is counted, as the next paragraph explains.

As each cycle of the clock enters IC2, it increments its internal counter and the values of that counter are shown by the states of pins 14, 11 and 6. After the first pulse, these three pins would have states corresponding to 001; after the second, 010; after the third, 011; after the fourth, 100; after the fifth, 101; after the sixth, 110. This sequence of 3-bit numbers represents a binary count from 1 to 6 in 'normal' parlance. These six states are used to illuminate the conventional pattern of dots on a die, using LEDs.

As the clock cycles are counted, the LEDs flicker as the die is 'rolled'. Resistors R4 to R7 are used to limit the current through the LEDs. When the counter stops, it can be in any of the positions shown in **Table 1**. Because of

Table 1 Dice number relative to counter output

Step	*Pins*			*Dice number*
	14	*11*	*6*	
1	0	0	1	4
2	0	1	0	2
3	0	1	1	6
4	1	0	0	1
5	1	0	1	5
6	1	1	0	3

the way in which the dots are grouped on the faces of a die, the wiring of the LEDs is simpler than it might otherwise be. You can see from Figure 1 that there are really only three sets of connections to the LEDs – one from each bit of the counter output. When pin 14 is at logic 1, four LEDs are lit, corresponding to the number four. For the number five, pins 14 and 6 will be at logic 1. For the number one, only pin 6 is at logic 1. For three, pins 11 and 6 are at logic 1, for six, pins 14 and 11 are at logic 1, and for two, only pin 11 is at logic 1. These conditions are summarised in Table 1.

Construction

Two pieces of Veroboard (of the strip type) are needed – one for the main circuit (**Figure 2**) and the other for the display LEDs (**Figure 3**). The display board is easier to build, so we will do that first. It measures 20 holes by 18 strips.

Cut the tracks as shown in Figure 3, using a 3 mm (⅛inch) twist drill rotated between thumb and forefinger. Insert and solder the Veropins, resistors and the wire links. Then solder the LEDs in place, making sure their polarities are correct. The LEDs are mounted proud of the board (**Figure 4**, which will help when you come to fix the board into a case.

The main board measures 32 holes by 18 strips. As before, remove the tracks in the places shown in Figure 2. Note that track 'L' is *not* broken under the position for IC2. Solder in the IC holders and the links. Solder in R1 and R2 vertically, and R3 horizontally. Then solder in C1, C2 and C3; these all being electrolytics, check their polarities. Solder in the Veropins and prepare the connections to those components not on the main board, using stranded, insulated wire. Check the circuit carefully, and read the handling precautions given earlier before carefully inserting the two ICs.

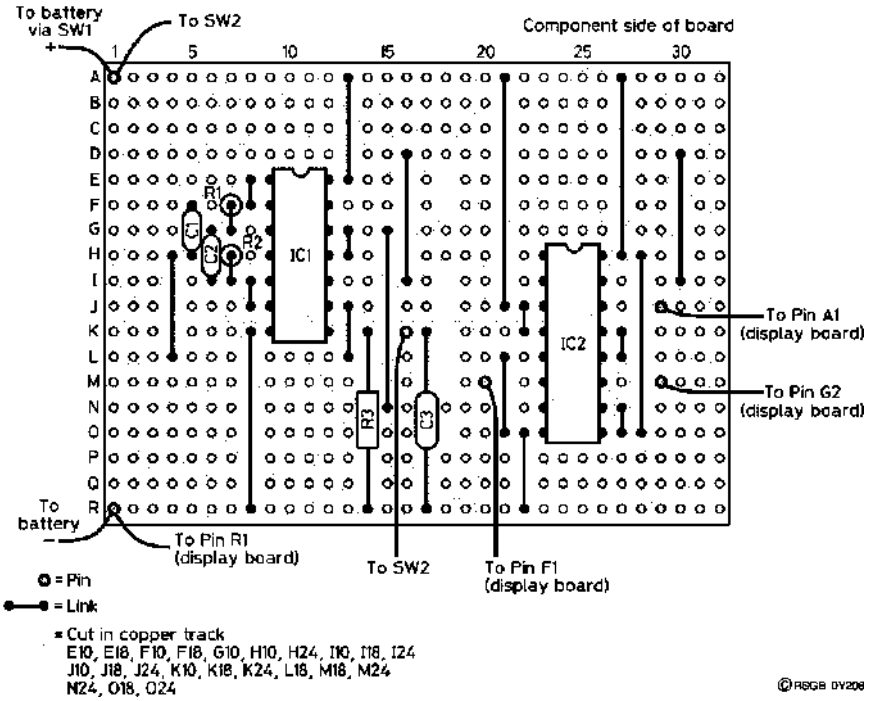

Figure 2 Main board, component layout

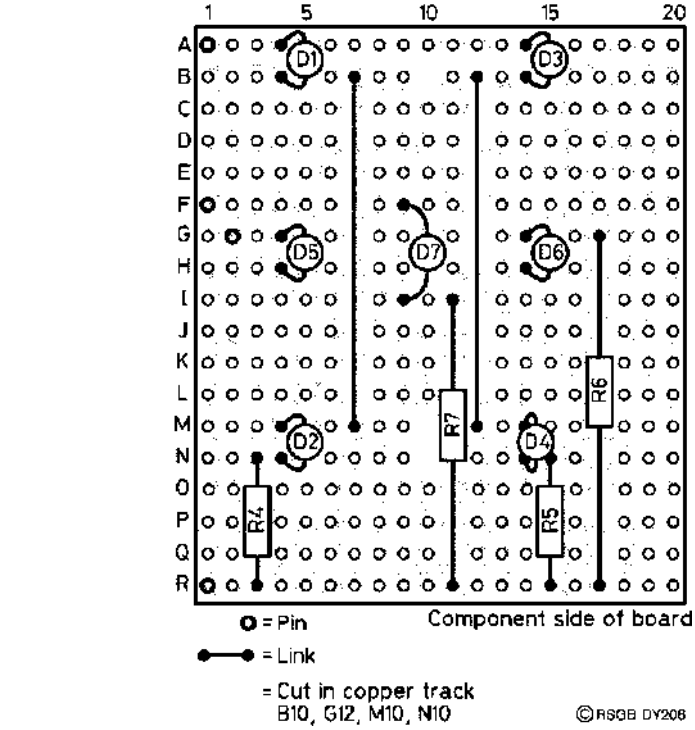

Figure 3 Board for the six LEDs

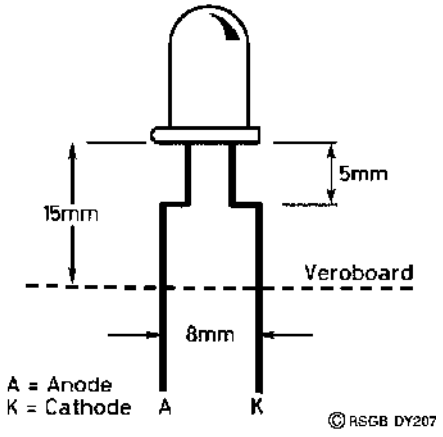

Figure 4 D7 lead bending

Testing and use

When the circuit is switched on, it is likely that the centre LED only will be lit. Press SW2, the 'throw' switch. All the LEDs should flicker, even after the switch is released, but only for a second or so. Then a standard pattern should show, signifying numbers between one and six. If this does not happen, switch off and check your circuit again. Are there any missing links? Are there any obvious dry joints (usually dull instead of shiny)? Can you see any solder bridges between tracks? Did you choose to ignore the handling precautions? If none of these results in a working circuit, try some fault-finding.

- Disconnect the lead to D7 on the main board (marked 'to pin F1' on Figure 2). Touch the lead on to the positive supply rail. D7 should light. Now transfer this lead on to pin 4 of IC1. If it flickers, then the oscillator is running (which it should).
- Transfer this lead to pin 10 of IC2. D7 should flicker when SW2 is pressed, but should be on permanently when it is released. This means that the correct signals are reaching IC2 from IC1.
- If one of the chains of LEDs (i.e. D1 and D2, D3 and D4, D5 and D6) does not light, you may have one *or both* LEDs the wrong way round.

When the die is working, you may care to experiment with the values of R1 and R2, but you should keep their values the same, i.e. R1 = R2. The larger the values of these, the more slowly the die will appear to 'roll'.

Finishing touches

On completion of the project, you will want to mount it in a smart case; any plastic box is suitable for this, with the display board mounted so that the

LEDs protrude through the top and are fixed to it using LED clips. The way in which you mount both boards to the case is entirely up to you.

Parts list

Resistors: all 0.25 watt, 10% tolerance, or better

R1, R2	5600 ohms (Ω)
R3	15 kilohms (kΩ)
R4–R7	470 ohms (Ω)

Capacitors

C1, C2	1 microfarad (μF) electrolytic, 16 V WKG
C3	68 microfarads (μF) electrolytic, 16 V WKG

Semiconductors

IC1	4011
IC2	4029
D1–D7	LEDs, any size and colour

Additional items

SW1	On-off switch SPST toggle
SW1	Push-to-make, non-latching
	Veroboard, 2 pieces, see text for sizes
	Veropins, 10
	Stranded insulated wire for general wiring
	Single-core insulated wire for links
	PP3 battery clip
	PP3 battery
	Plastic box to suit
	LED mounting clips (7)
	Means of mounting boards to box

Source

Components are available from Maplin.

63 The absorption wavemeter

Introduction

The purpose of the absorption wavemeter is to check that a transmitter is radiating within the correct waveband, and to detect any spurious *harmonic* emissions. A harmonic frequency is an integral multiple of the carrier frequency – e.g. if the carrier is at a frequency *f*, the harmonics are at frequencies 2*f*, 3*f*, 4*f* . . . and so on.

It can also be employed as a relative field-strength indicator, being used in experimentation with aerials. What it *cannot* do is to measure the transmitted frequency accurately; all it can do is to place the signal within a particular band, say the 7 MHz or the 18 MHz band (or their harmonics).

How it works

You may recognise the circuit of **Figure 1** as a crystal set with a meter replacing the headphones. It is simply the parallel combination of an inductance with a variable capacitance, which constitutes a resonant circuit with a variable frequency. A dial on the variable capacitor can be roughly calibrated with frequency. The fixed capacitor across the meter helps to improve the meter reading by making it read the peak value of the carrier wave rather than the average value.

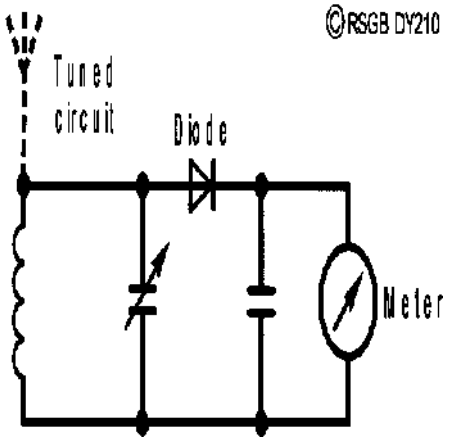

Figure 1 Absorption wavemeter circuit

When the wavemeter is situated in the vicinity of a relatively strong radio-frequency (RF) field, the inductor absorbs a small amount of energy from that field. If the circuit is resonant at the same frequency as that of the transmitter, an RF voltage is produced across the coil and is proportional to the strength of the RF field. The RF voltage is *rectified*, or *detected* (turned from AC into DC) by the diode and the second capacitor, and is displayed by the meter.

The tuned circuit

The formula for calculating the resonant frequency of a coil and capacitor is relatively simple. It is

$$f = \frac{1}{2\pi\sqrt{LC}},$$

where f is the resonant frequency (Hz),
L is the inductance (H), and
C is the capacitance (F).

If this formula puts you off, there is this slightly easier version:

$$f = \frac{159}{\sqrt{LC}},$$

where f is the frequency in **MHz**,
L is the inductance in **microhenries** (**μH**), and
C is the capacitance in **picofarads** (**pF**).

When a variable capacitor is specified, it is usual to quote its maximum capacitance, i.e. the value when the vanes are fully meshed. When the value of the capacitor is small, it is usual to quote its minimum capacitance also, the value when the vanes are fully open. If you use a variable capacitor of 10–100 pF with a 100 μH inductor, you will use the value of 10 pF to calculate the maximum resonant frequency, and the value of 100 pF to calculate the minimum resonant frequency, giving a tuning range of 1.6 MHz to 5 MHz. Check it yourself!

64 An HF absorption wavemeter

Introduction

An absorption wavemeter is basically a simple tunable detector circuit, such as would be used in a crystal set, but with the headphones replaced by a meter, in order to indicate the strength of the received signal.

The circuit

Figure 1 shows the circuit of the wavemeter. It is designed to cover all the HF bands from 1.8 MHz to 28 MHz in four switchable ranges. There is no built-in method of amplification, so a sensitive meter is needed in order to indicate sufficiently using the available absorbed energy. The meter does not need calibrating, it serves to produce only an indication of the absorbed power, *not* its absolute value.

An absorption wavemeter does not have outstanding selectivity, mainly because of the loading effect of the meter. This problem is ameliorated here (but only slightly) by the inclusion of R1 in series with the meter. It gives

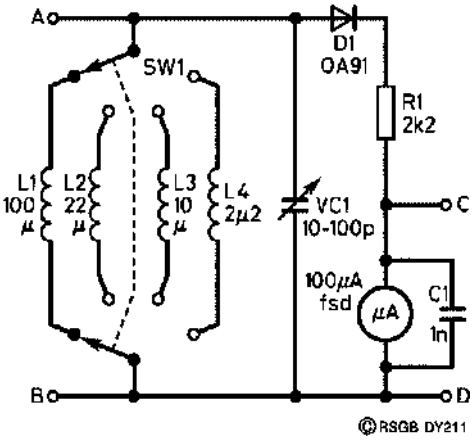

Figure 1 HF absorption wavemeter, circuit diagram

improved selectivity at the expense of a slight loss of sensitivity. The appearance of capacitor C1 across the meter is discussed in *The Absorption Wavemeter*, in the previous section.

Coils

These can be purchased (see the parts list) or hand-wound on short lengths of PVC water pipe or conduit, and the coil-winding details are given in **Table 1**. In theory, the 100 pF tuning capacitor would cover all the HF bands with only three coils, omitting the 22 μH coil. Sample calculations are explained in the previous article. However, its inclusion avoids the common problem of having some bands cramped at the extreme edges of the tuning scales.

Table 1 Close-wound coil values

L (μH)	No of turns	Span (mm)	SWG
PVC FORMER OF OUTSIDE DIAMETER 25 mm			
2.2	9	9	20
10	24	24	20
22	44	44	20
100	110	60	26
PVC FORMER OF OUTSIDE DIAMETER 20 mm			
2.2	10	10	20
2.2	9	5	26
10	32	32	20
10	24	12	26
22	63	62	20
22	41	21	26
100	134	70	26
PVC FORMER OF OUTSIDE DIAMETER 19 mm			
2.2	11	11	20
2.2	9	5	26
10	35	34	20
10	25	13	26
22	68	67	20
22	44	22	26
100	157	79	26

Construction

Hand-wound coils, using 19–25 mm PVC formers, have single-layer windings, with their ends secured by threading the wires through two small holes drilled in the formers at each end of each winding.

You may have wondered about the use of the two-pole switch SW1, as all the lower ends of the coils are grounded anyway. The answer lies in the ease of construction. Each coil can be mounted on the tags of the switch for support. If you are using the commercial coils, they are small enough to be accommodated on a miniature rotary switch; a larger rotary switch is required for hand-wound coils. The specification of a 6-way switch allows for the addition of extra frequency ranges at little extra cost. Rotary switches such as the 2-pole, 6-way variety have an adjustable end-stop which allows the number of ways to be set anywhere between 2-ways and 6-ways. Remove the nuts from the switch, and a 'washer' will fall out. It is not a washer, really, and has a little piece of metal bent over at right angles to the washer. This fits into one of 12 holes in the body of the switch, and prevents the shaft from turning through 360° and selecting the number of ways.

Calibration

This process needs a commercial amateur-bands transceiver, if it is to be done quickly and accurately.

- Connect the transceiver to a dummy load, and connect a piece of flexible wire from point A in Figure 1 and wrap two or three turns around the cable between the transceiver and the dummy load.
- Turn the transceiver power level control to minimum, and set the frequency at 1.81 MHz and the mode to FM or AM. Switch to transmit.
- With the wavemeter set to its lowest frequency range (i.e. 1.8–3.5 MHz), rotate the tuning capacitor until maximum deflection is obtained from the meter needle. Write the frequency on the inner ring of the wavemeter scale at that point.
- Switch off and retune the transmitter to 3.5 MHz. Repeat the above process.
- Repeat, using switch range 2 for 3.5, 7 and 10 MHz, range 3 for 7, 10 and 14 MHz, and range 4 for 14, 18, 21, 24 and 28 MHz.

An alternative source of calibration signal could be an HF signal generator, with a single-turn loop of wire at the remote end of its cable, and the wire from the wavemeter brought close to the loop.

Remember that the marks on the scale represent frequency *bands*, not precise frequencies.

Extending the range

If you would like to experiment with increasing the range to the lower VHF band, then 50 MHz should be achievable with an additional self-supporting coil (no former). Try three turns of 20 SWG enamelled copper wire of 25 mm ID (internal diameter). Wind it on some 25 mm PVC pipe, as before, then slide out the pipe! The same result could be achieved with four turns of 19 or 20 mm ID, or 12 turns of 7.1 mm ID.

Parts list

Resistor
- R1 — 2200 ohms (Ω) 0.25 watt, 10% tolerance

Capacitors
- C1 — 1 nanofarad (nF) min. ceramic
- VC1 — 100 picofarad (pF) variable

Inductors
- L1 — 100 microhenries (μH)
- L2 — 22 microhenries (μH)
- L3 — 10 microhenries (μH)
- L4 — 2.2 microhenries (μH)

Semiconductors
- D1 — Germanium OA91 or 1N4148

Additional items
- SW1 — Rotary 2-pole, 6-way
- Moving-coil meter, 50 or 100 μA FSD (any meter of this sensitivity will do)
- Plastic box, approx. 150 by 80 by 50 mm
- Connecting wire, coloured

65 A vertical aerial for 70 cm

Introduction

If the range of your hand-held transceiver is very limited, what you need is a vertical aerial mounted outside. This design is a half-wave dipole fed at the end instead of the middle. Because the impedance of the dipole is high at its ends (and low in the centre), a matching circuit is needed so that this high impedance can be matched to that of the low-impedance coaxial cable. All that is needed is a coil, which increases the *electrical length* of the aerial to $\frac{5}{8}$-wavelength. (Note that the *electrical* length (i.e. the length as it appears to an RF signal) is not necessarily the same as the *actual* length.)

Construction

The aerial element and the coil are made from a single piece of 1.5 mm welding (brazing) rod, and the dimensions are given in **Figure 1**. Wind the coil around a 4 mm rod or the shank of a twist drill. The lower end is filed to a point and then soldered into the centre conductor of a 4-hole panel-mounting BNC socket. (Try to obtain a good-quality BNC socket with PTFE insulation – the insulation of cheaper sockets is easily damaged.) Trim the element to 427 mm (top of element to top of coil) *after* the wire has been soldered to the socket.

The base coil causes the aerial to be rather 'whippy', so a piece of 5 mm plastic knitting needle can be cut to the length of the coil and then forced into it.

The radials are made from four lengths of 3 mm welding rod. These are bent and soldered into the four mounting holes of the socket, and then cut to the lengths shown in Figure 1.

Testing

Using a standing-wave-ratio (SWR) meter connected between your aerial and the transceiver, measure the SWR (or obtain some indication of the reflected power) on transmit. If it is greater than 1.5, switch off the transmitter, trim about 3 mm off the end of the element, and try again. Repeat the process until the measured SWR (or the reflected power) is as low as you can get it.

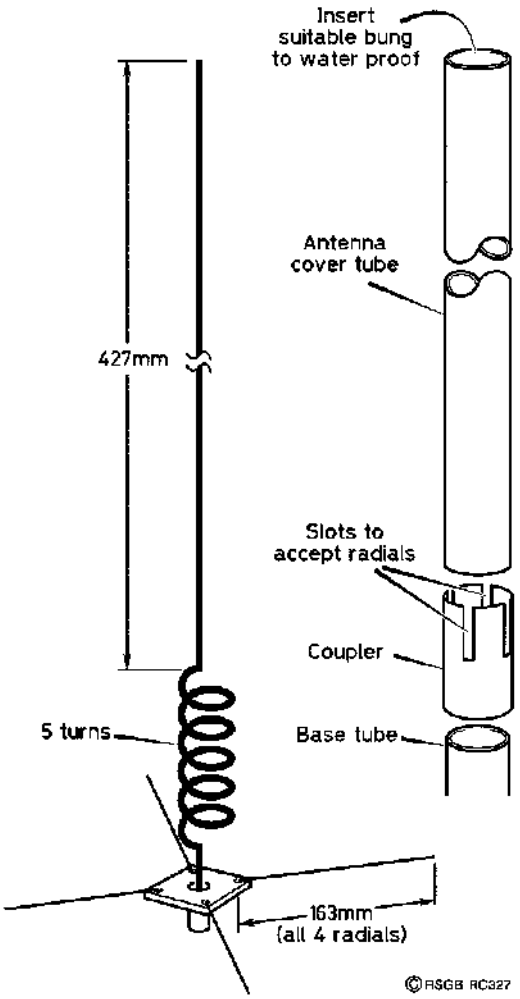

Figure 1 Construction of the 70 cm antenna

Installation

The aerial is made waterproof by enclosing it in a 22 mm diameter PVC waste water pipe. It is 'weldable', and available at plumbers' merchants, usually by the metre. A coupler is slotted to take the radials (Figure 1). File the BNC socket as required, so that it slides inside the coupler until the radials poke out of the slots. Cut a length of plastic tubing which is 30 mm longer than the aerial, and push it into the coupler. You will then need a plastic bung or screw-top to waterproof the top end.

Plastic welding solution is now applied to the joints, sealing the aerial inside the tube. The coupler has been weakened as a result of making the slots, so it is worthwhile applying PVC tape around this joint until the welding solution sets.

A support for the aerial is made from an off-cut of tube pushed into the lower end of the coupler and held with a self-tapping screw.

Parts list

1	4-hole panel-mounting BNC socket
1 m	3 mm brazing rod (may be available from a small garage)
1 m	1.5 mm brazing rod
1 m	22 mm PVC waste water pipe
1	22 mm straight coupler
	Plastic welding solution

66 A UHF corner reflector aerial

Introduction

The corner reflector is a well-known design and is capable of good performance on the VHF and UHF bands. At UHF, the practical implementation of the corner reflector is an ideal constructional project.

Some details

Expressed quite simply, the aerial consists of a $\frac{\lambda}{2}$ dipole (where λ is the standard symbol for wavelength, making a '$\frac{\lambda}{2}$ dipole' a half-wave dipole).

Nothing new in that, you might say. However, the interesting feature is the reflector, which is not the usual single element, but a 90° metal 'corner', acting rather like a parabolic dish as used for satellite signal reception. The wind resistance of this type of reflector makes it impractical so, to reduce the 'windage' quite significantly, we make the 'corner' from closely spaced rods, as illustrated in **Figure 1**.

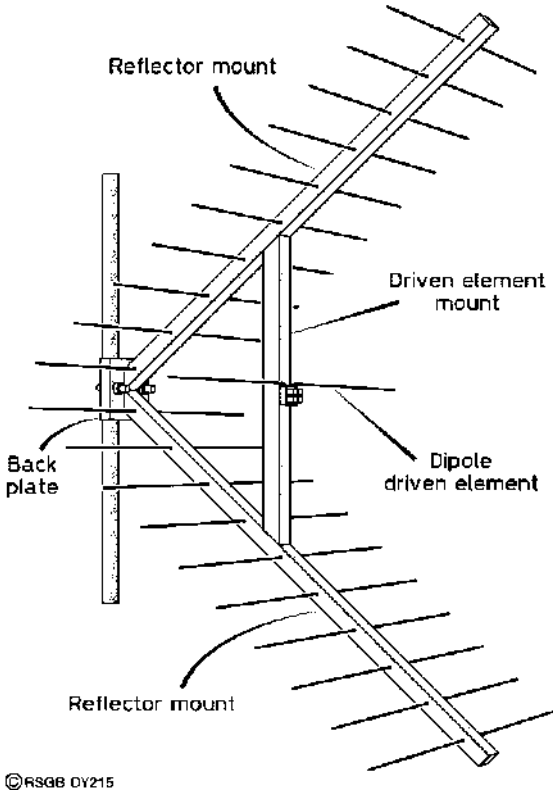

Figure 1 70 cm corner reflector antenna

The reflector consists of a number of 0.6λ rods, spaced from each other by 0.1λ. The aerial frame can be made of metal or wood, but wood is easier to work with, and mounting the elements to the frame is simpler. The prototype was made with wood of 20 mm by 15 mm cross-section, as **Figure 2** shows. The wood was varnished for protection. The elements were made from 1.5 mm diameter copper wire, because a large reel of the wire happened to be available. The wire diameter is not critical; tubing could be used just as successfully. 14 SWG hard-drawn copper aerial wire would be even better than that used in the prototype.

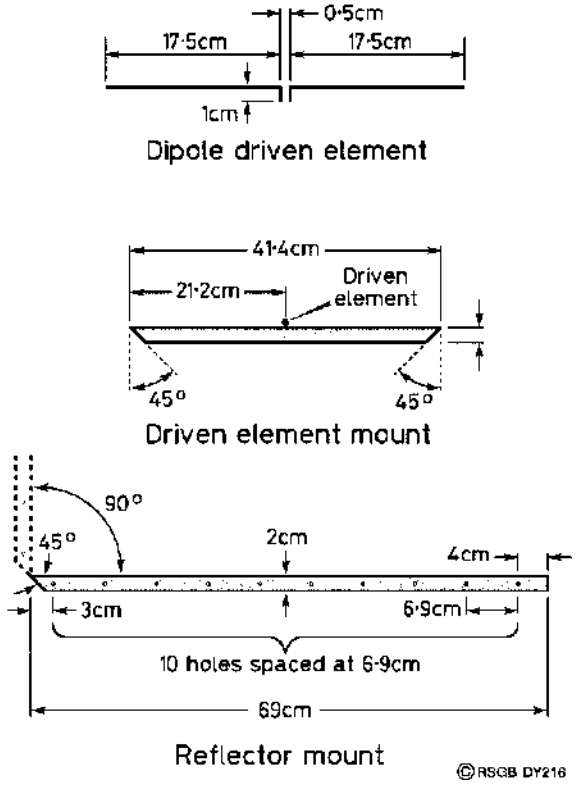

Figure 2 Driven element dimensions, together with boom dimensions for driven element and reflectors

Construction

This project is just as much a woodworking project as a radio project! Follow the instructions carefully, and you should have little trouble.

- Cut the booms for the reflectors, as shown in Figure 2. A mitre block is invaluable here in producing the 45° corners.
- Using the dimensions given on the diagram, mark the hole positions for the reflector elements, and then drill holes of a size which holds the elements firmly.
- Cut the driven element boom according to the diagram, and mark the point midway along the longer side, which will assist you later in positioning the driven element.
- Cut the back plate to size (about 120 mm by 80 mm). You may need to alter this size depending on the size of the U-bolt you will be using to clamp the aerial to the mast.

- If you want to be extra cautious in your construction, use the belt-and-braces approach, commonly known as 'screw-and-glue' to fix the booms to each other and to the back plate.
- Fix the reflector booms to the back plate first, then slide in the driven-element boom until it will go no further, then apply the wood glue and screw the two ends tightly to the reflector booms. Leave for the period prescribed by the glue manufacturers for the glue to harden.
- Varnish the whole structure.
- Cut the driven element to the correct size plus a couple of centimetres (the reason for this will be evident in the *Testing* section), and fix it to the centre of its boom (at the position you marked earlier) with a 'chocolate block' connector to which the coaxial feeder cable will eventually be connected.
- Cut and fix the reflector elements in place. If you find that these are a loose fit in the holes then, *for each element*, drill a pilot hole through the boom to intersect the hole for the element. File off the point of a woodscrew, and screw it gently into the pilot hole until it meets the element and grips it in place. You will now see why the point was filed off! Alternatively, you can glue the elements in place.

Testing

Place the aerial on a mast, clear of obstructions. Connect it to a transceiver with a length of coaxial cable, with a standing-wave-ratio (SWR) meter in circuit. Find a clear frequency, identify your transmission and ask if the frequency *really is* clear. If so, key the transmitter again and note the SWR. **Do not stand in front of any aerial when it is radiating!** The length of the driven element must be adjusted to obtain an SWR of less than 2. If you have to shorten the dipole, bend the ends over rather than cut them off. That way, if you go too far, your can lengthen them again! The dipole was initially cut too long intentionally, to allow for adjustment here! Bending the ends over also reduces the risk of physical damage to clothing, skin and eyes. You may like to consider applying the same technique to the reflector elements for that reason alone.

Moving on . . .

Once you have warmed to the idea of the corner reflector as an aerial, you might like to ring the changes regarding the reflector. How about replacing the 20 reflector elements with a wire mesh, such as garden centres sell as 'chicken wire'? Choose the finest mesh if there is a choice. Some extra support may be needed around the edges of the mesh, but you could go on to make a comparison of aerial gain between the two types, using the *UHF Field Strength Meter* described elsewhere in this book.

Materials

Stiff wire or thin-walled tubing for dipole and reflector
Frame – wood, 15 mm by 20 mm cross-section, lengths given in text
Back plate – stout plywood, dimensions given in text
U-bolt to suit mast
Wood screws
Wood glue
50 W coaxial cable for feeder
2-terminal 'chocolate block' for dipole connection to feeder
Varnish

67 A switched dummy load

Introduction

A dummy load is a pure resistor of value 50 ohms which can replace your transmitting aerial and enable you to operate the transmitter for test purposes without radiating a signal. It sounds simple enough, but there are two main problems. Firstly, it is impossible to delve into your junk box and emerge with a resistor that will dissipate 100 W PEP and still retain its marked resistance value. Secondly, a 'pure resistance' is very difficult to achieve. A pure resistance is a device which has resistance but no reactance. All common resistors have significant reactance at radio frequencies, particularly the wire-wound varieties, which have a helical (i.e. wound like a coil) construction. This is particularly annoying, because wire-wound construction is normally used for large-wattage resistors.

Although all resistors have *some* reactance, not all are quite as bad as the wire-wound type. Carbon film resistors are made by depositing a thin film of carbon on the surface of a small, hollow ceramic cylinder, the thickness of the film of carbon determining the value of the resistor. Provided the lead lengths are kept short, these resistors have a tolerably small reactance, and will be used in this project.

Bearing the load

A 2 W carbon film resistor is hardly going to withstand our 100 W PEP of SSB, so it is obvious that the design of our dummy load must be a little more

complex than a single resistor and a switch, despite what **Figure 1** might suggest! In fact, it uses 20 resistors, each of value 1000 Ω (1 kΩ). How does this solve our problem?

Perhaps a little theory is in order here, but no more than is required by the Radio Amateurs' Examination.

When two *equal* resistors of value r are combined in parallel (i.e. side by side), the total resistance, R_T, is given by:

$$\frac{1}{R_T} = \frac{1}{r} + \frac{1}{r}.$$

Adding $1/r$ to $1/r$ gives $2/r$, therefore:

$$\frac{1}{R_T} = \frac{2}{r}, \quad \text{i.e. } R_T = r/2.$$

So, by connecting *two* equal resistors in parallel, we get a combined resistance which is *half* the individual resistances. If we combine *three* in parallel, we get a *third* of the resistance, and so on.

Here, we are connecting *20* resistors of 1 kΩ in parallel, so we will produce an overall resistance of *one-twentieth* of the individual resistance, i.e. 1000/20 = 50 Ω, which is what we set out to achieve!

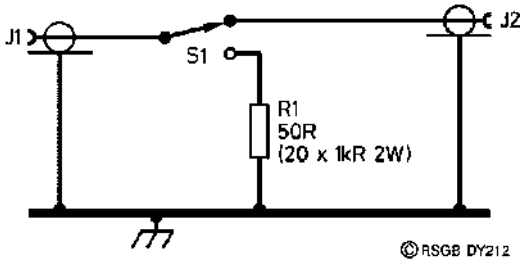

Figure 1 Basic circuit diagram

This is not the only advantage, though. Each resistor is capable of dissipating 2 W, so 20 of them will safely dissipate 40 W, for short periods at least. This power dissipation is approximately the same as 100 W PEP of normal speech, so the design should be capable of use in an 'average' amateur station. The power-handling ability of any dummy load can be improved by providing a 'heat sink' which helps to conduct the heat energy away from the resistors, thus lowering their temperature. One popular heat sink is a can of transformer oil, into which the resistors are immersed. This design uses a rather more mundane heat sink, but which is adequate for the job in hand.

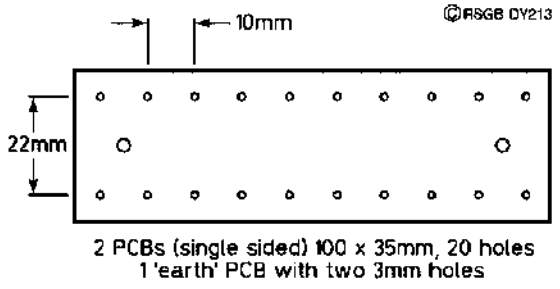

Figure 2 PCB resistor supports

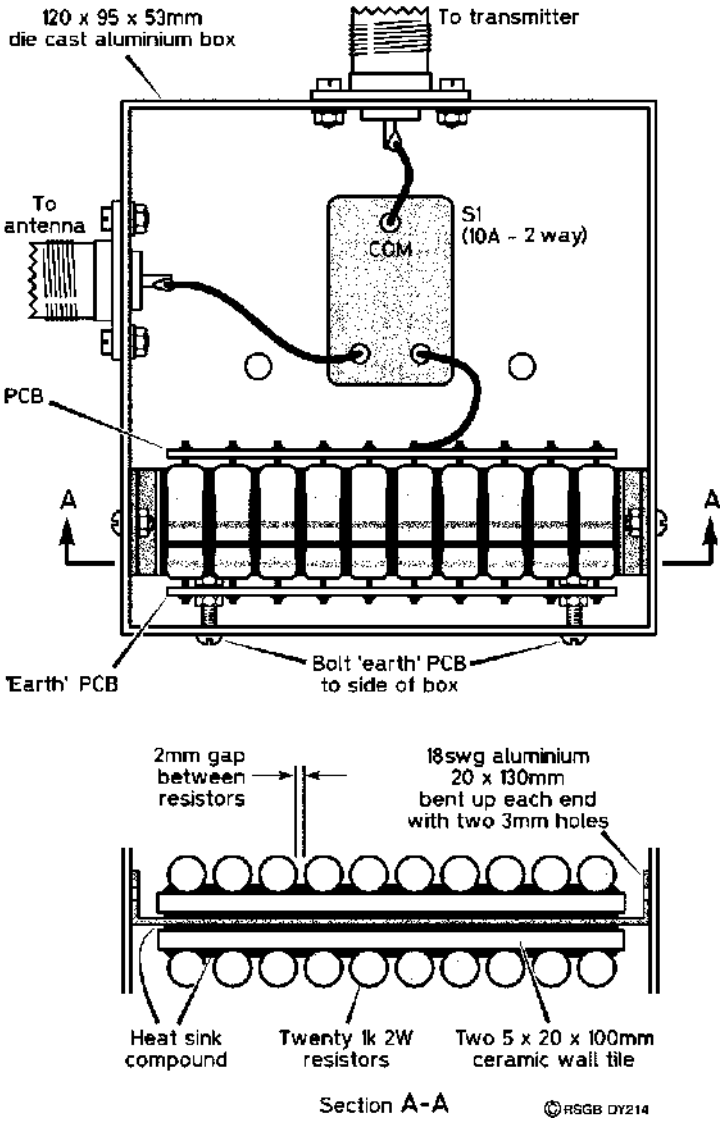

Figure 3 Switched dummy load, component layout

Pouring the heat away

Two basic PCBs are needed, the details being given in **Figure 2**. Both measure 11 × 35 mm. Each has a set of 20 holes of diameter about 1 mm to take the ends of the resistors. Only one of them has two 3 mm holes which are used for mounting the completed load. **Figure 3** shows how the heat sink is assembled. Solder one end of each resistor into the 'earth' PCB, and then mount this to the box using the two bolts as shown in the diagram. Between each rank of resistors is a 'sandwich' consisting of an aluminium strip and two pieces of ceramic wall tile, to act as a heat sink for the resistors. Heat sink compound is used to provide good thermal contact between the resistors and the tiles, and between the tiles and the aluminium strip. This is shown in the lower part of Figure 3. Thread the loose wires of the resistors through the holes in the second PCB, solder into place, and crop the protruding wires.

Switching

A changeover switch must be used so that the transceiver can be switched between the dummy load and the aerial without unscrewing connectors. For most purposes, an ordinary 10 A 230 V changeover switch will suffice, as found in many electrical shops and DIY stores.

Wire this into the circuit as shown in Figure 1 and Figure 3. Check your wiring. Put S1 in the 'dummy load' position. If you have a multimeter which includes an ohmmeter, measure the resistance across the socket, J1, before connecting it to the transceiver. It should be very near 50 Ω. With S1 in the 'aerial' position, there should be an infinite resistance across J1. Move your ohmmeter to read the resistance across J2. It should be infinite for both positions of S1. If all seems correct, close the box and your dummy load is ready for use!

Parts list

Resistors
- 1000 Ω (1 kΩ) 2 W carbon film, 20 required

Additional items
- 10 A 230 V changeover (SPDT) switch
- SO–239 sockets, 2 required
- Aluminium box 120 × 95 × 53 mm or similar
- Ceramic wall tile cut as required
- Aluminium strip, 18 SWG
- Nuts and bolts as required

68 A simple Morse oscillator

Introduction

This is an excellent project which uses the 'junk box' as its source of components. If you have trouble in finding the bits for this one, a good source of the components for this and many other similar projects is to be found with the parts list at the end of the project.

The circuit

This is shown in **Figure 1**, and uses an 'unknown' Plessey chip, which makes the overall circuit extremely easy to build. A 0.1 μF capacitor is connected between pins 7 and 8, a speaker (in the popular 8 to 25 Ω impedance range) is connected between pins 8 and 9. If a 9 V battery is connected with its positive terminal to pin 8 and its negative terminal to pin 1, 3 or 5, a tone will be produced in the speaker.

To make this circuit into a good Morse practice oscillator, it is necessary only to insert a Morse key into the supply rail from the battery.

However, there is another refinement which you may care to build into the circuit. The tone from the loudspeaker is different, depending upon which of pins 1, 3 or 5 you use. In the prototype, a single-pole changeover switch was used to select the tones from pin 1 or pin 3, and the Morse key would be connected to the circuit via a small jack socket. There is no need for an on/off switch, as the Morse key performs that function. The switch and the jack socket can be seen in the photograph.

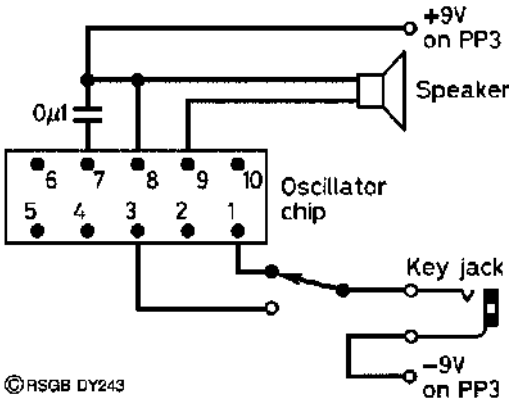

Figure 1 Morse oscillator, circuit diagram

The case

Almost any small loudspeaker will do; the higher the impedance the better. The 'impedance' is the figure usually printed on the rear of the speaker magnet. It is a value given in ohms (Ω). For simple circuits like this, you will usually find that the higher the impedance (within reason), the louder the sound it will produce. Speakers from old transistor radios will work, although their impedances can be rather low sometimes.

Any case big enough to house the components and the battery will be suitable. The prototype used a 'Walkman'-type speaker and case, and is shown in the photograph.

To use the circuit, simply attach a 3.5 mm jack plug to your Morse key, and insert it into the socket. Nothing should happen until you press the key, when a tone should be heard from the loudspeaker.

Another application

Try soldering the two wires of a 'twisted pair' to the 3.5 mm jack plug. Touching the wires together produces a tone from the speaker. This simple circuit can then be used as a 'continuity tester'. Touch the two wires to the ends of a fuse. If there is no sound, then the fuse is blown. There are many other such tests you could perform with this device – to check whether there really *is* a connection between one end of a wire and the other, for example.

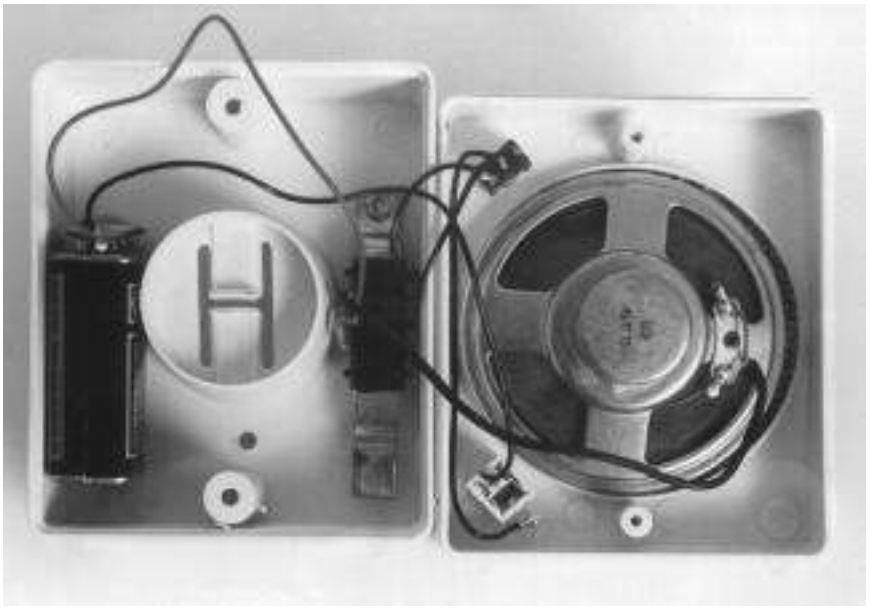

Warning

You must **never** make such tests on any equipment which is connected to the mains supply, even if it is switched off. If you want to make any such tests, make sure you are supervised by someone who understands what you are doing and is competent to advise and supervise you.

Parts list

Plessey oscillator chip
0.1 μF capacitor (disc ceramic)
Loudspeaker 8 to 25 Ω
3.5 mm jack socket (and 3.5 mm jack plug if needed)
Single-pole changeover switch

The Plessey oscillator chip is available from J. Birkett, 25 The Strait, Lincoln LN2 1JF, tel: 01522 520 767.

John Birkett may also provide a kit of parts (the chip, capacitor and loudspeaker).

69 A bipolar transistor tester

Introduction

This is a circuit which will test normal transistors, i.e. npn or pnp. It has the advantage of being able to test devices while they are still connected in their original circuits. However, when such tests are made, **the circuit containing the transistor under test must not be switched on**.

The circuit and how it works

The circuit runs from a 9 V battery such as a PP3 or six AA-type 1.5 V cells. Alkaline cells are to be preferred, as their electrolyte leakage properties are better. The circuit shown in **Figure 1** uses a single CMOS integrated circuit type 4001 or 4011. CMOS circuits require special handling precautions which are described in the project *Christmas Tree LEDs*, elsewhere in this book.

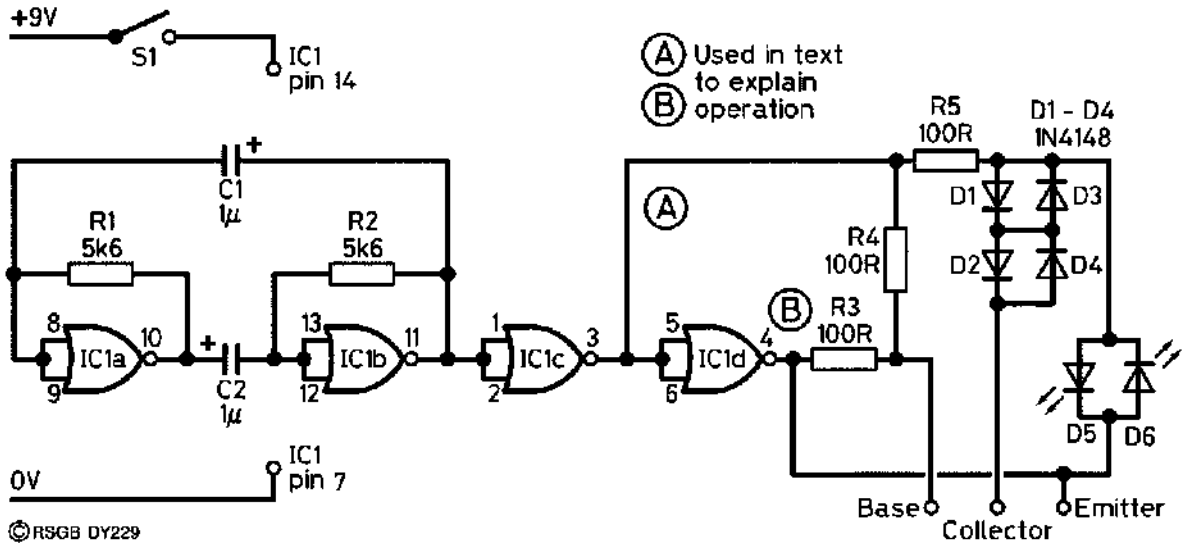

Figure 1 Transistor tester, circuit diagram

Inside the IC are four logic gates (see *Digital Logic Circuits*) which are all connected as inverters, which means that the output signal is always the logical 'opposite' of the input. The first two gates are connected as an oscillator; the circuit being the same as that used in *An Electronic Die*.

The output of the oscillator, at pin 11, is connected to the input of a buffer stage, IC1c, which helps to isolate the oscillator from the circuit that follows it. The buffer output appears on pin 3, which we shall label as *test point A* for future use. Another inverter, IC1d, follows this, its output at pin 4 being labelled *test point B*.

There are two LEDs connected back to back at the circuit output. These are D5 and D6, D5 being red and D6 being green. Whatever the output of the oscillator at any instant, one of the LEDs must be lit and the other unlit. With point A positive and point B zero, the red LED is lit, when A is zero and B is positive, the green LED is lit. Because the oscillator output is repeatedly switching from one polarity to the other, the lit LED is alternately red and green. They switch between the two colours much faster than we can see, so what we think we see are both LEDs lit together.

The two 100 ohm resistors, R3 and R4, provide the bias to the base of the transistor under test. When A is positive and B is zero, the base-emitter junction of the transistor will be forward-biased, and the transistor will switch on (if it is a working npn type). When the transistor is on, it effectively short-circuits D5 (the red LED) and it extinguishes. When point A is zero and B is positive, an npn transistor will be switched off and the

green LED (D6) will light. Thus, for a working npn transistor, only the green LED is lit.

If the transistor under test is a pnp type, it will switch on when A is zero and B positive, thus short-circuiting the red LED (D6). When A is positive and B zero, the transistor is off and the red LED (D5) is lit. Thus for a working pnp transistor, only the red LED is lit.

To summarise, the states of the LEDs indicate the following conditions:

- Both LEDs apparently lit: no transistor connected, or transistor permanently open circuit.
- Neither LED lit: a collector-emitter short-circuit is almost certain.
- Red LED alone: pnp transistor in working order.
- Green LED alone: npn transistor in working order.

Construction

The prototype tester was built on a piece of Veroboard measuring 15 strips by 18 holes. Cut the tracks using a track-cutting tool or a 3 mm (⅛ inch) twist drill, as shown in **Figure 2**. Notice that, in this diagram, there is no

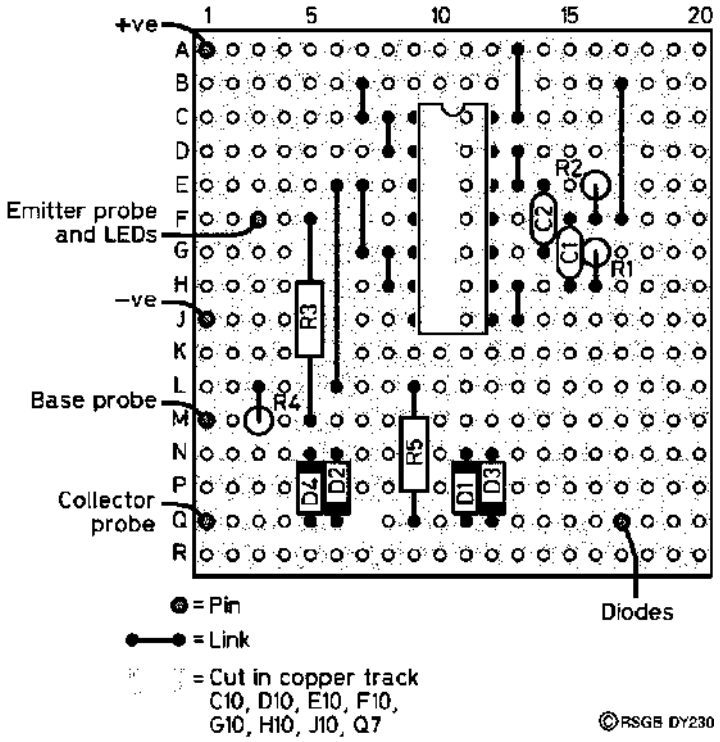

Figure 2 Transistor tester, component layout

track 'I', so try to avoid miscounting when you translate diagram positions to real positions on the board. Hold the board up to a strong light to ensure that there is no copper swarf shorting adjacent tracks together, and that you have made the cuts in the correct places.

Having done this, insert and solder Veropins for all the connections to be made to components not on the board itself. Then solder in the IC holder and the wire links. Then insert the other components in the order resistors, capacitors and diodes D1–D4. Some resistors are mounted vertically so that their connections are on adjacent tracks. Double check the diode polarities – it is easy to make a mistake when wiring diodes in anti-parallel! Next, connect up the off–board components, again making sure that the LEDs have the correct polarity. The probe leads for the emitter, base and collector should be made from different colours of wire and terminated in probe clips (small insulated crocodile clips).

Check carefully for dry joints and errant blobs of solder. Plug the IC into its holder, ensuring that it is inserted the right way round, as shown in Figure 2.

Testing

Without a transistor in circuit, and the battery connected, both LEDs should be lit. Connect a known good npn transistor and verify that the green LED lights. Now simulate two transistor faults: disconnect the base lead and both LEDs should light; remove the transistor and connect the emitter and collector leads together. Neither LED should light.

Repeat the tests with a known good pnp transistor. The results should be the same, except that the correct indication should now be a lit red LED. On your computer, make a small label of the bulleted list above, to fit on your tester showing the states of the LEDs and what they mean. It will act as a useful *aide mémoire* when you use the tester in future.

Using

The circuit will test transistors in isolation or in an existing circuit, i.e. prior to use. You can check the lead identifications in component catalogues such as the Maplin catalogue. The tester is ideal for going through the large bags of unmarked transistors that you can buy for a song at rallies. You can sort them into three piles – npn, pnp and dud!

Parts list

Resistors: all 0.25 watt, 10% tolerance or better

R1, R2	5600 ohms (Ω)
R3, R4, R5	100 ohms (Ω)

Capacitors

C1, C2	1 microfarad (μF) electrolytic, 16 V WKG

Semiconductors

D1–D4	1N4148 general-purpose silicon diodes
D5	Red LED
D6	Green LED

Integrated circuit

IC1	CMOS 4001 or 4011

Additional items

- Veroboard, 15 strips by 18 holes
- Veropins
- PP3 battery and connector (or 6 × AA cells in PP3 clip holder)
- Switch, SPST
- Connecting wire
- One each of known working npn and pnp transistors for test purposes.

Source

Components are available from Maplin.

70 The 'Yearling' 20 m receiver

Introduction

Published to celebrate the first anniversary of *D-i-Y Radio,* this excellent receiver design forms a suitable 'second receiver project' for those who have successfully completed the MW receivers earlier in this series. The receiver is powered from a PP3 battery or from a mains adaptor, and can be built with the help of an experienced constructor, on a prototype board. The circuit diagram and some of the components used are shown in the separate diagram. Headphones or a loudspeaker can be used and, once the radio is completed, a few simple adjustments will make the *Yearling* spring to life!

Building the receiver

Before starting the constructional process, start by identifying all the parts. One by one, tick them off against the parts list. Are their values correct? The varactor diode is a twin type (see circuit diagram overleaf), and must be cut *carefully* down the middle, producing two devices, D1 and D2, with two wires each.

First, solder the IC sockets, followed by the coils (inductors); L1 is pink inside the top, and L2 is yellow inside. Then, solder in the varactors; the lettering on D1 should be next to coil L1, and the lettering on D2 should face resistor R7. After those, the capacitors, wire links and resistors should be soldered to the board. Take care to wire the voltage regulator, IC3, correctly. Solder in the crystal X1 as quickly and deftly as you can – crystals do *not* take kindly to having their leads bent and being fried with a soldering iron! Make sure that the electrolytic capacitors C2, C12, C15 and C16 are fitted the right way round. Most electrolytic capacitors have only the negative lead marked.

Figure 1 shows the rear of the front panel, illustrating the connections from the board and antenna socket to the controls. All normal connecting wires are 22 SWG or thereabouts, with insulation. Their lengths should be about 15 cm, except for the battery lead to the switch, which is about 8 cm. It is recommended that you use different-coloured wire for each connection to a control. **Figure 2** shows this. The variable resistor section of VR5, the AF gain control, uses single screened cable connected to 0 V (ground) at the

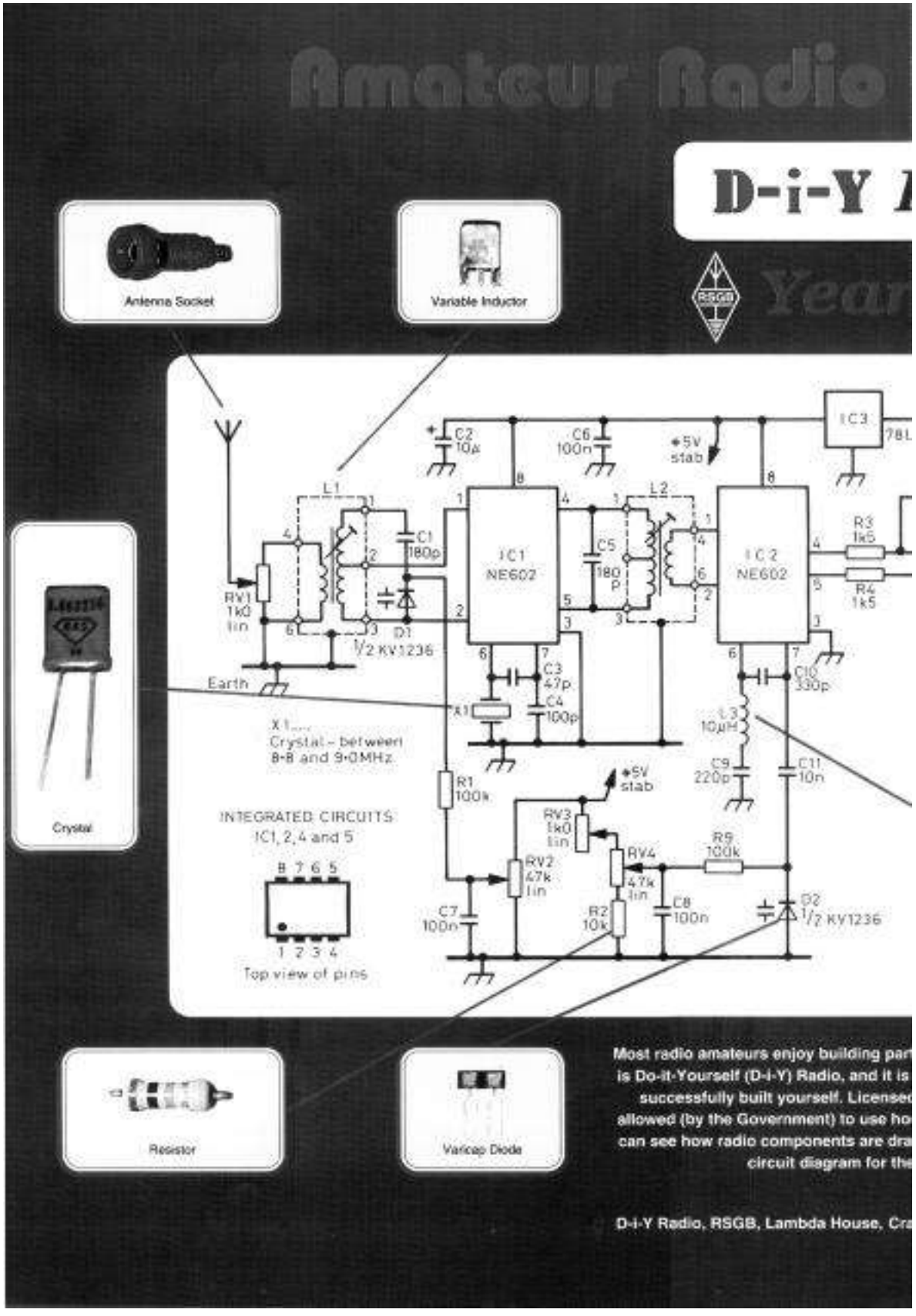
amateur radio
D-i-Y
Year
Antenna Socket
Variable Inductor
Crystal
Resistor
Varicap Diode
L1
L2
C1 180p
C2 10µ
C3 47p
C4 100p
C5 180p
C6 100n
C7 100n
C8 100n
C9 220p
C10 330p
C11 10n
RV1 1kΩ lin
RV2 47k lin
RV3 1kΩ lin
RV4 47k lin
R1 100k
R2 10k
R3 1k5
R4 1k5
R9 100k
D1 1/2 KV1236
D2 1/2 KV1236
IC1 NE602
IC2 NE602
IC3 78L
+5V stab
Earth
X1
L3 10µH
X1 — Crystal – between 8·8 and 9·0MHz
INTEGRATED CIRCUITS
IC1, 2, 4 and 5
8 7 6 5
1 2 3 4
Top view of pins
Most radio amateurs enjoy building part
is Do-it-Yourself (D-i-Y) Radio, and it is
successfully built yourself. Licensed
allowed (by the Government) to use ho
can see how radio components are dra
circuit diagram for the
D-i-Y Radio, RSGB, Lambda House, Cra

Do It Yourself

RADIO

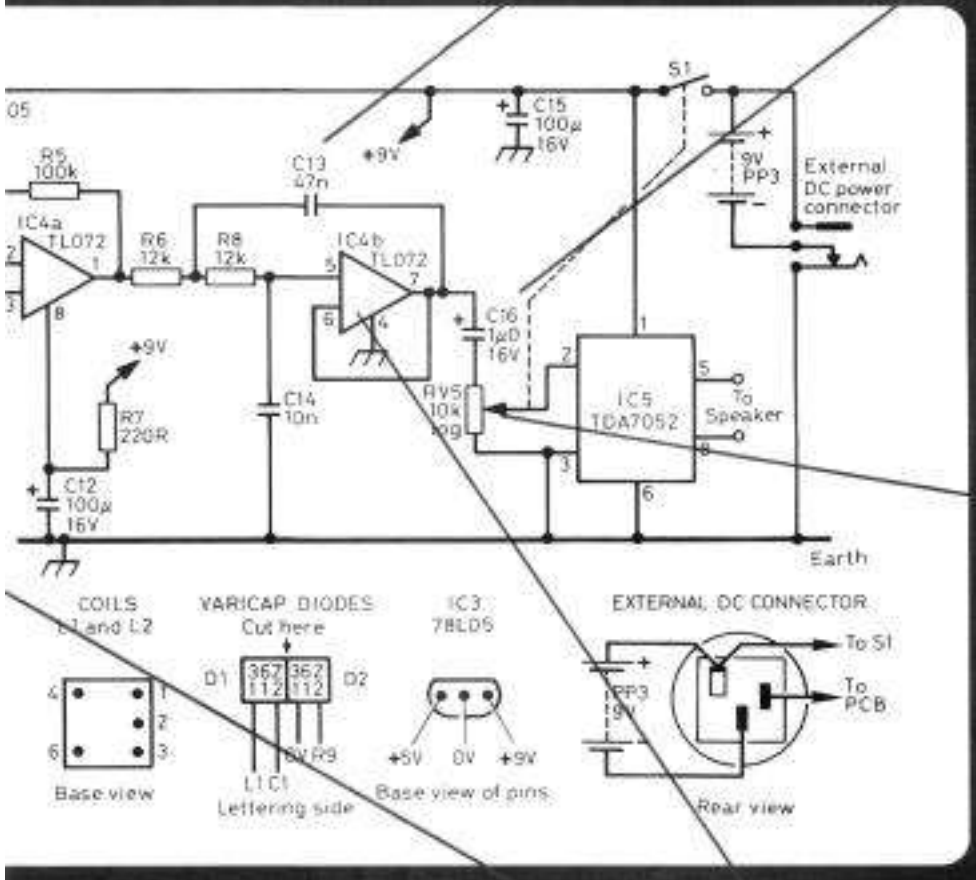

of their radio stations themselves, this very satisfying to use a radio you have radio amateurs are the only people me-built transmitters. On this page you wn on a circuit diagram. This is the full *D-i-Y Radio* Yearling.

nborne Road, Potters Bar, Herts. EN6 3JE

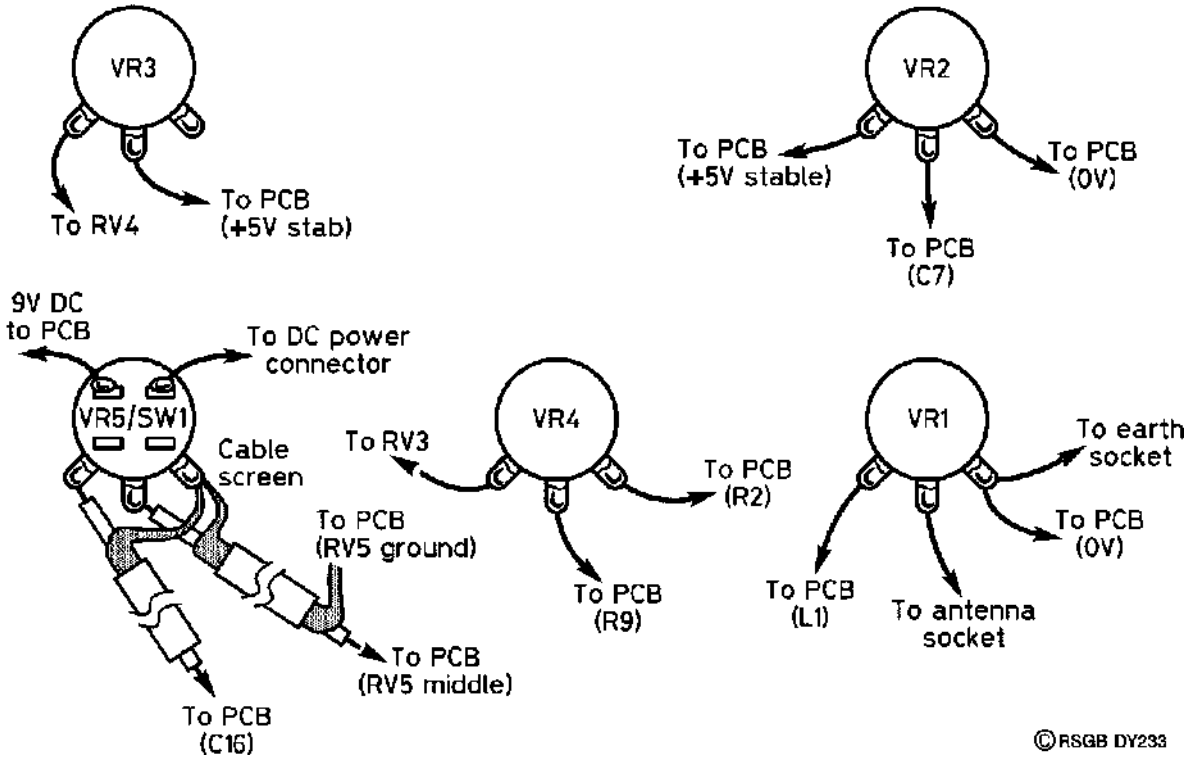

Figure 1 Rear view of the variable resistors. Check the connections carefully to make sure the wires fit the correct holes

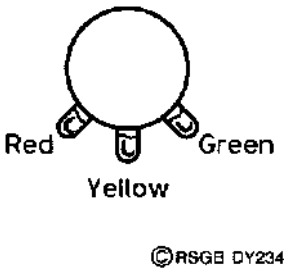

Figure 2 It is helpful to use different colour insulated connecting wires. Wires between each variable resistor and the board should be twisted together to give a neat wiring outfit.

board end. Now fit the ICs into their sockets. Make sure that they are the right way round (see circuit diagram) and that each pin lies directly above its corresponding socket before applying *gentle* pressure with the back of the board firmly supported.

Check that all the connections are correct (don't *assume* this – check the ends of each wire against the circuit diagram) and that all your soldered joints are shiny. Lastly, drill the five 10.5 mm diameter holes for the main controls. On the side of the case, a 6.3 mm diameter hole is needed for the speaker socket, and 8 mm holes for the antenna and earth sockets. The external power socket requires an 11 mm diameter hole.

Adjusting it

Before you can make adjustments, and in order to hear *anything* on your *Yearling*, you will need to connect an antenna (aerial) to the antenna socket. About 8 metres of wire, preferably outdoors and as high as possible, is all you need to connect to the socket. Connect the 3.5 mm jack socket for the speaker, and a 3.5 mm jack to your speaker leads. Connect a battery and switch on.

1. Using a very small screwdriver or, better still, a non-metallic 'trimming tool', *gently* screw in the core of L2 as far as it will go, but *don't force it*. Then unscrew it by three turns anticlockwise.
2. Set VR1, VR2 and VR4 to mid-position and rotate the core of L1 anticlockwise until the hissing noise you hear reaches a maximum intensity. Then adjust L2 for maximum noise.
3. If you now tune carefully with the main tuning control, VR4, you should hear some amateur Single-Sideband (SSB) speech signals. You may have to adjust the bandspread (fine tuning) control, VR3, to make the speech sound normal.
4. Having verified that everything is working, switch off and mount the controls on the front panel and the sockets on the side. To do this, it is much safer to disconnect all the controls and sockets, mount them in their final positions, and then wire them up again.
5. Fit the front panel knobs, connect your aerial and switch on again, checking that everything is working. Then, locate the cluster of CW (Morse) signals to be found at the bottom of the 20 metre band, set the bandspread control to mid-position and slacken off the main tuning knob. Turn the knob (but *not* the control!) until the pointer lies a little clockwise of 14.0 MHz. The SSB signals should now lie roughly between the dial centre and 14.35 MHz. Tighten up the knob.
6. Finally, fix the board to the rear panel, and secure the battery (if you are using one). Attach the rear panel to the back of the box, and you are finished!

Listening!

Make a habit of keeping the bandspread control in its centre position when searching for stations; then you can adjust it either way to make the signals readable. Unless you have a very big aerial, it is best to have the 'RF Gain' control, VR1, at maximum. Use the 'Antenna Tune' control, VR2, to give the best signal, and control the volume with the 'OFF/AF Gain' control. You will find some excellent DX stations with your *Yearling* receiver, and it will serve you well.

Parts list

Resistors (all 0.25 W, 5%)

R1, R5, R9	100 kilohms (kΩ)
R2	10 kilohms (kΩ)
R3, R4	1.5 kilohms (kΩ)
R6, R8	12 kilohms (kΩ)
R7	200 ohms (Ω)

Capacitors (all rated at 16 V or more, tolerance *at least* what is quoted)

C1, C5	180 picofarads (pF) polystyrene 5%
C2	10 microfarads (μF) electrolytic
C3	47 picofarads (pF) polystyrene 5%
C4	100 picofarads (pF) polystyrene 5%
C6, C7, C8	100 nanofarads (nF) or 0.1 microfarad (μF) ceramic
C9	220 picofarads (pF) polystyrene 2%
C10	330 picofarads (pF) polystyrene 2%
C11, C14	10 nanofarads (nF) or 0.01 microfarad (μF) ceramic
C12, C15	100 microfarads (μF) electrolytic
C13	47 nanofarads (nF) or 0.047 microfarad (μF) polyester, 5%
C16	1 microfarad (μF) electrolytic

Variable resistors

VR1, VR3	1 kilohm (kΩ) linear
VR2, VR4	47 kilohms (kΩ) linear
VR5	10 kilohms (kΩ) log with switch

Inductors

L1	Toko KANK3335R
L2	Toko KANK3334R
L3	10 microhenries (μH), 5%

Semiconductors

IC1, IC2	Philips/Signetics NE602 or NE602A
IC3	78L05 5 V 100 mA regulator
IC4	TL072 Dual Op-Amp
IC5	Philips TDA7052 audio amplifier

Additional items

D1, D2	Varactor diode Toko KV1236 (cut into two sections – see text)
X1	Crystal 8.86 MHz type (from Maplin, etc.)
4 off	8-pin DIL sockets for IC1, IC2, IC4 and IC5
2 off	4 mm sockets aerial (red) and earth (black)
1 off	3.5 mm chassis-mounting speaker jack socket
1 off	DC power socket for external supply (if required)
4 off	Red knobs with pointers
1 off	Tuning knob with pointer (e.g. 37 mm PK3 type)
1 off	Printed-circuit board or prototype board
1 off	Plastic case approx 170 × 110 × 6 mm (e.g. Tandy number 270-224)
1 off	Speaker 8–32 Ω impedance (or headphones)

71 Adding the 80 metre band to the Yearling receiver

Background

You will have noticed that your *Yearling* receiver has a dial which shows coverage of the 80-metre amateur band (3.5–3.8 MHz). This band is used for local contacts during the day, and contacts up to about 1600 miles in darkness. Longer distances are possible, particularly in the middle of winter.

The modifications

Only a few extra parts are required, as you may have noticed from the parts list. A low-pass filter, FL1 (one which passes low frequencies and rejects higher frequencies), is switched into the circuit on 80 m. The circuit of the

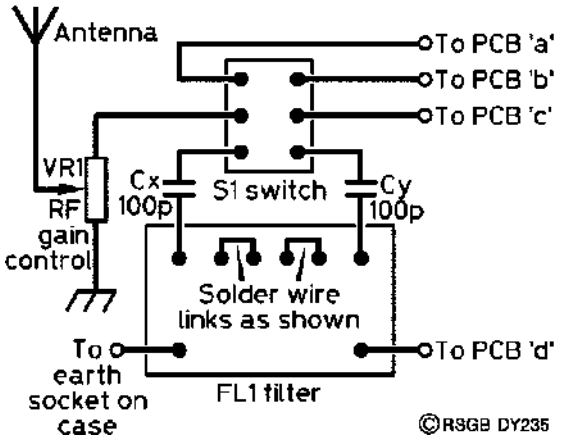

Figure 1 The circuit diagram shows the extra components for 80 m operation. Note the connections to the PCB 'a', 'b', 'c' and 'd'

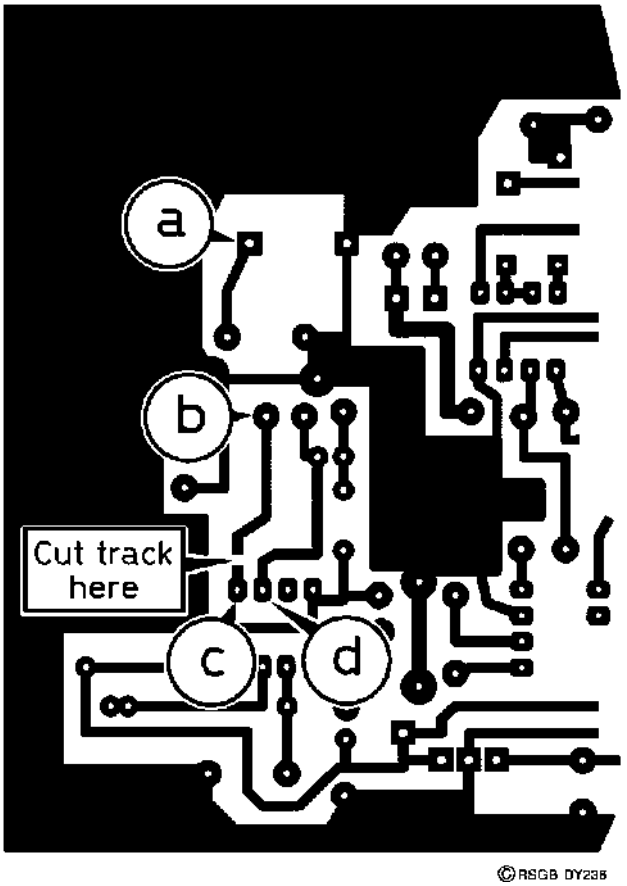

Figure 2 The underside of the PCB. Wires are connected from the switch and filter as shown

switch and its connections is shown in **Figure 1**. Before making the modifications, dismantle the receiver so that you have easy (and safe) access to the case and the track side of the PCB.

1. The first thing to do is to drill a 6.5 mm diameter hole in the side of the case into which the switch fits.
2. Then, using a sharp Stanley knife or scalpel, carefully cut the track on the PCB as shown in **Figure 2**, making a gap about 1 mm wide.
3. Using 10 cm lengths of different-coloured insulated wire, make the four connections, a, b, c and d, to the PCB, as shown in Figure 2.
4. Solder the two links on the filter, and then make the connections to the switch, capacitors and PCB. You will have to disconnect the existing wire between the RF gain control, VR1, and pin 4 of L1 on the PCB.
5. Lastly, check your new connections carefully, then mount the switch in the new hole and fix the filter to the bottom of the case with a little glue, as shown in **Figure 3**. Reassemble the circuit, and replace the back of the case.

More testing!

Firstly, switch your new switch, S1, into the 20 m position, to check that the original circuit still works! If you find that the 'Antenna Tune' control peaks at a slightly different position, don't worry.

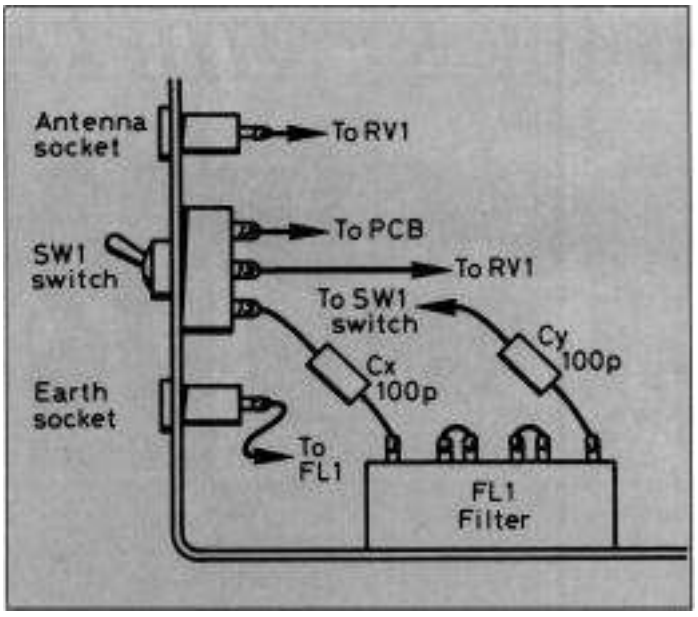

Figure 3 Internal view of the Yearling case. The filter FL1 is attached to the base with glue

Now switch to 80 m, and tune around the anticlockwise end of the dial; you should hear some SSB stations, particularly in the evenings and at weekends, when may people are on the air. At the other end of the travel of the tuning control, you should hear CW (Morse) stations.

The Radio Society of Great Britain broadcasts amateur radio news every Sunday morning on or about 3.65 MHz; the table below has the details. Finally, a good antenna is more important than ever for 80 metre reception – aim for more height and length, and then consider the project concerned with making an Antenna Tuning Unit (ATU)!

Parts list

Capacitors (all rated at 16 V or more, tolerance 10% or better)

Cx, Cy	100 picofarads (pF) polystyrene

Filter

FL1	Toko 237LVS1110 low-pass filter

Additional items

SW1	2-pole 2-way (changeover) toggle switch
7 off	Short lengths of insulated wire of different colours

The RSGB news broadcasts, GB2RS – Sunday mornings

Frequency (MHz)	*Local time*	*Reception area*
3.650	0900	SE England
3.650	0930	Midlands
3.650	1000	SW England
3.650	1100	Yorkshire
3.640	1130	Aberdeen
3.660	1130	Glasgow

The Midlands transmission is repeated at 1800 (6pm) local time on 3.650 MHz. All frequencies are approximate in order to avoid interference, and use lower sideband (LSB). If you also have a 40 metre receiver, there are GB2RS news broadcasts on 7.048 MHz at 0900 local time from Northern Ireland and from 1100 local time from the north midlands.

72 How the Yearling works

Introduction

The *Yearling* was designed to provide an introduction to *Amateur Radio* on the 20 m amateur band. Let's look at how the different sections (or 'stages') of a radio work, and how they fit together to form a complete receiver. **Figure 1** shows a block diagram which you can follow and compare with the circuit diagram of your *Yearling* receiver.

The antenna (or aerial)

Connected to your receiver, it will pick up not only amateur signals, but all other signals as well! This means that the receiver has to select the one signal that interests you, while rejecting all the others. The following stages do just that.

The RF filter

This stage (centred around L1) selects the band of radio frequencies (RF) containing the signal you want, in this case, those having wavelengths around 20 m. Signals from the 40 m band, for example, would not get through.

The crystal oscillator

This is an oscillator circuit designed around a quartz crystal (X1), and has a very stable frequency. It produces a single, very pure frequency to feed into the mixer. A crystal having a frequency between 8.800 MHz and 9.000 MHz is suitable for this circuit. The oscillator and mixer functions are both carried out inside IC1.

The first mixer

Yes, this stage 'mixes' two signals together. In this case, the two signals are (i) from the aerial via the RF Filter, and (ii) from the crystal oscillator. Two

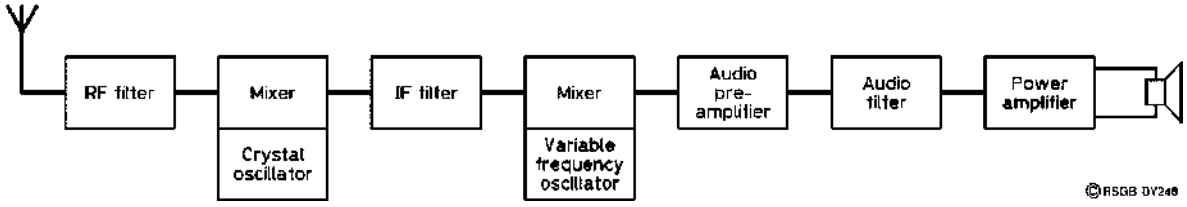

Figure 1 Block diagram of the Yearling, showing how the various stages fit together to make a complete radio receiver

bands of signals emerge from the mixer. The first is centred upon a frequency equal to the incoming signal frequency **added** to the crystal frequency, and the second is centred upon a frequency equal to the incoming signal frequency **subtracted** from the crystal frequency. Look at an example – if the signal is at 14 MHz and the oscillator at 9 MHz, then the mixer outputs will be 14 + 9 = 23 MHz and 14 – 9 = 5 MHz.

Intermediate frequency (IF) filter

It is the purpose of the IF filter (centred around L2) to select only one of these two bands of frequencies emerging from the mixer. In this case, it is the lower band of frequencies (around 5 MHz) which we select. This is because, in general, lower frequencies are easier to handle than higher ones.

Variable-frequency oscillator (VFO)

The VFO (part of IC2) enables us to tune into a particular station, and operates over a band of frequencies between 5 MHz and 5.35 MHz in this receiver. You will notice that IC1 and IC2 are the same type of chip, so that you will be expecting another mixer stage to be associated with the VFO. You are quite right!

The second mixer

This mixer obeys exactly the same rules as those of mixer 1. Sum and difference frequencies are produced, like this. Mixing is between the incoming IF signals (around 5 MHz) and the VFO signals (around 5 MHz), producing output frequency bands centred upon 10 MHz and 0 MHz. The use of the words 'band of frequencies' throughout this explanation is intentional. If all the signals were pure, there would be no bands; the bands are produced because of one thing – the modulation imposed on the pure

frequencies at the transmitter. So, the 'bands' contain the one thing that we want to extract from the signal, and that is the speech or Morse code that the signal contains. The band of frequencies at 0 MHz is just that – the audio frequencies we want in the loudspeaker. Because of this, the audio frequency output of the second mixer is selected and passed on for amplification.

The audio preamplifier

Preliminary amplification of the minute audio signal which emerges from the second mixer is provided by IC4a, which will respond only to audio signals, automatically rejecting the 10 MHz signal.

The audio filter

The bandwidth of normal speech when transmitted by an amateur station is around 3 kHz, so there is no advantage to be gained in amplifying frequencies greater than this. IC4b is known as a low-pass filter, because it passes (lets through) lower frequencies and rejects higher ones.

The power amplifier

IC5 produces the final audio amplification and provides enough power (about 350 milliwatts (mW) to drive a small speaker.

How does it work on 80 m?

If you have fitted the 80 m modification to your receiver, you are probably wondering how the circuit works at this different frequency. Firstly, the filter which you fitted selects the 80 m band instead of the 20 m band. The only other slight difference lies in the way the first mixer stage works. Its job is to produce sum and difference frequencies from the incoming signal and crystal frequencies. On 20 m, it did this by subtracting the crystal frequency (9 MHz) from the incoming frequency (14 MHz) to produce an IF output of 5 MHz. On 80 m, the incoming frequency (3.5 MHz) is subtracted from the crystal frequency (9 MHz) to produce an IF output of 5.5 MHz, which is still within the tuning range of the VFO in the next stage.

73 A field strength meter

Introduction

Having a reliable field strength meter is always useful. There are two basic types – the tuned variety (also known as an absorption wavemeter) and the broad-band variety. A project centred on the tuned variety can be found in this book (*An HF absorption wavemeter*), and the way it works is also presented (*The absorption wavemeter*). This project describes an untuned or broad-band type which is every bit as useful as the tuned type, when it is the level of RF in which you are principally interested.

With the possible exception of the meter, you may have all the parts needed in your junk box. The prototype was distinguished by its meter, found at a rally, and marked 'Safe', 'Dangerous' and 'Explosive' on its scale.

How it works

The basic field strength meter uses the circuit of a crystal set, but with a meter replacing the headphones. A better design, which is used here, is that of a voltage doubler, giving more sensitivity. **Figure 1** illustrates the voltage doubler circuit.

The AC input shown will be our RF input, which will be explained soon. Diode D1 will pass the positive half of the signal and use it to charge up C1 to the peak value of the signal. D2 uses the negative half of the signal to charge up C2 to the same value. Because C1 and C2 are in series, the peak voltage appearing across *both* of them (which is the DC output voltage) is equal to *twice* the peak input voltage, hence the name voltage doubler. If you're wondering why DC is present at the output when AC comes in at the

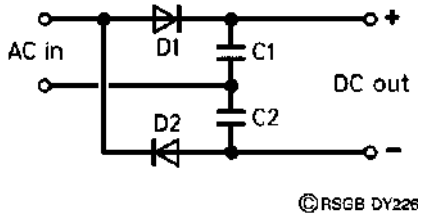

Figure 1 Voltage doubler circuit

input, remember that capacitors pass AC (RF) but block DC; thus the RF is shorted out through C1 and C2, but the steady voltage (DC) remains across the two capacitors. The voltage is thus proportional to the size of the RF signal applied at the input.

The circuit

The voltage doubler is converted into a field strength meter using the circuit of **Figure 2**. A piece of wire serves as the aerial to provide an RF signal across the radio-frequency choke (RFC). A choke is an inductor which is large enough to prevent the RF passing through it – it 'chokes' the RF. This produces the maximum RF signal at the input to the voltage doubler, and the DC output from it is measured on the meter.

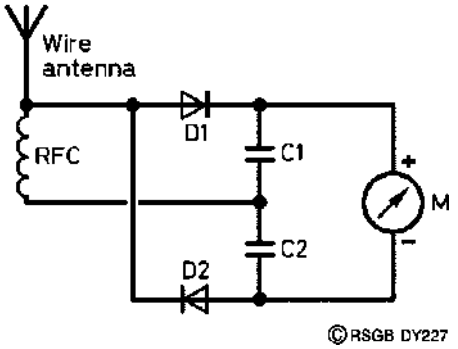

Figure 2 Field strength meter

The parts used are not very critical. The RF choke can have any value between about 1 mH and 2.5 mH. Almost any common diode such as the 1N914 or 1N4148 can be used for D1 and D2. The two capacitors could be any value between 1 nF and 100 nF (0.001 μF and 0.1 μF). The meter should be reasonably sensitive, with a full-scale deflection (FSD) in the range 50 μA to 100 μA. Look for VU meters at rallies – these are ideal.

Construction

The prototype circuit was made on matrix board. If you don't want to use pins with the board, simply push the component leads through the holes and make the connections on the underside of the board, either with the excess component leads themselves, or with ordinary connecting wire.

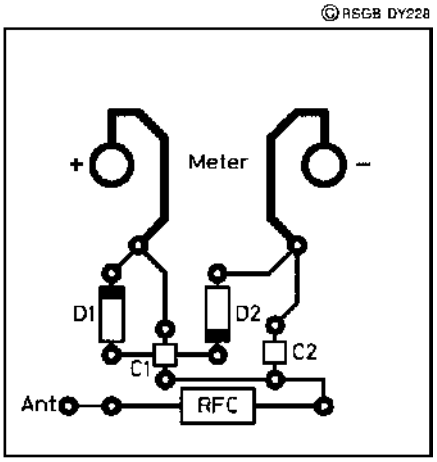

Figure 3 Board layout and interconnections

Figure 3 shows how the parts are placed and connected. The matrix board can be mounted directly on the meter using its terminal bolts!

In use

Needing no power supply other than an RF signal, just connect it all up and leave it to work! A short length of insulated wire is enough to pick up some RF and display it on the meter. Using a 200 μA meter, about 3 metres of wire gave a good deflection on the meter. To increase deflection, the wire can be wrapped around the aerial lead, provided that the wire is PVC covered and doesn't come into contact with the aerial wire.

This requires a little experimentation. Try a long piece of wire first and adjust its position until the meter needle kicks whenever there is a transmission. It is very reassuring to see the meter moving during a transmission. Although SWR meters also indicate power, they are usually set to read reverse power, and show little or no movement during transmission.

Parts list

D1, D2	1N914, 1N4148 or similar
C1, C2	10 nF disc ceramic
RFC	Miniature axial choke (1 mH)
Meter	Surplus VU meter or similar
Matrix board or similar	

Components are available from Maplin.

74 Preselector for a short-wave receiver

Introduction

A preselector is a simple RF tuned amplifier which is inserted between the aerial and the receiver. It provides some extra gain and may improve the overall performance of the receiver. This project uses a Field-Effect Transistor (FET) amplifier in grounded-gate mode.

The design has a tuned circuit at both the input and output which, with excessive gain and poor construction, would produce only one thing – oscillation! So, to avoid this happening, we will have only a low gain, and use a circuit which provides good isolation between input and output. The grounded-gate FET amplifier fulfils both these criteria. It will also cover a frequency range from about 7 to 30 MHz, which includes most of the HF amateur bands.

The circuit

This is shown in **Figure 1**. The signal from the aerial arrives at an RF transformer, the secondary of which is tuned with capacitor VC1a. The output from the tuned circuit is taken from a tap on the secondary to the source of the FET. The gate is grounded (earthed) and the amplified signal appears at the FET drain, which is then fed to the primary of another RF transformer, which is tuned by VC1b. The output to the receiver comes from the secondary of the RF transformer.

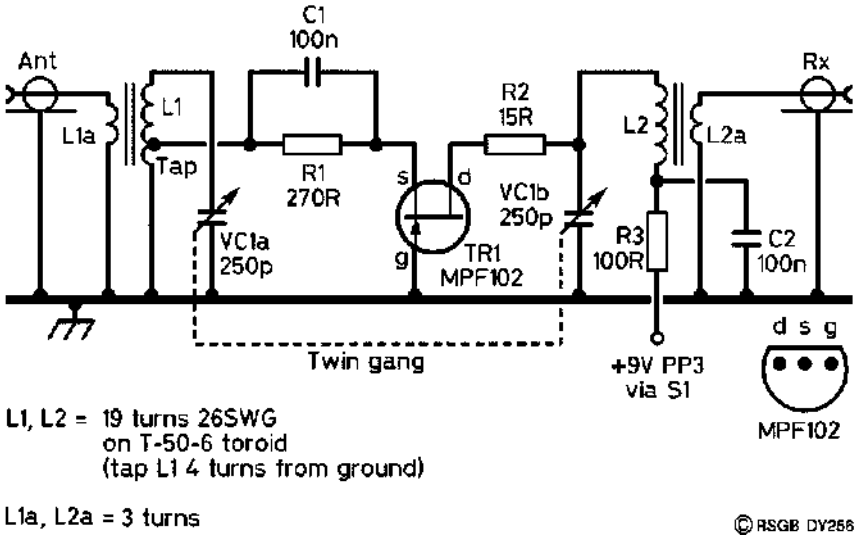

Figure 1 HF preselector, circuit diagram

Notice that the two RF transformers are identical, but they are used 'back to back', with the secondary of the first and the primary of the second being tuned. They are tuned with identical capacitors, fitted on the same shaft of a variable capacitor. We say that the two capacitors are 'ganged'. Because L1 and L2 are the same, and VC1a and VC1b are the same, both RF transformers should be resonant at the same frequency, no matter what that frequency is.

Construction

The final layout should look something like that shown in **Figure 2**. The external connectors and controls being two SO-239 sockets for connection to your receiver and aerial, a tuning control and its associated scale, and an on/off switch.

The circuit can be put together on a plain matrix board, using pins to anchor the components, or simply by pushing the component leads through the board and making connections on the underside. The layout of the prototype is shown in **Figure 3**. Mounting the board to the aluminium box is accomplished with bolts, solder tags and stand-off insulators.

Check your construction against the circuit diagram and against the layout diagram. Wire in the PP3 battery clip, put the switch in the 'off' position, and fit the battery. Testing can be carried out without fitting the top of the box.

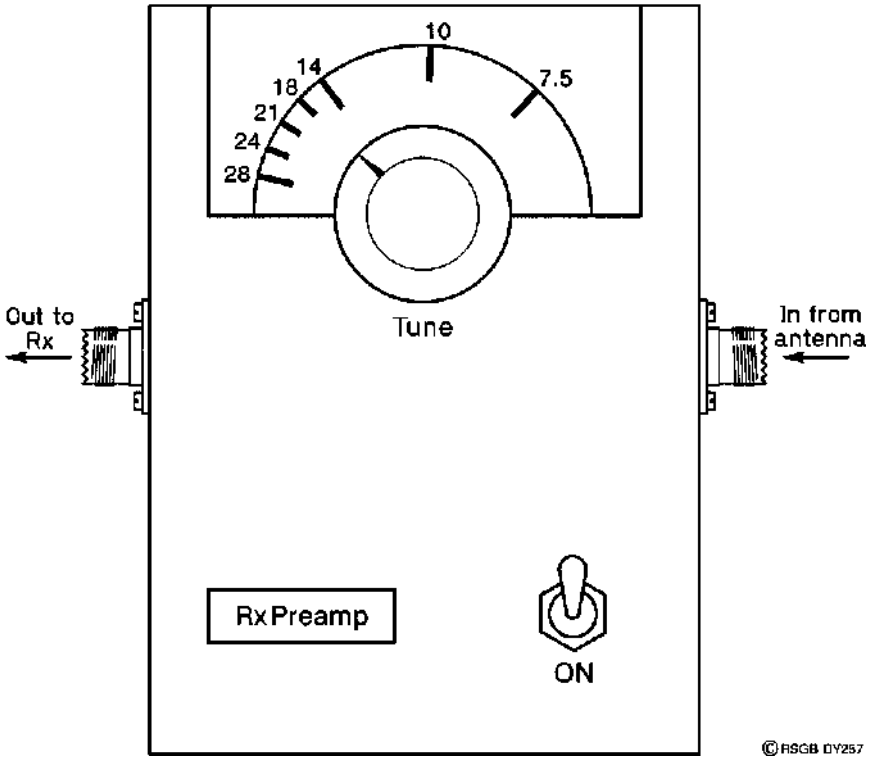

Figure 2 HF preselector, front panel layout

Testing

Don't fit your preselector yet. Tune your radio to a broadcast station, preferably a fairly weak one. Disconnect the aerial and fit your preselector between the aerial and receiver. Switch it on and rotate the tuning knob slowly. You should find a position where your original station is received more clearly than before. If it doesn't work at all, recheck your wiring. Is there a positive voltage on the drain of the FET? If not, work back towards the positive battery terminal. Is there a voltage at the junction of L2 and R2? Is there a voltage at the junction of L2 and R3? Is there a voltage at the junction of R3 and the battery lead? If there isn't a voltage at that point, then you have probably mounted your switch upside down, and it is off, not on! It's a common mistake.

Calibration

This is not obligatory, surprisingly enough. However, if having a frequency scale appeals to you, then using an RF signal generator (or using the services of a friend who has one) is the simplest solution. Feed in a weak modulated

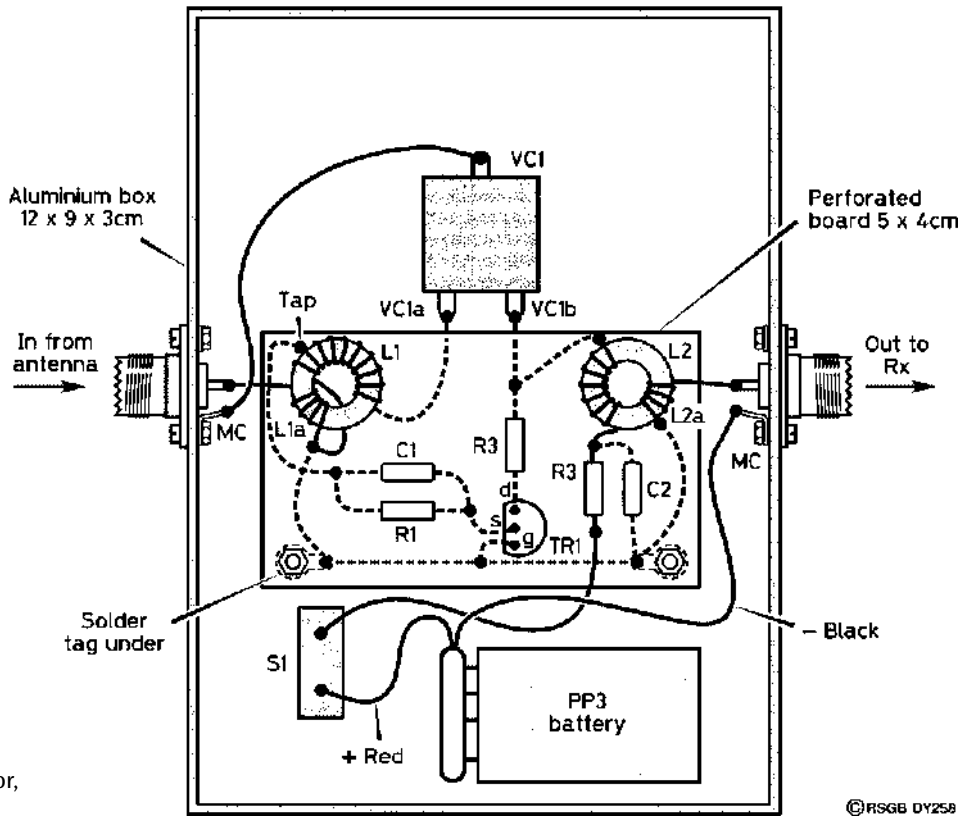

Figure 3 HF preselector, component layout

signal from the generator to the preselector, and rotate VC1 until the signal is maximum. Mark this frequency on your dial. Repeat the process for the frequencies shown on the dial in Figure 2.

If you have a commercial transceiver, feed its output into a dummy load (such as the type described in *A Switched Dummy Load*, elsewhere in this book) using a distinctive modulating signal such as an idling RTTY signal. Set the receiver to the same frequency with the preselector out of circuit. Insert it into the aerial lead, and search for the signal with VC1 until it gives the maximum deflection on your S-meter, then mark the frequency on your dial.

Parts list

Resistors: all 0.25 W carbon film or better

R1	270 Ω
R2	15 Ω
R3	100 Ω

Capacitors

C1, C2	100 nF (0.1 μF) ceramic
VC1	250/250 pF polyvaricon

Inductors

L1, L2	19 turns 26 SWG enamelled copper on T.50.6 toroid L1 has a tap 4 turns from ground end L1a and L2a – 3 turns wound over previous winding

Semiconductors

TR1	MPF102 FET

Additional items

Matrix board	To fit aluminium box (see Figure 3)
Aluminium box	12 × 9 × 3 cm
Battery and connector	PP3 9 V
S1	SPST on/off switch
Knob	As required
SO239	Sockets – 2 required

75 An audible continuity tester

Introduction

This is not the only continuity tester in this book. This alone attests to their use, so you may well want to experiment with several designs, then come up with one of your own! The very simplest form of continuity tester is probably a battery and a bulb in series, with the circuit being closed by connecting it to a fuse or other object being tested for continuity. The bulb could be replaced by a buzzer to give an audible indication. The current taken by the buzzer could damage some components, however. An ohmmeter can also be used, and is very popular for the purpose, as it indicates whether the circuit is low, medium or high resistance. This project has the advantages of indicating whether there is no continuity, some resistance or good continuity, and making an audible sound, so that you don't have to move your eyes from the circuit while making the test.

The circuit

Using only one integrated circuit, four components and a battery, this is a particularly simple circuit, as **Figure 1** shows. IC1 is usually used to flash an LED from a 1.5 V source, and to have a low current consumption. By changing the component values, IC1 is made to oscillate at audio frequencies, and we can hear these through the loudspeaker, LS1. Low-impedance speakers can be used, but result in an increased current drain, so the higher the impedance, the better.

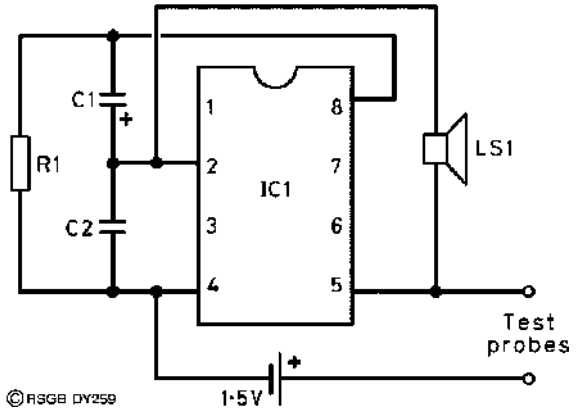

Figure 1 Continuity tester, circuit diagram

Construction

The layout of the circuit on Veroboard measuring 7 strips by 15 holes is shown in **Figure 2**. Start by making the four track cuts which will lie underneath the IC. Use a track cutter or a 3 mm (⅛ inch) twist drill rotated between thumb and forefinger for this. Solder the Veropins in place, followed by the wire link. Then solder in the IC holder, the resistor and the capacitors, making sure that the electrolytic capacitor, C1, is connected the correct way round.

Check, with the board against a bright light, that there are no shorted tracks, either by large blobs of solder or by copper swarf from the track-cutting process. Then insert IC1 into its holder the right way round. The probes can be ordinary connecting wire, the free ends being tinned with solder to prevent wire whiskers from touching components other than the one you are testing.

If you are happy that the circuit and the wiring appear to be correct, fit the battery into its clip. Nothing should happen until the probes are touched together, when you should hear a note from the loudspeaker. If nothing happens, all you can do is to recheck your circuit, as there is nothing else to go wrong!

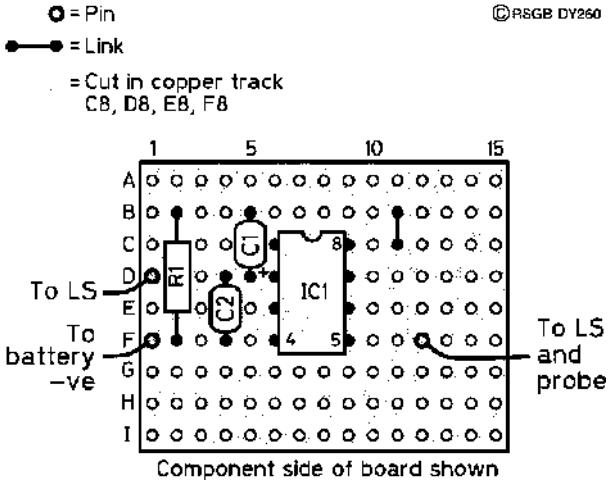

Figure 2 Continuity tester, component layout

Any box can be used; there is no justification for a metal case, unless you want to make use of something, which is to hand, such as a tobacco tin. Alternatively, any suitable plastic box will do.

Use

The tester will give different pitch notes for resistances of different values. The higher the resistance, the higher the pitch from the speaker. Try it with small inductors, and you will learn to recognise the different tones produced by the IC.

Safety notice

Using the continuity tester on components *in situ* is not advisable, as the results could be misleading. It can be dangerous to make measurements *in situ* on equipment, which is operating. If you must make such tests, always disconnect the equipment form its power source first.

Parts list

Resistor
R1 1000 Ω (1 kΩ), 0.25 W carbon, 10% or better

Capacitors
C1 10 μF electrolytic, 16 V
C2 0.1 μF subminiature polyester or ceramic

Integrated circuits
IC1 LM3909N

Additional items
Veroboard 7 strips by 15 holes
LS1 64 Ω miniature loudspeaker
IC holder
Veropins
Connecting wire
Test leads
1.5 V AA alkaline battery

76 An experimental 70 cm rhombic aerial

Introduction

Most commonly used aerials can be classed as *resonant* or *standing-wave* aerials. There is another class known as *non-resonant* or *travelling-wave*. Resonant aerials, such as the dipole, are narrow-band; this occurs because resonance occurs only over a narrow band of frequencies. Travelling-wave aerials, on the other hand, can operate over a wide band of frequencies.

The *rhombic* is an example of a non-resonant or travelling-wave aerial. It is often employed for fixed commercial and military short-wave radio links. Made with wire, it has a diamond shape when looking down on it from above. The four corners are supported on four masts. It is a very effective aerial, and has good gain, a quality which can be judged from the *polar diagram* shown in **Figure 1**. This has been obtained from a computer program, and so is the perfect shape for a rhombic aerial.

Theory (but only a little)

A polar diagram shows graphically the ability of an aerial to radiate (or receive) more effectively in one direction at the expensive of the radiation in other directions. Figure 1 shows the polar diagrams of two aerials, a simple 70 cm dipole and the rhombic described in this project. The dipole has the

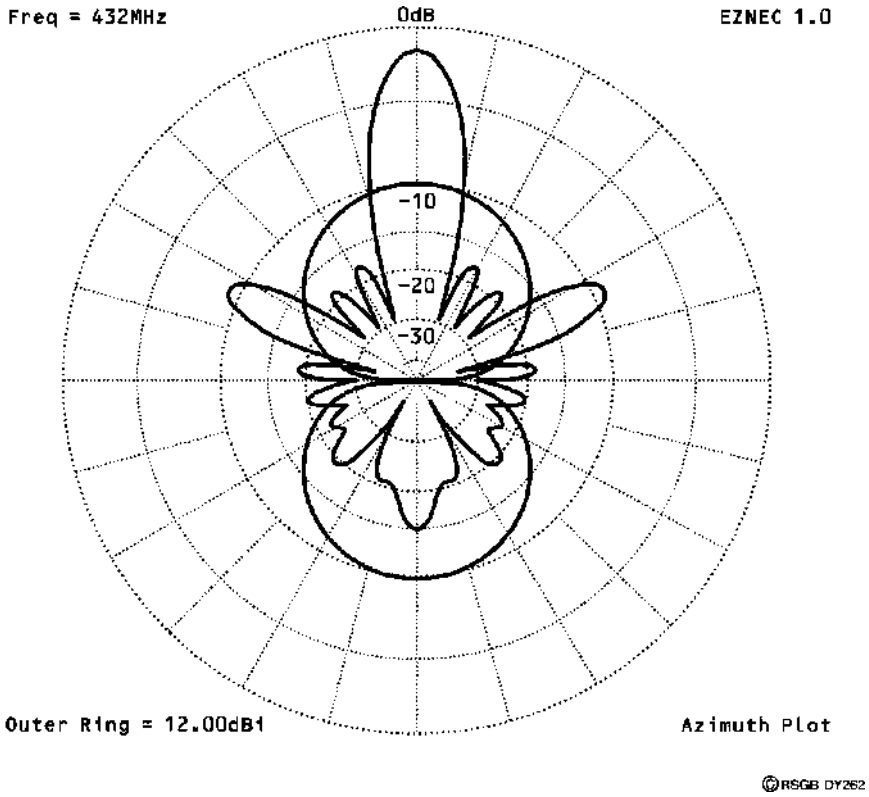

Figure 1 The horizontal polar diagrams of the small rhombic antenna and a dipole compared

well-known figure-of-eight shape, showing a symmetrical angular behaviour about the direction of the aerial and about a direction perpendicular to the aerial. That of the rhombic, on the other hand, is quite irregular by comparison, but is still symmetrical about one axis only, not two. It's this asymmetry that gives the rhombic its gain, by virtue of its *front-to-back ratio*. This is the ratio of the power radiated forwards to that being radiated backwards. Notice the large *lobe* (lump) at the top of the polar diagram; this is the direction in which the aerial transmits best. The lobe in the opposite direction has been reduced significantly, allowing more power to be directed forwards, not backwards

Problems

The rhombic is not found in every amateur's back garden, despite its attractions. To work best each edge of the diamond shape should be about two wavelengths long. Hence, a rhombic for the 20 metre band could be about 80 m from tip to tip! Another disadvantage is that, because of its size, it cannot be rotated.

It will operate well over a range of frequencies. An HF rhombic could work on the 7, 10, 14, 18, 21 and 28 MHz bands. One for the lower VHF frequencies could operate on the 50, 70 and 144 MHz bands.

Its large size is less of a problem at UHF. A portable rhombic can be made for 70 cm which can be used with a hand-held transceiver. The aerial design to be described here will give a gain of up to 9 dB relative to a dipole. This is written as 9 dBd, the second 'd' meaning 'relative to a dipole'. This is equivalent to improving your signal by 1.5 S-points at the receiver or (and you may be surprised by this) by fitting a linear amplifier to your transceiver that would take 5 W input and produce 40 W output to a normal dipole! Consider the relative costs of the two approaches to producing the same received signal. You will also receive everyone else's signals 1.5 S-points better than before!

Unlike the popular Yagi aerial, this design has no critical dimensions and can be folded up for transport by car or bicycle. It has a fairly high input (or feed) impedance, being fed usually by balanced twin feeder. To feed it with standard 50 Ω coaxial cable, a matching transformer in the form of a *balun* is required. A balun will convert the *bal*anced (symmetrical) aerial impedance to the *un*balanced and lower impedance of the coaxial cable. The details of how to build the balun, which in this case is a half-wave transformer, are included in the constructional details.

Construction

The aerial frame is made up of 1 cm × 2 cm strips of wood fixed to a plywood centre using 30 mm long M4 bolts, as shown in **Figure 2a**. The outer bolts fixing the front and side supports can be removed for folding prior to transportation, as shown in **Figure 2b**.

The wires are fixed to the front and rear supports using screw connectors, sometimes called 'chocolate block' connectors. Detail X and Y of Figure 2 show how this is done. The side supports have holes in the ends through which the wire is threaded.

The aerial must be mounted in the horizontal plane using a small shelf bracket attached to the centre plate, using the same bolts that hold the rear support. The other half of the bracket may be mounted to a vertical mast using screws or jubilee clips (hose clips).

The balun

Cut a 23 cm length of coaxial cable; this is to be our half-wave transformer. Cut and remove 2 cm from each end of the sheath. Make the braid into a pigtail at each end. Cut and remove 1 cm of the inner insulator from each

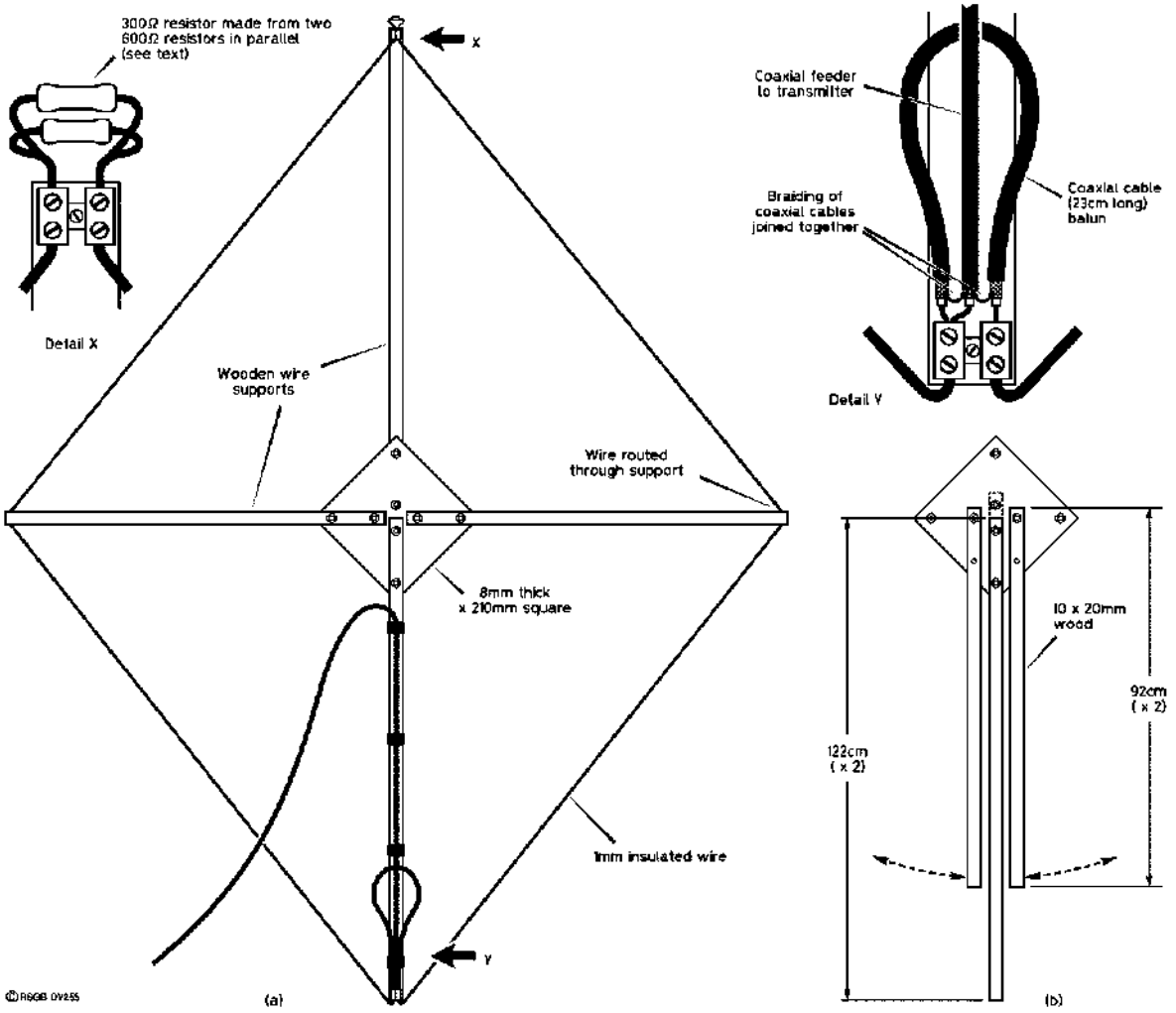

Figure 2 Construction of the UHF rhombic antenna

end, leaving 1 cm of the centre conductor exposed. Fasten this piece of cable to the chocolate block connector together with the coaxial feeder cable as shown in Detail Y of Figure 2. The braids of all three prepared ends are soldered together, but are not connected to anything else. The inner conductor of the feeder from the transceiver is soldered to one end of the centre conductor of the 23 cm piece, and is connected to one end of the rhombic by one side of the chocolate block. The other end of the half-wave transformer also goes to the chocolate block, where it is connected to the other side of the rhombic loop.

The opposite corner of the rhombic, as shown in Detail X of Figure 2, shows that the loop is broken at the chocolate block, and is 'terminated' by two 600 Ω resistors in parallel. This makes the aerial a broad-band travelling-wave device, and gives it its directivity and gain. There is a rule of thumb, which includes a safety factor, which says that the terminating resistor must be able to absorb one-half of the maximum transmitter output power. So, if you use two 2 W 600 Ω carbon resistors (*not* wire-wound resistors) in parallel, you can use a transmitter with an output of 8 W, which is more than adequate for 70 cm hand-helds.

Using the rhombic

Fit the aerial to a pole or mast in the horizontal plane, if you intend to use CW or SSB, but in the vertical plane if you want to concentrate on FM work. In the latter case, a wood or fibreglass pole is mandatory. Tune to a local repeater, whose signal strength you know. Rotate the aerial to face the repeater, and you should see that the signal strength is greatly improved! Verify the directional properties of the aerial by rotating it and observing the changes in signal strength on your S-meter.

77 Water level alarm

Introduction

This is a simple device which, when you have built it, you begin to wonder how you ever managed without it! It will sound a buzzer when the level of water reaches a particular point, which you can set and vary at will.

Detecting water

Water is not too difficult to detect electrically, because it is a conductor of electricity. Not a good one, but sufficiently so to carry enough current to control a warning circuit.

The circuit is shown in **Figure 1**. If you imagine a resistor placed between the ends marked 'water detector', the circuit is then recognisable as a transistor used as an electronic switch. Whether the switch is off or on depends on the value of this resistor. If the resistance is low, the transistor switches on and the buzzer sounds. If the resistance is high, the transistor switches off and the buzzer stops.

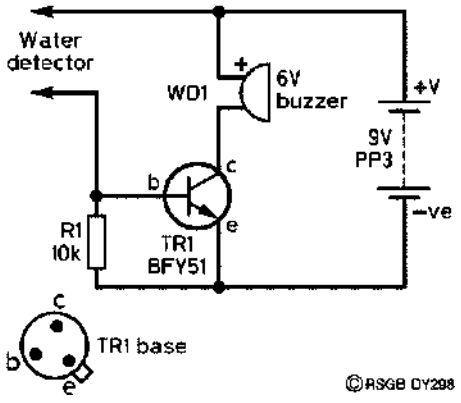

Figure 1 Circuit diagram of the water level detector

Construction

The unit is made in two separate sections – the detector board (**Figure 2**) and the main board (**Figure 3**). The main board is plain perforated board (without copper strips). The components are pushed through holes in the main board and connected together on the underside. The battery is held on with sticky tape. No on/off switch is used, as the circuit consumes virtually no current when it is not sounding the buzzer.

Unlike some buzzers, this type is polarised, and the red lead must go to the supply as shown in Figs 1 and 3.

The detector board is a piece of standard matrix board – the type with copper strips along one side. It measures 9 strips by 15 holes, and is wired in such a way that alternate strips are connected together, as Figure 2 shows. This gives a greater surface area for the water to touch, thus increasing the sensitivity of detection.

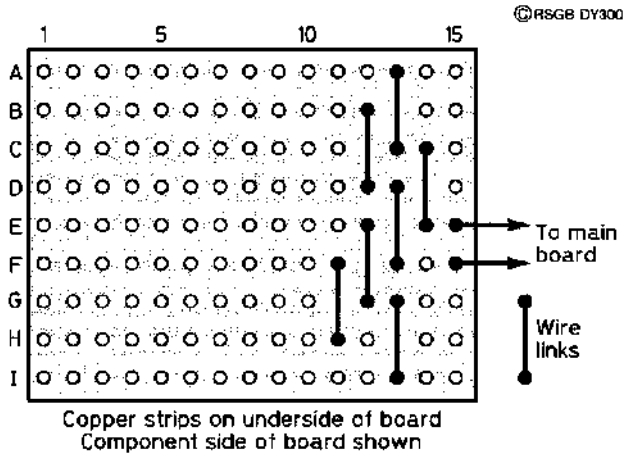

Figure 2 Layout of the main board

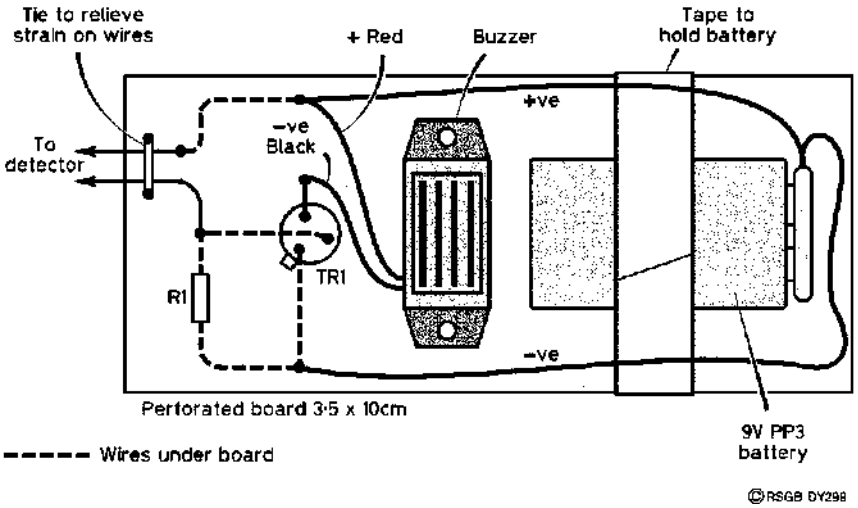

Figure 3 Water detector constructed from stripboard

The two boards are connected by ordinary twisted pair, enabling the detector to hang over the edge of the water container, with the buzzer circuit safely out of the way. When positioning the detector board, the left-hand edge (as shown in Figure 2) should face downwards, with the connecting-wire edge facing upwards. When the water level rises, the water causes current to flow between adjacent strips, and the higher the water, the lower the resistance between them. Eventually, the resistance will be low enough to turn on the transistor and sound the alarm.

Parts list

Resistor

R1	10 000 Ω (10 kΩ), 0.25 W

Semiconductor

TR1	BFY51

Additional items

WD1	6 V miniature buzzer (polarised)
	Battery PP3
	Battery connector
	Strip board 9 strips by 15 holes
	Perforated board 3.5 × 10 cm

78 A delta loop for 20 metres

Introduction

HF aerials take up a lot of room when they are straight. Space can be saved by bending them and, at the same time, giving them properties which are quite different from their original linear forms. The delta loops shown in the accompanying diagrams have the shape of the Greek upper-case letter delta (Δ) upside down. It can be upright, except that it is more practical to have the feed point at the bottom than at the top.

Putting the loop together

This is the design for a loop to be used on the 20 metre band. It is a very popular band and carries most of the amateur radio DX traffic. The aerial is light in weight and operates best if the top section is at least 30 ft above the ground, with the feeder point being about 6 ft above ground. All you need is some good wire, some polypropylene rope, some insulators and a method of matching the output of this 75 Ω balanced aerial to the 50 Ω unbalanced coaxial input of your transceiver or receiver.

Each of the three sides must be 7.2 m long. Using tent pegs or six-inch nails, mark out the three corners on the lawn, making sure that each pair of pegs or nails is exactly 7.2 m apart. Put the wire around the nails, together with two insulators on the wire for the two top corners. These insulators can be of the 'dog bone' variety, or of the home-made type, using a piece of flat plastic with holes in each end. The use of these is shown in **Figure 1**. Located at the positions of two of the tent pegs or nails, they must be secured at those points by any convenient means.

Now attach a support rope to the free end of each of the insulators, ready for suspension, as shown in the diagrams, from any convenient supports (house, tower, tree, etc.). The top section of the loop could be taped to a continuous piece of rope between the two supports. You might like to try this if you think it is easier. Then, when you find some dog-bone insulators, you can change the design and see if there is any noticeable change of performance.

Connecting to the radio

If you are the proud possessor of an aerial tuning unit (ATU) with a balanced output, all you will need is a length of twin cable soldered to the

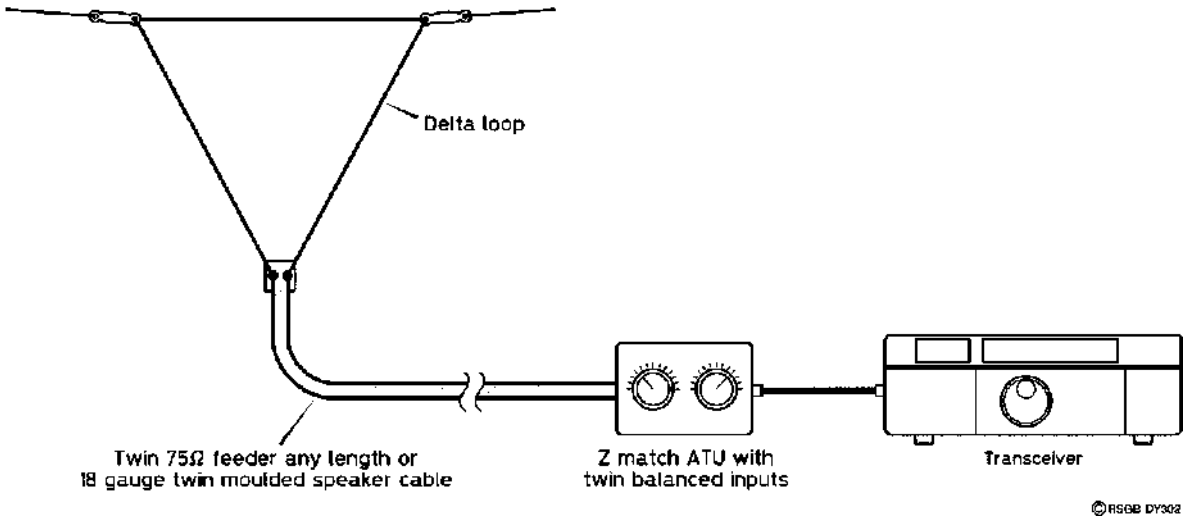

Figure 1 Multiband version of the delta loop connected to the ASTU using 75 Ω twin feeder

ends of your delta loop and connected to the balanced output terminals on the ATU, as Figure 1 shows.

Another way is to buy a ferrite-cored 1:1 balun, and use it as indicated in **Figure 2.** This produces an aerial which will operate over the whole range of amateur and commercial short-wave frequencies, when used with an ATU.

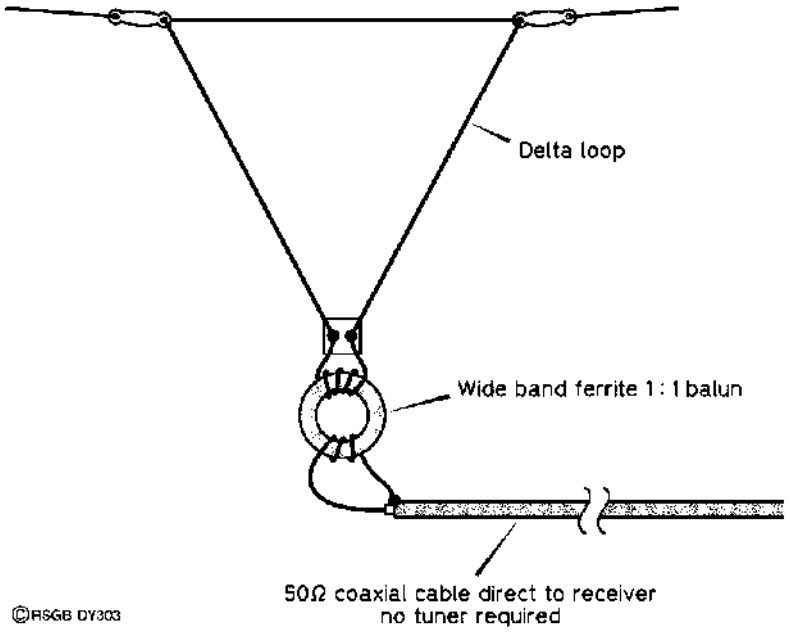

Figure 2 Multiband version of the delta loop using 75 Ω coaxial cable. This arrangement requires an ASTU if used with a multiband antenna

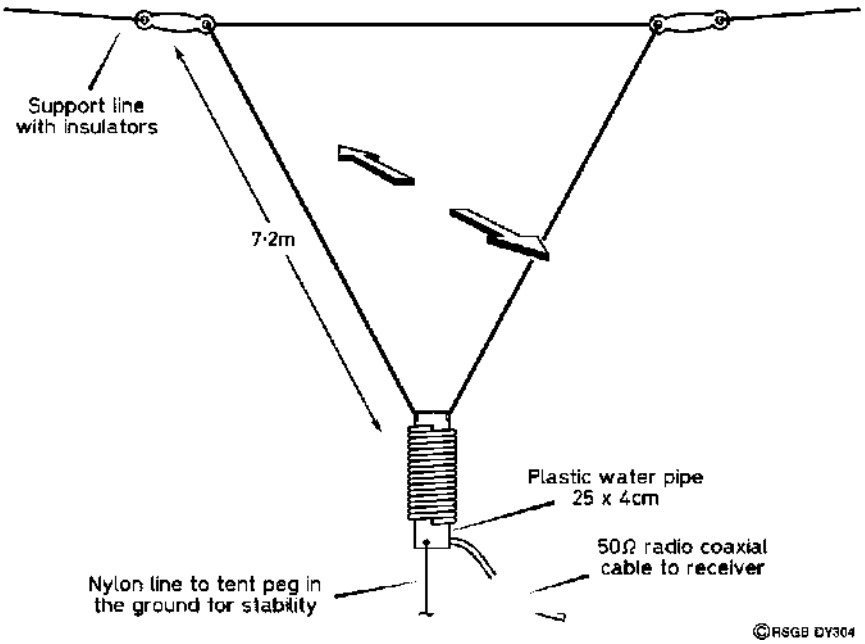

Figure 3 Single band version of the loop antenna using a coaxial balun. The direction of maximum signal strength is indicated by the arrows

However, since this aerial is designed to be a single-band type, there is a simpler answer to the problem of matching the aerial to your 50 Ω coaxial cable – **Figure 3** shows this. Make a tuned balun with a length of plastic water pipe, 25 cm long and 4 cm diameter and a piece of good-quality TV aerial cable. TV aerial cable has a characteristic impedance of 75 Ω, compared with the 50 Ω of the coaxial feeder that we usually use with amateur radio equipment. Use the type with a brown sheath and a closely knit earth braid, not the type having an earth foil inside the sheath.

The length we need for the balun is 3.8 m, but always allow between 3 and 4 cm extra for preparing the ends. Drill two small holes diametrically opposed in the top of the tube; these will be used to anchor the two ends of the delta loop, as shown in Figure 3. Drill another single hole in the bottom end of the tube, which will be used to anchor a nylon line going to the ground to add stability to the loop. Then, after drilling a pilot hole, drill a 5 or 6 mm hole near the top end of the tube, as shown in **Figure 4**. Prepare both ends of the coaxial cable, then feed one end into the tube, far enough for its ends to be soldered to the ends of the loop when the assembly reaches that stage.

Now, close-wrap the cable around the tube until only about 3 cm remain. Holding the cable tightly, drill another 6 mm hole beside the free end of the cable and feed it into this hole. At this point, feed the two ends of the loop into the top two holes and twist it back on itself. Figure 4 shows how this is done. Then, solder the ends of the coaxial balun to the ends of the loop.

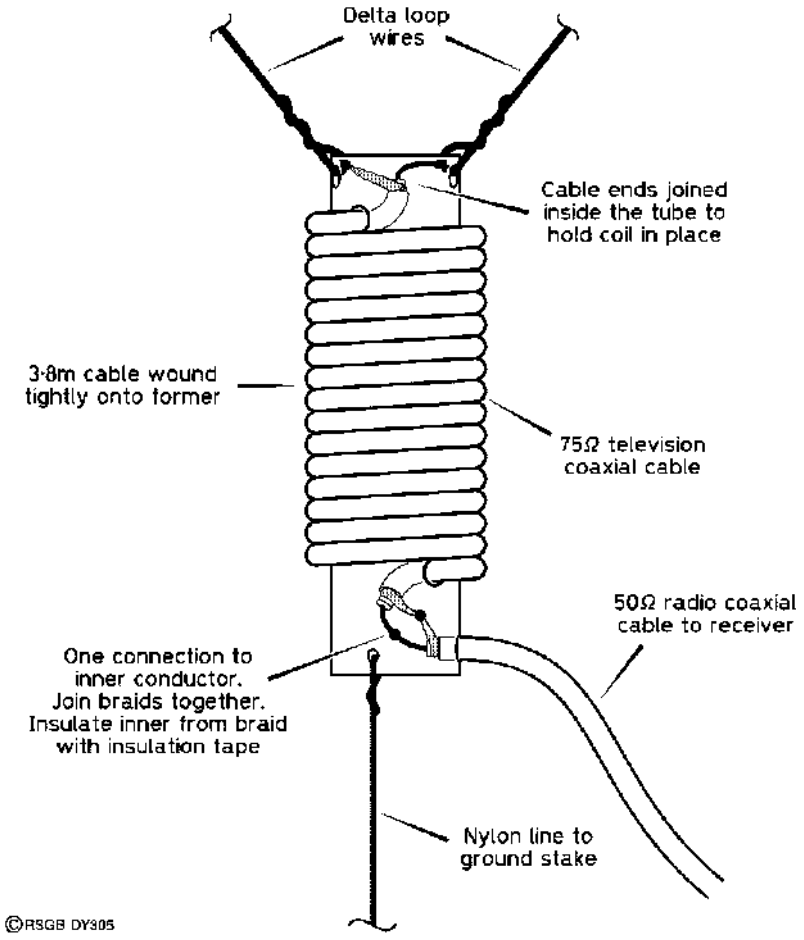

Figure 4 Construction of the balun

The bottom ends of the balun are then soldered to the 50 Ω coax which goes to your shack and to the transceiver.

Hoist the aerial into position carefully, being careful not to pull too hard on the support lines. Then, take the nylon line from the bottom of the balun to a peg in the ground. This adds stability to the aerial.

Using the delta loop

It is a directional aerial, as Figure 3 shows. It produces maximum power (and has maximum receive sensitivity) along a direction perpendicular to its own plane. Don't be too concerned with which direction it is pointing at first. Give it a try 'on the air' and see how it performs. Then you can contemplate how to point it in your favourite direction, to the USA, or Australia, for example.

Experimenting

You may want to enclose the balun in some sort of weatherproof container. Plastic ice cream containers are favourites for this sort of job. Seal all the holes where wires enter it with silicone sealant or self-amalgamating tape.

If you have used ordinary single-strand or multi-strand wire for your aerial, it will stretch over time under its own weight and that of the balun. Its operating frequency will fall slightly as a result. If you notice a significant difference, then dismantle it, remeasure and fix the sides and erect it again, perhaps facing a different direction. You can buy pre-stretched or hard-drawn wire for such purposes, if you feel that periodic tweaking of your aerial is a chore.

You can make a delta loop for different frequencies simply by scaling the lengths of wire for the loop and for the balun according to the design frequency. If your maths isn't quite up to this, enlist the help of someone well versed either in maths or aerial design!

79 A simple desk microphone

Introduction

A hand-held transceiver is usually the first type used by most novices. It is ideal when used out of doors, in the shack or mobile. However, using one in the shack with an outside aerial is not the best of solutions.

This article describes the design of a desk microphone which can be used either for transceivers using a common microphone and push-to-talk (PTT) line, or for those using a separate PTT line.

It is a simple design, using the barrels of two plastic pens, the lid of an old coffee jar, and the plastic sheath of a DIN plug.

Construction

The end caps and the ink tubes should be removed from two ball-point pens, leaving only the two plastic shells. One of them is used for the vertical microphone support, while the other is used to hold the microphone element.

The vertical support should have the pointed end shaped so that it holds the microphone support at a convenient angle, as **Figure 1** shows.

The base should be prepared next – see **Figure 2**. Four holes are required. Two, A and B, are small holes for the cable to be fed through. A third, C, is slightly larger and is used to take one of the plastic end caps. The fourth hole, D, is determined by the type of switch that you want to use for the PTT function.

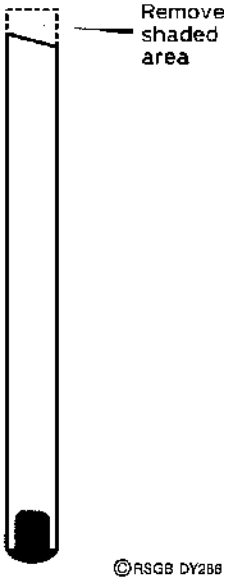

Figure 1 Vertical support made from ball-point pen shell

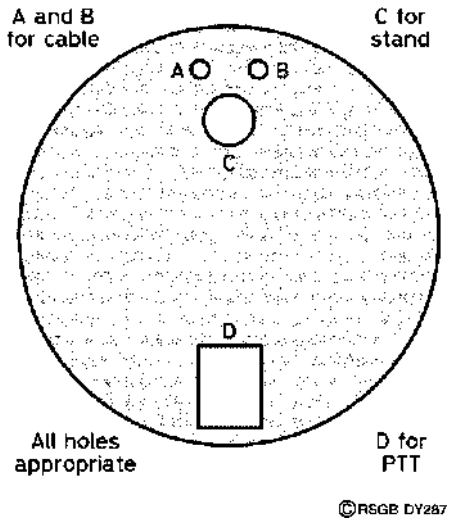

Figure 2 The microphone stand base

Some epoxy resin such as Araldite Rapid is used to mount the separate parts. Mix only a small amount at a time, and glue each part of the base assembly and allow to harden before moving on. Be sure to read and follow the instructions for the use of the glue to prevent accidents.

Firstly, glue the end cap to the base, feeding it underneath and pushing it up through hole C. Then, the vertical pen body is placed over the protruding end cap and glued into place, making sure that the top (shaped) end is pointing in the right direction to hold the other plastic tube carrying the microphone. While the glue hardens, place the DIN plug sheath on the second pen body. Place and glue this pen body on the shaped top of the vertical support, making sure that the whole assembly is supported while the glue sets. What you should have now ought to resemble **Figure 3**, but without the microphone and wiring. Leave everything to set for 24 hours.

Any switch of the press-to-make variety can be used for your PTT switch, but choose one which does not apply too much force to operate! If you find the whole assembly is too light and slides over your table, some plasticine can be pushed into the base when all the wiring has been completed.

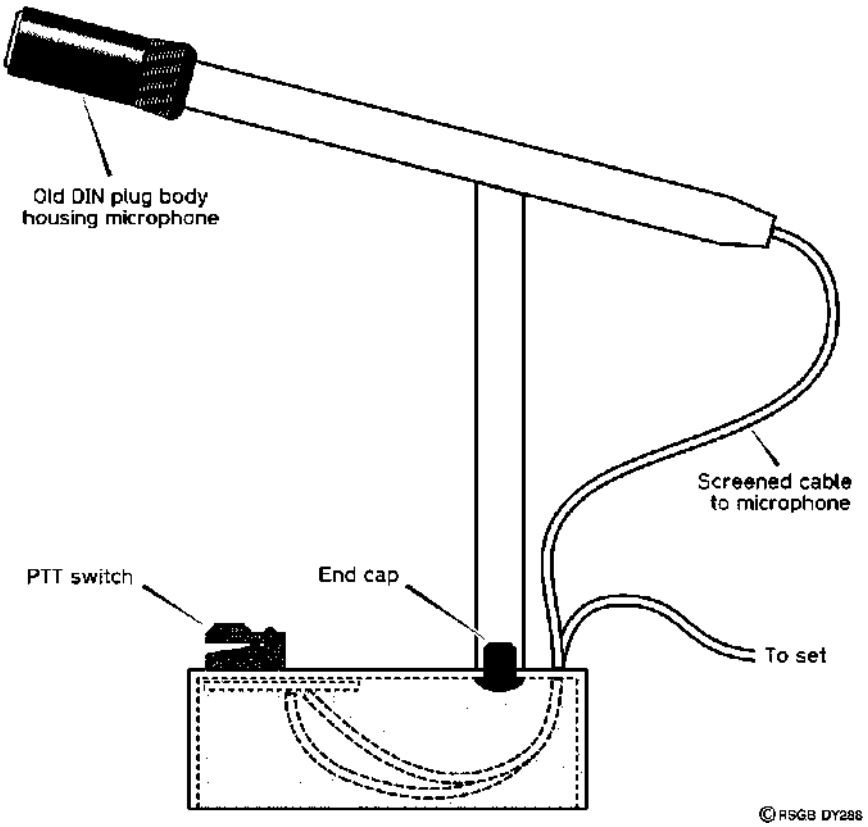

Figure 3 Complete microphone stand assembly

The circuit

A small electret condenser microphone is used, powered by a DC supply. Most hand-held radios use a single screened lead for both the PTT line and the microphone audio lead. In such cases, the circuit of **Figure 4** will operate the PTT function. Note that the PTT switch is in series with the audio lead from the microphone. If you find that the PTT switch does not switch your radio into transmit, reduce R1 from its normal value of 33 kΩ to 27 kΩ. You should find that the original value works with most hand-helds.

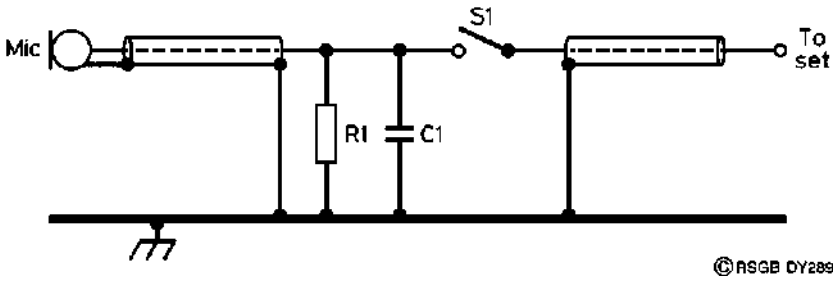

Figure 4 Wiring diagram for hand-held radios

For radios with a separate PTT lead, the circuit of **Figure 5** is used. However, a power supply is needed for the electret microphone. This can be a PP3 battery, or can (in most cases) be derived from the microphone socket on the transceiver. You will need to consult the makers' handbook for this information. Figure 5 shows the PTT switch wired in a 'ground-to-transmit' configuration, which is correct for most base-station transceivers. If you're in any doubt about what your radio needs, consult an experienced friend.

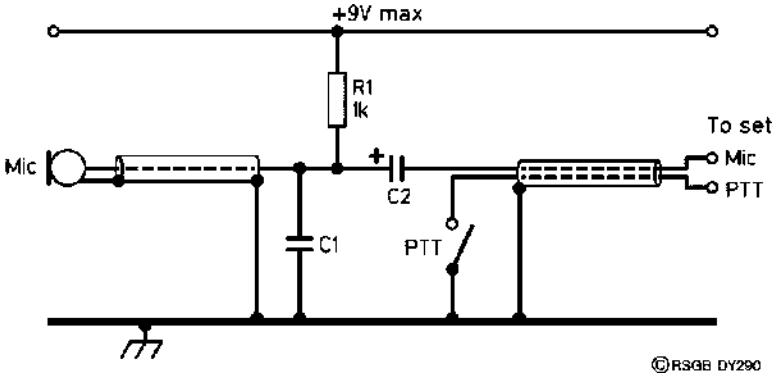

Figure 5 Wiring diagram for radios which use separate PTT lines

The last connections

The microphone element should be connected with screened cable. Tape (masking or insulating) should be wound around the electret insert until it is a snug fit inside the DIN plug sheath. Feed the screened cable through the barrel of the pen until it emerges from the far end. Poke it through hole B and make the connections under the coffee jar lid. The components can all be mounted on the PTT switch or on a small piece of Veroboard mounted under the top surface. The output lead emerges through hole A and is of sufficient length to reach your transceiver. A suitable plug needs to be fitted to it.

Parts list

Resistors: all 0.25 W carbon, 5% tolerance

R1 (Figure 4)	33 000 Ω (33 kΩ)
R1 (Figure 5)	1000 Ω (1 kΩ)

Capacitors

C1 (Figure 4 and 5)	0.1 microfarads (0.1 μF) disc
C2	10 microfarads (10 μF) electrolytic

Additional items

S1	Push-to-make
Mic	Electret microphone (Maplin type FS34W)
Screened cable	As required
Plug	As required by your radio
Veroboard	If required
PP3 battery and clip	If required

Two old plastic ball-point pens
Lid of coffee jar
Plastic sheath from DIN plug
Araldite or similar epoxy resin glue

80 Morse oscillator

Introduction

This is not the simplest Morse oscillator to build, but it differs from the simple circuits in that it produces a pure note, not a coarse, rasping sound. People who have practised Morse using a non-sinusoidal oscillator sometimes find that they have trouble copying Morse code with a pure tone. As the pure tone is the correct way to receive Morse code, it is important that you should learn to listen to the code from a pure oscillator – so here's one!

The twin-T

There are many oscillator circuits, and there are many variations of the twin-T oscillator that we are going to use. **Figure 1** shows one version of a very useful circuit. All oscillators must have positive feedback in order to work. The feedback determines the frequency of the note produced by the oscillator.

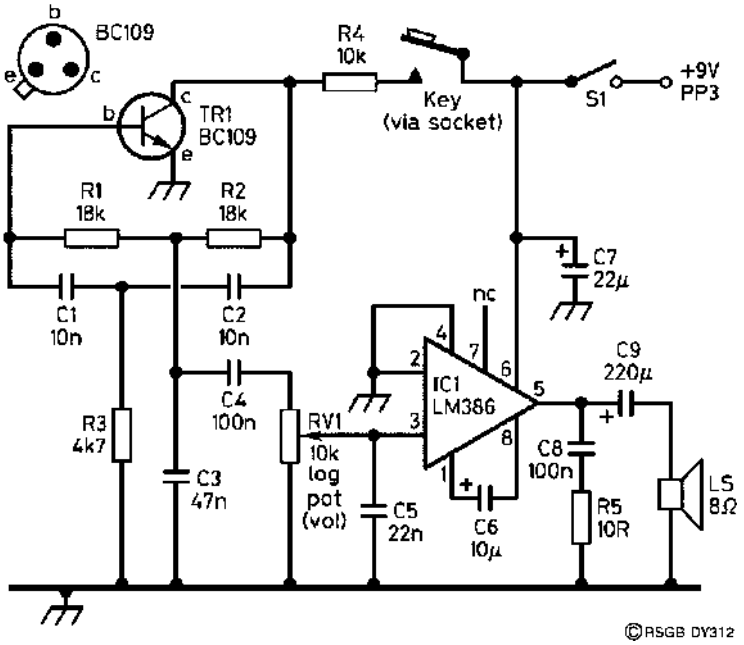

Figure 1 Circuit diagram of the sinewave oscillator and amplifier

Here, the feedback circuit looks like two letter Ts. If you look at Figure 1, one T is formed by R1, R2 and C3, the other by C1, C2 and R3 – hence the name 'Twin-T'. Notice that the two Ts are connected in parallel between the collector and base of TR1, so any signal appearing at the collector is fed into both Ts. What emerges is then fed back into the base, producing in turn a signal at the collector. And so it goes on, producing a sine wave output.

The oscillator output is fed into an integrated circuit amplifier for output via a small loudspeaker.

Putting it together

The prototype was constructed on plain matrix board (the type *without* the copper strips), as shown in **Figure 2**. The components have their leads pushed through the holes in the board, and connections are made underneath.

Build the amplifier circuit first, using a socket for IC1. Connect the 9 V supply and touch pin 3 with an ordinary piece of wire. If a buzz is heard from the speaker, all should be well. If not, check your circuit and make changes until it does.

Build the oscillator circuit, and connect its output to the volume control VR1 via C4. Set VR1 half-way along its travel and switch on. A note should be heard from the speaker when the Morse key is depressed. The component values making up the twin-T determine the frequency of the note. Try varying them if you think your note is too high or too low. Whatever changes you make, either to the resistors or the capacitors, always ensure that R1 = R2 and that C1 = C2.

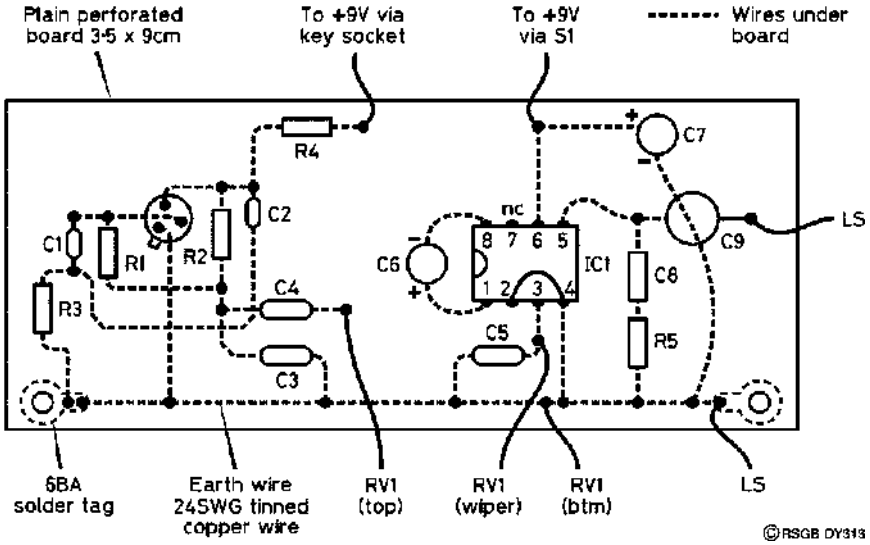

Figure 2 Component layout and interconnection diagram

Parts list

Resistors: all 0.25 W carbon film

R1, R2	18 000 ohms (18 kΩ)
R3	4700 ohms (4.7 kΩ)
R4	10 000 ohms (10 kΩ)
R5	10 ohms (10 Ω)

Capacitors

C1, C2	10 nF (0.01 μF)
C3, C8	47 nF (0.047 μF)
C4	100 nF (0.1 μF)
C5	22 nF (0.022 μF)
C6	10 μF electrolytic, 16 V WKG
C7	22 μF electrolytic, 16 V WKG
C9	220 μF electrolytic, 16 V WKG

Semiconductor

TR1	BC109

Integrated circuit

IC1	LM386

Additional items

VR1	10 kΩ log potentiometer with switch
LS	8 Ω loudspeaker

Matrix board 3.5 × 9 cm
Small jack socket for key input
Box
PP3 battery and clip

81 A simple 6 m beam

Introduction

The attraction of building your own aerials is an abiding feature of our hobby. You can *buy* almost any shape or size of aerial, but one you have made yourself can often work every bit as well as a commercial device costing ten times as much.

The design

This aerial, designed for use on the 6 m band, is essentially a two-element Yagi, with the elements bent in order to reduce the physical size. It is known

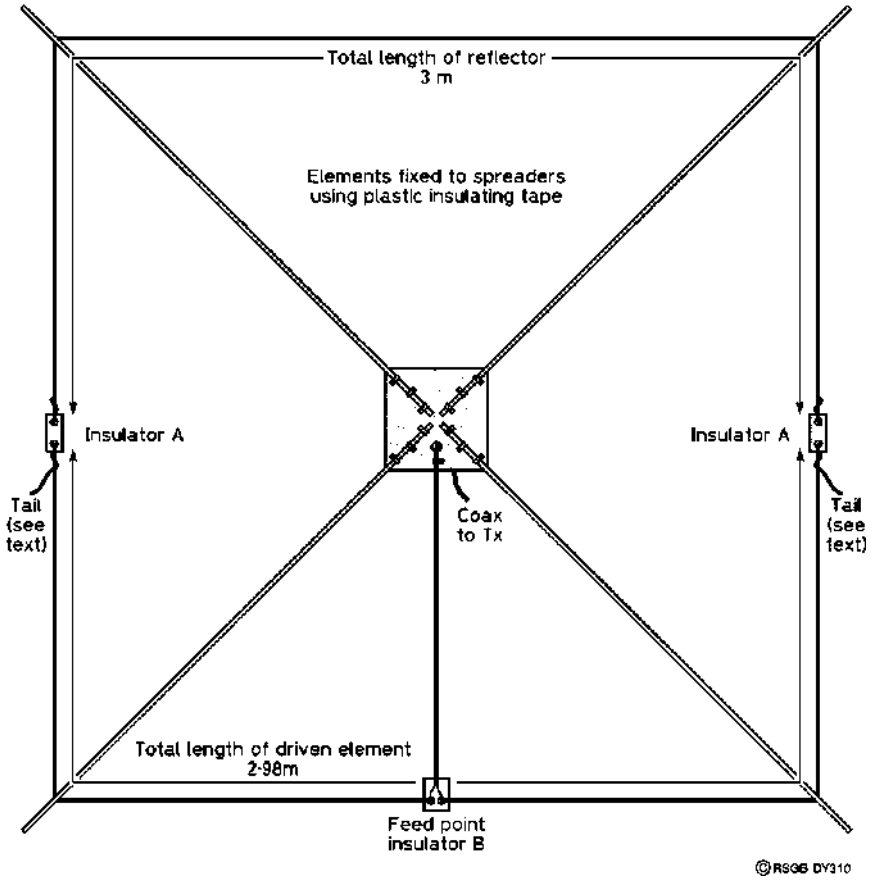

Figure 1 Plan view of the complete 50 MHz VK2ABQ antenna

as the VK2ABQ beam, and was designed originally for the 20, 15 and 10 m bands, principally because of its space-saving qualities. It is made using a wooden frame and wire elements, and is ideal for portable operation.

Tools ready?

The beam is shown in **Figure 1**. The driven element is the one whose centre is fed by the coaxial cable, and lies between the two insulators marked A and the feedpoint at B. The reflector is also anchored at the points A, and lies over the upper half of the frame.

The wooden centrepiece is used to support the cross-pieces and to mount the aerial on the mast, using a common shelf bracket. The cross-pieces, known as *spreaders*, can be wooden canes or dowelling, and are mounted to the centrepiece using cable clips and adhesive. **Figure 2** shows how this is done.

If the aerial is to be a permanent installation, the spreaders should be weatherproofed using a good-quality exterior varnish. The wire elements are PVC covered and fed through holes in the spreaders.

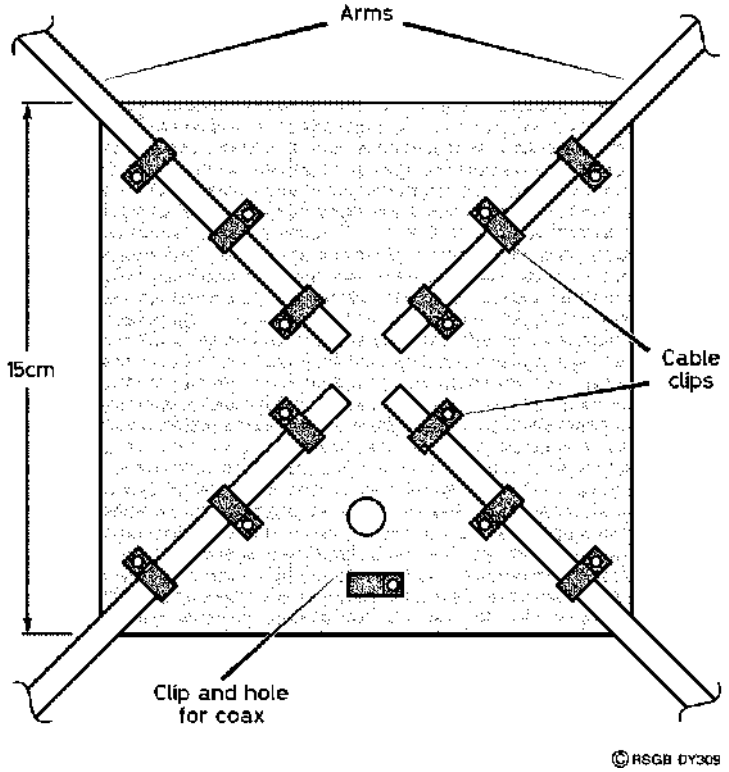

Figure 2 Centre support piece

The end insulators are made of drilled perspex, and the wire passed through the two holes and twisted, as shown in **Figure 3**.

Note: if you have not drilled holes in perspex before, take care! The drill bit must be well-lubricated because it generates a lot of heat (enough to melt the perspex and jam the drill). Never turn the drill for more than a few seconds at a time, and moisten the bit in between. Start with a pilot hole and use bits of increasing size until the hole is the size you want.

Another perspex insulator is used to secure the feeder to the aerial, as shown in Figure 3. The feeder then passes directly to the centrepiece, where it is fastened with a cable clip and then passes down the mast.

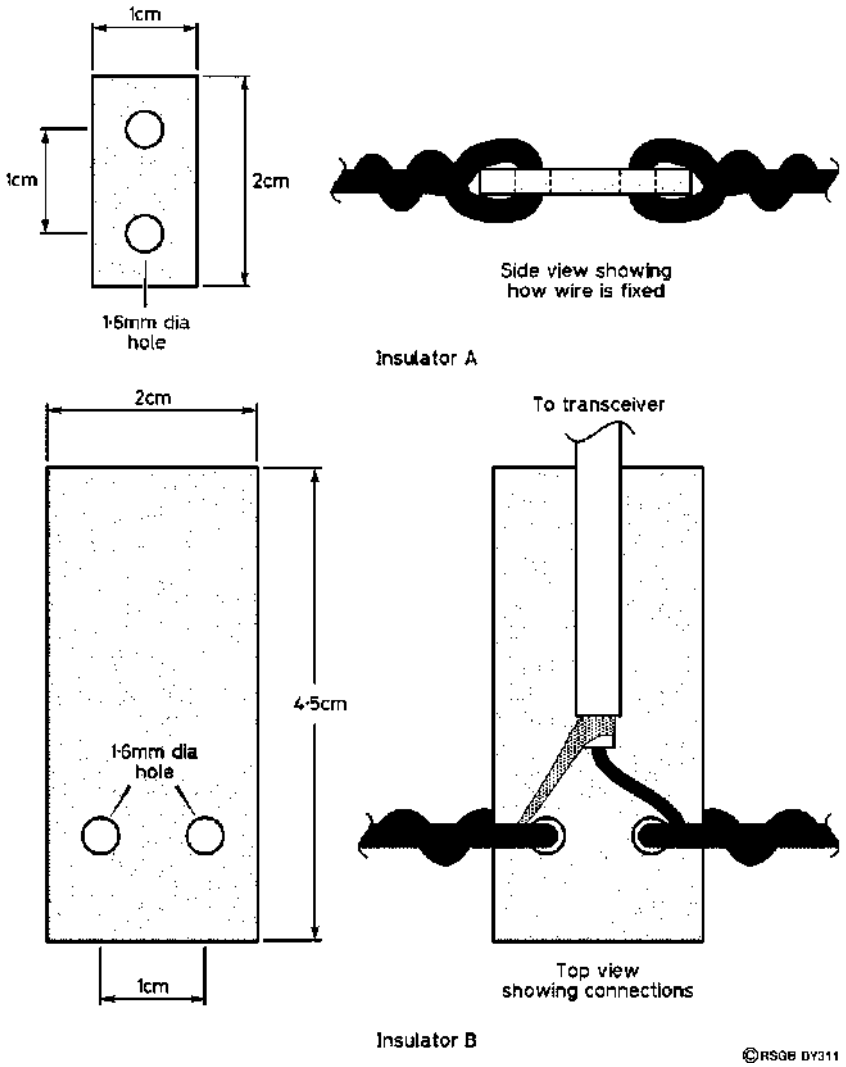

Figure 3 Details of insulators

Adjustment

The driven element (A–B–A) in Figure 1 is fixed to the end insulators in such a way as to have 'pigtails' which are about 10 cm long. Using an SWR meter between the aerial and the transmitter, trim the pigtails equally at each end for minimum SWR in that portion of the 6 m band in which you plan to work. Make sure that the transmitter is off when you trim the ends, as high voltages can be present there. Always listen on the frequency before you transmit and, when you do, ask if the frequency is in use and identify yourself. Use as little power as possible.

The prototype had an SWR of 1.2 at 50.2 MHz and performed well. If you look at Figure 1, which is a view of the aerial from above, you will immediately see that when the aerial is horizontal, it radiates with horizontal polarisation in a direction from the top of the page to the bottom. A metal pole or mast can be used for horizontal polarisation, but if you intend to use the aerial for vertical polarisation, it is much better to use a wooden or fibreglass pole.

Portable use

If you plan to operate portable with this aerial, the only real modifications you need are to the centrepiece and how it supports the spreaders. Instead of using glue and cable clips, nuts and bolts through the spreaders and centrepiece would allow the spreaders to be 'hinged' closed for transport.

Materials

Centrepiece	Hardwood, 15 × 15 × 25 mm
4 spreaders	110 cm long (cane or 6 mm dowel)
Wire	1.5 mm PVC-covered copper
50 Ω coaxial cable	RG58 or similar
Cable clips	6 mm (12 off)
Varnish	Polyurethane for waterproofing
Tape	Self-amalgamating, to waterproof all soldered joints
Insulators	See text

82 An integrated-circuit amplifier

Introduction

A simple audio-frequency amplifier is a very useful building-block in many more advanced electronic circuits. It is also a very useful piece of test equipment. To have one spare in the shack can be a life-saver at times.

Planning

Get into the habit of planning your project. How do you want it to look when it is finished. Do you want it in a box? Do you want it 'open-plan', with all the components on view?

The 'minimalist' approach to any project is simply a front panel and a baseboard, on to which all the components are fitted. In this case, the front panel would accommodate the loudspeaker, the volume control and the input and output jack sockets, and the baseboard would support the circuit board. Once you have decided these things, and know the size of the board, speaker and volume control, you can decided how big the panel and baseboard should be.

The amplifier

Instead of building the amplifier from discrete components (i.e. transistors), as was done in the project *An audio-frequency amplifier* (which you will find elsewhere in this book), we are going to use an integrated-circuit (IC) amplifier. External resistors and capacitors are still needed but, compared with the number of components *inside* the chip, these are very few indeed!

The IC we are going to use is the TBA820M. The circuit may look complicated, but with the use of a matrix circuit board it becomes quite simple. **Figure 1** shows the circuit diagram and **Figure 2** the layout on the board. The external connections to the PCB are shown in **Figure 3**.

To avoid having a separate switch to switch off the power supply when the amplifier is not being used, a volume control which incorporates a switch is used.

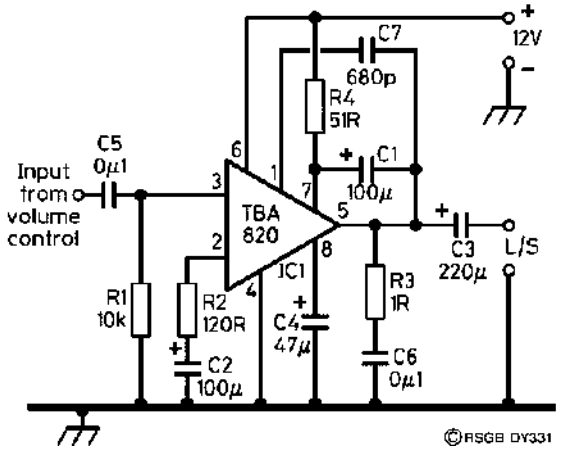

Figure 1 Audio amplifier, circuit diagram

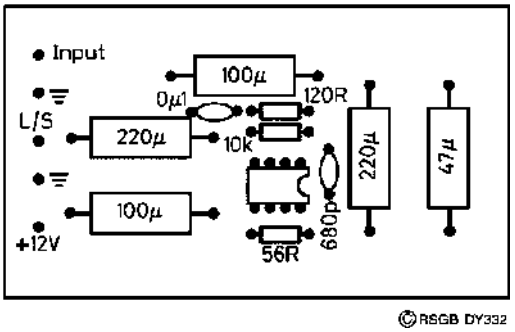

Figure 2 Audio amplifier, component layout

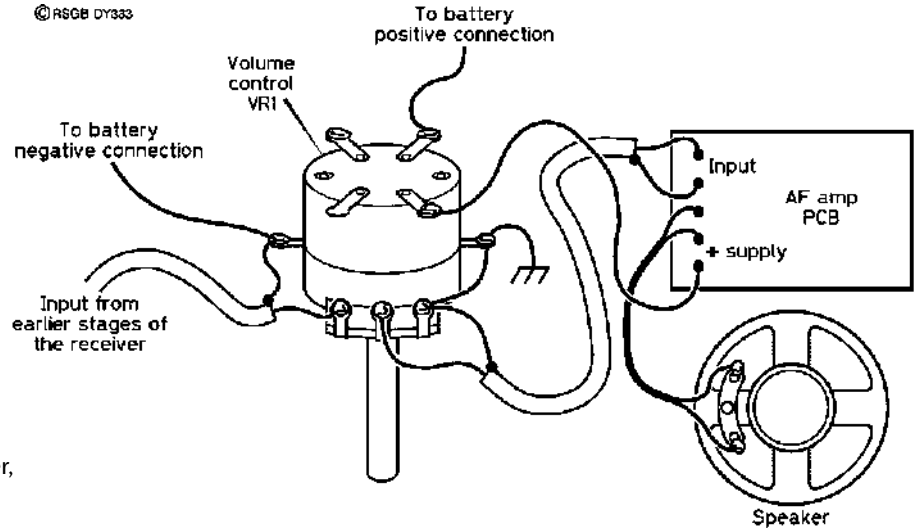

Figure 3 Connecting the circuit board to the speaker, volume control/switch and battery

What power supply?

If the amplifier is to be used only for short periods, as a test instrument, for example, then it can be run from a PP3 battery, which can be mounted on the baseboard. If you intend to use it often, then a connection to an external power supply is preferable. For this option, you may want to consider fixing two terminals to the baseboard for this connection.

83 A novice ATU

Introduction

Having an aerial tuning unit (ATU) is always useful. It is used for adjusting the aerial impedance, as 'seen' by the transceiver, to be the same as that of the transceiver itself, usually 50 Ω. This process is called *matching*, and ensures that the receiver and the power amplifier (PA) stage of the transmitter work efficiently.

This design is due to the late Doug DeMaw, W1FB, and uses readily available components. It will handle up to about 5 W, and operates over the frequency range 1.8 to 30 MHz.

Circuit evolution

The basic circuit of one type of ATU is shown in **Figure 1**. On transmit, the input signal at L1 is coupled into L2, which forms a resonant circuit with C1. The signal across the resonant circuit is fed to the aerial by C2. The combination of L2 and C1 helps to remove signal harmonics, because they are not at the resonant frequency and are shunted to earth. On receive, only those signals which are within the pass-band of L2 and C1 will pass into the receiver. This improves receiver performance by rejecting many out-of-band signals which the simpler receiver doesn't like.

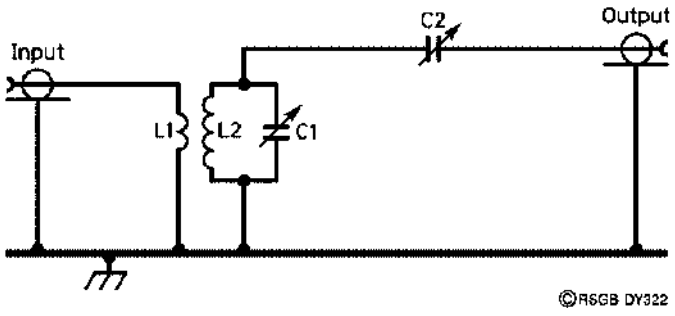

Figure 1 Basic circuit of the ATU

For this design, the all-important resonant frequency is chosen to be in the 80 metre band. If we want to make the circuit operate on other bands, we need to change either L2 or C1. It is easy to change L2 by using a set of switched inductors (L3–L5) as shown attached to S1 in **Figure 2**. Forget about S2 and L6 for the moment.

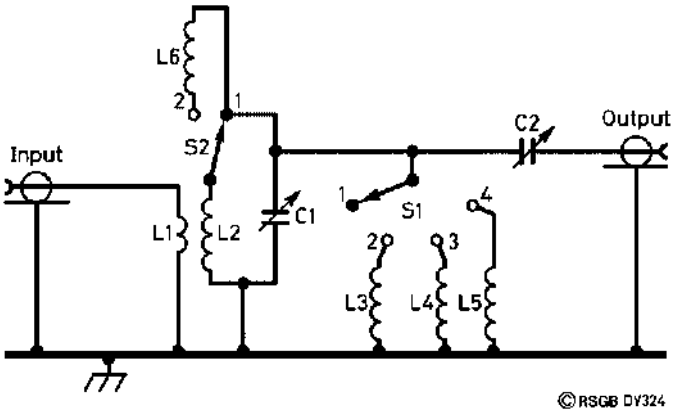

Figure 2 L6 added for 160 m

When S1 is in position 1, the circuit reverts to that of Figure 1. S2 should be brought into circuit only when S1 is in position 1. Looking at the way the circuit is drawn, you can see that when S2 is in position 2, we have two coils in series, which is equivalent to adding more turns to L2. More turns means more inductance, which lowers the resonant frequency still more, and gives coverage of the 160 m band.

Rather than having to remember to flick S2 to the correct position *and* move S1 to position 1 when we want to operate on 160 m, both functions can be combined into one rotary switch with two wafers. This circuit is shown in **Figure 3**.

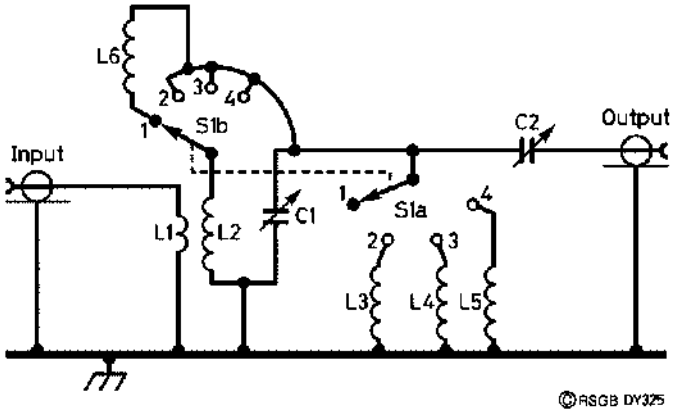

Figure 3 Two-pole switch for all bands

In all positions of S1a *except* position 1, the extra coil, L6, is shorted out. The two halves of the switch, S1a and S1b, move together, as the shaft is turned, so both halves are in position 1 at the same time, position 2 at the same time, and so on. The two switches, S1 and S2, are said to be *ganged*.

Construction

L1 is formed by winding four turns of 22 SWG enamelled copper wire over L2, as in **Figure 4**. L2 already exists on the purchased former. After scraping the enamel off the ends of the wire (with a sharp knife or sandpaper), one end of L1 must be soldered to one end of L2, as shown in Figure 4. The free end of L1 goes to the transceiver aerial socket.

All components except the capacitors are assembled on the switch. Note that the rotor of C1 is earthed, but neither side of C2 is earthed. This means that the metal shaft of C2 is not earthed, and touching it will detune the ATU. Using a plastic knob for C2 will minimise this effect. If you decide to use a metal box, take precautions to ensure that no part of C2 is in electrical contact with the box.

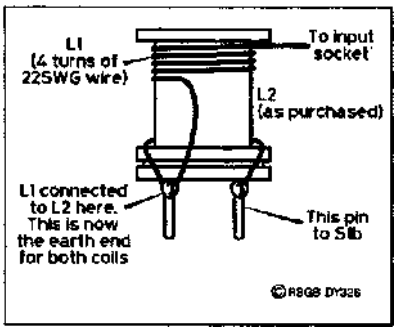

Figure 4 L1 is wound over L2 as shown

The capacitors are mounted using M2.5 screws. Make sure that the screws do not foul the vanes of the capacitor. If your screws are too long, a few washers between the box and the capacitor will solve the problem!

In use

The best indication of a good match is obtained with a standing-wave meter between the ATU and the transceiver. The controls are adjusted alternately to 'feel' your way to a better and better match.

For receive-only use, the same alternate adjustments are used, watching for the maximum signal strength on the S-meter or, for a very weak signal, making the signal from the loudspeaker as large as possible.

Parts list

Capacitors

C1, C2	350 pF variable

Inductors

L1	See text
L2	27 μH
L3	10 μH
L4	2.2 μH
L5	1 μH
L6	65 μH

Additional items

SO239 sockets (2 off)	
S1	2-pole 6-way rotary
Box	as required
Plastic knobs (2 off)	
Stick-on feet (4 off)	
M2.5 screws for capacitors	
Screws, nuts and washers for mounting the input and output sockets.	

84 CW QRP transmitter for 80 metres

Introduction

This is a relatively simple transmitter design having an output of 1 W. The design is not new, having been described before in other amateur radio publications. The components are all available new and the total cost should not exceed £15.

The circuit

Like other simple transmitters (see *An 80 Metre Crystal-Controlled CW Transmitter* and *A Breadboard 80 m CW Transmitter* elsewhere in this book) this one is crystal controlled. This assures frequency stability, but limits the usefulness of the transmitter. The key to increased frequency coverage without a conventional Variable Frequency Oscillator (VFO) is the use of a low-cost 3.58 MHz *ceramic resonator*. The 'pulling' range of a 3.58 MHz ceramic resonator covers the UK novice 80 m sub-band and some of the CW segment below 3.525 MHz.

A ceramic resonator is like a crystal, but not quite as stable in frequency. Its main advantage is its large pulling range.

The block diagram is shown in **Figure 1**. It is very similar to a crystal-controlled transmitter, and includes an oscillator, buffer and final amplifier.

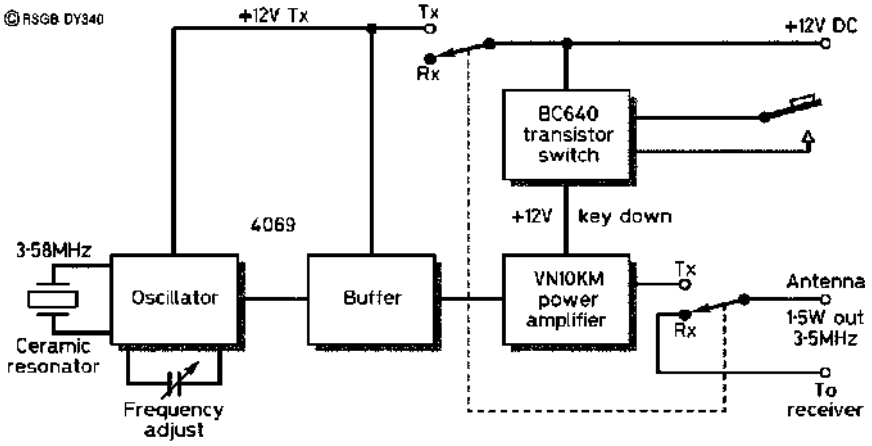

Figure 1 Block diagram of the ceramic resonator controlled 80 m CW transmitter

This amplifier is keyed, the oscillator remaining running all the time. This improves frequency stability because the oscillator is not being continuously stopped and started by the key. It is switched off while receiving, though, to avoid interference with the received signal. Transmit/receive switching is accomplished by a panel-mounted switch controlling both the aerial, oscillator and buffer switching.

Figure 2 shows the transmitter circuit diagram. An unusual aspect of this transmitter is the use of a digital CMOS integrated circuit (IC) type 4069 for the buffer and oscillator stages. The IC houses six inverters, four of which are used in the circuit. One is used as the oscillator, two are used for the buffer stage, and the fourth provides an output for a direct-conversion receiver, should one be added at a later date.

The frequency of the oscillator is changed by varying the capacitance in the ceramic resonator circuit. This is provided by VC1.

The power amplifier (PA) is a small MOSFET (metal oxide semiconductor field-effect transistor), TR1. This is capable of providing an output power of 2 W but, in this circuit, it is run conservatively to give 1.5 W. The output can be varied by changing the resistance (R5 + R6) in the gate circuit. Attempts

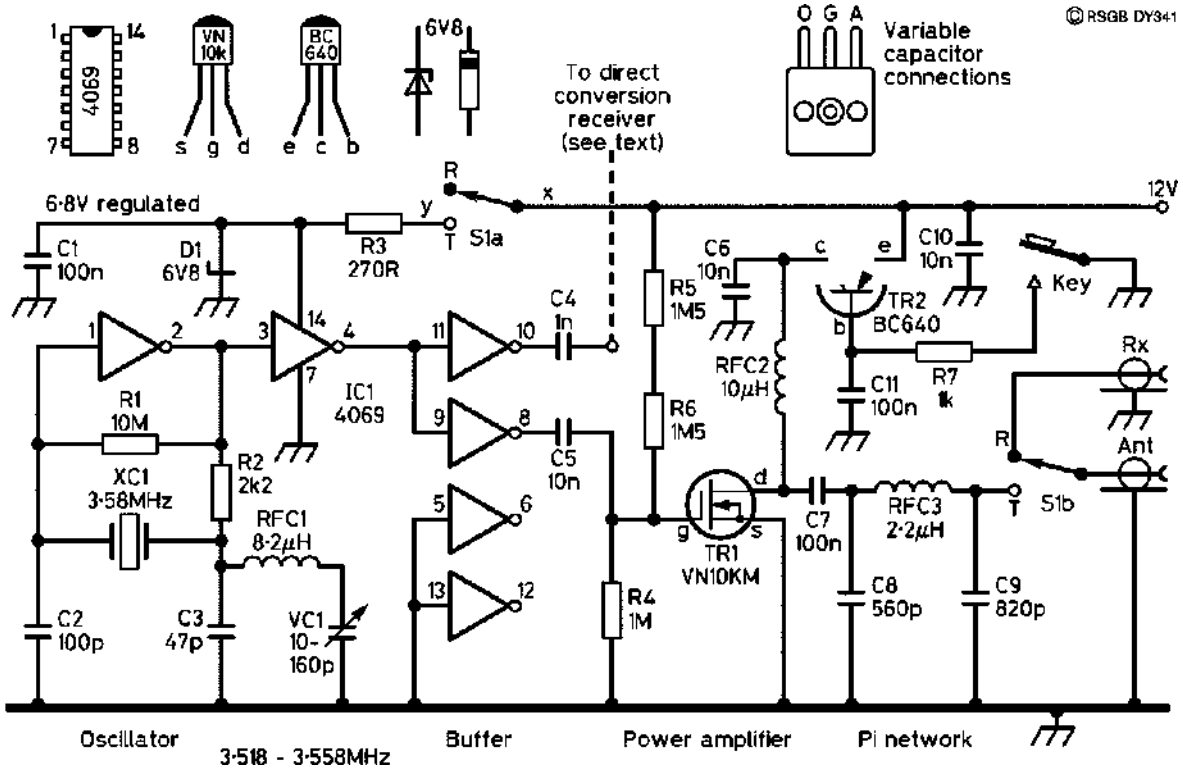

Figure 2 Circuit diagram of 80 metre transmitter

to raise the output power by decreasing the values of these resistors may result in immediate MOSFET failure.

A pi-network (C8, RFC, C9) provides impedance matching to 50 Ω, together with harmonic suppression. Like all inductors in this transmitter, the pi-network inductor is a pre-wound RF choke. A pi-network is so called because the components are arranged in the shape of the Greek letter pi (π).

Keying is carried out by a pnp transistor switch, TR2. Closing the key earths the base and supplies 12 V to the collector of TR2 and to the drain of the MOSFET, TR1, allowing the PA to operate.

Construction

You must house your transmitter in a metal box, to avoid hand-capacity effects and the radiation of spurious frequencies. Size is not important, provided it is large enough to accommodate the transmitter without cramping the components. You may want to allow space for future additions such as a direct-conversion receiver, break-in keying, sidetone or a small power amplifier. A good size is 5 × 15 × 15 cm. You can make your own box, buy it, or even use a biscuit tin!

Front and rear panel connectors can be fitted first. The choice of these is a personal matter, but a good working choice would be:

(a) Power socket – 2.1 mm panel socket – centre pin positive.
(b) Key socket – ¼ inch jack socket.
(c) Aerial and receiver connectors – panel-mounting SO239 type.

Particular attention must be paid to the mounting of the variable capacitor, VC1. Make sure the hole for the shaft is amply big enough, and if you use screws to mount the capacitor on the front panel, then make sure they are not too long, otherwise they will touch the vanes of the capacitor! Mounting can be by means of glue, sparingly applied and kept well away from the shaft.

A board size of about 6 × 10 cm is adequate. Component layout on the board is suggested in **Figure 3**. The prototype used ordinary matrix board, which is preferable to stripboard for a design like this; stripboard has undue capacitance between adjacent strips. Component leads are fed through holes in the board and are connected underneath. Make sure that leads and connections are rigid because, if they can move, there is always the danger of short-circuiting, and capacitance changes.

To facilitate construction, servicing and testing, it is advisable to use Veropins for connections to the variable capacitor, transmit/receive switch,

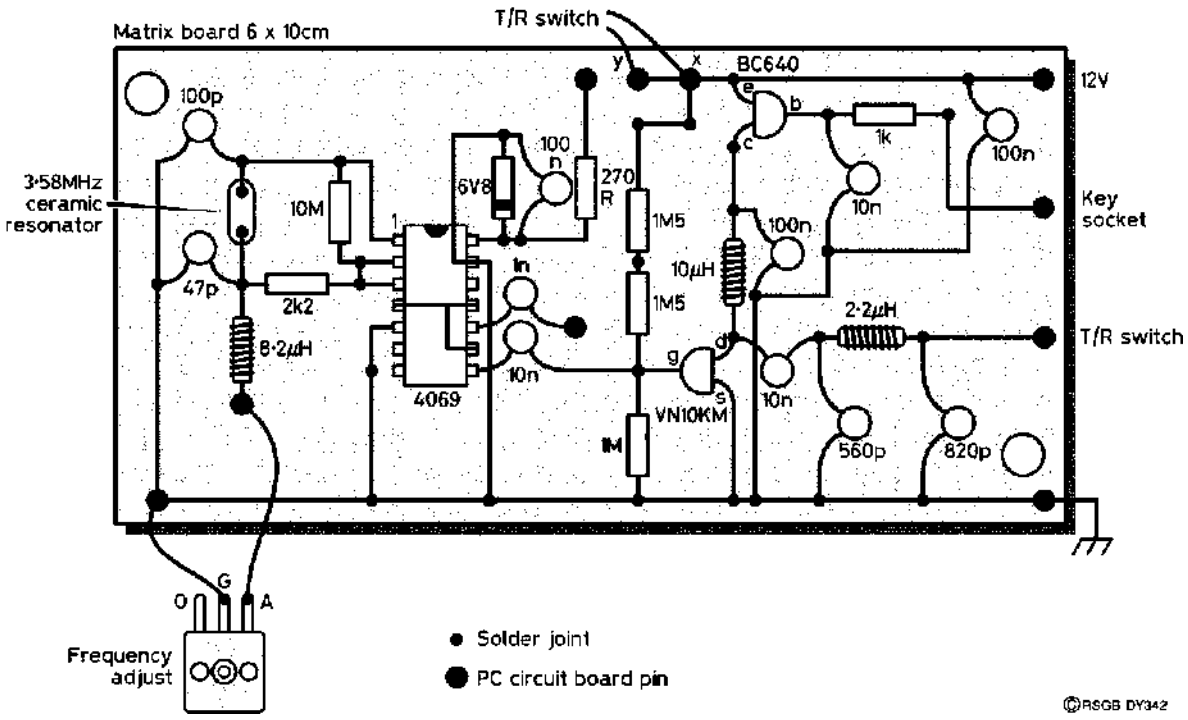

Figure 3 Component layout of the 80 metre transmitter. The transmit/receive switch is not mounted on the board and is not shown in this diagram

aerial and power sockets. Use screws and spacers to mount the circuit board to the box. Mounting the board horizontally assists troubleshooting.

Use a socket for the IC, and observe the CMOS handling precautions given in *An Electronic Die*, elsewhere in this book. When soldering the leads to the ceramic resonator, do it quickly – excessive heat damages the device. The earth lead running acoss the bottom of the board must be connected to the metal case by a short length of stout wire.

Testing

After carefully checking your wiring, both against the circuit diagram and the layout diagram, it is time to test your circuit. You will need a multimeter, an 80 m SSB receiver and a 50 Ω dummy load. A good design of dummy load can be found in the project *A Switched Dummy Load*, also in this book. An RF power meter and frequency counter will also be useful, although if your receiver has a digital frequency readout and S-meter, the latter two items are not really necessary. You will also need a 12 V 1 A power supply unit (PSU) to power the transmitter.

Switch the transmitter to receive and switch on the transmitter. No current should be consumed. Switch to transmit and check that pin 14 of IC1 is 6.8 V positive. With the dummy load connected to the aerial socket, press the key. The voltage on TR2 collector should now be 12 V, dropping to zero when the key is released.

Now check the operation of the oscillator. In transmit mode, you ought to be able to find a strong carrier signal with the receiver, even though the dummy load is connected. Adjusting the variable capacitor should change the frequency. At the lower end of the frequency range, you may find that the oscillator is unreliable in starting, because the circuit is attempting to pull the resonator too low in frequency. If this is the case, set the trimmer at the back of VC1 to minimum capacitance. If your version of VC1 has two trimmers, and you don't know which one to set, set them *both* to minimum capacitance. If there is still a problem, reduce the value of RFC1 to 6.8 or 4.7 μH.

In all probability, the unmodified circuit of Figure 2 will not require any of the changes outlined here. A coverage of 3.518 to 3.558 MHz should be possible, while preserving good frequency stability and reliable oscillation.

A signal probe (see *An RF Signal Probe*, elsewhere in this book) is useful for checking the operation of the oscillator and PA. Alternatively, an RF power meter or the receiver's S-meter can be used. With the PA running, the unit should draw between 200 and 300 mA. If TR1 becomes too hot to touch after a few seconds of transmitting, increase R5 or R6 to limit the transistor's heat dissipation. A small 6.3 V bulb connected across the aerial output is a simple way to check that the PA is working. An orange/white glow when the key is pressed is indicative of correct operation.

The final test is to monitor keying 'quality'. With your dummy load connected, press the key and listen to the note on the receiver's loudspeaker. Then operate the key, sending a string of dits, for example. What you hear should be free of chirps and clicks, as well as being stable in frequency. This test is sometimes better performed with no aerial connected to the receiver, thus preventing receiver overload and its associated plops. No problems should be encountered here.

Frequency tuning

A peculiarity of ceramic resonators is that, every now and again, their frequency changes abruptly by 100 Hz or so, then remains stable for some time. This is certainly noticeable in the received signal, but does not detract from the QSO and no characters are lost as a result. Try to keep the area around the ceramic resonator cool, to avoid temperature variations.

Parts list

Resistors: all 0.25 W, 5% tolerance

R1	10 megohms (MΩ)
R2	2200 ohms (2.2 kΩ)
R3	270 ohms (270 Ω)
R4	1 megohm (1 MΩ)
R5, R6	1.5 megohms (1.5 MΩ)
R7	1000 ohms (1 kΩ)

Capacitors

C1, C7	100 nF
C2	100 pF
C3	47 pF
C4	1 nF
C5, C6, C10	10 nF
C8	560 pF
C9	820 pF
VC1	10–160 pF variable

Inductors

RFC1	8.2 μH
RFC2	10 μH
RFC3	2.2 μH

Semiconductors

IC1	4069
TR1	VN10KM
TR2	BC640
D1	6V8 Zener

Additional items

- Matrix board (see text)
- 14-pin DIL socket
- Pointer knob
- Sockets (see text)

85 An audio booster for your hand-held

Introduction

The audio output from many hand-held transceivers and receivers usually leaves much to be desired, so this little amplifier was designed to increase the output at minimal expense.

All that is needed is a separate amplifier and bigger loudspeaker. This is accomplished using a single integrated circuit (IC), a few components, and a loudspeaker from the junk box. This circuit will enable the output from your hand-held to be heard easily in a car.

The circuit

This is shown in **Figure 1**. It uses only those components necessary to operate the IC amplifier. VR1 is the preset volume control, and varies the signal coming from the 'External speaker' jack on the hand-held before feeding it into the IC for amplification. C1 blocks any constant voltage present on the input.

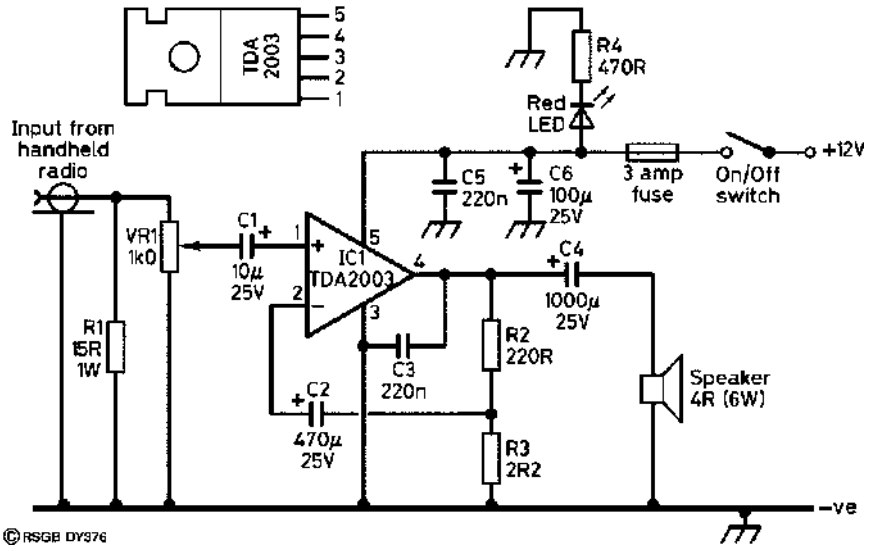

Figure 1 Circuit diagram of the audio amplifier. The power is derived from the cigarette lighter socket and the fuse is in-line with the lead

The IC output comes from pin 4 and is fed via the electrolytic capacitor, C4, to the loudspeaker. The circuit is provided with an on/off switch, fuse and LED to indicate when the circuit is switched on.

Construction

The box is made of aluminium. This is necessary to help to dissipate some of the heat generated by the IC. Do not build the circuit inside a plastic box unless you take special precautions! The IC has a metal mounting tab with a hole, specifically designed to be mounted to a metal box or other metal heat sink. Apply plenty of heat sink compound between the tab and the box, tighten the nut and bolt, and then wipe off any excess compound. The box will get slightly warm in operation.

The size of the box is not specified. You may want to decide on this when you find a loudspeaker. Choose one which will be able to handle 6 W

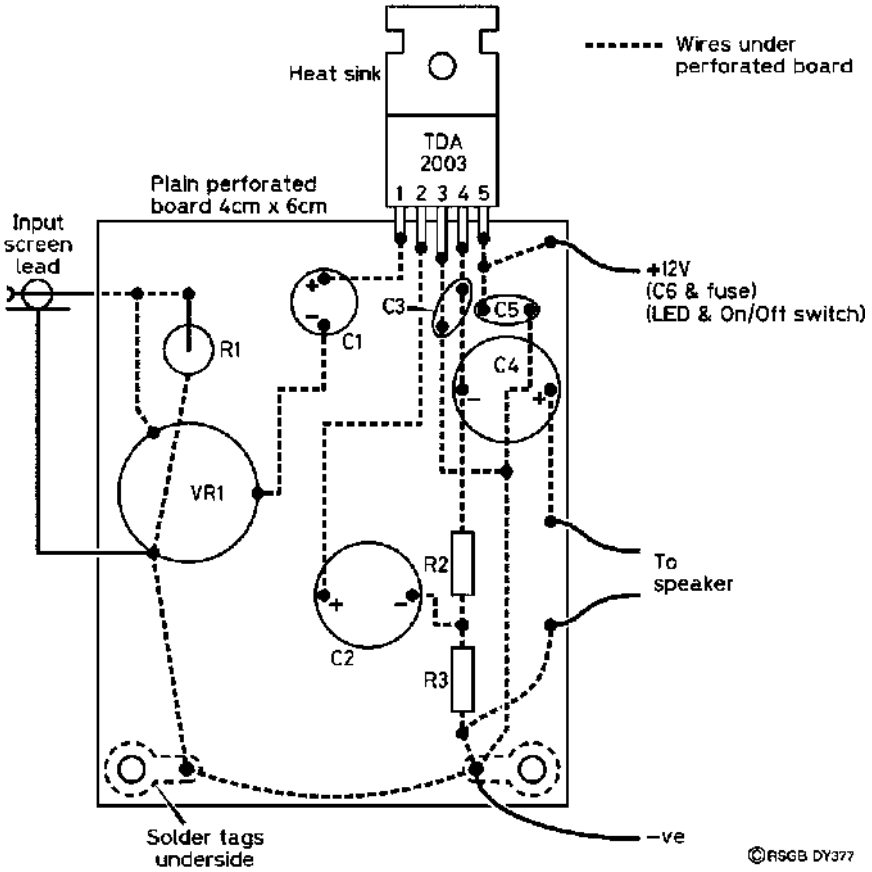

Figure 2 Layout of the components within the box

output. Drill all the holes in the box first. Holes for the speaker, input phono socket and the LED. The amplifier can be constructed on ordinary matrix board, which can be mounted inside the box with screws and spacers.

The layout is shown, for your guidance, in **Figure 2**. The components are mounted by pushing their leads through the holes in the board and making connections on the underside. The preset volume control, VR1, is set such that the hand-held's volume control is sufficient to control the final output over a good volume range. Use a screened lead from the 'External speaker' jack socket to the phono plug.

An external power supply is needed for this circuit. The normal dry battery which we usually use for small projects in this book will *not* work here, so you will need a proper mains power supply producing a stabilised 12 V. If you are going to use the unit principally in a car, then the cigar lighter socket can supply this voltage easily. Do make sure that the polarity is correct before you switch on!

When you plug the jack plug from your booster into the 'External speaker' socket on your hand-held, its internal speaker will be muted, so don't think that something dire has gone wrong! Adjust VR1 for a good volume range on your booster, when the volume control is turned on the hand-held.

Parts list

Resistors: all 0.25 W, 5% tolerance, unless otherwise stated

R1	15 ohms (15 Ω) 1 W
R2	220 ohms (220 Ω)
R3	2.2 ohms (2.2 Ω)
R4	470 ohms (470 Ω)
VR1	1000 ohms (1k Ω)

Capacitors

C1	10 µF 25 V
C2	470 µF 25 V
C3, C5	220 nF (0.22 µF) Mylar
C4	1000 µF 25 V
C6	100 µF 25 V

Semiconductor

LED	5 mm Red

Integrated circuit

IC1	TDA2003

Additional items
- Heat sink compound
- Nuts and bolts
- Loudspeaker 4 Ω 6 W
- 3 A fuse
- On/off switch (SPST)
- Matrix board 4 × 6 cm
- Solder tags
- Plugs and screened cable for connecting lead
- Aluminium box

86 A grid dip oscillator

Introduction

When an inductor and a capacitor are connected, whether in series or parallel, they form a circuit with a natural (or *resonant*) frequency. The circuit stores energy, and this energy is being constantly shifted from the inductor to the capacitor and back again.

The dip oscillator is a simple instrument used to measure the resonant frequency of a tuned circuit without having to make any direct connection to the circuit. The circuit is more commonly known as the *grid dip oscillator* (GDO), from the days when the active device in the circuit was a valve. The FET or Field-Effect Transistor operates in a way which is very similar to that of the valve, so it is not quite a misnomer to call this instrument a grid dip oscillator, too.

The circuit

The GDO uses a calibrated, tunable FET oscillator in the circuit of **Figure 1**. It has a frequency range of 1.6 to 35.2 MHz in four ranges using a set of plug-in coils, shown in **Figure 2**. When the oscillator coil, L1, is placed near an external resonant circuit, some of its RF energy is coupled into the external circuit. A gain in energy of the external circuit must mean a loss of energy in the GDO circuit, resulting in a change of current through TR1, which is measured by the meter, M1.

The current through TR1 is of the order of 5 to 8 mA, but the change of current may be only a few microamps. To measure a very small

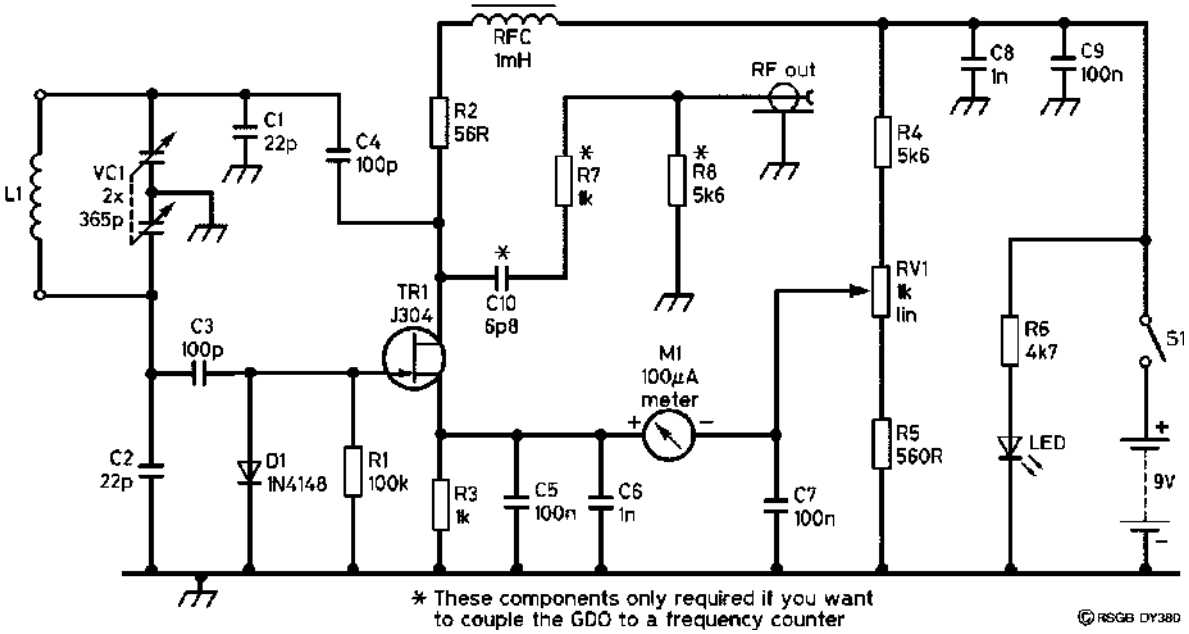

Figure 1 Circuit of an FET GDO. The coils are wound on DIN speater plugs, which provide both a plug-in base and a coil former

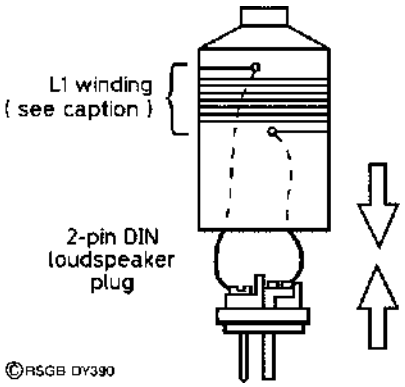

Figure 2 Details of coil construction:
Range 1: 1.6–4.0 MHz 55 turns of 30 SWG
Range 2: 3.3–7.9 MHz 27 turns of 30 SWG
Range 3: 6.3–4.0 MHz 14 turns of 26 SWG
Range 4: 11.9–4.0 MHz 7 turns of 24 SWG.

change superimposed on a much larger standing current, the method of *offset* can be used.

One connection to the meter goes to the source of the FET, while the other goes to a variable offset voltage set by VR1. M1 has a full-scale deflection (FSD) of 100 µA. If the current through TR1 changes, the voltage across R3 changes. When there is no resonance, the voltage at the wiper of VR1 is set to be very slightly greater than that across R3, and there is a 75% FSD meter deflection. When the voltage across R3 decreases very slightly, due to

external circuit resonance, a significant 'dip' in the meter deflection is produced, hence the name of the instrument.

The circuit is not difficult to make on standard matrix board. Provided you can follow a circuit and translate it into a good component layout, then this project is probably only an evening's work.

The most important part of the GDO is the tuning capacitor and its associated frequency-calibrated dial. New, air-spaced tuning capacitors can cost you up to £20, so it is worth delving around in junk boxes, or scouring the tables at a local boot sale or rally. The tuning capacitor from an old transistor radio should be perfect. It may even have a slow-motion drive and a dial which can be remarked for the project.

Choose a coil plug and socket arrangement that is practical. Think about crystal holders or phono plugs and sockets. The prototype shown in Figure 1 and Figure 2 used 2-pin DIN plugs, with the coil wound on the outside of the plastic plug cover. Figure 2 shows the coil construction and the winding details.

If you use a variable capacitor, VC1, with a value different from that shown in the parts list, then the frequency ranges will be different. This does not matter, as it will be taken into account during calibration.

Position VC1 so that the dial will be easy to see and to operate, while locating the coil socket as close to it as possible. **Figure 3** shows the traditional layout of the GDO.

Calibration

Because the GDO also radiates a very small amount of energy, a general coverage receiver can be used to calibrate the dial. Don't try to aim for great accuracy and clutter the dial with marks and figures! If you include C10, R7 and R8 in your circuit, you can connect a frequency counter directly to the GDO and leave it in circuit all the time.

The GDO in use

Always try to place the external tuned circuit with its coil coaxial with the plug-in coil, as shown in Figs 1 and 3. If the coils are at right angles, the GDO may not produce any resonance. Set the offset control to give about 75% FSD and slowly tune L1 through its whole range. If no dip occurs, you may have the wrong coil plugged in. When you eventually find a dip, move the external coil further away until only a minute dip is seen. You may have to retune the dip meter as you do this, but it gives a much more accurate reading of frequency.

Remember that you cannot 'dip' a coil by itself – there must always be a capacitor present.

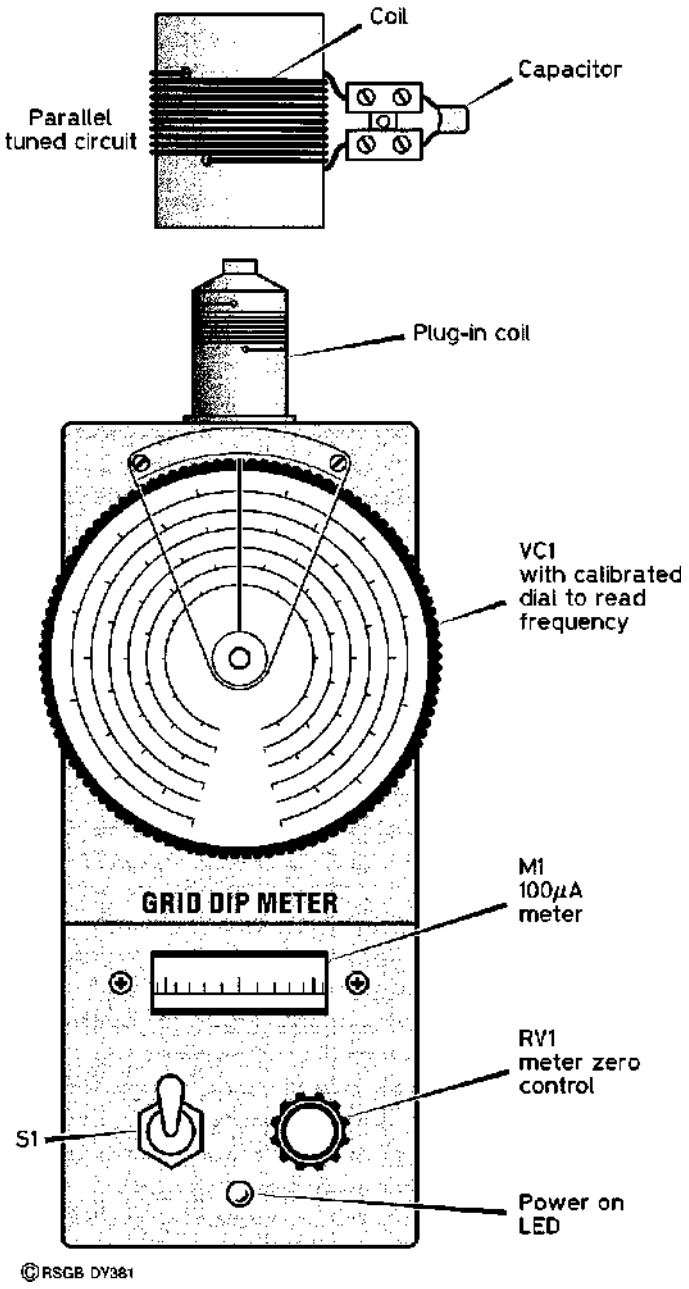

Figure 3 Layout of a typical GDO. The dial, meter and the location of the coil to the circuit under test can all be viewed at the same time. It is shown measuring resonance of a tuned circuit

Aerial resonance

Figure 4 shows how to check the resonance of a dipole aerial. Disconnect the coax feed at the aerial and place a short piece of wire, terminated with crocodile clips, across the centre insulator to short together the two ends of the aerial. By placing the GDO close to the shorting link, a dip should be seen on the meter while VC1 is turned. Alternatively, a loop in the element can be made around the coil, as in Figure 4, or the shorting link can be made long enough to loop over the coil. The latter method does not require tampering with the mounting and tensioning of the dipole wires.

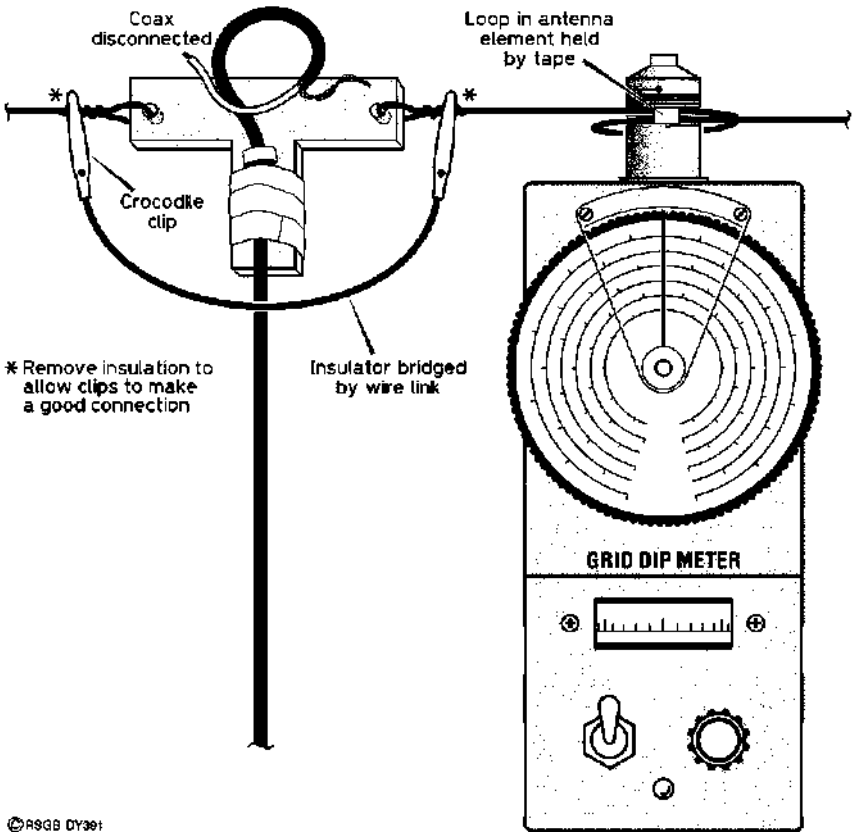

Figure 4 A wire antenna element can be looped into a single turn coil for increased coupling to the GDO

Parts list

Resistors: all 0.25 W, 5% tolerance

R1	100 000 ohms (100 kΩ)
R2	56 ohms (56 Ω)
R3	1000 ohms (1 kΩ)
R4	5600 ohms (5.6 kΩ)
R5	560 ohms (560 Ω)
R6	4700 ohms (4.7 kΩ)
R7	1000 ohms (1 kΩ)
R8	5600 ohms (5.6 kΩ)
VR1	1000 (1 kΩ) linear

Capacitors

C1, C2	22 pF
C3, C4	100 pF
C5, C7, C9	100 nF (0.1 μF)
C6, C8	1 nF (1000 pF)
C10	6.8 pF
VC1	2 × 365 pF

Semiconductors

TR1	J304 or similar
D1	1N4148
LED	

Additional items

L1	See Figure 2
RFC	1 mH
S1	SPST
M1	100 μA

Source

Components are available from Maplin.

87 A CW transmitter for 160 to 20 metres

Introduction

This very small transmitter is designed to work on any band from top band (160 m) to 20 m, with an RF output of 1 W. It will work on higher frequencies but with a reduced output.

The circuit

The three-transistor circuit is shown in **Figure 1**. It comprises a crystal oscillator using a BC182 transistor which drives a 2N3866 power amplifier (PA) keyed by a ZTX750 PNP transistor. The oscillator and PA are coupled by a capacitor and resistor; this provides a very small amount of positive bias to the PA.

The oscillator can be used as a basic crystal oscillator but, by including a variable series capacitor as shown in Figure 1, the crystal frequency can be 'pulled' slightly, making the oscillator a *variable crystal oscillator* (VXO).

Construction

The PCB layout is shown in **Figure 2** and in the photograph. Although the prototype was built around a PCB, this circuit is equally amenable to

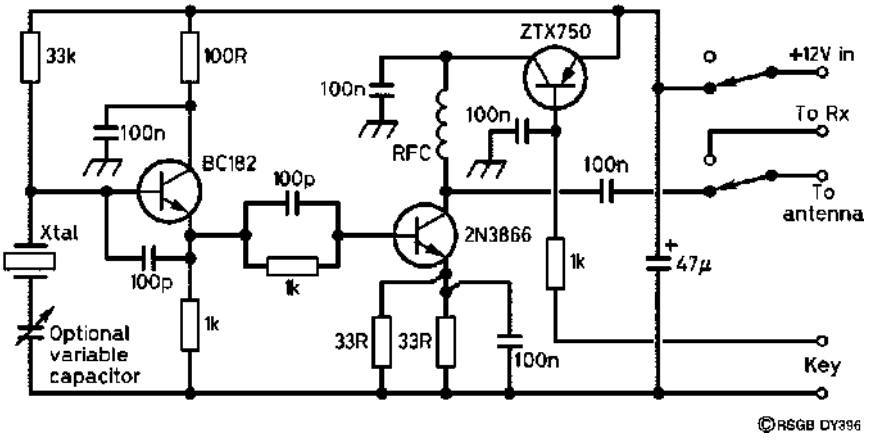

Figure 1 Transmitter circuit diagram

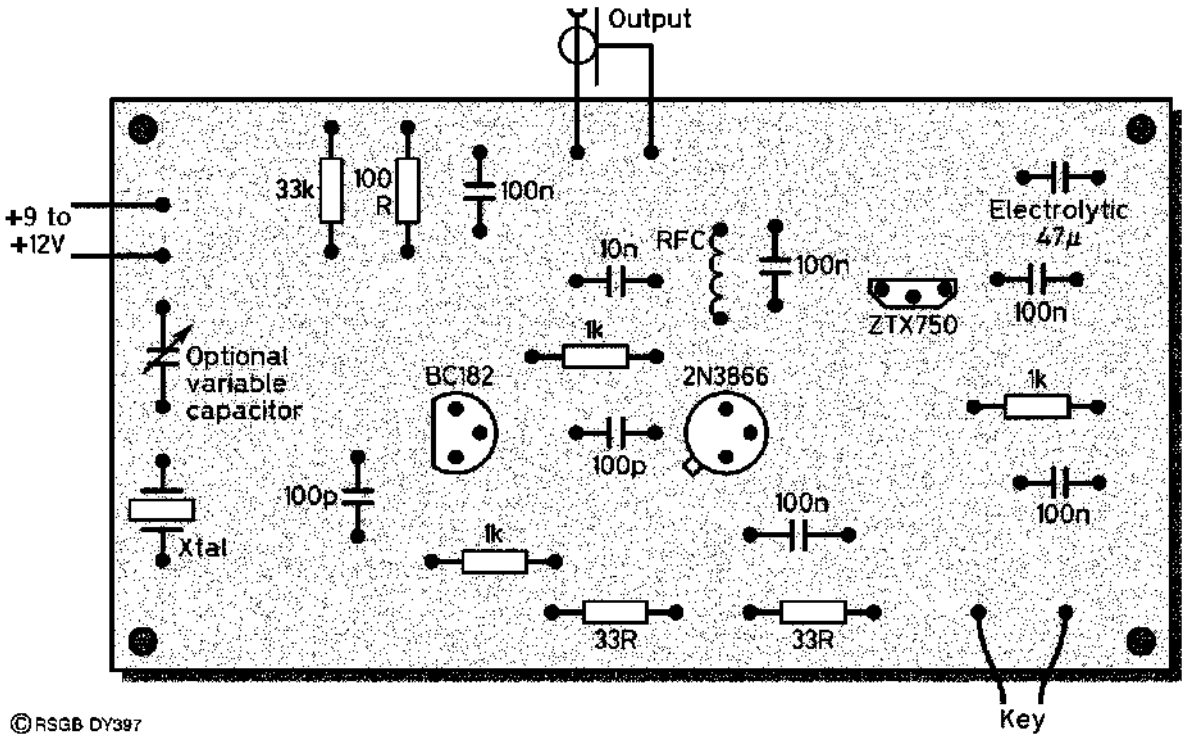

Figure 2 Component placing on the PCB. The external connections are also shown

construction on a matrix board. Populating the PCB is very simple, and you can expect to be able to do this in about one hour. The radio-frequency choke (RFC) is made by winding 10 turns of 33 SWG wire on a ferrite bead. The enamel coating of the wire is intended to vaporise when soldered into the board, thus obviating the need to remove the enamel manually with a knife or sandpaper. However, if you do have problems with the PA either not working or keying intermittently, it is suggested that you investigate the RFC connections immediately!

If you decide to make the VXO version, you will have to cut the track between the crystal and earth, and connect the variable capacitor (250 pF) across the break.

In use

After performing the usual checks on the accuracy of your circuit building and the wiring of the external components, it is time to connect a 12 V battery between the points shown in Figure 2. Do not switch on yet. An aerial needs to be connected to the output via an ATU and a crystal, of frequency matching that of the aerial, fitted. The variable capacitor should

give you a tuning range from about 14.058 to 14.064 MHz. 'Netting' (the process of tuning your transmitter to the same frequency as that of a received station) is achieved simply, because the oscillator is always running, and the leakage of the signal (despite the fact that the PA is not powered) is sufficient to bring the two frequencies to zero beat.

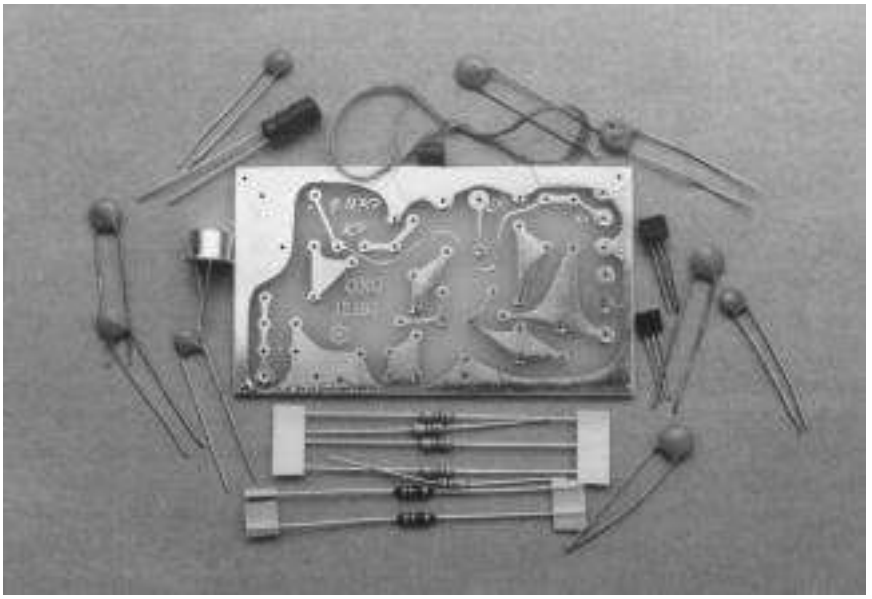

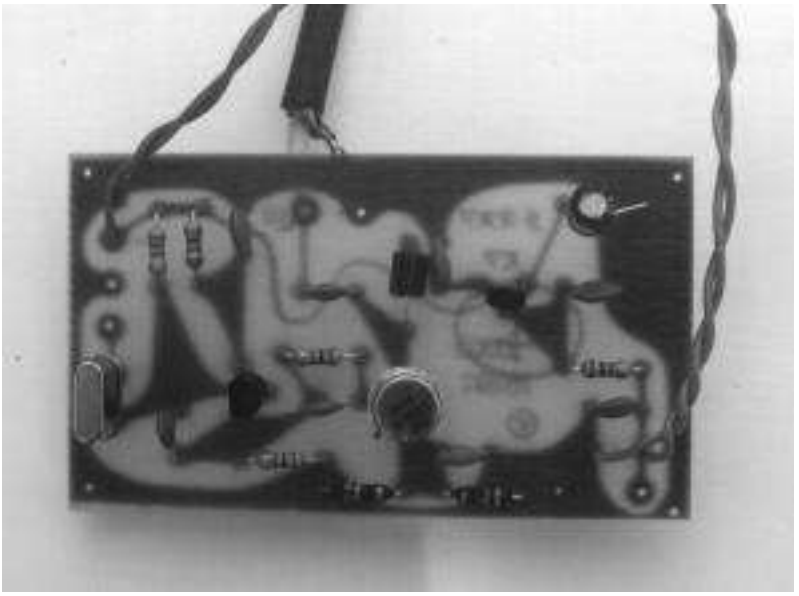

Warning

Note that the transmitter has no filtering; harmonics are not suppressed. It is strongly recommended that you use this transmitter in conjunction with the excellent low-pass filter described in the project *A 7-element low-pass filter for transmitters*, described elsewhere in this book.

88 Matching the end-fed random-wire aerial

Introduction

Many amateurs who do not have the space (or money) for a multi-band beam aerial, make use of the simplest possible alternative – the longest piece of wire that they can erect, with its end connected to the transceiver or receiver by an aerial tuning unit (ATU).

The length of the wire is not of major importance. Any length between 10 m and 80 m, with bends if necessary, will suffice. A good earth connection to the radio is just as important. Bends in the aerial wire can have some interesting effects on the directional properties of the aerial; V- or L-bends, or even a square shape are permitted. The only thing *not* permitted is to fold the wire back on itself in a tight hairpin bend!

Longish wire aerials

The term 'long wire' is usually used (incorrectly) to describe an end-fed aerial. How long is a piece of string? It depends what you mean by 'long'. In aerial parlance, it means 'long with respect to one wavelength'. Again, this depends on the band you are using. A long wire at 20 m is somewhat different from a long wire at 160 m. However, if you have sufficient real estate for a long wire on the 160 m band it must, by definition, be a long wire on all the other bands, too!

This should put you on your guard when analysing published data about feed-point impedance and the directional properties of a long wire aerial. Such theoretical data relate to a *real*, *ideal* long wire which is straight, horizontal, very high above perfect (conducting) ground, and not obstructed in any way. So your aerial doesn't quite match these criteria? Join the club!

Don't let this dampen your ardour when it comes to evaluating what the longish wire can do for you. The following should explain why.

Feed-point impedance

The impedance at the end of a longish-wire aerial can vary from a few tens of ohms to several thousand ohms, depending on the frequency in use and the wire length. It is also affected by factors such as bends, height above ground, proximity to buildings and wire diameter.

The actual value doesn't matter, provided we can make the aerial *appear* to have a 50 Ω impedance at the aerial socket of the transmitter. This process is what we call *impedance matching*, or simply *matching*. It maximises the power transfer from the transmitter to the aerial, and from the aerial to the receiver.

That is why an aerial tuning unit, or ATU, is almost (but not necessarily) obligatory.

The ATU

Many commercially produced HF receivers and transceivers have single 50 Ω coaxial sockets as their one and only means for connecting an external aerial. This means that an external aerial should have a 50 Ω feed impedance if it is to work efficiently, and it rules out most of the aerials being used by amateurs on the HF bands. Some means is necessary to change the aerial feed impedance to 'match' that of the transceiver. Such impedance-matching, or *Z*-matching (because *Z* is the symbol for impedance, just as *L* is the symbol for inductance) is the rôle of the ATU.

These can be bought and will accommodate either an end-fed or a coax-fed aerial. They can be bought ready for use or in kit form. Whether you want one for receiving only, or for use with a low-power (QRP) or high-power (QRO) transmitter, will determine what you need and how much you pay.

A simple single-band ATU

The simplest form of ATU is shown in **Figure 1**. It is simply a parallel LC (coil and capacitor) circuit, resonant at the chosen frequency, with taps on the coil for the aerial and the coaxial feed to the transceiver. If we assume the circuit is resonant, a high impedance exists at the top of the coil, and a low impedance at the bottom.

We said earlier that the end-fed longish wire presented an impedance which was high (or at least higher than 50 Ω). This explains why the aerial is tapped to the coil near the top, where the impedance is high, and the 50 Ω coax is tapped near the bottom, where the impedance is low.

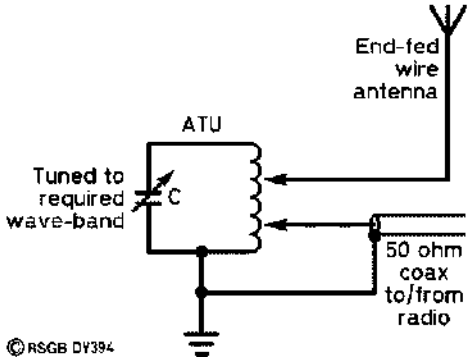

Figure 1 Parallel tuned circuit as single-band ATU for end-fed longish-wire antenna

Because the feed-point impedance of the aerial changes with frequency, so must the point at which the aerial is tapped to the coil to achieve impedance matching. The value of C must be changed also, to ensure that the circuit is resonant, and the 50 Ω tap will require tweaking also.

Setting up an ATU is quite simple. Make up an LC parallel-tuned circuit consisting of 50 turns of enamelled copper wire on an empty 35 mm film plastic container (or similar), tuned with a 500 pF variable capacitor. Make sure the enamel is removed from the ends of the wire before soldering.

Solder the inner wire of the coaxial cable from the radio to the first or second turn of the coil from its grounded end. Then solder the braid to the grounded end. Connect the aerial about one-third of the way down the coil from the top, removing the enamel at the connection point.

Adjust the variable capacitor for maximum noise or signal strength in the receiver. Then, try different tapping points from the aerial, to maximise the signal again. This matches the aerial impedance to that of the tuned circuit. Repeat the process with the coax tap, thus matching the impedance of the radio and the cable to that of the tuned circuit.

You will no doubt find that the tapping process on the coil was not easily accomplished, especially when the enamel must be removed at each tapping point without shorting adjacent turns together. It is therefore logical to produce a design where the taps have been prepared during the winding of the coil, and are selected with a rotary switch. To this end, the following multi-band design is described.

A multi-band ATU

The same type of coil design around a 35 mm film container is used (see **Figure 2**). The tapping points can be prepared in advance by a little judicious planning. Dismantle your original coil and measure the length of wire on it. It will be a little more than a calculation of $50 \times \pi D$ would suggest (where D is the diameter of the film container), due to the lack of tension in the coil and the wire diameter itself. You will need aerial tapping points at turns 1, 2, 3, 5, 10, 15, 20, 25, 30, 35, 40 and 45, corresponding to all the bands from 28 MHz to 1.8 MHz. The coaxial cable tap is fixed at turn 2 (an acceptable compromise). All the turns are counted from the earthy end.

Cut another piece of enamelled copper the same length as you used originally. Then, with the aid of an ordinary calculator, work out the positions of the points where the enamel must be removed for the taps. For example, turn 15 will have to be made $\frac{15}{50}$ of the way along the wire, turn 20 tap made at $\frac{20}{50}$ of the way along. So, if the length of wire is, say 4.7 metres, the two taps in question will be made at $\frac{15}{50} \times 4.7 = 1.41$ m and $\frac{20}{50} \times 4.7 = 1.88$ m from one end. This must be repeated for each of the tap positions, and the enamel removed ready for the wire to be soldered to it. With a

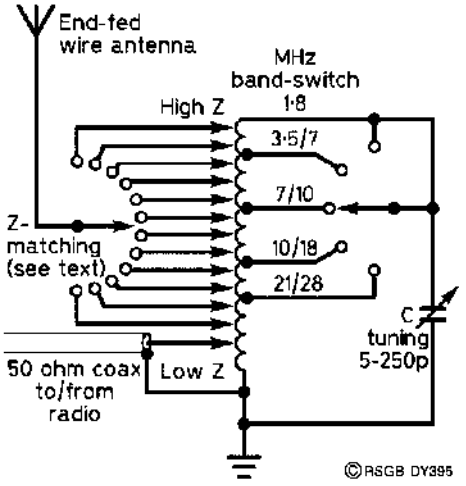

Figure 2 Simple multi-band ATU for end-fed longish-wire antennas

soldering iron, tin each tap point while the copper is shiny, thus ensuring a good, low-resistance connection. Do not solder on the taps yet.

The coil can now be wound as before. The taps can be soldered on, taking the lead from each one to the wafer of a single-pole 12-way rotary switch, the pole being connected to the aerial.

The tuning of the ATU is carried out by the same 250 pF capacitor, with a single-pole 5-way rotary switch used to select the band. Its tapping points will need to be chosen manually, using the method described earlier. Don't attempt to make new tapping points on the coil for this – use the taps available on the wafer of the other rotary switch, and find which is optimum for each band.

Notes

- For the aerial, use PVC-covered stranded tinned copper, of size 16/0.2 mm or 24/0.2 mm.
- Make the wire as long as possible, but anything over 10 m should be OK.
- Keep the wire as high as you can, in the clear and away from obstructions.
- Don't worry about bends, but don't use hairpin bends.
- Use a good insulator to attach your aerial – anything plastic will do.
- Anchor the wire near the point of entry to the building, but use a U-bend to prevent ingress of water.
- The wire can be brought in through the corner of a window, the PVC acting as an insulator. If you must drill a hole in the brickwork, make sure it slopes upwards from outside, so that water is deterred from entering.
- Use a good RF earth (as opposed to an electrical earth) such as half a dozen bare copper wires buried under the lawn in a fan shape. They should be joined together at the point of the fan and strapped to the earth connector of your ATU.

ARRL's

$19.95

RF Amplifier Classics

Practical design and construction details from the pages of *QEX* and *QST*.

Contents

HF/MF/VHF Amplifiers (1 to 54 MHz)

An Easy-to-Build 25-Watt MF/HF Amplifier	Gary Breed, K9AY
A Compact 1-kW 2-50 MHz Solid-State Linear Amplifier	H.O. Granberg, K7ES/OH2ZE
A Broadband HF Amplifier Using Low-Cost Power MOSFETs–Parts 1 and 2	Mike Kossor, WA2EBY
A 1.8 to 54 MHz 5-Watt Amplifier	Zack Lau, KH6CP
An Experimental Solid-State Kilowatt Linear Amplifier for 2 to 54 MHz	Joel Paladino, N6AMG
An All-Band, 1500-Watt-Output 8877 Linear Amplifier–Parts 1 and 2	Jerry Pittenger, K8RA
High-Efficiency Class-E Power Amplifiers–Parts 1 and 2	David Rutledge, KN6EK, et al.
A 100-W MOSFET HF Amplifier	William E. Sabin, WØIYH
The FARA HF Project	Jim Valdes, WA1GPO

VHF/UHF Amplifiers

A Compact "Brick" for 6 Meters	Pat Bunn, N4LTA
A 300-W MOSFET Linear Amplifier for 50 MHz	Richard Frey, K4XU
A No-Bandswitch, Dual-Band VHF Desktop Amplifier	Paul Hewitt, WD7S
An 8-Watt, 2-Meter "Brickette"	Bob Larkin, W7PUA
903-MHz Linear Amplifiers–Parts 1 and 2	Dave Mascaro, WA3JUF
25-Watt Linear Amplifiers for 144 and 220 MHz	Dave Mascaro, WA3JUF
A High-Power 2-Meter Amplifier Using the New 3CX800A7	David Meacham, W6EMD
A Quick Powerhouse	Russ Miller, N7ART
A Cathode-Driven Tetrode for 6 Meters	David Munyon, W7DVB
A UHF Amplifier—from Scratch	John Reed, W6IOJ
A Solid-State 6-Meter Linear Amplifier You Can Build	Tarmo Tammaru, WB2TMD
Build a 6-Meter "Mini-Lini"	Wilson Hoag, WA5OLT
A Grounded-Grid Kilowatt Amplifier for 432 MHz	Stephen J. Powlishen, K1FO

Microwave Amplifiers

A Quarter-Kilowatt 23-cm Amplifier–Parts 1 and 2	E.R. "Chip" Angle, N6CA
A 2-W 13-cm Amplifier	Zack Lau, KH6CP
1296-MHz Solid-State Power Amplifiers	Al Ward, WB5LUA

Amplifier Maintenance

Amplifier Care and Maintenance	Ward Silver, NØAX

Foreword

If antenna gain alone is not sufficient to bridge the path between two stations, the alternative is to increase RF power. Hams have been aware of this fact since the earliest days, and that is why RF power amplifier projects have always been popular.

In *RF Amplifier Classics* we have assembled a collection of articles published in *QST* magazine, and its sister technical journal, *QEX*. The collection spans the early 1980s through 2003 and includes many prominent authors. In those few instances where an author provided a design revision (or correction) after the article was published, that revision is *included* in the article as presented in this book.

See the leatest issue of *QST* for other ARRL RF design-related publications, or visit our on-line bookstore at **www.arrl.org/catalog**. Please take a few minutes to give us your comments and suggestions on this book. There's a handy Feedback Form for this purpose at the back, or you can send e-mail to **pubsfdbk@arrl.org**.

Our thanks to the many authors whose work appears in this book. Without their willingness to share their knowledge with the amateur community, *RF Amplifier Classics* would not be possible.

Dave Sumner, K1ZZ
Executive Vice President
Newington, Connecticut
August 2004

By Gary Breed, K9AY From *QST*, February 1994

An Easy-to-Build 25-Watt MF/HF Amplifier

Do you need a medium-power linear amplifier for SSB or CW? Congratulations—you just found it!

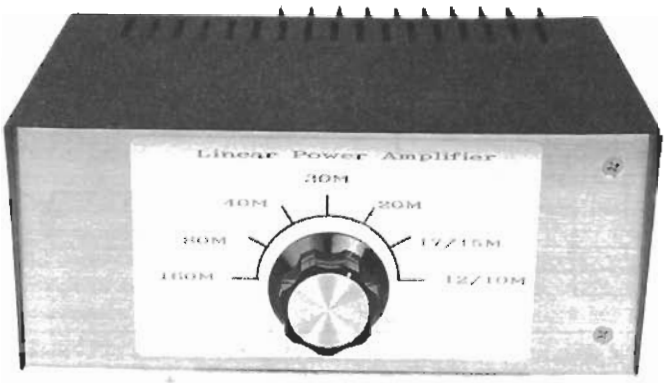

Here's a 25-W, 1.8- through 30-MHz, class-A linear power amplifier that's simplicity itself. What makes it simple is the use of a self-biased transistor module requiring few external components. To control harmonic output, a set of five-section low-pass filters is included. Power-supply requirements are +28 V at 2.5 A and —5 V at 200 mA.[1] With a gain of about 13 dB, a 1- to 1.4-W driving signal is all that's needed to deliver 25 W output. Gain is flat within ±0.75 dB across the covered frequency range.

If 25W isn't enough for you, it's easy to directly apply the design information to build a 50-W amplifier—all you do is use a larger transistor module! Another step toward project simplicity is the availability of kits. Each kit contains all the major components for either a 25- or 50-W version.[2]

Amplifier Design

When designing a power amplifier, the first step is to select the right transistor(s). Excellent bipolar-junction transistors (BJTs) and field-effect transistors (FETs) are available from well-known companies such as Motorola, M/A-COM PHI, SGS-Thomson, Philips, Mitsubishi and others. A number of smaller companies also make power transistors, usually for more-specialized applications. MicroWave Technology, Polyfet RF Devices, and Directed Energy may be company names unfamiliar to you, but they all make power transistors for MF and HF applications.

In this amplifier, I use the SLAM-0111 from MicroWave Technology.[3] I didn't choose it because of its gain, its efficiency, or even its price; I selected it because it's very easy to use. The device consists of two power JFETs (the particular specialty of MicroWave Technology), operating in push-pull. Since JFETs behave similarly to triode vacuum tubes, the company dubbed them *Solid State Triodes*. SLAM (Solid-state-triode Linear Amplifier Module) devices include thick-film bias resistors in the package with the transistors. These resistors set the gate bias for class-A operation, and establish a 50-a input impedance. At the rated power and supply voltage, the push-pull output impedance is also 50 Ω!

With such convenient input and output impedances, matching the devices to a 50-Ω system merely requires 1:1 balun transformers at the input and output. Because the bias voltage is internally generated, the only other external circuitry required is a suitably bypassed and isolated 28-V power supply.

Circuit Description

The amplifier schematic is shown in Fig 1. The balun driving the gates of the push-pull transistors is a conventional transformer. The primary and secondary windings are each three turns of #28 wire, wound on a two-hole ferrite balun core of 73 material (μ_i = 2500). These transformers are broadband enough to provide 1.8- to 30-MHz operation and offer dc isolation with no additional components. The input-transformer primary is center-tapped and bypassed to provide access to the gates for external dc bias (more on this later).

The output transformer is constructed in the same manner as the input transformer—it's just larger. Two ferrite beads of 77 material (μ_i = 2000) make a two-hole core, with primary and secondary windings of three turns each, using #24 hookup wire. The primary (transistor side) is center-tapped and bypassed to provide dc voltage to the drains. Feeding dc through a center-tapped transformer eliminates the need for the usual bifilar RF choke seen in push-pull amplifiers—another reduction in the component count. Multiple bypass capacitor values (0.01, 0.1 and 10 µF) are used to cover the MF/HF range. That's the basic amplifier block: two transformers, a SLAM device, and a few bypass capacitors!

Class-A Operation Notes

By definition, transistors operating in class A conduct over the entire 360 degrees of the signal (that's all the time, of course). This operational mode assures that the transistor is always operating in the linear region of its input-to-output transfer characteristic. To do this, the device must be biased to handle the maximum signal at all times.

Obviously, this class of operation is pretty inefficient, since full current is drawn whenever the amplifier is on. A "perfect" transistor operating class A can only be 50-percent efficient, and real transistors

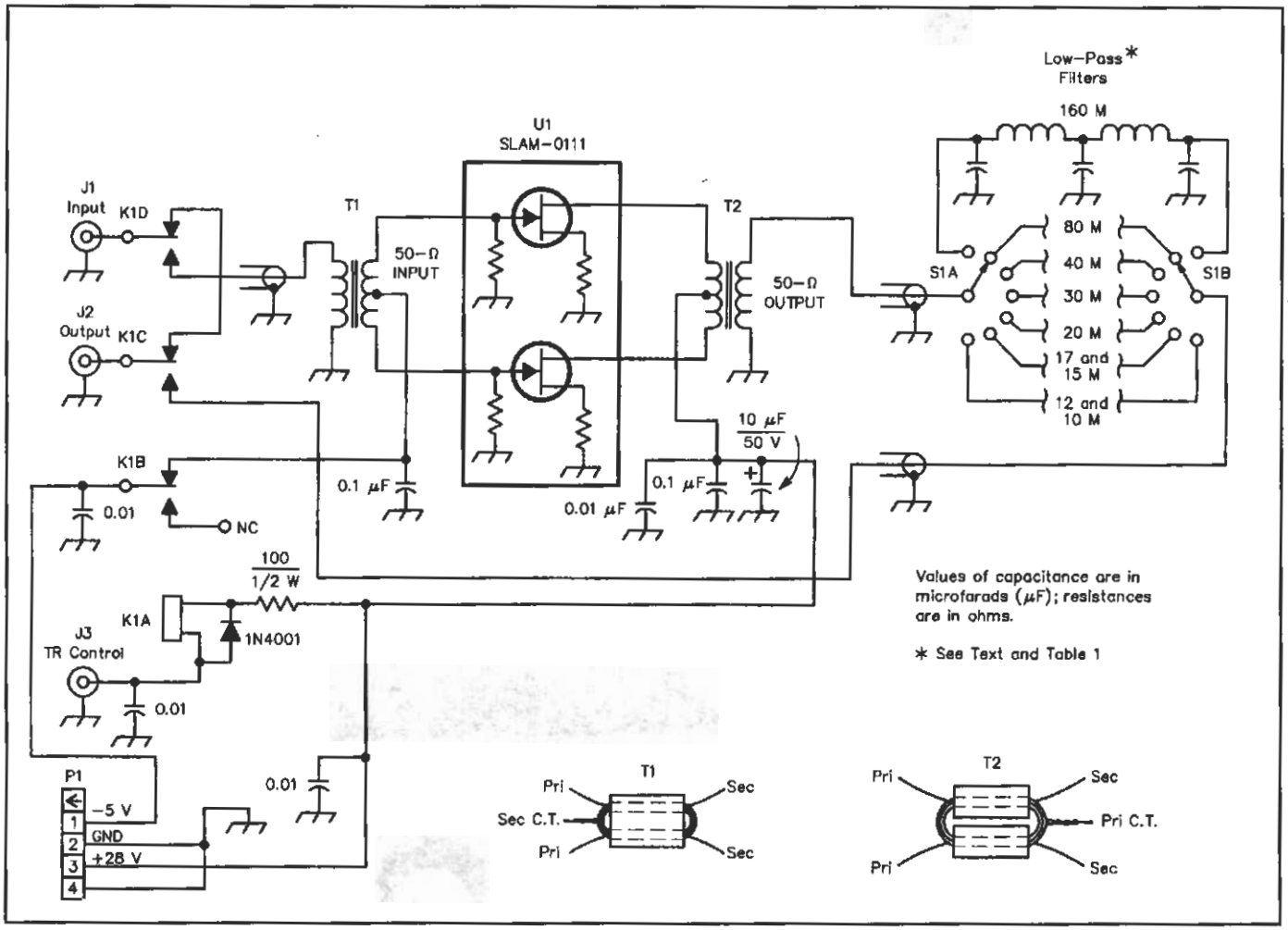

Fig 1—Schematic diagram of the 25-W class-A amplifier. Unless otherwise specified, resistors are 1/4-W, 5%-tolerance carbon-composition or film units. Equivalent parts can be substituted.

J1—Panel-mount BNC socket.
J2—SO-239 connector.
J3—Phono jack.
P1—4-pin male Jones plug.
K1—3PDT relay with a 24-V dc coil. A surplus Potter & Brumfield KHP series 4-pole relay is shown in Fig 6; one pole is unused. (All Electronics catalog number 4PRLY-24N [$4] or Ocean State Electronics R12-17D3-24 [$10.90] are suitable. See the Part Suppliers List on pp 35-40 of *The 1994 ARRL Handbook* for addresses and telephone numbers. —Ed.)
S1—2-pole, 7-position ceramic rotary switch. My switch is made from two surplus CRL 11-position switch wafers and an indexing assembly providing selectable stops. The wafers are spaced about 1 1/2 inches apart. CAL PA-200 series switch wafers and PA-300 series shaft and indexing assemblies are suitable (switches are available from Newark Electronics; tel 312-784-5100, fax 312-784-5100, ext 3107, to locate your nearest Newark distributor).
T1—Primary: 3 turns #28 AWG; secondary, 3 turns #28 AWG, center-tapped. Core: Fair-Rite #2873002402 balun (Amidon BN 73-2402).
T2—Primary, 3 turns #24, center-tapped; secondary, 3 turns #24. Core: two Fair-Rite #2677006301 beads (Amidon FB 77-6301).
U1—SLAM-0111 ultralinear 25-W, class-A, self-biased power FET module or SLAM-0122, 50-W version (Microwave Technology, 4268 Solar Way, Fremont, CA 94538, tel 510-651-6700, fax 510-651-2208).
Misc: RG-174 coax, enclosure (3 1/2 x 7/8 x 5 1/4 inches [HWD]), heat sink (3 x 4 1/8 x 1 3/8 inches [HWD]), PC-board material, knob, mounting hardware.

do no better than about 40 percent. This amplifier draws 2.5 A from a 28-V power supply for an input power of 70 W. When it is providing 25 W, it's 36-percent efficient. (When there is no input, it's 0-percent efficient!)

To help reduce the heat generated by an amplifier that requires 70 W, a negative bias can be applied to the gates when not transmitting. A bias of —5 V results in a 0.25-A standby drain current instead of the full 2.5 A. The internal bias resistors are about 50 ~ on each gate, and dissipate a maximum of I W. Under these biasing conditions, the resistors each dissipate 0.5 W. Don't try to cut off the transistors completely with greater bias voltage! You'll risk burning out the resistors.

Some may ask, "If class A is this power hungry, why use it?" In a word: linearity. If you want excellent linearity (which means minimum distortion caused by harmonics or intermodulation), class A is the way to go. For example, all small-signal amplifiers for receivers and low-level transmitter stages operate class A because they must handle signals without distortion. However, they operate at very low power, so power dissipation is rarely an issue. This power amplifier further minimizes distortion by using push-pull operation, which cancels even-order distortion products in the output and makes the next part of the design easier than usual.

Harmonic Filter Design

As mentioned previously, the amplifier uses several low-pass filters to cover the nine MF/HF amateur bands. Each filter was initially designed for a cutoff frequency 20 percent higher than the upper end of their respective 160, 80, 40, 30, 20, 15 and 10-meter ham bands. The 15-meter filter is also used for 17 meters, and the 10-meter filter for 12 meters.

With no filtering, even-order harmonics (2nd, 4th, etc) are more than 40 dB below the carrier, the result of good push-

Table 1
Filter Circuit and Comparison of Ideal and Final Component Values.

	Ideal Filter Values			*Actual Filter Values*		
Cutoff Freq. (MHz)	*C1, C5 (pF)*	*C3 (pF)*	*L2, L4 (µH)*	*C1, C5 (pF)*	*C3 (pF)*	*L2, L4 (µH)*
2.40	1521	2620	4.55	1470 (1000 + 470)	2880 (2200 + 680)	4.41 (30 t on T50-2)
4.80	761	1310	2.27	830 (560 + 270)	1430 (1000 + 430)	2.37 (22 t on T-50-2)
8.76	417	718	1.25	430	820	1.25 (16 t on T-50-2)
12.18	300	516	0.900	300	560	0.960 (14 t on T-50-2)
17.22	212	365	0.634	220	370 (270 + 100)	0.706 (12 t on T-50-6)
25.74	142	244	0.424	150	240	0.460 (10 t on T-50-6)
35.64	102	176	0.306	100	180	0.314 (8 t on T-50-6)

In some cases it is necessary to parallel two smaller-value capacitors to obtain the proper values of capacitance for C1, C2 and C5
The inductors are wound on T-50-2 or T-50-6 cores. Inductors for the 160- and 80-meter filters are wound with #26 AWG wire in order to fit all turns on the cores; the other inductors are wound with #22 wire.

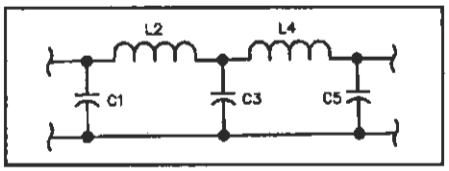

Fig 2—Schematic of the filter used for each band.

pull balance using factory-matched transistors. The 3rd and 5th harmonics are more than 15 dB down. To reduce the 3rd harmonic to at least 50 dB below the carrier, a five-section Chebyshev filter with low passband ripple is an appropriate choice. This type of filter has a good SWR in the passband, and a smooth roll-off characteristic. The design process began by creating ideal designs using a public-domain filter design program.[4]

Ideal designs rarely correspond to standard capacitor or inductance values that can be realized with a discrete number of turns on common toroid cores. Using a circuit analysis program,[5] the ideal designs were analyzed to see the effects of such realworld limitations on harmonic rejection and SWR performance.

First, the ideal component values were entered into the program, and varied ±20 percent to see which ones had the greatest effect on performance. C1 and C5 (see Fig 2 and Table 1) were found to be least sensitive to variations, L2 and L4 were moderately sensitive; varying C3 had the greatest effect on both passband and stopband performance. The ideal capacitor values were then replaced with standard capacitor values or—in some cases— parallel combinations of two common capacitor values. Inductors were given the near~st value available for coils wound on either T-50-2 or T-50-6 toroid cores. The final filter designs are the result of trade-offs between inductance, capacitance and filter performance. Table 1 shows the filter topology, along with a comparison of the original ideal filter component values and the values selected for the finished unit.

Construction

I built my amplifier and low-pass filter modules on single-sided PC boards, using pads to mount the components. No holes are drilled (except for mounting screws) and all leads are attached by soldering them to the pads. The PC-board patterns for the amplifier and filters are available (see Note 2).

Fig 3 shows the amplifier-assembly parts. This assembly is mounted to a heat sink (see Figs 4 and 5) capable of dissipating more than 40 watts without excessive temperature rise. (This assumes a worst case of 50-percent transmitting time, and 7-watts dissipation in standby.) A cutout in the middle of the amplifier board allows placement of the SLAM device. The PC board leaves a conducting path around the ends of the SLAM to maintain a ground potential across the entire board. Four mechanical components make up the amplifier assembly. The first is a 0.1875-inch-thick aluminum base plate to which the SLAM is mounted. Next are two aluminum 0.1-inch-thick spacers, which are placed between the base plate and the circuit board. These spacers set the proper distance from the base plate to SLAM leads. The SLAM is installed through the top of the PC board, and its leads are soldered to the traces on top of the board.

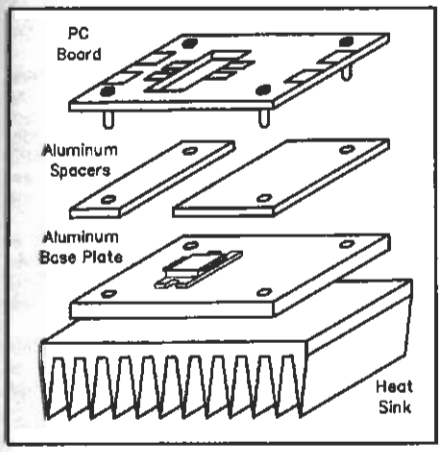

Fig 3—Mechanical assembly of the amplifier-module PC board, aluminum spacers and heat sink.

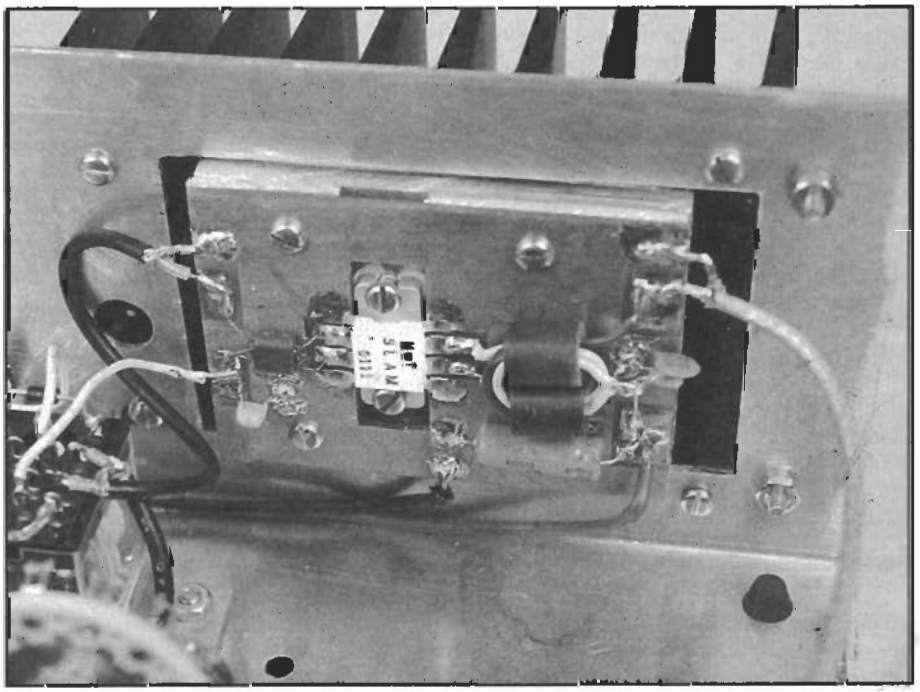
Fig 4—The assembled amplifier-module PC board in position and secured to the heat sink (see Fig 5, next page).

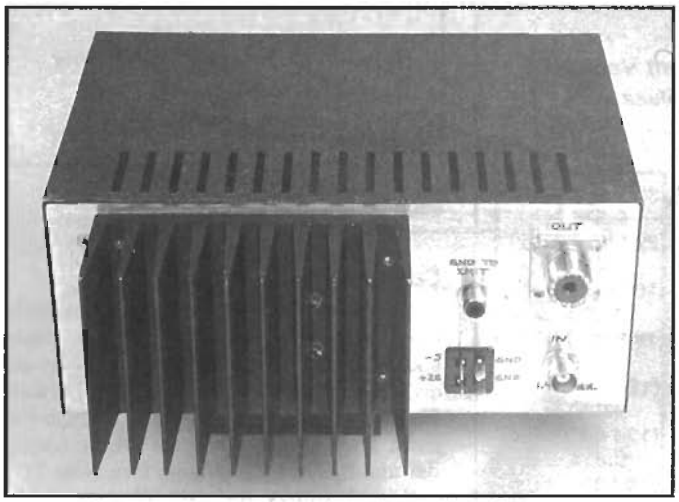

Fig 5—Rear view of the completed amplifier showing the hefty heat sink.

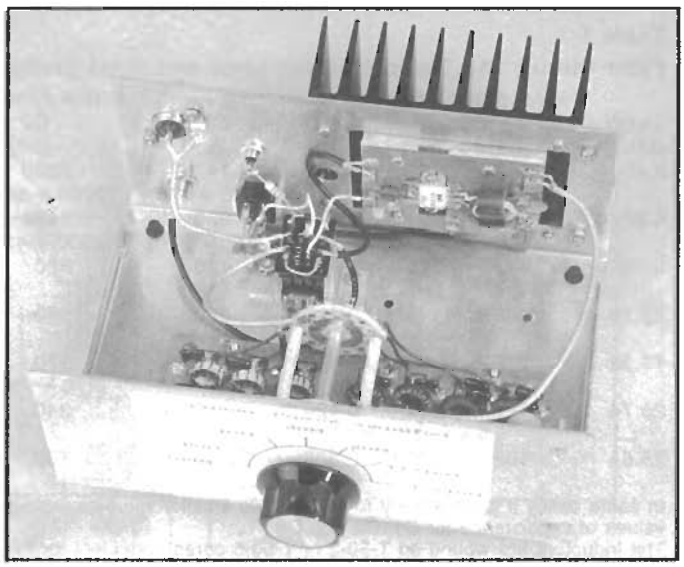

Fig 6—This interior view of the amplifier shows its simple and clean layout. The band switch is centered on the front panel. Immediately beneath the band switch is the filter assembly. Behind the switch and to the left is the TR relay, K1. A four-pin Jones plug power connector is mounted on the rear panel behind and to the left of the relay. On the bottom, near the outside lip of the rear panel, is J1. Above it is J2, with J3 to its right. Most of the rear panel—from its middle to the right lip—is occupied by the SLAM IC PC board and the aluminum spacers secured to the heat sink mounted on the rear panel's exterior. Rubber feet on the cabinet bottom help prevent scratching the supporting surface beneath and keep the amplifier from sliding. The band-switch knob center section is 1⅛ inches in diameter; the skirt flares to a diameter of 1½ inches.

Construction is easiest if the transformer connections to the SLAM are not soldered until after the SLAM is installed. This eliminates the possibility that the transformer connections will get in the way when you try to solder the SLAM into place. As with any power device, place a thin coating of thermal compound between the SLAM and the base plate, and between the base plate and the heat sink. Solder bypass capacitors directly to the transformer center tap and to the ground plane, with the minimum possible lead lengths.

The low-pass filter board is constructed one filter at a time. First, install the capacitor at the center (C3), then the inductors L2, L4), and finally the end capacitors (C1, C5). All inductors are wound with even spacing over three-quarters of the core circumference. Simply solder the capacitors to the pads and ground plane. Silver-mica capacitors were used in the prototype because they were on hand. Ceramic-disc capacitors with 200- to 500-V ratings will work equally well.

If the band switch is located close to the filter board (see Fig 6), short lengths of hookup wire can connect the filters to the switch wafers.

A spacious box houses the filter and amplifier assemblies, along with a TR relay that also switches the standby bias. Power and relay control leads are bypassed where they enter the enclosure.

Before final assembly, I gave the panels of the case a brushed look using a sanding block with oiled sandpaper. Band markings for the switch (see the title-page photo) are drawn on a large, adhesive-backed label attached to the front panel.

Performance

Amplifier gain ranges from 12.5 to 14 dB between 1.8 and 30 MHz. The gain flatness is basically a function of the input and output transformers. (It's possible to make the amplifier gain flat within 1 dB from 1 MHz to 100 MHz using transmission-line transformers and frequency compensation.) The required drive power for 25 watts output is 1.0 to 1.4 watts.

On-the-air performance is excellent. Besides low distortion in the SSB mode, a small advantage of linear amplification is a complete absence of rise and fall distortion of a CW waveform, which sometimes occurs in class-C amplifiers.

Summary

This project shows how new RF products can make home construction of amateur equipment very easy. Home-brewers can benefit from a growing trend in RF product engineering: reducing development time by using "super components" that require few external components and little engineering time to design them into a product.

A secondary purpose of this project is to show how even simple software tools can be used to speed up design. The programs used to design the amplifier's low-pass filters are inexpensive, and accurate at frequencies in the MF/HF bands. In this case, they made it possible to examine tradeoffs among standard-value components for seven different filters, without having to build, measure and tweak each one.

The result is a linear power amplifier with good gain and performance. Its uncomplicated design leaves little room for error, and no fancy test equipment is needed to successfully build it. Projects this easy can make an old-timer forget about the "simpler" days of vacuum tubes!

Notes

[1]Power supplies are available from Marlin P. Jones & Assoc, mc, PO Box 12685, Lake Park, FL 33403-0685, tel 407-848-8236; fax 1-800-432-9937.

[2]Parts kits for this project are available from Crestone Engineering, PO Box 3702, Littleton, CO 80161, tel 303-770-4709. Each kit includes all electronic and mechanical components for the amplifier module and lowpass filter assembly, includin9 circuit boards, heat sink and rotary band switch. Kits do not include an enclosure, connectors, or TR relay. A 25-W kit using the SLAM-0111 is $115; a 50-W kit using the larger SLAM-0122 is $190. Add $6 per kit for shipping. Payment may be made by check, money order, VISA, MasterCard or American Express.

PC board patterns for the amplifier and filters are availablefreefrom the ARRL. Send your request to the Technical Department Secretary, ARRL, 225 Main St, Newington, CT 06111. With your request for the BREED AMPLIFIER PC-BOARD TEMPLATE, enclose a business-size envelope with one First-Class stamp.

[3]Microwave Technology, 4268 Solar Way, Fremont, CA 94538. Their products are distributed by Richardson Electronics, 40W267 Keslinger Road, LaFox, IL 60147, tel 708-208-2200.

[4]Mike Ellis, "A Comprehensive Filter Design Program," RF Design, July 1991. The program is available from the RF Design Software Service, PO Box 3702, Littleton, CO 80161-3702, tel 303-770-4709 (part #RFD0791, $15 postpaid).

[5]NOVA, a shareware program by Robert Stanton, also available from the RE Design Software Service (part #RFD-0391 ,$15 ppd).

By H.O. Granberg, K7ES/OH2ZE

From *QEX*, July 1990

A Compact 1-kW 2-50 MHz Solid-State Linear Amplifier

Solid-state high-power linear amplifiers are becoming more and more popular in the field of ham radio as the prices of HF power transistors continue to fall. 250-W devices are now available for almost half the price they were selling for a few years ago. RF power FETs are still more expensive, but eventually their prices will also fall, although not as fast since they are still novelty items and the manufacturing yields are low due to ESD problems and requirement for cleaner facilities for wafer processing.

General

It is much easier to design wideband power amplifiers with FETs than bipolar transistors mainly due to their higher input impedances at least up to VHF. Their input impedance also varies less with frequency than that of bipolar devices and changes in the output load line are reflected back to the input to a lesser degree because of the much lower value of feedback capacitance (collector to base vs drain to gate). Practically all RF power FETs on the market today are of the enhancement MOS type, meaning that positive voltage at the gate in respect to the source is required to turn the device on.

The 1-kW amplifier described here would be difficult, if not impossible, to design to cover four and a half octaves with comparable performance using inexpensive bipolar transistors. In addition, a series of power splitters and combiners would be required to reach high power levels. Biasing to class AB linear operation is also much simpler with FETs since the gate does not draw any dc current, whereas a current equal to $I_C(peak)/h_{FE}$ must be supplied to the base of a bipolar device. One example of this and the splitter-combiner complexity is presented in the Application Note AN-758 by Motorola, Inc.

This article features a state of the art extremely compact design using a pair of FETs rated for 600 W of power output each. It would be capable of a power output of 1.2 kW as a push-pull circuit, but with the output matching employed, which is optimized at around 800 W, the unit starts saturating at around 1 kW at a 50-V dc supply, resulting in high IM distortion. Similarly at a 40-V supply, it would be usable up to 800 W. The type output matching transformer employed allows only integers as 1:4, 1:9. 1:16, etc. The 1:16 impedance ratio transformer would make the output matching optimized at 1400 W, which would result in a poor efficiency at 1200 W and lower power levels. The only way to compensate for this would be to adjust the supply voltage accordingly, in this case 45-46 V. However, the 1:16 ratio transformer of this type is physically much more difficult to fabricate than the lower ratio ones, and may not be available in the commercial market.

The Bias Regulator

The gate bias regulator (IC1 in Fig 1) allows the main supply voltage to be varied or the use of an unregulated supply while keeping the gate bias voltages and the FET idle currents constant. Since the maximum operating voltage of the regulator IC is only 40 V, a Zener diode (D1) is employed to keep it at a safe level. The regulator supply terminals are separated from the main power supply permitting the use of a separate bias supply if desired. There is also an option for a thermistor connection to stabilize the idle currents against temperature changes. The thermistor should be in a physical contact preferably with a mounting flange of one of the FETs. The gate voltages are individually adjustable (R1, R2) making gate threshold voltage matching of the devices unnecessary. In case of a device failure, such as a drain-gate short, D2 and D3 block the full supply voltage from being fed back to destroy the regulator. R10, R11 and C3, C4 are merely AC filters to protect the regulator from possibly strong RF fields. To set the idle currents, R1 and R2 must be adjusted to minimum. R3 is then adjusted for a regulator output voltage of about double the FET gate threshold voltages (IC1, pin 3). The current is monitored at the main supply voltage point while adjusting Ri for a desired idle current, typically 800 mA-1.0 A. R2 is then advanced until the current is doubled, resulting in equal idle currents for both devices. After this procedure, the settings of R1 through R3 should remain until one or both FETs must be replaced.

The RF Path

The amplifier is designed to operate into the industry standard 50-ohm input and output interface. The impedance matching to the low impedance levels of the FETs is accomplished with broadband RF transformers. Both the input transformer (T1) and the output transformer (T2) are of the so-called conventional type in contrast to transmission line transformers.[1,3,4] Both employ only one turn in the low impedance winding. T2 is far more critical than T1 because it determines the efficiency and the high frequency end gain characteristics, plus it must be able to handle a large amount of RF power. For increased bandwidth characteristics, its low impedance, one turn winding consists of three paralleled 10-ohm coaxial cables, resulting in a tight and controllable coupling between the primary and secondary. According to formulas given in Reference 2, approximately twice the present 4.7 cm^2 ferrite cross sectional area would be required in order for the core not to saturate with the calculated 127 gauss flux density. The saturation mainly occurs at the lowest frequencies, in this case at 2-3 MHz. Unfortunately most ferrite manufacturers do not give information on saturation flux densities that applies to applications such as this. However, it is known that high permeability ferrites, in

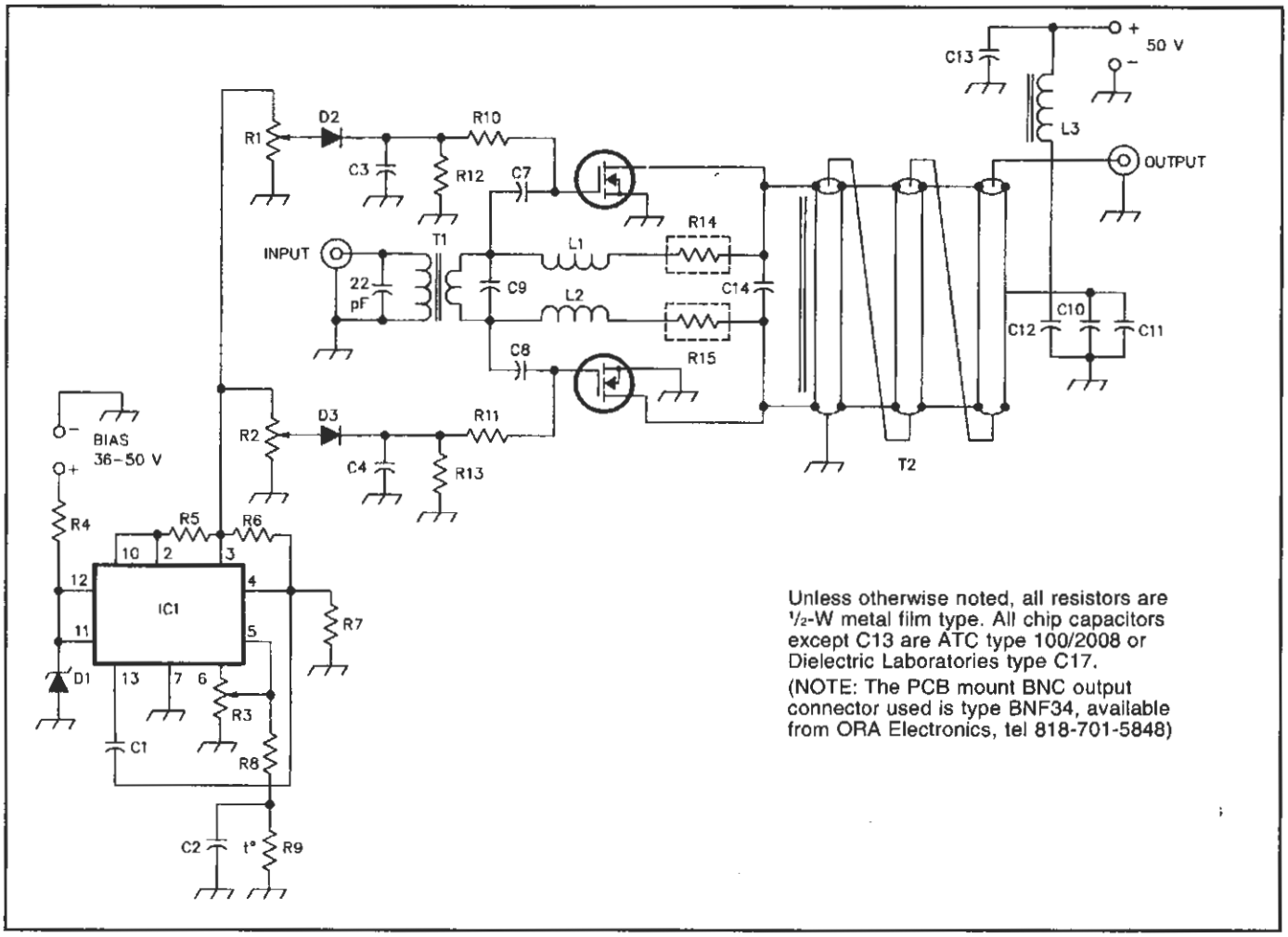

Fig 1—Circuit Diagram—2 to 50 MHz Amplifier 2-50 MHz Amplifier Components List

R1,R2—1 kΩ single-turn Trimpots
R3—10 kΩ single-turn Trimpot
R4—470 Ω, 2 watts
R5—10 Ω
R6,R12,R13—2 kΩ
R7—10 Ω
R8—Exact value depends on thermistor R9 used (typically 5-10 kΩ)
R9—Thermistor, Keystone RL1 009-5820-97-Di or equivalent
R10,R11—100 Ω, 1 W carbon
R14,R15—EMC Technology model 5308 or KDI Pyrofilm PPR 870-150-3 power resistors, 25 Ω
D1—1 N5357A or equivalent
D2,D3—1N4148 or equivalent
IC1 —MC1723 (723) voltage regulator
C1—1000-pF ceramic disc capacitor
C2,C3,C4—0.1-μF ceramic disc capacitor
C5—0.01-μF ceramic chip capacitor
C6,C12—0.1-μF ceramic chip capacitor
C7,C8—Two 2200-pF ceramic chip capacitors In parallel each
C9—820-pF ceramic chip capacitor
C10,C11—1000-pF ceramic chip capacitor
C13—0.47-μF ceramic chip capacitor or two smaller values in parallel
C14—Unencapsulated mica, 500 V. Two 1000-pF units is series, mounted under T2.
L1,L2—15 ηH, connecting wires to R14 and R15, 1.5 cm each #20 AWG
L3—10 μH, 10 turns #12 AWG enameled wire on Fair-Rite Products Corp ferrite toroid #5961000401 or equivalent
T1,T2—9:1 and 1:9 impedance ration RF transformers, types RF800-3 and RF2067-3 R, respectlvely (RF Power Systems, 3038 E Corrine Dr, Phoenix, AZ 85032)

general, saturate easier than low permeability materials. Thus, the lowest permeability material should be selected that will satisfy the minimum inductive reactance requirement at the lowest frequency of operation. The formula to calculate this is $NX_L = 2R_{S(L)}$, where: X_L=inductive reactance for one turn, N = number of turns, $R_{S(L)}$ = source or load impedance. Low permeability material is also less lossy at high frequencies, resulting in less heat generated in the transformer. T1, which must handle only 8-12 W of power, is made of higher permeability ferrite. This makes it possible to make the unit physically small as well. In Ti, the secondary consists of metal tubes (see Ref 1), where three turns of the primary wire is threaded through. Metal tubes are also used in T2, but only to hold the structure mechanically together.

At high-power levels generated with solid-state devices, which operate at relatively low voltages, the impedance levels automatically become low. This creates a problem for finding passive components, especially capacitors to handle the high RF currents involved. In vacuum tube circuits a similar problem exists, but in the form of high voltages. In this design, C14 gets the roughest treatment. It must be able to carry RF currents in excess of 10 amperes at the higher frequencies, although the voltage across it is only 75 V rms. At first, several good quality ceramic chip capacitors were tried in parallel, but temperature excursions caused them to crack resulting in AF arcs that burned the circuit board in the area as well. Finally, two unencapsulated mica capacitors (brand names such as Unelco, Underwood, Standex, Elmenco and Semco) were soldered in series by attaching the terminal tabs together, making it a sym-

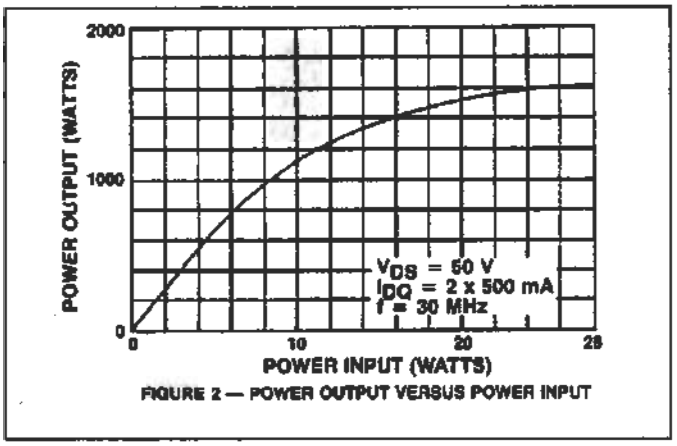

FIGURE 2 — POWER OUTPUT VERSUS POWER INPUT

Fig 2

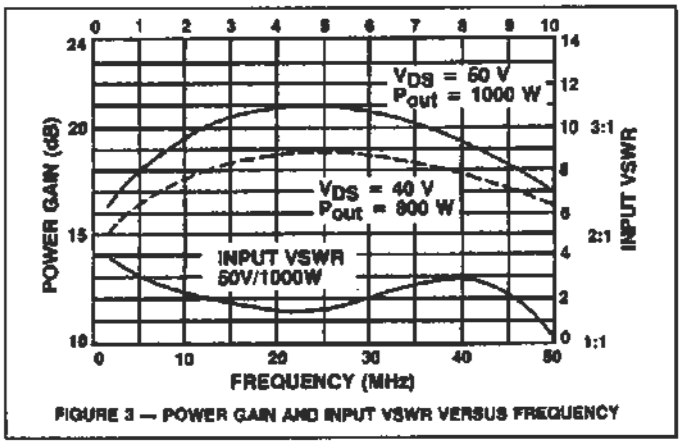

FIGURE 3 — POWER GAIN AND INPUT VSWR VERSUS FREQUENCY

Fig 3

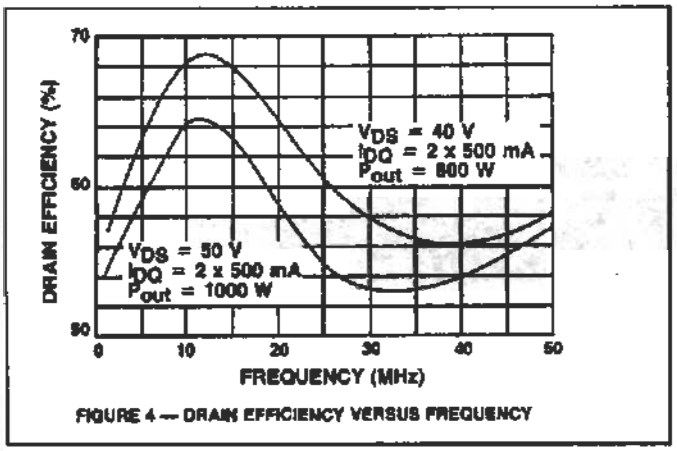

FIGURE 4 — DRAIN EFFICIENCY VERSUS FREQUENCY

Fig 4

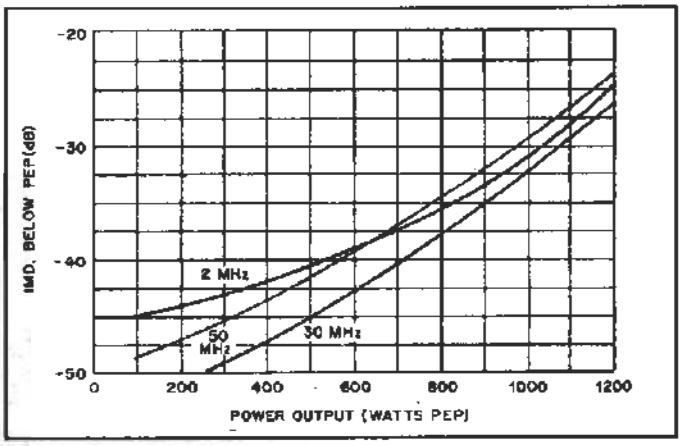

Fig 5

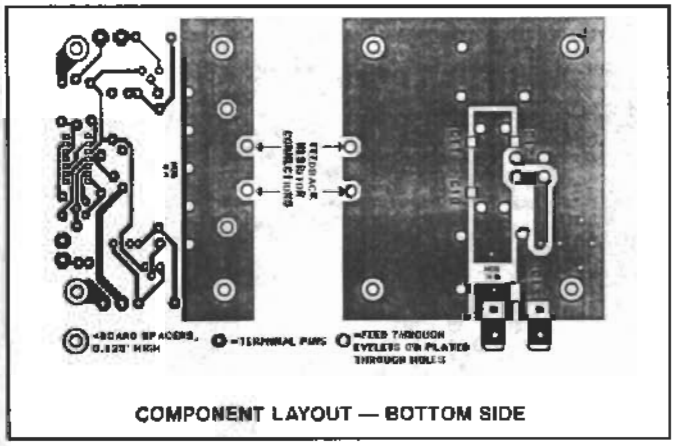
COMPONENT LAYOUT — BOTTOM SIDE

Fig 6

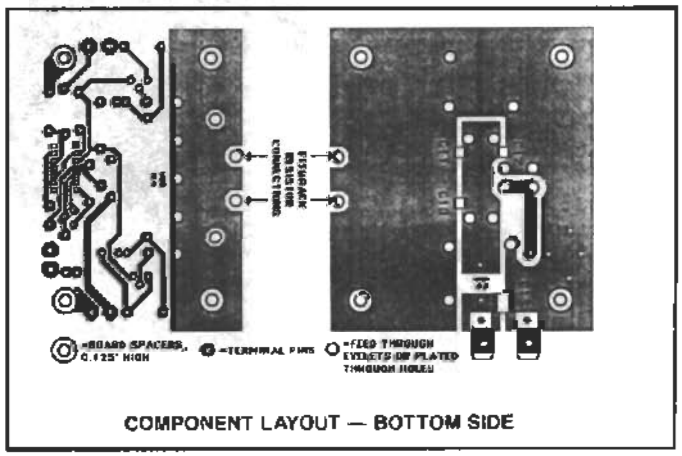
COMPONENT LAYOUT — BOTTOM SIDE

Fig 7

metrical structure. Since each is double the total value required and with double the number of plates, this increases the RF current carrying capability and provides a larger area to be soldered to the board metal foil to make the cooling more efficient. The low impedance winding terminals are then soldered to the tops of the capacitor metal casings, leaving the effective capacitance across the winding. For further fine tuning, an Arco (Elmenco) #469 or Sprague #GM-40900 compression mica trimmer can be soldered to the fronttop terminals of the transformer. Slot openings in the metal foil (Fig 7) located on each side of the output transformer, next to the drain terminals, were provided to increase the series inductance for certain highfrequency narrowband applications. This tunes out some of the FET output capacitance, resulting in increased efficiency. At lower frequencies (below 80 MHz) however, they only add to the IR loss and should be shorted. The location of C9 is also critical and should be placed approximately as shown in Fig 7. This will affect the input VSWR at frequencies above 30 MHz.

Bypass capacitors C10 through C12 must also be of good quality. The center tap of T2 should be free of AF if the circuit is balanced. This may not always be the case, in which case these capacitors will aid this function. L3 and C13 form an additional filter, ensuring that no RF energy is being fed back to the power supply. Switchmode power supplies especially are sensitive against RF and may actually get damaged from it.

Negative feedback is provided through the networks L1-R14 and L2-R15. Its purpose is to produce a relatively flat power gain versus frequency response. It also

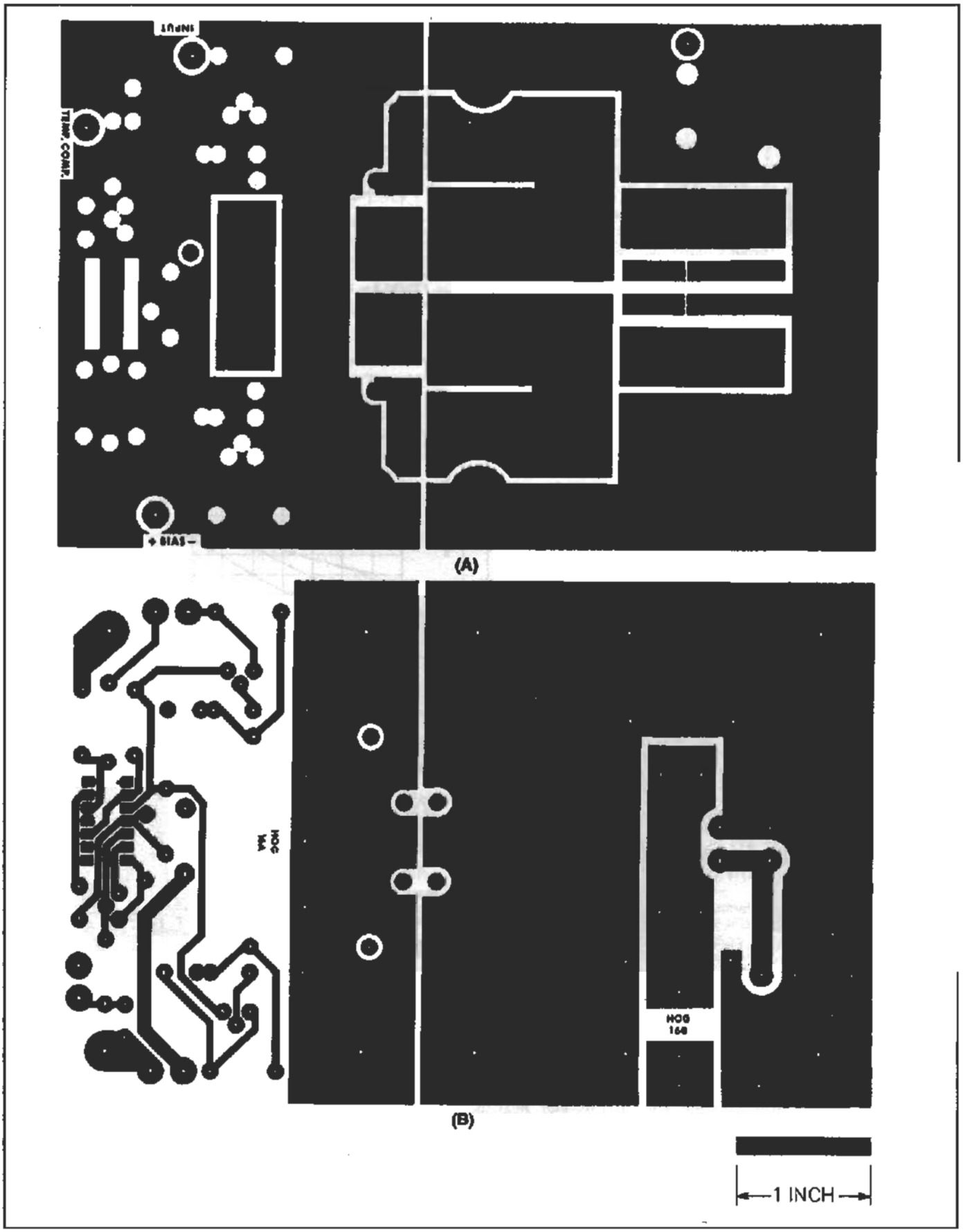

Figs 8A and 8B–Circuit Board–Top Side and Bottom Side

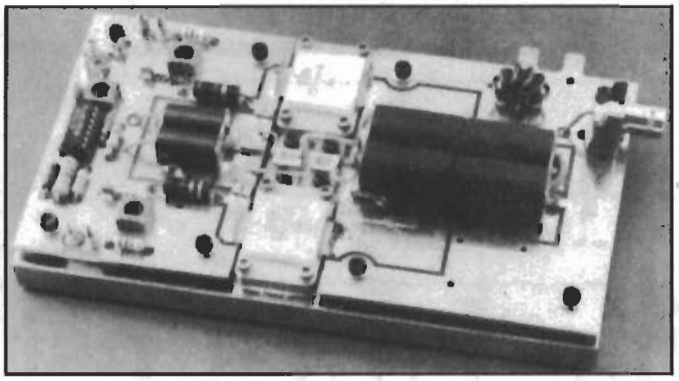

Fig 9—Amplifier mounted to the Heat Spreader.

improves the input return loss and helps to stabilize the amplifier at low frequencies, where the power gain would be 25-30 dB without it. The feedback is at its minimum at the high frequency end and at maximum at low frequencies, where most power is dissipated in R14 and R15. This power is roughly the difference in power input without the feedback between 2 and 50 MHz assuming a constant power output (in this case 25-30 W). A simple formula for calculating the feedback resistor values as well as their dissipation ratings is given in Reference 5. Reference 5 also includes information on physical construction of RF transformers such as used here.

Thermal Aspects

Assuming a 50% worst case efficiency for the unit, each FET dissipates 500 W of heat in an area of 1 x 1.5 inch. It is imperative that the transistors are mounted on the surface of a material with low thermal resistance such as copper. This is called a heat spreader as it is then attached to a heat sink made of material with poorer thermal resistance. It should extend about one inch beyond the edges of the FET mounting flanges at least on three sides. It is even more practical to make the heat spreader as large or larger than the amplifier itself. This would allow all circuit-board spacers to be an equal height of 0.125 inch. The thickness of the heat spreader should be a minimum of 0.375 inch. The heat spreader is then separately attached to the actual heat sink, which can be a 12-inch length of Wakefield Engineering type 4559 extrusion or equivalent[6]. Heat sink compound must be applied to all thermal interfaces and the recommended transistor mounting procedure should be followed, including the screw torque. Fig 9 shows the amplifier mounted to the heat spreader. Although the heat sink is not shown, one must be used for continuous operation and for test periods longer than a couple of minutes. For continuous operation, two 5-inch muffin fans under the heat sink will suffice. They will keep the device case temperature at below 80°C, and the die temperature, which equals to device thermal resistance x power dissipation + case temperature = 0.13 x 500 + 80, at less than 145°C, which is well below the 200-degree maximum recommended value. We must realize that the 500-watt dissipation is only valid when the unit is operated into a 50-ohm load. Under mismatched conditions, depending on the phase angle, the dissipated power may be lower or higher than this value.

Performance

Some of the amplifier performance characteristics are shown in Figs 2 through 5. Although at 30 MHz and above all harmonics are 25 dB or more below the fundamental, an output filter is required to comply with FCC regulations. However, it can be a simpler one than required for the low frequencies, where the third harmonic may be only attenuated 12-15 dB. In push-pull amplifiers, the even harmonics are not usually a problem since they are attenuated by the balanced operation of the circuit. Information on high power low-pass filters for applications as this can be found in Reference 7. These filters are automatically relay switched with BCD code available in most modern transceivers.

References

The circuit boards and other components for this design are available from Communication Concepts, Inc, 508 Millstone Drive, Xenia, OH 45385, tel 513-429-3811/ 220-9677.

[1]Motorola, Inc, Semiconductor Sector Application Notes AN-749 and AN-i 035.

[2]Hilbers, A.H., "Design of HF Wideband Power Transformers," Amperex (Philips) Application Laboratory Report EC06907 and ECO7213.

[3]Blocksome, Aoderick K., "Practical Wideband RF Power Transformers, Combiners and Splitters," *Proceedings of RF Expo*, February 1986.

By Mike Kossor, WA2EBY

From *QST*, March 1999

A Broadband HF Amplifier Using Low-Cost Power MOSFETs

Part 1—With only 1 W of drive, you'll get over 40 W out—from 160 through 10 meters!

Many articles have been written encouraging experimenters to use power MOSFETs to build HF RF amplifiers. That's because power MOSFETs—popular in the design of switching power supplies—cost as little as $1 each, whereas RF MOSFET prices start at about $35 each!

Over the years, I tucked away several of these articles, waiting for an opportunity to experiment with them. That opportunity came when I received a call from Al, W2OBJ. Al wanted a low-cost linear amplifier to use with his 5 W QRP transmitter when band conditions got poor. Ideally, the amplifier would generate at least 25 W on all the HF bands. Al's inquiry renewed my interest in the topic and provided the motivation I needed to get my project underway.

Al provided me with an extensive list of RF-amplifier construction articles that use power MOSFETs.[1-8] These articles provided useful information about MOSFETs and general guidelines for working with them, including biasing, parasitic-oscillation suppression, broadband impedance-matching techniques and typical amplifier performance data. It was clear from the performance data that Al's desire to get 25 W output from power MOSFETs on 1.8 to 30 MHz was going to be a challenge! The RF output power of most of the amplifiers described in the articles drops off to 10 W or less as frequency increases just to 14 MHz.

An Idea Brews

After hundreds of hours of experimentation, I came up with a design that exceeds our original objective: One watt of input power produces over 40 W of output (after harmonic filtering) from 160 through 10 meters. To the basic amplifier, I added an RF-sensed TR relay and a set of low-pass filters designed to suppress harmonic out-

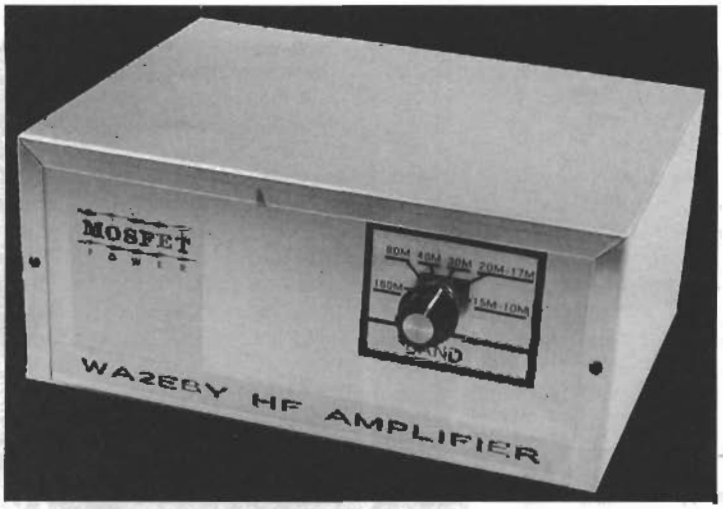

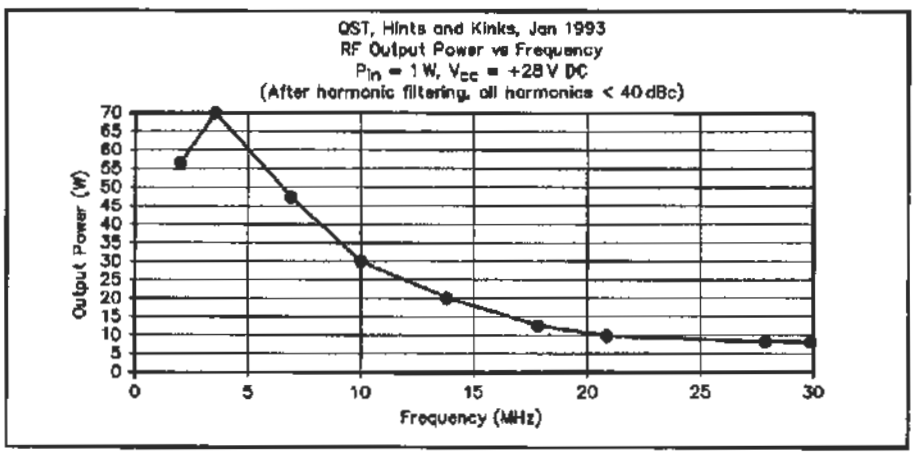

Figure 1—Jim Wyckoff, AA3X, "1 W In, 30 W out With Power MOSFETs at 80 M," Hints and Kinks, *QST*, Jan 1993, pp 50-51.

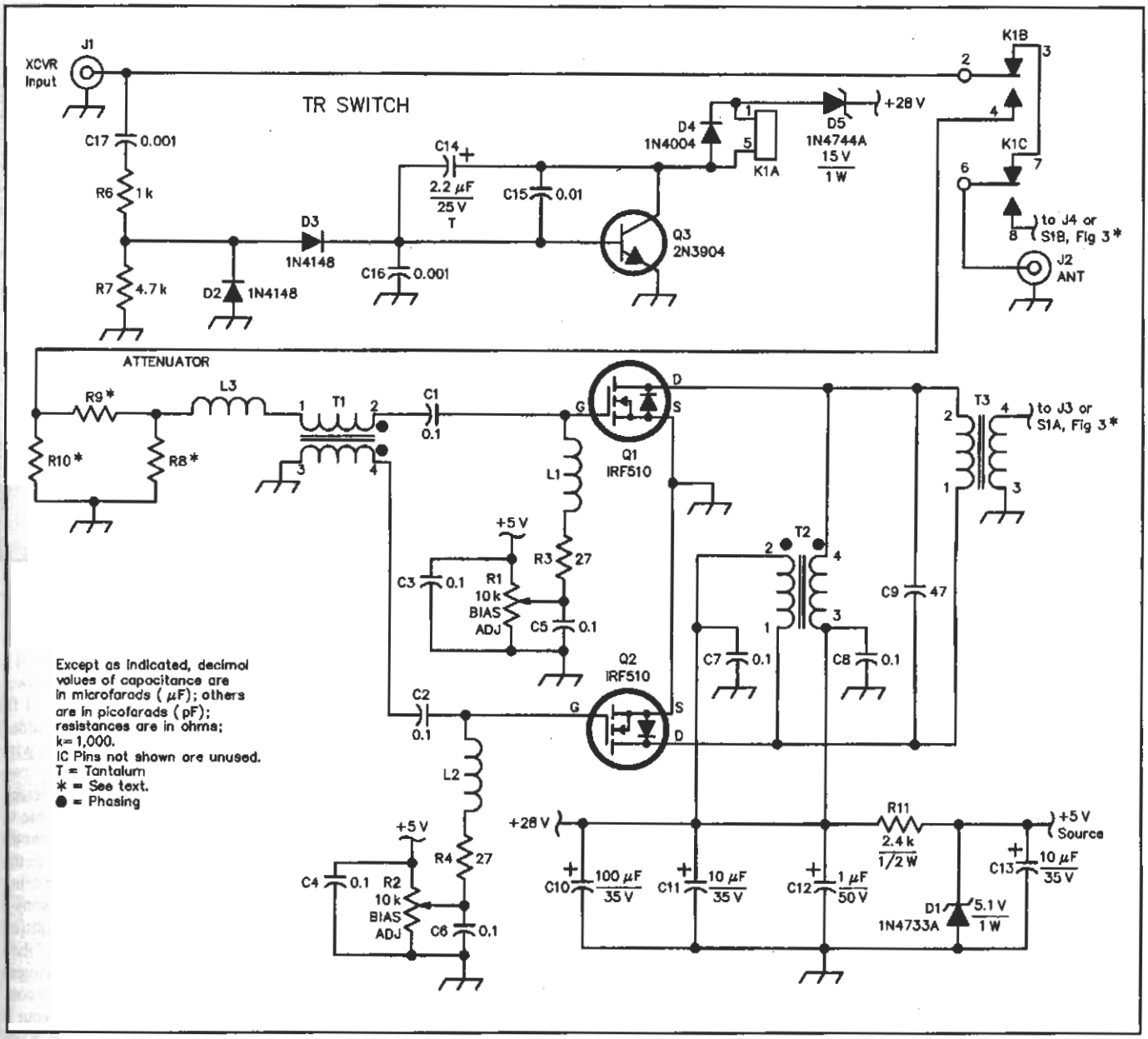

Figure 2—Schematic of the MOSFET all-band HF amplifier. Unless otherwise specified, resistors are 1/4 W, 5% tolerance carbon-composition or film units. Equivalent parts can be substituted. Part numbers in parentheses are Mouser (Mouser Electronics, 968 N Main St, Mansfield, TX 76063; tel 800-346-6873, 817-483-4422, fax 817-483-0931; **sales@ mouser.com**; **http://www.mouser.com**); see Note 9.

C1-C8—0.1 µF chip (140-CC502Z104M)
C9—47 pF chip (140-CC502N470J)
C10—100 µF, 35 V (140-HTRL35V100)
C11, C13—15 µF, 35 V (140MLR35V10)
C12—1 µF, 50 V (140-MLRL50V1.0)
C14—2.2 µF, 35 V tantalum (581-2.2M35V)
C15—0.01 µF chip (140-CC502B103K)
C16, C17—0.001 µF chip (140-CC502B102K)
D1—1N4733A, 5.1 V, 1 W Zener diode (583-1N4733A)
D4—1N4004A(583-1N4004A)
D2, D3—1N4148 (583-1N4148)
D5—1N4744A, 15 V, 1 W Zener diode (583-1N4744A)
J1, J2—SO-239 UHF connector (523-81-120)
K1—12 V DPDT, 960 Ω coil, 12.5 mA (431-OVR-SH-212L)
L1, L2—9 1/2 turns #24 enameled wire, closely wound 0.25-in. ID
L3—3 1/2 turns #24 enameled wire, closely wound 0.190-in. ID
Q1, Q2—IRF510 power MOSFET (570-IRF510)
Q3—2N3904 (610-2N3904)
R1, R2—10 kΩ trim pot (323-5000-10K)
R3, R4—27 Ω, 1/2 W (293-27)
R6—1 kΩ chip (263-1K)
R7— 4.7 kΩ chip (263-4.7K)
R8—130 Ω, 1 W (281-130); for 7 dB pad (5 W in, 1 W out)
R9—43 Ω, 2 W (282-43); for 7 dB pad (5 W in, 1 W out)
R10—130 Ω, 3 W (283-130); for 7 dB pad (5 W in, 1 W out)
R8, R10—300 Ω, 1/2 W (273-300); for 3 dB pad (2 W in, 1 W out)
R9—18 Ω, 1 W (281-18); for 3 dB pad (2 W in, 1 W out)
R11—2.4 kΩ, 1/2 W (293-2.4K)
T1—10 bifilar turns #24 enameled wire on an FT-50-43 core.
T2—10 bifilar turns #22 enameled wire on two stacked FT-50-43 cores.
T3—Pri 2 turns, sec 3 turns #20 Teflon-covered wire on BN-43-3312 balun core.
Misc: Aluminum enclosure 3.5∞8∞6 inches (HWD) (537-TF-783), two TO-220 mounting kits (534-4724), heat-sink compound (577-1977), amplifier PC board (see Note 9), heat sink (AAVID [Mouser 532-244609B02]; see text), about two feet of RG-58 coax, #24 enameled wire and #20 Teflon-insulated wire.

put and comply with FCC requirements. The amplifier is built on double-sided PC board and requires *no tuning*. Another PC board contains the low-pass filters. Power-supply requirements are 28 V dc at 5 A, although the amplifier performs well at 13.8 V dc.

Several of these amplifiers have been built and exhibit similar performance. Al has been using his amplifier on each of the HF bands, logging well over 500 contacts in 18 months. Signal reports indicate a noticeable improvement in readability (about two S units on average) over his 5 W rig. No indications of in-stability, CW key clicks or distortion on SSB have been reported. To make it easy for you to duplicate this project, PC boards and parts kits are available, all at a cost of about $100![9]

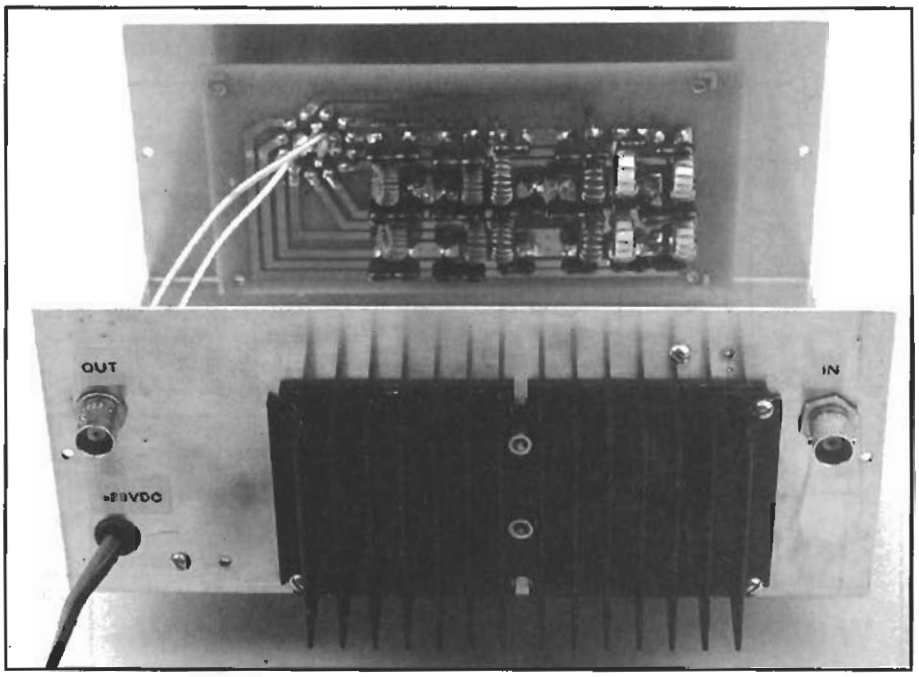

A rear panel view showing the heat sink.

An Overview of MOSFETs

MOSFETs operate very differently from bipolar transistors. MOSFETs are voltage-controlled devices and exhibit a very high input impedance at dc, whereas bipolar transistors are current-controlled devices and have a relatively low input impedance. Biasing a MOSFET for linear operation only requires applying a fixed voltage to its gate via a resistor. With MOSFETs, no special bias or feedback circuitry is required to maintain the bias point over temperature as is required with bipolar transistors to prevent thermal runaway.[10] With MOSFETs, the gate-threshold voltage increases with increased drain current. This works to turn off the device, especially at elevated temperatures as transconductance decreases and $R_{DS(on)}$ (static drain-to-source *on* resistance) increases. These built-in self-regulating actions prevent MOSFETs from being affected by thermal runaway. MOSFETs do not require negative feedback to suppress low-frequency gain as is often required with bipolar RF transistors. Bipolar transistor gain increases as frequency decreases. Very high gain at dc and low frequencies can cause unwanted, low-frequency oscillation to occur in bipolar transistor RF amplifiers unless negative feedback is employed to prevent it. Low-frequency oscillation can damage bipolar transistors by causing excess power dissipation, leading to thermal runaway.

MOSFET Limitations

Of course, MOSFETs do have their limitations. The high gate impedance and the device structure make them susceptible to electrostatic discharge (ESD) damage. Some easily applied precautions prevent this: Use a soldering iron with grounded tip; use a wrist strap connected to ground through a 1 MΩ resistor to bleed off excess body charge while handling MOSFETs and do all work on an anti-static mat connected to ground via a 1 MΩ resistor.

The sensitivity of a MOSFET's gate to static and high-voltage spikes also makes it vulnerable to damage resulting from parasitic oscillation. This undesired self-oscillation could result in excessive gate-to-source voltage that permanently damages the MOSFET's gate insulation. Another MOSFET limitation is gate capacitance. This parameter limits the frequency at which a MOSFET can operate effectively as an RF amplifier. I recommend reviewing the referents of Notes 1-3 if you are interested in more detailed information about MOSFETs.

Power MOSFET RF Amplifiers

Of the several power MOSFET amplifiers I built to check their performance, the one providing the best performance is the push-pull design described by Jim Wyckoff, AA3X, in *QST* (see Note 3). I used IRF510 power MOSFETs rather than the IRF511s specified. The performance of this power MOSFET amplifier design is summarized in Figure 1; its basic design is very similar to another amplifier described in the referent of Note 4, written 10 years earlier. That amplifier uses a pair of more-expensive MRF138 MOSFETs designed specifically for RF applications.

As Figure 1 shows, the Hints and Kinks amplifier performance is excellent from 1.8 MHz to 7 MHz and far exceeds the published figure of 30 W output on 3.5 MHz. As frequency increases above 10 MHz, however, output drops off rapidly, falling below 10 W above 21 MHz. (These levels were measured after harmonic filtering.)

Although the amplifier is identified as stable, my first attempt at duplicating the amplifier resulted in oscillations that destroyed one of the IRF510s. I was puzzled by this. At first, I thought the problem was caused by my substitution of the slightly more robust IRF510 MOSFETs for the called-for IRF511s. That idea proved wrong when my second attempt to power up the amplifier with IRF511 MOSFETs installed also resulted in a blown IRF511. (Thank goodness these are $1 power MOSFETs, not $35 RF MOSFETs!). I finally achieved good stability when I added a small amount of inductance in series with the MOSFET source to ground (just two turns of #24 wire, 0.125 inch diameter). With this added inductance, I was able to remove the ferrite beads from the circuit without any sign of instability. I believe the substitution of the IRF510 and minimizing source lead inductance are the reasons I obtained significantly higher RF output power and wider bandwidth than described in the referent of Note 3. This experiment underscores the need to observe *exact* construction techniques and physical layout if similar performance is to be expected. Even though I used PC board construction, I got significantly different results because my layout was not the same as the author's.

Modifying the Design

Although the amplifier performed better than expected, its bandwidth was significantly less than desired. Considerable experimentation (and I do mean considerable!) resulted in the circuit shown in Figure 2. This amplifier consists of two power MOSFETs operating in push-pull and employs an RF-sensed TR relay.

During receive, TR relay K1 is deenergized. Signals from the antenna are connected to J2 and routed through K1 to a transceiver connected to J1. (This path loss is less than 0.3 dB from 1.8 MHz through 30 MHz.) In transmit, RF voltage from the transceiver is sampled by C17 and divided by R6 and R7. D2 and D3 rectify the RF voltage and charge C16. Q3 begins conducting when the detected RF voltage across C16 reaches approximately 0.7 V. This energizes K1, which then routes the transmitted RF signal from J1

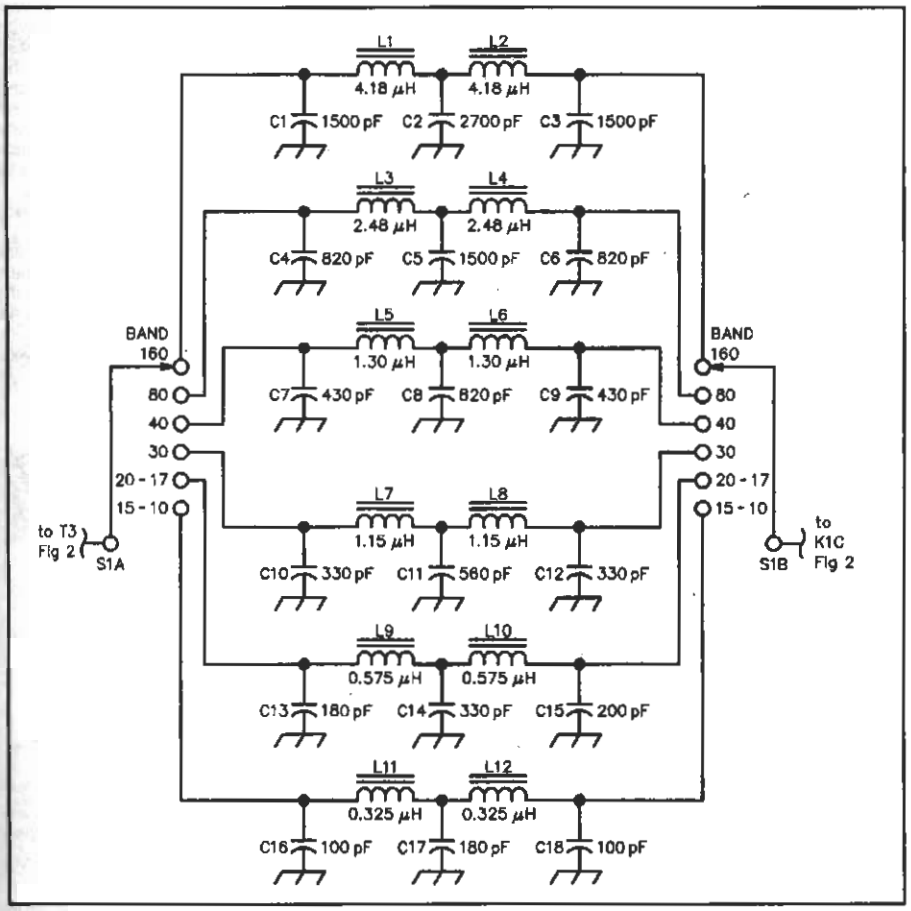

Figure 3—Low-pass filter schematic. In some cases, the actual filter component values differ from the calculated values of a standard 50 Ω-input filter. Such differences improve the impedance matching between the amplifier and the load. Capacitors are all dipped mica units.

C1, C3, C5—1500 pF (5982-19-500V1500)
C2—2700 pF (5982-19-500V2700)
C4, C6, C8—820 pF (5982-19-500V820)
C7, C9—430 pF (5982-15-500V430)
C10, C12, C14—330 pF (5982-19-500V330)
C11—560 pF (5982-19-500V560)
C13, C17—180 pF (5982-15-500V180)
C15—200 pF (5982-15-500V200)
C16, C18—100 pF (5982-10-500V100)
S1—2 pole, 6 position rotary (10YX026)
Misc: low-pass filter PC board (see Note 9)

to the input of the amplifier and sends the output of the amplifier to the antenna at J2. RF-sensed relay response is very fast. No noticeable clipping of the first CW character has been reported.

I made provisions to include an RF attenuator (consisting of R8, R9 and R10) to enable adjusting the amplifier input power to 1 W. (The parts list contains resistor values to reduce the output of 2 or 5 W drivers to 1 W.) The 1 W signal is then applied to the primary of T1 via an input impedance-matching network consisting of L3. T1 is a 1:1 balun that splits the RF signal into two outputs 180 degrees out of phase. One of these signals is applied by C1 to Q1's gate. The other signal is routed via C2 to Q2's gate. The drains of Q1 and Q2 are connected to the primary of output transformer T3, where the two signals are recombined in phase to produce a single output. T3 also provides impedance transformation from the low output impedance of the MOSFETs to the 50 Ω antenna port. Dc power is provided to the drains of Q1 and Q2 by phase-reversal choke, T2. This is a very effective method to provide power to Q1 and Q2 while presenting a high impedance to the RF signal over a broad range of frequencies. The drain chokes for Q1 and Q2 are wound on the same core, and the phase of one of the chokes (see the phasing-dot markings on T2) is reversed. C9 increases the bandwidth of impedance transformation provided by T3, especially at 21 MHz.

The 5 V bias supply voltage is derived from 28 V by Zener diode D1 and current-limiting resistor R11. Bypass capacitors C3, C4, C5, C6 and C13 remove RF voltages from the bias supply voltage. Gate bias for Q1 and Q2 is controlled independently. R1 adjusts Q1's gate-bias voltage via R3 and L1. R2 works similarly for Q2 via R4 and L2.

At low frequencies, the amplifier's input impedance is essentially equal to the series value of R3 and R4. L1 and L2 improve the input-impedance match at higher frequencies. The low value of series resistance provided by R3 and R4 also reduces the Q of impedance-matching inductors L1 and L2, which improves stability. Dc blocking capacitors C1 and C2 prevent loading the gate bias-supply voltage.

C14 keeps transistor Q3 conducting and K1 energized between SSB voice syllables or CW elements. Without C14, K1 would chatter in response to the SSB modulation envelope and fast keying. Increasing the value of C14 increases the time K1 remains energized during transmit. The reverse voltage generated by K1 when the relay is deenergized is clamped to a safe level by D4. D5 drops the 28 V supply to 13 V to power 12 V relay K1. D5 can be replaced with a jumper if K1 has a 28 V dc coil or if you intend to operate the amplifier with a 13.8 V dc supply.

Harmonic Filtering

Although biased for class AB linear operation, this amplifier (like others of its type) exhibits some degree of nonlinearity, resulting in the generation of harmonics. This push-pull amplifier design cancels even-order harmonics (2f, 4f, 6f, etc) in the output transformer, T3. Odd-order harmonics are not canceled. Second-order harmonics generated by the amplifier are typically less than 30 dBc (30 dB below the carrier) whereas third-order harmonics are typically only 10 dBc. FCC regulations require all HF RF-amplifier harmonic output power to be at least 40 dBc at power levels between 50 to 500 W. To meet this requirement, it is common practice for HF amplifiers to use low-pass filters. Separate low-pass filters are needed for the 160, 80, 40 and 30 meter bands. The 20 and 17 meter bands can share the same low-pass filter. So, too, the 15, 12 and 10 meter bands can share a common low-pass filter; see Figure 3.

Switching among the six filters can be a messy wiring problem, especially on the higher-frequency bands where lead lengths should be kept short for optimum performance. This problem is solved by mounting all six low-pass filters on a PC board. A two-pole, six-position rotary switch (S1) mounted directly on the same PC board manages all filter interconnections. One pole of S1 connects the amplifier output to one of the six filter inputs, while S1's other pole simultaneously connects the corresponding filter's output to the TR relay, K1. Only two coaxial-cable connections are required between the RF amplifier and the low-pass filter board.

Next Month

In Part 2, I'll wrap up with amplifier construction and adjustment, and discuss the amplifier's overall performance. See you then!

Notes

[1]Doug DeMaw, W1FB, "Power-FET Switches as RF Amplifiers," *QST*, Apr 1989, pp 30-33. See also Feedback, *QST*, May 1989, p 51.

[2]Wes Hayward, W7ZOI, and Jeff Damm, WA7MLH, "Stable HEXFET RF Power Amplifiers," Technical Correspondence, *QST*, Nov 1989, pp 38-40; also see Feedback, *QST*, Mar 1990, p 41.

[3]Jim Wyckoff, AA3X, "1 Watt In, 30 Watts Out with Power MOSFETs at 80 Meters," Hints and Kinks, *QST*, Jan 1993, pp 50-51.

[4]Doug DeMaw, W1FB, "Go Class B or C with Power MOSFETs," *QST*, March 1983, pp 25-29.

[5]Doug DeMaw, W1FB, "An Experimental VMOS Transmitter", *QST*, May 1979, pp 18-22.

[6]Wes Hayward, W7ZOI, "A VMOS FET Transmitter for 10-Meter CW," *QST*, May 1979, pp 27-30.

[7]Ed Oxner, ex-W9PRZ (SK), "Build a Broadband Ultralinear VMOS Amplifier," *QST*, May 1979, pp 23-26.

[8]Gary Breed, K9AY, "An Easy-to-Build 25-Watt MF/HF Amplifier," *QST*, Feb 1994, pp 31-34.

[9]Parts for this project are available in five modular kits. The following three kits are available from Mouser Electronics (Mouser Electronics, 958 N Main St, Mansfield, TX 76063; tel 800-346-6873, 817-483-4422, fax 817-483-0931; **sales@mouser.com**; **www.mouser.com**): Amplifier components (Mouser P/N 371-HFAMP1) consisting of the amplifier PC board and all PC-board-mounted components (except for the ferrite cores). Price: $35, plus shipping. Amplifier hardware kit (Mouser P/N 371-HFAMP2) consisting of the aluminum enclosure, two UHF connectors, two TO-220 mounting kits, AAVID heat sink and one container of heat sink compound. Price: $30 plus shipping. Low-pass filter kit (Mouser P/N 371-HFAMP3) consisting of the low-pass filter PC board, rotary switch and all PC-board-mounted capacitors (inductor cores are *not* included). Price: $35, plus shipping. Part-placement diagrams accompany the PC boards.

PC boards only are available from Mouser Electronics: HF amplifier board (#371-AMPPWB-2); filter PC board (#371-LPPWB-2). Price $15 each, plus shipping.

The following two kits are available from Amidon Inc (Amidon, Inc, 240 Briggs Ave, Costa Mesa, CA 92626; tel 1-800-898-1883, 714-850-4660, fax 714-850-1163): Amplifier ferrite kit (Amidon P/N HFAFC) containing the ferrite cores, balun core and magnet and Teflon wire to wind the transformers for the HF amplifier. Price: $3.50 plus shipping. Low-pass filter cores kit (Amidon P/N HFFLT) containing all iron cores and wire for the low-pass filters. Price: $4.50 plus ship.

[10]See Motorola Application Reports Q1/95, HB215, *Application Report AR346*.

Thermal runaway is a condition that occurs with bipolar transistors because bipolar transistors conduct more as temperature increases, the increased conduction causes an increase in temperature, which further increases conduction, etc. The cycle repeats until the bipolar transistor overheats and is permanently damaged.

By Mike Kossor, WA2EBY

From *QST*, April 1999

A Broadband HF Amplifier Using Low-Cost Power MOSFETs

Part 2—Let's put the finishing touches on this all-band HF amplifier!

Last month,[1] *I covered the history and development of this 40 W (average) amplifier. I'm sure you're anxious to get* your *amplifier finished and on the air, so let's get going!*

Amplifier Construction

The amplifier is constructed on a double-sided PC board with plated through holes to provide top-side ground connections. I used chip resistors and capacitors to simplify construction, but leaded capacitors may work if lead lengths are kept short. First, assemble all chip capacitors and resistors on the PC board. Tweezers help to handle chip components. Work with only one component value at a time (chip caps and resistors are very difficult to identify!). Chip capacitor and resistor mounting is simplified by tinning one side of the PC board trace with solder before positioning the capacitor or resistor. Touch the soldering iron tip to the capacitor or resistor to tack it in place. Finish mounting by soldering the opposite side of the component. *Don't apply too much heat to chip capacitors.* The metalized contacts on the capacitor can be damaged or completely removed if too much heat is applied. Use a 15 to 20 W soldering iron and limit soldering time to five seconds.

Mount axial-leaded resistors, diodes and remaining capacitors next. To avoid damaging them, mount inductors and transformers last. L1 and L2 are wound on a 0.25-inch drill-bit shaft. By wrapping the wire around the shaft 10 times, you'll get 9½ turns. The last turn arcs only a half-turn before entering the PC board. L3 is wound on a 0.190-inch diameter drill bit with 3½ turns wound the same way as L1 and L2. Mounting K1 is simplified by first bending all its leads 90° outward so it lies flat on the PC board. Use a wrist strap connected to ground through a 1 MΩ resistor to bleed off static body charge while handling MOSFETs, and do the work on an anti-static mat connected to ground via a 1 MΩ resistor. The gate input can be damaged by electrostatic discharge!

When winding T3, wind the primary first and add the secondary winding over the primary. Be sure to use Teflon-insulated wire for T3's windings; the high operating temperatures encountered will likely melt standard hook-up wire insulation.

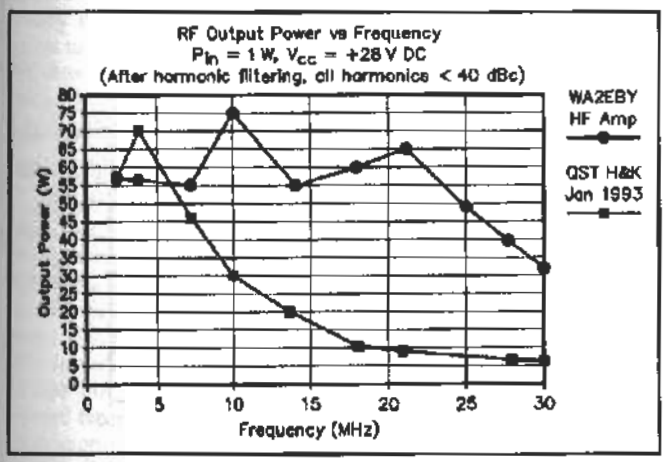

Figure 4—RF output power comparison of the Hint and Kink amplifier and this design.

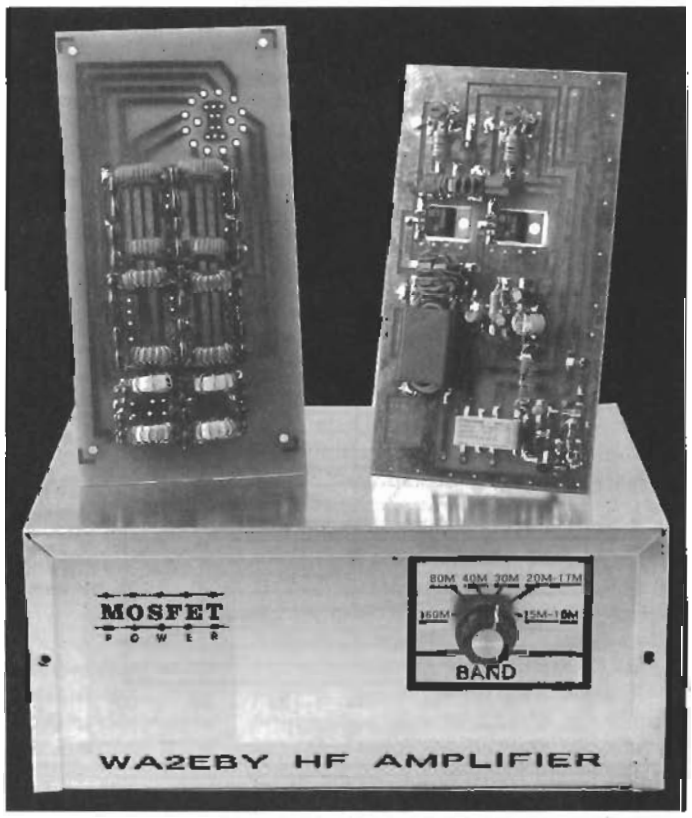

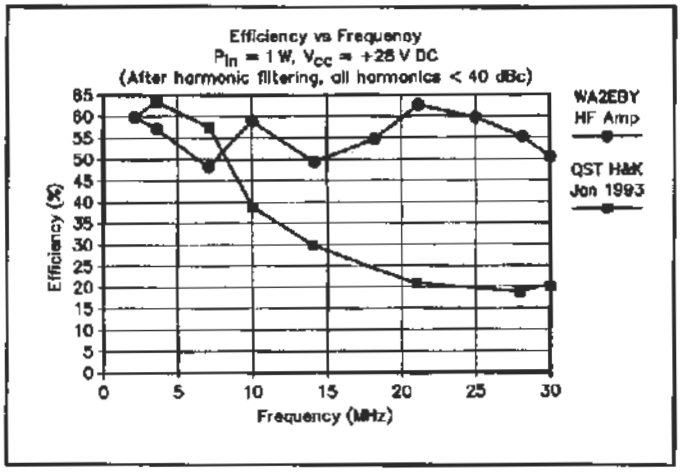

Figure 5—Efficiency comparison of the Hint and Kink amplifier and this one.

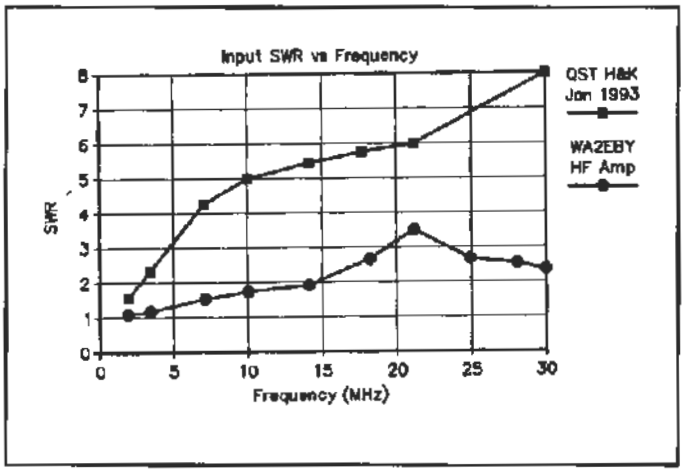

Figure 6—Input SWR comparison of the two amplifiers.

Heat Sinking

Together, Q1 and Q2 dissipate up to 59 W. A suitable heat sink is required to prevent the transistors from overheating and damage. I used an AAVID 244609B02 heat sink originally designed for dc-to-dc power converters. The amplifier PC board and heat sink are attached to an aluminum enclosure by two #4-40 screws drilled through the PC board, enclosure and heat sink at diagonally opposite corners. A rectangular cutout in the enclosure allows Q1 and Q2 direct access to the heat sink. This is essential because of the large thermal impedance associated with the TO-220 package (more on this topic later). Mark the locations of the transistor-tab mounting-hole location in the center of the heat sink in between the cooling fins. Disassemble the heat sink to drill 0.115 inch holes for #4-40 mounting screws, or tap #4-40 mounting holes in the center of the heat-sink fins.

Use mica insulators and grommets when mounting Q1 and Q2 to prevent the #4-40 mounting screws from shorting the TO-220 package drain connections (tabs) to ground. Coat both sides of the mica insulator with a *thin* layer of thermal compound to improve the thermal conduction between the transistor tab and the heat sink. Be sure to install the mica insulator on the heat sink *before* assembling the amplifier PC board to the enclosure and heat sink. The mica insulators are larger than the cut outs in the PC board, making it impossible to install them after the PC board is mounted.

Low-Pass Filter Construction

Inductor winding information for the low-pass filters is provided in Table 1.

Single Band

A PC-board trace is available on the amplifier PC board next to amplifier output (J3) to allow the installation of a single-band low-pass filter between the terminals of J3 and K1's input, J4. This is handy if you intend to use the amplifier on one band only. The input inductor of the low-pass filter connects from J3 to the single PC trace adjacent to J3. The output inductor connects in series between the single PC trace to J4. The three filter capacitors connect from J3, J4 and the PC-board trace near J3 to ground. *This single trace is not used when multiple filters are required.* Remember to remove the single trace adjacent to J3 on the amplifier PC board before attaching the amplifier board between the RF connectors on the enclosure's rear panel.

Multiple-Band Filters

Using the amplifier on more than one band requires a different approach. A set of

Table 1
Low-Pass Filter Inductor Winding Information
(Refer to Figure 3 in Part 1))

Inductor Number	*No. of Turns*	*Core*
L1, L2	30 turns	T-50-2
L3, L4	22 turns	T-50-2
L5, L6	16 turns	T-50-2
L7, L8	14 turns	T-50-2
L9, L10	11 turns	T-50-6
L11, L12	8 turns	T-50-6

Note: All inductors are wound with #22 enameled wire except for L1–L4, which are wound with #24 enameled wire.

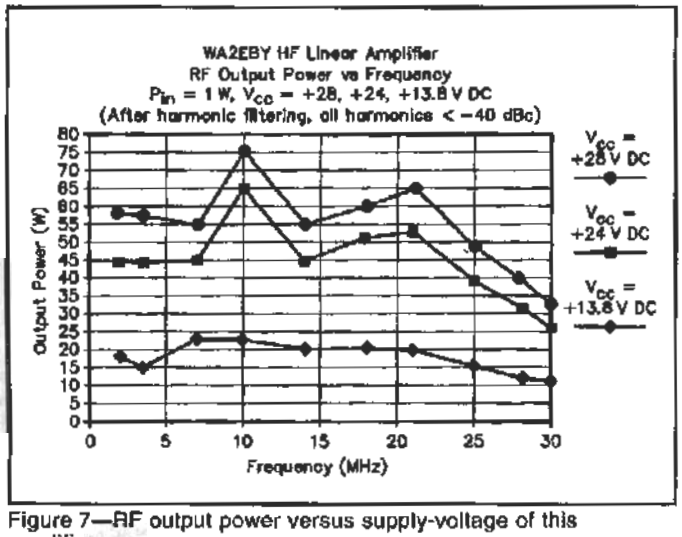

Figure 7—RF output power versus supply-voltage of this amplifier.

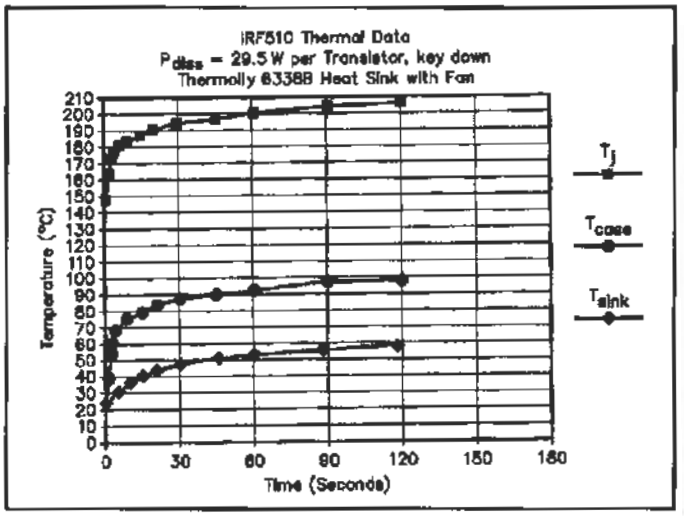

Figure 8—Thermal performance of the amplifier during key-down conditions.

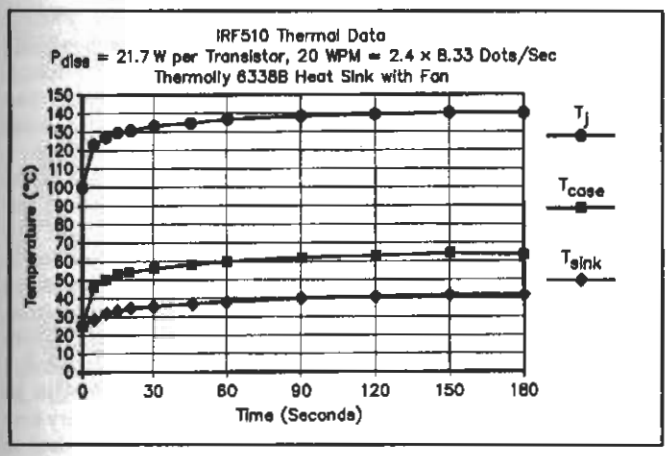

Figure 9—Thermal performance of the amplifier during simulated CW conditions.

six low-pass filters is built on a double-sided PC board with plated through holes to provide top-side ground connections. A PC-board mount, two-pole, six-position rotary switch does all low-pass filter selection. Silver-mica, leaded capacitors are used in all the filters. On 160 through 30 meters, T-50-2 toroids are used in the inductors. T-50-6 toroids are used for inductors on 20 through 10 meters. The number of turns wound on a toroid core are counted on the toroid's OD as the wire passes through the core center (*The ARRL Handbook* [12] provides complete details for winding toroids). Assemble one filter section at a time starting with the 160, 80, 40-meter filter, then the 30-meter filter. With the switch mounting position at your upper left, the filter input (C1) is near the top edge of the board and the filter output (C3) is near the bottom edge. *The last two filters are out of sequence;* the 15-10 meter filter comes *before* the 20-17 meter filter) and the inputs/outputs are reversed to simplify the PC-board layout. The input capacitors, C13 and C16, are mounted on the board *bottom edge*, and output capacitors, C15 and C18, are on the *top edge*.

Use care when assembling the rotary switch. All 14 terminals must fit through the PC board without damaging or bending the pins. Make sure there are no bent pins before you attempt assembly. Insert the rotary switch into the PC board. Do *not* press the rotary switch all the way into the PC-board holes flush with the ground plane! If you do, the top flange of the signal pins may short to the ground plane.

Bias Adjustment

The biasing procedure is straightforward and requires only a multimeter to complete. First, set R1 and R2 fully counterclockwise, (0 V on the gates of Q1 and Q2). Terminate the RF input and outputs with a 50 Ω load. Next, connect the 28 V supply to the amplifier in series with a multimeter set to the 0-200 mA current range. Measure and record the idling current drawn by the 5 V bias supply. The value should be approximately 9.5 mA (28 – 5.1 V) / 2.4 kΩ = 9.5 mA). Set Q1's drain current to 10 mA by adjusting R1 until the 28 V supply current increases by 10 mA above the idling current (9.5 + 10 = 19.5 mA). Next, adjust R2 for a Q2 drain current of 10 mA. This is accomplished by adjusting R2 until the 28 V supply current increases by an additional 10 mA (to 29.5 mA).

Amplifier Performance

With a 28 V power supply and 1 W of drive, the RF output power of this amplifier exceeds 40 W from 1.8 MHz through 28 MHz. Peak performance occurs at 10 MHz, providing about 75 W after filtering! A performance comparison between this amplifier and my modified version of the Hint and Kink amplifier mentioned earlier is shown in Figure 4.

As shown in Figure 5, this amplifier achieves an efficiency of better than 50% over its frequency range, except at 7 MHz where the efficiency drops to 48%. In contrast, the Hint and Kink amplifier delivers greater efficiency between 1.8 and 7 MHz, but it drops rapidly to only 20% as frequency is increased.

Figure 6 compares the input SWR of the two amplifiers. The Hint and Kink amplifier's SWR is acceptable (< 2:1) only at 1.8 MHz. This amplifier is better, however it, too, exceeds 2:1 above 14 MHz. The input SWR of this amplifier can be improved to better than 2:1 on all bands by adding a 3 dB pad (R8-R10 of Figure 2) at the input and supplying 2 W to the pad input. This keeps the amplifier drive at 1 W.

Figure 7 graphs this amplifier's RF output power as a function of drain supply voltage. During this test, the amplifier RF drive level was kept constant at 1 W. As you can see, even when using a 13.8 V dc supply, the amplifier provides over 10 W output (a gain of more than 10 dB) from 1.8 to 30 MHz.

Operation

The amplifier requires no tuning while operating on any HF amateur band. You must, however, *be sure to select the proper low-pass filter prior to transmitting*. If the wrong low-pass filter is selected, damage to the MOSFETs may result. Damage will likely result if you attempt to operate the amplifier on a band with the low-pass filter selected for a lower frequency. For example, driving the amplifier with a 21 MHz signal while the 1.8 MHz low-pass filter is selected will likely destroy Q1 and/or Q2.

The amplifier can also be damaged by overheating. This limitation is imposed by the TO-220 packages in which Q1 and Q2 are housed. The thermal resistance from junction to case is a whopping 3.5°C/W. This huge value makes it virtually impossible to keep the junction temperature from exceeding the +150°C target for good reliability. Consider the following conditions: key down, 1 W input, 53 W output on 7 MHz (worst-case band for efficiency). The amplifier consumes 28 V × 4 A = 112 W, of which 53 W are sent to the antenna, so 59 W (112 W – 53 W = 59 W) are dissipated in Q1 and Q2. Assuming equal current sharing between Q1 and Q2, each transistor dissipates 29.5 W. To keep the transistor junction temperature below +150°C requires preventing the transistor case temperature from exceeding 46.8°C (150 – [3.5 × 29.5]) while dissipating 29.5 W. Also, there is a temperature rise across the mica insulator between the transistor case and heat sink of 0.5°C/W. That makes the maximum allowable heat-sink temperature limited to 46.8 – (0.5 × 29.5) = 32°C. In other words, the heat sink must dissipate 59 W (29.5 from each transistor) with only a 7°C rise above room temperature (25°C). Even if the junction temperatures were allowed to reach the absolute maximum of 175°C, the heat sink temperature must not exceed 57°C. Accomplishing this requires a heat sink with a thermal resistance of (57 – 25) / 59 = 0.54°C/W. This is far less than the 1.9°C/W rating of the AAVID 244609B02 heat sink I used. The situation may seem bleak, but all is not lost. These calculations make it clear that the amplifier should not be used for AM, FM or any other continuous-carrier operation. The amplifier should be used only for CW and SSB operation where the duty cycle is significantly reduced.

Thermal performance of the amplifier is illustrated in Figure 8. Data was taken under dc operating conditions with power-dissipation levels set equal to conditions under RF operation. A RadioShack brushless 12 V dc fan (RS 273-243A) blows air across the heat sink. Key down, the maximum rated junction temperature is reached in as little as five seconds as illustrated in Figure 8. Prolonged key-down transmissions should be avoided for this reason.

Under intermittent CW conditions, the situation is very different. Transistor-case temperatures reached 66°C after operating four minutes under simulated CW conditions at 20 WPM (60 ms on, 60 ms off). The corresponding junction temperature is +141°C (based on an equivalent RMS power dissipation of 21.7 W per transistor). This keeps the junction temperature under the 150°C target (see Figure 9). One simple way to reduce power dissipation is

to reduce the power-supply voltage to 24 V. RF output power will decrease about 10 W from the maximum levels achieved with a 28 V supply.

From a thermal standpoint, the IRF510 power MOSFET is a poor choice for this RF amplifier application. Although I must say I am impressed with the robustness of these devices considering the times I spent testing them key down, five minutes at a time, without failure. Q1 and/or Q2 may need to be replaced after a year or so of operation because of the compromise in reliability. Considering their low cost, that is not a bad trade-off.

Stability

High gain, broad bandwidth and close input/output signal routing (within the TR relay) all work against stability. With a good load (< 2:1 SWR) the amplifier is stable from 1.8 MHz through 39 MHz. Oscillation was observed when the transmitter frequency was increased to 40 MHz. The output load match also affects stability. Oscillation was observed on 27.5 MHz when the load SWR was 3:1. This should not be a problem since the frequency is outside the ham bands. I spent a great deal of time trying to make this design unconditionally stable even with loads exceeding 3:1 SWR without sacrificing output power (gain) at 28 MHz without success. I did identify some reasonable compromises.

One of the easiest ways to improve stability and the input SWR seen by the RF source is to add an RF attenuator (pad) at the amplifier input. An attenuator is absolutely required if the transmitter (driver) provides more than 1 W to the amplifier. R8, R9 and R10 form an RF attenuator that attenuates the transmitter drive level, but does not attenuate received signals because it is only in the circuit when K1 is energized. To drive this amplifier with a 2-W-output transmitter requires use of a 3-dB pad. The pad improves the amplifier input SWR and the isolation between the amplifier's input and output. The drawback is that 1 W is wasted in the pad. Likewise, a 5-W driver requires use of a 7-dB pad, but 4 W are wasted in the pad. (Values for R8, R9 and R10 to make a 3-dB pad and a 7-dB pad are given in the parts list.) Installing a pad requires cutting the PC-board trace *under R9*, otherwise R9 would be shorted out by the trace. Make a small cut (0.1 inch wide) in the trace under R9 before soldering R9 in position. R8 and R10 have the same values, but may have different power ratings. Connect R10 between the RF input side of R9 and ground. Install R8 between the amplifier side of R9 and ground.

An impedance mismatch between the output of a 1-W-output driver and the amplifier input can be a source of instability. (Obviously, if the driving transmitter's output power is only 1 W, you can't use a pad as described earlier.) If you encounter stability problems, try these remedies: Place a resistor in parallel with L1 and L2 to decrease the Q of the amplifier matching network (try values between 50 and 220 Ω). Try reducing the value of L3 or eliminating L3 entirely. Both of these modifications improve stability, but reduce the amplifier's output power above 21 MHz.

Summary

This project demonstrates how inexpensive power MOSFETs can be used to build an all-band linear HF power amplifier. Frequency of operation is extended beyond the limits of previous designs using the IRF510 and improved input-impedance matching. Long-term reliability is recognized as a compromise because of the poor thermal performance of the low-cost TO-220 package.

If you have been thinking about adding an amplifier to your QRP station, this project is a good way to experiment with amplifier design and is an excellent way to become familiar with surface-mount "chip" components. I made arrangements with Mouser Electronics and Amidon Inc to provide parts kits for this project at a discounted price (see the parts list in Part 1). These parts kits make it very easy to get started and more economical to "homebrew" this project.

Acknowledgments

I want to thank the following individuals associated with this project: Harry Randel, WD2AID, for his untiring support in capturing the schematic diagram and parts layout of this project; Al Roehm, W2OBJ, for his continued support and encouragement in developing, testing, editing and publishing this project; Larry Guttadore, WB2SPF, for building, testing and photographing the project; Dick Jansson, WD4FAB, for thermal-design suggestions; Adam O'Donnell, N3RCS, for his assistance building prototypes; and my wife, Laura, N2TDL, for her encouragement and support throughout this project.

Notes

[11]Mike Kossor, "A Broadband HF Amplifier Using Low-Cost Power MOSFETs—*Part 1*," *QST*, Mar 1999, pp 40-43.

[12]R. Dean Straw, N6BV, *The 1999 ARRL Handbook for Radio Amateurs*, (Newington: ARRL), 76th ed, pp 25-23*ff*.

By Zack Lau, KH6CP/1

From *QEX*, May 1992

A 1.8 to 54 MHz 5-Watt Amplifier

Need a rugged and stable amplifier for your multiband QRP rig? Not only has the design been optimized on a pricey computer program called *Touchstone* (by eesof) for unconditional stability, it has actually survived a variety of poor loads—it was used to sweep filters with 5 W of RF. The gain of the two stage amplifier was measured to be between 28 and 30 dB in the amateur bands, though there is another dB of gain around 37 MHz.

For ruggedness and ease of design, a Motorola MRF 137 was selected as the final transistor. While the MRF 138 may be more linear, insufficient design information was available to ensure a stable design. While some amateurs will balk at the high cost of these devices ($24 in November 1991), such savings are easily lost if the cheaper device has a habit of blowing up. Also, one picks up a real clean SSB signal—the high-order IMD products are way down compared to typical bipolar amplifiers. For instance, the worst IMD on 3.5,7,14 and 28 MHz was –38 dB on 28 MHz, with the 5th order products 61 dB down (relative to PEP). The device was putting out 5-W PEP while being biased at 0.5 A (28-V supply).

Perhaps the biggest flaw is the power requirement—these FETs really like to see high voltages for best performance, and the MRF 137 is no exception. I biased the MRF 137 for 0.55 A and 28.2 V. It drew 0.6 A when putting out 4.6 W at 28 MHz. The driver runs off your normal 12-V supply.

The input amplifier shown in Fig 1a is pretty straightforward—a bipolar 2N5109 with the feedback networks adjusted to compensate the gain of the MRF 137. A series network of a 470-a resistor and a 12-pF capacitor was tacked between the collector and ground to ensure stability at all frequencies. The MRF 137 rolls off a few dB at 54 MHz, but the bipolar amplifier adequately compensates for this gain deficiency. The input return loss is better than 18 dB between 1.4 and 29.9 MHz, but degrades to 12 dB at 50 MHz. The input SWR was not tested with poor loads.

By itself, the MRF 137 amplifier stage shown in Fig 1b (see next page) makes an excellent 16-dB gain block between 1 and 32 MHz, having less than 0.5 dB of gain variation. The transmission line transformer on the input seems to help the input return loss/SWR, keeping these numbers above 18/below 1.3 to 1 between 1 and 50 MHz. I suppose that putting another transmission line transformer on the output could be used to get a more powerful amplifier with less gain over a similar frequency range, but this variation has not been investigated.

The simplest circuit board I could think of was used—I cut two pads in a piece of double-sided circuit board for the gate and drain leads. Then I wrapped the edges of the board with copper tape and soldered it down for good grounding. After making holes for the MRF 137 transistor and the mounting screws in the board and a spacer, made of 0.050-inch aluminum, I attached the spacer, the circuit board, and the MRF 137 to a heat sink tapped with 4-40 screw holes. Standard ground-plane construction was used to attach the other parts. The 2N5109 amplifier was built on its own ground plane—RF amplifiers work better if there isn't too much gain in one place. Three additional amplifiers were built by Mike Gruber, WA1SVF, for use in the lab. He noted that R8 had to be changed from 4.7 kΩ to 1 kΩ to bias the amplifiers at 0.5 amps. Apparently, the MRF 137s he used have a higher gate threshold voltage. Otherwise, performance was as expected.

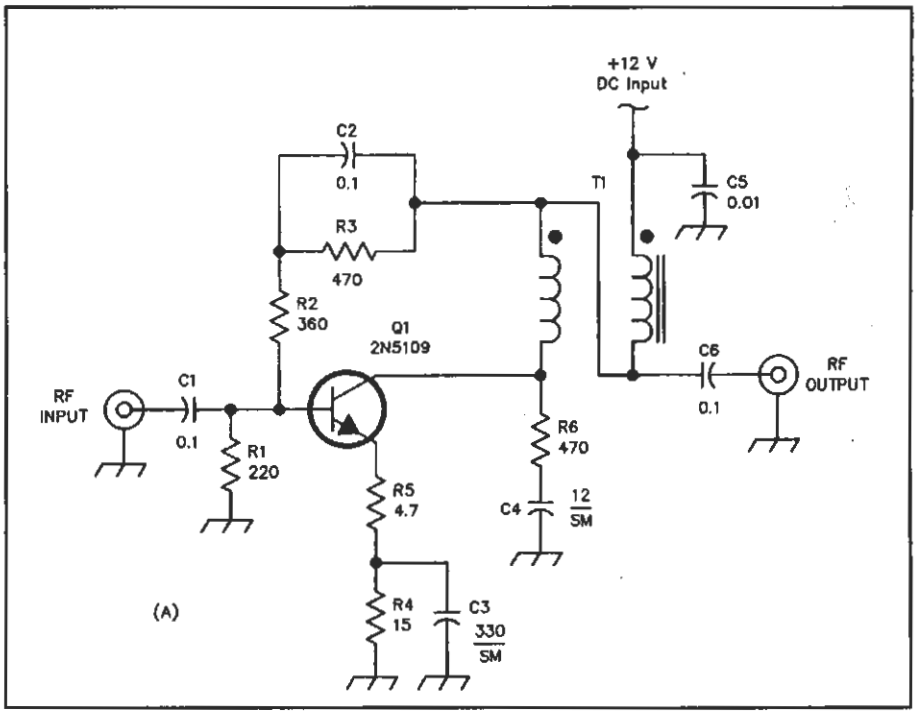

Fig 1a—Low-level amplifier designed to compensate for the gain rolloff from the power amplifier.
Q1—2N5109, 2.5-W heat-sinked RF transistor, f_T is 1200 MHz.
T1—15 turns bifilar #28 on FT-37-43 toroid core.

Fig 1b—5-W TMOS power amplifier.
L1—26 turns no. 26 enameled wire on T-44-2 toroid, 3.9 µh.
Q2—MRF 137 transistor.
R9—10-kΩ turn potentiometer for bias setting.
RFC1—21 turns of no. 26 enameled wire on FR-37-67 toriod.
T2—4 turns 25-Ω coax on FT-50-43 toroid core. The 25-Ω coax is actually two 50-Ω coax run side-byside. The prototype used RG-196/U coax.
U1—78L05 5-V regulator.

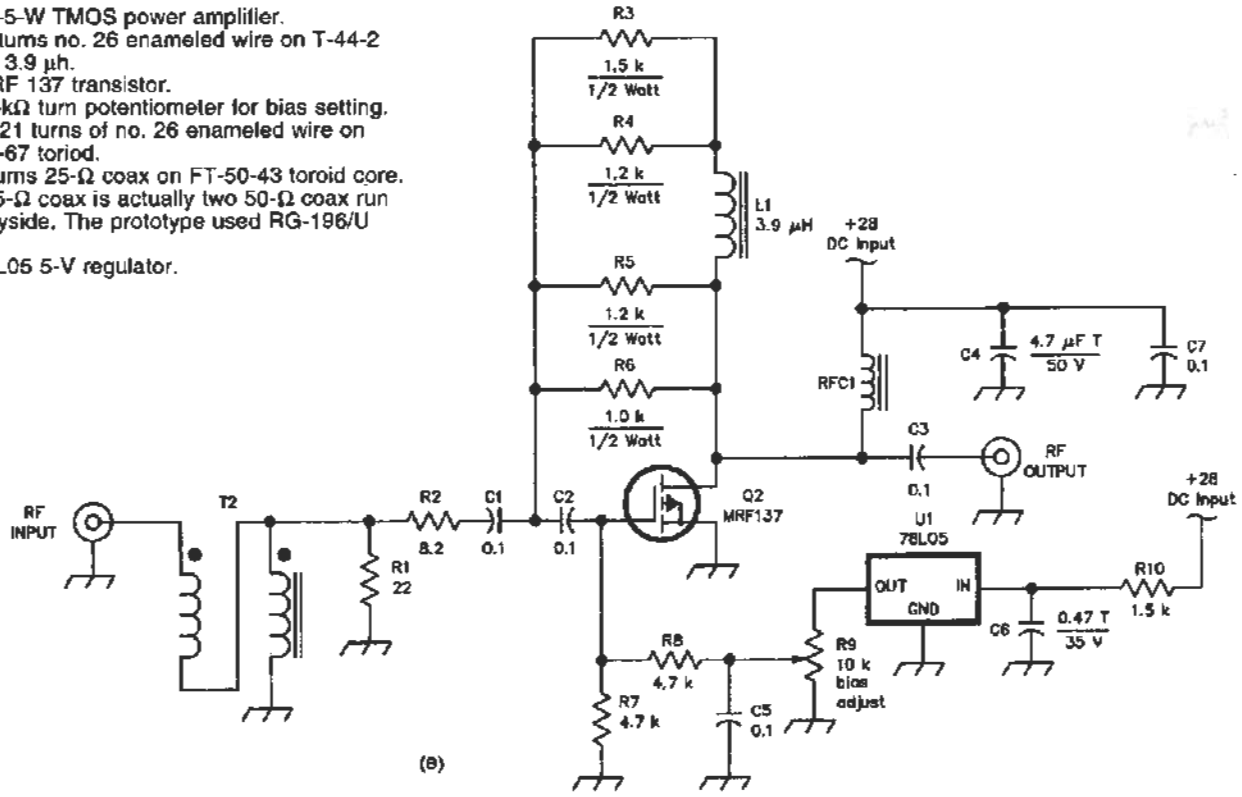

By Joel Paladino, N6AMG From *QST*, September 1992

An Experimental Solid-State Kilowatt Linear Amplifier for 2 to 54 MHz

Many kilowatt amplifiers could anchor a small boat, and don't cover 6 meters. Combined with its power supply, *this* kilowatt weighs less than 35 pounds.

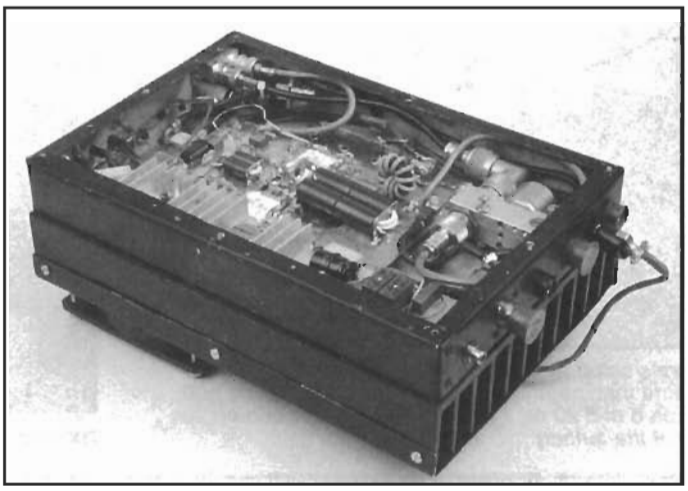

This article describes progress toward achieving a well-defined goal: building the smallest possible MF/HF/VHF amplifier capable of at least 1000 watts output. Nicknamed the Solid State Kilowatt (SSKW), the project has its roots in an article by Helge Granberg of Motorola in October 1986 *RF Design*.[1] Two water-cooled amplifiers of that design, built by Mike Staal (K6MYC) of M2, had many problems. Some of them were device-related; others, power-supply related. (More about these issues later.) In February 1990 I rebuilt one of the water-cooled units using the old design and two new transistors. Optimized for 50 MHz, this amplifier could just reach the 1000-watt level. After using it for three weeks of South Pacific DXpeditioning, I decided to construct an air-cooled unit. I spent the spring, summer and fall of 1990 building the SSKW and getting it ready for another DXpedition in the fall.

Circuit Description

Motorola's article reprint AR-347 describes the basic amplifier design. July 1990 QEX also carried an article about it.[2] Fig 1 shows the amplifier schematic. Briefly, the circuit consists of two MRF154 RF power MOSFETs in push-pull. Each of these transistors is capable of 600 watts output up to 100 MHz. The input and output transformers, 9:1 and 1:9, respectively, use cores of #67 ferrite material. The output transformer's 1:9 ratio is a compromise that is optimum at about 800 watts.

Incorporating the Motorola building block into a DXpedition-ready package required experimentation and problem-solving, as I described at the 1991 Central States VHF Conference.[3] Here's where the system stands today.

TR Switching

The SSKW includes TR relays that bypass the Fig 1 circuitry in receive mode. I designed their control circuitry to eliminate the possibility of the high RF fields in the amplifier compartment causing relay falsing problems, and to simplifies field repair by keeping parts count low. The relays are sequenced to allow the output relay to close before the amplifier puts out power. Because relays take a few milliseconds to operate, sequencing is necessary to keep the relay from hot-switching the amplifier output. (Hot-switching 1 kW will destroy a relay rapidly!)

This design has two small problems. For the short time it takes the amplifier's input relay to close on switching from receive to transmit, the exciter operates without a load. This can be remedied by delaying the exciter keying. The other problem is the relay's closure time changes as the relay heats. This can be solved two ways: Use external electronics to do the delay, or temperature-compensate for the resistance change.

SWR Protection

I haven't yet built SWR protection into the amplifier. In January 1983 *QST*, Helge Granberg described an SWR-protection circuit for a 2- to 30-MHz amplifier.[4] A phone conversation with Helge indicated that this circuit will work to 54 MHz, so it should suffice. How much mismatch the MRF154s can tolerate is unknown, however, so I don't

6-Meters: DXpeditioning with a Difference

Making the most of 6 meter DXpeditioning depends on knowing where and when to go If you want to work Europe from the Canary Islands summertime is best because sporadic E propagation is best then If you want to work the US from EA8 go when fall shifts into winter to take advantage of east/west F2 layer propagation It s always more exciting to go to a rare place but not necessarily more fun'

Once you ye decided on a DXpedition site plan your travel on the assumption that you II want to stay on site for at least two weeks This gives you about a 50% better chance of having good openings within a given month

Pay particular attention to the RF prospects of your accommodations Ideally you d be able to see ocean in all directions If that s not possible all s not lost A direct oceanic path isn t always the best propagation may be better over the backscatter path You II want to get your antenna up as high as possible to minimize radiation angle and AFI And consider EMI and NI possibilities carefully Some areas of the world use NTSC channel 2; others, PAL on channel 1—right in the middle of the band! If your RF gets into a resort's CATV system you II drive 60 televisions crazy rather than one or two.

Chapter 6 of *The ARRL Operating Manual* covers DXpedition power, health, licensing and logistical concerns in detail so see that book for more about those topics Ill add one thing though It helps to find a local ham with FAX capability as well as HF who can help you with questions on licensing and living accommodations

This can take 80% of the surprises out of the expedition!

Equipment

What I bring and use on 6-meter DXpeditions is based largely on the experiences of Jim Treybig, W6JKV, in his many years of 6 meter DXpeditioning. The core of the approach is pretty much this: Run as much power as permitted and bring as big an antenna as possible. There are practical limits to this, but let your ingenuity direct your thoughts. I consider 100 W as a minimum, 500 watts good and 1000 watts as optimum. High power lets you take advantage of scatter paths that simply won't work at 100 watts. It's very frustrating to hear a well equipped station that you cannot work!

Which Antenna?

A DXpedition antenna must be compact, light and reproducible The Yagi I use has six elements on a 30 foot boom. Optimized by Brian (K6STI) Beezley's Yagi optimization program *YO* it's fed with a T match and a half wave balun. Its boom folds down to two 40 inch sections, each 2 inches in diameter. Most of the element pieces fit inside the two 40-inch sections. The antenna is light enough to lift with one hand.

A rotatable antenna is *mandatory*. You'll need to turn your antenna to find the best direction of propagation. The antenna mast, 20 feet long overall, consists of 40 inch sections of 2-inch aluminum tubing joined with internal sleeves. The rotator is at the mast bottom and there's a slip ring at the mast top just below the Yagi (Having the rotator at the bottom makes putting the antenna up easier by minimizing weight at the upper end of the mast.)

I use Dacron rope for guying. How much rope should you

The author's setup at CN2JP, Rabat, Morocco. Efficiency counts more than neatness while you're busy making 900 contacts on 6 and 20 on 2-meter EME! *(DXpedition photos courtesy of the author)*

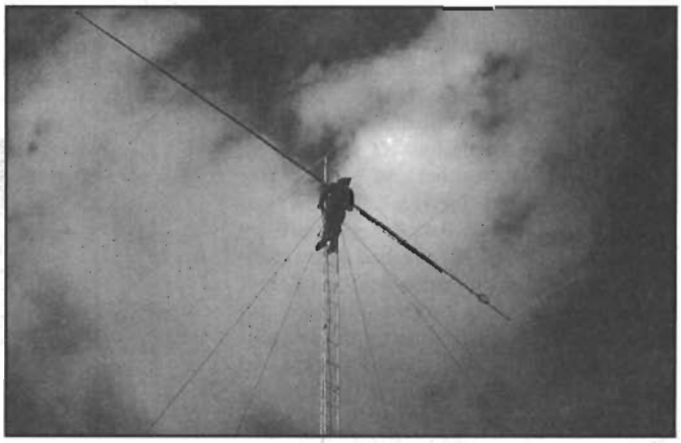

DXpeditioning would be no fun at all without antenna work!

want to use the SSKW to calibrate its own SWR-protection circuitry!

The amplifier's output can be reduced two ways: by turning down the exciter power via amplifier-generated ALC, or by reducing the amplifier bias. (These are enhancement-mode FETs, so positive bias is necessary to turn them on.) The ALC option is better because it does not affect the amplifier's linearity. A no-output-load condition must shut down the amplifier as quickly as possible.

Overdrive Protection

Overdrive can destroy power MOSFETs instantly, so a drive limit control is essential. A threshold detector should be incorporated. The SSKW's input includes a 5-dB attenuator so 100-watt exciters can drive the amplifier without damaging it. If the 5-dB pad fails to attenuate, or if the exciter puts out too much power, the amplifier must be shut down rapidly.

The amplifier must also be shut down if the transistors' flange temperature exceeds 40°C. Shutdown can be done two ways, depending on how the amplifier is used. The first way is to just turn down the bias, which changes the amplifier's linearity. The second way is to totally turn off the amplifier. This must be done gracefully so the amplifier does not shut down while producing full power. The following shutdown sequence is essential: (1) Turn down the bias; (2) open the input relay; and (3) open the output relay.

Bias

The SSKW's bias circuitry is straightforward. R8's value must be tailored to the particular MRF154s used. If the bias decreases too fast with rising temperature, increase the value of R8. The LM723's input voltage must never exceed 40 volts.

Output Filtering

Filtering must be added to make the amplifier comply with FCC signal-purity regulations. The reactance of these filters away from their intended passbands must be taken into account. Absorptive low-pass filters should be considered. Such filters dissipate harmonic energy as heat rather than reflecting it back to the amplifier transistors.

Packaging

I intended to make this amplifier as small and light as possible. Most of the amplifier's weight is its aluminum heat sink

take? Simple: Estimate what you need, multiply by 2.5 and you might make it! I usually bring two diameters, 3/16 and 1/8 inch.

Radios

Bring at least two radios: one for HF liaison (usually at 10 meters) and another for 6 meters. I recommend maximizing redundancy by taking two radios that both cover 10 and 6. At least one of the 6-meter rigs should include an excellent noise blanker for power-line problems and motorbikes. It must also be able to drive a kilowatt amplifier to full output on 6. (I use one Kenwood TS-680S and one ICOM IC-575.) Receive coverage between 10 and 6 meters is another plus. Where it's allowed, listening to nonamateur services between 45 and 50 MHz can be very important in determining the direction of propagation.

Additional Gear

Bring 12-volt supplies capable of operating at the line voltage and frequency at your DXpedition destination. The supplies should also be able to handle wide line-voltage variations around nominal. Carry two of them—one for each radio. I modify mine by adding line filtering and fusing. Parallel a standard receptacle of some kind with your supplies' rig plug or cable. Two-prong, polarized Jones plugs work well. You can use them on everything for quick setup and breakdown.

Bring a memory keyer for use as a beacon and in normal CW operation. Also consider taking a laptop computer. I now use a computer for logging, taking notes, calculating beam headings, and determining the footprint of the sun.

DXpeditioning is also about meeting people. Here's Tarik Skiredj, CN8ST, and friends.

Operating

Several operating subjects are of prime importance. Ten-meter liaison comes first. You must use 10 meters to get up-to-date propagation information and find out who's being heard. When you're feeling your way through a pile of stations, you can sometimes miss very rare propagation opportunities if you don't check 10 meters often.

Six-meter contact procedures come next. It's very difficult making everyone happy on 6 meters when you're the DX. You must set rules and stick to them. Pick a frequency and do your best to keep it when the band gets busy. Try to not work the same stations over and over again, especially during pileups. Your goal is to give as many people as possible a new country. Work each station as quickly as possible. Don't discuss names and grid squares—the time it takes just gives fewer people a chance to work you. Leave that info to the QSL cards! Which should you operate—phone or CW? The answer is "Probably both." CW penetrates weak conditions better than phone, and it gives more people at the edge of propagation a chance at working you. Then, when you go to phone, everyone who can will worK you again. I favor CW DXpedition operation because of my experiences on the non-DX end.

Should you operate on a single frequency or split? Go to split when there's a massive opening and you're being QRMed by people calling you. This usually happens during intense backscatter openings. Hams on the 10-meter liaison frequency can tell you when QRM gets too heavy.

Conclusion

Six-meter DXpeditioning is a blast. And the SSKW makes it even more fun: I can devote more weight to antennas!—*N6AMG*

and copper heat spreader. How much heat sinking is needed depends on the duty cycle required. I decided that a duty cycle of 50% or less was acceptable. The resulting weight for the package, 14 pounds, is very acceptable. The SSKW is 8 inches wide, 12 inches long and 5 inches high.

The key to making the package light was to use the smallest possible heat spreader. I decided to use enough ¼-inch-thick copper to surround each MRF154 with at least 1 inch of spreader. I machined the spreader flat and attached it to the heat sink, also machined flat. After attaching the copper to the aluminum, I resurfaced the copper again at the transistor contact points to insure flatness. I spread a thin layer of heat-sink compound between the copper and aluminum, and another layer between the copper and the transistors.

With two high-pressure, 24-volt fans blowing on the sink, the resultant duty cycle limit is a little less than 50%. These fans are in series across the amplifier's 50-volt supply. The small fan in the compartment is a 12-volt unit that just barely fits. (The compartment needs to be a little deeper.) A fan is necessary here, however, because compartment airflow dramatically keeps the output transformer's ferrite from getting hot.

A heat sink with more fins and a thicker base, but the same fin depth, would raise the duty-cycle limit. (The copper spreader should be made larger as well.) These changes would also make the amplifier heavier.

Construction Techniques

A milling machine is required for surfacing all of the amplifier's heat-conductive interfaces. Physical flatness is essential for maximum heat conductivity and to avoid warping the transistor cases. The Motorola bulletin specifies the torque of the screws on the MRF154s' flanges. Tightening these screws uniformly assures that the flanges won't warp during temperature cycling.

R14 and R15, the feedback resistors, are flange-mounted. Their beryllium copper leads cannot be flexed very many times before they break. (According to their manufacturer, that may be only once!) These two resistors just barely fit. So, make sure the two MRF154s are separated properly.

Power Supply

To keep the amplifier small and light, I use a switching power supply. A Lambda

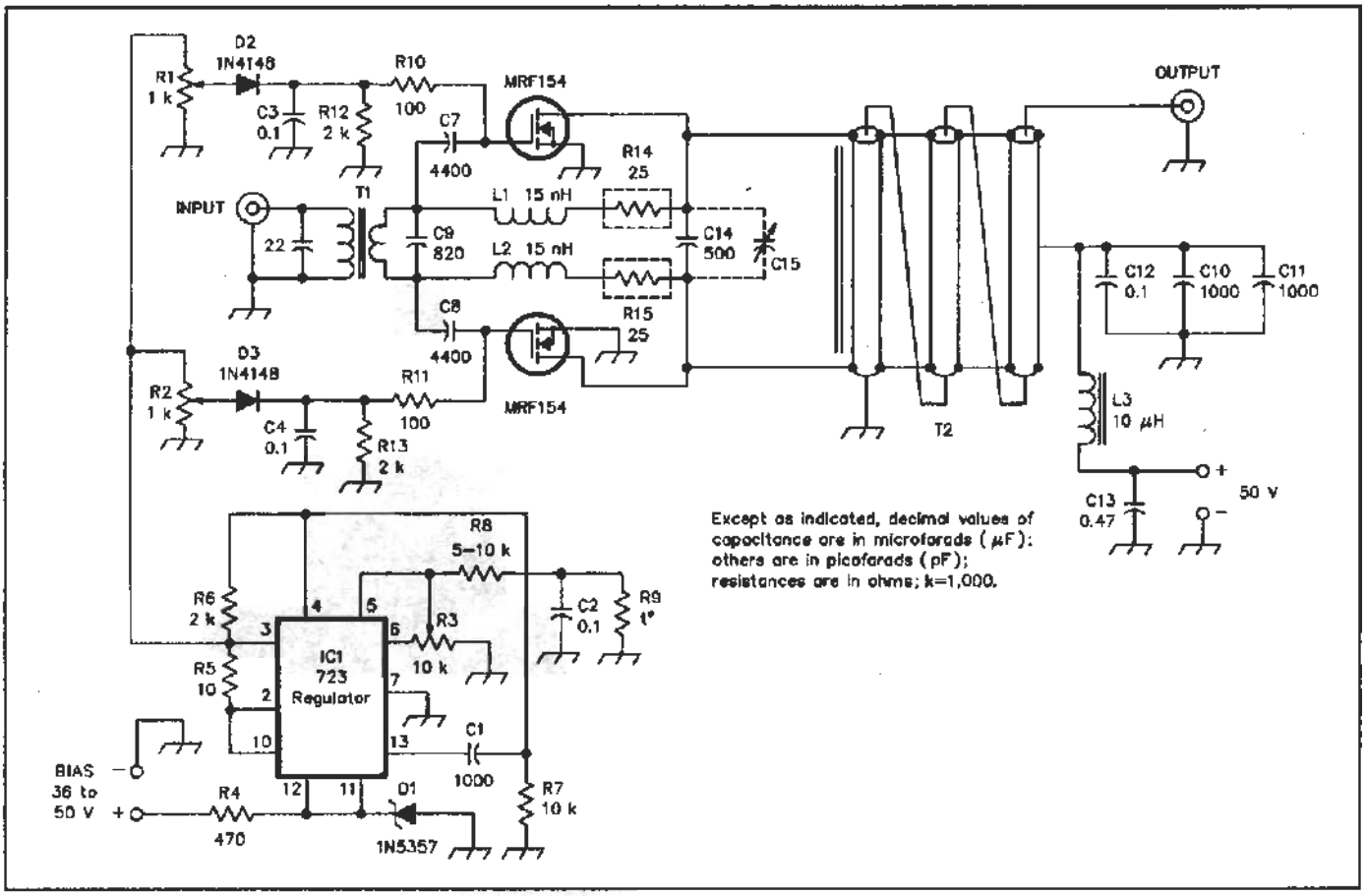

Fig 1—The basic SSKW circuit can produce at least 1 kW from 2 to 54 MHz. Duplicating this circuit requires additional information not given here. Output filtering is also necessary to ensure compliance with FCC emission-purity rules. See the text, Motorola Application Note AN-287, July 1990 *QEX* and the *1991 Central States VHF Conference Proceedings* for details. The *Central States* write-up includes SSKW performance graphs and spectrograms in addition to a diagram of the amplifier's relay-control circuitry.

LFS-50-48 (net weight, 20 pounds) does the job, with good results. Sized at 15 inches long, 7.5 inches wide and 5 inches high, it can source 50 amperes at 50 volts. This power supply produces significant radio noise up to 30 MHz, most of it radiating from the supply's ac-line leads. I EMI-filtered the supply's leads with good success. (We need better, RF-quieter switching supplies!) Because linear supplies generate little or no RF EMI, they are superior to switching supplies for fixed-station use.

Overshoot is a regulated power supply characteristic that's particularly troublesome in switching supplies. Overshoot occurs when a regulator responds too slowly to keep its output voltage down in response to short-duration, high-current loading. In a 50-volt switching supply, and depending on the load, overshoot transients of more than *100 volts* may result. I've seen overshoot destroy expensive transistors! The SSKW supply must be able to safely handle the variable power-supply demand that occurs during SSB and CW transmission.

Power-supply RF sensitivity is another consideration. Some power supplies are sensitive to RF. Their output voltages may vary with the presence and amplitude of RF on their input and output leads. The SSKW's supply must be free of such effects.

Hints and Kinks

Be careful when applying dc to the amplifier for the first time. Do not use a high-current supply for initial tests. Use a

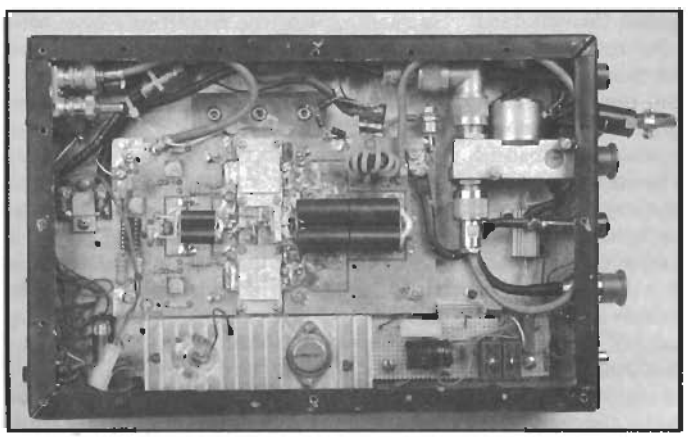

Two Motorola MRF154 RF power MOSFETS in push-pull make the SSKW perk. A 20-watt wxciter drives the amplifier to full output. (amplifier photos by Kirk Kleinschmidt, NTØZ)

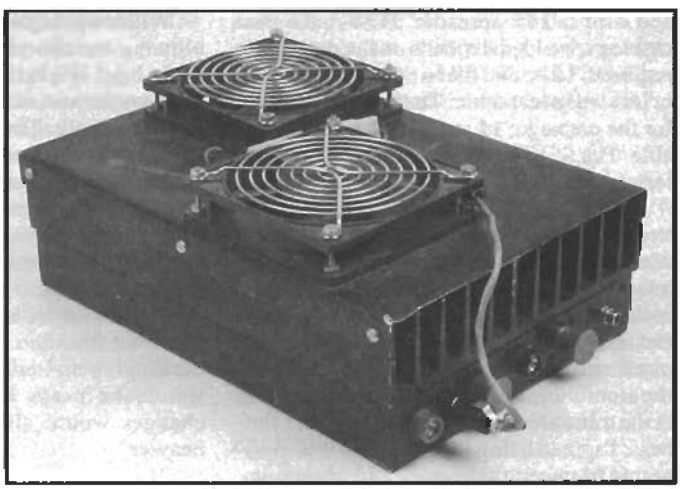

Without its two 24-volt fans, the SSKW's heat sink and spreader would have to be much larger.

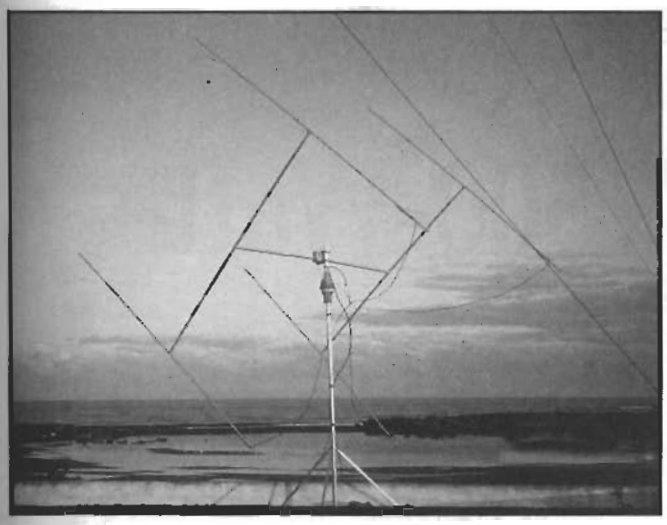

What luggage weight the SSKW amplifier conserves can be put to other uses—2-meter moonbounce gear, for instance. Operating as CN2JP, the author completed 20 EME contacts—Morocco's first—in November 1991. On the same trip, the SSKW performed like a heavyweight through 900 contacts with 56 countries on 6 meters.

Table 1
SSKW Performance Versus Frequency

Freq (MHZ)	Drive Power (W)	Power Output (W)	I_D (A)	Gain (dB)	Efficiency (%)	Input SWR	V_{cc} (V)
2	24.5	1000	39.1	16.1	51.2	1.41	50
4	21.0	1000	33.4	16.8	59.9	1.39	50
8	17	1000	32.4	16.8	59.9	1.39	50
15	15.5	1000	32.3	17.7	61.9	1.36	50
30	19.5	1000	41.5	17.1	48.2	1.87	50
50	29	1000	39.7	15.4	50.4	1.51	50

current-limited, 3- or 4-ampere supply to check the regulator and set the bias. The amplifier should have a reverse polarity protection diode rated at a voltage appropriate to the supply.

Make sure that you have a 50-ohm load on the amplifier output. The bias circuitry may not act correctly if there is no load. Slowly increase drive. Watch the output power and the current drain to make sure they are in line with efficiency. If the input match is bad, check C7 and C8. If the amplifier does not achieve its efficiency capability, RF that doesn't make it to the load may try to leave via the dc input line. This can cause C12 to explode off of the underside of the board. Also, under normal operation, the single unit Motorola specifies for C12 can barely handle the RF current that passes through it. I recommend paralleling 100-volt, 0.05- or 0.1-µF chip capacitors instead of using a single 0.1-µF chip.[5] This problem is difficult to analyze because C12 is on the underside of the board.

As mentioned earlier, the SSKW's bias circuitry may have to be tailored to the particular MRF154s used. One thing not mentioned on the schematics is the addition of an Arco 365 variable capacitor (C15 in Fig 1) across C14 to cancel some of the inductive reactance in the output transformer at 6 meters.

Performance

With a 50-volt power supply, the SSKW can produce over 1.1 kW from 2 to 54 MHz. At this power level, the MOSFETs' drain current runs at around 40 amperes, depending on the operating frequency. Table 1 shows amplifier performance data taken at six different frequencies. The SSKW can produce up to 1.5 kW below 30 MHz.

Especially below 30 MHz, the SSKW's harmonic output rises with output power. It may be possible to use only four low-pass filters to cover the 2 to 54 MHz range if a second harmonic of –40 dB can be tolerated. Since the transistors operate in push-pull, the second harmonic is usually not a problem.

Without its 5-dB input pad and operating with a 50-volt supply, the amplifier exhibits an input SWR of less than 2:1 (referred to 50 ohms) throughout its frequency range. Only below 5 MHz does its input SWR exceed 1.6:1. Inserting the 5-dB pad adds 10 dB of return loss and keeps the input SWR below 1.3:1 through the amplifier's operating range. I have not yet measured the amplifier's two-tone, thirdorder IMD performance.

Final Notes

For now, I can say that my goal of a compact, lightweight amplifier capable of at least 1 kW output is a reality. The SSKW has served me well in its intended DXpeditionary application. Nonetheless, the amplifier in its present form is still experimental. Before the SSKW could be acceptable for general use, output filtering and failureproof protection circuitry would have to be added. The next generation is on its way. The next project? Use the same 50-volt supply with power FETs capable of covering 144 to 432 MHz, and build it into a similar package!

Acknowledgment

I thank Helge Granberg for spending considerable time answering questions about this project.

Notes

[1]H. Granberg, "New MOSFETs Simplify High Power RF Amplifier Design," RF Design, Oct 1986, pp 43-48, 50, 52.

[2]H. Granberg, "A Compact 1-kW 2-50 MHz SolidState Amplifier," QEX, Jul 1990, pp 3-8.

[3]J. Paladino, "A Rapid Deployment Prototype Solid-State Kilowatt Linear Amplifier for 2 to 50 MHz Using MRF-154s," *1991 Central States VHF Conference Proceedings* (Newington: ARRL, 1991), pp 61-70. Available from the ARRL Bookshelf as #3614.

[4]H. Granberg, "MOSFET RF Power—An Update," Part 2, *QST*, Jan 1983, pp 30-33; also see Feedback, *QST*, Mar 1983, p 44. (Part 1 appeared in *QST*, Dec 1982, pp 13-16; also see Feedback, *QST*, Jan 1983, p 48.)

5American Technical Ceramics (ATC) has some new chip caps (the 900 series) that have higher voltage and current ratings than the capacitor Motorola specifies. I have samples but have not tried them yet.

By Jerry Pittenger, K8RA
From *QST*, September 1986

An All-Band, 1500-Watt-Output 8877 Linear Amplifier

Part 1—This rock crusher, rated for continuous full-legal-limit output, can be built at home. It is, however, a major project requiring dedication and commitment.

This article is the result of a 10-month project to build a legal-limit linear amplifier. The amplifier uses the popular EIMAC 8877 (3CX1500A7) high-mu power triode that can provide a continuous RF output of 1500 W to the antenna.

In recent years, I have built several different linear amplifiers, and I must admit that this previous experience was necessary to obtain the results achieved with this project.[1-4] I hope that by sharing this experience, others will benefit from it. Any amplifier design depends on the various components used and individual preferences. Therefore, you may not want—or be able—to duplicate this amplifier exactly.

The comment I receive most often from the amateur fraternity is about the high cost to build an amplifier like this. The criticism is valid. This amplifier is not inexpensive to build. Plan to spend from $1000 to $1200 for the RF deck, and another $500 to $600 on the power supply. If you really think about it, though, these costs are a bargain when you consider the performance and quality of the final product and the cost of an equivalent commercial unit.

This article is presented in two parts. In this part, I will describe the RF deck and power supply in general terms. Schematic diagrams and parts considerations are included. Part 2 gives detailed instructions for constructing the two units and considerations for the final testing and operation.

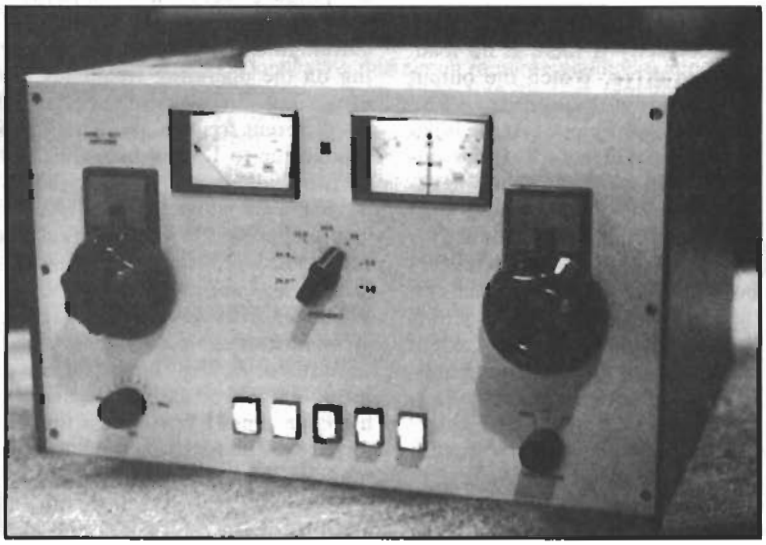

Table 1
Recommended Tools

- Drill press or drill fixture (with set of highspeed bits)
- Band saw capable of cutting 1/16-inch-thick metal
- Chassis punches (5/8 inch to 1 inch)
- Fly cutter, 2-inch radius
- Vise
- Set of taps
- Common handtools (screwdrivers, pliers, soldering iron and gun)
- Volt-ohmmeter
- Variable power supply (5-26 V, 1 A)
- Dip oscillator

Preliminary Thoughts

Finding Parts

Finding parts can be a big task. Even the most difficult parts to find, such as the vacuum variable capacitors, vacuum relays and door-knob capacitors are available, however, and appear for sale in the ads (*QST* Ham-ads and the Yellow Sheets), or at hamfests and flea markets.[5] Probably the best source of parts is other hams who are actively building equipment. Go talk to these people and let them know what you are looking for. It's amazing how others will help, and even let you into their personal stores. There are people, like myself, who like to build amplifiers. Once you learn who these individuals are, keep in touch with them. They can help find the key parts.

Parts that are not available in the surplus market can be purchased new. This will be necessary for some parts, such as

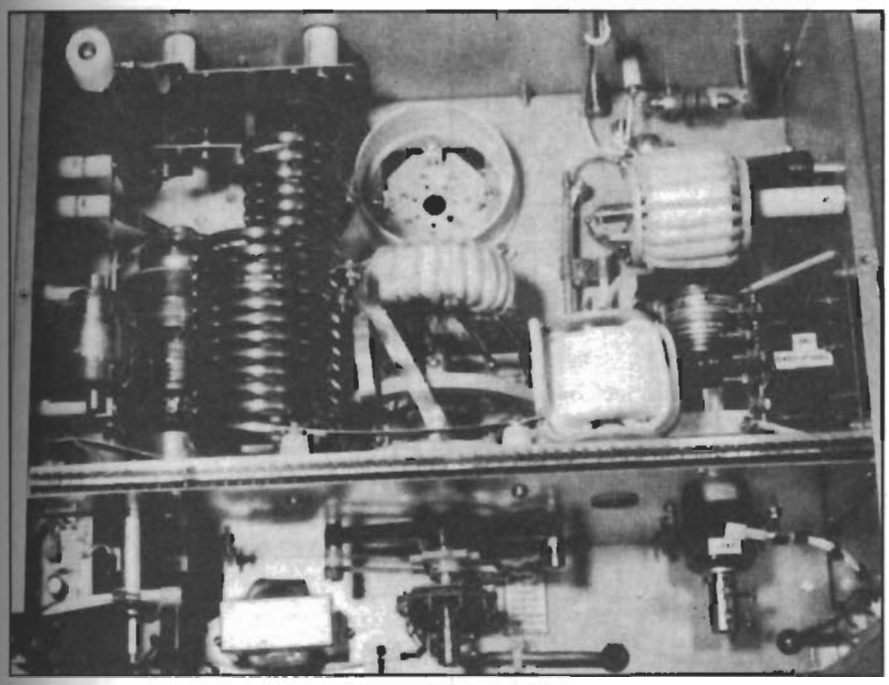

Fig 1—Top interior view of the 8877 linear amplifier RF deck.

cabinets, etc. Just remember that when you buy a new commercial amplifier, you pay the new price for every component.

Tools

A good assortment of hand tools, as well as some power tools, are necessary to complete this project. Table 1 shows the tools I recommend. In particular, I recommend that a drill press and band saw be available. You can do the job without all of the tools listed, but the job will be much more difficult.

Time

Time is probably the most valuable resource for most of us, and the one that may prove hardest to find. This project took well over 250 hours to complete. The key is to do each step right, and not hurry. Build the amplifier in a place where you can leave the project on the table and walk away. Plan each step and build in discrete modules. Work an hour or so whenever possible, and slowly, but surely, the modules will take shape. It is amazing how much you can accomplish using these small time segments. Also, great strides can be made on a Saturday or a Sunday. Commitment and consistency are the virtues required to finish the job.

RF Deck Circuit Description

The RF deck is designed to be a tabletop unit (see title photo). The power supply is remotely controlled and can be located almost anywhere. The amplifier design is based on proven circuitry. Included are all circuits required to provide a clean signal as well as adequate protection devices for the metal-ceramic 8877 tube.

Control Circuitry

Fig 2 shows the schematic diagram for the amplifier control circuitry and low-voltage power supply. The 117-V ac input from the high-voltage power supply enters the RF deck through a 5-conductor interconnecting control cable. Each control line is terminated in a pi-section filter as it enters the RF deck, to prevent RF from getting into the control cable and power supply. The pisection filters are constructed as an independent module.

The amplifier is powered up by the FIL ON/OFF switch, S1. Engaging S1 turns on the blower, filament power and 26-V dc power supply. The current inrush to the tube is limited by Ri, in series with the filament transformer primary. After approximately 1 second, K1 energizes and K1A shorts Ri thus providing full filament voltage to the tube. The K1 delay is controlled by R2 and C1 across the relay coil. R3, in series with the other leg of the filament transformer primary, is adjusted to provide the proper filament voltage (4.85 V ac) to the tube under load.

The 8877 requires a 3-minute warmup period to reach proper operating temperature. A solid-state timing circuit, formed by Q1 and Q2, locks the amplifier out of operation until the warmup period has elapsed. When the 26 V dc comes on, C2 charges through the 500-kilohm time-delay adjust and 1.2-megohm resistors. Q1 and Q2 form a high-impedance Darlington circuit, and the emitter of Q2 follows the voltage rise on C2. The high-impedance Darlington circuit is required to prevent the capacitor charge from draining through the transistors. After approximately three minutes, the potential at the emitter of Q2 reaches 18 V at which point the 4PDT relay, K2, engages. K2A applies 26 V dc to the K2 relay coil, removing the relay current load from Q2. The voltage also turns on the TIME pilot light located on the amplifier front panel to indicate that the warmup period is over. The same line also applies 26 V dc to S2B of the HV-ON push-button switch, which, when engaged, sends 26 V dc to the RF input/output relay circuits. K2B connects a 100-kilohm resistor across C2 to drain the charge from C2. This resets the 3-minute timer should the amplifier be turned off and immediately back on.

K2C and K2D are wired in parallel and apply 117 V ac to HV-ON switch S2A to energize the high-voltage power supply. The high-voltage power supply can't be turned on even if the HV-ON switch is engaged until after the 3-minute warmup period has ended. IN/OUT switch S3 allows the amplifier to be put in the standby mode with the amplifier turned on. Both HV-ON and IN/OUT front-panel push-button switches must be engaged to key the amplifier, thereby making it impossible to operate the amplifier without high voltage on the tube.

The amplifier is keyed by grounding the base of Q3 through the exciter TR-relay contact. A transistor is used to limit the current switched by the exciter VOX relay. This avoids a potential problem if the exciter VOX relay sparks on closure, which could damage the relay contacts. The "grid trip" break in the relay line causes the relays to drop out if the grid trip circuit actuates from too much grid current (approximately 120 mA). During normal operation, the grid trip break is shorted by a normally closed set of contacts on K3 (see Fig 3).

When the amplifier is keyed, the output RF relay must be closed before drive is applied to the tube—otherwise the tube will transmit for a brief period without a 50-ohm antenna load. This would not only be harmful to the tube, but also cause the grid-trip circuit to actuate. Therefore, a timing circuit, comprised of a 50-ohm resistor and i00-~iF capacitor, is included across the RF input relay K4 to allow vacuum relay KS time to close. The capacitor value depends on the relay used. Do not make the delay too long, since during the delay time, the exciter does not have a proper 50-ohm load. Check the time delay by placing a low voltage across the relay contacts and monitoring the contact closure on a dual-trace scope. I used a delay of about 20 ms..

RF Amplifier Circuit Design

The RF amplifier circuit is shown in Fig 3. The amplifier uses a tuned input network to minimize distortion products and provide a proper impedance match between the exciter and the tube. The input network is remotely switched, using small DPDT relays, to connect the correct pi-section for the selected band. A homemade switch deck is mounted on the band-switch shaft, in front of the subpanel, to ground the 12-V dc line for the proper input relay as selected by the main band switch. On 160 meters, the switch also controls a solenoid relay to add a 160-pF capacitance in parallel with the TUNE vacuum variable capacitor.

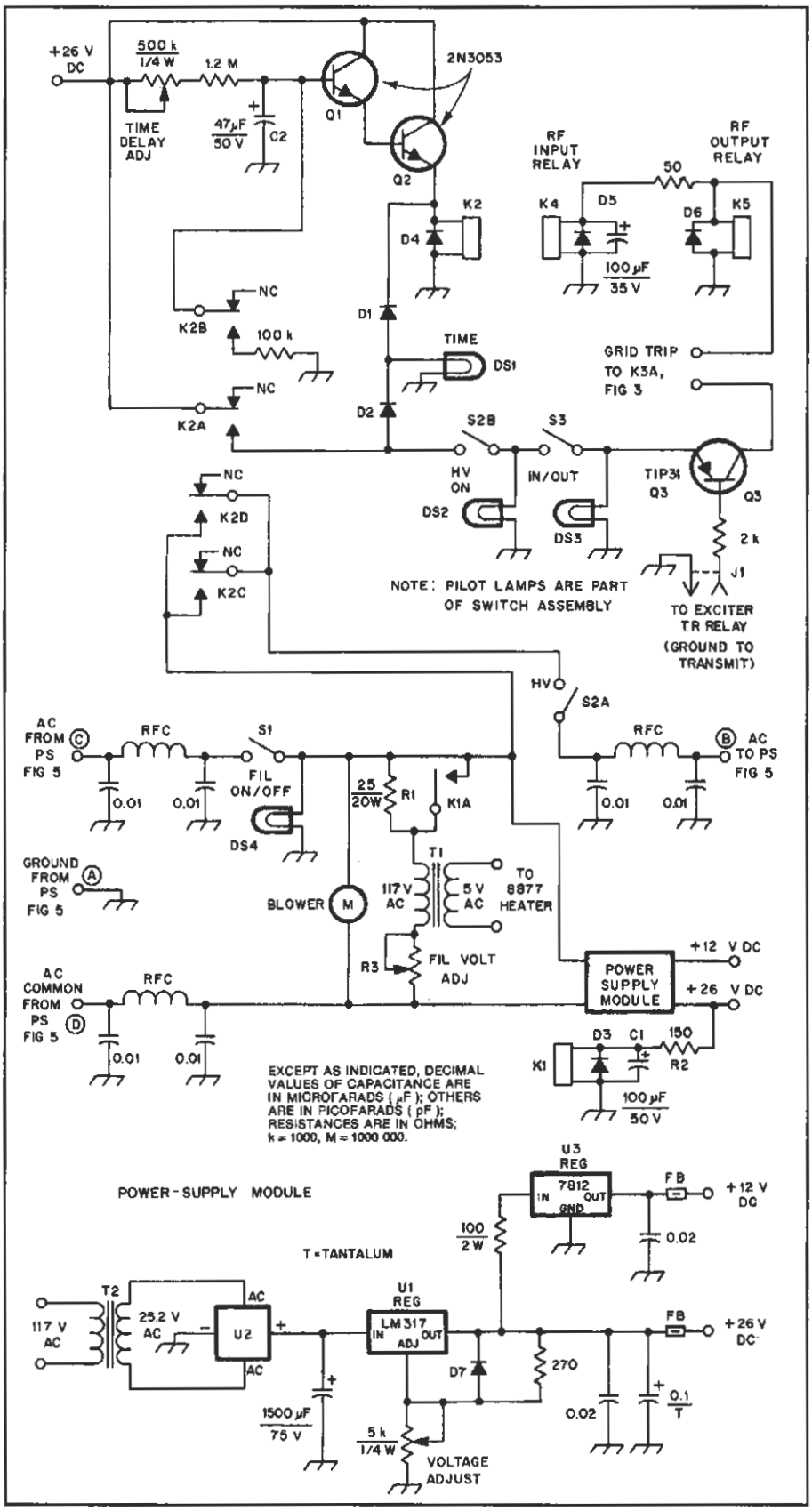

Fig 2—Amplifier control circuit and low-voltage power-supply schematic diagram. Part numbers shown in parentheses are Radio Shack.

B—Blower, Dayton 4C004-i.
D1-D6—Diode, 1 kV, 2.5 A.
FB—Ferrite bead.
K1-K4—4PDT 24-V dc relay, Potter & Brumfield KHU17D11.
K5—SPDT vacuum relay, 26-V dc coil.
Q1,Q2—2N3053 NPN transistor.
Q3—TIP31 NPN transistor (276-2017).
R1—25 Ω, 20 W.
R2—150 Ω, 2 W.
R3—25 Ω, 25 W variable.
RFC—10 turns no. 14 enam wire on ¼-in-diam ferrite rod.
S1,S3—Alco 16TL5-11 SPST.
S2—Alco 16TL5-22 DPDT.
S4—Alco 16TZ pilot light.
Ti—Filament transformer, 5.0 V ac, 10 A, Peter Dahl Co.
T2—25.2 V ac, 1.0 A, Stancor P6469.
U1—50-V, 4-A bridge rectifier.

An effective ALC circuit, adjustable from a front-panel control, is included to avoid overdriving the tube. This feature is essential in this amplifier because the drive requirement is only about 80 W for 1500-W output. The ALC circuit samples the RF drive level through a 27-pF mica capacitor to generate a dc voltage that is fed back to the exciter for drive-power control.

The grid-trip-protection circuit shuts down the amplifier if grid current exceeds 120 mA. This protects the tube from tuning errors or other problems such as losing the antenna, or a tube flashover during operation. Although grid current flows through all paths from ground to the B – line, most of the grid current goes through R1. The current passing through R1 develops a voltage drop. For example, if 100 mA of grid current is drawn through R1, 1 volt is developed (E = IR = 0.100 x 10). This voltage is used to turn on the transistor switch, Qi. When Qi turns on, the grid-trip relay, K3, energizes and opens the grid trip break in the RF relay control line to shut the amplifier down. R2 sets the current level at which Qi turns on. The front-panel GRID TRIP lamp goes out if the trip circuit is activated. The switch is reset by pressing S3.

The plate tank circuit uses a pi-L configuration because this design provides approximately 20-dB better harmonic suppression than the conventional pi design. The TUNE and LOAD capacitors are vacuum variable types to minimize space requirements and also optimize performance on 12 and 10 meters where small capacitance values are needed to achieve an acceptable tank-circuit Q. The 10- to 40-meter tank coil is homemade from ¼-inch copper tubing that is silver plated to minimize skin resistance. The 80-meter, 160-meter and L-coils are toroid designs to minimize space. Using a toroid for the L coil also helps isolate the L network from the rest of the tank circuit because of the toroid's self-shielding characteristics.

Metering circuits monitor plate and grid current, as well as filament voltage. Plate current is monitored by placing a meter in series with the B – line. Therefore, only a small dc voltage is across the meter. An additional position can be included on the FIL/GRID meter for plate voltage, but one is not shown in this design because a separate high-voltage meter is included in the power supply. It would be a good idea to include a high-voltage scale on the meter in case the RF deck is ever used with a different highvoltage supply. Grid current is monitored by measuring the voltage drop across R1. R3 is adjusted to give the cor-

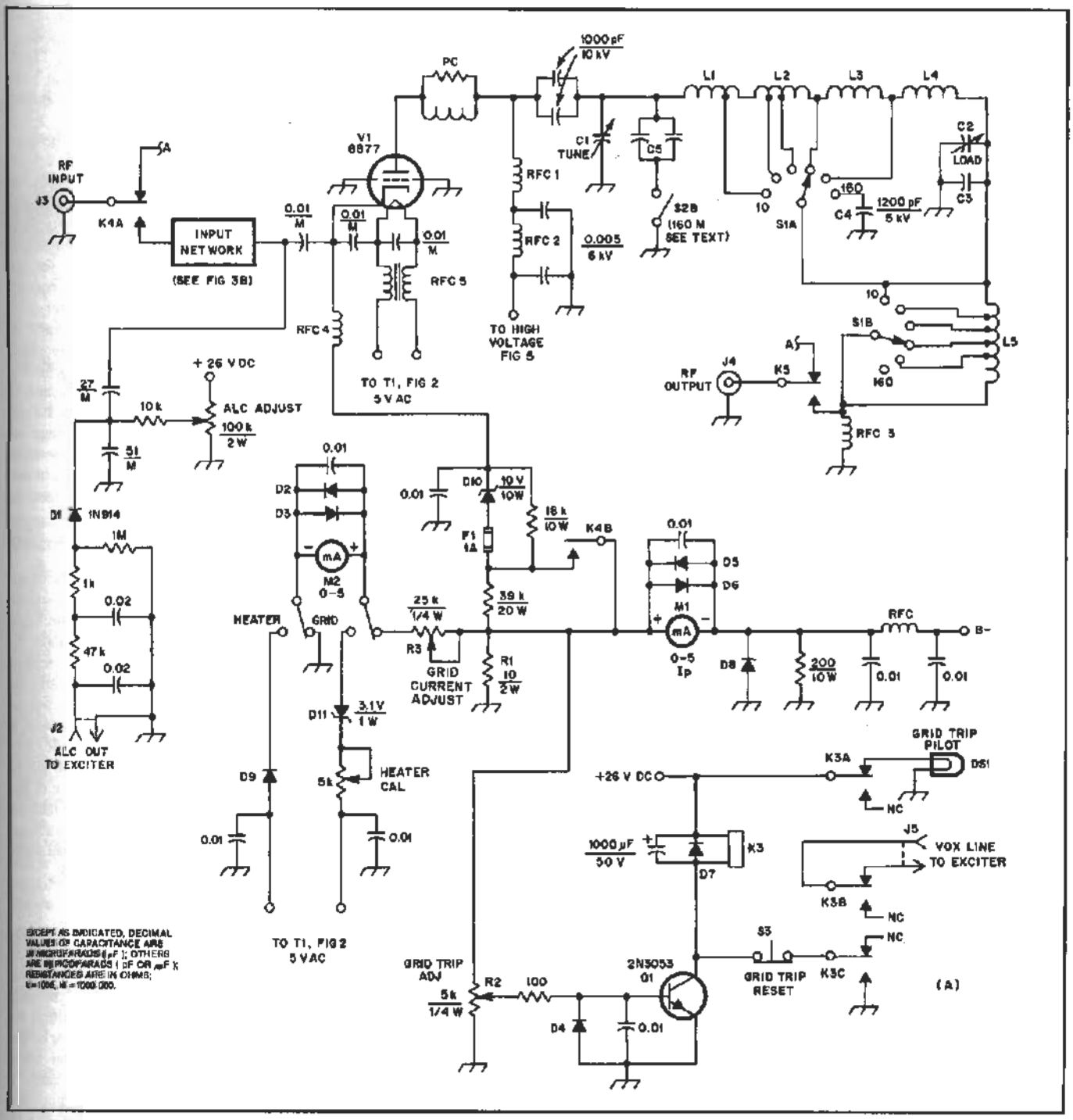

Fig 3—RF amplifier schematic diagram (see Part B on next page).

C1—Vacuum variable capacitor, 375 pF, 10 kV.
C2—Vacuum variable capacitor, 1000 pF, 10 kV.
C3—Mica transmitting capacitor, 100 pF, 5 kV.
C4—Mica transmitting capacitor, 3 × 400 pF, 5 kV.
C5—Fixed vacuum capacitor, 2 × 80 pF, 20 kV.
D1—Diode, 600 V, 1 A.
D2-D9—Diode, 1 kV, 2.5 A, HEP 170.
D10—Zener diode, 10 V, 1 W.
D11—Zener diode, 3.1 V, 1 W.
K1-K7—DPDT 12-V dc DIP relay (275-213).
K8—SPST 12-V dc relay (275-241).
RFC—10 turns no. 14 enam wire on ¼-in-diam ferrite rod.
RFC1—Plate choke, 2 A, Peter Dahl Co.
RFC2—Air-wound coil, 15 turns, ½-in diam.
RFC3—Choke, 1 mH, 800 mA.
RFC4—110 turns no. 20 enam wire on ½-in diam fiber rod.
RFC5—Filament choke, 18 bifilar turns no. 14 enam wire on ½-in-diam ferrite rod, 6 inches long.
PC—Three 150-ohm, 2-W carbon resistors in parallel with 2-inch horseshoe loop of ½-inch silver-plated strap.
L1-L5—See Table 2.
M1,M2—Simpson Wide-Vue panel meter, 01253 bezel and 01165 lighting kit (See text).
S1—9-position, 2-pole switch, Radio Switch model 88, 13-kV, 30-A.
S2—Solenoid-controlled switch; see text.
S3—SPST normally closed momentary switch, Alco 16TL-11 with 6T-2 red lens.

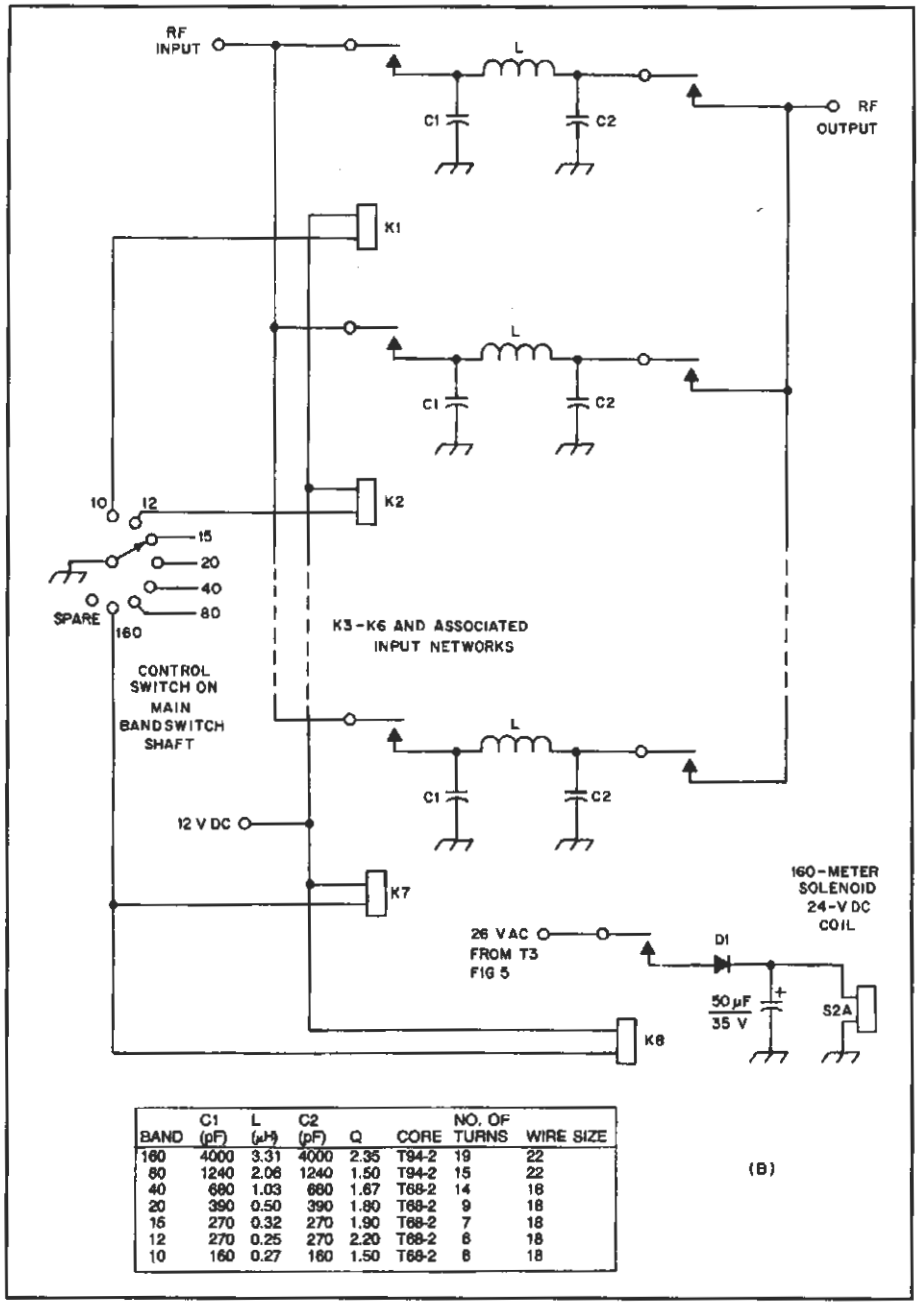

BAND	C1 (pF)	L (µH)	C2 (pF)	Q	CORE	NO. OF TURNS	WIRE SIZE
160	4000	3.31	4000	2.35	T94-2	19	22
80	1240	2.06	1240	1.50	T94-2	15	22
40	680	1.03	680	1.67	T68-2	14	18
20	390	0.50	390	1.80	T68-2	9	18
15	270	0.32	270	1.90	T68-2	7	18
12	270	0.25	270	2.20	T68-2	6	18
10	160	0.27	160	1.50	T68-2	6	18

Fig 3B—see previous page.

rect gridcurrent meter reading. Filament voltage is measured by converting the ac voltage to dc and displaying the dc voltage on M2. The 3.1-V Zener diode expands the meter scale by not allowing conduction until the voltage reaches 3.1 V.

A vacuum relay is used for the amplifier output. The relay is small in size, quiet and capable of handling large RF currents.

RF Deck Parts Selection

Finding all the parts for the RF deck is a major task. If you are planning to build an amplifier, begin collecting parts as soon as possible. It is the first step because the physical layout of the amplifier will depend on the components available. Don't try to exactly duplicate the components I used. For example, vacuum variable capacitors come in many different shapes and sizes, with different mounting provisions. Actually, the parts you find may be better than the parts used in my RF deck. As an example, a 1500-pF vacuum variable LOAD capacitor would be much better than the 1000-pF unit I used. Therefore, use whatever resources you have available to acquire the parts— but a word of caution! Do not compromise too much when gathering components. If you cannot find what you need on the surplus market, buy the parts new. It may cost a little more, but if the project is not done right, you will never be happy with the final result.

Vacuum Variable Capacitors

Vacuum variable capacitors are often difficult to locate at reasnable prices. Plan to spend about $50 for the TUNE capacitor and $75 to $100 for the LOAD capacitor if vacuum capacitors are used. The TUNE capacitor should be at least 300 pF at 7 kV, and the LOAD capacitor should be at least 1000 pF at 3 kV.

An air variable capacitor can be used for the LOAD control, if desired. The minimum capacitance for the LOAD capacitor is 112 pF for 10 meters, which is not difficult to obtain with an air variable type. A rating of 1 kV, minimum, is recommended. However, it is a different story for the TUNE capacitor. The minimum required capacitance is 26 pF. The direct inter-electrode capacitance of the 8877 tube in grounded-grid service is 10 pF; therefore, the TUNE capacitor must have a minimum value of not more than 16 pF for 10 meters.

This is nearly impossible with a 300-pF air variable. In addition, the voltage requirements for the TUNE capacitor make any air variable rather large. For these reasons, a vacuum variable is recommended for the TUNE capacitor.

Meters

Good-quality meters with bezels are essential for good appearance. The Simpson Wide-Vue® meters I used were purchased at a hamfest. The bezels were ordered directly from Simpson because they seldom appear on the surplus market. Actually, almost any meter movement can be used, so don't pass up a good meter just because it reads 50 V or 100 mA on the scale. Any meter with a movement from 100 µA to 5 mA can be used. This allows use of approximately 90% of the meters available on the surplus market. I will give instructions later for calibrating any meter to read whatever current or voltage is required.

RF Band Switch

Good RF band switches are very difficult to locate. More problems are experienced with arcing band switches than with any other amplifier component. If the band switch selected has insufficient voltage insulation, it will arc to the wiper rotor on the high-impedance 10-meter position when operating on the lower-frequency bands. I obtained the band switch for my amplifier from Radio Switch Corp.[6] The model 88 switch is a 2-pole, 9-position unit with a 13-kV peak flashover/30-A contact rating. This switch will not arc! Its list price is currently $107, and it is well worth the money!

Miscellaneous Parts and Materials

Many of the small parts (capacitors, relays and resistors) can be purchased at Radio Shack. Their parts selection is good, and continues to increase. You can usually find a store around the corner in almost any city. Pioneer Electronics is also a good source for commercial-grade components.[7] Good-quality PC-board material can be found at almost any hamfest. Don't compromise here—use G10 glass-epoxy board. As for coils? Make them. Complete "how-to" instructions are given later.

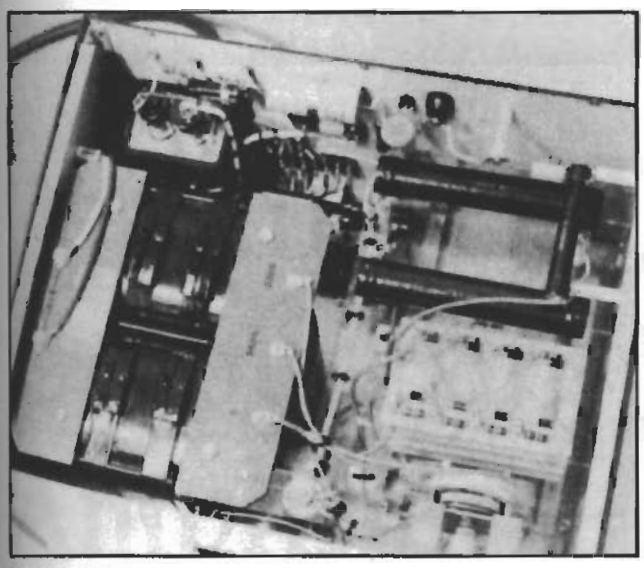

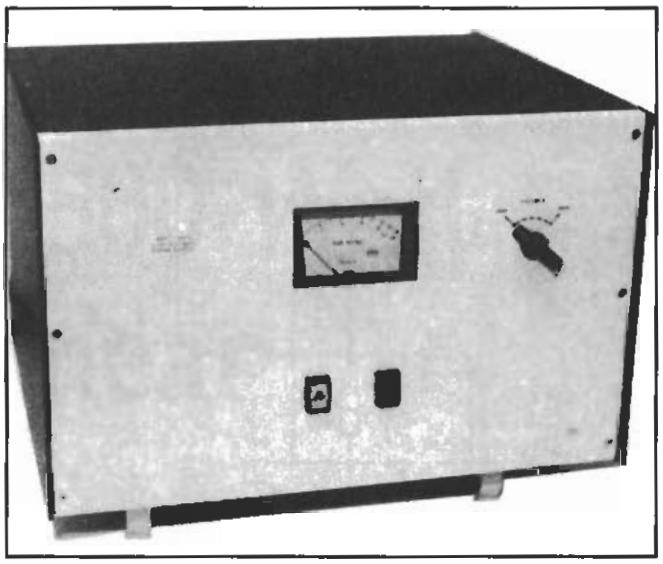

Fig 4—High-voltage power supply top interior view.

High-Voltage Power-Supply Circuit Description

The key to continuous duty in a high-power linear amplifier is the power supply. It must be able to deliver the required voltage and current on a continuous basis. Power supplies are usually the limiting factor in commercial linear amplifiers.

A WORD OF CAUTION IS IN ORDER. The power supply is a very dangerous piece of equipment! Give it proper respect. One mistake can be fatal. Use proper precautions in the construction and testing of this unit, and be careful to build a safe unit.

I recommend that the power supply be built first. The construction is not complex and it can serve as a training ground for amplifier building techniques, particularly for the first-time builder.

Power-Supply Design

The power supply is shown in Fig 4, and the schematic diagram is shown in Fig 5. The hypersil power transformer has a 234-V ac primary, and a 3300-V ac secondary that is tapped at 2600 V. This selection of two output voltages allows for a high- and lowpower capability. An alternative to this approach is to include a Variac® or Powerstat® autotransformer on the transformer primary.

The primary circuit of the power transformer includes a step-start circuit to protect the diode bank during the initial charge of C1, the 53-µF filter capacitor, when the power supply is turned on. Two 50-ohm, 25-W resistors, one in each leg of the primary, are shorted by time-delayed relays approximately 3 to 4 seconds after application of power. The more current drawn through the resistors at start up, the more voltage drop realized and this, in turn, protects the diode bank. The delay is provided by the time constant of the 500-ohm resistor and 100-µF capacitor. The relays must be dc types. Those I used have 90-V dc coils which allows power to be supplied from one 117-V leg of the primary. If 90-V relays can't be obtained, 24-V dc relays can be substituted. A 24-V dc power source must be provided if this is done.

The rectifier unit is a full-wave bridge with eight diodes in each leg. A 470-kilohm resistor and a 0.01-µF, 1-kV capacitor are wired in parallel with each diode to equalize the voltage and protect the diodes from voltage spikes.

The power supply is controlled remotely from the RF deck. A test switch has been incorporated to allow the supply to be energized without the RF deck. A shorted Cinch-Jones plug must be inserted into a socket in the rear of the supply for test switch S1 to operate.

Two pilot lights are mounted on the front panel. One pilot light is on whenever 234 V ac is present in the supply. The other lights when the power supply is activated.

A high-voltage meter is included on the front panel. The metering is done across a 25-ohm, 5-W resistor in series with the bleeder resistor. This voltage divider keeps the total high voltage off the meter. A 50-ohm, 50-W resistor in series with the high-voltage B+ circuit protects the tube and power supply from any current surge resulting from a tube flashover or other cause. In addition, a 0.6-ohm, 1-W resistor in series with the B+ line acts as a fuse resistor. A large current surge will cause the resistor to explode—an inexpensive protection device should a problem occur.

High-Voltage Power Supply Parts Selection

Transformer

It is important to find a good power transformer that can provide the proper operating voltages for the tube. Remember that some voltage drop will occur when current is drawn from the transformer. The voltage drop depends largely on the quality of the transformer (core and wire size), and can range from 200 V to over 1 kV. The transformer should have a 234-V ac primary. Transformers with 117-V primaries are usable only if two identical units can be wired in series to provide a 234-V primary. The secondaries can by wired in series or parallel, depending on the voltage requirements. Remember that the transformers must be identical.

The required transformer secondary voltage depends on the fmal voltage requirement of the tube and the power-supply circuitry. If a bridge rectifier is used, the power-supply high voltage will be about 1.4 times the secondary voltage. If a voltage doubler is used, the high voltage will be about 2.8 times the secondary voltage. A voltage doubler requires two filter capacitors, or more, so if a single oil-filled filter capacitor is to be used, the design can't be a voltage doubler. The *ARRL Handbook* contains circuits for both types of power supplies.[8]

The power-handling capability of a transformer can usually be estimated by its weight. As a rule, the heavier the transformer, the greater the power capability. The transformer for a 1500-W, continuous-duty amplifier will weigh 60-80 lb. The transformer used in this power supply was obtained from Peter Dahl Co.[9] The hypersil design provides a good ratio of power capability to size and weight. I have used several Peter Dahl transformer designs in the past and found them to be of excellent quality and reasonably priced.

Filter Capacitor

Enough filter capacitance is required to obtain good voltage regulation. What is enough? I have used as little as 18 µF and as much as 100 µF in power supplies. The required capacitance can be obtained with a single oil-filled capacitor or with a series string of computer-grade electrolytics. Either way, I recommend at least 25 µF be used, with at least a 10% voltage safety factor. The filter capacitor used in this power supply is a single oil-filled unit rated at 53 µF at 5kV dc. The capacitor was obtained

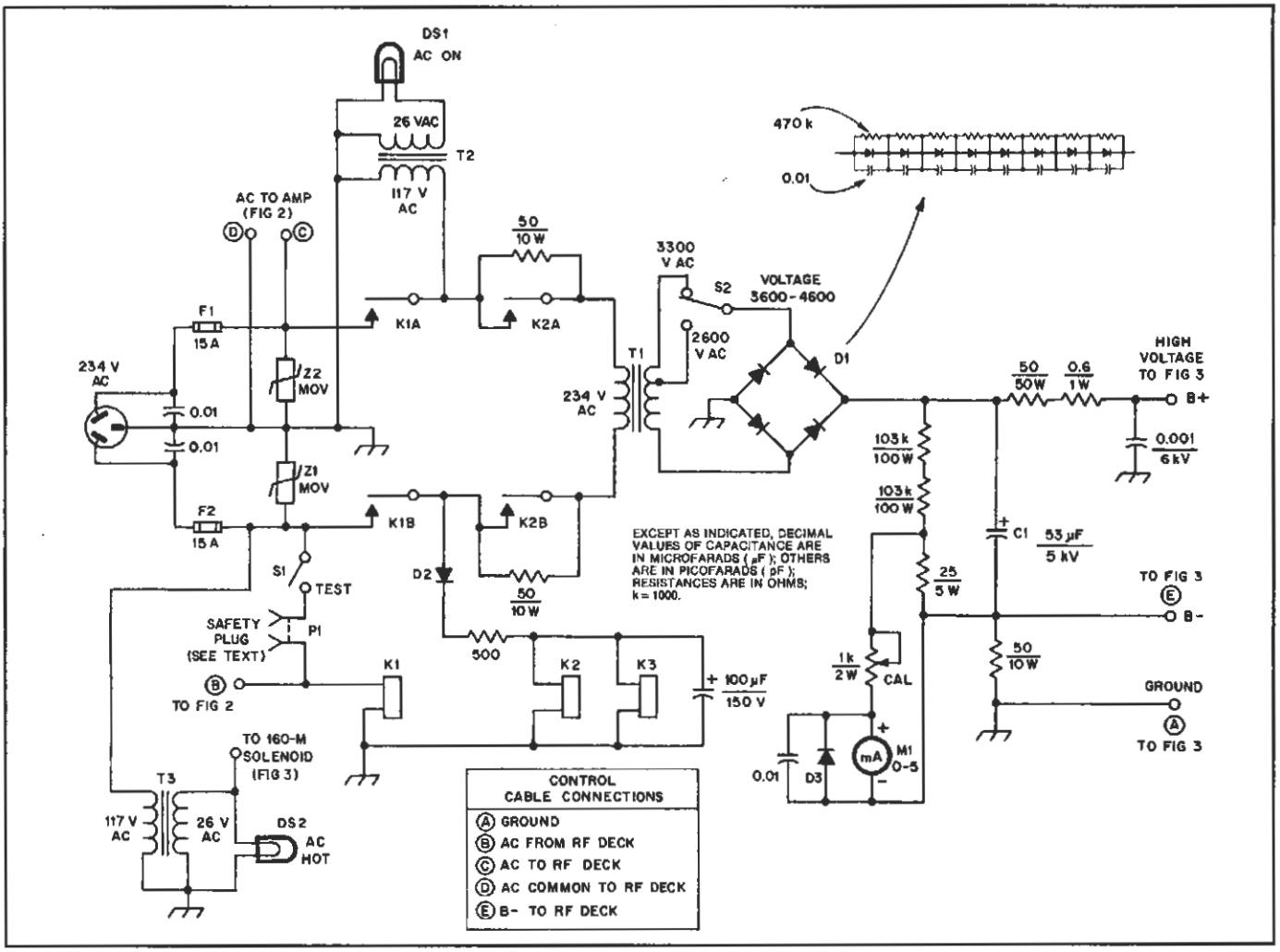

Fig 5—High-voltage power supply schematic diagram. Part numbers in parentheses are RadioShack.

C1—Oil-filled capacitor, 53 µF, 5 kV, Peter Dahl Co.
D1—Diode bridge rectifier assembly, Peter Dahl Co, see text.
D2,D3—Diode, 1 kV, 2.5 A.
F1,F2—Fuse, 15 A.
K1—2PDT mercury plunger relay, Dayton 6X598-3.
K2,K3—SPDT relay, Potter Brumfield PRD1 DYO/9OVDC.
M1—High-voltage meter, 3½-inch Simpson Wide-Vue, 01253 bezel and 01165 lighting kit.
Z1,Z2—MOV transient suppressor, 117 V ac (276-568)
P1—Two-pin Cinch-Jones socket and plug (274-201 and 274-202)
P2—Eight-pin Cinch-Jones connector.
S1—SPST switch (275-690)
S2—Modified 6PST switch, Fair Radio Sales.
T1—Power transformer, 2600/3300-V ac sec, Peter Dahl Co.
T2,T3—Transformer, 26 V ac, 300 mA (273-1386)
Miscellaneous
Pilot lamp—Alco 16TZ, 6T-4 (yellow) and 6T-2 (red) lenses.
Cabinet—CTS model MCLS 10-17-14 black and white, SPP 10-14 black side panels.

from Peter Dahl Co, and is physically very small for the voltage and capacitance rating.

Diode Bridge Rectifier

The full-wave, diode-bridge rectifier is made up with 1000-PIV diodes rated at 3 A. The unit is a commercial module sold by Peter Dahl Co. Each diode string is built on a separate glass-epoxy board. The module is supplied with 1-inch angle brackets on each end, but because of space restraints, the angle was removed and the module was mounted in a vertical position using two Nylon bolts.

Should you decide to build the rectifier assembly, use good-quality diodes, such as HEP-170s or 1N5408s. Be sure to parallel each diode with a 470-kilohm resistor and a 0.01-µF, 1-kV capacitor.

High- Voltage Switch

The transformer has two taps on the secondary to provide a high- and low-voltage capability. The front-panel VOLTAGE 3600-4600 switch is fabricated from a 6-position, heavy-duty ceramic switch (Radio Switch Corp p/n 65). The switch detent and all but the second and fifth contacts are removed. New stops are fabricated from glass-epoxy board. Full high voltage appears across this switch, and therefore, it must be well insulated. The switch is mounted on two pieces of ¾-inch Plexiglas® to provide 2-inch spacing from any chassis or panel ground. A fiber shaft protrudes from the switch through the front panel. To protect the contacts, this switch must never be actuated when the power supply is on.

Construction Details

Next month, I will describe the unique construction details for building this high-power linear amplifier and power supply. In the meantime, should you be so inclined, get out there and find the parts! Remember that you should build the power supply first, so concentrate on those components.

Notes

[1]J. L. Pittenger, "Modular Linear Amplifier for the High-Frequency Amateur Bands," *Ham Radio*, Jan 1981.
[2]J. L. Pittenger, "A 3CX800A7 Linear Amplifier," *Ham Radio*, Aug 1984.
[3]J. L. Pittenger, '3CX1200A7 10 to 80 Meter Amplifier," *Ham Radio*, Aug 1985.
[4]W. I. Orr, ed, Radio Handbook (Indianapolis: H.W. Sams, 1975), 20th edition, Sect 22-4, "A Modern 3-1000Z Linear Amplifier for 80-10 Meters."
[5]Ham Trader Yellow Sheets, PO Box 2057, Glen Ellyn, IL 60138-2057.
[6]Radio Switch Corp, Rte 79, Marlboro, NJ 07746, tel 201-462-6100.
[7]Pioneer Standard Industrial Electronics, 1900 Troy St, Dayton, OH 45404, tel 513-236-9900.
[8]M. Wilson, ed, *The 1986 ARRL Handbook* (Newington: ARRL, 1985).
[9]Peter Dahl Transformer Co, 4007 Fort Blvd, El Paso, TX 79930, tel 915-566-5365.

By Jerry Pittenger, K8RA

From *QST*, October 1986

An All-Band, 1500-Watt-Output 8877 Linear Amplifier

Part 2—Here's what you've been waiting for: detailed instructions for building a 1500-W RF deck and power supply.

Last month I described the circuitry and parts required for the 8877 linear amplifier and high-voltage power supply. This month I will cover the construction of both units. The power supply construction details are given first. Assuming that we have all the required parts in hand, we can determine the physical design of the power supply. To avoid costly mistakes, it is important to do adequate upfront planning before the first hole is drilled.

Power Supply Construction

Meter Selection and Labeling

Any meter with a movement from 100 µA to 5 mA can be used for the high-voltage meter. This meter measures the voltage across the 25-ohm resistor at the bottom (B–) end of the bleeder string (see Fig 5 in Part 1). The more sensitive the meter, the higher the resistance setting of the variable 1-kilohm calibration resistor. The setting of the resistor is a simple Ohm's law problem. The maximum power-supply voltage on the meter scale causes a current equal to the meter-movement rating to flow through the meter, and thus give a full-scale reading. For example, the maximum scale on the meter in this supply is 5 kV dc. The meter has a 5-mA movement; therefore, if the supply is at 5 kV, 5 mA must flow through the calibration resistor and the meter for a fullscale reading. Looking at the complete bleeder string, the total resistance is the sum of the two 103-kΩ bleeder resistors plus the 25-ohm resistor, or 206,025 ohms. At 5 kV, approximately 24 mA (5000/206,025) flows through the string. The value of the calibration resistor, therefore, was selected to allow 5 mA through the meter and 19 mA through the 25-ohm resistor. Using Ohm's law, the value of the resistor should be approximately 95 ohms (19 mA x 25 ohms/5 mA). The required wattage rating of the resistor is 0.23 W (I^2R = 0.005 × 0.005 × 95), and a 1-kΩ, 2-W potentiometer was used. The meter used originally had a 0-50 scale. The scale was changed to read 0 to 5 kV.

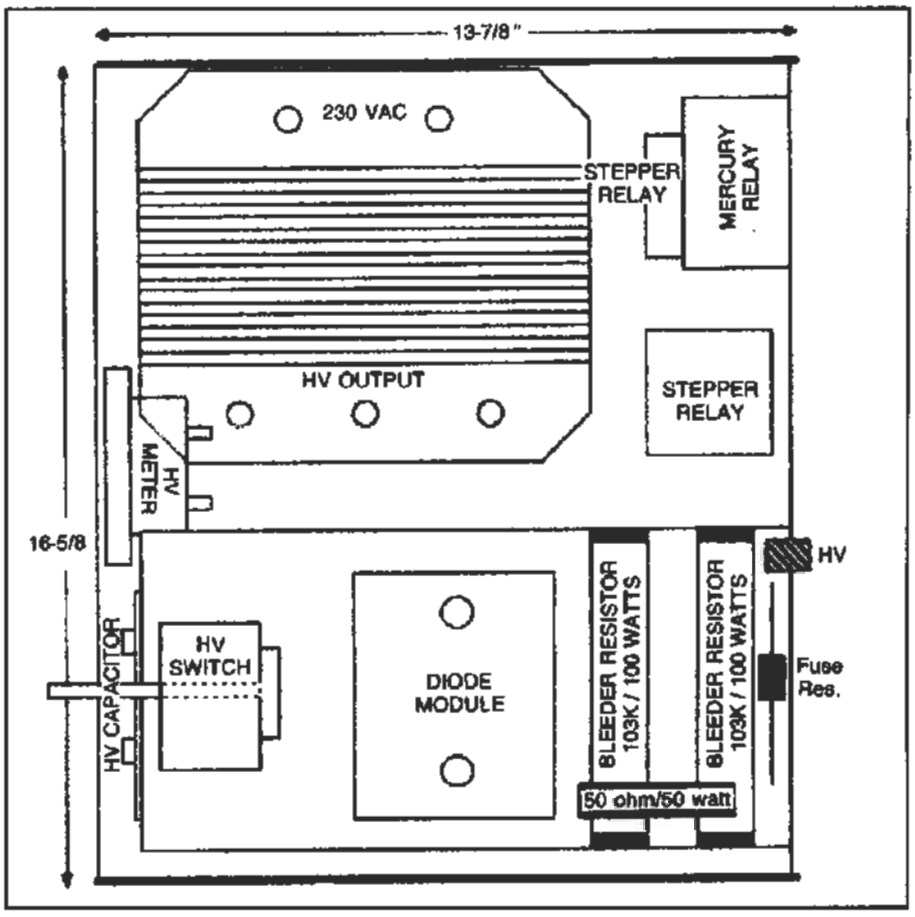

Fig 6—Typical computer-prepared layout drawing. Some component labels have been enlarged for legibility.

Panel/Chassis Layout

I do all my layouts with an Apple® Macintosh computer. An example of this layout is shown in Fig 6. A manual method may be used, instead. Cut out a piece of poster board the size of the front panel or chassis, as well as all the major components. Shuffle the pieces until you get an acceptable layout. This may seem like a lot of extra work, but "one picture's worth 1000 words." You will save time in the long run by going through this procedure, and not have to correct errors that otherwise are certain to occur. The panel layout should be symmetrical. Align switches and center meters. Make sure that components are properly spaced to accommodate the physical size of the parts behind the panel.

The computer-generated or manual layouts serve as a guide during construction, but are by no means sacred. Once you start putting the parts in place, you probably will make minor changes. Go ahead and make the changes, but always update the documentation.

Front-Panel Assembly

You probably will not be ready to cut metal until you are 3 to 4 months into the project. Do the front panel first, since the parts locations are fixed for symmetry. Parts behind the front panel can be moved to accommodate the front-panel design.

Cover the front panel with 3-inch-wide masking tape. The tape not only protects the panel from scratches, but also provides a way to lay out the panel with a pencil or pen. Before any holes are drilled, place all the major parts in their proper place in the cabinet to be sure that nothing obstructs the area behind the panel. Remember you have only one chance. Miss and it means a new panel, or cabinet!

Remove the front panel from the cabinet and center punch the panel where holes are to be drilled, as marked on the tape. Carefully drill a very small hole at each punch mark to serve as a guide, then cut the holes to final size. Holes up to approximately 7/16 inch can be drilled with either a hand drill or a drill press. Holes larger than 7/16 inch should be made with chassis punches. The meter hole is rectangular and is cut with a nibbler after drilling an access hole. Cut the meter hole about 1/32 inch smaller than needed and finish with a large file to straighten the edges. Be careful using the file—it is very easy to let the file slip out of the hole and make a big scratch in the panel. The meter hole doesn't have to be perfect since a meter bezel is used.

After the front-panel metal work is complete, carefully remove the masking tape. The front panel should be labeled before mounting the components. Labeling is done with dry-transfer lettering available from art stores or Radio Shack. Apply the labeling by laying the letter or figure on the panel in the proper position and rubbing over it with a soft pencil. The character will be transferred to the panel. If a mistake is made, the character can be removed with masking or Scotch® tape. There is a mattefinish spray available to protect the lettering. I do not recommend using this spray. It will peel if bumped and does not work well.

The parts can now be mounted on the panel. The cabling to the front panel is connected through nylon multipin connectors (available from Radio Shack) to allow easy panel removal. The same technique is used in the RF deck.

Rear-panel Assembly

Placement of parts on the rear panel is not as critical as on the front panel. Attention should still be paid to symmetry, however. I have found that it is best to mount rear-panel parts after the major parts have been mounted inside the cabinet. The rear panel is drilled and labeled in a manner similar to the front panel. The black rear panel requires white lettering. White lettering kits are available at art supply stores and some electronics suppliers.

Fig 7 shows the inside rear panel of the power supply. The control and power cables enter the rear panel and are routed directly to barrier strips. Each terminal is labeled for clarity. The rear panel is accessible by removing the front panel and the transformer. It sounds like a big job, but it can be accomplished in about 10 minutes. It is necessary to provide good strain relief for the cables. Immediately inside the rear panel, a piece of 3/4-inch aluminum angle stock is mounted, to which each cable is clamped. Large rubber grommets are used in the holes for cable protection.

Major Chassis Assembly

Power-supply components are extremely heavy and a good supporting structure is required. The 1/16-inch-thick bottom cover supplied with the cabinet is replaced with a 1/4-inch-thick base plate to provide an adequate foundation. The heavy plate is cut to size on a commercial metal shear. After the transformer, relays and filter capacitor are mounted, rubber-wheeled casters are bolted to the bottom so that the supply can be rolled, rather than carried from place to place.

The cabinet sides are formed by two removable panels. Parts can be mounted to the inner panel using countersunk screws and then covered with the 1/8-inch painted cover plate to provide a professional appearance. A 1/4-inch-thick sheet of Plexiglas® is mounted above the filter capacitor to support the high/low voltage switch, the diode bank and the bleeder resistors. The Plexiglas is supported by drilled and tapped holes for no. 6-32 countersunk screws in the rear and side panel. A post of 1/2-inch aluminum bar stock supports the front-left corner of the Plexiglas.

The mercury-wetted power relay is mounted on the rear panel and must be positioned vertically. Mercury-wetted relays have a tendency to buzz if mounted on a solid surface. Use a rubber grommet to make a bushing in each mounting hole, or mount the relay on a rubber pad. The stepstart relays, K2 and K3, are also mounted on 1/4-inch-thick rubber sheet to minimize noise.

Once the major components are mounted, wire them together, performing as much testing as possible along the way.

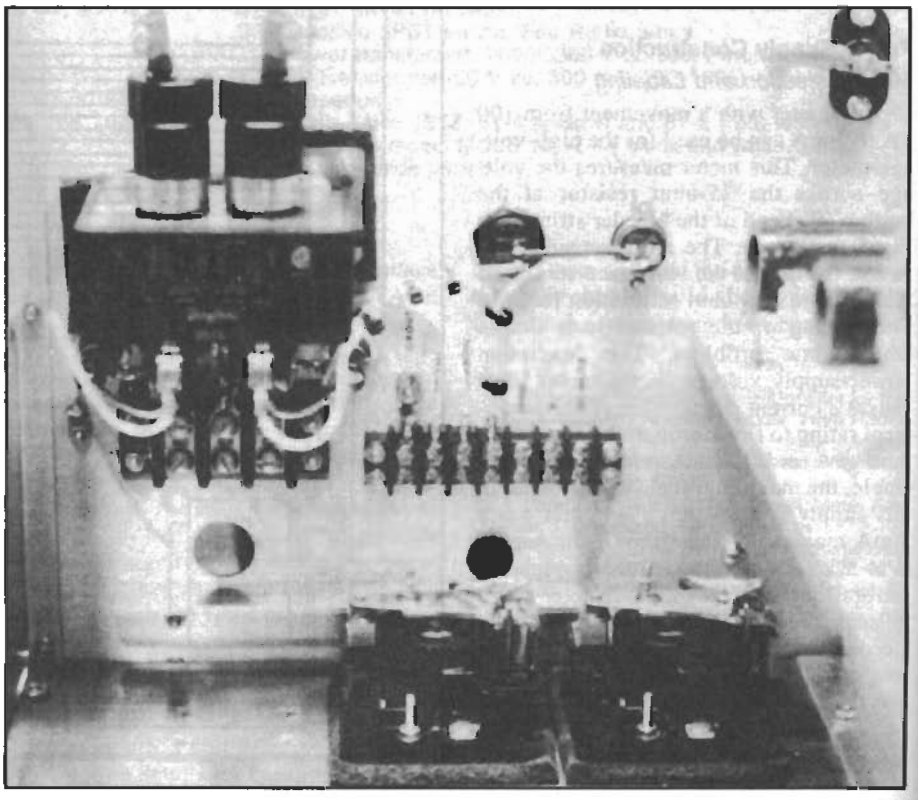

Fig 7—Interior view of rear panel. Note the mercury plunger relay mounting. Relays K2 and K3 are at the lower right.

Front- and rear-panel components are mounted and wired before those that are mounted to the cabinet sides and base plate.

Power-Supply Testing

When you are satisfied that the power supply has been correctly wired and carefully checked, go have a cup of coffee and come back later when your mind is fresh and check the wiring one more time. *Remember that this power supply can be a lethal device. One wrong move could be fatal.*

Final testing of the power supply is accomplished in three steps. Remove the wiring from the primary of the transformer and place a temporary line cord with a small variable autotransformer directly from a 117-V ac line to the primary. Turn the 117 V on and slowly run the variable autotransformer up. At 117 V, the power supply should be reading half-scale voltage. This test verifies that the diode bank and filter capacitor are correctly wired. Now is a good time to calibrate the front-panel meter. Using the variable auto-transformer, set the output voltage at a level that another VOM can measure accurately. For example, most VOMs can measure 1 kV. Adjust the calibration resistor so that the front-panel meter reads the same as the VOM.

The second test checks the primary 234-V ac circuitry. With the 234-V lines still disconnected from the primary, plug the power-supply line cord into a 234-V source. Remember that the shorted two-contact plug must be inserted into the rear-panel socket. Turn the power supply on with the test switch and listen for a 3- to 4-second time delay for the step-start relays. Check that 234 V appears across the two wires disconnected from the primary.

The final test is to try the entire power supply with 234 V applied to the primary. Check the high- and low-voltage indications on the front-panel meter.

Power-Supply Performance

The design results in a husky supply that delivers about 4.6 kV and 3.8 kV (no load) on the high- and low-voltage positions, respectively. In either position the power supply drops less than 400 V under full load. This is the performance you need to achieve full-power capability and good linearity.

RF Deck Construction

The physical design of the RF deck requires planning long before construction begins. Again, I used the Macintosh computer for my initial "paper design," but the same process can be done using paper and pencil. The important thing is to lay out the major components so that everything fits properly before starting to drill holes and cut metal. You must have all the major components in hand before doing the physical design, so you know what you have to work with.

Fig 8 shows the scaled Macintosh designs for the front, top and bottom views of

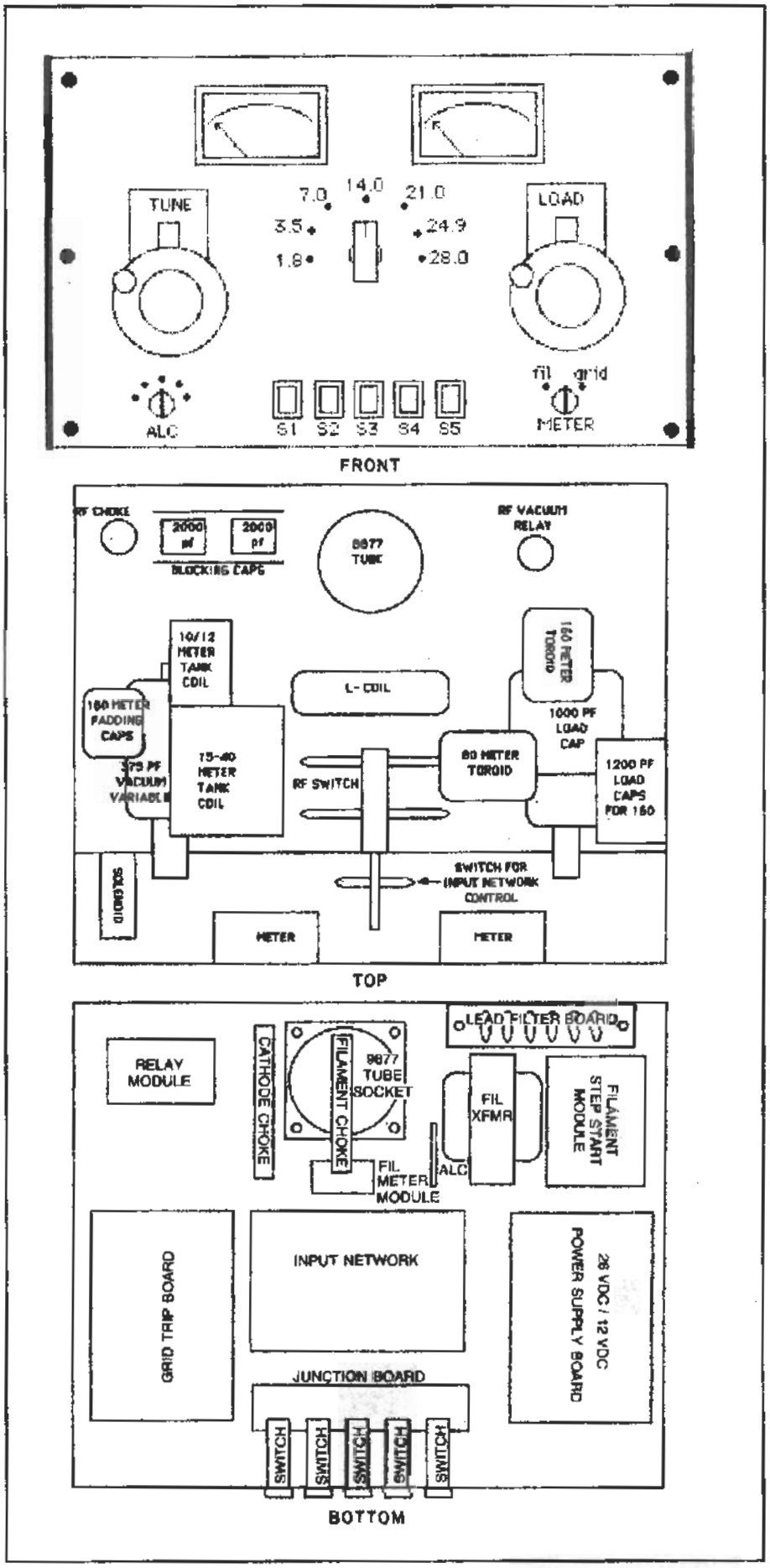

Fig 8—Scale layouts of the RF deck front, top and bottom views, as prepared on the Macintosh computer. Some component labels have been enlarged for legibility.

the amplifier. It is necessary to match the designs so that the front-panel controls end up at the right place on the panel. Everything must be drawn to scale to obtain the relative positions of the components. When designing the bottom and top layouts, only the major circuit boards and components like the grid trip, input network, low-voltage power supply, coils, capacitors and filament transformer are considered. The smaller components can be fitted in later. It is important that the unit be designed with maintainability in mind. Every component, large and small, must be accessible after the unit is completed. The amplifier was constructed in the following steps. Each major step is discussed in more detail later.

- Fabricate, build and test all printed circuit boards for the RF deck.
- Cut the holes in the front panel.
- Perform the major metal work on the subpanel and chassis plate.
- Mount the vacuum capacitors and band switch to the subpanel.
- Mount the PC boards, filament transformer and tube socket to the chassis plate.
- Wire and test the under-chassis control circuits.
- Fabricate and install the RF tank circuit.
- Label and calibrate meters.
- Complete the front panel and mate it to the chassis and cabinet.
- System test the amplifier with the power supply.

Printed-Circuit Board Fabrication

Making PC boards can be tedious, but with a little practice, good results can be obtained. Grouping interconnected circuits on the same PC board minimizes the cable harness between modules in the amplifier. In this design, nine PC board modules are required.

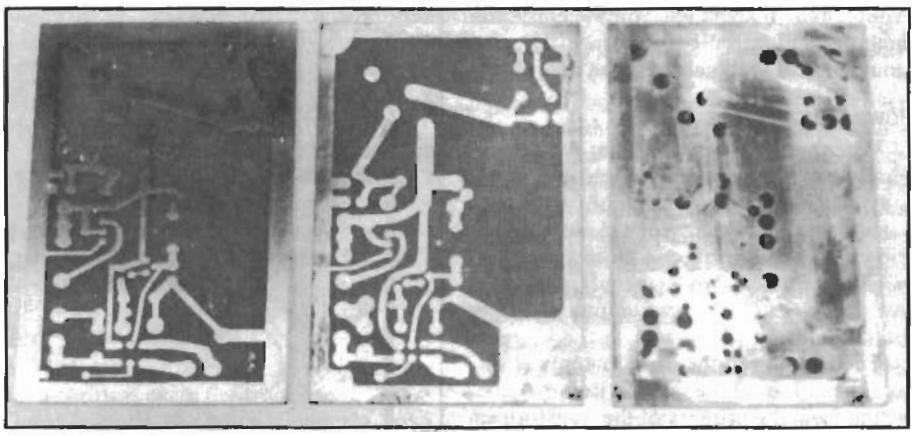

Fig 9—Things don't always work out. Three attempts were made to fabricate the grid-trip and bias PC board. The good board at left was subsequently damaged, requiring a fourth effort.

	Board Size
1) Input network	4" × 6"
2) Low-voltage power supply and timer circuit	4" × 6"
3) Grid-trip and bias circuit	4" × 6"
4) Switch bank harness interface to front panel	1" × 6"
5) Filament step-start circuit	2 3/4" × 3 3/4"
6) RF input/output relay timing circuit	2 3/4"
7) Line filters for control cable and blower	1 3/4" × 5 1/4"
8) Filament-voltage-meter circuit	1 1/8" × 2"
9) ALC circuit	1 3/4" × 2 1/4"

All boards, except nos. 4, 7, 8 and 9, are mounted on 1/2-inch channel to the chassis plate. Therefore, the PC board layouts include a ground strip on the edges of each board to mount the boards to the channel.

The Macintosh computer, with a software package called "Draw," was used to lay out the circuit boards. The design of PC boards with the computer is beyond the scope of this article. PC boards can also be laid out using pencil and paper. Once the design is laid out to scale, the layout must be transferred to the board. First wash the board with a mild detergent to remove all grease and dirt. Using tape and special dry transfers (Radio Shack p/n 276-1577), copy the design onto the board. The transfers are not exact, and the hand drawing only serves as a guide. Submerge the board into an etching solution to remove the exposed copper. I use ferric-chloride etchant. A flood lamp over the etching tray warms the solution and speeds the etching process. Agitate the solution occasionally. The final result should be a nicely etched board ready for drilling the holes for mounting parts. Believe me, however, it doesn't always go as planned.

Fig 9 shows three tries at making the grid-trip and bias board. Actually the third board, on the left, was damaged, and a fourth was necessary. However, once you get the hang of it, it usually goes well.

After etching the board, polish it with

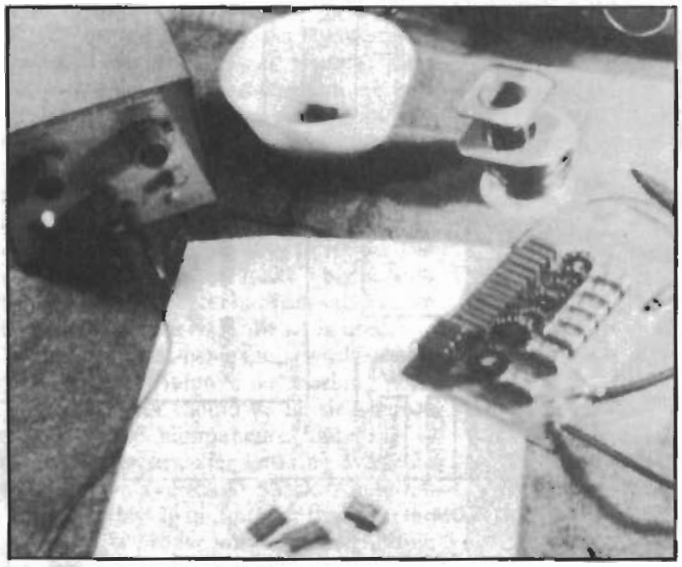

Fig 10—In-process testing of the input-network PC board. Each coil was trimmed to produce a 1:1 SWR into a 50-ohm load. Note the power supply required to actuate relays.

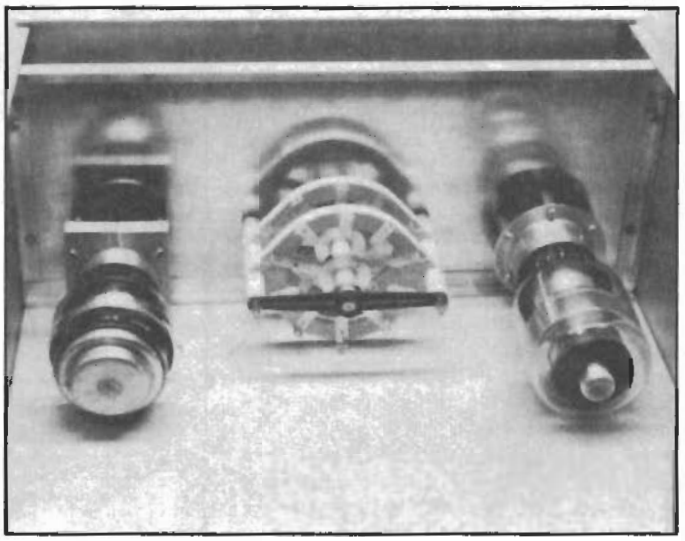

Fig 11—Subpanel installation in the cabinet. Note position of chassis plate, vacuum variable capacitors and band switch. Aluminum angle stock is used to mount the subpanel to the chassis plate and cabinet sides.

fine steel wool and drill the component mounting holes with a small drill. Use dry transfers to label the connections required to the board, before mounting parts. This will avoid wiring mistakes when the wiring harness is installed. Finally, mount and solder the components onto the board.

Test each board as much as possible before final assembly. For example, Fig 10 shows the input network being tested by hooking up coaxial cable and running 100 W through each section into a 50-ohm dummy load. The coils were adjusted at this time to give a flat 1:1 SWR. A power supply is needed to energize the relay for the pi-section being tuned.

Front-panel Fabrication

Cover the front panel with masking tape to protect it from scratches, and mark the mounting positions of the components. Take your time with this step since it is hard to recover if an error is made. Mark the front panel where the holes are to be cut and carefully drill a small pilot hole followed by the correct hole size. The holes for the band switch, capacitor control shafts, ALC control and multimeter switch are $^3/_8$-inch diameter and can be made with a regular drill bit. The holes for the power switches are $^5/_8$-inch diameter and require a chassis punch. The meter-mounting holes are the most difficult to make. The rectangular cutouts are marked about $^1/_{32}$-inch smaller than required to protect against overcutting. Use a nibbler to cut the holes carefully, then file them to the exact size of the meter bezels. Be careful that the file doesn't slip and scratch the panel (disaster!). Using a large file will help avoid this tragedy.

I recommend doing all the front-panel metal work at one time to ensure proper component layout. When the metal work is complete, leave the masking tape on the panel for protection as it will be used as a template to locate the parts mounted behind the front panel.

Chassis and Subpanel Metal Work

This amplifier design has very little metal work that requires more than a hacksaw and a file. The chassis plate was purchased with the cabinet. The only other panel, except for front and rear panels, is the subpanel that mounts perpendicular to the chassis plate, and 3 inches behind the front panel. The subpanel shields the meter compartment from RF and serves as a mounting support for the band switch, vacuum capacitors and 80-meter toroid coil.

The chassis is mounted 3½ inches from the bottom of the cabinet to allow room under the chassis plate for the filament transformer. Therefore, the subpanel is cut to 6¾ × 16½ inches. Referring to Fig 11, ½-inch aluminum angle is attached with screws to each edge of the subpanel to provide a mounting flange to the chassis plate and cabinet side walls. The top piece of angle stock provides a mounting surface for a piece of gold-plated finger stock that seals the subpanel to the cabinet top plate.

Two large holes are required. A 3-inch-diameter hole is required in the chassis plate for the tube socket. A 5-inch-diameter hole is cut in the cabinet top plate and aligned directly above the tube socket to vent the air flowing from the tube and chimney. Use a large fly-cutter, available at most hardware stores. For safety, the fly-cutter should be used only on a drill press—never with a hand drill. Therefore, if you don't have a drill press, find a friend who has one. Before cutting the large holes, use 3-inch masking tape to cover the chassis plate and top panel to mark where the holes are to be drilled, and to protect the surfaces. For safety, clamp the panels onto a board and the base of the drill press before drilling.

Cut a piece of perforated aluminum stock to be slightly larger than the hole in the cabinet top panel. Clean the perforated metal well, and spray with paint to match the cabinet color. Fasten the perforated piece to the inside top panel with several small countersunk screws painted to match the cabinet.

Mounting Vacuum Variable Capacitors and Band Switch

The vacuum variable capacitors and band switch are mounted to the subpanel, but their control shafts must be aligned with the front panel design. Allow enough slack in the positioning of these components to perform precise alignment with the front-panel holes when the front panel is installed. To mark the hole positions on the subpanel, slide the subpanel against the rear of the front panel while both the front panel and chassis plate are bolted into place in the cabinet. Cover the subpanel with masking tape and mark the exact centers of the holes for the components. Drill the two holes in the subpanel for the vacuum variable capacitors with hole saws. Mount the vacuum variable capacitors and band switch on the subpanel.

Mounting Major Components to the Chassis Plate

The major components (PC boards, filament transformer and tube socket) are mounted toihe chassis plate as shown in Fig 12. The PC boards are first mounted to ½-inch aluminum channel using sheet-metal screws for easy removal. Cover the bottom of the chassis plate with masking tape. Position and mark the PC boards, filament transformer and tube socket according to the planned physical layout. Drill the mounting holes in the chassis plate, then redrill the holes from the top with a countersink bit to allow flat-head countersunk screws to be used for mounting. This retains the flat surface on top of the chassis plate. With the ½-inch channels on the PC boards, mark the hole positions on the bottom of each channel with a pencil, using the predrilled chassis-plate mounting holes as a template. Remove the channels from the PC boards, mount the channels on the chassis plate, and remount the PC boards on the channels.

Under-Chassis Wiring

Complete the under-chassis wiring, according to the schematic diagram, using Teflon®-insulated wire. The nylon connectors near the front of the chassis connect to the front-panel power switches, the ALC potentiometer and the multimeter switch. This allpws the front panel to be easily removed for rear-panel access. The small board in the front center of the chas-

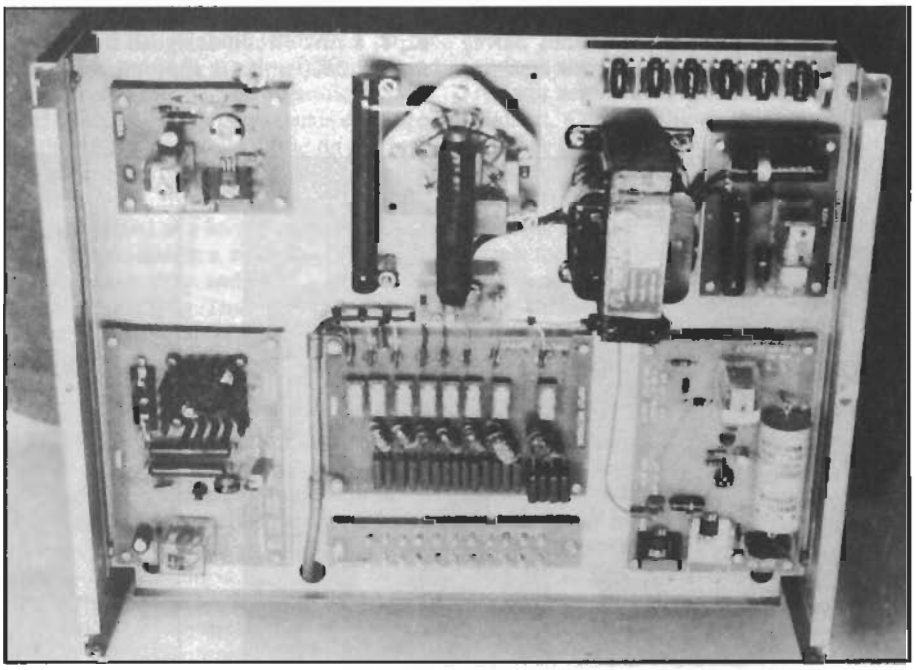

Fig 12—Bottom view of the RF deck showing placement of PC boards, transformer and tube socket.

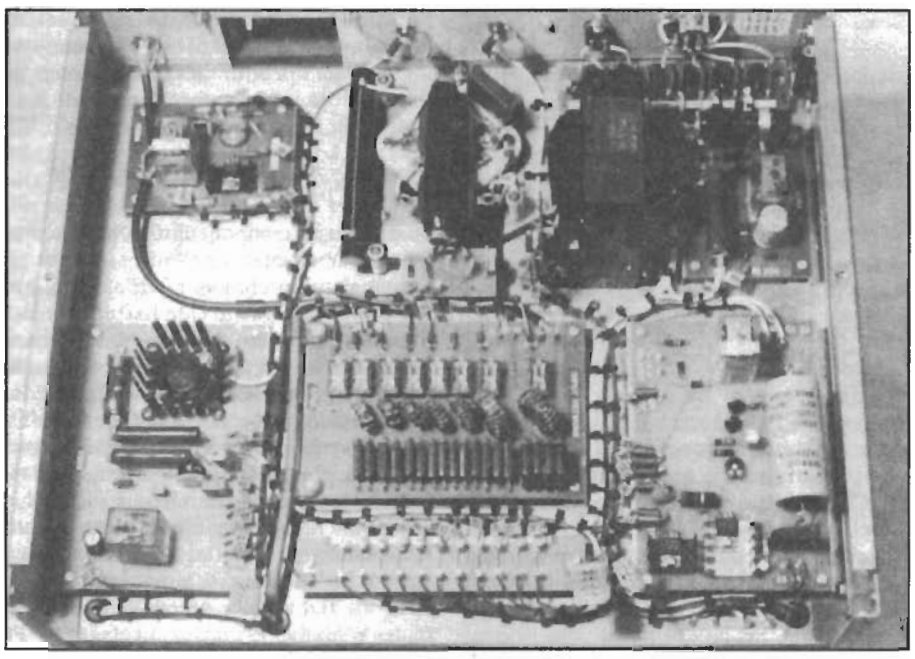

Fig 13—Bottom view of the RF deck showing harness wiring in place.

sis provides an easy way to mate the 12-pin nylon connector going to the power switches with the wiring harnesses under the chassis plate (see Fig 13). When making the PC boards, try to put all the connections to the board on one side. This allows access to the boards for maintenance without removing the wiring. Just unscrew the board from the channel and fold the board upward.

Each wire is labeled at each end with numbered tags, because the Teflon wire used is mostly the same color. A version of the schematic diagram was maintained with the wire numbers noted for easy wire tracing. The final wiring is cabled into harnesses with plastic cable ties. Don't be afraid to use plenty of ties, but at first only put a tie every inch or two. The ties will undoubtedly be cut several times during wiring to put in missing wires that are overlooked. When all wiring is complete and tested, put a cable tie every ½ inch on the major harnesses.

Amplifier Tank Circuit

The plate tank-coil set is shown in Fig 14. Before making the coils, detennine the tankcircuit parameters for the given tube plate impedance. The plate impedance can be determined from Eq 1.

Plate impedance = plate voltage/ (1.57 × plate current) (Eq 1)

Assuming the amplifier runs at 60% efficiency, the input power required for 1500-W output is approximately 2500 W. With 3200 V on the 8877 plate, plate current will be approximately 781 mA. From Eq 1, a tank circuit designed for approximately 2600 ohms is appropriate. A table of pi-L network component values is contained in Hoff's article, and the values used in this amplifier are summarized in Table 2.[10]

The 80- and 160-meter coils are wound on an assembly of three T225-2 toroid cores taped together with Scotch no. 27 glass-cloth tape. Use plenty of tape to provide good voltage insulation from the cores. The 80-meter coil is wound with 11 turns of no. 10 wire covered with Teflon sleeving. The 160-meter coil is wound with 19 turns of no. 12 wire, also covered with Teflon sleeving. The cores of both coils are mounted from 1 to 2 inches from the mounting wall on ceramic insulators. Each coil is sandwiched between two pieces of fiberglass material held together by a ceramic standoff running through the middle of each toroid (see Fig 15). Wind all coils in the same direction (clockwise or counterclockwise), to avoid a "bucking" action between coils.

The 10- through 40-meter coil is made from ¼-inch soft copper refrigerator tubing. Clean the tubing using fine steel wool (000) until the surface is smooth and bright. Use a piece of pipe with an OD equal to the desired coil ID and carefully wind the copper tubing around the pipe. After the smaller diameter part of the coil has been wound, change the pipe to a larger diameter, and wind the larger part of the coil. The inductance of the coil can be easily checked using a known fixed-mica capacitor with low internal inductance and a dip meter. After determining the resonant frequency, calculate the inductance using Eq 2.

Inductance = $1/(4 \pi f^2 C)$ (Eq 2)

Always wind the inductor with a few extra turns and then remove turns until the desired inductance is achieved. The induc-

[10]I.M. Hoff, "Pi Network Design for High Frequency Power Amplifiers," *Ham Radio*, Jun 1978.

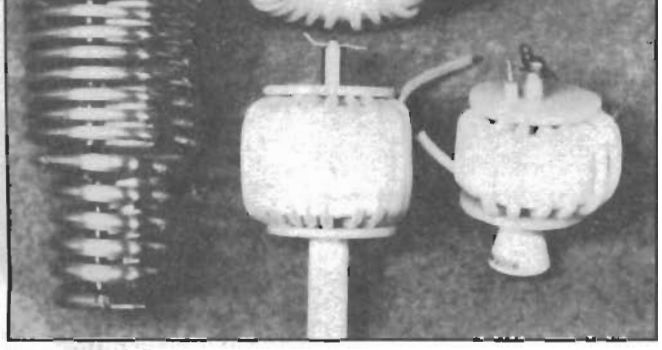

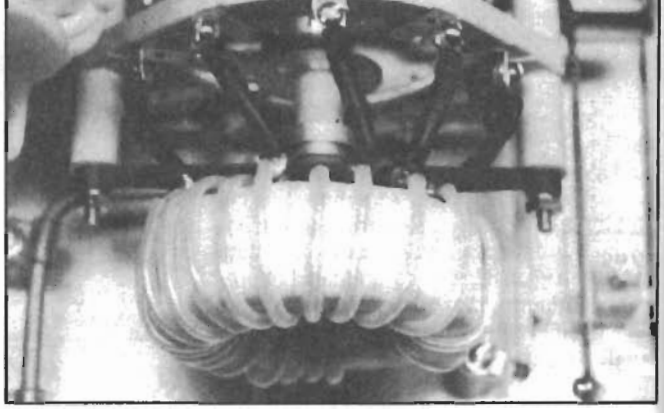

Fig 14—Plate tank coil set. Above: the various coils of the tank circuit. Right: the L toroid mounted on the rear of the band switch.

Table 2

Pi-L Network Design Parameters (See Fig 3, Part 1)

Freq (MHz)	C1 (pF)	L1-L4 (μH)	C2 (pF)	L5 (μH)	Q
1.8	462	22.02	2121	8.90	13.1
3.5	244	10.99	1132	4.45	13.4
7.0	113	6.03	503	2.44	12.4
14.0	55	3.08	245	1.24	12.2
21.0	37	2.05	164	0.83	12.2
24.9	30	1.70	130	0.70	12.0
29.7	26	1.48	112	0.60	12.0

L1, 10-12 rneters—6 turns ¼-inch silver-plated copper tubing, 2-inch outside diameter, 2 inches long. 10-m tap at 3 turns.

L2, 15-40 rneters—12 turns ¼-inch silver-plated copper tubing, 3¼-inch outside diameter, 4 inches long. 15-m tap at 2 turns, 20-m tap at 4 turns, 40-m tap at 12 turns.

L3, 80 meters—11 turns of no. 10 wire in Teflon sleeving over three T225A-2 iron-powder toroidal cores taped together with Scotch no. 27 glass-cloth electrical tape.

L4, 160 meters—19 turns of no. 12 wire in Teflon sleeving over three T225A-2 toroidal cores taped together with Scotch no. 27 glass-cloth electrical tape.

L5, L Coil—20 turns of no. 20 wire in Teflon sleeving over two T300-2 iron-powder toroidal cores taped together with Scotch no. 27 glass-cloth electrical tape. Tap as follows:

Band	10-12	15	20	40	80	160
Turn no.	2	3	4	6	10	20

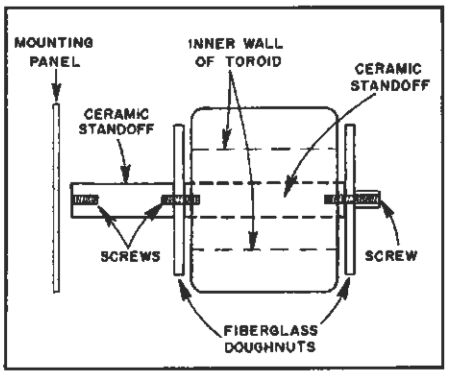

Fig 15—Mounting details of 80- and 160-meter toroids.

tance measurement is only an approximate value because there is always stray inductance introduced by the interconnecting leads and the band switch.

The copper tubing is silver plated only after the ends are configured to match the mounting lugs in the amplifier. Silver plating is simple with the right materials. Go to a photographic lab and get a couple of gallons of used fixer solution. Fixer solution is not usable when it becomes saturated with silver. The labs usually sell the spent fixer for silver recovery, so you may have to pay for it. Clean the coil by giving it another brushing with steel wool, wash it thoroughly in a mild detergent and rinse it well before plating. Put the fixer solution in a large plastic container and submerge the coil in it. A bright silver plate will form within seconds. The silver plate is not very thick, but it is sufficient to keep the copper from tarnishing. The coil taps are small wrap-around clamps made from silver-plated ½-inch-wide copper strap. Plate about 2 inches of copper strap, then drill a hole in one end for a no. 8-32 screw. Using a short piece of ¼-inch tubing as a jig, bend the end sharply around the tubing with a pair of duckbill pliers. Drill a second, matching hole, but squeeze the clamp in to provide a tight fit around the coil stock. Install the clamp with a flat washer on each side to provide a compression fit. The clamp should fit tightly. Don't solder the clamps until after the amplifier is tested. When the tap location is verified, heat the clamp and coil with a large solder gun and flow solder into the connection. After soldering the coil taps, spray the coil with a thin coat of clear plastic to retain the bright silver finish.

The L coil is wound on a pair of T300-2 toroid cores taped together with glass-cloth tape. The coil is mounted on the back of the band switch and supported by the connections to the coil. The leads are not soldered to the band switch, but are held in place with no. 6-32 screws.

Other major considerations in the RF tank circuit are the TUNE and LOAD capacitors. The TUNE capacitor is a 375-pF vacuum variable. Table 2 shows that though this capacitor will easily cover 10 through 80 meters, it is too small for 160 meters. One solution is to use a 500-pF vacuum variable, but units in this size class are not readily available in the surplus market, and you probably don't want to buy a new one at approximately $500. I solved the problem by switching in an additional 160-pF capacitor in parallel with the vacuum variable for 160 meters.

A 24-V dc solenoid, mounted on the subpanel, grounds a pair of 80-pF fixed vacuum capacitors. The solenoid is powered by a small 12-V relay that is energized by the 160-meter control line on the input network control switch. The grounding strap is made from a stiff piece of brass stock obtained at a hobby shop. A hinge is made by soldering a small piece of brass tubing to the strap and putting a solid rod through the tubing. The rod is supported on each end by a small piece of Plexiglas and allowed to pivot, thus forming a hinge. A piece of flexible braid is connected from the brass strap to ground for a good connection. The strap is held in the open position by a small spring pulling the strap back toward the subpanel. The contacts on the strap and the vacuum capacitors are from a 25-A power relay and soldered in place. A piece of ¼-inch brass bar stock is used to mount the contact on the vacuum capacitor side and to absorb the shock from the closure. A rubber grommet on the brass strap, where the rod from the solenoid hits the strap, also absorbs some of the shock. This scheme works smoothly and once thought out, took about one evening to install.

The LOAD capacitor is a 1000-pF, 3-kV unit with a fixed 100-pF, 5-kV fixed mica transmitting capacitor in parallel. This provides a total of 1100 pF for 80 meters. On 160 meters, the band switch adds an additional 1200 pF in parallel to provide a total of 2300 pF. The 1200-pF capacitor consists of three 400-pF mica transmitting capacitors in parallel.

Marking and Calibrating Meters

Any meter with a movement from 100 μA to 5 mA can be used for the front-panel meters. Use two identical meters, if possible, for esthetic reasons. In a very clean environment, begin by removing any internal meter shunts (on ammeters), or any series resistors inside the meter (on voltmeters) to obtain only the basic meter movement. Nothing else need be done for the multimeter, since the calibration resistors are a part of each metered circuit. A shunt resistor must be made for the plate-current meter. Wind about 2 feet of no. 22 enameled wire on a 2-W resistor of any value over 50 ohms, soldering the wire ends to the resistor terminals. Mount the resistor across the meter terminals to form a shunt. Connect the meter in series with another meter of known calibration and an adjustable power source. Trim the enameled wire 1 inch at a time until the meters read the same. If the meter being calibrated reads too low, the wire is too short. When the meters read the same, slip a piece of heat-shrink tubing over the resistor and seal the shunt.

Carefully remove the plastic face cover and the calibrated face plate from the meter. Do this in a clean environment because the magnet in the meter will attract metal shavings that could damage the movement. With a pencil eraser, rub off the original meter lettering, but not the analog scale tick marks. With small dry-transfer letters put the new numeric scale on the meter. Be careful not to bend the pointer when reassembling the meter.

Mounting the Front Panel

Remove the masking tape from the

panel, and carefully label the front panel with dry-transfer lettering before mounting any components. Mount the meters, potentiometer and switches in place, and complete the wiring. Wire nylon connectors to the power switches, ALC control, multimeter switch and meters to mate with the connectors in the RF deck. This will result in a totally removable panel.

When mounting the front panel to the cabinet, give careful attention to aligning the vacuum-capacitor and band-switch shafts. Loosen the component mounting screws and mate the shafts, then retighten the screws. Continue the alignment process until the controls operate smoothly.

Rear-Panel Assembly

Up to now, nothing has been done to the rear panel. Mount the panel and decide where the components should mount to obtain short connections. Lay the rear panel out in the same way as the front panel, and cut the necessary holes.

Mount the blower off the rear panel, located to allow good circulation of air up to the front of the under-chassis area and back to the tube socket. Positioning of the blower is not critical as long as air is not directly blown across the tube socket, which could cause backpressure.

Mount all components to the rear panel, and mount and wire the panel to the RF deck. The rear panel is not easily removable like the front panel.

Testing the Amplifier and Power Supply

Testing is the *big* moment and the climax of several months' work. First hook up the power-supply control cable and the ground cable. Leave the high-voltage cable off. Test the control circuits to ensure that the power supply can be turned on from the RF deck and the 3-minute time delay works. Make sure that the tube filaments are on. This isn't as easy as with a glass tube, which allows you to see the filaments glow. Let the tube run for about 10 minutes, then turn the power off. Immediately remove the tube and feel if the base is hot.

Test the amplifier first on 20 or 40 meters, since these bands use the midrange of the TUNE and LOAD capacitors. With high voltage applied to the tube, first key the amplifier with no input drive power. The resting idle current should be between 100 and 200 mA on the plate-current meter.

Now apply a little drive power to the tube. The plate current should rise. Move the TUNE and LOAD controls until power output is indicated on a wattmeter. Increase the drive while adjusting the TUNE and LOAD controls to achieve about 20 mA grid current and 650 to 700 mA of plate current, to realize 1500 W output. If the amplifier works properly on this band, proceed to the other bands and repeat the tests.

Efficiency should be at least 60% on all bands, except perhaps 10 and 12 meters, where efficiency may drop to 55%. If efficiency is poor, try moving the coil taps, but recognize that moving the taps also changes the Q of the coil. Decreasing the inductance and increasing the capacitance in the tank circuit will increase the Q. The amplifier may provide more power output over a larger frequency range with a lower tankcircuit Q, but harmonic suppression will also decrease and the amplifier could start generating interference or not meet FCC standards.

I must warn you one last time. *This device could kill you in one instant if you get tied into the high-voltage circuit. Put a good ground on both power supply and RF deck, and treat the equipment with proper respect!*

Conclusion

I have spent many enjoyable hours operating with this amplifier/power supply combination, with nothing but good signal reports. It was an exhausting task, but now that it's finished, I'm glad I did it. Try building one and you'll see what I mean.

By David Rutledge, KN6EK, et al. From *QST*, May 1997

High-Efficiency Class-E Power Amplifiers

Part 1—With 3 to 12 W of drive, you can push 300 to 500 W CW out of an $11 transistor! The trick is to use Class E.

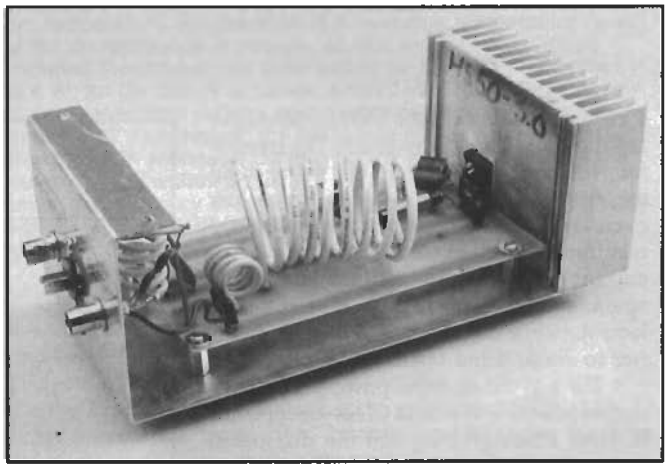

These 300 and 500-W 40-meter amplifiers evolved from a series of undergraduate student projects at Caltech. Our goal was to design an inexpensive amplifier that amateurs can easily duplicate.[1] The amplifiers use inexpensive, readily available power MOSFETs that can be driven by a QRP transceiver; in our case, the NorCal 40A. A block diagram of our setup is shown in Figure 1. The components of the station are shown in Figure 2.

Our 300-W amplifier uses an International Rectifier (IR) IRFP440; the 500-W amplifier employs an IRFP450. These transistors are widely used in switching power supplies, but we have not seen them previously reported for use as RF amplifiers. The MOSFETs have a maximum drain voltage of 500 V, with maximum RMS drain currents of 8.8 A for the IRFP440, and 14 A for the IRFP450. Both transistors are available from Digi-Key: The 440 costs $8; the 450 costs $11.

Class-E amplifiers are extremely efficient—about 90%. Because of the low loss, no cooling fan is required. No TR switch is needed; the received signal is piped through the amplifier itself. Even without an external filter, the amplifiers meet the FCC requirements for spurious emissions. They can be built and tuned up with an RF power meter, a multimeter, oscilloscope and a dummy load. Tune-up consists of adjusting an input coil for matching and an output coil to set the power level.

Operational Classes

In addition to the well-known Class A, B, and C operational modes, there are Class D and E.[2] In Class D and E, the devices operate as switches, half the time completely on, and the other half completely off. But transistors are not perfect switches. The MOSFETs have a resistance of about 1 Ω when on, and a capacitance of several hundred picofarads when off. Losses are greatly reduced in switching amplifiers, but there is a penalty: The output power no longer depends on the *drive power*, but rather on the *supply voltage*. This means that switching amplifiers are *not* linear amplifiers, and they are *not* suitable for SSB without additional limiting and modulating circuits. However, they are fine for CW, FSK and FM.

In a Class-D amplifier, a pair of transistors switch on and off, out of phase across an output transformer. Fred Raab, WA1WLW, recently developed a Class-D power amplifier that produces 250 W on 40 meters with an efficiency of 75%.[3] However, Class-D amplifiers are relatively complex. On the other hand, the Class-E circuit has significant advantages for the homebrewer because only one transistor, without gate bias or output transformer, is needed, and it can be driven by a low-power transceiver.

The Class-E Amplifier

The Class-E amplifier was invented and patented by Nathan Sokal, WA1HQC, and Alan Sokal, WA1HQB, in 1975.[4] It minimizes heat loss by having as little overlap as possible between voltage and current. Figure 3 shows an idealized Class-E circuit. As the switch opens and closes, the current alternately flows in the switch and in the load network. The switch voltage and current waveforms are shown in Figure 4. It may be easiest to understand the waveforms by starting at the beginning of the off-time interval. When the transistor turns off, the current flows into the resonant load network, and there is a transient voltage that rises and falls. With a properly de-

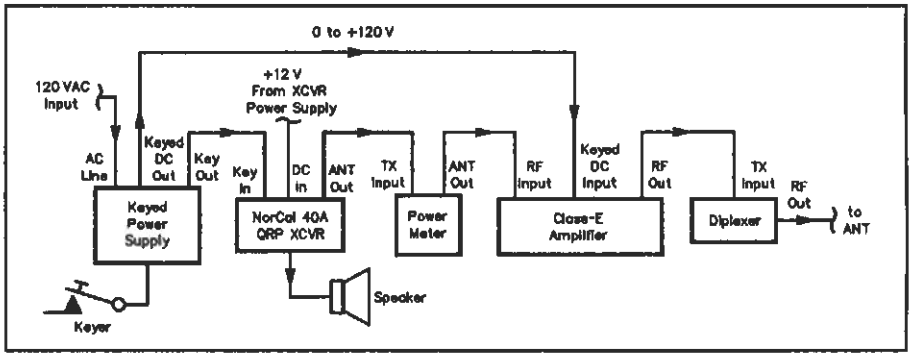

Figure 1—Block diagram of the Class-E amplifier station.

Figure 2—The components of the Class-E amplifier station. Clockwise from bottom left: the diplexer, amplifier, resonant speaker, NorCal 40A and keyed power supply. The latter houses the keyer and a pulse-stretching and shaping circuit.

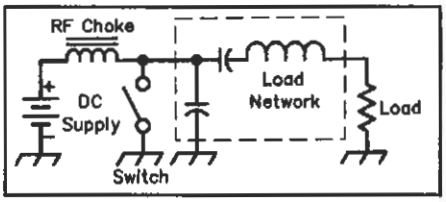

Figure 3—An idealized Class-E amplifier. The transistor is represented by a switch that opens and closes at RF.

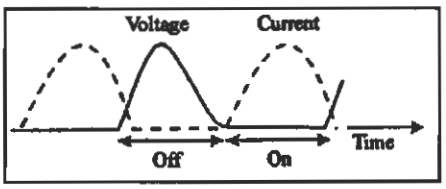

Figure 4—Class-E voltage and current waveforms. Class-E amplifiers reduce loss by keeping the overlap between voltage and current low.

signed load network, the voltage returns to zero smoothly with zero slope. The transistor switches on when both the voltage and the current are small, keeping losses low even if the switching is slow or slightly mistimed. Once the transistor turns on, the current rises smoothly until it switches off again, and the cycle repeats. The resonant load network does limit a Class-E amplifier to single-band operation.

For a given dc input power, the power output of a 90% efficient Class-E amplifier is three times greater, and the dissipated power is seven times smaller, than that of a 30% efficient Class-A amplifier. This means that for a given dissipated power, we can get *21 times* more power from a Class-E amplifier.

The Caltech Power Amplifiers

Both amplifiers have a common diagram (Figure 5) and PC board, but use components with different values. Several components are added to the basic Class-E circuit for matching and filtering. The MOSFET's gate impedance is rather low, and primarily capacitive, with a reactance of about 4 Ω. There is also a resistive component of about 2 Ω from parasitic series resistance in the gate itself, and the drain *on* resistance that is capacitively coupled to the gate. T1 reduces the 50-Ω impedance of the drive circuit to about 2 Ω to match the low resistance of the gate and sets the dc bias to 0 V. L1 is adjusted to cancel the gate capacitance; the input SWR is typically 1.5:1. C1 shunts L1 at high frequencies to reduce ringing in the VHF range. The 0-V gate bias ensures that the transistor is off when it is not driven, because this is far below the threshold voltage, which is about 4 V. We have never seen oscillations in these amplifiers.

C3 and L2 form a resonant network that produces the rising and falling voltage waveform needed for the Class-E ampli-

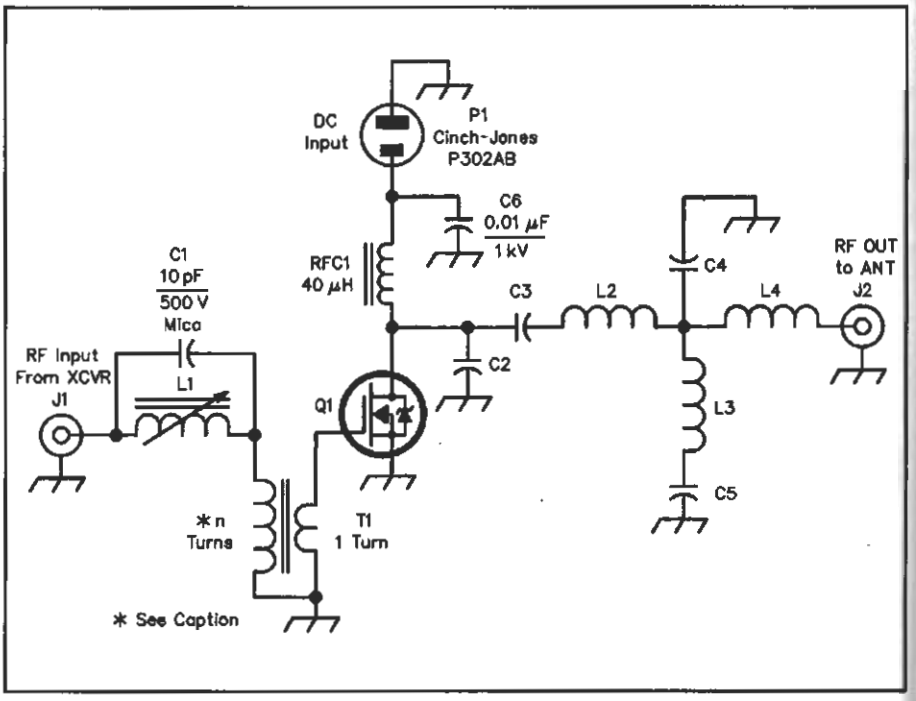

Figure 5—Circuit diagram and parts list for the amplifiers. Mica capacitors are available from Newark. L2, L3 and L4 are made with #10 THWN solid, insulated house wire sold in hardware stores. T1's core is an RF400-0, available from Communications Concepts (see Note 1 for supplier information). L1 is a Toko 10K (2.2 µH), available from Digi-Key. RFC1 is a J. W. Miller type 5240, available from Newark.

C1—10 pF, 500 V mica
C2—300 W, 270 pF; 500 W, 390 pF; (For C2 through C5, Cornell Dubilier mica capacitors, type CDV19, 1 kV, 5%
C3—300 W, 1500 pF; 500 W, 2000 pF
C4—300 and 500 W, 100 pF
C5—300 W, 680 pF; 500 W, 820 pF
C6—0.01 µF, 1 kV ceramic disc
J1, J2—BNC or SO-239 connectors
L1—2.2 µH, Toko 10K; available from Digi-Key.
L2—300 W, 9 turns; 500 W, 8 turns #10 THWN wound on 1¼-inch-OD plastic-pipe form; spread turns to fit holes in PC board.
L3—300 W, 4 turns; 500 W, 3 turns #14 THWN wound closely spaced on a ½-inch-diam drill bit
L4—300 W, 5 turns; 500 W, 5 turns #14 THWN wound on a ½-inch-diam drill bit form, turns spaced to occupy 1 inch
P1—Cinch-Jones P302AB
Q1—IRFP440 for 300-W amplifier; IRFP450 for 500-W amplifier; (use International Rectifier transistors only)
RFC1—40 µH, 3 A
T1—Pri: 300 W, 5 turns; 500 W 6 turns #26 stranded hook-up wire; wound on RF400-0 core, available from Communications Concepts
Misc: Berquist K10-104 insulating pad (thermal resistance of 0.2-K/W, 6-kV breakdown rating); available from Digi-Key.

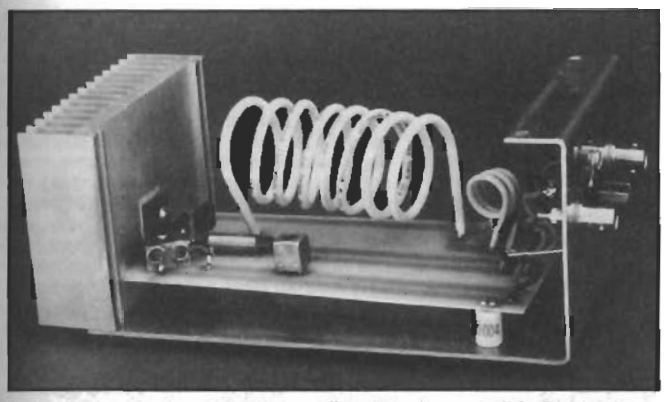

Figure 6—Inside the 500-W amplifier. The large coil is L2; L3 is the small coil. The circuit board is mounted on ½-inch standoffs. BNC connectors are used for the RF input and output. No harm is done if the RF input and output are accidentally interchanged.

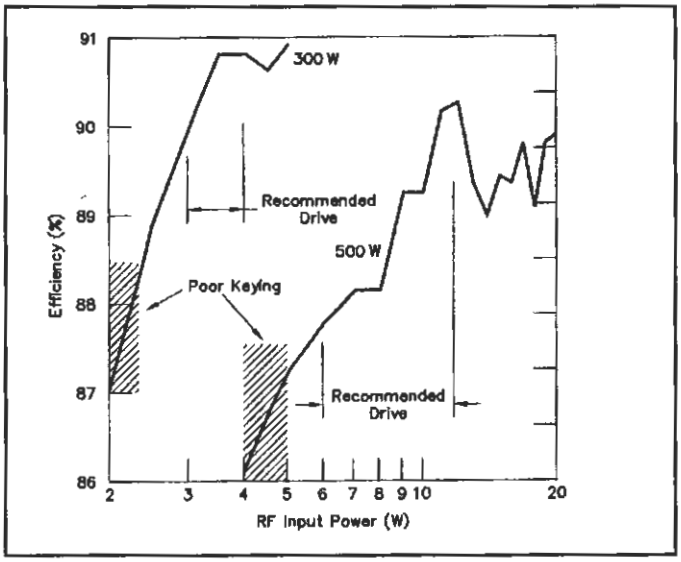

Figure 7—The measured efficiency plotted against RF input power. These measurements were taken with the heat sink at room temperature. In operation, the heat-sink temperature rises and the *on* resistance increases, so that the efficiency drops somewhat. Recommended drive power for the 300-W amplifier is 3 to 4 W; for the 500-W amplifier, 6 to 12 W. The dc input power was calculated from voltage and current measurements made with Fluke 87 multimeters; the RF output power was determined with a Bird 43P wattmeter using a 500-W element. Bird lists the accuracy of this wattmeter as ±25 W, but we were able to improve the accuracy of the measurement to an estimated 1% by thermal calibration. RF input power was measured with a Diamond SX-200 wattmeter.

fier. C5 and L3 act as a notch filter for the second harmonic. Without the notch filter, the second harmonic is typically between -25 and -30 dBc instead of the -40 dBc that the FCC requires on HF. In addition, C5 and L3 transform the 50-Ω antenna impedance to about 10 Ω, the appropriate load for a Class-E amplifier. RFC1 converts the 0 to 120-V dc input from the power supply to a current source, and C6 helps keep RF energy out of the power supply.

C4 and L4 form a low-pass filter to remove VHF harmonics. Without the filter, there are several harmonics at levels from -40 to -60 dBc in the frequency range from 130 to 210 MHz. With the filter, the VHF harmonics are reduced to the -70 to -80-dBc level.

Amplifier Construction

The 500-W amplifier is shown in Figure 6 with its cover removed. The transistor is mounted on a 3∞4⅛-inch heat sink with 1-inch fins (type HS50-3.0 from RF Parts, with a thermal resistance of 2 K/W with no fan) with a #6-32 bolt and nut. The transistor generates most of the heat (about 10% of the dc power) in the amplifier, so it must have good thermal contact to the heat sink. Because the transistor's case reaches high voltages, it must be electrically isolated from the heat sink. We use a Kapton pad manufactured by Berquist that has a thermal resistance of 0.2 K/W and a breakdown voltage of 6 kV. The heat-sink surface must be free of burrs, and the transistor should lie flat on the surface with minimal stress on the leads. If a torque screwdriver is available, International Rectifier recommends a mounting torque of 10 inch-pounds. The heat-sink baseplate is an aluminum L bracket bent from 0.050-inch-thick aluminum sheet. A U-shaped enclosure cover is made of 0.016-inch-thick aluminum sheet. A hole in the cover allows insertion of a plastic screwdriver for tuning L1.

Solder Q1 and C2 flush to the PC board to reduce VHF ringing on the gate signal. Good electrical contact is needed between Q1's source lead and the heat sink. Use a #6-32 bolt and nut, with washer spacers so that the source lead does not bend. Scope-probe pigtails soldered to Q1's gate and drain leads poke through holes in the baseplate. Rubber grommets in the holes prevent the pigtails from shorting to the chassis.

L4, L3 and L2 are made by winding solid insulated wire on pipe and drill-bit forms. Orient the coils at right angles to each other to reduce coupling between them. L2 has a 7-MHz Q of 350; L3 and L4, a Q of about 170. For C2, C3 and C5, use only 1-kV mica capacitors—even 500-V capacitors fail spectacularly with a burst of flame. If a 1-kV, 100-pF capacitor is not available for C4, substitute a series-connected pair of 500-V, 200-pF mica capacitors. For best filtering, mount C4 and L4 directly on the center pin and ground lug of J2. Mount L4 with its axis vertical to reduce coupling to the other coils.

The NorCal 40A Driver

For a driver, we use a NorCal 40A,[5] but its 2-W output is not enough to drive these amplifiers. Fortunately, the NorCal 40A can be modified to deliver greater power output.[6] We recommend 3 to 4 W drive for the 300-W amplifier, and 6 to 12 W for the 500-W amplifier. These drive levels give an efficiency in the 90% range (Figure 7). Drive levels lower than these give poor efficiency; higher drive levels increase the dissipated power without improving efficiency. Don't drive the 300-W amplifier with less than 2.3 W, and the 500-W amplifier with less than 5 W. At these low power levels, the transistor may not turn on fully at all supply voltages, subharmonic spurious components may be generated, and the amplifier may not key properly.

The recommended drive powers produce peak gate voltages of between 15 and 20 V. International Rectifier specifies a maximum peak gate voltage of 20 V to avoid rupturing the gate. Although the drive levels are close to this limit, experience shows them to be quite safe. The 20-V limit is more appropriate for the low frequencies used in power supplies than for RF voltages. In controlled tests, we've pushed the 300-W amplifier to 60-V gate-voltage peaks, *three times* the manufacturer's voltage limit, without damage.

Next month, we'll discuss the keyed power supply, keying waveform shaper and tune-up. Join us!

Notes

[1]A package of amplifier parts *only*, including PC board, components, connectors, heat sink and chassis is available at cost from Puff Distribution, Department of Electrical Engineering, MS 136-93, Caltech, Pasadena, CA 91125. Price: $50 for US orders, $60 for foreign orders. The price includes tax and shipping by surface mail. Make payment by check or money order only to "Caltech-Puff Distribution." Foreign checks must be drawn on a bank with a US branch office. Please provide your Amateur Radio call sign and specify which amplifier (the 300 or 500 W unit) you want. For more information, contact Dale Yee by e-mail at **yee@systems.caltech.edu**, fax 818-395-2137, or you can download an order form from: **http://www.systems.caltech.edu/EE/Faculty/rutledge/poweramp.html**. We do not offer power-supply components. Those parts are available from Communication Concepts, 508 Millstone Dr, Beavercreek, OH 45434-5840, tel 513-426-8600; Digi-Key, PO Box 677, Thief River Falls, MN 56701-0677, tel 800-344-4539, **http://www.digikey. com**;

Newark Electronics, (many branches throughout the US; check your telephone book for a branch near you); main office: 4801 N Ravenswood Ave, Chicago, IL 06040-4496, tel 800-463-9275, 312-784-5100, fax 312-907-5217; RF Parts, 435 South Pacific St, San Marcos, CA 92069, tel 800-737-2787; Mouser Electronics, 2401 Hwy 287 N, Mansfield, TX 76062, tel 800-346-6873, 817-483-4422, fax: 817-483-0931 e-mail **sales@mouser.com**; **http://www.mouser.com**.

A template package is *not* available from the ARRL.

[2]Historically, amateurs have built high-power amplifiers with vacuum tubes rather than transistors to avoid complicated power-combining networks and many low-power transistors. See Dick Ehrhorn, W4ETO, "RF Power Amplifiers and Projects," *The 1996 ARRL Handbook*, Chapter 13. Exceptions to this are the elegant designs by Helge Granberg, K7ES/OH2ZE (SK). *RF Application Reports*, published by Motorola Inc, in 1995, contains over 20 Application Notes and Engineering Bulletins written by Helge Granberg on amplifiers with output powers of 20 to 1200 W. Communication Concepts sells the boards and components for these amplifiers. *Radio Frequency Transistors*, by Norm Dye and Helge Granberg, published by Butterworth-Heineman, Boston, 1993, is recommended reading. Joel Paladino, N6AMG, adapted one of Granberg's transistor amplifiers (see "An Experimental Solid-State Kilowatt Linear Amplifier for 2 to 54 MHz," *QST*, Sep 1992, pp 19-23). However, the power transistors alone cost $900! This led us to look for a less-expensive way to make transistor power amplifiers.

[3]Fred Raab, WA1WLW, "Simple and Inexpensive High-Efficiency Power Amplifier," *Communications Quarterly*, Winter 1996, pp 57-63.

[4]Nathan Sokal, WA1HQC, and Alan Sokal, WA1HQB, "Class-E, A New Class of High-Efficiency Tuned, Single-Ended Switching Power Amplifiers," *IEEE Journal of Solid-State Circuits*, Vol SC-10, Jun 1975, pp 168-175. This paper by father and son is a classic in the radio engineering literature, and is still the basic reference for the Class-E amplifier.

[5]The NorCal 40A designed by Wayne Burdick, N6KR, is available in kit form for $129 from Bob Dyer, KD6VIO, at Wilderness Radio, PO Box 734, Los Altos, CA 94023-0734, tel 415-494-3806, **http://www.fix.net/jparker/wild.html**. The NorCal 40A Web address is: **http://www.fix.net/~jparker/norcal.html**.

[6]A number of NorCal 40 modifications were published in *QRPp*, the magazine of the Northern California QRP club that first made the NorCal 40 kit available. For information on subscriptions to *QRPp* and back issues, contact Jim Cates, 3241 Eastwood Rd, Sacramento, CA 95821. Wayne Burdick, N6KR, suggests increasing the supply voltage for more power. If you do this, increase the voltage rating of Zener diode D12 to accommodate a larger peak collector voltage. For 3 W output, we use an MRF237 at Q7, the PA. To further increase the power to 7 W, we reduced L7 from 18 turns to 11 turns, and L8 from 18 turns to 14 turns. We replaced C45 and C47 with 560-pF, 300-V mica capacitors, and C46 with a 1500-pF, 100-V mica capacitor. For other approaches to raising the output power, see Dave Meacham, W6EMD, "5 Watts from your NorCal 40A," *QRPp*, Mar 1995, pp 6-7, and Ron Manabe, KN6VO, "Increasing the Output Power of the NorCal 40," *QRPp*, Jun, 1994 pp 42-45. Ron reports an output power of 7 W.

By David Rutledge, KN6EK, et al. From *QST*, June 1997

High-Efficiency Class-E Power Amplifiers

Part 2—Class-E operation permits low-cost MOSFETs to develop considerable power.

Last month[7] we talked about Class-E amplifier fundamentals and began construction of a 40-meter unit. Now we'll tackle the power supply, keyed-waveform shaper and develop some power.

A Keyed Power Supply

Nonlinear Class-E operation sharpens the CW keying envelope, causing annoying key clicks. To prevent this, we key the power supply to shape the supply voltage. A separate 4×7×12-inch (HWD) enclosure houses the dc supplies, a stretcher circuit that delivers a stretched pulse to the driver and a shaper that produces the shaped pulse for the amplifier. Figure 8 shows how these circuits connect.

So that the RF drive does not end before the shaping pulse, the keying pulse to the NorCal 40A driver is stretched a few milliseconds. The stretcher (Figure 9) takes a keyer's CMOS logic signal and provides a buffered keying waveform to the shaper and a stretched keying waveform to the NorCal 40A driver. Dc supplies (Figure 10) provide 12 V dc to run the ICs and 0 to 120 V dc for the amplifier. A wave shaper (Figure 11) gives this 0 to-120 V dc supply voltage a controlled rise and fall time to avoid key clicks. Figure 12 shows the keyed power supply with its cover removed.

There are other advantages to using a keyed power supply to control the output power. The amplifier power dissipation is low at all supply voltage levels, so that loss is kept low throughout a keying pulse. Because the keyed power supply also acts as a solid-state TR switch, a relay is not needed. This is because the supply voltage is zero except during key down. (This feature works well with the NorCal 40A, because it, too, does not use a relay for switching.) At zero voltage, the drain-to-gate capacitance in a MOSFET is quite large, and the signal from the antenna is fed through the amplifier with a loss of only about 7 dB. The NorCal 40A receiver sensitivity is excellent,[8] and a 7 dB signal loss does not hurt reception at all. A 7-dB loss degrades the MDS to −130 dBm, still far below typical 40-meter antenna noise levels of −90 to −110 dBm. On the positive side, with 7 dB attenuation, the receiver is less susceptible to intermodulation distortion from other signals in the 40 meter band.

In addition, the amplifier reduces AM broadcast signals by about 20 dB. The 7-dB loss does need to be made up at the audio end. For this, we mount a 2-inch-diameter speaker in a cardboard mailing tube cut to resonate at 650 Hz for CW reception. This gives a sound level that is quite adequate.[9]

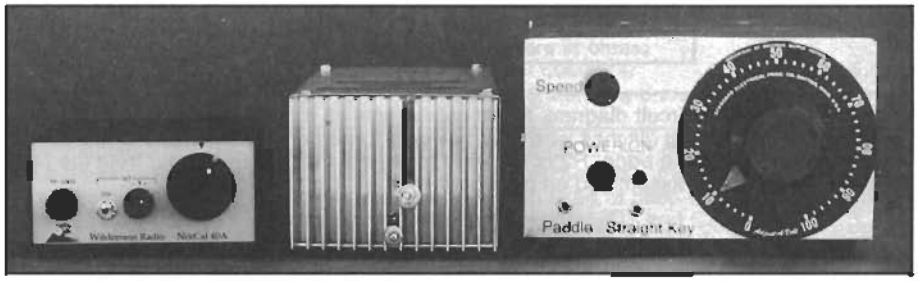

Transceiver, amplifier, and power supply for a 40-meter, 500-W station. The NorCal 40A transceiver driver is on the left, a 500-W amplifier is in the center and the power supply on the right. The amplifier's heat sink and transistor mounting screws are visible. The large dial controls the variable autotransformer, varying the RF output power.

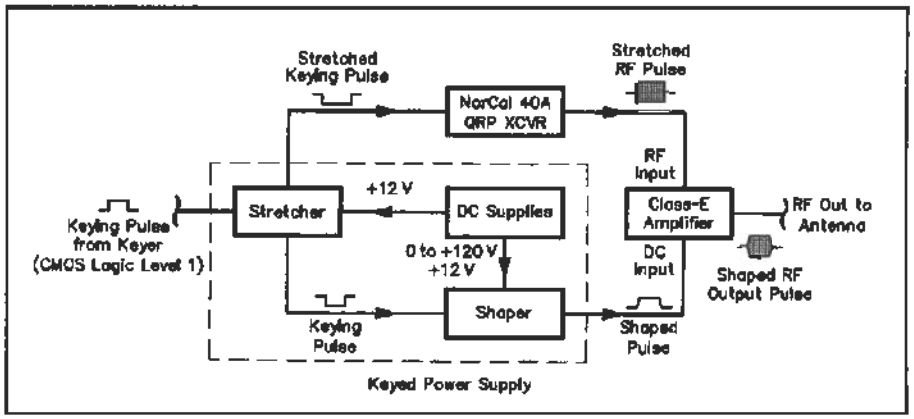

Figure 8—Block diagram showing the connections between the stretcher, dc supplies, shaper, NorCal 40A and the Class-E Amplifier. The stretcher, the dc supplies, and the shaper are in the keyed power supply. Power supply keying is done by a Curtis keyer IC (not shown) that provides a CMOS logic-level 1 during key down. The Curtis keyer IC and application note are available from MFJ Enterprises Inc, Box 494, Mississippi State, MS 39762, tel 800-647-1800, 601-323-5869, fax 601-323-6551; e-mail **mfg@mfjenterprises.com**; **http://www.mhjenterprises.com**.(Keyer circuits using Curtis ICs can be found in recent editions of *The ARRL Handbook*.—*Ed.*)

The Diplexer

For greater reduction of spurious emissions, we recommend following the amplifier with a band-pass diplexer (see Figure 13) to terminate out-of-band spurious components in a 50 Ω load.[10] Our diplexer (in a 3.5×6×10-inch [HWD] box) uses the equivalents of a 100-pF series capacitor, an 1800-pF shunt capacitor and air-wound inductors. Stretch or compress L2 to achieve minimum SWR. The measured loss of 40-meter signals was extremely low, only 4%. Our experience shows that a diplexer can reduce all spurious components to more than –55 dBc.

Tune-Up

Refer to Figure 3 in Part 1. There are two amplifier coil adjustments. First, with the cover on and the dc input off, L1 is set for minimum input SWR with full RF input. Typically, the SWR can be reduced to 1.5:1. If it cannot be brought below 2:1, try adding or subtracting a turn from L1.

Output power is peaked by stretching or squeezing L2. Note: For safety, the amplifier's cover should always be attached when the RF drive is applied. The cover also significantly lowers the inductance of L2. Be sure to turn off the supply voltage before you touch *any* amplifier parts! A high RF voltage will burn the skin. RF burns are deep and heal slowly. Having a keyed power supply helps here, because the amplifier supply voltage is zero except during key down.

Attach a dummy load and power meter to J2. With the RF input applied continuously, slowly increase the dc input voltage, while monitoring the gate and drain voltages using an oscilloscope with 10× high-impedance probes. (You should see waveforms similar to those in Figure 15, although the peak drain voltage should be about half of

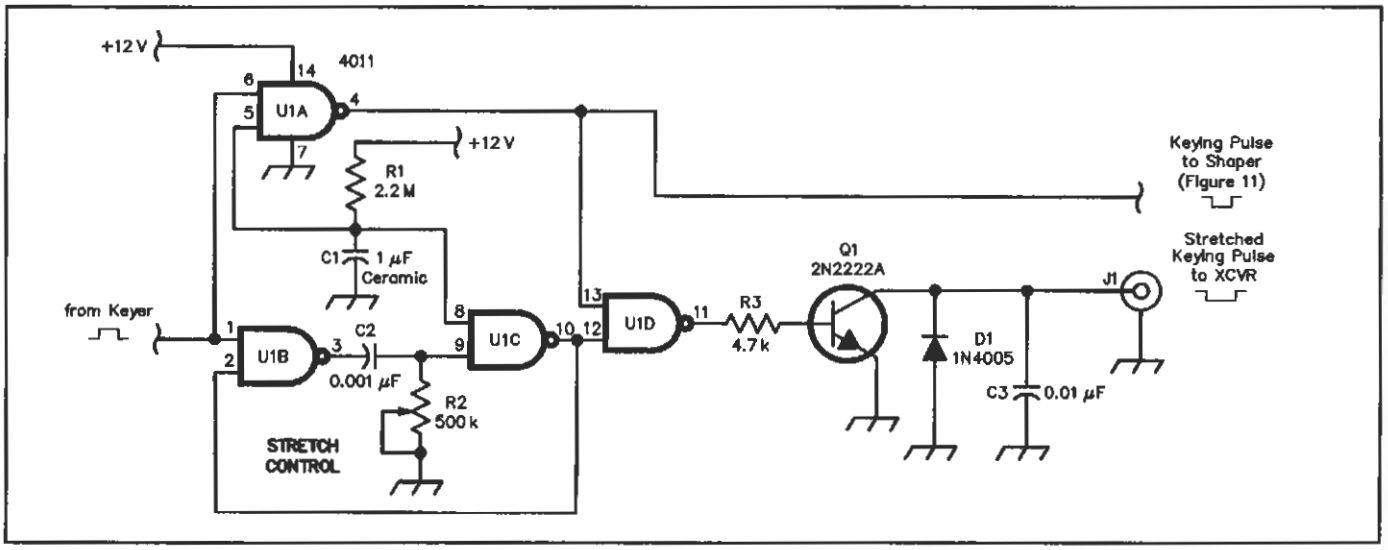

Figure 9—Stretcher circuit diagram. **NAND** gate A acts as a buffer and produces a keying pulse for the shaper. One input has an RC delay to prevent keying glitches when the power is turned on. Gates B and C are connected by an RC network that causes a pulse to be triggered on a falling edge. R2 is adjusted to ensure that the RF output from the NorCal 40A lasts longer than the shaping pulse. The components are assembled on perfboard.

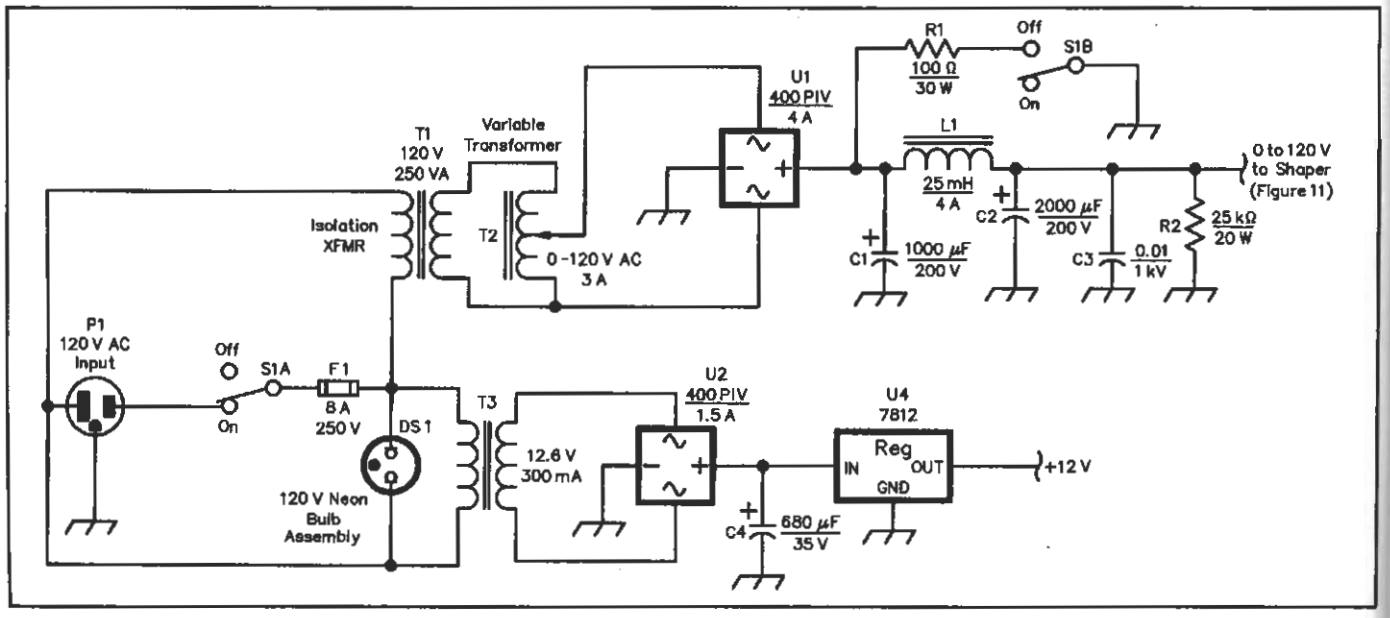

Figure 10—Dc supplies diagram. There are two isolated supplies: one with an unregulated 0 to 120-V output controlled by an autotransformer, and another with a +12-V regulated output. Two bleeder resistors help keep capacitor voltages at safe levels when the supply is turned off or its output reduced. The 4-A bridge rectifier is an RS404LR by Diodes, Inc, available from Digi-Key. The Panasonic 1000 and 2000-µF electrolytics in the filter are available from Digi-Key. The Stancor C-2686 25-mH choke is available from Newark. We scrounged the isolation transformer and variable autotransformer from old equipment. Look for them at swap meets, or purchase equivalents from Newark (Magnetek N55M 250-VA isolation transformer and the Staco 291 3-A variable autotransformer).

that in the figure.) The RF output should begin to rise. Increase the dc input until the forward RF output power is 25% of full power. Make sure the output SWR is 1.5:1 or less. Measure the dc input voltage, and adjust L2 to give 25% power at 60 V dc. Stretching L2 reduces its inductance and increases the output power, but usually lowers the amplifier's efficiency. Squeezing L2 reduces the output power and usually increases amplifier efficiency.

Increase the dc input voltage until the amplifier reaches maximum output power. The dc voltage should now be between 115 and 120 V, and the peak drain voltage of the RF-stage MOSFET should be between 380 and 420 V. Larger peak drain voltages run the risk of transistor failures. Lower voltages may indicate an excessive drain current, which can lead to a failure. If the voltage is too high, stretch the coils a bit more. If the voltage is too low, squeeze the coils. Check the RF drive and input SWR again. You may find that they have changed somewhat and that readjustment is needed. Measure the dc supply current and voltage, and calculate the amplifier efficiency to ensure that it is 85% or above. Use a 0.001-µF capacitor to bypass the voltmeter terminals because an RF voltage there can cause a significant measurement error. (In addition, you should realize that RF power meters often have error factors as high as 10%.)

Keyed-Waveform Shaping

The keying envelope is controlled by the three potentiometers in the shaper and stretcher circuits. R3 in the shaper circuit sets the rise time, R4 sets the fall time. R3 also helps control the power supply droop as the amplifier is keyed. R2 of Figure 9 determines the stretch in the pulse that keys the NorCal 40A, so that it does not stop transmitting before the end of the shaped

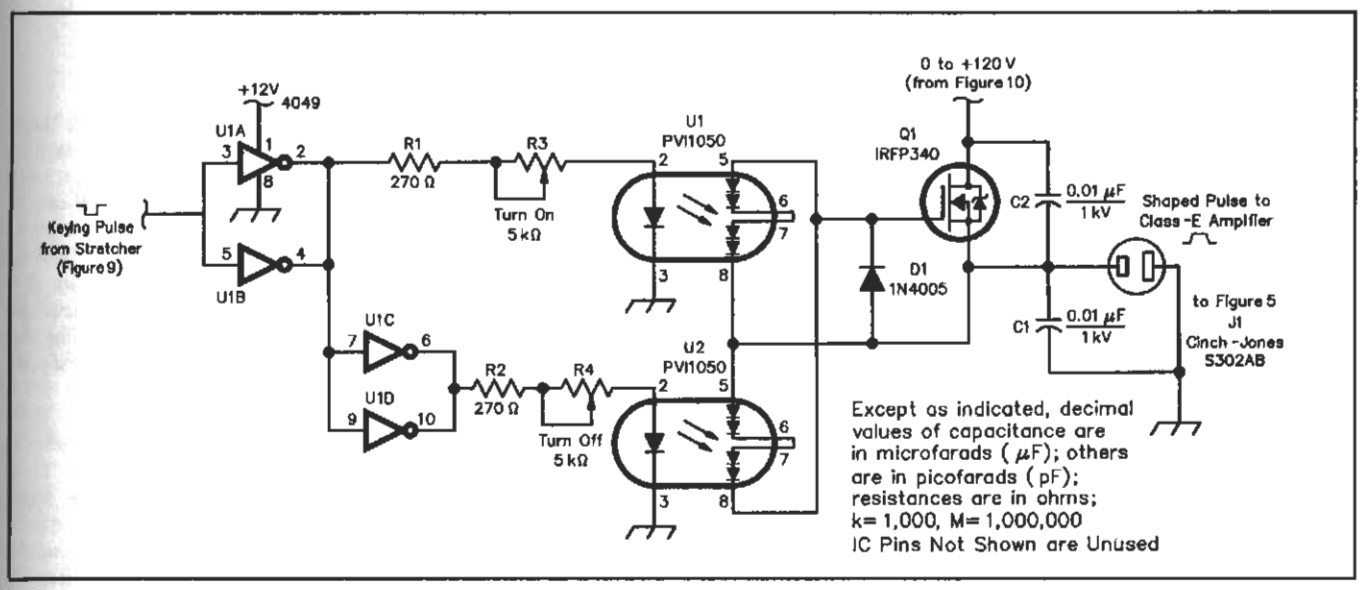

Figure 11—Shaper circuit diagram. A pair of optically isolated MOSFET drivers (type PVI1050) turn Q1 on and off to bring the supply voltage up and down. Keying waveform rise and fall times are adjusted by R3 and R4, which control the current to each MOSFET driver. The 270-Ω resistors limit the LED current to a safe level. The TURN-ON potentiometer is also used to keep the overshoot from the unregulated power supply to a reasonable level. D1 prevents Q1's gate voltage from drifting negative. C1 and C2 are RF bypasses. To keep the supply voltage from appearing across exposed contacts, a female socket is used at J1. All components are available from Digi-Key. Point-to-point wiring on perfboard is used.

Figure 12—The keyed power supply with the cover removed, viewed from the side. T1 is mounted on the back plate, along with the fuse and connectors for the dc output, a keying line to the NorCal 40A and the ac line input. The **TUNE** switch keys the amplifier for testing. The variable autotransformer is on the left, mounted to the front panel. In the center foreground, mounted to the base plate, is L1, the 25-mH choke. Mylar sheets are taped to the perfboards for electrical isolation. The large components are attached directly to the box. The IRFP340 is mounted on the bottom of the box using a Berquist K10-104 Kapton insulating pad, #6-32 screw and a torque of 10 inch-pounds. The other shaping circuit components are mounted on perfboard. Layout is not critical.

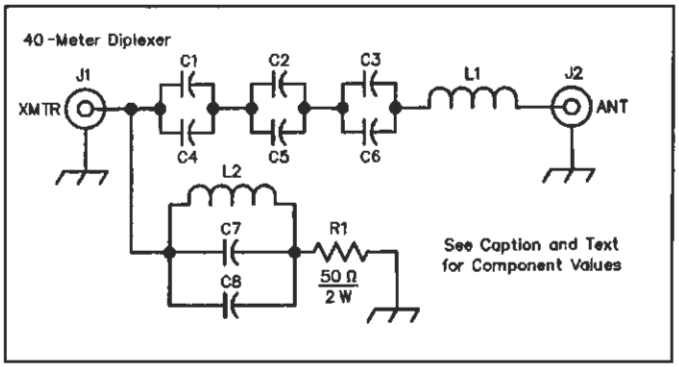

Figure 13—Schematic of our diplexer. It uses six 150 pF capacitors, two 910-pF capacitors and air-wound inductors made of 3/16-inch-wide copper tape (see Note 1).

C1-C6—150 pF, 1 kV mica 5%-tolerance (Cornell Dubilier type CDV19; available from Newark Electronics, see Note 1)

C7, C8—910 pF (same type as above)

L1—24 turns of 3/16-inch-wide copper tape, 1 3/8 inch ID; see Note 1.

L2—4 turns of 3/16-inch wide copper tape, 1 inch ID; see Note 1.

R1—50-Ω, 2-W (approx) termination, Jameco part number 71458; available from Jameco Electronics, 1355 Shoreway Rd, Belmont, CA 94002, tel 415-592-8097; fax 415-592-2503 and 415-595-2664)

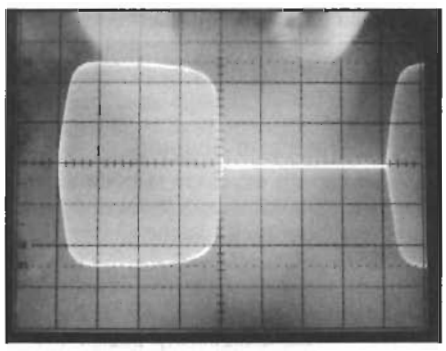

Figure 14—Keying waveform of the 500-W amplifier at 30 WPM. The horizontal axis is 10 ms per division. The rise and fall times are about 3 ms.

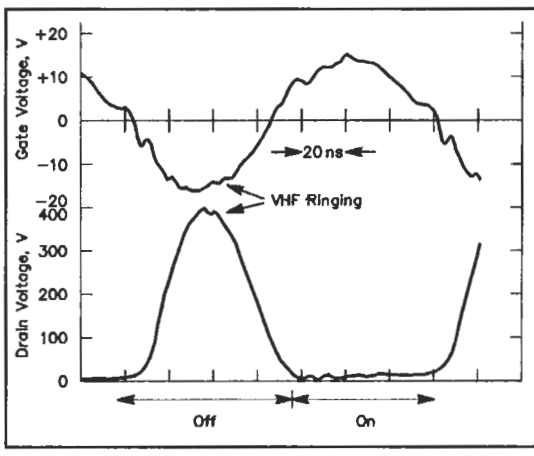

Figure 15—Drain waveform and ringing. Oscilloscope trace of the gate and drain voltages of the 300-W amplifier with 3 W drive. The dc supply voltage is 120 V; the input SWR is 1.6:1. Time scale is 20 ns per division; the transistor off and on times are shown. The transistor is off when the gate voltage is below the threshold, typically 4 V, and on when the gate voltage is several volts above the threshold. Peak gate voltage is 16 V, and the peak drain voltage is 400 V, safely within the manufacturer's ratings of 20 and 500 V, respectively.

pulse. We recommend using a keyer with adjustable weighting to offset the pulse stretching. The potentiometer settings interact somewhat, and there are variations at different sending speeds, so it is best to set them at the speed you commonly use. Adjust the controls for rise and fall times between 2 and 5 ms, and for a smooth keying envelope. Figure 14 shows keying at 30 WPM with rise and fall times of about 3 ms.

VHF Ringing

In many Class-E amplifiers, ringing in the VHF range can be seen on the gate and drain waveforms (Figure 15). This ringing can be quite pronounced, with bumps several volts high on the gate or drain or both. The bumps disappear when the RF input is removed, and that is why we refer to this as *ringing* rather than *oscillation*. We have compared measured spectral plots with *PSPICE* simulations and believe that the waves are driven by the sudden turn-on and turn-off of the transistor, acting rather like the gong of a bell.

We notice two distinct time periods and frequency ranges for the ringing. During the time the transistor is on, the ringing frequency is about 80 MHz. This appears to be a resonance of the external drain capacitor combined with the internal inductance of the capacitor and the transistor and may indicate a mismatched load. The on-ringing is usually small if the load is matched so that the drain voltage comes smoothly to zero before the transistor turns on.

The ringing while the transistor is off covers a broad range of frequencies—from 130 to 210 MHz. If the output low-pass filter is removed, the ringing can be seen easily on a spectrum analyzer at levels between −40 and −60 dBc. The off-ringing appears to be caused by a resonance of the external drain capacitor and its internal inductance, together with the transistor's internal drain capacitance and its inductance. The internal drain capacitance varies greatly with the drain voltage, so that the frequency is modulated as the drain voltage rises and falls. The low-pass filter reduces these harmonics to the −70 to −80 dBc range.

On the Air

The amplifiers meet the FCC requirements for spectral purity [confirmed in the ARRL Lab—*Ed.*]. NorCal 40A designer Wayne Burdick, N6KR, emphasizes that it is important to correctly tune the bandpass filter following the transmit mixer to minimize spurious emissions from the NorCal 40A.[11]

These amplifiers are excellent for chasing DX, schedules and "ragchews," particularly at this low point of the sunspot cycle. The amplifiers require no warm-up, no tune-up, and produce no fan or relay noise. We can vary the power from 1 W to full power via the variable autotransformer. The antenna SWR should be 1.5:1 or better because the amplifier is not protected against large mismatches. With a high SWR, the transistor will probably overheat. Check the dc voltage when the amplifier is delivering full power to the antenna to ensure that it remains between 115 V and 120 V. Readjust the coils if the voltage is too high or too low.

Our most common problem has been a poorly mounted PA transistor. If the transistor is not flat against the heat sink, heat transfer is poor and the transistor becomes quite hot; efficiency suffers (becoming usually less than 85%) and the amplifier may not reach full power. The output power may also drift downward, a sign that the transistor temperature is increasing and that the transistor is under stress.

Component temperature can be a good diagnostic tool. For the 500-W amplifier, our experience is that for CW QSOs longer than 30 minutes, the temperature of C3, C5 (Figure 5) and the heat sink rises to about 60× C. For the 300-W amplifier, the heatsink temperature is about 50× C. This is hot to the touch, and it can be checked with a lab thermometer. The temperature will vary according to your operating style, and if the temperature is higher than you like, you can add a fan.

The Future

We see room for improvements: protection against antenna mismatches and employment of an inexpensive keyed *switching* power supply that is as lightweight as the amplifiers. Finally, it would be interesting to develop Class-E amplifiers for the other bands. We have built a 250-W amplifier for the 20 meter band that exhibits an efficiency of 88% with 10 W drive. We believe that Class-E amplifiers provide amateurs with good building challenges and operating fun at modest cost.

Acknowledgments

This work began as senior theses by Joyce Wong and Meng-Chen Yu at Caltech, and many of their ideas appear here. John Davis was supported by a scholarship from the James Irvine Foundation and the Army Research Office. Eileen Lau, Kai-Wai Chiu, and Jeff Qin received Caltech Summer Undergraduate Research Fellowships funded by the ETO Corporation and the Caltech Gates Grubstake Fund. We appreciate the help from all the people at the ETO Corporation, particularly Dick Ehrhorn, WØID; Don Fowler, W1GRV; Tim Coutts; Chip Keen and Frank Myer. Mitsu Sakamoto, JA4FVE, of Kurashiki, Japan, sent us off-the-air recordings over the Internet. We would like to thank Wayne Burdick, N6KR; Wes Hayward, W7ZOI; and Bill Bridges, W6FA, for their advice.

Notes

[7]Eileen Lau, KE6VWU, et al, "High-Efficiency Class-E Amplifiers—*Part 1*," *QST*, May 1997, pp 39-42. The amplifier enclosures are 3⅛×4⅛×7⅛ HWD.

[8]Rick Lindquist, KX4V, "Low-Power Transceiver Kits You Can Build," Product Review, *QST*, Jun 1996, pp 45-50.

[9]See J. B. and R. V. Heaton, "An Electro-Acoustic CW Filter," *QST*, Apr 1983, pp 35-36; Wally Millard, K4JVT, "A Resonant Speaker for CW," Hints and Kinks, *QST*, Dec 1987, p 43; and Richard Clemens, KB8OAB, "More on Resonant Speakers," Hints and Kinks, *QST*, Jan 1989, p 37.—*Ed.*

[10]David Newkirk, WJ1Z (now W9VES), and Rick Karlquist, N6RK, "Mixers, Modulators, and Demodulators," *The 1996 ARRL Handbook*, Chapter 15, p 15.22.

[11]Telephone conversation with Wayne Burdick. This tuning is done by carefully adjusting C50 to peak the output power.

By William E. Sabin, W0IYH

From *QEX*, November 1999

A 100-W MOSFET HF Amplifier

We had the power supply in Mar/Apr[1] and the diplexer filters in Jul/Aug,[2] here's the main event: a reliable FET power amplifier that needs only 10 dBm of drive to produce a pristine 100 W output.

The two-stage amplifier described in this article and shown in Fig 1 is intended for SSB/CW/Data operation on all nine HF amateur bands. An input (R_{in}≈50 Ω) of about 10 mW (+10 dBm) is amplified to 100 W (PEP or average), continuous duty, with a gain of 40 1.0 dB from 1.8 to 29.7 MHz. Third-order, two-tone intermodulation distortion (IMD) products are 35 to 40 dB below 100 W, and higher-order products are also within the high-quality range for amateur SSB equipment, as shown in Fig 2. The main goal for this amplifier is to operate as a driver, with low adjacent-channel interference, for a legal-limit 1500-W linear amplifier. At this power level, adjacent-channel reduction is especially important. And, of course, it is used in the barefoot mode as well.

The power supply (40 V at 8 A) for the push-pull, class-AB MRF150MP (matched-pair) MOSFET output stage was described previously (see Note 1). Six diplexer filters (see Note 2) also known as invulnerable filters provide more than adequate harmonic attenuation for all nine HF bands. They present a broadband load impedance to the MOSFETs that helps to assure freedom from regeneration and oscillation, and good IMD performance. A resistive load impedance between 45 Ω and 55 Ω is recommended for best performance.

The MRF 150 was chosen because it is designed for linear, class-AB SSB operation and because it has high gain (gm) at the 30-MHz end of the HF spectrum. A desirable feature of the MOSFET power transistor is its ability to achieve low values of the higherorder IMD products.[3,4] As mentioned previously, these products contribute to adjacent channel SSB interference. The first stage uses high-gain, class-A push-pull MRF426 (matched-pair) BJTs that require 13.5 V at about 1.0 A from a separate supply. This supply is also the main supply for other system components. Matched pairs of both transistors are available for a small extra fee from at least two sources.[5,6] They are both listed in the current Motorola manual.[7]

One main idea for this amplifier is to operate it in a very low-stress manner that helps assure a low probability of failure for a very long time, which offsets the initial cost of the high-quality transistors. The MRF150 is a 50-V transistor operated at 40 V; the MRF426 is a 28-V transistor operated at 13.5 V. The required input level is low enough that most of the amplification at the signal frequency occurs in one gain block. Because of the good layout, circuit design and decoupling, the 40-dB gain value does not result in any stability problems.

The balanced amplifier greatly reduces even-order harmonics—especially the second—prior to any output filtering, as shown in Fig 3 for a 7.0-MHz signal. It should be 40 dB or more below a 100-W CW signal for each amateur band. This reduction has been found reliable, once achieved. The lowlevel signal source that drives this amplifier must have at least 50 dB of second-harmonic attenuation, since this amplifier will not suppress that harmonic. This is easy to accomplish, but must be considered during the equipment system design (see Fig 9) and while bench-testing the amplifier as shown in Fig 4.

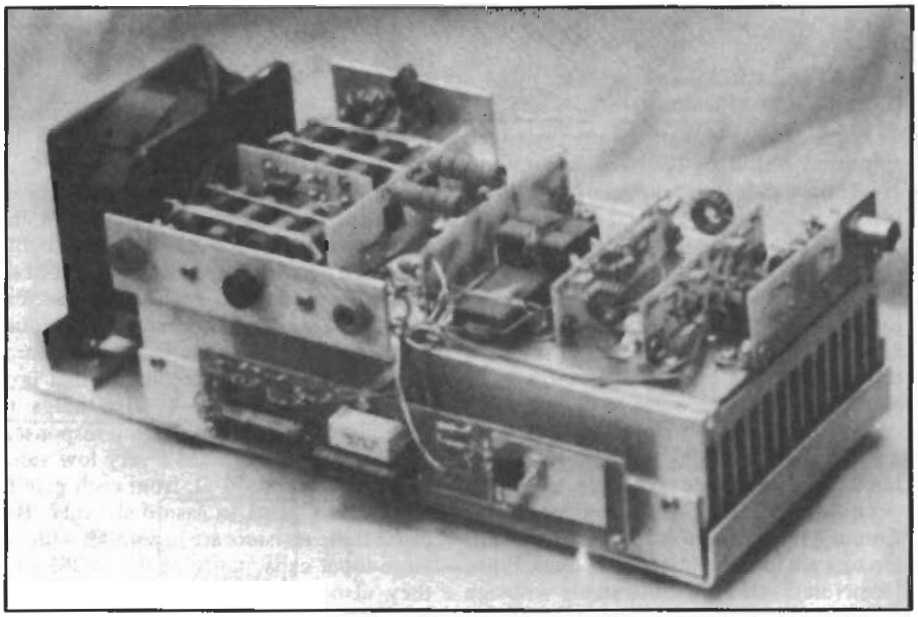

Fig 1—The 100-W broadband amplifier.

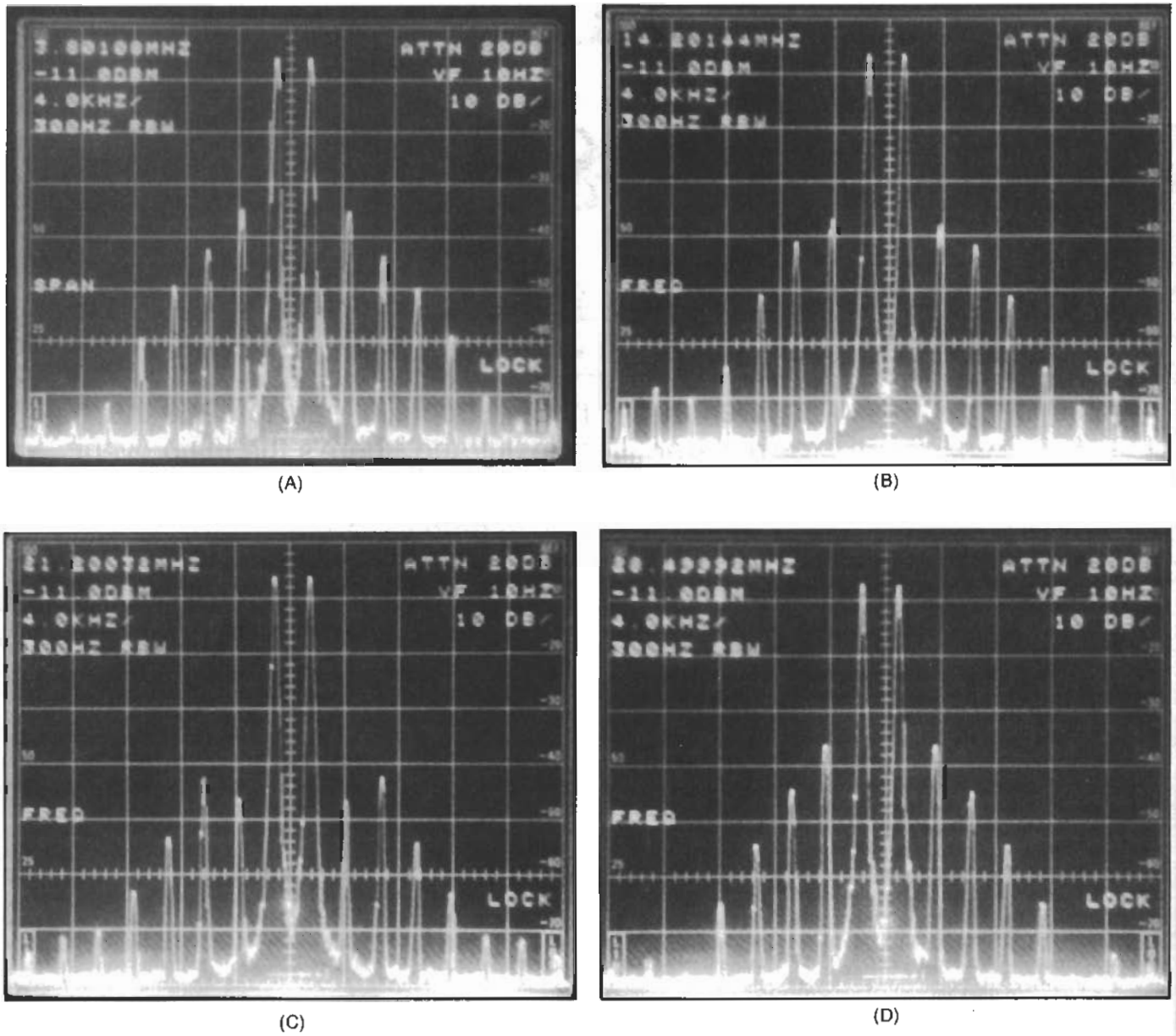

(A) (B)

(C) (D)

Fig 2—Two-tone IMD products: (A) 3.8 MHz, (B) 14.2 MHz, (C) 21.2 MHz, (D) 28.5 MHz.

Circuit General Discussion

Fig 5 is the schematic of the two-stage amplifier. It utilizes 1:1 choke baluns and 1:4 (impedance) step-up and step-down transmission line (Guanella) transformers. The choke baluns significantly improve the balance of the input and output stages. Notice also that T2, T3 and T4 have floating center taps rather than bypasses to ground. This is recommended to improve the even-harmonic balance[8] (verified). T4 and T5 run slightly warm as compared to conventional transformers that get quite hot. The 5-W feedback resistors get warm, but their large surface area limits their temperature rise. They also receive cooling air from the fan. All power resistors in the RF circuits are the excellent metal-oxide types (see Note 5) that are quite stable with age and temperature, and have very low reactance at 30 MHz (measured). Metal-film 1% resistors are used in several critical locations.

The first stage has resistance and inductance loading from collector to collector. A powerful free-running oscillation in the first stage at about 32.5 MHz was being triggered occasionally at the moment of dc supply turn-on while a fairly large 28.0 to 29.7 MHz input was present. The loading reduces stage gain and suppresses the parasitic collector circuit resonance that produced the oscillation. It also helps to flatten the amplifier frequency response.

The second stage has a very low value of RF resistance, 15 Ω, from each gate to ground that helps to assure stability. Because these resistors are in parallel with the large input capacitance of the MOSFETs, they also help to flatten the frequency response. Both stages have negative feedback networks that further assure stability and flatness of frequency response.

Two biasing networks are employed. The LM317 provides a highly regulated gate voltage for the second stage. The FET dissipation and linearity are very sensitive to this voltage; the bias voltage for SSB is fine-tuned for best signal purity using two-tone tests and a spectrum analyzer. Note the four 562-a resistors. If the LM317 fails short circuit, the voltage on the FET gates does not exceed 6.8 V, which will not damage the gates. The large drain current that results from this failure also does no damage because the 40-V power supply has current limiting and voltage fold-back that prevent harmful FET dissipation. The FETs are thus kept well within the safe-operating-area (SOAR) as defined in data sheets[9] (verified). It is important that each 56241 resistor from gate to ground be permanently attached directly between the gate and

source tabs of the FETs themselves so that the gates are never floating. Wrap the resistor leads around the tabs so that they cannot come loose. This avoids accidental static charges that might ruin them. On the other hand, it is better to tack and not wrap the base-collector and gate-drain signal leads so that they can be easily disconnected. We want to be able to test individual segments of the circuitry easily. In my experience, the MRF150 has proven to be a rugged transistor, much more so when operated conservatively and with the power-supply safeguards that I mentioned.

The LM317 provides about 5.8 V for the particular pair of FETs that I used. Individual pairs of FETs will probably require an adjustment of this voltage for idling current and for IMD products that resemble Fig 2. The adjustment procedure is described later. This bias value is set to emphasize the reduction of the higher-order products rather than third- and fifth-order products. These lower-order products do not contribute as much to adjacent channel interference; in fact, an SSB speech processor will make them worse anyway. The higher-order products need to be reduced and the MRF150 has this capability.

The 2N3906 PNP transistor is a bias-current source. The value of this current is determined by the 4.7-Ω resistor and the base-to-ground voltage of the 2N3906. The two 562-Ω resistors force equal base currents into the MRF426s. This helps to assure equal performance. The 0.47-Ω resistor is part of a negative-feedback bias loop. If collector current increases, the voltage across this resistor increases and this reduces the base current. Thermal runaway is avoided by this strategy because the reduced base bias restricts the current increase to a small value. Because of the low dissipation of the MRF426s and the good heat sink, this method is very effective. These transistors are also well inside their SOAR requirements. This stage is very linear and contributes almost nothing to the overall IMD products. To verify this, it is necessary to turn off the drain voltage to the MRF150s and connect a spectrum analyzer across one of the 15-Ω resistors.

The diplexer filter method was decided uponafter a lot of experimentation with other low-pass filter methods as a solution that is free of problems caused by complex interactions between the filters and the output transistors. A special peculiar problem is discussed later. The MRF150 has high gain into the VHF region; the diplexers eliminated all problems associated with this fact. This approach is recommended as a simple way to assure correct operation for HF amateur-band operation of these high-frequency MOSFETs. I was able to get good enough operation with the more conventional low-pass filters, but this approach was by far the most satisfactory for an amateur-band amplifier, as confirmed by swept-frequency tests at all power levels into a 50-Ω load. More about complex loads later.

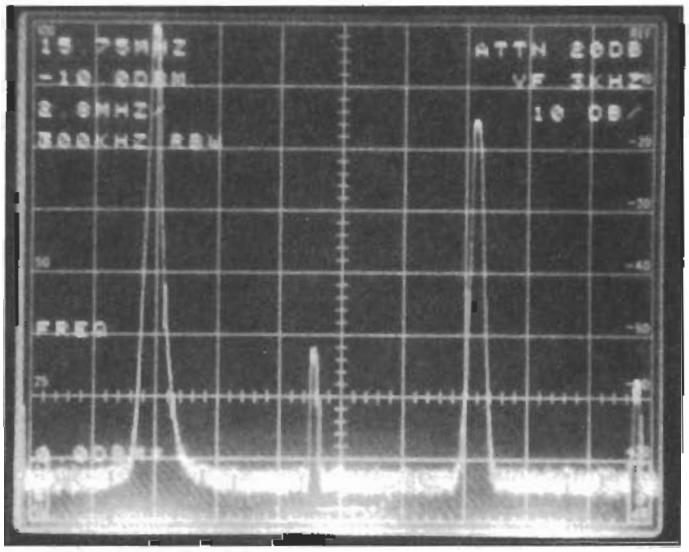

Fig 3—Wideband spectrum for a 7-MHz signal.

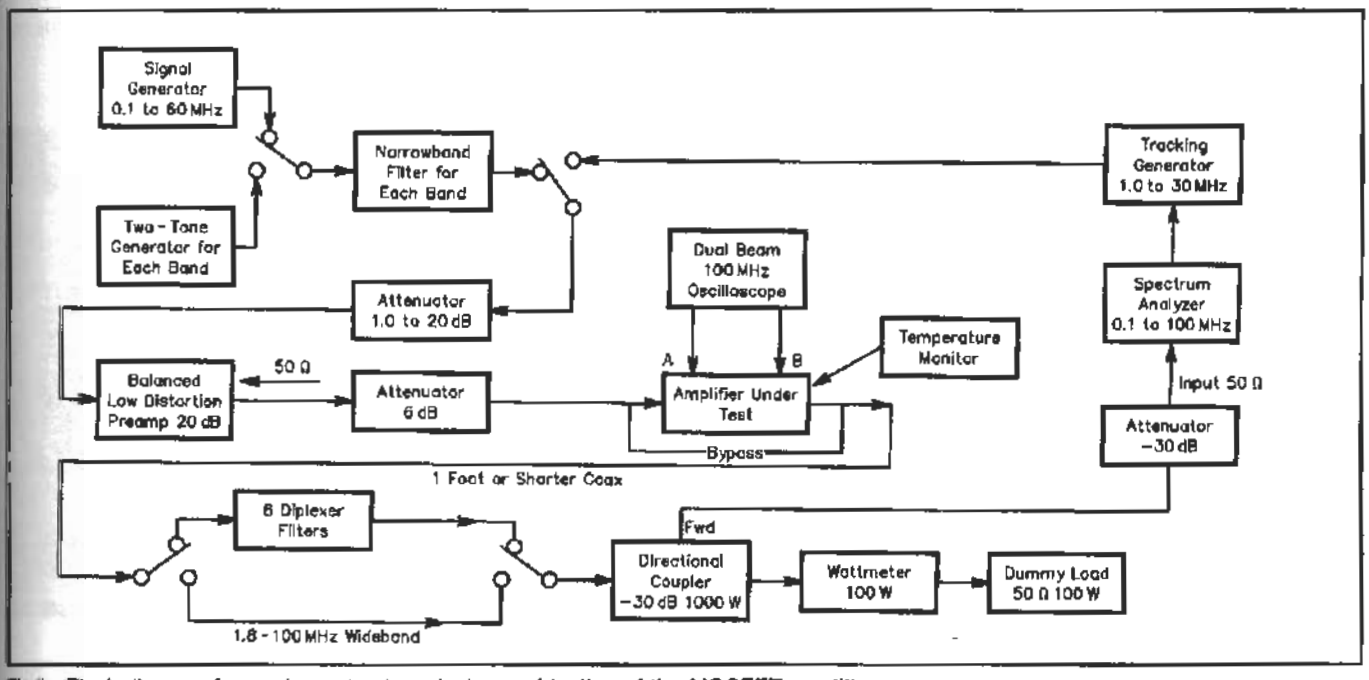

Fig 4—Block diagram for equipment setup, design and testing of the MOSFET amplifier.

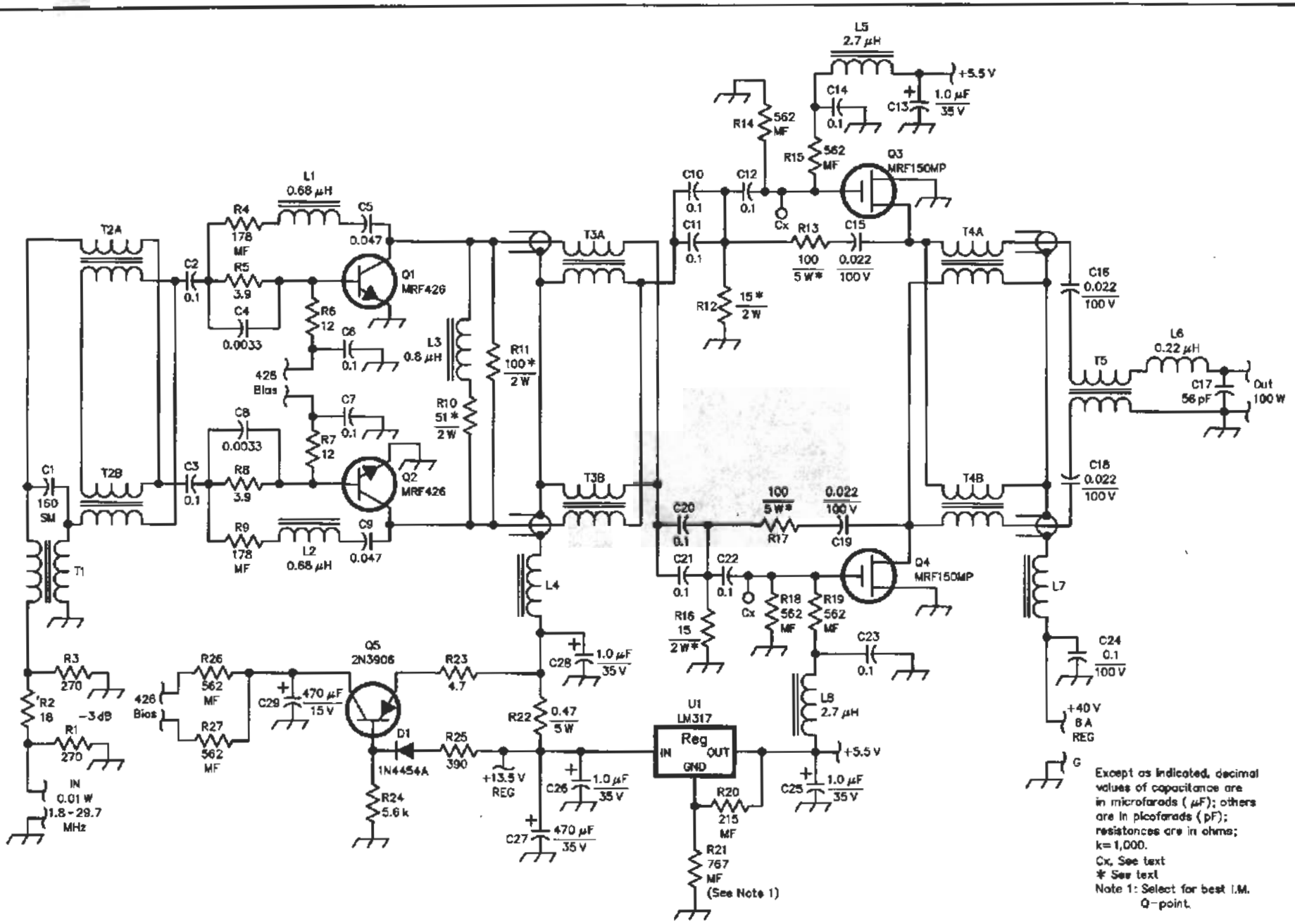

Except as indicated, decimal values of capacitance are in microfarads (µF); others are in picofarads (pF); resistances are in ohms; k= 1,000.

Cx, See text

* See text

Note 1: Select for best I.M. Q-point.

Fig 5—(left) Schematic diagram of a two-stage, 100-W amplifier. Unless otherwise specified, use 1/4 W, 5%-tolerance carbon composition or film resistors. Resistors marked with an asterisk are metal-oxide units. MF indicates metal-film resistors. Both the MRF426 and MRF150 devices are matched pairs. All capacitors are 50 V, unless otherwise indicated.

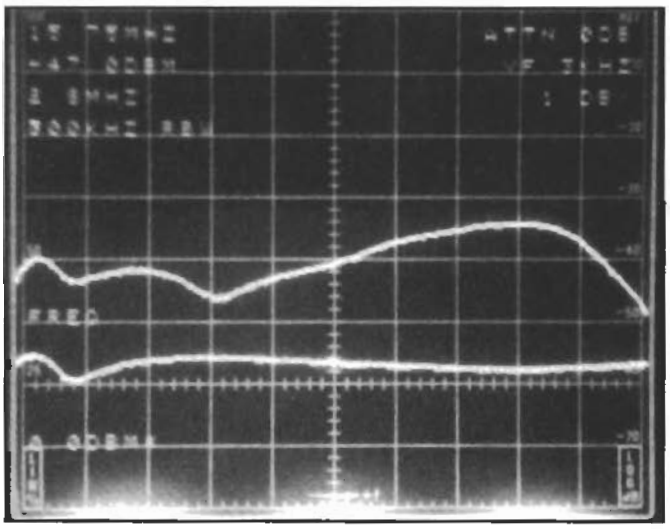

Fig 6—Gain variation, 1.8 MHz to 29.7 MHz, 1.0 dB per division vertical scale—The lower trace is a reference sweep that bypasses the 100-W amplifier—The response bump at low frequency is an artifact of the tracking generator.

Frequency Compensation

The bipolar transistors have gain values that decrease as frequency increases. The MOSFETS have large capacitances that also affect frequency-response roll-off. It was a major exercise to design networks that flatten the response from 1.8 to 29.7 MHz. Fig 5 shows the approach. The idea is to compensate smoothly from input to output in such a way that neither of the two stages is over-driven at any frequency. The criterion for this is to check IMD products and harmonics during the design process, which involves approximate analysis (see the MOSFET Stage Simulation sidebar) and negative feedback.[10] Beyond about 32 MHz, the gain falls off fairly rapidly (but not too rapidly). This is also desirable.

When testing the frequency response using the test setup of Fig 4, it is necessary to measure the frequency response of the signal path from tracking generator to spectrum analyzer while bypassing the 100-W amplifier. This reference response is then compared with the response with the amplifier in the path, as shown in Fig 6. Note the vertical scale: 1.0 dB per division. For the most credible results and ease of measurement, it is very desirable that the impedance looking back from the input be 50 Ω.

Signal Level Testing

We want to verify that the first stage is operating normally by measuring its RF voltages at 4.0 MHz. The class-A first-stage input impedance is close to 50 Ω, and the input level is +10 dBm. Temporarily disconnect the signal leads to the gates of the FETs. The voltage at each output of T3 is about 1.35 V. Reconnect the gate signal leads. The final output over the entire range into an unfiltered, wide-band 50-Ω load is then observed using the setup in Fig 4. A spectrum analyzer with tracking generator is very valuable for this. The accuracy of the wattmeter should be verified or calibrated by some means at both the 100-W and the 25-W levels (the power of each tone of a two-tone, 100-W PEP signal) in each amateur band.

If the second stage is working correctly, the output power is 100 W, or 71 V RMS across 50 Ω. These procedures assure that both stages are working properly and amplifying as intended. Because of the variations in the fabrication of the transistors, the total gain can vary a decibel up or down despite the use of negative feedback in each stage. I suggest the 3-dB attenuator at the input not be modified for simplicity reasons.

The drain-to-drain load impedance of the class-AB output stage is 12.5 Ω and the CW output power is 100 W, so the drain-to-drain ac voltage is 35.4 V. Fig 7 shows the dual-trace scope waveforms (chop mode) on each drain, superimposed on the 40-V supply, and also the drain-to-drain waveform that is confined to the linear region. The third-harmonic content is visible. It is interesting to note that although these waveforms show considerable non-linearity, the fundamental component is quite linear with respect to the gate signal level. I also found that a 50-V dc supply created more heat, but at 100W, did not improve linearity enough to make it worthwhile. The 35.4 V ac also appears across the two series-connected 100-Ω feedback resis-

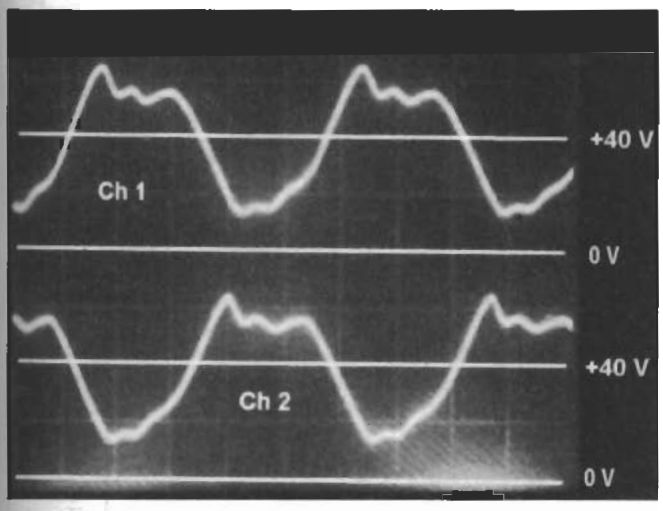

(A)

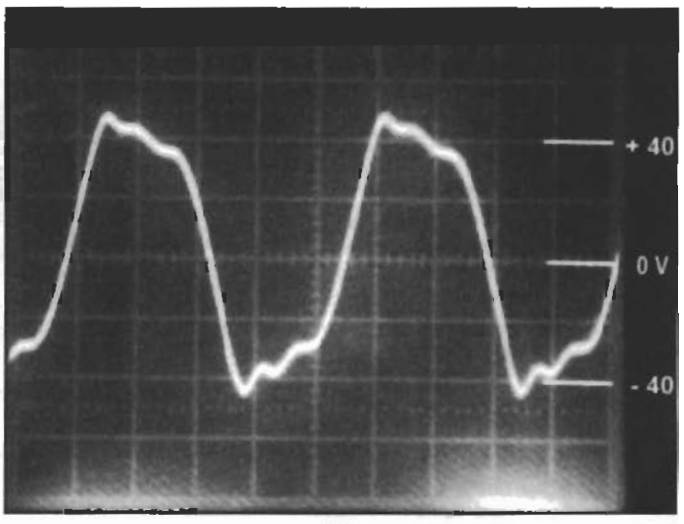

(B)

Fig 7—(A) drain and (B) drain-to-drain oscilloscope waveforms.

tors; they dissipate about (35.42)/200 = 6.3 W, or 3.2 W per resistor (64% of the 5 W rating).

A broadband, untuned power amplifier with flat frequency response and low distortion is not, by necessity, especially energy-efficient (ratio of RF output power to dc power). The output stage is less than 40% efficient for this reason. For SSB use, where the average power is not more that 25 W, even with speech processing, this is no problem at all. For continuous key-down at 100 W, the cooling fan is more than adequate.

Here is an important caution about using oscilloscope probes at the FET drains and the output connector: A 10:1 probe could be damaged (it happened to me) if used directly at this RF voltage level, especially at the upper end of the HF range. Use instead the homemade probe described previously (see Note 2) with a 50-Ω terminating resistor.

The quality of balance is checked by looking at the second harmonic on a spectrum analyzer using the setup in Fig 4 with the diplexer filters out of the signal path. At 100 W output, check the harmonics in each of the nine amateur bands. Capacitor C_x in Fig 5 is used (if needed) to improve the secondharmonic phase balance on the higher amateur bands. If the value is not well below 40 dBc, use C_x at one gate or the other to achieve 45 dBc. Extra pads are provided on the PC board for this capacitor. A value of between 22 pF and 56 pF should be adequate. Overkill is neither necessary nor desirable: The output filters will do the rest. For each decibel of power output below 100 W, the second harmonic normally drops about two decibels.

Construction Notes

Fig I shows how my version of the amplifier is constructed. A 0.125-inch (or 0.062-inch) double-clad PC board, 3.25 × 8.0 inches, is firmly attached to the heat sink. I suggest using this compact size for best reproducibility. The heat sink shown may not be presently available from RF Parts (see Note 5), but I also purchased a Model 99 sink from CCI (see Note 6) that is 6.5×12 inches. This can be easily tailored to the appropriate size with a band saw that has a metal-cutting blade. Pieces of angle and sheet aluminum can then be creatively fashioned to accommodate the fan (RadioShack #273-242) and the PC board that contains the bias circuitry. The transistors are bolted directly to the heat sink (through cutouts in the PC board) using heat-sink compound and tapped (and carefully deburred) #4-40 holes. Careful mounting of the transistors is essential. The main PC board has small sections of copper removed underneath the base and collector tabs of the MRF426s and underneath the gate and drain tabs of the MRF150s, so that accidental grounding is avoided. Use a hobby knife to define the areas and a hot soldering iron to peel off the copper.

A bottom cover is advised, as shown, so that air is funneled through the heat-sink fins efficiently. For a 100-W, continuous, single-tone output, the exhaust air temperature reaches 50°C. I used a RadioShack #22-174 multimeter with its temperature probe mounted inside the fins to monitor temperature during the design and testing phase.

The components are mounted on a set of seven small PC boards, six of which are mounted vertically (as shown) and bolted to the drilled-andtapped heat sink through the PC board, using #4-40 screws and small angle brackets. I used stiff, right angle #6 solder lugs that worked out very nicely. The seven PC boards are cut from a single 4×6-inch two-sided PC board, shown in Fig 8. The bias circuit board has a ground plane; the others do not. This set of boards is available from FAR Circuits.[11]

I chose this method because it is easy, makes the amplifier more compact, reduces stray L and C that can degrade the wideband frequency response and reduces stray couplings that can impair stability and harmonic balance. It also allows the ground plane to be one continuous surface, which is a plus factor. This approach worked out very well and I recommend it as a simple approach.

Temperature Rise

The cooling fan is important. This amplifier, as designed, should have the fan running, and I have found that a simple and reliable way to keep everything safe. It has been tested at 100 W continuously, for sev-

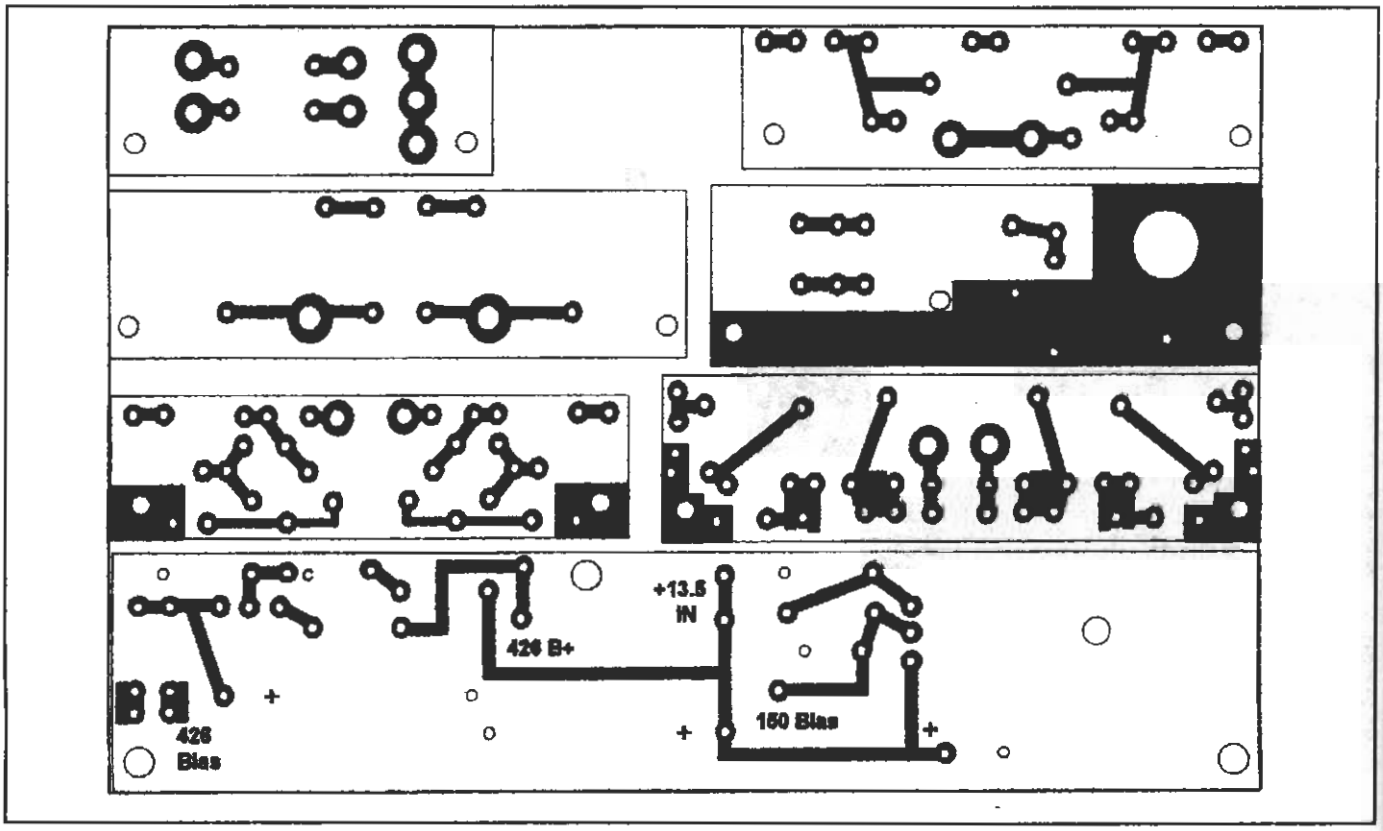

Fig 8—Etching pattern for a 4×6 inch (finished size) PC board that provides the seven individual boards.

MOSFET Stage Simulation

A simplified analysis of the second MOSFET stage is presented (Fig A) to illustrate the effect of the resistive negative feedback of the 100-Ω resistors and the 40-pF gate-to-drain capacitance. The simulation diagram shows the voltage-controlled current sources with a G_m of 6.0 S, which is assumed constant over frequency. The gate-to-source capacitance is 360 pF and the drain-to-source capacitance is 200 pF. These numbers are from the MRF150 data sheets.

The frequency plot (Fig B) obtained from the ARRL Radio Designer program shows the gain, MS21 (dB), with (lower trace) and without (middle trace) the 100-Ω feedback resistors. The gain variation is reduced from about 6 dB to about 1.5 dB. In this simplified model (good enough for this illustration), the gain drop is caused by the capacitors, especially the 40-pF capacitor whose influence is greatly magnified by the Miller effect. If this 40-pF capacitance is eliminated from the simulation, the frequency response variation—even without the feedback resistors—is less than 1.0 dB, as seen on the upper trace.

If the power output at 15 MHz is to be held constant, the turns ratio of the output transformer and the value of the feedback resistors can be manipulated to achieve that end. The simulation shows that a turns ratio of 1:$\sqrt{2}$ and a resistor value of 120 Ω does this. The FET load impedance is now 25 Ω instead of 12.5 Ω. The increased voltage gain makes the Miller effect greater and increases the gain variation (lower trace) to 2.3 dB. The drain-to-drain voltage is now 50 V instead of 35 V, and this results in higher drain efficiency for the MOSFETs. However, the push-pull 1:$\sqrt{2}$ -turns-ratio transmission-line transformer is not as simple as the 1:2 that uses 25-Ω coax, and for me, that was the determining factor.

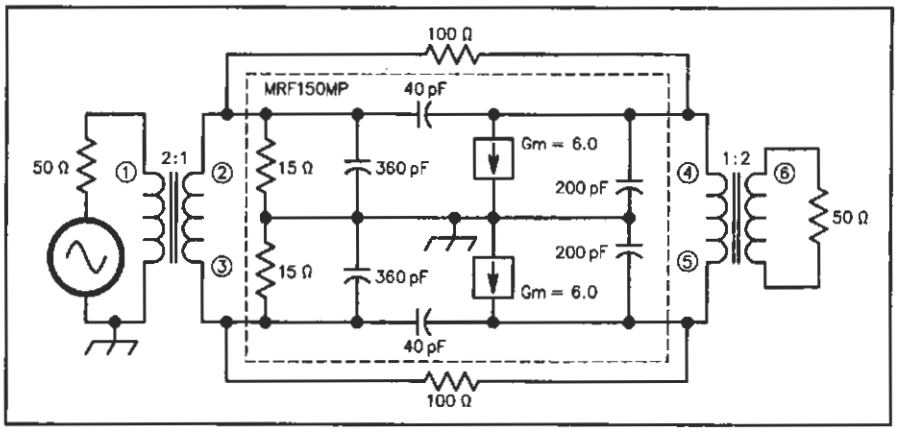

Fig A—A circuit used to analyze the PA output stage with ARD.

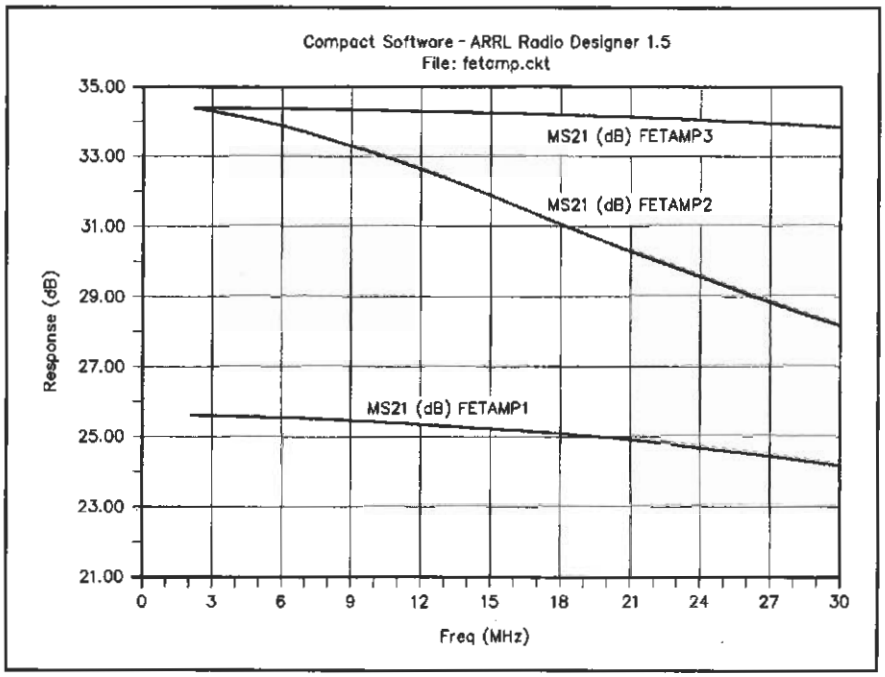

Fig B—The analysis results.

eral hours. The MOSFETs well separated on a good heat sink and with efficient airflow do not have a temperature-controlled gate-bias arrangement because I did not find it necessary at this power level. Because of the spread in threshold voltage of individual matched pairs, a one-time adjustment of gate bias is needed. The following simple procedure is used:

- Replace R21 with a resistor decade box set at 750 11.
- Place a 0-10 A meter in the +40-V line.
- With *no* signal input, switch on the amplifier and let the current reach its final value, which should reach about 1.5 A as the FETs warm up.
- Adjust the resistor value until DD is 1.5 A. After each adjustment, allow time for the FETs to reach a steady current value. This final value is not critical, but should be within 10%.
- Check the two-tone IMD at 100 W PEP (50 W average) and make further small changes, if needed, to resemble the IMD patterns in Fig 2.

In this amplifier, we are able to use the self-limiting feature of the MOSFET. This approach would not be appropriate in higher-power, higher-temperature amplifiers because of thermal runaway possibilities, where the decrease with temperature rise of the gate threshold voltage exceeds the decrease of the dc transconductance.[12,13] If fan reliability is a concern, add a thermal cutout switch to the +40-V line.

Load Impedance

Swept- and fixed-frequency tests at many signal levels and voltage valuesusing various values of parallel conductance and capacitive/inductive susceptancedid not reveal instability problems at SWR values less than 2:1. A tendency to oscillate in a peculiar manner occurred in the 20.0 to 29.7 MHz range, but only with input signal applied (a driven oscillation) and certain values of drive level, supply voltages less than 30 V, SWR of 3:1 or more, and a certain range of shunt capacitance at the output of the amplifier itself or at the output of the 12/10 meter diplexer. The instability shows up as a Christmas tree pattern in which discrete, uniformly-spaced 2- to 4-MHz sidebands appear on the main carrier. It is due to a parametric effect[14] involving the voltage-variable capacitances of the MOSFET transistors that is somehow enhanced by the shunt test capacitance. Shunt inductance did not produce the problem. The amplitude modulation of the carrier by the low-frequency oscillation is clearly visible on an oscilloscope. The low-frequency oscillation itself can be seen on a spectrum analyzer. At SWR values less than 2:1 and drain voltages greater than 35 V (40 V is recommended), the safety margin is large. The 0.22-μH,

56-pF network at the output greatly assisted with this problem. A coax cable from the PA to the diplexer assembly that is a foot or less duplicates my test setup. Under these conditions, there is no stability problem on any band caused by load-impedance values that my testing could identify. Actually, a resistive load between 45 Ω and 55 Ω is recommended for best SSB linearity, as mentioned previously. While driving a high-power linear amplifier to its rated two-tone SSB output, adjust its input impedance to 50 Ω resistive as closely as possible on each band, using a 50-Ω directional wattmeter. A broadband (untuned) solid-state driver amplifier such as this one requires such attention to load value for best results as compared to pi-network vacuum-tube PAs that can transform a fairly wide range of complex load impedance values to the correct tube plate load resistance at resonance.

It is difficult to achieve stability in a broadband, transistor power amplifier. Having done so, it is still wise to operate into the correct 50-Ω load as closely as possible. The monitoring of forward and reflected power in Fig 9 is helpful for this and assures clean, stable and reliable operation. This circuitry will cut back the drive level to a value that protects the output stage from excessive drain current or gate drive. Incidentally, the first stage goes into saturation far below the level that would damage the MOSFETs.

System Design

Fig 9 suggests a system implementation of the amplifier. For the flattest frequency response of the complete system from 1.8 to 29.7 MHz, the circuitry that drives this amplifier should also have a flat response and a 50-Ω output resistance—both easy to achieve. If it is not perfectly flat or not exactly 50 Ω, it may be necessary to slightly adjust the drive level on each band, which is not difficult. As mentioned before, the second-harmonic production of the circuitry preceding this amplifier must be of sufficiently low level (50 dBc) that balanced, push-pull operation is necessary. Narrow-band resonator filters are also very commonly used for amateur-band harmonic reduction in low-level exciter circuitry.[15,16]

The directional coupler detects excessive forward and reflected power. Both of these are displayed on a panel meter. The directional couplers forward port is also a

Parts List

C1—160 pF SM
C2, 3, 6, 7, 10-12, 14, 20-23—0.1 µF, 50-V CK05
C4, 8—0.0033 µF, 50-V CKO5
C5, 9—0.047 µF, 50-V CKO5
C13, 25, 26, 28—1.0 µF, 35-V tantalum
C15, 16, 18, 19—0.022 µF, 100-V CK05
C17—56 pF SM
C24—0.1 µF, 100-V CKO5
C27—470 µF, 35-V aluminum
C29—470 µF, 15-V aluminum
D1—1N4454A or equivalent
L1, 2—0.68 µH, T50-2 core, 10 turns #26 AWG
L3—0.80 µH, T50-2 core, 12 turns #26 AWG
L4—BN-43-3312, 4½ turns #22 hookup wire
L5, 8—2.7 µH molded
L6—0.22 µH, T50-2 core, 5 turns #26
L7—2 FB-43-5621 cores, 1½ turns #12 stranded
Q1, 2—MRF426 matched pair
Q3, 4—MRF150 matched pair
Q5—2N3906 PNP
R1, 3—270 Ω, ¼ W, 5% tolerance
R2—18 Ω, ¼ W, 5% tolerance
R4, 9—178 Ω, ⅛ W metal film, 1% tolerance
R5, 8—3.9 Ω, ¼ W, 5% tolerance
R6, 7—12 Ω, ¼ W, 5% tolerance
R10—51 Ω, 2 W metal oxide
R11—100 Ω, 2 W metal oxide
R12, 16—51 Ω, 2 W metal oxide
R13, 17—100 Ω, 5 W metal oxide
R14, 15, 18, 19, 26, 27—562 Ω, ⅛ W metal film, 1% tolerance
R20—215 Ω, ⅛ W metal film 1% tolerance
R21—767 Ω, ⅛ W metal film 1% tolerance, test selected
R22—0.47 Ω, 5W wire-wound
R23—4.7 Ω, ¼ W 5% tolerance
R24—5.6 kΩ, ¼ W, 5%
R25—390 Ω, ¼ W, 5%
T1—BN-43-202, 2½ turns #32 AWG, bifilar
T2A, B—BN-43-202, 2½ turns #32 AWG, bifilar
T3A, B—BN-43-3312, 2½ turns 25-Ω miniature coax*
T4A, B—(2) FB-43-5621, 1½ turns 25-Ω miniature coax*
T5—(2) FB-43-5621, 2½ turns 50-Ω miniature coax
U1—LM317 adjustable voltage regulator

Notes

*Microdot D260-4ii8-0000 available from Communication Concepts, Inc.
All cores are available from Amidon.
Closely matched transistor pairs are from RF Parts (see Note 5).

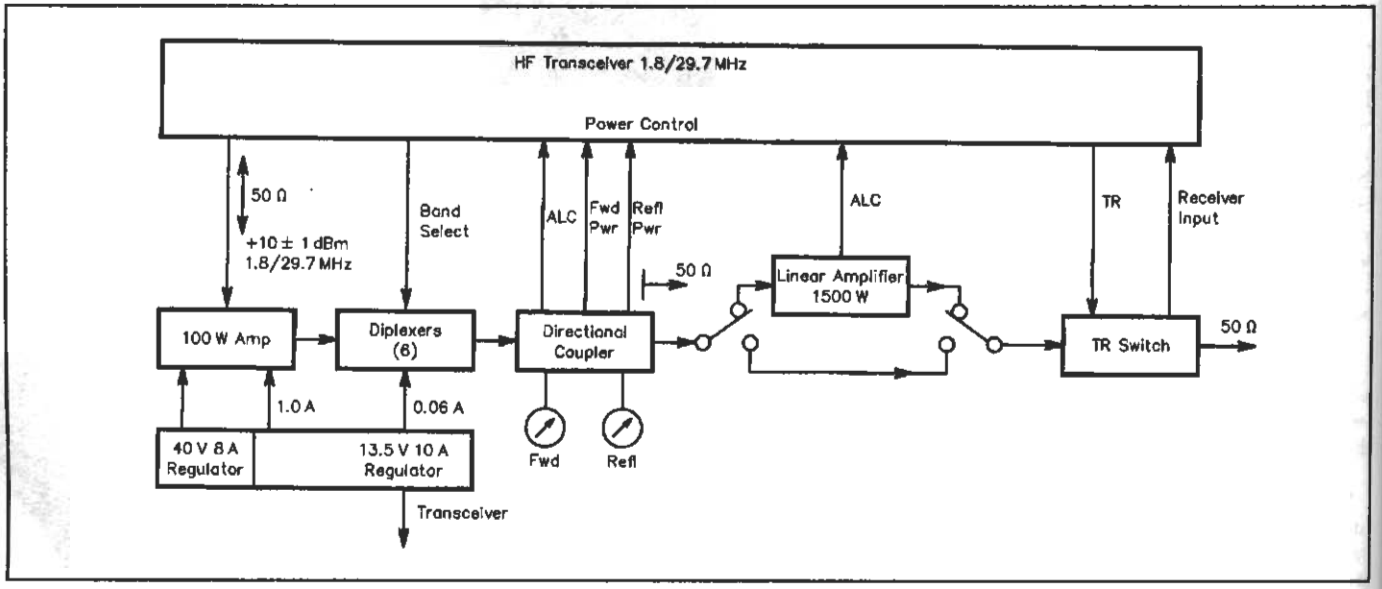

Fig 9—System implementation of the 100-W amplifier.

source of ALC voltage. These control voltages are fed back to the appropriate gain-controlled stages in the exciter. Gain control of the transistors in the 100-W amplifier is not recommended because changes in base or gate bias will degrade amplifier linearity, IMD products and possibly the flat frequency response. There are better ways to accomplish the gain-control task, such as preferably in a lowlevel IF amplifier. With respect to IMD, we are trying to control the odd-order curvature of the MOSFET transfer characteristic—especially for the higher-order products—by setting the gate-bias point. The bias value is found by looking at IMD on each amateur band and selecting the best compromise value. This was discussed previously in this article.

The diplexer filters are linked to the other band-switch circuitry so that the correct filter is always switched in. The TR relay is at the output of the diplexers. Do not hot-switch the diplexer filters because this might damage the inexpensive relays.

Conclusion

In conjunction with the power supply (see Note 1) and the diplexer filters (see Note 2), the amplifier described here is a basic module for homebrew equipment that should satisfy the requirements for a 100-W power level, a 1.8 to 29.7 MHz bandwidth and a high-quality signal. It should run trouble-free for a very long time. The initial cost of the four transistors is about $180, but they will last indefinitely if cared for properly. The ones that I use were abused considerably during the experimentation and continue to work perfectly. The approach that I suggest is best implemented with diplexer filters and a preamplifier that has very low second-harmonic output and low IMDboth easy to get at +10 dBm. The payoff for me is excellent performance and reliability, once the design was completed.

This project is suggested for the homebrew enthusiast who has at least some part-time access to lab-quality test equipment. Others who do not care to build may find the article, together with numerous other sources, interesting background information regarding MOSFET power-amplifier design and test methods.

Any attempt at building and testing this amplifier should also use the 40-V power supply in the referent of Note 1 or something similar. The automatic current limiting at 8 A, the automatic reduction of drain voltage, the short-circuit limiting to 4 A and the manual control down to 24 V help to protect the MOSFETs from mishaps that are bound to occur.

Notes

[1]W. Sabin, WØIYH, "Power Supply for a MOSFET Power Amplifier," *QEX*, Mar/Apr 1999, pp 50-54.

[2]W. Sabin, WØIYH, "Diplexer Filters for an HF MOSFET Power Amplifier," *QEX*, Jul/Aug 1999, pp 20-26.

[3]N. Dye and H. Granberg, *Radio Frequency Transistors* (New York: Butterworth-Heinemann, 1993), pp 42-43.

[4]W. Sabin and E. Schoenike, *HF Radio Systems and Circuits* (Tucker, Georgia: Noble Publishing Co, 1998), Chapter 12, Solid State Power Amplifiers, by R. Blocksome. This chapter is highly recommended regarding solid-state SSB power amplifiers. This book is also ARRL Order No. 7253. ARRL publications are available from your local ARRL dealer or directly from the ARRL. Mail orders to Pub Sales Dept, ARRL, 225 Main St, Newington, CT 06111-1494. You can call us toll-free at tel 888-277-5289; fax your order to 860-594- 0303; or send e-mail to **pubsales@arrl.org**. Check out the full ARRL publications line on the World Wide Web at **http://www.arrl.org/catalog**.

[5]RF Parts Co, 4355 Pacific St, San Marcos, CA 92069; tel 760-744-0700, 800-737-2787 (orders only), fax 760-744-1943; **rfp@rfparts.com**, **http://www.rfparts.com/**.

[6]Communication Concepts, Inc. (CCI), 508 Millstone Dr, Beavercreek, OH 45434; tel 937-426-8600, fax 937-429-3811; **cci.dayton@pobox.com**, **http://www. communication-concepts.com/**; ask for a catalog.

[7]*Motorola Wireless Semiconductor Solutions, Device Data*, Rev 9, Vol. II; Motorola #DL110/D. The data book is available from RF Parts (see Note 5). (A Motorola Selector Guide is available at **http://www.motsps.com/books/sguides/pdf/sg46rev18.pdf**. There is a MRF150 page at **http://www.mot-sps.com/products/rf_and_if/rf_transistors/high_power/power_mosfets/mrf150.html**. A MRF426 datasheet (MRF426/D)is available at **http://www.zettweb.com/CDROMs/cdrom013/pdf/mrf426rev0.pdf**, which is not a Motorola site—*Ed.*)

[8]Dye and Granberg, pp 113-115.

[9]*Motorola Wireless Semiconductor Solutions*; see pp 4.2-133 for the MRF151, similar to the MRF150. (See Note 7 for an MRF150 URL—*Ed.*)

[10]Dye and Granberg, Chapter 12.

[11]The set of boards costs $12 plus shipping and handling. FAR Circuits, 18N640 Field Ct, Dundee, IL 60118-9269; tel 847-836-9148 (Voice mail), fax 847-836-9148 (same as voice mail); **farcir@ais.net**, **http://www.cl.ais.net/farcir/**.

[12]Dye and Granberg, Chapter 4.

[13]H. Granberg, Wideband RF Power Amplifier, *RF design*, Feb 1988; also *Motorola RF Application Reports*, AR313, p 424.

[14]Dye and Granberg, similar top 124, Fig 7.7.

[15]*The ARRL Handbook* (Newington, CT: 1995-2000 editions), ARRL Order No. 1832; pp 17.60–17.66 and Fig 17.69. See Note 4 for purchasing information.

[16]W. Sabin, WØIYH, "Designing Narrow Band-Pass Filters with a BASIC Program," *QST*, May 1983, pp 23-29.

By Jim Valdes, WA1GPO

From *QST*, June 2003

The FARA HF Project

Would you like an economical and relatively easy to build 30 W HF amplifier? For about $130 worth of parts you can give that QRP rig an extra 12 dB of muscle!

One of the larger and more active radio clubs in the Cape Cod, Massachusetts area is the Falmouth Amateur Radio Association (FARA). Some of its members are affectionately referred to as the "hackers"—those who enjoy the construction phase of Amateur Radio. The renewed interest in low power (QRP) radios in the 2 to 5 W output range resulted in the desire for a 10 to 12 dB gain RF linear amplifier producing 30 to 40 W of output power. Commercial amplifiers capable of being driven with less than 50 W below 30 MHz are prohibited by FCC regulations.[1] As a radio amateur, you are permitted to construct one amplifier per year for your personal use. The amplifier described here is relatively easy to fabricate, given a basic knowledge of electronics and some familiarity with hand tools. This article describes in detail the construction of a 12 dB, nominal 30 W output, 1.8 to 30 MHz RF power amplifier. It is intended for 12 to 14.7 V dc operation, making it ideal for mobile use.

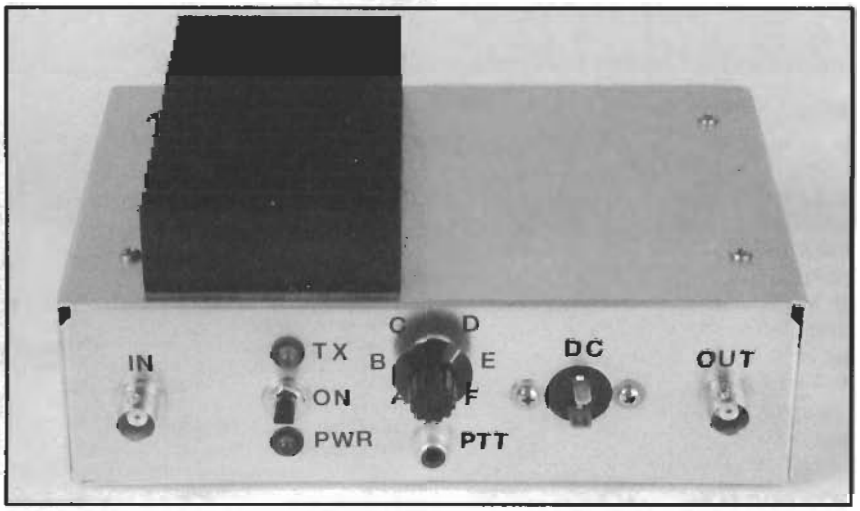

Figure 1—The completed 30 W amplifier. The band switch takes care of output low-pass filter switching.

Amplifier Description

The design of the amplifier is based upon common engineering practices. Ideas gathered from researching the handbooks published by the ARRL and The Radio Society of Great Britain (RSGB), as well as articles published in *QST* and other journals formed the basis of the design. This amplifier uses readily available components...many of the earlier designs were based on the Motorola MRF series of RF devices that are no longer available or are prohibitively expensive.

The amplifier is housed in a 5 × 7 × 2 inch aluminum box. It consists of two stacked circuit boards—an RF amplifier and a low-pass filter. The completed amplifier is shown in Figure 1. Figure 2 is the schematic diagram of the RF assembly together with the amplifier and low-pass filter parts list and Figure 3 is the low-pass filter schematic. The amplifier can be driven by 2 to 5 W at the RF input; an input attenuator consisting of R1, R2 and R3 must be selected (as noted in Figure 2) to ensure the proper drive level (2 W) for the push-pull (2SC2312C device types) class AB amplifier stage. T1 is wound on a small binocular core with a 4:1 ratio as detailed on the schematic. The low impedance secondary is a single turn center tapped; it carries the bias voltage to the output transistors. The bias voltage is derived from the LM317 regulator, which is operated as a switched current source. The LM317 is switched on when the internal PTT line is activated. Bias voltage is developed across the FES8J diode, which is in intimate thermal contact with the output transistors. The output transformer (T2) is also wound with a 4:1 ratio; it has a single-turn sense winding. The single-turn feedback winding provides some degree of negative feedback to flatten the gain and stabilize the input impedance over the HF frequency range. The RC network in the input base circuit establishes the overall gain. The 6.8 W series resistors determine the gain below 14 MHz, while the 4700 pF capacitors are effective above 14 MHz.

Figure 4 shows the output power versus frequency characteristics of the amplifier, including the second and third harmonic response. All measurements were made with an IFR1600S Communications Service Monitor. In all cases, harmonics were greater than 40 dB down referenced to the fundamental frequency (–40 dBc), and the amplifier meets current FCC requirements for spectral purity.[2] Note that the gain starts to decrease above 21 MHz, rolling off from a nominal 30 W to 20 W at 29 MHz. On 10 meters this still represents 10 dB of gain, a worthwhile improvement. The dc voltage to the output transistors is decoupled by the pi network at the center-tapped primary of the output transformer, T2. This winding carries substantial current and should be wound with #18 Teflon covered wire. Any IR drop in the dc circuit will severely degrade the amplifier performance. TR switching is provided by relay K1. The PTT line can be operated manually (pulled to ground) or RF activated switching circuitry can be installed to eliminate the need for external keying controls. The value of C12 (3.3 µF) determines the SSB time constant for the RF activated switch.

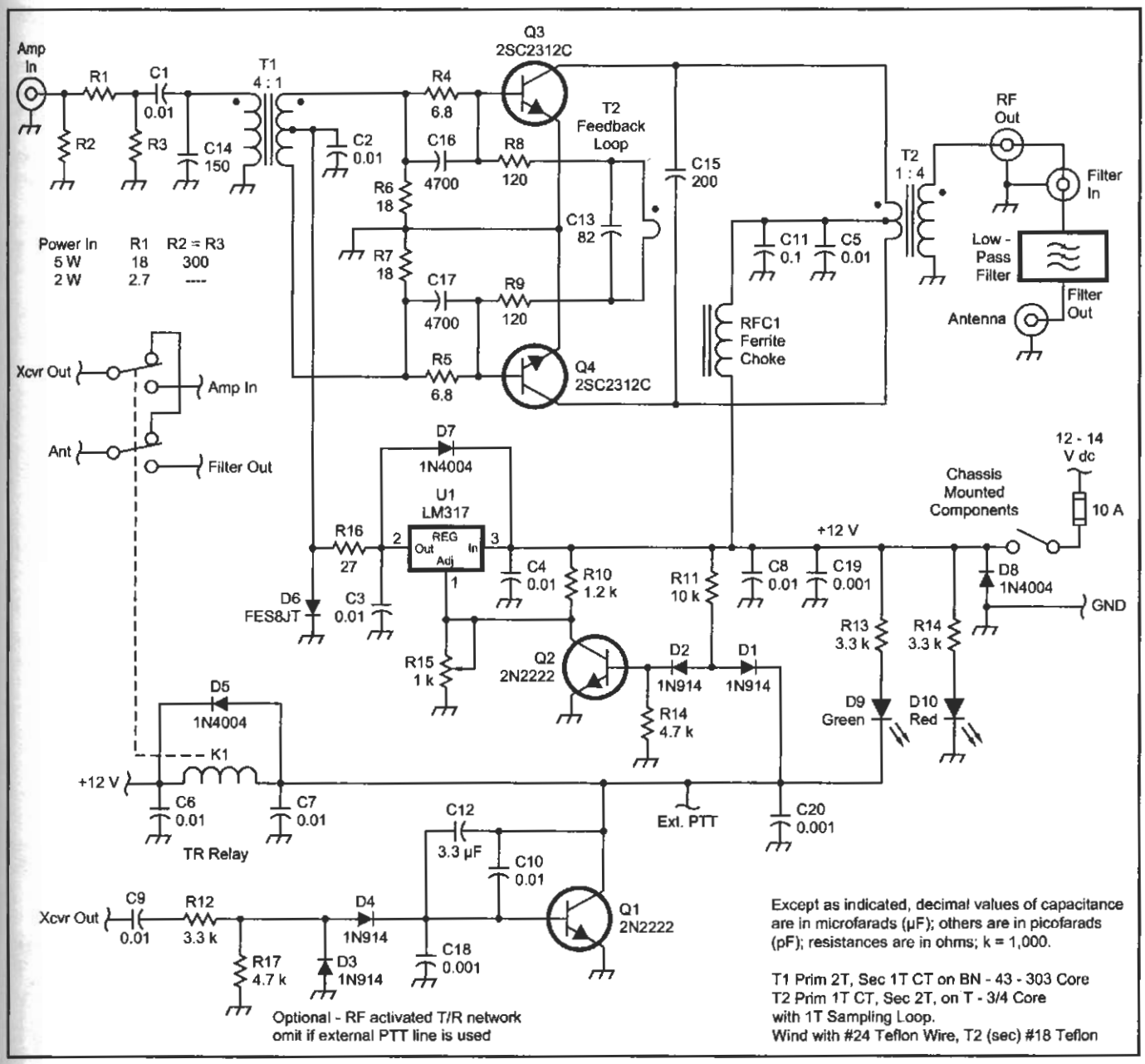

Figure 2—The RF amplifier schematic and parts list. (M) denotes Mouser Electronics, 1000 N Main St, Mansfield, TX 76063; tel 800-346-6873; **www.mouser.com**. (RF) denotes RF Parts Co, 435 S Pacific St, San Marcos, CA 92069; tel 800-737-2787; **www.rfparts.com**. (A) denotes Amidon, Inc, 240 Briggs Ave, Costa Mesa, CA 92626; tel 800-898-1883; **www.amidon-inductive.com**. (F) denotes FAR Circuits, 18N640 Field Ct, Dundee, IL 60118; tel 847-836-9148; **www.farcircuits.net**.

RF Amplifier Board
C1-10—0.01 µF capacitor, (M) 140-100Z5-103Z.
C11—0.1 µF capacitor, (M) 80-CK06BX104K.
C12—3.3 µF capacitor, (M) 80-C340C335M5U.
C13—82 pF capacitor, (M) 5982-15-500V82.
C14—150 pF capacitor, (M) 5982-15-500V150.
C15—200 pF capacitor, (M) 5982-15-500V200.
C16, 17—4700 pF capacitor, (M) 140-50P5-472K-TB.
C18-20—0.001 µF capacitor, (M) 140-100Z5-102Z.
D1-D4—1N914 diode, (M) 610-1N914.
D5, D7, D8—1N4004 diode, (M) 583-1N4004.
D6—FES8JT diode, (M) 625-FES8JT.
D9—LED, green, with mount, (M) 512-HLMP4719.
D10—LED, red, with mount, (M) 512-HLMP4700.
K1—Relay, 12 V dc coil, DPDT, (M) 551-MR-12USR.
Q1, Q2—Transistor, switching, 2N2222, (M) 511-2N2222A.
Q3, Q4—Transistor, RF, 2SC2312C, (RF) 2SC2312C.
R1—300 Ω, 1 W, (M) 281-300.
R2, R3—18 Ω, 1 W, (M) 281-18.
R4, R5—6.8 Ω, ¼ W, (M) 30BJ250-6.8.
R6, R7—18 Ω, ¼ W, (M) 30BJ250-18.
R8, R9—120 Ω, ¼ W, (M) 30BY250-120.
R10—1.2 kΩ, ¼ W, (M) 30BJ250-1.2K.
R11—10 kΩ, ¼ W, (M) 30BJ250-10K.
R12-14—3.3 kΩ, ¼ W, (M) 30BJ250-3.3K.
R15—1 kΩ, potentiometer, (M) 531-PTC10H-1K.
R16—27 Ω, 1 W, (M) 281-27.
R17—4.7 kΩ, ¼ W, (M) 30BJ250-4.7K.
RFC1—RF choke, (RF) VK-200-3R.
T1—Transformer core, (A) BN-43-303.
T2—Transformer core, (RF) T-¾ core.
U1—IC, LM317T, (M) 512-LM317T.

Misc
2—TO-220 mounting kit, (M) 534-4724.
2—TO-220 thermal insulator pad, (M) 526-NTETP0006.
PC board, FARA RF amplifier, (F).

Low-Pass Filter Board
(see Figure 3 for component delineation)
2—100 pF capacitor, (M) 5982-15-500V100.
3—180 pF capacitor, (M) 5982-15-500V180.
3—330 pF capacitor, (M) 5982-15-500V330.
2—430 pF capacitor, (M) 5982-15-500V430.
1—560 pF capacitor, (M) 5982-15-500V560.
3—820 pF capacitor, (M) 5982-15-500V820.
3—1500 pF capacitor, (M) 5982-19-500V1500.
1—2700 pF capacitor, (M) 5982-19-500V2700.
12—0.01 µF capacitor, (M) 140-100Z5-102Z.

[continued on next page]

[continuation of Figure 2]

12—Relay, 12 V dc coil, DPDT, (M) 655-T7NS5D1-12.
1—Switch, 1 pole, 6 pos, (M) 10-YXX026.
HF Filter Kit, (A) HFFLT. Contains the cores and wire necessary to build the low-pass filters.
PC board, FARA LP Filter, (F).

Chassis Parts

Chassis box, Bud, (M) 563-AC-402.
Chassis cover, Bud, (M) 563-BPA-1589.
Heat sink, (M) 532-244609B02.
4—4-40 hex-type standoff, (M) 534-2201.
9—4-40 × ¼ pan head screw.
4—4-40 × ½ pan head screw.
6—4-40 flat washer.
9—4-40 lock washer.
2—4-40 nut.
2—8-32 × ¼ pan head screw.
2—8-32 lock washer.
2—BNC socket, chassis mount, (M) 161-9323.
RCA-type socket, female, chassis mount, (M) 161-1005.
Switch, toggle, SPDT, (M) 10TC320.
Jones-type socket, chassis mount, male, 2 pin, polarized, (M) 538-13023.

The low-pass filter assembly utilizes relays to select the proper filter network for the various frequency ranges. Relays were chosen to simplify the RF switching and to minimize cost. The six filters cover the nine amateur bands from 1.8 to 30 MHz; the frequency ranges and circuit constants are as noted on the LPF schematic diagram. The inductor cores and wire to wind the coils are available as a kit of parts from Amidon.[3] The L/C constants are the same as those recommended by WA2EBY for the MOSFET RF amplifier in *The ARRL Handbook*.[4] The filters are not used when the amplifier is off or when the PTT line is not activated—this permits multi-band listening and limited VHF use when a wide frequency transceiver is in use (like the Yaesu FT-817). There is no provision for ALC feedback, so caution must be exercised so as not to overdrive the amplifier.

Construction Hints

Although no step-by-step instructions are provided, a few hints will ease the assembly process. The circuit boards pictured are the prototype assemblies; they are not solder-plated. However, the available circuit boards (from FAR Circuits) are plated but do not have plated through-holes, so through-holes must be pinned and soldered.[5] Detailed drawings of the PC boards, the parts layout, coil-winding data and chassis templates can be found at **www.arrl.org/files/qst-binaries/faraamp.zip**. Saul, K1BI, the FARA Webmaster has also set up a site for the project. It can be found at **www.falara.org/tektalk/tektalkfs.html**. The circuit boards as they appear before wiring can be seen in Figure 5.

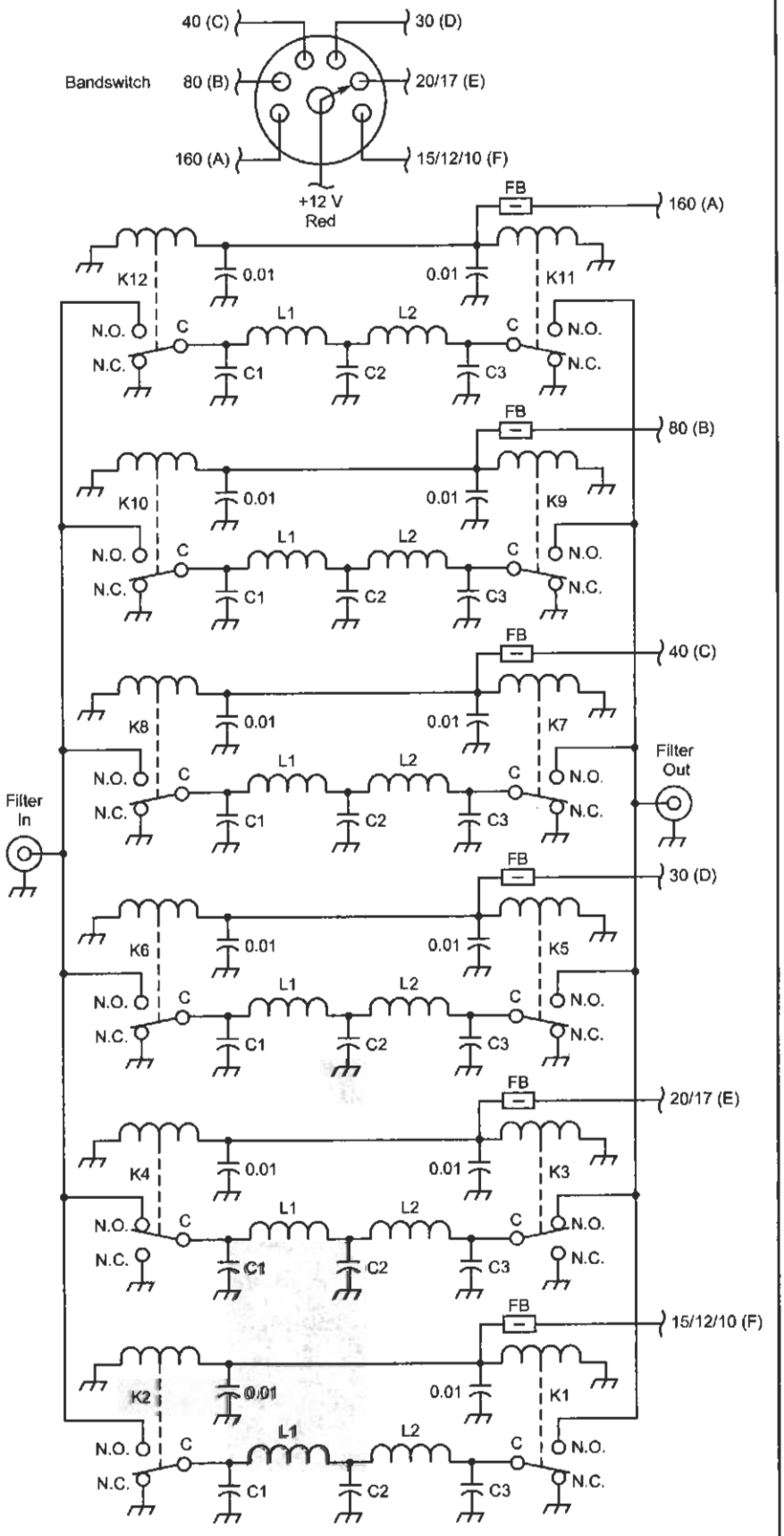

Cores T - 50 - X Amidon
L in number of turns (#22)
C in pF
Band (E) Shown Selected.
K3, K4 Energized.

Band	L1/2	C1/3	C2	Core
160 (A)	30	1500	2700	2
80 (B)	22	820	1500	2
40 (C)	16	430	820	2
30 (D)	14	330	560	2
20 - 17 (E)	11	180	330	6
15 - 10 (F)	8	100	180	6

Figure 3—The low pass filter (LPF) schematic.

Circuit Board Preparation

• Given the large ground plane area, the boards must be clean or you will experience difficulty when soldering to the foil. Plated boards are best; they are easier to solder. Some solder flux may improve the solderability of the board, but be sure to use *only* rosin core solder and a *non-corrosive* flux.

• Carefully inspect all soldered connections for cold solder joints. Good soldering technique is crucial to the performance of the amplifier.

• Periodically, the flux should be removed from the board during the construction phase with a suitable chemical cleaner.

• There are a number of holes to be drilled and pinned on each board; these are noted on the parts placements diagrams. Wires should be inserted through the board, bent into the shape of a "Z," formed flat against the board, soldered and cut.

• The four corner holes on each board must be sized as a clearance hole for the 4-40 mounting hardware.

• Components should be mounted flush to the board—fixed capacitors should be mounted as close to the foil as possible.

• The large rectangular blocks on the RF board must be trimmed in order to mount the RF output transistors and the bias diode.

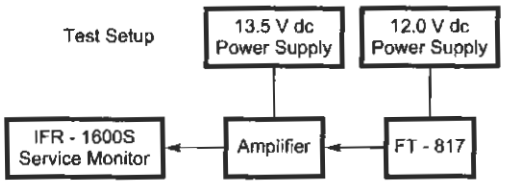

FT - 817, Power Output = 4.6 Watts ± .2 W (with −3 dB Pad)

FARA Amplifier Output Characteristics

Frequency (MHz)	RF Output (W)	2nd Harmonic (dB)	3rd Harmonic (dB)
1.8	23	−44	−43
3.5	33	−55	−63
7.2	33	−60	−50
10.1	28	−62	−45
14.2	31	−60	−50
18.1	31	−60	−52
21.2	30	−50	−47
24.9	25	−60	−53
28.4	21	−60	−56

Figure 4—Amplifier output data, including second and third harmonic response.

RF Amplifier Circuit Board

A view of the completed RF board can be seen in Figure 6. The following suggestions pertain to the amplifier board.

• Wind the secondary winding on T2 and mount it to the circuit board first.

• The emitters of the 2SC2312s (Q3, Q4) are intended to be grounded through a hole on the pad. The following modification is advised—bend a thin brass or copper strap into a "U" shape and solder it on both sides of the board. This lowers the impedance to ground.

• Next, mount the smaller fixed components, the resistors and capacitors.

• The semiconductors and the relay mount last.

• Do not mount D6, Q3 and Q4 until the assembly is fixed in the chassis and positioned relative to the heat sink.

Low-Pass Filter Circuit Board

This is a double-sided board; the reverse side is a ground plane with clearance etches for the various components. The LPF board can be seen in Figure 7. It may be necessary to form the capacitor leads slightly to conform to the hole spacing.

• Mount the filter components first, followed by the bypass capacitors and the jumper wires. Refer to the schematic for component values by frequency range.

• The relays mount last. Do not overheat their mounting pins when soldering.

• Do not mount the LPF assembly until the initial tune-up is completed. It is recommended that you pre-wire the band switch. It mounts between the two circuit boards when they are installed in the chas-

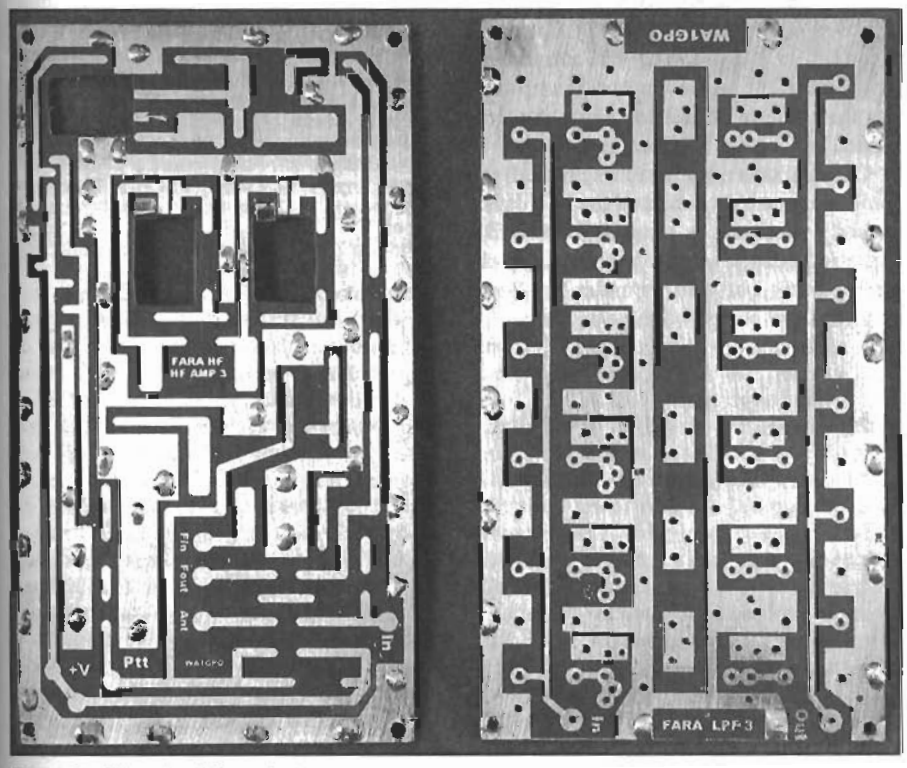

Figure 5—The circuit boards before wiring. The RF board is on the left and the LPF board is to the right. Note the pinned and soldered holes.

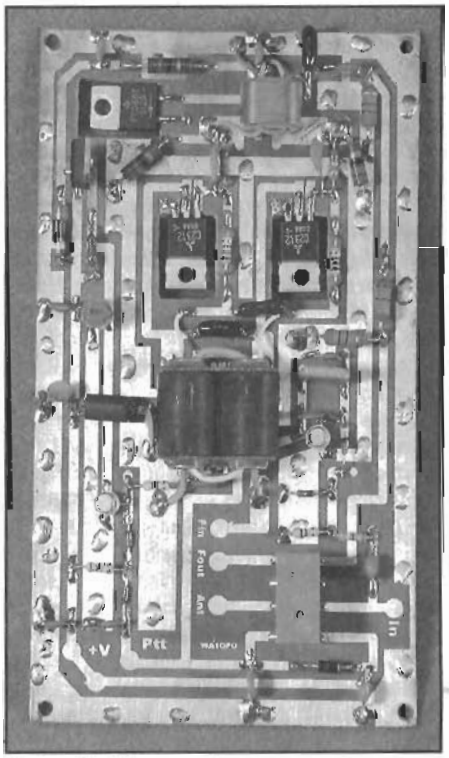

Figure 6—The completed RF assembly board.

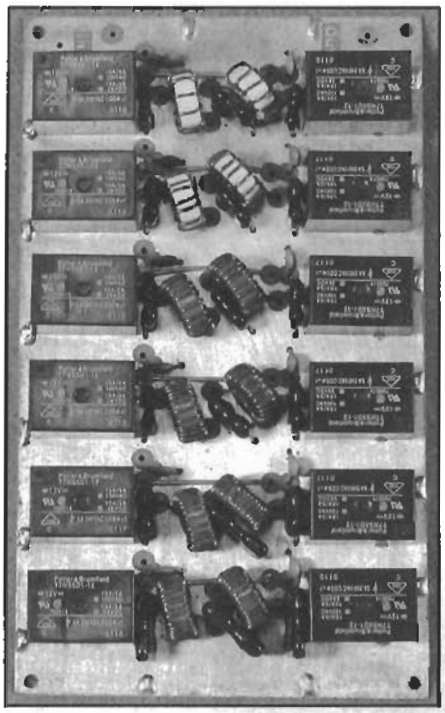

Figure 7—The completed LPF board. Note the relays that are used as filter switches—they are selected by the band switch.

sis and it is difficult to get to.

Chassis, Panel and Heat Sink

Full size templates for the chassis and panel can be found on the Web site. Trim the templates to size and fold and tape them to the aluminum box and heat sink. It is important to center punch the holes and drill a small pilot hole at each location. Enlarge the holes to size according to the dimensions. Letter the panel with dry transfer lettering available at office supply stores. Spray on several light coats of clear lacquer to protect the lettering. Mount the heat sink and the panel components, but do not mount the bandswitch at this time. Mount the RF amplifier board using a couple of 4-40 flat washers as spacers between the chassis and the circuit board at each corner. Install the 4-40 standoffs to hold the assembly in place. Mount D6, Q3 and Q4, using the TO-220 thermal pads and hardware to isolate the transistor mounting tab from the chassis. It is not necessary to isolate D6. Use RG-174 miniature coaxial cable for the internal RF connections.

Tune-up and Testing

As this is a broadband design there is no tune-up; only the bias adjustment needs to be set. A 12 to 14 V dc current limited variable supply is recommended for initial adjustment and testing. Use a dummy load at the amplifier output. Drive levels refer to the attenuator output, if used.

- Connect a temporary jumper between the F_{in} and F_{out} pads on the RF board.
- Preset R15 (1 kΩ potentiometer) so that the wiper is at ground.
- Apply 12 V dc and ground the PTT line (the relay should pull in).
- Briefly drive the input with 1 W at 14 MHz and note the power output.
- Again apply 1 W and increase bias (R15) until the output increases about 15%.
- Increase drive to 2 W and note the power output (about 25 W).
- Increase voltage to 14.7 V dc; note the output with 2 W of drive (about 35 W).

Remove power; remove the temporary jumper; mount the band switch; connect and install the LPF board. Verify that the power output over the range of 1.8 to 29 MHz is as expected. A view inside the bottom of the amplifier, with the LPF board visible, is shown in Figure 8.

Final Comments

The FCC has placed strict limitations on power amplifiers used below 30 MHz. Please review the appropriate FCC regulations before constructing this amplifier.[6] Kits offered for sale, even partial amplifier kits that require additional parts, are prohibited by current FCC regulations.[7]

Construction time, assuming that all the components are on hand and the boards are properly prepared, is about 4 hours. SSB operation results in the heat sink barely getting warm, and cooling under key-down conditions is more than adequate.

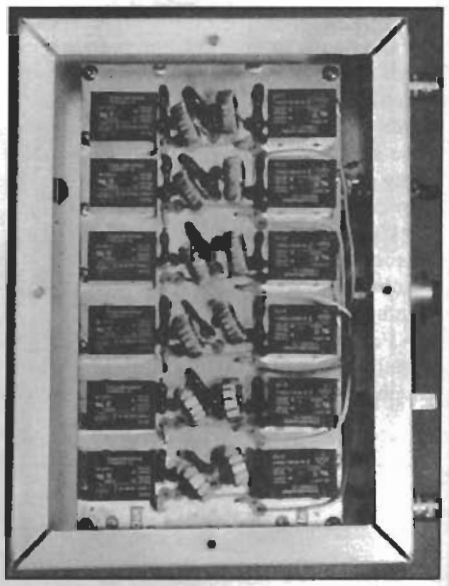

Figure 8—A bottom view inside the completed amplifier. The LPF board is mounted below the RF assembly.

A project of this scope is more fun when others participate. Harry, W2RKB, provided the necessary prodding to get it started. He also fabricated the circuit boards and the filter assemblies for the prototype amplifiers. Dave Hosom assisted with the photographs. A generous thank you is extended to them both. Give the FARA amplifier a try... it's a practical and rewarding project!

Notes

[1]Federal Communications Commission, Sec 97.315.
[2]See Note 1.
[3]Amidon Associates, Inc, 240 Briggs Ave, Costa Mesa, CA 92626; 800-898-1883; **www.amidon-inductive.com**.
[4]*The 2003 ARRL Handbook*, pp 17.91-17.97.
[5]FAR Circuits, 18N640 Field Court, Dundee, IL 60118; tel 847-836-9148; **www.farcircuits.net**.
[6]Federal Communications Commission, Sec 97.3 (19).
[7]See Note 6.

By Pat Bunn, N4LTA

From *QST*, October 1990

A Compact "Brick" for 6 Meters

Does your six-meter signal need some extra kick? This inexpensive amplifier bridges the gap from 10 to 100 watts.

Most transceivers available for the 6-meter band provide 10 W output. This power level provides satisfactory communications during good sporadic-E openings, but is not adequate for making long-haul contacts on meteor scatter or during F-layer openings. For the average station, an output level of 100 W seems to be a reasonable compromise between a 10-W exciter and a kilowatt amplifier. Unfortunately, 50-MHz amplifiers in this power class are not readily available.

I began operating on the 6-meter band a few years ago, near the lowest point in sunspot cycle 21. Sporadic E kept my interest high, and soon it became evident that I needed an amplifier. Being a builder at heart, I decided to "roll my own" and began to search the Amateur Radio literature for design examples. I found very few solid-state amplifiers, and only one in the 100-W class.[1]

I built the amplifier as specified, and I got good results. My 6-meter effectiveness made a quantum leap! One highlight was working Europe with a 12-foot-boom Yagi. The amplifier performed so well that several of my friends asked me to build them duplicates of it. With each revision, I tried to add design innovations, including on-board TR relays, a carrier-operated-relay (COR) circuit and transistor biasing, as well as low-pass filtering and more compact packaging. The product of these efforts is described in this article. At least 25 of these units have been constructed and are now in use. Several of these amplifiers have been used on DXpeditions, in beacon service, and as drivers for kilowatt-class amplifiers, and results have been excellent.

If you are looking for a low-cost 100-W amplifier, this proven design would make a nice addition to your 6-meter station. This circuit can also be adapted for use with an MRF140 FET, which produces over 160 W output with less than 10 W drive. See the sidebar for more details.

Circuit Highlights

The amplifier circuit, shown in Fig 1, is a single-stage, 10-dB-gain, class-B design using the popular Motorola MRF492 transistor. The RF circuitry is based on a test circuit in Motorola's RF Device Data book.[2] Input and output impedance matching is done with low-Q lumped circuits rather than with broadband transformers. The amplifier's bandwidth is about 1.5 MHz, which covers the DX portion of the 6-meter band with plenty to spare. And, the output network has a secondary dip at about 53 MHz, allowing CW/SSB work and FM operation without the need to retune the amplifier. The narrowband nature of the matching networks helps reduce harmonics. A half-wave low-pass filter in the output circuit further reduces harmonic content to meet current FCC specifications (see Fig 2).

The COR circuit is based on a high-gain operational amplifier that provides the sensitivity required for SSB operation. This circuit is much more effective than the Darlington-transistor COR circuits found in most commercial amplifiers. It works well with low-power SSB rigs that do not have easily accessible PTT lines, although a separate PTT input is also included.

The amplifier PC board[3] is mounted in a die-cast aluminum box (Hammond 1590R, Bud CU-247 or Jameco® part no. B5006) with an extruded-aluminum heat sink bolted to the bottom. (I used a 6-inch length of Wakefield no. 1527 heat sink. Any aluminum heat sink with similar dimensions should work fine.) The completed amplifier is operated inverted, with the removable lid serving as the bottom. The enclosure is painted flat black and labeled with white rub-on lettering. Stick-on rubber feet are attached at the corners of the bottom cover. The finished product

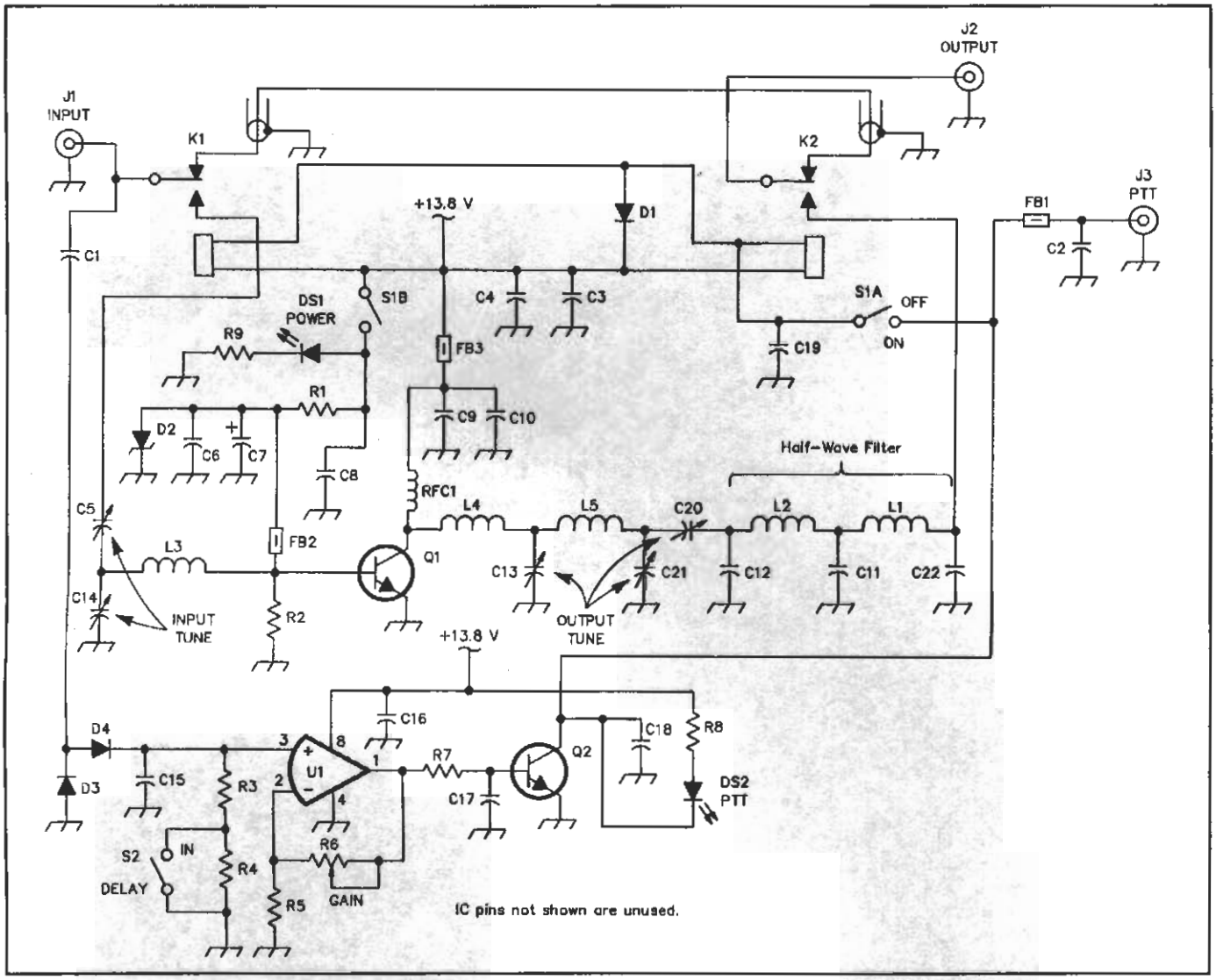

Fig 1—Schematic of the 100-W 6-meter amplifier. Liberal use of bypass capacitors and ferrite beads helps ensure stability and keeps RF out of the power supply.

C1—10 pF, ceramic disc.
C2—0.01 µF, polyester film.
C3, C10—0.001 µF, ceramic disc.
C4, C6, C8, C9, C15-C19—0.1 µF, polyester film.
C5—9- to 180-pF mica compression trimmer, Arco no. 463.
C7—1000 µF, 6.3 V, aluminum electrolytic.
Cli —120 pF, 100 V, silver mica.
C12, C22—62 pF, 100 V, silver mica.
C13, C14, C20—50- to 380-pF mica compression trimmer, Arco no. 465.
C21—25- to 280-pF mica compression trimmer, Arco no. 464.
D1—1N4002.
D2—1N1200 stud-mount diode.
D3, D4—1N4148.
DS1—Green LED.
DS2—Red LED.
FB1, FB3—Ferrite bead, Amidon no. FB43-901 or similar.
FB2—VK-200 wide-band choke, 2½ turns no. 24 solid wire on Amidon no. FB43-5111 ferrite core.
J1, J2—Female RF connector (UHF, BNC, N, etc).
J3—Phono jack.
K1, K2—SPDT relay, 12-V dc coil, Omron no. G5L112P-PS-DC1 2. Available from Digi-Key.
L1, L2—4 turns no. 14 enam wire, 7/16 in. diam, 3/8 in. long.
L3—2 turns no. 14 enam wire, 3/8 in. diam, 1/2 in. long.
L4—no. 14 U-shaped wire loop, 3/8 in. diam, 9/16 in. finished length.
Q1—MRF492.
Q2—2N2222A.
R1—5-W bias resistor (see text).
R2—10 Ω, ½ W, carbon comp.
R3, R5—10 kΩ, ¼ W, carbon comp.
R4—1 MΩ, ¼ W, carbon comp.
R6—100-kΩ PC-board potentiometer.
R7-R9—1 kΩ, ¼ W, carbon comp.
S1—DPDT miniature toggle.
S2—SPST miniature toggle.
U1—LM358.

Miscellaneous

Suitable die-cast-aluminum enclosure and heat sink.
Pair of binding posts or other suitable dc-supply connector.
Two 1- x 3-in. strips of double-sided foam tape.
Two LED holders.
Seven no. 4-40 x ¼ in. machine screws.

looks professional, and also does a good job of cooling the power transistor and bias diode.

Construction

The amplifier is assembled on a double-sided printed circuit board. All RF components are surface-mounted on the component side of the PC board (see Fig 3). The COR components, including the relays, connect to traces on the other side of the board. The remaining non-component-side foil serves as a ground plane, and is electrically connected to the component-side ground plane via platedthrough holes. If you make your own PC board, you can replace these plated-through holes with no. 18 AWG wires soldered to both sides of the board, or, preferably, copper rivets such as those available from Frontier Microwave and Down East Microwave.[4] The relays also mount in plated-through holes. The PC-board patterns and part-placement overlay are available from the ARRL Technical Department Secretary.[5]

Drill the case for the switches, connectors and indicators you'll use. Begin PC-

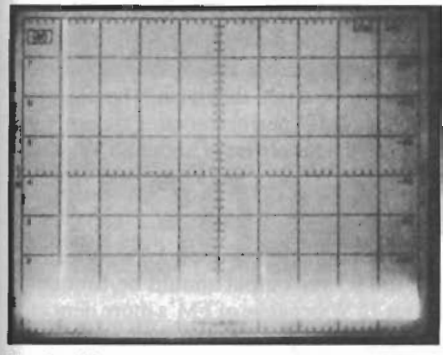

Fig 2—Worst-case spectral display of the 100-W 6-meter amplifier. Vertical divisions are each 10 dB; horizontal divisions are each 10 MHz. Output power was approximately 100 W at 50.2 MHz. All harmonics and spurious emissions are at least 60 dB below peak fundamental output when the amplifier is tuned as described in the text. The 100-W amplifier complies with current FCC specifications for spectral purity for equipment in this power-output class and frequency range. Better spectral purity can be obtained by using an external output filter (see the referent of note 1 for a suitable filter circuit).

board construction by mounting the parts that are soldered to traces on the other side of the board. This includes the COR parts and relays, the RG-174 jumper, and diode Dl. Make sure that the diodes and Q2 are properly oriented.

The solder-side parts are surface-mounted. Keep lead lengths to a minimum (no more than 1/4 inch) on these parts. The bypass capacitors should have the shortest possible leads, and should be surface-mounted on the PC board.

Wind the coils using 1/4- and 3/8-inch drill bits as temporary forms. Cut the coil leads to 1/4 inch, bend them 90°, scrape the insulation off the ends and solder the coils to the board. Some of the coils may need to be compressed or spread during tune-up to get maximum output power, so allow for this when mounting them. Use Fig 3 as a guide. Mount the mica trimmers by bending the solder tabs parallel to the board and surface-mounting them. (Some trimmers have extra tabs that may short to the PC board; I cut these off with side cutters Io eliminate this risk.) When surface-mounting the larger components, a high-wattage soldering gun is useful, but be careful: The traces may separate from the PC board if excessive heat is used.

When the PC board is complete, temporarily place the MRF492 in its mounting hole in the PC board, making sure to orient the transistor properly (the beveled lead is the collector). Place the PC board inside the box assembly. Carefully mark the transistor-mounting holes and the single PC-board mounting hole on the enclosure, through the PC board. Remove the PC board from the case, then drill and tap these holes for no. 4-40 hardware. Mark and drill the heat sink using the enclosure as a guide.

Drill and tap four more no. 4-40 holes, near the corners of the case, through the case and into the heat sink. Apply heat-sink compound between the die-cast box and the heat sink, then use no. 4-40 screws in these holes to secure the heat sink to the case.

Place the PC board into the case/heat-sink assembly again, and mark the location of the stud-mounted bias diode. Remove the board and drill and tap a 3/8-inch-deep no. 10-32 hole in the case/heat-sink assembly. The diode's threaded stud is more than 3/8 inch long, and should be carefully cut off (with a hacksaw) to 5/16 inch.

The rear of the PC board must be insulated from the box assembly, because many of the COR-circuit traces on the underside of the board are not at ground potential. I use 1/8-inch-thick double-sided foam tape to cover the solder-side traces and to support the board away from the case. Make sure the component leads are cut off closely at the rear of the PC board so that they don't punch through the foam tape and short to the box assembly. Mount the board inside the case, then screw the bias diode snugly into its mounting hole in the case/heat sink assembly.

Solder the MRF492 onto the board as the last step, *after* the transistor case has been mounted in the board and screwed into place. (This eliminates the possibility of cracking and ruining the $15 device!) Be sure to use a liberal amount of silicone heat-sink compound between the transistor and the box.

Mount the front-panel LEDs, switches and the RF connectors of your choice to the box. Any suitable RF connectors can be used. The connectors are wired to the PC board with no. 18 tinned bus-wire jumpers. Make these as short as possible. I used no. 24 insulated hookup wire to connect the switches and LEDs to the PC board. Finally, mount the dc-power binding posts to the rear panel. These are wired to the PC board with no. 18 bus wire run through FT-43-801 ferrite beads.

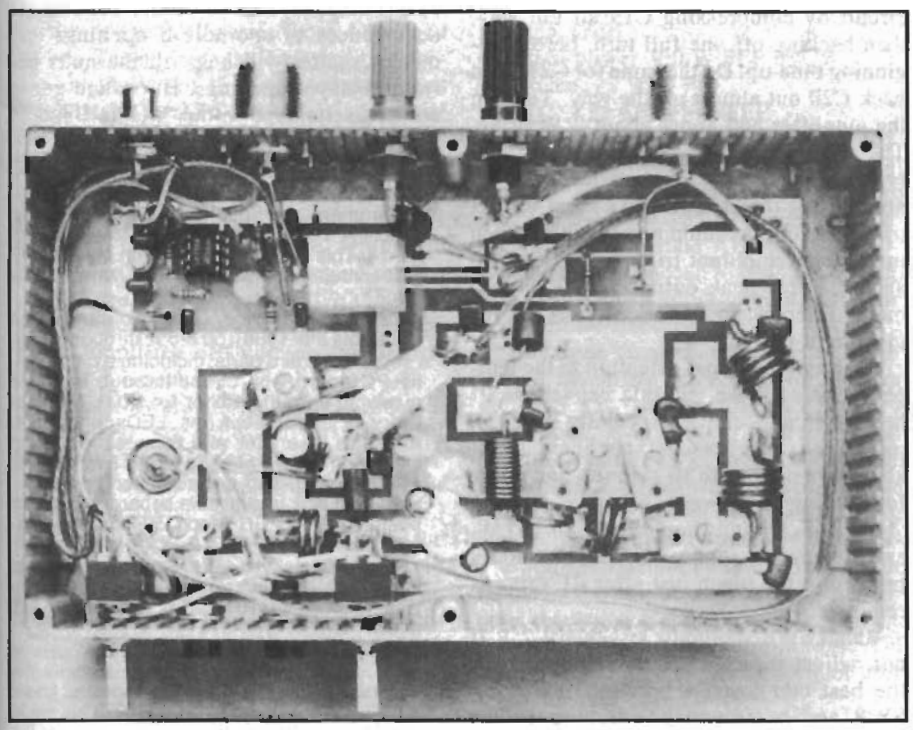

Fig 3—This inside view of the 100-W amplifier shows the circuit's simplicity. On the PC board, counterclockwise from upper left: the COR circuit; input-matching and bias networks, switches and indicators (lower left); MRF492 (lower center); collector choke and output network (lower right). The TA relays and connectors are at the upper center, and bias resistor R1 is just to the left of center.

Initial Testing

After the switches, LEDs and connectors have been wired, carefully check all connections. Make certain that the jumper from the PC board to bias diode D2 is connected! If all looks good, connect the amplifier to a 13.8-V power supply capable of sourcing 1 A. (If you have one, a small, current-limited power supply is best for testing.) If your power supply does not have reliable current metering, a meter capable of measuring 0-500 mA should be placed in series with the positive supply lead.

With the amplifier turned off, turn on the power supply. The meter should indicate 0. Turn on the amplifier and note the total indicated current. It should be between 50 and 300 mA. If it is much greater than 300 mA, quickly turn off the power supply and look for problems.

If the current is within these limits, you can go about setting the operating bias. This involves changing the value of RI until the collector current is between 75 and 175 mA. Note that this is not total circuit current, which includes the diode

Using a MOSFET to Get More Power from the Basic MRF492 Amplifier Circuit

The MRF492 amplifier circuit described in the main text is easily modified for use with an MRF140 VMOS power FET, which has about 15 dB gain and over 160 W output—substantially more than the MRF492. Even the device cases are the same, so the changes required to operate this circuit with an MRF140 are quite straightforward. Specific details of the modifications required, including a schematic diagram, are available from the author for an SASE.

The main differences between the devices are that the MRF140, a MOSFET, needs different biasing and a higher supply potential (28 V) than the MRF492, and is more expensive ($88 versus $15 for the MRF492, at this writing). But if you have a 28-V supply and need more than 100 W or have a 5-W exciter, the change is probably worthwhile. The MRF140 is easily biased with a three-terminal regulator (an LM317T works well), and requires very few component changes other than those in the bias circuit. An additional capacitor and inductor are also required at the MRF140's gate.

Because the modified amplifier requires a 24- to 28-V supply, different TR relays must be used, or, alternatively, 12-V-coil relays can be wired in series. (The COR circuit needs no modification because the LM358 works fine at 28 V.)

Good heat sinking is more critical to amplifier performance at the higher power level, so I used a 3- × 5- inch slab of 1/8-inch-thick copper between the device and the case as a heat spreader. A larger heat sink and/or forced-air cooling are also desirable.—*N4LTA*

current and POWER LED current. The best way to measure collector current is to lift FB3 and insert a milliammeter in series with the collector-supply lead at that location. An alternative method is to use the following equation to approximate collector current:

$$I_C = I_{TOTAL} - [(V_{R1} \div R1) + ([V_{CC} - 1] \div 1000)]$$

where

I_C = collector current in milliamperes
V_{R1} = measured voltage across R1
V_{CC} = measured supply voltage

This equation lets you calculate collector current by subtracting the current through R1 ($V_{R1} \div R_1$) and the current through the **POWER** LED ($[V_{CC} - 1] \div 1000$) from the total supply current.

Using either method, substitute different resistors at R1 until the collector current falls into the 75- to 175-mA range. In almost every case, a 5-W resistor of 82, 91, 100, 110, 120 or 130 Ω will bring the current into that region. (I have never had to substitute more than three resistors to arrive in this bias-current range.) These 5-W resistors can be purchased for less than $0.40 each, so, although a 200-Ω, 5-W wire-wound potentiometer could be used for R1, all six resistors can be purchased for far less. And, these days, high-wattage potentiometers are hard to find.

Tune-Up

When the bias current has been set, the amplifier can be initially tuned. For this procedure, the amplifier should be connected to a power supply capable of delivering at least 15 A at 13.8 V. A power meter capable of indicating at least 100 W at 50 MHz should be connected at the amplifier output, and the meter's output to a 50-Ω load. It is also desirable to measure input power from the exciter, as well as amplifier-input SWR, but these can be measured after initial tune-up if two meters aren't available.

Set the input-circuit trimmers (CS and C14) near midrange. Because the output circuit can be tuned several ways for the proper impedance transformation, it's important to preliminarily adjust the output circuit by compressing C13 all the way, then backing off one full turn, before beginning tune-up. Do the same for C21, then back C20 out almost all the way. Turn on the amplifier and apply about 2 W drive. The COR should sense the input RF and switch immediately into transmit. Using a nonmetallic tool, tune the two input-circuit trimmers for maximum power output, then tune the three output trimmers (C13, C20 and C21) for peak output. These adjustments interact, so continue tweaking for maximum power.

During tuning, pay attention to the temperatures of these variable capacitors. If heating is noticeable (especially in C13), reset these capacitors and start again. Limit key-down periods to 10 seconds, and allow for cooling in between. Increase drive to about 9 W. Output should be 95 to 105 W, and the output-tuning capacitors should be cool to the touch just after RF drive is removed.

Input SWR should be less than 1.2:1. If not, adjust the input-circuit trimmers for the best compromise between low input SWR and maximum power output. The amplifier is now ready for operation. Some MRF492s seem to be "hotter" (exhibit more gain) than others; I have seen some devices produce 115 W easily and others strain to put out 95 W. On the air, the difference is so slight that it can't be detected. For best IMD performance, I recommend running the amplifier at about 85 W output on SSB.

FM Operation

This amplifier also works well on FM, but the power output should be limited to about 75 W because of FM's more demanding duty cycle. As mentioned earlier, the amplifier's bandwidth characteristic is double-humped; if it's tuned up at 50.1 MHz, the second hump falls in the 53-MHz area, allowing for SSB and FM operation without retuning.

If the amplifier is to be used for beacon, CW or FM operation exclusively, I suggest you configure it for class-C operation. Efficiency in class-C operation is in the 72% range, versus 60% for class B. To configure the amplifier for class-C use, connect the inductor using FB2 (the multi-hole ferrite bead) from Q1's base to ground, and eliminate all of the other bias components, including D2. If you like, you can add a panel switch to change between class-C and class-B operation.

The amplifier should never be operated class C on SSB. Doing so results in severe distortion.

Conclusion

I hope that you enjoy building this project, and will be motivated to try 50-MHz operation. As I write this, Japanese stations are being worked on the East Coast, and all continents are frequently heard. In the years to come, the regular occurrences of sporadic-E openings and meteor scatter will help fill the nulls between F-layer openings. Hurry and get in on the excitement on the "Magic Band"!

Notes

[1]T. Tammaru, "A Solid-State 6-Meter Linear Amplifier You Can Build," *QST*, May 1982, pp 11-14. This circuit was based on an MRF492 test circuit in Motorola's *RF Device Data* book.

[2]*Motorola RF Device Data*, Fourth edition (Motorola Inc: 1986), pp 3-552 through 3-555.

[3]A set of PC-board parts, including a high-quality PC board with plated-through holes, is available from the author for $100 (UPS delivery included). Switches, LEDs, enclosure, terminals, heat sink and connectors are not included. The PC board alone is available for $17 postpaid, and a black anodized-aluminum heat sink is available separately for $12 postpaid. (The ARRL and *QST* in no way warrant this offer.)

[4]Frontier Microwave, AD 1, Box 467, Ottsville, PA 18942, evening tel 215-795-2648; Down East Microwave, RR 1, Box 2310, Troy, ME 04987, tel 207-948-3741.

[5]Send a business-size SAE with return postage for 1 ounce with your request. Specify the information package for the 6-meter linear amplifier from October 1990 *QST*. This package includes full-size etching patterns for the front and rear sides of the amplifier PC board and a part-placement overlay.

By Richard Frey, K4XU

From *QEX*, May 1999

A 300-W MOSFET Linear Amplifier for 50 MHz

Everyone is looking to go QRO on 6 meters. Build this "almost a brick" to boost your signals from 15 to 300 W.

In an earlier article, I described a 50 MHz, 125 V, 250 W, class-C amplifier using ARF448AJB highvoltage MOSFET devices.[1] This paper describes an improved version of an amplifier that is capable of class-AB linear operation. The design changes required and the procedures involved are explained and demonstrated. Complete descriptions of the amplifier and its construction are presented, as well as the measured performance.

High-voltage, high-power MOSFETs have been shown to be very capable RF power amplifiers.[2] The metal-gate architecture of the ARF series from Advanced Power Technology has raised the frequency limits for this type of device to 100 MHz. The APT448A/B is typical of the series. It has a 68,000square-mil die with a breakdown voltage rating, BV_{dss} of 450 V. The device is provided in the inexpensive TO-247 plastic package, and is available in common-source symmetric pairs. Like all MOSFETs, the gate threshold voltage, V_{th}, has a negative temperature coefficient. This makes operation as a linear amplifier difficult or impossible without compensation.

When forward biased with a constant gate voltage, the quiescent drain current rises as the temperature of the die increases. Operating at the typical drain voltage for these parts, about one third of the rated BV_{dss}, the power dissipation caused by the increasing 'dq results in "hot spotting" and subsequent thermal runaway. This is an unstable system. The dissipation increases so rapidly that the outside surface of the case does not follow internal junction temperature well. As a result, a bias-compensation scheme that uses temperature sensing cannot keep up with the V_{th} shift, and the device is destroyed.

The power dissipation within the die is a direct function of the operating voltage. By lowering the operating voltage, the thermal loop gain can be reduced to a point where the gatethreshold shift can be compensated. Thermal stability can be achieved by sensing the case temperature. Linear operation thus becomes practical at 100 V and below. While this is less than 25% of the rated BV_{dss} and produces less gain, a very rugged and useful linear amplifier is the result.

Amplifier Description

The following were the design goals for the amplifier:

- Frequency range 50 to 51 MHz
- Input SWR < 1.5:1
- Gain> 13dB
- Output power 300 W PEP or CW
- Efficiency> 50%
- IMD3 > 25 dB below PEP

A push-pull topology was chosen for best output power and minimum harmonic content. The previously reported class-C design used V_d = 125 V. Since this is too high for reliable class-AB operation, 80 V was eventually chosen for this design. This is a compromise between gain, efficiency and thermal stability.

Since the gate input impedance is very low, it magnifies the effects of any stray inductance in the gate matching circuit. In a push-pull design, it is critical to maintain absolute symmetry between the two sides. This fact was demonstrated during the initial design work. One preliminary design had a slight asymmetry in the PCB artwork. The amplifier exhibited low efficiency, hot ferrite in the output transformer balun and poor distortion characteristics with asymmetrical IMD product amplitudes. This clearly demonstrates the benefit of symmetrically packaged devices.

A multiple-aperture ferrite bead was chosen for the input transformer. Brass tubing was used for the secondary, and the primary was wound inside the brass tubes to provide a very broadband balanced transformer design with minimum leakage reactance. Several cores and construction methods were evaluated, and this well-tried design proved best.

The typical HF push-pull amplifier employs a bifilar choke to decouple the drain-voltage feed. As frequency and power increase, this feed method becomes less practical because the need to reduce the number of windings to offset the stray capacity and the need to prevent core saturation conflict. In this design, a powdered-iron toroid was chosen for the feed choke core. This proved far superior to any of the ferrite cores evaluated. It is inexpensive and easy to reproduce.

Design

Three main areas must be addressed. The input matching must provide a balanced feed to a pair of low-impedance gates. The output must be matched to a suitable load impedance, and then transformed to a 50-Ω unbalanced load. The bias must be thermally compensated to track the negative temperature coefficient of the gate bias threshold.

The input is reasonably straightforward. Each gate input is 0.2 +*j*0.5, as estimated from the data sheet. The push-pull topology puts these two impedances in series, which makes the matching less difficult. A Smith Chart[3] program makes the actual design easy. The program used here is *WinSmith*.[4] The two gate impedances are added in series, and a network synthesized to transform the resulting impedance up to 50 Ω. The Smith Chart program only works with single-ended circuits, so the center tap was added later. See Fig 1.

The input-transformer design was chosen for its simplicity and relative ease of construction. Of several attempts using different material permeabilities, multiple beads and different conductor types, this proved to be the best and most consistent performer. The core is a Fair-Rite[5] "multi-

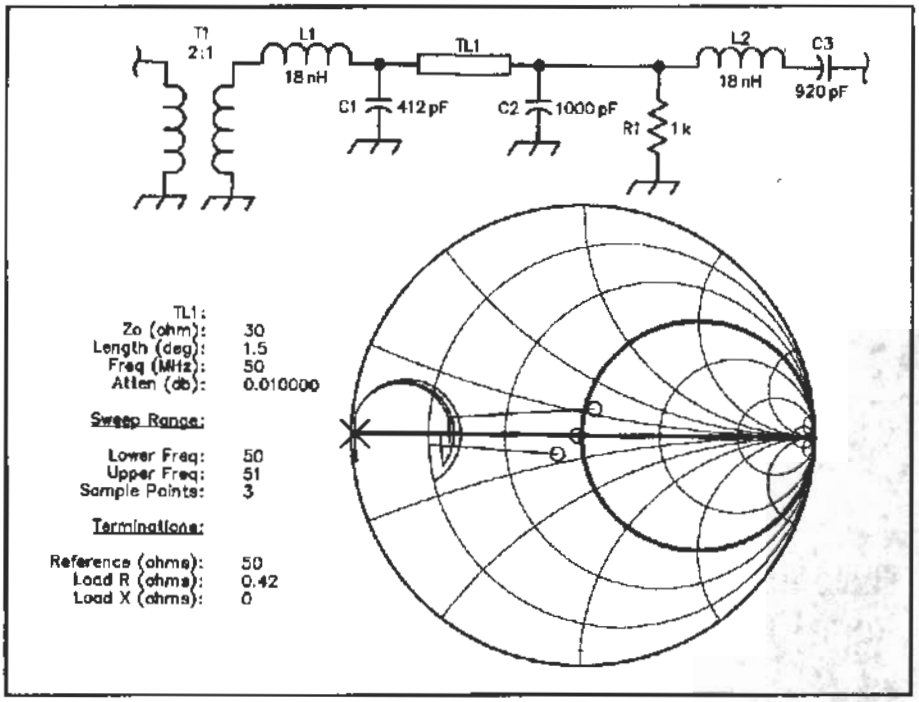

Fig 1—Input matching network and calculation.

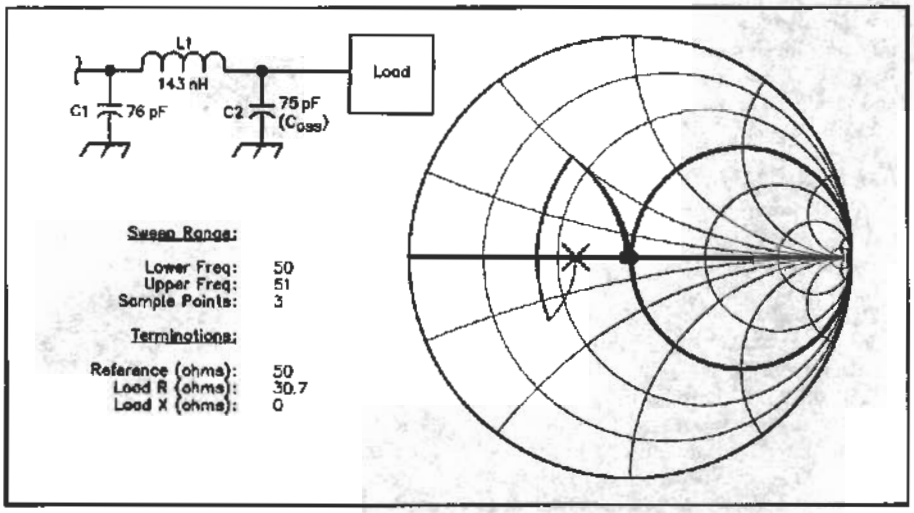

Fig 2—Output matching network and calculation.

aperture" core, part number 2843010402. The type-43 material has a μ_i of 850. At 50 MHz, type-61 material (μ_i of 125) would also be satisfactory. This transformer is essential to provide balanced drive to the gates of the MOSFETs. The secondary winding is $^3/_{16}$-inch brass tubing. Copper shim stock forms the connections to the brass tubing at each end of the transformer secondary. The two-turn primary is wound inside the tubing. This construction provides a very reproducible transformer with minimum leakage reactance and a very broad frequency response. It would be a suitable input transformer for a broadband amplifier covering 1 to 100 MHz.

The leakage reactance of the input transformer—referred to the secondary—is about 18 nH and is represented as Li on the simplified input schematic in Fig 1. The gate load is represented by the "Load R," L2 and C3. Using all three parts of the gate impedance allows proper evaluation of the network bandwidth. A pi network consisting of C1, TL1 and C2 is used to step-up the gate load to the 12.5 Ω needed by the transformer and compensates for T1's leakage reactance. Notice that the net stray inductance of the gate is almost enough to effect a match with a single shunt capacitor. This has actually been done, but it was not easy to fit all the parts in the available space; so it was judged unacceptable here. To transform the network into the required balanced configuration, the series TL1 is split into two equal parts; the shunt capacitors remain the same, and a neutral center tap is provided at the transformer secondary.

Because of the high currents circulating in the input network, it is imperative that C2 be a larger-sized, class-1 dielectric (C0G or NP0) capacitor. It must be a leadless, surfacemount chip type, or the value will need to be adjusted. The input tuning capacitor, a 900 pF mica compression trimmer, is mounted directly to the end of the input transformer.

The output network is also straightforward. The proper load impedance for class

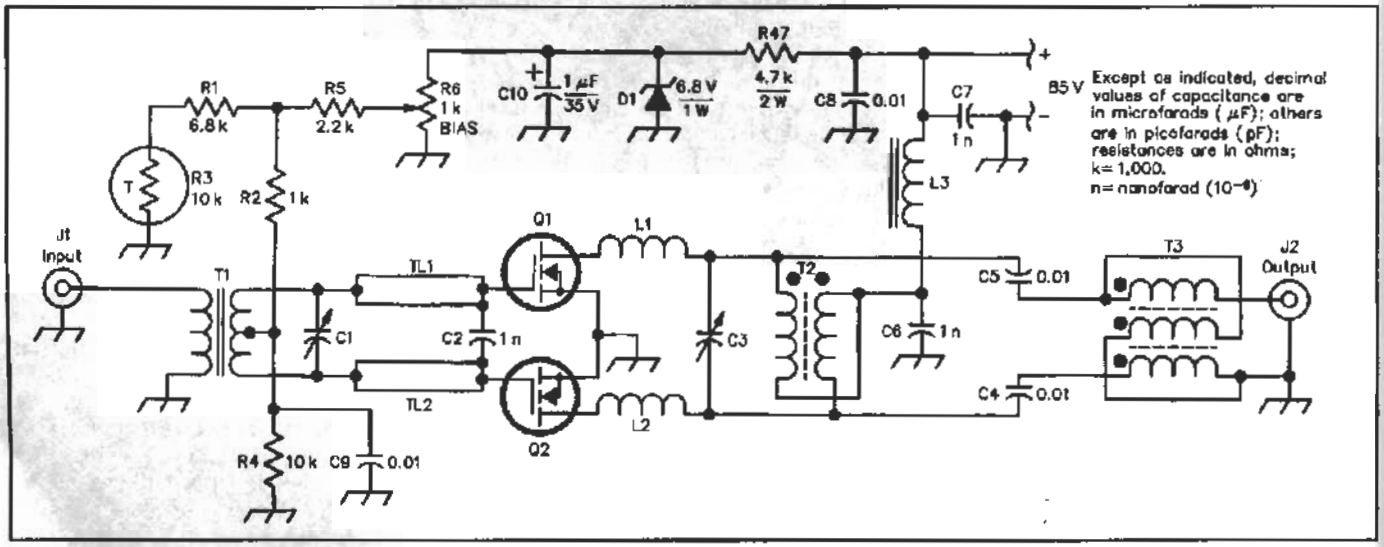

Fig 3—50 MHz amplifier schematic diagram.

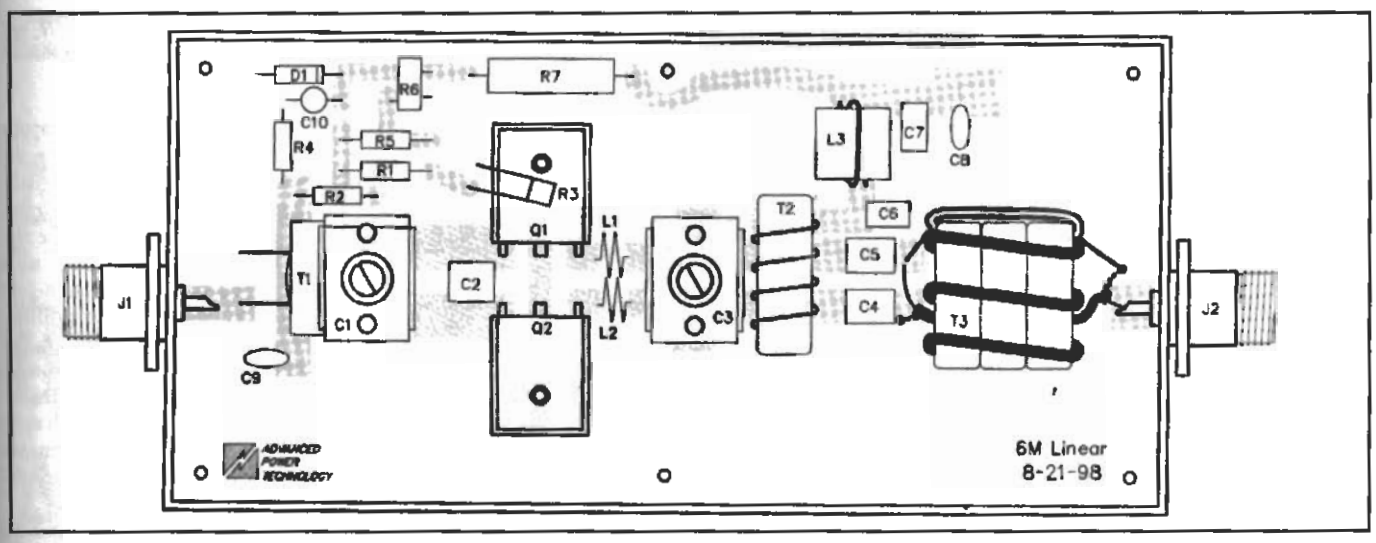

Fig 4—Amplifier parts layout.

AB is calculated from the formula:

$$R_L = \frac{0.98\,V^2_{dd}}{2P_o} \qquad \text{(Eq 1)}$$

This is the load for each device, and P_O is one half of the total in a push-pull circuit. It is shunted by the output capacitance, C_{oss}. As was done for the gate circuit, both output impedances are series-connected to represent the total output impedance. The result for both devices in push-pull is 30.7 Ω in parallel with 75 pF, half the output capacitance of a single device. Though the design goal was 300 W PEP, the amplifier was actually designed for a 400 W load line. This gives a good compromise between efficiency and linearity.

In a classical design, a suitable transformer would be used to set the load impedance, and either the output power or the operating voltage would be adjusted to fit the available turns ratio. Normally, in a low-voltage HF design, the output capacitance is ignored because it is shunted by a much smaller load resistance. At 50 MHz, the effects of the output capacitance must be compensated, so a slightly different approach was taken in this circuit.

WinSMITH was used again to design the output matching. See Fig 2. The output impedance of 30 Ω is rotated south by the effect of the shunt output capacitance, C2. Two options present themselves for compensation. Some additional shunt capacitance could be added to further reduce the equivalent series real part to 12.5 Ω, a series L used to resonate the resulting series C, then a 4:1 transformer used to go to 50 Ω. However, building a reproducible low-loss 4:1 balanced transformer was very difficult, and compensating its leakage reactance further complicates the design. The second option was used: The equivalent series output capacitance was resonated first, then more series inductance was added to rotate the load all the way up to the 1/50-mho conductance circle. Finally, a shunt capacitor was used to resonate the added X_L. The extra L and shunt C form an L-network, which transforms the 20-Ω equivalent series output impedance up to 50 Ω. This results in an easily duplicated design with a smooth, low-Q match.

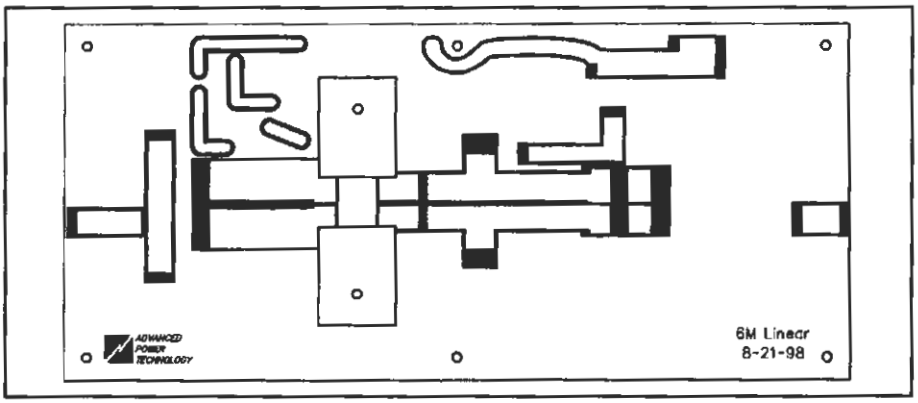

Fig 5—PCB artwork (not to scale, original size 3.35 (7.00 inches).

The dc feed to the drains is provided through a shunt bifilar choke. At this frequency, most ferrite materials exhibit too much loss to be used at this impedance level. A powdered-iron core works famously here.

The balun-transformer function is provided by a simple coax and wire transformer. Two of the windings are provided by 50-Ω Teflon coax, and the third balancing winding by an additional single wire.

The bias network requires some explanation. Power MOSFETs have normal lot-to-lot variations in gate threshold voltage, V_{th}, forward transconductance, G_{fs}, and other parameters. A number of devices were checked for V_{th}, and they were all very close. They were all from the same die lot. The die lot number is marked on the package. For comparison, devices from another lot were checked and were uniformly a half a volt lower. Were this the case for the devices to be used in the amplifier, a dc block would need to be added to each side at the transformer, and the bias-feed network duplicated for each device. Since these devices were uniform, the additional complication of individual gate-bias adjustments was omitted in this design.

Because the gate-bias voltage required to maintain a particular value of idling drain current decreases as the temperature of the die increases, it is necessary to thermally compensate the gate-bias source, or the devices will "run away." A commonly available NTC resistor tracks the temperature of the case. (Refer to Fig 3.) This bias circuit has been in the literature for many years.[6] The ratio of R1 to R3 in part determines the degree of compensation. A smaller value of R1, or a larger value of R5, will increase the thermal sensitivity. A drop of thermally conductive glue keeps the thermistor in contact with the case. Proper operation is indicated when the set value of I_{dq} does not change after the heat sink gets hot from prolonged operation.

Construction

Refer to Fig 4 for the parts layout. A photo master of the artwork is shown in Fig 5. The original size of the artwork is 3.35x7 inches. The circuit board is 1-ounce-copper, double-sided 1/16-inch G-10 PCB material. All four edges of the board and the three sides of the two rectangular cutouts for the transistors are wrapped with copper-foil tape that was soldered in place to

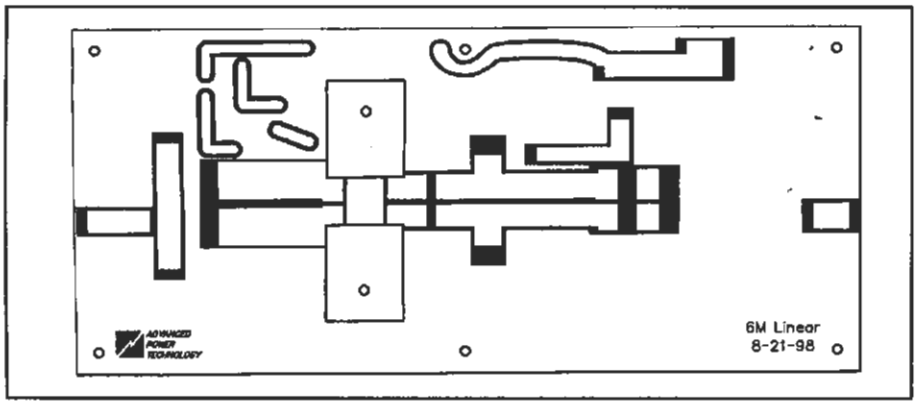

Fig 6—SSB IMD performance.

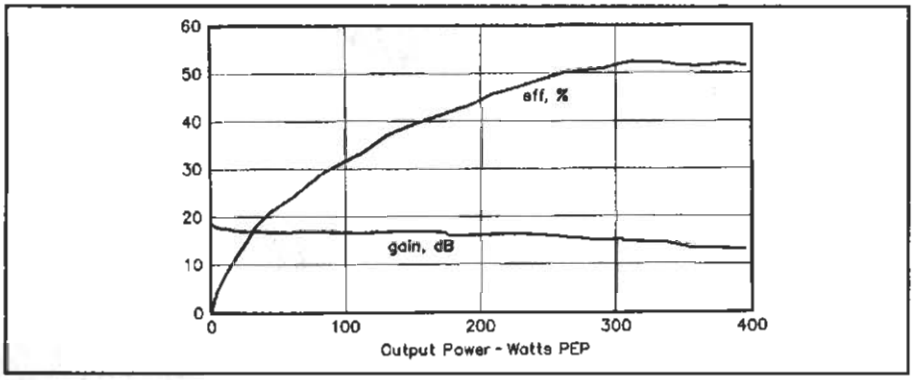

Fig 7—Amplifier efficiency and gain.

Table 1—Amplifier Parts List

C10—1μF, 35 V electrolytic capacitor
C1—215-790 pF Arco[8] #469 mica compression trimmer
C2, C6, C7—1000 pF, 500 V NPO chip cap, KD9 #2020N102J501P
C3—20-180 pF Arco #463 mica compression trimmer
C4-C5, C8-C9—0.01 μF, 500 V chip capacitor
D1—6.8 V, 1 W Zener diode
L1-L2—≈70 nH, 3t #18 AWG enameled wire 0.31-inch diameter 0.25-inch long
L3—2t #20 AWG on Fair-Rite #284301 0402 bead μ_i = 850
Q1 —ARF448A
Q2—ARF448B
R3—10 kΩ NTC Fenwal[10] #140-103LAG-RB1
R6—1 kΩ, 0.5W 10-turn trimmer
T1—Primary 2t #20 PTFE, Secondary 3/16-inch brass tube on Fair-Rite #2843010402 balun core
T2—6t bifilar #20 PTFE on Amidon #T-94-2 toroid μ_i = 10
T3—3t RG-316 coax, 3t #20 PTFE on three Fair-Rite #5961001801 toroids μ_i = 125
TL1, TL2—30-Ω printed line, 0.6 inches long

provide a low-impedance continuous ground plane. The two cutouts for the transistors and the six mounting holes are the only holes in the board. All of the parts are surface mounted, which permits the board to be mounted directly to the heat sink.

This amplifier was built on a 7-inch length of AAVID #60765 heat-sink extrusion.[7] It is 3.5 inches wide, 1.5 inches deep and has nine fins. With 50 CFM of air blown across it, the devices will easily maintain thermal stability in a 30°C environment. The heat sink is not big enough for anything but very intermittent use without a fan to assure adequate airflow across the fins. The input and output connectors are each secured by two #4-40 screws and holes tapped into the base of the heat sink. A cover is recommended for safety; fairly high RF voltages are present.

Power Supply

Power for the amplifier needs to be fairly well regulated, since any ripple will show in the output signal as undesired 120-Hz AM. For on-air testing at the author's home, a very simple power supply was constructed using a 500 W, 120 to 240 V isolation transformer to drive a full-wave, centertapped rectifier circuit with 50,000 μF of filtering. Under SSB conditions, this is adequate. For CW, it needs some better regulation or the output power will sag over the length of a dash, and there will be some detectable hum. A regulated supply capable of providing 80 V at 6 A is needed.

Performance

This is the first-known, class-AB application of the ARF448 parts. Until now, the only other linear application is in a pulsed-mode linear amplifier for magnetic-resonance imaging. The SSB performance was encouraging because these devices were developed to serve the ISM plasma-generation market and no attention to linear performance was given in their design. The IMD performance with 200 mA of quiescent bias was better than expected. (See Fig 6.) The amplifier was tested with up to 0.5 A of I_{dq}. While the IMD performance improves somewhat at this level, the efficiency degrades significantly.

The gain and efficiency objectives have been met, as shown in Fig 7. The gain is 14.3 dB at 300 W PEP. The efficiency peaks at 51% at the same power. Under single-tone conditions, the drain efficiency is 61% at 250 W. The bandwidth of the amplifier is determined by the input network. The Smith-Chart plot of the input impedance shows the tracks for 50, 50.5 and 51 MHz. With the network adjusted for best match at 50.5 MHz, the SWR at the ± 0.5 MHz bandwidth points is 1.3:1. It would be difficult to increase this SWR bandwidth enough to cover the full 4 MHz of the amateur 6-m band without resorting to resistive loading, which would then reduce the available gain.

Conclusion

This paper has presented a 50 MHz, 300-W PEP linear amplifier using plastic-packaged, high-voltage MOSFET transistors. This is the first-known implementation of a full-duty-cycleclass-AB amplifier using these transistors. The design challenges, approaches to their solution and the resulting amplifier performance are shown. The parts, construction and mechanical layout all have been described in sufficient detail to permit duplication. The new line of plastic-packaged RF power transistors from APT offers designers a new cost-effective solution for efficient layout and performance.

Notes

[1]R. Frey, *A 50 MHz, 250 W Amplifier Using Push-Pull ARF448A/B*, APT9702, Advanced Power Technology Inc.
[2]R. Frey, "A Push-Pull 300 Watt Amplifier for 81.36 MHz," *Applied Microwaves and Wireless*, April 1998.
[3]Smith Chart is a trademark and property of Analog Instruments Co, New Providence, New Jersey.
[4]*WinSMITH*, copyright Eagleware Corp, 1995, available through Noble Publishing, Inc.
[5]Fair-Rite Products Corp, PO Box J, One Commercial Row, Walikill, NY 12589.
[6]H. Granberg, "Wideband RF Power Amplifier," *RF Design*, February 1988.
[7]AAVID Thermal Technologies Inc, Box 400, Laconia, NH 03247.
[8]Arco Electronics, 5310 Derry Aye, Agoura Hills, CA 91301.
[9]KD Components Inc, 2151 Challenger Way, Carson City, NV 89706.
[10]Fenwal Electronics, Inc, 450 Fortune Blvd, Milford, MA 01757.

By Paul Hewitt, WD7S

From *QEX*, July 2000

A No-Bandswitch, Dual-Band VHF Desktop Amplifier

An old design idea together with new tubes yields legal-limit output on 6 and 2 meters from a small box.

Dual-band VHF amplifiers are by no means new in Amateur Radio. Several designs have appeared over the years, both commercial and homebrew.[1,2] The most recent commercial design was the Henry Tempo 6N2, now out of production for more than 20 years. There has never been a desktop capable of the new 1500-W PEP amateur power limit for both the 6- and 2-meter bands, until now. The amplifier I describe was designed primarily for meteor-scatter and weak-signal work, but the conservative design of the power supply and cooling system makes it well suited for EME (moonbounce) also. The amplifier uses a pair of Svetlana 3CX800A7s, operating in class AB2-push-pull on 2 meters and AB2-parallel on 6 meters. Features include: legal-limit output, no key-down time limit, no band switching, either-or operation, 50-60 W of drive for 1500 W PEP output on both bands, small size and light weight. In an effort to make this design easier to duplicate, off-the-shelf com-ponents and materials were used wherever possible. If you prefer not to "roll your own," Alpha Power should have a commercial version available soon.

Output Tank Circuit and Construction Details

Since this was a new tank design, I decided to use a box-in-a-box approach for the layout to make adjusting and debugging much easier. This should also make duplication of the tank circuits much easier for those of you who wish to use a separate, outboard power supply. The tank compartment (See Figs 1, 2 and 7) starts with a 7×7×2-inch Bud chassis with two surplus 11-pin ceramic sockets[3] mounted three inches apart (center-to-center) and four inches from the rear of the chassis. The sockets are mounted 1/4 inch below the chassis in 2 1/2-inch-square holes with each socket oriented at 45° to the hole (Fig 3). This is similar to an Eimac 2216 socket for the 8877. The Eimac #1906 chimneys were used in the normal manner. This is probably the upper frequency limit for this mounting scheme due to possible instability problems at UHF. One problem encountered while mounting the sockets this way is the small amount of tube exposed above the chimney to grasp for removal. This is easily solved by connecting several 1/4-inch-wide hose clamps together end to end, then clamping them to the anode cooler to serve as a temporary handle.

The front, top and sides of the tank com-

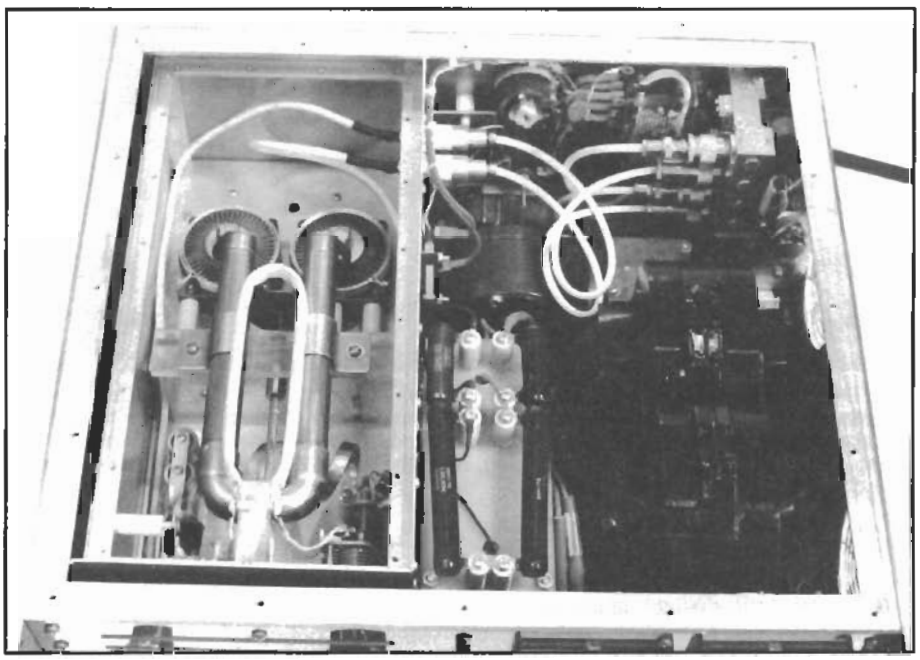

Fig 1—A top view of the amplifier. The plate transformer in the front right and high-voltage power assembly next to it occupy the majority of the control side with the blower, filament and control transformers sitting just behind. The tank compartment with the cover removed shows the plate line on its Plexiglas stand.

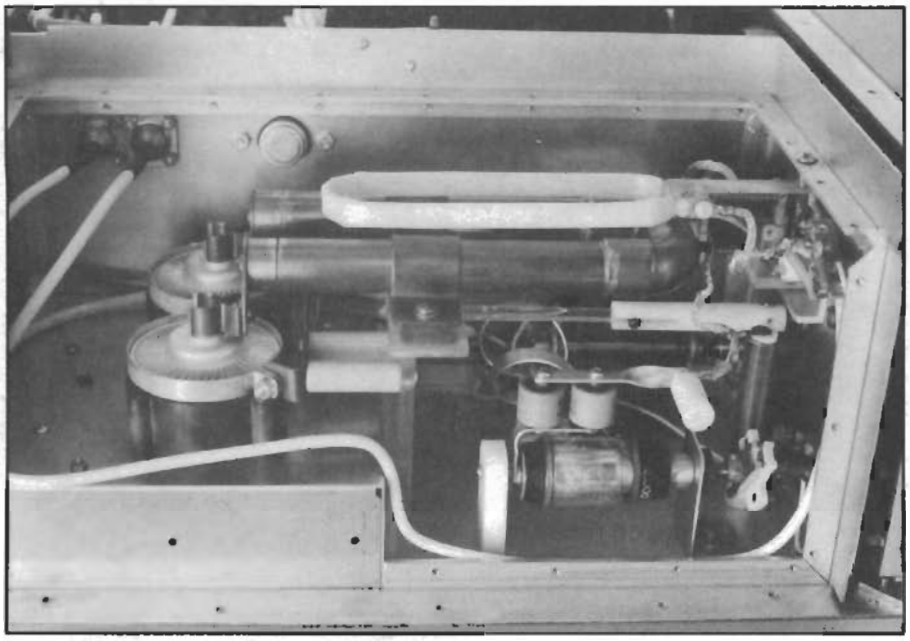

Fig 2—Side view of tank compartment. The 2-meter load capacitor on its ceramic standoffs mounted to the Plexiglas stand is in the center with the 6-meter tank coil just visible below the spline shaft assembly. The 6-meter tune capacitor on its L bracket is in the lower right front.

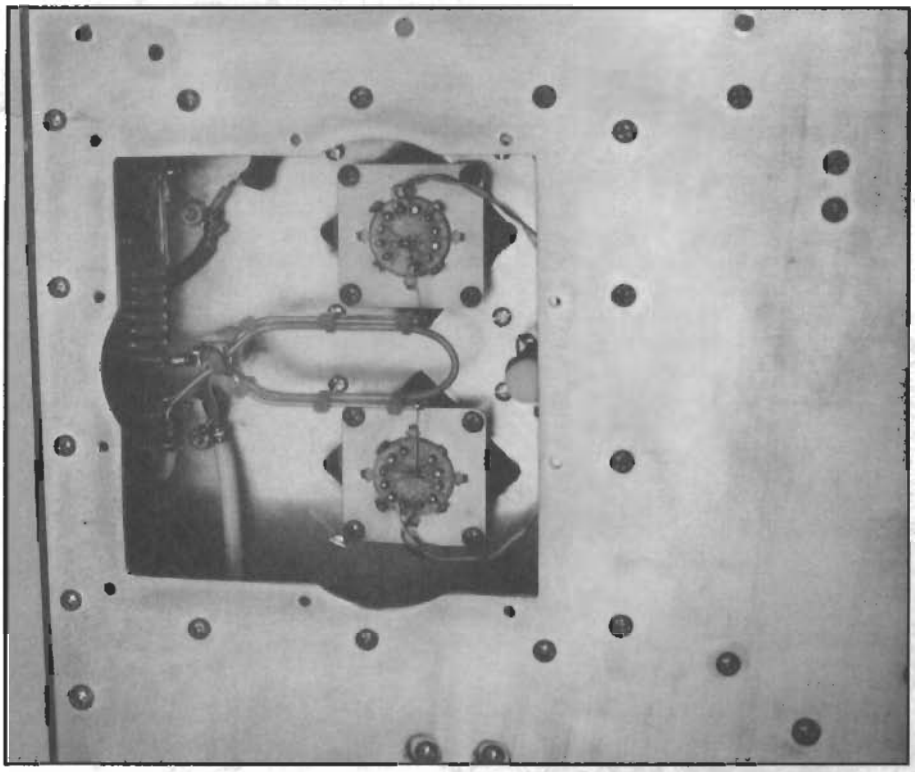

Fig 3—Bottom view of amplifier with cathode compartment cover removed The filament choke is to the right with the 2-meter input network visible centered between the tube sockets. Both input tuning capacitors are mounted on the rear panel and one of the 6-meter input coils is just visible on the left. Note the use of coax for exciter lines to keep feedback paths minimized.

partment are all made from 1/16-inch aluminum with 1/2×1/2×1/8-inch aluminum angle brackets at all corners. The completed compartment measures 7×6 1/4×14 1/2 inches (WHD). The front and right-side compartment panels extend to the top of the main cabinet cover to keep inlet and outlet air separated. The compartment cover (not shown) has 176 0.2-inch holes above the tubes for cooling exhaust. When this box is attached to the floor of the main cabinet, it leaves a 4×7-inch hole at the back before the rear panel is attached. This opening serves as access for a dip meter when checking the 2-meter tank resonance and tuning range.

The 2-meter tank circuit consists of a shorted λ/4 balanced line section, tuned by a homebrew split-stator capacitor at the tube end of the line. Designing this type of tank circuit is made very pain-less with information and design exam-ples provided in references.[4] There are several advantages of using a push-pull tank circuit instead of a parallel arrangement at 144 MHz. In the push-pull arrangement, C_{out} and C_{in} of the tubes are in series, allowing a total C_{out} and C_{in} that is one quarter of that with the parallel arrangement. This allows lower values of loaded Q, resulting in higher efficiency and reduced compo-nent heating, minimizing thermal drift. The low value of C_{out} in this case allows the use of a λ/4 line in place of a λ/2 line, increasing bandwidth and decreasing size.

The line section, L2 of Fig 4, is made from 3/4-inch type-K copper pipe; the shorted end is made from one standard 90° copper elbow and one "street" 90° copper elbow. The open ends of the line are closed with brass plugs of the same outside diameter as the pipe, with a portion machined to fit inside the pipe. Standard copper pipe caps could be substituted for these plugs. The total length of the line section is 7 3/4 inches, from the ends to the inside of the shorted end. The plate-to-anode connections are made with 1/16-inch copper plate fastened between copper fuse clips on the anode connectors and threaded holes in the ends of the brass plugs.

The line section is supported by a Plexiglas stand and held in place by two copper clamps. The stators of the 2-meter **TUNE** capacitor, C3, are sup-ported by 1 1/2-inch ceramic standoffs attached to the Plexiglas stand (Fig 5). A 3/8 ×5/8-inch ear from each stator attaches to a 3/8-inch-wide strap around each of the tubes' anode coolers. The rotor of C3 is a two-inch disk of 1/16-inch copper, which is mounted to a piece of 1/4×28 brass all-thread rod. The threaded rod is held by a brass fitting (tapped for 1/4×28) that is attached to the Plexiglas stand. The threaded rod is coupled to a sliding spline shaft consisting of 1/4-inch Plexiglas rod inside a 1/2-inch piece of Teflon rod that has been drilled through the center. The Teflon tube is attached to a short piece of 1/4-inch stainless-steel rod that exits the tank compartment through a 1/4-inch panel bushing. This shaft is coupled to the turns counter with a synchronous gear belt (Fig 6). This shaft relocation via the gear belt serves only to improve the front-panel appearance; it may be omitted if desired.

The 2-meter tank circuit is coupled to the antenna by an adjustable reso-nant link. The link position is adjusted by a #10-24 screw through a threaded Plexiglas block, to which the link is attached (Fig 2). One end of the adjusting screw is supported by the top-cover angle bracket and the other end by a 2-inch-long piece of 1/2-inch angle mounted to the front panel of the compart-

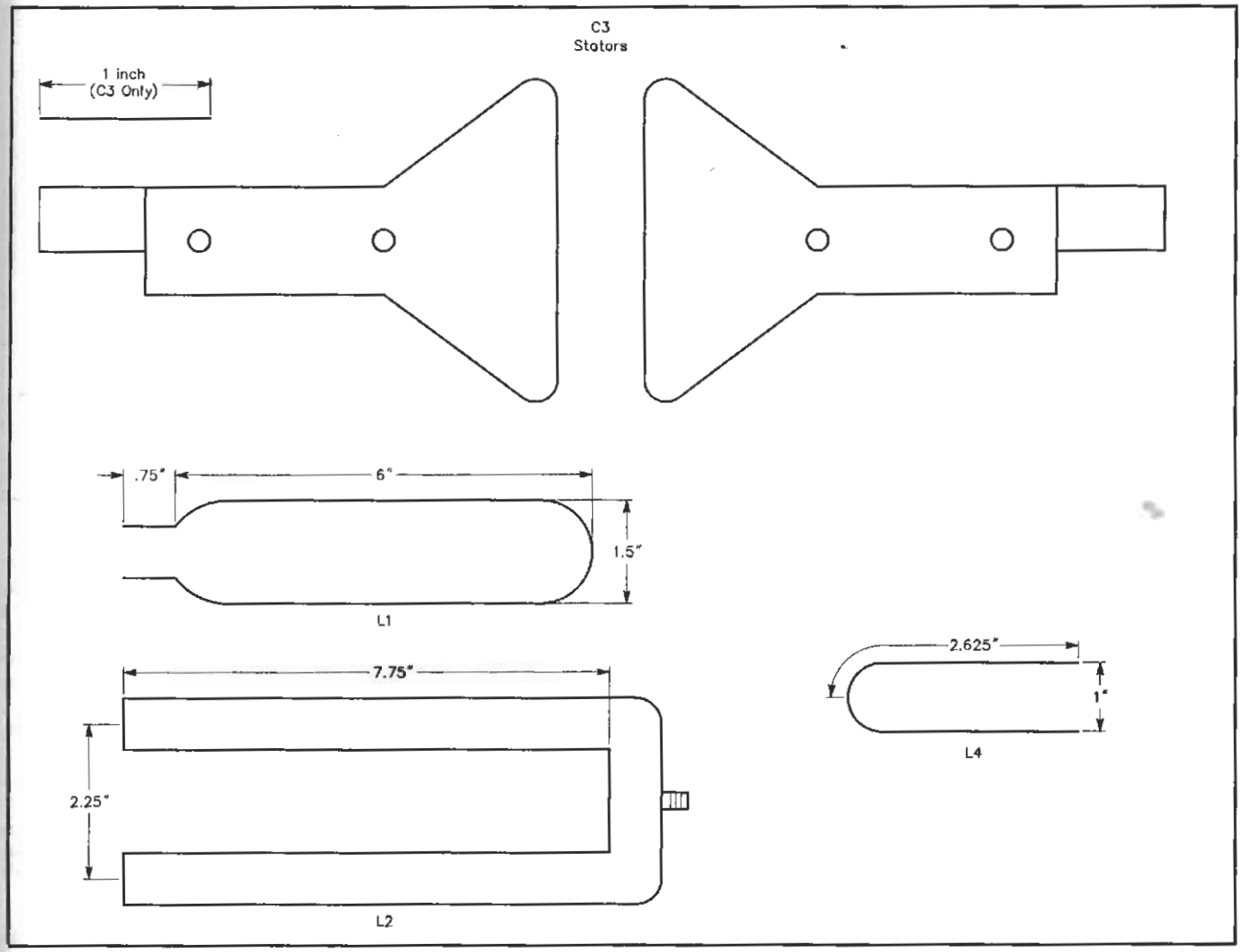

Fig 4—Details of 2-meter input and output tank indicators and the 2-meter TUNE capacitor stators.

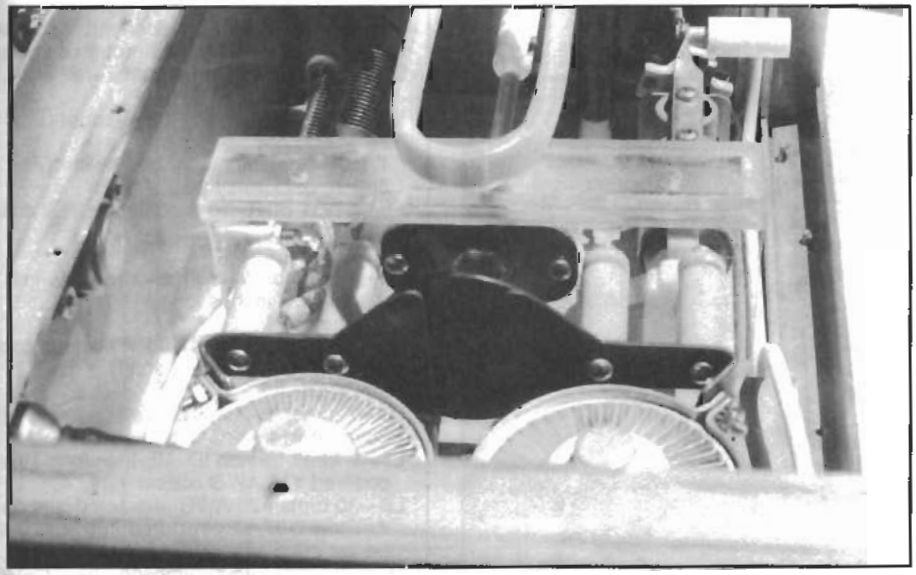

Fig 5—Rear view with the plate line removed showing the 2-meter TUNE capacitor.

ment. The link is made from $^3/_8 \times ^1/_{16}$-inch silver-plated copper strap, covered with a $^3/_8$-inch Teflon sleeve; it is attached to the Plexiglas block with four #10-32 nylon screws. Silver-plated coax braid attaches the link to the 2-meter **LOAD** capacitor, C2, and the isolation relay, K3. The link-adjustment screw is accessed through $^3/_8$-inch hole in the main cabinet top cover during initial setup, then the hole is covered with a plastic plug.

As with all push-pull circuitry, the key to successful operation is symmetry. All stray capacitance must be divided equally between both sides of the line and tubes. Also, try to keep ferrous materials out of the tank compartment to prevent imbalance.

The 6-meter tank is a normal π network designed for a plate-load resistance of 1150 W with a loaded Q of approximately 22. The design parameters are shown in Table 1. The input of the π network is connected to the center of the shorted end of the balanced line section where a #10-32 brass stud has been soldered in place. This is the low-impedance point of the line section, and anything but a dead short can be attached here without affecting the performance of the line.[5] To verify that the physical center of the line is also the RF center, couple a dip meter to the line and tune for a dip around 144 MHz. Then without moving the dip meter (DM), touch the tip of a lead pencil at points along the line until you find the spot that has the least effect on the DM. This is the attachment point for the plate choke and the 6-meter tank.

To keep the loaded Q of the π network as low as possible, full 51-54 MHz opera-

Table 1—Print out of operating parameters for the 6-meter input and output networks

The values for the PI matching network were calculated with Elmer (W5FD) Wingfield's new formulas found in the more recent ARRL handbooks.
FREEWARE Courtesy of KD9JQ
Triode Amplifier Program Version 2.0
For Grounded Grid Operation

(2) USER Biased 3CX800A7 at 50.0 MHz Rated for FORCED AIR

DC Plate Volts	=	2150.0	V (2500 V Max)
Max Plate Voltage	=	2150.0	V
Peak Plate Swing	=	1900.0	V
Min Plate Voltage	=	250.0	V
Plate Current Peak	=	3.368	A
Plate Current DC	=	1.119	A
Grid Current DC	=	0.063	A
Cath Current Peak	=	3.651	A
Design Plate RL	=	1128.1	Ω
RL for Matching	=	1154.8	Ω
Plate Dissipation	=	805.5	W (1600 W Max)
Grid Dissipation	=	3.2	W (8 W Max)
Cathode Bias	=	8.2	V
Conduction Angle	=	187.8	Degrees
Peak Grid Voltage	=	36.8	V
Zin @ Cathode	=	24.6	Ω
Pin Drive (PEP)	=	41.0	W
P0 @ Plate (PEP)	=	1600.0	W
P0 to Load (PEP)	=	1637.9	W
DC Power Input	=	2405.5	W
Efficiency	=	66.5	%
Power Gain	=	16.0	dB
Cath to Grid Cap	=	52.00	pF
Plate to Grid Cap	=	12.20	pF

T Match Input

RS	=	50.0 Ω
L2	=	0.521 µH
CI	=	44.924 pF
L1	=	0.422 µH
RFC	=	0.195 µH
Zin	=	22.6 –*j* 9.9 Ω
QL	=	5.0

Pi Match Output

RP	=	1154.8 Ω
CI	=	50.0 pF
L1	=	0.2377 µH
C2	=	232.0 pF
RL	=	50.0 Ω
QL	=	22.0

tion was not attempted. The 6-meter **TUNE** capacitor, C1, operates very near its minimum capacitance because of strays and the C_{out} of both tubes. These strays account for a large portion of the 6-meter tune capacitance, which causes the majority of the tank circulating current to flow through the blocking caps, C7-C8. I used parallel Centralab 858 "door-knobs" for the blocking capacitors and I haven't experienced any problems. Capacitors with larger current ratings (such as HT-57s) would be a better choice for longer duty cycles.

The 3-30 pF vacuum-variable capacitor is mounted to the floor of the tank compartment with an L-bracket bent from 1/16-inch aluminum. Use the bearing retainer nut to attach the capacitor to the bracket, but be sure to add shims to the bearing to make up for space lost by the thickness of the bracket, or backlash will occur. The other end of the capacitor is supported by a #6-32 brass screw in the end of the capacitor that passes through a piece of Teflon bar stock mounted to the floor of the cabinet. A #6-32 hex nut holds the end of L3 and a piece of 3/8-inch strap (which supports C7 and C8) tight to the end of the vacuum cap. The other end of L3 is supported by a 1/2×1-inch Teflon standoff. Silver-plated braid ties this end to the 6-meter **LOAD** cap, which is mounted on the sidewall of the tank compartment.

Setting the Output Tanks

The 6-meter tank can be checked for tuning range with an SWR analyzer at the output connector. Connect a 1.1 kΩ, noninductive resistor from one of the tube anodes to ground to simulate the 1100-W plate-load resistance. You should be able to achieve a 1:1 match at both ends of the desired tuning range. Some stretching or compression of L3 may be required to bring the tuning range to 50-51 MHz. Be sure the top cover of the tank compartment is in place, as the stray capacitance it introduces accounts for a portion of the tuning capacitance for 6-meters.

The 2-meter tank was set up entirely

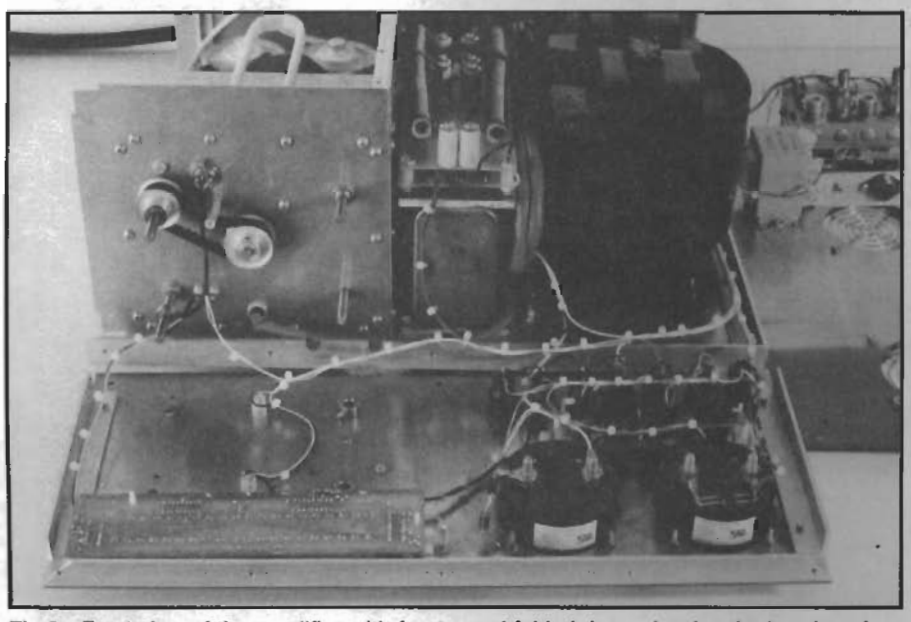

Fig 6—Front view of the amplifier with front panel folded down showing the location of high-voltage power-supply components at right and the gear-belt layout on the left. The bar-graph display PC board is visible in the lower left with the control board just beyond the two panel meters.

Fig 7—RF deck schematic. Unless otherwise specified, use 1/4 W, 5%-tolerance carbon composition or film resistors. See Table 3 for part-supplier contact information.
C1—3-30 pF vacuum-variable capacitor
C2—150 pF air-variable, 1400 V capacitor
C3—Split-stator air-variable (see text and Fig 4)
C4—325 pF air-variable, 1400 V capacitor
C5, C6—4.3-75 pF APC-style air-variable trimmer capacitor
C7, C8—1000 pF, 5 kV doorknob capacitor
C9—2500 pF, 2.5 kV feedthrough capacitor
D1—8.2 V, 50 W stud-mount Zener diode, 1N2806B
K3—Jennings RJ1A SPDT vacuum relay, 26.5 V dc coil
K4, K5—DowKey model 260B with "C" option, coax relay 26.5 V coil
K6—SPDT relay, 10 A contacts, 24 V dc coil
L1—See Fig 4
L2—See Fig 4
L3—2 turns of 3/8×1/16-inch strap, 1 1/2-inch diameter, 2 inches long
L4—See Fig 4
L5—8.5 inches of #14 Teflon covered copper wire with 6 inches tied tightly inside L4
L6—7 turns, 1/2-inch ID×1 1/8-inch long Teflon covered #14 AWG copper wire
L7—9 turns 1/2-inch ID×1 1/2-inch long Teflon covered #14 AWG copper wire
L8—30 turns #26 AWG enameled wire on an Amidon T-37-17 powdered-iron core over center conductor of coax
M1—0-2 A, 3.5-inch Simpson panel meter
M2—0-100 mA, 3.5-inch Simpson panel meter
RFC1—36 turns #18 AWG enameled wire, tight-wound on 1/2-inch-diameter Teflon rod
RFC2, RFC3—Ohmite Z-50
RFC4—Ohmite Z-144
V1, V2—Svetlana 3CX800A7

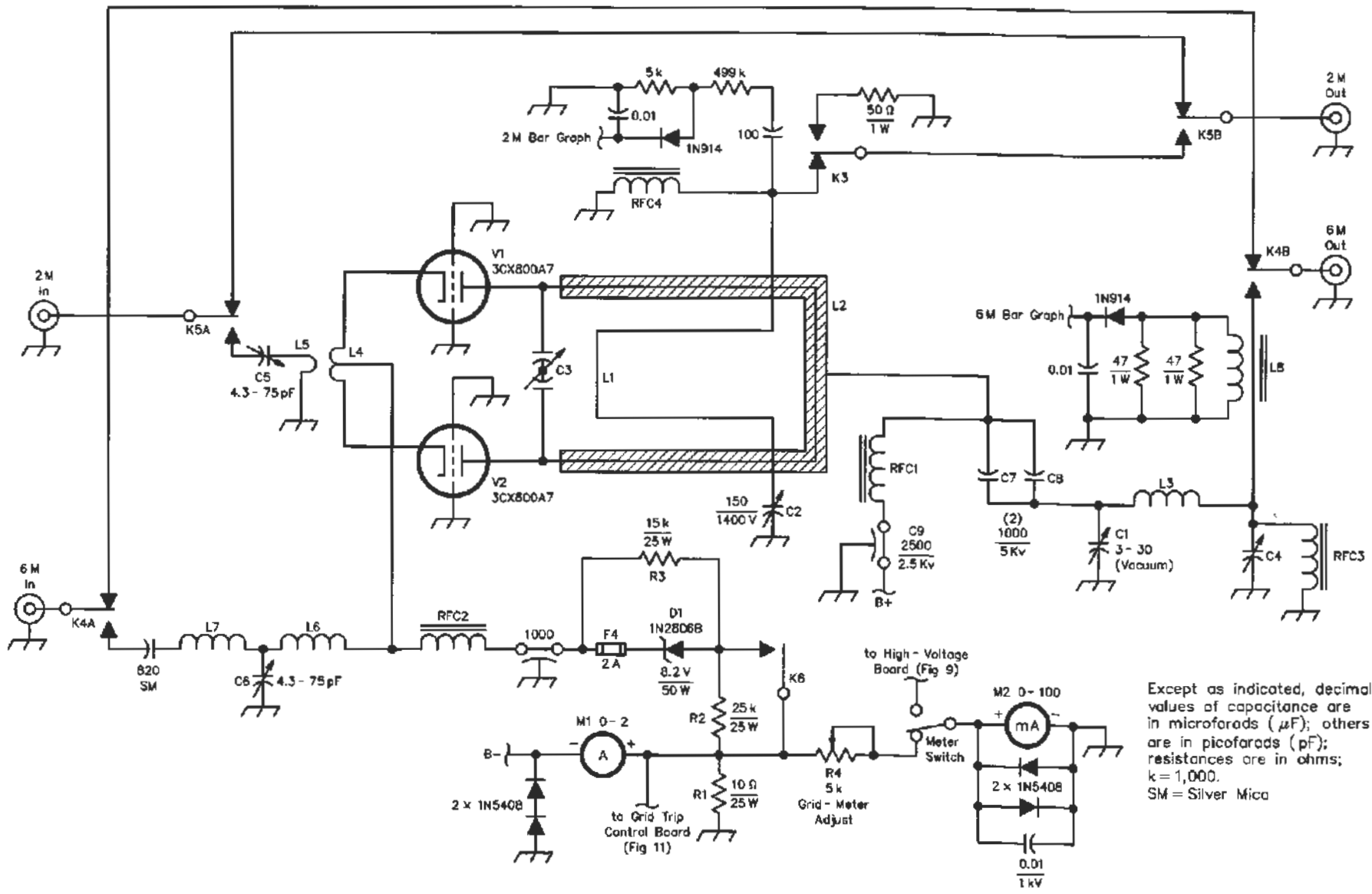

Except as indicated, decimal values of capacitance are in microfarads (μF); others are in picofarads (pF); resistances are in ohms; k = 1,000.
SM = Silver Mica

with a dip meter inserted through the opening in the back of the compart-ment. Set the output link about 3/8-inch from the top plane of the line; this is close to the final position and adds stray capacitance. To keep loaded Q low, try to set the line length so it doesn't take very much tune capacitance to resonate the line at 144 MHz. Start with a line section a little longer than shown and carefully trim it to resonance. Remem-ber that 1 inch of line length equals approximately 10 MHz of tuning range! The tank should resonate at 144 MHz with about 1/4 inch of space between the plates of C3. When the desired tuning range is found, install a 1/4×28 lock nut on the threaded shaft of C3 to stop travel at the upper frequency limit. This will prevent accidental tuning of the tank to the third harmonic of 50 MHz, which could potentially damage the front end of a 2-meter exciter. Remember that the isolation of most coax relays is very poor at 144 MHz: It was only 35 dB with the DowKey 260B used here. For this reason, a Jennings RJ1A vacuum relay, K3, was added in series with the 2-meter transfer relay. The vacuum relay disconnects the 2-meter link from the coax and terminates the coax in a resistive load during 6-meter operation. Make sure the electrical length of the coax between the relays is more than $\lambda/10$ and less than $3\lambda/8$ at 144 MHz. With these safety measures in place, third-harmonic energy at the 2-meter input port was measured at –17 dBm during 1500-W 6-meter operation.

Input Networks

The 2-meter input network consists of a single tuned-link, air-core transformer (Figs 3 and 4). This coupling method requires slightly more drive than a link-

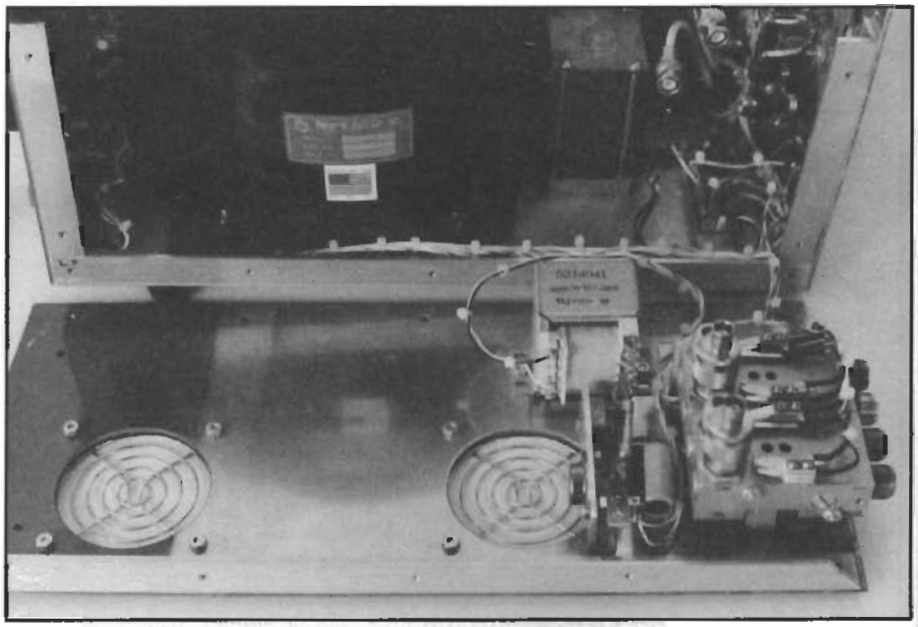

Fig 8—View of the right-hand side panel folded down showing the two transfer relays and the low-voltage power supply. The filament transformer is visible to the right of the plate transformer. Note the use of 80-mm fan covers for the cooling air inlets.

Table 2—Operating parameters of the amplifier

Plate voltage no load, 2350 V	
Plate voltage @ 1 A, 2150 V	
Zero signal plate current, 35 mA	
6-Meter drive, single tone, 49 W	
6-Meter power output,1420 W	
6-Meter plate current, 980 mA	
6-Meter grid current, 75 mA	
Apparent efficiency, 67.4% (feed-through power not subtracted)	
2-Meter drive, Single tone, 50 W	
2-Meter power output, 1275 W	
2-Meter plate current, 950 mA	
2-Meter grid current, 68 mA	
Apparent efficiency 62.4% (feed-through power not subtracted)	

Table 3—Parts suppliers

Fair Radio Sales Co, Inc
1016 East Eureka St
PO Box 1105
Lima, OH 45804
tel 419-227-6573, 419-223-2196
fax 419-227-1313
e-mail **fairadio@wcoil.com**
URL **http://www.fairradio.com/**

Mouser Electronics
2401 Hwy 287 N
Mansfield, TX 76063
tel 800-346-6873
fax 817-483-0931
e-mail **sales@mouser.com**
URL **http://www.mouser.com/**

Newark Electronics
4801 N. Ravenswood Ave
Chicago, IL 60640-4496
tel 800-463-9275, 773-784-5100
URL **http://www.newark.com/**

Peter W. Dahl Co, Inc
5869 Waycross Ave
El Paso, TX 79924
tel 915-751-2300
fax 915-751-0768
e-mail **pwdco@pwdahl.com**
URL **http://www.pwdahl.com/**

RF Parts Co
435 S Pacific St
San Marcos, CA 92069
tel 760-744-0700, 800-737-2787
(orders only)
fax 760-744-1943
e-mail **rfp@rfparts.com**
URL **http://www.rfparts.com/**

Surplus Sales of Nebraska
1502 Jones St
Omaha, NE 68102-3112
tel 402-346-4750, 800-244-4567
(Orders only)
fax 402-346-2939
e-mail **grinnell@surplussales.com**
URL **http://www.surplussales.com/**

Svetlana Electron Devices
8200 S Memorial Pkwy
Huntsville, AL 35802
tel 256-882-1344, 800-239-6900
fax 256-880-8077
e-mail **sales@svetlana.com**
URL **http://www.svetlana.com/**

coupled, half-wavelength resonant line, but saves a lot of space. Two references[6, 7] give formulas and rules of thumb for designing this type of transformer, but it still required a lot of "cut and try" before suitable sizes for L4 and L5 were found. The loaded Q of the resonant input link is approximately 3.5 before the coupled-in resistance from the secondary modifies it. The degree of mutual coupling of air-core transformers is an elusive value that makes the final loaded Q difficult to calculate. The input tuning capacitor, C5, could be changed to a 25-pF unit since the one used here turned out to be much larger than needed. Both sides of C5 are above chassis ground; it requires a nonmetallic screwdriver to adjust.

Six-meter drive and B– are applied to the center tap of L4, providing parallel cathode drive for 50-MHz operation. A common T network, with a loaded Q of five, matches the 50-W line to the 24.6-Ω input impedance of the parallel tubes. All the cathode pins of the sockets are tied together with buss wire in a star pattern. One-inch-long bus-wire leads connect the ends of L4 to the center of the bus-wire stars on the sockets. Again, symmetry is all-important in balanced operation.

Both input networks were set up with an antenna analyzer and two 50-W carbon resistors to simulate the input load impedance. Tack-solder the resistors from cathode to ground on each socket with the shortest-possible leads. Short leads are very important on 2 meters because lead inductance and stray capacitance become quite significant. The resistors present

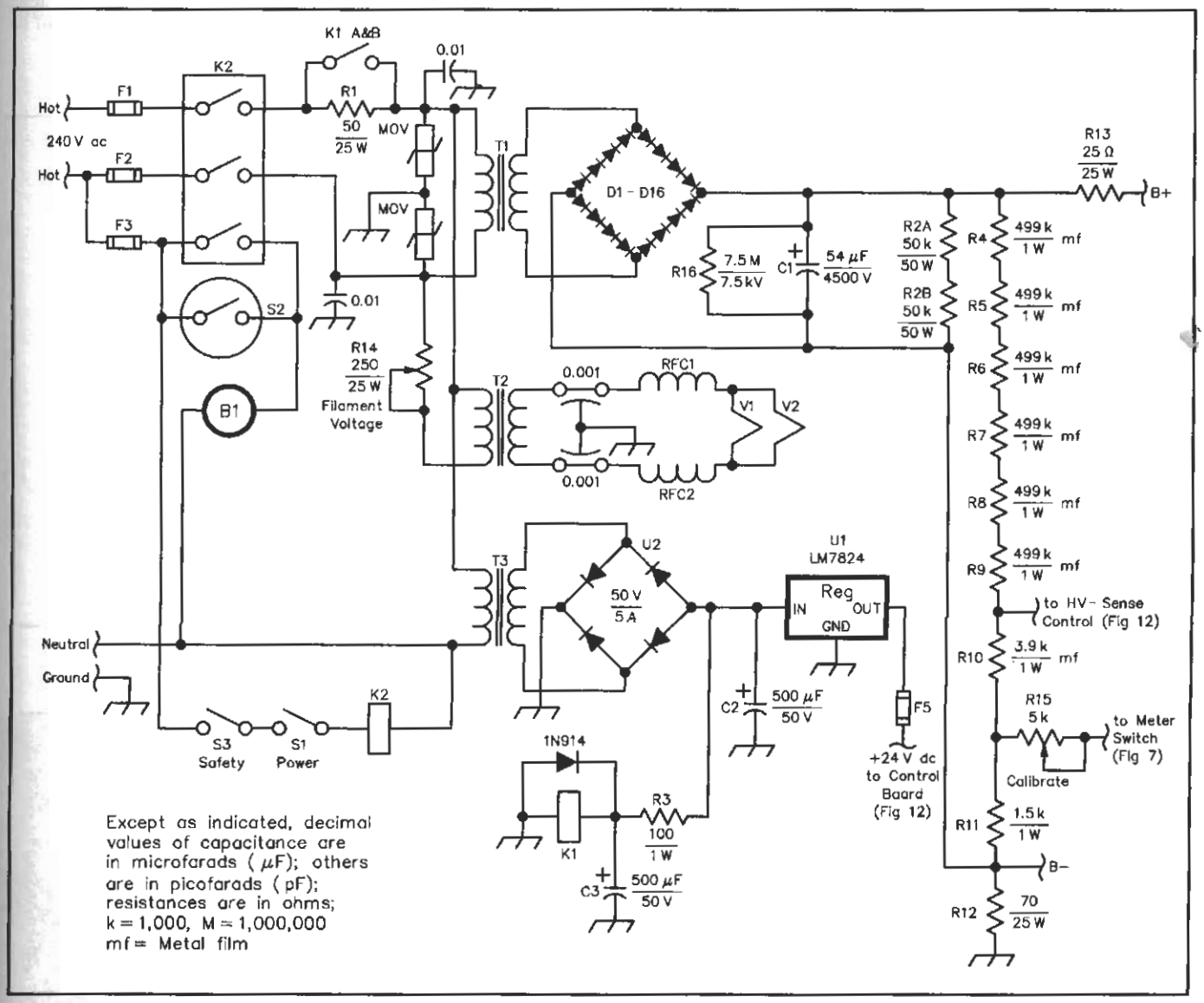

Fig 9—Power-supply schematic. Unless otherwise specified, use 1/4 W, 5%-tolerance carbon composition or film resistors. See Table 3 for part-supplier contact information.

B1—Dayton #4C761 squirrel-cage blower
C1—54 μF, 4500 V oil-filled electrolytic capacitor
C2, C3—500 μF, 50 V electrolytic capacitor
D1-D16—1N5409 1200 PIV, 3 A Silicon rectifiers, four diodes per string
F1, F2—20 A, 250 V ceramic fast-blow fuse
F3—3 A, 250 V fuse
F5—2 A slow-blow fuse
K1—DPST relay, 25 A contacts, 24 V dc coil
K2—3PST relay, 25 A contacts, 120 V ac coil
MOV—130 V metal oxide varistor, V130LA5
R1—150Ω 25 W wire-wound resistor
R2A, R2B—50 kΩ 50 W wire-wound resistor
R3—100 Ω, 1 W carbon resistor
R4-R9—499 kΩ, 1 W metal film resistor
R10—3.9 kΩ, 1 W metal film resistor
R11—1.5 kΩ, 1 W metal film resistor
R12—70 Ω, 25 W wire-wound resistor
R13—25 Ω, 25 W wire-wound resistor
R14—250 Ω, 25 W rheostat
R15—5 KΩ, 10-turn potentiometer
RFC1, RFC2—12 bifilar turns of #18 AWG enameled wire on 1/2-inch-diameter Teflon rod
S1—SPST 5 A lighted panel switch
S2—Temperature snap-disc control Grainger # 2E245
S3—SPDT 5 A microswitch
T1—Peter Dahl plate transformer: 240 V primary, 1800 V, 1 A CCS secondary
T2—240 V primary, 16 V, 5 A secondary
T3—120 V primary, 20 V, 2 A secondary
U1—LM7824 TO-3 case
U2—5 A, 50 V rectifier bridge

25 W to the parallel 6-meter network and 100 W to the 2-meter push-pull network. Con-nect the analyzer to the respective input ports and adjust each network for lowest SWR. Some adjustment of the 6-meter input coils (L6 and L7) may be required to achieve a 1:1 match. If the 2-meter network does not present a good match, some adjustment in length of L4 and L5 may be necessary. Again, the covers must be in place and tubes must be in their sockets when measuring the match. Both filament leads and the filament choke must be in their final positions because the cathode-to-filament capacitance affects input tuning at 144 MHz. Remember, this analyzer method only gets you close to the final tuning points; settings will be different under live conditions. Finally, don't forget to remove the temporary resistors from the cathode and tank circuits after the initial adjustments are done.

AC Mains and Low-Voltage Power Supplies

Several protective measures are built into the amplifier to protect the tubes and the operator. The ac mains are brought into the amplifier with four-conductor cord to keep the neutral and ground separated per the *NEC* (Fig 9). Three fuses are used to keep the blower's ac source separate from the fused plate transformer. This was done so the blower's cool-down delay still functions after a high-voltage fault, which removes ac from the entire amplifier in dual-fuse designs. A thermal snap switch in the tank compartment keeps the blower running after shutdown or a high-voltage fault if the exhaust air has been above 110°F and is not yet below 90°. This only happens after several minutes of continuous operation. You may want to use a switch with slightly higher ratings (120°F on, 110°F off) if your shack is often warmer than the 90° off point used here. The 3CX800A7's filaments dissipate only 20 W each during cutoff and natural convection is more than enough to cool the tubes when shut off.

AC voltage for K2, the main control relay, is also taken from F3, the blower fuse, to make sure blower voltage is available before the amplifier can be powered up. A safety switch that closes when the top cover is in place supplies ac to S1, the main power switch. Power-supply inrush protection is provided by K1, which closes approximately one second after K2 and effectively removes R1 from the transformer primaries. The delay period is set by R3 and C3. There are two MOVs across the ac lines after the contacts of K2 and K1. Arcing at the relay contacts can and will produce voltage spikes and spike protection on the fuse side of K2 will not always save the high-voltage diode strings and other components. Filament voltage is adjusted at the primary of T2 by R14, a 250-Ω, 25-W rheostat. Filament voltage is measured at the filament choke via two leads brought to the back panel of the amplifier. Purists may want to measure voltage at the filament pins, but the low filament-current demand of these tubes makes the voltage drop between the sockets and the choke negligible. The rheostat also provides passive filament-inrush protection.

The low-voltage supply—consisting of T3, U1 and U2—supplies regulated 24 V at 1 A. The bridge rectifier and 24-V regulator are mounted to a piece of ¾×1-inch aluminum angle that is placed directly in the cooling-air inlet path (Fig 8).

High-Voltage Power Supply

The high-voltage power supply consists of a Peter Dahl Hypersil plate transformer and a full-wave bridge rectifier with capacitor input filter. The supply is capable of producing 2150 V at 1 A CCS. The entire supply is assembled as one piece, then in-stalled on the floor of the main cabinet next to the plate transformer (Fig 6). The oil-filled filter capacitor is sandwiched between two 3×6½-inch pieces of Plexiglas, in turn held together with four #10-24×5-inch-long flat-head screws. The rectifier strings and high-voltage-meter multiplier resistors are mounted to a 3×6½-inch PC board supported by ¼-inch spacers on the same four screws. A 3×6½-inch piece of fiberglass board holding the two bleeder resistors, B+ current limit-ing resistor and B– float resistor tops off the

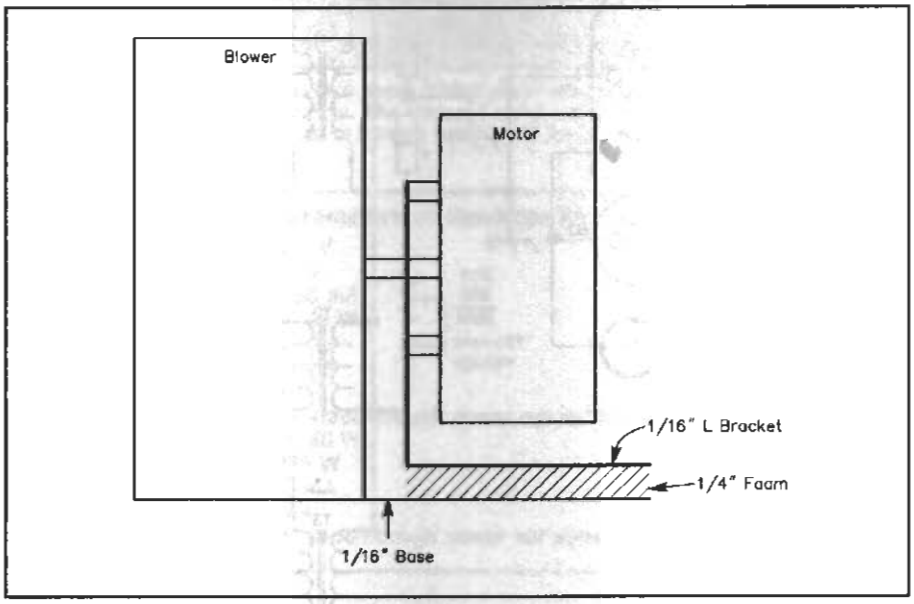

Fig 10—Layout of the blower modifications for sound reduction.

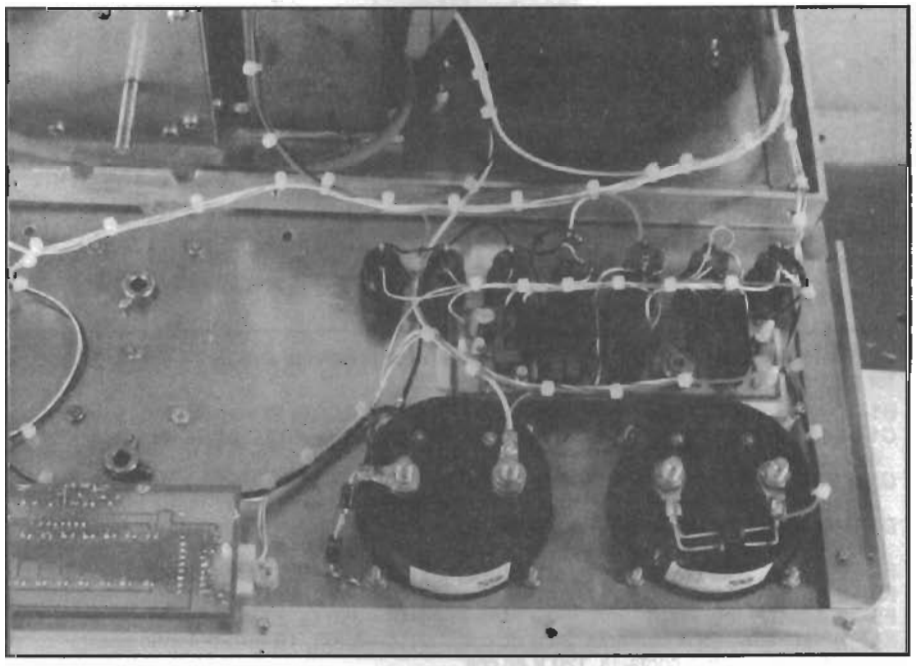
Fig 11—View of control board.

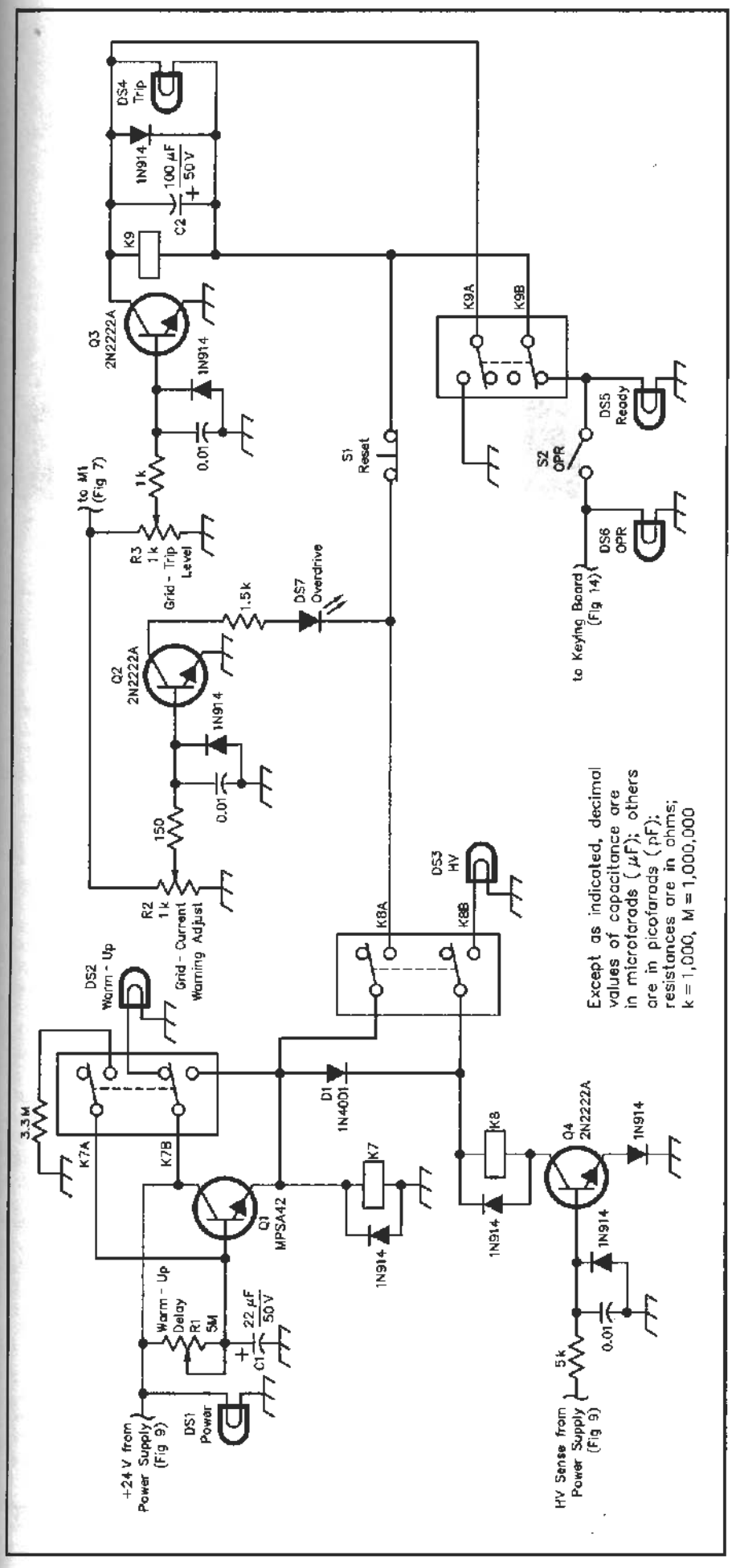

Fig 12—Control schematic. Unless otherwise specified, use ¼ W, 5%-tolerance carbon composition or film resistors. See Table 3 for part-supplier contact information.
C1—22 µF, 50 V electrolytic capacitor
C2—100 µF, 50 V electrolytic capacitor
DS1—24 V lamp part of S1 (see Fig 9)
DS2, DS3, DS5—24 V panel light
DS4—24 V lamp part of S1
DS6—24 V lamp part of S2
K7, K8, K9—DPDT 5 A DIP relay, 24 V dc coil
R1—5 MΩ PC-mount potentiometer
R2, R3—1 kΩ PC-mount potentiometer
S1—Normally closed momentary-contact lighted panel switch
S2—SPST lighted panel switch

stack. All of the power resistors on the top board are mounted on one-inch ceramic standoffs. High voltage is routed to the tank compartment with test-lead wire and a high-voltage feed-through capacitor. The diode strings do not use equalizing resistors or capac-itors as they are from the same batch and there is plenty of PIV headroom. Spike protection for the string is in the transformer primary, where it belongs. The high-voltage supply has three bleed-down paths for the filter capac-itor: the bleeder resistors, the high-voltage meter multipliers and a 7.5 MΩ, 7.5-kV resistor at the terminals of the capacitor itself. Even with these redun-dant safety measures, *never* assume that they are working. *Always follow standard safety procedures when working with any high voltage, including the ac mains: It can kill you.*

Cooling

Whole-cabinet cooling is accomplished via a Dayton model 4C761 squirrel-cage blower. Cooling air is drawn into the cabinet at the right-hand side through two 2¾-inch holes, one on each side of the plate trans-former. This removes heat from the bleeder resistors and other components before it enters the blower inlet. The Svetlana 3CX800A7 datasheet recommends airflow of 11 cfm at a back pressure of 0.2 inches (of water), for 600 W dissipation at sea level and 25°C inlet air temperature per tube. For two tubes, this is 22 cfm at 0.2 inches for 1200 W of dissipation. At a 1500-W output level with 60% efficiency, the tubes only dissipate 960 W.

The socket sub-mounting method I used resulted in a back pressure of 0.2 inches with this blower, as measured on my bench with a home-brew manometer. Since the blower is rated for 43 cfm at 0.2 inches (sea level assumed), there should be plenty of headroom for different elevations and inlet air temperatures. Remember that the above calculations are for continuous dissipation, while SSB and CW operation rarely approaches 50% of these values.

The mounting flange at the bottom of the blower was cut off so the outlet can align with the 2-inch-tall cathode chassis. The blower motor was taken off its squirrel

cage and mounted to an aluminum L bracket. The squirrel cage was mounted to a 4×4-inch piece of 1/16-inch aluminum that supports the L bracket through a piece of 1/4-inch foam (Fig 10). This sound-isolation method was borrowed from Alpha Power Inc, and it works very well.

Control Board and Metering

The control PC board (Fig 11) is mounted on nylon standoffs just below the panel meters and above the row of switches and panel lights. As with most indirectly heated, oxide-coated cathodes, a warm-up period is required; for the 3CX800A7, a minimum of three minutes is recommended. When the amplifier is turned on, regulated 24 V is applied to the warm-up

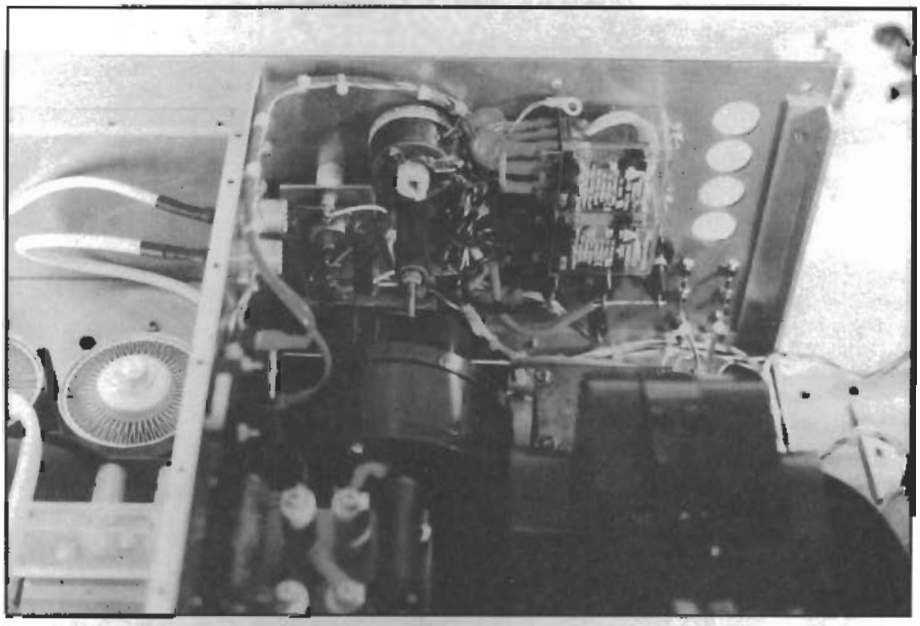

Fig 13—(right) View of panel showing K1 and K2. The bias heat sink and assembly is visible below the filament rheostat.

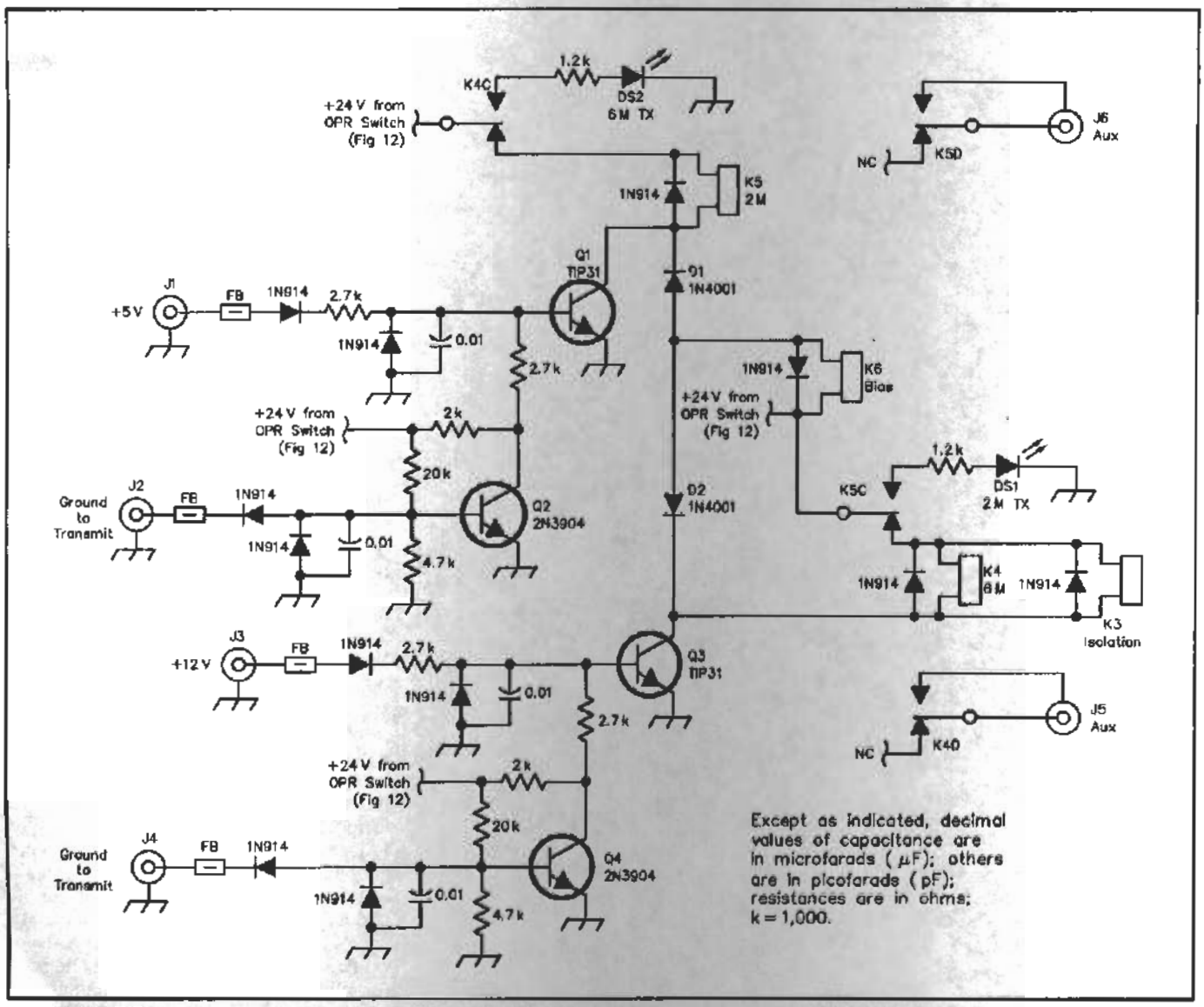

Fig 14—Schematic of the dual keying-circuit PC board. Unless otherwise specified, use 1/4 W, 5%-tolerance carbon composition or film resistors. See Table 3 for part-supplier contact information.

delay circuit consisting of Q1, R1 and C1 (Fig 12). When sufficient voltage appears at the base of Q1, relay K7 closes, with one set of contacts latching the relay on while the other set of contacts resets C1. If high-voltage is present, Q4 is switched on and K8 closes, lighting DS3 and supplying 24 V to the rest of the amp-lifier. Diode D1 was added between the field of K8 and the field of K7 to make sure K7 closes first. The proximity of the control board to the magnetic field of the plate transformer affects the timing of K7 slightly.

With the low grid-dissipation rating of these tubes, grid over-current protec-tion is necessary. Grid current is mea-sured as voltage drop across R1 of Fig 7, a 10-Ω, 25-W wire-wound resistor. R3 on the control board is set to fire K9 with Q3 at a grid current of 120 mA. One set of contacts latches the relay on; the other set interrupts the 24-V line to the **OPR** (operate) switch. Capacitor C2—across the field of K9—stops relay chatter on voice peaks. Lamp DS4 is part of the grid-reset switch S1, and it lights while K9 is energized. A second grid-current-sensing circuit, using Q2, is set to light DS7 on the front panel at 75 mA. This LED is used as a grid-current warning indicator and can be set at the grid-current level you prefer. The trip points of these two circuits and the grid-current meter reading are ad-justed while the amplifier is discon-nected from the ac supply.

To do so, connect a 24-V external supply to the 24-V bus of the amplifier after the timing circuit. Connect the positive lead of a variable-voltage dc supply to the ungrounded side of R1 of Fig 7 through an accurate dc milliammeter. Connect the external-supply negative lead to the chassis. With the grid-current panel meter disconnected, slowly increase the voltage of the bench supply until the milliam-meter reaches the set points of 120 mA for grid trip and 75 mA for the warning LED. Adjust R3 and R2 (Fig 12), respectively, to set the trip points. After the trip points are set, reconnect the grid-current meter and adjust R4 (Fig 7) for a full-scale reading of 100 mA using the same method as for the trip points. This "cold" method of setting grid trip points is a lot safer for the tubes than removing B+ and then applying drive to induce grid current.

The panel meter, M2, serves as the high-voltage meter as well as the grid-current meter. The calibration of the high-voltage portion was "roughed in" with the amplifier off and all voltages removed. A 1.5-V dc supply was connected to the multiplier side of R15 on the high-voltage rectifier board, then R15 is adjusted for a full-scale reading on M2. This corresponds to a full-scale reading of 3000 V. Meter calibration was then checked with a high-voltage probe and an accurate DMM, after the amplifier was turned on.

Plate current is measured directly in the B– line of the high-voltage supply, which is held slightly above ground by R12 on the power-supply assembly. Both meters are protected by 1N5408 diodes; two series-connected diodes on the B– bus keep it below approximately 1.4 V and two more are connected back-to-back from the multimeter to ground.

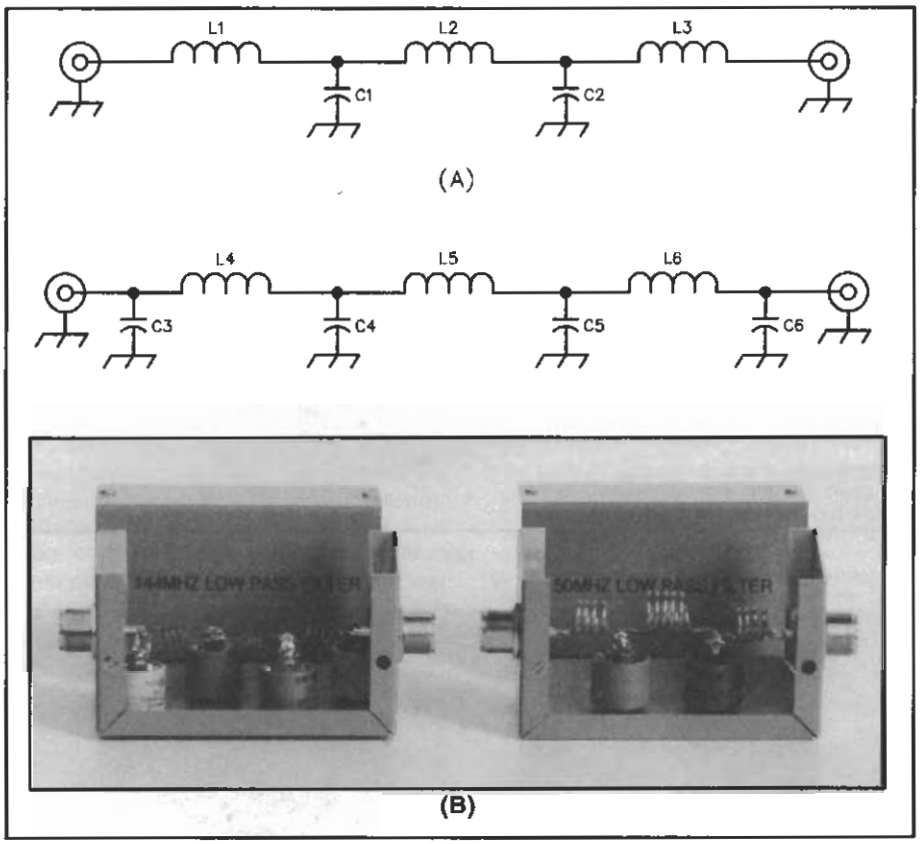

Fig 15—Details of the 2- and 6-meter low-pass filters. See Table 3 for part-supplier contact information.

50 MHz
C1, C2—50 pF doorknob capacitor
L1, L3—4 turns #14 AWG copper, 5/16-inch ID×1/2-inch long
L2—5 turns #14 AWG copper, 5/16-inch ID ×5/8-inch long

144 MHz
C3, C6—25 pF doorknob capacitor
C4, C5—40 pF doorknob capacitor
L4-L6—3.5 turns #16 AWG silver-plated copper wire, 1/4-inch ID×5/16-inch long

There are relative-output bar-graph displays for each band above the tune and load controls. These displays use two LM3914 bar-graph drivers per 20-segment display. A current-transformer pickup unit is used for 6 meters and a voltage-sensing pickup for 2 meters. The dual-bar-graph-display schematic can be found in Forrest Mims' book[8] and the 6- and 2-meter pickups are shown in Fig 7. The displays look appealing but turned out to be more trouble than they are worth, since I still use external wattmeters while I tune. The bar-graph displays' rapid response time would be better suited for plate- and grid-current meters.

Bias and Keying

Operating bias is developed across D1 of Fig 7, an 8.2-V, 50-W stud-mounted Zener diode. The Zener, along with K6, R2 and R3, is mounted on a 2×3-inch piece of 0.100-inch aluminum that serves as a heat sink (Fig 13). The entire assembly is mounted on two 1/2-inch Teflon stand-offs on the back panel of the cabinet. The 2-A cathode fuse is mounted on the back panel alongside the ac-line fuses.

The keying PC board is mounted on the rear floor of the main cabinet (Fig 8). The PC board contains keying circuits for both 6 and 2 meters (Fig 14). Because they are identical, I'll only describe the operation of one.

At rest, Q2 is biased on, holding the base of Q1 low. Grounding J2 will take the base of Q2 low, turning it off. This allows voltage to appear at the base Q1, turning it on and energizing K5. Alternatively, applying +12 V to J1 will also turn Q1 on, keying the amplifier. Both keying inputs are logic-compatible. The bias relay is energized through D1 or D2, which comprise a two-input **OR** gate. Each transfer relay is a DowKey #260B with the "C" option, which is a pair of DPDT signaling switches. Each of the relays' supply voltages is routed through one of the opposite relay's normally closed signaling contacts. This mechanical **EXCLUSIVE-OR** gate keeps the amplifier from being simultaneously keyed on both bands. The normally open contacts are used to light transmit LEDs on the front panel; these are mounted between their respective tune and load controls to help eliminate confusion while tuning.

With this type of transfer relay, input and output relay sequencing is obviously

(A)

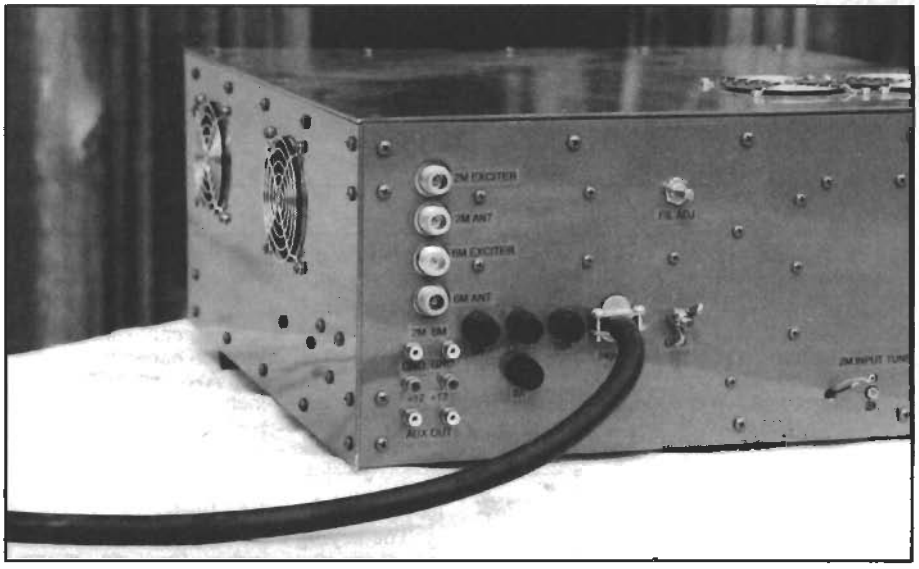

(B)

Fig 16—The completed amplifier ready for its ride to the mountain top. (A) Front view, (B) back panel.

not an option, and hot switching of the relays will result unless preven-tive measures are taken. One option is to key the amplifier and let it key the exciter. Each relay's spare set of signaling contacts was brought to the back panel for this possible use. Another option, which I employ, is to use an outboard keying sequencer. The sequencer takes care of my mast-mounted preamplifiers as well as the exciter-amplifier timing. A suitable sequencer can be found in the references.[9] When using separate exciters for each band, the spare set of signaling contacts can be used for audio muting of the unkeyed exciter while transmitting.

General Construction Notes

The entire amplifier cabinet was built using common hand and power tools. All aluminum was cut with carbide saw blades in a radial arm saw and table saw. Blades with a 5° negative hook angle seem to work best for aluminum. The main amplifier cabinet measures 18×16×7½-inches (WDH). The plate transformer determined the cabinet height. The entire cabinet is built from 0.100-inch aluminum sheet and ¾×¾×⅛-inch aluminum angle stock. All outside corners are secured with #8-32 pan-head screws tapped into the angle stock. The area under the plate transformer and high-voltage supply assembly was beefed up with a second layer of 0.100-inch aluminum on the cabinet floor. A square hole cut in the cabinet floor provides access the cathode compartment; it is normally covered with a piece of 1/16-inch aluminum. All round holes were cut with chassis punches. The cabinet was painted with Dupont Chromaclear, which is a two-step (color coat/clear coat) automotive paint. After the base coat was applied over the primer, dry transfer lettering was applied to the front panel controls and Brothers P-touch labels were applied to the rear panel. Two coats of clear were applied over the base coat to finish the job.

All interior wiring was done with scrap Teflon-coated wire. The wiring harnesses were arranged so that all side panels can be removed and laid flat next to the chassis for ease of alignment and debugging. The intern-al coax runs were made with Teflon-dielectric coax to handle these high power levels, most other coax falls short, particularly at 144 MHz.

Adjustment and Operation

Use an ohmmeter to check the ac paths and RF deck for possible shorts and wiring mistakes. Be sure to blow out the entire cabinet with compressed air to remove any hidden debris. Set the filament-voltage rheostat to maximum resistance. If you haven't already done so, apply 24 V from an external supply to the 24-V bus and check the timing, control and keying circuitry for proper operation. Connect the amplifier to a suitable ac mains supply and connect an accurate DMM to the filament-voltage test points. Connect a 2-meter exciter and dummy load. Turn on the main power switch and quickly set the filament voltage to 13.5 V, or slightly less. *Never* operate the filaments below the 12.9-V recommended minimum. Be sure to check the filament voltage again after 5 to 10 minutes to detect any thermal drift in the rheostat. Verify that the plate is at approximately 2375 V.

Both tank circuits should be set to the tuning values found during initial setup. After the three-minute delay has elapsed, key the amplifier with no drive and check for a cathode idling current of approximately 30-50 mA. Apply a little 144-MHz drive and tune C5 in the input circuit for minimum reflected power. The 2-meter output link should be preset approximately ½ inch above the top plane of the balanced line. Still with little drive, adjust the 2-meter tuning capacitor for maximum power output. Adjust the 2-meter load capacitor for peak output power and then leave it there until you are finished. Next, adjust link spacing as you would a load capacitor. Keep increasing the drive while increasing the link coupling for maximum power output, without exceeding grid-current limits and while also touching up the main tune capacitor, C3. Once the desired output power level is reached, check the link coupling by slowly decreasing the coupling until a slight decrease in output power is observed. Then increase the coupling slightly past the point where output power peaks and grid current is reduced to within operating limits. This should be very close to critical coupling, which will result in maximum efficiency. Go back and touch up the input network for minimum reflected power. The link is now set for operation and any further tuning adjustments can be made with C2 and C3.

Tune the 6-meter tank circuit the same way you would any other p net-work: by slowly increasing drive and tuning for maximum power output and best efficiency while touching up the input network for lowest reflected power. Then increase

loading until a 2% decrease in power output is observed.

With values of loaded Q below 30 in the output tanks, there is no way to keep harmonics below the 60-dB-down figure required by the FCC without outboard filtering. Harmonic filters are a very small price to pay for the higher efficiency, lower drive require-ment and reduced thermal drift that the lower loaded Q provides. I've included descriptions of two suitable filters from the references;[10,11] they are very easy to build. The silver-mica capacitors originally in the filters have been replaced with surplus door-knob capacitors for better power-handling capability. With both filters installed all harmonics and spurious signals are more than 70 dB down from the fundamental.

Final Thoughts

This amplifier was completed just before the summer E-skip season and was immediately put on the air. On-the-air signal reports were all good, and they compared well to the 8877 amplifier I normally use. Close in IMD testing was done with the help of NN7DX who is located nine miles away, over flat ground. Results showed no excessive signal bandwidth while our antennas were positioned to bring signals down to S-9 levels during 1500-W output testing. The amplifier runs cool to the touch even after several hours.

The biggest problem encountered with the operation of the amplifier had to do with interfacing with certain exciters. Some of the new multiband exciters provide multiple antenna ports that can be configured for HF, 6- and 2-meter outputs, but provide only one buffered keying line. The ICOM-746 is built this way, but it does provide two unbuffered keying lines: one for HF and 6 meters and one for VHF. The ICOM-706-series radios also provide two unbuffered lines but only two antenna ports. Both of these radios require some sort of external switching for the keying line—and the antenna line in the case of the '706—if this amplifier and an HF amplifier are both used. ICOM does provide band logic as a variable voltage at the radio's **ACC** plug. I've designed a simple decoder/buffer that uses this logic and the radio's internal power supply to automatically switch the keying line between HF, 6- and 2-meter amplifiers. The buffer will sink up to 3 A of relay current. It also selects from three separate ALC input lines for those of you that employ sequencers using the ALC line for transmit inhibit. The decoder is described in "Automatic Amplifier Selection for the ICOM IC-746, -736 and -706MKII Transceivers," *QST*, May 2000, pp 33-36. With the decoder in place, amplifier selection with an IC-746 becomes totally automatic when changing bands between HF, 6 and 2 meters. For the IC-706 series, an additional coaxial relay can switch one of the antenna ports between HF and 6 meters to allow automatic selection. The decoder also works with the ICOM IC-736, choosing between HF and 6 meters. Although not verified, I've been told that the Yaesu FT-847 does have separate buffered keying lines for each of its four antenna ports, making interface to this amplifier easy. Performance figures for the amplifier are listed in Table 2 and the completed amplifier is shown in Fig 16. Enjoy!

Acknowledgements

Thanks to Marv Gonsier, W6FR, and Roy Scanlon, NN7DX, for help in reviewing the text.

Notes

[1]C. M. Maer Jr, WØIC, "The Perseids Powerhouse," *QST*, Oct 1959, p 32.

[2]R. M. Richardson, W4UCH, "A Kilowatt Amplifier for 6 and 2 Meters," *QST*, June 1973, p 16.

[3]The surplus sockets have a built-in 0.005 µf grid/screen bypass capacitor. RF Parts has a limited supply of these sockets. Substitutes include Johnson #124-0311-110 (with a grid collet) and Eimac SK1900.

[4]G. R. Jessop, G6JP, *VHF/UHF Manual*, 4th edition, (Hertfordshire, England: Radio Society of Great Britain, 1983) Chapter 3.

[5]E. P. Tilton, W1HDQ, *The Radio Amateur's VHF Manual*, (Newington: ARRL, 1972) p 77.

[6]R. D. Straw, Ed., *The 1999 ARRL Handbook* (Newington: ARRL, 1998), pp 6-46 and 6-47.

[7] R. Myers, W1FBY, *The 1975 ARRL Handbook* (Newington: ARRL, 1974), p 46.

[8]F. M. Mims III, *The Forrest Mims Engineer's Notebook*, (San Diego, California: Hightext Publications Inc, 1992) p 107.

[9]*The 1999 ARRL Handbook*, pp 22-53 through 22-56.

[10]I. White, G3SEK, Editor, *The VHF/UHF DX Book*, Vol 1 First Edition (Buckingham, England: DIR Publishing, 1992) p 12-35.

[11]R. Schetgen, KU7G, Ed. *The 1993 ARRL Handbook*, (Newington: ARRL, 1992) p 31-37, Fig 95.

By Bob Larkin, W7PUA

From *QST*, June 2000

An 8-Watt, 2-Meter 'Brickette'

Put 20 mW into this little amplifier and get a 26-dB increase in transmitted power! Although the amplifier was designed initially for use with the DSP-10 transceiver, any 20-mW-output 2-meter exciter can enjoy the boost!

The DSP-10 transceiver[1] can be used with UHF/microwave transverters or as a very-QRP all-mode rig on 2-meters. The rig's 20-mW power output is sufficient for "barefoot" QSOs with locals, but that's hardly a big signal at any distance. Adding this little amplifier increases your fun quotient by raising the power level to 8 W, the high end of the QRP plateau. This brickette can also be used to drive an even higher-power, cascaded amplifier. Being a linear amplifier, it's suitable for use on all modes, including SSB, CW and FM.

The amplifier's front panel is quite simple, consisting of five monitoring LEDs. Knowing that everything is working correctly justifies the small amount of circuitry needed to operate these lights. The functions monitored include dc power on, transmit/receive status, power output, SWR and dc overvoltage. All amplifier control is done at the transceiver. Two RF cables connect to the transceiver output and receiver input, avoiding the need for an input relay in the amplifier.

This amplifier isn't limited to use with the DSP-10; any 2-meter transmitter that can deliver an output of 20 mW to drive the amplifier should work fine. In some cases, it might be desirable to use an input TR relay; there is sufficient room in the amplifier for adding one.

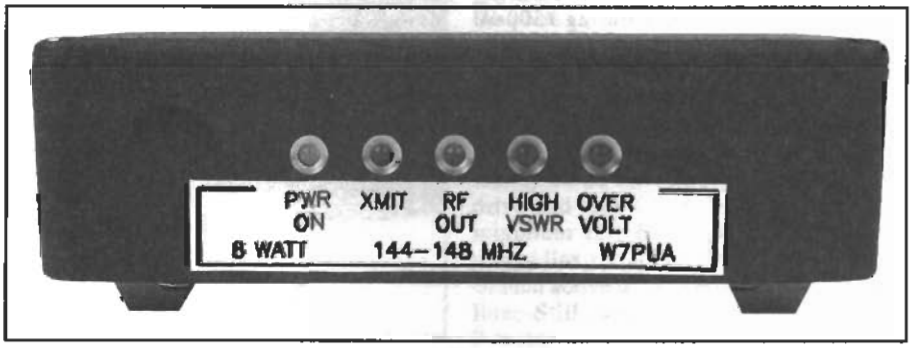

The five LEDs on the Brickette's front panel signal the amplifier's operating status. The power-output (**RF OUT**) and SWR (**HIGH VSWR**) LEDs vary in brightness depending on the forward and reflected power levels.

Circuitry

At the heart of this amplifier is an integrated power-amplifier module, manufactured by Mitsubishi. Such modules are used in many commercially manufactured transceivers and using one here makes amplifier construction and alignment simple. Within the module are two cascaded linear-amplifier transistors, along with their associated matching networks and biasing circuits for class AB operation. The module has 50-Ω input and output impedances. All we need to do is add a circuit to turn on the bias supply during transmit, install a low-pass filter for harmonic control and include an antenna-switching relay. To monitor amplifier operation, we tack on some simple circuitry.

Refer to the schematic in Figure 1. At the input pin of the RF module, U1, we apply 20 mW of drive. Blocking capacitors for the RF input and output ports are included within the module. Bypass capacitors on the three power leads are external, however. Ferrite beads, L6 to L8, prevent problems that might occur if RF gets on the power leads.

An **L** network consisting of L1 and C4 improves the impedance match to the module. Adding the network increases the output power by about 0.25 dB. Following the amplifier is a directional coupler (discussed later). Next is a five-pole low-pass filter. For simplicity, it is configured with the same coil and capacitor types as are used in the directional coupler. This filter attenuates the second and higher-order harmonics.

Separate connectors are available on the DSP-10 for the transmitter output and the receiver input. This simplifies adding the antenna relay for the amplifier since no switching is required at the amplifier input. A miniature relay is adequate at the amplifier output. Providing an isolation of about 30 dB, the relay, along with the PIN attenuator that is part of the DSP-10, provides plenty of protection for the receiver.

A lumped-element directional coupler, consisting of L2, L3 and C5 to C10, delivers power samples of the forward and reflected output signals. This directional coupler works quite well, providing a coupling of about −28 dB and a directivity[2] of 20 dB, but only over a narrow (12-MHz)

bandwidth. For our application, this is adequate. Two diode detectors, built around D6 and D7, generate low-level dc signals that indicate the forward and reflected powers. These signals, in turn, are amplified by two sections of op amp U2. The resulting voltages are displayed on two LEDs, green for **RF OUT** (forward) power and red for **HIGH VSWR** (reflected) power. The LEDs serve as rough indicators of proper amplifier operation.

The **OVERVOLTAGE** indicator lights when the dc supply voltage exceeds 14.5 V, but does not automatically shut down the amplifier. The idea here is to supply a warning mechanism. When RF is not applied to the amplifier, it is quite resistant to supply overvoltage. As long as the supply overvoltage condition sets an alarm light, an observant operator will defer applying RF until the voltage is reduced.

Amplifier control is handled by the DSP-10. That transceiver has software-controlled relay sequencing, providing +5 V during transmit. Q2 and Q3 drive the antenna relay from this control. A ferrite bead, L11, and C24 keep RF at the antenna relay from getting back into the control circuits. D10 shunts the inductive kick from the deactivated relay coil. An LED, D2 (**XMIT**), across the relay displays the amplifier TR status.

Q4 provides an output that can control a follow-on amplifier. This output is an open-collector, ground-on-transmit type, compatible with many commercial and homebuilt amplifiers. For added driver-circuit protection, a reverse-voltage shunting diode, D11, is used.

Building the Amplifier

You could build the amplifier on a scrap of PC board. In fact, my first version is built that way (see the sidebar). For many builders, however, a PC board[3] is a more convenient way to assemble the project and that is shown in the photos.

This PC board is double-sided, with plated through holes. The backside is a solid ground plane allowing the board to be fastened directly to the aluminum enclosure. Such construction works very well for RF boards because a low-inductance ground path can be maintained throughout, reducing any interactions between the various circuits. However, this mounting method does not allow component leads to extend beyond the bottom surface of the board. I dealt with this primarily by using surface-mount parts[4] and by carefully bending the component leads so they behave like surface-mount parts.

All of the chip resistors, chip capacitors, diodes, surface-mount ICs and ferrite-bead chips are soldered to their board pads conventionally. Install the amplifier module *after* the board is mounted in the box. The antenna relay, fuse clips and the variable resistor all have their leads bent away from their host. Avoid making any bends close to the component body; make the bends at a point about $^1/_{16}$ inch away from the component body. This approach eliminates mechanical stress on the lead attachment. These components end up about $^1/_{16}$ inch above the board's top surface after they are soldered in place.

Figure 2 shows the construction of the four toroidal inductors, L2 through L5. Experience shows the inductor values are quite repeatable if the turns are always distributed in the same manner around the core. As the turns are pushed closer together, the inductance increases considerably. The matching-network coil, L1, is noncritical and it should be wound as shown in the part list and Figure 2; it should need little, if any, adjustment.

The LEDs all have long leads and are soldered to the board after bending the lead ends by about $^1/_8$ inch. Be sure to keep track of the LEDs' longer (anode) leads: Those leads connect to the current-limiting resistors.

Putting the Board in a Box

Once the PC board is assembled, use it as a template for marking the hole locations in the enclosure, a standard Hammond die-cast box. Mount the board flat against the box bottom using #4-40 hardware. Because there will likely be some mold marks and box-identification letters where the board and RF module lie, make the enclosure's inner-bottom surface reasonably flat; you can do this with 60-grit sandpaper. Bend the leads of the five LEDs to apply a slight forward pressure on the lights as they slide into the holes in the box front. That holds the LEDs in alignment without needing adhesive.

Take care when tightening the PA module mounting screws to be sure that no pressure is applied to the ends of the module cover. The leads from the module need some trimming. They are above the board and need forming to get to the board level for soldering. Don't apply pressure at the edge of the module cover when doing this. You may need to hold each lead with needle-nose pliers to keep from damaging the case. It should be possible for the leads to reach the board surface within $^1/_8$-inch of the cover.

Three short pieces of 50-Ω coax attach the board to J1, J2 and J3. Solder lugs under the jacks provide for ground connections at one end and PC-board pads take care of the other end of the coax.

Three leads run between connectors J4, J5 and J6 and the PC board. Each of these leads has a bypass capacitor (C28, C6 and C27, respectively) at the connector. Short, low-inductance leads are important on these capacitors. To help keep the RF signals inside the box, a small inductor wound on a ferrite core (L14, L15 and L16) is placed on each wire. Position these inductors close to their connectors. If #22 or #24 stranded hook-up wire with thin insulation is used, it's possible to wind the coils with the hook-up wire.

Turning on the Amplifier

Now, to see it work! First, connect a 50-Ω noninductive dummy load to the amplifier output.[5] If you have a variable-voltage power supply to use for initial testing, slowly raise the dc supply voltage from 0 V to 13.8 V. Otherwise, you'll need to rely on the power-supply fuse as protection from any serious construction errors when apply-

Did the Amplifier Always Look Finished?

No, it didn't. Some people may be able to put a finished amplifier on a PC board and have it work fine. I don't seem to be able to do that!

My first step in designing the amplifier was to search for suitable RF modules, mostly via the Internet. Once I selected the M57732L as having suitable power, gain and dc operating voltage, I drew a schematic in my notebook. Originally, the circuit had automatic shutdown for high SWR and full voltage regulation to deal with overvoltage. This looked too complex. It was necessary to cut off the drive to the amplifier, and the regulator had to be a low-dropout type (for these, the difference in voltage between the input and the output need be only a fraction of a volt). I couldn't find an integrated regulator that met my requirements and the thought of building one using op amps and transistors used more parts than I could justify.

I opted for simplification, putting alarm lights on for SWR and overvoltage and turned the automatic part over to the operator! A new schematic resulted, not unlike that of Figure 1. I went to the *ARRL Radio Designer*† and simulated the directional coupler and low-pass filter. A little playing around with the simulation showed that a single inductor value could be used for both subcircuits.

Next, I built the "breadboard" version using scraps of PC board. Testing showed that almost everything worked as expected. The **overvoltage** light did not have snap action, though. That was caused by using a resistor where the ferrite bead, L13, is now. I ran the input voltage temporarily up to 16 V and everything continued to function. Next, I left the amplifier running for an hour and nothing overheated. I checked the intermodulation products and harmonics and found them to be at satisfactory levels.

It was now time to layout the PC board. The experience of putting the breadboard together allowed a smarter final layout. The first version was on two boards and some of the connectors ended up on the front panel. This was all worked out for the final design. —*Bob Larkin, W7PUA*

†ARRL order no. 6796. ARRL publications are available from your local dealer, or directly from the ARRL. See the ARRL Bookcase elsewhere in this issue, or check out the ARRL Web site at: **http://www.arrl.org/catalog/**.

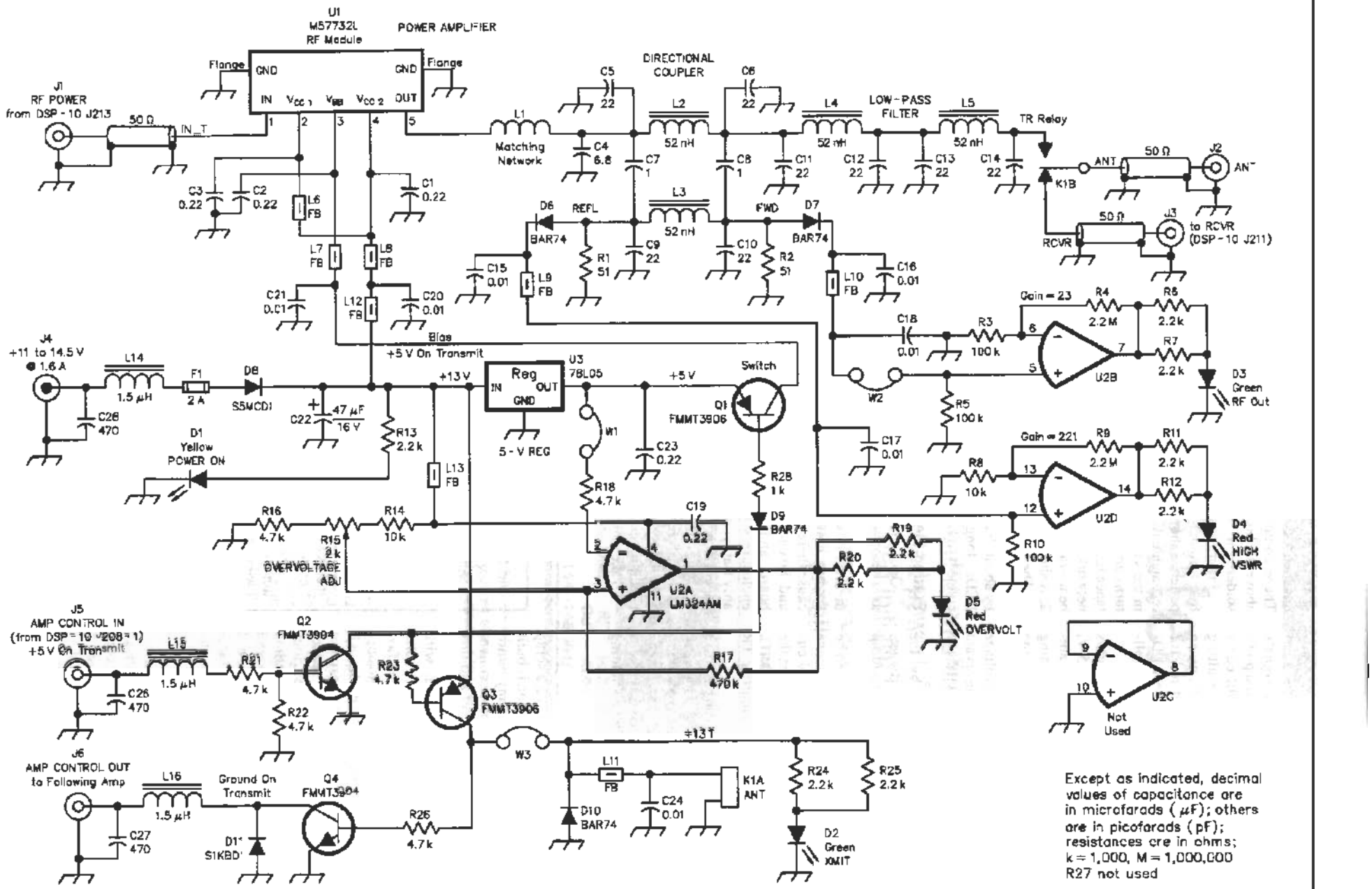

Except as indicated, decimal values of capacitance are in microfarads (μF); others are in picofarads (pF); resistances are in ohms; k = 1,000, M = 1,000,000
R27 not used

Figure 1—Schematic of the 8-W amplifier. All resistors are 5% 1206 chips. These are available in small quantities from Mouser Electronics (Xicon). Unless otherwise noted all capacitors are either 1206 or 0805 chips (either size fits on the board). Capacitors less than 470 pF are NP0, while values from 470 pF and up are any general-purpose ceramic, such as X7R or Z5U. Component sources listed here are generally only a few of several that manufacture equivalent parts. If the amplifier is built without a pre-made PC board, change the chip components to leaded types. Component designations for the LEDs differ from *QST* style. Parts used in the amplifier are available from one or more of the following sources. Source abbreviations used in the parts list precede the company name: (DK) Digi-Key Corp, 701 Brooks Ave S, Thief River Falls, MN 56701; tel 800-344-4539, 218-681-6674; **http://www.digikey.com**; (ME) Mouser Electronics, 958 N Main, Mansfield, TX 76063; tel 800-346-6873, 817-483-4422; **http://www.mouser.com**; (RS) RadioShack—see your local distributor; **http://www.radioshack.com**; (RP) RF Parts, 435 South Pacific St, San Marcos, CA 92069; tel 800-737-2787, 760-744-0700; **http://www.rfparts.com**.

C22—47 µF, 16 V surface-mount electrolytic (DK PCE3033CT)
C26, C27, C28—470 pF, 50 V, leaded ceramic (ME 140-50P2-471K)
D1—Yellow T1 LED (DK160-1079)
D2, D3—Green T1 LED (DK 160-1080)
D4, D5—Red T1 LED (DK 160-1078)
D6, D7, D9, D10—BAR74 diode (DK BAR74ZXCT)
D8—5-A, 50-V power rectifier, SMC package (DK S5ACDICT)
D11—1-A, 100-V power rectifier, SMB package (DK S1BBDICT)
K1—SPDT 12-V dc miniature relay, Omron G5V-1-DC12 (DK Z774)
L1—2t, #20 or 22, 1/8-inch ID; see Figure 3.
L2-L5—52 nH; 5 turns, #26 enameled wire on a T-25-17 toroid; see Figure 3.
L6, L7, L9, L10, L11, L13—Ferrite SMT bead, 1206, 600 Ω at 100 MHz, Stewart HZ1206B601R (DK 240-1019-1)
L8, L12—Ferrite SMT bead, 3 A, 1206, 100 Ω at 100 MHz, Stewart HI1206N101R (DK 240-1008-1)
L14-L16—1.5 µH, 5 turns #22 or #24 enameled wire on an FT-23-43 core; see text.
F1—2-A, 5x20-mm fuse (DK F948) with two clips (DK F058)
J1, J5, J6—Phono jacks (RS 274-346)
J2, J3—BNC jack (RS 278-105)
J4—5.5-mm OD, 2.1-mm ID power connector (RS 274-1563)
Q1, Q3—FMMT3906 PNP transistor, SOT23 (DK FMMT3906CT)
Q2, Q4—FMMT3904 NPN transistor, SOT23 (DK FMMT3904CT)
R15—2 kΩ adjustable resistor, Bourns 3329H-1-202 (DK3329H-202)
U1—RF amplifier module, Mitsubishi M57732L, (RP M57732L)
U2—LM324AM dual op-amp (DK LM324AM)
U3—78L05 5-V positive regulator, SO-8 package (DK LM78L05ACM)
Misc: PC board, enclosure 3.7x4.7 x1.3 inches, Hammond 1590BB (DK HM152), hardware.

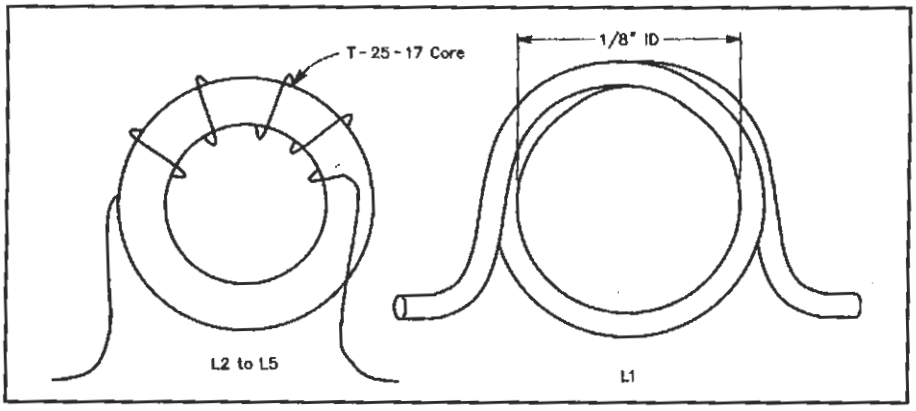

Figure 2—Coil details. Arrange the turns on the four toroids as shown here. L2 and L3 might need to have their turns spacing adjusted during tune-up.

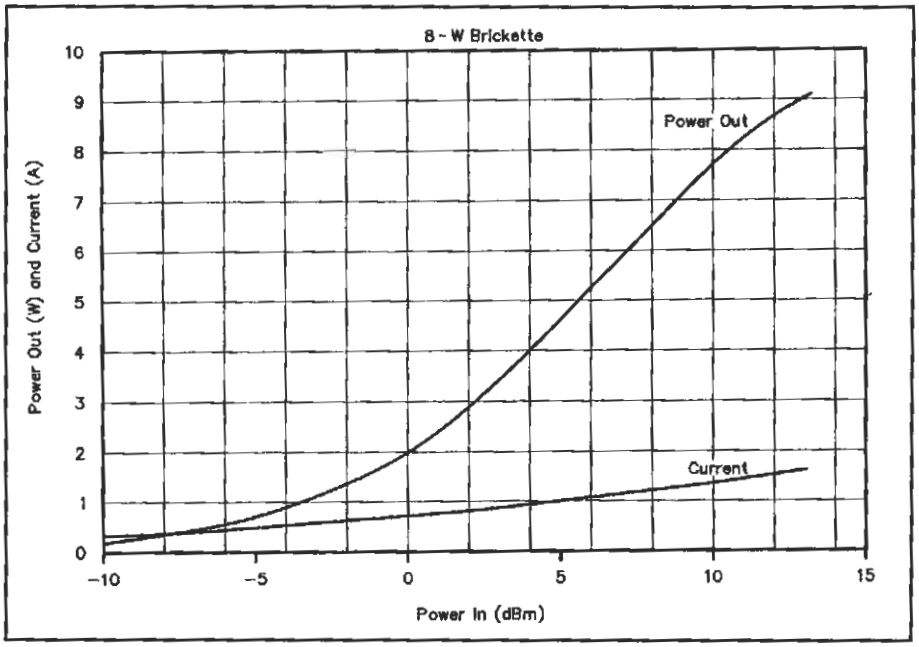

Figure 3—Measured power output and dc-supply current as a function of drive power. Notice that the output-power scale is not in decibels. This makes the output appear less compressed than it really is. The 1-dB compression point is at about 4 W.

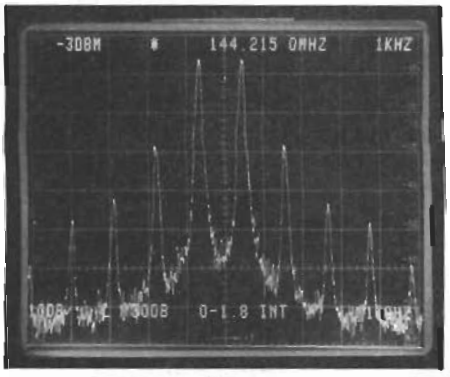

Figure 4—Measured intermodulation distortion with a PEP output of 8 W. Third-order products are down about 28 dB from peak power, fairly typical of this amplifier type. Perhaps more important is that the fifth and higher-order products continue to drop off as the order increases. These higher-order products are farther from the operating frequency and thus generally more disruptive to nearby stations. The current drawn during this two-tone test was 670 mA.

ing the full 13.8 V. At full voltage, the current drawn by the amplifier during receive should be about 10 mA. Next, set the **OVERVOLTAGE** alarm. Adjust the voltage at the wiper terminal of R15 to 4.68 V.[6] If you can vary the dc supply voltage, the **OVERVOLTAGE** LED should light at about 14.5 V.

When making the following adjustments, it is necessary to adjust the turns spacing on the toroidal inductors. For safety, *do this only when no RF drive is applied.*

Connect the TR control to the DSP-10 and connect J1, the amplifier's RF input, to the DSP-10 antenna connector. In CW mode, increase the DSP-10's RF power slowly until the **RF OUT** LED (D3) glows. Then adjust the turns spacing on L2 and L3 to extinguish the **HIGH VSWR** light (D4). This indicator is about 10 times more sensitive than the **RF OUT** LED, but it should be possible to extinguish the **HIGH VSWR** LED completely. Continue this adjustment process while increasing the drive power. You can measure the voltage at the output of the SWR op amp

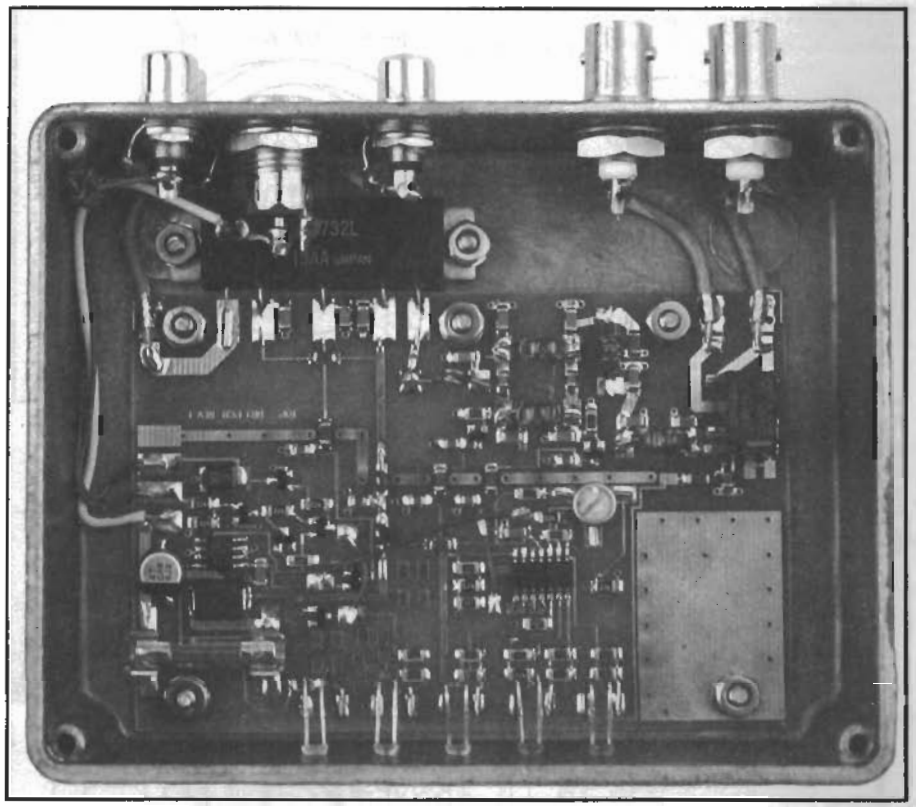

Pretty outside and pretty inside, the Brickette's construction reflects a caring hand. At the top-left rear the RF-amplifier module can be seen fastened to the base of the enclosure, which serves as a heat sink for the module. The relay is at the upper-right and a kludge area is visible at the lower right behind the front panel.

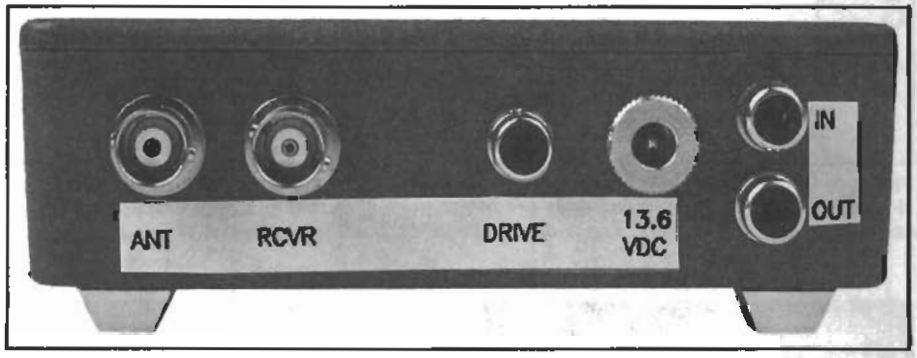

This rear-panel view of the 8-W Brickette shows compact but uncrowded I/O connectors clearly labeled.

(U2 pin 14) and continue to minimize this voltage, although the **VSWR** LED is not lit.

Optimize the amplifier matching by measuring the power output as indicated by the dc voltage at U2 pin 7 and adjusting L1's turn spacing (and perhaps changing the value of C4) for maximum output at high drive. Don't expect major changes with these adjustments as the amplifier is inherently quite well matched.

While in transmit, check that the bias voltage at pin 3 of U1 is about 4.9 V and that the idling current with no RF drive applied is about 140 mA.

Performance

Figure 3 shows the power output and current level for various drive levels. The CW output is over 8 W for the two devices that I tested. When tested with a two-tone input signal and an output of 8 W PEP, the IMD level is down 28 dB for third-order products and 43 dB for fifth-order products (see Figure 4). The strongest harmonic is the second (at about 292 MHz) and this is 65 dB down from peak output, more than enough to meet FCC 2002 requirements.[7]

Concluding Thoughts

Several areas on the PC board have either a ground plane section or pads for mounting transistors, resistors and other components. These areas are available to you to use for modifications or additions to the amplifier (perhaps you have an application that needs an input TR relay or you need a different control circuit).

Now you're ready to get on the air with a medium-sized signal. You can increase power even further by cascading another amplifier. Or, use some of the signal processing in the DSP-10 to work deeper into the noise. QRP power levels have pushed the idea of "working smarter instead of harder."

Notes

[1]Bob Larkin, W7PUA, "The DSP-10: An All-Mode 2-Meter Transceiver Using a DSP IF and PC-Controlled Front Panel," *QST*, —*Part 1*, Sept 1999, pp 33-41, —*Part 2*, Oct 1999, 34-40, —*Part 3*, Nov 1999, pp 42-45. Additional information on that project is available on the author's Web site, **http://www.proaxis.com/~boblark/dsp10.htm**. Any future information about this amplifier project will be placed at this Web site.

[2]The directivity of a coupler is the difference, in decibels, between the forward signal and the reflected signal, when the coupler is properly terminated in its designed load, in this case, 50 Ω. Couplers constructed from transmission lines have high directivity over a very wide frequency range. These lumped-element couplers are restricted in the frequency range where their isolation is high, but offer simplicity instead.

[3]Gerber files for making the PC board can be obtained from the author. Alternatively, unpopulated PC boards are available from Mashell Electric, PO Box 5, Eatonville, WA 98328. Price: $20 each in the US, $21 in Canada (air mail) and $22.50 (air mail) elsewhere. These boards have plated through holes, a solder mask on the component side and a silk-screened legend. Check their Web site **http://members.aol.com/w7slb/w7slb.htm** for details.

[4]See Sam Ulbing, N4UAU, "Surface Mount Technology—You Can Work with It!", *QST*—*Part 1*, Apr 1999, pp 33-39; —*Part 2*, May 1999, pp 48-50; —*Part 3*, Jun 1999, pp 34-36; —*Part 4*, pp 38-41. Additional comments from Avery Davis, WB4RTP, can be found in the *QST* Technical Correspondence, Feb 2000, p 70. Surface-mount techniques are used for the DSP-10 transceiver. Some people were initially concerned about dealing with the tiny components, but after constructing the board, most builders felt that it went well.

[5]A satisfactory dummy load for 144 MHz can be constructed from four 200-Ω, 3-W metal-oxide resistors. Arrange them in parallel around a coax connector. Short leads are important. *Do not use wire-wound resistors.*

[6]The **OVERVOLTAGE** alarm triggers when the dc supply voltage is greater than 14.5 V. If an adjustable dc supply is available, you can set this directly. Alternatively, set the voltage at the wiper of R15 to 0.360×(V – 0.6), where V is the dc supply voltage.

[7]Larry Price, W4RA, and Paul Rinaldo, W4RI, "WARC97, An Amateur Radio Perspective," *QST*, Feb 1998, pp 31-34. By these rules, an 8-W 2-meter transmitter must suppress the harmonics by at least 52 dB. Greater amounts of suppression are required for higher power levels.

By Dave Mascaro, WA3JUF

From *QST*, June 1990

903-MHz Linear Amplifiers

Part 1—Looking for a gain block or two for your 903-MHz station? Here are *eleven* of them to cover just about any need you may have, from a simple receiving preamplifier to one with 23 dB gain and over 4 W output!

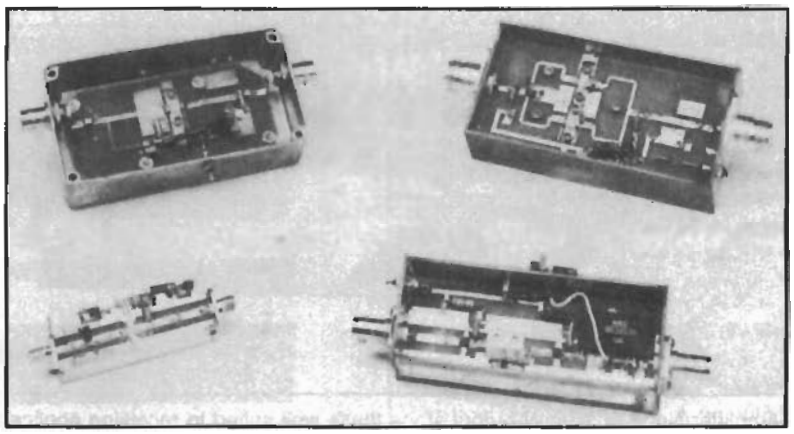

The 33-cm Amateur Radio band (902-928 MHz) is becoming well populated in many areas of the country. Propagation on 33 cm has traits similar to both 432 MHz and 1296 MHz, but has characteristics all its own at times, making it a very interesting band. It's pleasantly surprising what you can do with a few watts on 903 MHz with high-gain loop-Yagi antennas.

Articles have been published on transverters, amplifiers and receivers for 33 cm. I described a 759-MHz local oscillator[1] intended to be used with a 144-MHz IF for operation on 903 MHz. If you've built the transmit section of a transverter that gets you to the 10-mW level, or if you've purchased a commercial transverter such as Down East Microwave's low-power, no-tune unit,[2] you'll need to bring your transmitter power up to a usable level. Instead of showing a typical transmit-amplifier chain, many of which have been described in Amateur Radio literature, I will discuss eleven different gain blocks, for several different gains and power levels, in this two-part series.

I suggest that you build each amplifier in its own enclosure, rather than trying to build more than one amplifier in one box to eliminate connectors or reduce size. If you are building your own equipment, you probably aren't too concerned about size and compactness, and having separate enclosures makes for much easier tuning and troubleshooting. Many transistors used in 1296-MHz projects are suitable for use at 903 MHz; some even have more gain at 903.

Transistors with SD prefixes used in the following designs are manufactured by SGS-Thomson Microelectronics.[3] Some of these transistors don't operate at 12 V. Again, in building your own equipment, this shouldn't be a major problem. Gains listed are averages for several different devices tried. All of the amplifiers can be driven harder than indicated—for CW or FM operation only—but should be used at or below their rated power output for SSB work. All the designs can be used at lower power output; they are all linear amplifiers.

Construction

All of the amplifiers are built using similar techniques. Each design uses common $^1/_{16}$-inch-thick, G-10, double-sided, fiberglass-epoxy PC board for the microstrip circuitry. The ground-plane side of each PC board is unetched.

The microstrip boards can be made using what I call the "X-ACTO®-etch" method. This involves using a piece of clear tape as the resist. (Four-inch-wide clear tape is available at stationery stores.) After drawing the pattern on the board with a pencil or fine-tipped marker, cover it on both sides with clear tape and cut the pattern in the tape with an X-ACTO knife. Then, remove the tape from the areas to be etched and etch the boards in ferric chloride in a crock pot on low heat. Do this in a well-ventilated area! Etching takes about half an hour without agitation. The crock pot is a no-mess way to etch boards. Only an inch or so of ferric-chloride solution is needed. Of course, you can also use a photographic method to make boards, as I do for multiple or complicated boards.

After the PC board is etched, clean it with steel wool and drill holes at all dc- and RF-ground points using a no. 50 drill. No holes are needed for component leads, as all components are mounted on the microstrip side of each PC board. RF grounds must be located as close to the areas to be grounded as possible, to ensure low-inductance ground paths. There are at least two ways to do this. One is to install a rivet in each hole, flare it with an awl or ice pick, then flatten it by tapping with a small

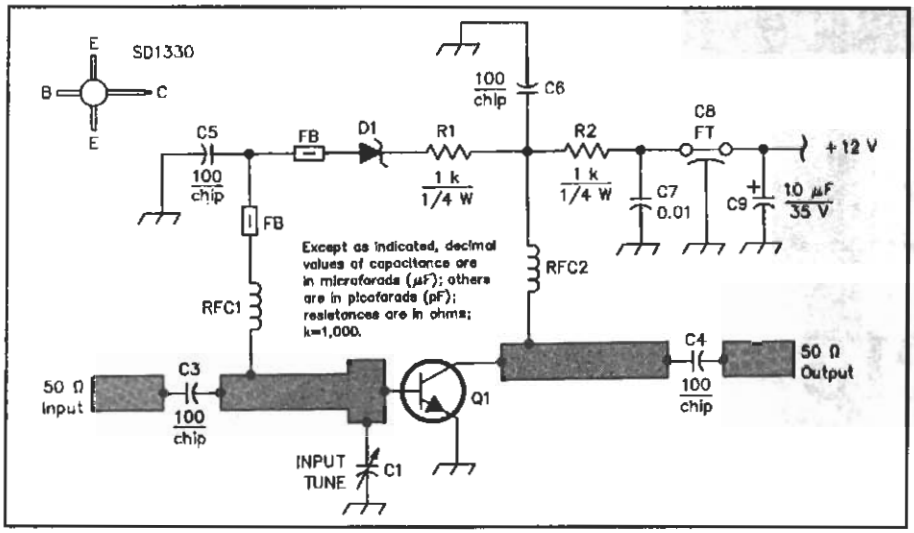

Fig 1—Schematic of the SD1330 receive preamplifier/low-level transmit stage. RFC1 and RFC2 consist of 8 turns of no. 24 enam wire closewound on a 0.1-inch-ID form (such as a 0.1-inch drill). D1 is a 9.1-V, ½-W Zener. C1, a 12.5-pF trimmer, is available from Mouser (part no. 24AA071).

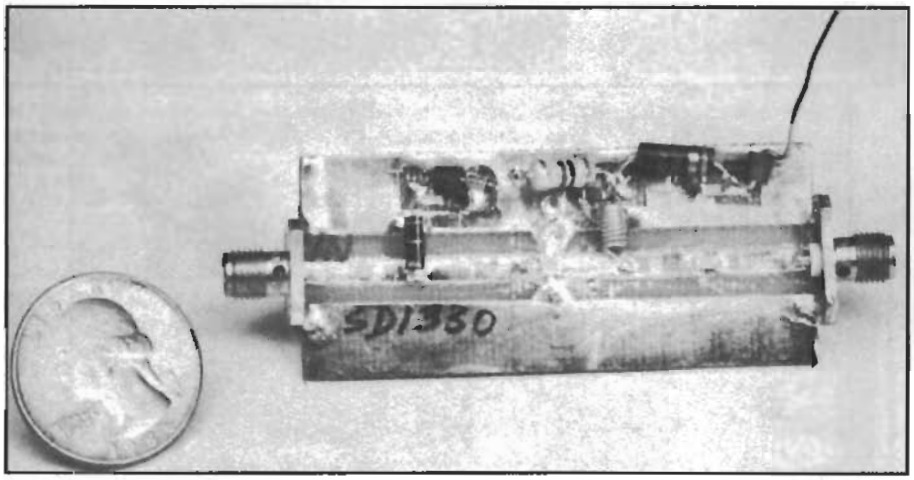

Fig 2—Amplifier No. 1, a 10-mW-output stage that's well suited to receiving applications, in prototype form.

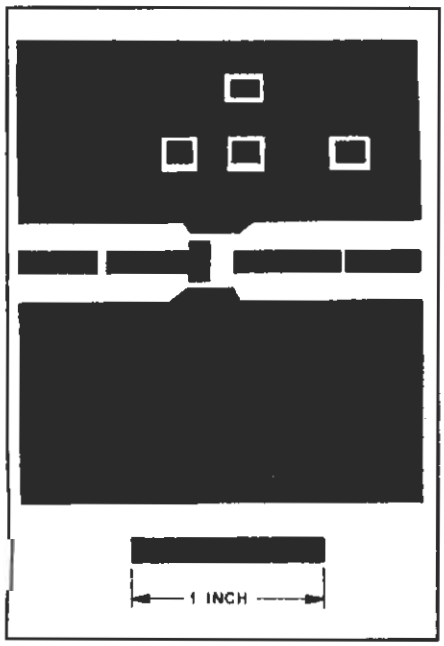

Fig 3—Full-scale PC-board artwork for the 10-mW SD1330 amplifier. Black areas represent unetched copperfoil. All parts are mounted on the foil side of the board. Crop the finished boards as necessary.

hammer on an anvil or other hard surface. Then, solder the rivets on both sides of the PC board. Alternatively, pieces of bus wire can be used for grounding.

Because parts placement is quite straightforward, I haven't provided parts-placement drawings for all of the designs. The schematics and PC-board artwork should provide all the guidance you'll need to assemble the boards. I can help with any questions that you might have when building any of the amplifiers.

All of the amplifiers described, except those operating under the 300-mW level, require some heat sinking. A small brass sheet is sufficient for the studded parts, but a finned heat sink an inch or two square is needed for the flanged-device amplifiers. Thermally conductive compound is required between the devices and their heat sinks. For studless devices, a small piece of brass shim stock soldered from the bottom of the device to the ground-plane side of the PC board should work fine.

An easy way to enclose an amplifier like those described is to make a housing using double-sided PC board or brass sheet for the four walls and bottom cover. The amplifier PC board makes the top cover. Input and output connectors (N, BNC or SMA) can be bolted or soldered to the end walls with their center pins soldered directly to the microstrip input/output lines in an end-launch configuration. When using PC-board material for housings, mount the side walls in such a way that the grounding is continuous from the connectors to the ground-plane side of the amplifier board.

Various die-cast aluminum boxes, such as Bud CU-123 and CU-124 and the Hammond 1590 series, also work great for enclosing these designs. Die-cast boxes usually provide sufficient heat sinking for amplifiers operating at less than 2 W output. Device studs or flanges should be attached directly to the boxes in these cases. All component leads must be kept as short as possible. This also applies to trimmer caps. Mount them flush to the PC board so that they act as capacitors—not as inductor/capacitor combinations. Use multiple rivets (or bus wires) to ground the trimmers.

Components

Use ceramic chip capacitors for the dc blocks and high-frequency bypassing. Some of the larger-value bypass capacitors, like 0.001 µF and 0.01 µF, are available in chip form also. These epoxy types are good for all the designs described here. I use inexpensive chip caps from Mouser Electronics.[4] Chip caps and Johanson piston trimmers are available from Microwave Components of Michigan.[5] Transistors are available from RF Parts[6] and RF Gain, Ltd.[7] Components, rivets and PC boards are available from Frontier Microwave.[8]

Tune-Up

In most of these amplifiers, the quiescent collector current (I_{cq}) initially will have to be checked and set with no drive applied.

To check bias current, disconnect the cold end of the collector choke and insert a milliammeter in series with the choke. Adjust I_{cq} by changing the value of the collector-bias resistor or by changing the collector voltage. All amplifiers requiring 12 V can be powered directly from low-current, 12-V dc sources (a three-terminal, 12-V regulator, for example). Amplifiers running on 14-18 V dc or 21-23 V dc can be powered by an LM317T (or LM317K) adjustable regulator. Set the regulated voltage to a minimum, and adjust it upward from minimum while monitoring I_{cq}. Idling collector current can be adjusted to suit your gain and power-output requirements.

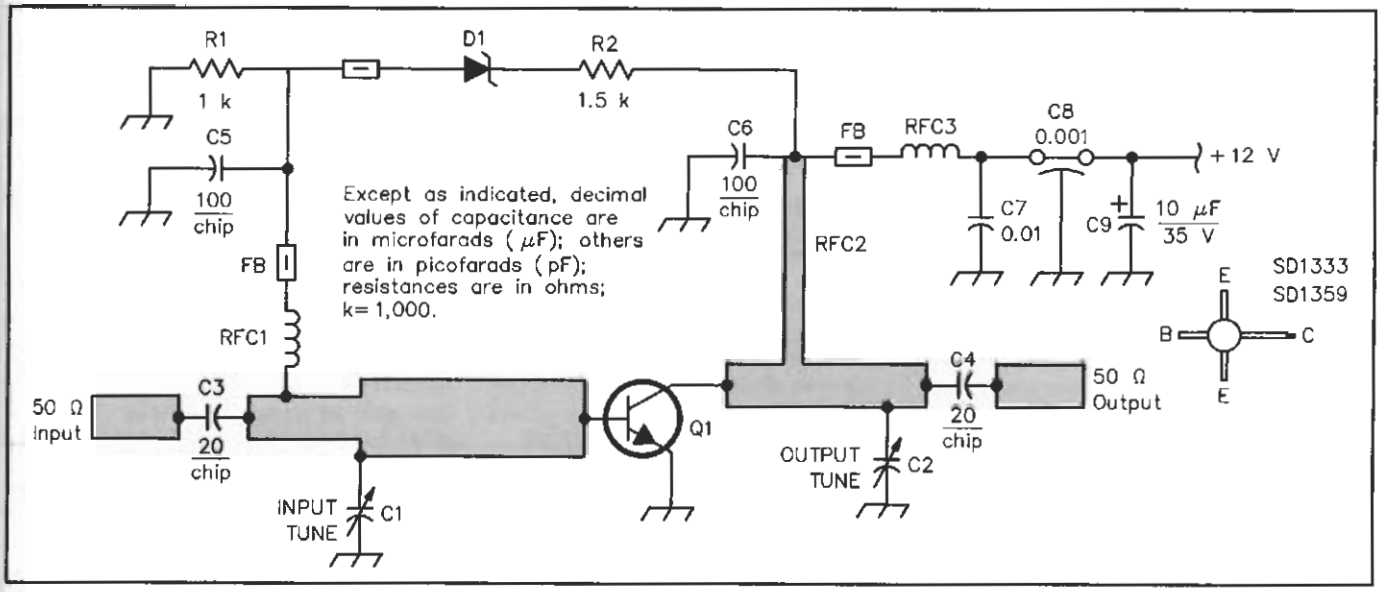

Fig 4—Schematic of the SD1333 and SD1359 amplifiers (Amplifiers No. 2 and No. 3). All components except Q1 are common to both designs (see text).

C1, C2—12.5-pF trimmer, Mouser no. 24AA071.
C7—0.01-μF disc ceramic.
D1—9.1-V, ½-W Zener.
RFC1, RFC3—8 turns of no. 24 enam wire, 0.1 inch ID, closewound.

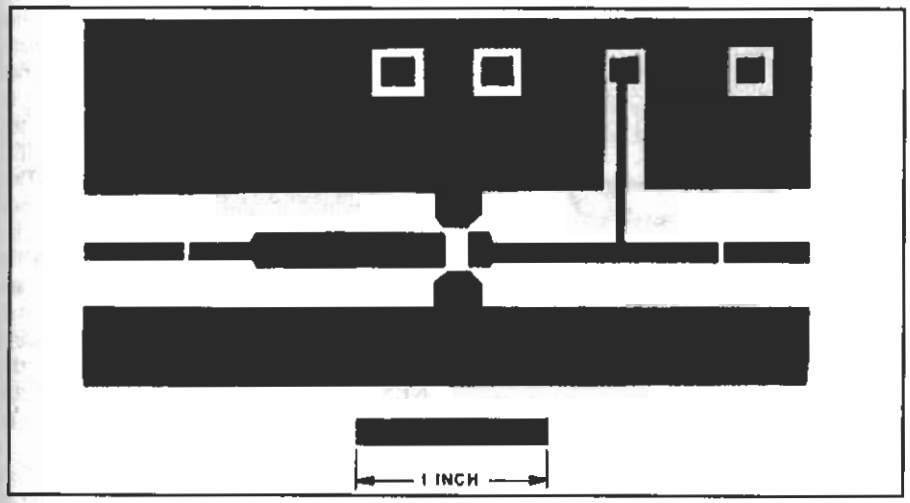

Fig 5—Full-scale PC-board network for the 100- and 250-mW amplifiers. Black areas represent unetched copper foil. All parts are mounted on the foil side of the board.

Amplifier No. 1: A Receive Preamplifier or 10-mW-Output, 13-dB-Gain Transmit Stage

The amplifier shown in Figs 1 and 2 is a low-power stage using an SD1330, Motorola MRF901 or NEC NE64535. This stage is best suited to the receiving side of a transverter. With a noise figure (NF) of 2 dB, it makes a fine front end by itself. With a good, low-noise GaASFET preamplifier in front of it, you'll have all the sensitivity you need in front of the receive mixer. For transmitting applications, where a low noise figure isn't important, an MMIC amplifier would be better because it is a lot easier to build for the same results.

The SD1330 amplifier is built on 0-10 double sided board; the artwork appears in Fig 3. After etching the board, install rivets at the RF and dc grounds. To mount the device, drill a hole in the PC board the size of Q1's macro-X case. This allows all four leads to be soldered to the microstrip without bending them.

The idling current for this amplifier should be set to 5 mA or less for good noise figure. The idling current is kept constant for different transistors and over different voltages and temperatures by current-limiting resistors R1 and R2 and Zener diode D1. Tune the input trimmer for best NF or maximum gain if an NF-measurement setup isn't available.

Amplifier No. 2: 10 mW In, 100 mW Out

The SD1333 transistor, a macro-X plastic-packaged device used in this design, delivers 100-125 mW. This device is capable of a reasonable noise figure (2-3 dB) and good dynamic range, which allows it to be used as a second stage (following a GaAsFET preamplifier) in a receiving system. (Motorola's BFR96/MRF961/MRF962 also work well in this circuit; the BFR96 has slightly less gain.) Fig 4 shows the amplifier schematic and Fig 5 shows the full-scale artwork.

Zener-diode bias is used for simplicity and some temperature compensation. Set the quiescent current to 40-50 mA (not critical) by varying R1. A pot can be used initially, then the pot can be replaced by a fixed-value resistor. Or the collector voltage can be varied slightly.

After the rivets are installed in the PC board, drill a hole the diameter of Q1's molded package in the PC board. Mount the device in the board so its unbent leads are soldered directly to the microstrip board. Use the small variable capacitors to tune for maximum gain.

Amplifier No. 3: 9 dB Gain, 250 mW Out

This unit is a slightly higher-power version of the previous amplifier, using an SD1359 or Motorola TRF559 plastic-packaged device. The artwork and schematic are identical to that of Amplifier No. 2. Idling current, 40-50 mA, can be optimized by adjusting the collector supply between 10 and 13 V to set the stage gain.

After the PC-board rivets are installed, drill a hole in the PC board to accept Q1. Mount the device in the board so its unbent leads are soldered directly to the microstrip board. Tuning is as discussed with Amplifier No. 2.

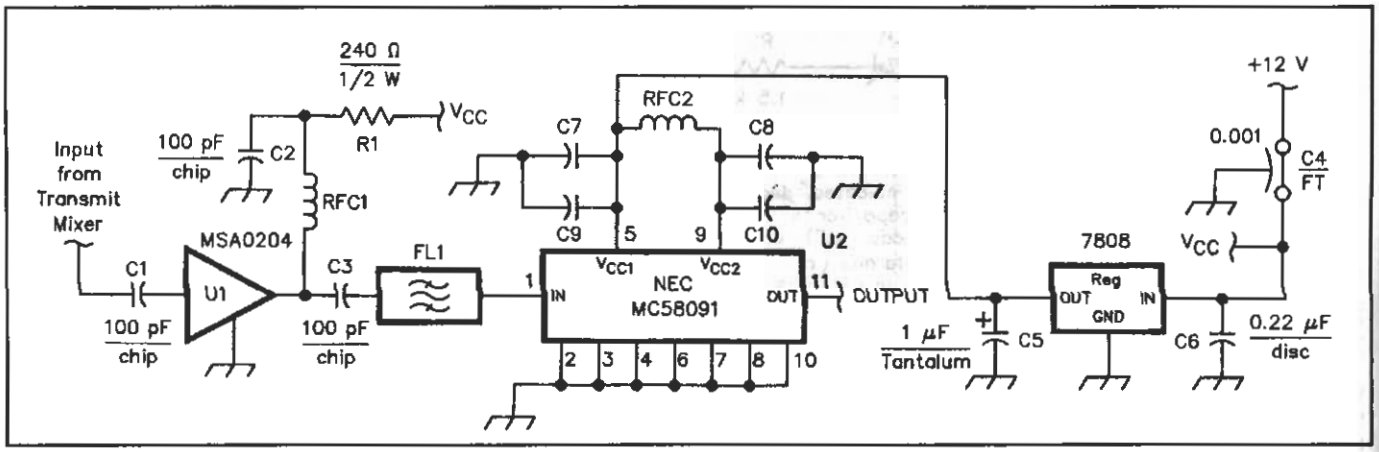

Fig 6—Schematic of the MSA 0204/MC5809L amplifier.

C7, C9—100-pF chip.
C8, C10—0.01-μF ceramic disc.
FL1—Two-stage Toko helical filter (Digi-Key no. TK23318).
RFC1—8 turns of no. 24 enam wire, 0.1 inch ID, closewound.
RFC2—1-μH molded choke.

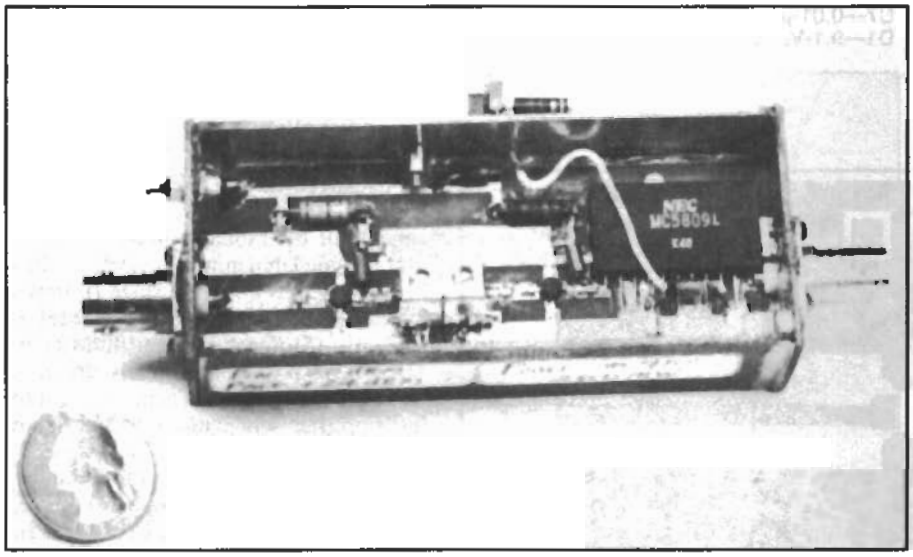

Fig 7—The 200-mW-output MSA 0204/MC5809L amplifier. In this prototype, I used MSA 0204 stages before and after the helical filter to provide addiional gain. The biasing components (the 7808 and associated parts) are mounted on the outside of the enclosure for convenience.

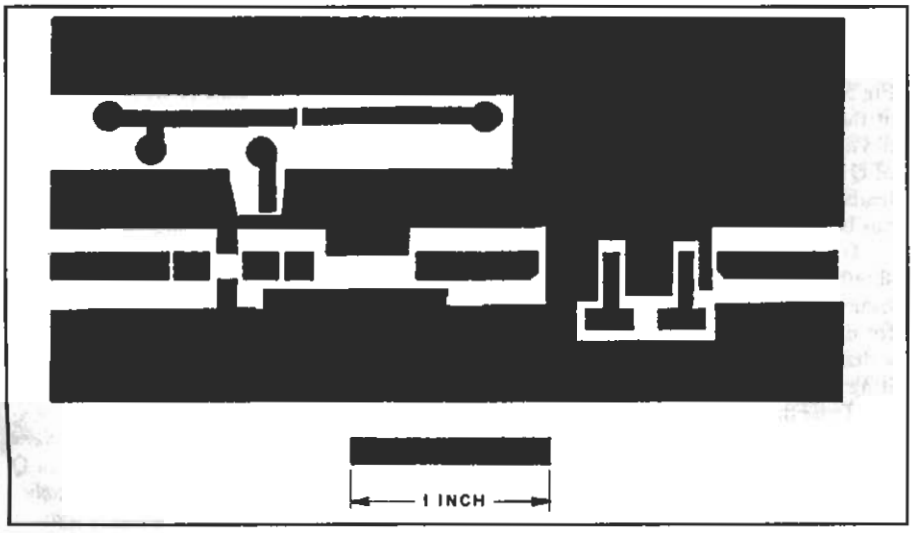

Fig 8—Full-scale PC-board artwork for the 200-mW amplifier. Black areas represent unetched copper foil.

Amplifier No.4:0.8 mW In, 200 mW Out

The amplifier shown in Figs 6 and 7 is a high-gain unit that can be used to follow the output of your 903-MHz transmit mixer. An Avantek MSA 0204 or Mini-Circuits MAR-2 MMIC is used for the first stage, followed by a Toko two-stage helical filter.[10] (In the prototype amplifier shown in Fig 7, I used two MMIC stages, in addition to the helical filter, before the final stage.) The output stage is an NEC MC5809L thick-film hybrid module. This NEC hybrid module is one of four such units intended for hand-held cellular telephones operating in the 800- to 960-MHz range. The MC5809-series amplifiers are rated at 150 mW minimum power output at 7.5 V dc. Using a more readily available power source (a 7808 regulator), the NE5809s I tried were linear at over 200 mW output. These hybrid amps are easy to use and are stable into any load.

The full-scale PC-board artwork is shown in Fig 8. The helical filter is used between stages to clean up the transmitter signal by filtering out the local-oscillator and image frequencies, but isn't required for applications where such filtering is done in other stages. A three-stage Toko filter[11] will also fit on the board, and could be used for better filtering. The filter leads are bent to the side to allow soldering to the PCboard traces. See Fig 9 for parts placement.

This amplifier is easy to build and get working. Because both active stages and the filter are designed for 50 Ω in and out, the amplifier uses 50-Ω microstrip throughout. No trimmer capacitors are needed and no bias adjustments are necessary—just apply the dc voltages and the drive signal, and peak the helical filter for maximum power output at 903 MHz!

Because more gain is available from this design than I needed, I tried mixing two signals at the input of the first stage. Using a T connection at the input of the first stage,

I used the circuit to mix a 759-MHz local oscillator with a 144-MHz IF signal. The 903-MHz output signal was about 175 mW and was fairly clean. Using MMIC amplifiers for gain blocks, almost anything can be used as a mixer!

Amplifier No. 5: 35 mW In, 350 mW Out

The amplifier shown in Fig 10 is practically as simple as an MMIC amplifier. The transistor, an SD1598, produces more than 350 mW output when mounted in a 50-Ω line. The SD1598 (originally another part number) was designed by Bill Olson, W3HQT, years ago, when he was employed by Solid State Microwave (now SGS-Thomson Microelectronics). I've used this transistor, which I refer to as a "hot 2N3866," in amplifiers and frequency multipliers at frequencies from 144 MHz to 3.3 GHz. The SD1598 is in a studded package and the SD1598-1 is a studless package; either style is suitable for use at 903 MHz. I've built two-stage SD1598 amplifiers with 50-Ω lines that work from 400-1300 MHz. Such a two-stage amplifier fits nicely into a 1.5 × 3.6 × 1-inch Bud CU-123 die-cast box. Gain is 10 dB per stage at 903 MHz and 8-9 dB per stage at 1296 MHz.

PC-board artwork isn't necessary for this amplifier, as the 50-Ω line can be easily made on a piece of G-10 PC board using an X-ACTO knife and a straight edge. A 50-Ω line on 0-10 PC board is about 0.1-0.11 inches wide. After cutting the edges of the 50-Ω line, cut another line about a quarter inch from, and parallel to, the 50-Ω line on each side of the 50-Ω line. Using a soldering iron, heat the quarterinch-wide strips between the 50-Ω line and the outer sections and remove them with the knife or a needle-nose pliers. Leave some copper near the transistor for connecting Q1's emitter leads to the microstripline.

Drill a hole in the board for the transistor such that the leads of the transistor can be soldered flush to the microstripline and ground foils. This is important: Excessive lead lengths drastically reduce the gain of this amplifier. Attach a small heat sink to the stud of the device.

The SD1598 can be powered by a 12- to 18-V supply, depending on the gain and power output required. Use an LM317T voltage regulator in the power supply, and vary the voltage to set the gain of this lowlevel stage. This is an easy way to match the drive levels needed by the following stages.

Set Q1's quiescent current, I_{cq}, to 30-50 mA. Vary R1 to get the correct idling current. This bias current is not critical, and depends on the device and the collector voltage used. Tune up is simple: Adjust C8 for maximum power output.

Amplifier No. 6: 100 mW In, 1 W Out

A pair of SD1598s and a Wilkinson power divider/combiner combination are used in this design. The schematic for the combined amplifier is shown in Fig 11, and the PC-board artwork is shown in Fig 12. I didn't make an effort to terminate the 75-Ω Wilkinson divider/combiner; the amplifier works fine as is. Power sharing between the two devices is excellent, and a 3-dB improvement in power output is available over a single device. Saturated power output is well over 1 W.

The supply voltage and idling currents are the same as single-device Amplifier

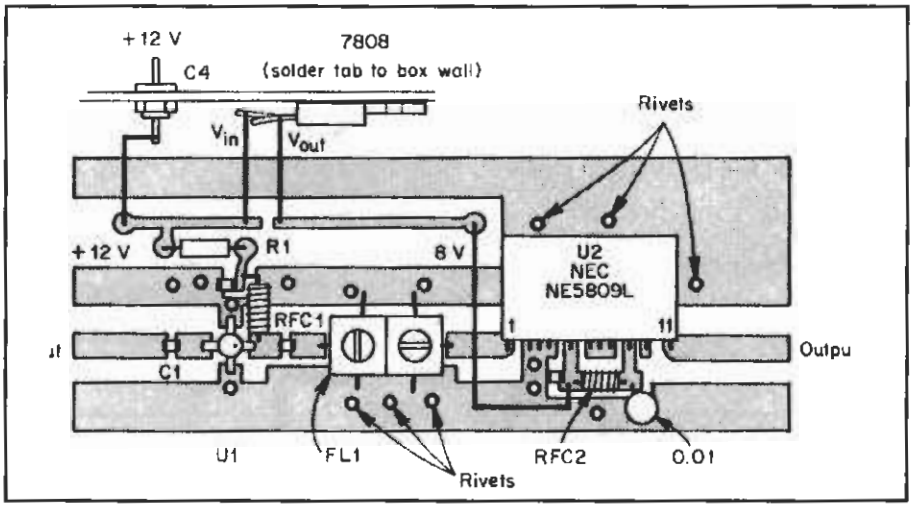

Fig 9—Parts-placement diagram for the 200-mW amplifier. All parts are mounted on the foil side of the board. Note the locations of rivets. At each V_{cc} lead on the MC5809L (pins 5 and 9), install a 100-pF chip capacitor and a 0.01-μF disc to ensure proper bypassing.

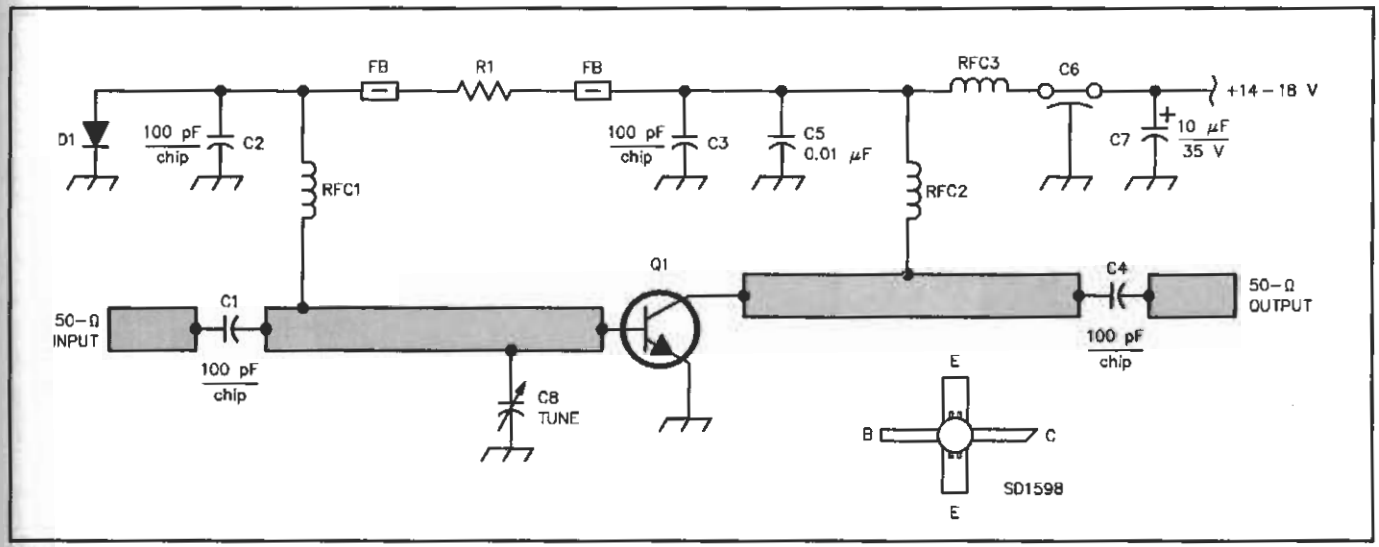

Fig 10—The 350-mW amplifier. Glue D1 to Q1's ceramic body for thermal composition.

C6—0.001-μF feedthrough.
C8—0.6- to 8-pF Johanson piston trimmer.
D1—1N4001.
Q1—SD1598.
R1—1.5-1.6 kΩ, ½ W.
RFC1, RFC2—8 turns of no. 26 enam wire, closewound, 0.1 inch ID.

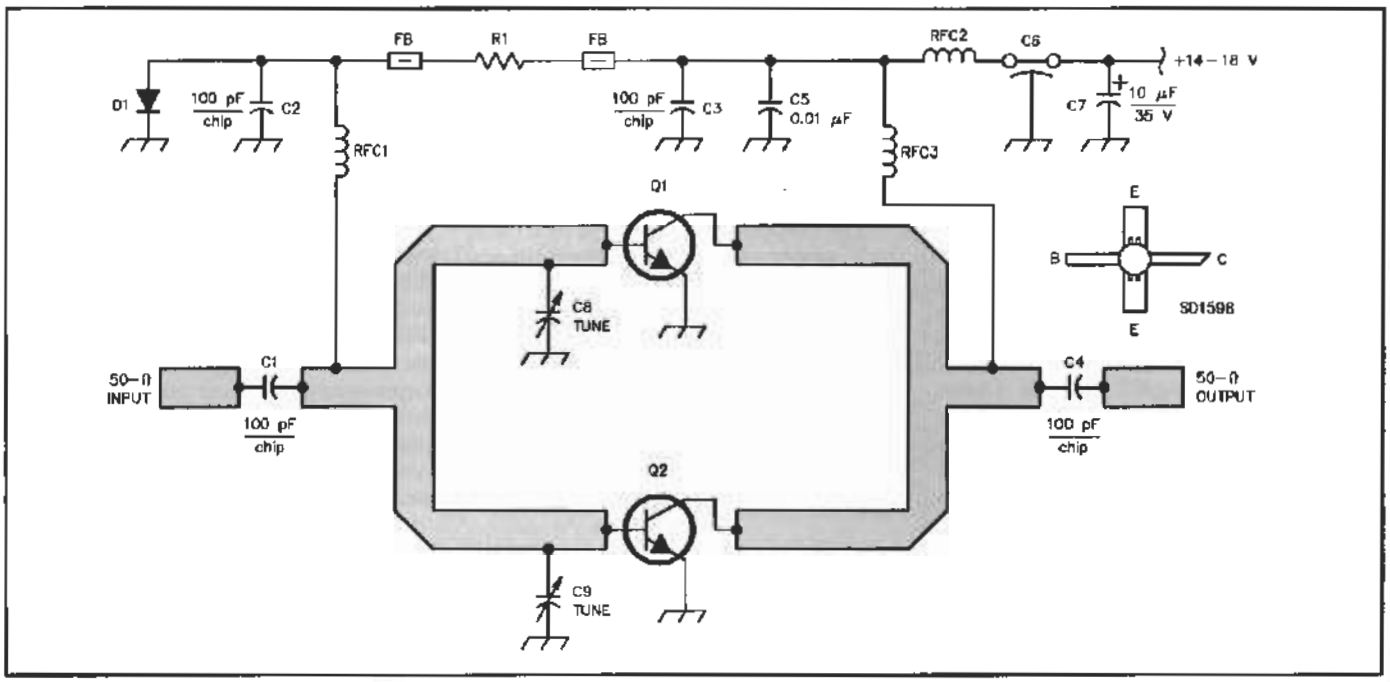

Fig 11—The 2x SD1598 amplifier. Glue D1 to Q2's ceramic body for thermal composition.

C8, C9—0.6- to 8-pF Johanson piston trimmer.
D1—1N4001.
Q1, Q2—SD1598.
R1—1.5-1.6 kΩ, ½ W
RFC1, RFC3—8 turns of no. 26 enam wire, closewound, 0.1 inch ID.

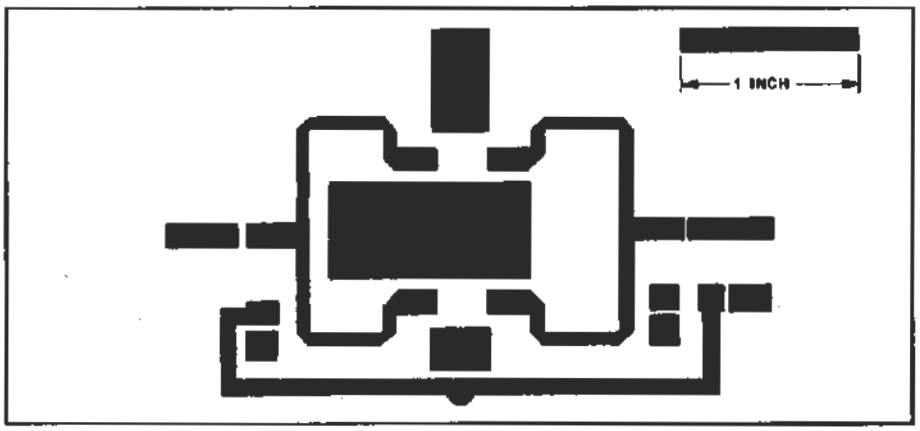

Fig 12—Full-scale PC-board artwork for the 2x SD1598 amplifier. Black areas represent unetched copper foil.

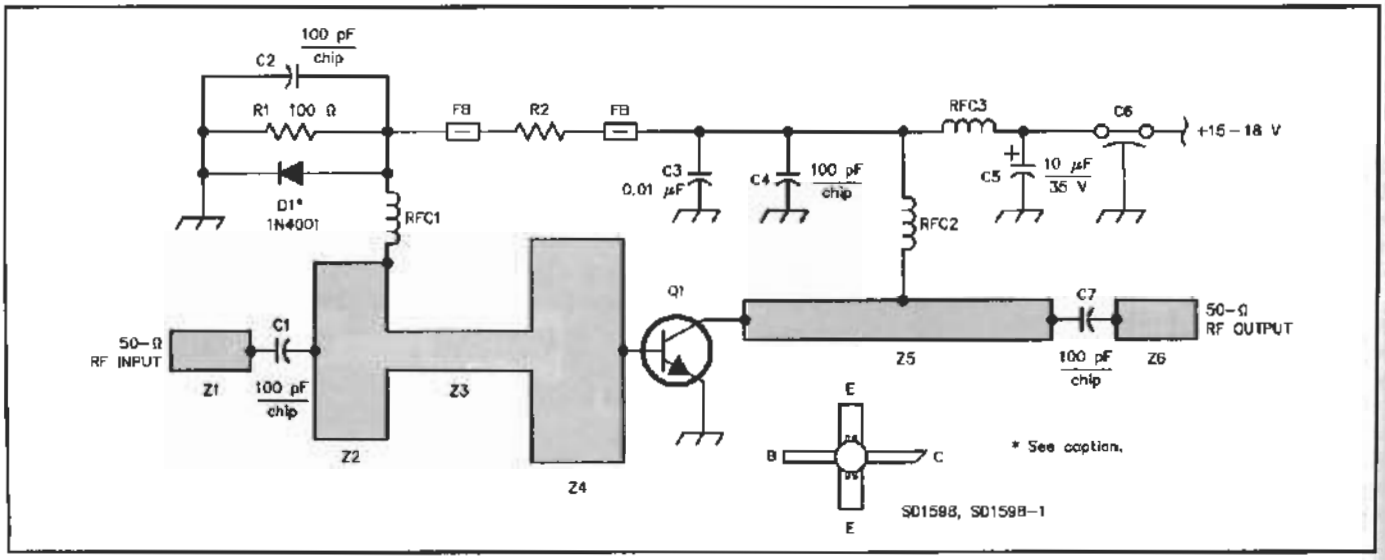

Fig 13—The 500-mW broadband amplifier. For power levels over 500 mW output, glue D1 to Q1's ceramic body for thermal compensation. RFC1 and RFC2 are implemented as PC-board traces.

Q1—SD1598 or SD1598-1.
R2—1.5-1.6 kΩ, ½ W
RFC3—8 turns of no. 28 enam wire, closewound, 0.1 inch ID.
Z1-Z5—Microstriplines. See text and Fig 14.

No. 5 (Fig 10). If this amplifier is mounted in a die-cast box, no additional heat sinking is required; If not, a small heat sink should be attached to the stud of each device. Adjust C8 and C9 for maximum power output.

Amplifier No.7: 12dB Gain, 500mW Out

The amplifier shown in Fig 13 is a broadband design that's been around for about 6 years. Bill Olson, W3HQT, designed it as a 1296-MHz amplifier. (The 1296-MHz version differs in that it has a small piston trimmer on the output circuit, about an inch from Qi's ceramic cap.)

This amplifier is a very versatile design; it works from 900-1300 MHz and has a power gain of 10-13 dB over this range. I built two test amplifiers for this design: one for the studded transistor and one for the flanged version. Over a dozen different devices were tried in these test circuits, both at 903 MHz and at 1296 MHz. Classes A, AB, C and pulsed-class-C operation were all tried, and all worked well.

The studded SD1598 is used in this design. Full-scale artwork appears in Fig 14; Fig 15 shows parts placement. As with the other designs, rivets are used at all dc and RF grounds. After the rivets are soldered in place, drill a hole in the board for the device. Trim Q1's leads with scissors, then solder them directly to the microstriplines and ground foils. If the amplifier is to be mounted in a die-cast box, the box will provide sufficient heat sinking. If you use another mounting method, attach a small heat sink to Q1's stud.

Power output for SSB is 500 mW, and

Fig 14—Full-scale PC-board pattern for the broadband 500-mW SD1598 amplifier. Black areas represent unetched copper foil.

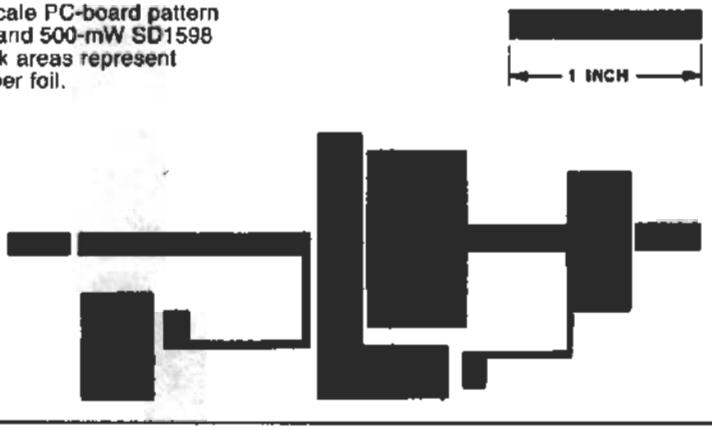

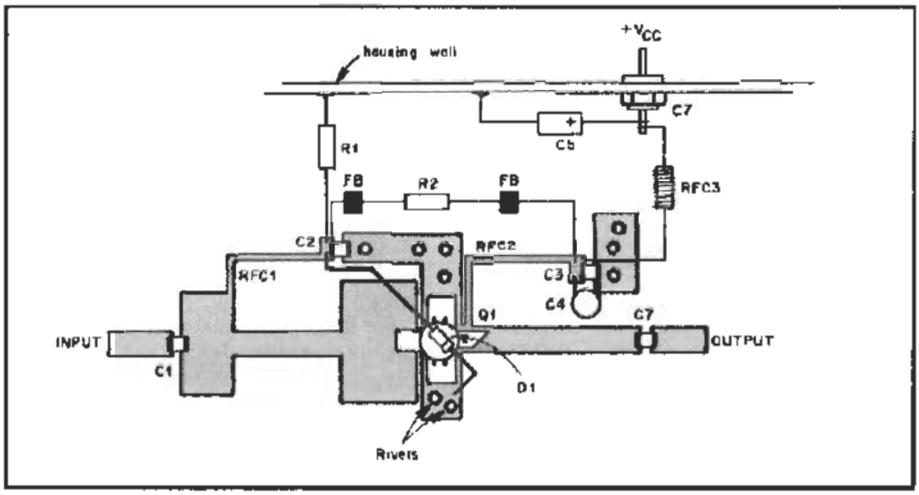

Fig 15—Parts-placement diagram for the broadband 500-mW SD1598 amplifier. The PC-board edges are not shown. All components are mounted on the foil side of the PC board (except those mounted to the enclosure).

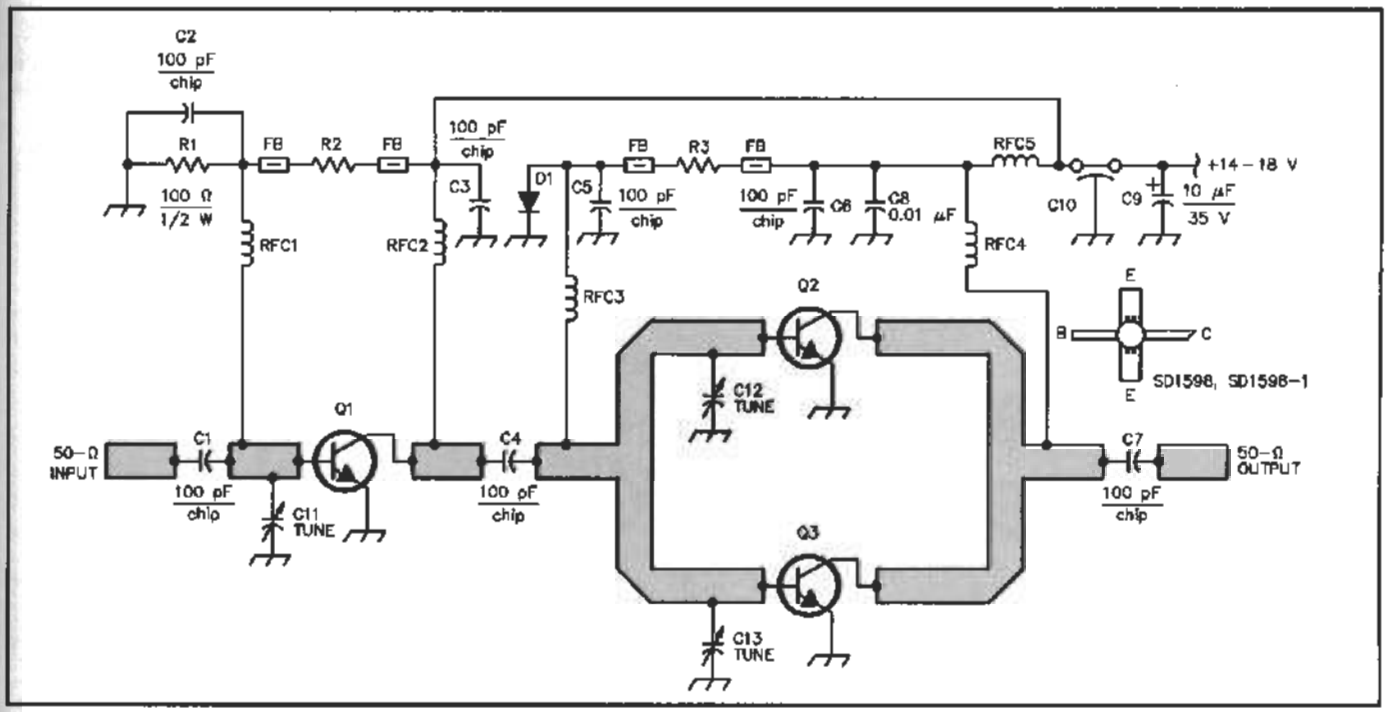

Fig 16—The two-stage, 1-W SD1598 amplifier. Glue D1 to Q2's ceramic body for thermal compensation.

C10—0.001-μF feedthrough.
C11, C13—0.6- to 8-pF Johanson piston trimmer.
Q1—SD1598 or SD-1598-1.
Q2, Q3—SD1598.
R2, R3—1.5-1.6 kΩ, ½ W.
RFC1-RFC5—8 turns of no. 24 enam wire, closewound, 0.1 inch ID.

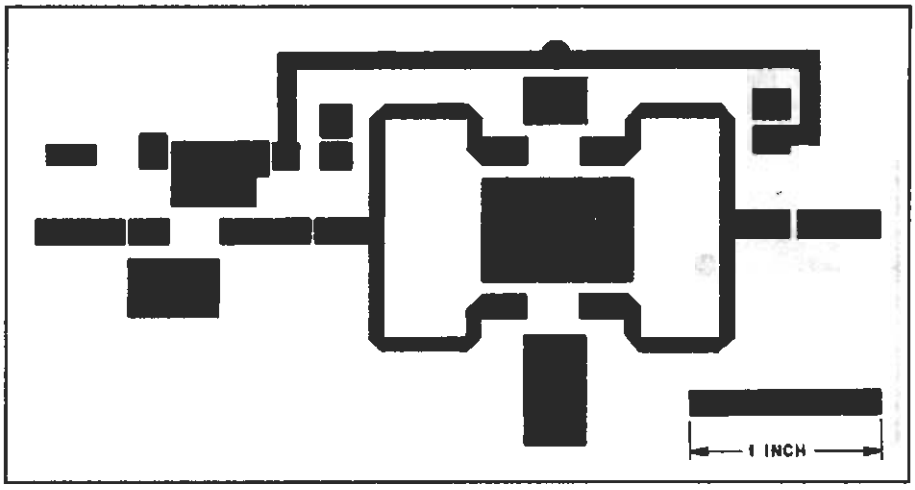

Fig 17—Full-scale PC-board pattern for the two-stage, 1-W SD1598 amplifier. Black areas represent unetched copper foil.

up to 1 W for CW and FM, depending on the device. In applications where the device will deliver over 500 mW, a 1N4001 (D1) diode can be glued to Q1 for thermal stabilization, as shown pictorially in Fig 15. Power gain at 1 W output is 7 dB or so. By varying R2, set Q1's I_{cq}, for 30-50 mA for power levels up to 500 mW, and 15-20 mA for higher levels.

For low-level stages (up to 200mW out), you can use the SD1598-1 studless part in this circuit. Solder the studless device to the microstrip, then solder a piece of hobby brass to the device's gold-plated bottom area and to the ground plane. This provides enough heat sinking to dissipate a few hundred milliwatts.

At 903 MHz, no output trimmer capacitor is required. Some improvement in the output match can be achieved by trimming the width of the output line by a few thousandths of an inch with an X-ACTO knife.

Amplifier No. 8: 10 mW In, 1 W Out

A second 1-watt amplifier, this one using a pair of SD1598's driven by a single SD 1598, is shown in Fig 16. This design is similar to that of Amplifier No.6, with the addition of a driver stage. The artwork appears in Fig 17.

For the driver transistor, you can use an SD1598-1 studless device, as Q1 must provide only a hundred milliwatts or so. The driver is mounted in a hole in the PC board. A small piece of brass shim stock is soldered to the bottom of the device and to the ground-plane side of the PC board for heat sinking.

This amplifier runs on 14-18 V dc. The idling current for each device is around 30-50 mA. Again, the supply voltage can be provided by an LM317T regulator. Adjust R2 and R3 to individually set each device's idling current. Then, tune the amplifier by adjusting C11, C12 and C13 for maximum output. Vary the supply voltage to optimize the required power output or gain.

The 2.4 × 4.4 × 1-inch Bud CU-124, or an equivalent die-cast box, is a suitable enclosure for this amplifier. Mount the connectors on the ends of the box, and place the amplifier PC board inside the box body, instead of on the inside of the cover. The box provides sufficient heat sinking for this amplifier.

Next month, I'll describe three more 903-MHz linear amplifiers, including two 4-W units.

Notes

[1]D. Mascaro,"A 759-MHz Local Oscillator," *QEX*, May 1988, pp 12-15.

[2]No-tune transverters, as well as antennas and microwave components, are available from Down East Microwave, Box 2310, RR 1, Troy, ME 04987, tel 207-948-3741. Catalog available.

[3]The amplifiers in this article use transistors manufactured by SGS-Thomson Microelectronics, 211 Commerce Dr, Montgomeryville, PA 18936, tel 215-362-8500.

[4]Mouser Electronics, 2401 Hwy 287 N, Mansfield, TX 76063, tel 817-483.4422. Catalog available.

[5]Microwave Components of Michigan, 17141 Merriman, Romulus, MI 48174, evening tel 313-753-4581. Parts list available.

[6]RF Parts, 1320 Grand Ave, San Marcos, CA 92069, tel 619-744-0728.

[7]SGS-Thomson Microelectronics transistors are available through RF Gain Ltd, 100 Merrick Rd, Rockville Center, NY 11570, tel 800-645-2322. $50 minimum order.

[8]Frontier Microwave, RD 1, Box 467, Mink Rd, Ottsville, PA 18942, evening tel 215-795-2648.

[9]D. Mascaro,. "A Transverter Band-Switching Display and Universal Power Supply," *QEX*, Aug 1987, pp 8-14.

[10]Available from Digi-Key Corp, 701 Brooks Ave South, PO Box 677, Thief River Falls, MN 56701-0677, tel 800-344-4539. Catalog available.

11Toko filters and other components are available from Steve Kostro, N2CEI, Box 341A, RD 1, Frenchtown, NJ 08825, evening tel 201-996-3584. Parts list available.

By Dave Mascaro, WA3JUF From *QST*, July 1990

903-MHz Linear Amplifiers

Part 2—Did you like the projects in Part 1? Here are three more amplifiers to suit your 903-MHz, 50-ohm gain-block needs.

In Part 1, I covered construction methods for building the 903-MHz linear amplifiers described in this twopart series. The amplifiers described this month cover a higher power range than those in Part 1, starting with a 2-W-output design, and finishing with a pair of 4-W output units (one with 13 dB gain, the other with 23 dB gain).

Amplifier No. 9: 100 mW In, 2 W Out

The transistor used in this amplifier, an SD1853, is a class-A device in a "strip-pac" flanged package. The PC-board artwork is shown in Fig 18, and the schematic appears in Fig 19. The parts-placement

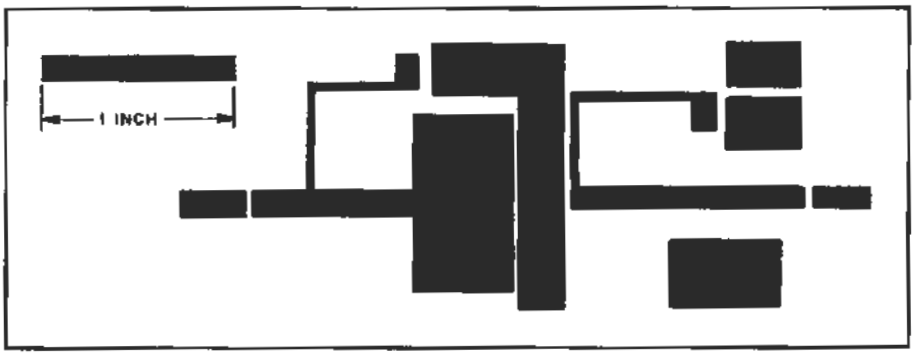

Fig 18—Full-scale PC-board pattern for the 2-W SD1853 amplifier. Black areas represent unetched copper foil.

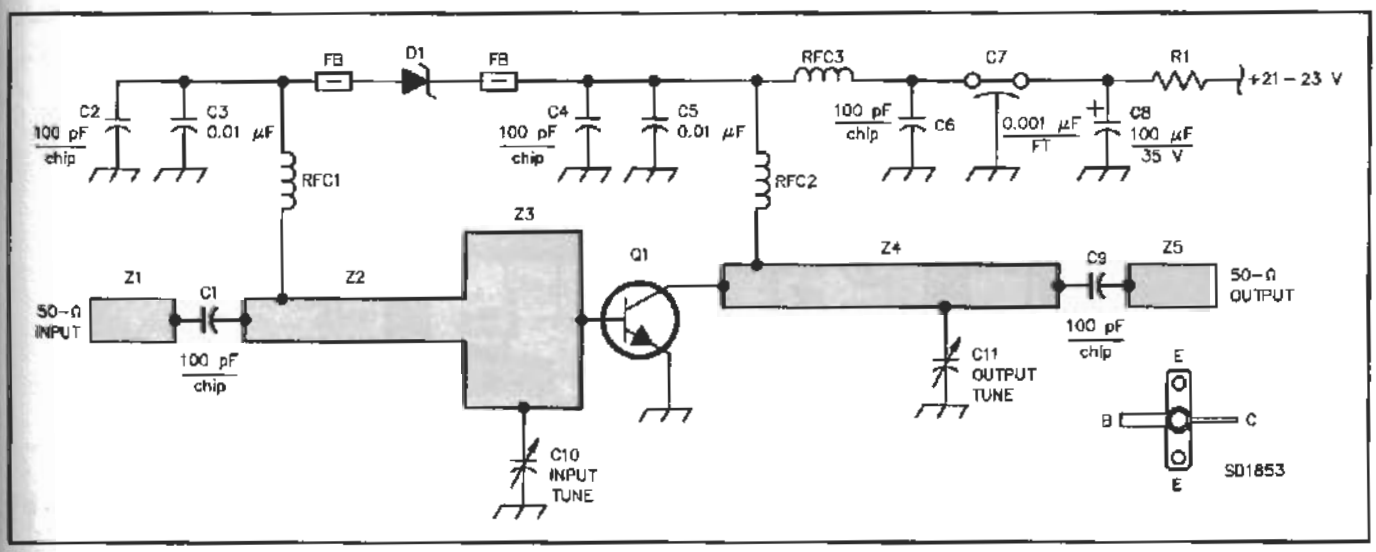

Fig 19—The 2-W SD1853 amplifier. RFC1 and RFC2 are implemented as PC-board traces.

C10, C11—0.3- to 3-pF Johanson piston trimmer.
D1—1N4747A 20-V, 1-W Zener.
Q1—SD1853.
R1—2-3 Ω, 1 W.
RFC3—8 turns of no. 26 enam wire, closewound, 0.1" ID.
Z1-Z5—Microstriplines. See text and Fig 18.

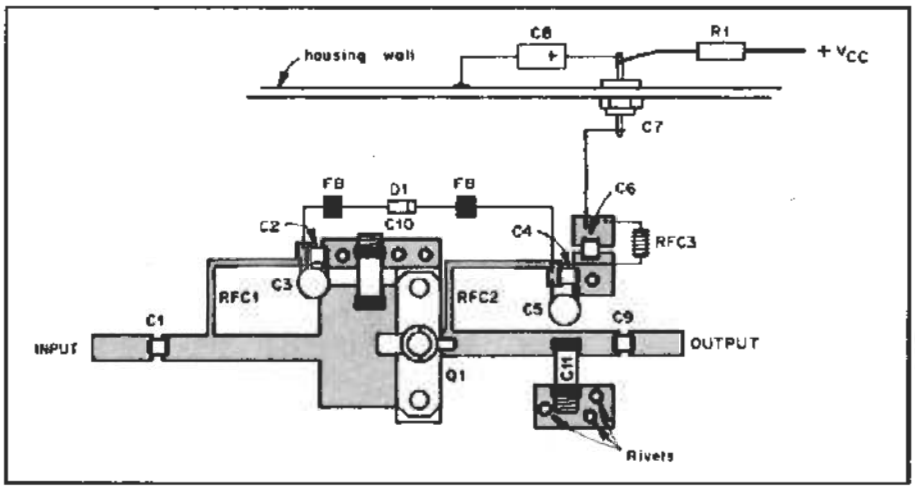

Fig 20—Parts-placement diagram for the 2-W SD1853 amplifier. The PC-board edges are not shown. All components are mounted on the trace side of the PC board (except those mounted to the enclosure).

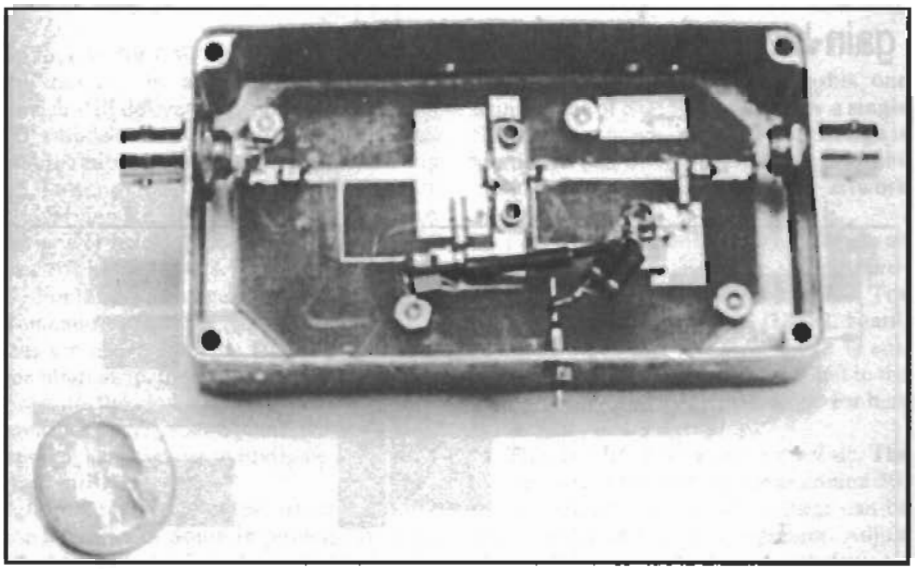

Fig 21—The prototype 2-W amplifier.

diagram is shown in Fig 20, and a photo of my prototype appears in Fig 21.

After the board is etched and rivets are installed, cut a hole and file its edges to accept Q1's flange. The SD1853 must be mounted to a heat sink. (A Bud CU-124 or equivalent die-cast box is adequate.) Use a piece of G-10 PC board between the amplifier board and the heat sink, to allow the device to be mounted flush to the microstrip. The device flange is the emitter, and a low-inductance ground connection is a must. Make this connection by using a piece of copper-foil tape soldered to the microstrip ground plane and placed between Q1's flange and the heat sink. Mount the transistor to the heat sink with no. 4-40 screws. Use heat-sink compound between Q1 and the heat sink.

An LM317T (or LM317K) adjustable regulator can be used to supply the voltage required by this amplifier. Use a 10-turn pot for the ADJUST control; smooth adjustment of the supply voltage to this amplifier is a must. Insert a milliammeter in series with current-limiting resistor R1, and slowly adjust the regulator output up from minimum until the idling current is 200-225 mA without RF drive applied. The exact supply voltage depends on the beta of

Fig 22 (below)—The 4-W, 2 x SD1853 amplifier.
C4-C6—0.3- to 3-pF Johanson piston trimmer.
D1—1N4747A 20-V, 1-W Zener.
Q1, Q2—Sd1853.
R1—2-3 Ω, 1 W.
RFC1, RFC2—8 turns of no. 26 enam wire, closewound, 0.1" ID.
Z1-Z5—Microstriplines. See text and Fig 23.

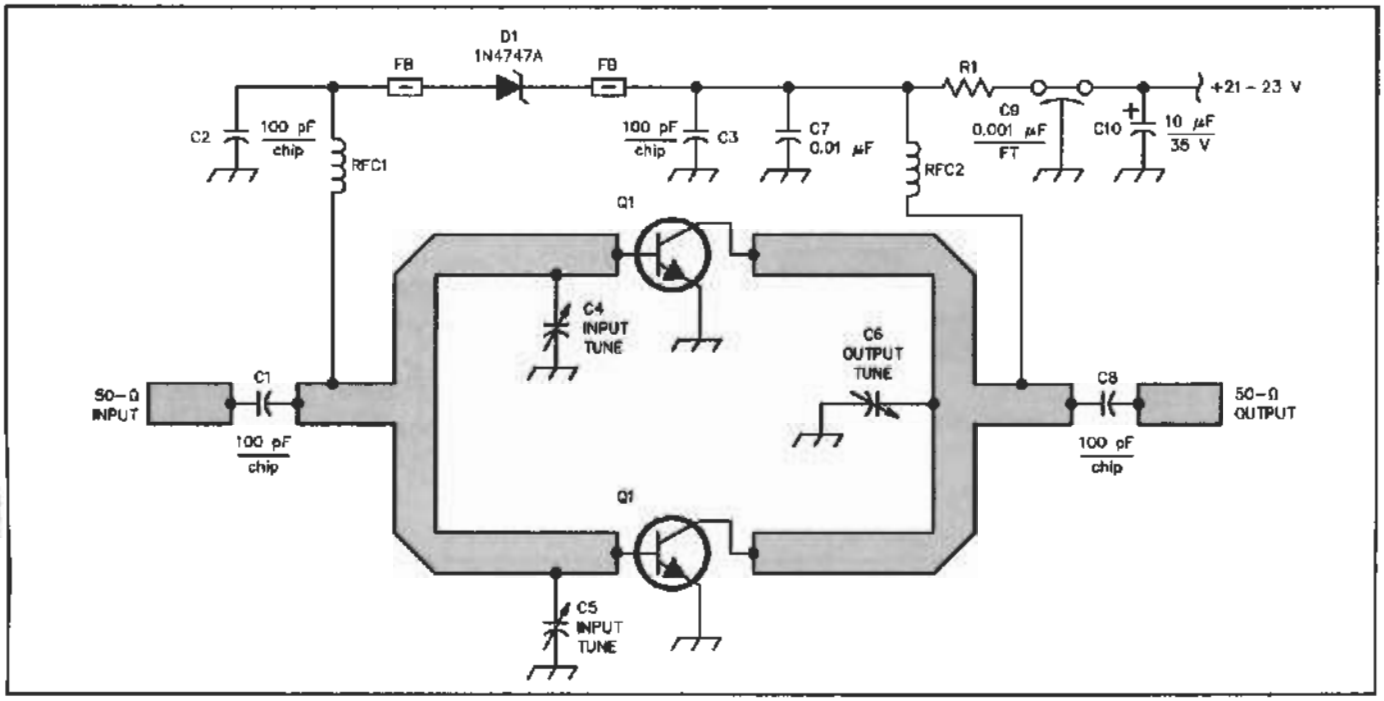

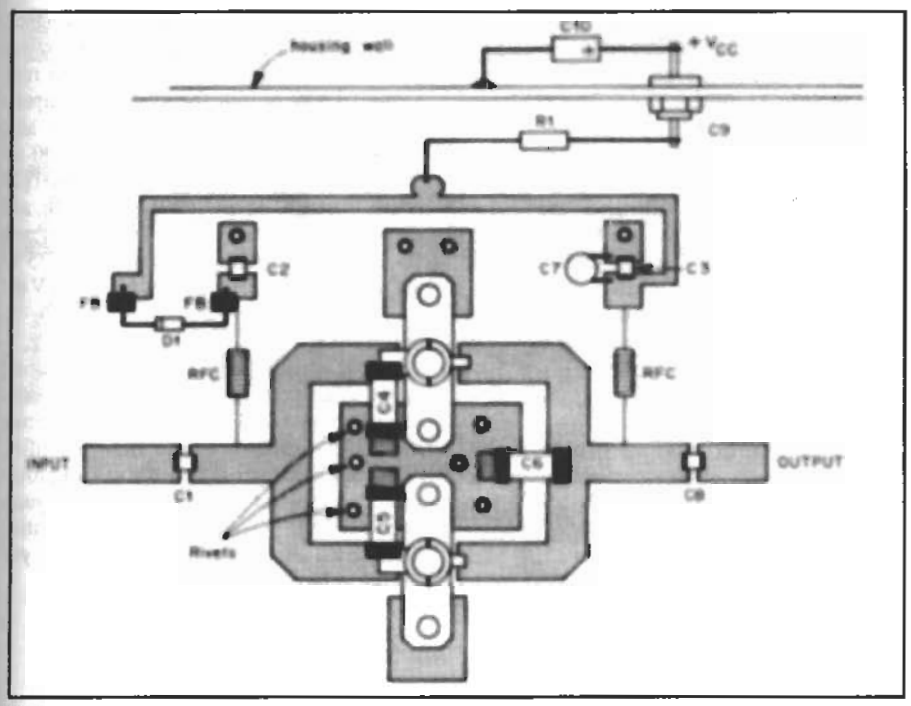

Fig 23—Parts-placement digram for the 2 x SD1853 amplifier. The PC-board edges are not shown. All components mount to the trace side of the PC board (except those mounted to the enclosure).

Q1, the value of R1, and D1's breakdown voltage. Idling current can be adjusted slightly to optimize gain and/or power output. The supply voltage must be removed during receive to minimize device heating.

Tune-up is simple. Apply drive and tune C10 and C11 alternately for maximum power output. If you have access to a return-loss bridge or network analyzer, you may want to trim the width of Z2 to improve the input return loss. Verify stability (as indicated by no output and no change in supply current) by tuning the trimmers through their ranges with no input signal applied.

Amplifier No. 10: 200 mW In, 4 W Out

This high-gain design consists of a pair of SD1853s combined in a Wilkinson power divider/combiner. As before, I made no effort to terminate the 75-Ω Wilkinson divider/combiner with balancing resistors. It worked just fine without them. Even the 1296-MHz version, which uses the same board layout, worked well in this configuration.

Fig 22 shows the schematic of this class-A amplifier, and Fig 23 shows parts placement. The PC-board pattern, the same

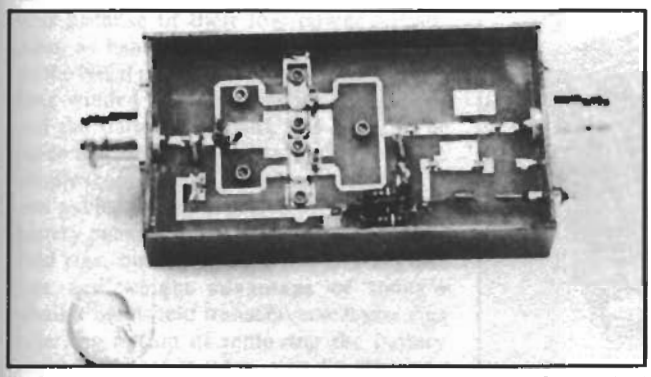

Fig 24—This prototype 4-W amplifier was built on a PC board with a spare driver stage that's bypassed with a brass strip.

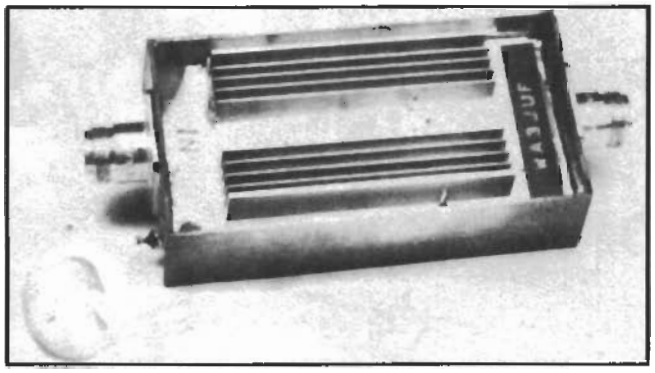

Fig 25—The 4-W amplifier's heat sink, bolted directly to the devices, must be positioned such that cooling air can flow over it during amplifier operation.

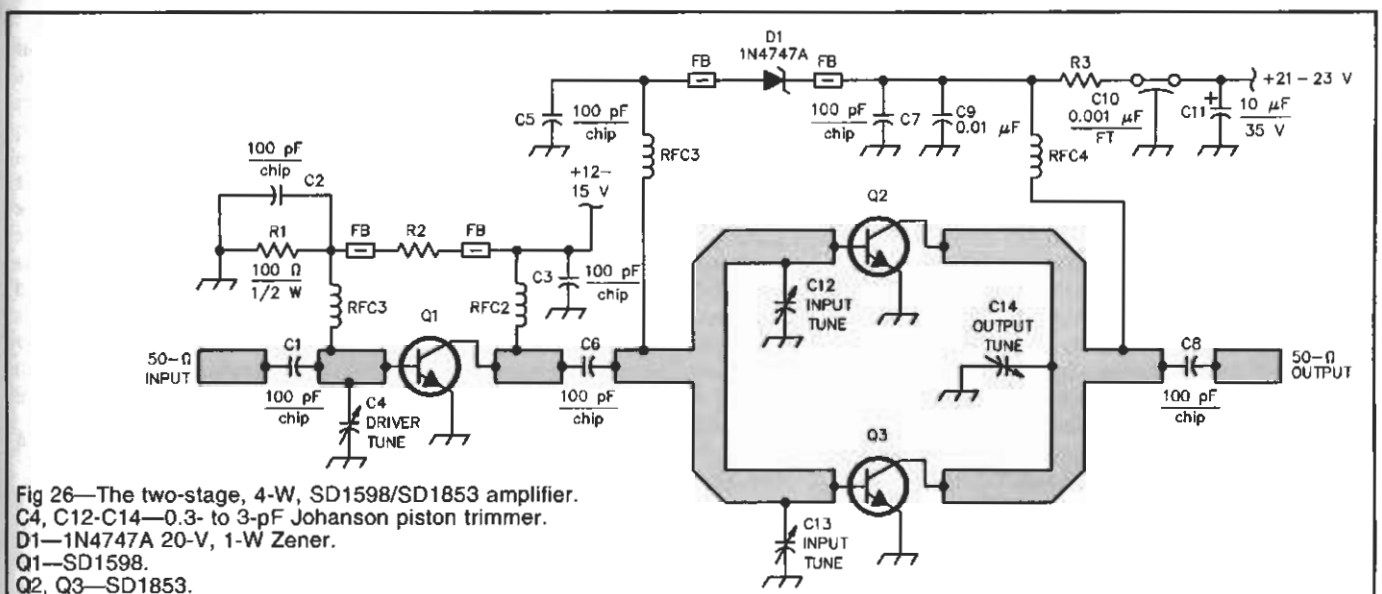

Fig 26—The two-stage, 4-W, SD1598/SD1853 amplifier.
C4, C12-C14—0.3- to 3-pF Johanson piston trimmer.
D1—1N4747A 20-V, 1-W Zener.
Q1—SD1598.
Q2, Q3—SD1853.
R2—1.5-1.7 kΩ, ½ W. See text, Part 1, June 1990 *QST*, p 24.
R3—1-2 Ω, 2 W.
RFC1-RFC4—8 turns of no. 26 enam wire, closewound, 0.1" ID.

as that for Amplifier No. 8, is shown in Fig 17 (shown in Part 1). The board's driver-stage traces are by-passed with a brass strip in this amplifier. Fig 24 shows my prototype mounted in a PC-board enclosure. A single base-bias source, using a current-limiting resistor and Zener diode, feeds both devices. Total idling current, measured in series with R1, is 400-450 mA.

The same mounting arrangement used with the single-SD1853 amplifier (Amplifier No. 9) applies to this unit. The device flanges must have low-inductance ground connections. Mount the transistors to a heat sink about 2 × 3 inches with 1/2 inch or taller fins, as shown in Fig 25. Again, the supply voltage is switched on only during transmit. To tune this amplifier, adjust C4, C5 and C6 alternately for maximum output.

Amplifier No. 11: 20 mW In, 4 W Out

A second 4-W amplifier, using a pair of SD1853s driven by a single SD1598, is shown in Fig 26. The final stage is Amplifier No. 10, and the driver is the same as that used in Amplifier No. 8. The PC-board artwork is shown in Fig 17; the parts placement can be done using Figs 23 and 16 as guides.

The power-supply and bias adjustments are the same as those for the previously described amplifiers using these devices. Transistor mounting is also the same as before, but extra heat sinking is required with this unit because of the class of operation and the power output.

Higher Power Output

Higher-power devices usable at 903 MHz are available from several manufacturers. NEC's NEL1320 (2SC3542) produces 18-20 W linear output at 903 MHz. These devices also work on the 1296-MHz band. These transistors, as well as single- and dual-stage amplifiers based on them, are available from Down East Microwave (DEM). (The DEM two-stage 3318PA runs around 18 W output for about 1 W input).

SGS-Thomson Microelectronics also makes high-power devices for the 800- to 960-MHz range. For example, the SD1423 is a 4-W-in, 30-W-out class AB device, and the SD1660 is a class-AB transistor that runs a whopping 120 W output for about 35 W drive. Both of these devices run on 28 V dc.

Summary

As I've shown in this two-part series, there's really nothing difficult about building your own 903-MHz equipment—from the local oscillator to the final amplifier. This ease of construction is a vast improvement over what it was just a few years ago—and the 903-MHz band's population has grown as a reflection of that. See you on the microwaves!

By Dave Mascaro, WA3JUF

From *QST*, August 1988

25-Watt Linear Amplifiers for 144 and 200 MHz

Do you need more punch from your hand-held or portable rig for 2 meters or 220 MHz? These little amplifiers can supply it!

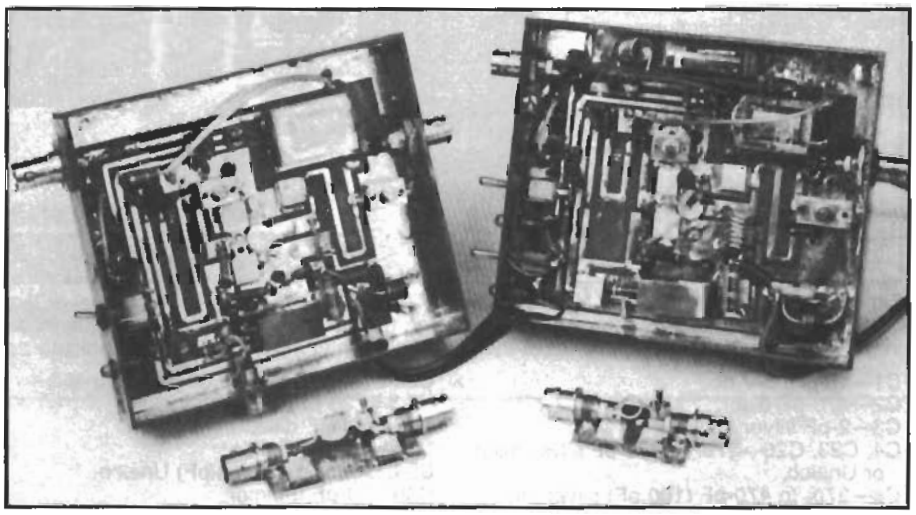

Many hams have 2-meter and 220-MHz hand-held rigs and low-power portable SSB rigs these days. Unfortunately, many of these radios have limited usefulness because of their low power output. Also, as hand-held radios get smaller, so do the NiCd packs that power them—a few long-winded transmissions on high power and the battery is dead! The low-power mode is usually good only for short-range simplex operation, or repeater use when you're close to the repeater. High-capacity battery packs are available for most hand-held rigs, but using them takes away the size and weight advantage of today's smaller hand-held transceivers. Some rigs offer the option of removing the battery pack and plugging the unit directly into 12-V dc, which gives you a small, lightweight rig, but you're still stuck with relatively low power.

The solution to this problem is the addition of a linear amplifier. An amplifier after the hand-held transceiver or portable rig that can give you 25 to 30 W of output power (depending on the output of the driving rig) without imposing large weight, cost and current-drain constraints is a great addition to your VHF station. An amplifier also allows you to use the same low-powered rig in the house and in the car with high power output. You can mount an amplifier under the seat or in the trunk of your car, and minimize the possibility of theft by taking the radio with you when you leave the car.

Amplifier Design

The amplifiers described in this article are capable of 25 to 30W of RF output for the drive power available from common handheld and portable rigs. The 2-meter and 220-MHz designs are so similar that we can describe them both in one discussion. The differences in the designs are covered in detail. Design, assembly, tuning and use of the amplifiers is virtually identical for both versions. Both versions even use the same PC board! (Note that two different boards are shown in the lead photo—they were prototypes of the fmal board design.)

Receiving preamplifiers are included in both units. They, too, are quite similar, differing only in some component values.

This power amplifier uses a single SD1274 bipolar transistor manufactured by Thomson Components/Mostek Corp.1 The device is operated class AB for all-mode operation. Nominal dc power-supply voltage is 13.8. The amplifier will operate on any dc supply voltage between 12 and 14.5 (the typical automobile supply voltage range).

The main amplifier PC board is a microstripline design on standard 1/16-inch-thick, double-sided, G-10 fiberglass-epoxy board. Input and output tuning capacitors are provided for maximizing gain and power output in a given band segment. If desired, the amplifiers can be tuned for broadband operation with only a slight reduction in power output across the operating frequency range.

The 2-meter and 220-MHz amplifiers are narrow-band designs. The 2-meter version gives 25 W output for 2 W of drive from 138 to 150 MHz, with a single tuning setting. When tuned for narrow-band operation, the amplifier gives about 20 W output for 1 W of drive. With the Kenwood TH-21AT on high power, my 2-meter amplifier puts out 25 W. On low power, I can adjust the amplifier for a maximum narrow-band gain, which gives about 7 to 8 W output. Efficiency is 50 to 60%, depending on tuning and power output.

The tuning range of the 220-MHz amplifier is 200 to 230 MHz. When tuned for narrow-band operation, the amplifier gives about 16 W output for 1 W of drive. Driving the amplifier with my ICOM IC-3AT on high power (about 1.5 W), the amplifier puts out 20 W. With the IC-3AT on low

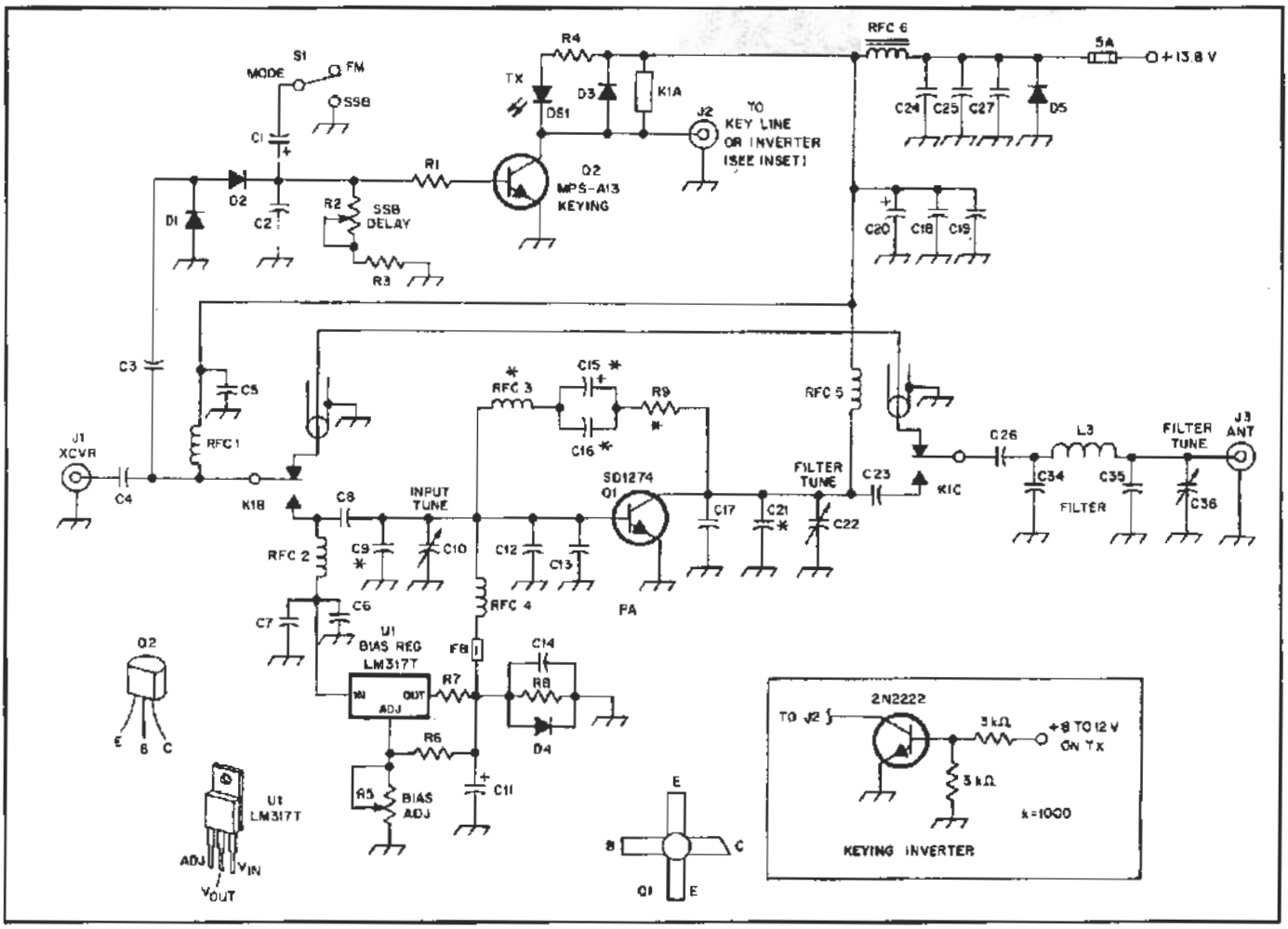

Fig 1—Schematic of the 25-W VHF amplifiers. The 5-A fuse is included in the power lead (external to the amplifier). Be extremely careful when mounting the power transistor—see text for precautions. In the parts list below, values for the 220-MHz version are given in parentheses where they differ from those in the 2-meter version. Asterisks indicate parts not used in the 220-MHz version.

C1—15-µF, 6-V dc.
C2—470-pF disc.
C3—2-pF silver mica.
C4, C23, C26—270- to 470-pF silver mica or Unelco.
C8—270- to 470-pF (100 pF) silver mica or Unelco.
C5, C7, C14, C16, C19, C24—0.01-µF disc.
C6—0.22-µF disc.
C9—43-pF silver mica or Unelco.
C10—Arco 404—4 to 60 pF (Arco 403—4 to 40 pF).
C11, C15—1-µF, 15-V tantalum.
C12—180-pF (120-pF) Unelco.
C13, C18—220-pF Unelco.
C17—68-pF (51-pF) Unelco.
C20—10-µF, 35-V electrolytic.
C21*—33 pF silver mica or Unelco.
C22—Arco 404—4 to 60 pF (Arco 402—1.5 to 20 pF)
C25—0.1-µF disc.
C27—0.001-µF disc.
C34, C35—25-pF (18-pF) Unelco.
C36—10-pF trimmer.
D1, D2—1N4148 or 1N914.
D3, D4—1 N4001 or equiv.
D5—ECG 581 or equiv.
DS1—LED.
FB—Ferrite bead.
K1—Omron LZN2O3-UA-DC12 DPDT relay.
L3—3 turns (1 turn) no. 18, closewound, 0.2-in. (¼-in.) ID.
Q1—Thomson/Mostek SD1 274.
Q2—MPS-A13 NPN Darlington.
R1, R4—1.5-kΩ, ¼ W.
R2—500-kΩ, 10-turn potentiometer.
R3—10-kΩ, ¼ W.
R5—100-Ω miniature potentiometer.
R6—270-Ω, ¼ W.
R1, R8—10-Ω, ½ W.
R9*—15-Ω, ¼ W.
RFC1, RFC2, RFC4—0.47-µH molded choke.
RFC3*—0.15-µH molded choke.
RFC5—6 turns (5 turns) no. 16 enam, ¼-in. ID.
RFC6—VK200/4B ferrite choke.
S1—Miniature SPDT toggle.
U1—LM317T voltage regulator

Miscellaneous

2 BNC or N connectors (see text).
4 × 4 × 1½-in. heat sink.
5-A fuse and in-line holder.
2 × 1-in. scrap of thin sheet brass.

power (about 150 mW), I can tune the amplifier to give 4W output. Efficiency is about the same as the 2-meter version.

The saturated power output for both versions is more than 35 W in FM operation. The maximum FM power input is 4 W. Minimum power input for proper RF sensed keying operation is 100 mW.

The Power-Amplifier Circuit

See Fig 1. K1 is similar to relays used in VCR RF circuits. I have switched up to 40 W at 2 meters and 35 W at 220 MHz with these relays. They present a good match to 50 Ω. The loss through the amplifiers (when not in use) resulting from these relays is less than 1 dB. This is typical for 2-meter and 220-MHz amplifiers.

In addition to switching the transmitted and received signals, the relays also switch the dc supply voltage. In the transmit mode, K1 switches 13.8 V dc to the input of the bias regulator, U1. The regulator IC and its associated resistors (R7, R8) and bias diode (D5) supply a stiffer bias voltage to the base of Q1 than the more-common voltage-divider bias networks. This low-impedance bias source keeps the bias voltage constant over the range of RF drive levels. With a voltage-divider bias network, bias voltage can be upset by the base-emitter rectification (self bias) developed by the RF driving signal. In such a case, over-driving the amplifier causes the base bias to decrease, resulting in non-linear amplification. This effect is limited with the regulator-type bias

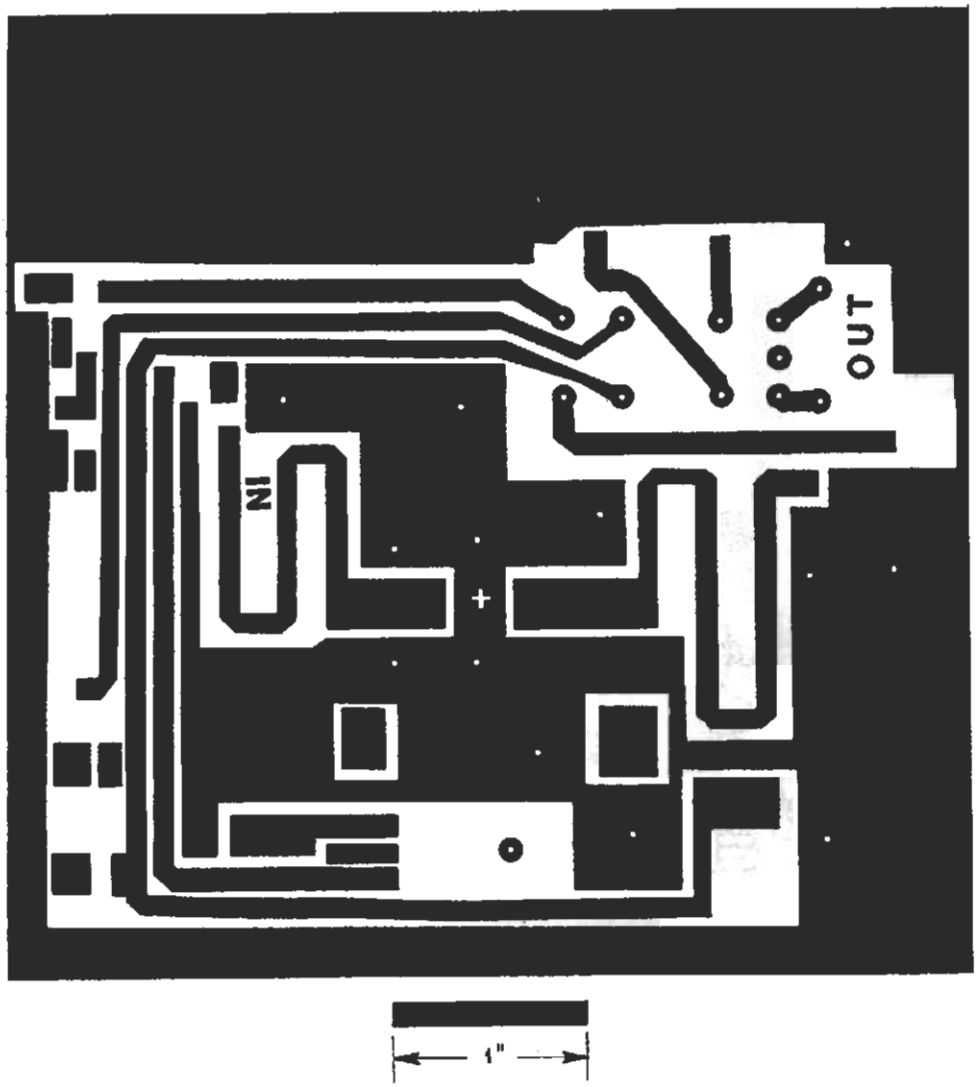

Fig 2—Main PC-board layout for the 2-meter and 220-MHz amplifiers. Artwork is full scale. Because this is a microstripline design, do not change the geometry or routing of board traces. The board must be drilled for rivets, mounting hardware and transistor mounting at the locations marked. The transistor-mounting hole is 0.38-in. diam and should be drilled at the + near the center of the PC board. All other holes (except for the relay-mounting holes near the output microstripline) are for rivets and no. 4-40 mounting hardware.

circuit used in these amplifiers.

TR switching is accomplished by an RF sensing circuit. A small amount of RF is sampled by C3 and rectified by D1 and D2, which turns on keying transistor Q2. Q2 pulls in K1, which switches the amplifier into the line.

When S1 is in the SSB position, a short drop-out delay is added in the RF-sensed-keying circuit to keep the amplifier keyed during brief pauses in speech. This delay is adjustable by varying R3. In the FM position, no delay is needed. S1 does not change the class of operation of Q1—it merely switches in the delay circuit.

The switching relays are wired so the amplifier can remain in-line at all times, with or without the supply voltage connected. Applying the supply voltage allows you to use the amplifier and preamp. Without the supply voltage connected, all transmitted and received signals pass through the amplifier.

The spectral output of these amplifiers is quite good, but to ensure clean signals, I've added filters to the output of each unit. Although there isn't much extra room for the filter components inside the amplifier cabinet, you can mount them on the back cover or in another small enclosure. The filters, shown in the title photo, are very simple to build and tune.

Construction

Each amplifier consists of two PC boards: the power-amplifier board and the preamp board (if used). After the PC boards are etched, holes are drilled with a no. 50 bit for installation of tinned grounding rivets at all RF and de grounds (see Fig 2).[2] Install the rivets on the board as follows: After inserting the rivets, flare the inserted end with an awl. Next, flatten the rivet by tapping it lightly with a hammer, using an anvil or other solid surface under the PC board as a support. Solder the rivets on both sides of the PC board. Alternatively, pieces of wire can be soldered through the board—but because the wires will not be flush with the board, mounting the heat sink may be difficult.

Drill the holes for Q1 and the board-mounting screws as indicated in Fig 2. No holes are needed for component mounting because all parts are mounted on the trace side of the PC board. All the components except the preamp board are mounted next. (The preamp board is mounted after the amplifier has been tested, to prevent possible damage to the preamplifier.) Connect a piece of miniature 50-Ω Teflon® or RG-58 coaxial cable between K1 and the amplifier-input microstripline (see Fig 3).

After drilling or milling holes for Q1 in a suitable heat sink (see Fig 4), tap the mounting holes in the heat sink for no. 4-40 hardware, and mount the PC board to the heat sink. Trim the four leads of Q1 to about half their original length to make mounting easier.

Q1 can be mounted in one of several ways. The distance between the underside of the leads of Q1 and the heat-sink mounting area of Q1 is larger than the thickness of $^1/_{16}$-in. G-10 board material. Because of this, the heat sink must be milled (see Fig 4), or small pieces of copper or brass must be soldered under each lead of Q1 to make up the difference in height. Alternatively, a second piece of G-10 material can be cut to the same size as the amplifier PC board

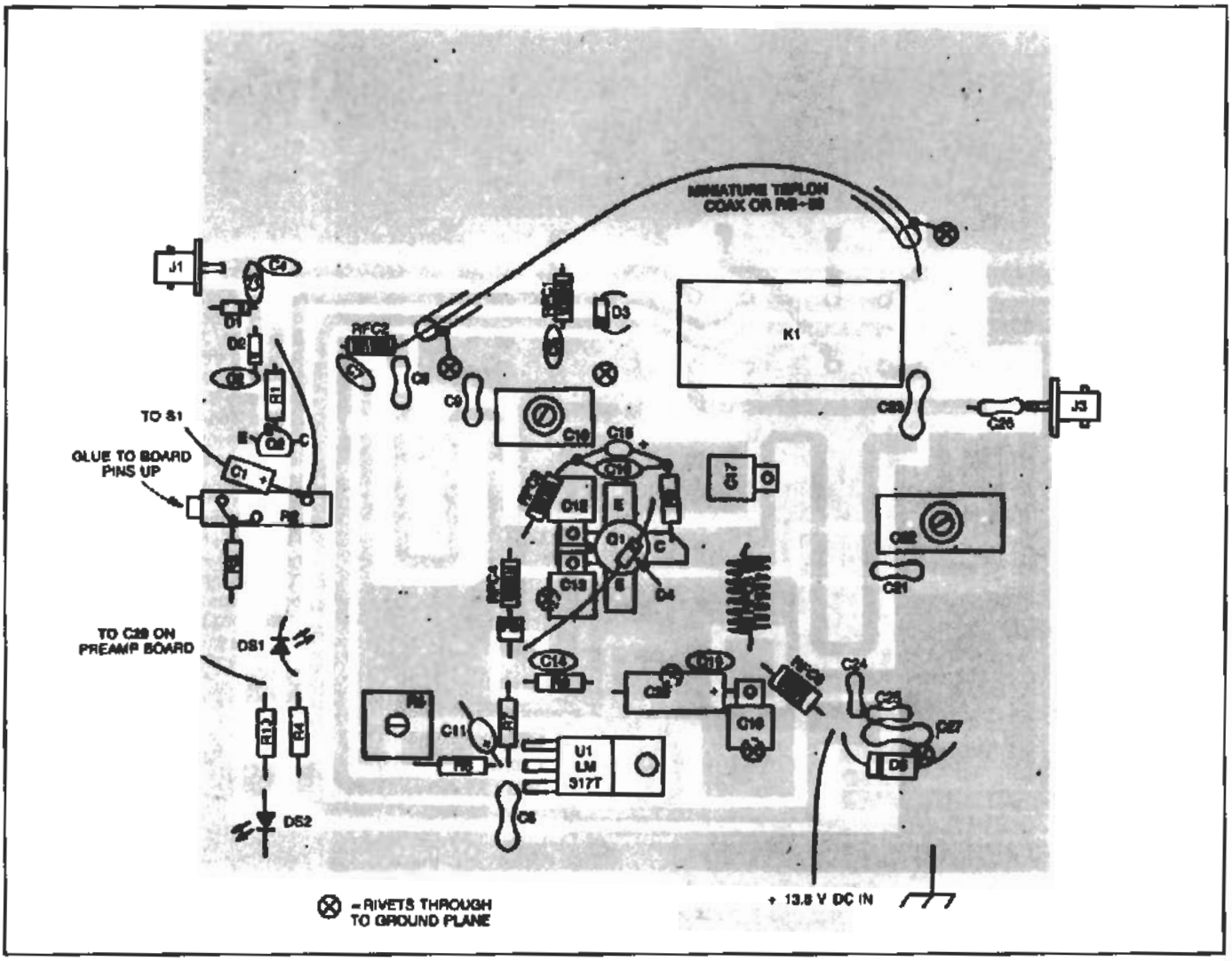

Fig 3—Parts-placement diagram for the VHF amplifiers. All parts are mounted *on the foil-trace side* of the PC board. The power-transistor mounting stud passes through the board and into the heat sink. D5 is epoxied to the ceramic cap of Q1. R2 (10-turn potentiometer) is epoxied to the PC board as indicated, with the pins facing up.0

and used as a spacer between the PC board and heat sink.

Be careful not to crack the body of Q1 where the leads of the device meet it—this can release beryllium-oxide (BeO) dust, *which is lethal*. The leads of the transistor can be bent down slightly to the PC board without affecting RF performance, but never force them in the opposite direction after the transistor has been tightened to the heat sink. Mount the transistor to the heat sink *first*, then solder its leads to the board, and *not vice versa*. Use thermally conductive compound between Q1's mounting surface and the heat sink.

Cut a piece of hobby-store sheet brass about as wide as the bias regulator IC and twice as long as the body of the device. This will be a heat sink for the bias regulator. When mounting the regulator IC, use thermally conductive compound between it and the brass sheet, and between the brass and the main PC board. After tightening the IC hardware to the PC board, bend the brass sheet in a U shape over the IC, leaving enough clearance for heat to escape between the IC and the brass heat sink. This heatsink arrangement can be seen near the bottom center of each amplifier in the lead photograph.

The Preamplifier Circuit

The high gain and low noise figure (NF) of a GaAsFET preamp are not necessary in amplifiers in this power class. I designed the preamp circuit (Fig 5) to use an inexpensive U310 FET. It has more than enough gain to overcome the losses of the amplifier switching circuits and the feed line to the amplifier. The preamp has more than 12 dB gain and noise figure of about 2 dB.

When S2 is closed, K2 closes, activating the preamplifier by applying the dc supply voltage to the drain circuit of Q3 and to the preamp ON LED, DS2. In the transmit mode, K1 switches off the supply voltage to K2, allowing K2 to drop out.

The preamp circuit is optional, and I didn't include it on the main amplifier PC board. If you're not going to build the preamp, solder foil-tape or wire jumpers between the two points on the main amplifier PC board where the preamp connects during assembly.

Building the Preamplifier

The schematic of the preamplifier circuit is shown in Fig 5. As mentioned earlier, although some component values differ between the 2-meter and 220-MHz versions, the two are essentially the same in all other respects. Components that have different values for the two versions are marked with asterisks on the schematic and the parts list. Unlike the main amplifier PC board, most preamp components are mounted through the board and soldered on the bottom side. The PC-board layout and parts-placement diagrams are shown in Figs 6 and 7, respectively.

As with most FET VHF preamplifiers, a shield is necessary between the input inductor and the active device. Solder a piece of scrap brass sheet to the ground foil between these circuit elements. (This preamp shield can be seen in the right-hand amplifier in the lead photo, just behind L1.)

After building the preamplifier, tune it

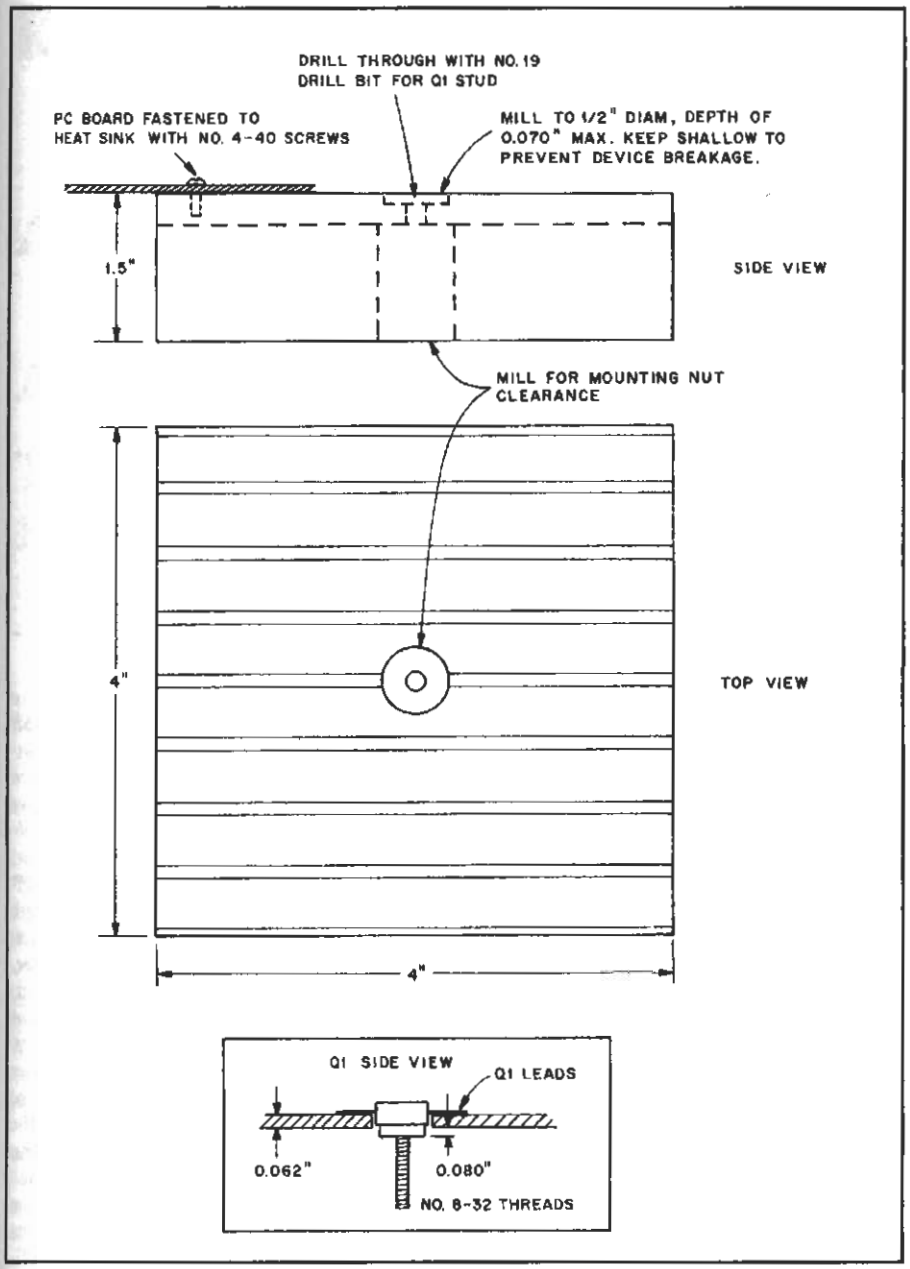

Fig 4—Heat-sink drilling dimensions for the VHF amplifiers. Overall heat-sink size isn't critical, but should be close to the dimensions shown. As an alternative to milling the heat sink to accept Q1, a piece of 1/16-in. double-sided PC-board material can be used as a shim. Be careful not to stress the transistor lead-to-body connections during mounting.

for maximum gain with a signal generator or an on-the-air signal. If one is available to you, use a noise-figure meter and tune the preamp for best NF.

Building the Output Filters

I built the output filters for each amplifier on scraps of PC-board material. The construction is shown in the title photo. After building the filters, it's a good idea to use some silicone sealant on the coil (especially in the 2-meter filter) to hold the coil turns in place. Install the filter in a suitable enclosure, or in the amplifier cabinet.

To tune the filters, you'll need a receiver capable of receiving the second harmonic of the fundamental (288 MHz for the 2-meter filter, and 440 MHz for the 220-MHz filter), and a signal generator or an on-the-air signal. Connect the filter between the antenna (or signal generator) and the receiver, and tune C36 for minimum second-harmonic signal level.

Enclosures

I used the main amplifier PC board as the top cover for the unit (with the heat sink mounted on it). I made the sides and bottom cover of the enclosure from PC-board material. The side walls are soldered to the amplifier board, and the bottom cover is attached to the side walls with small brackets (also made of PC-board material) soldered to the bottom cover. Alternatively, the amplifier can be mounted in an aluminum enclosure.

Although I used BNC connectors for RF input and output, N connectors can also be used. Make the connections from the input connector to the PC board with a piece of no. 16 wire or a 1/8-inch-wide strip of brass to the input microstripline. At the output, connect dc-blocking capacitor C26 between the microstripline and the antenna connector. Check the board for proper component placement and good solder joints, and get ready to tune up the amplifier!

Amplifier Tune-Up

As with the amplifier-circuit design and description, the tune-up procedure is very similar for both. The only difference is the exciter you use. Here's how to tune either version.

Disconnect RFC4 from the base of Q1. Connect a voltmeter to the free end of RFC4. Apply 13.8 V dc to the amplifier supply voltage leads. Using the voltmeter, verify that R5 is mounted so that output of U1 increases with clockwise rotation of R5. Turn R5 fully counterclockwise (minimum U1 output voltage). Reconnect RFC4.

Set the quiescent (no-drive) current to Q1 as follows: Disconnect one end of RFC6 and connect an ammeter in series with it. Apply 13.8 V dc to the amplifier through a 5-A fuse. Turn the preamp off. Do not apply RF drive during this adjustment. Using a clip lead, ground the collector of Q2. This should actuate K1. Check the TX LED, DS1, for operation. (If K1 actuates and the TX LED does not light, the LED may be installed in reverse.) Slowly adjust R5 for an idling current (through RFC6) of 75 to 100 mA. The amplifier should be stable; instabilities are indicated by erratic variation of Q1's quiescent current as R5 is adjusted.

Disconnect the ground lead of Q2. Q1's collector current should drop to zero. If the collector current does not drop to zero, the amplifier is unstable. If all is well, remove the ammeter and reconnect RFC6. If the amplifier is unstable, check all bypass capacitors and solder connections.

Apply about 100 mW of drive to the amplifier and check that the COR and delay circuits work properly. Adjust C10 and C22 for maximum power output. Increase drive power and retune for maximum output. After fmal assembly, tune the amplifier for the desired frequency and power level.

Final Assembly

The preamplifier board can now be installed on the main PC board. Mount the preamp on its edge (refer to the title photo and Fig 3) and solder the input and output microstriplines in place. Solder the ground foil of the preamp board to the ground foil of the main board in a few places to support the preamp board. Connect S2 and DS2 to the preamp board with hook-up wire (see Figs 5 and 6 for connection points). Apply power and check for proper operation of S2, K2 and DS2.

The enclosure can now be painted if you wish. Use masking tape to cover the connectors and heat sink. (Mount the LEDs and switches after painting.) You may want to

Fig 5—Schematic of the preamplifier circuit. K2 is identical to K1 on the main amplifier board. S2 and DS2 are mounted on the front panel of the amplifier. In the parts list below, values for 220-MHz version are given in parentheses where they differ from those of the 2-meter version.

C28, C29, C33—0.01-µF disc.
C30—2-pF silver mica.
C31, C32—20-pF trimmer.
DS2—LED.
D6—1 N4001.
L1, L2—5 turns (4 turns) no. 16 enam, 0.3-in. ID.
K2—Omron LZN2O3-UA-DC12 DPDT relay.
Q3—U310 FET.
R10—1.5-kΩ, ¼ W.
R11—91-Ω, ¼ W.
RFC7, RFC8—0.47-µH molded choke.
S2—Miniature SPDT toggle.

Miscellaneous

1 × ½-in. strip of thin sheet brass

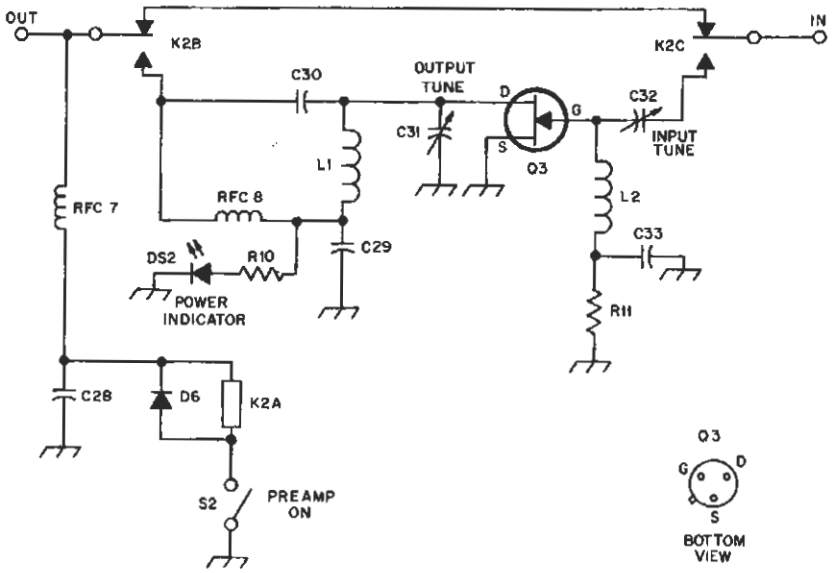

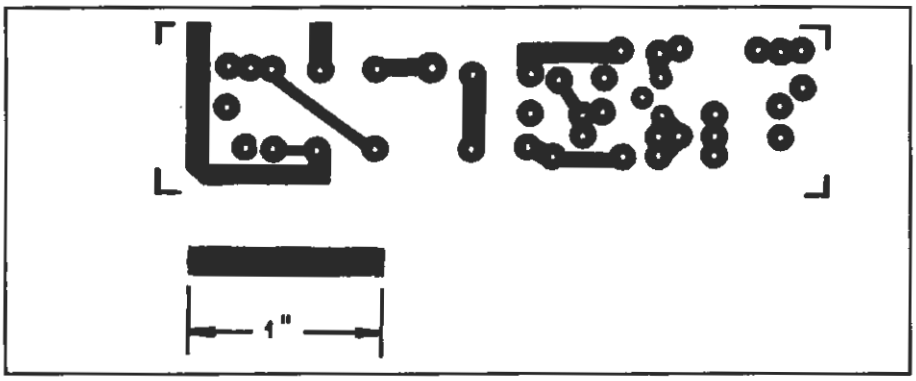

Fig 6—Full-size PC-board layout for the preamplifier circuit. Unlike the power-amplifier PC board, most of the preamplifier components are mounted on the non-trace side of the board.

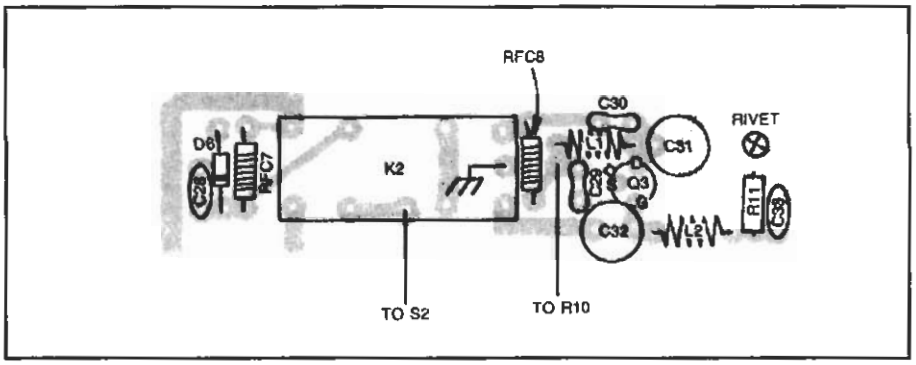

Fig 7—Parts-placement diagram for the VHF preamplifier. Mount all components on the unetched ground-plane side except for C30 and C31. Use a drill to clear the foil away from all mounting holes on the ground-plane side of the board (except for through-board ground connections). Solder all ground connections on both sides of the PC board (see text for rivet-installation instructions). Solder a brass-strip shield to the ground foil between L1 and Q3 on the component side of the PC board.

add stick-on rubber feet to the bottom cover to keep it from sliding around and being scratched.

Amplifier Operation

The 2-meter amplifier works very well with my Kenwood TH-21AT hand-held and ICOM IC-202S SSB/CW transceiver. I use one in my shack and one mobile—both at more than 25 W output. I drive the 220-MHz version of the amplifier with an ICOM IC-3AT (in its high-power mode).

Limit the amplifier power output to 25 W during linear operation. *All SSB amplifiers have a rated linear power output that should not be exceeded, even though the amplifier may be driven above that level. To keep your signal clean, do not overdrive any amplifier.* For exciters with fixed power outputs that would overdrive the amplifier, use the loss of a length of RG-58, or a discrete attenuator, between the radio and the amplifier to prevent overdrive. The gain of the preamplifier (if used) will overcome the attenuator or cable loss during receiving.

When using any amplifier or transverter in the shack, it is a good practice to "hard key" it. Hard keying is simply forcing the amplifier or transverter into the transmit mode with a switch closure or an applied voltage. To do this, run a keying line from the exciter to the amplifier. (Ground the collector of Q2 to hard key these amplifiers.) I added a phono jack to the 220-MHz amplifier to facilitate hard keying. If a positive voltage is used for keying, a 2N2222 transistor inverter can be used between the transceiver and the collector of Q2 (see the inset in Fig 1).

Summary

These amplifiers have served me well in the car and at home. After building one of these amplifiers, you'll probably find what I did: They're so handy to have around, and so easy to build, that you can't build just one!

Notes

1Thomson Components/Mostek Corp, Semiconductor Division, Commerce Dr, Montgomeryville, PA 18966. Thomson transistors are available through RF Gain, Ltd, 100 Merrick Rd, Rockville Center, NY 11570, tel 516-536-8868 or 800-645-2322.

2The following parts are available from Frontier Microwave, RD 1 Box 467, Ottsville, PA 18942: 100+ tinned rivets: $2; relays (K1, K2): 2 for $8. Prices include shipping. The ARRL and *QST* in no way warrant this offer.

By David D. Meacham, W6EMD

From *QST*, April 1984

A High-Power 2-Meter Amplifier Using the New 3CX800A7

Tired of hearing exotic DX on 2 meters but not being able to work it? Build this amplifier, and you'll transform your pip-squeak signal into a real rockcrusher.

The 3CX800A7 triode recently announced by Varian EIMAC has a plate dissipation rating of 800 W and modest cooling requirements. Its oxide cathode gives high emission with only 20 W of heater power. With full ratings up to 350 MHz, this tube is a scaled-up version of the 8874 — a proven performer in amateur and commercial gear.

The amplifier described here is based on a design presented by Raymond F. Rinaudo, W6ZO, in January 1972 QST. Most of the changes in the new amplifier (Fig. 1) are designed to accommodate the larger size of the 3CX800A7 and its attendant higher capacitances and currents. A plate-current meter is not included because my station power supply is already well metered. However, there is room on the front panel of the amplifier for a plate-current meter if another builder wishes to add one. Other changes to Rinaudo's design are minor.

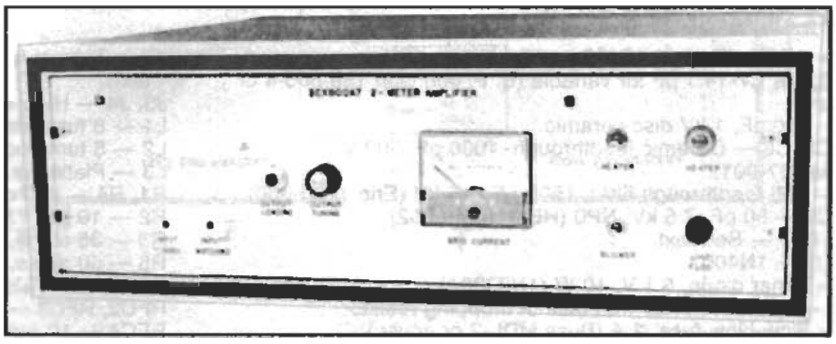

Construction

The amplifier chassis is mounted on a standard 19-inch wide, 5¼-inch-high aluminum rack panel (Bud No. SFA-1833).[1] A 5 × 13 × 3-inch aluminum chassis (Bud No. AC-422) is spaced 1¾ inches behind the panel by two aluminum end brackets. A 3½ × 4½ × 1-inch aluminum chassis (Bud No. AC-1402) houses the input circuitry and is mounted on the larger chassis between it and the front panel. The right-hand end bracket has a large lip on the rear for mounting the heater transformer and connectors. Fig. 2 shows mechanical details of the chassis and end brackets. The cabinet chosen is a lightweight aluminum unit made by TenTec (No. 19-0525).

Input Circuit

In the cathode-driven configuration, the input impedance of the 3CX800A7 appears as a nominal capacitance of 26.5 pF in parallel with a resistive component that varies with operating conditions but is typically about 49 ohms. The computerdesigned input circuit of this amplifier operates at a loaded Q of about 2.1. It can be set anywhere in the 2-meter band for a VSWR of less than 1.3:1. C1 and C2 are predominantly matching and tuning controls, respectively; there is some interaction between them, however. When the input is tuned at 144.5 MHz, the input VSWR will he less than 1.4:1 from 144 to 145 MHz.

The tube socket is an EIMAC SK-1900 or a Johnson part No. 124-311-100. Its center is mounted 2 inches from the end of the input box, adjacent to the mounting bracket. The tube pins and input circuit are cooled by a small amount of air admitted to the input box from the pressurized output box. Three holes, made with a no. 50 drill, provide adequate flow. These holes are spaced in a close triangle and are located diagonally across from the variable capacitors. Air exhausts through the tuning holes. Fig. 3 shows details of the input circuitry.

The heater circuit includes two chokes, feedthrough capacitors, the filament transformer, a voltage-dropping resistor and a switch. The chokes are wound with a turn-to-turn spacing of about one-half the wire diameter. They are self-resonant (parallel resonant) just above the 2-meter band. Nominal heater voltage for the 3CX800A7 is 13.5 V. The closest available commercial transformer has a 14.0-V secondary, so R3 is used in the primary. Switching is set up so that the blower must be on before the heater can be activated. Conversely, this arrangement allows the blower to be left on after switching off the heater—a highly recommended practice.

Cathode bias is provided by a 5.1-V Zener diode, D3. R1 prevents the cathode voltage from soaring if the Zener fails. F2 will blow if excessive cathode current is drawn. R2 nearly cuts off plate current on receive. Because the grid is at dc ground, the negative supply lead must be kept above

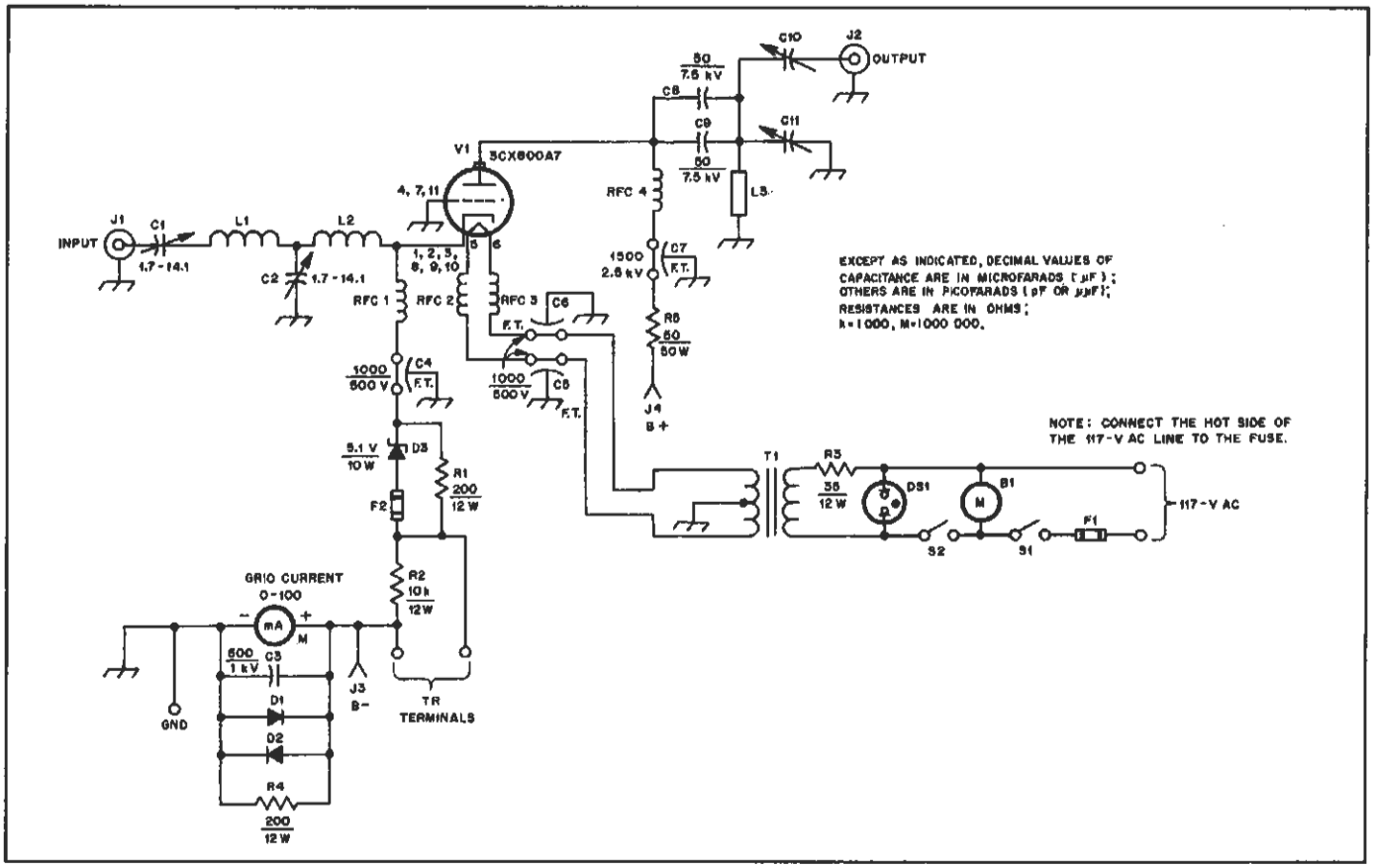

Fig. 1 — Schematic diagram of the 3CX800A7 amplifier.

B1 — Blower (Dayton 4C012 or equiv.); see text.
C1, C2 — 1.7-14.1 pF air variable (E. F. Johnson 189-505-4 or equiv.).
C3 — 500.pF, 1.kV disc ceramic.
C4, C5, C6 — Ceramic feedthrough, 1000 pF, 500 V (Erie 357-001).
C7 — EMI feedthrough filter, 1500 pF, 2.5 kV (Erie 1280-060).
C8, C9 — 50 pF, 7.5 kV, NP0 (HEC HT-50 852).
C10, C11 — See text.
D1, D2 — 1N4001.
D3 — Zener diode, 5.1 V, 10 W (1N3996A).
DS1 — NE51 in holder with built-in dropping resistor.
F1 — Slow-blow fuse, 2 A (Buss MDL-2 or equiv.).
F2 — 1.5 A fuse (Buss AGC 1½ or equiv.).
J1 — BNC bulkhead feedthrough connector (UG-492 A/U).
J2 — Type N female connector (part of C10 assembly — see text).
J3, J4 — High-voltage connector (Millen 37001 or equiv.).
L1 — 8 turns no. 16 tinned wire, 3/8-in ID, 11/16 in long.
L2 — 6 turns no. 16 tinned wire, 3/8-in ID, 11/16 in long.
L3 — Plate line, 1 5/16 in wide, 8 3/16 in long. See text and Fig. 4.
R1, R4 — 200 ohms, 12 W.
R2 — 10 kΩ, 12 W.
R3 — 35 ohms, 12 W.
R5 — 50 ohms, 50 W.
RFC1 — 1.0 μH choke, 300 mA (Miller 4602).
RFC2, RFC3 — 11 turns no. 20 HF wire on 3/8-in Noryl rod.
RFC4 — 10 turns no. 16 tinned wire, 1/2-in ID, 1 3/16 in long.
T1 — Filament transformer, 14.0-V, 2-A secondary (Triad F-215X or equiv.).

ground for grid-current metering by M1. R4 keeps the negative side of the plate supplyirom rising if M1, D1 and D2 all open up. D1, D2 and C3 protect the meter from transients and RF voltages.

Output Circuit

The output tank circuit is a silver-plated quarter-wave strip line (Fig. 4) foreshortened by the tube, loading and tuning capacitances at, and near, its open end. It operates at a loaded Q of approximately 20. The silver-plated anode collet (Fig. 4) is made of 0.062-inch-thick brass sheet with Tech-Etch 134B finger stock soldered on the inside. It is supported by two Teflon® standoffs ½-inch in diameter and 1 inch long. At the far end of the line, a silver-plated shorting block contacts the chassis and the strip line. This block (Fig. 4) is made from 7/16-inch-thick brass 1 15/16 inches wide and 1 inch high. EIMAC CF-800 fmger stock is screwed and then soldered on both top and bottom. The chassis and stripline are both slotted to allow 5/16 inch of shorting-block travel to set the tuning range of the capacitive-tuning paddle. A 1-inch-long Teflon standoff supports the center of the line.

The tuning (C11) and loading (C10) paddles are 1 3/16-inch-diameter discs made from silver-plated, 1/16-inch-thick brass. They are spaced 1 3/8 inches center-to-center. The output loading paddle is nearest the tube, and its center is 1 13/16 inches from the tube cooler surface. Spacing between the paddle and line during operation is about 0.135 inch. The output tuning boss, EIMAC part No. 720362, is tapped for a 1/4-28 threaded rod. The output loading control and output connector are two separate EIMAC assemblies combined into one unit. They are available from EIMAC as Support Assembly No. 720361 and Sliding Probe Assembly No. 720407. For this amplifier, the outer conductor was lengthened to reach the front panel. The grid collet is also available from EIMAC as part No. 720359.

In addition to RFC4 and feedthrough capacitor C7, an energy-absorbing resistor (R5) is wired in series with the dc plate supply. This resistor will protect the tube and power supply in the event of a highvoltage arc. It provides necessary protection while dissipating only 12.5 W at 500-mA dc plate current.

Cooling

The blower specified provides a measured 25 CFM airflow through the output box and tube cooler at 0.42 inch of water-column static pressure. This amount of cooling is sufficient for 800 W of plate dissipation at sea level with inlet air temperatures up to 35° C. It is adequate for the same dissipation at 5000 feet of altitude with

inlet-air temperatures up to 25° C.

Not evident from the photographs is the care taken to separate outgoing hot air from incoming cool air. This is accomplished by the addition of a simple dividing wall inside the cabinet running from the rear chassis cover of the output box to the rear of the cabinet. The material used is rigid fiberglass insulation — the kind you cut with a saw. It provides a measure of blower-noise suppression in addition to assuring cool inlet air.

Hot air leaving the anode cooler is directed to a homemade "honeycomb" RFI filter through a chimney made from rolled-up Teflon sheet. The filter is made of brass tubing and sheet with the honeycomb material soldered in place. See Fig. 5 for construction details. This filter acts as a waveguide-beyond-cutoff having high attenuation at 144 MHz.

The equation for calculating attenuation by this type of filter is

$$A_a = 32\ D/d \qquad \text{(Eq. 1)}$$

where A_a = aperture attenuation (dB), D = length of pipe, and d = inside diameter of pipe. In this case, the "pipe" is each cell of the honeycomb. The basic material for the honeycomb is cadmium-plated brass heat-radiator core.[2] Each hexagonal-shaped cell has a width between flat sides (diameter) of 0.100 inch. The material is 1/2-inch thick. Plugging these values into the equation yields an A_a of 160 dB—more than enough! From a practical standpoint, it is usually sufficient to make cell length at least three times the nominal cell diameter.

Tune-up

Initial work may be done with a dip meter, particularly on the output circuit. With the tube in place, but with no voltages applied, the shorting block on the end of the plate line should be set to give a paddle-tuning range that straddles the desired operating frequency. Bear in mind that when the tube is "hot," the resonant frequency will be somewhat lower than it is without electron flow.

The input-tuning capacitor can be dip-meter resonated with the matching capacitor set at one-half mesh for a start. Further work here must be done "hot" with a VSWR measuring device on the input.

Set the initial spacing between the output paddle and the plate line to 1/8-inch. Connect the output to a 50-ohm dummy load capable of handling at least 700W at 144 MHz through an accurate VHF wattmeter, such as a Bird model 43. Connect a driver capable of delivering about 20 W to the input through a VSWR-measuring device.

The heater of the 3CX800A7 should be run for at least three minutes before applying plate voltage. After the warm-up, short the TR terminals and apply about 1000 V to the plate. This should result in a small amount of idling plate current. Next, apply enough drive to produce a rise in plate current, and adjust the plate tuning for a peak in output power. Now tune and match the input circuit for minimum input VSWR. Next, adjust the output loading paddle for maximum power output while keeping the plate current dipped with the plate tuning paddle. Apply full plate voltage and higher drive power, and then repeak the output tuning and loading controls. Touch up the input tuning and matching, and the amplifier is ready for service.

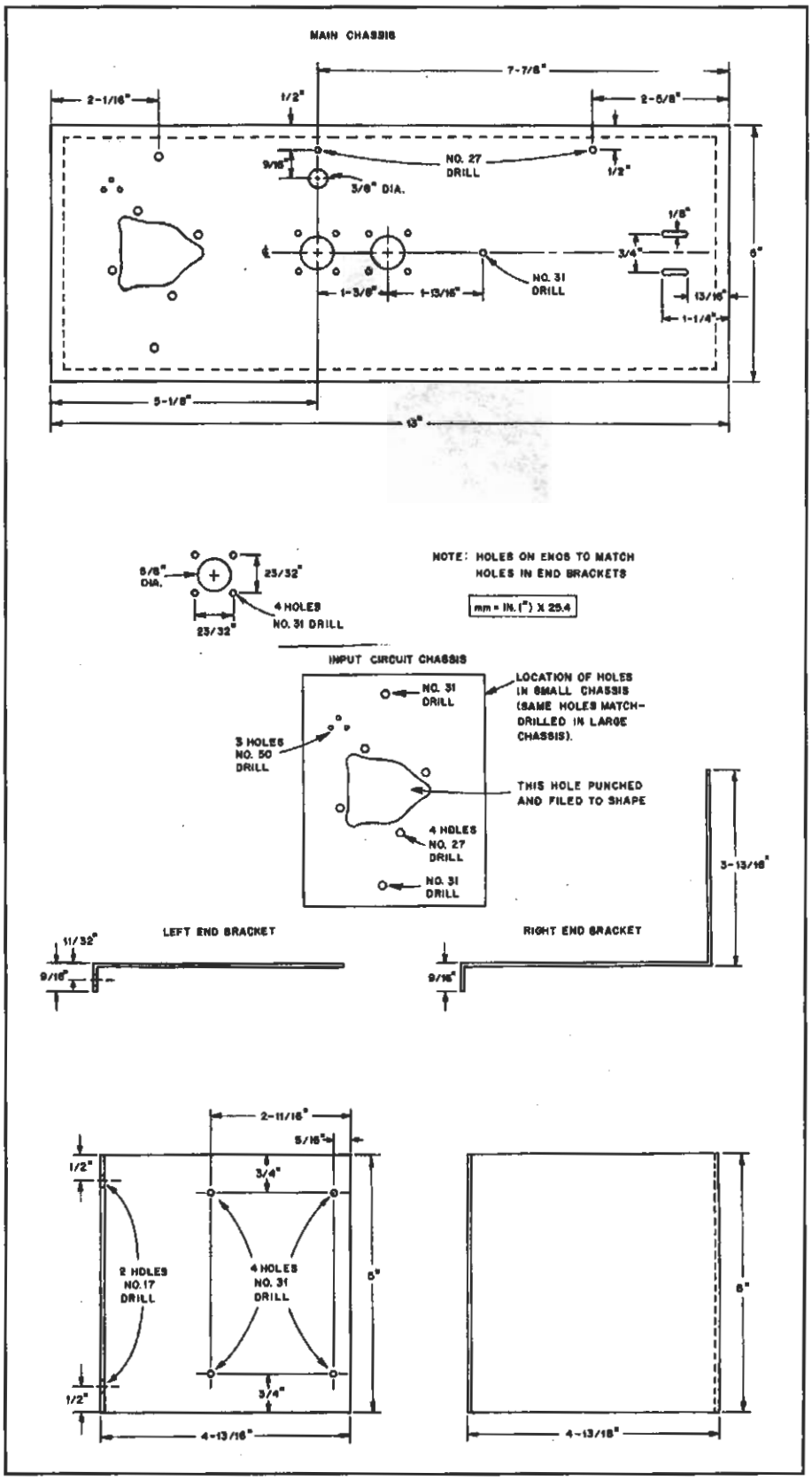

Fig 2—Mechanical details of the chassis and end brackets. The end brackets are made from 0.032-in aluminum, 5052 alloy or softer.

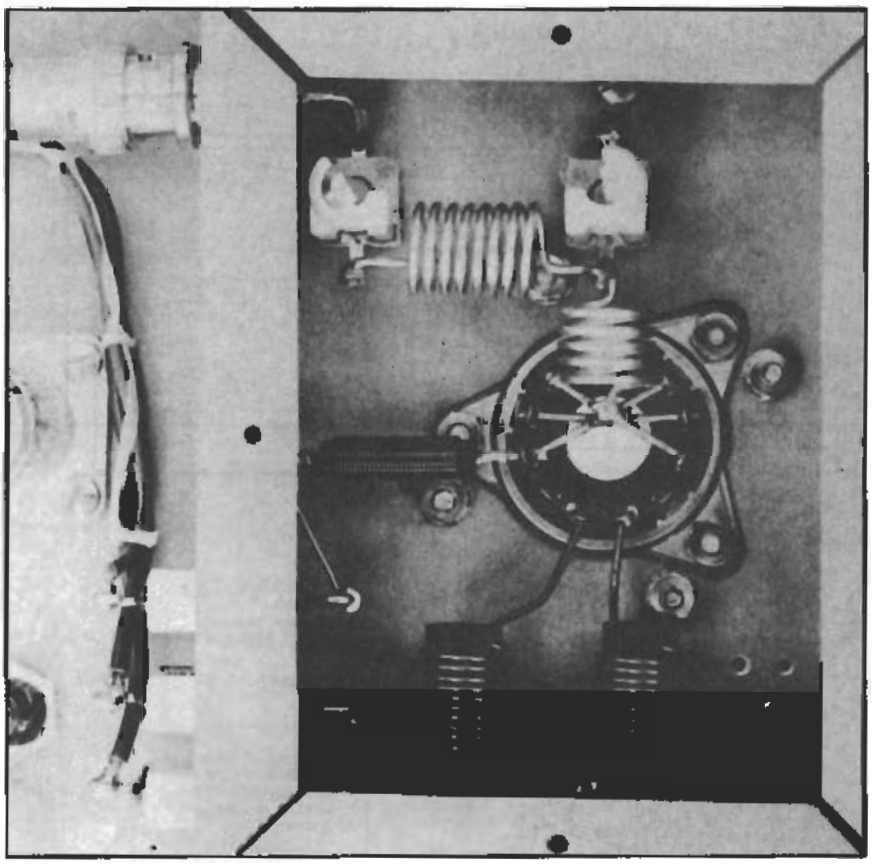

Fig 3—Close-up of the input circuitry and tube-socket wiring. Keep all leads as short as possible.

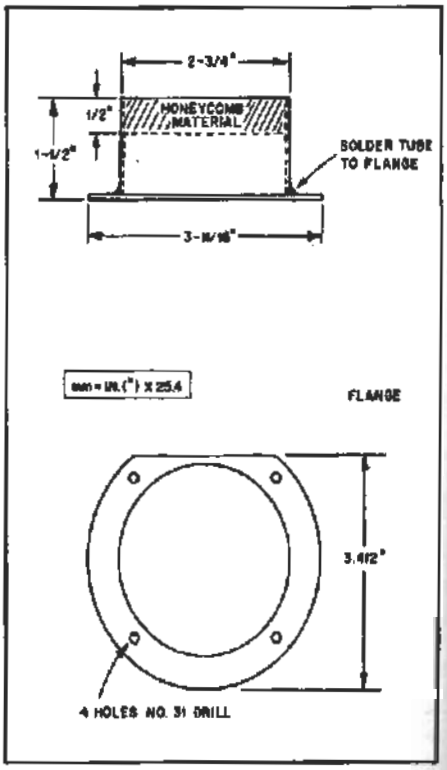

Fig 5—Mechanical details of the exhaust air RFI filter. The honeycomb material is soldered inside a 2¾-in OD, 0.065-in wall brass tube. The flange, which bolts to the chassis, is made from 0.125-in-thick brass sheet.

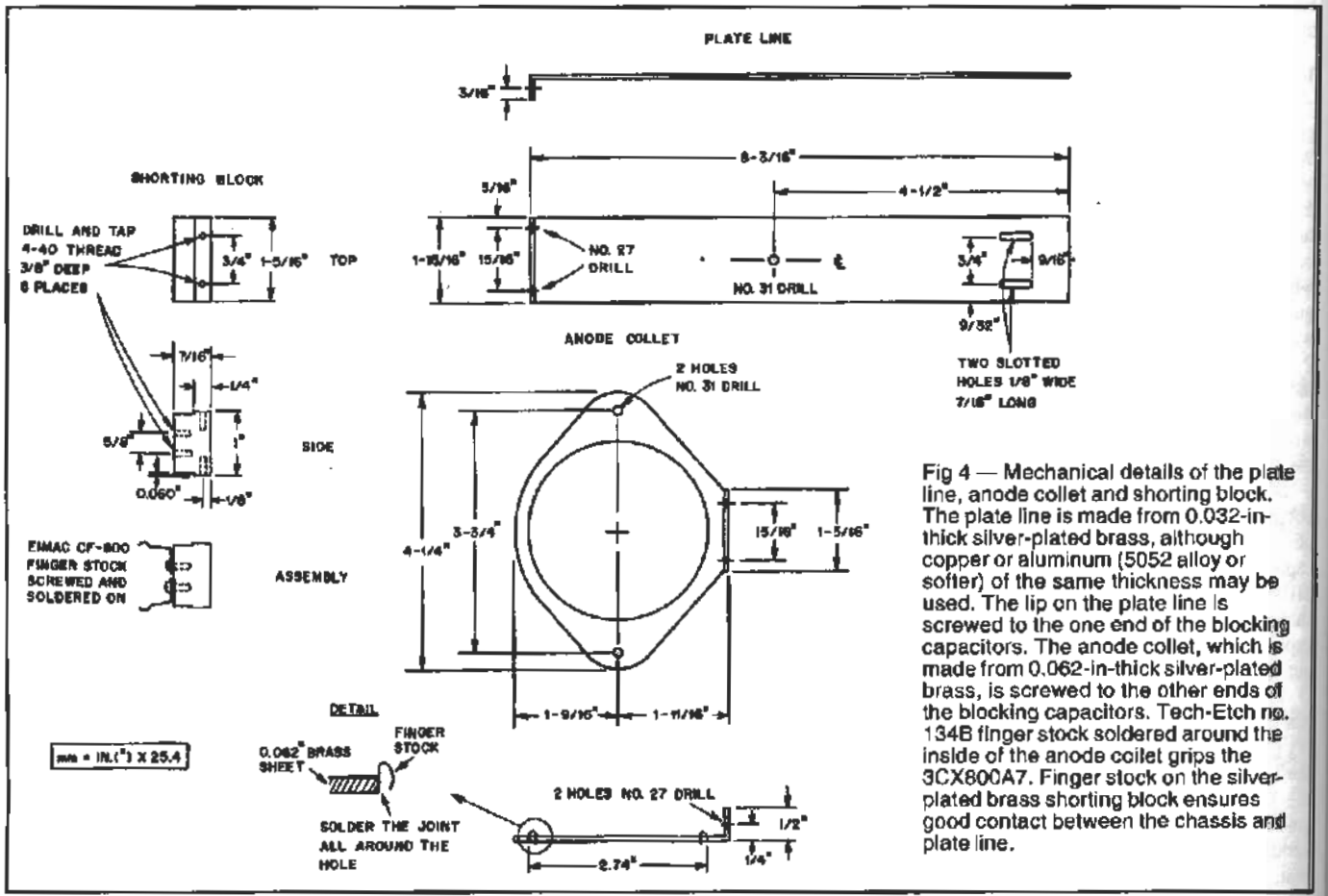

Fig 4 — Mechanical details of the plate line, anode collet and shorting block. The plate line is made from 0.032-in-thick silver-plated brass, although copper or aluminum (5052 alloy or softer) of the same thickness may be used. The lip on the plate line is screwed to the one end of the blocking capacitors. The anode collet, which is made from 0.062-in-thick silver-plated brass, is screwed to the other ends of the blocking capacitors. Tech-Etch no. 134B finger stock soldered around the inside of the anode collet grips the 3CX800A7. Finger stock on the silver-plated brass shorting block ensures good contact between the chassis and plate line.

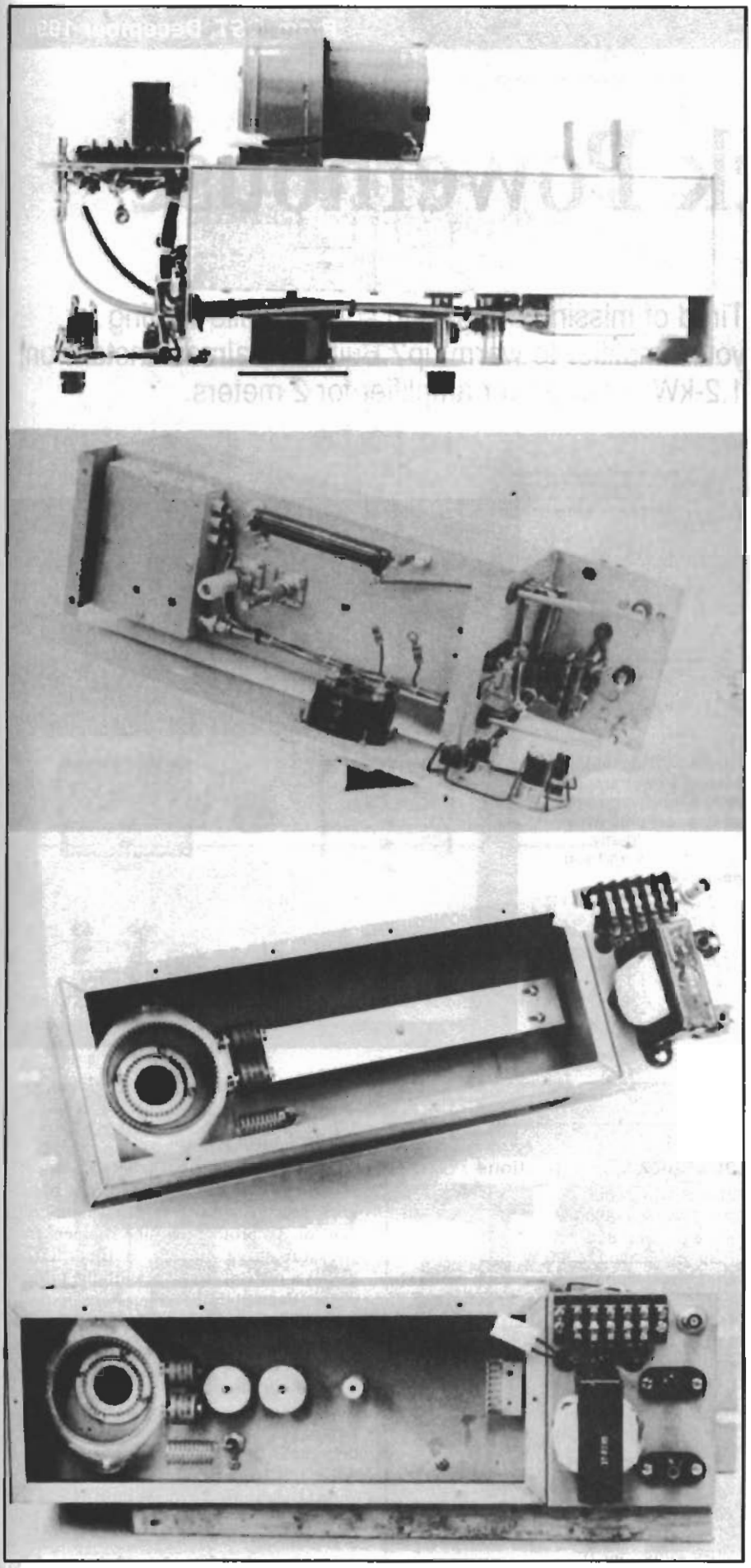

Fig 6—Various views of the completed 3CX800A7 amplifier.

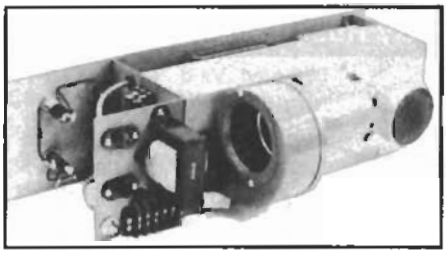

Fig 7—Rear view of the amplifier with the plate-compartment cover in place. Note the honeycomb RFI filter at the hot-air exhaust.

Table 1

Operating Conditions for the 3CX800A7 Amplifier

Plate supply voltage	2200 V
Zero-signal plate current*	65 mA
Single-tone plate current	500 mA
Grid bias (Zener bias)	–5.1 V
Single-tone grid current*	40 mA
Driving power	18.5 W
Output power	707 W
Gain	15.8dB
Efficiency**	64%

*Values may vary considerably from tube to tube.

**Actual tube efficiency is about one percent higher because of power loss in the 50-ohm series resistor in the plate lead (R5).

A few words of caution are in order. Remember that the heater voltage must never be applied without the blower running, and that the heater must warm up at least three minutes before applying plate voltage. Never exceed 60-mA dc grid current, even during tune-up. Also, because of the relatively low grid dissipation of the 3CX800A7, RF drive must never be applied unless plate voltage is applied to the tube and a suitable load is connected to the output. Following these simple rules will substantially increase tube life and amplifier reliability.

Typical Operating Conditions

With Zener-diode bias, the 3CX800A7 is best operated in Class AB2 for linear service. The data in Table 1 represent measured performance in linear service at 144 MHz. Complete data sheets are available from EIMAC. This amplifier is easily capable of conservative operation at 700-W output. Two of these tubes will run at the 1500-W output legal limit.

This amplifier uses straightforward construction techniques and is easily duplicated. Any builder will be rewarded with a great deal of satisfaction and a reliable amplifier.

Notes

[1]mm = in x 25.4; m = ft x 0.3048.

[2]One source for the honeycomb radiator core material is Technit West Division, 320 North Nopal St., Santa Barbara, CA 93103.

By Russ Miller, N7ART
From *QST*, December 1994

The Quick Powerhouse

Tired of missing a new grid square while waiting for your amplifier to warm up? Build this almost-instant-on, 1.2-kW linear power amplifier for 2 meters.

It's that typical, early summer afternoon, when, out of the blue comes co-channel interference to the low-band (channels 2 through 6) TV channels. Time to turn on the 2-meter receiver. Whoops! There's a sporadic-E opening, and stations are booming in from over 1000 miles away. Quickly, I hit the switches to warm up my linear amplifier. Time marches on, and now the amp is ready—only took 3 or 4 minutes. But that juicy, far-away clatter via sporadic E is gone! Woe is me!

Having had this happen more than once, I was delighted to find that Eimac was producing a new tube with an almost-instant-warm-up filament that functions well at 2 meters—the 3CX1200Z7.[1] The Z7 is different from the 3CX1200A7 by virtue of its external grid ring, redesigned anode assembly and a 6.3-V ac filament. One advantage to the 3CX1200Z7 is the wide range of plate voltages that can be used, from 2000 to 5500. This amplifier looks much like the easily duplicated W6PO design,[2] except for the plate collet and the addition of some control circuitry. The plate collet is adapted from the W6PO 222-MHz design.[3] The RF deck is a compact unit, designed for table-top use (Figure 1). Table 1 gives some data on the 3CX1200Z7; Table 2 lists CW operating performance for this amplifier.

Figure 1—This table-top 2-meter power amplifier uses a quick-warm-up tube, a real plus when the band suddenly opens for DX and you want to join in.

Input Circuit

The tuned-filament T network matches the 50-Ω drive source to the filament input impedance, providing a very low input SWR. Tuning is easy and docile. Grid bias is provided by an 8.2-V, 50-W Zener diode. Cutoff bias is provided by a 10-kΩ, 25-W resistor. A relay on the control board shorts out the cutoff-bias resistor, to place the amplifier in the TRANSMIT mode.

I didn't use a tube socket. Instead, I bolted the tube directly to the top plate of the subchassis, using the four holes (drilled to clear a #6 screw) in the grid flange. Connections to the heater pins are via drilled and slotted brass rods. The input circuit is contained within a 3½×6×7¼-inch (HWD) subchassis (Figure 3).

Table 1
3CX1200Z7 Specifications

Maximum Ratings

Plate voltage: 5500 V
Plate current: 800 mA
Plate dissipation: 1200 W
Grid dissipation: 50 W

Table 2
CW Operating Data

Plate voltage: 3200 V
Plate current (operating): 750 mA
Plate current (idling): 150 mA
Grid current: 165 mA
DC Power input: 2400 W
RF Power output: 1200 W
Plate dissipation: 1200 W
Efficiency: 50%
Drive power: 85 W
Input reflected power: 1 W

Control Circuit

The control circuit (Figure 4) is a necessity. It provides grid overcurrent protection, keying control, and filament surge control. To protect the tube filament from stressful surge current, a timer circuit places a resistor in series with the primary of the filament transformer. After four seconds, the timer shorts the resistor, allowing full filament voltage to be applied. C2 and R4 establish the time delay.

Another timer inhibits keying for a total of 10 seconds, to give the internal tube temperatures a chance to stabilize. C1 and R3 determine the time constant of this timer. After 10 seconds, the amplifier can be keyed by grounding the keying line. When the amplifier is not keyed, it draws no plate current. When keyed, idle current is approximately 150 mA, and the amplifier only requires drive to produce output. A

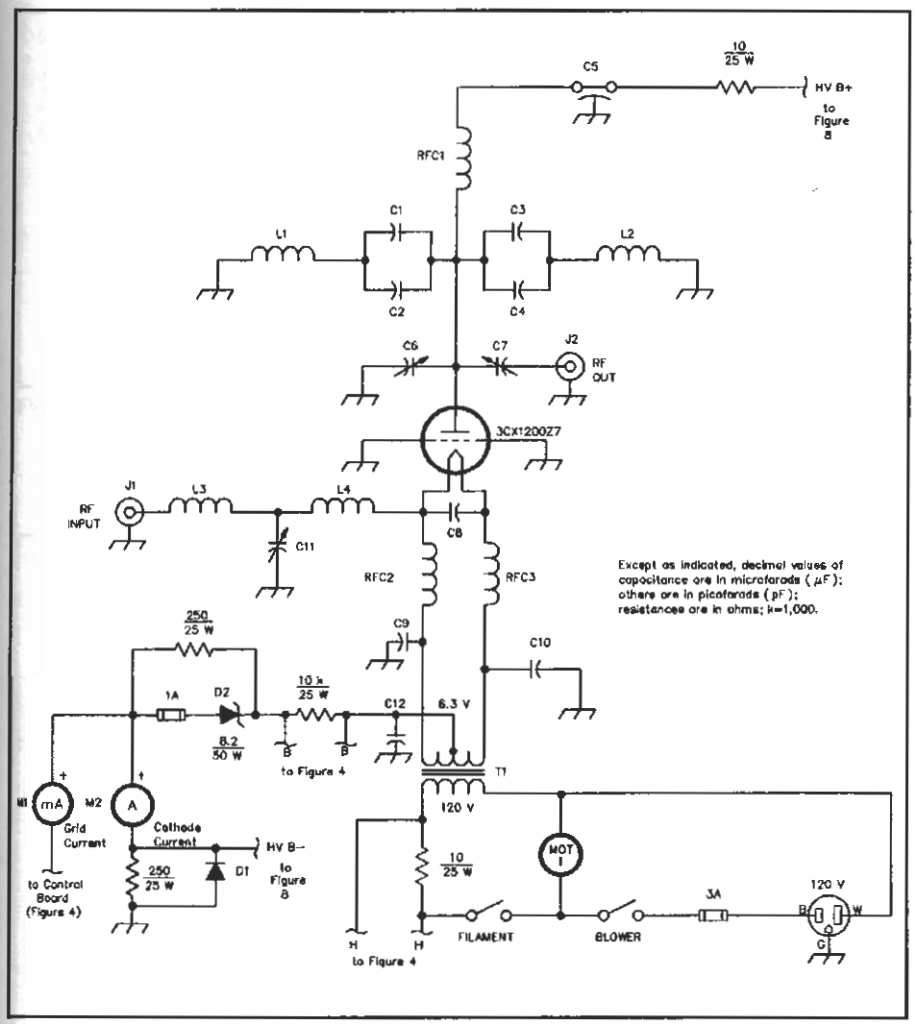

Figure 2—Schematic diagram of the 2-meter amplifier.

C1-C4—100 pF, 5 kV, type 850
C5—1000 pF, 5 kV
C6—Anode-tuning capacitor; see text and Figure 5 for details
C7—Output-loading capacitor; see text and Figure 7 for details
C8-C10—1000-pF silver mica, 500 V
C11—30-pF air variable
C12—0.01 μF, 1 kV
D1—1000 PIV, 3-A diode, 1N5408 or equiv
D2—8.2-V, 50-W Zener diode, ECG 5249A
J1—Chassis-mount BNC connector
J2—Type-N connector fitted to output coupling assembly (see Figure 7)
L1, L2—Plate lines; see text and Figure 6 for details
L3—5 t no. 14, 1/2-inch diameter, close wound
L4—3 t no. 14, 5/8-inch diameter, 1/4-inch spacing
RFC1—7 t no.14, 5/8-inch diameter, 1 3/8 inch long
RFC2, RFC3—10 t no. 12, 5/8-inch diameter, 2 inches long
T1—Filament transformer. Primary: 120 V; secondary: 6.3 V, 25 A, center tapped Available from Avatar Magnetics (Ronald C. Williams, W9JVF, 240 Tamara Trail, Indianapolis, IN 46217, 317-783-1211); part number AV-539
M1—Grid milliammeter, 200 mA dc full scale
M2—Cathode ammeter, 2 A dc full scale
MOT1 —140 free-air cfm, 120-V ac blower, Dayton 4C442 or equivalent.

Sources for some of the "hard to get parts" include:

Fair Radio Sales, 1016 E Eureka, Lima, OH 45802, tel 419-227-6573;

Surplus Sales of Nebraska, 1502 Jones Street, Omaha, NE 68102, tel 402-346-4750.

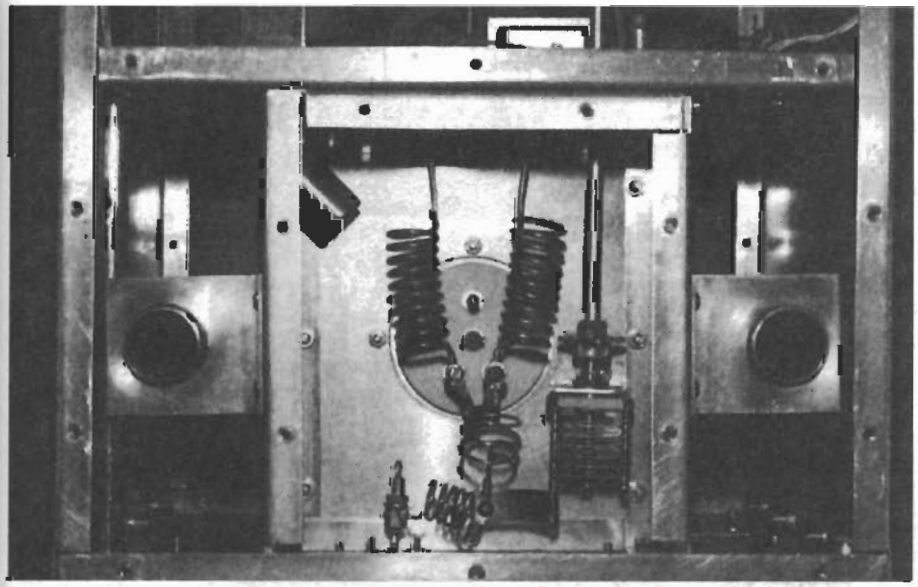

Figure 3—This view of the cathode-circuit compartment shows the input tuned circuit and filament chokes.

safety factor is built in: the keying circuit requires +12 V from the high-voltage supply. This feature ensures that high voltage is present before the amplifier is driven.

The grid overcurrent circuit should be set to trip if grid current reaches 200 mA. When it trips, the relay latches and the NORMAL LED extinguishes. Restoration requires you to press the RESET switch.

Plate Circuit

Figure 5 shows an interior view of the plate compartment.The anode collet is patterned after the one used in the W6PO 222-MHz amplifier. The differences are small. A 4×2 1/4-inch tuning capacitor plate and a 2×2-inch output coupling plate are centered on the collet. These parts are the same size and shape as those used on the 2-meter W6PO amplifier. The remaining difference is the diameter of the hole for the 3CX1200Z7 anode. Sufficient clearance must be left for the fingerstock. The hole diameter will be approximately 3 5/8 inches.

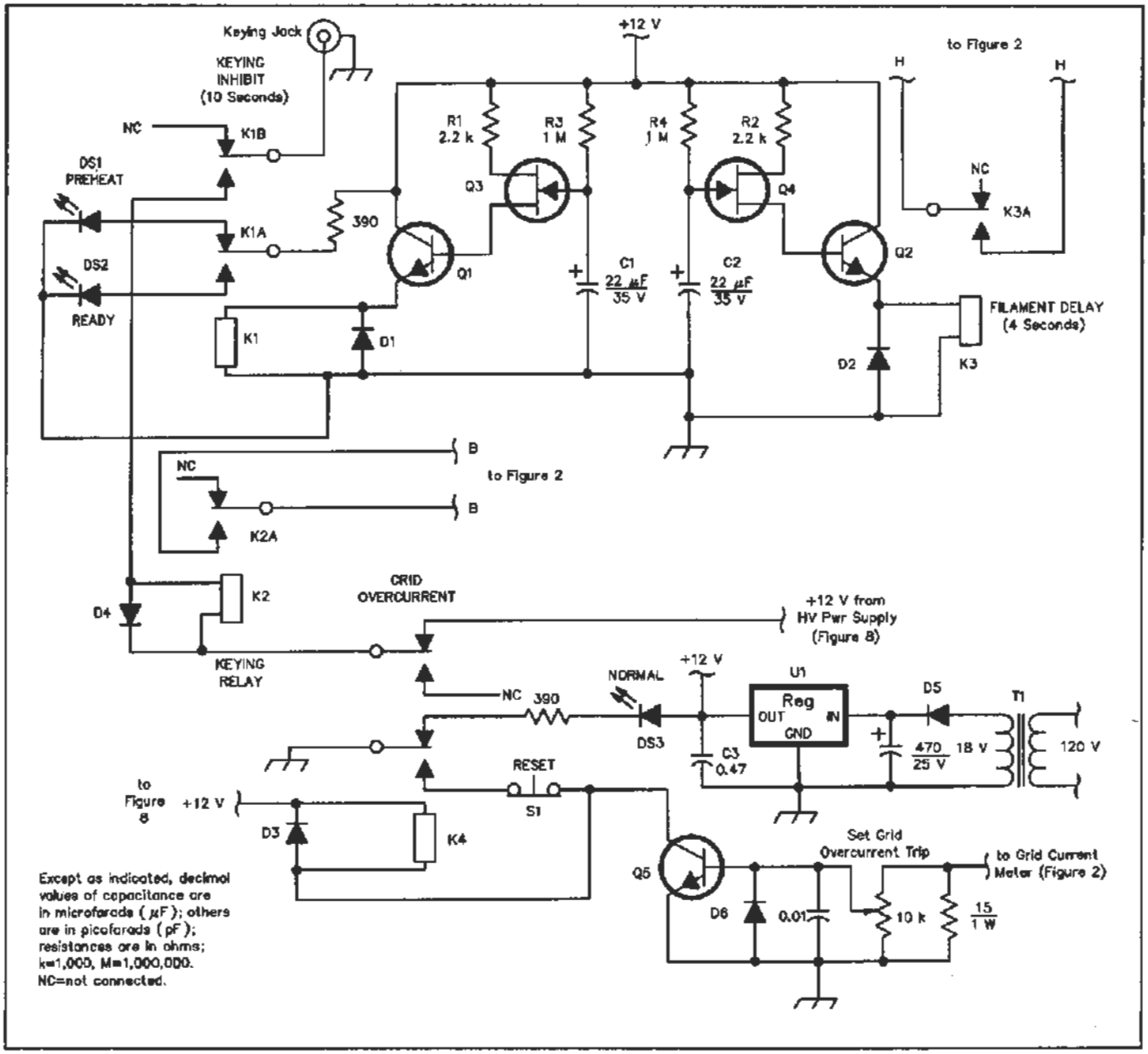

Figure 4—Schematic diagram of the amplifier-control circuits.

C3—0.47-µF, 25-V tantalum capacitor
D1-D5—1N400i or equivalent
D6—1N4007 or equivalent
DS1—Yellow LED
DS2—Green LED
DS3—Red LED
K1—Keying-inhibit relay, DPDT, 12-V dc coil, 1-A contact rating (RadioShack 275-249 or equivalent)
K2—Amplifier keying relay, SPDT, 12-V dc coil, 2-A contact rating (RadioShack 275-248 or equivalent)
K3—Filament delay relay, SPST, 12-V dc coil, 2-A contact rating (RadioShack 275-248 or equivalent)
K4—Grid-overcurrent relay, DPDT, 12-V dc coil, 1-A contact rating (RadioShack 275-249 or equivalent)
Q1, Q2, Q5—2N2222A or equivalent
Q3—MPF102 or equivalent
Q4—2N3819 or equivalent
S1—Normally closed, momentary pushbutton switch (RadioShack 275-1549 or equivalent)
T1—Power transformer, 120-V primary, 18-V, 1-A secondary
U1—+12 V regulator, 7812 or equivalent

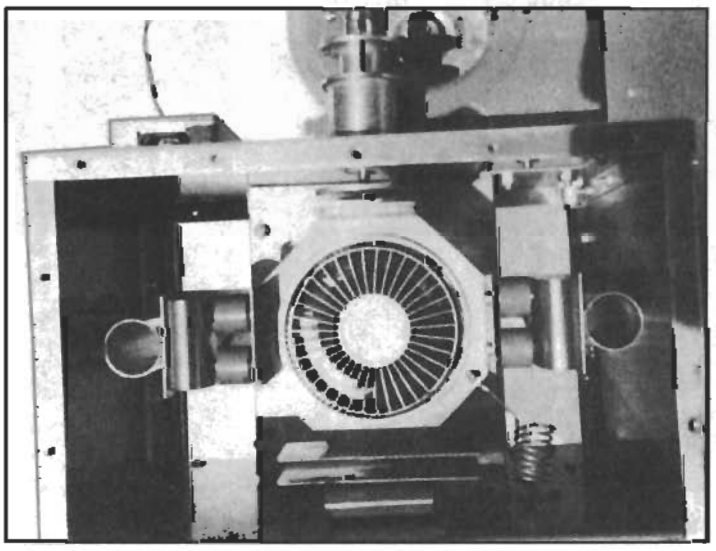

Figure 5—This top view of the plate compartment shows the plate-line arrangement, C1-C4 and the output coupling assembly.

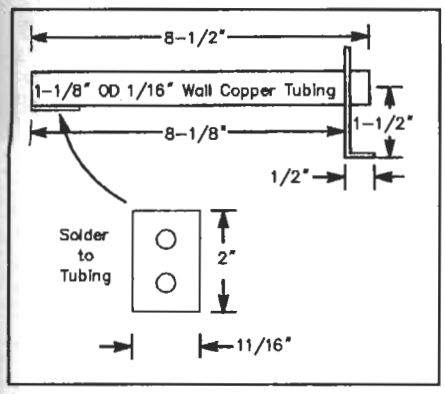

Figure 6—Plate line details.

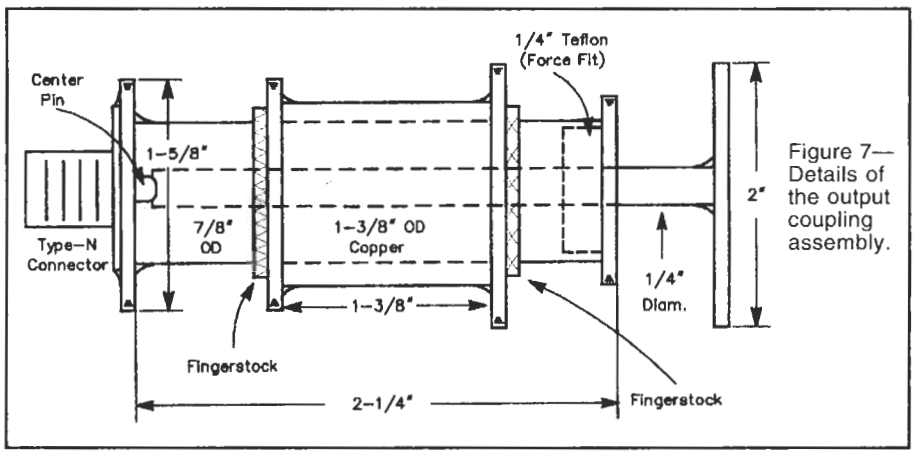

Figure 7—Details of the output coupling assembly.

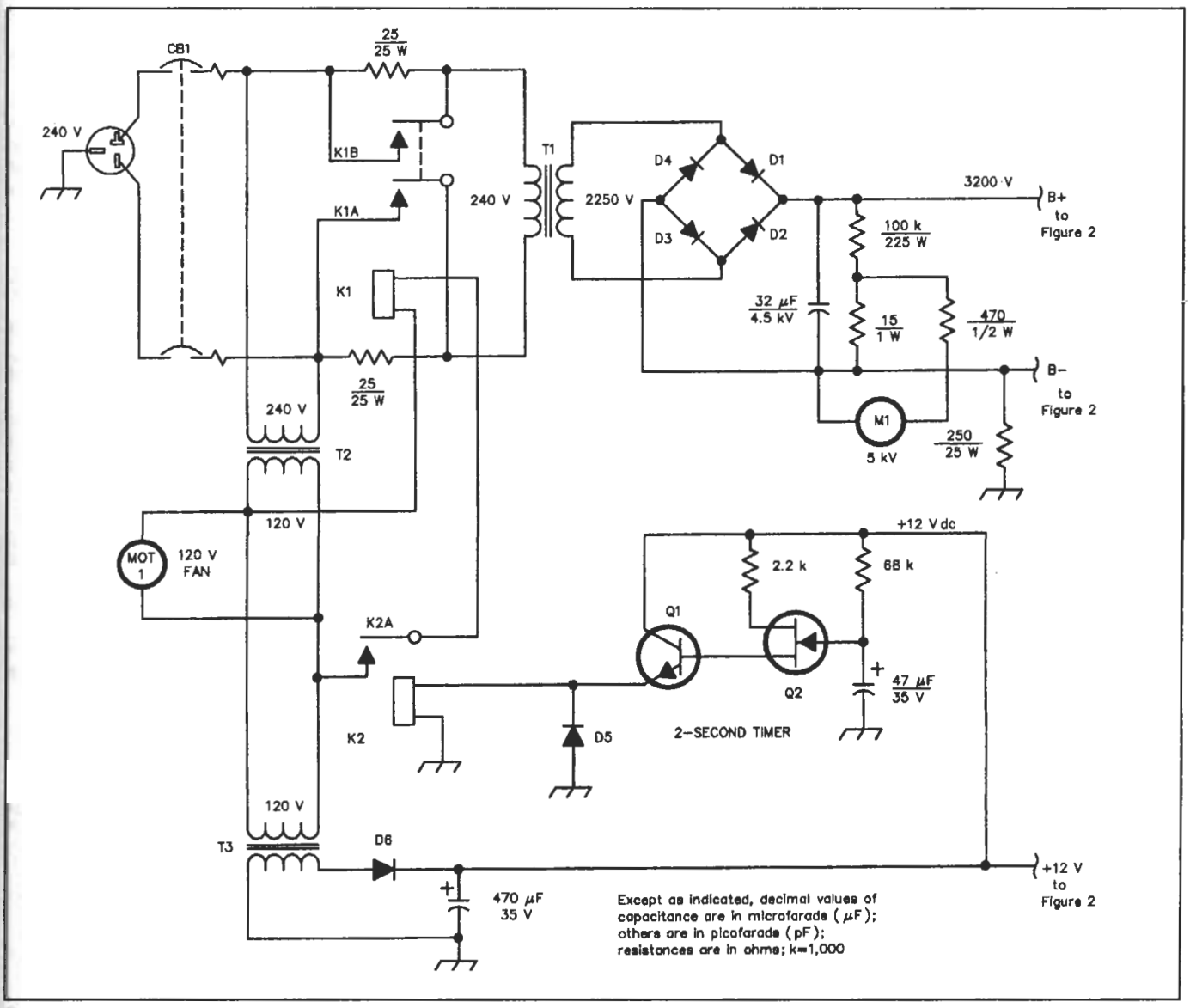

Figure 8—Schematic diagram of the high-voltage power supply recommended for use with the power amplifier.

D1-D4—Strings of 4 each, 1000-PIV, 3-A diodes, 1N5408 or equivalent
K1—DPST relay, 120-V ac coil, 240-V-ac, 20-A contacts (Midland Ross 187-321200 or equivalent)
K2—SPDT miniature relay, 12-V dc coil (Radio Shack 275-248 or equivalent)
M1—High-voltage meter, 5 kV dc full scale (1-mA meter movement used with series resistors shown in drawing)
MOT1—Cooling fan, Torin TA-300 or equivalent
Q1—2N2222A or equivalent
Q2—MPF102 or equivalent
S1—20-A hydraulic/magnetic circuit breaker (Potter and Brumfield W68X2Q12-20 or equivalent)
T1—High-voltage power transformer, 240-V primary, 2250-V, 1.2-A secondary (Avatar AV-538 or equivalent)
T2—Stepdown transformer, Jameco 112125, 240-V to 120-V, 100 VA
T3—Power transformer, Jameco 104379, 120-V primary; 16.4 V, 1-A secondary (half used)

Figure 6 is a drawing of the plate line and Figure 7 is a drawing of the output coupling asssembly.

Cooling

The amplifier requires an air exhaust through the top cover, as the plate compartment is pressurized. You can fashion a chimney from a 3½-inch waste-water coupling (black PVC) and a piece of 1/32-inch-thick Teflon sheet. The PVC should extend down from the underside of the amplifier cover plate by 1⅛ inches, with the Teflon sheet extending down ¾ inch from the bottom of the PVC.

The base of the 3CX1200Z7 is cooled by using bleed air from the plate compartment, which is directed at the tube base, through a ⅞-inch tube set into the sub-chassis wall at a 45° angle.

The recommended blower will supply more tban enough air for any temperature zone. A smaller blower is not recommended, as it is doubtful that the base area will be cooled adequately. The 3CX1200Z7 filament draws 25 A at 6.3 V! It alone generates a great deal of heat around the tube base seals and pins, so good air flow is critical.

Construction

The amplifier is built into a 12×12×10-inch enclosure. A 12×10-inch partition is installed 7¼ inches from the rear panel. The area between the partition and the front panel contains the filament transformer, control board, meters, switches, Zener diode and miscellaneous small parts. Wiring between the front-panel area and the rear panel is through a ½-inch brass tube, located near the shorted end of the right-hand plate line.

High voltage is routed from an MHV jack on the rear panel, through a piece of RG-59, just under the shorted end of the left-hand plate line. The cable then passes through the partition to a high-voltage standoff insulator made from nylon. This insulator is fastened to the partition near the high-voltage feed-through capacitor. A 10-Ω, 25-W resistor is connected between the insulator and the feed-through capacitor.

The plate lines are connected to the dc-blocking capacitors on the plate collet with 1¾×2-inch phosphor-bronze strips. The bottom of the plate lines are attached to the sides of the subchassis, with the edge of the L-shaped mounting bracket flush with the bottom of the subchassis.

When preparing the subchassis top plate for the 3CX1200Z7, cut a 2 11/16-inch hole in the center of the plate. This hole size allows clearance between the tube envelope and the top plate, without putting stress on the envelope in the vicinity of the grid flange seal.

Table 3
Power Supply Specifications

High voltage:	3200 V
Continuous current:	1.2 A
Intermittent current:	2 A
Step/Start delay:	2 seconds

Exercise care in placing the movable tuning plate and the movable output coupling disc, to ensure they cannot touch their fixed counterparts on the plate collet.

Operation

When the amplifier is first turned on, it cannot be keyed until:

- 10 seconds has elapsed
- High voltage is available, as confirmed by presence of +12 V to the keying circuit

Connect the amplifier to a dummy load through an accurate power meter capable of indicating 1500 W full scale. Key the amplifier and check the idling plate current. With 3200-V plate voltage, it should be in the vicinity of 150 mA. Now, apply a small amount of drive and adjust the input tuning for maximum grid current. Adjust the output tuning until you see an indication of RF output. Increase drive and adjust the output coupling and tuning for the desired output. Do not overcouple the output; once desired output is reached, do not increase loading.

When you shut down the amplifier, leave the blower running for at least three minutes after you turn off the filament voltage. I found the 3CX1200Z7 to be an excellent tube. I tried it with exessive drive, plate-current saturation, excessive plate dissipation—all the abuse it's likely to encounter in amateur applications. I had no problems, but I don't recommend you repeat these tests!

A Companion Power Supply

A good, solid-state high-voltage power supply is a necessity to ensure linearity in SSB operation. Specifications of the power supply I built are given in Table 3. Figure 8 is a schematic diagram of the supply. A power supply for a high-power linear amplifier should operate from a 240-V circuit, for best line regulation. I have specified a special, hydraulic/magnetic circuit breaker that doubles as the main power switch. I don't recommend you substitute a regular switch and fuses for this breaker, as fuses won't operate quickly enough to protect the amplifier in case of an operating abnormality. The bleeder resistor dissipates about 100 W, so I included a small fan to remove the excess heat.

Power Supply Construction

The power supply can be built into a 17×13×10-inch cabinet. The power transformer is quite heavy, so use ⅛-inch aluminum for the cabinet bottom, and reinforce it with aluminum angle for extra strength. The diode bridge consists of four legs, each containing five diodes.

Power Supply Operation

When the front-panel breaker is turned on, the two, 25-Ω resistors in the primary circuit limit inrush current as the filter capacitor charges. After two seconds, K1 activates, shorting both resistors and allowing full line voltage to be applied to the transformer.

As with all high-voltage power supplies, you must be extremely careful! Before opening the cabinet, remove the ac-line plug from its receptacle, and confirm that the filter capacitor is discharged before working on the supply.

Conclusion

This amplifier is a reliable and cost-effective way to generate a big 2-meter signal—almost as quickly as a solid-state amplifier.

To ensure that the output of my amplifier meets current spectral purity requirements, I use a high-power version of the half-wave output filter that appears as Figure 16 on page 39-10 of the 1993 and 1994 editions of *The ARRL Handbook*. Although I did not make spectral measurements of the output, I can run full output while my wife Mary Lou watches TV in a nearby room of our home.

Another suitable filter is the one that appears in the 1990 *ARRL Handbook* (Figure 150, on page 31-72) as part of the description of "A Legal-Limit 2-Meter Tetrode Amplifier."

Notes

[1]Suggested retail price of the 3CX1200Z7 is $625. You can obtain it from: Henry Radio, 2050 S Bundy Dr, Los Angeles, CA 90025, tel 310-820-1234; Richardson Electronics, 40 W 267 Keflinger Rd, La Fox, IL 60147, tel 708-208-2200; RF Parts, 435 South Pacific St, San Marcos, CA 92069, tel 619-744-0700.

[2]W. Orr, Editor, *Radio Handbook*, 23rd ed. (Indianapolis: Howard W. Sams and Co., 1987), pp 18-2 through 18-7.

[3]This project is also described in the *Radio Handbook*, pp 18-11 through 18-15.

By David Munyon, W7DVB

From *QST*, September 1984

A Cathode-Driven Tetrode for 6 Meters

Stability, power, low cost: Is this what you're looking for in a 6-meter do-it-yourself project? If so, look what's here!

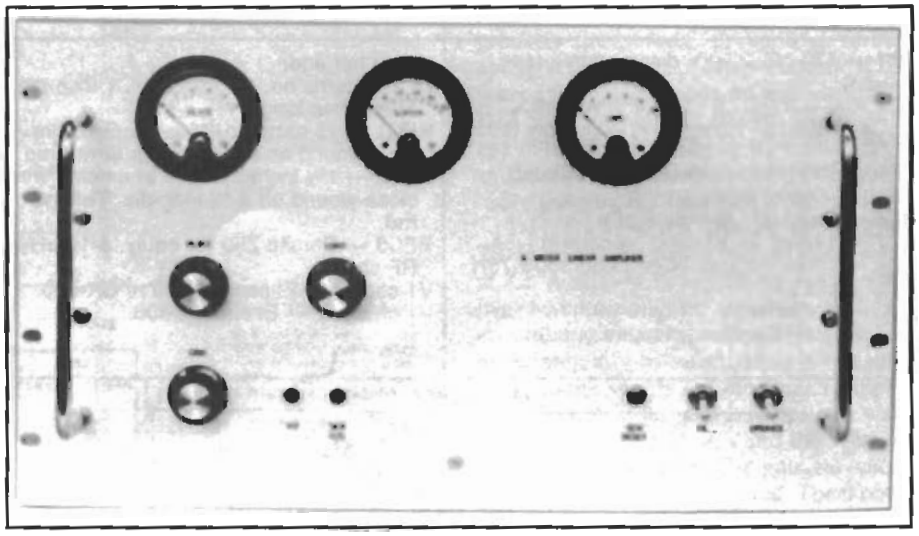

The advantages of grounded-grid amplifiers are numerous and have been proven over the years. They include: simplicity of design, good thirdorder IMD characteristics, inherent stability (generally without the need for neutralization) and noncritical tuning. The only requirement is abundant driving power. Usually, this is a small price to pay, unless the driver you intend to use is one of the many popular, low-power (10- to 25-W-output) VHF transceivers. Also, with the tremendous increase in the use of 100%-duty-cycle modes such as RTTY and SSTV, many of us would rather not operate our exciters at half to full bore while driving an amplifier. If you're willing to sacrifice only one of the aforementioned advantages—simplicity—the remaining attributes of grounded-grid operation can be made available at a considerable reduction in driving power.

Enter the Tetrode

For many years, tetrodes (most often connected as triodes) have been used in grounded-grid circuits. But we have good reasons to consider the tetrode as a cathode-driven performer in its own right. First, the drive requirements are reduced. A 4-400A requires 40W of drive power for full output when triode connected. Only half that amount is needed to drive its class-AB1 counterpart. The second reason is cost. Tetrodes are still available as hamfest and surplus items at a fraction of their original cost. (Some of the newer triodes cost more than the exciters that drive them!)

But not all tetrodes can be triode connected. All of the external anode family of tubes, and a few others, have internal geometry that allows the control grid dissipation to be greatly exceeded if the tube is operated as a triode. Therefore, those tubes should be cathode driven only as tetrodes. The usual way to do this is to ground the control and screen grids to RF with low-inductance bypass capacitors, and then place operating voltages on them. The cathode can be driven in a normal fashion, and the tube operated in any class consistent with linear service. Class-AB1 has the lowest drive requirements and is the easiest with which to work.

Tetrode Vs. Triode

I concede that the addition of a screen element complicates the overall circuit, especially if the screen-circuit provisions are made properly. But, the circuit need be no more complex than that of its grid-driven equivalent. The cathode-driven tetrode requires grid bias and a well-regulated screen supply. Also, there is no correct way to load a tetrode without a meter to monitor the screen-grid current. This device is invaluable and should not be omitted for the sake of economy.

No discussion of the screen-grid circuit would be complete without some mention of an overcurrent-protection circuit. Several solutions have been offered in the past (including the use of no protection circuit!), and each has its disadvantages. Sensitive relays are expensive and their use can have an adverse effect on screen-voltage regulation. Current-limiting supplies do an excellent job of protecting the tube, but do not inform you when something is wrong. Since screen current is extremely sensitive to minor plate-voltage excursions and plateloading conditions, the builder has to be absolutely certain that these are correct, and that plate voltage is always present with screen voltage, if the screen-protection circuit is to be eliminated. The protection circuit is well worth the small cost involved. This amplifier incorporates an inexpensive and simple circuit that contains none of the disadvantages mentioned earlier.

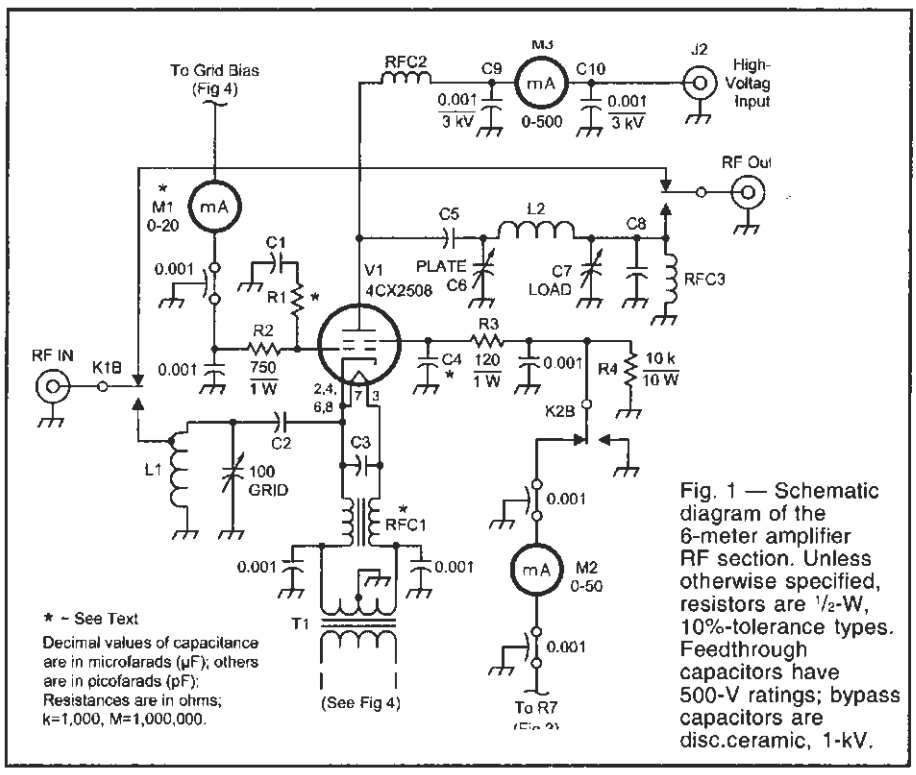

Fig. 1 — Schematic diagram of the 6-meter amplifier RF section. Unless otherwise specified, resistors are ½-W, 10%-tolerance types. Feedthrough capacitors have 500-V ratings; bypass capacitors are disc.ceramic, 1-kV.

C1 — 470-pF, 2.5-kV disc-ceramic (see text).
C2, C3 — 0.001-μF, 500.V silver mica.
C4 — Part of tube socket assembly (see text).
C5 — 500-pF, 5-ky ceramic (Centralab 858S-500 or equlv.).
C6 — See text (approx. 6 pF).
C7 — 140-pF air variable, receiving type.
C8 — 75-pF ceramic (Centralab 850S-75N or equiv.).
L1 — 4½ turns no. 14 bare wire, ½-inch-dia, 1½ inches long, tapped one turn from hot end.
L2 — 6 turns no. 10 bare wire, 1-inch-dia, 1½ inches long.
RFC1 — 15 turns no. 16 enameled wire closewound on a ½-inch-dia ferrite rod.
RFC2 — 1⅝ inches no. 22 enameled wire close-wound on a ⅜-inch-dia. Teflon® rod.
RFC3 — Ohmite Z50 (or equiv. 5-10 μH RF choke).
V1 socket — Eimac SK-600 or SK-620.
V1 chimney — Elmac SK-606.

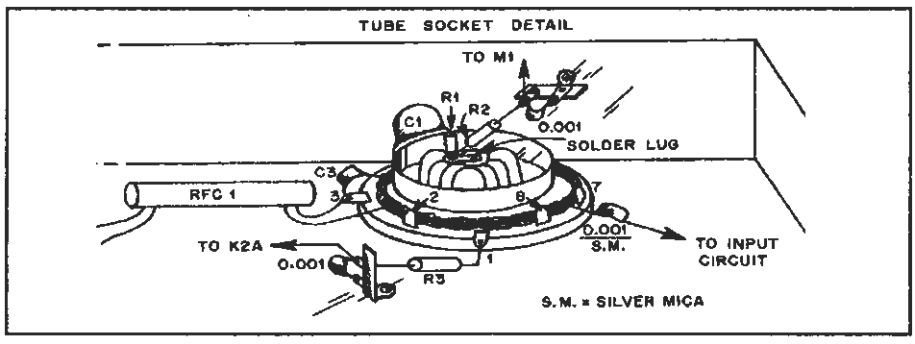

Fig 2—Tube socket detail. See text.

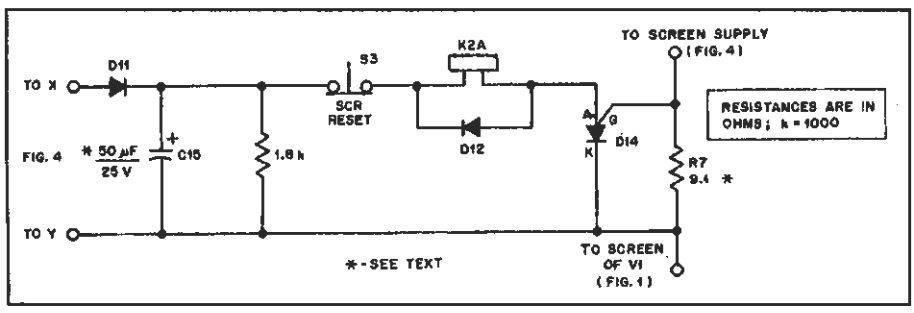

Fig 3—Screen overcurrent-protection circuit. Resistors are 1/2-W, 10%-tolerance types.

D11, D12—1-kV, 2.5-A silicon diodes.
D14—4-A, 200-V SCR (Jameco C106B1, ECG 5455 or equiv.).
K2—DPDT 12-V dc relay, 1-A contacts (see text).

A Cathode-Driven 4CX250B

I became aware of the cathode-driven tetrode years ago while trying to get a 4-1000A to wotk on 50 MHz. The results were so good that, when it came time to build an amplifier for my new solid-state transverter, I decided that building a grid-driven amplifier would be a giant step backward.

The 4CX250B is an excellent tube for 6-meter use. This tube has a high plate-dissipation rating for its small physical size, has reasonable power-supply requirements, and requires approximately 10 W of drive in a cathode-driven, class-AB1 configuration. (If much more drive is available, an appropriate attenuator must precede the input circuit.) The only differences between this design and its grid-driven equivalent are the filament/cathode and control-grid circuits.

Filament/Cathode Circuit

In Fig. 1, notice that the cathode and one of the filament connections are tied together. Normally, the isolation created by the physical separation of the two elements is sufficient to ensure stability, and a filament choke would not be required. I felt that this would not be the case on 50 MHz, and a call to Eimac confirmed it. At Bill Orr's recommendation, I tied the cathode and filament together, and fed the filament through a choke. The cathode impedance is approximately 120 ohms. In the interest of best linearity and minimum, drive requirements, a tuned input circuit is used. The tank coil is tapped to present an input impedance of 50 ohms.

There are many sockets designed for use with this family of tubes. I recommend that you use one that incorporates a built-in screen bypass capacitor (1100 or 2700 pF); either one will do. A few of these types of sockets are so constructed that the four cathode pins are grounded internally; do not use one of these. An Eimac SK-600 or SK-620 socket is recommended. The four cathode pins (2,4, 6, 8) and one of the filament pins (7) of the socket must be wired together to form one low-inductance connection. The easiest way to do this is to carefully bend pins 1 and 3 parallel to the chassis, and then strap together pins 2, 4, 6, 7 and 8. Make certain that this strap forms a complete circle around the socket. For strap material, I use some stretched and flattened shield braid removed from RG-58 coaxial cable. All connections made to the cathode, or the filament (pin 7), can be made anywhere along this ring. See Fig. 2 for details.

Grid Circuit

The tube grid is accessed through the socket center connector and is bypassed to ground by C1. The capacitance of C1 is not as important as its physical size. C1 should be a high-voltage, disc-ceramic type (2 kV or more), whose body nearly spans the distance between the connection points. This provides for an absolute minimum lead

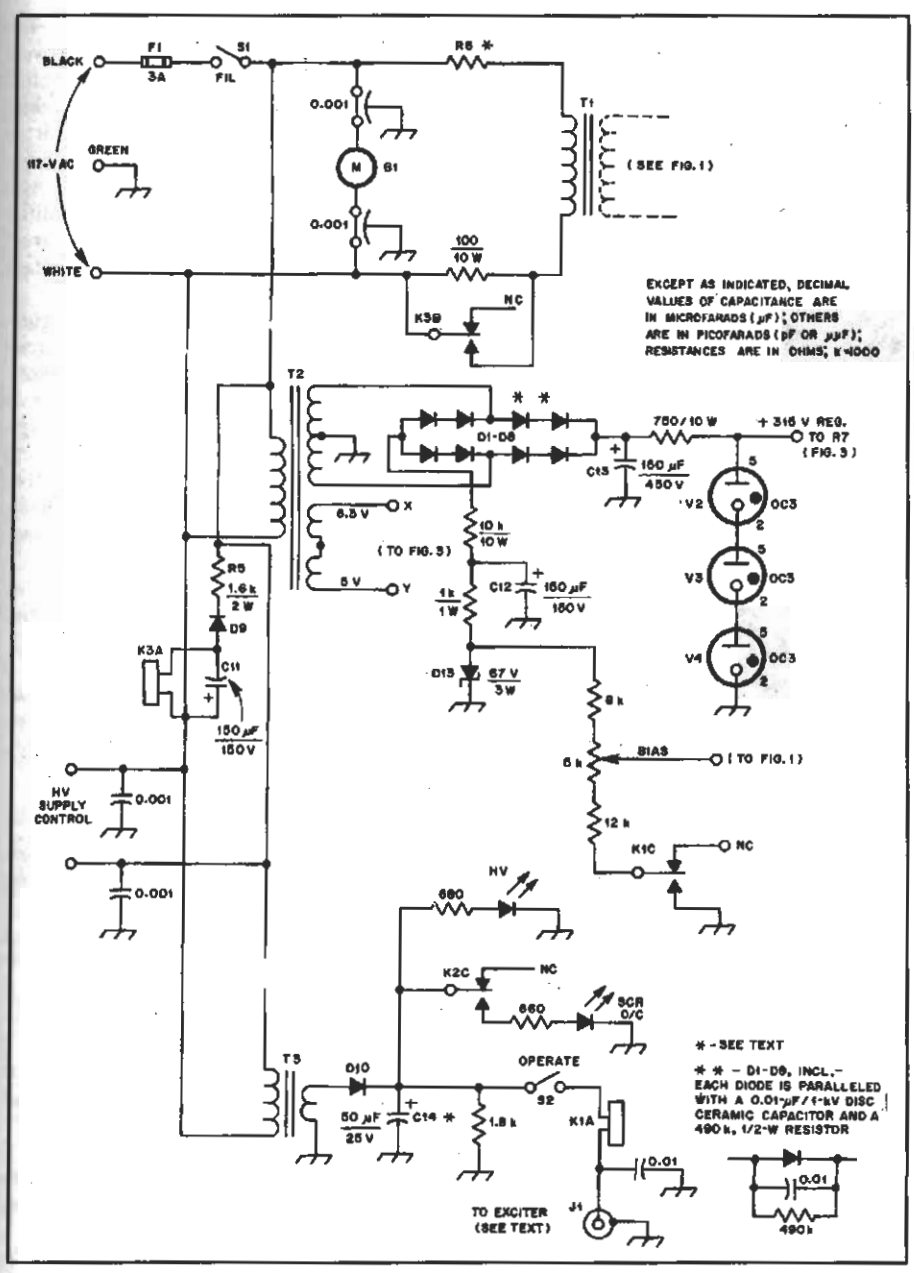

Fig. 4 — Power-supply section of the 6-meter amplifier. Unless otherwise specified, resistors are 1/2-W, 10%-tolerance types; feedthrough and bypass capacitors have 500-V ratings.

B1 — Squirrel-cage blower, 56 CFM (minimum), 117-V ac motor.
D1-D10, incl. — 1-kV, 2.5-A silicon diodes.
D13 — 87-V, 5-W Zener diode.
K1 — 3PDT 12-V dc relay, 5-A contacts.
K3 — SPST 234-V ac relay, 3-A contacts (see text).
T1 — 117-V primary; 6-V. 2.6-A secondary (see text).
T2 — 117-V primary; 580-V c.t., 75-mA secondary with 6.3- and 5-V filament windings (see text).
T3 — 117-V primary; 12-V. 1-A secondary.

length. Use a solder lug on the grid pin, and solder the other capacitor lead directly to the inside of the air duct on the tube-socket bottom.

When my amplifier was first tested, I found that the plate current idled at about 40 mA, and was completely independent of grid voltage. This self-biasing was traced to a parasitic in the grid circuit, and was eliminated by the addition of a series-connected resistor, R1. If you wish to experiment, R1 should be a 1/2-W, carbon-composition resistor with a resistance value that is the minimum required for complete stability. R1 should be placed as shown in Fig. 2; I found that a 3.9-ohm resistor kept my amplifier unconditionally stable.

In the interest of stability, don't use chokes in place of R2 and R3 in the grid and screen circuits. M1, the grid-current meter, can have a range of from 0-1 mA to 0-20 mA or so, and is included only to ensure that grid current is never drawn, and the operation remains class-AB 1.

Screen Circuit

Relay contacts K2B are part of the screen overcurrent-protection circuit, the operation of which will be discussed later. Because the 4CX250B draws negative screen current on occasion, the screen-current meter should ideally be of the zero-center type. As these meters are expensive and not readily found, a standard meter can be pressed into service by using bleeder string, R4. Notice that 15 mA of bleeder current is drawn through the meter whenever K2 is open (normal). This offsets the actual zero reading of the meter to the 15-mA position and allows a negative current of 15 mA to be metered. This is more than adequate for the 4CX250B. If a zero-center meter is used, R4 may be eliminated unless the screen supply shunt regulator is replaced by a series regulator. In that case, the bleeder would be necessary to offset the effects of secondary emission.

For the overcurrent-protection circuit (Fig. 3), an SCR (D14) seems to be a natural. A very small gate voltage, developed across R7 by the screen current, turns on the SCR and causes K2 to close. This removes screen voltage from the tube and grounds the screen, preventing further abuse. A second set of relay contacts (K2C) is used to light a front-panel-mounted LED. D14 continues to lock out the screen voltage until the SCR is reset by removing its anode voltage. This is done by momentarily pushing the RESET switch, S3.

D11, C15 and the filament windings of T2 provide dc power for a 12-V relay at K2. A relay with a different voltage rating can be used if this supply is modified accordingly. The value for R7 was found experimentally by substituting a variable, low-voltage supply for the screen supply. A 0-100 mA meter and load resistor were placed in series with R7, and the voltage, slowly increased until the gate threshold was reached and the SCR fired. The threshold current was noted, and R7 varied until the desired current would trigger the SCR. With R7 equal to 9.1 ohms, the SCR fired consistently at 45 mA.

Since 15 mA of the current drawn through R7 will be bleeder current, this allows a maximum of 30 mA for screen current, which is well below the 12-W screen dissipation rating for the tube. Note that the entire overcurrent-protection circuit is hot with screen voltage, so proper precautions must be taken during construction. I built the protection circuit on a PC board, but it could have just as easily been chassis-mounted using terminal strips.

Construction

The amplifier is built on a 3 × 8 × 17-inch chassis; a 3 × 5 × 7-inch chassis houses the output network components. A 10 1/2- × 19-inch rack panel is used for the amplifier front panel. The general physical layout should be followed, as it is well dictated by the flow of the circuit. All RF leads should be kept as short as possible, especially the bypass capacitor leads. Keep the dc leads cabled and

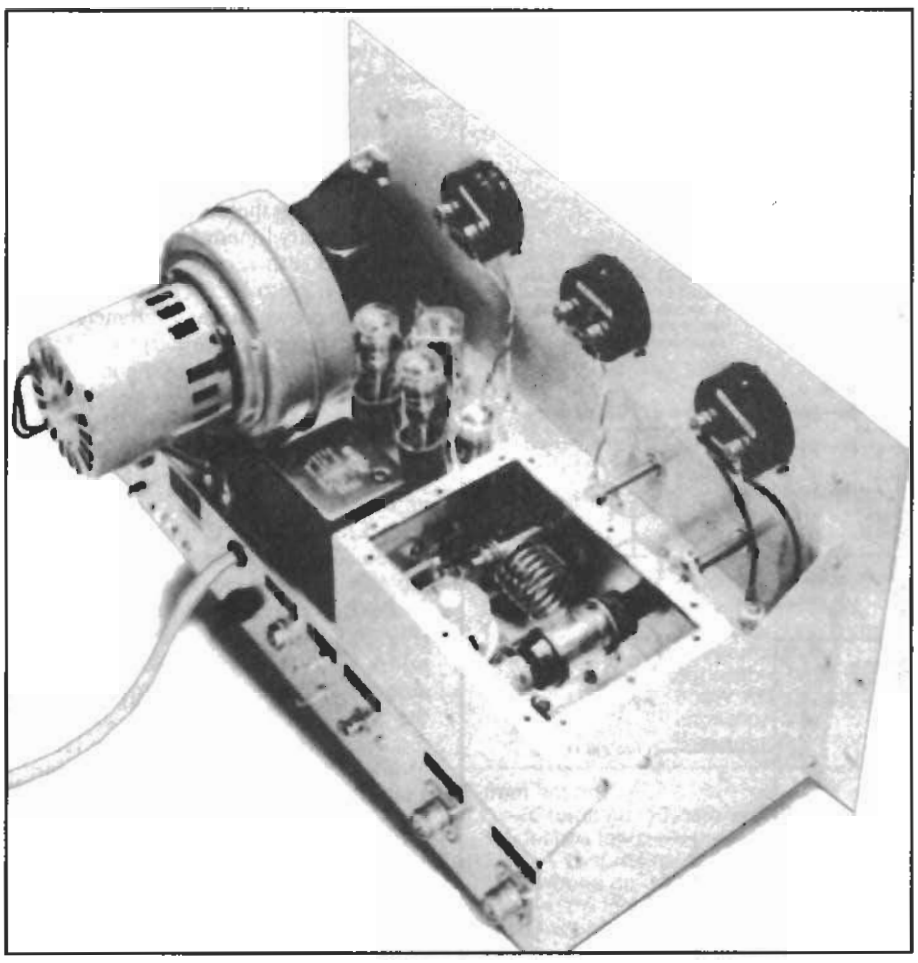

Fig 5—The final-amplifier-compartment cover has been removed for this photo.

as far away as possible from the RF leads. Most power-supply components are mounted on a fiberglass terminal board that is secured against the side of the chassis.

K3, D9, C1 1 and R5 (Fig. 4) constitute a time-delay circuit for filament inrush-current protection, and can be included if you feel that this is important. As it stands, the delay is approximately 1 second, which is more than ample. The 234-V ac relay is used on dc, and closes at about 70 V. The charging rate of C11 is controlled by its capacitance and the ohmic value of R5, and can be varied by changing their values.

Ideally, the input and output relays should be coaxial types; however, I used a single open-frame, 3PDT type and encountered no problems. The center pole is used for control (K1C), as that increases the isolation between the input and output circuits. In grid-driven amplifiers, I have never been able to use an open-frame relay for input and output switching. Because of the lower gain of this cathode-driven amplifier, I find no evidence of feedback or instability. Don't use plug-in type relays in their original form for K1. Remove the case, plug and connecting wires, and bolt the relay directly to the chassis. Use coaxial-cable braid to make the RF connections. The power supplies (Fig. 4) are of standard design. They may be replaced by any supplies yielding similar voltages, and need not reside on the same chassis as the amplifier. The high-voltage supply should produce 2-kV dc under load. Si turns on all supplies, including the external high-voltage supply. S2, the STANDBY/OPERATE switch, supplies power to K1, which allows the amplifier to be placed in operation; otherwise, the amplifier is simply bypassed.

If a 6.3-V ac filament transformer is used for T1, R6 will have to be.included to drop the filament voltage to 6 V. The ohmic value of R6 will have to be determined experimentally. Use a resistor with the highest wattage rating practical for good voltage stability. With an accurate voltmeter, measure the filament voltage at the tube socket with the filament choke in place, as there will be a slight voltage drop across the choke. Nothing will cause a 4CX250B to "go south" quicker than high filament voltage, and that means anything in excess of 6 V.

The filament choke (RFC1) consists of 15 bifilar turns of no. 16 enameled wire wound on half of an Amidon $^1/_2$-inch-diameter ferrite rod. The rod can be cut to a proper length by filing a small groove around its circumference, and then breaking it clean. Cover the rod with heat-shrink tubing or electrical tape before and after winding the choke. This will keep the rod and winding together, and make it self-supporting by its four leads.

The meters I used all have 0-1 mA movements and homemade shunts. The original meter-face calibration marks were carefully erased, and new ones applied using dry-transfer labels. Most such labels are ideal for panel marking, but are a bit too large for meter-face use. Your local stationery store should have transfers with smaller-sized numbers. During amplifier operation, care should be taken to avoid accidental contact with the plate-voltage meter, as it has high voltage on it.

Most VHF amplifiers have a higher-than-necessary Q in the output circuit because of the use of high minimum-capacitance air-variable capacitors. This is acceptable providing the rest of the output components are heavy-duty types and can handle the higher circulating currents. (Fhe small vacuum variable I used is admittedly first class, and it may not be used by many other builders.) Rather than using an air-variable capacitor, a homemade two-disc system is a preferred choice. If you can find a neutralizing capacitor with plates of 2-inch diameter or so, that would be ideal. If you must use an air-variable capacitor, use one with the least minimum capacitance; remove all unnecessary plates leaving just enough to do the job.

Tune-Up

Before the tube is placed in the socket, close S1 and check that all of the operating voltages are correct. Ground the bottom end of the bias string at K1C, and check that the BIAS potentiometer range will supply –50 to –60 V; then set it at –55 V. J1 should be connected to the external-circuit control jack of your exciter so that it is grounded when your exciter is keyed. Open Sl and make certain all voltages have bled down, then install the tube. Close S1 and S2. After the tube warms up, with no drive applied, key the exciter and adjust the BIAS potentiometer so that the plate idling current is exactly 100 mA.

While the tube is idling, rotate all the tuning controls throughout their respective ranges. If there are no sudden plate-current increases, the amplifier is stable. With a small amount of drive applied, tune the GRID and PLATE controls for maximum output. Once you are satisfied that both of these controls will provide resonance, apply full drive and retune the plate to resonance. Increase loading slowly, retuning the PLATE control each time, until a screen current of 5 mA (the meter actually reads 20 mA) is indicated. Observe how sensitive the screen current is to the operation of the LOAD control, and that it is by far the best indicator of plate resonance. If grid current is indicated, you're overdriving the amplifier.

Adjust the drive level and the plate TUNE and LOAD controls so that the platecurrent meter indicates 250 mA and the screen-current meter indicates 5 mA at resonance. Under these conditions, this amplifier develops a power output of about 310 W. With modulation, voice peaks should not exceed 150 mA on the plate-

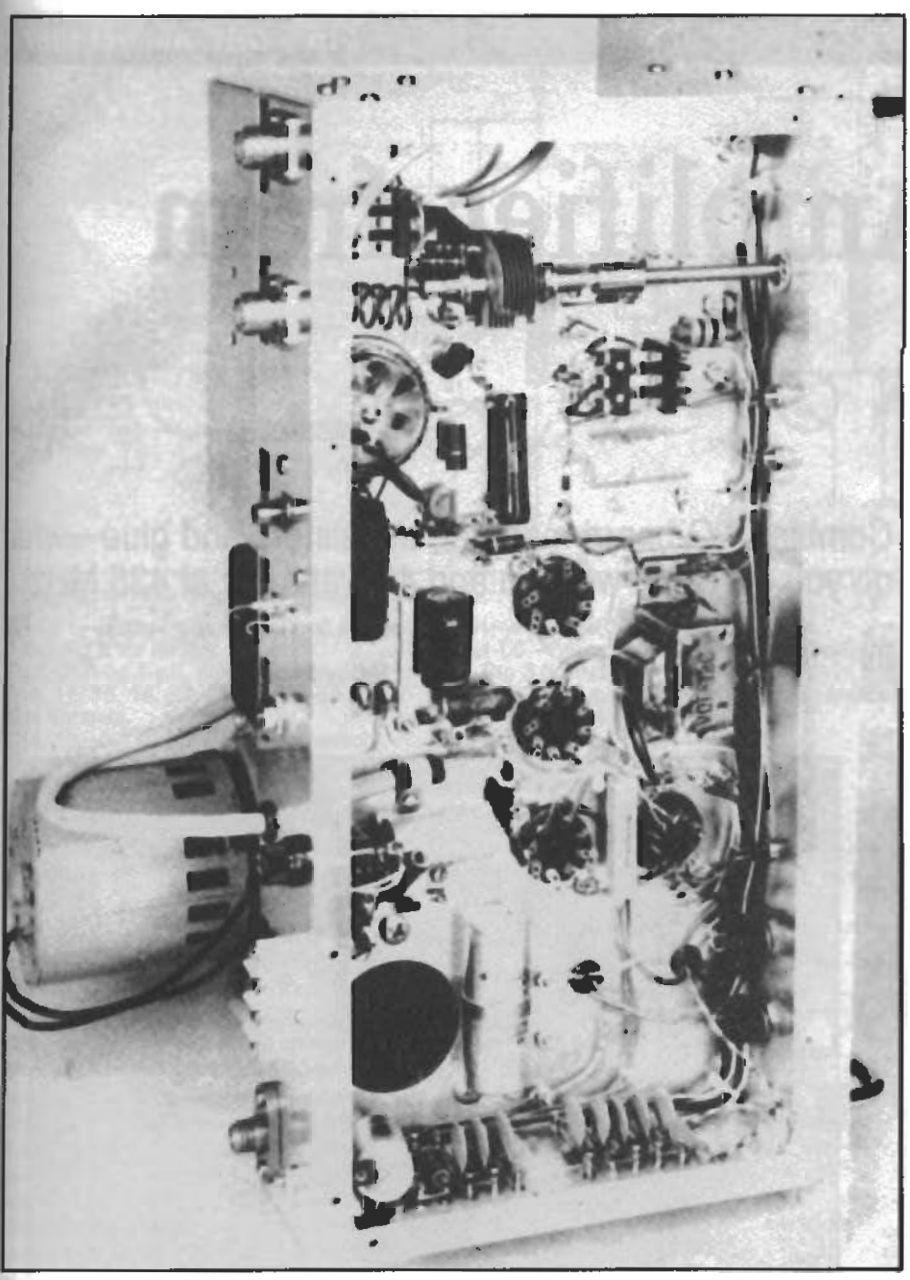

Fig 6—A bottom view of the 6-meter amplifier. The screen-protection circuit is mounted on the PC board to the right of the tube socket.

current meter, and a small amount of negative screen current is normal.

Summary

This amplifier has been in operation now for over a year, and all reports of its operation have been complimentary. I hope that this amplifier will be duplicated by many who had previously resigned themselves to grid-driven designs. Much of the material presented here is general enough to encourage interest in the cathode-driven tetrode as a viable alternative to the grounded-grid triode. I will be glad to answer all letters of inquiry regarding this amplifier; please include an s.a.s.e.

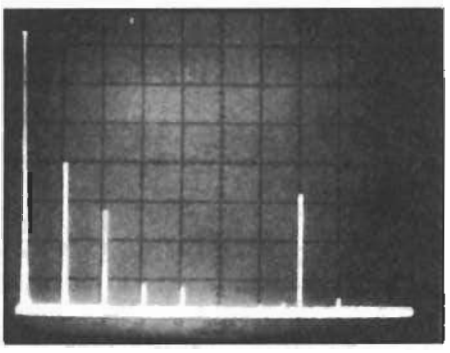

Fig 7—Spectral photo of the 6-meter amplifier without external filtering. Vertical divisions are each 10 dB; horizontal divisions are each 50 MHz. The fundamental (second pip from the left) has been notched approximately 40 dB by means of notch cavities to prevent analyzer overload. The seventh harmonic is approximately 48 dB below peak fundamental output.

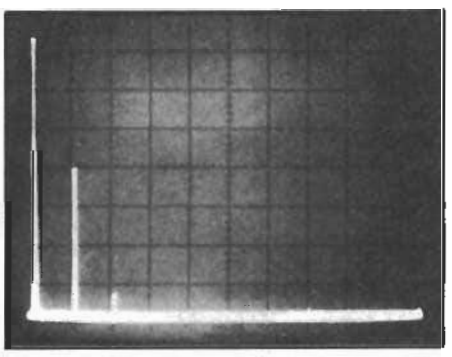

Fig 8—The addition of a simple filter (see Fig 9) at the amplifier output provides for excellent harmonic attenuation, and its use is recommended. All conditions are otherwise the same as those of Fig 7.

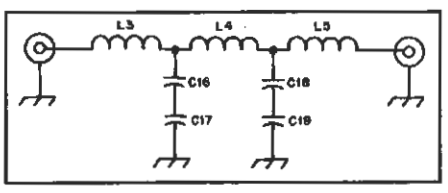

Fig 9—This simple harmonic-suppression filter, or one of similar characteristics, should be used at the output of the amplifier. The filter may be contained in a $2^1/_4 \times 2^1/_4 \times 5$-in (HWD) aluminum box.

C16-C19, incl.—110 pF, 1-kV silver-mica capacitors.
L3, L5—4 turns no. 14, $^5/_{16}$-in-ID, $^1/_2$ in long.
L4—5 turns no. 14, $^7/_{16}$-in-ID, $^5/_8$ in long.

By John Reed, W6IOJ

From *QST*, August 1987

A UHF Amplifier–from Scratch

Combine PC-board material, transistors and glue—what do you get? Two watts in and 45 watts out at 435 MHz!

Most UHF RF equipment designs involve undefined reactance. For example, the self-inductance of a variable capacitor, or simply the method of attaching a 50-ohm cable to the circuit may constitute reactance that is critical to the operation of the circuit. The result is that complete success in duplicating a circuit is not likely unless the components and layout are exactly the same as in the original. This is nearly always a limiting factor for the do-it-yourselfer wanting to duplicate a project. This class-C UHF amplifier project uses homemade components that anyone can assemble. Tests show that their use has resulted in little or no compromise in the performance of the amplifier over a design using far more expensive commercial parts. My amplifier shows more than 45 W output with less than 2 W input at 435 MHz. The output stage efficiency is approximately 60%, and includes a double-tuned filter for improved spectral purity.

The key to this design is the glue-down stripline technique I have used in many other UHF projects.[1] This method permits easy modification of stripline parameters for optimizing circuitry. Striplines are cut from double-sided, glass-epoxy PC board having the same dimensions that you would choose using the etched-PC-board method. One side of the stripline is smeared with glue (Radio Shack all-purpose adhesive, 64-2307) and firmly pressed against the common base PC board. Parts can be soldered to the stripline immediately (without waiting for the glue to dry). No dc connection is required between the glueline foils, and changes can be made within minutes by lifting the glue-down stripline with a knife and replacing it with one having altered dimensions. This project gives another example of how stripline parameters can be varied to optimize a circuit: homemade variable capacitors.

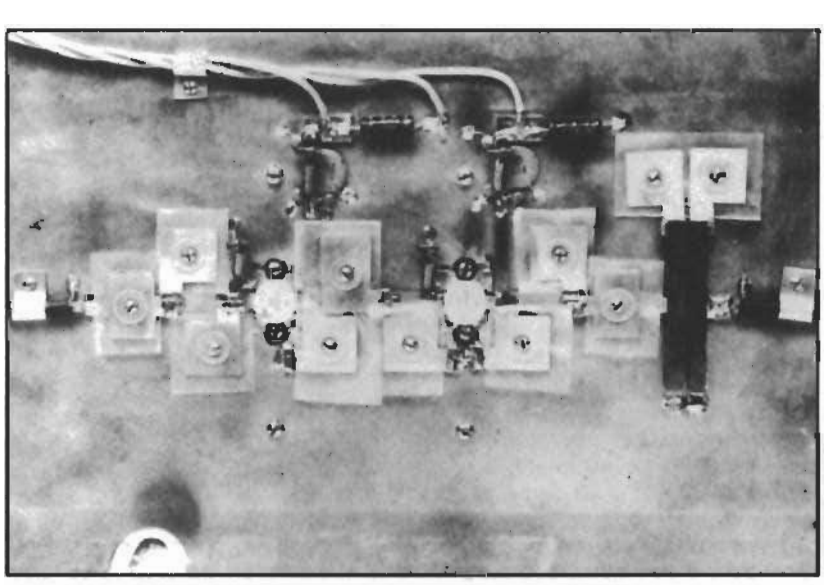

Circuit Details

See Fig 1. The two-stage amplifier uses an MRF641 (driver) and an MRF646 (final).[2] They were chosen primarily because of their availability in the surplus market. These are controlled-Q devices with a combined minimum gain of 12.6 dB. Although the output stage is rated at 45 W, typical saturated output with a 13.6-V collector supply is about 60 W (including drive power).

The home-brew compression-type variable capacitors, shown in Fig 2, dictated the overall design. I made them as small as possible (to minimize selfinductance), but kept them large enough to provide the necessary capacitance. The nominal $^5/_8$-inch-square compression plate results in a maximum capacitance of about 10 pF. The material used for the capacitor plates is 0.031-inch-thick Reynolds sheet aluminum, which is available at most hardware and home-supply stores. [Hobby store sheet brass works well in this application, is also commonly available, and is far easier to solder; it is a good alternative to aluminum—Ed.] The capacitor dielectric material is 2.7-mil polyethylene from a Dow Ziploc® heavy-duty freezer bag. Although I have tested this dielectric at a much higher voltage than it is subjected to in this application (at a high-impedance point in a vacuum-tube VHF amplifier), double thickness is used as a safeguard. The insulator between the adjustment screw and compression plate is made from plastic polymer. Most clear plastics used for miscellaneous household applications are of this type. I use plastic from a box used in packaging a tube of Grumbacher acrylic artists paint. Glass-epoxy insulation will work also, but at the higher-voltage

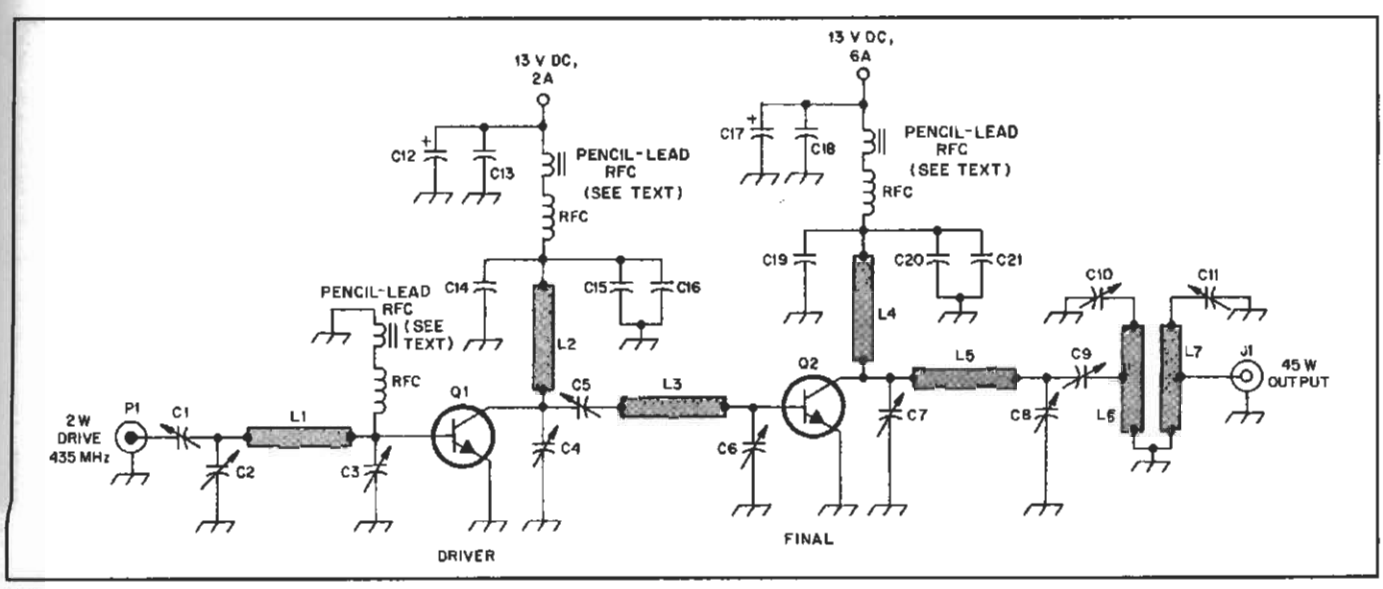

Fig 1—Schematic of the 435-MHz 45-W amplifier.

C1-C11—Homemade capacitors; see text and Fig 2 for details.
C12, C17—4.7-µF, 35-V electrolytic.
C13, 15, 16, 18, 20, 21—0.001-µF, 50-V disk ceramic.
C14, 19—0.1-µF, 50-V disk ceramic.
J1—Female BNC connector.
L1-L5—Glue-down striplines; see text and Fig 3 for details.
L6, L7—Air-gap striplines; see text and Fig 4 for details.
P1—Male BNC connector.
Q1—MRF641.
Q2—MRF646.
RFC—10 turns, no. 26 enameled copper, air-wound, 3/16-in diameter.

applications (especially at C10 and C11) there will be some loss and component heating.

Once I settled on the capacitor configuration, the input and output stripline characteristics were determined experimentally for optimum matching to Q1 and Q2. The related glue-down stripline and pad details are shown in Fig 3. The L2 L4 1/8-inch-wide striplines act as RF chokes, making the inductance associated with the subsequent disc-ceramic capacitors uncritical. The pads include a number of the capacitor stators (C1, C4, C5, C6, C7 and C9). Foils which contact stator-adjustment screws are reamed out to approximately 1/8-inch diameter to isolate the no. 2-56 screw from the stator. I did this with a large drill (3/8-inch). Screw contact with the bottom foil may also cause adjustment irregularities, so the foil was reamed appropriately. The stator plates must be completely deburred to prevent puncturing the plasticbag dielectric.

The amplifier output is coupled through C9 to a 1:1 inductively coupled, double-tuned filter. This 50-ohm filter consists of two striplines that are mounted parallel to each other and close together above the base PC board, as shown in Fig 4. Their close positioning establishes the necessary mutual coupling. Each line is tuned to resonance with a variable capacitor.

As indicated in Fig 1, dc-supply decoupling is identical for both stages. The 0.1-µF disk capacitors eliminate a bothersome low-frequency instability mode. RF chokes following these capacitors include two-turn sections with pencil-lead cores to minimize the possibility of parasitics. The 4.7-µF capacitors eliminate low-frequency power-supply instability problems.

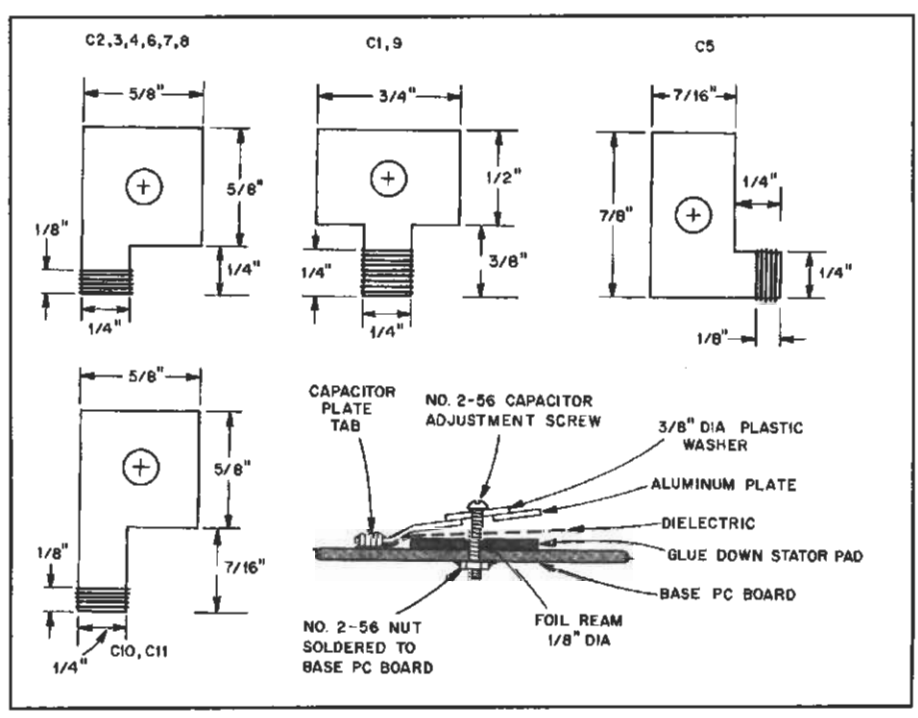

Fig 2—Variable-capacitor construction details. The "rotor" plates are made from 0.031-inch Reynolds aluminum sheet stock and polished with 320-grit sandpaper to ensure that no burrs are left that may puncture the dielectric material. Plate center holes are 3/16-inch diameter. Connections are made to the capacitors by means of no. 26 tinned copper wire, tightly wrapped (and crimped in a vise) around the tab on the capacitor and soldered to the appropriate circuit board connection. Make these connections carefully to ensure good electrical contact. See text for details on the dielectric and washer materials.

Assembly

The transistor-lead configurations are slightly modified to accommodate the glue-down striplines. Both the base and collector leads are bent up into an S shape so that the lead will overlap the stripline by approximately 1/16 inch when the transistor and stripline are mounted flush with the base PC board. The leads are only 0.005-inch thick and can be bent easily with long-nose pliers. Care must be taken to minimize stress at the lead-ceramic junc-

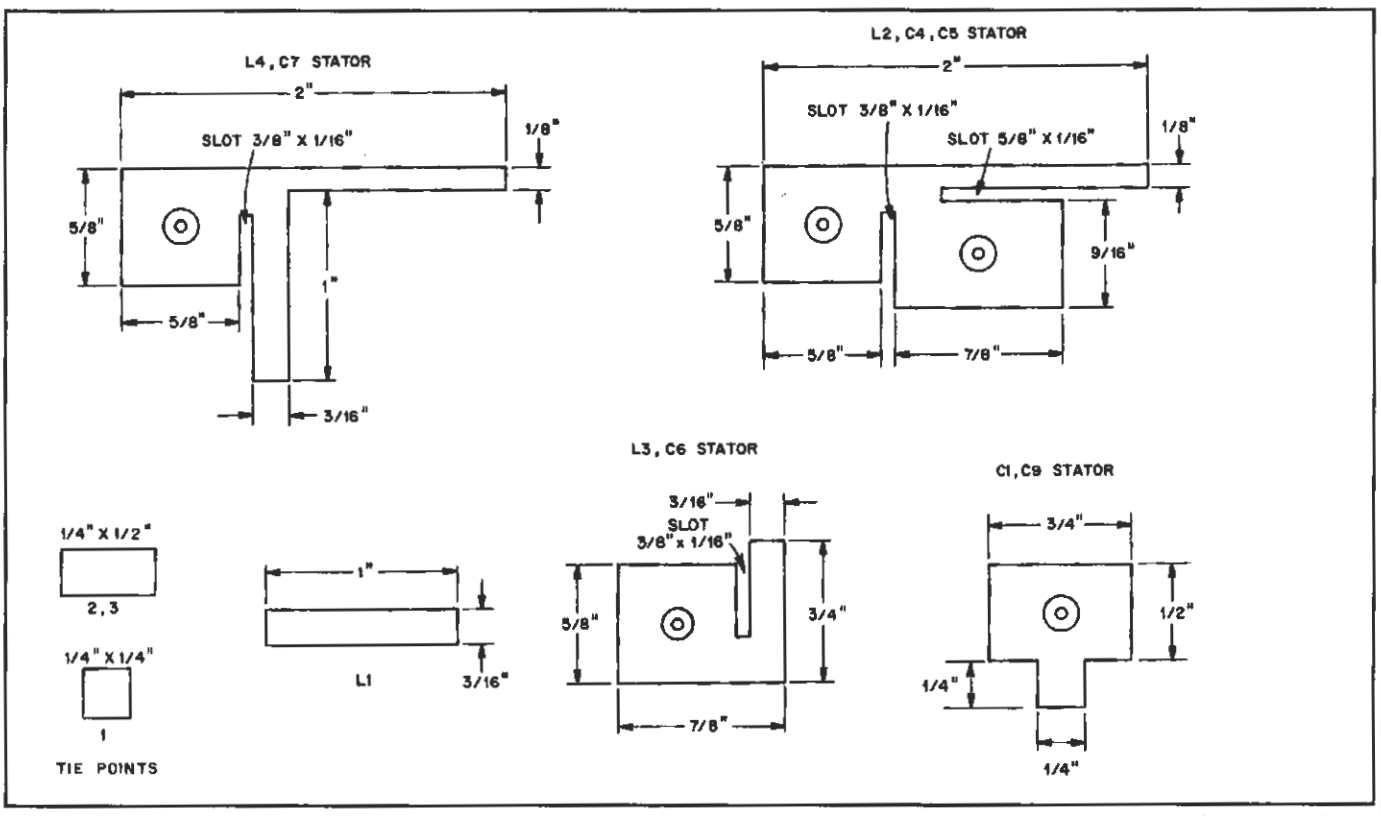

Fig 3—Glue-down stator pad construction details. Slots are cut with a hacksaw and then polished with a pattern file. The material is 0.062-inch-thick double-sided glass-epoxy circuit board material.[6] After cutting and filing, the pads must be polished with fine steel wool to remove any burrs.

tions. Also, 3/32 inch of each emitter lead must be cut off with scissors to allow room for the glue-down pads.

Details of the mounting arrangement are shown in Fig 5. My transistor mounting method was dictated by the dimensions of an old 1/8-inch-thick aluminum panel (with many miscellaneous holes), which I pressed into service as a heat sink. First, I mounted each transistor on separate aluminum subbases. I then fastened the sub-bases to the heat sink. Thermally conductive compound is used between the transistors and the subbases and between the sub-bases and the heat sink. This arrangement permits removal of the heat sink without disturbing the transistor mountings when I need access to the bottom PC-board foil. Note that the base PC board cutout includes notches at the base and collector leads of the transistors to prevent shorting to the common foil.

Detailed assembly like that shown in Fig 6 is easy once the transistors are mounted. Simply smear glue on the pads and fit them into position. Start by positioning L1, followed by the C1 stator, then C1, C2 and C3. Drill holes in the base PC board for the no. 2-56 capacitor-adjustment screws as you go along. At the same time, solder the no. 2-56 nuts on the reverse side (using a screw to hold them in position). Bend the capacitor tabs to make certain the plates will be flush with the stator, inserting the capacitor dielectric as the final step. Make certain the dielectric has been pushed in between the capacitor plates as far as possible (maximum safety margin), and use an awl to puncture the dielectric at the adjustment-screw position. The adjustment screw can then be easily started through the dielectric.

Operation

UHF transistors are great devices, but they can be damaged permanently with just one voltage transient. For example, an accidental short by a probe during a troubleshooting exercise, or the discharge of a probe capacitor at the transistor's base lead can be disastrous. Another common problem is instability that causes selfoscillation and excessive collector voltage (no insta-

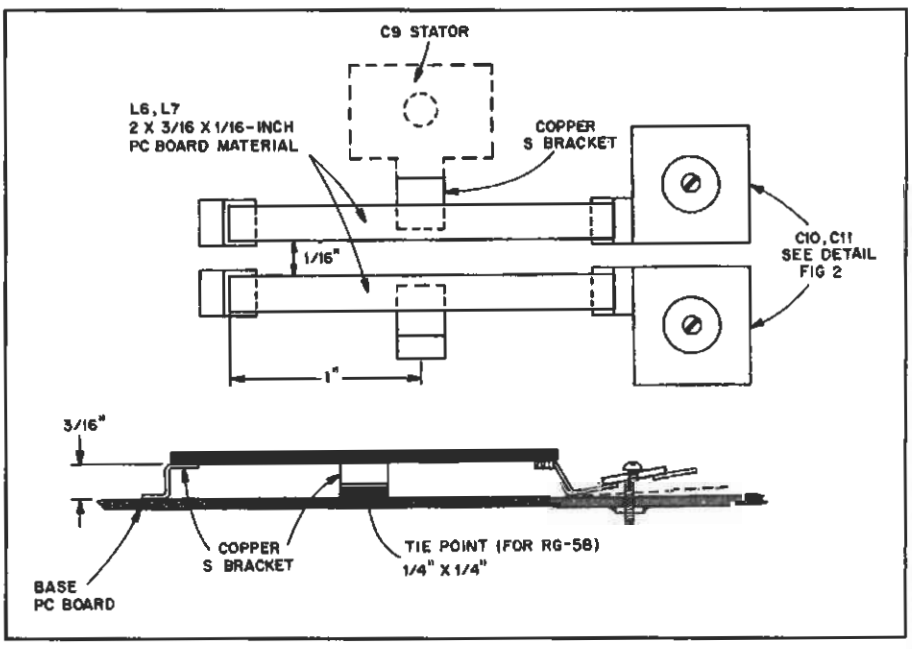

Fig 4—Construction details of the double-tuned output filter. The assembly is supported by copper brackets and parts of the variable capacitors.

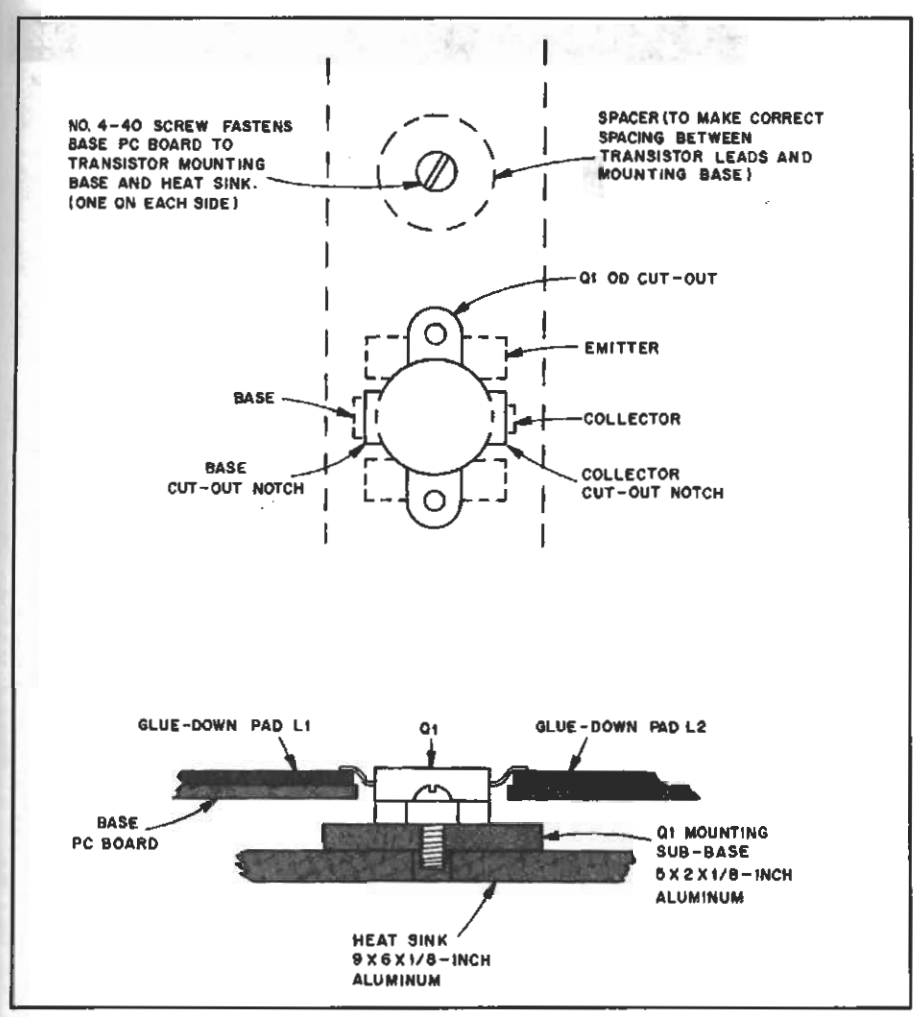

Fig 5—Pictorial of transistor mounting method. The same scheme is used for both the driver and final transistors.

bility modes are evident in the amplifier described here). These possible failure modes can be avoided by limiting the collector supply to 5 V (or less) during tune-up, as practically all instability modes will be evident at this lower potential (particularly if the input drive is varied over a wide range). Following alignment at 5 V, it is surprising how little readjustment is required when the collector potential is increased to 13 V. (If you can't reduce your power supply voltage, you may want to use a 2N3055 as a pass transistor, driving it with an LM317T regulator [Radio Shack 276-2041 and 276-1778, respectively].) This low-voltage test procedure is mentioned in Motorola Application Note AN-548A.[3]

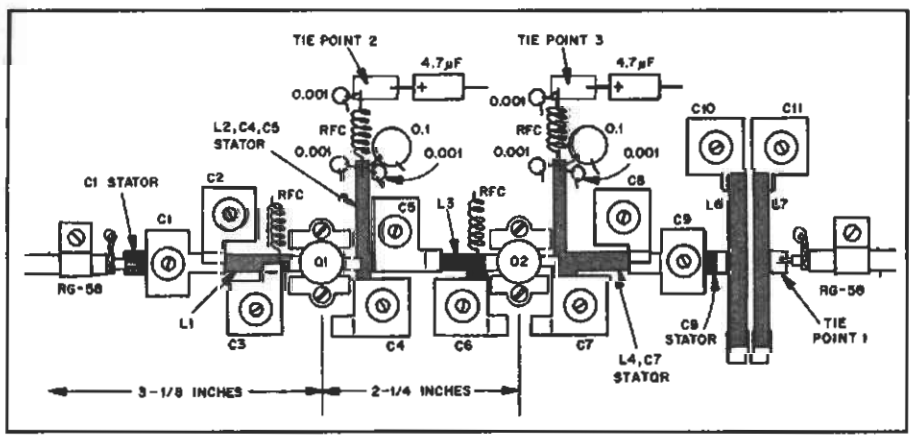

Fig 6—Circuit board layout of the completed amplifier. Begin construction by measuring the center-to-center distance from Q1 to Q2 and then mount the transistors, working away from them as you mount the other components. Use great care when mounting and soldering the transistors into the circuit to avoid damaging them. The PC board measures 9½ in. x 6 in., and is made from double-sided, glass-epoxy material (Meshna PCB28—see note 1).

Initial Tune-Up

The dummy load/power-measuring assembly and narrow-band peak detector pick-off assembly used in tune-up are the same as the ones that I used with my 15-W transmitter.[4] The dummy load consists of ten ½-W resistors connected in parallel and arranged in a circle to minimize self-inductance. Power measurements were made by calibrating dummy-load temperature rise with a dc input (ambient air-temperature conditions, no forced-air cooling). This information is then compared to the temperature rise of the dummy load resulting from the RF output of the amplifier. The "thermistor" used for measuring the temperature rise is a 1N34A (reading the reverse resistance).

Under key-down conditions during alignment, I place a blower at the chassis end to assist the limited heat-sink capabilities of the amplifier. Also, the dummy load requires forced-air cooling, as it becomes very hot in about two minutes under keydown conditions.

Miscellaneous lengths of RG-8/M and RG-58 were used as attenuators to increase power measurement capability of this system.[5] In testing the 45-W amplifier, I used a total cable attenuation of 6.4 dB. This increases the power-measurement capability by 4.4 times.

With a 5-V collector supply and 2 W of drive, first tune the input capacitors for maximum Q1 collector current, then tune the remaining capacitors for maximum power output. The output should be about 8 W. Increase the collector supply to 13 V; minor readjustment will probably be required. My final measurements showed an output of 48 W.

Summary

This is a well-behaved amplifier. After completing an experimental version on the breadboard, I built a new assembly using the data in this article. Alignment of this final model was completed without any problems, and operation is flawless. The glue-down stripline technique is very reliable in this application, and is simple to use.

Notes

[1]J. Reed, "A Simple 435-MHz Transmitter," *QST*, May 1985, pp 14-18, 45.

[2]These transistors are available from RF Parts Company, 1320-16 Grand Aye, San Marcos, CA 92069, tel 619-744-0728.

[3]This note is reproduced in *Motorola RF Device Data* (fourth edition, first printing, 1986) on pages 6-61 through 6-65. Thus book is available from Motorola Literature Distribution, PO Box 20912, Phoenix, AZ 85036, tel 602-994-6561. Cost is $4.75 (plus 15 percent of the total for shipping).

[4]See note 1.

[5]My 435-MHz measurements indicated that the RG-8/M I used has an attenuation of 9.0 dB per 100 feet (specified as 7.5 dB per 100 feet at 400 MHz); the RG-58 has 15.3 dB per 100 feet (specified as 12.0 dB per 100 feet at 400 MHz).

[6]Available from John J. Meshna, Jr. Inc, 19 Allerton St, Lynn, MA 01904, tel 617-595-2275.

By Tarmo Tammaru, WB2TMD — From *QST*, May 1982

A Solid-State 6-Meter Linear Amplifier You Can Build

Does your 6-meter signal need a little more punch? This amplifier will solve your problem—without breaking the bank!

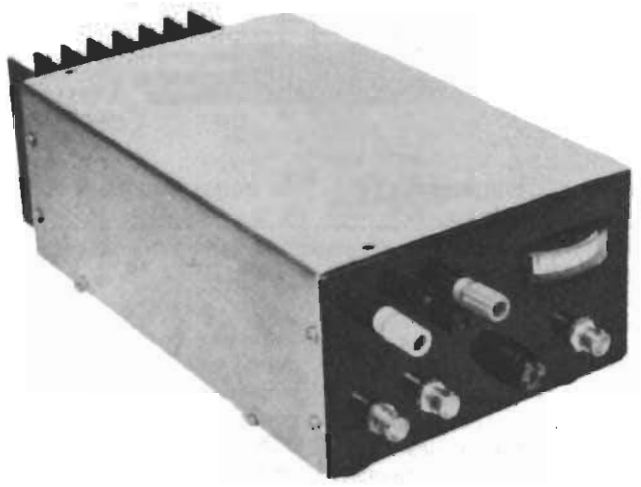

The new breed of 8-to 10-W, solid-state vhf transceivers offer compactness and relative freedom from TVI. However, there are times when 10 W will not do the job. This amplifier can correct that situation. I used it during the September vhf QSO party and was able to work every station I heard, except one.

The transistor used in the amplifier is a Motorola MRF-492, which is designed for use as an fm amplifier in the "vhf low" public-service band. In this service, the nominal output is rated at 75 W with a 12.5-V collector supply. The manufacturer's data sheet shows a maximum output of 120 W at 16 V. Hence, in ssb service, I felt it would be safe to operate at the 100-W PEP level from a 13.5-V supply. Although no numbers are given, the MRF492 is claimed to have "load mismatch capability at high line and rf overdrive."[1]

Circuit Description

The amplifier schematic diagram is shown in Fig. 1. Since I do not believe in "reinventing the wheel," the output matching network was taken directly from the Motorola data sheet. This network, incorporating L2 and L3 in the signal path, should provide excellent harmonic rejection. The network transforms the 50-Ω load impedance to the optimum transistor load of $0.6 + j1.0\ \Omega$. Note that this unit, like most rf amplifiers, does not have a 50-Ω output impedance. We simply adjust the output network to obtain the rated power into a 50-Ω load. Fig. 2A is an amplifier output spectral display. While the harmonic suppression is good, additional filtering is required before using the unit on the air. A simple, 5-pole, lowpass filter was placed at the amplifier output, and the resulting spectrum is shown in Fig. 2B. The low-pass filter circuit is given in Fig. 3.

Because the data sheet does not give values for input impedance in Class B service, the input circuit was derived basically by trial and error (the second version worked). The T matching network transforms the highly capacitive input impedance of approximately 1 Ω to a 50-Ω nonreactive load for the exciter.

In a Class B amplifier it is necessary to forward bias the base-emitter junction. There are basically two ways of doing this: the shunt diode method, and the emitter-follower method. The latter method undoubtedly results in lower inter-modulation products, but I have destroyed too many transistors using that method to try it with a $20 device. Forward bias is achieved by using the shunt regulator diode D1. This diode must be connected to the same heat sink as the MRF492, Q1. The voltage across D1 is adjusted to give a Q1 collector current of 100 mA with no drive applied. Do not attempt to set the bias point by measuring the base voltage of Q1 — use a milliammeter in the collector supply lead. I used an unmarked, surplus, 15-A rectifier diode for D1. Almost any diode will work, including power Zeners. I prefer a stud-mounted diode because it is easy to place in contact with the heat sink. Just be sure the polarity is such that the cathode is connected to the case. Several Motorola application notes specify a 1N4997 for this application. Unfortunately, this is a press-fit device. In any case, the heat sink must be grounded.

Parts Procurement

All parts, with the possible exception of an adequate heat sink, are readily available. The MRF492 has recently been advertised by Westcom[2] and Semiconductor Surplus.[3] RFC1 is a Nytronics shielded ferrite choke, designed to reduce coupling

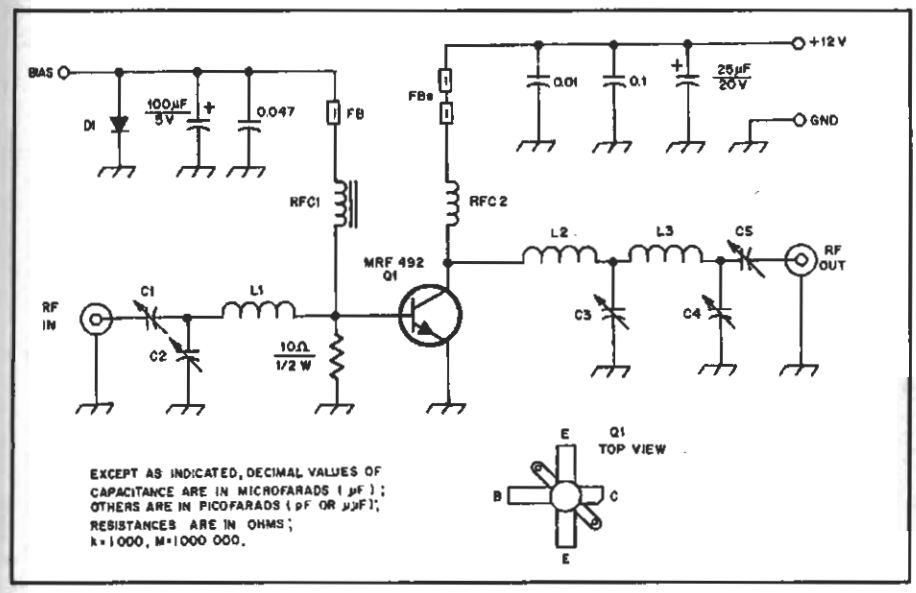

Fig. 1 — The schematic diagram of the amplifier circuit board. Decimal value capacitors are disc ceramic and oolarized caoacitors are electrolytic. Resistors are 10% carbon type.

C1 — 9-to 180-pF mica compression trimmer, Arco 463 or equiv.
C2, C4, C5 — 50- to 380-pF mica compression trimmer, Arco 465 or equiv.
C3 — 80- to 480-pF mica compression trimmer, Arco 466 or equiv.
D1 — 15-A, 50-V rectifier diode (see text).
Fb — Ferrite bead, Radio Shack 273-1571 assortment or equiv.
L1 — 2 t. of no. 14 bare copper wire, $^{19}/_{32}$-inch iD, $^{3}/_{16}$-inch long.
L2— Half loop of no. 14 bare copper wire, $^{19}/_{32}$ inch high, $^{13}/_{32}$ inch long (see photograph).
L3— 2 t. of no. 14 bare copper wire, $^{13}/_{32}$-inch ID, $^{1}/_{4}$-inch long.
Q1 — Motorola rf power transistor, MRF492.
RFC1 — 6.8 µH, Nytronics SWD 6.8 or equiv. (see text).
RFC2 — No. 16 enameled wire, close wound over full length of a 330-Ω, 2-W carbon resistor.

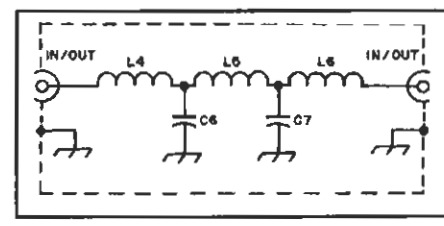

Fig. 3 — A simple low-pass filter for use with the 6-meter amplifier. The design information for this filter was taken from the 1982 ARRL *Radio Amateur's Handbook*. If the filter is mounted outside the amplifier cabinet, it should be enclosed in a metal box for shielding.

C6, C7 — 82-pF, 1000-V sliver-mica capacitor.
L4, L6 — 4 t. of no. 14 enameled wire. $^{3}/_{8}$-inch ID, $^{3}/_{4}$-inch long with $^{1}/_{8}$-inch leads (approximateiy 0.1 µH).
L5 — 6 t. of no. 14 enameled wire, $^{3}/_{8}$-inch ID, $^{1}/_{2}$-inch iong with $^{1}/_{8}$-inch ieads (approximately 0.2 µH).

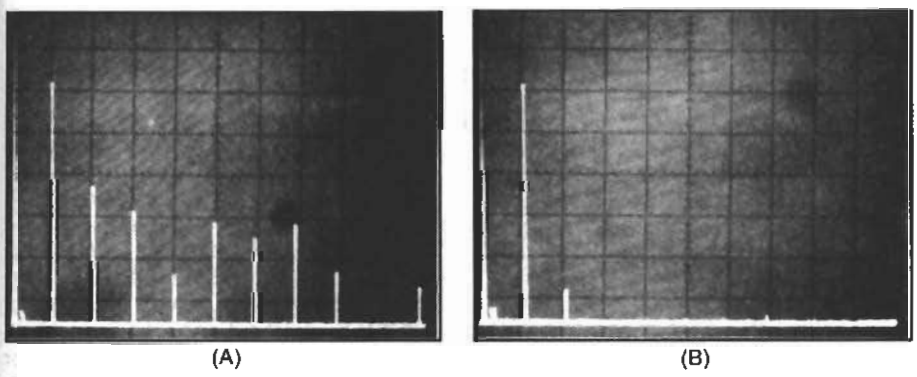

(A) (B)

Fig. 2 — The amplifier output matching network provides some harmonic suppression (A). To further reduce harmonics, a simple low-pass filter should be used (B). With the filter, au harmonics and spurious signais are more than 60 dB below the carrier, thus meeting current FCC spurious emission requirements for commercial equipment. In these displays, the carrier level has been reduced by means of a notch fiiter to avoid anaiyzer overload. Vertical divisions are each 10 dB and the horizontal divisions are each 50 MHz. These measurements were made in the ARRL lab.

between the base and collector circuit. The J. W. Miller 9250-682 should be as good. A toroidal inductor of 1 to 10 µH would also be suitable, since it is across an impedance of 1 Ω. Arco trimmers should be available from your local jobber. I used a surplus heat sink, measuring $3^{1}/_{2} \times 4^{1}/_{2} \times 1^{3}/_{4}$ inches, which is quite adequate for ssb.[4] Anything much smaller will require a fan. Remember, it must be flat on one side. A replacement heat sink for any of the 80- to 100-W 2-meter amplifiers would be ideal.

The Circuit Board

All the components shown in Fig. 1 mount on, or through, the circuit board (Fig. 4). Use double-sided glass epoxy board and cut away narrow channels to separate the various land (foil) areas. To form the channels, use a steel ruler and a sharp utility knife to cut through the foil. Next, pull a hot soldering iron along the strip of foil to be removed. You should see it curl up and away from the board. Start at one end, and pry up with the knife if it gets stuck. You will have to drill two holes, slightly more than $^{1}/_{2}$ inch in diameter, through the board to provide clearance for Q1 and D1. Use a small round file to make the two clearance areas for the flanges of Q1. Connect the ground foils on the top and bottom of the board together by placing short lengths of wire through holes drilled in the board. Place the wires close to the transistor emitter tabs and near each corner of the board. Use pieces of the same type of wire you used to make the inductors, and drill the holes just large enough to pass the wire. Solder the wire on both sides.

Assembly

Make sure you have all the parts on hand before you solder anything to the board. This will ensure that everything fits properly. To keep the inductors in place, I drilled holes through the board and stuck the ends of the wire into the holes. You will have to remove the foil from around these holes on the bottom of the board to keep from shorting the inductors to ground. A large drill bit works fine for this. Center the board on the heat sink, and drill the mounting holes for Q1 and D1. Although you may be able to use screws and nuts to attach Q1 and D1 (depending on the heat sink design), a better method is to tap the holes for the desired screw thread. Mount the board to the heat sink near the corners, shimming it with washers to the same depth as the Q1 mounting flange. Drop Q1 in from the top of the board. The tabs of Q1 should rest just above the top of the board when the flange is in contact with the heat sink. Do not put any upward pressure on the transistor tabs. Never cut or file an rf power transistor body — they contain berillium oxide. It is highly toxic in powdered form and could be inhaled or absorbed through the skin.

Fasten Q1 to the heat sink before sol-

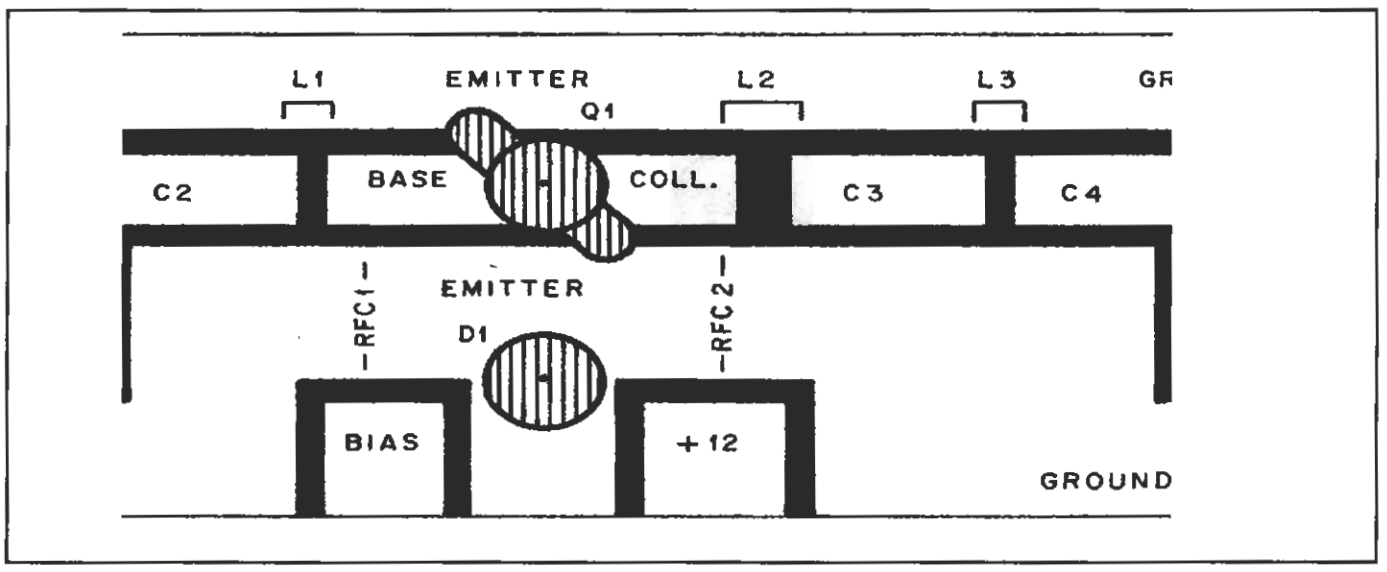

Fig 4—Full-scale circuit-board pattern and parts-placement guide for the 6-meter amplifier. Black represents those areas where copper has been removed by cutting or etching. The 10-ohm base resistor is connected between the base and ground foils, and is positioned next to RFC1.

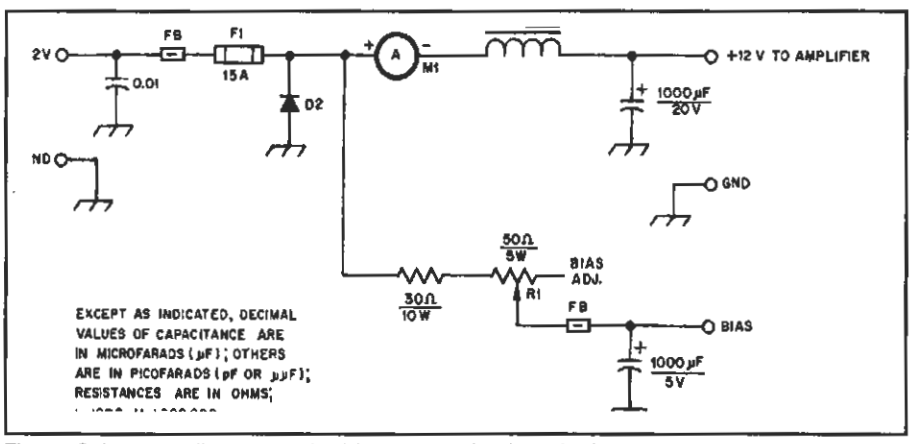

Fig 5—Schematic diagram of the bias-adjust circuit and other components not mounted on the circuit board. Decimal-value capacitors are disc ceramic, and polarized units are electrolytic type. Resistors are wire-wound type.

D2—20-A, 50-V rectifier diode.
RFC3—One turn of wire through a TV balun core (part of Radio Shack 273-1571 assortment or equiv.).

dering it in place. Use thermal grease when mounting Q1 and D1. Be sure to solder the full length of the tabs to the board, right up to the body of the transistor. This is especially important for the emitter tabs, because nanohenrys of inductance here translate to decibels of gain loss.

Break off the little tabs on the sides of the mica compression trimmers. Bend the ends of the mounting terminals with pliers to aid in soldering the trimmers to the board. In doing this, be sure the adjusting screw will not touch the board when it is all the way down. C2, C3 and C4 should be oriented so that the screw is connected to the ground end of the capacitor. For C1 and C5 let the screw end be the 50-Ω side.

Putting It All Together

I installed the circuit board and heat sink on the back wall of a 3½ × 6 × 10-inch Minibox. This is much larger than necessary, but does provide room for relays and a receiving preamp for an eventual remote installation. I usually discard the top (plain U-shaped) half of these boxes and bend up a new piece that fits over the other half, instead of sliding into it.

Fig. 5 shows the biasing circuit and other chassis mounted parts. Control schemes for use with a transceiver are described by Kapplin[5] and Ridpath[6] (also see the ARRL *Radio Amateur's Handbook*). D2 does not have to be heat sinked. It only has to last long enough to blow the fuse in case the wrong supply polarity is inadvertently applied. On the other hand, the 50-Ω bias adjust control (R1) gets quite warm, and should be mounted to the enclosure. In wiring the bias circuit, attach one wire from R1 to D1 and another wire from D1 to the bias point on the circuit board; all other connections are made to the circuit board. If R1 were connected to the circuit board, with a strap going to D1, you would almost certainly damage the transistor if the strap to D1 broke.

Alignment

It is necessary to set the bias before aligning the rf circuits. For an initial check, disconnect the wire between D1 and the circuit board (R1 is connected to D1). Apply power and measure the voltage across D1. It should be possible to lower it to 0.65 V, or less, by varying R1. Set R1 for the lowest voltage and connect the wire from D1 to the circuit board. Now reduce the resistance of R1 until the collector current is 100 mA. Be sure you are measuring collector current and not total supply current (you have about 300 mA flowing into D1).

For aligning the trimmers you will need, at least, an SWR indicator and a 50-Ω dummy load. You will, of course, not know how much power you are getting unless you also have a wattmeter. Connect the amplifier output to a dummy load and apply about 1 W of drive to the input through the SWR indicator. Adjust C1 and C2 for an SWR of 1:1. With CS snug, but not tight, adjust C3 and C4 for minimum collector current. With the SWR indicator or wattmeter connected between the output and the dummy load, adjust all the trimmers for maximum output. If more than one setting gives the same power, pick the one that corresponds to the lowest collector current. Slowly bring up the drive and keep readjusting all the trimmers. With 8 W of drive you should get an output of 100 W. The collector current will be approximately 15 A. Readjust the input for a 1:1 SWR at full power. This may, or may not coincide with maximum gain and you may have to compromise.

During testing you might consider using a harmonica to generate a multitone signal to reduce the average power dissipation (keep the speech processor off). If at any time the heat sink gets so hot you cannot hold your hand on it for five seconds, let it cool off. As a rough indication of power output, I found that at 100 W, a

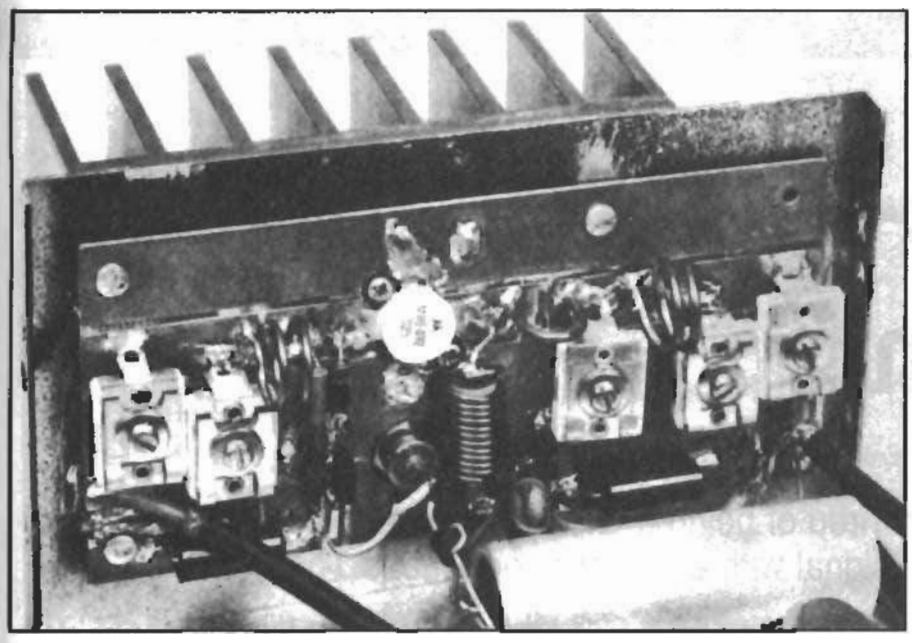

Interior view of the 6-meter amplifier showing the parts arrangement used by the author. The input matching network is at the right of the photo.

Drake DL 300 dummy load become too hot to hold after two minutes of key-down operation. To prevent rf burns, do not touch the dummy load while rf power is applied.

To maintain linearity, adjust the output circuits for 100 W, even if you are going to operate at 75 or 80 W. I evaluated the amplifier linearity by making two-tone IMD measurements with a spectrum analyzer. At a PEP output of 100 W, the third-order products were 25 dB below the PEP. At 80-W PEP they were down 30 dB. In over 100 contacts, I have not received any adverse comments on the signal quality.

Notes

[1]Motorola Inc., *Motorola Rf Data Manual*, 2nd ed. (Phoenix, AZ: Motorola Inc., 1980), p. 6-15.

[2]Westcom, 1320 Grand Ave., San Marcos, CA 92069.

[3]Semiconductor Surplus, 2822 N. 32nd St., No. 1, Phoenix, AZ 85008.

[4]mm = inches x 25.4.

[5]S. Kapplin, "Boots for QRP Rigs," *QST*, July 1981, pp. 15-20.

[6]I. Rildpath, "T-R Switching with PIN Diodes," *QST*, March 1981, pp. 19-21.

By Wilson Hoag, WA5OLT From *QST*, April 1982

Build A 6-Meter "Mini-Lini"

Tired of being a QRP station? Boost your low-level signal with a pair of sweep tubes.

Is low power enough for equality on 6 meters? Perhaps, but it has long been my contention that some stations are more equal than others! One of the great features of 6 meters is the ability to make contacts with just a few watts when the band is open. As solar activity begins to decline, band openings will be shorter and less frequent. This amplifier will add punch to your QRP signal.

The current offerings of solid-state 6-meter transceivers and transverters provide operating ease and good signal quality, but at the expense of rf power output. This, coupled with the paucity of linear amplifiers, resulting from the infamous amplifier ban, has caused an overall reduction in the average power output on 6 meters.

When I acquired my first solid-state rig (an IC-551) some time back, my tendency was to use its scan feature to locate a signal and then work the station with a 240-watt tube-type rig. A minor panic occurred when the tube rig "rolled over and died" midway through the '79-'80 F2 season. The Mini-Lini resulted from that panic.

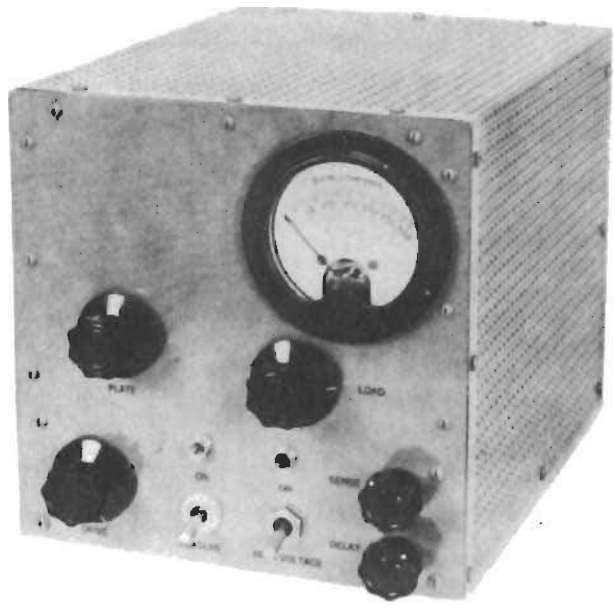

Design Approach

The amplifier was designed to be compatible with common power supplies, use a readily available tube, provide push-to-talk operation with the IC-551 and have approximately the same rf output as most tube-type transceivers. Fortunately, a design incorporating most of these features had been developed by Ed White, WA5RIA.[1] The major changes I made were in the methods of switching and bias adjustment. The tube used is the 6JB6, which is inexpensive, available and "happy" at 50 MHz. The biasing arrangement, an idea borrowed from Doug DeMaw,[2,3] allows the tubes to be matched for safe parallel operation. This amplifier provides about 50 watts of output when driven by a 10-watt exciter. More than one year of almost daily use has been trouble free and productive (42 states, including KH6 and KL7, plus JA and several Europeans).

Circuit Details

The circuit is conventional and typical of many low-band amplifiers. The original design used a capacitive input, but I thought that the parallel-tuned input method shown in Fig. 1 would provide more output when used with other QRP drivers. This was proven in practice: The amplifier delivers about 20 watts of output when driven by an IC-502. The potential problem of operating unmatched tubes in parallel has been avoided by biasing each tube individually. Component values shown will allow coverage of the entire 6-meter band.

The output network will not reject harmonic energy, and the second harmonic, as measured in the ARRL lab, was less than 40 dB below the fundamental (Fig. 2). This works out to a healthy 5 mW at 100 MHz. Most fm receivers in the neighborhood will detect this easily. FCC requirements for a commercial amplifier at this frequency are to have all spurious radiation at least 60 dB below the fundamental.

To meet this requirement (and to prevent a lot of RFI complaints) a 7-pole Chebyshev low-pass filter was built from data given in the 1982 *Radio Amateur's Handbook*, pages 6-11 and -12. Details of a filter with 0.01-dB of ripple and a 60-MHz cutoff frequency are given in Fig. 3. The coils can be wound on toroids, or be air-core types. Amidon T44-10 (or larger) cores should be adequate. The number of turns required will depend on core size or coil diameter, and can be calculated from data given on pages 2-12 and 2-30 of the *Handbook*. This filter reduced the second harmonic output to more than 65 dB below the fundamental (completely gone for all practical purposes). See Fig. 4.

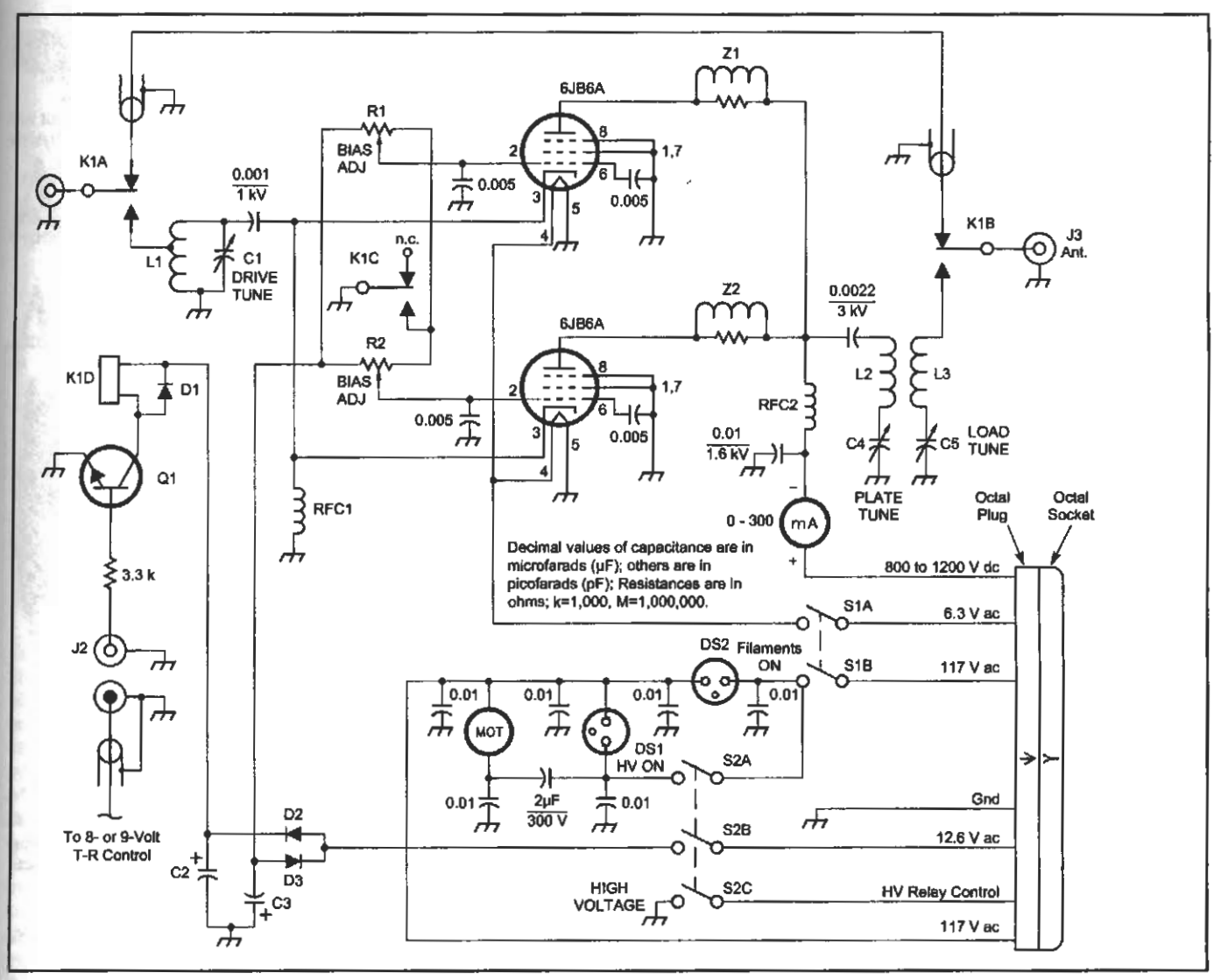

Fig. 1 — Schematic diagram of the 6-meter linear amplifier. The tube filaments can be wired In series, eliminating the need for a separate 6.3.V supply.

C1 — 50-pF miniature air variable, Cardwell 148-4 or equiv.
C2, C3 — 220-µF electrolytic, 50 V.
C4 — 25-pf air-variable, wide-spaced Hammarlund HF30X or equiv.
C5 — 100-pF air variable, Johnson 149-5 or equiv.
D1 — 1N914.
D2, D3 — 1 A, 50 V.
J1, J3 — SO-239.
J2 — Phono Jack.
K1 — 3pdt 12-V dc coil, rf type preferred, or KRP14DG.
L1 — 6 turns no. 14 enameled wire, ½-inch ID × 1-inch long, tapped at approximately 1½ turns.
L2 — 5 turns no. 12 enameled wire, 1½ inch ID × 2½ inches long.
L3 — 2 turns no. 12 enameled wire, 1½ inch ID × ½-inch long.
mA — 0-300 mA dc meter.
MOT — 117-V fan motor.
P1 — Chassis-mount octal plug.
Q1 — NPN power transistor, TIP31 or equivalent, (RS no. 276-2017).
R1, R2 — 10-kΩ, 2-W potentiometer.
RFC1 — 300-µH choke with ferrite bead on the ground lead.
RFC2 — 83 turns no. 28 enameled wire on a ½-inch diameter ceramic form. The coil is 2 inches long.
Z1, Z2 — 1 turn no. 16 enameled wire on 47-Ω, 2-W resistor.

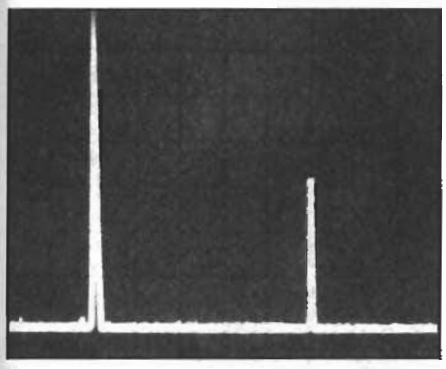

Fig 2—Spectral display of the amplifier output. Vertical divisions are each 10 dB, and horizontal divisions are each 10 MHz.

Construction

It should be possible to duplicate this amplifier for $40 or less, depending on the status of your junkbox. Oddly enough, the tube sockets proved to be the most difficult component to locate, since they are not a common catalog item. The 6JB6 uses a 9-pin NOVAR socket, and the best source turned out to be a shop that specialized in TV replacement parts. Tuning capacitor C4 is a junkbox item of questionable parentage. Any spacing greater than about 0.060 inch (mm = inches × 25.4) should be okay. RADIOKIT of Greenville, New Hampshire would be a good source for all of the variable capacitors.

My amplifier is constructed on an 8 × 10 × 2½ inch chassis (BUD AC-1418) for a base, with 8 × 8-inch end panels. The panels were flanged with ½ × ½-inch aluminum channel for attachment of a cane-metal cover for safety and TVI protection. Component placement is not critical, but all component leads should be as short as possible. The resulting layout was determined largely by some mid-project design changes aimed at making the unit compatible with a newly acquired IC-502. Visible on the lower-right front panel are potentiometers that were reserved for control of a planned rf-operated T-R relay.[4]

The tube sockets are modified slightly to ground the necessary tube elements. Copper washers, cut from flashing copper, fit inside

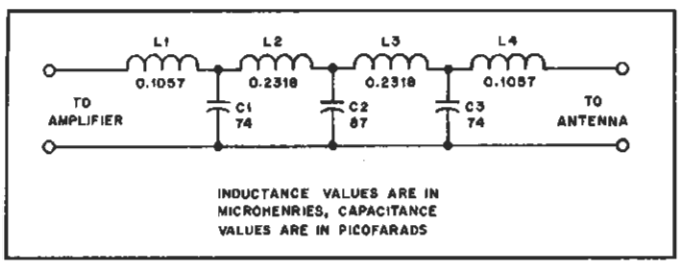

Fig 3—Schematic diagram of a 7-pole Chebyshev low-pass filter. Capacitors are silver-mica units, combined in parallel or series to obtain the design values. The text has information about winding the inductors.

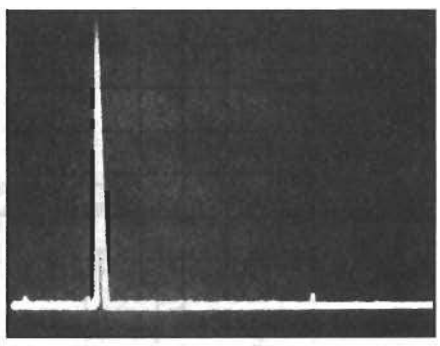

Fig 4—Spectral display of the amplifier output with a 7-pole Chebyshev filter. Vertical divisions are each 10 dB, and horizontal divisions are each 10 MHz.

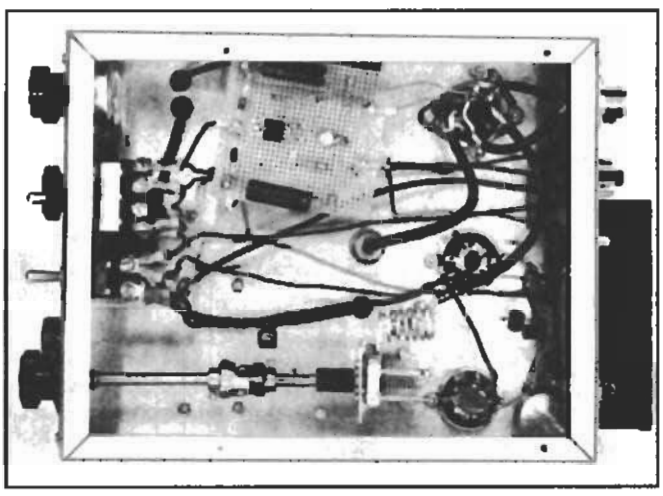

Fig 5—Bottom view of the amplifier chassis. Note the washers on the tube sockets, used to provide a ground connection for the appropriate pins.

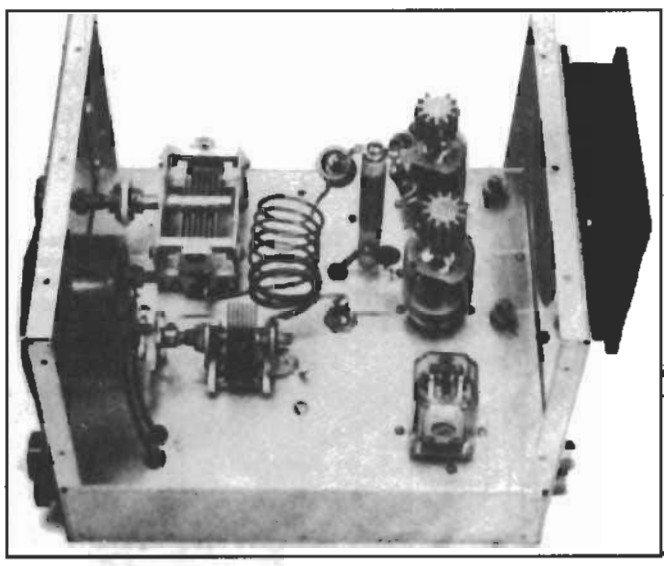

Fig 6—Top view of the Mini-Lini chassis. Large heat-dissipating plate caps and a fan help maintain cool operation of the tubes.

the pins on the underside of the sockets. Pins 1, 4, 7, 8 and 9 are bent over and soldered to the washer. The washers are grounded to the chassis with short pieces of no. 14 wire on opposite sides of the socket. Pins 2 and 6 of both tubes are bypassed to ground by connecting 0.005-µF disc-ceramic capacitors from these pins to the copper washers (Fig. 5). The control grids are raised above dc ground while providing a path for rf return. It also permits us to apply a dc bias to the control grid. This will establish the class of operation and cut the tubes off during receive, if desired.

Coils L1, L2 and L3 are wound with solid TW-insulated house wire from the local hardware store. I stripped the insulation from the wire before winding L1 and L2, but left it on L3 to prevent accidental contact with L2. The inside diameters shown are more the result of available cylindrical shapes than any electrical calculation. Coil spacing was adjusted, with the tubes in place, using a dip meter to ensure resonance at the proper frequency.

Heat-dissipating plate caps and a small fan provide cooling for the tubes. See Fig. 6. No thermal distress has been evident under any operating condition. The fan can be wired through S1 or S2, depending on whether cooling is desired during standby operation. Power connections to the fan should be isolated from the chassis.

A possible modification, shown on the schematic diagram, involves the use of a 3pdt relay for K1. The ground legs of R1 and R2 can be wired through one of the normally open contacts. This lifts the potentiometers above ground in the receive mode, applying full bias voltage and cutting off the tubes.

The bias voltage source and relay driver are "hard wired" on a small piece of perf board. The signal for T-R switching is applied to J2. This + 8-V signal is obtained from pin 6 of the IC-551 accessory socket. For use with other rigs, a 9-V battery, wired through a foot switch, works well. Current drain on this battery is low. An rf-operated T-R relay could be used in place of the directly keyed one described in this article. S2 disables the relay driver by removing the 12.6-V ac source in the standby position to permit straight-through operation.

Tune-Up and Operation

Initial tune-up is simple and ordinary. Connect a dummy load and the power supply to the appropriate jacks. Any high-voltage power supply that has an output of 750- to 1200-V dc should be satisfactory. Turn on S1 and allow the heaters to warm up for a minute or more. Switch S2 to turn on the other voltages. Actuate K1 to ground the bias resistors, R1 and R2. Adjust R1 and R2 to obtain 15 mA of idling current for each tube (30 mA total).

Connect the exciter to the amplifier through an SWR indicator. Actuate K1 and apply a small amount of drive. Adjust the position of the tap on L1 for minimum SWR. Be sure to remove all voltages each time you move the tap position!

Next, apply drive to the amplifier and adjust C1, C4 and C5 for maximum power output. For those lacking a wattmeter, an SWR indicator set in the FORWARD position can be used in the line between the amplifer and the dummy load.

Conclusion

The Mini-Lini should be ideal for those looking for more output from their solid-state rigs. Typical operating parameters are 50 watts out for 10 watts of drive, with 1050-V dc on the plates. Reports of signal quality have been complimentary. Enhance your "equality" and come join the fun on 6! I would be happy to answer any questions about the amplifier — enclose an s.a.s.e., please.

Notes

[1]The design was taken from personal correspondence with Ed White, WA5RIA.

[2]D. DeMaw, "Some Ground Rules for Sweep-Tube Linear-Amplifier Design," *QST*, July 1968, p. 30.

[3]D. DeMaw, "Some Thoughts About TV Sweep Tubes," *QST*, Feb. 1980, p. 11.

[4]D. DeMaw and J. Rusgrove, "An RF-Sensed Antenna Change-over Relay," *QST*, Aug. 1976, p. 21.

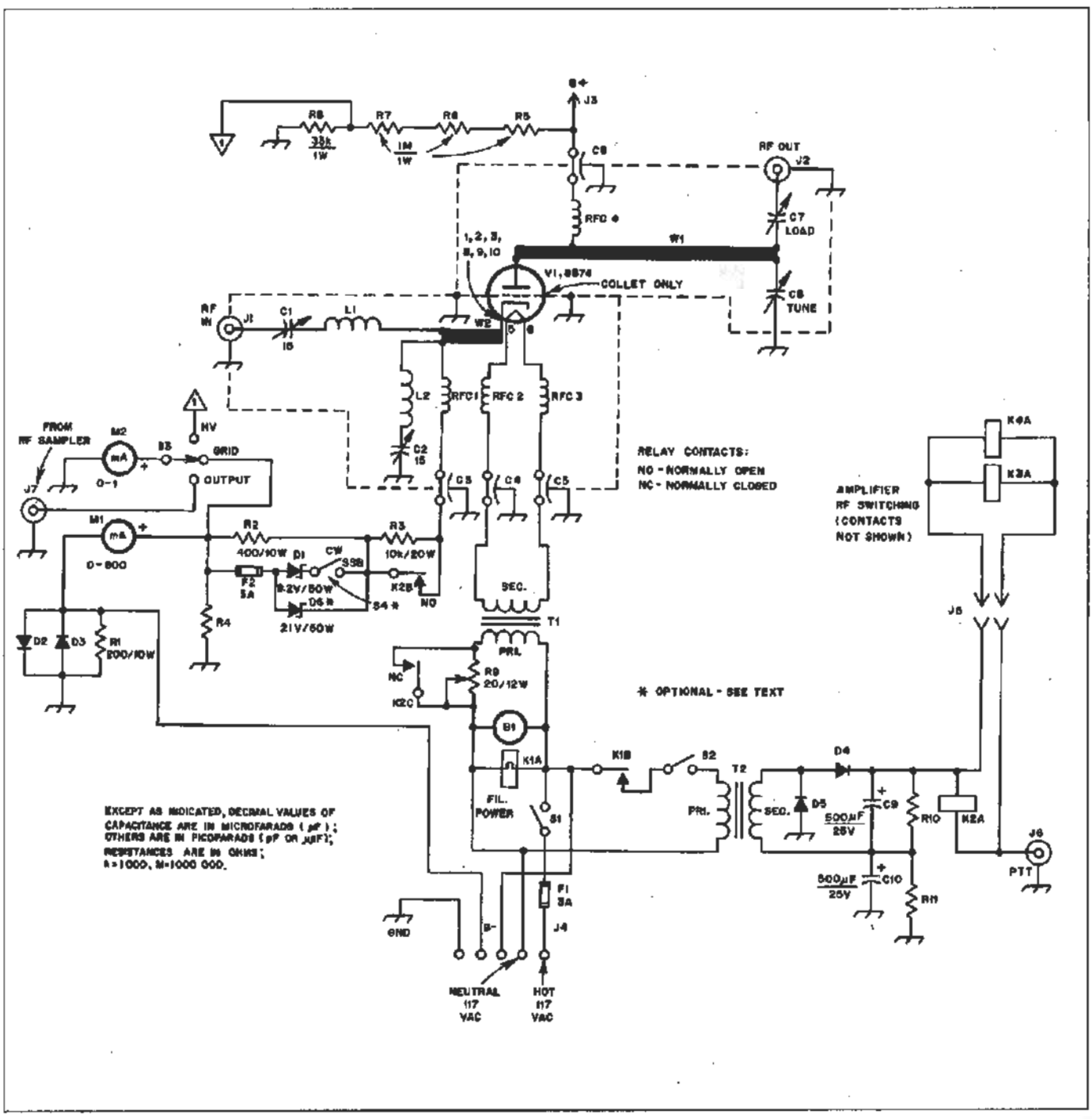

Fig. 1 — Schematic diagram of the amplifier.
B1 — 50-ft^3 (1.4-m^3)/min blower, Ripley Sk2754-2A or equiv.
C1, C2 — Air-variable capacitor, 15 pF, E.F. Johnson 189-0565-001, 160-0107-001 or equiv.
C3-C5, incl. — Feedthrough capacitor, 500 pF, 300 V.
C6-C8, incl. — Homemade "flapper" capacitor. Details of construction in text and Fig. 3.
C9, C10 — Electrolytic capacitor, 500 µF, 25 V.
D1 — 50-watt, 8.2-volt Zener diode, IR Z-3307-C or equiv.
D2-D5, incl. — 1-A, 1000-PIV diode, 1N4007 or equiv.
D6 — 50-watt, 21-volt Zener diode (optional — see text).
F1, F2 — 3AG fuses.
J1 — Chassis mount BNC female connector, UG-1094/U.
J2 — Chassis mount N female connector, UG-58A/U.
J3 — High-voltage connector, Millen 37001.
J4, J5 — Power connectors, as available.
J6, J7 — RCA phono jacks.
K1 — Time-delay relay, 90 second, normally open contact, Amperite 115N090T.
K2 — Control relay, 28-volt coil, 1-A 4pdt contacts.
K3, K4 — Coaxial relays equipped with suitable connectors. K4 should have N connectors, K3 may be BNC or N.
L1 — 3½ turns no. 16 enam. wire, ¾-inch (19 mm) long, ¼-inch (6 mm) diameter.
L2 — 1½ turns no. 16 enam. wire, ⅝-inch (16 mm) long, ¼ inch (8 mm) diameter.
M1 — 1-mA meter movement with shunt to provide 600-mA full-scale deflection.
M2 — 1-mA meter movement with shunts to provide 90-mA (grid current) and 3-kV (plate voltage) full-scale deflection.
R4 — Grid-current shunt.
RFC1 — 10 turns no. 18 enam. wire, close wound, ¼ inch (6 mm) diameter.
RFC2, RFC3 — 10 turns no. 16 enam. wire, close wound, ¼ inch (6-mm) diameter.
RFC4 — 5 turns no. 16 wire, one inch (25 mm) long, ¼ inch (6 mm) diameter.
S1 — Toggle switch, spst.
S2 — Toggle switch, spst.
S3 — Rotary switch, single pole, three position.
S4 — Toggle switch, spst (optional, see text).
T1 — Filament transformer, 6.3-volt, 3-A, Stancor P-6466 or equiv.
T2 — Transformer, 12.6 volts, 1 A.

By Stephen J. Powlishen, K1FO

From *QST*, October 1979

A Grounded-Grid Kilowatt Amplifier for 432 MHz

Stable, linear operation for tropo or moonbounce DX... that's the end result of this project.

In the last few years I've built several high-power 432-MHz amplifiers that used tubes from the 4CX250 family. While they worked well in Class C, their performance when biased for linear operation left something to be desired. My previous experience with grounded-grid triode amplifiers on 2 meters was so good that I decided to try the same approach on 70 cm. An Eimac 8874 high-mu triode was selected for this design and a crude prototype was built in a few evenings. After the design was verified, the amplifier described in this article was built. It is stable, compact and delivers over 500 watts output while requiring only a high-voltage supply and a source of about 25 watts of drive. The amplifier has been trouble free in over three years of heavy usage.

Circuit Description

A schematic diagram of the 432-MHz kilowatt is given in Fig. 1. W1 is a half-wavelength stripline which is tuned and loaded by C6 and C7 respectively. Plate choke RFC4 is connected at the approximate electrical center of the plate line. C8 functions as the plate-bypass capacitor. The half-wavelength cathode line is comprised of W2, L2 and C2. L1 and Cl serve to match the tube input impedance to the amplifier 50-ohm input. As the grid is grounded for dc as well as rf, D1 is used to develop operating bias at the cathode. R3 is switched in to supply near-cutoff bias during standby periods. Ml is used solely to monitor plate current in the high-voltage supply negative-return Lead. M2 is switched to read grid current, high voltage and relative output. The latter function is by means of an external line sampler.[1] With the exception of the multimeter functions the metering and bias circuits are similar to those in a 220-MHz amplifier.[2]

Separate coaxial relays attached to the

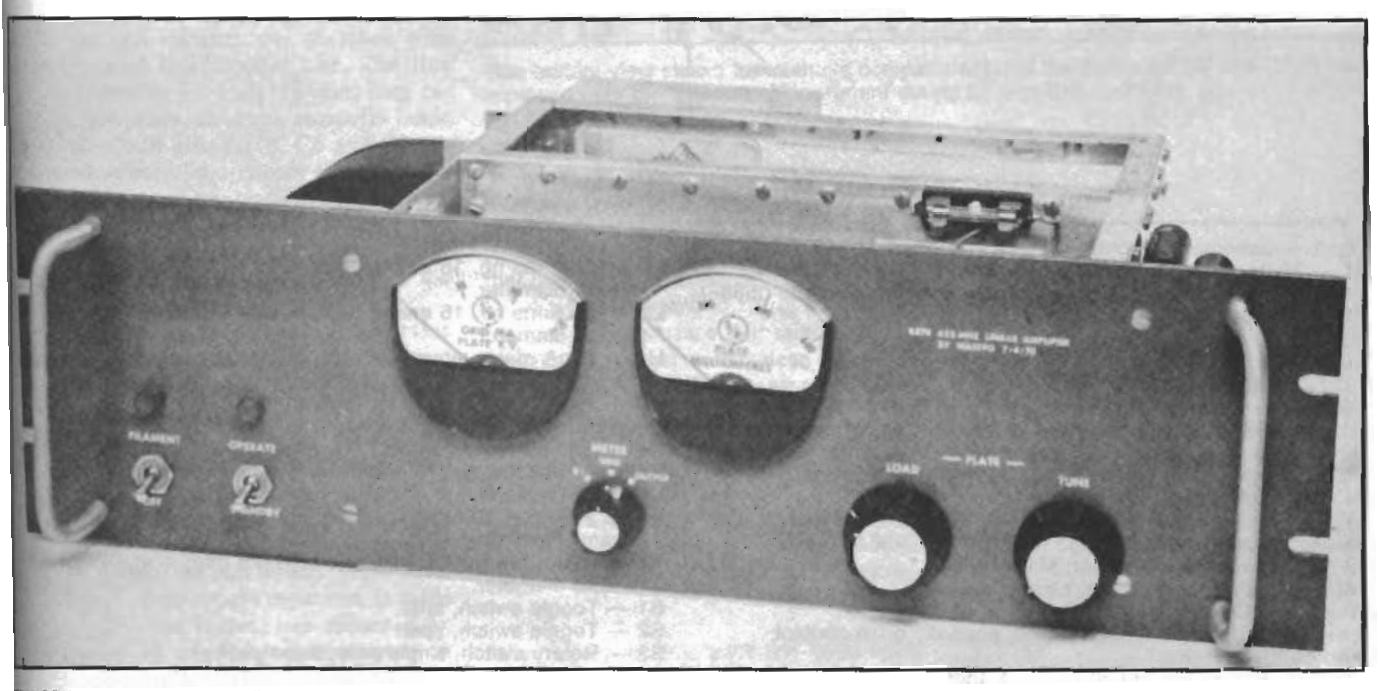

The high-power uhf amplifier. The toggle switches control filament power and standby/operate functions respectively. Multimeter function is selected with the switch located between the meters, while the plate tuning and loading controls are at the right. Modern knobs and homemade meter faces give the amplifier a commercial appearance.

input and output terminals allow the amplifier to be switched in and out of the line in a manner popular with hf amplifiers. Time-delay relay K1 prevents the amplifier from being switched into service for 90 seconds after the tube heater is energized, allowing the element to reach operating temperature. A normally closed contact of K2 applies full voltage to the heater during standby periods. The voltage is reduced during operation as recommended by the manufacturer.

Construction

Plate and cathode-compartment construction is from 0.032-inch (0.8-mm) thick aluminum sheet attached to 1/2-inch (13-mm) aluminum angle stock. Some angle stock may be anodized, giving the surface a dull appearance. This material must be lightly sanded to remove the anodized metal, which is a poor conductor. Holes are drilled in the angle stock to allow attachment of the covers; these are tapped for no. 4-40 screws. Details of the 10.5 × 4 × 3-inch (267 × 102 × 76-mm) plate compartment may be seen in the top view photo. Construction of the cathode compartment is similar, and may be seen in the photo of the underside. It measures 4 × 4 × 1 3/4 inches (102 × 102 × 44 mm). The aluminum brackets holding the rf enclosures to the front panel also serve as end covers for the compartments. Compartment spacing from the panel is four inches (102 mm). A 5 1/4 × 19-inch (133 × 483-mm) rack panel is used.

The plate line was fabricated from a piece of 1/16-inch (1.6-mm) thick brass. Fig. 2 gives detailed information for making the line. In addition to brass, lines were made from copper, both unplated and silver plated, with no discernible difference in efficiency. Double-sided G-10 printed circuit board would probably work as well. Best thermal stability was obtained with the unplated solid-copper line. The line is supported by 1.5-inch (38-mm) long ceramic insulators, although standoffs made of Teflon will also serve. C6 and C1 are made from beryllium-copper sheet. Details of their construction appear in Fig. 3. These "flappers" are moved with fishing line which is tied to 1/4-inch (6.4-mm) fiber shafts. These shafts may be seen in the underside view.

The anode collet (Eimac no. 008294) is secured to the bottom of W1 with standard 60/40 solder. Use no. 4-40 screws and nuts to hold the collet in place during the soldering operation. The grid collet (Eimac no. 882931) is attached to the chassis with eight no. 4-40 machine screws and nuts. A poor ground connection for the grid will greatly increase the amplifier drive requirements or make the unit totally inoperative.

C8, the plate-bypass capacitor, is made from two brass plates, one mounted on either side of the plate compartment. A 0.005-inch (0.13-mm) thick piece of Teflon sheet is used for the dielectric material. While this Teflon thickness may seem inadequate, it is rated at 1000 volts per mil (0.03 mm) thickness. It is necessary to coat the dielectric with Dow Corning type DC-4 silicone grease to fill in any imperfections in the surface that might allow a leakage path and subsequent capacitor breakdown. This silicone grease has dielectric properties similar to Teflon* A no. 8 (4-mm) brass screw is used to hold the plates in place, and also acts as the high-voltage feedthrough terminal. A 3/8-inch (10-mm) diameter washer was sliced from a Teflon rod and used to center the screw in the hole. Fig. 4 gives details of the remain-

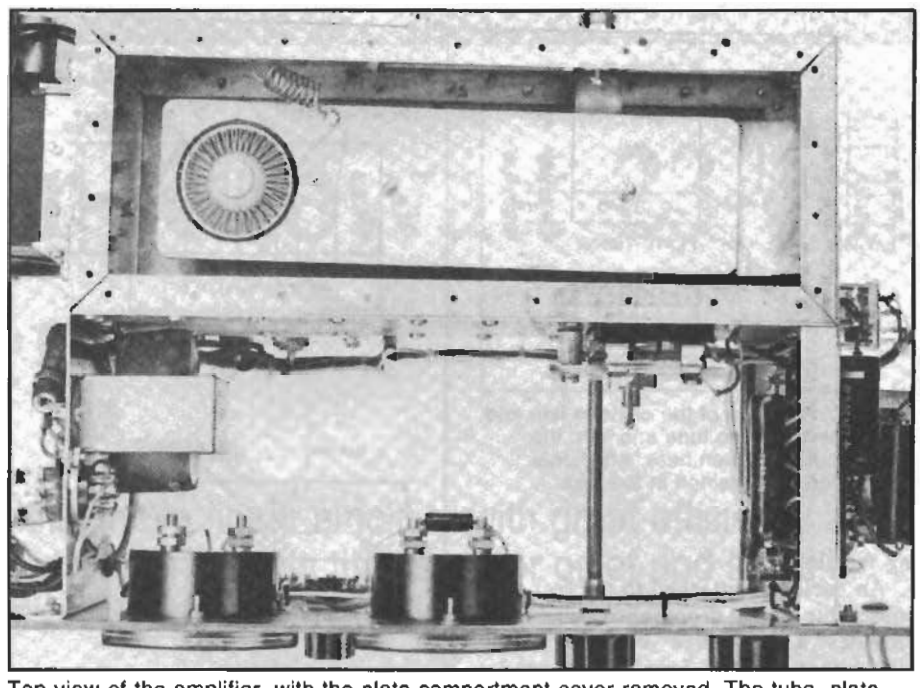

Top view of the amplifier, with the plate compartment cover removed. The tube, plate line (W2) and RFC4 may be seen at the top of the photo. Note the large number of holes drilled in the plate compartment to receive the cover hold-down screws. A tight seal is required to prevent rf and air leaks.

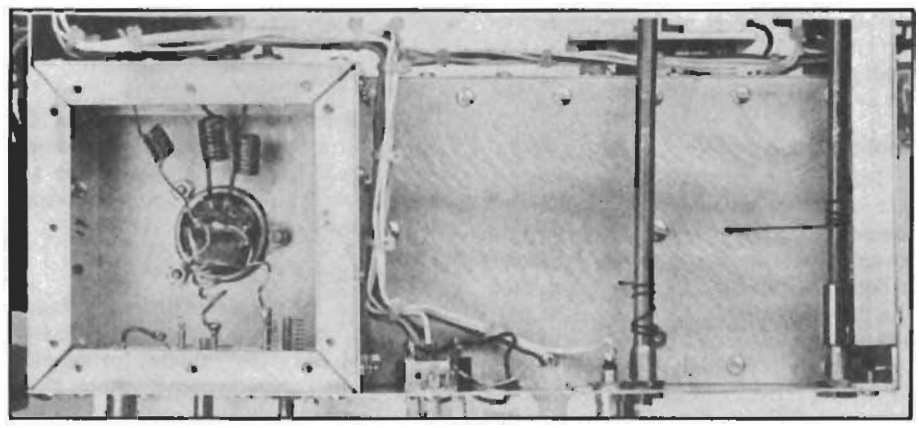

This bottom view shows the cathode compartment and the shafts for C6 and C7. A cover is placed over the cathode compartment during tuneup and operation.

*Alternatively, an Erie 2498-001-X5U0-102M 1000-pF 4-kV feedthrough capacitor may be used. This component is available from ARCOS, P.O. Box 546, East Greenbush, NY 12061.

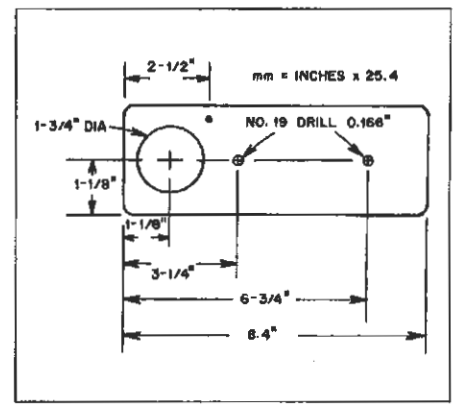

Fig 2—Dimensions of the plate line are given here. The line may be constructed from 1/16-inch (1.6-mm) thick copper or brass. Corners of the line should be filed to give a 3/16-inch (5-mm) radius.

By E.R. "Chip" Angle, N6CA

From *QST*, March 1985

A Quarter-Kilowatt 23-cm Amplifier

Imagine, a linear amplifier with great efficiency and long-term stability that is super quiet and small in size. Sounds like HF? Not exactly...

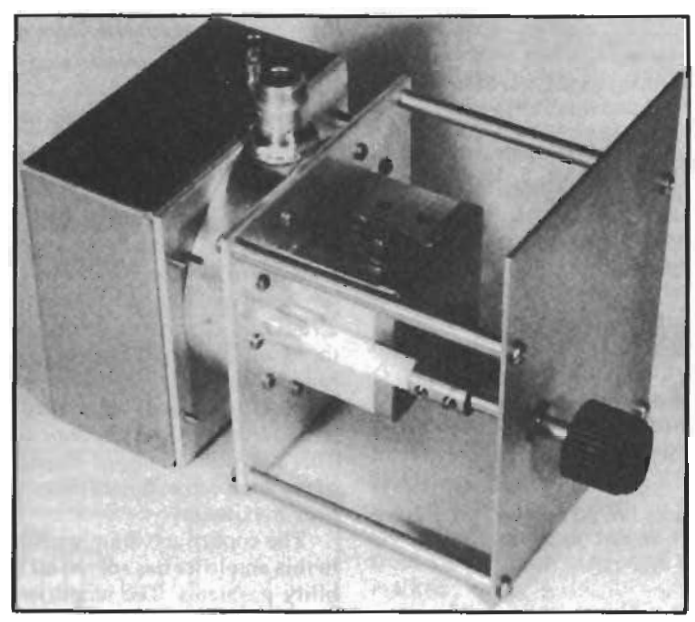

To me, there is nothing more frustrating than having to dig through a construction article to find out exactly what performance you can expect from the finished product. So here it is:

1) Grounded-grid 7289/2C39 cavity amplifier, single tube.

2) Linear operation (what you put in, you get out, only more of it).

3) Covers 1240 to 1300 MHz.

4) Power. gain ranges froth 12-20 dB depending on output power, input power, loading, anode voltage and grid bias voltage.

5) 50-ohm input and output — no stub tuner required.

6) Power output greater than 200W with about 12-W drive.

This is Part 1 of a two-part article. In this installment, I describe the design and construction of the RF deck. Part 2 describes power-supply construction, testing and operation.

This amplifier is a tried and proven design. Much development work has gone into this project. The amplifier works well, is reliable and can be duplicated. More than 50 of these amplifiers have been built to date. I have successfully worked many 1296-MHz EME (earth-moon-earth) stations with one of these amplifiers and a 384-element loop-Yagi array during the past year. Amplifiers of this design were used on both ends of the first California-to-Hawaii QSO on 1296 MHz. Another unit has logged more than 20,000 hours of continuous operation at the KH6HME beacon.

General Design Approach

A cavity amplifier is similar to a conventional amplifier designed for lower frequencies. The tube anode excites a resonant circuit, and power is in turn coupled into a load, usually 50 ohms. Instead of using coils and capacitors, as at lower frequencies, the cavity provides the resonant circuit necessary to tune the amplifier output.

The anode cavity of this amplifier is a squat cylinder. Cylinder height is set by mechanical tube requirements. The inside diameter of the cylinder sets the highest resonant frequency. Any capacitance added from the top to the bottom of the cavity will lower its resonant frequency, as will increasing the cavity diameter.

This amplifier uses 1/8-inch-thick copper plates for the cavity top and bottom, and a thick-wall aluminum ring, cut from tubing, for the walls.[1] This heavy construction virtually eliminates all resonant-frequency variations caused by thermal and mechanical changes.

Fig. 1 is a schematic diagram of the cavity amplifier. The circuit is simple. Filament voltage and cathode bias enter the RF deck through feed-through capacitors (C4, C5) and RFC1 and 2. High voltage is fed to the anode through RFC3. C8, the anode bypass capacitor, is homemade from Teflon® dielectric sandwiched between a copper plate and the chassis.

The input pi network easily tunes the entire band at any power level. it is made from two Johanson piston trimmer capacitors and a "coil" made from copper wire. An input cavity is not necessary at 23 cm.

Output coupling is through a rotatable loop that serves as a variable loading control. This allows amplifier-tuning flexibility; it may be tuned for maximum gain or for maximum power. Light loading can produce stable power gains of up to 20 dB.

Amplifier tuning is accomplished with a homemade cylindrical coaxial capacitor with Teflon dielectric (C6). There are no moving metal parts to cause erratic performance. The Teflon rod/tube screws in and

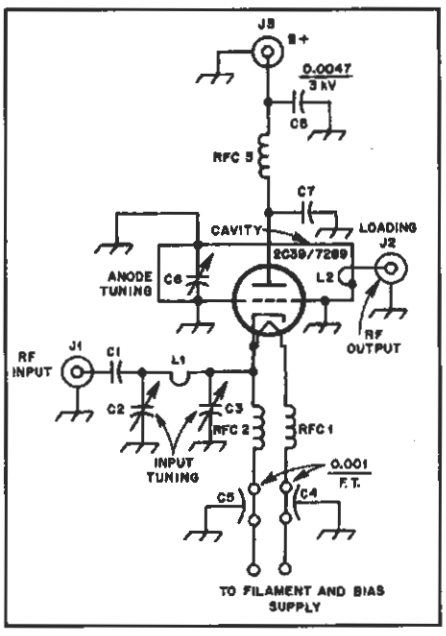

Fig. 1 — Schematic diagram of the 23-cm amplifier.

C1 — 3-pF dipped mica capacitor.
C2, C3 — 1- to 10-pF piston trimmer capacitor (Johanson no. 3957, 5201 or equiv.).
C6 — Anode-tuning capacitor. See text and Fig. 11.
C7 — Anode-bypass capacitor, 90 pF. Homemade from copper plate and Teflon sheet. See text and Figs. 5, 12 and 15.
C8 — Disc ceramic, 0.0047-μF, 3-kV capacitor.
J1 — 5-mm SMA connector, chassis mount, female.
J2 — Modified Type-N connector. See text and Fig. 7.
J3 — Female chassis-mount BNC connector.
L1 — Loop of no. 18 bus wire soldered between C2 and C3. See Fig. 15.
L2 — Output-coupling loop. Part of output-connector assembly. See text and Fig. 7.
RFC1, RFC2 — 5 turns no. 20 bus wire, 3/16-inch ID.
RFC3 — 3 turns no. 20 bus wire wound on a 20-ohm, 1-W carbon-composition resistor.

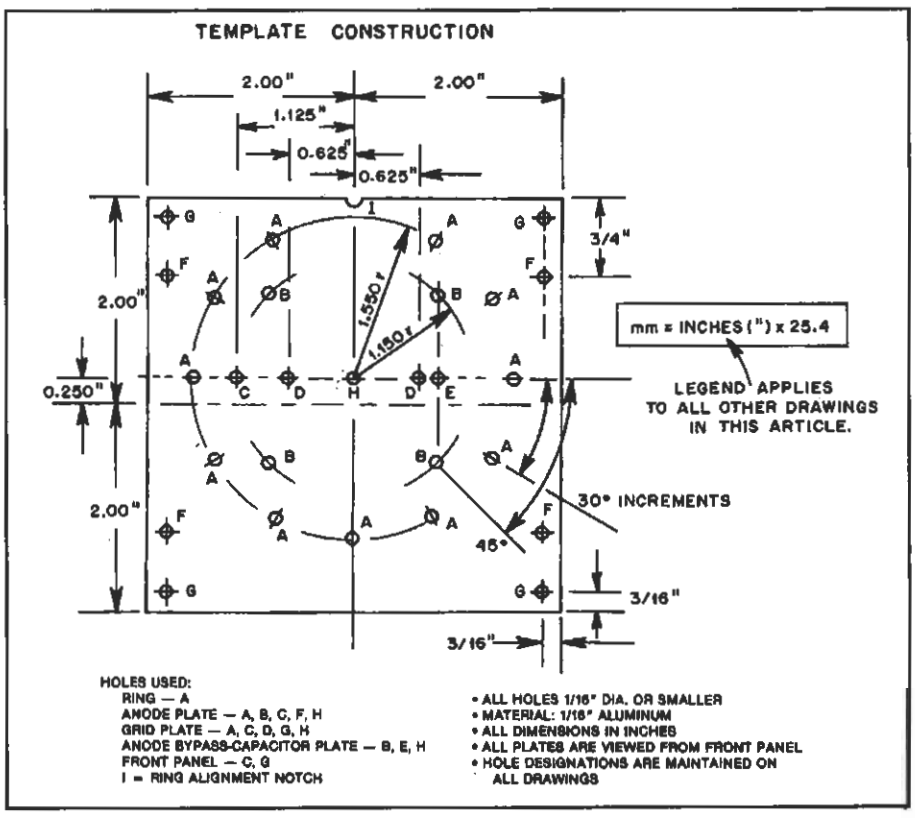

Fig 2—Complete dimensions for the aluminum template.

out of the coaxial capacitor, increasing or decreasing the capacitance by changing the amount of Teflon dielectric inside the cylinder. With the rod all the way in, the dielectric is all Teflon; with the rod all the way out, the dielectric is all air.

Teflon has a relative dielectric constant (relative to air = 1) of 2.05, which means that the value of the capacitor with the rod all the way in is twice the value of the capacitor with the rod all the way out. Full capacitance will pull the resonant frequency of the amplifier down to 1240 MHz. Use of only one tuning adjustment means the amplifier will have more gain because cavity shunt capacitance has been minimized.

Thermal Considerations

The cavity walls are formed by a thick-wall aluminum ring, which is sandwiched between two thick copper plates. RF and thermal properties of these two metals are reasonably close, whereas brass is rather poor in both respects. The 7289/2C39 tube used in this amplifier is being run at 2-2½ times its normal dissipation rating; therefore it's important to have a cavity that remains thermally stable.

Most previously described amplifiers have used sheet brass in their construction. This has usually meant constant retuning of resonance to maintain output power at or near maximum.

The copper and aluminum construction in this amplifier has solved all thermal stability problems. The amplifier can easily be run key down for over an hour at 200-W output without retuning. This, of course, is obtained only with a good tube and water cooling. A practical water cooling system will be described in Part 2 of this article.

Water cooling keeps the internal structure of the tube thermally stable. When air cooling is used for output levels of 100 to 150 W, output power fluctuations are a direct result of internal tube changes. These changes vary from tube to tube and must be tested for. In some cases, otherwise perfectly good RF tubes have had poor thermal stability. Such tubes can make good drivers at lower power levels.

"Using Simple Hand Tools Will . . ."

Hand tools are great if you are skilled and patient. Most people want to hurry up and finish their new project. If that's you, then have a machine shop make all of the parts, leaving you only the final assembly. It should cost about $200. The parts are not difficult to fabricate, but the process is time consuming. If you have the time and patience to do it yourself, this amplifier can be very inexpensive.

Gathering the Materials

All of the materials used in this amplifier are fairly common and should be available from suppliers in most metropolitan areas. Some suppliers have "short sale" racks, where they sell odd pieces cut off standard lengths or sheets at reduced prices. The parts for this project are small enough to be fashioned from cutoff stock. Surplus-metal houses have some great buys, so start there if one is nearby.

The key to successfully completing this project is careful layout work before cutting or drilling any parts. Invest in a can of marking dye, a sharp scribe, an accurate rule, vernier calipers and several center punches. These tools are available at any machinists' supply shop. The marking dye will make cutting and filing lines much easier to see. Measure all dimensions as carefully as you can and then recheck them before cutting. Mark with a sharp scribe because the sharper the scribe, the finer the marked line, and the finer the marked line, the closer your cut will be to where it should be. Remember—the accuracy of your drilled holes is only as good as your center-punching ability, so use a fine punch for the first mark and then a bigger one to enlarge the mark enough for drilling.

Access to a drill press is a must. It's extremely difficult to drill holes accurately with a hand drill. Although they are

not absolutely necessary, you should have access to a lathe or milling machine.

Other tools that will aid you with this project are a nibbling tool, a set of punches, a new set of files and some sharp drill bits. If you don't already have one, purchase a file card to clean metal shavings out of your files as you work. Clean, sharp files are faster and more accurate to work with. You'll also need an assortment of sandpaper for the final finish work.

The Template Approach

I highly recommend fabrication of a single template for marking and drilling the anode plate, anode bypass capacitor, cavity ring, grid plate and front panel. The template shown in Fig. 2 has all of the holes for these parts. If you use the template, you'll only have to make the careful measurements once — after that, it's simple to mark and drill the rest of the parts.

The template approach offers several other advantages. A template makes it much easier to maintain accuracy between the anode plate, cavity ring, grid plate and front panel; these parts will fit perfectly because they were all drilled from the same master. The template approach also makes it possible to set up a small production line if you decide to build more than one of these amplifiers and combine them for higher power, or if a friend wants to build an amplifier along with you.

See Fig. 2 for complete template dimensions. Start with a piece of 1/16-inch-thick aluminum stock that is larger than you need and degrease it with soap and water. Dry it off and spray it with marking dye. Scribe a 4-inch square on the stock and cut the template to size. A shear will make this job much easier, but it can be cut with hand tools and filed to size.

Carefully measure and scribe all holes. Note that holes A and B are on the circumference of circles. Use a compass to scribe the circles, and then locate the holes. After you have marked and checked all holes, centerpunch and drill them. The holes should be drilled with a 1/16-inch or smaller bit. Recheck all measurements. If you goof, start again. The time you spend making the template as perfect as you can will save you much time and aggravation when you make and assemble the other parts.

When you finish the template, mark the front side for future reference. All plates made from the template are marked and drilled from the front side (as viewed from the front panel).

Making the Copper Plates

Once you have completed the template, it will be easy to make the copper plates. The anode plate, grid plate and anode-bypasscapacitor plate are all made from 1/8-inch-thick copper. See Figs. 3, 4 and 5 for the dimensions of these pieces.

Measure and cut the three plates to the proper dimensions. Carefully break (deburr) all sharp edges to avoid small cuts to your fmgers and hands.

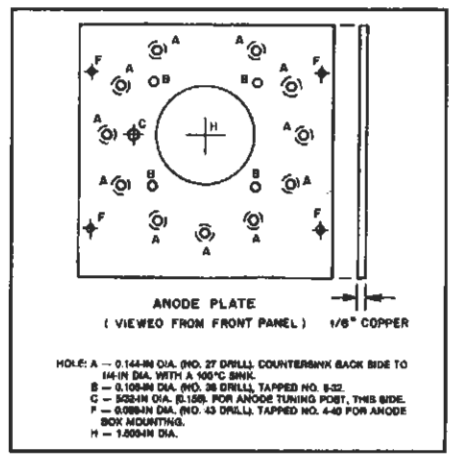

Fig 3—Drilling details for the anode plate. See Fig 2 for additional information on hole location.

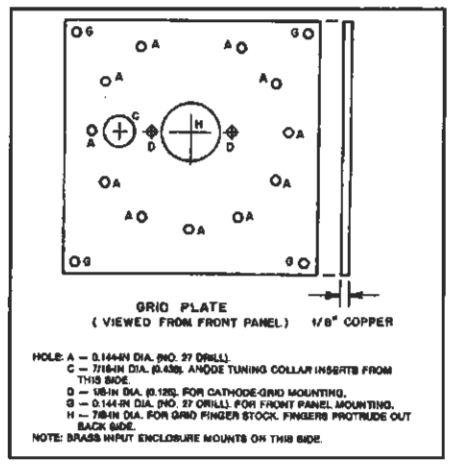

Fig 4—Drilling details for the grid plate. See Fig 2 for additional information on hole location.

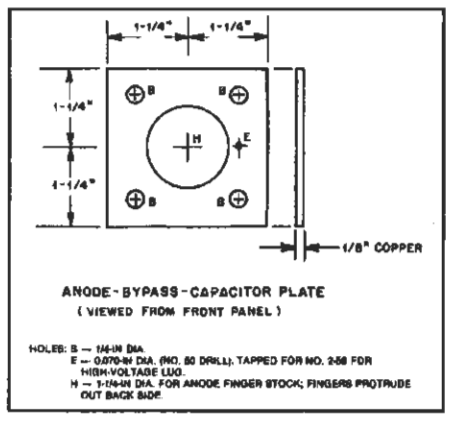

Fig 5—Drilling details for the anode bypass capacitor plate. See Fig 2 for additional information on hole location.

Clean the plates with alcohol and spray them with marking dye. Clamp the aluminum template to each plate, and carefully scribe the correct holes. Remember that all plates do not have the same holes. The anode plate uses holes A, B, C, F and H; the grid plate uses holes A, C, D, G and H. The anode-bypass-capacitor plate uses holes B, E and H.

Use a small center punch to punch all holes lightly. If they then look accurate, enlarge them enough for drilling.

Copper isn't the easiest metal to work with. It's very stringy, and drilling it can be frustrating. You'll need the proper drill bits for best results. Special drills can be purchased, or you can use a grinder to carefully remove the sharp points on the outer edge of the cutting surface of each side of a standard drill bit. This will eliminate any tendency for the copper to grab. Practice on an old bit and be sure to grind it symmetrically. Modified drill bits can still be used on aluminum and other metals.

Always start with a smaller drill and work up to the final hole size. It's safer and more accurate. The larger holes can be cut with a flycutter, or you can drill a series of smaller holes around the inside of a larger hole and file to finish. Either way is fme. Use lots of cutting fluid to lubricate the drill bit, and wear safety glasses and an old shirt. Remember, some cutting fluids are not to be used on aluminum.

Start with a no.50 (0.070-inch) or smaller bit and drill pilot holes at each of your punched marks. The details for finishing each hole are listed in the drawings. Some holes are countersunk or tapped. Pay attention to the details, and take your time.

When you are through drilling, you must deburr each hole. Copper is soft, so it tends to rise up around the hole during drilling and deburring. Use a flat file for the initial cut, and then remove any remaining material with a countersink. File the copper plates flat again; a flush fit on both sides of the aluminum ring is important.

When all copper work is done, you should be able to stack the plates and see all pertinent holes align correctly. Enough tolerance is included in the dimensions to accommodate minor errors. After the holes are drilled, it can be difficult to tell which side of each plate is which, so mark the front side of each plate with a permanent marker.

Machining the Ring

The aluminum ring that forms the cavity wall is cut (sliced) from a length of 3 1/2-inch OD tubing with a 3/8-inch wall thickness. See Fig. 6. The tubing ID is about 2 3/4 inches. The dimensions of the ring are the most critical in this amplifier. Tolerance of the ring thickness is ± 0.005 inch to maintain full band coverage.

The ring can be hacksawed or bandsawed out of the tubing, but take extreme care to be accurate. Cutting tubing straight isn't easy. Clamp the tubing to prevent rotating on the band saw. The final finish cut is best done on a lathe or milling machine, but careful filing will work.

Once the ring is the correct thickness, deburr the sharp edges and spray it with marking dye. Notice that the outside and inside diameters are not concentric. This is normal for large tubing. Lay the ring flat and fmd the thickest wall section. Scribe a

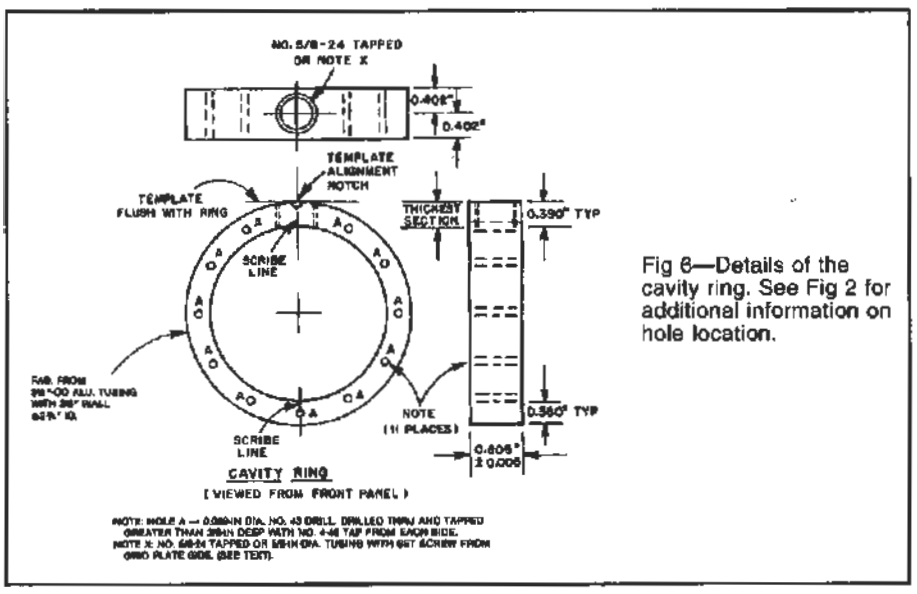

Fig 6—Details of the cavity ring. See Fig 2 for additional information on hole location.

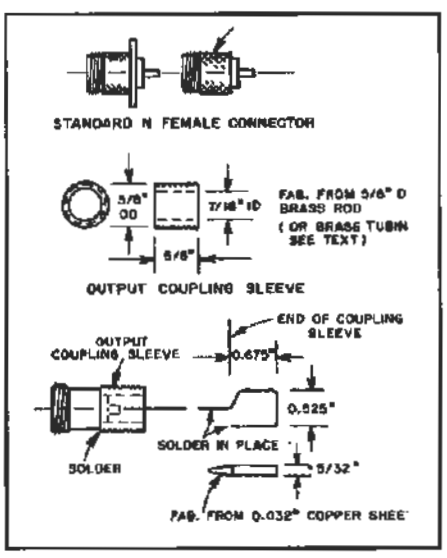

Fig 7—Output-probe/connector assembly details.

line across the wall at this point, across the center of the ring and across the wall on the other side. The scribed lines on each side of the ring will be used to align the template. The output connector will be placed at the thick wall section.

Carefully align notch 1 on the template with the line scribed on the thickest wall section on the ring. Clamp the template onto the ring. Mark each of the 11 holes labeled A on the template. After you mark the holes and remove the template, check alignment with the copper plates just in case. If everything lines up, center punch all eleven holes on one side of the ring only, and drill each hole completely through the ring. Use lots of cutting fluid. File the ring flat before and after deburring, taking care not to change the wall thickness. Tap each hole to accept no. 4-40 machine screws. Each hole will have to be tapped to a depth of at least $^3/_8$ inch from both sides because long taps don't exist. The inside of the ring doesn't need to be polished.

The hole for mounting the output connector can now be drilled. There are two ways to mount this connector, and either scheme works fine. Read ahead to the section on making the output connector for more information. The first method of mounting the connector involves tapping the ring with a no. $^5/_8$-24 tap and using a lathe to cut matching threads on the output connector coupling sleeve. Large taps are expensive, but a tap and die for Type-N connectors are handy if you do much building.

If you don't have access to a lathe or a large tap, the second method is easier. Make the output connector coupling sleeve from $^5/_8$-inch-OD brass or copper tubing, and drill the ring to just clear it. Then drill and tap the grid-plate side of the ring above the output connector to accept a setscrew. Also, drill a clearance hole in the grid plate for the setscrew. Use the setscrew to secure the output connector.

Output Connector

A standard Type-N chassis-mount female connector (silver plated) is used for the output probe/connector. See Fig. 7. First, remove the flange with a hacksaw and file flush with the connector body. Next, make the output-coupling sleeve that is right for your application (threaded orunthreaded, depending on how you fabricated the ring). The sleeve will be the same length in either case. The output-coupling loop is fashioned from a piece of 0.032-inch-thick copper sheet that is $^5/_{32}$ inches wide. Bend it to the dimensions shown in Fig. 7. We will solder the output connector together later.

Grid Compartment

The grid compartment measures 2 inches square by 1 $^1/_2$ inches high. See Fig. 8. It is made from brass and can be sawed out of square tubing or bent from sheet. The cover can be made from any material.

I use two small PC boards (Fig. 9) for

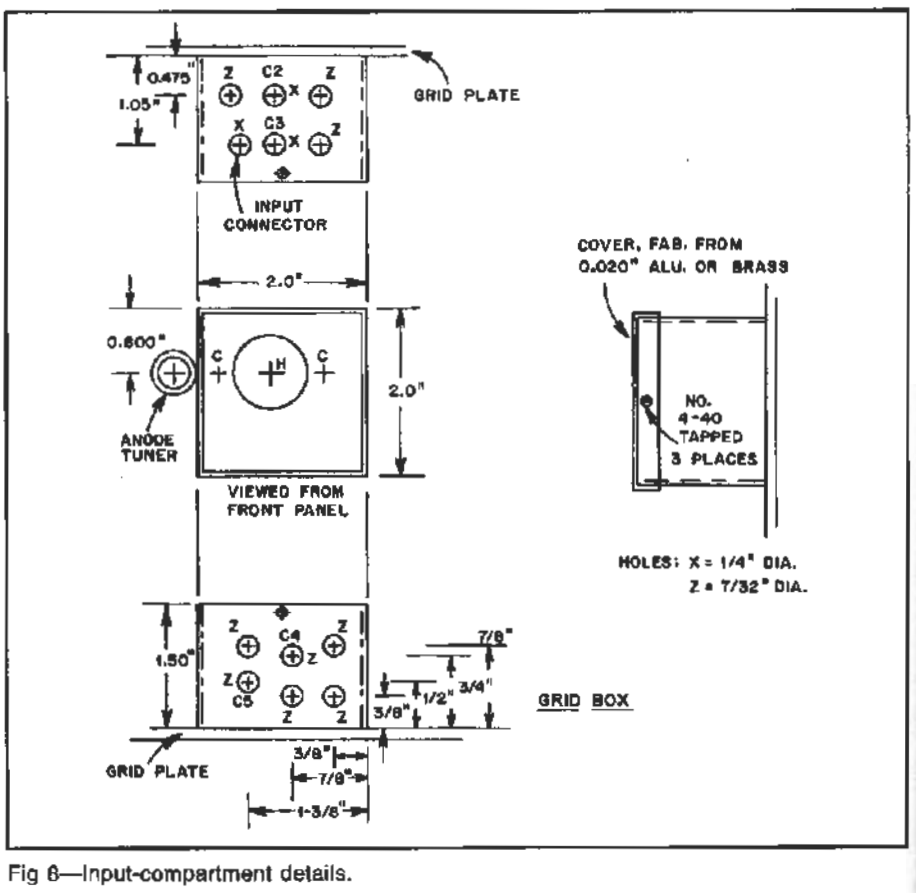

Fig 8—Input-compartment details.

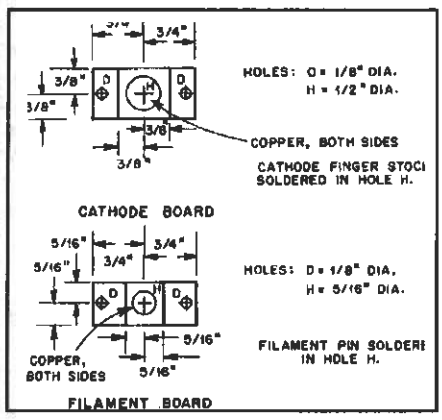

Fig 9—Cathode and filament PC-board details.

holding the fmger stock that makes contact with the filament pin and cathode ring on the 2C39 tube. These boards are cut from $^1/_{16}$-inch-thick, double-sided G-10 glass-epoxy stock. The copper pattern is identical for both sides of each piece. Mark and drill or file the holes first, and then cut the boards to size. Small boards are difficult to hold while drilling them. Mark each side of each board and score the copper foil with a sharp knife.

The unwanted copper can be removed easily by heating the foil with a soldering iron and lifting it off. Use a flat file to deburr the boards. Do not use a countersink because the copper foil must be as close to the holes as possible to facilitate soldering the finger stock in place.

The input connector that I use is a 5-mm SMA type. This is an excellent RF connector, especially for low-power UHF applications. I highly recommend use of an SMA, but any small screw-on connector will do. If you really feel you have to use a BNC then do so, but it's a lousy connector at frequencies above 200 MHz. Remember to move the connector hole to accommodate its larger size.

The input connector must be as close as possible to the first input capacitor. The lead length of the input dc blocking capacitor must be as short as possible. The 3-pF capacitor is series resonant at 1200 MHz only with short ($^1/_{16}$-inch or less) leads.

Miscellaneous Bits and Pieces

There are still several small, but very important parts to fabricate. The front panel I use is shown in Fig. 10. It is made from a piece of $^1/_8$-inch-thick aluminum sheet. Some builders may wish to mount the amplifier on a rack panel. Wash and dry your front-panel material and spray it with marking dye. Clamp it to the template and mark the holes. Check the hole alignment with the copper grid and anode plates. If all lines up correctly, center punch and drill the holes. The only front-panel control is for the anode tuning capacitor, which is adjusted by a $^1/_4$-inch shaft protruding through a $^3/_8$-inch panel bushing in hole C.

The anode tuning collar, shown in Fig. 11A, is made from a piece of $^1/_2$-inch OD brass rod. This rod has a $^3/_8$-inch hole drilled through its center, and it is turned down to $^7/_{16}$-inch OD for half its length. The inside of the $^1/_2$-inch-OD end is tapped to a depth of $^1/_4$ inch to accept $^3/_8$-24 threads. This collar will be inserted into hole C on the grid plate.

Fig. 11B also shows the anode tuning post. It is simply a length of $^5/_{32}$-inch-OD brass rod that inserts into hole C on the copper anode plate. This rod will form one plate of the anode tuning capacitor.

The anode tuner (Fig. 11C) is machined from a piece of $^3/_8$-inch-OD Teflon rod. One end of the rod is drilled out with a no. 21 drill. The outer wall of this end is threaded with a no. $^3/_8$-24 tap. This is the end that will thread into the anode tuning collar and slip over the anode tuning post. The other end is turned down to fit inside a $^1/_4$-inch shaft coupler.

Fig. 12 shows the remaining parts. The tuning shaft (A) is made from a piece of $^1/_4$-inch brass rod. A coupler (B) to connect the tuning shaft to the anode tuner may be purchased or made. This also applies to the front-panel spacers (C). The Teflon dielectric for the anode bypass capacitor (D) is made from 0.010-inch-thick Teflon sheet. Use the template to locate holes B and H. Teflon washers and inserts (F) are used to insulate the mounting hardware for the anode bypass capacitor from the chassis. The inserts are made from $^1/_4$-inch-OD Teflon rod. The washers are made from Teflon sheet. Sharpen a piece of $^3/_8$-inch aluminum tubing and chuck it up in a drill press. This tool will cut neat, round washers from the sheet.

The box that encloses the anode compartment (Fig. 13) is fabricated from a Bud AU-1083 utility cabinet. Clean the chassis and spray it with marking dye. Secure the template to the side of the enclosure that contacts the anode plate and scribe the holes labeled F. Make sure that these holes line up with the holes on the copper anode plate. If they do, center punch and drill them to size. If air cooling is used, the blower will mount to this box.

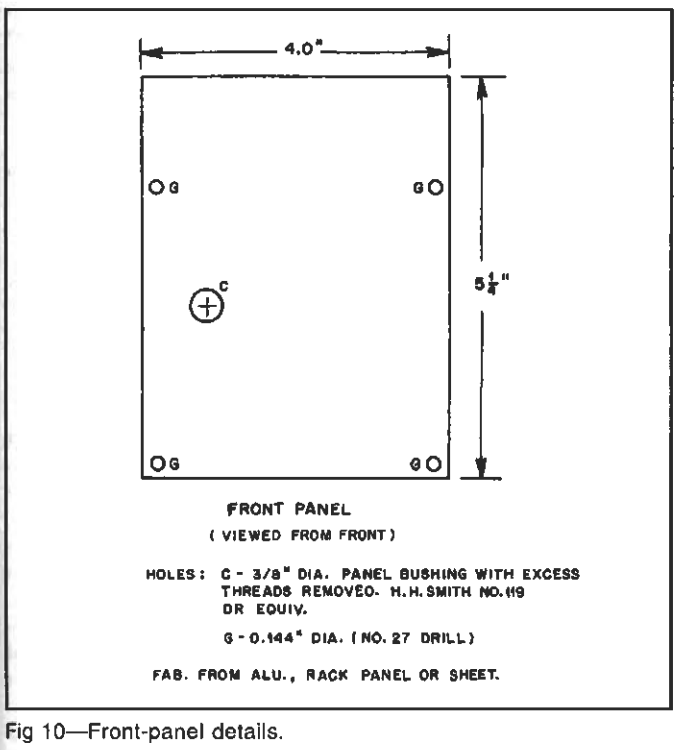

Fig 10—Front-panel details.

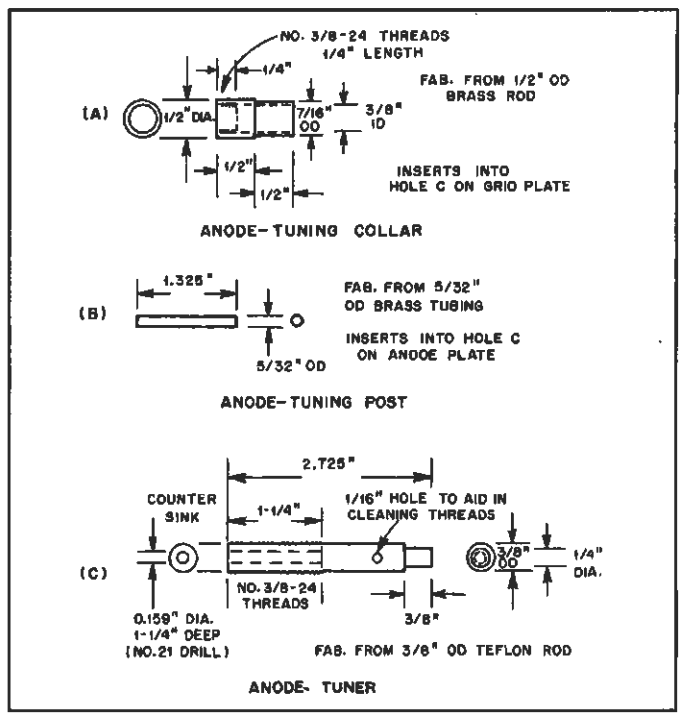

Fig 11—Anode-tuning capacitor details.

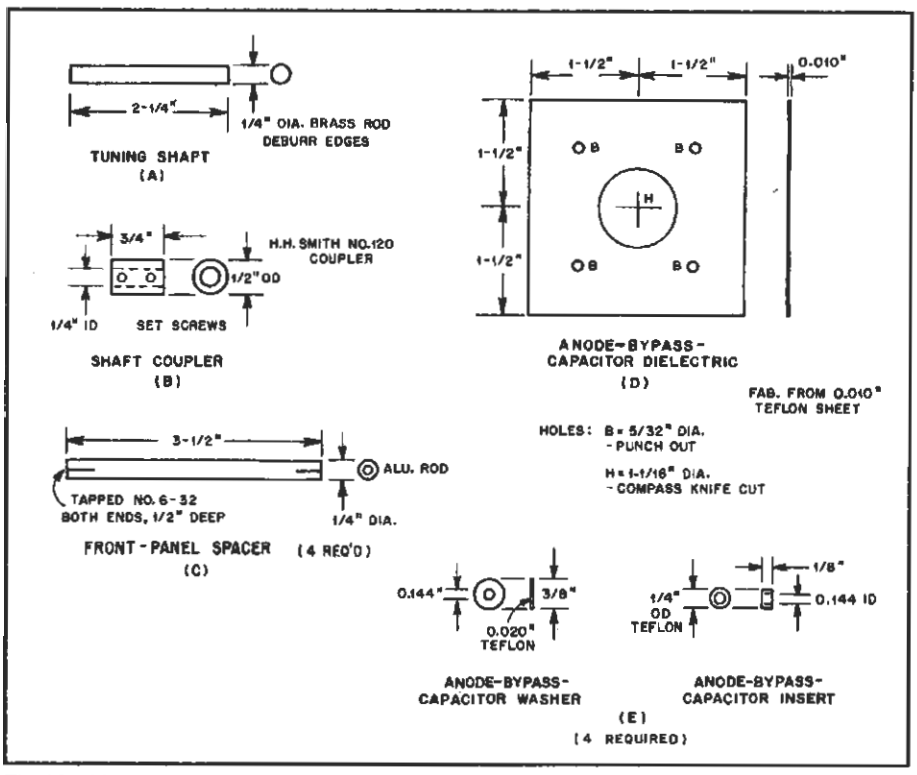

Fig 12—Miscellaneous parts necessary to complete the amplifier.

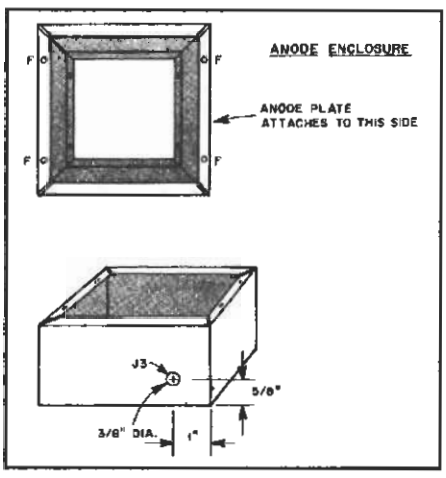

Fig 13—Anode-enclosure details.

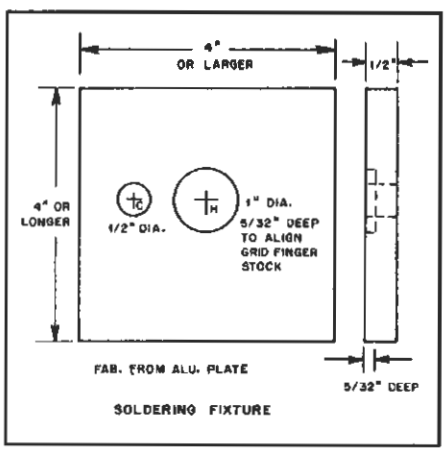

Fig 14—Dimensions of the soldering fixture. See Fig 2 for more information on hole location.

Soldering the Subassemblies

Once all copper and brass parts are drilled and deburred, they should be cleaned with alcohol and Scotch-Brite®, a nonmetaffic pot cleaner, and washed in alcohol again. Set the pieces aside and avoid touching them. Fingerprints will inhibit soldering.

I have found that the best way to solder the heavy brass and copper parts is to first build the soldering fixture shown in Fig. 14. This soldering fixture, made from $^1/_2$-inch-thick aluminum plate, will evenly heat the entire assembly to be soldered. Even heating will allow you to do a much better soldering job than you could otherwise.

The soldering fixture should be preheated on a stove or hot plate until bits of solder placed on its surface just melt. At this point, reduce the heat slightly. Avoid excessive heat. If the copper parts placed on the fixture suddenly turn dark, it's too hot.

Solder the grid plate assembly first. You will need the copper grid plate, grid finger stock, anode tuning collar and brass input compartment.[2] Look at the drawings again to be sure that you know which parts go where. Insert the grid finger stock into hole H on the grid plate. As viewed from the front-panel side, the curved fingers will protrude out the back side, away from you. Apply liquid or paste flux and set the grid plate in the soldering fixture. The finger stock will fit in hole H in the fixture, allowing the grid plate to rest flush with the surface of the fixture. Next, apply flux to the anode tuning collar and insert it in hole C of the grid plate. Part of the tuning collar will slip into hole C in the soldering fixture. Make sure the collar seats flush with the grid plate. The flux should start to bubble.

Carefully apply solder directly to the joints of the installed parts. The solder should melt almost immediately and flow bright and smooth. Next, place the square brass input compartment in place and apply flux. In a few seconds, it can be soldered by running solder around the joints, inside and outside. If you have trouble getting it to flow on both sides, merely tap the brass box aside ($^1/_{16}$ inch) and return it to its original position.

Now comes the hard part — getting the soldered assembly away from the heat without disturbing the alignment. A pair of forceps is recommended, but long pliers will do. Carefully lift the assembly off the soldering fixture and set on a cooling rack. Do this without moving any part. The cooling rack can be any two pieces of metal that will allow clearance for the protruding parts. You can expedite cooling by using an ordinary hair dryer in the "cool" position to gently blow air across the assembly.

While the grid assembly is cooling, assemble the output connector. See Fig. 7. Place the modified Type-N female connector, threaded end down, on the soldering fixture. Apply flux to the top and install the output coupling sleeve. Allow both parts to heat before applying solder. Carefully remove the soldered output connector from thefixture. When it has cooled, solder one end of the loop to the center pin of the N connector and the other to the output coupling sleeve.

Now place the anode plate on the soldering fixture and allow to heat. Apply flux to hole C. Insert the anode tuning post ($^5/_{32}$-inch-OD brass tube) and allow to heat; apply solder. Remove the parts and cool. Next, solder the finger stock in hole H on the anode bypass capacitor plate.[3]

This completes the work with the soldering fixture. Be sure to let it cool off before handling! Save the fixture for future construction; you never know when you might want it again.

The anode plate and the anode-bypass-capacitor plate must be filed and then sanded flat on their butt surfaces to assure that there are no solder bumps or sharp points to puncture the Teflon dielectric. This must be done after soldering. The Teflon sheet is adequate insulation for many times the anode potential of this amplifier, but only if the surfaces it separates are smooth!

Next, clean the cathode and filament PC boards. Install the fmger stock in hole H of the cathode board. Apply flux to both sides of the board. Heat with a hot iron and apply solder around the circumference of hole H, soldering the finger stock on both sides of the board. Use the same technique to install the filament pin.[4]

After all parts have cooled, use a spray can of flux remover to clean them. Slight scrubbing with Scotch-Brite pot cleaner will finish them nicely. Congratulations: You have finished the pieces and are now

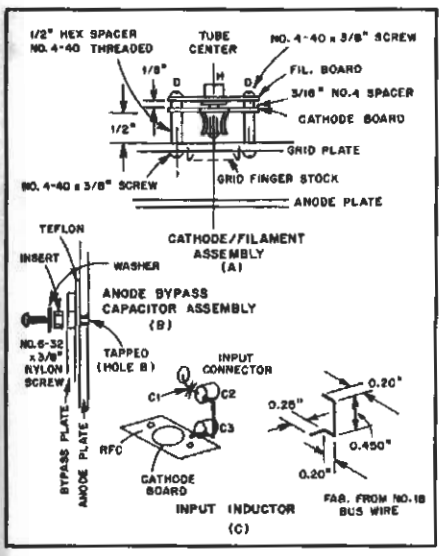

Fig 15—Assembly details for the filament and cathode boards (A), the anode-bypass capacitor (B) and the input pi network (C).

ready to bolt the amplifier together.

Silver Plating

Over the years, many people have pushed silver plating as the only way to go. You may wish to silver plate the amplifier components before soldering them together, but I do not think it's necessary. I ran several tests to prove how much various types of plating affect performance of this amplifier. Remember that the RF skin conductivity of aluminum and copper is pretty good at 23 cm; they are much better than brass.

Four amplifiers were built for this test. They were plated as follows:

1) Nickel plated
2) Tin plated
3) Silver plated
4) Unplated

There was no difference in performance among the tin-plated, silver-plated and unplated versions. The nickel-plated amplifier exhibited 3-dB less gain.

In other words, it is not necessary to silver plate this amplifier; however, it does improve appearance by making the parts a similar color. Silver does tarnish, especially with fingerprints. The decision to plate or not to plate is up to you.

Assembly

After fabrication of all parts, assembly is simple. Figs. 15 through 17 show assembly details. Loosely fasten the grid and anode plates to the ring. Mount the input connector and capacitors on the input compartment. Loosely install the cathode and ifiament boards and their respective spacers. See Fig. 15A.

Now insert a 7289/2C39 tube. This will center up all finger stock. Place the Teflon anode tuner in its collar on the grid plate and screw it most of the way in. Now tighten all of the screws. The 7289/2C39 tube should slide in and out snugly, and the anode tuner should screw in and out smoothly.

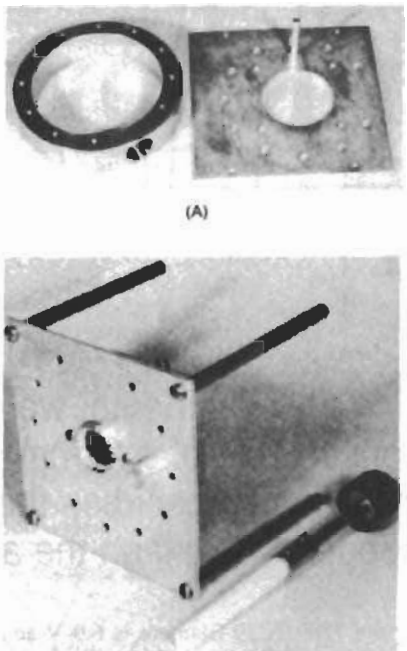

Fig. 16—The completed cavity ring and anode plate with anode tuning post soldered In place are shown at A. The photo at B shows the grid plate with finger stock, input compartment and anode tuning collar soldered in place. The completed anode tuner Is at the right. C shows the cavity ring attached to the anode plate. The anode-bypass capacitor is ready for installation. At D, the interior of the cavity as seen from the grid plate side is visible. The output probe/connector assembly is installed. The anode bypass capacitor and anode enclosure have been installed on the anode plate.

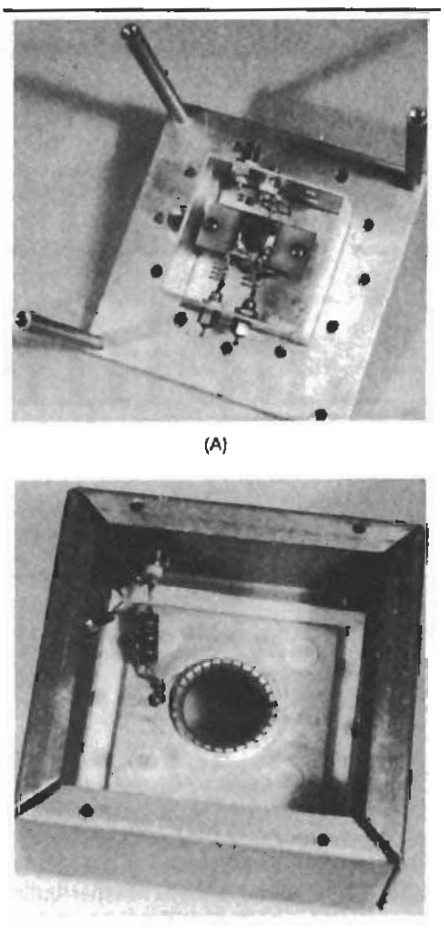

Fig 17—At A, the interior of the completed input compartment is visible. The photo at B shows the interior of the anode compartment with the anode bypass, RFC3, C8 and J3 installed.

The Teflon sheet and anode bypass capacitor plate can be installed now (Fig. 15B). Assemble the remaining input components, the filament feed-through capacitors and RFC5 (Fig. 15C). Screw the output probe into the cavity ring (or push in the probe and tighten the setscrew, depending on which method you chose). Install the high-voltage connector and other parts in the anode box. Mount the amplifier on the front panel and install the anode tuner shaft. This completes the assembly. Part 2 of this article will describe a complete power supply for the amplifier, a practical water cooling system, testing procedures, microwave radiation safety hazards, and amplifier tune-up and operation.

Notes

[1]mm = in x 25.4.

[2]The finger stock for this project is manufactured by Instrument Specialities, P.O. Box A, Delaware Water Gap, PA 18237. Contact them for the name of the closest distributor. The part numbers for this amplifier are: anode bypass capacitor plate, no. 97-70A; grid plate, no. 97-74A; cathode board, no. 97-420A; filament board, no. 97-280A.

[3]See note 2.

[4]See note 2.

By E.R. "Chip" Angle, N6CA

From *QST*, April 1985

A Quarter-Kilowatt 23-cm Amplifier

Part 2—Last month, we described the design and construction of a 23-cm cavity amplifier. This installment describes the rest of the components needed to put it on the air.

After you complete Construction of the cavity amplifier described in March *QST*, you are ready to assemble the rest of the components needed to put it on the air. This month, I will discuss the filament, bias and high-voltage supplies; a whisper-quiet, high-efficiency water-cooling system; testing and hookup; and, finally, tune-up and operation.

Power Supplies

The filament and bias supplies for the cavity amplifier are shown schematically in Fig. 1. The manufacturer's specification for the 7289/2C39 filament is 6.0-V ac at 1 A. I have found that the use of a standard 6.3-V ac, 1-A transformer only slightly increases the tube emission without much loss of tube life. The filament should be allowed to warm up before operating the amplifier, so the filament, bias and high-voltage supplies incorporate separate primary switches.

Biasing

Many biasing schemes have been published for grounded-grid amplifiers. Fig. 1 shows a bias network that satisfies all of the following operating requirements:

1) external bias supply referenced to ground

2) low-power components

3) variable bias to accommodate tube-to-tube variations

4) TR switchable with relay contact or transistor to ground

5) bias-supply protection in case of a defective or shorted tube.

U2 provides a variable bias-voltage source, adjustable by R1. The output of U2 drives the base of Q1, which is used to increase the current-handling capability of

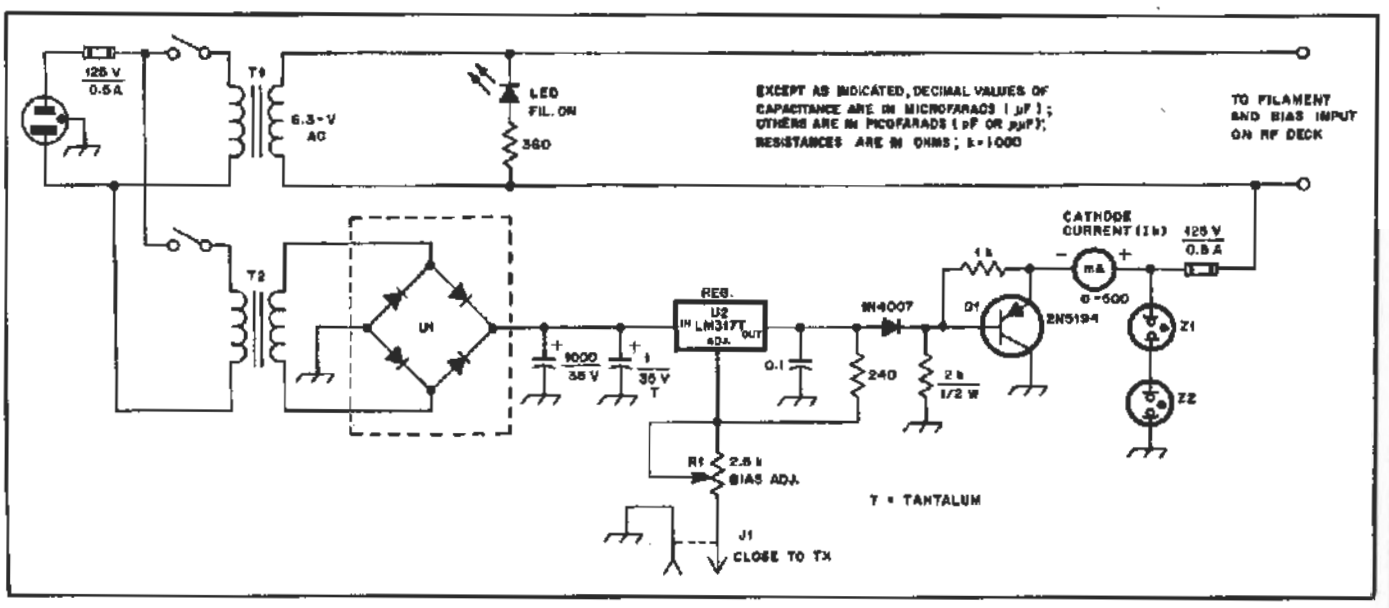

Fig 1—Schematic diagram of the cavity-amplifier filament and bias supplies. All resistors are ¼-W carbon types unless otherwise noted.

J1—Female chassis-mount photo connector.
T1—Filament transformer. primary, 117 V; secondary, 6.3 V at 1 A.
T2—Power transformer. Primary, 117 V; secondary, 24 to 28 V at 50 mA or greater.
U1—Bridge rectifier, 50 PIV, 1 A.
U2—Adjustable 3-terminal regulator (LM317T or equiv.).
Z1, Z2—20-V unipolar metal-oxide varistor (General Semiconductor SA20 or equiv.) or two 20-V, 1-W Zener diodes.

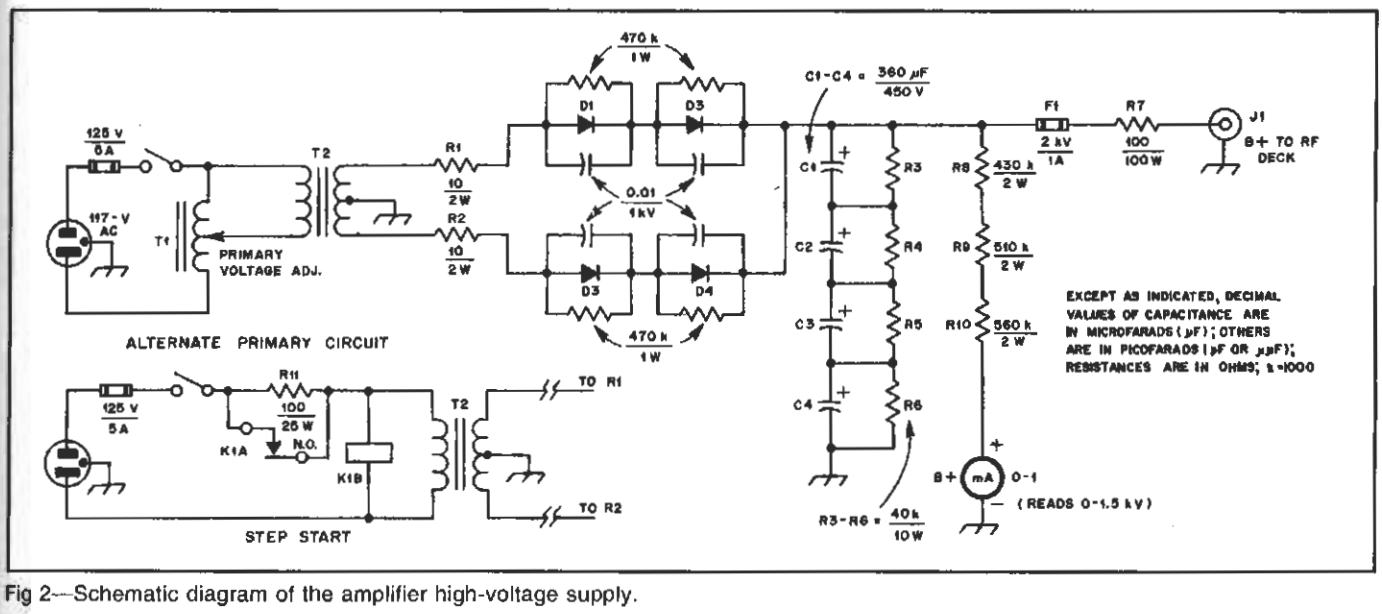

Fig 2—Schematic diagram of the amplifier high-voltage supply.

C1-C4—Electrolytic capacitor, 360 µF, 450 V.
D1-D4—Silicon rectifier, 1000 PIV, 3 A.
F1—High-voltage fuse, 2 kV, 1 A.
J1—Chassis-mount female BNC or MHV connector.
R3-R6—Wirewound resistor, 40 kΩ, 11 W.
T1—Variable autotransformer, 500 VA.
T2—High-voltage transformer. Primary, 117 V; secondary, 900 to 1050 V at 500 mA.

the bias supply. Q1 must be mounted on a heat sink. J1 is connected to the station TR switching system so that R1 is grounded on transmit and disconnected on receive. The approximate range of the bias supply is 6 to 20 V. Z1 and Z2 provide protection for Q1 in case of a shorted tube. The amplifier can be run without Z1 and Z2 if you keep the anode voltage below 1100 V.

High-Voltage Power Supply

A safe, reliable high-voltage power supply is described here. Of course, you can use any readily available HV supply; keep in mind, however, that the 7289/2C39 anode potential should never exceed 1400-V dc at full load and that the amplifier will withstand 1900-V dc at low cathode current and cutoff-bias conditions. For maximum power output, assuming adequate drive power is available, anode voltage under full load should be about 1200- to 1400-V dc.

Fig. 2 is a schematic diagram of the high-voltage supply. A power transformer (T2) that delivers 900- to 1050-V ac is ideal. The type of rectifier circuit used will depend on the type of transformer chosen. Each leg of the rectifier is made from two 1000-PIV, 3-A silicon diodes connected in series. Each diode is shunted with a 0.01-µF capacitor to suppress transient voltage spikes, and a 470-kΩ equalizing resistor.

Filtering is accomplished with a string of four 360-µF, 450-V electrolytic capacitors connected in series. R3-R6 equalize the voltage across each capacitor in the string and serve as bleeder resistors. Of course, a single oil-filled capacitor may be used here if available. Whatever type of filter you use, the total capacitance should be about 80 µF at a voltage rating of at least 1500-V dc. This value allows adequate "droop" of the anode voltage under high-current loads to protect the amplifier in case of RF overdrive or a defective tube.

Protective Circuitry

Some type of start-up protection should be incorporated in the primary. Fully discharged filter capacitors look like a dead short at supply turn-on. Initial surge current (until the capacitors charge) may be high enough to destroy the rectifiers. R1 and R2 provide some surge-current limiting, but either of the two primary configurations shown in Fig. 2 should be used. T1, a variable autotransformer (Variac and Powerstat are two common trade names), is ideal. In addition to allowing you to bring the primary up slowly (and charging the capacitors gradually), it also allows full control of amplifier output power by varying anode voltage.

The second method, a "step-start" system, uses a resistor in the T2 primary to limit the turn-on surge current. When the capacitors have charged, K1 is energized, shorting out R11 and applying full voltage to the T2 primary.

F1 and R7 protect against high-voltage arc-overs or short circuits. If sustained overcurrent is drawn, F1 will open and remove B+ from the RF deck. Use a high-voltage fuse here; standard fuses may arc when blown and not interrupt the B+ .R7 provides current limiting to protect the amplifier and power supply in case of a high-voltage arc.

Safety

An HV meter should always be used to monitor the status of the power supply. The values for R8-R10 shown in Fig. 2 will give a 1500-V dc full-scale reading on a 0-1 mA meter. RG-58 or -59 coaxial cable should be used for the high-voltage interconnection between the power supply and the RF deck. Ground the shield at both ends for safety and a good dc return.

Safety must be observed when working with all power supplies. These voltages are lethal! Always disconnect ac power and then discharge the filter capacitors before working on the power supply. Never guess or make assumptions about the status of a power supply. Assume it is hot.

Metering

Cathode-current monitoring is all that's really necessary for observing amplifier dc performance. Cathode current (I_K) is the sum of the plate (I_P) and grid (I_G) currents. Normally, when this amplifier is driven to 300- or 400-mA I_K, the grid current will be around 40 to 50 mA. The inclusion of a grid-current meter is not really necessary and only makes biasing and TR switching complicated.

Cooling

Desired output power and the level of drive power available will dictate what type of cooling to use. For intermittent duty (SSB, CW) at output levels less than 50 W, air cooling is satisfactory. Any small blower may be easily mounted to the aluminum box surrounding the tube anode. For high-duty-cycle modes and/or output levels greater than 50 W, water cooling is highly recommended. Greater than twice the normal air-cooled output power can be obtained from a water-cooled tube, and water cooling is quiet.

Tube Modification and Water Jacket

The first step is to remove the air radiator from the tube. The air radiator screws on, so it may simply be unscrewed without damage to the tube.

First, place a hose clamp around the tube anode. Secure the radiator fms in a vise and grip the hose clamp with a pair of large

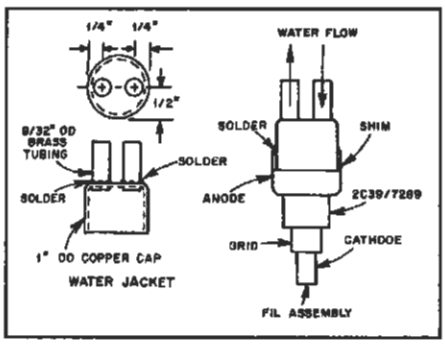

Fig 3—Details of the solder-on water jacket.

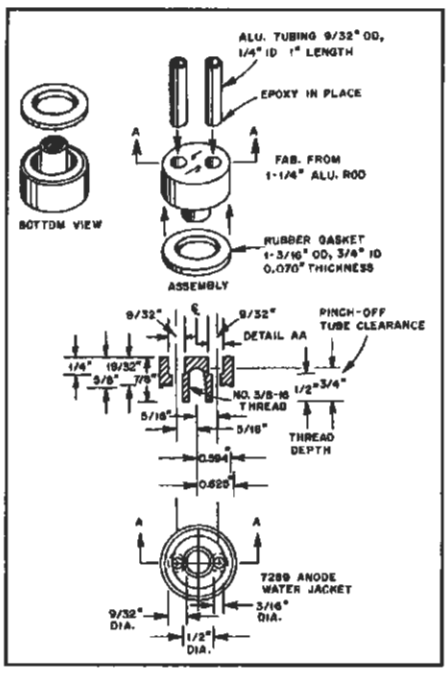

Fig 4—Details of the screw-on water jacket.

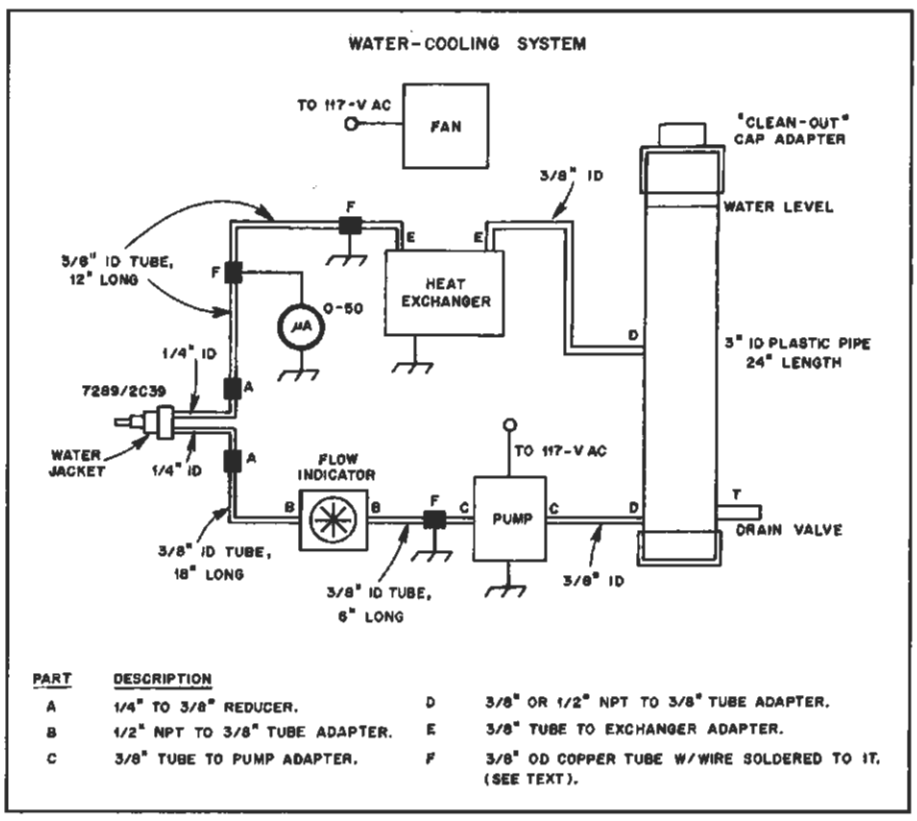

Fig 5—Details of the water-cooling system. Recommended pumps are: (1) Little Giant Pump Co. Model 1-42A or larger, available from most hardware stores; or (2) Calvert Engineering, Cal Pump Model 875S (160 gal/h), available from Calvert, 7051 Hayvenhurst Ave, Van Nuys, CA 91406, tel. 213-781-6029. The flow indicator (Model 15C; requires two 1/2-inch NPT adapters) is available from Proteus Industries, 240 Polaris Ave, Mountain View, CA 94043 tel. 415-964-4163.

pliers. Gently unscrew the tube from the radiator. If the hose clamp slips slightly, tighten it.

Some 7289/2C39 tubes use an air radiator that is attached with setscrews. To remove the radiator, simply remove the setscrews and pull the radiator off.

The air radiator will be replaced with a water jacket that allows water to be circulated past the tube anode and through a radiator, where it is cooled and circulated past the tube anode again. I have successfully used two different types of water jackets; both are described here.

The water jacket shown in Fig. 3 will work with any type of 7289/2C39. It is fabricated from a 1-inch-OD copper tubing cap and two short pieces of 9/32-inch-OD brass tubing. The copper tubing cap should be available from a local hardware store or plumbing supply house. Brass tubing is available from many hobby stores and metal supply houses.

Mark and drill the copper cap so that the brass tubing is a snug fit. Thoroughly clean the parts until they shine. Push the tubing into the holes in the end cap and degrease the assembly with alcohol. Using plenty of flux, solder the seam around each section of tubing. Allow the jacket assembly to cool.

Meanwhile, thoroughly clean the 7289/2C39 anode to a bright finish. Check the water jacket for fit. In some cases, you'll have to use a 0.005- to 0.010-inch-thick copper shim to fill the gap between the copper cap and the tube anode. This shim helps eliminate pin holes in the solder.

Using plenty of flux, solder the water jacket to the tube anode. Solder it quickly with a hot, high-wattage iron. Allow the tube to cool in the air after soldering to avoid thermal shock and possible breakage. After the tube has cooled, use plenty of alcohol to remove all traces of flux from the tube and water jacket.

The second type of water jacket is shown in Fig. 4. This jacket will work only with 7289/2C39 tubes that have a screw-on air radiator. It is designed to thread onto the tube anode just like the air radiator did. This jacket is machined from a piece of 1 1/4-inch aluminum rod. The water inlet and outlet tubes are made from 9/32-inch-OD, 1/4-inch-ID aluminum tubing that is epoxied in place. A rubber gasket seals the jacket against leaks.

If you have access to a lathe, you should have no trouble duplicating the jacket. You could have one made up at a local machine shop. Complete screw-on water jackets are also available from the author.

After you unscrew the air radiator from the 7289/2C39, check for and remove any burrs from the tube anode. The anode surface must be flat if the rubber gasket is to be effective. Screw the water jacket onto the tube. Tighten by hand only. Do not use any tools, or you could damage the tube or jacket! Do not use the water inlet and outlet tubes for leverage—they have thin walls and break easily.

Water System

Fig. 5 depicts the complete water-cooling system. Recommended pumps and accessories that have proven reliable and effective are listed in the caption.

Any small pump, such as a fountain pump, that can deliver 160 to 200 gallons per hour can be used here. Most inexpensive pumps are not self-priming, which means that they won't pump water if they have air in the rotor. Although water can be forced through the pump for the initial prime, my system uses gravity priming. The water reservoir is a 2-foot length of 3-inch-OD plastic pipe that is available from hardware or plumbing stores. The outlet is at the bottom, and the inlet about halfway up the column. The inlet is located here to eliminate aeration that ionizes the water and reduces its effectiveness. The outlet

Microwave Radiation Safety

Intense RF radiation concentrated on body tissues can produce heat damage; the extent and penetration will depend on the radio frequency in use and on exposure duration. You should be aware of the approximate intensity of RF radiation of the transmitting equipment and antennas you come in contact with.

RF intensity is commonly expressed in milliwatts per square centimeter (mW/cm^2), which is the power flowing away from a source through a unit sampling or interception area at some specified distance. Although the United States as yet has no federal RF protection standard, a useful interim guide is the 1982 standard of the American National Standards Institute (ANSI '82). The most stringent level in this standard is 1 mW/cm^2 for frequencies between 30 and 300 MHz. Above 300 MHz, the protection level rises until it reaches 5 mW/cm^2 at 1500 MHz. Beyond 1500 MHz, the recommended level remains at 5 mW/cm^2. These levels represent the average power density allowed over any six-minute period and are for the sum of all polarizations from a given source.

At 1296 MHz, where one wavelength (λ) equals 23 cm, a thick resonant dipole feeding a calibrated power meter with matched coaxial cable (itself free of pickup) may be used to obtain an indication of power density. A reasonably lossless resonant dipole has an effective aperture of $\lambda^2/8$; at 23 cm this is 66 cm^2. The power meter reading in milliwatts, divided by 66, is the indicated power density. For this to be a reliable indication, the dipole must be positioned far enough from the RF source to be in its far field. For a small source, the distance should be at least $\lambda/2$, and here that would be about 12 cm (45 inches). The dipole should be oriented for alignment with the dominant polarization. Note that the power meter must be capable of readings well below 1 mW.

This arrangement would be useful for checking leaks along the coaxial route that the high power (here 250 W) takes to a load, be it dummy load or antenna. Cable connectors may not be tightly secured, or they may be faulty. For equipment operating in the SHF region, waveguide flanges may not be clamped properly.

Direct measurement of electric field strength near an antenna (with a calibrated instrument, preferably one with the indicating meter shielded and possibly positioned at the center of the sampling dipole) is another way to check for adequate protection. A field strength of 60 V per meter (V/m) corresponds to 1 mW/cm^2; 134 V/m corresponds to 5 mW/cm^2. At a distance 60 cm (2 feet) from an isolated dipole fed with 26 watts, the field strength would be about 60 V/m. This is a far-field field strength for all frequencies where the half wavelength is less than 60 cm, or for frequencies above 250 MHz. For full 250 watts applied to the dipole, the 60 V/m level occurs at a distance of 1.8 meters (6 feet), and at this distance this holds for all frequencies above 80 MHz.

With SSB or CW keying, the fields during Amateur Radio operation are highly intermittent, and usually include considerable pauses or intervals for listening. These factors reduce the average power density over the six-minute averaging period.

Further information on RF safety and protection estimates can be found in Chapter 7 of *The Satellite Experimenter's Handbook*, published by the ARRL. The following rules of good practice for RF protection are recommended:

- Never operate an RF amplifier with equipment shielding removed.
- Never handle antennas with RF power applied.
- Never guess that RF levels are safe. Take the time to consult a reliable reference for an estimate, or measure levels carefully. Allow a "cushion" of about 6 dB (factor of four in power density). If possible, borrow an RF radiation monitor (after learning how to use it), or consult with a ham who is well informed on RF protection.
- Never look into an open end of a power waveguide; never point a powered directive antenna (a beam or a paraboloid, for example) toward people. Keep all VHF and UHF transmitting antennas as high as possible, distant from humans.
- Use good-quality, well-constructed coaxial cable and connectors to avoid RF leaks.
- Think RF and electrical safety first; test later!
- Watch *QST* for news on RF measurement techniques and progression, protection standards and proposed federal and state RE regulations.—*David Davidson, W1GKM*

directly feeds the pump. The pump and the reservoir outlet port should be mounted in the same plane. The pump should be oriented so that air bubbles will rise into the impeller output port and can be blown out once the pump starts running.

Flow Indicator and Heat Exchanger

Water cooling is best described as "super quiet." There is no noisy fan to reassure you that the tube is receiving adequate cooling. If water flow is reduced or cut off during amplifier operation, tube damage is virtually assured.

Flow interlocks and switches to shut down the amplifier if water flow is reduced are hard to find and expensive. Flow indicators, however, are inexpensive and reliable. A flow indicator has a spoked rotor that turns as water passes through the unit. If the wheel is turning, there is water flow; if not, you have a problem. Changes in flow rate can be observed by watching for speed changes in the rotor. A small lamp illuminates the flow indicator, making it easy to see rotation. The flow indicator should be mounted where it can be seen from the operating position and monitored during operation.

Heat exchangers, or radiators, remove the heat from water as it passes through. For this application, a small automobile transmission-oil cooler works great. Most auto- parts stores and speed shops have a good selection. Pick one that is similar in size and aspect ratio to a whisper fan (approximately 4 × 4 × 1 inches). Some come with mounting brackets. Look for a cooler with the input and output ports on the top so air bubbles will rise to the top and move on without becoming trapped. Trapped air degrades cooler performance.

If you use the amplifier for high-duty-cycle modes such as ATV or FM, or for long, slow-speed CW transmissions (EME, for example), you should use a small axial whisper fan to increase the effectiveness of the heat exchanger. A fan isn't necessary during normal operation, or even for sustained operation at moderate power levels, but I highly recommend one if you plan prolonged operation at maximum power. Locate the fan so the warm exhaust air won't heat up other equipment.

Hoses and Fittings

Most hardware stores carry a complete line of brass fittings and adapters that can be used for this project. Brass, however, will eventually corrode and pollute the water supply. Plastic fittings are cheaper and don't corrode, but they are harder to find. Recreational vehicle suppliers are my main source for these parts. They are used extensively in drinking water systems for mobile homes and travel trailers. Procure the fittings when you have the rest of the parts in hand, as there are many variables to consider.

You can use any relatively soft, thin-wall vinyl tubing for all water lines. The main runs are made from $^3/_8$-inch-ID hose, while $^1/_4$-inch-ID stock is used to connect to the 7289/2C39 water jacket. The $^1/_4$-inch-ID tubing fits snugly over the $^9/_{32}$-inch-OD inlet and outlet tubes on the water jacket, so no clamps are required. All other hose connections should be secured with stainless-steel clamps to prevent leaks. Any leaks mean air in the system and deterioration of cooling performance.

Safety

The tube anode, and hence the water jacket and water, are in direct contact with the high-voltage supply, so some safety precautions must be observed. Approximately 12 to 18 inches of tubing should run between the 7289/2C39 jacket and any other component in the cooling system. This will allow enough resistance in the water to provide adequate current limiting, should the water contact any components that are grounded.

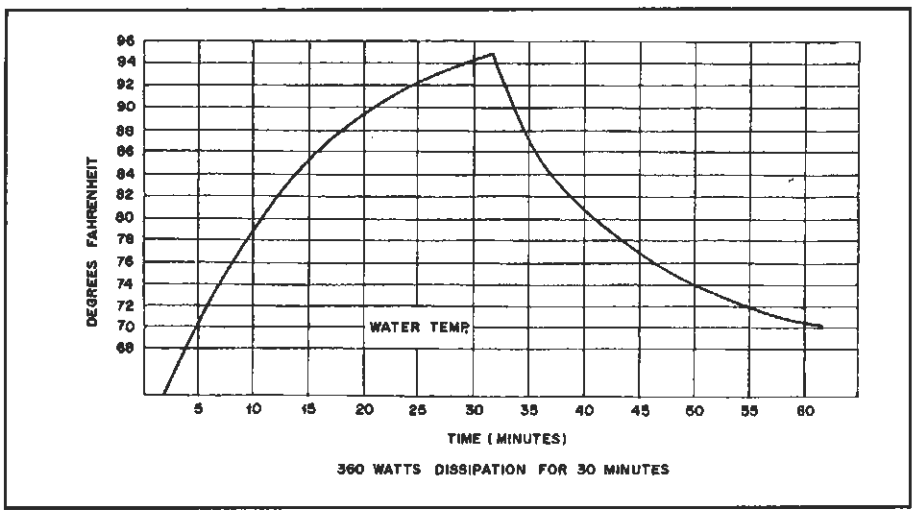

Fig 6—Performance graph of the water-cooling system.

It is best to ground the water supply at the pump. Do this by replacing a short section of the tubing that runs to the flow indicator with a piece of brass or copper tubing. Solder a wire to this metal tubing and connect the other end of the wire to your station ground. Use at least 24 inches of vinyl tubing between the anode cooling jacket and the ground point.

On the warm-water side of the 7289/2C39, run 12 inches of vinyl tubing to a small metal fitting or short section of metal tubing, and then another 12 inches of vinyl tubing to a grounded point (this can be at the heat exchanger). You can measure the water leakage current to ground by placing a microammeter between the metal fitting that connects the two vinyl hoses and ground. Leakage current should be less than 10 μA with clean water and an anode potential of 1 kV. As the water ages, the leakage current will rise; when this happens, replace the water.

Grocery stores carry distilled water for use in steam irons. It may be deionized and not truly distilled, but it works fine for about four to six months in this application. Filters can be purchased from scientific supply houses, but they're not really worth buying because deionized water is so cheap.

Do not use tap water under any circumstances! When you turn on the water system for the first time, run a gallon of water through it for half an hour to wash out fabrication impurities. Replace with clean water before using the system to cool the amplifier.

Water was chosen because it's inexpensive, nontoxic, nonflammable and easy to clean up if you have a leak. Better liquid coolants are available, but they are toxic. Don't use them!

Cooling Performance

I have used water-cooling systems for several years with no problems whatsoever. Fig. 6 is a graph of several transmit/receive cycles on a water-cooled, 500-W output, 23-cm power amplifier. For this test, I used two of the amplifiers described in this artide coupled with a pair of hybrid combiners. This particular cooling system used 1 gallon of water. Experiments indicate that, during extended operation, the water temperature rises only 30° to 35°F above ambient room temperature. Typically, the tube anode and water average 10° to 15°F above ambient during casual operating.

Flow rates in this system are typically $^1/_3$ gallon per minute per tube, which is more than adequate. At this rate, more than 300 W of dissipation from a single inefficient 7289/2C39 were required to boil the water in the water jacket. The water should not be allowed to boil because this will heat the rubber gasket.

Tubes

It is not really necessary to buy a new 7289/2C39. Used tubes can be found surplus for around $1 to $5 and, in many cases, will perform as well as a new tube. Most used tubes have been sitting around for several years, so it's a good idea to run them through the dishwasher to clean them up and then run the filaments for about 24 hours. This will restore operation in many cases.

If you buy a new tube, you should be aware that the 7289/2C39 is being run far in excess of its ratings in this amplifier. The manufacturer's warranty will not cover tubes run in this application.

Contrary to popular opinion, glass tubes will work. Physically, they are not as rugged as the ceramic version, but the glass-to-metal seal seems to provide better shelf life than the ceramic seal. The glass tubes make great driver tubes and will work fine for power levels up to 100-W output. Pulse tubes (7815, 7211) are not recommended because of their poor thermal stability at high power levels. Also, they generally are 30 to 40 MHz lower in resonant frequency in this amplifier compared to the 7289/2C39. Some 7289 tubes can be as much as 30 MHz lower in frequency. Minor length adjustment of the anode-tuning post may be required to accommodate amplifier and tube differences.

Tube Insertion

Extreme care must be exercised when inserting the 7289/2C39 tube. Never force the tube in place, as damage (bending) of the cathode finger stock may result. Observe the layout of the finger stock to get an idea of how the tube inserts. Carefully position the tube so it is straight as you gently push. It should slide in snugly without any solid resistance.

Testing

After you have completed all of the parts for the amplifier, it's time to test everything before hooking it all together. Test the water-cooling system by turning it on and watching for steady water flow as indicated on the flow meter. The tube and water jacket can be removed from the cavity amplifier for this test.

Check all of the power-supply voltages first without connecting them to the RF deck. Then, without the tube in place, hook the bias and filament supplies to the cavity and check the voltages again at the tube fmger-stock connections. Connect the high-voltage supply to the RF deck and bring the voltage up slowly with a variable autotransformer. Monitor the high voltage on the anode-bypass-capacitor plate, and look and listen for any possible arcing between the anode-bypass-capacitor plate and ground. Use extreme care when measuring and testing the high-voltage supply. If everything looks okay with the power supplies, shut them off and disconnect them.

You can make a safe, low-power test of the cavity resonance without applying any voltage. With the tube in place, insert a 2-inch-long coupling loop on the end of a piece of coaxial cable between the spring fingers of the anode down into the cavity. Connect the amplifier output probe/connector to a device capable of detecting low-level RF at 23 cm (for example, a spectrum analyzer or microwattmeter). Feed a signal from an L-band signal generator into cable attached to the wire coupling loop that you inserted into the cavity. Set the signal generator for various frequencies in the 23-cm band and tune the amplifier anode tuner. There will be sharp peak in output at cavity resonance.

This testing method can be used to determine cavity tuning range, anode-bypasscapacitor effectiveness and resonance of various tube types for use in this amplifier. Any cavity amplifier can be tested completely without ever applying high voltage. The better your test equipment, the easier the amplifier is to test. If all dimensions were followed strictly, the amplifier will tune as designed.

Amplifier Hookup

Installation and operation of this amplifier is relatively straightforward, but

as with any amplifier, several precautions must be followed. If these are adhered to, the amplifier will provide years of reliable service.

The amplifier is designed to be operated in a 50-ohm system and should never be turned on without a good 50-ohm load connected to the output connector. Never operate it into an antenna that has not been tuned to 50 ohms!

Drive power to the amplifier should *never* exceed 15 W. *Never* apply drive power in excess of 1 W unless all operating voltages are present and the tube is biased on. Otherwise, the tube grid-dissipation rating will be exceeded and you will probably ruin it.

As in all TR-switched systems, some type of interlock or sequencing of transmit and receive functions should be incorporated. In most systems, the sequence for going into transmit is something like this: First, switch the antenna changeover relay from the receiver to the power amplifier. Next, bias the power amplifier on. Last, key the exciter and apply drive to the amplifier. To go to receive, unkey the exciter, remove operating bias from the amplifier and switch the antenna relay back to the receiver.

If the antenna relays are switched while the power amplifier is operating and putting out power, damage to the relay contacts and/or the amplifier is likely. If there is a momentary removal of the antenna while the power amplifier is biased on, oscillation may occur. This can damage the TR relay, the tube or even the receive preamplifier.

Tune-up and Operation

This is it — the big moment when you will see your project come to life! Connect an accurate UHF power meter and a 50-ohm antenna or load to the amplifier output connector. A Bird Model 43 wattmeter with a 100- or 250-W, 400-1000 MHz slug will give reasonable accuracy, depending on the purity of the drive signal. Apply filament power and tube cooling, and allow 3 to 5 minutes for the filaments to warm up. Turn on bias supply (the amplifier will draw maximum current if the anode voltage is applied without bias). Apply 300 to 400 V to the anode. There should be no current flowing in the tube as indicated on the cathode-current meter. Ground J1 on the bias supply to apply transmit bias and observe cathode current. As R1, the bias control, is turned clockwise, quiescent idling current should increase. Set for about 25 mA.

Apply 1 W of RF drive power. Turn the anode tuner while observing the RF output power meter and tune for maximum output. The output should go through a pronounced peak at cavity resonance. Adjust C2 and C3 on the input tuning network for maximum amplifier output. If possible, use a directional wattmeter between the driver and the amplifier input to check that best input SWR and maximum amplifier output occur at roughly the same setting.

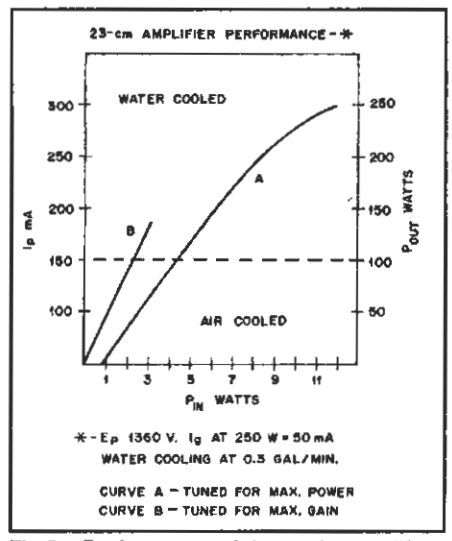

Fig 7—Performance of the cavity amplifier under different drive and plate-current conditions.

Depending on the amount of drive power available, you may want to tune the amplifier for maximum power output or maximum gain. Fig. 7 shows what you can expect from different drive levels.

Once the amplifier is tuned for best input SWR and maximum output with 1 W of drive, anode voltage and drive power can be increased. Increase both in steps; be sure to keep the anode tuner peaked for maximum output power. When you get to the 100-W output level, very carefully readjust the input circuit for maximum output. The input capacitor closest to the cathode is critical and should need to be rotated less than 90 degrees maximum. Maximum output power will be roughly coincident with best input SWR.

Increase the drive power and keep the anode tuner peaked for maximum output. Increase the drive until you reach the desired output level, but *do not exceed 400-mA I_K!* At 1400-V dc and 350-mA I_K, output power with a good tube should be about 230 to 250 W. At lower anode voltages, I_K will be higher for the same output power. Higher anode voltages result in higher gain, lower drive levels, lower grid current and lower plate current for a given output power.

The anode tuner's tuning rate is approximately 5 MHz per turn. Clockwise rotation of the tuner lowers the resonant frequency of the cavity. This control will require readjustment as you make large frequency excursions within the 23-cm band (for example, if you go from 1296 weak-signal work to the 1269-MHz satellite segment). You should also check the input SWR if you move more than 15 MHz. Generally, amplifier tuning does not change much after initial setup. You should be able to turn it on and use it without retuning as it heats up. Slight adjustments may be necessary, however, depending on cooling, inherent thermal differences from tube to tube and duty cycle of the operating mode. Always keep the anode tuner peaked for maximum output, and check it from time to time, especially while you are first learning how the amplifier operates.

The output loading control is the output connector and probe assembly. Loading is changed by minor rotational adjustment of the N connector. First loosen the jam-nut (or setscrew) slightly. While observing output power and keeping the anode tuner peaked, rotate the loading control ±30 degrees maximum for greatest output power. This should be done only once and should not need repeating unless another tube is installed. Even then it may not be required.

Conclusion

This cavity amplifier for the 23-cm band is capable of safe, reliable operation at output powers in excess of 200 W. More than 50 of these amplifiers are in operation, and you can build one, too. I would like to thank Mike Stahl, K6MYC, Bill Troetschel, K6UQH, William Jungwirth, AA6S, Lem Moeschler, W6KGS and Joseph Cadwallader, K6ZMW, for their help and encouragement during the development of this project.

References

Laakmann, "Cavity Amplifier for 1296 MHz," QST, Jan. 1968, pp. 17-22.
Laakmann, "Kilowatt Amplifier for 1296 MHz," *Ham Radio*, Aug. 1968, pp. 8-17.
"Power Amplifier for 23 cm," *VHF Communications*, April 1976, p. 222.
"Power Amplifier for 24 cm," *VHF Communications*, March 1978, p. 175.
Stefanskie, "1270 MHz ATV Power Amplifier," *Ham Radio*, June 1977, pp. 67-73.
Tech Report #6, Crawford Hill VHF Club, July 1971.
Tech Report #13, Crawford Hill VHF Club, Dec. 1972.

By Zack Lau, KH6CP/1 From *QEX*, May 1994

A 2-W, 13-cm Amplifier

This amplifier uses a resistively stabilized Hewlett Packard ATF-44101/AT-8 140 power GaAs FET running class A to provide 14 dB of gain and a 2-W output. It wasn't too difficult to choose the device—there aren't that many linear devices that cover the 2.3 GHz band at this power level. Unfortunately, it is fairly pricey; the circa 1990 price was around $90. But since this transistor has been around a long time, it may be available surplus. Several hundred were sold at the bargain price of $3 each about a year and a half ago. I bought a few—I should have bought more.

Even if you do buy your FETs at bargain prices, you still will want to ensure that they are biased safely. As has been pointed out many times in the literature, having the negative gate bias supply fail while the drain supply is applied may result in the destruction of the device. Thus, designers have devised elaborate protection schemes to shut off the drain supply if the gate supply fails.

Fig 1 shows a simpler power-supply circuit. The drain supply is controlled by an ordinary 723 voltage regulator with current limiting. The current limiting protects the device—instead of the expensive FET getting hot and seif-destructing, the cheap TIP 30 power transistor gets warm. Doing this eliminates the need for complex shutdown circuits to handle a failed bias supply. While there are more modern regulator chips than the 723, they aren't significantly better for this application. In fact, some are "improved" to the point where they are tougher to use. For example, chips with better current-sensing circuits often require special low-value resistors. While you could use the copper wire table in the *ARRL Handbook* to make your own low-value resistors from wire, it makes more sense to me to use a 723 with standard, readily available parts.

The gate bias supply is produced by an NE555 timer running as an oscillator and driving a voltage inverter. An LM337 adjustable 3-terminal voltage regulator controls the gate supply. Now, you have to be a little careful using adjustable voltage regulatorswith bias supplies. While I haven't experienced this myself, it is entirely possible that a noisy potentiometer could momentarily present an open circuit between the wiper and the resistance element. Conceivably, in some circuits, this could result in voltage spikes at the output of the voltage regulator as the voltage is adjusted. The cure for this is to wire the potentiometer so that it never presents an open circuit, even with an intermittent wiper, as I've done with R9 in Fig 1.

For some other GaAs FET circuits, it may be advantageous to use an active-bias supply which operates inside the feedback loop of the current limited supply. This allows the bias point to be unaffected by temperature variations. The current limiting acts as a failsafe, protecting the transistor if a more negative gate supply voltage is unable to turn off the transistor. I've successfully used this circuit when only a milliamp of bias current was needed. Due to the high current required by the gate circuit of the 2-W amplifier, I decided it was impractical to active-bias the FET in this application; the ICL7660 can't provide the needed current. But there are highercurrent versions of this chip, for those who don't mind the price.

RF Design

I found the AT-8 I40 rather difficult to get unconditionally stable. I ended up placing a 10041 chip resistor from gate to ground, which resulted in pretty good stability, except around 2.3 GHz. Unfortunately, it doesn't appear possible to dc decouple this resistor without adversely affecting stability, so quite a bit of bias current is needed. Because of this, it is conceivable that you may find a FET that needs too much gate voltage for a typical 10041 chip resistor to handle. Whether this is the case with a particular FET depends on both the threshold voltage and the transconductance of the device. The threshold voltage can vary quite a bit, particularly in older devices, though the manufacturers have tightened up this specification in recent data books. Worst case would be a large negative threshold voltage and a high transconductance. Stacking chip resistors in parallel might be a solution, though this might also invite unwanted parallel resonance effects, similar to what is seen with paralleled capacitors.

While in-band stability is not too critical, since the source and load impedance matching is usually pretty good at the operating frequency, I used a series resistor in the gate decoupling line to make the amplifier unconditionally stable, according to

Table 1—Measured Amplifier Performance

Input to MGF 1801 driver (dBm)	*Driver Output (dBm)*	*AT 8140 Output (dBm)*	*AT 8140 Gain (dB)*
–7.0	5.7	19.8	14.1
0.0	12.5	26.6	14.1
3.0	15.5	29.7	14.2
4.0	16.5	30.8	14.3
5.0	17.5	31.7	14.2
6.0	18.4	32.6	14.2
7.0	19.2	33.3	14.1
8.0	20.3	33.9	13.6
9.0	21.2	34.1	13.1
10.0	22.1	34.6	12.5
13.0	24.2	34.9	10.7

The 1-dB compression point is at 34.1/33.2 dBm output.
Comparing measurements made using an HP8563E spectrum analyzer against those made with an HP 453B/8481A power meter, a signal that measures 4.7 dBm on the spectrum analyzer reads out as 3.8 dBm on the power meter. The values listed are from the spectrum analyzer, taking into account a 30.2-dB, 25-W Bird attenuator inserted between the amplifier and the analyzer.

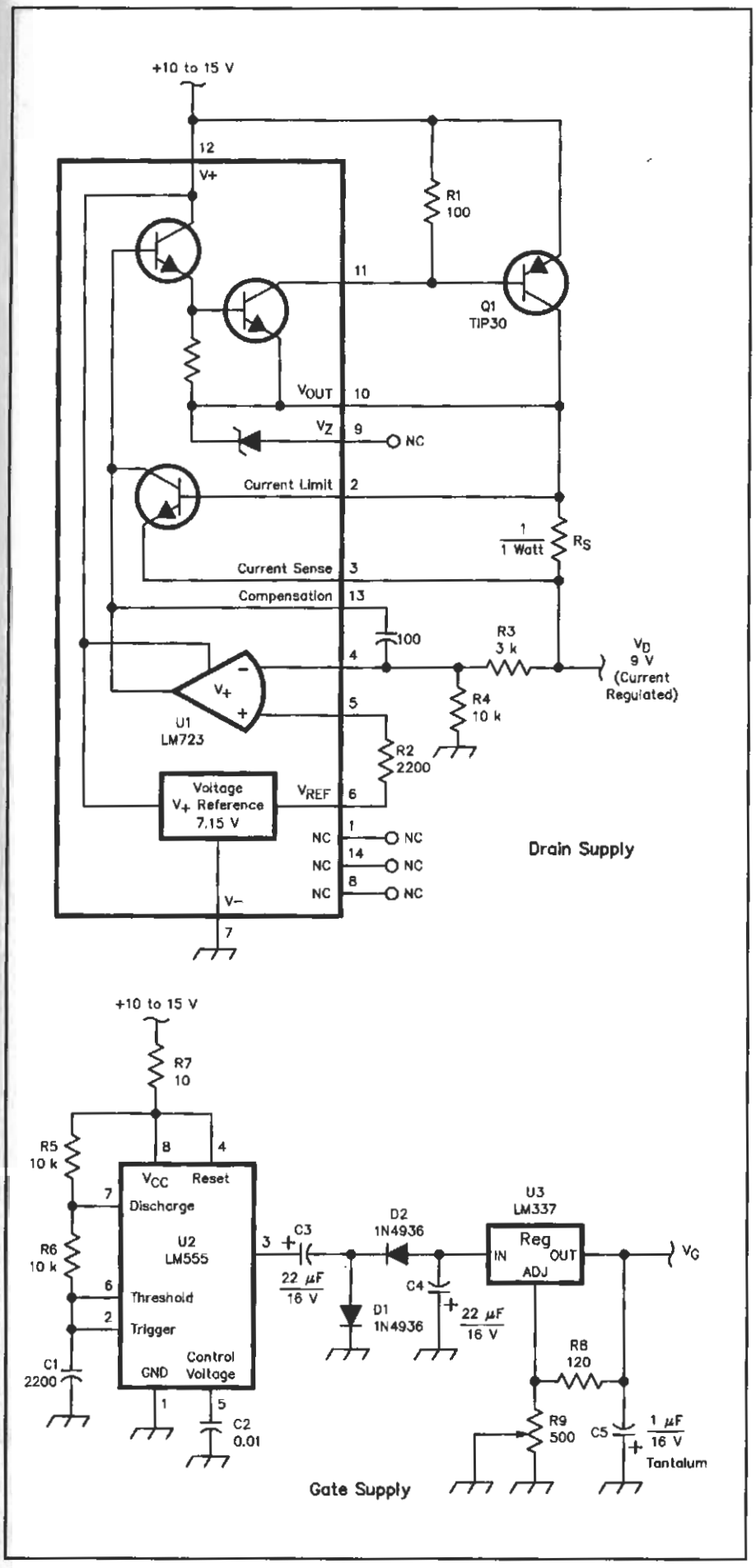

Fig 1—Power supply for the 2-W, 13-cm amplifier.

the computer model. This series resistor also improved the input match bandwidth, an important consideration if you don't want to tune the amplifier. Of course, improving the bandwidth with resistance also reduces the gain. The loss isn't too bad, however, seeing as this design is within a few dB of the maximum stable gain the data sheet specifies. The design was optimized with 150 Ω of series resistance, but I decided that such a high value was unwise. To accommodate such a high series resistance, it is entirely likely that the negative supply voltage would have to be more negative than the VGS limit. Then, if the 10041 resistor were to fail opencircuited, the supply could damage the gate of the transistor. For this reason, I chose to use a 5041 series resistor. I didn't reoptimize the design for 50 Ω of series resistance, since the likely improvement was small compared to the variations I've seen when optimizing the unit on the bench.

Finally, I discovered that additional gate circuit bypassing was required at audio frequencies to prevent the circuit from oscillating. This was done with a 1-µF capacitor that is not shown in the computer model. This frequency range wasn't covered by the model.

Several dB of additional saturated output power was obtained by modifying the output network with foil tabs. AT-8140s saturate at about 2.2 W output with around 200 mW of drive. An advantage to optimizing the circuit by modifying the 5041 striplines at the input and output of the amplifier is that the stability should not be adversely affected. But the board does have to be made larger to accommodate such tuning.

The original design was optimized using *Microwave Harmonica*, with the results shown in Table 2 and Fig 6. After I tweaked the output network to get maximum output power, I entered the changed circuit components into the computer and analyzed the circuit, resulting in the analysis shown in Table 3 and Fig 7. Table 1 shows the performance of the circuit in its final configuration.

Construction Notes

To ground the drain bypass capacitor and the gate resistor, I cut slots in the board and connected the pads to the ground plane with 1-mil copper foil. Copper foil was also used to connect the gate bypass capacitor, although in this case I trimmed the board so that it wasn't necessary to cut a slot.

For high-quality grounding without lots of tiny screws, I decided to try using a heat spreader made out of 1-mil copper foil. I cut a hole in the circuit board for the FET and then carefully soldered the foil across the hole in the circuit board, taking care not to put any solder where it would interfere with heat-sinking action. I didn't want any air pockets, as they are extremely poor conductors of heat. Then, after attaching the board to a piece of 0.25-inch sheet aluminum with suitably tapped holes, I used a scribe to punch holes for the 0-80 screws to

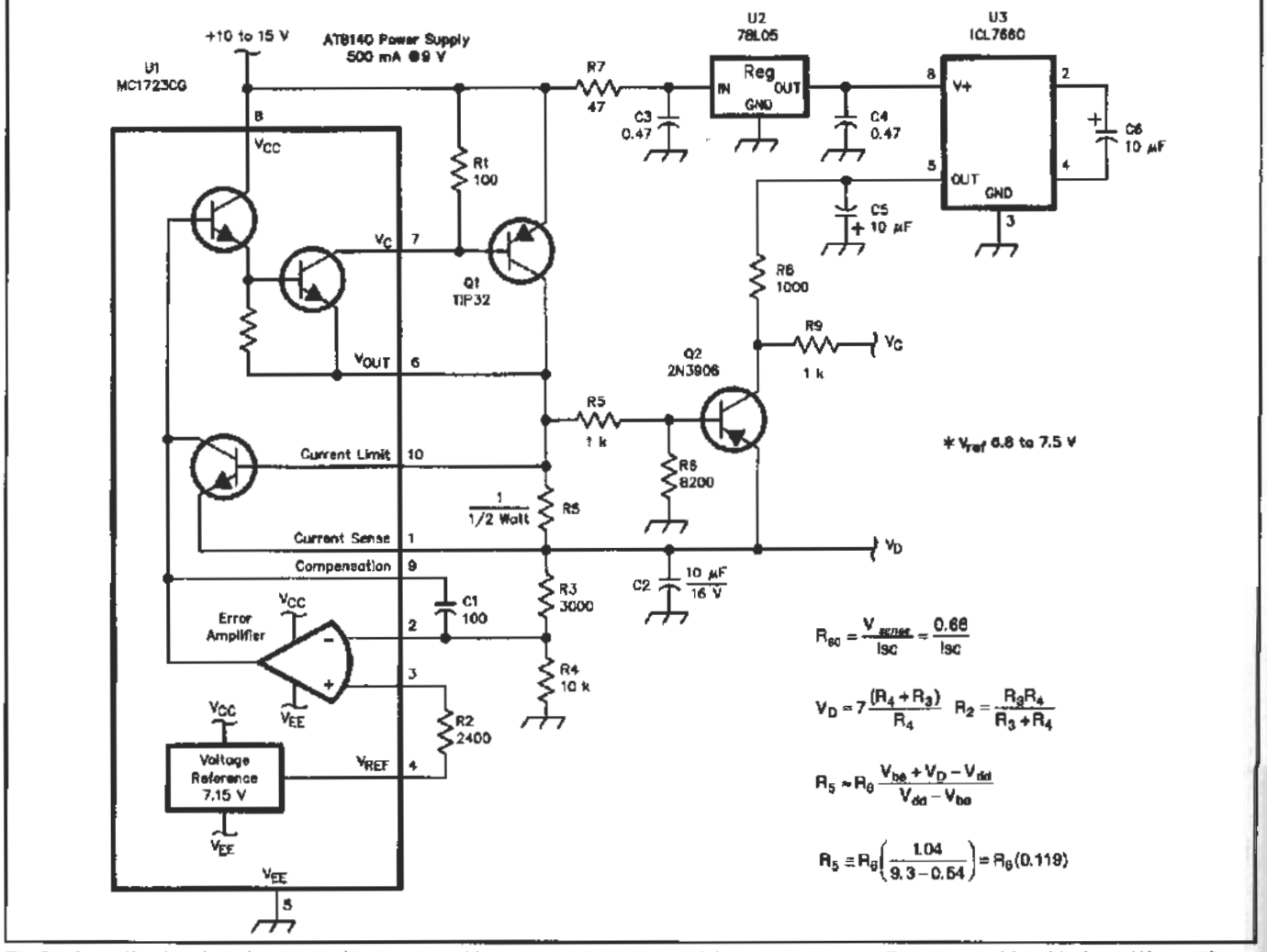

Fig 2—An active biasing circuit suitable for use with amplifiers that draw minimal gate current. Do *not* use this with the 2-W amplifier.

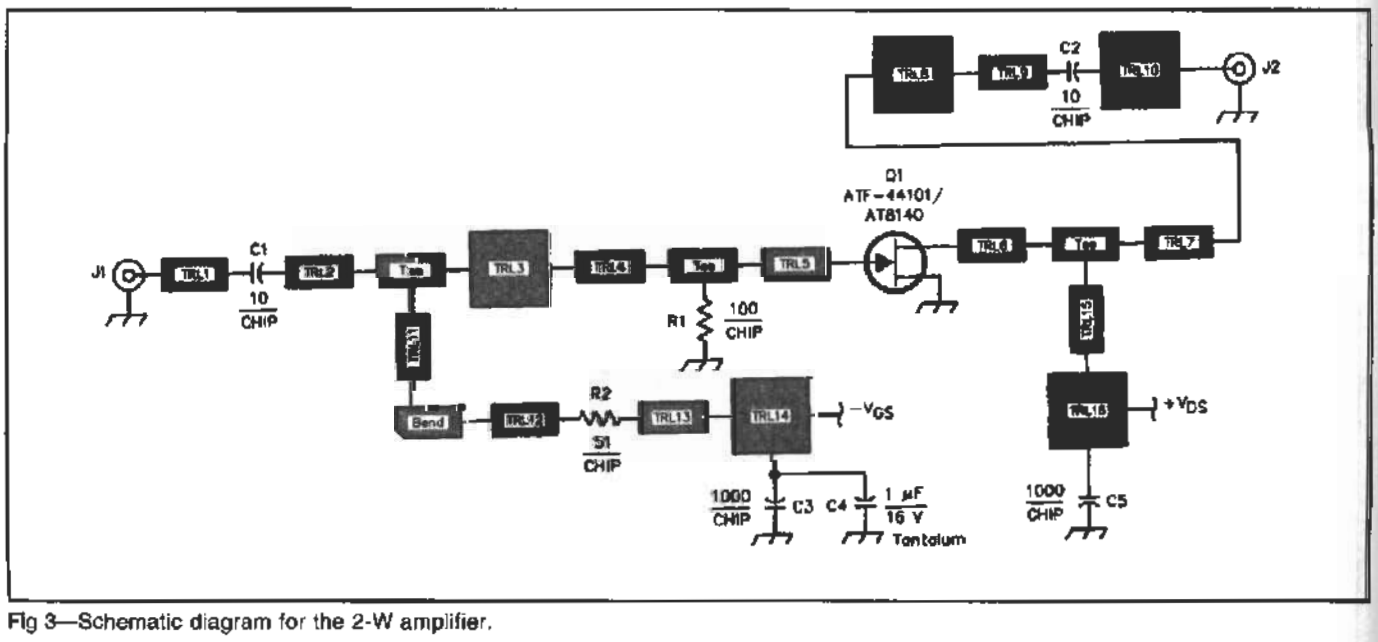

Fig 3—Schematic diagram for the 2-W amplifier.

C1, C2—10-pF, high-quality porcelain chip capacitors. I used 55-mil capacitors, although 100-mil capacitors should work just fine.
C3, C5—1000-pF NP0 chip capacitors
C4—1-µF, 16-V tantalum capacitor.
J1, J2—SMA jacks.
Q1—Hewlett Packard ATF-44101/AT-8410 medium power GaAs FET. This device must be properly heat-sinked. The absolute maximum channel temperature is 175°C. The case-to-junction thermal resistance is 23°C/W.
TRL1-16—Microstriplines etched on 0.031-inch-thick, ε_r = 2.55 Teflon circuit board.

Table 2—*Microwave Harmonica* Analysis (Original Circuit)

MICROWAVE HARMONICA PC V5.5 File: \mh\2304\qexamp.ckt 22-DEC-93 17:54:54

Freq GHz	MS11 dB AMP	PS11 deg AMP	MS21 mag AMP	PS21 deg AMP	MS12 mag AMP	PS12 deg AMP	MS22 dB AMP	PS22 deg AMP	MS21 dB AMP	K AMP
1.000	-0.70	-167.5	2.084	19.3	0.017	-53.7	-6.01	-128.7	6.38	1.64
1.100	-0.57	-177.2	1.980	0.1	0.018	-71.2	-5.35	-139.0	5.97	1.43
1.200	-0.47	173.3	1.941	-17.8	0.020	-87.3	-5.02	-148.2	5.76	1.27
1.300	-0.40	164.0	1.945	-35.0	0.022	-102.6	-4.96	-156.6	5.78	1.17
1.400	-0.36	154.7	1.999	-52.0	0.024	-117.7	-5.13	-164.3	6.01	1.09
1.500	-0.38	145.2	2.110	-69.2	0.028	-132.9	-5.59	-171.8	6.48	1.05
1.600	-0.48	135.2	2.288	-87.3	0.032	-148.9	-6.43	-177.6	7.19	1.02
1.700	-0.73	124.6	2.542	-106.8	0.039	-166.3	-7.84	178.8	8.10	1.01
1.800	-1.26	113.0	2.872	-128.6	0.047	174.0	-9.91	-177.3	9.16	1.01
1.900	-2.31	101.1	3.248	-151.5	0.056	151.3	-11.05	-156.6	10.21	1.01
2.000	-4.14	90.9	3.547	178.8	0.064	125.8	-8.31	-138.3	11.00	1.02
2.100	-6.75	87.5	3.682	149.7	0.070	98.9	-5.06	-141.0	11.32	1.04
2.200	-9.11	95.3	3.655	121.2	0.073	72.6	-3.15	-153.0	11.26	1.06
2.300	-10.01	108.4	3.587	91.9	0.075	47.6	-2.42	-167.3	11.09	1.07
2.304	-10.02	108.9	3.585	92.8	0.075	46.6	-2.41	-167.9	11.09	1.08
2.400	-10.08	120.9	3.503	66.5	0.078	22.4	-2.72	177.8	11.08	1.09
2.500	-9.15	137.4	3.638	36.0	0.082	-5.9	-4.55	162.9	11.22	1.11
3.000	-0.30	98.5	0.945	-114.5	0.025	-146.5	-1.26	-164.2	-0.49	1.17
4.000	-0.74	28.9	0.159	140.2	0.006	122.2	-0.11	150.2	-15.96	1.91
5.000	-2.01	-15.1	0.071	59.8	0.003	56.4	-0.08	123.6	-22.98	13.43
6.000	-0.78	1.8	0.044	120.4	0.003	135.4	-0.07	100.6	-27.30	9.68
7.000	-0.36	-60.0	0.158	60.8	0.014	86.8	-2.73	123.5	-16.02	8.12
8.000	-0.77	-109.6	0.086	-76.3	0.010	-50.3	-0.74	73.6	-21.26	16.53
9.000	-3.99	178.3	0.630	151.2	0.004	-174.8	-0.10	53.3	-30.56	50.93
10.000	-1.70	-138.8	0.816	5.4	0.003	45.4	-0.10	33.1	-36.06	75.19
11.000	-0.67	163.8	0.924	-91.2	0.006	-46.2	-0.47	12.8	-32.44	53.16
12.000	-0.95	116.5	0.831	106.0	0.010	152.8	-0.48	-0.6	-30.15	33.01

Table 3—*Microwave Harmonica* Analysis (Optimized for Output Power)

MICROWAVE HARMONICA PC V5.5 File: bigexamp.ckt 22-DEC-93 18:09:28

Freq GHz	MS11 dB AMP	PS11 deg AMP	MS21 mag AMP	PS21 deg AMP	MS12 mag AMP	PS12 deg AMP	MS22 dB AMP	PS22 deg AMP	MS21 dB AMP	K AMP
1.000	-0.72	-168.6	2.386	39.7	0.020	-33.3	-17.28	-86.0	7.55	1.63
1.100	-0.67	-179.3	2.331	20.4	0.022	-50.9	-15.61	-117.3	7.35	1.42
1.200	-0.64	172.6	2.299	2.0	0.023	-67.5	-14.05	-142.9	7.23	1.27
1.300	-0.64	163.7	2.294	-15.7	0.026	-83.3	-12.69	-165.0	7.21	1.17
1.400	-0.66	155.0	2.314	-32.9	0.028	-98.6	-11.48	175.0	7.29	1.09
1.500	-0.71	146.5	2.365	-49.9	0.031	-113.6	-10.42	156.4	7.48	1.05
1.600	-0.79	137.8	2.453	-66.8	0.035	-128.4	-9.50	138.6	7.79	1.02
1.700	-0.91	128.9	2.588	-83.8	0.039	-143.3	-8.71	121.3	8.26	1.01
1.800	-1.10	119.4	2.786	-101.2	0.045	-158.5	-8.08	103.9	8.90	1.01
1.900	-1.42	108.8	3.073	-119.8	0.053	-174.6	-7.62	85.7	9.75	1.01
2.000	-1.98	96.3	3.482	-139.1	0.063	167.9	-7.46	65.7	10.84	1.02
2.100	-3.10	80.3	4.065	-161.7	0.078	147.5	-7.86	41.8	12.10	1.04
2.200	-5.77	57.1	4.815	170.7	0.096	122.2	-9.64	9.1	13.65	1.05
2.300	-14.58	10.6	5.418	135.8	0.113	89.5	-15.23	-52.9	14.68	1.07
2.304	-15.31	6.6	5.428	134.2	0.113	88.0	-15.85	-57.2	14.69	1.07
2.400	-19.67	-157.1	5.138	96.3	0.111	52.3	-13.32	176.5	14.22	1.09
2.500	-4.22	165.0	4.086	61.5	0.092	19.6	-7.41	139.7	12.23	1.11
3.000	-0.53	96.9	1.222	-35.2	0.032	-67.2	-2.33	21.6	1.74	1.17
4.000	-0.75	29.2	0.494	-155.6	0.019	-173.6	-1.06	-79.0	-6.11	1.69
5.000	-1.99	-15.1	0.261	93.6	0.013	90.6	-1.04	-169.9	-11.67	11.23
6.000	-0.98	1.9	0.137	130.1	0.010	135.1	-0.55	136.4	-17.28	7.89
7.000	-0.39	-60.0	0.101	160.7	0.009	178.7	-0.92	-3.1	-19.91	8.22
8.000	-0.75	-109.9	0.196	-1.0	0.023	25.0	-6.65	-66.0	-14.17	14.18
9.000	-4.01	178.4	0.126	-132.4	0.018	-98.4	-1.60	-147.6	-18.01	39.98
10.000	-1.70	-138.8	0.076	53.9	0.015	93.9	-2.18	130.1	-22.42	57.57
11.000	-0.66	163.8	0.071	-60.9	0.017	-15.9	-8.01	29.7	-22.92	50.28
12.000	-0.97	116.5	0.092	168.5	0.030	-145.5	-8.93	160.9	-20.71	31.18

Fig 4—Parts placement diagram for the 2-W amplifier. Points labeled XX should be connected to the ground plane using copper foil.

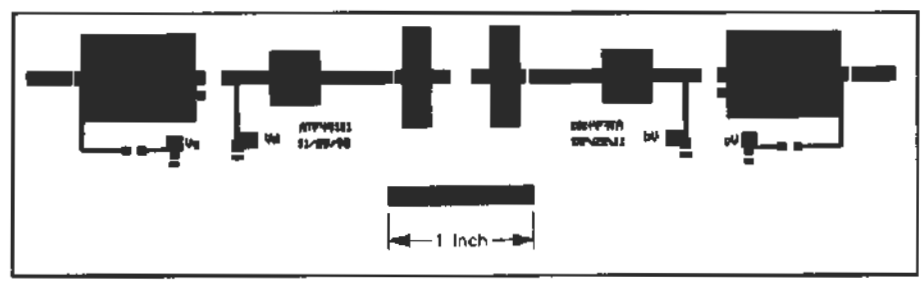

Fig 5—Etching pattern for the 2-W amplifier. Use 0.031-inch-thick, ε_r = 2.55 Teflon circuit board.

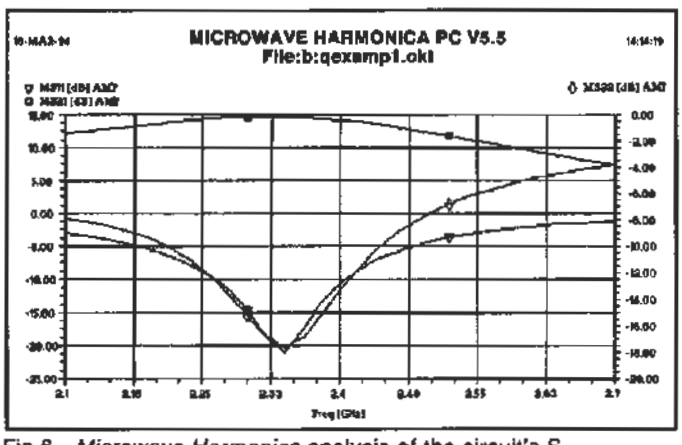

Fig 6—*Microwave Harmonica* analysis of the circuit's S parameters after computer optimization.

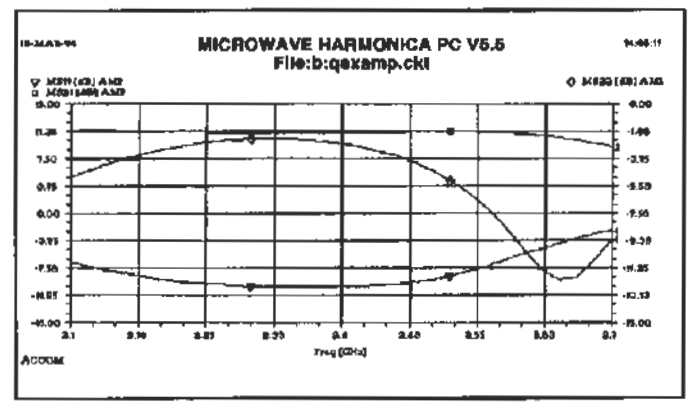

Fig 7—After the output network was optimized on the bench for maximum output power, *Microwave Harmonica* produced this analysis of the resulting circuit.

mount the FET. Ideally, clean holes would be punched into the copper, but I couldn't figure out a way to do that with the tools I have available. I used 0-80 screws, which are the largest screws I've found that will fit in the mounting holes. While I've used smaller screws in the past, I prefer using the largest screws possible since taps generally get tougher to use as they get smaller. I built one amplifier using 0.125-inch thick 6061 aluminum, but found that to be too thin to easily make the tapped holes for attaching the connectors and brass strips, although the finished mounting plate was stiff enough.

By Al Ward, WB5LUA

From *QST*, December 1985

1296-MHz Solid-State Power Amplifiers

Explore the DX possibilities of the 23-cm band with these modern amplifiers.

With the ever-increasing number of ready-to-go 1296-MHz transverters available on the market today, there is a great demand for a simple and economical way to generate higher power than the typical 0.5 to 1 W output these transverters provide. If 1 W or less is used to drive a typical 2C39/7289 stripline or cavity amplifier, the low output power is often disappointing. A tube-type amplifier run with 1 kV on the plate typically offers a gain of 10 dB. This means that, at best, you can expect 5- to 10-W output from your 1-W or less input.

A popular way of generating higher power is to cascade two tube-type amplifiers for 50- to 100-W output. Here I will show you an alternative: two solidstate amplifiers that can replace the tubetype driver amplifier and provide 10- to 20-W output—enough to drive a two-tube amplifier to full output.

The NEC NEL1306 and the NEL1320 1300-MHz power transistors are an economical solid-state approach to generating moderate power levels (10-20W) at 1269 and 1296 MHz. These amplifiers can be used for terrestrial or sateffite work. When OSCAR 10 was designed, it was thought that 10 W into a modest gain antenna (20 dBi) would produce usable signals from the sateffite. Unfortunately, there were some problems, and the sensitivity of AO-10 was not as originally expected for the Mode-L uplink. These amplifiers can, however, be used as a driver for a higher-powered tube amplifier for Mode-L service. If all goes according to plan with the launch of AMSAT-OSCAR Phase IIIC, 10 to 20 W with a 20-dBi gain antenna will produce acceptable downlink signals.

The NEL1306 is rated for 6-W output at 1296 MHz at the 1-dB compression point; the NEL 1320 is rated at 20 W. These devices offer several advantages for amateur experimenters. They were designed for collector voltages of 12- to 13.6-V dc, making them ideal for portable and mobile operation. Although the price may seem high to someone familiar with HF parts, these devices are less expensive than most microwave power transistors. The NEL 1306 is in the $26 price range, while the NEL1320 costs about $42. California Eastern Laboratories makes these transistors available in single-lot quantities, so you don't have to be "in the business" to get your hands on them.[1]

The performance of the amplifiers I built and tested is shown in Table 1. The NEL1306 is a good buy. With 1.5-W input, 6- to 8-W output can be achieved. When the amplifier is tuned up at lower power levels, power gain can be as high as 10 dB. With 200-mW drive from my homemade transverter, an output power level of 2 W is attainable.[2]

Power gains as high as 17 dB are possible with a two-stage amplifier (an NEL1306 driving an NEL1320). With a mere 200 mW of drive, 10-W output is possible. When the pair of amplifiers is driven with 1 W and tuned for maximum power output, the 1-dB compression point of 18 W will be achieved.

Circuit Details

The basic design, shown schematically in Fig. 1, is an adaptation of a circuit described in the NEL1300 series data sheet. The design incorporates 30-ohm quarter-wavelength microstriplines on the input and output. C3, C4, C7 and C8, along with L1, form a pi network that matches the low input impedance of the device to 50 ohms. CS, C6, C9 and C10 and the 30-ohm transmission line (L2) form an output pi network that maximizes power transfer to 50 ohms. C10 is not always necessary, depending on variations among devices and circuit-board material.

I designed the amplifiers for 0.031-inch-thick, double-sided glass-epoxy circuit board. A 30-ohm line in this dielectric equates to a line width of 0.121 inch, which is equivalent to the width of the collector and base leads of the NEL1300 series

Table 1
Typical Operating Conditions for the 1296-MHz Solid-State Power Amplifiers

Device	*NE130681-12*	*NEL132081-12*
P_{out}(1-dB compression point)	7W	18W
Gain (1-dB compression point)	6 dB typ.	5 dB typ
Collector efficiency	40-50%	40-50%
Idling current	50 mA	150 mA
I_C @ 1-dB compression point	1.1 A	3.0 A
V_{CC}	13.5 V	13.5 V
Power input	14.9 W	40.5 W

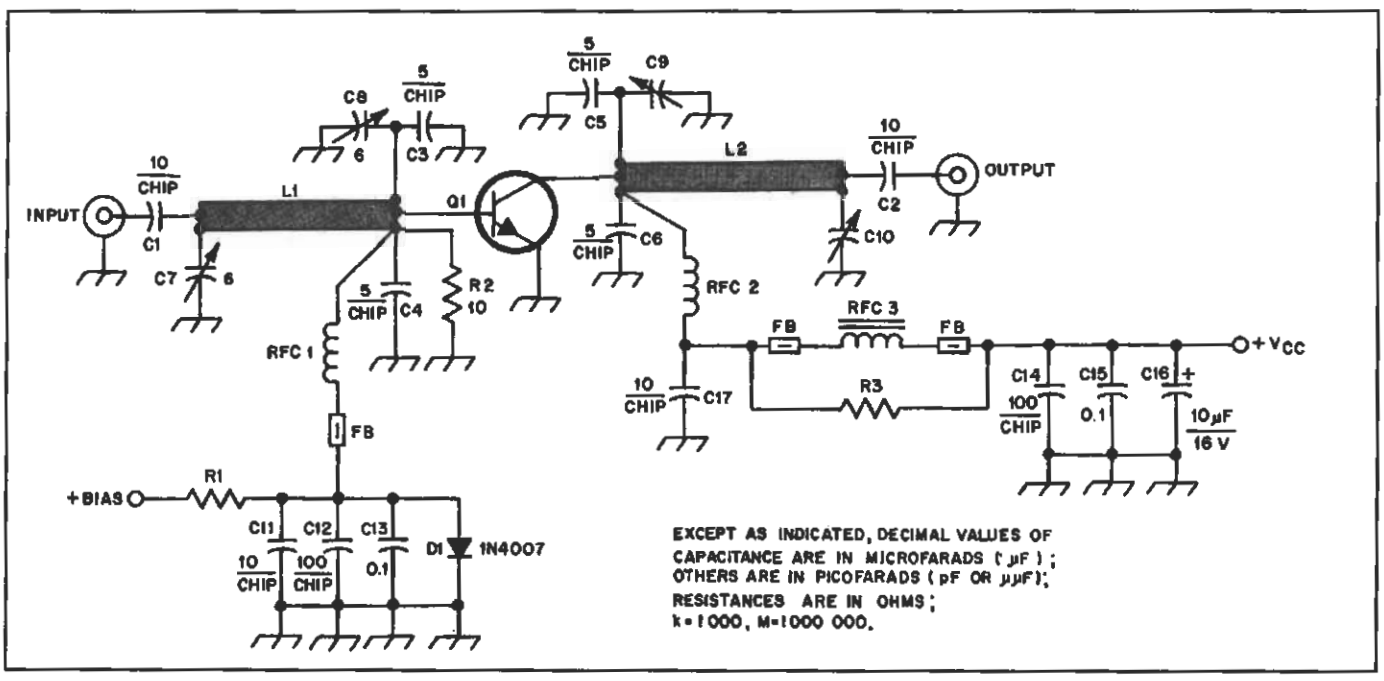

Fig. 1—Schematic diagram of the NEL1306 and NEL1320 1296-MHz solid-state power amplifiers. The schematic is identical for both versions. Component values are the same except as noted.

C1, C2, C11, C17—10-pF chip capacitor.
C3, C4, C5, C6—3.6- to 5.0-pF chip capacitor.
C7, C8—1.8- to 6.0-pF miniature trimmer capacitor (Mouser 24AA070 or equiv. See text).
C9, C10—Same as C7 and C8 for the NEL1306 amplifier. For the NEL1320 version, 0.8- to 10-pF piston trimmers are used (Johanson 5200 series or equiv.).
C12, C14—100-pF chip capacitor.
C13, C15—0.1-µF disc ceramic capacitor.
C16—10-µF electrolytic capacitor.
D1—1N4007 diode.
L1, L2—30-ohm microstripline, 1/4-wavelength long (see text).
Q1—NEC NEL130681-12 (6 W) or NEL132081-12 (18 W) transistor.
R1—82- to 100-Ω resistor, 2-W minimum. Vary for specified idling current.
R2—10-Ω, 1/4-W carbon-composition resistor with "zero" lead length. See text.
R3—15-Ω, 1-W carbon-composition resistor.
RFC1—3t no. 24 wire, 0.125 inch ID, spaced 1 wire diam.
RFC2—1t no. 24 wire, 0.125 inch ID, spaced 1 wire diam.
RFC3—1-µH RF choke; 18t no. 24 enam. close-spaced on a T50-10 toroid core.

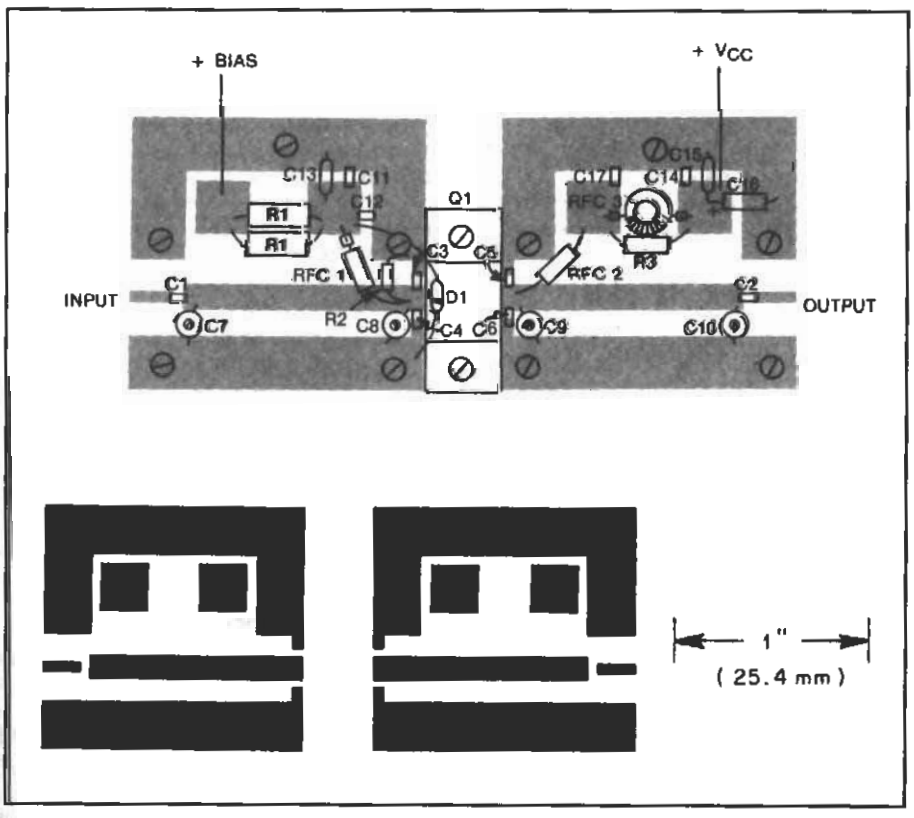

Fig 2—Parts-placement diagram and full-size etching pattern for the solid-state 1296-MHz power amplifiers. All components mount on the etched side of the board. The same PC boards are used for each version.

devices. This minimizes the discontinuity between L1, L2 and Q1.

Bias is provided by R1, R2 and D1. R1 can be optimized, if desired, to adjust the collector idling current.

I selected RFC1 and RFC2 by choosing the lowest possible reactance that will not affect power gain or output power. The RF chokes and the 10-pF bypass capacitors afford adequate decoupling at the frequency of operation. The values of RFC1 and RFC2 are purposely made different to avoid oscillations caused by bias-choke coupling.

After building several of these amplifiers, I noticed that the transistors sometimes generated low-frequency spurious signals. Although these signals were very low in amplitude and caused no problems, they were annoying. I found that I could eliminate them by keeping the high-frequency RF chokes in the collector circuit as small as possible and adding the parallel R3/RFC3 combination, as well as bypass capacitors C14, C15, C16. RFC3 must be capable of handling 1 A for the NEL1306 and 3 A for the NEL1320, so I made special RF chokes to withstand the current.

Construction

Identical construction techniques are used for both amplifiers. Most of the components are mounted to the PC board, and

the board and transistor are mounted to an aluminum base plate made from 1/4-inch-thick stock. PC-board layout is shown in Fig. 2. Two separate boards are used—one for the input side and one for the output—and they are mirror images of each other. The copper is retained on the bottom side and serves as a ground plane. The grounded areas on the top side must have a good connection to the bottom ground plane for low-inductance grounding of the transistor emitter leads, matching capacitors and bias circuitry. Etched PC boards and partial parts kits for this project are available from A & A Engineering.[3]

Several effective methods of connecting the top and bottom ground planes are summarized here.

1) Plated-through holes at the critical grounding areas mentioned earlier.

2) Use of pins or screws that penetrate through the circuit board into the aluminum base plate at the critical areas.

3) Use of "wrap-around" foils on all edges of the ground plane.

Plated-through holes are often used in the commercial and military electronic marketplace but are not so easily reproduced in the average builder's circuitboard shop. I've found that the best technique for the home builder is a combination of methods 2 and 3. First, wrap thin copper or brass foil around the board edges and then solder the foil to the top and bottom. Sometimes called "shim stock," thin sheet metal is often available from hobby shops or metal suppliers. Next, drill holes through the board and use no. 4-40 screws to tie the circuit board to the base plate at the critical areas shown in Fig. 2.

The transistor must be mounted so that its leads lie flat against the PC board. This poses a slight problem, since the transistor leads protrude from the device 0.165 inch above the bottom of the flange, and the PC boards are only 0.031 inch high. There are a couple of ways around this problem. They work equally well, so choose the method that is easiest for you.

If you have access to a machine shop, you can mill out a 0.240-inch-wide by 0.090-inch-deep slot in the aluminum base plate to clear the transistor flange. This is a simple task on a milling machine, and you can probably find a local machine shop that will do small jobs when business is slow. The other method is to mount the transistor to the base plate and use a piece of 0.090-inch-thick aluminum sheet to bring the input and output PC boards up to the right height. The 0.090-inch dimension allows a wrap-around foil and solder buildup of 0.040 inch, maximum.

I used 1-inch-long screws to secure the transistor to holes drilled and tapped in the aluminum base plate. The extra screw length that protrudes from the bottom of the base plate allows the use of an external heat sink, which is suggested if continuous operation is desired.

The clearance holes in the NEL1300 devices are for no. 4-40 hardware. I drilled out the holes to accept no. 6-32 screws to make the assembly more rugged, although this may not be necessary. Be careful if you decide to drill out the holes to accept no. 6-32 hardware; the transistor flange is soft copper, and you could damage the device. Use a small vise to hold the transistor flange during the drilling operation.

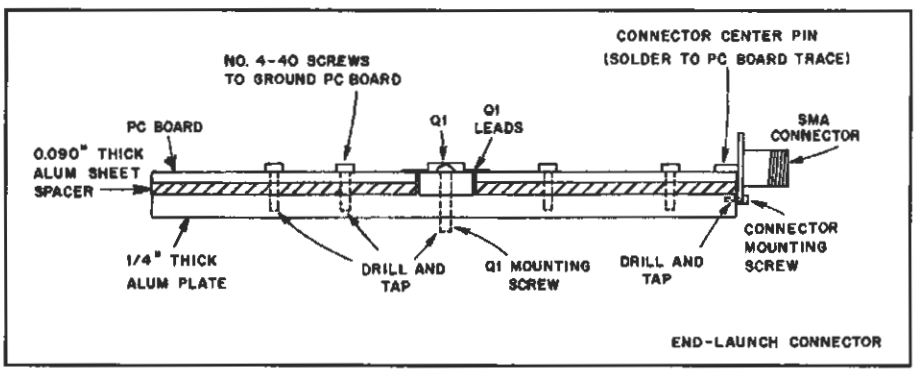

Fig 3—Construction details for the solid-state 1296-MHz power amplifiers. See text for additional information.

Solder the components to pads on the board using surface-mounting techniques. Silver solder (2%) is recommended for the chip capacitors, but 5N63 will work fine. Use a 15-W iron and solder quickly to avoid burning the metallization off the capacitors.

The transistor leads should be soldered in place only after the circuit boards and transistor have been firmly bolted down to the base plate. This is necessary to minimize any buildup of stress in the transistor leads. Chip capacitors C3, C4, C5 and C6 should be soldered directly onto the leads of Q1 to ensure the shortest possible lead length. Keep D1 close to Q1. Thermal compound will enhance heat transfer to D1 to ensure minimal drift in idling current with temperature changes.

In the original design of these amplifiers, Johanson piston-trimmer capacitors (5200 series or equiv.) were used for C7, C8, C9 and C10. These capacitors are fairly large, and in some instances the coupling between the bodies of C8 and C9 was enough to cause an in-band oscillation. Smaller variable capacitors should be used if at all possible. I've used a 1.8- to 6.0-pF miniature ceramic trimmer capacitor, Mouser Electronics part number 24AA070, in the input and output networks of the NEL1306 amplifier and in the input network of the NEL1320 amplifier with no performance degradation.[4] I did use the Johanson piston trimmers in the output network of the NEL1320 amplifier because of the high RF currents involved.

The PC board makes use of end-launch SMA-type connectors. Fig. 3 illustrates this technique. Four-hole, flange-mount SMA connectors can be mounted to the edge of the base plate using two of the four mounting holes. Drill and tap the base plate for no. 2-56 hardware. Be careful—it's easy to accidentally cross-thread orovertorque the no. 2-56 hardware.

An alternative approach is to mount the amplifier in an aluminum die-cast box (Bud CU-124B or Hammond 1590B) and run miniature 50-ohm coaxial cable such as RG-174 from the amplifier board to the connector. The amplifiers shown in Figs. 4 and 5 use standard SMA connectors mounted to the walls of the metal box. BNC or Type-N connectors should work equally as well. When preparing each end of the coaxial cable, try to keep the pigtail leads as short as possible (1/8 inch or less); otherwise the mismatch will be difficult to tune out.

I compared the performance of an amplifier with end-launch connectors to that of another that used the approach just described. I could measure no difference in gain or 1-dB compression point.

Considerable effort was put forth to make sure the amplifiers are stable. The devices have fairly high gain at the frequency of operation, so layout and good construction practices are very important. Here are some construction hints that can help ensure amplifier performance and stability.

1) Use the smallest (physical) size variable capacitors that will still handle the RF current.

2) Use wrap-around ground foils as noted. Grounding screws are required at the critical RF-ground areas near the shunt variable capacitors, shunt bypass capacitors and Q1 emitters.

3) Connect braids from the coaxial-cable jumpers to the same ground as the shunt variable capacitors.

4) Use as little lead length as possible on R2—less than 1/8 inch.

5) In some instances when the large piston trimmers are used, a shield approximately 3/4 inch high mounted on top of Q1 and grounded via the mounting screws can improve isolation between C8 and C9.

Tune-up and Operation

Measuring RF power at 1296 MHz can be difficult. I used a calibrated 20-dB directional coupler along with enough attenuator pads to allow power to be read with a Hewlett Packard HP430C power meter and an HP477B thermistor mount. Even better is the HP431 power meter with its associated HP478A thermistor mount (a newer version of the HP430C that does not

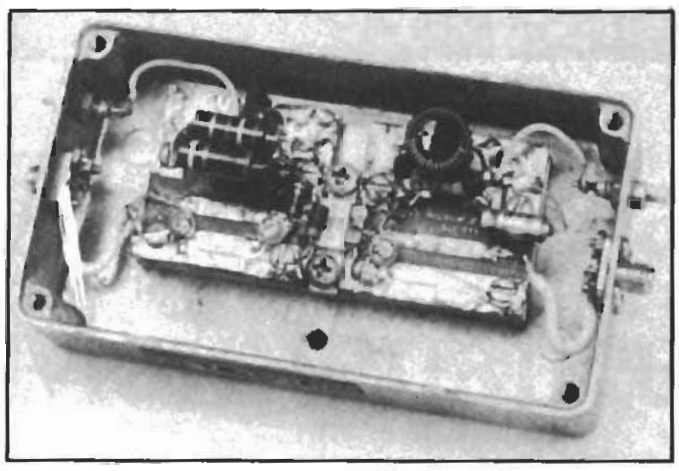

Fig 4—This NEL1306 amplifier was built inside a die-cast box. Miniature coaxial cable runs to the connectors.

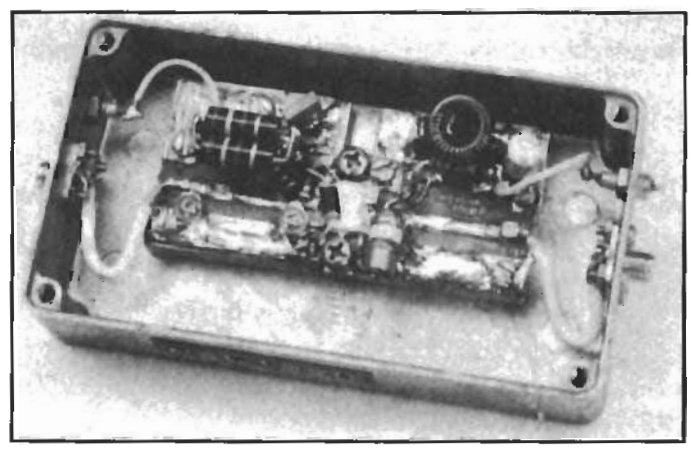

Fig 5—The NEL1320 amplifier is virtually identical to the NEL1306 version of Fig 4, except for the capacitors on the output strip line. C10 was not necessary on this version.

suffer from temperature-drift problems). Bird offers several low-power elements for the popular model 43 in this frequency range. Bird 400-1000 MHz elements are common, and they can be used with decreased accuracy.

Begin initial setup of each amplifier by terminating the input and output in good 50-ohm loads. I recommend that you use a fuse in the collector lead of Q1 to protect the device until you are sure everything is working normally. Start with all capacitors at minimum. Apply 12- to 13.5-V dc to the V_{CC} and bias terminals. The collector idling current should be as shown in Table 1. Vary the value of R1 for correct idling current.

For the NEL13O6 amplifier, start out with 50 to 100 mW of drive. Adjust the output network for maximum power output and then peak the input network for maximum output power. Increase drive and repeak both matching networks for rated performance as shown in Table 1. Similarly, start out with approximately 1 W of drive for the NEL1320 and follow the same procedure. After a minute or two of operation at maximum power output, remove RF drive power and check to see that the collector idling current has not increased more than 25% over the initial setting. Keeping D1 in close contact with Q1 will minimize drift in idling current with temperature changes.

If you're going to use transistor switching to apply dc to the power amplifier stages during transmit, consider the following technique. Apply 13.5-V dc to the V_{CC} terminal during receive and transmit. Use a series transistor switch to apply 13.5-V dc to the bias terminal during transmit. A power transistor capable of carrying only a few hundred milliamperes of bias current, as opposed to several amperes of collector current, will be required. More important, the voltage drop across the transistor switch in the V_{CC} line will be eliminated. This will ensure maximum power output of the NEL1300 devices by keeping V_{CC} at 13.5-V dc.

Switching the bias port off during receive is important for another reason. Normally during receive periods, the amplifier is left unterminated. Sometimes the input port is also left open. Depending on the length of the unterminated 50-ohm cable on the amplifier ports, the unit may show signs of instability if it is drawing idling current.

Several amateurs in the Dallas area have duplicated these amplifiers with no problems. Other amplifiers of this design are in use in different parts of the country. The NEL1300 series amplifiers offer a simple and inexpensive means of generating medium power on 1296 MHz. You'll be amazed at what you can work with 18 W that you can't with 1 W.

I wish to thank everyone who offered technical advice, especially Wes Atchison, WA5TKU, for helping with the construction and evaluation of the prototype amplifiers.

Notes

[1]NEC transistors are available from California Eastern Laboratories, 3260 Jay St., Santa Clara, CA 95050, tel. 408-988-3500.

[2]Complete construction details for this transverter may be found in Chapter 32 of the *1986 ARRL Handbook*.

[3]A & A Engineering, 7970 Orchid Dr., Buena Park, CA 90620, tel. 714-521-4160.

[4]Mouser Electronics, 11433 Woodside Ave., Santee, CA 92071, tel. 619-449-2222.

By Ward Silver, N0AX
From *QST*, September 2003

Amplifier Care and Maintenance

With few moving parts, your amplifier can be easy to overlook. Here are some ideas for taking care of amplifiers.

Amplifiers come in all shapes and sizes, large and small, light or heavy, tube or solid-state, VHF or HF. Regardless, they all need a little TLC from time to time. They can cost as much as top-of-the-line radios, so it's important that they get a little maintenance on a regular basis.

While this article focuses on amplifiers that use vacuum tubes, many of the ideas presented here can and should be applied to any amateur amplifier—HF or VHF/UHF. Solid-state amplifiers operate at lower voltages and generally have fewer points of failure, but they still need occasional maintenance.

Safety First

It is important to review good safety practices.[1] Tube amplifiers use power supply voltages well in excess of 1 kV and the RF output at full throttle can be hundreds of volts, as well. Almost every voltage in an amplifier can be lethal! Take care of yourself and use caution!

- *Power Control*—Know and control the state of both ac line voltage and dc power supplies. Physically disconnect line cords and other power cables when you are not working on live equipment. Use a lockout on circuit breakers. Double-check visually and with a meter to be absolutely sure power has been removed.
- *Interlocks*—Unless specifically instructed by the manufacturer's procedures to do so, never bypass or "rig" an interlock. This is rarely required except in troubleshooting and should only be done when absolutely necessary. Interlocks are there to protect you.
- *The One-Hand Rule*—Keep one hand in your pocket while making any measurements on live equipment. The hand in your pocket won't give current a chance to flow through you. It's also a good idea to wear shoes with insulating soles and work on dry surfaces. Current can be lethal even at milliampere levels—don't tempt the laws of physics.
- *Patience*—Repairing an amplifier isn't a race. Take your time. Don't work on equipment when you're tired or frustrated. Wait several minutes after turning the amplifier off to open the cabinet—capacitors can take several minutes to discharge through their bleeder resistors.
- *A Chicken Stick*—Make this simple safety accessory shown in Figure 1 and use it whenever you work on equipment in which hazardous voltages have been present. The ground wire should be heavy duty (12 gauge minimum) due to the high peak currents (hundreds of amperes) present when discharging a capacitor or tripping a circuit breaker. When equipment is opened, touch the tip of the stick to *every* exposed component and connection that you might come in contact with. Assume nothing—accidental shorts and component failures can put voltage in places it shouldn't be.
- *The Buddy System and CPR*—It's always a good idea to use the buddy system when working around any equipment that has the potential for causing serious injury. The buddy needn't be a ham, just anyone who can be nearby in case of trouble. Your buddy should know how to remove power and administer basic first aid. Since hams work around electrical equipment frequently, it would be a good idea to have your buddy or someone in the household know CPR, as well.[2]

Cleanliness

The first rule of taking good care of an amplifier is cleanliness. I realize that 90 percent of ham shacks have just failed the first rule. Amplifiers need not be kept sparkling new, but their worst enemy is heat. Excess heat accelerates component aging and stresses those expensive tubes and transformers. There are two areas to keep clean—the inside and the outside.

Outside the amplifier, you need to prevent dust and obstructions from blocking the paths by which heat is removed. This means keeping all ventilation holes free of the ever-present dust bunnies, pet hair and

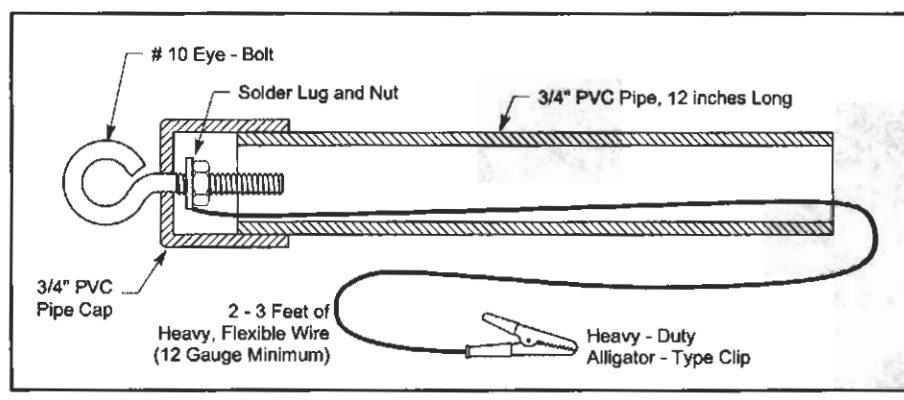

Figure 1—The "chicken stick" is a great way to ensure that everything inside the amplifier that should be discharged actually is. It can be a life saver.

insects. Fan intakes are particularly susceptible to inhaling all sorts of "goop." Get out the vacuum cleaner and clean not only the amplifier, but the surrounding areas. Don't even think about letting liquids anywhere near the amplifier. One spilled cup of coffee can cause hundreds of dollars of damage.

Keep papers or magazines off the amplifier—even if the cover is solid metal. Paper acts as an insulator and keeps heat from being radiated through the cover. Amplifier heat sinks must have free air circulation to be effective. There should be at least a couple of inches of free space surrounding an amplifier on its sides and top. If the manufacturer recommends a certain clearance, mounting orientation or air flow, follow those recommendations.

Just as the outside needs to be kept clean, so does the inside. High voltage (HV) circuits attract dust like crazy. The dust slows heat dissipation and will eventually build up to the point where it arcs or carbonizes. Our friend the vacuum cleaner should make another appearance to remove any dust or dirt. If you find insects (or worse) inside the amp, try to determine how they got in and plug that hole. Window screening works fine to allow airflow while keeping out visitors. While you're cleaning the inside, this is a great time to perform a visual inspection as described in the next section.

Vacuuming works best with an attachment commonly known as a "crevice cleaner." Figure 2 shows a crevice cleaning attachment being used with a small paintbrush to dislodge and remove dust. Don't use the vacuum cleaner brush attachment; they're designed for floors, not electronics. Some vacuums also have a blower mechanism, but these rarely have enough punch to clean as thoroughly as a brush. Besides, that dust you blow all over is going to wind up in some other equipment, so it's best to take it out of circulation, so to speak. The brush will root dust out of tight places and off components without damaging them or pulling on connecting wires.

If you can't get a brush or attachment close enough, a spray can of compressed air will usually dislodge dust and dirt. If you use a rag or towel to wipe down panels or large components, be sure not to leave threads or lint behind. Never use a solvent or spray cleaner to wash down components unless the manufacturer advises doing so—you might leave behind a residue or damage the component.

Visual Inspection

Once the amplifier has been cleaned, it's time for a visual inspection. Remove any internal covers or access panels and...*stop*! Get out the chicken stick, clip its ground lead securely to the chassis and touch every exposed connection. Now, using a strong light and possibly a magnifier, look over the components and connections. Amplifiers have far fewer components than transceivers do, so it's quite feasible to look at every component and insulator. Look for cracks, signs of arcing, carbon traces (thin black lines), discoloration, loose connections, melting of plastic, and anything else that doesn't "look right." This is a great time to be sure that mounting and grounding screws are tight. While you're in there, does anything smell burnt? The nose can quickly detect the odors of toasted transformer, cooked capacitor or roasted resistor. Learn the smells of healthy and not-so-healthy components.

Make a note of what you find, repair, or replace—even if it's absolutely nothing. If you don't keep a shack notebook, start one. A simple spiral notebook with notes about maintenance, wiring, color coding, antenna behavior and so forth can be a big timesaver.

Electrical Components

An amplifier contains many heavy-duty HV and RF components. These can be expensive and hard to replace, so it's important that you take good care of them. Let's start with the power supply.

There are three basic parts to amplifier power supplies—the ac transformer and line devices, the rectifier/filter and the metering/regulation circuitry. Transformers need little maintenance except to be kept cool and be mounted securely. Line components such as switches, circuit breakers and fuses, if mechanically sound and adequately rated, are usually electrically okay, as well.

Rectifiers and the capacitors that filter the HV dc require occasional cleaning. Look for discoloration around components mounted on a printed circuit board (PCB) and make sure that all wire connections are secure. HV capacitors are generally electrolytic or oil and should show no signs of leakage, swelling or outgassing around terminals.

Located at the output of the filter, components that perform metering and regulation of voltage and current can be affected by heat or heavy dust. If there has been a failure of some other component in the amplifier—such as a tube—these circuits can be stressed severely. Resistors may survive substantial temporary overloads, but may show signs of overload, such as discoloration or swelling.

Amplifiers contain two types of relays—control and RF. Control relays switch ac and dc voltages and do not handle input or output RF energy. The usual problem encountered with control relays is oxidation or pitting of their contacts. A burnishing tool can be used to clean relay contacts. In a pinch a strip of ordinary paper can be pulled between contacts gently held closed. [Avoid the temptation to over-clean silver-plated relay and switch contacts, as the author points out later. It is easy to remove contact plating with excessive polishing and while silver-plated relay and switch contacts may appear to be dark in color, oxidized silver (black) is still a good conductor. Once the silver's gone, it's gone; contact erosion will then be pervasive.—*Ed.*] If visual inspection shows heavy pitting or

S. COHEN, N1SC; R. SCHETGEN, KU7G

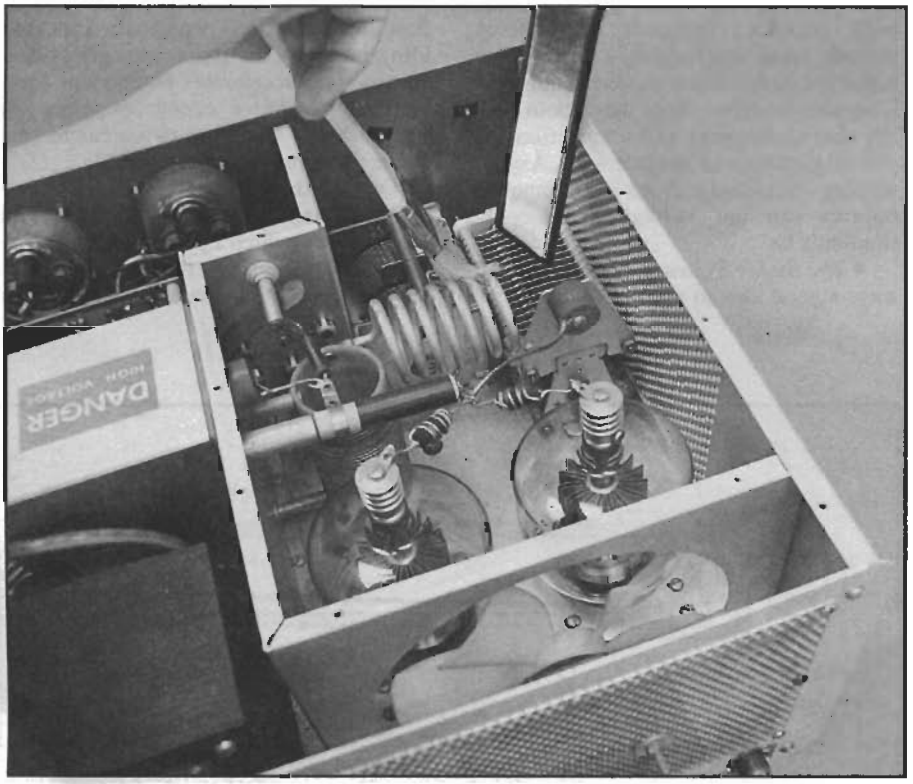

Figure 2—A small paintbrush and a vacuum cleaner crevice attachment make dust removal easy.

discoloration or resistance measurements show the relay to have intermittent contact quality, it is best replaced.

RF relays are used to perform transmit-receive (TR) switching and routing of RF signals through or around the amplifier circuitry. Amplifiers designed for full break-in operation will usually use a high-speed vacuum TR relay. Vacuum relays are sealed and cannot be cleaned or maintained. When you replace RF relays, use a direct replacement part or one rated for RF service with the same characteristics as the original.

Cables and connectors are subjected to heavy heat and electrical loads in amplifiers. Plastics may become brittle and connections may oxidize. Cables should remain flexible and not be crimped or pinched under clamps or tie-downs. It's a good idea to gently wiggle cables while watching the connections at each end for looseness or bending. Connectors can be unplugged and reseated once or twice to clear oxide on contact surfaces. Carefully inspect any connector that seems loose. Be especially careful with connectors and cables in amplifiers that have RF decks that are in separate enclosures from those of their power supplies. Those interconnects are susceptible to both mechanical and electrical stress and you don't want an energized HV cable loose on the operating desk. Check both the soldered electrical integrity and the mechanical stability of those cables and make sure they are tightly fastened.

As with relays, switches found in amplifiers are either control function orientated or RF routers. Adequately rated control switches, if mechanically sound, are usually okay. Bandswitches are the most common RF switch—usually a rotary phenolic or ceramic type. A close visual inspection should show no pitting or oxidation on the wiper (the part of the switch that rotates between contacts) or the individual contacts. Arcing or overheating will quickly destroy rotary switches. Figure 3 is a photo of a heavy-duty band switch that has suffered severe damage from arcing. Slight oxidation is acceptable on silver-plated switches. Phosphor-bronze contacts can sometimes be cleaned with a light scrub from a pink pencil eraser, but plating can be easily removed, so use caution with this method and be sure to remove any eraser crumbs. Rotary switch contacts cannot be replaced easily although individual wafer sections may be replaced if an exact matching part can be obtained.

Amplifiers use all types of capacitors and resistors. When replacing them, be sure to use a part rated for the use to which it will be put. Voltage and power-handling ratings are particularly important, especially of those handling high RF currents. An RF tank capacitor replacement should be checked carefully for adequate RF voltage and current ratings, not just dc. HV resistors are generally long and thin to prevent arcing across their surfaces. Even if a smaller (and cheaper) resistor has an equivalent power rating, resist the temptation to substitute it. In a pinch, a series string of resistors of the appropriate combined value can be used to replace one HV unit. Don't use carbon resistors for metering circuits, use metal or carbon film types. The carbon composition types are too unstable.

If you are repairing or maintaining an old amplifier and manufacturer-specific parts are no longer available, the ham community has many sources for RF and HV components. Fair Radio Sales and Surplus Sales of Nebraska are familiar names.[3] Hamfests and Web sites such as **www.eham.net** or **www.k1dwu.net/hamtrader** often have amplifier components for sale. You might consider buying another amplifier of the same type in non-working condition for parts use.

Tubes

The single most expensive component in an amplifier is usually the vacuum tube that performs the amplification. Good maintenance of tubes starts with proper operation of the amplifier. Follow the manufacturer's instructions for input drive levels, duty cycles, tuning and output power level. Frequently check all metered voltages and current to be sure that the tubes are being operated properly and giving you maximum lifetime. Penta Labs has an excellent Web page on maintaining power tubes.[4]

The internal mechanical structures of tubes generally do not deal well with mechanical shock and vibration, so be gentle. The manufacturer may also specify how the amplifier is to be mounted, so read the operating manual.

Tubes generate a lot of heat, so it's important that whatever cooling mechanism employed is kept at peak efficiency. Airways should be clean, including between the fins on metal tubes. All seals and chimneys should fit securely and be kept clean. Wipe the envelope of glass tubes clean after handling them—fingerprints should be removed to prevent baking them into the surface.

On metal tubes that use finger-stock contacts, be sure the contacts are clean and make good contact all the way around the tube. Partial contact or dirty finger stock can cause asymmetric current and heating inside the tube, resulting in warping of internal grids and possibly causing harmonics or parasitics.

Plate cap connections and VHF parasitic suppressors should be secure and show no signs of heating. Overheated parasitic suppressors may indicate that the neutralization circuit is not adjusted properly. Inspect socket contacts and the tube pins to be sure all connections are secure, particularly high-current filament connections. Removing and inserting the tubes once or twice will clean the socket contacts.

Adjustments to the neutralizing network, which suppresses VHF oscillations by negative feedback from the plate to grid circuit, are rarely required except when you are replacing a tube or after you do major rewiring or repair of the RF components. The manufacturer will provide instructions on making these adjustments. If symptoms of VHF oscillations occur without changing a tube, then perhaps the tube characteristics or associated components have changed. Parasitic oscillations in high-

H. WARD SILVER, N0AX

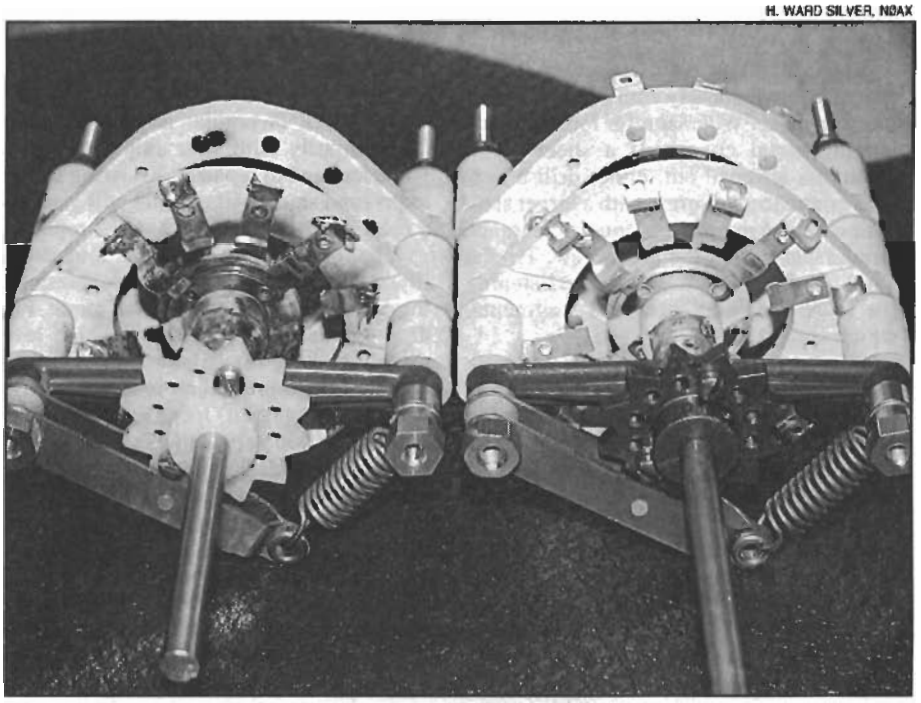

Figure 3—The band switch section on the left clearly shows the signs of destructive arcing.

power amplifiers can be strong enough to cause arcing damage. Perform a visual inspection prior to re-adjusting the neutralizing circuit.

Metering circuits rarely fail, but they play a key part in maintenance. By keeping a record of "normal" voltages and currents, you will have a valuable set of clues when things go wrong. This is perfect information for the shack notebook. Record tuning settings, drive levels, and tube voltages and currents on each band and with every antenna. When things change, you can refer back to the notebook instead of relying on memory.

Mechanical

While the amplifier is primarily an electronic beast, it has a significant number of mechanical parts that affect its well-being. Thermal cycling and heat-related stresses can result in mechanical connections loosening over time or material failures.

Switch shafts, shaft couplings and panel bearings all need to be checked for tightness and proper alignment. All mounting hardware needs to be tight, particularly if it supplies a grounding path. Examine all panel-mounted components, particularly RF connectors, and be sure they're attached securely. BNC and UHF connectors that are mounted with a single nut in a round panel hole are notorious for loosening with repeated connect/disconnections.

Rubber and plastic parts are particularly stressed by heat. If there are any belts, gears or pulleys, make sure they're clean and that dust and lint are kept out of their lubricant. Loose or slipping belts should be replaced. Check O-rings, grommets and sleeves to be sure they are not brittle or cracked. If insulation sleeves or sheets are used, check to be sure they are covering what they're supposed to. Never discard them or replace them with improperly sized or rated materials.

Enclosures and internal shields should all be fastened securely with every required screw in place. Watch out for loosely overlapping metal covers. If a sheet metal screw has stripped out, either drill a new hole or replace the screw with a larger size, taking care to maintain adequate clearance around and behind the new screw. Tip the amplifier from side to side while listening for loose hardware or metal fragments, which should all be retrieved.

A great time to clean the front and back panels and get gummy finger deposits off before they cause permanent finish damage is during maintenance. If the amplifier is missing a foot on the cabinet or an internal shock mount, replace it. A clean unit with a complete cabinet will have a significantly higher resale value than a dirty, grubby one, so it's in your interest to keep the equipment looking its best.

Shipping

When you are traveling with an amplifier or shipping it, some care in packing will prevent needless damage. Improper packing can also result in difficulty in collecting on an insurance claim, should damage occur. The original shipping cartons are a good method of protecting the amplifier for storage and sale, but they were not made to hold up to frequent shipping. If you travel frequently, it is best to get a sturdy shipping case made for electronic equipment.[5]

Some amplifiers require the power transformer to be removed before shipping. Check your owner's manual or contact the manufacturer to find out. Failure to remove it before shipping can cause major structural damage to the amplifier's chassis and case.

Tubes should also be removed from their sockets for shipment. It may not be necessary to ship them separately if they can be packed in the amplifier's enclosure with adequate plastic foam packing material. If the manufacturer of the tube or amplifier recommends separate shipment, however, do it!

Cleaning and Maintenance Plan

This discussion should have given you plenty to think about. It's easy to defer maintenance, but as with a vehicle, performance and lifetime are improved if a regular program is put into place. For amateur use, there is little need for maintenance more frequently than once per year. If there is a period of the year in which you are most active, put a note on the calendar about six weeks in advance to "open the hood," giving you time to obtain and replace any components.

Consider the maintenance requirements of your amplifier and what its manufacturer recommends. Sit down with your amplifier's manuals and make up a checklist of what major steps and tools are required. When maintenance time rolls around, you'll be prepared and be able to perform the job in the most efficient manner.

Troubleshooting

A benefit of regular maintenance will be familiarity with your amplifier should you ever need to repair it. Knowing what it looks (and smells) like inside will give you a head start on effecting a quick repair.

The following discussion is intended to illustrate the general flow of a troubleshooting effort, not be a step-by-step guide. Figure 4 shows a moderately-high-level troubleshooting flow chart. Before starting on your own amplifier, review the amplifier manual's "Theory of Operation" section and familiarize yourself with the schematic. If there is a troubleshooting procedure in the manual, follow it, of course.

You might be surprised how many "amplifier is dead" problems turn out to be simply a lack of ac power. Before even opening the cabinet of an unresponsive amplifier, be sure that ac is really present at the wall socket and that the fuse or circuit breaker is really closed. Assuming that ac power is present, trace through any internal fuses, interlocks and relays all the way through to the transformer primary terminals.

Hard failures in a high voltage power supply are rarely subtle, so it's usually clear if there is a problem and what components are involved. When you repair a power supply, take the opportunity to check all related components. If all defective components are not replaced, the failures may be repeated when the circuit is re-energized.

Rectifiers may fail open or shorted—test them using a DVM diode checker. An open rectifier will result in a drop in the HV output of 50 percent or more but will probably not overheat or destroy itself. A shorted rectifier failure is usually more dramatic and may cause additional rectifiers or filter capacitors to fail. If one rectifier in a string has failed, it may be a good idea to replace the entire string as the remaining rectifiers have been subjected to a higher-than-normal voltage.

High voltage filter capacitors usually fail shorted, although they will occasionally lose capacitance and show a rise in ESR (equivalent series resistance). Check the rectifiers and any metering components—they may have been damaged by the current surge caused by a shorted filter. Power transformer failures usually manifest themselves by insulation failures with consequent arcing of the windings. Either can result in the unmistakable aroma of overheated transformer. A failed transformer is generally not repairable.

Along with the HV plate supply, tetrode screen supplies occasionally fail, too. The usual cause is the regulation circuit that drops the voltage from the plate level. Operating without a screen supply can be damaging to a tube, so be sure to check the tube carefully after repairs.

If the power supply checks out okay and the tube's filaments are lit, check the resting or bias current. If it is excessive or very low, check all bias voltages and dc current paths to the tube, such as the plate choke, screen supply (for tetrodes) and grid or cathode circuits.

Having exhausted power supply and dc problems, you will then turn to the RF components or "RF deck." There is a natural tendency to forge ahead and swap in a known-good tube or tubes. Don't! Tubes are expensive and if the problem is elsewhere, you may damage the spares. Wait to swap tubes until you are sure that the tube is likely to be defective.

Check the input SWR to the amplifier. If it has changed (you did write down the normal SWR and drive levels, didn't you?) then you likely have a problem in the input circuitry or one or more tubes have failed. Perform a visual check of the input circuitry and the band switch, followed by an ohmmeter check of all input components.

If input SWR is normal and applying drive does not result in any change in plate current, you may have a defective tube, tube socket, or connection between the input circuits and the tube. Check the TR

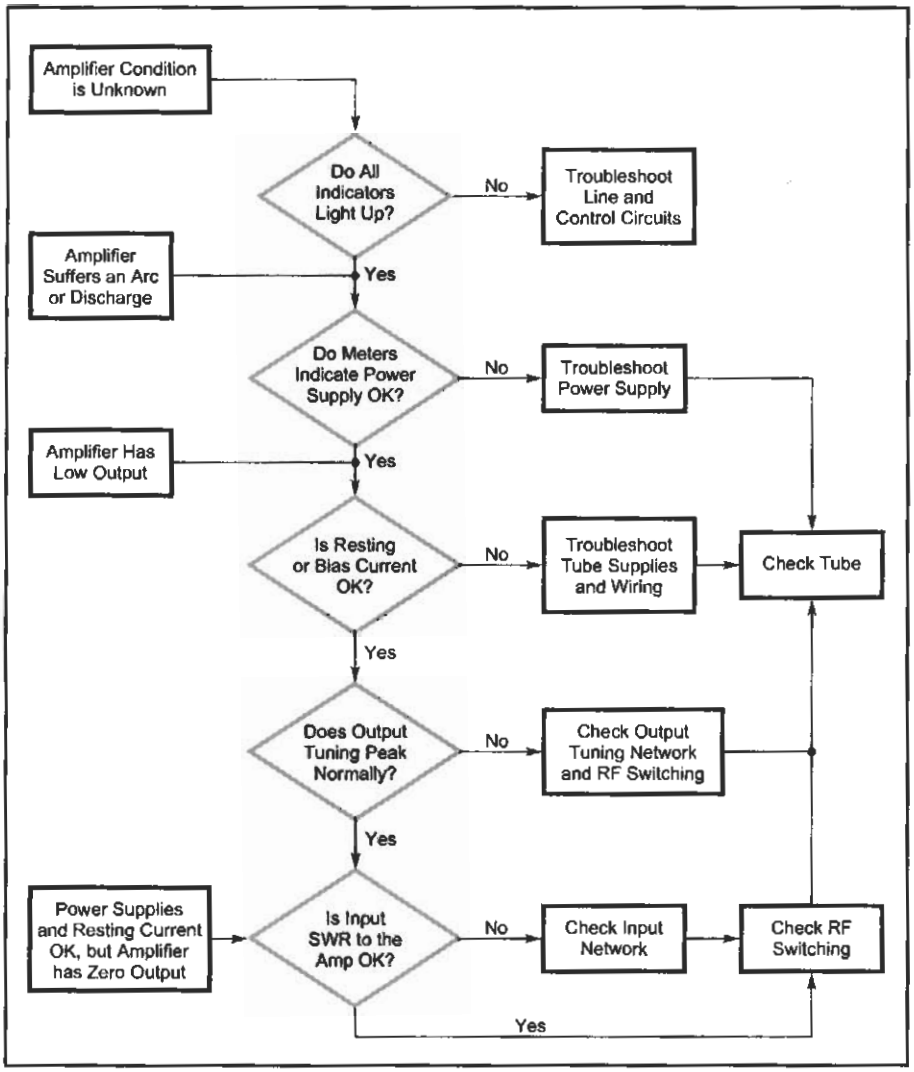

Figure 4—This moderate-level flow chart is a good way to identify amplifier problems quickly in lieu of a misplaced or nonexistent manufacturer's troubleshooting procedure.

control circuits and relay. If plate current changes, but not as much as normal, try adjusting the output tuning circuitry. If this has little or no effect, the tube may be defective or a connection between the tube and output circuitry may have opened. If retuning has an effect, but at different settings than usual, the tube may be defective or there may be a problem in the tuning circuitry. A visual inspection and an ohmmeter check are in order.

The key to finding the trouble with your amplifier is to be careful and methodical, and to avoid jumping to false conclusions or making random tests. The manufac-turer's customer service department will likely be helpful if you are considerate and have taken careful notes detailing the trouble symptoms and any differences from normal operation. There may be helpful guidelines on the manufacturer's Web pages or from other Internet resources. Sometimes there is more than one problem—they work together to act like one very strange puzzle. Just remember that most problems are very simple and can be isolated by careful, step-by-step tests.

Summary

Amplifiers have been part of ham radio for many years. They are simple, reliable pieces of equipment that respond well to basic care and common sense. Take the time to know your amp—inside and out. If you take care of it, it will reward you with reliable service and maximum tube lifetime.

Notes

[1]Chapter 9 of the current *ARRL Handbook for Radio Communications* is an excellent source of safety information. Available from your local dealer or the ARRL Bookstore. Order no. 1921 (softcover), no. 1948 (hardcover). Telephone toll-free in the US 888-277-5289, or 860-594-0355, fax 860-594-0303; **www.arrl.org/shop/**; **pubsales@arrl.org**.

[2]Instructions for CPR can be found at: **about-the-web.com/spiritworks/web/Kaiser/html/adult.htm**.

[3]Two sources of HV and RF parts include Surplus Sales of Nebraska (**www.surplussales.com**) and Fair Radio Sales (**www.fairradio.com**). Others can be found at the ARRL Technical Information Service database (**www.arrl.org/tis/tisfind.html**).

[4]Penta Labs, "Tube Maintenance & Education" (**www.pentalaboratories.com/maintenance.asp**).

[5]Pelican (**www.pelican-shipping-cases.com**) and Anvil (**www.anvilsite.com**) make excellent shipping cases suitable for carrying amplifiers and radio equipment.

Build safe and reliable amplifiers. Produce loud and clean signals.

Planning to build an amplifier compares well to the work of a cook searching for a recipe and all the ingredients. Find the right design, and then locate the parts and components to begin building.

Shorten your discovery work with *ARRL's RF Amplifier Classics*! Use this book to find classic tube and solid-state designs at power levels from 5 W to 1.5 kW. Included are two-dozen amplifier projects and articles published in ARRL's popular journals between 1980 and 2003. There are amps for HF, MF, VHF and microwave. These are high quality works from respected authors such as Gary Breed, K9AY; Jerry Pittenger, K8RA; Bill Sabin, WØIYH; Al Ward, W5LUA; Dave Meacham, W6EMD and others.

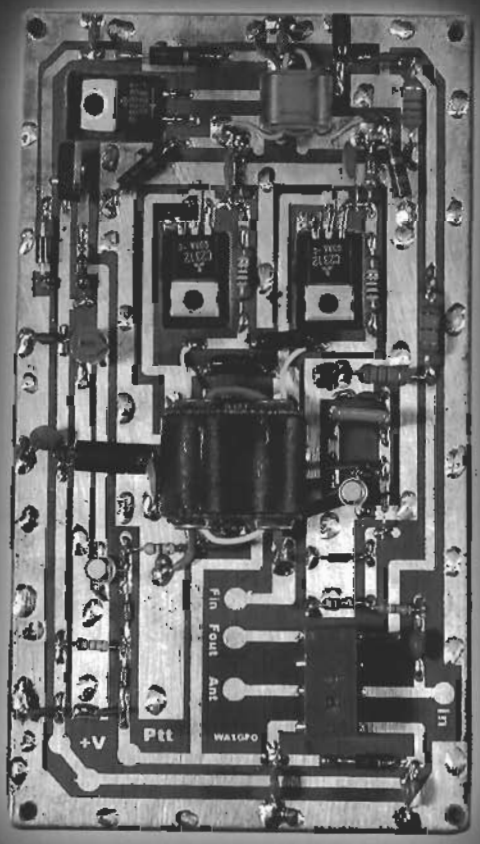

Turn dreams of constructing your first amp or next brick into reality!

ARRL The national association for AMATEUR RADIO
225 Main Street,
Newington, CT 06111-1494 USA
ARRLWeb: www.arrl.org/

ISBN 0-87259-931-0
51995 >
EAN
9 780872 599314

ISBN 0-87259-931-0 ARRL Order No. 9310

The ARRL Guide to Antenna Tuners

A Radio Amateur's Guide to Antenna Matching

Joel R. Hallas, W1ZR

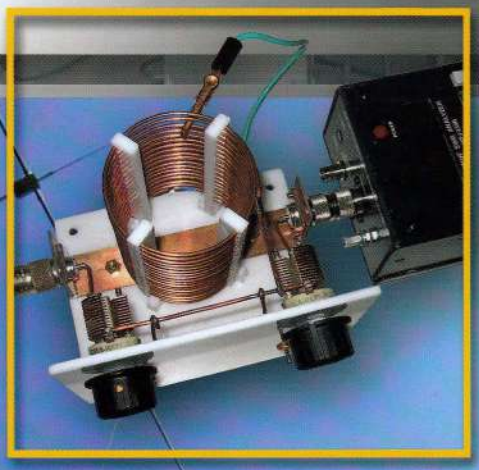

The ARRL Guide to Antenna Tuners

A Radio Amateur's Guide to Antenna Matching

Joel R. Hallas, W1ZR

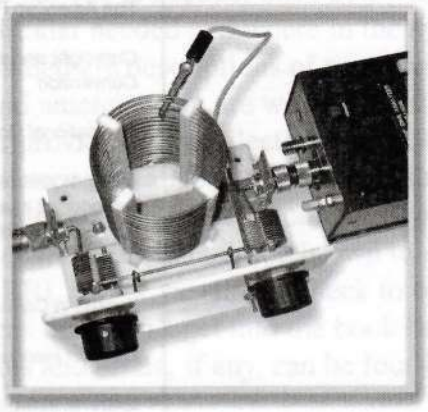

On the Cover

The group of special purpose antenna tuners made by the late George Badger, W6TC, is shown beneath his rotary antenna system. The inset shows a general purpose L-network antenna tuner built by Barry Shackleford, W6YE, who took both photos. Both are discussed in Chapter 15.

Production
Michelle Bloom, WB1ENT
Jodi Morin, KA1JPA
David Pingree, N1NAS

Cover
Sue Fagan, KB1OKW

Copyright © 2010-2012 by
The American Radio Relay League, Inc.

Copyright secured under the Pan-American Convention

International Copyright secured

All rights reserved. No part of this work may be reproduced in any form except by written permission of the publisher. All rights of translation are reserved.

Printed in Canada

Quedan reservados todos los derechos

IBSN13: 978-0-87259-098-4

1st Edition
2nd Printing

Foreword

Antenna Tuners are mystical devices that are sometimes needed between antenna systems and transmission lines or radios to make everything play the way it's supposed to. They are the subject of considerable confusion and misunderstanding by many Amateur Radio operators.

This book is intended to assist readers who have a basic knowledge of antennas, such as conveyed by *Basic Antennas — Understanding Practical Antennas and Designs*, in gaining an understanding of whether or not they need an antenna tuner in their station.[1] If it turns out one is needed, this book will help the reader decide the type of tuner needed and where in the system it should be applied. Also provided are descriptions of appropriate applications of such devices and antennas that are well suited for such use.An additional chapter provides data collected from ARRL Laboratory product reviews of representative antenna tuners to assist in tuner selection. Design methodology and specific design details are also provided for those who wish to build their own tuners.

As with all ARRL books, be sure to check to see if there are any last minute changes that didn't get into the book before it went to the printer. Updates and errata, if any, can be found at **www.arrl.org/product-notes/**.

David Sumner, K1ZZ
Executive Vice President
Newington, Connecticut
October 2010

[1]J. Hallas, W1ZR, *Basic Antennas — Understanding Practical Antennas and Designs*, Available from your ARRL dealer or the ARRL Bookstore, ARRL order no. 9994. Telephone 860-594-0355, or toll-free in the US 888-277-5289; **www.arrl.org/arrl.store/**; **pubsales@arrl.org**.

Acknowledgements

I would like to offer my special thanks to the ARRL production and editorial staff who made this book come together smoothly. In addition, thanks go to my long-suffering wife Nancy, W1NCY, who put up with the countless hours of my writing to make this happen.

I especially appreciated the tireless efforts of ARRL Technical Advisor Barry Shackleford, W6YE, who carefully examined every page of the manuscript in an effort to make sure there were neither technical nor grammatical errors and that all points were made clearly.

About the ARRL

The national association for Amateur Radio

The seed for Amateur Radio was planted in the 1890s, when Guglielmo Marconi began his experiments in wireless telegraphy. Soon he was joined by dozens, then hundreds, of others who were enthusiastic about sending and receiving messages through the air—some with a commercial interest, but others solely out of a love for this new communications medium. The United States government began licensing Amateur Radio operators in 1912.

By 1914, there were thousands of Amateur Radio operators—hams—in the United States. Hiram Percy Maxim, a leading Hartford, Connecticut inventor and industrialist, saw the need for an organization to band together this fledgling group of radio experimenters. In May 1914 he founded the American Radio Relay League (ARRL) to meet that need.

Today ARRL, with approximately 150,000 members, is the largest organization of radio amateurs in the United States. The ARRL is a not-for-profit organization that:

- promotes interest in Amateur Radio communications and experimentation
- represents US radio amateurs in legislative matters, and
- maintains fraternalism and a high standard of conduct among Amateur Radio operators.

At ARRL headquarters in the Hartford suburb of Newington, the staff helps serve the needs of members. ARRL is also International Secretariat for the International Amateur Radio Union, which is made up of similar societies in 150 countries around the world.

ARRL publishes the monthly journal *QST*, as well as newsletters and many publications covering all aspects of Amateur Radio. Its headquarters station, W1AW, transmits bulletins of interest to radio amateurs and Morse code practice sessions. The ARRL also coordinates an extensive field organization, which includes volunteers who provide technical information and other support services for radio amateurs as well as communications for public-service activities. In addition, ARRL represents US amateurs with the Federal Communications Commission and other government agencies in the US and abroad.

Membership in ARRL means much more than receiving *QST* each month. In addition to the services already described, ARRL offers membership services on a personal level, such as the ARRL Volunteer Examiner Coordinator Program and a QSL bureau.

Full ARRL membership (available only to licensed radio amateurs) gives you a voice in how the affairs of the organization are governed. ARRL policy is set by a Board of Directors (one from each of 15 Divisions) elected by the membership. The day-to-day operation of ARRL HQ is managed by a Chief Executive Officer.

No matter what aspect of Amateur Radio attracts you, ARRL membership is relevant and important. There would be no Amateur Radio as we know it today were it not for the ARRL. We would be happy to welcome you as a member! (An Amateur Radio license is not required for Associate Membership.) For more information about ARRL and answers to any questions you may have about Amateur Radio, write or call:

ARRL—The national association for Amateur Radio
225 Main Street
Newington CT 06111-1494
Voice: 860-594-0200
Fax: 860-594-0259
E-mail: **hq@arrl.org**
Internet: **www.arrl.org/**

Prospective new amateurs call (toll-free):
800-32-NEW HAM (800-326-3942)
You can also contact us via e-mail at **newham@arrl.org**
or check out *ARRLWeb* at **http://www.arrl.org/**

Table of Contents

Chapter 1	Why Might I Need an Antenna Tuner
Chapter 2	A Look at a Typical Configuration
Chapter 3	So Just What is an Antenna Tuner?
Chapter 4	Tuning an Antenna Tuner
Chapter 5	The Internal Tuner — How Does it Help?
Chapter 6	An External Tuner at the Radio
Chapter 7	Transmission Lines and Loss
Chapter 8	Moving the Tuner to the Back 40
Chapter 9	Transmission Line Choices for Low Loss
Chapter 10	Balanced versus Unbalanced Lines
Chapter 11	So What's a Balun, an Unun, a Choke?
Chapter 12	Balanced Antenna Tuners
Chapter 13	Antennas that Work Well with Tuners
Chapter 14	A Survey of Available Tuners
Chapter 15	Making Your Own Tuner
Appendix A	Using Decibels for Loss Calculations

Chapter 1

Why I Might Need an Antenna Tuner

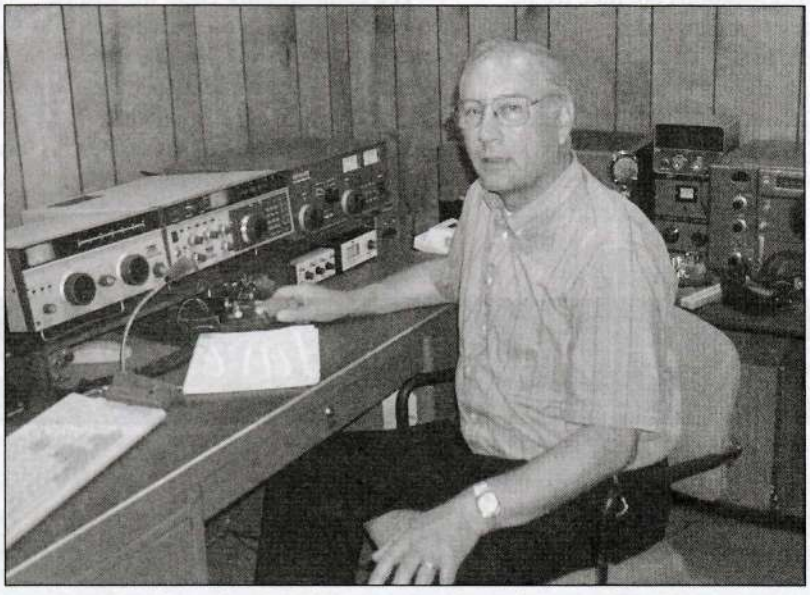

Amateur Radio station W1ZR, home station of the author. The unit on the far left is an early Ten-Tec 238 manual antenna tuner.

Contents

Radio Incompatibility? 1-2
Does My Antenna Have to be a Resistor? 1-2
So What's the Problem? 1-3
What Happens if the Radio and Antenna Aren't Matched? 1-3
So What Can We Do? 1-4
What's in a Name? 1-5
Review Questions 1-6

To transmit radio signals, you need a transmitter, often the transmitter side of a *transceiver* — a combined transmitter and receiver — and an antenna. Of course you will need a few other things such as legal authority to transmit, from the FCC in the US, a power source and an information source, such as a telegraph key, microphone or PC. In this book we will focus on the interconnection between the transmitter and the antenna, leaving the other topics to other books.

You might notice that, in spite of the book's title, we didn't mention antenna tuners — a device that goes between the transmitter and antenna. This is because, strictly speaking, an antenna tuner isn't necessary, at least not in all cases. The antenna tuner is only required if the transmitter can't put its output power into the antenna because of an incompatibility between them.

Radio Incompatibility?

A radio transmitter comes with a set of specifications. For proper operation, the owner is responsible to ensure that the requirements listed in the specifications are met. Some are straightforward, such as "power required: 13.8 V dc at 20 A max." If we plugged such a radio into a 120 V ac outlet, we wouldn't have a right to expect it to operate properly — in fact we might expect to see smoke and flames. We would need an intermediate device, called a power supply, to transform the 120 V ac in our outlet to the 13.8 V dc our radio wants.

The compatibility issue we will be considering here is one relating to the *ANTENNA IMPEDANCE* specification. While not all transmitter specifications include an explicit antenna specification, most will say something like *ANTENNA IMPEDANCE, 50 Ω (Unbalanced)* or possibly *ANTENNA IMPEDANCE, 50 Ω (Unbalanced) with SWR of 2:1 or less.* These specifications indicate the load that the antenna system must present to the radio for proper operation. We will discuss the different parts of this specification and what they mean as we go forward. As with the power supply, if the antenna doesn't meet the specification's requirements, we might need an intermediate device — possibly an antenna tuner.

Does My Antenna Have to be a Resistor?

The indication "50 Ω" does sound a lot like a resistor. The radio will be very happy to put its power into an actual 50 Ω resistor, in fact that's how we often test a radio when we don't want the radio signal to go out over the air. Unfortunately, a resistor absorbs the transmitter power and turns it into heat — it does not make a good antenna.

In a properly designed antenna, it is often the case that the antenna's radiating properties will be converted into a load that acts like a 50 Ω resistor to the radio, but actually radiates the power as radio waves.

So What's the Problem?

It would seem that we can solve our incompatibility problem by just buying (or building) an antenna that has a compatible specification of a 50 Ω resistive impedance and connecting it to our radio. This is quite true, and can be very successful — within certain constraints (see **Figure 1-1** for the ideal case). This compatible case is referred to as a *matched* system. Unfortunately, the real world rears its ugly head in a few ways:

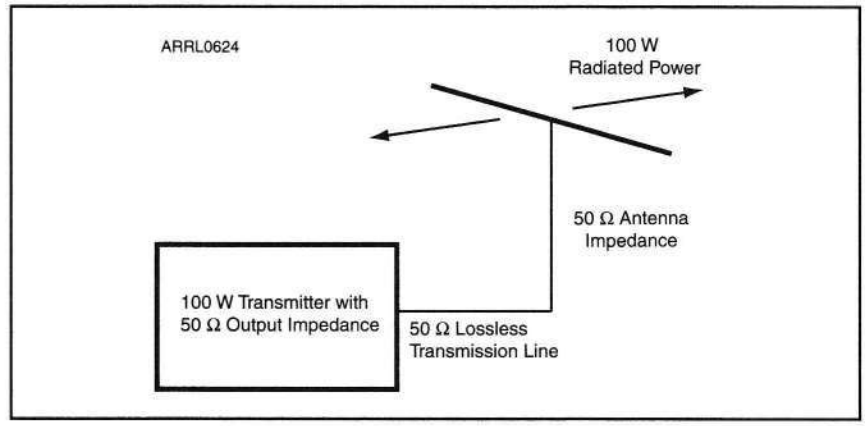

Figure 1-1 — Radio and antenna system with matched impedances.

- The biggest issue is that any antenna will have its particular design impedance on a single frequency. This is not an issue with many radio services — broadcast stations, for example — that operate on a single assigned frequency. Some services, such as the Amateur Radio service, operate within assigned bands. Shifting frequency from one end of the band to the other can result in a significant change in antenna impedance.
- A real antenna is always installed at some height above the local terrain. The electrical properties of the soil and the height above ground will have a significant impact on antenna impedance. For example, perhaps the simplest antenna, a half wave horizontal dipole has an impedance that varies from around 40 to 100 Ω as it moves from 0.1 to 0.35 λ (wavelengths) above ground.

What Happens if the Radio and Antenna Aren't Matched?

Most radios can tolerate a certain amount of mismatch from an antenna system without any problems. This is often specified in terms of standing wave ratio (SWR), a measure of mismatch. Often the allowed value is 2:1; which, for a 50 Ω system, would represent resistive values of 25 or 100 Ω (50/2, or 50 × 2).[1] Note that while the radio will operate without damage at this level of mismatch, it may not operate quite as well as if it were matched.

A mismatched load impedance in early solid state transmitters could result in damage to components in the power amplifier stages due to higher voltages or currents than it was designed to handle. Modern transceivers have *fold-back* circuitry that senses the mismatch and reduces transmitter power to avoid damage. Note that while the transmitter will not be damaged, and still can be used, it will put out less power, sometimes beginning to fold back at an SWR as low as 1.5:1. This is perhaps the most common reason that we might notice our 100 W transmitter actually putting out 25 W.

[1]In addition to these two resistive values, there is a whole set of combinations of resistive and reactive impedance components that will also result in an SWR of 2:1.

So What Can We Do?

Perhaps not surprisingly, one solution to this issue is something that is generally called an *antenna tuner*. The antenna tuner is a variable impedance transforming device that can transform the impedance of an antenna system so that it appears to the transmitter as a 50 Ω load, while causing almost all of the transmitter power to be radiated from the antenna, just as if everything were matched.

As shown in **Figure 1-2**, the antenna tuner can be placed directly at the transmitter and connect directly to an antenna. In many cases, a *transmission line* is used between the transmitter and the antenna. We will discuss transmission lines in more detail later, but for now be aware that a transmission line is frequently used if the transmitter and antenna are not in the same place. As shown in **Figures 1-3** and **1-4**, the antenna tuner can be placed at either the antenna end or the radio end of a transmission line interconnecting the radio and antenna. It could even be put at an intermediate point.

Much of this book will discuss the details of the different configurations and requirements of antenna tuners and where they are located, so you can make the most informed decision on what type of tuner to buy or build and where to install it.

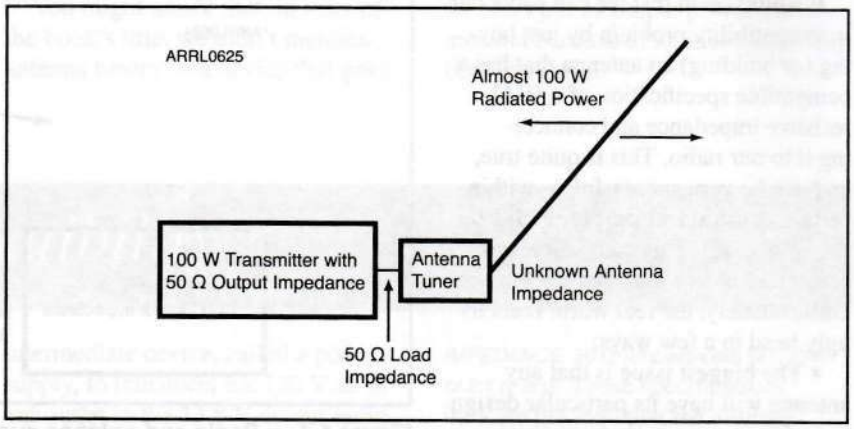

Figure 1-2 — Antenna tuner collocated with the radio and the antenna. All the transmitter power reaches the antenna except for any loss in the tuner, generally less than 5%.

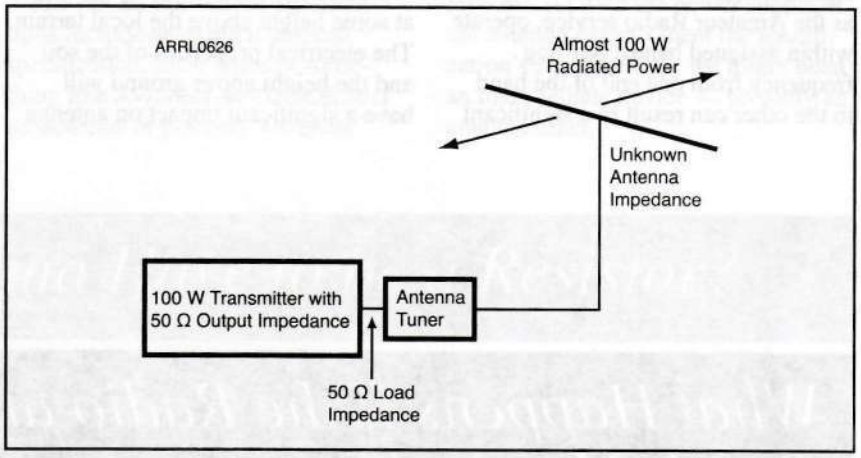

Figure 1-3 — Radio and antenna system with tuner located at the radio end of the transmission line.

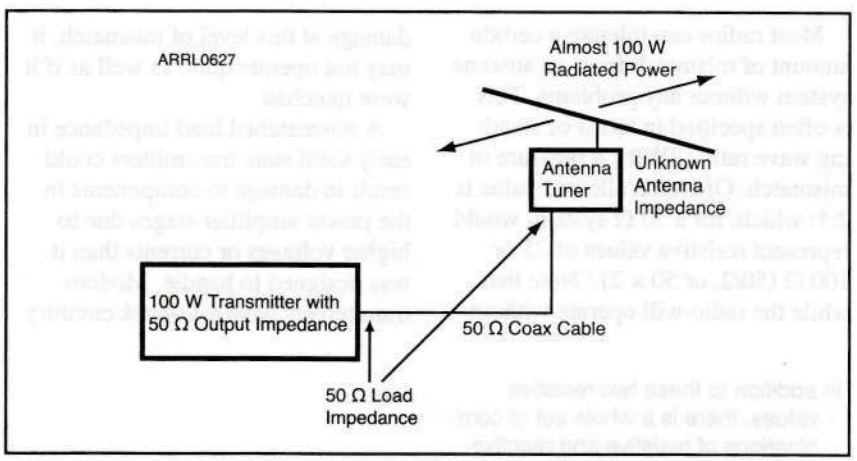

Figure 1-4 — Radio and antenna system with tuner located at the antenna end of the transmission line.

What's in a Name?

Over the years there has been some discussion of what to call this device I call an *antenna tuner*. There are those who would say that *antenna tuner* is a misnomer because it doesn't actually tune the antenna, but really tunes the transmission line in most applications.

Over the years many other terms have been used to describe this device. You will see references to an *antenna coupler*, *antenna tuning unit* (ATU) and a *transmatch* — all within various ARRL magazines and books. They all mean the same thing and refer to the same type of device.

The best name I've heard for this function is *antenna system matching device*. Since that doesn't resolve itself to an easy to pronounce acronym, throughout this book I will use the most common term *antenna tuner* with neither apology nor regret.

Review Questions

1-1 Under what conditions is there no requirement for an antenna tuner in a transmitting system?

1-2 How can you tell if an antenna tuner is needed?

1-3 What are the likely consequences of not having an antenna tuner, or having a misadjusted antenna tuner?

1-4 If an antenna tuner is properly adjusted on one frequency, what must be done if the operating frequency is changed?

Chapter 2

A Look at Typical Configurations

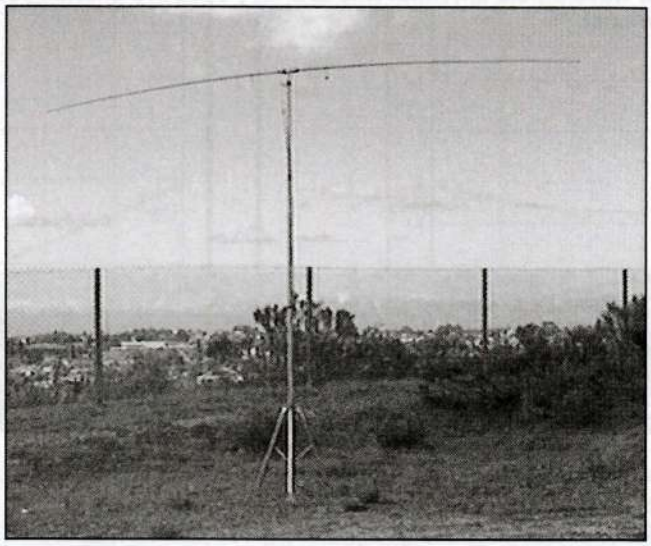

The classic half-wave dipole — an antenna mainstay at many amateur stations.

Contents

A Transmission Line — The Piece in the Middle 2-2
Dipole for the 40 Meter Amateur Band 2-3
The Dipole for the 80 Meter Amateur Band 2-4
Fractional Bandwidth 2-5
Review Questions 2-6

A very popular antenna for a new radio amateur is called a *half-wave dipole*. This antenna is easy to construct from two pieces of wire with a total length of about 468/f, where f is the frequency in MHz and the result is in feet. The antenna is often fed with 50 Ω coaxial cable as shown in **Figure 2-1**. Generally, the antenna length is trimmed equally on each side of center until the closest match to 50 Ω is found. While it will function as shown, more predictable performance is often obtained by inserting a device between the inherently balanced antenna and unbalanced (with respect to ground) coaxial cable to provide an appropriate transition between them. This device is generally called a balun — for balanced to unbalanced transition. We will discuss this in detail later in the book.

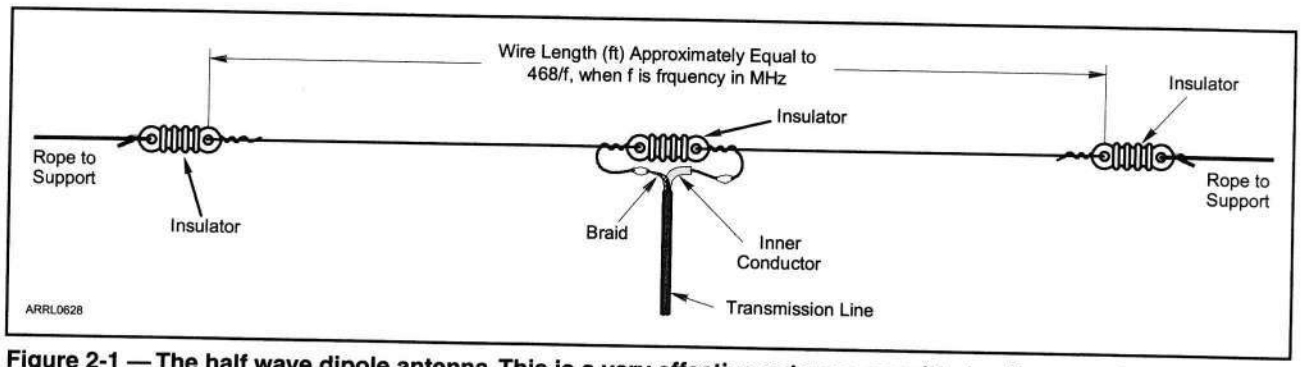

Figure 2-1 — The half wave dipole antenna. This is a very effective antenna, considering its ease of construction and low cost.

A Transmission Line — The Piece in the Middle

In most cases the antenna and radio are located in separate areas. Most often, the optimum location for the radio is somewhere that a person can comfortably operate a radio. For many types of radio systems, this means indoors. The antenna, on the other hand, is typically located outside so it can radiate with minimal obstructions and with at optimum height above the terrain.

It is possible to meet both requirements if an antenna is connected to the radio system through a *transmission line*. An ideal transmission line conveys energy from one end to the other in a totally transparent manner. A real transmission line, on the other hand does so with some limitations:

- Each type of transmission line has a characteristic impedance, Z_0. If the transmission line is terminated with an impedance equal to the Z_0, the same impedance will be seen at any length of line. Fortunately, there are many types of line that have a Z_0 of 50 Ω, so such a line connected to an antenna with a 50 Ω impedance will present a 50 Ω load to the radio no matter the length of the line. It is worth mentioning briefly at this point that if the line is terminated in an impedance other than its Z_0, the impedance at the far end in general will be neither the terminating impedance nor the Z_0 of the line.

These topics will be covered in much more detail later, but it's good to have an idea as we go through the basics.

- Real transmission lines have some associated losses. Thus not all the power put into the bottom by the transmitter comes out at the antenna. The attenuation is higher with increasing frequency, for a given type of line. The attenuation is also directly proportional to line length. In addition, the attenuation increases with standing wave ratio (SWR, a measure of mismatch) — another reason to have a matched system, if possible. We will discuss this phenomenon later.
- SWR is generally determined by measuring the ratio of reflected power to forward power. An SWR of 1:1 results in no reflected power. If the line has significant attenuation, both the power getting to the antenna, and any reflected power will be attenuated. Thus a measurement of SWR at the radio end will appear to be lower than the real SWR at the antenna end.

Dipole for the 40 Meter Amateur Band

If we were to make a dipole of the form of Figure 2-1 for the center of the US 40 meter band, we would use the formula 468/f, with the f equal to 7.15 MHz to result in a starting length of 65.45 feet, or 65 feet, 5.4 inches. As noted previously, this will vary with height, but let's say we get it all correct and have a height that provides close to a 50 Ω load at that frequency. If we then measure the standing wave ratio (SWR) across the band, 7.0 – 7.3 MHz, we would observe a set of SWR data very much like that plotted in **Figure 2-2**.[1,2]

Note that, as desired, we observe an almost perfectly matched condition (SWR of 1:1) at our design frequency of 7.15 MHz. Note also that as we change frequency across the band, our SWR rises to 2:1 at each band edge. Thus, even though our antenna is only closely matched at the band center, if the transmitter can operate at full power with a 2:1 SWR, this antenna will be usable across the band, if trimmed very carefully.

[1]Notes appear on page 6.

What About Height?

We have previously mentioned that changing height will also change the

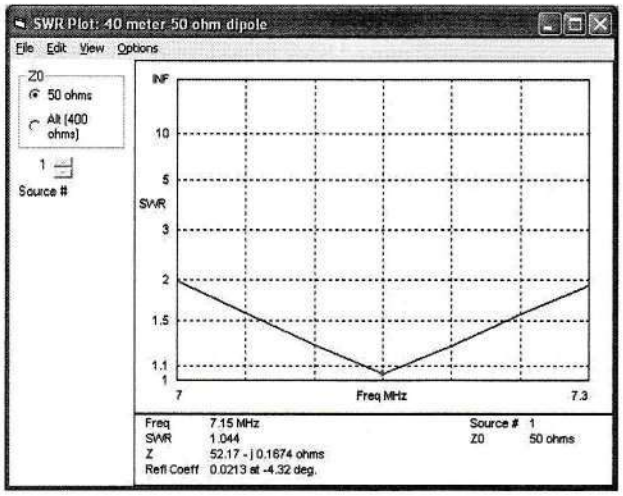

Figure 2-2 — Plot of SWR of a 40 meter dipole with height and length adjusted for 50 Ω at 7.15 MHz.

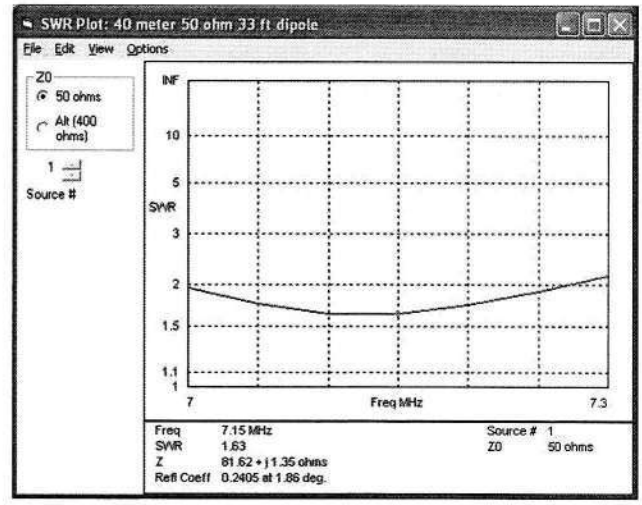

Figure 2-3 — Plot of SWR of a 40 meter dipole with height set to λ/4, about 33 feet.

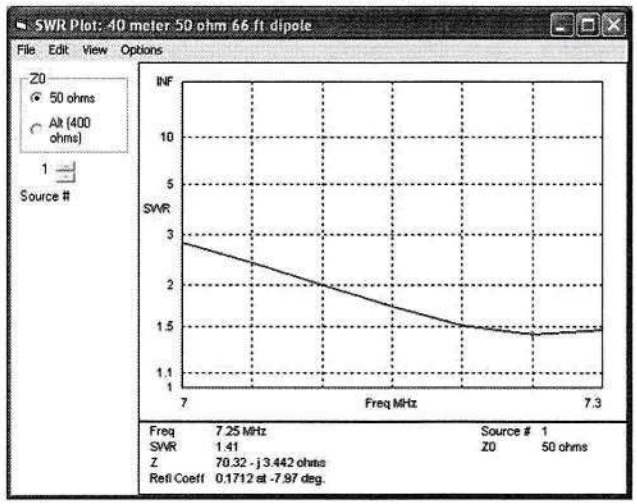

Figure 2-4 — Plot of SWR of 40 meter dipole of Figure 2-3 raised to a height of λ/2, about 66 feet. Note the change in frequency of minimum SWR. It could be tuned back to mid-band by lengthening.

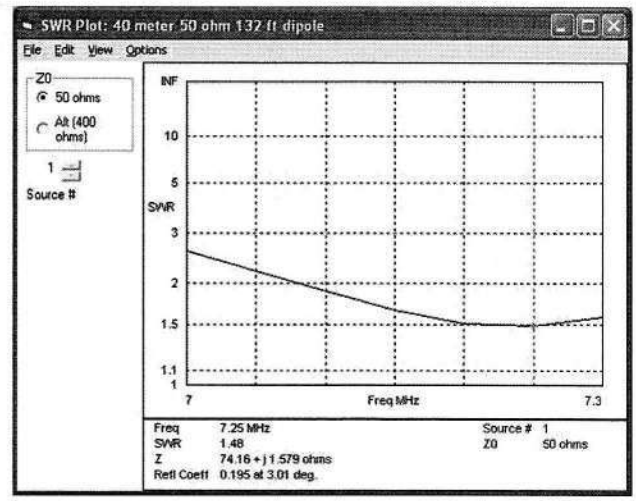

Figure 2-5 — Plot of same antenna raised to 1 λ, about 132 feet.

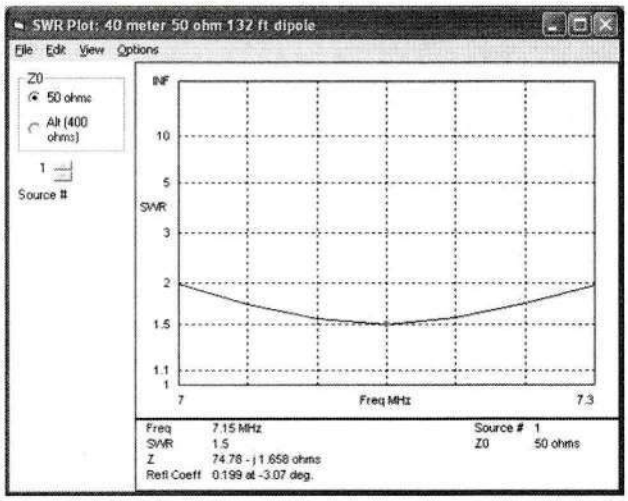

Figure 2-6 — Plot of SWR of a 1 λ high 40 meter dipole trimmed for mid band.

antenna impedance. In fact it will also change the resonant frequency of the antenna. To obtain the plot in Figure 2-2, we lowered the antenna to a height of 12 feet. While such an antenna will operate, the combination of its direct signal and the signal reflected from the ground will result in most of the radiation going skyward. This makes it suitable for short and medium range communication. In many cases antennas are raised higher to increase low angle radiation to support communication over longer distances.

Impedance and Resonant Frequency at Greater Height

Figs 2-3 through **2-5** are a series of SWR plots of the same antenna as it is raised, first to 33 feet (λ/4), then 66 feet (λ/2) and finally 132 feet (1 λ). Observe the two phenomena happening as the antenna is raised — first, the impedance is changing and second the resonant frequency (frequency at which the impedance is resistive) is changing. Note that the impedance shown is that close to the resonant frequency.

To improve the SWR, we can adjust the length by making it long enough so that the resonant frequency is moved back to mid band. The result is shown in **Figure 2-6**. Note that the antenna now has an SWR range across the band of 2:1 or less so it might still work well across the band without a tuner. Note that to achieve this result, it must be very carefully trimmed.

A Dipole for the 80 Meter Amateur Band

A dipole for 80 meters (don't worry, this is the last example) has a very different result. The US 80 meter (sometimes called 75 and 80 meters) band is wider than 40 meters, covering 3.5 to 4 MHz. The result, again with the height lowered and length adjusted to match 50 Ω at mid band is shown in **Figure 2-7**. This is a very different result from our 40 meter dipole's impedance over the band. The SWR at the band edges is now above 7:1, and the bandwidth over which the SWR is 2:1 or less, the SWR bandwidth, is about 150 kHz — about half what it was on 40 meters.

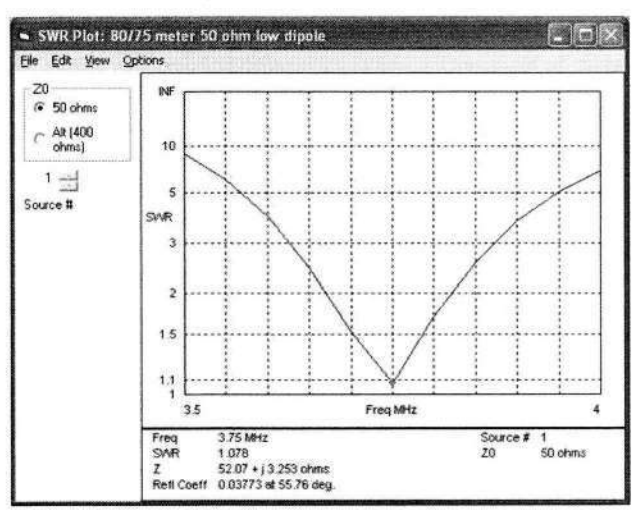

Figure 2-7 — Plot of SWR of a 80/75 meter dipole with height and length adjusted for 50 Ω at 3.75 MHz.

Fractional Bandwidth

The reduced bandwidth on 80 meters illustrates a few interesting principles. First, for a band this wide at this frequency, it would take at least three dipoles with slightly different lengths to cover the whole band if we didn't have a device to transform the impedance to a value we wanted — an *antenna tuner*. Second, we note that the key factor is not the bandwidth itself, but rather the fraction (or percentage) of the center frequency that we wish to be able to cover.

In the case of 40 meters, we were able to cover a bandwidth (7300 – 7000) of 300 kHz with an SWR of 2:1. This is the fraction 300/7150 = 0.042, or 4.2%. Note that on 80 meters we had about 150/3750 = 4%. We can use this as a predictor of whether a single thin dipole can cover each amateur band with the results shown in Table 2-1.

Clearly, the problem is most pronounced on 80 meters, perhaps why we chose that example. In addition, 160, 10 and 6 meters are wider than our threshold, as is the 70 cm band. Fortunately, the higher three of these bands have operations divided by mode, so that it is not unreasonable to have, for example, a horizontal 6 meter antenna centered at the low end for CW and SSB operation and a separate vertical antenna for FM designed for the high end. Many operators, however, like to work all portions of 160 and 80 meters, so that can be an issue.

Table 2-1

Percentage Bandwidth of Each HF and VHF US Amateur Band.

Band (Meters)	*Upper Frequency (kHz)*	*Lower Frequency (kHz)*	*Bandwidth (kHz)*	*Bandwidth (%)*
160	2000	1800	200	10.5
80	4000	3500	500	13.3
60	5407	5330	77	1.4
40	7300	7000	300	4.2
30	10,100	10,150	50	0.5
20	14,000	14,350	350	2.5
17	18,068	18,168	100	0.6
15	21,000	21,450	450	2.1
12	24,890	24,990	100	0.4
10	28,000	29,700	1700	5.9
6	50,000	54,000	4000	7.7
2	144,000	148,000	4000	2.7
1.25	222,000	225,000	3000	1.3
70 cm	420,000	450,000	30,000	6.9

Notes

[1]This plot was obtained using an antenna modeling program named *EZNEC*. We will call upon this program repeatedly throughout the book. Several versions of *EZNEC* antenna modeling software, including a free trial version, are available from developer Roy Lewallen, W7EL, at **www.eznec.com**.

[2]For an introduction to *EZNEC* modeling, see Appendix A of J. Hallas, W1ZR, *Basic Antennas — Understanding Practical Antennas and Design*. Available from your ARRL dealer or the ARRL Bookstore, ARRL order no. 9994. Telephone 860-594-0355, or toll-free in the US 888-277-5289; **www.arrl.org/arrl-store**; **pubsales@arrl.org**. See chapters 2-6.

Review Questions

2-1 Under what conditions might a ½ wave dipole not be compatible with a radio system?

2-2 Why can a transmission line tend to mask a high SWR?

2-3 If a dipole should be able to cover a complete amateur band, but doesn't because the minimum SWR is higher than the middle of the band, what can you do to improve the situation?

2-4 If you have no antenna tuner, how many separate dipoles would be required to cover the entire 10 meter amateur band with an SWR of less than 2:1?

Chapter 3

So Just What Is *an Antenna Tuner?*

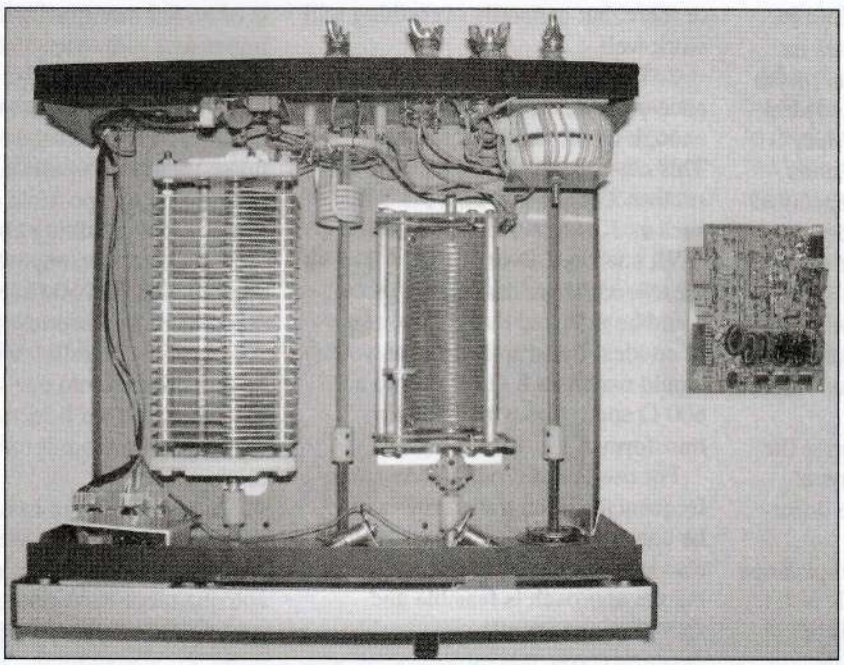

On the left, inside view of a manually tuned 1500 W L-network HF tuner (Ten-Tec 238); on the right, a computer controlled 100 W automatic tuner (Elecraft KAT3) designed to fit inside the compact Elecraft K-3 HF and 6 meter transceiver.

Contents

What's In an Antenna Tuner..... 3-2
Antenna Tuner Controls..... 3-3
Sidebar — A Quick Discussion of Standing Wave Ratio 3-4
Where are the Knobs on an Automatic Antenna Tuner? 3-8
What's the Best Tuner for You? 3-9
Review Questions..... 3-10

As noted in Chapter 1, *the antenna tuner is a variable impedance transforming device that can transform the impedance of an antenna system to appear to the transmitter as a 50 Ω load, while causing almost all of the transmitter power to be radiated from the antenna, just as if everything were matched.* This sounds like just what we need to solve the problem of using an antenna system that has an SWR that the transmitter doesn't like to deal with.

While an antenna tuner may well be just what we need — they come in many flavors, shapes and sizes — not to mention specification ratings. Much of this book will deal with how to choose the best type of antenna tuner, as well as to determine the best place in the system to locate it.

What's In an Antenna Tuner?

In order to perform its transformation function, an antenna tuner must deal with any load that is within its specified limits (everything has its limits — no antenna tuner can match absolutely everything!). As noted in the sidebar, an SWR greater than 1:1 happens if the load of the antenna system is different from the specified output load impedance of the transmitter, 50 Ω for most current designs. Table B in the sidebar shows some representative values of resistance and capacitive or inductive series reactance that result in various values of SWR.

Note that we could categorize the load impedance into four general categories that could all have different solutions:

1. The load is a resistive impedance of 50 Ω. In this case the SWR is 1:1 and we don't need an antenna tuner at all. We could bundle with this all loads that work well with the transmitter without change — perhaps those with an SWR of less than 2:1. There may be a bit of extra loss here or there, but generally everything will work well.

2. The load is a resistive impedance other than 50 Ω , and not close enough to allow proper operation. This could be loads with a 2:1 SWR such as 25 Ω or 100 Ω, a 3:1 SWR such as 16.7 Ω or 150 Ω, or a 10:1 SWR such as 5 Ω or 500 Ω. All of these loads share the fact that they could be matched through the use of an ideal transformer, just as you would match an 8 Ω speaker to a 600 Ω audio line with an audio transformer.

For use in radio rather than audio frequencies, such transformers must be constructed differently to avoid also introducing reactive components, but the approach is feasible and sometimes encountered. One classic example is the matching arrangement employed in a wideband antenna often used at HF called a rhombic. It offers an almost resistive load of around 600 Ω over a 4:1 frequency range and is often fed through a wideband 12:1 impedance ratio transformer by a 50 Ω system. **Figure 3-1** shows the idea. While most folks would call it a transformer rather than an antenna tuner, there's no question that it is performing one possible class of the function we're talking about.

3. The load is composed of a combination of a 50 Ω resistive component and a series reactance. A load with a parallel reactance can be transformed into one with a series reactance, but we'll focus on the series version since it may be easier to visualize.

This makes for an easy to imagine antenna tuner. If the series reactance of the load is inductive ($+X_L$), all the antenna tuner need contain is a component with a capacitive reactance of the same magnitude, ($-X_C$). The series combination of the two is just 0 Ω reactive, so the resultant is the

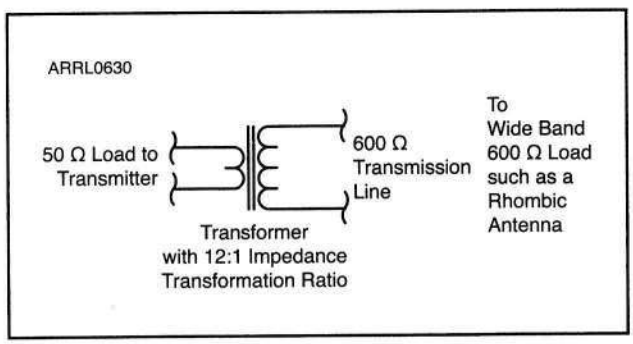

Figure 3-1 — A wide-band impedance transformer can serve the function of an antenna tuner for a resistive load.

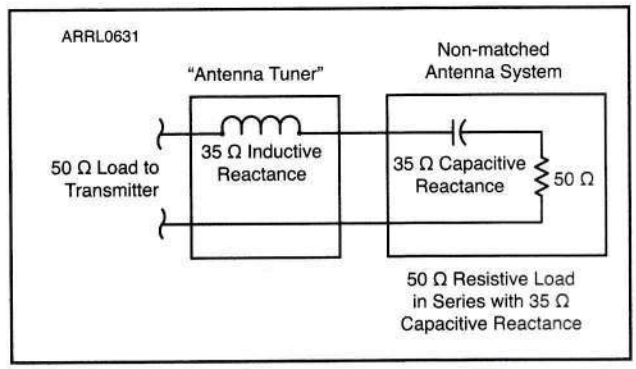

Figure 3-2 — Antenna tuner for special case of reactance in series with resistive part equal to Z_0.

resistive component —50 Ω as shown in **Figure 3-2**.

Note that, unlike the wideband transformer, this will likely work only on a single frequency. If the antenna has an inductive reactance, it will tend to increase with frequency ($X_L = 2 \times \pi \times f \times L$), at least over a limited frequency range. In order to keep the total impedance resistive, we will need a variable capacitor, so we can adjust the capacitive reactance to match the changing inductive reactance of the load. Note that our "antenna tuner" now has a knob on the front, and is starting to look more like an antenna tuner.

4. The load is a combination of resistive and reactive components that have an SWR greater than we can deal with and that falls in none of the other three categories. This is the general case — the one all general purpose antenna tuners must deal with, at least over some range of SWR.

There are a number of circuit configurations that can be employed that will do a combination of cancelling the reactance and transforming the resistive impedance. We have cataloged them in **Figure 3-3** so you will recognize the configurations as we discuss them. In many cases, if constructed of the same quality components, they will provide equivalent performance. As with all general purpose devices, there are certain advantages and disadvantages of each, and some may be more appropriate for some applications than for others.

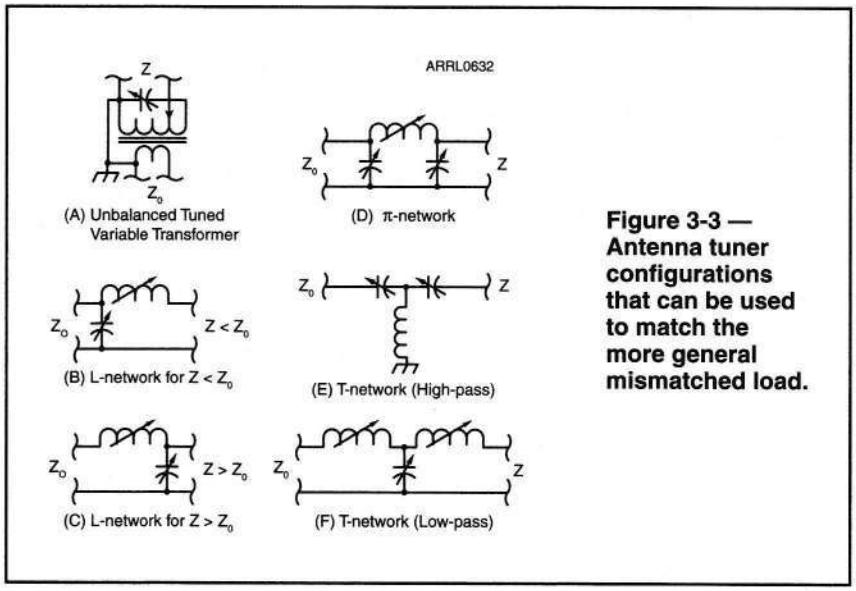

Figure 3-3 — Antenna tuner configurations that can be used to match the more general mismatched load.

Another categorization that can be made is whether the tuner is designed to feed an unbalanced load, typically fed with coaxial cable or a single wire against ground, or is intended to feed a balanced load such as a dipole fed with balanced open wire transmission line. Each of these configurations can be adapted to either task, however, we will defer that discussion until later.

Antenna Tuner Controls

Not surprisingly, many of the different manual antenna tuner configurations have different control arrangements.

L-Network Tuner Controls

The L-network has two primary adjustments, an inductor and a capacitor. In the Ten-Tec 238 tuner shown in **Figure 3-4**, and in most L-network tuners, each control is adjustable throughout its entire range on any band, providing maximum flexibility. In addition, there is a switch to move

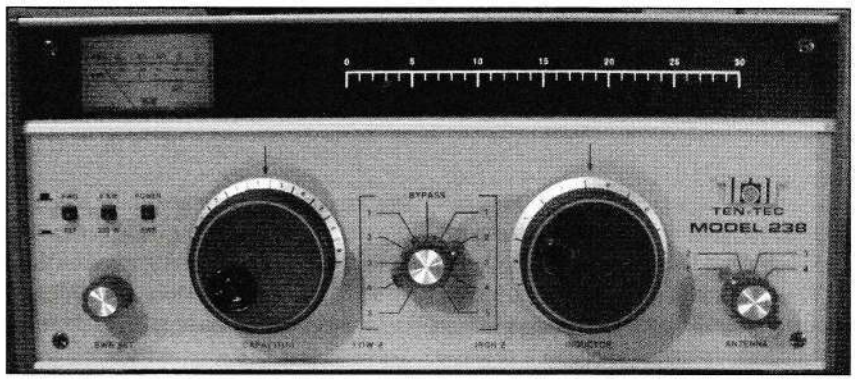

Figure 3-4 — Front panel view of an L-network tuner, an early version of the Ten-Tec 238.

A Quick Discussion of Standing Wave Ratio

We discussed standing wave ratio in Chapter 2 and noted that a matched antenna system has a standing wave ratio (SWR) of 1:1. That is the case in which there are no standing waves and all energy from the transmitter is delivered to the load with no reflections on the transmission line. This is a very straightforward situation that is easy to understand. Getting into the details of this topic can get lengthy and there are entire books devoted to the topic.[A] Fortunately, we won't need to get that deeply involved to understand antenna tuners and their applications. Still, we need to have some idea about SWR, what it means and what its consequences are to understand, when and if it is a problem and how to solve it.

The Matched Transmission Line

If we were to connect a battery to a long real transmission line with no load and monitor the current that would flow with a high speed oscilloscope we would notice an interesting effect. The combination of the line series inductance and shunt capacitance, and to a lesser effect the wire resistance, would result in an initial current that would flow, even though there is an open circuit at the far end.

The current will continue to flow until the signal propagates to the end of the line and returns. When it reaches the end of the line (traveling somewhat slower than the speed of light) a *reflected* wave of the opposite polarity will propagate back because there can be no current flow at the open circuit. When the reflected wave returns to the source end of the line the combination of the forward and reflected wave will result in zero current — just what we would expect for an open transmission line.

The ratio of the applied voltage to initial current is an impedance and we call this the characteristic impedance or Z_0 of the transmission line. This is the current that would flow into an infinite length of line no matter what is at the far end. Note that we didn't say anything about signal frequency here, this is strictly a matter of the way the line is constructed, especially the capacitance and inductance that is distributed along its length. For the usual low loss line, ignoring resistance, we can determine Z_0 as follows:

$$Z_0 = \sqrt{L/C}$$

where L and C are the inductance and capacitance per unit length, typically per foot or per meter. These values can often be found in many manufacturers' specification sheets.

The Matched Transmission Line

If, instead of having an infinite line, we put a resistor with a resistance equal to the line Z_0 on the far end of the line it will absorb the power as it arrives and there will be no reflection. The voltage and current relationship at the signal end of the line will appear as if it were the same resistor, just located at the source.

This is exactly what we wanted! If the source is a radio designed to drive a 50 Ω load, Z_0 is 50 Ω and our load is an antenna with an impedance of 50 Ω, we get just what we want — to our transmitter it appears as if the antenna is connected directly to the antenna. There is no reflected power, the SWR is 1:1 and all is well with the world.

The Mismatched Transmission Line

There are an infinite number of cases in which a transmission line is terminated, not with its Z_0, nor with an open or short, but with some other impedance. This results in a reflection of a signal that is smaller than the signal that was sent down the line. It is important to note that this signal does not represent lost power, because it is re-reflected from the transmitter back up to the line. It is true that the power delivered to the antenna will equal the forward power less the reflected power, however, because the power is re-reflected at the transmitter so the numbers go up together. This is illustrated in **Table A** for the case of perfect (lossless) transmission line, assuming the transmitter can put power into the SWR shown.

So What's the Big Deal

The key is the two reasonable assumptions noted above. Let's discuss each:

■ Transmission lines are not lossless, and their losses increase with increasing SWR as we will discuss. Whether or not that's a problem depends on the line

Table A

Example of Net Transmitted Power with 100 W Transmitter versus SWR with Lossless Transmission Line

SWR	*Reflection %*	*Forward Power*	*Reflected Power*	*Antenna Power*
1:1	0	100	0	100
2:1	10	111	11	100
3:1	25	133	33	100

the variable capacitor between the two ends of the inductor to allow tuning of both high and low impedance loads.

This particular tuner uses a rotary inductor (see **Figure 3-5**) for adjustment of inductance. The coil turns with rotation of the shaft on the left end. As it turns, its point of connection to the small wheel on the top in the picture is moved up and down the coil. It requires about 30 turns of the knob to adjust from the minimum to the maximum amount of inductance. Some tuners use a switched inductance instead. The switch allows a quicker change of settings, but does not provide for values of inductance between the switched taps. This is not generally a problem, although there are some loads that can't be tuned to a 1:1 SWR at some frequencies — still close enough works. Note that there is no bandswitch, on this model, since any available adjustment

type, frequency and SWR as we will discuss later.

■ Often a more serious problem is that somewhere in the range of SWR in Table A, typically by an SWR of 2:1, transmitters will reduce power to avoid damage due to the higher current or voltage that results from the higher than specified SWR.

Note that the second problem is not a fundamental issue of SWR itself, but rather a design choice made by transmitter designers. Still, for transmitters that we may choose to use, it is a real problem that we have to deal with.

What Kind of Load Results in High SWR

Any load that is different from Z_0 of the transmission line will result in a SWR greater than 1:1. For the case of the frequently encountered 50 Ω coaxial cable, that means any load that is not 50 Ω resistive. This can mean a load that is resistive with a value of other than 50 Ω or a load that is resistive, but also has capacitive (–X) or inductive (+X) reactance, or any of an infinite number of combinations of the two. Some examples of loads with different SWRs are shown in **Table B**.

Note that it is very easy to determine the SWR for the resistive case — it's just Z_0/R or R/Z_0 depending on whether the load is greater or less than the Z_0.

Thus it is important to know not just the resistive part, but also the equivalent series inductive or capacitive reactance to determine the SWR.

Determining SWR from Impedance Data

While the case for resistive loads is simple, the case for loads with reactance or complex loads is well — more complex. Still, there are at least three ways that I know of to determine the SWR of a complex load, not counting measuring with an SWR meter, as follows:

■ Use the software TLW (Transmission Line for Windows) that comes packaged with recent editions of The ARRL Antenna Book.[B] If you plug in the R and X values and the appropriate transmission line Z_0, it provides the SWR at each end of the line. You can select which end of the line has the measured Z (input or load). This is very handy since it will also calculate the line loss.

■ This may be the most simple calculation to make graphically with a Smith Chart.[C] Recall that if the Z is just resistive (X=0), the SWR is either Z_0/Z or Z/Z_0, depending on whether the Z is lower or higher than the Z_0. Recall also that a circle on a Smith Chart represents constant SWR. Thus if you enter the Z on the Smith Chart and draw a circle centered on the chart center, it will show the transformed Z for any length of line. Either point at which the circle crosses the resistive axis can be used to calculate the SWR as described above.

Table B

Impedance of Loads that Result in Different SWRs.

For Ideal 50 Ω Coaxial Cable

R (Ω)	*X (Ω)*	*SWR*
50	0	1:1
25	0	2:1
100	0	2:1
50	±35	2:1
30	±18	2:1
16.7	0	3:1
150	0	3:1
50	±58	3:1
30	±40	3:1
5	0	10:1
500	0	10:1
50	±142	10:1
250	±250	10:1

■ If you have neither computer nor Smith Chart, you can compute the SWR directly. This can be found, for example, in a book I had as a text many years ago, a classic by the late John Kraus, W8JK, *Antennas*. In the first edition it is in the appendix on page 507. The calculation is done in two steps:

1. Find the voltage reflection coefficient σ:
   $\sigma = (Z-Z_0)/(Z+Z_0)$
   Note that the Z is a complex number, so the calculation is a bit tedious.
2. Find the SWR = $(1 + |\sigma|) / (1 - |\sigma|)$
   where $|\sigma|$ indicates the magnitude of the complex reflection coefficient, σ, found in step 1.

Notes

[A] W. Maxwell, W2DU, *Reflections*, check his Web site for information on availability of the latest edition at **w2du.com**.

[B] R. D. Straw, Editor, *The ARRL Antenna Book*, 21st Edition. Available from your ARRL dealer or the ARRL Bookstore, ARRL order no. 9876. Telephone 860-594-0355, or toll-free in the US 888-277-5289; **www.arrl.org/shop**; **pubsales@arrl.org**.

[C] Paper copies of 50 Ω Smith Charts are available from your ARRL dealer or the ARRL Bookstore, ARRL order no. 1341. Telephone 860-594-0355, or toll-free in the US 888-277-5289; **www.arrl.org/shop**; **pubsales@arrl.org**.

is usable on any band — you just crank until you are within range. It may even be helpful for upper body development.

The capacitor can be a single, or multiple section type or a combination of a variable and fixed capacitors. In my tuner, the switch that moves the capacitor from one end of the inductor to the other has additional positions that switch in fixed capacitors in parallel to extend the tuning range. The fixed and variable combination allows somewhat finer tuning, but in multiple steps. A larger variable with a multi-turn vernier dial may be equivalent, and may be quicker to adjust.

An advantage of the L-network tuner is that there is only a single combination of L and C that will match a given load. As noted below, some tuners can offer more than one, but only one is optimum.

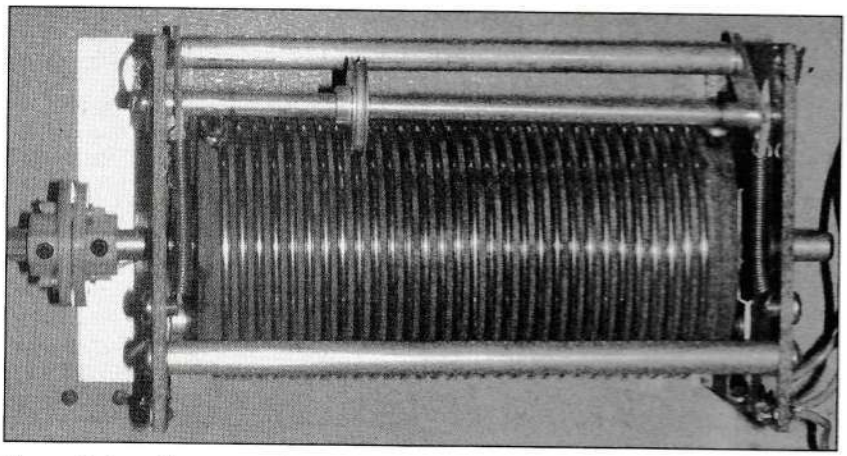

Figure 3-5 — Close up of a rotary inductor.

Pi- and T-Network Tuner Controls

Pi- and T-network tuners have three tuning controls — usually one inductor and two capacitors. Pi-network tuners that started out in the age of vacuum tube transmitters with pi-network output circuits often are built with similar components and are thus bandswitched as in the Drake MN-2000 tuner shown in **Figure 3-6**. In this tuner, the bandswitch sets the inductance to a preset coil tap for the middle of the expected range and the capacitors on both ends are used to provide the closest match. This configuration can be useful, but generally has less tuning range than those with adjustable or switched inductors in small increments.

Note that a pi-network tuner set to minimum capacitance on either of the capacitors essentially becomes an L-network tuner, with the high or low impedance determination dependent on which capacitor is set to around zero.

With either the pi- or T-network tuners, sometimes multiple very different settings can be found that will tune a particular load. In general, a setting with the minimum inductance is more efficient since the wire resistance of the inductor can dissipate power.

Tuned Transformer Tuner Controls

The tuned transformer is essentially the same as an output circuit from an earlier, before the pi-network, kind of transmitter. It typically has a balanced tuned circuit designed to resonate on a particular band (there weren't as many back then) using a fixed inductor and variable capacitor. The typically balanced transmission line was tapped symmetrically on the coil — close to the center for low impedance loads, close to the ends for high impedance loads. Small clips were generally used to provide load connection points. Very low impedance loads were connected in series with the center of the inductor.

Any reactance in the load would detune the tuned circuit that would then be readjusted by retuning the variable capacitor. The usual transmitter side connection was a link of a few turns that could be mechanically moved in and out of the center of the coil to provide adjustable coupling.

It was actually simpler to adjust than describe. Once the tap points were located for a particular band using the usual single antenna, the clips were fixed in place, and this became just one more coil to be changed while changing frequencies. Both transmitters and receivers of the pre WW2 era often had plug-in coils that required changing each time a band change was desired.

The 1950s era E. F. Johnson *Matchbox* antenna tuner (see **Figure 3-7**) was a radical design change to the tuner transformer type of tuner. This was the era in which transmitters and receivers were generally bandswitched and the Matchbox was an effort to make antenna tuning just as easy. What made the matchbox unique was a patented differential capacitor design that allowed a variable capacitance to be made of two capacitors — one that increased and one that decreased as it was rotated.

A pair of these were placed across the tuner resonant circuit allowing the transmission lines in the middle of each to be tapped across the resonant circuit using capacitive "taps" instead of the previous inductive taps. This allowed a continuously adjustable impedance setting to be made from the front panel. The bandswitching allowed bands to be changed without changing coils. This was very popular at the time, and they are still popular today. They do have some limitations, principally that they only work on the amateur bands of that day, not 30, 17 and 12 meters — although they may

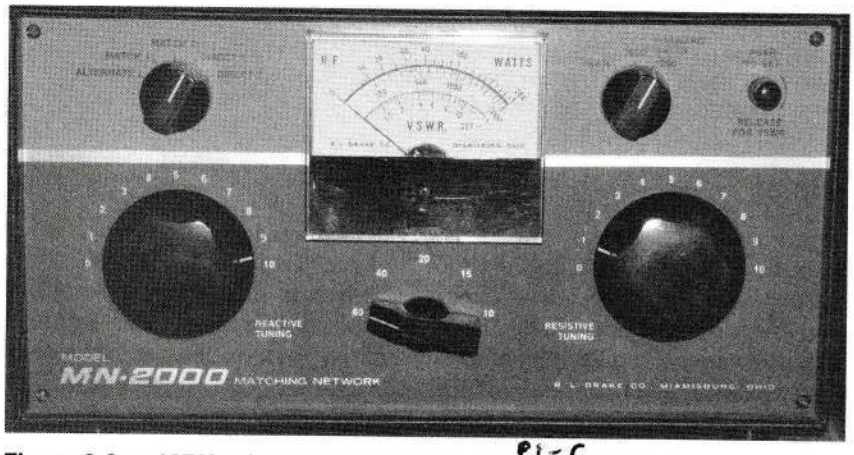

Figure 3-6 — 1970's vintage bandswitched ~~pi-network~~ Pi-C tuner.

THE DRAKE MN-2000 IS NOT A PI-TYPE CIRCUIT BUT A PI-C CIRCUIT WITH THE INPUT CAPACITOR AND THE COIL BEING FIXED (BAND-SWITCHED) AND THE TWO OUTPUT CAPACITOR BEING VARIABLE. THIS IS VERY CLEVER DESIGN, THE Q IS

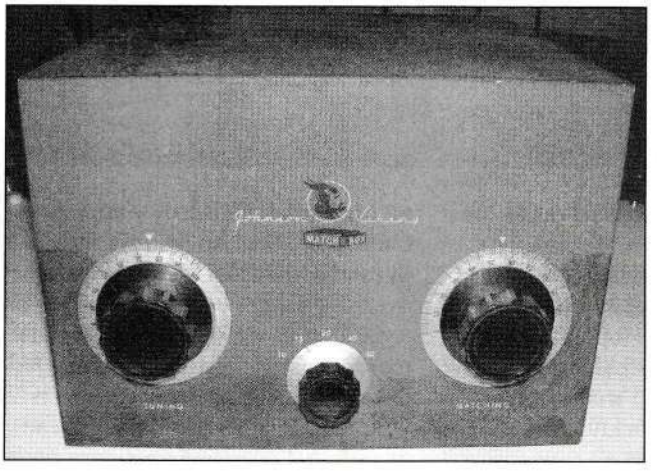

Figure 3-7 — 1950's vintage E. F. Johnson *Matchbox* antenna tuner.

drive some loads on the higher bands by setting to an adjacent band.

Antenna Tuner Metering

Many antenna tuners include metering, either directional power meters or an SWR bridge. These can be used to monitor progress while adjusting the antenna tuner — either for minimum reflected power, or for minimum SWR. Arguably, this is somewhat redundant if the connected radio transmitter also has SWR or reflected power measurement capability, although some meters in tuners may be more sensitive or easy to read.

While there is certainly no harm in having redundant metering, if your radio meter is easily visible from the antenna tuner location, and has sufficient sensitivity to allow proper tuning, there isn't much benefit in my opinion. The early transceivers, and especially pre-transceiver transmitters, did not generally include that function, perhaps explaining why most tuner manufacturers still provide them. For most users with metering in the transmitter, transmission line current meters on the output side of the tuner would actually be more useful. To my knowledge, alas, no tuner manufacturers now include these.[1,2]

Tuner Limitations

All tuners are composed of combinations of inductors and capacitors in various combinations. Since the impedance at a high SWR can vary widely, the tuner needs to have a wide range of values in order to be able to accommodate all possibilities at every frequency within its range. It is generally the case that the lower the frequency, the more inductance and capacitance will be required. Thus the maximum available inductance and capacitance, generally determines the low frequency limit of operation.

In the case of high power tuners with large components, it is not unusual for tuners that cover down to 160 meters (1.8 MHz) to be in larger enclosures simply because the size of the components is larger. In a similar way, it is the minimum capacitance and inductance that sets the high frequency limit. In this case, one must often look beyond the specified values of the components themselves and look to the stray capacitance of wires and component frames to the cabinet, as well as the inductance of connecting wires between components. Some tuners have trouble matching loads on 10 meters (28 to 29.7 MHz in the US) that would be easy to match at lower frequencies for this reason.

Increasing power with high SWR can result in very high currents and voltages within the tuner, requiring large components for high power tuners. The large components, in addition to making the box much bigger, also make the control of stray inductance and capacitance more of a challenge for the designer.

[1]Notes appear on page 9.

CONSTANT (18) OVER THE TUNING RANGE AND THERE IS ONLY ONE MATCH FOR A GIVEN IMPEDANCE IN CONTRARY TO THE T-TUNER.

Where are the Knobs on an Automatic Antenna Tuner?

Automatic antenna tuners don't generally have tuning knobs. Instead, they have a microcontroller that monitors SWR or reflected power and uses an algorithm to step through allowable values of L and C until a match is found. Any of the tuner topologies in Figure 3-3 could be used in an automatic tuner with an appropriate control mechanism.

Some automatic tuners use rotating variable capacitors and rotary inductors, just as in many manual tuners. In fact some are adaptations of manual tuners with servo motors and controllers added on as an additional physical and logical layer.

I do think it is safe to say, however, that the majority of auto tuners use a set of discrete components instead of variable ones. A range of inductance is provided by using relays to switch different sizes in series to reach the desired value. Similarly, a range of capacitance can be provided by having multiple capacitors switched in parallel. By having values available in a series such as 1, 2, 4, 8, 16, 32, 64, 128, 256 for example, any value from 1 to 511 (either pF or μH) can be obtained in steps of 1 unit. Thus any needed resolution and range can be easily provided.

While such switching, if done manually with toggle switches, might make us go over the top, it's duck soup for a microprocessor. The hard part may be defining a computer algorithm that can quickly find the right values without trying all combinations. Fortunately, that just needs to be done once and is provided "free" with the tuner. Most auto tuners can find a suitable match within a defined threshold, often 1.5:1, within a few seconds with no additional information about the antenna being tuned.

Many auto tuners have the capability to memorize the appropriate settings for a particular load once it's found. There are two approaches to this, both can be quite successful:

Memory stored by frequency. Perhaps most commonly found in tuners is the storage of tuning data based on frequency. Of course, this requires that the tuner measure the frequency before it can tune.[3] Most tuners have a number of frequency "bins" of a certain bandwidth, for example perhaps 25 kHz. If the frequency is within that bin, the last successful setting from a frequency within that bin will be used. If it doesn't meet the threshold, the tuner will start tuning over.

Obviously, the smaller the bin, the more successful the tune is likely to be, assuming the same antenna is used. On the other hand, this depends on previous operation within the bin, so it takes longer to accumulate data for all bins. Most tuners seem to have it about right, in terms of trade off.

Memory stored by past success. A different approach is to just keep track of the last number of successful tuner settings, independent of frequency. Let's say the tuner remembers the last 100 successful tuner settings. It just very quickly tries all those before it initiates its regular tuning algorithm. It is quite likely that recent conditions will be repeated. This approach is particularly advantageous for a single port tuner that is switched between multiple antennas making multiple successful tuner settings appropriate within a single frequency bin. Of course an advantage for the manufacturer is that the tuner doesn't need to measure or otherwise determine transmitting frequency.

What's the Best Tuner for You?

The best tuner for a particular application will depend largely depend on your antenna system and operational needs. Automatic antenna tuners inside transceivers are convenient and don't require extra space or wiring. Check the specs carefully, many do not cover a wide impedance range (many are spec'd at 3:1, although some may do better than spec). Interestingly, the internal tuners from Elecraft, FlexRadio and Ten-Tec do provide wide range (to 10:1 SWR) tuning, perhaps others will follow in this direction. The other disadvantage of internal tuners is that you will need a tuner with a higher power rating if you use, or consider using a linear amplifier. A high power tuner will work fine at low power, if the linear is in your plans.

Manual Tuners often offer antenna switching and control functions, not present in many auto tuners. Manual tuners also often provide continuous tuning to allow setting the controls for an exact 1:1 SWR, although that doesn't really provide a significant benefit.

Automatic tuners have a number of advantages and not many disadvantages. Some can be operated remotely at or near the antenna to reduce system losses. Either of the memory tuner types can reduce the tuning time for previously encountered antennas from a few seconds to a few tenths of seconds. Arguably either is significantly quicker to get into operation than a manual tuner, even with recorded dial settings.

The rest of the book will explore these issues in more detail.

Notes

[1]E. Nichols, KL7AJ, "Keeping Current with Antenna Performance," *QST*, Feb 2009, pp 34-36.

[2]P. Danzer, N1II, "A Simple Transformer to Measure Your Antenna Current," *QST*, Sep 2009, p 35.

[3]Internal, or brand specific tuners have the advantage that the frequency information can be made instantly available from the radio circuitry.

Review Questions

3-1 What are two reasons to provide a matched, or nearly matched, load to a transmitter?

3-2 What is the SWR of a 50 Ω cable with a 500 Ω resistive load? How about a 500 Ω transmission line with a 50 Ω resistive load?

3-3 If a 100 W output transmitter is connected to a lossless antenna system with a 3:1 SWR and it can deliver its full power, how much power reaches the antenna? How much power is reflected from the load?

Chapter 4

Tuning an Antenna Tuner

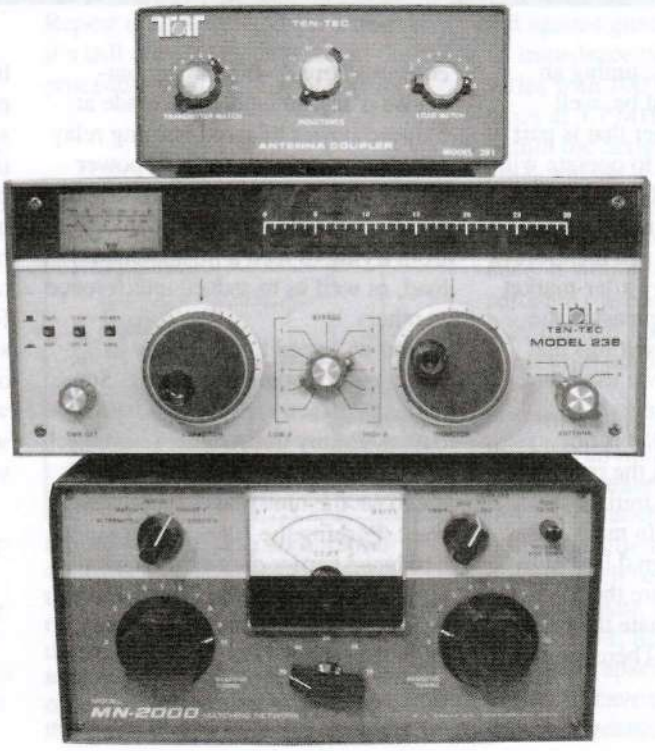

Tuning controls of three manual tuners. On top, a 100 W Pi-network, in the middle a 1500 W L network tuner and on the bottom a bandswitched 1000 W Pi-network tuner.

Contents

Tuning an Automatic Tuner 4-2
Tuning a Manual Tuner 4-3
A Simple Transformer to Measure Antenna Current 4-6
Review Questions 4-7

By now we, hopefully, know what an antenna tuner is, and why it may be a good idea. The next question should be "how do we work it?" The answer to this depends a bit on the type of tuner and your configuration. In all cases, the most important rule is: *Don't interfere with other users of the band!* This is an issue because all types of tuners require the transmission of RF for at least the final adjustment.

This is because tuning is considered complete only if the SWR is close to 1:1, and it takes a signal to be able to measure SWR. Even if the signal is of a reduced amplitude, people have been known to make worldwide contacts with transmitters running less than 1 W, so don't assume a low powered TUNE signal won't go anywhere.

If you are worried about loosing track of the current frequency that has a particularly desirable station; just put it in memory, tune off the frequency, adjust the tuner and, when tuning is complete, recall the desired frequency from the memory. You should be good to go, and you won't ruin it for someone else.

Tuning an Automatic Tuner

As its name implies, tuning an automatic tuner should be, well *automatic*. If it's a tuner that is part of the radio, or designed to operate with the radio, there is likely a TUNE button that reduces power, sends a carrier on the desired frequency and then forces the tuner to tune. Many after-market automatic tuners first measure the frequency and try the settings that worked the last time you used that frequency, or one close to it.

If the tuner is one that is not designed to work with the radio, you generally will need to initiate the process in some way. In many cases, if a transmitted RF signal is sent to the tuner it will measure the SWR and automatically initiate the tuning process if it needs to. There are two concerns here — first, many tuners want adjustments to be made at reduced power to avoid burning relay contacts — second, reduced power should also be used during tuning to avoid potential transmitter damage from trying to feed a mismatched load, as well as to reduce interference to others.

You will need to find a way to easily reduce power for tuning. Some radios do exactly that with a TUNE button. On my transceiver, I have such a button and a menu selection allows me to set the tune power to any level I want. Pushing the TUNE button sends a reduced carrier out of the transmitter until I push it again. This button is also useful to start tuning a linear amplifier. If you don't have a TUNE button, you may need to manually reduce power and then hit a key to send a signal. Note that I said *key*, as in radiotelegraph mode. Hitting the push-to-talk button on a SSB voice transmitter will switch to transmit, but not put out a signal until you start talking — so that doesn't work well for this application. If your transmitter supports AM voice, it will usually put out a carrier of about 25% of full PEP when keyed, so that is a possibility as well, although that is usually somewhat more power than desired.[1]

[1]Transmitters such as the early R. L. Drake vacuum tube series use controlled carrier in AM mode and may not put out a carrier without speech.

Tuning a Manual Tuner

To tune a manual tuner, you can actually start with the transmitter turned off. First look at the instruction manual and see if it provides suggested settings for each band. While your actual settings will be somewhat different, since you will have a different impedance on each band, they should make a good starting point. Hopefully the controls on your tuner have calibration marks on each control, if not, imagine an analog clock face on each control.

Next, practice tuning your tuner into a dummy load. Even though the tuner usually isn't needed to match the 50 Ω dummy load to the transmitter, if the tuner is in line, the tuner will require just as careful adjustments to tune into that load. Try the tuner on each band and record the settings.

Adjusting a Manual Tuner

Most manual antenna tuners have three controls. If it's a Pi- or T-network, they will all be adjustable inductors or capacitors, usually one of the former and two of the latter. An L-network will just have one of each but will usually have a switch to move the variable capacitor between the input and output side of the inductor as shown in Figure 3-3 in Chapter 3. Because the three controls interact to some degree, finding the right settings can be arduous, can stress the transmitter and can also cause interference to others as you try to find the right settings, hence the recorded table. I provide the following suggestions.

- Many antenna tuner instruction manuals have tables of typical values for each band. Use these as a starting point.
- Practice tuning your antenna tuner into a dummy load, as discussed above.
- First tune as close as you can using the receiver as an indicator. If there are signals on the band, adjust for maximum S-meter indication. If there are no signals adjust for loudest band noise or meter indication.
- If you have an antenna analyzer, use it instead of the radio to find settings that offer a matched load to the radio port as shown in **Figure 4-1**.
- If you can't quite get to a 1:1 SWR, shift one of the controls off its minimum position and adjust the other one (or two) for minimum. If the result is better, move the first control a bit more in the same direction. Repeat until it starts to get worse. If it's still not satisfactory, repeat the procedure with a different control.

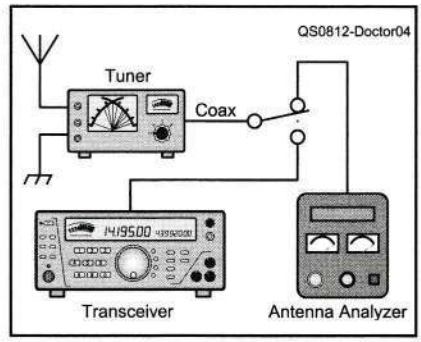

Figure 4-1 — Using an antenna analyzer to adjust your antenna tuner reduces both stress to your radio and interference to other users of the band. The coax switch shown can be used to switch the output of the antenna tuner to either the radio or the antenna analyzer.

- If there are multiple settings yielding a match, as there will likely be with T- and Pi-network tuners, select the one with minimum inductance — it will be more efficient because inductors tend to have more loss than air variable capacitors. The following example illustrates the point.

A fairly typical "random" length of wire likely to be matched with an antenna tuner would be 57.5 feet long fed against ground. This would have an impedance of 25.6 Ω resistive in series with 100 Ω capacitive reactance at 3.7 MHz — a 10:1 SWR, just within the design range of most wide range tuners. A low-pass L-network tuner will just have a single value of L and C that would mach this impedance. It would be, according to *TLW* software (discussed later in detail), 5.29 µH and 1000 pF. The loss in the L-network tuner would be 0.11 dB or 2.5%.

With a high-pass T-network tuner, there are an infinite number of combinations of tuner components that can result in a satisfactory match. Setting one value requires the other two components each be set to a particular value to obtain a match. As shown in **Table 4-1**, listed by selected value of output capacitor, not all combinations will have the same efficiency. It shows dramatically that by having a

Table 4-1

Examination of High-Pass T-Network Tuner Efficiency as a Function of Tuning: Load 25.6 Ω Resistive in Series with 100 Ω Capacitive at 3.7 MHz.

Capacitor Output (pF)	*Intput (pF)*	*Inductor (µH)*	*Loss (dB)*	*Loss (%)*
5	9.2	130.6	8.5	85.9
10	12.5	82.1	5.4	71.3
30	25.7	34.4	2.4	41.7
50	37.5	22.5	1.6	29.9
100	63.2	12.8	0.9	18.4
200	102.6	7.8	0.5	11.5
500	171.2	4.7	0.3	6.8
1000	223.2	3.7	0.23	5.2
2000	264	3.2	0.19	4.4
5000	297	2.6	0.17	3.9

Table 4-2

W1ZR Antenna Tuner Settings Table

Antenna Tuner Settings — 100 Ft Dipole (4)

					AMP SET	
FREQ	*C*	*IMPED*	*L*	*SWR*	*Load*	*Tune*
1.8	8.0	L5	4 - 9.9	2.5	0.0	8.0
3.55	5.6	H1	20 - 6.9	12.0	4.0	5.8
3.8	1.0	H1	18 - 1.9	9.8	8.8	4.7
5.3	4.3	H1	12 - 9.5	5.8		
7.0	1.2	H2	6 - 5.0	4.6	7.8	2.7
7.2	8.5	H1	8 - 1.0	5.6		
10.1-.15	8.8	H1	4 - 6.3	4.4		
14.0	2.0	H1	4 - 5.6	4.0	7.0	1.5
14.2	1.3	H1	4 - 6.4	3.7	7.0	1.4
18.068-.168	4.1	H1	2 - 7.7	2.9	7.0	2.0
21.0	3.0	L1	2 - 6.5	3.7	6.2	1.5
21.2	2.6	L1	2 - 6.2	4.3		
21.3	2.5	L1	2 - 6.3	4.5	6.0	1.3
24.890-.990	1.5	H1	1 - 1.8	1.8		
28.0	1.0	L1	3 - 5.4	1.6	5.0	2.0
28.5	1.0	L1	2 - 9.6	2.5	4.5	2.0
29.0	1.0	L1	2 - 6.0	3.6		

Antenna Tuner Settings — Tri-Band (2)

					AMP SET	
FREQ	*C*	*IMPED*	*L*	*SWR*	*Load*	*Tune*
10.1-.15	4.0	L1	9 - 1.3	5		
18.068-.168	3.3	L1	4 - 8.2	5	7	2.0

Antenna Tuner Settings — Ground Plane (3)

					AMP SET	
FREQ	*C*	*IMPED*	*L*	*SWR*	*Load*	
3.6	10.0	L1	9 - 1.7	2.3	4	5.8

high inductance value, the loss will be higher than if an inductor with a lower value were used. All combinations will provide a 1:1 match to the transmitter which will happily pump power into the system. While some values would likely not be realizable at 3.7 MHz, the reactances all would be easily employed at 30 MHz. A 1500 W transmitter with the 86% loss of the first entry would dissipate 1290 W in the tuner as heat. The tuner would likely melt before your eyes!

Note that Table 1 indicates that the highest efficiency is with the lowest inductance value — often the case. It also can happen that the high Q of a low inductance solution can result in large circulating currents resulting in additional loss. The best way to be sure is to measure the relative current going from the tuner to the antenna. The solution with the highest current will be the most efficient.

The actual value of the current isn't usually significant since the antenna impedance is unknown. For any given antenna on a given frequency, what is important is that you have the solution that provides the most current towards the antenna with the transmitter operating into its design load and within ratings. Unfortunately, I am not aware of any tuners now available that provide for the measurement of antenna current. RF ammeters are available on the surplus market and one is available from MFJ. Alternately, a fairly simple antenna current transformer project article in *QST* described how to make your own. It is reproduced in the following sidebar.

Once you have a match, reduce the inductance, retune the capacitors, and see if you can still obtain a match with an even higher current. Once you have the settings for a particular antenna, you won't need to measure the current again unless something changes in the system.

•Record your data! All manual antenna tuners I've seen have calibrated scales on their front panel for each control. As soon as you have a match, write down the settings you found for future reference and use them for a starting point next time. I find that having a set of dial readings for at least the phone and CW portions of the band is useful. **Table 4-2** is the actual table that I use at my station. Note that there are separate table segments for three different antennas. The fourth position is connected to a dummy load for testing and amplifier adjustment purposes.

The Controls in My Table

Since there's a bit more here than you might need, let me explain the columns I have included in my chart. The tuner I use is an early Ten-Tec 238 with front panel layout shown in the chapter title (center) figure. This is a 1.5 kW rated L-network tuner that provides four antenna connection ports, one of which (# 4) can be set up for either a balanced or unbalanced load using an internal balun on the output side.

• FREQ is the approximate frequency that I made the adjustment for.

•C is the approximate setting of the variable capacitor dial. It has 10 divisions, but I "eyeballed" how far between the marks the setting was to get the tenths position.

•IMPED is a switch that can set the configuration for high (H) or low (L) impedance and has five fixed capacitor settings for each, hence the numbers 1 through 5, in addition to the letter.

•L is the setting for the variable inductor. The inductor setting has two numbers because it is a multiple turn rotary inductor. The first number is the value of the TURNS scale, while the second is the knob setting from the skirt on the knob.[2]

[2]Current models of this tuner have an improved drive for the rotary inductor that provides a single reading for the L value.

- SWR is the SWR measured with the tuner bypassed. This doesn't play a part in the tuning, but is useful as a check to make sure the antenna hasn't changed or fallen down since it was installed. The tuner will just as happily tune the antenna if it breaks and falls down, but the signal won't go as far.
- The two AMP SET adjustments are for my linear amplifier tuning controls. They share the spreadsheet because, as with the antenna tuner, if I change bands or modes, they need adjustment. These columns save having an additional piece of paper on the operating desk. If you don't have a linear amplifier you don't need these.

Your tuner may have different control labels, and you may not want to include all my data, however, it should give you a starting point for your own record keeping. I maintain my records on a PC spreadsheet, although any convenient medium can be used. A small set of data might fit on a 3 × 5 (or perhaps 5 × 7) inch file card. The spreadsheet has the advantage that it can be easily updated as antennas are changed or added. In my experience, amateur stations are never quite done!

A Simple Transformer to Measure Your Antenna Current

SWR doesn't give you the whole story — you need an RF current meter.

Paul Danzer, N1II

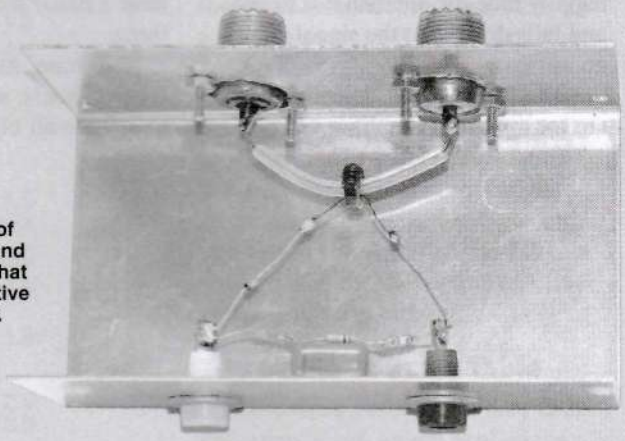

Figure 1 — View of the transformer and simple circuitry that make up the relative RF current meter.

In a recent *QST* article, Eric Nichols, KL7AJ, presented a good idea — monitoring the RF current into your antenna system to insure optimum tuning.[1] Actually, it was the second time it was mentioned to me — George Peters, K1EHW, suggested the same thing to me several months before. At the end of Eric's article, he proposed using a current transformer to do the monitoring.

Making a Current Transformer

This could be as simple as a turn of wire through a ferrite core and several turns of wire around the core to form a transformer.[2] The output of the transformer would be proportional to the current through the wire.

Making it Happen

This seemed simple enough, and the result of one hour's work is shown in Figure 1. The core used was a T37-6. T37 designates the size (0.37 inches OD), picked so the insulated center conductor of RG-58 (or RG-59) would fit comfortably through the core center. The –6 designation relates to the frequency application of the ferrite mix, in this case 2 to 50 MHz.

Searching the ARRL suppliers' data base, it appears that Alstar Magnetics offers this core; an alternate would be a Palomar F37 with mix 61. There is no criticality here — if you want to try it, strip a core from any old source — perhaps from a junked PC power supply or computer cable. It may not be the most efficient RF transformer ever built, but if it works it will do the job.

Wrap 20 turns of 24 gauge enameled wire as the transformer secondary. The secondary is connected to half wave rectifier consisting of a silicon diode (1N914), a 10 kΩ resistor as the load and a 0.1 μF capacitor as a filter (see Figure 2). A high-impedance voltmeter (the $10 variety) is connected to the two pin jacks to serve as an indicator.

The unit shown was tested with a 100 W transmitter on all bands from 80 through 10 meters. Performance across each band was relatively uniform, considering the probable variation of SWR and power though the feed line as the frequency was varied.

Hook up the rest of the circuit as shown in Figure 2 and connect a meter to the terminals.

What we Have

The object here was not to get an exact measure of the antenna current. What I wanted was a relative measure, so I could see if anything was going wrong, or use it as a way to adjust my antenna tuner for the maximum signal to the antenna. Commercial stations use a current meter, mounted at the connection of the feed line to the antenna, to monitor output. Since they know the antenna impedance and their meters are calibrated, they can determine precise power into the antenna.

If you enjoy low power (QRP, typically 5 W or less) or very low power (QRPP, less than 1 W) operation, more turns may be needed and can easily be added.[3] Similarly, if your meter does not have enough sensitivity, more turns may be called for. If after assembly the core is not firmly in place, held by the friction of the secondary on the primary wire, a drop of glue can be used to secure it all together.

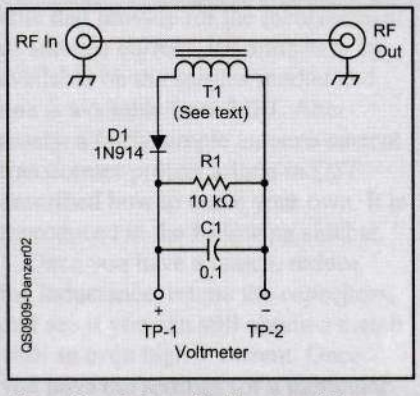

Figure 2 — Schematic diagram of the relative RF current meter. Nothing about the circuit is critical. See text for parts information.

Putting it to Use

The current meter consumes a miniscule fraction of the output power, so, can be left in the line, or removed when not in use. You may even find a meter case and a surplus meter at a hamfest that will work with it to give continuous indication without tying up your bench meter. I suggest writing the relative current indication for each band in your log. Later, if something seems amiss, it is then an easy job to compare your readings to the recorded ones to find out if the problem is in your antenna system.

Notes

[1]E. Nichols, KL7AJ, "Keeping Current with Antenna Performance," *QST*, Feb 2009, pp 34-36.

[2]Each pass through the center of a toroid counts as a full turn.

[3]Low power operators may obtain better results using a germanium diode, such as a 1N34, in place of the silicon diode due to its lower forward voltage drop.

ARRL Member Paul Danzer, N1II, was first licensed in 1953, and now holds an Amateur Extra class license. Paul has been operating 40 meter CW almost constantly since he first started. He uses his years of experience as an electronic engineer to design and build small, one-night ham radio projects. Currently he is a Professor of Computer Science at Housatonic Community College in Connecticut. He can be reached at **n1ii@arrl.net**.

From September 2009 QST © ARRL

Review Questions

4-1 Why is it important to listen to the operating frequency before you start the tuning process?

4-2 Why is it a good idea to manually initiate tuning with your auto-tuner before transmitting on a new frequency at full power?

4-3 If there are more than one set of tuner settings that provide a 1:1 SWR, which should you choose?

Chapter 5

The Internal Tuner — How Does it Help?

The Yaesu FT-2000 transceiver, one of many modern transceivers equipped with an automatic internal antenna tuner.

Contents

The Flavors of Internal Tuners 5-2
Tuner Impedance Range 5-2
Impedance Limits of Internal Tuners 5-3
That Coax Connector 5-3
Coax Loss — If Things Seem Too Good to Be True 5-3
What Else is Going to be in Your Station? 5-3
Review Questions 5-4

So far, our discussions about antenna tuners have made it appear that they are a separate device that is inserted between a transceiver and an antenna system. While that's often true, we should also consider the case of a transceiver that has an internal, almost always automatic, antenna tuner.

The idea of an automatic antenna tuner is that it can sense the SWR and adjust the tuner to minimize it. This is most commonly accomplished by a configuration consisting of a collection of inductors and capacitors that can be switched in or out of a matching network until the lowest SWR is obtained. A few automatic tuners actually rotate the shaft of a variable capacitor using an electric motor as the driving element.

The Flavors of Internal Tuners

Some transceivers offer an internal tuner as an extra cost option, in many cases one that can be added if needed. In other cases, the transceiver with tuner is essentially a separate model that has to be specified at the time of purchase. Other transceiver lines come only with or only without an internal tuner. Thus, if you're in the process of deciding on your next (or first) transceiver it's good to think carefully about your requirements before you make a decision. **Figures 5-1 – 5-3** illustrate radios with some of the choices.

Figure 5-1 — The Elecraft K-3 is an entirely modular design, including the option of a wide-range internal antenna tuner.

Figure 5-2 — The ICOM IC-7600 is only available with a built in antenna tuner.

Figure 5-3 — The Kenwood TS-480 is available as either a 100 W version with internal tuner (TS-480 SAT) or 200 W version without (TS-480 HX).

Tuner Impedance Range

As noted previously, all antenna tuners have limits on the range of impedances that they can transform to the desired load — almost always 50 Ω. In many cases the range of values is dependent on the frequency, often narrower on 6 meters than on the HF bands. Most tuner designs are limited on the low frequency end by the maximum values of the inductors and capacitors, and on the high frequency end by their minimum values, often the minimum capacitance of the elements to the metal case.

Thus it is often the case that the range of impedance values that the tuner is able to match is greater in the middle of the range than on the ends — typically 80 or 160 meters on the low end and 10 or 6 meters on the high end. Most manufacturers provide a single specification such as "tunes SWR at least 10:1" or "matches from 5 to 500 Ω." Note that the latter specification is not as general as the first — does it mean it only matches

resistive loads? Probably not, since it would be hard to design a tuner that just did that, nor would it be very useful. I tend to think that both ratings actually mean the same 10:1 SWR.

If they deliver on their promise, that would mean that they would actually tune the 10:1 range on the highest and lowest bands, and actually tune a wider range in the middle — and many seem to do just that.

Impedance Limits of Internal Tuners

While most external tuners have rating similar to the 10:1 discussed above, many transceivers have internal tuners rated at a 3:1, or 16.5 to 150 Ω tuning range. This seems to be particularly true of the radios provided by the large Japanese companies — ICOM, Kenwood and Yaesu. In contrast, the US made HF transceivers, Elecraft, FlexRadio and Ten-Tec, offer internal tuners specified to tune a 10:1 range.

The tuners with a 3:1 range are intended to deal with a matched antenna operated somewhat away from its design frequency. A look at the SWR plots in Chapter 2 provides the idea. While a 3:1 range will easily cover a 40 meter dipole across the whole band, it will only cover about 300 kHz of the 500 kHz width of 80 meters with a standard 80 meter wire dipole (see Figure 2-7).

The tuners with a tuning range of 10:1 or greater are what I call *wide range* tuners. These tuners can not only deal with an 80 meter dipole across the whole band, but can be used to match a whole spectrum of antenna types ranging from random, non resonant, wires to dipoles fed on multiple bands and exotic high gain antennas such as V beams or rhombics.

That Coax Connector

All current internal tuners terminate on the back of the radio in a coax connector, just as do radios without a tuner. This is a signal that they are intended to drive into coax fed *unbalanced* antenna systems. We will discuss the various benefits of balanced and unbalanced transmission lines a bit later, however, it is worth pointing out that many external tuners are set up to drive either. If your antenna system is balanced, you will need to make the transition from coax to balanced line outside the radio, tending to reduce the "all in one box" benefit of the internal tuner.

Coax Loss — If Things Seem Too Good to Be True...

It is tempting to try to use the antenna tuner to "force fit" an antenna to work on a band other than the one it's designed for. This can often appear to work, but appearances can be deceiving. Let's take one example.

Say you have a 20 meter dipole fed with 100 feet of RG-58 coaxial cable. The antenna works very well on 20 meters, and requires just a bit of trimming with the tuner for proper operation. So far so good.

All of a sudden sunspots reappear after years of absence and 10 meters is wide open with great signals world wide (sooner or later it's bound to happen). You have no antenna for 10 meters, so try using your 20 meter dipole. Wonder of wonders, it actually tunes with the internal tuner — a perfect match! You hear your neighbors working distant stations right and left, but no one hears you — what's the story?

This is an interesting case that provides a cautionary tale, as well as outlines one of the challenges of designing multiband antennas. On 20 meters, our dipole (depending on height) will have an SWR of around 1:1. The 100 feet of RG-58 coax will have a loss of about 37% (less than 2 dB), not noticeable in most cases, and all will be fine.[1]

Move to 10 meters and the 20 meter dipole will no longer provide a good match. In fact, my model indicates that its impedance will be 3836 Ω resistive in series with 790 Ω capacitive reactance — an SWR of 81:1! The high SWR increases the loss of the transmission line to about 15 dB. That means that of our 100 W, only 3.1 W will reach the antenna — that explains why we aren't being heard as well as our neighbors!

The perhaps more interesting aspect of this is that the power reflected by the mismatched antenna also is reduced by 15 dB on its way back to the tuner. Because of this, the tuner only sees an SWR at the bottom of the cable of about 3:1 and will happily adjust for a match. Thus the radio is happily transmitting, but 97% of its power output is heating up the transmission line.

What Else is Going to be in Your Station?

Another consideration as to whether an internal tuner will be your best choice is whether you have, or expect to have, a linear amplifier following your transceiver. For some types of operation, being able to select whether you transmit 100 or 1500 W can make a big difference.

If you have a linear amplifier and need a tuner, you will need an antenna tuner on the output side of your linear. A tuner in your transceiver can adjust for a mismatch in the input side of the amplifier (rarely needed), but can't help with tuning the antenna system. That has to be done at the output of the amplifier — and at the higher power level. If the amplifier is turned off, the radio's tuner can be used to match the antenna, but you will want to disable it when you switch to high power.

Thus, if you have or expect to have, a linear amplifier as a part of your station; you may want to consider a transceiver without a tuner and instead purchase a tuner with a power rating that can handle your linear. Note that this is mostly a monetary statement, since there is no harm in having the additional tuner in your transceiver. It can be turned off if you don't need it. I actually have one in my transceiver and another following the linear. I find the transceiver's internal tuner handy when I take my transceiver on vacation and am forced to use "antennas of opportunity."

[1]We will use decibels (dB) to express gain and loss ratios throughout the book. If you need a refresher on the topic, please see Appendix A.

Review Questions

5-1 What are some of the advantages of an internal antenna tuner in a transceiver?

5-2 What kind of antennas can be tuned with a tuner that can tune an SWR of 3:1?

5-3 Why isn't an antenna that can be tuned with an internal tuner always effective?

Chapter 6

An External Tuner at the Radio

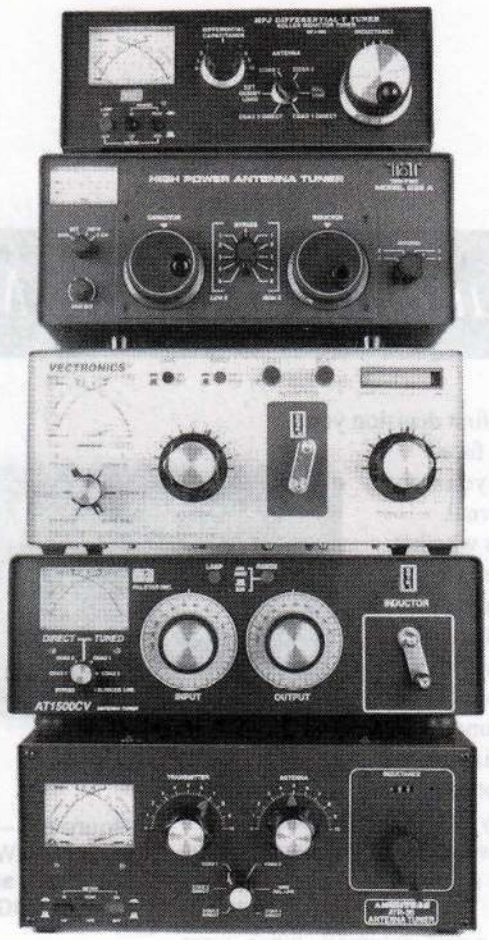

Five high power (1 kW or higher rating) manual tuners, one choice for an external tuner to place near the transceiver

Contents

Automatic versus Manual Tuners 6-2
Review Questions 6-4

In place of an antenna tuner that is built into the transceiver, another option is to have one next to the radio. Note that this is the functional equivalent of an internal tuner, and shares the potential problem of appearing to work well with an inappropriate antenna, as described in the previous chapter.

There are many available choices for such a device, including automatic tuners from some radio manufacturers that integrate directly with radio controls. There are others from after market manufacturers that offer additional features and, in some cases, are less expensive than internal tuners. While you do have to have an extra box on or near your radio, external tuners may offer some significant advantages:

- As discussed in Chapter 3, they can have a wider tuning range than many internal tuners.
- If you think you may want to add (or if you have) a high powered linear amplifier, you can select a tuner compatible with the higher power.
- Some external tuners offer both balanced and unbalanced outputs.
- Some external tuners offer multiple switched connections so different antennas can be quickly brought on line.
- If you have multiple radios, they can be switched to the tuner input so only one tuner is needed.

Automatic versus Manual Tuners

The first decision you will be faced with if you want an external tuner is whether you prefer an automatic or a manual one. As the name implies, an automatic antenna tuner finds the optimum, or near optimum, settings by itself. The manual tuner usually has three controls that require adjustment to obtain the best match.

Figure 6-1 — High power (1 kW or greater) automatic antenna tuners from Palstar, LDG and MFJ).

In the past, automatic tuners were not available at high power levels, so those with high powered stations had no choice but to use manual tuners. That is no longer the case, as automatic tuners are available at all legal amateur power levels (See **Figure 6-1**). Over the years, the ARRL has tested many manual and automatic tuners as part of *QST* product reviews. I was surprised to find that to our level of measurement precision, there was not a big difference in efficiency between tuners in the two groups. Still, there are some benefits to manual tuners and many amateurs are happy with the results they receive.

Automatic Antenna Tuners

To operate an automatic, you just feed it some power, hit a TUNE button and listen and watch while it finds satisfactory settings. Many tuners can do this in tens of seconds the first time and often remember the settings so the next time it takes just a few seconds or less for that antenna at that frequency.

In my experience there's not a lot not to like about an automatic antenna tuner. I have a number of them for particular applications, although I still use a manual tuner for my main station tuner. The key is to select a tuner that will operate with your radio — some are radio independent, while some work with the same radio controls that would operate one from the manufacturer of the radio.

One issue with some automatic tuners is just what happens if they sense a mismatch as you operate. Most automatic tuners are rated to tune at reduced power to avoid excessive arcing at relay contacts. If you change frequency or even if the wind blows your antenna around and the tuner starts tuning, the results could be dramatic. Some allow disabling the auto tune function once you have it tuned, others automatically cut back on power. In my opinion, it's better to

be able to take control yourself.

Manual Antenna Tuners

Manual tuners do often provide an additional level of control capability. Some have switch selectable outputs for multiple balanced and unbalanced antenna connections. One can be dedicated to a dummy load, if you don't (yet) have enough antenna connections to fill up the jacks. Manual tuners often provide SWR and power metering independent of that of the radio.

Most automatic tuners tune until they reach what they consider a reasonable match, perhaps 1.5:1. Hopefully it is a value that will allow your radio to operate at full power. The manual tuner let's you set it to whatever threshold you think is best — although if your transmitter can put out full power, it won't make much difference.

Review Questions

6-1 What are three potential benefits of using an external tuner at the radio rather than an internal tuner in the radio?

6-2 What are the benefits of an internal tuner?

6-3 What limitation is common to either internal or external tuners located at the radio?

Chapter 7

Transmission Lines

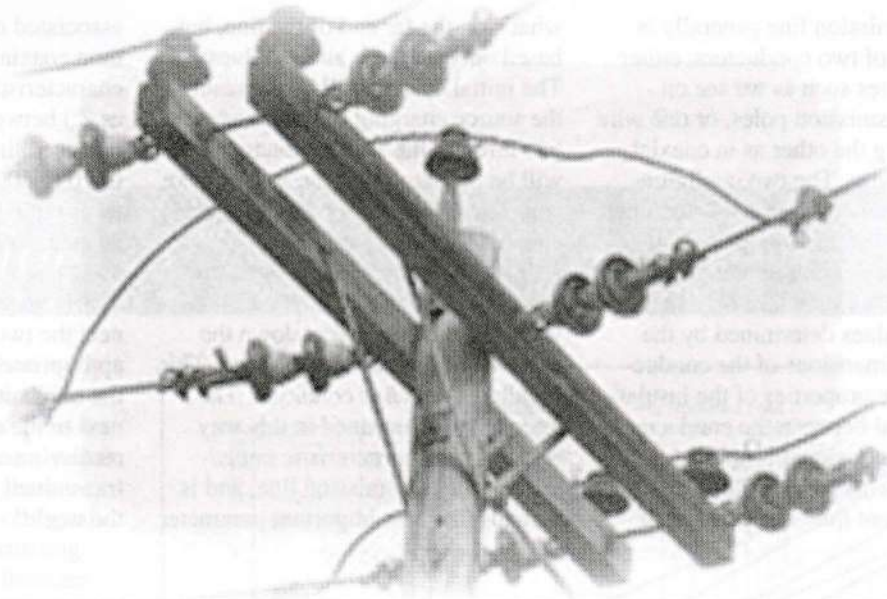

Transmission lines come in many forms, serving many applications.

Contents

Characteristic Impedance 7-2
Propagation Velocity 7-3
Attenuation 7-3
What Can We Do to Reduce Transmission Line Loss? 7-5
Sidebar: Determining the Input Impedance of an Unmatched Transmission Line 7-6
Review Questions 7-7

As we have mentioned previously, frequently the antenna and radio are not in exactly the same place. There are some notable exceptions, particularly in portable hand-held systems and various microwave communications and radar systems. In most other cases, optimum performance requires the transmitter and receiver to be at some distance from the antenna. It may also be a matter of combat survival, especially if your enemy is equipped with anti-radiation weaponry designed to home in on a signal. The component that makes the interconnection is called a *transmission line*.

Transmission lines are used in places besides radio systems — for example, power distribution lines are a kind of transmission line, as are telephone wires and cable TV connections. In addition to just transporting signals, transmission lines have some important properties that we will need to understand to allow us to make proper use of them. This section will briefly discuss the key parameters.

Characteristic Impedance

A transmission line generally is composed of two conductors, either parallel wires such as we see on power transmission poles, or one wire surrounding the other as in coaxial cable TV wire. The two configurations are shown in **Figure 7-1**. Either type has a certain inductance and capacitance per unit length and can be modeled as shown in **Figure 7-2**, with the values determined by the physical dimensions of the conductors and the properties of the insulating material between the conductors. If a voltage or signal is applied to such a network, there will be an initial current flow independent of what's on the far end of the line, but based only on the L and C values. The initial current will be the result of the source charging the shunt capacitors through the series inductors and will be the same as if the source were connected to a resistor whose value is equal to the square root of L/C.

If the far end of the line is terminated in a resistive load of the same value, all the power sent down the line will be delivered to the load. This is called a *matched* condition. The impedance determined in this way is called the *characteristic impedance* of the transmission line, and is perhaps the most important parameter associated a transmission line. Common coaxial transmission lines have characteristic impedances (referred to as Z_0) between 35 and 100 Ω, while balanced lines are found in the range of 70 to 600 Ω. What this means to us as radio people, is that if we have an antenna that has an impedance of 50 Ω and a radio transmitter designed to drive a 50 Ω load, we can connect the two with any length of the appropriate 50 Ω coaxial cable and the transmitter will think it is right next to the antenna. The antenna will receive most (see next section) of the transmitted power and all is well with the world!

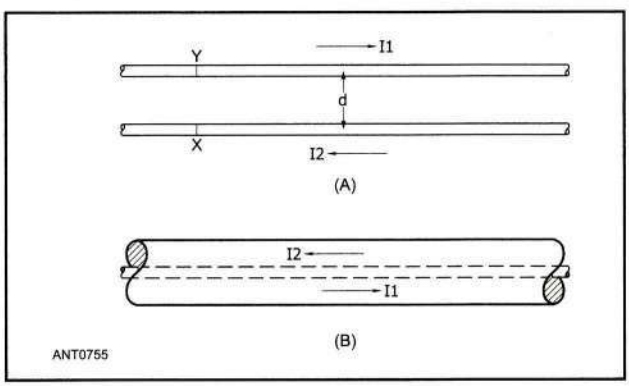

Figure 7-1 — Parallel wire and coaxial transmission lines.

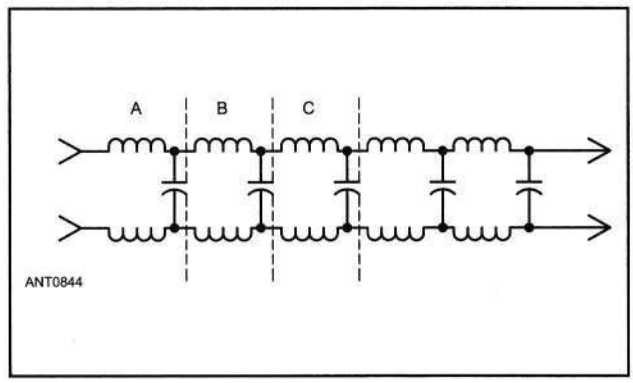

Figure 7-2 — Lumped constant equivalent of an ideal transmission line.

Propagation Velocity

Signals in air dielectric transmission lines propagate at almost the speed of light in air. Other dielectric materials between the conductors cause the signals in transmission lines to slow down just as we observe with light rays traveling through water. In many cases, this is not a matter of concern, since we often only care that the signals get out the other end, however, there are some exceptions.

The velocity can be shown to be reduced by a factor of one over the square root of the relative dielectric constant of the insulating material. Some cable specifications provide the relative velocity as a fraction of the speed of light. If not, and you know the material, most engineering handbooks include tables of properties of materials. For example, polyethylene is a common cable insulating material and has a relative dielectric constant of 2.26. The square root of 2.25 is 1.5, so the propagation velocity in polyethylene insulated coaxial cable is about $3/1.5 \times 10^8$ or 2×10^8 m/sec.

Some applications actually use coaxial cables to provide delayed signals in pulse and other applications. Having a way to accurately predict the delay just by knowing the cable characteristics and measuring the length of the cable can save a lot of lab time.

Attenuation

The ideal transmission line model shown in Figure 7-2 passes all input power to a matched load at the output. A real transmission line also has resistance associated with the wire conductors and some loss of signal due to the nature of the insulating material. As transmission lines are made larger, the resistance is reduced and as the dielectric material gets closer to low-loss air, the losses are reduced. The skin effect causes currents to travel nearer to the surface of the conductors at higher frequencies, and the effective loss thus increases as the frequency is increased.

Figure 7-3 provides some real world examples of the losses as a function of frequency for the most common types of transmission line. Note that the loss increases linearly with length and the values are for a length of 100 feet. Note also that the losses shown are for transmission lines feeding into loads matched to their Z_0. As will be discussed shortly, losses can increase significantly if the line is not matched. The "open wire"

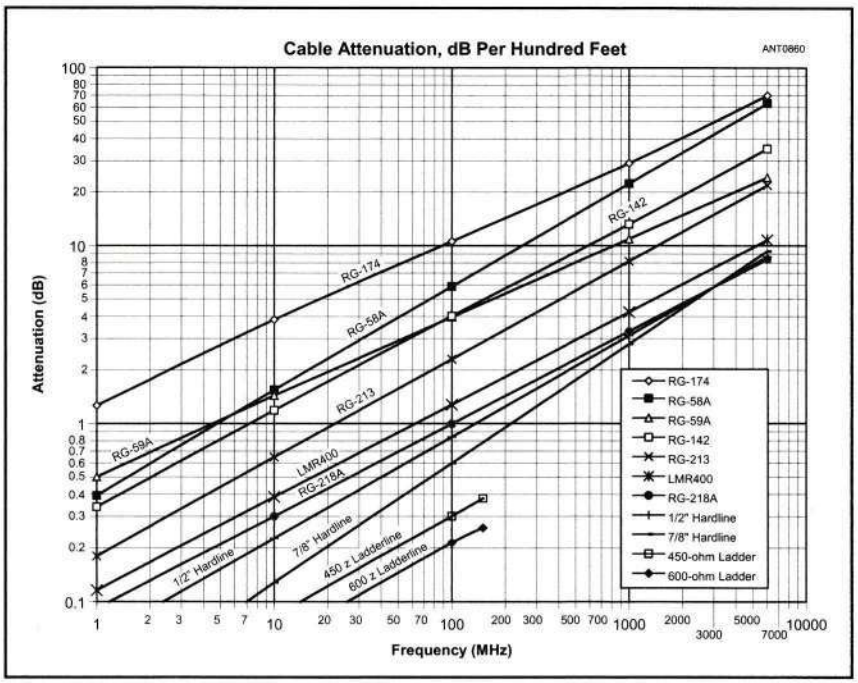

Figure 7-3 — Loss of some typical transmission lines in dB per 100 feet as a function of frequency. The RG-58 transmission lines are 50 Ω polyethelene insulated coaxial cable slightly less than ¼ inch in diameter. The RG-8 through RG-216 are 50 and 70 Ω polyethelene insulated transmission lines with a diameter somewhat less than ½ inch. The "hardline" types have a foam dielectric very near to air.

line shown consists of two parallel wires with air dielectric and infrequent spacers, typically resulting in a Z_0 of around 600 Ω. While the losses of such a line are low, they only work well if spaced from metal objects and lossey material and not coiled up, while coaxial cables have higher loss, all the signal is within the outer conductor and they can be run in conduit, coiled up, placed next to other wires and are therefore much more convenient to work with.

Sometimes a long straight run of open wire line will be transformed to 50 Ω at the ends with coaxial cable used at the antenna and radio ends to take advantage of the benefits of both.

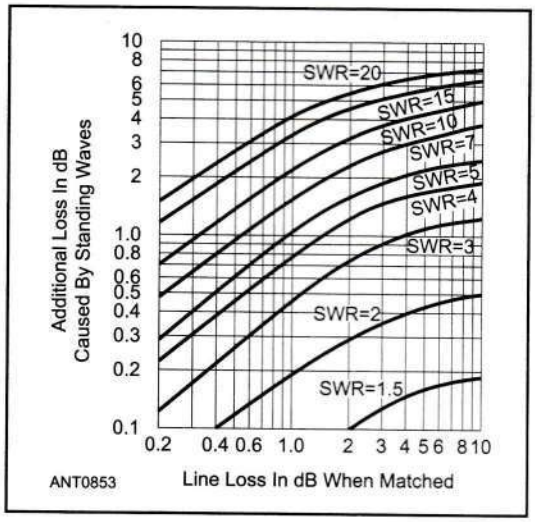

Figure 7-4 — Additional loss of a transmission line when mismatched. This loss needs to be added to the loss in Figure 7-3 for mismatched lines.

Lines with Unmatched Terminations

In our discussions so far, we have been talking about transmission lines feeding terminations matched to their characteristic impedance. In that case, the voltage-current relationship at the load will reflect the impedance of the load — not the characteristic impedance. Along the line the voltage and current will vary with distance providing a load to the transmitter end that is generally neither that of the far end Z_L, nor the Z_0 of the transmission line. The transmitter load can be calculated knowing the Z_L, the Z_0 and the electrical length of the line as discussed in the sidebar.

The ratio of maximum voltage on the line to minimum voltage on the line is called the *standing wave ratio* or SWR. A matched line has an SWR of 1:1, a 50 Ω line terminated with a 25 or 100 Ω load will have an SWR of 2:1. There are a whole family of complex impedances that will also have a 2:1 SWR, by the way. The computation is easier with resistive loads.

There are some interesting special cases with a mismatched line. The load impedance, resistive or complex, repeats every λ/2, for example. The impedance goes to the opposite extreme in odd multiples of a λ/4. For example our 25 Ω load would get transformed to 100 Ω in λ/4 or ¾ λ transmission line sections and vice versa. This effect can be used to our advantage if we wish to transform impedances at a specific frequency. In this case, the line is actually acting like a kind of antenna tuner.

A generally less desirable effect of mismatched lines is that the losses increase. This is easy to see, if voltages and currents are higher, we might expect losses to increase as well. **Figure 7-4** provides the additional loss for a mismatched line that needs to be added to the matched loss in Figure 7-3. As is evident, the combination of matched loss and high SWR results in dramatic increases in loss. This is why antenna designs that don't use matched transmission lines often use air-dielectric lines.

What Can We Do to Reduce Transmission Line Loss?

By now you should have a clear understanding of what can happen to a signal if applied to an antenna system through even a relatively short length of coaxial cable that has a high SWR. Depending on the matched loss, length and SWR, much of your signal can disappear before it gets to the antenna.

The insidious aspect of this is that while this is happening, the SWR at the radio with a collocated or internal tuner looks great — a perfect match and easy to get it. Losses are like that — they tend to result in a wide SWR bandwidth, as does a dummy load. Not a good thing if you want to communicate over the air. Fortunately, there are three fairly straightforward approaches to solving this problem:

- Change the antenna to one with either a wide enough bandwidth to cover all frequencies of interest, or one that covers multiple amateur bands with low SWR. This is not a topic for a book on antenna tuners, but is covered in many books on antennas.[1,2]
- Move the antenna tuner to, or close to, the antenna location. This is the subject of Chapter 8, or;
- Use a transmission line that has low enough matched loss so that even a high SWR doesn't result in high losses. This is the subject of Chapter 9.

Notes

[1]J. Hallas, W1ZR, *Basic Antennas — Understanding Practical Antennas and Designs,* Available from your ARRL dealer or the ARRL Book-store, ARRL order no. 9994. Tele-phone 860-594-0355, or toll-free in the US 888-277-5289; **www.arrl.org/arrl-store/**; **pubsales@arrl.org**. See Chapter 11, "Wideband Dipole Arrays;" Chapter 12 "Multiband Dipole Arrays" or Chapter 21 "Log Periodic Dipole Arrays," for example.

[2]R. D. Straw, Editor, *The ARRL Antenna Book,* 21st Edition. Available from your ARRL dealer or the ARRL Bookstore, ARRL order no. 9876. Telephone 860-594-0355, or toll-free in the US 888-277-5289; **www.arrl.org/arrl-store/**; **pubsales@arrl.org**.

Determining the Input Impedance of an Unmatched Transmission Line

The input impedance of a transmission line of any length with any terminating impedance can be determined in a number of different ways.

The most straightforward way is through direct calculation. Unfortunately, this is also perhaps the most time consuming and perhaps most error prone method, at least until you have it set up on a spreadsheet or other program that can handle he hyperbolic function.

My favorite way to determine the input impedance, standing wave ratio (SWR) as well as the line loss, is to use *TLW* (*Transmission Line for Windows*) software that comes with *The ARRL Antenna Book*.[3] The main screen is shown in Figure 7-A performing an analysis of an antenna with a complex load impedance fed through 100 feet of coaxial cable.

The antenna input impedance (74.3 + *j*16.1) is inserted in the LOAD box. The + *j*16.1 indicates an inductive reactance with a value of 16.1 Ω at the frequency of interest (10.1 MHz). A –*j* value would indicate a capacitive reactance, which would be entered with a minus sign. The output impedance through 100 feet of RG-58A 50 Ω coax is provided at the bottom in both rectangular (69.02 – *j*6.23) and polar coordinates (69.53 @ –5.15°), along with the SWR at line input (1.40:1) and output (1.62:1) as well as line loss (1.661 dB) — both for the matched case (1.555 dB) and the additional loss due to mismatch (0.106 dB). That's about everything I could think to ask, except which pile in the basement has the RG-58A!

A third way to evaluate the input impedance is through a graphical method. A Smith chart, see Figure 7-B, can be used to determine the input impedance of a transmission line. This was very commonly used before the personal computer became ubiquitous. In addition to the accuracy limitations due to the input and output resolution inherent in a chart, the Smith chart assumes that the line is lossless. This may result in significant errors depending on the amount of line loss.

[3] *TLW* is supplied with *The ARRL Antenna Book*, 20th Edition, available from the ARRL Bookstore at **www.arrl.org/catalog/** order number 9043 — $39.95.

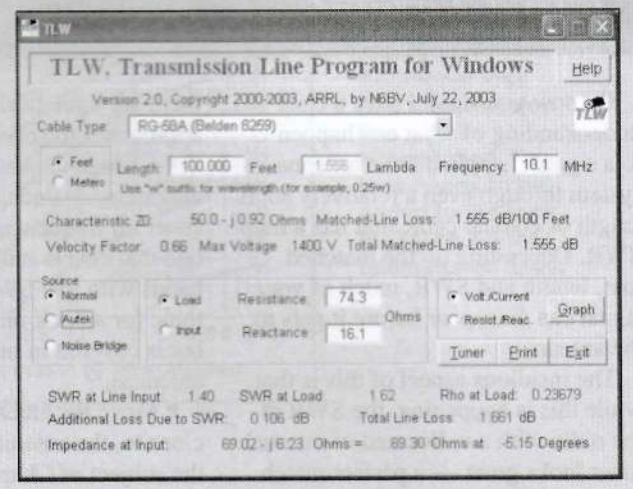

Figure 7-A — The main screen of *TLW* (*Transmission Line for Windows*) software is shown performing an analysis of the condition of the L/D of 10,000 case.

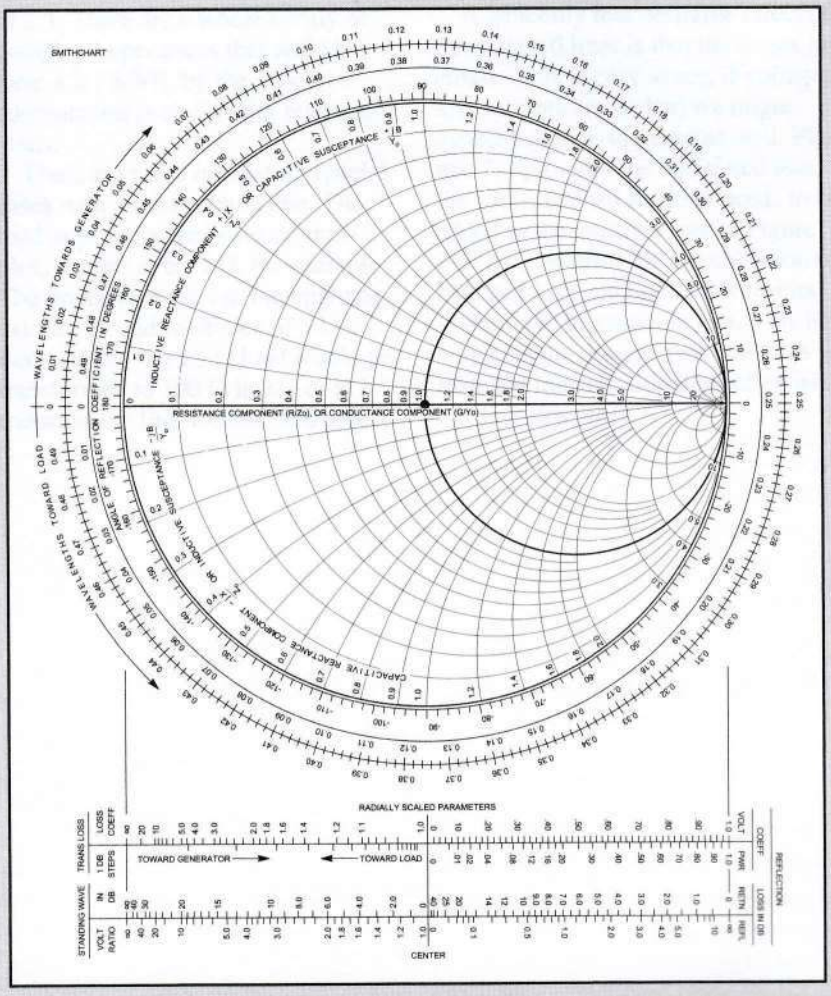

Figure 7-B — A Smith chart used for the graphical determination of the input impedance of a lossless transmission line.

Review Questions

7-1 Describe three reasons it might be desirable to have a transmitter and an antenna in different locations.

7-2 If you want to make a $\lambda/4$ section of RG-213 for our 10 MHz system, how long would you make it?

7-3 A 1000 W transmitter at 15 MHz is feeding a matched load through 200 feet of RG-8 transmission line. How much power reaches the antenna? Repeat if the frequency is 150 MHz. Repeat both cases if the antenna has an SWR of 3:1.

Chapter 8

Moving the Tuner to the Back 40

Automatic antenna tuners designed for remote mounting. On top, one from SGC, beneath a model from LDG.

Contents

An Example of Using a Remote Tuner to Minimize Loss.... 8-2
Intermediate Steps 8-4
Remote Antenna Tuners — the Downside..... 8-5
Review Questions..... 8-6

Some automatic antenna tuners are designed to be mounted remotely, rather than being collocated with the radio. We can take advantage of this in order to minimize losses in the transmission line between the antenna system and the transceiver. With the tuner at the antenna end, the load at the antenna end of the transmission line provides very close to a 1:1 SWR. The line will then have only the matched loss between the radio and the tuner, not the additional loss due to mismatch.

An Example of Using a Remote Tuner to Minimize Loss

Figure 8-1 shows the configuration of a transceiver with a remote automatic antenna tuner at the antenna. Let's assume that the transmission line is RG-58 and that it is 100 feet between the radio and the tuner plus the tuner is connected directly to the feed point of the coax fed antenna.

We will again use the example from Chapter 4 of a 20 meter dipole tuned by the tuner to operate on 10 meters where its impedance will

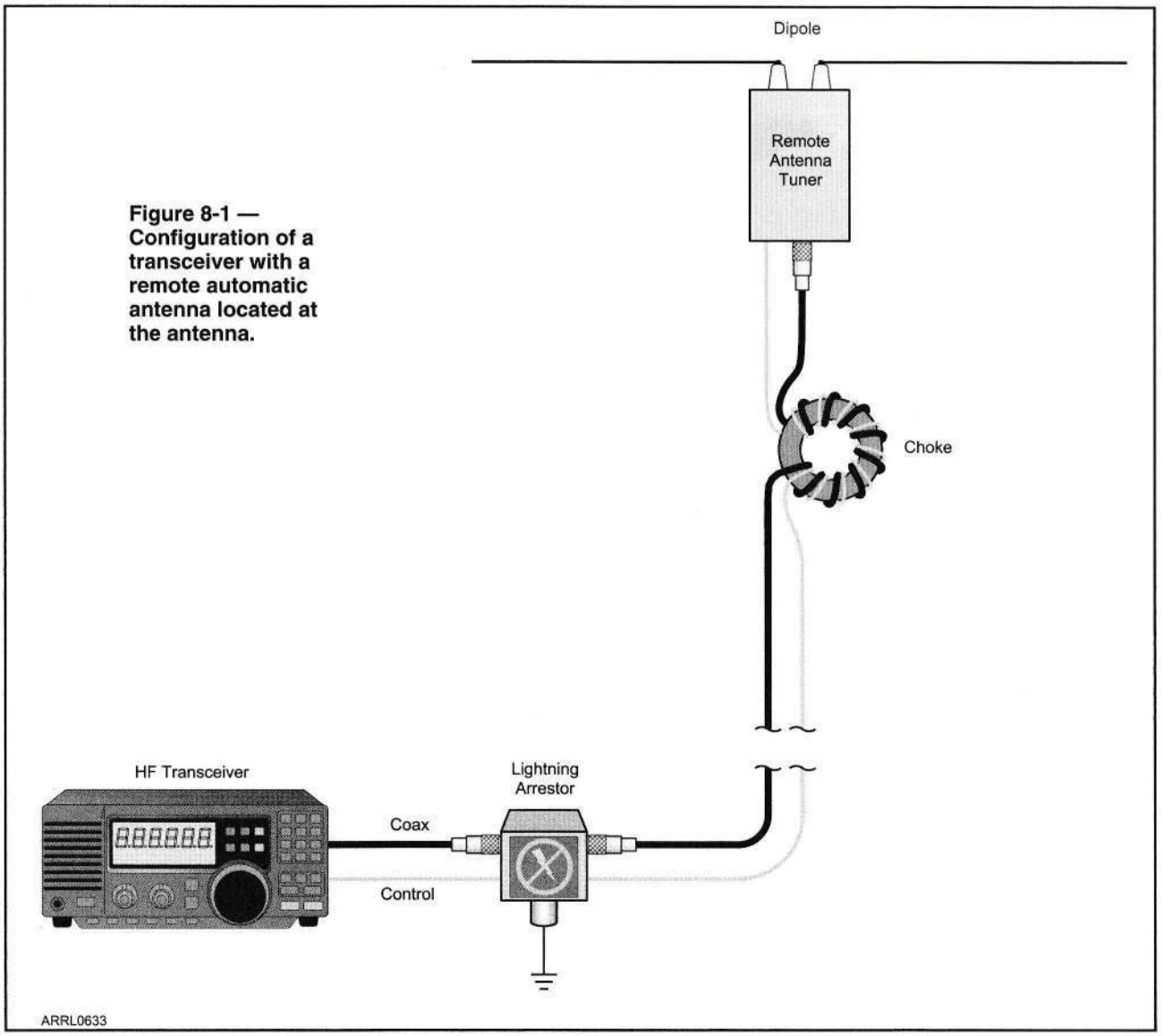

Figure 8-1 — Configuration of a transceiver with a remote automatic antenna located at the antenna.

Table 8-1

Comparison of System Losses for Remote and Collocated Tuners — RG-58

Loss Element	*Tuner at Radio*	*Remote Tuner Beneath Antenna*
Loss in 100' Cable (dB)	14.7	2.9
Percent Power Lost (%)	96.6	48.1
Power to Antenna at 100 W (W)	3.4	51.9

Table 8-2

Comparison of System Losses for Remote and Collocated Tuners — LMR-400

Loss Element	*Tuner at Radio*	*Remote Tuner Beneath Antenna*
Loss in 100' Cable (dB)	8.62	0.66
Percent Power Lost (%)	86.3	14.1
Power to Antenna at 100 W (W)	13.7	85.8

be 3836 Ω resistive in series with 790 Ω capacitive reactance — an SWR of 81:1. **Table 8-1** provides the comparison in loss for a 100 W output transceiver, in each case assuming the antenna tuner contributes no loss. While this is slightly optimistic, that loss is usually very small. The result is rather dramatic and illustrates why just hitting the TUNE button on your internal tuner may not provide satisfactory results even if the resulting radio SWR ends up at a perfect match.

Perhaps you will also not be satisfied with moving your tuner to the antenna and still losing almost half your power in the RG-58. The lesson here is that RG-58, while available and relatively inexpensive, is not the best choice for even a 100 foot run at 28 MHz. Of course, it's much worse as you move to VHF, and keep in mind that it effects both transmit and receive signals.

One of the lowest loss flexible coaxial transmission lines that fits the usual UHF coax connectors is Times Wire LMR-400. There are similar cables by other manufacturers. **Table 8-2** repeats the exercise shown in Table 1 with the lower loss cable. Note that while there is measurable loss even for the matched case, it is less than 1/10 of an S-unit, so hardly noticeable, and much less than the loss for the tuner located at the radio that will result in about a 1.5 S-unit reduction on the receiving station's meter.[1]

[1]Notes appear on page 5.

Intermediate Steps

Not all antenna systems are structured in a way to allow a tuner to be at a feed point. An example might be a dipole suspended between two supports with a transmission line hanging in the middle. In this case, it is tempting to consider a short coax run from the antenna itself to the tuner as shown in **Figure 8-2**. This arrangement may also be necessary if the tuner is not waterproof and requires shelter from the elements.

This is a feasible arrangement; however, while a substantial portion of the loss can be eliminated in this way, the loss in the section between the tuner and the antenna can still be surprisingly high. For example, for the RG-58 case of Table 8-1, a 30 foot run between the antenna and the tuner would have a loss of 4.4 dB, or 64% of the power, leaving only 36 W from your 100 W transmitter to be radiated — if it got to and through the tuner without other losses.

A better way to accomplish this in many cases will be to use a section of the low loss transmission line discussed in Chapter 9 between the antenna and the tuner.

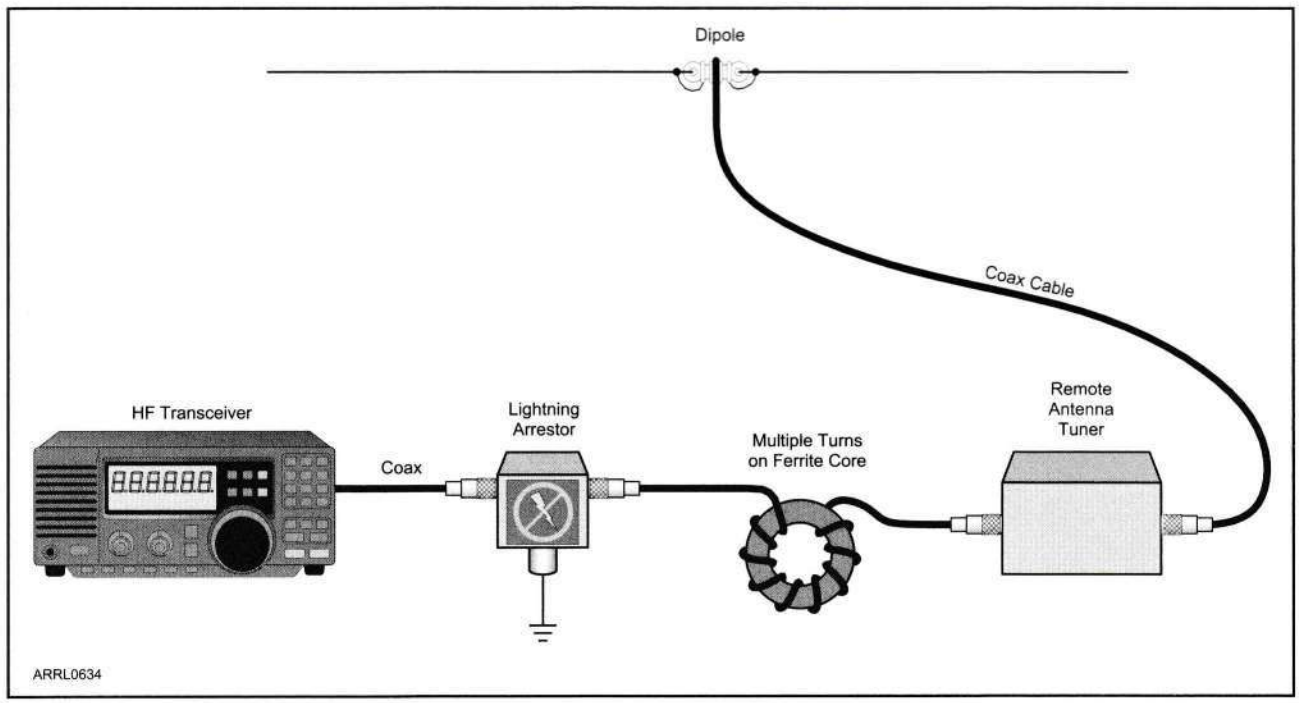

Figure 8-2 — Configuration of a transceiver with a remote automatic antenna located beneath the antenna.

Remote Antenna Tuners — the Downside

The use of a remote antenna tuner has a few disadvantages. I currently use three in various station locations and am quite happy with them in spite of the downsides:

- One remote tuner is located near my main basement station. I share antennas with my spouse (Nancy, W1NCY), who has an upstairs station. With an automatic tuner that can be patched to antennas from the W1ZR main station, she has access to any W1ZR antenna with low loss in the 100 foot coax run to her desktop setup.
- On our sailboat, I use an insulated backstay as an HF antenna. This non-resonant system has a high SWR on all bands and requires a tuner at the feed point to feed it against ground. I have a short lead from a corner under the lazerette beneath the antenna feed with another short lead to the engine block where a ground connection is available. Not only does it work well on all HF bands, but by keeping the radiating portion of the system in the corner of the boat, I minimize interference between the radio and marine navigation systems.
- I also have a remote tuner in the trunk of my car for my mobile HF system. Typical HF mobile antennas have very narrow SWR bandwidths. By using a remote antenna tuner at the antenna base, I can cover entire bands, or even tune to lower frequency bands than the antenna is designed for. While this sort of operation isn't as efficient as adjusting the antenna itself, it is much easier than making adjustments while driving at highway speeds!

There are a few aspects of remote tuner operation that might be disadvantageous for some. One is the fact that in most such installations the tuner becomes integrated into a particular antenna structure. If we have multiple antennas, each will need its own tuner — a potentially expensive proposition.[2] It also is the case that in addition to providing coaxial cable to the tuner, one must also provide operating power and sometimes control signals to the tuner. Some tuner manufacturers package the coax, power and control into extension cable assemblies that can be used for this purpose. Another possibility is to use a *bias-T* to insert the power onto the coax cable, sharing it between the two functions.[3]

Notes

[1]The Collins Radio established, now industry standard, S-meter calibration is that S-9 equals 50 µV at the antenna terminals and each S-unit represents a change of 6 dB. To say that not all amateur S-meters follow this standard would be an understatement.

[2]Remotly controlled antenna switches may be used to solve this problem, although commercial units cost as much as some remote 100 W antenna tuners.

[3]S. Ford, WB8IMY, "Short Takes — MFJ-4712 Two-Position Remote Antenna Switch," *QST*, Sep 2006, p 48.

Review Questions

8-1 Why is the quality (loss) of a transmission line more important in the mismatched than the matched case?

8-2 If using an internal tuner in a transceiver, why might the SWR *before* tuning be an important indicator of antenna system efficiency?

8-3 Why is the SWR *before* tuning insignificant if an antenna located tuner can match to the transmission line Z_0?

Chapter 9

Transmission Line Choices for Low Loss

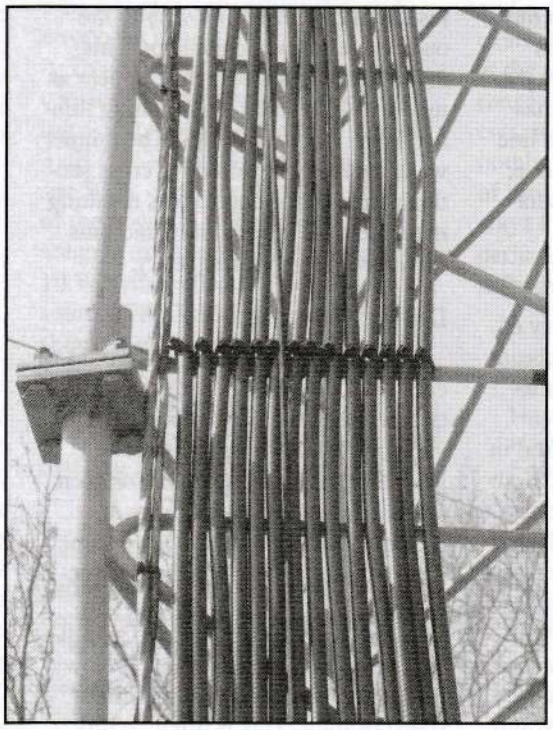

Coaxial cables going up one of the towers at W1AW, the ARRL Headquarters station

Contents

Hello Real World! 9-2

How Can We Determine Loss? 9-3

How is Transmission Line Made? 9-4

I Know What's Happening at the Shack —

Sidebar: What's Happening at the Other End of my Feed Line? 9-5

Review Questions 9-6

The ideal transmission line accepts the output power (as well as received signal) from its source and delivers it to its destination load without loss. If the characteristic impedance (Z_0) is the same as the source and load impedances, it delivers it with the same ratio of voltage to current. That means, for all practical purposes, the ideal transmission line is invisible to the system. Devices connected to both ends act as if they were collocated, except for the delay in signal arrival time, unimportant except in special circumstances.

Hello Real World!

Unfortunately, ideal transmission lines don't exist, although for many applications we can come remarkably close. The primary issue in most cases is loss. We just don't get as much power to the far end as we put in. There are three primary mechanisms that result in transmission line loss. They are conductor resistance, dielectric loss and leakage or radiation.

Conductor Resistance

Figure 7-1 shows the geometry of the two primary types of transmission line. At (A) is a balanced transmission line, while at (B) we have coaxial cable of the type discussed in the earlier chapters of the book. Both propagate signals down the line as currents with their associated electric and magnetic fields. In a properly terminated transmission line, the magnitude of I_1 will equal that of I_2 with the result that fields at some distance will cancel. In the case of coaxial cable they cancel at the shield, while for balanced line they exist for some distance around the line.

The action of the currents in an ideal line can be modeled as shown in Figure 7-2 in Chapter 7. The model can be analyzed with reasonable accuracy in comparison to real cable if there are at least 10 sections per wavelength, and if the inductors and capacitors are modeled as real elements, including the resistance of the wire and the dielectric loss of the capacitors.

For the case of dc, the wire loss just equals the dc resistance of the wire, a function of its diameter and material. As frequencies increase, *skin effect* results in the current moving to the outer edge of each conductor. This makes the wires electrically appear as tubes, with the tube walls getting thinner as the frequency rises. The thinner walls decrease the effective cross sectional area of the conductors resulting in an increase in resistance and thus increased loss with frequency.

Dielectric Loss

An ideal transmission line would consist of conductors with the insulation between them a perfect lossless vacuum. While some transmission lines approach this, with air (or even special gasses) as the primary dielectric, real lines always have some lossey material between the conductors.

A lossey dielectric has two significant effects on signals: First, it slows the signal to some fraction of the speed of light. This is often an important consideration in multielement driven antennas that rely on accurate phasing of signals, but does not enter into this discussion.

Second, dielectric loss results in yet another contribution to line loss, and this also increases with increasing frequency.

Radiation or Leakage Loss

While generally less significant a loss factor than the previous two, some signal is lost in a real line due to it leaving the transmission line before it reaches the intended load. In a sense this is more a misdirected signal than a lost signal, and, because the signals end up in undesired places, the interference to other systems may be more important than the slight reduction in signal delivered to the desired load. Still, for either reason it can represents a significant issue for real lines.

In the case of coaxial cable, a portion of the shield resistance (depending on the shield coverage) results in a current that appears on the outside of the shield. The outer shield current actually makes the outside of the shield act as an antenna with resulting radiation detectable along the length of the shield. For balanced transmission line, the fields cancel wherever the distance to both wires is the same. For a perfectly installed line, that means all the places on a plane centered between the conductors and perpendicular to the line between them.

If the line is not perfectly installed, there will be some unbalance between the capacitance of each wire to ground resulting in a current unbalance that results in radiation. A similar effect occurs if the load is not perfectly balanced. Even in the case of perfect balance, there is some radiation in directions in which the distance to the wires is different. If the spacing is a small fraction of a wavelength, this radiation is diminished within a few times the wire spacing.

How Can We Determine Loss?

Transmission line loss is a design parameter that is specified by each manufacturer for their cables. The line loss is generally specified over the usual operating range at a number of frequencies, often 1, 10, 100, 1000 and 10,000 MHz.

Matched Loss

Figure 7-3 shows the *matched* loss per 100 feet of representative transmission line types. As you make choices of transmission line, it is important to note that this data is representative — the variation between attenuation of different manufacturers, and even different part numbers from the same manufacturer, can be striking. Check the manufacturer's Web page for the data sheet of the transmission line you are considering to be sure you know what you are getting.

For lengths other than 100 feet, the loss scales linearly. For example if a line has a matched loss of 2 dB at 100 feet, the same line, at the same frequency, will have a loss of 1 dB if 50 feet long, and 5 dB if 250 feet long.

Additional Loss Due to Mismatch

By now it should come as no surprise to find that a mismatched line has more loss than a matched one. The additional loss due to mismatch is a function of both the mismatch and the loss if matched. Figure 7-4 shows the additional loss in dB that occurs as a result of a line not being matched.

Note that the SWR shown is the SWR as measured, or calculated, at the load not the SWR measured at the transmitter end of the cable. This is particularly important in the case of a lossey line since the loss will reduce both the power reaching the antenna and the power of the reflected wave that is used to determine the SWR. This can give very optimistic, and erroneous results.

To give an example of this effect, consider a 100 W transmitter driving a 100 feet of coax with a loss of 3 dB (50% loss). The antenna will see 50 W of power. Lets say 20% of the power is reflected due to the antenna mismatch. That will result in 10 W being reflected back toward the source. The 3 dB loss results in 5 W showing up as reflected power at the bottom of the cable. This is quite different than if the 100 W were applied to the antenna on lossless line — in that case, a reflected power of 20 W, not 5 W, would, show up at the SWR measurement device.

Table 9-1 summarizes what we have at the two locations. Note the rather distressing result. A very acceptable measurement of an SWR of 1.6:1 at the bottom of the coax is the result of an unpleasant SWR of 4:1 at the antenna. In this example, our 100 W of power results in only 40 W radiated from the antenna — yet all of our measurements make us think we're doing well. Unfortunately, this example is not unusual, especially at the upper end of HF into the VHF range. If it happens at higher frequencies, it is usually more evident since nothing much ends up going in or out of the system! The sidebar discusses ways that this can be calculated, and perhaps avoided, through the use of software.[1]

[1]J. Hallas, W1ZR, "I Know What's Happening at the Shack — What's Happening at the Other End of my Feed Line?" *QST*, Feb 2007, p 63.

Table 9-1
Forward and Reflected Power and SWR as Seen at Each End of a Transmission Line with 3 dB Loss

Measurement	*Bottom of Cable*	*Top of Cable*
Forward Power (W)	100	50
Reflected Power (W)	5	10
Indicated Reflection Coefficient	0.224	0.447
Indicated SWR	1.6	4.0

How is Transmission line Made?

You may wonder what is it about transmission lines that makes their loss performance so different. It all comes down to how and of what they are made. **Figure 9-1** shows typical construction techniques of parallel and coaxial transmission line types. Not shown are lines with mostly air as a dielectric, the lines with the least loss. Parallel line, so-called open-wire line, consists of two parallel bare wires with occasional spacers designed to keep them apart and at about the same distance. The traditional insulators were ceramic, however, recent lines have used plastic or PVC spacers. Mostly air-dielectric coax is sometimes encountered. Such cable that I've seen is formed from two concentric copper tubes with ceramic donut shaped spacers every foot or so.

The characteristic impedance of cable is a function of conductor diameter and spacing. Thus as line gets larger, each conductor gets larger for the same Z_0 and thus the resistance is reduced, resulting in lower loss with larger cable.

The balanced line (more next chapter) has progressively less attenuation as the Z_0 gets higher (the ratio of series resistance to load resistance goes down) and as the polyethylene dielectric is replaced by air, partially in the case of window line (C) and more completely in open wire line described above.

Coaxial cable loss is similar in that foam dielectric is part polyethylene and part air. The lines with double (E) and solid metal (F, G) shields have lower resistance and much less leakage.

Perhaps not surprisingly, all the factors that make line have lower attenuation, make it more expensive. Still, in most systems, for reasonable distances, transmission line cost is a small part of total system cost, and often provides a worthwhile investment.

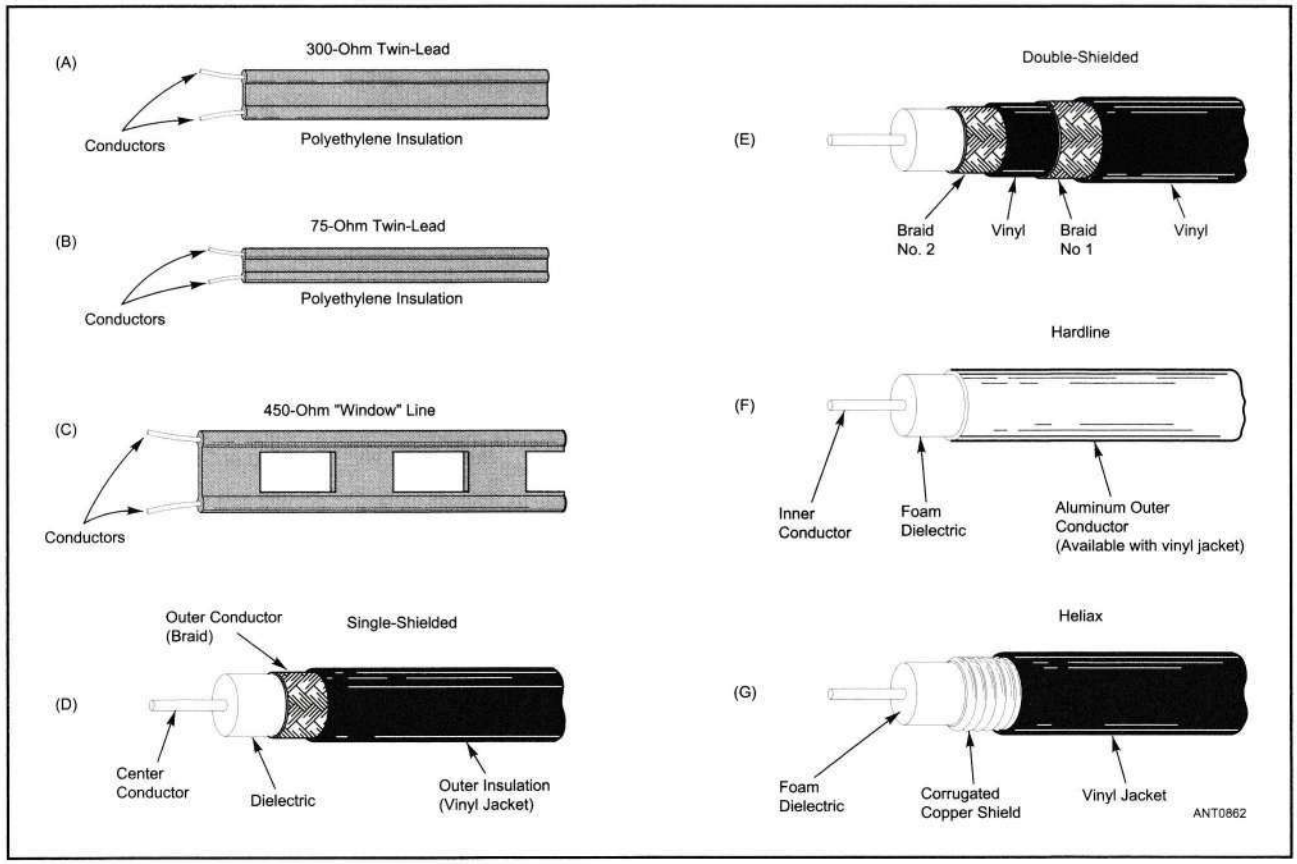

Figure 9-1 — Construction techniques used in making flexible transmission lines.

I Know What's Happening at the Shack — What's Happening at the Other End of my Feed Line?

If you want to find out — here's the easy way using TLW.

Joel R. Hallas, W1ZR
Technical Editor, QST

I'm told that one of the more frequent questions received by *QST's* "Doctor" has to do with folks wanting to determine the impact of transmission line losses on the effectiveness of their antenna system. These questions are often along the lines of "I measure an SWR of 2.5:1 at the transmitter end of 135 feet of RG-8X coaxial cable. My transceiver's auto-tuner can tune it to 1.1, but how can I tell what my losses are?" or "How much difference will I have if I have a tuner at the antenna instead of using the built-in tuner?"

These are important questions that almost every amateur operator is faced with from time to time. An approximate answer can be obtained by using the graphs found in any recent edition of The ARRL Antenna Book showing the loss characteristics of many transmission line types, plus adding in the effect of an SWR greater than 1:1. The SWR at the antenna end can be determined from the bottom end SWR and the cable loss. Using these graphs requires a bit of interpolation or Kentucky windage, but can result in useful data.

But There's an Even Better Way!

Packaged with each of the last few editions of *The ARRL Antenna Book* is a CD containing the pages of the whole Antenna Book as well as some very useful software. The program that I use almost daily is one written by Antenna Book Editor R. Dean Straw, N6BV, called *TLW* for Transmission Line for Windows.

TLW provides a very easy to operate mechanism to determine everything I usually need to know about what's happening on a transmission line. When you open the program, you are presented with a screen as shown in Figure A. This has the values plugged in from the last time you used it, often saving a step. Let's take a quick tour of the inputs:

Cable Type — This allows you to select the cable you would like to analyze. A drop-down box provides for the selection of one of 32 of the most common types of coax and balanced lines. An additional entry is provided for User Defined Transmission Lines that can be specified by propagation velocity and attenuation.

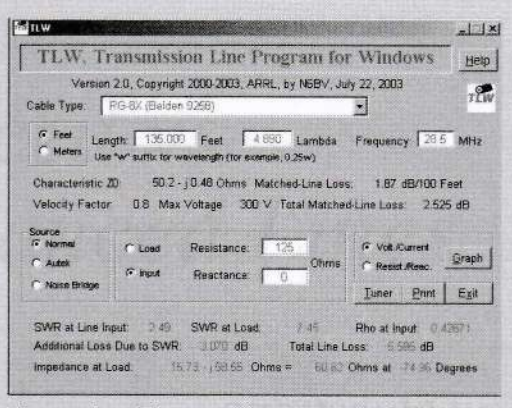

Figure A — The opening screen of *TLW*, illustrating the process described in the article.

Length — In feet or meters, your choice.

Frequency — This is an important parameter when dealing with transmission line effects.

Source — This defines the form of the input impedance data. Generally, you can use NORMAL.

Impedance — The impedance can be specified as what you measure, resistive (real) and reactive (imaginary, minus means capacitive). This could come from your antenna analyzer at either end of the transmission line. Note, if you only know the SWR, not the actual impedance, all is not lost — see below.

Now for the Outputs

SWR — The SWR is provided at each end of the cable. This is an important difference that many people miss, important even with a moderate SWR at the transmitter end, as we'll see — the SWR at the antenna will be much higher due to the cable loss. With TLW, you instantly know the SWR at both ends, and the loss in the cable itself

Rho at Load — This is the reflection coefficient, the fraction of the power reflected back from the load.

Additional Loss Due to SWR — This is one of the answers we were after.

Total Loss — And this is the other, the total loss in the line, including that caused by the mismatch.

But Doctor, What if I can Only Measure the SWR — Not the Actual Impedance?

Often the only measurement data available is the SWR at the transmitter end of the cable. Because the losses are a function of the SWR, not the particular impedance, you can just put in an arbitrary impedance with that same SWR and click the INPUT button. An easy arbitrary impedance to use is just the SWR times the Z_0 of the cable, usually 50 Ω. For example, you could use a resistance of 125 Ω to represent an SWR of 2.5:1. This is what we've done in Figure A, using 135 feet of popular Belden RG-8X.

The results are interesting. Note that the 2.5:1 SWR as seen at the radio on 28.5 MHz results from a 7.45:1 SWR at the antenna — perhaps this is an eye-opener! Note that of the 5.6 dB loss, more than half, or 3.1 dB, is due to the mismatch. Note that if we used something other the actual measured impedance, we can't make use of the impedance data that TLW provides. We can use the SWR and loss data, however, but that's probably what we wanted to find out.

We can now do some "what ifs." We can see how much loss we have on other bands by just changing the frequency. For example, on 80 meters, with the same 2.5:1 at the transmitter end, the SWR at the antenna is about 3:1 and the loss is slightly more than 1 dB. We could also plug in an impedance calculated at the antenna end and see what difference other cable types would make. For example, with the same 28.5 MHz SWR of 7.45 at the antenna and 135 feet of 1/2 inch Andrew Heliax, we will have a total loss of 1.5 dB at 28.5 MHz. Note that the SWR seen at the bottom will now be 5.5:1 and our radio's auto-tuner might not be able to match the new load.

But Wait There's More!

You can also click the GRAPH button and get a plot of either voltage and current or resistance and reactance along the cable. Note that these will only be useful if we have started with actual impedance, rather than SWR.

Pushing the TUNER button results in a page asking you to select some specifications for your tuner parts. TLW effectively designs a tuner of the type you asked for at the shack end of the cable. It also calculates the power lost in the tuner and gives a summary of the transmitted and lost power in watts, so you don't need to calculate it!

When you've finished, be sure to hit the EXIT button, don't just close the window. Otherwise TLW may not start properly the next time you want to use it.

Review Questions

9-1 What parameters make a difference in the matched loss of transmission line, mismatched loss?

9-2 Why is it important to know the SWR at the load, rather than at the transmitter to determine transmission line loss?

9-3 Does coaxial cable or parallel line transmission line tend to have the lowest matched loss?

Chapter 10

Balanced vs Unbalanced Lines

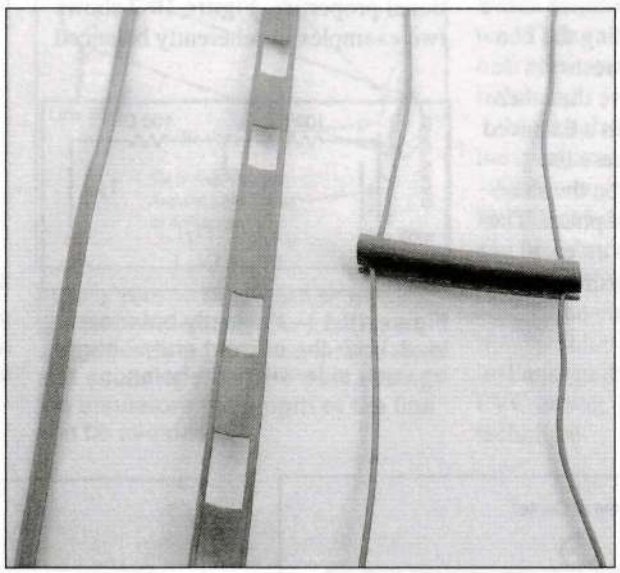

View of three popular types of balanced line. On far left, TV type 300 Ω twinlead, nominal 450 Ω "window" line and 600 Ω open-wire line.

Contents

What's the Story About Balanced Line? 10-2
The Benefits of Balanced Line 10-3
The Downside of Balanced Line 10-4
What About Unbalanced Currents on Coax? 10-4
What Happens If I Feed my Dipole Directly with Coax? 10-5
Review Questions 10-6

The careful observer might have noted that in Figure 7-3, in Chapter 7, the lowest loss line was not the fancy, expensive "hardline" coax, but rather the much less expensive balanced open-wire and window line. This is a hard combination to beat — low cost and low attenuation, which explains its popularity. The other side of the coin is that most current radio equipment is designed to operate with unbalanced coaxial line.

What's the Story About Balanced Line?

Before we can go too far, we need to discuss what we mean by balanced and unbalanced. By a balanced system, we mean one in which the two sides are at the same impedance above ground. For example feeding the non ground end of two 100 Ω resistors (see **Figure 10-1**) that have the other end grounded will result in a balanced 200 Ω system. In such a case the voltage on each side will be the same magnitude but 180° out of phase. The magnitude of the currents on each side will also be the same since the voltages and resistances are equal.

Note that the system would be balanced whether or not the ground connection were there. No current flows in the ground lead of the perfectly balanced system, so it could be removed without changing the operational properties. **Figure 10-2** shows two examples of inherently balanced

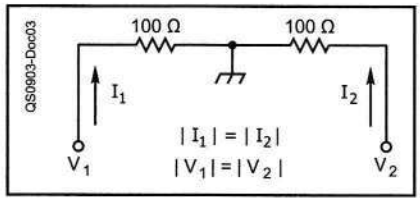

Figure 10-1 — Perfectly balanced load, both the current and voltage on each side will be in balance.

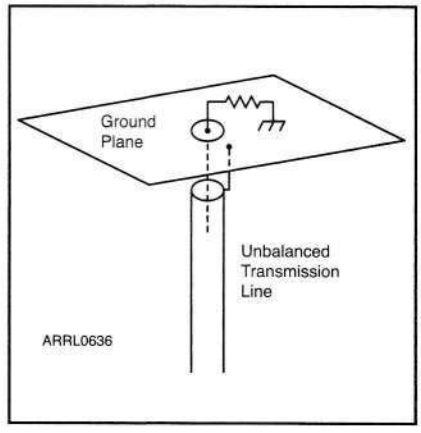

Figure 10-3 — Unbalanced resistive load. The signal is applied with reference to ground.

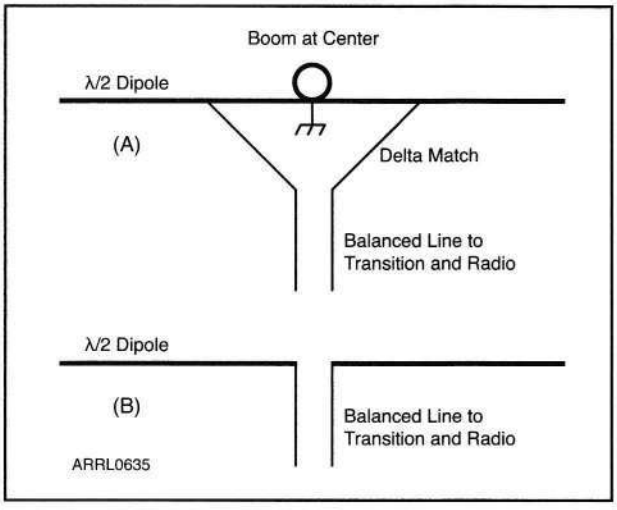

Figure 10-2 — Two examples of inherently balanced antennas, one (delta matched dipole) with a central ground (A) and one (split dipole) without (B).

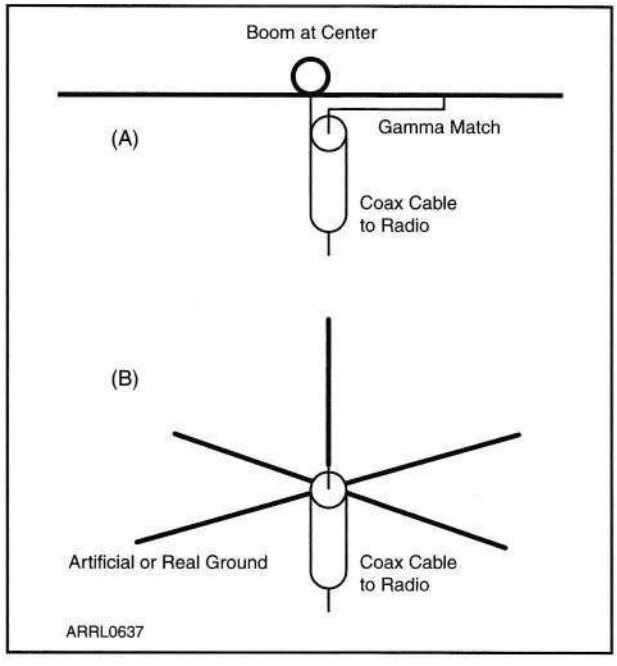

Figure 10-4 — Two examples of inherently unbalanced antennas, a gamma matched dipole at (A) and a vertical monopole at (B).

antennas, one with a central ground (A) and one without (B). The ground in the first is not actually necessary, but can be beneficial for lightning protection purposes. For both cases, we note that some kind of transition is required to shift to an unbalanced system for connection to the radio. The types of transition will be the subject of the next chapter.

An unbalanced system, on the other hand, is fed with respect to ground. That is, one side of the load is at ground potential. **Figure 10-3** is an example of an unbalanced resistive load, and **Figure 10-4** is shows two antennas with inherently unbalanced feed points.

The Benefits of Balanced Line

As noted earlier, balanced line has two primary benefits in comparison to coaxial cable. Most balanced lines, especially those with large portions of air dielectric, such as window line or ladder line, have a significantly lower matched loss than most coaxial cables. Even though their characteristic impedance is often higher than desired for many antenna systems, the total of matched and mismatched loss is generally much less than the loss of coax — particularly if the coax is not well matched to the impedance of the load.

Balanced line is often very conveniently connected to balanced antennas and is most often encountered in that application. It is also frequently found in very long runs from unbalanced antennas in which the losses (or cost) of coax would be prohibitive. In that case, it may be worth the effort to transition (Chapter 11) from unbalanced to balanced near the antenna and then back at the radio end.

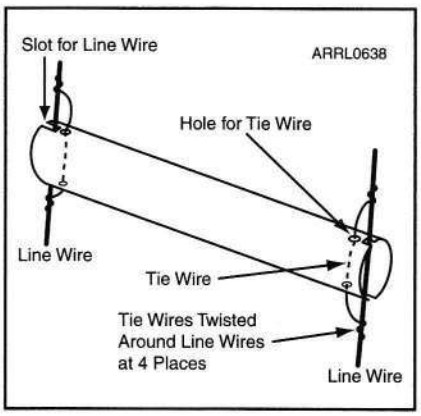

Figure 10-5 — One method of making homemade low loss open wire line. By putting the line in slots and securing with tie wires, sliding the insulators the length of the line can be avoided.

Most balanced line is relatively inexpensive when compared to coax — often an important consideration. Excellent homemade open wire line can be fabricated at low cost from two rolls of wire (stranded works best, in my experience, particularly if subject to flexing) and insulators made from inexpensive household PVC tubing. **Figure 10-5** shows one technique.

The Downsides of Balanced Line

As with most aspects of life, there are downsides of balanced line as well as benefits. While coax cable, with its fields contained within the shield, can be rolled, buried (if it has a direct burial rating) or installed within or near pipes without impacting performance, this is not true of balanced line. With balanced line, the fields conveying the signal down the line are significant not only between the wires but outside as well for a distance of a few times the wire spacing. This means that balanced line can't be placed on the ground, run in metal ducts, run through lossey material or rolled up, without causing additional loss.

While fields at a distance from balanced line are small, nearby fields can cause interference to other systems, particularly those interconnected by wiring. In addition, on receive, balanced line can pick up interfering signals from computers and other systems if run too close to them.

Another potential issue, particularly with the twinlead or window line variants of balanced line is a change in characteristics when wet. Rainwater can accumulate on the web material between the conductors resulting in a change to the dielectric properties of the line.[1]

There are a few things that can be done if this is a problem:

- Some have been known to carefully cut away some of the web to reduce the water collection surface. To avoid weakening the line, don't cut into the wire if you try this.
- In the "old days," some amateurs waxed their twinlead. This was reputed to cause the water to bead up and run off. Remaining water would be concentrated in droplets leaving most of the dielectric clear. I haven't seen any data on how effective this actually is, nor have I heard of any modern amateurs having the patience to actually do it!

In many cases, these potential problems can be largely avoided through careful planning and installation design. If not, it is sometimes efficient to make a transition to coax cable for some portion of the transmission line run.

[1] B. Allison, WB1GCM, J. Hallas, W1ZR," A Closer Look at Window Transmission Line," *QST*, Nov 2009, pp 66-67.

What About Unbalanced Currents on Coax?

In the above section, it probably sounded as if the fields in coax are completely within the coax, thus avoiding the downsides of parallel or balanced line. That is true for the ideal case of properly terminated coax, however, there are at least three ways in which coax can suffer the same limitations as balanced line in this regard. In all cases, this results in currents on the outside of the shield. I have listed them in order of likelihood and severity, based on my experience.

- The coax is not terminated in a properly unbalanced load. This happens if the coax shield is not connected to a ground reference at the antenna. The result is that the current to the shield splits between the inside and outside of the shield.
- The coax run is coupled to the antenna such that the net coupling is not balanced at the cable. For a center fed antenna, coax should be run perpendicular to the antenna element so the coupling from each side cancels. If not, even with proper termination, there will be currents induced on the outside of the shield. For some antennas, monopoles or off center fed antennas for example, it is almost impossible to avoid such coupling.
- The coax shield itself can be leaky. The shield of most coax is not perfect and some is far from it. The specification sheets often list "percent coverage" indicating how well the shield covers the center conductor. Cables with lower numbers will be leakier than those with higher coverage. The current tends to increase as it is coupled over longer distances.

In many cases, the effects of such currents are small, but be aware that they exist and check them out if strange problems appear. A quick test is to note the antenna tuning or SWR as you run your hand along the cable. With properly installed and isolated coax, the tuning shouldn't change.

What Happens If I Feed my Dipole Directly with Coax?

Many amateurs connect their coax directly to a balanced center fed dipole — center conductor to one side, shield to the other as shown in **Figure 10-6**. This is a topic of some controversy with as many folk swearing that it works fine, as there are those who say it causes problems.

The reason for the disagreement may be that there are actually people who end up in both camps because of the dimensions of their system. Recall that due to skin effect, the currents on the inside of the shield of a coax cable are within a small thickness from the inside wall. Thus the outside of the coax acts like a completely different conductor — it's as if the insulated coax were installed in a pipe that is connected to the shield at the antenna end.

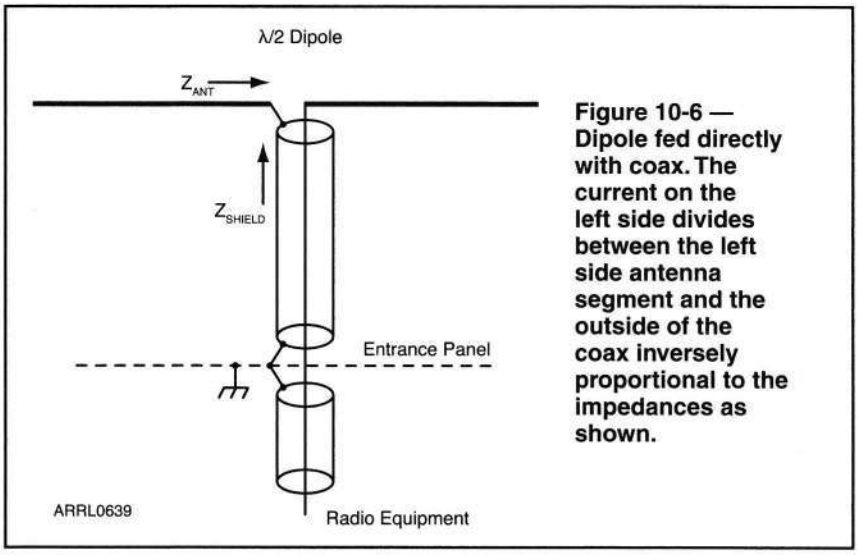

Figure 10-6 — Dipole fed directly with coax. The current on the left side divides between the left side antenna segment and the outside of the coax inversely proportional to the impedances as shown.

If the half wave dipole in Figure 10-6 had a center impedance of 50 Ω, typical for relatively low dipoles, the balanced antenna would act like a 25 Ω load to each connection of the coax, Z_{ANT} in Figure 10-6. The impedance of the outside of the shield at the antenna is a bit less obvious. This impedance depends on the impedance to ground at the bottom of the cable, usually at a ground level and grounded entrance panel, and the length of the cable between the antenna and the ground terminal.

Just as with an antenna wire or transmission line, this impedance varies depending on electrical length. If the ground impedance is low and the length is a multiple of a half wave, the impedance at the top will repeat and also be low. On the other hand, if the length is an odd number of quarter wavelengths, the impedance will reverse and be high. Lengths in between will result in intermediate values of impedance, both resistive and reactive.

If the impedance at the top of the shield is of the same order as the half dipole impedance, the current will divide between the two paths. This can have three effects:

- If the ground at the bottom is not of a very low impedance, RF currents can enter the radio room and cause a number of strange equipment problems such as feedback or transmitter lockup.
- The radiation from the transmission line will distort the antenna pattern, usually adding an omnidirectional vertical component. For a single element antenna, this may not be all bad, since it may tend to fill in the nulls that otherwise would be in some directions. For a directional array, however, such radiation will reduce both forward gain and front-to-back ratio — not good things.
- If the transmission line runs past sensitive electronic systems, fire or intrusion alarm wiring, computers or telephone systems, for example, the radiation may cause harmful interference in either direction.

Note that for a low impedance antenna, such as our dipole and most coax fed antennas, there are a small number of lengths that will result in such problems. With a multiband antenna the possibilities of problems increase directly with the number of bands covered. Thus it is not surprising that many don't think any precautions are necessary. Still, it can't hurt to avoid them, much of the subject of the next chapter.

Review Questions

10-1 Under what conditions is unbalanced transmission line most appropriate for antenna to radio connections?

10-2 Repeat question 10-1 for balanced transmission line.

10-3 Why do some people report problems with balanced antennas connected directly to coax while others observe no difficulties?

Chapter 11

So What's a Balun, an Unun, a Choke?

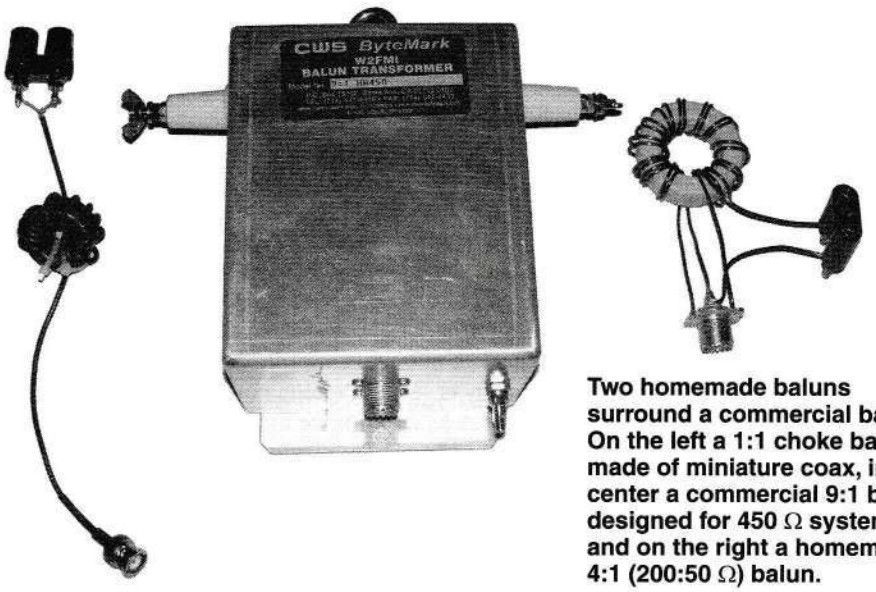

Two homemade baluns surround a commercial balun. On the left a 1:1 choke balun made of miniature coax, in the center a commercial 9:1 balun designed for 450 Ω systems and on the right a homemade 4:1 (200:50 Ω) balun.

Contents

When are Baluns Necessary? 11-2
What Do We Mean by Balanced to Unbalanced? 11-3
Balun Location 11-4
The Different Balun Configurations 11-5
Selecting Baluns for Use in Your System 11-7
Review Questions 11-8

Baluns are devices that provide a transition between unbalanced and balanced systems, impedance transformation or a combination of both. The name *balun* comes from *BAL*anced to *UN*balanced and each part is pronounced the same way as in the separate words.

Sometimes you will encounter an *unun.* The unun (*UN*balanced to *UN*balanced) provides an interconnection between two unbalanced systems, either to change the system impedance, to force all currents into the inside of a coaxial transmission line or usually both.

A *choke* refers to an inductance that offers a high impedance over a particular frequency range. A choke wound with coaxial cable has its high impedance only to currents on the outside of the coax shield, the inductances of the inner conductors effectively cancel. As we will discuss, such a choke can be used either as a balun or an unun.

When are Baluns Necessary?

We have discussed unbalanced line such as coax cable, balanced line such as twinlead, window or ladder line as well as balanced and unbalanced loads. We should point out that virtually all transmitters or transceivers built since the 1950s are designed to work into an unbalanced load — made evident by the coaxial connector used for the antenna connection.[1]

There are many antennas designed to operate with a coaxial cable connection. These antennas can be connected directly to the radio with coaxial cable if they present the desired load to the transmitter. In this case, no transition is required, the entire system is unbalanced. This system can work well and neither an antenna tuner, nor a balun, is required for proper operation. The one exception occurs if there is coupling from the antenna to the transmission line, resulting in undesired coax shield current in which case a common mode choke is recommended.

[1]The shift to the use of coaxial cable happened because coaxial cable became available after WW2 coincidentally with the popularity of broadcast television. Transmitters with shielding, filtering and coaxial RF connections were less likely, if properly designed, to cause interference problems with TV sets.

What's Wrong with this Picture?

The unbalanced antenna, unbalanced transmission line and unbalanced radio make a simple and straightforward arrangement that is easy to operate. Unfortunately, in many cases, the antenna only provides an appropriate match over a narrow frequency range — often narrower than an amateur band, for example. This has two effects:

- If the SWR at the transmitter reaches a higher value than the transmitter can operate into, it will usually reduce the power output to avoid damage to internal components.
- While the losses for matched coaxial cable can be made acceptable by selecting the proper cable for the frequency and length, the losses generally go up quickly with increasing SWR. As noted previously, this actually makes the SWR at the transmitter look better; however, significant power may be lost (turned into heat) in the cable.

Many amateurs choose instead to use a balanced antenna fed with lower loss balanced line in this case. As will be discussed later, this often makes what would be a single band antenna, if fed with coax, into a multiband antenna. We then are faced with a balanced load and an unbalanced transmitter output connector.

What Happens if We Plug the Balanced Line into our Coax Connector?

While not recommended. you can actually make the connection, if pressed. Arguably, it is not much worse than the previously discussed case of hooking unbalanced coax line to a dipole antenna. In this case, however, the shield side of the transmitter output is connected to ground and a fraction of your output power will flow in that direction radiating within the room instead of towards the desired direction. If the ground is not solid, you can end up with RF on all your equipment, causing various strange and sometimes uncomfortable effects.

What do We Mean by Balanced to Unbalanced?

The balun makes the transition from an unbalanced system, such as the transceiver, to a balanced system, such as a balanced transmission line. A balun can be used between a balanced dipole and a coaxial cable to avoid the problem of current being driven down the shield of the coax, or it can be used between the unbalanced transmitter and a balanced line to result in the current going towards the antenna as shown in **Figure 11-1**.

As noted previously, sometimes a balun is also used to transform impedances. For example, in the case of a 50 Ω antenna, a 50 Ω transmitter and the use of low loss 450 Ω transmission line, a balun with a 9:1 impedance transformation ratio allows a straightforward interconnection as shown in **Figures 11-2** and **11-3**.

Of course there is still no such thing as a free lunch. In order to use the low loss balanced line in this configuration, the added loss in each of the two baluns must be considered as part of the equation. Measurements I've taken of commercial HF 9:1 baluns have indicated that losses of about 0.5 dB each should be anticipated. It doesn't usually take too long a run of line before the balun loss is compensated for by the higher loss of the coax. This depends on both length and frequency.

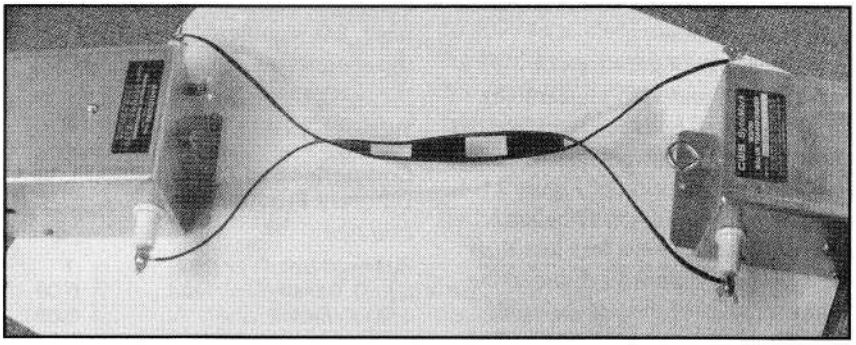

Figure 11-3 — Photo of a model of the system of Figure 11-2 using commercial 9:1 baluns. The twist in the window line is intentional. An occasional twist reduces wind effects and tends to maintain balance in the system if near objects.

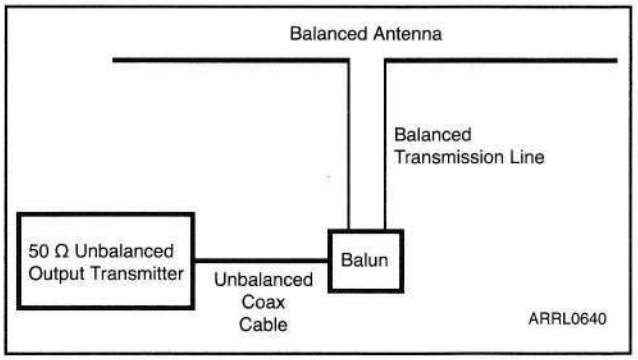

Figure 11-1 — A balun inserted between the unbalanced output of a transmitter or transceiver and a balanced antenna system.

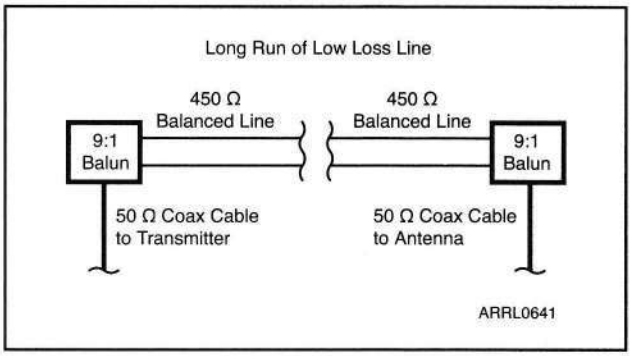

Figure 11-2 — The use of baluns with a 9:1 impedance transformation ratio makes it easy to use low loss 450 Ω balanced transmission line for long runs.

Balun Location

A balun can be inserted anywhere in a system between a coaxial connection and the balanced load. As shown in **Figures 11-4** and **11-5**, the connection between an unbalanced radio and a balanced dipole can include a balun at either end of the transmission line run. Here we have used a dipole with a *delta match* adjusted to provide a 450 Ω balanced load at the antenna.

While the configurations of Figures 11-4 and 11-5 appear to be equivalent, and both can work well as shown, there are advantages to each:

- The configuration of Figure 11-4, using a long run of 450 Ω balanced line, will usually have less loss than the system in Figure 11-5 due to the characteristics of the transmission line. The difference will depend on the frequency, line length and type of coax. Some representative loss figures are shown in **Table 11-1**.
- Using coaxial cable for the run, as in Figure 11-5, has its own advantages. The principal one is that coax is less fussy about how it is placed than is balanced line. While coax can be run in metal conduit, coiled up and some types can be buried — this is not the case with balanced line. With properly installed coax, the fields are entirely within the coax, making it insensitive to its surroundings. Parallel conductor balanced line, on the other hand, has significant fields between the conductors and extending out to a few times the wire separation in all directions. In order to obtain the benefits of such line, it needs to be spaced that far from metal structures and lossey media.

Note also that it is not necessary to have the run entirely with one type of line. For example, a long aerial run of balanced line can be transitioned to coax near the radio with a short run of coax going through conduit or other balanced line hostile environments.

Table 11-1

Comparison of Transmission Line Losses of Different Lines at Different Frequencies

Line Type	*Matched Loss at Frequency (MHz, dB per 100 feet)*			
Balanced Line	*1*	*10*	*100*	*1000**
300 Ω Transmit Twinlead	0.09	0.3	1.1	3.9
450 Ω Window Line	0.02	0.08	0.3	1.1
600 Ω Open Wire Line	0.02	0.06	0.2	0.75
Coax Cable	*1*	*10*	*100*	*1000*
RG-58	0.37	1.4	5.3	20
RG-213	0.18	0.7	2.5	8.6
LMR-400	0.12	0.39	1.3	4.2

*Spacing may be too wide for efficient operation at this frequency.

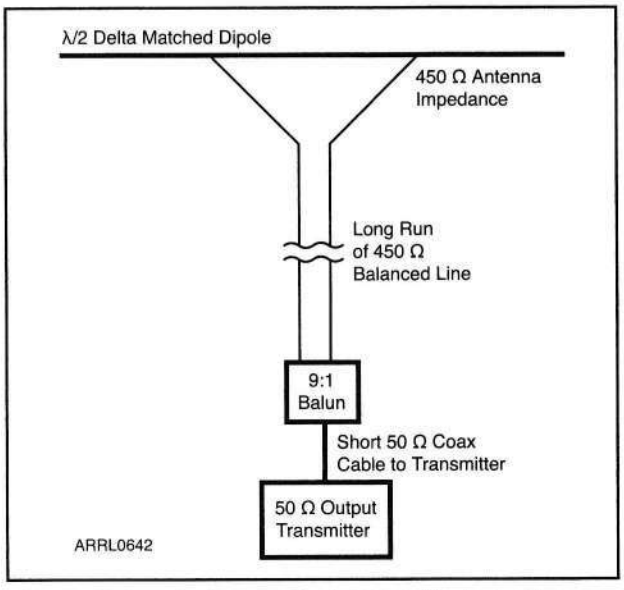

Figure 11-4 — Delta matched 450 Ω dipole fed by low loss 450 Ω balanced line to a 9:1 balun at the transmitter.

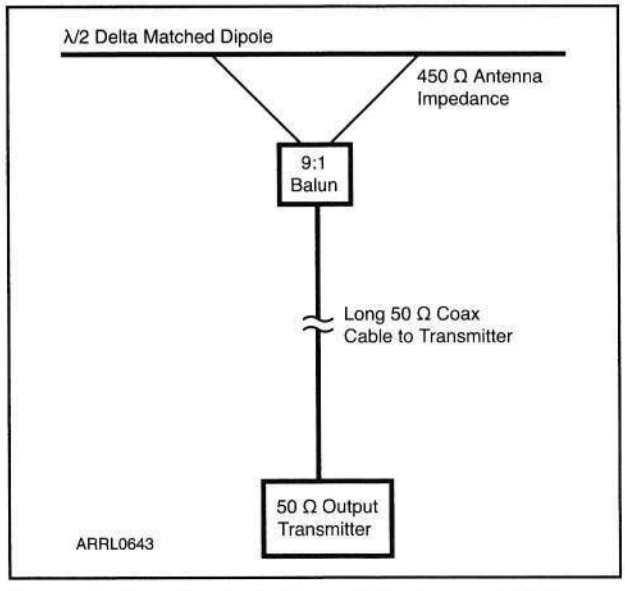

Figure 11-5 — Dipole fed by a 9:1 balun and 50 Ω coaxial cable to the transmitter.

The Different Balun Configurations

There are a number of different balun configurations. They range from simple chokes that force (most of) the current that otherwise would be on the shield of coax to the intended load to more complex devices that combine balanced to unbalanced transitions and impedance transformations in a single device. The following is a summary of the more common types.

Choke Baluns

Choke baluns are found on the coax side of a balanced to unbalanced transition. As noted previously, if a balanced load, such as a dipole antenna, is fed directly by coax, the current on the shield side of the connection will split between the connected half dipole and the outside of the shield in a ratio inversely proportional to the two impedances. The idea of the choke balun is to increase the impedance of the outside of the shield by adding inductance and thus reducing the current that flows down the outside of the shield. If no current were to flow down the shield the current to the each side of the antenna would be the same as if the coax were a balanced line on the antenna side.

Air wound coax loops — The simplest form of choke is just a coil of coaxial cable as shown in **Figure 11-6**. Note that for the so called *differential mode* signal, the desired signal inside the coax, this coil just acts like a few feet of transmission line. The *common mode* signal, any undesired signal on the outside of the coax, sees the effect of the coil inductance.

This configuration has been evaluated at length with results reported in *The ARRL Antenna Book*.[2] An example is a six turns in single layer coil of coax with a diameter of 4.25 inches. This coil will have an impedance ranging from 514 Ω at 14 MHz to 1079 Ω at 29 MHz, very suitable for feeding a dipole or triband Yagi, for example. Such coils are sometimes scramble wound rather than being wound in a single layer. While

[2]R. D. Straw, Editor, *The ARRL Antenna Book,* 21st Edition. Available from your ARRL dealer or the ARRL Bookstore, ARRL order no. 9876. Telephone 860-594-0355, or toll-free in the US 888-277-5289; **www.arrl.org/arrl-store**; **pubsales@arrl.org**.

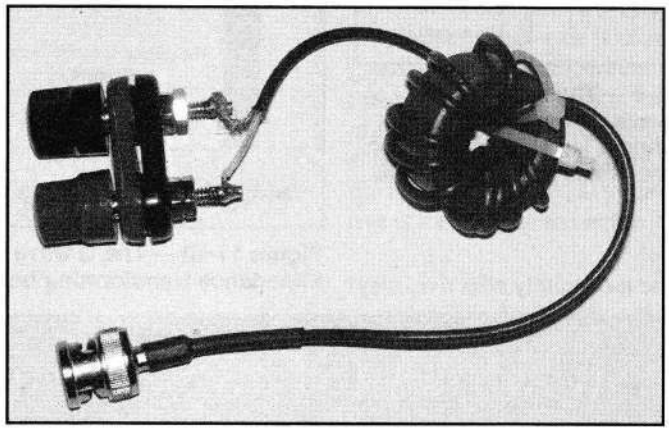

Figure 11-7 — Choke balun made by passing multiple turns of coax through a ferrite toroidal core.

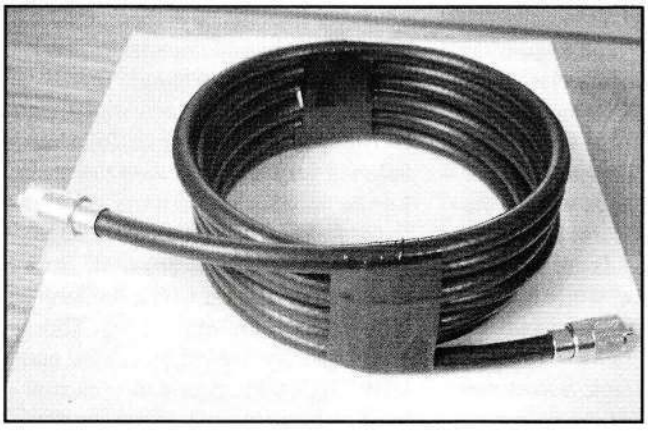

Figure 11-6 — Choke balun made from a coil of coax. Such a balun can be effective over about a 2:1 frequency range.

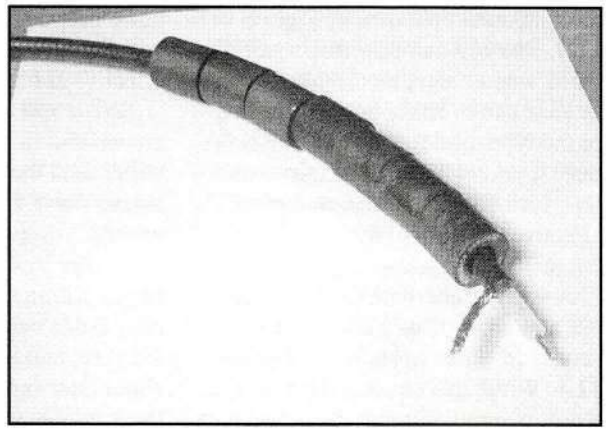

Figure 11-8 — Using multiple single turn "coils" in series — a good solution for large diameter or stiff coax.

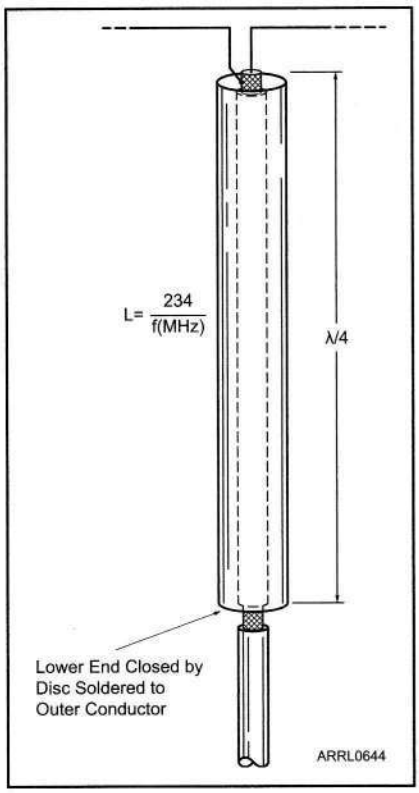

Figure 11-9 — The bazooka quarter wave choke balun made by providing a shorted line section around the shield of a coax cable.

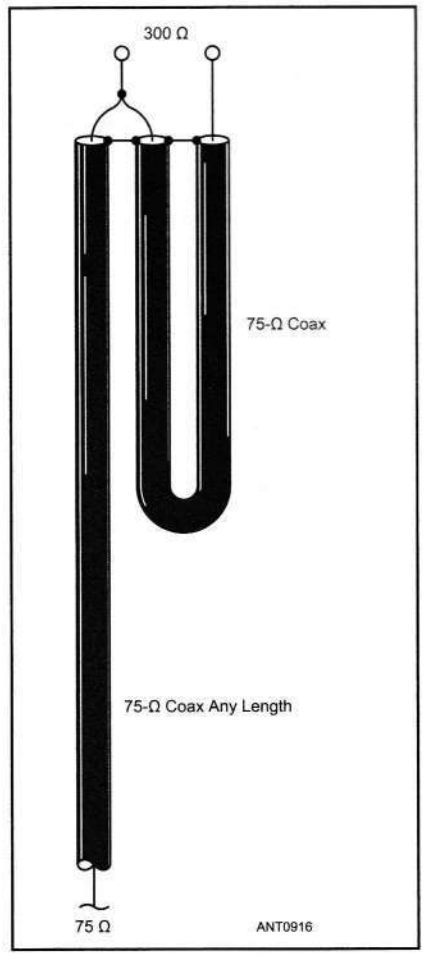

Figure 11-10 — The ½ wave 4:1 impedance transforming balun.

they can be moderately effective, they usually suffer at higher frequencies due to excessive capacitance between turns. The only other effect of the coax coil is any attenuation due to the additional length of coax, in this case about 7 feet.

Ferrite toroid coils — The effectiveness of a choke coil can be improved by winding it on a ferrite toroidal core, as shown in **Figure 11-7**. The coil can be either a pair of wires wound together around the core or coax cable, either extra thin coax, or the type used for the transmission line. A coil of 12 turns of thin coax on a type FT240-61 core makes an effective choke over the range from 1.8 to 30 MHz.

A popular alternate method is to use a number of single turn ferrite "coils" in series as shown in **Figure 11-8**. While this can be effective, it is worth pointing out that the inductance of N such inductors in series equals N times the inductance of a single inductor. On the other hand, the inductance of multiple turns through a single toroid goes up by the square of the number of turns. Still if the coax is thick, or hard to bend tightly, this is a very workable solution. It has the additional advantage that the capacitance between "turns" is less than with a coil, so it will tend to be more effective at higher frequencies.

Ferrite rod coils — Some baluns are wound on sections of ferrite rod rather than the toroid, donut shaped, cores. These can work as well as the toroids, however, the toroids have the advantage that the fields are contained within the core, while the rods have fields between the ends outside the core, making them more fussy about their surroundings. Sometimes the available space will point towards one versus the other. All other things being equal, I prefer the self shielding toroids, if feasible.

Transmission line sections — A quarter wave long section of transmission line, shorted at the far end, has a high impedance at the near end. This property can be used as a choke at the particular frequency that the line section is that length (or odd multiples). This is called a bazooka, due to the use of large concentric structures as shown in **Figure 11-9**. This is a particularly popular arrangement at VHF and higher, since the dimensions are reasonable and wideband properties of the ferrite baluns and chokes are often not required.

Transformer Baluns

The half-wave coax loop — One of the early forms of transforming balun was also made of coax cable, this time an electrical ½ wave long. This cable was formed into a loop with one end on each side of the balanced load as shown in **Figure 11-10**. The unbalanced line was connected to one side of the balanced load.

The half wave loop provides a copy of the signal from the coax feedline delayed by 180°, and thus out of phase. Each of the two signals see an impedance of half of total 300 Ω load, or 150 Ω. Because the impedance on a halfwave (or multiple) of a transmission line repeats itself, the loop will bring the 150 Ω impedance back to the feedline junction. The parallel combination of the two 150 Ω signals at the feedline junction is thus ¼ of the total load or 75 Ω. Note that since a half wave length of transmission line repeats whatever impedance is there, this will transform any impedance to ¼ the value on the single frequency.

The half-wave loop transforming balun is very efficient, with the only loss or imbalance a result of the loss in the loop of coax. A disadvantage is that they only operate on (or close to) the frequency at which the loop is ½ wave (or multiples) long. These are frequently used to feed VHF and UHF Yagis that operate on a narrow band of frequencies making the narrow bandwidth irrelevant.

Ferrite transformers — Broadband

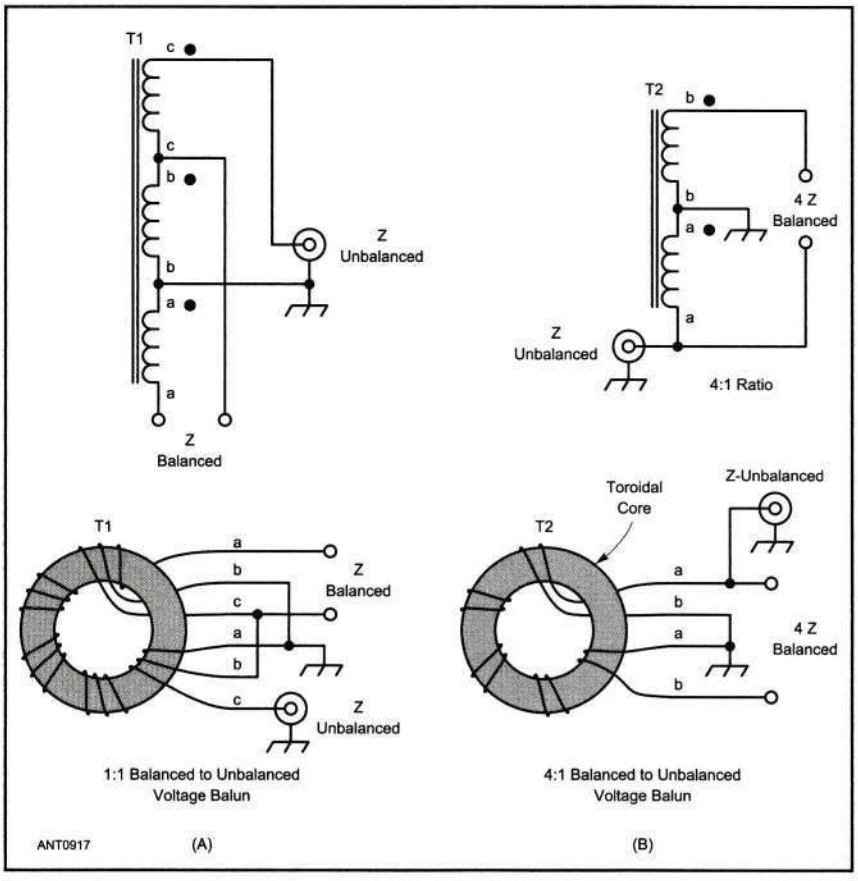

Figure 11-11 — Schematic and pictorial view of a broadband ferrite core 4:1 impedance transforming balun.

baluns can be made using the same kind of ferrite structures described previously as transformers. They frequently are made with multiple windings that can be connected in series or parallel to provide multiple transformation ratios. The 4:1 balun shown in **Figure 11-11** is an example of such a balun that functions similarly to the ½ wave coax loop balun.

Current and Voltage Baluns — Depending on the details of their design, a balun can be made to force either the current *or* the voltage on the balanced side to equal each other. Note that in a perfectly balanced load, in which each side has the same impedance to ground, if the voltages are equal so will be the currents and vice versa.

Unfortunately, in our real world, often an intended balanced load, isn't quite. For example, an otherwise balanced antenna may become unbalanced if one side is closer to the ground, or to a metal structure, than the other. If the balun is intended, as most are, to keep currents off the outside of coax shields, then by forcing the currents to be equal your objective is most likely to be met.

Selecting Baluns for Use in Your System

Within the constraints listed above, any of the general type of baluns described can be selected for use. Most baluns have a specified input and output impedance and power rating. These should be matched to your application. The transformation ratio does not apply for any impedance, rather for the design center of the balun. For example a 4:1 balun designed to transform a 200 Ω balanced load to 50 Ω coax, can not counted on to provide a 4:1 transformation to a 2000 Ω balanced load.

In practice, the transformation is likely to be close to the specified ratio for perhaps a 4:1 mismatch — in the previous case that would be from 50 to 800 Ω. Outside of that range, they may continue to function as a balun, however, the transformation ratio will be different and the losses will tend to increase.

A mismatch will also increase the stress on the balun. The current or the voltage will be higher by the square root of the SWR or mismatch ratio and thus the ratings should be increased appropriately. After use (with power off) a good check at a 100 W or higher power station is to put a finger on the balun to check the temperature. Any increase above ambient is cause for reconsideration.

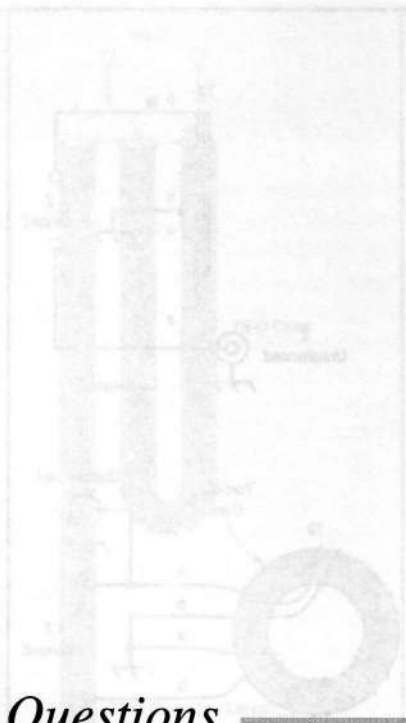

Review Questions

11-1 Provide three reasons for using a balun.

11-2 What are the relative advantages of having a balun at a balanced antenna feed point versus having a long run of balanced line to a balun near the transmitter?

11-3 What are the consequences of operating a balun at an impedance far from its design point?

Chapter 12

Balanced Antenna Tuners

A classic 275 W E. F. Johnson "Matchbox" balanced antenna tuner from the 1950s. Still a viable tuner useful to 750 W PEP and available at hamfests and auction sites. A 1 kW model, useful above the US legal limit, was also offered.

Contents

What's a Balanced Tuner? 12-2

A Balanced Tuner versus an Unbalanced Tuner with a Balun 12-3

Another Possibility — The "Hot" Tuner 12-4

Review Questions 12-5

We've been talking about antenna tuners and balanced line in the same sentence, even though we haven't addressed the issue of the kind of tuners to use with a balanced load. Now it's time.

What's a Balanced Tuner?

While we haven't specifically addressed the question, the tuners we've been talking about so far have been really what could be called *unbalanced* tuners. You can usually spot an unbalanced tuner by its input and output connector arrangements. In some cases, they have a coax connector for unbalanced cable on both the radio and antenna system sides. Other unbalanced tuners have a coax connector for the radio side and a single terminal intended for a wire antenna and another for a ground connection.

Some unbalanced tuners have another pair of connectors that are designated for "balanced loads" but the transition occurs after the tuner function using an internal balun. While these can be useful for driving balanced loads, as we will discuss, they are really two distinct pieces, an unbalanced tuner followed by a balun.

Enter a Truly Balanced Tuner

The tuner configurations shown in Figure 3-3, in Chapter 3, are all inherently unbalanced since ground is on one side of each. Any of them can be converted to a balanced configuration by essentially providing a mirror image on the other side of ground. The configurations of Figure 3-3 are shown in balanced form in **Figure 12-1**. A quick look at the figure will indicate that we now have something we probably didn't want — a balanced to balanced tuner!

The one configuration that can be easily transformed to a balanced to unbalanced tuner is the tuned transformer in Figure 12-1 (A). This is because the transformer coupling to the radio (left) side of the transformer does not maintain the same ground reference. Thus one side of the primary (left) winding can be grounded resulting in an unbalanced connection. This is exactly what the 1950s era Johnson Matchbox did, perhaps explaining why it is still in demand today.

Unbalancing One Side

The other configurations in Figure 12-1 require a balun on the 50 Ω side to fit into coaxial fed systems. While this may seem about the same as putting the balun on the antenna side of the tuner (more in next section), the difference here is that we transform the widely variable balanced antenna system impedance on the right side to a 50 Ω balanced load on the left in Figure 12-1. We then can use a 1:1 50 Ω balun to transform to unbalanced for coax connectivity. Alternately, some tuners are designed to transform to a 200 Ω balanced load, to be followed by a 4:1 balun for connectivity to 50 Ω coax.

In either the 1:1 or 4:1 case, we have the advantage that the baluns are operating at their design impedance. They will offer minimum loss and will operate with their expected transformation ratios.

There's Always a Price

A possible downside of the balanced antenna tuner designs is that the nature of the beast requires significantly more — but not quite twice — as many components as the same unbalanced configuration. The usual antenna tuner components, for medium to high power tuners, are both large and pricy. This results in ramifications in terms of both cost and size. There is, after all, still no such thing as a free lunch.

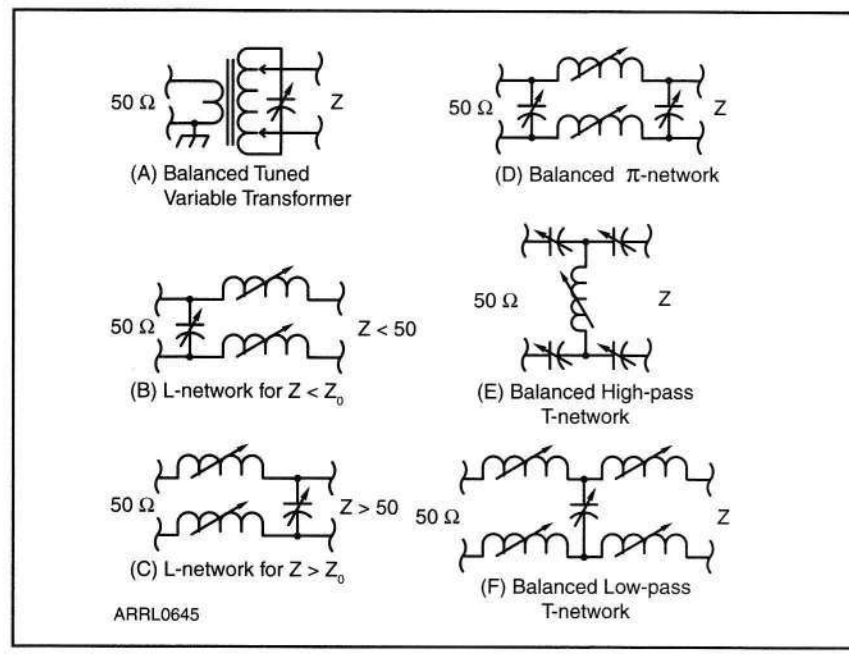

Figure 12-1 — Configurations of balanced antenna tuner versions of the unbalanced tuners in Figure 3-3, in Chapter 3.

A Balanced Tuner versus an Unbalanced Tuner with a Balun

As you look over the features of commercial antenna tuners, you will see many with "balanced outputs." In most cases, these are inherently unbalanced tuners, with a balun on the antenna side to transform to a balanced load. Many people, including your humble servant, have been happily using such tuners for years — so what's the problem?

Well, the simple answer is — there may not be a problem! If the impedance at the bottom of your balanced feed line (generally quite different from either the antenna impedance or the transmission line characteristic impedance, if the line is not matched to the antenna) can transform to an unbalanced impedance through the balun without difficulty — there is no problem — you're done!

On the other hand, if the impedance at the balun is very different from its design point, you may have a number of problems, most significantly loss in the balun. While balun loss is not great in its own right — toroid cores are not very good heat radiators. Any balun loss will transform itself into heat and may destroy the balun's ferrite core in the process.

The Good News Is

While there are exceptions, many unbalanced tuners, including those with a balun for balanced loads, offer additional features compared to many "balanced" tuners. My fairly typical unbalanced L-network tuner, for example, has three outputs for unbalanced coax terminations and a fourth that can either be coax or balanced, using an internal 4:1 balun on the output side. In addition to my main balanced multiband antenna, I have a few other antennas that are fed by coax. Thus the tuner provides a convenient point for them all to come together with easy switching between them. With a single switch on the tuner, I can instantly select any of the four antennas — either through the tuner, or bypassing the tuner, if they are matched systems. Most balanced tuners just provide a connection to a single balanced antenna system.

In terms of keeping common mode RF currents out of your station, it really doesn't matter which side of the tuner has the balun — its choking impedance has the same effect.

If it Doesn't Play

If an unbalanced tuner with a balun doesn't work well with your antenna system on a particular band, you may be able to recover. The fact that it doesn't tune usually means that the balanced line has a high SWR (if it were matched, to say 450 Ω, the tuner and balun combination could probably handle it without difficulty). Because of the nature of the mismatched line, changing the length will have a profound effect on the impedance as seen by the tuner. Try inserting about ⅛ wavelength of line and see what happens. Be sure to observe the usual cautions about balanced line — such as not coiling it up.

Another Possibility — The "Hot" Tuner

Impedance transformation through an unbalanced tuner will not "know" it is unbalanced unless one side of the tuner is grounded. Thus it is quite possible to use an inherently unbalanced tuner into a balanced load if it is isolated from ground. This can be accomplished as shown in **Figure 12-2** for a remote automatic tuner.

The configuration in **Figure 12-3** makes this quite convenient, however, it can also be accomplished using a manual tuner in the station. The difficulty with the tuner in the station is that it generally is designed so that the cabinet is at what it thinks is "ground" potential. If it is isolated from ground, the whole cabinet is at the potential of half the RF voltage feeding the antenna. This can be uncomfortable for the operator, unless she uses oven mitts to make adjustments. An unsuspecting cat can get quite a curl as it passes by during a transmission!

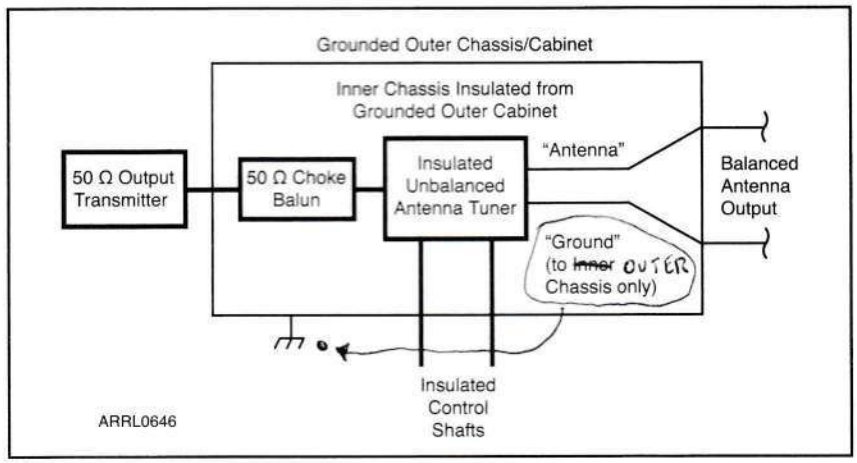

Figure 12-3 — Manually tuned version of an unbalanced tuner isolated from ground driving a balanced load. Note the insulated additional layer of cabinetry.

The hot chassis problem has been solved by at least one published design in which what would be the cabinet is insulated from and inside an additional cabinet with insulated shaft extensions on the controls as shown in **Figure 12-3**. I'm not aware that this has been offered as a commercial product, however, it is feasible — if not simple to implement.

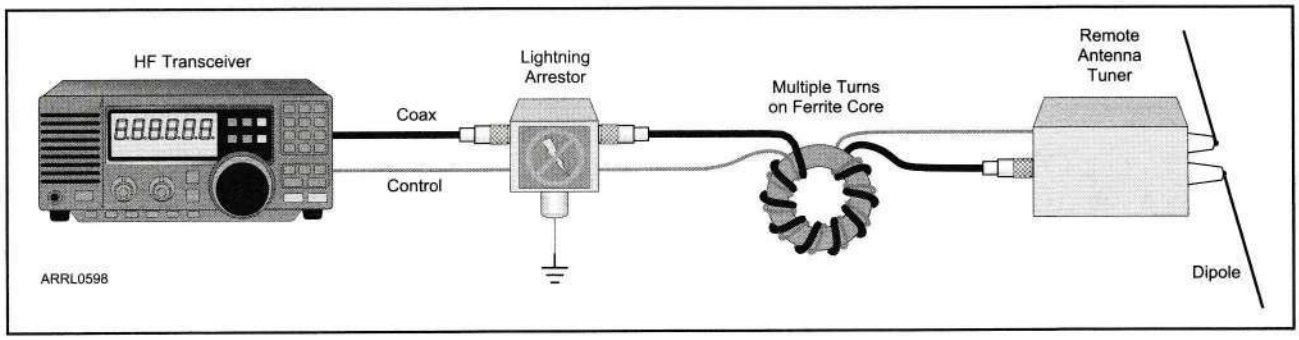

Figure 12-2 — Unbalanced tuner isolated from ground driving a balanced load. The common mode choke on the radio side maintains the balance on the antenna side. Note that it is necessary to provide a choke on all ~~balun~~ REMOTE TUNER connections, as shown, in order to elevate the whole tuner above RF ground.

Review Questions

12-1 Why might an inherently balanced tuner be a good idea?

12-2 What difference does it make whether a balun is on the input or output of an antenna tuner?

12-3 What kind of problems might you have using an unbalanced tuner with a balanced load?

Chapter 13

Antennas That Work Well with Antenna Tuners

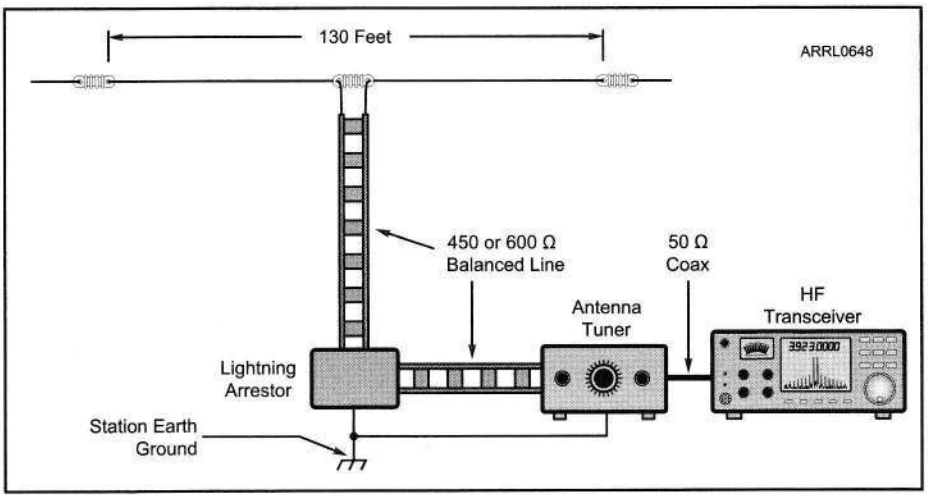

The center-fed Zepp is a very popular antenna with those having a wide-range antenna tuner.

Contents

The Coax Fed Dipole 13-2
Tuned Yagi Arrays 13-3
Single Wire Fed Antennas 13-4
The Vertical Monopole 13-5
Balanced Antenna Systems 13-7
Mobile Antenna Systems 13-8
Review Questions 13-10

There's no magic antenna that goes well with a tuner — in fact, virtually any antenna can benefit from a tuner under some circumstances. Here we will discuss how a tuner can increase the flexibility and usefulness of some popular antennas.

The Coax Fed Dipole

In Chapter 2, we discussed the nominally matched dipole and the limitations on its bandwidth within a given SWR. For example, to have a single low 80 meter dipole be useful across the entire band, we may need to deal with an SWR as high as a 10:1 as shown in Figure 2-7, in Chapter 2, although at many heights, the SWR will not rise beyond 5 or 6:1 at band edges. Most other examples shown in Chapter 2 have more reasonable SWR characteristics. Still, in many cases an SWR higher than 2:1 may be encountered, requiring an antenna tuner to permit proper transmitter operation at band edges.

A Dipole Operated on an Odd Harmonic

A special case of the dipole is one used on its third harmonic. A very popular amateur antenna is a 40 meter (7 to 7.3 MHz in the US) dipole also operated on 15 meters (21 to 21.450 MHz). This is often stated as if it were a straightforward arrangement, however, it is just a bit more difficult to achieve than would be implied by some. A tuner makes it much easier. The difficulties arise particularly due to two factors:

- The nominal impedance of a ¾ λ dipole in free space is about 110 Ω, rather than 72 Ω for a λ/2 dipole. While the actual impedance will vary above and below this number, depending on height above ground, this often gives us a higher SWR than 2:1 to start with.
- The third harmonic of 7.15 MHz, the center of the 40 meter band, is 21.45 MHz, the very top of the 15 meter band.

Figure 13-1 shows the modeled SWR of a wire 40 meter dipole cut for mid band at a height of 40 feet. **Figure 13-2** shows the SWR of the same antenna operated on 15 meters. Obviously, this isn't going to work out as well as some folks hypothesize.

Many wide range tuners could compensate for the SWR at the transmitter. As discussed in Chapter 7, however, the losses in a coax cable with a 10:1 SWR at 21 MHz may result in more loss than can generally be tolerated, although it certainly could be used in a pinch. Because the losses in mismatched coax are less at lower frequencies, the concept can be salvaged by optimizing the dipole as a 15 meter ¾ λ dipole with the results shown in **Figures 13-3** and **13-4**.

Note that the lengthened antenna has an SWR of less than 3:1 across all of 15 meters, significantly reducing the transmission line loss associated with Figure 13-2. While the SWR on 40 meters is no longer delightful, it is reasonable from a transmission line loss standpoint. The resulting antenna can work well with some nominal "3:1" SWR tuners that work beyond

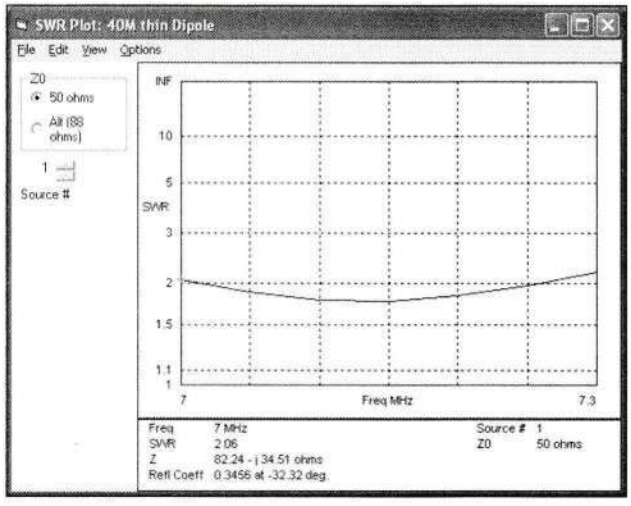

Figure 13-1 — 50 Ω SWR of a 40 meter dipole at 40 feet cut for mid band.

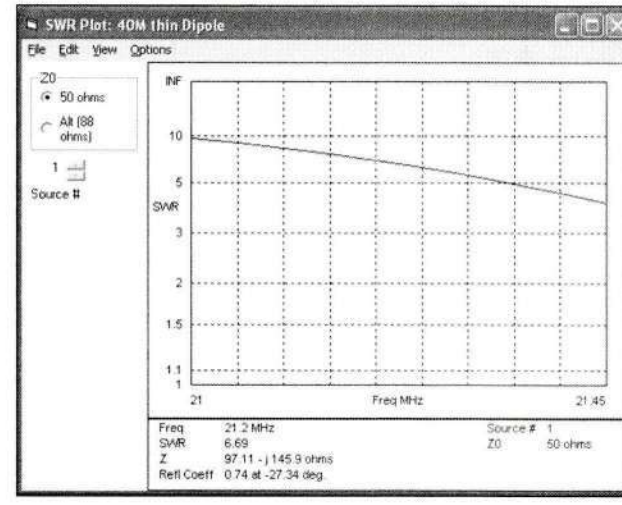

Figure 13-2 — SWR of the 40 meter dipole of Figure 13-1 across 15 meters.

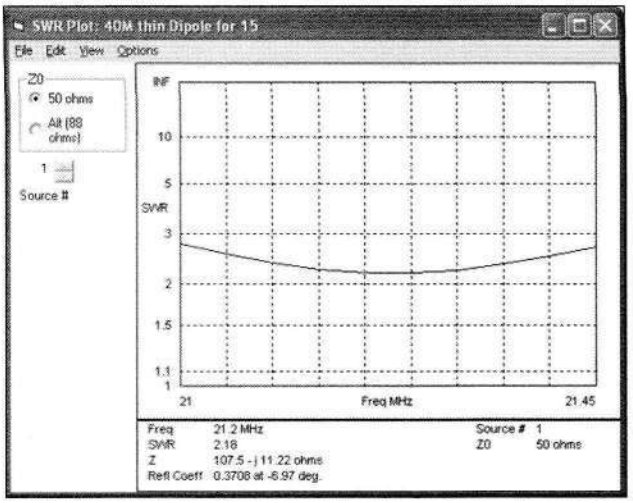

Figure 13-3 — SWR of the 40 meter dipole of Figure 13-1 lengthened to be optimized for 15 meters across 15 the 15 meter band.

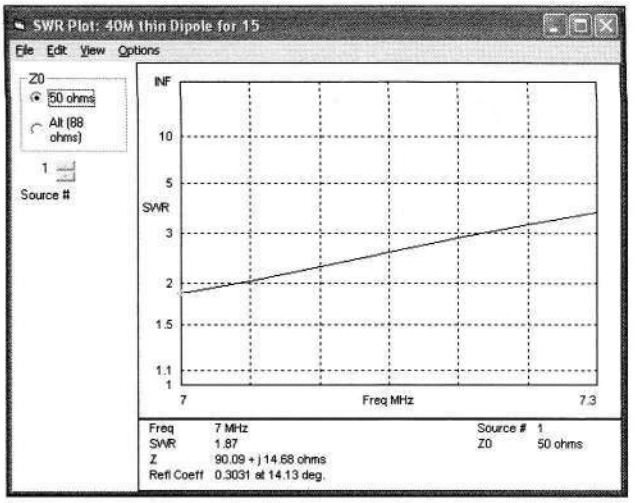

Figure 13-4 — SWR of the lengthened (15 meter optimized) 40 meter dipole of Figure 13-3 across 40 meters.

their specs, and is an easy job for wider range tuners.

Dipoles Can Benefit

The preceding examples illustrate ways in which a simple dipole can benefit from an antenna tuner. For any dipole, the tuner can compensate for imperfect length adjustment, often a convenience. The one caution is that even if the tuner can match the resulting impedance, the loss in the mismatched transmission line between the tuner and the antenna can be an issue, even if all seems well at the transmitter. Take another look at Chapter 7.

Tuned Yagi Arrays

We often think of the popular HF Yagi beam antenna as one that is fed directly with 50 Ω coax with low SWR and without any need for a tuner. This is certainly the sense one gets from the specification sheet, yet some highly tuned Yagis, particularly those operating on multiple bands, have trouble providing a close match from band edge to band edge, particularly if optimized for the CW or SSB segment. In most cases, even though the SWR may be marginal at the far edge, there is still beneficial gain and front to back ratio. This is exactly the place for a limited range internal tuner to be applied, since the SWR is often less than 3:1. My sense is this is what they had in mind when these 3:1 tuners were designed — compensating for the just out of tune coax fed dipole or Yagi.

Single Wire Fed Antennas

There are a number of antennas that are designed to be fed as a single wire, without any transmission line. Some are field expedients, however, others are well thought out designs that can offer excellent performance.

Single Wire Antennas

Single wire antennas go back to the very beginning of amateur radio — the days before anyone thought of a transmission line. The most commonly used transmitting antenna in the early days was a short vertical (we're talking below 200 meters, so everything was short!) with top capacitance loading of multiple horizontal wires. They were used on shipboard, shore and ham stations alike, and worked well enough to get the signals through.

These days, a "random length" single wire is often used as an easy to deploy temporary antenna or, for some, using very thin wire, as an unnoticeable stealthy antenna if neighbors or deed restrictions object to "antennas." They can be effective, especially if fed against a good ground system, and if they are at least λ/4 long at the lowest frequency. Such a λ/4 wire fed against ground even has a name! This is called a Marconi antenna, and yes. it dates back more than a century.

Random wire antennas will still work if shorter, but ground losses rapidly reduce efficiency as lengths get much shorter than λ/4.

The success of such single wiere antennas depends on all the usual factors including height, length, and ground conditions all played against desired frequency and geographical coverage. With a ground mounted radio and a higher wire antenna, there will always be some vertically and often horizontally polarized radiation as well. The combination can provide a useful mix of coverage, although the coverage in any direction will not be as good as that of an antenna designed for the job.

The key element in making such an antenna play is a wide range antenna tuner that can match the widely variable load of the single wire on multiple bands to the 50 Ω that modern radios require. So we have a place here for the antenna tuner, the question is "which place."

Antenna Tuner at the Shack — This can work and has been done, but in the most successful implementations, the antenna tuner is near the boundary between indoors and out. In some stations, that boundary is within or at the edge of the shack eliminating the distinction.

A portion of a radiating antenna inside a building is generally asking for some kind of trouble. First there is the RF safety issue as applied to any people inside the structure. Even if your transmit power level does not require a formal assessment, you are not released from the requirement to not expose people to excessive levels of RF. Second, your indoor receiving antenna will pick up electrical noise from other equipment in the building. Third, if the building contains any sensitive electronic systems, your signal has a good chance of causing trouble, such as setting off fire alarms, or getting in to a television receiver while a spouse is watching an important show. In any case, any radiation that occurs within the building structure is not likely to help you get your signal where you want it.

None of this is to suggest that indoor antennas can't be used, however all of the above issues need to be considered. Here we are talking about an antenna that is partly inside a building, and partly outside. The point is that having as much as possible outside is generally a better solution.

Antenna Tuner at the Antenna — The antenna tuner can also be located at the antenna, if it's remotely tuned or sometimes remotely switched. Some remote tuners are waterproof, while others will need a waterproof enclosure to make them last. With the tuner at or near the antenna feed point, matched coax can run from the tuner back to the station, as discussed previously. By running the coax from the station out to the antenna feed point, the issues of radiation within the building can be largely avoided.

This is the configuration used for

Table 13-1

Random Wire Antenna Lengths that Should be Avoided Due to Resonance and High Impedance.

Band (Meters)	*0.5 λ*	*1 λ*	*1.5 λ*	*2 λ*	*2.5 λ*	*3 λ*
160	234 to 260	468 to 520	702 to 780	936 to 1040	1170.0 to 1300.0	1404.0 to 1560.0
80	117.0 to 133.7	234.0 to 267.4	351.0 to 401.1	468.0 to 534.9	585.0 to 668.6	702.0 to 802.3
40	64.1 to 66.9	128.2 to 133.7	192.3 to 200.6	256.4 to 267.4	320.5 to 334.3	384.7 to 401.1
30	46.1 to 46.3	92.2 to 92.7	138.3 to 139.0	184.4 to 185.3	230.5 to 231.7	276.7 to 278.0
20	32.6 to 33.4	65.2 to 66.9	97.8 to 100.3	130.5 to 133.7	163.1 to 167.1	195.7 to 200.6
17	25.8 to 25.9	51.5 to 51.8	77.3 to 77.7	103.0 to 103.6	128.8 to 129.5	154.6 to 155.4
15	21.8 to 22.3	43.6 to 44.6	65.5 to 66.9	87.3 to 89.1	109.1 to 111.4	130.9 to 133.7
12	18.7 to 18.8	37.5 to 37.6	56.2 to 56.4	74.9 to 75.2	93.6 to 94.0	112.4 to 112.8
10	15.8 to 16.7	31.5 to 33.4	47.3 to 50.1	63.0 to 66.9	78.8 to 83.6	94.5 to 100.3
6	8.7 to 9.4	17.3 to 18.7	26.0 to 28.1	34.7 to 37.4	43.3 to 46.8	52.0 to 56.2

many marine HF antennas. On a sailboat, the typical HF antenna is an insulated backstay fed by a remote single wire tuner located near the antenna base and fed against the ship ground system, including salt water, if possible.

But Watch Out for Tricky Lengths! — The so called *random length* wire antenna is not really random since any antenna does have a specific length. Such an antenna will work better at some lengths than others, making it best if not entirely random in its installation. The problems most often show up if the length happens to be a multiple of λ/2. At this length, the impedance hits a maximum, often in the 1000 to 2000 Ω range, depending on the usual factors. This results in an SWR of 20 to 40:1, higher than even a wide range tuner promises to deal with.

The impedance gets somewhat lower with each multiple of a λ/2, but may still be a problem. A second concern is that the voltage on the end at the tuner is high. The voltage can be nearly 500 V_{RMS} with a 100 W transmitter. This can stress tuner capacitors as well as pose a safety hazard to unsuspecting people. Instead of the shock experienced by coming in contact with dc or 60 Hz ac, contact with RF results in a painful burn that is usually slow to heal.

While it sounds like it should be an easy task to select a length, the multiplicity of bands without harmonic relationship makes it difficult to find a length that won't be likely a problem on some band. A look at **Table 13-1**, indicating approximate λ/2 resonant lengths for each band, along with multiples, provides a list of lengths to avoid for the amateur bands. There are so few lengths available, that sometimes it makes sense to just try the length that fits the available spot and, if it has problems tuning on a band, add a few feet and try again.

The Vertical Monopole

A popular antenna with those who like to operate long distances on the lower HF and MF bands is a vertical monopole. This can perhaps be considered a special case of the random wire antenna, except that it is generally of specific electrical length — typically λ/4 or ⅝ λ, depending on frequency and available supports. While a λ/4 vertical monopole can usually be fed directly with 50 Ω coax against ground, the other lengths do require matching networks or an antenna tuner for operation with a transmission line. A low impedance ground is a requirement for efficient operation of such antennas.

A 43 foot tall vertical made from wire or tubing is a very popular antenna in some quarters. It is a ⅝ λ long monopole on 20 meters and thus provides the optimum low angle radiation from a single vertical radiator (see **Figure 13-5**), yet can provide excellent low angle performance on 40 meters where it is somewhat longer than λ/4, as well as on 80 meters where it is somewhat less than λ/4, but generally a manageable height. All the lengths share a complex feed point impedance that responds nicely to a remote tuner at the base, although at these frequencies, a short run of high quality coax may have sufficiently low in loss to be suitable for use with a tuner at the station.

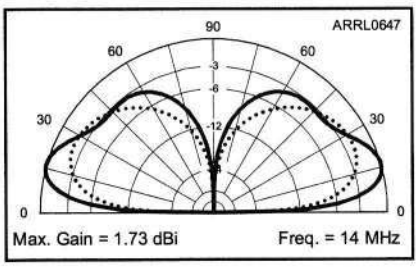

Figure 13-5 — Vertical radiation patterns of a 43 foot, ⅝ λ, vertical on 20 meters (solid) compared to a ¼ λ monopole. Note the increased radiation at low elevation angles. THE DOTTED PATTERN IS FOR THE 1/4 λ MONOPOLE.

Inverted L

A popular variant of the vertical monopole, particularly on the lower frequency bands, is the inverted L. A λ/4 monopole for 160 meters, for example, needs to be around 130 feet long — a bit of a stretch for most as a vertical arrangement. The inverted L is obtained by taking the same length of wire and going as high as feasible, then bending the remainder horizontally. The antenna has the appearance of an upside down letter L — hence its name.

The lower (vertical) portion has the highest current and will thus provide low angle radiation very similar to that of a full sized monopole. At the λ/4 frequency, the inverted L can often be fed directly by 50 Ω coax with a reasonable SWR. An additional advantage of this arrangement, if fed with a wide range tuner at its base, is that it will provide low angle vertically polarized radiation at higher frequencies up to the frequency at which the vertical portion is just longer than ⅝ λ. Note the earlier concerns about feeding an antenna that is a multiple of λ/2, and if multiband operation is in the plan, make the inverted L longer than λ/4 on the lowest band.

The Bobtail Curtain

An interesting, inexpensive and surprisingly effective directional array called the Bobtail Curtain is composed of three λ/4 vertical elements fed in phase and driven from the single wire center element as shown

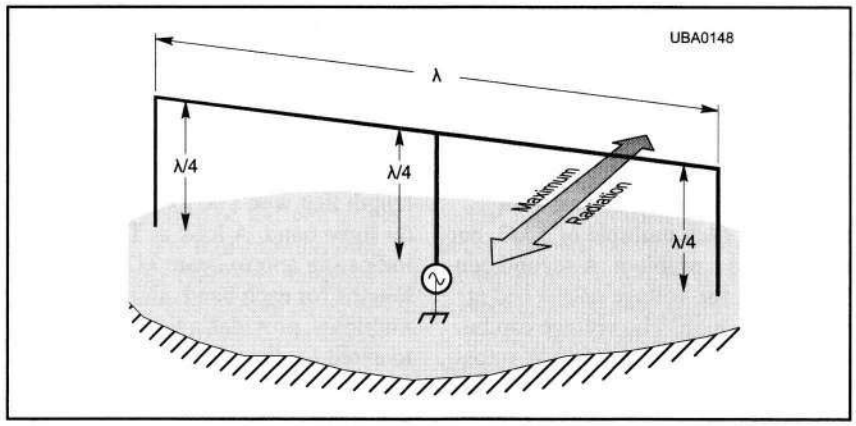

Figure 13-6 — The Bobtail Curtain three element vertical phased array fed by a single wire.

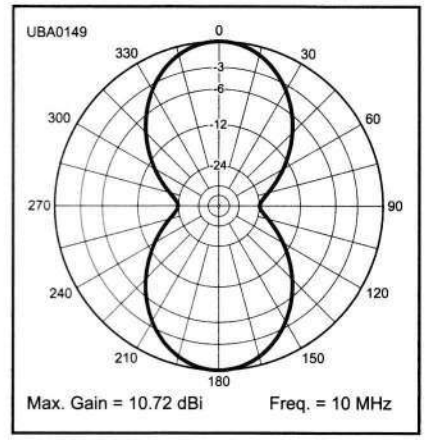

Figure 13-7 — Azimuth pattern of a Bobtail Curtain array at 10° elevation. Note the high gain over 60° on each side, broadside to the array.

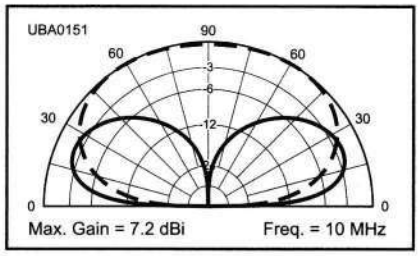

Figure 13-8 — Elevation pattern of a Bobtail Curtain array (solid) compared to a full wave center fed antenna on the same supports (dashed). Note the superior low angle coverage.

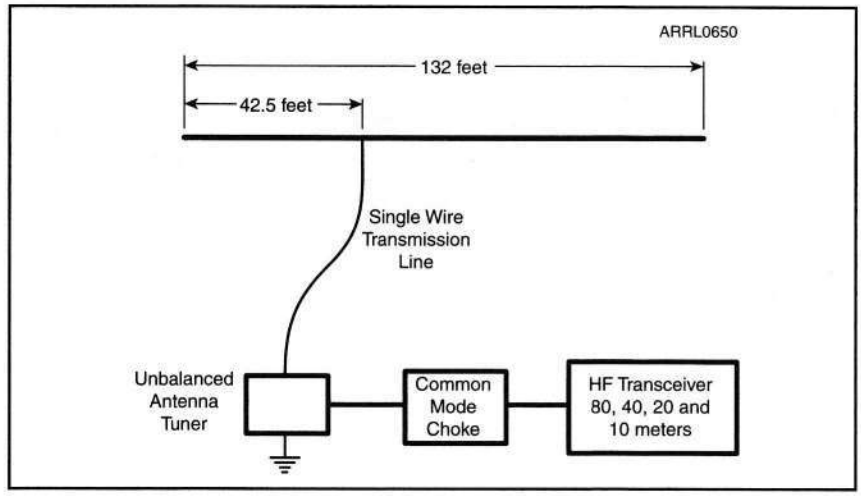

Figure 13-9 — Single wire fed Windom antenna configuration for 80, 40, 20 and 10 meters.

in **Figure 13-6**.[1] This antenna is composed of just four pieces of wire, yet provides significant gain in two fixed directions as shown in **Figure 13-7**. The low angle gain of this antenna favors long distance communication (see **Figure 13-8**) and is higher than that of horizontal antennas of the same height.

The Bobtail Curtain can be fed by a single wire tuner located at the source shown in Figure 13-6, although the impedance is quite high, as discussed in the previous section. Making the middle wire a few feet longer may make it usable with most wide range tuners. The antenna can be used on other bands as a kind of top loaded monopole, although the results will not be in the same league as those at its design frequency.

Single Wire Fed Windom

An unbroken half wave antenna off-center fed by a single wire was quite a popular multiband radiator in the 1930s, following publication of a note by Windom in *QST*.[2] The Windom antenna, as shown in **Figure 13-9,** with a fundamental frequency in the lower portion of 80 meters, was said to operate equally well on 40, 20 and 10 meters, thus covering all the amateur HF bands of the day.

There is some controversy over just how well this antenna works as a horizontal antenna; however, there is no question that it can work. Figure 13-9 shows a choke or current balun in the coax from the tuner to the radio, since there will likely be significant common mode current that should be kept out of the radio room.

[1]For more about the Bobtail Curtain array, see J. Hallas, W1ZR, *Basic Antennas — Understanding Practical Antennas and Designs,* Chapter 15. Available from your ARRL dealer or the ARRL Bookstore, ARRL order no. 9994. Telephone 860-594-0355, or toll-free in the US 888-277-5289; **www.arrl.org/shop/**; **pubsales@arrl.org**.

[2]L. Windom, W8GZ, "Notes on Ethereal Adornments," *QST*, Sep 1929, pp 19-22, 84.

Balanced Antenna Systems

For many amateurs, the antenna tuner really earns its keep by matching balanced systems for multiple bands. The classic system is one that is often called a center-fed Zepp, although there are some who suggest it really should have different names on different bands.

The Center-Fed Zepp

This antenna is actually a half-wave dipole if fed on its lowest band. The difference between it and the usual dipole is that it is fed with low-loss balanced transmission line, such as open wire line or window type line. Since it doesn't really need to be resonant to work well, and thus can be almost any length, a more accurate name might be the *not always resonant tuned feeder dipole*. Still more folk will know what you mean if you call it a center-fed Zepp (CFZ). The configuration is shown in **Figure 13-10**.

For the case in which it is resonant at its half wave frequency, the radiation pattern is the same as any half-wave dipole at the same height. The difference is that the SWR on the transmission line will be in the range of 4:1 to 10:1 depending on the height of the antenna and the transmission line type. While the loss with this kind of mismatch would be a problem with coax, it isn't with low loss line. Including the loss due to mismatch, the total loss is comparable or even less than most matched coax situations at the same frequency.

The antenna can easily be fed with a wide range antenna tuner, preferably a balanced antenna tuner, but usually also with an unbalanced tuner equipped with a balun. The antenna will work very well on higher bands — into the VHF range. There may be some lengths of transmission line that will result in an impedance that the tuner can deal with on all bands.

The antenna patterns become fairly complex at higher frequencies. For resonant antennas, there are generally 2 × N main lobes where N is the number of full wavelengths.

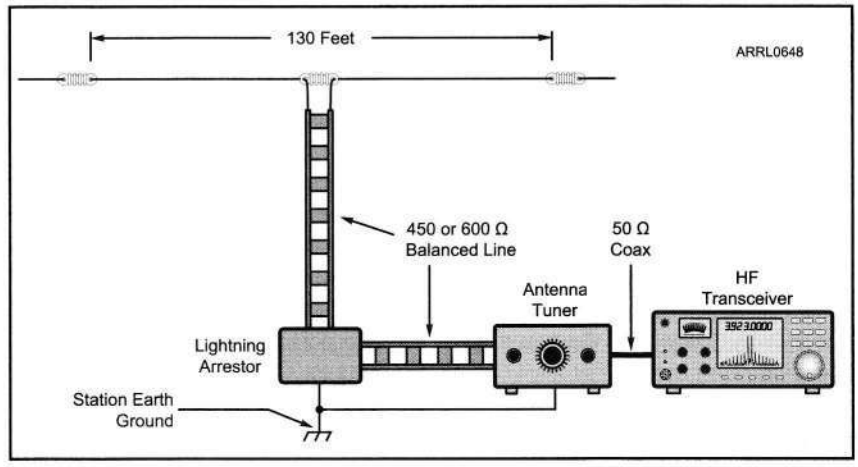

Figure 13-10 — Traditional center-fed Zepp antenna. With the length shown, the antenna will work well from 80 through 6 meters, and may even tune on 160 meters. The antenna length is not critical, however, it works best if close to λ/2 on the lowest operating frequency as described in the text.

As mentioned, the antenna has no particular need to be resonant anywhere to work well. The impedance is easier to match if the antenna is at least a half wave long at its lowest frequency, but there is nothing magic about that length. I use a 100 foot long dipole, center fed with 450 Ω window line quite successfully on all bands from 80 through 6 meters, for example.

Another popular length is 86 feet. This provides the optimum gain on 20 meters in single lobes in each direction perpendicular to the wire. While the lobes are sharp compared to a dipole, 35.6° on either side compared to 83°, the gain at the peak is more than 3 dB higher than a dipole.

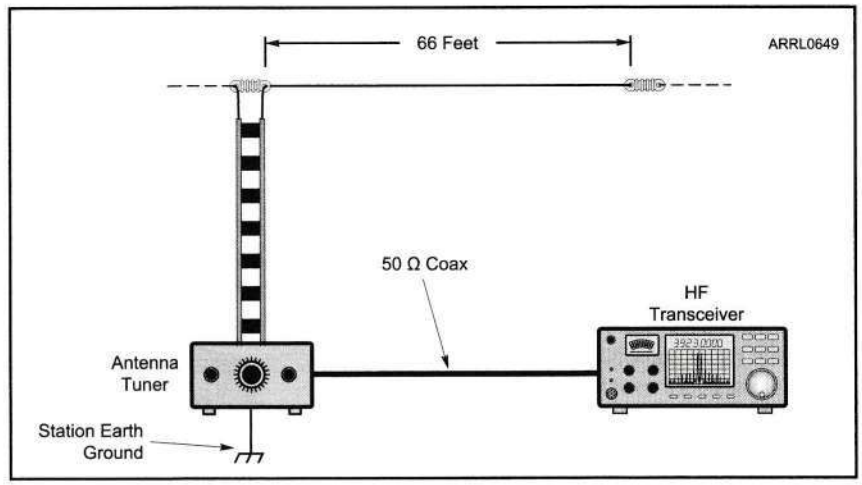

Figure 13-11 — End-fed Zepp antenna for 40, 20, 15 and 10 meters. This works as a horizontal antenna if the length is a multiple of λ/2 on each frequency used. On other frequencies the feed line will also radiate, usually with vertical polarization, and precautions must be taken to keep common mode currents from the radio equipment. Lightning arrestor not shown.

This length will usually be useable from 80 meters through the higher frequency bands, although some transmission line lengths may have problems with some wide range tuners on 80 meters.

If there are problems matching particular impedances, usually an extra 10 feet or so of the transmission line will change the impedance enough to make the match possible. Be sure to check the other bands to make sure you haven't just moved the problem around. Usually a length can be found that will work on all bands. Be sure to avoid coiling up the excess balanced line. Always keep it off the ground and away from metal — at least three or four times the distance between the conductors.

The End-Fed Zepp

A half wave antenna fed on the end with a λ/4 matching section of low loss balanced line is called an end-fed Zepp. This is often a convenient antenna if the station is close to a property boundary, making a center-fed antenna a difficult proposition. The matching section transforms the high impedance on the end, typically close to 2000 Ω, to a relatively low impedance that can be fed by a transmitter, or a narrow range tuner. This is the original Zeppelin antenna that was deployed beneath the aircraft's gondola. It is also popular as a VHF vertical called a "J-antenna."

Some have had better results by providing a λ/10 or so of wire as a counterpoise on the other side of the transmission line, particularly if using it on multiple bands. On bands at which the antenna is a multiple of λ/2, it provides mostly horizontal polarization with minimal common mode current on the transmission line. It can be made to work on bands at which it is not resonant, however, there will be a pronounced lack of balance on the transmission line.

While the λ/4 matching section is a key part of the original Zepp design, it is not necessary if a wide range antenna tuner is provided to perform the matching as shown in **Figure 13-11**.

The unbalanced line currents result in two effects.

- First, the line will radiate. This may not be a terrible thing, if the line is in the clear, but can cause problems if it is running near other equipment.
- Second, the line will bring common mode current into the station. This can usually be addressed through a common mode choke at the point at which a transition to coax is made. Make sure the coax run is short, since the mismatch will result in much higher losses in coax.

Mobile Antenna Systems

Antennas used in vehicles operate under the same principles as antennas in other applications, however, they often provide unique challenges. Antennas for MF and the lower portion of the HF region must be shortened considerably in order to be practical on most motor vehicles, large ships are a notable exception. In addition, unlike the usual antenna environment, these antennas are usually quite close to both the radio equipment as well as the vehicle body. With the exception of aircraft antennas, most mobile antennas are also quite close to the ground.

While none of the above differences by itself results in major problems, they all lead to certain limitations in

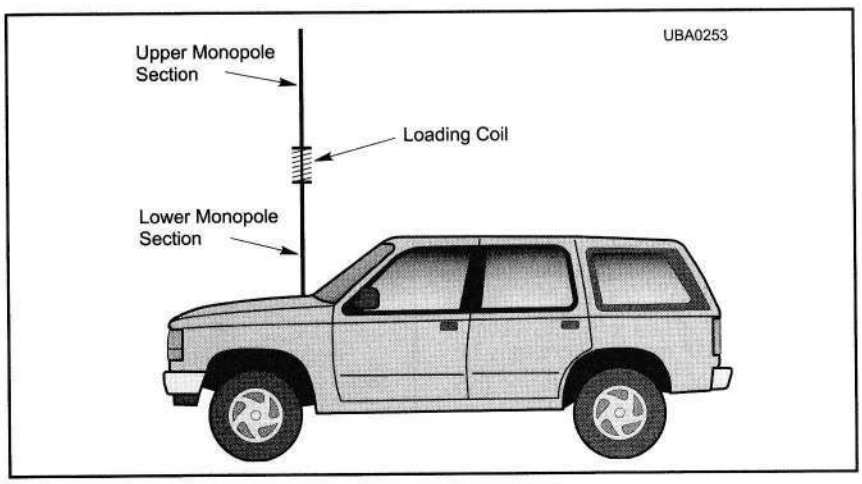

Figure 13-12 — Typical vehicle mounted monopole for the lower HF range. Because of practical limitations to do with garages, tunnels and trees, lengths tend to be 8 feet or less, from about ⅛ to 1/32 wavelength. The center loading shown improves efficiency.

antenna design and performance.

HF Mobile Antennas on Land Vehicles

The lower HF bands, especially 80, 40 and 20 meters, are popular with mobile operators. Depending on the sunspots and time of day, one or more can usually be counted on for reliable medium to long range communication. The usual antenna is a relatively short monopole antenna mounted on, and fed against, the vehicle body as shown in **Figure 13-12**.

As in the antenna in Figure 13-12, center loading is often used because it results in higher current in the lower section and thus less loss, although base loading, or even just using a solid whip with a tuner at the base are often encountered. A limitation of such an antenna is its SWR bandwidth, a typical case shown in **Figure 13-13** — much narrower than a full size antenna.

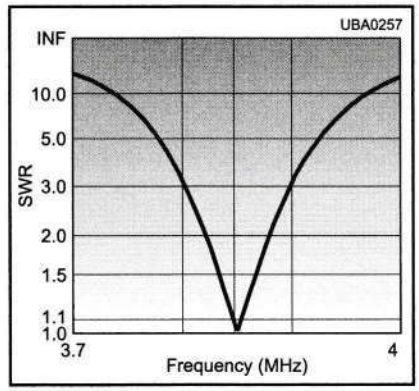

Figure 13-13 — Typical SWR plot of a mobile antenna of the type shown in Figure 13-12. The 2:1 SWR bandwidth is likely to range from 20 to 50 kHz, with antennas having less efficiency tending to have wider bandwidth.

This makes the shortened mobile antenna a good candidate for a wide range antenna tuner. The tuner can be used to allow full band coverage to be obtained. I have even used a tuner to allow a 40 meter mobile whip to be used on 80 meters, although it is not as efficient as the center loaded 80 meter arrangement.

HF Mobile Antennas on Other Vehicles

Those using HF on boats or aircraft do not generally share the same size restrictions as on land vehicles. Often either will use a convenient length of wire, for example the insulated backstay on a sailboat, or a wire from a short mast to a handy surface on an aircraft, to form an antenna similar to the random wire described earlier. This is almost always accompanied by a remote, usually automatic, antenna tuner very near one end or the other of the wire. This system can work very well if fed against the aircraft body or a metal hull. On my fiberglass sailboat, I feed it against the ship ground system.

Review Questions

13-1 Under what circumstances can an antenna tuner be of benefit in feeding a simple coax fed $\lambda/2$ dipole?

13-2 Why is it important to use low-loss transmission line such as window or ladder line if using a dipole on multiple bands?

13-3 What are the possible consequences of common mode currents on a transmission line?

Chapter 14

A Survey of Available Tuners

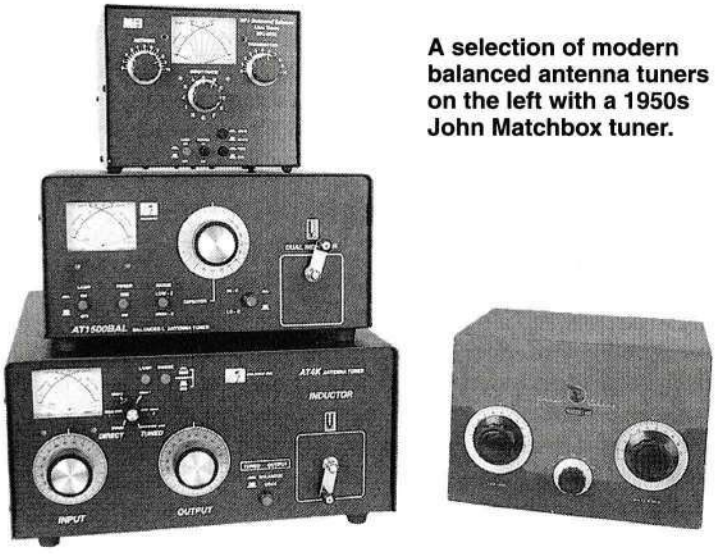

A selection of modern balanced antenna tuners on the left with a 1950s John Matchbox tuner.

Contents

Key Tuner Parameters 14-2
Product Review Testing 14-4
Selected QST antenn Tuner Product Review Articles
QST Reviews Five High Power Antenna Tuners 14-5
Automatic Antenna Tuners — A Sample of the Field 14-12
Medium to High Power Auto Antenna Tuners —
The Evolution Continues 14-19
A New Generation of Balanced Antenna Tuners..... 14-26
Review Questions..... 14-36

Key Tuner Paramaters

Virtually every configuration of antenna tuner, capable of operation at every legal power level, is available commercially from one or more vendors. This can make selecting a commercial tuner a bit of a challenge, just as it is much tougher to select a meal from a restaurant with many good choices, compared to just a few.

Fortunately, the choices can be quickly reduced if one can make a few decisions on key tuner parameters. I will try to organize them in a way that will help make the selection easier. The following are the major decisions to be made, in this person's opinion:

What Frequencies Do You Want the Tuner to Cover?

When talking about antenna tuners, we almost always are talking about the HF range, although there are also some tuners for VHF bands. This means that we want to cover the amateur bands from 80 through 10 meters — that's a *given*. Most current amateur transceivers also cover 160 meters. Is that of interest? If so, because it often doubles the size of many tuner components, it will likely add significantly to the cost and size of a tuner, all other things being equal. The 160 meter band is gaining in popularity since it provides interesting operational conditions at the bottom of the sunspot cycle, as I write this. If you have room for effective 160 meter antennas, having a tuner that supports operation here may be a good choice.

On the other end of the spectrum is 6 meters. More and more current amateur "HF" transceiver cross into operation on our lowest VHF band. This band is also quite popular now since there are long distance modes that don't depend on sunspot activity. If you have, or expect to have, a dedicated 6 meter antenna, the chances are that it will be suitable to be fed directly with 50 Ω coax and a tuner will not be needed. On the other hand, if you will need to use your all band tuner fed antenna, such as the center-fed Zepp, on this band, you will want to include that capability in your tuner.

The other frequency decisions may be more subtle. Operation on 10 meters is sometimes a problem with larger tuners that have trouble ending up with sufficiently low minimum inductance and capacitance to provide the same impedance coverage on 10 meters as on the other bands — check the specifications to get an idea. In a similar vein, some tuners don't have quite enough maximum inductance or capacitance to provide the tuning capability to cover 80 (or 160) meters with the same range as on the other bands.

How Much Power Do You Expect to Run?

For any given tuner design, there is no factor that influences tuner cost and size more than power level. This should not be a surprise since higher power means higher voltage and current stress on the components within. The obvious answer might be to pick a tuner with a power rating equal to the most power that your transmitter can put out — but be careful, there are four issues hidden here:

- The power rating is based on the manufacturer's SWR specification (if they did a proper design job). If it says a tuner is good for an SWR of 10:1, typical for a wide range tuner, and you tune an antenna with a 20:1 SWR, you may be able to get a match, but either the voltage or the current in the tuner can be higher by a factor of $\sqrt{(20/10)}$, or 1.41 times. That may explain the arcing, or the burning smell, you observe on some frequencies! The answer may be to go somewhat higher in power rating than you expect to actually run.
- So you now have that shiny new 100 W transceiver — you love it to death and can't imagine that you will ever need more power. You buy a 100 W antenna tuner (or better a 200 W tuner, as discussed above) and happily make many contacts with your stealthy antenna. Now you decide to try for DXCC and notice that the DXpedition in Outer Slovenia can almost hear you, but can't quite copy your call letters. A bigger antenna is out of the question — the only solution is a high power amplifier. Oops, now you have an almost new 100 W tuner that you can no longer use.
- In addition to taking up more space, and more lawnmowing money, high power tuners often, because of the physical size of the components, have trouble providing the tuning range some antennas need on the higher bands. Some switch out portions of the circuit on higher bands to avoid the problem, but some don't. Keep your eye on that ball, if looking at higher power tuners.
- On the plus side, higher power tuners usually have inductors that are wound with heavier wire. This reduces losses, although it may not be noticeable in the test results.

Do You Want a Balanced or Unbalanced Tuner?

If you expect to be feeding single wire or coax-fed antennas, an unbalanced antenna tuner will be fine. If you want to feed an antenna such as a center fed Zepp with balanced line, you will need to have some provision to feed a balanced load. This can be handled in one of three ways:

- A fully balanced tuner is ideally suited to matching to balanced loads within its matching range. These are available in multiple power ranges and can work quite well. A disadvantage of these is that many do not include all the switching options of many unbalanced tuners — not a problem if you expect to use a single antenna.
- Many inherently unbalanced

tuners include an output connection through an internal balun. These work best with balanced loads within about 4:1 SWR of the balun design impedance. Most use 4:1 baluns designed for a 200 Ω load. That means they will work reasonably well with resistive loads from 50 to 800 Ω, and with complex loads of a similar SWR. They will also work outside that range, although their response can be a bit unpredictable. If they don't get hot, they are probably putting the power where you want it.

•The same kind of balun can be added outside of an unbalanced tuner if you decide to move from coax to a balanced feeder system. The same concerns as noted above apply. However there are some advantages such as that you can custom design the balun for the impedance that each antenna has, and you can have the balun some distance from the station equipment — but watch out for mismatched coax losses if the distance is more than a few feet.

Do Your Want a Remote or Local Tuner?

An antenna tuner that is located next to the radio in the station area offers a lot of plusses in terms of control and monitoring. Some antennas, however, really want the impedance matching performed at the antenna. A big consideration here is that if the tuner is located with the antenna, it usually can only operate with that single antenna, although remote switching is possible. If the antenna tuner is near the radio, switching between antennas systems is usually much easier — sometimes provided within the tuner, sometimes outside — but always within reach.

Do you Want a Manual or an Automatic Tuner?

A manual tuner requires adjusting two or three controls (and often switches) every time either frequency is changed, typically by around 50 kHz, depending on what band is selected or what type antenna is used. The adjustments can be tedious, although recording them makes returning to a proper tune under previously encountered conditions fairly easy.

An automatic tuner, on the other hand, just requires a push of the button to obtain a tune. Many have some sort of memory arrangement so they can quickly return to previous settings. The tuning usually takes a few seconds the first time, a fraction thereafter. While it is possible to imagine a remote manual tuner, to my knowledge, all remote tuners are of the automatic flavor. So if you want remote, you get automatic.

The idea of an automatic tuner sounds pretty good, and it is. There are just a few items to be aware of, as noted below:

•In general, an auto tuner will make a match within its specified SWR threshold, often 1.5:1, but check and compare with your radio's requirement. With your manual tuner, you can usually find a 1:1 setting. If the radio will put out its full power into the load, this is not worth worrying about.

•Watch out for tuners that initiate a tune on their own. Some can be just *too* automatic to suit me. You tune your radio 25 kHz off your previous frequency to capture a neat DX station, start to call, and hear your antenna tuner relays clacking. Chances are the up and down tuning will result in the station missing some part of your call sign.

Of more concern, if there is no circuitry to prevent it, many automatic tuners that can handle 100 W, for example, want tuning to occur at a lower power level to avoid burning relay contacts. If it starts up while you are operating, you can easily hit it at full power before you know what's happening. In the mobile environment, this can also happen as you pass that 18 wheeler with a giant piece of aluminum detuning your antenna (it can also serve as a reflector, if you get it in the right place!).

•I once thought that the small components in the usual compact automatic antenna tuner would result in more losses compared to the larger components, especially inductors, in the usual manual tuners. To my surprise, following the test results presented below, this does not seem to be the case, although it might be buried in the 5% minimum loss, below which we don't report due to measurement uncertainty. If it is a loss of that level (0.2 dB), in my opinion, it should not be part of the decision process.

Product Review Testing

The American Radio Relay League (ARRL), the US Amateur Radio organization publishes a monthly magazine, *QST*, for its members. In addition to its many technical and general interest features, each month's issue includes detailed reviews of products of interest to its readers. These Product Reviews generally include laboratory evaluation of equipment operational parameters using professional grade, independently calibrated test instruments. Over the years, we have had many such reviews of antenna tuners and I have reproduced the results from some here.

While many of the reviews include currently available equipment, some models covered are no longer available as new equipment. Even so, it may be of benefit in two ways:

- There is an active used equipment market in Amateur Radio equipment. This may provide a way to knowledgeably purchase an antenna tuner at a lower cost.
- In some cases, manufacturers have made relatively small changes to equipment, so data on previous models may be directly applicable.

ARRL Lab Antenna Tuner Testing Methodology

The following method was used in the ARRL Lab to measure the loss of the tuners presented below. Two test fixtures were built which would hold combinations of high power 50 Ω "non-inductive" carbon resistors (one fixture for parallel combinations and one for series), one shown in **Figure 14-1**. Even with the non-inductive resistors, some net fixture inductance was apparent at some frequencies, so a variable capacitor was used to compensate. The fixture accuracy was measured using the Lab's vector impedance meter.

Each fixture used an input connection (for the tuner) and an output connection. The output connection went to a 50 Ω input power attenuator, which took the place of one of the resistors in the load (for the series loads, it was always the one on the ground side of the network). The output of the power attenuator was connected to a high accuracy laboratory wattmeter, and the actual attenuation was measured for each frequency. The tuners were matched at low power, then 100 W of RF was applied at the input, with the output being measured by the Lab's wattmeter.

Each tuner was connected to the load fixture at each resistive impedance level for testing in the ARRL Lab. A 100 W RF source fed the input of the tuner. The resistive load was connected to the antenna output. The load was connected to a 50 Ω. power attenuator, which took the place of the final resistors. This is a close-up of the parallel load test fixture. The variable capacitor was used to compensate for fixture inductance encountered at some frequencies. While complex impedance loads could have been tested as well, the additional data points would have made testing impractical. We believe that the results at a particular SWR should be representative of other loads with the same SWR.

Note that the reviews were conducted over a period of a few years and the data taken, as well as the presentation, varied slightly from review to review. Please make sure that you are comparing equivalent data.

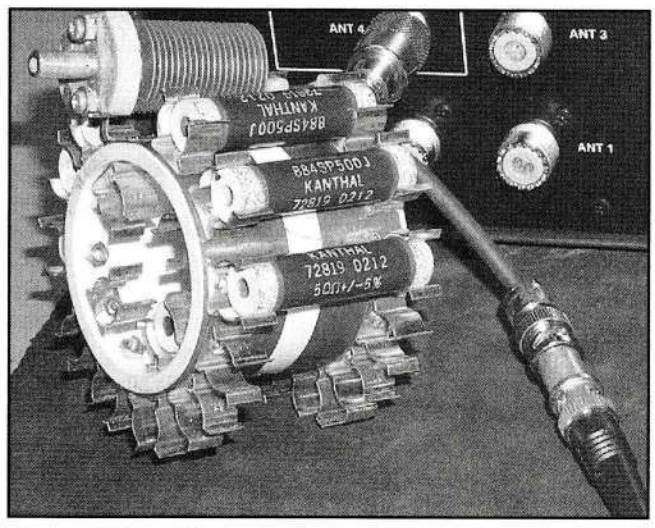

Figure 14-1 — Close up of test figure used to test antenna tuner efficiency into loads from 50 Ω down using paralleled 50 Ω noninductive loads.

QST Reviews Five High Power Antenna Tuners

Reviewed by Jim Parise, W1UK
ARRL Technical Advisor
QST *February, 2003*

One piece of gear that finds its way into most everyone's shack at one time or another is an HF antenna tuner. First of all, the name antenna tuner is something of a misnomer. It does not tune the antenna at all, but acts as an impedance transformer that provides your transmitting equipment with the proper load, usually 50 Ω.

Who needs an antenna tuner? Well, anyone who has the need to match an antenna with an impedance outside the range of their transmitter or amplifier's output circuits. Modern transceivers often have built-in tuners that are capable of matching SWR mismatches up to 3:1. Beyond that they need help, and if you use an amplifier you most surely will need one. Many hams find themselves with limited antenna choices and the desire to operate on frequencies other than what they were designed for, or use non-resonant multiband antennas that require a tuner. The five HF tuners we tested are all in the kilowatt class, meaning the manufacturer rates their power handling capability at 1 kW output or more.

With the wide range of frequencies in the HF spectrum and the huge diversity of antenna types in use, tuners are expected to perform under an incredible number of possible combinations. Some are more efficient at it than others. A measure of a tuner's ability to transform impedances efficiently is energy loss. Under extreme conditions a tuner can get quite hot or arc over at power levels well under the manufacturers rating. Heat in a tuner is a product of loss. RF energy being dissipated as heat is lost power that will not find its way to your antenna and onto the air.

Tuner losses generally get higher as the impedance of the load decreases. If a ham were running 1500 W into a tuner that was 50% efficient, 750 W would be dissipated in the tuner. Most of the loss in a tuner occurs in the coil, and no coil can withstand 750 W of power. A high-power tuner could probably be safely used at 50% efficiency and 100 W, but hams should be careful with high SWR and high power, or a tuner failure is a real possibility. Each tuner was tested into resistive impedances that ranged from 6.25 to 400 Ω, and their respective percentage of loss and 1.5 SWR bandwidth measured. The tuners were also used in everyday communications on all bands at power levels up to 1 kW, matching a G5RV fed with balanced ladder line and a 160 meter inverted L fed with coax.

The characteristicvs of the five uners tested are described in **Table 14-1**. Each tuner is described separately below.

Table 14-1
Comparison of Five Antenna Tuners

	Ameritron ATR-30	*MFJ MFJ-986*	*Palstar AT1500 CV*	*Ten-Tec 238A*	*Vectronics HFT-1500*
Circuit Type	T-network	T-network	T-network	L-network	T-network
SWR/wattmeter	Cross-needle	Cross-needle	Cross-needle	Single-needle	Cross-needle
Balun type	4:1 current	4:1 current	4:1 voltage	4:1voltage	4:1 voltage
Manufacturer's claimed PEP rating	3000 W	3000 W	1500 W	2000 W	2000 W
Manufacturer's claimed Matching range	35-500	35-500	20-1500	5-3000	Not specified
Physical dimensions (HWD) in inches	5.25x13x14.4	4.1x11x15.2	4.5x12.5x12	5.5x13x11	5.5x12.5x12

AMERITRON ATR-30

The ATR-30 (**Figures 14-2, 3, 4**) is Ameritron's legal limit T-network antenna tuner offering. It is housed in a plain, all black aluminum enclosure with a scratch resistant coated front panel. A look under the cover reveals two large variable capacitors and an air core edge wound silver plated roller inductor. Like most of the other tuners reviewed here, the capacitors are adjusted with vernier reduction drives, and although they tune smoothly, they require a lot of force to turn. The roller inductor is adjusted with a plastic lever type knob and is quite stiff to crank. The roller itself is a pinch roller, and the physical resistance in turning the crank may be offset by lessoned contact resistance.

The balun is constructed with three large cores and wound with wire covered with Teflon tubing. The cross-needle meter displays both average and peak power in switchable 300 W or 3 kW ranges. The wattmeter requires dc to function. It is illuminated by either a 12 V barrel connector on the back panel or a 9 V battery accessible through a trap door on the bottom of the unit. With 12 V, both the meter and inductor turns counter are illuminated. When a 9 V battery is used, the meter will function, but the panel lamps will not light.

Finding a match on 80 meters on the G5RV required quite a bit of time finding the right combination of capacitor tuning and inductance, and the stiff controls didn't make it much fun. Finding the sweet spot on the higher bands was much easier. There are three coax outputs on the ATR-30, including two that may be switched direct or through the T-network and a third direct only. Single or balanced feed lines connect to large ceramic binding posts with wing nuts. Test results are summarized in **Table 14-2**.

Manufacturer: Ameritron, 116 Willow Rd, Starkville, MS 39759; tel 662-323-8211; fax 662-323-6551; **www. ameritron.com**. 2003 price: $599.95.

Table 14-2
Ameritron ATR-30 Loss and Bandwidth Test Results

SWR	*Load (Ω)*		*160 m*	*80 m*	*40 m*	*20 m*	*10 m*
8:1	6.25	Power Loss %	20	12	<10	<10	<10
		1.5 SWR BW	1	3	>5	4	>5
4.1	12.5	Power Loss %	15	<10	<10	<10	<10
		1.5 SWR BW	3	4	>5	>5	>5
2:1	25	Power Loss %	10	<10	<10	<10	<10
		1.5 SWR BW	4	>5	>5	>5	>5
1:1	50	Power Loss %	<10	<10	<10	<10	<10
		1.5 SWR BW	>5	>5	>5	>5	>5
2:1	100	Power Loss %	<10	<10	<10	<10	<10
		1.5 SWR BW	>5	>5	>5	>5	>5
4:1	200	Power Loss %	<10	<10	<10	<10	<10
		1.5 SWR BW	>5	>5	>5	>5	5
8:1	400	Power Loss %	<10	<10	<10	<10	<10
		1.5 SWR BW	>5	>5	>5	>5	3

Notes
Power losses are expressed as a percentage. A 21% loss of power is 1 dB.
The 1.5-SWR Bandwidth (SWR BW) represents the bandwidth over which an SWR of 1.5:1 or less was maintained as a percentage of the measurement frequencies (1.8, 3.5, 7.2, 14.2 and 29.7 MHz).

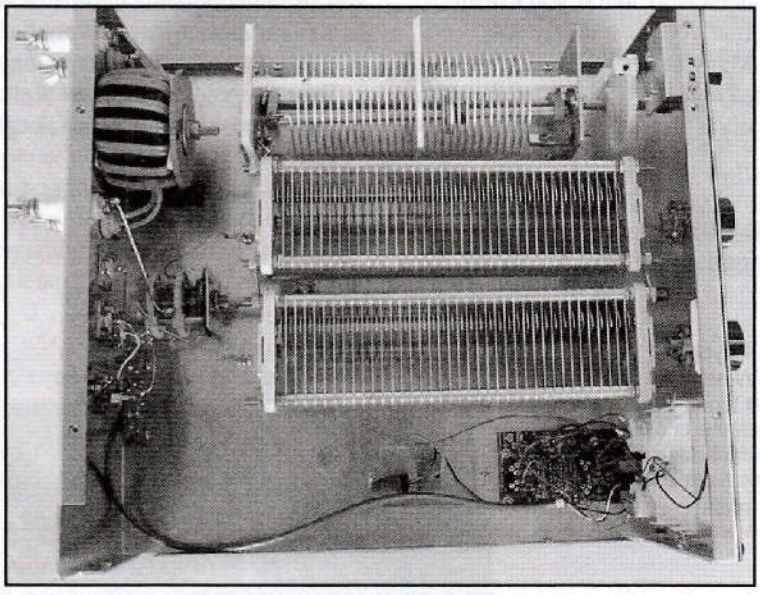

Figure 14-3 — Interior circuitry of the Ameritron ATR-30.

Figure 14-2 — Front panel of the Ameritron ATR-30.

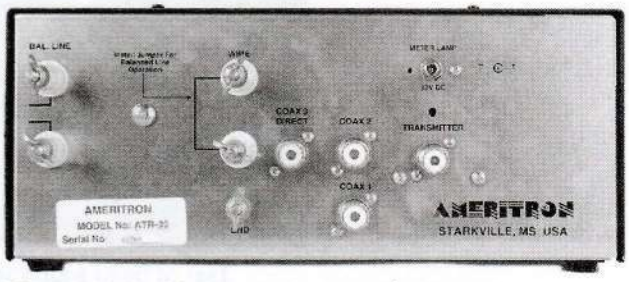

Figure 14-4 — Rear panel connections on the Ameritron ATR-30.

MFJ-986

The '986 is one of more than 20 antenna tuner products offered by the prolific MFJ (in 2003). It is rated for 1500 W PEP within the 35-500 Ω impedance range, positioning it alongside the '989C as one of their high power units. Unlike the traditional T-network with a pair of variable capacitors, the '986 (**Figures 14-5, 6, 7**)makes use of a single variable capacitor and a wire wound air core roller inductor with a three digit turns counter. The tuner uses what MFJ describes as a "differential" capacitor. It has two discrete sets of fixed plates and one variable set, with a single capacitor control, forming a T-network with the inductor.

The cabinet is narrow and extends nearly 18 inches deep. The cross-needle meter has a high (3000 W) and low (300 W) setting switched by a front panel button, and it can display average and peak power as well as SWR. Providing 12 V to the connector on the back panel brightly illuminates the meter. Both the capacitor and roller inductor are directly driven. The inductance knob has a finger depression, which are often found on a transceiver's tuning knob. It is somewhat awkward to turn due to binding. The tuner had a tendency to creep around the operating desk when the inductor is rapidly turned. A check inside revealed several loose screws holding the inductor to the chassis. Tightening these did improve the smoothness somewhat.

The '986 provided a match to both antennas quickly, but arced over on 80 meters with the inverted L at 900 W. While this tuner does provide ease of use, one should give careful consideration to the loss figures in the tables. During operation the meter developed an intermittent problem with both needles going off scale even with very low power applied and a low SWR. Movement of the SWR bridge circuit board on the inside back panel seemed to correct the problem.

Two coax outputs are provided that can be switched to bypass the tuning circuit, as well as a third output for a dummy load. Balanced and single-wire feed lines connect to large ceramic feed through posts with wing nuts. A 4:1 two-core current balun is provided at the output. Test results are summarized in **Table 14-3**.

Manufacturer: MFJ Enterprises, Inc, PO Box 494, Mississippi State, MS 39762; tel 800-647-1800; fax 662-323-6551; **www.mfjenterprises.com**. 2003 price: $329.95.

Table 14-3
MFJ-986 Loss and Bandwidth Test Results

SWR	*Load (Ω)*		*160 m*	*80 m*	*40 m*	*20 m*	*10 m*
8:1	6.25	Power Loss %	47	31	21	16	13
		1.5 SWR BW	1	1	2	4	>5
4.1	12.5	PowerLoss %	33	22	14	12	11
		1.5 SWR BW	1	1	4	5	>5
2:1	25	PowerLoss %	25	20	10	<10	10
		1.5 SWR BW	1	2	4	>5	>5
1:1	50	PowerLoss %	22	12	<10	<10	<10
		1.5 SWR BW	2	3	>5	>5	>5
2:1	100	PowerLoss %	15	10	<10	<10	19
		1.5 SWR BW	3	5	>5	>5	>5
4:1	200	PowerLoss %	11	<10	<10	<10	<10
		1.5 SWR BW	3	>5	>5	>5	>5
8:1	400	PowerLoss %	10	<10	<10	11	16
		1.5 SWR BW	3	>5	>5	>5	5

Notes
Power losses are expressed as a percentage. A 21% loss of power is 1 dB.
The 1.5-SWR Bandwidth (SWR BW) represents the bandwidth over which an SWR of 1.5:1 or less was maintained as a percentage of the measurement frequencies (1.8, 3.5, 7.2, 14.2 and 29.7 MHz).

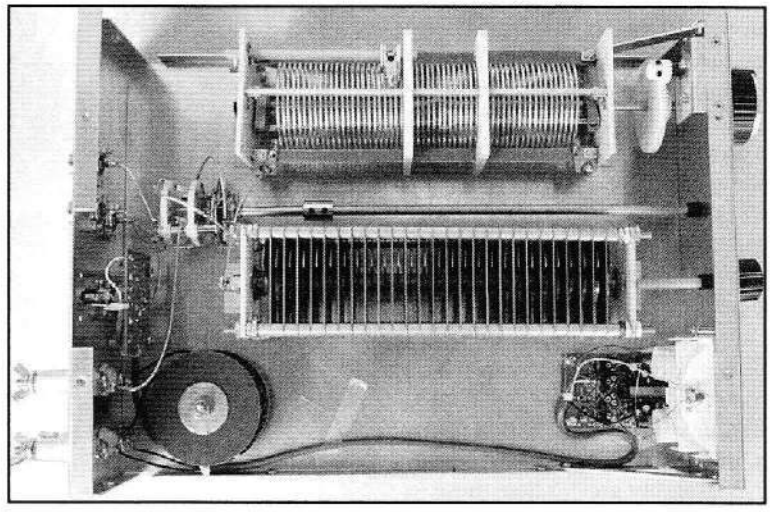

Figure 14-6 — Interior circuitry of the MFJ-986.

Figure 14-5 — Front panel of the MFJ-986.

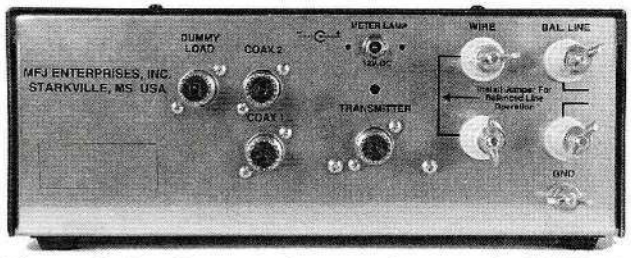

Figure 14-7 — Rear panel connections on the MFJ-986.

PALSTAR AT1500CV

The Palstar AT1500CV (**Figures 14-8, 9, 10**) is a T-network tuner solidly constructed in a compact aluminum enclosure. Inside, the metering and SWR bridge circuitry are encased in their own aluminum boxes. The moderately sized variable capacitors are mounted side by side and feature large calibrated dials and silky smooth vernier tuning that allows for precise adjustment. Palstar indicates that newer units incorporate a roller bearing assembly which makes inductor adjustment smoother. The roller inductor is quite large. It is an air core silver plated edge wound coil with heavy-duty ceramic forms. Control of the inductor is via a lever handle and mechanical turns counter. It is not as smooth as some of the other tuners and tends to lurch as it is rotated during fine adjustments. The cross-needle meter displays SWR and average forward and reflected power in 300 and 3000 W ranges, with no option for peak power metering. It is illuminated with 12 V from an included wall adapter.

Achieving a 1:1 SWR on the G5RV was possible on all bands from 80 through 10 meters at its rated power maximum of 1000 W single tone. Similar results were noted on the inverted L. Although the tuning chart provided in the manual does not include settings for 30 meters, the tuner easily matched both antennas on that band. This tuner has a solid feel to it and doesn't creep around while making adjustments.

In laboratory tests, the AT1500CV had more difficulties on 160 meters than on other bands. A 1:1 SWR was only obtainable with the 25 and 50 Ω loads, the power losses at 160 meters were measurably greater than those on other bands at the same loads. The variable capacitors are 240 pF maximum, which explains the 160 meter performance. The tradeoff results in lighter weight.

Antenna connections on the back panel include three coax inputs. Two are available direct or through the tuning network and one is bypassed

Table 14-4
Palstar AT1500CV Loss and Bandwidth Test Results

SWR	*Load (Ω)*		*160 m*	*80 m*	*40 m*	*20 m*	*10 m*
8:1	6.25	Power Loss %	No Match	25	16	12	12
		1.5 SWR BW		1	2	>5	3
4.1	12.5	Power Loss %	No Match	16	13	<10	11
		1.5 SWR BW		2	4	>5	>5
2:1	25	Power Loss %	21	13	<10	<10	<10
		1.5 SWR BW	2	3	>5	>5	>5
1:1	50	Power Loss %	13	<10	<10	<10	<10
		1.5 SWR BW	3	>5	>5	>5	>5
2:1	100	Power Loss %	No Match	<10	<10	<10	13
		1.5 SWR BW		>5	>5	>5	>5
4:1	200	Power Loss %	No Match	<10	<10	<10	12
		1.5 SWR BW		>5	>5	>5	>5
8:1	400	Power Loss %	No Match	<10	<10	<10	<10
		1.5 SWR BW		>5	>5	>5	5

Notes
"No Match" means that a 1:1 SWR could not be obtained.
Power losses are expressed as a percentage. A 21% loss of power is 1 dB.
The 1.5 SWR Bandwidth (SWR BW) represents the bandwidth over which an SWR of 1.5:1 or less was maintained as a

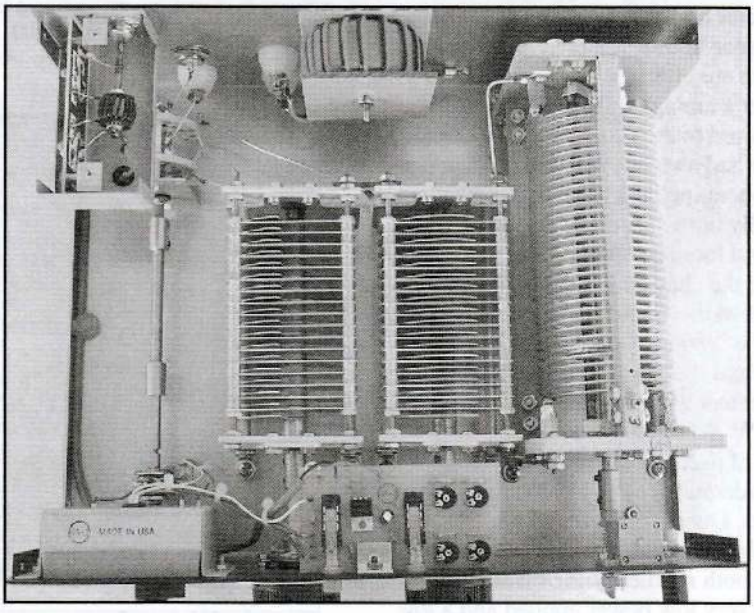

Figure 14-10 — Interior circuitry of the Palstar AT1500CV.

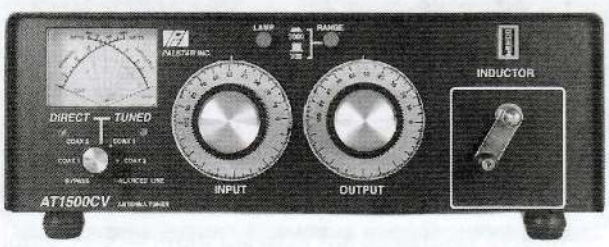

Figure 14-8 — Front panel of the Palstar AT1500CV.

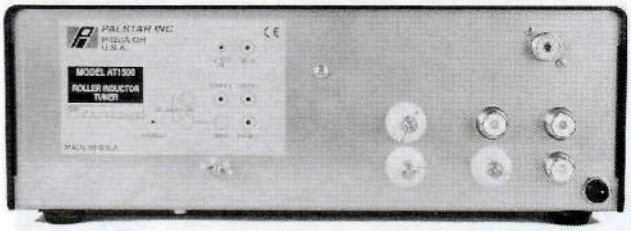

Figure 14-9 — Rear panel connections on the Palstar AT1500CV.

straight through. The bypass output can also be used with an optional 4:1 balun available for $39.95 [2003]. Balanced or single wire feed lines are attached to Delrin terminal posts with wing nuts.

Longer threaded material on the terminal posts would be a welcome improvement and make attachment of larger gauge wire much easier. In one isolated circumstance during lab testing, our engineer felt an RF bite on 10 meters through the metal portion of the inductor crank. This did not seem to be a pervasive problem, and Palstar indicates that the grounding on the crank has also recently been improved. Test results are summarized in Table 14-4.

Manufacturer: Palstar, Inc, 9676 N Looney Rd, PO Box 1136, Piqua, OH 45356; tel 937-773-6255; fax 937-773-8003; **www.palstarinc.com**. 2003 price: $429.95, optional 4:1 balun $39.95.

TEN-TEC 238A

The Ten-Tec 238A (**Figures 14-11, 12** and **13**) is the only tuner in our roundup to utilize an L-network. Using an innovative switching arrangement, the '238A actually provides five different circuit configurations to maximize efficiency. A look at the low loss figures in the table confirms this. The well-constructed tuner makes use of a single variable capacitor and a smooth turning wire-wound roller inductor to match impedances up to 3000 Ω. Additional capacitance can be switched into the circuit by means of a front panel switch. Five settings each are available for high and low impedances, as well as a bypass choice. A ceramic feed through post on the back panel provides a connection to add an additional 1000 pF capacitor (included with the tuner) to the circuit for matching 160 meter antennas. The small dual use meter can be switched to display SWR or RF power in either a 2000 or 200 W range. The meter lamp is powered by 12 V on the back panel.

The '238A handily matched all bands on both test antennas at full legal limit power. On 10 meters using the G5RV, the capacitor and inductor controls were a bit sensitive to small adjustments. One minor complaint: Measuring forward power in the high power range on the meter caused the indicator to slap the right extreme position during CW keying.

In laboratory tests, the '238A did not match on 160 meters into a 6.25 Ω until 2700 pF of external capacitance was added. Ten-Tec indicates they will provide additional capacitors to purchasers at no extra charge. Also, the power losses on 10 meters were considerably greater than those on other bands. However, the '238A performed very admirably on most other bands, quite often exhibiting the least losses on given band and load combinations.

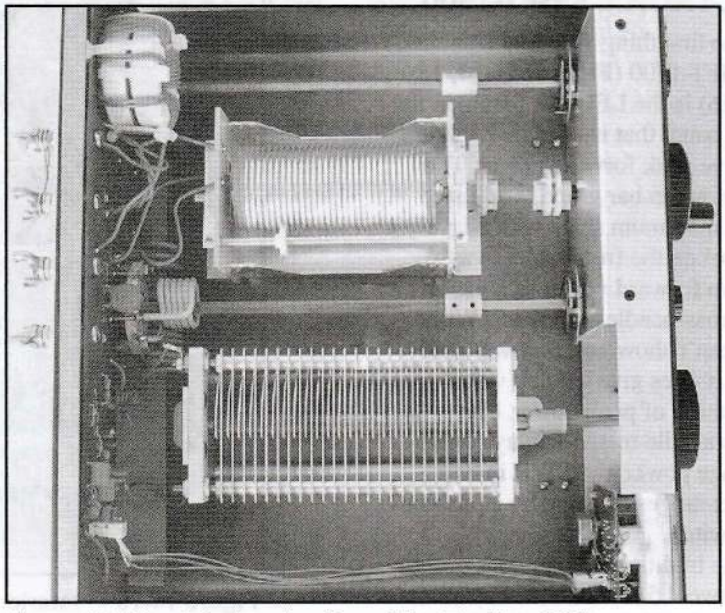

Figure 14-13 — Interior circuitry of the Ten-Tec 238A.

Figure 14-11 — Front panel of the Ten-Tec 238A.

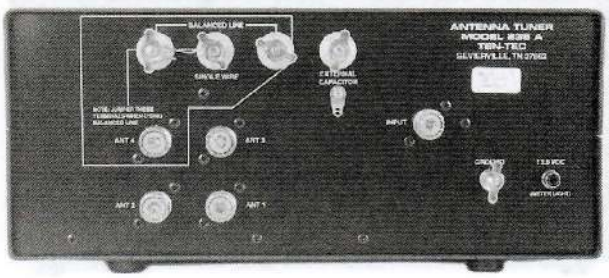

Figure 14-12 — Rear panel connections on the Ten-Tec 238A.

Table 14-5
Ten-Tec 238A Loss and Bandwidth Test Results

SWR	*Load (Ω)*		*160 m*	*80 m*	*40 m*	*20 m*	*10 m*
8:1	6.25	Power Loss %	No Match	<10	<10	<10	28
		1.5 SWR BW		>5	>5	>5	2
4.1	12.5	Power Loss %	<10	10	<10	<10	22
		1.5 SWR BW	>5	>5	>5	>5	2
2:1	25	Power Loss %	<10	10	<10	<10	17
		1.5 SWR BW	>5	>5	>5	>5	3
1:1	50	Power Loss %	<10	<10	<10	<10	<10
		1.5 SWR BW	>5	>5	>5	>5	>5
2:1	100	Power Loss %	<10	<10	<10	<10	20
		1.5 SWR BW	>5	>5	>5	>5	4
4:1	200	Power Loss %	<10	<10	<10	<10	20
		1.5 SWR BW	>5	>5	>5	>5	4
8:1	400	Power Loss %	<10	<10	<10	10	13
		1.5 SWR BW	>5	>5	>5	>5	1

Notes

"No Match" means that a 1:1 SWR could not be obtained, even with the included 1000 pF external capacitor attached. A match on 160 m at 6.25 was achieved with 2700 pF of external capacitance; the power loss was less than 10%, and the 1.5 SWR BW was greater than 5%.

Power losses are expressed as a percentage. A 21% loss of power is 1 dB. The 1.5-SWR Bandwidth (SWR BW) represents the bandwidth over which an SWR of 1.5:1 or less was maintained as a percentage of the measurement frequencies (1.8, 3.5, 7.2, 14.2 and 29.7 MHz).

The four-position antenna switch on the front panel allows selection of four coax outputs or a balanced/random wire. The balanced output and one coax connector share position four. A two-core balun is provided for matching the balanced output. The '238A is the only one of the five tuners reviewed here without an air-core inductor. The inductor here has a linen phenolic core.

Since we purchased our review unit, Ten-Tec has produced a substantially identical antenna tuner, the '238B. The Tennessee manufacturer is now selling only the '238B model. Test results are summarized in **Table 14-5**.

Manufacturer: Ten-Tec, 1185 Dolly Parton Pky, Sevierville, TN 37862; tel 865-453-7172; fax 865-428-4483; **www.tentec.com**. 2003 price: $475.00 ('238B).

VECTRONICS HFT-1500

The first thing you notice about the HFT-1500 (**Figures 14-14, 15** and **16**) is the LED bar graph on the front panel that is used to display relative peak forward power. The bright green bar graph is adjusted to its maximum scale with a level control on the front panel to a known forward power reading on the cross-needle wattmeter. While it doesn't show actual power readings, it does give a quick visual indication of peak power. The cross-needle meter displays only average power and SWR in two power ranges selected by a pushbutton switch.

The traditional T-network design uses two 4.5 kV variable capacitors adjusted with large comfortable

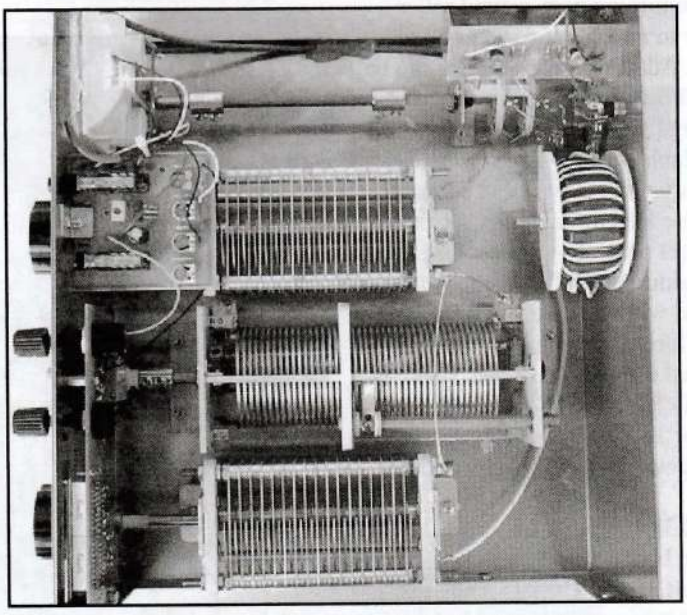

Figure 14-16 — Interior circuitry of the VECTRONICS HFT-1500.

Figure 14-14 — Front panel of the VECTRONICS HFT-1500.

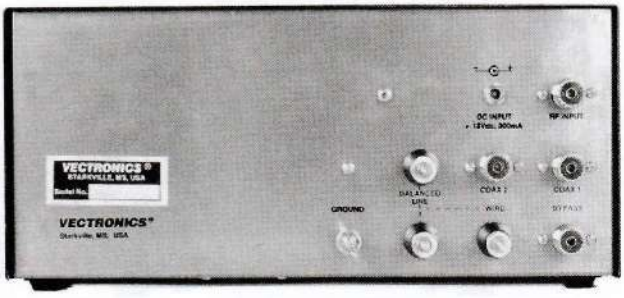

Figure 14-15 — Rear panel connections on the VECTRONICS HFT-1500.

Table 14-6
Vectronics HFT-1500 Loss and Bandwidth Test Results

SWR	*Load (Ω)*		*160 m*	*80 m*	*40 m*	*20 m*	*10 m*
8:1	6.25	Power Loss %	45	42	16	15	8
		1.5 SWR BW	1	<1	2	5	>5
4.1	12.5	Power Loss %	32	31	11	<10	<10
		1.5 SWR BW	>5	>5	3	>5	>5
2:1	25	Power Loss %	19	24	<10	<10	<10
		1.5 SWR BW	2	1	>5	>5	>5
1:1	50	Power Loss %	12	<10	<10	<10	<10
		1.5 SWR BW	3	>5	>5	>5	>5
2:1	100	Power Loss %	12	<10	<10	<10	<10
		1.5 SWR BW	3	>5	>5	>5	>5
4:1	200	Power Loss %	<10	<10	<10	<10	<10
		1.5 SWR BW	4	>5	>5	>5	>5
8:1	400	Power Loss %	<10	<10	<10	11	16
		1.5 SWR BW	4	>5	>5	>5	4

Notes
Power losses are expressed as a percentage. A 21% loss of power is 1 dB.
The 1.5-SWR Bandwidth (SWR BW) represents the bandwidth over which an SWR of 1.5:1 or less was maintained as a percentage of the measurement frequencies (1.8, 3.5, 7.2, 14.2 and 29.7 MHz).

knobs and very smooth vernier tuning. This tuner stays put on the desk while you utilize a lever handle and gear driven five digit mechanical turns counter to adjust the air wound roller inductor.

Tuning the 160-meter inverted L and the G5RV on all bands except 10 meters was easily accomplished, with no problems handling 1 kW. In the field, the best SWR that could be obtained on 10 was 2.33:1; this is possibly due to the additional "loading" when a human touches the all-metal inductor crank. The ARRL Lab adjusted the inductor with a wooden pencil in some cases to obtain a match.

The HFT-1500 provides two coax inputs and a third that completely bypasses the tuning network. The balanced and single wire inputs are Delrin terminal posts connected to a large single core 4:1 voltage balun. In some circumstances during lab testing, our engineer felt RF bites through the metal portion of the inductor crank. Later units feature a metal shaft bushing that provides a better ground. This was not experienced in field testing, but tuner adjustments were not made at high power. Test results are summarized in **Table 14-6**.

Manufacturer: Vectronics, 300 Industrial Park Rd, Starkville MS 39759; tel 662-323-5800; fax 662-323-6551; **www.vectronics.com**. 2003 price: $459.95.

Automatic Antenna Tuners — A Sample of the Field

Reviewed by Joel R. Hallas, W1ZR
QST *Technical Editor*
QST *May, 2004*

Automatic antenna tuners can provide a quick and easy method of matching multiband or nonresonant antennas quickly and effortlessly. Performance is on par with manual tuners and there is now a selection available providing a fit to most requirements. A few years back, we surveyed the antenna tuner market in these pages. All those tuners were manual ones.

A few automatic tuners were available at that time, but they were the exception rather than the rule. Since then, a number of manufacturers have focused their attention on automatic antenna tuners and it seems as if there's now one for every application.

For this review we selected representative tuners from a number of manufacturers (see **Figure 14-17**). There are two general configurations: those providing remote tuning, with the tuner intended to be near the antenna, and those intended to be collocated with the station equipment. For those manufacturers having models in each camp, we selected one of each.

As noted in the specifications, each tuner is different and they don't exactly line up head-to-head, so a direct comparison is not always appropriate. Still, for each we will provide the basic data you would need to decide if one of these is a good fit for your needs. If you like the looks of a particular manufacturer, but the tuner reviewed doesn't exactly meet your requirements, check their Web page or your dealer for other models at different power levels or with different features.

For this review we stuck to those at the 100 to 200 W level and tried for a representative self-contained and remote tuner from each manufacturer. For these tests, we looked at units designed to work with any radio. In addition to these, most HF radio manufacturers offer external auto tuners designed to operate exclusively with their radios. One manufacturer, LDG, also offers tuners with the capabilities to operate with specific radios' commands. Many HF radio manufacturers also offer internal auto-tuners as a part of their transceivers. We generally review these as a part of the radios. We elected to stick to general purpose models for this review.

Those selected for this test include the RT-11 and Z-100 from LDG, the MFJ-991 and from SGC the SG-237 and MAC-200.

Remote vs Collocated Autotuners

It's probably worth a paragraph or two to discuss the relative merits and appropriateness of the two configurations. If the antenna(s) to be matched terminate right at the station equipment, without a transmission line (or with a very short one), there is no particular advantage to having a remote tuner.

On the other hand, that setup often results in problems with "RF in the shack," or EMI within the house. I have one antenna setup of that form and whenever I use it, the RF resets the kitchen FM radio, causing it to lose track of time and memory. Most find it a better solution to have the antenna system stop somewhere outside the house and have a transmission line interconnect the radio and antenna.

With a remote tuner, the matching can be at or near the antenna, resulting in a well matched transmission line coming back to the radio. With the tuner at the radio, the matching takes place near the radio, and the SWR on the line out to the antenna will often be high. Note that in both cases the radio will be provided a good match and will happily put full power into the system. With the remote tuner, often more of the power will be radiated by the antenna and less will be dissipated as heat by the transmission line.

Some radios now come with automatic tuners as part of the radio. These can be functionally equivalent to the local tuner. The separate tuner does offer two advantages over the

Figure 14-17 — Automatic tuners from LDG, MFJ and SGC — ready for test.

internal tuner — it can support multiple radios, and most can match a higher SWR than many of the internal tuners. The key factor in deciding between a local and a remote tuner then becomes how much of the transmitter power actually reaches the antenna system and how much will heat up the transmission line. This is a function of operating frequency, SWR and line length.

The place to start the analysis is with *The ARRL Antenna Book*.[1] Figure 23 in Chapter 24 provides the attenuation in 100 feet of *matched* transmission line for each of the common types. Table 14 in the same chapter provides the *additional* loss for the non-matched case as a function of SWR and matched loss. [The same data is in Chapter 7 of this book.] Using the two tables, you can determine the total loss of your transmission line.

If the loss is acceptable, you can tune at the transmitter end. If not, by tuning at the antenna end you can eliminate most of the additional loss due to mismatch.

An example might be helpful. A multiband antenna such as my G5RV might have a 5:1 SWR on parts of 10 meters. If we feed it with 150 feet of RG-58 cable we have a matched loss of about 3.5 dB and the 5:1 SWR adds about another 2 dB for a total of 5.5 dB loss or about 71% of our power heating up the line! By moving the tuner to the antenna end of the coax, we reduce that to 55%. Another option is to change the transmission line (my solution immediately after making that calculation!).

If we go with lower loss RG-8 instead, we have a matched loss of about 2 dB (1.3 dB per 100 ft) and the SWR adds about another 0.3 dB for a total of 2.3 dB, or a loss of about 41% of our power. With the tuner at the antenna, the total loss would be the 2 dB or 37%—not much of a difference. Note that I didn't consider the tuner losses here, under the assumption that they would be the same at either location. The numbers get much more grim as the SWR goes up, by the way.

Two notes of caution—first, if you measure the SWR at the shack end of the cable, it will appear better than it is, due to the cable loss; second, the matched loss from Figure 23 is the *best* matched loss for new and dry cable. The actual loss can only go up from there, especially if the cable came from some dark corner of your basement, or worse, from an unknown source at a flea market.

Note that all of these tuners are designed for unbalanced (coax) cable between the tuner and the radio and, with the exceptions noted, unbalanced operation on the antenna side (coax or single wire antennas) as well. In order to use these tuners with a balanced load, it is best to decouple the ground side of the tuner from the transmission line. A coax choke can be used, or a balun (balanced to unbalanced transformer) can be employed. If you are using a balun, it is best to keep the line impedance within a SWR of about 4:1 (with respect to the usual 200 Ω impedance of a 4:1 balun) to avoid heating, loss and possible balun damage. A subsequent planned review will look at the special class of unbalanced to balanced tuners that sidestep this issue in an elegant way and are once again appearing on the market.

A word or two about the data shown may be in order. Please note that we used the same precision resistive load set for each tuner. In most cases, this includes data outside the manufacturers' specification range. We measured at a single frequency in each band, and for 6 meters we just measured the case with a 1:1 load for all the tuners that claimed operation there.

[1]Notes appear on page 14-35.

LDG RT-11 and Z-100

A look at LDG's Web page, **www.ldgelectronics.com**, will show you their selection of tuners and accessories. In addition to the RT-11 remote control tuner and the Z-100 local tuner, tested (see **Figure 14-18**), they offer an autotuner rated at 1000 W. As this review was being prepared in 2004, they also announced a much more feature rich desktop unit to complement the very basic, but lower cost Z-100.

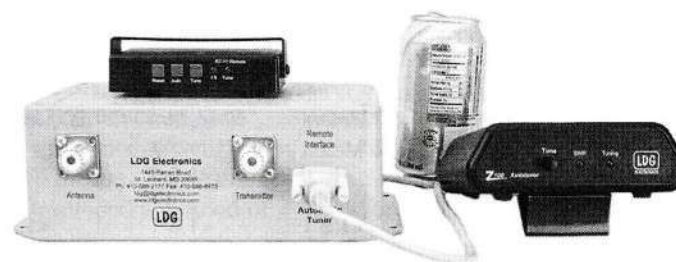

Figure 14-18 — LDG RT-11 (left) with control box and Z-100. A 12 ounce beverage container provides scale.

LDG RT-11

The RT-11 is a rugged, weatherproof tuner designed to be used inside or outdoors. It has coax connectors on input and output and is rated at 125 W from 1.8 to 30 and 50 W to 54 MHz. It is rated to match antennas with an SWR of 10:1 to 30 MHz and 3:1 from 50 to 54 MHz. This unit has an optional remote control designed to be used up to 100 feet from the tuner (15 foot cable supplied).

The remote control provides the ability to force a new tune, set for semi or full auto operation, keep the unit from tuning and allows bypassing of the tuner (straight through operation for matched antennas or out of band receive). In addition, LED indicators let you know the status and whether the SWR is below 1.5:1. One caution with the remote, the mounting bracket screws are not captive so you may want to use double-sided tape to secure it to a surface.

The RT-11 also has a jack to allow interfacing to radios designed to control proprietary tuners by emulating their commands. Special cables are offered to hook to various Alinco, ICOM, Kenwood and Yaesu radios for this purpose.

In my trials at home, I found that the RT-11 effortlessly tuned every antenna I had on all bands with a very low SWR, always well below 1.5:1. The tuning seemed to take about 5 seconds and hit the result the first time.

While automatic operation is possible without radio interface or remote control, I would have trouble imagining it and would suggest the remote for those without a compatible radio. For one thing, once tuned, it won't automatically restart the tuning process until the SWR reaches 3:1, a value that might cause many radios to "fold back" (reduce power) significantly.

The manual mentions that tuning should take place at the 25 W level, with full power applied only after tune is achieved, so that relay life will not be reduced. They also indicate that if a radio has the common power output fold back with high SWR it will automatically reduce power appropriately. I wouldn't count on that providing sufficient reduction, especially as the match is approached; I would instead manually reduce power while tuning.

LDG Z-100

The Z-100 is a self contained desk top unit with a 125 W rating (50 W on 6 meters). This unit is the first of a new series of tuners being released by LDG, with others providing additional features and controls. This is a basic unit corresponding to its low price, but none the less provides the needed tuning functions with straightforward "one button" operation. It includes memory of the settings for the last 200 matches made and tries those before it branches to its *unknown tune* algorithm. This is a clever idea that avoids the need to measure frequency. It is particularly useful for the case in which more than one antenna is used, since it really doesn't care — if it made the match before it will do it again, in a fraction of a second.

A feature of this unit is that it only draws power when actually tuning. Upon completion, the relays remain latched without power required until

Table 14-7
LDG RT-11 Remote Automatic Antenna Tuner

Manufacturer's Specifications	*Measured in ARRL Lab*
Input SWR range: to 10:1 (3:1 on 6 meters).	See below.
Output SWR range: not specified.	See below.
Frequency coverage: 1.8 to 54 MHz.	As specified.
Input power: 0.1 to 125 W, 50 W on 6 meters.	Tested at 50 W on HF, 20 W on 6 meters.
Power requirements: 11 to 14 V dc, 7 to 250 mA.	Idle 0 mA, max 140 mA at 13.8 V dc.

Measured power loss into resistive loads (%) / Input SWR at match:

SWR	*Load (Ω)*	*160 Meters*	*80 Meters*	*40 Meters*	*20 Meters*	*10 Meters*	*6 Meters*
16:1	3.125	No Match	No Match	27	22	<10	
				<1.5:1	2.6:1	<1.5:1	
8:1	6.25	No Match	17	17	19	20	
			<1.5:1	<1.5:1	<1.5:1	<1.5:1	
4:1	12.5	11	11	12	13	26	
		<1.5:1	<1.5:1	<1.5:1	<1.5:1	<2:1	
2:1	25	<10	<10	<10	<10	23	
		<1.5:1	<1.5:1	<1.5:1	<1.5:1	2.1:1	
1:1	50	<10	<10	<10	<10	<10	21
		<1.5:1	<1.5:1	<1.5:1	<1.5:1	<1.5:1	2.1:1
2:1	100	<10	<10	<10	<10	17	
		<2:1	<1.5:1	<1.5:1	<1.5:1	<1.5:1	
4:1	200	<10	<10	<10	<10	15	
		<2:1	<1.5:1	<1.5:1	<1.5:1	<1.5:1	
8:1	400	<10	<10	<10	<10	28	
		<1.5:1	<1.5:1	<1.5:1	<1.5:1	<1.5:1	
16:1	800	<10	12	<10	<10	19	
		<1.5:1	<1.5:1	<1.5:1	<1.5:1	<1.5:1	

Table 14-8
LDG Z-100 Desktop Automatic Antenna Tuner

Manufacturer's Specifications	*Measured in ARRL Lab*
Input SWR range: to 10:1 (3:1 on 6 meters).	See below.
Output SWR range: not specified.	See below.
Frequency coverage: 1.8 to 54 MHz.	See text.
Input power: 0.1 to 125 W, 50 W on 6 meters.	Tested at 50 W on HF, 20 W on 6 meters.
Power requirements: 7 to 18 V dc, 250 mA.	Idle 0 mA, max 160 mA at 13.8 V dc.

Measured power loss into resistive loads (%) / Input SWR at match:

SWR	*Load (Ω)*	*160 Meters*	*80 Meters*	*40 Meters*	*20 Meters*	*10 Meters*	*6 Meters*
16:1	3.125	No Match	No Match	15	10	<10	
				<1.5:1	<1.5:1	<1.5:1	
8:1	6.25	No Match	13	15	15	20	
			2.6:1	<2:1	<1.5:1	<2:1	
4:1	12.5	No Match	<10	<10	<10	<10	
			<1.5:1	<1.5:1	<2:1	<1.5:1	
2:1	25	<10	<10	<10	<10	17	
		<1.5:1	<1.5:1	<1.5:1	<1.5:1	<1.5:1	
1:1	50	<10	<10	<10	<10	<10	20
		<1.5:1	<1.5:1	<1.5:1	<1.5:1	<1.5:1	<2:1
2:1	100	<10	<10	<10	<10	<10	
		<1.5:1	<1.5:1	<1.5:1	<1.5:1	<1.5:1	
4:1	200	<10	<10	<10	11	<10	
		2.1:1	2.2:1	<1.5:1	<1.5:1	<1.5:1	
8:1	400	<10	<10	<10	11	<10	
		<1.5:1	<1.5:1	<1.5:1	<1.5:1	<2:1	
16:1	800	11	14	15	33	43	
		2.2:1	2.3:1	<1.5:1	<1.5:1	<1.5:1	

the next tune is requested. This is particularly appealing for portable low power operations in which every milliamp-hour is carried in.

The operation of this tuner is fundamentally different from the others in that it will only tune when the TUNE button is pushed. This has an advantage in that it will not start tuning inadvertently on high SWR, potentially applying full power during tune. Upon changing frequency, the operator can decide whether or not to initiate the tune cycle. By pushing the button for less than 0.5 seconds, the tuner goes to bypass. Between 0.5 and 3 seconds the tuner will attempt to find a match from memory (typically less than half a second), and only initiate a full tune if needed. If the button is pushed for more than 3 seconds a full tune cycle is initiated, ignoring any memorized settings.

This is easier to deal with than it sounds since the LEDs provide a confirmation of tuning mode. A green LED also indicates if the match is less than 1.5:1 or between 1.5 and 2:1. An early production unit exhibited some inconsistent tuning results on 6 meters. The manufacturer has developed a method of improved internal decoupling that solved this problem and the results reflect that change. LDG states that this will be included in future production units and that anyone having problems with 6 meter tuning on early units should contact them directly.

Manufacturer: LDG Electronics Inc, 1445 Parran Rd, PO Box 48, St Leonard, MD 20685; tel 877-890-3003; fax 410-586-8475; **www.ldgelectronics.com**. 2004 prices: RT-11 Tuner, $209; Remote head, $39; Z-100, $149; 12 V power cube for either tuner, $10.

MFJ-991

Figure 14-19 — MFJ-991 Autotuner.

MFJ has recently announced a series of autotuners. All are in the typical indoor/ colocated configuration, but with the available remote kit (ordered, but not received in time for the review) can be used as a remote tuner if kept out of the weather. They offer the MFJ-991 (tested, as shown in **Figure 14-19**) 150 W rated tuner, a tuner with similar features rated at 600 W and a 300 W autotuner with digital display, balun and two port antenna switch. As with the LDG, the MFJ tuners require their tuning be accomplished at reduced power.

The MFJ-991 front panel provides full control capability and forward and reflected power metering with "crossed-needle" SWR measurement display. Two features of the '991 are not found on other tested units and are worth mentioning. First, the '991 has the capability to allow manually adjusting the C and L values of the tuner while in receive. This is helpful if you are using your radio for receive only and wish to attempt to match in order to increase signal strength. The second feature is the ability to select the SWR threshold at either 1.5 or 2:1.

In our testing the tuner went to the best match it could find in either case. The difference was in how far you could change frequency before it would automatically retune when you transmitted. If your radio can tolerate a 2:1 SWR, this could provide a benefit. The '991 could tune my G5RV on all bands and remembered the last setting for each frequency (1000 memories), with a one-click reset. Tuning the first time on a frequency was typical of the cycle time of the other units. This unit sounded somewhat louder (it has 18 heavy duty relays) than the other test samples, although not an issue for the single click associated with a memorized tune.

The MFJ-991 can interoperate with ICOM and Alinco tuner control commands. Appropriate interface cables are available from MFJ.

In addition to the obvious controls and indicators, there are some subtle ones as well. There are a number of meter "signals" sent to the operator that will not be clear without a cruise through the manual. For example, if you forget to reduce power before tuning, the power meter swings to full scale and the tuner is bypassed. If you toggle between 1.5 and 2:1 SWR threshold, the meter briefly jumps up to indicate that SWR.

Manufacturer: To order, or for your nearest MFJ dealer, call MFJ Enterprises at 800-647-1800 or order at **www.mfjenterprises. com**, fax 662-323-6551; or write MFJ Enterprises, Inc, 300 Industrial Park Rd, Starkville, MS 39759. [2004] Price: $220.

Table 14-9
MFJ-991 Desktop/Remote Automatic Antenna Tuner

Manufacturer's Specifications	*Measured in ARRL Lab*
Input Impedance range: 6 to 3200 Ω.	See below.
Output SWR range: 1.5:1 or 2:1 selectable.	See below.
Frequency coverage: 1.8 to 30 MHz.	As specified.
Input power: 5 to 150 W.	Tested at 50 W.
Power requirements: 12 to 15 V dc, 1.0 A.	Idle 90-300 mA, max 500 mA at 13.8 V dc.

Measured power loss into resistive loads (%) / Input SWR at match:

SWR	*Load (Ω)*	*160 Meters*	*80 Meters*	*40 Meters*	*20 Meters*	*10 Meters*
16:1	3.125	No Match	27	20	15	<10
			<1.5:1	<1.5:1	<1.5:1	<2:1
8:1	6.25	12	14	15	24	19
		<1.5:1	<1.5:1	<1.5:1	<1.5:1	2.6:1
4:1	12.5	<10	<10	<10	<10	12
		<1.5:1	<1.5:1	<1.5:1	<1.5:1	<1.5:1
2:1	25	<10	<10	<10	<10	<10
		<1.5:1	<1.5:1	<1.5:1	<1.5:1	<1.5:1
1:1	50	<10	<10	<10	<10	<10
		<1.5:1	<1.5:1	<1.5:1	<1.5:1	<1.5:1
2:1	100	<10	<10	<10	<10	<10
		<1.5:1	<1.5:1	<1.5:1	<1.5:1	<1.5:1
4:1	200	<10	<10	<10	<10	<10
		<1.5:1	<1.5:1	<1.5:1	<1.5:1	<1.5:1
8:1	400	<10	<10	<10	11	11
		<1.5:1	<1.5:1	<1.5:1	<1.5:1	<1.5:1
16:1	800	<10	16	<10	<10	23
		<1.5:1	<1.5:1	<1.5:1	<1.5:1	<1.5:1

SGC SG-237 and MAC-200

SGC has been making automatic antenna tuners for many years, and offers a wide selection. Until recently, they concentrated on remote tuners, usually the weatherproof type, at power ratings of 100 to 500 W. More recently, they have introduced a number of variations of their SG-237, a board version to build into your own radio or antenna cabinet, an open enclosure model for remote but indoor use and one with controls and indicators intended for portable use. They have recently released a Multiple Antenna Controller, MAC-200. The units we tested were an SG-237 (one that has fed the backstay of my sailboat for some years) and a relatively new combination unit, the MAC-200 (as shown in **Figure 14-20**).

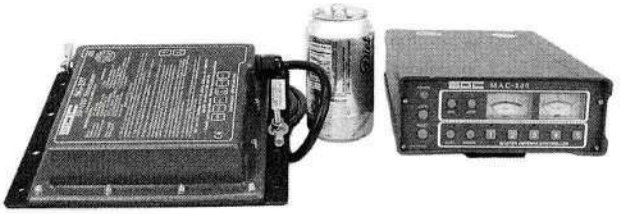

Figure 14-20 — SGC SG-237 (left) and MAC-200.

SGC SG-237 Autotuner

The SG-237 was the first in a series of SGC tuners that were much more compact than their previous (and continuing) line, the SG-230 (200 W, 1.6-30 MHz), SG-231 (100 W, 1-60 MHz) and SG-235 (500 W, 1.8-30 MHz). The SG-237 is rated at 100 W PEP, both for operation and for tuning (40 W continuous carrier power). The transmitter connection is via a 9 foot combined RF, control and power cable (25 and 50 foot extensions are available), while the antenna connection is via a single ceramic insulated terminal. While the tuner is designed to feed a single wire against ground, I have successfully employed mine into coax fed antennas as well as loops and single wires.

This is a rugged unit in a compact waterproof aluminum enclosure that can slide in almost anywhere. It needs no remote control box to work, and I've used mine that way for years. An optional remote control is offered (and we tested with it) to provide a positive indication of match and to allow a lockout or a forced reset. The lockout can be handy in a portable or mobile environment to avoid the tuner attempting to retune due to the temporary proximity of outside objects while in motion, for example.

The '237 provides a memory function that uses the measured transmitter frequency to result in the tuner settings last used to successfully tune to that frequency. This means that instead of taking 5 to 10 seconds to tune, the previously stored settings for a frequency are applied in milliseconds and used if the resulting SWR

Table 14-10
SGC SG-237 Remote Automatic Antenna Tuner

Manufacturer's Specifications	*Measured in ARRL Lab*
Input SWR range: corresponding to a minimum 7 foot antenna above 3.5 MHz, 23 feet above 1.8 MHz.	See below.
Output SWR range: 1.4:1 typical.	See below.
Frequency coverage: 1.8 to 60 MHz.	As specified.
Input power: 3 to 100 W.	Tested at 50 W.

Power requirements: 10.5 to 18 V dc, 300 mA. Idle and tuning 270 to 480 mA at 13.8 V dc.

Measured power loss into resistive loads (%) / Input SWR at match:

SWR	*Load (Ω)*	*160 Meters*	*80 Meters*	*40 Meters*	*20 Meters*	*10 Meters*	*6 Meters*
16:1	3.125	21	21	19	No Match	<10	
		<1.5:1	<1.5:1	<1.5:1		<1.5:1	
8:1	6.25	16	18	20	24	23	
		<1.5:1	2.1:1	<1.5:1	<1.5:1	<1.5:1	
4:1	12.5	11	12	15	17	23	
		<1.5:1	<1.5:1	<1.5:1	<1.5:1	<1.5:1	
2:1	25	<10	11	21	18	26	
		<1.5:1	<1.5:1	<2:1	<2:1	<1.5:1	
1:1	50	<10	<10	<10	<10	12	29
		<1.5:1	<1.5:1	<1.5:1	<1.5:1	<1.5:1	<1.5:1
2:1	100	<10	<10	<10	13	14	
		<2:1	<2:1	<1.5:1	<1.5:1	<1.5:1	
4:1	200	No Match	<10	<10	16	10	
			2.1:1	<1.5:1	<1.5:1	<1.5:1	
8:1	400	No Match	<10	10	16	18	
			2.1:1	<1.5:1	<1.5:1	<1.5:1	
16:1	800	<10	<10	14	30	58	
		<1.5:1	<1.5:1	<1.5:1	<1.5:1	<2:1	

is less than 2:1. In some cases they won't be right (and a new tune will be initiated), if a different antenna is used, for example, but their concept is that this tuner is out where the antenna is and thus should see the same impedance for a given frequency each time that frequency is employed.

SGC MAC-200 Multiple Antenna Controller

This device combines a 200 W autotuner, a five port automatic or manual antenna switch, power and SWR meters and a balun in one compact package. This is a nice unit and quickly grew on me in operation. It has enough controls and indicators to keep me entertained even when the bands aren't open.

For some time, most manual tuners have had provisions for switching antennas as well as tuning them. This is very handy, since even those with just one antenna should have a dummy load to switch to for tune up. I have no numbers, but I would guess more hams have more than one HF antenna than have only one. I don't have fancy HF antennas, but I have a G5RV I use on 80 through 10, a Lazy-H, perpendicular to the G5RV for 30 through 10 meters and a 70 foot wire vertical for use when it makes sense (not often in my part of New England).

With the MAC-200, I can memorize which antenna to use on which band. It switches antennas on the first dot of a CW string (full power—no problem) and I'm there. As noted, at my station, on some bands the antenna is a function of the direction to the distant station, I can just touch the MANUAL button and I can select a different antenna by touching a button numbered 1 to 5.

As configured, antenna one is intended for balanced feed, antenna two has a terminal for a single wire feed, and three through five are terminated in UHF (SO-239) coax connector jacks.

The separate meters for power and SWR are handy. The SWR meter is especially convenient in that it computes and indicates SWR independent of power level without an adjustment. The manual warns that the meters are not of the precision type and I can attest to that. Their meter indicated 80 W while my Bird 43 showed 100. This is still very useful to let you know if all is well.

This is a handy unit, in a cabinet matching the cross section of the SGC-2020 transceiver (but somewhat longer), it can be made to fit in most shacks. In mine it can slide beneath the shelf that holds my equipment three inches above the desk, for example.

The one limitation some may have is it provides a "typical" match of 2:1. Well 2:1 is fine for some transmitters, while others may start to "fold back" above 1.5:1 and this may be a problem if yours is in that group. On the other hand, looking at the data it is clear that most of the time it was below 1.5:1 with our loads.

Our original unit remembered which antenna to use on each band, but didn't memorize tuner settings. A warranty replacement unit had a flawless memory function.

Manufacturer: SGC Inc, 13737 SE 26th St, Bellevue, WA 98005; tel 425-746-6310; fax 425-746-6384; **www.sgcworld.com**. 2004 price: SG-237, $360; Smartlock remote control, $59; MAC-200, $360.

Table 14-11
SGC MAC-200 Desktop Automatic Antenna Tuner and Controller

Manufacturer's Specifications	*Measured in ARRL Lab*
Input impedance range: 5-1000 (feed line) 0.2-5000 (long wire).	See below.
Output SWR range: 2:1 typical.	See below.
Frequency coverage: 1.8 to 60 MHz.	As specified.
Input power: 1.5 to 200 W.	Tested at 50 W.
Power requirements: 10 to 18.5 V dc, 230 mA. Idle 240 mA, max 490 mA at 13.8 V dc (meter light off)	Idle 280 mA, max 530 mA at 13.8 V dc (meter light on)

Measured power loss into resistive loads (%) / Input SWR at match:

SWR	*Load (Ω)*	*160 Meters*	*80 Meters*	*40 Meters*	*20 Meters*	*10 Meters*	*6 Meters*
16:1	3.125	No Match	39	24	<10	<10	
			<2:1	<2:1	<1.5:1	<1.5:1	
8:1	6.25	No Match	16	18	15	30	
			<1.5:1	<1.5:1	<1.5:1	<1.5:1	
4:1	12.5	<10	<10	<10	18	27	
		<1.5:1	<1.5:1	<1.5:1	<1.5:1	<1.5:1	
2:1	25	<10	<10	<10	<10	25	
		<1.5:1	<1.5:1	<1.5:1	<1.5:1	2:1	
1:1	50	<10	<10	<10	<10	12	27
		<2:1	<1.5:1	<1.5:1	<1.5:1	<2:1	<2:1
2:1	100	<10	<10	<10	<10	14	
		<1.5:1	<2:1	<2:1	<2:1	<1.5:1	
4:1	200	<10	<10	<10	<10	14	
		<1.5:1	<1.5:1	<1.5:1	<1.5:1	<2:1	
8:1	400	<10	<10	13	15	17	
		<1.5:1	<1.5:1	<1.5:1	<1.5:1	<1.5:1	
16:1	800	No Match	22	14	25	31	
			<1.5:1	<1.5:1	<1.5:1	<1.5:1	

Medium to High Power Auto Antenna Tuners — The Evolution Continues

Reviewed by Joel R. Hallas, W1ZR
QST *Technical Editor,*
QST *August 2006*

We last looked at a selection of automatic antenna tuners in May 2004 (see previous section). At that time, we picked four examples, two designed for remote operation and two desktop units. While different in many ways, they all were limited to 100 to 200 W. Higher powered automatic antenna tuners have been available, but they were either built into high powered amplifiers (ICOM or Yaesu, for example), were designed for remote operation as in the SGC SG-235, or have been discontinued, as in the case of the Ten-Tec 253.[2]

High powered automatic antenna tuners initially appeared in the 1980s — the Heath 2500, J.W. Miller AT2500, and Daiwa CNA-1001 — but they were not as sophisticated as the units reviewed here, requiring some manual adjustment or presetting of the inductor for best operation.[3,4,5]

Modern solid state transceivers and linear amplifiers with their "no tune" output stages have been well received, especially by those of us who grew up in the vacuum tube era.

The typical transmitter of that time required careful adjustment of the transmitter TUNE, LOAD and DRIVE controls, at a minimum, every time we changed frequency. Failure to do it right could result in destruction of the final amplifier tubes — sometimes a pricey proposition. The other side of the coin is that those transmitters could be adjusted to match antenna loads with a much higher SWR than the current crop of radio gear.

The modern no-tune feature generally means "no tune if the SWR is 1.5:1 or less," something that often doesn't fit with real world antennas and wide amateur bands. The answer has been an antenna system matching unit, often called an antenna tuner, even though many would argue that it doesn't really tune the antenna — rather it transforms the impedance at the bottom of an antenna system to the 50 Ω the radio equipment wants to operate into. Setting semantics aside, it seems that the controls we used to have to adjust haven't disappeared but have moved from the radio to another box — the antenna tuner.

Enter the Automatic Antenna Tuner

To extend the no-tune concept all the way to the antenna requires a no-tune, or *automatic*, antenna tuner. As noted, these have been generally available for some time at the power levels of modern transceivers, Each of these tuners can effectively add an automatic antenna matching system to your medium to high power HF station, at least up to their power limits. Honor the caveats and you will appreciate the freedom they provide.

For this review we have selected three desktop models that span the medium to high power range and highlight some other differences as well. While they all fill the same spot in a station block diagram, they are quite different in several respects and thus should not be directly compared on a 1:1 basis. Rather, determine if one or more will meet your needs, desires and budget.

All of the tuners reviewed in the 2004 report shared the same adjustment mechanism — fixed inductors and capacitors switched by relays. The LDG and MFJ tuners reviewed here share that architecture as well, but with beefier components designed to meet the higher power requirements of their ratings. The Palstar AT-Auto is of a completely different design, a T network with a differential variable capacitor, half on each side of a shunting rotary inductor. The Palstar makes its adjustments via stepper motors rather than relays. Interestingly, while standalone tuners have tended to be of the relay type, many internal tuners have used motor driven capacitors. Motor driven components were also used in the high powered automatic tuners from the 1980s mentioned previously, so this is a time-tested approach. We'll look at each tuner in alphabetical order. These tuners from LDG, MFJ and Palstar offer the convenience of automatic tuning at medium to high power levels.

Figure 14-21 — Medium power tuners from Palstar, LDG and MFJ.

LDG AT-1000 Automatic Memory Antenna Tuner

The LDG AT-1000 sits squarely in the middle of the pack, both in terms of price and power rating. The 1000 W level fits nicely with a good selection of popular, not quite legal limit, linear amplifiers, including a couple announced at Dayton in 2006. All of the tuners reviewed here cover 160 through 10 meters, but the AT-1000 offers operation on 6 meters at the 100 W level as well.

The LDG, in common with the other units, has memories to allow a rapid return to the last previously matched settings. In the case of the AT-1000, there are 200 memory locations and the tuner will reset to them in less than half a second. If the antenna you are tuning does not have a memorized setting that works, the tuner can spend up to 8 seconds finding a match, but will remember for the next time.

The LDG approach to memory management is different from some. Some others tuners store settings based on frequency. This is a great approach if you will be tuning a single antenna for each band. In the LDG AT-1000, the last 200 successful matches are stored independent of frequency. A new match request quickly cycles through the 200 to see if a match is found before it begins its tune algorithm. This is a particularly beneficial approach if you switch the tuner output to different antennas on the same band, since it doesn't have to relearn parameters for a particular frequency every time you change antennas. It also avoids the need for frequency measuring circuitry within the tuner.

The AT-1000 has a fairly Spartan front panel that doesn't immediately show its capabilities. LDG has made

Table 14-12
LDG AT-1000

Manufacturer's Specifications

Maximum power, 1000 W SSB, 750 W CW, 500 W digital, 100 W 6 meters.
20 W while tuning (100 W with foldback), 75 W (3:1 SWR), 125 W (1:1 SWR).
Minimum power for tuning: 5 W.
Frequency range: 1.8 to 54 MHz.
Tuning time: 1 to 8 seconds. 0.5 second if memorized
Input impedance: 6 to 800 ..
Power required: 11 to 15 V, 1 A.
Dimensions (height, width, depth): 3 × 13 × 9 inches.
Weight: 6 pounds.

Measured power loss into resistive loads (%) / Input SWR at match. Tested at 50 W.

SWR	*Load (Ω)*	*160 m*	*80 m*	*40 m*	*20 m*	*10 m*
16:1	3.125	No match n/a	No match n/a	No match n/a	No match n/a	No match n/a
8:1	6.25	No match n/a	No match n/a	* **	20 1.6:1	22 **
4:1	12.5	12 2.3:1	* **	* **	* **	18 2.2:1
2:1	25	* **	* **	* **	* **	* **
1:1	50	* **	* **	* **	* **	* **
2:1	100	* **	* **	* **	* 2.1:1	* **
4:1	200	* **	* **	* **	* **	* **
8:1	400	16 2.1:1	* **	* **	22 2.1:1	17 **
16:1	800	No match n/a	18 **	17 **	55 **	No match n/a

*Power loss less than or equal to 10%.
**Matched SWR less than or equal to 1.5:1.

Figure 14-23 — Rear panel connections on the LDG AT-1000.

Figure 14-22 — Front panel of the LDG AT-1000.

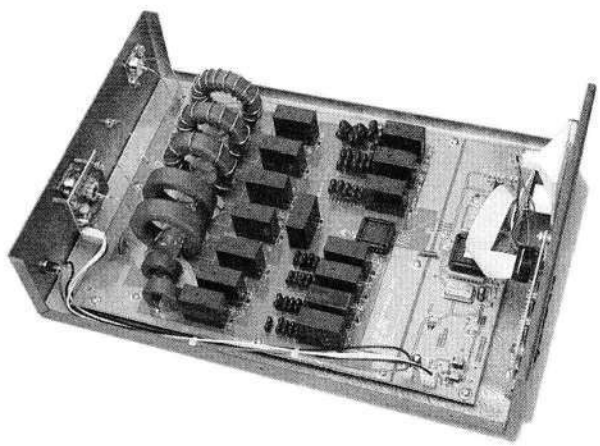

Figure 14-24 — Interior circuitry of the LDG AT-1000.

maximum use of the cross needle wattmeter on the front panel, going further with information delivery than I would have imagined with such a straightforward display. The cross needle wattmeter has two scales, reading forward (1000 W) and reflected (180 W) power simultaneously. The point at which the meter pointers cross is a third scale directly reading in SWR. So far it's just like every other cross needle meter we've seen.

What sets the AT-1000 apart is that LDG has additional indicator functionality that appears as a set of semaphore signals between tuner and operator. Each needle is driven independently in this mode and each can vary in speed and position as it fills you in on the tuner's condition and status. For example, if during a tuning cycle, both arms quickly raise fully (in surrender?) it means too much power has been supplied to allow it to safely tune. It then switches to bypass mode and goes on break until you reduce power and restart the tuning cycle.

Another feature is the ability to change the inductance and capacitance parameters manually. This can be a benefit in at least two ways. First it allows manual fine trimming of the tuning in case you want a better SWR than the tuner finds automatically. Manual tuning can also be used to peak up the receive signal strength if you're listening to a station on a frequency that you can't transmit on. This could include shortwave broadcast frequencies or bands or segments for which you don't yet have license privileges.

How'd it Work? At my station the AT-1000 did everything I asked of it without problems. My antennas tuned satisfactorily on all bands. Memorized settings were recalled without difficulty in a fraction of a second. The 15 page multicolor manual does a good job of describing how to set up and use the tuner. A table of "meter bounce codes" is included, and you will likely want to keep a copy at hand, unless your memory is much better than mine. ARRL Lab test results are shown in **Table 14-12**.

Manufacturer: LDG Electronics, 1445 Parran Rd, St Leonard, MD 20685; tel 410-586-8475; **ldg@ldgelectronics.com**; **www. ldgelectronics.com**. 2006 price: $599.

MFJ-994 Intellituner Automatic Antenna Tuner

At first glance, the MFJ-994 appears to be a very similar tuner to the AT-1000. It has almost the same controls and indicators as the LDG tuner, although they are on opposite sides of the front panel. It makes use of a similar set of semaphore indications. The major differences are:

- The MFJ tuner has a lower maximum power rating (600 vs 1000 W PEP and 300 vs 750 W CW) and a correspondingly lower price.
- The '994 provides an interface to allow operation using the TUNE button on Alinco, ICOM, Kenwood or Yaesu radios equipped to control an antenna tuner. An accessory cable is required to activate this function.
- The '994 has more memory locations, all indexed by frequency.
- The '994 offers a choice of two power meter scales, 3000 or 300 W forward power with corresponding 600 or 60 W reflected power at full scale.

During the review process, we determined that the MFJ-994 has now been superseded by the MFJ-994B. The functionality and operation are similar, with the same tuning and switching elements. The main difference seems to be the memory management function, with the B

Figure 14-26 — Rear panel connections on the MFJ-994.

Figure 14-25 — Front panel of the MFJ-994.

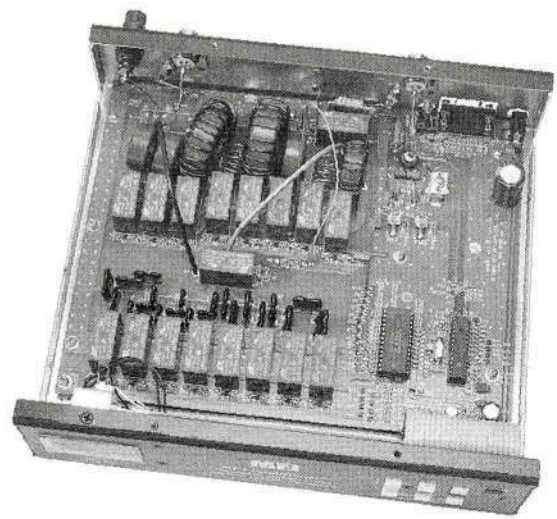

Figure 14-27 — Interior circuitry of the MFJ-994.

Table 14-13
MFJ-994

Manufacturer's Specifications

Maximum power, 600 W PEP SSB, 300 W CW, 20 W while tuning (100 W with foldback).
Minimum power for tuning: 10 W.
Frequency range: 1.8 to 30 MHz.
Input impedance: 12 to 800.
Power required: 12 to 15 V, 1 A.
Dimensions (height, width, depth) 2.8 × 10.1 × 9.2 inches.
Weight: 3.7 pounds.

Measured power loss into resistive loads (%) / Input SWR at match. Tested at 50 W.

SWR	*Load (Ω)*	*160 m*	*80 m*	*40 m*	*20 m*	*10 m*
16:1	3.125	No Match	No Match	10	12	*
		n/a	n/a	2.6:1	2.2:1	2.0:1
8:1	6.25	13	13	*	13	15
		2.4:1	1.8:1	**	**	2.2:1
4:1	12.5	*	*	*	*	15
		**	**	**	**	1.8:1
2:1	25	*	*	*	*	*
		**	**	**	**	**
1:1	50	*	*	*	*	*
		**	**	**	**	**
2:1	100	*	*	*	*	*
		**	**	**	**	**
4:1	200	*	*	*	*	*
		**	**	**	**	**
8:1	400	*	*	*	14	*
		**	**	**	**	1.8:1
16:1	800	*	17	16	11	*
		**	**	**	1.8:1	1.7:1

*Power loss less than or equal to 10%.
**Matched SWR less than or equal to 1.5:1.

model including a virtual memory function said to store up to 10,000 frequency data points versus 1000 in the earlier '994. The other difference noted in the specs is that the new one can tune with a minimum of 2 W, versus 10 W in the original.

The MFJ has some control flexibility hidden behind its few buttons. The "tuned" threshold can be set to either 1.5:1 or 2:1. With the 1.5:1 setting, the match is closer, but it will take a bit longer to find. While 2:1 should happen more quickly, some radios won't put out full power into a 2:1 load. It's nice to have the choice. An "auto tune" function is also provided that causes the tuner to activate if the SWR goes above your threshold by a user selectable 0.5, 1.0 or 1.5. This is handy as you change frequency, but be careful it doesn't drop into tuning mode while you are at full power. Pushing in the AUTO button unambiguously disables the auto tune function, entirely avoiding this concern.

In Summary The MFJ-994 did everything just as promised. It showed no problem handling the 600 W we could deliver, the only tuner of the group that we could test to the limit! It was too quick for me to stopwatch the tuning speed, but my sense was, as expected, that the frequency based memories were a bit quicker if all operations were using the same antenna. It also appeared that the MFJ relays were a bit quieter than the other relay operated tuner, but that could have been because there were generally fewer cycles needed before it was matched. ARRL Lab test results are shown in **Table 14-13**.

MFJ provided a comprehensive 23 page, well illustrated, instruction manual that was clear in its description of how the unit operated and what to expect of it.

Manufacturer: MFJ Enterprises, 300 Industrial Park Rd, Starkville, MS 39759; tel 662-323-5869, fax 662-323-6551; **www. mfjenterprises.com**. 2006 price: $359.95. Auto tuner radio interface cables: MFJ-5124A for Alinco, $19.95 MFJ-5124I for ICOM, $19.95 MFJ-5124K for Kenwood, $59.95; MFJ-5124Y for Yaesu, $59.95.

PALSTAR AT-AUTO

As noted previously, the AT-Auto is of a different architecture than the other tuners in this review. Palstar is noted for its line of high quality manual antenna tuners, so it should not be a surprise that Palstar decided to build its first auto tuner using the same type of in-house constructed parts that have been successful in their other offerings.

This is a large and complex device with features that I haven't seen before in any tuner. The first feature you might notice is the cross needle wattmeter that takes up the left side of the front panel. This is the same display and circuitry built into their PM2000A standalone wattmeter. It provides both average and peak forward and reflected power readings at full scale power levels of 3000/600 (forward/reflected) and 300/60 W. This is an upgrade to the Palstar WM150 wattmeter reviewed in July 2002 with the addition of a PEAK HOLD setting with a 2 second hold time.

The right side of the panel includes a two-line liquid crystal display (LCD), a knob for manual tuning (more later), MANUAL/AUTO and SELECT buttons. It is on this side of the panel that interesting things happen. As with most auto tuners, you apply power and it starts to match your antenna to 50 Ω. What's different with the AT-Auto's tuning sequence is that it first measures frequency, tells you the operating frequency and then politely asks you to turn off your transmitter while it finds a close match. It has a default set of L and C values for each frequency and runs its quiet motors until they are in range. It then asks for another dose of RF to refine the tune. Every time it does this, like a good smart machine, it memorizes its settings and uses them the next time you use that frequency. This approach minimizes interference to others.

A well thought out and, to my knowledge, unique feature of this tuner is its use of a radio interface. This, and many other auto tuners, make use of a radio's tuner interface to initiate the tuning sequence and cause a reduced-power tune signal to be sent from the radio. The AT-Auto has an additional connection from the radio's CAT (computer interface) port. The CAT port provides frequency data from the radio to the tuner. As you tune the receiver, the tuner indicates the frequency and follows along with either its default or memorized values. This means that, if you've been on that frequency before, the tuner will be tuned before you hit the key or PTT! If you haven't been there before, it will use its default values and still be pretty close.

This is particularly handy if you are listening to a frequency at which you aren't licensed to transmit, for example WWV or shortwave broadcast frequencies. The cable for ICOM radios is provided. You do have to think a bit while you use it (yes we have to be even smarter than our smart devices!). The CAT frequency data reflects the frequency of whichever VFO is active. If you are operating split frequency, it will tune back and forth between the two VFO frequencies as you switch between them. This is not likely much of an issue if you are operating in the typical "up five" (VFOs just 5 kHz apart) environment, but could be a disaster if you are operating cross-band split for some reason. The solution — while you have the VFO on your transmit frequency and the tuner properly tuned, tap the MANUAL/AUTO button so that it will be in manual mode and the automation will take a break.

The CAT function, as we wrote this, is available only for radios that support ICOM's CI-V protocol. Palstar expects to have cables and software upgrades to allow interoperation with Kenwood and Yaesu radios soon. Speaking of software, Palstar kindly provides a 9-pin serial cable designed to allow you to install

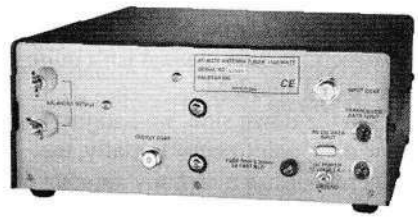

Figure 14-29 — Rear panel connections on the Palstar AT-Auto.

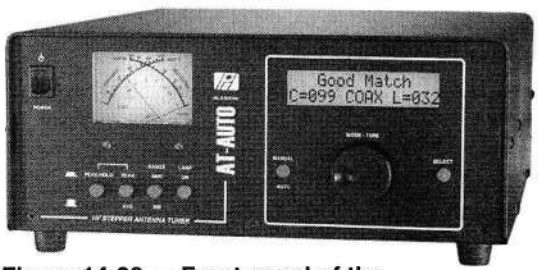

Figure 14-28 — Front panel of the Palstar AT-Auto.

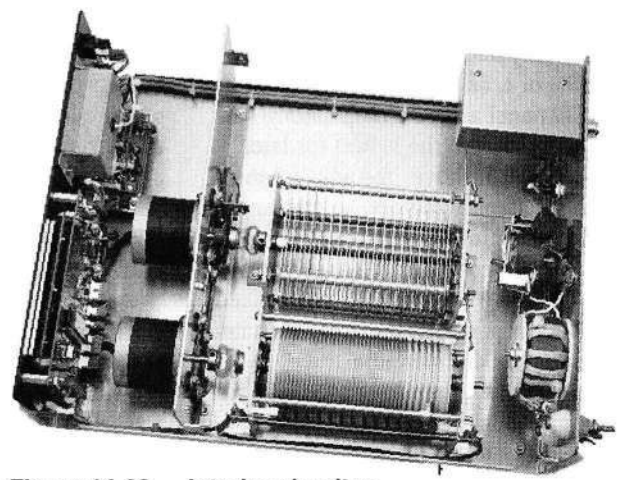

Figure 14-30 — Interior circuitry of the Palstar AT-Auto.

upgraded software when it is available. As we write this, there is no information on how to do this in either the manual or on the Palstar Web site. On the other hand, there is no new software either, so presumably when there's something new to download, they will tell us how to do it. We did successfully download upgraded software for their ZM-30 Antenna Analyzer during that review, so they seem to be able to deal with the process. We understand from Palstar that revised firmware to improve 10 meter operation has been developed and will be available shortly.

Another nice feature of the AT-Auto is that it has provisions for switch selection (via the front panel SELECT button) of either a balanced (through a 4:1 balun at the output) or an unbalanced (coax connected) antenna. The switch doesn't just insert the balun, but provides two completely independent antenna connections, so both can be always available. The memory associates the settings with each antenna port separately, so if you switch between antennas while on the same band, it thoughtfully remembers the settings for each.

New production tuners will also include BYPASS selection. A factory upgrade is said to be available for early production units. Want to do it Yourself? Poke the MANUAL/AUTO button and you are into manual tuning mode. The single knob below the LCD display is used to change the inductance or capacitance. It comes up ready to tune the C; push the knob in briefly and it changes the L. The value of L and C are displayed on the LCD panel as you change them, so you can record the values for later reference. It moves the adjustments via the stepper motors, so minimum effort is required — no heavy cranking needed.

So how'd it work? We really liked the concept of this tuner. By its nature it can provide finer adjustment than the relay types we have seen, although their resolution could be made arbitrarily fine with additional relays and smaller increments of C and L, and higher cost. We also liked the quietness of the motors compared to the clacking relays. The downside can be tuning time. As noted above, with a CATconnected radio and memorized settings it rapidly follows you as you tune. A change in bands can take longer. We measured the following times to retune between bands:

From (Meters)	*To*	*Tune Time (Seconds)*
80	40	11
40	30	4
30	20	3
20	15	2
15	10	2
160	10	45

The times shown are between memorized settings. To tune from a default setting to a finely tuned condition takes about 2 additional seconds if there isn't already a memorized setting for the frequency. It seems especially quick with the CAT function, since it feels like it's all tuned and waiting for you to catch up!

The AT-Auto comes with a well illustrated 20 page manual. The manual assumes you know why you wanted an antenna tuner and where you are going to connect it. This wasn't much of a problem since it has such an informative display, although, if you're expecting "open left flap, remove tuner from box..." type instructions, this manual isn't quite up to that standard.

On the down side, we had just a few disappointments. Initially, the tuner wouldn't match my antenna on 12 and 10 meters. On 12 meters, my measured SWR was 6:1 at the tuner. While it couldn't find a perfect match, and announced MATCH NOT FOUND! on the LCD panel, it actually got to within a 2.4:1 SWR, which my radio found acceptable. On 10 meters my antenna showed an SWR of 3:1 and the best the tuner could do was 2.78:1. In both of these cases, the LCD panel noted that the inductance was at L=000.

This suggested to me that it was the particular value of complex impedance rather than the SWR that was causing the problem. I put in an additional 6 feet of 50 Ω coax to move "around the Smith Chart" and the tuner was then able to find a perfect match in both cases. This is a good trick to keep in mind if faced with this kind of problem with any tuner. The indicator was very helpful in pointing me in the right direction.

A less significant problem was that the frequency metering system required more power to determine the frequency on the higher bands. On 160 through 15 meters, the 10 W that the ICOM transceiver put out in TUNE mode was plenty to allow the frequency to be read and the tune function to be initiated. On 12 and 10 meters, at 10 W, I received a FREQUENCY ERROR CHECK CARRIER LEVEL message on the LCD. It took more power to allow the frequency to be read. This was no problem with another transceiver that allows me to crank it up as far as I want when the TUNE button is pressed, but the ICOM had a fixed level. A quick fix is to switch to AM or FM mode to put out more power. Just hit the bar on your PTT microphone or use a straight key in CW mode.

Upon further investigation, I found that it worked fine on all bands with 10 W to a matched load. At some impedances, apparently there was not enough signal for the measuring circuits. Another workaround would be to manually set it within range and then let the AT-Auto fine tune to perfection. A handy feature of this tuner is that it can be tuned at 1500 W with no relay contacts to burn. This is good since it sometimes notices a bit of reflected power and trims the adjustment after you turn on the amplifier. ARRL Lab test results are shown in **Table 14-14**.

Manufacturer: Palstar Inc, 9676 N Looney Rd, Piqua, OH 45356; tel 800-773-7931, fax 937-773-8003; **info@palstar.com**; **www.palstar.com**. 2006 price: $1195.

In Summary

Each of these tuners did what they said they would over most of their frequency range and each could be of benefit to operators using higher power than that handled by other automatic antenna tuners. Some care needs to be taken with their operation, beyond that found in the lower

Table 14-14
Palstar AT-Auto

Manufacturer's Specifications
Maximum power: 1500 W single tone.
Frequency range: 1.8 to 30 MHz.
Input impedance: 160 to 20 meters, 1200 ±j1200; 15 to 10 meters 1000 ±j1000.
Tuning time: 1-30 seconds.
Dimensions (height, width, depth): 5.5 × 12.5 × 16 inches.
Weight: 25 pounds.

Measured power loss into resistive loads (%) / Input SWR at match. Tested at 50 W.

SWR	*Load (Ω)*	*160 m*	*80 m*	*40 m*	*20 m*	*10 m*
16:1	3.125	54	33	19	*	No Match
		**	**	**	**	n/a
8:1	6.25	42	24	15	12	No Match
		**	**	**	**	n/a
4:1	12.5	30	17	14	*	No Match
		**	**	**	**	n/a
2:1	25	24	12	*	*	26
		**	**	**	**	**
1:1	50	16	*	*	*	*
		**	**	**	**	**
2:1	100	13	*	*	*	20
		**	**	**	**	**
4:1	200	11	*	*	12	43
		**	**	**	**	**
8:1	400	12	*	11	23	42
		**	**	**	**	**
16:1	800	16	25	24	55	49
		1.6:1	**	**	**	**

*Power loss less than or equal to 10%.
**Matched SWR less than or equal to 1.5:1.

powered units, because of the power involved and particularly because of the difference between "tuning power" and "operating power." Each unit is specified to be tuned using reduced power from the exciter at somewhere in the 10 to 100 W range.

Each tuner finds a match at that power level and then it should be safe to switch on the linear amplifier — but is it? With the MFJ and Palstar tuners, there were conditions under which it would initiate the tuning cycle again at full power, even after being within specification at the lower tuning power. The reason is likely a combination of a larger sample of RF to make reflected power measurement and nonlinearity of the detectors, not surprising for analog circuitry. Different tuners will react differently under this circumstance. The Palstar actually doesn't mind tuning at 1500 W and will calmly trim up without a whimper. The MFJ tuner will note that it is tuning above the specified tuning power spec and switch to bypass — whoops, you had the linear pre-tuned with a dummy load so that it would be ready to go, and now it sees a 9:1 SWR, or whatever your antenna has, going directly to the amplifier. This could cause a catastrophic reaction in your amplifier! The LDG tuner is different in this regard. It only initiates a tune cycle if the TUNE button is pressed.

So what to do? There are two potential solutions. One, manually trim up the tuning for an even lower SWR using the L and C up and down buttons. If the reflected power is fully nulled, it should avoid this problem. The other approach is to switch the tuner to manual mode after it finds its initial match. That will prevent it from automatically retuning while high power is applied. Or do both. Arguably this changes tuner operation from "auto" to "semi-auto," but I recommend it for any high power relay switched tuner. The consequences of not doing so could be extreme to either the amplifier or the relay contacts or both.

A New Generation of Balanced Antenna Tuners

Reviewed by Joel R. Hallas, W1ZR
QST *Technical Editor*
QST *September 2004*

A new breed of antenna tuner available in different flavors from multiple manufacturers addresses concerns about using baluns with high SWR to feed balanced antenna systems. Paul Danzer's article in the April 2004 issue of *QST* brought to paper a concern many of us have had for some time — the use of baluns at the output of antenna tuners.[6] As noted in his article, if the balanced load is near the balun's design impedance (typically 200 Ω for the usual 4:1 balun) all is well.

Unfortunately, the typical random sized center fed antenna with random length ladder line feed has an impedance at the feed point that varies dramatically with frequency. The result can be heating and loss (and occasional damage) at the balun. These effects were well documented in a series of *QST* articles by Frank Witt and later in a performance evaluation of unbalanced tuners with both balanced and unbalanced loads.[7,8]

So How Do We Fix the Problem?

As Danzer noted, the classic solution has been the use of an inherently balanced tuner. The commercially manufactured E.F. Johnson Matchbox tuners of the '50s worked reasonably well in their day, and over the bands that they covered (we didn't have the 60, 30, 17 and 12 meter bands back then). Now at least three manufacturers have begun offering balanced antenna tuners of a different configuration. For this review we selected the MFJ-974H and the Palstar AT1500BAL and AT4K. Interestingly, each of the three uses a different architecture, and each is different from the design of the old Matchbox!

In addition to those units, SGC has announced a low power self-contained auto-tuner, the SG-211, which shares the design concept of the AT4K and will be the subject of an upcoming Short Takes column. We thought it would be good to evaluate the performance of the medium and high-power units and provide a comparison to the old Johnson tuner.

What's in the New Tuners?

Glad you asked! As noted, each of the tuners uses a different design configuration. Each can be directly compared to some of the common unbalanced configurations. Note that the power ratings and price of the Palstar tuners put them in a different category from the MFJ units and thus, direct comparisons may not be appropriate. Both the MFJ and the Palstar AT1500BAL are fully balanced tuners — the MFJ a dual T section design with shunt L, and the Palstar a dual L section with shunt C. The Palstar AT4K tuner takes a completely different approach. It uses the insulated unbalanced scheme suggested in Paul's article and described in detail in *The ARRL Antenna Book*.[9]

The relationship of the designs to their more commonly encountered unbalanced configurations are shown in simplified schematics in **Figures 14-32** through **14-33**. The other differences between the units are in their ratings. The MFJ tuner covers 160 through 6 meters, while the Palstar tuners top out at 10 meters. Both Palstar tuners are rated at 1500 W or greater (the AT4K has a reduced rating below a 25 Ω load) while the MFJ tuner is rated at 300 W PEP, 150 W CW.

The ratings of the Johnson Matchboxes were established in a day when amateur power levels were specified based on average dc power *input*, rather than the current PEP RF *output*

Figure 14-31 — From the top the MFJ-974H, the Palstar AT1500BAL and AT4K. On the right, they are being scrutinized by their logical ancestor, the Johnson Matchbox.

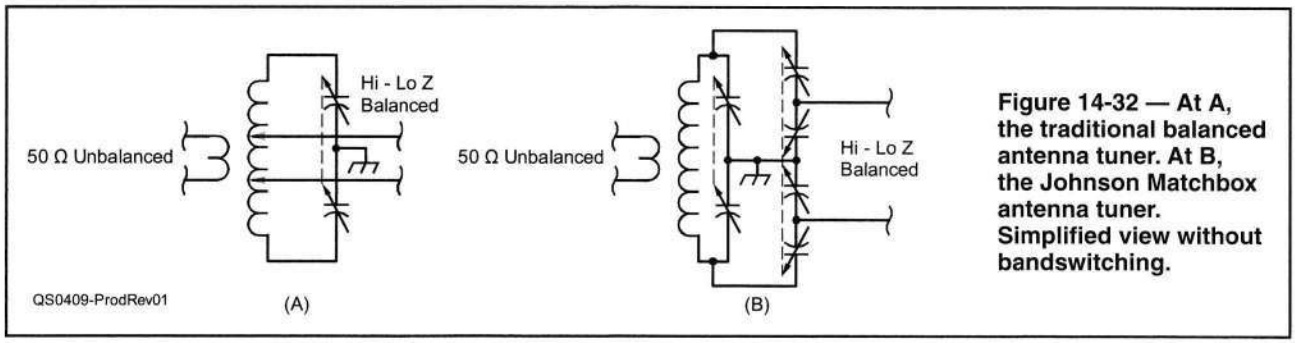

Figure 14-32 — At A, the traditional balanced antenna tuner. At B, the Johnson Matchbox antenna tuner. Simplified view without bandswitching.

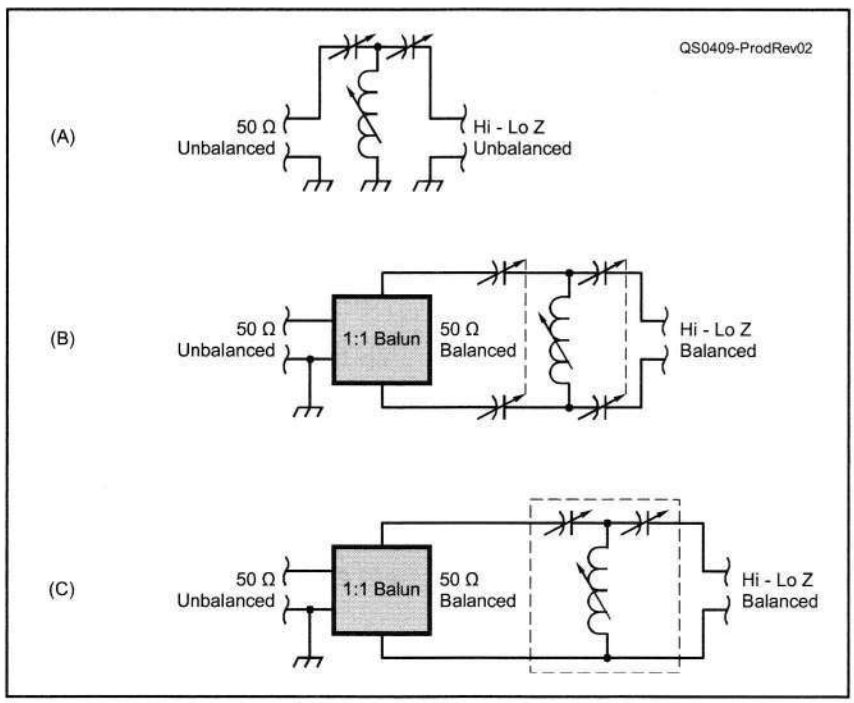

Figure 14-33 — At A, an unbalanced T-network tuner. At B, a balanced T-network tuner. At C, an unbalanced T-network tuner for balanced loads.

power. A "275 W" Johnson matchbox was thus rated to work with transmitters running 275 W dc input, or about 200 W average output. This was in the day of plate modulated AM service, so that rating further translates to 800 W PEP under today's rules. Similarly, a "kW Matchbox" would likely be rated today as a 3 kW PEP tuner.

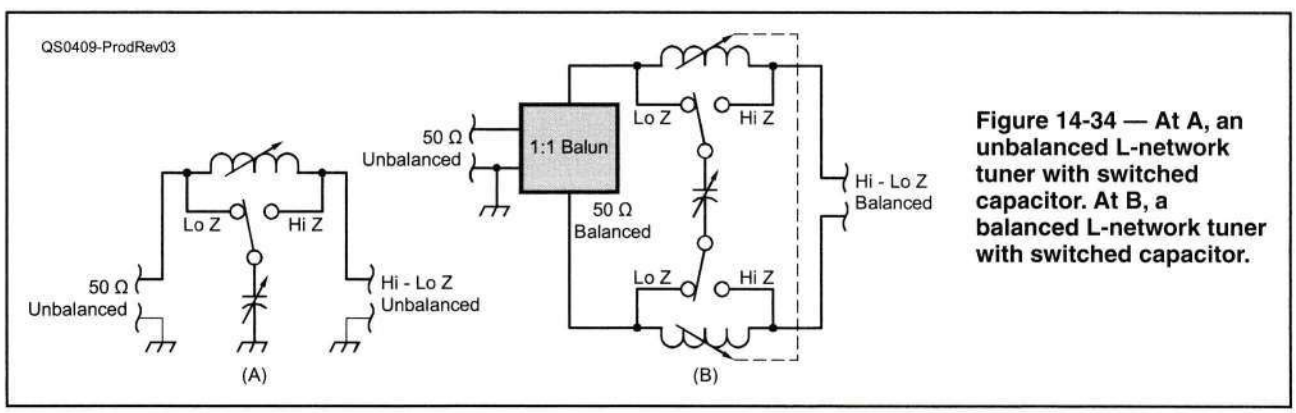

Figure 14-34 — At A, an unbalanced L-network tuner with switched capacitor. At B, a balanced L-network tuner with switched capacitor.

MFJ-974(H) Balanced Antenna Tuner

MFJ provides two versions of their '974, with ('974H) and without ('974) the capability to cover 160 meters. Both are rated at 300 W PEP, and 150 W CW. At only 7½ inches wide, it takes up a small amount of desk space. Interestingly, it has about the same shape as the old 275 W Johnson Matchbox, but is 1 to 2 inches smaller in each dimension. As noted above, this unit uses a T section design as in **Figure 14-33B**, so it is not necessary to switch capacitors from one side to the other as the impedance changes from high to low.

The inductor is varied by selecting among 12 steps. The H model has an extra inductance for 160 meters that changes the tuning range as needed. A cross-needle two-range (30 and 300 W full scale) power/SWR meter can be set to read peak or average power. Both the power level and null matched the meter on my transceiver quite closely. The capacitors are direct (1:1) drive, with plastic gearing between the ganged units. I found them easy to turn and to get a null. I used the old trick of tuning for maximum receive signal, first with the L switch, then with the capacitors.

MFJ provides a page of nominal settings by band that you may find helpful. When you switch to adjusting the tuner while transmitting, be sure to note their caution about not changing the inductor switch with power applied. You may burn the contacts otherwise. I also make it a practice to always tune at reduced power to avoid hitting my finals with a heavy mismatch at full power. When you have it set, turn up the power and confirm that all is well.

One caution that applies to all T section tuners is to note that multiple settings can result in low SWR. Unfortunately, some will have higher losses than others. The rule of thumb is to use the setting with the smallest inductance (the L switch position on

Table 14-15
MFJ-974H Balanced Antenna Tuner

Manufacturer's Specifications	*Measured in ARRL Lab*
Input load range: 12 to 2000 Ω.	See below.
Output SWR range: Not specified.	See below.
Frequency coverage: 1.8 to 54 MHz.	See below.
Input power: 150 W average, 300 W PEP.	Not tested.
Size: 6 × 7.5 × 9 inches (HWD).	

SWR	*Load (Ω)*		*160 Meters*	*80 Meters*	*40 Meters*	*20 Meters*	*10 Meters*	*6 Meters**
		Power Loss %	55	41	32	20	16	
8:1	6.25	SWR BW %	0.9	0.6	1.0	2.0	2.0	Not Tested
		Imbalance**	0	0	0	0	0	
		Power Loss %	40	33	23	<10	10	
4:1	12.5	SWR BW %	0.6	0.9	1.4	2.8	3.4	Not Tested
		Imbalance	0	0	0	0	0	
		Power Loss %	25	22	<10	<10	<10	
2:1	25	SWR BW %	0.8	1.1	3.2	4.9	2.4	Not Tested
		Imbalance	0	0	0	0	0	
		Power Loss %	22	15	32	20	<10	<10
1:1	50	SWR BW %	1.1	1.4	2.1	2.1	12	10
		Imbalance	0	0	0	0	0	0
		Power Loss %	18	<10	<10	<10	<10	
2:1	100	SWR BW %	1.1	1.7	4.1	7.0	25	Not Tested
		Imbalance	0	0	0	0	0	
		Power Loss %	17	<10	<10	<10	<10	
4:1	200	SWR BW %	1.1	2.8	2.5	9.1	10	Not Tested
		Imbalance	0	0	0	0	0	
		Power Loss %	12	<10	<10	<10	<10	
8:1	400	SWR BW %	1.5	3.4	7.5	7.0	3.7	Not Tested
		Imbalance	0	0	0	0	0	
		Power Loss %	10	<10	<10	<10	<10	
16:1	800	SWR BW %	1.9	4.3	8.3	7.7	3.7	Not Tested
		Imbalance	0	0	0	0	0	
		Power Loss %	<10	<10	<10	10	11	
32:1	1600	SWR BW %	2.1	2.6	5.6	4.4	3.0	Not Tested
		Imbalance	0	0	0	0	0	

Notes
Power losses are expressed as a percentage. A 10% power loss represents less than half (0.46) a dB.
The SWR bandwidth is the percentage of the measurement frequency that can be changed with the SWR staying under 1.5:1.
*The ARRL test fixture is only usable at 50 . on 6 meters.
**As defined in F. Witt, "Evaluation of Antenna Tuners and Baluns—An Update," *QEX*, Sep-Oct 2003, pp 3-14.

this tuner) and highest capacitance that will provide a match. One limitation of the switched rather than roller inductor is that you can't get values in between. I didn't find that much of a problem, as I was always able to get to 1.5:1 or better SWR with my antennas.

As you make adjustments, I suggest you log the settings for each frequency in a table such as the one supplied in the back of the manual. You may want to make photocopies or set up a spreadsheet so you will be able to repeat the process for your next antenna. If you find that you can't get a match at some frequency, try adding 6 feet of ladder line at a time. The different length will move the impedance around and may solve the problem, but you will have to retune on the other bands and hope to find a length that will tune properly on all bands.

Balanced loads are connected via standard (¾ inch) spaced multipurpose binding posts. These accept wire ends, or dual banana plugs, a handy connector for balanced feed lines at this power level. The '974H also provides a capability to match unbalanced loads and provides a coax connector for that purpose. It is necessary to provide a jumper between the lower balanced load binding post and the ground terminal to complete the unbalanced hookup. Note that the output is not switched, so an antenna should be connected to either the coax connector or the balanced jacks, but not both.

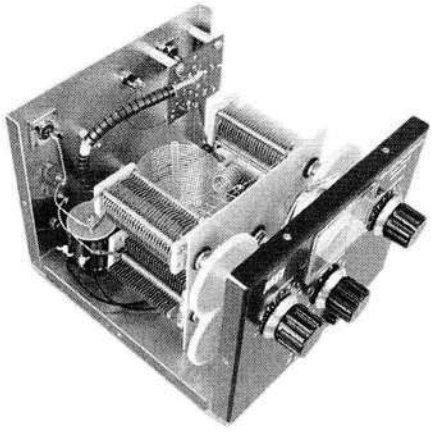

Figure 14-35 — MFJ-974H, inside view.

Note that while the '974 is specified to match a wide range of impedances on 6 meters, neither the Lab nor W1ZR could test at any impedance other than 50 Ω. I tried the unbalanced connection arrangement with my coax-fed G5RV. It worked fine until I tried it on 160 meters, not one of the bands the antenna is supposed to operate on. I was able to quickly find a match at low power. When I turned up the power past 70 W, arcing was evident inside the unit. I opened it up and was surprised to find that rather than the expected arcing tuner element, I found the arcing source was at the metering circuit board. Measured Lab data is shown in **Table 14-15**.

The unit went back to MFJ for repair under their warranty. Upon return, it worked fine at 100 W (my maximum power with the transceiver) and I was told by MFJ that a signal wire had been dressed too close to the meter board and arced. It was repositioned and MFJ installed the intended tie-wrap to hold it away from the meter board. The tuner was retested and had exhibited no problems.

Manufacturer: MFJ Enterprises Inc, 300 Industrial Park Rd, Starkville, MS 39759; tel 800-647-1800; fax 662-323-6551; **www.mfjenterprises.com**. 2004 price: MFJ-974, $179.95; MFJ-974H, $199.95.

Palstar AT4K Antenna Tuner

Unlike the other tuners in this review, the AT4K might best be described as an unbalanced tuner designed to feed unbalanced or balanced loads. This sounds contradictory, but really isn't, as described in footnotes 1 and 6. If you just think of this tuner as a "four-terminal black box" (see **Figure 14-33C**) connecting a balanced load to a balanced source, followed by a 1:1 balun going to the transceiver, you may get the picture.

An unbalanced T section, isolated from ground within the box, performs the required impedance transformation to match the impedance at the bottom of the balanced transmission line to 50 Ω to operate properly through the internal balun. This tuner also provides a heavy duty relay to connect the common points of the input, output and inductor to the chassis to convert it to a typical T section tuner for unbalanced loads.

An additional feature, not found in any of the other tuners in this review, is antenna switching capability. The AT4K has a single pair of balanced output terminals, but also has three coax outputs. Two can be tuned, or switched to straight through, while the third provides straight though operation only. This is a great spot to connect a dummy load, or a well matched Yagi.

The inside view gives a sense of the heavy duty construction of this massive tuner. The rotary inductor is fabricated from silver plated strip stock, rather than the usual wire, and the rolling contact is designed to grip a significant portion or the coil, not just the edge. The inductor is driven by a smooth turn-count dial reading out to 1/10 of a turn and resetable in

Table 14-16
Palstar AT4K Balanced/Unbalanced Antenna Tuner

Manufacturer's Specifications	*Measured in ARRL Lab*
Input load range: 8 to 2000 Ω.	See below.
Output SWR range: Not specified.	See below.
Frequency coverage: 1.8 to 30 MHz.	See below.
Input power: 2500 W single tone.	Not tested.
Size: 5 × 15 × 16 inches (HWD).	

SWR	*Load (Ω)*		*160 Meters*	*80 Meters*	*40 Meters*	*20 Meters*	*10 Meters*	*6 Meters**
		Power Loss %	24	14	10	10	34	
8:1	6.25	SWR BW %	1.1	2.6	6.4	4.9	0.5	
		Imbalance	0.6	0.7	0	0.6	5.2	
		Power Loss %	12	<10	<10	<10	18	
4:1	12.5	SWR BW %	1.9	4.0	17	8.5	0.7	
		Imbalance	0	0.4	0	0.4	1.7	
		Power Loss %	<10	<10	<10	<10	<10	
2:1	25	SWR BW %	3.0	7.4	39	21	1.5	
		Imbalance	0	0.2	0	0.5	0	
		Power Loss %	<10	<10	<10	<10	<10	
1:1	50	SWR BW %	5.5	16	69	42	3.0	
		Imbalance	0.3	0	0	0.4	0.3	
		Power Loss %	<10	<10	<10	<10	<10	
2:1	100	SWR BW %	6.1	26	49	44	10	
		Imbalance	0.4	0	0	0	0	
		Power Loss %	<10	<10	<10	<10	37[1]	
4:1	200	SWR BW %	6.9	22	24	32	0.8	
		Imbalance	0.5	0	0	0	3.4	
		Power Loss %	<10	<10	<10	<10	Note 1	
8:1	400	SWR BW %	7.8	15	14	15		
		Imbalance	1.5	0.3	0	0		
		Power Loss %	<10	<10	<10	<10	Note 1	
16:1	800	SWR BW %	7.2	10	10	8.5		
		Imbalance	2.6	0.5	0	0		
		Power Loss %	<10	<10	<10			
32:1	1600	SWR BW %	4.4	6.9	5.6	No Match	No Match	
		Imbalance	4.9	0	0			

Notes

[1]According to the owner's manual for the AT4K, the matching range is limited on 10 meters. In testing, it was found that matches (SWR <1.5:1) could be obtained on 10 meters with some higher impedance loads by using a large amount of inductance. However, it is very likely that the tuner was close to self-resonance under these conditions, and this type of operation should be avoided due to the high losses in the tuner.

Power losses are expressed as a percentage. A 10% power loss represents less than half (0.46) a dB.

The SWR bandwidth is the percentage of the measurement frequency that can be changed with the SWR staying under 1.5:1.

between marks. As with its sister units, the capacitors are driven by 5:1 reduction drives with 0 to 100 logging scales.

One design challenge with a tuner built of these large parts is to keep the minimum capacitance low enough so the unit will meet specifications at 10 meters. As shown in the data, Palstar has done a reasonably good job with this, but the limitations should be noted. I found that this unit could match all my antennas, balanced or unbalanced, except on 17 and 10 meters where not all impedances are within range. Again, a change in transmission line length may move your impedance to a value within the tunable range.

Figure 15-36 — Palstar AT4K, inside view.

The metering was consistent with my other wattmeters, both in position of reflected null and forward power. I was able to easily return to a previous setting using the resolution of the dial scales. Measured Lab data is shown in **Table 14-16**.

Palstar AT1500BAL Balanced Antenna Tuner

The Palstar AT1500BAL is of the configuration shown in **Figure 14-34B**. It is a legal limit device and a look inside makes me believe that it can handle serious power. The rotary inductors, two edge-wound silver plated ball-bearing monsters, driven by a toothed fiberglass belt and turns counting dial take up a lot of the interior space. The rest is largely occupied by a 450 pF 4.5 kV variable driven by a smooth 5:1 vernier dial.

The inductors and capacitor are made in-house and work very well. I was particularly impressed with the resetability of the controls. The turns counter reads out to tenths of a turn, and can be easily reset to ½ a tenth out of the 32 turns end-to-end. The vernier drive has a dial with 100 divisions and no perceivable backlash. Once you make up a table of tuning values by frequency, retuning should be a snap. I found the tuner easy to use at W1ZR, matching all reasonable antenna configurations I tried. I am only able to test at the 500 W level and, as expected, encountered no difficulties.

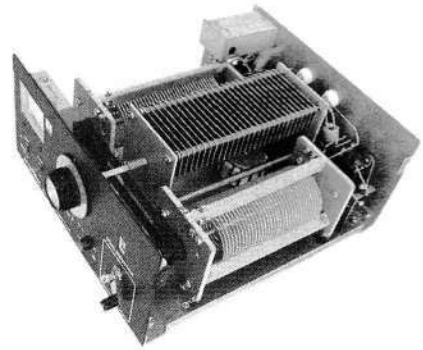

Figure 14-37 — Palstar AT1500BAL, inside view.

The cross-needle meter (300 and 3000 W full scale ranges for forward average power) agreed closely with those on my equipment. One note, on many tuners, power is only required for meter lighting. On this unit, relays are used — both to switch capacitors from one end to the other and to switch in additional capacitance. The tuner will work only in the "high impedance/ no extra capacitance" mode if you neglect to plug in the

Table 14-17
Palstar AT1500BAL Balanced Antenna Tuner

Manufacturer's Specifications	*Measured in ARRL Lab*
Input load range: 160 to 20 meters, 2500 ± j2500 Ω.	See below.
20 meters 1000 ± j1000 Ω; 10 meters, 500 ± j500 Ω.	See below.
Output SWR range: Not specified.	See below.
Frequency coverage: 1.8 to 30 MHz.	See below.
Input power: 1500 W PEP.	Not tested.
Size: 6.5 × 12.5 × 15 inches (HWD).	

SWR	*Load (Ω)*		*160 Meters*	*80 Meters*	*40 Meters*	*20 Meters*	*10 Meters*	*6 Meters**
Power Loss %			<10	<10	<10			
8:1	6.25	SWR BW %	No Match	No Match	9.9	6.6	5.4	
		Imbalance	0.3	0	0			
		Power Loss %	<10	<10	<10			
4:1	12.5	SWR BW %	No Match	No Match	1.3	1.3	10	
		Imbalance			0	0	0	
		Power Loss %	<10	<10	<10	17	<10	
2:1	25	SWR BW %	1.5	46	42	19	13	
		Imbalance	0	0	0	0	0	
		Power Loss %	<10	<10	<10	<10	<10	
1:1	50	SWR BW %	>100	>100	>100	>100	20	
		Imbalance	0.3	0	0	0	0	
		Power Loss %	<10	<10	<10	<10	<10	
2:1	100	SWR BW %	>100	54	58	56	61	
		Imbalance	0	0	0	0	0	
		Power Loss %	<10	<10	<10	<10	<10	
4:1	200	SWR BW %	>100	29	26	30	3.7	
		Imbalance	0.2	0	0	0	0	
		Power Loss %	<10	<10	<10	<10	13	
8:1	400	SWR BW %	17	23	18	20	1.7	
		Imbalance	0	0	0	0	0	
		Power Loss %	<10	<10	<10	<10	18	
16:1	800	SWR BW %	11	11	13	13	4.0	
		Imbalance	0	0	0	0	0	
		Power Loss %	<10	<10	<10	<10		
32:1	1600	SWR BW %	5.6	8.0	7.8	5	No Match	
		Imbalance	0	0	0	0		

Notes
Power losses are expressed as a percentage. A 10% power loss represents less than half (0.46) a dB.
The SWR bandwidth is the percentage of the measurement frequency that can be changed with the SWR staying under 1.5:1.

supplied wall-wart or connect an external 12 V dc supply. I found I needed to exercise both relays to tune my antenna on all bands.

Just after we purchased the AT1500BAL tuner for evaluation, Palstar added the AT1KBAL tuner to their line. In spite of their product numbers, they both are specified to handle the US legal limit. There is a key difference, however. The AT1KBAL tuner has the capacitors on the output side only. This results in a tuner that is designed to match from around 100 Ω up and is similar to an early balanced tuner described by Measures.[10,11]

Palstar has informed us that later this year they will replace the AT-1500BAL and the newer (and not tested) AT1KBAL with a new balanced tuner, the model BT1500A. This tuner will share the basic architecture and design of the AT1500BAL. It will make use of a new switched two-section variable capacitor designed to reduce minimum capacitance. This is intended to improve the tuning range, particularly on 10 meters. It will also have the inductors driven in tandem, removing the requirement for the drive belt and said to make for smoother tuning. Palstar expects to offer the BT1500A as their only balanced tuner once material for the others is exhausted. Measured Lab data is shown in **Table 14-17**.

Manufacturer: Palstar Inc, 9676 N Looney Rd, PO Box 1136, Piqua, OH 45356; tel 937-773-6255; fax 937-773-8003; **www.palstar.com**. 2004 prices: AT4K, $895; AT1500BAL, $695.95; AT1KBAL, $595.

E. F. Johnson Matchbox Antenna Tuners

Before WW II, the E. F. Johnson Company of Waseca, Minnesota, manufactured high quality variable capacitors, inductors and ceramic parts for electronics. By 1950 they were advertising their innovative Viking I transmitter in *The ARRL Radio Amateur's Handbook* and the next year their Matchbox antenna tuner for $48.95. A kW version was advertised in 1957. These tuners were based on the classic prewar balanced tuned circuit tuner (**Figure 14-32A**), but with an added twist. While the classic tuner of the day used plug-in coils to change bands, and manually attached tap points on the coil to change impedances, the Matchbox was bandswitching and had a unique differential capacitor arrangement to adjust the transformation ratio from the front panel, as shown in **Figure 14-32B**.

Models were available with and without SWR metering and the units included a TR relay useful for the typical separate transmitter and receiver setups of the day. By the '60s, the typical amateur antenna system had become one designed for resonant matched operation using coaxial cable without antenna tuners. Radios moved from AM to SSB, and Johnson changed their focus from amateur equipment to the commercial two-way FM radio market.

Their tuners are still a popular item at flea markets and on electronic auction sites. While not exactly a part of this review, Matchbox data reported by Witt in his earlier article is presented for comparison. As noted in the tables, the Matchbox tuners work well, but over a typically smaller impedance range than their modern counterparts. They also do not have band switch positions for any of the newer bands, although there is enough tuning range so they can typically cover 17 and 12, but not 30 or 60 meters. Within these limits, however, they can still be put to good use. Until the units discussed in this review became available, the Matchboxes were the only commercial tuner

Table 14-18
E. F. Johnson 275 W Matchbox, Balanced Antenna Tuner

Manufacturer's Specifications	*Measured in ARRL Lab*
Input load range: 25 to 1250 Ω.	See below.
Output SWR range: not specified.	See below.
Frequency coverage: 80, 40, 20, 15 and 10 meters	See below.
Input power: 275 W dc input.	Not tested.
Size: 7 × 10 × 10.5 inches (HWD).	

SWR	*Load (Ω)*		*80 Meters*	*40 Meters*	*20 Meters*	*15 Meters*	*10 Meters*
		Power Loss %					
4:1	12.5	SWR BW %	No Match	No Match	No Match	No Match	No Match
		Imbalance					
		Power Loss %				<10	<10
2:1	25	SWR BW %	No Match	No Match	No Match	4	4
		Imbalance				0	0
		Power Loss %	<10		<10	<10	<10
1:1	50	SWR BW %	2	No Match	>5	>5	3
		Imbalance	0	0	0	0	
		Power Loss %	<10	<10	12	11	<10
2:1	100	SWR BW %	2	4	>5	>5	3
		Imbalance	0	0	0	0	0
		Power Loss %	11	<10	<10	<10	11
4:1	200	SWR BW %	2	4	>5	>5	3
		Imbalance	0	0	0	0	0
		Power Loss %	12	<10	<10	<10	11
8:1	400	SWR BW %	2	4	>5	>5	3
		Imbalance	0	0	0	0	0
		Power Loss %	10	<10	<10	<10	11
16:1	800	SWR BW %	2	4	>5	>5	3
		Imbalance	0	0	0	0	0
		Power Loss %	10	<10			
32:1	1600	SWR BW %	2	4	No Match	No Match	No Match
		Imbalance	0	0			
		Power Loss %	10				
64:1	3200	SWR BW %	2	No Match			
		Imbalance	0				

Notes
Power losses are expressed as a percentage. A 10% power loss represents less than half (0.46) a dB.
The SWR bandwidth is the percentage of the measurement frequency that can be changed with the SWR staying under 1.5:1.

in wide use specifically designed to work with balanced antenna systems. Measured data from Frank Witt is shown in **Tables 14-18** and **14-19**.[12]

Notes

[1]R. D. Straw, Editor, *The ARRL Antenna Book*, 21st Edition. Available from your ARRL dealer or the ARRL Bookstore, ARRL order no. 9876. Telephone 860-594-0355, or toll-free in the US 888-277-5289; **www.arrl.org/shop**; **pubsales@arrl.org**.

[2]The SG-235 is a 500 W version of the SG-230 with similar specifications, except needing a longer antenna. The SG-230 was reviewed in *QST* in November 1993.

[3]P. Pagel, "Product Review: Heath SA-2500 Antenna Tuner," *QST*, Mar 1985, pp 39-41.

[4]L. Aurick, "Product Review: J.W. Miller Automatic Antenna Tuner Auto-Trak Model AT2500," *QST*, Jul 1981, pp 42-43.

[5]S. Gerli, "Product Review: Daiwa CNA-1001 Automatic Antenna Tuner," *QST*, Nov 1981, pp 41-42.

[6]P. Danzer, N1II, "Open Wire Feed Line—A Second Look," *QST*, Apr 2004, pp 34-36.

[7]F. Witt, AI1H, "How to Evaluate Your Antenna Tuner—Parts 1 and 2," *QST*, Apr 1995, pp 30-34 and May 1995, pp 33-37.

[8]R. Lindquist, N1RL, "Product Review—QST Compares: Four High-Power Antenna Tuners," *QST*, Mar 1997, pp 73-77.

[9]R. D. Straw, Editor, *The ARRL Antenna Book*, 21st Edition. Available from your ARRL dealer or the ARRL Bookstore, ARRL order no. 9876. Telephone 860-594-0355, or toll-free in the US 888-277-5289; **www.arrl.org/shop**; **pubsales@arrl.org**.

[10]Most center-fed antennas longer than 0.5 Ω are likely to meet this criterion. Very short antennas, or some low impedance driven arrays (8JK, for example) may have problems with this configuration, depending on feed line length.

[11]R. Measures, AG6K, "A Balanced Balanced Antenna Tuner," *QST*, Feb 1990, pp 28-32.

[12]See Note 7.

Table 14-19

E. F. Johnson kW Matchbox, Balanced Antenna Tuner

Manufacturer's Specifications	*Measured in ARRL Lab*
Input load range: 50 to 2000 Ω.	See below.
Output SWR range: not specified.	See below.
Frequency coverage: 80, 40, 20, 15 and 10 meters	See below.
Input power: 1000 W dc input.	Not tested.
Size: 12.5 × 17.25 × 11 inches (HWD).	

SWR	*Load (Ω)*		*80 Meters*	*40 Meters*	*20 Meters*	*15 Meters*	*10 Meters*
		Power Loss %				15	<10
4:1	12.5	SWR BW %	No Match	No Match	No Match	1	3
		Imbalance				0	0
		Power Loss %			<10	13	<10
2:1	25	SWR BW %	No Match	No Match	2	2	4
		Imbalance			0	0	0
		Power Loss %		<10	<10	<10	<10
1:1	50	SWR BW %	No Match	2	2	2	4
		Imbalance		0	0	0	0
		Power Loss %	<10	<10	<10	<10	<10
2:1	100	SWR BW %	1	2	2	2	4
		Imbalance	0	0	0	0	0
		Power Loss %	<10	<10	11	<10	<10
4:1	200	SWR BW %	1	2	2	2	4
		Imbalance	0	0	0	0	0
		Power Loss %	<10	<10	<10	14	11
8:1	400	SWR BW %	1	2	2	2	4
		Imbalance	0	0	0	0	0
		Power Loss %	10	<10	<10	11	11
16:1	800	SWR BW %	1	3	2	2	4
		Imbalance	0	0	0	0	0
		Power Loss %	10	<10	<10		
32:1	1600	SWR BW %	1	2	2	No Match	No Match
		Imbalance	0	0	0		
		Power Loss %	10				
64:1	3200	SWR BW %	2	No Match	No Match	No Match	No Match
		Imbalance	0				

Notes

Power losses are expressed as a percentage. A 10% power loss represents less than half (0.46) a dB.
The SWR bandwidth is the percentage of the measurement frequency that can be changed with the SWR staying under 1.5:1.

Review Questions

14-1 What are some of the key issues to keep in mind if selecting a commercial tuner?

14-2 What is the major advantage of an automatic antenna tuner?

14-3 Why might it be important to use a remotely tuned antenna tuner near the antenna feed point?

Chapter 15

Building Your Own Tuners

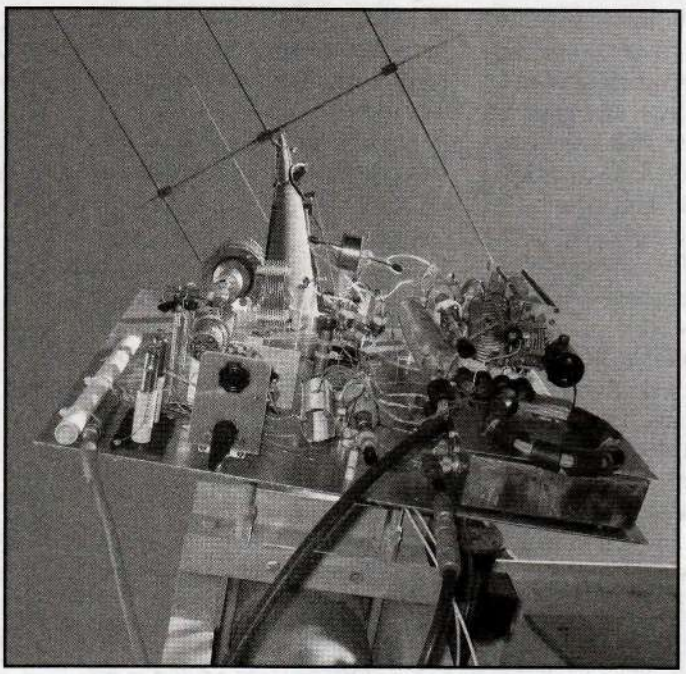

Contents

Why Build a Tuner.....15-2
Special Purpose Tuners.....15-2
Home Built General Purpose Tuners.....15-7
Review Questions.....15-12

Why Build a Tuner

A quick look at the schematic diagram of a basic manual antenna tuner (see Chapter 3), not counting metering and switching functions, reveals perhaps the simplest of amateur equipment schematics. A tuner has very few parts, and very few connections. That should make it easy to duplicate — and it does. Unfortunately each of the parts can be quite expensive and perhaps hard to find. On the other hand, if you have — or can easily obtain — the needed parts, there is no reason not to try building one or more tuners.

Special Purpose Tuners

Most of the tuners we have discussed heretofore have been of the general purpose variety. That is, they were designed to match varying loads on multiple frequencies from a single box. In any given amateur station, that may not be what is needed. You may have a need to match your particular antenna system to your particular radio on a particular frequency. That describes a "tuner" that needs no knobs or controls — just a fixed matching network.

The fixed network is more common than we may think. Every Yagi antenna with a gamma, T or hairpin match at the driven element has essentially done exactly that. Each is a matching network located at the antenna to provide a match from the antenna to the transmission line for a low loss run to the radio.

In a similar way, we can provide a network for each of our antennas that provides needed matching. The chapter title figure, a shot of a collection of specialized antenna matching systems at, W6TC, the advanced Amateur Radio station of the late George Badger, illustrates the point. None of those networks looks quite like any of the usual commercial antenna tuners of the last chapter! Another shot of this collection of networks, annotated with descriptions of each tuning element is shown in **Figure 15-1**.

Designing Your Special Purpose Tuner

While the usual circuit design and analysis tools of an electronic engineer can be used to design an impedance matching network, it can be a much simpler proposition for the amateur with a few software and hardware tools. The steps are straightforward:

•*Determine the (complex) impedance that the antenna system will present to the radio or transmission line.*

Determining the impedance can be done in a number of ways. The best approach is probably to measure the impedance at the location that will have the tuner by using an antenna analyzer. Such analyzers include tun-

1 — RG-213 coax cable from shack to input of vacuum relay box behind board (37) to connect to SteppIR Yagi antenna or 30, 40, 60, 80 and 160 meter loop tuners.
2 — RG-213 coax cable to SteppIR antenna.
3 — Coax connector to 30 and 40 meter balun (38).
4 — 30 meter tuning inductor.
5 — 30 meter vacuum variable capacitor.
6 — 30/40 meter vacuum relay connected to loop.
7 — 30/40 meter vacuum relay connected to loop.
8 — 40 meter phone/CW vacuum relay.
9 — 40 meter phone/CW inductor.
10 — 40 meter tuning capacitor.
11 — Motor drive for 40 meter tuning capacitor.
12 — 40 meter tuning inductor.
13 — 40 meter matching inductor.
14 — Coax connector to 60 meter balun.
15 — 60 meter balun.
16 — 60 meter tuning inductor.
17 — 60 meter tuning vacuum variable capacitor.
18 — 60 meter vacuum relays.
19 — 80 meter coax connector to 80 meter balun.
20 — 80 meter balun.
21 — Motor drive for 80 meter vacuum variable capacitor.
22 — Limit switches for 80 meter vacuum variable capacitor.
23 — 80 meter vacuum variable capacitor.
24, 25 — 80 meter tuning and matching inductors.
26 — 80/160 meter vacuum relay.
27 — 160 meter open end vacuum relay.
28, 29 — Connection to loop on tower.
30 — 160 meter receive vacuum relay.
31-33 — 160 meter receive RC network.
34 — Spark gap protector for 160 meter receive RC network.
35, 36 — 25-pair control cable to shack.
37 — Vacuum relay switch box to connect to SteppIR Yagi or loop.
38 — 30 and 40 meter balun.
39, 40 — Feed-through to 80 and 160 meter radial system.
41 — Remote motor control.
42 — Control shaft for 30 meter vacuum variable capacitor (5).
43 — Motor control relay.
44 — 160 meter balun.
45 — Manual control for 60 meter vacuum variable capacitor.
46 — Connector to 160 meter balun.

PHOTO AND ANNOTATION BARRY SHACKLEFORD, W6YE

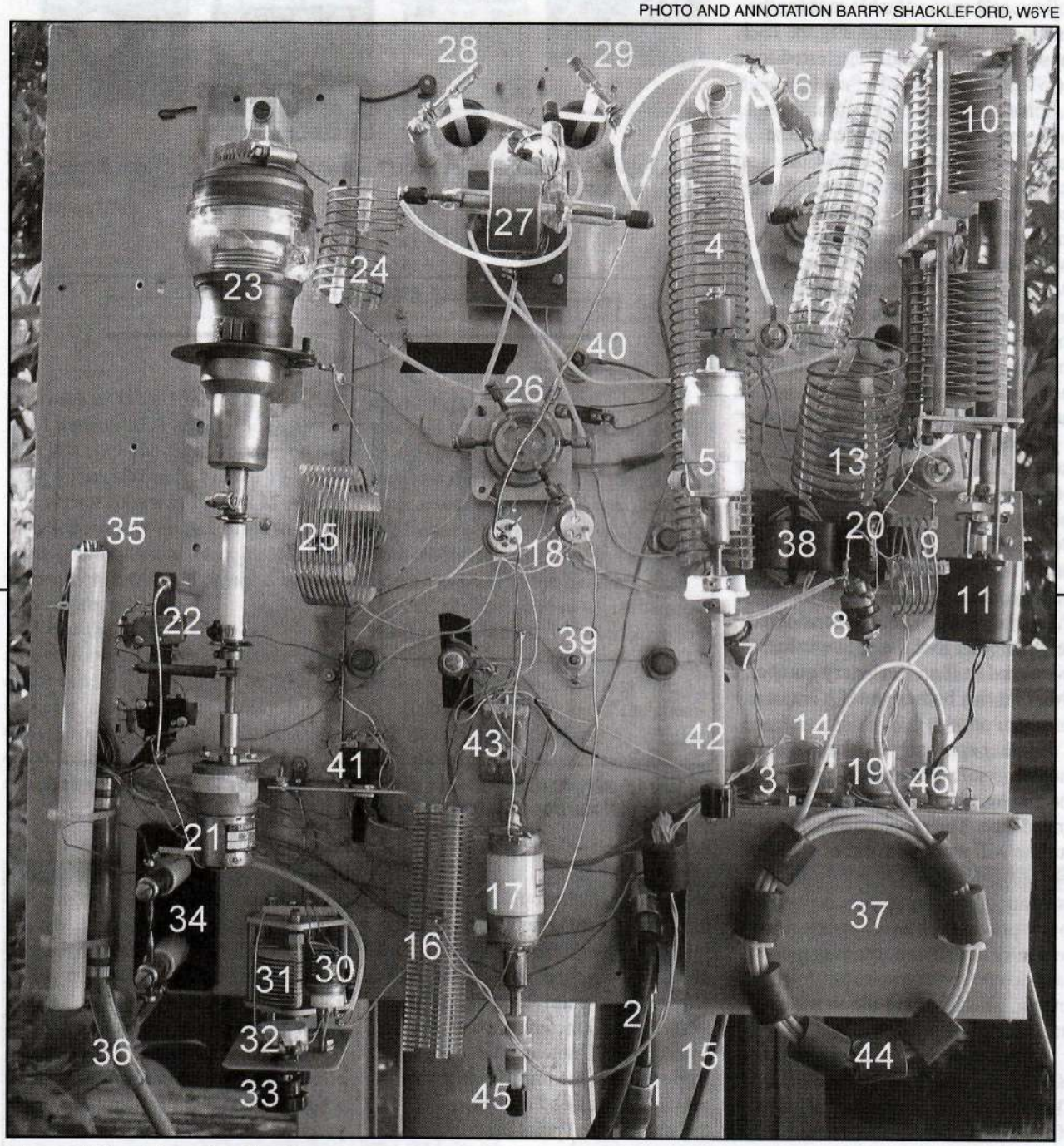

Figure 15-1 — Example of perhaps the extreme in homemade antenna tuning arrangements. This collection of remotely controlled special purpose antenna tuners, all on an outside panel (cover removed for photo), was made to switch between and tune the multiple antenna systems of the late George Badger, W6TC, the designer and builder. The annotations refer to the elements in the list below.

The tuner panel includes separate remote controlled matching networks and connections for each of the HF bands from 30 to 160 meters. It is mounted at the base of the tower. At the top of the tuner panel are two connectors that connect to the two lower ends of the 30, 40, 60, 80 and 160 meter loop that extends from the left connector up to the 5 foot fiberglass boom extension on the left, up and over the 8 foot fiberglass mast extension at the top to the boom extension on the right, then down to the right connector.

able RF generators and displays that indicate actual complex (resistive and reactive) impedance, not just SWR. These are available from a number of manufacturers for a few hundred dollars, and are a valuable tool for the antenna inclined amateur. **Figure 15-2** shows a sampling that were tested for a *QST* product review.[1]

Some analyzers provide the resistive value of the impedance and the magnitude, but not the sign of the reactive part. In order to design a matching network, it is important to know whether the reactance is positive (inductive) or negative (capacitive). Fortunately, it is usually easy to determine this. Just make a slight change in frequency and note the change in the value of reactance. If the reactance goes up as the frequency goes up it is inductive (+). If it goes down with increasing frequency, it is capacitive (–). This only works if the reactance does not go to zero between the two data points. Note that many programs use a lower case italicized letter *j* as part of the reactive value. This indicates that it should be mathematically considered perpendicular to the resistive value, or calculated as if an imaginary number. Don't let this bother you if it is not a familiar concept.

Another approach is to use antenna modeling software to determine the antenna, or the antenna system, impedance. The procedure I will outline will work with either. While modeling will result in a reasonable estimate of the impedance, it is rare that it provides an exact result, since generally not all conditions (ground parameters, for example) are fully known. This is what I did in the example that follows.

A third approach is to rely on manufacturers' or other published data. This also has its limitations in terms of the effect of the actual conditions at your location.

Figure 15-3 provides the basis for a short example of how this process can easily be conducted. The antenna under consideration is a dipole cut for the low end of the 40 meter amateur band. Instead of feeding it directly

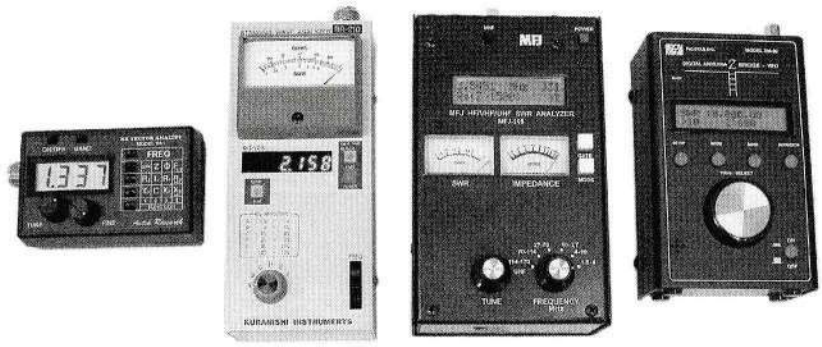

Figure 15-2 — A sampling of hand held antenna analyzers from Autek, Kuranishi, MFJ and Palstar.

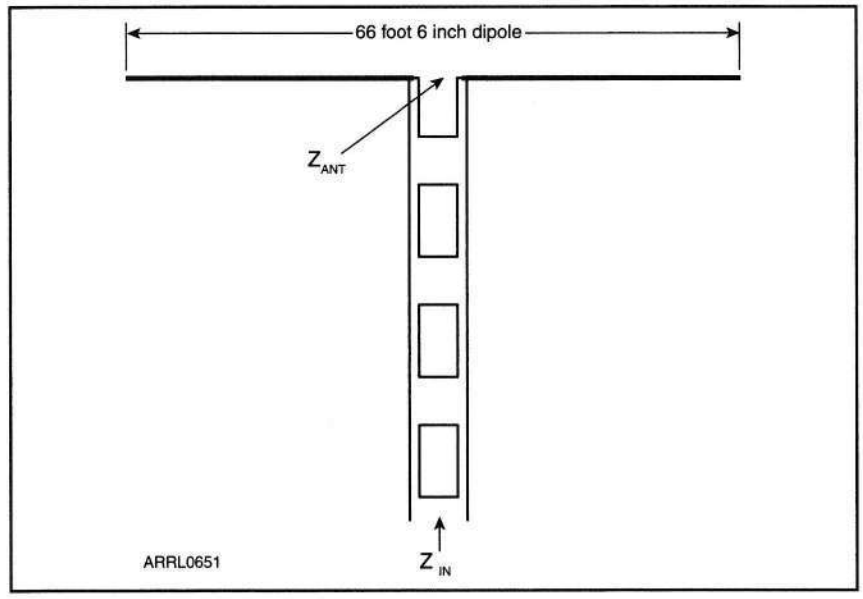

Figure 15-3 — 40 meter dipole used as the example for the determination of a special purpose matching network.

with coax, which would likely not require a matching network, we have selected to use 70 feet of nominal 450 Ω window line, so it can be fed efficiently on multiple bands. In order to use it on 40 meters, we determine (using *EZNEC* antenna modeling software) that the impedance at the center and each end of the band at the antenna feed point is as shown in **Table 15-1**.[2]

We then use the transmission line analysis program *TLW*, furnished with recent editions of *The ARRL Antenna Book*, to determine the impedance at the bottom of the mismatched transmission line as shown in **Table 15-2**.[3] Note that we could have gone directly to Table 15-2 using many antenna analysis programs that are equipped with transmission line models. My version of *EZNEC* included an early transmission line capability that did not take losses into account, so I used *TLW* instead. Since we need *TLW* for the next step, it wasn't any extra effort. One hint about using *TLW* — when finished don't just close the program window — click on the EXIT button to avoid problems with it starting properly next time.

•*Design a network that will transform the impedance to the desired impedance of the radio or transmission line.*

There are many techniques that could be employed to design a matching network to match any of the im-

1Notes appear on page 11.

Table 15-1
Impedance Predicted at the Antenna (Z_{ANT}) as Shown in Figure 15-1.

Frequency(MHz)	*Resistive Part (Ω)*	*Reactive Part (Ω)*	*50 Ω SWR*
7.0	82.3	–34.0	2.0
7.15	88.0	–0.37	1.8
7.3	94.1	+33.1	2.2

Table 15-2
Impedance Predicted at Bottom of the 70 Foot Transmission Line (Z_{IN}) as Shown in Figure 15-1.

Frequency(MHz)	*Resistive Part (Ω)*	*Reactive Part (Ω)*	*450 Ω SWR*
7.0	87.7	+82.9	4.9
7.15	103.3	+148.6	4.6
7.3	236.5	+229.7	4.3

pedances in Table 15-2 to our desired 50 Ω transmitter. Perhaps the easiest is to just click the TUNER button on the *TLW* screen shown in **Figure 15-4**. The screen shown in **Figure 15-5** will then appear, providing a place to input some common parameters including transmitter power and physical component properties.

While the design power is a straightforward parameter, some of the other terms may not be. The inductor and capacitor Q are related to the losses in the components. Typically, the biggest loss in an HF tuner, especially one with an air dielectric capacitor(s), is due to coil wire resistance. If you are buying a coil, it will likely specify the Q. If not, you can measure the impedance of the coil on your antenna analyzer at the operating frequency. The Q is just X_L/R, both available on an antenna analyzer screen.[4] Values in the hundreds are typical, and the good news is the program results are not very sensitive to the value of Q. A 100% change in Q, in this example, results in less than a 0.5% change in the value of the specified inductor and capacitor — smaller than the usual component tolerance, thus we specify a Q of 200 and the resulting design should be fine for most real inductors.

The OUTPUT STRAY CAPACITANCE value represents the capacitance of the wiring and components on the output side to the chassis. All wiring and components in the usual metal chassis or cabinet have capacitance to the metal walls. This is most important as the frequency goes up. Values in the tens of picofarads are common depending largely on component size and placement.

The other choice on this screen is the TUNER NETWORK TYPE. There really isn't too much to say about this — pick the one you like best, or better yet — try them all. I am somewhat partial to the low-pass L-network because it only has two components and provides some attenuation of harmonic signals. It also has only one solution for any load — more later. Pick any one to start, you will likely want to look at them all to find which one has components that are available or easiest to obtain.

If you pick any configuration besides the L-network, it will ask you for a value to use for the capacitor on the output side (towards antenna). It will try to design a tuner for any value you pick. If it can't make a tuner work with your value it will suggest making it larger or smaller. Make note of the power loss and try different values of output capacitor

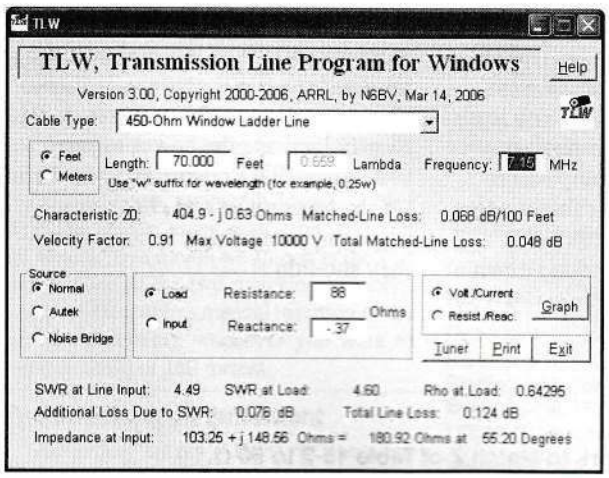

Figure 15-4 — Input screen of *TLW* transmission line analysis software used to determine the impedance at the bottom of the mismatched transmission line of Figure 15-1.

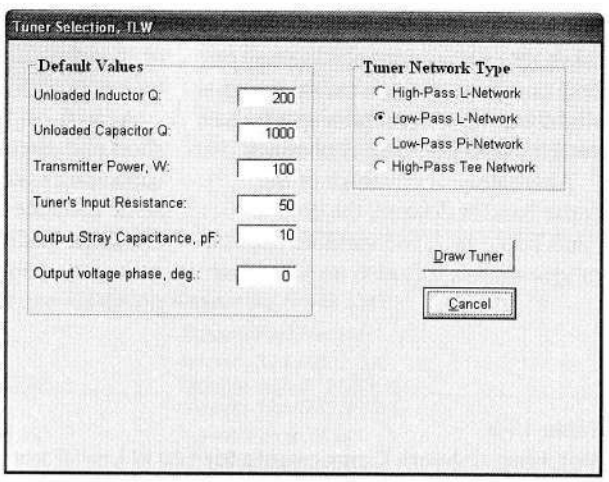

Figure 15-5 — Antenna tuner Input screen of *TLW* software. Note the tuner configuration selected, LOW-PASS L-NETWORK, the power level, 100 W, that determines component ratings as well as the other parameters as described in the text.

until you achieve a design that has an acceptable amount of loss and reasonably sized components. This illustrates the fact that the three element tuners — Pi- and T-network — have more than one set of adjustments that will provide a satisfactory match to the radio. Unfortunately, while they will all look good to the radio, some will have more loss than others.

Push the DRAW TUNER button. The screen shown in **Figure 15-6** should appear providing the design details for the low-pass L-network tuner I selected. In addition to the component values needed to provide the match, the table above the schematic provides information on component stress levels and other key data. The primary selection criterion can be found by looking at the resulting tuner designs (next paragraph) in each configuration and seeing which ones have component values that are reasonable, and even better, that you have on hand. A look at the resulting efficiency, expressed as POWER INTO LOAD, may also help you select a preferred topology.

Table 15-3 shows the resulting design for the middle and both edges of the 40 meter band. This design can be used as a starting point for a single frequency, single load, matching network. I say starting point because even with careful analysis there are a few variables that are not known exactly, including actual component values — typical tolerances are ±10% — for example. This is often taken into account by making one or both components variable, or trying slightly different component values until the desired result is obtained.

Alternately, if coverage of the entire band is desired, the components could be made variable over the ranges shown. It is also possible that the values for the middle of the band will provide a satisfactory match over at least a portion of a band without requiring change. This can be determined by trial and error, or simulated in an antenna analysis program by using modeled lumped "loads" at the bottom of the transmission line.

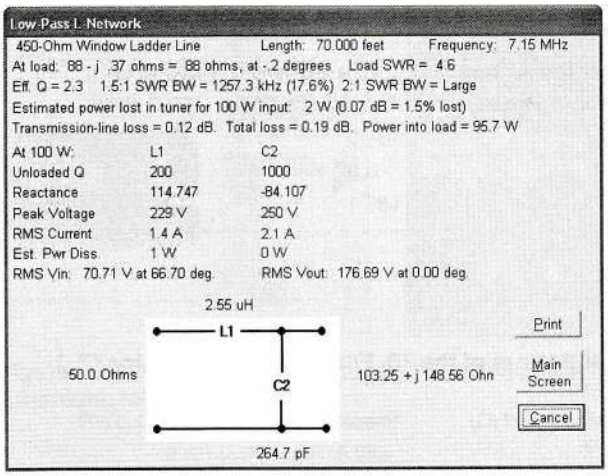

Figure 15-6 — Antenna tuner output (design) screen of *TLW* software. Note the tuner schematic with parts values shown. The data and table above provide additional important information.

•*Build and test the network.*

As noted, the hardest part is often finding the needed components, especially those needed for high power networks. Hamfest flea markets are often a good source for such items, although they often come with a level of uncertainty regarding ancestry and component value. Again, the trusty antenna analyzer can be used to measure the reactance. Fixed or tapped inductors can be easily wound using plastic rod or tubing as a form. *The ARRL Handbook* provides a source of formulae for winding the desired inductance.

As with all RF projects, keep leads short and direct. To minimize stray capacitance, keep the components some distance from the cabinet edges. Use high quality connectors and make sure you have provided direct connectivity for all needed interconnections.

The best way to test the network is to start with the antenna analyzer. With the network connected to the proper place on the transmission line, the impedance should read close to 50 Ω at the design frequency. Now take *swept frequency* type data by measuring the impedance and SWR every 25 or 50 kHz. By plotting these on a graph, you should have a good idea of what the network will do and whether or not it will work across the range. If it isn't quite right, make a small change in one value and repeat the sweep. You should see an indication of the extent and direction of the change. Since there are only two or three components, you should quickly converge on your result.

Next hook it to your radio tuned to an unused frequency and note the transceiver's SWR reading. It should be close to that of the analyzer. Slowly increase the power to just below the level you designed to. Turn off the transmitter and check to see if any components have become hot — they shouldn't!

Table 15-3
Matching Network Components for 100 W Low-Pass L-Network to Match Z of Table 15-2 to 50 Ω.

Frequency(MHz)	*Inductance (μH)*	*Inductor Current (A_p)*	*Capacitance (pF)*	*Capacitor Voltage (V_p)*	*Efficiency (%)*
7.0	1.72	1.4	339.4	181	96.1
7.15	2.55	1.4	264.7	250	95.7
7.3	3.28	1.4	205.2	317	95.4

160 and 80 Meter Matching Network for Your 43 Foot Vertical — *Part 1*

The popular 43 foot vertical works best with matching at the antenna base — here's a way to do it for our two MF bands.

Phil Salas, AD5X

I've recently made the move to a 43 foot vertical for much of my lower frequency operations. This length antenna offers higher radiation resistance than shorter loaded monopoles. Increased radiation resistance improves efficiency by reducing the effects of ground losses, especially when you have an electrically short antenna — a characteristic of even a 43 foot antenna on 160 and 80 meters. If fed with a 1:4 unbalanced to unbalanced transformer (unun), a 43 foot antenna has a reasonable compromise SWR on 60 through 10 meters, which means that cable and unun losses are pretty much negligible on these bands.

This antenna is really not a good performer on 160 meters, and to a lesser extent on 80 meters, unless you provide matching right at the antenna base. This is due to the high capacitive reactance and still relatively low radiation resistance of a 43 foot antenna on 160 and 80 meters. This makes the mismatch so bad that it is almost impossible to efficiently match from your shack. If you can match the antenna system from your shack, you will throw away a lot of power in your coax and unun due to the very bad mismatch at the antenna.

I thus started experimenting with matching networks and wound up with two external impedance matching devices designed to significantly reduce SWR related coax losses and unun mismatch losses, and to help the inside tuner match on 160 and 80 meters. This month we'll look at the simpler version of the two matching networks. This version requires manual insertion of the matching network whenever you want to operate on 80 or 160 meters.

The Matching Requirement

According to my AIM4170C antenna analyzer, my 43 foot vertical antenna has a capacitive reactance of about 580 Ω on 160 meters. This will vary based on the particular construction of your 43 foot vertical, its proximity to other objects, and other factors. The reactance will almost certainly be in the 550 to 650 Ω range. This amount of capacitive reactance needs approximately 50 μH of inductance in order to resonate the antenna. On 80 meters, approximately 9 μH is needed to resonate the antenna. A 50 μH high Q inductor is going to be large. For this first solution, I elected to go with a toroidal inductor in order to keep the matching unit as compact as possible.

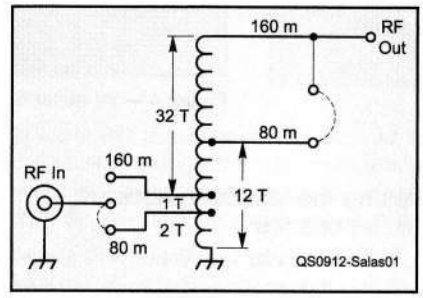

Figure 1 — Schematic diagram of the two band matching unit. 80 meter connections shown with dashed lines.

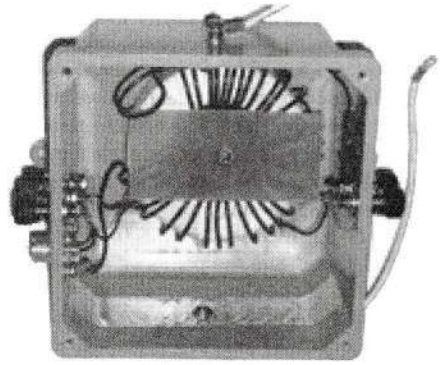

Figure 2 — T400A-2 160 and 80 meter matching unit.

Toroid Inductor Matching Solution

This compact design will handle the full legal limit on 80 and 160 meters for low duty cycle SSB and CW modes. The inductor consists of 35 turns of #14 AWG solid copper insulated house wiring wound on a T400A-2 toroid core. The antenna feed point is tapped two turns from the ground end for 80 meters, and three turns from the ground end for 160 meters. You should start with 38 turns total on your toroid, but then remove turns as necessary to get the network to resonate where you want it in the 160 meter band (more on this later).

I mounted the toroid assembly in a 6 × 6 × 4 inch NEMA enclosure using a 2½ inch long #10 machine screw and associated hardware along with a 2 × 4 inch piece of unplated fiberglass PC board material. Before you mount the toroid, prepare

Table 1
160 Meter Toroid Impedance Matching Assembly Parts List

Description	*Source/Part Number**
Banana plug (4 required)	Mouser 174-R802-EX
Binding post, black (4 required)	Mouser 164-R126B-EX
Binding post, red	Mouser 164-R126R-EX
NEMA Enclosure, 6 × 6 × 4 inch	Lowes/Home Depot
Glass cloth tape, 3M #27	ACE Hardware
SO-239 connector	Mouser 601-25-7350
Toroid, T400A-2 powdered iron	Amidon T400A-2

*Amidon parts are available from **www.amidoncorp.com** and Mouser parts from **www.mouser.com**.

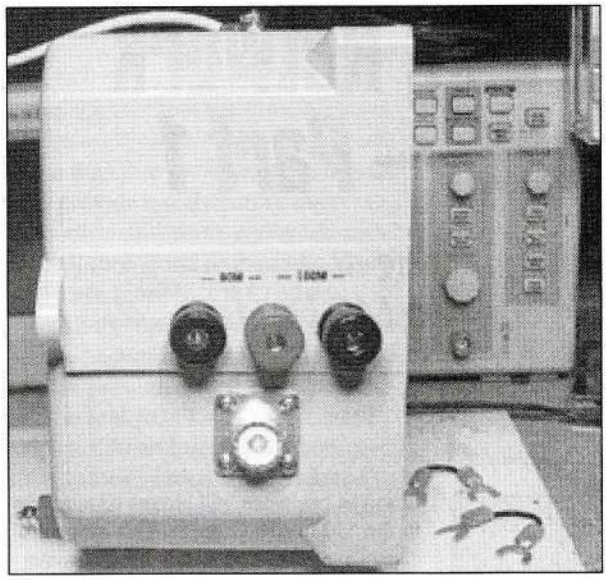

Figure 3 — 160 and 80 meter input tap points.

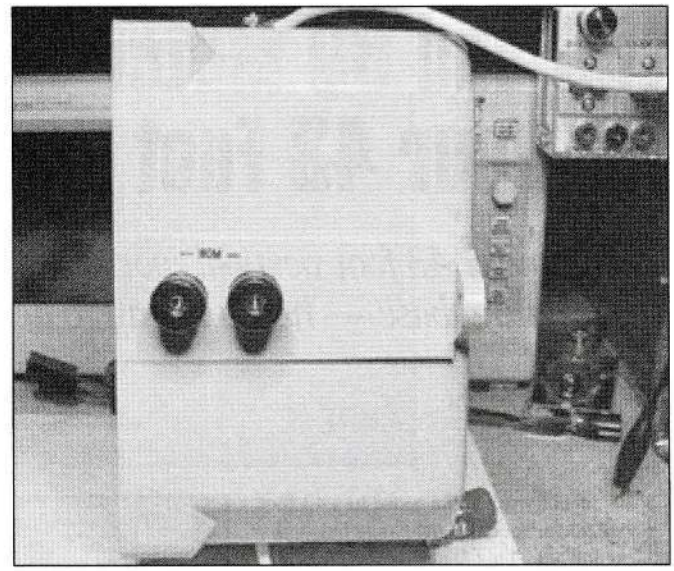

Figure 4 — 80 meter coil shorting jacks.

it by scraping the insulation off the outside second, third and 11th through 13th wire turns. Because of the high voltages possible at legal limit power levels, especially on 160 meters, wrap the toroid with two layers of 3M #27 glass cloth electrical tape for added insulation between the #14 AWG wires and the toroid core.

Figure 1 is the schematic of the matching assembly, Figure 2 shows the internal details of the assembly, and Table 1 lists the parts necessary. To select between 160 and 80 meter operation, I used external jumpers across binding posts as shown in Figures 3 and 4. Stainless steel #8 hardware (screws, washers, lockwashers and nuts) are used for the matching unit ground and RF output terminals. Internal to the matching unit, I used a 2 inch wide strip of aluminum duct repair tape as a good low impedance ground between the UHF connector and the ground screw on the bottom of the case. Finally, I used #14 AWG stranded insulated wire for all internal connections.

Tuning the Matching Network to Resonance

Your particular installation will almost certainly require you to change the resonant frequency of the matching network. This is because there will be some variations of the antenna impedance based on your particular antenna physical construction, proximity to other objects and final length, as well as your desired operating frequency range. The design is such that the overall inductance is too large for 160 meters, so the network should resonate at or below the lower band edge. Therefore, you will need to remove one or more of the upper inductor turns in order to resonate the network for the desired frequency on 160 meters.

To do this, first solder wires from the second and third turn tap points on the coil to the two outer binding posts by the SO-239 connector. The input tap points tend to be fairly noncritical and will probably be the same for all installations. Now solder a short wire from the SO-239 center pin to the middle binding post. Next, externally jumper the middle binding post to the 160 meter binding post (third turn).

Connect the matching assembly to the base of your 43 foot vertical and see where the minimum SWR point is on 160 meters using your antenna analyzer. If the resonant frequency is too low, remove a turn of wire and see where the minimum SWR point is again. You'll see about a 50 kHz upward move in frequency per turn of wire removed. When you have your desired resonant point on 160 meters, it is time to move to 80 meters. Externally jumper the input tap middle binding post to the 80 meter binding post (second turn), and use a clip lead to short from the top of the coil to turn number 12 and see where your minimum SWR frequency occurs. Move the tap point up or down until your resonance point (lowest SWR) is where you want it. Solder a wire from this tap point to one of the binding posts. Solder another wire from the top of the coil to another binding post. Now you will be able to externally jumper these binding posts to select either 160 or 80 meters.

My final test results for 160 and 80 meters are shown in Figures 5 and 6 as measured with my RigExperts AA-200 antenna analyzer connected directly to the matching network input at the base of the antenna. I'm a CW operator, so I favor resonance in the lower part of these bands, but you can adjust for your favorite portion of each band. The 2:1 SWR bandwidth on 160 meters is about 50 kHz, and about 150 kHz on 80 meters. Even a 3:1 SWR on these bands results in negligible SWR related cable losses for any reasonable length cable and is easily matched with my MFJ-998 in-shack tuner or most transceivers' internal tuners.

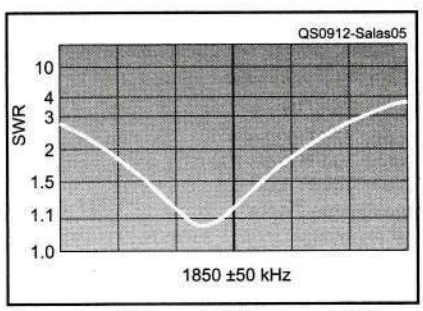

Figure 5 — Measured SWR across 160 meters indicating a 2:1 SWR bandwidth of approximately 50 kHz.

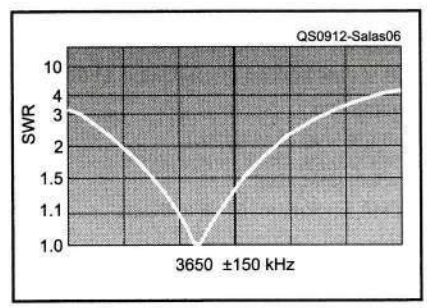

Figure 6 — SWR across 80 meters indicating a measured 2:1 SWR bandwidth of about 150 kHz.

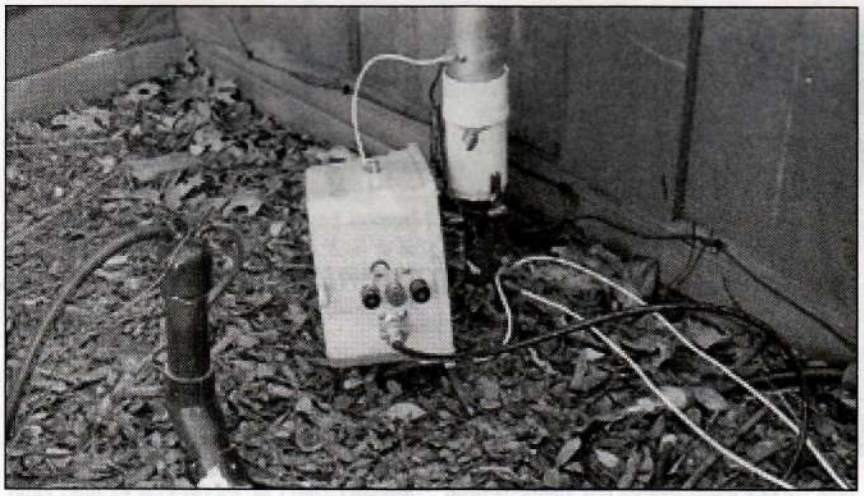

Figure 7 — Matching unit at the base of the author's 43 foot antenna. In this view, it is strapped for 80 meters.

Operation

Using the matching unit is simple. Just disconnect your normal unun when you want to operate on 160 or 80 meters and connect this matching unit to the base of the antenna. Select either 160 or 80 meters with the external straps. You can connect both the unun and this matching unit to the antenna at the same time, and just leave off the ground wire from the unit that is not used. The matching unit connected to the base of my 43 foot vertical is shown in Figure 7.

Conclusion

The matching network discussed in this article will permit very effective operation of your 43 foot vertical on the 160 and 80 meter bands. In Part 2, we'll look at a remotely switchable 160, 80 and 60 through 10 meter base matching unit. It is more complex, but it is also more convenient. Until then, see you on top band!

Amateur Extra class operator and ARRL Life Member Phil Salas, AD5X, was first licensed as WN3BCQ in 1964. Ham radio became the reason he subsequently pursued a career in electrical engineering. Phil earned BSEE and MSEE degrees from Virginia Tech and SMU, respectively, and worked in new product development for the next 33 years. Phil is now retired and spends his days split between ham radio related projects and enjoying time with his wife, Debbie, N5UPT. You can reach Phil at 1517 Creekside Dr, Richardson, TX 75081 or at **ad5x@arrl.net**.

160 and 80 Meter Matching Network for Your 43 Foot Vertical — *Part 2*

This dual band matching section design provides for remote band changing.

Phil Salas, AD5X

In Part 1, I described a simple 160 and 80 meter base matching assembly for a 43 foot antenna. While that unit is very effective and inexpensive to build, it is also a little inconvenient in that you must connect it when it is needed, and you must also manually enable 160 or 80 meter operation using straps. This month, we'll look at a more versatile matching assembly that is completely remote-controllable for operation on all bands. Again, this base matching network will significantly eliminate SWR-related coax losses and unun mismatch losses, and assist inside tuners in providing a match on 160 and 80 meters.

The All Band Matching Solution

As discussed in Part 1,[1] a 43 foot vertical antenna requires approximately 50 µH of inductance to resonate the antenna. On 80 meters, approximately 9 µH is needed for resonance. For the matching solution shown in Figure 1, I used an MFJ 404-0669 air wound coil and two Array Solutions RF-30 relays for up to full legal limit matching on all bands from 160 to 10 meters. A 2.1 × 5.5 mm dc power jack located below the SO-239 connector provides for relay control voltage inputs of 0 V, +12 or –12 V dc. The control input MOVs and bypass capacitors are mounted on a 6 terminal strip inside the matching assembly.

The matching unit operates as follows: With no control voltage applied, the inductor is disconnected and the unun is connected across the antenna feed point thereby preserving the original compromise SWR on 60-10 meters.

When +12 V is applied, the inductor is connected across the antenna feed point and inductor turns are shorted to resonate the antenna on 80 meters.

When the voltage is reversed, the short across the coil is removed and the matching section resonates the antenna on 160 meters. In both the 160 and 80 meter cases, the unun secondary taps into the inductor at the 200 Ω point, providing a proper match to the unun on these bands. This keeps the unun secondary voltage reasonable, and the feed line and unun losses very low as well.

I built the matching unit into an 8 × 8 × 4 inch NEMA weatherproof box available from home supply stores (see Figure 2). This box is too small to fit the entire inductor length needed, so I split the inductor into two pieces as can be seen in Figure 1. The long inductor section consists of 61 turns, and the short inductor section consists of 12 turns. While I preferred the more compact size of this box, you may wish to use the larger 12 × 12 × 4 inch NEMA box that can contain the full uncut inductor length needed.

All internal wiring uses insulated #14 AWG stranded wire. I attached the wires to the coil tap points using the MFJ coil clips called out in the parts list. You can solder the wires directly to the coil, but this is difficult due to the #12 AWG size of the coil wire and the spacing of the turns. The coil is mounted with #8 stainless steel screws, washers, lock washers and nuts also used for the ground and antenna feed terminals. Figure 1 shows the final matching unit with all components mounted. Note the terminal strip with the MOVs and bypass capacitors.

Since the antenna is unbalanced, a current balun or voltage unun is typically used. A voltage unun should be wired as shown in Figure 2.

Relay Connections

Some comments are necessary regarding the relay connections. See the sidebar on the *QST* binaries Web site for a discussion of how high the peak voltage across the full coil can be on 160 meters. As you can see, I connected relay contacts in series to increase the overall breakdown voltage. Also, the tap points on the inductor provide additional voltage above ground, which helps with the overall breakdown voltage.

The main concern is with the contact-to-coil 5.3 kV peak breakdown rating. When I examined the relays, I observed that the outer SPDT contacts are connected via insulated internal wires that are well separated from the coil by 0.1 to 0.2 inches. The problem is with the center SPDT relay common wire, which is in contact with the coil. While the coil and common wire are both insulated, there is no air-gap separation between them. This common wire-to-coil contact is obviously what

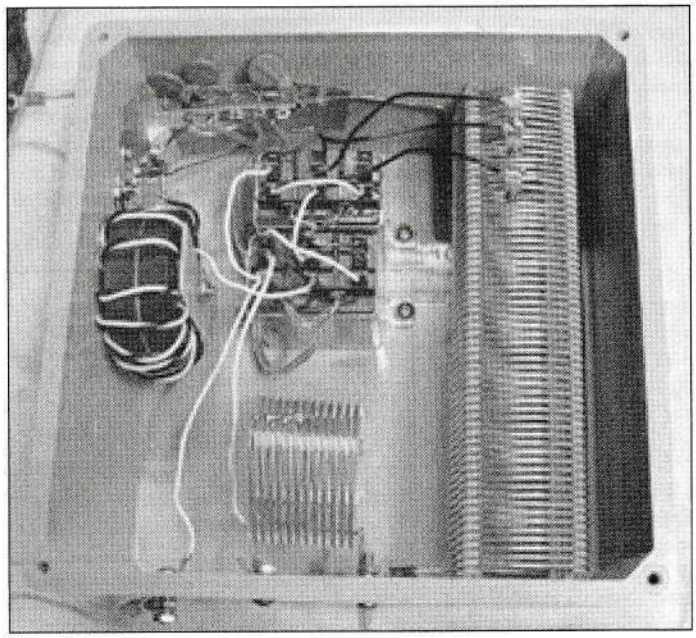

Figure 1 — All parts mounted in the NEMA enclosure.

[1]Notes appear on page 35.

determines the breakdown voltage rating. The way I got around this problem was to use the center SPDT relay contacts for the lowest potential interfaces as indicated in the schematic (Figure 2).

For the switched control voltage input, I used a 12 V, 1 A wall wart to keep the +12 V control voltages separate and isolated from the regular station voltage. This is to eliminate any possibility of shorting the main power supply when the control voltage polarity is flipped.

I mounted the switch in a small plastic box that I attached to my transceiver support shelf. The unlabeled center-off position is for 60 through 10 meter operation. The separate switch you see in the photo is for controlling other outdoor accessories, as I have two voltage feeds going out to my antenna location.

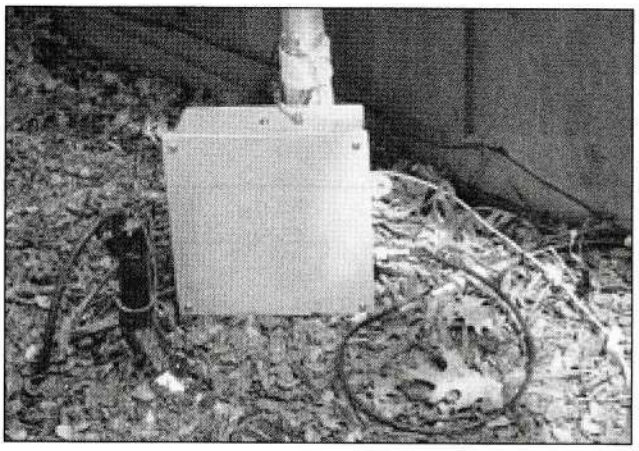

Figure 3 — The completed all band remotely controlled switching and impedance matching network mounted at the antenna base.

Matching Network Resonance

As with the previous matching network, you will almost certainly need to adjust the resonant frequency of the matching network due to variations in particular antenna physical construction, proximity to other objects and final length, as well as your desired operating frequency range. The overall starting inductance is too large for 160 meters, so the network will resonate at or below the lower band edge. Therefore, you can simply short one or more of the upper (short coil) inductor turns in order to tune the network higher to your desired 160 meter frequency.

To do this, first leave off the wire leads that attach between the relay contacts and the tap points on the coil. Build up short jumpers using the test-clips and micro-clips (perfect for the coil turn taps) called out in the parts list, and attach these between the relay contacts and coil, using the suggested tap points shown on the schematic.

Connect the matching assembly to the base of your 43 foot vertical (see Figure 3). Then enable 160 meter operation by applying –12 V dc, and jumper turns on the 12 turn inductor with a short clip lead until you find your desired 160 meter resonance point. Next, move the 160 meter relay tap point until you get minimum SWR. Now permanently short the turns on the short coil by soldering a piece of #16 AWG buss wire across these turns.

As you can see from my photos, I needed to short six turns on this coil. Next enable 80 meter operation (apply +12 V to the relays assembly) and select the coil shorting point for your desired resonant frequency and the tap point for best SWR. Finally remove the test clips leads, attach the coil clips, and solder wires between the coil clips and relay.

The 2:1 SWR bandwidth on 160 meters is about 50 kHz, and about 150 kHz on 80 meters. Even a 4:1 SWR on these bands results in negligible SWR related cable and unun loss, and is easily matched with my MFJ-998, an in-shack tuner.

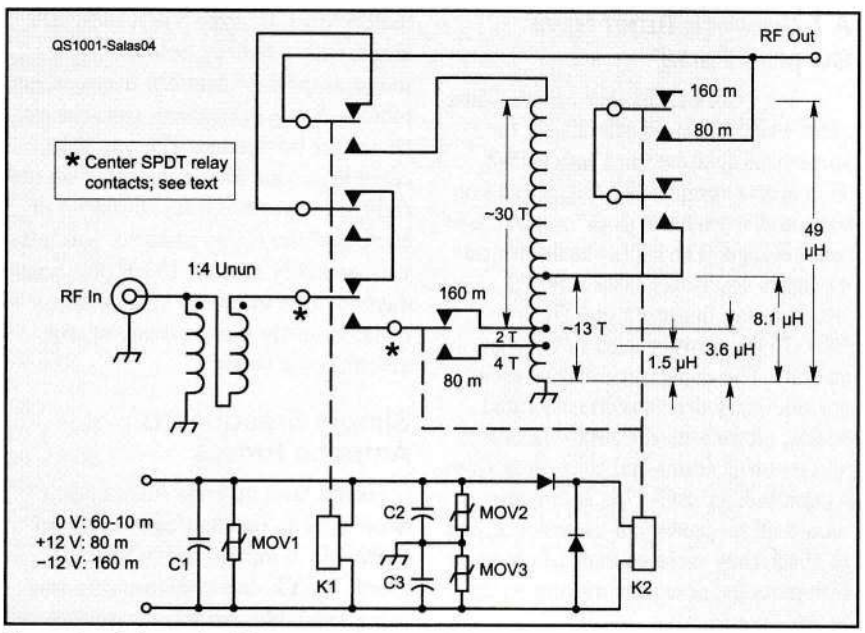

Figure 2 — Schematic of the remotely controlled matching network. The parts list is on the QST binaries version.[2]

Operation

Operation of this matching unit couldn't be simpler. When no control voltage is applied, the antenna functions as it always has on 60 through 10 meters. For 80 meter operation, apply +12 V dc, and for 160 meter operation apply –12 V dc. The matching unit connected to the base of my 43 foot vertical is shown in Figure 10.

Conclusion

The matching network discussed in this article will permit very effective operation of your 43 foot vertical on all bands from 160 through 10 meters. Although on 10, 12 and 15 meters the elevation angle of the peak is higher than optimum for DX, it will still allow contacts. Feel free to experiment a little. You might prefer to use the toroid from Part 1 in this design instead of the air-core inductor. If you are not running more than about 500 W, the less expensive RF-10 relays are all you will need. Have fun, and I'll see you on the low bands.

Notes

[1]P. Salas, AD5X, "160 Meter Matching Network for Your 43 Foot Vertical — *Part 1*," *QST*, Dec 2009, pp 30-32.

[2]**www.arrl.org/files/qst-binaries**.

See Part 1 for Phil's bio. You can reach Phil at 1517 Creekside Dr, Richardson, TX 75081 or at **ad5x@arrl.net**.

Home Built General Purpose Tuners

There are a number of approaches to the design and construction of general purpose antenna tuners. Perhaps the easiest is to replicate existing successful designs, although finding the exact parts called for is sometimes a problem. Fortunately, the exact values are not very critical. It is also possible, if somewhat tedious, to go through the *TLW* based procedure described above at the extremes of frequency and mismatch to determine the range of values needed and then construct a tuner with variable and/or switched elements, often in combination, that will cover the needed range.

I have done this for the most popular configurations, see **Figure 15-7**, the high-pass T-network, Pi-network and low pass L-network with the results shown in **Tables 15-4** through **15-6**. I have provided the values for matching loads with a 10:1 SWR, the usual spec for a wide range tuner. In addition to the resistive loads at 5 and 500 Ω, I have made runs for moderate reactive loads of 25 ± *j*25 Ω and extreme reactive loads of 250 ± *j*250 Ω, all with approximately a 10:1 SWR.

As noted in Chapter 4, the Pi- and T-network tuners have multiple solutions for any load, while the L-network has a single solution. It is worth stressing this in case you use one, whether a commercial unit or a home-built one. Look again at Table 4-1, in Chapter 4, to get the idea.

Such "HF" tuners sometimes include the MF 160 meter amateur band as well as the 80 through 10 meter HF bands. I have provided data for 160, 80 and above the top of 10 meters so you can decide which way you want to go. Note that the addition of 160 meters makes a big difference in the component values required, one reason it often is not included. In addition, in some cases the larger inductor and capacitor(s) may have too high a minimum value to allow proper operation on 10 meters.

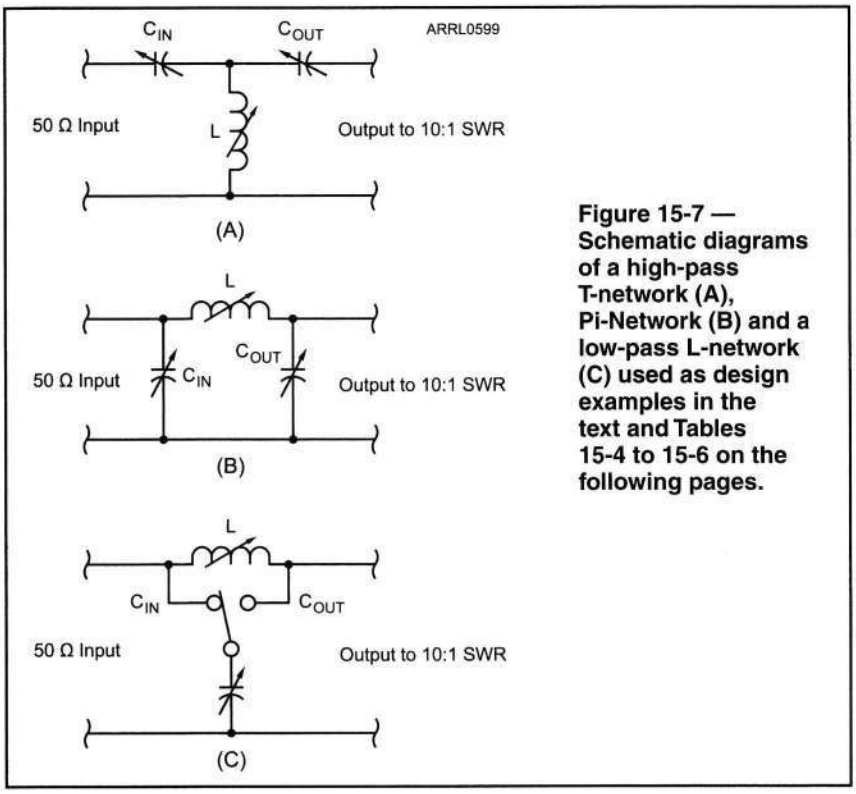

Figure 15-7 — Schematic diagrams of a high-pass T-network (A), Pi-Network (B) and a low-pass L-network (C) used as design examples in the text and Tables 15-4 to 15-6 on the following pages.

A T-Network Tuner from Surplus Parts

A T-network tuner that I made some years back and used effectively for some time is shown in **Figure 15-8**. This is an example of a "use what you have and see what it does" approach to tuner design. The unit is built around a chassis and panel from a WW2 surplus plug in tuning unit from a BC-375 transmitter used in bomber aircraft. The capacitor controls nice 4:1 planetary drives with calibrated scales, along with the rotary indicator and its turns count dial also came from a cannibalized BC-375. Today they would all be preserved as antiques, but in 1965, they were sources of cheap or free parts for new transmitting equipment.

Figure 15-9 shows the inside of the tuner, including a home built "Monimatch Mark II" type SWR indicator, along with a battery holder for the meter amplifier.[5] Modern transceivers include SWR indication, so these may no longer be needed. The variable capacitors, one above the other on the right side, were of a few hundred pF each, and the rotary inductor (on left) was probably around 15 μH. In those days, no one knew for sure — but it successfully matched any of my antennas for years.

Simple Breadboard Antenna Tuners

Home-built antenna tuners don't need to be as mechanically complex as my old T-match. Barry Shackleford, W6YE, has constructed a few using available variable capacitors and inductors fabricated in his workshop. While these won't handle full power,

Table 15-4

Component Requirements for High-Pass (Shunt L) T-Network Antenna Tuners at 10:1 SWR

Frequency/Z (Ω)	*Capacitor*		*Inductor (μH)*	*Capacitor Voltage (V_p)*		*Efficiency (%)*
1.8 MHz	*Input (pF)*	*Output (pF)*		*100 W*	*1500 W*	
5	1136	3000	2.1	180	710	96
500	548	500	13.9	323	1250	98
25 + *j*100	343	300	10.3	790	3070	92
25 – *j*100	170	300	20	1040	4030	86
250 + *j*250	308	200	10.5	380	1470	98
250 – *j*250	337	300	16.9	525	2030	96
Frequency/Z (Ω)	*Capacitor*		*Inductor (μH)*	*Capacitor Voltage (V_p)*		*Efficiency (%)*
3.5 MHz	*Input (pF)*	*Output (pF)*		*100 W*	*1500 W*	
5	563	1500	1.1	190	720	96
500	265	200	7.3	343	1330	98
25 + *j*100	275	200	3.5	613	2373	95
25 – *j*100	104	200	8.6	880	3403	88
250 + *j*250	333	100	5.6	381	1475	98
250 – *j*250	136	100	10.8	670	2600	94
Frequency/Z (Ω)	*Capacitor*		*Inductor (μH)*	*Capacitor Voltage (V_p)*		*Efficiency (%)*
30 MHz	*Input (pF)*	*Output (pF)*		*100 W*	*1500 W*	
5	79	200	0.12	160	640	96
500	29	50	0.77	370	1470	97
25 + *j*100	91	30	0.24	400	1560	98
25 – *j*100	24	100	0.46	440	1710	93
250 + *j*250	36	100	0.9	300	1150	98
250 – *j*250	29	100	0.6	360	1410	97

Table 15-5

Component Requirements for Low-Pass (Series L) L-Network Antenna Tuners at 10:1 SWR

Frequency/Z (Ω)	*Capacitor*		*Inductor (μH)*	*Capacitor Voltage (V_p)*		*Efficiency (%)*
1.8 MHz	*Input (pF)*	*Output (pF)*		*100 W*	*1500 W*	
5	5254	n/a	1.34	100	390	98
500	n/a	536	13.5	310	1210	98
25 + *j*100	n/a	1408	12	290	1120	98
25 – *j*100	1760	n/a	11	100	390	97
250 + *j*250	n/a	713	13	310	1210	98
250 – *j*250	n/a	359	13	310	1210	98
Frequency/Z (Ω)	*Capacitor*		*Inductor (μH)*	*Capacitor Voltage (V_p)*		*Efficiency (%)*
3.5 MHz	*Input (pF)*	*Output (pF)*		*100 W*	*1500 W*	
5	2700	n/a	0.69	100	400	98
500	n/a	275	6.8	310	1200	98
25 + *j*100	n/a	720	6.2	290	1120	98
25 – *j*100	926	n/a	5.6	100	390	97
250 + *j*250	n/a	367	6.8	310	1210	98
250 – *j*250	n/a	184	6.8	310	1210	98
Frequency/Z (Ω)	*Capacitor*		*Inductor (μH)*	*Capacitor Voltage (V_p)*		*Efficiency (%)*
30 MHz	*Input (pF)*	*Output (pF)*		*100 W*	*1500 W*	
5	315	n/a	0.08	100	390	98
500	n/a	32	0.79	310	1210	98
25 + *j*100	n/a	85	0.72	290	1120	98
25 – *j*100	140	n/a	0.58	100	390	97
250 + *j*250	n/a	43	0.79	310	1210	98
250 – *j*250	n/a	22	0.79	310	1210	98

Table 15-6
Component Requirements for Low-Pass Pi-Network Antenna Tuners at 10:1 SWR

Frequency/Z (Ω)	*Capacitor*		*Inductor (μH)*	*Capacitor Voltage (V_p)*		*Efficiency (%)*
1.8 MHz	*Input (pF)*	*Output (pF)*		*100 W*	*1500 W*	
5	5256	500	1.4	100	390	98
500	2602	1000	9.6	310	1200	96
25 + *j*100	966	1500	12.5	280	1110	97
25 – *j*100	3410	500	7.5	280	1100	96
250 + *j*250	1931	1000	11.3	310	1210	97
250 – *j*250	1284	500	12.9	310	1210	97
Frequency/Z (Ω)	*Capacitor*		*Inductor (μH)*	*Capacitor Voltage (V_p)*		*Efficiency (%)*
3.5 MHz	*Input (pF)*	*Output (pF)*		*100 W*	*1500 W*	
5	2706	500	0.7	100	390	98
500	1287	500	5.1	310	1200	96
25 + *j*100	643	800	6.2	280	1110	97
25 – *j*100	1886	300	3.7	280	1430	95
250 + *j*250	934	500	6.0	310	1200	97
250 – *j*250	859	300	6.2	310	1200	97
Frequency/Z (Ω)	*Capacitor*		*Inductor (μH)*	*Capacitor Voltage (V_p)*		*Efficiency (%)*
30 MHz	*Input (pF)*	*Output (pF)*		*100 W*	*1500 W*	
5	321	200	0.08	100	390	98
500	118	50	0.7	310	1200	97
25 + *j*100	103	100	0.7	290	1100	97
25 – *j*100	205	30	0.5	285	1100	96
250 + *j*250	71	50	0.8	310	1200	97
250 – *j*250	77	30	0.8	310	1200	97

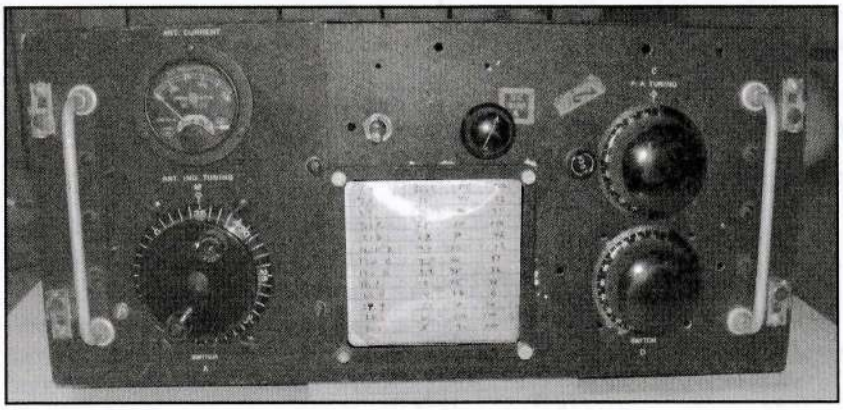

Figure 15-8 — Front view of an early homemade antenna tuner. The unit is completely built of surplus parts. Note the handy tuning chart that was part of the BC-375 transmitter tuning drawer.

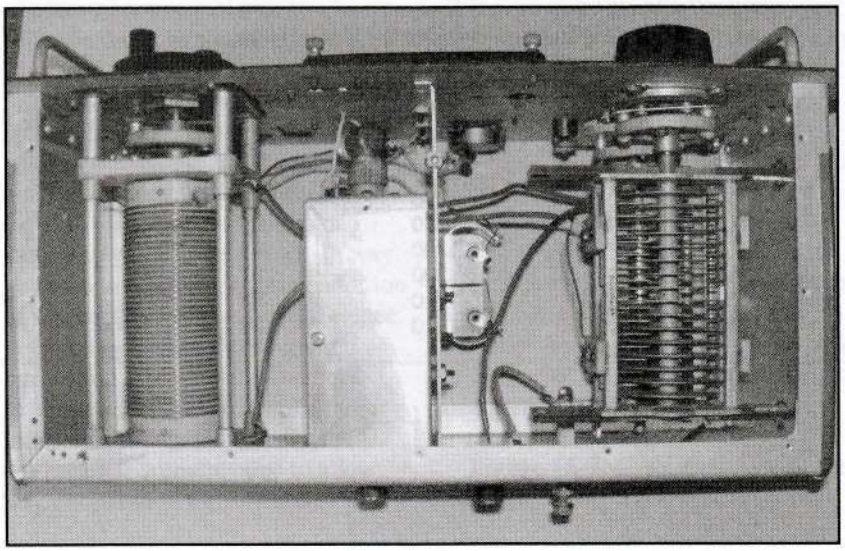

Figure 15-9 — Inside view of the home brew T-network tuner. The SWR meter (in 2 × 2 × 5 inch box in left partition) and associated circuitry would likely not be needed to use with current transceivers.

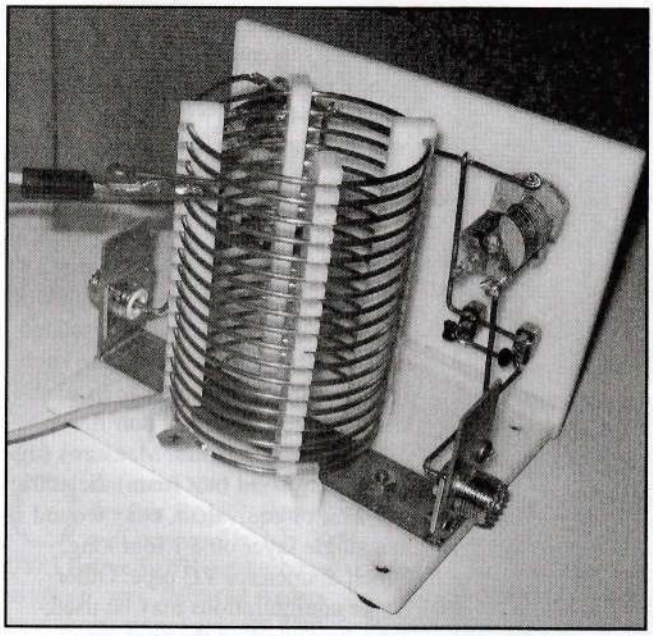

Figure 15-10 — Homebrew breadboard T-network tuner made by Barry Shackleford, W6YE. This tuner uses smaller variable capacitors with a voltage rating appropriate for 100 W use. The inductor was homemade, as described in the text. Note the inductance can be changed by moving (with transmitter off) the alligator clip to a different turn.

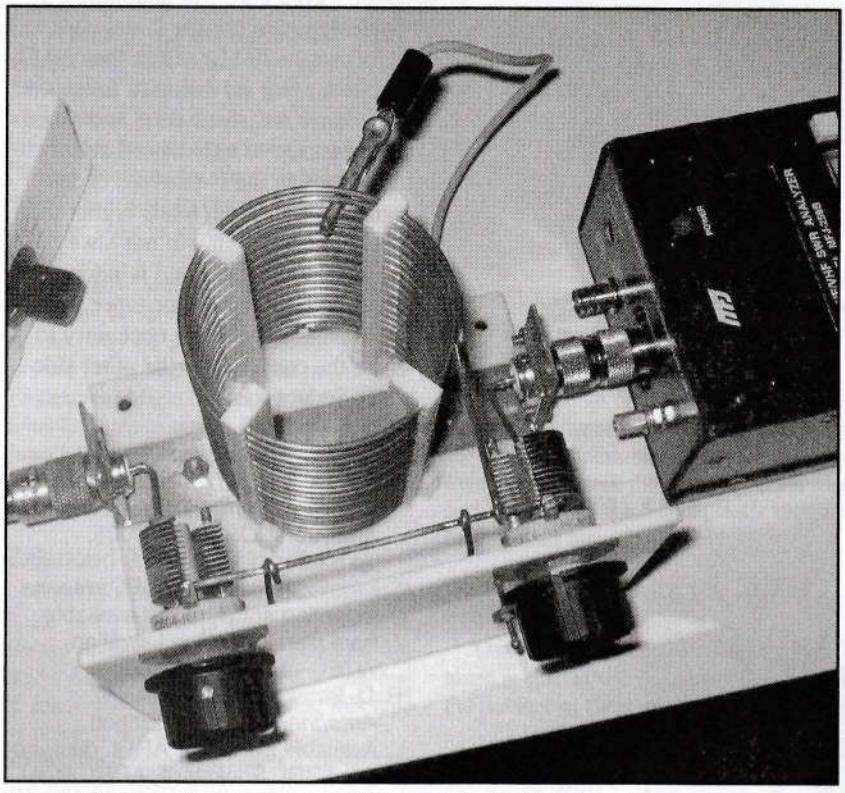

Figure 15-11 — Another view of Shackleford's T-network tuner.

they should be fine at the 100 W level. **Figures 15-10** and **15-11** show a T-network tuner that Barry made. Note the simplicity of construction. The only complication may be the homemade inductors. Barry used acrylic stock, cut and notched with his table saw, using a jig to set the spacing. You could use any technique that allowed the turns to be spaced so that his alligator clip tuning method can be employed. Barry stretched the wire before winding to work harden it and then secured it in his form with hot glue.

Barry also made the L-network tuner shown in **Figure 15-12**. This uses two capacitors in parallel, one an old broadcast three-gang unit, making up the single capacitor for the L-network. The smaller capacitor makes it easy to make fine adjustments, once you're close with the larger unit.

Making Tuners for Balanced Loads

Many tuners; home made as well as commercial units, provide for balanced loads by including a balun between an unbalanced tuner and the balanced load. This is an appropriate approach if the load is within perhaps 4:1 of the typical 200 to 50 Ω balun often used for the purpose. If beyond that range, the balun does not perform very well and losses and even damage may result.

A different approach was presented by Richard Measures, AG6K, in a *QST* article some years back.[6] Measures presented a design that first transformed the balanced antenna system load to 50 Ω balanced and then made the transition from balanced to unbalanced using a 1:1 choke balun operating at its design impedance.

Measures used a balanced L-network to perform the transition to 50 Ω and followed it with a coax choke. The schematic is shown in **Figure 15-13**, with a photo of his breadboard version, less balun, in **Figure 15-14**. He went on to show an elegant design suitable for remote control using stepper motors with remote position indicators, available on the ARRL members Web site. However, for many, a duplication of his breadboard design may be more feasible.

Measures found that inductors in the range of 15 to 20 μH maximum inductance were suitable, with a 5 A current rating for 1.5 kW use. Inductors may be found at hamfests, or are available from MFJ (**www.mfjenter-**

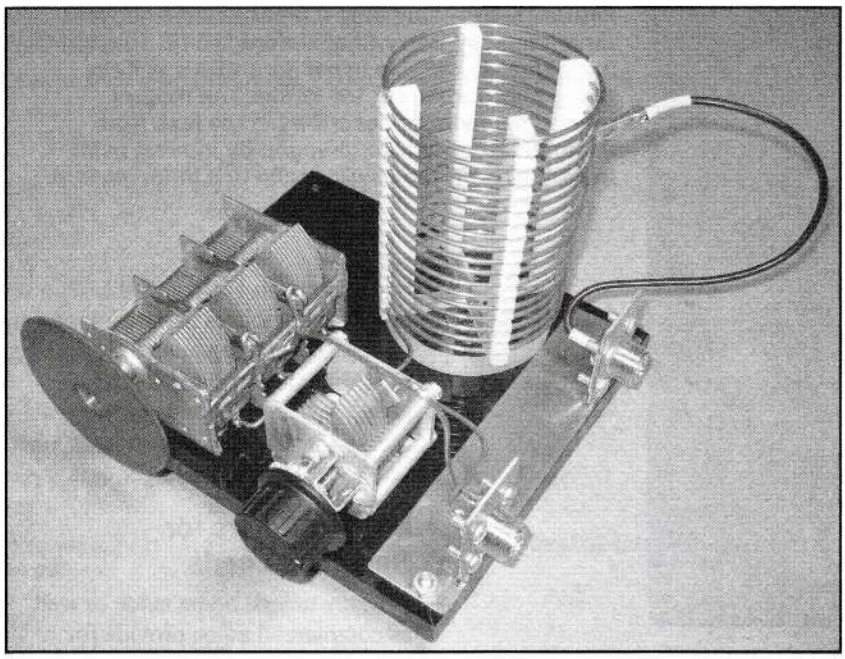

Figure 15-12 — An L-network tuner made by Barry Shackleford, W6YE. The two capacitors are in parallel making a single equivalent capacitance with the smaller one used for fine adjustment.

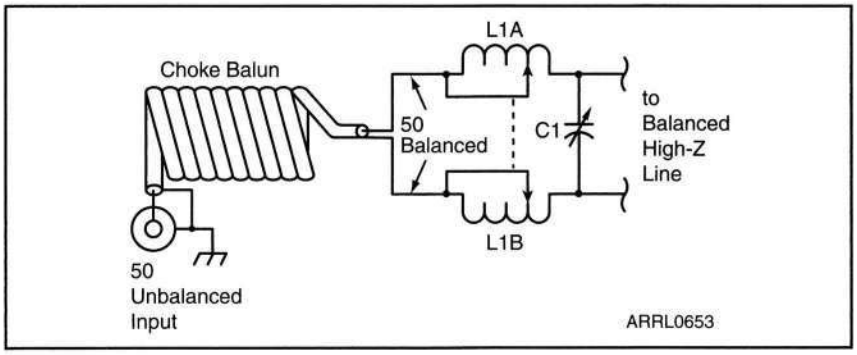

Figure 15-13 — The balanced L-network tuner designed by Richard Measures, AG6K.

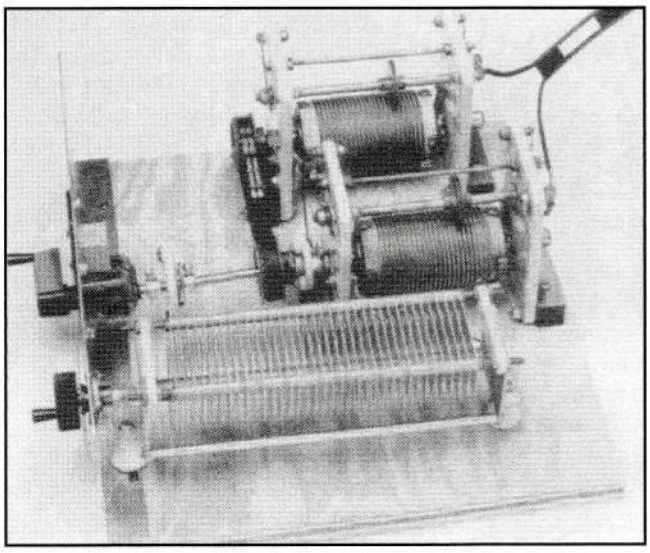

Figure 15-14 — Photo of Measures' balanced L-network tuner. The choke-balun is not shown.

prises.com). Suitable sprockets and drive belts to couple the inductors together are available from McMaster-Carr (**www.mcmaster.com**), or they may be coupled end-to-end with some loss of symmetry.

Capacitors should be in the 200 to 300 pF range, with a 1.5 kV rating if used at the 1.5 kW level. Note that both sides of the capacitor are hot with RF, so to avoid burns use an insulated shaft coupling on the way to the knob. Trust me, the set screw in an insulated knob will get you if you don't!

For the choke balun, Measures suggests using solid (not foam) dielectric RG-213, or equivalent, coax wound in a single layer on a 1 foot long, 5 inch diameter, PVC pipe. Other choke configurations may be used, including winding the coax on a ferrite toroid core. An adaptation of the design is to use the L-network to transform to 200 Ω, rather than 50 Ω, and then use a 4:1 balun to finish the impedance transformation and make the transition to unbalanced coax.

As shown, the L-network is designed to transform loads higher then 50 Ω. This is often, but not always the case with ladder and window line systems. If a lower impedance load is encountered, it will be necessary to move the capacitor to the other side of the inductors.

Notes

[1]J. Hallas, W1ZR, "Product Review — A Look at Some High-End Antenna Analyzers" *QST*, May 2005, pp 65-69.

[2]Several versions of *EZNEC* antenna modeling software are available from developer Roy Lewallen, W7EL, at **www.eznec.com**.

[3]R. D. Straw, Editor, *The ARRL Antenna Book,* 21st Edition. Available from your ARRL dealer or the ARRL Bookstore, ARRL order no. 9876. Telephone 860-594-0355, or toll-free in the US 888-277-5289; **www.arrl.org/arrl-store**; **pubsales@arrl.org**.

[4]Note that the value of R will be higher than the dc resistance because of skin effect.

[5]L. McCoy, W1ICP (SK), "The Monimatch," *QST*, Feb 1957, pp 38-40.

[6]Richard Measures, AG6K, "A *Balanced* Balanced Antenna Tuner," *QST*, Feb 1990, pp 28-32.

Hairpin Tuners for Matching Balanced Antenna Systems

Balanced Transmatch designs for 28 to 450 MHz.

John Stanley, K4ERO

Once more, the advantages of ladder line for HF antennas were well presented in July 2008 *QST*.[1] Before WWII surplus brought us cheap coax, balanced feeders were almost always used for VHF as well. In the January 1942 *QST* reproduction that was included with The 2007 ARRL Handbook, we find that both home-brew and commercial VHF gear all used balanced lines.[2] For a given cost, open wire ladder line, window line or even TV twin lead can give you a lower loss installation than trying to buy large diameter coax in an effort to keep the losses to an acceptable level. This is dramatically demonstrated by comparing losses in various line types.[3] So, we wonder, why do so few present-day operators use ladder line or twin lead on the VHF frequencies? Might one reason be the lack of suitable *antenna tuners* (transmatches) for those bands? If balanced tuners were available, would ladder line be as popular at VHF as it has become at HF?

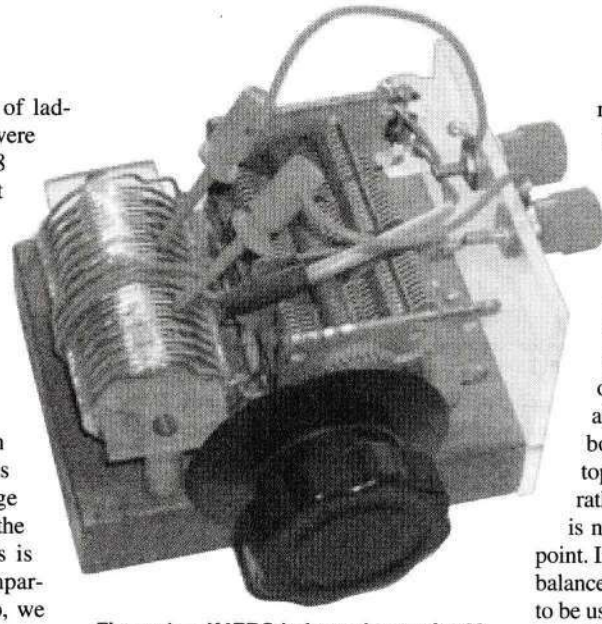

Figure 1 — K4ERO balanced tuner for 60 through 15 meters.

Balanced Tuners for HF Use

The ARRL Handbook, *The ARRL Antenna Book* and other ham publications have always included designs for balanced tuners.[4,5] Adam Nathanson, N4EKV, has one of many good Web sites showing this type of tuner at **www.n4ekv.com/tuners.asp**. I have used tuners like this for years with good results. Figure 1 shows the one I use at up to 100 W on the HF bands.

As noted in Volume 6 of *The ARRL Antenna Compendium*, I lean toward tuners with a fixed link and tapped coil.[6] The match is found by tuning the capacitor and adjusting the output side to connect to a variable number of turns, keeping the taps equidistant from the coil ends. Other versions use the taps for coarse tune and a variable capacitor in series with the link for finer tuning.

Balanced Tuners for the Higher Frequencies

One of the problems with this type of tuner is that as the frequency goes higher, the number of turns on the coil goes down rather quickly. By the time you get to 28 MHz, there may be only four turns on the coil. This means that the adjustment *steps* available are very limited. You can tap to either two or four turns, or if you are willing to unbalance the tap positions, or can access the opposite side of the coil, you could use one or three turns. In either case, the operation is compromised. Another approach is to connect one tap to the bottom of the coil, instead of to the top, effectively using fractions of a turn rather than whole turns, but this often is not feasible from a mechanical standpoint. In addition the symmetry and thus the balance are affected. If this type of tuner is to be used on 10 meters and higher, we need to rethink the design.

Figure 2(A) is a schematic of the conventional tapped link coupled tuner. Figure 2(B) is a representation of what I call a *hairpin* tuner. The electrical properties are essentially identical, but the physical layout of the hairpin type is optimum for the higher frequencies. By making the main inductor in the shape of a hairpin, or shorted transmission line, instead of a single layer solenoid coil, as is used in the conventional design, the tuner becomes much easier to build and adjust. The use of a short short-circuited transmission line section as an inductor is nothing new. It has been used for VHF/UHF circuits for many years.

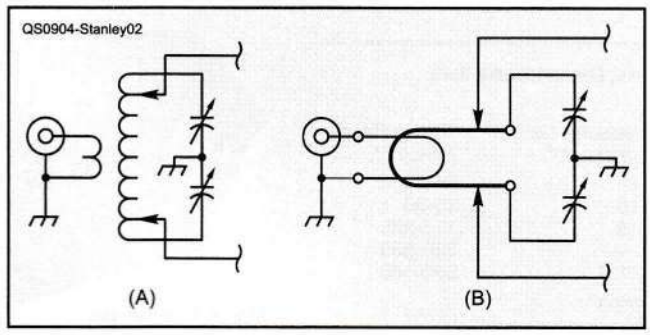

Figure 2 — Balanced tuner configurations. At (A) conventional tapped coil based tuner, at (B) the hairpin equivalent.

Building Hairpin Tuners

For some time I have been using a hairpin inductor in a balanced tuner for 6 and 10 meters, and recently I built one for each of the 144, 220 and 432 MHz bands. The approach is the same on each frequency. A section of transmission line was used instead of the coil typically used on lower frequencies.

[1]Notes appear on page 36.

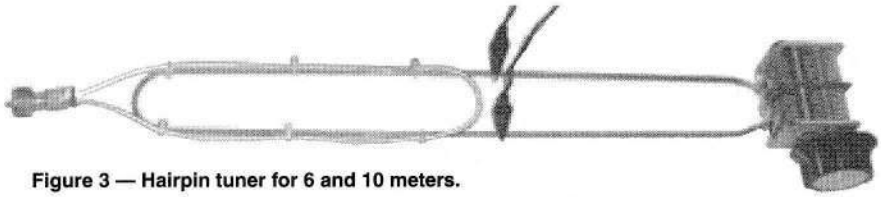

Figure 3 — Hairpin tuner for 6 and 10 meters.

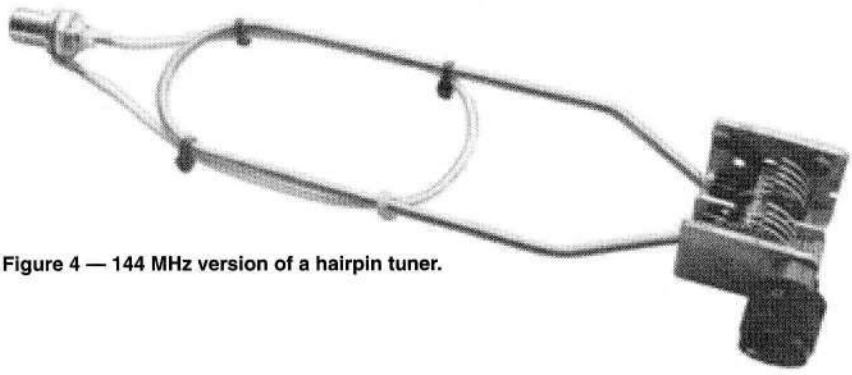

Figure 4 — 144 MHz version of a hairpin tuner.

The capacitor was a split stator or butterfly design. The input link is a single turn inductor that overlaps a portion of the main transmission line inductor and the output taps were taken at whatever point of the hairpin that gives the best match.

The advantage of this layout is that moving the taps to any point on the hairpin is the same as tapping on different numbers of turns on a coil, except that with the hairpin, it is very convenient to make the adjustment in as fine a step as may be desired. In all of my designs, the coupling loop is held to the main hairpin by cable ties. This allows some adjustment of the coupling loop, but holds the loop sufficiently snug so that it is not likely to move around accidentally. Use less loop coupling for higher Q with more selectivity and more loop coupling for lowest loss.

Making them Play

The frequency tuning range percentage will depend on the capacitor used. For widest range, select one with a high minimum to maximum capacitance ratio. All of the capacitors I have tried have provided adequate range to cover the desired amateur band. The range can be extended to cover a second band by putting fixed capacitors in parallel with the variable tuning capacitor. For example, the 6 meter version, shown in Figure 3, works for 10 meters with the addition of a parallel 40 pF fixed ceramic capacitor, while the 220 MHz version, shown in Figure 5, works fine on 2 meters with the addition of a 12 pF ceramic. As it is, the 2 meter version just makes it to 222 MHz, so two bands are possible without switching caps. A single tuner could also work on 10 and 6 meters without switching by careful component selection.

Capacitor Options

The most difficult component to find will likely be the split stator capacitor. There are ways of designing your own capacitor and it is made easier because of the relatively small capacitance required at these frequencies. For all of the designs shown here, I took capacitors from my well stocked junk box. You less well equipped folks will have to search at a hamfest or check out the basement of one of the local old timers. Commercial capacitors are available, but the price may shock you. You could also choose to use a single section capacitor instead of the split stator. In that case, the capacitor shaft and frame will be "hot" and must be floated above ground. You will have to tune it via a long insulated shaft. And, of course, the balance will be somewhat compromised. The method does work and a suitable single section capacitor may be easier to find, however . Alternatively you could use a pair of identical capacitors to ground if you adjusted them each to the same setting or worked out a common shaft arrangement. Fussy, but it could work. Target dimensions and component values for the bands in this range are shown in Table 1.

Inductor Choices

The length of the hairpin will depend on the value of your capacitor. The values below represent tuners I have built and should give you a good starting point. Match the hairpin width to the spacing of the capacitor terminals, or bend the ends of the hairpin in or out at the capacitor end in order to make the connections. Spacing does affect the inductance value so keep it close to what you see in the photos.

My inductors are ⅛ inch diameter brass rod, but they could be soft copper tubing or wire in sizes from 12 gauge up to ¼ inch. Brass welding rods from the hardware store could also be used. A smaller diameter means the hairpin should be shortened a bit as the inductance per inch will be higher. The links should be insulated wire, either enameled or PVC coated or, best of all, Teflon insulated. The 6 meter tuner in Figure 3 uses the shield of Teflon coax as the link. My links do not make electrical contact anywhere with the main hairpin. The coax shield and center of the hairpin could both

Table 1

Hairpin Tuner Component Values, Dimensions and Frequency Range

Band	*Capacitor Value (pF/Section)**	*Inductor Length (Inches)***	*Tuning Range (MHz)****
10 Meters	95-170	15	26-34
6 Meters	15-90	15	36-90
2 Meters	3-20	6	110-225
222 MHz	3-10	4	220-330
432 MHz	3-4	1.5	390-440

*Effective capacity is ½ of the value/section.
**All inductors made of ⅛ inch brass rod.
***Range may by reduced or shifted by reactive loads.

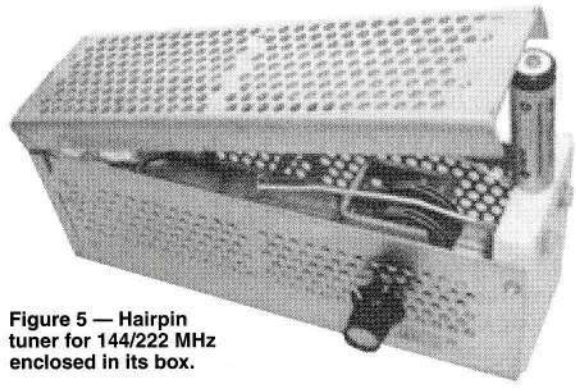

Figure 5 — Hairpin tuner for 144/222 MHz enclosed in its box.

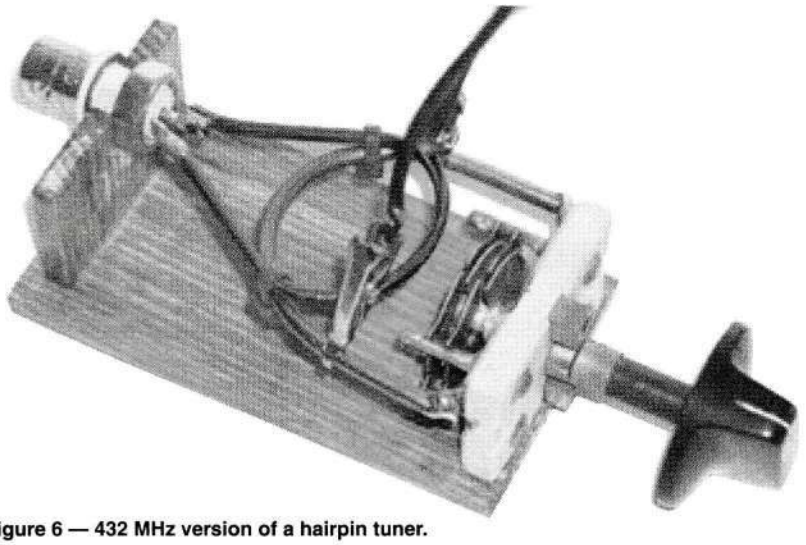

Figure 6 — 432 MHz version of a hairpin tuner.

be grounded to a chassis, if desired.

Tuning Up

Tuning consists of setting the taps to an intermediate position and adjusting the capacitor for minimum SWR. If SWR is not as low as desired, move the taps a bit either towards or away from the capacitor and readjust the capacitor. You should be able to find tap settings that allow the SWR to be reduced to 1:1.

Safety Considerations

Note that neither of the tuners described above are shown installed within a chassis of any kind. This is to show the construction more clearly. Also, I must admit that during tests, I got away with this because I used low power and am very careful not to touch the *hot* parts of the circuit. I also have a non-metallic operating desk. The open construction is useful during experiments.

I definitely do not recommend this approach for general use. You will want to put your tuner in a shielded box of some kind, probably with a hinged lid to allow you to move the taps as shown in Figure 5. You should *never* adjust the tap clips with power applied. The tuning shaft should be brought out through the enclosure where an insulated knob should be installed for tuning even though with a split stator capacitor the shaft should be at ground potential. For high power, the use of a suitable enclosure is essential, especially if the tuner is to be installed close to the operating position. This is to prevent RF burns from contact as well as exposure to excess RF levels.

Remember that your body is more susceptible to pick up from VHF fields than is the case at HF. If you put the tuner well away from the operating position in a place that is protected from access by family members or pets, you may be able to use a somewhat more open construction as is sometimes done with conventional home brew tuners. Radiation from an unenclosed tuner of any type can be enough to cause interference with nearby electronics devices and could cause fires if anything flammable comes in contact with the hot parts of the circuit.

These tuners have been tested with 100 W on 10 and 6 meters, 50 W on 2 meters and 20 W on 70 cm, the maximum output of my rig. For higher power, the designs can be scaled, remembering that the bigger it gets, the lower the frequency for the same geometry. Thus, a design similar to that used here for 432 MHz, but three times larger, would probably work fine with a full kW, but on 144 MHz. Since my 20 W, 432 MHz design uses an inductor that is about as short as is practical (see Figure 6), getting up to 1 kW at 432 MHz, might prove difficult with this design. At the least, a different type of capacitor would be required.

I hope that these simple to build and adjust tuners will start a trend towards greater use of balanced feeders on the higher frequencies just as ladder line has become the favorite for many on the lower bands.

Notes

[1]J. Hallas, W1ZR, "Getting on the Air—Your Second HF Antenna," *QST*, Jul 2008, pp 69-70.

[2]B. Goodman, W1JPE, "Receivers for 112-Mc. Emergency Work," *QST*, Jan 1942, pp 18-25, 74-75.

[3]*The ARRL Handbook for Radio Communications*, 2009 Edition, Figure 21.4. Available from your ARRL dealer or the ARRL Bookstore, ARRL order no. 0261 (Hardcover 0292). Telephone 860-594-0355, or toll-free in the US 888-277-5289; **www.arrl.org/shop**; **pubsales@arrl.org**.

[4]See Note 3, p 21.13.

[5]R. D. Straw, Editor, *The ARRL Antenna Book*, 21st Edition, p 25-3. Available from your ARRL dealer or the ARRL Bookstore, ARRL order no. 9876. Telephone 860-594-0355, or toll-free in the US 888-277-5289; **www.arrl.org/shop**; **pubsales@arrl.org**.

[6]J. Stanley, K4ERO, "The Filtuner," *ARRL Antenna Compendium, Volume 6*. Available from your ARRL dealer or the ARRL Bookstore, ARRL order no. 7431. Telephone 860-594-0355, or toll-free in the US 888-277-5289; **www.arrl.org/shop**; **pubsales@arrl.org**.

John Stanley, K4ERO, holds an Amateur Extra class license and has been licensed for over 50 years. He has worked as a broadcast engineer most of his life, mainly with religious shortwave stations in many parts of the world. He graduated from MIT in 1962 with a BSEE degree. John is an ARRL Technical Adviser. He and his wife, Ruth, WB4LUA, live in Rising Fawn, Georgia. You can reach John at 524 White Pine Ln, Rising Fawn, GA 30738 or at **jnrstanley@alum.MIT.edu**.

Review Questions

15-1 What are some major challenges involved with building an antenna tuner?

15-2 Under what conditions is a special purpose tuner a viable option?

15-3 Why might you decide not to include 160 meters in your tuner design?

APPENDIX A

Making Sense of Decibels

Joel R. Hallas, W1ZR

Much of the technical data found in *QST* and other ARRL publications is expressed in decibels, generally shown as *dB*. Contrary to the belief of some, this is not done to mystify beginners, but rather is intended to make comparisons easier and avoid the use of very large or small numbers.

So What's this Decibels Business All About?

Decibels are just a way of expressing ratios, often power ratios. If we are looking at the gain of an amplifier stage, the pattern of an antenna or the loss of a transmission line we are generally interested in the ratio of the power out to the power in, or the ratio of the power in front of a beam antenna to that coming from the back. These are some of the places that we will find the results expressed in dB.

Decibels are a logarithmic function. Logarithms are a handy mathematical tool based on exponents. An important feature of logarithms is that multiplication can be performed by adding the logarithmic quantities instead of multiplying them. Similarly, divisions can be accomplished by subtracting in the same manner. This becomes a benefit if you are dealing with multiple stages of amplification and attenuation — as we often are in radios — snatching a minuscule signal from the ether — amplifying and processing it so we can hear it out the loudspeaker. Instead of having to multiply and divide at each stage to keep track of the progress of our signal processing — often with signal levels with many zeros to the right of the decimal point — we can just tally all the dB and have total gain of the system.

So How do We Compute the Decibels?

The *deci* in decibels refers to a factor of 1/10, as in *deciliters* for 1/10 of a liter, while the *bel* relates to the idea of a logarithmic ratio, originally used to define sound power.

- To convert a power ratio into decibels, just:

1. Find the base 10 logarithm of the power ratio.
2. Multiply by 10.

For example, if we have an amplifier with a power gain of 275, we find the logarithm of 275 (see below, if you don't do logs in your head) to be 2.44. We multiply by 10 and the result is that a power gain of 275 can be represented as 24.4 dB.

- To convert decibels to a power ratio, we do the opposite:

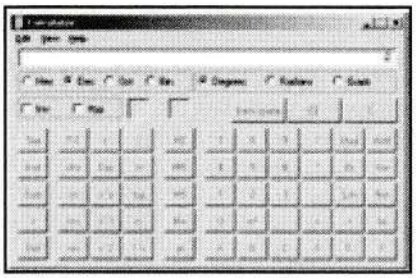

Figure 1 — The *Windows Scientific Calculator* ready to calculate the effect of a 2 dB cable loss.

1. Divide by 10.
2. Find the base 10 antilog of the result.

Note that the base 10 antilog of a number is just 10 raised to the power of the number. This is also something you probably don't do in your head, so let's see how to easily perform the computations.

Understanding a few characteristics of logs will help avoid problems interpreting results. Note that a gain of 0 dB means that there is no change to the signal — not that the signal has vanished! The other important fact is that a power ratio of less than one (a loss rather than a gain) is represented as a negative number in decibels.

Enter the *Windows Scientific Calculator*

In the *very* old days, engineers and technicians used tables to make accurate logarithmic calculations, and mechanical slide rules if three significant digits was sufficient precision.[1] Starting around 1970, scientific calculators became available. Initially they were expensive typewriter-sized devices that were typically shared within an engineering department. Within a few years pocket-sized units were available for less than $200, and now everyone could make calculations to a precision of nine significant digits, whether warranted by the data accuracy or not. Tables and slide rules were relegated to the pages of history with spark transmitters.

The dawn of the reasonably priced personal computer seemed to push the fancy scientific calculator out of sight only about 10 years later. Unfortunately, for many functions a calculator may be a better choice, and decibel calculations may be one. The calculations may be easily performed on a PC by putting the equations in cells of an Excel spreadsheet, but not everyone can do that without a lot of thought.

If you have a suitable scientific calculator, that should easily make the calculations. Not all have an ANTILOG button, but if not, they will likely have a button that says X^Y, which can be used as above. If you don't have a handheld calculator, you may not know that there is a very capable one included as an "accessory" within the Microsoft *Windows* operating system! Just click START then ALL PROGRAMS then ACCESSORIES. You should find an icon for the *Windows Calculator*. You could open it, but why not drag it onto your desktop first.

On first opening, you may find a four-function grocery store type calculator. Have no fear, just click on VIEW then SCIENTIFIC to get the one you want. It should look about like Figure 1.

Give it a Test Drive

Let's say you have a mismatched coax cable with a loss of 2 dB. You may want to know how many of the 100 W from your transmitter actually reach your antenna. Remember a 2 dB loss is a "gain" of –2 dB! We'll go through the inverse dB calculation of column 2. Using your *Windows Calculator*, either hit 2 on your keyboard, or:

- Click on the 2 on the calculator "keypad," then:
- Click on the +/– key; the display should show – 2, as in Figure 1.
- Click on the / key to select the "divide by" operation. Enter the digits 1 and 0 for the number 10 and hit ENTER or =. Make note of the result (–0.2) or store it in memory (M+).
- Enter the digits 1 and 0 for the number 10.
- Click on X^Y to raise 10 to a power.
- Enter your earlier result, –.2 and hit ENTER.
- The display should show 0.63095734448 01932494343601366223 4 or about 0.63. That is the fraction of your power left after a 2 dB loss. That means your antenna sees 63 W and 37 W is heating your transmission line.

While you are using the *Windows Scientific Calculator* look over its other features. It provides painless conversion between decimal and binary, octal or hex numbers, for example.

Joel R. Hallas, W1ZR, is QST *Technical Editor. He can be reached at* **w1zr@arrl.org**. QST

[1]See, for example, *Standard Mathematical Tables*, CRC Press, any edition. In addition to tables of logarithms and trigonometric functions, it includes many handy formulas from geometry, trigonometry and calculus.

From April 2007 QST © ARRL

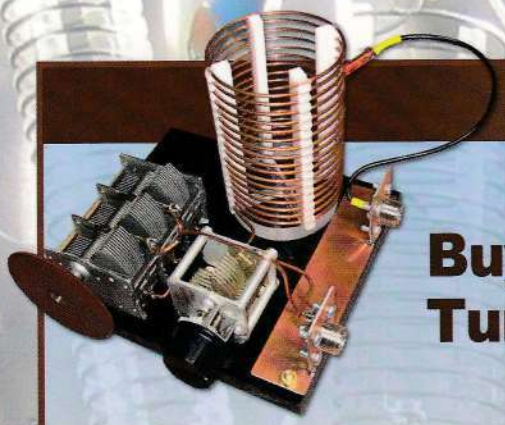

Buy or Build the Best Tuner for Your Station.

Antenna tuners are devices often misunderstood in the Amateur Radio world. While not every station requires an antenna tuner to transmit radio signals, often an incompatibility between the transmitter and the antenna system results in poor performance. An antenna tuner between them is the way to obtain efficient operation.

The ARRL Guide to Antenna Tuners discusses the details of the different configurations and requirements of antenna tuners. It explores the design, construction and applications of the different types available. You'll learn if one is necessary in your station, what type of tuner is needed and where to install it for maximum improvement. This book will give you a better understanding of your antenna system and the way it can be enhanced through the selection and use of the appropriate antenna tuner.

Contents:

- Why Might I Need an Antenna Tuner
- A Look at a Typical Configuration
- So Just What is an Antenna Tuner?
- Tuning an Antenna Tuner
- The Internal Tuner—How Does it Help?
- An External Tuner at the Radio
- Transmission Lines and Loss
- Moving the Tuner to the Back 40
- Transmission Line Choices for Low Loss
- Balanced versus Unbalanced Lines
- So What's a Balun, an Unun, a Choke?
- Balanced Antenna Tuners
- Antennas that Work Well with Tuners
- A Survey of Available Tuners
- Making Your Own Tuner

Joel Hallas has been a radar and telecommunications systems engineer, engineering manager, telecommunications executive and college teacher, and is now Technical Editor of ***QST***, the monthly journal of ARRL, the national association for Amateur Radio. He has earned BS and MS degrees in electrical engineering. Joel is a radio amateur, and holds the license call sign W1ZR.

***ARRL** — devoted entirely to Amateur Radio*

ARRL has books, software, online courses and other resources for licensing, operating and education. Look for these other popular ARRL titles:

- ***The ARRL Antenna Book***
- ***Basic Antennas: Understanding Practical Antennas and Design***
- ***The ARRL Antenna Designer's Notebook***

Published by:

ARRL *The national association for* ***AMATEUR RADIO™***

225 Main Street
Newington, CT 06111-1494 USA
www.arrl.org

ISBN 978-0-87259-098-4
52295
9 780872 590984
USA $22.95 ARRL Order No. 0984

PART II—
BUILDING AND USING
BALUNS AND UNUNS

Chapter 7

The 1:1 Balun

Sec 7.1 Introduction

In this chapter I will introduce the most popular broadband Balun in amateur radio use—the 1:1 Balun. This topic been discussed in the amateur radio literature since the publication of Turrin's 1964 article.[8] Although Turrin's Balun is really a version of Ruthroff's, which was introduced in his classic 1959 article,[9] the real beginning of the broadband 1:1 Balun dates back to Guanella's classic paper of 1944.[3] Guanella's objective was to design a broadband 16:1 Balun to match the balanced output impedance of 960 ohms of a push-pull, 100-watt vacuum-tube amplifier to the unbalanced load of a matched 60-ohm coaxial cable. Use of his approach for 1:1, 4:1, and 9:1 Baluns has produced the designs of choice. They are presently called current or choke Baluns.

This chapter begins with an introduction to the technology of transmission line transformers. Other topics discussed include: 1) when to use a Balun; 2) highlights of significant articles in the professional and amateur radio literature; 3) high-power, medium-power, and low-power designs; and 4) isolation transformers. The latter is presented here for the first time. The chapter closes with a brief summary of the significant points included within.

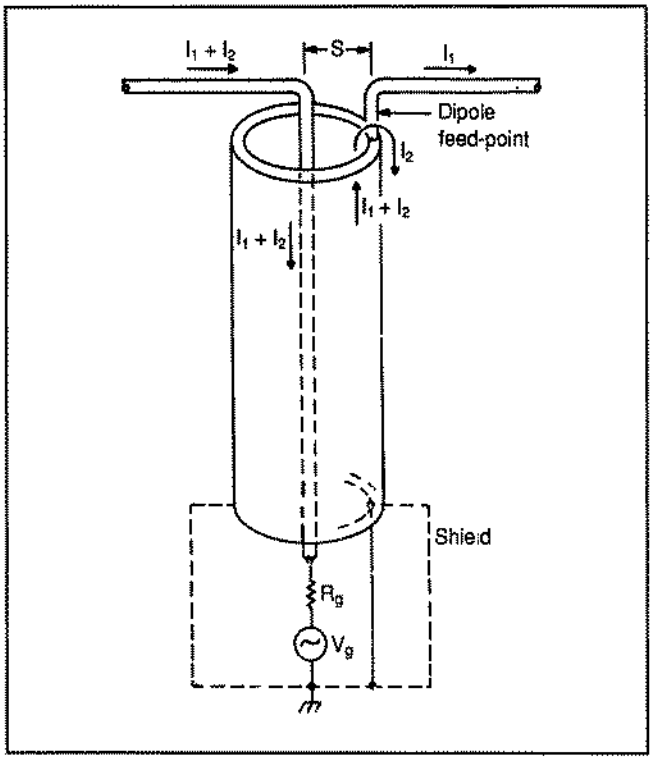

Figure 7-1. *An illustration of the various currents at the feedpoint of a dipole. I_1 is the dipole current and I_2, the inverted L (imbalance) current.*

Sec 7.2 When to Use a Balun

Baluns have taken on a more significant role in the past few decades with the advent of solid-state transceivers and Class B linear amplifiers with unbalanced outputs. That is, the voltage on the center conductor of their output chassis connectors varies (plus and minus) with respect to ground. In many cases, coaxial cables are used as the transmission lines from these unbalanced outputs to antennas like dipoles, inverted Vs, and Yagi beams that favor a balanced feed. In essence, they prefer a source of power whose terminals are balanced (voltages being equal and opposite) with respect to actual ground or to the virtual ground that bisects the center of the antenna. The question that is asked most frequently is whether a 1:1 Balun is really needed.

To illustrate the problem involved and to give a basis for my suggestions, I refer you to **Figure 7-1**. Here we have, at the feedpoint of the dipole, two equal and opposite transmission line currents with two components each—I_1 and I_2. Also shown is the spacing, s, between the center conductor and the outside braid. Theoretically, a balanced antenna with a balanced feed would have a ground (zero potential) plane bisecting this spacing. However, because a coax-feed is unbalanced and the outer braid is also connected to

ground at some point, an imbalance exists at the feedpoint giving rise to two antenna modes. One lies with I_1, providing a dipole mode; the other lies with I_2, providing an inverted L mode.

If the spacing, s, is increased, the imbalance at the feedpoint becomes greater—giving rise to more current on the outer braid and a larger imbalance of currents on the antenna's arms. Several steps can be taken to eliminate or minimize the undesirable inverted L mode (that is, eliminate or minimize I_2). The obvious choice is to use a well-designed Balun that not only provides a balanced feed, but also minimizes (by its choking reactance) I_2—if the coaxial cable does not lie in the ground plane that bisects the center of the dipole. The other step is to ground the coaxial cable at a quarter-wave (or odd-multiple thereof) from the feedpoint. This discourages the inverted L mode because any radiating element will want to see a high impedance at these lengths instead of the low impedance of a ground connection.

I conducted experiments with Baluns on a 20-meter half-wave dipole at a height of 0.17 wavelengths, which gave a resonant impedance of 50 ohms. VSWR curves were compared under various conditions. When the coaxial cable was in the ground plane of the antenna (that is, perpendicular to the axis of the antenna), the VSWR curves were identical with or without a well-designed Balun—no matter where the outer braid was grounded. A significant difference was noted only when the coaxial cable was out of the ground plane. When the cable dropped down at a 45-degree angle under the dipole, a large change in the VSWR took place. This meant that the inverted L mode was appreciable.

It should also be mentioned that the direction of I_2, the imbalance current, can depend upon the side on which the coaxial cable is out of the ground plane of the dipole. For example, if the cable comes down under the right side in **Figure 7-1** (that is, the angle between the horizontal arm and the coax is less than 90 degrees on the right side and more than 90 degrees on the left side), then the direction of I_2 can be reversed by the imbalance in the induced currents on the outside of the braid. By the same token, by having the coaxial cable coming down on the other side, the value of I_2 is only increased in magnitude.

However, feeding a Yagi beam without a well-designed 1:1 Balun is a different matter. Because most Yagi designs use shunt-feeding (usually by hairpin matching networks) in order to raise the input impedance close to 50 ohms, the effective spacing (s) is greatly increased. Furthermore, the center of the driven element is actually grounded. Thus, connecting the outer braid (which is grounded at some point) to one of the input terminals, creates a large imbalance and a real need for a Balun. An interesting solution, which would eliminate the matching network, is to use a step-down Balun designed to match 50-ohm cable directly to the lower balanced-impedance of the driven element.[2]

In summary, if you concur with the theoretical model of **Figure 7-1**, my experiments performed on 20 meters, and the reports from radio amateurs using dipoles and inverted Vs without Baluns, then it appears that 1:1 Baluns are really needed for: a) Yagi beam antennas where severe pattern distortion can take place without one, and b) dipoles and inverted Vs that have the coaxial cable feed lines out of the ground plane that bisects the antennas, or that are unbalanced by their proximity to manmade or natural structures. In general, the need for a Balun is not so critical with dipoles and inverted Vs (especially on 40, 80, and 160 meters) because the diameter of the coaxial cable connector at the feedpoint is much smaller than the wavelength.

If my model, which assumes that a part of the problem when feeding balanced antennas with coaxial cable is related to the size of the spacing, s (shown in **Figure 7-1**), then the possibility exists for using Ununs for matching into balanced antennas with impedances other than 50 ohms and with small values of s. For example, half-wave dipoles at a height of about a half-wave, quads, and center-fed 3/2-wave dipoles—which all have impedances close to 100 ohms—could very well be matched to 50-ohm cable by a 2:1 Unun. As I will show, they are considerably easier to construct than 2:1 Baluns. Furthermore, Genaille[10] has recently shown considerable success using Ununs in this kind of application.

To wind up this section, I would like to comment on an article published by Eggers,[11] WA9NEW, concerning the use of a Balun with a half-wave dipole. While at North Carolina State University, he conducted an experimental investigation of pattern distortion without a Balun at 1.6 GHz in an RF anechoic chamber (which simulates "free space"). Briefly, his results showed that, with a Balun (bazooka type), the antenna radiation pattern compared very favorably with the classic "figure-eight." Without the Balun, the radiation pattern was severely distorted.

Even though the author expressed difficulty in obtaining accurate measurements at this very high frequency, I have a question regarding the validity of performing the experiment in the first place. From the photograph in the article, it appears that conventional coaxial cable and connectors were used in the experiment. If we assume an effective diameter of 0.375 inches for these components, then scaling up to 3.5 MHz (457.14 fold) results in a coaxial cable with a diameter of 14.28 feet! I am quite sure that the large spacing, s, of 7.14 feet would bring about a noticeable imbalance resulting in appreciable pattern distortion even at 3.5 MHz.

Sec 7.3 Highlights of Significant Articles on 1:1 Baluns

Although there have been many articles on 1:1 Baluns published in the professional and amateur literature, I have selected for review a few that I believe have had the most impact on 1:1 Baluns for amateur radio use. As you will see, even though I consider some of the amateur articles significant, their impact upon the use and understanding of these devices has not always been positive. In fact, in some cases, the opposite has been true.

In the professional literature

There are actually only two significant articles in the professional literature that provide the fundamental principles upon which the theory and design of this class of transformers are based. It can be said that succeeding investigators simply extended the works of the authors of these two articles.

The first presentation on broadband matching transformers using transmission lines was given by Guanella in 1944.[3] He coiled transmission lines forming a choke such that only transmission line currents were allowed to flow, no matter where a ground was connected to the load. His single, coiled transmission line resulted in a 1:1 Balun. It is shown schematically in **Figure 7-2A**. Prior to this, RF Baluns were achieved by the use of quarter and half-wave transmission lines, and as a result, had narrow bandwidths. Guanella then demonstrated broadband Baluns with impedance transformations of $1{:}n^2$ where n is the number of transmission lines he connected in a series-parallel arrangement.

Several important points should be made regarding Guanella's 1:1 Balun shown in **Figure 7-2A**. With

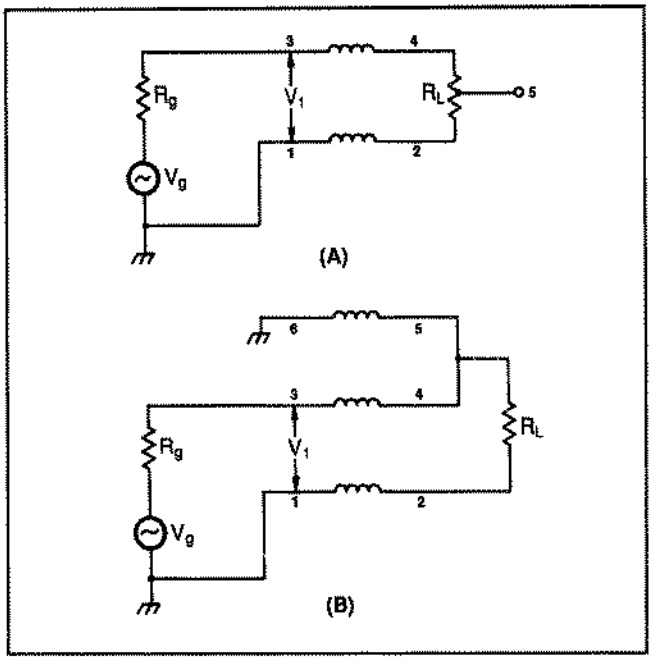

Figure 7-2. *Two versions of the 1:1 Balun: (A) the Guanella Balun and the basic building block; (B) the Ruthroff Balun as originally drawn.*

sufficient choking reactance, the output is isolated from the input and only flux-canceling transmission line currents are allowed to flow. With matched or very short transmission lines, the grounding of terminal 5 (actually or virtually like the center of a dipole) results in terminal 4 becoming $+V_1/2$ and terminal 2 becoming $-V_1/2$—creating a balanced output. This type of Balun has lately been called a "current" or "choke" Balun. A significant feature of this model is that a potential gradient of $-V_1/2$ exists along the length of the transmission line. This gradient, which exists on both conductors, accounts for practically all of the loss in these transformers because the loss mechanism is voltage dependent (a dielectric-type loss). All transmission line transformers have some sort of voltage gradient along their transmission lines and are, thus, subject to the same type of losses. Furthermore, the theory and loss mechanism is the same whether the transmission lines are coax or twin-lead, or coiled around cores, or threaded through ferrite beads. Additionally, it was shown[2] that higher-impedance Baluns or Baluns subjected to higher VSWRs have more loss because the voltage gradients are also larger.

The second significant article on broadband transmission line transformers was published by Ruthroff.[9] His 1:1 Balun, which is shown as originally drawn in

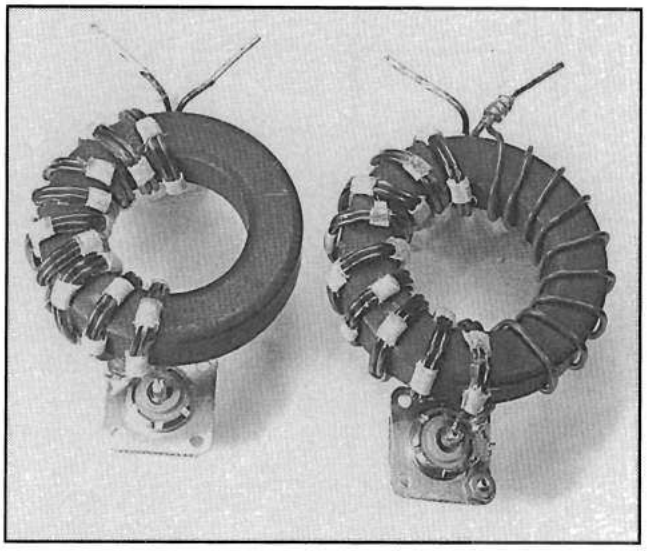

Photo 7-A. *The two basic forms of the 1:1 Balun that first appeared in the professional literature. The two-conductor Guanella Balun is on the left and the three-conductor Ruthroff Balun is on the right.*

Figure 7-2B, used an extra winding to complete (as he said) the path for the magnetizing current. Even though his schematic drawing appeared to look like a trifilar winding, his pictorial in the article clearly showed that the third winding (5-6) was on a separate part of the toroid. With an equal number of turns, it forms a voltage divider with winding (3-4) placing terminal 4 at $+V_1/2$ and terminal 2 at $-V_1/2$. In his classic paper, Ruthroff also presented his form of the 4:1 Balun (which is also different from Guanella's), a 4:1 Unun, and various hybrids. **Photo 7-A** shows the two basic forms of the 1:1 Balun that first appeared in the professional literature. The two-conductor Guanella 1:1 Balun is on the left and the three-conductor Ruthroff Balun is on the right. As was mentioned before, the Guanella Balun has also been called a "current" or "choke" Balun.

Before moving on to the significant articles in the amateur radio literature, some mention should be made of the differences between the two basic forms shown in **Photo 7-A**. Guanella's 1:1 Balun came to be known as the *basic building block* for this whole class of broadband transformers. This term was coined by Ruthroff as he showed its 1:1 Balun capability when the load was grounded at its center (terminal 5), and as a phase-inverter when the load was grounded at the top (terminal 4). By connecting terminal 2 to terminal 3 and connecting the bottom of the load to ground, Ruthroff demonstrated his very popular 4:1 Unun. I call this type of arrangement the bootstrap connection. By grounding terminal 2, there is no potential drop along the transmission line and, therefore, no need for magnetic cores or beads. This arrangement, which turns out to be an important function for extending the high frequency performance of this class of transformers, I call the "phase-delay" connection.

Thus, with the flexibility shown by Guanella's basic building block, a 1:1 Balun is now realized that not only presents a balanced power source to a balanced antenna system, but can also prevent an imbalance current (an inverted L antenna current) by its choking reactance when the load is unbalanced or mismatched or when the feedline is not perpendicular to the axis of the antenna.

Interestingly enough, except at the very low end of the frequency response of the Ruthroff 1:1 Balun where autotransformer action can take place, his Balun takes on the characteristics of the Guanella Balun. The reactance of the third winding becomes great enough to make it literally transparent. This is not the nature of the trifilar-wound (voltage) Balun, which is sensitive to unbalanced and mismatched loads over its entire passband because it is actually two tightly coupled transmission lines. This distinction was not recognized by most of those who published in the amateur radio literature.

In the amateur radio literature

R. Turrin, W2IMU—1964

The first presentation in the amateur radio literature on 1:1 Baluns using ferrite cores was by Turrin in 1964.[8] Turrin, who was a colleague of Ruthroff's at Bell Labs, took his small-signal design (which used No. 37 or 38 wire on toroids with ODs of 0.25 inches or less) and adapted it to high-power use. This was done by using thicker wire, larger cores, and (very importantly for high efficiency[2]) low permeability ferrite. Ruthroff used lossy manganese-zinc ferrites with permeabilities of about 3000 because efficiency was not a major consideration.

Figure 7-3 is a pictorial and a schematic of Turrin's design. As you can see, the third wire (winding 3-4) is placed between the two current-carrying wires (windings 1-2 and 4-5). **Photo 7-B** shows (on the left) his actual design using a ferrite core; a popular design (on the right) using a powdered-iron core is available in kit form from Amidon Associates, Inc. Both Baluns use 10 trifilar turns of a single-coated wire like Formex™ or Formvar™ on a toroid. Turrin's design

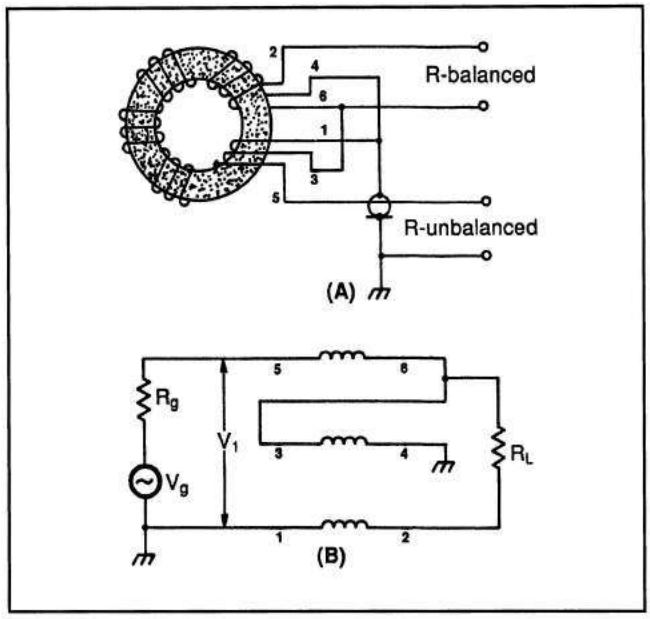

Figure 7-3. *(A) A pictorial of Turrin's 1:1 Balun, and (B) a schematic of his Balun.*

uses a ferrite toroid with an OD of 2.4 inches and a permeability of 40. The Amidon Associates' Balun uses a powdered-iron toroid with a 2-inch OD and a permeability of only 10. Both Baluns are specified to handle 1000 watts of power from 1.8 to 30 MHz.

Figure 7-4 shows the response curves for these two Baluns when terminated with 50-ohm loads. The response curve for a popular 1:1 rod-type Balun that uses the same schematic and wire is also shown. It has 8 trifilar turns, tightly wound on a rod of 0.5-inch diameter, 2.5 inches long, and with a permeability of 125. The rod-type Balun is shown in **Photo 7-C**.

Several important features should be brought out regarding the results shown in **Figure 7-4**. They are:

1. All Baluns had insufficient choking reactance and, hence, poor low-frequency responses. The powdered-iron version was especially poor. They all showed a drop in the input impedance and an inductive component at 2 MHz. This meant flux in the cores and an undesirable condition—especially for ferrite, which is a nonlinear material. Ferrite cores could not only suffer damage, but they could also generate spurious frequencies under these conditions. In fact, the same condition could occur at 4 MHz with a VSWR of 2:1! Therefore, I don't recommend any of these Baluns for use on 160 or 80 meters.

2. The major problem at the low-frequency end is the role of the third winding (3-4) in **Figure 7-3B**. It has been claimed[12] that the third winding improves the low-frequency response (over the two-conductor Guanella 1:1 Balun) because it enables autotransformer action at the low end. However, recent measurements I have made on two-conductor Guanella Baluns and three-conductor Ruthroff (or Turrin) Baluns, with loads grounded at their centers, show insignificant differences. This type of load approximates the actual condition when feeding a balanced antenna system. The negative feature of the third winding (3-4) is that, at the low-frequency end, there can be insufficient reactance to prevent harmful flux in the core because of a direct shunting path to ground. With the two-conductor 1:1 Balun, the only flux-inducing current is that of the imbalance current (the inverted L mode), which is usually far smaller.

3. Another important feature of the curves shown in **Figure 7-4** is the effect of the characteristic impedances of the coiled transmission lines. For example, a bifilar winding (wires tight together) on a toroid with spacing between adjacent bifilar turns exhibits a char-

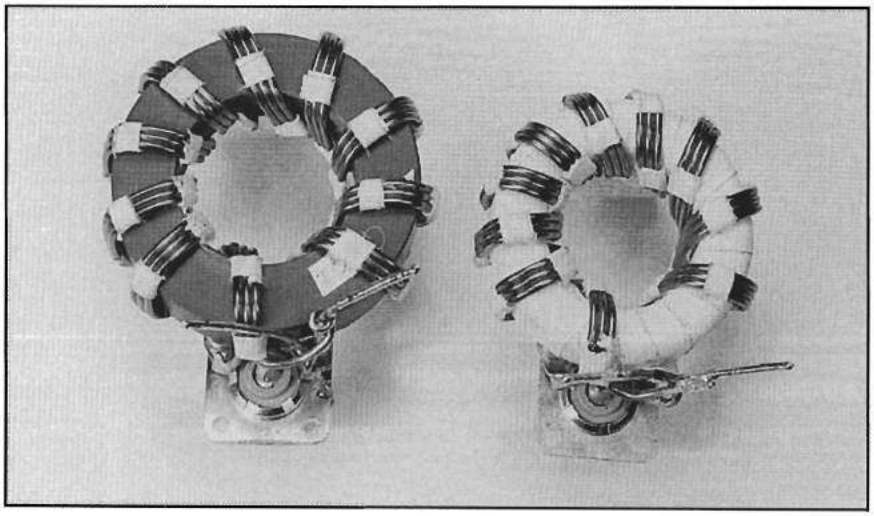

Photo 7-B. *Two versions of Turrin's design: On the left, the 1:1 Balun that has appeared in the amateur radio literature; on the right, a 1:1 Balun that has been readily available in kit form from Amidon Associates, Inc.*

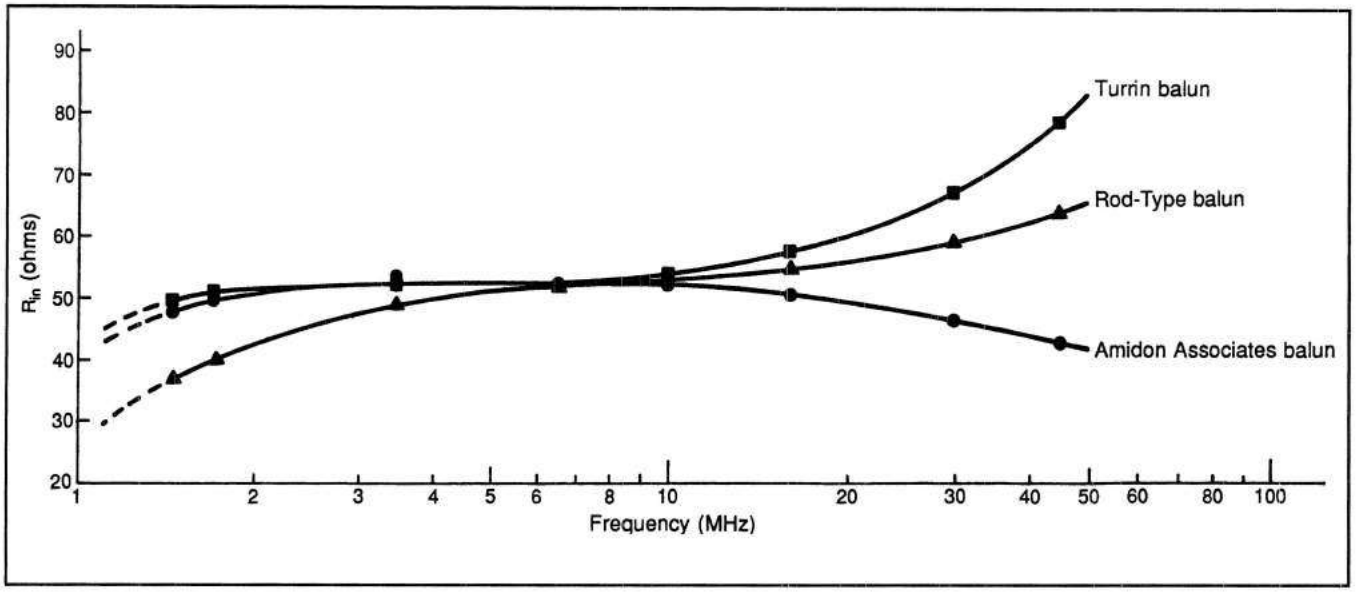

Figure 7-4. *The input impedance versus frequency, when terminated with 50 ohms, for the Turrin, typical rod-type, and Amidon Associates 1:1 Baluns.*

acteristic impedance of about 45 ohms. When wound on a rod with no space between adjacent bifilar turns, the characteristic impedance drops to about 25 ohms. With the third winding (3-4) between the other two as shown in **Figure 7-3B**, the characteristic impedance is raised to approximately 70 ohms in the toroidal case and to about 47 ohms in the rod case. If the toroidal Baluns were terminated in 70 ohms and the rod Balun terminated in 47 ohms, the high-frequency responses would be practically flat to at least 30 MHz. The difference in high-frequency response between the two toroidal Baluns (with 50-ohm loads) is due to the differences in the lengths of their transmission lines. The transmission line on the powdered-iron core is appreciably less because the OD, as well as the cross-sectional area, is smaller.

4. The trifilar-wound form of the 1:1 Balun also has an additional undesirable property. Its high frequency response is sensitive to unbalanced and mismatched loads. This is because the third wire now forms two tightly coupled transmission lines. It is unlike the Ruthroff version shown on the right in **Photo 7-A**. In his second article,[12] Turrin pointed out this important distinction.

J. Reisert, W1JR—1978

The next significant article on 1:1 Baluns was published by Reisert in 1978.[7] Reisert proposed winding some of the smaller (but still high-powered) coaxial cables around a 2.4-inch OD ferrite toroid with a permeability of 125. The windings also included a crossover, which is shown in **Figure 7-5** and **Photo 7-D**. In addition, he recommended various numbers of turns, depending upon the low-frequency requirement. For example, he suggested 12 turns to cover 3.5 MHz, 10 turns for 7 MHz, 6 for 14 MHz, and 4 for 21 and 28 MHz. Because the characteristic impedance of the coaxial cable is the same as the coax feedline, the Balun only introduces a foot or two of extra length to the feedline. This is true in the HF and VHF bands. The coaxial cables recommended in the article were RG-141/U, RG-142/U, and RG-303/U.

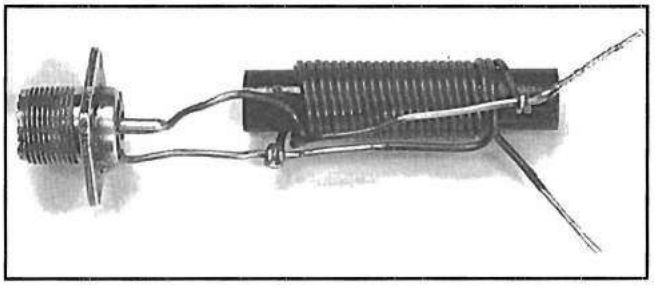

Photo 7-C. *A typical rod-type Balun.*

From the articles that followed in the amateur radio literature, it became apparent that few recognized all of the important features of Reisert's Balun. They are listed below.

1. An efficient, low-loss ferrite was used.
2. The Baluns had sufficient choking reactances for the various low-frequency requirements.

3. The characteristic impedance of the coiled transmission line was the same as that of the feedline, thus eliminating the extra transformer action of a length of transmission line with a different characteristic impedance.

4. The Balun is a form of Guanella's two-conductor 1:1 Balun, which is not prone to core flux and, hence, saturation and the generation of spurious frequencies. It is also not susceptible to mismatched and unbalanced loads as are the Turrin and "voltage" Baluns.

After constructing several of Reisert's Baluns and comparing them with other Guanella designs, I found that the crossover winding had virtually no effect up to 100 MHz (the limit of my equipment). In regards to Reisert's VSWR comparison with a rod-type Balun when feeding a triband Yagi beam on 20 meters, I found that his Balun had a lower VSWR (practically 1:1) at the best match point. The rod-type Balun had a best VSWR of about 1.3:1, but at a slightly higher frequency. He attributed the higher (and somewhat flatter) VSWR curve of the rod-type Balun to its greater ohmic loss. Because the rod-type Baluns I have investigated used the same low-loss ferrite that Reisert's did, I suspect that the differences in the VSWR curves were mainly due to the mismatch loss introduced by the rod-type Balun.

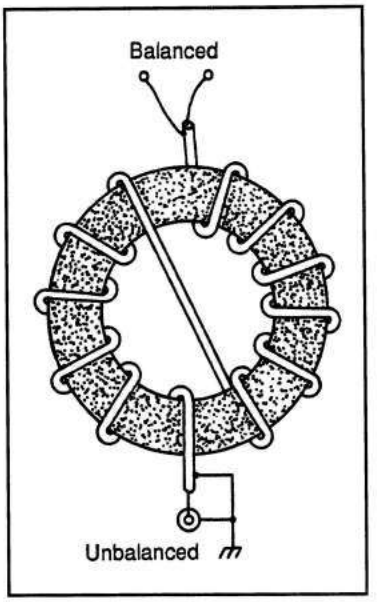

Figure 7-5. *A pictorial of the crossover used in Reisert's 1:1 Balun.*

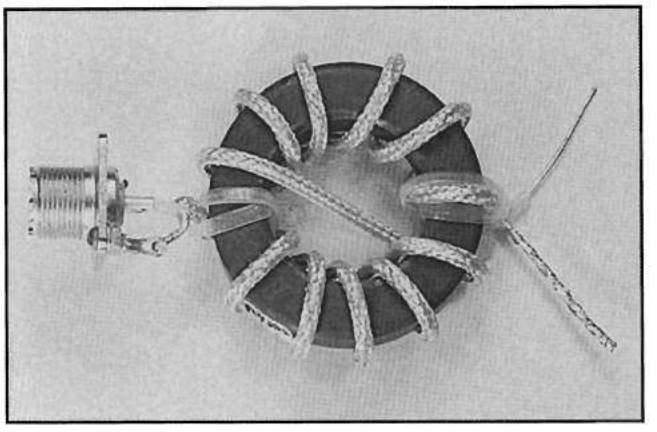

Photo 7-D. *A Reisert, W1JR, 1:1 Balun.*

G. Badger, W6TC—1980

Badger published an in-depth, two-part series[13,14] in *Ham Radio* magazine in 1980 on air-core Baluns and Ununs. I am sure it was instrumental in advancing the technology of this class of wideband transformers. An article by Orr[15] also shows that there are many other radio amateurs who see the advantages of air-core transformers.

What are the claims for air-core Baluns over their ferrite-core counterparts? First and foremost, proponents of air-core Baluns claim they don't suffer the consequences of saturation that leads to spurious frequencies, heating, and ultimate damage. Secondly, it's said that they are not subject to arcing from the windings to the core.

What are the claims for the ferrite-core Baluns over their air-core counterparts? Simply put, they have wider bandwidths and are more compact.

After reading Badger's two-part series, I found that my curiosity was piqued by his experimental data on harmonic distortion due to saturation in a ferrite-core 1:1 Balun. Although many have expressed concerns regarding saturation in ferrite-core Baluns, Badger's data could very well provide the only results available. He used the two-tone test method, which combined two RF sources of 2.001 and 2.003 MHz, amplified it to 2 kW PEP and then fed it through a commercial 1:1 rod-type ferrite Balun. The data showed considerable distortion in the 3rd order and 9th order distortion products. In other words, appreciable nonlinearity took place at this high power level.

Several questions come to mind regarding these measurements. What was the low-frequency response of the commercial 1:1 rod-type Balun Badger used? From my measurements on a rod-type Balun (**Figure 7-4**), I found a drop in the input impedance and an inductive component at 2 MHz. This indicates flux in the core and a problem when using this Balun at 2 MHz. Because many rod-type 1:1 Baluns have been used over the years, it would have been instructive if he had also made these measurements at 4 and 7

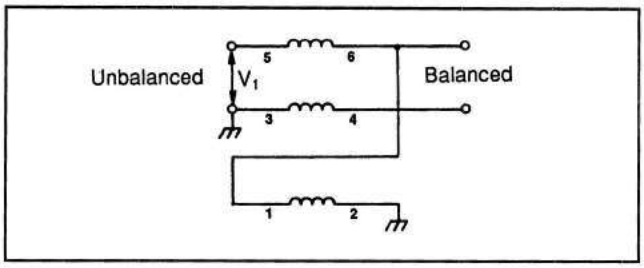

Figure 7-6. *Schematic of Badger's 1:1 Balun with a compensating winding (1-2). Winding (3-4) is the outer-braid of the coax and winding (5-6) is the inner conductor.*

MHz. They would have given the readers a safe lower-frequency limit for these Baluns.

I wondered why Badger didn't make similar measurements on Reisert's 1:1 Balun, which he included in his articles. As noted earlier, I consider Reisert's 1:1 Balun a very good design! I am sure that no distortion products would have been found at 2 MHz with this Balun. The end result is that Badger chose a poor ferrite-core design for making his comparisons. This helped to contribute to an undeserved reputation for the ferrite-core Balun.

Badger also suggested placing an insulated wire in parallel with the coax winding on Reisert's 1:1 Balun. He called this a compensating winding, which provided a superior balanced output. The third winding (1-2) is shown **Figure 7-6**. Winding (5-6) is the inner conductor and winding (3-4), the outer braid. Later experiments by myself and others have shown that a well-designed two conductor (Guanella) 1:1 Balun has a completely satisfactory balanced output for antenna applications. Furthermore, it does not suffer from an unbalanced and/or mismatched load and core saturation. Incidentally, Badger's schematic of **Figure 7-6** now adds up to four different versions of the 1:1 Balun. They are the two-conductor version of Guanella's and the three, three-conductor versions of Ruthroff's, Turrin's, and (now) Badger's.

Badger and Orr also mentioned the Collins Balun in their articles. This Balun is comprised of a dummy length of coax wound as a continuation of the original coiled coax winding. Interestingly, it is connected as a Ruthroff 1:1 Balun (**Figure 7-2B**), which also uses a third winding. Because there is appreciable coupling between the two coiled windings, the Collins Balun should also be susceptible to mismatched and/or unbalanced loads. Badger claimed it was, by far, the best 1:1 Balun he had ever used. Again, it would have been very informative if he had compared it with the Reisert Balun (without the compensating third wire).

M.W. Maxwell, W2DU—1983

One of the more significant articles on 1:1 Baluns was published by Maxwell[4] in 1983. Maxwell introduced, what he called, the "choke" Balun. It was formed by placing high-permeability ferrite beads over about one foot of small (but high-powered) coaxial cables similar to the ones used in the Reisert Balun. **Photo 7-E** shows the W2DU "choke" Balun removed from its plastic enclosure.

Maxwell compared his Balun with (what he termed) a "transformer-type" Balun by measuring the input impedances versus frequency when the outputs were terminated in 50 ohms. The "transformer-type" Balun didn't yield a true 1:1 impedance transfer ratio, which he claimed was due to losses, leakage reactance, and less than optimum coupling. Because Maxwell gave no description of the "transformer-type" Balun, I assumed it was the popular rod-type Balun shown in **Photo 7-C**. As you can see in **Figure 7-4**, this Balun has a poor low-frequency response. Furthermore, it is really optimized for a load of 47 ohms and not 50 ohms.

What Maxwell failed to realize was that his Balun was a form of Guanella's two-conductor type. That is, it is both a choke (a lumped element) and a transmission line (a distributed element). Additionally, Guanella's theory applies whether the transmission lines are coiled (about a core) or beaded, twin-lead or coaxial cable. From Ruthroff's classic paper,[9] which extended Guanella's work,[3] we became aware of the

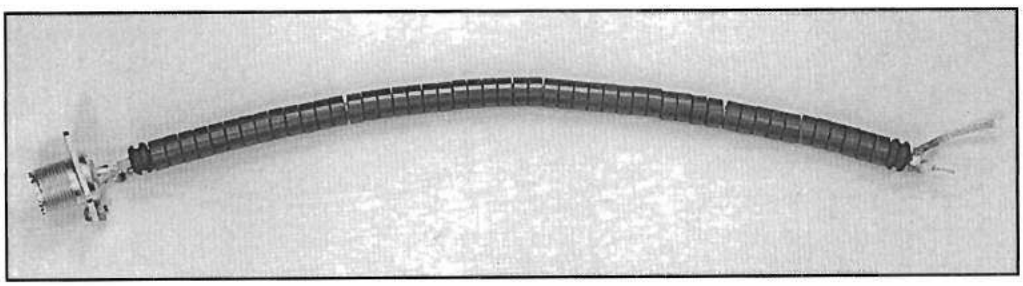

Photo 7-E. *The Maxwell, W2DU, "choke" 1:1 Balun.*

voltage drops along the lengths of the transmission lines. From very accurate insertion loss measurements,[2] we learned that the losses were mainly in the magnetic medium—and that they were related to the voltage levels and the permeabilities. Maxwell didn't take into account these latter findings. He used lossy high-permeability beads (2500) and assumed that the main loss was in the transmission line. He claimed that the CW power-handling capability of his Balun was 3.5 kW at 50 MHz and 9 kW at 10 MHz—the same as the coaxial cable itself. I seriously question these power ratings. Ironically, it is very likely that Maxwell's Balun had more real loss than the so-called "transformer-type" Balun!

R.W. Lewallen, W7EL—1985

There is very little doubt that Lewallen's interesting article[6] in 1985 contributed significantly to the better understanding and design of 1:1 and 4:1 Baluns. In it, he coined the (now very popular) terms "voltage" and "current" Baluns. The "voltage" Balun, a three-conductor type, has output ports which have voltages that are balanced to ground. It is brought about (see **Figure 7-6**) by the voltage-divider action of windings (5-6) and (1-2). Because we have two tightly coupled transmission lines in the passband with the same potential gradients, terminal 6 is at $+V_1/2$ and terminal 4 at $-V_1/2$ where V_1 is the input voltage. The "current" Balun, on the other hand, is a two-conductor Balun that produces equal and opposite currents on the output ports for any form of load impedance.

Lewallen conducted a series of experiments on 10 meters to compare the performances of "voltage" and "current" Baluns under balanced and unbalanced conditions. In the unbalanced (nonsymetrical) condition, the dipole was lengthened by five inches on one side and shortened by five inches on the other side. He then obtained a figure of merit for both Baluns (as well as for the case without a Balun) defined as the ratio of the average magnitude of the currents at the feedpoint over the magnitude of the imbalance (the inverted L) current. The magnitudes of the currents were obtained by current-probe toroids. Measurements were made at the antenna feedpoint and at a half-wave (physically) from it.

The "current" Balun consisted of 15 turns of very small RG-178/U coax on an FT82-61 core (a ferrite toroid with an OD of 0.825 inches and a permeability of 125). The "voltage" Balun had 10 turns of RG-178/U coax with a No. 26 wire in parallel (closely coupled) on the same toroid. The schematic is shown in **Figure 7-6**.

Lewallen concluded (and I agree) that his experiments clearly showed that the "current" Balun gave superior performance at every measured point in each experiment. However, the "voltage" Balun still improved the balance over the no-Balun case. He also concluded that other experiments should be performed in order to better compare the two forms of the Balun. One is to ascertain the difference when the feedline is placed nonsymetrical with respect to the antenna (to induce an imbalance current into the feedline). Others include determining the optimum point in the feedline to place the Balun, and testing the various kinds of core and beaded Baluns.

Although Lewallen's article pretty much speaks to Badger's proposal of adding a third wire to Reisert's Balun for better balance (i.e., avoid it), there are some comments and questions I have regarding his experiments and findings. They are:

1. Why didn't Lewallen use Reisert's Balun as the "current" Balun and Badger's suggested third-wire design as the "voltage" Balun? These would have been more realistic designs for comparisons. Instead, he used very small structures (which will only find use in QRP operations) and, as such, have higher frequency capabilities. Also, because the "voltage" Balun only had 10 turns (and hence a shorter transmission line and a poorer low-frequency response), it was favored in the comparisons on 10 meters. Had Lewallen used transmission lines of equal lengths on Reisert's cores, the differences between the two Baluns would have been even more dramatic.

2. It would also have been very useful if Lewallen had made comparisons between a "current" Balun that could handle the full legal limit of amateur radio power (again like the Reisert Balun) and "voltage" Baluns using Turrin's schematic (**Figure 7-3**) with rod and toroidal cores which have been readily available for nearly three decades.

3. Additionally, comparisons should not only be limited to 10 meters. Because 1:1 "voltage" Baluns are configurations of coupled transmission lines with various characteristic impedances, their performances with mismatched and unbalanced loads are more sensitive to the higher frequencies than their "current" Balun counterparts. Therefore, making similar measurements on 20 meters would also provide more useful information.

4. Even though Ruthroff's classic 1959 paper[9] has been the industry standard over the years, his 1:1

Balun design has been practically nonexistent in the amateur literature. Turrin mentioned its advantage over his first design in his second article.[12] But Turrin's first design has prevailed in our amateur literature. Because Ruthroff's design has the third conductor on a separate part of the toroid, it has the balanced output mentioned by Badger,[13] but still retains the flexibility of the Guanella[3] Balun. In other words, as the frequency is increased, the choking action of the third wire makes it practically transparent. This enables it to handle any form of load impedance. It would have been informative if Lewallen had pointed this out and also noted that Ruthroff's 1:1 Balun, although looking like a "voltage" Balun, is really a "current" Balun.

5. Lewallen and the others who have published in the amateur radio literature have failed to reference the first presentation on what are now known as "current" or "choke" Baluns, made by Guanella[3] in 1944. Even though Guanella used coiled transmission lines without a magnetic core, his theory on how these devices work is still applicable today.

J.S. Belrose, VE2CV—1991

The last article on 1:1 Baluns I considered worth mentioning was written by Belrose[5] in 1991. In it, he described the W2DU Balun by Maxwell and how his technique of threading coaxial cable through ferrite beads could be easily applied to 4:1 and 9:1 Baluns.

What immediately grabbed my attention in this article was the *deck head* (the editor's comments), which included highly complimentary remarks regarding the beaded-coax Balun. In essence, it said, "In this breakthrough article, W2DU's peerless 1:1 current-Balun design serves as the basis for excellent ferrite-bead-choke current Baluns capable of 4:1 and 9:1 impedance transformation."

However, if one reads the article carefully, it becomes apparent that this is not what Belrose said. His words were, "The *current Balun* of the *type* developed by Walt Maxwell, W2DU—a Balun consisting of ferrite beads slipped over a length of coaxial cable—is the best so far devised (italics mine)." He did not say that W2DU's Balun was "peerless." In fact, in the article he said just the opposite. He pointed out that the W2DU Balun's main disadvantage is that the beads are lossy at HF and heating becomes a concern when the transmitting power exceeds 125 watts! For high power (that is 1-kW CW), Belrose recommended Roehm's[16] designs, which use lower permeability (850) beads nearest the Balun's balanced output (where most of the heating takes place).

However, I do question two of the advantages he claims for the W2DU Balun. They are:

1. Its excellent power-loss and impedance-versus-frequency characteristics are much superior to those of a bifilar current Balun wound on a ferrite toroid.

2. It has excellent power-handling capability, and can function quite satisfactorily when working into highly reactive loads. This is so because the magnetic flux produced hy currents flowing on this Balun's wires cannot saturate its ferrite beads.

Belrose ohtained evidence for advantage number 1 by comparing the input impedance and power loss versus frequency of the W2DU Balun with a commercial Balun when they were terminated in 50 ohms. The commercial Balun was a bifilar wound toroidal type used in a differential-T tuner. What Belrose failed to realize was that the commercial Balun had heavily insulated wires, resulting in a characteristic impedance greater than 100 ohms. Thus, he was actually comparing a 50-ohm transmission line with a longer line that had a characteristic impedance in excess of 100 ohms! As expected, his input impedance versus frequency curve for the commercial Balun was even more severe than that of the Turrin Balun shown in **Figure 7-4**.

Advantage number 2 is based upon the premise that the magnetic flux produced by currents on the W2DU Balun's wires cannot saturate the ferrite beads, while the windings of a bifilar wound toroidal current Balun can. This is an incorrect assumption because the magnetic flux of a two-conductor type Balun, like the beaded-coax or the bifilar-wound toroidal Balun, is generated by the imbalance (inverted L) current and hence is *much* lower than the transmission line currents. This is especially true with sufficient choking reactances. The perception that the toroidal type Balun still transmits the energy to the output circuit by flux linkages, could very well lead to this mistaken impression.

For high power beaded-coax Baluns, Belrose referred to designs by Roehm,[16] who increased the power capability of this type of Balun by using lower permeability beads near the balanced output. He also increased the length considerably. For operation from 80 meters to 10 meters, Roehm used 28 inches of beaded coax. For 160 meters to 10 meters, he used 36 inches of beaded coax. Belrose's suggestion of connecting beaded coaxes in parallel on the low-imped-

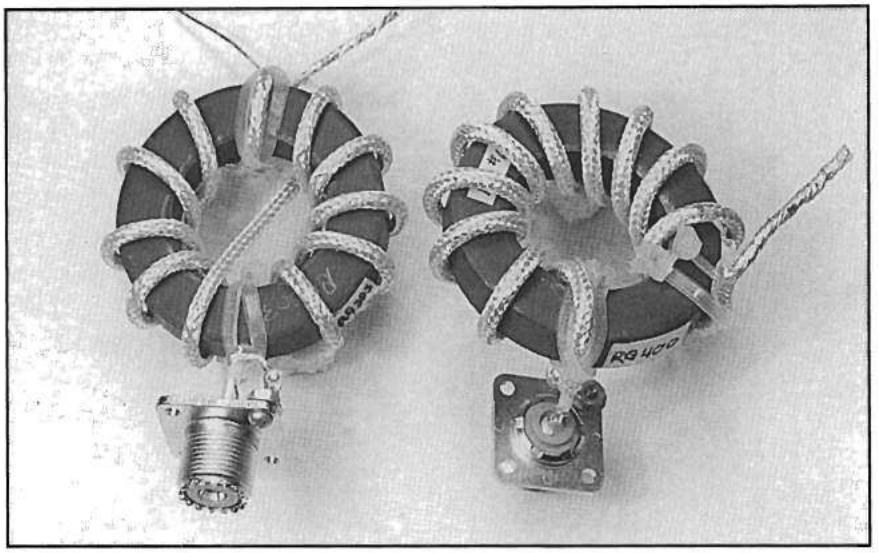

Photo 7-F. *Two versions of Reisert's 1:1 Balun. The Balun on the left uses the crossover shown in Figure 7-5. The Balun on the right is continuously wound. Both have the same electrical performance in the HF band.*

ance side and in series on the high impedance side to obtain a broadband 4:1 transformation ratio would require transmission lines with characteristic impedances of 100 ohms. This means, for a high power 4:1 Balun using beaded transmission lines, about 56 inches of beaded line would be required for the 80-meter to 10-meter operation and 72 inches for the 160-meter to 10-meter coverage. For a 9:1 Balun, it would be necessary to increase these lengths by 50 percent!

It remains to be seen what Belrose would have said or done if he had compared the W2DU Balun of Maxwell's with the W1JR Balun of Reisert's. He certainly couldn't claim the advantages listed in his article for the W2DU Balun. Would he still have claimed that the type of Balun developed by Maxwell is the best so far devised? Given the evidence, I doubt it.

Sec 7.4 High-, Medium-, and Low-power Designs

In this section I'll present my latest 1:1 Balun designs. Except for one Balun that appeared in the June 1993 issue of *CQ*, the others appeared for the first time in the magazine's April 1994 issue. Because I have favored Reisert's design throughout this chapter, the first Baluns described here are my versions of his technique of coiling small (but high power) coaxial cable around a low-permeability ferrite toroid. For my wire versions, I could have used all sorts of adjectives to describe them like Guanella, two-conductor, choke, and current. However, in the process of writing this section, I thought Belrose's adjectives were the most direct. Using his words, I call my wire versions of the 1:1 Balun simply—*bifilar toroidal Baluns*.

Photo 7-F shows two versions of Reisert's Balun. The one on the left uses the crossover shown in **Figure 7-5**. Because no difference in performance at HF was noticed without the crossover, a continuous-wound version is also shown on the right. The main advantage in the HF band with the crossover winding is purely mechanical. Having the input and output connections on opposite sides of the toroid is not only more convenient, but it also offers a much stronger method of mounting.

For operation from 1.8 to 30 MHz, 10 turns of small coax like RG-303/U, RG-142B/U, or RG-400/U are wound on a 2.4-inch OD ferrite toroid with a permeability of 250. If the use is limited from 3.5 to 30 MHz, then a permeability of 125 is recommended because it would yield a slightly higher efficiency at the high end. If one wants the highest possible efficiency and limits the operation from 14 to 30 MHz, then a permeability of 40 is recommended. With loads grounded at their centers, these conditions were found to give ample margins (handle a VSWR of 3:1 without any appreciable flux) at their low frequency ends.

For ease of winding, I found TY-RAP™ Cable Ties *very* useful. Two were used at each end. Removing the covering on the outer braid also helps. Because about 24 inches of cable is wound on the toroid, I recommend you start with at least 32 inches. Of the three cables noted above, I found RG-303/U cable the easiest to wind and connect. Although it only has a single-thickness braid (the others have double-thickness braids), its power rating is still the same—9 kW at 10 MHz and 3.5 kW at 50 MHz.

The next high power design is shown in **Photo 7-G** mounted in a 4 inch long by 3 inch wide by 2.25 inch

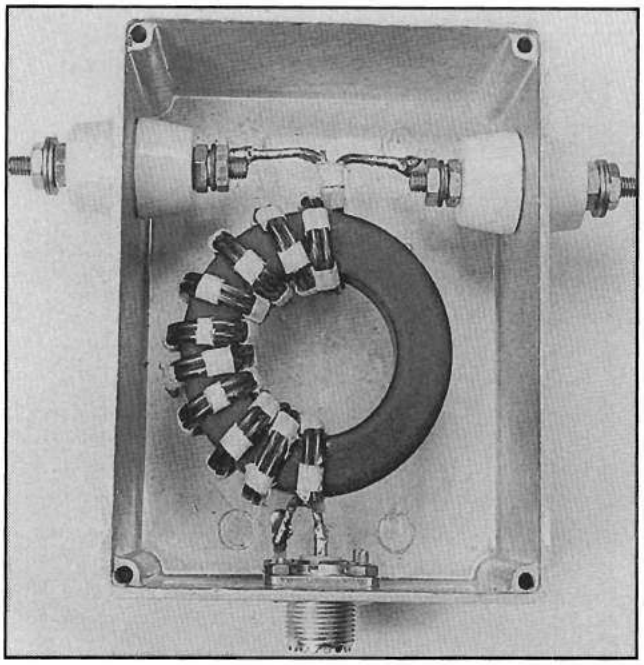

Photo 7-G. *My high-power design of a bifilar toroidal (Guanella/current) 1:1 Balun mounted in a 4 inch long by 3 inch wide by 2.25 inch high Bud aluminum box.*

high Bud CU 234 aluminum box. It has 10 bifilar turns of No. 12 H Thermaleze wire on a 2.4-inch OD ferrite toroid. As with the Reisert versions, a permeability of 250 is recommended for 1.8 to 30 MHz, 125 for 3.5 to 30 MHz, and 40 for 14 to 30 MHz. One wire is also covered with two layers of Scotch No. 92 polyimide tape in order to raise the characteristic impedance to 50 ohms. With this added insulation, the voltage breakdown of this twin-lead transmission line compares very favorably with RG-8/U cable (4000 volts). In order to preserve the spacing, the wires are also clamped together about every 1/2 inch with strips of Scotch No. 27 glass tape 3/16 inches wide and a little over 1 inch long.

Two "economy" versions of the high power bifilar toroidal Balun are shown in **Photo 7-H**. The one on the left shows the windings crowded on one-half of the toroid. The one on the right provides the same positions of the input and output connections by using the crossover. Their performances are identical. Both Baluns have 10 bifilar turns of No. 14 H Thermaleze wire on a 2.4-inch OD ferrite toroid. The choices of permeability, which trade off bandwidth for efficiency, are the same as those used in the two previous high power designs. The word "economy" here refers to economy in labor—this Balun is actually very easy to construct.

This "economy" Balun, which also handles the full legal limit of amateur radio power, has a small tradeoff in high frequency response. Because no extra insulation is used, the characteristic impedance of two tightly clamped No. 14 H Thermaleze wires is 45 ohms. With one layer of Scotch No. 92 tape, it increases to 50 ohms. But for most of the HF band, the difference in performance between Baluns using transmission lines of 45 and 50 ohms should be negligible. Even without the extra insulation, the voltage breakdown should compare very favorably with the smaller, high-power coaxes used in the Reisert versions (1900 volts).

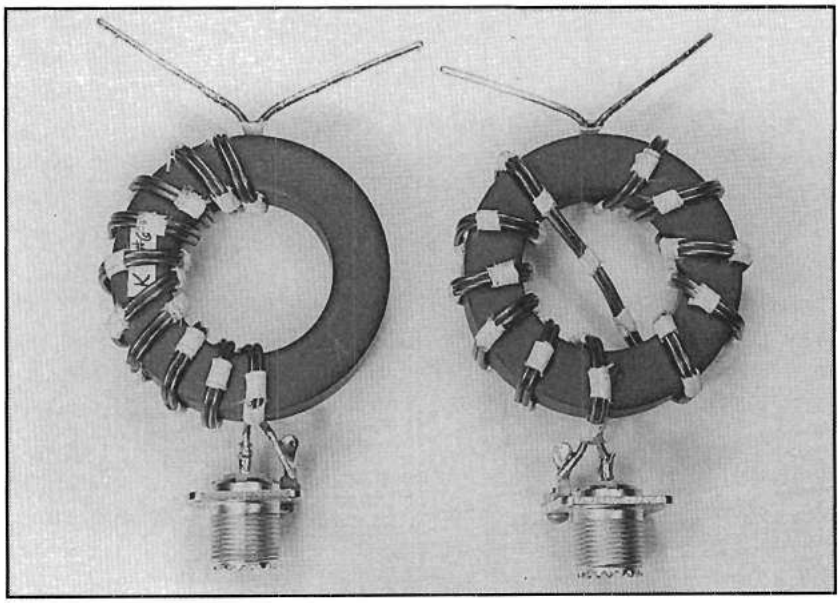

Photo 7-H. *Two "economy" versions of the high-power bifilar toroidal (Guanella/current) 1:1 Balun. The one on the right uses Reisert's crossover technique.*

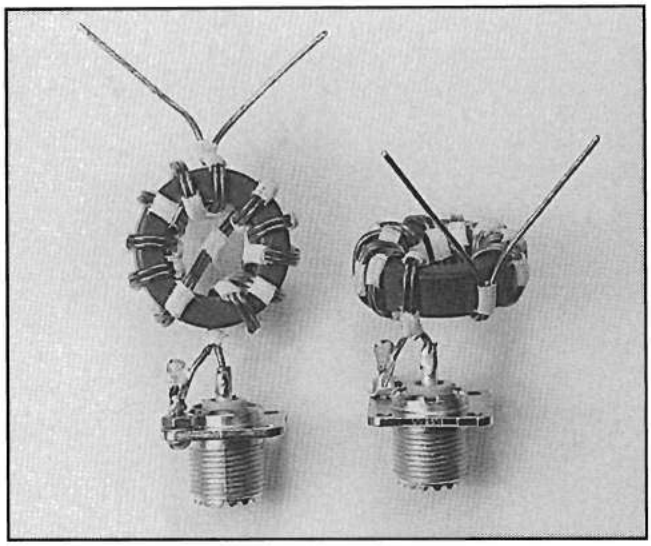

Photo 7-I. *Two low-power versions of the bifilar toroidal (Guanella/current) 1:1 Balun capable of handling the output of practically any HF transceiver. The Balun on the left has the crossover.*

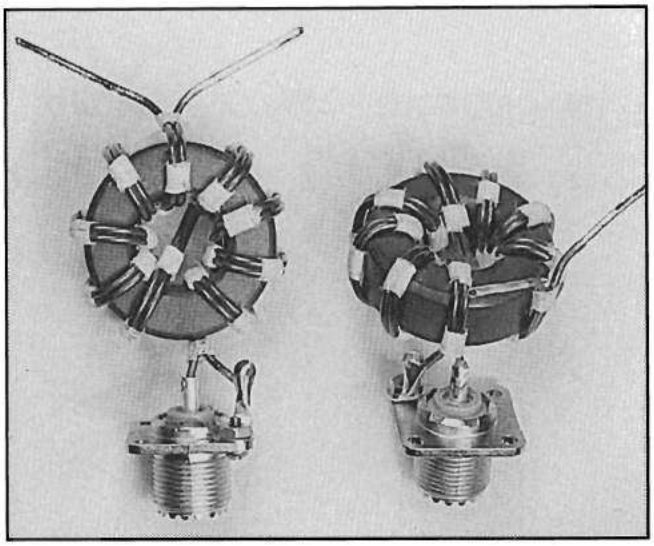

Photo 7-J. *Two medium-power versions of the bifilar toroidal (Guanella/current) 1:1 Balun capable of handling the full legal limit of amateur radio power when the VSWR is less than 2:1. The Balun on the left has the crossover.*

Photo 7-I shows two low-power versions of a bifilar toroidal Balun capable of handling the output of practically any HF transceiver. One has a crossover winding and the other, a continuous winding. They both have 10 bifilar turns of No. 16 H Thermaleze wire on a 1.25-inch OD ferrite toroid with a permeability of 250. Since efficiency is not a major problem in low-power use, I found no reason to suggest the other two versions, which use lower permeabilities. It is also interesting to note that two tightly clamped No. 16 H Thermaleze wires have a characteristic impedance close to 50 ohms. Therefore, this small Balun (particularly with its short leads) has a very good high frequency response.

Photo 7-J shows two medium-power versions of a bifilar toroidal Balun capable of handling the full legal limit of amateur radio power under controlled conditions—when the VSWR is less than 2:1. Being smaller than its larger (2.4-inch OD) counterpart, its heat-sinking capability and, hence, power rating is less. As before, one Balun uses a crossover while the other doesn't. Each has 8 bifilar turns of No. 14 H Thermaleze wire on a 1.5-inch OD ferrite toroid. The ferrite permeabilities and expected bandwidths are the same as the other high-power Baluns. Because the average magnetic path length in the core is about two-thirds that of the 2.4-inch core, only 8 bifilar turns are required in order to produce a similar low-frequency capability. Even though the characteristic impedances of their bifilar windings are 45 ohms, their responses on 10 meters should be somewhat better than the "economy" models because the lengths of their transmission lines are shorter (18 compared to 24 inches).

And now a few words on what sort of efficiency one can expect in trading-off low frequency response by using lower permeability ferrite cores. From earlier studies,[2] it was found that the efficiency (with sufficient choking, so only transmission line currents flow) is related to the permeability, the voltage drop along the length of the transmission line, and the frequency. The higher the permeability and/or voltage drop, the greater the loss. Additionally, the higher the permeability, the greater the loss with frequency. It was also found that a permeability of less than 300 was necessary in order to obtain the very high efficiencies of which these devices are capable.

Here are some efficiencies that might be expected from ferrites under matched conditions, based on the results of the studies:

1. With 250 material, an efficiency near 99 percent at 1.8 MHz and 97 percent at 30 MHz.
2. With 125 material, an efficiency near 99 percent at 3.5 MHz and 98 percent at 30 MHz.
3. With 40 material, an efficiency of 99 percent at 14 MHz and at 30 MHz.

When a Balun is exposed to a high impedance resulting in a VSWR of 2:1, the voltage, and hence loss, increases by about 40 percent. With a VSWR of

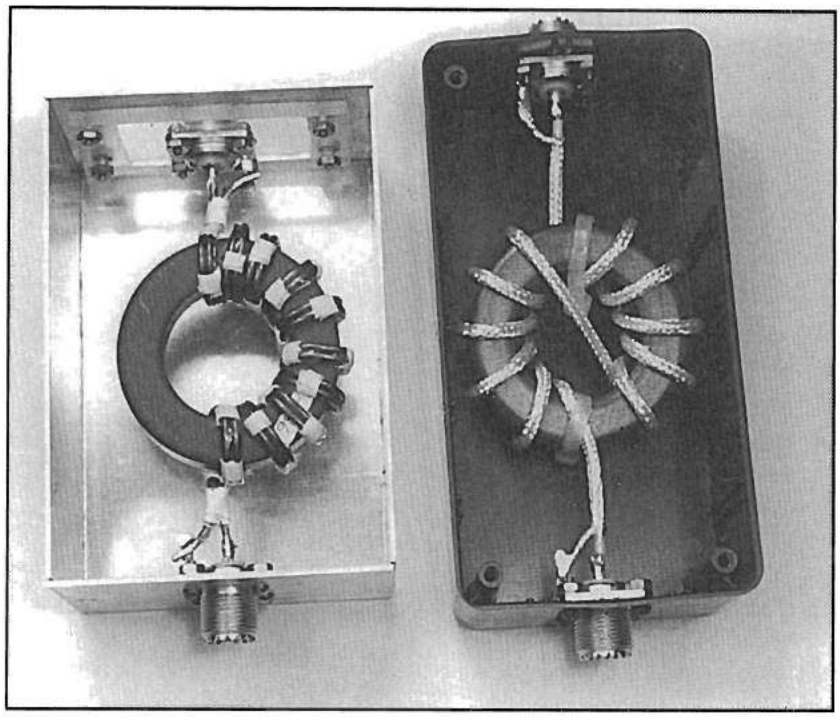

Photo 7-K. *Two examples of mounting the high-power 1:1 Guanella Balun in enclosures that allow isolation transformer operation.*

4:1, the loss doubles. With a VSWR of 10:1, the loss is more than three-fold. Since limited data was obtained in this study,[2] these increases in losses with increases in VSWR could very well be even greater.

Sec 7.5 Isolation Transformers

As was shown in the preceding sections, the 1:1 Guanella (current/choke) Balun is in reality a two-conductor RF choke, or an isolation transformer. However, practical Balun designs don't usually lend themselves to isolation use for mechanical reasons. They cannot be conveniently inserted into a coaxial cable system. Therefore, the objective is to mount the "Guanella Baluns" in enclosures that will allow them to perform as isolation transformers.

Photo 7-K shows two examples of enclosures that should accomplish the mission. The example on the left shows one of the high-power units mounted in a 5 inch long by 3.5 inch wide by 2.25 inch high aluminum enclosure. The output connector (on the top) is insulated by a 0.125-inch-thick piece of plastic. The one on the right shows another high-power unit mounted in a 6 inch long by 3 inch wide by 2 inch high plastic enclosure, which is available from Radio-Shack. The descriptions of the high-power units are given in the preceding section.

These isolation transformers can be used as Baluns when inserted in a coaxial cable one-half wavelength (physically) from a half-wave dipole[6] or between a coaxial cable and a balanced L-C tuner.[16] They should never be inserted in a coaxial cable system that presents a high impedance and, consequently, a high voltage. This could be harmful to the unit.

Note that the high-power unit on the left in **Photo 7-K** can also be used as a filament choke in a Class B linear amplifier. Its low-frequency response is much better than any rod-type, assuring 160-meter operation. Obviously, it would not be mounted in the aluminum enclosure shown in the photo. In addition, the two layers of Scotch No. 92 tape would not be required because the characteristic impedance of the winding is unimportant and the voltages involved are quite low.

By the way, the designs discussed above can be used as phase-inverters. Simply connect the hot lead on one side to the ground on the other side.

Sec 7.6 Summary

In investigating the 1:1 Balun, I was quite surprised to see the ferrite- and powdered-iron-core designs that have been available in the literature and off-the-shelf since 1964. They not only had poor low- and high-frequency responses, but they were also susceptible to flux in the cores at their low-frequency ends. Furthermore, since they only used single-coated wires, they were also prone to voltage breakdown. No doubt, these designs are responsible for the poor reputation that the Balun has had for many years.

It wasn't until 1978, when Reisert published his article, that a Balun which had all of the attributes of a good design became available. Namely:

a) It is efficient because it uses a low-permeability core.

b) It has sufficient choking reactance to meet its low-frequency requirement.

c) It is not prone to flux in the core (and, hence, saturation) because it has no third winding.

d) It has a 50-ohm characteristic impedance and maintains a 1:1 transformation ratio with a 50-ohm load.

e) It has a good voltage breakdown capability (1900 volts).

f) It can handle a mismatched and/or unbalanced load.

However, succeeding investigators failed to see the advantages of Reisert's design and proposed their own. Surprisingly, they belonged to two distinct groups. One group favored "air-core" Baluns and the other, "choke" (beaded-coax) Baluns.

The main argument given by the "air-core" followers was that their Balun would never experience problems with saturation, while the "ferrite-core" Balun would. However, the Reisert Balun is a current/choke type Balun that could only have flux in the core due to the imbalance (inverted L) current, which is much smaller than the transmission line currents. In fact, with any degree of choking reactance by the coiled transmission line, the imbalance current is essentially negligible. Therefore, saturation is not a concern with a Balun like Reisert's. In all fairness, it should be noted that it is a different story with the 4:1 current/choke and voltage Baluns. All three of these types of Baluns have a "magnetizing inductance" in their low-frequency models and hence a possibility of saturation with a poor design.

The advocates of the "choke" 1:1 Balun claim that their beaded-coax Balun can't saturate while the bifilar (current) toroidal Balun can. This is untrue; they are basically the same kind of structure, and neither has a third conductor which could allow a flux-causing current at the very low-frequency end. But of all of the attributes listed above for the Reisert Balun, the first one has the "choke" Balun at a disadvantage in the HF band. Because its transmission line is not coiled about a toroid, it does not have the multiplication factor of N^2 (due to mutual coupling), where N is the number of turns, while the toroidal Balun does. Therefore, higher-permeability beads are required in order to obtain sufficient choking reactance. This results in lower efficiency.

Finally, it should be pointed out that the 1:1 Balun using the small, but high-power, coaxial cable is capable of 5-kW operation in the HF band. Because of current crowding, the bifilar toroidal Balun, even with No. 12 wire, has shown excessive wire heating at this level. Therefore, No. 10 or No. 8 wire, with added layers of Scotch No. 92 tape in order to obtain a 50-ohm characteristic impedance, is recommended.

Chapter 8

The 4:1 Balun

Sec 8.1 Introduction

Chapter 7 in this book discussed the most popular of all Baluns—the 1:1 Balun designed to match 50 ohms unbalanced to 50 ohms balanced. It not only gave a review of the history, theory, and design of these broadband transformers, but also my viewpoint on published articles advocating later designs using coaxial cable wound around a toroid, threaded through ferrite beads, or just plain coiled in air (an air-core Balun). As was noted, I am in considerable disagreement with many of the claims advanced for these later 1:1 Baluns.

Chapter 8 deals with the next most popular Balun —the 4:1 Balun designed to match 50 ohms unbalanced to 200 ohms balanced. Baluns matching 50 ohms unbalanced to 12.5 ohms balanced are also included. It begins with a little information on the history and design of these Baluns, followed by high- and low-power designs and comparisons with other Baluns that have been on the market or in the amateur literature. Guanella's approach to the design of a 4:1 Balun is particularly noteworthy. It not only yields an excellent Balun design, but also an Unun (unbalanced-to-unbalanced transformer) with practically the same performance. His design could very well be called a *Balun/Unun*. As in the first chapter, this one also closes with a brief summary of the significant points.

Sec 8.2 A Little History and Design Information

There are really only two classic papers that have established the principles upon which the transmission line transformer (the Balun being a subset thereof) is based. The first one was written by Guanella in 1944. Guanella proposed the idea of coiling a transmission line to isolate the input from the output, resulting in the (now popular) *current* or *choke* Balun.[3] The second was by Ruthroff in 1959, whose analysis of these transmission line transformers is the present industry standard.[9] Ruthroff also introduced the Unun and the hybrid transformer.

Interestingly enough, both Guanella and Ruthroff had different approaches to their 1:1 and 4:1 Balun designs. Guanella used a two-conductor 1:1 Balun design, while Ruthroff used a three-conductor design. Ruthroff's third conductor (which was said to increase the low-frequency response over the two-conductor Balun[12]) lay on a separate part of a toroidal core. Investigators who followed failed to recognize this fact. Their comparisons were made with a three-conductor Balun that had the third wire in parallel with the other two, which then formed two coupled transmission lines. This gave rise to the term *voltage* Balun—an inferior design.[6]

However, the differences between Guanella's and Ruthroff's approaches to 4:1 Baluns were even more striking. Guanella connected coiled transmission lines in a parallel-series arrangement, so in-phase voltages were summed at the high impedance side. His Balun has been called a *current* Balun.[6] Ruthroff, on the other hand, obtained a 4:1 transformation ratio by summing a direct voltage with a delayed voltage that traversed a single transmission line in a phase-inverter connection (see **Chapter 7**). His Balun has been called a *voltage* Balun. The distinction between the operation of these two Baluns was also overlooked by practically everyone who followed.

This section reviews the two different approaches taken by Guanella and Ruthroff in obtaining 4:1 Baluns. Of particular importance are the descriptions of the potential drops along the lengths of the transmission lines when the loads are grounded at various points. These voltage drops are not only relevant to the ohmic losses in the Baluns, but also to their electrical performances. These descriptions were quite

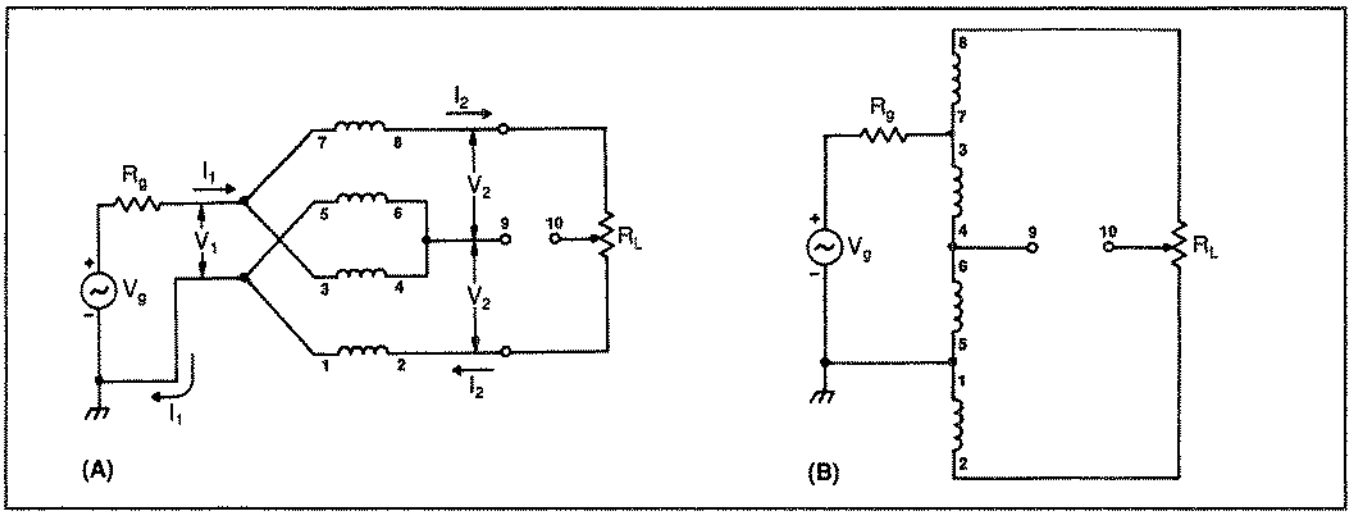

Figure 8-1. *Electrical models of the Guanella 4:1 Balun: (A) high-frequency, (B) low-frequency.*

possibly presented for the first time in the second edition of my book *Transmission Line Transformers*.[2]

Sec 8.2.1 Guanella's 4:1 Balun

Figures 8-1A and **B** show the high- and low-frequency models of Guanella's method of connecting transmission lines in parallel-series to obtain a 4:1 Balun. The high-frequency model (**Figure 8-1A**) assumes that the choking reactances of the coiled (or beaded) transmission lines are sufficient to isolate the input from the output, so only transmission line currents are allowed to flow. This occurs when the reactance of windings 3-4 and 5-6 (which are in series) is much greater than R_g (at least by a factor of ten.[2] If two cores are used, the reactance is the sum of the reactances of windings 3-4 and 5-6. If a single core is used, the reactance is twice as large because of the mutual coupling between the windings. The other advantage of Guanella's method (besides only using one core) is that shorter transmission lines can be used, resulting in better high-frequency performance.

As with all transmission line transformers, the objective is to have the transmission lines see loads equal to their characteristic impedances, resulting in "flat lines." This yields the highest frequency response. Because each transmission line in **Figure 8-1A** sees one half of the load, R_L, the optimum value of the characteristic impedance is $R_L/2$. Consequently, the input impedance, V_t/I_1, is simply the impedance of two identical transmission lines connected in parallel. It follows that the impedance transformation ratio is the load, R_L, divided by the input impedance.

Because the Guanella 4:1 Balun sums voltages of equal delays from identical transmission lines, his Balun is only limited in high-frequency performance by the deviation of the characteristic impedance of the transmission lines from the optimum values and the parasitics not absorbed into the characteristic impedance of the lines. I (and practically everyone else) had overlooked the simple and important statement, "a frequency independent transformation," which appeared in Guanella's 1944 article[3]—a fact that is evidenced by the scarcity of his designs in the literature. Another interesting aspect of the Guanella 4:1 Balun is the analysis of his Balun when the load is floating or grounded at different points. This leads to the determination of the voltage gradients that exist along the transmission lines and the various functions of which his 4:1 design is capable. Assuming a matched load or very short transmission lines resulting in $V_2 = V_1$, they are as follows.

Floating Load

With terminal 10 (which is at the center of R_L) floating, the potential gradient along the top transmission line in **Figure 8-1A** (windings 5-6 and 7-8) is $-1/2V_1$; along the bottom transmission line (winding 1-2 and 3-4) it's $-3/2V_t$. The voltage to ground on terminal 9, V_{90}, is $-1/2V_1$. Because the bottom transmission line (in **Figure 8-1A**) has a voltage drop along its length three times greater than the top transmission line, it results in three times more loss because losses in transmission line transformers are voltage dependent (dielectric-type losses).[2]

Even though a single-core Guanella 4:1 Balun maintains the voltages (stated above) when feeding a folded dipole (of about 200 ohms) which has a virtual-ground potential at terminal 10, it still feeds equal currents to each side of the antenna because of the series-connection at its output. Since the output voltages are not balanced to ground, a reactive component is probably introduced into the input impedance. Additionally, the choking reactance of the windings also prevents antenna currents from flowing on the outside of the coaxial cable feedline.

Load Grounded at Center

When two cores are used and terminal 10 (the center of R_L) is grounded, the voltage gradient along the top transmission line in **Figure 8-1A** is zero, and along the bottom transmission line it is $-V_1$. The voltage to ground on terminal 9 (V_{90}) is also zero. In fact, the core for the top transmission line isn't needed. It merely acts as a mechanical support for the top transmission line, which now only operates as a delay line. Also, all of the loss now occurs in the core of the bottom transmission line where a longitudinal potential gradient exists. Furthermore, the low-frequency response, as seen from **Figure 8-1B**, is now determined by the reactances of windings 1-2 and 3-4. This means that the low-frequency response with a floating load is better by a factor of two over the case where the load is grounded at its center.

But the single-core case is a different matter. Since the potential at terminal 9 (V_{90}) wants to be at $-1/2V_1$, connecting a ground directly to the center of R_L causes an imbalance that renders the single-core Balun unusable. If the ground were placed at a point 25 percent below terminal 8 (50 ohms from terminal 8 with a 200-ohm load), no difference would be noted from a floating load. This condition also exists when two cores are used.

Load Grounded at the Bottom

It is when the load is grounded at the bottom (at terminal 2), that we have what is probably the most interesting case. The 4:1 Balun (with two cores) is now converted into a very broadband Unun (unbalanced-to-unbalanced transformer). Because the bottom transmission line in **Figure 8-1A** has no potential drop along its length, it only acts as a delay line. The voltage to ground at terminal 9 (V_{90}) is $+V_1$, and the voltage gradient along the top transmission line is $+V_1$. This results in a voltage of $2V_1$ across the load. The low-frequency response is now determined by the reactances of windings 5-6 and 7-8. This is just the opposite of the Balun case when the center of the load was grounded. A single-core 4:1 Guanella Balun can also be converted to an Unun by putting a 1:1 Balun (for isolation) in series with the 4:1 Balun.[2]

There is a reason for claiming a very broadband response for a Guanella Unun (converted from his Balun)—the two in-phase voltages are now summed at the high-impedance side. The only other competition for a 4:1 Unun design is that of Ruthroff's,[9] where a direct voltage is summed with a delayed voltage that traversed a single transmission line (and, hence, had a built-in, high-frequency cut-off). In fact, very little information can be found in the literature on a *Guanella 4:1 Unun*.

Sec 8.2.2 Ruthroff's 4:1 Balun

Figures 8-2A and **B** show the high- and low-frequency models of Ruthroff's approach for a 4:1 Balun. The high-frequency model (**Figure 8-2A**) assumes that the

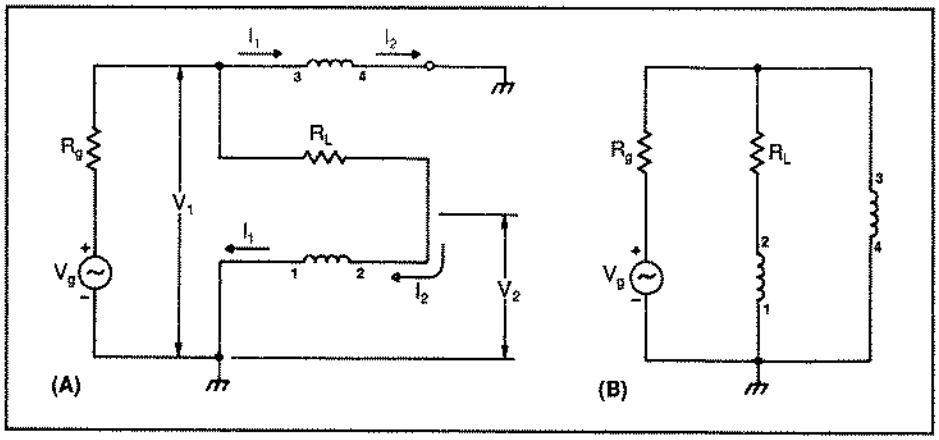

Figure 8-2. *Electrical models of the Ruthroff 4:1 Balun: (A) high-frequency, (B) low-frequency.*

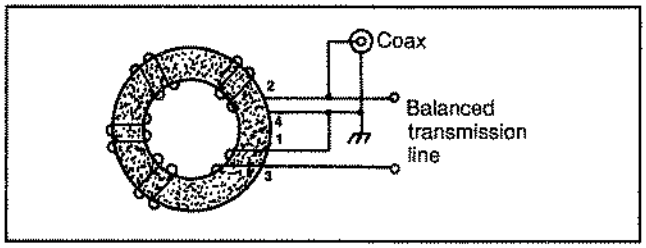

Figure 8-3. *A pictorial of the connections for a 4:1 Ruthroff (voltage) Balun.*

choking reactance of the coiled (or beaded) transmission line is sufficient to isolate the input from the output, so only transmission line currents are allowed to flow. This occurs when the reactance of winding 3-4 (or 1-2, because they are the same) is much greater than R_g (at least by a factor of ten^2).

As **Figure 8-2A** indicates, the transmission line is connected in a *phase-inverter* function (see **Chapter 7**). That is, a $-V_1$ voltage gradient now exists along the length of the transmission line. Therefore, the voltage across R_L now becomes $V_1 + V_2$. Although Ruthroff analyzed his 4:1 Unun in his classic paper,[9] his results also apply to his Balun with a floating load, because both devices sum a direct voltage with a delayed voltage. In essence, he used loop equations on the input and output and transmission line equations to eliminate one set of variables (I_2 and V_2). Ruthroff also used a maxima technique (setting a derivative to zero) to solve for the optimum characteristic impedance of the transmission line. As in the Guanella case, he found the optimum value to be $1/2R_L$.

An inspection of **Figure 8-2A** shows that the left side of R_L (terminal 3) has a direct voltage (V_1) to ground, and the right side (terminal 2) a delayed voltage ($-V_2$) to ground, which traveled the length of the transmission line. Also note, that if the line is electrically one-half wavelength long, the output is *zero*. As a result, Ruthroff's design (which has a built-in cut-off) is sensitive to the transmission line length.

I have recently unearthed another interesting aspect of Ruthroff's design.[2] If the center of the load is grounded, the high-frequency performance is vastly improved. The built-in high-frequency cut-off is eliminated and the Balun appears to take on the character of a Guanella Balun that sums voltages of equal delays. A closer inspection reveals that the input impedance now consists of two impedances in parallel: one consisting of $R_L/2$, and the other of a "flat line" terminated by $R_L/2$. As a result, the currents are not in phase!

Surprisingly, when matching into a folded dipole with an input impedance of 200 ohms, Ruthroff's Balun exhibits a high frequency response that is much greater than expected (see later sections). Because the folded dipole has a *virtual* ground at its center, the Balun could very well be summing voltages of equal phases.

Sec 8.2.3 Amateur Radio History and Design

Looking back at old issues of amateur radio handbooks (I don't have a complete set), I found that the first presentation on broadband 4:1 Baluns appeared in the 1955 edition of *The ARRL Handbook*. The section was called "Coil Baluns." The schematic diagram was that of Guanella's, shown in **Figure 8-1A**. What surprised me was that this section appeared to use many of the important words contained in Guanella's article.[3] It mentioned that the choking action of the coiled transmission lines should be great enough to isolate the input from the output at the lowest frequency of interest. It also included the requirement on the characteristic impedance of the coiled transmission lines; namely, that the characteristic impedance should be equal to $R_L/2$, where R_L is the load.

However, the section also included two other statements which are not correct in light of today's design practices. One recommended that the length of the winding in each coil be equal to about a quarter wavelength. The other stated that the principal application is in going from a 300-ohm balanced load to a 75-ohm coaxial line. With magnetic cores, the lengths of the windings are now considerably shorter than a quarter wavelength, and the applications include a host of different impedance levels.

Recent issues of the handbooks now include the 4:1 broadband *coil Balun* (along with the same write-up that appeared in the 1955 issue), and one with windings on ferrite cores. They are now called 4:1 air-core current Baluns and "just plain" 4:1 current Baluns (ferrite cores being assumed). Unfortunately, what is lacking in the description of the 4:1 current Balun is information on the importance of the characteristic impedance of the windings and the value of the permeability of the ferrite cores. The literature states that 8 to 10 turns (of No. 14 Formvar-coated, close-spaced—I guess) on a toroidal core or 10 to 15 turns on a rod are typical values for the HF range. Ferrites with permeabilities from 850 to 2500 are also sug-

gested. Nothing is mentioned regarding the dimensions of the cores.

In essence, there's very little information available today in our handbooks that would help one understand and construct the "popular" *current* Balun. Even the choices of recommended ferrites to be used are found wanting. Accurate loss measurements[2] have shown ferrites with permeabilities of 850 to 2500 to be lossy in Balun and Unun applications. Only when the permeabilities of ferrites are 300 or less will Baluns and Ununs exhibit the very high efficiencies of which they are capable.

Even though the 4:1 *voltage* Balun has actually had a shorter history than the *current* Balun, considerably more construction detail (including an actual photograph) has been available in the amateur radio handbooks. As far as I can tell, the first presentation took place between 1965 and 1968. In looking through succeeding issues (including the 1993 issue), I find the write-up hasn't changed much (if any) over the years. The 4:1 Balun from the handbooks and a commercial rod-type are described and compared with my designs in the succeeding sections.

Sec 8.3 4:1 Ruthroff Balun Designs

As mentioned above, the schematic of Ruthroff's Balun is shown in **Figure 8-2A**. A pictorial representation is shown in **Figure 8-3**. **Photo 8-A** (on the left) shows my construction of a design close to the one shown in the handbook's photographs. It has 10 close-spaced, bifilar turns of No. 14 Formvar-coated wire on a 2.4-inch OD ferrite toroid with a permeability of 40. **Figure 8-4** shows a plot of the input impedance versus frequency when the 200-ohm load is center-tapped-to-ground (which is close to the actual case when matching into balanced antenna systems). As you can see, when compared to a design that has the proper characteristic impedance of the winding and sufficient choking, the response is very poor. Although this Balun has been rated at 1000 watts of RF power from 1.8 through 60 MHz, I would suggest it not be used below 6 MHz for fear of excessive flux in the core (especially when the magnitude of the load is greater than 200 ohms). Also, above 14 MHz, the transformation becomes considerably greater than 4:1.

My design, on the right in **Photo 8-A**, has 14 bifilar turns of No. 14 tinned copper wire on a 2.4-inch OD ferrite toroid with a permeability of 125 or 250. The wires are threaded through No. 13 Teflon tubing with

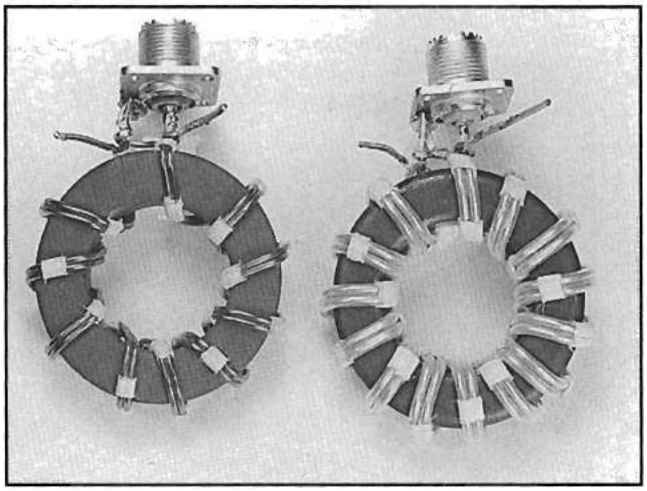

Photo 8-A. *Two designs of the 4:1 Ruthroff (voltage) Balun. The one on the left is taken from the amateur radio handbook. The one on the right is my improved version.*

a wall thickness of 20 mils. As you can see by its excellent high frequency response in **Figure 8-4**, the characteristic impedance of the bifilar winding must be very close to the ideal value of 100 ohms. **Photo 8-B** shows two different views of my design mounted in a 4 inch long by 3 inch wide by 2.25 inch high Bud CU 234 aluminum box. The Balun, which is placed equidistant between the top, bottom, and sides of the enclosure, is securely mounted by soldering its leads to the two feedthrough insulators and the SO-239 chassis connector.

It should be mentioned that if the Balun is to be used mainly on the lower portion of the HF band (including 160 meters), then the 250 permeability ferrite is recommended. Even though the difference in low frequency response between permeabilities of 125 and 250 doesn't show up in **Figure 8-4**, the 250 permeability would provide an extra safety margin (from flux in the core) at the low frequency end. The trade-off lies in giving up a little in efficiency (about 1 percent) for an increase in the safety margin (a factor of 2) at the low end.

Incidentally, the handbooks also state that the Balun can be used between a balanced 300-ohm point and a 75-ohm unbalanced line. Because I suspected this statement as well, I again measured the input impedances versus frequency of both Baluns when terminated in a 300-ohm center-tapped-to-ground load. **Figure 8-5** shows the deterioration that takes place, especially at the high end. Even a Balun that is well designed for a 50:200-ohm impedance level is not recommended

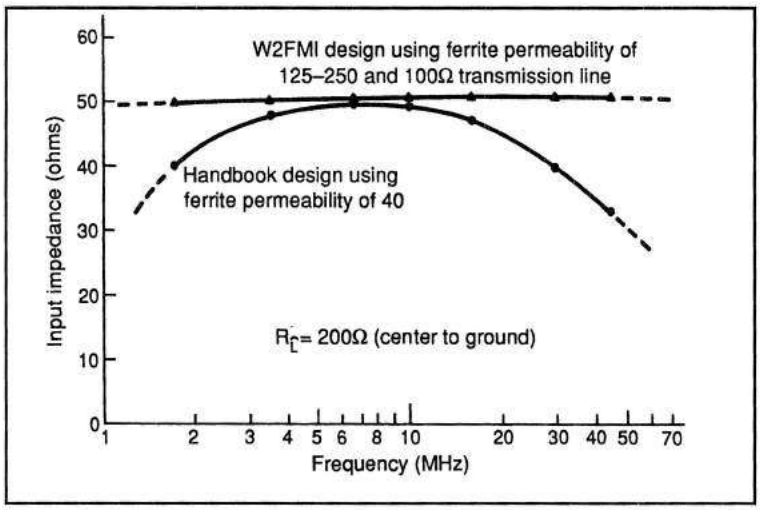

Figure 8-4. *The input impedance versus frequency for a 4:1 Ruthroff (voltage) Balun design from the amateur radio handbook and one optimized for the 50:200-ohm level. The load is grounded at its center.*

Figure 8-5. *The input impedance versus frequency for the two Ruthroff Baluns of Figure 8-4, but with a 300-ohm load. Note the deterioration of the W2FMI design, which was optimized for the 50:200-ohm level.*

for the 75:300-ohm level. Because the length of the transmission line becomes significant beyond 10 MHz, standing waves then change the impedance ratio due to the mismatch with the Balun's transmission line. My design also shows more safety margin at the low end. I'm surprised that these simple measurements weren't made many years ago.

However, the Balun shown in the handbook does have one interesting feature. It uses a very low permeability ferrite (40), which has been shown by very accurate insertion loss measurements[2] to yield efficiencies in Baluns (and Ununs) of *99 percent* at the

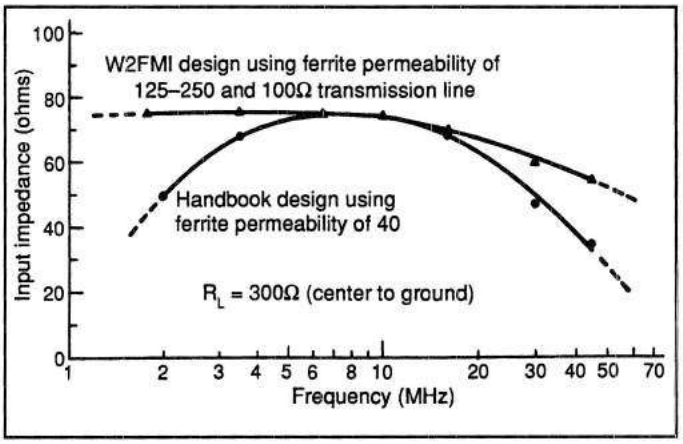

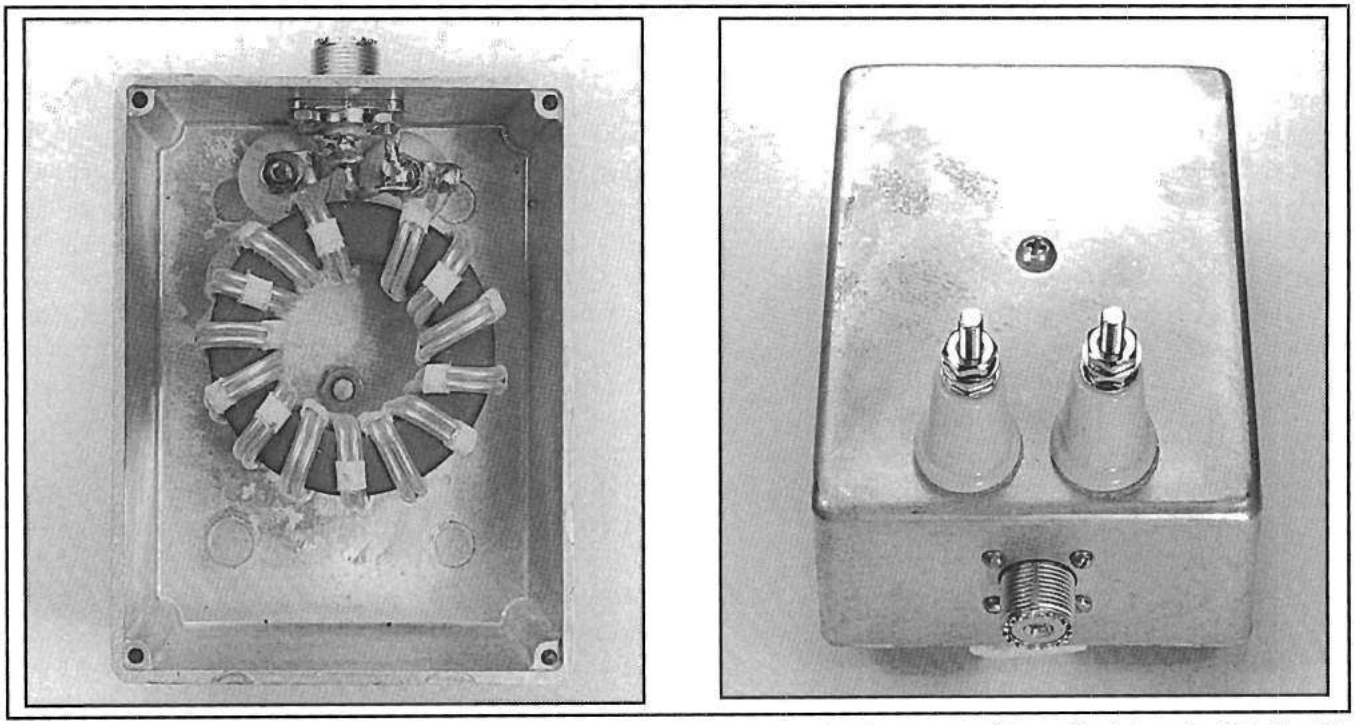

Photo 8-B. *Two different views of the optimized version of the 4:1 Ruthroff Balun mounted in a 4 inch long by 3 inch wide by 2.25 inch high Bud CU 234 aluminum enclosure.*

50:200-ohm impedance level! This is even a percent or two better than the ferrite with a permeability of 125. Because this ferrite permeability is so low, the major problem lies in obtaining sufficient choking reactance at the lowest frequency of interest, so that only transmission line currents are allowed to flow.

The design chosen (in order to exploit this very high efficiency) is shown **Photo 8-C**. It uses 14 bifilar turns of the same wire, as with my previous Balun shown on the right in **Photo 8A**, on two 2.4-inch OD cores (bound together with No. 27 glass tape) with permeabilities of 40. The unmounted view shows how the two cores are bound together by glass tape. The other views attempt to give an example for mounting the Balun. The Balun is supported by two acrylic end pieces which are, in turn, held fast to the enclosure by a long bolt. The Balun is placed equidistant between the top, bottom, and sides of a 5 inch long by 3.5 inch wide by 2.25 inch high aluminum enclosure. A few washers at the point where the bolt comes through the enclosure help to position the Balun between the top and bottom.

When matching 50 ohms (unbalanced) to 200 ohms (balanced), the response of this Balun is practically the same as mine, shown in **Figure 8-4** using a single core. From 1.7 to 30 MHz, it can certainly handle the full legal limit of amateur radio power with an efficiency close to 99 percent. However, if the operation of this Balun is restricted to the HF band only (that is, from 3 to 30 MHz), then it could be rated conservatively at 10 kW of peak power and 5 kW of average power. It would be an ideal Balun for a log-periodic beam antenna.

Finally, **Photo 8-D** shows three different views of a low power 4:1 Ruthroff (voltage) Balun designed to handle the output power of any HF transceiver easily. It has 10 bifilar turns of No. 18 hook-up wire on a 1.5-inch OD ferrite toroid with a permeability of 250. The enclosure is a 2.75 inch long by 2.125 inch wide by 1.625 inch high CU 3000-A minibox.

Section 8.4 4:1 Guanella Balun Designs

Photo 8-E shows two high-power Guanella 4:1 Baluns designed to match 50-ohm coaxial cable to loads of 200 ohms. They both use No.14 H Thermaleze wire with a covering of Teflon tubing giving characteristic impedances very close to 100 ohms (the objective). Their responses are flat from 1.5 MHz

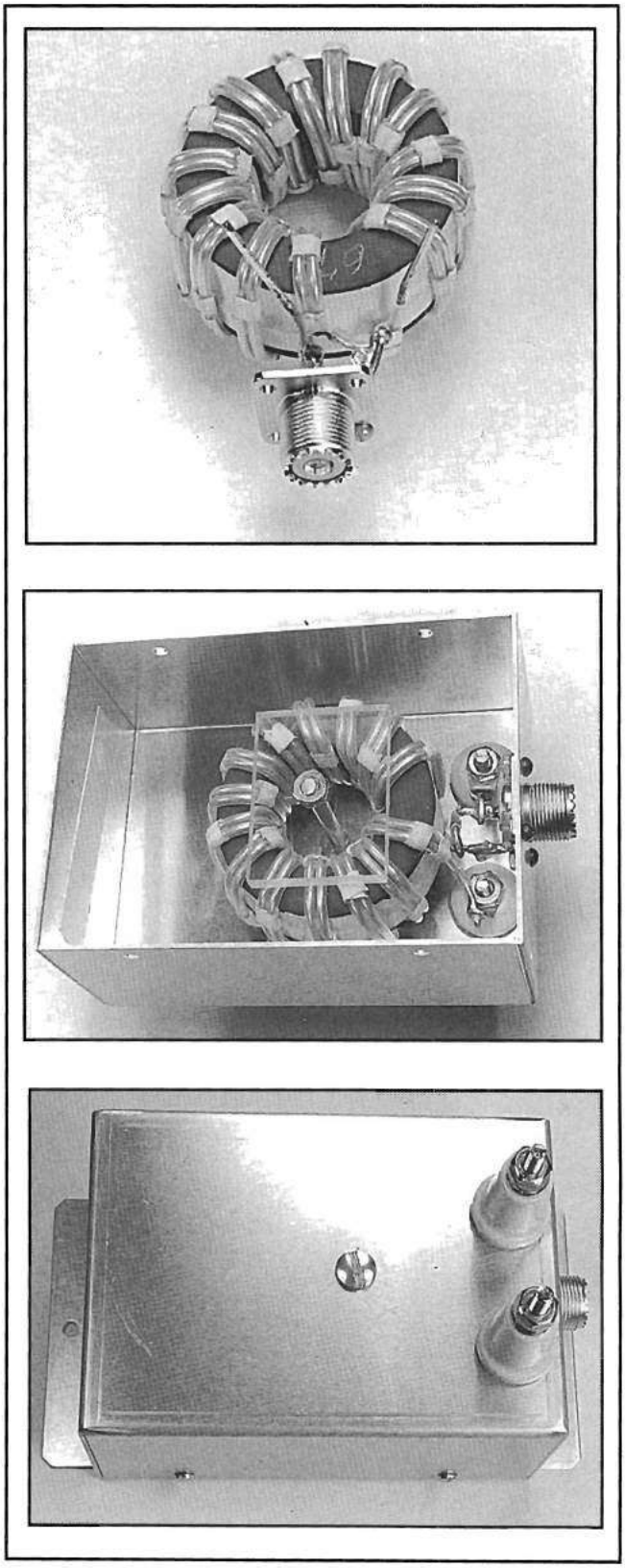

Photo 8-C. *Three views of the very high-power 4:1 Ruthroff Balun using two low-permeability (40) ferrite cores. Dimensions of the aluminum enclosure are: length, 5 inches; width, 3.5 inches; height, 2.25 inches.*

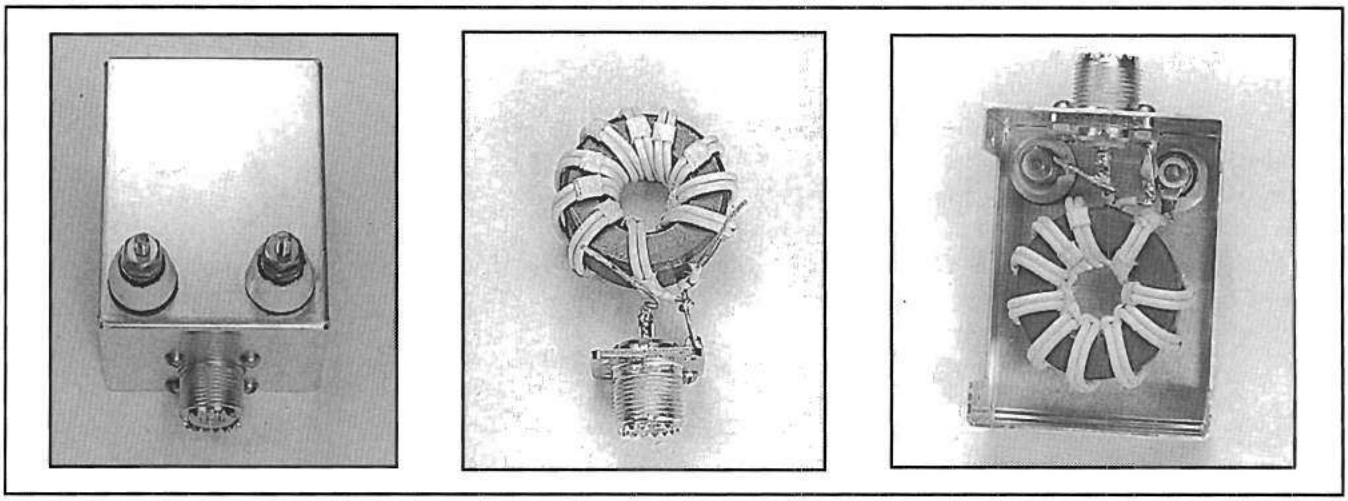

Photo 8-D. *Three views of the low-power 4:1 Ruthroff Balun designed to handle the output of any HF transceiver. The aluminum enclosure is a 2.75 inches high by 2.125 inches wide by 1.625 inches high CU 3000-A minibox.*

to well beyond 30 MHz. Both can easily handle the full legal limit of amateur radio power.

The single-core version (on the left) has 8 bifilar turns on each of its two transmission lines. The dual-core version (on the right) has 16 turns on each core. The wires are clamped together with strips of Scotch No. 27 glass tape placed about every 3/4 inch. The cores are 2.4-inch OD ferrite toroids with a permeability of 250. The connectors are on the low-impedance sides. For ease of connection, the dual-core version has one winding clockwise and the other, counterclockwise. Also, in the dual-core case, the spacing between the two cores (which isn't critical) can be as small as 1/4 inch.

These transformers can also be wound with ordinary No. 14 (solid) house wire. The several samples I tried yielded characteristic impedances close to 100 ohms (and, thus, were acceptable). The major difference lies in the voltage-breakdown capability. Units wound with Teflon-sleeved No. 14 H Thermaleze wire have been reported to withstand 10,000 volts without breakdown! Obviously, this is beyond the capability of ordinary house-wire.

Photo 8-F shows a Guanella (current) 4:1 Balun mounted in a 5 inch long by 4 inch wide by 3 inch high CU 3005-A minibox. It has 14 bifilar turns of No. 14 H Thermaleze wire on each of the two 2.4-inch OD ferrite toroids with permeabilities of 250. Each wire is covered with Teflon tubing, resulting in a characteristic impedance close to 100 ohms (the optimum). The windings also employ a crossover after the seventh turn, as shown in **Figure 8-6**. For ease of con-

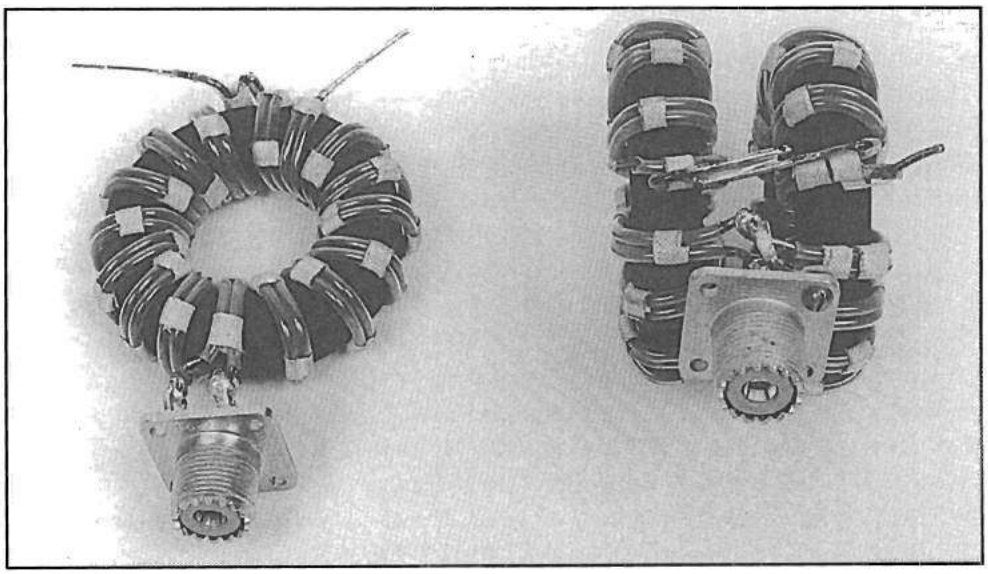

Photo 8-E. *Two high-power versions of the Guanella 4:1 Balun. The Balun on the left uses a single core while the one on the right uses two cores. The connectors are on the low-impedance sides.*

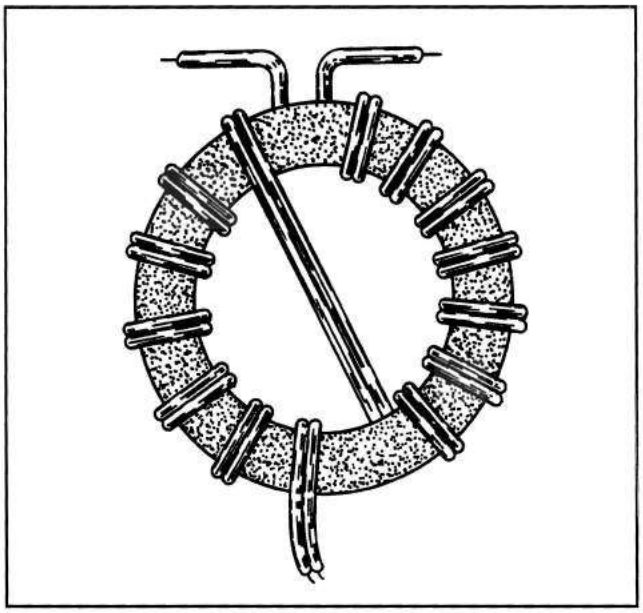

Figure 8-6. *Construction of a crossover placing input and output connections on opposite sides of the toroid.*

nection, one toroid is wound clockwise and the other, counterclockwise. The spacing between the toroids can be between 1/4 and 1/2 inch.

When matching 50-ohm cable to a balanced load of 200 ohms, the transformation ratio is constant (within 2 percent) from 1.5 to 45 MHz. This Balun can also handle the legal limit of amateur radio power. It would probably perform satisfactorily if wound with ordinary No. 14 house wire (solid), or with Teflon-covered No. 14 tinned wire. However, the design in **Photo 8-F** has withstood peak pulses of 10,000 volts! Considering this fact, it might be worthwhile to take the extra effort and use Teflon-covered No. 14 H Thermaleze wire.

A single-core version using two coiled transmission lines on a single core looks interesting and should be investigated. It results in balanced currents and unbalanced voltages. I would use two coiled transmission lines with 7 bifilar turns of the same wire on the same core as above.

Photo 8-G shows two low-power Guanella 4:1 Baluns designed to match 50-ohm coaxial cable to loads of 200 ohms. They both use No. 20 hook-up wire (solid) giving a characteristic impedance very close to the objective of 100 ohms. Their responses are flat from 1.5 MHz to well beyond 50 MHz. They are conservatively rated at 150 watts of continuous power and 300 watts of peak power. They have been exposed to 500 watts of continuous power (in a matched condition) for a considerable length of time with virtually no rise in temperature.

The single-core version (on the left) has 7 bifilar turns on each of its two transmission lines, while the dual-core version (on the right) has 14 turns on each core. The wires are clamped together about every 1/2 inch with strips of Scotch No. 27 glass tape. The cores are 1.25-inch OD ferrite toroids with a permeability of 250. The connectors are on the low-impedance sides. As above, the dual-core version has one winding clockwise and the other, counterclockwise.

Photo 8-H is a step-down version of the Guanella 4:1 Balun and uses two ferrite rod-cores 3/8 inch in diameter and 3.5 inches in length. Core permeabilities are 125. It uses the schematic of **Figure 8-1A,** but with the generator (which is grounded) on the right side and the load (ungrounded) on the left side. This 4:1 Balun is designed to match 50-ohm coaxial cable (on the right side) to a balanced load of 12.5 ohms. Each rod has 13.5 bifilar turns of No. 14 H Thermaleze wire. Again, for ease of connection, one rod is wound clockwise and the other, counterclockwise. The response is flat from 1.5 MHz to well over 30 MHz. This Balun is fully capable of handling the legal limit of amateur radio power. The connector is on the high-impedance (50 ohms) side. Beaded versions of Guanella's step-down 4:1 Balun also look very promising for operations on the VHF and UHF bands. The technique requires minimizing the parasitics in the interconnections. Some examples will be shown later.

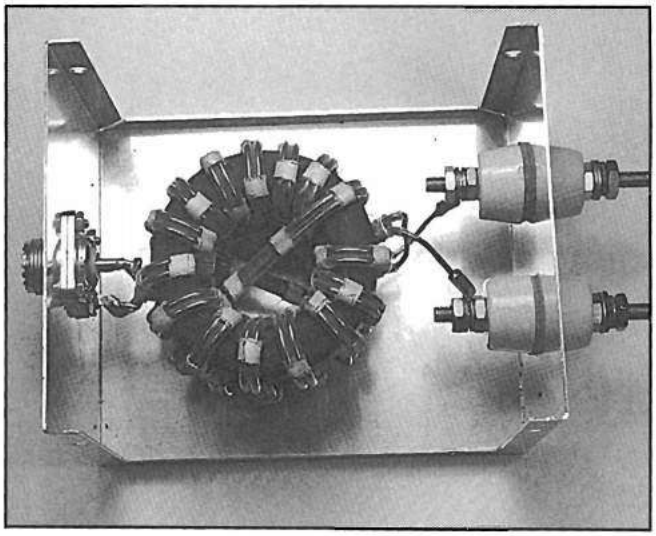

Photo 8-F. *A 4:1 Guanella Balun using the crossover connection of Figure 8-6 and mounted in a 5 inch long by 4 inch wide by 3 inch high CU 3005-A minibox.*

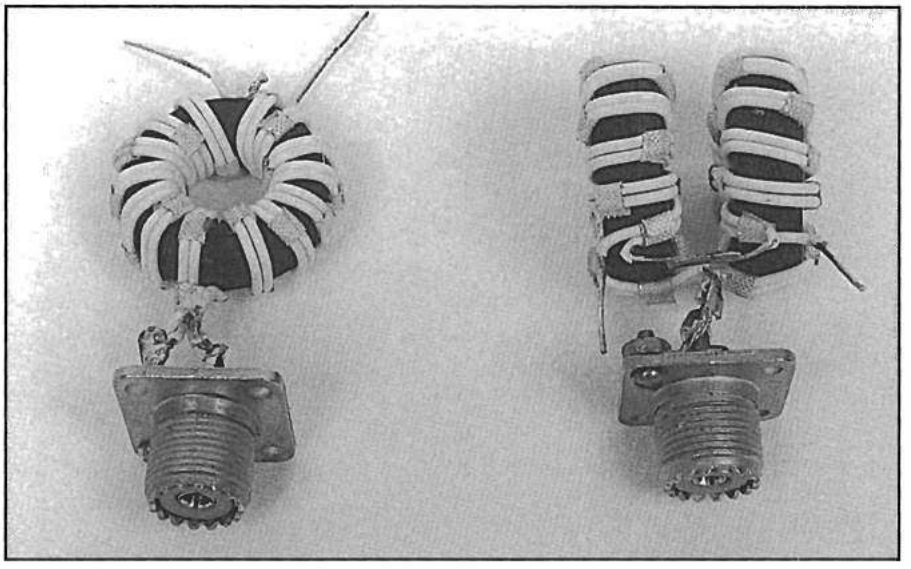

Photo 8-G. *Two low-power versions of the Guanella 4:1 Balun. The Balun on the left uses a single core while the one on the right uses two cores. The connectors are on the low-impedance sides.*

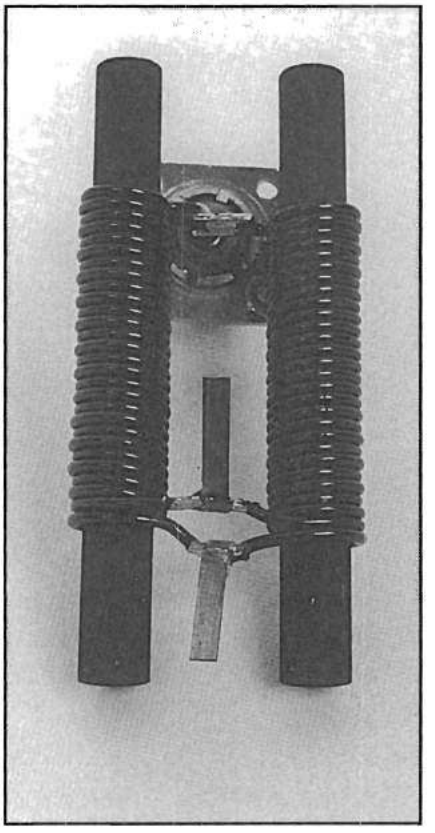

Photo 8-H. *A dual rod-core 4:1 Guanella step-down Balun designed to match 50-ohm cable to a balanced load of 12.5 ohms. The connector is on the 50-ohm unbalanced side.*

It should be mentioned again that the three dual-core Baluns above also make excellent broadband Ununs. They only sacrifice a little in low-frequency response. However, because of their conservative designs, they can still handle the 160-meter band.

Sec 8.5 Comparisons with Other Baluns

After completing the study on 4:1 Baluns, I thought it would be interesting to characterize other Baluns that are commercially available, or that have been recently described in the amateur radio literature. My findings are as follows.

The 4:1 Rod-type Ruthroff Balun

Photo 8-I shows a photograph of the typical rod-type 4:1 Balun, which was practically the only one available for the past three to four decades. The Balun in the photograph is the **HI-Q Balun.** It is the Ruthroff design (now called a *voltage* Balun[6]) with 10 bifilar turns of No. 14 wire on a 1/2-inch diameter ferrite rod 2 inches in length. In terminating this Balun with 200 ohms, the useful range was found to be from 7 to 15 MHz. Below 7 MHz, the input impedance showed a considerable inductive component—indicating autotransformer action and flux in the core (which could be harmful). Above 15 MHz, the transformation ratio increased and became complex. The optimum impedance level was found when matching 100 ohms to 25 ohms (indicating a characteristic impedance of the windings of only 50 ohms). The useful frequency range at this impedance level increased to 3.5 MHz to 30 MHz.

When matching 50-ohm coaxial cable to a 20-meter folded dipole at a height of 0.17 wavelengths (resulting in a resonant input impedance of 200 ohms), the VSWR curve was indistinguishable from that of the best Guanella 4:1 (current) Baluns.[6] This Balun also presented no difficulty in handling the full power limit. However, on 10 meters, the difference due to a very low characteristic impedance of the coiled transmission line became evident. **Figure 8-7** shows the poor VSWR curve of the rod-type Balun when compared to other Guanella and Ruthroff Baluns with characteristic impedances close to the optimum value of 100 ohms. The rod-type Balun with all of its inadequacies, which include voltage-breakdown, is certainly *not* recommended.

The high-power Ruthroff Balun is close to McCoy's design.[17] It uses 11 bifilar turns of No. 14 H Thermaleze wire on a stack of three T200-2 cores. The wires

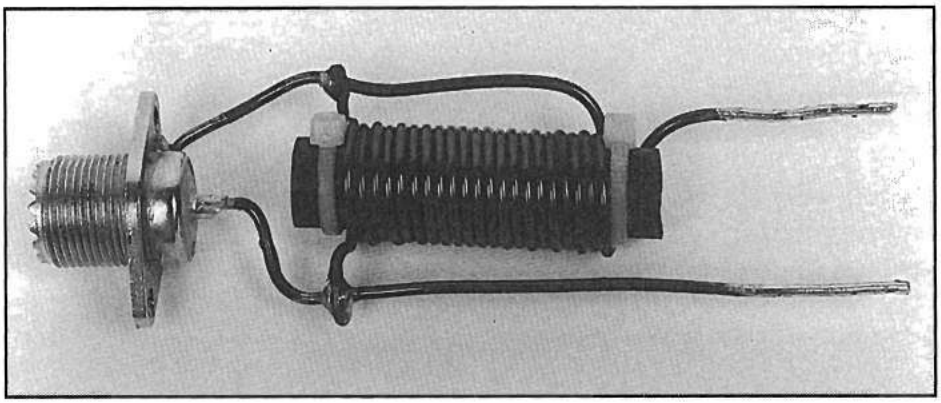

Photo 8-I. *A typical 4:1 rod-type Ruthroff (voltage) Balun (HI-Q).*

are also covered with 20-mil wall Teflon tubing yielding a characteristic impedance close to 100 ohms. I differ with McCoy's design because I feel the characteristic impedance of his transmission line could be closer to 50 ohms. His Balun and others that use powdered-iron cores will be described further in the next chapter on Baluns for antenna tuners.

The low-power units in **Figure 8-7** used 14 bifilar turns of No. 18 hook-up wire on 1.25-inch OD ferrite toroids with a permeability of 250. The transmission lines of the low-power Baluns were just under 20 inches, while those of the high-power Balun were 50 inches in length.

As can be seen in **Figure 8-7**, there are **very** small differences between the VSWR curves of the two low-power Baluns and the high-power Ruthroff (voltage) Balun. The differences could very well be attributed to the small variations in the characteristic impedances of the windings. Very likely, the most important information gleaned from **Figure 8-7** is that, when feeding a balanced dipole with a virtual ground-plain bisecting it, the Ruthroff Balun takes on the character of a two-core Guanella Balun. In other words, the Ruthroff Balun loses its built-in high-frequency cut-off!

4:1 Current Baluns

I also characterized several so-called *current* Baluns[6] that recently appeared on the market. These are my findings:

a) They are the dual-core (toroids) version of the Guanella Balun, which sums voltages of equal delays.

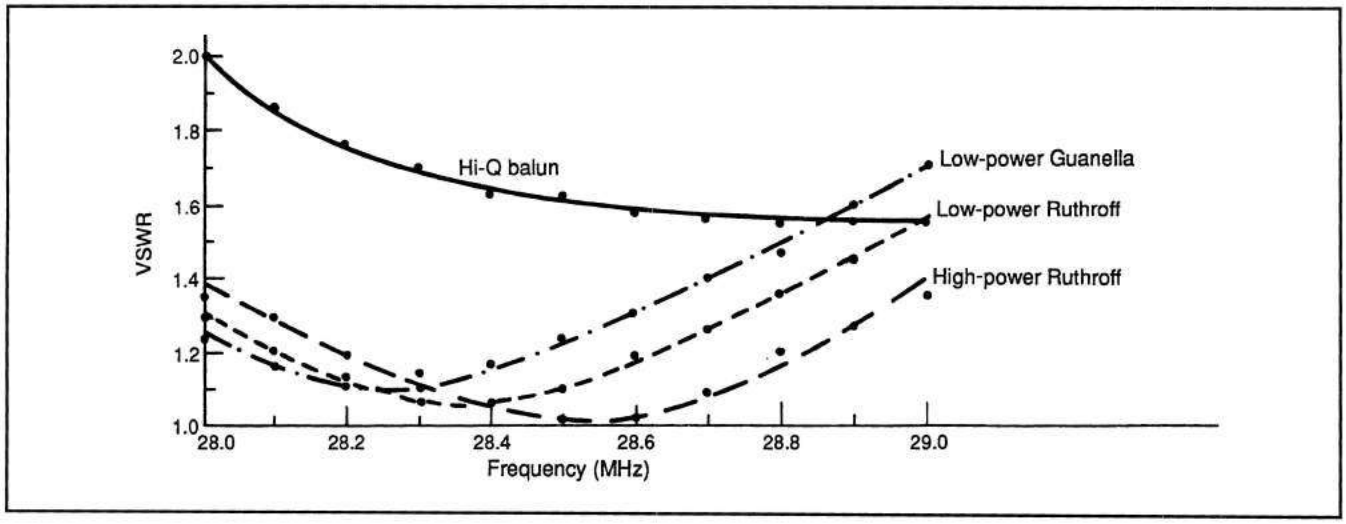

Figure 8-7. *Plots of VSWR curves on 10 meters for four different 4:1 Baluns. The high-power Ruthroff Balun is actually McCoy's design with a 100-ohm characteristic impedance winding (and is described in the next chapter). The Hi-Q Balun is shown in Photo 8-I. The comparisons show the importance of having the optimum value of the characteristic impedance of the windings and that the high-power Balun with its much longer transmission line indicates a Guanella-type operation.*

b) The electrical performances of these Baluns are vastly superior to the rod-type Balun described earlier.

c) These Baluns should meet their electrical and power-rating specifications.

d) My only criticism is that they could have more of a safety margin at the low-frequency end, where excessive core flux (due to higher than expected impedances) could take place. More inductance in the windings is recommended.

The Beaded-coax 4:1 Balun

A design in an amateur radio journal[5] advocated using beaded coaxial cable (of 100 ohms) in a 4:1 Guanella design. Various claims were advanced for this approach. I constructed one of these Baluns using No.14 wire with Teflon sleeving, resulting in the required 100-ohm characteristic impedance. Here are my findings:

a) The Balun had excellent margins at both the high- and low-frequency ends. The performance of this Balun verified the analysis (expressed earlier) with the high- and low-frequency models and the subsequent voltage gradients. In fact, the high-frequency performance exceeded the capability of my simple test equipment.[2]

b) The major disadvantage is in efficiency. Because high-permeability (2500) beads are required in order to obtain the required choking reactance in the HF band, this Balun had considerably more loss than coiled-type Baluns using low-permeability (less than 300) ferrite toroids.[2] A soak-test[2] (transformers connected back-to-back and about 500 watts applied into a dummy load) with the dual-core low-power unit in **Photo 8-G** showed that the smaller Balun ran considerably cooler! The beaded transmission line technique is recommended mainly for Baluns (and Ununs) operating at low impedance levels or on the higher-frequency bands.

Sec 8.6 Summary

Unlike the 1:1 Balun, the 4:1 Balun matching 50 ohms unbalanced to 200 ohms balanced has had no real standard for comparison in the amateur radio literature. As **Chapter 7** showed, Reisert's Balun in his 1978 article[7] had all of the attributes of a good 1:1 design. Therefore, he set a legitimate standard for others to follow or even attempt to exceed. Also shown were some of my variations in his design for increased efficiency and ease of construction.

However, **Chapter 8** has illustrated that the designs in the amateur literature (particularly the handbooks) are found lacking in bandwidth, or efficiency, or both. Even the 4:1 Baluns on the commercial market can be improved. This is *especially* true of the rod-type Balun that has been available for decades!

In the process of investigating the 4:1 Balun for my series of articles in *CQ* and *Communications Quarterly*, I have arrived at some designs that could provide the beginnings of standards for this device. They are included in this chapter and are:

1. For *balanced* applications like matching 50-ohm cable to the 200-ohm balanced input impedance of folded-dipole or log-periodic antennas, I recommend the single-core, Ruthroff design of **Photo 8-A**. It is capable of handling the full legal limit of amateur radio power. For a higher-power capability and a little less bandwidth, I recommend the Ruthroff design shown in **Photo 8-C**. These designs are presently called *voltage* Baluns.[6]

2. For unbalanced applications like the OCFD (off-center-fed dipole), or a dipole that could be unbalanced by surrounding structures or by construction errors, I recommend the two-core Guanella design of **Photo 8-E** or **Photo 8-F**. It is a much more flexible unit that can operate successfully as a Balun when the load is grounded at its center (**Figure 8-1A**), or as an Unun when the load is grounded at the bottom. Although not shown, it can even be grounded at the top, yielding a 4:1 phase-inverter.

3. For low-power 4:1 Baluns, there really have been no designs in the literature for comparisons. Therefore, by default, the designs in this chapter are suggested as standards. Applications of the single-core Ruthroff Balun and the two-core Guanella Balun are the same as their higher-power counterparts.

I am sure there are some who don't agree with the recommendations proposed above. The Guanella (current) Balun appears to be the main Balun of choice. The question is: Why use a two-core Guanella (current) Balun when a single-core Ruthroff (voltage) Balun will do? They both have the same power ratings! For those who disagree with my views, designs, or recommendations, I encourage them to (as the classic TV commercial used to say) *put it in writing*. Then we will all benefit from the new information.

Chapter 9

Baluns for Antenna Tuners

Sec 9.1 Introduction

The 4:1 Balun, matching 50 ohms (unhalanced) to 200 ohms (balanced), has found its most popular use in antenna tuners. Because the Balun rarely sees a resistive load of 200 ohms in this application, the primary objective is to take the balanced impedance (with respect to ground) of the input to an open-wire (or twin-lead) feedline and transform it into an unbalanced impedance which has one side grounded and can be transformed into 50 ohms by an L-C matching network. This was well described in two *CQ* articles by McCoy.[17,18]

As **Chapter 8** has shown, there are two different forms of the 4:1 Balun. One uses two transmission lines wound on separate cores (or threaded through ferrite beads in some cases) and connected in parallel at the 50-ohm side and in series at the 200-ohm side. This design was first presented by Guanella in 1944,[3] and is presently called a *current* Balun.[6] The other design, using a single transmission line wound around a core and connected in a phase-inverter configuration, was introduced by Ruthroff in 1959.[9] This design, which has recently been called a *voltage* Balun,[6] is now perceived as the inferior design.

This chapter presents another view of the 4:1 Balun. It not only includes the optimum design considerations for antenna tuner use, but also the design parameters for multiband antenna systems using center-fed dipoles with open-wire or twin-lead feedlines. Also included are my views on the G5RV antenna, the tuner using a 1:1 Balun before the L-C matching network, and the special cases of Ruthroff's 4:1 design matching into a load that is actually or virtually grounded at its center.

Sec 9.2 The Two Forms of Antenna Tuners

Three of the more common items in amateur radio jargon are VSWR, antenna tuners, and multiband antennas (especially the G5RV). These have appeared upon the scene because of the ease at which bands can now be changed and the narrow limits in the range of matching impedances with modern rigs.

The concept of using a wire antenna on many different bands isn't new. Designs have been around for more than six decades. In fact, satisfactory circuits have also been available which couple transmitters to balanced lines that present loads different than the transmitter output impedance. These were known as series and parallel-tuned circuits.[19] The transforming of a balanced impedance to an unbalanced impedance was accomplished by the isolation provided by magnetic coupling. Energy was transmitted from one circuit to the other by either having two coils in close proximity or by "link" coupling. However, these methods of coupling have fallen by the wayside, together with rock-bound rigs, plug-in coils, separate

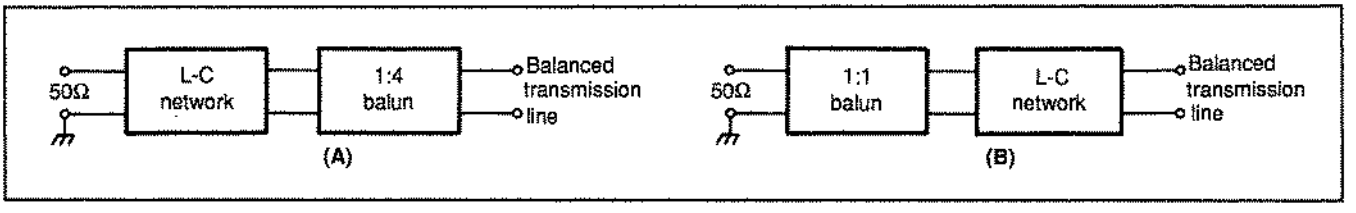

Figure 9-1. *The two basic forms of the Transmatch (antenna tuner): (A) the more popular design using an unbalanced L-C network and a 1:4 Balun; (B) a 1:1 Balun and a balanced L-C network.*

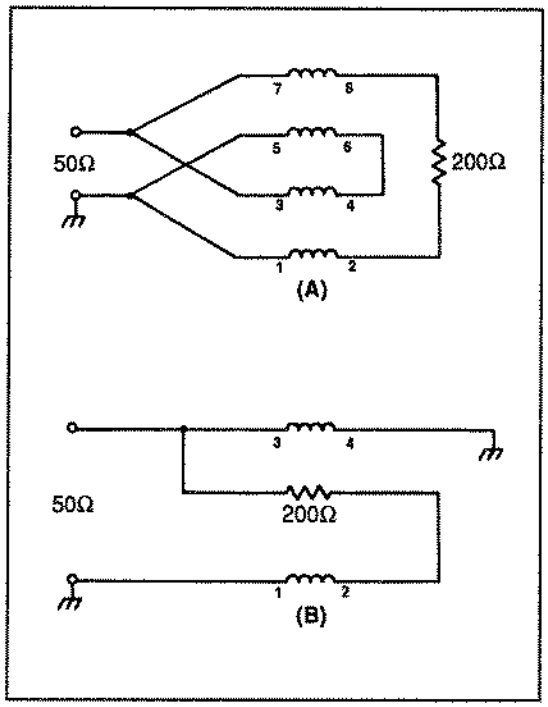

Figure 9-2. *The two basic forms of the 1:4 Balun: (A) the Guanella (current) Balun; (B) the Ruthroff (voltage) Balun.*

Figure 9-3. *The frequency response of a 4:1 Ruthroff (voltage) Balun with the load floating and with its center grounded. In the grounded case, the high-frequency response is similar to that of a 4:1 Guanella (current) Balun.*

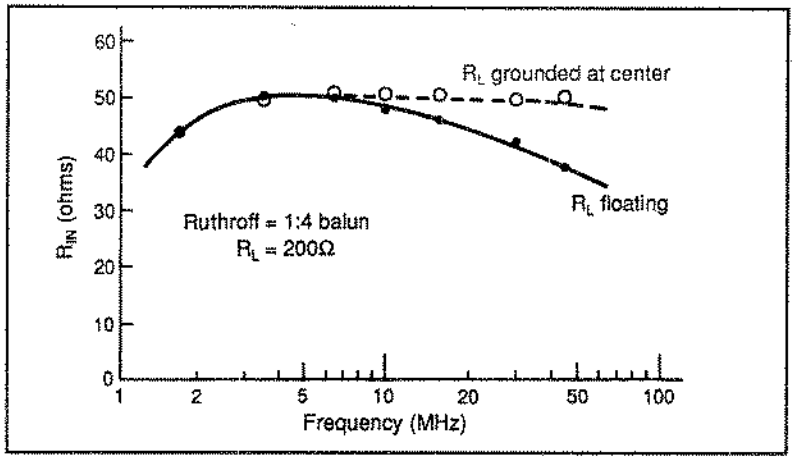

receivers and transmitters, and (sad to say) the exciting flashing of mercury-vapor rectifiers.

Today, the *transmatch* is most often used to convert the reactive/resistive load presented by an antenna system to a nonreactive, grounded 50-ohm load. The transmatch is also commonly known as an antenna tuner. The isolation role, that of converting a balanced impedance to an unbalanced one, is now provided by the Balun transformer.

There are two basic forms of the transmatch, and they are shown in **Figure 9-1**. **Figure 9-1A**, which shows a 4:1 Balun between the L-C network and the balanced transmission line, has been the most popular. In some designs, a 1:1 Balun has been used. In either case, this form of antenna tuner places the burden on the Balun, not on the L-C network. Depending upon the dimensions of the antenna and open-wire (or twin-lead) transmission line, the Balun can see very high impedances that may be harmful. In turn, the L-C networks are simple because of their unbalanced nature. Among the most popular networks are L, pi, T, Ultimate, and SPC types.[20–23] An added advantage to this approach is that the Balun can be placed outside the operating area and connected to the L-C network by a coaxial cable.[17,18]

On the other hand, **Figure 9-1B** takes the complexity out of the Balun and places it on the L-C network. With a balanced network, the 1:1 Balun should see a lower voltage drop along the length of its transmission line (and, hence, less loss[2]) because its load is always close to 50 ohms. Additionally, the choking requirements of a 1:1 Balun are considerably less than that of the 4:1 Balun in **Figure 9-1A**.

Roehm has addressed the problems related to this form of transmatch in an article.[16] In fact, he suggests a design using an unbalanced T network and a 1:1 beaded-coax Balun. Although a balanced L-C network is inherently more complex and costly, it would be interesting to see its comparison with Roehm's unbalanced design. Additionally, a comparison with a 1:1 Balun using 50-ohm twin-lead or coaxial cable wound around a ferrite toroid with a permeability of less than 300 would also be useful. Because the 1:1 beaded-coax (choke-type) Balun requires ferrite beads with permeabilities considerably greater than 300, it has more loss.[2]

In any event, the basic form of the transmatch using the design in **Figure 9-1B** looks promising and merits further investigation.

Sec 9.3 Another View of the 4:1 Balun

This section presents my views and the results of my work on a 4:1 Balun designed for use in the very popular "antenna tuner" shown in **Figure 9-1A**. Because the Balun may be exposed to harmful high voltage conditions in this application, the efficiency and

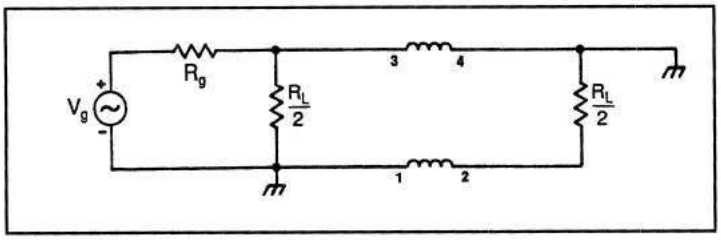

Figure 9-4. *Suggested model of the 4:1 Ruthroff (voltage) Balun when the load, R_L, is grounded at its center.*

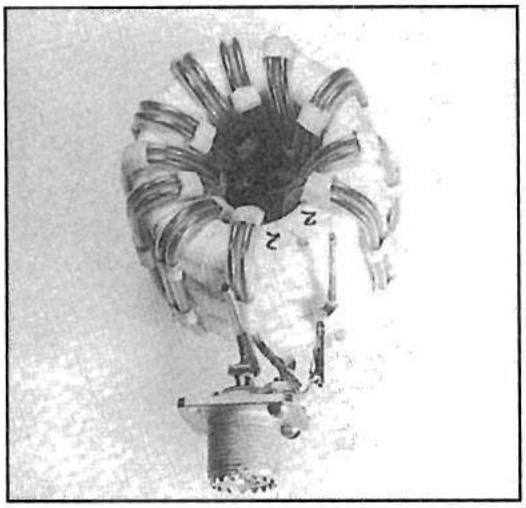

Photo 9-A. *The high-power Ruthroff 4:1 Balun used in the comparison with other Baluns (see Figure 9-7, and Figure 8-7 of Chapter 8). Except for some difference in the characteristic impedance of the bifilar winding, it is essentially the McCoy 4:1 Balun.*

ruggedness of the core materials are important considerations. Experiments have shown that losses in Baluns are related to the impedance level[2] (and, hence, voltage level), and the permeability of the materials. Therefore, the losses are of a dielectric-type and not of a current-type, as in conventional transformers. Moreover, it is well known that powdered-iron is a more rugged and linear material than ferrite. A very important question to ask is which form of the 4:1 Balun should be used in this application—Guanella's or Ruthroff's? My conclusions may surprise many readers.

As was mentioned at the beginning of this chapter and above, there are two basic forms of the 4:1 Balun. They are shown in **Figure 9-2A** and **B**. **Figure 9-2A** is Guanella's approach. It uses two coiled transmission lines (on separate cores) connected in parallel on the 50-ohm side and in series on the 200-ohm side. This has recently been called a *current* Balun.[6] In order to have "flat" transmission lines and obtain the highest frequency response, the characteristic impedance of the coiled transmission lines should be equal to the loads they see—namely, $1/2R_L$ and, in this case, 100 ohms.

As Guanella said in his classic paper,[3] this Balun is literally "frequency independent." At the low frequency end, the reactance of the coiled transmission line should be much greater than 100 ohms (in this case) in order to assure that the energy is transmitted from input to output by an efficient transmission line mode. Beaded transmission lines aren't recommended for use on the HF band at these impedance levels because of excessive dielectric loss.

Figure 9-2B shows Ruthroff's approach, which uses a single transmission line connected in the phase-inverter configuration (see **Chapter 7**). By grounding terminal 4, a voltage drop of $-V_1$ appears across the length of the transmission line. As a result, terminal 3 is at $+V_1$ and terminal 2 is at $-V_1$—a 4:1 transformation ratio.

It is when the load is actually grounded at its center that we see a very interesting feature of this approach. A simple impedance measurement will show that the high frequency response is *vastly* improved and that the Ruthroff (voltage) Balun appears to take on the character of a Guanella (current) Balun! **Figure 9-3** illustrates the measurements of the input impedance of a Ruthroff 4:1 Balun with the load floating, and when it is grounded at its center. These measurements (with a simple resistive bridge) were made on my design using a powdered-iron core, which will be described later.

A model for the Ruthroff 4:1 Balun, when the load is grounded at its center, is provided in **Figure 9-4**. If the characteristic impedance of the transmission line in the 4:1 Balun is 100 ohms (the optimum value if the load is 200 ohms), then the generator sees $R_L/2$ in parallel with a $R_L/2$ from a "flat" line. As a result, the generator sees its match of 50 ohms—even though the currents in the loads are not in phase!

However, when the Balun is connected to a center-fed, folded dipole, or log-periodic beam antenna with 200-ohm input impedances, the virtual ground-plane bisecting the antennas presents an interesting case. Because there is no metallic connection to the center of the load, the currents in both halves of the antennas are in phase. This is unlike the situation in **Figure 9-4**, where the current in the load on the right is delayed compared to the current in the load on the left. As is evident in **Figure 8-7** of **Chapter 8**, the VSWR curve

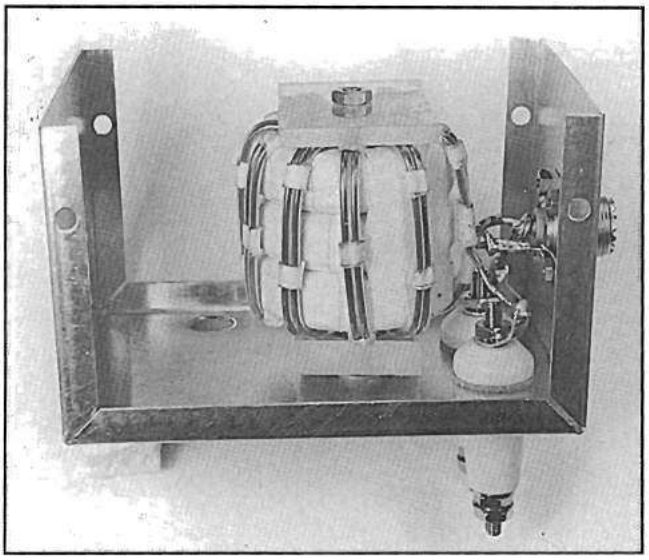

Photo 9-B. *The Balun of Photo 9-A mounted in a 5 inch long by 4 inch wide by 3 inch high minibox.*

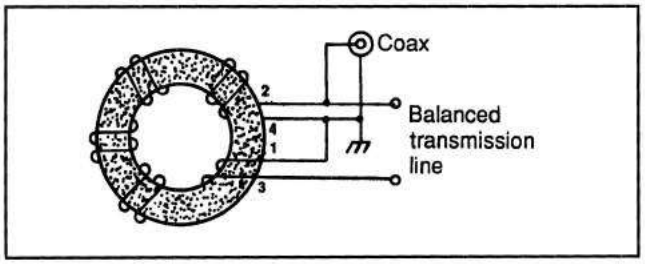

Figure 9-5. *A pictorial of the connections for a 4:1 Ruthroff (voltage) Balun.*

for the high-power Ruthroff Balun has practically the same shape as those of the two lower-power units—even though its transmission line is more than two and one half times longer.

Because the high-frequency response of a Ruthroff 4:1 Balun with a floating load is highly dependent upon the length of the transmission line, **Figure 8-7** suggests that, in the virtual ground case, the Balun acts as a Guanella Balun which sums voltages of equal phases. It also suggests that the effective electrical length of the transmission line is one-half of its actual length. I am quite sure that this model of Ruthroff's Balun was not proposed by him or by others that followed. However, it should be remembered that this condition only exists in the *balanced* case. With an unbalanced load, the Balun should introduce a reactive component that will limit the high frequency response. In the unbalanced case, the Guanella Balun with two cores is the Balun of choice.

Sec 9.4 Some "Hardy" 4:1 Designs

Photos 9-A and **9-B** show two views of a Ruthroff 4:1 Balun, much like McCoy's design, which has been used in his highly popular transmatch.[22] **Figure 9-5** shows a pictorial representation of the connections. It has 11 bifilar turns of No. 14 H Thermaleze wire on three (stacked) T200-2 cores. The cores are powdered-iron material with a permeability of 10. The OD

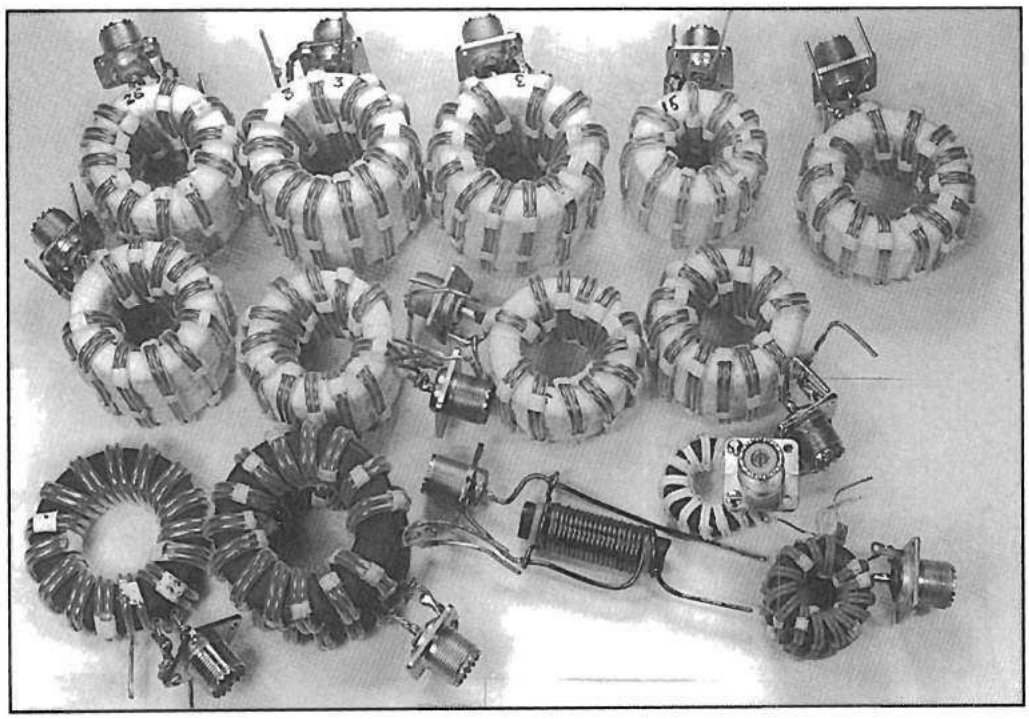

Photo 9-C. *The various Baluns used in the study of 4:1 Baluns for antenna tuners.*

is 2 inches. The wires are also covered with a 15-mil wall Teflon tubing, yielding a characteristic impedance close to the optimum value of 100 ohms.

I differ with McCoy's design here, because the characteristic impedance of his Balun could be closer to 50 ohms. **Photo 9-B** shows the Balun mounted in a 5 inch long by 4 inch wide by 3 inch high minibox. Because McCoy didn't use a thickly insulated wire, he wound a layer of Scotch No. 27 glass tape on each toroid before stacking. This was followed by another layer in the stacking process. With Teflon sleeving over the wire, the extra insulation provided by the glass tape could be dispensed with.

In order to improve the low-frequency response of McCoy's Balun, I made a study of higher permeability powdered-iron cores. **Photo 9-C** shows the various Baluns used in the study. The object of this study was to determine the best core material for a 4:1 Balun to be used in antenna tuners where they can be exposed to high impedances (and, hence, hostile environments). I knew, as the result of very accurate insertion loss measurements[2] that loss with ferrite materials was related to the voltage drop along the length of the transmission line and to the value of the permeability. Permeabilities of 40 (No. 67 ferrite) exhibited the lowest loss. The results taken on a single powdered-iron material—No. 2 material with a permeability of 10—also showed the very same low loss. Because powdered-iron material has been known to be more rugged and linear than ferrite material, this suggested that other powdered-irons with greater permeabilities should also be investigated.

I investigated four other powdered-irons with permeabilities of 20, 25, 35, and 75. Their designations were Nos. 1, 15, 3, and 26, respectively. Comparisons were made on input impedances (with the outputs terminated in 200 ohms) and temperature rises (when handling 500 watts of power). The power test showed, convincingly, that No. 26 material was not to be used because it showed a definite rise in temperature while the other three didn't. However, all four materials showed a definite lower input impedance than the No. 2 material, which has a permeability of 10. As expected, the higher the permeability, the larger the difference with No. 2 material. Although an input impedance measurement does provide some indication of loss because it appears as a shunting path to ground, a very accurate insertion loss measurement would provide a more precise indication of the trade-off that can be made in efficiency for low frequency response.

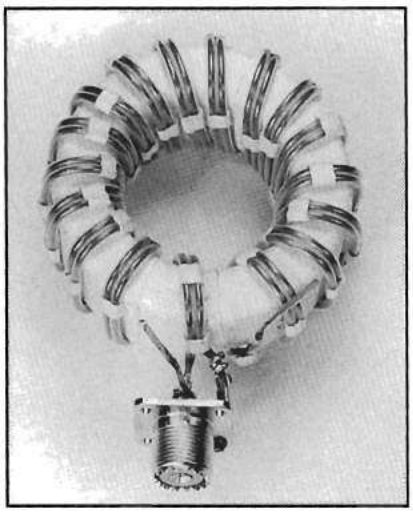

Photo 9-D. *An improved 4:1 Ruthroff design for antenna tuners.*

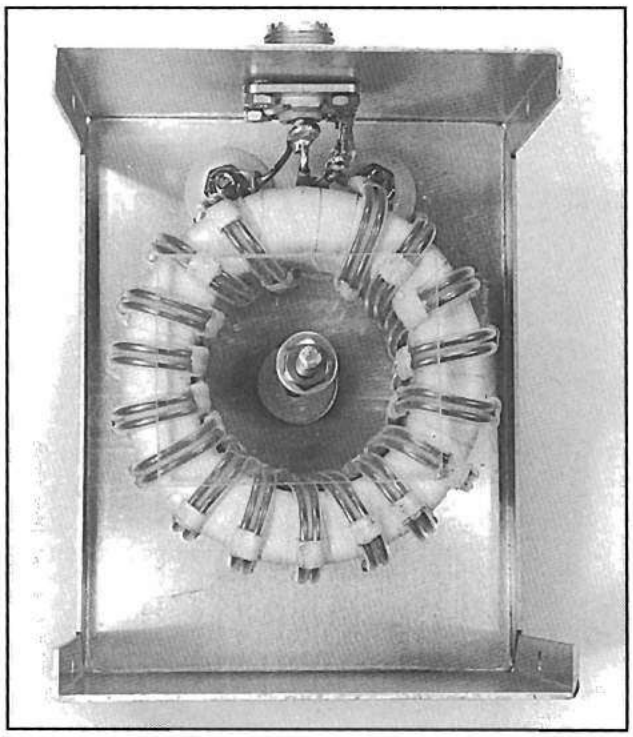

Photo 9-E. *The improved 4:1 Ruthroff Balun mounted in a 5 inch long by 4 inch wide by 3 inch high minibox.*

Because my simple loss measurements indicated that the higher permeability powdered-irons had more loss than the No. 2 material, I decided to design a 4:1 Ruthroff Balun using this material—but with a larger core and more turns than the McCoy[17,18] Balun. Although McCoy's design has enjoyed considerable success over the years, I felt that a larger inductive reactance was desirable in order to assure better performance on the lower frequency bands (particularly 160 meters).

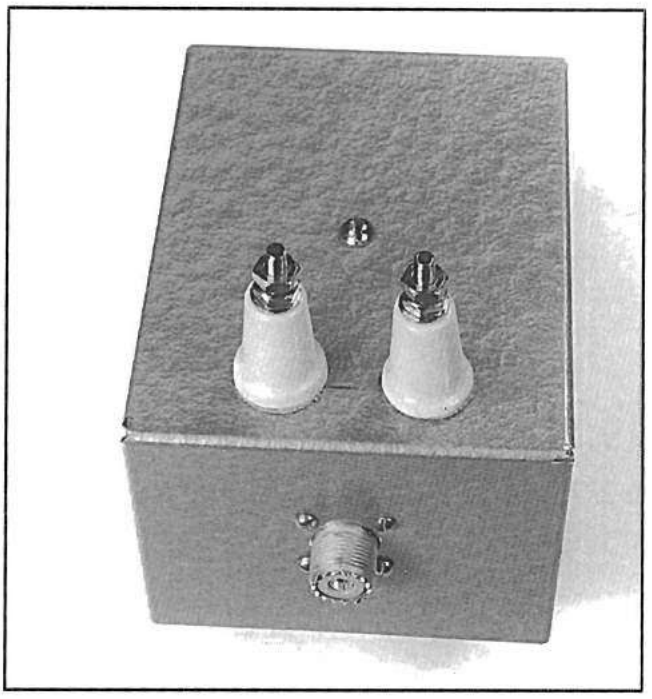

Photo 9-F. *The top view of the 4:1 Balun of Photo 9-E.*

The specific design is shown in **Photo 9-D**. It has 17 bifilar turns of No. 14 H Thermaleze wire on a T300A-2 powdered-iron core, which has an OD of 3 inches and a permeability of 10. With this number of turns and a larger cross section than the three T200-2 cores, the low frequency response improved by a factor of about two over the McCoy Balun, which has 10 to 12 turns on a stack of three T200-2 cores. Furthermore, the wires are also covered with 15-mil wall Teflon tubing, resulting in a characteristic impedance of 100 ohms (the objective). This well-insulated transmission line has been reported to handle 10,000 volts without breakdown. **Figure 9-3** illustrates the performance of this Balun (under a matched condition) when the load is floating and when it is center-tapped-to-ground. **Photo 9-E** shows the Balun mounted in a minibox 5 inches long by 4 inches wide by 3 inches high. **Photo 9-F** shows the top view of the mounted Balun.

Because the Balun with the larger core and more turns showed an improvement by a factor of two in the low-frequency response over the McCoy Balun, I constructed an even larger design. This is shown in **Photo 9-G**. It has 21 turns of the same wire on a T400A-2 core with an OD of 4 inches and a permeability of 10. Even though **Photo 9-G** shows the toroid wrapped with Scotch No. 27 glass tape, as mentioned earlier, this extra insulation isn't required because the wires are covered with Teflon sleeving.

Figure 9-6 shows the comparisons in the input impedances versus frequency of these three "hardy" Baluns when they are terminated in 200-ohm loads grounded at their centers. As can be seen, the low-frequency response of the Balun with the most turns and largest core is the best. Even though the Balun with the 3-inch core has a poorer low-frequency response, it is an improvement over the McCoy Balun and should find considerable use in transmatches. **Figure 9-6** also shows that the high frequency responses of these Baluns with the loads grounded at their centers are remarkably similar. This is especially interesting, as the length of the transmission line on the larger

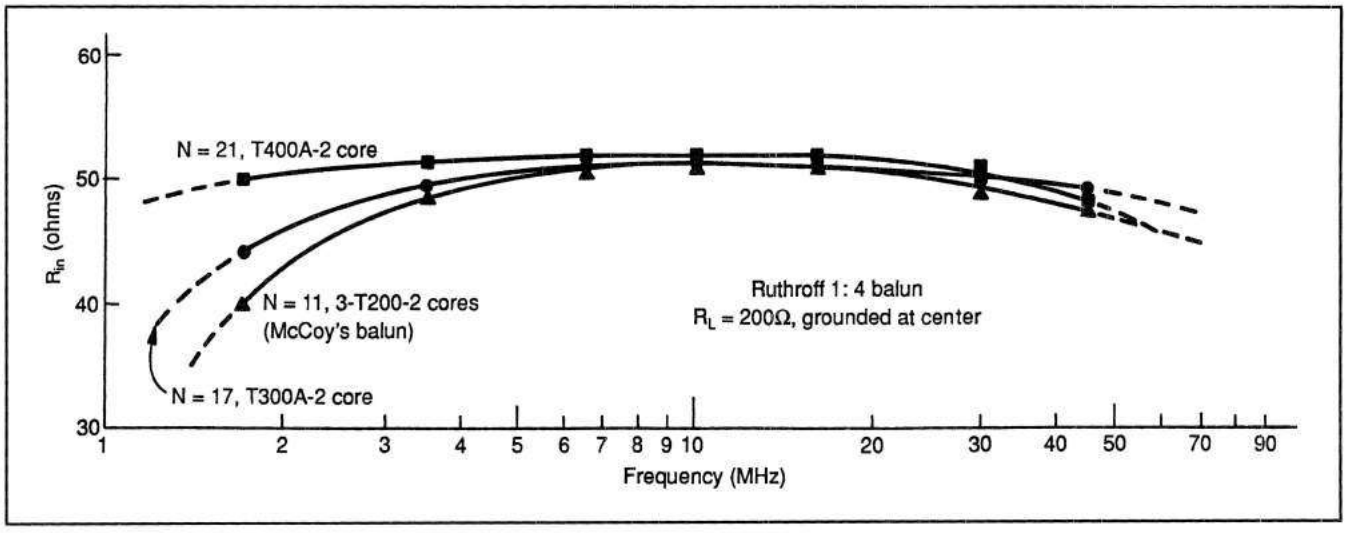

Figure 9-6. *A comparison of the performance of the McCoy 4:1 Balun with Baluns having larger cores and more turns.*

Balun (with the T400A-2 core) is more than twice as long as the other two (115 inches compared to 50 and 55 inches). If it is correct that my model of a Ruthroff (voltage) Balun feeding a balanced antenna or transmission line takes on the character of a Guanella (current) Balun because of the virtual ground, then this large Balun could have many applications.

Sec 9.5 Multiband Dipoles

Antenna tuners have been known to work well for some radio amateurs and not for others. This is due to the differences in the dimensions of their antenna systems. With high impedances seen by the 4:1 Baluns in the antenna tuners, the Baluns not only fail to provide a good balanced-to-unbalanced conversion, but they can also be damaged by excessive heating. The high current, low impedance condition seen by the Balun isn't a problem. Therefore, the object in multiband antenna design is to provide the most favorable impedances for the Baluns, especially on the three lowest frequency bands—40, 80, and 160 meters. Usually on the higher frequency bands, the impedances seen by the Baluns are not as high and the Balun's choking reactances are greater (assuring balanced-to-unbalanced conversion). This section discusses three cases of multiband center-fed dipole designs. They are 1) the "worst case" design, 2) a smaller design—the G5RV, and 3) a larger design. Others may have better designs for multiband operation, but it's clear that the "worst case" design ought to be avoided. **Figure 9-7** shows the symbols for the dimensions of the center-fed dipoles.

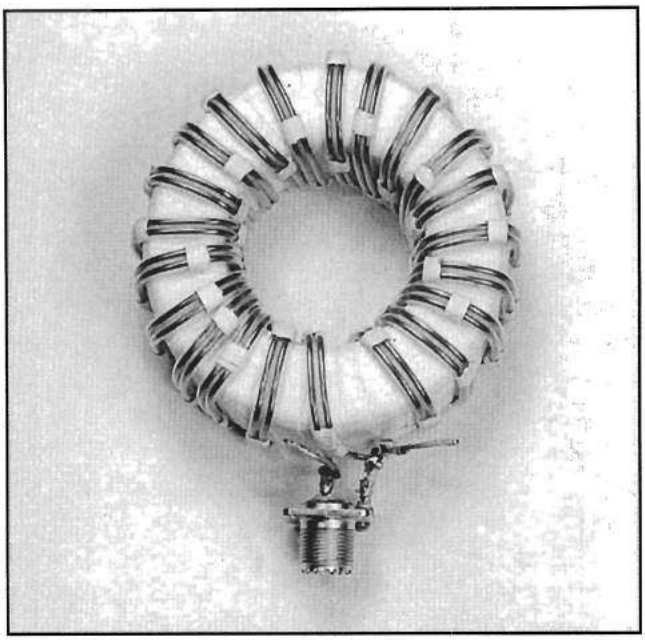

Photo 9-G. *A large 4:1 Ruthroff design using a 4-inch OD powdered-iron core and 21 bifilar turns.*

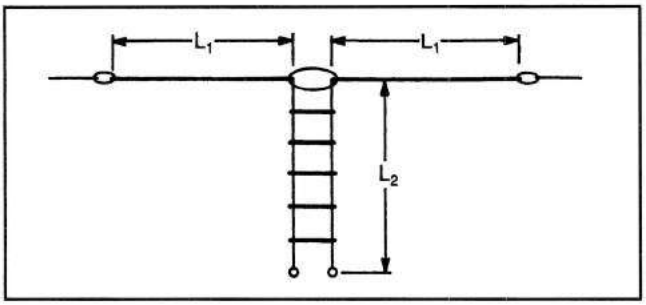

Figure 9-7. *The symbols used for the dimensions of a center-fed dipole with open-wire feeders (or twin-lead with appropriate consideration of velocity factors).*

Sec 9.5.1 The "Worst Case" Design

Apparently, an 80-meter dipole with a quarter-wave open-wire (or twin-lead) feedline is a logical design for a multiband dipole. In **Figure 9-7** this would mean that $L_1 = L_2 = 59$ to 67 feet, depending upon the favorite operating frequency. If one were to use 450-ohm twin-lead with "open windows," L_2 would be diminished by 10 percent; with 300-ohm TV twin-lead, it would be diminished by about 20 percent. This would make a good antenna system on 160 meters. Because $L_1 + L_2$ is close to a quarter-wave, the current at the input to the feedline is at its highest value and the impedance at its lowest—a very favorable condition for the Balun. In fact, a 1:1 Balun at the feedpoint would probably do a good job.

However, what does the input to the feedline look like on 80 meters? If 450-ohm feedline is used, the 4:1 Balun sees a quarter-wave 450-ohm feedline terminated in approximately 50 ohms. Transmission line theory tells us that the Balun would see 4050 ohms—an impossible condition for most Baluns. The situation becomes worse on 40 meters, where we may have a center-fed, full-wave dipole with a half-wave transmission line (a 1:1 matching transformer). In this case, the Balun could see an impedance approaching 10,000 ohms—a more than impossible condition! Although high impedances would also be seen on 10, 15, and 20 meters, the conditions are not quite as severe because the Balun's choking reactances are usually greater and the impedances lower. In essence,

the "worst case" design for a 4:1 Balun is the "best case" design (except for 160 meters), if one still uses inductive coupling to a parallel-tuned circuit.[19]

Sec 9.5.2 A Smaller Design—The G5RV

Varney,[24] G5RV, designed a multiband center-fed antenna system capable of operation on all HF bands from 3.5 to 30 MHz. In contrast to multiband antennas designed as half-wave dipoles on 80 meters (the "worst case" design), the full-size G5RV antenna was designed as a three-half-wave antenna on 14,150 MHz with a 1:1 transmission line matching transformer. It was possible to accomplish this using the dimensions of 51 feet for L_1 and 34 feet for L_2. For 450-ohm twin-lead with "windows," L_2 would he 31 feet; for 300-ohm TV ribbon, L_2 would be 28 feet. Consequently, the input impedance at the hase of the matching transmission line was about 100 ohms on 14,150 MHz, and a manageable impedance for 50 or 80-ohm coaxial cable.

However, with a total length for $L_1 + L_2$ of 85 feet, the impedances at the input to the transmission line on 40, 80, and 160 meters are also manageable. Even though they have a reactive component on these bands, they aren't so high that a well-designed 4:1 Balun in an antenna tuner can't handle them easily. Varney also showed that the highest impedances occurred on the 18-, 21-, and 28-MHz bands. However, this doesn't present a problem with the design shown in **Photo 9-D** because it uses an efficient core material, and it also has the highest reactances of its windings at these frequencies.

Varney[24] also wrote, at considerable length, on the unsuitability of a Balun being used to connect the base of the 34-foot open feeders to a coaxial cahle feedline. He stated that if a Balun is connected to a reactive load with a VSWR of more than 2:1, its internal losses would increase. Varney also mentioned heating of the wires and saturation of the core. Evidently Varney was not familiar with McCoy's design, which uses a powdered-iron core (with a permeability of 10) that can withstand VSWRs considerably greater than 2:1—without showing any temperature rise. Furthermore, the wire doesn't heat up; however, the core itself does via dielectric heating. Additionally, with sufficient choking reactance, Baluns can handle (equally) the resistive and reactive components of an impedance.

Finally, after observing the voltage and current distributions on all of the bands, it appears that a 2:1 (100:50-ohm) Balun might he an interesting one to try on the G5RV antenna. It could he that many of the bands would not require the added matching of an antenna tuner. If some of the bands require an antenna tuner in order to be used, then I would suggest using a "hardened" Balun. That is what I call McCoy's approach, which uses efficient and hardy powdered-iron cores. A 2:1 Balun, comprised of a 1:2 Unun in series with a 1:1 Guanella (current) Balun, could be easily designed and built (see **Chapter 10**).

Sec 9.5.3 A Larger Design

Even though the G5RV antenna can be made to operate on 160 meters with a suitable antenna tuner, an antenna system larger than the "worst case" design can provide better operation on the 40-, 80-, and 160-meter hands. As you might expect, an antenna system about twice as large as the G5RV offers these advantages. Suggested dimensions are $L_1 = 80$ feet and $L_2 = 100$ feet. If the feedline is 450-ohm twin-line with "windows," then $L_2 = 90$ feet. If it is 300-ohm TV ribbon, then $L_2 = 82$ feet. As with the G5RV, it's the total length of $L_1 + L_2$ that presents favorable or unfavorable impedances to the 4:1 Balun in the antenna tuner. Therefore, L_1 and L_2 could hoth be 90 feet, as well. Only very small differences in performance would be noticed between these two systems, particularly on the lower-frequency bands. Obviously, other combinations totaling 180 feet are also possible. In the G5RV case, it's 85 feet.

Sec 9.6 Summary

After reading this chapter, one might think that I have set this technology back a few years by advocating voltage Baluns and powdered-iron cores. I have even questioned the professional literature. However, my conclusions were based upon three experimental results. These were: 1) measurements with my resistive bridge on input impedances of 4:1 Ruthroff (voltage) Baluns with loads floating and center-tapped-to-ground, 2) VSWR measurements on folded dipoles with various 4:1 Baluns (large and small and, therefore, with many different lengths of transmission lines), and 3) McCoy's success with his 4:1 Balun. Also, as this chapter points out, it helps to have the dimensions of a multiband, center-fed dipole, and feeders favor the operation of a 4:1 Balun

in antenna tuners. And, *yes*, there is a "worst case" antenna design!

As in many investigations, supplying answers to some questions can lead to others that appear to be important. Specifically, for powdered-irons, how would permeabilities in the 20 to 35 range perform? Simple impedance measurements showing lower values on input impedances, indicate that there is more loss than with a permeability of 10; but accurate insertion loss measurements are needed in order to tell the complete story—the trade-off in efficiency for low-frequency response.

Finally, low permeability ferrite-like No. 67 material with a permeability of 40 looks interesting for use in Baluns for antenna tuners. Accurate insertion loss measurements[2] have also shown the very same high efficiency that was exhibited by powdered-iron having a permeability of 10. With a sufficient number of turns on an appropriate size core, a Balun made of this material could be practical. Even though the amateur radio literature still refers to the problem of core saturation, there has been only one recorded case. This was on 2 MHz with a rod-type 1:1 Balun where insufficient choking reactance exists.[13,14]

Chapter 10

1.5:1 and 2:1 Baluns

Sec 10.1 Introduction

There are many applications for broadband Baluns with impedance transformation ratios close to 1.5:1 and 2:1. Two applications involve matching 50-ohm cable to balanced loads of 75 or 100 ohms, which are the input impedances of a half-wave dipole at heights of 0.22 or 0.34 wavelengths above ground. Another, is the matching of 50-ohm cable to the 100-ohm input impedance of a quad antenna. An interesting, and somewhat unexpected, application is the matching of 50-ohm cable directly to the input impedance of the driven element of a Yagi beam antenna of 33 or 25 ohms. This would eliminate the common hairpin matching network presently used to raise their input impedances to 50 ohms.

There are many versions of these two Baluns. They include: 1) high- and low-power designs, 2) designs matching 50-ohm cable to higher or lower impedances, 3) series- or parallel-type designs, 4) single- or dual-core designs, 5) dual-ratio designs, and 6) HF and VHF designs. The series-type Baluns use an Unun (unbalanced-to-unbalanced transformer) in series with a Guanella (current) Balun. More details on these Ununs are provided in later chapters. In this chapter, you'll read about many high-power designs capable of handling the full legal limit of amateur radio power. They are optimized for sufficient margins in choking reactance at their low frequency ends, and in efficiency throughout their passbands. Two of the 2:1 Baluns are specifically designed for 2-meter operation.

Sec 10.2 1.5:1 Baluns

In this section, I'll present two series-type 1.5:1 Baluns (actually 1.56:1, which should be close enough). They both use 1.56:1 Ununs in series with Guanella 1:1 Baluns. **Figures 10-1A** and **B** show their schematic diagrams. **Figure 10-1B** has an extra input (to a tap), which provides another ratio of 1.33:1.

The left-hand side of **Photo 10-A** shows a design using **Figure 10-1A** mounted in a CU 3006 minibox 5.25 inches long by 3 inches wide by 2.25 inches high (RadioShack has carried a similar enclosure). The 1:1.56 Unun has 4 quintufilar turns on a 1.5-inch OD

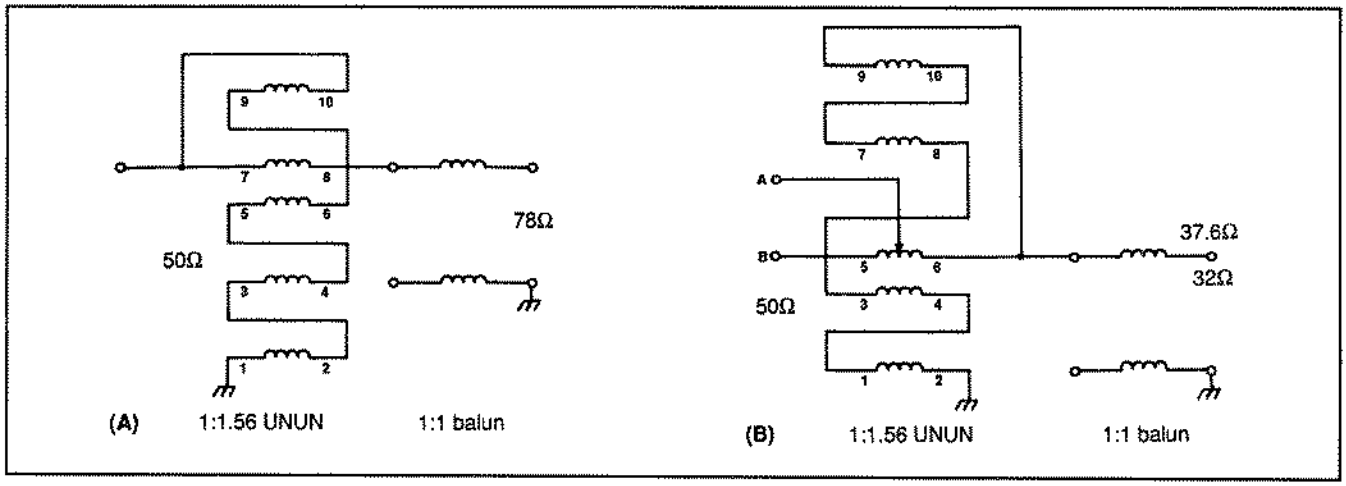

Figure 10-1. *Schematic diagrams of two 1.56:1 Baluns: (A) step-up, 50:78 ohms; (B) step-down, 50:37.6 ohms—connection A, 50:32 ohms—connection B.*

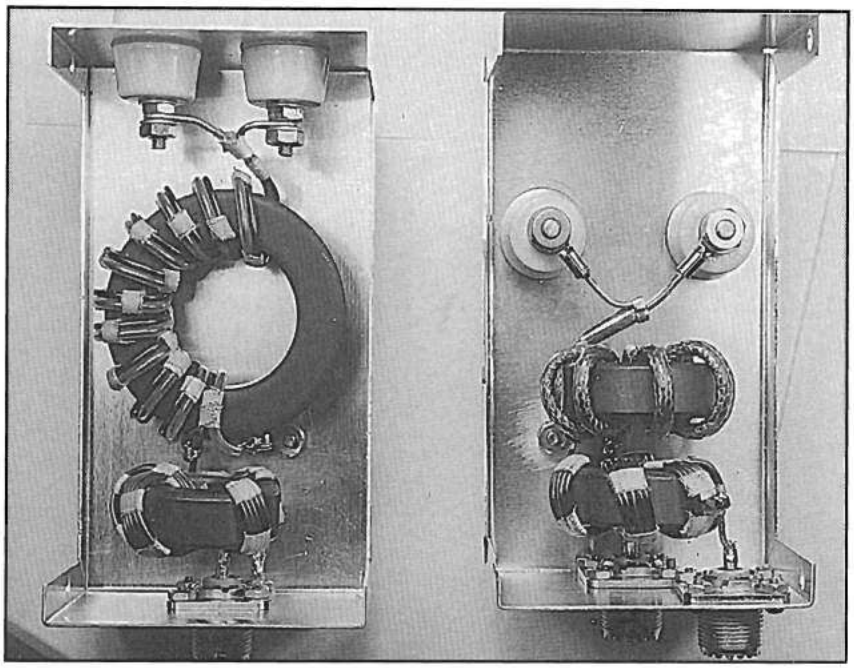

Photo 10-A. *Baluns using the schematic diagrams of Figure 10-1. Balun on the left matches 50-ohm cable to a balanced load of 78 ohms. Balun on the right matches 50-ohm cable to balanced loads of 37.6 or 32 ohms.*

ferrite toroid with a permeability of 250. Winding 7-8 is No. 14 H Thermaleze wire and the other four are No. 16 H Thermaleze wire.

The 1:1 Guanella Balun has 11 bifilar turns of No. 14 H Thermaleze wire on a 2.4-inch OD ferrite toroid with a permeability of 250. One wire is covered with Teflon tubing, resulting in a characteristic impedance very close to 78 ohms (the optimum value).

When matching 50-ohm cable to a balanced load of 78 ohms, the impedance transformation ratio is literally flat (within a percent or two) from 1.5 MHz to 40 MHz! You might be interested to know that (separately) the 1:1 (75:75-ohm) Balun would make an excellent isolation transformer for 75-ohm hardline, and the 1.56:1 (78:50-ohm) Unun an excellent match between 75-ohm hardline and 50-ohm cable.

The right-hand side of **Photo 10-A** shows a design using **Figure 10-1B** mounted in a similar enclosure. The 1.56:1 Unun has 5 quintufilar turns on a 1.5-inch OD ferrite toroid with a permeability of 250. Winding 5-6 is No. 14 H Thermaleze wire and is tapped at one turn from terminal 5. The other four wires are No. 16 H Thermaleze.

The 1:1 Guanella Balun has 7 turns of homemade coaxial cable on a 1.5-inch OD ferrite toroid with a permeability of 250. The inner conductor is No. 14 H Thermaleze wire and is covered with Teflon tubing. The outer braid, which is from a small coaxial cable or from 1/8-inch tubular braid, is also tightly wrapped with Scotch No. 92 tape to preserve the low characteristic impedance.

In matching 50-ohm cable to a balanced load of 37.6 ohms (connection A), or to a balanced load of 32 ohms (connection B), the response is essentially flat (within a percent or two) from 1.5 to 30 MHz.

Sec 10.3 2:1 Baluns

The 2:1 Balun lends itself to more choices in design than the 1.56:1 Balun. This is especially true because the parallel-type design, which provides a 2.25:1 Balun with the widest possible bandwidth, can easily be employed. The 1.56:1 Balun is at a disadvantage here. This section presents many Baluns using both series and parallel-type designs.

Sec 10.3.1 Series-type Baluns

Figure 10-2 shows circuit diagrams for two versions of the series-type Balun. **Photo 10-B** shows a design using **Figure 10-2A** mounted in a CU 3005-A minibox 5 inches long by 4 inches wide by 3 inches high. The 1:2 Unun has 7 trifilar turns on a 1.5-inch OD ferrite toroid with a permeability of 250. The output tap is located 6 turns from terminal 5. Winding 5-6 is No. 14 H Thermaleze wire and the other two are No. 16 H Thermaleze wire.

The 1:1 Guanella Balun has 14 bifilar turns of No. 14 H Thermaleze wire on a 2.4-inch OD ferrite toroid with a permeability of 250. Both wires are covered with Teflon tubing, which results in a characteristic impedance of 100 ohms (the optimum value). A crossover, placing 7 turns on one side of the toroid

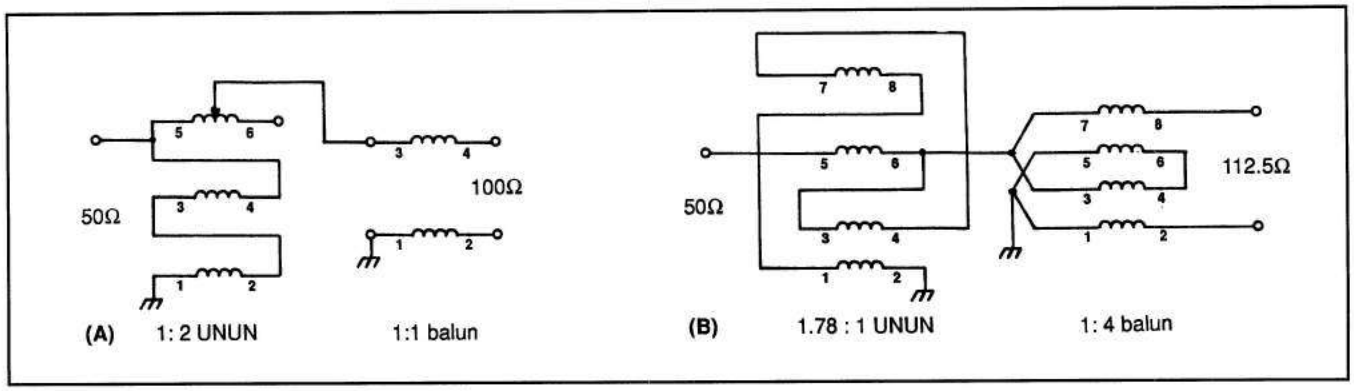

Figure 10-2. *Schematic diagrams of two versions of the series-type Balun: (A) 1:2 (50:100 ohms) Balun; (B) 1:2.25 (50:112.5 ohms) Balun.*

and 7 turns on the other, is used so the output and input are on opposite sides of the toroid. **Figure 10-3** is a drawing of the crossover. Although this technique has no electrical advantage at HF, the mechanical advantage is obvious.

When matching 50-ohm cable to a balanced load of 100 ohms, the response is literally flat (within 2 to 3 percent) from 1.5 to 30 MHz. By connecting the output of the Unun to terminal 6 instead of to the tap, the Balun would match 50-ohm cable to a balanced load of 112.5 ohms with about the same response.

Photo 10-C shows two slightly different versions of series-type 2.25:1 Baluns using the circuit of **Figure 10-2B**. Both have the same 1.78:1 step-down Unun, which has 5 quadrifilar turns on a 1.5-inch OD ferrite toroid with a permeability of 250. Winding 5-6 is No. 14 H Thermaleze wire, and the other three are No. 16 H Thermaleze wire. Each version also has 8 bifilar turns of No. 14 H Thermaleze wire on both of the 1.5-inch OD ferrite toroids, with a permeability of 250.

The differences are: 1) the Balun on the left in **Photo 10-C** has one layer of Scotch No. 92 tape on one of the wires in each bifilar winding and a crossover after the fourth turn, and 2) the Balun on the right has two layers of Scotch No. 92 tape on one of the wires on one toroid and no extra insulation on the wires of the other toroid. Therefore, one of the windings in the 1:4 Guanella Balun has a characteristic impedance a little less than 50 ohms and the other a little greater than 50 ohms, resulting in a canceling effect. Furthermore, the crossover isn't used in this design. The Balun on the left is mounted in a CU 3006 minibox 5.25 inches long by 3 inches wide by 2.25 inches high. The Balun on the right is mounted in a CU 3015-A minibox 4 inches long by 2 inches wide by 2.75 inches high.

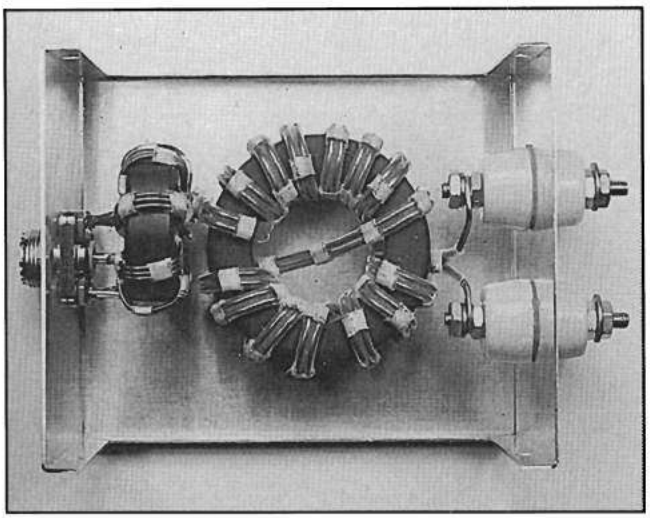

Photo 10-B. *A series-type Balun using the schematic diagram of Figure 10-2A designed to match 50-ohm cable to a balanced load of 100 ohms.*

The performance of these two Baluns is essentially the same. When matching 50-ohm cable to balanced loads of 112.5 ohms, the responses are essentially flat (within 2 to 3 percent) from 1.5 to 30 MHz.

From preliminary measurements on series-type 2:1 Baluns, the Balun in **Photo 10-B** is the one I'd recommend for matching 50-ohm cable to balanced loads of 100 ohms, while the Baluns in **Photo 10-C** would be best for matching to balanced loads of 112.5 ohms. Also, by replacing the 1.78:1 Unun in **Figure 10-2B** with a 2.25:1 Unun, and not adding any extra insulation to the windings of the 1:4 Balun, it's possible to obtain an excellent Balun matching 50-ohm cable to a balanced load of 89 ohms.

Figure 10-4 shows the schematic diagram of a series-type Balun designed to match 50-ohm cable to balanced loads of 25 or 22.22 ohms. **Photo 10-D**

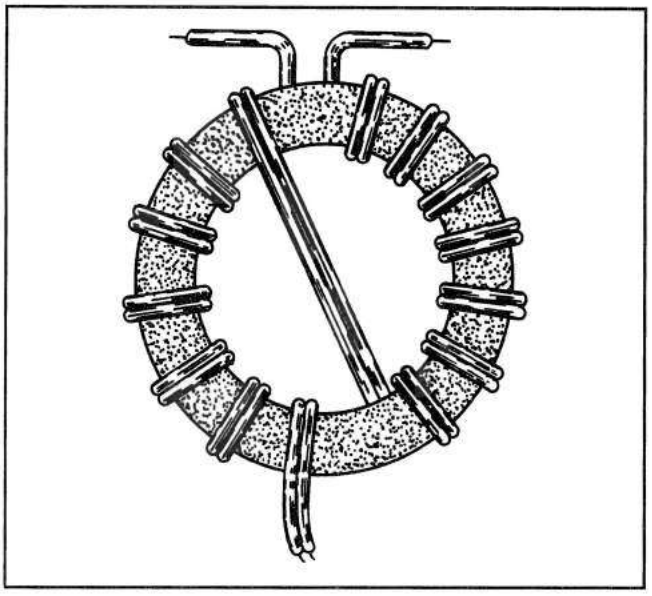

Figure 10-3. *Construction of a 1:1 Guanella Balun with a crossover placing the input and output terminals on opposite sides of the toroid.*

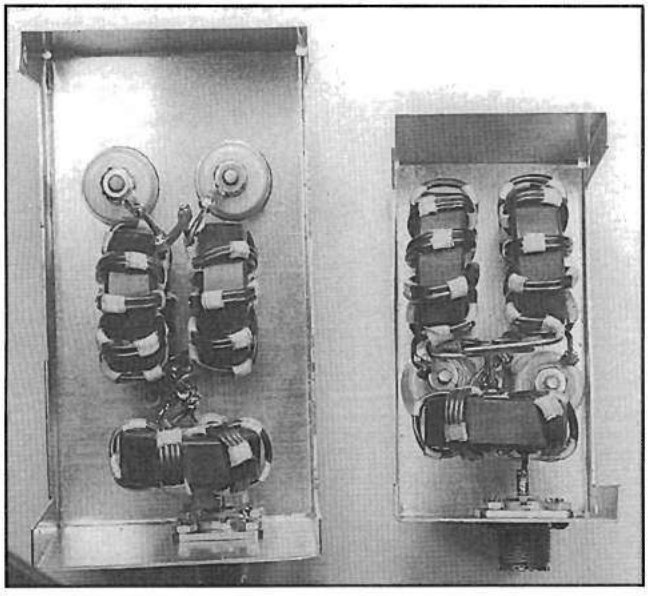

Photo 10-C. *Two series-type Baluns using the schematic diagram of Figure 10-2B designed to match 50-ohm cable to balanced loads of 112.5 ohms.*

shows two versions of this dual-ratio Balun. The Balun on the left, for its Unun, has 6 trifilar turns of No. 14 H Thermaleze wire on a 1.5-inch OD ferrite toroid with a permeability of 250. Winding 3-4 is tapped one turn from terminal 3, yielding the 2:1 ratio. The 1:1 Guanella Balun has 6 turns of homemade coaxial cable on a similar toroid. The inner conductor is No. 12 H Thermaleze wire and is covered with Teflon tubing. The outer braid, from a small coax or from 1/8-inch tubular braid, is tightly wrapped with Scotch No. 92 tape to preserve its low characteristic impedance.

In matching 50-ohm cable to balanced loads of 25 ohms (connection A) or to 22.22 ohms (connection B), the response is essentially flat (within a percent or two) from 1.5 to 30 MHz.

The Balun on the right in **Photo 10-D** has similar windings on a single 2.4-inch OD ferrite toroid with a permeability of 250. Its performance is quite comparable to the Balun on the left.

Sec 10.3.2 Parallel-type Baluns

As you saw in the previous section, the series-type Baluns presented here are combinations of Ununs with ratios of 1.33:1, 1.78:1, 2:1, and 2.25:1 in series with Guanella 1:1 or 4:1 Baluns. The Ununs, which are really an extension of Ruthroff's[9] bootstrap technique for obtaining a 4:1 Unun, sum direct voltages with delayed voltages that traverse a single transmission line. Therefore, the Unun eventually limits the high-frequency response of the series-type Balun.

On the other hand, the parallel-type Balun is an extension of Guanella's technique of summing voltages of equal delays. Instead of simply connecting transmission lines in parallel-series, the parallel-type Balun connects Guanella Baluns in parallel-series. As I noted in **Reference 25**, two 4:1 Guanella Baluns can be connected in parallel-series, yielding very broadband ratios of 6.25:1. This section shows how a 1:1 Guanella Balun can be connected with a 4:1 Guanella Balun in parallel-series, yielding a very broadband ratio of 2.25:1.

Figure 10-5 is the schematic diagram of the high-frequency model of a 2.25:1 Unun which is used for analysis purposes. Because the current through the load is $3/2I_1$, the transformation ratio is $(3/2)^2$, or 2.25:1. Therefore, if the impedance seen on the left side is 50 ohms, a matched impedance on the right side is 22.22 ohms. Because two thirds of the 50 ohms appears across the input of the Guanella 1:1 Balun, its optimum characteristic impedance is 33.33 ohms. Similarly, this is also the value of the optimum characteristic impedance for the windings of the 4:1 Balun. Because the 1:1 Balun wants to see 33.33 ohms on its output (a matched condition) and the 4:1 Balun wants to see 66.66 ohms, placing these two values in parallel results in the confirming value of 22.22 ohms.

If the 50-ohm generator is placed on the right side in **Figure 10-5**, the circuit becomes a step-up Unun matching 50 ohms to 112.5 ohms (on the left). If the ground is removed on the left side, the transformer becomes a Balun. A similar analysis as above, shows that the optimum characteristic impedance of the three bifilar windings now becomes 75 ohms.

Photo 10-E shows a parallel-type 2.25:1 Balun designed to match 50-ohm cable to a balanced load of 112.5 ohms. It has 9 bifilar turns of No. 14 H Thermaleze wire on each of the three toroids that have a 1.5-inch OD and a permeability of 250. Also, one of the wires on each toroid is covered with Teflon tubing, resulting in a characteristic impedance of 75 ohms (the optimum value). When operating as a Balun, the response is essentially flat from 7 MHz to over 45 MHz. As an Unun, the flat response is broadened from 1.5 MHz to over 45 MHz.

Because the coiled wire, parallel-type Balun didn't provide any real advantage over the series-type Balun (in fact, the low-frequency response was poorer), I investigated the beaded transmission line version for possible use in the VHF band. **Figure 10-6** shows a schematic diagram of one using coaxial cable. Obviously, twin lead could be substituted for the coaxial cable. **Photo 10-F** shows both versions.

The top design in **Photo 10-F** has 4 inches of 3/8-inch OD ferrite beads with a permeability of 125 on each of the three 75-ohm transmission lines. It is designed to match 50-ohm cable on the right to a balanced load of 112.5 ohms on the left (with the ground on terminal 1 removed). The transmission lines consist of two No. 14 H Thermaleze wires separated by the Teflon tubing covering one of them. When matching 50-ohm cable to a balanced load of 112.5 ohms, the response is essentially flat from 30 MHz to over 100 MHz (the limit of my bridge).

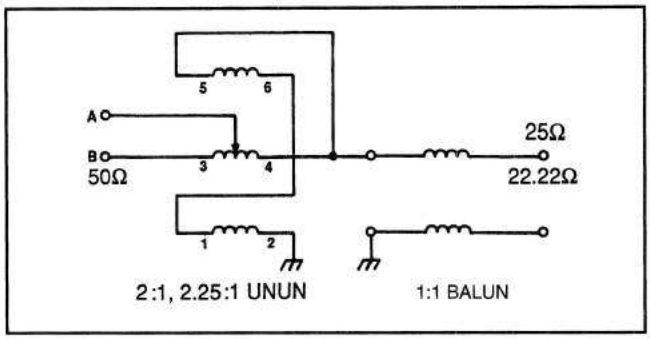

Figure 10-4. *Schematic diagram of a dual-ratio series-type Balun. Connection A matches 50-ohm cable to a balanced load of 25 ohms. Connection B matches 50-ohm cable to a balanced load of 22.22 ohms.*

The bottom design in **Photo 10-F** also has 4 inches of 3/8-inch OD ferrite beads with a permeability of 250. However, they are now threaded by homemade coaxial cable with a characteristic impedance of 33.33 ohms. It is designed to match 50-ohm cable on the left to a balanced load of 22.22 ohms (with the ground on terminal 2 removed). The inner conductor of the coax is No. 14 H Thermaleze wire and is covered with

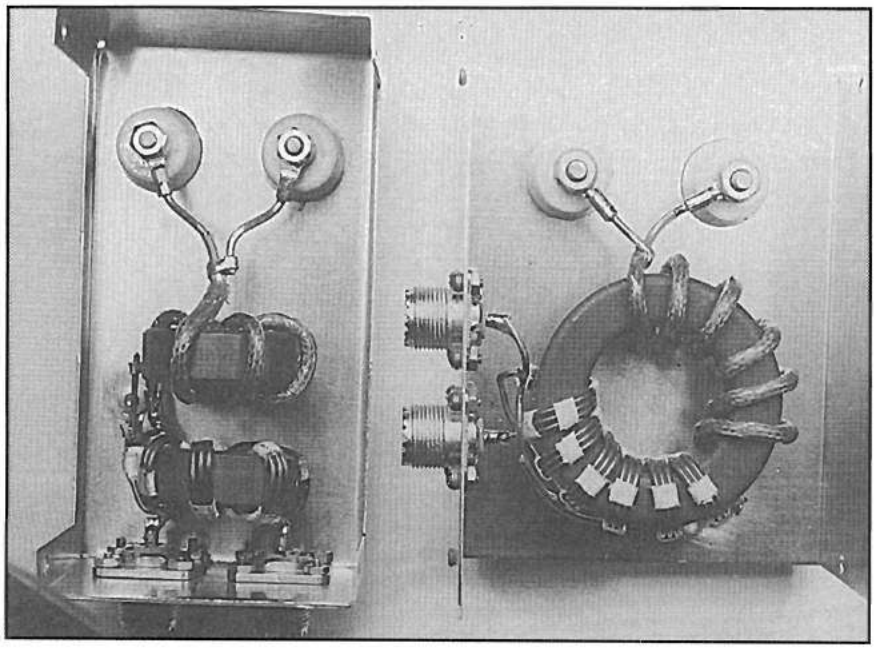

Photo 10-D. *Two series-type Baluns using the schematic diagram of Figure 10-4 designed to match 50-ohm cable to balanced loads of 25 ohms or 22.22 ohms.*

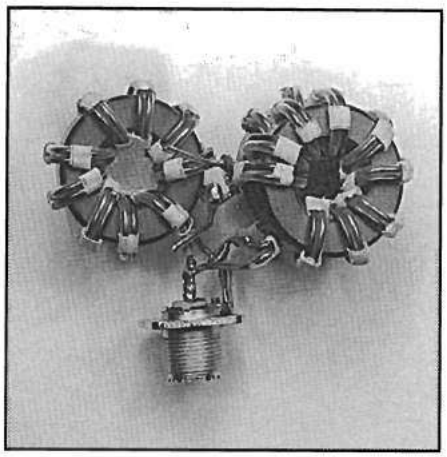

Photo 10-E. *Parallel-type 2.25:1 Balun matching 50-ohm cable to a balanced load of 112.5 ohms.*

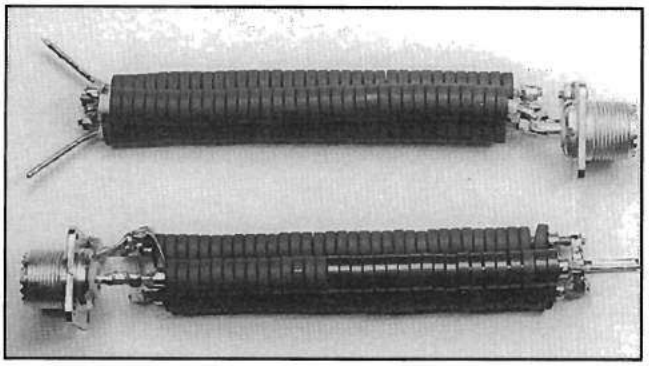

Photo 10-F. *Beaded transmission line versions of the 2.25:1 parallel-type Balun for operation in the VHF band. The top Balun matches 50-ohm cable to a balanced load of 112.5 ohms. The bottom Balun matches it to a balanced load of 22.22 ohms.*

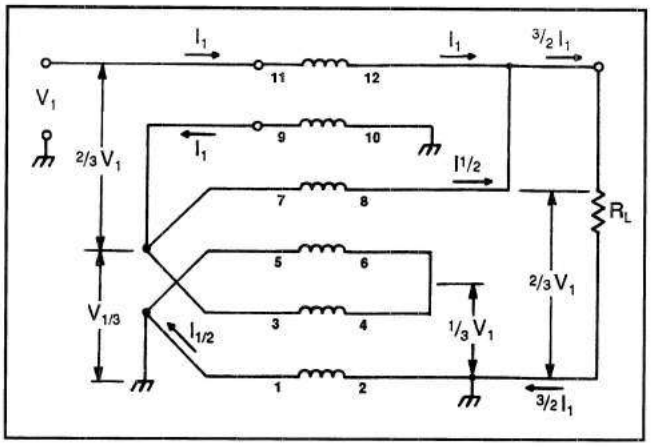

Figure 10-5. *High-frequency model of the parallel-type 2.25:1 transformer. Connections shown are for Unun operation.*

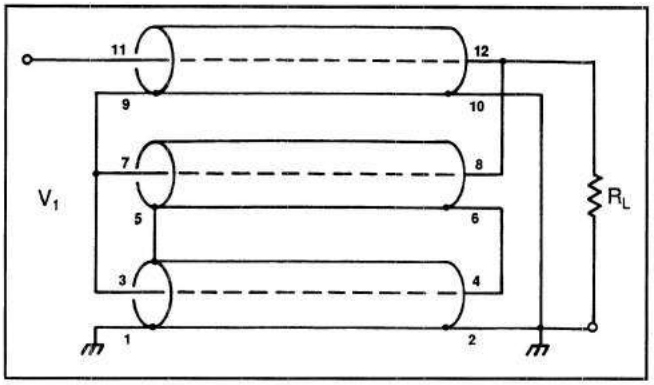

Figure 10-6. *The coaxial cable version of the parallel-type 2.25:1 transformer of Figure 10-5.*

Teflon tubing. The braid is from small coaxial cable or from 1/8-inch tubular braid. The braid is also tightly wrapped with Scotch No. 92 tape in order to preserve the low characteristic impedance. When matching 50-ohm cable to a balanced load of 22.22 ohms, the response is essentially flat from 14 MHz to over 100 MHz (again, the limit of my bridge).

Sec 10.4 Closing Comments

In closing, I'd like to make a couple of comments regarding parallel-type Baluns.

First, if you are interested in a 1.78:1 ratio, replace the 1:4 Balun in **Figures 10-5** and **10-6** with a 1:9 Guanella Balun (three transmission lines connected in parallel-series). This would yield an output current of $4/3I_1$ and a ratio of $(4/3)^2$, or 1.78:1. If you replace the 1:4 Balun with a 1:16 Guanella Balun (four transmission lines connected in parallel-series), the output current will be $5/4I_1$, with a ratio of $(5/4)^2$, or 1.56:1.

Second, because the parallel-type Balun is really an extension of Guanella's technique of summing voltages of equal delays,[26,27] the high-frequency response is mainly limited by the parasitics in the interconnections. Therefore, beaded transmission lines offer the best opportunity for successful operation on the VHF band. It is also recommended that the ferrite beads have permeabilities of 300 or less[2] in order to achieve the very high efficiencies of which these transformers are capable.

Chapter 11

6:1, 9:1, and 12:1 Baluns

Sec 11.1 Introduction

This chapter is a combination of two articles I wrote for *Communications Quarterly*. One, on the 6:1 and 9:1 Baluns, appeared in the Winter 1993 issue and the other, on the 12:1 Balun, ran in the Summer 1993 issue. I combined these two articles here because the three Baluns discussed have much in common. Commonalities include: 1) They are the most difficult to construct and are, therefore, the most expensive; 2) two of them, the 6:1 and 12:1 Baluns, use Ununs in series with Guanella Baluns; 3) two of them use the 9:1 Guanella Balun—the 12:1 Balun with a series 1.33:1 Unun; 4) they are generally associated with two-wire transmission lines with characteristic impedances of 300, 450, and 600 ohms, respectively; 5) when matching 50-ohm cable to higher impedances, they have more loss than the Baluns in the preceding chapters; and 6) the optimum application of these Baluns requires a more critical understanding of the trade-offs in low-frequency response for efficiency.

Like the 2:1 Balun in **Chapter 10**, the 6:1 (actually 6.25:1) Balun also comes in two forms: the series-type, which offers better low-frequency response in the HF band, and the parallel-type, which has a vastly greater high-frequency capability. The parallel-type 6:1 Balun, together with the 9:1 Guanella Balun (which is also a parallel-type), offer the potential for designs capable of efficient and broadband operation on the VHF and UHF bands.

Sec 11.2 6:1 and 9:1 Baluns

Many radio amateurs associate the use of the 6:1 and 9:1 Baluns with 300-ohm twin lead feeding folded dipoles, 450-ohm "ladder" line feeding single or multi-band antenna systems. However, what is neglected (in some cases) is the effect of the height of these antennas above earth and the length of the transmission lines feeding them.

Broadband 6:1 and 9:1 Baluns are considerably more difficult to construct than the more common 1:1 and 4:1 Baluns. This is especially true when matching 50-ohm cable to impedances of 300 and 450 ohms. Furthermore, there are some important trade-offs in low-frequency response for efficiency.

From what I could gather "on the air" or talking to radio clubs, I have determined what I believe are probably two of the most common misconceptions regarding the use of these Baluns:

1. 6:1 Baluns. In free-space, the folded dipole with 300-ohm twin-lead has a resonant impedance close to 300 ohms. The dipole also has this value at a height of about 0.225 wavelength above ground. However, it's only 200 ohms at a height of about 0.17 wavelength and 400 ohms (the maximum) and at 0.35 wavelength. In many cases, the 4:1 Balun would actually do a better job of matching.

2. 9:1 Baluns. Some are unaware of the relationship between the impedance at the input of a transmission line, the characteristic impedance of the line, and the impedance at the end of the line. Just because a transmission line has a characteristic impedance of 450 ohms doesn't necessarily mean that a 9:1 Balun will perform a satisfactory match to 50-ohm cable. Far from it. For example, if the line is terminated by a half-wave dipole with an impedance of 50 ohms, the 9:1 Balun would see 50 ohms when the line is a half-wave long and 4050 ohms when it's a quarter-wave long! Broadband Baluns cannot be designed to handle impedances as high as 4050 ohms. It's very likely that a well-designed 50:450-ohm Balun would experience (particularly on 80 and 160 meters) harmful flux in the core *and* excessive heating because of the large voltage drop along the length of its transmission lines. This problem of presenting very high (and harmful) impedances to Baluns is quite prevalent with multi-band antenna systems.

Clearly, there are many applications for 6:1 and 9:1 Baluns. They not only include matching 50-ohm cable

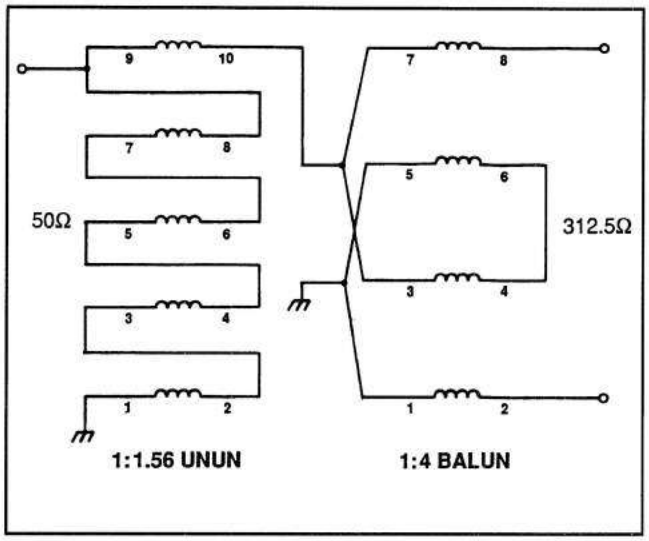

Figure 11-1. *Schematic diagram of the series-type Balun with a 1:6.25 ratio designed to match 50 to 312.5 ohms.*

to balanced loads of 300 and 450 ohms, but also to balanced loads of 8 and 5.6 ohms, as well. Furthermore, many of the designs in this chapter will perform almost as well in Unun (unbalanced-to-unbalanced) applications. The trade-off (which is usually very small) is in low-frequency response. Additionally, these Baluns could be used to exploit the low-loss properties of 300- and 450-ohm twin-lead where very long transmission lines are used. This is especially important at 14 MHz and above.

In the pages that follow, I'll present a variety of Baluns matching 50-ohm cable to 300 ohms (actually to 312.5 ohms, a 6.25:1 ratio) and to 450 ohms, as well as 50-ohm cable to 8 and 5.6 ohms. Also included are two different versions of 6.25:1 Baluns. One is a series-type using a 1.56:1 Unun in series with a 4:1 Guanella Balun and the other a series-parallel arrangement using two 4:1 Guanella Baluns. Because the series-parallel Balun adds voltages of equal delays, you'll find its high-frequency capability is much greater.

The 9:1 Balun is a conventional Guanella Balun with three transmission lines connected in series at the high-impedance side and in parallel at the low-impedance side. Therefore, it also sums voltages of equal delays. Some of the comparisons and analyses of these 6.25:1 and 9:1 Baluns were probably published for the first time in my Winter 1993 *Communications Quarterly* article.

Sec 11.2.1 6.25:1 Series-Type Baluns

Figure 11-1 shows the schematic diagram of a series-type Balun designed to match 50-ohm cable to a balanced load of 312.5 ohms. It consists of a 1:1.56 Unun in series with a 1:4 Guanella Balun. The overall ratio of 1:6.25 should satisfy most of the 1:6 requirements. **Photo 11-A** shows three examples. All three Baluns use the same step-up Unun that has four quintufilar turns on a 1.5-inch OD ferrite toroid with a permeability of 250. Winding 9-10 is No. 14 H Thermaleze wire and the other four are No. 16 H Thermaleze wire. Because this Unun sums only one delayed voltage with four equal direct voltages, it has an excellent high-frequency response.[2]

The Balun on the left in **Photo 11-A** has eight bifilar turns of No. 18 hook-up wire on each transmission line of its 1:4 Balun. The wires are further spaced with No. 18 Teflon tubing providing a characteristic impedance close to 150 ohms (the optimum value). The ferrite toroid has a 2.4-inch OD and a permeability of 250. When matching 50-ohm cable to a floating

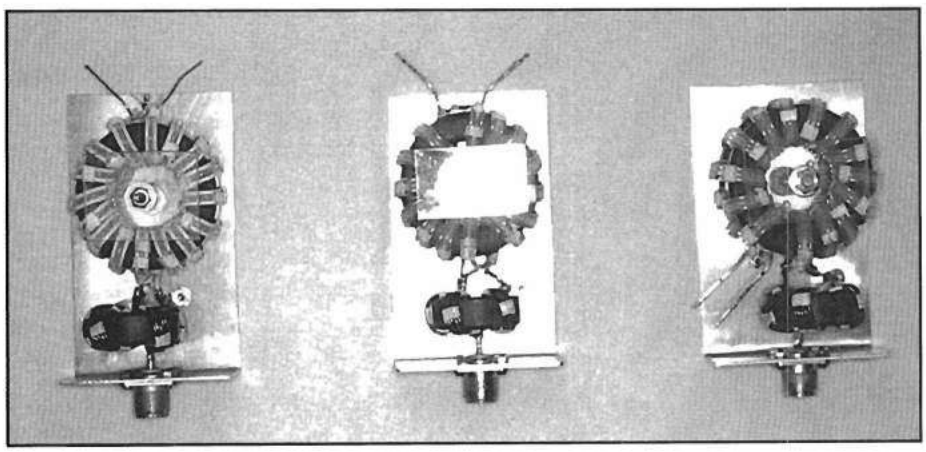

Photo 11-A. *Three examples of series-type 1:6.25 Baluns. The Balun on the right, with a double-core 1:4 Balun, has both a balanced voltage and current output. The other two only have balanced-current outputs.*

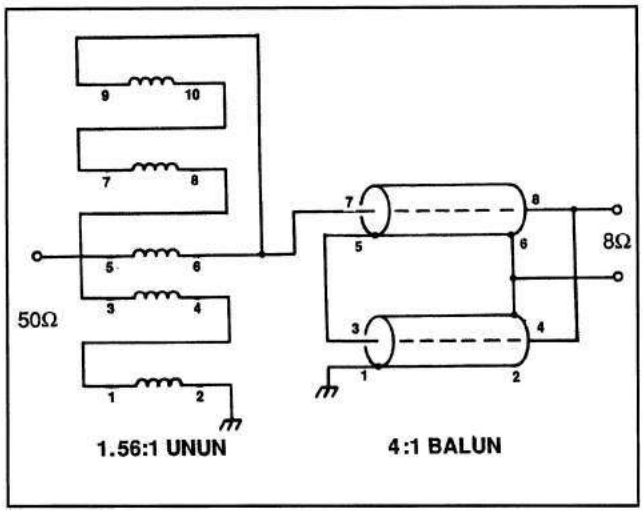

Figure 11-2. *Schematic diagram of the series-type Balun with a 6.25:1 ratio designed to match 50 to 8 ohms.*

load of 312.5 ohms, the response is essentially flat from 1.7 to 30 MHz. Under matched conditions, 500 watts of continuous power and 1 kW of peak power is a conservative power rating. Because the 1:4 Balun in this series-type 1:6.25 Balun uses only one core instead of two, this transformer should never be used when the load is grounded at its center. Also, it is not recommended for balanced antennas. This series-type Balun presents balanced currents, but does *not* present balanced voltages.

The Balun in the center of **Photo 11-A** has seven bifilar turns of No. 16 SF Formvar wire on each transmission line on its 1:4 Balun. The wires are covered with Telfon sleeving and further separated by No. 16 Teflon tubing. Like the Balun on the left, the characteristic impedance is also close to the objective of 150 ohms. The toroid also has a 2.4-inch OD and a permeability of 250. When matching 50-ohm cable to a floating load of 312.5 ohms, the response is essentially flat from 3.5 to 30 MHz. Over this frequency range, this Balun can easily handle the full legal limit of amateur radio power. Because this Balun also presents balanced currents and not balanced voltages, it should not be used when the loads are balanced to ground or grounded at their centers.

The Balun on the right in **Photo 11-A** has 14 bifilar turns of No. 16 SF Formvar wire on each of the two toroids of the 1:4 Balun. The wires are also covered with Teflon sleeving and further separated by No. 16 Teflon tubing. For ease of connection, one core is wound clockwise and the other counterclockwise. The two cores are spaced 1/4 inch apart with acrylic sections. When matching 50-ohm cable to a 312.5 load that is either floating, balanced to ground, grounded at its center, or grounded at its bottom (a broadband Unun), the response is essentially flat from 1.7 to 30 MHz. Under this matched condition, it can easily handle the full legal limit of amateur radio power. Furthermore, this is a true Balun because it presents equal currents and equal voltages. If one were to measure the voltages-to-ground, when matching into a balanced load, one would find them to be equal and opposite. The other two 1:6.25 Baluns using single-core 1:4 Baluns, would have equal currents but not equal voltages (see **Chapter 8**). Because they are easier to construct, it would be interesting to compare them with a true Balun.

Figure 11-2 shows the schematic diagram of a series-type Balun designed to match 50-ohm cable to a balanced load of 8 ohms (perhaps a short-boom Yagi). It consists of a 1.56:1 step-down Unun in series with a Guanella 4:1 step-down Balun. The overall ratio is 6.25:1. **Photo 11-B** shows two examples. Both Baluns use the same step-down Unun, which has four quintufilar turns on a 1.5-inch OD ferrite toroid with a permeability of 250. Winding 5-6 is No. 14 H Thermaleze wire and the other four are No. 16 H Thermaleze wire. The interleaving of the wires is such that the performance is optimized for matching 50 to 32 ohms.

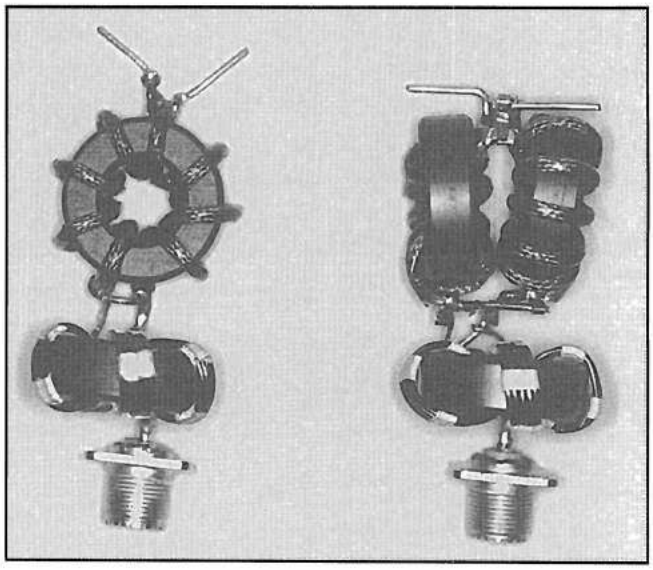

Photo 11-B. *Two examples of the series-type 6.25:1 Balun optimized at the 50:8-ohm level. The Balun on the left is designed to match into a floating 8-ohm load. The Balun on the right is designed to match into an 8-ohm floating, center-tapped-to-ground or grounded load (Unun).*

The Balun on the left in **Photo 11-B** has four turns of low-impedance coaxial cable on each transmission line on the single-core 4:1 Balun. The inner conductor is No. 14 H Thermaleze wire, and it has two layers of Scotch No. 92 polyimide tape. The outer braid is from a small coax (or 1/8-inch tubular braid) and is tightly wrapped with Scotch No. 92 tape to achieve the 17-ohm characteristic impedance (the optimum value). The ferrite toroid has a 1.5-inch OD and a permeability of 250. When matching 50-ohm cable to a floating load of 8 ohms, the response is flat from 1 to 40 MHz. In a matched condition, this Balun can easily handle the full legal limit of amateur radio power.

The Balun on the right in **Photo 11-B** has six turns of the same coaxial cable on each of the two cores of the Guanella step-down Balun. The cores also have a 1.5-inch OD and a permeability of 250. The performance of this Balun is practically the same as the above with the single-core 4:1 Balun. The important differences are that this 6.25:1 Balun also performs equally well whether the load is center-tapped-to-ground, balanced-to-ground, or grounded at the bottom (a broadband Unun). This is the one recommended for feeding a short-spaced Yagi beam antenna.

Sec 11.2.2 6.25:1 Parallel-Type Baluns

The 6.25:1 series-type Baluns described in the preceding section consisted of a 1.56:1 Unun, which is an extension of Ruthroff's bootstrap approach for Ununs,[9] in series with a Guanella 4:1 Balun.[2] The upper-frequency limit for this combination is really set by the Unun, which sums a delayed voltage with four direct voltages. The parallel-type 6.25:1 Baluns described in this section are really extensions of Guanella's approach, which sums voltages of equal delays. Therefore, the upper-frequency limit is mainly dependent upon the parasitics in the interconnections.

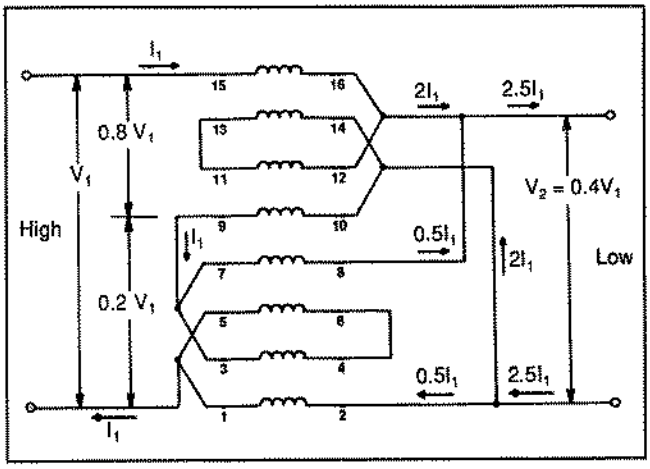

Figure 11-3. *Schematic diagram of the parallel-type Balun (and Unun) with a 6.25:1 ratio. The currents and voltages are shown for analysis purposes (see text).*

The 6.25:1 parallel-type Balun uses two 4:1 Guanella Baluns connected in parallel on the low-impedance side and in series on the high-impedance side. As you will see, one of the Baluns is reversed, giving the desired ratio of 6.25:1. Other combinations can produce different fractional-ratios (other than $1{:}n^2$ where n is 1, 2, 3, . . .), like 2.25:1 and 1.78:1. Because very little practical design information is available regarding this family of very broadband Baluns,[26,27] this section also includes my high-frequency analysis of the 6.25:1 parallel-type Balun. It should also be pointed out that very little sacrifice in performance occurs whether the load is grounded at its center or at the bottom (as an Unun).

Figure 11-3 shows the coiled-wire version of the 6.25:1 parallel-type Balun. For analysis purposes, the voltages and currents are also shown. As can be seen, the top 4:1 Balun is connected as a step-down Balun, while the bottom 4:1 Balun is connected as a step-up Balun. The Baluns are in series on the high-impedance side (on the left) and in parallel on the low-impedance side (on the right). As **Figure 11-3** illustrates, the lower 1:4 Balun adds a current of $0.5I_1$ to the load, resulting in a total current of $2.5I_1$. Thus, the impedance transformation ratio is 2.5^2, or 6.25:1.

For maximum high-frequency response, each transmission line should see a load equal to its characteristic impedance. In other words, they should be "flat" lines. If the high side on the left is 50 ohms, then 40 ohms appears on the input of the top Balun and 10 ohms on the input of the bottom Balun. Consequently, the optimum characteristic impedance for *all* transmission lines is 20 ohms. On the low-impedance side on the right, the top Balun wants to see 10 ohms, while the bottom Balun wants to see 40 ohms. Because 10 ohms in parallel with 40 ohms equals 8 ohms, each Balun conveniently sees its ideal load and a broadband ratio of 6.25:1 is obtained.

If the Balun is required to match 50-ohm cable (on the right side) to a balanced load of 312.5 ohms (on the left side), the same analysis shows that the optimum characteristic impedance of all the transmission lines is 125 ohms.

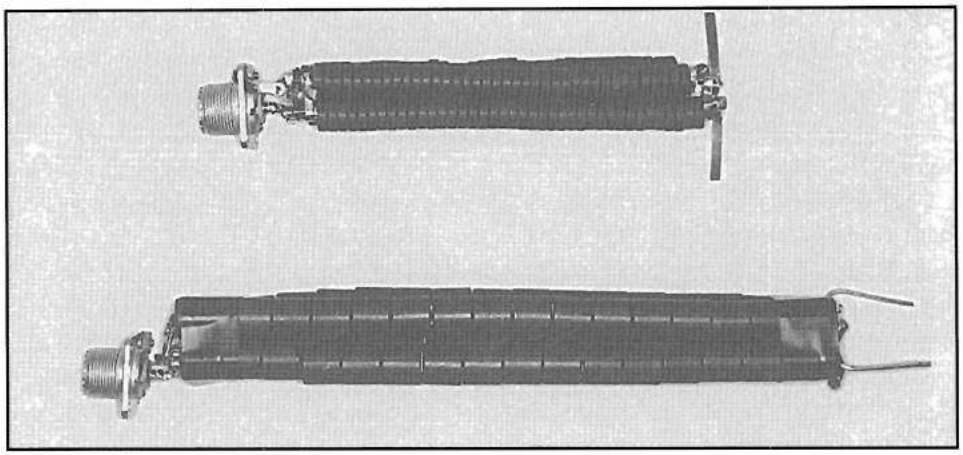

Photo 11-C. *Two beaded-line versions of the parallel-type 6.25:1 Balun (and Unun). The top transformer is designed to match 50-ohm cable to 8 ohms. The bottom transformer is designed to match 50-ohm cable to 312.5 ohms.*

Because the parallel-type Balun (or Unun) sums voltages of equal delays and, therefore, has no built-in high-frequency cut-off, it has a real advantage over the series-type Balun on the VHF bands and above. Furthermore, beaded transmission lines with low-permeability ferrite beads (125 and less) can be used, resulting in high efficiencies. On the HF band, where coiled windings are generally used, the series-type Balun is preferred because of its simplicity.

Photo 11-C shows two beaded-line 6.25:1 transformers. The top Balun, designed to match 50-ohm cable (on the left) to 8 ohms (on the right), uses low-impedance coaxial cable lines. The schematic diagram is shown in **Figure 11-4**. It has 5 inches of 0.375-inch OD beads (permeability 125) on four coaxial cables with characteristic impedances of 20 ohms. The inner-conductors of No. 12 H Thermaleze wire have two layers of Scotch No. 92 polyimide tape. The outer braids, from small coaxial cable or 1/8-inch tubular braid, are also wrapped tightly with the same tape in order to preserve the 20-ohm characteristic impedance. When matching 50 ohms to 8 ohms, the response is essentially flat from 10 MHz to beyond 100 MHz (the limit of my simple bridge). Under this matched condition, this Balun can easily handle the full legal limit of amateur radio power. Furthermore, it has practically the same performance when operating as an Unun (both terminals 1 and 2 grounded). In the Unun application, the bottom transmission line has no voltage along it and, therefore, requires no beads.

The bottom Balun in **Photo 11-C**, which is designed to match 50-ohm cable to a balanced load of 312.5 ohms, has 8 inches of 0.5-inch OD beads on 125-ohm twin-lead transmission lines. The ferrite beads also have a permeability of 125. The wires are No. 14 H Thermaleze wire and are covered with Teflon sleeving. They are further separated by No. 18

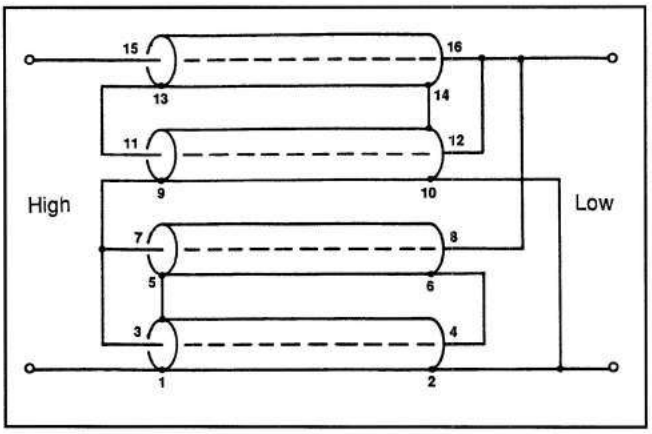

Figure 11-4. *Schematic diagram of the coaxial-cable version of the parallel-type 6.25:1 Balun (and Unun).*

Teflon tubing. When matching 50-ohm cable (on the right side) to 312.5 ohms (on the left side), the response is essentially flat from 20 MHz to over 100 MHz. Under this matched condition, this Balun can also easily handle the full legal limit of amateur radio power. Additionally, this transformer performs practically as well when used as an Unun.

Sec 11.3 9:1 Baluns

The broadband 9:1 Balun, matching 50-ohm cable to a balanced load of 450 ohms, is one of the most difficult ones to construct because high-impedance transmission lines (150 ohms) are required for maximum high-frequency response, and greater reactances are needed in order to isolate the input from the output. So one can appreciate the task at hand, this section also provides a brief review of the theory of these devices.[2]

Figure 11-5 shows the high- and low-frequency models of the Guanella 9:1 Balun that connect three

transmission lines in series at the high-impedance side and in parallel at the low-impedance side. Because Guanella's Baluns (which can be easily converted to Ununs) sum voltages of equal delays, they offer the highest frequency capability.

The high-frequency model (**Figure 11-5A**) assumes there is sufficient choking reactance in the coiled (or beaded) transmission lines to isolate the input from the output and only allow transmission line currents to flow. Under this condition, the analysis is rather straightforward as it only involves transmission line theory. Simply stated—the maximum high-frequency response occurs when each transmission line is terminated in a load equal to its characteristic impedance, Z_0. Thus, the transmission lines in the 9:1 Balun have no standing waves. Because each transmission line sees one third of the load, the optimum value of Z_0 is $R_L/3$. Except for parasitics in the interconnections and self-resonances in coiled windings, Guanella's approach is literally "frequency independent."

On the other hand, the low-frequency analysis of the Guanella 9:1 Balun is most important because it reveals the major difficulty in designing them for low-loss, wideband operation. **Figure 11-5B** is the model for determining the low-frequency response. It assumes that no energy is transmitted to the load by a transmission line mode. Although the terminology and analysis is the same as that used for conventional autotransformers, the similarity ends when there is sufficient choking reactance to only allow for the efficient transmission line mode.

As with conventional transformers, one can analyze the low-frequency response of the 9:1 Balun from either the low- or high-impedance side. By putting the generator on the low-impedance side in **Figure 11-5B**, I've chosen to analyze it from that side. With the output open-circuited, the generator sees four coiled (or beaded) lines connected in series-parallel. The net result is that the generator sees the reactance of only *one* coiled (or beaded) line. To prevent a shunting current to ground (and/or autotransformer operation), the reactance the generator sees should be much greater than R_g (at least by a factor of 10 at the lowest frequency of interest). The inductance of the coiled or beaded line that prevents the unwanted currents is still known as the magnetizing inductance, L_M.

What's important to note here is that the low-frequency model of the Guanella 4:1 Balun does not have the series-parallel combination of coiled or beaded lines.[2] Only two lines, which are in series, exist in its model. Therefore, for a two-core Guanella 4:1 Balun having the same number of turns (and same cores) as a 9:1 Guanella Balun, its low-frequency response is better by a factor of two!

Another advantage that goes to the Guanella 4:1 Balun when matching 50 to 200 ohms, is in the number of turns that can be wound on the same cores. Since 4:1 Baluns require characteristic impedances of 100 ohms (instead of 150), the width of the transmission lines is considerably less, thus allowing for more turns. Also, as will be shown later, the efficiency of the 4:1 Balun is greater because the potential drops

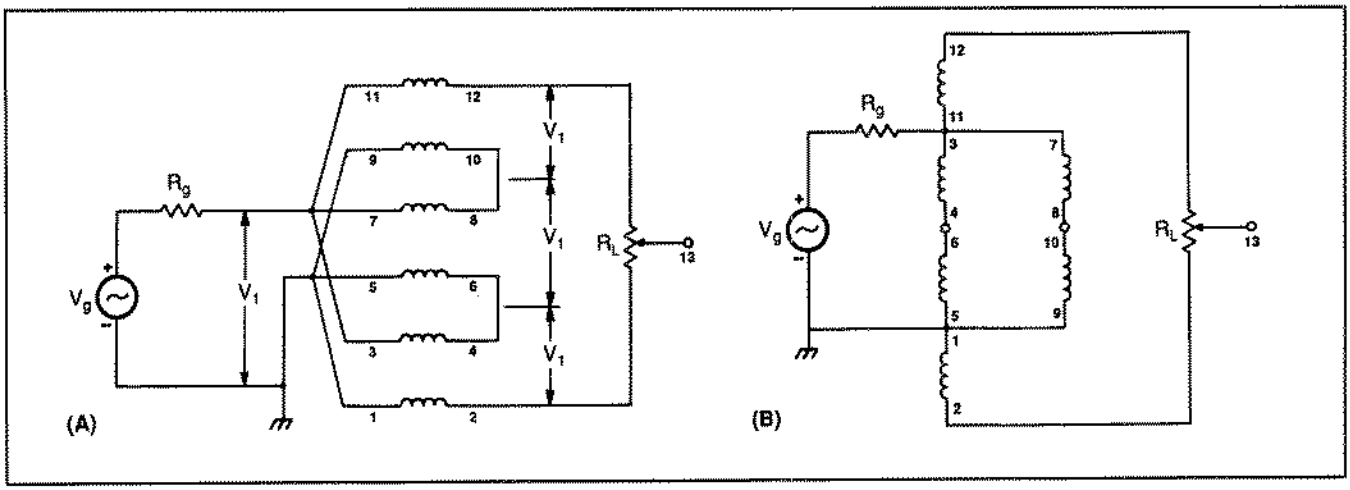

Figure 11-5. *Models of Guanella's 1:9 Balun. The high-frequency model, (A), assumes that $Z_0 = R_L/3$, and therefore V_2, the output of each transmission line, equals V_1. The low-frequency model, (B), assumes no energy is transmitted to the load, R_L, by a transmission line mode.*

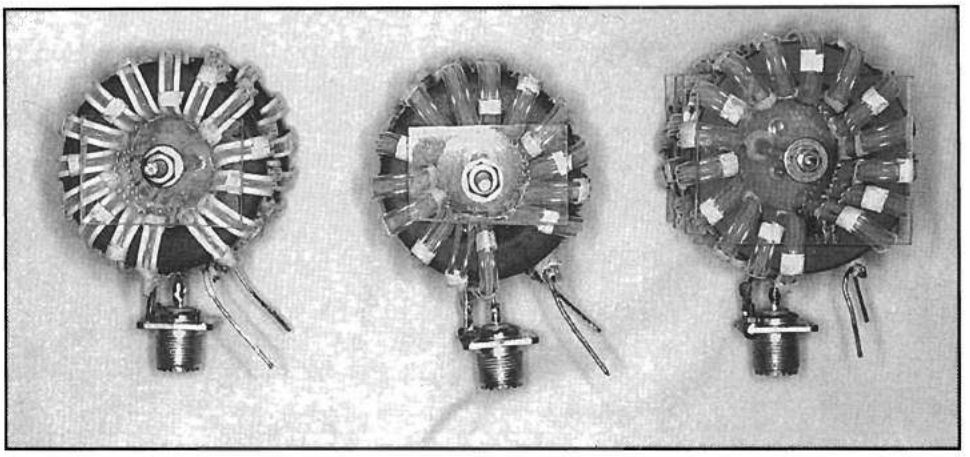

Photo 11-D. *Three broadband Guanella 9:1 Baluns designed to match 50-ohm cable to 450 ohms. The transformer on the left, using No. 18 hook-up wire, can handle 500 watts from 1.7 to 45 MHz. The transformer in the center, using No. 16 wire, can handle 1 kW from 3.5 to 45 MHz. The transformer on the right (with larger cores), using No. 16 wire, can handle 1 kW from 1.7 to 45 MHz.*

along the transmission lines are lower (less dielectric loss). Finally, as you can see from **Figure 11-5B**, by also grounding terminal 2 (Unun operation), windings 1-2 and 3-4 are both shorted—degrading the low-frequency response because L_M is reduced by one third.

Another interesting analysis with Baluns and Ununs concerns the potential gradients (voltage drops) along the transmission lines. Because the loss with these transformers, when transferring the energy via a transmission line mode, is a dielectric-type (voltage dependent), the higher the gradient, the greater the loss. The interesting cases occur when the load is: a) floating, b) grounded at the center, and c) grounded at the bottom (an Unun).

Floating load. With terminal 13 in **Figure 11-5A** ungrounded, the top transmission line has a gradient of $+V_1$ and the bottom transmission line has a gradient of $-V_1$. The center transmission line has a gradient of zero. Therefore, the center transmission line only acts as a delay line and doesn't require a magnetic core or beads. As a result, the top and bottom cores (or beads) account for the dielectric loss.

Load grounded at the center. With terminal 13 grounded at the center of the load, the top transmission line has a gradient of $+V_1$, the bottom transmission line has a gradient of $-V_1$, and the center transmission line has a gradient of $-V_1/2$. This configuration results in about 25 percent more loss because of the extra gradient along the center transmission line. Incidentally, this condition exists when matching into balanced systems like 450-ohm transmission lines or antennas because they have virtual grounds at the center of the loads they present.

Load grounded at the bottom. With terminal 13 grounded at the bottom of the load (an Unun), the top and center transmission lines have gradients of $+V_1$. The bottom transmission line has no gradient and, therefore, no loss. It only acts as a delay line and thus requires no magnetic core or beads.

Sec 11.3.1 Some Practical 9:1 Balun Designs

Photo 11-D shows three versions of the broadband Guanella 9:1 Balun designed to match 50-ohm cable to 450-ohm loads. The transformer on the left has 15 bifilar turns of No. 18 hook-up wire on each of the three ferrite toroids with a 2.4-inch OD and permeability of 250. The wires are further separated by No. 16 Teflon tubing, resulting in a characteristic impedance close to 150 ohms (the optimum value). The cores in this Balun, as well as the other two that follow, are spaced 1/4 inch apart by sections of acrylic. In matching 50 to 450 ohms, the response is essentially flat from 1.7 to 45 MHz. In this matched condition, this transformer can easily handle 500 watts of continuous power and 1 kW of peak power.

The transformer in the center of **Photo 11-D** has 14 bifilar turns of No. 16 SF Formvar wire on each of the three ferrite toroids with a 2.4-inch OD and permeability of 250. The wires are covered with Teflon sleeving and further separated by No. 16 Teflon tubing. The characteristic impedance is also close to the optimum value of 150 ohms. In matching 50 to 450 ohms, the response is essentially flat from 3.5 to 45 MHz. In this matched condition, this transformer can easily handle 1 kW of continuous power and 2 kW of peak power. **Photo 11-E** shows this Balun mounted in a minibox 6 inches long by 5 inches wide by 4 inches high.

The transformer on the right in **Photo 11-D** is designed to handle 1 kW of continuous power and 2 kW

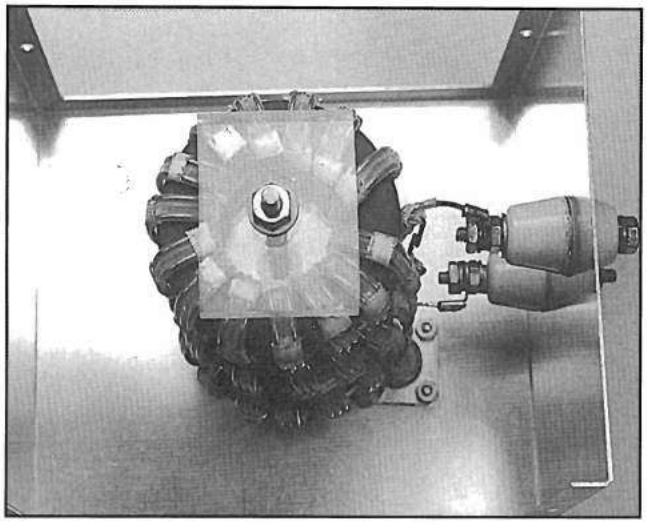

Photo 11-E. *The Guanella 9:1 Balun shown mounted in a large minibox.*

of peak power from 1.7 to 45 MHz. Because this transformer uses larger cores with slightly higher permeabilities (2.68-inch OD and 290 permeability), which are not as popular as those used in the other two Baluns, it is much more expensive to construct. It has 16 bifilar turns of No. 16 SF Formvar wire on each toroid. The wires are covered with No. 16 Teflon sleeving and further separated with No. 16 Teflon tubing. In matching 50 to 450 ohms, the response is flat from 1.7 to 45 MHz.

Finally, **Figure 11-6** shows the schematic diagram of a 9:1 Balun (or Unun) using coaxial cables wound around ferrite cores or threaded through ferrite beads. This form of the transformer is especially useful when matching 50-ohm cable to 5.6 ohms because the choking reactance of the magnetizing inductance, L_M, only need be much greater than 5.6 ohms. **Photo 11-F** shows two different designs.

The transformer on the top has 9 1/2 turns of low-impedance coaxial cable on each rod. The rods are 1/2 inch in diameter, 2 1/2 inches long, and have a permeability of 125. The low-frequency response of this Balun is quite insensitive to the length and permeability of the rods.[2] The inner conductors of the coaxial cables are No. 12 H Thermaleze wire with two layers of Scotch No. 92 tape. The outer braids are made from small coax (or 1/8-inch tubular braid). They are further wrapped with Scotch No. 92 tape to preserve the low-impedance of 17 ohms. In matching 50-ohm cable to 5.6 ohms, the response is essentially flat from 1.7 to 30 MHz. The optimum impedance level was found when matching 40 to 4.45 ohms. The addition of another layer of Scotch No. 92 tape would optimize this transformer at the 50:56-ohm level, and the high-frequency response would exceed 100 MHz. This transformer is very efficient and should handle the full legal limit of amateur radio power easily.

The bottom transformer in **Photo 11-F** is designed to match 50-ohm cable to a load of 5.6 ohms in the VHF band. It uses 3 1/2 inches of beads on three low-impedance coaxial cables. The ferrite beads have an OD of 3/8 inch and a permeability of 125. The inner conductors of the coaxes are No. 12 H Thermaleze wire with one layer of Scotch No. 92 tape. The outer conductors are from small coaxes or 1/8-inch tubular braid, and are also tightly wrapped with Scotch No. 92 tape to preserve the low characteristic impedance. In matching 50-ohm cable to 5.6 ohms, the response is essentially flat from 7 MHz to over 100 MHz (the limit of my test equipment). This 9:1 Balun (which can be used as an Unun) can handle the full legal limit of amateur radio power under matched conditions, because of the low-permeability beads and the low-voltage gradients along the lengths of its transmission lines.

Sec 11.4 Concluding Remarks on 6:1 and 9:1 Baluns

One of the most important properties of broadband Baluns and Ununs (which all use ferrites) is their capability of having extremely high efficiencies. Knowing the loss mechanism in these transformers and the trade-off in low-frequency response for efficiency allows one to optimize their applications. In the paragraphs that follow, I'll discuss the losses and

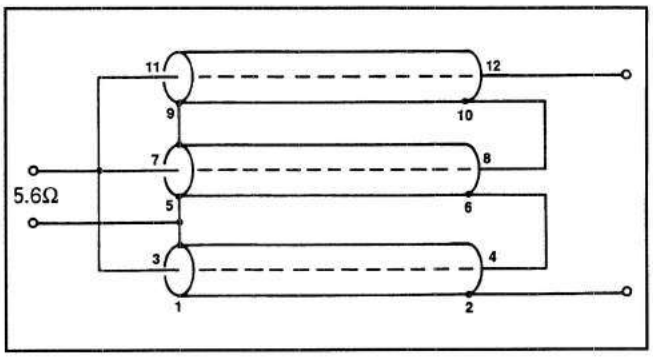

Figure 11-6. *Schematic diagram of a coaxial cable (beaded or coiled) 9:1 Guanella Balun (or Unun). This design is especially useful in matching 50-ohm cable to 5.6 ohms over a very wide bandwidth.*

trade-offs involved with the transformers presented in the preceding sections. The approach used here should be applicable to all forms of transmission line transformers. This section ends with a review of two articles that contained 9:1 Baluns. As you'll see, I have some rather different views on the claims made in these articles.

Accurate measurements on many broadband Ununs have found the losses to be related to the permeability and the impedance level.[2] Permeabilities greater than 300 resulted in excessive losses. Because these losses are unlike the conventional transformer whose losses are current-dependent, it can only be assumed that their losses are voltage dependent; in other words a dielectric-type loss. Therefore, higher-impedance transformers have higher voltage gradients along their transmission line and, thus, have greater losses. Additionally, it was found that the higher the permeability, the greater the loss with frequency. Taking into account the accurate measurements and the factors noted above, I offer these loss values for the transformers in the preceding sections:

1.56:1 Ununs. The 1.56:1 Ununs (either step-up or step-down) used in series with Guanella 4:1 Baluns to form 6.25:1 Baluns have the lowest potential gradients along their transmission lines. Voltage drops of only about 0.2 V_1, where V_1 is the input voltage, exist along their transmission lines. Accurate measurements have shown losses, in a matched condition, of only 0.04 dB. If the cores, which have a permeability of 250, were replaced with cores having a permeability of 125, the losses could be as low as 0.02 dB over much of the passband. The low-frequency response would still be acceptable at 1.7 MHz. This Unun is a natural for matching into 75-ohm hard line when long transmission lines are required.

6.25:1 and 9:1 Low-impedance Baluns. Baluns matching 50-ohm cable to 8 or 5.6 ohms, also have very low voltage drops along their transmission lines. Generally, they are about twice that of the 1.56:1 Unun. Therefore, the losses with these Baluns should be on the order of 0.1 dB in their passbands.

6.25:1 High-impedance Baluns. The losses in the series-type Baluns are mainly in the 1:4 Guanella Baluns, which have potential gradients of about 1.25 V_1, where V_1 is the input voltage. From previous measurements at this impedance level, the suggestion is that the losses (with ferrites of 250 permeability) should be about 0.1 dB at 7 MHz and 0.2 dB at 30 MHz. By using toroids with permeabilities of 125, the losses could be 0.07 dB and 0.15 dB, respectively. However, with a permeability of 40, the losses could be as low as 0.05 dB within the passband. However, one must consider the sacrifice in low-frequency response incurred when using these lower-permeability ferrites. With a permeability of 125, it's poorer by a factor of 2. With a permeability of 40, it's poorer by a factor of 8! The 6.25:1 parallel-type Balun in this article uses ferrite beads with a permeability of 125 and, therefore, should have losses similar to its series-type counterpart.

9:1 High-impedance Baluns. As was shown in the preceding section, the potential gradient along two of the transmission lines is V_1, where V_1 is the input voltage. The third transmission line, with a balanced load (or as an Unun), has no potential gradient and, consequently, no loss in its core. Because the loss with the series-type Balun mainly exists in one core, the loss with the 1:9 Balun should be a little less than twice as great. With ferrite cores of 250 permeability, the suggested losses are 0.2 dB at 7 MHz and 0.4 dB at 30 MHz. With cores of 125 permeability, the losses are about 0.14 and 0.28 dB, respectively. Again, by using cores with permeabilities of 40, the losses are practically negligible—approximately 0.1 dB within its passband.

As in the case of the 1:6.25 Baluns above, similar trade-offs occur in the low-frequency response. That is, if 125 permeability cores are used, the low-frequency response is poorer by a factor of 2; with 40 permeability cores, it's poorer by a factor of 8. The major difference here is that the low-frequency performance of the

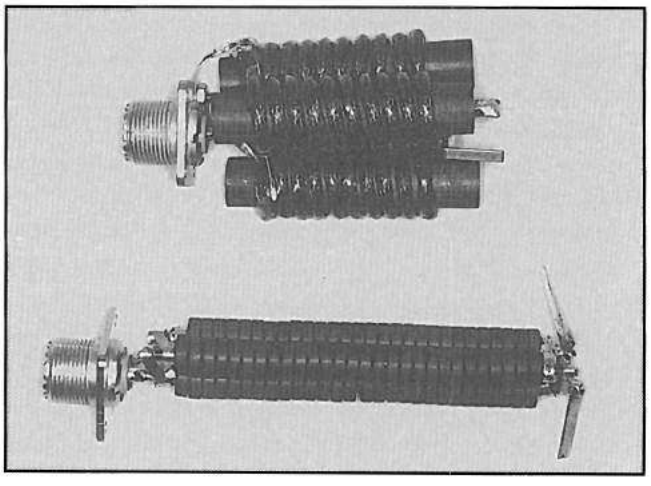

Photo 11-F. *Two versions of the coaxial-cable 9:1 Guanella Balun (or Unun) designed to match 50-ohm cable to 5.6 ohms*

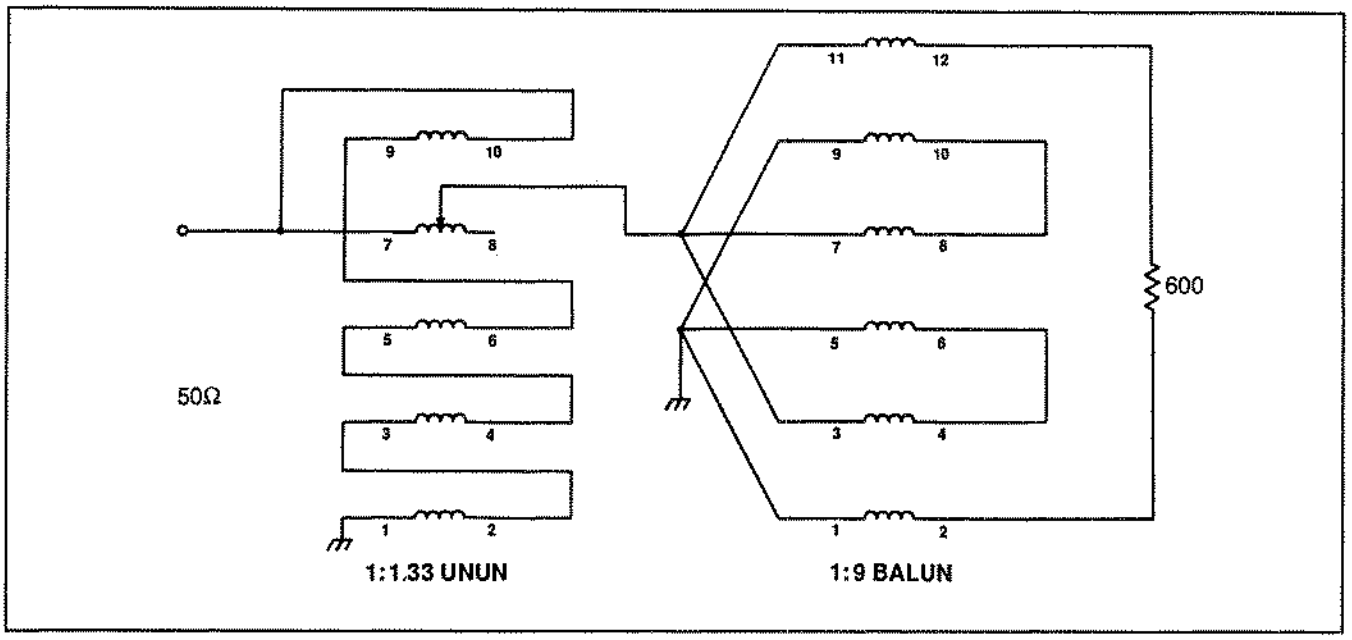

Figure 11-7. *Schematic diagram of the series-type 12:1 Balun using a 1:1.33 Unun in series with a 1:9 Guanella Balun.*

9:1 Balun, as seen by its low-frequency model, isn't as good as the 4:1 Balun that controls the low-frequency response of the series-type 1:6.25 Balun. Additionally, it should be pointed out that all of the suggested losses for the transformers in this chapter are for matched conditions—that is with VSWRs of 1:1. If the VSWR is 2:1 due to a load twice as large as the objective, the input voltage to the Balun increases by about 40 percent. Therefore, the losses should increase by close to the same percentage.

In closing this section, I would like to report my findings on two recent articles in amateur radio journals that also described 9:1 Baluns matching 50-ohm cable to 450 ohms. One[5] advocated using three 150-ohm coaxial cables threaded through high-permeability ferrite beads—a 9:1 Guanella Balun. Because of the low voltage-breakdown capability of the coaxial cable and the high loss found by accurate measurements on Ununs using these high-permeability ferrites, the design was suspect. I built a copy of the design and found it to be, as expected, unable to handle any appreciable power. The second article[28] advocated using 14 trifilar turns of "magnet wire" on a 2-inch OD powdered-iron core (permeability of 10). This Balun was also constructed and tested. Again, as was expected, when matching 50-ohm cable to a floating load of 450 ohms, the 9:1 Balun barely reached a true 9:1 ratio at 7 MHz. Above 7 MHz, the ratio became greater than 9:1 and also introduced a reactive component. Below 7 MHz, there was insufficient choking reactance to prevent flux in the core. My three objections to this design are: 1) a trifilar design has a poor high-frequency response because it sums a direct voltage with a delayed voltage that traverses a single transmission line and a delayed voltage that traverses two transmission lines, 2) the characteristic impedances of the transmission lines are only 50 ohms (the objective is 150 ohms), and 3) the low-frequency response is poor because of the low-permeability powdered-iron core. I do not recommend either of the designs in these two articles.

Sec 11.5 12:1 Baluns

Over the years, the broadband, 12:1 Balun has been of special interest to users of rhombic and V antennas. With the aid of this Balun, certain advantages over multi-element arrays can be fully exploited. Rhombics and Vs are easier to construct, both electrically and mechanically, and there are no particularly critical dimensions or adjustments. Furthermore, they give satisfactory gain and directivity over a 2-to-1 frequency range. These antennas have also been found to be more effective in reception. Because their designs can present input impedances of 600 ohms, and very long lengths of highly efficient 600-ohm open-wire line can be used between the shack and the antenna, an efficient and broadband 12:1 Balun is a natural for

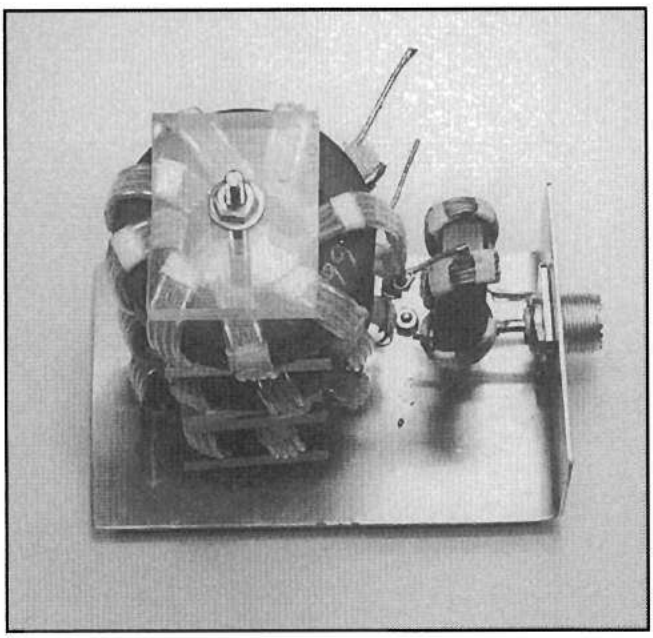

Photo 11-G. *Top view of the high-power 12:1 Balun.*

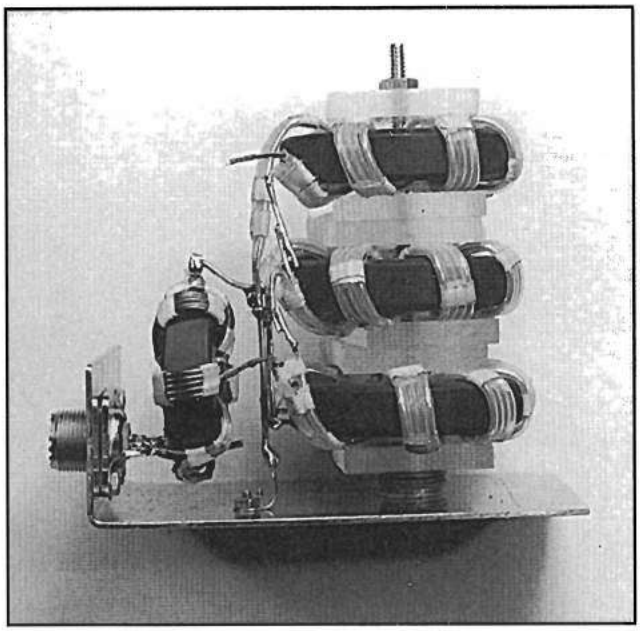

Photo 11-H. *Side view of the high-power 12:1 Balun.*

this application. However, to my knowledge, satisfactory Baluns have not been available for this use.

I will present two versions of a series-type Balun designed to match 50-ohm cable to a balanced load of 600 ohms. One is a high-power unit designed to handle the full legal limit of amateur radio power over a bandwidth of 7 to 30 MHz. The other is a medium-power unit capable of handling approximately one-half the legal limit of amateur radio power from 3.5 to 30 MHz. Both Baluns use a 1:1.33 Unun in series with a 1:9 Guanella Balun.

As you will see, these Baluns are not especially easy to design and construct. The major difficulties lie in trying to obtain sufficient choking reactances in the coiled windings to meet the low-frequency requirements, and large enough characteristic impedances of the windings to meet the high-frequency requirements. Because a coiled winding with a characteristic impedance of 200 ohms (the objective) is practically impossible to obtain with any reasonable wire size and number of turns, I used the compensating technique first described in my book.[2] Because the characteristic impedances of the 9:1 Guanella Balun are somewhat less than 200 ohms, a compensating effect (and hence higher frequency response) can be obtained by having a higher (than the normal objective) characteristic impedance of the windings in the 1:1.33 Unun. Earlier work (also described in my book) presented a 12:1 Balun using a 1:3 Unun in series with a 1:4 Ruthroff Balun. The Baluns presented in this section using a 1:1.33 Unun in series with a Guanella 1:9 Balun, are much improved designs.

Sec 11.5.1 A High-power 12:1 Balun

Figure 11-7 shows the schematic diagram of the series-type 12:1 Balun used in both the high- and medium-power versions. **Photo 11-G** shows a top view of the high-power Balun. **Photo 11-H** shows a side view.

The 1:1.33 Unun has 5 quintufilar turns on a 1.5-inch OD ferrite toroid with a permeability of 250. Winding 7-8 is No. 14 H Thermaleze wire and the other four are No. 16 H Thermaleze wire. Winding 7-8 is also tapped at 3 turns from terminal 7.

The 1:9 Guanella Balun has 8 bifilar turns of tinned No. 16 wire on each of the three toroids. Each wire is covered with Teflon tubing and further separated by two Teflon tubings. The characteristic impedance of the windings is about 190 ohms (the objective is 200 ohms). The ferrite toroids have an OD of 2.4 inches and a permeability of 250. The spacing between the toroids is 1/2 inch.

In matching 50-ohm cable to a balanced load of 600 ohms, the response is literally flat (within a percent or two) from 7 to 30 MHz. Within this bandwidth, it is capable of handling the full legal limit of amateur

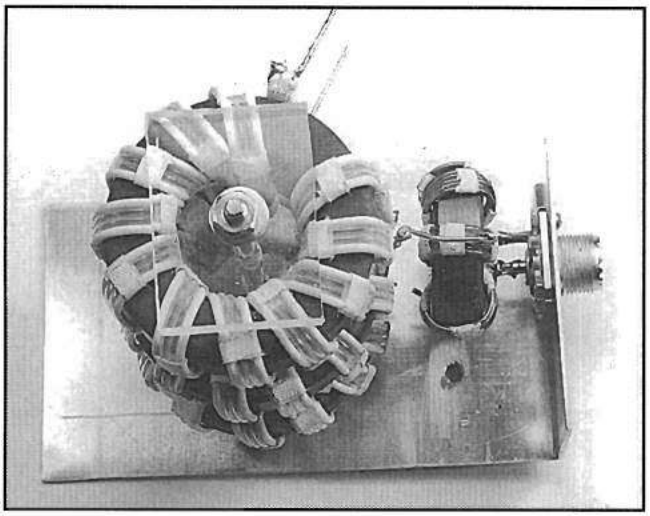

Photo 11-I. *Top view of the medium-power 12:1 Balun.*

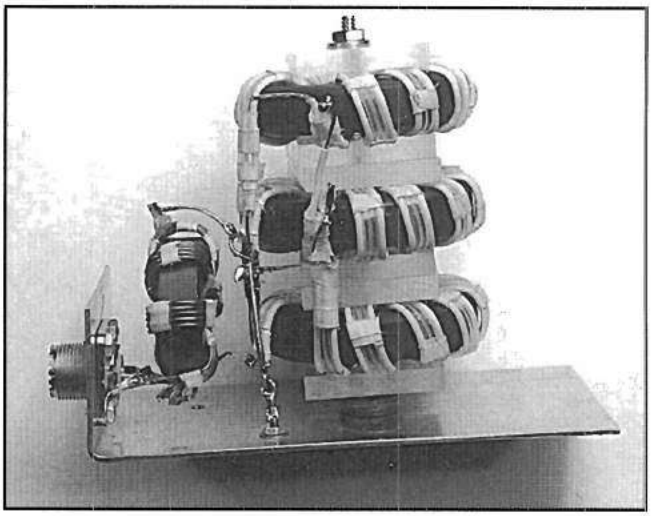

Photo 11-J. *Side view of the medium-power 12:1 Balun.*

radio power. In a matched condition, the expected insertion loss is about 0.25 dB.

Sec 11.5.2 A Medium-power 12:1 Balun

Photo 11-I shows the top view of the medium-power 12:1 series-type Balun. **Photo 11-J** shows the side view. This Balun also has the same 1:1.33 Unun as described earlier.

The 1:9 Guanella Balun has 11 bifilar turns of No. 18 hook-up wire on each toroid. The wires are further separated by two No. 18 Teflon tubings. The characteristic impedance of the windings is about 170 ohms. The toroids have an OD of 2.4 inches and a permeability of 250. The spacing between the toroids is also 1/2 inch.

In matching 50-ohm cable to a balanced load of 600 ohms, the response varies less than 5 percent from 3.5 to 30 MHz. Within this bandwidth, the Balun can handle about one-half the legal limit of amateur radio power. As with the high-power version, the expected insertion loss is also 0.25 dB.

Sec 11.6 Concluding Remarks on 12:1 Baluns

Many of the concluding remarks from the discussion on 6:1 and 9:1 Baluns (**Sec 11.4**) also apply to 12:1 Baluns; therefore, I won't repeat them here. But the following four remarks are specific to 12:1 Baluns and warrant mentioning:

First, high-impedance transmission line transformers like the 12:1 Balun are particularly sensitive to metallic enclosures. If a minibox were to be used, I would suggest the one shown in **Photo 11-E**, which is 6 inches long by 5 inches wide by 4 inches high. Smaller metallic enclosures would reduce the characteristic impedances of the windings and affect the high-frequency response. Even the spacing between cores had to be increased from 1/4 inch (for a 50:450-ohm Balun) to 1/2 inch. The subchassis shown in the photographs were used because they provided the necessary electrical and mechanical support.

Second, the 12:1 Baluns described in this section also make excellent Ununs, albeit with some compromise in the low-frequency response. I would suggest using the high-power unit only between 14 and 30 MHz and the medium-power unit only between 7 and 30 MHz.

Third, for the readers interested in VHF operation, I would suggest the parallel-type approach described in the earlier section on 6:1 Baluns. In this case, a 9:1 Guanella Balun is connected in series-parallel with a 1:4 Guanella Balun. This would produce a broadband ratio of 12.25:1. By using 170-ohm twin-lead (about 10 inches long) threaded through ferrite beads with a permeability of 125, it appears that it is possible to match 50-ohm cable to a balanced load of 612.5 ohms throughout the VHF band.

Fourth, by using torids with a permeability of 125 in the 1:9 Guanella Baluns (of the 12:1 Baluns), the insertion loss would be reduced by around one half (0.12 dB), with a trade-off in low-frequency response. The high-power unit would now cover about 10 to 30 MHz, and the medium-power Balun would cover about 7 to 30 MHz.

Chapter 12

The 4:1 Unun

Sec 12.1 Introduction

From an analysis standpoint, the 4:1 Unun can be said to have received the most attention in the literature. It began with Ruthroff's introduction and complete analysis of this device in his classic paper published in 1959.[9] Ruthroff's paper then became the industry standard for this class of devices known as *transmission line transformers*. These are devices that transmit the energy from the input to the output by an efficient transmission line mode, and not by flux linkages (as in conventional transformers).

However 15 years earlier, Guanella had introduced, in his classic 1944 paper,[3] the first broadband Baluns by combining coiled transmission lines in a series-parallel arrangement, yielding ratios of $1{:}n^2$ where n = 1, 2, 3,... and so on. It has also been shown that Guanella's technique also lends itself to Ununs as well.[2] In fact, in this chapter, you will see that his technique of summing voltages of equal delays promises to yield high-power designs capable of operating on the VHF and UHF bands.

The 4:1 Unun also exemplifies (more than any other transformer) the many choices that can be made in its design. These include: 1) Ruthroff's or Guanella's designs, 2) wire or coaxial cable transmission lines, 3) coiled or beaded lines, 4) rods or toroids, 5) low-power or high-power designs, 6) HF, VHF, or UHF designs, and 7) the trade-offs in efficiency for low-frequency response or for high VSWR. The 4:1 Unun is the most prevalent of all the Ununs. It finds extensive use in solid-state circuits and in many antenna applications involving the matching of ground-fed antennas—where impedances of 12 to 13 ohms must be matched to 50-ohm coaxial cable. This chapter provides information on many 4:1 Unun designs.

Sec 12.2 The Ruthroff 4:1 Unun

Figure 12-1 illustrates two versions of Ruthroff's approach to obtaining a 4:1 unbalanced-to-unbalanced transformer (Unun). As can be seen, one uses a coiled wire transmission line, while the other uses a coiled coaxial cable. Depending upon the frequency, beaded transmission lines may also be used.

Ruthroff's design uses a single transmission line connected in, what I call, the bootstrap configuration. That is, terminal 2 is connected to terminal 3, lifting the transmission line (at the high-impedance side) by the voltage V_1. If the reactance of the coiled winding or beaded line is much greater than R_G, then only flux-canceling transmission line currents are allowed to flow. It is also apparent that the output voltage is the sum of a direct voltage, V_1, and a delayed voltage,

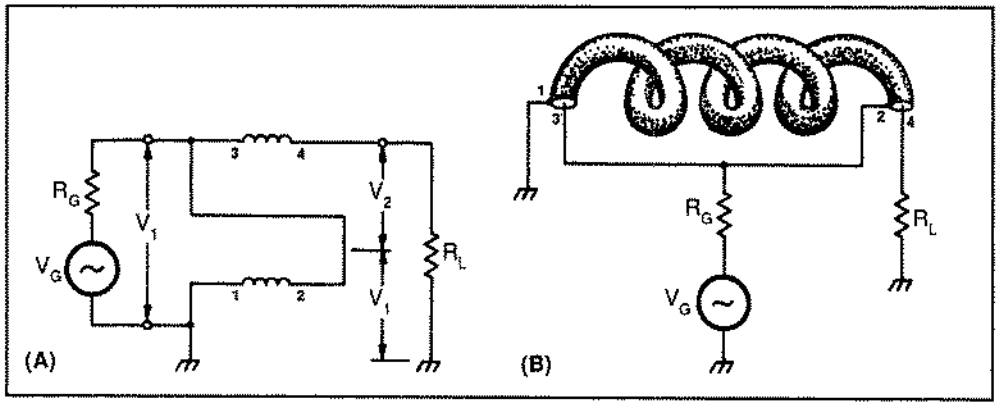

Figure 12-1. *The Ruthroff 4:1 Unun (R_L=4R_G): (A) coiled bifilar winding; (B) coiled coaxial cable.*

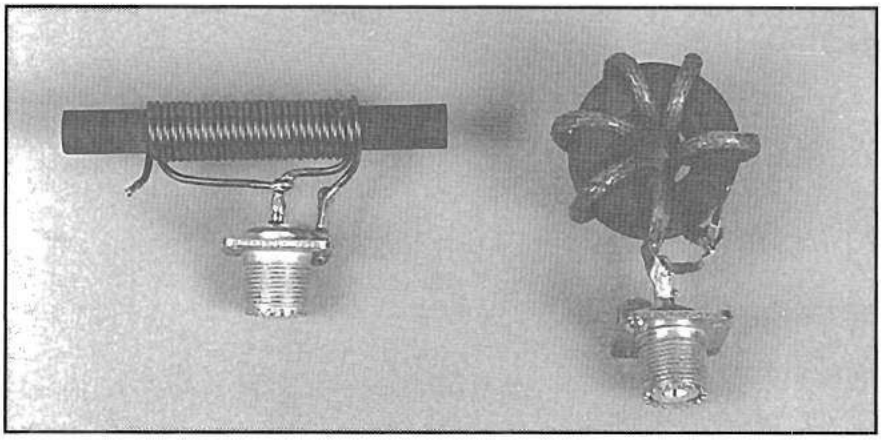

Photo 12-A. *Two versions of the Ruthroff 4:1 (50:12.5-ohm) Unun: coiled wire rod (on the left); coiled coaxial cable toroid (on the right).*

V_2, which traverses a single transmission line. This delay in V_2 eventually limits the high-frequency response. For example, if the electrical length of the line is a 1/2 wave, the output is zero. Ruthroff also found that the optimum value of the characteristic impedance of the transmission line (for maximum high-frequency response) is $R_L/2$.

Therefore, the electrical length and characteristic impedance of the transmission line play major roles in Ruthroff's design. Because his work was mainly concerned with small-signal applications, Ruthroff was able to obtain broad bands of a few tens of kilohertz to over a thousand megahertz. This was possible because he used a few turns (5 to 10) of fine wire (Nos. 37 and 38) on high-permeability toroids as small as 0.08 inches in OD. As a result, the phase-delay with these very short transmission lines was very small. However, large-signal (power) applications present an entirely different picture. For operation in the HF band (including 160 meters), transmission lines vary between one to three feet in length (depending upon impedance level). Consequently, phase-delay can play a major role, as will be seen in the following examples.

Sec. 12.2.1 50:12.5-ohm Ununs

Photo 12-A shows two examples of efficient and broadband 4:1 Ununs matching 50 to 12.5 ohms. The rod version (on the left) has 14 bifilar turns of No. 14 H Thermaleze wire on a low-permeability (125) ferrite rod 0.375 inches in diameter and 3.5 inches long. The connections are shown in **Figure 12-1A**. The cable connector is on the low-impedance side. The response is flat from 1.5 to 30 MHz. In a matched condition, this Unun can easily handle the full legal limit of amateur radio power. Because a tightly wound rod Unun yields a characteristic impedance very close to 25 ohms (the optimum value), this is quite likely the easiest one to construct that covers the above bandwidth.

The toroidal version (on the right in **Photo 12-A**) has 6 turns of homemade, low-impedance coaxial cable on a 1.5-inch OD ferrite toroid with a permeability of 250. The connections are shown in **Figure**

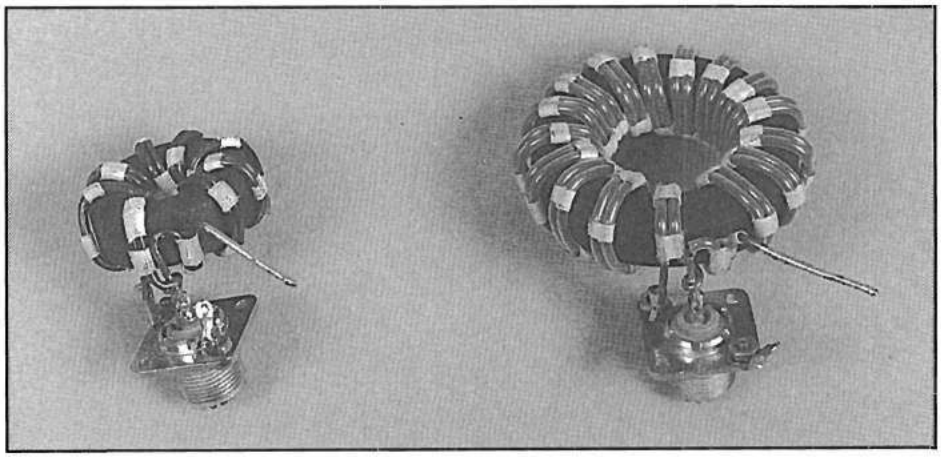

Photo 12-B. *Two higher-impedance Ruthroff 4:1 Ununs: 100:25-ohm (on the left); 200:50-ohm (on the right).*

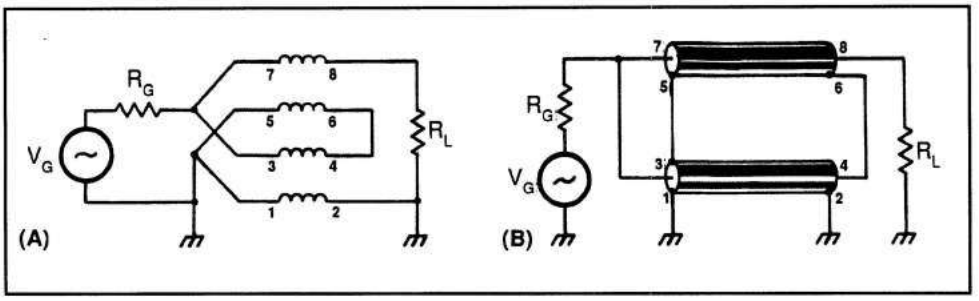

Figure 12-2. *The Guanella 4:1 Unun (R_L=4R_G): (A) coiled bifilar windings; (B) coiled or beaded coaxial cables.*

12-1B. The cable connector is on the low-impedance side. The inner conductor is No. 14 H Thermaleze wire and is covered with Teflon tubing. The outer braid is from a small coaxial cable (or from 1/8-inch tubular braid) tightly wrapped with Scotch No. 92 tape in order to obtain the desired characteristic impedance. In matching 50 to 12.5 ohms, the response is flat from 1.5 to 50 MHz. Because the current is evenly distributed on the inner conductor, this small Unun has an exceptionally high power capability—at least 5 kW of continuous power and 10 kW of peak power (in a matched condition).

Sec 12.2.2 100:25-ohm Unun

In some combiner applications, an Unun matching 100 to 25 ohms is required. The smaller toroidal version, pictured on the left in **Photo 12-B**, shows a Ruthroff design that can satisfy many of these requirements. It has 8 bifilar turns of No. 14 H Thermaleze wire on a 1.5-inch OD ferrite toroid with a permeability of 250. One wire is also covered with a single layer of Scotch No. 92 tape, providing a characteristic impedance close to the desired value of 50 ohms. In matching 100 to 25 ohms, the response is essentially flat from 1.5 to 30 MHz. This Unun can easily handle the full legal limit of amateur radio power.

Sec 12.2.3 200:50-ohm Unun

When dealing with this type of Balun, the Ruthroff approach cannot yield the broadband response of the lower-impedance designs shown above. Because more turns are required in order to obtain the necessary choking reactance, and a 100-ohm characteristic impedance that requires more spacing between the wires is used, the cores must be considerably larger. This results in longer transmission lines. Consequently, the high-frequency response is now limited by the greater phase delay of this high-impedance Unun.

The larger transformer, shown on the right in **Photo 12-B** is my optimized version of a Ruthroff 200:50-ohm Unun. It has 16 bifilar turns of No. 14 H Thermaleze wire on a low-permeability (250) 2.4-inch OD ferrite toroid. Each wire is covered with Teflon tubing, resulting in a characteristic impedance of 97 ohms. Because of the long transmission line (36 inches), the impedance transformation ratio (in matching 200 ohms to 50 ohms) varies from 4 to 4.44 from 1.5 to 30 MHz. A conservative power rating (under a matched condition) is 2 kW of continuous power and 4 kW of peak power. Because this higher-impedance Unun has a larger voltage drop along the length of its windings, its loss (a dielectric-type[2]) is a little greater than the lower-impedance Ununs described earlier. In a matched condition, the efficiency is about 97 percent, while the others experience efficiencies of 98 to 99 percent.

Sec 12.3 The Guanella 4:1 Unun

Even though Guanella's investigation[3] was directed toward developing a broadband Balun to match the balanced output of a 100-watt, push-pull, vacuum-tube amplifier to the unbalanced load of a coaxial

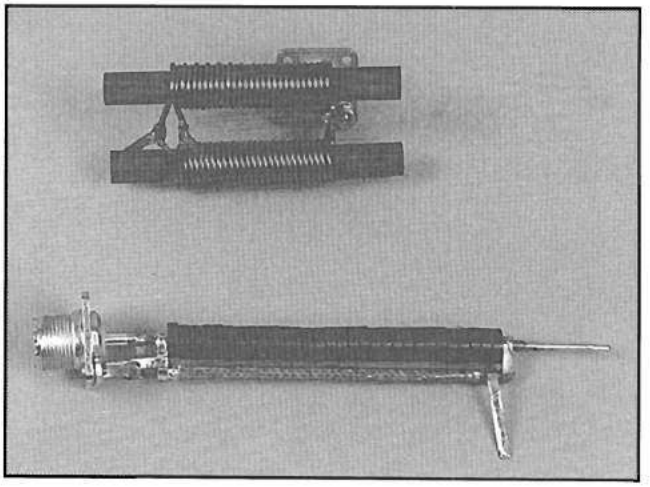

Photo 12-C. *Two Guanella 4:1 (50:12.5-ohm) Ununs: rod version (on the top), 1.5 to 50 MHz; beaded version (on the bottom), 10 MHz to over 100 MHz.*

cable, his technique of connecting transmission lines in a parallel-series arrangement has only recently been recognized as the design for the widest possible bandwidth in an unbalanced-to-unbalanced application.[2] Some have labeled his approach the "equal-delay network".[26] The major difference in Guanella's approach (from Ruthroff's) is that by summing the equal-delay voltages of coiled (or beaded) transmission lines, he minimizes the dependence of the high-frequency response on the lengths of the transmission lines. As was mentioned before, Ruthroff's method of summing a direct voltage with a delayed voltage that traversed a single transmission line has a limited application, especially with high-power, high-impedance Ununs (like 200:50 and 300:75 ohms).

Furthermore, Guanella's approach is also important in designing high- and low-impedance Baluns and Ununs with impedance transformation ratios other than 4:1. Connecting three transmission lines in parallel-series results in a 9:1 ratio, four in a 16:1. Also by connecting a fractional-ratio Unun in series with his Baluns, or by using various combinations of parallel-series transmission lines,[26,27] Ununs and Baluns are now available with a continuum of ratios from 1.36:1 to 16:1. Moreover, these ratios now make it possible to match 50-ohm cable to impedances as low as 3.125 ohms and as high as 800 ohms. A major factor in the success of these designs rests in the understanding of the low-frequency models of these various transformers.[2] This section looks at the 4:1 Unun using Guanella's approach. As in the Ruthroff case, the optimum value of the characteristic impedances of the transmission lines for a Guanella 4:1 transformer is also $R_L/2$.

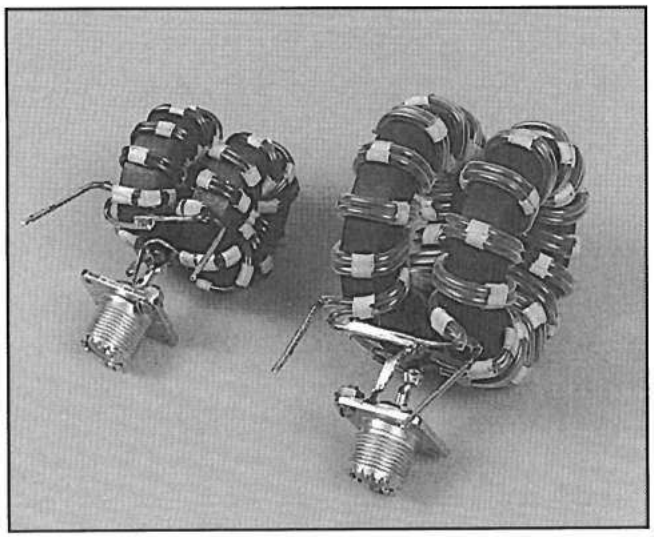

Photo 12-D. *Two higher-impedance Guanella 4:1 Ununs: 100:25-ohm (on the left); 200:50-ohm (on the right).*

Sec 12.3.1 50:12.5-ohm Ununs

Figure 12-2 shows the schematic diagrams of the coiled-wire and coaxial cable (coiled or beaded) versions of 4:1 Ununs using Guanella's technique of connecting transmission lines in parallel-series arrangements. As can be seen in **Figure 12-2**, the lower transmission lines are grounded at both ends and, therefore, have no potential drop along their lengths. Thus, the coiling or beading has no effect. The core only acts as a mechanical support and the beads can be removed. In essence, the bottom transmission line plays the important role of a delay line. In addition, the low-frequency response of this form of Unun is solely determined by the reactance of the top coiled or beaded transmission line.

The top Unun in **Photo 12-C** shows a rod version of Guanella's 4:1 Unun. There are 13.5 bifilar turns of No. 14 H Thermaleze wire on low-permeability (125) ferrite rods 0.375 inches in diameter and 3.5 inches long. For ease of connection, one winding is clockwise and the other is counterclockwise. The cable connector is on the high-impedance side. In matching 50 to 12.5 ohms, the response is flat from 1.5 to over 50 MHz! This Unun, in a matched condition, is capable of handling the full legal limit of amateur radio power. Furthermore, with the 50-ohm generator on the right (in **Figure 12-2A**) and a 12.5-ohm balanced load on the left (perhaps a Yagi beam), this transformer makes an excellent step-down Balun.

The bottom transformer in **Photo 12-C** shows a beaded-coax version of a 50:12.5-ohm step-down Unun designed for 2-meter operation. It has 3.5 inches of beaded coax on the top transmission line (**Figure 12-2B**) and no beads on the bottom transmission line. (Actually, the bottom rod in **Figure 12-2A** can also be removed with no change in performance.) The beads are low-permeability (125) ferrite. The inner conductor of the coaxial cable is No. 12 H Thermaleze wire with about 3.5 layers of Scotch No. 92 tape (two 0.5-inch tapes wound edgewise like a window shade), providing a characteristic impedance close to the optimum value. The outer braid is from a small coaxial cable (or from 1/8-inch tubular braid). This homemade coax is further wrapped tightly with Scotch No. 92 tape in order to preserve its low characteristic impedance. The cable connector is on the low-

impedance side. The response of this Unun is essentially flat from 10 to 100 MHz (the limit of my bridge). It can also (easily) handle the full legal limit of amateur radio power.

Sec 12.3.2 100:25-ohm Unun

The Unun on the left in **Photo 12-D** is a Guanella version that matches 100 to 25 ohms. There are 8 bifilar turns of No. 14 H Thermaleze wire on each 1.5-inch OD low-permeability (250) toroid. One toroid is wound clockwise and the other is wound counterclockwise. One of the wires (on each toroid) is covered with one layer of Scotch No. 92 tape. The cable connector is on the low-impedance side. The response is flat from 1.5 MHz to well over 30 MHz. This Unun can also handle the full legal limit of amateur radio power.

It is interesting to note that when used as a Balun (the ground removed from terminal 2), and placed in series (on the left side) with a 1.78:1 Unun (see **Chapter 13**), this compound arrangement provides an excellent Balun for matching 50-ohm coaxial cable directly to quad antennas having impedances of 100 to 110 ohms.

Sec 12.3.3 200:50-ohm Unun

The transformer on the right in **Photo 12-D** is an excellent Unun (or Balun with terminal 2 removed from ground) for matching 50 to 200 ohms. It has 14 bifilar turns of No. 14 H Thermaleze wire on each low-permeability (250) toroid with a 2.4-inch OD. Each wire is covered with Teflon tubing, providing a characteristic impedance of 98 ohms (which is quite good because the optimum value is 100). Again, for ease of connection, one winding is clockwise and the other is counterclockwise. When operating as an Unun or a Balun and matching 50 to 200 ohms, the response is essentially flat from 1.5 to 30 MHz. A conservative power rating (in a matched condition) is 5 kW of continuous power and 10 kW of peak power. This transformer has been reported to handle peak pulses of 10,000 volts!

Summary

Since its introduction by Ruthroff in 1959,[9] the 4:1 Unun has been the most popular transmission line transformer matching unbalanced impedances to unbalanced impedances. As I mentioned at the beginning of this chapter, there are many choices to consider when designing these broadband and efficient transformers. One of the most important choices involves whether to use the Ruthroff or Guanella approach. In fact, the Guanella design should probably be designated a *Balun/Unun*. Recently, it has become the design of choice in the higher frequency bands. From the designs presented in this chapter, I offer the following recommendations:

1. For Ununs in the HF band with impedance levels of 100:25 ohms and lower, the Ruthroff approach is recommended because of its simplicity.
2. For high impedance levels in the HF band (like 200:50 and 300:75 ohms), the Guanella approach is recommended.
3. For low-impedance operation on the VHF band, the beaded-coax Guanella approach is recommended.
4. For high-impedance operation on the VHF band, the coiled-wire Guanella approach appears to be the preferred choice, and should be investigated first. Obviously, the number of turns should be reduced from the examples shown in this chapter because the reactance of the winding is proportional to the frequency.
5. For high-power use on the HF band, the Ruthroff Unun with low-impedance coaxial cable on a toroid (on the right on **Photo 12-A**) is recommended. It is easy to construct and can very likely handle more than 5 kW of continuous power.
6. Also, at high-impedance levels, one might consider using lower permeability ferrites for higher efficiencies. Look at permeabilities of 125 and 40.

Chapter 13

1.33:1, 1.5:1, and 2:1 Ununs

Sec 13.1 Introduction

Little practical design information has been available on Ununs with impedance transformation ratios of less than 4:1 (these are called *fractional-ratio* Ununs). However, many important applications can be found for efficient and broadband Ununs with ratios like 1.33:1, 1.5:1, and 2:1. Some examples include the matching of 50-ohm coaxial cable to: a) vertical antennas, inverted Ls, and ground-fed slopers (all over good ground systems), b) 75-ohm hardline cable, c) a junction of two 50-ohm coaxial cables, d) shunt-fed towers performing as vertical antennas, and e) the output of a transceiver or class B linear amplifier when an unfavorable VSWR condition exists.

These three Ununs also play an important role in making other useful Baluns possible. Examples given in earlier chapters include: a) connecting a 1.5:1 Unun (50:75 ohms) in series with a 1:1 Balun (75:75 ohms) results in a broadband 1.5:1 Balun (50:75 ohms); b) connecting a 2:1 Unun (50:100 ohms) in series with a 1:1 Balun (100:100 ohms) results in a broadband 2:1 Balun (50:100 ohms); c) connecting a 1.5:1 Unun (50:75 ohms) in series with a 4:1 Balun (75:300 ohms) results in a broadband 6:1 Balun (50:300 ohms), and d) connecting a 1.33:1 Unun (50:66.7 ohms) in series with a 9:1 Balun (66.7:600 ohms) results in a broadband 12:1 Balun (50:600 ohms).

It has been shown[2] that a continuum of ratios can now be obtained with Ununs matching 50-ohm cable to impedances as low as 3.125 ohms and as high as 800 ohms. In addition, by using higher-order windings (trifilar, quadfilar, etc.), Ununs can be constructed with two broadband ratios like 1.5:1 and 3:1, or 2:1 and 4:1. Furthermore, by tapping some of the windings of these higher-order Ununs, multimatch transformers can be constructed with many broadband ratios. As a result of this class of fractional-ratio Ununs, a continuum of Ununs and Baluns is now available to match 50 ohms unbalanced to unbalanced or balanced impedances as low as 3.125 ohms and as high as 800 ohms.

My first attempt to obtain ratios less than 4:1 was made by tapping one of the wires in a Ruthroff 4:1 bifilar Unun. My experiment met with only moderate success.[2] An adequate low-frequency response with a 1.33:1 ratio was difficult to obtain. Also, the 2:1 ratio had considerably greater loss than higher or lower ratios. Recently, I found that higher-order windings (trifilar, quadrifilar, etc.), some with taps, provide much wider bandwidths and higher efficiencies. This

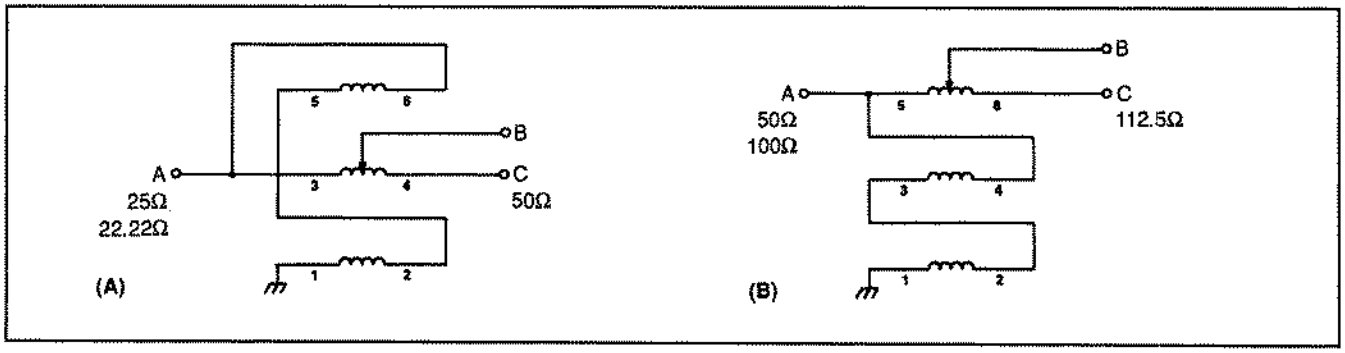

Figure 13-1. *Schematic diagrams: (A) matching 50 to 25 ohms (B-A) and 50 to 22.22 ohms (C-A); (B) matching 100 to 50 ohms (B-A) and 112.5 to 50 ohms (C-A).*

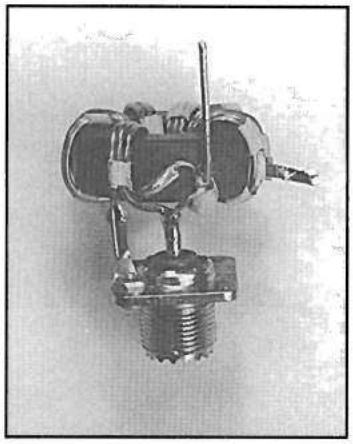

Photo 13-A. *Bottom view of the 2:1 Unun designed to match 50 ohms to 25 ohms or 22.2 ohms (Figure 13-1A). The connector is on the low-impedance side.*

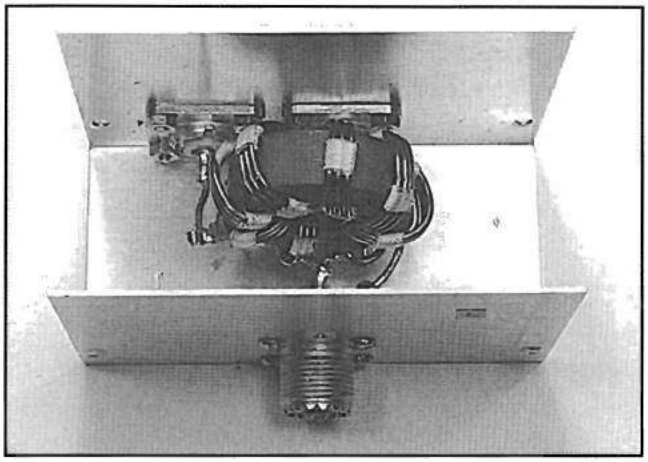

Photo 13-B. *The 2:1 Unun mounted in a 4 inch long by 2 inch wide by 2.75 inch high minibox.*

chapter describes fractional-ratio Ununs using these higher-order windings.

The next section discusses the practical aspects of the 2:1 Unun. This Unun is not only one of the more useful transformers, but it also serves as a good introduction to the trifilar and quadrifilar designs. What follows is an introduction to the most difficult fractional-ratio Unun—the quintufilar design, which results in very broadband 1.33:1 and 1.5:1 Ununs. A more complete discussion appears in **Part I** of this book.

This chapter closes with construction tips. As you will see, these Ununs can be difficult to construct.

Sec 13.2 2:1 Ununs

Figure 13-1A shows the schematic diagram of an Unun designed to match 50-ohm cable to an unbalanced load of 25 ohms (2:1 ratio with connections A-B) or 22.22 ohms (2.25:1 ratio with connections A-C). It has 6 trifilar turns of No. 14 H Thermaleze wire on a 1.5-inch OD ferrite toroid with a permeability of 250. Winding 3-4 is tapped at 5 turns from terminal 3. **Photo 13-A** is a photograph showing the various connections. The connector is on the low-impedance side. **Photo 13-B** shows the transformer mounted in a CU-3015A (4 inches long by 2 inches wide by 2.75 inches high) minibox. In matching 50 ohms to either 25 or 22.22 ohms, the transformation ratio is constant from 1 to 30 MHz.

Because the transmission lines are very short, this Unun does quite well as a step-up transformer. That is, when matching 50 ohms (on the left side) to 100 ohms (connections A-B) or 112.5 ohms (connections A-C) on the right side, the transformation ratio is constant from 1 to 15 MHz. Because of the extremely high efficiency of this transformer (98 to 99 percent under matched conditions), this small version can easily handle the full legal limit of amateur radio power.

Figure 13-1B shows the schematic diagram of an Unun designed to match 50-ohm cable to an unbalanced load of 100 ohms (2:1 ratio with connections A-B) or 112.5-ohms (2.25:1 ratio with connections A-C). It has 7 trifilar turns on a 1.5-inch OD ferrite toroid with a permeability of 250. The top winding 5-6 is No. 14 Thermaleze wire and is tapped at 6 turns from terminal 5. The other two windings are No. 16 H Thermaleze wire. **Photo 13-C** shows the various connections. The connector is on the low-impedance side. In matching 50-ohm cable to 100 ohms (A-B) or 112.5 ohms (A-C), the transformation ratio is constant from 1 to 30 MHz.

Again, because the transmission lines are very short, this Unun does quite well as a step-down transformer. In matching 50-ohm cable (on the right side) to 25 ohms (A-B) or 22.22 ohms (A-C), the transformation ratios are constant from 1 to 15 MHz. As above, this transformer can easily handle the full legal limit of amateur radio power.

Although the quadrifilar Unun shown in the schematic diagram in **Figure 13-2** and in **Photo 13-D** has an impedance transformation ratio of 1.78:1, it should also satisfy many of the 2:1 requirements. This Unun, which is designed to match 50-ohm cable to an unbalanced load of 28 ohms, not only has a very broadband response (1 MHz to over 50 MHz), but also offers other possible wideband ratios that will be covered in succeeding chapters.

Specifically, the Unun has 5 quadrifilar turns on a 1.5-inch OD ferrite toroid with a permeability of 250. Winding 5-6 is No. 14 H Thermaleze wire and the other three are No. 16 H Thermaleze wire. Like the

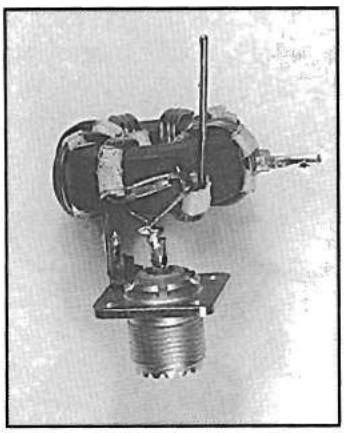

Photo 13-C. *Bottom view of the 2:1 Unun designed to match 50 ohms to 100 ohms or 112.5 ohms (Figure 13-1B). The connector is on the low-impedance side.*

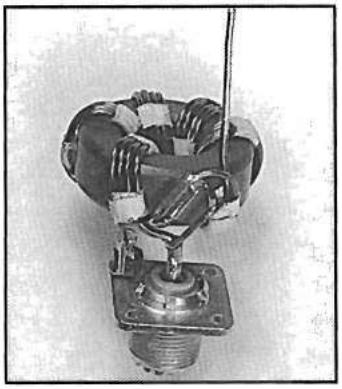

Photo 13-D. *Bottom view of the 1.78:1 Unun designed to match 50 to 28 ohms. The connector is on the low-impedance side.*

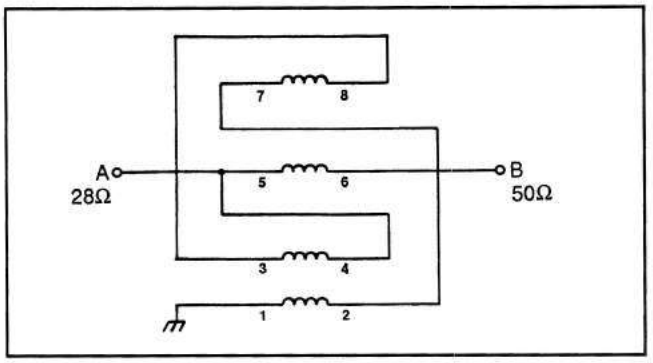

Figure 13-2. *Schematic diagram of the quadrifilar Unun designed to match 50 to 28 ohms (1.78:1 ratio).*

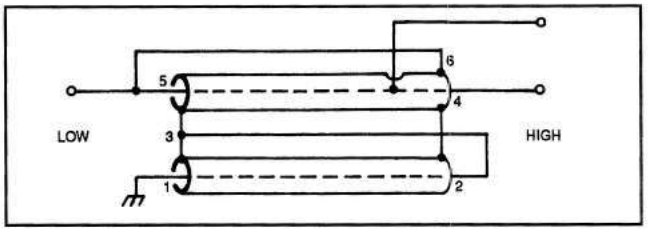

Figure 13-3. *Schematic diagram of a tapped-trifilar Unun that uses two sections of coaxial cable, yielding impedance ratios of 2:1 and 2.25:1.*

two 2:1 Ununs described above, this one also easily handles the full legal limit of amateur radio power.

As with most coiled Ununs that have little spacing between adjacent turns, current-crowding (between adjacent turns) can eventually limit the power-handling capability of these devices. It's possible to improve the ability for handling higher currents by using thicker wires, or by using coaxial cables where current-crowding is nonexistent. **Figure 13-3** shows the schematic diagram of a tapped-trifilar transformer that uses two sections of coaxial cable yielding impedance ratios of 2:1 and 2.25:1. **Photo 13-E** shows two trifilar toroidal transformers using low-impedance coaxial cables with their outer braids connected in parallel and acting as the third conductor. These transformers are conservatively rated at 5 kW of continuous power.

The smaller transformer in **Photo 13-E** has 7 trifilar turns of low-impedance coax on a 2-inch OD toroid with a permeability of 290. The No. 14 H Thermaleze wire inner conductors have four layers of Scotch No. 92 tape. The outer braids are made from small coaxial cables (or 1/8-inch tubular braid), and are also wrapped with Scotch No. 92 tape in order to preserve the low characteristic impedances. The inner conductor of the top coax in **Figure 13-3** is tapped at 6 turns from terminal 5. When matching 50 ohms to 22.22 ohms or 25 ohms, the impedance ratio is constant from 1 to over 50 MHz.

The larger transformer in **Photo 13-E** also has 7 trifilar turns, but on a 2.4-inch OD toroid with a permeability of 125. The inner conductors of No. 14 H Thermaleze wire now have a 15-mil wall of Teflon sleeving, yielding the low-impedance coaxial cable. The outer braids are the same. Because the ferrite permeability is lower and the lengths of the transmission lines are longer than those of the smaller unit, this transformer's bandwidth is not quite as good. When matching 50 to 22.22 ohms (this particular Unun doesn't have a tapped winding), the impedance ratio is constant from 1.7 to 30 MHz.

Although not shown, these very high-powered 2:1 Ununs can also be easily designed to match 50-ohm cable to unbalanced loads of 100 and 112.5 ohms. This is done by using small but high-powered coaxes like RG-303/U, RG-141/U, or RG-142/U.

Sec 13.3 1.5:1 Ununs

Figure 13-4 shows three basic forms of a quintufilar 1.56:1 Unun that should satisfy most of the 1.5:1 requirements. As can be seen, the only difference in

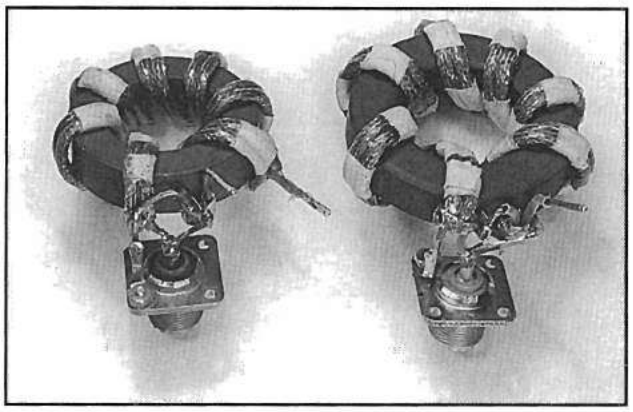

Photo 13-E. *Two toroidal transformers using coaxial cable and designed to match 50 to 22.22 ohms (2.25:1). The smaller transformer is also tapped, yielding a match of 50 to 25 ohms (2:1).*

the schematic diagrams is in the interleaving of the windings. This is done to optimize the performance of these Ununs at the various impedance levels. Schematic A is optimized for matching 50 to 75 ohms. Schematic B is optimized for matching 32 to 50 ohms. Schematic C, while optimized for matching 40 to 62 ohms, still yields quite broadband ratios at both 50:75 and 32:50-ohm levels. It should be a useful, general-purpose Unun.

Photo 13-F is a photograph of the bottom views (showing the connections) of the three different designs. They appear in the same order as the schematics of **Figure 13-4**; i.e., a) the Unun on the left is designed to match 50 to 75 ohms, b) the Unun in the center is design to match 32 to 50 ohms, and c) the Unun on the right is designed to work quite well at both impedance levels. The SO-239 connectors are all on the low impedance side of the Ununs.

All three transformers have four quintufilar turns on a 1.5-inch OD ferrite toroid with a permeability of 250. Their differences are:

1. **50:75 ohms** (on the left on **Figure 13-4** and **Photo 13-F**).

Winding 9-10 is No. 14 H Thermaleze wire. The other four windings are No. 16 H Thermaleze wire. When matching 50 to 75 ohms (actually to 78 ohms), the transformation ratio is constant from 1 to over 30 MHz. In matching 50 ohms (on the right side in **Figure 13-3A**) to 32 ohms, it is still constant from 1 to 15 MHz.

2. **32:50 ohms** (in the center in **Figure 13-4** and **Photo 13-F**).

Winding 5-6 is No. 14 H Thermaleze wire. The other four windings are No. 16 H Thermaleze wire. When matching 32 to 50 ohms, the transformation ratio is constant from 1 to over 30 MHz. In matching 75 ohms (on the right side in **Figure 13-3B**) to 50 ohms, it is still constant from 1 to 15 MHz.

3. **50:75 ohms; 32:50 ohms** (on the right in **Figure 13-4** and **Photo 13-F**).

Winding 7-8 is No. 14 H Thermaleze wire. The other four windings are No. 16 H Thermaleze wire. In matching 32 to 50 ohms, the transformation ratio is constant from 1 to 30 MHz. In matching 75 ohms (on the right side in **Figure 13-3C**) to 50 ohms, it is still constant to 21 MHz. This is quite a good general-purpose design.

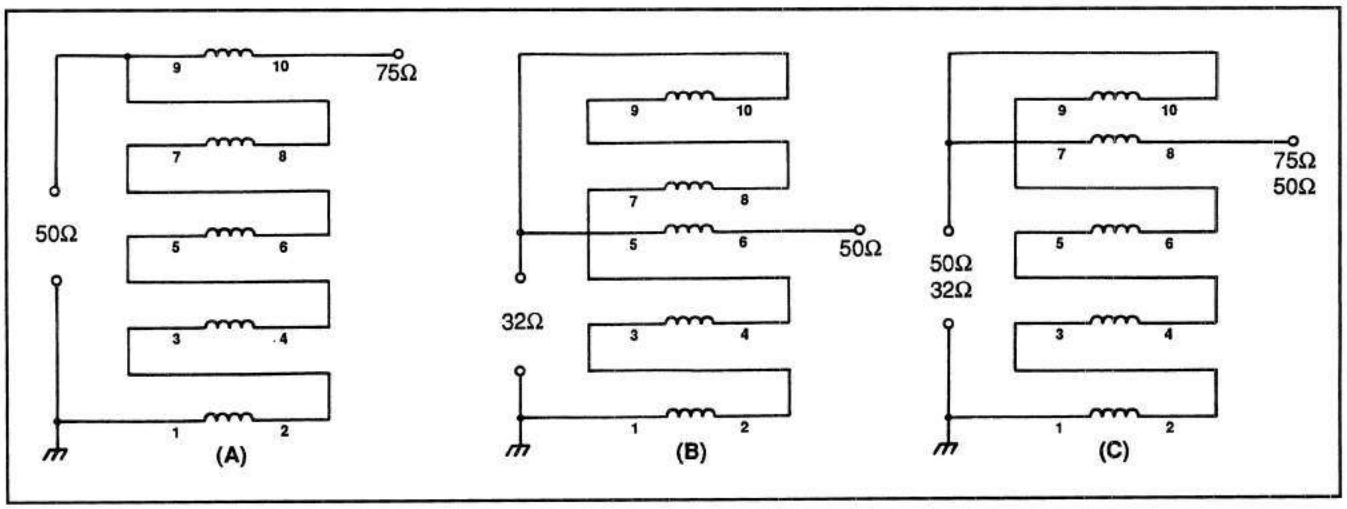

Figure 13-4. *Three basic forms of a quintufilar 1.56:1 Unun: (A) optimized to match 50 to 75 ohms, (B) optimized to match 32 to 50 ohms, and (C) optimized to match 40 to 62 ohms, resulting in a good general-purpose design.*

Even though a small toroid (with only a 1.5-inch OD) is used, these Ununs are still very sturdy transformers. Because their efficiencies are so high (98 to 99 percent), they can easily handle the full legal limit of amateur radio power.[2] Furthermore, the windings carrying the majority of the current (80 percent) are all No. 14 wire. Only when well-designed Ununs are subjected to very high VSWRs will excessive heating occur. Ununs (and Baluns) should never be exposed to these severe conditions.

Sec 13.4 A 1.33:1 Unun

The circuit shown in **Figure 13-5** evolved after many attempts were made at obtaining a broadband match of 50 to 66.7 ohms (1.33:1). **Photo 13-G** shows the bottom view of an actual design. The SO-239 connector is on the low impedance side. **Photo 13-H** shows the Unun mounted in a CU-3015A minibox.

Specifically, this Unun has five quintufilar turns on a 1.5-inch OD ferrite toroid with a permeability of 250. Winding 5-6 is No. 14 H Thermaleze wire and is tapped at three turns from terminal 5 (**Figure 13-4**). It is also covered with one layer of Scotch No. 92 polyimide tape, optimizing the performance at the 50:66.7-ohm level. The other four windings are No. 16 H Thermaleze wire.

In matching 50 to 66.7 ohms (A-B), the transformation ratio is practically constant from 1 to 30 MHz. The ratio only decreases by 3 percent across the band. In matching 50 to 32 ohms (C-A), the transformation ratio is constant from 1 to 30 MHz. In matching 75 to 50 ohms (C-A), the ratio is constant from 1 to 15 MHz. In matching 50 to 37.6 ohms (B-A), the ratio is constant from 1 to 15 MHz. As you can see, the Unun has some useful broadband multimatches.

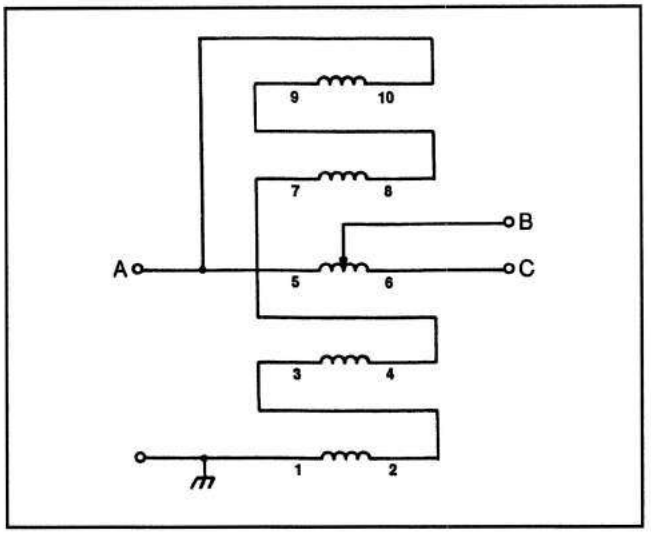

Figure 13-5. *Schematic diagram of a quintufilar Unun specifically designed to yield a broadband 1.33:1 ratio (66.7:50 ohms; connection B-A). Connection C-A also yields a broadband 1.56:1 ratio (50:32 ohms).*

As in the cases of the other three Ununs, this tapped-Unun also easily handles the full legal limit of amateur radio power. Like the 2:1 Unun, for higher power capabilities, thicker wires or a three-coax quintufilar design can be used.[2]

Sec 13.5 Construction Tips

Most of my Unun designs use the bootstrap connection that sums direct voltages (on the high-impedance side) with a delayed voltage, which traverses a single transmission line.[2] Therefore, in order to achieve the very wideband responses, small toroids (which allow the shortest transmission lines) are used. The small 1.5-inch OD toroids offer this advantage. Furthermore,

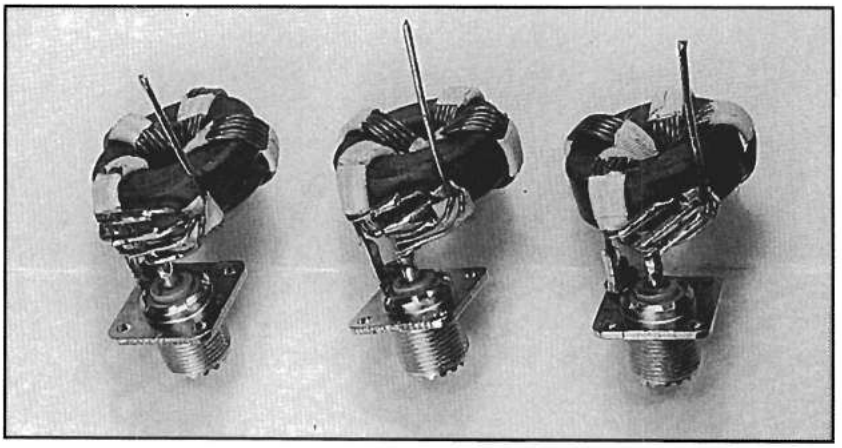

Photo 13-F. *Photograph of the three different Unun designs shown in Figure 13-4: A) on the left, 50:75 ohms, B) in the center 32:50 ohms, and C) on the right, a general purpose design matching both impedance levels quite well.*

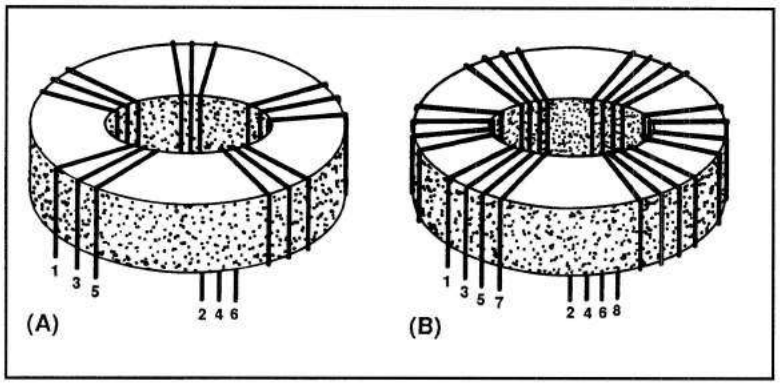

Figure 13-6. *Pictorials of higher-order windings: (A) trifilar and (B) quadrifilar.*

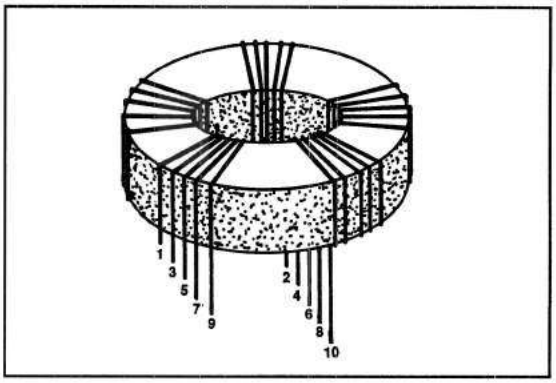

Figure 13-7. *Pictorial of a quintufilar winding.*

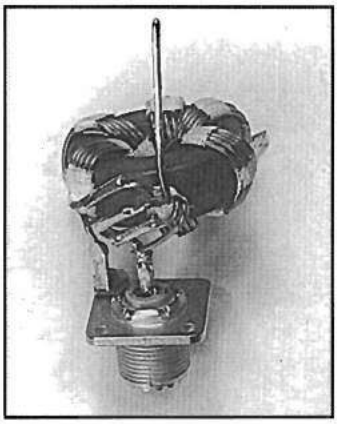

Photo 13-G. *Photograph of the 1.33:1 Unun (66.7:50 ohms). This transformer also has a broadband 1.56:1 ratio (50:32 ohms).*

quintufilar (and higher-order windings) Ununs are also eventually limited in their high-frequency responses by self-resonances. Shorter winding lengths keep these self-resonances well out of the HF band. For the Ununs in this chapter, they occur between 45 and 65 MHz, with **Figure 13-4A** having the higher value.

There is also a mechanical advantage in using the smaller toroids. You'll find that the popular CU-3015A minibox makes an excellent enclosure for the 1.5-inch OD toroid. Furthermore, because ferrite is a ceramic and, therefore, unaffected by moisture, no special precautions need be taken for out-of-doors use. Potting the transformer in plastic is unnecessary. One must only keep the Unun out of a pool of water.

Because well-designed transformers have virtually no flux in the core, their power ratings are mainly determined by the ability of the transmission lines to handle the voltages and currents. Furthermore, it can be shown that the losses in these transformers are related to the voltage gradients along the transmission lines.[2] Thus, they are dielectric-type ferrite losses. This means that the efficiency can be severely degraded with very high VSWRs since higher voltage gradients occur under these conditions.

Several suggestions can be made regarding the construction of Ununs using these higher-order windings (trifilar, quadrifilar, etc.). They are:

1) Make a ribbon out of the wires and wind them all at the same time. This keeps the wires as close as possible, resulting in the maintenance of the optimum characteristic impedance of the transmission lines. I found that strips made with 1.25- by 0.375- to 0.55-inch glass tape (Scotch No. 27), clamped about every 1/2 inch, hold the wires in place very well. The starting lengths of the wires should be about 5 inches longer than one would calculate knowing the number of turns and the length around each turn.

2) Because work-hardening of the copper wire takes place in coiling it around a toroid, a pair of pliers and

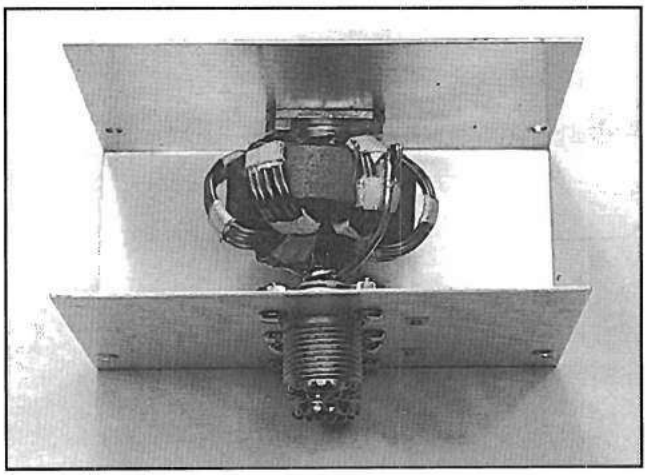

Photo 13-H. *The 1.33:1 Unun mounted in a CU-3015A minibox.*

a strong thumb (and arms) are indispensable tools. It takes considerable effort to wind these transformers. Also, because these designs have adequate margins at their low-frequency ends, some space between the windings and the toroids can be tolerated.

3) It is helpful to recognize the various patterns that appear at the ends of the windings. **Figure 13-6** shows a drawing of the trifilar and quadrifilar patterns and **Figure 13-7** shows the quintufilar pattern. Note that terminal 1 and terminal 6 or terminal 8 or 10 are the outside terminals of the patterns. Also, note that terminal 1 is always grounded in the schematic diagrams.

4) Tapping windings can be one of the more difficult tasks in constructing these transformers. Winding a tapped transformer is also more difficult. I found that the edge of a small, fine file does the best job in removing the insulation. About 1/8 to 1/4 inch is removed around the wire. It also helps to remove some of the copper. Then a flat 1/8-inch copper strip or No. 14 wire flattened on one end is soldered to the bare wire. The soldered connection is then rendered smooth using the edge of the file. Finally, two pieces of Scotch No. 92 polyimide tape are placed on the joint to insulate it from the neighboring turns. I also found that a tap placed one turn from the end of the winding is best made approximately 4 inches from the end of the wire (when the wire is straight).

Finally, a comment should be made about low-power Ununs. Practically all of the transformers in this chapter can be easily designed for low-power use. Designs capable of handing the full output of HF transceivers can be readily constructed. Cores with an OD of 1.25 inches are recommended. The same number of turns, but with one size smaller wire, is also recommended. Because smaller cores and thinner wires are used, these lower-power units are not only easier to construct, but they also have wider bandwidths due to the shorter lengths of the windings.

Chapter 14

Dual-Ratio Ununs

Sec 14.1 Introduction

Earlier chapters in this book on Ununs have basically covered single-ratio transformers. Broadband ratios of 1.33:1, 1.5:1, 2:1, and 4:1 were the design objectives. The 1.33:1 ratio was obtained by tapping a 1.5:1 (actually 1.56:1) quintufilar-wound Unun. The 2:1 ratio was obtained by tapping a 2.25:1 trifilar-wound Unun. Although these transformers can be considered to have two broadband ratios (1.33:1 and 1.56:1 or 2:1 and 2.25:1), their two ratios were not different enough for many practical applications. This is especially true of antennas where the input impedance varies with frequency.

My earlier work[2] and an article by Genaille[10] have shown that a host of ratios (less than 4:1) can be obtained by tapping the bifilar winding of a Ruthroff 4:1 Unun.[9] However, the bandwidths obtained using this technique are quite limited with each ratio and are highly dependent upon the impedance level. This is particularly true when a rod core is used because it requires more turns (resulting in longer transmission lines) in order to obtain the necessary choking reactance that isolates the input from the output. Furthermore, ratios around 2:1 exhibit more loss because autotransformer action also enters into the matching process.[2]

By using quadrifilar and quintufilar windings on small 1.5-inch OD cores, and connecting them in such a way that the characteristic impedances of the windings are near optimum, two very different and broadband ratios matching 50 ohms to lower impedances are obtained. Furthermore, because the transmission lines in these transformers are so very short (8 to 9 inches in length), these transformers do quite well in matching 50 ohms to higher impedances (as step-up transformers).

This chapter presents two Ununs which have two broadband ratios that differ by a factor of two! One has a 1.5:1 and a 3:1 ratio (actually 1.56:1 and 2.78:1). The other has a 2:1 (actually 1.78:1) and a 4:1 ratio. Also, this chapter introduces the novel tech-

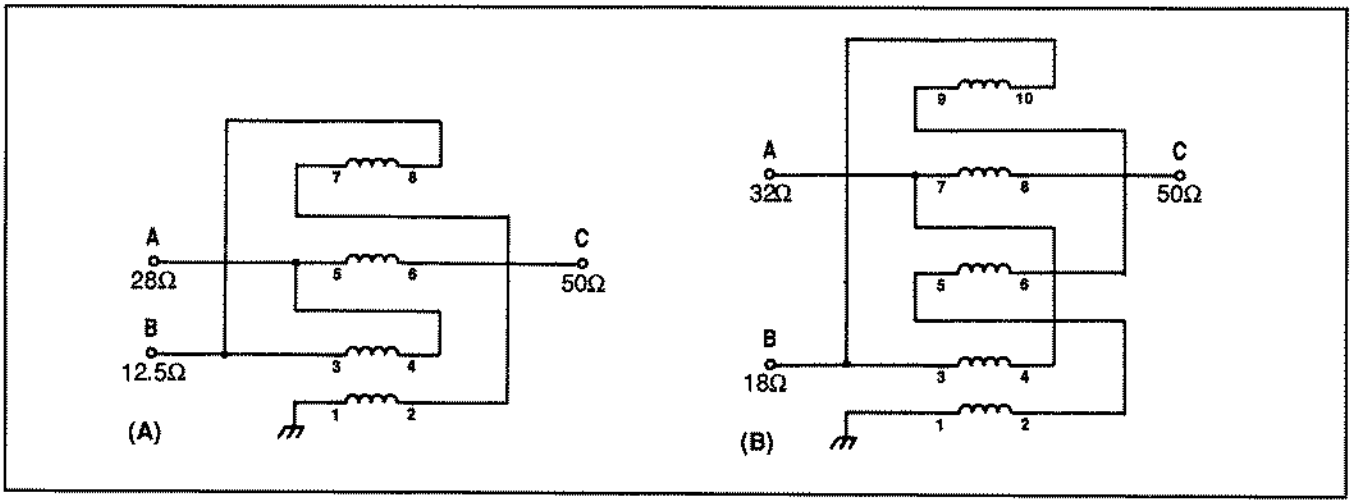

Figure 14-1. *Schematic diagrams of dual-ratio Ununs: (A) 1.78:1 connection C-A, 4:1 connection C-B; (B) 1.56:1 connection C-A, 2.78:1 connection C-B.*

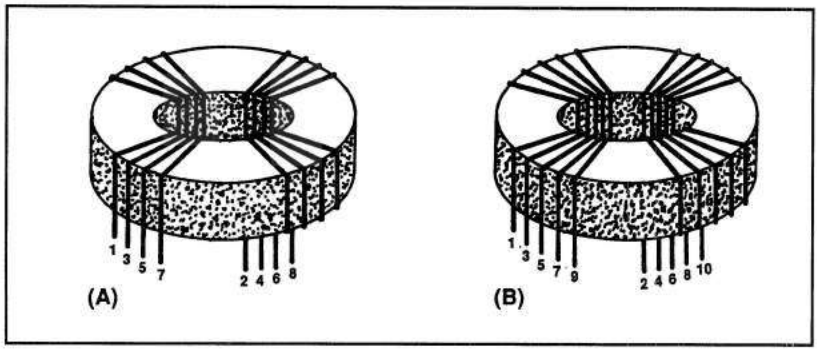

Figure 14-2. *Pictorials of higher-order windings: (A) quadrifilar, (B) quintufilar.*

nique of connecting these two transformers in parallel on their 50-ohm sides, resulting in four very broadband ratios.

Sec 14.2 2:1 and 4:1 Ratios

Figure 14-1A shows the schematic diagram of the quadrifilar Unun yielding ratios of 2:1 (actually 1.78:1) and 4:1. **Figure 14-2A** provides a pictorial of its windings. On the left in **Photo 14-A**, you see the bottom view of an Unun. The cable connector is on the 28-ohm (1.78:1) side. This Unun has four quadrifilar turns of No. 14 H Thermaleze wire on a 1.5-inch OD toroid with a permeability of 250.

In matching 50 to 28 ohms (connection C-A), the response is flat to within 1 percent from 1 to 30 MHz. From 1 to 50 MHz, it's flat to within 2 percent. In matching 50 to 12.5 ohms (connection C-B), the response is flat to within 3 percent from 1 to 30 MHz.

Because very short transmission lines are used, this transformer performs quite well as a step-up transformer. In matching 50 to 200 ohms (connection B-C), the response is flat to within 3 percent from 1.5 to 10 MHz. In matching 50 to 89 ohms (connection A-C), the response is flat to within 5 percent from 1.5 to 30 MHz!

Sec 14.2.1 Construction Tips

Start with about 14 inches of straightened wire. Form the wires into a ribbon with clamps of Scotch No. 27 glass tape every 1/2 inch. I found that strips 3/16 inch wide and about 1.5 inches long do a good job. The clamps should be long enough to go around the wires twice. After winding, connect terminals 2 and 7. Then connect terminals 3 and 8. Finally, connect terminals 4 and 5. Because work-hardening takes place quickly, you will find that a pair of pliers and a strong thumb (and arms) are necessary tools. You will also find that winding these exceptionally performing transformers is not easy. As in all endeavors, practice really pays off.

Sec 14.3 1.5:1 and 3:1 Ratios

Figure 14-1B shows the schematic diagram of the quintufilar Unun yielding ratios of 1.5:1 and 3:1

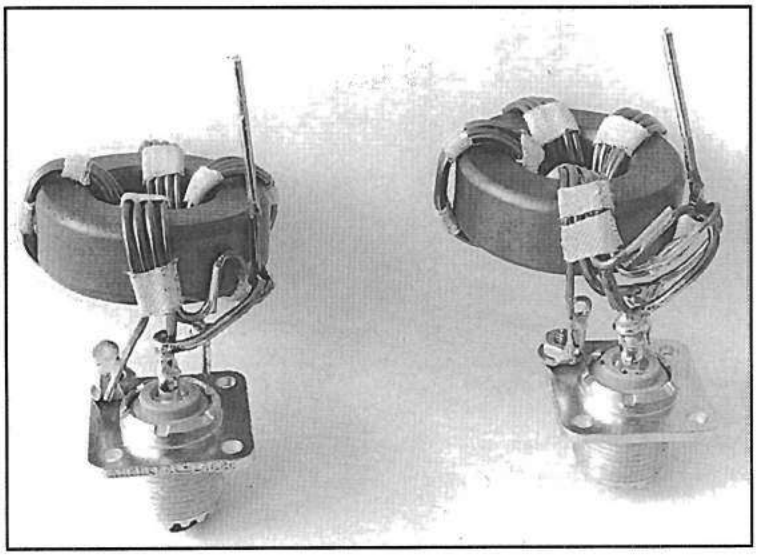

Photo 14-A. *On the left, a quadrifilar Unun with ratios of 1.78:1 and 4:1; on the right, a quintufilar Unun with ratios of 1.56:1 and 2.78:1.*

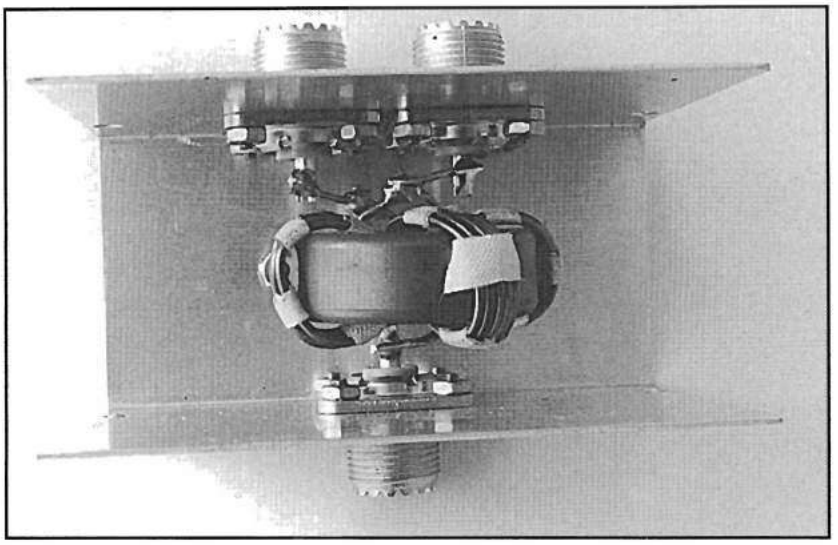

Photo 14-B. *The dual-ratio quintufilar Unun mounted in a 4 inch long by 2 inch wide by 2.75 inch high minibox.*

(actually 1.56:1 and 2.78:1). **Figure 14-2B** is a pictorial of its windings. On the right side in **Photo 14-A** you see a bottom view of an Unun. The cable connector is on the 32-ohm (1.56:1) side. This Unun has four quintufilar turns on a 1.5-inch OD toroid with a permeability of 250. Windings 3-4 and 7-8 are No. 14 H Thermaleze wire. The other three are No. 16 H Thermaleze wire. Winding 7-8 also has two layers of Scotch No. 92 polyimide tape, which optimizes the 1.56:1 ratio.

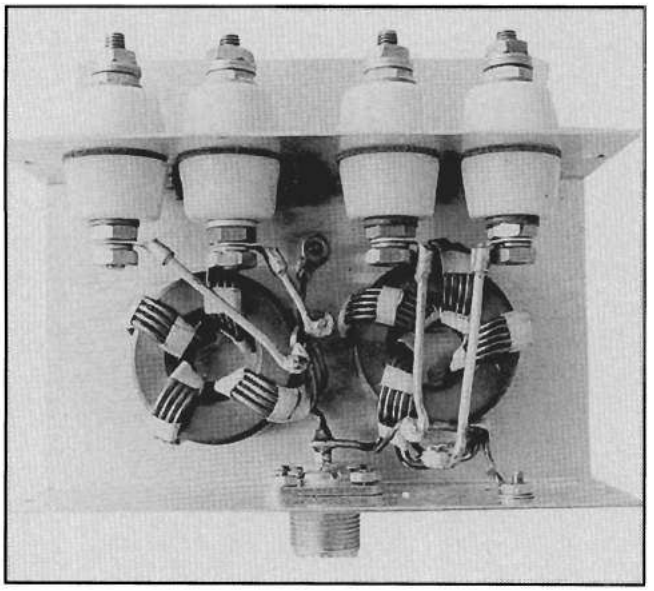

Photo 14-C. *The two dual-ratio Ununs connected in parallel on their 50-ohm sides providing four broadband ratios close to 1.5:1, 2:1, 3:1, and 4:1. The quadrifilar unit is on the left and the quintufilar unit is on the right. The enclosure is a 5 inch long by 3 inch wide by 2 inch high minibox.*

In matching 50 to 32 ohms (connection C-A), the response is essentially flat (less than 1 percent variation) from 1 MHz to over 40 MHz. Without the two layers of Scotch No. 92 tape, the response varies by 4 percent from 1 to 30 MHz. When used as a step-up transformer matching 50 to 78 ohms (connection A-C), and with the two layers of Scotch No. 92 tape on winding 7-8, the response is flat to within 5 percent from 1 to 15 MHz. Without the extra insulation on winding 7-8, the response is flat to within 5 percent from 1 to 7.5 MHz.

In matching 50 to 18 ohms (connection C-B), the variation in response is less than 3 percent from 1 to 40 MHz. The response is the same whether winding 7-8 is covered with the extra insulation or not. As a step-up transformer matching 50 to 139 ohms (connection B-C), the response is flat to within 3 percent from 1 to 10 MHz (with or without the extra insulation on winding 7-8). **Photo 14-B** shows this Unun mounted in a 4 inch long by 2 inch wide by 2.75 inch high minibox. The two cable connectors on the low impedance side could be replaced with feedthrough insulators for antenna use.

Sec 14.3.1 Construction Tips

Prepare the ribbon as was described for the quadrifilar Unun. If you choose to use the two extra layers of Scotch No. 92 tape on winding 7-8, make sure this winding is on the outside position of the ribbon (refer to **Figure 14-2B**). I found the best order in which to connect the wires is as follows: first, connect terminal 2 to 5; second, connect terminal 6 to 9; third, connect terminal 3 to 10; and, finally, connect terminal 4 to 7.

As was mentioned before, because a small toroid is used in order to achieve the best response (due to shorter transmission lines), this transformer also requires considerable strength and patience in the winding proeess.

Sec 14.4 Parallel Transformers

One of the most pleasant surprises I received with these efficient and broadband transformers was to find that they can be connected in parallel on their 50-ohm sides and still possess the same performance levels. Because the loading effect of one transformer on the other is minimal (like a short length of transmission line), the transformer that is properly terminated takes the power, while the other one is transparent. This lets you obtain four very wideband ratios with the two dual-ratio Ununs described in this chapter. Obviously, this technique eliminates one transmission line. Furthermore, Baluns can also be connected this way for feeding, with a single coaxial cable, beams and dipoles with different resonant impedances.

Photo 14-C shows two transformers connected in parallel on their 50-ohm sides using the two dual-ratio Ununs described in this chapter. As was mentioned, it now yields four wideband ratios very close to 1.5:1, 2:1, 3:1, and 4:1. I have used this matehing network to feed a host of ground-fed antennas (over a good ground system). In one case, I had a 10-, 15-, and 20-meter trap vertical, slopers for 40 and 160 meters, a 12-meter vertical, and an inverted L for 80 meters all matehed to a single coaxial cable at the same time. It was a simple matter of connecting each antenna to the output terminal that presented the best match (lowest VSWR). Tbis teehnique is actually an extension of connecting dipoles for different bands, in parallel. The antenna that presents the correct impedance takes the power, and the others are essentially transparent. In many eases, I found that only one transformer with two broadband ratios performed adequately.

Chapter 15

Multimatch Ununs

Sec 15.1 Introduction

Broadband multimatch Ununs capable of high-power applications have been the goal of many designers over the years. Some have resorted to using conventional autotransformers with tapped windings to obtain the many impedance transformation ratios. However, these attempts met with little success because of the device's limited bandwidths and efficiencies. Others (including myself)[2] have tried tapping a bifilar Ruthroff Unun.[9] Although these designs yielded the high efficiencies of transmission line transformers, they had limited bandwidths. Furthermore, their best bandwidths (for the various ratios) occurred at odd impedance levels. In other words, they didn't meet the objective of broadband operation with one of the input or output ports at 50 ohms.

Chapter 14 presented two Ununs which had two broadband ratios that differed by a factor of two. One had a 1.5:1 and a 3:1 ratio (actually 1.56:1 and 2.78:1). The other had a 2:1 (actually 1.78:1) and a 4:1 ratio. This chapter describes two multimatch designs that are capable of many more broadband ratios. For the most part, both are capable of broadband operation from 1.7 to 30 MHz.

One Unun has the following five ratios (which are close to): 1.5:1, 2:1, 4:1, 6:1, and 9:1. Because the two lower ratios work well in either direction (that is stepping up or down from 50 ohms), this design can match 50-ohm cable to impedances as high as 100 ohms (actually 112.5 ohms) and as low as 5.6 ohms over the frequency range. As a result, it has seven usable applications. Furthermore, because this is a transmission line transformer that cancels out the flux in the core, losses (in a matched condition) of only 0.04 to 0.08 dB can be expected.

The novelty in this design lies in the use of a trifilar winding (with one winding tapped) on a very small ferrite toroid, resulting in the shortest possible lengths of transmission lines. The windings are also connected in such a manner as to optimize their characteristic impedances from an overall standpoint.

I have used the adjective *ultimate* to describe the second Unun design. Although it might be risky business, I assume that this design will meet one of the most common definitions for this adjective—namely, *beyond which it is impossible to go*. For many of us, the classic use of this adjective was made by Lew McCoy in describing his popular transmatch.[22] Although there have been some improvements to Lew's design, his use of this definite (and strong) adjective can be said to have withstood the test of time. I hope my use meets with similar success.

While the tapped-trifilar design provides five broadband ratios and seven practical applications, the *ultimate* design presented in this chapter goes well

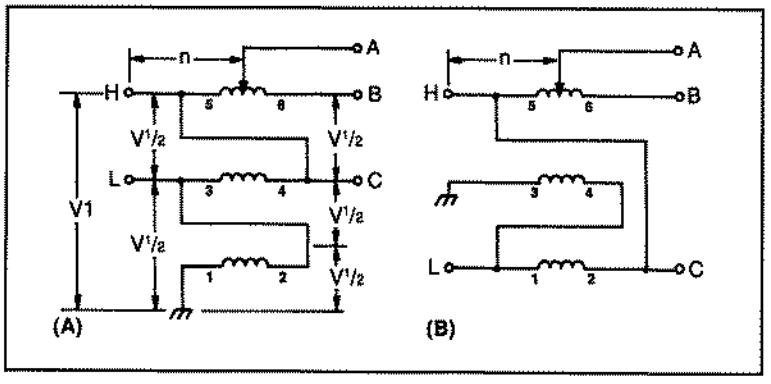

Figure 15-1. *Circuit diagrams for the 5-ratio Unun: (A) diagram for analysis; (B) transposed windings for best overall performance.*

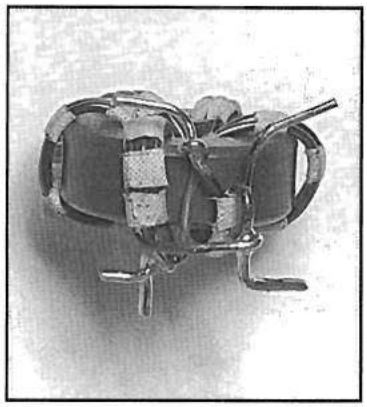

Photo 15-A. *Bottom view of the 5-ratio Unun of Figure 15-1B. The upper-left lead is terminal C. The upper-right lead is terminal B. The lower-left lead is terminal H. The lead pointing straight down is grounded (terminal 3). The lower-right lead is terminal L.*

beyond this number. It uses a tapped-quadrifilar design that yields the following 10 broadband ratios: 1.36:1, 1.56:1, 1.78:1, 2.25:1, 3.06:1, 4:1, 6.25:1, 9:1, 12.25:1, and 16:1. Because the four lower ratios also work quite well in either direction, this design offers *fourteen* applications in matching 50-ohm cable to impedances as high as 112.5 ohms and as low as 3.125 ohms. It also has the advantage of using a small low-loss toroidal core. Additionally, the windings are also interleaved in a pattern that optimizes their characteristic impedance.

However, this achievement comes at a price—*difficulty*. The 5-ratio Unun, which uses a trifilar winding, is considerably easier to wind. In addition, the quadrifilar 10-ratio Unun has two of its windings tapped, while the 5-ratio Unun has only one (see **Chapter 13** on tapping windings). If you have had little experience in winding Ununs or Baluns, attempt simplified versions of these two multimatch Ununs first. These versions eliminate the tapping of the windings. For the trifilar Unun, the remaining ratios would be: 2.25:1, 4:1, and 9:1. For the quadrifilar Unun, they would be: 1.78:1, 2.25:1, 4:1, 9:1, and 16:1.

For those interested in the design considerations of these broadband multimatch transformers, a brief review is presented in each section. These sections are followed by others describing high-power designs capable of handling the full legal limit of amateur radio power. Finally, the remaining sections present low-power designs capable of handling the output of any HF transceiver. Because transmission line transformers can be made so efficient in matching 50 to 100 ohms or less, their small sizes will surprise many readers. Therefore, the combination of using small ferrite toroids with the maximum allowable permeability (less than 300) for high efficiency,[2] and with sufficient turns to meet the low-frequency objective, results in the excellent performance exhibited by the designs in this chapter.

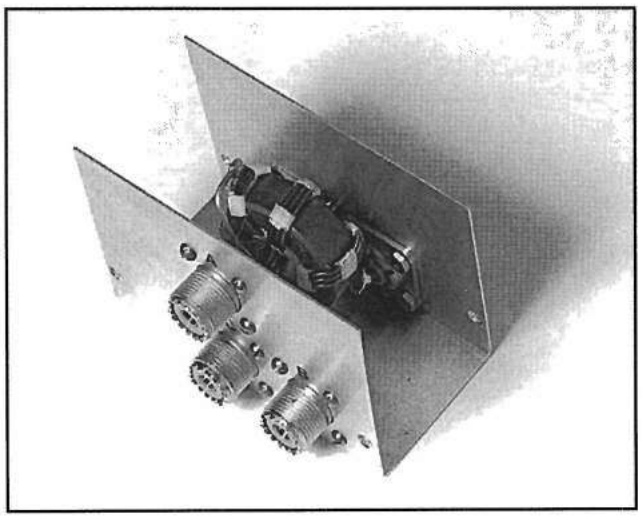

Photo 15-B. *The high-power unit mounted in a 4 inch long by 2 inch wide by 2.75 inch high minibox.*

Sec 15.2 The 5-Ratio Unun

Let's first look at **Figure 15-1A** because it is the easiest form of the trifilar-wound Unun to explain. For example, if the input voltage to ground, V_1, is connected to terminal H, the output terminal B, has a voltage to ground of $3/2V_1$. This results in a transformation ratio, g, of $(3/2)^2$ or 2.25:1. This should satisfy most 2:1 requirements. If the output is at terminal A to ground, then the output voltage is:

$$V_o = V_1 + V_1(n/2N)$$
$$= V_1(1 + n/2N) \qquad \text{(Eq 15-1)}$$

where:
N = the total number of turns on the winding
n = the number of turns from terminal 5.

The transformation ratio, g, then becomes:

$$g = (V_o/V_1)^2$$
$$= (1 + n/2N)^2 \qquad \text{(Eq 15-2)}$$

If the input voltage to ground, V_1, is connected to terminal L, then terminal C has twice the voltage of V_1—resulting in a 4:1 ratio. Terminal B has three

times the voltage resulting in a 9:1 ratio. With terminal A, the output voltage is:

$$V_o = 2V_1 + V_1(n/N)$$
$$= V_1(2 + n/N) \qquad \text{(Eq 15-3)}$$

The transformation ratio, g, then becomes:

$$g = (2 + n/N)^2 \qquad \text{(Eq 15-4)}$$

Sec 15.2.1 A High-power 5-Ratio Unun

After several attempts at rearranging the windings of **Figure 15-1A** for the best overall performance (optimizing the effective characteristic impedances of the windings), **Figure 15-1B** evolved. **Photo 15-A** shows the bottom view of an Unun, using the circuit of **Figure 15-1B**, capable of handling the full legal limit of amateur radio power. **Photo 15-B** shows the unit mounted in a CU-3015A minibox. It has five trifilar turns on a 1.5-inch OD ferrite toroid with a permeability of 250. Winding 5-6 is tapped at two turns (n = 2) from terminal 5.

If the 9:1 ratio matching 50 to 5.6 ohms (connection B-L) is to be used at full power, then winding 3-4 should be No. 12 H Thermaleze wire. If not, then all windings can be No. 14 H Thermaleze wire.

A listing of the expected performance across the band from 1.7 MHz to 30 MHz, with the various ratios, is as follows:

9:1 (B-L); 50:5.6 ohms
Ratio is within 1 percent!
5.75:1 (A-L); 50:8.7 ohms
Ratio decreases by 5 percent.
4:1 (C-L); 50:12.5 ohms
Ratio increases by 15 percent (the greatest deviation of all the ratios).
2.25:1
a) (B-H); 50:22.22 ohms
Ratio decreases by 4 percent.
b) (H-B); 50:112.5 ohms
Ratio increases by 8 percent.
1.44:1
a) (A-H); 50:35 ohms
Ratio decreases by 10 percent.
b) (H-A); 50:72 ohms
Ratio increases by 2 percent.

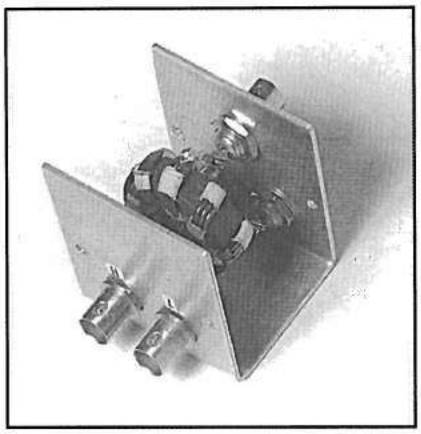

Photo 15-C. *The low-power unit mounted in a homemade 2 inch long by 1.5 inch wide by 2.25 inch high minibox.*

Several comments should be made regarding the expected results shown above. First of all, the greatest deviation from a flat response at any ratio occurs when matching 50 to 12.5 ohms (connection C-L; a 4:1 ratio). If an accurate insertion loss measurement was made at this ratio and impedance level, the result would show an insignificant difference across the band. Secondly, the major part of the deviations for all ratios occurs beyond 15 MHz (the effect of standing waves). Finally, the higher ratios should *never* be used to match 50 ohms to 450 ohms, 288 ohms, and 200 ohms, respectively. The characteristic impedances and choking reactances *do not* allow for broadband operation under these conditions.

Sec 15.2.2 A Low-power 5-Ratio Unun

Photo 15-C shows a low-power unit mounted in a homemade 2 inch long by 1.5 inch wide by 2.25 inch

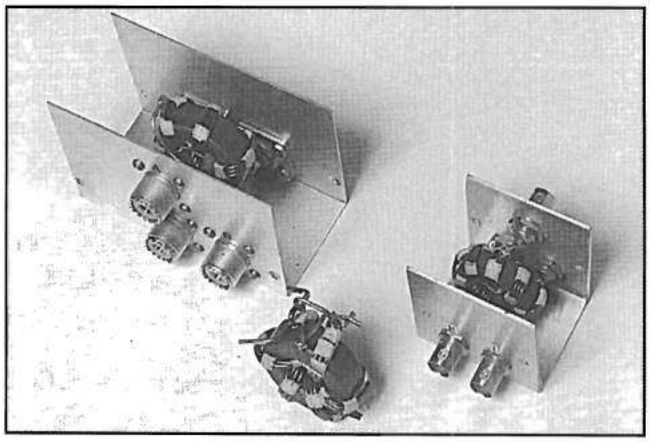

Photo 15-D. *The three 5-ratio Ununs together. From left to right, the high-power unit mounted and unmounted, the low-power unit.*

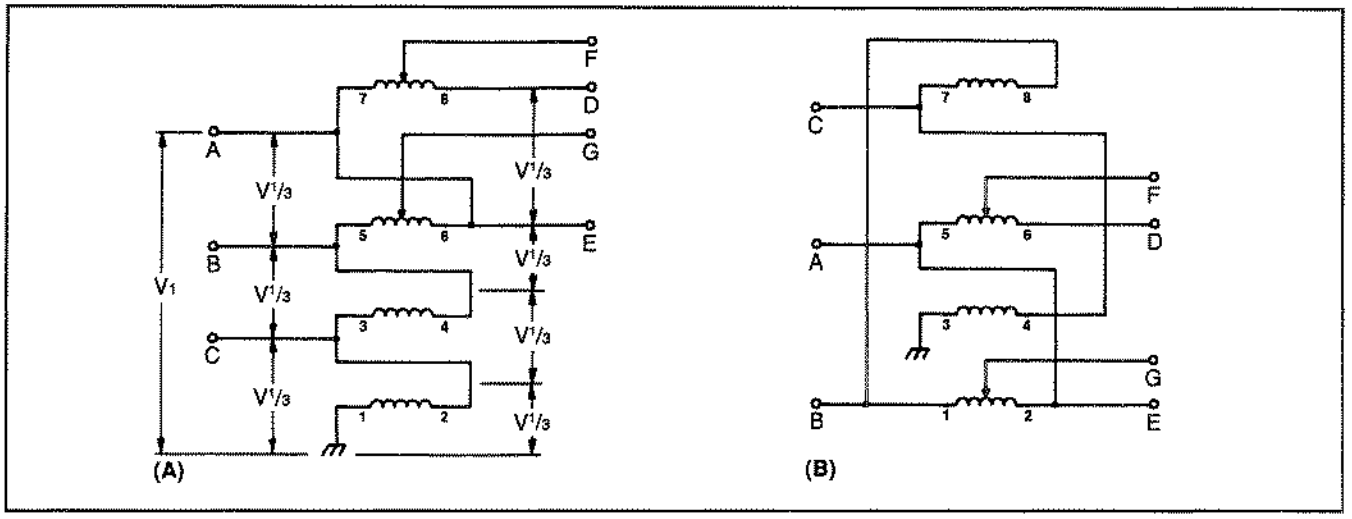

Figure 15-2. *Circuit diagrams for the 10-ratio Unun: (A) diagram for analysis; (B) transposed windings for best overall performance.*

high minibox. It has six trifilar turns of No. 16 H Thermaleze wire on a 1.25-inch OD ferrite toroid with a permeability of 250. The tap on winding 5-6 is located three turns from terminal 5, yielding ratios of 6.25:1 and 1.56:1 instead of the 5.75:1 and 1.44:1 ratios of the high-power unit. In actual use, these differences should be negligible.

Because this Unun has shorter transmission lines than its high-power counterpart, the deviations of the ratios across the band are even smaller. It is also interesting to note that, if No. 14 H Thermaleze wire was used in winding 3-4, this very small Unun could very well be rated at 500 watts of continuous power!

Photo 15-D shows all three 5-ratio Ununs together.

Sec 15.3 The 10-Ratio Unun—The Ultimate Multimatch

Figure 15-2A is presented here because it is the easiest form of a quadrifilar-wound Unun to explain. With the input voltage, V_1, connected to the various terminals on the left (the low-impedance side), and with very short transmission lines compared to the wavelength, we have the following transformation ratios:

1. V_1 connected to terminal A

a) At terminal D the output voltage V_o is $4/3V_1$. Therefore, the transformation ratio, g, with connection A-D is:

$$g = (4/3)^2 = 1{:}1.78 \qquad \text{(Eq 15-5)}$$

b) At terminal F the output voltage is:

$$V_o = V_1(1 + n/3N) \qquad \text{(Eq 15-6)}$$

where:
N = total numher of turns
n = number of turns from terminal 7.

The transformation ratio with connection A-F then becomes:

$$g = (V_o/V_1)^2 = (1 + n/3N)^2 \qquad \text{(Eq 15-7)}$$

2. V_1 connected to terminal B

a) At terminal E the output voltage is $3/2V_1$. Thus, the transformation ratio with connection B-E is:

$$g = (3/2)^2 = 1{:}2.25 \qquad \text{(Eq 15-8)}$$

b) At terminal G the output voltage is:

$$V_o = V_1(1 + n/2N) \qquad \text{(Eq 15-9)}$$

where n = number of turns from terminal 5.

The transformation ratio with connection B-G becomes:

$$g = (V_o/V_1)^2 = (1 + n/2N)^2 \qquad \text{(Eq 15-10)}$$

c) At terminal D the output voltage is $2V_1$. The transformation ratio with connection B-D is:

$$g = (2)^2 = 1{:}4 \qquad \text{(Eq 15-11)}$$

d) At terminal F the output voltage is:

$$V_o = V_1(3/2 + n/2N) \qquad \text{(Eq 15-12)}$$

where n = number of turns from terminal 7.

The transformation ratio with connection B-F, then, is:

$$g = (V_o/V_1)^2 = (3/2 + n/2N) \qquad \text{(Eq 15-13)}$$

3. V_1 connected to terminal C

a) At terminal E, the output voltage is $3V_1$. The transformation ratio with connection C-E becomes:

$$g = (3)^2 = 1{:}9 \qquad \text{(Eq 15-14)}$$

b) At terminal G, the output voltage is:

$$V_o = V_1(2 + n/N) \qquad \text{(Eq 15-15)}$$

where n = number of turns from terminal 5.

The transformation ratio with connection C-G is:

$$g = (V_o/V_1)^2 = (2 + n/N)^2 \qquad \text{(Eq 15-16)}$$

c) At terminal D, the output voltage is $4V_1$. The transformation with connection C-D becomes:

$$g = (4)^2 = 1{:}16 \qquad \text{(Eq 15-17)}$$

d) At terminal F the output voltage is:

$$V_o = V_1(3 + n/N) \qquad \text{(Eq 15-18)}$$

where n = number of turns from terminal 7.

The transformation ratio with connection C-F is:

$$g = (V_o/V_1)^2 = (3 + n/N)^2 \qquad \text{(Eq 15-19)}$$

Sec 15.3.1 A High-power 10-Ratio Unun

Figure 15-2B evolved after several attempts at rearranging the windings of **Figure 15-2A** for best overall performance (optimizing the effective characteristic impedances of the windings). **Photo 15-E** shows the bottom view of an unmounted Unun using the circuit of **Figure 15-2B**. The top-left lead is terminal E. The top-right lead is terminal D. The bottom-left lead is terminal B. The center lead (connected to the SO-239 connector) is terminal A.

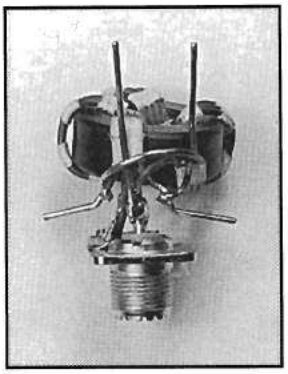

Photo 15-E. *Bottom view of the 10-ratio Unun. The connector is on terminal A.*

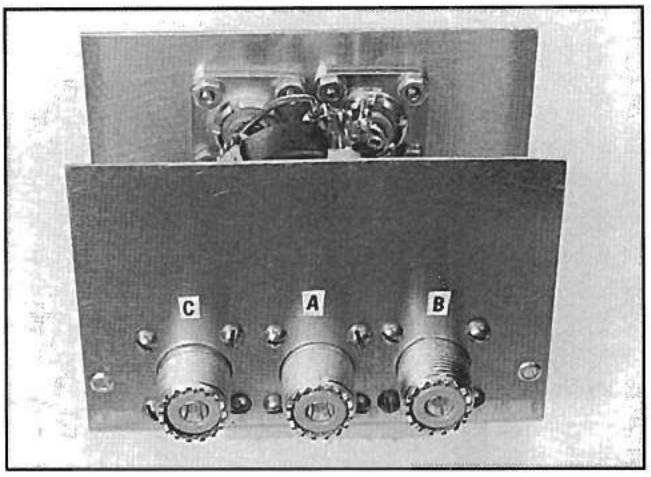

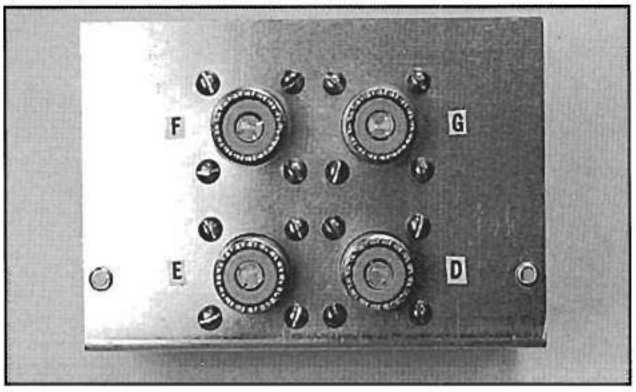

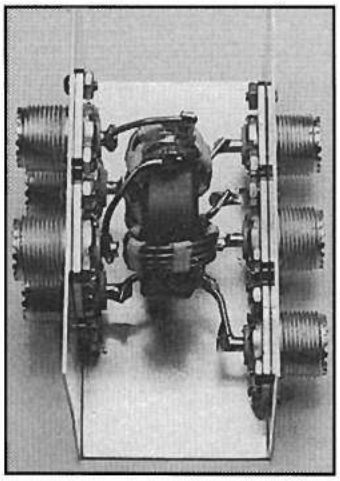

Photo 15-F. *Three different views of the 10-ratio Unun mounted in a 4 inch long by 2 inch wide by 2.75 inch high CU-3015A minibox.*

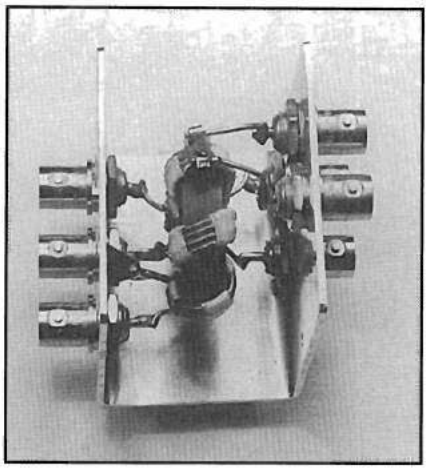

Photo 15-G. *The low-power unit mounted in a homemade 2.25 inch long by 1.5 inch wide by 2.25 inch high minibox.*

The bottom-right lead is terminal C. Below these three bottom leads is a ground connection (terminal 3 in **Figure 15-2B** to the SO-239 connector. **Photo 15-F** shows three different views of this high-power unit mounted in a 4 inch long by 2 inch wide by 2.75 inch high CU-3015A minibox.

This 10-ratio Unun has four quadrifilar turns of No. 14 H Thermaleze wire on a 1.5-inch OD ferrite toroid with a permeability of 250. Winding 5-6 is tapped at 2 turns from terminal 5 and winding 7-8 is tapped at 2 turns from terminal 7.

If the 9:1 ratio (connection C-E), the 12.25:1 ratio (connection C-F), and the 16:1 ratio (connection C-D), are to be used at the full legal limit of amateur radio power, then I suggest that winding 3-4 be replaced with No. 12 H Thermaleze wire. If not, then these three ratios should be used at lower power levels (of 500 watts continuous and 1 kW peak). It should also be mentioned that using No. 12 wire for winding 3-4 adds a greater degree of *difficulty* to the construction process.

A listing of the expected performance across the band from 1.7 to 30 MHz, with the various ratios, is as follows:

16:1 (D-C); 50:3.125 ohms
Ratio is constant up to 21 MHz. It then decreases by 15 percent.
12.25:1 (F-C); 50:4.08 ohms
Ratio is constant.
9:1 (E-C); 50:5.56 ohms
Ratio increases by 5 percent.
6.25:1 (G-C); 50:8 ohms
Ratio is constant.
4:1 (D-B); 50:12.5 ohms
Ratio decreases by 5 percent.
3.06:1 (F-B); 50:16.3 ohms
Ratio decreases by 10 percent.
2.25:1
a) (E-B); 50:22.22 ohms
Ratio increases by 4 percent.
b) (B-E); 50:112.5 ohms
Ratio increases by 50 percent (the greatest deviation across the band of any of the ratios).
1.78:1
a) (D-A); 50:28.1 ohms.
Ratio is constant.
b) (A-D); 50:89 ohms.
Ratio increases by 15 percent.
1.56:1
a) (G-B); 50:32 ohms
Ratio increases by 10 percent.
b) (B-G); 50:78 ohms
Ratio increases by 40 percent.
1.36:1
a) (F-A); 50:36.8 ohms
Ratio decreases by 9 percent.
b) (A-F); 50:68 ohms
Ratio increases by 1.5 percent.

Sec 15.3.2 A Low-power 10-Ratio Unun

Photo 15-G shows a low-power unit mounted in a homemade 2.25 inch long by 1.5 inch wide by 2.25 inch high minibox. It has five quadrifilar turns of No. 16 H Thermaleze wire on a 1.25-inch OD ferrite toroid with a permeability of 250. The tap on winding 5-6 (**Figure 15-2B**) is at three turns from terminal 5 and on winding 1-2; it is three turns from terminal 1. Because the number of turns is different from the high-power unit, so are the ratios that use the taps. In this case, they are a little larger. Specifically, the tapped ratios are now: 1:12.96, 1:6.76, 1:3.24, 1:1.69, and 1:1.44. If the taps were at two turns from terminals 5 and 1, the ratios would be a little less than those of the high-power unit. You can play with the equations in the first section of this chapter and arrive at many different ratios.

Because this Unun has shorter transmission lines than its high-power counterpart, the deviations of the ratios across the HF band are generally smaller. Also, if winding 3-4 (in **Figure 15-2B**) were replaced with No. 14 H Thermaleze wire, this low-power unit could very well be rated at 500 watts of continuous power for all ratios!

Chapter 16

Ununs for Beverage Antennas

Section 16.1 Introduction

The Beverage antenna[19] is well known by 160-meter enthusiasts for enhanced signal-to-noise ratios when there are high levels of interference and atmospheric noise. If erected properly, Beverages also have excellent directivity. However, they are quite inefficient and, therefore, not generally suitable as transmitting antennas. Important considerations with Beverages are the terminating resistor (for the more common single-wire version) and the input matching Unun (unbalanced-to-unbalanced transformer). The terminating resistor and the impedance ratio of the Unun are determined by the characteristic impedance of the antenna acting as a long transmission line with one good conductor and one poor conductor (the earth). This line is generally between 400 and 600 ohms, and theoretically given by:

$$Z_o = 138 \times \log(4h/d) \qquad \text{(Eq 16-1)}$$

where:
Z_o = characteristic impedance of the Beverage
h = height of the wire above ground
d = diameter of the wire.

This chapter presents low- and high-power versions of multimatch Ununs designed to match 50-ohm cable to unbalanced loads from 450 to 800 ohms. The low-power unit, which is capable of handling continuous power levels up to 100 watts, is specifically designed for the Beverage antenna when it is performing as a receiving antenna. The high-power unit, which is capable of handling 1 kW of continuous power, can be used with the Beverage or any other traveling wave antenna when used as a transmitting antenna. Also presented are high-power designs capable of flat response, including the entire AM broadcast band. These multimatch Ununs could be of interest to designers of high-power amplifiers for the broadcast band. A little theory on how these devices are designed is also provided.

Sec 16.2 A Little Theory

Transmission line transformers[2] (the Unun being a subset thereof) are known for having greater bandwidths and efficiencies than their counterparts, the conventional transformers. Design considerations for the two types of transformers are also vastly different. Transmission line transformers use chokes and transmission lines, while conventional transformers use flux linkages.

High-impedance Ununs (and Baluns), which match 50 ohms unbalanced to impedances as high as 800 ohms, lie at about the edge of this technology's capability. The reasons are: 1) the windings require more turns because higher reactances are needed for isolating the input from the output, and 2) they require higher characteristic impedances in the transmission lines because the loads they see are greater. Therefore, when winding one of these devices, you'll *just* run out of space on your toroidal cores when trying to satisfy the low frequency and high frequency objectives. Incidentally, beaded transmission lines are not recommended at these impedance levels because of their excessive losses.

There are two methods for obtaining broadband operation at these high impedance levels. One uses Guanella's 9:1 and 16:1 Baluns, which are converted to Unun operation.[2] The other uses higher-order windings (quadrifilar in this case) on a single core, which is an extension of Ruthroff's bootstrap approach.[2] The Guanella approach, which uses coiled transmission line connected in series at the high-impedance side and in parallel at the low-impedance side, results in very broad bandwidths—but with difficulty in meeting low-frequency objectives. Low-frequency models[2] show that, with ratios above 4:1,

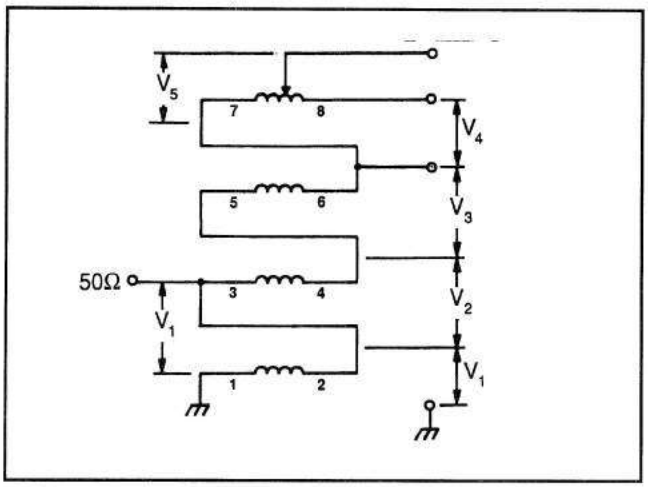

Figure 16-1. *Schematic diagram of the quadrifilar design, using Ruthroff's approach for high-impedance, low-frequency Ununs like the Beverage matching transformer.*

some of the coiled windings are connected in parallel, resulting in reduced reactances. However, with the Ruthroff approach, all of the inductances (at the low-frequency end) end up mutually aiding each other. However, Ruthroff's approach suffers at the high-frequency end because a direct voltage is summed with three voltages that traverse various lengths of transmission lines. As a result, Guanella's approach of summing voltages of equal delays is preferred for the higher frequency bands, and Ruthroff's approach is most often used for the lower frequency bands. This chapter presents designs using Ruthroff's approach.

Figure 16-1 shows the schematic diagram of a quadrifilar-wound Unun. If the lengths of the transmission lines are very short compared to the wavelength (therefore, phase delay and standing waves are negligible), then:

$$V_1 = V_2 = V_3 = V_4 \qquad \text{(Eq 16-2)}$$

at terminal 6,

$$V_o = V_1 + V_2 + V_3 = 3V_1 \qquad \text{(Eq 16-3)}$$

and the impedance ratio becomes:

$$g = (V_o/V_1)^2 = 9 \qquad \text{(Eq 16-4)}$$

At terminal 8, it becomes:

$$g = 16 \qquad \text{(Eq 16-5)}$$

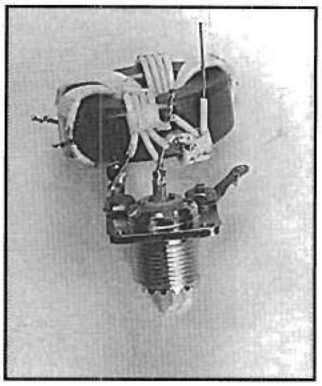

Photo 16-A. *The bottom view of the low-power Beverage antenna Unun.*

The voltage at the tap in winding 7-8 is:

$$\begin{aligned} V_o &= 3V_1 + V_5 \\ &= 3V_1 + n/NV_1 = V_1(3 + n/N) \\ &= V_1(3 + n/N) \end{aligned} \qquad \text{(Eq 16-6)}$$

where:
N = total number of turns
n = number of turns from terminal 7

The impedance ratio, using the tapped winding, becomes:

$$g = (V_o/V_1)^2 = (3 + n/N)^2 \qquad \text{(Eq 16-7)}$$

When the lengths of the transmission lines are significant, then important phase delays can occur and reduce the high frequency response. As you can see in **Figure 16-1**, V_2 travels one transmission line, V_3 travels two transmission lines, and V_4 travels three transmission lines. Additionally, the high frequency response is further diminished if the characteristic impedances of the transmission lines are not at their optimum values (which is hard to do at these impedances levels). Even with these major flaws, the Ruthroff approach is better for Beverage antenna use because this antenna's greatest advantages are on the lower frequency bands (80 and 160 meters).

Sec 16.3 A Low-power Design

Photo 16-A shows the bottom view of a 5-turn quadrifilar-wound Unun designed to handle 100 watts of continuous power with constant ratios from 9:1 to 16:1 in the 40- and 80-meter bands. It uses the Ruthroff approach of **Figure 16-1** and is shown here to give the reader a method for making the various interconnections. For operation on the 80- and 160-meter bands, I would use 6 quadrifilar turns on a 1.5-

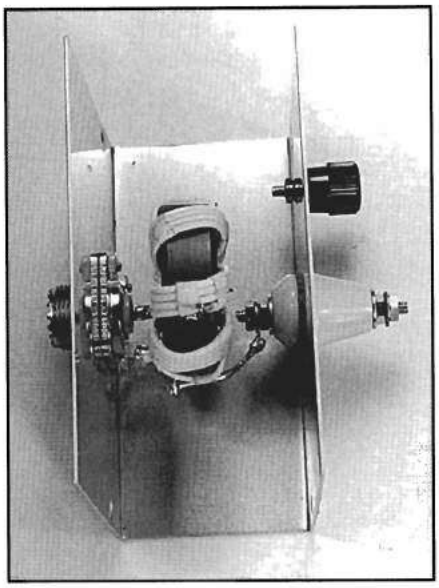

Photo 16-B. *The low-power Beverage antenna Unun mounted in a 4 inch long by 2 inch wide by 2.75 inch high minibox.*

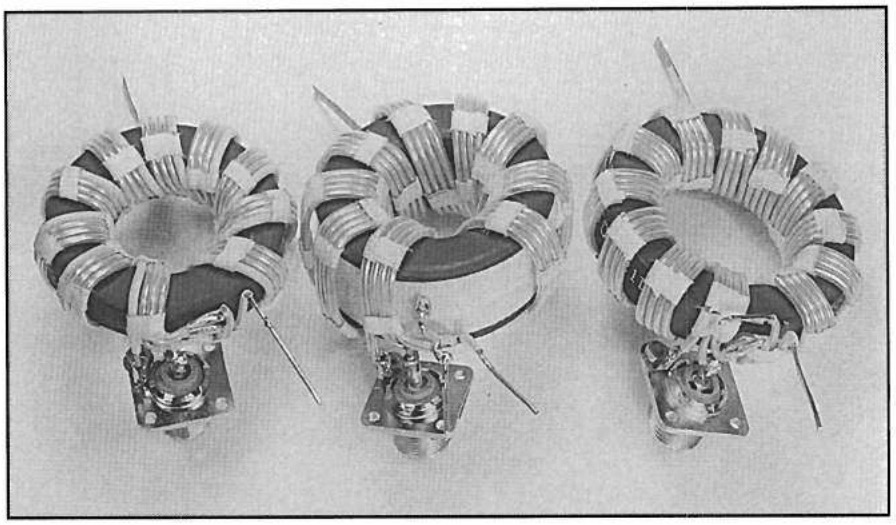

Photo 16-C. *Three high-power, low-frequency Ununs using a quadrifilar design with Ruthroff's approach. The one on the left is designed to cover the 80- and 160-meter bands. The other two are designed to cover the 160-meter and AM broadcast bands.*

inch OD ferrite toroid with a permeability of 250. The bottom winding is No. 20 hook-up wire and the other three are No. 22 hook-up wire. Winding 7-8 is tapped at 2 turns from terminal 7, yielding a 11.11:1 ratio, and at 3 turns from terminal 7, yielding a 12.25:1 ratio. Therefore, with outputs also at terminals 6 and 8, this Unun matches 50-ohm cable to loads of 450, 555.6, 612.5, and 800 ohms.

Photo 16-B shows the unit mounted in a 4 inch long by 2 inch wide by 2.75 inch high minibox. The output (the feedthrough insulator) is connected to one of the taps. A grounded binding post is also shown.

Sec 16.4 High-power Designs

Photo 16-C shows three high-power designs. The one on the left is specifically designed to cover the frequencies generally used with traveling wave structures like the Beverage antenna. This design has 10 quadrifilar turns on a 2.4-inch OD ferrite toroid with a permeability of 250. Winding 1-2 is No. 14 tinned copper wire, and the other three are No. 16 tinned copper wire. The wires are also covered with Teflon sleeving. Winding 7-8 is tapped at 5 turns from terminal 7, yielding a ratio of 12.25:1. When matching 50-ohm cable to loads of 450 ohms (terminal 6), 612.5 ohms (the tap), and 800 ohms (terminal 8), the variation in response is less than 5 percent from 1.5 to 4 MHz. At 6.5 MHz, the variation (which is an increase in the impedance ratio) increases to about 20 percent. **Photo 16-D** attempts to provide a better view of the connections.

The other two high-power Ununs in **Photo 16-C** are specifically designed to cover the broadcast and 160-meter bands. The one in the center has 9 quadrifilar turns (of the same wires as above) on a stack of two 2.4-inch OD ferrite toroids with permeabilities of 250. The tap on winding 7-8 is now at 4 turns from terminal 7, yielding a ratio of 11.86:1. When matching 50-ohm cable to 450 ohms (terminal 6), 593 ohms (the tap), or 800 ohms (terminal 8), the response is literally

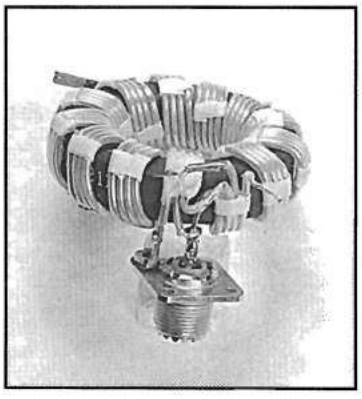

Photo 16-D. *The bottom view of the high-power Beverage antenna Unun.*

flat from 0.5 to 2 MHz. At 4 MHz, the ratios increase by about 6 percent. At 7 MHz, they increase by about 20 percent.

The Unun on the right in **Photo 16-C** illustrates another way of obtaining the same performance as above. In this case, the design has 12 quadrifilar turns (of the same wires as above) on a 2.68-inch OD ferrite with a permeability of 290. The tap on winding 7-8 is at 6 turns from terminal 7, yielding a 12.25:1 ratio (instead of 11.86:1 as above). Although the performance of this design is practically the same as the one above (using the two 2.4-inch OD cores), it is a much more expensive design because the 2.68-inch OD core is not nearly as popular. However, if a broadband, high-power and high-impedance Unun (or Balun) is required to cover 1.5 to 30 MHz, then these expensive 2.68-inch OD ferrite cores are very likely the *only* alternative!

Chapter 17

Concluding Remarks

Sec 17.1 Introduction

As I've often said, there is little information that deals with aspects of design and applications of practical hardware. Most companies are reluctant to publish their results for fear of giving away their hard-earned secrets. Textbooks only contain a few paragraphs on the subject. Therefore, very few people fully understand this technology, and, as a result, it is still far from reaching its full potential.

This book not only contains my designs, which have appeared in series written for *CQ* and *Communications Quarterly*, but also my views on other articles that have appeared in the amateur radio literature.

In the process of converting and combining the articles into appropriate chapters, one section in my article in the *CQ*, March 1993 issue entitled "Dual-Ratio Ununs," stood out as having broader applications. It is entitled "Reflections on Power Ratings" and is presented here. This information is followed by a section on misconceptions and one on the "state of the art."

After reading this book, some might think I was overly critical and didn't agree with any of the designs or explanations (or both) presented in the amateur radio literature. This is quite true. In taking this stand, I was hoping to provoke, in return, critical comment on my work. In this way, we can help our amateur friends—and perhaps even our professional friends—by advancing the understanding and application of these very useful transformers.

Sec 17.2 Reflections on Power Ratings

Power rating is one of the most controversial and least understood specifications for the transmission line transformer. As of today, no professional group has yet set the standard for this specification (as well as any other) for this popular class of matching transformers. In fact, manufacturers of ferrites, which are mainly the materials used with these devices, only specify them for their uses as conventional transformers and inductors, or microwave devices.

It is well known that power ratings for practically all conventional devices are based upon catastrophic failures (usually exceeding a voltage or current limit), and failures over a relatively short period of time due to an excessive rise in temperature.

With transmission line transformers, there are really two catastrophic-type failures that can occur. One is voltage breakdown. If the device is misterminated with a high impedance (especially an open circuit), a breakdown of the insulation can occur. This is particularly true of the 1:1 Balun (50:50 ohms) that is terminated with the very high impedance of a full-wave dipole or inverted V. Using heavily coated wires (but still maintaining a characteristic impedance close to 50 ohms), or small but high-power coaxial cable, can help under these conditions.

The second catastrophic failure occurs at the low-frequency end of the transformer's passband, when the energy is not completely transmitted to the output circuit by a transmission line mode. This takes place when the reactance of the coiled or beaded transmission line is not sufficient to prevent conventional transformer currents or shunting currents to ground. Under these conditions, harmful flux can take place in the core or beads. Nonlinearities can also occur if the flux becomes appreciable. The objective in design at the low-frequency end is to have a margin of safety such that, with a termination of about three times (hence VSWR of 3:1) that of a matched condition,[2] no flux will appear in the core or beads.

The failure due to an excessive rise in temperature is the least understood of the two because it involves the failure mechanism in transmission line transformers when only transmission line currents are allowed to flow. Unlike the conventional transformer whose

losses are current dependent (wire, eddy current, and hystereis losses), the transmission line transformer's losses are voltage dependent (a dielectric-type). That is, the greater the voltage drop along the length of the transmission lines, the greater the loss. Furthermore, it can be shown that only low-permeability ferrites (less than 300) yield the extremely high efficiencies of which these transformers are capable.[2]

Because all transmission line transformers have voltage drops along their transmission lines, we must look at their high-frequency models to determine the magnitude of these drops and, hence, the temperature rise that can be expected. Here are some examples:

If V_1 is the voltage that appears on the 50-ohm side of the transformer, then:

1) For a quintufilar-wound Unun, the longitudinal voltage-drop is $V_1/5$ in matching to lower impedances (like 32 or 18 ohms) and $V_1/4$ in matching to higher impedances (like 78 or 139 ohms).

2) For a quadrifilar-wound Unun, the longitudinal voltage-drop is $V_1/4$ in matching to lower impedances (like 12.5 or 28 ohms) and $V_1/3$ in matching to higher impedances (like 89 or 200 ohms).

3) For a trifilar-wound Unun, the longitudinal voltage-drop is $V_1/3$ in matching to lower impedances (like 22.22 or 25 ohms) and $V_1/2$ in matching to higher impedances (like 100 or 112.5 ohms).

4) For a bifilar-wound Unun, the longitudinal voltage-drop is $V_1/2$ in matching to a lower impedance of 12.5 ohms and V_1 in matching to a higher impedance of 200 ohms.

Because the quintufilar-wound Unun has the lowest voltage drop, it is expected to have the highest efficiency. Furthermore, it can be seen that the highest efficiencies occur in matching to lower impedances. Very accurate measurements[2] have shown that 4:1 Ununs, using ferrite cores with permeabilities of 125, have exhibited losses of only 0.02 to 0.04 dB in matching 50 to 12.5 ohms from 1 MHz to over 30 MHz. Even though the Ununs in this book have mostly used permeabilities of 250, and should have slightly greater losses, many use higher-order windings (trifilar, quadrifilar, and quintufilar) and, hence, have lower longitudinal voltage drops. Therefore, they should have losses of only 0.02 to 0.04 dB, as well.

When matching at the 1 kW level, the figures above mean that only 5 to 10 watts would be dissipated in the Unun. As a heatsink, these small transformers should be able to handle this loss easily. In fact, they should be able to handle several times this level of continuous power. Also, because they use heavily coated wires, their peak power ratings should be greater by more than a factor of two!

Another important power rating consideration is to determine what happens when the transformers are misterminated. Because the losses being considered now are dielectric-types and, hence, voltage-dependent, the harmful terminations are greater than that for which the transformers were designed. For example, if the termination is three times greater (a VSWR of 3:1), the voltages along the transmission lines would increase by a factor of 1.73. This means the losses would practically double. The Ununs described in this series, when matching to impedances lower than 50 ohms, should easily handle this mismatch. Obviously, mismatches in the range of 10:1 would result in much lower efficiencies and should be avoided.

The analysis of the losses in Baluns follows the same pattern. The voltages are as follows: under matched conditions for a 1:1 Balun (50:50 ohms), $V_1/2$; for a 4:1 Balun (50:200 ohms), V_1; for a 9:1 Balun (50:450 ohms), $1.5V_1$; and for higher-impedance Baluns it could be $2V_1$. The higher voltage drops, together with high VSWRs, means that high-impedance Baluns (and Ununs) have more loss and require larger structures to dissipate the heat. It should also be pointed out that there is a tradeoff in efficiency for low-frequency response with Baluns (and Ununs) when matching 50 ohms to higher impedances like 200 ohms, 300 ohms, 450 ohms, and higher. This is done by using permeabilities of 125 and lower.

Finally, I thought it might be useful to give some general guidelines as to what efficiencies you might expect with Baluns and Ununs when using ferrite cores or beads with a permeability of 250. Here are some expected efficiencies when matching 50 ohms to various loads under matched conditions:

Loads	**Efficiency**
50 ohms or less	98 to 99.5 percent
50 to 100 ohms	97 to 98 percent
100 to 200 ohms	96 to 97 percent
200 ohms and above	93 to 96 percent

As I mentioned earlier, these efficiencies would be reduced by a percent or two with a VSWR of 3:1, which increases the loss by a factor of about two. Also, the efficiencies can be increased by a percent or two with high-impedance loads (greater than 100 ohms) by resorting to lower permeability ferrites that

trade off efficiency for low-frequency response. In closing, I would like to say that high-permeability manganese-zinc ferrites should be avoided because of their much higher losses. Furthermore, their losses are highly frequency dependent, while low-permeability nickel-zinc ferrites are not.

Sec 17.3 Misconceptions

From recent discussions on the air and phone calls concerning Baluns, I think the most *expensive* misconception regarding Baluns is the assumption that a 9:1 (450:50 ohm) Balun would match 50-ohm cable (or the output of a linear or transceiver) to 450-ohm twin lead, without considering the effect of its termination. In truth, the 9:1 Balun would *only* see 450 ohms if the line were terminated in 450 ohms. In reality, if the line were terminated in a 50-ohm dipole, the Balun would see 50 ohms when the line is a half-wave long and 4050 ohms when is a quarter-wave long. The 9:1 Balun is clearly useless in this application.

By far, most misconceptions regarding Baluns are due to the many radio amateurs who perceive these devices as conventional transformers that transmit the energy from input to output by flux linkages and not as transmission line transformers, which transmit energy by an efficient transmission line mode. This is clearly shown by the writers who have compared their "new" coaxial cable (coiled about a toroid or threaded through ferrite beads) Baluns with Baluns using wire transmission lines coiled about a ferrite rod or toroid. They claim their Baluns are better because the others: 1) were limited by leakage inductance, 2) did not exhibit true 1:1 impedance transformations, 3) were prone to core saturation, 4) added a reactive component to the input impedance, 5) were susceptible to unbalanced and mismatched loads, and more importantly, 6) had *more* loss.

If the writers had accepted the correct model for these devices (given to us by Guanella and Ruthroff), which shows that they are really chokes (lumped elements) and configurations of transmission lines (distributed elements), then there are several parameters they should have considered in their comparisons. They are: 1) the characteristic impedances and lengths of the transmission lines (the high-frequency capability), 2) what form of the 1:1 Balun or 4:1 Balun is used by the other Balun, 3) the low-frequency capabilities (safety margins), 4) power capabilities, and finally 5) efficiencies.

Now, had the writers used the proper parameters in their comparisons, they would have found that mismatch loss was mistaken for real (ohmic) loss; high-frequency response was limited by standing waves, and not leakage inductance or shunting capacitance; the beaded-coax Balun had *more* loss than a well-designed Balun using wire or coax transmission lines coiled about a toroid; and that their comparisons were made with either the trifilar (voltage) 1:1 Balun or the Ruthroff 4:1 Balun, which are inferior designs.

In fact, the perception that the transmission line transformer is actually a conventional transformer is so prevalent, that a new name for this class of devices should be considered—*broadband transmission line matching networks*. This name (without the word *transformer*) would help in dispelling inaccurate perceptions and in standardizing the schematic diagrams. It would place the coiled or beaded transmission lines (in the high-frequency models) horizontally, and eliminate the phasing or polarity dots.

Sec 17.4 The State of the Art

Until very recently, the radio amateur had only two types of Baluns available in the literature and on the market. They were the so-called 1:1 and 4:1 "voltage" Baluns. As was shown in **Chapter 7**, the comparisons by others with new 1:1 designs using coaxial cable (called "current" Baluns) were made with an inferior trifilar-wound Balun, instead of Ruthoff's design that appeared in his 1959 paper and became the industry's standard. Ruthroff's third conductor on his 1:1 Balun was on a separate part of the toroid, thus giving it practically the same characteristics as the Guanella ("current") Balun. These articles on newer designs not only gave a new language to our Baluns, but also presented questionable statements regarding their performances. It would be interesting if the authors of these articles compared their Baluns with well-designed Ruthroff or Guanella Baluns using 50-ohm bifilar windings or coaxial cables on low-loss ferrite toroids (less than 300 permeability). I am quite sure their claims would be greatly diminished.

As was noted in **Chapter 8**, the 4:1 voltage Balun appeared in the amateur radio journals about 25 years ago (the same time as the "inferior" 1:1 voltage Balun). Considerable design information appeared in the handbooks of the time regarding the construction and performance of this Balun. Furthermore, this information also stayed the same over these many

years. As was shown in **Chapter 8**, the design was found lacking. However, with some rather simple changes, like doubling the cross-sectional area of the core, increasing the number of turns from 10 to 14, and using extra insulation on the wires to increase the characteristic impedance of the coiled transmission line from about 50 to 100 ohms (the objective), a much better design emerged. In fact, for balanced antenna systems, this new design might well be described as "peerless."

A 4:1 Guanella (current) Balun has now appeared in our handbooks. This more flexible Balun uses two transmission lines wound on separate cores and connected in series at one end and in parallel on the other. Literally, no design information is given on its construction. What is offered are recommendations for the permeability of the ferrite cores. Values from 850 to 2500 are proposed. However, use of these high permeabilities would result in lossy Baluns.

I also found it interesting, in my work on these devices, that the classic papers of Guanella[3] and Ruthroff[9] are still the cornerstones of this technology known as *transmission line transformers*. To be sure, some of us have extended the work of these two by using better measuring equipment, creating more complicated configurations, and finding new applications. However, it is apparent from the articles published in the amateur radio journals and discussions on the air and at club meetings that most radio amateurs still perceive these devices as conventional transformers. They don't look at these devices as Guanella and Ruthroff did—as chokes and transmission lines. As a result, there has been a lack of good design information in our literature.

There are many new and useful designs possible with this technology, as discussed in **Part I** of this book. They include: higher power levels, applications on the VHF and UHF bands and above, and new Baluns and Ununs with ratios other than $1{:}n^2$ where $n = 1, 2, 3, \ldots$, etc. This book presents some designs* and suggestions for higher-power and higher-frequency applications.

I see two reasons for the lack of emergence in this technology. They are:

1) This subject is not adequately covered in any college textbook, and it generally has not been of interest to academics who rightfully view their role as basic research and not applications. As a result, there are few graduates with any skill in the design of transmission line transformers—in contrast to the areas of transmission line, waveguide, and antenna theory.

2) The professional societies don't receive enough application papers. Although much of the research and development work performed in industry is highly innovative, important to the advancement of the technology, and certainly publishable in scientific journals, corporations are often reluctant to allow publication for fear of "aiding" their competition. It has been stated[29] that in the past few decades, the submission of application papers to the technical journals of the IEEE has declined. In fact, a survey by one of the technical societies showed that 85 percent of the submissions now come from universities, not industry!

In order to assist technologies, like *transmission line transformers*, which are far from reaching their potential applications, IEEE has instituted a program called *Emerging Practices in Technology* (EPT). The object of the EPT program is to facilitate the development of new standards by disseminating and making available various EPT papers to the broadest possible audience worldwide. The papers on practices in various areas of technology are peer reviewed by relevant IEEE Technical Committees, and have the potential for standardization in the future. The papers (mine is **Reference 30**) are published by the IEEE Standards Press.

FOOTNOTE

*Kits and finished units available from Amidon Associates, Inc., 240 Briggs Ave., Costa Mesa, CA 92626.

References

1. Jerry Sevick, W2FMI, *Transmission Line Transformers*, 1st edition, Amateur Radio Relay League, 1987.

2. Jerry Sevick, W2FMI, *Transmission Line Transformers*, 4th edition, Noble Publishing Corporation, 2001.

3. G. Guanella, "Novel Matching Systems for High Frequencies," *Brown-Boveri Review*, Volume 31, September 1944, pages 327–329.

4. Walt Maxwell, W2DU, "Some Aspects of the Balun Problem," *QST*, March 1983, pages 38–40.

5. John Belrose, VE2CU, "Transforming the Balun," *QST*, June 1991, pages 30–33.

6. Roy Lewallen, W7EL, "Baluns: What They Do and How They Do It," *The ARRL Antenna Compendium*, Volume 1, Amateur Radio Relay League, 1985, pages 12–15.

7. Joe Reisert, W1JR, "Simple and Efficient Broadband Balun," *Ham Radio*, September 1978, pages 12–15.

8. Richard H. Turrin, W2IMU, "Broad-Band Balun Transformers," *QST*, August 1964, pages 33–35.

9. C. L. Ruthroff, "Some Broad-Band Transformers," *Proceedings of the IRE*, Volume 47, August 1959, pages 1337–1342.

10. Richard A. Genaille, W4UW, "How to Build a Multi-Tap Unun," *CQ* May 1992, pages 28–32.

11. Bruce Eggers, WA9NEW, "An Analysis of the Balun," *QST*, April 1980, pages 19–21.

12. Richard H. Turrin, W2IMU, "Application of Broad-Band Balun Transformers," *QST*, April 1969, pages 42, 43.

13. George Badger, W6TC, "A New Class of Coaxial-Line Transformers, Part 1," *Ham Radio*, February 1980, pages 12–18.

14. George Badger, W6TC, "A New Class Of Coaxial-Line Transformers, Part 2," *Ham Radio*, March 1980, pages 18–29, 70.

15. Bill Orr, W6SAI, "Radio Fundamentals: The Coax Balun," *CQ*, November 1993, pages 60–65.

16. Albert Roehm, W2OBJ, "Some Additional Aspects of the Balun Problem," *The ARRL Antenna Compendium*, Volume 2, Amateur Radio Relay League, pages 172–174.

17. Lew McCoy, W1ICP, "Let's Talk About Wire," Part 1, *CQ*, January 1993, pages 42–45.

18. Lew McCoy, W1ICP, "Let's Talk About Wire," Part 2, *CQ*, February 1993, pages 32–42.

19. Gerald Hall, K1TD, Editor, *The ARRL Antenna Book*, 16th edition, Amateur Radio Relay League, 1991, Chapter 25.

20. George Grammer, W1DF, "Simplified Design of Impedance-Matching Networks," in three parts, *QST*, March, April, and May 1957.

21. D.K. Belcher, "RF Matching Techniques, Design and Example," *QST*, October 1972, page 24.

22. Lew McCoy, W1ICP, "The Ultimate Transmatch," *QST*, July 1970, pages 24–27, 58.

23. Warren Bruene, W5OLY, "Introducing the Series-Parallel Network," *QST*, June 1986, page 21.

24. Louis Varney, G5RV, "The G5RV Muliband Antenna...Up-to-Date," *The Antenna Compendium*, Volume 1, Amateur Radio Relay League, pages 86–90.

25. Jerry Sevick, W2FMI, "6:1 and 9:1 Baluns," *Communications Quarterly*, Winter 1993, pages 43–51.

26. D. Meyer, "Equal-Delay Networks Match Impedances Over Wide Bandwidths," *MICROWAVES & RF*, April 1990, pages 179–188.

27. S.E. London and S.V. Tomeshevich, "Line Transformers with Fractional Transformation Factor," *Telecommunications and Radio Engineering*, Volume 28/29, April 1974.

28. Carl Markle, K8IHQ, "Wideband RF Baluns," *73 Amateur Radio Today*, September, 1992, pages 20–23.

29. S. Maas, D. Hornbuckle, D. Masse, "Applications Papers for the *MTT Transactions*," Summer 1992, IEEE MTT-S Newsletter, pages 3, 5.

30. Jerry Sevick, W2FMI, "Design and Realization of Broadband Transmission Line Matching Transformer," *Emerging Practices in Technology*, IEEE Standards Press, 1993.

Index

Amidon Associates, Inc...18, 30–32
  kits...30–31, 88
Antenna modes
  dipole mode...28
  inverted L mode...28, 31
Antenna tuners, Baluns for...55–63
Autotransformers...6, 9, 19, 21, 30–31, 52, 76, 97, 101

Badger, George...33–36, 89, 114
  two-tone test method...33
Baluns
  air-core...33, 41, 43, 46
  and dipoles...27–29, 35, 40, 45–46, 52–55, 57, 61–62, 65, 71, 100–111, 113
  and inverted Vs...27–28, 111
  and log-periodics...49, 54, 57,
  and multiband dipoles...61
  and quads...28, 65, 87
  and rhombics...80
  and Yagis...27–28, 33, 65, 73–74, 86
  attributes of a good design...41
  Balun/Unun...43, 87
  beaded-coax...36, 41, 54, 56, 86–87, 113
  bifilar toroidal...37–39, 40
  broadband...27, 29, 65, 71, 74, 78, 83, 85, 115
  coil...46
  Collins...34
  commercial...33, 36, 47, 52–54
  choke...4, 19, 27, 29–30, 34, 36–37, 40–41, 43, 56
  current...4, 27, 29–30, 35–36, 38–41, 43, 46–47, 50, 52–55–57, 61, 62, 65, 113–114
    bifilar current type...36
  dual-core...50–54, 65
  dual-ratio...65, 68–69
  economy...38–39
  ferrite core...30–31, 33–34, 39, 41, 46, 49, 78–79, 110
  for antenna tuners...55–63
  for 2-meter operation...65
  fractional-ratio...74
  "hardened"...62
  HF designs...65
  high-impedance...15, 79–80
  high-power...27, 37–40, 49–53, 57–58, 65, 81–82
  HI-Q...52–53
  low-power...27, 37, 39, 43, 50–54, 65
  medium-power...27, 37, 39, 81
  misconceptions about...113
  parallel-type...65, 66, 68–71, 74–75, 79, 82
  RF...29, 115
  rod-type...4, 31–34, 40, 47, 52–54, 63
  series-type...16, 65–69, 72–75, 79–82
  single-core...45, 50–51, 54, 73–74
  step-down...28, 51–52, 65, 73–74, 86
  step-up...65, 74
  three-conductor...30–31, 34–35, 43
  toroidal...32, 36–39, 41
  transformer-type...34–35
  trifilar-wound...30, 32, 113
  two-conductor...30–31, 33–37, 53
  VHF designs...65
  voltage...33, 35–36, 43, 47, 52, 54–55, 62, 113
  when to use...27–29
  "worst case" design...61–63
  1:1...2, 4, 15–16, 27–41, 43, 45, 54–56, 61–66, 68, 71, 89, 111–113
    articles on...29
    bifilar toroidal...37–39, 41
    in amateur radio literature...30–37
    trifilar-wound...30, 32, 113
    using ferrite cores...30, 112
  1:4...5–7, 11–12, 16, 21–22, 55–56, 67, 70, 72–74
  1.5:1...65–70, 89
  1.56:1...65–66
  1:6...72
  1:6.25...16, 72–73, 79–80
  1:9...15–16, 70–71, 76, 78–82
  2:1...28, 62, 65–71, 89
  4:1...5, 7, 27, 30, 35–37, 41, 43–62
    history...43–44
    beaded coax...54
    current...53
  6:1...71–82, 89
  6.25:1...71–75, 79
    high-impedance...74, 79
    low-impedance...74, 79

9:1...27, 36–37, 71–82, 89
high-impedance...79
low-impedance...79
practical designs...77–78
12:1...71–82, 89
16:1...27, 107
50:450-ohm...71, 82
Balun/Unun...43, 87
Beach umbrella antenna...Preface
Belrose, John...36–37, 115
Beverage antennas...107–110
Bootstrap...5, 7, 10–11, 13, 17, 21–22, 30, 68, 74, 83, 93, 107
Broadband matching transformers...29
Broadband transmission line matching networks...113

Characterization...17–20
Cores
air...33, 41, 43, 46
ferrite...30–31, 39, 46, 49, 78–79, 110, 112, 114
geometry of...17
low permeability...41
magnetic...17, 30, 36, 46, 77
materials...18
powdered-iron...30, 32, 40, 53, 57–62, 80
rod...3–4, 17–18, 51–52, 97
toroidal...3, 11, 17, 35, 43, 46, 102, 107
Crossover...32–33, 37–39, 50–51, 66–68,

Delay line...4–5, 20, 22, 45, 77, 86
Dipole antennas...27–29, 35, 40, 45–46, 52–55, 57, 61–62, 65, 71, 100, 111, 113

Eggers, Bruce...28, 114

Ferrite
Balun...33
beads...4, 7, 29, 34, 36, 43, 55–56, 69–70, 75, 78–80, 82, 113
high-permeability...34–35, 54, 80
core...30–31, 39, 46, 49, 78–79, 110, 112, 114
efficiencies...39
low-loss...32–33, 113
low permeability...30, 37, 48, 54, 63, 75, 86, 112
manganese-zinc...4, 30, 113
nickel-zinc...18, 113
rod...11, 20, 52, 84, 86
toroids...13, 17, 31–32, 35–39, 47, 49–51, 53–54, 56, 66–68, 72, 74, 77, 81, 84–85, 90, 92–93, 101–104, 106, 109, 113
Flux canceling...21, 29, 83
Floating load...44–46, 58, 72–74, 77, 80
Fractional-ratio Ununs...86, 89–90

Genaille, Richard...28, 97, 115
Guanella, G.
basic building block...3–5, 10–11, 16, 21–22, 29–30
classic paper of 1944...3–5, 23, 27, 43, 57, 83, 114–115
current/choke Balun...4, 27, 30, 36, 38–40, 43, 50, 54, 56
dual-core Balun...52–53
equal-delay approach...11, 13, 22, 86
single-core Balun...44–45, 49–52
two conductor...30–31, 33–34, 37, 40, 43
1:1 Balun...4, 29–31, 33–34, 38–40, 43, 65–66, 68
1:4 Balun...5–7, 11, 16, 21, 56, 67, 72, 79, 82
1:4 TLT...5–7, 22
1:4 Unun...5, 7, 20–22
1:9 Balun...15–16, 70, 76, 80–82
4:1 Balun...5, 7, 27, 43–45, 49–54, 56–57,68, 72–74, 76, 79, 114
4:1 Unun...7, 45, 83, 85–86
9:1 Balun...27, 71–72, 75–82, 107
16:1 Balun...27, 86, 107
G5RV antenna...55, 61–62, 115

Hairpin matching networks...28, 65
HI-Q Balun... 52–53

Imbalance current...28, 30–31, 35, 41
Inverted V antennas...27–28, 111
Isolation transformers...4, 27, 40, 66

L-C matching network...55
L...56
pi...56
T...56
Ultimate...56
SPC....56
Lewallen, Roy...35–36, 115
1:1 Balun...35
4:1 Balun...35
current Balun...35
voltage Balun...35
Link coupling...55
Loads
balanced...46, 51–52, 65–70, 72–75, 79, 81–82, 86
center-tapped-to-ground...47, 60, 62, 73–74
floating...44–46, 56–58, 60, 62, 72–74, 77, 80
grounded at bottom...4, 45, 54, 73–74, 77
grounded at center...3–4, 30–31, 37, 45–46, 54–55–57, 60, 73–74, 77
mismatched...30, 32–35, 41, 113

reactive...36, 62
unbalanced...27, 30, 33–35, 41, 58, 85, 90–91, 107
Log-periodic antennas...49, 54, 57

Magnetizing inductance...17–18
Materials, core...18
Maxwell, Walt...34–37, 115
choke Balun...34
transformer-type Balun...34–35
1983 article...34
McCoy, Lew...52–53, 55, 57–60, 62, 101, 115
Multiband antennas...55, 61–62
dipoles...61
Multimatch transformers...89, 102

Orr, Bill...33, 115

Phase-delay...30, 37, 39, 73, 85, 87, 94, 108
Phase-inverter...4–6, 21, 30, 40, 43, 46, 54–55, 57
Pi network...56
Polarity dots...113
Power ratings...35, 54, 94, 111–112
loads and efficiencies...112–113

Quad antennas...28, 65, 87

Reisert, Joe...32–35, 37–38, 41, 54, 115
crossover...32–33, 37–39
Rhombic antennas...80
Roehm, Albert...36, 56, 115
Ruthroff, C.L.
bifilar Unun...89
bootstrap...5, 7, 10–11, 13, 15, 17, 21–22, 30, 68, 74, 83, 93, 107
broadband transmission line transformers...22, 29
classic paper of 1959...23, 27, 30, 34–35, 43, 46, 83, 113–115
high-frequency model...5, 45
hybrid transformer...43
maxima technique...46
phase-inverter configuration...21, 55, 57
three-conductor Balun...30–31, 34, 43
trifilar-wound Balun...15, 30, 32, 113
voltage Balun...43, 52, 54–55, 62, 113
1959 article...1, 4, 9, 10, 17, 29, 42, 57, 61, 87, 88
1:1 Balun...3–4, 29–30, 34, 36, 43, 113
1:4 Balun...5–7, 22, 56, 81
1:4 TLTs...6
1:4 Unun...5–6, 9, 11, 16, 21
4:1 Balun...30, 43, 45–50, 53, 55–59, 61–62, 113
rod-type...52–53
4:1 bifilar Unun...89, 97
4:1 Unun...30, 45–46, 68, 83–84, 87, 97
100:25-ohm Unun... 84–85
200:50-ohm Unun...84–85

Series and parallel-tuned circuits...55
Single-core Balun...45, 50–51, 54, 73–74
Step-down transformers...90
Step-up transformers...90, 97–99

Terman, Frederick E...22–23
Toroids...17, 20–21, 30, 51, 69, 73, 79, 81–82
cores...3, 11, 35, 46, 107
current-probe...35
ferrite...13, 17, 31–32, 35–39, 47, 49–51, 53–54, 56, 66–68, 72, 74, 77, 81, 84–85, 90, 92–93, 101–104, 106, 109, 113
powdered-iron...17, 31
4C4...9, 18
Transformation ratios...37, 41, 43–44, 51–52, 57, 65–66, 68, 74, 85–86, 89–90, 92–93, 101–105
Transformers
air-core...33
Balun...56, 115
bifilar, tapped...9
broadband...30, 43, 100
multimatch...89, 102
conventional...21, 57, 76, 79, 83, 107, 111, 113–114
equal-delay...12
flux linkages...21, 83, 107, 113
hybrid...43
isolation...4, 27, 40, 66
matching...29, 61–62, 108, 111
multimatch...63, 76
parallel...100
step-down...90
step-up... 90, 97–99
toroidal...17, 91
transmission line...3, 5, 21, 23, 27, 29, 43–44, 79, 82–83, 101–102, 107, 111–115
unbalanced-to-unbalanced...43, 45, 65, 83, 107
wideband..33
Transmatch...55–56, 58, 60, 101, 115
Transmission lines
balanced...56
beaded...17, 34, 37, 54, 57, 69–70, 75–76, 83, 86, 70, 107, 111, 113
coax...29, 34, 83, 113
coiled...5, 17, 29, 31, 33–34, 36, 41, 43–44, 46, 51–52, 57, 76, 83, 86, 107, 111, 114

coupled...30, 32, 35, 43
currents...27, 29, 36, 39, 41, 44, 46, 49, 76, 83, 111
flat line...44, 46, 47, 57, 69, 74
half-wave...29, 61
high-impedance...75, 82
ladder line...71
matched...29, 62
McCoy...53
open-wire...5, 56
quarter-wave...29
theory...61, 76
twin-lead...29, 34, 38, 56, 75
very short...29, 44, 84, 90, 97–98, 104, 108
Transmission line transformers (TLTs)
book by W2FMI...12, 44, 81, 115
broadband...10, 13, 22, 29–30, 43, 100, 102, 113, 115
catastrophic failures...111
coiled wire...12
equal-delay...12
isolation transformers...4, 27, 40, 66
low-ratio...9, 13
power ratings...111–113
trifilar-wound...15
technology of...27, 113–114
with 1:1 ratios...3–4
with 1:4 ratios...5–7
with ratios greater than 1:4...15–16
with ratios less than 1:4...9–13
1:1...5
1:4...5–7, 21–22
1:9...21
1:16...21
Turrin, Richard
articles...27, 30–32, 36, 115
Baluns...27, 31–34, 36

Ultimate multimatch...104–105
Ununs
air-core...33
bifilar...89, 101, 112
broadband ratios...89, 92, 97, 99, 101
broadband...45, 52, 73–74, 79, 89
coiled...91
dual-ratio...97–100
1.5:1 and 3:1 ratios...98–99
2:1 and 4:1 ratios...98
for Beverage antennas...107–110
low-power design...108–109
high-power designs...109–110
for 2-meter operation...86
fractional ratio...86, 89–90
high-impedance...85–86, 107, 110
high-power...83, 109–110
input-matching...107
low-power...83, 95
multimatch...101–107
parallel transformer...100
parallel-type...74–75
quadrifilar...67, 90–91, 94, 98–99, 102, 104, 106, 108–109, 112
tapped...102
quintufilar...12, 16, 65–66 72–73, 81, 90–94, 96–99, 112
step-down...67, 73, 86
step-up...69, 72, 79, 90
trifilar...10, 66, 68, 89-90, 94, 97, 102
tapped...91, 101–102, 112
1:1.33...16, 80–82
1:1.5...22
1:2...22, 62, 66
1:3...81
1.33:1...71, 89, 93–94
1:4...5–7, 9, 11, 16, 20–22
1.5:1...89–93
1.56:1...65–66, 72, 74, 79, 91–92
quintufilar...66, 91-93, 97–98, 102
2:1...28, 89–95
4:1...7, 30, 45-46, 68, 83–87, 97, 112
5-ratio...102–103
high-power version...103
low-power version...103–104
9:1...78–79
10-ratio...102, 104–105
high-power version...105–106
low-power version...106
quadrifilar...102
50:12.5-ohm...84–85
100:25-ohm...85
200:50-ohm...85

V antennas...80
Varney, Louis...62, 115
Vertical antennas...89
shunt-fed towers performing as...89

Wideband transformers...33
Wire antennas...55

Yagi antennas...27–28, 33, 65, 73–74, 86

$4.95

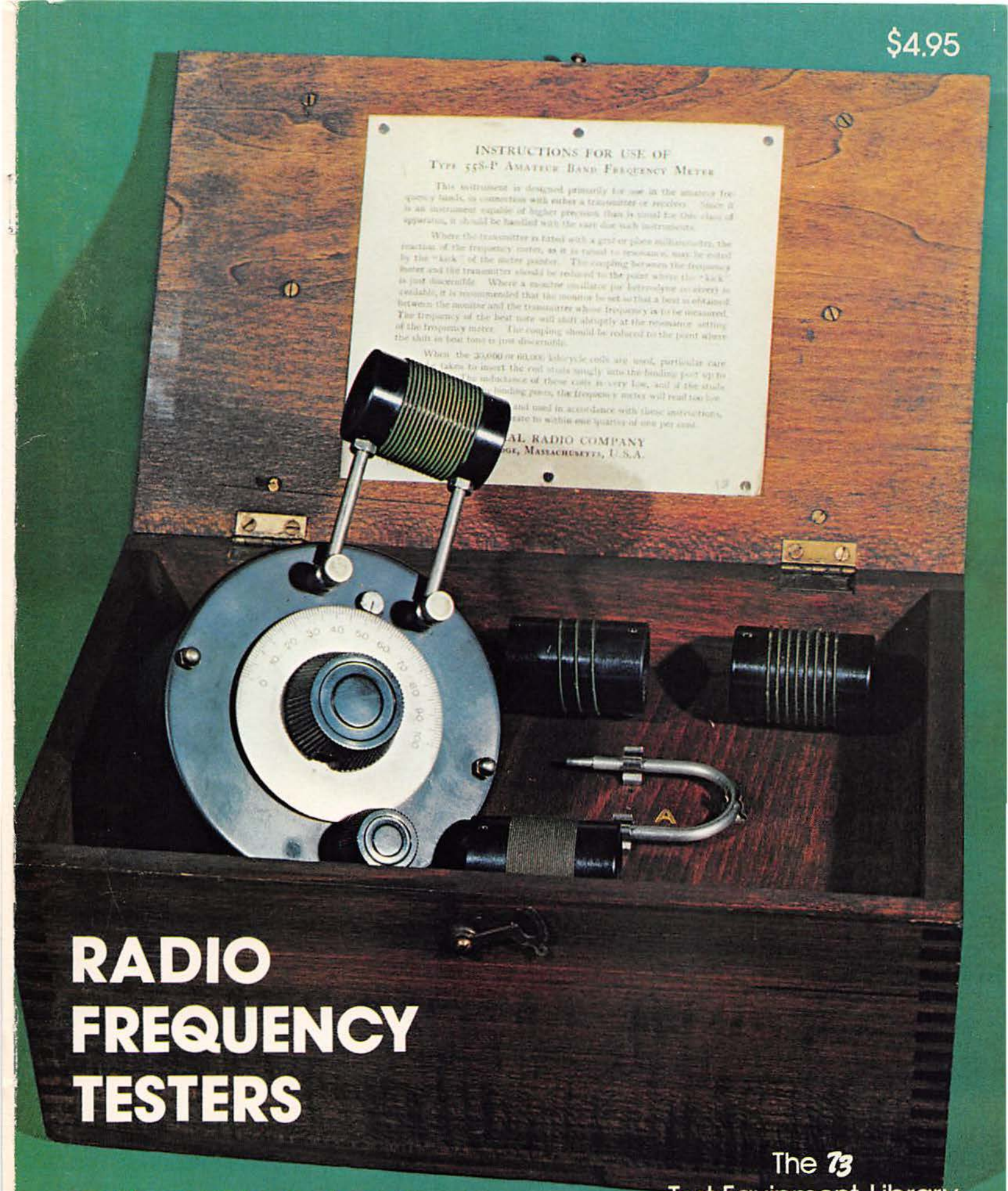

RADIO FREQUENCY TESTERS

77 Pieces of Test Equipment You Can Build!

The 73 Test Equipment Library volume III

Table of Contents

The 73 Test Equipment Library

Volume III: Radio Frequency Testers

Chapter I: What is Your SWR, OM?		
SWR Power Meter for 80 Thru 10m Bands	W6VAT	5
An Etched Circuit SWR Bridge	WA5SWD	6
Checking Your SWR Indicator	W5EHC	8
Home Brew Bridge Calibration	W4OAB	8
Mini SWR Bridge	W2EEY	8
VSWR Supreme	W4BRS	9
A Simple VHF SWR Meter	W2EEY/K3EZ	10
Directional Coupler and VSWR Bridge for VHF and UHF	WA6SXC	13
A Slotted Line for 1250 MHz	WA8CHD	14
Some Directional Wattmeters and a Novel VSWR Meter	G3PDM	16
SWR Bridges Using Zero-Center Meters	W2EEY/K3EZ	18
Chapter II: How to Measure RF Impedance		
The Antennascope – An Effective Tool	VE3CEA	21
How to Build an Antennascope	WA1CCH	22
The Mark III RF Impedance Bridge	W6CRT	22
Measure RF Impedance with Your SWR Bridge	W2AOO	26
Use Your GDO and Z Meter	WØBMW	27
Chapter III: Measuring RF Power Output		
Measuring RF Output	WA6CPP	30
Light Bulbs as RF Indicators	WB2GQY	30
Build Yourself a Light Wattmeter	Henry	32
Low Power Light Wattmeter	K1CLL	33
Yet Another Light Wattmeter	K5CXN	34
A Low Cost RF Wattmeter	WA3AJR	35
RF Power Measurement Using Hot Carrier Diodes	W6AJF	36
VHF Dummy Load Wattmeter	K9STH	38
Chapter IV: Measure Your Field Strength and Frequency		
The RF Sniffer	K5JKX	39
A Useful Accessory for the Ham Shack	W2WHX	40
Two Thru Twenty FSM	W7OE	40
An Amplified, Calibrated Signal Strength Meter	VE3CES	41
Frequency Measuring Equipment at Microwave Frequencies	WA9VFG	42
Frequency Meter-1 to 10 GHz Amateur Microwave	K1CLL	43
Lambda Lines	W2DXH	46
Chapter V: RF Signal Generators		
Zero-Beating with a Frequency Meter	WB4TBX	48
Hand Calibrate the BC-221 Frequency Meter	Henry	48
High Accuracy VHF Frequency Measurements	W5WGF	49
Transistorized LM Meter	W5SOT	50
An I-F Spotter	W5WGF	52
430-470 kHz Sweep Frequency Generator	WA5SWD	53

An Armstrong Sweeper	W2EMF	54
A New Broom	K6JHJ	54
Low Cost Signal Source	VE3GFW	55
Receiver Tweaker	K6UAW	56
Citizen Band Alignment Aid	WA5SWD	56
FET Chirper	K6QKL	57
UHF Signal Source	K1CLL	58
Crystal Controlled Signal Source with Infinite Attenuator for 144, 432 and 1296 MHz	K1CLL	59
Low Cost 220 MHz Signal Generator	K1CLL	60
UHF Signal Generator	K6MIO	62
Lab Type IF/RF Sweep Generator Using ICs	K4DHC	63
100 kHz Thin-Line Pulse Generator	W2DXH	70
Chapter VI: Crystal Calibrators		
All Band Band-Edge Marker	WA2HRZ	74
The Multical	K9VXL	74
100 kHz Marker Generator	W7CJB	75
All Band Frequency Marker	W1KNI	75
Poor Man's Universal Frequency Generator	W2EEY	76
Calibrate that Calibrator	W2KPE	78
A Simple Frequency Deviation Meter	K6BJ	78
Chapter VII: GDOs		
The Indicating Oscillator	KH6AF	80
The Little Gate Dipper	W5ETT	81
The Great Dipper	WAØAYP	83
The Great Dipper-Modification	WAØAYP	85
Etched Circuit UHF Dipmeter	W1JJL	86
UHF Grid Dipper	WA6BSO	87
Wide Range VHF-UHF Dipper	K1CLL	91
Extra Services from Your Grid Dip Oscillator	WA4UZM	94
GDO to Find C	G3OGR	94
GDO Coil Extension	WAØABI	94
Chapter VIII: Noise Generators		
Simple Noise Generator	K9ONT	96
A Crystal Diode Noise Generator	W5TEV	96
Temperature Limited Diode Noise Generator	Thomas	97
Calibrated Noise Generator for 432	W6GXN	98
Another Way to Measure Noise Figure	K5JKX	99
Chapter IX: Attenuators and Dummy Loads		
Low Power Attenuators for the Amateur Bands	WB6AIG/WA6RDZ	102
S-Unit Attenuator	WA5SWD	103
The Ever-Useful T-Pad	K5JKX	103
Combination Dummy Load/Attenuator Network	W2EEY	104
The Minican	W6JTT	106
The Tiny Terminator	K5JKX	106

Chapter I

What is Your SWR, OM?

SWR POWER METER FOR 80 THRU 10m BANDS

James Lee W6VAT

With the declining sunspots, usage of the lower frequency bands is definitely increasing. The resulting increased QRM is helpful to no one and only efficient equipment and operating procedures will result in a maximum number of QSO's. The SWR/PWR meter described here won't make you a better operator, but it can help you be sure that you are delivering the most rf to your antenna from your rig. Fig. 1 shows a front view of the meter.

The basic circuit is a directional coupler switched to sample either forward or reverse voltage and a voltmeter to read this voltage.

This type of coupler has an output proportional to length, power, and frequency. The longer it is, the more output it gives. Since it puts a small impedance "bump" in the line, the length of the coupler should be limited to not over 1/20 wavelength at the highest frequency, or it may begin to contribute noticeably to the SWR itself. For a given power, if the frequency of the rf flowing through the coupler is reduced, the maximum coupler output is reduced. This means that you can get full scale readings on 10 M with a lot less power than on 80 M. The meter described here gives half scale deflection on 40 M, at maximum sensitivity, with about 350 watts of forward power. If your rig is a KW this meter will fill the requirements for SWR/PWR measurements nicely. It can be left in the line at all times to monitor SWR or Power delivered to the antenna or other load. If desired, a Barker and Williamson type 551A coaxial switch can be used to insert the meter in the line for test purposes and then switch it out during operating periods.

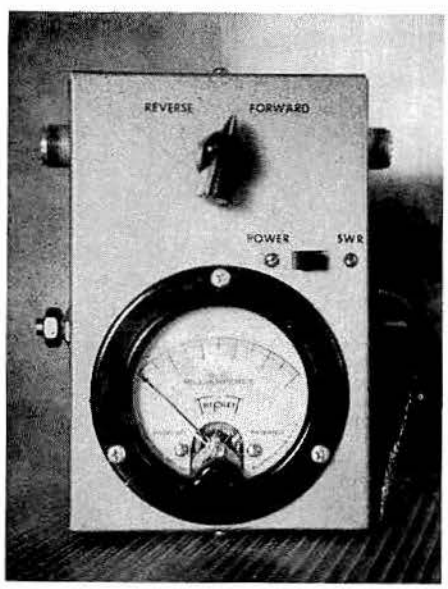

Construction

The unit is built in a gray hammertone LMB type 141 box. The dimensions of this box are 3" x 4" x 6". Fig. 2 shows the parts placement and should answer any questions concerning layout.

The coax directional coupler is made from a 14" length of RG-8/U. The outer covering is slit lengthwise with a knife and peeled off. Take care here not to cut into the woven braid. The woven braid is then bunched toward the center to loosen it. Next, a length of #22 enameled wire is passed through the braid at about 2¼" from one end and run under the braid next to the inner insulation. It is brought out at the other end, again 2¼" from the end of the shield braid. When this is done, smooth the braid back to its original position carefully to avoid scratching the enamel on the #22 wire. The #22 enameled wire should lay as straight as possible under the braid. It should have no slack nor should it twist around the inner insulation to any great degree. The ends of the shield braid are trimmed back far enough to be soldered to Amphenol 83-1H hoods. The inner insulation is trimmed off so as to expose about 3/16" of the inner conductor. The inner conductors are then soldered to Amphenol 83-1R female type chassis mount coax connectors. The coupler may now be set aside and the rest of the meter constructed.

Potentiometer R_1 is mounted on 1/16" x 1" x 4" piece of bakelite and positioned approximately in the center of the box to minimize capacity to ground. The metal rear cover is removed from the pot for the same reason. The pot ground lead is to the center of the coax and is wire in last. The diode D_1 should be protected from damage by heat when soldering it in the circuit. Long nose pliers gripping the leads near the body of the diode are satisfactory. The directional coupler is the last item soldered in place. As can be seen in the photos—the coax connectors are mounted from the inside of the box. When the #22 enameled leads are soldered to S_1 they should be the same length, and again, take care not to scratch the enamel or a short circuit may occur and you'll have to do it all over again.

Calibration

There are any number of ways to calibrate the SWR/PWR meter, but the way most hams will use is their own rig and a suitable dummy load. Though very limited in power, a 2 watt 50 ohm resistor such as made by Ohmite, IRC and others, mounted inside an Amphenol 83-1SP male coax plug makes a very good dummy load. Although not completely non-inductive, this dummy load is far superior to such real unknowns as light bulbs, electric iron heating elements, etc. This particular load is 50 ohms shunted by 6 mmfd over the range of 3-30 mc. It is a good dummy load—though a low power one.

With the back cover off, attach the dummy load to J_2, the load jack. Set R_1, the Sensitivity Control, to maximum and S_1 to FORWARD. Next apply power by hooking your rig (or

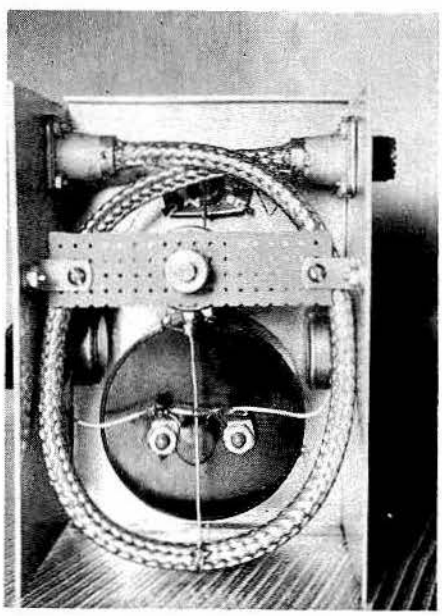

other rf source) to J_1, the transmitter jack. Make sure that the rf applied is 28-30 mc, or, the highest frequency you operate in the 3-30 mc region. This meter is sensitive to frequency. Stray capacities and other unbalances will have their greatest effect at the highest frequencies. In any event, calibrate the unit on the highest frequency your rig will tune in the 3-30 mc region. With power applied, set R_2 so the meter reading is at least half scale and switch S_1 to REVERSE. This will result in a lower meter reading. R_1 should then be adjusted for a minimum reading on the meter. Using the suggested load, you will not get a complete null, but the null should not be much more than 50 ua for half scale deflection in the FORWARD position on S_1. Don't put too much power into the dummy load since excessive dissipation can ruin it and change its characteristics greatly. If you have a higher power dummy load whose characteristics you know accurately, by all means use it, but remember a light bulb is not a good load. Once nulled, lock the nut on R_1 taking care not to disturb the setting. Replace the back cover and using the dummy load, recheck the null to make certain that it has not shifted.

Using The Meter

To make SWR measurements you need only insert it in the line and set S_1 to FORWARD and S_2 to SWR. Adjust the sensitivity control for at least a half scale reading. Then switch S_1 to REVERSE and read the value. SWR is then calculated by the following:

$$SWR = \frac{I_{fwd} + I_{rev}}{I_{fwd} - I_{rev}}$$

For example:

let $I_{fwd} = 500$ ua and $I_{rev} = 50$ ua, then

$$SWR = \frac{500 + 50}{500 - 50} = \frac{550}{450} = 1.22:1$$

The meter is useful for tune-up purposes where exact SWR is not needed. Just keep the FORWARD reading at a constant value and tune for minimum REVERSE readings. The exact SWR can be calculated when you have found the lowest REVERSE position.

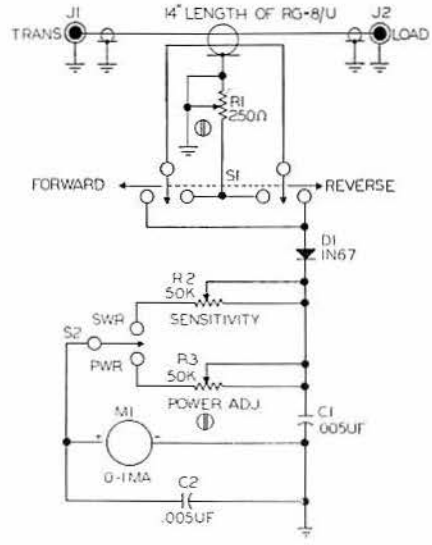

The POWER position may appear to be essentially the same as the SWR position and it is. When measuring power into a load of known fixed value you only need to know the voltage across (or the current through) the load. The POWER position on S_2 is used with S_1 set to FORWARD. R_3 is merely set to a scale reading that is convenient for all bands if only a relative reading is used. If a good 50 ohm high power dummy load is available, you may make accurate calibrations by using a VTVM plus high frequency detector probe and measuring the actual voltage across the load. Just put a T-connector on the load jack J_1. Put the dummy load on one arm of the "T" and read the voltage at the other arm. 200 volts across a pure resistive load of 50 ohms is equal to 800 watts of power. If your rig delivers a key down 800 watts to a load then you could set R_3 at 0.8 ma on the scale, etc. The scale will not be precisely linear, particularly at low powers, but if enough resistance is used at R_3 the effects should be minimum. Since the coupler voltage is frequency sensitive one setting of R_3 will not hold for all bands. If desired, R_3 could be replaced with a switch and a number of selected resistors (one for each band). This would keep the scale factor constant between bands. This could be done for R_2 as well, but complicates an otherwise simple device

Operation

Once calibrated, the meter is very simple to use. Just hook it in the line at some convenient point and apply power. With S_1 set to FORWARD and S_2 set to SWR, adjust R_2 for at least a half scale reading. Switch S_1 to REVERSE and you will then be able to continuously monitor your reverse power. For power measurements, set S_1 to FORWARD and S_2 to PWR. Apply power and the meter will be monitoring your forward power continuously. R_3 is a screw driver adjusted pot. It can be set, and locked at a point which allows operation on all the bands you operate. The scale reading on each band will be different, but once set, these readings can be jotted down in your log book and any change quickly noted. This meter is also an excellent device for the antenna "tinkerer," or if you have coax coupling between stages in your rig it can be used to provide proper power transfer. Best of all, it is not expensive nor difficult to construct. Try one and you won't be without one again.

AN ETCHED CIRCUIT SWR BRIDGE

Ed Lawrence WA5SWD

Several of these boards have been etched and units assembled, and all have been satisfactory. I have used mine, with a 200 microamp meter, from a kw on the low bands up to a "Twoer," with no problems with sensitivity.

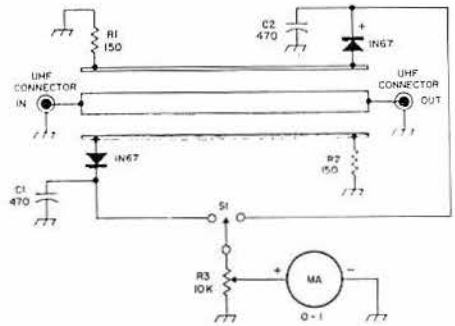

Schematic diagram of SWR bridge.

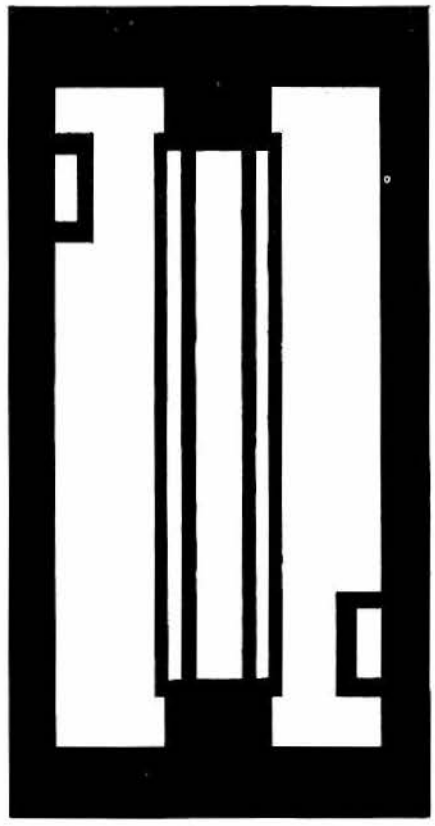

Since Bud Miniboxes are commonly available, I scaled this board to fit into the Bud

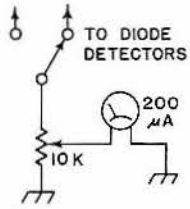

Fig. 1. Metering circuit for the etched circuit SWR bridge.

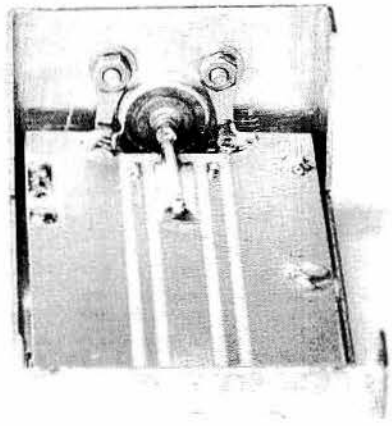

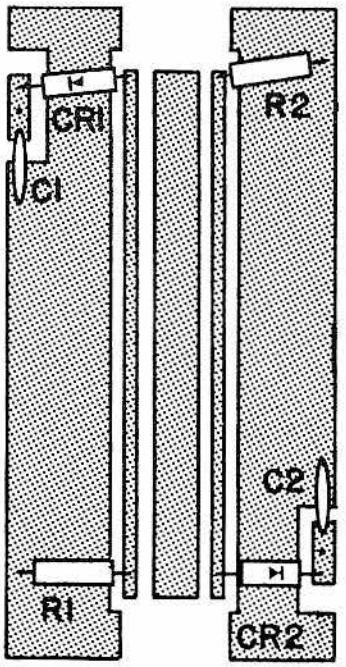

Fig. 2. Layout for the printed circuit board.

Minibox CU 2102A or CU 3002A. If you want to include the metering in the same package, the CU 2103A or CU 3003A should be used to give more room.

If you use the CU 2102A, center the coax connectors on the ends. If the CU 2103A, mount the connectors .8 inches from the open end. I used solder lugs bent at right angles to mount the P. C. Board to the chassis. The photograph shows the mounting much better than 10,000 words.

The meter sensitivity control circuit shown has a wider control range than the one shown in the *ARRL Handbook*, since the pot shunts the meter at low settings. This action could be accentuated by putting a fixed resistance in series with the meter movement, at the expense of sensitivity.

Although the virtues of operating transmission lines with low standing wave ratios (SWR) have been discussed many times in the past, evidently the economics of maintaining low SWR's are not readily apparent, particularly if the frequency of operation is low and the transmission line short. This has been reflected in various pseudo-technical QSO's where many have been led to the utter disregard for standing wave ratios. Most members of the amateur fraternity exist on limited budgets at best and when a significant portion of that precious transmitted power is eaten up by transmission line losses and misinterpreted standing wave ratios for naught, something should be done.

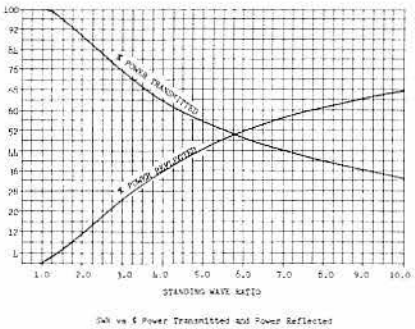

SWR vs % Power Transmitted and Power Reflected

Figure 1

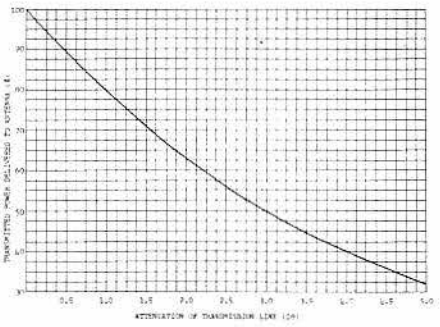

Figure 1
Attenuation vs Power transmitted.

A look at the graph in Fig. 1 will show you the percentage of power reflected for various standing wave ratios. For instance, if you are presently tolerating an SWR of about 5.8:1 (not uncommon in many ham shacks), 50% of the power which reaches the antenna is actually reflected back down the transmission line, heating up the final tank and causing TVI. Nor is only the transmitted signal effected, a high SWR will similarly degrade the received signal. This is particularly important in the reception of the extremely low level signals often encountered in DX and VHF operating. Stereophonic buffs should take heed too. A recent report by the IEEE (Institute of Electronic and Electrical Engineers) Professional Group on Broadcasting noted that a high SWR on receiver antenna inputs causes a reduction of stereo quality.

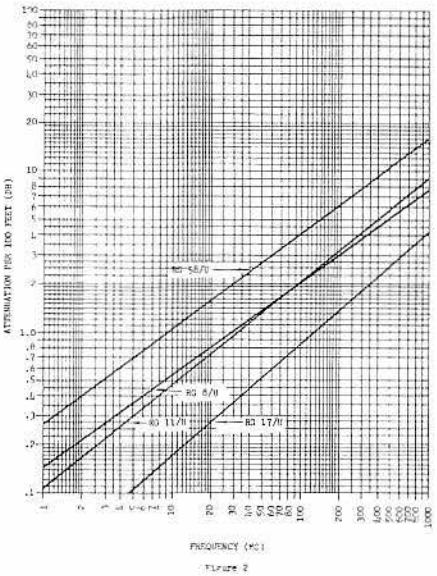

Figure 2
Attenuation vs frequency.

Many of the amateur stations on the air today make use of RG8A/U coaxial cable. Its excellence is proven out by its extensive use by the military, but a look at the loss graph (Fig. 2) for this cable indicates that it is not completely lossless! Even at 4 mc it has approximately 0.3 db loss per 100 feet, and on six meters there is a loss of 1.4 db for the same length. A look at Fig. 3 indicates that on 75 meters only 94% of the transmitted power is delivered to the antenna if 100 feet of RG8A/U is in use. At 50 mc the loss has sky rocketed to 26% for the same length of line. However, there is one big hooker for these conditions to exist: the SWR must be 1:1. For any other value of SWR there will be further line losses as shown in Fig. 4 because standing waves have the property of multiplying attenuation. This graph indicates that if a transmission line is operating at an SWR of 3.7:1, the line loss will be multiplied by a factor of two. For the previously mentioned situation on 50 mc, an additional 24% loss could be expected with an RG8A/U line operating at an SWR of 3.7:1.

It should be obvious by now that the use of an SWR bridge in the line at all times is very advantageous in the maintenance of a low SWR at the operating frequency. However, contrary to popular belief, the SWR bridge does not tell all. Since there is loss or attenuation in any length of transmission

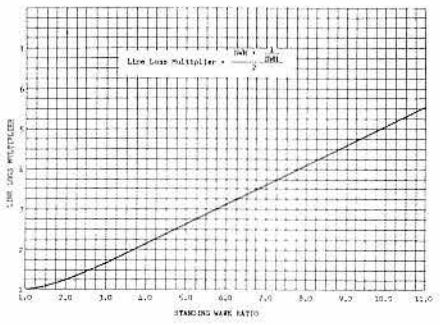

Figure 4
Line loss multiplier vs SWR.

line, the reflected wave will be attenuated in the same matter as the transmitted or incident signal. Because the standing wave ratio is the ratio of the incident wave to the reflected wave, attenuation of the reflected wave will give erroneous SWR measurements when the SWR bridge is conveniently located at the transmitter. In this location the bridge will see the full power of the transmitter, but only a portion of the reflected signal. In some cases where the length of the transmission line is excessively long, the reflected wave will be attenuated to such a degree that the SWR will appear to be very close to 1:1, while in reality it will be a good deal higher. This fact is graphically represented in Fig. 5.

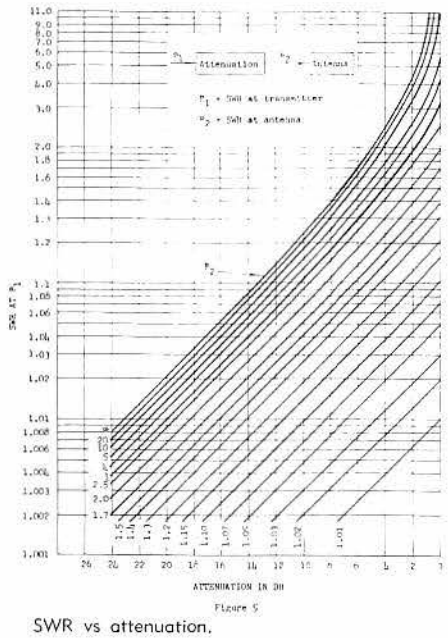

SWR vs attenuation.

For example, 143 feet of RG8A/U at 50 mc would result in approximately 2 db attenuation. If an SWR bridge inserted in the line at the transmitter indicated an SWR of 2:1, this graph shows that an SWR of 3:1 exists at the antenna. A look at Figs. 3 and 4 will indicate that a 3.3 db loss (2 db times 1.65 multiplier) occurs, amounting to 47% loss of transmitted power in transmission line losses. Of the remaining 53% power arriving at the antenna, 24% will be reflected back down the line. A little simple arithmetic will show that of the total power transmitted, only 30% will be radiated! This simple mathematical fact should make the merits of low standing wave ratios immediately obvious if we wish to get the most out of our equipment. By keeping transmission lines short and by insuring that the SWR is as close to 1:1 as practicable, line losses will be minimized, maximum power will be delivered to the antenna and more successful and reliable radio communications will result.

CHECKING YOUR SWR INDICATOR

Carl Drumeller W5EHC

Many articles have been published on how to build and even some on how to calibrate a VSWR indicator. The calibration instructions usually tell you to terminate the indicator's output with a purely-resistive 52-ohm load and then to adjust the device so that a maximum forward and minimum reflected meter deflections are obtained. Sometimes they'll go further and tell you to reverse the device and recheck for opposite indications.

This is all very well. It assures you that the VSWR indicator will be telling you the truth when it says "All's well!" while looking into an utterly-flat transmission line. It doesn't tell you a thing about what the indicator will have to say when it gets tangled up with a line that has a wildly-mismatched termination.

As most transmission lines, in actual practice, are terminated in loads which are not only mismatched in the matter of resistance but also in the inclusion of a considerable magnitude of reactance, it would be well to explore the indications you'll get under realistic circumstances. After all, these are the situations under which you'd want to take corrective steps. Accurate indications of undesired conditions, therefore, are imperative if intelligent remedial actions are to be taken.

Fortunately, some quite enlightening tests are made easily. All you'll need are some lengths of coax transmission line (the same as you're using in your antenna feedline) equipped with male fittings at each end and a few female-to-female junctions. Select the frequency at which you want to make the test. Usually it's wise to make the test on the highest frequency band you plan to use. With this in mind, make up three one-eighth wavelength sections of transmission line and mount the male fittings on the ends of each section.

If your antenna presents an unmatched load to your transmission line, you may elect to skip over this paragraph and go directly to the next one. If it does not (Ah, you dreamer!), you'll need another piece of transmission line. It should be fairly long, perhaps a half wavelength. Put a male fitting at one end and attach a termination, which is deliberately made to be a sad mismatch, at the other end. Don't just mismatch it by using too high or too low a value of resistance. Throw in some reactance, too! You might use a resistor with an inductor in series. Or, you might try a capacitor in series with the resistor. Or, you could use either an inductor or a capacitor in parallel with a resistor. In fact, it would be best to experiment with all four!

Now that you have a transmission line available that you know is mismatched, you're ready to start the test. The first check (the "control", you might call it) is made with everything normal. That is, you'll have the transmitter feeding directly into the VSWR indicator's transfer box and the transmission line (either the one to your antenna or the substitute line to the mismatched load) attached to the output of the transfer box. Note the VSWR indicated. Also note your transmitter; insure that it's tuned to resonance and is adjusted to a power you can maintain throughout the first portion of the tests. Jot down these indications. Now, insert an eighth-wave section between the transfer box and the transmission line and without making *any* other changes or adjustments, note the VSWR. Repeat these steps, adding an additional eighth-wave section each time until you've used all three. Did you detect any change in VSWR? If there was even the slightest change, your VSWR indicator is not trustworthy!

Now for two more checks. Try varying the transmitter power output. Does this have any effect upon the indicated VSWR? If it does, your VSWR indicator is not trustworthy! Then try varying the transmitter output tuning, deliberately throwing the stage out of resonance. Does this have any effect upon the indicated VSWR? If it does, your VSWR indicator is not trustworthy!

Few VSWR indicators under the $150 class will pass these basic tests. If yours doesn't, don't be perturbed. You have an instrument that still has a useful field of application. You can use it as a comparative indicator. For instance, if you're adjusting the gamma match at an antenna, it'll serve quite well; in this application, you're holding all of the significant variables constant, with the exception of one (the gamma match), the effect of which you want to observe. Your tests will have shown you the parameters you'll have to hold constant for any other than simple comparisons. In all probability, you will have found that measurements taken with different (electrical) lengths of transmission line are invalid. Also, it's probable that, owing to the non-congruity of diode curves, measurements will have to be taken at precisely the same level of rf power if accurate comparisons are to be made.

If you'll keep its very real limitations in mind, you'll find that even an inexpensive VSWR indicator has excellent potentials for useful measurements. But don't ask it to perform at levels that even its expensive siblings can't attain!

HOME BREW BRIDGE CALIBRATION

Clifford Honess W4OAB

This table is useful for all homebrew SWR bridges and gives the % reflected power and the % full scale reading in the reflected mode, when the meter is set at full scale in the forward mode.

SWR	% Pwr. Refl.	Refl. Rdg. in % of Full Scale
1.1	.2%	4.8%
1.2	.8	9.1
1.3	1.7	13.1
1.4	2.8	16.7
1.5	4.0	20.0
1.6	5.3	23.1
1.7	6.7	25.9
1.8	8.2	28.6
1.9	9.7	31.1
2.0	11.0	33.3
2.1	12.6	35.5
2.2	14.0	37.5
2.3	15.5	39.4
2.4	17.0	41.2
2.5	18.4	42.9
2.6	19.7	44.4
2.7	21.1	45.9
2.8	22.5	47.4
2.9	23.8	48.7
3.0	25.0	50.0
4.0	36.0	60.0
5.7	49.0	70.0
9.0	64.0	80.0
19.0	81.0	90.0

MINI SWR BRIDGE

John Schultz W2EEY

Most SWR meters today are of the coupled variety which can be left in a transmission line while a transmitter is operated at full power. However, for a number of prolonged

tune-up operations, involving antenna matching systems, for instance, such couplers have several disadvantages.

On 160 and 80 meters, especially, a reasonable amount of power is necessary to produce full deflection—up to 100 watts with some configurations. With a very low-powered transmitter, making adjustments at this power level certainly may damage the output tube or tank-circuit components with a high SWR. This will not be the case with higher-powered circuits but, in any case, a signal strong enough to cause needless QRM will be radiated.

Another disadvantage of the coupled SWR meter, if it is home constructed, is that it must be carefully calibrated since its response is very dependent upon the mechanical configuration of the coupling circuit. This is unlike the bridge-type SWR meter (described in this article) where a standard SWR curve may be used with a good degree of accuracy.

The above factors, plus the fact that I didn't need an SWR meter continuously in the transmission line, led me to construct the little resistance type SWR bridge shown in the photograph. It is just about as simple and inexpensive a unit as can possible be built.

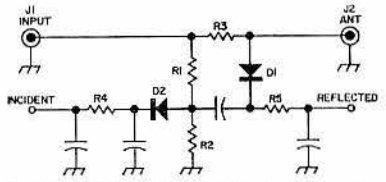

Fig. 1. SWR Bridge Circuit. See text for values of R_1, R_2 and R_3. R_4 and R_5 may be any matched value from 10 k to 47 k. D_1 and D_2 are IN34, IN54, or similar types. All capacitors are disc ceramic, .005 MF, 100V.

Construction

Two SO-239 coax chassis connectors are joined back to back by two 1¼ inch threaded hex spacers. The two four-lug terminal strips are mounted at the ends of one of the spacers. The wiring of diodes D_1 and D_2 as shown in Fig. 1, should be such that the incidental voltage-measuring point appears on the terminal strip mounted on the "input" SO-239 connector, in order to avoid confusion in measurement. Short leads, of course, should be used but hardly anything else is possible with only 1¼ inches between connectors.

Some attention must be paid to the components used if accurate readings are to be obtained. Resistor R_3 must closely match the impedance of the coaxial line used (52 or 75 ohms). For 52-ohm lines, a suitable resistor (within ½ to 1 ohm) can usually be found from a group of standard 10% tolerance, 47-ohm resistors; and for 75-ohm lines, from a group of 68-ohm resistors. Resistors R_1 and R_2 can have any value from about 30 to 100 ohms, but it is important that they are as closely matched as possible. One trick which may be used to affect very small resistance changes is to file "V" notches in

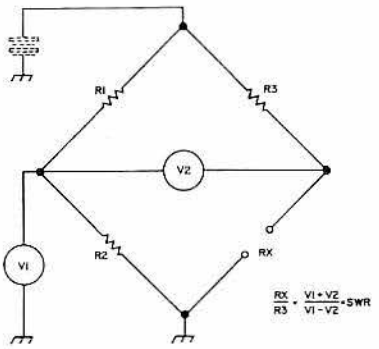

Fig. 2. Simplified diagram of SWR Bridge. V_1 represents incident voltage and V_2 the reflected voltage.

a composition resistor to raise its resistance. Two-watt units are suggested for these resistors because of their longer-term stability and endurance in case too much input power is applied.

Resistors R_4 and R_5 serve as linearizing resistors so that almost any meter with a basic movement of 1 mA or less can be used as an indicator. The lower dc voltage ranges on almost any VOM will work fine. These resistors as well as diodes D_1 and D_2 should be checked to see that they match reasonably well (the resistors within a few precent and the diodes within a few percent for their forward and reverse resistance readings).

Calibration

There are really no adjustments that can be made to the bridge, and calibration really consists of checking the balance. Fig. 2 is the dc circuit of the bridge (a simple Wheatstone bridge with resistance arms). If the balance of the bridge is good, V_2 should be the same when points R_X are opened or shorted so long as V_1 is held constant. This can be checked on the actual bridge by applying an input at the highest frequency of interest (6 or 10 meters), shorting J_2, and checking that incident and reflecting voltages are the same. The same is done with J_2 open. If the voltages are not equal, the difference can be taken as an indication of how accurate the SWR readings will be. If the difference is too great, R_1 or R_2 will have to be changed for a better match or the mounting of the components changed to reduce stray couplings.

A further check is to connect a known 52 or 75 ohm resistor across J_2. The reflected voltage should, of course, read zero.

Operation

As noted in Fig. 2 the actual SWR is a simple function of the incident and reflected voltage readings. Fig. 3 presents this function in graphical form. The incident voltage is simply adjusted for some convenient value, say 10 volts reading on the dc scale of a VOM (possible with most SSB transmitters by adjusting the carrier balance control with no audio input). The reflected voltage is then read as a percentage of the incident voltage and the SWR found from Fig. 3. The input power required to operate the bridge is essentially independent of frequency, being about 1-2 watts maximum.

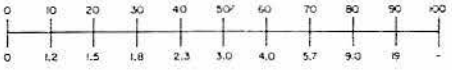

Fig. 3. SWR values for selected reflected voltage readings taken as % of incident voltage reading.

It should be remembered that such a bridge can measure only the resistive portion of an impedance. When using it to adjust a circuit, if a SWR minimum null but not a zero reading for reflected voltage can be obtained, it indicates some reactive component must still be present.

VSWR SUPREME

E. L. Klein W4BRS

One of the most valuable tools used by the amateur is the Voltage Standing Wave Ratio Meter. It ranks with the grid-dipper and the plate current meter as an indispensable instrument around the ham shack. We know that the VSWR meter is very handy in indicating relative power output when tuning a transmitter, particularly when the plate dip is not too discernable. It is most useful, however, in proving that the last available watt has reached the antenna where it can do some good.

Why a good match?

Although a good copper connection is made all the way to the antenna, an efficient transfer of power may not be achieved because of a mismatch between the characteristic impedances of the various portions of the transmission system. The interesting thing is that the "match" is different for each frequency because the antenna is essentially a single frequency device.

We can appreciate the importance of a proper match between the transmitter and the antenna when we are told, for example, that a VSWR of 3 to 1 causes a power loss of nearly 3 dB for 200 feet of RG-8/U coaxial line at 30 MHz. The table below provides

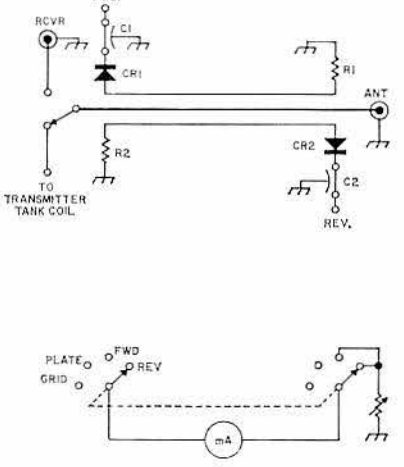

Fig. 1 Schematic of basic VSWR Meter and associated switching circuits.

Table I

VSWR	Power Loss (dB)	Transmitter Power Needed to Provide 1 kW at the Antenna
1.5:1	2.1	1600 watts
2:1	2.3	1700
3:1	2.8	1900
4:1	3.3	2000
5:1	3.7	2300
7:1	4.5	2800
10:1	5.3	3400

Additional power needed to compensate for a poor impedance match between transmitter and antenna. Figures are based upon 200 feet of RG-8/U cable at 30 MHz.

the real reason why we should be concerned with the impedance match. Notice how much the transmitter power would have to be increased to make up for a poor match between the transmitter and the antenna. Incidently, this match involves each and every part of the total transmission system including connectors, antenna relay, low-pass filter, balun, etc., as well as the transmission line itself and that particularly critical point at which it is connected to the antenna.

A new approach

Most VSWR meters today are an external accessory to the transmitter. But this practice is not good. Coaxial connectors are expensive and cause unwarranted mismatch and power loss. Meter faces usually end up behind the transmitter or in some other inaccessible location. When switching from forward to reverse, the little accessory box scoots across the table leaving scratches and a distraught operator.

The transmitter plate current meter is no longer a plug-in accessory. Why should the VSWR meter be? (Believe it or not, plate meters used to be plugged in with phone jacks.) Using the simple design described here, the home constructor as well as the commercial manufacturer can now build the VSWR meter into the transmitter in the smallest possible space and at only pennies of cost.

The circuit

Nothing is new about the circuit. It has been adequately described in the past in magazine articles and handbooks. However, for the convenience of the reader, the VSWR meter circuit is reproduced in **Fig. 1** for handy reference. Terminating resistors R1 and R2 should be 33 ohms for a 50-ohm transmission line when the physical configuration, as shown here, is used. One-half watt or smaller size resistors may be used. Diodes CR1 and CR2 are any matched pair of silicon diodes or germanium. The types which are enclosed in glass cases are the easiest to use because of their small size. The ohmmeter can be used to select and match the diodes of the ten-cent surplus variety found in advertisements in ham magazines such as *73*. Bypass capacitors C1 and C2 are 1500 pF Centralab type FT-1500.

Physical components

Parts used in this VSWR meter are illustrated in **Fig. 2**. The brass tubing is about 5 to 7 inches long and of 5/16 inch outside diameter. This size tubing fits snugly around the inner polyethelyne insulation from RG-8/U coaxial cable. About 10 inches of coax is stripped of its outer jacket and braid. The inner insulation is trimmed to extend 1/8 inch past each end of the brass tubing. Two large solder lugs are selected to fit over the 1/4 inch threaded shank of the bypass capacitors. These lugs should be of the long variety so they may be shaped and soldered to the brass tubing as shown in **Fig. 3**. Two 8-inch pieces of #22 enameled copper wire are also required.

Assembly

After soldering the lugs to the brass tubing about 5/8 inch in from each end, the bypass capacitors are assembled to the lugs. Place several fiber washers under the ring nuts prior to tightening them down on the threaded shank of the capacitors. This permits careful soldering of the capacitors to the lugs without danger of also soldering the nuts in place.

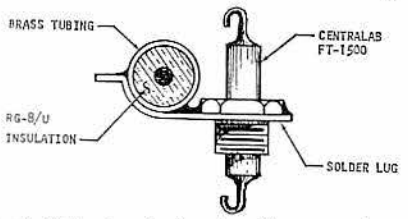

Fig. 3 Solder lug is shaped to fit one-quarter way around the brass tubing.

Two small grooves are now cut 180 degrees apart for the total length of the polyethelyne insulation. A small wood carving gouge or carefully manipulated razor blade can be used for this purpose. These grooves provide a space for the enameled copper wire which is held in place when assembling as shown in **Fig. 4**. Prior to this operation, the wire should be stretched and work-hardened by jerking it between two pairs of pliers. Be sure that the plane described by the two wires lies at right angles to the chassis on which the unit is mounted. This permits all resistors and diodes to have equal lead lengths.

When the inner assembly has been tugged and shoved into place within the brass tubing, the #22 wire ends are trimmed, stripped and soldered to their respective resistors and diodes. Much care should be exercised at this point to prevent melting the insulation or damaging the near zero-length component leads.

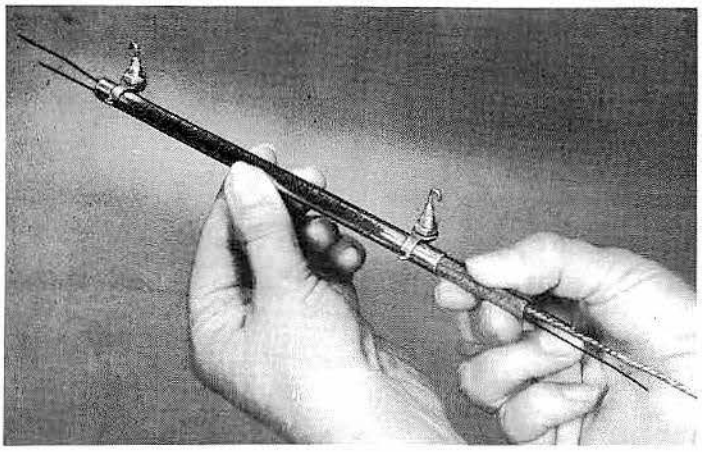

Fig. 4 Assembling the inner components into the brass tubing.

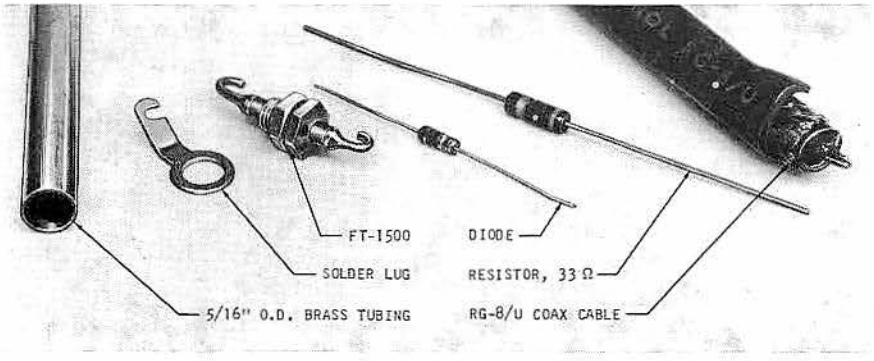

Fig. 2 Component parts used in making the VSWR sensing unit.

Application

A completed sensing unit for the VSWR meter is shown mounted on a typical chassis in **Fig. 5**. It will be noted that no conventional box or housing is used because the total outside of the unit is at ground rf and dc potential, save for the component connections at each end. By mounting the bypass capacitor in the chassis, the low-voltage rectified current fed to the meter switch is

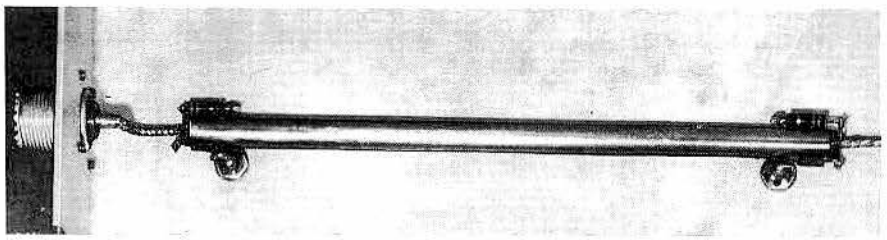

Fig. 5 Finished VSWR sensing unit mounted on a typical chassis.

isolated from high-power rf on the other side of the chassis. It can readily be seen that the finished sensing unit occupies no more space than would be used by a coaxial lead running from an antenna relay to the antenna connector on the chassis.

A further refinement is shown in **Fig. 6.** Complete isolation of the high-power rf is provided by the coaxial hood. Impedance discontinuity is also minimized by use of the hood, which was designed for this purpose and is readily available.

Length of sensor

The dimensions given for the length of the sensor element, including its outer tubing and inner conductor, are not critical. They are, however, directly related to the power of the transmitter with which the VSWR meter is used. For example, with a one kilowatt high-frequency CW transmitter and a 0-1 milliammeter as the indicating meter, the length of the sensor can be as short as 2-3 inches. A sensor which is constructed approximately 7 inches long, as illustrated in this article, will work fine with the same meter on a 25-200 watt high frequency transmitter. If meters with higher current ratings are used, a longer sensor is required, and, conversely, a more sensitive meter would provide adequate full-scale deflection with a shorter sensor element. Obviously, it is impracticable to vary the length of the sensor element in order to vary the sensitivity of the VSWR meter as a whole. It is for this reason that the adjusting resistor is provided in series with the meter. For VHF use, the sensor can be shorter.

All that has been said above can be depicted graphically. **Fig. 7** shows the generalized relationship between the sensor length and transmitter power with which it is used. The two curves represent different meter sensitivities. A 0-1 milliammeter offers a good compromise. With a 5-7 inch long sensor and the proper series resistor, all powers normally encountered in amateur work can be handled. However, if space requirements so dictate, a shorter sensor unit can be employed with some small sacrifice in accuracy.

Terminating resistor

Small variations in mechanical construction and lead dress will have an effect on the value of the terminating resistors, R_1 and R_2. Also, a carbon resistor does not display the same reactance at high frequencies as its measured resistance at dc. The value of the 33-ohm resistor was therefore determined empirically.

To verify the proper value of the terminating resistors, the test set-up shown in **Fig. 8** is used. A radio-frequency source of approximately 10 to 20 watts is required. A transmitter exciter stage operating on the 10-meter band is preferred for this purpose. Ten meters, or even fifteen meters, will provide better accuracy than one of the lower frequency bands. A dummy load is also required. This load must be capable of dissipating the power of the radio-frequency source used in making the test. Three or four 2-watt carbon resistors of the proper value in parallel to provide 52 ohms will suffice if the power is not left on continuously.

In making the test, the selector switch is first placed in the "forward" position. With power applied, immediately adjust the sensitivity control so that the meter reads full scale. Upon switching to the "reverse" position, the meter should read near zero and be at or below the 1:1 calibration point on the meter scale. Several resistors may be substituted until the proper value is found. The important thing to remember is that both of the resistors should be simultaneously substituted and that they must be as near identical as possible as measured on a reasonably good ohmeter. Lead lengths should also be as short as possible and of identical length.

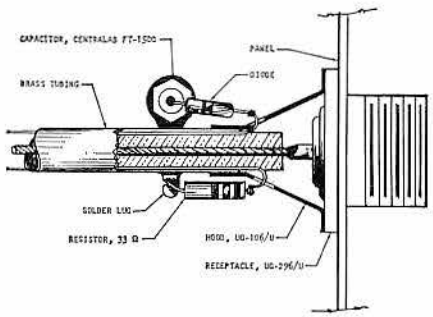

Fig. 6 Recommended chassis connection for output of VSWR meter sensing unit.

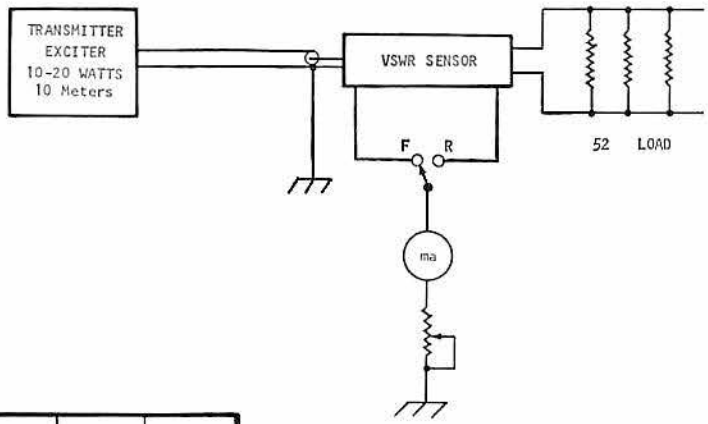

Fig. 8 Test set-up for verifying the proper value of the terminating resistors which are a part of the sensor unit. The value of the dummy load should match the characteristic impedance of the sensor unit and have a total wattage rating nearly equal to the source power.

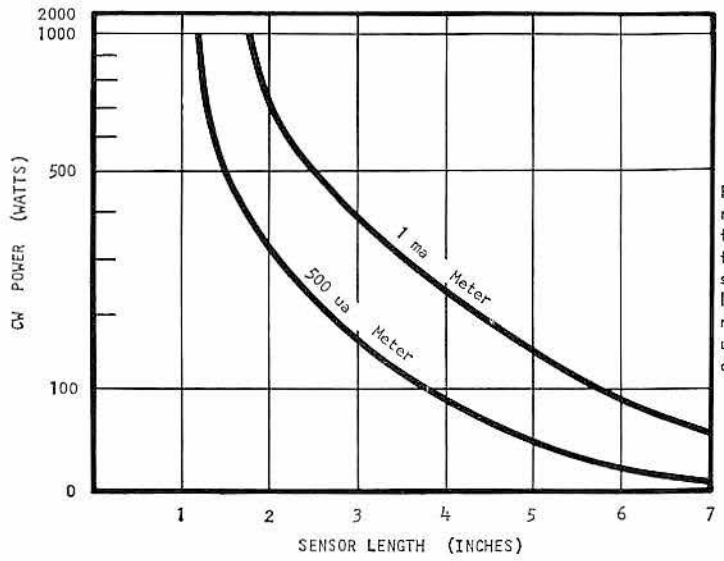

Fig. 7 The approximate relationship between sensor length and transmitter power is shown for two commonly used meter movements. Other meter values may be used as discussed in the text.

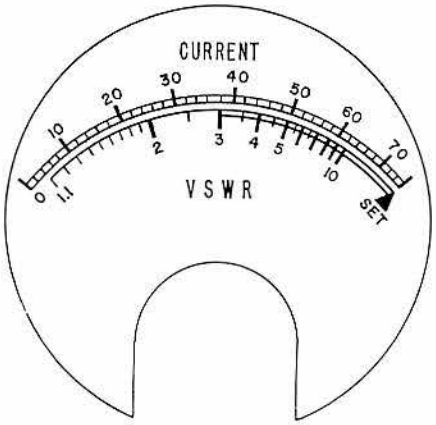

Fig. 9 Full-size photomaster of the VSWR meter dial. A multi-purpose meter was used in the author's transmitter so that the grid and plate currents could also be read on the upper scale.

The dial scale

Using the standard formula for calculating VSWR, it is possible to calibrate the meter face as follows:

$$\text{VSWR} = \frac{\text{forward} + \text{reverse}}{\text{forward} - \text{reverse}}$$

Fig. 9 is a full-scale illustration of a meter face used with the *VSWR Supreme*. This scale fits the Triplett Model 327, as well as a number of other meters of the same size category. A word of caution—don't assume that the scale calibration, or linearity will be the same for all makes of meters. The individual meter movement selected should be checked by using the above formula and marking off radials representing 4-5 different VSWR values. With the scale from your meter at the center of an oversized radial(s) drawing, it is possible to verify the angular placement of each VSWR calibration point.

The *VSWR Supreme* is truly a novel approach to an old standby. Using the construction methods outlined in this article, it is possible to fabricate the sensor unit so that it occupies the smallest possible space. This sensor can now be built into a transmitter and take up no more room than the coaxial lead which it replaces.

A SIMPLE VHF SWR METER

John Schultz W2EEY/K3EZ

I recently wanted to do some work on a 2 meter antenna and since no other instrument was handy, started to use an SWR meter manufactured for use on the high frequency bands. After some erratic results, it was decided to check the SWR meter accuracy on 2 meters with some carbon resistors to simulate different SWR's. The results readily confirmed that the SWR meter was useless at VHF unless one didn't care whether a SWR was really 1:2 or 1:5. Rather than purchase another SWR meter, it was decided to construct one that would render reasonable results, within 10% accuracy or so, on the VHF bands, particularly 144 and 220 MHz.

There is nothing basically new in the circuitry of the SWR meter to be described. What is different about it is that it utilizes a particularly simple and inexpensive method of construction that yields reasonable results. It can be constructed as a completely self-contained SWR meter or only the pickup element can be constructed and used with an external meter. The circuitry as shown here for the meter utilizes two meter movements so one can read forward and reflected power simultaneously and avoid the annoyance of having a forward-reflected switch arrangement for a single meter.

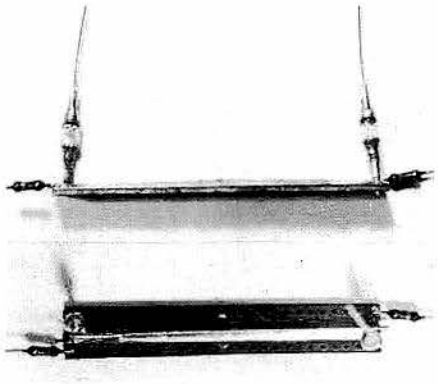

The heart of the SWR meter is a carefully constructed pickup element. Details of construction are discussed in the text but the photo shows how closely the diodes and terminating resistors must be soldered to the pickup element.

Pickup Element

The "heart" of any SWR meter of the reflectometer type is the pickup element. Many elaborate forms for such elements have been devised which involve complicated mechanical construction. Such complicated construction does become necessary if very accurate results are desired and if the meter is to maintain linearity over a very wide frequency range. However, over a smaller frequency range and with some minor sacrifice in accuracy, the construction of a pickup element can be greatly simplified. Basically, the pickup element should not cause any discontinuity in the transmission line section in which it is inserted but yet be long enough so enough voltage can be picked up in both the forward and reflected directions to make the meter usable with even low power transmitters.

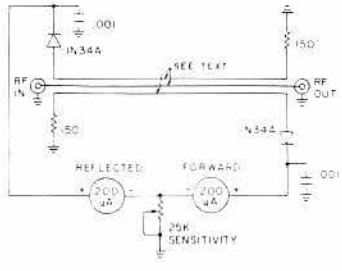

Fig. 1. SWR meter circuit. Two identical meters should be used (current range and internal resistance).

The pickup element I devised is shown in the photo. It is a 2-7/8" long piece of alternate grid pre-punched perf-board stock. The board is about 7/16" wide and within this width contained 4 separate copper strips spaced about 1/16" or less apart. The center two strips are soldered together to act as the inner conductor continuation of a coaxial line section. To solder the two inner strips together tack solder a bare piece of hookup wire between the two strips and then cover the entire two strips with solder.

Without the use of pickup wire, it will be nearly impossible to develop a smooth solder flow between the strip. Each outer strip acts as a pickup element for the SWR meter circuit shown in Fig. 1. The terminating resistor and diode are soldered to each end of the outer strip as shown in the photo and with minimum excess lead length to the strip. The use of a heat sink on the diode is necessary to prevent damage during soldering.

Mounting The Pickup Element

The pickup element made from the board stock is mounted between two approximately spaced SO-239 chassis connectors. The center strip of the board is soldered at each end to the center post of the SO-239 connector. The terminating resistor at each end is grounded as directly as possible to a ground lug held in place by one screw of the SO-239 mounting hardware. These details are shown in Fig. 2. It is important that the terminating resistor be grounded in this manner with minimum lead length. The enclosure in which the pickup element is contained should just be wide enough to accommodate the SO 239 connectors so that when the enclosure is secured together, the pickup element is boxed in by a metal surface on each side except directly above it. Many chassis or enclosure types are suitable for this purpose and the overall size of the enclosure will depend, of course, on the meter used and sensitivity control placement. These details are not covered here because they can be made as desired. They will not affect the basic accuracy of the meter as long as the pickup element is properly mounted and enclosed. The bypassing of the pickup rectifier diodes must also be done with as short leads as possible on the bypass capacitor. As shown in Fig. 2, a two lug terminal strip (one lug grounded)

mounted on the side wall of the enclosure immediately at the cathode end of the diode will perform this task very well. The length of the IN34A diodes is such that the bypass capacitor cannot be connected to the same ground lug used for the terminating resistor. The leads on the capacitor would be too long and it will be ineffective.

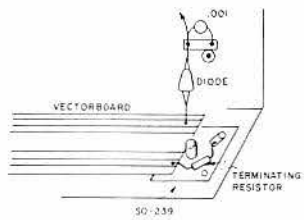

Fig. 2. Center strip of vector board is soldered to center post of SO-239. Other components are mounted at each end of board as shown (only one end shown here).

Operation and Results

The dual meter circuit of Fig. 1 reads forward and reflected power simultaneously. The sensitivity potentiometer is set to read full scale on the forward meter and the SWR read directly from the reflected meter. The latter meter can be calibrated for various SWR's by the use of small carbon resistors (100Ω to simulate a 1:2 SWR in a 50Ω line, etc.). Usually, it is only necessary to calibrate the reflected meter for SWR's of 1.5, 2 and 3 at the frequency of interest. Calibrated in this manner, the accuracy of measurement will be roughly 10% and is certainly good enough for most general antenna work. A particularly nice meter display can be made if one can find a two meter movement in one enclosure. I purchased a surplus stereo VU meter which had dual 200 μA movements and used it in the SWR meter.

The sensitivity of the SWR meter is such that transceivers of the 1-2 watt output class can easily be used with it on the VHF bands. The basic meter, of course, can also be used on the lower frequency bands as well and it will retain good accuracy. The only problem on the lower frequency bands is that the pickup strips are so short that more transmitter power has to be used to activate the meter than is usually convenient to use during antenna experiments. No exact tests were made but probably 70–100 watts would be needed to use the meter on as low a band as 80 meters. The meter was used and checked, however, on 40 meters. The accuracy of the meter remained very good and full scale deflection of the forward level meter required a power level of 60 watts. Being an in-line type meter, it can be left permanently in line when used on any band with a minimum of loss.

DIRECTIONAL COUPLER AND VSWR BRIDGE FOR VHF AND UHF

Bob Kolb WA6SXC

The aerospace industry has fostered the development of many new components and materials. Hams, being the kind of people they are, are quick to see practical applications for these materials that never occur to design engineers. I have often heard the criticism that it is impractical to publish articles or design ham gear with these new or expensive materials, because most OM's don't have access to them. Yet I've often been dismayed when I learn of an application for a piece of surplus equipment after it is no longer available. For this reason I feel that we should publish any application that is practical regardless of how immediately it can be used. Sooner or later, the material will show up on the surplus market and then we'll know what use can be made of it.

Reliable test equipment for the VHF-UHF bands is difficult to come by on a low budget. The literature is full of "relative" measuring devices but few pieces of homebrew gear are engineered for repeatable performance. Several directional couplers have been built according to the description in this article and each has measured to within ±.5 dB of the designed value. This is due in part to the mechanical rigidity and close tolerance of RG-141 "coaxitube." No special tools are required outside of a cheap pair of vernier calipers. The tools used to make the original coupler were an Xacto knife, file, soldering gun, vernier calipers and a vise. Don't let the calipers scare you. If you're not after a closely calibrated device they may be omitted.

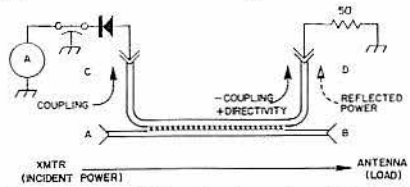

Fig. 1. A typical directional coupler. This device is the heart of a VSWR bridge, and can also be used for many other applications.

The design goal was a directional coupler with about 30 dB directivity in the passband with a low insertion loss. Each milliwatt measured at the coupling arm equals one watt through the main line. Such a device is the heart of a good quality VSWR Bridge. The measured values were 30.3 dB coupling and 38 dB directivity at 432 MHz. Data presented in the graph was taken using HP608C and 614A signal generators and a General Microwave R. F. Power Meter. The measured insertion loss was 0.2 dB.

Resolution of the smallest possible VSWR is limited by directivity. Few of the handbook VSWR bridges or the low cost type attractive to the CB trade achieve as much as 20 dB directivity. Thus the minimum discernable VSWR is approximately 1.7:1. With 38 dB directivity, 1.02:1 VSWR's can be accurately measured.

Directivity may be defined as the isolation of arm D from arm A, over and above the coupling as shown in the **Fig. 1.** Coupling is achieved by removing part of the jacket between adjacent coax conductors. If the input is at arm A, incident power can be sampled 30 dB down at arm C but appears −68 dB at arm D. Reflected power entering arm B is sampled −30 dB at arm D while at arm C it is −68 dB. It stands to reason if the directivity is low, one cannot tell with certainty if he is measuring incident or reflected power. Port D may be used as the dc return for a detector at port C and vice versa.

This device will have its fundamental passband where the length exposed between the two lines is $\lambda/4\sqrt{\epsilon_r}$. It will also have a passboard at $(2n-1)\ \lambda/4\sqrt{\epsilon_r}$ or at three, five, seven, etc., times the frequency for which it is a quarter wave. Hence a coupler designed at 432 MHz is usable at 1296 MHz.

This coupler has also been used to measure relative power and modulation at 2 meters where its coupling factor for incident power is approximately −40 dB but the directivity is poor, hence arm D must be terminated in 50 ohms. It's a real aid for tune up and will give a good indication of increased power with AM modulation right in the r.f. line. RG141 will handle 500 watts of rf up to 2000 MHz.

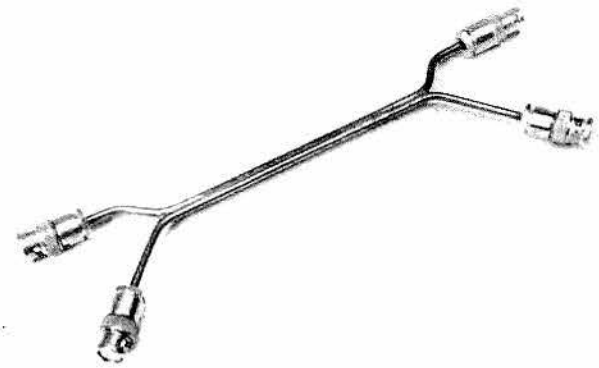

This UHF directional coupler is very simple to make, yet offers excellent performance on the 70 and 23 cm bands.

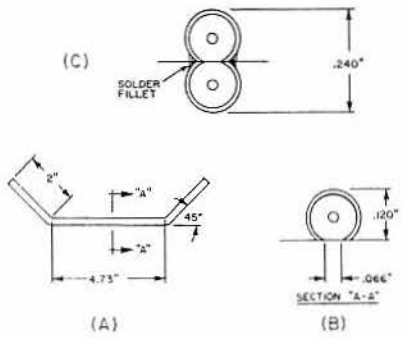

Fig. 2. Details of the construction of the UHF directional coupler.

The formula for determining coupling length is

$$\frac{c}{4fo\sqrt{\epsilon_r}} = \frac{\lambda c}{4\sqrt{\epsilon_r}} \quad \text{or} \quad \frac{300 \times 10^8 \text{ cm}}{4 \times fo \times \sqrt{2.1} \times 2.54 \text{ cm/in}} = \frac{\lambda \text{ c inches}}{4\sqrt{\epsilon_r}}$$

$\sqrt{\epsilon_r}$ for Teflon $= \sqrt{2.1} = 1.449$

From these calculations $\frac{\lambda \text{coupling at 432}}{4}$ MHz is 4.73 inches. With an Xacto knife cut two pieces of line 8.73 inches long and carefully bend them so that they form the shape shown in **Fig. 2A.**

Clamp the bent coax into the vise and file away the copper jacket taking care that the filed surface is smooth and flat. A belt or stationery disc sander works well too. A cross section of the filed piece should look like **Fig. 2B.** Next fit the two pieces together so that a cross section would look like a figure 8 and secure in a vise. Heat with a soldering gun only. Do not use a torch. Avoid excessive heating. Flow solder between the two lines as shown in **Fig. 2C.** The "arms" can now be bent into any convenient configuration provided enough allowance is made at the ends for connector assembly. A good rule to follow is a minimum bend radius of half an inch although a quarter inch radius is permissible. The arms should be approximately two inches long.

RG 141 has the same cross section as RG 58/U *without* the vinyl jacket therefore any connector that will accept RG 58/U can be used on RG 141 provided a sleeve is made up to make a snug fit in the clamping nut. A special adaptor is made by Kings for this purpose and sells for 45 cents. The connector assembly is shown in **Fig. 3.** Three RG 88E/U and one RG 89C/U connectors were used on the coupler shown in the photo.

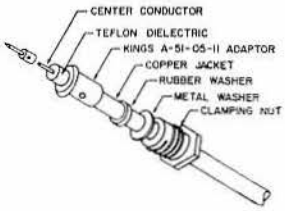

Fig. 3. Use of Kings A-51-05-11 adapter for using GR-141 with standard BNC connectors.

Fig. 4 gives the measured directivity and coupling for this type of directional coupler at both 70 and 23 cm. You can see that performance is quite satisfactory.

Fig. 5 lists a number of applications for a directional coupler. The detectors in the measuring instruments should be suitable for use at 500 or 1300 MHz.

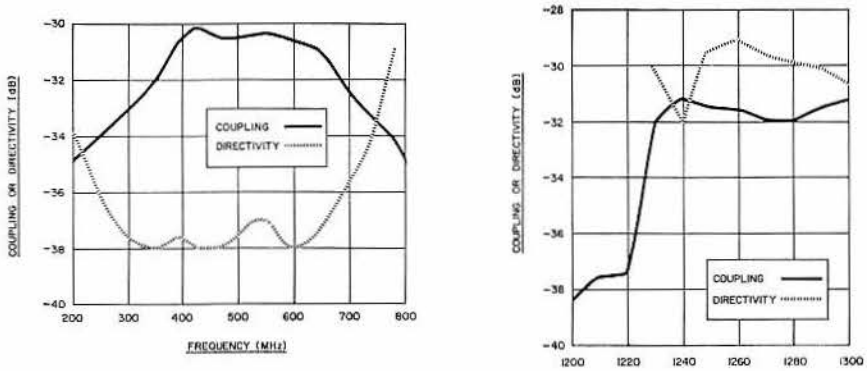

Fig. 4. Coupling and directivity for a directional coupler similar to the one discussed in the text. This device used a coupling wavelength of 4.635 inches rather than the 4.73 inches specified in the text. The only effect of the longer wavelength is to center the curves on 432MHz instead of about 500 MHz.

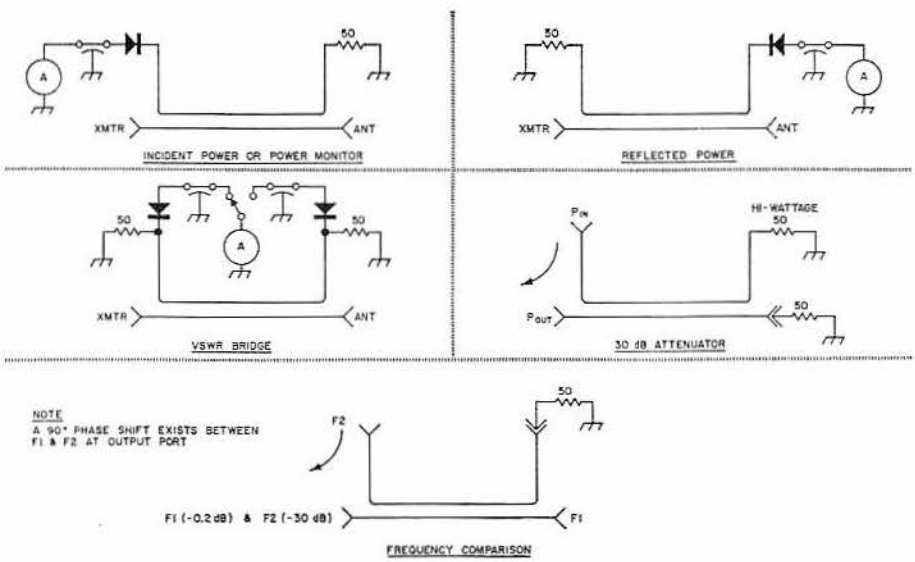

Fig. 5. Applications of the directional coupler described in the text. Unlike most pieces of ham-made test equipment, this one is good at 450 and even 1300 MHz.

A SLOTTED LINE FOR 1250 MHz

Silas Smith WA8CHD

The SWR bridge is a very useful—and sometimes badly neglected—tool. Especially on 1250 mc with only two or three watts of power, you should measure your SWR and do something about it if necessary. I recently joined the 23 cm boys, though I have only worked 1234 mc so far. My first attempt to communicate with W8VKQ on the other end failed but after two evenings of diligent work with a meagre amount of test equipment we made contact. It would have been a lot easier with test equipment good in the 1250 mc range since most hams are not equipped to measure frequency and adjust their rigs at these frequencies.

After that experience, I made the slotted line indicator described in this article. The cost is next to nothing and it's easy to build, but it does a good job. The unit is built around a one inch thin wall copper tube 10¼" long (Fig. 1). This tube has a ⅛" slot cut lengthwise for 7½", about ¾ wavelength at 1250 mc. This is long enough to get a fair sampling of the standing wave or null points.

Three other pieces of 1" copper pipe are needed. Two are 5/16" long and one is 1⅜" long. The two 5/16" pieces each have ¼" cut out and are reshaped to fit inside the 1" tube. These two pieces were each soldered to 1/16" plates as in the detail in **Fig. 1.** This process makes two cup-like structures which should

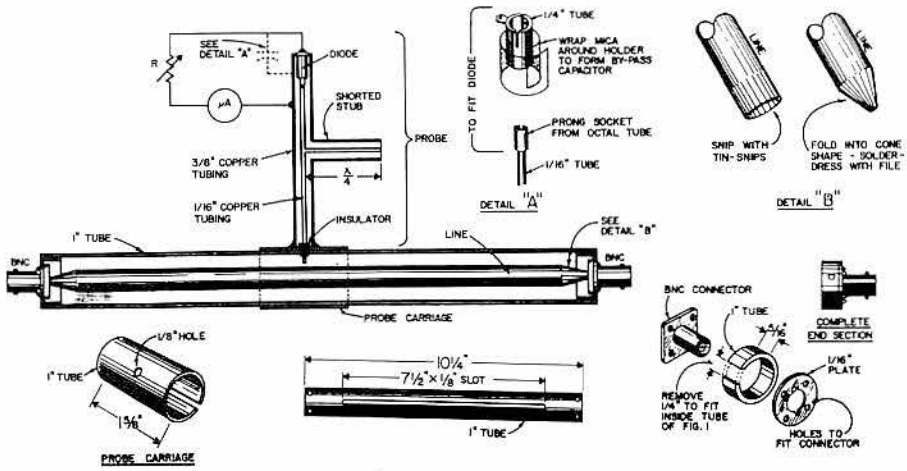

Fig. 1. The slotted coaxial line and probe for 1215 to 1300 mc described in this article.

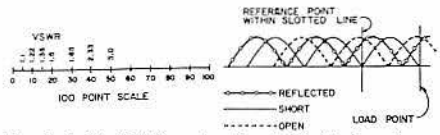

Fig. 5, Left. VSWR scale. Fig. 6, Right. Impedance measurements.

fit within the end of the 1" pipe. Drill nine holes in each cup: four holes for attaching the cup to the slotted line, four to fit the BNC connector mounting plate and one ¾" hole to pass the main body of the connector. File two notches for the connector ears. You can fasten the cups to the slotted tube with small sheet metal screws, threaded holes or nuts soldered to the back of the holes.

The 1" x 1⅝" piece of pipe is for the probe carriage. It is cut lengthwise on one side, slipped over the 1" tube, centered, and a ¼" hole drilled through it over the slot in the 1" tube.

The probe is built from ⅜" and ¼" brass tubing from your hobby shop. At the probe end is an insulator from a coax fitting and on the other end is a jack made from an octal tube socket. A small piece of ¼" brass tubing is used to make the diode socket (see detail A). A piece of 22 gauge wire is inserted in the probe end of the 1/16" tubing and soldered. A 1N21 diode works very well.

Use **Fig. 2** to choose the proper size for the line in the center. Each end of this line should be tapered and soldered to the coax fitting as in detail B. The center conductor should be 7/16" for 50 ohms or 5/16" for 73 ohms.

The meter used should have a range that permits a full scale reading and should be calibrated with some scale.

Uses: Measuring frequency

Frequency can be measured with the slotted line in two ways: the distance between null points at one half wavelength ($\lambda/2$) or the distance between peaks. See **Fig. 3.** Measuring between the nulls is preferable since the peaks are very broad. If your line is flat, the peaks and nulls may be very small, so you may have to induce a mismatch in the line. Likewise, you may have to induce a mismatch to get the two nulls to fall within the 7½" of the line. The easiest way to induce a mismatch is a short in the line.

Measure the distance between the nulls carefully with a centimeter rule. Twice this distance divided into 30,000 will give you your frequency in megacycles. It would be a good idea to check this against a standard or at least avoid operating too close to the edge of the band.

Measuring VSWR

Measuring voltage standing wave ratio (VSWR) with the slotted line is easy, too. We are looking for a ratio of E_{min}, the minimum voltage on the line, and E_{max}. The ratio:

$$\frac{E_{max}}{E_{min}} = \text{VSWR}$$

However, there is a slight complication of vectors in E_{max} and E_{min}, so that to find them, you must first determine the highest voltage read on the meter, E_1 and the lowest voltage read on the meter, E_2 with the same setting of the shunt resistor, as the probe carriage is slid along the line. Now, $E_{max} = E_1 + E_2$ and $E_{min} = E_1 - E_2$ so that

$$\text{VSWR} = \frac{E_1 + E_2}{E_1 - E_2}$$

An even simpler method is to set the meter to full scale (100) at the highest reading, and reading the VSWR directly from **Fig. 5.**

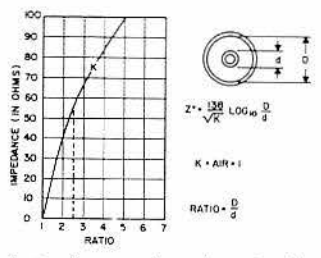

Fig. 2. Ratio of outer tube to inner line for various impedances.

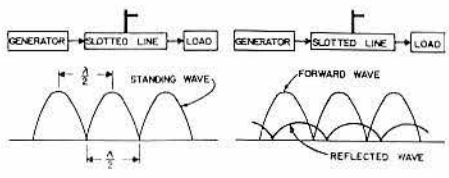

Fig. 3, Left. Measuring frequency. Fig. 4, Right. Measuring VSWR.

Impedance measurements

It's a little harder to measure impedance, but even it's not bad if you do it step by step. First, consider the high impedance on your line when your antenna is open or shorted. Perhaps you don't think of it as a change in impedance. This is what we are looking for. Remember that there is a definite relationship between impedance and frequency. **Fig. 6** shows the voltage relationship between a short and open. On a short set the probe for a null point, usually the first null from load end of the slotted line. This will be our reference point. You will note that when the load point is open there is a shift of 90° or a quarter wavelength either side of the reference point. This adds up to one half wavelength. Any impedance between infinity and zero ohms will lie somewhere along the half wavelength of the line. It will be noted that an open is equidistant from the reference point toward the generator and toward the load, however the line has moved toward the load (capacitive reactance). To measure this reactance, we replace the load that we measure with a short. We set our probe to the first minimum reading from the load end of the slotted line. Mark this spot with a scribe. This is our reference point. Now we remove the short and add our load under measurement. It will be noted that the voltage has moved upward. Move the probe toward the load. If the voltage goes down, you are heading in the right direction. If the voltage starts to go up change direction toward the generator. Move the probe as above to the new null point and note the direction that the probe has been moved.

Here's a step-by-step example. First, you'll need the frequency and wavelength, VSWR, direction of probe, distance between reference point and new null, and impedance of the slotted line.

Let's say as we measured the frequency, the distance between the null points was 12 cm. This is half the wavelength, so the wavelength is 24 cm. The frequency is 30000/24 or 1250 mc.

Let's say we read 80 as a maximum and 20 as a minimum on a point scale in measuring the VSWR:

$E_{max} = E_1 + E_2 = 80 + 20 = 100$
$E_{min} = E_1 - E_2 = 60$

$$\text{VSWR} = \frac{100}{60} = 1.66$$

Or set E_1 to 100 by adjustment of R, then E_2 would read 25 on the meter, a VSWR of 1.66 by **Fig. 5.**

As in **Fig. 6,** the probe was moved toward the load.

Let's assume the distance from the reference point to the new null was 2 cm. What part of a wavelength is 2 cm? Wavelength is 24 cm, so 2/24 = .083 wavelengths.

This is a movement of .083 wavelengths toward the load.

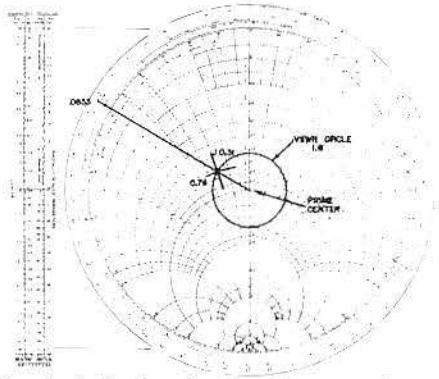

Fig. 7. Smith chart for determining impedance.

The slotted line used has an impedance of 50 ohms.

We are now ready to plot this information on the Smith chart (**Fig. 7**, better get out your magnifying glass).

Draw the VSWR circle at the prime center with a radius of 1.6.

Draw a line from .083 wavelength toward the load from the prime center.

At the intersection of the circle and line, follow the constant resistance circle to .74 and the capacitive reactance circle to .31. Our load impedance is then:

$Z_L = Z_0\ (.74 - .31j)$

$Z_L = 50\ (.74 - .31j)$

$Z_L = 37 - 15.5j$

Well, there are some of the things your slotted coax line can do besides telling you that you're on the air. A commercial version would cost $750. I guarantee that you'll get your dollar's worth out of this one as it costs less than $1 to build. I hope that it helps you get on 1250 mc.

SOME DIRECTIONAL WATTMETERS AND A NOVEL VSWR METER

P. G. Martin G3PDM

Most conventional reflectometers cannot be used for accurate power measurement because their sensitivities are frequency dependent. This is due to the use of combinations of reactance and resistance in the sampling circuits which detect the transmission line current and voltage.

This basic problem can be solved by the use of conventional lumped components instead of the distributed parameters of a transmission line. The line voltage can be sampled by two resistors or two capacitors used as a voltage divider, rather than one resistor and some distributed capacitance. The line current can be monitored by a properly designed current transformer instead of an inductance and resistance. High frequency current transformers consist of primary and secondary windings on a ferrite or iron dust toroidal core, with a low value of load resistance across the secondary winding.

All SWR bridges and directional wattmeters need to generate two dc voltages proportional to the forward and reflected voltages or currents of the transmission line. To achieve this one has either the current detector or the voltage detector providing two antiphase signals so that addition and subtraction can be performed.

A Frequency-Independent Directional Wattmeter

M. B. Allenson G3TGD, has designed a wattmeter using the above principles, where the low resistance in the current transformer secondary circuit is split into two equal parts. The center connection is taken to the voltage sampling point so that sum and difference voltages are available at the ends of the transformer secondary winding, see Fig. 1.

With two meters, this circuit can be used as a versatile calibrated directional wattmeter over the freqnecy range 100 kHz to 70 MHz, with an accuracy of about 10 per

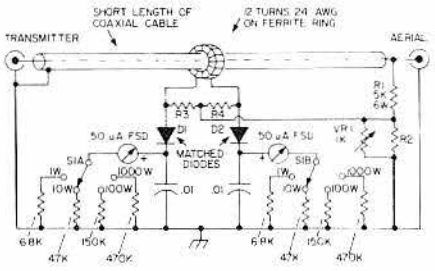

Fig. 1. Circuit of the basic frequency-dependent directional wattmeter due to G3TGD. The two meters indicate forward and reflected powers.

cent. Precise calculations of SWR and transmitter efficiency can be made.

Maximum sensitivity with a 50 μA meter is less than five milliwatts, but with the multiplier resistors specified in Fig. 1, full scale deflection corresponds to power of 1, 10, 100 and 1000 watts. Calibration is non-linear, because the instrument samples

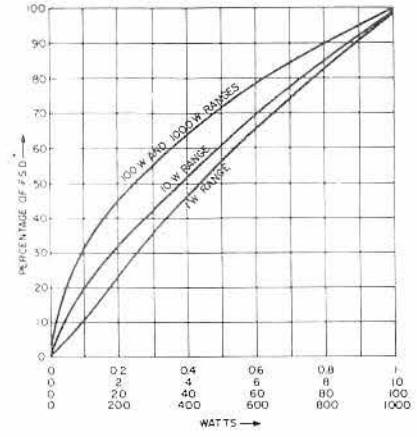

Fig. 2. Calibration curves for the instrument described in Fig. 1.

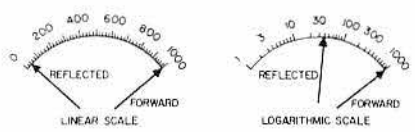

Fig. 3. Linear and logarithmic scales. The inherent advantages of the logarithmic form are immediately obvious.

voltage, and power is proportional to voltage squared.

Unfortunately, two transmission line impedances are in common use in coaxial systems: 50Ω and 75Ω. As it is not possible to design instruments whose sensitivities are independent of line impedance, some component values must depend on the impedance in use. For simplicity, only one of the voltage driver resistors need be changed, but instrument calibration will be different. By changing the current transformer resistors as well as one of the voltage divider resistors, the calibration is the same for both line impedances. This technique has been adopted here, and the calibration curves in Fig. 2, are correct for 50 or 75Ω lines provided the resistor values in Table I are used.

The Logarithmic Wattmeter

The basic instrument can be simplified by including a logarithmic network so that the power range switch is redundant and a single meter scale can be used for powers from, say, one watt to 1000 watts. A logarithmic scale has the 1, 10, 100 and 1000 watt points equally spaced (see Fig. 3).

The advantage of a logarithmic instrument is that one can measure very low reflected powers and very high forward powers simultaneously with the same percentage accuracy, without having to switch meter ranges.

It is simple to add a reasonably accurate *wide-range* logarithmic network to the meter in Fig. 1 (see Fig. 5). The basis of its

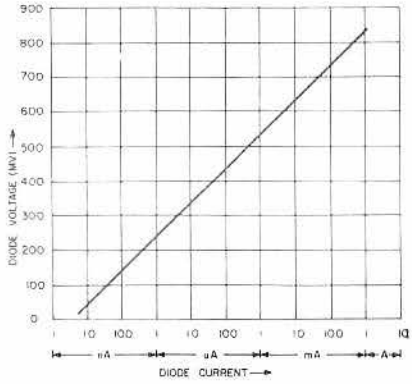

Fig. 4. Smoothed experimental plot of the current /voltage characteristic of a 1N4002 silicon junction diode, showing its logarithmic properties.

operation is that the voltage dropped across a forward-biased p-n junction diode is proportional to the logarithm of the current passing through it (see Fig. 4). To reduce the potential dynamic range of the circuit, a relatively insensitive meter is used, and a small resistance is added in series with the logarithmic diode to restore a logarithmic form to the scale (see Fig. 6).

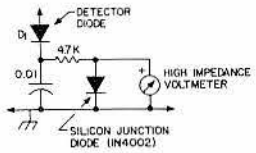

Fig. 5. Basic wide-range logarithmic converter.

An experimental logarithmic wattmeter is shown in Fig. 7. Figure 8 gives the calibration scale for 50 or 75Ω lines, provided the correct resistors are used (Table I).

A Direct-Reading SWR Meter

A particularly useful device would be an instrument giving a direct measurement of the standing wave ratio on a transmission line, independent of the absolute power levels or the frequency in use. Such an instrument, with its single meter, would be ideal for incorporation into transmitters and transceivers (especially with the physically small sampling circuits associated with it).

The swr can be expressed in terms of the forward and reflected voltages according to:

$$\text{swr} = \frac{E_f + E_r}{E_f - E_r} \qquad (1)$$

We wish to generate this function electronically, so that outputs of the two detectors can be used to generate a meter current proportional to SWR. This would be rather tedious, though not impossible.

Conveniently, manipulation of equation (1) shows that:

$$\frac{E_f}{E_r} = \frac{\text{SWR} + 1}{\text{SWR} - 1} \qquad (2)$$

which although not proportional to SWR, is a mathematical function of it only. Electronic division of E_f by E_r is easily done by taking logarithms and subtracting. That is:

$$\log \frac{E_f}{E_r} = \log E_f - \log E_r$$

Table I

	Ω	Ω
Line impedance	50	75
R3 and R4	27	33
R2	220	180

Values for R2, R3 and R4 to be used in 50 and 75Ω transmission lines.

In Fig. 9, the two silicon diode voltages are proportional to the logarithms of their currents, which in turn are proportional to the forward and reflected voltages. The two diode voltages can be subtracted directly by connecting a meter between them, rather than from each one to chassis.

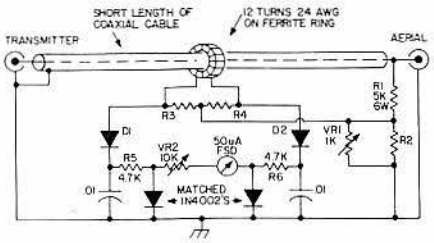

Fig. 6. Circuit of the logarithmic directional wattmeter. D3 and D4 are matched (see text).

The meter cannot be calibrated linearly in SWR, because of equation (2), and because the circuit does not take anti-logarithms after subtracting the logarithms. The outcome of this is beneficial: the SWR meter is increasingly sensitive as the standing wave ratio approaches 1:1. This is where one wants most sensitivity: to make the final

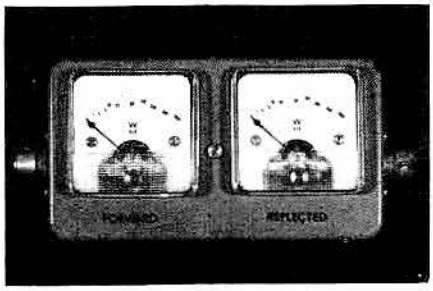

Fig. 7. An experimental logarithmic wattmeter.

adjustments to aerial arrays, to measure the variations in SWR over a band, and so on. Fig. 10, shows a calibration curve for SWR meters. Naturally the meter sensitivity cannot be completely independent of the power level in use. Accuracy falls when the reflected power is less than about half a watt (this corresponds to an SWR of 1.05:1 when the forward power is 1 kW).

A differential amplifier could be added to the circuit of Fig. 9, to enable a less sensitive meter to be used.

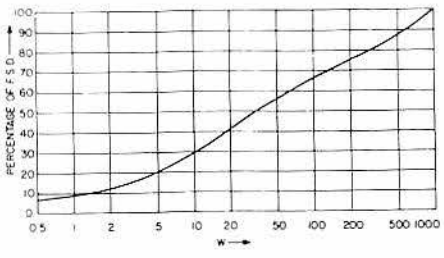

Fig. 8. Calibration curve for logarithmic wattmeters.

Construction of the Instruments

Layout of the sampling circuits is fairly critical, see Fig. 11. The input and output sockets should be set a few inches apart, and connected together with a short length of coaxial cable. The coax braid must be grounded at one end only, so that it acts as an electrostatic screen between the primary and secondary windings of the toroidal transformer. Twelve turns of 24 AWG enamelled wire, equally spaced around the circumference of the ring, form the secondary winding. The primary is formed by simply threading the ring onto the coax.

A suitable ferrite ring is the Mullard FX1596, made in England, although other types are suitable. The FX1596 has an outside diameter of half an inch, and is designed for wideband rf applications between 5 and 20 MHz. The main requirement is that the ferrite material should maintain a high permeability over the frequency range in use.

Other components in the sampling circuits should have the shortest possible leads. R1, R2 and R must be non-inductive solid carbon types: for high power levels (about 100 watts) R1 should consist of two or three 2 watt carbon resistors in parallel. VR1 should be a miniature skeleton potentiometer to keep stray reactance to a minimum, although it may be dispensed with by trying various fixed resistors for R2 until the reflected indication under matched conditions is zero.

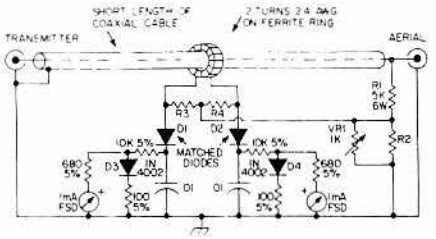

Fig. 9. Complete circuit for a power-independent, frequency-independent direct-reading SWR meter.

The detector diodes need to be matched for similar voltage drop, using the circuit in Fig. 12. Point contact germanium types with a PIV rating of 80 volts or so are recommended.

Logarithmic diodes should be modern medium-current silicon junction types, such as conventional rectifier diodes. The 1N4002 is specially recommended for its good logarithmic properties. Log diodes should also be matched with the circuit in Fig. 12.

The 0.01 μF decoupling capacitors should be a disc ceramic type.

In designing a toroidal transformer different to that specified, several factors should be borne in mind. As the number of secondary turns increases, the self-capacitance rises and causes the response to fall at high

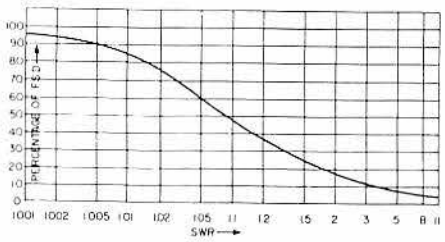

Fig. 10. Calibration curve for SWR meters of the type described in Fig. 9.

frequencies. Failure of this nature causes the reflected power indication to rise; in other words the directivity of the instrument falls. If the 27Ω resistors are raised appreciably in value, the instruments will eventually become frequency sensitive.

The ratio of the voltage sampling resistors (R1 and R2) in the HF designs is determined by the sensitivity of the current sensing circuit, and the two sampling voltages must be equal in magnitude under matched conditions. VR1 provides fine adjustment of the ratio. Absolute values of the resistors can be varied considerably, bearing in mind that as their values increase the stray capacitance across them may need to be compensated for.

Useful Equations

Let the line current be I amps, the line voltage be V volts, and the characteristic impedance of the transmission line be Z_O. Then $V = IZ_O$.

If the current transformer has a ratio of 1:n, and each of the resistors in its secondary circuit has a value of RΩ, then the rf voltage across each of them is given by:

$$V_{(i)} = \frac{IR}{n} \qquad (3)$$

The voltage detector output is obviously

$$V_{(v)} = \frac{VR_2}{R_1 + R_2} = \frac{R_2}{R_1 + R_2} IZ_O$$

Which is, to a good approximation,

$$V_{(v)} = \frac{R_2}{R_1} IZ_O \qquad (4)$$

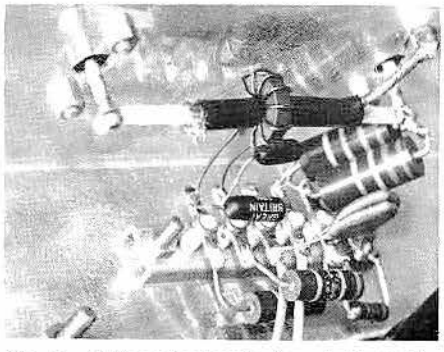

Fig. 11. Photograph showing layout of sampling circuits used in an experimental swr meter.

The main design equation for all the HF instruments is therefore:

$$R_2 = \frac{R.R_1}{n.Z_O}$$

where the value for R2 includes the effect of VR1, if fitted.

The dissipation of some of the components specified is quite high. For those planning different circuits, the following equations express the dissipation of R1 and the current transformer resistors R:

$$W_{(R1)} = \frac{Z_O.W}{R_1} \text{ watts,}$$

where W is the transmitter output power.

$$W_{(R)} = \frac{W.r}{n2.Z_O} \text{ watts.}$$

In the instruments described, $W_{(R1)}$ is about 5 watts, and $W_{(R)}$ 2 watts for a transmitter power of 500 watts.

Calibration

If any of the instruments are built exactly as described, and used in systems of the correct impedance, the calibration given in Figs. 2, 8 and 10 will be sufficiently accurate for most purposes. For those designing their own circuits, the following procedure is recommended.

Test equipment needed includes a high power rf source (a transmitter) and an rf voltmeter. The instruments can be calibrated with less accuracy without the rf voltmeter. The wattmeters are calibrated by feeding power through the meter into an appropriate dummy load (50 or 75Ω). VR1 is set for minimum reflected power indication, and the power scale is marked according to the rf voltage appearing across the load. If an rf voltmeter is not available, a peak-reading type can be made with a diode, capacitor and dc voltmeter. As the detector output is equal to the peak rf voltage applied to it, equation (4) leads to:

$$V_{(det)} = 2.8 \text{ V } \frac{R_2}{R_1} = 2.8 \sqrt{WZ_O \frac{R_2}{R_1}}$$

It would be difficult for most amateurs to obtain sufficient high power carbon resistors to calibrate an SWR meter by means of deliberate mismatching. An indirect method is therefore recommended.

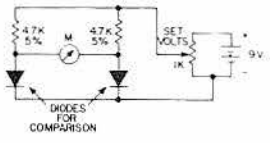

Fig. 12. Hookup circuit for matching detector diodes for equal forward voltage drop, and silicon junction diodes for similar logarithmic properties. The meter should be as sensitive as possible (say 50 μA fsd), and should not deflect appreciably as the voltage is varied between zero and nine volts.

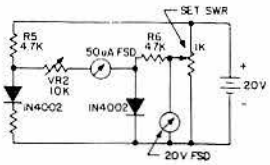

Fig. 13. Circuit used to calibrate SWR meters(see text).

Disconnect R5 and R6, Fig. 9, from the detectors, and connect them instead as shown in Fig. 13. One voltage is fixed at about 20 volts, and the other is varied between zero and 20 volts. The ratio of these voltages corresponds to a definite SWR which can be determined from equation (1). Before carrying out this procedure, however, VR2 should be set for full scale deflection of the meter under matched conditions at the highest power level to be used.

Conclusions

All of the instruments described in this article have been tested under actual operating conditions, on all amateur bands between 1.8 MHz and 30 MHz. Power levels used varied from 100 to 1200 watts. With the components specified, the instruments will sustain power levels well above the kilowatt level for periods of tens of seconds.

It is hoped that by introducing frequency independent directional wattmeters, one will be able to make useful comparisons of absolute power levels and accurate assessments of standing wave situations. The logarithmic scales are an added convenience, and the direct-reading SWR meter offers a saving in meters.

SWR BRIDGES USING ZERO-CENTER METERS

John Schultz W2EEY/K3EZ

The basic coaxial cable swr meter, which samples both the forward and reflected voltages on a transmission line, is an essential instrument in setting up an amateur station. Although a low transmission line swr in itself doesn't guarantee that an antenna system will work, knowing what the swr is remains an essential bit of information in evaluating the status of the transmitter/antenna interface.

The virtues of the usual coaxial line swr meter – economy and simple circuitry – are offset by the awkwardness involved in using the instrument: that is, switching back and forth between "forward" and "reflected" switch positions and adjusting a sensitivity control for sull-scale deflection in the forward position. This awkwardness of operation is partly relieved by dual-instrument swr meters so the forward/reflected switch is no longer necessary – but the cost of the instrument increases. The awkwardness of

operation can be completely relieved by special dual movement meters with crossing pointers and/or special circuitry, but then the cost really soars.

Another approach is the usage of some different circuitry to detect the swr which can then activate a zero-center meter so one can peak up the antenna coupler, etc., for minimum swr on a transmission line with the same ease as one tunes an FM entertainment receiver for a zero-center reading on the discriminator meter. In the end analysis, practically no line is set up for any specific swr, but simply for the lowest swr that can be achieved. So, why not make the process as simple as possible? Circuitry to do this has actually been available for many years and was especially developed for use with the automatic servo-tuning of military transmitters. The zero output when tuning conditions were correct, and the plus or minus output when they were not, allowed, after sufficient power amplification, the activation of motors to tune transmitter PA task circuits, coupling circuits, etc. Now, with the economical availability of toroids and imported zero-center meters, zero-center swr type circuits can be applied to amateur usage and meet the criteria of being easy to construct and economical. They offer a real challenge to the conventional type of swr meter, especially when one is using a multiband antenna and tuner arrangement, or just leaves an swr meter in a transmission line to verify that the line swr is holding constant. In the former case, one usually knows the approximate transmitter/tuner settings on each band, and the swr meter is used to peak up the adjustments. Such peaking-up, as mentioned before in the case of an FM receiver, is certainly facilitated by just having to look at a zero-center meter. In the latter case, a zero-center meter will more readily reveal slight changes in transmission line swr from an established norm. Perhaps the only place where a conventional swr meter is still to be preferred is when one is

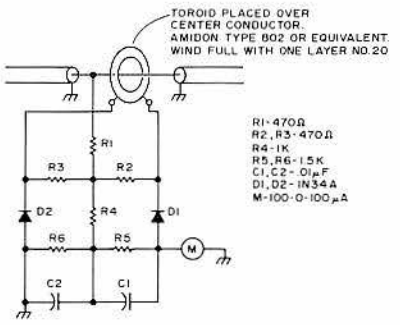

Figure 1.

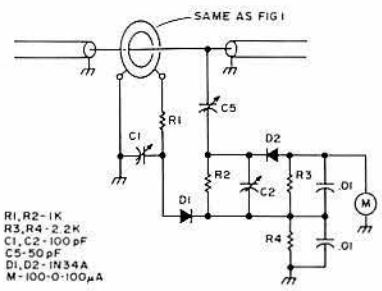

Figure 2.

dealing with experimental antennas where extreme swrs exist and a conventional swr meter can help to more quickly obtain "ballpark" antenna coupler or loading coil settings. The zero-center type circuits operate on a slightly different basis than the conventional swr meter circuits, and just a brief review of transmission line operation will be helpful to understand the different basis for the functioning of the two types.

If a transmission line is attempting to deliver power to a load, both voltage and current values exist along the line. If the antenna load impedance is resistive and equals that of the line impedance, all the power feed into the line reaches the antenna less any power loss in the line itself because of the line's inherent loss. If the load is not equal to the line impedance or reactive, part of the power the line tries to deliver is rejected by the load and reflected back along the line. This sets up standing waves of voltage and current which are not in phase with the original voltage and current waves the transmitter is trying to "pump" into the line.

Conventional swr meters sample a portion of the voltage or current wave traveling towards the load and a sample of that traveling back from the load. The relative amplitude of the two samples is the swr and, of course, the desired condition is that there be no reflected wave from the load. If there is no reflected power from the load, the line is often referred to as being "flat." This term is a bit misleading. Although the reflected power may be zero under matched conditions, the power flowing to the load via the line will still set up normal sine wave distributions of voltage and current along the line.

Another way to sense that the load is matched to the line is to determine first of all that the phase difference between the voltage and current on the line is zero and that the ratio of the in-phase voltage and current is correct for the impedance of the line being used. If there is no reactance present in the load, there will be no phase difference between voltage and current, as in any ac circuit feeding a resistive load. If the load is not only non-reactive but also of the correct resistance, the ratio of voltage and current on the line will have a definite relationship correct for a given line impedance. The zero-center meter circuits are designed to monitor both of these line conditions.

Practical Circuits

Two separate circuits are used to monitor the line conditions just described. One could switch a separate zero-center meter between the two line monitor circuits but with imported zero-center meters available for as low as $1.50, it is hardly worthwhile to do so. (A good source of the 100-0-100uA meters needed is Edlie Electronics, 2700 Hempstead Turnpike, Levittown NY 11756. Their meters with order number DA798 or DA792 cost only $1.50 but they have a $7.50 mail order minimum.) Also, for many installations, it is not necessary to use both circuits. For instance, in a home installation feeding a set of various fixed antennas, it would probably be of primary interest to have the impedance monitor circuit (voltage/current ratio). Once the antennas have been set up and operate satisfactorily, one would primarily just be interested to know that some impedance condition on the line has not changed. In a mobile installation, where some reactance cancelling L or C needs to be adjusted with frequency changes, it would be of prime interest to have the phase monitor circuit once the installation has been initially set up for a correct impedance match, and the reactance cancelling component only needs adjustment during actual operation.

Phase Monitor

Fig. 1 shows the circuit of the phase monitor. It is a basic discriminator circuit. The voltage on the transmission line to ground is sampled via R1. The current on the line induces a voltage in the windings on the toroid placed in the line which, of course, is 90° out of phase with the voltage sample. The voltage proportional to the line voltage is divided across R1 and R4 (C1 and C2 are rf bypass capacitors). The voltage proportional to line current (across the toroid winding) is divided between R2 and R3. Referenced to the center point of R2 and R3, these voltages are 180° out of phase with respect to each other and either one is 90° out of phase with respect to the voltage across R4. The voltages across R2 and R4 are rectified by D1 and, because of the diode

polarity, produce a voltage with the polarity indicated across R5. Similarly, R3 and R4 and D2 produce a voltage of opposite polarity across R6. When the transmission line current and voltage are in phase, the voltages across R5 and R6 are equal and opposite, and the resultant voltage output which drives the meter is zero. For an out-of-phase condition, some output voltage exists whose magnitude indicates the amount of the phase difference and whose polarity would indicate whether the line voltage leads or lags the line current.

One could actually calibrate the output meter for different magnitudes and directions of phase difference, but this would be very tedious and not of real use for just checking the adjustment of a line for reactance cancellation. The only calibration that has to be checked is to excite the circuit into a resistive dummy load and to be sure that the zero-center feature works. If it does not, it indicates that some unbalance has been introduced during construction or some of the components (R2/R3 and R4/R5) are not closely enough matched. If the meter excursions off zero center become too violent with a high power transmitter, some additional resistance can be introduced in series with the meter to limit the maximum current flow.

Impedance Monitor

Fig. 2 shows the circuit of the impedance monitor, which is also a form of discriminator circuit. Samples of the transmission line voltage and current when they achieve the desired ratio produce an output voltage from the circuit which is zero. As in the previous circuit, a toroid placed around the center conductor of the transmission line develops by transformer action a voltage proportional to the line current. A sample of the line voltage to ground is taken via the variable capacitor C5. Unlike the previous circuit, both the sampled voltages are rectified, producing voltages across load resistors R3 and R4, without paying any attention to the phase differences between the sample voltages. It is only the amplitude of the sample voltages which determines the amplitude of the voltage across R4 (for the line voltage) or across R3 (for the line current). Because of the diode polarities, the voltages across R3 and R4 are of opposite polarity. They will cancel when equal, producing zero output voltage, and since C5 is variable, this condition can be set to occur at any desired line voltage to current ratio.

The difficulty with this circuit is that the sample voltages generated by the toroid transformers and the C5 coupling are frequency dependent. The rest of the components in the circuit (R1/C1 and R2/C2) are there to help eliminate the frequency sensitive output of the coupling elements over a reasonable range.

C5 is set with C1 and C2 at mid-range to provide a zero voltage output from the circuit on 20m when the line is terminated in a resistive load equal to the line impedance. Going to 10m, C2 is adjusted to restore balance and on 80m, C1 is used to restore balance. The adjustment has to be gone through several times before a good balance is achieved over the entire HF range. It would be possible to calibrate the meter with different value load resistors for different swrs. For high value loads, the meter would move off center in the opposite direction for low value loads. But, such calibration would only hold true for non-reactive loads.

Construction

Many conventional swr bridge circuits have been described over the last year or two in amateur literature where a toroid transformer, rather than a parallel wire to the center conductor of a coaxial line, has been used as a pickup element. The construction of such units applies equally well to the circuits shown here. It is only the circuitry following the pickup element that is really different, plus the added R1 pickup in Fig. 1, or the C5 pickup in Fig. 2. Note that it doesn't matter on which side of the toroid these pickups are placed. However, as in any rf circuit, all leads must be kept as direct and as short as possible. The circuits shown are for the HF range, but by changing the toroid and values of the bypass capacitors, they can be extended, by experienced experimenters, into the VHF range.

Chapter II

How to Measure RF Impedance

THE ANTENNASCOPE – AN EFFECTIVE TOOL

W. R. Carruthers VE3CEA

There are two types of antennas, commercial and amateur. A commercial antenna is generally designed for one frequency, has many acres of ground around it, no obstructions and miles of heavy copper cable buried underground to provide an "effective" ground. These antennas work as designed – very well. The amateur antenna, on the other hand, is just that – an amateur design and construction.

This antenna is subject to all ills, roof tops, buildings, trees, TV masts, house electric wiring, telephone wires and what not. It's a wonder they work at all! But they can be made to work and thousands of amateurs make them work. They make them work by pruning or lengthening the feeder cable and by using an antenna coupler. These are always empirical steps, the "let's cut and try and see what happens" method. How much better it would be, and a time saver too, if we tested our antenna systems electrically and *knew* what was happening and then could take intelligent action to put the whole antenna system into resonance.

This fact is well known – an antenna can only accept power and radiate properly when it is operating at its resonant frequency. This is no problem for the commercial people who operate at one frequency. The amateur, however, wants to "roam the band" and may wish to operate over frequencies hundreds of thousands of cycles wide, even megacycles wide. How can he do this with a fixed antenna system? The answer is, he can't! But he can construct an antenna system for a certain frequency and take the penalty of reduced radiation when he moves far away from it. However this actually works very well, because each amateur has his own particular part of a band in which he likes to operate – and his friends tend to stay there too. On this particular spot, the amateur works diligently to "put out a good signal."

The question arises – how can we make sure our antenna system is radiating well at the particulaf frequency we wish to use? One answer is to use electrical test equipment to show us what is happening on the whole antenna system, which includes the antenna and the feed line.

One of the most useful devices for this purpose is the rf bridge, generally called the Antennascope. It is a simple device, inexpensive to construct and very effective in results. It is usually powered by a grid dip oscillator. Such bridges should be used at the junction of the feed line and the antenna and will show the resonant frequency of the antenna itself and the radiation resistance at the feed point.

Making such measurement up in the air is a difficult thing for the average amateur and impossible for those whose antennas are supported at the ends. If we are willing, however, to accept a small degradation in results, we can use the *rf* bridge at the station end if we have a half wave, or multiple of a half wave, feed cable. At every half wave point on a feeder cable the voltage and current vectors are in phase, which simply means that the electrical condition seen at the end of the cable is repeated every half wavelength in the cable. We can use the *rf* bridge then, at the station end of the feed line, if we are willing to agree that the results will not be 100% but reasonably close to it. The results will be affected by all the various factors that affect amateur antenna resonance and these effects may give us some peculiar results, but they can be overcome and the final results may be quite valuable to us.

Let me give you an example to illustrate what I'm talking about and to show you how effective the use of the *rf* bridge can be: –

A friend of mine constructed a 40 meter inverted V antenna, held at the feed point 40' up on his beam tower, 66' legs down to supports which held the ends about 8' off the ground. Feed line was 100' of Twin Amphenol cable, velocity factor .68. The antenna was difficult to feed, swr was high, radiation was poor. He asked me to have a look (electrical) at it. I took my grid dip meter, *rf* bridge and vtvm.

The first thing done was to check the feed line length. 1/2 wave length at 7.1 MHz was 492 x .68/7.1 or 47.1 feet. Two 1/2 wave lengths (to get into the station) would be 94.2 feet.

The first conclusion was that the feed line was 5.8 feet too long.

Next Test No. 1 was made using the *rf* bridge with results as shown in **Fig. 1**, the results being shown in table form and also plotted in graphical form.

It was obvious from this graph that the antenna system was resonating outside the

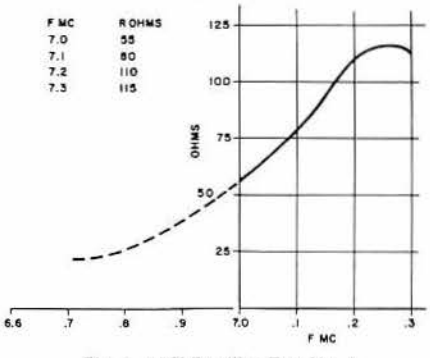

Fig. 1. 100' Feedline Test No. 1.

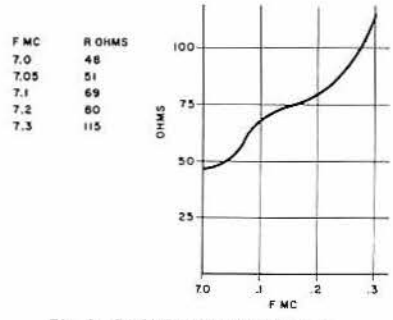

Fig. 2. 94.2' Feedline Test No. 2.

band as shown by the dotted lines. This test was repeated and the results were taken down to 6.4 MHz. They showed the system to be resonant at 6.6 MHz.

Test No. 2 was made next using the feed line cut to 94.2 feet. Fig. 2 shows the results.

It was obvious the resonant point of the system was rising.

Test No. 3 was made next, cutting the feed line to 91.2 feet long. Fig. 3 shows the results.

F MC	R OHMS
7.0	43
7.1	46
7.2	76
7.3	81

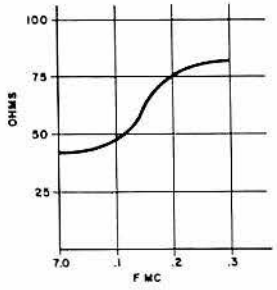

Fig. 3. 91.2' Feedline Test No. 3.

The resonant point was rising, but not far enough yet.

Test No. 4 was made using the feed line cut to 88.2 feet long. Fig. 4 shows the results. It was obvious that we were very

F MC	R OHMS
7.0	45
7.05	47
7.1	51
7.2	60
7.3	75

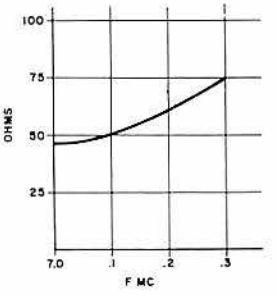

Fig. 4. 88.2' Feedline Test No. 4.

close to the resonant frequency of 7.1 MHz which my friend wished to use.

Test No. 5 was with 85.2 feet in the feed line. Fig. 5 shows the results.

F MC	R OHMS
7.0	78
7.1	61
7.2	60
7.3	66

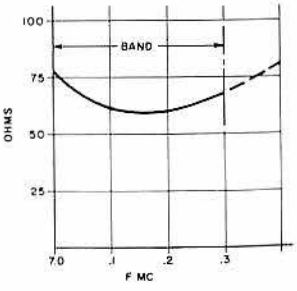

Fig. 5. 85.2' Feedline Test No. 5.

Test No. 6 was with the transmitter (300 watts CW) and antenna coupler connected. There was no trouble in loading and no trouble in balancing the coupler to obtain an swr of 1 to 1 ratio.

The results on the air were interesting, 5/9+ reports to the Eastern half of the U. S. A., 5/8 reports to Germany etc. *Conclusion:* The results shown above are not precise, nor can they be expected to be precise. There are too many unknown factors entering the electrical picture, such as those which required a shortening of the feed line, in this example, to somewhat less than a half wave length. But the bridge showed us the overall picture and suggested what was required to be done. The on-the-air results show that it was giving us a good picture and a result that was very satisfactory for my friend's needs.

Why not construct an *rf* bridge and check you own antenna system? I suggest it will pay off and be very informative to you, showing you what your antenna system looks like electrically and what to do to bring your whole system to the resonant frequency you wish to obtain. . . . VE3CEA

HOW TO BUILD AN ANTENNASCOPE

Paul Franson WA1CCH

A type of simple bridge used for measuring antenna impedance is called the Antennascope, shown in Fig. 1. This bridge is designed for low power operation – a grid dip meter usually gives plenty of power. It should be built very compactly with short leads. The potentiometer should be of high quality; an Allen-Bradley Type J is fine. The bridge can be calibrated with regular composition resistors. Simply connect the resistors in turn to the antenna terminal and adjust the pot until the meter reading dips to zero. Then mark the value of the resistor by the pot pointer. In use, the meter reading will not null completely except for resistive loads, so it will not read zero for reactive antennas. Nevertheless, the minimum reading will occur at the approximate impedance reading. Remember that all antenna bridges should be used between the antenna and the transmission line.

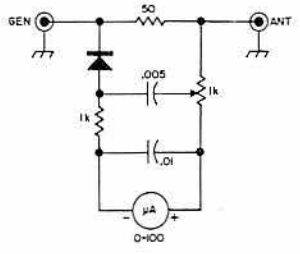

Fig. 1. The Antennascope is a simple antenna impedance bridge. It should be constructed compactly for best high frequency use.

THE MARK III RF IMPEDANCE BRIDGE

Mark Cholewski W6CRT

NEED to measure the input impedance of that new beam? Or maybe to find out just what is the Q of the coils in your final? Or even to determine how much signal is being soaked up by your coax? If you ever want to do these, or any similar jobs, then the Mark III RF Impedance Bridge is the thing for you.

You can build it for a total cost of about $30 (exclusive of sheet metal) and, if you follow instructions closely, it will be accurate to closer than 10 percent throughout its operating range. Unlike the more common resistive-bridge and reflectometer methods of measuring impedance, the Mark III operates equally well at resonance or far away. It will measure both resistance and reactance present in resistors, capacitors, inductors, antennas, and transmission lines at any frequency between 2 and 30 mc.

Before we start into the actual construction of the Mark III, one thing must be emphasized. Accuracy can be assured only if the components, circuit, and parts layout are absolutely duplicated. The original instrument's calibration was obtained through tedious laboratory techniques. If you make any changes, the calibration curves will no longer apply. However, if instructions are followed to the letter you need have no worries about accuracy. A test model, built by W6BJU following these instructions, checked out to 2 percent accuracy at 2 mc and 10 percent at 30 mc.

Construction of the Mark III divides into three major sections: Preliminary metalwork, actual wiring, and calibration. Each will be described separately. Ready? Let's go!

Preliminary Metalwork

1. Cut, drill, and bend to shape from soft aluminum shields S1, S2, and S3 as shown in Figs. C1, C2, and C3.
2. Cut, drill, and tap plexiglas insulators I1, I2, and I3 from bulk rod stock as shown in Figs. C4 and C5. When tapping plexiglas, use water as lubricant.
3. Cut, drill, bend, and solder tubular shields S1A, S2A, and S3A as shown in Fig. C6. Copper or brass may be used; aluminum should be avoided because of solding difficulties.
4. Assemble shielded resistor assembly R2/S4 as shown in Fig. C7. The copper tubing must be drilled out to clear the body of R2. When soldering, hold the assembly in a vise to protect R2 from excessive heat.
5. Cut, drill, bend to shape, and solder box shields S1B, S2B, and S3B as shown in Fig. C8.
6. Drill S5 (a 3x4x6 LMB unpainted chassis box) as shown in Fig. C9.
7. Cut, drill, and bend to shape shield partition S5A as shown in Fig. C10.

Shielded Transformer

While classified under the "preliminary metalwork" section for reasons which will become obvious, construction of the shielded transformer is the most critical part of the entire project. Before proceeding, read and re-read steps 8 through 24 and be sure that you understand them fully. Take special care when soldering—three transformers were built for the original instrument before a non-shorted one was achieved.

8. Cut to length, drill, and tap transformer mounting insulator 14 from 5/16-inch plexiglas rod.

9. Cut and drill two bobbin-end washers as shown in Fig. C12 and solder them to a length of copper tube as also shown. Then cut halfway through the bobbin with a hacksaw.
10. Pull the shielding from an 18-inch length of RG58/U. Save 8 inches for step 19 and use the rest in step 11.

11. Solder one end of the 10-inch shielding into the U-shaped slot on the bobbin end, using an aluminum rod or small drill to keep the inside of the shielding open. It must pass

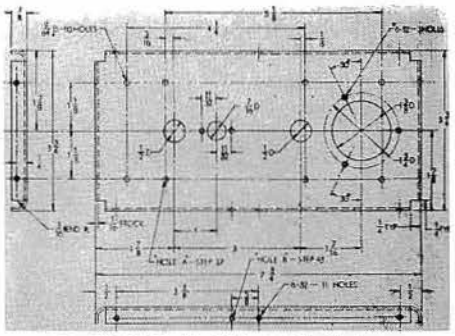

C1—Shield S1 (1 REQ), Mat'l Aluminum

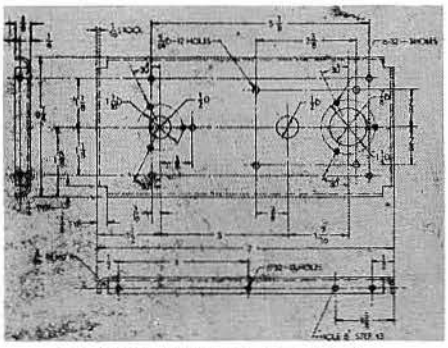

C2—Shield S2 (1 REQ), Mat'l Aluminum

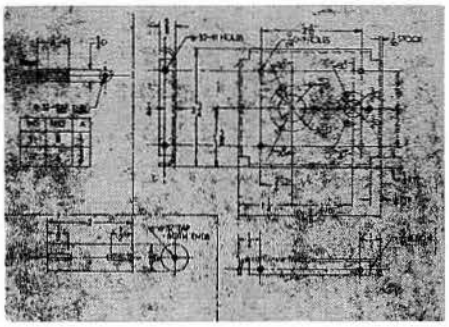

C4 — Insulators, Mat'l Plexglas rod
C5 — Insulator 13 (8 REQ), Mat'l Plexiglas rod

C3—Shield S3 (1 REQ), Mat'l Aluminum

No. 26 plastic-covered wire. Clean off all metal burrs and solder splatters.

12. Wind 48 turns of No. 26 plastic-covered hookup wire on the bobbin in three lays of 16 turns each. Solder the start of the winding at point A (see Fig. C12) and wind in the direction shown by the arrow.

13. The last turn will end at the shielding attached in step 11. Feed the free end of the wire into the shielding, draw the turns tight, and secure the winding with plastic tape.

14. Cut a piece of brass or copper shim stock as shown in Fig. C13 to a length which will wrap around the bobbin but will not allow the ends of the shim stock to touch each other.

15. Tin the shim stock along the edges.

16. Place the wound bobbin in a vise, wrap the shim stock around it, lining up the free ends of the shim with the slot cut in step 9, and solder the shim to the bobbin ends. Caution.

Do not overheat the winding; the plastic covering melts easily and a short is almost impossible to detect.

17. Connect an SO-239 coax connector and UG-177/U hood to the shielded primary lead as shown in Fig. C15.

18. Wind one turn of ¼-inch diameter half-hard copper tubing around a 1-inch diameter form. Saw the tubing as shown by "phantom lines" in Fig. C14. Drill as shown in Fig. C14 and clean off all burrs.

19. Locate the 8-inch piece of shielding left over from step 10.

20. Using same technique as in step 11, solder one end of the shielding into the ⅛-inch hole. Clean off all solder splatter and burrs.

21. Solder one end of another length of No. 26 plastic-covered hookup wire to point A (see Fig. C14) and wind three turns inside the tubing in the direction shown.

22. Feed the free end of the hookup wire through the shielding. Bend the tubing into final shape as shown in Fig. C14. Pull up the three turns snugly, making sure that the plastic coating is undamaged.

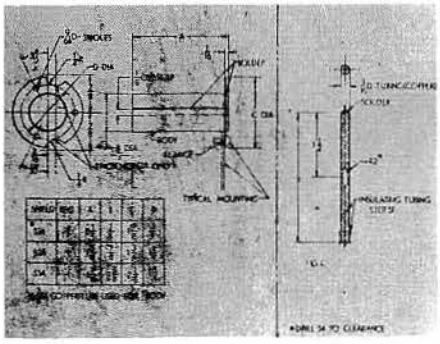

C6—Tube shield, Mat'l .010 Brass

C7 — Shield Assembly S4

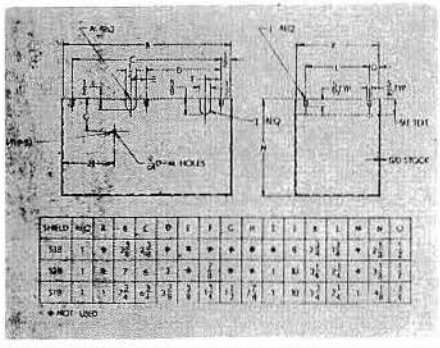

C8—Shield can, Mat'l Aluminum

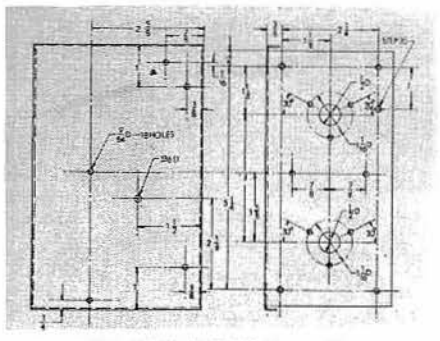

C9—3X4X6 LMB Shield can S5

23. Connect a male phono plug to the free end of the shielded wire as shown in Fig. C15. Length of the wire is critical.

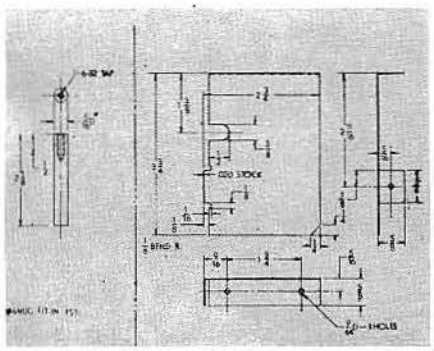

C11 — Insulator 14, Mat'l Plexglas

C10—Shield Partition S5A, Mat'l Aluminum

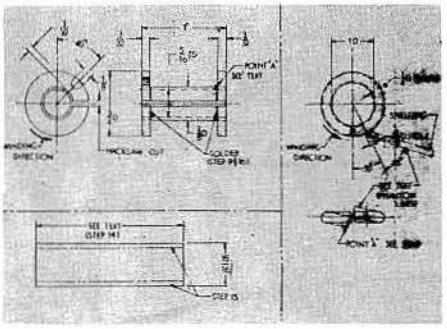

C13—Shield PS1A, Mat'l .005 Brass or Copper
C12 — Primary bobbin PS1, Mat'l Brass or Copper

C14—Shield PS2, Mat'l copper

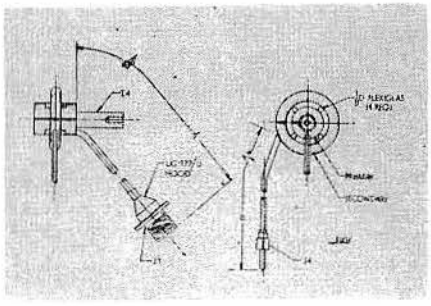

C15—Transformer assembly

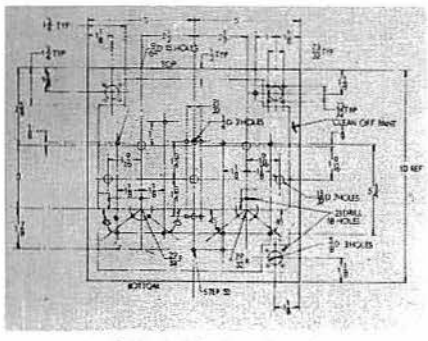

C16—Inside view of panel

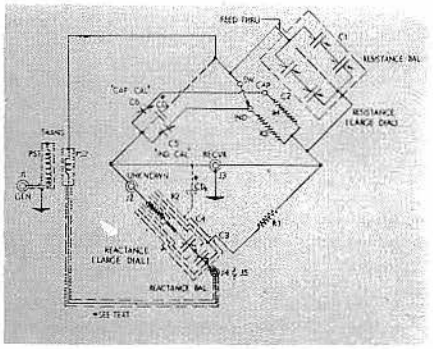

Fig. 1—HF. RF. Bridge Mark III Schematic

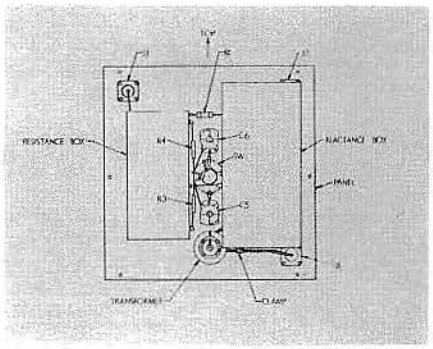

Fig. 2—Inside view

24. Using four pieces of ⅛-inch diameter plexiglas rod as spacers, assemble the primary and secondary shielded windings as shown in Fig. C15. Attach insulator I4 to the transformer by cementing it into the bobbin hole with Duco. Cement both windings to spacers with Duco and allow to dry overnight. This completes the transformer.
25. Remove top and bottom from the 8x10x10 utility box. Remove all paint from flanges; clean to bare metal to provide adequate rf shielding on reassembly.
26. Remove paint from inside of bottom plate for ½ inch in from each edge.
27. Remove paint from inside of top plate as shown in Fig. C16 by "phantom lines."
28. Drill the top plate as shown in Fig. C16.

Note that drawing shows INSIDE surface of plate.

29. Cut shafts of all four variable capacitors to ⅜-inch length. Remove all trimmer capacitors.
30. Tap the threeholes on the face of each capacitor, using a 6-32 tap. Take care not to damage the first stator plate; a bottom tap may be necessary. Attach three type I2 insulators to C1 and C2, using ¼-inch-long 6-32 set screws as shown in Fig. 3. This completes preliminary metalwork.

Actual Wiring

31. Attach C1 and C2 to shield box S5 using six ¼-inch-long 6-32 machine screws. Connect stator lugs of C1 to those of C2 with No. 18 tinned wire, as shown in Fig. 3.
32. Mount two soldering lugs as shown in Fig. 3 and connect remaining stator lugs to them, using No. 18 tinned wire.
33. Press the Erie CF-408 feed-thru into the 0.136-inch diameter hole in S5. Solder a short No. 18 tinned lead from the inside terminal of this insulator to the wire installed in step 31, as shown in Fig. 3.
34. Attach shield partition S5A, using three ¼-inch-long 6-32 machine screws. One of the screws installed in step 32 must be temporarily loosened and removed.
35. Attach four type I3 insulators to shield box S5 as shown in Figs. 3 and C9.
36. Attach three more soldering lugs to S5 as shown in Fig. 3, using ¼-inch-long 6-32 machine screws.
37. Attach four type I3 insulators to shield platform S1, using the 4¼-inch-spaced holes in S1 and 6-32 screws. Attach S1A to S1, using 6-32 screws from the inside of S1. Attach the female phono socket to S1 in the 7/16-inch diameter hole. Attach four type I1 insulators, using ¼-inch-long 6-32 screws. Do not tighten the screw in the hole marked "Hole A" in Fig. C1; this screw will hold a cable clamp later. See Fig. 4 for details of insulator placement.
38. Attach four type I1 insulators to shield platform S2, using the 2⅜-inch-spaced holes in S2 and ¼-inch-long 6-32 screws. Attach S2A to S2. Attach capacitor C3 with 1-¼-inch-long 6-32 screws, using two nuts on each screw as shown in Fig. 4. Mount a soldering lug under one nut as shown. Align the capacitor by adjustment of the mounting screws and nuts.
39. Solder a No. 18 tinned wire to the female phono socket and pass the wire through the corresponding hole in S2. Attach S2 to S1 with ¼-inch-long 6-32 screws going into the type I1 insulators attached to S1 in step 37.
40. Attach C4 to shield platform S3 using ⅜-inch-long 6-32 screws with dual nuts (same as in step 38). Attach S3A to S3.
41. Connect two of the stator lugs of C4 with No. 18 tinned wire as shown in Fig. 4. Slide shield assembly S4 into S3A. Center assembly S4 in S3A, using a piece of ¼-inch-long insulating tubing. Make certain that opposite ends of S4 and S3A are even as shown in Fig. 4, and cement tubing in place with Duco. Solder the shorted end of resistor R2 (which is in S4) to the wire connecting stator lugs of C4.
42. Attach shield platform S3 to S2, using ¼-inch-long 6-32 screws going into the type I1 insulators installed on S2 in step 38.
43. Place a ¼-inch-long 6-32 screw in the flange of S3 as shown in Fig. 4, with a soldering lug. Connect this lug to the stator lug of C3 with No. 18 tinned wire. Using ¼-inch-long 6-32 screws, mount a soldering lug in Hole B (see Fig. C1) of S1 and another in S2 as shown in Fig. C2. These lugs are mounted in a direction opposite to that of the platform flanges.
44. Attach the "unknown" ground lug to the panel next to the "unknown" coax connector hole, as shown in Fig. C16. Attach the "receiver" coax connector to the panel, from the inside. Attach the "IND-CAP" switch to the center of the panel, using an extra nut to position the switch as far as possible from the panel. Orient the switch as shown in Fig. 5. Place a soldering lug under each nut. Mount C5 and C6, using ⅜-inch spacers between the capacitor frames and the panel. Connect the

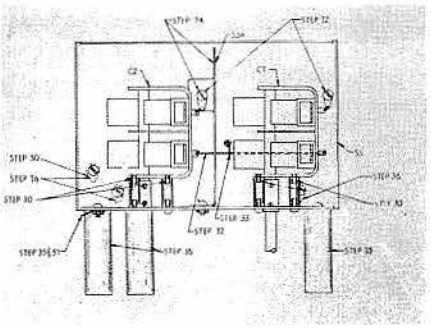

Fig. 3—Resistance box—Inboard view

rotors of C5 and C6 to the lugs of the switch with No. 18 tinned wire as shown in Fig. 5.
45. Solder a 2½-inch length of No. 18 tinned wire to the "COMMON" terminal of the switch. Connect the stators of C5 and C6 to the remaining switch terminals, as well as resistors R3 and R4. Complete connections are shown in Fig. 5.
46. Attach the "unknown" coax connector to

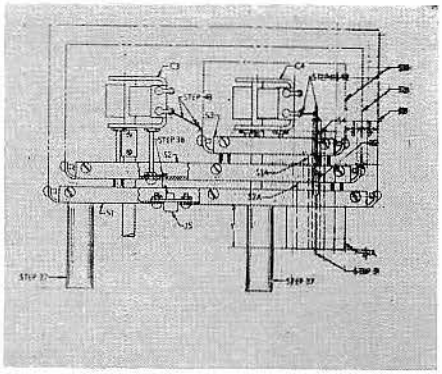

Fig. 4—Reactance Assembly—Inboard view

the panel, placing a soldering lug under one mounting screw. Connect the "unknown" ground lug to this soldering lug to provide a good bond.
47. Mount panel bearings for capacitors C2 and C4. Mount the special panel bearings furnished with the Johnson Vernier Dial assemblies in place. Attach the two large dials to dummy shafts and mount the dial indicator in the position you prefer. Remove the large dials and dummy shafts after placing the dial indicators.

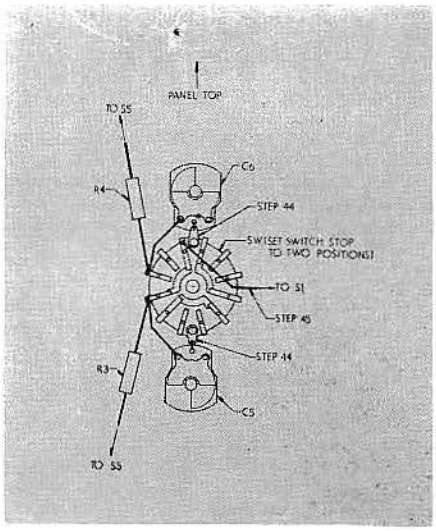

Fig. 5—Switch Assembly

48. Mount S5 at the left side of the panel (as shown in Fig. C16) and mount the assembly of S1, S2, and S3 at the right side. See Fig. 2.
49. Attach shaft couplers to the four capacitors. Cut the plexiglas shafts to length and mount them in place. Attach the large vernier dials. Set the dial of C2 so that it reads "0" at minimum capacity. Set the dial at C4 so that it reads "100" at maximum capacity. Mount the two Calrad dials on the panel, setting them so that they both read "0" at maximum capacity. Attach the knob to the "IND-CAP" switch.
50. Connect resistor R1 (270-ohm deposited-carbon) from the soldering lug on S2 to the lug in line on S5. Connect R3 (220 ohms) and R4 (100 ohms) to the soldering lugs on S5 which were installed in step 36. R3 will be the resistor nearest the bottom of the panel.
51. Connect a No. 18 tinned-wire lead from the "detector" coax connector to the lug on S5. Connect a No. 12 (note different wire size) lead from the "unknown" connector to the free end of R2. *Make sure that* R2 *is not shorted to any shield.*
52. Attach the transformer, completed in step 24, to the bottom of the panel as shown in Fig. 2. Attach the coax connector connected to the transformer to the panel in the "signal generator" hole. In the hole between the transformer and the connector, mount a cable clamp to hold the shielded primary lead. Secure the

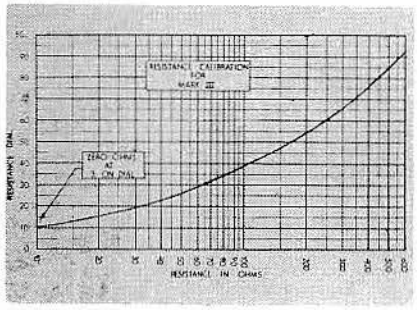

Fig. 6

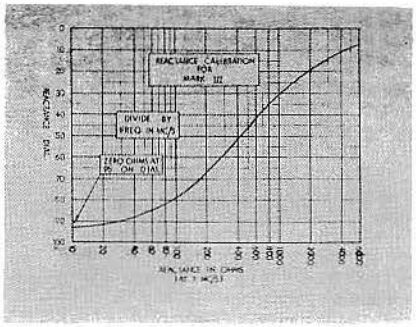

Fig. 7

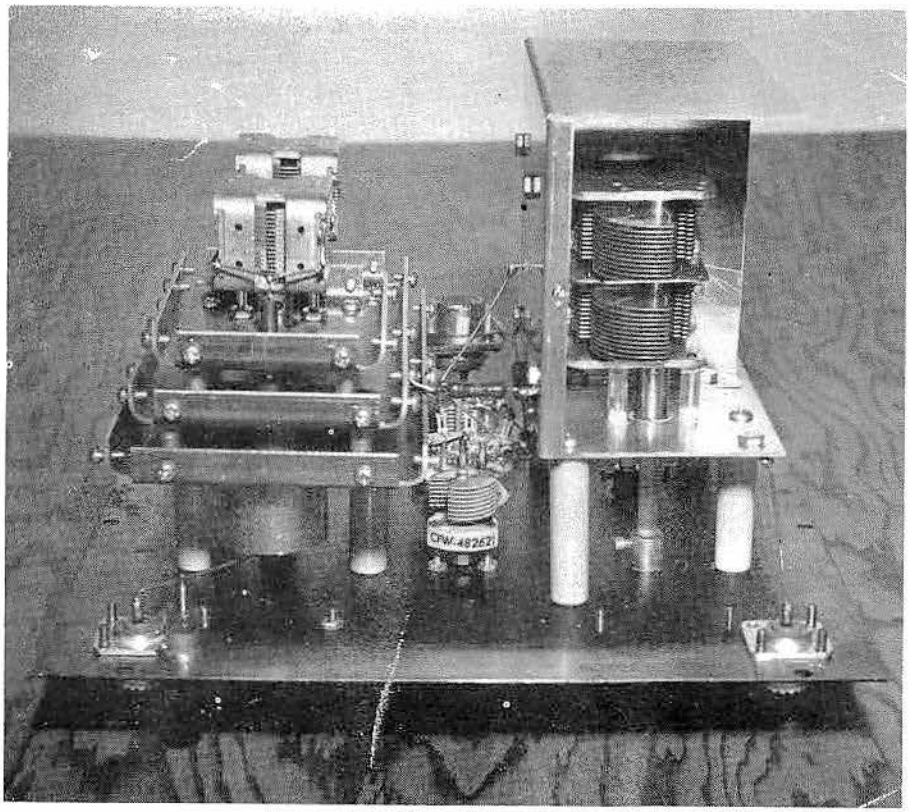

shielded secondary lead with another clamp held by the loose screw installed in step 37.
53. Mount a soldering lug to S1B with a ¼-inch-long 6-32 screw, placing the lug in the direction of the box opening.
54. Place ¼-inch-long 6-32 screws in all remaining tapped holes in S1, S2, and S3. Starting with S3, place all shield boxes in place and secure screws. Connect a No. 18 tinned lead from the soldering lug installed in step 53 to the Erie feed-thru on S5. Set C5 and C6 to mid-capacity.
55. Attach four rubber feet to the bottom plate of the case and four more to the bottom side of the utility cabinet. Restore the front plate in place and secure with the sheet-metal screws provided. This completes construction of the bridge. After calibration, it will be ready for use.

Calibration and Use

Since the Mark III is a null-type instrument (adapted from the Schering bridge circuit) it can only be used with a signal generator and a detector. Both must be shielded; however, a Heath SG-8 will do nicely as the signal generator and any decent communications receiver will serve as the detector. For best results, it

should be calibrated with the signal generator and receiver with which it will be used.

56. Connect the bridge to the signal generator and the receiver, using coax cable from the panel connectors to each.

57. Set both the signal generator and the receiver to 2 mc.

58. Short the "unknown" terminal and ground terminal using a banana plug in the connector or a coaxial short made by soldering the pin of a PL-259 connector to the shell through a copper disc.

59. Set the "IND-CAP" switch to "CAP."

60. Set the "Reactance" dial to 15.

61. Set the "Resistance" dial to 5.

62. Tune the signal generator, only, for maximum signal in the receiver.

63. Using the two small "balance" dials, reduce the signal in the receiver to the lowest level possible. This is the "null" or "balance" condition. The dials will interact, and multiple adjustment will be necessary. However, all receiver and signal generator adjustments must be left alone during this step.

64. Replace the short across the "unknown" connector with the 620-ohm deposited-carbon "test" resistor.

65. Using only the large "resistance" and "reactance" dials, null out the signal once more. Record the final reading of the "resistance" dial. If this reading is 95, you are extremely lucky and the first half of the calibration is complete. If not, proceed with step 66.

66. If the "resistance" dial reading is less than 95, increase the capacity of C6 slightly and repeat steps 60 through 65. If the reading is larger than 95, decrease the setting of C6 and repeat steps 60 through 65. Continue this process until the reading comes out at 95.

67. When capacitive calibration is complete, set the "IND-CAP" switch to "IND," and the "reactance" dial to 30.

68. Repeat steps 60 through 65; if the final reading of the "resistance" dial is other than 95, proceed with step 69.

69. If the reading is less than 95, increase the capacity of C5 slightly and repeat steps 60 through 65. If the reading is larger than 95, decrease the setting of C5 and repeat. Continue until the reading is 95. This completes calibration, and the curves shown here can be used for readings.

Using the Mark III

To use the Mark III, set the instrument up as described in step 56 of the calibration procedure. Set the signal generator to the desired frequency and short out the "unknown" terminal of the bridge as described in step 58.

If you're measuring an inductive impedance, set the "IND-CAP" switch to "IND," the reactance dial to 95, and the resistance dial to 5. Null the signal with the small balance dials.

Now remove the short and connect the unknown. Rebalance the bridge using the large dials, note the readings, and convert the readings to ohms by use of the calibration curves.

These initial values must be corrected. The reactance value is corrected by dividing the value read from the curve by the frequency (in mc) at which the reading was taken. The resistance value is corrected by obtaining the correction factor due to frequency from Fig. 8 and multiplying the reading by this factor.

If you're measuring a capacitive impedance, set the switch to "CAP." Then estimate the reactance of the unknown and set the large reactance dial to a value just larger. Set the resistance dial to 5 and short out the "unknown" connector. Null the signal with the short and again with the unknown, the same as for an inductive impedance.

Correct the resistance reading in the same manner as for an inductive impedance. However, the reactance reading is corrected differently: Subtract the value taken from the calibration curve from the value originally set on the reactance dial. Now divide this remainder by the frequency (in mc) at which the reading was taken. The result is the true value of capacitive reactance.

A few minutes' practice will make operation of the Mark III far more simple than the detailed directions would indicate; in practice, you can make a reading in less time than it takes to read these paragraphs.

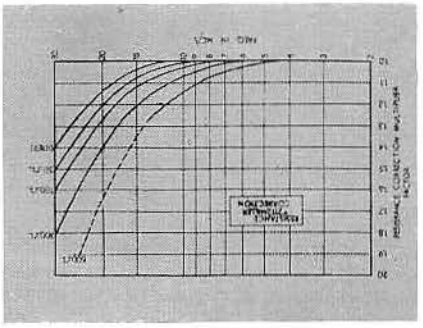

Fig. 8

Parts Substitutions and Design Changes

Since few hams are content to build a "Chinese copy" of someone else's design, a few words on the effect of changes are necessary.

Naturally, the Mark III doesn't represent the only possible—or even necessarily the best—way in which such a bridge can be built. Any part, or all, may be changed. However, any such change will invalidate the calibration curves, and is not recommended unless the builder has access to laboratory equipment.

Even then, before making any substitutions, these three design articles should be read and fully understood:

"A Radio-Frequency Bridge for Impedance Measurements From 4000 KC/S to 60 MC/S," D. B. Sinclair, Proceedings of the I.R.E., November, 1940, pages 497-502.

"A High Frequency Model of The Precision Condenser," D. B. Sinclair, General Radio Experimenter, October-November, 1938, pages 1-7.

"The Effect of Stray Capacitances to Ground in Substitution Measurements," M. Reed, Wireless Engineering, May, 1936, page 284 ff.

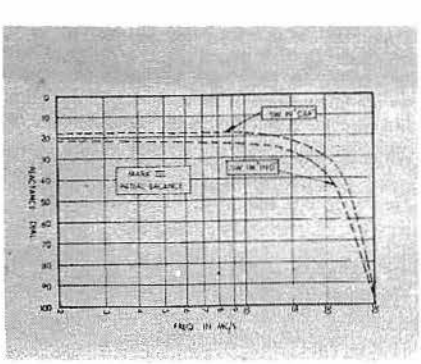

Fig. 9

Parts List

Quan.	Item	Description	Cat. No.
1 ea.	C1, C2	Hi-Q, 10-365 mmf/sect.	2112
1 ea.	C3, C4	Miller, 10-365 mmf	2111
1 ea.	C5, C6	50 mmf air padder (good quality)	APC-50
1 ea.	J1, J2, J3	SO-239 Panel coax connector	
1	J4	Phono plug	
1	J5	Phono socket	
1	R1	Aerovox 1% 1/2W 270 ohm "Carbofilm"	Type-CP
1	R2	330 ohm 5% 1/2W Carbon Resistor	
1	R3	220 ohm 5% 1W Carbon Resistor	
1	R4	100 ohm 5% 1W Carbon Resistor	
1	Test	Aerovox 1% 1/2W 620 ohm "Carbofilm"	Type-CP
1	SW	Centralab 3p; 1 Sect; 2-3 Position (reset stop to two positions only)	2506
*2	Dials	E. F. Johnson Vernier (0-100 CW)	116-285-1
2	Brgs	E. F. Johnson Panel Bearings	115-255
4	Cplrs	Metal ¼ shaft couplers	
3	Rod	¼ inch diameter plastic rod x 12"	
1	Rod	⅛ inch diameter plastic rod x 6"	
2	Rod	⅜ inch diameter plastic rod x 12"	
2	Dials	"Calrad" 1-13/32 inch Vernier Dial	VD-36
1	BP	Binding Post (ground lug)	
1	Case	Bud carrying case 10"x10"x8"	CC-1100
1	Box	LMB box (plain) 3" x 4" x 6"	
1	Hood	UG 177/U coaxial cable hood	
1	Insul.	Erie feed-thru insulator	CF-408
1	Short	PL-259 coaxial male connector	
2	Clamps	Walsco clamp for ⅛ to 3/16 cable	7502-N

Of the above list the critical parts are: C1, C2, C3, C4, J2, R1, Test resistor, Case, LMB box, UG 177/U, Erie feed-thru.

* This author hand engraved these dials per Figs. 6 and 7.

MEASURE RF IMPEDANCE WITH YOUR SWR BRIDGE

Warren McDowell W2AOO

So far, the great majority of antenna impedance bridges that we have found in construction articles are devices that function only with a low power rf source. The run-of-the-mill impedance bridge is designed to operate with a grid dipper as the source of rf excitation. Operation with tube type dippers is generally intended as the transistor dippers produce an rf level that is too low for excitation of this bridge type.

The conventional antenna bridge cannot be left in the transmission line continually as excessive rf energy would soon destroy the device. This means that each time measurement of antenna impedance is desired, the transmission line must be opened and the bridge inserted and grid dip excitation applied. Grid dippers are not necessarily the most accurate rf source for a specific frequency in an amateur band . . . therefore the station receiver must monitor the dipper output for any bridge accuracy. A low power bridge will not often present the true operating impedance of the antenna . . . especially antennas with parasitic elements. A bridge that operates under full transmitter power will present a much more accurate picture of your antenna system at a specific frequency.

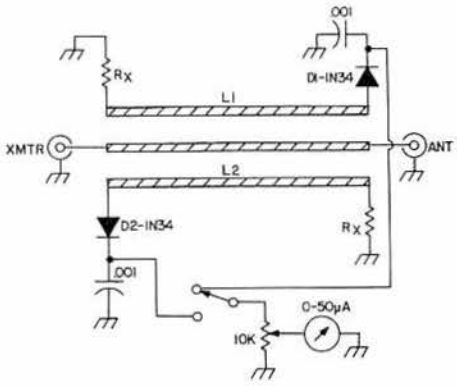

Fig. 1. Conventional swr bridge.

Inspiration for the "In Line" full power bridge came from information concerning the standard swr bridge. Just about every amateur has in his possession some sort of swr bridge and the great majority are of the type illustrated in Fig. 1. This bridge consists of a section of transmission line near which are placed two inductors. These inductors are actually two bridges along with their associated diodes and resistors. One of the bridges reads forward power and the other reflected power. The resistors (Rx) at the end of the inductors L1 and L2 are critical for accurate bridge null (balance) and therefore must be the proper value for the specific transmission line used. For the average swr bridge the value for Rx is 100Ω for 75Ω line and 150Ω for 50Ω transmission line. Considering that resistor Rx is critical for the impedance of the line in use, varying the value of Rx and devising a system of calibration for Rx would enable us to determine the impedance of a line when a null is achieved on the bridge meter.

The "reflected" inductor which is L1 in Fig. 1 is the portion of the bridge circuit we are interested in for impedance measurements. The value of Rx and the transmission line must balance the bridge for a null to be realized. Any variation from the above parameters will mean changing the value of Rx so that the bridge again balances at a new impedance value.

By experimenting with various values of resistance at Rx, it was determined that a 1000Ω potentiometer represents a fair value. The 1000Ω potentiometer is inserted in place of Rx on inductor L1 (see Fig. 2). This is the inductor with the diode pickup located toward the load or antenna end of the swr bridge.

Make sure that all leads to the 1000Ω potentiometer are short and that the metal case (shell) of the potentiometer is well grounded. Excessive lead length or inductance will create inaccuracy of the device. The position of the potentiometer will be determined by the physical layout of your particular swr bridge. It must be set at a point where the shaft can be extended through the front panel of your swr bridge. Allowance must also be made for a dial or other indicating device which can be calibrated in ohms (impedance) on the front panel. It might even be desirable to mount your entire present bridge in another larger case so that all functions can be accommodated.

Calibration of this in-line bridge was the major problem. An ordinary grid dip meter will not provide sufficient excitation for readings. With full power applied, especially a kilowatt, it becomes difficult to find resistive dummy loads of various values to calibrate the bridge. Even with 100W of rf, proper resistive load values are not common.

The solution to the calibration problem came to us in the form of an (ouch!) CB transmitter. A CB transmitter is fortunate if it is able to put out 3W of rf and at the same time is well within the frequency range of an swr bridge. The most important fact is that a CB transmitter will provide adequate excitation for calibration of the bridge with ordinary 5W 5% carbon (garden variety) resistors. For calibration, a good assortment of these resistors is necessary. Use values such as 5, 27, 47, 75, 100, 150, 220 and 470Ω. Intermediate values can be then interpolated on your scale. The calibration procedure is simple . . . first borrow your neighbor's CB, then attach the 5W resistors across the antenna coax connector of the bridge and excitation of the CB transmitter is applied to the remaining connector on the bridge. The bridge sensitivity should be set for a middle scale reading of the meter and the 1000Ω potentiometer is varied until you reach a null on the meter. Mark the value of the calibration resistors on the potentiometer scale (dial). Do this for all of the available resistors and your bridge will be in fair calibration.

At this point we should mention that this system does not measure reactive components in the antenna system. If your antenna is reactive, either inductive or capacitive, the meter will present a shallow, poorly defined null at the operating frequency. A sharp, well defined null will indicate a purely resistive impedance.

When using the bridge in its former function as an swr bridge, set the resistance dial to the value of your transmission line. When measuring impedance, vary the dial for maximum dip on the meter and read the resistance (impedance) directly.

As a final point, it is wise to insert the swr/impedance bridge at a half-wave or an even multiple of a half-wavelength from your antenna. At half-wave points from the antenna, the antenna impedance is repeated. This will enable your measurements to be much more accurate. When determing half-wavelength points, take into consideration the velocity factor of your particular coax.

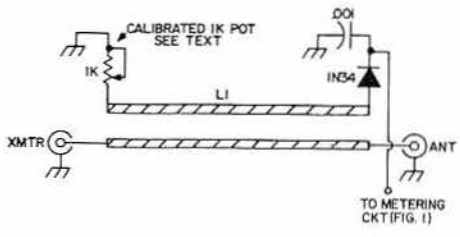

Fig. 2. The modified bridge leads to 1K pot should be as short as possible and shell (case) of pot grounded.

USE YOUR GDO AND Z METER

Denys Fredrickson WØBMW

The GDO is one of the most versatile pieces of test equipment available. Yet there are many hams who don't know how or when to use one. The writer will try to describe and explain some of its various functions.

The GDO is basically a variable high frequency oscillator with a frequency range of approximately 550 kc to 250 Mc. It may also be used as a diode detector or wave meter. The GDO gets its name from the fact that a meter measures the grid current and when the oscillator circuit is coupled to a resonant circuit a reduction in grid current is obtained. This is called the grid dip. However, when it is used as a wavemeter and coupled to an rf source, an increase in current is obtained at resonance.

The GDO and impedance meter can be used to accomplish the following:

1. Determine the resonant frequency of tuned circuits, including antennas.
2. Determine the impedance of circuits, receiver inputs and antennas.
3. Determine the length of half-wavelength or quarter-wavelength transmission or tuning stub lines.
4. Determine the "Q" of a circuit or component with the aid of a VTVM.
5. Determine the resonant frequency of individual coils, capacitors or crystals that are within the range of the GDO.
6. Determine the rf frequency of energized circuits.
7. Monitor a radiated rf signal with the aid of headphones.
8. Neutralize rf stages.
9. Locate parasitic oscillations.
10. To align receivers and television sets.
11. Determine where BCI and TVI is entering the radio or television receivers.
12. Determine unknown inductance.
13. Determine unknown capacitance.

Now if you will step into the lab we will try to demonstrate how these instruments can be put through their paces. Let's begin with

the simple functions and then gradually creep up to those which are more complex so they don't scare us before we get started.

An oscillator-detector

Simply plug in a pair of headphones (if GDO has facilities for them) and "zero-beat" with the radiating signal. This then will be the frequency of the radiating signal.

Crystal frequencies

Connect a one turn loop of wire across the crystal and couple the GDO close enough to get a dip of the meter when resonance is obtained. It is always wise to check lower frequencies to be sure it is the fundamental frequency that is being indicated.

Frequency determination

Generally the GDO has a switch which is used to remove the plate voltage from the tube. The tube will then serve the function of a diode and the meter as a diode load. When a peak deflection of the meter is obtained this will indicate the frequency of the radiating signal.

Resonance of an RF choke

When an rf choke is used as a parallel or shunt fed circuit, it must be free of self resonance over the operating frequency range of that circuit or it may burn up. The popular pi tank circuit is an example. Place a short circuit across the choke and then determine its self resonant frequency by coupling the GDO close enough to indicate a dip on the meter when the resonant frequency is obtained.

Neutralization

Apply plate power to the exciter stages and filament power only to the stage being neutralized. Use GDO as a wavemeter and couple close to the tank coil in the stage being neutralized. Vary the frequency of the GDO until maximum reading is obtained and then adjust the neutralization for minimum GDO meter reading. The circuit being neutralized may have to be retuned and the above procedure repeated with a closer coupling of the GDO to the Tank coil.

IF alignment

Tune the GDO to the desired frequency and couple it close to the if coil to be aligned. Adjust the if coil until a dip is observed on the meter. The if coil will then be tuned to the desired frequency.

Inductance and capacitance checking

To determine the value of an unknown capacitor, connect it across a known inductance and use the GDO to find the resonant frequency of the circuit. With these known values a reactance chart will give the value of the capacitor. Some GDO's supply a chart which corresponds to the coils supplied with the GDO as the known inductances. To determine the value of an unknown inductance, connect a known capacitance across the coil and use the GDO to find the resonant frequency. Again, the reactance chart may be used or the following formula (which may be used for either inductance or capacitance) for resonant circuits:

$$L = \frac{1}{39.48\ (f^2)\ C} \quad \text{or} \quad C = \frac{1}{39.48\ (f^2)\ L}$$

Where f = cycles per second
L = inductance in henries
C = capacitance in farads

The inductance of an air core coil can be estimated by the following formula:

$$L = \frac{(rN)^2}{9r + 10w}$$

Where L = inductance in microhenries
N = number of turns
r = radius of coil in inches
w = length of coil in inches

Q measurements

Connect a condenser across the coil so the tank circuit resonates at the desired frequency. Connect a VTVM across the tuned circuit and tune the GDO until maximum reading is obtained on the VTVM. The GDO coupling may be changed until a convenient value is obtained on the VTVM and then it must not be moved during the remainder of the test. Note the resonant frequency f_c then detune the GDO to a lower frequency until the VTVM reads 70.7 percent of its original or peak value and call this frequency f_1. Now detune the GDO to a higher frequency until the VTVM again reads 70.7 percent of its original or peak value and call this frequency f_2. The Q is then calculated by using the following formula:

$$Q = \frac{f_c}{f_3}$$

Where f_c = is the center of resonant frequency
f_3 = the difference between f_1 and f_2

Parasitic oscillations

By using a pair of headphones with the GDO, the parasitic oscillation frequency may be determined. Turn the power off of the stage being checked and then use GDO to find the circuit which resonates at the parasitic frequency by moving the GDO slowly around the wiring. When a "dip" is observed, moisten the finger and touch an ungrounded point of the circuit. If a change in the dip is observed, it indicates that it is the portion of the circuit that would be a likely suspect.

BCI and TVI locator

Most of the BCI and TVI problems can only be resolved at the receiver, either by installation of filters, resistors or condensers or a combination of all three. The problem is—where is the rf entering the receiver? Use the GDO tuned to the frequency which produces the greatest amount of interference. Probe around with the GDO until the most sensitive spot is located, which is indicated by watching or listening to the receiver interference. After the point of entry is determined then the appropriate corrective action can be accomplished.

Antenna measurements

Space does not permit to discuss all types of antennas and adjustments so only a few will be mentioned to give some idea on the use of the instruments. At this point it should be mentioned that inductive type coupling should be used between the GDO and antenna when checking near the current maximum point and capacitive coupling when checking near the voltage-maximum point.

The beam antenna has gained tremendous popularity in recent years plus many headaches for those striving to obtain the maximum effectiveness. Most of the headaches can virtually be eliminated by using the GDO and Impedance meter (Z-meter). Let's take a look at a 3 element yagi and see what has to be done to obtain a good adjustment. The element lengths must be physically adjusted or electrically loaded to obtain resonance at the desired frequencies and the feed point impedance must match the impedance of the transmission line. These two points are not the only considerations for beam adjustment but they are the most important factors. The GDO can be inductively coupled to each element and the elements adjusted until each one is resonant at the desired frequencies. It is best to make the measurements while the antenna is in operating position. This is very difficult to do in many cases but let's assume you can. After the elements have been adjusted, the feed point must be adjusted to match the line. The Z-meter and GDO will be used to accomplish this adjustment. The Z-meter is basically a resistance type bridge with a calibrated potentiometer as one of the bridge arms. Connect the Z-meter directly to the antenna feed point. Couple the GDO to the Z-meter inductively thru a couple loops of wire connected to the other terminals of the Z-meter. Tune the GDO to the resonant frequency of the beam and adjust the Z-meter to the dip or null. If the impedance indicated by the Z-meter is not the same as the transmission line then readjust the matching network and redip the Z-meter until the impedances are equal.

Now—if you can't adjust the antenna in the operational position you still can determine the resonant frequency and the impedance by standing on the good old Terra-Firma. The procedure is a little more involved but effective. First—we must have a means of electrically connecting the instruments to the antenna. This is best accomplished by a transmission line a half-wave or a multiple of a half-wave in length. Determine the height of the antenna above ground and calculate how many half-wave lengths of line will be required by using the following formula for a half-wave length of line:

$$L = \frac{(492)\ (K)}{f}$$

Where L = feet
f = megacycles
K = propagation constant
(RG/8 is .66)

This is an approximate length so be sure and cut it extra long because now we will find the exact physical length. Why an exact physical length? A halfwave length of transmission line will reflect the resistance placed across the output at the input end of the line, i.e. if a 50 ohm non-reactive resistor is placed across one end of a half wave or multiple length thereof, the GDO and Z-meter will indicate 50 ohms at the other end of the line. Cut the line somewhat longer than calculated above, short one end and connect the Z-meter to the other end of the line. NOTE: Keep twin lead off the ground and away from metal objects. Set the Z-meter to zero impedance and couple the GDO inductively to the Z-meter. Adjust GDO frequency until the fundamental frequency causes the Z-meter to dip or indicate a null. The frequency indicated should be lower than the desired frequency. Simply cut a few inches of cable off, short the end again and readjust the GDO. Repeat this procedure until the desired frequency (which should be the same as the resonant frequency of the antenna) is obtained. You will then have an electrically halfwave length of line or a multiple thereof.

Coax or twin-lead may be used for the halfwave length line when checking the impedance of the antenna. Connect the line to the antenna, hoist the antenna up to its operating position and adjust both the Z-meter and GDO for the null indication. If the antenna is not resonant at the desired frequency, the driven element should be readjusted a measured amount and then note the frequency change. This will give you an idea how much the resonant frequency changes with a corresponding element change. Now adjust the matching network to the desired impedance. This will be accomplished when the Z-meter dips at the desired impedance with the GDO set at the resonant frequency of the Antenna.

What would you do if your 100 foot coax cable developed a short someplace along the line? Replacing the whole line would be too expensive. Simply connect the Z-meter to one end of the line, adjust the Z-meter for zero impedance and then adjust the GDO for lowest frequency which will produce a null on the Z-meter. Use this frequency in the formula given for a halfwave length line and carefully calculate the length which will be the distance from the input end to the short.

A quarter wave length tuning stub can also be determined by using the procedures just outlined for the halfwave length line except a quarter wave line reflects a short at the input when the output end is electrically open. Now that we have mentioned the quarter wave length line, some may be wondering just what useful purpose does it serve. The quarter wave tuning stub (as it is sometimes called) may be used for antenna matching, TVI elimination or matching two units which have different impedances. The quarter wave matching stub can be used as a matching device on antennas which is explained in most antenna handbooks. It may also be used to eliminate an interfering frequency from entering the TV. This is accomplished by connecting a quarter wave stub to the TV antenna terminals which is a quarter wave in length at the interfering frequency.

Another use for the quarter wavelength matching stub is to permit maximum signal transfer between the source and a load which have different impedances. If the signal source impedance was 100 ohms and the load impedance was 52 ohms, a 72 ohm quarter wavelength of line would give a good impedance match. Hold it just a minute, how in the world did we come up with that 72 ohm business? Simple—another formula will give us this information.

$$Z_o = \sqrt{Z_s\ Z_a}$$

where Z_o = Impedance of quarterwave matching stub
Z_s = Impedance of the source
Z_a = Impedance of the load

Very little has been said concerning the various methods of GDO coupling. Actually—only two types of coupling are used; inductive and capacitive. Capacitive type coupling may be used on shielded coax cable, the ends of antenna elements and generally where the voltage maximum exists. To obtain the greatest accuracy, the GDO should be loosely coupled. Parallel coupling to inductors can be used to obtain maximum coupling.

Chapter III

Measuring RF Power Output

MEASURING RF OUTPUT

Paul Schuett WA6CPP

So your new Bandjammer 5000-Q is rated at 752W peak power. Big deal. How much of this is getting out where it counts?

It's easy to find out by inserting an rf ammeter in series with the line. A more exact reading would be to have the rf ammeter at the antenna input terminals, but that might be impractical when it comes to reading the meter (although you could put a diode there and a remote-reading meter in the shack).

Recently I found an rf ammeter at one of the mail-order surplus houses for $2.95. I installed this in a little cabinet, put two coax connectors on the back (in and out) and now can read rf current in the line, into the dummy antenna, or wherever it is going.

Remember the formula $P=I^2R$? Square the reading on the meter, multiply by the impedance of the line you're using, and you have the power past that point. At the antenna, you could determine the antenna resistance and take the current reading at that point.

For those who have difficulty with mental computations and can't find a pencil, the following chart fives the computed power levels present in matched 50 and 70 Ohm coaxial lines for various levels of rf current:

RF Current Amperes	Power Output in Watts 50 Ohm Line	70 Ohm Line
0.5	12.5	17.5
1.0	50	70
2.0	200	280
3.0	450	630
4.0	800	1120
5.0	1250	1750

When tuning up the rig, place the ammeter on the antenna side of any tuning or matching devices and tune for maximum current.

Inside wiring is extremely simple. Note ground wire installed to insure continuity of the shield circuit.

The completed instrument showing the coax connectors on the rear.

It's amazing to learn how much (or how little) current these rigs produce. For instance, my Swan 250-C puts 1.35A into a 50Ω line. My friend's SB101 from Heathkit put out 0.7A until we worked on the antenna – then it put out about 1.25A. My Heathkit SB401 puts anywhere from 2 to 0.6A into a 50Ω Cantenna, depending on what band it's on.

Commercial stations determine their power by the antenna current. Knowing the antenna resistance at the operating frequency, they multiply that by the current squared. If the antenna resistance is 62½Ω, 4A rf would be 1 kW into the antenna. 126.48A would be 1 MW.

Remember the ammeter does insert a little reactance in the line (I never leave it in all the time), and the calibration changes with frequency, although you can tell what side of the ballpark you are on. An rf ammeter in the shack makes a nice piece of test equipment.

LIGHT BULBS AS RF INDICATORS

John Houser WB2GQY

The major appeal to the amateur – as well as some commercial applications – of light bulbs as rf power indicators is low cost. To this must be added the universal availability of bulbs and screwbase sockets for pennies.

As low cost is of primary interest to well over 50% of those interested in any project, and as I have always had an insatiable desire to find out the why's and wherefore's of standard light bulbs as rf power indicators, I decided it might be the opportune time to do a resarch project and determine once and for all just which bulbs might be suitable and which might not be, and also to determine whether light bulbs would make *good* rf power indicators, or poor, and to find out what precautions might have to be taken if one decided he was going to take this low-cost path of determining his transmitter output power rather than go for a more expensive power output meter.

Also, power output meters in the higher wattage ranges become quite expensive compared to the $2 to $5 which might be expended in a light bulb indicator. In general, porcelain screw bases are available for from 12¢ to 25¢ each, and bulbs from 15¢ to 65¢ each, and not more than four of each are necessary for up to 3 KW power indication.

Table 1 lists most of the common types of electric light bulbs readily available. One look at this table immediately reveals why such light bulbs might not be such good rf power indicators as some folks may have thought they were in the past. It also reveals that some very special precautions have to be taken in using them, or the user may find he has overloaded his transmitter and burned up a few components which might be expensive to replace.

Table 1

Variation in Resistance, Cold to Hot State, Common Variety of Electric Light Bulbs.

Bulb Rating Watts At 115V	Cold Filament Resistance	Hot Filament Resistance	Ratio Cold to Hot Filament Res. (Approx.)
7.5	166	1750	1 to 10
25	40	529	1 to 13
40	27	331	1 to 12
60	20	219	1 to 11
100	9	132	1 to 15
150	6	83	1 to 14
200	4.5	65	1 to 14
250	3.5	53	1 to 15
500	2	26	1 to 13
750	1+	17.7	1 to 15

Table 2

Possible Configurations for Various Power Outputs at Various Impedance Terminations

A. – Nominal 70 to 73Ω Impedance Loads:		
175W Load:	3–60W bulbs in parallel	(73Ω)
	OR	
	7–25W bulbs in parallel	(70Ω)
3,000W Load:		
	4–750W bulbs in series	(71Ω)
B.) Nominal 50 to 55Ω Impedance Loads:		
250W Load:	4–60W bulbs in parallel	(54.9Ω)
500W Load:	2–150W bulbs in series, both paralleled by	
	1–150W bulb	(55Ω)
1,000W Load:	2–500W bulbs in series	(53.6Ω)
2,250W load:	3–750W bulbs in series	(53.1Ω)

The extremely high ratio of cold to hot filament resistance in all types of these bulbs immediately struck me as being the most undesirable factor in using them.

It is very easy to see, for instance, that if one wished to use a 250W bulb for indication on a 250W transmitter, and he computed the resistance at 250W to be 53Ω, (which it is, but only when *hot*), he would assume he had just about a perfectly matched indicator to plug in in place of his 52.5Ω feed line.

However, from this table, it is apparent that this 53Ω resistance is attained *only* at full brilliance and wattage, and the actual cold resistance is only 3.5Ω. In other words, if the bulb were connected to the antenna terminals of the transmitter, and the transmitter keyed full power, the transmitter would be looking into *not* 53Ω, but 3.5Ω, which is a lot of difference, and an extremely low value for any pi network to match.

For a few seconds, until the filament attained full brilliance, the transmitter would be subjected to a terrific overload, due to this impedance mismatch.

Therefore the first precaution which might be emphasized in using light bulbs would be *not* to key the transmitter at full power with a cold bulb, but to gradually bring the power from some lower value to full power as the bulb attains full brightness (and hot, matching resistance).

Not until I got into this project did I realize the very high ratio of resistance of these filaments from the cold to hot state; I don't suppose very many people do. It also brings to mind how the house electric meter must jump every time a bulb is snapped on in the house. This is not an ad for those light dimmers being sold at all the electrical stores, but it sure brings to mind that power bills could be cut appreciably through their use, i.e., bringing the bulb gradually to full brilliance instead of just snapping on a switch.

Getting back to the bulbs, Table 2 gives in various configurations series, and/or parallel combinations which would be most likely to give the amateur a load for a particular transmitter power output, in nominal impedances near 52 and 72Ω. If the configuration mentions 200W, this does not mean that it would be suitable for indicating the output of a 100W output transmitter, because at half brightness, the resistance offered by the bulb is not identical to that at full brightness.

While a differance of an ohm or two would not be serious, nor would a difference of as much as five, or even ten watts, at high power levels, at low power levels less than 100W, for instance, such differences would be seen to become increasingly serious from the matched impedance standpoint. The configurations given match quite a variety of standard line impedances and a wide range of power outputs. Matches can be obtained for RG-8, 11, 17, 13, 58 and 59 type cable.[1]

One may not realize without measurement that the lead length of the filament support wires alone inside the 25–150W bulbs is very close to 18 cm. Even though they are coiled on a 2 to 1 ratio, the filament is inductive in every sense of the word. At higher frequencies, the filament support wires would appear inductive, and to these factors must be added the parallel capacity of the screwbase shell and the central base contact wafer. Even though such capacity is small, it would become significant at most amateur frequencies above the 30 MHz range. Though the 22 cm total wire path would perhaps indicate a bulb could be used up to 300 MHz, such is not at all the case.

It is easy to see that the sometimes suggested trick of using a capacitor in series with a light bulb as a load should be approached with caution, for it would be very easy indeed to run into a series resonant circuit which might result in damage to the transmitter to which such circuit were connected.

In the course of my preparation of this article, I discussed the ramifications with a number of interested hams. Some of them suggested I extend the research to include the use of the smaller types of indicator (pilot) bulbs as loads for testing out transmitters with power outputs in the 1W to 20W range, not only just for amateur applications, but also with a view to using them as loads in testing FM transmitters.

When one considers that there are well over 100 types of these small bulbs, rated from .001W to 2W, and if all of these were to be considered individually, it could take a vast amount of time – and eventually one would end up with perhaps only five or so of these bulbs that would be at all suitable, so such research was not included in this article. However it did open up a field in which there may be a demand for information and may be the subject of a subsequent article.

Frequency Ranges

The use of standard screw-base ceramic or steatite porcelain light bulb sockets is entirely feasible for all of the configurations shown and will handle all amateur bands, 160 through 10. Naturally the leads from socket to socket should be as short as possible in either the series and/or parallel configurations. I found these leads can be kept to approximately 2 cm for such interconnections. Likewise, the coax termination lead should be kept to 2 cm or less.

If extra precautions as to lead lengths are observed, and the bases of the bulbs removed to enable connections directly to the stem wires, it would appear reasonable to suspect that these bulbs might be used for 6, 5, and perhaps 2 meter bands, but it is also quite evident the 2 meter band would be the practical limit.

One should be able to conjecture that light bulbs as power rf indicators are not quite the equal of well-designed power output meters which maintain their rated impedances over a very wide power output range – bulbs do not – but then, they *are* cheap in comparison.

Visual comparison of brightness is completely satisfactory for comparison purposes.

For instance, a 500W bulb connected to the 115V mains should show the same brilliance as one of the 500W bulbs as used in the 1 KW load.

Actually a transmitter supposedly putting out 2,000W PEP is putting out something less than 1,000W with average voice modulation; it would be more of the order of 500–750W average power. Remember that the light bulb is only going to show average power output, not peak, and as ham transmitters are limited to 1,000W dc input to the final amplifier, one cannot expect much more than 500–750W output (average) unless the efficiency of the final amplifier stage approaches 85% which is very unusual, although I am hearing lately that certain high-power transistors are in development which will deliver such high efficiency figures; a bit above that which heretofore has been obtainable with tubes. You should be hearing a lot more about these super-efficiency transistors in the near future; and I expect them to be appearing in certain ham transmitters within a year or so.

Naturally a CW transmitter with the final operated Class C may deliver as much as 850W with 1,000W dc input, while a DSB transmitter on phone could not be expected to deliver more than 650W with Class A or B modulation.

The research and conclusions I reached on this project brought to mind the old subject of using light bulbs in series with primaries of transformers to reduce the secondary output voltages, which is a trick which has been used for years by hams and others. The information contained herein indicates they are not only quite suitable for such usage, but in fact make quite ideal voltage regulators of a sort.

In fact, the question immediately arises as to why bulbs would not make rather ideal voltage regulators for high voltage supplies if used as a variable-resistance dc regulator in the dc leg. This again opens up a field which might bear intense investigation.

[1] Solid Dielectric RF Transmission Lines, W8LUQ, *Radio News* Oct. 1946.
Line Matching: Table of Power and Voltage Loss in DB, *Radio News* Feb. 1947.

BUILD YOURSELF A LIGHT WATTMETER

Carl Henry

Every week brings something new in the hectic field (or pasture) of electronics. Attempting to solve old problems with new components is an interesting pastime for electronics enthusiasts, but they must be careful not to put their foot in the wrong thing. One of the new components is the cadmium sulphide/selenide photocell. A semiconductor sensitive to light is not an entirely new concept, since selenium cells have been around for some time, but the degree of sensitivity makes the cadmium cell stand out.

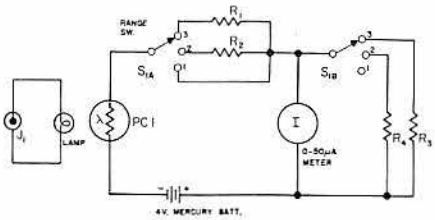

Fig. 1. Circuit of Light Wattmeter.

In measurements especially, there are many possible applications for cadmium photocells. One measurement in particular is usually difficult for the amateur, and this is power measurement. There is a way of using cadmium photocells to measure power, and I call this circuit a "light wattmeter". Operation is just as the name implies, that is, the power is used to generate light which is measured by the photocell.

You have probably realized by now that we are going to use a light bulb as a load. Now this is frequently done in amateur circles, but no one will go out on a limb as to its accuracy. Except me. We know that the ordinary lamp filament has a positive temperature coefficient. Fig. 5 illustrates the variation of a typical lamp filament resistance with input power. By keeping this in mind, fairly good accuracy can be had. Of course, if you use a different lamp, the curve will still apply, but the resistance will be different.

You can run your own graph, however, by using the setup shown in Fig. 2. Either dc or ac can be used, and since the lamp has little inductive or capacitive effect, the readings taken will be good to better than 100 mc. After you have a graph on the lamp you are using, you can effect any kind of impedance match you wish.

Using a lamp as a load simplifies the problem of power measurements because loads for this service are hard to come by. Power resistors are too inductive, and when they approach 1000 watts, they become downright expensive. However, even a 1000 watt lamp is not too expensive.

Fig. 1 shows the circuit that I used as the basis of this article. A standard 150 watt lamp was used here as a load. The photocell is mounted about five inches from the bulb. A wooden box houses the wattmeter, completely sealed internally against extraneous light. Figs. 3 and 4 illustrate the variation of resistance of the photocell with variation of power applied to the lamp. Even very small amounts of power are measureable, if the cell

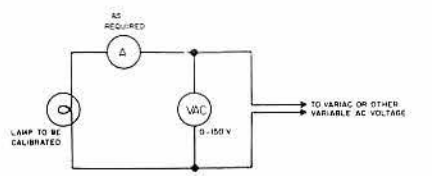

Fig. 2. Method of calibrating lamp and determining resistance.

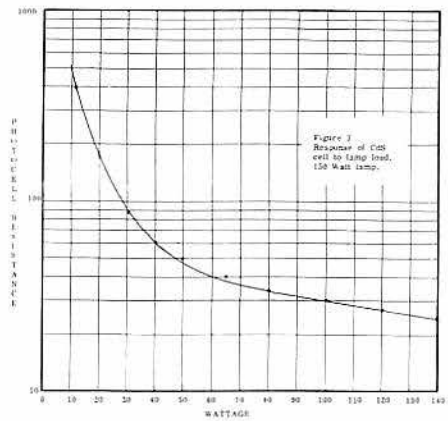

Fig. 3. Response of CdS cell to 150 watt lamp.

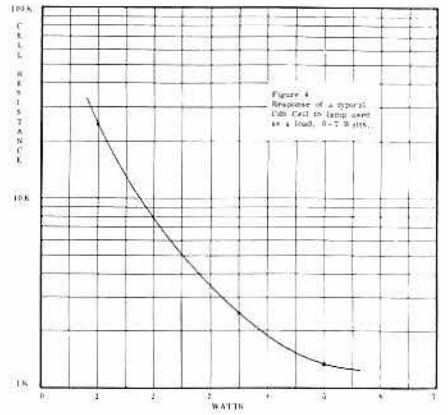

Fig. 4. Response of cell to 7 watt lamp.

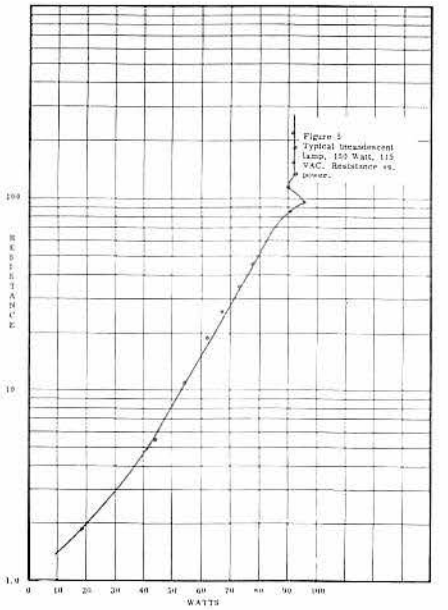

Fig. 5. Resistance versus power input, 150 watt lamp.

is shielded from external light.

The wires from the input connector to the lamp are kept as short as possible by removing the lamp base and soldering the lamp wires directly to the coaxial connector. Switch S1 selects three ranges, which can be set by the builder to anything he desires. In my case I used three ranges which cover from 0.5 watt full scale to 250 watts full scale. With some photocells a 1.35 volt mercury battery can be used instead of the 4 volt battery shown. Also, I used a 50 microamp meter, because of convenience (mine), but even a 10 ma meter will work. Don't exceed the rated power dissipation of the photocell, and remember this may derate with increasing ambient temperature. One thousand watts in a box can be a lot of ambient temperature.

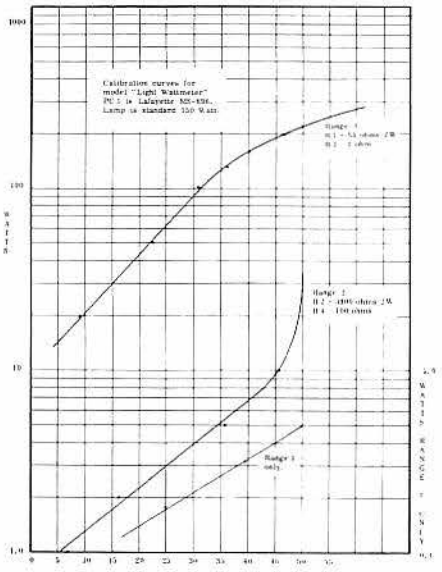

Fig. 6. Calibration curve for Light Wattmeter.

Getting back to the accuracy, if I were to tell you what the meter would read with such and such a lamp, and a given power input, your calibration would be off ten to twenty per cent when the construction was finished. The best way of getting a good calibration is something you've heard before; "if you want a job done right around here you've got to do it yourself".

Now obviously you can't calibrate the wattmeter at 14 mc, because this is what you are trying to measure to start with. Luckily the light from the lamp filament is primarily a power function, and it doesn't matter whether this is dc power, or 100 mc power.

So, to calibrate the wattmeter, apply ac or dc as you wish. Measure the input voltage and current, and read the meter. Make a graph of input power vs. meter reading, and there you have it. Fig. 6 is the graph that I use with the circuit in Fig. 1. Keep the impedance variation in mind, and select a lamp with the power impedance so that standing waves won't eat up lots of your power. As a dummy load and approximate power indictor this is not too critical, of course. But if you wish accurate power measurements, your impedance should be approximately matched.

LOW POWER LIGHT WATTMETER

Bill Hoisington K1CLL

This article describes a very useful gadget for determining the rf power output of solid-state VHF–UHF transmitters in the difficult range to measure, from about 10 mW up to 5 watts. It does not read watts directly; but by a simple comparison of calibrated pilot light brilliance, it will tell you how many watts you are putting out, to within less than 5%. It allows you to check power increases and estimate your efficiency quite close.

Principle Involved

We'll start right in with this part because, while this unit is not by any means a "trick," it does not read rf directly. You first light a pilot light as a good dummy load, matching it into the rf tank circuit of your transmitter by the normal means, also noted here.

You then switch on a second bulb of the same type by means of a battery, controlling the light output with a $1.30 wirewound potentiometer in series, as shown in Fig. 1. This pot must be previously calibrated in milliwatts, as by the method of "volts times milliamperes equals milliwatts." You then match the brilliance of the bulb lit up with rf or its dull glow at some 18 to 25 milliwatts if you're just getting your transmitter going, and read the watts on the wattmeter dial. It's astonishing how well it works, how repeatable it is, and how you wouldn't be without it once you build and calibrate it.

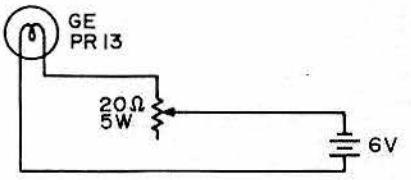

Fig. 1. The circuit supplies the brilliance "standard" for comparison. When the "standard" lamp is mounted adjacent to the dummy load, the pot permits variation of the standard to match the load. If the resistance is panel-marked in watts, a good power indication is achieved.

Brilliance Standard

Figure 2 tells almost the whole story at a glance. You can, of course, put as much calibration on the dial as you have time for. It is quite important to orient the bulb filaments in the same relation to your eyes for best matching. There isn't much in back of the panel except one 6V battery which can be obtained in any hardware store.

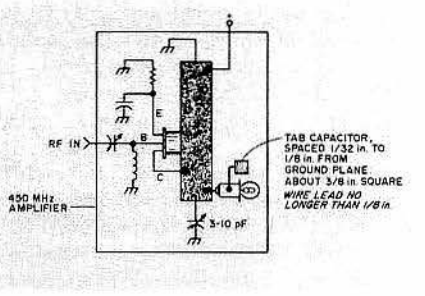

Fig. 3. Matched pilot light load for the UHF version.

RF Matching

Not that it is particularly critical, but be sure and note the need for a large range of series capacitors for the rf pilot lights as you go up in frequency. This can be seen clearly in Figs. 2 and 3. The block diagram, Fig. 2, shows a 6 meter setup. As you go up in frequency the series capacitance drops. A good matched load on 432 MHz can be obtained as shown in Fig. 3. I sometimes remove the tin base from the bulbs, but this is not an absolute neces-

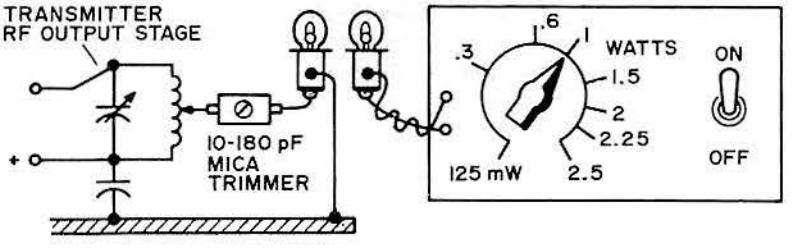

Fig. 2. A series capacitance loads the rf indicator for comparison. The capacitance value will decrease inversely with frequency increases.

sity. It is important to vary the amount of coupling, and thus the series capacity, by spacing the tab capacitor closer or further away from the ground plane, as detailed in Fig. 3. You also can use as many bulbs as you can solder onto a tuned rf inductor, even though they don't all light up with the same brilliance. You can match them all up, but you don't have to. Just check the wattage, or milliwattage, of each one and add them up for the total.

The number 48 or 49 bulb, listed at 2V and 60 mA, is rated at 120 mW, and glows dim at about 12 to 15 mW; so it can be used for low-power receiver oscillators, etc. With two other bulbs found in hardware stores, connected and matched to the rf inductor, such as the PR13 (5V at 500 mA), you can read correctly up to 5W. From there on up you're on your own, although a good variable 115V dc supply can be made up to work around 50 to 100W. I generally use a variety of 115V bulbs of different wattage, light them up with rf, and use their rated wattage.

YET ANOTHER LIGHT WATTMETER

John Meisner K5CXN

Many VHF operators would like a cheap, accurate instrument to measure rf power. The same desire is frequently expressed by operators of the HF bands. Here is a very simple wattmeter which when used with a 50Ω transmission line or load has all of the following desirable characteristics:

1. Easily calibrated to good accuracy (±5%) with your multimeter and a variable dc source;
2. Perfectly flat from dc to 450 MHz;
3. Insertion VSWR less than 1.05
4. Power readings in the 2 to 50 watt range (higher power can be measured with slight design changes);

The operating principle of this wattmeter is stark simplicity. A pilot lamp across the rf line senses a small portion of power in the line and glows brighter with increasing power. An appropriately located photovoltaic cell connected to a microammeter measures the light output which is proportional to the power flowing in the line. Of course a good deal of nonlinearity is involved in the various elements – both the lamp's resistance and its spectrum output change with heating; output of the photovoltaic cell varies considerably with both the amount and frequency of the light shining upon it. Some of these factors tend to cancel out however, because the photovoltaic cell produces some current with only infra-red lamp output at low power levels before the lamp even produces a visible glow, and the cell tends to saturate, increasing its output quite slowly at more intense illumination levels.

Probably the biggest single requirement of any wattmeter is that it must be capable of being inserted into a transmission line without disturbing the operating conditions in the line (low insertion VSWR). It might be argued that hanging a lightbulb across a transmission line will seriously affect the line impedance. Ordinarily, this is true, but the undesirable changes can be minimized and indeed approach an insignificant level if the resistance of the lamp filament is very large when compared to the line impedance. In general, a factor of 15 or more times the line impedance is sufficiently large to produce negligible effects. In the case of the suggested 10V, .014 Ampere pilot lamp, the mismatch produced in the line gives a VSWR of 1.05:1 at the power level of 1 watt. This mismatch decreases rapidly with increasing power. It falls to well below 1.01:1 at 50 watts. Another point of interest with regard to this particular choice of lamp is that it is a long-life type with a life expectancy of 10,000 hours. This implies two advantages: (a) The lamp will operate at well over its rated voltage without burnout (50.0V at 50 watts), and (b) the interior of the lamp envelope will resist darkening which would negate the wattmeter calibration. In addition, the filament structure of this type of lamp is a single-strand straight tungsten wire. The coiled type of filament structure introduces undesirable inductance into the circuit which can distort wattmeter readings in the UHF range.

The wattmeter shown is constructed in two boxes for the sake of convenience. The sensor can be located in the transmission line at any point and the meter can be placed beside the transmitter. For test work, the whole unit could easily be put into a single box. Coaxial fittings and cable were used for interconnection, but since dc only flows in this circuit, any type of wiring would be satisfactory.

The photovoltaic cell used in this wattmeter is a unit obtained from the local Allied/Radio Shack store. (Catalog No. 276-115.) Output of the cell is rated .5V at .6 mA in sunlight.

Since the cell generates considerably more than 20 mA under moderate illumination, a switching arrangement is incorporated into the wattmeter to shunt it into progressively higher current ranges with increasing power. Alternatively, a 50 or 100 milliammeter could be used with less switching at a sacrifice of sensitivity in the 1–3 watt range.

Calibration of the wattmeter is a simple process. By solution of the formula $P = V^2/R$ for voltage, the following tabulation is made for a 50Ω line impedance:

VOLTAGE (rms or dc)	POWER (Watts into 50Ω)
7.07	1
10.00	2
12.24	3
14.14	4
15.71	5
17.32	6
18.71	7
20.00	8
21.21	9
22.36	10
31.62	20
38.71	30
44.71	40
50.00	50

Using the tabulation, fasten a metered variable dc supply into the wattmeter according to the following diagram. Now simply note the reading on your wattmeter for each of the selected voltages in the table and tabulate this reading with the corresponding power in watts in a table of your own. It may even be possible to remove the front of the meter case and mark new calibrations directly on the dial. This was not possible with some hermetically sealed meters. It is best to disconnect the wattmeter from the antenna feedline for this calibration. If the meter is left with a transmission line attached and the antenna happens to be fed through a balun device with near zero resistance, the power supply, and perhaps the balun, will suffer.

It must be pointed out again that this power meter is intended for use either with 50Ω coaxial line systems with low VSWR or with 50Ω dummy loads. A coaxial line that is not "flat" (unity VSWR) or a dummy antenna that does not look like" 50Ω, which is the case with

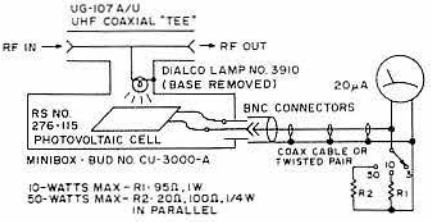

Fig. 1. Schematic diagram.

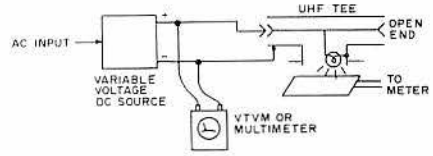

Fig. 2. Calibration diagram.

most HF loads used at VHF or UHF, may cause distorted power readings. If you have doubt about your transmitter's power output when using this meter, you should check it while using a known 50Ω load rated at the transmitter's output frequency.

I mentioned before that this power meter was easily adaptable to higher power readings. To upgrade the meter, the only change required is to insert the correct higher voltage pilot lamp having low current, long-life specifications. Suggestions for some of these are the following Dialco Lamps:

Part No.	Max Power Level (Watts)
24CS	100
48CS	200
60PSB	340
120PSB	800

A LOW COST RF WATTMETER

Mark Leavey WA3AJR

You say you just finished building that 2 meter rig and want to find out how much power you're running but can't afford to buy a wattmeter? You've been calling "CQ 80 QRP" all day with your quarter-watt wonder and nobody is answering? Then get yourself up, go down into the workshop, and build yourself a neato-keeno handy-dandy wattmeter.

If we are going to build a wattmeter, let's consider what we want. Accuracy and ease of calibration, as well as simplicity in construction are prime requisites. The meter described here is as accurate as components allow, and it's easy to build. The calibration is logarithmic, which means that a simple graph is possible, and easier than changing the meter scale.

For the mathematicians, I will present the formulas upon which this device is based, and ways of modifying it; for those of you who avoid math whenever you can, look at the graphs and skip these few paragraphs.

To spare undue complexity, assume 51Ω line – other values can be dealt with later. Perhaps the easiest parameter to measure, and one that is proportional to power, is rf voltage. A voltmeter can be made most easily with a series resistor and a 0–1 mA meter. Now let's plunge into the actual calculations.

Assume W is the full-scale meter reading in watts, Z is the line impedance, E is the voltage measured, I is the full-scale meter reading in amps of the basic meter, and R is the value of the series resistor in ohms. We know that the voltage (IR) is equal to the square root of "impedance times

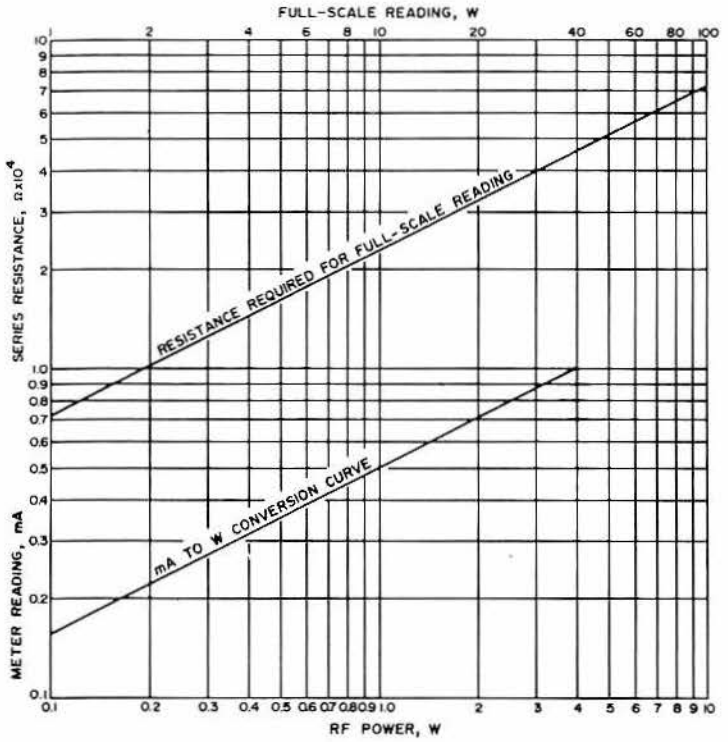

Fig. 1. Logarithmic plots for determining power. The upper curve gives resistance values for determining what the full-scale meter deflection will be (remember to multiply the series resistance value shown on the chart by 12 kΩ). The lower curve will allow you to determine your precise power out if you use a 0–1 mA meter.

power," or 14.270V. Now, since the voltage and the current (.001A because the full-scale movement is 1 mA) are known, simple division yields 14,270. The resistor value, then, is 14.270 kΩ. The upper portion of Fig. 1 is a graph that will enable the nonmathematician to choose the value of the resistor for full-scale readings up to 4 kW, with 51Ω line and a 0–1 mA meter.

Why 4 kW with an amateur power limit of 1 kW? A look at the bottom half of Fig. 1 will explain. Although this is the calibration of the prototype, for 4W full scale, it will double for 40, 400, or 4000W. A half-scale reading, 0.5 mA, corresponds to 1W (1 kW, etc.). This spreads out the range below 1 kW for ease of reading and measuring.

Now get out that soldering copper and gas pliers, and build it. As the schematic

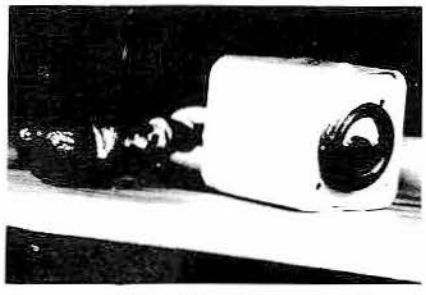

Front view of unit.

(Fig. 2) shows, the circuit is a basic rectifying type rf voltmeter. The prototype was built in a small can of the plug-in-module variety that was scrounged from the junkbox. About the only critical part is the series resistor. The capacitors in the prototype were mica, but ceramic disks would work as well. The diode can be a 1N34A, 1N270, 1N52, 1N38A, or just about anything else. Use the old ham's rule of thumb: "When in doubt, try it out!"

Two sockets might prove more convenient rather than one with a coaxial tee as shown. Conventional minibox construction or building into a new or existing rig will be more than adequate. Point-to-point wiring is used to permit compactness and reduce lead length.

"Fine," you say, "but I don't have a huge mound of test equipment. How do I calibrate it?" That is the beauty of it – you don't! If the series resistor is accurate, the meter will be self-calibrating to a log scale. Remember, you know R and Z, and the full-scale W. Now assume a half-scale

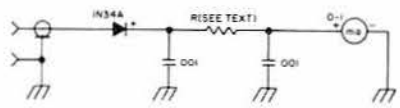

Fig. 2. Schematic diagram of the simple, accurate, and easy-to-build rf wattmeter.

Connection to transmitter with dummy load (see text).

reading, I = 0.0005, and calculate W for half-scale. Plot these two points at 1.0 and 0.5 mA on Fig. 1, and connect by a straight line, which you may extend the length of the graph.

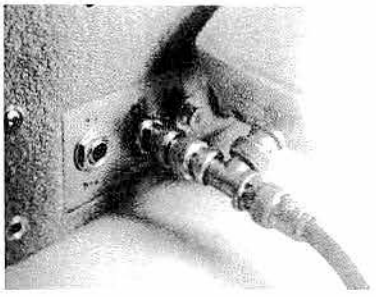

Connection to transmitter with antenna connected.

Install the meter through a coaxial tee at your antenna connector, or through some other predetermined means, and terminate with a dummy load. The one seen in the picture is three 150Ω resistors in parallel, dipped in epoxy, shielded with a copper braid, and installed on a BNC plug. Apply power and read the meter. That's it! The meter can be used with an antenna if your swr is below about 1.2:1.

So what did I promise? A low-cost, rf wattmeter that is inexpensive enough for the Novice, practical and useful enough for the General, and "Extra" accurate. Go raid the junkbox, and add a worthwhile piece of gear to your shack.

RF POWER MEASUREMENT USING HOT CARRIER DIODES

Frank Jones W6AJF

Two rf wattmeters are shown here, one with a range of 25 mW to 10W and the other covering the range of 5 to 300W. Both are useful from low radio frequencies on up through 450 MHz.

The low-power version (Fig. 1) makes use of a 20W Sierra dummy antenna built into the meter case, though the metering circuit only goes up to 10W. If the maximum is to be 20W, the reference meter reading could be about 45 μA instead of 30. The minimum power reading would be doubled. In this wattmeter, the power range potentiometer is calibrated and only a reference line on the meter is used when making rf measurements. The dummy 50Ω antenna resistor is rated up to 1000 MHz so is excellent from 450 MHz down.

The range potentiometer had an audio (nonlinear) taper. By connecting the "high" resistance end to the diode, the watt range scale is spread out quite well in the 0.1–10W range. The hot carrier diode, an HP 2900, has a 10 PIV rating, which means that the rms rf voltage across it should be less than 3V for safe operation. At 10W of rf power, the rms voltage would be a little over 22V, which means a voltage

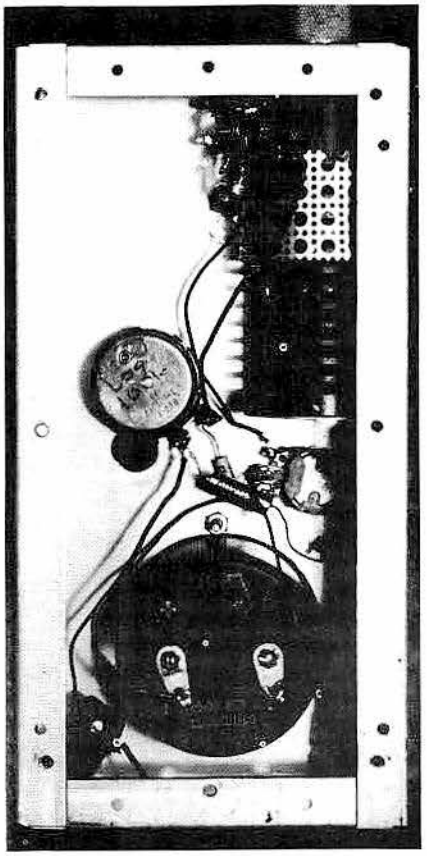

Bottom view of 10W unit with the rf dummy antenna clamped in one corner.

Top view of low powered rf wattmeter covering .025 to 10W. Built into a 8x4x2 chassis with wire screen bottom plate for ventilation.

divider is needed to keep the applied diode voltage down to about 2V. An HP 2800 diode with a 75 PIV rating would be more desirable, especially if the meter was to be calibrated for 20W maximum. This diode is about $1 and has a little higher capacitance, which would require a different shunt capacitance across parts of the resistor divider to make the device work with the same power range calibration.

The divider should use ½W resistors of the carbon or metal film type, since these units are part of the rf circuit. It is better to use three ½W 300Ω resistors in the string rather than a single 900Ω 2W resistor: this is because the rf resistance characteristic is usually better in ¼ or ½W types in certain ranges of resistance. Every resis-

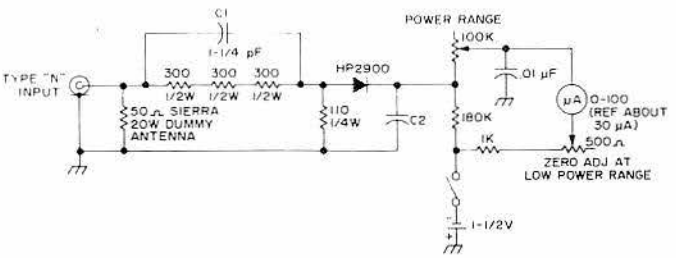

Fig. 1. .025 to 10W RF wattmeter.

tor has some inductance and shunt capacitance which becomes part of the voltage divider. The diode shunt capacitance is in parallel with that of the 110Ω ¼W resistor in Fig. 1. However, nearly any combination of resistor sizes can be equalized within 10 to 20% over the desired frequency range. This divider is across the 50Ω dummy antenna, so should not shunt the value down to less than 49 or 48Ω. This divider has to dissipate a little rf power also. Its total resistance should be at least 20 times as high as the dummy antenna load resistor.

The values shown in Fig. 1 are just about the minimum that should be used. Too high values makes it more difficult to extend the frequency range to the upper end, though it can be done, as was discovered in the higher-powered wattmeter of Fig. 2.

All diodes are poor rectifiers at applied rf voltages below their forward bias values of 300–700 mV (peak). By using a forward dc bias voltage to make the diode conduct at least 5 or 10 mA, the detection sensitivity is increased as much as 5 or 10 times. This requires a small battery, a couple of fixed-value resistors, and an adjustable pot to balance this current out of the meter when measuring rf powers below 100 mV. If the power range is limited to a minimum of ¼ or ½W , no bias circuit is needed in this 10W instrument. The range scale in either case has to be hand calibrated.

A low-powered radio transmitter or exciter can be used as a 10W power source when calibrating the power range pot scale. The transmitter can use stage detuning to reduce power outputs down to the lower values needed. Many swr meters have watts of power calibration and one of these can be put in the coax line to the rf wattmeter for calibration service. A more accurate calibration can be made by comparing the power readings against some reliable commercial rf wattmeter within its frequency range and calibration charts. This scheme is usually necessary for checking the calibration at VHF or UHF. Another method is to use an accurate rf voltmeter across the dummy antenna connection to ground and read the power values in watts = E^2/R. For example, 5V (rms) squared is 25; and divided by 50Ω is equal to 500 mW.

The Sierra 50Ω dummy antenna has no connection available at the high end of the resistor, which terminates in a type N fitting. The metering circuit has to connect to this point as close as possible by getting into the inner conductor of a coax fitting, or by drilling a 3/8 or ½ in. hole through the shell of the dummy antenna close to the rf fitting end. This can be done and the first 300Ω resistor in the voltage divider soldered to the inner connection to the large 50Ω resistor. A long 1/8 in. diameter soldering iron tip is needed. The divider resistors, diode, and four .001 μF stud-mounted bypass capacitors were all mounted around this large hole in tapped 6-32 holes for the four capacitors. Larger values of bypass capacitors can be shunted across these 0.001 μF values to ground to extend the frequency range down to low rf or even af values. For example, a .02 μF capacitor shunt would allow operation to 2 MHz. A miniature 50 or 100 μF electrolytic shunt would function at audio frequencies down to 300 Hz. The diode must have a low-impedance path to ground over the desired frequency range to function as a peak rectifier and get as much dc output voltage as possible for the meter circuit. The microammeter in series with a variable range resistor is simply a dc voltmeter. The diode rectifier converts rf voltage to dc, so the diode should be equally efficient over the whole rf range.

The 5–300W unit was built to use with a large dummy antenna rated up to 500 MHz, which is a massive unit external to the box shown in the photographs. Quite a bit of rebuilding went into this device to make one calibration of the range potentiometer fit all frequencies from 450 to 2 MHz. The input and output coax fittings had to be finally mounted so the inner conductor tips could be soldered together and the resistor divider connected to this point. The latter consisted of two 4300Ω 2W carbon resistors and a 68Ω 1W resistor in series to a copper sheet inside of the aluminum box.

The watt range variable resistor was a 500 kΩ linear potentiometer which was limited to a lower value by shunting it from the moving arm to the diode connection end with a 220 kΩ resistor. This gave a maximum power reading of 300W when

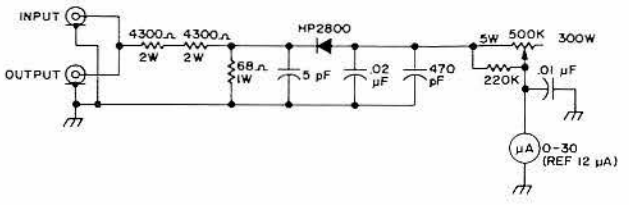

Fig. 2. 5 to 300W RF wattmeter metering circuit. External 300 or 400W during antenna load.

Top view of 5 to 300W metering circuit for use with external high powered dummy antenna.

the reference line was drawn on the meter face at 12 μA. The import, low priced, 0–30 μA meter had a large meter scale. A smaller 0–50 μA meter would have been usable, since the meter is used only as a reference. The range pot knob is adjusted when rf power is applied to run the meter reading up to the line drawn on the meter scale face.

The circuit shown in Fig. 2 was equalized to within about 15% error over the range of 2 to 450 MHz by shunting a 5 pF capacitor across the 68Ω resistor in the rf divider.

Calibration of this device was made at 144 MHz using a transmitter having up to 400W available carrier output. The meterizing unit was connected to a large Bird rf wattmeter at the external fittings of the latter. Several thermocouples had to be used to cover the wide range of power for the calibration. This required reading a chart curve for each Bird wattmeter reading and using correction factors for frequency in order to obtain the actual watts of rf power. Now, the large unit is used without the thermocouples, charts, rf choke, etc. simply as a dummy antenna. The new metering circuit connects directly into the antenna fitting, with a few feet of 50Ω coax over to the transmitters being tested.

This power measuring device can be used in any 50Ω coaxial line to monitor the actual power going toward the antenna. The swr in the line should be low, or near unity, in order for the calibration to be reasonably accurate.

VHF DUMMY LOAD WATTMETER

Glen Zook K9STH

The unit

The unit described herein is similar to some 60 watt units which may be found around many commercial two-way radio shops. This dummy load has provision for connection to an external relative output meter. This external output meter may become an accurate wattmeter if the following criteria are met:

1. Frequency bandwidth of ±10% of calibration frequency.
2. RF output kept within power dissipation of dummy load.
3. Accurate initial calibration.

These criteria may be easily met in amateur vhf operation if only one band is considered for each set of calibration data. Since most vhf amateurs operate on 50 mhz, 144 mhz or 432 mhz, the ± 10% frequency limitations may be easily met. This limitation gives a 10 mhz bandwidth at 50 mhz, 29 mhz bandwidth at 144 mhz, and 86 mhz at 432 mhz. The limitation to the power ratings of the dummy load is only common sense, for if a resistive network is overloaded, the impedance may be drastically increased, caused by damage to the load resistors. The calibration limitation may be overcome if a standard, previously calibrated unit, or commercial unit is used.

The unit consists basically of 16 220 Ohm resistors in a series parallel arrangement. The metering circuit consists of a germanium diode pickup with necessary rf filtering. The meter movement is generally a vom, but any 50 ua meter movement should suffice. Exact physical layout is not extremely critical, but it is suggested that the layout be made similar to the unit shown in the accompanying photographs. This unit is acceptable for 60 Watt output transmitters without modification. The power capability may be increased to about 200 Watts if the resistive network is suspended in 1 quart of oil. If this is done, care must be taken to keep the metering circuit out of the oil. The lead from the diode to the resistive network must, of course, be partly submerged, but keep the diode itself out of the oil. I do not personally use this arrangement, but I know of two units which have been in use at a large Southeastern two-way radio shop for several years. The same shop has incorporated a range switch with several meter shunts for various maximum scale power readings. This feature is especially useful to the amateur vhf FM operator who may be working with equipment of from ½ to 250 Watt outputs. The schematic appears as Fig. 1, and the basic circuit for various meter shunts as Fig. 2.

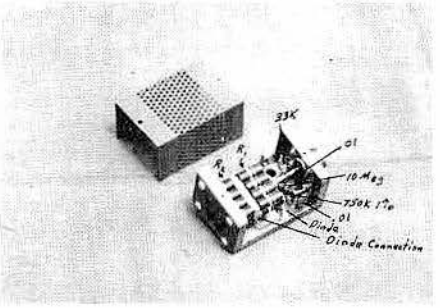

Parts layout and interior view of Dummy Load – Wattmeter

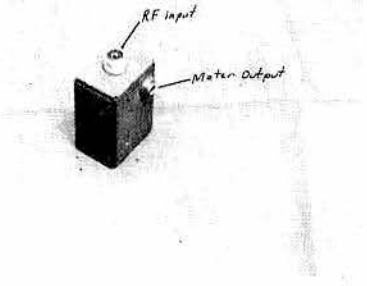

External view.

Calibration

Calibration is best accomplished by using a Bird "Thruline" or similar commercial vhf inline wattmeter. Second choice is a Bird "Termaline" or similar dummy load-wattmeter. In both cases, a graph should be created by plotting meter divisions on the horizontal axis, and power on the vertical axis. The meter shunt should be placed at minimum resistance and increased to give maximum reading at the desired power level (this holds primarily true for units using the metering circuit of Fig. 2) or, if a vom or vtvm is being used the range switch should be placed on a high voltage setting and reduced a setting at a time until the desired reading is obtained. The transmitter should be adjusted for various power levels on the standard wattmeter and the voltage or current reading on the new meter recorded on the graph. In the case where the standard meter is of the dummy load-wattmeter type, it will be necessary to switch the coax from one unit to the other. Do not retune the transmitter, for each unit will present almost the same load to the transmitter (50 ohms). Take the reading and record as with an inline type of meter. The points on the graph should now be connected with a smooth curve (use of a draftsman's

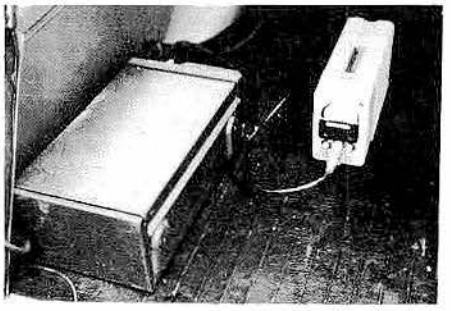

Using the Dummy Load – Wattmeter to check output of FM unit.

range switch is used, it will be necessary to calibrate for each switch position. Also, if multi-band use is expected, the graphs must be made for each band. Use of the wattmeter now requires only the connection to the transmitter, setting of range switch to the proper level, and reading the graph.

Uses

The uses of this dummy load-wattmeter are as varied as the amateur mind can devise. One very important use is determining the losses of 50 ohm coax. Measure the output of the transmitter at the transmitter. Then measure the output at the end of the length of coax. The losses in the line become apparent. The loss in db may be calculated by the standard power ratio formula, 10 $\log_{10}$ Power out of coax/Power into coax.

Another use is the determination of efficiency of final amplifier stages. This efficiency may be calculated by Power out (measured by dummy load-wattmeter)/Power in (measured by plate current/plate voltage meter) x 100%. A third use is determining once and for all which amateur really has the most output. This list may be expanded by the builder to suit his own tastes.

Conclusion

This dummy load-wattmeter is not a Bird "Termaline" nor should it be regarded as a substitute for any other laboratory equipment. However, with a little care in calibration, (assuming a 5% accuracy standard is used for initial calibration) the accuracy should be within 10%, and this, my friend, is not bad for a wattmeter costing less than $10.

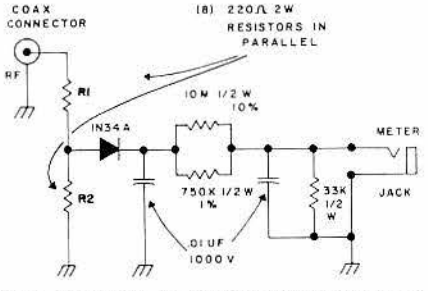

Fig. 1. Schematic. R1 and R2 consist of eight resistors each, in parallel.

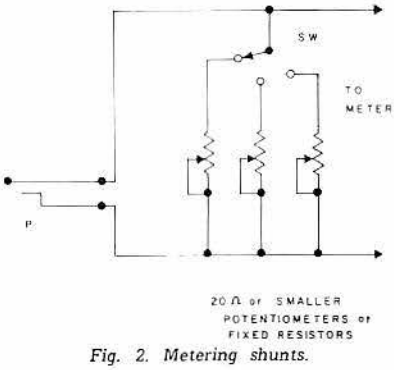

Fig. 2. Metering shunts.

Chapter IV

Measure Your Field Strength and Frequency

THE RF SNIFFER

Jim Kyle K5JKX

Every now and then there's a need to know if any rf is present in a circuit. Frequency isn't so important—the question is simply. "Is there rf here?"

Your grid-dipper can frequently answer this, if used in the wavemeter mode, but occasionally it's not sensitive enough—particularly if you're working with a receiver oscillator where power is measured in microwatts.

Here's an rf Sniffer which will indicate the slightest trace of rf in a circuit. In addition to checking receiver oscillators, it's a perfect gadget to ensure perfect neutralization of a transmitter final.

Connect the components as shown in the schematic. Use long-nosed pliers as a heat sink between the diode and the solder joint when wiring, to prevent diode damage. Note that the pickup loop of 14 gauge wire is insulated with a strip of spaghetti.

Mount capacitor and diode on back of meter with shortest possible leads. Attach pickup loop directly to negative meter terminal; it's stiff enough to do without other mechanical support.

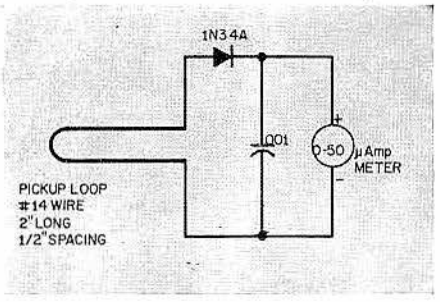

Amplifier Neutralization—Couple the Sniffer to the antenna terminal with a temporary two-turn link around the pickup loop. Remove plate and screen voltage from the final amplifier. Apply drive. Adjust neutralization for minimum indication on the Sniffer—but don't expect to be able to get it down to zero.

Oscillator Checking—Place the pickup loop near the oscillator coil. If the oscillator's working, the Sniffer will indicate rf. Touching either the grid or plate lead (use an *insulated* tool for this test, not your fingers) should reduce the Sniffer's indication.

Receiver Troubleshooting—Check the oscillator as described above. If it's okay, next check the mixer plate coil by placing the Sniffer pickup loop near it. If you get an indication here, move to the first if stage and place the pickup loop near the plate pin of the tube socket. Proceed through the receiver until you lose the indication. The trouble is somewhere between the last indication and the point at which it disappeared.

Field Strength Meter—Couple a short antenna to the pickup loop by two turns of wire around the loop. Field strength will be indicated in a comparative manner by the meter. It cannot be calibrated, but proves useful in tuning mobile or beam antennas, etc.

SWR Measurement—(Parallel lines only). Move the Sniffer long the line. Mark maximum reading and minimum reading over a half-wavelength. Divide minimum into maximum. The quotient is, roughly, your VSWR. This method is by no means exact, but will indicate whether the line is under or over a 2:1 SWR.

UHF Frequency Measurement—Set up Lecher wires. Couple the rf Sniffer lightly to the tank circuit instead of using a flashlight bulb. Use Lecher wires in normal fashion, reading Sniffer indications for maximum and minimum. This is much more exact than the normal methods.

Improvised Grid-Dipper—If you have a signal generator available, it can be used with the rf Sniffer to serve as a "grid-dip" meter to locate resonance for any tank circuit. Couple both the generator and the Sniffer lightly to the unknown tank. Vary generator frequency. A sharp rise in Sniffer indication indicates the resonance point.

THE PINK TICKET REJECTOR

A. D. Taylor GW8PG

Hams sometimes get into trouble with the FCC because they have made a mistake in tuning a frequency multiplier or PA stage. For example, if the multiplier stage following a 3.5 MHz oscillator is accidentally tuned to 10.5 MHz instead of 7 MHz, the PA can be loaded on 10.5 MHz; and if this is done even a short transmission is likely to produce an unwanted "QSL" from the FCC! Mistakes like this can be prevented by using the simple, easily built absorption wavemeter shown in Fig. 1. Only one coil is required in this meter, the low frequency range being obtained by switching a padding capacitor in parallel with the variable tuning capacitor. With switch S1 open the tuning range is approximately 6.8 to 30 MHz, and with S1 closed it is approximately 3.5 to 6.8 MHz.

Construction of the wavemeter is simple. It can be put together in a metal utility box, on a wooden panel and baseboard, or even in a cracker can of the right size. The coil can be wound on any type of ¾ in. diameter form. If nothing else is handy, a short length of dowel could be used. The coil winding consists of 7 turns of 20-gage wire, close wound. Both the tuning capacitor (C1) and the padding capacitor (C2) should be 500 pF components, but the values of the other components are not critical.

Any meter having a full-scale deflection between 100 μA and 1 mA can be used. If the wavemeter is built in a metal box, L1 must be mounted outside the box. A slow-motion drive is not needed. If C1 is fitted with a pointer type knob and a cardboard scale is cemented onto the front panel, the calibration points can be written on the scale in ink.

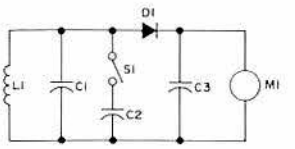

Fig. 1. L1 – 7 turns 20 gage enameled copper wire, close-wound on a ¾ in. form; C1 – 500 pF variable capacitor; C2 – 500 pF fixed capacitor; C3 – Fixed capacitor, any value between 1000 pF and 0.01 μF; D1 – Silicon or germanium; M1 – Moving coil-meter (100 mA–1 mA).

When it came to calibrating the wavemeter I thought of a simple method that I have not seen described before. I soldered about 2 in. of wire onto one end of L1, and about 10 ft of wire onto the other end. I then connected the short lead to the antenna terminal of my receiver and strung the 10 ft of wire up as a temporary antenna. I then tuned the receiver to a steady signal at each frequency at which I wanted a calibration point, and adjusted C1 until the strength of the received signal suddenly dropped sharply, indicating that the wavemeter was tuned to the frequency of the signal. I was then able to mark this frequency on the cardboard tuning scale. The drop in signal strengh was very sharp so calibration was easy. Once enough calibration points had been obtained the temporary wires were unsoldered and the wavemeter was ready for use.

The only frequency which may require a little adjustment is 30 MHz. If the wavemeter will not tune as high as this, push the top turn of coil L1 about 1/8 in. away from the other turns. This should reduce the inductance sufficiently; a spot of cement will hold the turn in its new position.

To use the wavemeter for checking a transmitter, bring coil L1 close to the tank coil of the stage being checked, apply power to the stage and rotate C1 until a maximum reading is obtained on the meter. The output frequency of the stage can then be read off from the wavemeter tuning scale.

The wavemeter can also be used as a radiation meter for tuning up single-wire antennas. If it is tuned to the transmitter output frequency and placed near to the antenna wire, maximum reading on meter M1 will indicate maximum output power from the transmitter.

Many readers will have realized that the calibration method I suggest uses the principle of the rejector circuit. That is why I have called the little gadget "the pink ticket rejector"!

A USEFUL ACCESSORY FOR THE HAM SHACK

Rex Morris W2WHX

BECAUSE we are dealing with something we cannot see, namely electrons and electromagnetic radiation (we only see their effects), we must acquire the ability to use test equipment, in order to understand and find our way in this invisible realm.

The piece of test equipment about to be described is one of the more useful instruments that the amateur should have in the shack. While this instrument serves primarily as a field strength meter, it will also serve as a phone monitor, neutralization indicator and a sensitive wavemeter.

Referring to the circuit diagram, meter M1 is a sensitive instrument which indicates the pressure of rf when the device is used as a

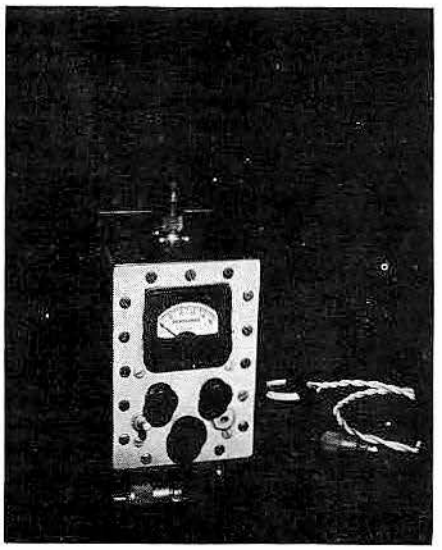

field strength meter, wavemeter or neutralization indicator.

To use this instrument as a wavemeter, a pickup loop is substituted for the short whip antenna at the top. Switch S1, the band switch on the right of the panel, is placed on the proper position. Coil L1 tunes the vhf range of approximately 90 mc to 170 mc (2 meters). L2 tunes 28 mc to 100 mc (10 meter and six meter bands). L3 tunes to 7 mc to 30 mc (40, 20, 15 and 10 meter bands). L4 tunes from 2 mc to 7 mc (80 and 40 meter bands). With switch S1 on the proper tap, condenser C2, on left of panel, is used to peak the reading on meter M1. Using a calibrated dial, frequency may be read directly. Toggle switch S2 is a high-low range switch for meter M1, providing a means of keeping the meter on scale and protecting it against burn-out. Potentiometer R1 (center of panel) is a vernier shunt control, also for keeping the meter on scale.

For use as a phone monitor, rf should be fed into the input jack with a link or pick-up wire. Once again the LC circuit is resonated to the frequency we desire. Earphones inserted in jack J2 will open the meter circuit and allow you to monitor the signal. Switch S2 is placed in the Hi position.

Field strength readings can be taken by using a short pickup antenna. Again the LC circuit should be tuned to resonance. Meter M1 will give an indication of field strength.

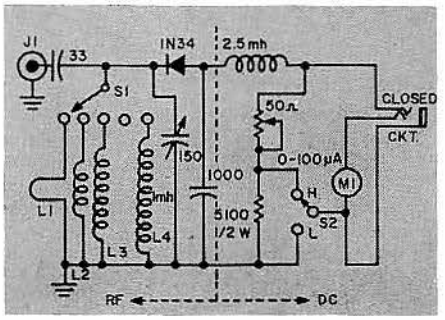

With switch S2 in the Hi position the meter is very sensitive and potentiometer R1 is a variable shunt providing much range of scale adjustment. For use as a remote reading field strength meter an external microammeter (with up to 200 feet of wire) may be plugged into J2. For making transmitter adjustments this is a very desirable feature.

Now notice that one position on the bandswitch S1 is vacant, this vacant position provides a very broad band—low sensitivity position for those extremely high rf fields where even R1 and S2 cannot provide enough attenuation.

Neutralization measurements are made by coupling the instrument through a pick-up link to the tank coil involved, with S2 in the Lo position. When the instrument is tuned to resonance it becomes a very sensitive rf indicator. It is so sensitive that it will readily be seen that complete neutralization exists in theory only.

As in all simple gadgets there are a few simple construction techniques which make the difference between gadget and instrument. In this case the important thing to keep in mind is that from the antenna to the crystal is the rf portion, and from the crystal to the jack J2 is the dc portion (with audio superimposed). With this in mind, construction is such that the two parts are separated, thereby giving some measure of protection from rf energy to the very sensitive microammeter M1. Also note the extensive use of sheet metal screws on the aluminum case. The only rf we want to enter the case is the rf we are attempting to measure via the antenna jack. Note again, we have here an instrument for detecting electromagnetic radiation, from approximately 170 mc to 2 mc. We now have an instrument for visualizing what cannot be seen.

The usefulness of this instrument is limited only to one's ability to apply it and interpret the results it gives. These only come with experience, trial and error and determined application.

Coil Data

L1—One turn hairpin loop.
L2—5 turns of #18 enamel wire space wound 1" dia.
L3—24 turns #22 cloth covered wire, close wound, 5/8" dia.

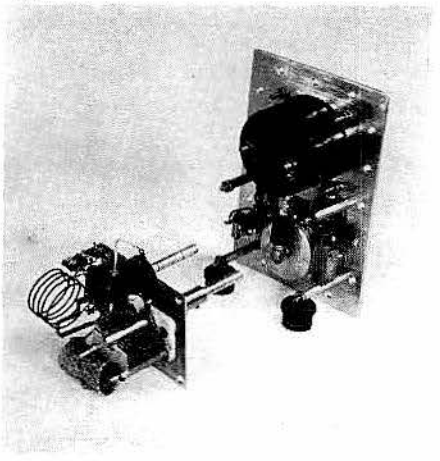

TWO THRU TWENTY FSM

Howard Pyle W7OE

I used a small LMB aluminum meter cabinet with a hole for a 2" meter; any equivalent cabinet can of course be used. With a small enclosure such as this (4"x4") the meter occupies the face of the cabinet and all controls are on the rear. Using a somewhat larger housing both the meter and the control knobs can be placed on a front panel if you prefer.

Rather than wind up the three coils I found that the J. W. Miller Company RF chokes with minor modifications were admirably suited for a compact job. One each of their catalog numbers 4606, 4588 and 4580 were required to cover the three frequency spreads from 2 through 20 meters. The #4606 coil should have five turns carefully removed, to cover the 10-20 meter bands; remove three turns from #4588 for six meters and two turns

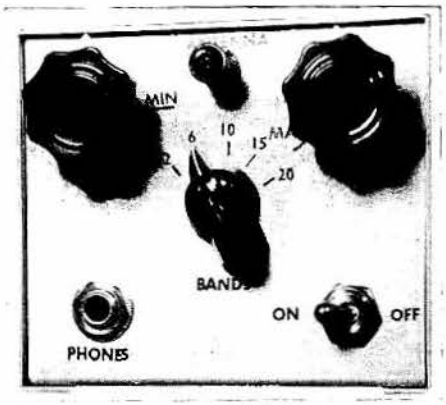

from the #4580 coil to handle 2 meters. These can all be resonated with a 50 pf midget variable tuning capacitor; a Hammarlund HF-50 or the equivalent is excellent. Any of the small multi-point selector switches can be used for band switching. A JBT lever switch type SS-14-ILS will handle the job or, if you prefer a rotary switch you can use a Mallory type 3215J as I did, leaving two positions unused. (I might want to add a couple of coils and try 40 and 80 later!).

Resistors R-1 and R-2 shown in the schematic, need be only ½ watt. A single flashlight cell will serve for the battery although I chose a 1.4 volt mercury transistor battery to conserve space. Other items shown on the schematic are obvious and all parts are readily available from most electronic parts distributors as well as from the electronic mail order houses.

Build this little F/S meter and know what your VHF outputs are doing. If you want to check your modulation quality, a phone jack may be added as shown, making this little gadget really versatile.

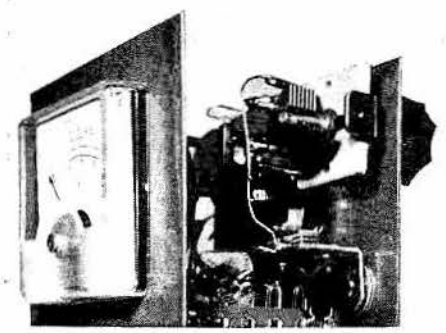

Side view of the FSM.

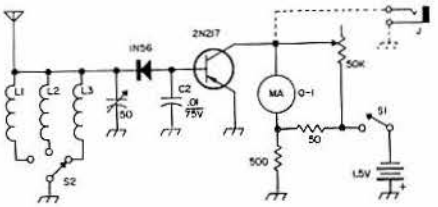

Fig. 1. The bandswitching, transistorized field strength meter for two through twenty meters.

AN AMPLIFIED, CALIBRATED SIGNAL STRENGTH METER

J. L. Iliffe VE3CES

Recently, I had the problem of tuning a four element quad. As you may or may not be aware, these beasties are supposed to be tuned from the rear for minimum signal. A quick check showed none of my friends had a signal strength meter, so I prepared to degrade myself and buy one. A look at a few prices convinced me to build.

Since I wanted some other information on the quad, like front to back ratio and the effect of more or fewer elements, I decided to add a calibrated attenuator and enough gain to make a fairly wide input range. It also had to be cheap!

The result is shown in Fig. 1.

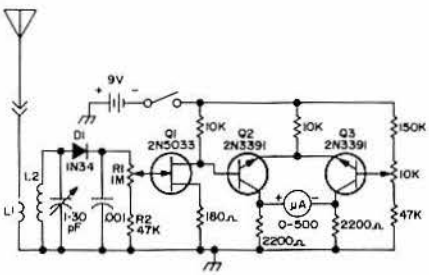

Fig. 1. Diagram of the field strength meter.

To use the normal rf attenuator method of switched T-pads requires complicated shields and quite a few resistors. Also the attenuator has to be terminated in its characteristic impedance to read correctly. To bypass this problem I first detect the rf, then attenuate the dc. This has the added advantage that the circuit is no longer frequency sensitive.

The incoming rf is tuned by C1-L2. C1 can be any small variable. I used both sections of a dual 15 pF because my local surplus store has them for 60¢. For VHF use only 1 section.

L2 is wound on a plastic pill bottle about 1" in diameter and tapering to 7/8". To cover 13–24 MHz, I used 11 turns spaced over about an inch. L1 is 2 turns over top of L2. I tried bandswitching with another pill bottle fastened on the other side of the shield from L2. The idea was to bandswitch another frequency range but I find it more convenient to wind on coils as needed. Use the grid dipper to get you in the ballpark. I have used this meter as high as 72 MHz without trouble. D1 can be any diode. I used a 1N34 because I could then specify it and know it would work, but I tried a computer type which also worked. If you prefer the meter to peak rather than dip, reverse D1.

Rectified rf from D1 is put on the top of R1, the calibrated attenuator. R2 in series with R1 gives the 0 dB point at its junction. For a 30 dB range, R2 is 47K if R1 is 1 MΩ This doesn't quite fill the range but is close. Changing the value of R2 will change the range but 30 dB is considerably more than the F/B ratio of most beams.

Q1 is a 2N5033 FET. The high input impedance of Q1 allows us to set the calibration of R1 directly by dc voltage measurements on the VTVM since it does not draw any base (gate) current. It is a p-channel device. If you use an n-channel type you will have to change the entire biasing of the circuit and also reverse D1.

Q2 and Q3 form a differential amplifier to drive the meter. Q2 is necessary to avoid loading Q1 and I had quite a bit of trouble balancing the meter against battery voltage changes until I added Q3. It will now operate from 8.5–9.2 volts with no trouble. The 10K pot in Q3's base centers the meter. The meter I used is a 250 μA tuning meter with no markings on it except a red/white/blue bar. This is all you need since we calibrate on R1, not the meter.

Operation

The meter is quite sensitive and with a two foot antenna I could get a reading several hundred feet behind my quad at 60 watts input. First tune the input (which is quite sharp) with the attenuator set at zero. This is the least sensitive position. Now set the meter for a convenient reading near the center scale with the incoming signal still on using R3. Adjust your antenna. When you feed it power again the reading will not be quite on scale on the meter but turning up R1 will allow you to put the meter back to the original position. Do not touch R3. The reading on R1 is now the increased gain in dB needed to bring the signal back to its original strength. In other words, the decrease in signal strength.

Note that during measurements you need a received signal to use R1. With no signal the meter will be off scale.

I have also used the meter to align oscillators and doublers in my two meter receiver. A probe can be made for this from two turns of wire on the end of a piece of coax. The high gain available allows the pickup loop to be quite far away which reduces detuning. Adjustments show up well on the meter.

FREQUENCY MEASURING EQUIPMENT AT MICROWAVE FREQUENCIES

Silas Smith WA9VFG

This article is not intended to give the theory, but rather a practical solution to the building and use of wavemeters at micro-wave frequencies.

In microwave work, frequency is one of the most important measurements. It must be understood the wave length in the devices described here is not the exact frequency wave length. A well-constructed wavemeter that has been calibrated can be very precise. They can be within 1.5 MHz at 10 GHz or less than half of a MHz at 1250 MHz. Temperature has some effect on the frequency. Most commercial wavemeters are constructed of Invar, a metal that changes very little with temperature. Some parts are of bi-metal construction to compensate for temperature. For the average experimenter, brass and copper will have to suffice. Although silver plating is desirable, it isn't an absolute necessity. Frequency at microwave frequencies can be measured by three methods: wavemeters, slotted lines, and frequency comparisons. All of these methods are used commercially. The frequency comparison is usually used in the laboratory to calibrate the wavemeter and the slotted line. As a general rule, any method of frequency measurement used at lower frequencies can also be used at the microwave frequencies, but are not always practical. The resonate cavity as a wavemeter is used in microwave measurements.

There are three types of cavity wavemeters: the transmission type, Fig. 1A and 1B, the reaction type, Fig. 1C, and the assorption or absorption type, Fig. 1D. All are resonate cavities. The way in which the wavemeter is used determines the type.

All wavemeters are adjusted for maximum readings except the assorption type. The assorption is adjusted for a dip in power output. The most popular wavemeter used by the beginner is the open circuited transmission line type, Fig. 2. This type of wavemeter is the equivalent of lecher wires. (Open circuit refers to the standing wave within the cavity, not the physical construction except as it pertains to the frequency wave length.) The practical physical dimensions are not many. The inner circumference of the main tube should be less than one wave length at the highest frequency to be measured. The rod should be small compared to the tube. If inductive coupling is used, the inductive coupling should be close to the shorted end. For probe coupling, the probe should be close to the middle. The open circuited transmission line is generally used in two ways. This type can be used "in line' (Fig. 1B) as it has very little loss when it is resonated. However, it should be removed from the line before transmitting, as it will act as a narrow band filter. The half wave length is the measurement between the two successive points at which the generator will load to maximum, as the rod is inserted or withdrawn.

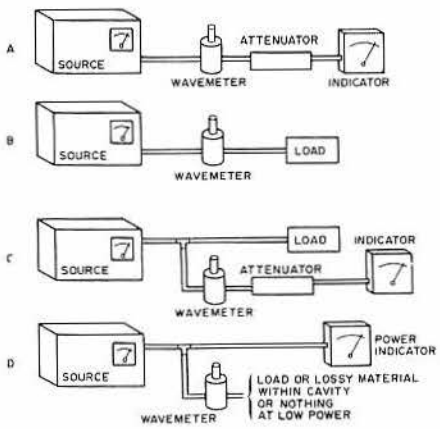

Fig. 1.

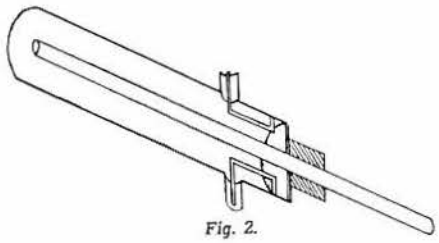

Fig. 2.

Another method in the use of the open circuited transmission line calls for the use of an additional circuit, as in Fig. 3. The circuit is a simple crystal diode detector connected to a microampmeter. The diode and condenser are usually built into the connector, as the leads should be kept as short as possible. The half wave length measurement is made on the rod between two successive maximum readings on the meter, as the rod is inserted or withdrawn. See Fig. 1A and 1B for the setup.

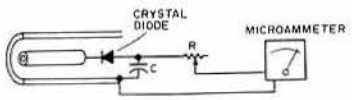

Fig. 3.

The quarter wave coaxial cavity is actually a shorted coaxial line one quarter wave length long (Fig. 4, 5, 6). As illustrated in these figures this type makes a very good cavity to use as a standard. To calibrate, a chart is made of the micrometer settings at different frequency wave lengths from a calibrated source generator. Don't tell them so, but the Public Relations Department of the Telephone Company may help you here, if they have any microwave technicians close by. The quarter wave coaxial cavity can be either physically open or closed. If closed, the closed end should extend at least a quarter of an inch beyond the center conductor at its lowest frequency. The closing of the end will lower the resonate frequency. Probe (capacitance) coupling as used for coupling in Fig. 5 will shorten the center conductor, and loop (inductive) as used in Fig. 4 will lengthen the conductor. In Fig. 4 we change the length of the center conductor to change its one quarter wave length. In Figs. 5 and 6 the center conductor remains the same, and we change the resonate frequency by capacitance. This method makes it necessary to construct the center conductor very short as compared to the full quarter wave length as in Fig. 4. These devices are not longer, so caution must be used when calibrating. The closed wavemeter as indicated in Fig. 7 is a shorted coax line at each end. The wavemeter uses a shorting plunger which is movable along part of its length. If used as the quarter wave coaxial cavity, the center conductor must be longer than a quarter wave length.

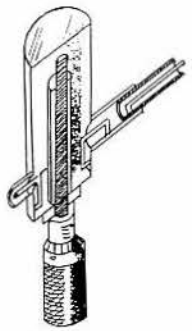

Fig. 4.

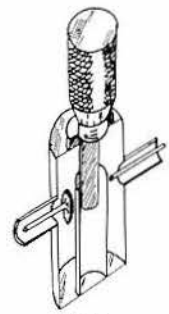

Fig. 5.

Up to this point we have covered most of the wavemeters that could be used from around 144 MHz up to approximately 3000 MHz. 1000 MHz to 3000 MHz are usually called the lower microwave frequencies. If the inner circumference of the outer tube is kept less than one wavelength, these wavemeters will operate in the desired TM mode.

There are four ways to couple energy into a wavemeter, loop (Fig. 4), probe (Fig. 5), direct (Fig. 6) and slit (Fig. 8). The most commonly used is the loop, as it has very little effect upon the electric field. The usual methods for changing loop coupling is to change the size and orientation of the loop. Loop coupling is usually placed in the high current area of the wavemeter. Capacitative coupling is changed by the size of probe and the distance from the center conductor. Capacitative coupling is usually placed at the high voltage portion of the wavemeter. As in Fig. 5, a small probe – say ½ in. piece of No. 22 wire, for example – may require an external voltage amplifier. The smaller the probe, the less effect on the resonate fre-

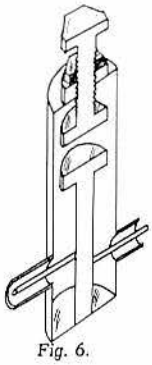

Fig. 6.

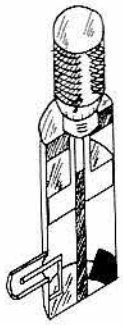

Fig. 7.

quency of the wavemeter. In direct coupling as in Fig. 6 the primary concern is impedance. To increase the impedance, move the coupling up the line away from the shorted end. To decrease the impedance, move the coupling down the line toward the shorted end. Slit coupling (Fig. 8) can be a small hole or a series of small holes or a slit. Its purpose is to allow a certain amount of leakage. In all forms of coupling, it is desirable to use loose coupling, as the wavemeter will have less effect on the system, and the Q of the circuit will be higher.

Above 3000 MHz, usually only the tunable wavemeter is used. The cavity is one quarter wave length long. The cavity can be coupled in three ways: loop, probe and slit. Because of the high frequencies, the slit is usually used, and the meter is most often

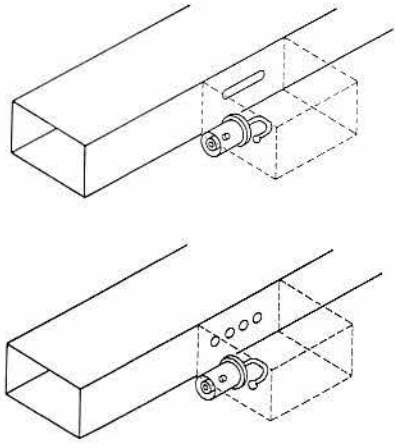

Fig. 8.

kept as an assorption meter. In the assorption method, the wavemeter should be detuned when not in use. Some of the cavity wavemeters have a little lossy material added to absorb some of the energy, as in Fig. 7. Lossy material can be made from graphite impregnated cloth in epoxy.

There is one other type of wavemeter that can be briefly mentioned; it is the reference wavemeter. The reference wavemeter is of any design as described, but would be constructed more like Fig. 6. It can be locked when adjusted to a selected frequency and used as a reference standard. The micrometer assemblies can be made from any micrometer with additional parts welded on. I constructed one using an oversized tube over the main cavity, and dimpled it at various places around its circumference until it fit smoothly over the cavity, and I used a piece of 3/8 threaded brass pipe as the main adjusting screw. I am sure you can come up with a good one without any backlash. This wavemeter spread the 1250 MHz band out to over 100 inches by rough measurements. I haven't calibrated it, so I can't say for sure just how far. There are three nice veeder root counters in the APX 6 which would make excellent wavemeters plus sliding contact material. One could even use the entire cavity.

The last method of microwave measurement that we will look at is the slotted line

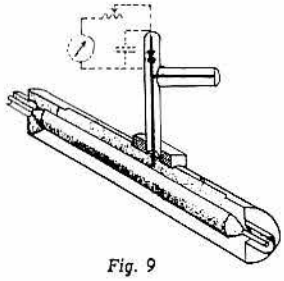

Fig. 9

(Fig. 9). The slotted line is a section of coax line along which is cut a slot. A probe, which is a simple crystal detector with a one quarter wave length shorted stub for a dc return path, is moved along near the center conductor of the slotted section. In this case we are looking for two successive minimum readings along the line. The distance between these readings is one half wave length. A slotted line should also be calibrated. If calibrated at one spot near the intended frequency to be measured, a chart will not have to be made – just a K factor obtained. The distance between two successive readings times the K factor should equal the frequency half wave length. There are a few accessories that can be either built in or used

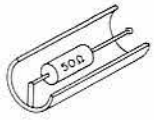

Fig. 10

externally. One is a coax attenuator shown in Fig. 4. It will slide in and out of the other half. It too can be calibrated if one wishes. A 50Ω resistor can be used for an impedance match for 50Ω lines if inductive coupling is used such as in Fig. 10 and when the loop is small. The line stretcher (Fig. 11) is useful with the slotted line. It merely consists of two coax sections, one sliding into the other.

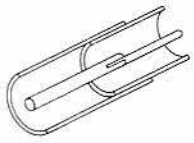

Fig. 11.

FREQUENCY METER – 1 to 10 GHz AMATEUR MICROWAVE

Bill Hoisington K1CLL

A quarter wave coaxial cavity is used up to about 5 ghz, and from there to over 10 ghz the three quarter mode is used. A complete explanation of these types of operation is given.

The same type of unit can be used as a very good tuned mixer from 1 to 10 ghz.

The Coaxial Cavity

The basic circuit of the coaxial cavity is shown in **Fig. 1.** A cylindrical outer cavity wall encloses a round rod some 4 inches long which is the center conductor–this center conductor is grounded at one end.

The Shape of the Cavity

The exterior shape of the cavity is shown in Fig.2. and is seen to be rectangular in cross section, with two thin walls and two thick side walls. Believe me, this configuration was not arrived at in one day! De-

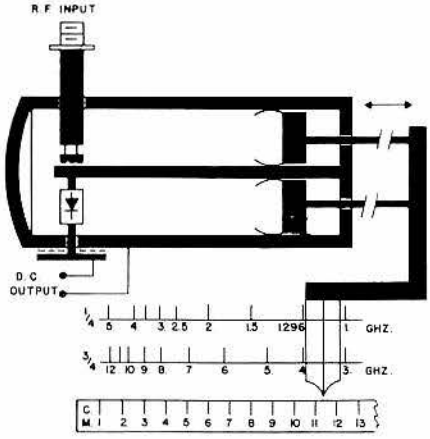

Fig. 1. Basic coaxial cavity.

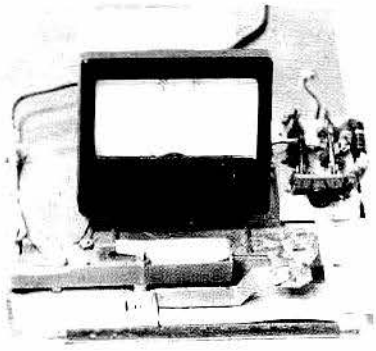

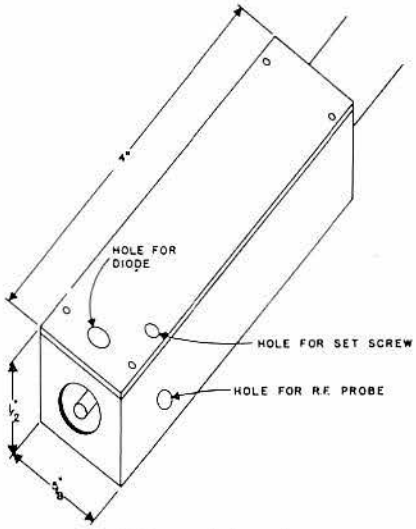

Fig. 2. Shape of the cavity.

signing tuners for X Band, I gaily started in with sections of thin-wall round pipe, the way I'd always done on uhf. The first thing you run up against is, how do you make the diode bypass capacitor? Machine out a curved saddle piece to fit exactly over the outer wall? Possible, but too expensive. And then how do you introduce the rf probe coupling into the cavity? Add on a "saddle" with a hole in it? These considerations and others, such as mounting (more saddles?) led to the abandonment of the pipe as a shape for microwave cavities; but not until a lot of time had been spent on the above mentioned items.

Diode holder and capacity

Looking at **Fig. 3.** you will see the first answer arrived at; but only after weeks and weeks of making different types and shapes. The center conductor is slightly flattened and drilled out to fit the diode prong. An 8/32 copper machine screw is drilled out to fit the other prong, then slotted with a fine

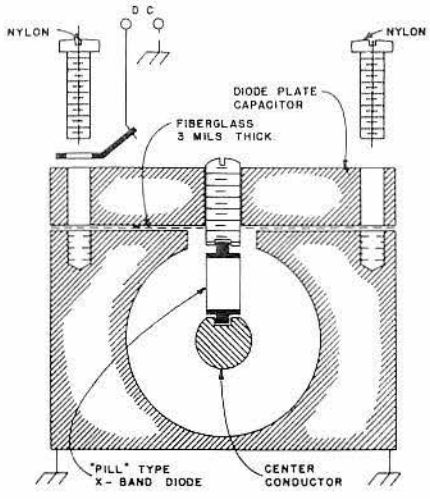

Fig. 3. Diode holder and capacitor.

jeweller's saw, and then compressed slightly to an inside diameter a shade less than the OD of the diode prong. In this way the copper screw will hold the diode as you insert it into the cavity. Believe me, that helps!

The second answer is also evident from **Fig. 3.** as the diode bypass capacity can now be made efficient at X-Band. As mentioned before, you cannot "buy" a capacitor "good for X-Band. You can make it though, as shown in **Fig. 3.**, if the cavity body has been designed correctly for it. One of the thin wall sides of the cavity is drilled out (or machined out) just wide enough to clear the diode and it's holder, which is the 8/32 copper screw. The copper capacitor plate, which is thick enough to take at least a half dozen 2/56 threads, is drilled and tapped for the 8/32 screw, and clearance drilled in the corners for the 2/56 mounting screws. A soldering lug for the dc connection is used under one of these, and a three mil (three thousandth of an inch) thick sheet of fiberglass cut out to fit, larger than the plate. This helps to keep metal particles from lodging inside the tiny crack that might be there if the fiberglass sheet did not extend out beyond the plate all the way around. You can begin to see some of the detail needed at X-Band.

Further reasons for the rectangular cross-section now show up in **Fig. 4.**, which details the rf probe connections. This item was also very troublesome in first models using pipe

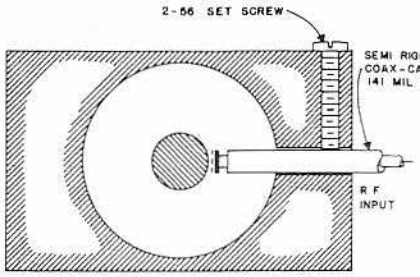

Fig. 4. RF probe connector detail.

walls, where "more saddles" was the only solution. All "saddles" are eliminated by the rectangular shape. Small semi-rigid cable is used for the connector. I have some short lengths with X-Band antennas connected to them for use as "In-Space" pick-ups, feeding directly into the wavemeter cavity. There is at times an advantage in this type of "energy collection" (antennas) which will be taken up later.

Fig. 5. shows detail of the treatment of the cavity end of the rf cable, or probe. The outer conductor is cut away for about one quarter inch in length and removed. About a sixteenth or so of the Teflon is left, which is then removed from the center conductor. A

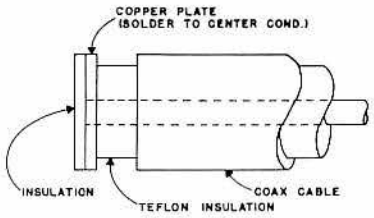

Fig. 5. RF probe detail.

thin copper washer (which I generally cut out of sheet copper since the hole to solder the center conductor is quite small) is then soldered to the center conductor, making the "capacity probe", as shown in **Fig. 5.**

Mylar tape or other good insulation is fastened to the side of this washer facing the center conductor. With this insulation in place you can push the probe all the way in, while testing, and still not have a dead short. Different thicknesses of fiberglass sheet can also be cemented on, to make up more permanent types of fixed capacitors, of different values.

For some uses, particularly in this one as a wavemeter, loose coupling is desired, but it must be securely locked with the set screw, otherwise your dial calibration and frequency reading will suffer.

Plunger fingers

Here is the most difficult item. It is hoped to have stock pieces made up for this work that you can purchase at reasonable cost. The fingers should be made of tempered beryllium-copper, which is not easy to work with.

Fig. 6. shows some details of the plunger and fingers. I assume, having been told so by "well-informed sources" (mechanical engineers) that these units should be made in a machine shop by competent machinists. Maybe so, as the ones I have made here in the shack by hand tend to lose their tension if not handled carefully.

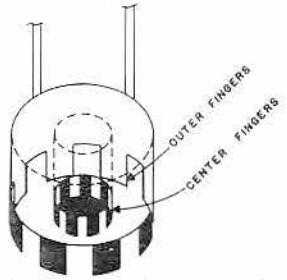

Fig. 6. Plunger details: A)End view, B)Outer fingers, C)Center fingers.

Fig. 7. shows the desired fit for these fingers. The plunger body should be an easily slide-fit *inside* the ¼ inch cavity, and the center hole in the plunger after the fingers should also be an easy fit *over* the center conductor.

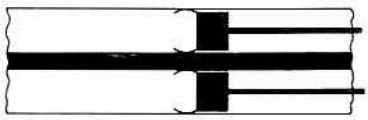

Fig. 7. Desired shape and curvature of the plunger fingers.

Two steel push rods lead back from the plunger through small holes in the back end of the cavity (see Fig. 1.); these terminate in the brass block which is furnished with a pointer for the frequency scale. Maximum extension of the plunger should be up against the end piece, as a positive reference point for the dial, in case of trouble after calibration. This point should be indicated on the scale as "minimum frequency" in order to reset the pointer if it should ever become displaced after calibration.

The diode

At present, the diode used is an X-Band "pill package," with a prong at each end as shown in Fig. 3. These are point-contact diodes, like the famous 1N23 ceramic cartridge types of World War II fame, only a lot smaller. Referring again to Fig. 3. always make sure that the ceramic part of the diode is, as nearly as possible, in the open space between the inner and outer conductors. This space is where the rf is! It is also important to make sure that there is as much metal surface continuity as possible along the cavity wall, across the fiberglass sheet X-Band capacitor insulation onto the diode capacitor plate, and from there over to the diode holder and onto the metal end of the diode.

The rf is at a maximum between the inner and outer conductors, which is an air space of a sixteenth of an inch. and that is where the diode should be.

The diode rf bypass capacitor, formed by the diode plate and the flat top of the cavity body, need only have a capacity which is relatively small; anything over about 20 pF is sufficient. What it *must* have is the proper *lack* of inductance! The details of how this act has been covered in previous paragraphs, and if you follow those details you will find little or no rf on the *outside* of the diode capacity plate or the dc lead from it.

X-Band is not just short waves. It is really short; like a quarter wave at X-Band equals 9/32 of an inch as you can plainly see, if you get one (or more) of those little plastic millimeter rulers in a stationery store for 5 or 10¢. Be sure and get some, by the way, if you're going to do anything above two meters.

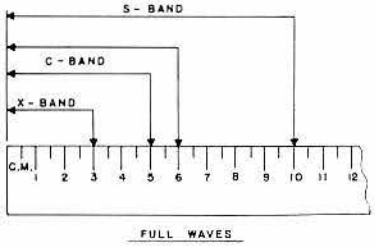

Fig. 8. Full waves for S, C and X-Bands on millimeter scale.

Fig. 8. shows the millimeter scale, with s, C, and X-Band plainly showing.

A handy wavelength-frequency chart is included here for your convenience, which is useful from the khz range way up *above* X-Band. See Fig. 9. Get to know the easy reciprocals, like 1 centimeter equals 30,000 mhz, 3 centimeters equals X-Band, 10 centimeters equals S-Band (3,000 mhz), 1,000 mhz equals 30 centimeters, etc. Very useful!

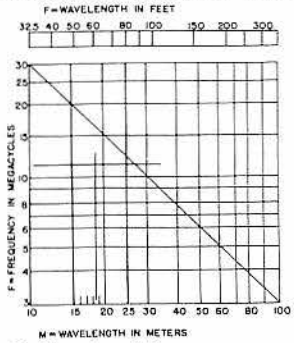

Fig. 9. Wave-length/frequency converter. Use of multiplying factors such as those at the bottom of the graph will cover any portion of the electromagnetic-wave spectrum.

The 3/4 mode and harmonics

Don't worry about that word "mode." Generally when something odd takes place in a cavity or waveguide, certain types of engineers tend to fall back on obscurantism (I seem to have fallen for that S64 word. It just means covering up). They say, "It jumped mode", or, "Spurious showed up."

Here's the straight dope. Fig. 10 shows the quarter wave "mode" of operation. Starting at 1 ghz you will find *one* point of maximum dc output. If the oscillator under measurement is "running hard" with lots of 2nd and 3rd harmonic energy content, these will be found at 2 and 3 thousand megahertz, and possibly higher ones, which should drop steadily in power as you go up. The diode itself may cause some of these if hit too hard with the rf input.

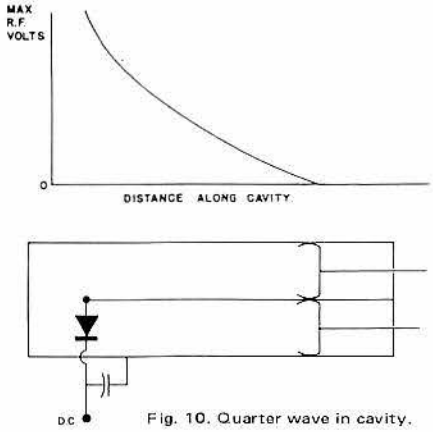

Fig. 10. Quarter wave in cavity.

Fig.11. shows the 3/4 wave mode, which is a very "natural" type of operation. Don't forget that in an instrument of this kind you are looking for standing waves and you want them to be of the greatest amplitude possible (within reason). So, if you tune the cavity by the plunger so that it measures

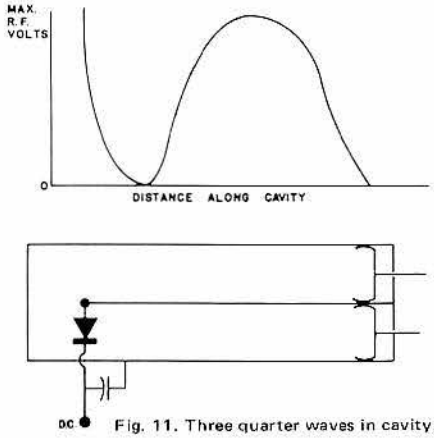

Fig. 11. Three quarter waves in cavity.

some three quarter waves on it (allowing for length-loading of the diode on the first quarter), you will find two peaks on the meter due to the situation shown in Fig.11. The higher the Q, and the lower the losses along the line, the more quarter waves can be found. For the 4 inch cavity shown, three quarter waves at S-Band are the longest that will fit.

A check on this operation is easy. Using the millimeter scale on the "dial', take several readings between maximums, for example, 22, 37, 51, and 67, add the spacings together, which comes to 45 millimeters, divide by three (the number of samples), and you will find an average of 15 millimeters for the waves which are standing on the center conductor (or "along the cavity", if you prefer) and there you are, 15 millimeters for the half wave, 3 centimeters for the full wave. Which is X-Band at 10,000 mhz or 10 ghz.

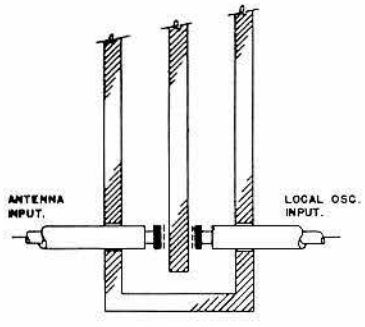

Fig. 12. Double input detail.

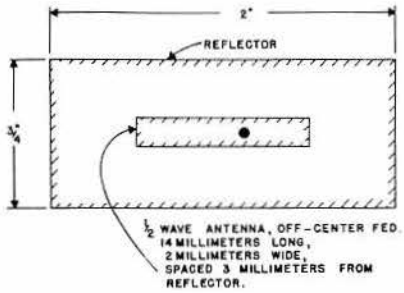

Fig. 13. Test antenna—X-Band "two-element".

If you find numbers which are not well known, you can find the frequency on the chart, at least close enough to put you in one of the microwave amateur bands, such as 5,650 or 10,500 mhz.

Use as a Microwave Mixer

This same type of cavity can be used from 1 to 10 ghz as a mixer for the front end of a superhet receiver covering those frequencies.

This application will only be touched on briefly here as the whole receiver is detailed in another article in *73 Magazine*.

Fig. 12. shows how to do it, so you can plan on this use, and make more than one, if you wish to.

Looking at Fig. 12., you can see how useful it is to have *two* thick sides on the cavity, one for rf input and one for the local oscillator input.

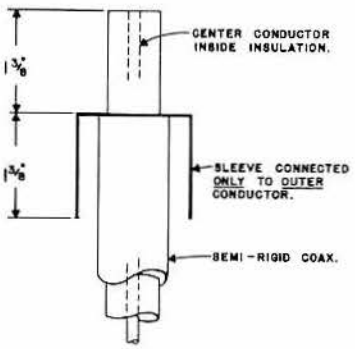

Fig. 14. Test antenna—S-Band. Dimensions suitable for amateur S-Band 2,400 mhz (omni-directional).

Conclusion

That about covers the details and some uses. The whole unit can be mounted on a piece of copper-clad, along with a 50 ma meter, the dial scale, and the centimeter-frequency chart. I broke down on this one and used a "regular" small microwave input connector for the rf. (Instead of an "RCA Phono Jack".) For connections to other units, such as oscillators and multipliers, small flexible cable may be used.

Fig. 13 shows a test antenna for X band, not the best in the world but good enough for a starter. With a lens in front it really picks up signals. Fig. 14 shows an S band antenna for the 2,400 MHz amateur frequencies.

LAMBDA LINES

James Ashe W2DXH

Over the past few years, new kinds of commercial gear and military surplus have made it quite easy to generate VHF frequencies. But the problem of measuring the frequencies has not become any easier for amateurs short on calibrated instruments. Of course this means the newcomer to VHF! What can he do to find what ballpark a circuit is radiating in, if there are no accurate devices available? When this problem came up recently, a simple solution appeared quite by accident. It was so simple, in fact, that its simplicity must be the feature that has kept it out of the ham publications. Another first for 73!

The traditional solution to the rough frequency measurement problem is to make up a Lecher Wire system. There is some question about the value of one of these in the modern ham shack. Narrow-band crystal-controlled techniques guarantee frequency and stability once the multipliers are tuned properly. In the old modulated oscillator days things were not that stable . . . so why go to all that carpentry and construction work for what fairly well promises to be a use-it-once gadget? Particularly when a little reflection (pun intended!) may bring out a cheaper, faster and better arrangement?

Ham and commercial builders of VHF gear have been using tuned stubs for years to match impedances, tune out frequencies, tune in others, etc. Yet it seems to have occurred to very few workers indeed that it might be possible to cut stubs to length accurately enough to serve as frequency standards. Apparently this can be done, with an accuracy of about 5%! This compares very favorably indeed with the performance of lower-frequency grid dip meters and some signal generators. It's pretty good for a pencil and yardstick operation: the only other items required are some understanding of how it works and a piece of 300 ohm twin lead. Belden #8235 recommended. You can calibrate that new GDO for 432 at a cost of just a few cents!

Theory

Many kinds of things show a property of tuning sharply to a certain frequency. This property is called resonance. We hear it when a struck piece of metal rings, and see it in the pendulum of an old grandfather clock. The grid dip meter shows a drop in grid current of an oscillator when a nearby resonant circuit steals energy from the oscillator. And it is the nearby resonant circuit that is the subject of this article.

The basic circuit is the quarter-wave stub. A little browsing around in the handbooks and earlier issues of 73 and other ham magazines will tell you lots about quarter wave stubs. The important practical points are that the stub resonates at certain frequencies, and that at these frequencies it can be dipped at its shorted end in the same way as any other resonant circuit.

But the term 'quarter-wave' has to be taken with a grain of salt. The tuned stub will be shorter than a free-space quarter wave, because the dielectric has a slowing-down effect on the rate at which the RF bounces end-to-end along it. Suppose you laid out a mile or so of twin-lead and transmitted a signal, at the same time sending off a reference signal by space wave. The reference signal would arrive at the other end first, in about 5.35 microseconds. The twin-lead signal would arrive a full microsecond later, about a 20% delay. Since this applies even to short lengths of twin-lead, the delay must be taken into account for accurate measurements. Also, there is a considerable difference in velocity factors between different brands and qualities of twin-lead.

Crystals are often used in overtone oscillators for generating stable VHF frequencies. The various modes of oscillation are pictured in the handbooks. Tuned lines will also show overtone resonances, and in the case of large uncertainty, it might just happen that reasonable errors could lead to a consistent but very wrong result. A halfwave line will resonate at a frequency f, and also at 2f, 3f, and so on. Note both odd and even multiples! All other resonant lines have a similar overtone resonance property. The problem is slightly aggravated by the convenience of using relatively long lines at the higher frequencies because they are easier to handle. The solution is to cut a pair of lines whose collections of resonant frequencies have only one resonance in common. The recommended lengths are a half-wave and a three-quarter wave line.

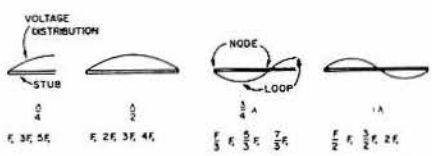

Fig. 1. Four kinds of tuned stubs, taking their fundamental resonances as the frequency producing the illustrated voltage distribution. This shows that none of them has a unique resonant frequency.

Fig. 1 shows four basic tuned lines. Just which resonance is an overtone and which is not depends somewhat on the application. The simplest way out of this problem in semantics is to say that the three-quarter wave line really doesn't have that resonance at f/3, ignore the quarter and fullwave lines, and stick to the remaining two for test work.

At 432 MHz a wave in free space is about 27.3 inches long. Suppose we are using Belden #8235 twin lead, which Belden says has a velocity factor or propagation constant of 0.77. The twinlead wavelength than is 27.3 times 0.77 or 21 inches. The halfwave stub must be 10.5 inches long, shorted on both ends; and the three-quarter wave stub 15.75 inches long, shorted at one end. These are convenient lengths, not too long to use on the workbench, nor so short that percentage accuracy in cutting becomes a big question.

Using the stubs

The commercially available grid dip meters are not noted for accuracy. It's commonly estimated that the scale calibration can be

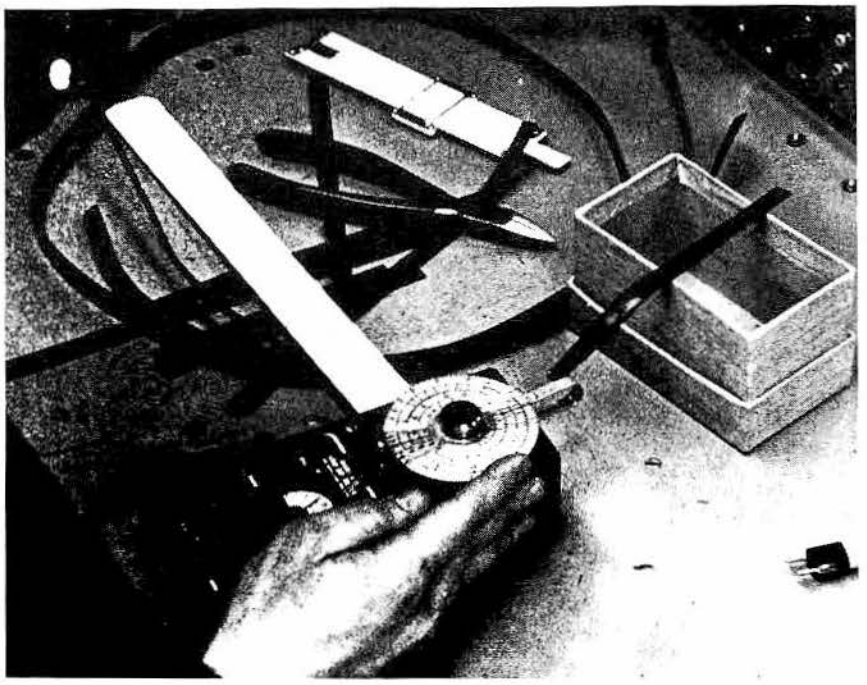

Fig. 2. Some overtone resonances of a halfwave stub (shorted at both ends). F1, F2, F3 and F4 should be 1F, 2F, 3F, 4F.

trusted to within about 20%. With some care, calibration points taken from twin-lead resonators appear to be good to about 5%. The first precaution is accurate construction. Cut the strips slightly long, short one end of each, and cut the three-quarter wave line to length. Then go more carefully at the other end of the halfwave line, which must be shorted at both ends. It should not be too hard to get the correct lengths within one sixteenth inch.

When making frequency checks, the lines must be held off the workbench an inch or two. Use small boxes or pieces of cardboard. Probably the better part of a foot distance is in order if the workbench is of metal or has a copper surface. At two meters, a perceptible change in calibration can be detected if the line is laid out on a wood surface! It's very good practice to make up lines for two meters or lower, and practice dipping them. Some refinement of technique will certainly be required before a halfwave and a three-quarter wave line can be made to dip at the same point on a standard dip meter. Once the trick is mastered, it can be carried up to the higher frequencies.

The lines are dipped in the same way as any coil. Because they have a very high Q, there will be a tendency for the dip oscillator to pull, or to seem to give different readings when tuning down to frequency and tuning up to frequency. The remedy is less coupling: move the dip meter a little further away from the line and try again. Dip the stub at its shorted end!

But what was that trick for calibrating a dip oscillator, mentioned earlier? Can't make up a pair of lines for each frequency. No need to! That's simply the reliable way for finding the right ballpark. When you're there, you can set the lines aside, make up another three-quarter wave resonator cut for the lowest frequency, and after marking that point on the scale, trim the stub up to the next calibration frequency. Throw the remainder away when done calibrating.

The half-wave stub is also useful as a tuned coupler. Suppose you want to tune an oscillator to a particular frequency but have nothing to indicate at that frequency. Loosely couple the RF into one end of the half-wave stub, and take it out the other end with a hairpin loop, through a diode to a 50 μA meter. You will only get a reading at the resonant frequency of the half-wave stub. Simple!

Chapter V

RF Signal Generators

ZERO-BEATING WITH A FREQUENCY METER

Jim Harrison WB4TBX

After putting an LM-18 in service, I found it a nuisance to plug in headphones every time it was necessary to adjust the corrector control to produce Zero Beat at one of the crystal check points. I hooked up a phone plug to the plate winding of an audio output transformer, and then connected a small loudspeaker to the secondary winding. I leave the phone plug inserted in the LM phone jack at all times. After using this setup for a while, it occurred to me that the last few cycles either side of zero beat might not be audible, so I tried a parallel hook-up off the primary side of the transformer. The other end of the cable was connected to the Vertical input of an oscilloscope. Now, when adjusting the corrector control for zero beat, you will see low amplitude sine waves even after you can no longer hear the beat note. You tune out the sine waves until you have a perfectly straight reference line on the scope. The Heterodyne oscillator is then corrected to calibration much more accurately than trusting to the ear alone. The principle is not new, yet the idea may not have occurred to some people. Any old scope will do, as the frequencies are in the audio range.

Another bit of frustration occurred when trying to adjust the corrector knob. I would pass the zero beat point time and time again, due to the stiffness of the control. Remember, these units are built for ship-board use, and loose controls cannot be tolerated. I dug up a small vernier tuning drive, similar to the Jackson Planetary-Vernier drive, (about 5 to 1 ratio). I mounted this drive on a right-angle aluminum bracket and attached it to the LM using the two screws on the upper right side of the unit. Bore holes slightly oversize to allow for accurate alignment of the control shaft so that it will not bind. Cut out a portion of the bracket so the "High-Low" knob can be moved. The precise Zero beat adjustment can now be made very easily with the reduction drive.

HAND CALIBRATE THE BC-221 FREQUENCY METER

Carl Henry

At present many amateurs have an opportunity that may not repeat itself. I refer to the many army and navy surplus frequency meters now available, through MARS and surplus sales. Many of these meters have the original calibration chart missing, and are considered virtually useless. This is demonstrated graphically by prices, the frequency meters with charts costing $100, the meters without charts selling for one-third this amount. Meters without charts are worth more than this would seem to indicate. It is no great job to calibrate one of these meters, but it is time consuming. A little care is required, but you do not need to be a super technician or electronic engineer to do the job. Neither is elaborate equipment required.

Essential to the calibration are several items not commonly available around the shack, but easy to build. Figure 1 illustrates the first requirement. This is a 10 kc multivibrator, which will operate from a 100 kc xtal calibrator, and give 10 kc markers up to 20 mc. I am assuming here that you have or can beg, borrow, or steal a 100 kc calibrator, this being a common item. In fact, some receivers have them built in. Using this 10 kc marker source, the high band of the frequency meter can be calibrated. Interpolation to 1 kc points is then possible, and if care is used an accuracy of better than 0.005% will result.

Fig. 2 shows a simple beat detector that can be used with earphones to get an exact zero beat. It took about ten minutes to wire up a 1629 (army surplus magic eye tube) temporarily for this purpose, and it is certainly worth while in the interest of increased accuracy.

With your equipment assembled, connect the frequency meter to its power supply. Allow at least one hour for proper warm-up so that all equipment will stabilize, including the 100 kc calibrator and 10 kc multivibrator. Set the CALIBRATE control on the frequency meter to center, and be especially careful not to move it until the calibration is complete. After the warm-up period the 100 kc calibrator should be zeroed against WWV, at as high a frequency as possible. The 10 kc multivibrator must be checked to see that it gives nine beats between each 100 kc beat. This can be done with your communications receiver, and it will be easiest to do it on as low a frequency as possible, say 600 to 700 kc. Now type several sheets of paper, listing the high range of your frequency meter by 10 kc points. If you are in doubt as to the range, check it with your receiver. To do this set the dial to the low end of its range, turn on the internal xtal, and zero in on the strongest beat at or near the low end. Turn off the internal xtal oscillator and find the signal from the frequency meter with your receiver. Note the frequency. Tune your receiver until you reach another harmonic from the frequency meter. The difference between the first and second readings is the frequency of the meter at the low end

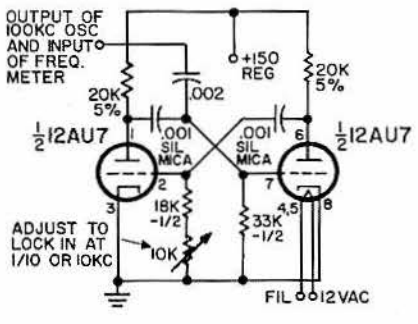

Figure 1. 10 kc multivibrator for use with 100 kc crystal oscillator, providing 10 kc beats with frequency meter.

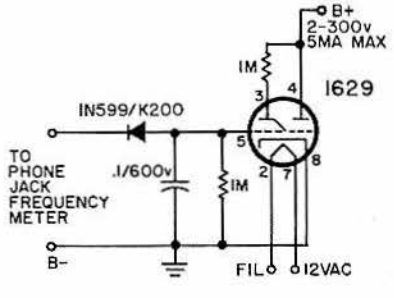

Figure 2. A simple zero-beat indicator for use in conjunction with headphones.

of its dial. Now do the same thing at the high end, and you have the primary coverage of your frequency meter. Most have a range of 125 to 250 kc on the low band and 2 to 4 mc on the high band.

When you write up the frequency range by 10 kc points, leave a space between notations, since you will be adding information here later. Now, using the 100 kc xtal, check the high band of the frequency meter at 100 kc points, listing the dial readings. Now go back and check the dial at 10 kc points, listing all the dial readings. The checks should agree with the 100 kc checks at every tenth point. This is a handy method of cross checking yourself. You might note that on equipment of this type, always approach the final reading from below. If you pass the zero beat point, don't jockey the dial back and forth for zero beat. Go back below the beat by 5 kc or so and approach again from below. This procedure will help to eliminate error from dial backlash.

After your 10 kc points are all listed, interpolate to 1 kc points. This is the hardest part of the job, and is very time consuming. A big pot of coffee and a patient and loving XYL will be a big help here. The patient XYL can be replaced with an adding machine if you have one available, but you'll still need the coffee.

The difference between each 10 kc point must be listed. Note this in the space you left on your sheets. Each 1 kc will be 10% of this, so add 10% to the 10 kc listing for 11 kc, 10% more for 12 kc, 10% more for 13 kc, and so on. When you reach the next listed 10 kc point, the calculated listing and the measured listing must agree, another cross-check. This will take 2000 individual additions.

After the high band is finished, you may wish to calibrate the low band in the same fashion. Referring to Figure 1, change the grid-plate capacitors to 0.01 mfd. This will put the multivibrator at approximately 1 kc intervals. If you have trouble syncing the multivibrator, you may have to build another to operate at 10 kc, and sync the 1 kc from this. No trouble should be had with a strong output xtal calibrator, however. Calibrate the multivibrator as before, except with 1 kc intervals instead of 10 kc.

A calibration book can be prepared when you finish. It is a good idea to file all your original calculations and papers, should the book ever be destroyed. The frequency meter is now as good as any with original calibration book, at a good saving of money.

HIGH ACCURACY VHF FREQUENCY MEASUREMENTS

Howard Burgess W5WGF

Accurate frequency measurements can be a problem for the amateur with a limited budget. However with some home construction and careful operation the average ham can make VHF frequency measurements to an accuracy better than .00015% at two meters. This is the equivalent of measuring the distance from New York to Los Angeles with an error of only 25 feet. Many commercial units cannot equal this figure. The same method can also be used for HF and UHF measurements.

There are many ways to measure frequency but few of them are satisfactory for use at the very high frequencies. The well known hetrodyne frequency meter becomes unstable when its oscillator is operated at VHF. It can no longer be held or read to any degree of accuracy. The oscillator can be operated at a low frequency and one of the harmonics used at VHF, but any error in the oscillator will be multiplied by the number of the harmonic used. A frequency meter that can be held to within 200 hertz at 4 MHz will be off by 7.4 kHz at the 148 MHz harmonic.

A second method of much greater accuracy uses low frequency crystals which are referenced to a known standard such as WWV. The harmonics of these oscillators will be quite accurate and useful far into the UHF region. However this system has its limitations. Even when used with multivibrators and harmonic amplifiers it produces only spot frequencies.

Although neither of these two methods is satisfactory when used alone, they can be combined to make an accurate and versatile system. If you haven't guessed it by now, the system works like this. A crystal oscillator operates on 5 MHz. This oscillator can be kept to zero beat with WWV with very little effort. With a simple harmonic amplifier following it, strong markers are available every 5 MHz far into the UHF region. To fill in between the 5 MHz points, and get full tuneable coverage, all that is required is to add the output of a stable low frequency VFO to the proper marker. Example: To measure 146.25 MHz just add 1.25 MHz from a calibrated tuneable oscillator to the 145 MHz harmonic of the crystal. The same results can be had by using the 150 MHz marker and substracting 3.75 MHz.

The tuneable low frequency oscillator of this hetrodyne system can be any stable, calibrated, oscillator that will give the desired frequencies. A good signal generator can be used but better yet is the old faithful BC-221 frequency meter. The crystal oscillator that supplies the 5 MHz markers should be designed for high stability. However, even simple crystal-controlled units can be kept zero beat with WWV for periods long enough to make most measurements.

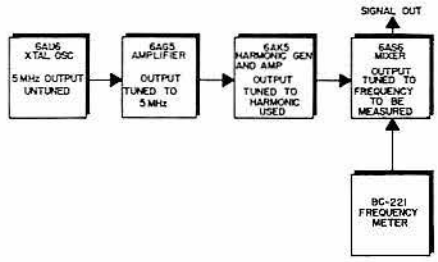

Fig. 1. Block diagram of the VHF frequency meter.

Earlier we quoted a figure of .00015% or better for the accuracy of this system. Perhaps we should show how this is possible. The crystal oscillator can be held to near zero beat with WWV but due to propagation errors in the signal of WWV, we can never be sure that our crystal is closer than 2 parts in 10 million. This would be 2 hertz of error at 10 MHz or an uncertainty of 29 Hz in the 145 MHz marker. The BC-221 is normally considered to be a .05% instrument. This would be an error of about 1.75 kHz at 3.5 MHz. However with care in calibration, and reading it is not difficult to reduce this value to 200 hertz or less. In a hetrodyne system the error of the VFO is not multiplied at VHF but is just added to the error of the crystal marker used.

The total error at 2 meters is 29 Hz contributed by the crystal and 200 Hz by the VFO for a total of 229 Hz. This is a little more than 1.5 hertz per million hertz for a tuneable system. Of course these values are approximate and with careful operation they can be reduced by 50% or more.

In the 146.25 MHz example used earlier, the VFO was required to furnish less than 1% of the total output. To put it another way, the only wobble is in the smallest cog and its contribution is so small it can't shake up the machinery too much.

The circuit shown in **Figs. 1 and 2** has been used for monitoring MARS, CAP, and several other services. The crystal oscillator is quite stable but can be tuned enough to zero with WWV. Tuning is done with C1. One stage of harmonic amplification is sufficient to give strong signals well above 150 MHz. The plate circuit of this amplifier stage is tuned to the harmonic to be used. This feeds one input

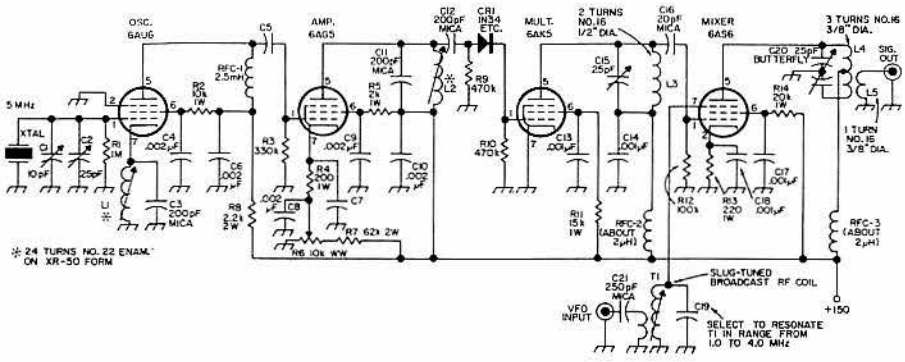

Fig. 2. Schematic of the oscillator, multipliers and mixer for using a BC-221 on the VHF ham bands.

grid of the mixer. The other grid of the mixer is driven by the output of the BC-221 frequency meter. The tuned circuit shown in this grid resonates broadly in the 2-4 MHz range of the BC-221. This helps to keep the higher harmonics of the BC-221 out of the mixer.

The output of the mixer is resonated to the desired operating frequency. This will be either the sum or difference of the two input signals. The level of the output signal can be controlled by R6.

Operation of this system is simple. The "cook book" would read as follows:

1. Couple the output to the antenna of the VHF receiver.
2. Determine the crystal harmonic and VFO frequency that will give the frequency of the signal to be checked.
3. Tune the VHF receiver to the signal to be checked.
4. Tune the BC-221 until the output of the frequency monitor zero beats the received signal.
5. If required, peak the tuned circuits in the monitor for maximum output and adjust R6 as needed.
6. The frequency of the received signal will be the crystal harmonic plus (or minus) the reading of the BC-221.

Many details cannot be covered in one story due to lack of space. The operator will have to determine the most effeceive method of coupling to this particular receiver. He will also have to explore the many combinations of frequencies which can be used. These and many other questions cannot be included at this time. However those who require such a system as this will probably be capable of filling these details.

One word of caution is in order. With two oscillators that are rich in harmonics, there can be many unwanted "birdies." These present no problem after the operator has gained experience but the new user should be very cautious. Many times an unwanted beat can be eliminated at a critical spot by changing the two frequencies that are being mixed (shift from sum to difference).

Perhaps we should emphasize that this system is a "trade off" where the amateur can trade his skill and patience for highly accurate measurements with simple equipment.

A TRANSISTORIZED LM METER

Charles Landahl W5SOT

The last word may never be written about the BC-221 and LM frequency meters. The LM is particularly attractive because it is in the smaller package. With transistors replacing tubes, it has features most everyone wants – it is rugged, portable, and accurate, to name a few. I will describe a conversion of an LM-15 frequency meter in which field-effect transistors replace tubes; the power supply becomes a standard 9V transistor radio battery and the current drain is less than 3 mA when all functions are energized. In addition, I offer calibration information which will be of interest to anyone having a BC-221 or LM without the official calibration book. I bought an LM-15 for a temptingly low price (Fair Radio Sales Co., Lima, Ohio, $14.95). The set is sold in the "as is" condition with tubes and crystal but without calibration book. It is a good idea, but not necessary, to start with a set which is working before making the change to FETs. Resistance measurements will show if the circuits are complete. Important values are marked on the schematic of Fig. 1.

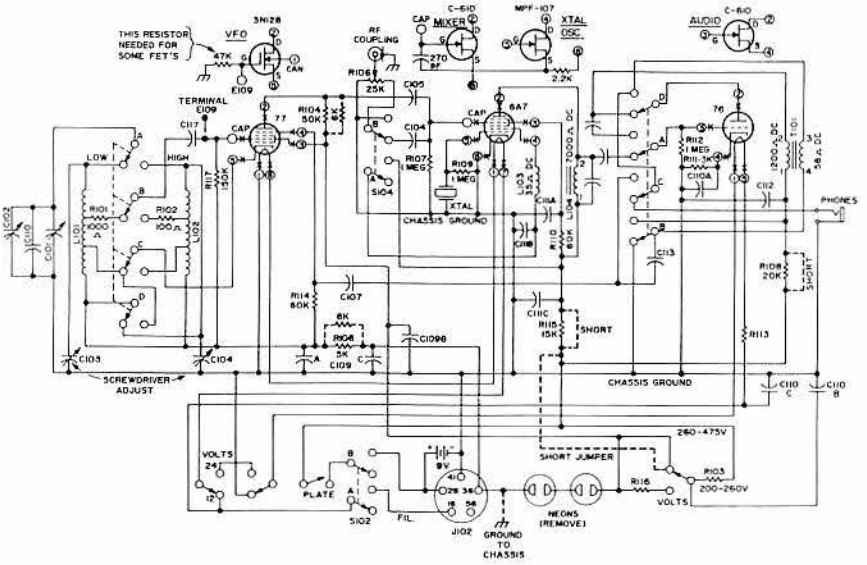

Fig. 1. Modified schematic of frequency meter.

Smash Tubes

The most difficult part of my conversion was getting up the courage to smash the tubes! I wanted the bases for mounting transistors. Place the tubes one at a time in a paper sack, hold the top closed and with a metal object, strike the glass through the paper. The flying glass is caught and collected for disposal. Scrape and clean the mastic from the inside of the tube bases. Should you choose to mount a transistor socket in the wall of each tube socket, you can use the original wires; otherwise, unsolder the old wires and replace the needed ones with about 2 in. of sturdy new tinned wires. The appropriate tube base pin connections are shown in Fig. 2. Actually there is no preferred mounting scheme. Use whatever appeals to you.

Check for clearance between socket and walls. My conversion used transistor sockets mounted on metal plates which were bolted to the wall of the salvaged tube bases. This allowed FET substitution to determine which ones would work best in the several circuits of the LM. All FETs used are N-channel.

Modification

With cover removed and the LM in the upright position, front panel toward you, on the left side wall, look through two oblong machined slots and see mounted on a phenolic board a 50 kΩ plate resistor. Parallel it with about 6 kΩ. Turn the LM upside down, panel toward you. On the underside, two resistors must be shorted and a jumper wire made up and connected. Short R115, which is a 15 kΩ wirewound resistor, quite visible on a phenolic board at the left of the 1000 kHz crystal can. Run an insulated wire from a terminal of this shorted resistor to the 260–470V tap contact of the link switch. This wire can be about 6 in. long and conveniently passes through a wall slot behind the crystal socket. The link switch and its terminals are on a phenolic board in the compartment aft of the crystal socket. The jumper wire will cross near the grid resistor, R109, of the crystal oscillator. While there, change the 100 kΩ (R109) to 1 MΩ. Next, unfasten the screws holding the phenolic board located to the left of the power plug. Tip up the board and short across R108. This is a 20 kΩ composition resistor which is in the plate voltage line to the audio amplifier. Also, at the power plug, locate pin 36. Short it to chassis ground. On most sets pin 36 is the ground return for the vfo cathode. The circuit was closed through external connections in a power supply. You have completed the surprisingly few changes needed to make the LM work on FETs and a 9V battery.

The VFO

With FET source connected to pin 5, drain to pin 2, can to pin 1 (if needed), plug the FET into the vfo socket. Connect

a solid wire between terminal E109 and the gate of the FET. (Terminal E109 held the grid cap wire for the vfo tube.) Connect a 9V battery to the power plug pins. PLUS to 26 and MINUS to terminal 41. If you have a milliammeter in the battery lead, it should read about 1.5 mA when you turn on the FIL and PLATE switches. Provided you were fortunate in the choice of FET, you should hear a clear CW signal in your receiver. Set your receiver to 2 MHz or 4 MHz. You may need to connect a wire from the rf coupling post on the front of the LM to your receiver antenna. Rotate the LM dial between 0300 and 0600 on the readout. Your vfo will be on the low end of 125–250 kHz or 2–4 MHz depending on the position of the low or high band switch. The XTAL and MOD switches should be off. The FET selected for the vfo may require a 47 kΩ resistor between gate and chassis ground. I found this to be true for the RCA 3N128, 3N142,and *one* of the two 40559A FETs. On the other hand, one RCA 40559A and one of several 2N3085 silicon N-channel FET from Poly-Paks worked beautifully without adding 47 kΩ to the gate.

Apparently junction and insulated-gate field-effect transistors have slightly different characteristics which show up in this peculiar vfo circuit. My own choice is the 3N128 with the additional resistor on the gate. You may find it necessary to "tune" the source, drain, and gate resistances in order to have your vfo working well with a particular FET. I used potentiometers across the various elements to arrive at the recommended values. My vfo works reliably from 10V down to 6V and the maximum drain current is 1.5 mA.

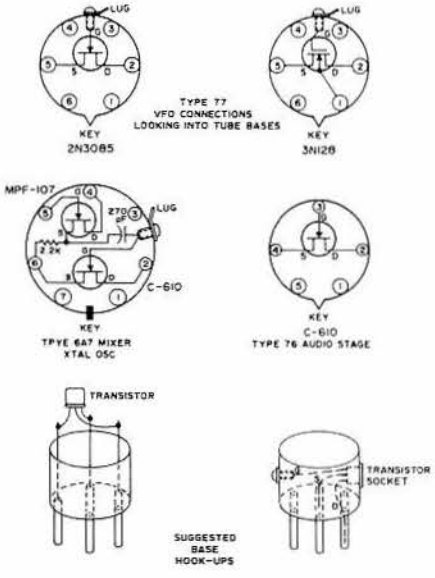

Fig. 2. Suggested semiconductor hookups for tube sockets.

Caution

Other oscillator hook-ups may occur to you, and they will work – but the tuning range and linearity of the vfo will suffer! Linear tuning is most important, so stick with that shown.

The AFO and AF Amplifier

The audio oscillator and amplifier wasn't as fussy as the vfo. I used a Radio Shack 276-664 FET – it is said to replace a C-610 or 2N3088. I found that the Poly-Paks "hobby" FET 92CU588 will work equally well. In making up the socket, gate goes to tube pin 3, source to cathode pin 4, and drain to plate pin 2. That is all there is to this one. Plug in the FET. When you next turn on the 9V power, the milliammeter will barely increase a few hundred microamps as you switch on the modulation control. At this moment a rather pleasant 500 Hz tone will appear on the vfo frequency no matter which harmonic you have tuned in on receiver. Your modulator is finished. The audio amplifier is too, for that matter. You just won't hear anything in the headphones until you complete the crystal oscillator and the mixer circuits.

Crystal Oscillator

The reference oscillator is not much trouble. You have already changed the gate resistor from 100 kΩ to 1 MΩ. Actually this change may not be necessary because some crystals are more active and will oscillate well with the original resistor. Mine went into oscillation better with the higher value. The FET you select for this circuit can be one of several. Mine is a Motorola MPF-107. I found the Radio Shack 276-112 and the Poly-Paks 2N3085 also work, but draw more current. Whichever you choose, the gate connects to base grid pin 5, source to cathode pin 6 *through* a 2.2 kΩ resistor. Drain hooks to plate pin 4.

Now, when 9V is turned on, MOD off, XTAL on, you should hear the crystal oscillator signal every 1000 kHz on your receiver. The milliammeter should increase about 1.5 mA or less when XTAL is turned on. If you don't hear the crystal frequency, bring the receiver antenna wire close to the crystal FET. We still haven't made the connection which adds the crystal-oscillator signal to the rf coupling post on the front of the LM. Assuming you have all circuits in working order up to this point, we move to the mixer.

Mixer

There is no single FET substitute for a pentagrid converter tube. The dual-gate MOSFET comes closest; however, use of one would have defeated my goal of simplest conversion. Therefore, four N-channel FETs are needed to do the work of three tubes, but what a saving in power supply! The mixer concerns itself only with beat frequencies occurring between the reference oscillator, vfo, or an external signal – all audio work. Thus, a hobby FET was selected. I used the Poly-Paks N-channel FET. A Radio Shack C-610 replacement will also work. Connect source to chassis ground through pin 6 of the tube socket; the drain connects to plate pin 2, gate to mixer grid cap wire through the lug in tube socket wall.

Finally, connect a capacitor (200–300 pF) from the top of the 2.2 kΩ crystal oscillator source resistor to the gate of the mixer FET (grid cap wire). You are in business.

With 600Ω phones plugged into the LM, you should hear all the necessary beat frequencies occurring between the vfo and the crystal oscillator as you tune the vfo through its range. XTAL must be on and the MOD switch off. Otherwise, the audio amplifier becomes the modulator and you hear nothing in the LM phones.

What Next?

With the beat notes loud and clear you are ready to calibrate. This is quite the most fun part of the work because the linear tuning rate of the LM is almost unbelievable. The slow rate is due to the series combination of the A section of C109, C101, tuning L101 or L102. The amount of the matter is that one revolution of the 100-division circular dial produces about 3 kHz change on 125–250 kHz range, and about 50 kHz per revolution on the 2–4 MHz range. The actual calibration of my unit was 2.89 kHz and 45.17 kHz per revolution.

The linearity can be checked by how little you need to vary the "corrector" for each zero-beat checkpoint. Each LM or BC-221 will be slightly different. Now, when you consider that the vernier allows you to split one division into tenths, then it is clear that you can set a frequency to better than 0.5 kHz over the range of the frequency meter. May I repeat:

1 dial revolution of
100 div = 45.17 kHz
1 division = 0.4517 kHz
1/10 div = 45 Hz

Therefore, all you need is a checkpoint at which to zero the vfo and start counting revolutions, divisions and tenths of divisions to accurately set any frequency within the two ranges of the vfo. I found it useful to construct graphs on K&E 358 11L graph paper. The grid is 10 X 10 (per 0.5 in.). The paper has 20 units vertical and 30 horizontal. This allows graphing 100 division and leaves room for 10 vernier

divisions on the right hand end of the paper. Use the crystal checkpoints listed in Table I to locate *your* dial settings. Once graphed, a frequency can be selected directly from the chart, or, depending on the accuracy desired, interpolated between checkpoints.

Table I. Crystal Checkpoints

KHz	VFO	XTAL	Approximate Dial Settings
Low Band			
125	8	1	0320
150	20	3	1192
166.667	6	1	1750
200	5	1	2935
222.222	9	2	3700
250	4	1	4647
High Band			
2000	1	2	0396
2250	4	9	0945
2500	2	5	1493
2750	4	11	1050
3000	1	3	2606
3250	4	13	3150
3500	2	7	3711
3750	4	15	4262
4000	1	4	4812

It is obvious from this discussion that the low band of the LM is fabulous. You can squeeze down to about 3 Hz by use of the vernier scale. By the way, hidden behind two cover plates just beneath the corrector knob, are "high" and "low" padder capacitors. These were used when vfo tubes were replaced to bring calibration book values into usefulness. The padders should be set near the middle of their range.

Make it Handy!

Fasten a handle to the case, strap on a 9V battery, go forth and have fun with your rejuvenated frequency meter. I use mine for its intended purposes as well as a band-edge marker and keying monitor.

AN I-F SPOTTER

Howard Burgess W5WGF

If you have ever tried to find the *if* frequencies of unfamiliar and inoperative pieces of surplus gear with no schematic, it is a waste of time to tell you how rough it can be. Even a single *if* transformer from the junk box can be a problem if it has no part number or identification.

Of course in some cases a grid dip meter can be used to find the operating frequency. However, few grid dippers cover the important *if* frequencies below 2 mc. To complicate things, if a dipper is used on a shielded transformer above 2 mc, the resonant frequency of the transformer may be shifted if the shield is removed.

If these problems sound familiar to you, we would like to suggest a little gadget that can help solve them. With just two resistors, two

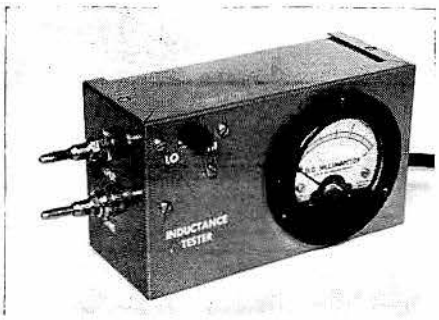

The if spotter. The switch for changing the coupling capacitor is at the upper left marked "HI" and "LO." The posts on the end are X1 and X2.

capacitors, and a tube, don't expect it to give a digital read-out to all your questions, but it can put you in the ball park.

The principle of operation is as simple as the construction. The tuned circuit in question is merely made to oscillate at its resonate frequency. The frequency can then be determined by tuning in its radiated signal on the ham receiver. To set the unknown coil into oscillation requires the use of a simple "two terminal" oscillator. Such an oscillator is shown in the schematic of Fig. 1. When any tuned circuit is connected to the two points marked X, the circuit will oscillate at its resonant frequency.

In this oscillator the twin triode is a tube such as the 12AT7. The section V2 furnishes the necessary feedback and eliminates the need for extra coils or feedback connections.

The construction is simple. The unit could have been built in a larger case with its own power supply and would have become a nice piece of bench equipment. However, due to the few parts required and the small amount of plate power used (3 mils at 90 volts) it was built as an overgrown probe. The power is robbed from another piece of test equipment or the receiver.

As a probe it can be used on the work bench to test individual coils and transformers or it can be held in contact with the various transformers in a receiver.

There is only one point of caution that should be observed in construction. The lead from the grid contact of V1 to the X1 post should be kept as short and direct as possible with the least capacity to ground. This lead becames part of the oscillating tuned circuit and limits the upper frequency to which the unit will operate.

The coupling capacitor from the grid of V1 to the plate of V2 furnishes the feedback required to maintain oscillation. To reduce the loading on the tuned circuit, this capacitor should be held to the smallest value that will sustain oscillation. Because of the wide range over which this instrument operates, a switch is provided to change values. With the capacitors shown, operation is possible from about 60 mc down to well below 50 kc. The larger value is used at the lower frequencies and is switched in only when required. With coils of medium Q the switching point is around 3 to 5 mc.

The connectors X1 and X2 can be almost any kind of posts. The ones shown on the unit here are banana plugs. These can be used as test points, or alligator clips can be slid over them for use in clipping to coil leads.

The meter shown is a three mil meter and is used to read the total plate current of both halves of the tube. This will indicate when the circuit is oscillating. When the tester is not oscillating the meter will indicate a current of about 1 mil (with 90 plate volts). Under oscillating conditions the meter will rise to as much as 3 mils with a high Q coil. The actual amount of current is not so important as the fact that the upward shift indicates that the coil is not open and is oscillating. A 5 or 10 mil meter will serve the purpose just as well.

As the pictures show, this unit was built in

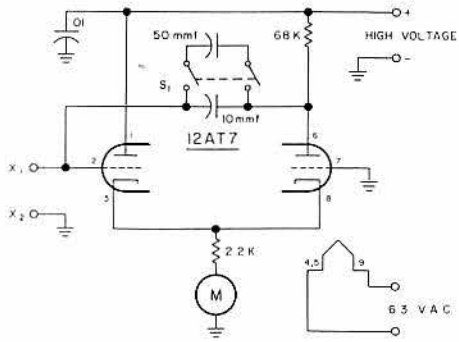

FIGURE 1

Circuit diagram of the if spotter

.01 Ceramic capacitor
50 pf Mica capacitor
10 pf Ceramic
68 K ½ watt carbon resistor
22 K ½ watt carbon resistor
Milliammeter in range of 3 to 10 ma
Slide action Double Pole-Single Throw switch (S1)
2 Banana plugs (x1 and x2)
12AT7 tube
Minibox (size depends on type of meter used)
9 pin miniature tube socket

a small 5" x 3" x 2" box. The unit will work just as well if it is built on a small piece of peg board with a couple of leads run out to the multimeter. This is for the man in a hurry.

When the unit is finished, apply power with the "X" points open (no coil across them). Because of the open grid of V1, the meter will drift about. After the tube has had time to warm up, short the X posts with a heavy piece of bus or copper. The meter will now come to rest somewhere around 1 mil. This is the "no oscillation" current and should be kept in mind as a reference point for future use. Now remove the short and connect almost any kind of an LC circuit across the posts. The meter reading will now rise from the "no oscillation" value indicating that the coil is oscillating. Do not use the large coupling capacitor unless the circuit refuses to oscillate with the smaller value.

To check a single *if* transformer, all that is necessary is to hook one of the *tuned* coils

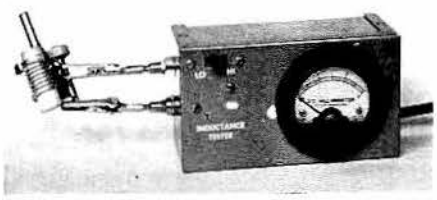

Checking a ten meter tank circuit

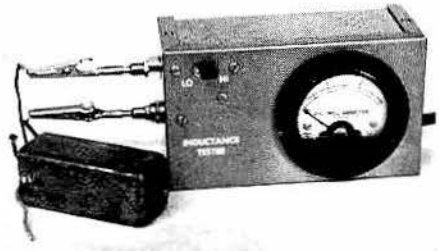

Checking an if transformer

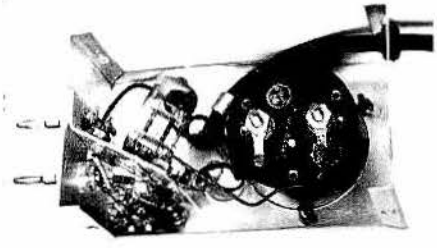

Inside view showing extreme simplicity of the "Spotter." The tube is mounted at an angle to keep the grid lead to the "unknown" as short as possible.

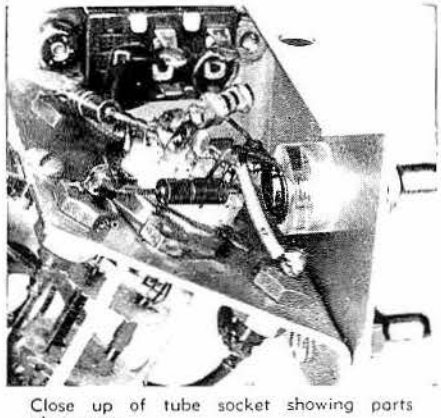

Close up of tube socket showing parts placement.

to the input terminals of the tester. Some transformers have a number of terminals which may not go directly to the tuned circuit inside. To obtain oscillation there must be both a dc and an rf path between the two pots.

If the transformer is one whose frequency falls in the range below the broadcast band it is quite convenient to have one of the surplus receivers that covers the range down to 200 kc. However the check can still be made with a regular broadcast receiver. All that is necessary is to find the harmonics of the tester as they fall in the broadcast band. They will be separated by a value equal to the frequency of the coil being tested. As an example, if a signal is spotted at 900 kc and the next one higher is found at 135 kc, it is a pretty good bet that the transformer is operating on 450 kc (1350 − 900 = 450).

To find the operating frequency of an *if* stage it is not necessary to have the amplifier in operating condition or the tubes hot. Just connect the two contacts across the primary or secondary of the transformer in question and watch for signs of oscillation on the meter. Some transformers have a portion of the bias system inside of the can. This can usually be overcome by connecting the tester from grid to ground of the tube in the stage being tested.

In addition to checking transformers it can also be useful in testing the range over which a transmitter tank will tune. Just make sure that the high voltage is turned off and connect the probe across the tank to be tested. Now you can tune the tank and follow its entire usable range with the receiver. If the tank being checked happens to be the final, the meter on the probe will indicate when the antenna is brought into resonance.

This little tester was built to do just one thing—sort out some old *ifs* in the junk box. After we tried it we found that it would do a lot of useful chores around the ham shack. With proper care and feeding, it can probably learn to do tricks that we haven't even thought of.

430-470 kHz SWEEP FREQUENCY GENERATOR

Edward Lawrence WA5SWD

Here is a simple sweep frequency generator for aligning the most common *if* strips. The unit has only one transistor because the sweep voltage is taken from the oscilloscope it is used with. Most general purpose oscilloscopes have a sawtooth output jack. By using this sawtooth, the frequency is locked to the position of the trace.

The oscillator is made to deviate in frequency in step with the voltage applied to the base bias circuit, either the sweep voltage or the dc voltage applied at the control point. If no sweep or control voltage is applied, the oscillator runs at the center frequency, and may be used as a conventional signal generator.

The 2.5 mh choke and the two 150 pf capacitors form a very broad tank circuit, so it is easy to FM the oscillator without a great change in amplitude. As to how the change in base voltage causes the frequency shift, I am not quite sure. All I know is that it is quite linear and is a positive shift (**Fig. 3**). That is, an increase in base voltage causes an increase in frequency. Also, a change in collector supply voltage will shift the frequency, so be sure to use a stable supply.

Since an rfc is used as part of the tank, you may have to compensate for a variation in center frequency by changing the 150 pf capacitors to some other value to get 455 khz as your center value.

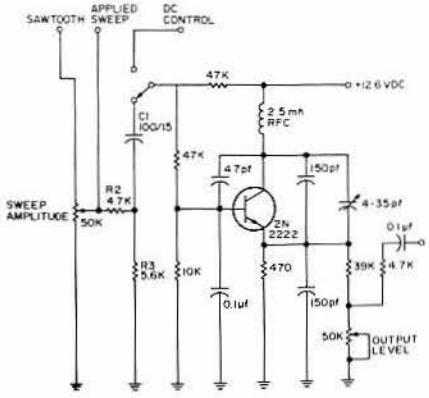

Fig. 1. Sweep generator circuit diagram.

If you do, then run a plot of dc control voltage vs frequency and adjust the voltage divider R2 and R3 so that 1 volt P-P at the sweep pot wiper gives plus and minus 5 khz (10 khz total). This is not as hard as it sounds. Just listen for the harmonics on a broadcast band radio. For instance, the second harmonic of 430 khz is 860 khz, and the second harmonic of 470 khz is 940 khz, both handy on the BC radio. Note the dc voltages at the control point required to obtain these frequencies. Take the difference and divide by four. The answer is the P-P voltage required to shift the oscillator plus and minus 5 khz. Then apply a low, known ac voltage to the wiper of the sweep pot with the switch in the *sweep applied* position. Adjust the value of the divider resistors to get the proper fraction. In my case it was 0.43.

It is advisable to run the sweep rate as slowly as possible, in order to display the response curve as accurately as possible. The sharper the skirts, the more slowly the generator must pass through the bandpass. With this generator, the amount of frequency deviation is controlled by the P-P amplitude at the sweep pot arm. If you are looking at the response of a regular *if*, you would set the sweep amplitude high to see the entire response curve. As far as an accurate display is concerned, this is fine, since the slope of the skirts is shallow. But if you were looking at the response of a sharp filter, you could not tolerate such a wide sweep, because the fast rate-of-change would tend to skew the display. To correct this, reduce the sweep amplitude to reduce the frequency deviation down to the edges of the skirts of the response curve. This reduces the rate of change and minimizes the skewing of the display. Also, it is better to display the *if* before detection, if possible, to prevent the detector time constant from possibly distorting the display.

If you have the sweep generator set up as described, then it is easy to set the sweep for a known deviation, and then procede to read the 3 or 6 db points from the face of the scope. Be sure to disable the AGC for this test.

For those who aren't familiar with the setup for obtaining the response curve display, refer to **Fig. 2.** and the following outline.

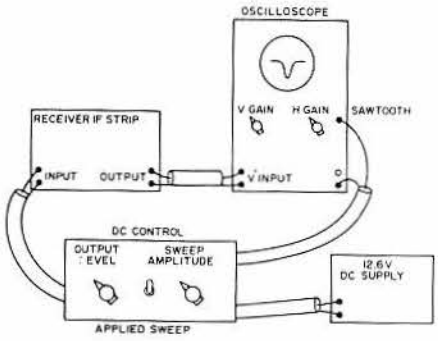

Fig.2. Interconnections of sweep generator.

First, hook up the equipment as in Fig. 1 Set *horz gain* for desired sweep width. Adjust *sweep amplitude* pot on generator for desired frequency range. Set *output level* to mid-range. Adjust the *vert gain* for the desired pattern height.

If we wish to change the total frequency deviation and the horizontal display width at the same time, use the scope's *horz gain* control. This presumes that the amplitude of the sawtooth output is also varied by the *horz gain* control.

If we wish to change the frequency spread and not change the width of the scope display, adjust the *sweep amplitude* control. This allows you to take a better look at the sidelobes or any ripples in the passband, depending on how the controls are adjusted.

You don't have to use a sawtooth to sweep with if it isn't handy.

Sixty hz can also be used, but it will probably skew the passband you are trying to display, so I don't recommend it. One note here: when the sweep generator is first turned on, or the setting of the sweep amplitude is changed, the frequency will drift for a few seconds. This is due to the charge on C1 changing to a new level. C1 is large to couple the low frequency sweep with as little distortion as possible.

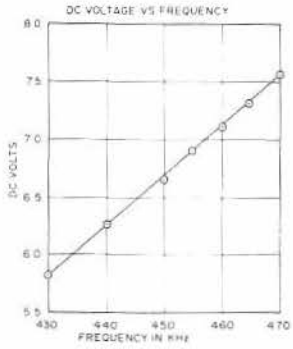

Fig.3. Sweep frequency vs dc voltage.

DC CONTROL VOLTS	FREQUENCY
5.86	430
6.27	440
6.69	450
6.90	455
7.12	460
7.33	465
7.55	470

AN ARMSTRONG SWEEPER

Al Donkin W2EMF

Sometime ago while experimenting with SSB crystal filters at 480 kc, it occurred to me that a manually swept Armstrong oscillator with a pot coupled to the tuning capacitor for 'scope sweep voltage would save point by point frequency measurements with a BC221 while adjusting the filter for minimum in-band ripple. A circuit was hurriedly developed, and the results were even better than expected. Simple though it may be, I'm sure anyone who is working with crystal filters will appreciate its usefulness. The effects of tuning and "diddling" were immediately visible in the in-band ripple and the skirts down to about 20 db could be observed with a few twists of the knob.

With this encouraging experience, a sturdier

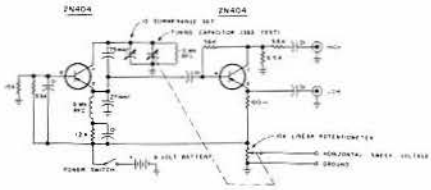

model was constructed. The circuit was assembled on a small piece of Vector-board, with the tuning capacitor and batteries mounted in a $5 \times 7 \times 3$" aluminum chassis. An aluminum bracket was bent to hold the "sweep" pot and mounted behind the tuning capacitor, spaced to accomodate the mechanical shaft coupling. The Vectorboard was also mounted on the bracket.

The oscillator circuit is simple, using a 1 mh rfc for the tank inductor. The range of the circuit as shown is about 400 kc to 500 kc, at center frequency. The tuning capacitor is a Hammerlund MC-50-M with two of the rotor plates removed, resulting in a range of approximately 7-25 mmfd. An untuned amplifier provides isolation of the oscillator from the reactance of the load. I used 2N404 transistors but most PNP *if* transistors will work.

In addition to sweeping crystal filters, I have found this little box handy as a general purpose low frequency oscillator and sweeper for receiver *if*'s. The persistency of most oscilloscopes produces a much better display than might be expected, and it certainly beats the point by point method of plotting filter responses.

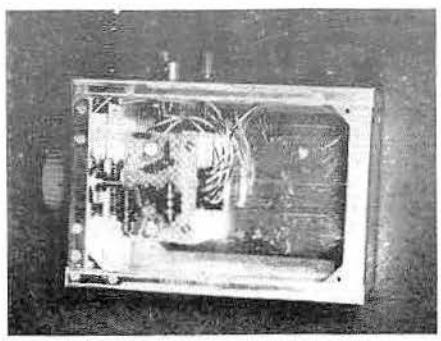

A NEW BROOM

Dick Gridley K6JHJ

This unit is a sweep generator of simple design, with many uses. Besides being useful for filter alignment, as shown in the diagram, it is useful for optimizing receiver and transmitter performance.

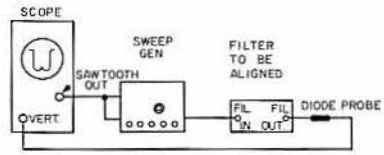

The heart of the rig is an inexpensive item called the Vari-Cap by International Rectifier Corp. Two are discussed here, the 6.8SC20 and the 100SC2. The 6.8SC20, according to the manufacturer, will vary its capacitance from 50 mmfd at .lv to 2.5 mmfd at -200v. The 100SC2 will vary from 600 mmfd at .lv to 100 mmfd at -10v. These units each cost less than $3.00. The construction is not critical in any way, nor is layout a problem—just use good ham practices. Any power supply delivering 150 v dc at 60 ma regulated will do. The oscillator tank must be grounded and I did have some trouble until I removed the unused winding from the 455 *if* transformer used for the oscillator tank.

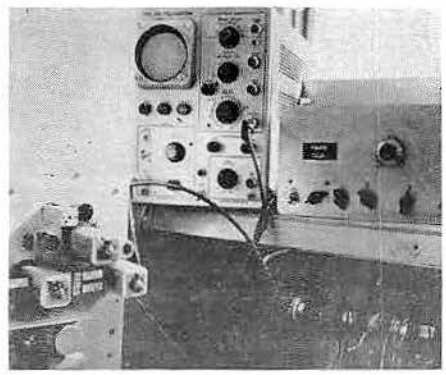

Sawtooth energy is applied to R1 which regulates the amount to be amplified by V1. R2 linear control merely puts a portion of regulated voltage on the Vari-Cap and thus sets the capacity of Vari-Cap close to its center, so the sawtooth pulse creates a linear frequency swing. This circuit gives about 6 kc sweep. I have used TV horizontal coils for L1 and increased C1 and C2 to .003 for 85 kc and 50 kc operation. However, to get enough swing at low frequency, the Vari-Cap was changed to a 100 SC2. For 200 kc to 10 mc the 6.8SC20 gives plenty of sweep.

A note here about scopes. Most of the average do not go below 15 cycles and the sweep rate should be about 10 cycles. Some do not have a sawtooth output jack. The sawtooth output can be picked off the sync circuit. I found the best point is on the feed side of the sync pot through a .25 mfd capacitor. Some scopes have a couple of jack pins to add capacity externally, some don't. You will find little trouble adding about .25 mfd across the slowest speed.

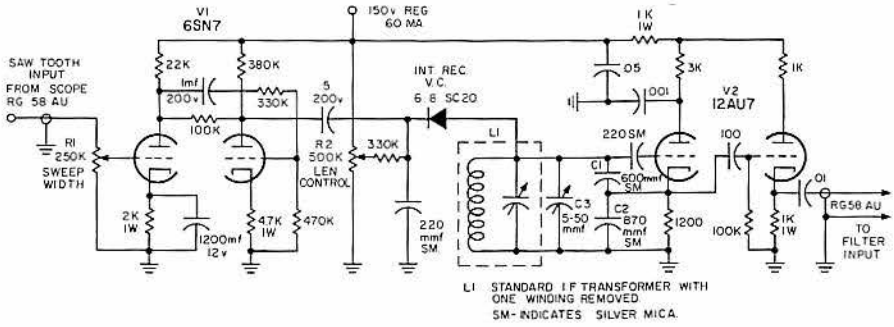

The use of the rig is simple. Plug the lead from R1 into the scope's sawtooth output. Couple the output from the cathode follower section of V2 to the filter input through a .001 mfd capacitor. The vertical input of the scope is connected to the filter output through an rf probe. Adjust R1 and R2 about ½ open. With C3 about ½ meshed, adjust the trimmer in the *if* can to put you in the ball park, and then use C3 for fine adjustments of frequency. Additional minor adjustments of R1 and R2 may be necessary. Of course, when used to align a receiver, the diode probe is unnecessary if the input to the scope is picked off of the diode detector. It goes without saying that it is necessary to plot an index for the scope bezel so that a ready reference is available for band pass width and depth of skirt.

Some one now says "This is just like setting ye old TV—*if* band pass." That it is. The only difference here is the frequency and the sweep generator cost was junk and $5.00.

The unused switch, shown in the photo, was installed to select one of three frequencies. However, this rig has been used on about six. I don't think I ever will decide which three to use. The unidentified tube is a 6U8 used as a 1 kc audio oscillator with cathode follower output.

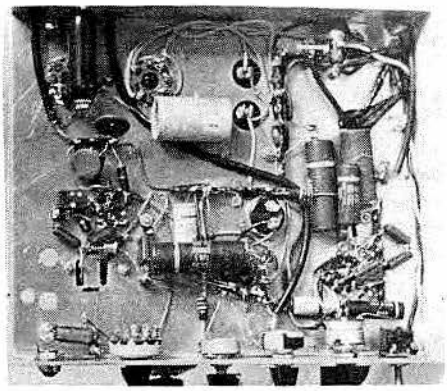

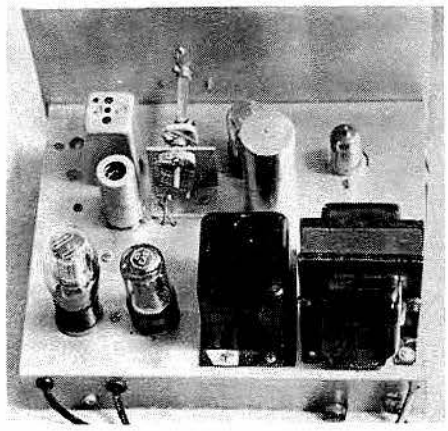

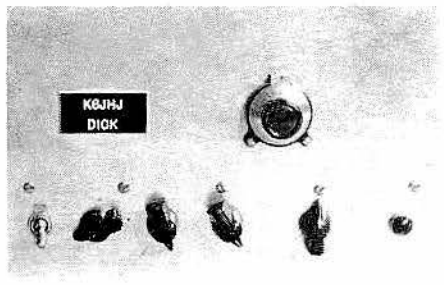

LOW COST SIGNAL SOURCE

Howard White VE3GFW

For many years the Measurements Corporation Model 80 signalgenerator has been the industry standard for tuning rigs. Many hams have wanted to have a laboratory-grade signal source of this type but the $800 price tag is prohibitive. This article describes a signal source that has many of the same features as the 80 except that it only costs 1% as much. That's why I call this the Model 0.8.

You wonder at some of the features of the marvelous little device? To briefly list them, it has:

- Variable output from about 80 nV to 50 mV of rf power.
- Frequency range from 1.8 to 450 MHz so you can cover 160 through ¾ meters.
- Crystal-control frequency stability.
- Fairly clean output signal.
- A 51Ω antenna load.
- Safety feature to prevent the destruction of the device in case a transmitter is accidentally loaded into it.

The Circuit

The circuit is the combined brainchild of many ham engineers and technicians in our local 2m FM club – the Toronto FM Communications Association. More than 300 of these units have been built in the past two years, so the circuit has been exceptionally well tested in the field.

The unit consists of a single 2N5130 NPN transistor oscillator configuration. Other transistors, such as the 2N706, can be used in this circuit with slightly different biasing arrangements; however, the 2N5130 appeared to give the cleanest output signal.

Output level can be varied from less than 80 nV (the best we could measure) to 50 mV. It is controlled by a 1 kΩ pot in the transistor collector circuit. Power is obtained from a 1.5V penlight cell bypassed for rf by a 0.1 μF capacitor.

My present "0.8" signal source has been used intermittently for more than a year without any degradation of output. However, remember to shut the unit off when you're finished with it; the battery doesn't last forever.

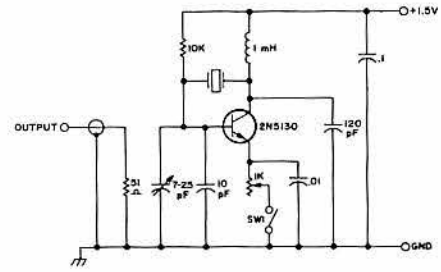

Fig. 1. Schematic diagram of the "Point Eight" Signal Source, the "poor man's Model 80."

The unit is built on a PC board. The parts layout is almost exactly the same as that of the schematic shown in Fig. 1. The electronic components are placed on the copper side of the board. The on-off switch-level control, frequency adjustment, output jack, and crystal socket are on the other side (Fig. 2). The unit can be packaged in a minibox.

Almost any crystal in the 1.8–12 MHz will oscillate in this unit. The output is rich in harmonics to 450 MHz, so you can tune up any receiver from 160 to ¾ meters.

The output impedance of the signal source is 51Ω, a value which simulates a perfect antenna load to the receiver. This is the manner in which this is accomplished: A 51Ω, ½W resistor is connected across the terminals of an RCA phono jack. No physical connection is made to the circuit except through the common

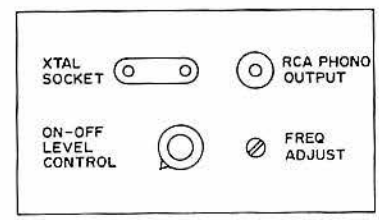

Fig. 2. Minibox layout of the signal source panel.

ground of the PC board. The maximum output level depends on the lead lengths of the resistor. (The unit has plenty of output when the lengths are about ½ in. long.) This design has an added safety feature, too; if by accident you load a transmitter into the unit, all that is destroyed is the ½W resistor.

Operation and Uses

These units were originally designed to tune up 2m FM receivers. The procedure is quite simple. You connect the signal source to the antenna input on your receiver. Plug in a transmit crystal, and adjust the frequency control for a zero reading on the discriminator. Adjust the output level to the desired signal strength (below first limiter saturation) and tune up the receiver.

There are a myriad of other uses for the signal source. Using a 3.5 MHz crystal, you have a band edge marker. With the transmit crystals on a Twoer or any other transmitter you have instant frequency spotting without modifying the circuit of the transmitter. Of course, the signal source can be used to tune up any receiver, peak tuned circuits, be an rf source for an antenna noise bridge, and so on.

RECEIVER TWEAKER

Malcolm Oakes K6UAW

I've found that the singlemost piece of needed test equipment by the amateur on FM is a receiver alignment generator. Most of us, however, do not have access to a signal generator. (Come on now, you wouldn't really call that *TV thing* a signal generator would you?)

The unit to be described is a very functional device that will allow you to scrape every ounce of sensitivity from your receiver. The generator can be built so small you can carry it around in your shirt pocket. Compactness, combined with its battery-powered portability make it ideal for servicing mobile receivers. Stability? It's crystal controlled and is as good as the rock you plug in (you obtain the rock from your transmitter). Output reactance? Nearly zero degrees, allows proper tuning of rf stage. The attenuator shown does not have a great deal of dynamic range due to distributed capacity of the potentiometer. However, I said before, the unit was "functional" and it is just that. The signal can be attenuated into the noise and brought up to approximately a 30 uv level; overly sufficient for a normal alignment.

Construction

The circuit layout is not particularly critical, and if laid out in a manner similar to the schematic, no problems should be encountered. The attenuator section should be completely shielded away from the oscillator and multiplier stages, so rf leakage will not be a problem. A crystal socket should be provided so the unit is versatile for any frequency. However, if you plan on using it on only one channel and can spare a crystal, build it with the crystal inside. Two glass piston screwdriver adjusted trimmers must be provided (to "rubber the crystal" and tune the output to resonance) as front panel controls.

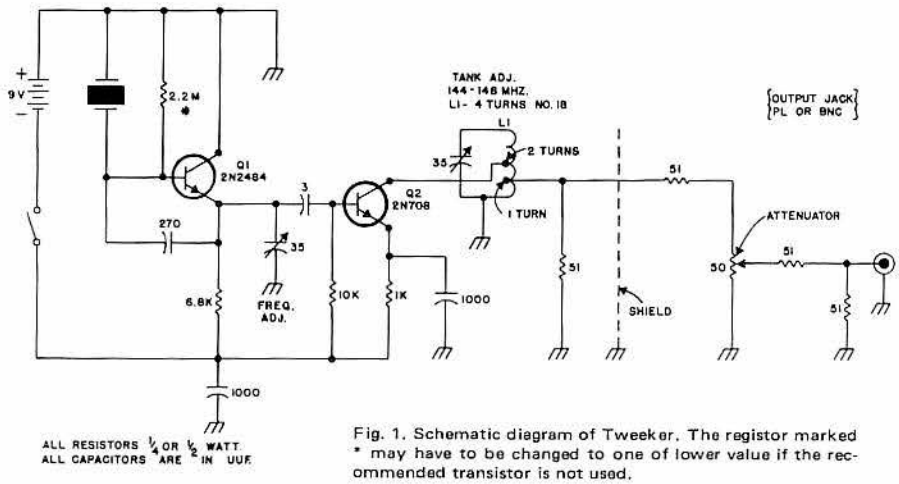

Fig. 1. Schematic diagram of Tweeker. The registor marked * may have to be changed to one of lower value if the recommended transistor is not used.

Circuit

Transistor Q1 in the first stage is a crystal oscillator which is very loosely coupled to Q2 the multiplier. This stage is biased into "class C" so as to multiply the 6 mhz crystal 24 times, up to the two-meter band. (3 mhz crystals will also work at a multiplication of 48.) Another important function of this stage is to attenuate the oscillator output (about 6-7 volts peak-to-peak) to a level usable at the two-meter frequency for alignment – 30 to 40 uv. The potentiometer adjusted attenuator takes the signal down to a level as desired by the operator.

I developed this unit for use on two meters. Several have been built and all work fine. But, for those of you who need a six-meter generator, this same circuit should work fine with the only modification needed being the final tank frequency. (A few more turns on the coil and a slightly larger trimmer capacitor.)

Adjustment and operation

Connect the output of the generator to your rig. Plug in a crystal and tune for zero (with frequency adjustment) on the discriminator (center frequency). Now, looking at the first limiter voltage, peak the final tank. Attenuate the generator as necessary to avoid saturation of the limiter. Repeat as necessary until a definite peak is reached.

If the generator will not go down into the noise with the attenuator control, the final tank may be detuned as necessary to provide the desired range on the attenuator.

CITIZENS BAND ALIGNMENT AID

Edward Lawrence WA5SWD

It is obvious that the front end of a receiver should be tuned to respond equally well across the band, and thus have consistent sensitivity at any frequency in the band, if maximum usefulness is to be obtained. The usual method of insuring reasonable results is to tune at the middle, and check the ends. This is rather spotty, at best, as it would be better to check all channels. This is involved since you must set both frequency and amplitude 23 times in a single pass.

Naturally, a good sweep generator could be used, and the rf-mixer tracking set with it instead, but this was not available to me at the time. The circuit in Fig. 1 was originally a super-regenerative receiver taken from the GE Transistor Manual. These, as is well known, tend to spray a lot of rf back out the antenna. With this in mind, I listened with a communications receiver and noted strong modulation products about 100 kHz above and below the "carrier." Deducing this to be caused by the quench frequency, I brilliantly decided to drop the quench frequency into the audio range, by increasing the capacitance across the base bias resistor. Lo and behold! Suddenly the entire Citizens Band was alive and jumping with a mass of "line noise," which at first appeared to be like

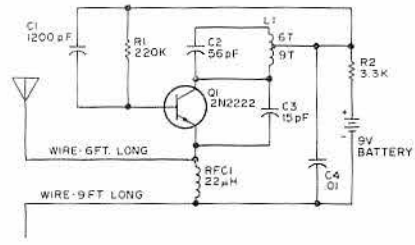

Fig. 1. Schematic of the alignment aid. L1 is 15 turns No. 22 tapped at 9 turns from the collector end. No switch is shown, so remove battery when not in use.

73 LIBRARY

NEW REPEATER ATLAS

Hundreds of new listings . . . listed by both location and frequency . . . dual listing, invaluable for your car . . . find those repeaters as you travel. This is the ONLY complete list of repeaters being published. Almost 3000 repeaters listed in this issue . . . repeaters from all over the entire world. only $1.95

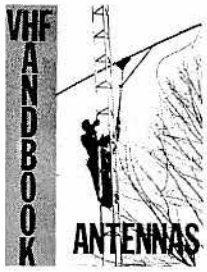

VHF ANTENNA HANDBOOK

The NEW VHF Antenna Handbook details the theory, design and construction of hundreds of different VHF and UHF antennas . . .

A practical book written for the average amateur who takes joy in building, not full of complex formulas for the design engineer. Packed with fabulous antenna projects you can build. $4.95

73 VERTICAL, BEAM AND TRIANGLE ANTENNAS by Edward M. Noll W3FQJ

Describes 73 different antennas for amateurs. Each design is the result of the author's own experiments: each has actually been built and air-tested. Includes appendices covering the construction of noise bridges and antenna line tuners, as well as methods for measuring resonant frequency, velocity factor, and standing-wave ratios. 160 pages. $5.50

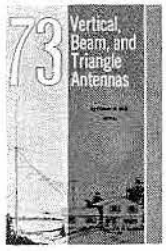

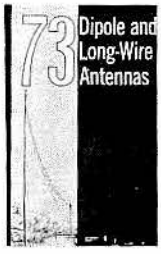

73 DIPOLE AND LONG-WIRE ANTENNAS by Edward M. Noll W3FQJ

This is the first collection of virtually every type of wire antenna used by amateurs. Includes dimensions, configurations, and detailed construction data for 73 different antenna types. Appendices describe the construction of noise bridges, line tuners, and data on measuring resonant frequency, velocity factor, and swr. 160 pages. $5.50

2M FM HANDBOOK

Contains almost every conceivable circuit that might be needed for use with a repeater. All circuits explained in detail. All aspects covered, from the operator to the antenna. $5.95

Practical Test Instruments You Can Build

37 simple test instruments you can make — covers VOMs, VTVMs, semiconductor testing units, dip meters, wattmeters, and just about anything else you might need around the test lab and ham shack. $4.95

IC OP-AMP COOKBOOK

by Walter G. Jung. Covers not only the basic theory of the IC op amp is great detail, but also includes over 250 practical circuit applications, liberally illustrated. 592 pages, 5½ x 8½, soft bound. $12.95

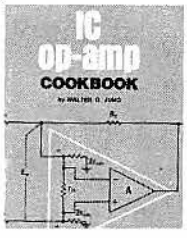

RF AND DIGITAL TEST EQUIPMENT YOU CAN BUILD

RF burst, function, square wave generators, variable length pulse generators — 100 kHz marker, i-f and rf sweep generators, audio osc, af/rf signal injector, 146 MHz synthesizer, digital readouts for counters, several counters, prescaler, microwavemeter, etc. 252 pages. $5.95.

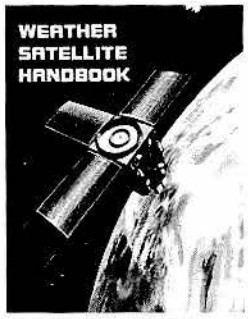

WEATHER SATELLITE HANDBOOK

Simple equipment and methods for getting good pictures from the weather satellite. Antennas, receivers, monitors, facsimile you can build, tracking, automatic control (you don't even have to be home). Dr. Taggart WB8DQT $4.95.

SSTV HANDBOOK

This excellent book tells all about it, from its history and basics to the present state of the art techniques. Contains chapters on circuits, monitors, cameras, color SSTV, test equipment and much more.
Hardbound $7 Softbound $5

FASCINATING WORLD OF RADIO COMMUNICATION

Interesting stories of the history of radio pioneering and discovery. Also includes the fundamentals of broadcast band DXing. A must for every radio amateur. $3.95.

TEST EQUIPMENT LIBRARY

A multi-volume anthology that you won't find anywhere for three times the price! The editors of *73* present a complete guide to testing that is both basic and complete and aimed at everyone from beginners to amateur Extras. Everything from how to test diodes to frequency counters. Plus a cumulative index . . . all in *73*'s all new TEST EQUIPMENT LIBRARY Vol. I — Vol. III.

Vol. I — Component Testers — $4.95
Vol. II — Audio Frequency Testers — $4.95
Vol. III — Radio Frequency Testers — $4.95

1001 PRACTICAL ELECTRONIC CIRCUITS

Tab's new 1001 circuits is available for only $9.95 ppd. The next time you want a circuit for just about anything, eat your heart out that you didn't send for this book the first time you read about it. You'd better order the book right away, before they run out. $9.95

VHF PROJECTS FOR AMATEUR AND EXPERIMENTER

A must for the VHF op. Opening chapters on operating practices and getting started in VHF, both AM and FM, followed by 58 chapters on building useful test equipment, modifying existing and surplus gear. $4.95

Hewlett Packard 6384 A power supply

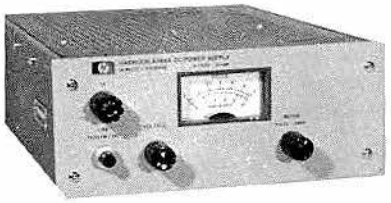

SPECIFICATIONS:

DC Output: 4 to 5.5 Vdc @ 8 Amps
Load Regulation: 2 mV no load to full load
Line Regulation: 2 mV for line changes between 104 and 127 Vac at any output voltage and current within specifications
Ripple & Noise: Less than 5 mV peak to peak
Crowbar, Factory Set at 6.25 V, Automatic cutback limit circuit and overvoltage crowbar protection.

HEWLETT PACKARD 6384A Power Supply $99.95

Power design 1210 regulated power supply

Output: 0 to 12 V @ 0 to 10 Amps
Regulation: 0.01% or better.
Ripple and Noise: Less than 500 uV rms. Voltage Controlled, Metered.

POWER SUPPLY 1210 - Regulated Power Supply - $149.00

a full range, 5-function 3½ digit multimeter

DC CURRENT: 0 to ±1.999/19.99/199.9/1999 mA
AC CURRENT: 0 to 1.999/19.99/199.9/1999 mA
RESISTANCE: 0 to 199.9 Ω through 19.99 Megohms (6 ranges!)

ACCURACIES

DC VOLTS: ±0.2% F.S. ±0.2% of reading
(1000V range: ±0.5% F.S. ±0.5% of reading).
AC VOLTS: ±0.7% F.S. ±1% of reading
(1000V range: ±0.7% F.S. ±2% of reading).
DC CURRENT: ±0.5% F.S. ±0.8% of reading
(1000 mA range: ±0.5% F.S. ±1.8% of reading).
AC CURRENT: ±0.5% F.S. ±1.3% of reading
(1000 mA range: ±0.5% F.S. ±2.3% of reading).
RESISTANCE: ±0.5% F.S. ±0.8% of reading
(10 megohm range: ±0.5% F.S. ±1.8% of reading).

RANGES
DC VOLTS: 0 to ±1.999/19.99/199.9/1500 Volts
AC VOLTS: 0 to 1.999/19.99/199.9/1000 Volts

DATA PRECISION MODEL 134 – $169.00

AST/SERVO SYSTEMS, INC.
20 Republic Road, North Billerica MA 01862
(617) 667-8541

NEW 73 BOOKS

TEST EQUIPMENT LIBRARY
Vol. III, Radio Frequency Testers

Radio frequency waves are the common denominator of Amateur Radio so here is a book for all hams. No matter what your specific interest, such items as SWR, antenna impedance, line impedance, RF output and field strength should interest you. This book not only gives detailed instructions on testing these items but includes sections on signal generators, crystal calibrators, grid dip oscillators, noise generators, dummy loads and much more. It's a must for all up-to-date shacks.

Test Equipment Library
Vol. III, Radio Frequency Testers *$4.95*

TEST EQUIPMENT LIBRARY
VOL. II, Audio Frequency Testers

HOW'S YOUR SPEECH POWER? YOUR SHIFT? YOUR SYNC?

You can find out easily with a little time and a junk box full of parts. It's all right there in the new Volume II of the 73 Test Equipment Library . . . Audio Frequency Testers . . . jam packed full of all kinds of audio frequency test equipment. So if you're into SSB, RTTY, SSTV, etc., this book is a must for you . . . good book for hi-fi addicts and experimenters too!

Test Equipment Library
Vol. II, Audio Frequency Testers *$4.95*

BUILD YOUR OWN TEST EQUIPMENT!

SAVE A BUNDLE!

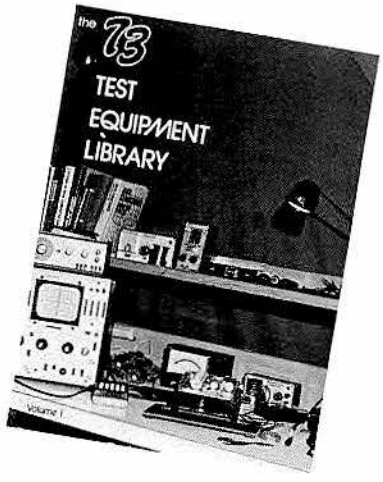

TEST EQUIPMENT LIBRARY
VOL. I, Component Testers

Just out is Volume I of the 73 Test Equipment Library . . . how to build transistor testers (eight of 'em), diode testers (3), IC testers (3), voltmeters and VTVMs (9), ohmmeters (8 different kinds), inductance (3), capacity (9), Q measurement, crystal checking (6), temperature (2), aural meters for the blind (3) and all sorts of miscellaneous data on meters . . . using them, making them more versatile, making standards, things like that. Invaluable book, ridiculously low priced.

Test Equipment Library, Vol. I, Component Testers *$4.95*

Send me:
☐ Vol. I .....Component Testers @ $4.95
☐ Vol. II ..... Audio Frequency Testers @ $4.95
☐ Vol. III ..... Radio Frequency Testers @ $4.95

☐ Cash enclosed ☐ Check enclosed

☐ BankAmericard ☐ Master Charge ☐ American Express

Card # _____ Interbank # _____ Expiration date _____

Name _____ Signature _____

Address _____

City _____ State _____ Zip _____

73 magazine • Peterborough NH 03458

Meshna

New England's #1
Surplus Dealer For Over 20 Years.

Send for our latest catalog.

Meshna PO Box 62 E. Lynn, Mass. 01904

Fig. 2. Full size PC board layout (foil side).

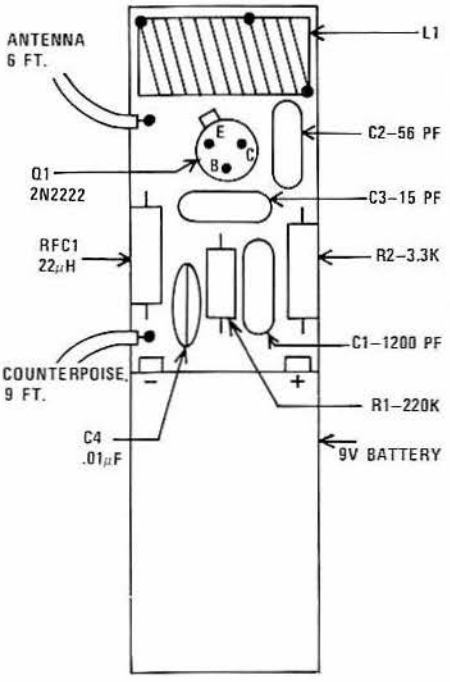

Fig. 3. Component side parts placement.

natural noise. Then I turned on the BFO, which showed it to be many, many, many closely spaced "carriers." I presume the lower quench frequency develops a much larger bias swing on the base of the transistor, FM'ing it across the entire band. This stuff is concentrated in the region of 27 MHz, with very little spill-over into 10 or 15 meters, although the level across the design range is rather constant. The nearly constant rf level is what I needed to simplify tuneup of the front ends of the units I was working on.

Figure 2 is the layout of the P.C. board I made to facilitate reproduction of this useful circuit for a few interested friends and Fig. 3 is the component layout.

I used 6 ft of wire as an antenna connected to the emitter side of the rfc, with 9 ft of wire on the battery side of the rfc as a counterpoise. Since this made it a bit large, I carefully hung it vertically in a handy tree nearby. Of course, since this put a strong signal on every channel into every CB receiver within 300 yards, I limited the use of this device to avoid unnecessary interference to the deserving users of the band. However, one fellow accidentally launched his into a tree too high to recover with an over-ambitious heave, and it ran for about a month in the dead of winter in a nameless northern city, helping every CBer for miles around align their sets! It only draws about half a milliamp from a 9 volt battery.

Since I am sure many others would like to align their 11 meter receivers for optimum results, I am presenting this circuit as a very low cost and worthwhile aid.

FET CHIRPER

Chuck Hines K6QKL

The Chirper is an automatically keyed, crystal controlled, signal source which may be used to optimize the signal-to-noise ratio of a receiving converter. Homebrew or commercial, converters are a common thing around an amateur station. And, most of the VHF Tribe have read thru a jungle of esoterica dealing with low noise front ends, the velvet beauty of FET's on Two, noise generators and eternal truth, and how to copy 20 db below the noise by the selective use of liquid helium. With a kind of relentless evolution converters have been getting better and better, noise figures become lower, and the prices of suitable front end devices are dropping by the hour. But when it comes to aligning these converters the scene is one of wretchedness. A black art at best, the job is taken up with an enduring combination of blunt instrument and myth. The latter have a certain charm. Are you convinced your converter is in top notch condition because you can "hear noise" when you attach the antenna – or better yet, when you place a 50 ohm resistor across the input? Try putting a complete short across that same input. Shorts aren't much good as noise sources. You'll find the short gives about the same change in noise level as the 50 ohm termination. What has changed is the impedance the front end "sees". The same is partially true of the noise from the antenna. Neither is indicative of the performance of the converter. Peaking the system up for maximum on either a weak signal or on noise gets you nowhere. The diode noise generator which every VHF book of substance describes is a good and useful tool when used properly. The assumption is that everyone already knows full well how to use it and does so. Few in fact do.

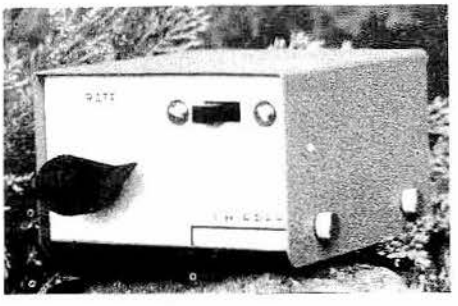

I'm sure you've read of it before in many places, but a little redundancy is in order. The noise with which you are concerned is the noise generated *internally* by the first tube, transistor, or other active device the signal encounters upon its arrival at your converter. By fiddling with the external reactances, adjusting the voltage and current and otherwise manipulating the things soldered to the device, one may minimize the internally generated noise. At the same time the reason the front end exists is to amplify the signal. One usually desires as much amplification possible, short of smoke and oscillation. Minimum noise and maximum amplification is the game. Though the two are not quite mutually exclusive a certain amount of compromise takes place. Thus, the signal to noise ratio. When aligning a converter's first stage every adjustment effects *both* signal and noise. Given a constant signal source coupled into the converter thru an appropriate impedance, the job is finished when the front end has been adjusted for the greatest *difference* between signal and noise of which it is capable.

The Chirper is designed to help you do all this by letting you see what effect each adjustment has on both signal and noise. The TIS34 oscillates at a frequency controlled by the crystal. With the constants shown, that can be anywhere between 8.2 and 36 MHz. The variable capacitor must be adjusted for resonance. It isn't particularily critical but its setting peaks the *rf* output at either the fundamental or some harmonic. For 6 meters an 8.35 MHz crystal is used. A 9.0 MHz rock will pin the meter when the

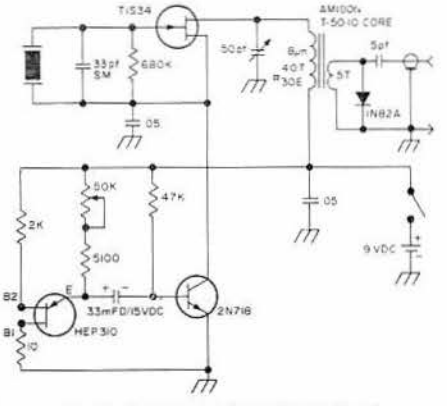

Fig. 1. Schematic of the FET chirper.

Chirper is connected into a 2 meter converter. The Amidon toroid is wound with No. 30 enameled, 40 turns for the primary and 5 turns for the secondary. After it is wound, spread the turns to fill the toroid and paint it with Q dope. The diode and 5 pF coupling capacitor are connected with the shortest possible leads, the diode being grounded at the *rf* connector. The harmonic output is excellent and quite useable at 1200 Mhz.

The oscillator is turned on and off by a multivibrator combination of unijunction and NPN transistor adapted from the *G. E. Transistor Manual.* The rate at which the multivibrator cycles is determined by the large value capacitor, in this case 33 mF. The polarity of the capacitor is critical. Observe it. To increase the cycling rate, decrease the capacitance; and, to decrease the rate, put in a larger value. Mine cycles a little under once per second. A value somewhere between 30 and 40 mF should suit your needs. You are better off scrounging some odd value from a defunct computer board because of the tolerance problem. If it says 33.2 mF, its probably pretty close to that value. Otherwise you're dealing with tolerances of plus 100% and minus 50% or something equally grotesque. The 50K pot determines the portion of the cycle during which the oscillator is On and is mislabeled rate on the Chirper shown. The HEP-310 is generally available and inexpensive. Other unijunctions were not tried. On the other hand almost any NPN of reasonable quality will work in place of the 2N718. A number of 2N388 and 2N3478's were tried and behaved well. It's a good place to use those transistors you've replaced with FET's. Use something with a Beta of 50 or better for best results. The 5100 ohm resistor in series with the pot is for current limiting. It's deletion will increase battery drain with no increase in Chirper performance. Normal current from the 9 volt battery is around 5 mA.

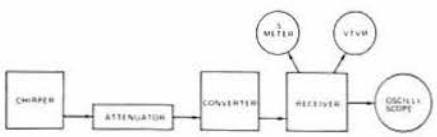

Fig. 2. Test set-up for converter alignment.

Construction is non-critical and pretty much a matter of taste. Mine is built on a piece of vector-board and mounted in a Suzurando box, model M-1N. It measures 3¼ X 2 X 4" and there is still room inside for additions. It sells for 330 yen, about 92c. A slide switch is used to turn the power on and off. Paint one well of the slide switch with red paint – Testor's Pla, a model plastic paint, is good – and the switch will indicate its position. Red for On and black for Off. It saves batteries. Check your work and the polarity of the large capacitor. Re-check the connections to all the semi-conductors. With four different kinds of devices things can become confused. Set the pot to the middle

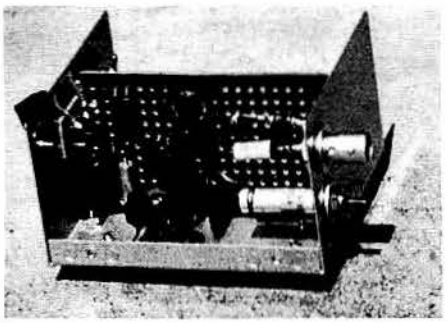

of its range. Insert a crystal in the socket. Connect the Chirper to your converter, turn the switch on and adjust the variable capacitor for the highest reading on your S-meter. The oscillator will turn on and off. Varying the pot will extend or diminish the amount of time the oscillator is on. Whatever you do, *don't connect the chirper to an external antenna.* The harmonic content is high and even at this power level is sufficient to cause severe interference to television receivers within a two block radius.

For converter alignment, the test set-up is illustrated in Fig. 2. The Chirper is fed to the converter thru an attenuator for two reasons. First, the power output of the Chirper is too high on six and two. You don't want to align with a forty over nine signal. Something around S-5 to S-7 is desired. Second, the attenuator maintains a 50 ohm termination for the converter. A converter cannot be aligned with a floating input impedance. Fixed and variable attenuators of excellent quality are available thru surplus and homebrew data is available. See *73,* January 67, p. 40 for one that will do the job. Turn the receiver avc off. The read-out options are diverse. The best is probably a scope connected to the *if.* A vtvm can be used, connected to the audio output. And, the S-meter can be used with the avc on *fast.* This will vary with the receiver and it's particular time constants. What needs to be avoided is avc pumping that interferes with your readings.

Turn the Chirper on, adjust the attenuator for a convenient signal level. When the oscillator is on, you're reading signal. When the oscillator is off, you're reading noise (on the scope, vtvm, S-meter, etc.). As you make adjustments on your converter, observe the effect on both signal and noise. Adjust for the greatest difference between the two. Turn the Chirper off and re-check the converter neutralization. If necessary, re-neutralize the converter and go thru the whole thing again. Talking about it makes it seem somewhat complex. It really isn't and the whole business won't take long once you've done it. It will become quickly apparent that highest signal level and lowest noise level do not coincide. You can vary the bias, voltage, etc., and observe the effects of each on the signal-to-noise relationship. You can, in short, optimize your converter's performance.

A number of things can be done with the Chirper. There is room in the box to build another oscillator section connected to the transistor collector, operating in parallel and simultaneous with the first oscillator. By appropriate choice of crystal and attenuation, both signals can be introduced into the converter in order to adjust the mixer for minimum cross modulation.

Or, instead of using an oscillator at all, you can use the switching section of the Chirper to key a noise generator on and off. This has a certain attraction where an integrating network is used prior to a vtvm. In this case noise is used as a signal.

In spite of it's name, the Chirper is remarkably stable. Chirp becomes apparent from two meters or so, but is no problem. Build one and take the myths out of your converter.

UHF SIGNAL SOURCE

Bill Hoisington K1CLL

The UHF experimenter learns early that the UHF ham bands don't always furnish a signal when you need them. When I build receivers and converters for 432 and 1296, I find that I need a small signal generator for alignment and band spotting. Not much power is needed for this work, so transistors are the ideal choice for generating the signal. This signal source is in three parts, a 432 source, a tripler to 1296 and a modulator.

The 432 Driver

I started with a low-cost 27 mc crystal that I found in my junk box. (Never mind how it got there!) I used my usual phase-reversing crystal circuit followed by a bunch of doublers. Lower-priced transistors were used in the early stages and the UHF ones saved for later. You really need good ones on 1296! Each doubler is biased from rectification of rf from

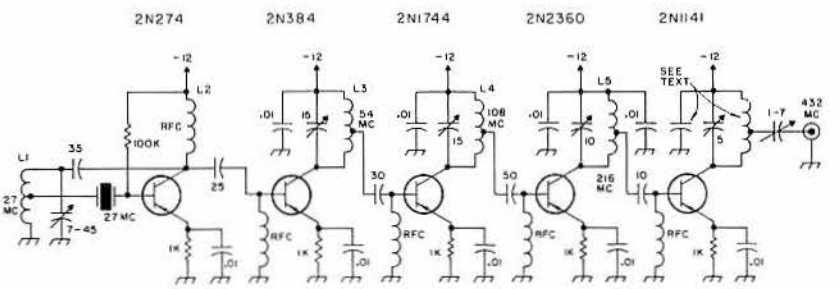

Fig. 1. Schematic diagram of the 432 mc signal source. The transistors aren't critical in most cases and other UHF and VHF ones will work fine.

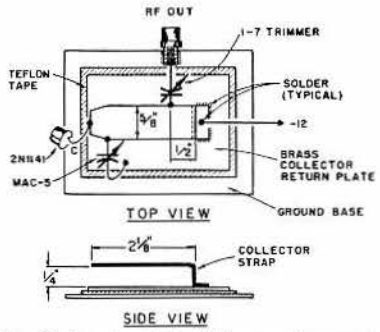

Fig. 2. Details of the 432 mc collector circuit.

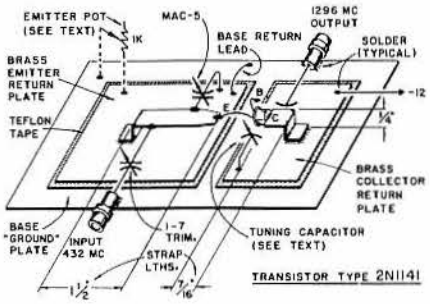

Fig. 5. Pictorial layout of the 1296 mc tripler.

the previous stage. If you need more output than this circuit gives you, use less than a 1 k resistor in the emitter, but watch out for high collector current. Fig. 1 shows the schematic of the 432 mc generator and Fig. 2 gives details of the 432 mc collector circuit.

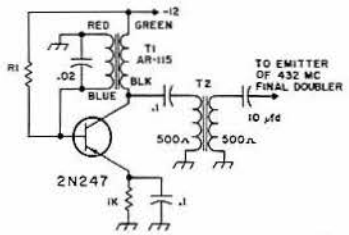

Fig. 3. The tone oscillator for the 432 mc signal source.

The tone modulator

This is a crude modulator (Fig. 3), but it works. The modulation transformer is not absolutely necessary, but seems to improve results. You can apply the modulation almost anywhere for this application, but modulating across the 1 k emitter resistor gave the cleanest sound with the doubler used.

Now to 1296

I built this tripler to 1296 just for the fun of it. But it worked quite well. I normally don't hold with triplers at this frequency, but it's an easy way to get 1296 mc energy from the 432 mc driver. The transistor I used was a Motorola 2N1141. It's several years old and there are better ones that are far cheaper now. But it does work on 1296. I couldn't get it to work with grounded emitter, but grounded base is fine. Fig. 4 gives the schematic but Fig. 5 gives the details, which are vital. The input on 432 tunes very nicely. But I had to reduce the emitter resistor in the doubler to 432 to get enough drive. It ended up at 200 ohms. The collector circuit is short, but tunes smoothly. The 1296 mc output registers 100 a in the 1296 cavity in the May 73.

You might try a small amount of modulation on the 1296 mc tripler. Also a waveguide attenuator. Be seeing you on 23 cm.

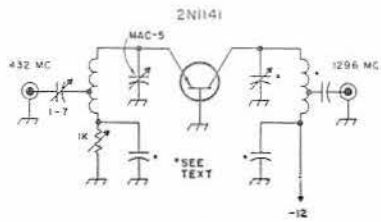

Fig. 4. Schematic of the 1296 mc tripler.

CRYSTAL CONTROLLED SIGNAL SOURCE WITH INFINITE ATTENUATOR FOR 144, 432 AND 1296 MHz

Bill Hoisington K1CLL

One of the most useful test-equipment gadgets the homebrewer can build is a signal generator. The one described here is of commercial quality and it can be completely contained inside a waveguide. Positioning, by sliding along the waveguide, provides a variable-strength stable signal of one millivolt, one microvolt, one nanovolt, or less, dropping down gradually to a true zero. It does this in a perfectly smooth fashion without steps or jumps so that every fraction of a decibel in lower noise figure shows immediately on the slide dial. What's more, the slide can be calibrated so that FM'ers can use the device for directly measuring receiver sensitivity in tenths of a microvolt.

In building a 6 meter receiver recently for maximum absolute sensitivity I naturally had to check especially on the first-stage rf transistor and circuit for minimum noise figure. (For this type of work you *must* have a signal generator capable of being attenuated out of sight with any receiver you can buy for any money.) The usual generators on the market under $100 do not do this. And many of the very expensive generators get so leaky that they have to be used 200 ft from the receiver. At any rate, the generator described here can be made up quickly and at low cost, and it *is* stable, reliable, and infinitely variable.

Waveguide

The only possible difficulty might be in obtaining the piece of waveguide needed. The piece I used is 4¼ in. wide by 2 1/8 in. high, and is 24 in. long. If you have a choice, get a piece a little longer. You could make up this item out of brass or copper if you had to, because in this case it is not used to *carry* energy but to *attenuate* it, so the worse you make it the better!

The waveguide *must not* have any holes in it and should be reasonably smooth inside; otherwise your dial would not read smoothly in attenuation. You *could* use copper or aluminum drain pipe, although I have not tried them yet. Working directly on the rf, this attenuator is good for any kind of modulation, including SSB, FM, pulse, or what have you.

Construction

Figure 1 shows the basic idea. When the signal generator plate is close to the

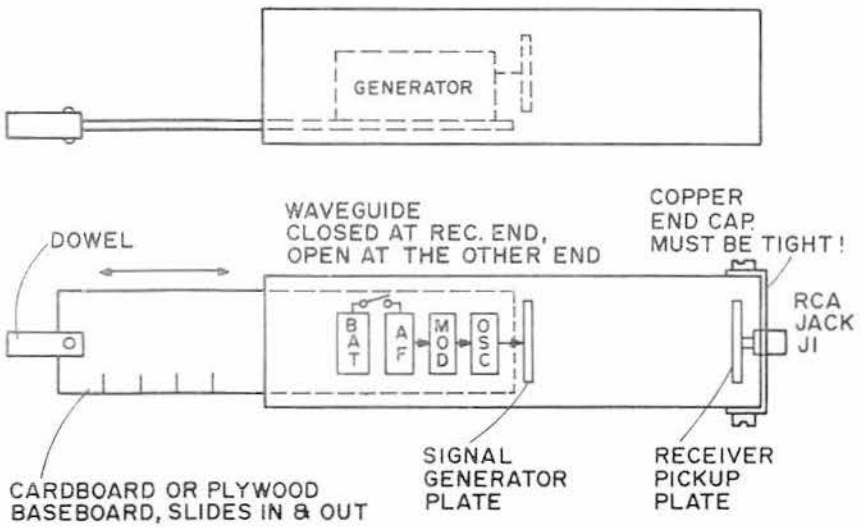

Fig. 1. Sketch shows plan-view layout of unit inside waveguide attenuator. The oscillator unit is mounted on a flat wood or cardboard strip that can be calibrated to give accurate indications of output signal.

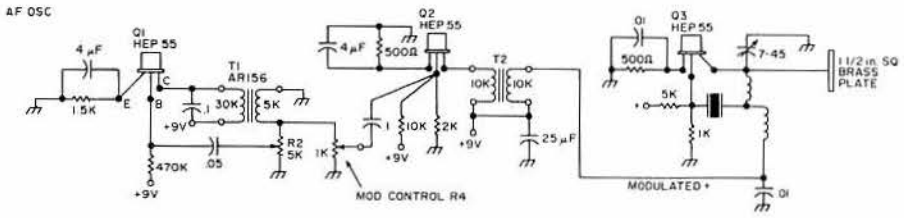

Fig. 2. Schematic of generator. This entire assembly about 3 x 4 in. including small 9V battery and switch must be entirely inside the waveguide. No wire or metal of any kind can be brought outside.

receiver pickup plate, you can get about 100 mV of signal into the receiver, and it is handy for checking diode receivers. When the two plates are about 8 in. apart, the signal is just detectable on a good receiver. Additional spacing between plates amounts to "waveguide beyond cutoff." I do not believe that there is any receiver in the world that can pick up the signal much beyond the 8¾ in. point.

Pretty soon in your receiver "peaking" work you get to that signal that may be but a tenth of a microvolt or so, and you begin dreaming about cryogenic front ends, masers, and such. As mentioned, every fraction of a decibel lower in noise figure, every improvement in sensitivity comes out rigorously and relentlessly on that slide dial. You can easily check which of your low-noise transistors is really low, whether that MOSFET will do a better or worse job for you, and in which circuit.

As you go up in frequency you may have to make smaller and smaller oscillators in order to fit in smaller waveguides to get the cutoff effect. (That will not be a problem if you read 73; the May issue described a "postage-stamp-sized" rf generator that is an ideal candidate for the signal source.)

Circuit

A crystal oscillator, an af oscillator, and a simple class A modulator do an excellent job to start with. Figure 2 shows the present unit as used on 6 meters. It must be stressed again that no wire or other piece of metal may be allowed to reach the outside from this assembly. I'm making up another for 2 meters soon (still my favorite band) and will try one on 450 a little later.

Audio

A controlled-feedback transformer-coupled af oscillator does a good job in furnishing a sine wave. A Motorola HEP55 is used for the oscillator, with feedback to the base from the collector through transformer T1, controlled by resistor R2. Audio output is taken off the 5 kΩ winding of T1, is fed through R4 the modulation control, and then to the base of af modulator Q2. Transistor Q2 is set up for low-power class A operation because not much modulation is needed for the signal generator. Transformer T2 is an old 5W unit from "tube-type portable" days. The secondary of T2 feeds a modulated +9V signal to Q3, the crystal-controlled 50 MHz oscillator.

This rf oscillator is one of my negative-feedback jobs with phase reversal in the crystal. A 1½ in. square plate is tied onto the collector, radiating energy to the receiver pickup plate facing it inside the waveguide. This energy is rapidly attenuated as you move the plates apart, and should be impossible to detect after some 9 or 10 in. of separation.

Once again, do *not* bring any wires or any other metal or conductor out from the oscillator assembly. If you want an outside controlled switch or other control, bring it out as a wooden dowel handle.

That's about it. Tune everything up outside the waveguide on the bench; when you're satisfied, plug your best 6 meter receiver into J1, push the oscillator plank along the waveguide (or rather I should say pull it along) away from J1. You'll get a surprise! Hope this helps you with your low-noise receiver work. It did a lot for me.

LOW COST 220 MHz SIGNAL GENERATOR

Bill Hoisington K1CLL

This article describes the design and construction of an easy to build, inexpensive, crystal controlled signal generator for the 220 MHz band, including a very low cost attenuator that goes from a quarter volt down through 1/20th of a microvolt and on to a real zero (of rf power). It is very useful for receiver front-end tuneup, low noise tests, and as a portable field generator for overall antenna tests through the receiver. For signal identification purposes, af and FM modulation are included.

If you really want to fight for a low-noise front end, this piece of equipment will be of great assistance to you, because the attenuation really is infinite and without any difficult bypassing or shielding.

Design of the attenuator.

Infinite attenuation is achieved here by the use of a 50¢ piece of aluminum tubing, as shown in Fig. 1. You cannot drive 220 MHz signals more than a few inches down inside of a piece of aluminum tubing. By putting *everything* – battery, on-off switch, circuit and all – on the movable generator strip and sliding it in and out of the tubing, you avoid all touchy, difficult and expensive bypassing, costly attentuator pots, shielding, etc., and provide a simplified means of varying the attenuation with stable, smooth, easy repeatability. Calibration is of the slide rule variety and also simple as far as writing down the microvolts on the scale is concerned.

This principle is older than radio tubes; in fact Sir Oliver Lodge used it in his 1890 microwave work.

Attenuator Construction Details

Figure 1 tells most of the story, with details in Figs. 2 through 9. An adequate rf seal can be made at the pickup end of the aluminum tubing, standard TV masting, 1¼ O.D., by 2 or 4 tabs in one end as in Fig. 3 and bending them back as shown, then cutting off the excess tubing. Install the pickup, plate, output jack, and end plate as shown in Fig. 1. I used time-saving external mounts for fastening it down to the wood baseboard as shown in Figs. 2 through 5. Drill a ¼ in. hole for a screwdriver as in Fig. 2, and use angles for the pickup end. Figure 2 also shows the scale in use for attenuation settings, and Fig. 3 shows pointer details.

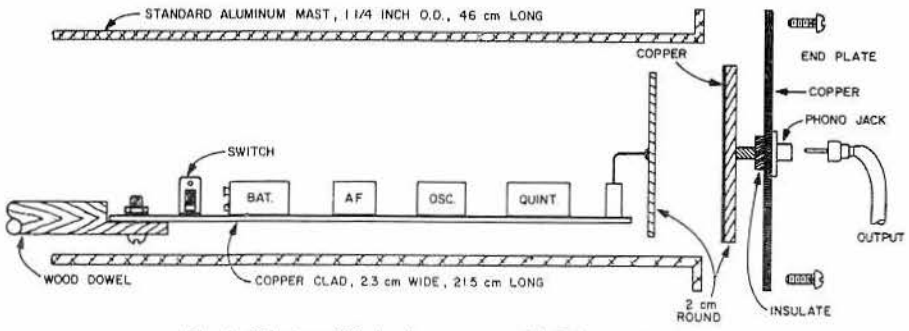

Fig. 1. Sideview, 220 signal generator and infinite attentuator.

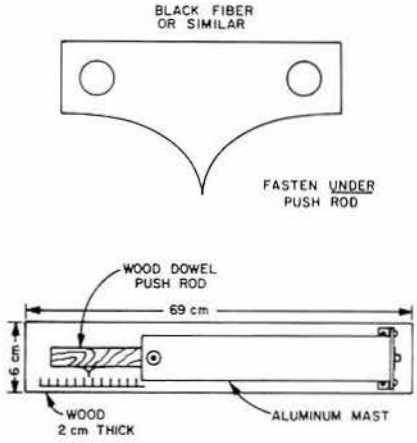

Fig. 2. Top view of the 220 signal generator and details of the calibration pointer.

Figures 6 and 7 show pictorials of the layout, top view and side view.

The Generator

Nothing too fussy here, but attention to details will assure reliable af and rf oscillation at low power and low battery drain and good frequency multiplication. Figure 8 shows the schematic with the details of the two oscillators, the crystal in the 44 MHz range, and the quintupler. The af uses a standard circuit which, however, has one item to watch. Contrary to a transformer coupled circuit, which is seldom mentioned, this twin-T job has a nasty trick of not starting every time. However a small cap from collector to ground cures this and makes it 100% reliable in that respect. The emitter being grounded, I suppose this establishes the correct in-phase relation with the collector, in which both of these elements should be in phase. You can put a small trim pot af gain control between the modulator and the oscillator if you wish, watching out for dc voltages of course. As shown here, there is plenty of modulation for signal identification, both AM and FM.

Referring to Fig. 8, at the left is the af oscillator. It is not down symmetrically, but you can note the two 22K resistors and the two .02 frequency settling caps, along with the .05 and the 2.2K terminating the lines. All of these set the frequency, and to change the frequency you should vary all of them in at least their approximate present ratios. It is around 500 cycles as shown. Do not forget the "starting cap" from collector to ground.

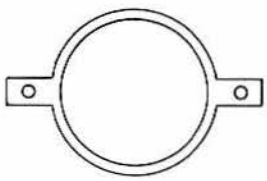

Fig. 3. Cable end view tubing.

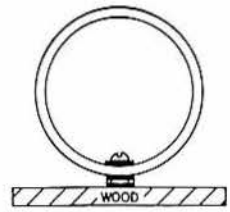

Fig. 4. Open end view.

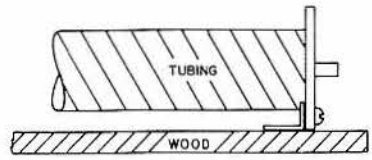

Fig. 5. Side view.

The output goes to the antenna plate on the forward end of the baseboard plank. When this plate is moved all the way in so that it is only ¼ in. from the cable pickup plate in the end of the aluminum tube, a full scale reading may be obtained on a 50 microamp meter on the output of a tuned diode detector (see Fig. 9). My first model here has marks on the scale (see Fig. 2) for 1 rf stage; 2 rf stages; mixer (feeding into a good i-f strip); mixer plus 1 rf, etc. At the 1 rf plus mixer, you begin to hear all the repeaters within 100 miles or so. With 2 rf plus mixer (followed by a sensitive i-f of course) you are really getting sensitivity. This is where you put a scope in line in order to have an electronic comparison point for signal coming out of the noise purposes, and then can really get into the low-noise bit, if you have a hermit location. Just happens I have one here. When I hear the noise of a car, it's a visitor!

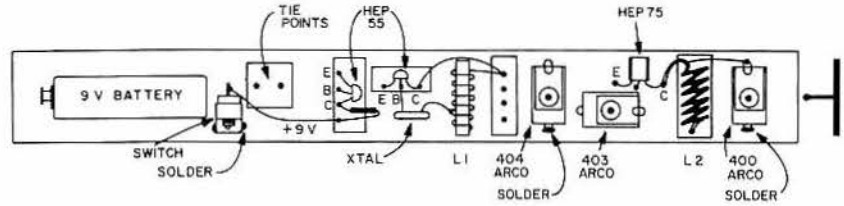

Fig. 6A. Layout, top view.

This audio is fed to the base of the multiplier where it provides some AM and some FM modulation for signal identification purposes. When working with receiver oscillators, and in particular with high-ratio multipliers, this is very important. It may also be locked into any old scope sync for noise figure and sensitivity comparisons. The scope sync gives a reference point where the signal to noise ratio will always be the same, without resorting to guess work. The crystal oscillator is my old tried and true crystal phase-reversing job, which uses negative feedback from the collector coil, which, after going through the crystal, reverses phase and becomes positive, thus assuring oscillation but *only* on the crystal frequency. A HEP 75 (similar to the famous 3866) is used for the quintupler. A lot more output is noted with this powerful but smooth operating old faithful, still good to 450 MHz.

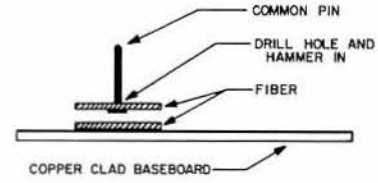

Fig. 6B. Tie-point construction.

Output

You will see for yourself as soon as you start testing that the attenuator is smooth-working and stepless, and that true infinite attenuation is at hand. An rf input state (pre-amp) with a noise figure a fraction better than another shows right away on the scale. For example, adjustment of the fixed bias voltages on the two gates of a 3N200 or 3N201 shows right away on the scale as the

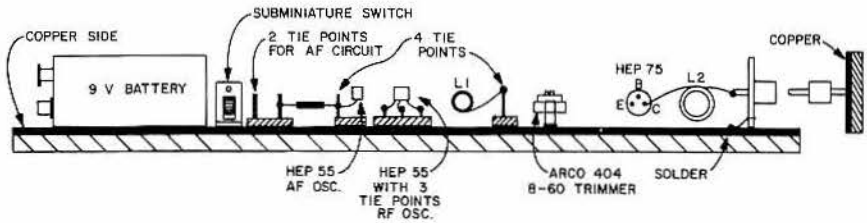

Fig. 7. Side view of the signal generator, 220 MHz.

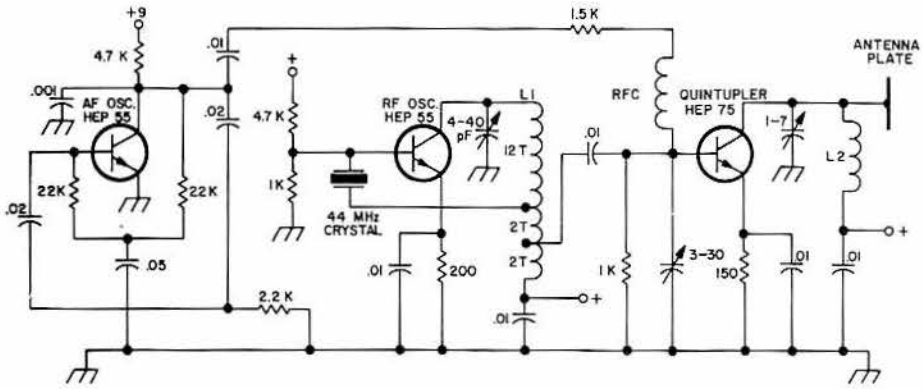

Fig. 8. Schematic. L1 = 16 turns No. 26 output tap at 2 turns, crystal feedback tap at 4 turns, from cold end. Wound on phenloic form .6 cm O.D. L2 = 6 turns No. 18 bare, air wound, .6 cm O.D., 2.5 cm long between tie points. RFC = about 40 turns No. 40, on phenolic form .3 cm O.D., 1 cm long (not critical).

push-rod is moved in and out and the signal is locked onto the scope. This work you can do right on the bench and at low cost.

There is quite a bit of mechanical work in the unit, depending on just how much "finish" you want it to have. You can also bring a dowel rod for "on and off" use. Do not, under any circumstances, bring out a *conductor*. You *can* do this, but only with an extreme amount of filtering, which is not part of this article. Be sure to set up the baseboard, antenna plate and battery first, and get them working mechanically. With a drawn-out shape like this I generally start with a longer piece of copper-clad than needed, build from one end, and then cut off what is left over. Understandably, once you have made the first one you can always see, after it is done, many ways of improving it. However, someone has to make the first one, and that's generally my job.

Antenna and Field Tests

Out of the tubing, and with a small antenna connected via a one turn link around the quadrupler coil and then to ground, returning L2 for maximum output, this little rig puts out a lot of signal on 220. Especially if you reduce the oscillator emitter resistor! Up to several volts of rf can be obtained in a tuned diode receiver if you push things along, which is around 5 to 10 mW. If you place this generator out in a field several hundred yards or more away, you can then line up your antenna on the car or house, check antenna cables, antenna input alignment, and match or mismatch for lowest noise figure, etc.

Front end alignment should first be done with a relatively broadband i-f strip on 10.7 MHz. Be sure nothing metallic on the generator strip protrudes enough to touch the inner wall of the tubing, or "scratch" will occur in the high gain receiver. A piece of thin fiberglass or other insulating sheet wrapped around the whole generator movable plank is a good precaution.

Once again I include a 220 MHz tuned diode detector, which is an absolute must for frequency multiplication, especially quintupling and such, where the other unwanted harmonics are as little as 20% away from the desired frequency. Figure 9 shows this piece of test equipment in pictorial schematic form. Remember, shape is of considerable importance as you go from VHF into UHF. It is quite easy to make the square trough line out of an old piece of copper clad. Or even a new piece! And this particular one described and shown in Fig. 9 goes very well to over 450 MHz and thus is very nice for the next band also. If you make it just as I've shown it, it will do a good job for you.

Calibration will present some difficulties, so line up some other lads around who are already on these bands and get your calibration that way.

So good luck, friends, more coming – lot's more! Keep reading.

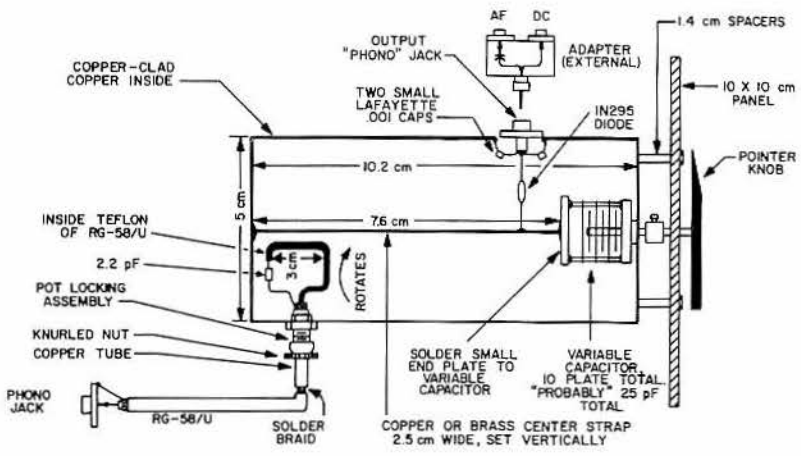

Fig. 9. Tuned diode detector, 160–460 MHz.

UHF SIGNAL GENERATOR

Jim Kennedy K6MIO

Several requirements were the basis for the design of this signal generator: operation on both 432 mc and 1296 mc, high stability e.g., crystal control, variable rf amplitude, provision for insertion of various types of modulation, and lowest possible cost consistent with satisfactory operation.

I had a 27.005 mc overtone crystal left over from a brief period of disillusionment about CB and, since 27 times 6 is 432 which times 3 is 1296, this seemed a likely place to start.

Fig. 1 shows the final result. The overtone oscillator is voltage regulated and is left operating at all times when the generator is on. The crystal is mounted underneath the chassis to protect it from rapid temperature changes from drafts, etc., further enhancing the stability.

The use of diode multipliers at 432 mc and 1296 mc greatly simplifies developing UHF rf.

Direct coupling the modulation into the cathode of the last vacuum tube multiplier provides a modulation input that will accomodate almost any signal from audio to video, or even pulse.

A four position mode switch on the front panel allows the choice of carrier, no carrier, carrier with 60 cycle modulation and finally carrier with external modulation.

Construction

Building the unit presents no special problems except getting it all under the chassis. The 5 x 9½ x 2½ chassis doesn't leave much useful

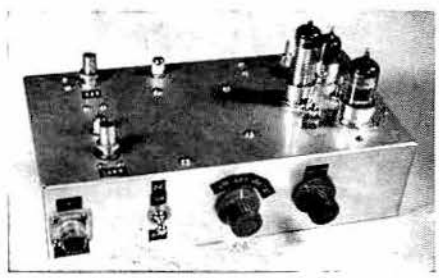

Front view of signal generator.

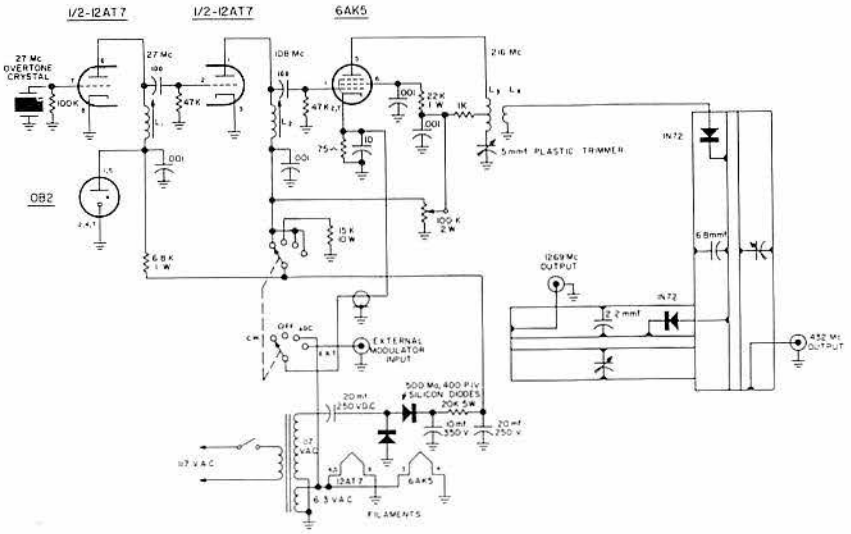

FIGURE 1

L1—10 turns # 28, 3/8" slug form.
L2—3 turns #28, 3/8" slug form.
L3—10 turns #18, 1/2" dia.
L4—3 turns #18, 1/4" dia.

room to spare, but it does make for a very compact device.

The lengths of the diode multiplier tuned lines were determined primarily by the space available and bear only the slightest relation to the wave lengths involved; hence, it was necessary to pad both lines with additional capacitances in order to resonate them properly.

Both lines were folded from 1/32 inch brass sheet stock. The inner conductors are made from ¼ inch brass tubing. The 432 line is 1" x 1" x 7". The input diode is tapped onto the inner conductor 1¼ inches from the other end. The signal output loop is about 1¼ inches long. The output diode is tapped 2 inches from the loop end of the line.

The tuning capacitor is made by soldering a 10-32 nut over a hole in the middle of the line shell. This provides the threads for the 10-32 screw which actually serves as the capacitor.

Round ½ inch disks are soldered to the bottom of the center of the inner conductor and to the end of the turning screw to provide additional range.

The 1296 line is similar except it is only 3⅝ inches long. The multiplier diode is tapped on the inner conductor ⅝ inches from one end. The signal output loop is about ¾ inches long and is located at the other end of the line. The tuning capacitor is identical to the one used in the 432 line.

The 15K 10 watt resistor in the carrier OFF position limits the no load voltage from exceeding the ratings on the filter capacitors.

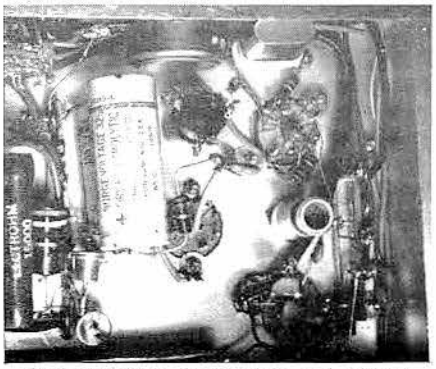

Closeup showing the oscillator and vacuum tube multipliers.

Operation

The tune up of the tube stages can be easily accomplished with a grid dipper. The UHF stages should only need to be peaked with a converter and receiver.

Shields on all tubes and a bottom cover on the chassis are important requirements if stray leakage at the signal frequency or lower harmonics is to be eliminated as a possible source of measurement error. These were removed for the photographs but are always used in practice.

For best results it is a good idea to employ a 50 ohm (or 75 ohm as the case may be) pad between the signal generator and the equipment under test. This will insure that the generator will appear as a resistive load as much as possible. This is necessary if the generator is to duplicate the conditions presented to the receiver by a good antenna.

This pad can take many forms. The two easiest ways to make one would be to use sufficient lengths of some lossy coax. At 432 mc higher, 20 or 30 feet of RG-58 (or RG-59) seems to be quite adequate for most applications. The other approach would involve building a conventional resistor pad into a male and female BNC connector soldered back to back. Fig. 2 shows such a pad.

Aside from receiver testing, this device has

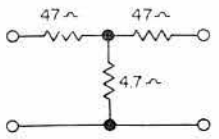

FIGURE 2

Fig. 2. 20 db 52 ohm pad. Resistors mounted in BNC connector.

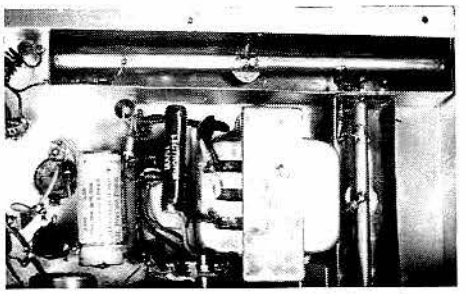

Closeup view showing details of diode multipliers lines.

several other uses to which it can be put. It is also useful as a signal source for antenna tests and it may be used as frequency standard.

This last use can be of great value at UHF because of the persistent problem of crystal tolerance versus frequency multiplication. A converter can easily be 40 or 50 kc or more off of the indicated frequency at 1296 mc. This can be quite a problem if you are hunting for a moonbounce signal through a 5 cps filter.

Though not shown on the diagram or in the pictures, it was found that a 50 mmfd variable capacitor connected across the crystal was sufficient to reduce 27.005 mc to the 27.000 . . . mc required to put the generator on 432.00 . . . and 1296.00 . . . mc. It will probably be necessary to retune the oscillator plate circuit for best operation; some loss in output will be encountered but this should not be a serious problem. However, if such operation is contemplated, it might be of some advantage to obtain a 27.002 mc crystal and employ a smaller variable capacitor.

In order to make the frequency standard really something of a standard, a 1 mc calibration oscillator should be employed. Some harmonic of the oscillator (5 mc, 10 mc, etc.) should be zero beated against WWV. The signal generator should then be zero beated against the 27 mc harmonic of the 1 mc calibrator—presto!—a 432-1296 mc frequency standard.

Though there are many refinements which can be made, the unit described has done a yeoman service in all the varied tasks asked of it.

LAB TYPE IF/RF SWEEP GENERATOR USING ICS

Ray Megirian K4DIIC

Just about every kit-type sweep generator on the market starts life out at around 3 or 4 MHz and ends up at 200 MHz or so. This always made analysis or display of 456 kHz i-f amplifier response characteristics a tedious step-by-step plotting procedure or required time out to rig up a temporary gimmick to do the job. No more. The sweep generator to be described here will do the job with ease and precision. Even if you do not intend to duplicate the instrument, you may find parts of it useful for other applications.

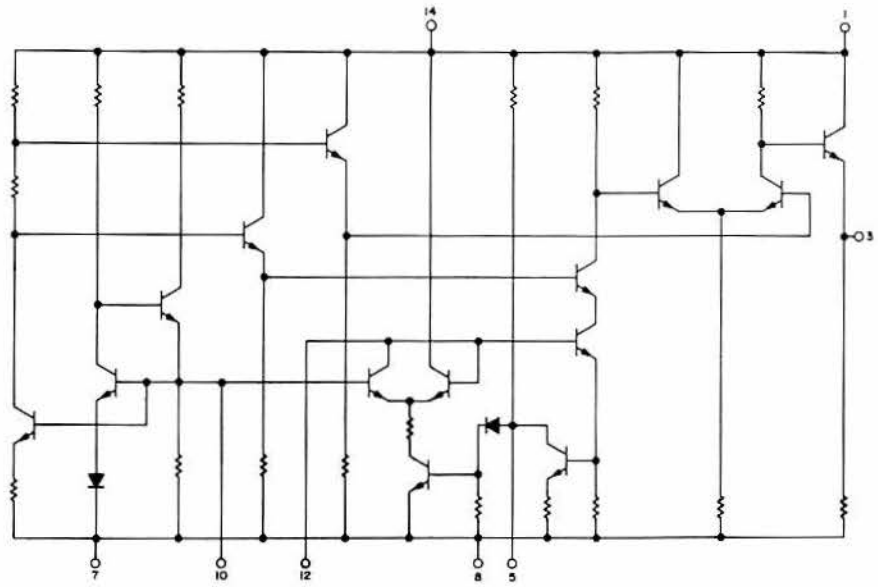

Fig. 1. Schematic of the MC1648 IC.

The generator covers a frequency range of from 400 kHz to 30 MHz in five bands. It can be operated in the CW mode as well as swept, thus allowing it to be used as an ordinary signal generator. Maximum output is 350 mV p-p across 50Ω. When sweeping, the return trace may be blanked or not, as desired. Two calibrated dials are provided for setting the start and stop frequencies and the maximum sweep width would be the entire band in use. The frequencies covered by the five bands are: 400 to 900 kHz, 850 kHz to 2.3 MHz, 2 to 6 MHz, 5 to 15 MHz and 10 to 30 MHz. Sweep time is variable between 20 ms and 6 seconds per sweep. A step attenuator in conjection with a vernier control provide a maximum attenuation of the output of 120 dB. An input is provided for a post-injection marker system built into the unit. A synchronous ramp with gain control is provided for driving the oscilloscope horizontal sweep. Blanking pulses are also brought out to a connector in case they are needed for synchronizing external equipment.

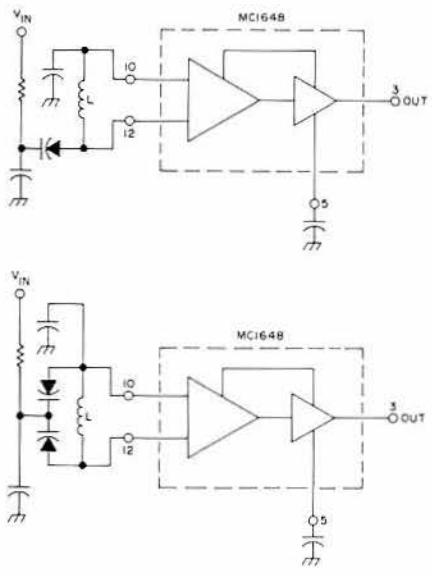

Fig. 2. Tuning the MC1648 with a single diode (A) and using back-to-back diodes (B).

A New IC

The heart of the generator is a new Motorola IC, the MC1648 emitter-coupled oscillator. It was intended for use in phase-locked loop systems operating in excess of 150 MHz, but may be used in many other applications such as this one. The device provides output of high spectral purity and incorporates an internal agc system which simplifies design of the sweep generator by eliminating the need for external leveling. A buffer amplifier and emitter-follower output are also incorporated on the chip, eliminating the need for external amplifiers. Figure 1 is a schematic of the MC1648 IC. Figure 2 illustrates two methods for tuning the oscillator. The device is packaged in a 14-pin DIP and requires a 5V dc supply. Since it was intended to be used with Motorola MECL III logic, either polarity is permissible. A positive supply is used here, connected to pins 1 and 14 with 7 and 8 grounded.

All the information covered by the data sheet for the MC1648 dealt with operation from 10 MHz up to about 180 MHz. Since I was interested in going as low as 400 kHz, I had to do some experimenting with tank circuits. My best results were obtained with the use of cup cores for the two lowest bands. I also found that ordinary molded iron core rf chokes of the miniature variety did an excellent job the rest of the way. Use of these tiny components made possible a very compact 5-band assembly.

The VCO

In order to facilitate shielding and simplify construction, electronic band switching is employed. Figure 3 is the schematic for the rf portion of the generator. The 2N4391 J-FET has a low 'on' resistance and works very well as a switch. One of these transistors is placed in series with each tank circuit

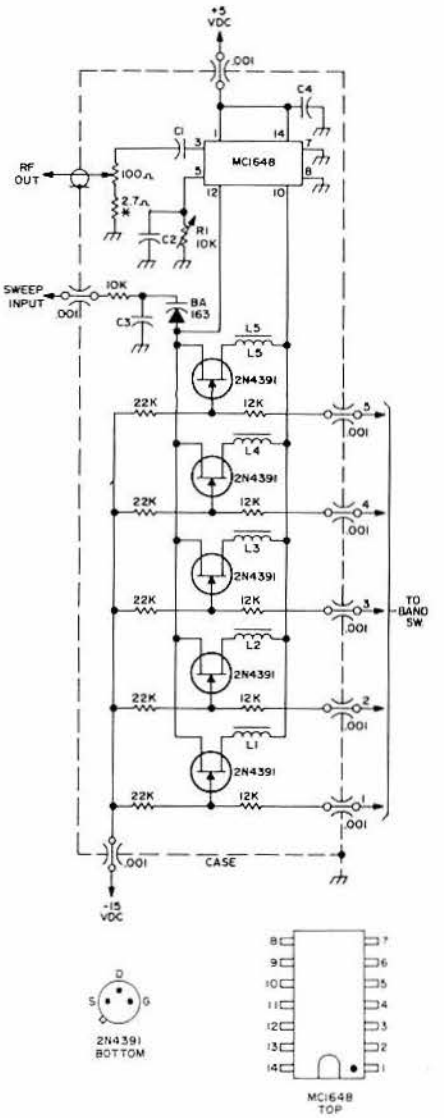

ALL RESISTORS - 1/4W, 5%
L1 - 28 TURNS NO. 30 AWG ENAMEL.
L2 - 12 TURNS NO. 28 AWG ENAMEL.
(L1 & L2 MOUNTED IN CUP CORE - See Text)
L3 - 18 μH MINIATURE MOLDED RFC.
L4 - 4.7 μH MINIATURE MOLDED RFC.
L5 - 1.1 μH MINIATURE MOLDED RFC
C1, C2 - TYPE 150D TANTALUM - 2.2 μF/20V.
R1 - BECKMAN 89PR10K 15-T TRIMMER.

* - SELECTED PART - See Text.

Fig. 3. Schematic of the rf assembly using dc band switching.

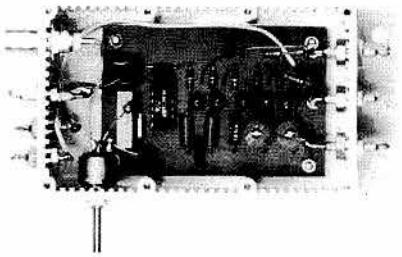

Completed rf assembly ready for mounting in the cabinet. A plastic version of the 2N4391 was used with a considerable savings in parts cost.

and can be turned on by application of a positive voltage at the gate. This allows the use of a strictly dc-operated remote switching arrangement. The entire assembly is built on a 2 x 3 in. pc board and mounted in a Pomona Model 3306 enclosure with a Model 3328 bottom mounting plate.

A BA163 tuning diode by ITT is used to sweep the oscillator. Although it is intended for bc band use, it performs admirably at these higher frequencies and its high capacitance ratio allows wide sweep excursions. If you are planning to use this oscillator for VHF applications, a more suitable diode would be in order. According to the data sheet on the MC1648, typical maximum output frequency is 225 MHz.

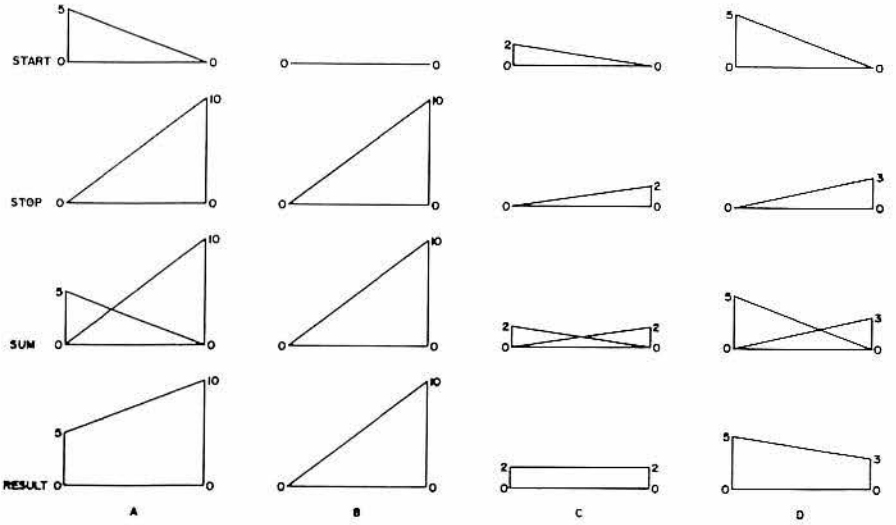

Fig. 5. Pictorial demonstration of ramp generation.

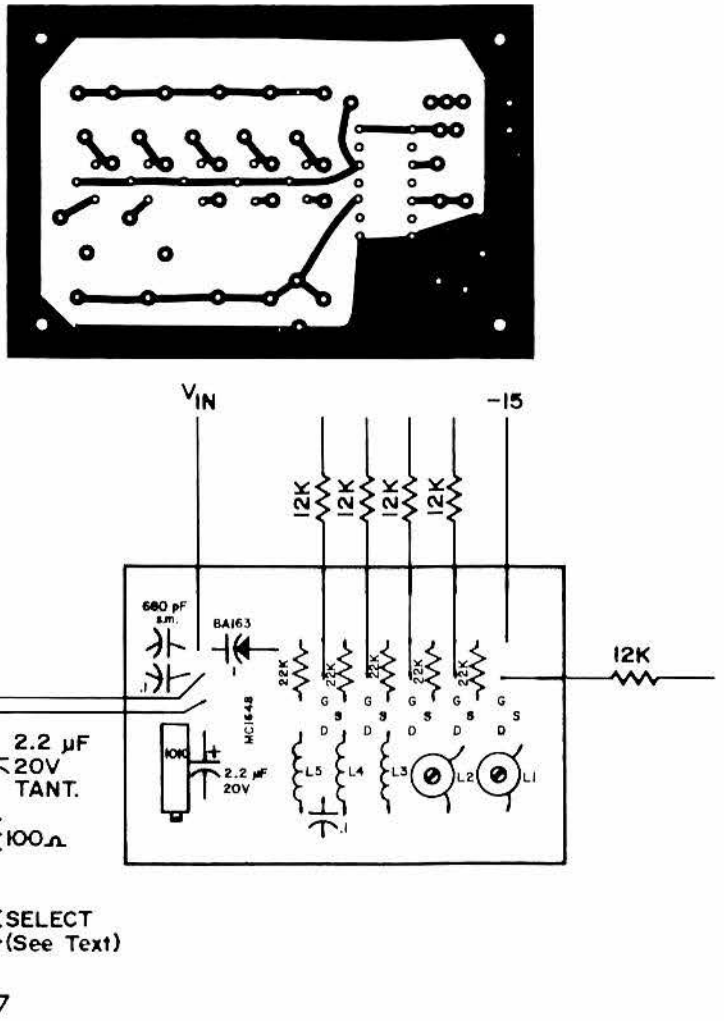

Fig. 4. (A) Foil side of rf pc board. (B) Location of parts on component side.

The vernier attenautor is a 100Ω RV6 style potentiometer mounted inside the enclosure. A coupling and extension shaft are used to bring the control out to the front panel. The value of the resistor at the bottom end of the pot will have to be selected so that a range of 20 dB is provided with full swing of the control. Since end resistance varies from one control to another, an exact value will have to be arrived at experimentally.

The output from the VCO is a square wave. If sine wave output is desired, the agc characteristic may be modified by introducing resistance between pin 5 and ground. The small trimmer incorporated on the board is used for this purpose. It was my experience, however, that this may introduce instability with some MC1648s. Although the trimmer was left in, the one in my unit is turned to maximum resistance where it has no effect and left there. It would do no harm to leave it out altogether since no other changes would be needed.

If any readers are contemplating exact duplication of this generator, you will find the cup cores I used are no longer available. These were Ferrox-cube part number 332P133B4-3C and are obsolete. I had a large number of these on hand left over from another project and saw no sense in buying more. I am sure some of the presently available cup cores will make excellent substitutes. Those used here are about 3/8 in. in diameter and are ungapped. You may have to experiment with the number of turns in the coil to obtain the coverage you require. One handy trick you can pull with a cup core is to rotate the slots in each half so that fractional turns are produced when the coil wires are brought out separately through the

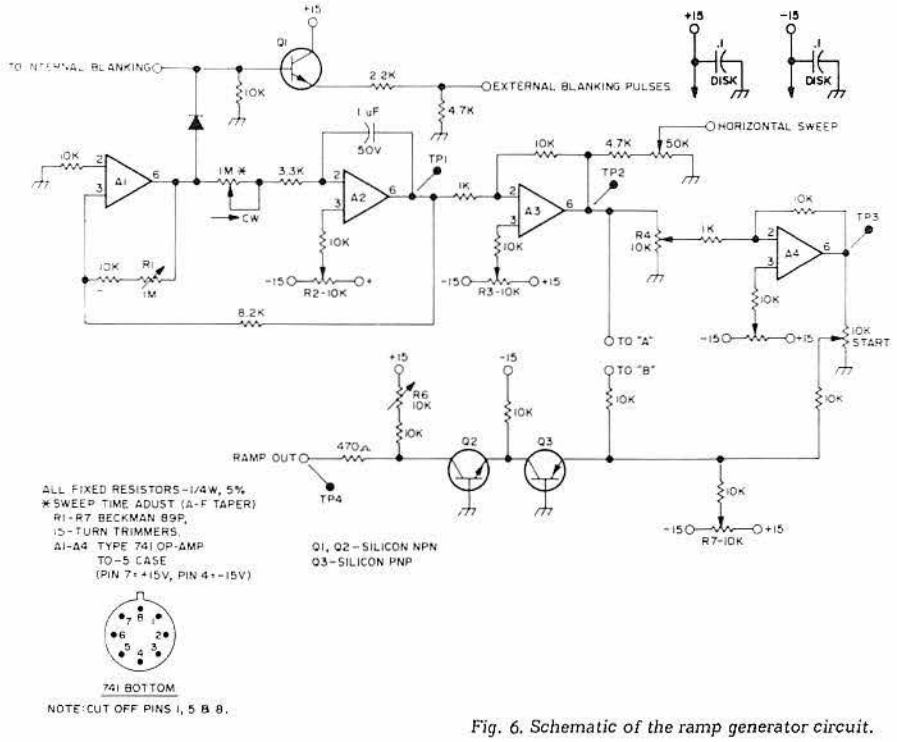

Fig. 6. Schematic of the ramp generator circuit.

two spaced holes. Exerting pressure on the core by means of the mounting screw will also shift the frequency and is almost like having a slug to tune. Increasing pressure seems to raise the frequency. The rf chokes used for the higher bands may also vary slightly from piece to piece and several may have to be tried to get the desired coverage. There isn't much we can do to alter the frequency where the chokes are used. Of course, slug-tuned coils may be used if the pc layout is modified. I do not recommend their use on the two lowest bands, however, since my results were rather unsatisfactory with this sort of tank circuit.

One final point would be in order before leaving the VCO. Note that the 10 KΩ resistor going to the tuning diode, the 2.2 μF rf output capacitor and each of the 12 KΩ resistors going to the transistor gates are not mounted on the board. One end of each has a hole provided on the board and then the component itself is used to make the connection to its final destination. This saves board space and eliminates separate wires. The small resistor at the bottom of the vernier attenuator is similarly mounted between the board and the bottom lug on the control. These points are more clearly seen in the photo. Also note that the cup cores are fastened directly to the board by means of 1-72 screws into threaded holes.

The Ramp Generator

In contrast with kit-type sweep generators that use the 60 Hz line for sweeping the oscillator, laboratory instruments have internal circuitry designed for this purpose. In our case, as with most sweep generators, a voltage ramp is used to control the oscillator during the sweep period. The circuitry has been arranged so that we can adjust the starting point (dc level) of the ramp independently of the stopping point. This simply means that we can set the frequency at which the sweep starts as well as the frequency at which it stops. We can also control, over a fairly wide range, the time it takes for a complete sweep. In this case, the sweep time is continuously adjustable between 20 ms and 6 seconds per sweep.

To get a better idea of how the ramp generator produces the results we've described above, let's look at Fig. 4. Note that a negative-going linear ramp (start) is combined with a positive-going linear ramp (stop) to produce the resultant ramp being applied to the varactor diode. If either input ramp is zero, the resultant will be the same as the single ramp since adding zero to anything will not change its value. Naturally, if both are zero, the output will be zero and the oscillator output frequency will be constant during the sweep period. The same is true whenever both ramps are of equal amplitude, except that the output will be a steady voltage other than zero. Also note that the resultant ramp could have a negative slope if the 'stop' input is lower than the 'start' input, and the oscillator would obviously sweep down in frequency rather than up.

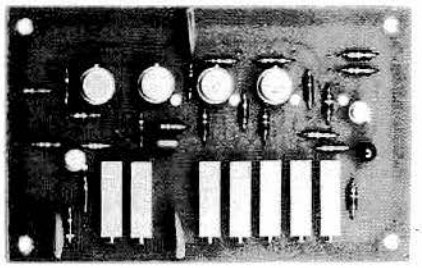

The ramp and blanking generator pc assembly. The leads going to external points will go in the holes visible on the board.

The schematic for the ramp generator is shown in Fig. 6. Operational amplifiers A1 and A2 form a triangle wave generator with A1 acting as a threshold detector and A2 as an integrator. One half of the triangle (negative-going) represents the sweep period while the other half represents the retrace time. Since a square wave is generated at the output of A1, we have a convenient source of blanking voltage built right in. This signal is positive during the sweep period and is connected to the band switch when Swept I (blanked retrace) operation is selected. During retrace the square wave drops to zero and actually disconnects the tank circuit until the next sweep starts. An emitter-follower, Q3, buffers the square wave output for external use.

The output of inverting amplifier A3 is a positive-going ramp during the sweep period and is used for both the 'stop' signal and horizontal sweep for the oscilloscope. Since an additional inversion takes place in the output of A4, the negative-going ramp at this point is used as the 'start' signal. These two ramps are applied across front panel controls which have 6:1 reduction drives and are fitted with dials calibrated in frequency for the five operating bands. The outputs from these two pots are fed to summing amplifier Q1, where the output will be the resultant ramp we discussed above. Because the output Q1 is in the negative region (PNP transistor), a second common-base (NPN) amplifier is used to shift the output back to where it will always be positive.

The ramp and blanking generator is constructed on a pc board 2.6 x 4.1 in. in size. For convenience, all the trimmer resistors were mounted along one edge. As seen in the photo, this board was mounted by means of two small brackets in a vertical position with the trimmers facing up. To simplify pattern layout, unused pins 1, 5 and 8 on each of the four 741 opamps were clipped off right at the case. Color-coded wires were connected to all necessary points on the board before it was mounted, with the leads made long enough to reach their destinations. For those interested in building this unit, a detailed procedure for setting up the ramp generator will be given later.

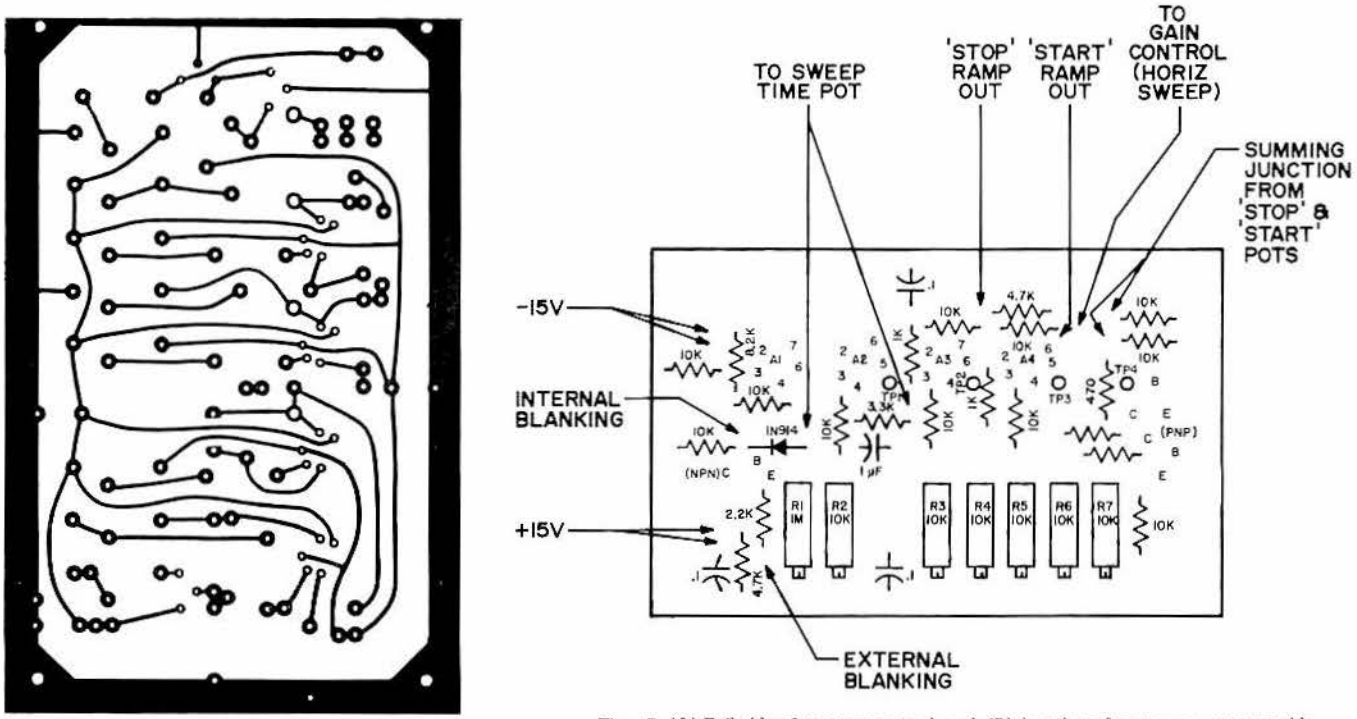

Fig. 7 (A) Foil side of ramp generator board. (B) location of parts on component side.

The Mixer/Amplifier

In order to provide a means for displaying frequency markers, a mixer and amplifier circuit was built into the sweep generator. The schematic for this circuit is shown in Fig. 6. A marker generator was not included inside the sweeper because other rf generators were available for use as markers and the added expense seemed unnecessary. Because the mixer board was to be installed inside a shielded box, dc gain control was resorted to as with the band switching discussed earlier. A 2N4391 is used as a variable resistor to control the signal input to the amplifier stage. This in turn controls the size of the marker being displayed on the curve. A 2N3819 FET is used in a simple mixer circuit which worked the best of several tried. Incidentally, the PNP and NPN transistors used here and on the ramp generator board are unknown surplus silicon units.

The pc board for the mixer is 1.5 x 2.9 in. and is mounted in a Bud CU-124 die-cast aluminum box. Note that here again some of the components are mounted between the board and their external connectors. These include both the 10 pF and 100 pF input capacitors to the 2N3819 and the 10 KΩ resistor going to the gate of the 2N4391.

The Power Supply

Figure 7 is a schematic for the power supply. Voltage requirements for the sweep generator are +15V, −15V and +5V dc. The current drawn by any of the above circuits runs no more than 30 or 40 mA maximum,

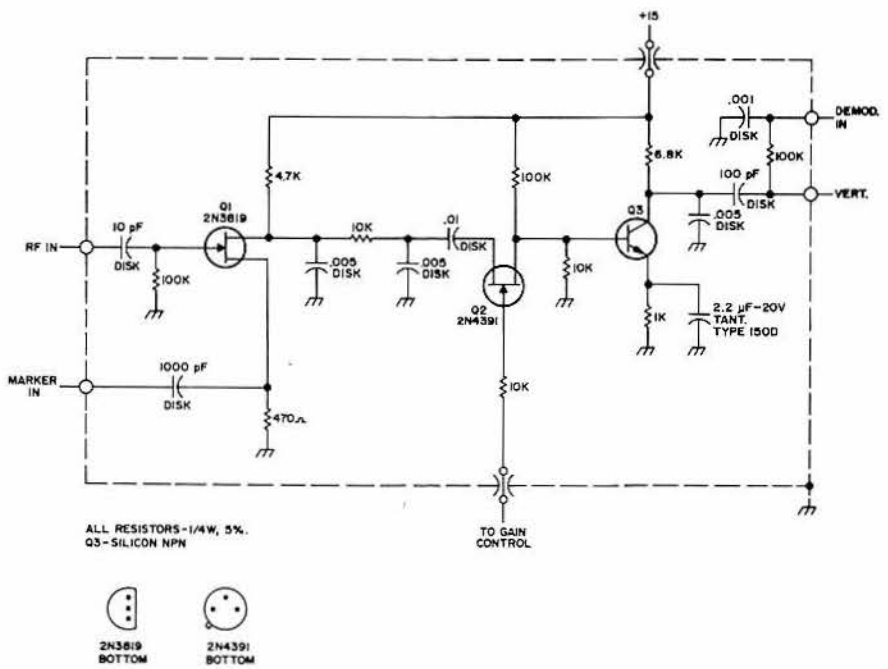

Fig. 8. Post-injection marker circuit with dc gain control of marker size.

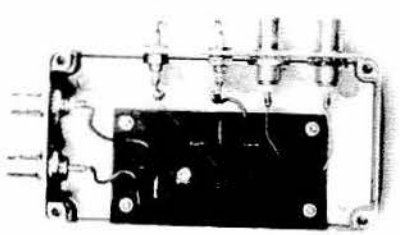

Completed mixer/amplifier board mounted in the die-cast housing.

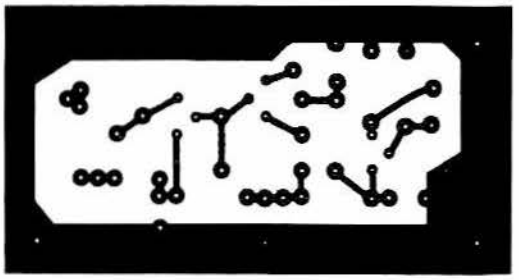

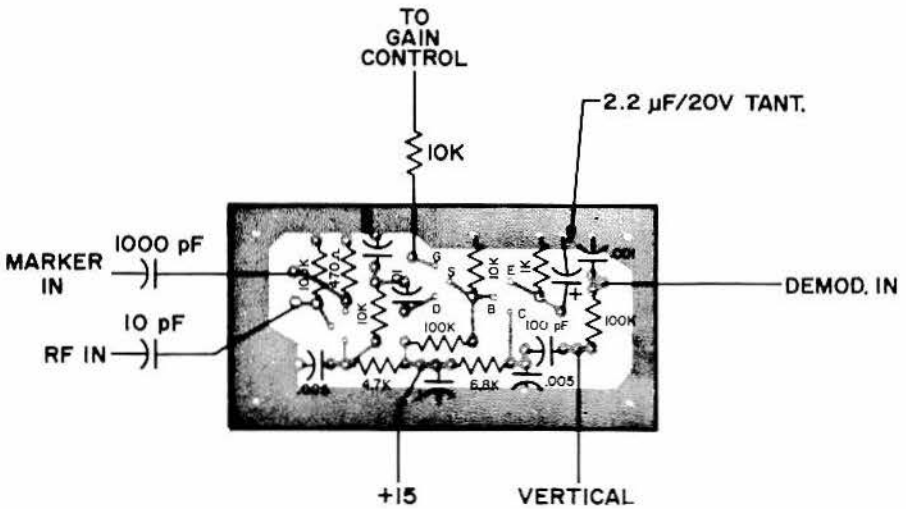

Fig. 9. (A) Foil side of mixer/amplifier pc board. (B) Location of parts on component side.

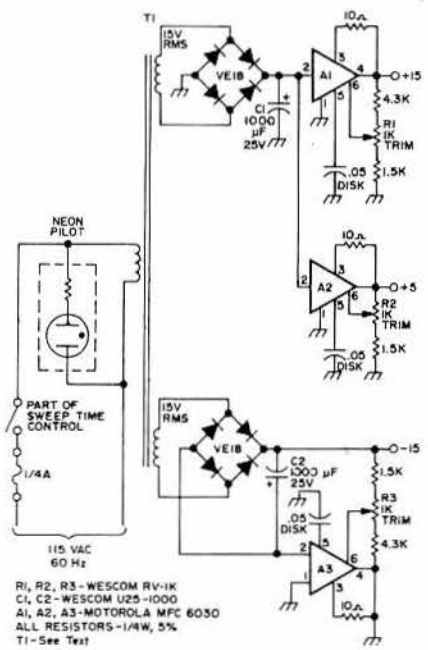

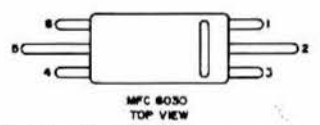

Fig. 10. (A) Foil side of power supply pc board. (B) location of parts on component side.

making the use of small IC voltage regulators ideal. Motorola MFC6030 (plastic) regulators are used in each supply and are overload protected against accidental short circuit. Varo type VE18 molded bridge rectifiers, together with 1000 µF filter capacitors, supply the dc input to the regulators. The +15V and +5V regulators are both fed from the same source. The power transformer was a surplus unit with a 30V CT secondary. The center tap was uncovered and the two leads separated so as to provide two independent 15V windings. A small trimmer is provided in each supply for voltage adjustment.

The pc board for the power supply is 2.6 x 4.1 in. All components but the transformer are mounted on the board. The transformer is mounted directly on the chassis. Relative placement of the various components making up the complete generator can be seen quite clearly in the photo.

Control Circuits

Figure 8 is the wiring diagram for the control circuitry. Note that for CW operation of the generator, a dc voltage is applied to the varactor by way of the Start pot. In order for the dial calibration to be valid in either mode, the dc level applied to the control must be exactly the same as the peak amplitude of the ramp during swept operation. As will be explained in the set-up

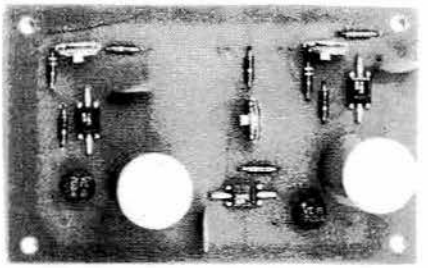

The power supply pc assembly.

procedure, the ramp will vary from a starting point of approximately +1.4V and peak at +12V. Resistor R1 in series with the +15V line is selected for a +12V level at the high end of the pot. R2 is selected for a level of +1.4V at the low end. The reason for the offset of 1.4V at the low end is because the pin to which the tuning diode is connected at the MC1648, sits at this level. The source of this bias is the drop developed across two forward-biased junctions within the IC and not from any external source. Once these dc levels have been set for CW with the fixed resistors, the ramp can be made to match by means of the trimmers in the ramp generator circuit.

The rest of the control circuitry is quite straightforward. In position 2 (Swept 1) of the mode switch, positive pulses from the ramp generator are fed to the band switch during the sweep period. When retrace occurs, the pulse drops to zero and the oscillator shuts off until the next sweep starts. In the CW and Swept 2 positions of the mode switch, a steady +15V is applied to the band switch and the oscillator runs continuously.

The final function performed by the mode switch is to route the dc for CW or the ramp for swept operation to the tuning diode. The two fixed resistors are mounted point-to-point behind the panel since all points are readily accessible within every short distances. The fixed resistors associated with the marker gain control are also mounted the same way behind the panel. The switches are ordinary rotary types and the potentiometers are all ordinary carbon controls. The Start and Stop controls as well as all gain controls have linear tapers. The Sweep Time pot is an audio taper type with built-in switch for ac power.

Setting Up the Ramp Generator

For best results, a calibrated dc scope is required to properly adjust the ramp generator. Test points have been provided on the pc board and short pieces of bare wire connected to each of these points make excellent tie points for the scope probe. The

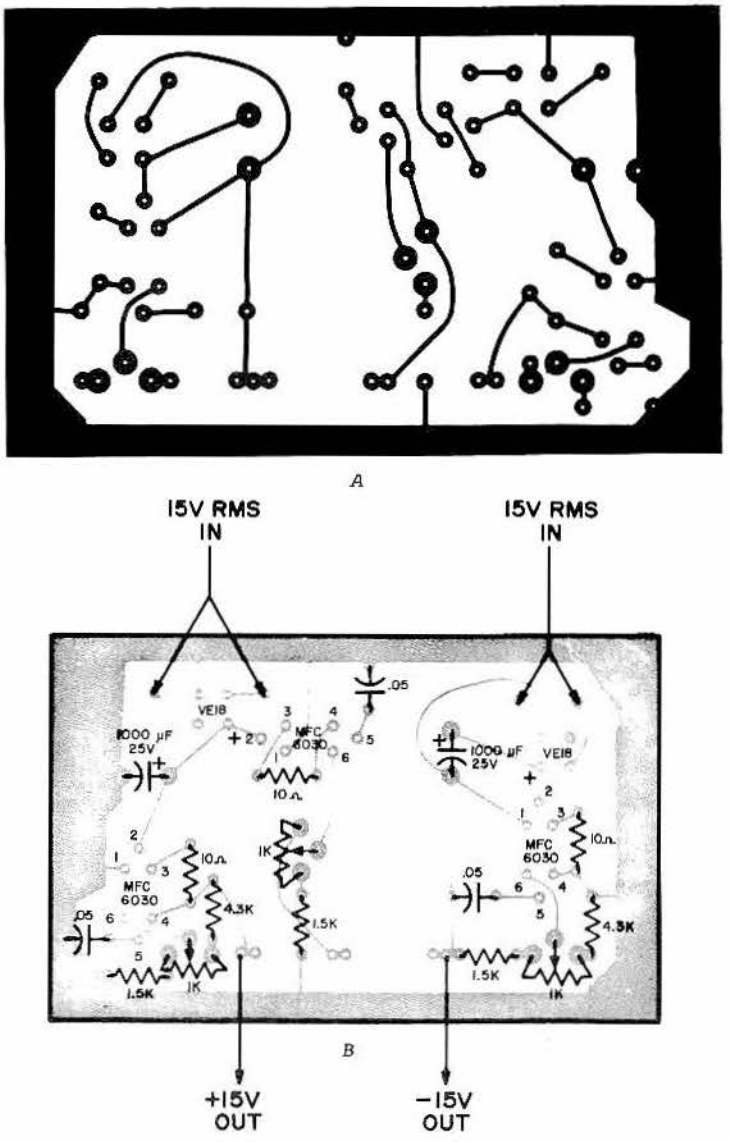

Fig. 11. (A) Foil side of power supply PC board. (B) Location of parts on component side.

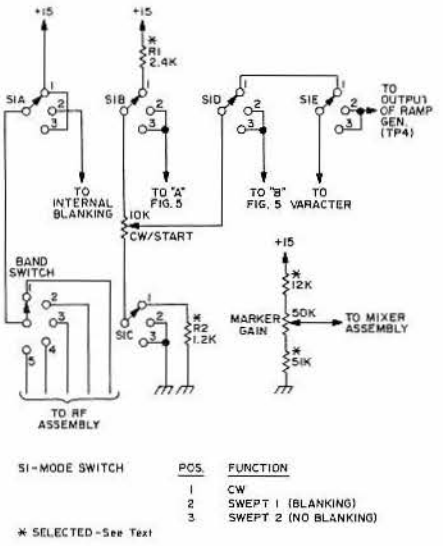

Fig.12 Control circuit wiring schematic.

circuit may be aligned either before or after installation. The Start, Stop and Sweep Time pots can be connected at the ends of their respective leads if the unit is checked outside the cabinet.

Set all seven trimmers to mid-range. Connect the scope to TP1 and adjust the horizontal for a full sweep of 20 ms. Set the Sweep Time control to minimum resistance and apply power. Some sort of triangular wave should be displayed. Adjust R1 for a 3V p-p amplitude of the waveform. Turn R2 cw until the negative-going portion of the triangle is 20 ms long. Since R1 and R2 interact, you will have to stop occasionally and reset R1 for proper amplitude. Once the ramp is set at 20 ms with the Sweep Time pot at minimum, the slow speed end will automatically be about 5 or 6 seconds with a 1 MΩ pot.

Transfer the scope probe to TP2 where a positive-going ramp should be seen. Set the starting point of the ramp to zero volts by means of R3. Amplitude of this ramp must be 10V. If it is not, go back and adjust R1 slightly until it is. If necessary, reset R2 for 20 ms trace length. As soon as a 10V, 20 ms, zero-based, positive-going ramp has been achieved at TP2, go on to TP3.

At TP3 there should be a negative-going ramp. Once again we require a zero base line or starting point. Adjust R5 to accomplish this. Amplitude should once again be 10V and is controlled by R4. Once you have a 10V, zero-based, negative-going ramp, move on to TP4.

Connect the probe to TP4 and set the Stop control to full cw. The Start pot should be at minimum setting. A positive-going ramp should be present at TP4. By means of trimmer R7, move the ramp up or down until the starting point is approximately +1.4V. Ordinarily the ramp will not go below zero but will flatten out as the positioning control is adjusted. This is due to clipping in the output amplifier. If the ramp generator is going to be used with another type of VCO, the ramp can be set to exactly zero if desired. In our case we can't as explained previously.

Because a substantial amount of capacitance change occurs in the tuning diode up to 12V, the final ramp amplitude is set to 12V by means of R6. Because R6 stretches the signal in a negative direction, R7 will have to be used to reset the base line at 1.4V. Other than for checking tracking between the CW and swept modes, this completes the alignment procedure for the ramp generator.

When the generator is finished, you can check the tracking by observing actual signals at the input to the VCO. Connect the scope probe to the feedthrough capacitor on the VCO assembly that goes to the tuning diode and set the Start control to maximum. Switch rapidly between the CW and Swept 1 positions of the mode switch. The CW input will be a straight line sitting at +12V while the swept input will be a ramp peaking at +12V. Next, turn the Start control to minimum and again compare levels. If the Stop control is also at minimum, both signals will be straight lines at +1.4V. If there is any substantial difference between the two modes, use R6 and R7 on the generator board to make the ramp agree with the dc levels. That completes all phases of the ramp set-up procedure.

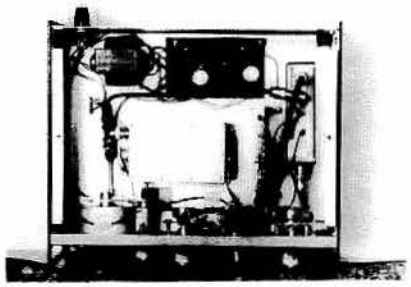

This bird's eye view of the interior shows the location of all major assemblies.

Construction

The cabinet used here is one manufactured by Sorensen Electronics in their Mod-U-Line series. These are the most reasonably priced instrument enclosures I've come across so far and I've used them for several projects. This one is a Model MCH-5129 with a CP-129 chassis plate. Dimensions are: 5¼ in. high by 12 in. wide by 9 in. deep.

The 5-step attenuator was picked up surplus from Fertik's Electronics for about $10. It is well made and designed for 50Ω systems operating up to 1 GHz. It has an integral female BNC output connector on the front face along with four threaded mounting holes for ease of installation. The input connector is a BNC male at the end of a short piece of coax.

All rf assemblies are interconnected inside the cabinet by means of coax cables. This is clearly evident in the photo.

The Start and Stop pots were mounted on brackets behind the front panel so that Jackson Brothers type 4511/DAF reduction drives could be installed for easier tuning. The two circular dials are slightly under 2 in. in diameter and were cut from sheet plastic. While operating in the CW mode, one of these was calibrated in pencil to provide a pattern for the finished product. A master was laid out using Rubylith® film and rub-on numbers. A negative of this was then made using 3M reversing film. From the negative a finished set of dials was printed on aluminum material of the presensitized variety. These were cut out and stuck to the plastic by means of their own pressure-sensitive adhesive backing. The nameplate was made from the same material. The two index pointers are clear plastic with hairlines scored on the inside surface. They are mounted on spacers directly over each dial. All remaining labeling was done with tub-on lettering.

Vendor Addresses:

Fertik's Electronics, 9th & Tioga Sts., Philadelphia PA 19140.

Sorensen Electronics Co., Inc., 418 Queens Lane, San Jose CA 95112.

Wescom, P.O. Box 2436, El Cajon CA 92021.

100 KHZ THIN-LINE PULSE GENERATOR

James Ashe W2DXH

Ordinary 100-kHz frequency standards are usually audible up to a few tens of megahertz. A good one might be usable at 50 MHz. The circuit described here uses a dual NAND gate to generate a 100 kHz signal whose harmonics are usable to 432 MHz or higher. And it can be built without benefit of special instruments and knowledge.

The thin line pulse

One rather surprising result of higher mathematics is that all repetitive signals are composed of harmonically related sine and cosine waves. For example, the familiar square wave is composed of a fundamental frequency, which sets its basic repetition rate, and of odd harmonics only of its fundamental, which contribute to its square corners. If the harmonics' amplitude or phase relationship is upset, the square wave is distorted. This feature makes the square wave very useful for amplifier testing, but its harmonic content is not very good for frequency standard applications.

Now suppose that we start adding up signals of F, 2F, 3F, and so on, phased in so that they all reinforce each other once per cycle. Let's say thay are all the same amplitude. What would we get? See Fig. 1A.

The five equal amplitude sine waves peak simultaneously at the beginning of the fundamental's cycle. Everywhere else, until near the end of the cycle, they are more or less out of phase. Trying to see what will happen, we try adding the first two frequencies. Fig. 1B, the result, might suggest something to a mathematician.

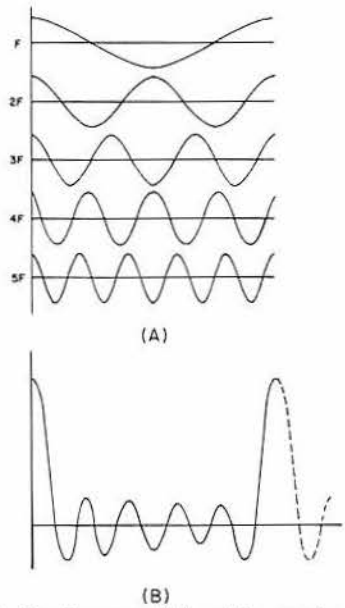

Fig. 1. Five sine waves (A) and the waveform as a result of point-by-point addition (B).

As the number of frequencies is increased, their amplitudes tend to average to zero everywhere except at the beginning of the cycle. Here, they all add up to a short, sharp pulse. It follows that a short, repetitive, one-sided pulse should contain odd and even multiples of the fundamental frequency.

An ideal thin line pulse has infinite frequency content.* No real signal could meet

External view of the 100 Hz thin-line generator.

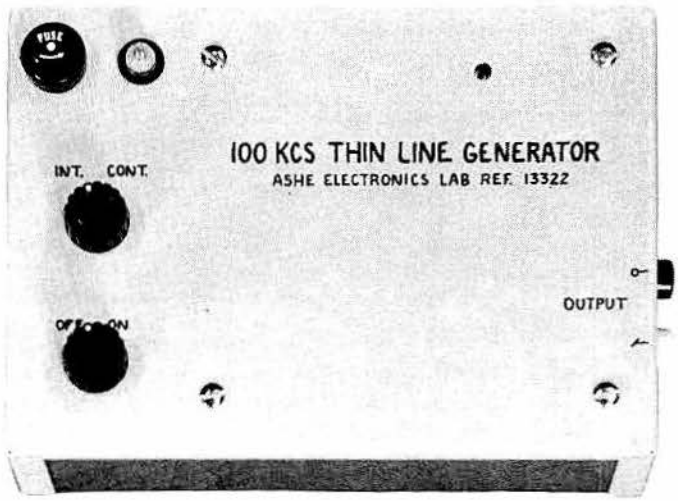

The finished sweep generator makes a professional appearance.

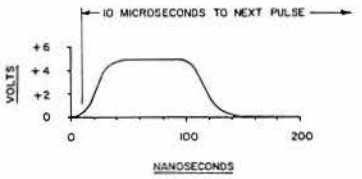

Fig. 2. Real circuit output as seen by a Tektronix 545A oscilloscope. A faster scope shows shorter rise-time and sharper corners.

this spec, but a fast digital IC can produce a very workable approximation. Fig. 2 shows a Tektronix 545A view of the generator output and tests with other scopes indicate the real pulse has better rise time and sharper corners than shown here.

If this pulse is viewed on a low-performance service variety scope, its appearance will be greatly changed. There will be an apparent loss in amplitude, since the pulse occurs and terminates before the slow circuitry can properly respond. The apparent duration is increased, also because of the slower viewing circuitry. And the fast pulse may excite circuit resonances, so that the thin line pulse appears as a damped oscillation. But these problems do not interfere with constructing the generator, because the very simple NAND gate circuitry contains no critical elements or adjustments.

How it works

There are four circuit sections, shown in Fig. 3. A 100-kHz crystal-stabilized oscillator sets the basic frequency, and a dual NAND gate circuit converts the oscillator output to a thin line pulse. A 1-Hz astable generates the output marking signal. A 6 volt dc power source is provided by a voltage doubler zener-regulated supply.

Multivibrator oscillators are not ordinarily very stable frequency sources. But if the oscillator is designed to run slightly below required frequency, and an appropriate crystal is connected between transistor base terminals, oscillations are stabilized at the crystal frequency.

The crystal does not change the multivibrator's style of operation. It synchronizes the astable to its own frequency, by triggering the OFF transistor into conduction shortly before normal RC turn-on. The output is a squarish wave with good fall time, but a long rise time as shown in **Fig. 4A.**

In passing through the first NAND gate the pulse is squared up and becomes slightly unsymmetrical. See **Fig. 4B.** A differentiating network, C7 and R11, converts the square wave into the pulses shown in **Fig. 4C.** These pulses, applied to the second NAND gate, reappear as the thin line pulses shown in **Fig. 4D.**

Since one CW signal sounds just like another and there may be several in the vicinity of a check point, a marker feature is required. This is provided by the 1-Hz astable, which paralyzes the second NAND gate part of the time. Its base bias resistors are unequal, giving a distinctive duty cycle to the output signal. A switch disables the astable if a continuous signal is required. **Fig. 5** shows the output when the second astable is operating: the output is locked in the up

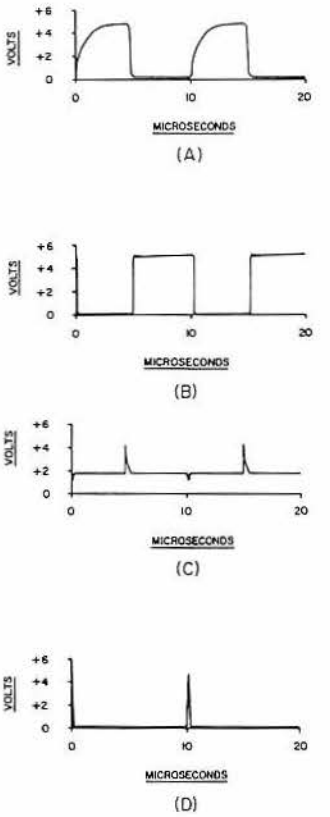

Fig. 4. Signals at four critical points in the generator, as displayed on a Tektronix 545A oscilloscope. They are shown in time coincidence.

condition during half of each 1-Hz astable cycle.

Sometimes an astable oscillator will refuse to start oscillating when it is turned on. It does not start because both transistors are in saturation. This reduces loop gain so that available noise cannot be amplified around the loop. It would never start without some strong, outside interference.

A pair of diodes, D1 and D2, provide a reliable remedy. The diodes are arranged so that base bias must come from whichever collector is at the higher voltage. If both transistors are in saturation, their collectors are at perhaps 1 volt, which cannot provide enough base current to keep the transistors in saturation. This contradictory situation does not arise in the real circuit, which starts reliably.

Additional diodes, D5 through D8, appear in the base circuit of the 1-Hz astable. These are protective diodes. The collector swing at turnoff of about 5 volts is conveyed powerfully to the opposite base through the large coupling capacitors C5 and C6. The reverse B-E breakdown voltage of these transistors is not known, so the diodes are provided to prevent the turnoff voltage exceeding 2 volts or so.

DC power for the Generator circuitry comes from a voltage doubler supply based on a low-current filament transformer. Its design is conventional, but a large capacitor, C12, is provided across its output to mini-

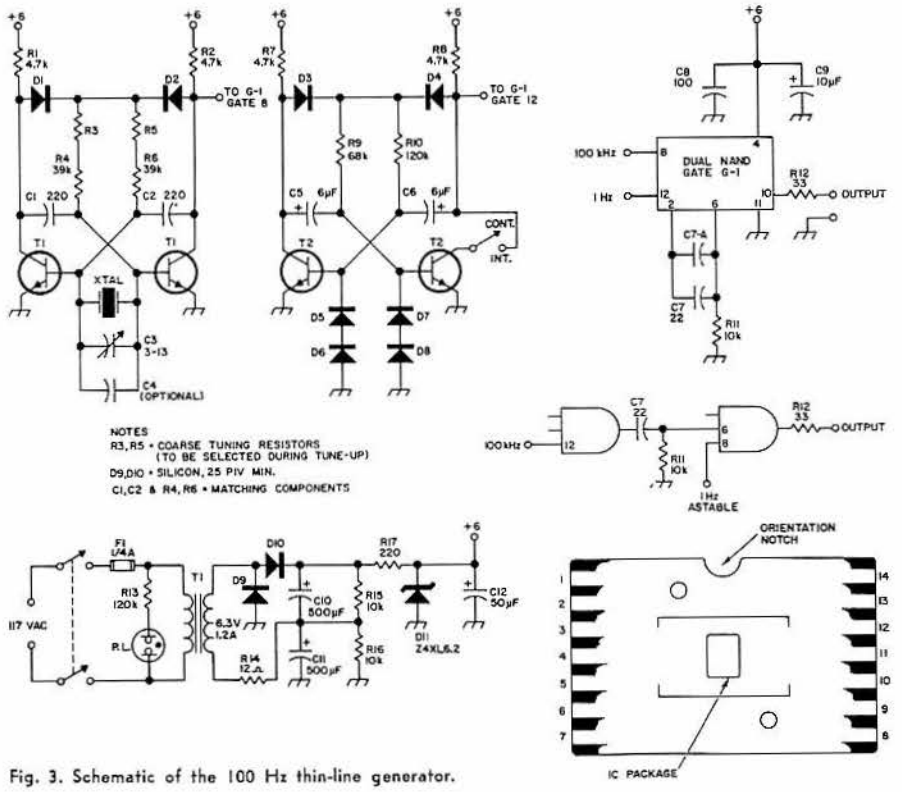

Fig. 3. Schematic of the 100 Hz thin-line generator.

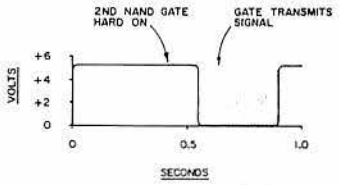

Fig. 5. The second NAND gate locks in its up position part of the time to produce an intermittent output.

mize noise on the supply line. The supply could be replaced with some batteries, shunted by a 50 μF or larger capacitor to absorb transients. The original breadboard ran very well, powered by four flashlight batteries.

Construction

The generator is built in a Premier #PMC 1008 3x5x7 inch heavy aluminum box. Its top cover was refinished in light green enamel, and four ⅜ inch grommets in the bottom piece serve as protective feet.

Inside the box, the 6.3-volt transformer and cheater cord connector are mounted on the left-hand wall. A pilot lamp, fuse, and two switches are mounted on the horizontal panel, at the extreme left. This leaves just enough open space for the two circuit boards which occupy most of the box. Two banana jack output connectors are placed on the right-hand side, just below the panel.

The circuit boards are cut to 4½ x 5 inches, from Vector $\frac{3}{32}$ inch pattern A stock and mounted parallel to the panel. The upper board is spaced an inch from the panel, and carries both astable oscillator circuits. The other board is mounted one half inch below, and carries the digital IC and the power supply circuitry. Assembled, the two boards make a sandwich with wiring sides together.

Both boards are mounted on the same four centers. These are through the second hole diagonally inward from each corner. The 1 inch 6-32 internally threaded spacers are modified by adding a short length of 6-32 threaded shaft to one end of each, simplifying assembly.

Component assembly on the boards is largely a matter of plugging in Vector T9.4 lugs. The finished product looks much better if some thought is given to facing the lugs in one of two directions. Mounting and transistor holes should be drilled and reamed to size before installing lugs.

The general arrangement puts all wiring on one side of the board and practically all components on the other side. This approach seems a little inflexible but is straightforward and looks good.

Possible board orientation problems may be overcome by working out a handling and wiring procedure that doesn't require constant reference to actual components. A good approach assumes that the board is only turned over an imaginary hinge at its bottom edge, so that top down when one side is up becomes bottom up when the other side is down. This preserves left-right relationships. Another useful convention is that all supply wiring goes to left-hand end of components.

Wiring is carried out one network (plus supply lines; ground lines; interstage lines, etc.) at a time, with prearranged color coding. Bare wire goes for short runs and where there is no chance of a short. Solder each lug when convenient. #22 solid wire fits the T9.4 lugs well, but flexible stranded wire is used for the four lines from one board to the other.

Transistors precede other components into the board, because they are convenient position markers. They are placed in their mounting holes in the board from the component side, and their leads brought to the T9.4 lugs. Then the other components are mounted on the boards. Diode and electrolytic capacitor mounting polarity should be double checked. The T9.4 lugs may need a little bending before they will take a good grip on the components, but no component soldering is done until everything is installed.

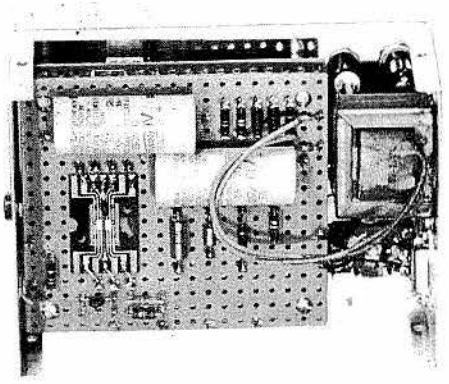

Inside the assembled thin-line generator showing the component side of the power supply and IC board.

Trimmer capacitor C3 is mounted on its tabs just under the top panel. Then a small screwdriver access hole is drilled over it in the panel, before painting, for vernier frequency adjustment after final assembly.

Certain components are matched before installation. An ohmmeter and a capacitor checker will do a satisfactory job of selecting C1 and C2, and R4 and R6, for equal values. These components are chosen alike for best symmetry of the 100-kHz oscillator operation. It might be good planning to leave these components unsoldered until tuning is completed, but everything else can be soldered to the board at this point. Note that the R3 and R5 sites do not get resistors until later.

Two optional capacitor sites are included. These are for C4, an additional and probably unnecessary padder across the crystal; and C7A, which can be added to increase the width of the thin line pulse.

Apparently, the digital IC comes in a specially designed package for testing before use. To mount the IC, solder a ⅜ inch piece of #22 wire in each of the T9.4 lugs carrying supply and signal voltages to the IC. Place the IC between the two rows of lugs, bend the wires against the proper terminals, and solder. No other mounting is required.

The original breadboard showed a lot of transient noise in its supply circuit. This originated from the IC, which was trying to get big chunks of current to manufacture pulses. Since the IC cannot deliver frequencies not available from the supply lines, very careful bypassing is indicated.

High-frequency bypassing consists of C9, a .01μF disc ceramic capacitor across the IC supply terminals on the wiring side of the board, and C10, a 100 picofarad capacitor soldered directly between supply terminals on the IC. The capacitor leads are provided with spaghetti insulation and placed for minimum open space between the capacitor leads and the IC's supply leads.

Testing before final assembly is very easy, because the odd appearing board layouts go together giving a structure that opens out like a book. The hinge is the four leads between boards. Leave transformer leads long, so that the circuit may be tested well free of its cabinet.

The upper half of the Premier box is prepared by a powerful cleaner which removes its original paint. After thorough removal of the cleaner, the metal is roughened with wet sandpaper, rinsed in vinegar solution and then clear water, leaving a very good surface that does not require priming for excellent paint adhesion. Watch out for greasy fingerprints.

Rustoleum #868 Green applied from a convenient spray can gives a fine finish. Follow instructions on the can. After drying, the fresh, clean enamel will take waterproof India ink, applied with a Leroy drafting pen. When the ink is thoroughly dry, a final coat of Rustoleum #717 Clear finishes the job. The enamel is soft at first, but hardens into a coat durable in normal lab use.

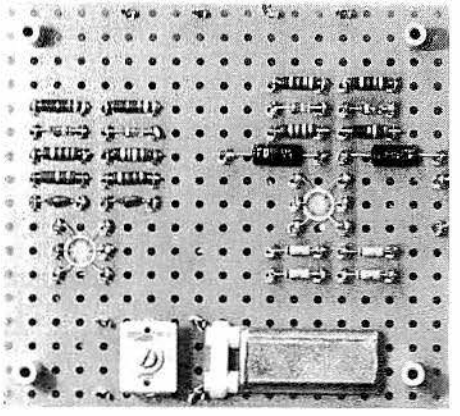

View of the component side of the astable oscillators board.

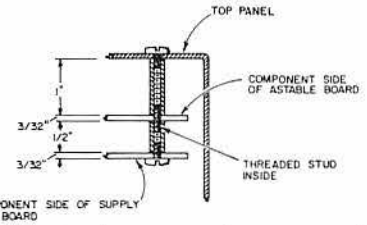

Fig. 6. Mounting dimensions and spacer assembly diagram.

Table of special parts

Crystal: 100 kHz parallel resonant 32 pF. shunt capacitance normally designed quartz crystal.

The following parts were obtained from Solid State Sales, P. O. Box 74, Somerville, Mass. 02143.

T1 & T2: 2N2060 type dual NPN transistor

D1, D2, D3, D4: fast point-contact Germanium diodes coded 1N59

D5, D6, D7, D8: fast point-contact Silicon diodes marked S284GM

G1: surplus digital integrated circuit Solid State Sales type G1. (comes with data sheet)

Tuning up

The generator should be zeroed to frequency before installation in its case. This is a two-step process. First, the 100-kHz astable base resistances are adjusted by choosing resistors for R3 and R5 to bring the oscillator frequency within trimmer range of 100 kHz, perhaps a few hundred cycles high at 15 MHz. Then the trimming capacitor brings the frequency to accurate coincidence with WWV.

To roughly zero the generator, set the trimmer capacitor, C3, at minimum capacitance. Identify WWV on a short-wave receiver, and tune around a bit to familiarize yourself with what's happening in the vicinity. It would be nice if things are fairly quiet.

Then put 4.7k resistors into the astable board at the R3 and R5 sites, turn on the generator, and look around for the signal. Depending upon actual values of C1 and C2, the signal may be on either side of WWV but is likely to be on the high side. If so, try again with resistors one size larger, which will lower the frequency. You should shortly find resistors that bring the frequency near enough to WWV for final zeroing with the capacitor. Verify tuning range on both sides of WWV.

Correct values for R3 and R5 may be approximated very quickly if a good triggered scope is available. Try selecting resistors for a period of 11.4 microseconds with the crystal removed.

Using the thin line generator

A breadboard test showed that (as might have been expected) there should be some way to distinguish generator signals from other CW signals. The continuous/intermittent feature provides the marking, and once the correct signal is located the generator can be switched to "continuous" for accurate work.

At low frequencies, the generator output and behavior resembles a conventional 100-kHz standard. The signal simply is not as strong. A greater difference appears at higher frequencies: the original model yields an audible beat note at 80-MHz from a diode mixer through an inexpensive audio amplifier. And another test shows a usable signal at 432 MHz: the 4,320th harmonic.

Some connection to the receiver or other detector is required. This is a natural consequence of a circuit design that puts the signal where it belongs, rather than spraying it all over the lab. A few picofarads coupling capacitance is sufficient at all frequencies.

Perhaps this circuit can be used for purposes other than a frequency standard. Its moderate amplitude but wideband output should be ideal for detecting changes in receiver sensitivity over a broad tuning range. In fact, with a little decoupling of the input leads and provision of a coax output connector the generator should do well as a stable, reliable small-signal source. A piece of adjustable waveguide-below-cutoff would make an excellent attenuator for work not requiring exact measurements. Another thought that occurs is possible further development by provision of some arrangement for detecting which harmonic is actually being heard.

Chapter VI

Crystal Calibrators

ALL BAND BAND-EDGE MARKER

Charles Berner WA2HRZ

This calibrator is complete with its own ac supply, eliminating the need for taking power from the receiver. If ac outlets are at a premium at your shack, the on-off switch and the line plug can be eliminated and the ac line connected across the receivers ac input so that the calibrator comes on whenever the receiver is turned on. A high density selenium rectifier was used and this contributes greatly to the compactness of the unit. The whole thing runs very cool and even after 24 hours operation, still isn't hot.

Wiring isn't too critical, but keep all leads short and direct. Using an octal socket for a xtal holder lets you use the unused pins as tiepoints and is recommended.

A Petersen type Z-2 xtal was used because it has a tolerance of .002%. This is one reason why no provision is made for "zeroing" the calibrator against a standard. The other is that there isn't any such standard as WWV for use. However, if this provision is desired, C1, the 56 mmfd capacitor, connected to pin 1 of the 6BH6 thru the 18K resistor, can be made variable. Also, if band edge markers are wanted for 50 mc and up, a 5 mc xtal may be substituted when this function is wanted and C1 made variable for "zeroing" against WWV.

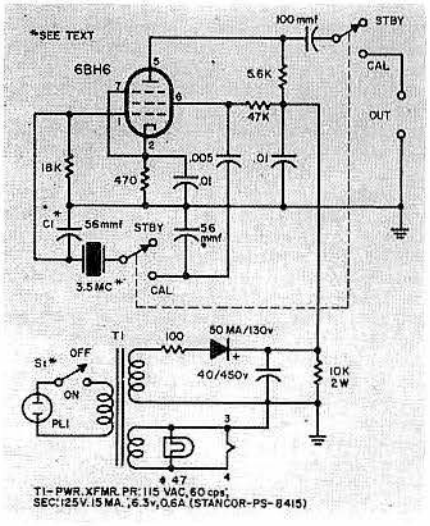

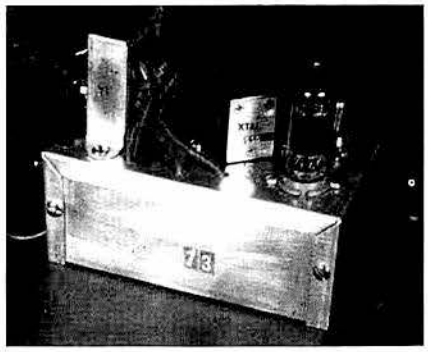

This gadget can also be used as a xtal activity checker by simply replacing the marker xtal with the xtal to be tested. Tuning your receiver should get you a strong signal at the xtal's fundamental if it is OK.

Table 1:

Band	Harmonic 3.5 mc	100 kc	Marker Frequency
80 meters	1	35	3.5 mc
40 "	2	70	7.0 mc
20 "	4	140	14.0 mc
15 "	6	210	21.0 mc
10 "	8	280	28.0 mc
6 "	15	525	52.5 mc
2 "	42	1470	147.0 mc
1¼ "	63	2205	220.5 mc
1¼ "	64	2240	224.0 mc

THE MULTICAL

E. R. Davisson K9VXL

What is the "Multical"? As the name implies, "multi" would suggest several uses, and "cal" might infer a calibrator of some sort.

Well, that's right, but there is slightly more significance to the name. "Multi" is also a short form term used to describe flip-flop circuits known as multivibrators.

By combining the basic characteristics of a free-running multivibrator (astable) with crystal control, you have a simple, stable, virtually-insensitive-to-temperature-changes, crystal calibrator for that receiver you have been wondering about.

The circuit uses no inductors and depends upon the crystal for the proper feedback for oscillations. Temperature stability is partially due to the absence of capacitors.

Transistor stage Q_2 operates with unity gain, whereas transistor Q_1 operates at considerably more gain. Both stages are operating as feedback amplifiers. The harmonic generator diode D_1 is a 1N128. Any general purpose diode may be used.

By using the multivibrator circuit, the waveform obtained is comparatively rich in harmonics and could be used without any further refinements. However, to insure useful harmonics through 30 MHz starting from a 100 kHz crystal, a harmonic generator consisting of R_6 and D_1 shown in **Fig. 1** was added. The capacitors C_1 and C_2 are used strictly for coupling and have no effect on frequency stability.

Crystals from 100 kHz up to 1 MHz may be used in the Multical with no changes. The circuit will oscillate from voltages as low as 2 volts and can be operated safely from voltages as high as 20 volts. This wide range of voltage operation allows the source to be obtained from virtually any place.

Output from the calibrator may be fed directly into the receiver's input, or may be coupled to a short whip antenna. With a whip antenna, close coupling to the receiver's input

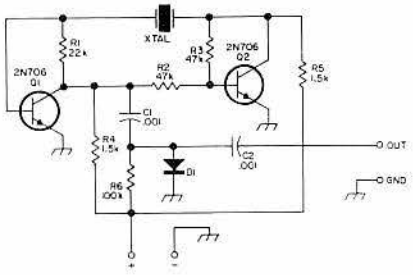

Fig. 1. Schematic of the Multical.

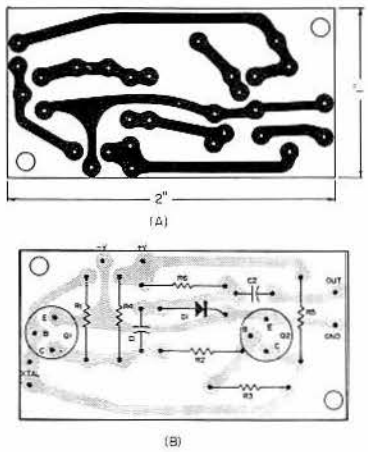

Fig. 2. Suggested printed circuit board layout for the Multical. A gives the copper side, B the component side. A board for the Multical is available for $1 from the Harris Company, 56 E. Main Street, Torrington, Conn.

may be required at higher frequencies. (Especially at the lower voltage levels.)

For the more ambitious builders, **Fig. 2** shows the printed circuit board layout for the Multical. Due to its small physical size (1" x 2"), room can probably be found even in the most compact of receivers. **Fig. 2A** shows the foil side, and **2B** shows the parts placement.

So the next time you wonder about the accuracy of your receiver calibration, give this simple circuit a try and you'll know for sure.

100 KHZ MARKER GENERATOR

W. W. Davey W7CJB

This useful piece of equipment generates usable harmonics from 100 kHz to 225 MHz. It is completely self contained and portable which makes it convenient not only to use in the ham shack, but also in the mobile unit or at a field day location. Its use lies mainly in accurately spotting band edges and 100 kHz calibration points throughout the ham bands.

Most modern day home receivers are equipped with calibrators, but these calibrators are of little use when needed to spot frequencies on VHF and UHF converters or portable equipment.

The generator is constructed in a 2¼ x 4¼ x 1½ inch handi-box. The parts are mounted on a vector board, and the entire unit is powered by one #216 nine volt battery or its equivalent.

Hints on construction First obtain some vector board. The piece I used was cut from the board supplied in a "GE experimenters aid hobbyist kit." The board must be cut to size before construction and will measure 3½ x 2 inches. This will allow room for the 9 volt battery in the end of the handi-box. Make sure the newly cut vector board will fit inside the handi-box before you start mounting parts. It might save a lot of trimming at a later date.

The parts layout is not critical. Components may be arranged as shown in the

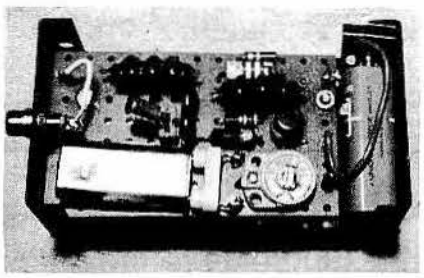

photo or in any other arrangement suitable to the components you may be using. I used sockets for the transistors, as I wanted to be able to experiment to see which transistors from my junk box would give the most output in the VHF and UHF bands. I ended up using the 2N404 for the oscillator and a 2N384 in the multiplier stage. I also found that Japanese 2SA83 transistors which had been removed from the *if* stages of a junked transistor radio, would work equally well in both sockets.

All components are mounted on the top of the Vector board with the exception of C4 and C5. For the most part, wiring can be completed with existing leads on components. The push-in terminals furnished with the GE experimenters kit were used for the battery connections, antenna connection and for mounting the crystal socket. The circuit board can be mounted to the handi-box with three 11/16 inch bushings. This leaves room for a slide switch to be mounted on the cover of the handi-box. Two of these bushings were purposely placed at the end of the board to form a sort of socket to hold the 9 Volt battery. The antenna output connector which is mounted on the handi-box is a switchcraft #3501FP phono jack. A small hole may be drilled in

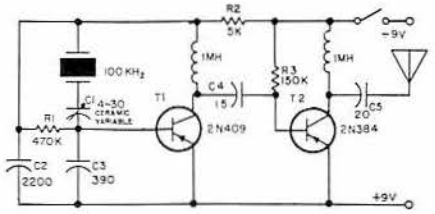

the bottom of the handi-box through which a screwdriver may be inserted for adjusting C1. For extreme accuracy C1 is adjusted to zero beat with WWV.

A 36 inch piece of insulated wire soldered into a phono plug may be inserted into the phono jack and used as a test antenna. The intensity of the markers may be varied by

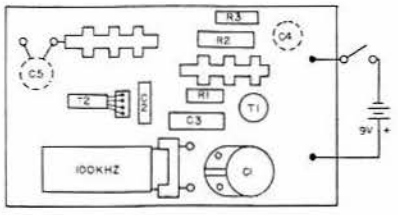

moving this test antenna near your receiver antenna lead-in. If you are using a coax lead-in you can couple by drilling a small hole in your coax relay so that the test antenna can be inserted near the relay armature. You will find that most SWR meters provide an easy method of coupling to the center conductor of the coax. As a last resort you can always couple to the receiver or converter antenna coil.

I have made very good use of this gadget to spot frequencies in the 144 and 220 MHz bands. It was well worth the time and effort it took to build it.

ALL BAND FREQUENCY MARKER

Kenneth W. Robbins WIKNI

Crystal controlled marker generators are useful adjuncts in any frequency determining situation requiring high accuracy, such as locating band edges, sub-bands and calibrating receivers. If you've been entertaining thoughts about construction of one, a version is described here which uses the new C/MOS integrated circuits powered by a 9 volt transistor radio battery. And instead of the usual rotary harmonic selector switch, a multi-pin IC connector strip and three test plugs serve as a miniature patch panel to enable various divisions of the reference crystal, with a maximum countdown of 256. "Rocks" from 100 kHz to 4 MHz oscillate readily in this circuit. In this model an FT241 xtal set to 400,000 Hz has been chosen for control and has usable receiver calibration divisions down to 2.5 kHz. The harmonic spectrum extends to at least 160 MHz, the tuning limit of a transistor superregen used in testing. When used in densely

Divide by	Output, kHz
1	400
2	200
4	100
8	50
10	40
16	25
20	20
40	10
80	5
100	4
160	2.5

Table 1.

occupied HF bands, an AM beeper can be switched on as an identification aid.

Referring to Fig. 1, one third of a hex inverter makes up a crystal controlled oscillator and buffer, another third is a slow rate pulser and the two remaining units function in the dividing section. These are all standard circuits described in RCA's COS/MOS Data Book #SSD-203. An emitter follower minimizes loading on the IC outputs, speeds up rise time to increase harmonic content, and provides a low impedance output. The AM

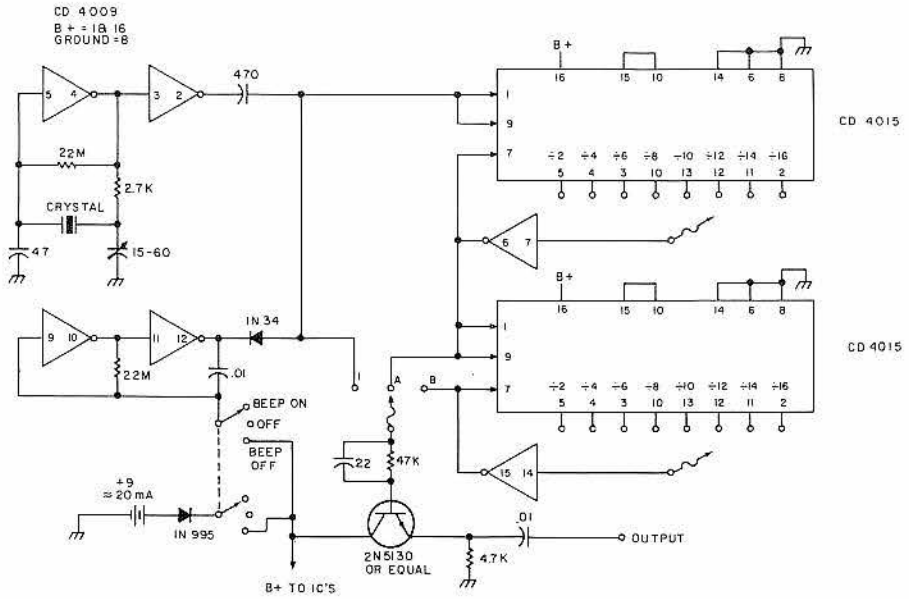

Fig. 1. Schematic.

beeper is a simple clamp that gates rf on or off to following stages.

Photo 1 shows all components mounted on Vector P pattern perf-board that fits inside a Bud minibox. Sleeving 3/8" (10mm) long is slipped over the wire trap terminals of the contact strip to space it up from the board. A DPDT center-off miniature toggle switch acts as one board to panel spacer. Diagonally across from it, a 4-40 threaded rod conducts emitter follower output up through the front panel via a 1/2" (13mm) insulating spacer and plastic shoulder washers. Two regular 4-40 screws and spacers complete the four corner mounting. This spacing allows the contact strip to project partly through a panel cutout so that it is mechanically secure without fastening.

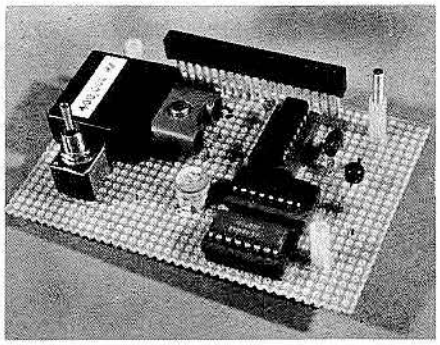

Photo 1.

Photo 2 (completed assembly) shows a stick-on label with patching connection call-outs for various division ratios. If only one crystal is employed, labeling could indicate most used frequencies instead. A typical frequency vs division listing for this model is shown in Table 1. You can easily make up a complete table of all possible ratios, remembering that each CD4015 shift register divides by even numbers ONLY, starting at 2 and ending at 16.

Uses to which a marker generator may be put have been described before: i-f alignment, BFO, scope linearity, etc. A type that divides down to the audio range like this one is especially useful in checking superhets. A very broad and flat spectrum of overlapping signals is generated and an audio tone will be heard no matter where the set is tuned. If its tracking and sensitivity are top-notch, the S meter will hold steady over the tuning range. Tracking adjustment amounts to tweaking for maximum meter reading or loudest audio tone. Then patch for 100 KHz markers and check calibration. It's a lot faster and easier than using a conventional signal generator.

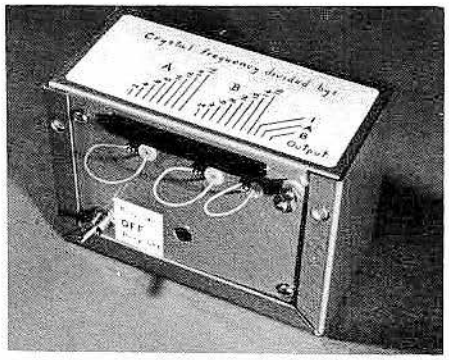

Photo 2.

1	CD4009	1	15/60pF trimmer
2	CD4015	1	.01 uF
1	1N34	1	xtal; see text
1	1N995	1	xtal socket
1	2N5130 or equiv.	1	Alco #MST205P switch
1	2.7k	1	Bud #CU-2115HG minibox
1	4.7k	1	Vector #44P29-062 perfboard
1	47k	1	#216 battery
2	22M	1	Battery connector
1	22pF	3	16 pin IC sockets
1	47pF	3	Augat patch pins or equiv.
1	100pF	1	20 pin contact strip
1	470pF		SAE #Series 7000

Table 2. Parts List.

POOR MAN'S UNIVERSAL FREQUENCY GENERATOR

John Schultz W2EEY

As precise frequency control and measurement becomes more and more a part of the amateur radio game, the need develops for test instruments that deliver a wide range of both rf and af signals of high accuracy. It would be ideal if everyone could have a frequency counter and a synthesizer type rf and af generator but that is hardly the case. Most amateurs must utilize their basic station gear along with selected accessory items to test out and adjust equipment. This article describes a very useful accessory item that for a modest cost goes a long way toward having some of the expensive test equipment just mentioned. The item to be described is somewhat like a grid-dip meter in that it is basically a simple type of oscillator but as one gets to know and use it, new uses for it are found and its versatility constantly expands.

Circuit Description

Figure 1 shows the circuit diagram of the test generator. Basically, it consists of a string of SN7490 decade counters which are used to divide down a selected input signal by a factor of 10 or 2. The input signal can come from a 1 MHz master oscillator, a special crystal oscillator for externally used crystals or from any external sine-wave source. The special crystal oscillator which uses a SN7400 will operate with almost any basic or overtone crystal in the hf range. It can be used for crystals in the low frequency and lower VHF range also by a simple

modification. One gate of the SN7400 crystal oscillator is used to drive a LED which will indicate that the crystal is oscillating so it serves as a crystal activity indicator as well. When an external sine-wave source is used, it is first coupled through a SN74121 multivibrator. This stage squares off the sine wave so it can better drive the subsequent frequency divider chain.

The frequency divider chain is fixed, although one could easily switch the individual SN7490 units to divide by different ratios when desired. This should be obvious by noting the wiring of the divide by 2 SN7490 with that of the divide by 10 units. However, the variety of frequencies which can be generated then with different input sources becomes confusing and more than would normally be needed.

The fixed divider chain follows the sequence: divide by 10, divide by 2, divide by 10, divide by 10. A separate branch after the first divide by 10 unit goes through two other divide by 10 stages. In the case of the divider chain being driven by the 1 MHz master oscillator, this results in the following output frequencies being simultaneously present: 1 MHz (basic oscillator output), 100 kHz, 50 kHz, 10 kHz, 5000 Hz, 1000 Hz and 500 Hz. With any other frequency input source you can easily calculate what frequency outputs the divider chain will bring in both the rf and af regions. Many surplus crystals will produce interesting frequencies of high stability in the af region that can be used for test purposes.

When using the special crystal oscillator, the LED will glow to indicate that oscillation is taking place. As shown with a 150 pF capacitor from one side of the crystal oscillator circuit to ground, the oscillator will work satisfactorily with hf crystals. Its range of oscillation can be extended to lf as well as high frequency overtone crystals by changing this capacitor. The value of capacitor required in picofarads is 500 divided by the frequency of the crystal in MHz. This value need, however, to be only approximate unless you require an absolutely square wave output from the unit.

When using the multivibrator input about a 1½ to 2V peak input, either sine-wave or approximate square wave is required.

Construction

The whole unit can be constructed on a piece of perforated board about 3 x 2 in. and made completely portable if powered by a 4½V battery (Burgess No.532) or just three D cells in series. This arrangement does not provide the absolutely best stability for the 1 MHz master oscillator but unless you intend to use the unit for marker frequency generation in the VHF range, it is a perfectly satisfactory arrangement. Alternatively, one could power the ICs from any standard 5.5V regulated supply used for IC digital circuitry.

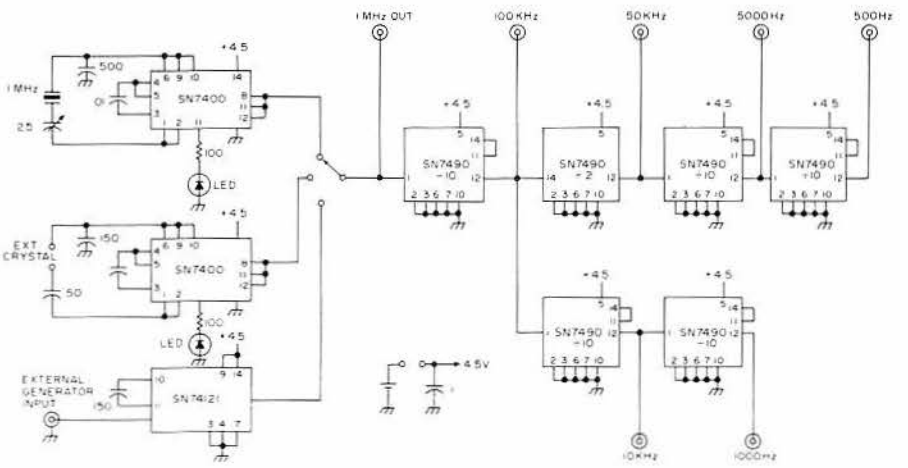

Fig. 1. Diagram of universal frequency generator. Output frequencies shown are for using 1 MHz oscillator.

I constructed my unit for battery powered operation and enclosed the unit in a small aluminum mini-box. The output of each divider was brought to a pin jack on the front panel of the unit.

One simple way to wire the relatively small number of ICs involved is to purchase perforated board which has hole spacing to fit standard DIP and preferably with a copper pad still left around each hole. The ICs are then placed on the board and the appropriate pins which either go to ground or to the 4.5V line bent in different directions. The ground line is run along one side of the IC and the 4.5V line along the other side and bare wire used to connect the appropriate pins to either line. Figure 2, illustrates the wiring for one of the divide by 10 ICs. When one starts this process on the board, it will be surprising how fast the wiring is completed. Individual insulated wire jumpers are used to make the input/output connections between ICs. The wiring is not critical and using a receiver to hear the markers, or an audio amplifier for the lower frequency outputs, one should be able to determine quickly if the circuit is working. The frequency of the 1 MHz master oscillator may be brought exactly on frequency using the 25 pF trimmer in the circuit and checking against WWV with a harmonic of the oscillator or by using a counter.

Applications

As I mentioned before, the applications that you can find for the generator really begin to unfold only after you have had it around the shack for awhile. Some of the applications would be:

1. A frequency marker generator for receiver calibration. The markers are usable up into the VHF range.

2. To extend the range of present rf or af signal generators into lower frequency ranges than they presently cover.

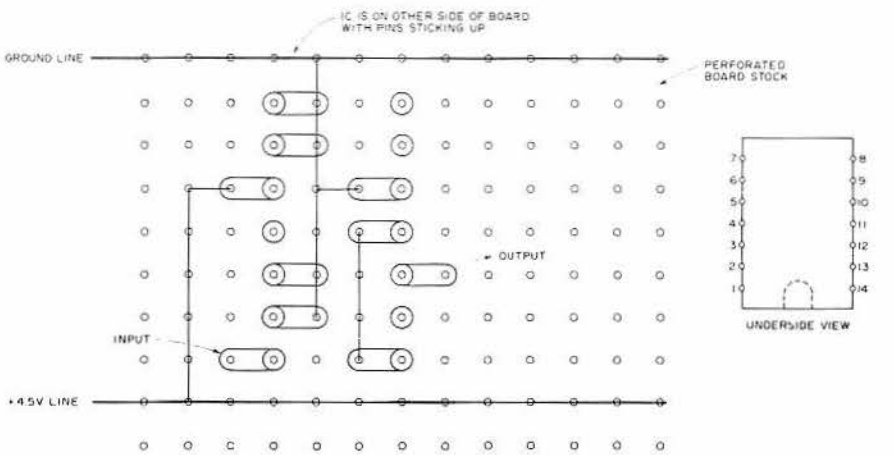

Fig. 2. Perforated board wiring of ICs. One SN 7490 divide by 10 unit is shown wired.

3. To perform stability checks on high frequency variable oscillators. The divider chain will always perform precisely and you can monitor the change in frequency of a higher frequency oscillator with a stable low frequency receiver.

4. A frequency generator to generate precise rf or af square wave signals at any frequency desired by choosing the proper crystal.

5. A crystal activity checker.

6. By taking two or more of the simultaneous outputs together via mixing diodes and a series tuned circuit resonant at the desired frequency, you can also mix the divider outputs to generate a variety of intermediate frequency outputs.

CALIBRATE THAT CALIBRATOR

Mitchel Katz W2KPE

Most modern receivers and transceivers in use today rely upon a 100 kHz crystal oscillator to calibrate the tuning dial. While some of the calibrators are built in, others come as outboard accessories. In any event the operation of each is the same.

By this time we all probably know what "zero beating" is. The 100 kHz oscillator in order to serve as a calibrator must be "zeroed" to some standard frequency such as the WWV carrier frequency on 5, 10, 15, 20, etc. MHz. With a CW or AM receiver, we can very easily tune through the zero beat point. On SSB receivers because one of the sidebands is missing we can only hear the one side as we approach zero. The other side of zero is greatly attenuated and may possibly not be heard at all. To further complicate matters for us in trying to calibrate the 100 kHz oscillator, as we can only hear down to about 20 Hz, we can't zero in any closer than this. Leaving the receiver at this point, we next turn on the 100 kHz calibrate oscillator. After a suitable warm up period, we turn the tune control of the oscillator and again adjust for a zero beat condition against the WWV frequency. With this method of calibration we have several possible sources of error. First in zeroing WWV with the receiver beat frequency oscillator and then zero beating the 100 kHz calibrator against the bfo. Each of these adjustments is limited to the lower limit of our hearing range, as well as the fact that we are obtaining the zero beat at a relatively low i-f frequency.

A more accurate method of calibrating the 100 kHz oscillator will now be discussed. After the receiver and calibrator oscillator have been warmed up for about 30 minutes, tune in WWV on a frequency that produces a fairly good, steady signal. Adjust the tuning for maximum reading on the S-meter. Having tuned in WWV, turn *off* the beat frequency oscillator. Now turn on the 100 kHz oscillator that is to be calibrated. If a harmonic of this oscillator is fairly close to the WWV frequency, a beat note will be heard. At this time adjust the calibrator "crystal tune" control and the S-meter will start pulsing from a maximum to a minimum value. The closer you get to dead center the slower the pulsing action will become. It is fairly easy to come down to 1 pulse per second with this method. If your receiver doesn't have a meter, you can also hear this pulsation very clearly. In any event you would always tune for the slowest pulse rate.

Note that with this method we have adjusted the calibrator frequency harmonic directly to the WWV carrier rather than to a low i-f. We have eliminated one zero beating step, and this, together with the fact that we are obtaining the zero beat at a much higher frequency, will provide greater accuracy.

Having described the method, here are a few points of general interest:

1. Before attempting any calibration let the equipment heat up for at least a half hour to stabilize.

2. After tuning in WWV, wait until the 400 Hz modulating tone goes off before adjusting the calibrator. If not, you may find later that you zero beat the 400 Hz instead of the carrier frequency!

3. The levels produced in the receiver by WWV and the calibrator oscillator should be about equal to produce a good beat between the two frequencies.

4. Use the highest WWV frequency that will produce a good, stable signal in the receiver. Certainly a 1 pulse per second beat at 20 MHz will provide greater calibration accuracy than 1 pps beat at 5 MHz or better yet than 455 kHz! The accuracy will be considerably greater and it is no more difficult to come by.

A SIMPLE FREQUENCY DEVIATION METER

John Reinartz K6BJ

A frequency-deviation meter allows one to read the deviation plus or minus that a received signal is off frequency. Depending on the meter range desired and used, a deviation of ten or less cycles can be read either high or low. Such a device is especially useful when used on MARS nets or when frequency checks are desired of any incoming signal and the answer must be in cycles low or high of a desired frequency. Those grinding their own crystals or desiring to compare crystals will find this device especially useful.

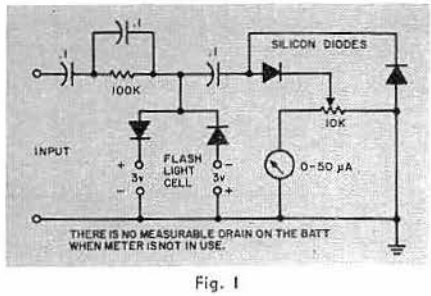

Fig. 1

Two fundamental circuits were investigated, one using diodes only and the other using transistors only. These are shown in Fig. 1 and 2 respectively. A 0-50 microampere meter should be used for the diode type and a 0-1 milliampere meter will serve nicely for the transistor type, although a 0-50 or 0-100 microampere meter will also serve nicely in the transistor type frequency-deviation meter system. Silicon diodes were used for the diode type and 2N123 for the transistor type. An input voltage of 25 is needed for the diode type and 7 volts or less for the transistor type depending on the meter sensitivity, being 2 volts when a 50 microampere meter is used.

Whatever scale reading is desired, be it 250 cycles low or high or 500 cycles low or high, the meter cover is removed and new figures are added below the meter scale with a zero in the center of the scale and maximum readings at each end of the scale as appropriate. Pencil markings will do. The 250 cycle can be read to 10 cycles per division and the 500 cycle scale can be read to 20 cycles per scale division. Each can be read to half these values or 5 and 10 cycles respectively.

In use, you set your frequency meter, LM or 221 either 250 cycles or 500 cycles lower

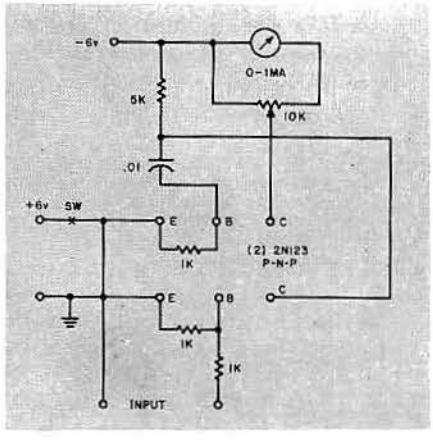

Fig. 2

than the frequency to be checked. If the frequency to be checked is right on, the frequency-deviation meter will read zero at the center of the scale on the meter; if the frequency is low, the meter will read low and if higher, the meter will read higher. The answer in cycles will be the value indicated by your new markings. In use the frequency-deviation meter is connected across the high impedance output of your receiver in the case of the diode type and across the low impedance output in the case of the transistor type.

In those cases where a definite frequency will be under observation, it will be found advantageous to grind or obtain a crystal that is adjustable to 250 cycles low or 500 cycles low, as appropriate, and to use it in the transistorized oscillator shown in Fig. 3. Any crystal holder that has an adjustable air gap will do. Some of the TCS surplus crystal holders have a three point adjustable top plate and are about the best obtainable. Since your

best and probably only method of adjusting the crystal is by the use of your LM or BC221, be sure that your frequency standard is accurate. It is best to use the low frequency position and with the 1 mc crystal switch on, tune the meter to that portion of the desired frequency less the mc part. For instance, to set the LM for a reading of 2,732,000 cycles, set the LM on the low frequency for 732,000 cycles or 732 kc. The 1 mc crystal will furnish the mc part of the reading. In my case I set the LM to 731.5 kc and adjust the crystal to that

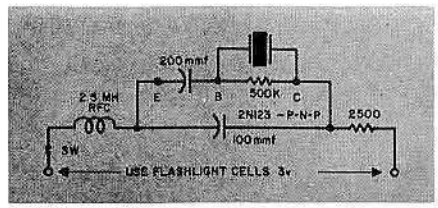

Fig. 3

frequency in the adjustable TCS holder. The transistorized oscillator holds the frequency to such a close tolerance it has not been necessary to make adjustments in weeks. A hand held push switch connected into the positive battery lead allows the oscillator to be turned on as needed to check the frequency of a MARS station on 2732 kc to an accuracy of plus or minus 10 cycles of that frequency. The frequency-deviation meter is of course checked against the 440 or 600 cycle tone of WWV, no other check is necessary since the scale is linear.

Chapter VII

GDOs

THE INDICATING OSCILLATOR

Ken Brown KH6AF

Relatives of this little gadget have been around a long time! Even the transistorized versions, which usually leave something to be desired. With an FET, however, we are back in business as with tubes, but with many advantages.

The range of this oscillator is fantastic. That is, without any circuit tricks or special handling. The low frequency end was carried down to the 1 MHz in order to cover the lowest ham band. The high end takes care of 250 MHz easily. This can be extended with a little more effort.

Use of a field-effect transistor (FET) allows operation more nearly like the tubes with which we are, perhaps, more familiar. However, we are not tied to the power lines, which alone makes it worthwhile.

A 2N4221 FET was used in this indicating oscillator. Very likely other FETs will work also. The MOSFETs also should be as good, if not better. The new ones with built-in diode protection would be much easier to handle.

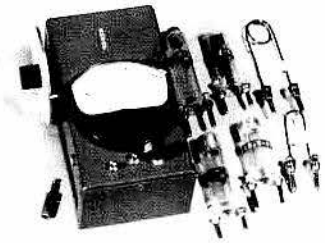

Standard banana plugs spaced ¾ in. make ideal bases for the coils. The lower frequency coils are wound on polystyrene forms.

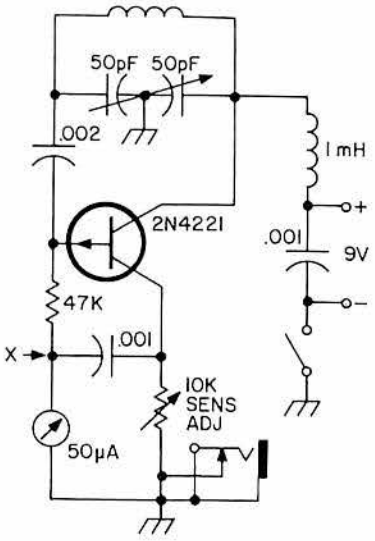

Fig. 1. Indicating oscillator circuit diagram.

The circuit (Fig.1) is not critical. However, the sensitivity control should not be bypassed. Layout could possibly be improved with a slightly larger box, allowing the dial to be placed on the face with the meter. It is a good idea to keep the layout symmetrical as far as possible, particularly the tuned circuit. This can be seen in the photo of the inside view. The box used was an LMB 532 EL with the cover reversed to allow for coil mounting insulator (polystryrene or other good rf insulating material). The meter should be a 50 μA movement; otherwise, a meter amplifier such as the one shown schematically in Fig. 2 will be necessary. This is no problem, as there is room for this amplifier on the circuit board.

A thumbwheel from a BC-375 tuning unit could be used very nicely as a dial. Three sides have been left clear for ease in placement of unit when in use. Plug-in coils makes for easy bank change and application to the job at hand. Standard-spaced banana pins allow for use with other accessories. Use 5/8 in. polystryrene tubing and stud-type banana pins.

A dual banana plug can be used during construction for setting the spacing accurately. The coils shown have the pins wired in place for stronger mechanical assembly. Drill a hole for about 24 AWG copper wire on each side of the pin studs which will lie along each side of the poly tubing. Use a number 59 or 60 drill. One wire is enough on each pin. Form a hairpin with about an inch of wire, push it through the drilled holes from the outside. Now twist tightly with longnose pliers, cut it off short, but not so short as to allow the wire to untwist! Then apply several coats of liquid "poly" cement. Be sure to move the coils frequently during the hardening period to make sure the liquid "poly" flows evenly over the stud and forms a slight fillet with the tube. Epoxy doesn't seem to work well with polystyrene. Neither Allied nor Newark list liquid polystyrene any longer, but your neighborhood hobby shop should be well stocked.

The lowest frequency coil (number 1, 0.95–2.2 MHz) was made from a Miller

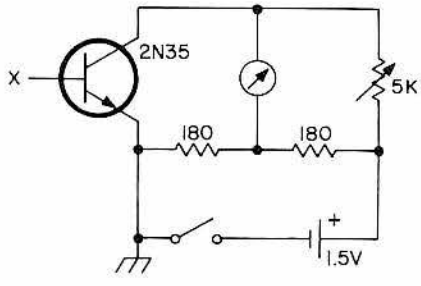

Fig. 2. This meter amplifier will increase the level of the signal so that a less-sensitive meter than 50 μA may be used.

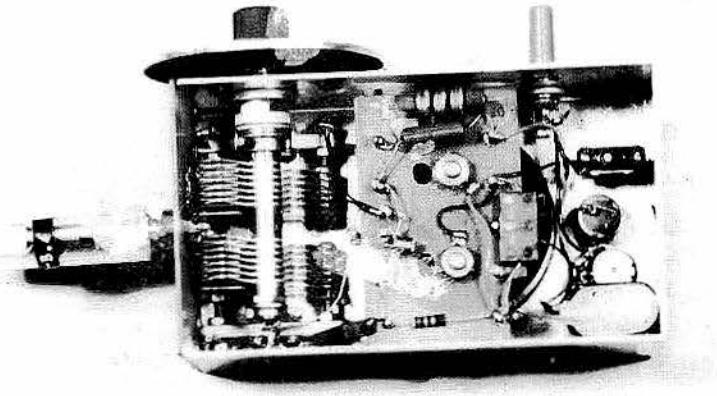

Interior view of oscillator with coil attached shows construction of the author's version.

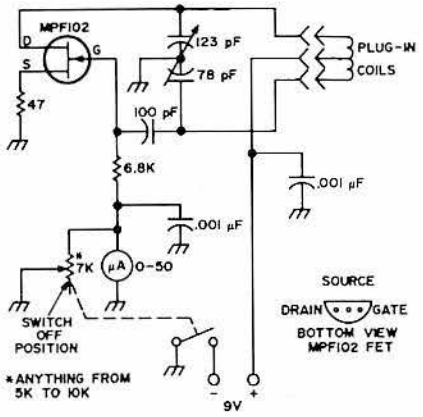

Fig. 1. Schematic diagram of the little gate dipper.

951 ferrite 0.5 mH choke with 6 or 8 turns removed – just enough to slip inside the poly tubing. Some reaming may be necessary. The number 2 coil (2.2–5.4 MHz) was made from a Miller ferrite antenna unit with the slug permanently installed in the top end and all lugs and mounting hardware removed. This coil was also mounted inside the poly tubing. The number 3 coil (5.4–13.5 MHz) consists of 32 turns of 28 AWG enameled wire, close-wound on the outside of the poly tubing. All coils are 2½ in. long with windings as near the end as practical. The number 4 coil (27–50 MHz) consists of 10 turns of 24 AWG enameled wire, close-wound. The number 5 coil (45–100 MHz) consists of 2 turns of 14 AWG enameled wire, self-supporting. The number 6 coil (60–270 MHz) is one hairpin loop 3/8 x 1 in.

A jack is provided for headphone use. The screwdriver-adjusted miniature pot is for zero adjustment of the meter amplifier. It can be seen in the photograph.

THE LITTLE GATE DIPPER

John Aggers W5ETT

Possibly you now own a grid dipper, but is it small, easy to handle, and cordless, making it completely portable? If not, you will want to build this gate dip meter. The cost is extremely low – only about $7. All parts are readily obtainable and construction is simple. The plug-in coil forms, using battery plugs and polystyrene tubing, are easy to make.

The Circuit

An MPF 102 FET is used in a modified Colpitts circuit. Except for the #1 coil, where a choke is used, the B+ is fed to the centertap of the coil. This is necessary to obtain a fairly constant gate current as the oscillator is tuned to its end frequencies. Drain current varies from 4 to 1 mA proceeding from 225 to 1.7 MHz. At the same time the gate current varies from 20 to well over 50 µA.

From this, it is apparent that the stronger the oscillations the smaller the drain current and the larger the gate current. In gate dip operation, as power is drawn from the oscillator the drain current will increase and the gate current will decrease or dip.

Limited wavemeter operation, obtained by switching off the B+, is accompanied by a slight shift in calibration. When the circuit picks up rf, the FET suddenly goes into oscillation using the rf as its battery. Thus, the amount of rf picked up must be large enough or there will be no oscillation and no meter indication. However, despite these deficiencies, it is still considered a useful mode of operation and for that reason has been included. It is only necessary to wire the sensitivity control so that the resistance is maximum when the switch is in the off position.

Construction

A natural finish aluminum minibox (4 x 2-1/8 x 1-5/8 in.) is used for the meter case. The variable capacitor came from an old transistor radio and measured 1 3/8 x 1/2 x 1 in. The shaft was already squared and tapped for a small screw. Since those listed in the catalogs have a plain or flat shaft, you will have to use a collar with setscrew, or drill and tap the shaft. The trimmer capacitors are not used and should be removed.

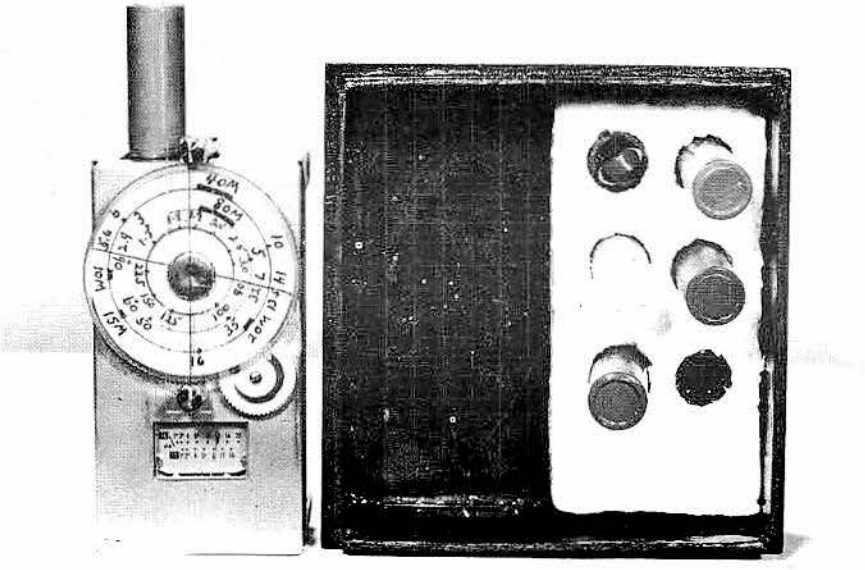

The little gate dipper with spare coils.

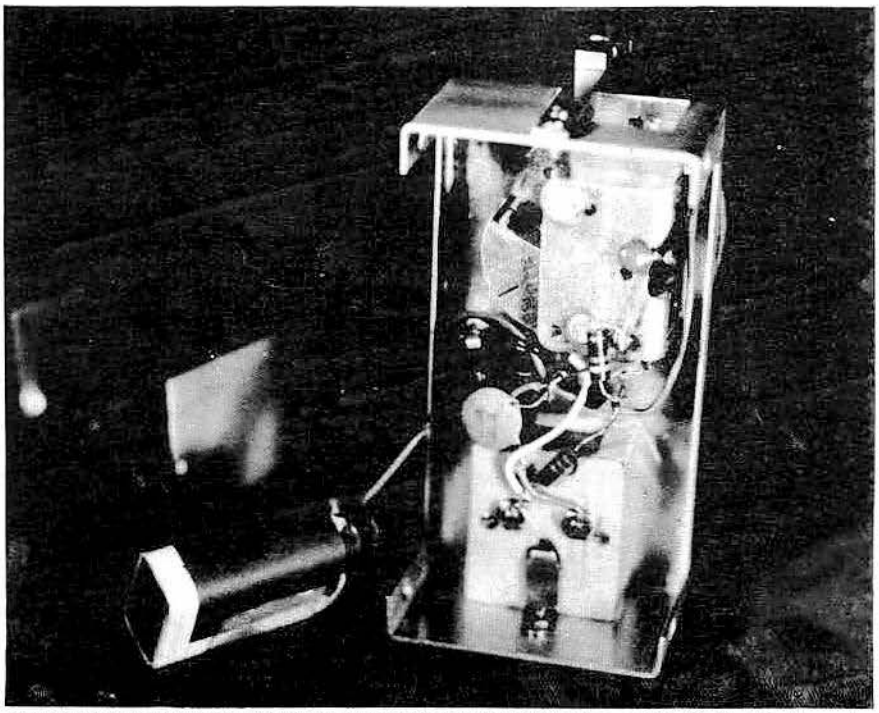

Meter is held against the front panel by a small bracket. The FET is the small black object in the center.

To make the coil socket you will need three pin receptacles from an octal socket, two pieces of 1/8 in. Plexiglas approximately 7/8 x 3/4 in., and one battery plug for a pattern. The pins of the battery plug form a triangle. I shall refer to the holes at the base as the outside holes. Drill holes in one piece of plastic to match the pins of the battery plug. Match the two pieces of plastic, clamp in a vise, and drill the two outside holes in the second piece. Bend the lug part of each socket pin to a right angle. Slip one over each outside pin of the battery plug. Using this as a jig, solder the lug portions to the stators of the variable capacitor. Remove the plug, and the pieces of plastic should fit down over the variable capacitor. The lug part of the center socket pin is brought out between the two layers of plastic.

File a small notch in the bottom piece to accommodate the lug. Before cementing the two pieces together and to the frame, make each hole slightly larger than the diameter of the socket pins. This will allow for expansion when the plug is inserted.

The dial is made of 2-1/4 in. diameter 1/8 in. Plexiglas. To give the dial a rough edge, for good thumb traction, I heated an old gear wheel and rigged up an arrangement to rotate the dial against it. The gear should have rather coarse teeth and rotate with the dial, or you will create flat spots.

The variable capacitor can now be mounted in the case. Position it so that the top and sides of the dial will be just about even with the edges of the case.

The dial marker is mounted on square aluminum posts. The top post (2 in. long) has 1½ in. of its length filed down to a 1/8 in. thickness to reduce its bulky appearance. To make the hairline, scribe a line in a ½ in. wide piece of plastic and fill in with a ballpoint pen.

The sensitivity control I used was already prepared for the knob shown. If you don't have one like it, use a dime-size pot and a setscrew knob. Any resistance from 5 to 10 kΩ will be fine.

Keystone light meters are available from Olson Electronics in a package of five ($3.99) or Transistors Unlimited Co. (75¢ each). Some modification of the meter is necessary. Remove the light cell and series resistor. Drill two holes, spaced ½ in. apart in the back of the case to pass 4–40 machine screws for easy soldering, make sure the heads and nuts are clean and free of any nickel plating. The screws should be filed even with nuts in order to make room for the battery. Solder the leads from the meter movement to the terminals, but be quick because the plastic case tends to melt in a hurry.

Wiring is just a here-to-there proposition, requiring no terminal boards or terminal lugs. The FET is soldered in place supported by its own leads. With reasonable care you should not damage it. A battery holder was found unnecessary; however, it is a good idea to wrap a layer of tape or stiff fiber paper around the battery to prevent the metal case from shorting out the meter terminals.

Coil Construction

Figure 2 and the photo give the necessary dimensions and show the parts needed to make the coil forms. The battery plugs are listed in the catalogs to fit #482 and

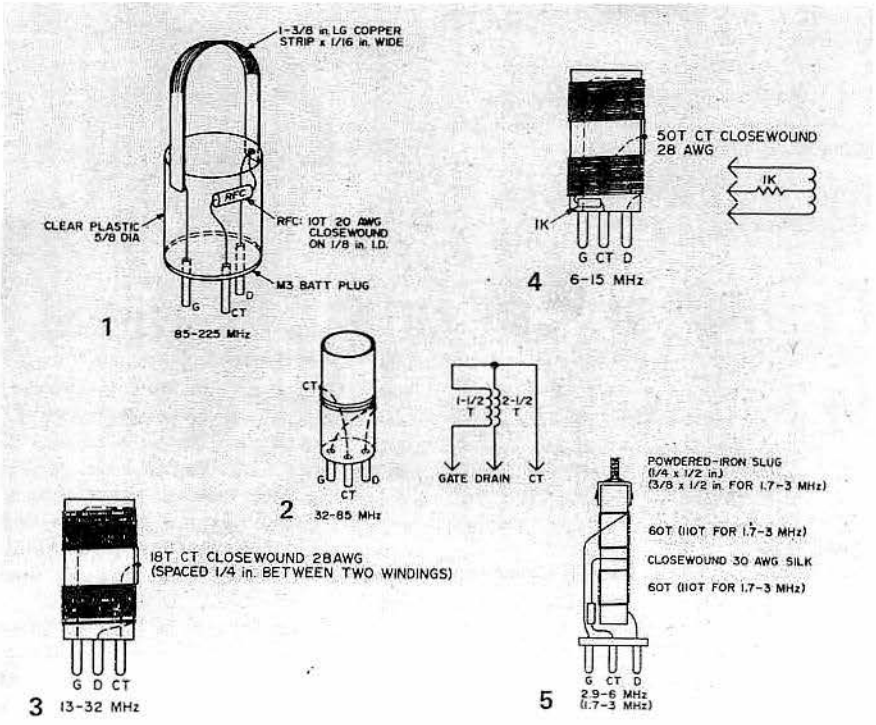

Fig. 2. Coil configurations for various frequencies of resonance.

M3 batteries. The center pin should be filed slightly shorter to make the plug seat evenly in the socket. While you are at it, file the nickel plating from the ends of all plug prongs. This will make for easier soldering.

Complete coil information is given in Fig. 2. However a little explanation may be in order. The irregular method of winding the #2 coil is necessary to reach 85 MHz and still maintain oscillation. With 4 turns close-wound the highest was too low. With the 4 turns spaced, oscillation ceased at the highest frequency. The 30 AWG silk wire was taken from a TV flyback transformer. The resistors in the centertap of the last three coils improve the meter's sensitivity slightly. They are mounted right next to the coil winding. With a slight groove filed inside the insulating sleeve, it should slip over the resistor.

The #6 coil is layer-wound as space permits and scrambled wound the rest of the necessary turns. The top winding of all coils should end near the very edge of the coil form. This will make for easier coupling to a tuned circuit. After the coils are checked out the insulating sleeves may be glued to the plug base.

Allow the glue to dry for several days before plugging the open ends of each coil with a small cardboard disk. The coils are painted with colored lacquers. Colored paper between the coil and the insulating sleeve will probably work just as well.

Calibration

For calibration purposes, you will need another indicating oscillator or dip meter. Operate it in the diode or wavemeter mode and loosely coupled to the gate dipper. I calibrated only 5 points on each scale plus any ham bands which appeared. Remember the dipper is not a frequency meter but something to get you in the ballpark.

Conclusion

The little gate dipper was checked against a well known commercial tube equivalent and, as near as I could tell, they were just about even. The battery should last for a long time because the current drain is extremely low.

THE GREAT DIPPER

John E. Boyd WAØAYP

Test equipment is essential in the ham-shack, as those of us have found when we attempted to get that new piece of home-brew perking for the first time. One of the most useful pieces of test equipment is the grid dip oscillator or simply, the GDO; besides being relatively inexpensive, it is particularly versatile. Need an indicating absorption wave meter? The GDO will do that. How about a modulated signal source? It handles that too. If you are interested in discovering its whole variety of uses, why not purchase one of several books on the subject.

Every item used in this GDO was selected with an eye toward the average home builder. There are no parts which must be specially purchased from the West Indies Export Company or similar outfit. Nearly all the parts, except for the meter, miniature pot, and mode switch, were obtained from the junkbox, or rather, from several junkboxes. If you insist on buying all new parts, total cost of the project will be about $20.

Circuit description

The grid-dip oscillator, in this case more properly termed an emitter-dip oscillator, gets its name from the fact that emitter current in transistor Q_1 decreases when the tuned circuit C_1-L_1 is in resonance with a nearby circuit. This decrease is easily seen by the dip of the meter indicating pointer.

When switched to the diode position, B+ is removed from the oscillator and the incoming rf is rectified by diode D_x; the voltage developed across the 2k resistor is amplified by the meter amplifier and monitored by the 0-1 mA meter. In switching to the signal position, B+ is removed from the meter amplifier but applied to the modulator, and a 1 kHz tone is available from one of the output jacks. In the modulated oscillator position, B+ is reapplied to the oscillator, and the oscillator is modulated by the 1 kHz tone.

Like a patch-work quilt, this GDO was built using circuits from already published articles or books and modified where necessary. The whole circuit is composed of three separate entities—oscillator, meter amplifier, and audio tone generator. The circuit is not particularly critical, but lead lengths and dress in the oscillator must follow good VHF practice, if stable VHF oscillation is to be maintained.

My operating time is spent on the various bands from 28 mHz to 432 mHz. Quite naturally, when I discovered that the GDO would

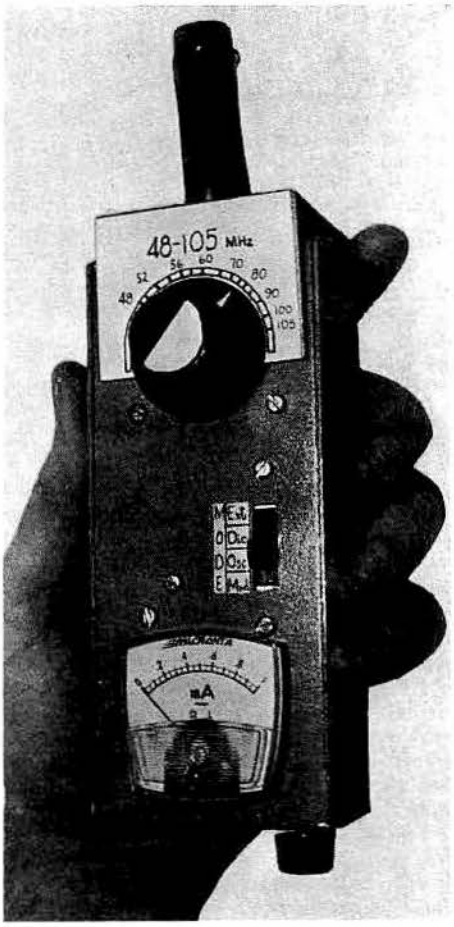

not oscillate satisfactorily over the entire range from 2 mHz to 200 mHz, I juggled values so that it would oscillate well at 216 mHz (for tuning frequency doublers to 432 mHz); then I tried to get as low in frequency as possible. Oscillation was vigorous to about 20 mHz. Coils and scales were then made to cover the respective ranges. It you don't do any homebrewing on the VHF bands perhaps you will find it necessary to

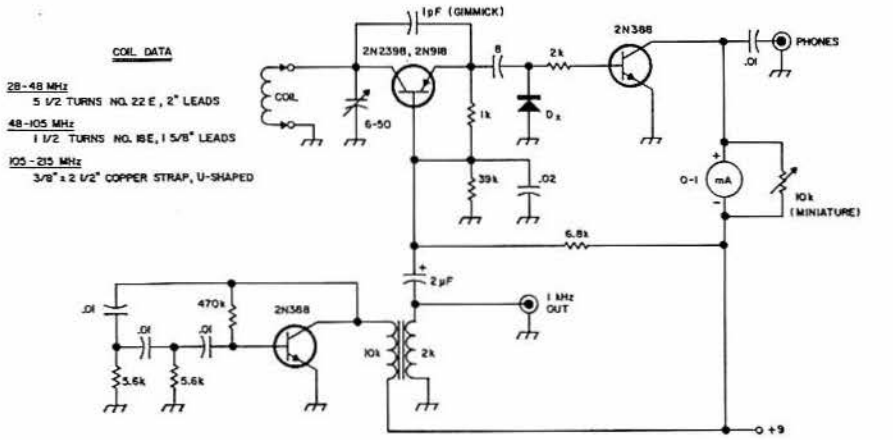

Fig. 1. Circuit diagram of the great dipper. Note that although the 2N2398 is a PNP transistor, the 2N918 is NPN, and if used as the oscillator transistor, problems would arise with voltage polarity. The diode D_x may be almost anything that you have available. The 1 pF gimmick capacitor consists of 1½" of twisted wire.

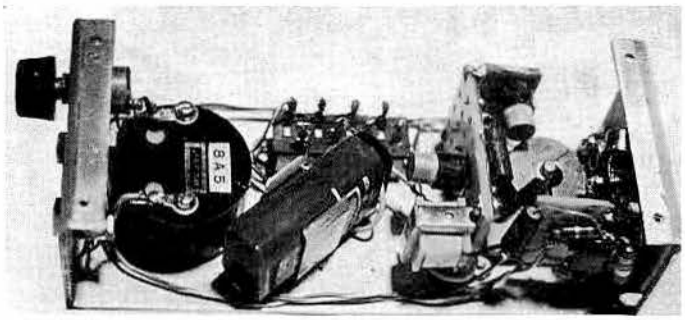

Internal construction of the great dipper. The modulator and oscillator boards are to the right—the oscillator transistor is mounted right next to the coil jacks.

change the value of the emitter-collector feedback capacitor, and to juggle the emitter and base resistor values in order to sustain oscillation at your desired frequencies.

Construction

Vector board was used, mainly because I wanted to experiment with component values; however, a printed circuit would be just as good, especially for something such as a club project. It can be seen from the photograph that the meter amplifier and audio oscillator are built on separate boards. This is due to the fact that I built several different amplifiers; the layout would look neater if they were on the same board. Positioning of the rf oscillator and capacitor C_1 as shown in the photograph is recommended, but the placement of other parts is not critical.

Fiberglass board is used as an insulator for mounting the banana jacks and plugs. It cuts and drills easily and appears to work fine. Three banana jacks were used, the third jack being used merely to provide mechanical rigidity. It could also be used, if necessary, to shunt additional capacitance across the emitter and collector on the lower frequencies.

Because a shear and a brake were available, I constructed my own chassis, consisting of two U-shaped pieces of 1/16" aluminum. Using the GDO is a breeze, for it fits the hand very comfortably; if placed on the workbench, it doesn't roll off each time it is bumped. The completed case (1¾" H x 2½" W x 6¼" L) is exceptionally rigid and imparts a reassuringly solid feel when handled. Commercially available miniboxes could be used if you don't have facilities available for rolling your own.

In building the rf oscillator, keep all the rf leads as short as possible; especially the short lead from C_1 to Q_1 and from circuit ground to chassis ground. It was found that false dips could be completely eliminated if a copper strap ¼" wide was added from the capacitor ground lug directly to chassis ground. Apparently the ground on the variable capacitor C_1 is not quite good enough at frequencies above 100 mHz. Various transistors were tried in the oscillator; the PNP type 2N2398 was found to be a good performer, as was the NPN type 2N918.

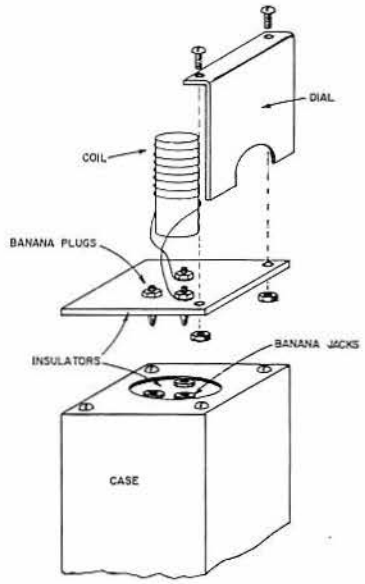

Fig. 3. Construction of the plug-in coil assemblies. The coil forms were made from the plastic containers which hold Polaroid print coater.

However, the use of the NPN type could lead to problems with battery polarity. Capacitor C_2 is a 1½" length of twisted wire positioned near the collector lead of Q_1. This slightly modified oscillator circuit is from a book describing, among other things, a transistorized GDO which you may wish to use as a reference.

To keep cost low, a 0-1 mA meter was used in conjunction with a simple meter amplifier. If you happen to have a 0-50 μA meter lying in the junkbox, that would work equally well, and the circuit could be simplified accordingly. Several circuits were built for the meter amplifier; the one chosen was a compromise between cost and performance. A germanium transistor was used because it requires less voltage to turn it on. Leakage is low, the pointer of the meter resting just off zero when no coil is in place. Further information can be obtained from January 1966 *73 Magazine*, which was the source for this circuit.

A transistorized audio tone generator is coupled by a 2 μF capacitor to the base of the oscillator transistor for modulation. This modulated oscillator allows the GDO to be used as a versatile signal source. An output jack is included on the panel to allow the 1 kHz tone to be used without turning on the oscillator.

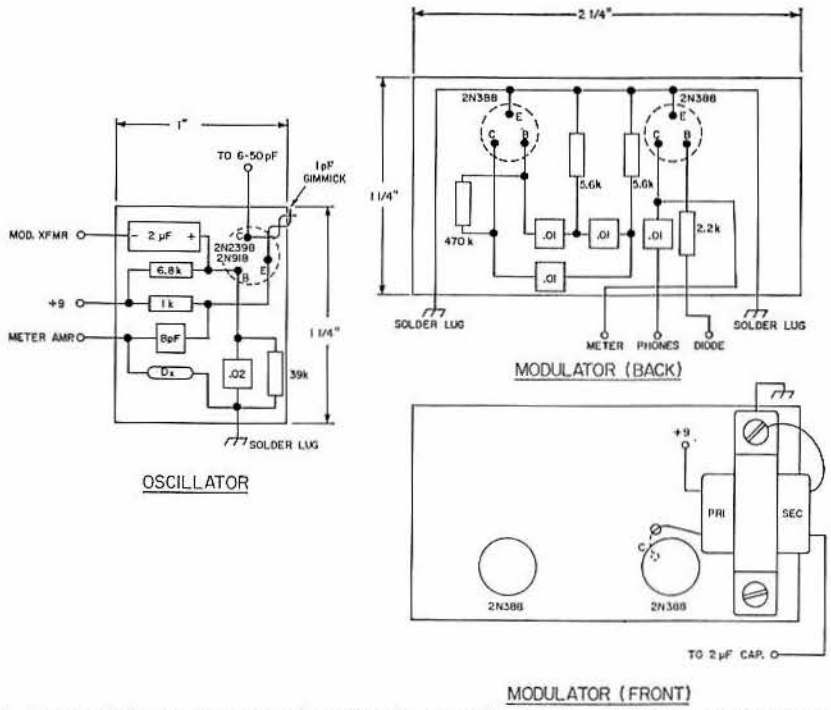

Fig. 2. Layout of the two circuit boards used in the great dipper. Although two boards were used in this case, the circuit could be easily adapted to one board, and even to printed circuitry.

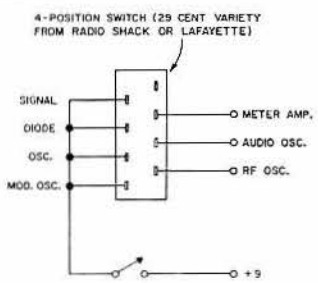

Fig. 4. Wiring the four-position slide switch for the great dipper.

The three plug-in coils for the Great Dipper. Three ranges cover from 28 to 216 MHz. The second harmonic of 216 MHz may be used for tuning up 432 MHz converters and such.

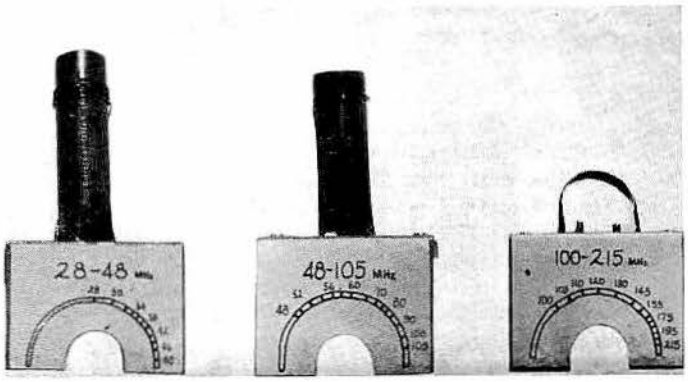

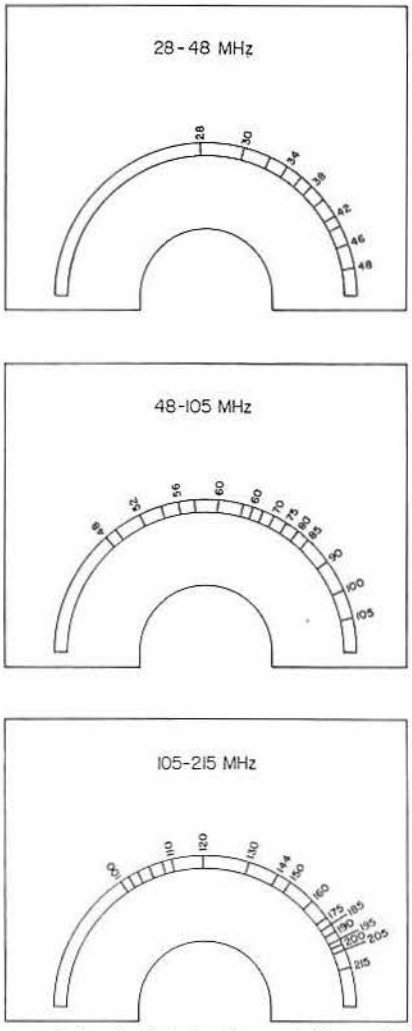

Fig. 5. Full-scale dials for the great dipper. If the construction shown in the photographs is followed closely, the calibration of these dials should be within several percent.

There are a couple of components which not everyone will want to duplicate. One, the sub-miniature 10k pot with SPST switch, was chosen because a very limited amount of space was available; if the unit is built on a larger chassis, the more commonly available *Midgetrol* could be used. The other, a four position switch used to select the desired mode, is a 29c variety available from Lafayette or Radio Shack. It has a peculiar switching arrangement and if you duplicate this project, several hours of experimenting could be eliminated by following the pictorial diagram included in this article. A disadvantage of this particular switch is that the meter does not indicate in the modulated oscillator position.

Using individual scales on each plug-in coil assembly greatly enhances scale legibility, reducing the chance of reading error and speeding frequency identification. This scheme; however, is not original. It was described in a 1957 issue of *Short-wave Magazine*, and is currently being used on a commercial GDO. It requires little additional effort to build the coil assembly in this manner and is, to me, well worth that extra effort. For want of anything else, the coil forms were made from the plastic tubes which contain the film coater supplied with each roll of Polaroid film.

Lastly, ease of tuning is accomplished largely through the use of a 1" skirted knob. Small knobs are simply too difficult to use comfortably.

Calibration and operation

It is best to calibrate this GDO by listening for the oscillator, modulated by the 1 kHz tone, on a general coverage receiver. An alternate method is to use another GDO, placing one in oscillate and the other in diode, tuning for either peak or dip. The scales which were used on this GDO will serve if parts and layout are followed closely.

To use this unit as a dipper, place the mode switch in oscillate, and place the dipper coil next to the coil under test. The turns of both coils should be parallel, and not at right angles to each other. To keep from pulling the oscillator frequency, keep the two coils separated as much as possible, while still maintaining a meter dip. This assures that dial accuracy will be kept high. If a coil is inaccessable, twist a pair of wires together, forming a two turn coil on each end; slip this coupling link over the two coils. Keep in mind that a coil, when it is in a circuit, may not dip at the same frequency as when it is out of this same circuit.

GREATER DIPPER – MODIFICATION

John E. Boyd WAØAYP

Introduction

To the uninitiated, a grid dip oscillator is neither glamorous nor exotic, even if it does happen to be transistorized. But to those who have ever tried to put a coil on frequency, one is worth its weight in microcircuits.

The original model of the *Great Dipper* proved to be a versatile, if unexciting, grid dip oscillator. Intended to be used mostly at VHF, the dipper was limited to frequencies above 28 MHz. To those who seldom operate above 10 meters, the lack of frequency coverage below 28 MHz was a definite handicap. Expanding the frequency coverage downward extends the dipper's usefulness considerably.

Component changes made were not extensive, nor were the physical dimensions of the unit changed. The schematic diagram of the modified circuit is shown in **Fig. 1**, and the pictorial diagram of **Fig. 2** is included to supplement the photographs printed in the original article.

Modification

First, the oscillator circuit board should be rotated 90 degrees from its original position so that transistor substitution or replacement can be made easily. A microwave diode might be substituted for the original glass computer-type diode; this results in better performance at VHF, but its effect cannot be accurately predicted. A 1N21 or 1N23 diode could be used in place of the D4900 called for in the schematic. Best oscillator performance over a wide frequency range results from using a 5 pF capacitor as the collector feedback coupler, but this was a compromise value. If operation is likely to be confined to either the HF or VHF segments of the radio spectrum, some experimentation with this capacitor should result in improved performance over that particular range. For experimentation, use a 3-12 pF or 4-30 pF trimmer.

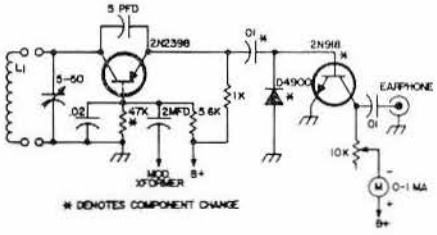

*Fig. 1. Schematic of modified circuit, with component changes indicated by *. L1: 13-23 MHz, 14½ turns No. 20; 22-44 MHz, 5¼ turns No. 24, 45-90 MHz, 1½ turns No. 24; 90-195 MHz, 2½ x 3/8 in.*

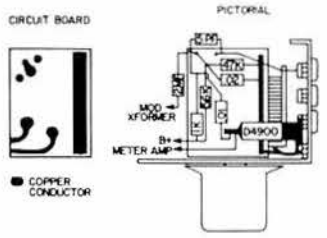

Fig. 2. Pictorial view of the dipper and its circuit board.

To perk up meter amplifier performance, the 2N388 meter amplifier is replaced by a 2N918, a relatively high gain, low leakage transistor.

Although the change was not made in this unit, a 6-100 pF (MAPC-100) variable capacitor could be substituted for the existing 5-50 pF unit. As can be seen from the full-size scales, frequency coverage is narrow on the 13-23 MHz plug-in coil. Those who frequently construct HF gear might benefit from the substitution.

Operation

Operation of the dipper is the same as before, except the frequency range is greater. Another coil must be wound for the 10-25 MHz range, but existing coils were not modified. Calibration is now different from before; full-size scales are included with this article for those who do not have a general-coverage receiver or another grid dip oscillator on hand for calibration.

Oscillation is still vigorous at 13 MHz, which indicates lower frequencies may be reached with a suitable coil plugged in. Similarly, oscillation is still noticeable at 195 MHz, so operation at higher frequencies may be possible.

Finishing Touches

Appearance of the dipper was improved after enlisting the help of a draftsman. The dial and meter scales were professionally inked. Figure 3 provides full-size copies of these scales.

To improve the legibility of the labels and scales, they were inked on yellow cards rather than on conventional white paper. It's a small point, but for those who use test equipment frequently, the black-on-yellow technique results in less eye strain.

ETCHED CIRCUIT UHF DIPMETER

Bob Corbett W1JJL

I made three models of the dipper. They cover 130-175 MHz, 175-250 MHz, and 250-480 MHz. The first two models use the same size inductor, with the 130-175 MHz model using a larger capacitor for tuning with a ceramic trimmer across it. This trimmer is not shown in the schematic; its value is 7-45 pF and it should be adjusted to cover the proper range.

The 250-480 MHz dipper uses a smaller inductor than the others. It also has a copper jumper (shown in the layout) that the lower frequency dippers don't have.

Each dipper is complete (including the battery) except for the meter. The meters were omitted to save space and money, but can be included if you wish to use a slightly larger case.

Each dipper uses one RCA 2N3478 NPN silicon transistor. These transistors cost only $1.90 apiece, but it's likely that other transistors that are even cheaper could be used. The 2N3478 has odd basing—the only reference is the short case-shield lead—so don't shorten any leads until you're sure that you can keep track of the connections.

The copper side of the board for the dipper is shown in Fig. 2 with the component side in Fig. 3. Use glass or Teflon based board. Paper or bakelite board probably wouldn't be satisfactory. Trim the board to the proper shape with a nibbler. The inductor should be coated with coil dope to keep from shorting it when you use it.

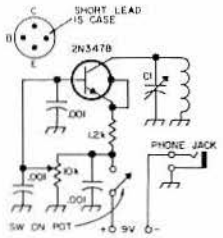

Fig. 1. The etched circuit dipper is very simple. The circuit is almost identical to the one described by WA1CCH in the December 1965 73, but the construction is quite different. C1 is Johnson 160-104 (9 pF) for the two higher frequency dippers, and 160-107 (14 pF) for the 130-180 MHz model. There is a trimmer across C1 in the 130-180 MHz model; see text.

To mount the boards, you'll have to cut a thin slot near the edge of the Minibox used as a case. One way to do it is to drill a number of holes of the proper size in a row, then use a file to finish the slot. You'll have to bend that side of the Minibox out to get the board in. It's held in place by an extra set of nuts on the shafts of the potentiometer and the tuning capacitor. Be sure to trim the leads projecting from the copper side of the board so that they won't touch the metal of the case. The battery is held in place with a simple clip made from scrap metal.

The dipper is very easy to use. But before we get to that, let's check it out and calibrate it.

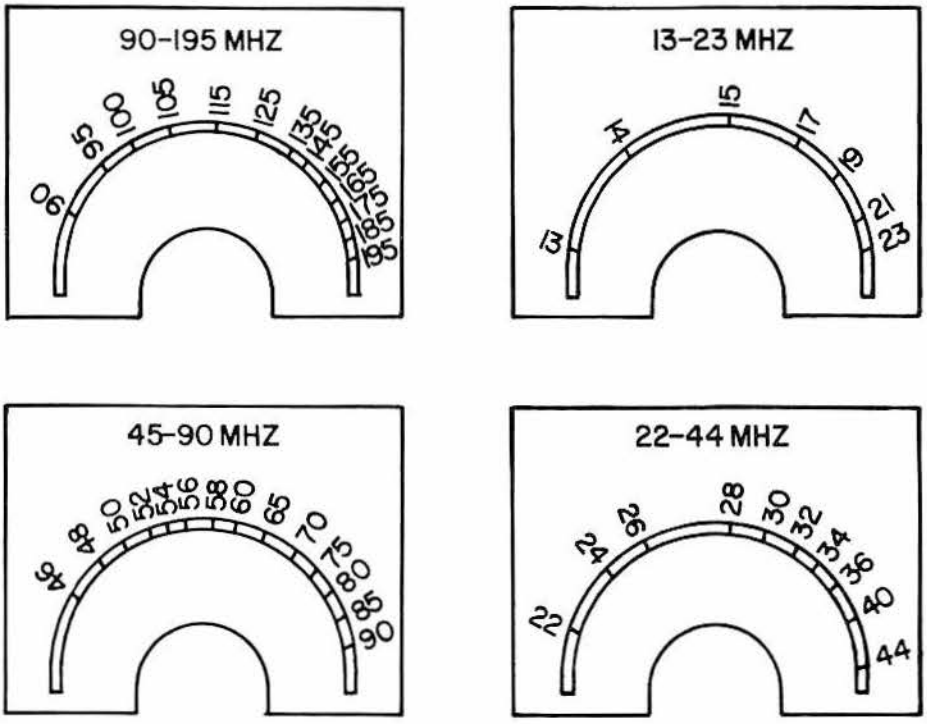

Fig. 3. Dial designs for the various MHz ranges, full size.

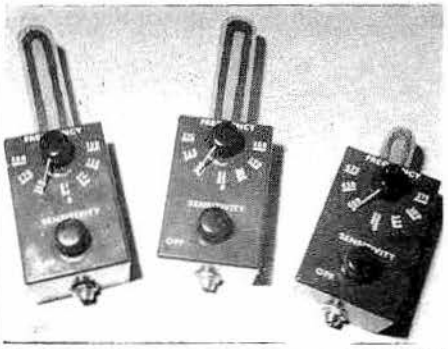

The three dippers shown here cover 130-480 MHz.

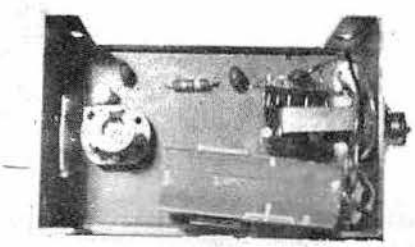

Here's the inside of one of the dippers.

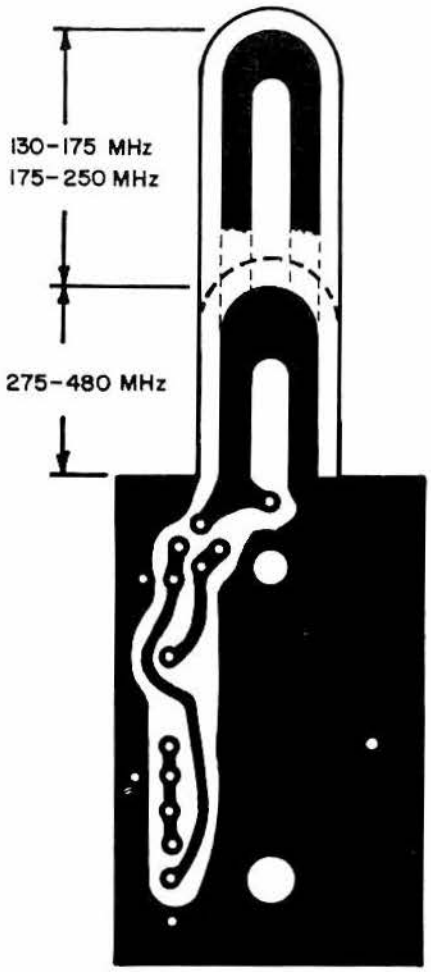

Fig. 2. The copper side of the etched circuit board used in the dipper. This layout is full size. Use board suitable for these frequencies: fiber glass or Teflon.

Plug a 2 to 5 mA meter into the meter jack. You can use a more sensitive meter if you shunt it with a resistor that gives the proper scale. Put the resistor across the meter jack terminals in the dipper if you use the meter for other things.

Turn on the dipper by twisting the potentiometer knob clockwise until it clicks. The meter should show very low current. As you turn the pot, the current should suddenly jump to about 1 mA. That means that the transistor is oscillating. If you touch the coil, the meter reading should drop and the dipper may stop oscillating completely. Now tune the capacitor through its range. There should be a little variation in current, but not too much.

Now you're ready to calibrate the dipper. The easiest method is a sensitive wave meter that covers the range, but it's quite easy to do the job with a TV set. A TV set covers 176 to 216 MHz (channels 7-13) for the low calibration. Then the second harmonics of the dipper tuning 235 to 445 MHz can be received on a UHF TV set (470-890 MHz). If you have a two meter receiver, that gives you another maker at 146 MHz. You can put on the panel markings with Ami-Tron or Datak rub-on lettering.

The dipper should be complete now, and ready for use. Bring the dipper near a resonant circuit in the dipper's range and tune the frequency control. You should get a prominent dip in current when both circuits are tuned to the same frequency. The amount of dip depends on the setting of the pot in the dipper, the distance from the tuned circuit, the Q of the circuit, and the type of coupling.

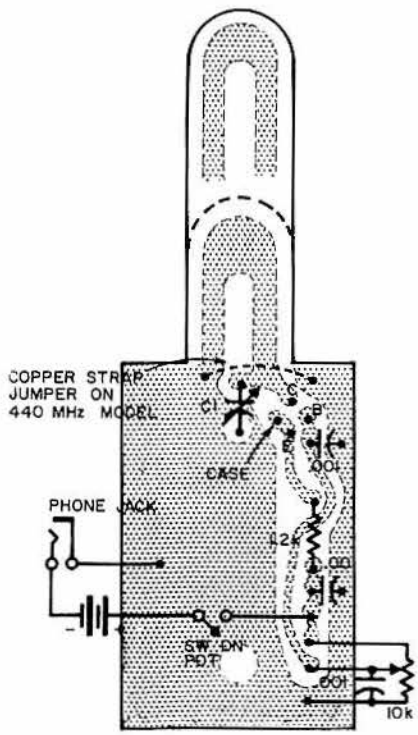

Fig. 3. Component side of the dippers. There is a 7-45 pF ceramic trimmer across C1 in the lowest frequency model. See the text.

In many cases it's easiest to leave the dipper stationary and tune the other circuit.

The dipper can also be used for monitoring AM transmitters by plugging a set of headphones in the meter jack and adjusting the tuning and pot. You can also use the dipper for determining the frequency of another oscillator. Simply tune the oscillating dipper with headphones plugged in until you hear a slight click. You probably won't be able to get a zero beat at these frequencies.

Be careful that you don't use the dipper around an energized transmitter of more than a few watts output or the dipper may be damaged.

These dippers are simple, inexpensive and non-critical to build. After you've build them, you'll wonder how you ever tried to build UHF equipment without a good dipper.

UHF GRID DIPPER

J. Fisk WA6BSO

When building or testing equipment for the 420 mc band, amateurs invariably run into the problem of, "Where am I?". It becomes a little difficult to tell whether you are actually in the band or somewhere nearby. The uninitiated will counter that you should be able to figure close enough, after all the band is 30 mc wide; but even the experienced old timer will confirm that this just isn't so.

The 420-450 mc amateur band falls between the VHF and UHF television assignments and there is very little to use for a frequency reference point. It is nearly impossible to tell exactly where you are without resorting to expensive commercial gear or lecher wires. Nor is the problem confined to the ¾ meter band; when building crystal controlled converters for 432 or 1296, it's nice to know that the last tripler is really tripling and not doubling or quadrupling. Even with a 45 or 50 mc crystal, it's quite easy to tune up on the wrong harmonic. Remember that a 40 mc change at 400 mc is analogous to a 400 kc change on 75 meters.

There are several commercial instruments that fill this requirement nicely, but the cost of the least expensive of these would buy a pretty respectable all band receiver. Occasionally suitable test equipment appears on the surplus market, but again, the price is prohibitive. The simple UHF grid-dipper described in this article was designed specifically to economically fill this need. It covers the frequencies

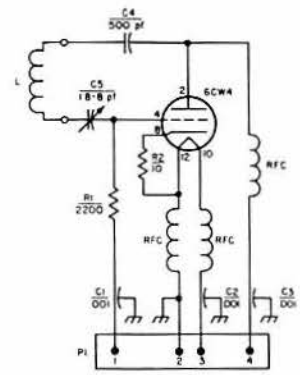

C1,C2,C3 STANDOFF BUTTON BYPASS CAPACITORS
C4 BUTTON CAPACITOR (SEE TEXT)
C5 E.F JOHNSON TYPE 160-104 VARIABLE
L PLUG-IN COIL
P1 AMPHENOL 91-MC4M MALE CABLE PLUG
RFC's 8-1/2" No 27 ENAMELED WIRE WOUND ON 1/2 W, 100 K COMPOSITION RESISTORS

Fig. 1. Schematic of the rf head of the UHF grid dipper.

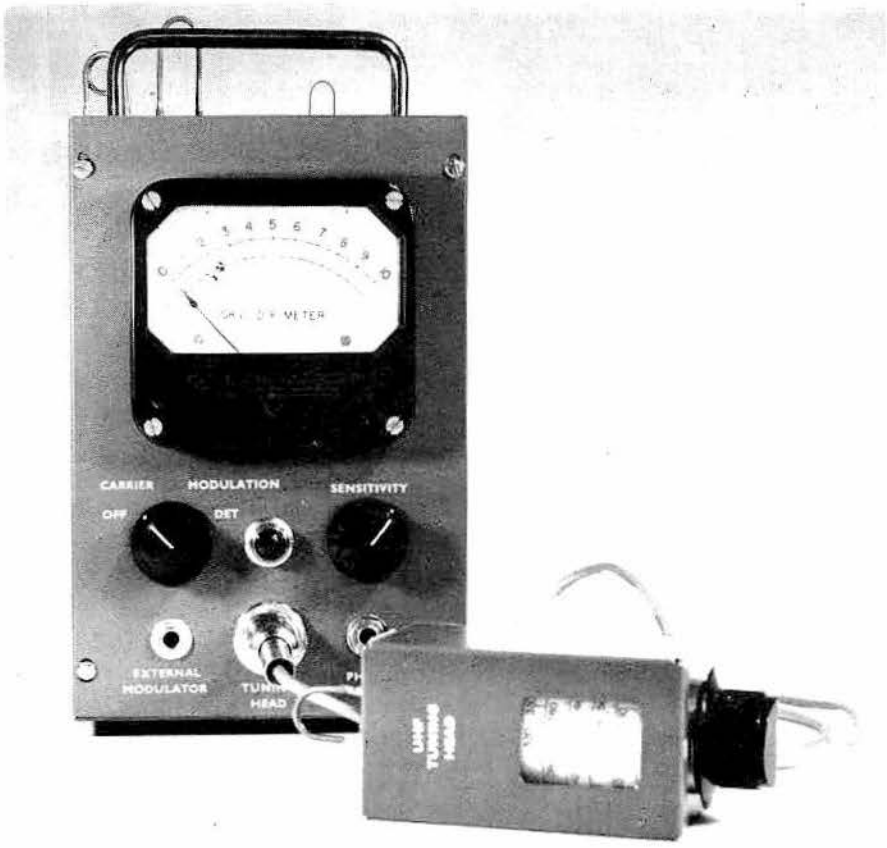

from 300 to 680 mc at a total cost that is comparable to a low-frequency kit-type grid-dipper. By using junk-box parts and smart horsetradesmanship this cost may be substantially reduced. I should hasten to point out that substitution of parts in the tuning head should be avoided if accurate dial calibration is desired.

This particular grid-dipper has been duplicated several times and in each case calibration has been within several percent of the original unit; at least as accurate as the familiar kit-type grid-dipper. This is helpful to the ham who does not have access to commercial equipment for calibration purposes. By using the layout and parts described in this article, the precalibrated dial illustrated in Fig. 8 may be used with a minimum of error.

Although an accessory power supply, modulator and indicator are included in this design, an enterprising ham could use the power supply and meter presently available in any lower frequency tube type grid-dipper. Although using a modified low-frequency dipper is simple and inexpensive, the power/indicator box specifically designed for the UHF tuning head has several features that are not available in inexpensive kit-type units. These include internal 1,000 cycle modulation, provision for external modulation, and voltage regulation which provides the necessary stability at the ultra high frequencies.

The rf tuning head

The heart of this instrument lies in the tuning head itself. There is nothing particularly new or different about the circuit, but at these frequencies stray inductance and capacitance in circuit layout and construction will seriously affect the end result. All the lead lengths must be as short as humanly possible and physical circuit layout must follow standard UHF practice. One of the big problems in building tunable oscillators at UHF is to obtain an oscillator that will tune from one end of the range to the other with no "holes," frequency jumping or instability. The series tuned 6CW4 nuvistor oscillator shown in Fig. 1 fills these requirements.

Insofar as possible, all the tuning head wiring is done on a point-to-point basis with the components mounted directly to the 6CW4 tube socket or button capacitor lugs as illustrated in Fig. 3. To obtain the desired accuracy with the precalibrated dial, this diagram should be followed as closely as possible.

To keep stray circuit inductance to a minimum, all wiring between the coil and tube socket is done with one-quarter inch wide strips of thin copper sheet. In addition, the rotor of the variable capacitor is connected to the 6CW4 grid (pin 4) with a short strip of the same material. The only tricky part of this wiring is the installation of the series capacitor C4. This capacitor is a 500 picofarad button type mounted as shown in Fig. 5. The "S" shaped bracket ("A") is made from a one-quarter inch wide copper strip, one and one half inches long and soldered to the mounting stud of the capacitor. Connection to the 6CW4 plate (pin 2) is made with the soldering lug on top of the button.

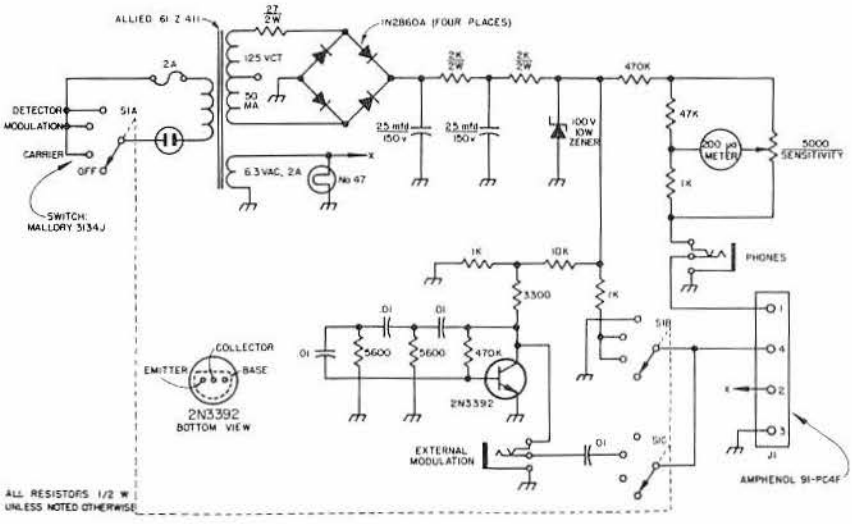

Fig. 2. Power supply and modulator for the UHF grid dipper.

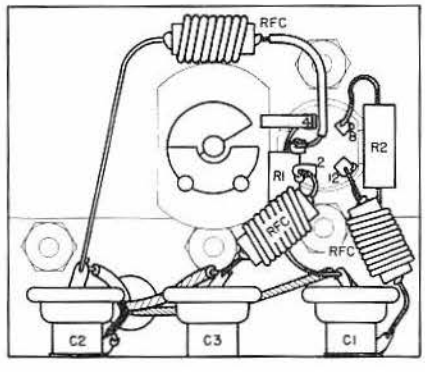

Fig. 3. Critical wiring around the 6CW4 socket.

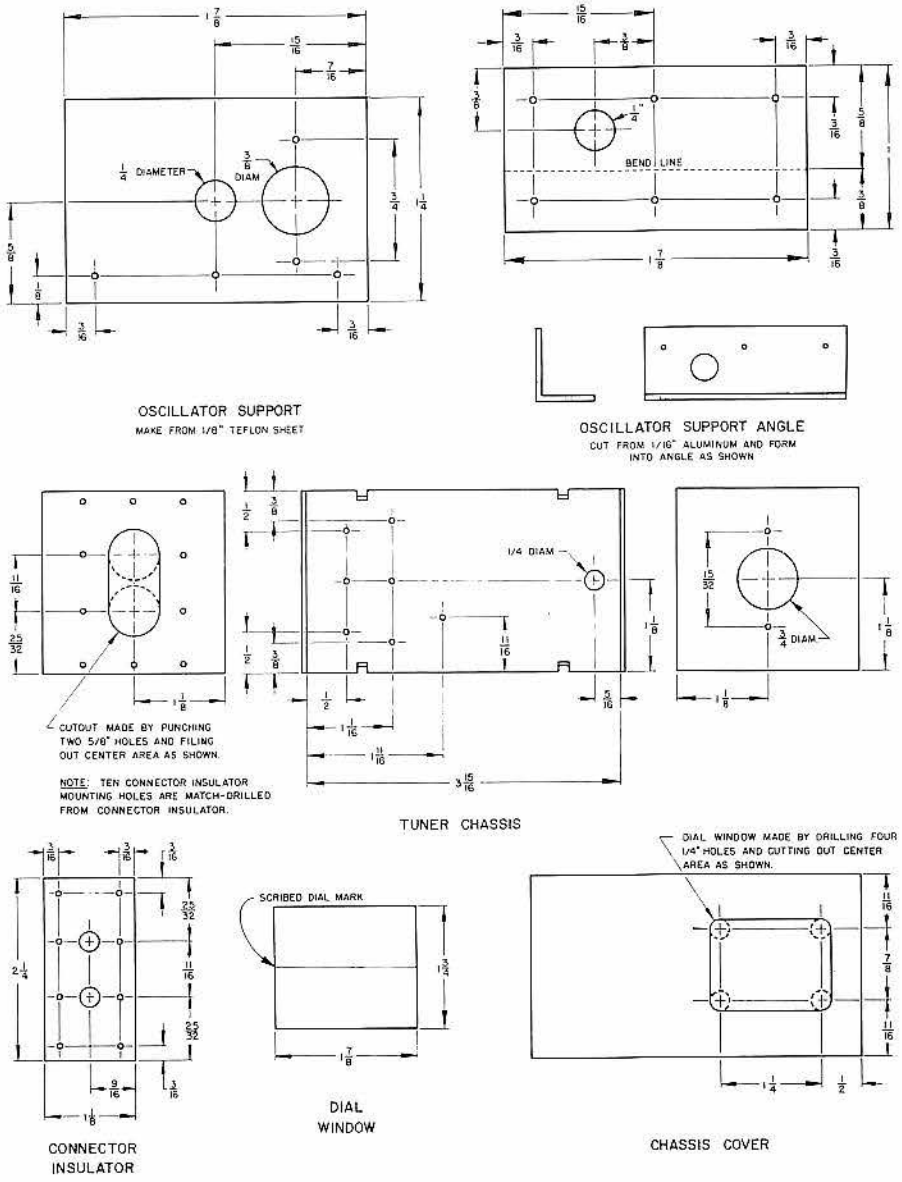

Fig. 4. Layout of the tuner chassis, chassis cover, dial, connector insulator, oscillator support and oscillator support angle.

Connection to the stator of the variable capacitor is accomplished with another short strip of thin copper as shown in **Fig. 5** ("B"). This piece of copper is bent so it touches both stator mounting pins when the unit is assembled; then it is soldered in place.

The oscillator and tuning mechanism are housed in a standard 2¼ × 2¼ × 4 inch chassis box laid out as shown in **Fig. 4**. Although the author's unit is based on an LMB type 107 chassis box, other manufacturers have similarly sized boxes which are equally suitable. The layout of the enclosure is straight-forward and no difficulty should be found in duplicating it. The dial and coil socket cutouts are made by drilling or punching round holes and then cutting out the area between them as shown in the drawing. This is easily done with an Adel "nibbling" tool. All of the small screw holes are drilled with a standard ⅛ inch drill to pass 4-40 screws; 5⁄32 inch holes will be required if 6-32 screws are used.

The dial window is cut from a sheet of 1⁄16 inch clear plastic to the dimensions shown in **Fig. 4**. A hairline is scribed in the center of this window; if a more distinct line is desired, this scribe mark may be filled in with black india ink. After the tuner enclosure is completed, this dial window is epoxied in place over the dial cutout.

The coil socket is made by installing two banana jacks (E. F. Johnson type 108-740) on 1 1⁄16 inch centers in the Teflon connector insulator illustrated in **Fig. 4** (if Teflon is not available, Polystyrene may be used). This "socket" is installed over the large oblong hole cut in the end of the chassis. The screw holes used for mounting the connector insulator are match-drilled to the holes in the insulator itself. In this way it is properly mated to the enclosure. Although nylon attaching screws were used in the original model, they are not necessary and regular metallic screws will not alter any of the oscillator's characteristics.

To reduce stray capacity to a minimum, the oscillator circuitry is mounted on an insulating sheet. Teflon was used for this purpose in the original unit, but epoxy board with the copper peeled off would be perfectly suitable. Sheet polystyrene is not too desirable in this location because of its susceptibility to heat. The envelope of the 6CW4 gets very hot and the ambient temperature within the confines of the small chassis is quite high.

The general layout of the Teflon oscillator support and associated support angle are also shown in **Fig. 4**. The angle is cut out from a piece of 1⁄16 inch aluminum sheet and bent in a vise to form the angle. When these two pieces are mated together, the metal angle will probably interfere with the lower nuvistor socket mounting screw. It must be drilled out using the hole in the oscillator support as a guide. This additional hole is not shown because its exact location will vary from unit to unit and depends upon the accuracy with which the parts are laid out.

The dial mechanism is not complicated, but it is hard to ascertain from the photographs exactly how it is put together. The exploded drawing of **Fig. 6** should help in this respect. The vernier mechanism is an Eddystone 10:1 planetary drive that provides both smooth

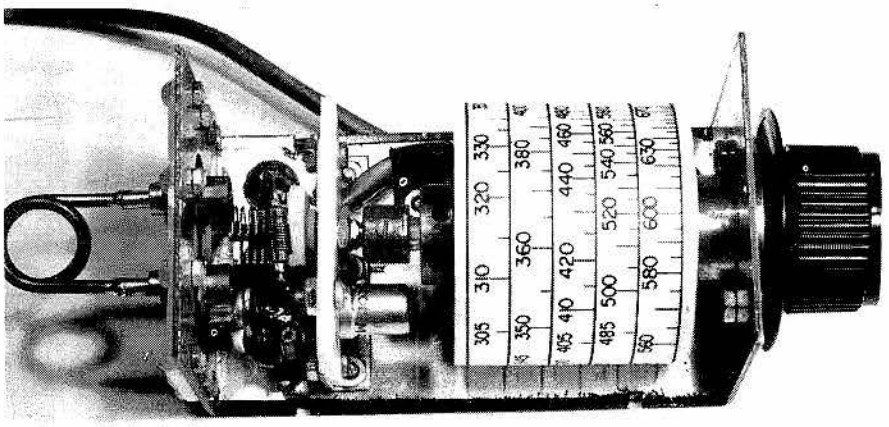

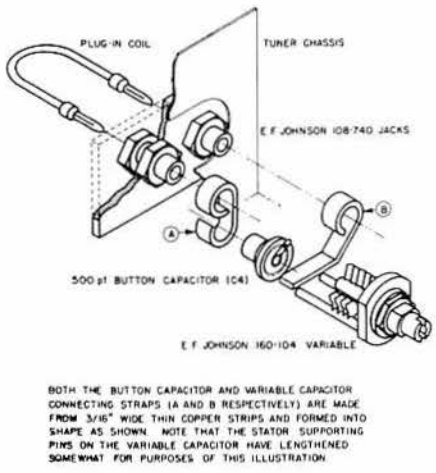

Fig. 5. Exploded view of the connections between the 6CW4 and the coil socket.

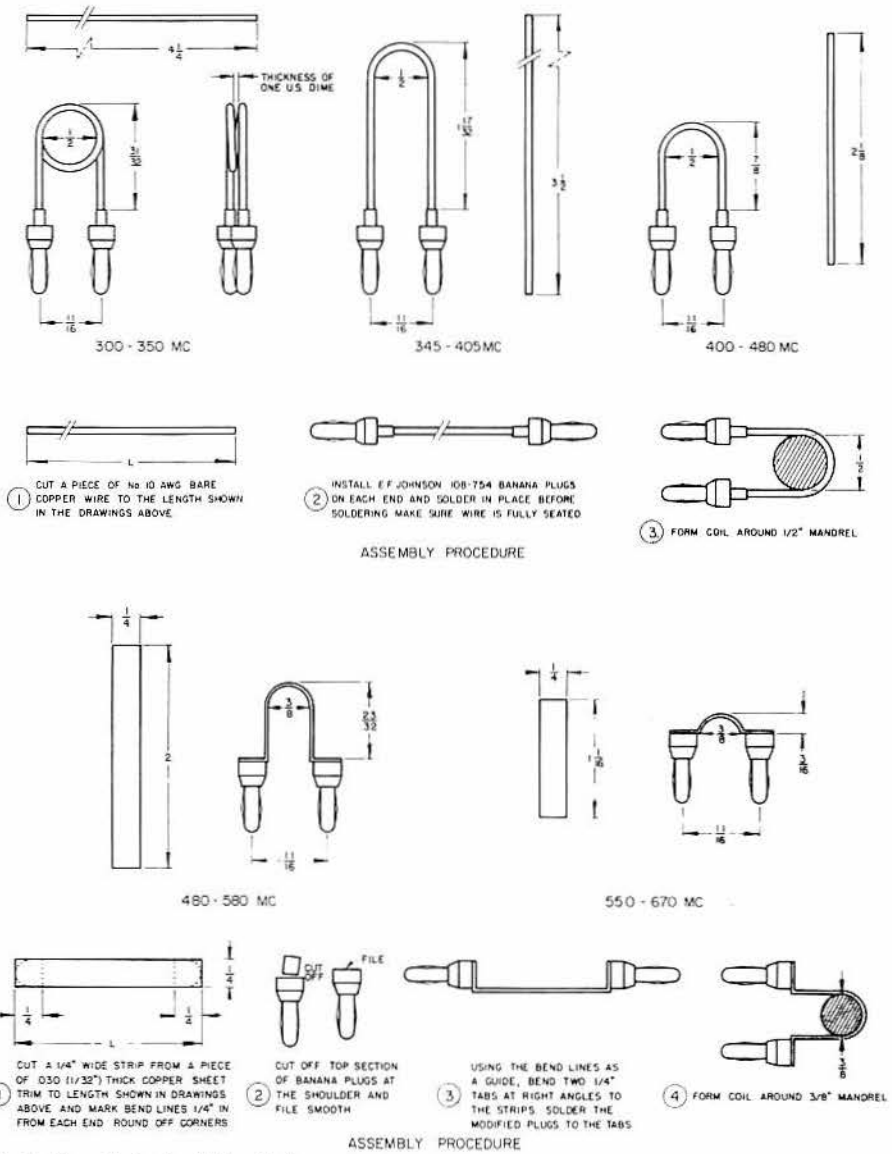

Fig. 7. The coils for the UHF grid dipper.

action and repeatability in a small package. Although this unit is manufactured in England, it is available from many of the larger electronics parts houses in this country.

Substitution of similar drives should be perfectly satisfactory as long as they don't extend more than one inch beyond the front panel of the tuner chasssis.

The vernier drive is connected to the variable capacitor through a ¼ inch polystyrene shaft 1-¾ inches long and the usual "¼ to ¼" shaft couplers. Polystyrene or some other insulator must be used here because the rotor of the capacitor must be isolated from ground. Because of the space limitations inside the enclosure, the coupler at the variable capacitor end of this shaft is only one-half of a standard coupler. A standard "¼ to ¼" coupler is sawed in two and one-half is epoxied to the end of the polystyrene shaft. Save the other half; it will be used for the dial drum hub.

The 8 pf variable capacitor was designed for screwdriver adjustment and its $^{3}/_{16}$ inch shaft must be made compatible with the standard coupler. This is accomplished with a bushing made from sheet copper. A short piece of ¼ inch wide, $^{1}/_{32}$ inch thick copper strap is formed around the capacitor shaft and takes up the slack between the shaft and the coupler.

The drum dial in the original unit was made from the metal top of a Johnson's Shoe Shine Kit (49¢ at the local grocer's), but any similar closed cylinder 1-$^{15}/_{16}$ inches in diameter and about 1-$^{11}/_{16}$ inches long should be suitable; other diameters will void the accuracy of the precalibrated dial. The "skirt" or bottom rim is cut off the metal can at the circumferential notch and a ¼ inch hole is drilled in the center of the top. The remaining half of the ¼ inch shaft coupler that was left over from the polystyrene shaft is then epoxied in place over the hole to provide a dial drum hub. Another hole is drilled in the side of the can $^{11}/_{16}$ inches from the top; this provides access to the shaft coupler on the rear end of the vernier drive.

The precalibrated paper dial may now be cemented in place. It's a good idea to cement a piece of white paper the same size as the dial between the dial and the drum, otherwise the label on the can will show through the paper dial. Rubber cement is recommended at this point to prevent excessive wrinkling and distortion of the dial.

When all of the dial parts are completed, they are put together as shown in **Fig. 6**. It's a little crowded in the small box, but all of the parts *will* fit. However, in order to get all of the dial machinery into the box in the right order, a correct assembly sequence must be followed. First the polystyrene shaft and coupler are inserted into the dial drum from the rear. Next insert the Eddystone drive assembly through the hole in the front panel and mate it with the end of the polystyrene shaft. Place the bushing over the capacitor shaft, attach the polystyrene shaft and tighten the coupler; also tighten the coupler at the back end of the Eddystone drive thru the access hole provided in the dial drum. Install the vernier drive mounting screws. Now completely mesh the capacitor plates, center the low edge of the dial in the window and tighten up the dial drum hub. Disassembly must be accomplished in reverse order.

The tuning head is attached to the indicator/power unit through a four-conductor cable three feet long. This cable is attached to the box with a plastic cable clamp mounted in a hole provided immediately adjacent to the oscillator support angle and exits through a rubber grommeted hole at the front end of the enclosure. There is not enough room at the rubber grommet to use a cable clamp, so the cable is epoxied to the box at this point. Before installing the cable, however, check for sufficient clearance between it and the dial drum. It will probably be necessary to route the cable along the corner of the chassis to gain enough clearance.

Power indicator modulator

The power/indicator unit is housed in a standard 9 x 6 x 5 inch utility box (Bud type AU-1040 or equivalent). The layout of this

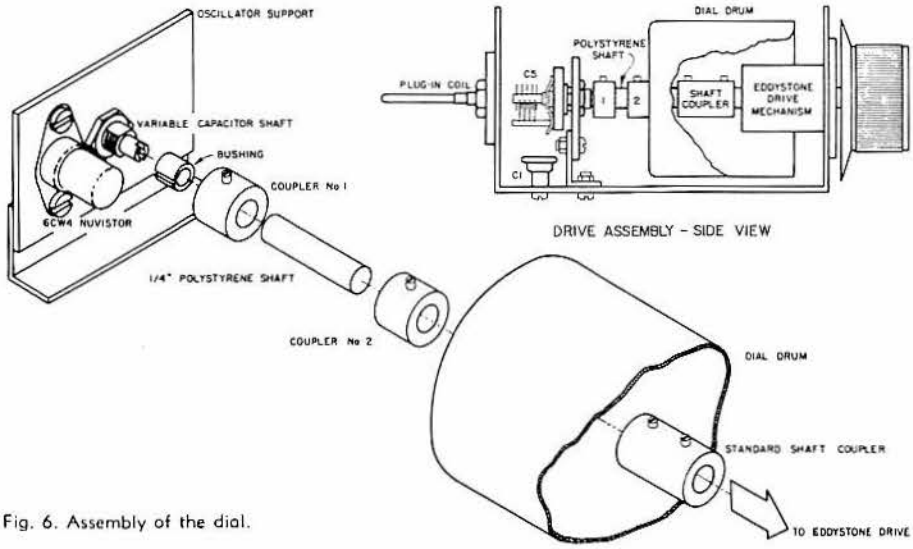

Fig. 6. Assembly of the dial.

circuitry is not at all critical, and just about anything that suits the builder may be used. The only particular caution that must be observed is with the transistorized 1 kc phase shift oscillator. This unit is built on a piece of perforated epoxy board (Vector 32AA18) 1-3/16 inches wide and 1-11/16 inches long. To preclude any 60 cycle pickup, this board is situated on the opposite side of the chassis from the power transformer.

In the author's case all the power/indicator components were mounted on a 4 x 5 x 1 inch aluminum chassis. This chassis was then mounted to the front panel of the utility box with the phone jack and power plug mounting nuts. Two large diameter holes (1-3/4 inch) are punched in the rear panel to provide access to the fuse holder and to pass the AC power plug. A chassis handle (Bud H-9168) on the top and rubber feet on the bottom just about complete the unit. There is one other addition however; five pairs of 5/32 inch holes, drilled on 11/16 inch centers along the rear edge of the top of the box provide convenient storage for the five frequency determining coils. A coat of spray paint and some Datak "Letraset" dry transfer labels are the finishing touches.

Calibration and operation

Without access to existing 420 mc equipment with known frequency characteristics, exact calibration in this band is impossible. However, this grid-dipper may be checked on the other ranges with the aid of an all-band television receiver. If the circuit layout and construction techniques described are closely followed, good correlation can be obtained and reasonable accuracy insured. The bands that are likely to be the furthest off are the lowest and the highest. In the lowest the coil spacing is quite critical and in the highest a slight change in length will move the frequency several megacycles. An accuracy of 2% at 600 mc is plus or minus 12 mc; close attention to the specified dimensions should provide accuracy better than this.

Operation of this grid-dipper is exactly the same as any lower frequency unit. It may be used in determining circuit resonance, detecting parasitic oscillations or as a signal generator. Because of its extended range, it has been found to be very useful in determining the series resonance point of rf chokes and ceramic bypass capacitors.

In the detect mode, this unit will indicate rf voltages as low as 50,000 microvolts. More sensitive operation may be obtained if it is used as an oscillating detector. In this case headphones are used and an audio beat note will be heard when the grid-dipper is tuned to the oscillator being checked. In the upper frequency ranges, it is usually difficult to obtain an actual beat note, and only a "tick" will be discernible when you tune by the frequency of the unknown energy.

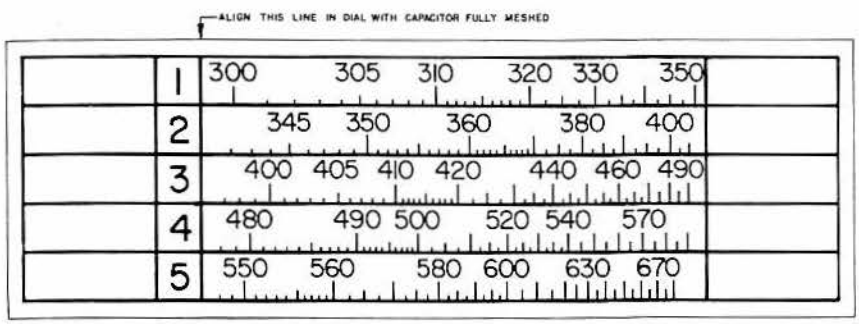

Fig. 8. Full size dial scale.

When the oscillator is tuned between 605 and 650 mc, there is sufficient second harmonic energy to provide a strong reference signal in the 1215 mc amateur band. This is particularly useful in the initial tune-up of converters for this band. Use of the internal 1000 cycle modulation aids in distinguishing the grid-dipper signal from other rf sources that are present throughout the spectrum.

WIDE RANGE VHF-UHF DIPPER

Bill Hoisington K1CLL

Most dippers for amateurs that I have seen so far, not counting the $400 ones, stop around 200 MHz just as you are about to enter the fascinating UHF region. We do have the 432 and 1296 bands, so let's become more familiar with them.

After all these years of "grid-dipping" we find ourselves without a grid; so it just becomes a "dipper". To retain the prestige of a hyphenated name we can call it a "dipper-generator". Most grid-dippers have been used as generators, but this one has built-in modulation, variable input-output coupling, controlled Q, and several other interesting features. Best of all, it goes all the way up to 1296 MHz.

When this little unit is completed it may be used as a dipper for determining the resonant frequency of VHF and UHF circuits, as an indicating frequency meter with an adjustable Q-multiplier, a field strength meter and modulation monitor, a sensitive regenerative receiver, or a CW and MCW signal generator. You can also use it as a harmonic monitor or as a frequency transfer unit from one transmitter to another.

Several circuits must be considered when building a wide band instrument such as this. For example, you should change circuits around 100 MHz and again at 600 MHz, give or take a few hundred. Below 100 MHz coils are good; from there to 600 MHz you can use ¼ wave resonators, and after that the ½ wave job becomes rapidly the best method, up to 1300 MHz.

Plug-in rf heads

I have made no attempt to cover the complete range from 130 to 1300 MHz with one oscillator. By using plug-in tuners you may vary the components to suit the frequency. On 50 MHz for example, you may use a low cost transistor, a coil, and a 25 or 50 pF capacitor. From 100 to 600 MHz you use a better transistor, a ¼ wave strap, and a 10 or 15 pF capacitor. In the microwave region up to 1296 MHz you use the best transistor you've got, ½ wave lines,

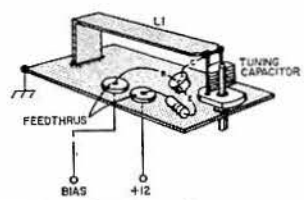

Fig. 1. Basic VHF/UHF oscillator circuit.

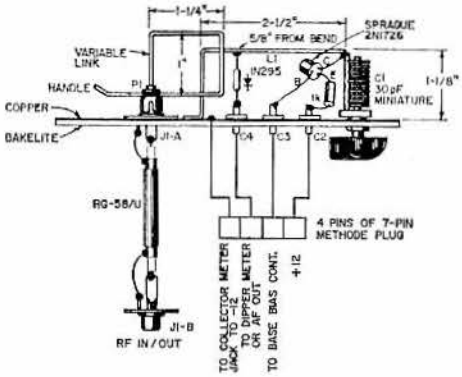

Fig. 2. 130 to 300 MHz tuning head.

and a small butterfly capacitor of 3 to 5 pF.

If you break the circuit at the right point, it simplifies things—then the two halves may be connected through a miniature 7-pin socket and plug as shown in Fig. 2. All four leads are reasonably dead to rf. You can leave out some of the audio if you like, but it's very handy to have a modulated signal. If you're running triple or quadruple conversion, it's nice to know by it's modulation which is the signal and which might be a *birdie*. As far as dials are concerned—it makes calibration and reading a lot easier to have only one band or range per dial.

130 to 300 MHz oscillator

Fig. 1 shows the basic ¼ wave circuit; Fig. 2 the complete rf unit with control, af output and modulation.

The circuit itself is very simplified, as seen in Fig. 1; there being only one inductance, L1, and no choke coils. This should make for a flat tuning oscillator without power dips as it is tuned over a 2 to 1 range in frequency, and it does just that. With a 2N1726 in the circuit there is a smooth power output curve from about one volt rf at 130 MHz down to ½ volt at 300 MHz.

The rf coupling jack J1 couples the rf energy both in and out. This is because L1 acts as either a detector resonator or an oscillator resonator, as required. Actually this rf jack can be used as shown in Fig. 2. P1 is a variable link to L1 and is plugged into J1; J1A has a few inches of cable between the white ABS plastic front panel and the copper clad bakelite sub-panel. Because the phono plug is rotatable, a nice variation in rf coupling can be obtained. The coax cable and J1B get the rf out to the front panel for easy use with antennas, probes, cables, etc.

The emitter goes to a 1K resistor then through a coaxial bypass capacitor which gets the dc in and out and leaves the rf behind. These feed-through type bypasses are very necessary—do *not* skimp on this item.

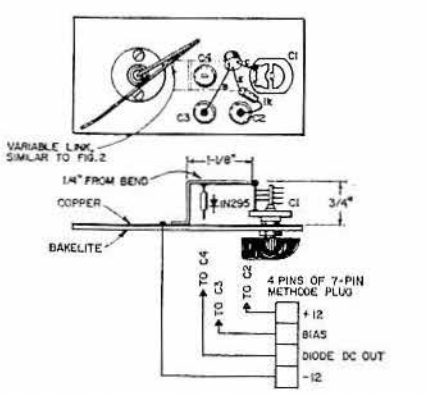

Fig. 3. 300 to 600 MHz oscillator with variable link.

300 to 600 MHz unit

Fig. 3 shows that this unit is essentially the same as the last, except for dimensions. I used a 2N1141 here although many others will work too. It tunes smoothly from 300 to 600 MHz; use the variable link feature as in Fig. 2.

900 to 1100 MHz

For this frequency range we need a little different approach. From Fig. 4 we can see that we now have two ½ wave lines on which low-voltage points can be found to attach the base and collector resistors. Most of the ¼ wave portion of the lines on the transistor end are actually inside the case. The places where the base resistor and the 500 ohm collector resistor are attached to the ½ wave lines can be found, or checked, by watching the rf meter and touching the lines with a pencil. At the proper point no change occurs in the rf output; sometimes it even increases.

The diode circuit of Fig. 6 is not ideal but it works. I have several of these around the shack and they work very well for detecting 1296 Mhz energy. Even ordinary hook-up wire will support the assembly of Fig. 6 about ¼ inch below the rf lines; you will soon find the best spot with the unit oscillating. The rf input jack and associated loop L3 are fastened so that L3 is in place over L1 and L2, and it's coupling can be varied in a semi-fixed fashion.

At this point we should mention that as a "dipper" the circuit is still working fine; also as a signal generator. It also serves as an rf detector but as the frequency gets up into the microwave ranges it is not quite as good as the tuned rf detectors featured in another article in 73 Magazine. Ideally, you should use the dipper on microwaves as a modulated generator and couple it into the unknown circuit; then a probe attached to *another* tuned detector should be coupled into the unknown circuit. There are quite a few variations using the dipper as an oscillator that you will find useful if you use a little ingenuity.

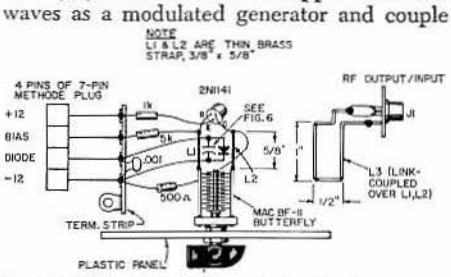

Fig. 4. 900 to 1120 MHz oscillator circuit.

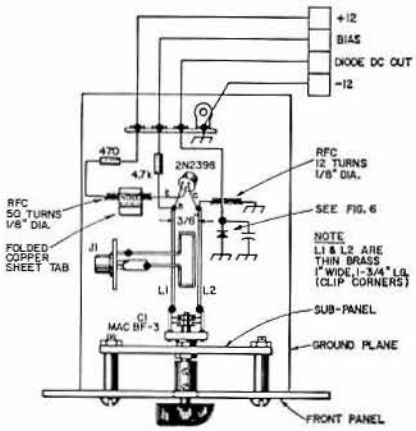

Fig. 5. 1200 to 1300 MHz oscillator and layout.

In the microwave detector line, my experience indicates that the plunger tuned coax cavity line is the best, the tuned trough line next, and the circuit of Fig. 5 next best. As a dipper, generator and regenerative receiver it is still good at 1296 MHz. Just to check, I plugged an antenna into J1, put an audio amplifier across the diode and copied a small transistor oscillator across the room. The base bias control works as a very smooth regeneration control. Smooth regeneration, as we will see later, is very important for maximum sensitivity when looking for harmonics and weak signals.

1200 to 1300 MHz unit

Fig. 5 shows the 1296 unit; I have used this circuit for many months as a dipper, variable-frequency generator, modulated-oscillator source, and as a regenerative receiver for 1296. In this circuit I used a negative dc grounded collector return. Don't short the base plate to the modulator base. Note that one end of the diode is tied to the base plate; this lead is brought out as the minus 12 volt lead. You can also use it ungrounded as in Fig. 4—you can use a 5th lead in the 7-pin plug and keep the diode isolated from the minus 12 volts. Suit yourself, just remember that *all* units have to use the same leads, as they all plug into the single modulator rf unit.

I just plugged a little 12 element Yagi antenna into this dipper and it works nice and smooth as a regenerative receiver. Please note, this is only for test purposes around the shack. You can hear with it, but not *that* good!

I had to put a choke in the cathode lead on this one, and tune it (the choke) with a piece of copper foil. A choke was needed in the collector lead too; after all this is the L-band microwave region.

The rf input jack J1 is mounted on a bakelite upright. Be careful of vertical metal

pieces attached to the base plate; they only need to be two inches long or so to become Marconi antennas on 1296! Bring the base resistor and the collector choke away from the lines in a perpendicular fashion—it helps.

The total length of the diode and it's two leads, from ground to the tiny .001 capacitor C2 is about 1½ inches; it is spaced about 3/16 from the ground plane. The bottom edges of the lines are about ½ inch from the ground plane.

The transistor presently in the unit is a selected 2N2398; about half of the dozen or so I have here go to 1300 MHz, a couple go to 1400, and the rest to 1100 or 1200.

Don't be alarmed that L1 and L2 are longer than those of Fig. 5, the smaller butterfly capacitor does that. You can make a choice as to capacity, length of brass, and desired rf range. You can use a 5 or 10 pF capacitor for C1, shorter lines, and tune over 1300 MHz. In fact, I have reached 1600 MHz with this circuit!

Modulation and control

Fig. 7 shows the circuitry for bias control, modulation and audio. Don't let it scare you. It's just the same old deal of doing what has to be done for control purposes, and from then on just turning the knobs to get what you want.

I have found that a very good plug and jack can be made by using an ordinary 7 pin socket and a Methode 7 pin bakelite plug. Unfortunately, I have never found a miniature tube with a bakelite base; they are always made of glass, so you will probably have to buy the 7 pin plug.

The minus 12 volt lead goes to the collector meter jack and then to the minus 12 volt of the power supply. This puts the rf panel ground at minus 12 volts and the audio af panel at plus 12. Of course, you don't have to ground the plus 12 on the audio panel, I just have that habit.

The base return goes through a 5K resistor and then to the bias control potentiometer. The diode dc/af output goes to af jack J2 and the meter M1 through the meter sensitivity control. This potentiometer is selected to suit the meter; I have used a 10 K unit with a 500 microampere meter. Note that part of this resistor should be used when af output is desired, otherwise the meter shorts out the af.

Audio modulation

You might think that just about everyone knows how to build an audio oscillator. Mine did oscillate, but the tone! And the wave-shapes, hoo-boy! I used an af transformer with the collector on one side and

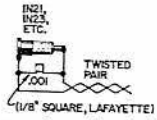

Fig. 6. RF detection loop for half-wave oscillators.

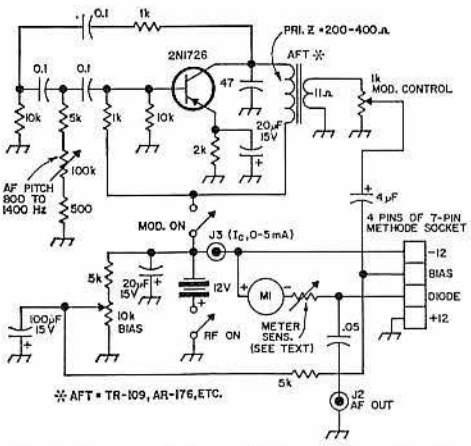

Fig. 7. Power control, modulation and audio circuitry. This circuit is used with all the rf heads.

the base on the other. So, once again to the handbooks and once again practically zilch. I did get the idea for a phase shift oscillator out of one of them, even if the circuit didn't work at first. After considerable experimentation I can recommend the circuit shown in Fig. 7. It works! In addition, the modulation may be adjusted to exactly 1000 MHz. This is very useful as many microwave test amplifiers have built-in narrow band af audio filters centered on 1 KHz. There is also a modulation gain control. This helps if a nice tone is desired.

Almost any small transistor output transformer will do the job for the af transformer, but don't go over 400 ohms impedance in the collector winding. Note the 1K resistor between the collector and the phase shift network; this reduces feedback to the base and may have to be increased or decreased depending on the gain of your transistor at 1000 Hertz.

I usually run the rf current (collector dc) between one and two mils with the 2N1726 transistors; other transistors may take more. A number 48 bulb in the collector lead may save you a $3 transistor. With the 2N1141 the rf output keeps climbing up to 4 or 5 mA collector current. You will readily find the best place to operate. When the collector mils keep climbing and the rf output starts to drop off, back off!

Operation

Dipper

As a general rule "dipping" is easier in the VHF region and gets more difficult as you go into the microwave region. On HF you couple one coil end on to the other; on VHF you bring it near, and on UHF you have to work to get the necessary coupling or use a probe.

With nothing near the dipper, swing the dial through the range to make sure it has no dips of it's own. The VHF/UHF units without chokes described here do not generally have such dips. Unwanted dips can be caused by chokes, resonant feed wire lengths, metal supports, and rf links and cables among other things.

When you do get a dip after coupling to the unknown circuit be sure and change the resonance of that circuit for a final check while watching the dipper meter. If the test circuit is a tuned circuit vary the tuning and see if the dipper will follow it—it *should*. If all else fails, use the dipper as a generator. Since it is very difficult to get the far end of a cable matched exactly over much of a frequency range, *expect* to find external dips in the dipper when using a cable.

Indicating frequency meter

Always keep the transistor plugged in and the base bias at zero so the diode is doing the work. When you advance the bias, collector capacity will cause the dipper frequency to change a little—more with some transistors than others.

For finding a weak signal you can use regeneration by turning up the base bias, but watch out for slight frequency changes. This regeneration can be very handy for finding weak oscillators or hard-to-find rf energy. Use the rf input loop with care; the least coupling is the best. Remember that some cables and terminations will detune L1.

Field strength meter and modulation monitor

The first part is obvious; use a small antenna or probe, get some signal in, and go ahead. Do not use any base bias to start with. If you are working with a very weak signal you might have to push the bias up for regeneration.

The modulation monitor is simply our often-described system of diode detector, transistor amplifier, and padded ear-phones. You can actually hear what your own transmitter sounds like to others. I use it on every new rig and after every circuit change. You don't need much of an antenna or probe when listening to your own rig; don't overload the diode when checking modulation. In fact, use light rf coupling and plenty of audio gain to hear yourself as others hear you.

Regenerative Receiver

Plug an audio amplifier into J2, Fig. 7, advance the bias control, and tune. I have heard several UHF TV stations from Massachusetts up here in Peterborough, so it is really sensitive. One nice feature of this circuit is that the regeneration turns into oscillation very smoothly. Stability is good too. You can heterodyne a crystal controlled two meter signal and copy CW with it. Not bad for a 144 MHz blooper!

To transfer signals from one transmitter (A) to another (B), just tune in A, then shut it off; listen for B and tune it in. That's all. Harmonic monitoring is easy: just tune over the suspected range in the regenerative condition. It is particularly good because only *one* frequency is present in the receiver. This is *not* the case when using a super-het receiver for monitoring harmonics.

Signal generator

One of the big features of this circuit is the presence of an rf meter right in the proper place circuit-wise. The modulation also helps, especially when running triple or quadruple conversion in a receiver. The modulation control is very convenient, at full on its spreads the signal across 20 or 30 kHz on a selective receiver. For checking a difficult to get at circuit, use a cable and probe, either capacitive or inductive, to get the signal into the unknown circuit.

I often use one of these units for antenna and receiver tests. I just plug a little two element beam into the rf jack and set it out away from the shack; often one or two hundred yards away. There is nothing like tuning up pre-amps with your antenna system connected. For antenna tests it is used in reverse.

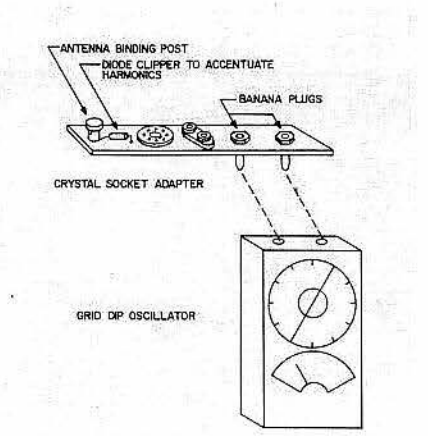

Crystal socket adapter for grid dip oscillator extends the unit's capability by enabling it to read crystal activity.

EXTRA SERVICES FROM YOUR GRID-DIP OSCILLATOR

W. B. Cameron WA4UZM

One of the handiest instruments around the average ham shack is the grid dip oscillator, but many hams do not get all of the advantages this little instrument can offer. Most people know that it is useful for finding the resonant frequency of an LC circuit, or for generating a signal someplace in the range, although it is not quite a substitute for a well calibrated signal generator in this respect.

Many people do not realize that the grid dip oscillator makes an excellent crystal calibrator as well. The typical grid dip oscillator uses a two-terminal coil and a two-section variable capacitor, connected in the form of a Colpitts oscillator circuit, with the variable capacitor providing the voltage division for proper feedback. This same circuit, with a quartz crystal replacing the coil, becomes a very satisfactory crystal oscillator. In this case, the variable capacitor becomes a trimming capacitor capable of putting the crystal on the proper frequency with considerable accuracy and also allowing a fairly wide latitude higher or lower for checking bandpass.

The meter reading gives an index of crystal activity. What is required is an adapter to match the pins of the crystal holders to the coil socket of the grid dip oscillator. I have made up such an adapter for my particular unit which consists of a 1½ inch by 4½ inch piece of masonite which carries two banana plugs to insert into the oscillator socket, and several different sizes of crystal holders, all connected in parallel, to accommodate any crystals I happen to have around the shack. I carry in my tool kit various assorted crystals. These give me spot frequencies for band edges and other reference points on all of the amateur bands.

In checking the higher frequency bands, I find it useful to add a diode clipper and have one permanently wired on the same adapter board. This is a 1N69 which simply goes from one side of the crystal to a terminal point at which I can attach an antenna or a lead to the input jack of the receiver. By simply attaching a short length of wire approximating a quarter wavelength at this frequency, I can provide a strong enough signal from the shack to enable me to check out my direction finding loop in the automobile fifty feet away.

In tuning up my 2 meter FM gear, I plug in a 3061.25 crystal (which is the transmitter oscillator crystal for my Link 2m FM unit) and then couple from the 1N69 to the input of the receiver. This provides a signal stronger than most of the local signals on the band, and adequate for initial tune-up. For finer adjustment of the i-f strip, I clip the lead from the 1N69 to the chassis close to the antenna input jack and the leakage provides a signal of the order of .2 μV, which is useful for final adjustment of the critical tuned circuits, the squelch control, and others. For best results, I leave the oscillator and the receiver on for a half hour or so to warm up, and then with the variable capacitor in the grid dip oscillator, I zero-beat the incoming signal of a station generally considered to be on frequency. Once this is done, I have a signal source on the bench with which to check the receiver for passband balance as indicated on the microammeter connected to the discriminator output.

GDO TO FIND C

F. C. Rayer G3OGR

Most amateurs have a grid dip oscillator lying around, and an easy accessory can allow it to be used to read the values of unknown capacitances up to about 1000 pF. This is useful for unmarked surplus, those with obliterated markings, or to find the swing of small variables. Or we may check the best value found in some circuit position with a preset or variable, then measure this and substitute a near value fixed capacitor.

Figure 1 is the circuit. C1 and C2 are on the lid of an insulated box, carrying also spring terminals for CX. The capacitors have good knobs with pointers. Coil L can be half a dozen turns of stout wire, self-supporting, or anything which comes within a convenient range of the GDO (say 2.5–10 MHz) with both variables fully closed.

To calibrate, close C1 and C2 fully. Tune the GDO for the usual dip. Note the frequency on the box for future use. Take a few 1% capacitors, such as 100 pF, 200 pF, and so on, up to a total of about 1000 pF. Clip one to CX. Open C2 to restore the dip on the GDO. Mark the capacitor value on C2 dial. Series and parallel capacitors give more values. For example, 100 pF plus 200 pF in parallel gives 300 pF, while 500 plus 200 gives 700 pF, and so on.

Restore C2 to its fully closed mark. Repeat to calibrate C1, this time using

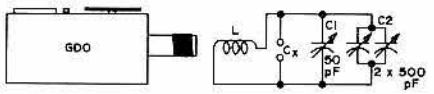

Fig. 1. GDO to find C.

capacitors such as 5 pF, etc., up to about 50 pF. When you see how the scales mark, estimate intermediate markings, to fill in.

Once calibration is finished, it is easy to find a capacitance value from about 2.5 to 1000 pF. Close C1 and C2. Put the GDO near L and tune the GDO for dip. Clip the unknown capacitor across CX. Open C1 or C2, as appropriate, to restore the dip. Read off the value from the scale. That's all there is to it!

GDO COIL EXTENSION

Bill Turner WAØABI

A grid dipper is a great piece of test equipment and belongs wherever rf equipment is to be designed, constructed, or serviced. All writings on the subject seem to be prefaced with this comment, and I hesitate to break tradition. Now that the formalities are over, we will proceed with the subject matter.

Probably the one most inconvenient feature of all grid dip meters is the physical size of the instrument. This holds true for the two unit commercial models as well as the more common self-contained types. It is not

so much that they are large but rather that the head will not always fit into the nooks and crannies which seem to be designed into most equipment. This situation will more than likely become more severe as integrated circuits come into more general use. At lower frequencies the coil assembly is usually long enough to reach to within shouting distance of the desired circuit, but as the frequency is increased the dipper coil shrinks to perhaps an inch protruding from the case. Try getting this even near a circuit buried 2 or 3 in. deep in a chassis and you will fully appreciate the magnitude of the problem.

There is a way of relieving the difficulty which requires neither a great deal of time nor expense. It is only necessary to put to use some basic theory which each of us was required to know in order to get a ham license. Required are perhaps a 3 ft length of small coax (RG 174/U), 6 in. of hookup wire and a ballpoint pen casing. The innards of the pen are removed, and the business end reamed slightly to accept the ends of a ½ in. diameter one turn link formed of hookup wire. Inside the barrel of the pen the ends are soldered to the coax, insulated, and cemented in place. The remaining wire is formed into a 2 turn link which fits snugly on the coil form of your grid dipper. This link is soldered to the opposite end of the coax and secured. Shrinkable tubing is perfect to cover the joint.

The next time you face this perplexing problem hold your head high and fear not. Merely slip the link over the coil form, place your probe so as to allow coupling into the desired circuit and proceed as usual. The only difference will be a more or less fixed load on the oscillator which doesn't affect its ability to indicate resonance. As always, best results are obtained with minimum coupling.

Chapter VIII

Noise Generators

SIMPLE NOISE GENERATOR

George Rubis K9ONT

As anyone knows that has done any work at all on receivers, whether it is a conversion or simply substituting a "hotter" tube in the front end, we get to the point where we begin to wonder if the adaptation was worth while or have we been fooling ourselves.

A noise generator using one of the noise diodes (IN21 or IN23) can give an indication if any improvement has been made.

The circuit is straight forward, but with one addition that others that I have seen do not have. The voltage is regulated by a Zener diode.

The reason is obvious to anyone who has worked with the simpler type of noise generator. The results are not always consistent from measurement to measurement and from day to day. The voltage and current vary with the setting of the variable resistance and due to the normal aging of the battery.

The Zener Diode eliminates this by maintaining a constant line voltage. In our particular instrument it is six volts. Of course we must use a battery in excess of six volts. Nine volts is a good value. I have found that used transistor radio batteries still have enough life in most instances to last for many tests.

One of the main requisites of a noise generator is that it must be shielded throughout. Therefore we must give some thought as to the placement of the various components.

A Mini-box 2¼ x 2¼ x 4 is an ideal size. As for a connector I used the SO-239 coaxial. I find that this connector allows more flexibility

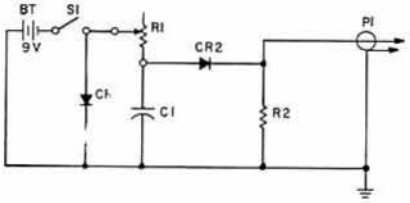

To avoid excess wear and tear on the zener diode and the battery a 200 ohm resistor should be inserted between the 9 v battery and S1.

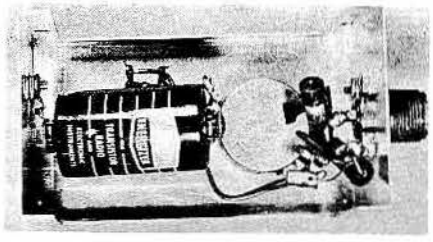

than any other. If a direct connection to the receiver is desired merely attach it through the double connector type DKF-2 made by Dow Key. On the other hand if it is desired to have the controls of the noise generator close at hand merely connect a length of Coax of eighteen inches or so. I haven't been able to discover that it has affected any measurements to any degree.

In the construction of this noise generator just remember a few basic rules. Keep all connections as short as possible. The noise diode and bypass condenser and resistor (50 or 75 ohms as the case may be) as close as possible to the output plug. Remember to use pliers to absorb the heat when soldering the leads of the diodes.

To mount the silicon diode, which has one large end and one small, we must improvise to a certain extent. For the small end a lug from one of the old tube sockets will do. For the large end use a small fuse clip.

Don't be too fussy about the variable resistor. For most purposes any value from 10M up to 50M can be used.

The battery you choose will determine the manner of mounting.

No need to give detailed instructions as to the use of this noise generator. There are ample instructions to be found in various magazines as well as handbooks.

. . . K9ONT

Parts List

2—¼ x 2¼ x 4 Minibox
Bt—9 volt battery
Cr1—6 Volt Zener Diode
Cr2—IN 21 or IN 23 Silicon Diode
R1—10M-50M Variable
R2—51 ohm or 75 ohm (according to your line)
C1—.001 to .005 disk ceramic
S1—S.P.ST. this may be on your variable resistance
P1—So-239

A CRYSTAL DIODE NOISE GENERATOR

Karl Tipple W5TEV

Most amateurs who do very much operating at the higher frequencies where receiver sensitivity rather than QRM often determines success eventually come to the conclusion that their present receiving equipment is not as sensitive as would be desirable and that a change is in order. And once that change has been made, whether it takes the form of a new converter or modification of existing rf stages, one nearly always wonders whether the new really *is* better than the old. Comparisons of signal strength with new and old equipment are erratic and unreliable at best and do not necessarily give the desired information since the absolute output level or "S" meter reading is not the problem. What is actually of concern is whether the signal to noise ratio of the receiving system has been improved. Or in other words, does a given rf signal produce an audio output signal from the new receiving equipment that is louder in comparison to the background noise than did the same input signal with the original receiving equipment. If it does, the noise figure of the new receiving equipment is smaller (better) and it should be possible to copy a weaker signal than before.

Unfortunately few of us own or have access to a signal generator of the proper frequency range, with an accurately calibrated attenuator and shielded output, for making the type of measurements mentioned above. For the majority of amateurs something less expensive and more readily available is needed. A crystal noise generator, which can be constructed for a few dollars and which will enable anyone to make before and after comparisons of noise figure, is such a device.

Briefly, the theory behind the use of the noise generator follows. The sensitivity of a receiver is highly dependent on the ability of the rf stages to amplify a weak signal as much as possible while adding a minimum amount of noise to the signal. Noise of this type will

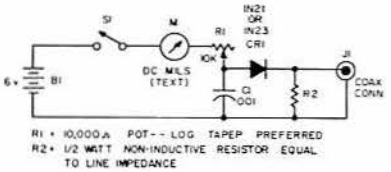

R1 = 10,000Ω POT--LOG TAPER PREFERRED
R2 = 1/2 WATT NON-INDUCTIVE RESISTOR EQUAL TO LINE IMPEDANCE

FIG. 1

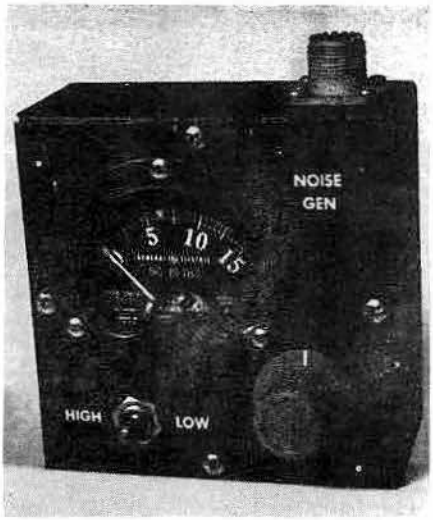

be heard at the receiver output as a familiar hiss or "rushing" sound. Now, if an external source of broadband or white noise (random noise independent of frequency) is connected to the receiver antenna terminals, an increase in noise or hiss will be noted at the receiver output. And if the noise generator output is adjusted to provide exactly twice as much receiver output noise as existed before the application of the noise generator, then the generator must be providing a noise signal equal to that generated in the receiver. Thus, if the receiver can be modified so as to reduce the noise generator signal required to double the receiver noise output, the noise figure of the receiver will have been improved.

A noise generator of the type described in this article can not be used for measurement of absolute noise figure without additional calibrating equipment. It can, however, be used for *comparison* of noise figures. It enables one to determine whether a receiver really has been improved and it can be used to determine which of a number of possible modifications will yield the best results in terms of minimum noise figure (maximum sensitivity). Use of the device will be discussed in more detail later.

A basic noise generator circuit is shown in Fig. 1. The noise is produced by CR1, a silicon diode of the 1N21 or 1N23 variety. These diodes have been widely available on the surplus market for several years. They are also readily available new at small cost; however as will be explained later, it may be desirable to use a surplus diode rather than a new one.

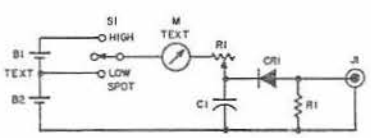

FIG. 2

R1 = 10,000 ohm pot—log taper preferred
R2 = ½ watt non inductive resistor equal to line impedance
Other parts same as Fig. 1

The current supplied to the diode from the battery and therefore the noise generated by the diode is determined by the setting of R1. The best value for R1 is necessarily a compromise since in its maximum resistance position it must limit the current to a low value but it must also not change resistance too rapidly at the low resistance end of the range or the normal operating range of the instrument will be limited to only a few degrees rotation of the R1 shaft. A 10,000 ohm log taper pot should prove satisfactory.

The value of R2 should be about the same as the transmission line impedance. A good value might be 56 or 68 ohms, although if it is desired to use the noise generator with equipment which normally operates from higher impedance lines, a larger value should be selected for R2. In this case one might compromise with a value of 100 ohms. C1 serves as bypass capacitor and may be either mica or disc ceramic.

A more elaborate arrangement was used in the construction of the unit shown in Photo. 3. A schematic of this generator appears in Fig. 2. Here a tapped battery (2 pencells) was used to minimize the range to be covered by R1. It should also be noted that the diode is shown reverse biased in Fig. 2. Many of the surplus diodes available have very poor reverse resistances, which will allow reverse bias operation, and when operated under these conditions will generate considerably more noise for the same bias current than when operated in the more conventional configuration shown in Fig. 1. The diode must have a reverse resistance of only a few thousand ohms or less if it is to work successfully in the reverse bias connection. Therefore unless the reader can obtain some surplus diodes and select one with a low reverse resistance, it will probably be necessary to operate the diode forward biased and to use the higher battery voltage of Fig. 1.

The meter range depends upon the battery voltage and the resistance of the diode in whichever connection it is used. The meter used in Fig. 2 was a 0-4 ma surplus meter. However, if the diode is operated in the forward biased connection a meter of somewhat higher current rating will probably be needed. Therefore, it is suggested that a low range meter be obtained and if more than full scale current is required for the diode to develop sufficient noise, a shunt resistance can be placed across the meter terminals to extend the meter range. An inexpensive meter can be used since all that is needed is a relative indication of current.

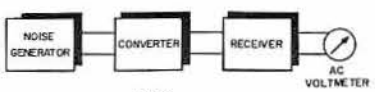

FIG. 3

For those not familiar with the IN21-1N23 type diodes it might be mentioned that they have no wire leads. The anode connection is a brass shell on one end of the unit and the cathode connection is a brass pin at the other end. Although external connecting wires might be soldered to the brass ends, there is danger that the diode will be over heated and destroyed by such techniques. It is safer to make connections by clamps made from small plate or grid caps or fahnstock clips.

It should be evident from the above discussion that there is nothing critical about the construction of a noise generator of this kind and that a number of different circuit variations are possible. Even if the device were constructed entirely of new components the cost should be less than $8 and with a little ingenuity the cost can be reduced substantially through the use of surplus parts.

Perhaps use of the noise generator can best be illustrated by considering an example of noise generator application. Suppose that you want to use either one of two available 6 meter converters with your low band receiver and that you wish to determine which converter will provide the best weak signal reception. A test set-up is shown in Fig. 3.

The ac voltmeter is used to measure the audio output of the receiver and may be either a multimeter or a VTVM. It can be connected across the speaker terminals or across the headphone line. Higher voltages can generally be obtained from the headphone output and this connection will probably have to be used if a multimeter without a very low ac range is used.

The measurements can be started by measuring the ac noise output voltage from the receiver with the noise generator turned "off". Then the noise generator should be turned "on" and the generator level adjusted until the output meter reading has doubled. At this point a note should be made of the noise generator setting. The above procedure can now be repeated with the second converter connected to the receiver. Whichever receiver-converter combination requires the smaller noise generator current setting to double the noise output is the combination that will provide the best weak signal reception.

The noise passed by the receiver is a function of the bandwidth of the receiver. Also the reading given by a particular output meter is dependent on its bandwidth. Therefore the bandwidth of the receiver should not be changed during measurements and the same output meter should be used thoughout a set of measurements.

The technique described above can also be used to determine which of a number of rf amplifier tubes will give the best performance. The noise generator can be used for alignment of rf stages.

For the man who constructs his own converters or receivers the device is a tremendous boon since such adjustments as determining the optimum antenna to grid coil coupling can be made simply by adjusting for maximum increase in noise when the generator is switched "on". (This technique gives the same results as adjusting for minimum noise generator setting to double noise output and it is a bit easier to use when adjustments must be made.) If the input circuit uses a single tapped coil instead of two coils, the best tap position can be determined.

The uses mentioned above are only a few of the possible applications of this noise generator, and for the amateur who constructs his own receiving equipment the device is indispensable.

TEMPERATURE LIMITED DIODE NOISE GENERATOR

F. L. Thomas

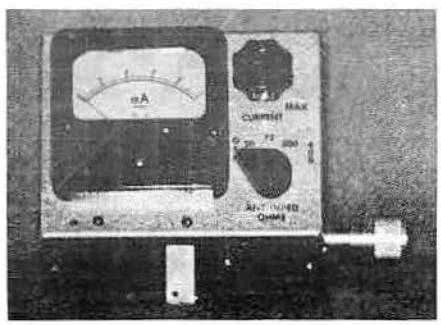

Recently I was confronted with the necessity for a good noise generator. All of the noise generator designs available in any of the

amateur publications at hand were of the crystal diode type. The disadvantage of this type of instrument lies in the fact that the current through the diode has no simple relation to the noise output. Unless expensive calibration equipment is on hand this type of generator is useful only on a comparative basis. Consequently it was decided that a temperature limited diode noise generator would be built.

The noise output of a temperature limited diode noise generator is simply related to the current flowing through the diode.[1] The noise figure of a receiver may be calculated directly from the magnitude of the current by the following equation:[2]

Noise figure in db.=10 log (20 I R)−(1)

Where I=current through temperature limited diode required to make the noise output power of the receiver double the value it was with no current through the diode.

R=antenna impedance

The actual noise generator is quite simple, consisting of half a 6AL5 with a milliammeter in the cathode leg and the appropriate resistance for the antenna circuit connected to the plate by means of a selector switch. The heater current is controlled by a 20 ohm potentiometer in series with the heater. The unit is battery operated for convenience. High current capacity, small sized mercury cells are used throughout. The whole unit is contained in a 3" x 4" x 5" Minibox.

Construction

The resistors are mounted on the switch, making the leads as short as possible. The tube socket is mounted on a small bracket screwed onto the side of the chassis, placed so that the distance from the switch is a minimum. The meter calibration potentiometer and the heater supply battery holders are mounted on another bracket placed over the meter as shown in the photograph.

Operation

To use the generator it is connected to the receiver antenna terminals, the AVC is turned off, and the audio output is measured with the generator off. The generator is then turned on and the current through the diode is increased until the power output is double what it was before. At this point the voltage output will only be 1.41 times the original. The current necessary to give this noise increase is noted and the noise figure calculated according to equation (1), or estimated from the figures given in Table I.

Noise Figure in db.	Current, ma., for antenna impedance of:			
	50Ω	72Ω	300Ω	600Ω
2	1.40	1.15	-	-
4	2.25	1.80	0.42	-
6	3.55	2.85	-	-
8	5.65	4.50	1.05	0.53
10	8.85	7.15	-	-
12	14.2	11.3	2.65	1.32
16	-	-	6.65	3.30
20	-	-	16.6	8.42

The unit described is useful for noise figures up to 13 db at 72 ohms. For higher noise figures a higher current capacity diode and a higher heater voltage and current supply is required, necessitating an ac operated power supply. With a suitable power supply a 6X4 may be satisfactorily operated up to a noise figure of about 22 db. In both cases the maximum noise is obtained by passing more

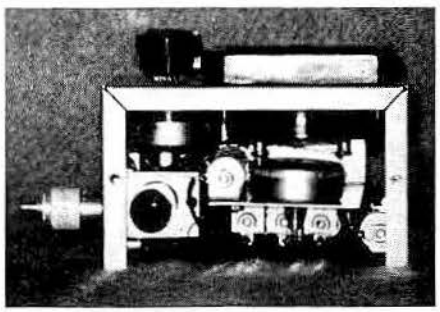

than the allowable average current through the diode. Consequently readings at these extremes should be made and the current lowered again in only a few seconds, or damage to the diode will result.

Table I shows the current readings for various noise figures with different antenna impedances.

The generator will operate satisfactorily up to at least 50 mc, and probably considerably higher.

Editor's Note: By substituting flashlight batteries for the mercury cells and a 20 mA meter instead of the 1 mA meter with a shunt across it, the cost of construction can be greatly reduced.

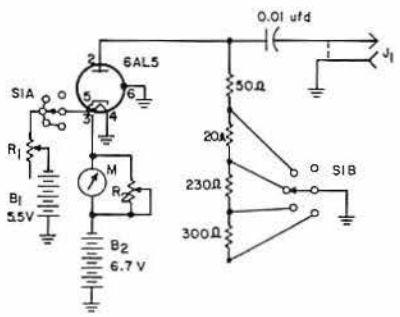

B1—four Mallory RM12 or RM12R in series (lifetime of this circuit should be greater than 10 operating hours)
B2—Mallory TR-135R
M—0-1 ma (Lafayette TM-60 or equivalent)
R1—20 ohm potentiometer
R2—20 ohm Potentiometer
J1—coax connector
S1—DP 5 pos miniature rotary switch

REFERENCES

1. Radiotron Designers Handbook, fourth edition, page 1307, reproduced and distributed by RCA Victor Division, Radio Corporation of America, Harrison, N. J., 1953.
2. Radio Engineering Handbook, fifth edition, page 19-10, Edited by Keith Henney, Published by McGraw-Hill Book Company, 1959.
3. Terman, F. E., Electronic and Radio Engineering, fourth edition, Published by McGraw-Hill Book Company, 1955.

CALIBRATED NOISE GENERATOR FOR 432

Hank Olson W6GXN

As pointed out in previous articles—the temperature-limited noise diode is the best tool for measuring the sensitivity of one's receiver. The measurement made with this device is "noise-figure" or "noise-factor" and this is the magic number by which you can compare your VHF or UHF receiver with Joe's down the street, or Sam's in Massachusetts. These measurements will be comparable between any two receivers because bandwidth, type of detector, and other miscellaneous features (different for each receiver) do not affect the measurement, if it's carefully made (that is, if one's measurement of 3 db power increase, when the diode is turned on, is true).

Past amateur articles on noise-diodes and their use in noise-factor measurement have only shown how to construct units for up to about 200 mc. The noise generators described previously, for amateur use, have used the 5722, the diode wired 24G (3C24), or the diode wired 801A, as their tungsten-filament diodes. The 15E and 01A have also been used occasionally as diode-wired triodes, too. Commercial UHF noise generators use a variety of tungsten-filament tubes, all of which are a bit expensive for most hams. If you can lay your hands on one of these tubes, used or otherwise surplus, by all means employ it in your noise generator. Table I is a list of such gems.

Philco:	L1262A
RCA:	R6212
Bendix:	6144
Marconi:	CV2171

Table I

The tube I used is a triode, a Western Electric 708A, originally designed for grounded-grid UHF amplifier service. The grid and filament are used as the diode elements, ignoring the plate altogether; the plate, if used, could only increase transit time and shunt capacity. The tube is used, as it was intended to be used, with the metal shell (grid) grounded. The 50 Ω load is connected in the filament cricuit; the filament power is fed in by means of a concentric inductor, which also tunes out the stray capacity of the tube.

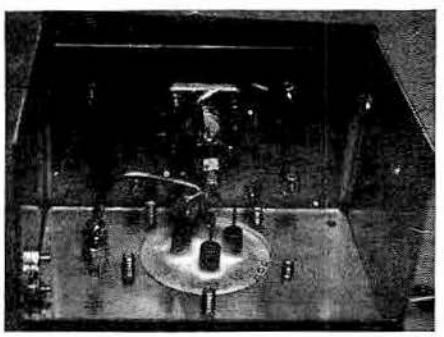

RF Circuitry.

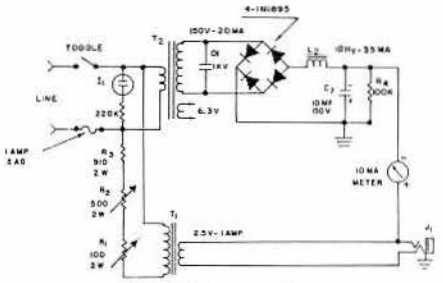

Fig. 1. Power supply.

C_1, a small "tweaker," adds in a tiny additional capacity to make adjustment to 432 mc easier; it makes tuning to anywhere in the 420 to 450 mc band possible. L_1 is constructed of a 1¾" length of ¼" copper tubing and has a piece of No. 20 teflon insulated wire inside it. The use of teflon insulated wire is only necessary because teflon will withstand the heat of soldering.

The effective circuit, then, is as in Figure 2.

At 432 mc, if $Cgk + C_1 = 3$ mmfd, then L must be 0.04 μh to be parallel resonant. The reactance of either $Cgk + C_1$ or L_1 is about 100 Ω, so the system has a Q of ½, and hence will be rather broad in its noise output spectrum—just as we want it to be.

The WE 708A tube was recently available from a Los Angeles surplus emporium at the price of 39 cents each or ten for a dollar. We bought a buck's worth, figuring some would be NG, but all were perfect and saturated well. One was lost in initial test, when we applied too much filament voltage; it was subsequently hack-sawed open to find out the details of its construction and to confirm connections. The details learned are presented in Figure 3 along with its saturation curve.

The filament is a single, fine, straight, tungsten wire through the grid helix. The grid helix is perhaps 1/16" diameter and is welded every turn to the shell. All this adds up to: good cylindrical diode configuration, close cathode-grid spacing to cut down transit time, and low grid to case inductance. In short, we have a nearly ideal noise diode for a dime a piece.

Construction details: The rf section of the generator is constructed on an aluminum plate bent into an L, the WE 708A protrudes through a 1⅝" round hole to expose its filament pins next to where the UG58A/U connector is mounted on the other side of the L. The WE 708A is held in place by five 8-32 binding-head screws that are tapped into the plate. The UG58A/U has four 200Ω, ½ w resistors soldered to it each at 90° to its neighbors to form a less inductive load, approximating a resistive sheet. These resistors are soldered to the UG58/U before it is mounted to the aluminum sheet to make soldering easier (less heat required). Then L_1 is formed and soldered from the WE 708A filament pin to C_3. The center filament lead of L_1 is fed through and soldered to the other filament pin and to C_4. C_2 is then soldered in; be sure this is the type called for or a similar low inductance stand-off ceramic. The rest is straight forward. Diode and power supply were each built in an LMB 141 box chassis. The details of wiring the diode circuitry are shown in Fig. 4.

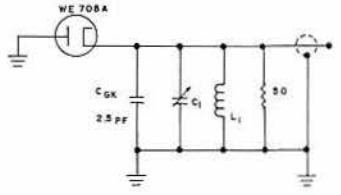

Fig. 2. Basic noise generator circuit.

A word about R_1 (the "fine" adjust) is worthwhile. Make *sure* this one is a 2w type A.B. (ohmite) molded carbon pot, if not both R_1 and R_2. This will make smooth diode-plate current adjustment easy; a wire wound pot will cause the plate current to vary in steps because of the effect of the pot's sliding contact sequencially contacting each wire (the same applies if you use a Variac).

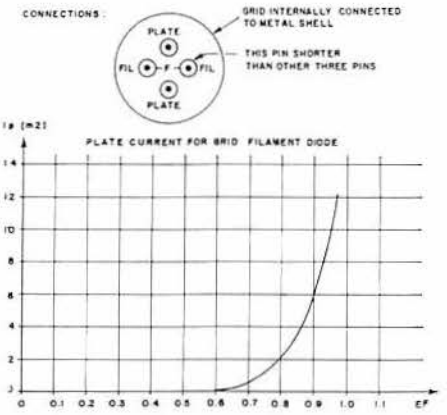

FIG 3

Fig. 3. Connections of 708A and graph of relationship between "plate" current and filament voltage.

To align on 432 mc, C_2 is temporarily removed and a UHF grid dip meter coupled to L_1, loosely. C_1 is adjusted for a dip at 432 mc. Then C_2 is reinstalled, and we should be ready for receiver checks.

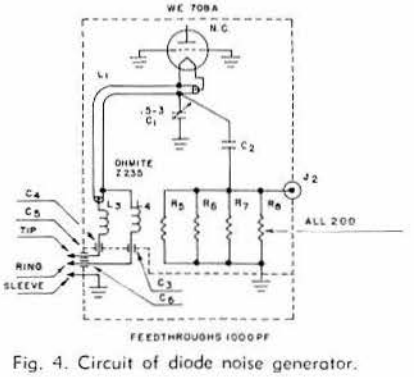

Fig. 4. Circuit of diode noise generator.

The above noise generator was compared with a Hewlett Packard 343A noise diode using my own 432 mc converter as the "to be measured" device. The results showed less than 0.5 db difference.

The author wishes to thank Gene Howell, W4RLU, for his photography of the unit.

ANOTHER WAY TO MEASURE NOISE FIGURE

Jim Kyle K5JKX

Many times it's been said, but it can always bear repeating. Noise figure is probably the least-well-known measurement in any amateur station.

At least a part of the difficulty with noise figure lies in the means usually employed to measure it. While it's not too difficult to figure out the power input to your final, or even the power *output* (often a surprisingly different figure), measurement of receiver noise figure tends to be a complicated and somewhat inaccurate process at best. It requires special equipment, and even then may be no more accurate than plus-or-minus 100 percent.

The classic means of measuring noise figure is to use a noise generator and crank in additional noise until receiver output is doubled. This means, of course, that the noise generator output is then exactly equal to the original noise, and if the noise-generator output is accurately known then the original noise is also known. All this has been gone into in detail in another article.

However, a noise generator with accurate calibration isn't so easy to come by, and an inaccurate noise generator doesn't do much good for measurement purposes (although it's fine for tune-up).

There *is* another way to do it, which is actually much more in line with amateur practice. This other way also requires some test equipment, but it might be more easy to come by.

Before we get into the details of the "other way" to measure noise figure, let's take another look at the reason for using noise-figure measurement as a yardstick for receiver sensitivity in the first place.

To start, we're really interested in the answer to the question "How weak a signal can I hear?" In the 3-30 mc range, the question can be answered directly—how many microvolts must the receiver have to give readable output?

As the vhf region is entered, though, the fractional microvolts become alarmingly small.

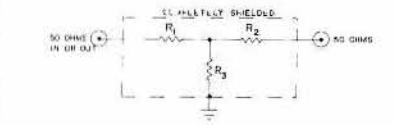

DB Loss	R1, R2	R3
3	8.2	150
6	16	68
9	24	39
20	39	10

All resistors composition, ½ watt, 5%

Fig. 1. Construction of T-pads

Somebody figured out that most of the problem lay in the receiver's own internal noise, and came up with the idea of a "perfect" receiver which would have no noise at all. This is a noise figure of 0 db. Now by comparing existing receivers to this perfect ideal, and comparing the internal noise in db, we had a way of discussing receiver sensitivity.

Since we're now talking about noise, which is equally present at all frequencies throughout the spectrum, we can see that the amount of noise present in a receiver's output is at least partially determined by how much of the spectrum we are looking at. A broad receiver has more noise output than a narrow one, all other things being equal. If you don't believe it, fiddle with the selectivity switch on your own rig and listen to the change of noise output.

This dependence of noise on bandwidth is another reason for using noise figure as a comparison. The *actual* amount of noise is cancelled out in the comparison, leaving only the relative amounts of noise in the "perfect" receiver and the receiver under test to be measured.

When all this became established, nobody

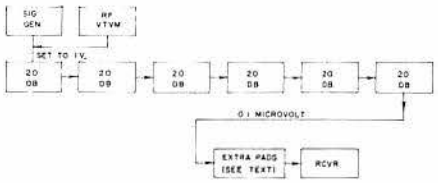

Fig. 2. Test set up.

was paying much attention to receiver bandwidth and it was felt that a true determination of the effective noise bandwidth of a receiver was much more complicated than the comparison measurement. However, in these days of SSB and special filters, that's not so true any more.

As you may have guessed by now, the "other method" of determining noise figure depends on a microvolt measurement and knowledge of the receiver's effective noise bandwidth. The only reason for converting the results back to noise figure is to allow comparison with measurements made in the more conventional manner.

With typical ham measurement techniques, the results won't be of National-Bureau-of-Standards accuracy. However, if you're reasonably careful, results using this method will be at least comparable in accuracy to those made with a homebrew noise generator. Ready? Let's go:

You'll need two items of test equipment (only one if you're really lucky). These are an rf signal generator covering the desired frequency range on fundamental output, and an rf VTVM reasonably accurate at the desired frequency. If you have access to a "microvolter" or similar laboratory signal generator, you won't need the VTVM.

In addition, you'll need a whole handful of 50 ohm T-pads; these can easily be put together in a hurry by following the schematic in Fig. 1. You'll probably need about 8 20-db pads, as well as one each in 3-db, 6-db, and 12-db values.

Turn on both the receiver and the signal generator and let them warm up. For protection against any leakage from signal-generator to receiver through the power lines, it's best to supply them from separate circuits and to use a power-line filter such as that used to eliminate rf interference between the power line and the unit.

Connect a string of six 20-db pads to the signal-generator output as shown in Fig. 2, and adjust output of the signal generator to 0.1 volt. If you have a microvolter or equiv-

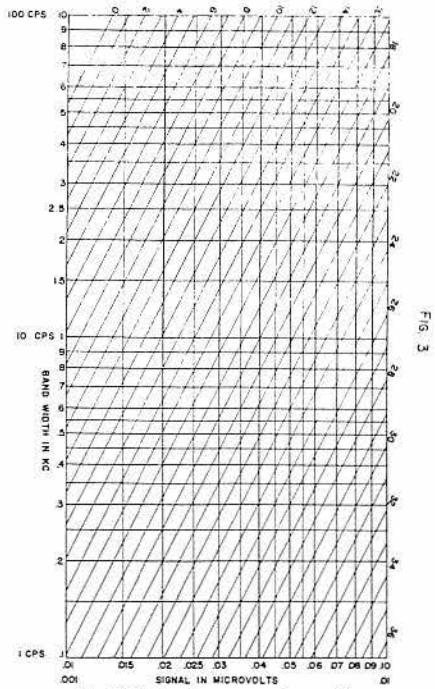

Fig. 3. Noise figure vs. microvolts.

alent, use only one 20-db pad and set generator output to 1 microvolt.

In either event, the output of the final T-pad will be a 0.1 microvolt CW signal. This should be more than adequate for any reasonably-sensitive receiver to allow spotting of the signal.

Switch the receiver's avc off and the bfo on, and place the selectivity switch in any position for which the selectivity is accurately known. The selectivity marked on the front panel will not be the effective noise bandwidth, but you can use it as a starting point to guesstimate the noise bandwidth. If your receiver uses a mechanical filter or other device with approximately the same skirt selectivity, effective noise bandwidth will be about 1½ times the bandwidth marked on the front panel. If it is one of the older types with reasonably broad skirts, noise bandwidth will be about 3 times the marked value. Both these correction factors are approximate, of course; if you have any means of measuring effective noise bandwidth, use it instead.

For a start, use a fairly broad selectivity position; this requires more signal and makes things a bit easier.

Now tune in the signal from the generator, leaving gain controls at maximum but tuning for maximum signal strength just as if it were the new state you need. The 0.1-microvolt signal should be easy to find.

Next step is to reduce the generator output by hooking in additional T-pads until you locate the point of "minimum discernible signal." The 3, 6, and 12 db pads may be hooked up in series in any combination to give you from 3 to 24 db additional attenuation in 3-db steps. Using another 20-db pad will give you from 20 to 44 db more attenuation, and the signal is sure to become too weak to copy before you reach 44 db below one-tenth of a microvolt!

The point of MDS is approximately equal to a 0-db signal-to-noise ratio for most of us, and is considerably easier to determine than would be a true output S/N ratio. When you find this point, record the db below 0.1 microvolt and the selectivity (in kilocycles) used.

Now switch to a different bandwidth on the receiver and repeat the test. Record its results also. For maximum accuracy, repeat each of the tests 10 to 12 times and average the result.

The signal level in microvolts corresponding to db below 0.1 microvolt is given in Table I. Locate it there and move to Fig. 3, the graph of signal versus bandwidth by noise figure.

Enter the graph from the side with effective noise bandwidth, and move across until you intersect the line corresponding to signal level in microvolts. The diagonal lines are noise figure; if one passes through the intersection point, read noise figure in db from it. If not, interpolate between the lines.

In reading Fig. 3, use the 10 kc-100 cps scale with the .01-.1 microvolt scale, and the 100 cps-1 cps scale with the .001-.01 microvolt scale. If your bandwidth-signal level combination falls off the graph to the left, use the

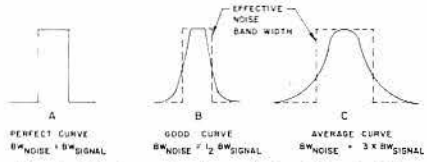

Fig. 4. Relation of noise and signal bandwidths.

lower signal-level scale with the *higher* bandwidth scale and subtract 20 db from the resulting noise figure.

In the happy event that all your errors (and our approximations) cancel out, you'll find the noise figure to be the same at both the narrow and the broad bandwidth positions. However, it's more likely that you'll measure different noise figures at different positions of the selectivity control. It's safest to take the highest noise figure measured as being closest to correct, but you can average them if you prefer. Either way, you will probably be within 1 db of the real figure—and this is as accurate as most noise-generator techniques can be, also.

That completes the measurement, but before we wind this up let's take a more detailed look at the idea of "effective noise bandwidth" which is such a key part of this measurement technique.

Most of us are familiar with the idea of a "perfect" curve for receiver selectivity such

as that shown at A in Fig. 4. Here the receiver has equal response over the desired band, and response drops to zero at the band edge. Such a curve is said to have a shape factor of 1, and is of course impossible to achieve in practice.

Now back to noise; it's spread out equally over the spectrum. A noise bandwidth of 1000 cycles per second contains 10 times as much noise as one of 100 cps. Thus "noise bandwidth" inherently has a shape factor of 1.

Since such a shape factor is impossible to achieve, it follows that "noise bandwidth" and actual receiver bandwidth must differ. If receiver bandwidth is measured at the —60 db points, the noise bandwidth will always be smaller than this receiver bandwidth. If receiver bandwidth is measured at the points where response drops 1 db below peak, the noise bandwidth will always be greater.

The mathematical expression for noise bandwidth is an integral equation involving differential gain, which is a cumbersome thing to solve. In general, the noise bandwidth of a receiver is said to be approximately equal to the bandwidth between points which are 3 db down from peak response.

In practice, if the shape factor (6 to 60 db) of the receiver is 2, the effective noise bandwidth will be approximately 1.3 times the 6-db bandwidth. If shape factor is between 2 and 10, noise bandwidth will be approximately equal to the square root of the shape factor (6 to 60 db) times the 6-db bandwidth. Few receivers have shape factors greater than 10.

db BELOW 0.1 MICROVOLT	MICROVOLTS
3	.07
6	.05
9	.035
12	.025
15	.018
18	.013
20	.01
21	.009
23	.007
24	.0063
26	.005
29	.0035
32	.0025
35	.0018
38	.0013
41	.0009

Table I.

The approximations quoted earlier (1.5 times marked bandwidth for SSB-selectivity receivers, 3 times marked bandwidth for others) are based on these relations. If you're really interested in calibrating your receiver's noise bandwidth for using this measurement technique, however, you might take a converter and have it measured for noise figure by the generator technique, then run this technique backwards to determine the effective noise bandwidth of your receiver in each position of the selectivity control.

The technique described here, incidentally, assumes that no audio filters are used following the detector. If they are, all results are off, since the effective noise bandwidth will have been changed in an unpredictable manner by the audio filters.

However, you can remove the audio filters from the hookup for measurement purposes, determine noise figure, then return the audio filters to the circuit and run the measurement backward to find out your effective noise bandwidth with filters present. Don't be surprised if it comes out in the region from 1 to 10 cycles per second; a good audio filter can work wonders with weak-signal reception.

For additional details on this technique of measuring noise figure, you can consult Reference Data for Radio Engineers, 4th edition, published by IT&T and available from Radio Bookshop, or any good radar text.

Chapter IX

Attenuators and Dummy Loads

LOW POWER ATTENUATORS FOR THE AMATEUR BANDS

George Daughters WB6AIG
Will Alexander WA6RDZ

In the evaluation of rf amplifiers, filters and many other devices, a variable attenuator is indispensable. This article describes attenuators built and tested by the authors. These attenuators are flat from dc to over 50 MHz and usable to over 450 MHz. They use low cost parts, are very simple to build, and are more accurate than ordinarily required in amateur applications.

The basic attenuator section is the symmetrical pi shown in Fig. 1. Resistance values are given by the relations:

$$R_1 = R_s\,(\sqrt{K} + 1)/(\sqrt{K} - 1)$$
$$R_2 = R_s\,(K - 1)/(2\sqrt{K})$$

where R_s is the characteristic impedance of the pad (equal to the source and load impedance) and K is the attenuation factor, P_{in}/P_{out}.

Resistor values for the most commonly used impedance (50 ohms) are shown in **Table 1.**

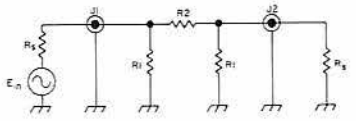

Fig. 1. Basic pi-network attenuator section.

Nominal attenuation in dB	R1 in ohms	R2 in ohms	Calculated attenuation in dB	Measured attenuation in dB
1	910	6.2	1.1	1.1- 1.2
2	430	12	2.1	2.1- 2.3
3	300	18	3.0	3.2
6	150	39	6.2	6.3- 6.6
10	91	68	10.2	9.6-10.1
20	62	240	19.6	19.5-19.7

Annenuation measured at 50 MHz and lower.

Table I. Resistor values for 50-Ω attenuators.

Notice that the use of standard value 5% half watt composition resistors allows accuracy within 1 dB of the calculated value of attenuation and within 1 dB of the desired nominal value.

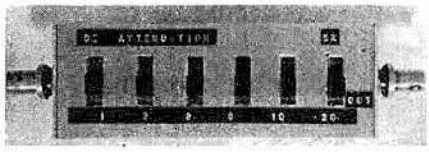

Amateur low-power attenuator made from inexpensive slide switches, 5% resistors and fiber glass, copper-clad board.

The attenuators are built in small channel boxes made of copper-clad etched circuit board material. Aluminum channel boxes commercially available would probably work equally well. Small, inexpensive DPDT slide switches (H. H. Smith No. 518 or equivalent) are soldered directly to the copper board and the resistors are soldered to the switch terminals (which have been cut short) with the shortest leads possible.

Two wiring variations have been tried, one with the series resistors (R_2) mounted between the switch wiper contacts (type B), and one with all resistors connected to the attenuator in terminals (type A). See **Fig. 2** and the photo of the interior of the attenuator. It was found that the latter arrangement, type A,

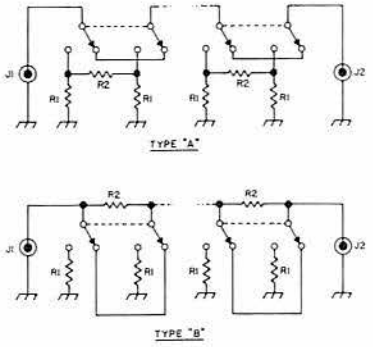

Fig. 2. Two types of attenuator construction. Type A has lower insertion loss than type B at high frequencies, so A is recommended. Resistors R1 and R2 are 5% composition, ½ watt. The switches are H. H. Smith 518 or equivalent. The connectors can be of any type to suit.

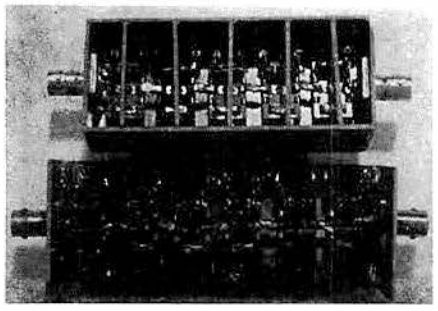

Details of attenuator construction. The top style, with complete shielding, is recommended.

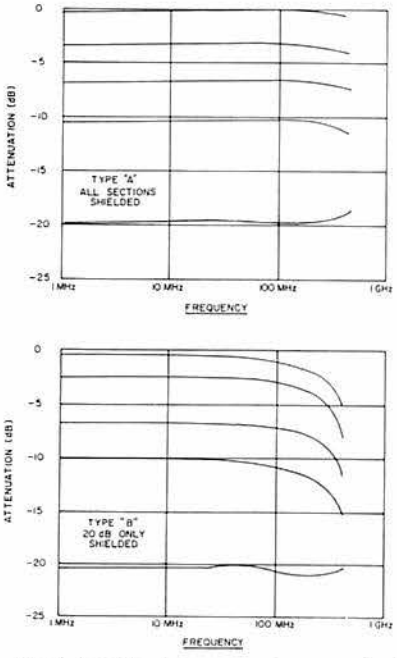

Fig. 3. Insertion loss versus frequency for the two types of attenuator construction: all sections shielded (A) and only the 20 db section shielded (B).

provided less insertion loss than the former at high frequencies, so this type of construction is recommended. Also note that dividing shields are desirable between input and output elements of a single section. These shields prevent capacitive feedthrough at the high frequencies, and are desirable on the high attenuation sections (anything over 10 dB) even at low frequencies. On the low attenuation sections, very little difference is evident below VHF. See Fig. 3 for the attenuation of the attenuators up to over 450 MHz. Building attenuators with greater than 20 dB attenuation per section by this method is not recommended for high frequency use.

S-UNIT ATTENUATOR

Ed Lawrence WA5SWD

Since the topic of "S meters" is a popular one among radio amateurs, a lot of time is spent describing these devices, usually along the lines of how generous or "Scotch" the meters are at the QTH of the parties in the QSO. After a few such QSO's, I decided to build an attenuator, calibrated in "S" units. My aim was to attain an accuracy of 1 db or better, using 5% ½w resistors and simple construction so it would be easy to duplicate.

As a sidelight, I started out by calculating both "tee" and "pi" pads, and used "pi" because all values of resistance are close to standard values, but (especially for high attenuation pads) the values for "tee" pads can get quite small; and expensive.

I figured the values required from the tables in the Allied's "Electronics Data Handbook", page 8, 5th edition. (Allied Radio, 75c, full of good info.)

Since "S" units are supposed to be 6 db, I figured data for steps of 1,2,4 and 8 times that amount, or 6,12,24 and 48 db. With these steps, any number from 0 to 15 "S" units of attenuation could be selected. However, 8 "S" units proved to be too much for one step, as shown by the lowered attenuation at 30 MHz, due to the inherent shunt capacitance of the resistor used in the series leg, plus the stray capacitance of the switch. So I removed the 8 "S" unit step and installed another 4 "S" unit step. This allows selected steps of attentuation from 0 to 11 "S" units.

Here are the values I calculated, and the actual values used, based on 51 ohms. The steps are switched in series, as required for the desired attenuation.

Resistance Values for 51 Ohm Attenuator:

"S" units	DB	R1 ideal	R1 actual	R2 ideal	R2 actual
1	6	154	150	38	39
2	12	85	82	96	100
4	24	58	56	405	390
8	48	51.5	51	6400	6800

After the attenuator was completed, the attenuation was measured at 3 kHz and at 30 MHz. With the test equipment available it was possible to measure more accurately at 30 MHz than at 3 kHz. Below is the data from the tests.

Atten Step "S" units	DB	Predicted atten DB	Measured at 3 kHz	Measured at 30 MHz
1	6	6.2	6.0	6.02
2	12	12.3	12.2	12.16
4	24	23.3	24.2	24.05
8	48	48.5	47.5	39.11

Now if we want to make an educated guess as to how far up we can expect good results, say 1 db error out of 24 db, then we can use the measured error in the 48 db step to calculate the capacitance across the series leg, and from that calculate the frequency where the 1 db error will occur. Go through the math if that is how you get your kicks, or take my word for it. It comes out to about 2 pF. And this will cause a reduction of 1 db at about 220 MHz. And since the resistor is

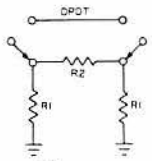

Fig. 1. Diagram for one step in the attenuator.

of a lower value for the smaller steps, they should hold their values to even higher frequencies, but I expect other factors would get into the act along the line somewhere. I will state that still works well at 2 meters.

If you want to get fancy, you can always figure the values for 1, 2 and 3 db steps and have from 0 to 72 db attenuation in 1 db steps.

Referring to the photos; you can see I built my attenuator in a Bud Minibox CU-2102-A, 4" X 2-1/8" X 1-5/8". Four steps is the maximum in this size box, unless different switches are used. Mine are Cutler-Hammer 7592K6. The shielding was made from transformer strap, but could be any soft copper available. Try a Hobby Shop and get the thin sheet that is used for embossing if all else fails.

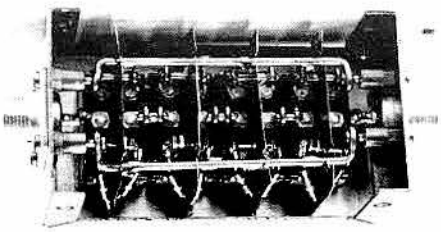

Looking inside the attenuator.

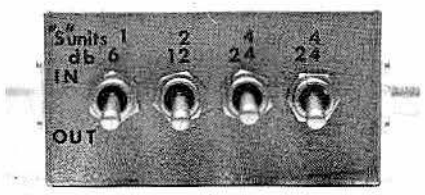

Front panel showing the switches for the various steps of attenuation.

Here are some of the uses an attenuator of this type is suited for:

Checking receiver "S" meter calibration.

Attenuating signals to aid in peaking receivers and converters.

Calibrating diode voltmeters for *rf* measurements.

Checking antenna gain. Or gain of that outboard *rf* stage.

P. S. My "S" meter lies, just as I thought!

THE EVER-USEFUL T-PAD

Jim Kyle K5JKX

Most of us have transmitters; let's hope that an equal number of us have receivers also. Antennas and microphones are usual station accessories, with a few determined diehards here and there clinging to the trusty old key. But how many of us have much in the way of test equipment?

Now and then somebody pops up with a VOM, and occasionally you can even find an operator who uses a scope. But the kind of special-purpose test gear you find in a well-equipped laboratory is almost always absent in the ham shack.

Which is more or less as it should be, since we're hams, not laboratory technicians. But with the present trends toward VHF, at least some specialized test gear is necessary. Otherwise, the regular station equipment can't be tuned for maximum performance.

One of the simplest such items is a noise generator, for getting the VHF receiver in perfect tune. This gadget has been described many times before, so we won't repeat it again —but we do have something which transforms the usual noise-generator lashup from a so-so item to an instrument capable of laboratory accuracy.

Before going into detail, let's look at the normal method of using a noise generator: you connect the generator to the antenna input, tie the converter to the receiver, turn the avc off, connect a voltmeter to the detector load resistor in the receiver (or put an ac voltmeter across the speaker leads), and measure the voltage produced by just noise. Then you turn on the generator and adjust it for a 3 db (1.4 times the voltage) increase in output; the object is to achieve the 3 db increase with the minimum amount of current flowing in the noise generator.

However, this technique of using the noise generator is pretty sloppy, since it assumes that the receiver's detector is absolutely linear for small signals—and this assumption is almost always incorrect.

A far better technique is to hook things up just as before, except now you place three T-pads in the line between converter and receiver. The T-pads on each end of the string serve merely to clamp the line impedance at 50 ohms, but the one in the center is built for precisely 3 db loss.

Now take the 3 db pad out and take your reading as before with the noise generator off; you don't have to turn off avc or hook up a voltmeter. The receiver's S-meter can be

used instead, since we're not measuring anything with the meter itself. It merely serves as an indicator so we can come back to the same point.

Then replace the 3 db pad in the line, turn on the generator, and crank it up until you get the same meter reading as before. Since you now have 3 db of added loss between converter and receiver you must have increased the noise power output of the converter by that same 3 db, and you could care less about the linearity of the detector!

This whole method is far from new, but previous descriptions of it have left something to be desired in the way of telling how to build the T-pad. The gadget is so simple that it must have seemed obvious to previous writers—but it does have its tricky points too.

For instance, since a T-pad consists merely of 3 resistors, it is pretty easy to just wire them up by their leads. But they are hanging in the receiver antenna lead, and present-day receivers are rather sensitive. If you happen to find a 20-meter signal, it's going to foul up your measurements!

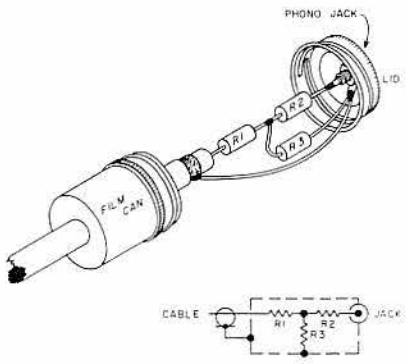

T-Pad construction details

One of the quickest ways to sidestep this problem is to shield the pad against all outside influences—but how do you shield anything so tiny?

The answer here is to use discarded 35-mm film cans, which all photographers who shoot 35-mm cameras have in abundance. The Kodak kind seem to work best. This type has a threaded cap, with a flat spot in its center just right for drilling a ¼ inch hole to take a single-hole-mounting phono jack. At the other end, a ⅜ inch hole can be punched and lined with a rubber grommet for coax cable to enter.

Next step is to place the jack in the hole in the lid, with its solder lug on the inside (be sure to clean the paint so that a good electrical contact will result). The T-pad can be assembled as shown in the drawing with shortest possible leads, and supported by its lead connecting to the jack. Thread a short length of RG-58 through the grommetted hole, and connect its center conductor to the other lead of the pad; the shield and shunt lead of the pad connect to the solder lug of the jack.

All that's left is to wire-brush the threads on the film can for good contact, and screw the lid down tight. Presto, a shielded T-pad. A phono connector should be put on the free end of the cable.

You can make up a whole bunch of these in various loss values, and get virtually any amount of loss you want by stringing them together. And this has a whole lot more use than just using with a noise generator . . .

For instance, when you want to test an antenna, arrange for a steady signal, strong enough to register on your S-meter with the back of the antenna pointed at it. Then swing the antenna in small steps, and bring the S-meter back to the same reading by inserting additional loss between converter and receiver with the T-pads. The difference between this and S-meter indications may amaze you.

Or if you are called upon to measure the difference in signal strength between two stations, the same approach can be used. Note the S-meter reading of the weaker, then knock the stronger one back to the same reading by putting T-pads in the converter-to-receiver line. Read the db off the pads and add them up.

You can even use this in place of an S-meter if you really want to know the signal-to-noise ratio of an incoming signal with accuracy; take a reading on noise, then knock the signal back to the same point. Total up the db, and there's your answer.

Though resistance values in the pad must be precise for absolute accuracy, the pad has an inherent tolerance of small errors and you should have better than 2 percent accuracy if you use 5-percent resistors. Specifically, a 10-percent error in the resistance value of any one arm produces less than ¾ db error in the pad loss, and less than 4 percent error in impedance. Using 5-percent resistors would, of course, cut these error limits in half.

If you want to follow the approach of using a string of these pads for all purposes in the shack, it's best to make them up on a "binary" approach since this gives you the maximum number of db values with the minimum number of parts. A basic assortment might be two 1 db pads, and one each of 2 db, 4 db, 8 db, 16 db, and 32 db. Using them in series in various combinations, you can get any whole number of db from 0 to 64, which pretty well covers the range of values you may ever need. For an example, to get 50 db you would use the 32 db pad, the 16, and the 2. For 60 db, you would use the 32, the 16, the 8, and the 4.

If the ability to increase loss in 1 db steps seems a bit exotic to you in view of the fact that 3 db is only half an S-unit, then you can use a binary progression in 3 db steps; this takes one 3 db pad, one 6 db, one 12 db, and one 24 db. The range is from 0 to 45 db, 3 db at a time.

For clamping a line's impedance, it's a good idea to use at least a 3 db pad and a 6 db unit might be even better. The lower-loss pads pads may not have the ability to swamp out impedance variations on their other sides.

About all that's left to make this complete is a chart of resistance values for various loss figures. Here it is; all are for use with a 50 ohm line; to use at any other impedance, multiply these values by the ratio of the new impedance to 50 ohms:

LOSS AMOUNT	R1, R2	R3
1 db	2.7	430
2 db	5.6	220
3 db	8.2	150
4 db	11	100
6 db	16	68
8 db	22	47
12 db	30	27
16 db	36	16
24 db	43	6.2
32 db	47	2.2

COMBINATION DUMMY LOAD/ ATTENUATOR NETWORK

John Schultz W2EEY

There are many instances when it is desired to use an existing transmitter as an exciter unit for a high-power linear amplifier. Many such linear amplifiers require a drive level that is only a fraction of the transmitter's output. To some degree, the transmitter can be detuned in order to reduce its output level, but this procedure is rarely possible when several orders of magnitude reduction in the power level are necessary. In such a case one can either internally modify the transmitter for a lower output level or use an alternator network between the transmitter and linear amplifier. In the latter case, the transmitter can be operated at its normal power input level and with its tuning controls at their normal settings.

The unit described in this article functions as both an *rf* attenuator and as a

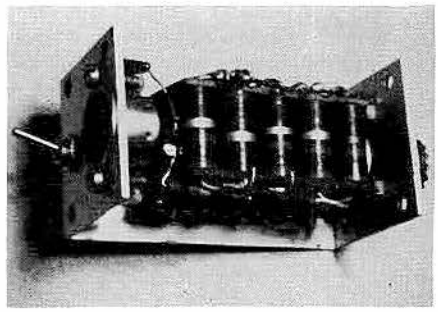
A simple method of construction is employed. Based mainly on "sandwiching" the resistors used between two pieces of vectorboard. Details are given in the text. SO-239 is used as coax input connector. The circuit function switch is located below the output connector.

dummy load. The latter capability allows a transmitter to be properly tuned alone for correct operation before it is used to drive a linear amplifier. An optional wattmeter circuit is included which when calibrated allows direct reading, in watts, of the full transmitter output or of the drive level supplied to the linear amplifier.

The unit described was built for use with a nominal 100 output transmitter used primarily for SSB service. The construction used, however, can be extended to other power levels for transmitters operating on 80-10 meters. Also, using the information

Power Reduction	Resistor Factors a	b
1/4 (6db)	.3	1.3
1/5 (7db)	.4	1.1
1/10 (10db)	.5	.7
1/20 (13db)	.6	.5

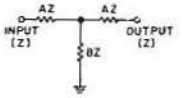

Fig. 1. Approximate resistor factors for "T" network attenuators over the ranges normally desired for exciter power output reduction.

supplied, the same type of attenuator/dummy load can be designed for other than 50 ohm transmission line systems. The attenuator was not designed as a precision network in order to allow the use of inexpensive resistors. However, the attenuation characteristics are quite satisfactory for the intended usage.

Besides its application as a power reducer when driving a linear amplifier, the unit can be used with a transmitter whenever a quick, known level of power output reduction is needed for operating purposes, approximate gain measurements, etc.

Circuit

Fig. 1 shows the circuit values for a generalized T network attenuator that can be used in any impedance unbalanced transmission line. The scaling factors are only shown for those power reduction levels most likely to be needed when driving a linear amplifier with a 75-200 watt transmitter, in order to avoid unnecessary detail. Factors for intermediate power reduction values can be found by interpolation to a satisfactory degree or one can consult an electronics handbook. The basis of the attenuator/dummy load network is to find the combination of resistor arms that will provide the desired attenuation and still be able to be connected together to form a dummy load of the correct value. Fig. 2 shows one possible combination. Each resistor bank has a value of about 20 ohms (5 resistors of 100 ohms each in parallel). In one position of the DPDT switch, the resistor banks are formed into a "T" network attenuator. In the other switch position, all three banks are placed in series as a dummy load connected across the input only. The resistance values which result are not exactly those shown in Fig. 1 for a 10db alternator. However, they are close enough to be effective and some tailoring of the individual legs is possible since each of the resistor bank values vary by a few ohms due to the tolerance of the resistors used. An optional voltmeter circuit is also shown in Fig. 2 connected to one pole of the DPDT switch. It can be used as a relative power output indicator or if calibrated, as described later, actually measure the power output of the transmitter and of the attenuator.

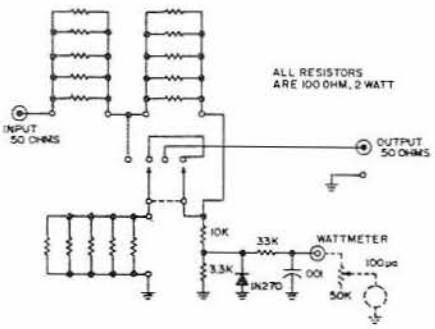

Fig. 2. Circuit of one possible dummy load/attenuator network providing about 10 db power reduction. Optional wattmeter circuit is also included.

Many variations of the basic idea are possible. Fig. 3 shows the use of four banks of 100 ohm resistors. All four are used to form an attenuator that comes reasonably close to the values required for 7db attenuation in a 50 ohm system. Only three are used in series for the dummy load function. In this case only a simple SPST switch is necessary to disconnect the output. The same *rf* voltmeter circuit as used in Fig. 2 may be added if desired. The switch, in fact, could be eliminated entirely if one were willing to disconnect the output termination in order to use the dummy load feature.

Whatever combination of resistance banks are used in order to achieve a desired attenuation value and the correct dummy load resistance, care must be taken that each resistance bank has sufficient power dissipation capability. The dissipation in each leg of the "T" network varies according to the attenuation level and can be calculated by Ohms Law. In general, a continuous power rating for a resistor bank equal to about one-third of the SSB peak power rating seems to suffice, including for quick tune-up on CW. For keyed CW service, the power rating should be increased to at least one-half the key-down power level.

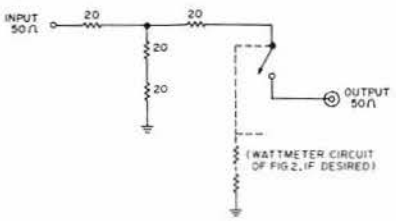

Fig. 3. Another dummy load/attenuator configuration possible with the 100 ohm resistor banks. It provides about a 1/5 power reduction (7db) when used as an attenuator.

Construction

The approach of using a relatively large number of 2 watt composition resistors is far less expensive than using specific value *rf* non-inductive resistors of 10-30 watts power rating. In quantities of more than 10, IRC type RC-2, 2 watt, 10% tolerance resistors cost about 9 cents each. So, one can achieve a 40 watt unit for less than $2 resistor cost. Banks composed of these resistors work well up to 30 mc as long as the interconnecting leads are kept short.

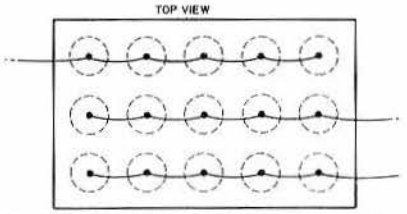

Fig. 4. Similar resistor banks are connected together on the underside of the assembly.

The photograph shows the construction used by the author for the circuit of Fig. 2. Similar construction can be used for larger size units as well. As shown in the photograph, the 15 resistors in rows of 5 each are sandwiched between two 1-1/8" x 1-7/8" pieces of vectorboard. None of the resistors physically touches. The wiring is done using the resistor leads. This construction is somewhat compact to expect full, continuous power dissipation from the unit but suffices for intermittent use. The frame measures 2¾" x 1½" x 1½". A cover is not absolutely necessary since the minor radiation that takes place is not important in this application. If a cover is used, it certainly should be of a perforated type to allow maximum air flow. A SD-239 connector is used at one end of the frame for the input. A dual connector is used at the other end, but normally one would use two RCA type phono jacks—one for the output and one for a meter circuit. The switch is located immediately below the output connector—a miniature Alco MST type.

Calibration

If it is desired to calibrate the voltmeter circuit as a wattmeter, it is necessary to use a probe and VTVM. Using the unit as a dummy load, the *rf* voltage is measured at the input and the power calculated. The 50K ohm potentiometer is used to set the meter at full scale for the highest power level used. The *rf* voltage is measured and the power level calculated in order to calibrate the meter for lesser power levels leaving the potentiometer at its "set" value. The same procedure is followed to calibrate the meter for the output power level by measuring the output *rf* voltage when the unit is used as a "T" attenuator and connected to a regular dummy load. The calibration should be made on the lowest frequency band used and rechecked on the highest frequency band used. If the readings differ significantly on the highest frequency band from those established, it may be necessary to add a few mmf capacitance across the diode in the voltmeter circuit in order to compensate for the slightest reactance present in the circuit.

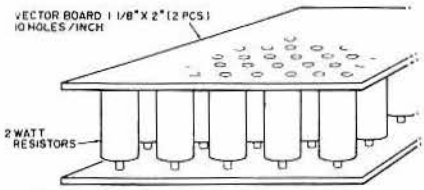

Fig. 5. Sketch showing details of resistor "sandwich" assembly.

Operation

When used between a transmitter and the 50 ohm input of a linear amplifier, the unit is first used as a dummy load for tune-up of the transmitter. The unit is then switched (with the transmitter unkeyed) to its attenuator position. In most cases, no returning of the transmitter should be necessary unless the input of the linear amplifier is particularly reactive.

Summary

The unit described is not intended as a precision attenuator or power measuring device. However, it will perform very well for its intended applications and costs far less than more sophisticated units performing the same functions.

THE MINICAN

Sam Kelly W6JTT

The Heathkit "Cantenna" has proven to be a major breakthrough in the field of dummy loads for ham use. Unfortunately, it isn't the most convenient thing to use on a small work bench with low power rigs! Borrowing their idea, I built this load for use with transmitters in the 5 to 15 watt range. The parts are few: a Campbell soup tin can, four one watt resistors, a UG-254-A connector, a short piece of 5/16 inch brass tubing and transformer oil.

Fig. 1 is a sketch of the assembled unit. The 50 ohm resistance was made up of three 15 ohm and one 5 ohm one watt carbon resistors.

First sand a can lid from a larger size can until it is free of paint. Drill a ½ inch hole through the center of the lid, and a ¼ inch hole on the perimiter. Mount the coaxial connector through the center hole. Solder a 1 inch length of 5/16 in. brass tubing over the ¼ inch hole. Solder the resistors as shown. Center the lid on the can and solder the lid to the can. Use a file to remove all rough edges. Mask the connector with masking tape and paint the can to prevent rusting.

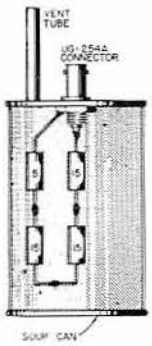

Fig. 1. Construction of the Minican. Main parts are a soup can, coax connector and resistors.

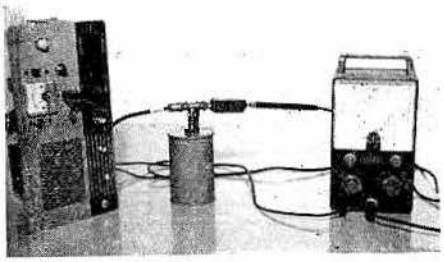

The Minican in use with the companion detector.

Fill the can with transformer oil. A good grade of automatic transmission fluid was used in one load with no degredation in performance. However, it probably is not advisable as the fluid has a relatively low ignition temperature and might create a fire hazard.

The load was tested by running it for five hours with an input of 15 watts of 50 MHz rf. The can became warm, but the resistors showed no signs of overheating.

A maximum VSWR of 1.5:1 was obtained at 234 MHz. The measurement was made at this frequency because an automatic test set was available.

A companion rf detector unit shown in Fig. 2 was built in a two inch section of ¾ inch square extruded brass stock. A Dage 394-1 BNC connector is mounted on one end for connecting to the RF circuit, while the DC output to the VTVM is a tip jack.

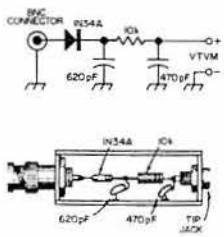

Fig. 2. Rf detector for use with the Minican.

THE TINY TERMINATOR

Jim Kyle K5JKX

HAVE you ever felt the need for a dummy load which would also indicate accurately the actual rf output power of a transmitter?

You can buy such a beastie, you know. The Bird *Termaline*, standard of the two-way communication industry, shouldn't set you back much more than a C-note . . .

But you can also build one at considerable less outlay, and that's what this article is all about.

As the photographs show, there's almost nothing to the "Tiny Terminator"—nothing, that is, but a 50-ohm load for any transmitter, which will absorb 20 watts for days on end and will handle 40 watts for brief periods (a minor modification can double these ratings), will *not* radiate rf into the ether after the fashion of the "standard" light bulb load, will allow accurate measurement of output power up past 225 mc, and can be built in less than two hours for less than $5.

You can see by the schematic that there's nothing to the device electrically; the tricks are all mechanical. Electrically, the Tiny Terminator consists of 20 (that's what we said) 1000-ohm 1-watt resistors connected in parallel, with a crystal diode running from the hot end of the composite resistor to the meter jack and a 27 mmfd capacitor bypassing the meter.

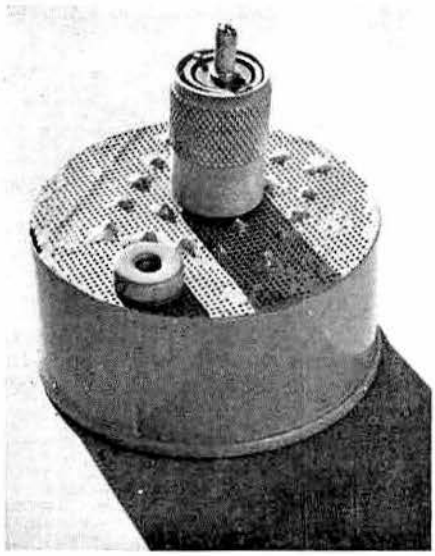

Mechanically, the big problem with a unit such as this is the problem of keeping the load resistive regardless of frequency. Resistor leads have inductance (about 25 millimicrohenries per inch) so we get rid of the leads as completely as possible. This is done by punching holes in a flat plate, passing the lead through the hole until the resistor is flush with the plate, and soldering rapidly with a hot iron (an Ungar 47-watt 1100-degree tip was used in building the model shown) so that the resistor body won't cook before the leads and plate are joined.

The flat plate has capacitance. This is avoided by keeping the plate shielded from outside influences, and separated as far as possible from its shield.

The shield, incidentally, is the bottom of 1½ inches of a Canada Dry cola, soldered all around the edge to the front resistor plate. This confines all rf inside the terminator.

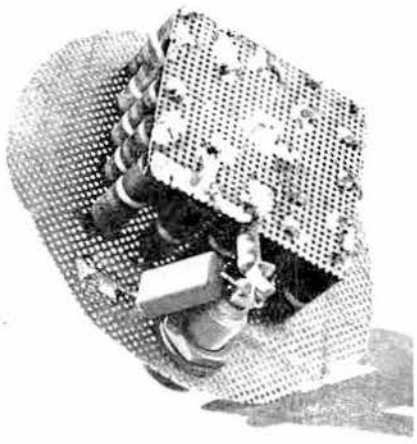

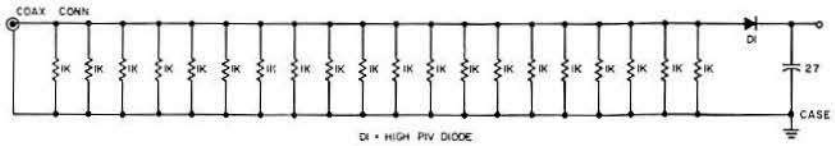

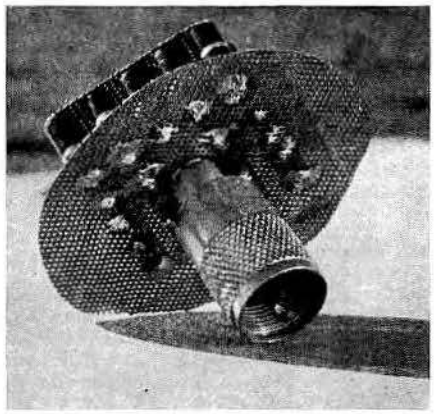

Addition of the crystal diode (a 1N34 was used, but a higher-voltage unit is recommended if you ever expect to measure power higher than 8 watts) and the bypass capacitor provide the power-measuring feature. These two components, in conjunction with an external voltmeter of at least 1000 ohms per volt sensitivity, provide you a peak-reading ac voltmeter. The voltage indicated on the meter will be equal to the peak value of rf voltage present across the load. Squaring the voltage and dividing by 50 (the resistance) will give you the *peak* power. Most power ratings are in rms values rather than peak; multiplying the indicated voltage by 0.707 before squaring will give you the rms power output.

The unit shown in the photos used perforated brass stock for the resistor plates; this happened only because a length of the brass was on hand in the junkbox at the time. A cut-out tin can lid will work equally well and will be much less expensive.

Not visible in the photos is the means of connecting the hot end of the resistor plate. A hole was punched in the middle of the hot plate and a length of No. 14 bare wire was soldered in, then filed off flush on the rear side. The bare wire was threaded through the coax connector and soldered to the center contact after checking for possible shorts.

The coax connector itself is held in place by a solder joint all around the rim of the cable-end aperture (see photo). This joint, if well made, provides plenty of strength.

Earlier, we mentioned that a minor modification would double the power rating. That modification is this: instead of 1-watt resistors, use the 2-watt variety. If you really want to go high-power, use 50 2700-ohm 2-watt resistors and have a terminator which will absorb 100 watts continuously and 200 watts ICAS. However, one that big will cost more—and you'll probably have to use a coffee can for the shield instead of the cola can used here.

1

Basic Principles of Radiofrequency Identification

CONTENTS

1.1 Basics of RFID 1
1.2 Passive versus Active RFID Systems 5
1.3 Functional Classification of RFID Transponders 6
1.4 Applications and Frequency Selection 7

Although the widespread use of radiofrequency identification (RFID) is recent, the technology itself is several years old. RFID was first developed during World War II in order to distinguish between friend and enemy aircraft. Several years later, thanks to the technological advances in microelectronics, wireless communications, and computer networks, RFID has come of age. It has now become a technology that is mature enough to be mass-marketed at competitive cost and become a critical player in the global market. This chapter introduces the reader to the different parts that make up a RFID system and provides an overview of the different concepts that will be described in depth in the upcoming chapters.

1.1 Basics of RFID

The basic function of an RFID system is to automatically retrieve the information that has been previously inserted into specific integrated circuits, as seen in Figure 1.1. RFID systems were first developed in automatic identification laboratories as a natural evolution of the different technologies they use. Different automatic identification systems use different methods to transmit the identifying information. For example, bar code technology uses light as the transmission media, while RFID systems use radio waves. In this context, the two main elements of RFID systems are the devices used to carry this information and the equipment used to automatically capture or retrieve the information.

The devices that store and carry the information are called *transponders* or *tags* and are shown in Figure 1.2. Although the industry commonly refers to them as *tags* mainly due to their physical shape and the fact that they are

© 2011 by Taylor and Francis Group, LLC

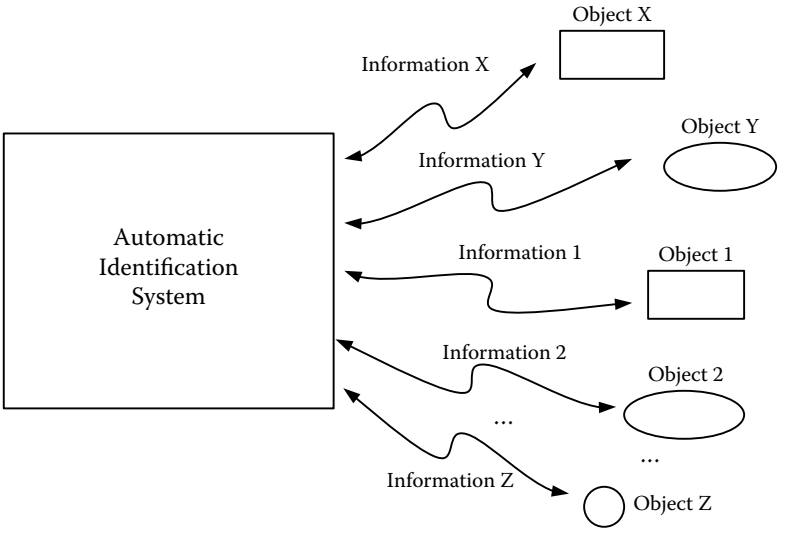

FIGURE 1.1
Information transfer in an automatic identification system.

FIGURE 1.2
Several types of transponders used in RFID systems.

© 2011 by Taylor and Francis Group, LLC

mostly used to tag pallets or cases of goods, the name *transponder* reflects better the function of these devices.

The device that is used to capture and transfer information is commonly called a *reader*, because in earlier RFID systems they were only able to read the information sent by the transponders. However, with the development of new functions and applications of RFID systems, the name *interrogator* reflects better the function of this subsystem. Therefore, this book will use the names *transponder* and *interrogator* when referring to these elements.

Transponders must have the circuitry needed to harvest power from the electromagnetic fields generated by the interrogator, the necessary memory elements, as well as the different control circuits. The simplest transponders contain only read-only memory (ROM), while more sophisticated transponders also include random access memory (RAM) and nonvolatile programmable read-only memory (PROM) or electrically erasable programmable read-only memory (EEPROM). ROM usually contains the identification string for the transponder and instructions for its operating system. RAM is normally used for temporary data storage when the transponder communicates with the interrogator. PROM or EEPROM is normally used to incorporate additional functionality depending on the application. The memory capacity of transponders ranges from a single bit to several kilobits. Single-bit transponders are typically used in retail electronic surveillance in which there are only two possible states: *article paid* and *article not paid*. Memory sizes of up to 128 bits are enough to store the individual transponder identification number with several check bits. Memories up to 512 bits are normally user programmable, in which in addition to the individual identification number the memory can hold additional information required by its application. Higher capacity memories can be seen as carriers for the transport of data files. They are also used in applications in which there are several sensors attached to the transponder.

Interrogators have vastly different complexity levels depending on the type of transponders they support as well as their specific purpose. In any case, they all must provide the basic functionality to communicate with the transponders, first by energizing them and second by establishing a communications link. The complexity of the communications link can also vary considerably depending on the desired reliability. The reliability of the communications link between transponder and interrogator can be enhanced by adding parity checks, error detection, and error detection and correction. However, the use of these schemes will result in a lower transmission rate. Figure 1.3 shows a picture of a basic interrogator in which it is possible to see the coiled antenna and some of the electronic circuits.

RFID systems contain more elements in addition to the transponder and interrogator. First, the communication between transponder and interrogator is not possible—or becomes extremely deficient—without the appropriate radiant elements that will transfer the information between these two subsystems in the form of electromagnetic energy. Both transponder and

© 2011 by Taylor and Francis Group, LLC

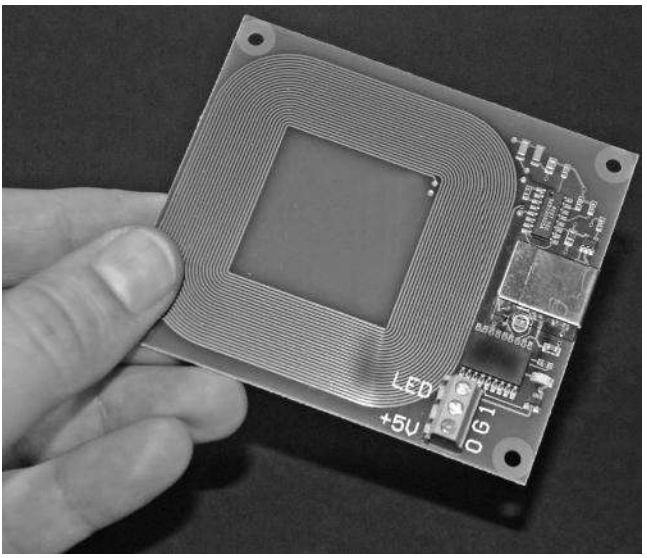

FIGURE 1.3
Basic RFID interrogator operating in the low-frequency (LF) range.

interrogator need to use the appropriate antennas to transfer information. As will be discussed in Chapter 2, the antenna dimensions in commercially available transponders and interrogators are much shorter than their ideal dimensions. This results in seriously limiting the transfer of energy between interrogators and transponders.

In addition to the transponders, the interrogators, and their antennas, the RFID system requires a *host computer* connected to the interrogator. This host computer provides a certain level of intelligence and acts like the interface between the RFID system and the ultimate application. Therefore, the interrogator must have the means to at least perform basic communication functions with the interrogator. A large number of today's applications require more than one interrogator running on a network rather than the single, stand-alone interrogator that was typical of earlier systems. Finally, an *edge server* is normally used between the host computer and the network in which the application is running.

In addition to these elements (shown in Figure 1.4), most of them hardware based, a typical RFID system contains several software elements. The *firmware* is the software that runs inside the interrogator in order to provide it with its basic functions. Some interrogators may also run one or more software *applications* that enhance the versatility of the interrogator. The name *middleware* encompasses the software applications that run in the background of the system, typically after the host computer. Finally, most applications require the use of one or several *databases* used to link the stored message

© 2011 by Taylor and Francis Group, LLC

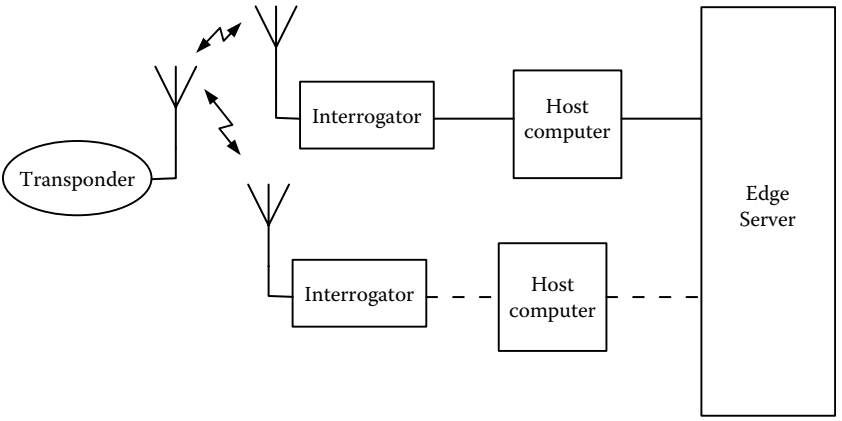

FIGURE 1.4
Basic structure of an RFID system.

sent by the transponder with more detailed information that can identify the transponder and provide additional information.

1.2 Passive versus Active RFID Systems

Passive RFID systems are those systems that use passive transponders. Passive transponders do not have an internal power source. They harvest the energy needed by their internal circuits from the electromagnetic field generated by the interrogator. For this reason, they have a short range, limited to a few feet and often, more realistically, to a few inches. Because they don't have an internal source of energy, the user does not need to worry about the status of the battery. Furthermore, their manufacturing and production costs are very low. The RFID transponders and systems described in this book are all passive.

Active RFID systems, on the other hand, use active transponders. Active transponders have an internal power source, typically a battery that allows broadcasting the signal to the interrogator. Because of not being limited to the power harvested by the antenna, they have an extended read range, typically several hundred feet. However, the inclusion of the power source increases their cost in two ways: the cost of the battery itself as well as the maintenance costs required to check the status of the internal power source and replace it when it has reached an unacceptably low level. The cost of an active transponder is approximately 100 times higher than the cost of a passive transponder. Active transponders typically operate in the ultra-high-frequency (UHF) and microwave ranges. A new type of active RFID transponder is

© 2011 by Taylor and Francis Group, LLC

linked to the use of RFID-enabled cell phones that can emulate an active tag. In this case, the problem of battery maintenance is solved as the user keeps the cell phone charged as part of its regular maintenance.

A third type of transponder is called *semipassive* or *battery-assisted transponder*. These transponders also include a battery, but contrary to active transponders, the battery is not used to generate the power to transmit the signal to the interrogator. Instead, the battery is used to support secondary functions like the data logging from different types of sensors. These transponders also harvest the energy from the electromagnetic field generated by the interrogator to power its internal circuits other than the sensing and data-logging parts.

1.3 Functional Classification of RFID Transponders

A functional classification of RFID transponders is based on their electronic product code (EPC) class. EPC is the application of one specific type of RFID technology within the consumer packaged goods industry. Within this classification, RFID transponders are divided into different classes and generations:

Generation 1, Class 0: Passive tags with read-only functionality. These are also called *write one, read many* (WORM) transponders. These transponders are programmed at the factory with their unique identification number. The user is not able to change it or include additional information.

Generation 1, Class 0+: These are also WORM transponders. They differ from Generation 1, Class 0 transponders in that it is the user who programs them. After they have been programmed by the user, no further programming or changing of data is allowed.

Generation 1, Class 1: These transponders were similar to Generation 1, Class 0 or 0+ transponders, but could be read by interrogators from other companies. Gen 1, Class 1 transponders have evolved into the different transponders from Generation 2.

Whereas Generation 1 transponders employ proprietary data structures and can be read only by interrogators manufactured by the same vendor, Generation 2 transponders are vendor neutral in their specifications. This means that as they have developed (following agreed upon standards), they can be read with interrogators from multiple vendors. These transponders provide additional features, for example the elimination of duplicate reads within the read range. They are also more reliable than Generation 1 transponders and support faster read rates. The user of Generation 2 transponders

© 2011 by Taylor and Francis Group, LLC

can access specific parts of their memory as these are rewritable transponders.

Generation 2, Class 1: These transponders are WORM transponders. They are also programmed at the factory, but they can be read with equipment from different vendors, support the higher read rates, and have more noise immunity than the Generation 1 transponders.

Generation 2, Class 2: These transponders are rewritable transponders. They can be written several times by the user using equipment different from the vendor's equipment.

Generation 2, Class 3: These transponders are the semipassive or battery-assisted transponders.

Generation 2, Class 4: This refers to active transponders.

Generation 2, Class 5: These transponders are essentially interrogators. Transponders that follow Generation 2, Class 5 must be able to power other transponders.

1.4 Applications and Frequency Selection

RFID systems come in different flavors from the point of view of the frequency they use. Selecting the most adequate frequency is a function of two variables: the technological developments of systems at the different operating frequencies—directly related to the cost of systems—as well as the properties of electromagnetic waves at those different frequencies.

The initial users of RFID systems found systems operating in the low-frequency (LF) range followed a few years later by systems operating in the high-frequency (HF) range. Therefore, their selection of systems was limited to these two broad frequency ranges even if those were not the most adequate for their specific applications. Recent years have seen an increase in the number of available RFID systems operating in the UHF range as well as a reduction of their economic cost. It is possible to expect a similar trend in upcoming years for RFID systems operating in the microwave range to become more available and more affordable. This will help the final users to make decisions on what type of RFID systems to deploy based on technical reasons rather than based on the availability and cost of these systems.

Table 1.1 presents a broad view of the frequency spectrum used by RFID systems as well as the most common frequencies for each band. It is necessary to note that Table 1.1 is not exhaustive because it is possible to find systems, within each frequency band, operating at other frequencies.

The LF band has been used by RFID systems for several years. This fact, together with the less stringent requirements of the electronics operating in this frequency range, has made these systems very cost-effective. Their

© 2011 by Taylor and Francis Group, LLC

TABLE 1.1

Commonly Used Frequency Band for RFID Systems

Frequency Band	Frequency Range	Typical Frequencies Used in RFID Systems
Low Frequency (LF)	100 kHz – 500 kHz	125 kHz 134.2 kHz
High Frequency (HF)	10 MHz – 15 MHz	13.56 MHz
Ultra High Frequency (UHF)	400 MHz – 950 MHz	866 MHz Europe 915 MHz United States
Microwaves (μW)	2.4 GHz – 6.8 GHz	2.45 GHz 3.0 GHz

major drawback is that due to the low frequency of the carrier, these systems can only communicate at low frequency rates. The main advantage of LF RFID systems is that electromagnetic waves operating in the LF range are the least affected by the presence of metals due to the penetration depth of these frequencies. This makes them ideal to be used in applications in which the transponders are surrounded by large metallic masses. Furthermore, LF waves can travel through water with minimal attenuation compared to waves of higher frequencies. This property makes them the frequency range of choice for the identification of animals due to their high water content. Most of these applications are based on implanting these transponders in livestock and pets. Figure 1.5 shows a picture of two different transponders that operate in the LF range in which it is possible to see the multiple loops used by these transponders.

RFID systems operating in the HF range can support higher read rates than LF systems. Although signals in the HF range are more affected by metal and have more attenuation when traveling through water, the transponders used for HF systems can be manufactured at a lower cost than the transponders operating in the LF range. This is due to the fact that the antennas for HF transponders can be made smaller, as shown in the two transponders seen in Figure 1.6. The need for less conductive material to construct the antennas results in a lower cost. Finally, the global uniformity across the world in the frequency of 13.56 MHz makes HF systems able to operate in any country.

While HF RFID systems operate at the single frequency of 13.56 MHz, UHF RFID systems can operate at different frequencies in the UHF band. Moreover, different countries have established different frequency ranges for their UHF RFID operation, making the compatibility between systems more difficult. For example, in North America the assigned band is from 902 MHz to 928 MHz, while in Europe it is from 860 MHz to 868 MHz and in Japan is from 950 MHz to 956 MHz. Other countries and regions have other different allocated frequency ranges. Despite this challenge and due to the developments in microelectronics that allowed the decrease in cost for these

© 2011 by Taylor and Francis Group, LLC

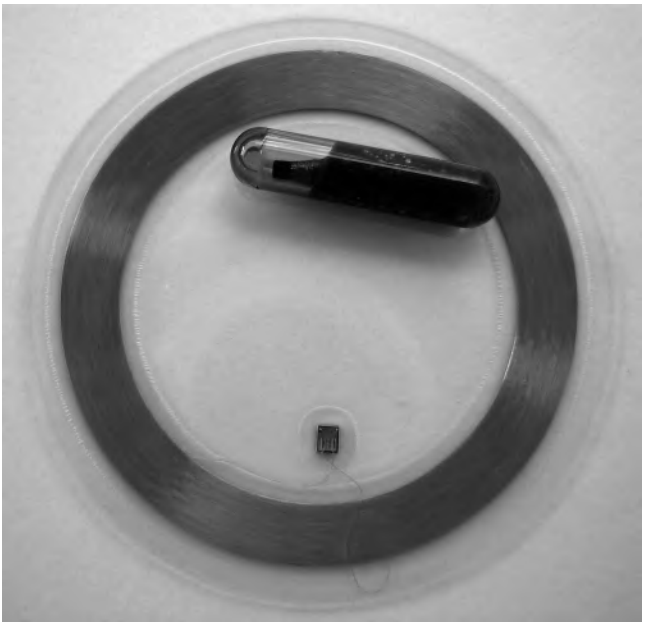

FIGURE 1.5
Low-frequency (LF) RFID transponders require antennas of several hundred feet of coiled wire.

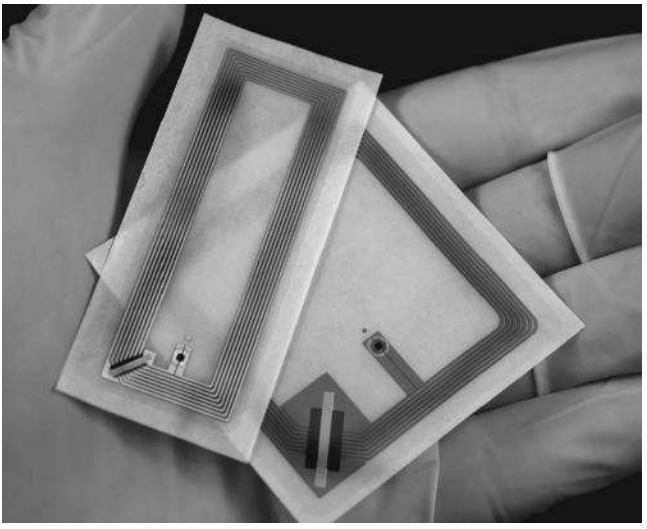

FIGURE 1.6
High-frequency (HF) RFID transponders can use shorter, smaller antennas.

© 2011 by Taylor and Francis Group, LLC

systems, UHF systems have established themselves as a viable alternative to the existing LF and HF systems. One of the main advantages of UHF RFID systems is that their higher carrier frequency allows for a much faster read rate of the transponder information, thus allowing the transmission of higher amounts of data. The communication between transponder and interrogator used in UHF systems is by electrical field instead of the magnetic coupling used by LF and HF systems. The antennas required by UHF systems can also be smaller than the antennas used for LF and HF systems, resulting in higher efficiency. These last two factors contribute to extended read ranges for UHF RFID systems. However, UHF systems also present several drawbacks compared to HF and LF systems. The antennas for transponders operating in the UHF range have very different physical dimensions depending on the parameters that the manufacturer wants to optimize in a given transponder. Figures 1.7 and 1.8 show examples of several UHF transponders in which it is possible to notice these differences.

UHF systems do not work well around metals as these reflect their electromagnetic waves. In addition, water absorbs UHF waves, making them unusable for animal implantation. Furthermore, the extended read range of UHF transponders may become a drawback for those applications that want to keep the read of transponders confined to a certain area.

Although 2.45 GHz is within the UHF range (UHF extends from 300 MHz to 3 GHz), the RFID systems operating in the frequency range extending from 2.45 GHz to 5.8 GHz are commonly called *microwave RFID systems*. In this frequency range, the propagation is limited to line of sight. Microwave signals are also attenuated by water and reflected by metallic objects. The cost of interrogators and transponders used in the microwave range is higher

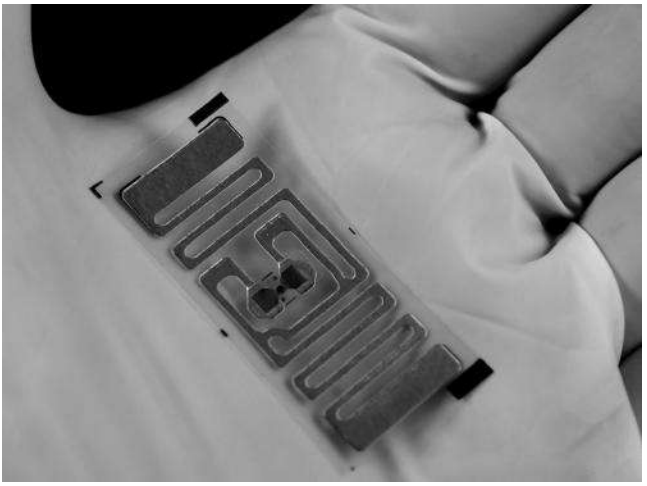

FIGURE 1.7
Ultra-high-frequency (UHF) RFID transponder.

© 2011 by Taylor and Francis Group, LLC

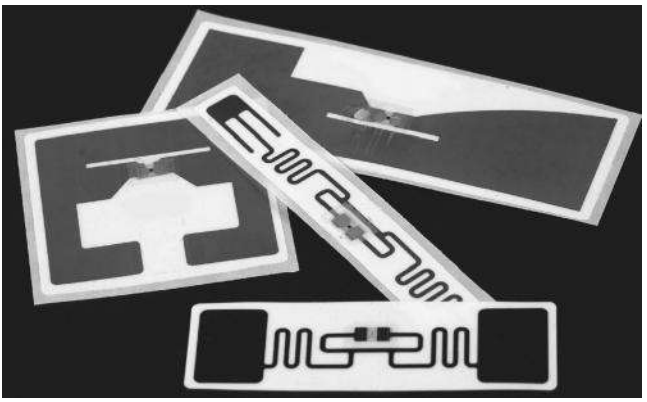

FIGURE 1.8
Several types of antennas used by ultra-high-frequency (UHF) RFID transponders.

than for any other type of system. On the positive side, it is possible to achieve very high read rates, and with the help from spread spectrum techniques, it is possible to achieve very high reliability rates and noise immunity. The higher end of the range, from 5.5 GHz to 6.8 GHz, is still currently under research and development.

© 2011 by Taylor and Francis Group, LLC

2

Antennas for RFID Transponders

CONTENTS

2.1 Review of Basic Antenna Theory for RFID Transponders 14
2.1.1 Antennas for RFID Transponders Operating in the LH and HF Regions 14
2.1.2 Inductance of Coil Antennas Operating in the LF and HF Regions 17
2.1.3 Antennas for RFID Transponders Operating in the UHF Region 24
2.2 Antenna Tuning for RFID Transponders 29
2.3 Antenna Matching for RFID Transponders 33
2.4 Antennas in Commercial RFID Transponders 37
2.5 The Connection between the Chip and the Antenna in RFID Transponders 43
2.6 Additional Factors That Affect the Performance of Antennas in RFID Transponders 47

The purpose of the antenna in the transponder of an RFID system is multiple: first, it has to collect power from the electromagnetic field generated by the interrogator. In addition, the antenna must transfer the collected power to its load that is the chip in the transponder in order to turn it on. Finally, the antenna must radiate the data signals generated by the chip back to the interrogator. The antenna should be optimized to minimize energy losses during this process by choosing the type and dimensions of the antenna suited for a specific application and matching its impedance to the impedance of the load. Because these requirements may lead to contradictory solutions, the designer of the system must evaluate them carefully when considering the possible solutions.

This chapter explores the design and performance considerations for antennas in transponders. It starts by presenting a basic review of antenna theory with special emphasis on the differences used for systems in the low-frequency (LF) and high-frequency (HF) ranges compared to the antennas used for ultra-high-frequency (UHF) systems. The chapter continues by describing the types of antennas found in commercial transponders. This is followed by considering the requirements for antenna tuning and

© 2011 by Taylor and Francis Group, LLC

antenna matching. The following section describes the different methods for attaching the antenna to the chip on the transponder. The chapter finishes with a review of other antenna factors that affect their performance.

2.1 Review of Basic Antenna Theory for RFID Transponders

2.1.1 Antennas for RFID Transponders Operating in the LH and HF Regions

Electrical current flowing through a conductor generates electromagnetic fields. From the point of view of the concepts described in this chapter, it is possible to distinguish two field regions. The first region is called the *far-field region*. In this region, the generated fields are radiated fields, meaning that the energy propagates through the space with an energy density proportional to the inverse of the distance. The second area is called the *near-field region*. In this area, radiated fields are not prevalent. Instead, attenuating fields, in which the strength of the field decreases with $1/r^3$, are dominant. Furthermore, the power in this region is reactive.

Given these two regions, it seems obvious that antennas for RFID transponders should be designed to operate in the far-field region. However, the boundaries between far-field and near-field regions depend on the relationship between the physical dimensions of the antenna and the wavelength of the propagating signal. In particular, the dimensions of the antenna should be comparable to the wavelength of the signal in order to achieve optimal performance. The wavelength of signals operating in the LF region is around 2.4 km (1.5 miles), while the wavelength for signals operating in the HF region is 24 m (78 feet). Therefore, at these frequencies it would not be practical to build antennas with dimensions similar to the wavelength of their signals. Any antennas that can be built in a practical manner for RFID transponders operating in the LF or HF ranges will be electrically small and therefore highly inefficient. In contrast, RFID signals operating in the UHF region have a wavelength of approximately 30 cm. Although this dimension is still very large for building practical antennas, the following sections will explore how they can be modified to obtain antennas for UHF transponders that will operate in the far-field region.

RFID transponders operating in the LF or HF frequencies cannot use dipole antennas because of the mismatch in dimensions. An alternative solution to this problem is to use a small-loop antenna instead of a dipole. While the near fields radiated by a dipole are mainly electrical fields, the near field from a loop antenna is a magnetic field. A small-loop antenna is a closed loop with a maximum dimension that is less than about a tenth of the wavelength of the signal. It can be shown that the small-loop antenna is the dual equivalent of an ideal dipole, thus making it suitable for antennas incorporated in transponders operating at LF or HF frequencies.

© 2011 by Taylor and Francis Group, LLC

Let's consider a conductor of infinite length carrying a magnitude of current of I amps. The magnetic field (B_Φ) measured at a distance of r meters from the conductor can be found using Ampere's law as

$$B_\phi = \frac{\mu_0 I}{2\pi r} \ (Weber / m^2) \tag{2.1}$$

where μ_0 is the permeability of free space ($4\pi 10^{-7}$ H/m).

However, a conductor of infinite length is not realistic. Its practical implementation is based on building a loop antenna by bending the original, finite wire, which carries a current of I amps in a circle with a radius of a meters. In practice, the wire is bent in such a way that produces a total of N turns as this allows using a longer wire with a relatively small diameter. In this situation, the value of the magnetic field in the z-coordinate direction (B_z) for a point located at a distance of r meters from the plane of the coil and located along the axis of the coil, as shown in Figure 2.1, can be found as

$$B_z = \frac{\mu_0 I N a^2}{2(a^2 + r^2)^{3/2}} \ (Weber / m^2) \tag{2.2}$$

where a is the radius of the loop in meters.

Assuming that the distance at which the field is measured, r, is much larger than the radius of the coil ($r^2 >> a^2$), equation (2.2) can be simplified as follows:

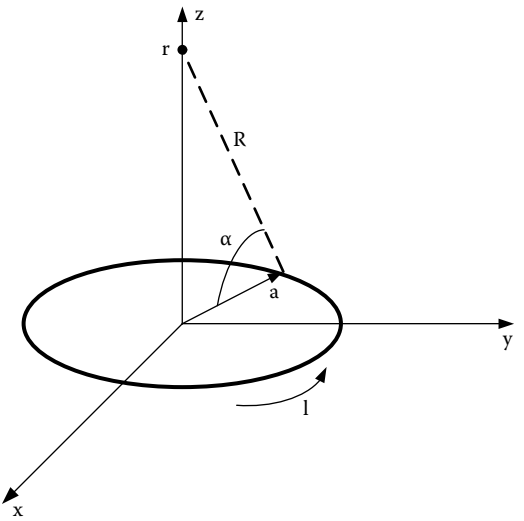

FIGURE 2.1
Magnetic field produced by loop antenna.

© 2011 by Taylor and Francis Group, LLC

$$B_z = \frac{\mu_0 I N a^2}{2 r^3} \ (Weber / m^2) \tag{2.3}$$

As shown by equation (2.3), the magnetic field created by the small-loop antenna is dependent on $1/r^3$. This causes a strong decrease of field intensity as one moves away from the location of the coil antenna, and will seriously limit the read range of transponders using this type of antenna. However, even with this limitation, the small-coil antenna is more desirable than an electrically small dipole.

The antenna in the RFID transponder has to be both a receiving antenna and a transmitting antenna. It has to collect enough energy from the electromagnetic field generated by the interrogator to be able to power its integrated circuit, and it also has to transmit the data signal generated by the chip back to the interrogator. The *reciprocity theorem* indicates that the receiving and transmitting patterns for a given antenna are identical, and therefore the same antenna can be used for either task.

The voltage induced in a coil consisting of N loops immersed in a time-variant magnetic field can be calculated using Faraday's law as

$$V = -N \frac{d\Psi}{dt} \tag{2.4}$$

with Ψ being the magnetic flux.

The magnetic flux, in turn, can be calculated as

$$\Psi = \int B \bullet dS \tag{2.5}$$

where

B = the magnitude of the time-variant magnetic field

S = the surface area of the coil

$\cdot$ = the inner product operator

Equation (2.5) indicates that the magnetic flux, and consequently the voltage induced in the coil, is dependent on the relative orientation between the coil and the magnetic field. This has some important implications at the time of using interrogators and transponders. Assuming that the magnetic field B was generated by the interrogator using another loop antenna, the maximum received voltage will occur when both coils are placed parallel to each other. Because the voltage generated in the coil that will be used to power the chip in the transponder is proportional to the intensity of the magnetic field (B), this voltage will also be dependent on ($1/r^3$). This is important because

© 2011 by Taylor and Francis Group, LLC

it limits the maximum distance between the interrogator and transponder coils that will produce the threshold voltage necessary to power the chip on the transponder.

Although the previous equations describe the full underlying relationships between the variables involved in this process, it is more desirable from a practical point of view to study how these equations evolve in specific cases. Assuming that the coil is specifically tuned to the frequency of the time-variant magnetic field, the induced voltage in the coil is as follows:

$$V_0 = 2\pi f N S Q B_0 \cos\beta \tag{2.6}$$

where

V_0 = the induced voltage in the coil
f = the frequency of the time-variant magnetic field
B_o = the intensity of the field
N = the number of loops in the coil
Q = the quality factor of the coil antenna
S = the area of the coil
β = the angle between the plane of the coil and the direction of the field

Keeping in mind that the magnetic field generated by the coil in the interrogator is perpendicular to its plane, and that equation (2.6) will be maximized when $\beta = 0$, the induced voltage will be maximized when the interrogator and transponder coils are placed parallel to each other. Once again, the limiting factor in equation (2.6) comes from the intensity of the magnetic field (B_0) decreasing with the cube of the distance between coils ($1/r^3$).

2.1.2 Inductance of Coil Antennas Operating in the LF and HF Regions

Because, as shown in equation (2.6), the induced voltage is proportional to the quality factor (Q factor) of the coil antenna, it is desirable to increase the Q factor as much as possible. This can be achieved by carefully choosing the value of the inductance of the antenna. This section discusses the values of inductance found in typical antennas operating in the LF and HF regions.

Typical RFID systems use inductance values for antennas in transponders of few mH, while antennas for the interrogators have typical values between 10 and 100 times lower. It is necessary to keep in mind that the calculation of inductance values presented here can only be considered as approximated values. These calculations do not take into consideration the finite value of the conductivity of the wire that results in Ohmic losses, and, more importantly, they do not take into account the distributed stray capacitances that appear in the coil. A more detailed and comprehensive analysis and calculations of inductance values in antennas are beyond the scope of this book, but

© 2011 by Taylor and Francis Group, LLC

they can be found in any book on electromagnetism. If the designer requires an accurate value of inductance, the best option is to measure it with a complex impedance meter. This instrument is also able to measure the Q factor of the antenna, providing good characterization of the antenna.

The inductance of the coil shown in Figure 2.2, made with a single layer of wire and with n turns and a core of air, is approximately:

$$L = \frac{d^2\, n^2}{18d + 40l}\,(\mu H) \tag{2.7}$$

where

d = the diameter of the coil in inches

n = the number of turns

l = the length of the coil in inches

Equation (2.7) shows the square relationship between inductance and number of turns; if the number of turns is doubled, the resulting inductance is quadrupled.

Example 2.1:

Calculate the number of turns required to achieve an inductance of 10 μH by winding a piece of wire over an air core with a diameter of 1 inch. The length of the resulting coil must be equal to 1.25 inches.

Solution:

In this situation, l = 1.25 inches, and d = 1.0 inches. Therefore, we can write

$$10 = \frac{(1.0)^2\, n^2}{18 \cdot 1.0 + 40 \cdot 1.25}$$

Solving for n gives n = 26.07 turns. Given the limitations of the approximation for equation (2.7) plus the stray capacitance issues mentioned earlier, a good starting point would be to choose 26 turns. In this case, the value of inductance that we would measure in practice is likely to differ from 10 μH. The designer would have to adjust the number of turns after measuring the actual value of inductance. A recommended procedure is to start by choosing a larger number of turns and therefore a larger number of inductance, and proceed by removing turns until the coil achieved the required inductance.

Although this type of structure to create the antenna for an RFID system is not the most commonly used, it is nevertheless employed in some applications, especially in those that required a hermetically sealed transponder. Figure 2.3 shows an RFID transponder operating in the LF frequency in which it is possible to see the coil antenna and its windings.

© 2011 by Taylor and Francis Group, LLC

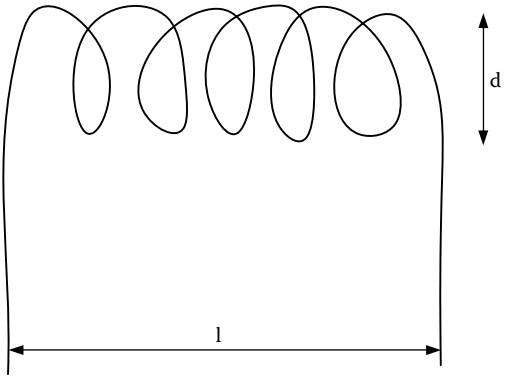

FIGURE 2.2
Single-layer, air-core coil.

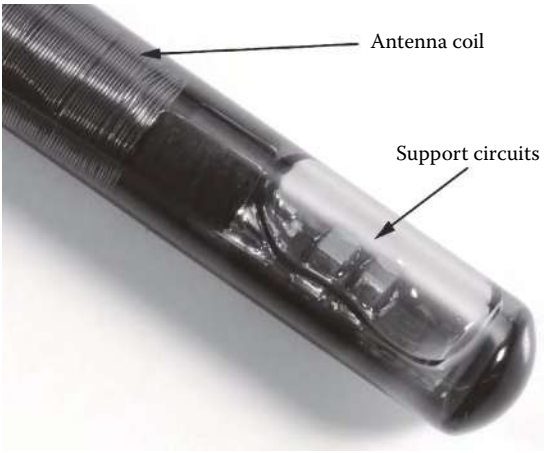

FIGURE 2.3
Detail of coil antenna in a commercial radiofrequency identification (RFID) transponder for the low-frequency (LF) range.

The practical problem associated with the use of this type of antenna is the three-dimensional space that it requires. Such antennas are not practical for applications that require a flat transponder, such as a credit card, and they are limited to applications that can support the tubular shape, for example in animal implantation. For this reason, the majority of transponders in the LF and HF frequency regions use antennas formed on a single plane, using several layers of conductor to achieve the desired inductance. Figure 2.4 shows this configuration for a multilayer circular coil with n turns.

© 2011 by Taylor and Francis Group, LLC

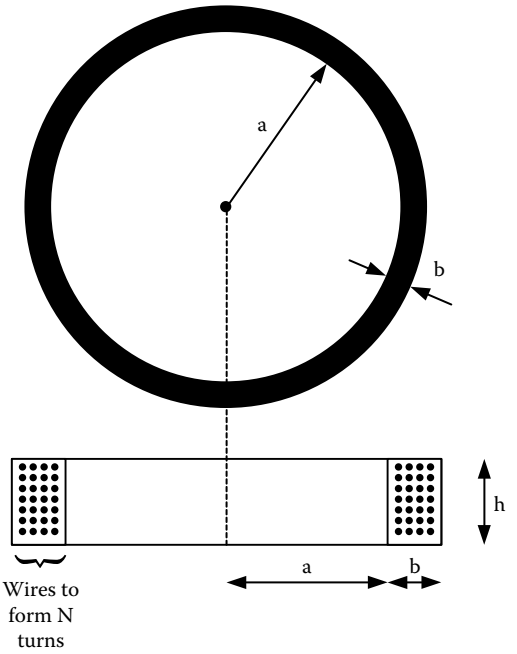

FIGURE 2.4
Multilayer, circular-coil, *N*-turn antenna.

The inductance of this coil is

$$L = \frac{0.31a^2 n^2}{6a + 9h + 10b} \quad (\mu H) \tag{2.8}$$

where

a = the radius of the coil in cm
n = the number of turns
b = the winding thickness of the coil in cm
h = the winding height in cm

This configuration allows building coils with the required amount of inductance with minimal thickness, therefore minimizing the transponder's footprint. A variation of this antenna that results in an even thinner antenna is the spiral wound coil with a single layer shown in Figure 2.5.

The inductance of a single-layer spiral antenna is

$$L = \frac{0.3937\, a^2 n^2}{8a + 11b} \quad (\mu H) \tag{2.9}$$

© 2011 by Taylor and Francis Group, LLC

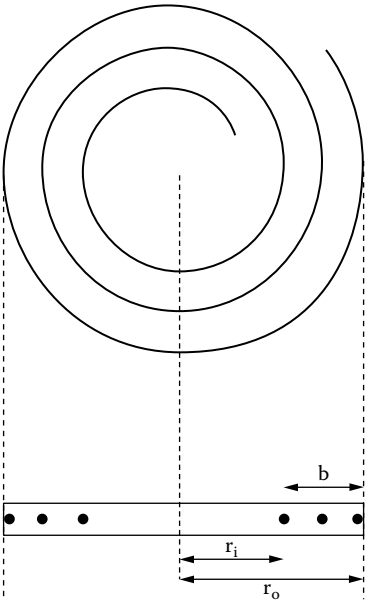

FIGURE 2.5
Single-layer, spiral-coil antenna.

where

a = the average radius of the coil in cm $\left(a = \frac{r_i + r_o}{2}\right)$

b = ro – ri in cm

n = the number of turns in the spiral

This structure results in a thinner antenna, although the number of turns in the antenna is limited to the number of turns that is possible to pack in a single layer. This limits the inductance of the antenna as this value depends on the square of the number of turns. Other forms of planar coil antennas are the multilayer square-loop coil antenna with n turns and the multilayer rectangular-loop coil antenna, also with n turns, shown in Figure 2.6.

The inductance for the planar multilayer square loop coil antenna with n turns, shown in Figure 2.6(a), is

$$L = 0.008\, a\, n^2 \left[2.3 \log\left(\frac{a}{h+b} \right) + 0.2235 \frac{b+h}{a} + 0.726 \right] (\mu H) \qquad (2.10)$$

where

n = the number of turns

a = the distance from the center of the coil to the side in cm

h = the thickness of the winding in cm

b = the width of the winding in cm

© 2011 by Taylor and Francis Group, LLC

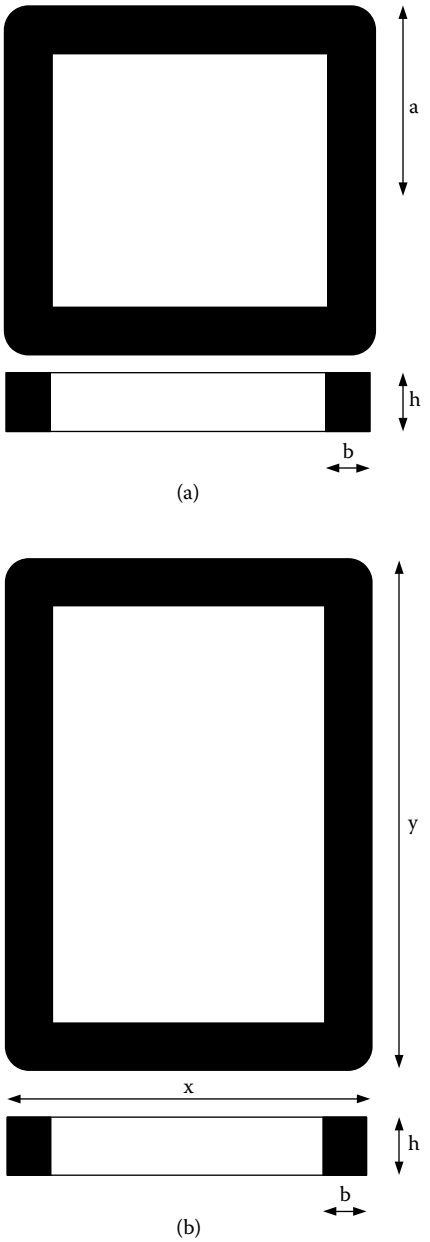

FIGURE 2.6
(a) Multilayer, square-coil antenna. (b) Multilayer, rectangular-coil antenna.

© 2011 by Taylor and Francis Group, LLC

The inductance for the planar multilayer rectangular-loop antenna with n turns, shown in Figure 2.6(b), is

$$L = \frac{0.0276\, n^2 \left(x + y + 2h\right)^2}{1.908\, \left(x + y + 2h\right) + 9b + 10h} \quad (\mu H) \tag{2.11}$$

where

x and y = the dimensions of the coil in cm

h = the thickness of the coil in cm

b = the width of the winding in cm

n = the number of turns

It is necessary to state once again that these equations, used to calculate the inductance of various coils are only approximations and need to be taken with some care. In particular, equation (2.11) is valid only when the dimensions x and y of the coil are quite different. For example, if the two dimensions of the coil in equation 2.11 (x and y) were identical, thus resulting in a square coil, the inductance values calculated by equations (2.10) and (2.11) will be different. These equations are provided as a starting point for the designer of antennas for RFID transponders.

Some antennas in transponders are configured as planar rectangular spiral structures, as shown in Figure 2.7. Figure 2.8 shows an example of a commercial transponder using this type of antenna.

There is not a full and closed equation to calculate the inductance of this type of antenna. However, its inductance can be calculated as the sum of the self-inductances for all the straight segments minus the sum of the mutual inductances existing in the arrangement. The mutual inductance is

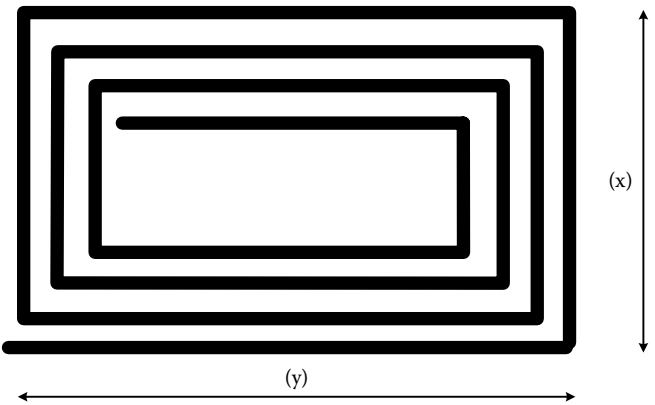

FIGURE 2.7
Single-layer, rectangular planar spiral antenna.

© 2011 by Taylor and Francis Group, LLC

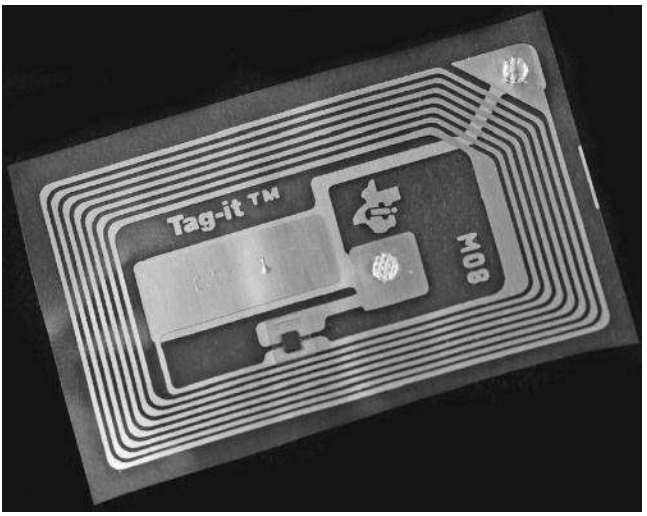

FIGURE 2.8
Commercial transponder using a planar, rectangular-spiral antenna.

the inductance that results from the magnetic fields produced by adjacent conductors. This mutual inductance will be positive when the direction of the current in the conductors is the same, and it will be negative when it is opposite.

2.1.3 Antennas for RFID Transponders Operating in the UHF Region

When the transponder is operating in the UHF region, the wavelength of the electromagnetic radiation is now comparable to the dimensions of the antenna. Because the antenna is no longer electrically small, a dipole can now be used. A *short dipole* is defined as a dipole whose length does not exceed one-fiftieth of the wavelength of the current signal. A short dipole, as depicted in Figure 2.9, produces an electric field that in near-field conditions has both radial and zenithal components, as given by equation (2.12):

$$E_r = \frac{2I_0 l}{4\pi} k^2 \eta_0 \, e^{-jkr} \left(\frac{1}{(kr)^2} - \frac{j}{(kr)^3} \right) \cos\theta$$
$$E_\theta = \frac{I_0 l}{4\pi} k^2 \eta_0 \, e^{-jkr} \left(\frac{j}{kr} - \frac{1}{(kr)^2} - \frac{j}{(kr)^3} \right) \sin\theta \qquad (2.12)$$

© 2011 by Taylor and Francis Group, LLC

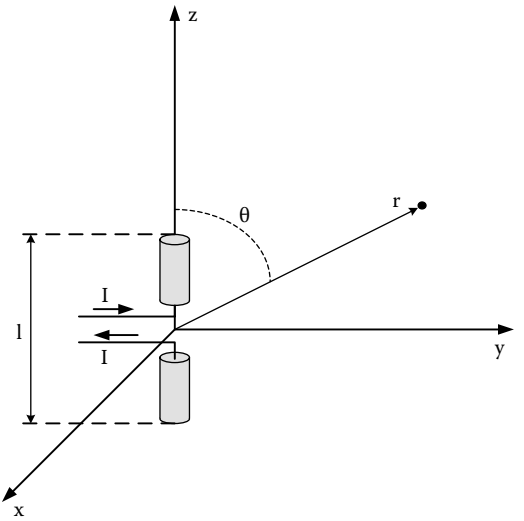

FIGURE 2.9
Electric field produced by a short dipole.

where

k = the wavenumber $\left(k = \frac{2\pi}{\lambda}\right)$

η_0 = the intrinsic impedance of free space $\left(\eta_0 = \sqrt{\frac{\mu_0}{\varepsilon_0}} \approx 120\pi\right)$

r = the distance for the center of the dipole at which the field is measured

θ = the zenith angle at which the field is measured

Assuming that the far-field approximation is valid ($r \gg \lambda$), the radial component of the electrical field can be neglected, and therefore equation (2.12) becomes

$$E_\theta = \frac{jI_0 l}{4\pi} k\eta_0 \frac{e^{-jkr}}{r} \sin\theta \tag{2.13}$$

The short dipole, however, does not radiate effectively because it has a very small radiation resistance, normally below 1 Ω, making it unsuitable for a good impedance match. Therefore, other dipole alternatives are preferred when possible, such as the half-wave dipole. The *half-wave dipole*, depicted in Figure 2.10, receives its name because its length equals half of the wavelength of the current signal traveling through the antenna.

A half-wave dipole also produces an electric field only in the zenith component that can be described by equation (2.14):

© 2011 by Taylor and Francis Group, LLC

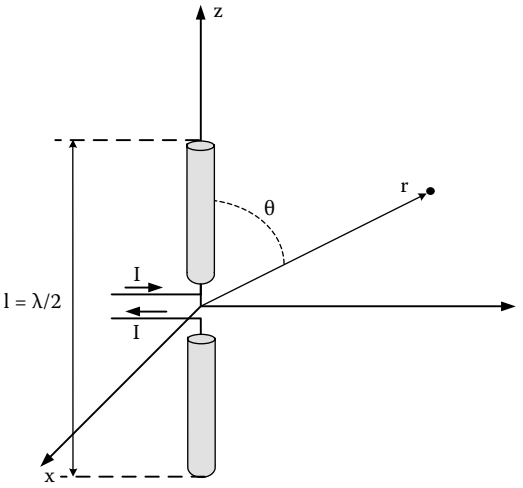

FIGURE 2.10
Electric field produced by a half-wave dipole.

$$E_\theta = \frac{j\,60 I_0}{r}\left(\frac{\cos\left(\frac{\pi}{2}\cos\theta\right)}{\sin\theta}\right)e^{-jkr} \tag{2.14}$$

One of the main advantages of the half-wave dipole is that its radiation resistance, around 73 Ω, is much larger than the radiation resistance of the short dipole. This makes the half-wave dipole better suited to match the impedance presented by its load, the integrated circuit in the transponder.

The wavelength for the typical UHF RFID frequency of 915 MHz is approximately 33 cm. Therefore, the length of a half-wave dipole is 16.5 cm. This value is valid only for free space; for an antenna mounted on an inlay, the actual value of its half wavelength decreases as the dielectric constant of the substrate increases. Although this distance is achievable, it presents some drawbacks. First of all, 16.5 cm may still be too large for some applications that require or would benefit from smaller transponders. More importantly, the power transfer characteristics for this antenna are very small and therefore require substantial matching approaches. Antenna matching is described in further detail in Section 2.2.

The space required by the antenna can be shortened while keeping the length of the conductors to the required 16.5 cm, for example by bending or even folding the wires that make up the dipole, as shown in Figure 2.11. This process can be repeated several times, bending the wires of the antenna in different directions as shown in Figure 2.12, which results in the structure known as the *meandered dipole*.

© 2011 by Taylor and Francis Group, LLC

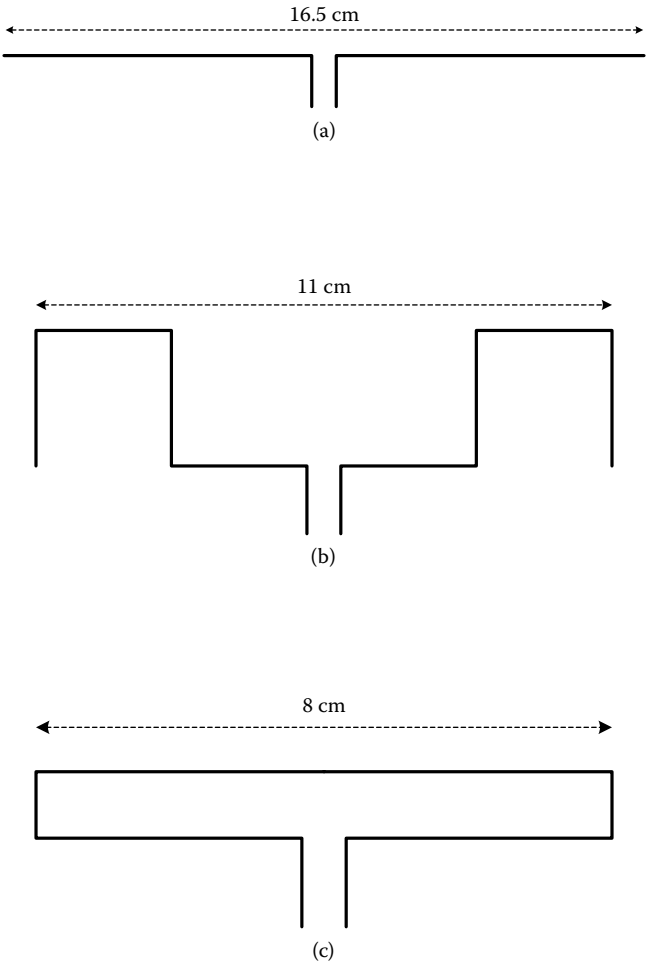

FIGURE 2.11
Strategies for reducing the size of ultra-high-frequency (UHF) antennas. (a) Original half-wave dipole. (b) Bent dipole. (c) Folded dipole.

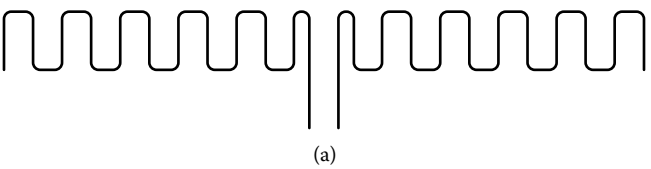

FIGURE 2.12
Examples of meandered dipole antennas. (a) Meandered dipole in a single direction. (b) Meandered dipole in two directions.

© 2011 by Taylor and Francis Group, LLC

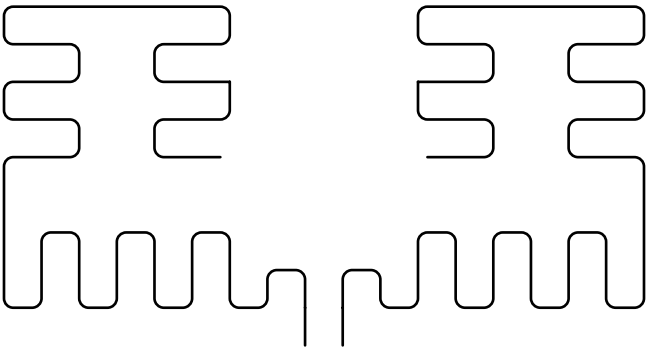

(b)

FIGURE 2.12 (Continued)
Examples of meandered dipole antennas. (a) Meandered dipole in a single direction. (b) Meandered dipole in two directions.

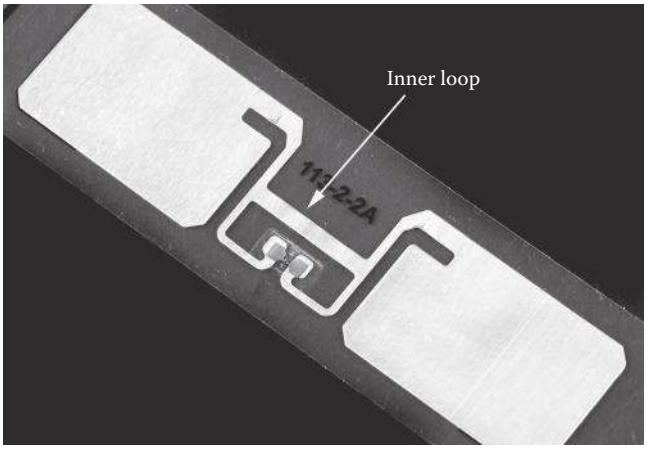

FIGURE 2.13
Detail of the inner loop used in some UHF antennas.

However, bending the dipole degrades the electrical characteristics of the antenna: the current lines flowing in opposite directions through adjacent paths have a canceling effect that in turn increases the radiation resistance of the antenna. Because this effect depends on the distance between the paths, the canceling effect becomes stronger when the antenna has multiple bends closely packed. In practice, the total length of a bent or meandered dipole is longer than the straight half-wave wavelength, although the total size of the antenna will be smaller.

Some antennas operating at the UHF range also incorporate a low DC resistance path closer to the center of the antenna known as the *inner loop*. This inner loop, shown in Figure 2.13, presents a series of advantages that makes its use common in this type of antenna.

© 2011 by Taylor and Francis Group, LLC

First, the inner loop presents a low DC resistance that helps reduce the potential of damage to the integrated circuit due to high-voltage electrostatic discharges that may occur in the antenna or its vicinity. Second, the inductance of the inner loop can be used in conjunction with the input capacitance of the integrated circuit to form a resonance circuit that will couple with the magnetic near field, producing enough voltage to power the integrated circuit. Near-field communications for UHF RFID systems, although not very common yet, are growing rapidly. Third, the inner loop can be used like a transformer to help match the impedance of the integrated circuit to the antenna. Finally, the impedance of the antenna can be lowered or increased by changing the width of the trace in the inner loop.

2.2 Antenna Tuning for RFID Transponders

Antenna tuning for RFID transponders operating at LF or HF frequencies attempts to make the antenna resonant at the frequency of transmission, thus maximizing the current or the voltage in the system. Because the antenna has a marked inductive component, resonance is achieved by placing a capacitor of the adequate value in series or in parallel with the antenna.

When the capacitor is placed in series with the antenna, the resulting series resonant circuit has an impedance minimum at the resonance frequency and therefore maximizes the current being delivered to its load. This type of configuration is typical for interrogators and will be studied in Chapter 4. When the capacitor is placed in parallel with the antenna, the result is a parallel circuit that exhibits an impedance maximum at the resonant frequency and therefore maximizes the voltage across its terminals. This is the typical configuration for transponders. The tuning capacitor in RFID transponders can be created over the same substrate as shown in Figure 2.14.

The resonant circuit can therefore be modeled as a parallel circuit, similar to the one shown in Figure 2.15, in which L represents the inductance of the antenna, C represents the capacitance of the capacitor that must be added, R represents the resistance of the load that is the integrated circuit that must be powered, and the value r represents the resistance of the coil. Because normally $r \ll R$, the value r will be ignored in the calculations needed to find the value of required capacitance. However, the resistance r of the inductor contributes to degrading the overall performance of the antenna. These effects will be studied in the last section of this chapter.

The complex impedance presented by the circuit shown in Figure 2.15, neglecting the Ohmic losses r, is

© 2011 by Taylor and Francis Group, LLC

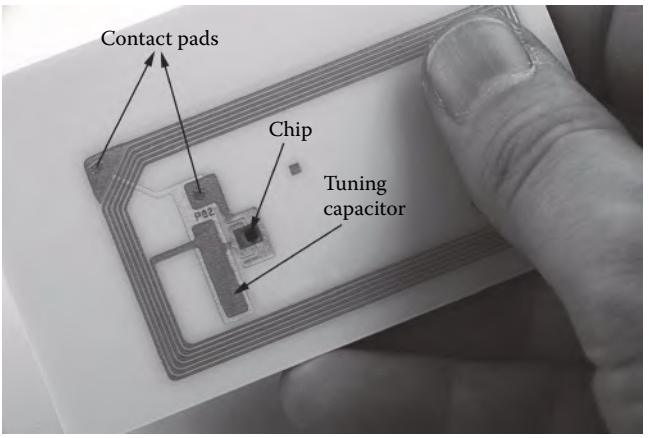

FIGURE 2.14
Tuning capacitor in the antenna of a high-frequency (HF) transponder.

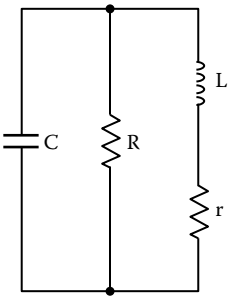

FIGURE 2.15
Parallel resonant model used to analyze antenna resonance. L: antenna inductance. C: external tuning capacitor. R: load (chip to energize). r: Ohmic losses in the antenna.

$$Z(j\omega) = \frac{\dfrac{j\omega}{C}}{\left(\dfrac{1}{LC} - \omega^2\right) + j\dfrac{\omega}{RC}} \tag{2.15}$$

where $\omega = 2\pi f$.

The resonant frequency for the parallel circuit is the frequency that creates the maximum for $Z(j\omega)$. This frequency is

$$\omega_o = \sqrt{\frac{1}{LC}} \quad or \qquad f_o = \frac{1}{2\pi\sqrt{LC}} \tag{2.16}$$

© 2011 by Taylor and Francis Group, LLC

From equation (2.15), it can be seen that at the resonant frequency, the impedance of the parallel circuit is real and equal to the value of the resistance of the load. This is the maximum value for the impedance.

Example 2.2:

Consider the value of inductance for the antenna in Example 2.1 (10 μH). Calculate the value of parallel capacitance required to make the antenna resonant at the typical RFID frequencies of (a) 125 kHz for LF systems and (b) 13.56 MHz for HF systems.

Solution:

Solving for C in equation (2.16) yields

$$C = \frac{1}{L(2\pi f)^2}$$

Therefore, the values of capacitance required for resonance are as follows:
$C_{125\ kHz}$ = 162 nF
and
$C_{13.56\ MHz}$ = 13.7 pF

The same calculations for resonant frequency can be applied to the devices that communicate data by tuning and detuning the antenna. This can be accomplished by using, for example, two capacitors or two inductors in the parallel RCL circuit. In order to detune the antenna, the controlling device can, for example, shorten one of the capacitors or inductors, resulting in a new resonant frequency. This, in turn, results in a minimal transfer of energy back to the interrogator.

The devices MCRF355 and MCRF360 from Microchip Technologies operate following this principle. Figure 2.16 shows one of the configurations used. Here, the antenna will be tuned when both inductors are active and will be detuned when the device shortens the inductor L_2.

Using equation (2.13), the resonant frequency when the antenna is tuned is $f_{\text{tuned}} = 1/2\pi\sqrt{L_T C}$, with L_T being the total inductance between point A and ground. When the device detunes the antenna by shortening inductor L_2, the new resonant frequency becomes $f_{\text{detuned}} = 1/2\pi\sqrt{L_1 C}$. Because $L_T > L_1$ ($L_T = L_1 + L_2 + 2k\sqrt{L_1 L_2}$, with k being the coupling coefficient between the coils), $f_{\text{tuned}} < f_{\text{detuned}}$.

The difference between the tuned and detuned frequencies must be chosen to maximize the Modulation Index and the read range. If it is necessary to choose the tuned and detuned frequencies such as $f_{\text{tuned}} < f_{\text{detuned}}$, this can be achieved by using the configuration shown in Figure 2.17.

The operation is similar as shown before. Here, $f_{\text{tuned}} = 1/2\pi\sqrt{L C_T}$, with $C_T = C_1 C_2 / C_1 + C_2$. The device detunes the circuit by shortening the capacitor

© 2011 by Taylor and Francis Group, LLC

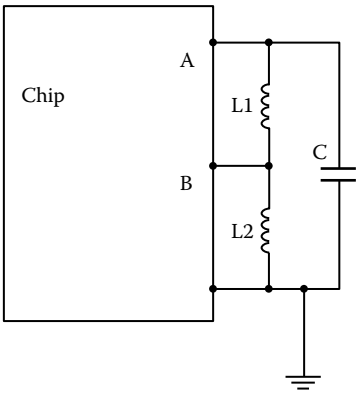

FIGURE 2.16
Tuned and detuned circuit using two inductors and one capacitor. This configuration results in $f_{\text{tuned}} < f_{\text{detuned}}$.

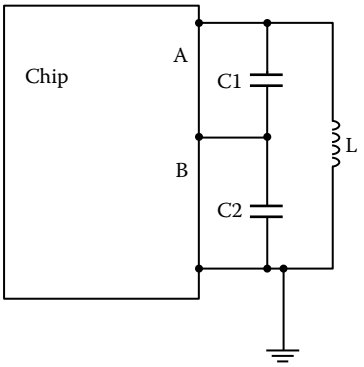

FIGURE 2.17
Tuned and detuned circuit using two capacitors and one inductor. This configuration results in $f_{\text{tuned}} > f_{\text{detuned}}$.

C_2, resulting in the following detuned frequency: $f_{\text{detuned}} = 1/2\pi\sqrt{L\,C_1}$. Because $C_T < C_1$, this results in $f_{\text{tuned}} < f_{\text{detuned}}$.

Equation (2.15) can also be used to calculate the bandwidth of the system defined as its –3 dB cutoff. This is

$$B = \frac{1}{2\pi RC} \quad (Hz) \tag{2.17}$$

An important parameter in a resonant circuit is its quality factor (Q), which compares the energy stored in the circuit with the energy that it dissipates:

© 2011 by Taylor and Francis Group, LLC

$$Q = \frac{f_o}{B} \tag{2.18}$$

Equation (2.17) can be rewritten taking into account the values of components in the resonant circuit by combining equations (2.16) and (2.17):

$$Q = R\sqrt{\frac{C}{L}} \tag{2.19}$$

Equation (2.6), found earlier, was used to calculate the voltage induced in the coil. Substituting equation (2.19) into equation (2.6) yields

$$V_0 = 2\pi f N S Q B_0 \cos\beta \quad = \quad 2\pi f N S R\sqrt{\frac{C}{L}}\, B_0 \cos\beta \tag{2.20}$$

This equation indicates that the voltage induced in the antenna transponder is inversely proportional to the square root of its inductance, and proportional to both the number of turns in the coil and its surface.

2.3 Antenna Matching for RFID Transponders

The purpose of matching an antenna to its load is to ensure that the antenna transfers the maximum amount of power to its load. In an RFID transponder, the load of the antenna is the integrated circuit that will be powered by the energy supplied by the antenna. Antenna matching is generally based on altering the complex impedance presented by the antenna at its operating frequency, by modifying its physical dimensions, inserting a reactive component, or a combination of both.

Consider a simple circuit, as shown in Figure 2.18. The power transferred by the voltage source V_s to the load resistance R_L is

$$P_L = \frac{R_L}{(R_L + R_s)^2}\, V_s^2 \tag{2.21}$$

The goal of power matching is to find a relationship between R_s and R_L that will maximize the power transferred to the load. In mathematical terms, this

© 2011 by Taylor and Francis Group, LLC

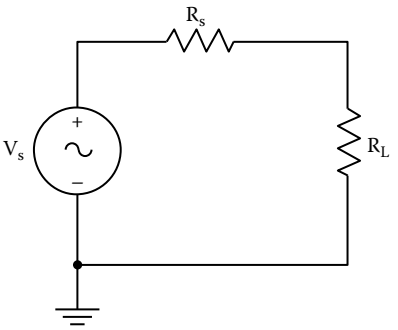

FIGURE 2.18
Simplified model for power transfer calculations.

is equivalent to finding the relationship between R_L and the rest of the circuit elements that will make the first derivative of equation (2.21) zero. That is,

$$\frac{dP_L}{dR_L} = \frac{(R_L + R_s)^2 - 2R_L\,(R_L + R_s)}{(R_L + R_s)^4} V_s^2 = 0 \quad \Rightarrow \; R_L = R_s \tag{2.22}$$

In a transponder, the voltage source models the voltage induced in the antenna, and the load models the integrated circuit that must be powered. These are not purely resistive elements such as those depicted in Figure 2.18, but they have resistance and reactance. Therefore, a more accurate model for this situation is shown in Figure 2.19.

Equation (2.23) shows the power transferred to the load that is the real part of the impedance of the integrated circuit:

$$P_L = \frac{R_{ic}}{2\left[\left(R_{ant} + R_{ic}\right)^2 + \left(X_{ant} + X_{ic}\right)^2\right]} V_{ant}^2 \tag{2.23}$$

There are now two conditions that must be met in order to transfer the maximum amount of power between the source (voltage generated by the antenna) and the load (integrated circuit to be powered). These are

$$\begin{cases} R_{ic} = R_{ant} \\ X_{ic} = -X_{ant} \end{cases} \tag{2.24}$$

Equation (2.24) can now be understood by saying that the amount of power transferred from the antenna to the integrated circuit will be maximum when their impedances are conjugate. This is an advantageous condition for RFID systems as the impedance of the antenna has an inductive behavior and the

© 2011 by Taylor and Francis Group, LLC

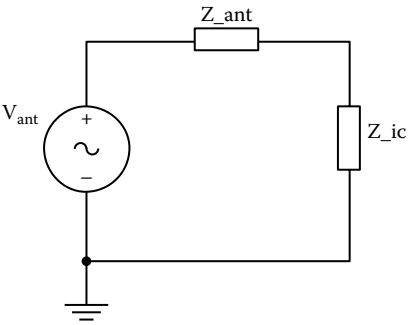

FIGURE 2.19
Model for power transfer calculations in an RFID transponder.

input impedance of the integrated circuit presents a capacitive behavior. The model shown in Figure 2.19 can be further refined as the model shown in Figure 2.20.

It is necessary to point out that the series impedance model used in Figure 2.20 is not the most common way to represent the input impedance of an integrated circuit or any other electronic device. Generally, input impedance is expressed using a parallel model with the input resistance and the input capacitance. However, to preserve the parallelism used in Figures 2.18 and 2.19, it is more convenient to express it using the series model. Given the values of parallel resistance and capacitance, it is possible to find their equivalent series values using equation (2.25):

$$\begin{cases} R_s = \dfrac{R_p}{1+\left(\omega R_p C_p\right)^2} \\ C_s = \dfrac{1+\left(\omega R_p C_p\right)^2}{\omega^2 R_p^2 C_p} \end{cases} \tag{2.25}$$

Example 2.3:

The specifications for the chip MCRF200 from Microchip used in RFID transponders indicate a parallel capacitance of 2 pF. Assuming a parallel resistance of 3 kΩ, find the equivalent series model at the frequency of 915 MHz.

Solution:

Equation (2.25) gives the following values of the equivalent series model:

R_s = 2.6 Ω and C_s = 1.96 pF. In general, the values of series and parallel capacitance will be approximately the same. However, the values of the series and parallel resistances are very different for each model.

© 2011 by Taylor and Francis Group, LLC

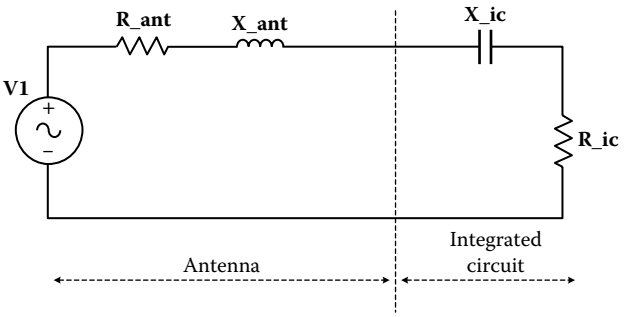

FIGURE 2.20
Series model for the transponder antenna and chip to be energized.

It is also interesting to calculate the gain or attenuation between the voltage delivered to the integrated circuit and the voltage generated by the antenna in the optimal case of maximum power transfer. Using the model shown in Figure 2.16, the voltage across the integrated circuit produced by the antenna can be calculated as follows:

$$V_{ic} \approx j\frac{1}{2\pi\omega R_{ic} C_{ic}} V_{ant} \tag{2.26}$$

Example 2.4:

Using the values given in Example 2.3, calculate the voltage gain or attenuation at the input of the integrated circuit at the frequency of 915 MHz.

Solution:

Using equation (2.26), V_{ic} / V_{ant} is equal to 34. This means that the voltage at the input of the integrated circuit in the transponder at the resonance frequency will be 34 times larger than the voltage generated by the antenna. In practice, this number will be lower because equation (2.26) has not considered factors such as the effect of the Q factor and other losses in the system. Typical voltage gains in practice are around 10 to 15. In any case, this represents an important benefit for the designer of the RFID system.

It is necessary to consider that, in practice, there will be some mismatch between the impedance of the integrated circuit and the impedance of the antenna as these will not be perfect conjugates. This mismatch will produce losses in the power being delivered to the integrated circuit, resulting in decreasing the sensitivity and read range for the transponder. This factor becomes more important for UHF antennas designed for global operations that have a frequency bandwidth of 860 MHz to 960 MHz rather than those

© 2011 by Taylor and Francis Group, LLC

designed for operation at a single frequency. In this case, the usual design approach is to place the matched frequency at the geometrical mean of the two frequency ends, resulting in 908 MHz. This will result, however, in mismatch losses at frequencies close to 860 MHz and frequencies close to 960 MHz.

2.4 Antennas in Commercial RFID Transponders

Coil antennas are used in the different type of encapsulated glass transponders, similar to Figure 2.21, operating in the LF region manufactured by Texas Instruments. Glass transponders are hermetically sealed, making them waterproof and therefore suitable to be immersed in water and other fluids.

These transponders are marketed toward access control, vehicle identification, container tracking, asset management, animal identification, and waste management applications, as described by the literature provided by their manufacturer. Texas Instruments has different versions of these transponders depending on the size of the memory in the chip and its ability to be rewritten by the user. The transponders are also available in different sizes, in particular lengths of 12 mm, 23 mm, and 32 mm. Figure 2.22 shows the different sizes of these glass transponders that operate at the central frequency of 134.2 kHz, corresponding to the LF range. Other operational characteristics of these glass transponders are listed in Table 2.1.

FIGURE 2.21
Glass transponder used for RFID applications in the LF range.

© 2011 by Taylor and Francis Group, LLC

FIGURE 2.22
Three commercial glass transponders of different sizes used for application in the LF range.

TABLE 2.1

Operational Characteristics of Glass Transponders

Main Operational Parameters Glass Transponders Texas Instruments – LF Region	
Modulation	FSK: 134.2 kHz and 123.2 kHz
Transmission Principle	Half Duplex
Read Range	Less than 100 cm
Maximum Operating Temperature Range	– 25°C to + 85°C
Read Time	Less than 70 ms
Case material	Glass
Protection	Hermetic seal
Weight	0.8 grams
Memory on board	4 different options depending on specific part number

Other transponders operating in the LF region use planar coil antennas similar to those shown in Figure 2.23. The dimensions of the larger transponder are 25 mm for the outer ring and 20 mm for the inner ring, while the dimensions for the smaller antenna are 14 mm for the outer ring and 9 mm for the inner ring.

These antennas consist of a length of conductor wire coiled multiple times in order to create the desired inductance. The manufacturer specifies their use for the same general type of applications as the glass transponders, with the advantage of being much thinner.

Antennas for transponders operating in the HF frequency (13.56 MHz) are normally planar antennas, having a structure similar to the planar antennas used in the LF region. However, because HF antennas require a lower

© 2011 by Taylor and Francis Group, LLC

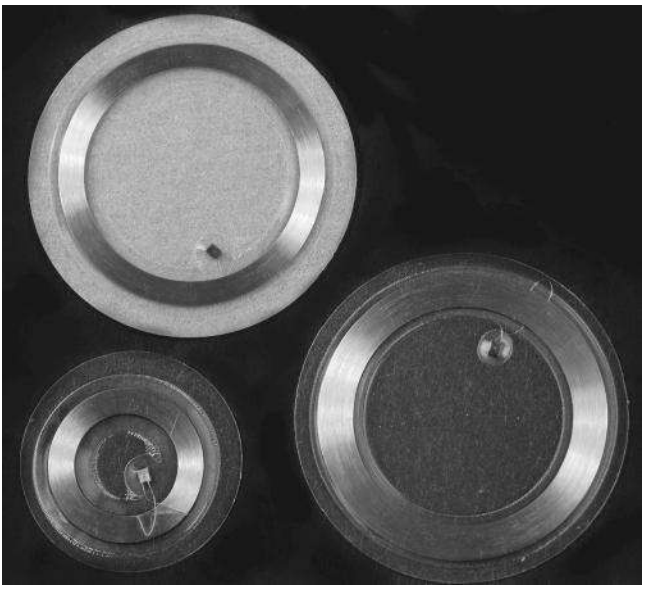

FIGURE 2.23
Commercial planar coil antennas.

inductance, the number of turns for these antennas is much lower, normally less than 10 turns. Planar antennas for RFID transponders operating in the HF region are also manufactured in different sizes and thicknesses depending on the intended application. Figure 2.8 showed a picture of an HF transponder manufactured by Texas Instruments under the name of Tag-it™. This type of transponder is marketed toward product authentication, library applications, supply chain management, asset management, and ticketing or stored value applications. The antennas are built over a polyethyleneterephthalate (PET) substrate giving a maximum thickness of 0.085 mm for the antenna area and 0.355 mm for the chip area. Figure 2.24 shows three antennas from this same family. The larger rectangular antenna has maximum dimensions of 75 mm × 45 mm and consists of seven turns; the small rectangular antenna has a maximum dimension of 39 mm × 22 mm and has six turns; the square antenna has maximum dimensions of 45 mm × 45 mm and contains nine turns.

The number and type of different antennas for transponders operating in the UHF region are higher as each commercial product has been optimized with an application in mind in terms of the different antenna parameters or the type of substrate better suited for a specific purpose. Figures 2.25, 2.26, and 2.27 show three examples of the diverse UHF transponders manufactured by Alien Technology.

Figure 2.25 shows the Alien ALN-9640 Squiggle® Inlay from Alien Technology. This is a general-purpose transponder used for packages that

© 2011 by Taylor and Francis Group, LLC

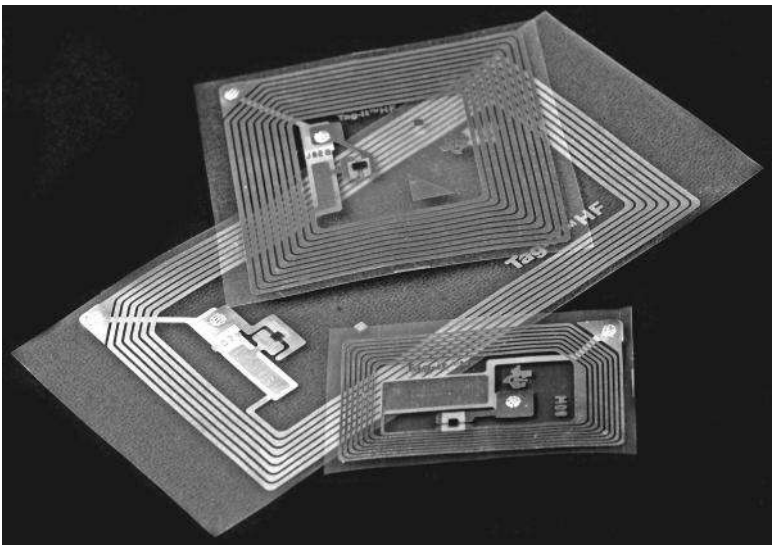

FIGURE 2.24
Diverse planar rectangular antennas used in commercial HF transponders.

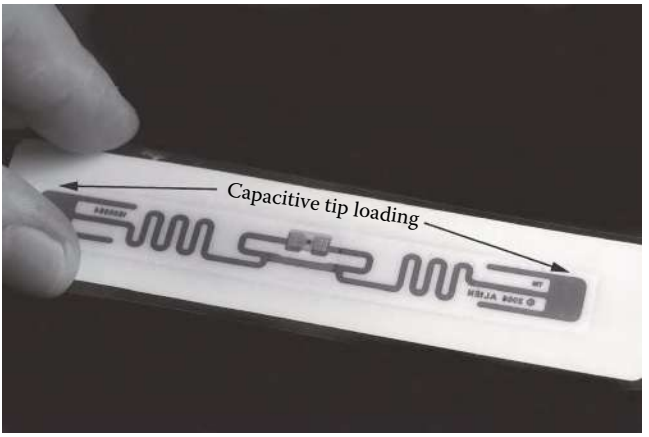

FIGURE 2.25
Commercial UHF transponder based on a meandered dipole and using capacitive tip loading.

include metal or water. The largest length dimension of this antenna is 98 mm, and the largest width of the overall antenna is 8 mm. This antenna exhibits a radiation pattern similar to a half-wave dipole. This antenna is based on a half-wave dipole that has been made shorter by bending the wires and adding shunt and series inductors to create the adequate resonant frequency for the integrated circuit that will be powered by the antenna. The large conductive areas located at each end of the antenna serve as capacitors

© 2011 by Taylor and Francis Group, LLC

used to increase the antenna capacitance. This technique is known as *capacitive tip loading*. Since the magnitude of capacitive reactance decreases as the capacitance increases, a tip-loaded dipole exhibits a more inductive behavior than a dipole of the same length without the additional capacitance at its ends.

Figure 2.26 shows the Alien ALN-9534 2x2 Inlay from Alien Technology. This antenna exhibits a more omnidirectional radiation pattern and is marketed toward item-level tagging applications such as apparel or baggage. The maximum dimensions of this antenna are 46 mm × 40 mm. This type of antenna, in which the conductors are thicker than the previously studied wire antennas, presents the advantage of having higher capacitance and lower inductance than the wire antennas, therefore making it easier to match to the characteristics of its integrated circuits. Furthermore, these antennas made with thicker conductors exhibit a wider bandwidth than the wire antennas.

Figure 2.27 shows the Alien ALN-9554 M Inlay from Alien Technology. This antenna exhibits a better omnidirectional radiation pattern and is marketed toward tagging plastic totes, pallets, and other reusable assets. The maximum dimensions of this antenna are 98 mm × 38 mm. This type of antenna presents the higher bandwidth for the same reasons described earlier. When using conductive inks to create the antenna, the additional ink required to create them results in a cost increase for this type of antenna.

Figure 2.28 shows an example of a meandered dipole antenna with an inner loop for use in the UHF range manufactured by RSIID technologies.

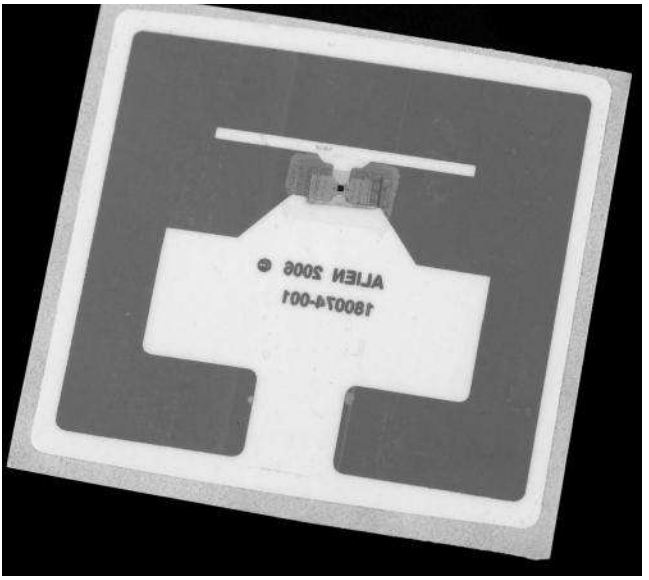

FIGURE 2.26
Commercial UHF transponder using a more omnidirectional antenna.

© 2011 by Taylor and Francis Group, LLC

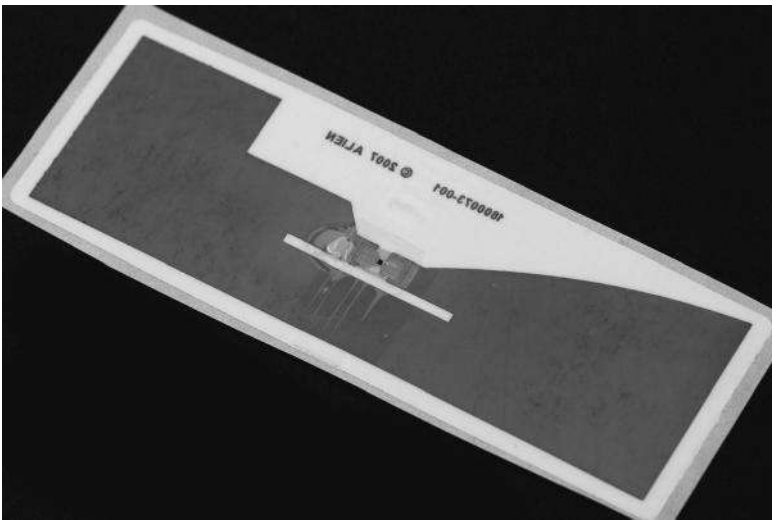

FIGURE 2.27
Commercial UHF transponder having a higher bandwidth response.

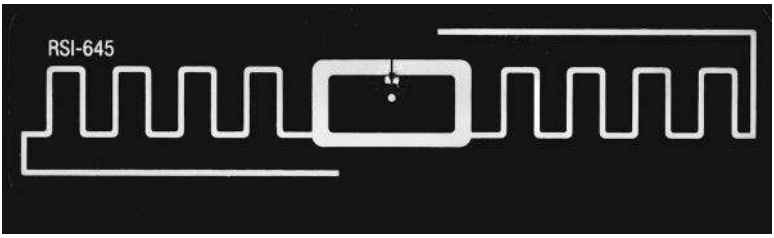

FIGURE 2.28
Meandered dipole antenna for UHF applications.

The maximum dimensions of this antenna are 67 mm × 13.5 mm, thus making it suitable for applications with limited available space. Figure 2.28 is just one example of the different configurations available for meandered dipoles.

Figure 2.29 shows a dual dipole transponder. These transponders have two dipole antennas to make them more insensitive to the orientation of the transponder in reference to the interrogator. The potential drawback of this approach is the additional space required by the transponder that may not be suitable for all products. Furthermore, the front end of the integrated circuit that will be powered by the antenna increases in complexity as it needs to respond to two different antennas. However, for longer range applications in which the position of the object can change, this type of antenna presents a clear advantage.

© 2011 by Taylor and Francis Group, LLC

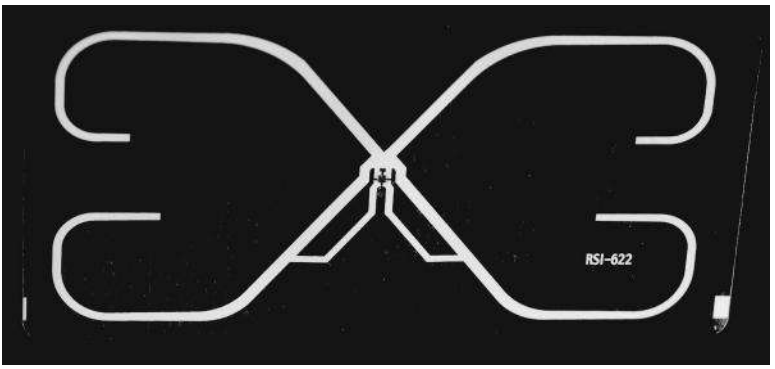

FIGURE 2.29
Dual dipole antenna for UHF transponders.

While the majority of transponders operating in the UHF range are powered by far-field electromagnetic radiation, in some cases the relatively large area that they require may be larger than the available surface in the transponder. The solution in this case is to use UHF antennas that operate in the near-field region, accepting the drawbacks associated with this mode of operation. These antennas operate based on the same inductive coupling principles used by LF and HF antennas. However, it is possible to add shunt and series inductors or capacitive tip loads to create what are known as *hybrid antennas*. These hybrid antennas, examples of which are shown in Figures 2.30 and 2.31, are able to operate in the near and far fields even though the performance in the far-field region is degraded compared to the performance of a typical dipole antenna.

2.5 The Connection between the Chip and the Antenna in RFID Transponders

A critical step in the manufacture of RFID transponders is the connection between the antenna and the integrated circuit in the transponder. There are main methods of doing this connection: chip-on-board and direct die attachment.

Chip-on-board (COB) is an assembly technology for semiconductors in which the electronic chip is directly mounted on and connected to its final board instead of undergoing the traditional packaging process for integrated circuits. This process reduces space requirements and cost, and also increases the performance of the system due to the decrease in connection lengths and increase in reliability. This approach is normally used for wire-wound antennas. During the COB process, the capacitor used to create resonance is also packaged in the device. The device is then covered in epoxy in such a

© 2011 by Taylor and Francis Group, LLC

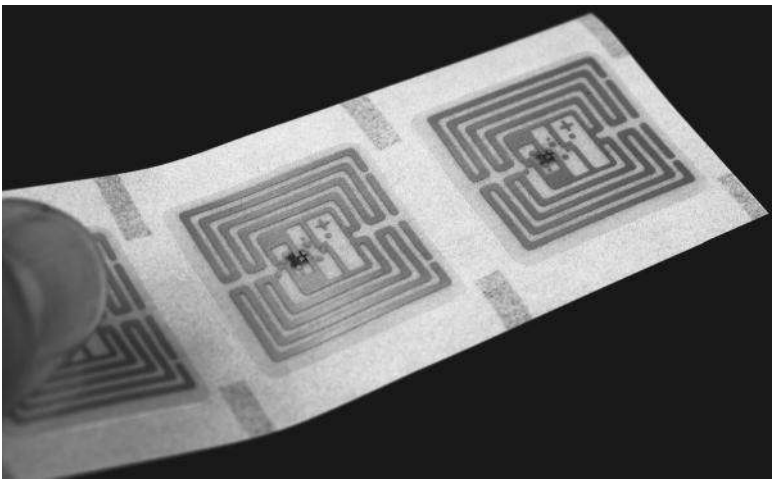

FIGURE 2.30
Hybrid UHF antenna able to communicate in near field and far field.

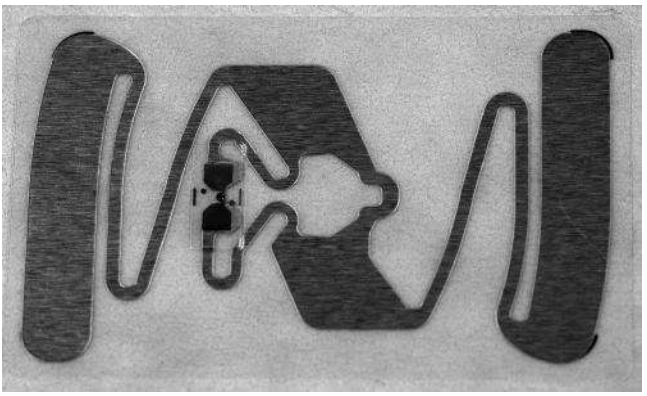

FIGURE 2.31
Hybrid UHF antenna with tip loading.

way that only the two cables to connect to the antenna emerge from the package, as shown in Figure 2.32. The majority of COB packages are used in cards that need to meet the requirements for standard thickness of these cards at 0.76 mm. With this requirement, the typical thickness of COB packages is about 0.41 mm. Although the COB package is designed to protect the internal silicon device during the card lamination process, it is necessary to be careful to prevent mechanical cracks on the device as a result of the mechanical pressures and hot temperatures.

Direct die attachment can be achieved using two techniques: wire bonding or flip-chip. Flip-chip is a technology for interconnecting semiconductor

© 2011 by Taylor and Francis Group, LLC

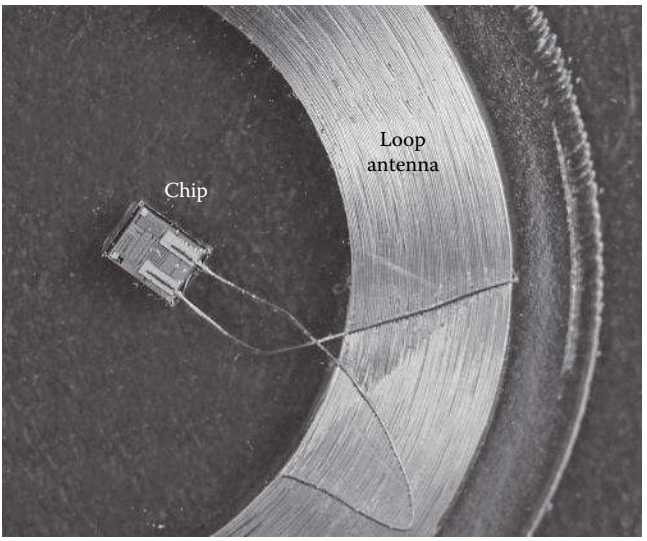

FIGURE 2.32
Connection of the antenna wires to the chip in the transponder.

devices by creating conductive bumps in the pads of the chip. In order to connect the chip, this has to be flipped so the bond pads are in contact with the matching pads in the circuit. In the wire-bonding technology, the chip is mounted upright and wires are used to connect the chip to the circuit. In the case of RFID transponders, the bumps or wires are connected to the antenna, thus being an ideal method to use for printed, etched, or stamped antennas. In this case, the resonance capacitor can also be etched on the substrate of the transponder, and therefore this technology does not require binding it with the chip as COB does. Figure 2.33 shows an example of this type of connection.

The choice between printing, etching, or stamping the antenna is a trade-off between cost and performance. The Q factor of the antenna, which as discussed earlier has a strong effect on the read range for the transponder, is inversely proportional to the resistance of the antenna. With this in mind, it is desirable to use an etched antenna instead of a printed antenna made of conductive material. The etching process is also less expensive than the printing process. For large antennas, however, etching and stamping waste too much unwanted material. In this case, a printed antenna becomes a more desirable solution. Figure 2.34 shows the general structure of the chip-to-antenna connection, independently of the specific technique being used. The antenna is connected between one of the terminals in the die and its ground connection (GND).

This connection creates a problem due to the crossing of the connection to the antenna with the ground ring around the die, creating a parasitic

© 2011 by Taylor and Francis Group, LLC

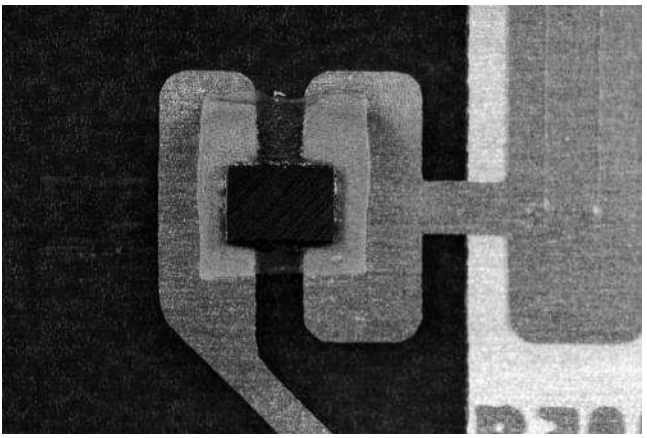

FIGURE 2.33
Direct connection between the chip and the antenna in the transponder.

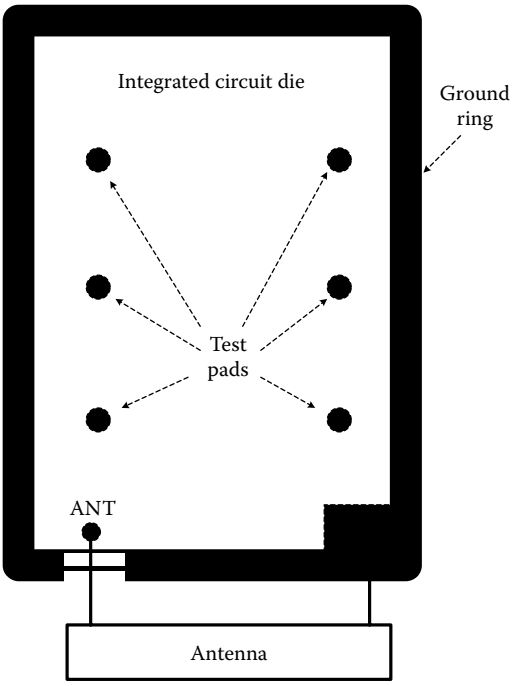

FIGURE 2.34
Strategy for reducing the stray capacitance when connecting the chip to the antenna in an RFID transponder.

© 2011 by Taylor and Francis Group, LLC

capacitance. Depending on the technology being used to make this connection, the parasitic capacitance can have a value of up to 20 fF, influencing the resonant frequency for the antenna. To limit this effect, the ground ring around the die is narrowed in the vicinity of the pad for the antenna connection, thus reducing the parasitic capacitance.

2.6 Additional Factors That Affect the Performance of Antennas in RFID Transponders

As discussed in the preceding sections, the quality factor of an antenna is influenced by its Ohmic losses. For the coil antennas used for transponders operating in the LF region, these Ohmic losses come from the wire used to build the coil. The resistance in DC of a conductor of length l, with a uniform cross-section S, is

$$R_{DC} = \frac{l}{\sigma S} \tag{2.27}$$

where σ is the conductivity of the material.

Because of the need to manufacture the antenna as small as possible, designers opt for choosing the narrowest possible diameter, resulting in an increase in its resistance as shown by equation (2.27). More important, however, for the design of antennas is their losses in AC. The density of AC current through a wire is not constant through its surface, but the current tends to flow through the outer section of the wire, thus decreasing its effective area. This is known as the *skin effect*. Similarly, the *skin depth* for a conductor is defined as the value of its depth at which the current density falls to 37% of the current density along the surface. As shown in equation (2.28), for a given material, its skin depth is dependent on the frequency of the AC current:

$$\delta = \frac{1}{\sqrt{\pi \mu \sigma f}} \tag{2.28}$$

where

δ = the skin depth

μ = the permeability of the material

σ = the conductivity of the material

f = the frequency of the AC current through the material

© 2011 by Taylor and Francis Group, LLC

Example 2.5:

Calculate the skin depth for copper wire at (a) 125 kHz and (b) at 13.56 MHz.

Solution:

Copper has a relative permeability of 1, so its total permeability is $\mu = 4\ \pi\ 10^{-7}$ H/m. Its conductivity is equal to $\sigma = 5.8\ 10^{7}$ mho/m. Therefore, equation (2.28) can be rewritten for copper as

$$\delta = \frac{0.066}{\sqrt{f}} \quad (m)$$

A. The skin depth of copper at 125 kHz is equal to 0.186 mm. This means that the current density of a point located 0.186 mm away from the surface of the conductor is only 37% of the current density on the surface.
B. The skin depth of copper at 13.56 MHz is equal to 0.018 mm. At this frequency, the skin depth is about one-tenth of the skin depth at 125 kHz. Therefore, at 135 MHz the majority of the current is flowing through the surface of the conductor.

The total resistance of a wire to AC current (R_{ac}) is a combination of its DC resistance (R_{DC}) and its skin depth (δ):

$$R_{ac} = R_{DC}\frac{a}{2\delta} \tag{2.29}$$

where a is the radius of the wire.

For etched coil antennas, commonly found in planar transponders, the AC resistance is given by equation (2.30):

$$R_{ac} = \frac{1}{(w+t)}\sqrt{\frac{\pi\mu f}{\sigma}} \tag{2.30}$$

where

w = the width

t = the thickness of the conductor on the substrate

Etching is a wasteful process as metal is removed from the substrate in order to create the antenna. Although some of the materials may be recycled, etching also requires large amounts of chemicals and energy to use in the process. To respond to this concern, newer processes based on conductive inks or copper deposits have been developed, especially for antennas operating in the UHF frequency range. Because of the higher conductivity of copper compared to silver-based conductive inks, antennas made with deposited copper can be substantially thinner than those made with conductive inks. In general, both materials can be effectively used to create antennas.

© 2011 by Taylor and Francis Group, LLC

3

Transponders

CONTENTS

3.1 The Analog Front End 50
3.1.1 Radiofrequency Stage 50
3.1.2 Power Management 54
3.2 Signals in the Transponder 57
3.2.1 Signal Encoding 57
3.2.2 Modulation and Demodulation 59
3.3 The Logic System 66
3.3.1 Data Memory 66
3.3.2 Cyclic Redundancy Check for Error Detection 75
3.4 Transponder Programming 77
3.5 Summary of Electrical Specifications for RFID Transponders 79
3.6 Mechanical Considerations and Transponder Assembly 81

The two main components of a transponder are its internal circuits and its antenna. The antenna, studied in Chapter 2, is used to collect energy from the electromagnetic fields in which the transponder is embedded as well as to transmit the information back to the interrogator. The integrated circuit, also known as the *chip* or *device*, is the key component in the transponder, and for this reason this chapter uses the names *transponder*, *chip*, and *device* interchangeably. The integrated circuits have the ability to store information to be transmitted to the interrogator, execute a series of commands, and, in some cases, store new information sent by a remote station.

This chapter describes the fundamental blocks that make up the transponder. Because there are a large number of transponders in the market, each one with its own specific differences, this chapter focuses on the functional blocks common to them using commercial transponders to illustrate these concepts. Therefore, the devices used in the examples should not be seen as an exhaustive list of transponders but just as examples used to illustrate specific concepts and ideas. This chapter starts by describing the analog front end commonly encountered in these devices. The analog front end contains the radiofrequency section that is necessary to match the electrical properties of the device to the electrical properties of the antenna as well as the circuits used for harvesting and managing the power necessary to turn on the device. This section is followed by the description of the main encoding and modulation methods commonly used by transponders. This is followed

© 2011 by Taylor and Francis Group, LLC

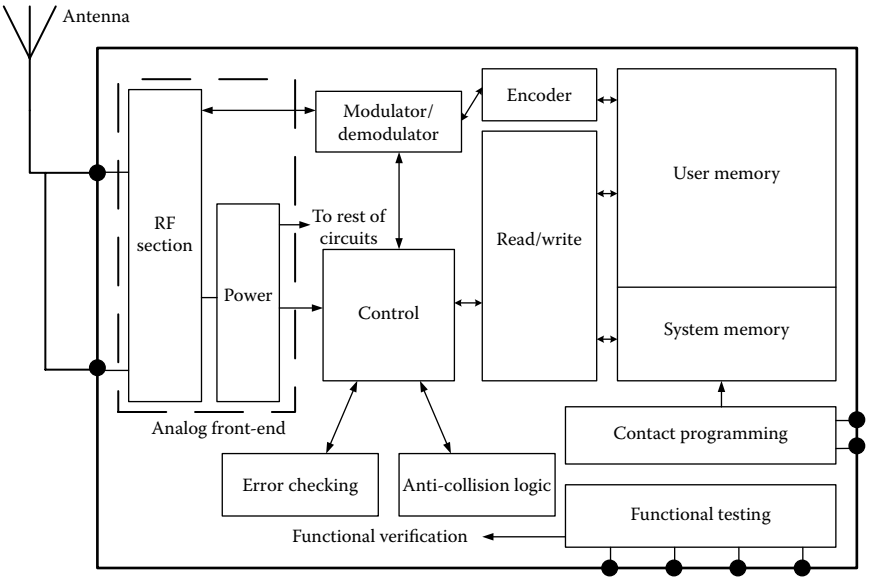

FIGURE 3.1
Block diagram of a generic RFID transponder highlighting its main functional components.

by the description of the different memory structures to store data and configuration parameters as well as the codes used to ensure the integrity of the digital data. The next section briefly describes the methods for programming the transponder by either a contact programmer or a contactless programmer. The last two sections in this chapter present a summary of the electrical and mechanical specifications found in commercial transponders as well as a description of their most common assembly methods.

Figure 3.1 depicts the block diagram of a basic and generic RFID transponder showing its main functional blocks. It is important to note that not all the blocks shown in the figure will be always present in any transponder depending on its use, intended application, and cost.

3.1 The Analog Front End

3.1.1 Radiofrequency Stage

When the transponder is immersed in an electromagnetic field of the appropriate frequency, a radiofrequency voltage appears across the antenna terminals. The task of the front-end stage is to rectify that radiofrequency voltage and convert it into a continuous voltage (DC) with a value high enough to power the rest of the circuits inside the device. Different transponders have

© 2011 by Taylor and Francis Group, LLC

different requirements regarding the minimum voltage required to become operational depending on their internal structure and fabrication technology.

The first step in the energy conversion process between the electromagnetic field and the DC voltage is the resonant circuit tuned to the frequency of the field. The different possible configurations for the external resonant circuit described in Section 2.2 are now studied, taking into account the structures used in commercial transponders. Figure 3.2 shows the possible alternatives for the external resonant circuit using two commercial devices: the MCRF355 and the MCRF450, both from Microchip Technology and both operating at 13.56 MHz.

Some devices incorporate one or two capacitors inside their integrated circuit, eliminating the need for using an external capacitor and therefore reducing the size required for the overall transponder inlay. Figure 3.3 shows the resonant circuit using commercial devices that incorporate one or two capacitors in their internal circuitry.

The devices MCRF360, MCRF451, and MCRF455 from Microchip Technology have a single internal capacitor with values of 100 pF, 95 pF, and 50 pF, respectively. The device MCRF422, also from Microchip Technology, has two internal capacitors of 50.6 pF and 65.4 pF. All these devices operate at 13.56 MHz.

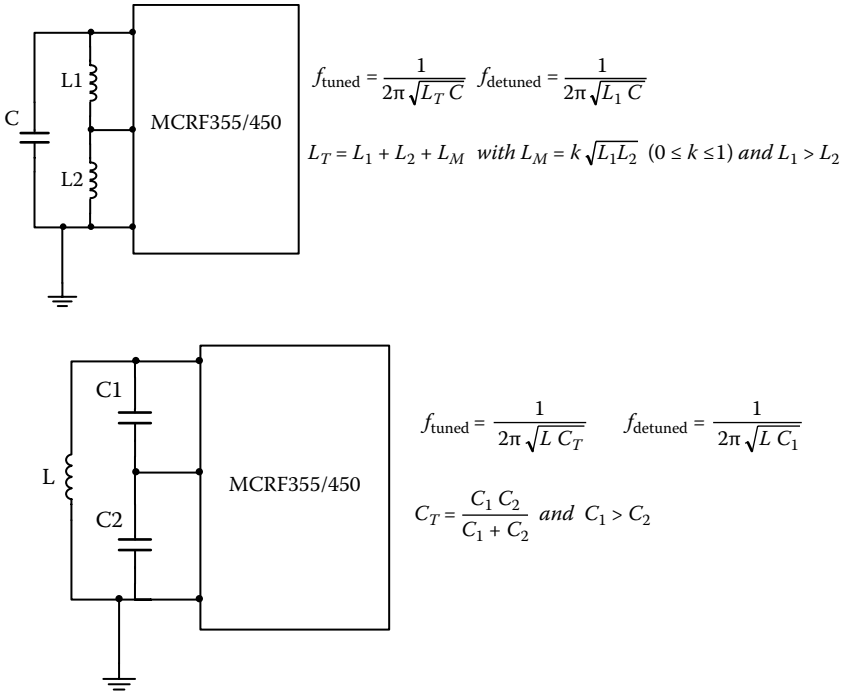

FIGURE 3.2
Alternatives for the external resonant circuit found in commercial transponders. These transponders require a capacitor in the inlay to create the resonant circuit. The inductor in the circuits models the antenna.

© 2011 by Taylor and Francis Group, LLC

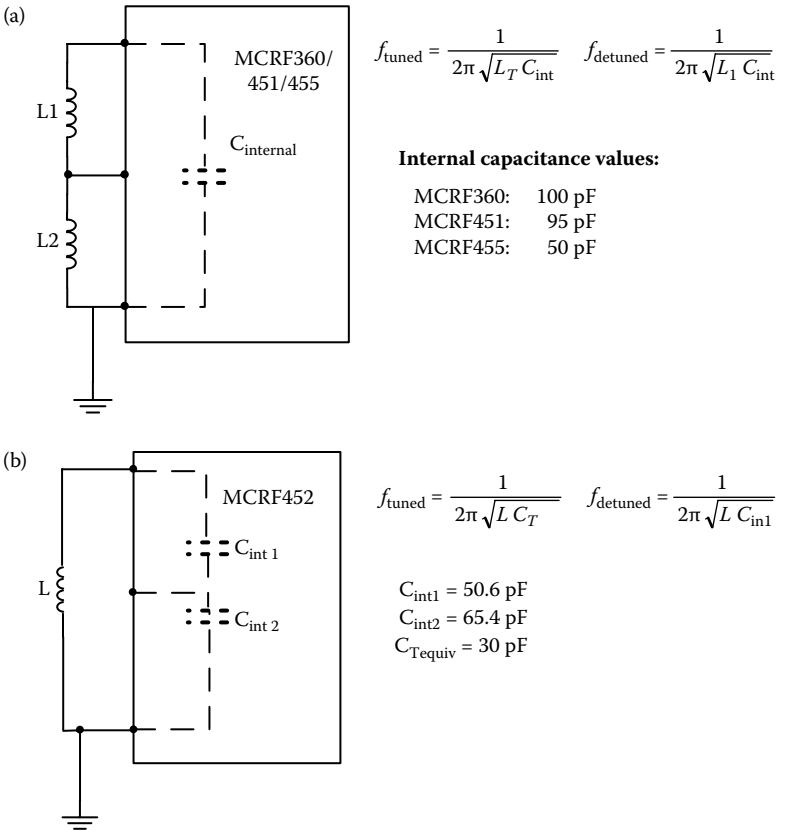

FIGURE 3.3
Alternatives for the external resonant circuit for devices that incorporate the resonance capacitor in the die of the integrated circuit. (a) Structure with a single internal capacitor. (b) Structure with two internal capacitors.

The path between one of the antenna connection nodes and ground, shown in Figures 3.2 and 3.3, is shortened according to a control signal. The path is shortened using a transistor, called a *modulation transistor*, that exhibits a low ON resistance, normally below 5 Ω and a very high OFF resistance of several MΩ. In this situation, the transponder exhibits two different resonant frequencies.

The resulting resonance frequency when the modulation transistor is OFF is chosen to be equal to the frequency of the electromagnetic field emitted by the interrogator. As shown in Figure 3.4, because of the resonance condition, the energy of the field is transmitted through the front end to the device, resulting in the radiofrequency voltage at the input of the device being maximal. This situation is called *uncloaking*. When the modulation transistor is turned ON, it shortens one of the inductors or capacitors, resulting in a resonant frequency for the circuit different from the frequency of the electromagnetic field. When it shortens one of the two inductors connected

© 2011 by Taylor and Francis Group, LLC

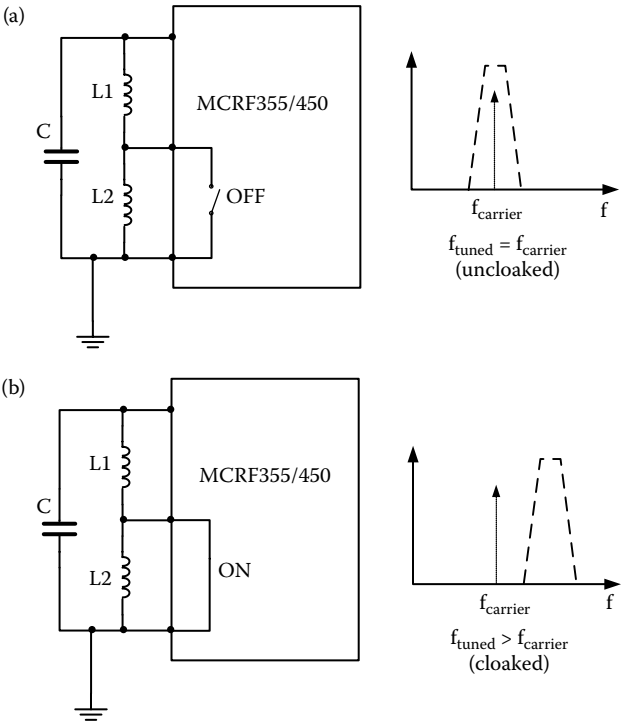

FIGURE 3.4
Cloaking and uncloaking modes produced by the control transistor in the transponder and the different resonant frequencies generated. (a) Uncloaked. (b) Cloaked.

in series, the resulting resonant frequency is higher than the frequency of the field; when it shortens one of the two capacitors connected in series, the resulting resonant frequency is lower. In any case, the frequency of the circuit and the frequency of the field are different, and therefore most of the energy of the electromagnetic field is rejected by the filter, resulting in the voltage generated at the input of the device being minimal, ideally zero. This situation is called *cloaking*. The same cloaking–uncloaking approach is used by the transponder to transmit data to the interrogator. Using this approach, the digital signal controls the modulation transistor.

Example 3.1:

Calculate the values of the external inductors needed to use in a transponder based on the MCRF451 device.

Solution:

The MCRF451 has an internal capacitance of 95 pF and operates at a frequency of 13.56 MHz. Using the equations shown in Figure 3.3, the total inductance

© 2011 by Taylor and Francis Group, LLC

necessary is L_T = 1.45 μH. With this inductance, the circuit resonates at 13.56 MHz, and therefore the energy from the electromagnetic field is passed to the device. The L_T = 1.45 μH of external inductance will be split between L_1 and L_2.

The value of L_1 can be calculated using the equations from Figure 3.3 now for the case of detuned frequency. The detuned frequency should be between 3 MHz and 6 MHz away from the tuned frequency. For the structure used by the MCRF451 device, the detuned frequency will be higher than the tuned frequency. Using for example a frequency shift of 4 MHz, the detuned frequency becomes 17.56 MHz, resulting in a value of L_1 equal to 864 nH. Assuming initially a value for the coupling coefficient between L_1 and L_2 equal to zero (k = 0), the required value for L_2 is 586 nH. It can be observed that $L_1 > L_2$ as it is required. In a more realistic situation, the value of the coupling coefficient will be between 0 and 1, resulting in a lower value for L_2.

3.1.2 Power Management

In order to be operative, the transponder needs to convert the radiofrequency voltage detected by the antenna into a DC voltage. The voltage required to bias the internal components in the transponder is higher than the voltage detected by the antenna. Therefore, the transponder requires the use of voltage multipliers to reach the values necessary by the biasing voltage.

A voltage multiplier is a circuit that converts a lower AC voltage into a higher DC voltage. Figure 3.5 shows the basic structure of a simple voltage multiplier called a *voltage doubler*.

Assuming initially ideal diodes for simplicity, diode D1 is forward biased during the phase of negative input voltage, while diode D2 is reverse biased and therefore capacitor C2 is disconnected from the rest of the circuit. In this stage, capacitor C1 charges to a DC voltage ideally equal to the amplitude of the AC signal. Afterward, during the phase of positive input voltage, the biasing of the diodes reverses: D2 is forward biased, and D1 becomes reverse biased. This causes capacitor C2 to be directly connected to the input of the AC signal. Taking into consideration the voltage at which capacitor C1 was originally charged, the DC voltage at capacitor C2 will be equal to twice the amplitude of

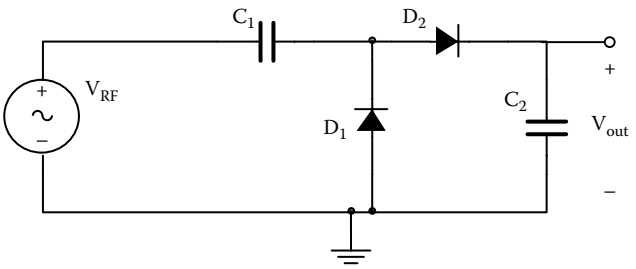

FIGURE 3.5
Structure of a single-stage basic voltage multiplier. V_{RF} models the voltage generated by the electromagnetic field in which the transponder is immersed.

© 2011 by Taylor and Francis Group, LLC

the input voltage. Considering now the minimum ON voltage for real diodes, the voltage at the output of the structure shown in Figure 3.5 is

$$V_{out} = 2(V_p - V_{ON}) \tag{3.1}$$

where

V_{out} = the output DC voltage,

Vp = the peak voltage detected at the antenna terminals

V_{ON} = the minimum direct voltage across the diode to turn it on

Figure 3.6 shows the intermediate signals observed at the different nodes in the voltage doubler structure. The voltage supply models the radiofrequency signal detected at the terminals of the antenna in the transponder. The graph of the output voltages shows how the output capacitor is being charged until it reaches the steady-state level predicted by equation (3.1). Once the transient disappears, the output voltage stabilizes and will remain at that level as long as the transponder is immersed in that electromagnetic field.

In practical RFID systems, because the RF voltage detected at the antenna terminals is relatively small, the voltage doubler structure shown in Figure 3.5 does not produce a high enough voltage to power the integrated circuit in the transponder. This situation can be resolved by connecting additional voltage doublers. The resulting structure is known as a *Dickson charge pump*, resulting in an output DC voltage equal to

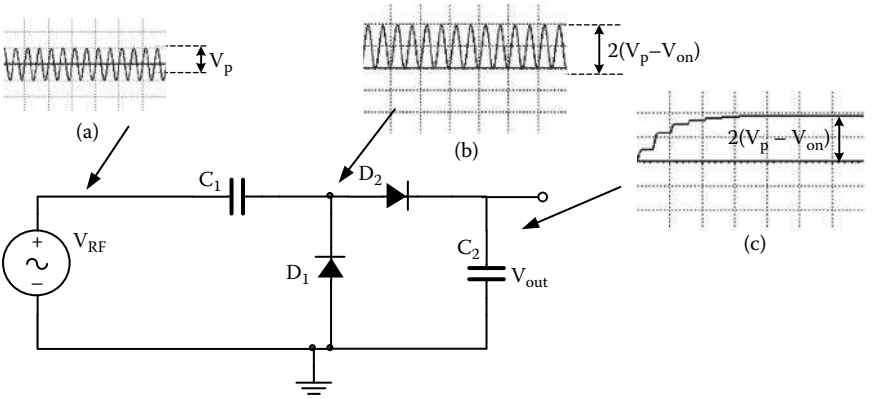

FIGURE 3.6
Signals observed at diverse points in the single-stage voltage multiplier. (a) Input signal. (b) Intermediate signal consisting of the input signal plus a DC component equal to its peak value. (c) Output signal. After the transient disappears, the output signal is a DC signal with a value equal to the double of the peak amplitude of the input signal.

© 2011 by Taylor and Francis Group, LLC

$$V_{out} = 2N(V_p - V_{ON}) \tag{3.2}$$

where N is the number of basic voltage doubler cells.

Figure 3.7 shows a three-stage Dickson charge pump. Its output voltage is equal to six times the peak voltage for the input minus the turn-on voltage for the diodes. Figure 3.8 shows the intermediate signals observed at several nodes in this structure. The sensitivity of the different graphs in volts per division has been kept the same to better observe how at each intermediate node, the AC signal has an additional offset equal to its peak value. The final DC output voltage is predicted by equation (3.2).

There is, however, a practical limit to the number of stages that is reasonable to consider for use in a practical application. As the number of stages increases, the number of required diodes increases by a factor of 2, and therefore the power dissipated by the charge pump also increases in the same ratio, decreasing the overall efficiency of the circuit. The efficiency of the charge pump is given by equation (3.3):

$$\eta_{pump} = \frac{P_{load}}{P_{load} + P_{consumed}} = \frac{V_{out}}{V_{out} + 2N V_{ON}} \tag{3.3}$$

where N is the number of stages in the charge pump.

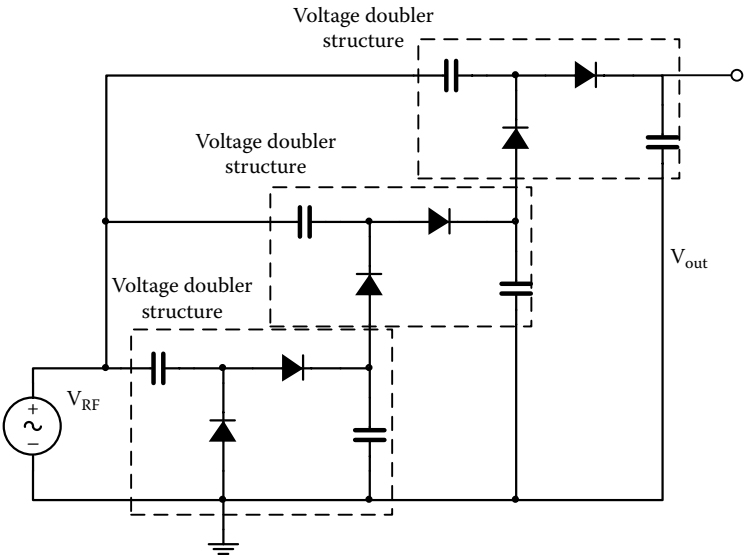

FIGURE 3.7
Dickson charge pump structure used to increase the DC voltage extracted from the radiofrequency signal generated by the electromagnetic field in which the transponder is immersed.

© 2011 by Taylor and Francis Group, LLC

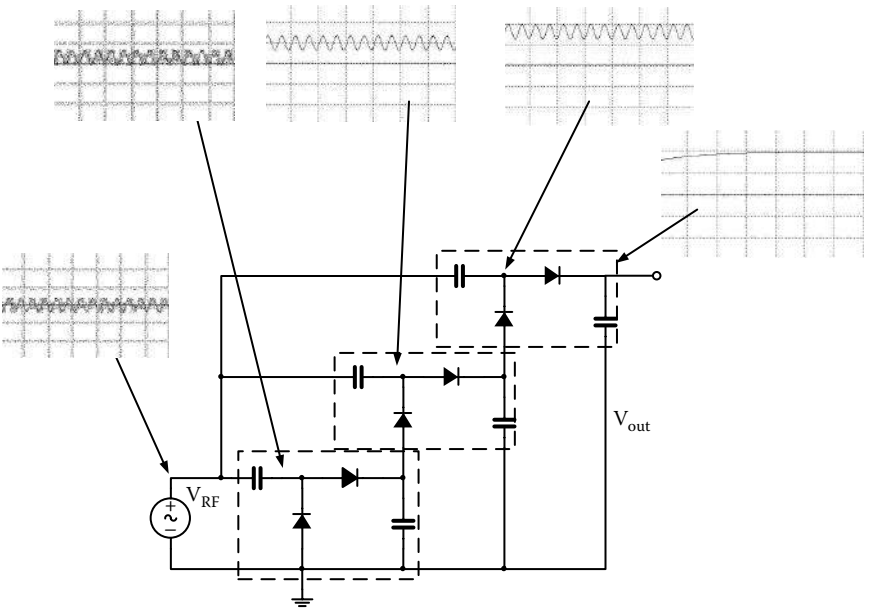

FIGURE 3.8
Signals observed at different points in the Dickson charge pump. After each stage, the overall signal increases its DC component until it only contains a DC component at the output of the last stage.

Equation (3.3) shows that the efficiency of the charge pump will increase by using diodes with a lower turn-on voltage. To this extent, several types of devices have been used and several more types are being currently investigated. The most common approach is to use Schottky diodes due to their electrical characteristics that make them extremely attractive for this purpose. However, using Schottky diodes increases the complexity of manufacturing the transponder, thus resulting in a higher cost. For this reason, the use of ultra-low-power complementary metal oxide semiconductor (CMOS) diodes appears to be an attractive alternative as they can be manufactured with the rest of the transponder and therefore they will not increase the cost of manufacturing the transponder.

3.2 Signals in the Transponder

3.2.1 Signal Encoding

The digital signals in the transponder are encoded using one or more of these common encoding schemes that are represented in Figure 3.9.

© 2011 by Taylor and Francis Group, LLC

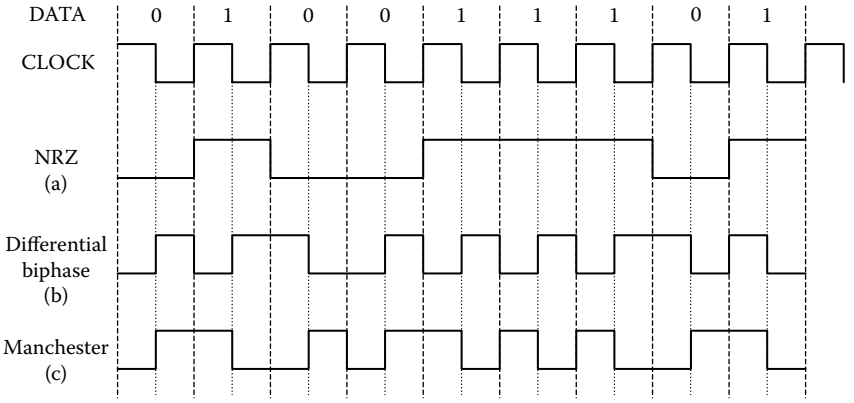

FIGURE 3.9
Common signal-encoding techniques. (a) Nonreturn-to-zero (NRZ): *1* represented by a high logic level; *0* represented by a low logic level. (b) Differential biphase: *1* represented by a change in level at the start of the clock period; *0* represented by no change in level at the start of the clock period. There is always a change of level at the middle of the clock period. (c) Manchester: *1* represented by a high-to-low transition at the middle of the clock period; *0* represented by a low-to-high transition at the middle of the clock period.

These encoding techniques are as follows:

NRZ (nonreturn to zero): There is no data encoding done. The 1's and 0's are clocked from the data array directly to the output transistor that will close or open the switch in the analog front end, as was shown in Figure 3.4. Although extremely simple, this encoding technique presents problems if the data to transmit have long strings of 1's or 0's because these may be misunderstood as the presence of a DC voltage in the line.

Differential biphase: Multiple encoding approaches using this method. This method embeds clocking information with the data and will help to synchronize the interrogator to the bit stream. In this approach, a level change occurs at the middle of every bit clock period. *1* is represented by a change in level at the start of the clock. *0* is represented by no change in level at the start of the clock.

Manchester code (biphase level, biphase_L, or split phase): This is a variation of the previous encoding method. There is not always a transition at the clock edge, but there is always a transition in the middle of the clock cycle, thus allowing one to extract the clock signal from the data signal. In Manchester code, a *1* is represented by a high to low level change in the middle of the clock. A *0* is represented by a low to high level change at the start of the clock. This type of encoding is used in the MCRF355/360 and the MCRF45X family of transponders manufactured by Microchip Technology.

© 2011 by Taylor and Francis Group, LLC

Example 3.2:

Assume that we are using a biphase-L format (Manchester) for encoding the digital data at a frequency of 70 kHz. The data bit *0* is sent by first detuning (cloaking) the device during 7 μs and then tuning (uncloaking) the device for an additional 7 μs. The data bit *1* is sent by uncloaking the device and then cloaking it for the same time periods.

3.2.2 Modulation and Demodulation

Modulation refers to changing one or more parameters in the carrier radiofrequency signal as a method to transmit the encoded signal. In practice, only one of the parameters (amplitude, frequency, or phase) of the radiofrequency is usually changed when transmitting simple digital data.

When the amplitude of the carrier changes depending on the encoded signal, the resulting modulated signal is called *amplitude shift keying*, or ASK. In this case, a high voltage in the envelope of the radiofrequency signal signifies a logic level *1*, while a low voltage in the envelope signifies a logic level *0*, following the appropriate signal-encoding method being used. ASK modulation is also known as *direct modulation* in RFID systems. ASK modulation offers the possibility of high data rates due to the simplicity of the process. The spectrum of the ASK signal is relatively narrow as it contains only energy at the frequency of the carrier signal and at each of the two sidebands. One sideband is located at the frequency of the carrier minus the frequency of the modulating signal, and the other sideband is located at the frequency of the carrier plus the frequency of the modulating signal. The bandwidth efficiency of a binary-modulated ASK signal is 1 bit/second/Hz. The detection of the ASK signal can be done using a coherent detector or a noncoherent detector. Noncoherent detection increases the simplicity of the overall system, although it reduces the ability to differentiate between the desired signal and noise. The immunity to noise can be increased by using a coherent detector, although the immunity to noise is overall lower than using an FSK or PSK modulation process. The bit error probability for noncoherent ASK modulation, assuming an additive white Gaussian noise limited channel, is

$$P\big|_{\substack{ASK \\ NONCOH}} = 0.5e^{\frac{-E_b}{4N_0}} + 0.5erfc\left(\sqrt{E_b / 2N_0}\right) \tag{3.4}$$

where

P = the bit error probability

E_b/N_0 = the average bit power

$erfc(x)$ = the complementary error function for the argument x

© 2011 by Taylor and Francis Group, LLC

Similarly, the bit error probability for coherent ASK modulation is

$$P\big|_{\substack{ASK \\ COH}} = 0.5 erfc\left(\sqrt{E_b / 2N_0}\right) \tag{3.5}$$

Figure 3.10 shows the bit error probability values obtained using equations (3.4) and (3.5) for different values of energy transmitted. From this graph it is possible to observe the decrease in bit error rates for coherent ASK modulation, which is especially significant when increasing the energy per bit transmitted.

When the encoding signal changes the amplitude of the carrier being transmitted, the resulting modulated signal is called *frequency shift keying*, or FSK. When the modulating signal is binary, FSK results in using two different frequencies for transmitting the digital data. The most common approach to FSK in RFID systems is called Fc/8/10: this means that a *0* is transmitted as an amplitude modulated clock cycle with a period corresponding to the carrier frequency divided by 8, and a *1* uses a period that corresponds to the carrier frequency divided by 10. Figure 3.11 shows the time representation for this FSK modulation.

The logic level *0* is transmitted by sending a total of eight cycles of the RF signal; the first four cycles have a higher amplitude than the last four cycles. The logic level *1* is transmitted by sending a total of ten RF cycles,

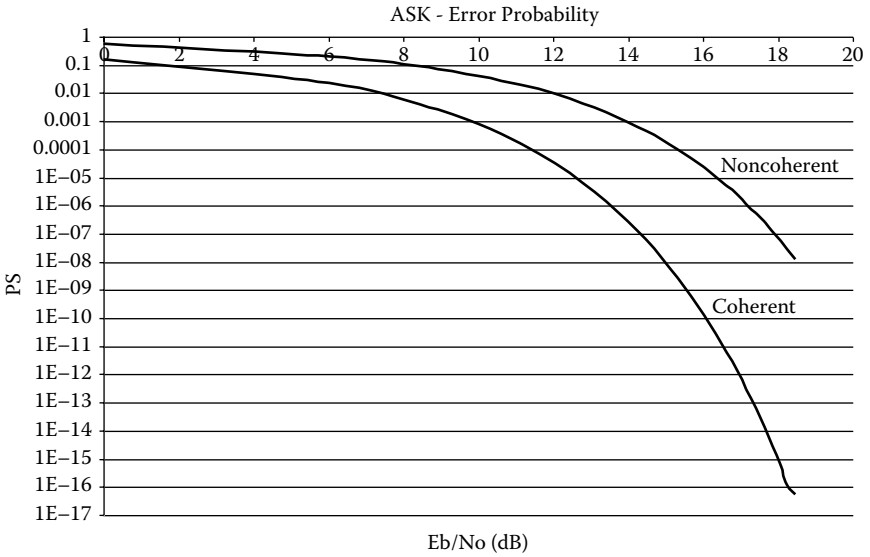

FIGURE 3.10
Error probability (Ps) for coherent and noncoherent ASK modulation as a function of the energy received (Eb/No).

© 2011 by Taylor and Francis Group, LLC

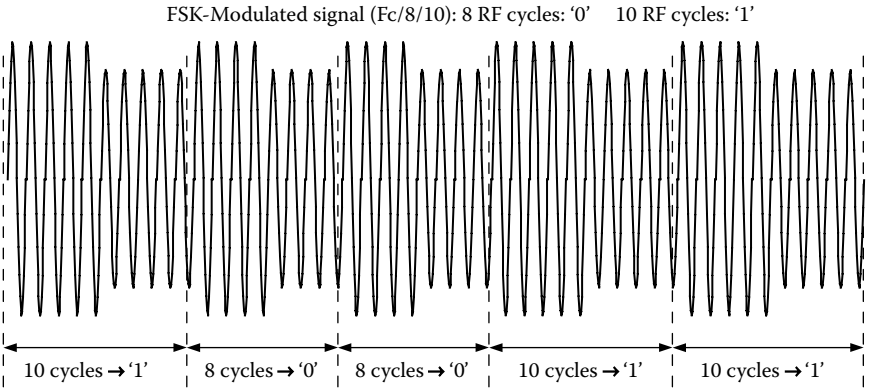

FIGURE 3.11
Structure of the FSK-modulated signal. The symbol *1* is represented by sending 10 RF cycles, while the symbol *0* is represented by sending 8 RF cycles. The message sent in the figure is *10011*.

with the first five cycles having a higher amplitude than the last five cycles. The change in amplitude between the first and second halves of the cycles allows one to count the number of cycles between transitions and therefore to differentiate between logic levels. In other words, the *1* and *0* are differentiated by looking at the number of periods between transitions.

Other FSK approaches used by other transponders are Fc/10/8, Fc/5/8, and Fc/8/5. Table 3.1 lists the relation between the encoding signal and the data transmitted.

The bandwidth required by the FSK signal is dependent on the existence or not of phase changes when changing frequencies. Obviously, in those FSK modulation approaches that exhibit abrupt phase changes, there will be more spectral components at higher frequencies, thus increasing the bandwidth. The bandwidth efficiency of a binary-modulated FSK signal depends on how the modulation process has been performed, but it approaches 2 bits/second/Hz. Similarly to ASK modulation, FSK signals can be recovered using noncoherent detectors or coherent detectors, with a coherent detector providing stronger noise immunity. The calculation of the bit error rate for FSK signals depends on the separation between the frequencies used to transmit the FSK signal. The optimal frequency selection occurs when these frequencies are a multiple of the frequency of the encoding signal. These are called *orthogonal frequencies*.

The bit error probability for noncoherent FSK modulation, assuming an additive white Gaussian noise limited channel, is

$$P\big|_{\substack{FSK \\ NONCOH}} = 0.5e^{\frac{-E_b}{2N_0}} \tag{3.6}$$

© 2011 by Taylor and Francis Group, LLC

TABLE 3.1

Different FSK Modulation Approaches

	Logic Level "0"	Logic Level "1"
Fc/8/10	8 RF cycles	10 RF cycles
Fc/10/8	10 RF cycles	8 RF cycles
Fc/5/8	5 RF cycles	8 RF cycles
Fc/8/5	8 RF cycles	5 RF cycles

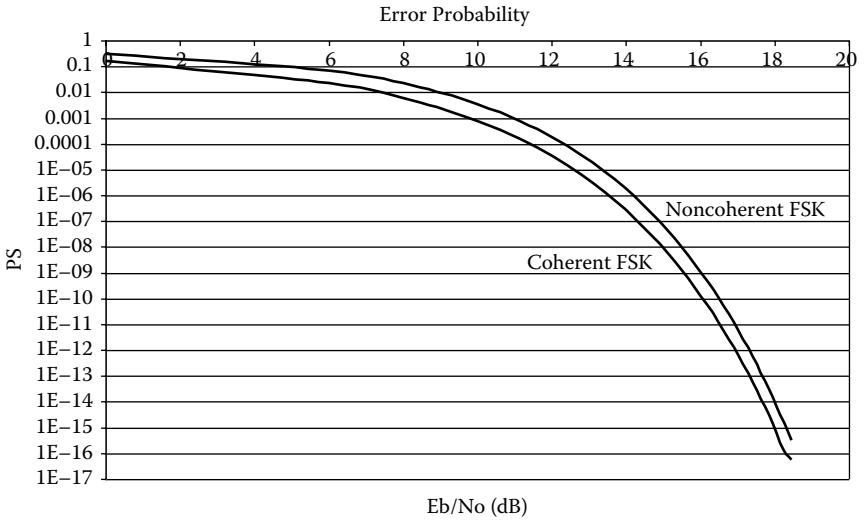

FIGURE 3.12
Error probability (Ps) for noncoherent FSK and coherent FSK as a function of the energy received (Eb/No).

The bit error probability for coherent FSK modulation is

$$P|_{\substack{FSK \\ COH}} = 0.5 erfc\left(\sqrt{E_b / 2N_0}\right) \tag{3.7}$$

Comparing equations (3.5) and (3.7) shows that if the two frequencies that make the FSK signal are chosen to be orthogonal, then the bit error rates for coherent ASK and coherent FSK signals are essentially the same. Figure 3.12 shows the probability of bit error as predicted by equations (3.3) and (3.4) for different values of energy per bit. This figure shows that the difference in performance between noncoherent detection and coherent detection for FSK signals is lower than for ASK signals. This has resulted in the widespread use of noncoherent FSK modulation due to its simplicity.

© 2011 by Taylor and Francis Group, LLC

Example 3.3:

Calculate the bit error rate for coherent and noncoherent ASK and FSK demodulation for the following signal-to-noise ratios (E_b/N_o): (a) 5 dB, (b) 10 dB, and (c) 15 dB.

Solution:

The bit error rates for each type of demodulation are given by equations (3.4) to (3.7). The first step is to express the signal-to-noise ratio in linear units. This results in the following values:

A. $E_b/N_o = 5$ dB ➔ $E_b/N_o = 3.16$ (linear units)
B. $E_b/N_o = 10$ dB ➔ $E_b/N_o = 10.0$ (linear units)
C. $E_b/N_o = 15$ dB ➔ $E_b/N_o = 31.6$ (linear units)

Bit error rates for noncoherent ASK demodulation are predicted by equation (3.4), resulting in the following:

With $E_b/N_o = 3.16$ (5 dB): $P_s = 0.264$ (approximately 1 error every 4 bits transmitted)
With $E_b/N_o = 10.0$ (10 dB): $P_s = 0.042$ (approximately 1 error every 24 bits transmitted)
With $E_b/N_o = 31.6$ (15 dB): $P_s = 0.185\ 10^{-3}$ (approximately 1 error every 5400 bits transmitted)

Bit error rates for coherent ASK demodulation are predicted by equation (3.5), resulting in the following:

With $E_b/N_o = 3.16$ (5 dB): $P_s = 0.037$ (approximately 1 error every 30 bits transmitted)
With $E_b/N_o = 10.0$ (10 dB): $P_s = 0.78\ 10^{-3}$ (approximately 1 error every 1300 bits transmitted)
With $E_b/N_o = 31.6$ (15 dB): $P_s = 9.47\ 10^{-9}$ (approximately 1 error every 100 million bits transmitted)

Bit error rates for noncoherent FSK demodulation are predicted by equation (3.6), resulting in the following:

With $E_b/N_o = 3.16$ (5 dB): $P_s = 0.103$ (approximately 1 error every 10 bits transmitted)
With $E_b/N_o = 10.0$ (10 dB): $P_s = 3.37\ 10^{-3}$ (approximately 1 error every 300 bits transmitted)
With $E_b/N_o = 31.6$ (15 dB): $P_s = 6.87\ 10^{-8}$ (approximately 1 error every 14.5 million bits transmitted)

Bit error rates for coherent FSK demodulation are predicted by equation (3.7), resulting in the following:

With $E_b/N_o = 3.16$ (5 dB): $P_s = 0.037$ (approximately 1 error every 30 bits transmitted)
With $E_b/N_o = 10.0$ (10 dB): $P_s = 0.78\ 10^{-3}$ (approximately 1 error every 1300 bits transmitted)
With $E_b/N_o = 31.6$ (15 dB): $P_s = 9.47\ 10^{-9}$ (approximately 1 error every 100 million bits transmitted)

© 2011 by Taylor and Francis Group, LLC

These results show that the performance of coherent demodulation has a much better performance than noncoherent demodulation. Even for relatively noisy signals, coherent ASK shows a much lower bit error rate than when the demodulation is performed noncoherently. Therefore, it seems obvious to choose a coherent demodulation scheme when using ASK. While coherent FSK demodulation also shows a lower bit error rate than noncoherent FSK demodulation, the difference is not as strong as in the ASK case. For this reason, a noncoherent FSK demodulation may be preferred as it will reduce the complexity of the system without excessively degrading its performance.

When the encoding signal changes the phase of the carrier, the resulting modulated signal is called *phase shift keying* (PSK), as shown in Figure 3.13. PSK is basically the same approach as FSK with the difference being that only one frequency is used. The information is encoded here in the change of phase between clock cycles. PSK also allows for different approaches on this encoding. Because the receiver is only looking for changes of phase, it is possible to transmit information in a smaller number of radiofrequency cycles, resulting in using faster data transfer rates compared to FSK.

Some devices like the MCRF200 and the MCRF250, both from Microchip Technology, support two PSK modulation modes called PSK_1 and PSK_2. In PSK_1, the phase of the RF signal changes when the encoding data change. This means that, for example, the phase of the RF signal will change when the encoding signal changes from *1* to *0* or from *0* to *1*. In

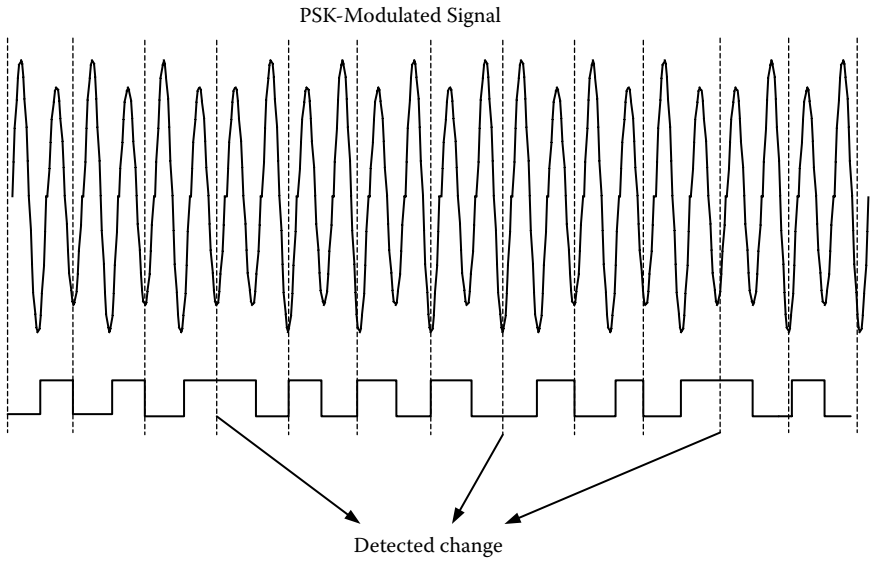

FIGURE 3.13
A generic PSK-modulated signal. The figure shows that the PSK signal requires less RF cycles to transmit the digital data.

© 2011 by Taylor and Francis Group, LLC

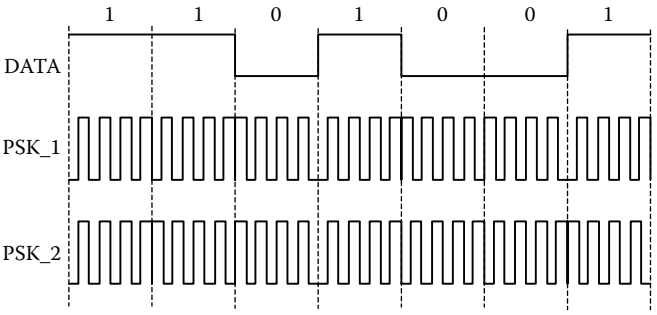

FIGURE 3.14
Two variations of PSK modulation. In PSK_1, the phase of the carrier changes every time there is a change in the symbol transmitted. In PSK_2, the phase of the carrier changes every time the symbol transmitted is *1*.

PSK_2, the phase of the RF signal changes every time the encoding data have the logic level *1*. For example, the phase will change when the encoding data change from *0* to *1* or from *1* to *1*, but it will not change when the encoding data move from *1* to *0* or from *0* to *0*. Figure 3.14 depicts these two PSK modulation approaches.

A third PSK modulation mode available in some other devices—for example, the T5557 from Atmel®—is based on a phase change on the rising edge of the encoding signal.

The spectral occupancy of the PSK signal is identical to the ASK signal assuming that there are no phase changes abruptly occurring at the symbol boundaries. However, in contrast to ASK and FSK, the detection of PSK signals requires a coherent demodulator. The bit error rate for PSK signals is

$$P\big|_{\substack{PSK \\ COH}} = 0.5 erfc\left(\sqrt{E_b / N_0}\right) \tag{3.8}$$

When comparing the different modulation methods and assuming equal average energy per symbol transmitted, the different PSK modulation approaches present the strongest immunity against noise. Coherent FSK modulation with orthogonal symbols or coherent ASK modulation is the next best approach followed by the noncoherent FSK modulation. Noncoherent ASK modulation exhibits the poorest performance. For example, a bit error rate of 10^{-6} requires a value of Eb/No slightly above 10 dB for a PSK signal, but it will require a value of Eb/No of about 18 dB for a noncoherent ASK signal. Similarly, an energy Eb/No of 10 dB will result in a bit error rate of 1.5 10^{-5} in using PSK, but the bit error rate will increase up to 1.5 10^{-2} when using noncoherent ASK. This represents moving from 1.5 errors every 100,000 bits transmitted (PSK) to 1.5 errors every 100 bits transmitted (noncoherent ASK).

© 2011 by Taylor and Francis Group, LLC

3.3 The Logic System

3.3.1 Data Memory

The memory of RFID transponders is divided into data memory and configuration memory. Data memory stores the information that will be transmitted back to the interrogator. Configuration memory stores data regarding the configuration parameters for the transponder. Memory varies in size, rewriting capabilities, structure, and characteristics similar to those found in memory used in other products. The size of the memory ranges from 1 bit to 64 kbits or even larger, with the most common values being around a few hundred bits. One of the most important differences between transponders is whether the data stored in their memory can be rewritten by the user. This gives rise to the distinction between *read-only* transponders and *read/write* transponders. Because memory types, sizes, and structures can greatly differ between different transponders, the following examples are not intended to be viewed as a comprehensive guide, but to highlight some of the most commonly used approaches to memory in transponders.

The device MCRF200 from Microchip Technology contains a memory of 140 bits; 128 bits are data bits, and the remaining 12 bits are used for the configuration register. This is a one-time programmable (OTP) device that operates as a read-only device once it is programmed. The data memory can be programmed by the user using a contactless programmer or can be directly programmed by the factory at the time of production. The configuration register can only be programmed at the time of production. The manufacturer specifies memory data retention better than 200 years.

Figure 3.15 shows the block diagram of this device. The EEPROM memory is addressed by the column and row decoders at the clock rate. The output from the memory array is a bit stream that is directly fed into the modulation control and modulation circuit in order to be transmitted back to the interrogator. Figure 3.16 shows the description of the different bits for the configuration register in this memory.

CB12 is the bit that allows programming the device. Once CB12 is set to 1, the device cannot be programmed or erased. Because the MCRF200 does not support anticollision, bit CB11 is always 0. However, for the device MCRF250 that is similar to the MCRF200 with the only exception that MCRF250 supports anticollision, its bit CB11 is always set to 1. CB10 is used to establish the transmission rate when PSK modulation has been selected. Bits CB9 and CB8 establish the modulation for the encoded data using the modulation types shown in Section 3.2.2. Bits CB7 and CB6 determine how the data are encoded, as described in Section 3.2.1. Bit CB5 is always set to 0. Bits CB4, CB3, and CB2 are used to set the baud rate at which data are transferred. The default timing (CB4 = CB3 = CB2 = 0) is MOD128, meaning that the transmission rate is set at 128 RF cycles for bit.

© 2011 by Taylor and Francis Group, LLC

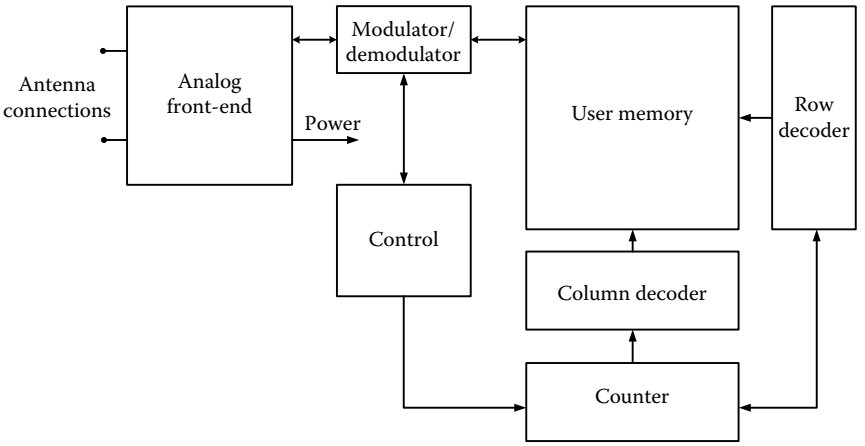

FIGURE 3.15
Structure of the circuitry for memory reading, writing, and control.

Because the MCRF250/251 device operates in the LF range, assuming a carrier frequency of 128 kHz, this setting will result in a transmission rate of 1 kHz. Conversely, the fastest transmission rate is MOD16, which will result in a transmission rate of 8 kHz. It is also important to keep in mind that MOD128 is the data rate used when programming the device. Finally, CB1 is used to specify the size of the data memory of 128 bits or 96 bits depending upon the needs of the user.

Example 3.4:

The configuration register for a MCRF 200 device is set to $08D. Describe the settings for the device.

Solution:

The binary values for the configuration register are shown as follows:

CB12	CB11	CB10	CB9	CB8	CB7	CB6	CB5	CB4	CB3	CB2	CB1
0	0	0	0	1	0	0	0	1	1	0	1

CB12 = 0. The device has not been programmed yet.
CB11 = 0. MCRF200 does not support anticollision; therefore, CB11 is set to 0.
CB10 = 0. Rate of PSK modulation is equal to half of the carrier frequency.
CB9 = 0 and CB8 = 1. The modulation chosen is PSK_1. This means that the phase of the modulation signal changes at the change of the encoded data.
CB7 = CB6 = 0. Data encoded using nonreturn to zero level (NRZ_L).
CB5 = 0. No special meaning because CB5 is always set to 0.
CB4 = 1; CB3 = 1; CB2 = 0. Baud rate is MOD32, resulting in a 4 kHz baud rate.
CB1 = 0. Memory size is 128 bits.

© 2011 by Taylor and Francis Group, LLC

Example 3.5:

State the configuration register for a transponder based on the MCRF250 device with the following parameters:

Blank (not programmed device)
Modulation: PSK_1.
PSK rate: Frequency half of the carrier frequency
Data encoding: NRZ_L
Baud rate: MOD 32
Memory size: 128 bits

Solution:

The MCRF250 is a device similar to the MCRF200, with the only difference being that it supports anticollision. Therefore, the configuration bit CB11 will be set to 1. The rest of the configuration bits have the same meaning as the MCRF200. The values of the configuration bits in this case are as follows:

CB12	CB11	CB10	CB9	CB8	CB7	CB6	CB5	CB4	CB3	CB2	CB1
0	1	0	0	1	0	0	0	1	1	0	1

Therefore, the hexadecimal value stored in the configuration register is $48D.

The devices MCRF355 and MCRF360, also manufactured by Microchip Technology, operate at the HF frequency of 13.56 MHz. They both have a total of 154 bits of memory that must be programmed using a contact programmer. This makes them act as read-only devices when they are used in the field but gives them the flexibility to be reprogrammed by the user when necessary. The data retention specified by the manufacturer is also better than 200 years.

The family of devices MCRF450/451/452/455 also operates in the HF frequency range at 13.56 MHz. As was discussed in Chapter 2, the different devices in this family use internal or external capacitors to modulate the radiofrequency signal. In discussing their internal memory structure, the concepts described for the device MCRF450 are also valid for the rest of the devices in this family. All of these devices have their memory organized in two areas: main memory and stored cyclic redundancy check (SCRC) memory. SCRC memory is used in the operation of the cyclic redundancy code necessary for the operation of the anticollision algorithm, as all of these devices support anticollision. The explanation of the CRC procedure is shown in Section 3.3.2.

The main memory of the MCRF450 and similar devices contains a total of 1024 bits and is structured in 32 blocks, each one with 32 bits. The SCRC memory is organized in 32 blocks, each one with 16 bits. Figure 3.17 shows the structure of the user memory in these devices.

The first three blocks (B0–B2) of the main memory are used to set up the operation of the device in a manner similar to a configuration register, while the remaining 29 blocks (B3–B31) are for user data. All the blocks of the main

© 2011 by Taylor and Francis Group, LLC

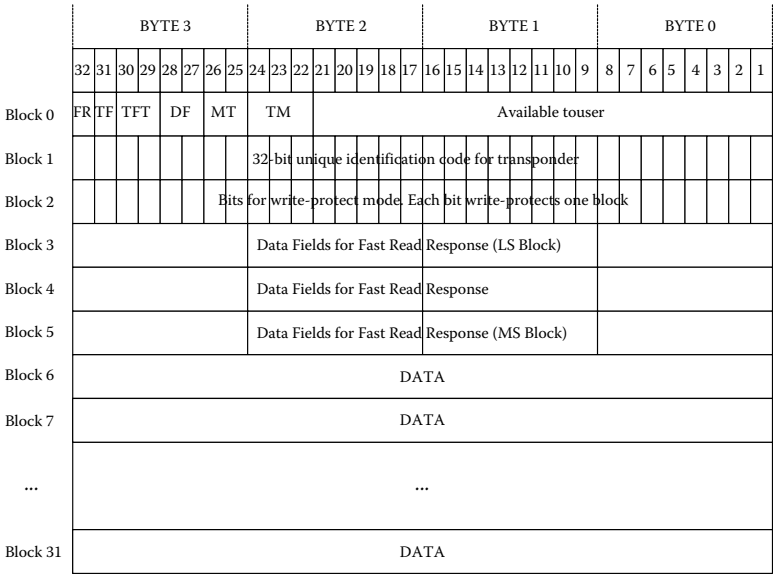

FIGURE 3.17
Structure of the user memory for the MCRF 450 family of transponders.

memory with the exception of Block 1, which contains the ID or serial number of the transponder, can be individually rewritten block by block by a contactless programmer. Block 1 is programmed at the factory and is protected against being rewritten. The main memory is read or written in blocks of 32 bits, with the exception of bits 30 and 31 in Block 0 that can be selected individually. Blocks 3 to 5 constitute the fast read field (FRF) that is used by the interrogator in the transmission of commands to the transponder.

Block 0 is split into 21 bits of general memory available to the user and 11 bits containing operational parameters for the transponder. These operational bits, shown in Figure 3.17, are as follows:

FR (Bit 31). When FR = 0, the transponder will respond to the *fast read bypass* (FRB) command but will not respond to the *fast read request* (FRR) command from the interrogator. When FR = 1, the previous situation is reversed. These interrogator commands are further explained and described in Chapter 6.

TF (Bit 30). TF = 0 sets the transponder in *interrogator talks first* (ITF) mode. This means that it will wait for an FRR command. TF = 1 sets the transponder in *tag talks first* (TTF) mode if FR = 1. In this case, the transponder will send a *fast read response* without waiting for an FRR.

TFT (Bits 29–28). These two bits set the value for the parameter TCMAX when the transponder is in TTF mode. TCMAX is the number of

© 2011 by Taylor and Francis Group, LLC

TABLE 3.2

Configurations for TFT Bits

Bit 29	Bit 28	TCMAX
0	0	1
0	1	2
1	0	4
1	1	Continuous

TABLE 3.3

Configuration for DF Bits

Bit 27	Bit 26	TCMAX
0	0	32 Bits
0	1	48 Bits
1	0	64 Bits
1	1	96 Bits

fast read responses that the transponder can send after an FRR command, as shown in Table 3.2. For example, TCMAX = 2 means that the transponder can send its response twice for acknowledgment. If TCMAX is set to continuous mode, the transponder will send its response approximately every 80 ms until it receives the correct response from the interrogator. This is the default mode.

DF (Bits 27–26). These two bits set the length of the data transmitted by the transponder according to Table 3.3. The default data length is 32 bits.

MT (Bits 25–24). These two bits are hardwired and cannot be changed by the user. At the current state of production, these two bits are both set to 0. The remaining values are reserved for future applications.

TM (Bits 23–22–21). These three bits set up the total memory size. These three bits are also hardwired. Currently, there are only two possibilities allowed: 000 and 001. The code *000* describes a transponder with 512 bits of memory, while the code *001* describes a transponder with a memory size of 1 kbit.

Block 1 contains a unique 32-bit identification number for the transponder. This identification word is serialized by the manufacturer.

Block 2 contains the bits that set each block in write-protect mode. Each bit corresponds to its 32-bit block. For example, bit 5 will set Block 5 as writable or write-protected. When the write-protect bit is set to 1, the block is writable; when the bit is set to 0, the block is write-protected. It is important to note that once a block is write-protected, it cannot be changed back to being

© 2011 by Taylor and Francis Group, LLC

writable. The transponders are shipped to the user with all the write-protect bits to 1 with the exception of bit 1. This means that Block 1, which contains the unique ID for the transponder, cannot be changed by the user. Bits 31 and 30 in Block 0 (bits FR and TF) are not write-protectable, thus allowing the user to change how the transponder is operating. Finally, it is also important to note that Block 2 can also be set to be write-protected.

Blocks 3 to 5 contain data bits for the fast response. The size of the fast response was set by bits 27 and 26 (bits DF) in Block 0.

The SCRC memory section is organized into 32 blocks, each one with 16 bits as shown in Figure 3.18. The blocks contain the CRC code for the corresponding memory block sent back to the interrogator in order to check for anticollision.

One of the family of transponders operating at 13.56 MHz manufactured by Atmel® has an internal user memory ranging from 1 kbit to 64 kbits with the distinct feature that this memory is encrypted, thus providing an additional layer of protection. The *CryptoRF EEPROM* family offers user memory of 1 kbit, 2 kbits, 4 kbits, 8 kbits, 16 kbits, 32 kbits, and 64 kbits. In addition to the user memory, all these devices have a configuration memory of 2 kbits. This configuration memory is used to store eight sets of passwords for reading and writing, four crypto key sets, security access registers for each user zone and password, and key registers for each zone. The transponders in this family also support anticollision. Figure 3.19 shows the block diagram for these types of devices. As shown in the figure, while the analog front end is similar to that of any transponder, it differs in the existence of authentication and password verification prior to the device sending data.

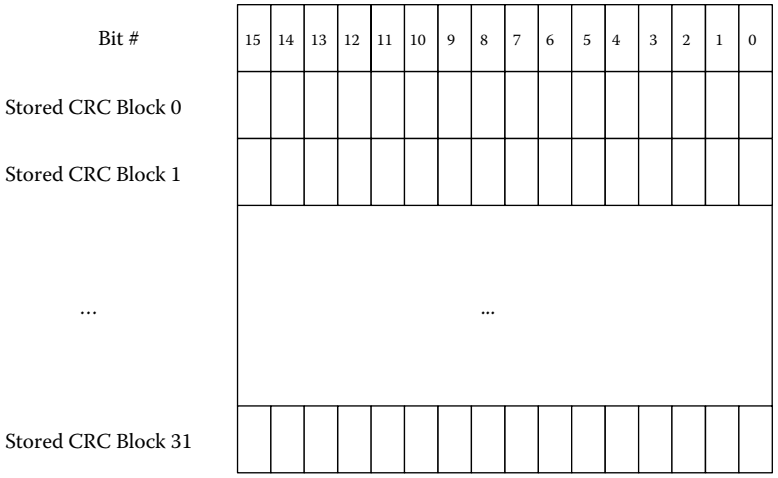

FIGURE 3.18
Structure of the stored CRC memory used in the MCRF 450 family of transponders.

© 2011 by Taylor and Francis Group, LLC

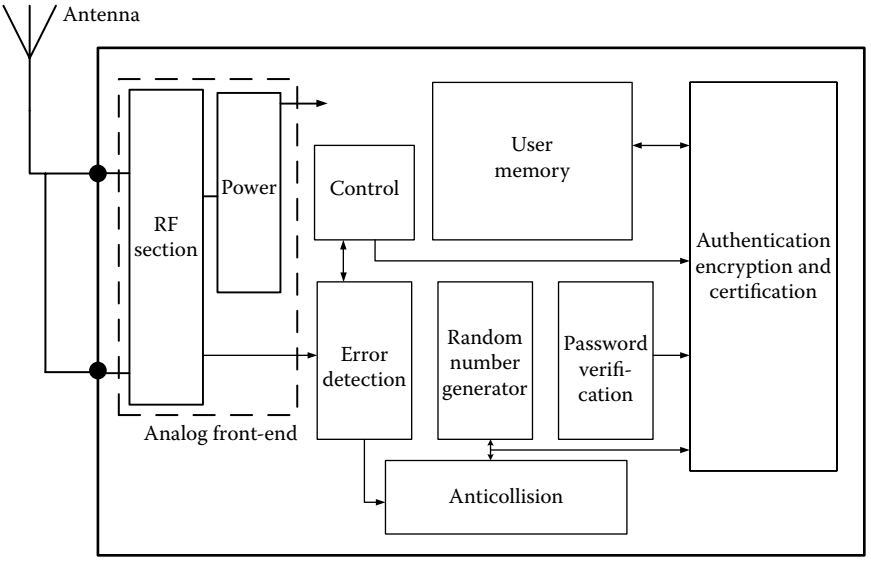

FIGURE 3.19
Transponder with encrypted memory showing the additional components needed for this process.

In the transponders with user memory size of 64 kbits, 32 kbits, or 16 kbits, the EEPROM user memory is divided into 16 user zones. Figure 3.20 shows the memory map for the 64 kbit memory transponder. As seen in the figure, each user zone is configured for storing 512 bytes (4096 bits), giving a total user memory of 64 kbits. For the 32 kbit transponder, its memory is also divided into 16 user zones, each one of 256 bytes (2048 bits); for the 16 kbit memory, the size of each user zone is 128 bytes (1024 bits).

The transponder from the same family with a memory of 8 kbits has a similar structure, although the memory is divided into eight different user zones. Each zone can store 128 bytes (1024 bits). The memory for the transponders with 4 kbits, 2 kbits, and 1 kbit of user memory are all divided into four user zones. For the 4 kbit memory, each user zone stores 128 bytes (1024 bits); for the 2 kbit memory, each user zone stores 64 bytes (512 bits); and for the 1 kbit memory, each user zones stores 32 bytes (256 bits).

In all cases, the access to the user zones is only possible after having some security requirements are met. These are defined by the user during the setup of the device. The initial state for the transponders in this family is to have all the security features disabled. The user must set up the level of protection by configuring the security requirements for the transponder. These security requirements are stored in the configuration memory.

All the transponders in the CryptoRF family have a configuration memory of 2048 bits. This memory stores passwords, keys, codes, and security

© 2011 by Taylor and Francis Group, LLC

	Address	Bit 7	Bit 6	Bit 5	Bit 4	Bit 3	Bit 2	Bit 1	Bit 0
User Zone 0	0								
	1								
	...	Total of 512 bytes (4096 bits) in Zone 0							
	512								
User Zone 1	0								
	1								
	...	Total of 512 bytes (4096 bits) in Zone 1							
	512								
User Zones 2 to 14	...								
User Zone 15	0								
	1								
	...	Total of 512 bytes (4096 bits) in Zone 15							
	512								

FIGURE 3.20
Memory map divided into 16 user zones, each one containing 4096 bits for a total of 65,536 bits (64 kbits).

definitions for each one of the user zones. The access rights to the configuration memory are defined in the control logic and cannot be altered by the user. The transponder can be programmed so each zone uses a different set of passwords. This is especially useful in the case of different users accessing the transponder. In addition, the transponders include three fuses that must be blown during the setup process. The fuses lock some of the portions of the configuration memory.

Atmel® also manufactures families of transponders that operate in the LF range, as well as in the UHF range. For example, the transponder ATA5558 can operate between 100 kHz and 200 kHz, while the ATA5590 operates in the UHF range from 860 MHz to 960 MHz. Both devices contain an internal EEPROM divided into a user memory of 1024 bits and a system memory of 320 bits. The user memory is organized in pages of 128 bits, and each page in blocks of 32 bits. Each one of the blocks must be programmed separately. Pages are protected against overwriting by the use of a lock bit that, as shown in Figure 3.21, is the most significant bit of each block.

The system memory in the ATA5590 transponder contains a page with the identification information for the transponder (Tag_ID page), a page with system-level information available to the user, and two blocks with system-level information for the manufacturer of the transponder.

© 2011 by Taylor and Francis Group, LLC

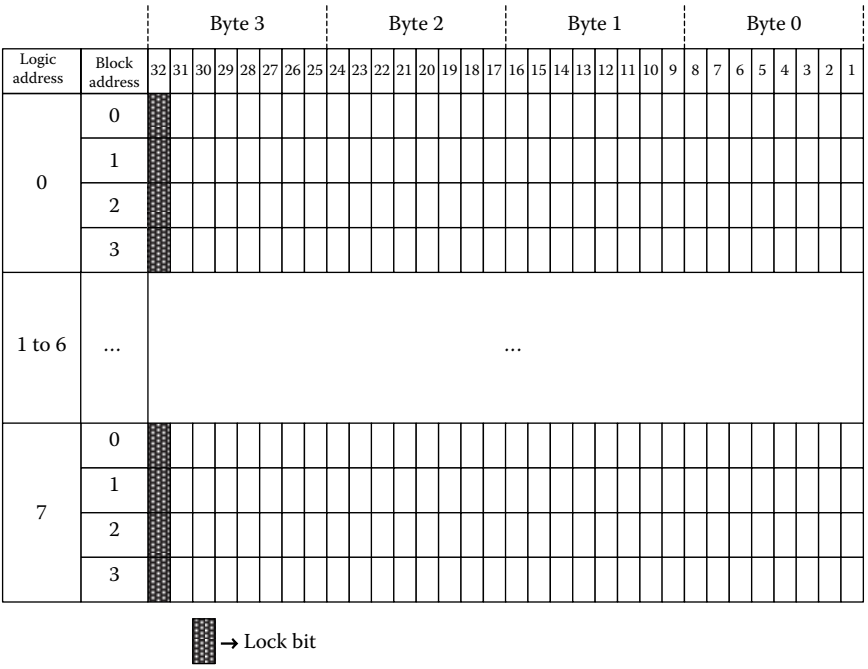

FIGURE 3.21
Memory map with lock bit. The lock bit is located at the MSB in each address.

3.3.2 Cyclic Redundancy Check for Error Detection

The cyclic redundancy check is the most used method for ensuring the integrity of the digital signals in some RFID transponders. In particular, CRC is used as a method of error detection in the digital stream transmitted and received by the transponders that support CRC. It is important to note that although the CRC algorithms detect the existence of errors, they do not make corrections.

The CRC method is based on appending additional information to the message being transmitted. This additional information is mathematically related to the message and therefore is redundant. At the receiving end, the receiver checks this additional information to verify that it agrees with the message being transmitted. This allows the receiver to determine with a certain degree of probability the existence of an error in the transmission. However, this method implies that not all errors are subject to detection. Simply stated, the CRC method is implemented by dividing the entire numeric binary value of the message by a constant. This constant is called a *generator polynomial*. The reminder in the division is then appended to the message. The polynomial that is used for the division is chosen from a family of polynomials with certain mathematic properties whose study is beyond the scope of this book. The transponders from Atmel and Microchip both use a polynomial known as the CRC-CCITT-16, although their specific

© 2011 by Taylor and Francis Group, LLC

implementation is somewhat different. This polynomial is also used in other digital transmissions such as CDMA and Bluetooth, among others. The CRC-CCITT-16 polynomial is

$$CRC - CCITT - 16: x^{16} + x^{12} + x^5 + x^0$$

Reading the polynomial from most significant bit (MSB) to least significant bit (LSB) (normal representation) results in a value of 1021 hexadecimals. We must take into consideration that CRC polynomials have always had their MSB equal to 1, and for this reason it is not considered in the calculation of their values. Reading the polynomial from LSB to MSB (reverse representation) results in the value of 8048 hexadecimals. Microchip Technology uses reverse representation, while Atmel® uses normal representation.

CRC can be hardware-implemented using shift registers and exclusive-OR (XOR) gates in the feedback process shown in Figure 3.22. The encoder shown in Figure 3.22 consists of 16 shift registers and the exclusive-OR gates. The initial value loaded into the shift registers is $FFF in the Microchip Technology approach and $000 for the Atmel approach. The encoder performs the exclusive-OR function and shifts the registers until the last bit of the data stream is entered. At that point, the CRC value of the data set is equal to the values in the shift registers. When the transponder transmits data, the calculated CRC value is attached to the data.

The receiver performs an identical process and verifies that the CRC code generated by the receiver is equal to the CRC code appended to the message. The advantage of the CRC method is that the current state of one of the shift registers is a result of considerable past history, as it has to go through a lengthy process. Therefore, it is unlikely that a burst of errors will produce a CRC code equal to the one generated in the absence of errors. In fact, the CRC-CCIT-16 code is able to detect all error bursts of 16 bits or less as well as 99.9% of error bursts of more than 16 bits.

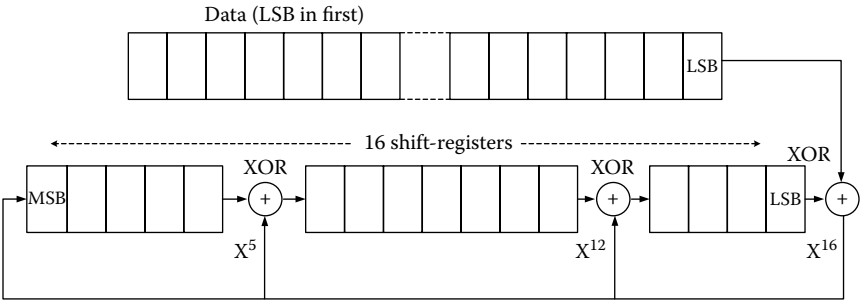

FIGURE 3.22
Structure of a generic CRC encoder using the CRC-CCITT-16 polynomial.

© 2011 by Taylor and Francis Group, LLC

Different manufacturers may also follow different approaches as to whether they append the CRC value with its LSB or MSB first. The specification documents for the transponders describe how the CRC value is attached to the data. The previous section described the structure of memory in some specific transponders. For example, the user memory for the MCRF450 family of transponders from Microchip Technology is divided into 32 blocks. When the interrogator tries to write data into any of these blocks, before doing any processing, the transponders check the CRC. If the CRC data are correct, the transponder proceeds with storing the data and the CRC in memory. Then, the transponder immediately transmits back the data and stored CRC to the interrogator for verification. If the CRC received by the transponder is incorrect, the transponder ignores the received message and waits for the next command with a valid CRC.

3.4 Transponder Programming

The programming of the transponders can be done by the manufacturer at the time of production or by the end user. *Programming the transponders* means to store a unique identification number in its memory, as well as to set up the configuration parameters for the communication between the transponder and the interrogator and additional parameters such as password protection. Transponders can be programmed using contact or noncontact methods.

The MCRF200/250 family of transponders manufactured by Microchip Technology is an example of a contactless programmable device. Because the MCRF200/250 family is made up of one-time programmable devices, the device can only be programmed when it is blank from the manufacturing process. Programming this device requires a specific sequence of radiofrequency signals applied following this sequence:

Initial, power-up RF signal (125 kHz for the MCRF200/250 family) lasting between 80 μs and 180 μs.

Absence of RF field lasting between 50 μs and 100 μs.

A continuous FSK signal that serves as a *verify* signal, lasting 131 ms. This signal is required for the transponder to be energized in order to output all the data contained in its 128 bits of memory. Because the device is blank at the time of programming, the output data are all *1*.

Programming data: After completing the verify mode, the device enters the programming mode. The device is programmed starting with bit 1 and finishing with bit 128. The symbol *1* is programmed by sending a low-power RF signal with an amplitude similar to the one used for the initial power-up. The symbol *0* is programmed by sending a high-power RF signal with an amplitude approximately equal to 2.2 times the amplitude used for the symbol *1*.

© 2011 by Taylor and Francis Group, LLC

Device response: After the 128 bits have been programmed, the device responds by transmitting the programmed data.

The MCRF355/360 family of transponders, also from Microchip Technology, has 154 bits of memory that can be programmed by using a contact programmer. Also, the memory in this family of devices can be reprogrammed. Figure 3.23 shows the pin diagram for this device.

Note that Pin 3 (Ant. A) and Pin 6 (Ant. B) are used to connect the external capacitors and inductors, as was shown in Figures 2.16 and 2.17, while Pin 5 (Vss) serves a ground. In order to program these devices, Pins 3, 6, and 5 are connected to ground, Pin 8 (Vdd) is connected to the positive voltage source, Pin 2 (CLK) is connected to the clock, and Pin 1 (Vprg) is connected to the signal that will be programmed in the transponder.

Some specific codes are used to carry out specific functions in the memory of the device. For example, because this device is reprogrammable, when the user wants to write new data into memory, the existing data must be erased first. This is done by sending the code 0111010100 through the VPRG pin, as shown in Figure 3.24.

Similarly, to start the programming sequence, the user must transmit the code 0111010010, followed by the data bits to store in memory. In total, there will be a total of 166 bits sent to the device: the first 12 bits are the command to program, and the remaining 154 bits are the data to be stored in memory. Finally, the data stored in memory can be read by transmitting the code 0111010110 to the device. After this code has been transmitted, the device will output the data stored in its memory.

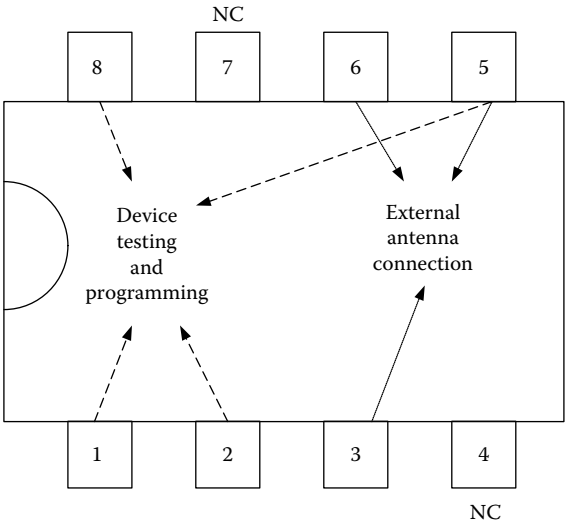

Pin	Function
1	VPRG
2	CLK
3	Antenna A
4	NC
5	V_{ss}
6	Antenna B
7	NC
8	V_{dd}

FIGURE 3.23
Pins for the MCRF355/360 transponders.

© 2011 by Taylor and Francis Group, LLC

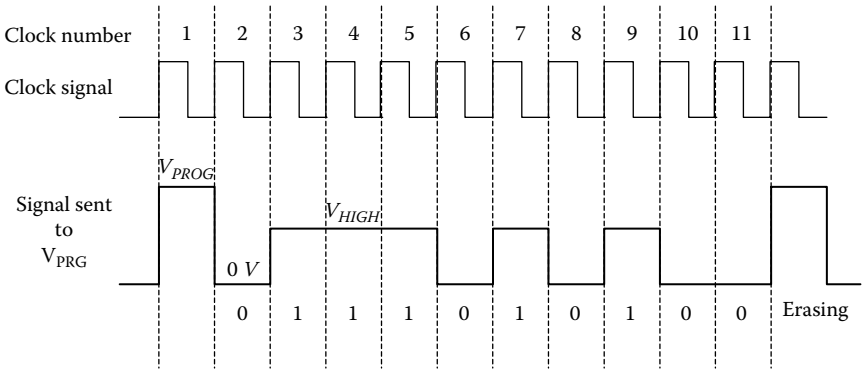

FIGURE 3.24
Code sent to erase existing data in memory using a contact programmer.

3.5 Summary of Electrical Specifications for RFID Transponders

The manner in which manufacturers specify the performance of their transponders varies greatly, not only among different manufacturers but also for devices from the same manufacturer. Tables 3.4 to 3.7 attempt to show the most important performance specifications from different manufacturers of RFID transponders. Table 3.4 does not pretend to be an exhaustive list of available devices, but just aims to show specific examples of device performance. The values of the parameters found in Tables 3.4 to 3.7 should be seen as somewhat typical performance values.

Table 3.4 shows the performance characteristics of three RFID transponders manufactured by Microchip Technology. The device MCRF200 is listed as a *125 kHz microID® Passive RFID Device*; the MCRF250 is exactly similar to the MCRF200 but incorporates anticollision; the MCRF355/360 family of devices is listed as *13.56 MHz Passive RFID Devices with Anti-Collision Feature*; and the devices in the MCRF450 family are listed as *13.56 MHz Read/Write Passive RFID Devices*.

Table 3.5 shows the electrical performance characteristics for four transponders manufactured by Atmel®. The ATA5567 device is listed as a *Multifunctional 330-Bit Read/Write RF Identification IC*; the ATA5570 is listed as a *Multifunctional 330-Bit Read/Write RF Sensor Identification IC*; the ATA 5558 is listed as a *1 kbit R/W IDID® with Deterministic Anticollision*; and the T5557 is listed as a *Multifunctional 330-Bit Read/Write RF Identification IC*.

Table 3.6 shows the performance parameters of two additional transponders from Atmel®. The device TK5530 is listed as a *read-only transponder*, while the TK5551 is listed as a *standards read/write ID transponder with anticollision*. The difference between these transponders and those evaluated earlier is

© 2011 by Taylor and Francis Group, LLC

TABLE 3.4

Summary of Electrical Parameters for Several RFID Transponders Manufactured by Microchip Technology

Parameter	MCRF 200/250	MCRF 350/360	MCRF 450/451/452/455
Operating frequency	100 kHz to 400 kHz	13.56 MHz	2 MHz to 35 MHz
Dynamic coil current	50 µA		
Operating current	5 µA	7 µA	20 µA
Maximum current through antenna pads	50 mA	40 mA	40 mA
Current leakage		10 nA	
Turn-on voltage	10 Vpp between antenna pads 2 V_{DC}		
Reading voltage		2.4 V	2.8 V
Testing voltage		4.0 V	
Programming voltage		V_{IH}: 2.8 V V_{IL}: 1.2 V	
Coil voltage while reading		4 Vpp	4 Vpp
Coil clamp voltage		32 Vpp	
Programming time	2 sec (for all 128 bit array)		5 ms (for a 32-bit block)
Sleep time		50 ms to 200 ms	
Modulation resistance		< 4 Ω	< 5 Ω
Internal capacitance	2 pF	100 pF	95 pF (MCRF451) 30 pF (MCRF 452) 50 pF (MCRF 455)
Data retention	200 years	200 years	200 years
Maximum storage temperature	-65°C to +150°C	-65°C to +150°C	-65°C to +150°C
Maximum ambient temperature	-40°C to +125°C		-40°C to +125°C
Maximum dissipated power			500 mW

[a] Blank spaces in the table indicate that the manufacturer did not provide information for that specific parameter.

that the ones shown below incorporate the coil for the antenna within the transponder. Moreover, the operating characteristics are given as strength of magnetic field instead of voltage or current.

Table 3.7 summarizes the most important characteristics of several transponders manufactured by Texas Instruments under their Tag-it™ commercial name. The manufactured has also chosen to specify their reading and writing thresholds as field intensity.

© 2011 by Taylor and Francis Group, LLC

TABLE 3.5

Summary of Electrical Parameters for Several RFID Transponders Manufactured by Atmel®

Parameter	ATA5567	ATA5570	ATA5558	T5557
Operating frequency	100 kHz – 150 kHz	100 kHz – 150 kHz	100 kHz – 250 kHz	100 kHz – 150 kHz
Supply current read mode	4 µA	4 µA	7 µA	4 µA
Supply current programming	40 µA		40 µA	40 µA
Maximum DC current	20 mA	20 mA	20 mA	20 mA
Maximum AC current	20 mA	20 mA	20 mA	20 mA
Coil voltage normal mode	3.6 V		4 V	4 V
Coil voltage Read / Write	> 6 V	> 10 V	> 6 V	> 6 V
Coil voltage Programming	> 8 V		> 6 V	> 8 v
Clamp voltage	17 V – 23 V	17 V – 23 V	7 V – 16 V	17 V – 23 V
Internal capacitance	78 pF	340 pF	78 pF	78 pF
Start-up time	< 1 msec	< 3 msec	< 3 msec	< 3 msec
Programming cycles	100,000 cycles	100,000 cycles	100,000 cycles	100,000 cycles
Data Retention	50 years	50 years	50 years	50 years
Maximum storage temperature	-40°C to +150°C	-40°C to +150°C	-40°C to +150°C	-40°C to +150°C
Maximum operating temperature	-40°C to +85°C	-25°C to +105°C	-40°C to +85°C	-40°C to +85°C
Maximum dissipated power	100 mW	100 mW	100 mW	100 mW

3.6 Mechanical Considerations and Transponder Assembly

The integrated circuits or chips in which the transponders are based are available in different packages. While commercial transponders use the chip-on-board (COB) technique described in Chapter 2, this package is not adequate for the development of prototypes. For this reason, most of the transponders are also available in the more common plastic dual-in-line packages (PDIPs) or small outline plastic packages (SOICs).

For example, some of the transponders described in this chapter, such as the MCRF200/250, the MCRF355/360, and the family of MCRF450 transponders, all manufactured by Microchip Technology, are available in these three packages (COB, SOIC, and PDIP). In their SOICs or PDIPs, these are available in eight pins; four of the pins are for testing purposes, two of the pins are for

© 2011 by Taylor and Francis Group, LLC

TABLE 3.6

Summary of Electrical Parameters for Several RFID Transponders Manufactured by Atmel®

Parameter	TK5530	TK5551
Resonance frequency	121.4 kHz – 129.2 kHz	120 kHz – 130 kHz
Inductance	3.95 mH	3.8 mH
Quality factor	13	13
Max field strength before modulation	2 A/m	4 A/m
Field strength operation	30 A/m (-40°C) – 17 A/m (+85°C)	30 A/m (-40°C) – 17 A/m (+85°C)
Field strength programming mode		50 A/m
Modulation Range	4.0 V (20 A/m) – 8.0 V (100 A/m)	4.0 V (20 A/m) – 8.0 V (100 A/m)
Programming time		16 ms per block
Data retention		10 years
Programming cycles		100,000 cycles
Absolute maximum field strength	1000 A/m	1000 A/m
Maximum storage temperature	-40°C to +125°C	-40°C to +125°C
Maximum operating temperature	-40°C to +85°C	-40°C to +85°C

connecting the transponder antenna, and the two remaining pins are not-connect pins. The devices ATA5570 and ATA5567/5558 from Atmel® are also available in COB packages and PDIPs, also using eight pins. The ATA5570 uses four not-connect pins, two pins for connecting the antenna, one pin for ground, and one pin for connecting the output of an external sensor. Because the ATA5567 and ATA5558 do not use an external sensor, their pinout is much simpler using six not-connect pins and two pins for connecting the external antenna. The dimensions of the COB version for all these transponders are 8 mm × 5 mm with a thickness of 0.4 mm. This extremely reduced size makes it ideal for incorporating the transponder and its antenna into the inlay. Transponders, especially in their COB form, are extremely sensitive to issues such as electrostatic discharge and their exposure to ultraviolet light that may result in erasing the contents in their memory cells. However, the use of X-rays for die inspection does not harm the device or erase their memory cell contents.

The process for assembling the whole transponder varies depending on the frequency range at which it will operate as well as the specifications for the final product. For transponders operating in the LF region, the assembly process starts by preparing the die and the capacitor and testing the functionality of the combined die-capacitor element. This is followed with preparing the antenna coil used in this frequency range and creating the inlay formed by the coil and the COB. After the inlay has successfully passed the test, the finished transponder is processed depending on the

© 2011 by Taylor and Francis Group, LLC

desired final product, such as card lamination and plastic molding. The last step in this process is a final functional test.

Transponders operating in the HF region can be assembled using three different methods. The first method, which results in the transponder with the COB, is based on the same assembly process as described earlier for LF transponders. A second method results in creating the transponder with direct wire bonding to the antenna that can be etched, printed, or stamped. This assembly method starts by preparing the die; preparing the antenna on the substrate etched, printed, or stamped; and then making the inlay by direct wire bonding to the antenna. After the inlay test, the finished transponder is created by using card lamination, plastic molding, or another method. The last step is a final functional test. The third method creates a transponder with a flip-chip process using a bumped die. The process starts by die bumping for flip-chip assembly, preparing the antenna on the substrate by etching, printing, or stamping it. The inlay is then created using the flip-chip process to attach the antenna to the die. This is also followed by the inlay test, and the finishing of the transponder by lamination or plastic molding. As always, the last step is a final functional test.

© 2011 by Taylor and Francis Group, LLC

4

Antennas for Interrogators

CONTENTS

4.1 Antennas for HF and LF Interrogators 86
4.1.1 Design of Antennas for HF and LF Interrogators 86
4.1.2 Antenna Matching 96
4.1.3 Multiple Antenna Systems 103
4.2 Auxiliary Elements for LF and HF Interrogator Antennas 104
4.2.1 Antenna-Tuning Indicators 104
4.2.2 Antenna Multiplexers 104
4.2.3 Preamplifiers 105
4.3 Antennas for UHF Interrogators 106
4.3.1 Design of Antennas for UHF Interrogators 106
4.3.2 Transmission Lines and Connectors for UHF Interrogators 111
4.4 Commercial Antennas for RFID Interrogators 114
4.4.1 Antennas for RFID Interrogators 114
4.4.2 Tuning Boards for Interrogator Antennas 116

This chapter describes the principles of design for interrogator antennas. The basic theory that describes the behavior of the antennas used in interrogators is the same that was used to describe the behavior of antennas used in transponders. However, in the case of antennas for interrogators, the size of the antenna is much less critical: because the interrogator has less size restrictions, the antenna can have larger dimensions. This results in an increased antenna performance. Furthermore, antennas for interrogators can be created with thicker conductors that can substation higher currents, resulting in stronger electromagnetic fields. The chapter starts by describing the basic principles used in the design of antennas for interrogators operating in the high-frequency (HF) and low-frequency (LF) bands. It continues by describing auxiliary elements such as tuning indicators, multiplexers, and preamplifiers used with those antennas in order to improve the overall performance of the system. The next section describes the basic principles used in the design of antennas in interrogators operating in the ultra-high-frequency (UHF) band. The last section in this chapter shows different examples of commercially available antennas for interrogators.

© 2011 by Taylor and Francis Group, LLC

4.1 Antennas for HF and LF Interrogators

4.1.1 Design of Antennas for HF and LF Interrogators

Antennas for interrogators operating in the HF and LF ranges are designed for parameters such as maximum read distance for transponders, transponder read rate, as well as regulations such as the maximum field allowed in some specific conditions. The majority of antennas used in HF and LF interrogators are variations of the coil antenna that generates a magnetic field. These antennas are typically called *portal antennas* because due to their physical dimensions and geometry, they can be placed in portals. A small number of antennas for HF and LF interrogators are based on a small dipole that generates an electric field. These antennas are normally called *stick antennas*.

In general, the distance at which a transponder can be read increases with the size of the antenna. However, this size cannot increase arbitrarily. This is due to the practical limitations in using an antenna of a large size and also to the limitations due to regulatory issues. Examples of these factors are the decrease in the signal-to-noise ratio as the size of the antenna increases; the potential for exceeding the regulatory limits of field strength; the need for shielding nearby electronic equipment to avoid unwanted interaction with the generated field; the increase in the area of null zones in which the generated field is zero; and the increase in the inductance of the antenna to a point that makes matching the antenna to the reader extremely difficult, if not impossible.

Interrogators working in the HF range expect an antenna tuned at the frequency of 13.56 MHz, with an input impedance of 50 Ω and a loaded quality factor (Q factor) of less than 20. Similarly, interrogators operating in the LF range expect an antenna tuned to the appropriate LF frequency, an input impedance of 50 Ω, and a loaded Q factor of less than 20. In both cases, for best performance, the match of the interrogator with the antenna should have a *voltage standing wave ratio* (VSWR) lower than 1.2.

The VSWR is a measure of how much of the energy sent through a transmission line is reflected back to the transmitter instead of being transferred to the antenna in order to be converted to the electromagnetic field. Standing waves occur as a result of the existence of incident and reflected waves. The ratio of reflected voltage to incident voltage is called the *reflection coefficient* and is denoted by the symbol Γ. Mathematically, the reflection coefficient is

$$\Gamma = \frac{E_r}{E_i} \tag{4.1}$$

where

Γ = the reflection coefficient

E_r = the reflected voltage

E_i = the incident voltage

© 2011 by Taylor and Francis Group, LLC

The reflection coefficient can also be expressed in terms of the impedance of the transmission line and the impedance of the load as

$$\Gamma = \frac{Z_L - Z_o}{Z_L + Z_o} \tag{4.2}$$

where Z_L = the impedance of the load and Z_o = the characteristic impedance of the transmission line.

Equation (4.2) shows that when the transmission line is terminated with a load with an impedance equal to its characteristic impedance, the reflection coefficient is zero. This means that all the energy present in the line has been transferred to the load. When the line is terminated with either an open circuit or a short circuit, the absolute value of the reflection coefficient is equal to 1. This indicates that none of the energy present in the line has been transferred to the load, but is being reflected back to the transmitter. For any other terminations, including complex impedance values, the value of the reflection coefficient is, in absolute value, between 0 and 1. This indicates that a portion of the energy present in the line has been transferred to the load and some other portion of the energy remains in the line.

The VSWR is defined as the ratio of the maximum voltage in the line (E_{max}) compared to the minimum voltage in the line (E_{min}):

$$VSWR = \frac{E_{max}}{E_{min}} \tag{4.3}$$

The VSWR can also be defined as a function of the reflection coefficient (Γ):

$$VSWR = \frac{1+|\Gamma|}{1-|\Gamma|} \tag{4.4}$$

Equation (4.4) shows that in the case of maximum reflection due to the transmission line terminated in an open or a short circuit, which results in $|\Gamma| = 1$, the value of the VSWR is infinity. Conversely, when the line is terminated with its characteristic impedance that results in $|\Gamma| = 0$, the value of VSWR is equal to zero.

Example 4.1:

The designer of a RFID system specifies a match between an interrogator and the antenna, resulting in a VSWR better than 1.2 using a 50 Ω coaxial cable as the transmission line. Calculate the maximum reflection coefficient and the allowed range of antenna impedance, assuming it is perfectly resistive.

© 2011 by Taylor and Francis Group, LLC

Solution:

The relationship between VSWR and the reflection coefficient is given by equation (4.4). Algebraic manipulation of this equation yields $|\Gamma| = 0.1$. This is the maximum value allowed for the reflection coefficient.

The relationship between the reflection coefficient and the impedance of the load is given by equation (4.2). When solving for the value of Z_L using this equation, it is necessary to consider the two signs associated with the previous result of $|\Gamma| = 0.1$ as the impedance of the load can exceed or be below the impedance of the line.

$\Gamma = 0.1$ results in $Z_L = 61\ \Omega$, while $\Gamma = -0.1$ results in $Z_L = 41\ \Omega$. Therefore, an antenna impedance ranging from 41 Ω to 61 Ω will result in a VSWR better than 1.2.

Note than the range of allowed load impedances is not symmetric referred to the impedance of the line (Z_o). There is more tolerance for values above Z_o than for values below Z_o.

A transmission line that is not perfectly matched (i.e., a VSWR value higher than 1) reduces the amount of power from the interrogator that reaches the antenna. More importantly, however, is the fact that a fraction of the power that remains in the transmission line can break down the dielectric of the line or increase its temperature due to the power dissipated. Therefore, it is critical to achieve the best possible matching.

Antenna analyzers are a very versatile and useful tool at the time of designing antennas and matching them to their transmission lines. Figure 4.1 shows an image of a low-cost antenna analyzer. The configuration of this analyzer is done through software, and the results are displayed and stored in a personal computer.

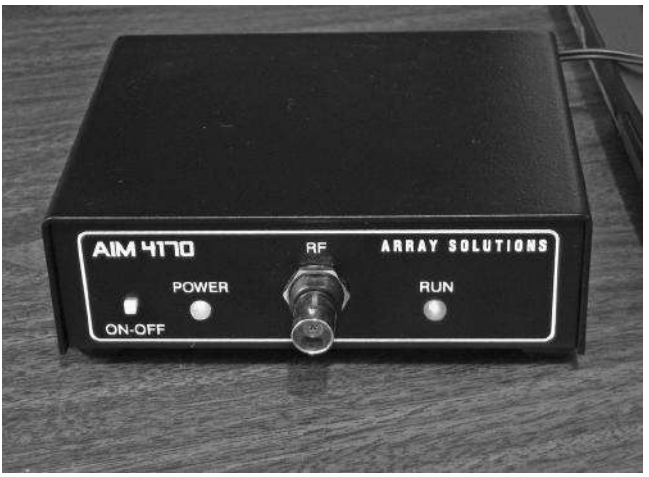

FIGURE 4.1
Antenna analyzer from Array Solutions. The control of the unit and the display of results are done by software.

© 2011 by Taylor and Francis Group, LLC

This unit shown in Figure 4.1 allows the measurement of the complex impedance of a transmission line or an antenna, the measurement of reflection coefficient, insertion losses, and other parameters of interest. The front panel only contains an ON/OFF switch, two light-emitting diodes (LEDs) that indicate whether the unit is energized and whether the unit is running a test, and a single Bayonet Neill-Concelman (BNC) connector. The back panel contains the power supply connection and a DB9 connector for a serial cable from the control computer to configure the instrument and transmit the results. The user can select the range of frequencies for the sweep-starting frequency, ending frequency, and step- or central frequency and bandwidth. This unit can also act as a fixed radio frequency source by generating a user-selected single frequency signal. The output values are shown graphically on the screen as conventional graphs (parameter versus frequency) or Smith charts. The data can also be stored as a text file for further processing. The graph can display one or more of the following parameters: impedance magnitude, impedance phase, reflection coefficient, return loss, stationary wave ratio, series load circuit, or parallel load circuit. Figure 4.2 shows an example of the output showing the magnitude and phase of a transmission line between 25 MHz and 40 MHz.

Figure 4.2 depicts the magnitude and phase of the impedance measured by the antenna analyzer for a transmission line with an electrical length

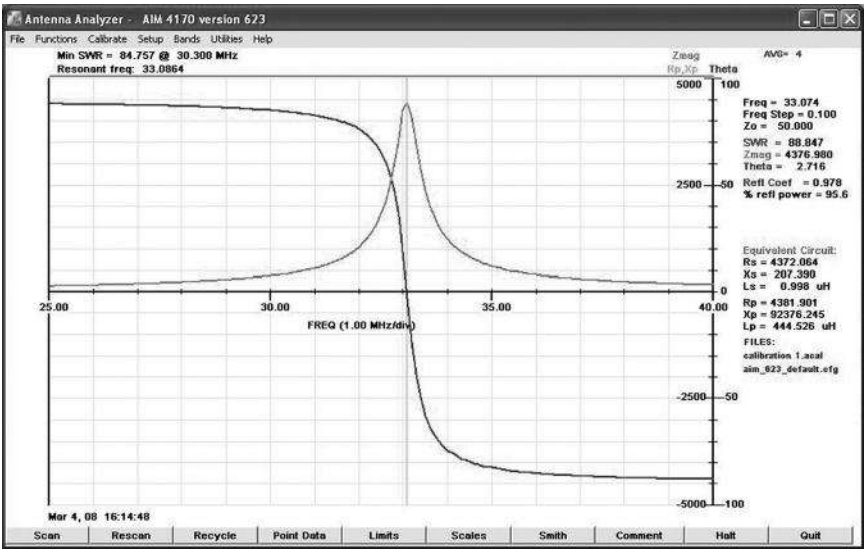

FIGURE 4.2
Frequency behavior of a transmission line terminated with a short circuit for frequencies around a quarter wavelength. This display shows the magnitude and the phase of the impedance at the near end.

© 2011 by Taylor and Francis Group, LLC

equal to one-quarter of the wavelength, terminated in a short circuit. Due to the impedance transformations at this specific electrical length, the theoretical value of the transformed impedance seen at the near end of the line is infinity. In practice, the losses of the line make the impedance have a large, yet finite, value. The output also displays other values described earlier in this section, such as the reflection coefficient and the VSWR, among others. Similar results could also be obtained using other commercially available antenna analyzers.

When designing the antenna, it is also necessary to take into consideration the write range of transponders that is about 70% of their read range. This is due to the higher amount of power needed to rewrite a transponder compared with just reading it. The orientation of the antenna with respect to the transponder is also a factor in determining the maximum read range in a given application. As shown in Figure 4.3, the field generated by the coil antenna does not have the same strength in all the spatial directions, but instead it has regions of maximum values alternating with regions of minimal strength.

An additional parameter that may limit the maximum read range of a system is the presence of metal objects in the vicinity of the antenna. Metal objects close to the antenna have the effect of detuning it, and therefore it loses its efficiency at the desired frequency. As the size of the antenna increases, the minimum required separation distance between the antenna and the metal objects also increases. For antennas operating in the HF frequency range, the minimum distance between antenna and metal has to be greater than 10 cm.

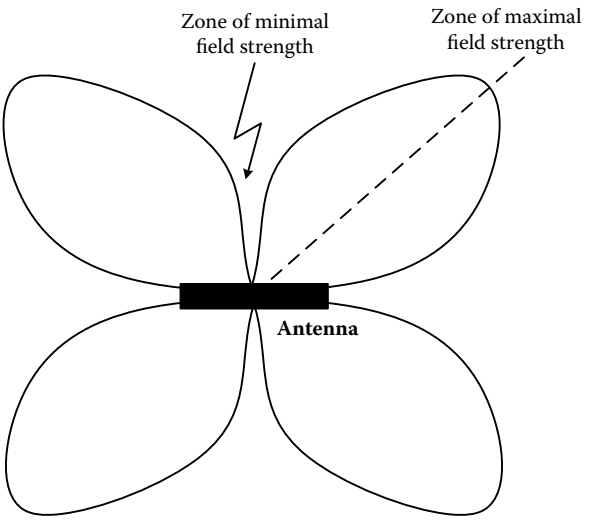

FIGURE 4.3
The radiation diagram for the loop antenna in the interrogator shows areas of maximum and minimum field strength.

© 2011 by Taylor and Francis Group, LLC

Even at 30 cm of separation, there is a considerable decrease in the reading range. When the distance between antenna and metal object reaches 50 cm, there is no measurable difference. Similarly, the presence of other antennas in the vicinity also affects the overall performance of the system.

Antennas can be built using any conductive material. However, they are normally built using copper or aluminum. The type of material used for the antenna and the dimensions of the tube or strip lines depend on the desired mechanical parameters of the antenna as well as the maximum inductance that must be matched to the interrogator. In addition to the conductors, the matching process requires the use of capacitors and resistors. These must be rated for the high voltages that may arise in resonant antennas as well as for the power that they must dissipate. Typical power values for these resistors range from 2 W to 50 W.

The dimensions of the antenna have an effect on the read distance between interrogators and transponders. The strength of the magnetic field for an electrically small-loop antenna is

$$B_z = \frac{\mu_0 I N a^2}{2\,(a^2 + r^2)^{3/2}} \quad (Weber / m^2) \tag{4.5}$$

with a being the radius of the loop and r being the radial distance from the center of the loop. To study the effects of the antenna radius, the rest of the parameters in equation (4.5) can be considered constant. Assuming that all antennas have the same amount of current and also the same number of turns, the only parameter that changes is the radius of the loop. Figure 4.4 depicts the values of magnetic fields for coils with three different radii (0.2 m, 0.4 m, and 0.8 m). Because the graph is only intended to highlight the dependence of the field with the distance from the center of the coil, it uses arbitrary units for the strength of the field depicted in the vertical axis.

It is interesting to note that, although larger coils produce stronger fields, this only happens after a certain distance threshold has been reached. In particular, for read distances closer to the antenna, the stronger fields are produced by the coils with the smallest radius. Antennas with smaller radii produce stronger fields in the vicinity of the antenna, but these fields decrease faster for longer distances. Therefore, the design of the antenna must consider the range of distances between transponders and the interrogator when selecting the size of the loop.

The resonant frequency of an antenna (ω_o or f_o) is

$$\omega_o = \sqrt{\frac{1}{LC}} \quad or \qquad f_o = \frac{1}{2\pi\sqrt{LC}} \tag{4.6}$$

© 2011 by Taylor and Francis Group, LLC

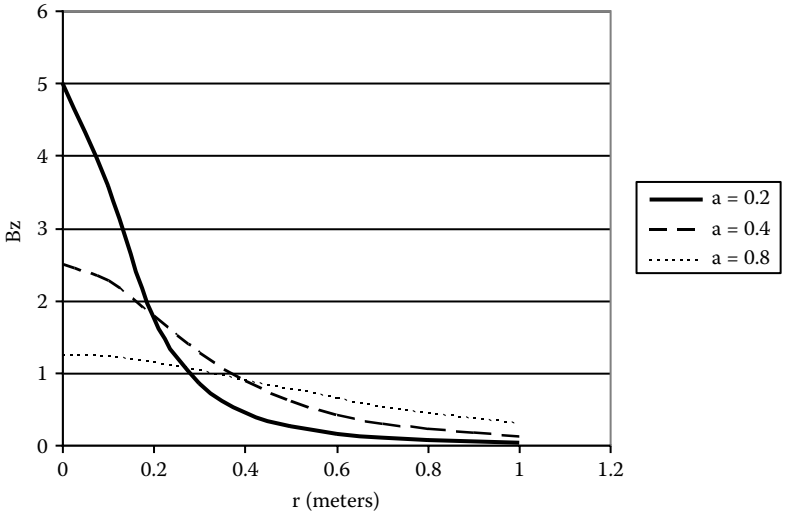

FIGURE 4.4
Strength of the magnetic field as a function of the distance from the coil for loop antennas of different diameters.

An antenna will reach its resonant frequency when its inductive impedance is equal to its capacitive impedance. The loop antenna has an inherently inductive behavior. Therefore, it needs an external capacitor to provide the capacitive impedance required for resonance. The value of this external capacitor can be calculated using equation (4.6). It is important to note that the capacitance and inductance of the antenna are inversely related. A problem may arise if the inductance of the antenna increases to a point that may make it difficult to use a capacitor of suitable value. For example, a loop antenna with an inductance of 5 μH operating in the HF range requires a matching capacitor of 27 pF. For these small capacitance values, the parasitic capacitances that have not been taken into account when modeling the antenna may contribute significantly to the overall capacitance and therefore modify its resonant frequency. It is then important for antennas to be designed with lower inductive values. This may require one to use, for example, low-resistance conductive tube instead of wire at the expense of increasing its physical dimensions.

The inductance of the antenna made with copper tube, shown in Figure 4.5, can be estimated as

$$L(\mu H) = 0.008\ a\left[\ln\left(0.707\,\frac{a}{d}\right) + 0.379\right] \tag{4.7}$$

where

L = the estimated value of inductance

d = the diameter of the tube in cm

© 2011 by Taylor and Francis Group, LLC

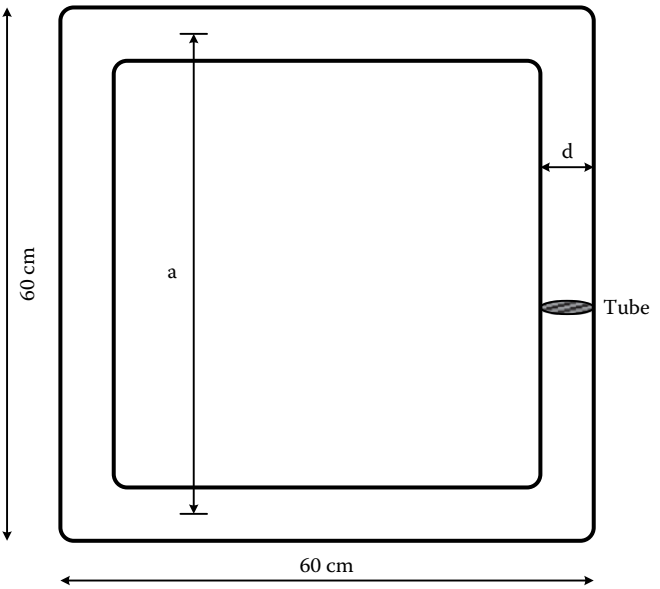

FIGURE 4.5
Basic structure of a loop antenna made with copper tube.

a = the length of the side of the antenna from center to center (as shown in Figure 4.5)

Example 4.2:

An interrogator operating at HF uses a loop antenna made of copper tube with a diameter of 2 cm, with a rectangular shape of 60 cm × 60 cm. Estimate the value of the inductance for the antenna. Estimate also the value of the capacitor required to tune the antenna for resonance.

Solution:

Using equation (4.7) with d = 2 and a = 59 yields L = 1.6 μH. This value of inductance can now be used in equation (4.6) to calculate the estimated value of capacitance. The estimated value of capacitance is 86 pF.

The previous equations provide an estimated value of antenna inductance. After the antenna has been built, its inductance must be measured in order to choose the correct value for the tuning capacitor. This can be done with an impedance analyzer that allows the selection of the measurement frequency. However, impedance analyzers are expensive and may not be available in most cases. In this case, a low-cost LCR (inductance [L], capacitance [C], and resistance [R]) meter that operates at the frequency of 1 kHz can give a reasonable approximation of the antenna inductance. The antenna analyzer shown in Figure 4.1 is another low-cost alternative for measuring

© 2011 by Taylor and Francis Group, LLC

the inductance of the antenna and the resonant frequency of the antenna-capacitor system.

The last parameter that needs to be calculated and measured when designing the antenna is its Q factor. The Q factor is a measure the frequency selectivity of an antenna. The Q factor is related to the range of frequencies above and below its resonant frequency that the antenna will be able to transmit or receive with losses below 3 dB. The Q factor can be estimated as

$$Q = \frac{f_r}{BW_{-3dB}} \tag{4.8}$$

where Q is the quality factor of the antenna, f_r is its resonant frequency, and BW_{-3dB} is the bandwidth of the antenna at 3dB of attenuation.

A high Q factor indicates an antenna that is very narrow in frequency, that is, highly selective. This may be good in order to reject interfering signals that otherwise would be detected by the antenna. However, the RFID signal has a certain bandwidth. If the antenna is too selective, it may distort the components of the transmitted signal that fall outside the selectivity of the antenna, as shown in Figure 4.6. A good experimental compromise is to choose a Q factor of around 20.

If the Q factor of the system made of the antenna and capacitor is higher than 20, it needs to be brought down by using a dampening resistor in parallel with the antenna in order to widen its bandwidth. This technique is shown in Figure 4.7.

The introduction of the dampening resistor produces Ohmic losses in the system, lowering the Q factor. The Q factor is related to the parallel resistance as

$$Q = \frac{R_{par}}{2\pi f L} \tag{4.9}$$

An additional problem arises when using equation (4.9) in order to select the value of the parallel dampening resistor: the value R_{par} in the equation is the combination of the external dampening resistor (R_{damp}) in parallel with the resistance of the antenna at the frequency of interest (R_{ant}). The measurement of the resistance of the antenna at the operating frequency is difficult and requires the use of expensive instrumentation. However, the Q factor for an antenna is relatively easy to measure experimentally with an antenna analyzer or using a radiofrequency signal generator and a spectrum analyzer. Therefore, the resistance of the antenna R_{ant} at the operating frequency can be calculated indirectly by measuring the Q factor of the antenna without an external dampening resistor. Once this value has been found, it is now possible to calculate the required value of the total parallel resistance R_{par} to achieve the desired value of Q. Because R_{par} is the parallel of R_{ant} and the

© 2011 by Taylor and Francis Group, LLC

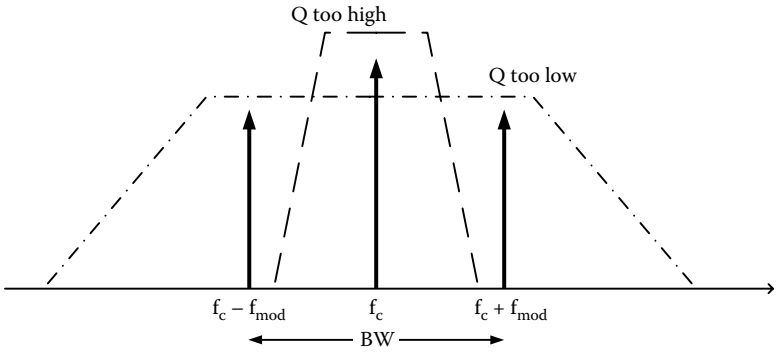

FIGURE 4.6
Q factor of an antenna and its relationship with the antenna performance. (a) A very low quality factor (Q factor) does not provide adequate selectivity. (b) A very high Q factor may reject components of the transmitted signal.

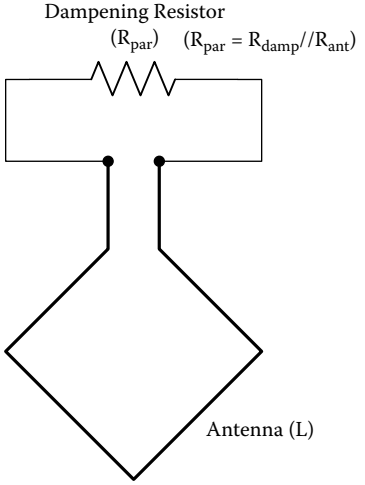

FIGURE 4.7
Dampening resistor connected in parallel with the antenna. This is used to lower the Q factor to the desired value.

external dampening resistor R_{damp}, it is now possible to estimate the value of this external resistor. Example 4.3 illustrates this procedure.

Example 4.3:

Consider the antenna for the RFID system from Example 4.2. Estimate the value of the external dampening resistor necessary for the system to achieve a Q factor of 20. The initial measurement of the Q factor for the antenna-capacitor system resulted in a value of 55.

© 2011 by Taylor and Francis Group, LLC

Solution:

Using equation (4.9) with a Q factor of 55, an inductance value for the antenna of 1.6 μH, and a frequency of 13.56 MHz results in a resistance equal to 7.5 kΩ. Because the Q factor of 55 was measured without the use of external resistors, the value of resistance obtained is the resistance of the antenna: R_{ant} = 7.5 kΩ.

Now, we must calculate the value of the total parallel resistance needed to reduce the Q factor to the desired value of Q. We use again equation (4.9) with the same operational parameters as before, with the exception that the new value for Q results in a resistance equal to R_{par} = 2.7 kΩ.

Considering that the total value of the resistance found above is equal to the resistance of the antenna in parallel with the dampening resistor ($R_{par} = R_{ant} // R_{damp}$), it is now possible to calculate the value of the external dampening resistor. This results in R_{damp} = 4.2 kΩ. Because this is not a standard resistor value, the designer should use the next standard value, which is 4.3 kΩ.

Therefore, the addition of 4.3 kΩ results in lowering the Q factor from its initial value of 55 to the desired value of 20. Because the value of inductance used for this calculation could be an estimated value, the design process involves measuring the Q factor with the external dampening resistor of 4.3 kΩ and adjusting its value if necessary to reach a Q factor of 20. Finally, it is also necessary to keep in mind that this external dampening resistor must be sized to dissipate the power transmitted by the interrogator.

4.1.2 Antenna Matching

Matching the impedance of the antenna to the impedance of the transmission line (normally a coaxial cable of 50 Ω) ensures that all the power from the interrogator is transferred to the antenna, and there is no power reflected in the line. In practice, a VSWR of 1.2 or lower is acceptable as the majority of the power is transmitted to the antenna. From the several approaches to match an antenna to its transmission line, the most widely used matching methods for interrogator antennas in RFID systems are gamma matching, T-matching, transformer matching, and capacitance matching.

Gamma matching is a technique based on connecting the two conductors of the coaxial cable that make up the transmission line to the two points in the antenna that exhibit a resistive impedance equal to 50 Ω. The shield of the coaxial cable is normally connected to the point in the antenna that is opposite to the gap used to connect the resonance capacitor and the dampening resistor. The central connector of the coaxial cable is then connected, by means of an additional conductor, to the appropriate point in the antenna as shown in Figure 4.8.

In practice, the point at which the central conductor of the coaxial cable is connected (point A) must be determined by experimentation. The designer of the system connects an antenna analyzer at the far end of the coaxial cable and moves point A until the antenna analyzer reads a VSWR value equal to 1. This indicates that the impedance of the antenna between point A and the connection of the central conductor is equal to 50 Ω. The value of the capacitor used to tune the antenna to the resonance frequency was

© 2011 by Taylor and Francis Group, LLC

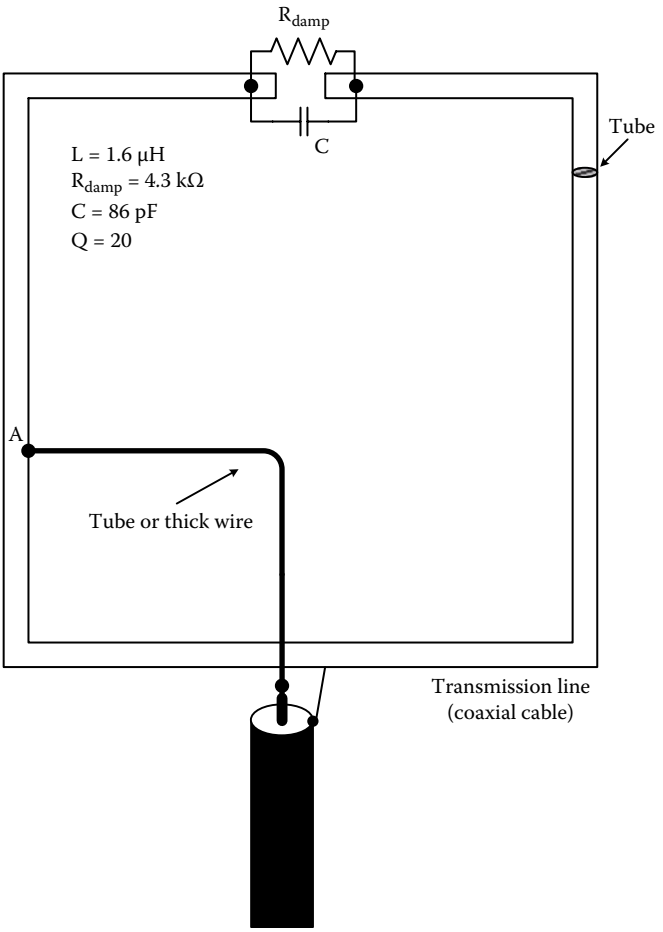

FIGURE 4.8
Connections for gamma matching.

determined using an approximation for the value of the antenna inductance. Therefore, a variable capacitor is initially used in order to tune the antenna to its resonant frequency. Once the correct value of capacitance has been determined, it is then possible to substitute the bulkier variable capacitor with a fixed capacitor.

T-matching is similar to gamma matching with the difference being that in T-matching, both the internal and external conductors of the coaxial cable are tapped to two points in the antenna, as shown in Figure 4.9. It is based on the fact that two points of the antenna, equidistant from the center, exhibit a purely resistive impedance.

The two tapping points are located symmetrically with respect to the gap used for connecting the tuning capacitor and the dampening resistor. The

© 2011 by Taylor and Francis Group, LLC

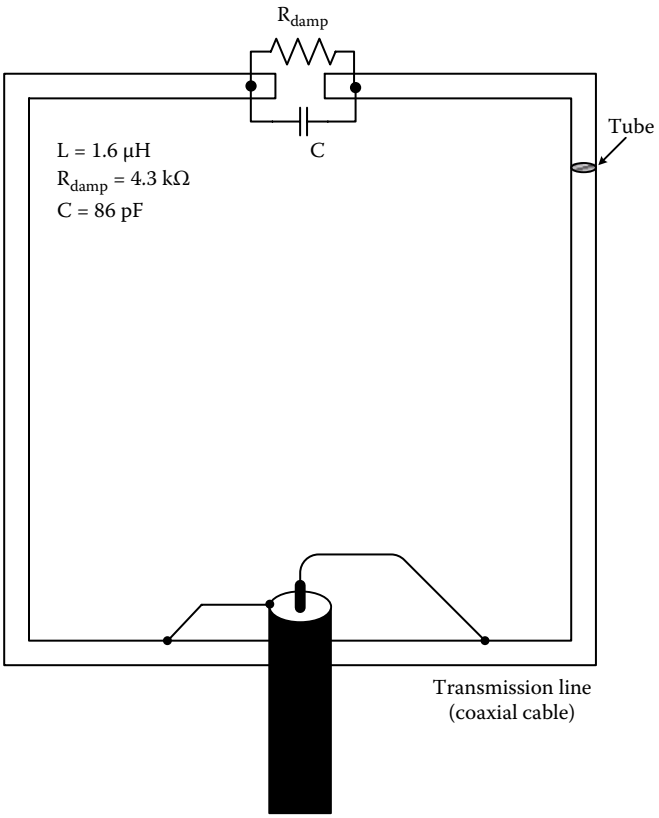

FIGURE 4.9
T-matching.

two tapping points are found by using an antenna analyzer until the VSWR value is equal to 1. Higher values of the Q factor results in the two matching points being closer together.

Transformer matching has the advantage that it electrically isolates the antenna from the interrogator, thus breaking the Ohmic continuity between these two parts of the system. This is useful when the RFID system is affected by noise as it breaks any ground loop that may exist. Figure 4.10 shows the electric diagram of transformer matching. It is important to note that the matching occurs at the gap in the antenna that is used to connect the resonance capacitor and the damping resistor instead of their opposite point, as it happens with gamma and T-matching.

Transformer matching requires the design of two elements: the matching transformer and a balum (balanced–unbalanced) transformer. The design of the matching transformer requires one to size the number of turns of the primary (N) that is connected to the transmission line and the secondary (M)

© 2011 by Taylor and Francis Group, LLC

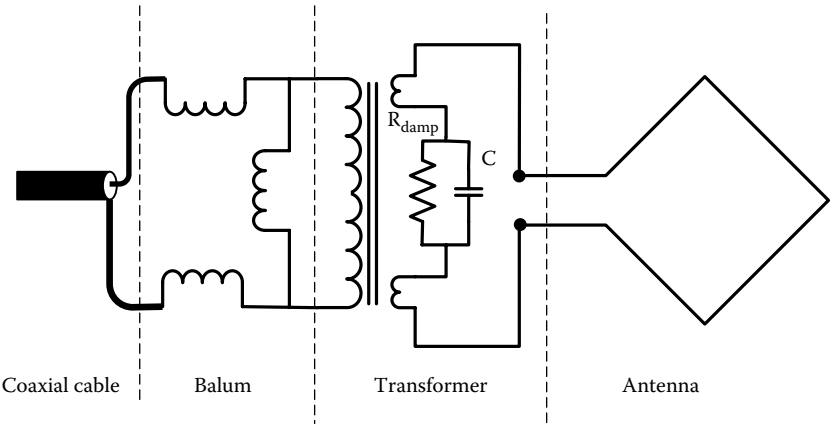

FIGURE 4.10
Transformer matching. Notice how the matching point is the same point at which the capacitor and resistor are connected.

that is connected to the antenna. The ratio of turns can be found using the following:

$$\left(\frac{N}{M}\right)^2 = \frac{Z_o R_{par}}{(2\pi f L)^2} \tag{4.10}$$

where (N/M) is the primary to secondary ratio of turns, Z_o is the impedance of the transmission line, R_{par} is the parallel resistance of the antenna and the dampening resistor, and L is the inductance of the antenna.

Example 4.4:

Using the values from the previous examples in this chapter, calculate the number of turns for the primary and secondary of the matching transformer. Assume a characteristic impedance of 50 Ω.

Solution:

Using equation (4.10) with R_{par} = 2.7 kΩ, L = 1.6 μH, and f = 13.56 MHz, the ratio of turns is equal to 2.7. Using, for example, M = 3 results in N = 8 windings.

The balum transformer is used to connect unbalanced transmission lines such as a coaxial cable to balanced antennas such as the loop antenna. Although they can be connected directly, as with the gamma matching, the common mode currents that appear in the antenna and line due to the unbalance may cause excessive noise and disturb the circuits. In this case, the connection of a balum transformer between line and transformer

© 2011 by Taylor and Francis Group, LLC

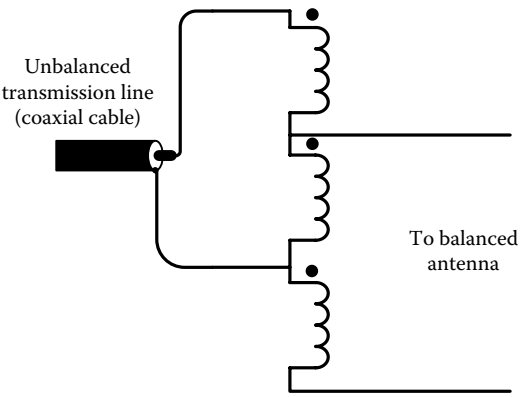

FIGURE 4.11
A balum is used to connect unbalanced transmission lines to balanced antennas.

solves these problems. The structure of a balum transformer is shown in Figure 4.11.

Both the matching transformer and the balum transformer are normally made with a toroid ferrite core. The balum transformer can be tested by connecting a 50 Ω load to the balanced side and measuring the VSWR through a coaxial cable connected to the unbalanced side. The VSWR should be close to 1.0.

Capacitance matching attempts to match the antenna and its transmission line by adding to external capacitors between the resonance capacitor and the dampening resistor, as shown in Figure 4.12.

Because of the stray capacitances inherent to the system, it is very difficult to predict the adequate values for the two matching capacitors, which requires extensive experimentation. Furthermore, for larger antennas, the values of the two matching capacitors tend to be very small, making the matching process very sensitive to stray capacitances. In Figure 4.12, the series combination of C_1 and C_2 must be equal to the capacitance value required to tune the antenna at the correct frequency.

The value of the matching capacitor C_{m1} can be estimated as

$$C_2 = C_{tuning}\sqrt{\frac{R_{par}}{R_{out}}} \tag{4.11}$$

where C is the total capacitance required for tuning the antenna, R_{par} is the equivalent value of the AC resistance of the antenna in parallel with the damping resistor, and R_{out} is the desired matching impedance, typically 50 Ω. The value of C_1 can be calculated through the series capacitance of C_1 and C_2.

© 2011 by Taylor and Francis Group, LLC

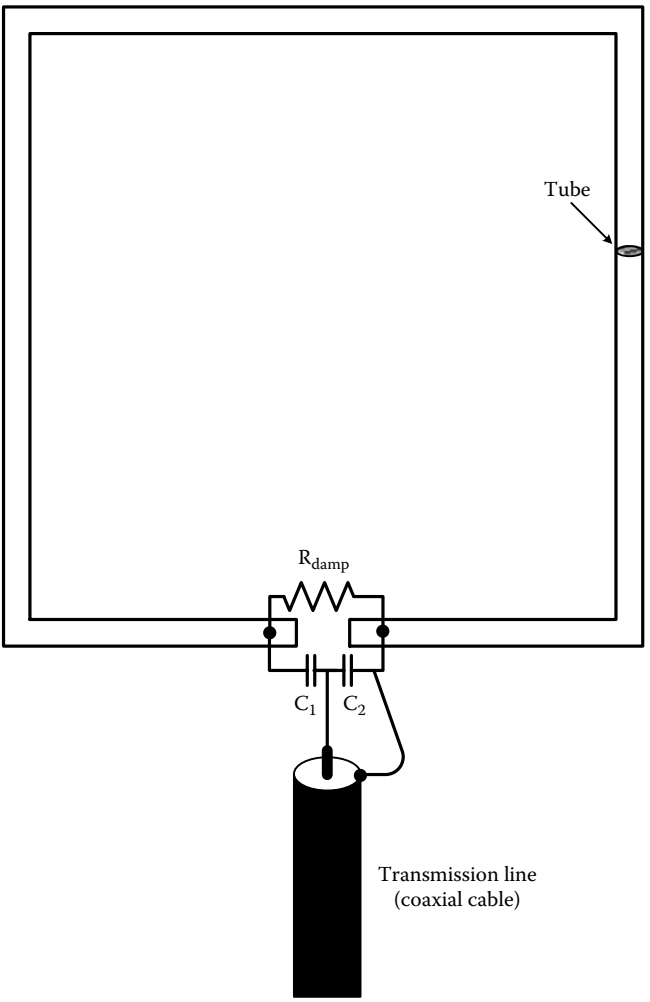

FIGURE 4.12
Capacitance matching.

Example 4.5:

The antenna used in Example 4.4 must be matched to a 50 Ω transmission line using capacitance matching. Calculate the values of the two matching capacitors required.

Solution:

The required tuning capacitor has a value of 86 pF, and the parallel resistance has a value of 2.7 kΩ. The required value for R_{out} is 50 Ω. Using equation (4.11) yields a value of C_2 = 632 pF. The equivalent series capacitance is 86 pF, allowing one to calculate the value of C_1 equal to 99 pF.

© 2011 by Taylor and Francis Group, LLC

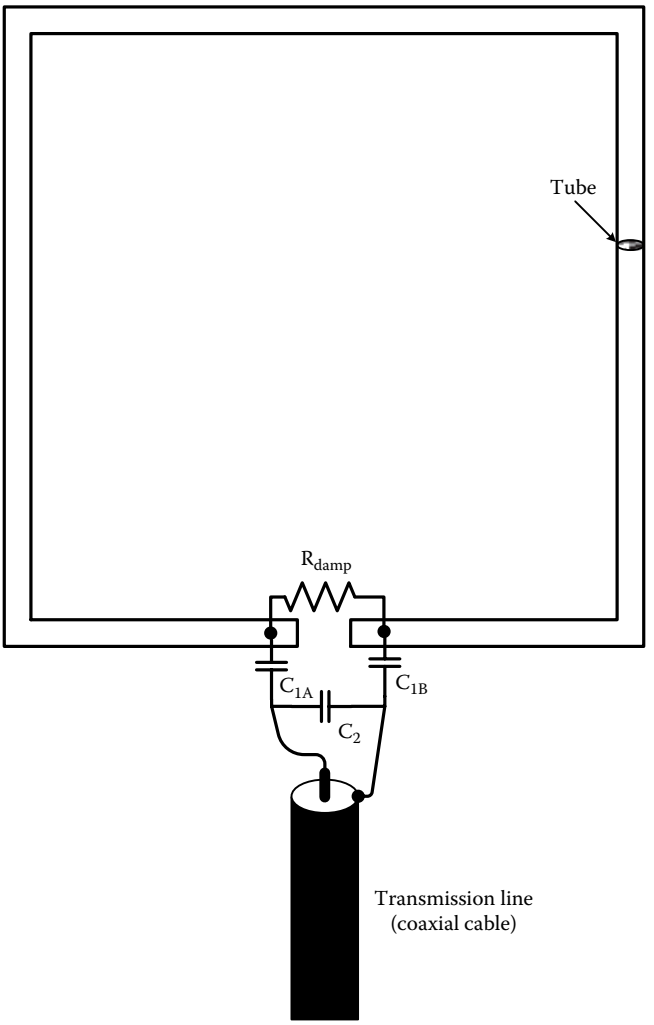

FIGURE 4.13
Balanced capacitance matching.

Some antennas require a matched capacitance so the capacitance seen by both conductors of the coaxial cable is the same. This can be achieved by using the structure shown in Figure 4.13. In this structure, the value of C_1 is doubled and added to each side of C_2.

Example 4.6:

Using the results of Example 4.5, calculate the capacitor values required for balanced matched capacitance.

© 2011 by Taylor and Francis Group, LLC

Solution:

From Example 4.5: $C_1 = 99$ pF and $C_2 = 632$ pF. To achieve balanced capacitance, $C_{1A} = C_{1B} = 198$ pF. C_2 remains at the same value of 632 pF.

4.1.3 Multiple Antenna Systems

It is not uncommon for several antennas to be located in close proximity. This may be due to different interrogators being close to each other or for multiple antennas to be connected to a single interrogator. When designed correctly, the mutual coupling between the antennas can enhance the performance of the overall system. However, a careless positioning of the multiple antennas may result in their mutual coupling, severely degrading their performance.

When several single-antenna interrogators coexist in close vicinity to each other, it is necessary to minimize their interaction with each other. The coupling between these antennas depends on the distance between them as well as their relative angles. Although the radiation pattern of a single antenna is well known and easy to predict, this radiation pattern becomes distorted due to the coupling. The best approach for locating the optimal placement of two or more antennas is by using an antenna analyzer in order to find the minimum of radiation by measuring the voltage generated in the nearby antenna.

A technique sometimes used to enhance the radiation pattern of the antenna in a single interrogator is to place another matched but unconnected antenna, opposite to the antenna connected to the interrogator. This connected antenna is a *driven antenna*, while the unconnected antenna is a *reflective antenna*. The combination of both antennas directs the energy from the driven antenna to a narrower area. Once again, an antenna analyzer should be used in order to determine the best arrangement between the two antennas.

Instead of leaving the second antenna unconnected, making it a reflective antenna, it is also possible to drive it with the signal from the interrogator by means of a splitter. In this case, the output of the interrogator is connected to the input of the splitter, and each output from the splitter is connected to a matched antenna. Splitters also offer the possibility to have the two output signals in-phase or out-of-phase. Splitters introduce losses, but when the two signals are connected in-phase, the reading distance between interrogator and transponders increases more than the reading distance with just one antenna without the losses from the splitter. The increase in the reading distance is at the cost of reducing the radiation pattern in the directions perpendicular to the arrangement of antennas. Therefore, this technique is only useful when the transponders are located only in known areas. When the signals fed to the two antennas are out-of-phase, the radiation pattern changes significantly, resulting in a pattern opposed to when the two signals are in phase. This gives the designer of the system the ability to configure the radiation pattern depending on the needs of the system.

Other techniques based on systems with multiple antennas are directed toward specific applications. In one of them, two identical antennas located

© 2011 by Taylor and Francis Group, LLC

in a crossed arrangement are connected to the output of a splitter but use different lengths of transmission line. In particular, if the different between lengths is a quarter of a wavelength, the two fields are shifted in 90°. This produces a field that changes the direction of its maximum, giving the appearance of a rotating field. Some other commercial antennas have an additional input that allows connecting an out-of-phase signal from a complementary antenna in order to maximize field strength in a single direction.

4.2 Auxiliary Elements for LF and HF Interrogator Antennas

4.2.1 Antenna-Tuning Indicators

Tuning indicators are used to facilitate the process of antenna tuning without the need to use antenna analyzers or other instrumentation. They present the advantage of being a self-contained system that has been optimized for specific interrogators and antennas. On the other hand, because of their specific nature, they can only be used with a limited number of antennas.

For example, Texas Instruments manufactures the RI-ACC-ATI2 antenna-tuning indicator used to help tune their LF antennas. The tuning indicator is connected to the interrogator and indicates to the user if the inductance or capacitance in the interrogator needs to be increased or decreased until the optimal value has been achieved. Some interrogators have a tuning capacitor, while some others have a tuning inductance that can be adjusted for optimal performance.

4.2.2 Antenna Multiplexers

Antenna multiplexers are used to connect multiple antennas to a single interrogator. This can be done to take advantage of the multiple coupling between antennas or when it is necessary to read data from multiple interrogators located at distant points not covered by a single antenna. The majority of multiplexers in the market work with two, four, or eight antennas. The multiplexer is connected between the radiofrequency output of the interrogator and the antennas, as shown in Figure 4.14.

It is not necessary for all the antennas connected to the multiplexer to have the same inductance. This presents the advantage of being able to choose the antenna most adequate for a specific application without having to physically connect and disconnect them from the interrogator. However, because most multiplexers do not include a tuning feature, each antenna must be tuned to the appropriate resonance frequency with their own individual tuning method described in Sections 2.2 and 2.3.

Antenna multiplexers are normally created by the manufacturers of interrogators, although there are some third-party companies that also

© 2011 by Taylor and Francis Group, LLC

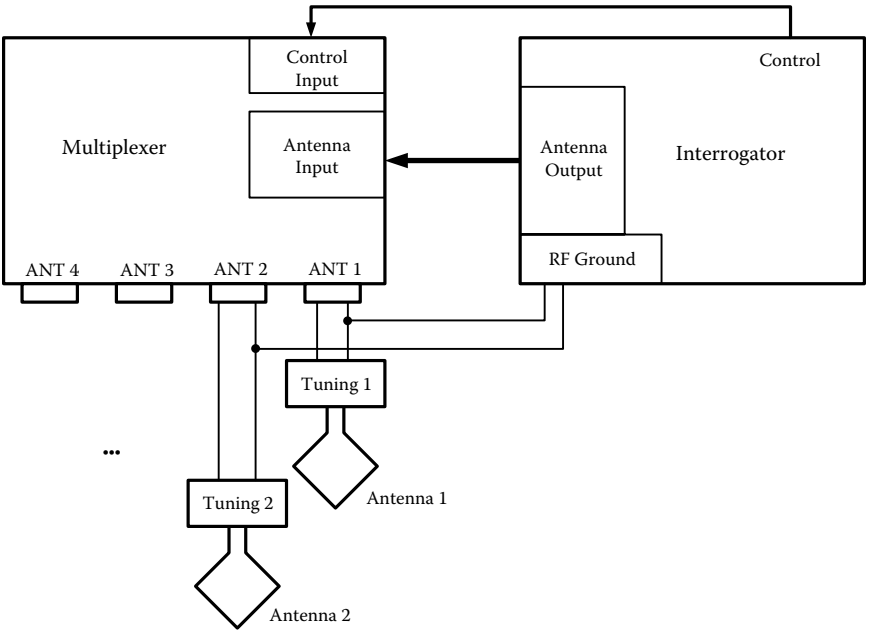

FIGURE 4.14
Multiplexer for connecting multiple antennas to a single interrogator.

manufacture them. For example, Skyetek manufactures multiplexers for the HF frequency range that can control four or eight antennas, having insertion losses lower than 0.7 dB and isolation between adjacent channels better than 45 dB.

4.2.3 Preamplifiers

Increasing the reading distance between interrogators and transponders requires a double approach. First, the electromagnetic field transmitted by the interrogator has to increase in order to generate enough power to turn on the distant transponders. This is relatively easy to do and is mainly limited by standards and regulations on maximum power and maximum allowed field strength. Second, reading distant transponders requires the interrogator to detect signals closer to the noise level. The increase in the detection sensitivity can be achieved with the use of preamplifiers, as shown in Figure 4.15.

The factor that limits the read range in RFID is ultimately the inherent noise that accompanies the signal received by the interrogator. A correctly designed preamplifier is able to increase the level of the signal without degrading the signal-to-noise ratio. The design of the main preamplifier is normally based on a low pass filter in order to reject the frequency generated by the field and

© 2011 by Taylor and Francis Group, LLC

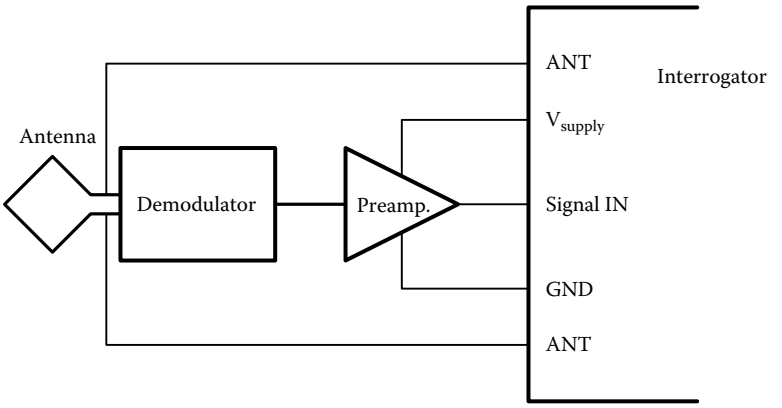

FIGURE 4.15
Preamplifier for extending reading distance.

allow the transmission of data. This stage is followed by an AC amplifier that increases the signal levels to the point that can be easily understood by the interrogator. The design of the preamplifier must consider the trade-offs between increasing the reading distance and the settling time required by the system. This means that the interrogator will be optimized for reading distance or for settling time, but cannot be optimized for both parameters.

Even when using preamplifiers, it is necessary to minimize the other potential sources of noise in the system. These can be the use of bad connectors between the interrogator and the antenna, improper installation of the transmission line between interrogator and antenna, an antenna that is not tuned correctly, the existence of interfering signals from nearby electronic equipment, and noise emanating from the power supply lines, among others. The designer of the RFID system should ensure that all these sources are minimized or at least known, and their values measured.

4.3 Antennas for UHF Interrogators

4.3.1 Design of Antennas for UHF Interrogators

Given the wavelength of signals in the UHF range, it is possible to design antennas for interrogators that operate in the far-field region as interrogators do not have the same space limitations of transponders. The resulting radiation pattern of two dipoles located at a short distance from each other can be easily modified by carefully arranging the distance between them as well as the phase shift of the signals that they radiate. A further modification of the radiation pattern comes from placing a large metal surface at a

© 2011 by Taylor and Francis Group, LLC

specific distance from the two dipoles. The metal surface acts like a shield that effectively removes half of the radiation pattern. Furthermore, if the distance between the antennas and the metal shield is one-fourth of the signal wavelength, the phase shift due to the distance between antenna and shield, combined with the phase shift created by the reflection in the metal shield, places the reflected signals in phase with the signals originated by the antenna. This, in turn, has the effect of doubling the power transmitted in the area away from the metal shield, as shown in Figure 4.16. It is necessary to remember that the increase of power in that specific direction comes at the expense of having no power in the area behind the metal shield, also known as a *passive reflector*. This structure is commonly used in *patch* or *flat* antennas.

An additional advantage of working in the far-field region is the possibility to take advantage of polarization. Polarized signals have their electric fields oscillating in a known and constant direction in space. This way, the signal recovered by the receiving antenna has a marked dependence on the geometrical relationship between the direction of the electric field and the direction of the antenna. Therefore, the energy recovered by the antenna in the interrogator ranges from a maximal value to zero depending on the relative orientation between the antennas in the interrogator and transponder. Using polarized signals allows discriminating between transponders. When the discrimination between transponders is

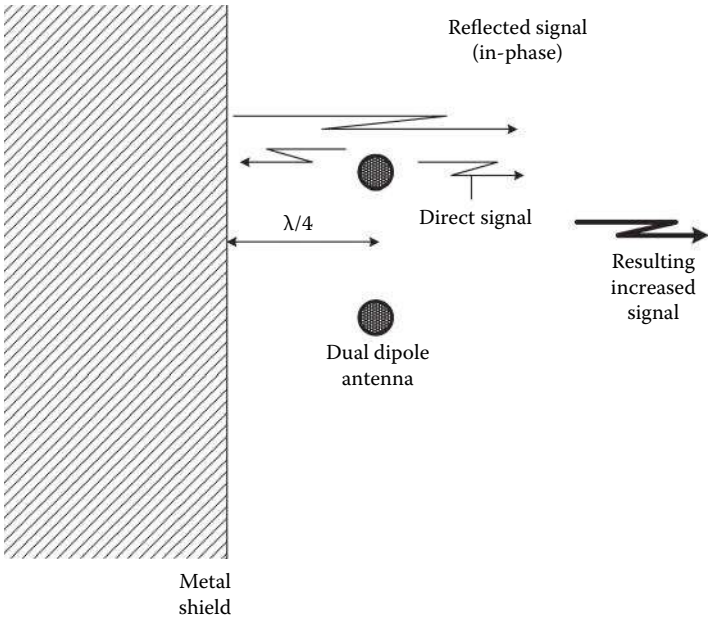

FIGURE 4.16
Metal shield increases effective radiated power in one specific direction.

© 2011 by Taylor and Francis Group, LLC

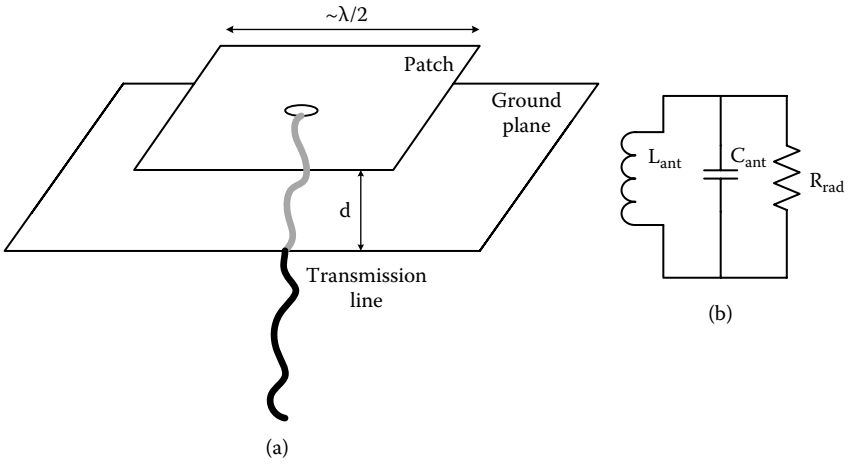

FIGURE 4.17
(a) Basic structure of a patch antenna. (b) Parallel equivalent circuit for a patch antenna.

not required, the use of dual dipole antennas in the transponders ensures that the interrogator will receive an adequate amount of energy.

The design of an antenna for the UHF RFID band represents an increased engineering challenge compared to designing it for the HF or LF bands because of the higher bandwidth needed for signals in the UHF band. It also becomes more difficult to maximize the performance of the antenna over the wider frequency range allocated for RFID systems in the UHF band. For this reason, while most of the HF and LF antennas follow the same basic design, engineers have developed several approaches to the design of UHF antennas for interrogators based on different performance parameters. This is especially critical for handheld applications in which the limited size of the antenna degrades its performance.

The patch antenna shown in Figure 4.17(a) is one of the most commonly used antennas for UHF interrogators. In its basic form, it consists of a metal patch of approximately one-half of a wavelength long and mounted over a ground plane. Figure 4.17(b) shows its equivalent electrical model.

Typical values for the equivalent circuit shown in Figure 4.17(b) are around 150 Ω for the radiation resistance of the antenna, between 9 and 10 pF for its capacitance, and from 2 to 4 nH for its inductance. The matching of the transmission line with a 50 Ω characteristic impedance to the relative high radiation resistance of the antenna is done by changing the location at which the transmission line feeds into the metal patch away from its center. The bandwidth of the patch antenna is a function of its dimensions and the separation between the metal patch and the ground plane. The type of dielectric used between the planes is also important, as dielectrics other than air will increase its equivalent capacitance.

© 2011 by Taylor and Francis Group, LLC

The patch antenna, by its very own design of using a ground reference as part of the antenna, is an unbalanced antenna. Because unbalanced antennas do not operate well when they are close to dielectric materials, and the human body can be essentially considered as a dielectric material at UHF frequencies, patch antennas are not the best choice for handheld interrogators. Furthermore, the size and weight limitations required by mobile and handheld interrogators further limit the use of patch antennas in these applications. A better solution for handheld and mobile interrogators are balanced antennas, that is, antennas with symmetric and opposed currents as shown in Figure 4.18.

When the antenna is fed using an unbalanced transmission line, such as a coaxial cable, it is necessary to use a balum transformer to match the unbalanced line to the balanced antenna. The basic theory behind this balum is the same as was described for HF and LF antennas. Although the structure shown in Figure 4.18 is technically feasible, an additional problem may arise due to the size required by half of a wavelength, especially for handheld interrogators. At the frequency of 915 MHz, the length of half of a wavelength is equal to 16 cm. While this is a very reasonable distance for a stationary antenna, it may be excessively large for applications involving handheld readers. In this case, it is possible to bend the dipoles in a similar way as is done for the antennas in transponders, as shown in Figure 4.19.

The reduction in size for the bent dipoles comes at the expense of degrading the electrical specifications of the antenna. In particular, its radiation resistance decreases and therefore the bandwidth of the bent dipole structure also decreases compared to the bandwidth of the regular dipole.

A different type of antenna used in UHF interrogators (either stationary or mobile) is based on the Yagi-Uda antenna. This structure, shown in Figure 4.20, consists of a driven element and two or more parasitic elements: one reflector and one or more directors. The parasitic elements direct the majority of the

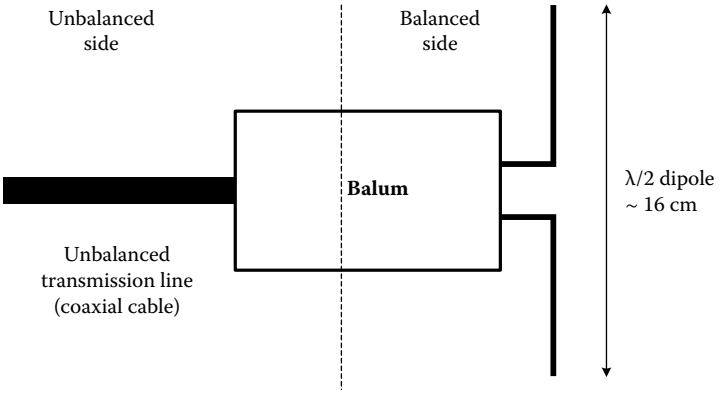

FIGURE 4.18
Balanced half-wavelength antenna.

© 2011 by Taylor and Francis Group, LLC

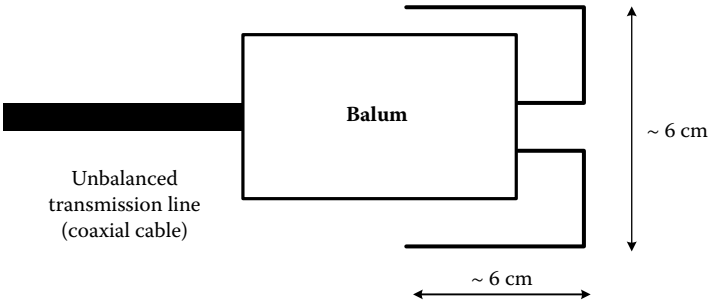

FIGURE 4.19
Bent dipole for a UHF interrogator antenna.

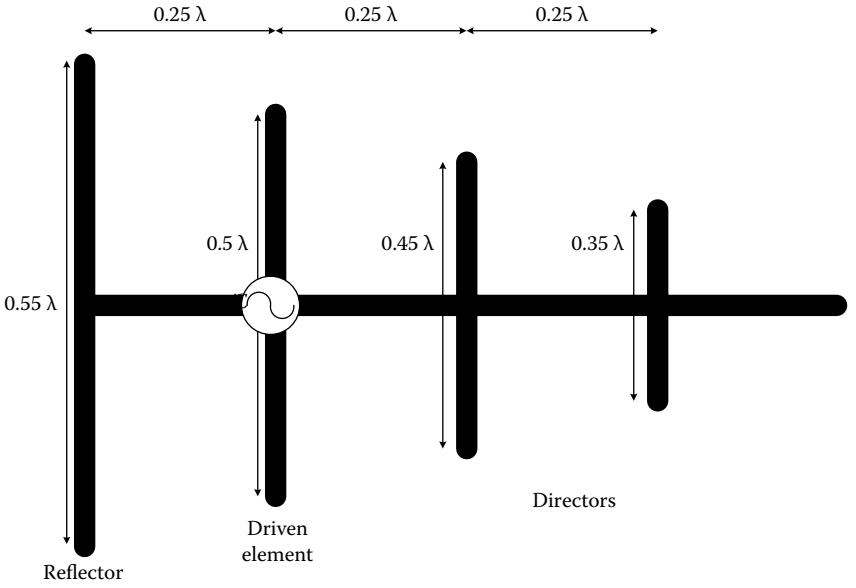

FIGURE 4.20
Yagi-Uda antenna.

energy radiated by the antenna toward the director. Therefore, this structure helps to minimize the interaction of the radiated field with a person who may be holding an antenna for handheld interrogators. Moreover, because this is a balanced antenna, this interaction between the energy radiated by the antenna and that radiated by the human body is further minimized.

In its original form, however, Yagi-Uda antennas can still be considered too large to use with handheld interrogators. In this case, it is possible to bend the dipole and longer elements, as described above. The existence of the parasitic elements will provide additional gain compared to the single dipole.

© 2011 by Taylor and Francis Group, LLC

4.3.2 Transmission Lines and Connectors for UHF Interrogators

Contrary to LF and HF systems, the coaxial cables and connectors typically used in UHF RFID systems have the potential to extremely degrade the signal they transmit. The main reason for this problem is the skin depth. *Skin depth* describes the effect that the current flowing through a conductor flows through a portion of its inner surface. Equation (4.12) shows that the skin depth (δ) is inversely proportional to the frequency of the signal:

$$\delta = \sqrt{\frac{1}{\pi \mu \sigma f}} \tag{4.12}$$

where δ is the skin depth, μ the magnetic permeability of the conductor, σ its conductivity, and f the frequency of the current flowing through the conductor.

Therefore, an increase in the signal frequency results in a smaller portion of the conductor being used to transmit the signal. For a typical conductor made of copper, the skin depth for an LF signal is 0.2 mm, the skin depth for an HF signal is 55 μm, and for a UHF signal it is 2 μm. Consider a copper conductor with a radius of 0.2 mm. At LF frequencies and below, the current will flow through all the conductor area. When the frequency increases to 13.56 MHz, only the first 55 μm are actually available as a path for the current. The effective area has been reduced to a half of the area available for an LF signal. Because the conductivity of the conductor depends on its area, the conductivity of this conductor at HF is about half of its conductivity at LF. The situation changes more dramatically at UHF frequencies, as the skin depth of 2 μm means that current can flow only through the outer 1 percent of the conductor. With this, the conductivity of the copper wire for UHF signals has been reduced in a factor of 62 compared to the conductivity at LF. This strong decrease in conductivity introduces considerable losses that may render the system unusable. Figure 4.21 further illustrates this situation.

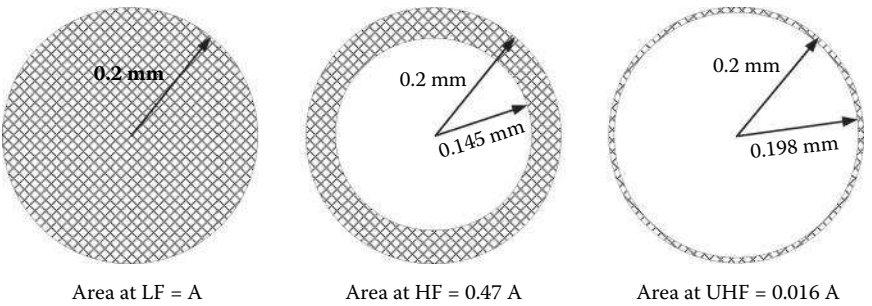

FIGURE 4.21
Skin effect at (a) low frequency (LF), (b) high frequency (HF), and (c) ultra-high frequency (UHF). Current flows through the shaded areas.

© 2011 by Taylor and Francis Group, LLC

With these considerations, the layout of the transmission line used to connect the UHF interrogator to its antenna becomes critical. The most effective approach to improving the performance of the system is to minimize the length of transmission line between the output of the interrogator and its antenna. It can also be possible to use transmission lines with larger diameter wires; however, the slight increase in effective area does not compensate for the additional cost of these lines or their increased rigidity. It is also important to choose a coaxial cable that has a continuous outer conductor instead of a multistrand ribbon for its shield.

The use of adequate connectors is also critical for RFID systems working in the UHF band. The BNC connectors that are commonly used in the LF and HF bands could be used without significant performance degradation in UHF applications. However, other types of connectors, specifically designed for higher frequencies, produce more reliable results. TNC connectors were conceived as a threaded version of the BNC connectors, being suitable for use up to 10 GHz. Type-N connectors are commonly used in high-frequency applications as they are suitable to carry signals up to 10 GHz and even 18 GHz with their recent enhancements. They are also mechanically robust and well suited for outdoor use. Figure 4.22 shows a male type-N connector, while Figure 4.23 shows a female type-N connector.

Because type-N connectors are available in 50 Ω and 75 Ω versions and the connectors are typically not labeled, it is very easy to confuse them, originating an impedance mismatch. Furthermore, the dimensions of their inner conductors are slightly different, so mismatching the connectors may

FIGURE 4.22
Male type-N connector.

© 2011 by Taylor and Francis Group, LLC

FIGURE 4.23
Female type N-connector.

FIGURE 4.24
Male and female subminiature version A (SMA) connectors.

also damage them physically. Subminiature version A (SMA) connectors, shown in Figure 4.24, are perhaps the most widely used microwave connector and are becoming more used in RFID systems. SMA connectors can transfer signals up to 18 GHz and have a 50 Ω impedance. The main problem using this type of connector is that they have not been designed to be connected and disconnected constantly, like for example a BNC connector. Even with the best of care, they cannot exceed a few hundred connections and disconnections.

© 2011 by Taylor and Francis Group, LLC

4.4 Commercial Antennas for RFID Interrogators

4.4.1 Antennas for RFID Interrogators

Antennas for interrogators are available from the same manufacturers that make transponders and interrogators, as well as third-party vendors that build interrogator antennas for specific applications. Some manufacturers offer systems in which the antenna and the interrogator are integrated together, as is the case with handheld RFID systems.

Texas Instruments manufactures two types of antennas for the LF band under the generic name of Series 2000. These antennas are divided into *gate antennas* and *stick antennas*. Table 4.1 shows the specifications of these antennas.

As shown on Table 4.1, gate antennas mainly differ in their size. Designers of RFID systems choose the size of the antennas based on the required application, depending on the area that they have to cover. The stick antennas S01C and S02C are identical, with the only difference being the length of their coaxial cable: 1 meter for S01C and 3 meters for S02C. Choosing between gate antennas and stick antennas is also application dependent. In general, gate antennas offer a larger read zone and more read distance, while stick antennas offer a more focused zone. Therefore, if for example it is necessary to distinguish between different transponders, stick antennas will be more useful due to their more defined radiation field.

Some manufacturers have designed HF antennas that are shaped in a particular way for a specific application. For example, Unified Transponder Concepts, Inc., produces several antennas specific for laundry systems. One of them is shaped like a garment portal to be used with standard garment racks for clothes with an embedded RFID transponder. Another example from the same manufacturer is an antenna in the shape of a chute, used for the detection and control of deposited items tagged with the appropriate transponders. In addition, they also manufacture the more traditional panel and handheld antennas. The power levels accepted by these antennas ranges from 1 W to 4 W, and they all exhibit a resistance of 50 Ω at 13.56 MHz.

TABLE 4.1

Specifications for Some Texas Instruments Series 2000 Antennas Operating in the LF Band (134.2 kHz)

	Model	Inductance	Dimensions	Weight
Gate Antennas	G01E	27 μH	0.7 m x 0.2 m	745 grams
	G02E	27 μH	0.2 m x 0.2 m	425 grams
	G04E	26 μH	1.1 m x 0.52 m	2500 grams
Stick Antennas	S01C	27 μH	0.14 m x 2mm (Ø)	134 grams
	S02C	27 μH	0.14 m x 2 mm(Ø)	185 grams
	P02A	116 μH	0.13 m x 21.3 mm (Ø)	105 grams

© 2011 by Taylor and Francis Group, LLC

TABLE 4.2

Specifications for UHF Antennas Manufactured by NetHome

	Dimensions (mm)	Gain	Polarization	Connector
NT-900-SPP	90 x 90 x 25	0 dBi	Right / Left hand	SMA
NT-900-MPP	120 x 120 x 25	0 dBi	Circular	SMA
NT-900-CP	200 x 200 x 25	6 dBi	Right / Left had	SMA
NT-900-FP	360 x 260 x 25	6 dBi	Circular	TNC

TABLE 4.3

Specifications for MTI Wireless Edge Antennas Operating in the 400 MHz Range

Model	Frequency (MHz)	Dimensions (mm)	Gain	Polarization	Connector
MT182018	430 – 440	305 x 305 x 25	3.5 dBi	Circular LH	N-type Female
MT182016	430 – 437	370 x 370 x 30	9 dBi	Circular LH	N-type Female
MT181033	430 – 440	305 x 305 x 25	3 dBi	Linear	N-type Female
MT182011	405 – 450	370 x 370 x 40	8 dBi	Linear	N-type Female

TABLE 4.4

Specifications for MTI Wireless Edge Antennas Operating in the 865 MHz to 870 MHz Range

Model	Dimensions (mm)	Gain	Polarization	Connector
MT242032	190 x 190 x 30	7 dBi	Circular LH or RH	N-type Female
MT242040	190 x 190 x 30	7.5 dBi	Circular LH or RH	N-type Female
MT242033	540 x 470 x 220	8.5 dBi	Circular LH or RH	N-type Female
MT242034	685 x 626 x 220	8.5 dBi	Circular LH or RH	N-type Female
MT242027	260 x 260 x 30	8.5 dBi	Circular LH or RH	N-type Female
MT242014	305 x 305 x 25	8.5 dBi	Circular LH or RH	N-type Female
MT242017	371 x 371 x 40	10 dBi	Circular LH or RH	N-type Female
MT243017	650 x 320 x 40	11 dBi	Circular LH or RH	N-type Female

There is a larger number of independent manufacturers for antennas operating in the UHF range. For example, the Korean manufacturer NetHom offers flat, patch antennas that operate in the 902 MHz to 928 MHz range and have an input impedance of 50 Ω, as shown in Table 4.2.

Another manufacturer, MTI Wireless Edge Ltd., offers a vast array of standalone antennas for a wide number of frequencies and applications. Table 4.3 shows specifications for their line of antennas in 400 MHz UHF RFID range. All the antennas shown in Table 4.3 have a maximum input power of 6 W and an input impedance of 50 Ω.

The same manufacturer also offers antennas that operate in the 865 MHz to 870 MHz frequency range, have an input impedance of 50 Ω, and have a maximum allowable power of 6 W. Table 4.4 shows the rest of the specifications for these antennas.

© 2011 by Taylor and Francis Group, LLC

TABLE 4.5

Specifications for MTI Wireless Edge Antennas Operating in the 2.4 GHz Range

Model	Dimensions (mm)	Gain	Polarization	Connector
MT343024	190 x 190 x 30	13 dBi	Circular LH or RH	N-type Female
MT344034	305 x 305 x 15	15.5 dBi	Circular LH or RH	N-type Female
MT345014	371 x 371 x 40	19 dBi	Circular LH or RH	N-type Female

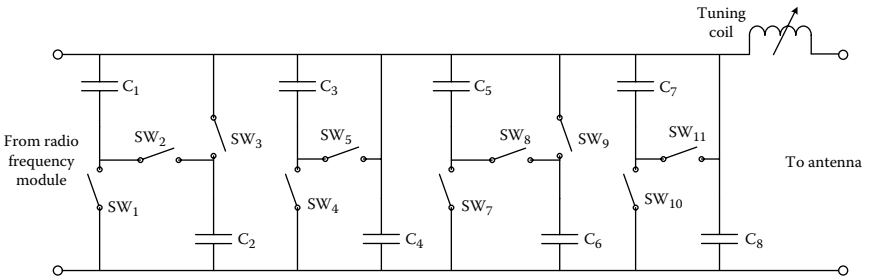

FIGURE 4.25
Schematic for the tuning board in the Series 2000 Reader from Texas Instruments.

It is also possible to purchase antennas similar to those shown in Table 4.4 dual polarized, that is, being both right-hand (RH) and left-hand (LH) circularly polarized. In this case, the antennas have two N-type female connectors, one for each polarization. Other models for antennas in the same frequency range of 865–870 MHz are available for linear polarization. In addition, this manufacturer also offers antennas for the 902–928 MHz and 950–956 MHz frequency ranges with dimensions and gains similar to those shown in Table 4.4 for either single or dual polarization.

Table 4.5 shows the specifications for a sample of antennas from MTI Wireless Edge Ltd. operating in the 2.4 GHz to 2.5 GHz frequency band and having an input impedance of 50 Ω.

Once again, antennas with similar dimensions and gains for the 2.4 GHz range are also available for single- and dual-linear polarizations.

4.4.2 Tuning Boards for Interrogator Antennas

Tuning boards are the circuits that are used to provide the high resonance needed to increase the strength of the field generated by the antennas in the system. Tuning boards can be found as stand-alone systems or as part of the interrogators. This subsection describes the Antenna Tuning Board that is part of the 2000 Series Reader System manufactured by Texas Instruments as an example of this type of circuits. As shown in Figure 4.25, the tuning board consists of a series of capacitors that are connected in parallel with the inductance of the antenna by means of several switches

© 2011 by Taylor and Francis Group, LLC

TABLE 4.6

Resulting Capacitance for Different Configurations of Switches in Tuning Board

Switch	Capacitance (nF)	Connection
SW1	33	C_2 ON
SW2	16.5	C_1, C_2 in series
SW3	33	C_1 ON
SW4	33	C_4 ON
SW5	16.5	C_3, C_4 in series
SW7	15	C_6 ON
SW8	7.5	C_5, C_6 in series
SW9	15	C_5 ON
SW10	10	C_8 ON
SW11	5	C_7, C_8 in series

(SW1–SW11) in the same board, thus allowing one to match a wide range of antenna inductances.

Table 4.6 shows the capacitive effect of each one of the switches in the tuning module. It can be seen that the lowest capacitance occurs when only SW11 is closed, resulting in a total capacitance of 5 nF. The highest capacitance that can be achieved with the board is equal to 139 nF, which occurs when SW1, SW3, SW4, SW7, SW9, and SW10 are closed.

The initial, coarse tuning adjustment is done with the capacitors, while the fine tuning due to the steps in the overall capacitance is done with the tuning coil located at the end of the tuning board. This process is repeated while monitoring the strength of the field generated by the antenna until it reaches a maximum.

© 2011 by Taylor and Francis Group, LLC

5

Interrogators

CONTENTS

5.1 Transmitter and Receiver 120
5.2 Modulator and Demodulator 126
5.2.1 Amplitude-Shift Keying (ASK) Modulation 126
5.2.2 Frequency-Shift Keying (FSK) Modulation 127
5.2.3 Phase-Shift Keying (PSK) Modulation 129
5.3 Long-Range Considerations 133
5.4 Interrogator Synchronization 134
5.4.1 No Synchronization at the Interrogator Level 134
5.4.2 Wireless Synchronization 135
5.4.3 Wired Synchronization 137
5.4.4 Combined Wired–Wireless Synchronization 137
5.4.5 Master–Slave Synchronization 137
5.4.6 Carrier Phase Synchronization 139
5.5 Structure of Commercially Available Interrogators 140
5.5.1 Interrogators for LF RFID Systems 140
5.5.1.1 Radiofrequency Modules 141
5.5.1.2 Control Module 144
5.5.2 Interrogators for HF RFID Systems 149
5.5.3 Single-Chip Interrogators 150

Interrogators have two basic functions: to generate and transmit the radiofrequency signal used to energize the transponders and to receive and decode the backscattered signal generated by the transponders. In addition, some interrogators may also transmit specific commands to the transponders. The interrogator also handles the bidirectional communication with a host computer used to process the information from the transponders and to issue commands to the interrogator. Figure 5.1 shows a basic block diagram of a generic interrogator with its basic constituent blocks.

If the transponder is able to accept commands from the interrogator, the radiofrequency signal generated by the interrogator has to be further modulated with the specific code; otherwise, the interrogator will only transmit the radiofrequency carrier. In either case, the radiofrequency signal is then amplified to specific power levels and passed through the tuning circuits before reaching the antenna. The antenna is also used to detect the backscatter signal generated by the transponder, which, after being filtered, is

© 2011 by Taylor and Francis Group, LLC

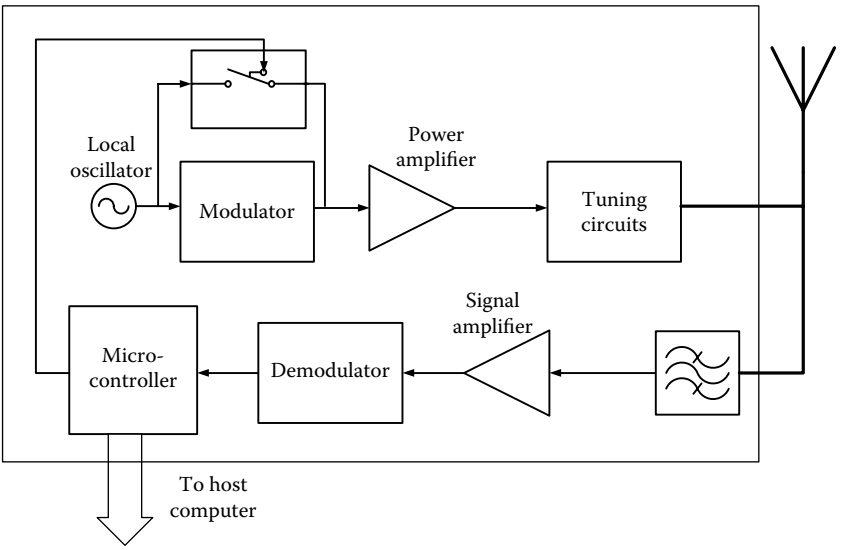

FIGURE 5.1
Basic block diagram of a generic interrogator.

then amplified and demodulated if necessary. The resulting signal is then sent to a microcontroller that will transmit it to the host computer using the appropriate communications protocol. The microcontroller also manages the timing for the interrogator to act as a transmitter or a receiver.

This chapter starts describing the transmitter and receiver sections in an interrogator. It continues by studying the most commonly used digital modulations in RFID systems. Afterwards, the chapter discusses issues related to extending the read range between transponder and interrogator as well as the requirements for interrogator synchronization when two or more interrogators coexist within the same general area. The last section in this chapter provides a description of the structure in different commercial interrogators.

5.1 Transmitter and Receiver

The basic structure of the transmitter section in the RFID interrogator contains an oscillator operating at the frequency of interest, a voltage or power amplifier, and the tuning circuits to match the impedance of the transmitter to the characteristics of the antenna. In addition to providing the radiofrequency signal to energize the transponders, some interrogators also transmit commands to the transponder. They can also be able to write new data into

© 2011 by Taylor and Francis Group, LLC

the transponder's memory. Transmitters in a RFID system must generate an accurate radiofrequency signal while minimizing the spurious radiation that they produce. *Spurious radiation*, common to all transmitters, is the amount of energy that falls outside the desired transmission band. In addition, they have to be as efficient as possible in order to reduce the amount of energy dissipated as heat. Excessive heat can severely reduce the life span of electronic components and must be reduced to acceptable levels.

For read-only transponders, the interrogator continuously transmits the radiofrequency signal and receives the response from the transponders. This mode of operation is known as *tag talks first*. When read/write transponders are being used, the interrogator must send commands for reading or writing them. For example, in the devices used by Microchip Technology, the interrogator uses amplitude modulation to transmit commands to the transponders. The communication starts by the interrogator sending specially timed gap pulses called *fast read request* (FRR) and *fast read bypass* (FRB). These gaps that are periods of time without electromagnetic field, are 175 μs wide, having a 100% modulation depth. The FRR or FRB pulses contain five of these gaps within 1.575 ms, as shown in Figure 5.2.

For RFID systems using magnetic coupling, one of the easiest approaches to drive the resonant circuit connected to the antenna is by using a D-drive circuit. Although either a full-bridge or a half-bridge will work correctly, most of the circuits use the half-bridge structure as it is less costly and easier to implement. Figure 5.3 shows a basic schematic for the half-bridge drive.

With a digital signal driving the circuit, the voltage at the node V_S is a square signal with voltages between V_{SS} and V_{DD}. Depending on the resonant quality factor (Q factor), the voltage across the antenna can reach a few hundred volts peak to peak. This is important to note at the time of selecting the electronic components used. An additional advantage of this structure is that although the driving digital signal has a very rich harmonic component,

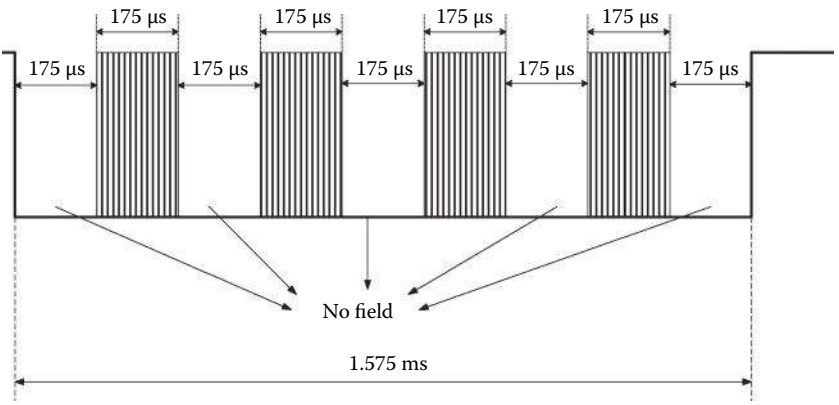

FIGURE 5.2
Fast read request (FRR) and fast read bypass (FRB) pulses.

© 2011 by Taylor and Francis Group, LLC

the signal across the antenna consists mostly of the fundamental component due to the filtering effect and the high Q factor value at the antenna. There are several devices commercially available that integrate the inverter and the two metal oxide semiconductors (MOSs) or metal oxide semiconductor field effect transistors (MOSFETs) in a single package. In addition to being able to operate at the high voltages generated, the capacitors used must have very low tolerance values due to the requirements for an elevated Q factor.

The typical rise and fall times for the signals using the circuit shown in Figure 5.3 range between 120 μs and 200 μs. This limits the data transmission rate that can be achieved. A modification of the circuit to increase transmission rates by reducing rise and fall times needs to accelerate the turn-on or turn-off response of the driver. This can be achieved by using the modified driver circuit shown in Figure 5.4.

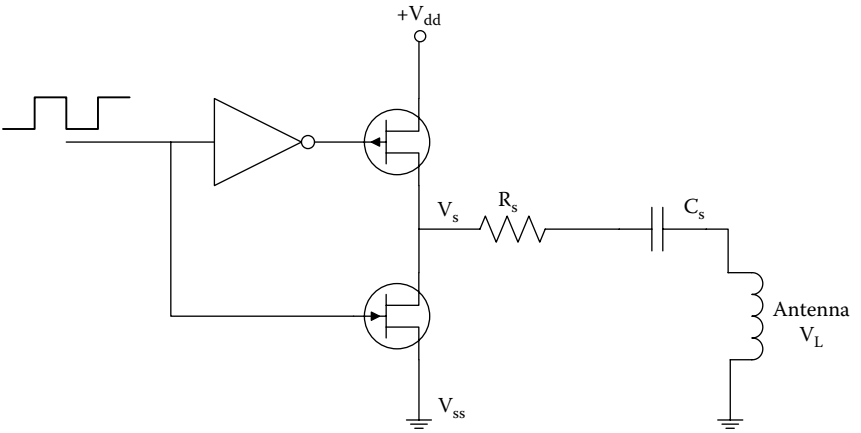

FIGURE 5.3
Half-bridge structure used to drive the resonant circuit.

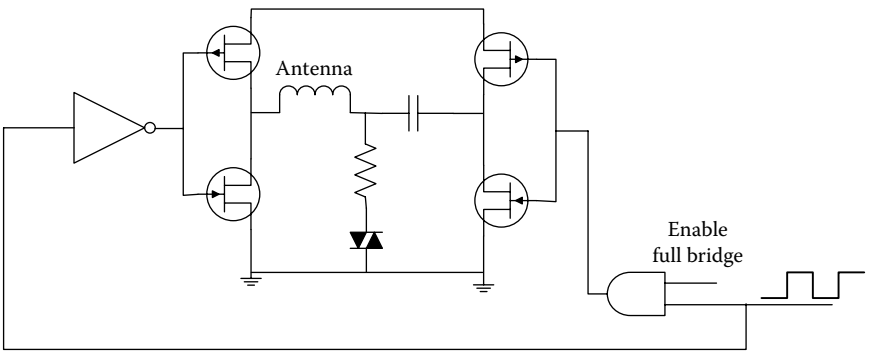

FIGURE 5.4
Modified bridge for increased transmission rates.

© 2011 by Taylor and Francis Group, LLC

The idea behind this circuit is to decrease the start-up time by starting the driver in full-bridge mode until the voltage has reached the desired value, at which point it can be switched back to half-bridge mode. Because the driver is started by driving the two half-bridges 180° out of phase, it effectively operates like doubling the input source voltage. With this structure, the circuit can respond up to three times faster. It is also necessary to keep in mind that the voltage across the capacitor will also increase and therefore the capacitor must be rated for that higher voltage. In order to reduce the electromagnetic interference generated by the circuit, the Triac is typically fired at zero.

The basic structure of the receiver in the RFID interrogator also contains a detector, typically an envelope detector, a signal amplifier, filters, and the appropriate pulse-shaping circuits. These circuits convert the distorted received signal at the output of the filters into pulses. These pulses are, in turn, connected to the input of a microcontroller that will send the appropriate data to the middleware or host computers for further processing.

Selectivity and sensitivity are key parameters for any radiofrequency receiver. *Selectivity* is defined as the extent to which a receiver can differentiate between the desired signal and unwanted signals present in its bandwidth. *Sensitivity* is defined as the minimum input signal that produces the minimal required output to be interpreted as information. Other important characteristics for receivers are their dynamic range, cross-modulation, and intermodulation distortion. *Dynamic range* refers to the range of signal levels simultaneously applied to the input for which the receiver will operate correctly. *Cross-modulation* and *intermodulation distortion* originate as a result of the nonlinear effects in the receiver that cause it to create new, undesired components.

For RFID systems with magnetic coupling, the transponder communicates with the interrogator by changing the value of the magnetic field. The transponder is magnetically coupled to the front end of the receiver in the interrogator. In this structure, changes in the magnetic field become voltage changes at the antenna in the interrogator. Figure 5.5 shows a basic block diagram following this approach. The peak detector extracts the envelope of the signal being transmitted. The peak detector is followed by a filter to remove the DC component of the envelope. A further low-pass filter removes the radiofrequency component, leaving only the envelope of the modulated signal. The output of the comparator is a digital signal with the information from the transmitted signal.

The peak detector must operate with the relative high voltages that may appear at the input of the tuning circuit. Moreover, it should not become a load to the tuning circuit either. Other requirements for the peak detector are to reduce the ripple in the carrier as much as possible, maintain the modulation of the signal, and possess low setting times, among others. It is not possible to optimize all these parameters simultaneously, thus requiring the designer of the system to find an acceptable compromise depending on its overall requirements.

© 2011 by Taylor and Francis Group, LLC

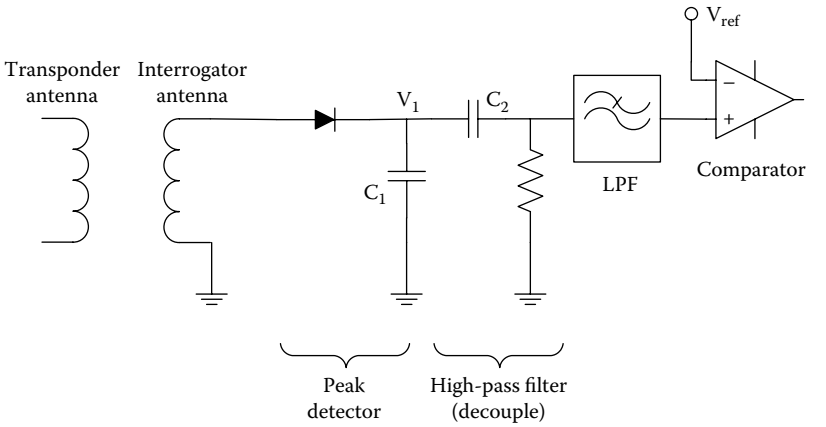

FIGURE 5.5
Basic structure for the detector in the RFID interrogator.

Example 5.1:

Discuss possible solutions for reducing ripple in the carrier.

Solution:

The ripple in the carrier can be reduced by increasing the value of the capacitor used in the peak detector. However, increasing the value of the capacitor will degrade the settling time for the detector, and will increase its loading effects. A possible solution would be to use an active peak detector. However, given the range of voltages expected at the input of the detector, the cost of the detector would significantly increase.

The voltage at node V_1 increases quickly when the input voltage increases due to the low impedance of the diode in forward mode. When the input voltage decreases, the voltage at node V_2 decreases extremely slowly due to the very high impedance presented by the diode in reverse conduction. This situation could be solved to some extent by placing a resistor in parallel with capacitor C_1 to help discharge it. However, this resistor has to be large enough for the peak detector to avoid loading the input circuits. A value of 10 MΩ is typically used.

The goal for the decoupling stage is to reject the high DC voltages present in the signal without excessive loading the front end. This stage should also have a fast dynamic response and stabilize quickly after detecting energy. The time constant of this stage is equal to the product of the resistance by capacitance C_2. The component values can be calculated by considering the delay time in establishing the communication after detecting the presence of radiofrequency energy as well as the minimum allowable voltage after the settling time. The cutoff frequency of the resulting high-pass filter has a strong effect in distorting and attenuating the digital signal that contains the information. With these conflicting requirements for the time constant, the

© 2011 by Taylor and Francis Group, LLC

simple RC circuit is not appropriate for removing the DC component of the received signal. Instead, it is necessary to use a circuit with either a nonlinear or a controllable time constant, as shown in Figure 5.6.

The diodes start conducting when the voltage across the resistor is above $(V_{REF} + V_{ON})$ or below $-(V_{REF} + V_{ON})$. This results in lowering the effective resistance seen by the circuit, and therefore it lowers its time constant. An additional benefit from using the diodes is that they protect the low-pass filter against positive or negative voltage spikes. The additional resistor R_2 is controlled by the switch. The switch is closed during transient periods and opened when data are being received by the circuit.

The low-pass filter stage is best implemented using an operational amplifier configured as an inverting amplifier, as shown in Figure 5.7. This structure not only allows controlling the gain in the pass band, but also minimizes its output impedance.

The cutoff frequency depends on the values of R_f and C_f. This frequency should be chosen at least two decades above the cutoff frequency from the DC blocker. It is also necessary to limit the gain of the filter to avoid the saturation of the operational amplifier. For some systems, the simple filter shown in Figure 5.7 may not provide enough attenuation at the desired frequencies. If this is the case, it can be substituted by a more complex filter. The three most common active filter topologies are Chebyshev, Butterworth, and Bessel filters. Chebyshev filters have the steepest transition between the pass and stop band, although they have ripple in the pass band. Butterworth filters have the flattest pass band, but their transition is not as steep as Chebyshev filters. Bessel filters have linear phase response with a smooth transition between

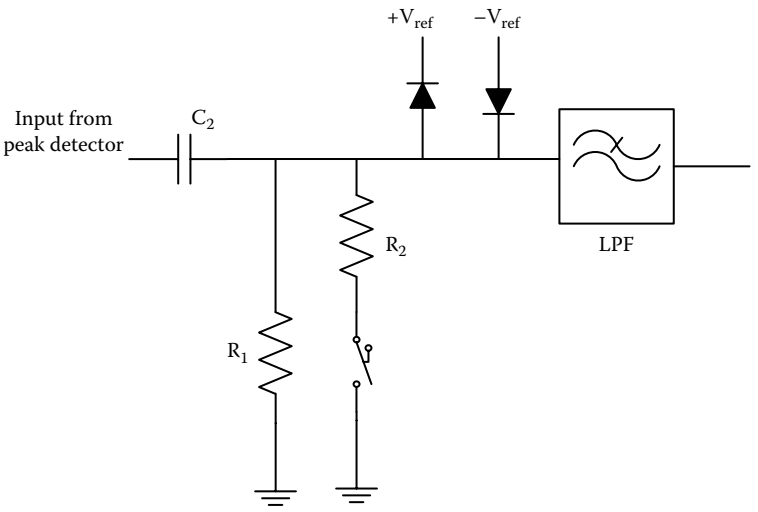

FIGURE 5.6
Circuit for implementing a nonlinear time constant.

© 2011 by Taylor and Francis Group, LLC

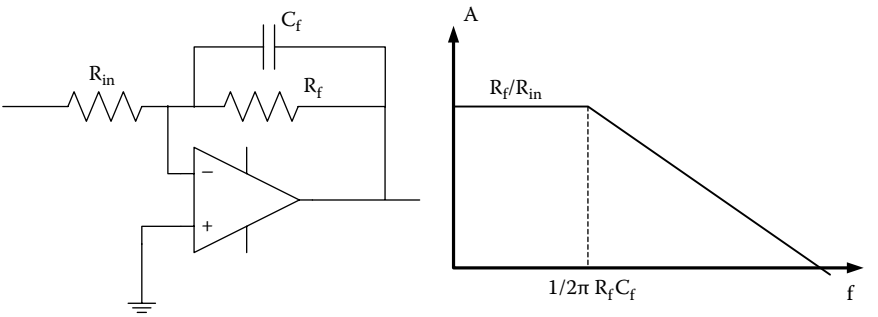

FIGURE 5.7
Low-pass filter stage.

pass band and stop band. When selecting one of these filter structures, it is necessary to consider not only their frequency response but also their transient response. For example, although Chebyshev filters have the best frequency response due to the fast transition between pass and stop bands, this results in an underdamped transient response with overshoot and ringing. Therefore, it has a very long settling time. Although Butterworth filters have a better transient response, they still exhibit some overshoot. The Bessel filter, although it has the worst frequency response, exhibits the best and fastest transient response and therefore is a very attractive candidate for this type of application.

The final stage is a comparator with some degree of hysteresis. The level of hysteresis is chosen to provide the required immunity against noise. The output of the comparator should be a digital signal that can be directly connected to the input of a microcontroller for further processing and transmission.

5.2 Modulator and Demodulator

5.2.1 Amplitude-Shift Keying (ASK) Modulation

Amplitude-shift keying (ASK) is the most basic form of modulation for digital signals. In ASK, data are represented as variations in the amplitude of the radiofrequency carrier. In binary ASK, there are only two symbols to be transmitted: the symbol *1* is normally represented by the full amplitude of the carrier, while the symbol *0* is represented by the minimal amplitude of the carrier. In this case, these two different symbols are represented by a single bit. In general, for *M*-ary ASK symbols, *n* bits are used to represent *M* symbols as

$$M = 2^n \tag{5.1}$$

© 2011 by Taylor and Francis Group, LLC

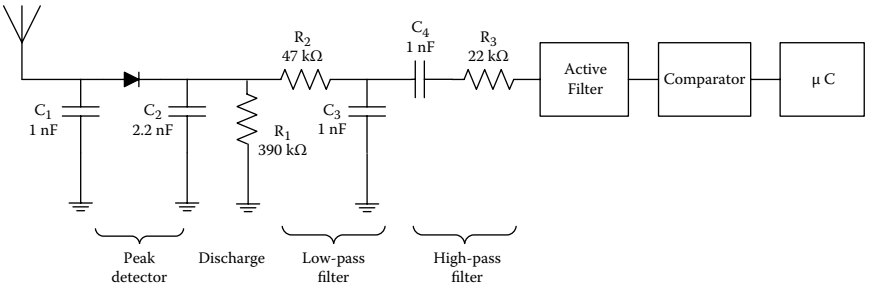

FIGURE 5.8
Detector in the receiver section of a commercial interrogator.

A *M*-ary ASK system requires distinguishing between *M* different amplitude levels for the radiofrequency carrier. While *M*-ary systems increase the transmission rate because each symbol encodes *n* different bits, the amplitude levels of the different symbols become closer to each other, making the system more susceptible to transmission errors. Therefore, there is a tradeoff between the transmission rate and acceptable transmission errors.

The ASK signal is demodulated by detecting the envelope of the carrier, normally using a half-wave rectifier. This detects the peak amplitude of the signal generated by the transponder and feeds it into an RC circuit that charges and discharges accordingly. The time constant of the RC circuit must be chosen with these two considerations: (1) it must be small enough so the voltage across the capacitor diminishes fast enough in order to keep with the changes in the envelope of the signal, and (2) it must be high enough to avoid excessive ripple in the detected signal. After the envelope has been detected, the resulting signal is passed through a low-pass filter and a signal-shaping circuit and finally fed into a microcontroller. Figure 5.8 shows the schematic of the detector in the receiver section of a commercially available interrogator working in the LF range at 125 kHz.

The capacitor C_1 provides the resonance for the inductance of the antenna. An additional advantage of this structure is that because C_1 is grounded, the carrier finds a path to ground. The diode and C_2 form the half-wave rectifier for which the resistor R_1 provides a discharging path. The time constant of this circuit is approximately 850 μs. The signal is further low-pass and high-pass filtered before entering the comparator for processing.

5.2.2 Frequency-Shift Keying (FSK) Modulation

Frequency-shift keying (FSK) is a form of modulation in which the digital signal to be transmitted changes the frequency of the carrier within a predetermined set of available frequencies. The most basic case, in which only two instantaneous frequencies can be transmitted, is called *binary FSK* (2FSK). For more complex systems, and in order to increase the bit transmission rate, the number

© 2011 by Taylor and Francis Group, LLC

of possible instantaneous carrier frequencies is higher, normally a power of 2. This situation is called *M*-ary FSK, where *M* represents the total number of different possible instantaneous frequencies, as shown in equation (5.1).

Binary FSK transmits two different frequencies f_0 and f_1 to represent a logic *0* or a logic *1* following an established protocol. The transmission of 2FSK can be easily accomplished by having two oscillators operating at frequencies f_0 and f_1, followed by a switch that selects one or the other based on the digital input. Although this is a simple procedure, it results in discontinuities of the carrier frequency at the time of switching, thus resulting in a greater prominence of high-frequency components that implies the need for a much wider bandwidth transmission. 2FSK can also be generated using the VCO approach as is done for analog signals. Because the digital modulating signal will never have a zero rise or settling time, this digital modulation is in fact an analog modulation with a very short transition time. In this case, the carrier has a continuous and smooth transition, therefore guaranteeing phase continuity and requiring a narrower spectrum for transmission. This method is known as continuous-frequency shift keying (CPSK) and can also be readily applied for multilevel modulation systems.

FSK signals can be detected by *noncoherent detection* or *coherent detection*. Noncoherent detection is based on simultaneously injecting the 2FSK signal into two band-pass filters, each one tuned to the transmitted frequencies, f_0 or f_1, as shown in Figure 5.9. In this case, the output of each filter is connected to an envelope detector and their outputs are combined to reconstruct the baseband modulating signal.

An alternative method for noncoherent FSK detection is based on injecting the FSK signal to the input of a phase-locked loop (PLL). The output of the internal *voltage-controlled oscillator* (VCO) will switch between frequencies following the signal at the output of the PLL, thus locking on to the incoming FSK signal so that the output changes between the logic levels of *0* and *1*, depending on the frequency of the incoming signal.

Figure 5.10 shows the basis for coherent detection of FSK signals. This approach requires the generation of two carriers with the same exact frequencies and phases as those used by the transmitter. In this case, only one

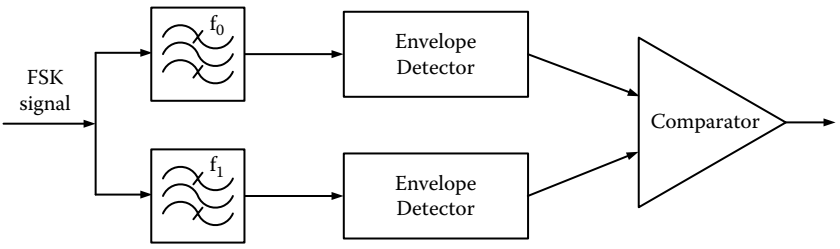

FIGURE 5.9
Noncoherent frequency-shift keying (FSK) demodulator.

© 2011 by Taylor and Francis Group, LLC

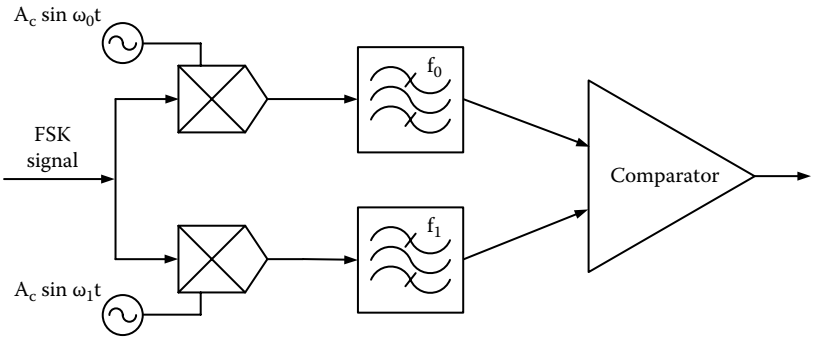

FIGURE 5.10
Coherent FSK demodulator.

of the filter outputs contains a signal at any given time. Therefore, after the addition of the two paths, the transmitting signal is recovered.

The coherent detection of FSK-modulated signals requires a more complex receiver than the noncoherent detection of the same signal, although it decreases the rate of errors for the transmission. Consequently, the designer of the system must consider the trade-offs between bit error rates and system complexity.

5.2.3 Phase-Shift Keying (PSK) Modulation

Phase-shift keying (PSK) modulation is one of the most effective methods to transmit digital signals. In PSK, the information is contained in the instantaneous phase of the modulated carrier. Usually, this phase is imposed and measured with respect to a known and selected phase of the carrier. For 2PSK, in which the modulating signal has two levels, the phase states are 0° and 180°. In *M*-ary modulation systems, the phase associated to each transmitted symbol is distributed equidistantly from each other around the 360° circle. When $M = 4$ ($n = 2$ bits), the resulting modulation is called *quadriphase phase-shift keying* (QPSK). QPSK, in which the phases are separated by 90°, is a common modulation used in communication systems.

Figure 5.11 shows a simplified version of one of the methods to generate a 2PSK signal. After the radiofrequency carrier is shifter by 180°, the resulting signal as well as the original signal are fed at the input of a 2-to-1 selector. This selector is driven by the digital signal. The output of the selector is either signal (a) or signal (b), depending on the value of the digital signal that controls the output of the selector.

PSK signals always require coherent demodulation, and therefore the PSK detector needs to know perfectly the phase of the unmodulated carrier. This requirement can be problematic as any phase error of the locally generated carrier reduces the effective voltage at the output of the detector in $\cos(\Phi)$, thus degrading the signal-to-noise ratio. A solution to this problem is by the

© 2011 by Taylor and Francis Group, LLC

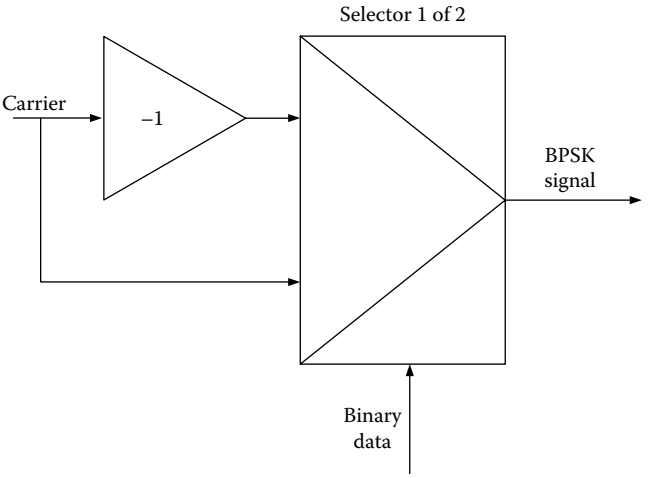

FIGURE 5.11
Binary phase-shift keying (2PSK) generation.

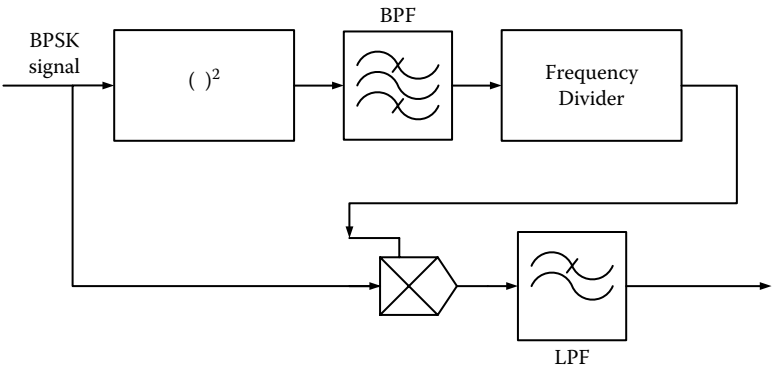

FIGURE 5.12
2PSK demodulation.

demodulator itself deriving a phase coherent reference to use in the demodulation process, as shown in Figure 5.12.

The output of the squaring circuit contains information at DC as well as at a double of the radiofrequency carrier. The band-pass filter eliminates the DC component. The frequency divider divides the frequency of the resulting signal by two and shifts its phase. The resulting signal is then multiplied by the original 2PSK signal that, after being filtered, will result in a DC signal with amplitude either positive or negative, thus shifted in 180°.

Figure 5.13 shows the generation process for QPSK signals. The digital-modulating signal $v_m(t)$ is connected to a 2-bit serial to parallel converter, so the resulting signals $v_1(t)$ and $v_2(t)$ change at half the rate of $v_m(t)$. This has the

© 2011 by Taylor and Francis Group, LLC

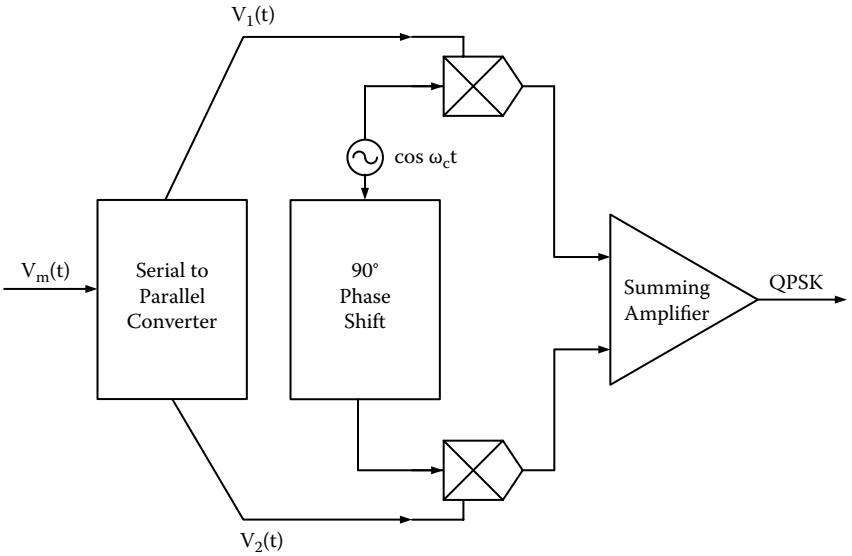

FIGURE 5.13
Quadriphase phase-shift keying (QPSK) generation.

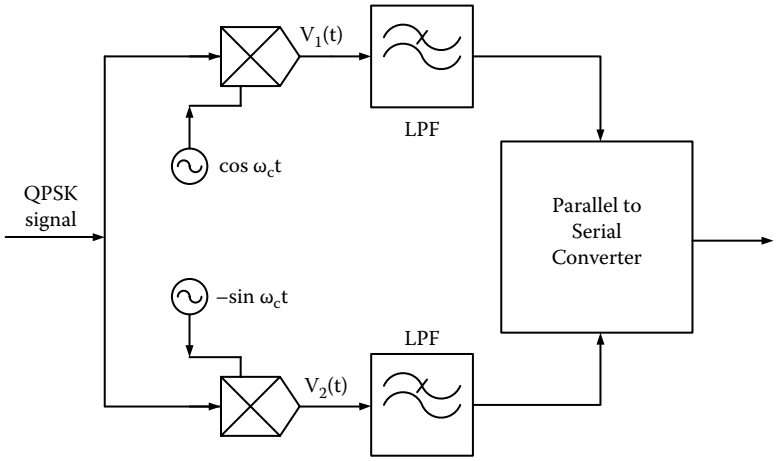

FIGURE 5.14
QPSK demodulation.

advantage of reducing the required transmission bandwidth as is the case of *M*-ary modulations. The output QPSK signal contains two components at the same frequency but shifted in 90°, and therefore there is no interference between them as they are in quadrature. That is, all the spectral components of the first term are 90° out of phase with those of the second term, making them independent from each other.

© 2011 by Taylor and Francis Group, LLC

The detection of the QPSK signal, as shown in Figure 5.14, follows an inverse process. The intermediate output signals $V_1(t)$ and $V_2(t)$ contain energy at DC as well as a frequency double the radiofrequency signal. This last component is eliminated by the low-pass filter, resulting in two separate streams of digital data. There are combined into a single data stream by the parallel-to-digital converter, thus recovering the original digital-modulating signal. QPSK modulation allows for sending information at twice the speed of 2PSK using the same bandwidth without compromising the performance of the system from the point of view of error rates.

Figure 5.15 shows a basic diagram of a 2PSK demodulator used in a commercial RFID interrogator operating in the LF range at 125 kHz. Capacitor C_1 provides the capacitance for resonance with the inductance of the antenna. The two diodes are used for detecting the envelope of the signal; each diode is on during half of the cycle. The 1 MΩ resistor is used to discharge the voltage store in capacitor C_2 used for the envelope detection. The envelope signal is fed into a series of active filters and pulse-shaping circuits not shown in Figure 5.15. The output of the last pulse-shaping circuit is a square wave at a frequency that is half of the radiofrequency carrier signal. This signal exhibits a 180° phase shifts according to the digital data sent by the transponders. This signal is now used as the clock for a D-type flip-flop. The input to the flip-flop is a signal at the same frequency derived from the transmitting signal. As the phase of the detected signal V_{out} changes, the output of the flip-flop also changes, thus recovering the digital information sent by the transponder.

One of the major problems with the design shown previously is that the phase of the returned signal can be, in certain conditions, unpredictable. For example, if the transitions of the incoming signal and the reference signal occur at the same time, the output of the flip-flop becomes unpredictable. This situation can be avoided with additional circuitry that intentionally shifts the phase between the signals to 90°, making it ideal for PSK detection.

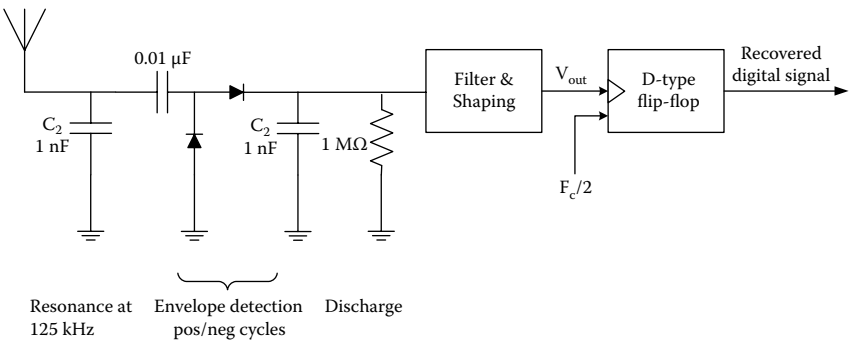

FIGURE 5.15
2PSK demodulator in a commercial interrogator.

© 2011 by Taylor and Francis Group, LLC

5.3 Long-Range Considerations

When evaluating the read range of transponders, it is necessary to understand that long-range operation may not always be a desirable condition. For example, in an environment where several interrogators communicate with their own transponders, it is necessary to ensure that a specific interrogator reads data from only the transponders that it has been assigned. Data from a distant transponder would then be treated like an interfering signal.

If long range is truly needed, it can be achieved by one or more of the following design considerations:

Increasing the transmitter output power. This can be achieved by designing the power amplifiers in the transmitter section in the interrogator with higher gain. Alternatively, when it is not possible to modify the interior of the interrogator, it is then possible to use an external preamplifier. In any case, it is necessary to comply with the limits set by the appropriate regulatory agencies on limits of power for different frequency range. Also, some regulatory agencies may also limit the ability of a user to modify a system that has already been approved and certified by the regulatory agency. This comes from the fact that the modification of the gain in the amplifiers can have effects on the frequency stability, spectral purity, and other characteristics of the transmitted signal that are specified by the regulatory agencies.

Modifying the size of the antenna. As described in Chapter 4, the size of the antenna and its quality factor (Q factor) affect the characteristics of the signal being transmitted and therefore the range at which transponders receive enough energy to activate their internal circuits. A correctly sized antenna becomes critical for long-range applications.

Optimizing the sensitivity of the receiver. Merely increasing the power in the transmitter section may not have a significant effect in the read range of the system if the signals generated by the transponder cannot be detected by the receiver. Therefore, interrogators to be used for long-range applications must have front-end amplifiers with high enough sensitivity that will allow them to detect the signals from the transponders at the longest distance from the interrogator that has been specified. In addition to the optimal design of the receiver, the sensitivity of the interrogator can be increased by reducing the amount of noise and interference added to the desired signal. This can be achieved by appropriate shielding of the front-end components, by placing the interrogator away from electrically noisy sources and using pass-band filters.

© 2011 by Taylor and Francis Group, LLC

5.4 Interrogator Synchronization

Synchronization is used to prevent interference between the interrogators in applications that have multiple interrogators operating in the same area. Synchronization is based on preventing interference by coordinating their transmission and reception windows. Synchronization is only required when the different interrogators are located physically close to each other. Therefore, when working with multiple interrogators, it is critical to determine if synchronization is required. However, the distance between interrogators alone is not sufficient to determine the need for synchronization. The electrical path between interrogators is affected by the presence of metallic structures such as buildings, the existence of conveyors, the layout of nearby power or data cables, and even the existence of reinforcing metal bars in concrete floors. Assuming only radiated signals, Texas Instruments has published some guidelines for the maximum distances that require synchronization for interrogators using some of their antennas as shown in Table 5.1. It is important to note that Table 5.1 assumes the two interrogators are using the same antenna type.

Table 5.1 shows that antennas with larger dimensions require more separation. Because this table assumes only radiated signals, in more realistic situations, this distance can be highly reduced due to the additional paths available to the different radiofrequency signals. This table can also be used as a starting point when working with interrogators using different antennas.

The next step, after determining that synchronization between interrogators is needed, is to decide on the method used to synchronize them. Although the following are the synchronization methods available to some of the Texas Instruments interrogators, the same methods are used by interrogators from other manufacturers.

5.4.1 No Synchronization at the Interrogator Level

This method can only be used with a single reader or in the case of synchronization by software. It represents the fastest method for receiving

TABLE 5.1

Separation between Interrogators After Which Synchronization Is No Longer Necessary Assuming Only Radiated Signals

Antenna Type	Antenna Dimensions	Minimum Separation Distance
S02-C (stick antenna)	Ø = 21 mm; l =140 mm	18 meters
G02-E (gate antenna)	200 mm x 200 mm	32 meters
G01-E (gate antenna)	715 mm x 170 mm	55 meters
G04-E (gate antenna)	1018 mm x 518 mm	105 meters

© 2011 by Taylor and Francis Group, LLC

information from the transponders. If all the interrogators are connected to the same network, the coordination can be carried out by the host computer issuing commands to read transponders simultaneously and buffering the results, or issuing different commands to different interrogators in turn. In any case, the coordination is done by the host computer rather than by the interrogators.

5.4.2 Wireless Synchronization

In wireless synchronization, when a specific interrogator detects increased energy at the frequency of the carrier, it assumes that this energy has been generated by another interrogator. This makes it stop itself before starting its own cycle. Obviously, this method only works when the background noise is low for the type of antenna being used. Larger antennas, which are more sensitive, present a clear disadvantage in this situation. When the environmental conditions change and there are additional reflections of signals in the immediate electrical environment, this approach is not valid either.

The receiver in each individual interrogator is adjusted in order to determine the level of background noise in the absence of signals from other interrogators. This determines the level after which the interrogator assumes that another interrogator is transmitting and therefore waits for a predetermined amount of time before starting its own cycle. This situation is illustrated in two situations depicted in Figure 5.16.

Figure 5.16(a) shows a time diagram involving wireless synchronization when the interrogator has not detected the presence of other signals. The interrogator starts by transmitting the radiofrequency signal for 50 ms that is used to energize the transponder. After the transponder is energized and recognizes the end of the radiofrequency energy burst, it starts transmitting its data for 20 ms. Once the transponder has finished sending its data, the interrogator waits for another 20 ms before starting the whole process again. This additional period is build as a precaution to avoid corrupting the data from other transponders to other interrogators. Because the interrogator does not detect any signals during this last 20 ms period, the whole cycle takes 90 ms.

In Figure 5.16(b), however, after the transponder has completed sending its information to the interrogator, the interrogator detects the presence of radiofrequency energy, and therefore responds by waiting 70 ms before starting its new cycle. This additional period gives enough time for the second interrogator to finish its own cycle. After the 140 ms have elapsed, the first interrogator starts its own cycle regardless of the presence of radiofrequency energy. This is done in order to prevent the interrogators always giving priority to other interrogators and therefore not being able to read their own transponders.

Wireless synchronization has the advantages that it does not need wires to interconnect the interrogators and all the interrogators are autonomous

© 2011 by Taylor and Francis Group, LLC

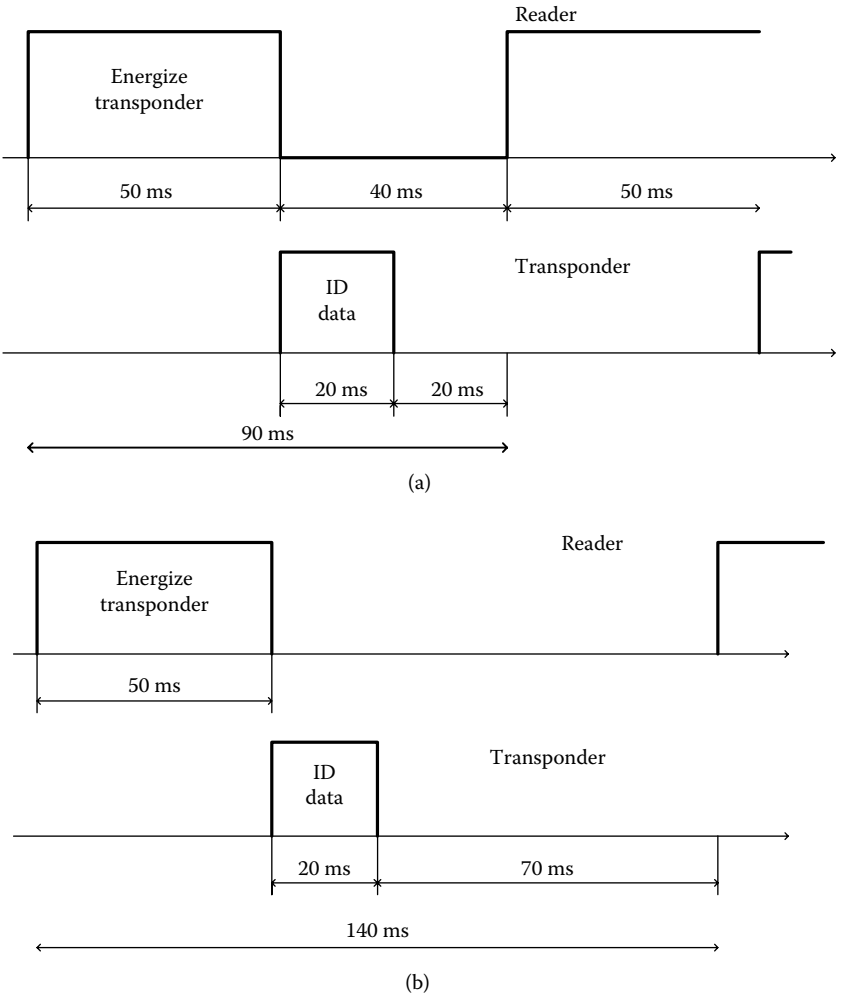

FIGURE 5.16
Wireless synchronization: (a) no other interrogators detected, and (b) delayed cycle due to other interrogators detected.

as there is not a master unit. It is very useful when handheld units have to coexist with fixed interrogators for these reasons. Wireless synchronization, however, is not adequate when large antennas are used in noisy environments because these large antennas are too sensitive to the background noise levels. Also, it cannot be used when the environmental conditions change, for example when vehicles enter or leave the read area as it changes the background energy. Finally, it cannot be used when other interrogators write data to the transponders.

© 2011 by Taylor and Francis Group, LLC

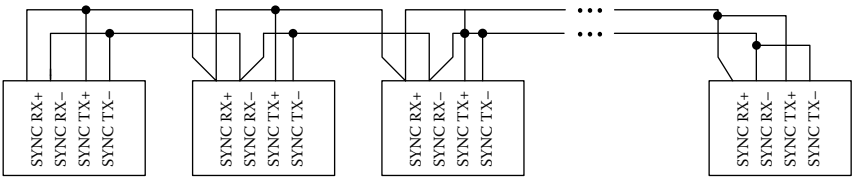

FIGURE 5.17
Structure of the control modules in interrogators using wired synchronization.

5.4.3 Wired Synchronization

The approach in wired synchronization is the same as for wireless synchronization with the only difference being that it uses wires to detect the presence of other interrogators instead of detecting radiofrequency energy. Therefore, the cycle for a single interrogator lasts 90 ms or 140 ms as described for wireless synchronization. This presents the advantage of being able to operate regardless of the environmental noise level, using a single twisted pair cable. This approach does not need a master unit. The main problem with wired synchronization is that if the power for a single interrogator fails, the bus fails and therefore the whole system fails. It is also not suitable for read/write transponders. Figure 5.17 shows the standard connection for the control modules of the interrogators using wired synchronization using the following nomenclature:

SYNC RX+: Noninverted data input
SYNC RX–: Inverted data input
SYNC TX+: Noninverted data output
SYNC TX–: Inverted data output
GND: Signal ground

5.4.4 Combined Wired–Wireless Synchronization

Using this approach, interrogators synchronized using a hard wire connection are also detecting the amount of radiofrequency energy to decide if another interrogator is already operational. This method resolves the individual disadvantages of each single approach.

5.4.5 Master–Slave Synchronization

In this approach, which is probably the most commonly used method of synchronization, one of the interrogators is configured as the master while the rest of the interrogators are configured as its slaves. Master–slave synchronization can be carried out using three variants:

© 2011 by Taylor and Francis Group, LLC

Master–slave without acknowledgment. This method is the fastest approach for reading transponders as it assumes that all the interrogators are part of the same synchronization bus. This requires the interrogators to have a synchronization bus that connects all the readers, using for example a single twisted pair as shown in Figure 5.18.

Once the master has finished a complete read cycle, it transmits a synchronization pulse in the bus. Any slave that has finished its own cycle is waiting for this pulse in order to start a new cycle, as shown in Figure 5.19.

This approach presents the advantage of needing only a single twisted pair. It also has the fastest read rate and can be used when transponders are rewritten by interrogators. It is necessary, however, to keep in mind that if the master fails, the rest of the units stop working. Also, if a slave reads a transponder and the master does not, the slave may miss the next pulse as it is busy processing the information from its transponder.

Master–slave with acknowledgment. In this approach, the master has to wait until all the slaves have completed their cycles before starting a new master cycle. This requires using four wires: two for the pulse from the master and two for the information from the slaves to the master, as shown in Figure 5.20.

All the interrogators are running free while buffering the data via a point of data connection. A slave will not respond to a command from the host computer unless it has received the pulse from the master. This method presents the advantage that all the interrogators wait for the slowest to be complete and all the units are able to write to the transponders. This happens at the price of using a twin twisted pair instead of a single.

Master–slave triggered synchronization. This is similar to the previous approach, although in this case, the pulse is generated by an external device instead of an interrogator in the chain. All the interrogators

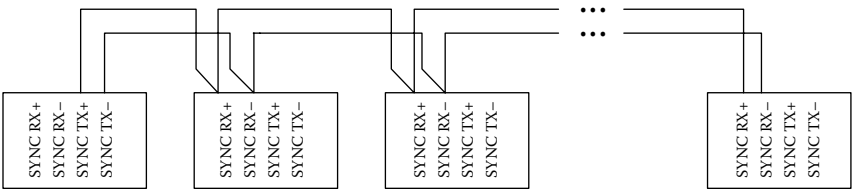

FIGURE 5.18
Structure of the control modules in interrogators using master–slave synchronization without acknowledgment.

© 2011 by Taylor and Francis Group, LLC

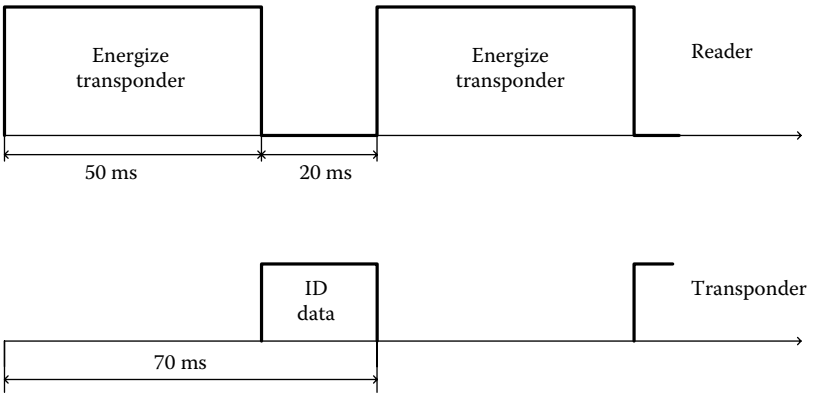

FIGURE 5.19
Master–slave synchronization without acknowledgment.

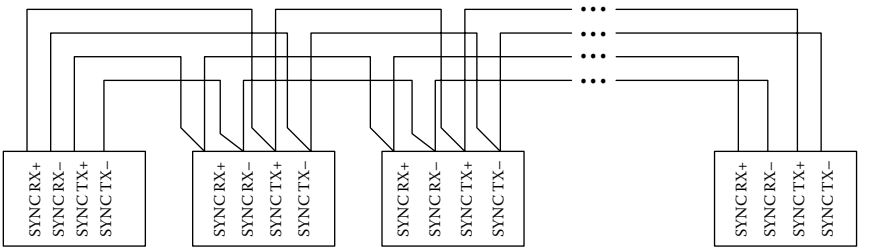

FIGURE 5.20
Structure of the control modules in interrogators using master–slave synchronization with acknowledgment.

are configured as slaves with the external master issuing the synchronization pulses at suitable intervals. This is required for interrogators that must read and write to multipage transponders in which different interrogators require different window times. In this case, the master has total control over the coordination of the devices in the chain. However, the master must be a more complex system and requires additional intelligence.

5.4.6 Carrier Phase Synchronization

This method is used when several antennas are located close together with the possibility that the field generated by each one of them may interact with the others. Because of the different transmission phases at each interrogator, the interaction may result in destructive interference. To avoid this effect, all the interrogators must be operated from the same carrier signal.

© 2011 by Taylor and Francis Group, LLC

5.5 Structure of Commercially Available Interrogators

Interrogators for RFID systems take different approaches depending on the specific needs of their intended application: from large and complex systems to single-chip interrogators. The following pages describe these different approaches through examples from commercial interrogators. It is necessary to view them just as specific examples as the number of available systems is higher, each one of them using a different approach. However, these examples provide valuable information about the structure of interrogators.

5.5.1 Interrogators for LF RFID Systems

The Series Reader 2000 from Texas Instruments is an example of a complex interrogator for an RFID system operating in the low-frequency range. Its main component is the S251B reader. This interrogator has a communications interface as RS232, RS422, or RS485; eight general-purpose input/output lines; two open collector outputs; one synchronization bus; one carrier phase synchronization bus; as well as a power connector and an antenna connector. Table 5.2 shows the electric specifications of the eight general-purpose input/output (I/O) lines in this unit.

This interrogator supports two different communication protocols: the ASCII protocol or Texas Instruments' own TIRIS protocol. The ASCII protocol that is used to send commands to the interrogator can only be used with the RS232 or RS422 interface. The TIRIS bus protocol is a binary protocol between a host computer and one or more interrogators.

The interrogator has two main modules: the *control module* and the *radio-frequency module*. The control module contains all the electronics needed for the communication between the interrogator and the host computer in order to control the radiofrequency module. It also has circuits used to optimize the performance of the antenna by correctly tuning the module. The radio-frequency module handles all the analog functions needed to generate the

TABLE 5.2

Electrical Specifications of S251B Reader (Texas Instruments)

Parameter		Minimum	Maximum
General Purpose I/O Voltage			
	Low Level	---	0.9 V
	High Level	3.15 V	5.25 V
General Purpose I/O Current			
	Low Level	----	25 mA
	High Level	----	16 mA
General Purpose I/O 1 to 4 Total output current		----	10 mA
General Purpose I/O 5 to 8 Total output current		----	10 mA

© 2011 by Taylor and Francis Group, LLC

signal that energizes the transponders, send commands to the transponders, and detect their responses. These two modules will be studied in deeper detail in Sections 5.5.1.1 and 5.5.1.2.

The synchronization bus operates in differential mode with a maximum data rate of 10 Mbits/s and allows for a maximum cable length of 1200 m. It can handle up to 32 different drives or receivers on the line. The outputs of the bus are protected against short circuits with a current limit of 150 mA to ground and 250 mA to the power supply. In addition, this unit contains three banks of dual in-line package (DIP) switches that allow for configuration changes. One of the banks is for setting up the control module, another bank for the settings of the communications protocol, and the third one for synchronization settings.

5.5.1.1 Radiofrequency Modules

The functions of the radiofrequency modules in the RFID system are to transmit the radiofrequency signal to the transponder via the antenna, to receive and demodulate the response of the transponder, and to write information to the transponder. Figure 5.21 shows a simplified block diagram of a generic radiofrequency unit in an interrogator.

For the modules that are part of the Series 2000 Reader manufactured by Texas Instruments, it is possible to distinguish the following submodules:

Power supply. This submodule provides the necessary voltage to power the rest of the electronics in the radiofrequency module. The majority

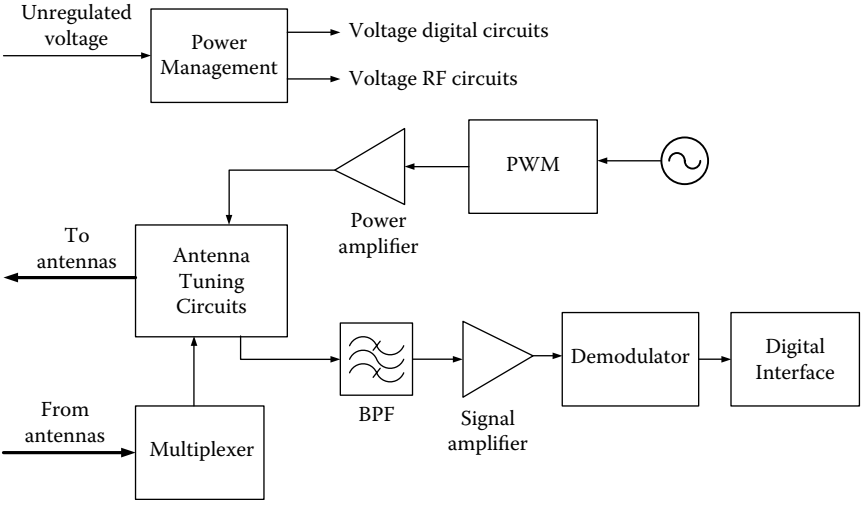

FIGURE 5.21
Simplified block diagram for the radiofrequency unit.

© 2011 by Taylor and Francis Group, LLC

of modules contain two voltage regulators, one to power the logic circuits and the other to power the rest of the module.

The manufacturer stresses not using a switching power supply, as at their typical frequency of operation their harmonics will create strong interfering signals.

Transmitter. The radiofrequency signal is generated by a crystal oscillator operating at the RFID frequency of 134.2 kHz. This signal is then fed into the pulse width modulator for which the user can select the width ratio between 3% and 50%. It is necessary to consider that decreasing this ratio also decreases the energy of the transmitted signal, thus providing a method to control the power transmitted by the interrogator.

Antenna circuit. The purpose of this submodule, shown in Figure 5.22, is to match the impedance of the transmitter to the impedance of the antenna in order to maximize the radiated power as well as its Q factor.

The circuit consists of the inductance of the antenna in series with an adjustable inductance for fine tuning as well as the capacitive part formed by the capacitors C_1, C_2, C_3, C_4, and C_{couple}. The switch is used to connect or disconnect C_4 for coarse tuning. It is necessary to connect several capacitors in series because of the high voltages that can be developed across the antenna terminals during resonance.

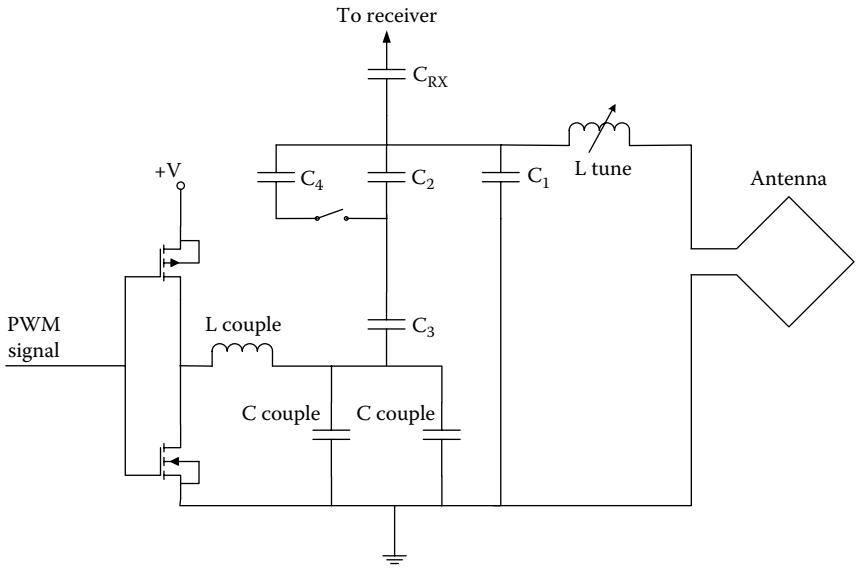

FIGURE 5.22
Antenna-tuning circuit.

© 2011 by Taylor and Francis Group, LLC

The capacitive resonator is driven by the *pulse-width modulation* (PWM) signal from the transmitter by two MOSFET power transistors through the inductor L_{couple}.

Receiver. The receiver in this module demodulates the FSK signals generated by the transponders, with a low symbol specified by a frequency of 134.2 kHz and a high symbol by a frequency of 123.2 kHz. The module can operate with a single antenna used for transmission and reception or with specific transmission and reception antennas. The path for the received signal depending on the type of antenna used is selected by the multiplexer at the front end.

Table 5.3 describes the different pins and its connections for the standard radiofrequency module in the Series 2000 Reader from Texas Instruments. Modules from other manufacturers have similar connections.

The most important electrical characteristics for these pins and connectors are shown in Table 5.4.

As shown in Table 5.4, the radiofrequency module incorporates a signal strength detector whose output is the RXSS- pin. This allows adjusting the threshold level for the detection of radiofrequency energy required by wireless synchronization. The adjustment is done by means of a potentiometer on the board. Different types of antennas require different threshold levels even if they operate in the same environment.

TABLE 5.3

Pins and Connectors in Standard Radiofrequency Module

Signal Name	Connection	Description
GND	IN	Ground logic circuits
TXCT-	IN	Transmitter control input for activation
VSL	IN	Supply voltage
RXDT	OUT	Receiver data signal output
RXSA	IN / OUT	Adjustment for receiver threshold level
RXCK	OUT	Clock output receiver
GNDP	IN	Ground power stage
RXA0	IN	Select signal for multiplexer
GNDP	IN	Ground power stage
RDTP	OUT	Test pin for receiver
VSP	IN	Supply voltage power stage
RSTP	OUT	Test pin for receiver
VSP	IN	Supply voltage power stage
RXSS-	OUT	Signal strength output in receiver
VD	IN / OUT	Internally regulated voltage
RCTP	OUT	Test pin for receiver

© 2011 by Taylor and Francis Group, LLC

TABLE 5.4

Summary of Electrical Characteristics Radiofrequency Module

Parameter	Min	Typ	Max	Unit
Internal regulated voltage	4.75	5.00	5.25	V
Supply current receive mode		9.0		mA
Supply current transmit mode		11.0		mA
Low level input voltage at TXCT- and RXA0	0		0.8	V
High level input voltage at TXCT- and RXA0	2.4		5.0	V
Low level output voltage at RXDT and RXCK	0		0.8	V
High level output voltage at RXDT and RXCK	4.0			V
Low level output voltage at RXSS-			0.8	V
Cable length for connection to control module		0.5	2.0	m
Number of slave modules that can be driven		1	5	
Inductance of antenna tuning coil	1.3	3.0	4.7	μH
Total antenna resonator capacitor	46	47	48	nF

This radiofrequency module, as well as most of the modules available in the market, can be used with the transmit–receive antenna or with special receive-only antennas. The type of antenna to be used is selected by a multiplexer in the receiver section.

5.5.1.2 Control Module

The control modules provide the functionality needed for the radiofrequency module to communicate with the rest of the devices. They control the Transmit and Receive commands from the radiofrequency modules according to the commands sent by the host computer. They also process the information from the transponders received by the radiofrequency modules, decode them, check their validity, and convert the signals to the protocol used for communication with the host computer. The control modules used in conjunction with the radiofrequency modules described in the previous section are available using the RS232C, RS422, or RS422/485 interfaces depending on the needs of the user. These control modules also handle the different synchronization methods described in Section 5.4 that need to be followed when more than a single interrogator is being used.

During the *charge time*, the control module activates the transmitter in the radiofrequency module. As long as this is active, the antenna resonates at the oscillator frequency and generates a radiofrequency field around its vicinity. This field charges the capacitor incorporated in the transponders energizing them. The typical length of the charge time is 50 ms. During this time, the receiver is disabled and cannot read any data. The charge time is followed by the *read time*, as shown in Figure 5.23. This time typically lasts 20 ms, during which the transponder sends the information back to the interrogator.

© 2011 by Taylor and Francis Group, LLC

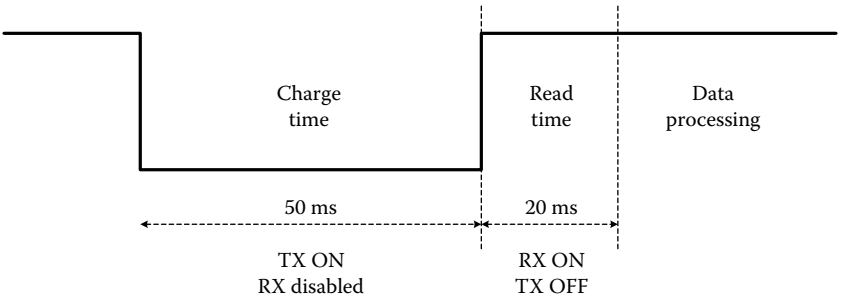

FIGURE 5.23
Charge and read times.

All the data formats consist of 128 bits. After being received by the radio-frequency module, they are checked by the control module. The different types of transponders supported by these interrogators are differentiated from each other by using different Start, Stop, and End bytes. The data structure for these transponders is shown in Figure 5.24. It is important to note that the first bit being transmitted is the least significant bit (LSB) and the last bit is the most significant bit (MSB).

The data structure for read-only transponders is shown in Figure 5.24(a). The data format starts with 16 pre-bits that are all set at zero, followed by the start byte ($7E). The next 64 bits are the identification data bits programmed into the transponder at the time of manufacturing; they cannot be changed by the user. The next 16 bits comprise the data protection bits (BCC). The following byte is the stop byte, which has the same structure as the start byte ($7E). Afterward, the transponder sends 16 end bits, all of them set to zero. During the last bit, the transponder discharges its capacitor, therefore deenergizing its internal circuits.

Figure 5.24(b) shows the data structure for read/write transponders. It also starts with the 16 pre-bits set at zero followed by the start byte that in this case is set at $FE. This tells the interrogator that the data come from a read/write transponder. The next 80 bits are the data bits that can be programmed by the user. The manufacturer recommends splitting these bits into 64 bits of data identification transmitted first and 16 bits for data protection bits (block check character, or BCC). The stop byte that is transmitted next has the same value as the start byte ($FE). The final 16 bits reflect the 16 LSBs of the read data that must be checked for validity by the control module. Once again, the last of these 16 bits makes the transponder discharge its capacitor and deenergize its internal circuits.

The data structure for the multipage read/write transponder is shown in Figure 5.24(c). The data start again with the 16 pre-bits set at zero, followed by the start byte with a value of $7E. This start byte is the same as for read-only transponders, meaning that the distinction between these two structures will be possible after the reception of the read address and read address frame

© 2011 by Taylor and Francis Group, LLC

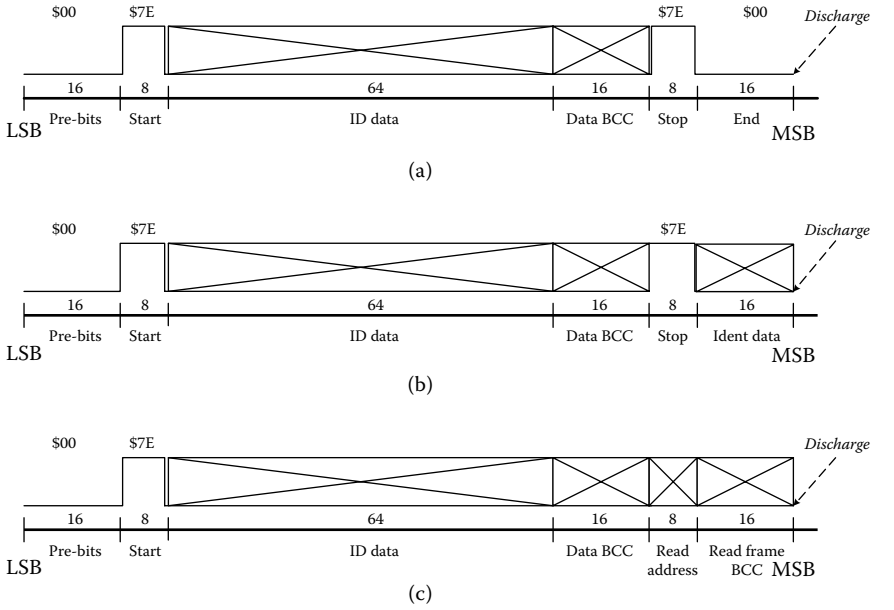

FIGURE 5.24
Data structure for several transponders: (a) read-only transponders, (b) read/write transponders, and (c) multipage read/write transponders.

BCC. The start byte is followed by 80 data bits that can be programmed by the user. The manufacturer also recommends splitting them into the first 64 data identification bits and 16 bits for protection data (BCC). The next 8 bits make up the read address byte; this contains a status field (2 bits), which is transmitted first, and a page field (6 bits). The 2 bits that make up the status field inform the control module about the function that the transponder has executed and the type of page that has been received. The final 16 bits make up the read frame BCC. One bit after having sent the first 128 bits, the transponder discharges the capacitor and deenergizes its internal circuits.

The function of the 16 pre-bits is to give enough time to the radiofrequency module to recover from the overload that it may have experienced during the 50 ms in which the transmitter has generated the radiofrequency signal. This is especially important because the transponders may start transmitting data immediately after having been energized. This period is known as the *waiting time*, lasting less than 1 ms.

After this time has elapsed, it is necessary to detect the first low-to-high transition for the start byte. After successful detection, the radiofrequency module synchronizes its clock and its data. The control module must also ensure that it receives all the high bits in the start byte. Otherwise, if a low bit is received, the process tops and the control module goes back to waiting for the detection of the low-to-high transitions. If the start byte has been successfully detected,

© 2011 by Taylor and Francis Group, LLC

the control module receives the next 80 bits and starts the generation of the cyclic redundancy check (CRC) to ensure the validity of the data. The last step in the decoding process is to determine whether the transponder that generated the data stream was a read-only transponder or a multipage read/write transponder as they both use the same start byte. This is done by checking the content of the CRC generator at the end of the process. If this value is equal to $0000, this indicates that a multipage read/write transponder originated the data. Otherwise, it indicates that it came from a read-only transponder. Figure 5.25 shows an overview of this sequence for the control module.

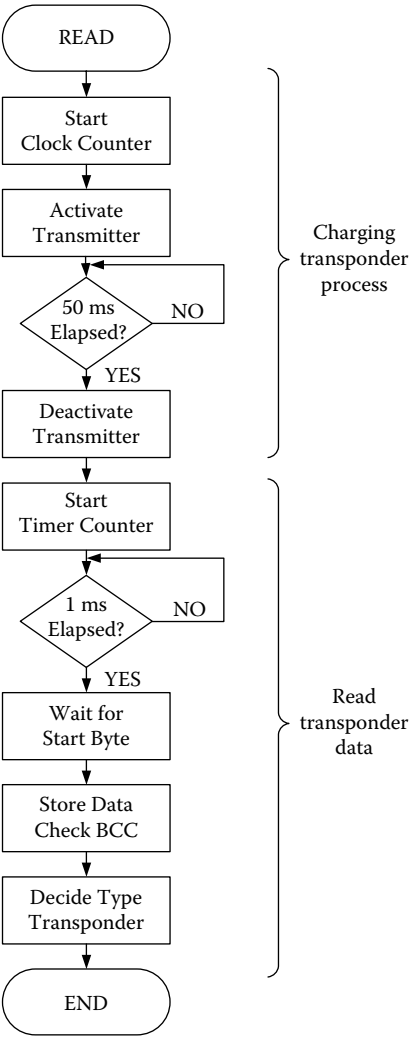

FIGURE 5.25
Control module sequence.

© 2011 by Taylor and Francis Group, LLC

The control module is also used to control the flow for writing to the transponder. Writing to the transponder is used to transfer commands, addresses, and data to the transponder. Before writing to the transponder, this must be energized. Therefore, writing to the transponder occurs after the transmitter has sent the 50 ms radiofrequency pulse to energize the circuits in the transponder. The actual process of writing is done by switching the transmitter off and on. To write a high bit, the transmitter is inactive during 1 ms followed by being active during 1 ms. To write a low bit, the transmitter is inactive during 0.3 ms followed by being active during 1.7 ms. The total time for writing a single bit is 2.0 ms.

To program the write data into the transponder's memory, the transmitter must be active for at least 15 ms immediately after the previously described write function has been executed. This is known as the *programming time*. Having the transmitter on for this time enables it to energize the circuits in the transponder. The write data format is shown in Figure 5.26.

All the data bits are transmitted to the transponder with the LSB first. The 8-bit write keyword ($BB) and the 8-bit write password ($EB) are sent to the transponder to initiate the transmission of the 80-bit data. The manufacturer recommends splitting the 80-bit data into 64-bit identification data transmitted first followed by 16 protection data bits (BCC). The write data format is terminated by a 16-bit write frame that must be set to $0300. After write frame, the transmitter will be active for 15 ms to allow the transponder to program the received data into its memory. The actual programming will only take place if the write keyword and write password bytes are received, the write data have the correct number of bits, and the radiofrequency field generated by the transmitter is high enough to produce the voltage required to program the transponder's memory. This voltage exceeds the voltage required to read the memory. Once after the programming time has elapsed, the transponder responds by sending the data that it has stored into its memory. This data follow the 128-bit format described previously in this section. If the read data received are structurally valid, they must be compared against the write data that were sent to the transponder to ensure that the correct data were written into the transponder. If the structure or the contents of the read data are not valid, the process must be repeated.

The last main function for the control module is to handle the synchronization tasks between different interrogators. For this to occur, a synchronization

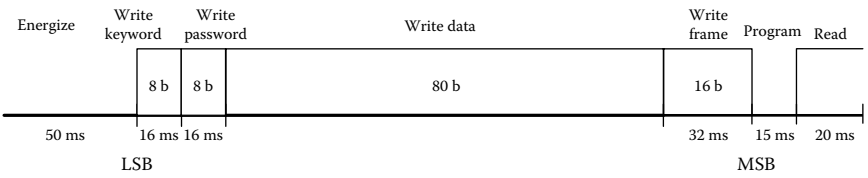

FIGURE 5.26
Format for writing data.

© 2011 by Taylor and Francis Group, LLC

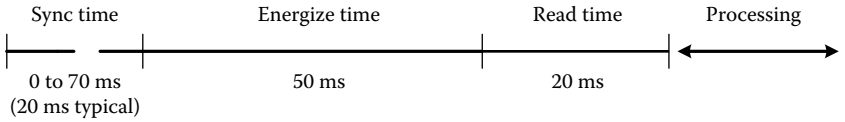

FIGURE 5.27
Synchronization sequence.

time must exist before the transmitter in the interrogator generates the radiofrequency signal to energize the transponders, as shown in Figure 5.27.

The synchronization allows the different interrogators in the overall system to detect each other and delay the activation of their own transmitters until other interrogators have finished their read functions. For this reason, the synchronization times vary depending on the number of interrogators in the application as well as the relative order of one interrogator in reference to the others in its vicinity.

5.5.2 Interrogators for HF RFID Systems

The Series Reader 6000 from Texas Instruments is an example of an RFID interrogator that operates in the HF range. The structure of the system is similar to the 2000 Series Reader described in the previous section. The Midrange Reader Module in this system provides the communication between transponder and interrogator. Output power levels can be adjusted between 100 mW and 1000 mW by means of a potentiometer placed on the radiofrequency module of the interrogator. The communication from the interrogator to the transponder is by ASK modulation, normally at 20%. The communication from the transponder to the interrogator is done by FSK modulation.

The TRF7960/1 also from Texas Instruments comprises multistandard fully integrated circuits containing the analog front end and the data-framing system. Their internal receiver enables them to modulate ASK and PSK, and it also includes automatic gain control and selectable bandwidth. In addition, the receiver includes a framing system allowing one to perform CRC checks, parity checks, or both. The output data are then sent to a microcontroller. The output of the transmitter only needs to be connected to the same impedance-matching circuit used for reception. Figure 5.28 shows the basic structure of the RFID system using this integrated circuit.

The receiver has two inputs that must be connected to an external filter. The external filter also converts the PSK modulation from the transponder into an amplitude-modulated signal. The two receiver inputs are multiplexed to two receiver channels: a main receiver and an auxiliary receiver. The main receiver contains a radiofrequency detection stage, a gain, a filter with automatic gain control, a digitizing stage, and an indicator for the strength of the received signal. The auxiliary receiver has a similar structure, although it is mainly used to measure the strength of the received signal.

© 2011 by Taylor and Francis Group, LLC

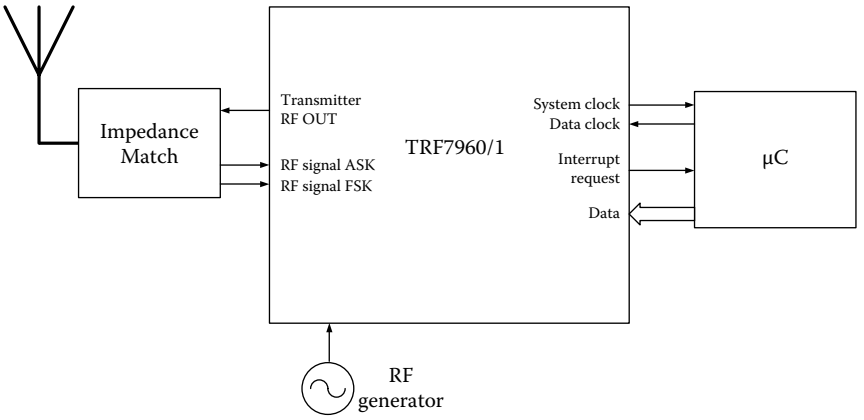

FIGURE 5.28
Structure of an interrogator using the TRF7960/1 circuits.

This is done by measuring the voltage of the demodulated signal and latching at its peak value.

The digital part of the receiver contains the bit decoders for the various protocols that supports the framing logic. The bit decoders convert the decoded signal into a bit stream. It has been specifically designed for maximum error tolerance, thus allowing the correct decoding of signals that have been partially corrupted due to noise or interference. The framing section packages the received bits into bytes, removing the control bytes sent by the transponder. This results in raw data that are sent to the microcontroller.

The transmitter contains the radiofrequency oscillator at 13.56 MHz, the processing circuits, and the radiofrequency power stage. The power levels available are 20 dBm (100 mW) or 23 dBm (200 mW) when the circuit is powered with 5V. When it is powered with 3 V, the available power levels are 15 dBm (33 mW) or 18 dBm (70 mW). The digital portion of the transmitter is very similar to that of the receiver as these circuits frame the command signals originated by the microcontroller.

5.5.3 Single-Chip Interrogators

In contrast to the complex systems described earlier, some interrogators have minimal components, normally an integrated circuit containing the transmitter and receiver and circuitry to communicate with a microcontroller or a microprocessor.

The core of the Series 6000 Reader from Texas Instruments is the RI-R6C-001 Integrated Circuit manufactured by the same company. This chip, whose block diagram is depicted in Figure 5.29, is a transceiver that provides the transmit and receive functions necessary for communication with transceivers operating at that frequency range.

© 2011 by Taylor and Francis Group, LLC

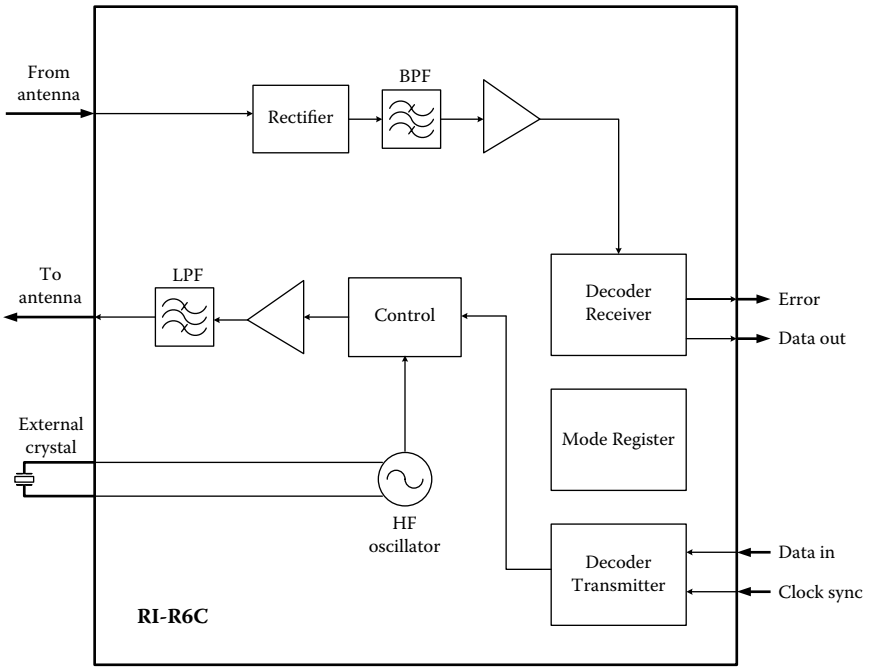

FIGURE 5.29
Simplified structure of the RI-R6C integrated circuit.

This transceiver integrated circuit communicates with its remote controller, normally a microprocessor, by a simple three-wire serial link. The communication between the transceiver and the transponders is generated by the microprocessor that sends the commands directly to the transceiver. The transceiver, in turn, applies the necessary carrier modulation and generates the radiofrequency signal.

The U2270B integrated circuit manufactured by Atmel® is another example of a single chip that serves as an interrogator. As shown in Figure 5.30, the U2270B incorporates an on-board power supply, an oscillator, tuning circuits, and other signal-processing circuits to produce an output that can be read by a microcontroller.

This specific chip has been designed to operate in the low-frequency range. It can be configured to work with different ranges of voltages for power supplies (from 5 V to 16 V). The low-pass filter in the receiver is a fourth-order Butterworth designed to remove the remaining energy of the carrier signal and other high frequencies after the demodulation process. The cutoff frequency can be selected by the user depending on the type of communication between the chip and the transponder that is being used. The possible choices are a Manchester code or biphase modulation typically at 5 kbaud.

© 2011 by Taylor and Francis Group, LLC

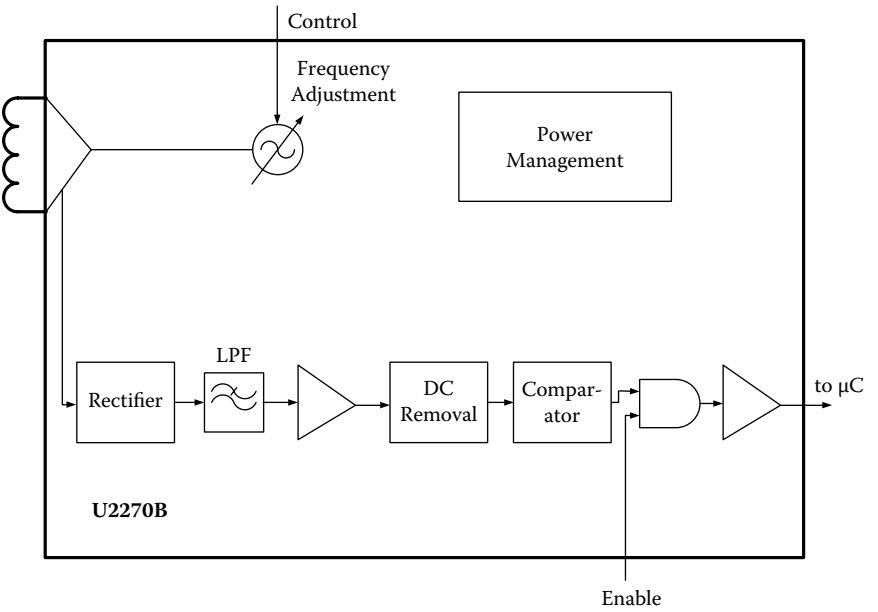

FIGURE 5.30
Simplified structure of the U2270B integrated circuit.

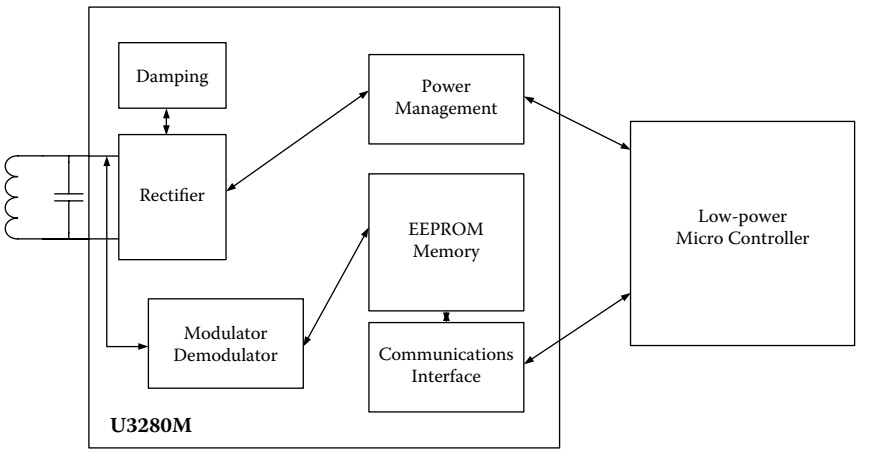

FIGURE 5.31
Simplified structure of the U3280M integrated circuit.

© 2011 by Taylor and Francis Group, LLC

One of the main applications of this chip is as an electronic immobilizer for the automotive industry in order to reduce auto theft. The interrogator and the associated microcontroller are located inside the vehicle, while the transponder with its unique identifier code is carried by the lawful owner or user in the vehicle. Unless the interrogator receives a valid code from a transponder, the microcontroller keeps the electronic ignition of the vehicle disabled. An additional benefit of this approach is that because the power to the transponder is supplied by the interrogator through the electromagnetic field it generates, the user of the vehicle does not need to worry about carrying fresh batteries like in traditional wireless fobs.

Atmel® also manufactures another chip, the U3280M shown in Figure 5.31, which, although marketed as a transponder interface for microcontrollers, functions as an interrogator. The chip can supply the energy required to power an external microcontroller and can also accept an external battery. The distribution of power is controlled by a power management circuit that either operates in automatic mode or is controlled by the microcontroller. The communication of this device with its microcontroller is carried out following a serial format. Modulation is carried out by changing the magnetic field generated by the antenna by varying its load. For example, a high logic level results in an increase of current through the antenna while the voltage becomes damped. The low logic level is generated by a decrease of current through the antenna that results in an increase in its voltage.

© 2011 by Taylor and Francis Group, LLC

6

Interrogator Communication and Control

CONTENTS

6.1 TIRIS Bus Protocol: Texas Instruments 155
6.2 ASCII Protocol for TIRIS Interrogators: Texas Instruments 159
6.3 Series 2000 Micro-Reader System: Texas Instruments 160
6.4 High-Frequency Interrogators: Texas Instruments..... 166
6.4.1 TIRIS Protocol for Series 6000 Reader System Interrogators... 166
6.4.2 Host Protocol for Tag-it™ Series 6000 Reader System Interrogators 166

Interrogators communicate with the host computers in order to transmit commands to the transponders and collect their information. This chapter explores some of the protocols used for linking interrogators with the host computers using as examples the different protocols employed by some interrogators manufactured by Texas Instruments. These examples show the basic communication processes between interrogators and their host computers as a stepping-stone to understand the control of interrogators from other manufacturers. The chapter starts by describing the TIRIS Bus Protocol, developed by Texas Instruments. It continues by studying how the ASCII protocol is used in some commercial interrogators. The next section explains the protocol used in some LF interrogators manufactured by Texas Instruments. The chapter ends by describing the communication protocols used in interrogators operating in the HF range.

6.1 TIRIS Bus Protocol: Texas Instruments

The TIRIS Bus Protocol is a proprietary protocol developed by Texas Instruments for communications between its interrogators or between interrogators and a host. This is a half-duplex byte-count protocol. It allows efficient communication between a single master and multiple slaves. The protocol allows communication with a single slave unit on a RS232 line and up to 31 slaves on a RS422 or RS485 line or using parallel links.

All the data transfers using the TIRIS protocol are initiated by the host; the slave units only send data upon request from the host unit, therefore

© 2011 by Taylor and Francis Group, LLC

eliminating the possibility of data collision on the bus. Furthermore, the protocol uses positive acknowledgment with the slave units indicating the reception of a message from the master. All the messages have the same format independently of the direction they travel. Table 6.1 shows the structure of an *N*-byte message using this protocol.

Command-message-codes describe the action that the master requires from the slave. Its most significant bit (MSB; Bit 7) is the *queued-response flag*, while the following seven bits contain the command code. When the queued-response flag is set to 1, it indicates to the destination unit that it should acknowledge and execute the command but its response should be queued until requested by the master. This is normally used with commands that have a delayed response in order to avoid suspension of the line activity. When the flag is set to zero, the response is immediate following the execution of the command.

TABLE 6.1

TIRIS Bus Protocol Format

Byte	Content
0	Start Mark[a]
1	Destination Address[b]
2	Source Address[c]
3	Message Code[d]
4	Data length
5	Data field (1)
6	Data field (2)
…	…
N + 4	Data field (N)
N + 5	MSB for CRC-field (1)
N + 6	CRC – field
N + 7	End Mark

[a] The *start mark* signifies the beginning of a message and is represented by $01. This corresponds to the ASCII character Start-of-Heading.

[b] The second byte, *destination address,* indicates the address of the unit to which the message is directed. The binary value of this byte corresponds to the ID of the destination address. The ID for the different units ranges from $00 to $FE, although the maximum number of units in a specific application is limited by the physical limitations of the link. Broadcast messages are indicated by using a destination address of $FF.

[c] The *source address* is the third byte in the message format. It indicates the ID of the unit sending the message.

[d] The fourth byte is the *message code* byte. This byte is used to define the content of the message. When the message is from the master to the slave, this byte is a *command-message-code*. When the message is from slave to master, this byte is a *response-message-code*.

© 2011 by Taylor and Francis Group, LLC

The response-message-code describes the acknowledgment that the slave unit has received the command. The four MSBs in the code are flags, while the four remaining least significant bits (LSBs) are the response code. The different flags are as follows:

The MSB (Bit 7) is the *error-flag*. When it is set to 1, it indicates that the slave has detected an error in the transmission or in the contents of the command. The error code is indicated in the last four bits.

Bit 6 is the *busy-flag*. When it is set to 1, it indicates that the slave is temporarily unable to accept commands.

Bit 5 is the *data-available-flag*. When it is set to 1, it indicates to the master that there is at least one message in the output queue in the slave. In order to read this message, the master must send the appropriate command.

Bit 4 is the *broadcast-received-flag*. When it is set to 1, it indicates that a broadcast message, issued previously, has been received correctly. The response to the broadcast command is placed in the queue. The master can read the response by issuing the appropriate commands at which point the flag is reset to 0.

Bits 5-8 in the Response-Message-Code byte indicate the type of response. Their meaning varies depending on the state of the Error-Flag bit as shown in Table 6.2.

Bit 5 in the TIRIS protocol is the *data length* byte. This byte shows the number of bytes that follow as data field. If the command or response does not require any data, this value will be zero.

The following N bytes in the TIRIS protocol make up the *data field*, with N being the value specified in the previous byte (Data Length byte). The content of this field depends on the message being sent.

The two bytes after the Data-Field bytes are *CRC-field* bytes. These bytes contain the Cyclic Redundancy Check values to ensure the integrity of the message. The TIRIS Bus protocol supports two methods of generating the CRC field. The first method is the Reverse CRC-CCITT algorithm that was described in Section 3.3.2. The second method supported by this protocol is called Longitudinal Redundancy Check (LRC). This is based on XORing each character with the previous value and storing the result in the LSB byte fin the CRC-Field. The MSB byte of the CRC-Field is generated by storing the 1's complement of the LSB byte. Using this method, if the MSB and LSB are ANDed together, the result should be zero. Consequently, any value different from zero indicates an error in the received message. This method is not as secure as the Reverse CRC method but it is faster.

The final byte is the *end mark* byte that indicates the end of the message. This is represented by $04 that corresponds to the ASC II character *end of transmission*.

© 2011 by Taylor and Francis Group, LLC

TABLE 6.2

Response Codes

Bit	Error-Flag = 0 Process Response		Error-Flag = 1 Error-Response	
0	Command Complete	A non-queued command received and executed correctly	Transmission Error	Slave received a message with its ID but found error on data
1	Accepted	A queued response command received correctly. Response will be placed on the queue	Command Invalid	Message received correctly but command code is not valid for this slave
2	Queue Empty	No message in the queue	Error – Data field length	Data field length wrong. Command not executed
3	Nothing to Resend	No information to resend available	Error - Parameter	Invalid parameter. Command not executed

Note: The following *N* bytes make up the *data field,* with *N* being the value specified in the previous byte (data length byte). The content of this field depends on the message being sent.

Using a two-wire, half-duplex circuit is not possible to execute flow control. Therefore, all the units in the bus must be able to receive and buffer the maximum length of the message at the operating speed for the line. When a unit is unable to handle correctly the incoming data, it cannot send an error message until the original message has ended. At that point, it can transmit the appropriate error message.

The data flow for the commands that do not require queuing from the slaves is always controlled by the master. The first steps for the master unit are to enable the transmitter, send the command message, and disable the transmitter. The slave unit, which is always monitoring the line, receives the incoming message and checks for the correct destination address. If the destination address is incorrect, it ignores the message and returns to monitoring the line. Because in this case the slave does not give any response to the master, the master will resend the command.

If the destination address is correct, the slave unit checks for errors in the message. If it detects errors, it sends an error response to the master, disables its transmitter, and returns to monitoring the line. Upon reception of the error response, the master unit processes the error code and resends the original command. If no errors are detected, the slave unit processes the command, sends the appropriate response message, disables the transmitter, and returns to monitoring the line. Upon reception of the response message, the master processes it and proceeds to transmitting the next command.

Broadcast messages transmitted by the master are not acknowledged in the normal way. After the master has sent the broadcast command, the slave checks for errors in the received message. If it detects errors, it ignores the message, sets the error flag, and returns to monitoring the line. If it does not detect errors, it sets the broadcast-received flag, processes the command, and places the response in its queue. The master accesses the special status bit in

© 2011 by Taylor and Francis Group, LLC

the response-code field in the slave's response to evaluate the correct reception of the previous message.

Example 6.1:

Describe the operations taken by a master unit that wants to initiate an operation on all slaves simultaneously.

Solution:

The master unit sends a command with a destination ID of $FF. The master unit then waits the expected operation time and proceeds to poll each individual slave. The master is looking for the *broadcast-received-flag* that verifies the correct reception of the command. The absence of this flag in a slave unit triggers the master to broadcast the command again.

Queued messages use a slightly different format from the format used by broadcast or immediate commands. The *N*th data field byte contains a sequence number, given by the master, that is used to have a reference when the queued messages are requested from the slave units. The slave unit indicates that a command requiring a queued response has been received and is being processed by sending a response message to the master with the accepted flag set. This response is not transmitted directly by the slave unit, but it is placed on its queue for the master unit to access it when ready.

When interrogators are asked to queue a response, these responses are placed in a 30-position circular buffer. The buffer has two pointers: store-next-message and read-next-message. Because of the circular structure of the buffer, it is not necessary to delete responses as they are overwritten when the pointer is incremented.

6.2 ASCII Protocol for TIRIS Interrogators: Texas Instruments

Some of the interrogators from Texas Instruments accept commands using a simple ASCII protocol. This ASCII protocol can only be used with a RS232 or RS422 communications line. Once the interrogator reinitializes, the first character to be transmitted is $02 (Start of Text, or STX), followed by $0D (Carriage Return) and $0A (Line Feed) through the serial interface. Any characters that may have been transmitted before the STX character are treated as random characters generated by the start-up process and therefore discarded.

Using this protocol, the interrogator can operate on four different modes: execute, normal, line, and gate. In execute mode, the interrogator triggers a single command, while in the other modes the read function is continuously triggered. The interrogators are also able to distinguish between three types of transponders: read-only, read/write, and multipage. The serial communications protocol from the interrogator to the host computer is

© 2011 by Taylor and Francis Group, LLC

introduced as a single character that describes the type of interrogator that originated the message: R (read-only), W (read/write), or M (multipage).

After receiving data from a transponder, the interrogator performs a data check. The result of this data check is one of the following: *identification received correctly*, *identification invalid*, or *no identification detected*. After receiving a correct identification, the interrogator proceeds to send the information through the bus. This is done by placing the identification string in a buffer that is accessed, read, and cleared by the host computer. The TIRIS protocol can distinguish between two groups of transponder identification: animal code numbers and industrial (nonanimal) code numbers.

6.3 Series 2000 Micro-Reader System: Texas Instruments

The Series 2000 RFID interrogators operate in the LF range. Table 6.3 describes the structure of an *N*-byte message sent from the host computer to the interrogator in these systems.

The following set of bytes are the *data field* bytes. These bytes only exist if required by the command field.

TABLE 6.3

Series 2000 Host-to-Interrogator Message Format

Byte	Content
0	Start Mark[a]
1	Message length[b]
2	Command Field[c] (1)
3	Command Field (2) - not always present
4	Data field (1)
5	Data field (2)
…	…
N + 3	Data field (N)
N + 4	BCC

Note: If the second command field is not used, the length of the message is *N* + 3 bytes. In addition, messages are limited to a total of 41 bytes.

[a] The first byte is the *start mark* that indicates the start of a message.

[b] The second byte is the *message length* byte that indicates the length, in bytes, of the command and data fields that follow.

[c] The third and fourth bytes (when the second command field byte exists) are the *command field* bytes. These bytes define the mode of operation for the interrogator and determine the operation that the interrogator must carry out on the transponder. Depending on the type of command, the information in the data fields may or may not be transmitted to the transponder. The meaning of the different bits for the command field (1) is described in Table 6.4.

© 2011 by Taylor and Francis Group, LLC

TABLE 6.4

Command Field (I) Bit Description

Bit	Description	Value	Operation
0 and 1	Operation Mode	00	Perform single command
		01	Read in continuous Normal Mode
		10	Read in continuous Line Mode
		11	Send interrogator software version
2	FBCC Calculation	0 or 1	1 = interrogator calculates FBCC
3	Power burst I	0 or 1	1 = duration determined in data field
4	Power burst pause	0 or 1	1 = duration determined in data field
5	Power burst II	0 or 1	1 = duration determined in data field
6	Data	0 or 1	1 = determined in data field
7	Command Expansion Field	0 or 1	1 = Command Field (2) is used

TABLE 6.5

Command Field (2) Bit Description

Bit	Description	Value	Operation
0	Special write timing	0 or 1	1 = Must be determined in data field.
1	Wireless synchronization	0 or 1	1 = Wireless synchronization being used.
2	Database consistency check (DBCC) calculation	0 or 1	1 = Interrogator calculates DBCC.
3 to 7	Reserved	0 or 1	Reserved.

The following set of bytes are the *data field* bytes. These bytes only exist if required by the command field.

The last byte in the message is the *block check character* (BCC) byte. This is a one-byte value that results from XORing each one of the bytes in the preceding message with the exception of the start mark byte.

As shown in Table 6.4, the existence of command field (2) is set by bit 7 of command field (1). Table 6.5 shows the meaning of the bits in command field (2) when it is present in the message.

Example 6.2:

Calculate the BCC for a message containing the following hex bytes: 04 23 38.

Solution:

BCC is calculated by XORing the bytes of the message. Start by first XORing 04 and 23:

04	0000 0100
23	0010 0011
XOR	0010 0111

The resulting value (0010 0111) is now XORed with 38:

Previous XOR	0010 0111
38	0011 1000
XOR	0001 1111

Therefore, the resulting BCC is $1F.

© 2011 by Taylor and Francis Group, LLC

The following three examples illustrate the structure of messages between the host computer and the interrogator for a variety of different commands and applications.

Example 6.3:

The following is the structure of a message transmitted from the host computer to the interrogator in commanding the interrogator to read a read-only transponder:

Byte	Code	Content	Description
0	$01	Start Mark	Start Mark
1	$02	Length	Two bytes follow (excludes BCC)
2	$08	Command Field (1)	Perform single command – Power burst
3	$32	Data Field (1)	Power burst for 50 ms to energize transponder
4	$38	BCC	BCC over previous bytes excluding Start Mark

Example 6.4:

The following is the structure of a message transmitted from the host computer to the interrogator in commanding the interrogator to write the following data in a read/write transponder.

00	0A	FE	32	66	00	00	01
MSB							LSB

Byte	Code	Content	Description
0	$01	Start Mark	Start Mark
1	$11	Length	17 bytes follow (excludes BCC)
2	$E8	Command Field (1)	Perform single command, no FBCC calculations, send power burst to energize transponder for reading and writing. Data command on following field
3	$06	Command Field (2)	Use wireless synchronization
4	$32	Data Field (1)	Power burst to energize transponder for reading (50 ms)
5	$0F	Data Field (2)	Power burst to energize transponder for writing (15 ms)
6	$0C	Data Field (3)	12 data bytes follow
7	$BB	Data Field (4)	Write Keyword
8	$EB	Data Field (5)	Write Password
9	$01	Data Field (6)	LSB of data to write
10	$00	Data Field (7)	Data to write
11	$00	Data Field (8)	Data to write
12	$66	Data Field (9)	Data to write
13	$32	Data Field (10)	Data to write
14	$FE	Data Field (11)	Data to write

© 2011 by Taylor and Francis Group, LLC

Byte	Code	Content	Description
15	$0A	Data Field (12)	Data to write
16	$00	Data Field (13)	MSB of data to write
17	$00	Data Field (14)	Write frame
18	$03	Data Field (15)	Write frame
19	$9C	BCC	BCC over previous bytes excluding Start Mark

Example 6.5:

The following is the structure of a message transmitted from the host computer to the interrogator in commanding the interrogator to read page 2 of a multipage transponder.

Byte	Code	Content	Description
0	$01	Start Mark	Start Mark
1	$04	Length	Four bytes follow (excludes BCC)
2	$48	Command Field (1)	Perform single command – Power burst with data
3	$32	Data Field (1)	Power burst for 50 ms to energize transponder
4	$01	Data Field (2)	One data field follows
5	$08	Data Field (3)	Write address specifying general read of page 2
6	$77	BCC	BCC over previous bytes excluding Start Mark

The structure of the messages sent from the interrogator to the host computer is described in Table 6.6.

The bytes following BCC are the *data* field bytes.

TABLE 6.6

Series 2000 Interrogator-to-Host Message Format

Byte	Content
0	Start Mark[a]
1	Message length[b]
2	Status[c]
3	Data field (1) LSB byte
4	Data field (2)
…	…
N + 2	Data field (N) MSB byte
N + 3	BCC

[a] The first byte is the *start mark* that indicates the start of a message.

[b] The second byte is the *message length* byte that indicates the length, in bytes, of the command and data fields that follow.

[c] The third byte is the *status byte*. This provides feedback about the preceding read or programming operation according to Table 6.7.

© 2011 by Taylor and Francis Group, LLC

TABLE 6.7

Description of Bits in the Status Byte

Bit	Value	Operation
0 and 1	00	Read Only transponder
	01	Read/Write transponder
	10	Multipage transponder
	11	Other transponder
2	0 or 1	1 = Start byte was successfully detected
3	0 or 1	1 = DBCC was successfully performed
4	0 or 1	1 = DBCC was successfully performed
5	0 or 1	1 = Software version for interrogator follows
6–7	Reserved	

TABLE 6.8

Description of Data Field Bytes

Type of Response	Number of Bytes in Data Field	Description
Read Only	8	Identification data. LSB first
Read/Write	8	Identification data. LSB first
Multipage	9	Identification data. LSB first and Read Address
Other	14	Complete transponder protocol without pre-bits assuming a successful start byte was detected
No Read	0	No data fields, no start byte. Status is $03
Software version	1	Software version. For example $12 means software version 1.2

The last byte in the message is the *BCC* byte. This is a one-byte value that results from XORing each one of the bytes in the preceding message with the exception of the start mark byte.

The length and meaning of the data field bytes are shown in Table 6.8.

Example 6.6:

The following is the structure of a message transmitted from the interrogator to the host computer after a successful read of a read-only transponder.

Byte	Code	Content	Description
0	$01	Start Mark	Start Mark
1	$09	Length	Nine bytes follow (excludes BCC)
2	$0C	Status	Valid RO, Start byte detected, DBCC is correct
3	$6A	Data Field (1)	Identification data (LSB)
4	$58	Data Field (2)	Identification data

© 2011 by Taylor and Francis Group, LLC

Byte	Code	Content	Description
5	$4C	Data Field (3)	Identification data
6	$00	Data Field (4)	Identification data
7	$00	Data Field (5)	Identification data
8	$00	Data Field (6)	Identification data
9	$00	Data Field (7)	Identification data
10	$00	Data Field (8)	Identification data (MSB)
11	$7B	BCC	BCC over previous bytes excluding Start Mark

Example 6.7:

The following is the structure of a message transmitted from the interrogator to the host computer after an unsuccessful read attempt.

Byte	Code	Content	Description
0	$01	Start Mark	Start Mark
1	$01	Length	One byte follows (excludes BCC)
2	$03	Status	Other, no Start byte detected, DBCC is not correct
3	$02	BCC	BCC over previous bytes excluding Start Mark

Example 6.8:

The following is the structure of a message transmitted from the interrogator to the host computer after successfully programming page 2 of a multipage transponder.

Byte	Code	Content	Description
0	$01	Start Mark	Start Mark
1	$0A	Length	Ten bytes follow (excludes BCC)
2	$1E	Status	Valid Multipaage, Start byte detected, DBCC is correct
3	$47	Data Field (1)	Identification data (LSB)
4	$C6	Data Field (2)	Identification data
5	$2D	Data Field (3)	Identification data
6	$00	Data Field (4)	Identification data
7	$00	Data Field (5)	Identification data
8	$00	Data Field (6)	Identification data
9	$00	Data Field (7)	Identification data
10	$00	Data Field (8)	Identification data (MSB)
11	$09	Data Field (9)	Read address specifying successful programming of page 2
12	$7B	BCC	BCC over previous bytes excluding Start Mark

© 2011 by Taylor and Francis Group, LLC

6.4 High-Frequency Interrogators: Texas Instruments

6.4.1 TIRIS Protocol for Series 6000 Reader System Interrogators

The Series 6000 Reader System interrogators are RFID interrogators operating in the HF band, manufactured by Texas Instruments. These interrogators use a RS232 line to communicate with the host computer. The data packet from the host to the interrogator is known as the *request*, while the data from the interrogator to the host are known as the *response*. All communication sequences are initiated by the host that is the primary station. Using this protocol, the host waits for the response before continuing, thus assuring that the host does not have to handle large sequences of open requests. This is a binary, byte-count-oriented protocol in which the data length is passed as a parameter in the message.

Table 6.9 shows the structure of the messages used by these interrogators for the request message (host to interrogator).

The contents of byte 5 (command flags) are used to control the actions of the interrogator. The meanings of the different bits in this byte are shown in Table 6.10.

The BCC, used to ensure the integrity of the message, is a 16-bit code calculated on all the bytes of the packet including the start mark. The BCC contains two parts: its least significant byte is a longitudinal redundancy check (LCR) calculated by performing a cumulative XOR operation on all the bytes of the packet. The most significant byte in the BCC is the one's complement of the LCR.

The structure of the message sent from the interrogator to the host (response) is shown in Table 6.11. Most of these bytes are similar to the bytes in the request message.

The data field in response messages is limited to a maximum of 23 bytes. The contents of byte 5 (command flags) are used to report on the actions of the interrogator. The meanings of the different bits in this byte are shown in Table 6.12.

The different error codes that the interrogator transmits to the host computer when bit 4 of the command flag byte is set to 1 are described in Table 6.13.

The contents of byte 5 (command flags) are used to control the actions of the interrogator. The meanings of the different bits in this byte are the same as for the request message shown in Table 6.10.

6.4.2 Host Protocol for Tag-it™ Series 6000 Reader System Interrogators

This protocol defines the communications between the Tag-it™ Series 6000 Reader System Interrogators and the host computer. It handles the communication between the host and the interrogator, and carries out the requests

© 2011 by Taylor and Francis Group, LLC

TABLE 6.9

Series 6000 Host-to-Interrogator Message Format

Byte	Content
0	Start of Frame[a]
1	Message length[b] - LSB
2	Message length - MSB
3	Node address[c] - LSB
4	Node address - MSB
5	Command flags[d]
6	Command[e]
7	Data[f]
8	Data
…	Data
N+6	Data
N+7	BCC[g]
N+8	BCC

[a] The first byte is the *start mark* that indicates the start of a message. This byte is equal to $01.

[b] The second and third bytes are the *message length* bytes that indicate the length of the whole packet, including the start mark.

[c] Bytes 3 and 4 constitute the *node address*. Its value is $0000.

[d] Byte 5 is the *command flags* byte. It controls the actions taken by the interrogator. The value of this byte is dependent on the command being transmitted.

[e] Byte 6 is the *command* byte. It specifies the actions that must be taken by the interrogator. The value of this byte is dependent on the command being transmitted.

[f] The following *N* bytes are the *data* bytes. These contain the parameters and the data for the command.

[g] The last two bytes are the *BCC* bytes used to ensure the integrity of the preceding message. BCC is performed on the previous bytes, including the start mark.

TABLE 6.10

Bit Functionality in Command Flag Byte (Request)

Bit	Description
0	Reserved for future use
1	Reserved for future use
2	Reserved for future use
3	Reserved for future use
4	1 = Command to be performed only on transponders with an address that matches the data section of the message
5	Reserved for future use
6	Reserved for future use
7	Reserved for future use

© 2011 by Taylor and Francis Group, LLC

TABLE 6.11

Series 6000 Interrogator-to-Host Message Format

Byte	Content
0	Start of Frame
1	Message length - LSB
2	Message length - MSB
3	Node address - LSB
4	Node address - MSB
5	Command flags
6	Command
7	Data
8	Data
…	Data
N+6	Data
N+7	BCC
N+8	BCC

TABLE 6.12

Bit Functionality in Command Flag Byte (Response)

Bit	Description
0	Reserved for future use
1	Reserved for future use
2	Reserved for future use
3	Reserved for future use
4	Error flag. 1 = command was unsuccessful. Data section of response packet contains the code of the error
5	Reserved for future use
6	Reserved for future use
7	Reserved for future use

TABLE 6.13

Error Codes

Code	Description
$01	Transponder not found
$02	Command not supported
$03	Packet BCC invalid
$04	Packet flags invalid for command
$05	General write failure
$06	Write failure because of locked blocks
$07	Transponder does not support command
$0F	Undefined error

© 2011 by Taylor and Francis Group, LLC

for commands as well as their responses. Additionally, the protocol manages some aspects of the functionality of the reader and enhances the functionality of basic transponders by requesting the execution of compounded commands. This protocol is intended for point-to-point, half-duplex communications in which the host is the primary station. In some situations, however, the host may receive responses without sending a request first. This is a binary, byte-count-oriented protocol in which the data length is passed as a parameter in the message. Similar to the TIRIS protocol, the message from the host to the interrogator is called a *request*, while the message from the interrogator to the host is called a *response*.

The communication between host and interrogator is performed using a frame structure. The frame structure is essentially the same for requests and responses with the exception of the flag as they have different meanings. Requests use control flags, while responses use status flags. In this protocol, the length of the message data is limited to 4091 bytes. Table 6.14 describes the structure of the request and response frames.

In *pass-through-service* mode, the interrogator passes the information that it has received from the host to the transponder immediately without doing any other action. When the interrogator receives a response from the transponder, it also passes it directly to the host without further action. If the interrogator does not receive a response from the transponder in a specified period of time, it sends a message to the host with the error flag set and the

TABLE 6.14

Structure of Request and Response Frames

	Description	
Byte	**Request Frame**	**Response Frame**
1	Start Code[a]	Start Code
2	Data Length[b]	Data Length
3	Data Length	Data Length
4	Service Code[c]	Service Code
5	Control Flag	Status Flag
6	Message Data	Message Data
…	Message Data	Message Data
N-1	Message Data	Message Data
N+6	BCC	BCC
N+7	BCC	BCC

[a] The first byte contains the *start code*. This is the start frame delimiter using the value $D5.

[b] The next block is the two *data length* bytes that specify the number of data bytes that follow that block. The minimum length is 4 bytes (the service code, control flag, and two BCC bytes), while the maximum length is limited to 4095 bytes.

[c] The *service code* indicates the type of command that is being sent, as shown in Table 6.15.

© 2011 by Taylor and Francis Group, LLC

TABLE 6.15

Service Codes

Code	Description
$01	Pass-through Service
$02	Single Service
$03	Compound Service
$04	Ancillary Service

appropriate error code. Using pass-through service, the host directly controls the transponder.

In *single-service* mode, after receiving a request from the host, the interrogator analyzes and verifies it before formatting and sending a single command to the transponder. Also, when the interrogator receives a response from the transponder, it analyzes it, verifies it, formats it, and sends a unique response to the host.

The *compound-service* mode is used by the host to instruct the interrogator to perform specific actions on transponders using the transponder protocol. The difference between these actions and the actions from a single-service request is that in compound service, the interrogator performs complex operations involving multiple commands before returning a response to the host computer. After receiving a compound-service request, the interrogator also analyzes and verifies it before sending the appropriate commands to the transponder. The interrogator also analyzes and verifies all the responses received from the transponder before sending a single response to the host. This response, however, may consist of more than one frame depending on its size. Compound service increases the performance of the system because, for example, it takes less time to send a single command to read four blocks of memory and transmit the information to the host, rather than issuing four different reading commands while transmitting the intermediate information to the host after each one has been performed.

Ancillary-service mode is used to instruct the interrogator to perform certain actions that do not involve communication with the transponder. Examples of such actions are interrogator reset, read interrogator version, and perform interrogator diagnostics. They are also used to upload new software versions in the interrogator or to set up new communication parameters.

Table 6.16 lists the available service codes with the exception of the pass-through-service codes as they are defined by the transponder protocol. The different transponder protocols are described in Chapter 7. The different commands are described in further detail in the next sections of this chapter. Table 6.16 can also be used to understand the type of commands available for each service code.

For control flags, four of the bits in byte 5 are used to specify instructions to the interrogator or they carry information about the message, as shown in Table 6.17.

© 2011 by Taylor and Francis Group, LLC

TABLE 6.16

Commands Available for Different Service Codes

		Service Code		
Command	**Command Code**	**Single**	**Compound**	**Ancillary**
Tag Version	$03	$02		
Read Block	$12	$02		
Read Multiblock	$02	$02	$03	
Read Block SID	$FE		$03	
Read Multiblock SID	$FD		$03	
Write Block	$05	$02		
Write and Lock Block	$07	$02		
Write Multiblock	$06	$02	$03	
Lock Block	$08	$02		
Lock Multiblock	$09	$02	$03	
Repeat Last Request	$01			$04
Send Last Request	$02			$04
Stop Continuous	$04			$04
Start Synch	$05			$04
Reader Reset	$10			$04
Reader Version	$11			$04
Reader Diagnostic	$12			$04
Read Reader Setup	$13			$04
Start Flash Loader	$16			$04
Factory Lock Block	$3D	$02		
Write SID Code	$3E	$02		
Factory Programming Off	$3F	$02		

The next byte, byte 5, is the *control flags* byte. This byte has a different meaning depending on the direction of the message. For Request Frames (host-to-interrogator), byte 5 is called the *control flag byte*. For response frames (interrogator-to-host), byte 5 is called the *status flag byte*.

For status flags, four of the bits in byte 5 are used to provide information about the result of the request, as shown in Table 6.18.

Bit 0 (exception flag) indicates whether the request was successfully routed to the interrogator. When bit 0 is reset to 0, it indicates that no exception occurred and the request was completed satisfactorily. When bit 0 is set to 1, it indicates that an exception occurred. In this case, the error code that describes the exception can be found in the first byte of the message. These errors are shown in Table 6.19.

Bit 1 (more flag) informs the interrogator whether more data follow (bit 1 = 1). Bit 2 (emulation flag) informs the interrogator whether the transponder completed the request using a compound command to emulate a complex command (bit 2 = 1). Bit 3 (auto-repeat flag) informs the interrogator where

© 2011 by Taylor and Francis Group, LLC

TABLE 6.17

Bits for Control Flags

Code	Description
0 (LSB)	Reserved
1[a]	More Flag
2[b]	Emulation Flag
3[c]	Auto Repeat Flag
4[d]	BCC Flag
5 to 7	Reserved

[a] When bit 1 (more flag) is set to 1, it indicates to the interrogator that it should expect more frames until the host sends a frame in which bit 1 is reset to 0. When bit 1 is reset to 0, it indicates to the interrogator that there are no more data associated with the request either in a single message or at the end of a series of messages.

[b] Bit 2 (emulation flag) indicates the interrogator if it is allowed to emulate a complex request by sending multiple single requests. This results in substituting a complex command with a compound command. When bit 2 is set to 1, this means that if the command cannot be performed using the current transponder version, the interrogator will attempt to use a compound command. When bit 2 is reset to 0, the substitution is not allowed.

[c] Bit 3 (auto-repeat flag) specifies whether or not the interrogator should automatically repeat the execution of the request. When Bit 3 is set to 1, auto-repeat is on. In this case, the interrogator will execute the request, send the response it has received from the transponder back to the interrogator, wait for a specified amount of time, and send the request again. This process is repeated until it receives another instruction with bit 3 reset to 0.

[d] Bit 4 is the BCC flag. It specifies the type of block code check used to ensure the integrity of the message. When bit 4 is reset to 0, the message uses CRC-CCIT, while when bit 4 is set to 1, the message uses LRC. Although LRC is simpler to implement and requires less processing time than CRC, it does not offer as much protection as CRC.

TABLE 6.18

Bits for Status Flags

Code	Description
0 (LSB)	Exception Flag
1	More Flag
2	Emulation Flag
3	Auto Repeat Flag
4	BCC Flag
5 to 7	Reserved

© 2011 by Taylor and Francis Group, LLC

TABLE 6.19

Error Messages Associated to Exception Flag

Code	Description
$00	Reserved
$01	Request data corrupted and not executed
$02	Application not supported
$03	Data format error and request aborted
$04	Continuous mode not available for this request
$05	Reserved
$06	Reserved
$07	Reserved
$08	Reserved
$09	Reserved
$0A	Reserved
$0B	Reserved
$0C	Reserved
$0D	Reserved
$0E	Reserved
$0F	Undefined error and request aborted

TABLE 6.20

Structure of Single Service Messages

Length	Description
5 bytes	Frame
1 byte	Command
1 byte	Format
1 byte	Synch
≤ 4088 bytes	Message Data
2 bytes	Frame

the transponder performed the request once (bit 3 = 0) or continuously (bit 3 = 1). Bit 4 (BCC flag) specifies the method used to generate the BCC byte: CRC (bit 4 = 0) or LRC (bit 4 = 1).

The next byte or set of bytes are the *message data* bytes that carry the actual message. The actual format of the message depends on the type of command that was specified in the service code byte. In pass-through-service messages, the interrogator is transparent to the request from the host to the transponder. The communication from the host to the transponder uses the transponder protocol. Because this is a bit-oriented protocol, it may be necessary to add the necessary bits to the message to ensure that the whole frame falls within a byte-oriented protocol. These are called *pad bits*. The structure for single-service messages is shown in Table 6.20.

© 2011 by Taylor and Francis Group, LLC

TABLE 6.21

Format Byte for a Request Message

Bit	Name	Description
0 (LSB)	Reserved	
1	Code Extension	0 = No extension code 1 = Code extension used
2	Addressing	0 = Not addressed 1 = Addressed. Address contained in first 4 bytes of data field
3	Format	0 = Fixed format 1 = Variable format
4	Transmitter control	0= Turn transmitter off after executing command 1 = Leave transmitter on
5	Reserved	
6	Reserved	
7 (MSB)	Reserved	

TABLE 6.22

Format Byte for a Response Message

Bit	Name	Description
0 (LSB)	Error	0 = No error 1 = Error occurred. Status code is first byte of data field after any address information
1	Code Extension	0 = No extension code 1 = Code extension used
2	Addressing	0 = Not addressed 1 = Addressed. Address contained in first 4 bytes of data field
3	Format	0 = Fixed format 1 = Variable format
4	Reserved	
5	Reserved	
6	Reserved	
7 (MSB)	Reserved	

The structure for single-service messages is shown in Table 6.20.

The format byte contains information about the format and status of the message. The contents are different depending on whether the message is a request or a response. Table 6.21 shows the description of the format byte for a request message, while Table 6.22 shows the description of the format byte for a response message.

Table 6.23 shows the meaning of the synchronization codes for both request and response messages.

The structure for compound messages is shown in Table 6.24.

Tables 6.25 and 6.26 show the structure of the format byte for request messages and response messages, respectively.

© 2011 by Taylor and Francis Group, LLC

TABLE 6.23

Synch Byte for a Request or for a Response Message

Bit	Name	Description
0–2	Synchronization type	000 = No synchronization 001 = Master Slave synchronization (Master) 010 = Master Slave synchronization (Slave) 011 = Cascaded synchronization
3	Action on "No Transponder"	0 = All responses sent to host 1 = "No transponder" responses not sent to host
4	Alternate Operation during continuous mode	0 = All valid data responses sent to host 1 = Identical responses sent to host only once
5	Reserved	
6	Reserved	
7	Reserved	

TABLE 6.24

Structure of Compound Messages

Length	Description
5 bytes	Frame
1 byte	Command
1 byte	Format
1 byte	Synch
≤ 4088 bytes	Message Data
2 bytes	Frame

TABLE 6.25

Format Byte for a Request Compound Message

Bit	Name	Description
0 (LSB)	Reserved	
1	Reserved	
2	Addressing	0 = Not addressed 1 = Addressed. Address contained in first 4 bytes of data field
3	Format	0 = Fixed format 1 = Variable format
4	Transmitter control	0= Turn transmitter off after executing command 1 = Leave transmitter on
5	Reserved	
6	Reserved	
7 (MSB)	Reserved	

© 2011 by Taylor and Francis Group, LLC

TABLE 6.26

Format Byte for a Response Compound Message

Bit	Name	Description
0 (LSB)	Error	0 = No error 1 = Error occurred. Status code is first byte of data field after any address information
1	Reserved	
2	Addressing	0 = Not addressed 1 = Addressed. Address contained in first 4 bytes of data field
3	Format	0 = Fixed format 1 = Variable format
4	Reserved	
5	Reserved	
6	Reserved	
7 (MSB)	Reserved	

TABLE 6.27

Structure of Ancillary Messages

Length	Description
5 bytes	Frame
1 byte	Command
≤ 4090 bytes	Message Data
2 bytes	Frame

Note: Because this type of command does not involve communication with the transponder, it does not require the format or sync bytes present in the other types of messages. The last two bytes contain the BCC code of either CRC or LRC. This is performed over all the preceding data with the exception of the start-of-frame byte.

The description of the synchronization bit is the same as for single messages that was shown in Table 6.23. The structure of ancillary messages is shown in Table 6.27.

The method of flow control demands for each request to receive a response. The flags in the response message indicate the presence of an error or other exceptions. After a certain time without receiving a response, the request can time out. The control is done by the host that acts as the primary station. Data lengths are variable for each message, although the maximum data length in a single message is 4091 bytes.

© 2011 by Taylor and Francis Group, LLC

7

The Air Communication Link

CONTENTS

7.1 Communication Protocols 178
7.1.1 Communication Protocols for Systems Operating in the LF and HF Ranges 178
7.1.2 Communication Protocols for Systems Operating in the UHF Range 181
7.2 The Communications Link 184
7.2.1 Elements of the Communications Link 184
7.2.2 Forward Link 186
7.2.3 Return Link 189
7.3 Transponder Operating Modes 191
7.3.1 Transponders Operating in the LF and HF Bands 191
7.3.2 Transponders Operating in the UHF Bands 193
7.4 Arbitration for Transponders 196
7.4.1 Principles of Arbitration 196
7.4.2 Principles of Anticollision 197
7.4.3 Deterministic Anticollision Procedures 199
7.4.4 Aloha-Based Anticollision Procedures 200

This chapter describes the communication methods used to transfer information from the interrogator to the transponder and from the transponder to the interrogator. The communication from interrogator to transponder is usually known as the *forward communications link*. This consists mostly of commands sent from the host computer to the transponder via the interrogator. It also contains the data to be written for those transponders whose memories can be rewritten. The communication from transponder to interrogator is known as the *return link* or the *backscattered communication*. This consists mostly of the transmission of the data stored in the transponder's memory.

While there are several standards that specify the critical elements of the communications protocol, the implementation of these standards especially varies not only among different manufacturers but also among different products from the same manufacturers. Therefore, this chapter does not pretend to be a comprehensive collection of all the air communication methods employed by RFID systems. Instead, this chapter explores the most common

© 2011 by Taylor and Francis Group, LLC

approaches to the communication between these elements of the RFID system using specific systems as general examples. This should give the readers the basic information while preparing them to search for more specific details if they so require.

This chapter starts by describing the different air communication protocols followed by the study of the elements that make up the forward and the return communications link. It continues by talking about the different modes of operation available to transponders. The last section in this chapter describes the different arbitration methods and the anticollision procedures that allow effective communication when there is more than a single transponder in the radiofrequency field.

7.1 Communication Protocols

7.1.1 Communication Protocols for Systems Operating in the LF and HF Ranges

The T5557 is a transponder with a 300-bit memory manufactured by Atmel® that operates in the low-frequency range and is similar to other transponders from different families of manufacturers. The communication between transponder and interrogators starts with the chip in the transponder being initialized after it has reached its threshold voltage. Afterward, the chip will be ready or will experience an additional delay of 67 ms depending on the status of one of its configuration bits. In read mode, the data from the memory are transmitted serially by modulating the load across the antenna terminals, starting with bit 1 from block 1. This process continues until the last bit from the specified number of blocks has been transmitted. The number of blocks to be read is defined by one of the bits in the transmitted command.

The transmission from the transponder to the interrogator uses amplitude-shift keying (ASK) modulation by switching a load connected to the antenna terminals on and off. Figure 7.1 shows the waveform across the load for different types of coding.

The transponder has the ability to insert a special pattern in order to synchronize the interrogator before transmitting the first block. This pattern consists of four bit periods in which the modulation is turned off and on, as shown in Figure 7.2.

In order to write data to the transponders, the interrogator uses on-off keying. It interrupts on and off the electromagnetic field generated as shown in Figure 7.3. The time between the gaps is used to encode the data to be transmitted: 24 periods of the RF field for a *0* and 54 periods of the RF field for a *1*. The process finishes after the transponder has detected that there is no gap

© 2011 by Taylor and Francis Group, LLC

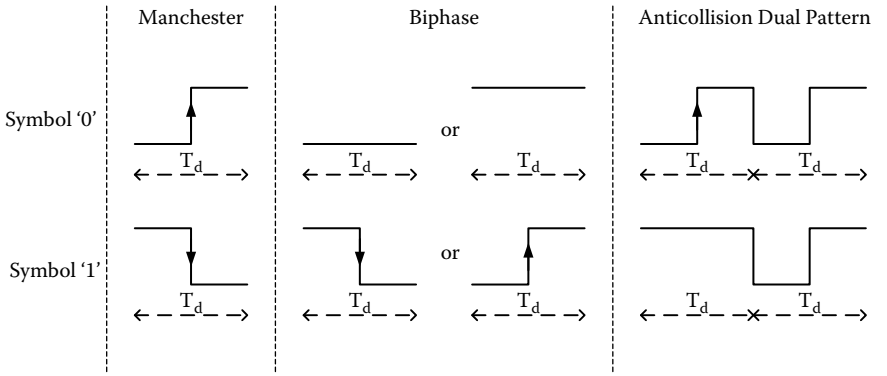

FIGURE 7.1
Waveforms across load for different types of coding.

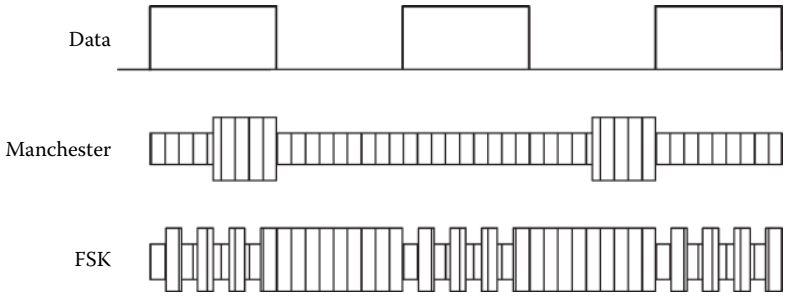

FIGURE 7.2
Synchronization patterns for Manchester and frequency-shift keying (FSK) modulations.

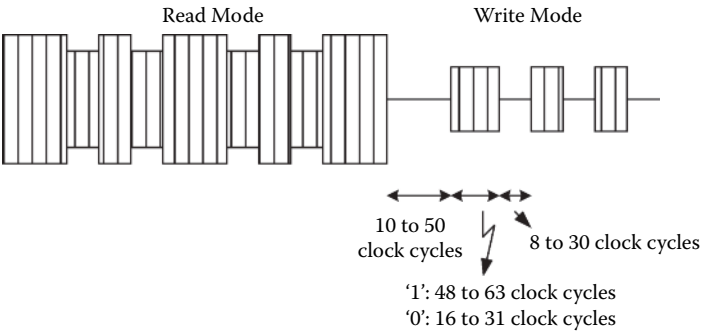

FIGURE 7.3
Gap sequences used in data transmission.

© 2011 by Taylor and Francis Group, LLC

for more than 64 periods. The initial gap triggers the communication from the interrogator to the transponder. This initial gap can be accepted at any time after the system has been initialized.

After the initial gap, the transponder expects to receive a valid command sequence. A standard write command needs the operation code, the lock bit, the 32 bits that make up the data, and the 3-bit address. Writing to a protected transponder requires the additional 32-bit password that is placed between the operation code and the data address bits. The password bits are compared bit by bit with the contents of the password stored in memory. If the bits do not match, the transponder returns to read mode. The complete writing process is shown in Figure 7.4.

After all the information has been correctly received, the transponder can be programmed. There is, however, a delay of one clock period between the end of the writing sequence and the start of the programming. The typical programming time is 5.6 ms, including the reading for data verification. Figure 7.5 displays the voltage measured across the antenna after programming a memory block.

For the Tag-it™ family of transponders manufactured by Texas Instruments, the communication between interrogator and transponder is done by amplitude modulation of the carrier. This allows the interrogator to generate enough energy to power the chips on board the transponders while simultaneously sending data. The encoding for the logic symbols *1* and *0* is done

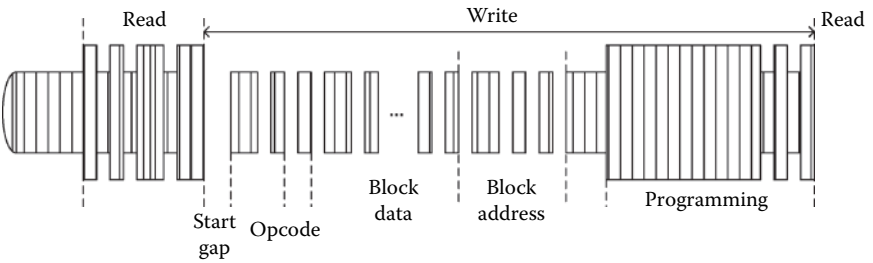

FIGURE 7.4
Writing sequence.

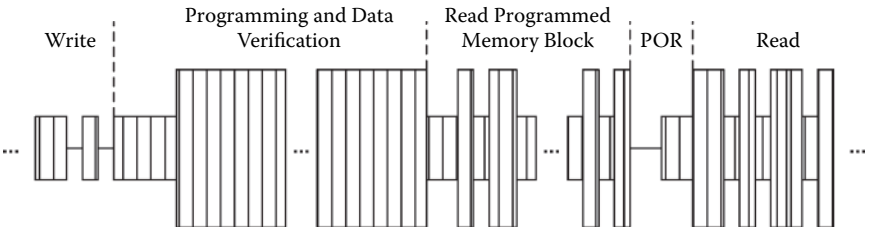

FIGURE 7.5
Voltage across antenna terminals after programming a block.

© 2011 by Taylor and Francis Group, LLC

by pulse width modulation: *1* is encoded as a power burst lasting 150 μs, while *0* is encoded by power bursts lasting 100 μs. Data are framed between a start-of-frame (SOF) signal and end-of-frame (EOF) signal. SOF consists of a 50 μs burst followed by a standard duration pulse, terminating with a 150 μs pulse. The EOF signal consists of a 50 μs burst followed by a standard duration pulse, terminating with a 100 μs pulse.

The communication between the transponder and the interrogator uses the modulation of the antenna as it tunes and detunes the signal to generate the backscattered information. The signals being transmitted are encoded using a Manchester code, taking advantage of the clock frequency being embedded in the transmitted signal. With the load modulation, a Manchester high level is represented by a frequency of 423.75 kHz, while a Manchester low level is represented by a frequency of 484.29 kHz.

7.1.2 Communication Protocols for Systems Operating in the UHF Range

Transponders operating in the UHF range manufactured by Atmel® are based on the *interrogator talks first* (ITF) approach to establish communication with the interrogator. The communication always starts with a forward message, that is, a message from the interrogator to the transponder. After receiving this initial message, the transponder responds by backscattering a message to the interrogator. This is known as the *return link*. This backscatter communication is done using a binary phase-shift keying (2PSK) modulation based on changing the imaginary part of the input impedance in the transponder as a function of the message between sent.

The communication is based on a system of frames, as shown in Figure 7.6. The first frame is the header frame that is used to adjust the timing. The second frame is the data frame that is used to transport the data. The length of this frame depends on the command sent and the addressing mechanism being used. The last frame is the end-of-transmission (EOT) frame that marks the end of the transmission. Once the transmission has finished, the interrogator enters into listening mode after having received another header frame.

While the interrogator is transmitting data, the transponder remains in listening mode. During the transmission of the interrogator header frame, it is possible for the transponder to operate in full duplex. It transmits data back to the interrogator in a loop until the EOF frame is sent.

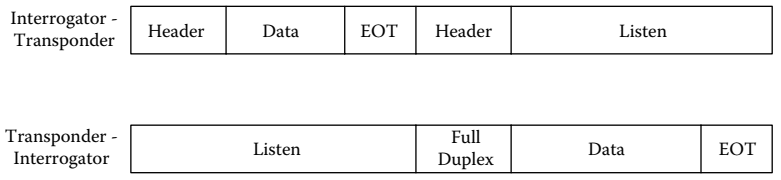

FIGURE 7.6
Frame communications during default transmissions.

© 2011 by Taylor and Francis Group, LLC

The communication between transponder and interrogator must be reliable even in the noisy environments in which these systems normally operate. To improve the reliability of the communication link, the interrogator transmits periodic clock ticks to the transponders, ensuring reliability because it helps to block other radiofrequency sources. In addition, the link between transponder and interrogator operates synchronously, and because the interrogator controls the speed and modulation ticks, the resulting transmission has a higher signal-to-noise ratio than an asynchronous communication.

The general structure of the frames is different between the forward or return link as well as the type of commands that it carries. All the frames start with a header frame. The data frame in the forward link depends on the type of command carried, as shown in Figure 7.7, which shows frames for different types of commands. Data frames contain the command and its cyclic redundancy check (CRC), data-setting parameters, address information, and data for programming. For example, short commands consist of 6 bits and its 2-bit CRC, while long commands consist at least of the command fame, the CRC, and the parameter field. In the transmission of a long command, these frames are followed by a CRC frame of 16 bits. The transmission ends with an end-of-transmission frame that is made of two EOF symbols.

Figure 7.8 shows the general structure for the return link frames. The communication link starts with a header frame that is used to obtain reference symbols, adjust modulation, and set the timing for the EOF characters. This is followed by a data frame, a CRC frame 16 bits long, and an

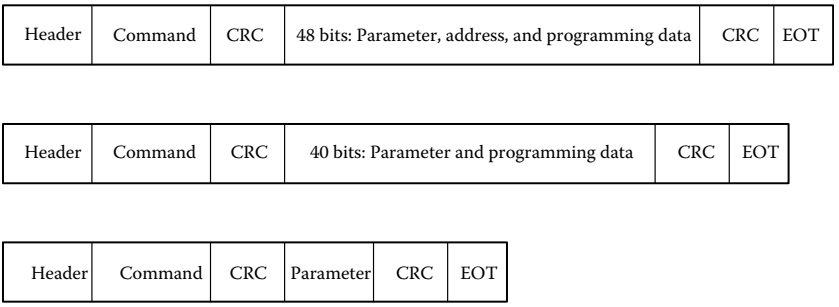

FIGURE 7.7
Examples of data frames in a forward link.

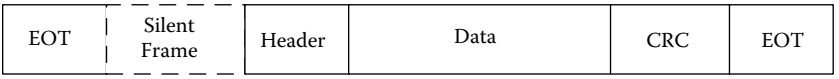

FIGURE 7.8
General structure for return link frames.

© 2011 by Taylor and Francis Group, LLC

end-of-transmission frame. The data frame can have a length of 8 or 16 bits depending on the type of data carried. The silent frame shown in Figure 7.8 is only used during programming. During the silent frame period, the interrogator only transmits a continuous wave. The length of this period depends on the strength of the electromagnetic field.

The general structure of the communications flow for these transponders is shown in Figure 7.9. The transponder is continuously waiting for a notch indicating the presence of the external field. After it has been received, it will check for a valid header frame that indicates the beginning of a transmission. After the header frame has been received correctly, the transponder performs several additional verifications while transmitting the different parts of the message, including checking for the anticollision requests. The process ends after receiving the EOF data.

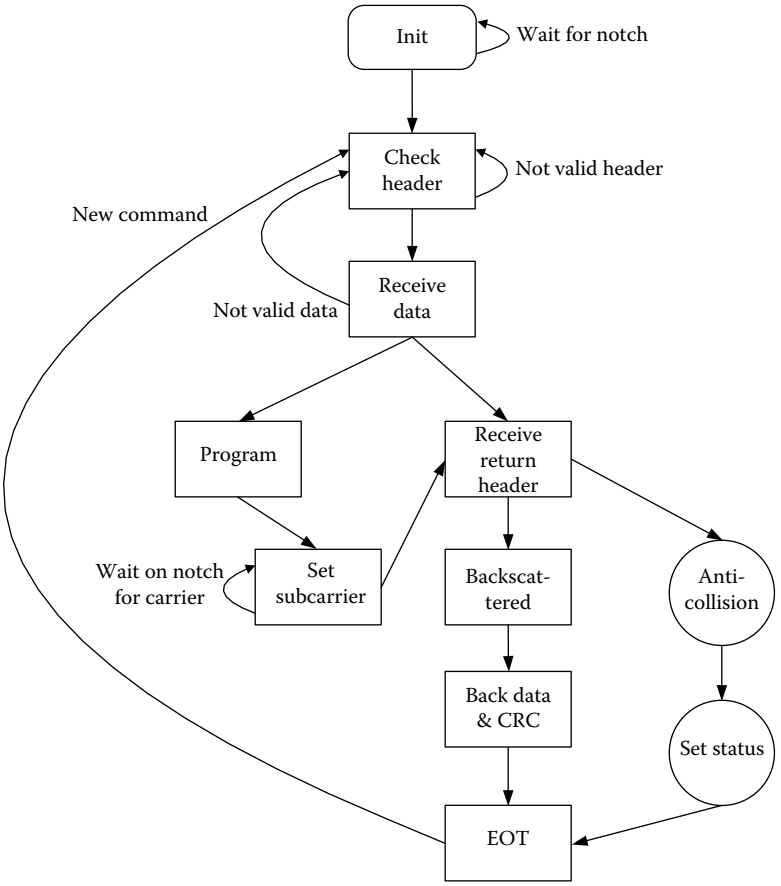

FIGURE 7.9
General structure of communications flow.

© 2011 by Taylor and Francis Group, LLC

7.2 The Communications Link

7.2.1 Elements of the Communications Link

Because the transponder is powered by the electromagnetic field generated by the interrogator, it must measure the strength of this field continuously. If the strength of the field decreases in such a way that causes the voltage after the rectifier to be lower than a certain threshold, the circuits in the transponder activate an internal reset. For voltages higher than this threshold, the oscillator and the rest of the circuits in the transponder circuit are enabled. Figure 7.10 shows the time events between the different signals involved after the transponder is turned on for some transponders manufactured by Atmel®.

The duration of the power on reset (POR) period depends on how fast the signal ramps up. This in turn depends on the strength of the electromagnetic field. After the POR has executed, there is an additional waiting period called the *band gap* that is needed for stabilization of the rest of the internal circuits before the signal to enable the oscillator switches its state. Finally, there is a delay of 64 clock cycles (approximately 160 μs) before the oscillator in the transponder achieves operational status.

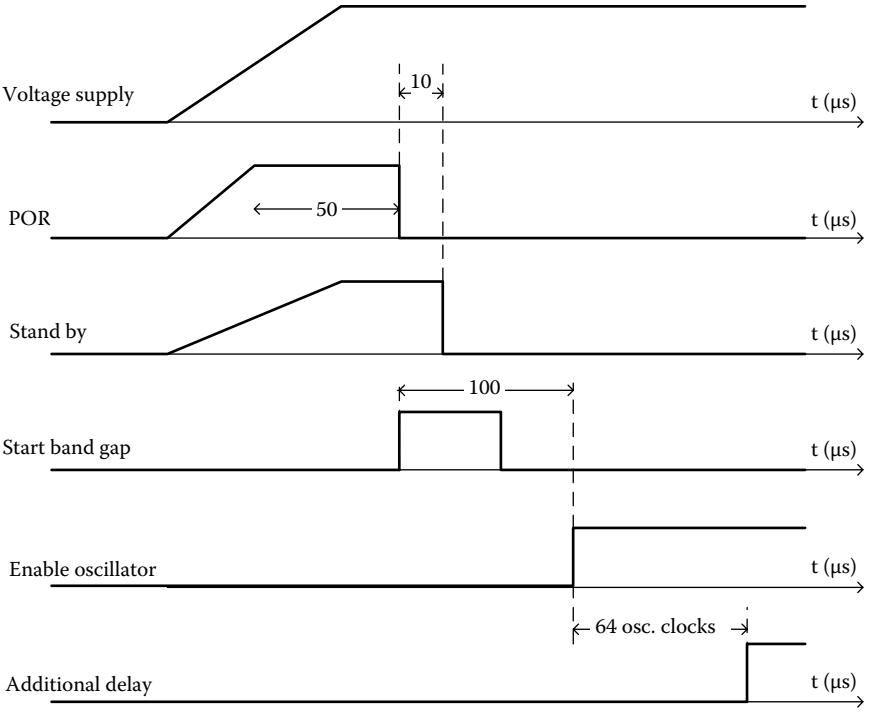

FIGURE 7.10
Chronogram of signals during power up.

© 2011 by Taylor and Francis Group, LLC

When the electromagnetic field decreases, the voltage after the internal rectifier also decreases. Once it reaches a certain threshold level, the oscillator stops. This results in lowering the current required by the circuit that in turn results in the voltage supply decreasing with a lower slope as shown in Figure 7.11. Finally, if the voltage decreases below another threshold, the circuit executes a reset. The difference between the two voltage levels allows for taking into account variations in the strength of the field without having to execute a reset.

The communication between transponder and interrogator normally happens in a noisy environment. Therefore, the designers of the system must ensure bit error rates as low as possible. This is achieved by using a combination of several techniques including generating notches in the system clock, making the return link synchronous to notch signals generated by the interrogator, using different coding techniques, and using CRC to protect the integrity of the data. CRCs for commands are 2 bits long, while CRCs for data are 16 bits long. Figure 7.12 shows the concept of notch timing, which results from generating notches at periodic intervals in the signal generated. For a typical value of signal level between 450 mV and 600 mV, T_1 lasts 4 µs and T_{notch} lasts 2 µs.

Other techniques include using *pulse interval encoding* to define the symbols *1* and *0*, whose timing and timing differences are controlled by the interrogator as an additional element to increase the robustness of the link. The fact that the return link is synchronous to the interrogator allows it to close the communication as soon as it detects a transmission error.

The communication from the interrogator to the transponder is known as the *forward link*, while the communication from the transponder back to the interrogator is known as the *return link*. The forward link carries the different type of commands to the transponder, while the return link carries the data from the transponder to the interrogator. These data will only be available for those commands that require the return of data. Because the

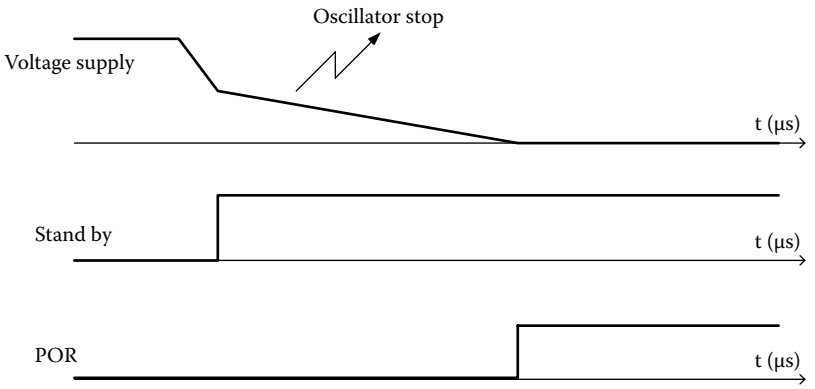

FIGURE 7.11
Chronogram of signals during power down.

© 2011 by Taylor and Francis Group, LLC

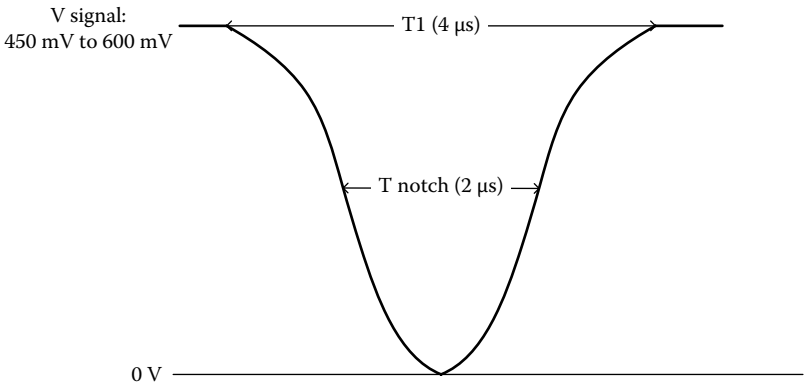

FIGURE 7.12
Notch timing chronogram.

handover mechanism from the forward to the return link happens synchronously, there is no need to wait for a cycle between them. Once the forward link sends its last frame that consists of an end-of-transmission message, the transponder is ready to transmit its return link header.

Texas Instruments RFID systems operating at low frequency use a frequency of 134.2 kHz to encode a low bit and a frequency of 123.2 kHz to encode a high bit. Because each bit uses 16 radiofrequency cycles to transmit, the duration of a low bit is different from the duration of a high bit. The low bit needs 119.9 µs to transmit, while a high bit needs 129.2 µs. The interrogator sends information to the transponder to transfer commands, addresses, or data. The writing process is always initiated by turning the radiofrequency transmitter on for a period of time of up to 50 ms. Afterward, the interrogator starts sending the bits that make up the command and associated data. Write bits last 2 ms. The differentiation between high and low bits is based on the duty cycle for each one of these bits. As shown in Figure 7.13, a high bit has a duty cycle approximately equal to 50%, while the low bit has a duty cycle approximately equal to 20%. The program phase consists of a continuous radiofrequency field for the duration of this period.

7.2.2 Forward Link

The forward header in most Atmel® transponders has four symbols, as shown in Figure 7.14. This header is accepted by the transponder if the length of the symbols *check1* and *EOF** is larger than the length of the symbol *0**.

Figure 7.15 shows that the information being transmitted is encoded in the timing between pulses. After the frame has been accepted and the

© 2011 by Taylor and Francis Group, LLC

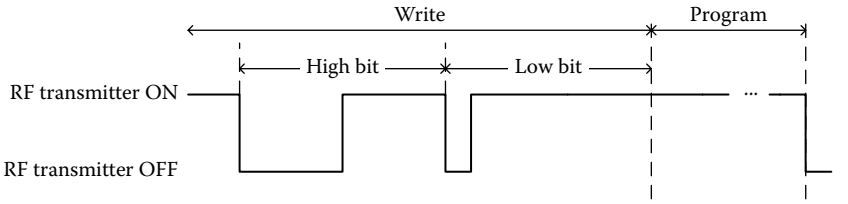

FIGURE 7.13
Write and program signals.

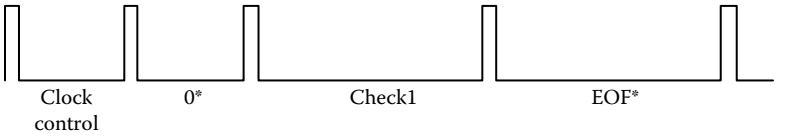

FIGURE 7.14
The four symbols in the forward header.

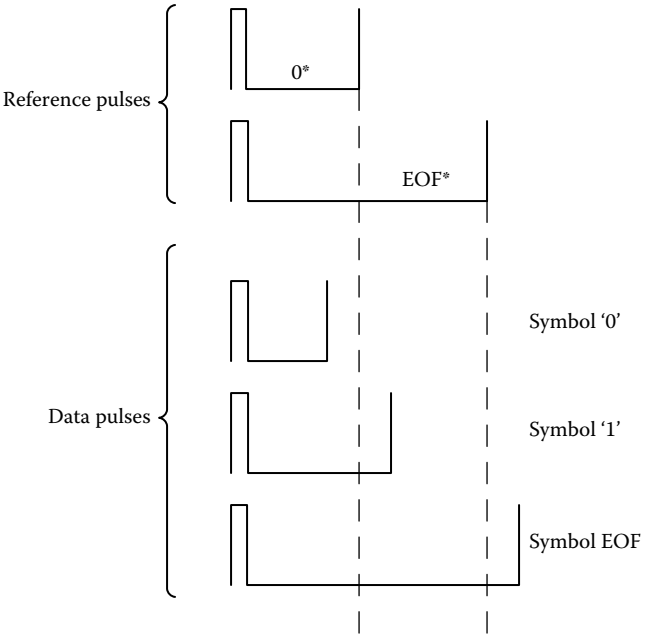

FIGURE 7.15
Pulse timing used to encode information.

© 2011 by Taylor and Francis Group, LLC

interrogator transmits data, the transponder measures the time between two pulses or notch signals. This is used by the transponder to decide whether the received symbol is a *0* or a *1* by comparing its length with the length of the symbols *0** and *EOF**, as shown in Figure 7.15.

This figure shows that a symbol will be interpreted as a *0* if its timing is shorter than the time that was sent in the Header for the symbol *0**. A symbol will be interpreted as a *1* if the time used by that symbol is longer than for the symbol *0** but shorter than the time used in the header for the symbol *EOF**. Finally, EOF will be interpreted for a symbol that lasts longer than the *EOF** symbol. This approach increases the reliability of the link as the transponder does not have to measure absolute but relative time intervals.

The communication from the interrogator to the transponder for the Series 2000 Texas Instruments RFID systems is based on transmitting bursts of energy of specific duration at specific intervals. For example, the commands used to read read-only or read/write transponders consist of an initial power burst lasting 50 ms followed by a period of 20 ms in which the radiofrequency field is turned off. In fact, all these transponders use the 50 ms power burst as the initial identifier for an upcoming command in addition to providing the energy to power the transponder. The following are some examples of formats for the different commands supported by these transponders. Figure 7.16 shows the protocol to transmit the command used to program a rewritable transponder.

The command starts with the 50 ms power burst followed by the specific command keyword and the password if necessary. These are followed by the 80 data bits used by this family of transponders and the 16 bits that make up the write frame. The last information being sent is the PBII, after which the transponder will read the new data stored in its memory to be verified by the interrogator. Figures 7.17 and 7.18 show the communication protocols for the commands *lock page* (of multipage transponders) and *selective read page* (of multipage transponders), respectively.

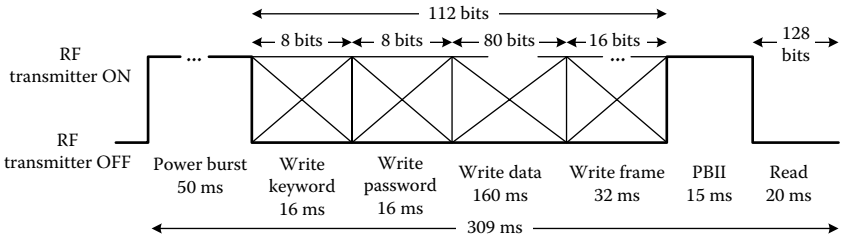

FIGURE 7.16
Protocol used to transmit a command to program a rewritable transponder.

© 2011 by Taylor and Francis Group, LLC

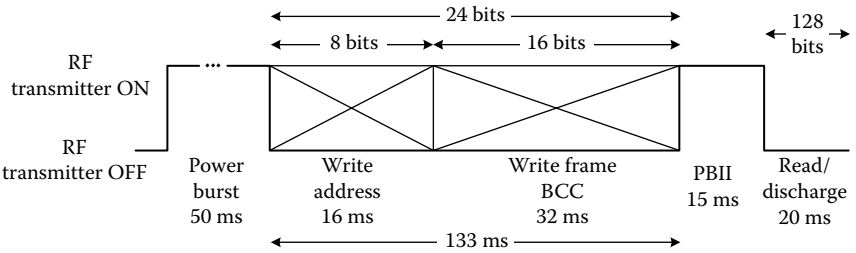

FIGURE 7.17
Protocol for the *lock page* command.

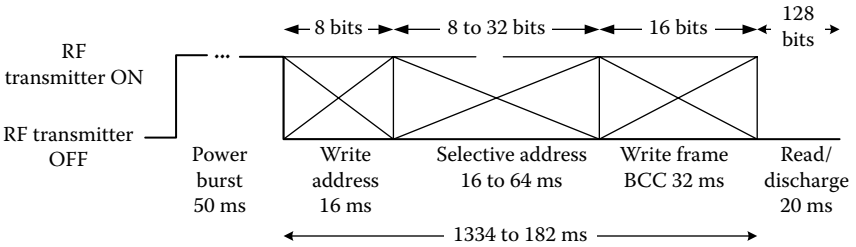

FIGURE 7.18
Protocol for the *selective read page* command.

7.2.3 Return Link

The return link in the majority of Atmel® transponders uses synchronous communication and angular modulation (binary PSK) in order to increase the signal-to-noise ratio and reduce the bit error rates because the return signals have extremely low power values. The synchronicity occurs as the transponder transmits its signal between two notches from the signal generated by the interrogator.

The return link starts with the return link header that is used to provide the timing information for the signal similar to the forward link header. Figure 7.19 shows the structure of the return link header for different types of coding styles used for the communication. In any case, the return link header always contains four symbols. The function and structure of each one of these symbols are shown in Table 7.1.

The return link header waits for a notch in the radiofrequency field generated by the interrogator before starting the generation of the reference timing. The data in the return link can be encoded using any of these coding techniques: bit stream (raw data), notch-locked non-return-to-zero-inverted (NRZI) encoding, soft-locked NRZI, FM0, and 3phase1. The EOT frame contains two EOF symbols.

© 2011 by Taylor and Francis Group, LLC

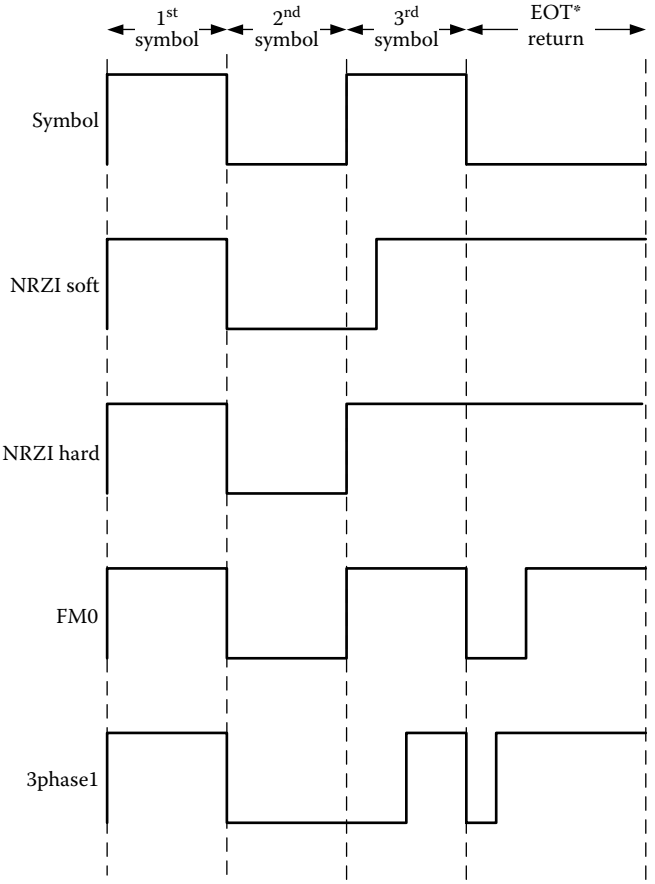

FIGURE 7.19
Structure of the return link header for different coding styles.

TABLE 7.1
Function of the Symbols in the Return Link Header

Symbol	Function	Additional Comments
1st	Main timing and power management	Used by interrogator to affect transmission rate of return link
2nd	Timing Reference	Used for anticollision control
3rd	Same timing as symbol 4	When using NIRZ, modulation is on
4th	Timing reference for EOF detection	

Figure 7.20 shows the transmission protocol used by the transponder to send information back to the interrogator as its response to a Read Data command for Texas Instruments transponders using their TIRIS protocol. All parts of this message are transmitted, with the least significant bit (LSB) being the first bit transmitted.

© 2011 by Taylor and Francis Group, LLC

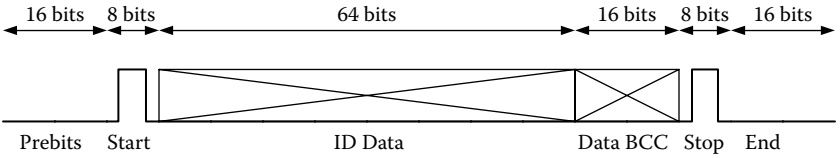

FIGURE 7.20
Transponder data sent back to the interrogator.

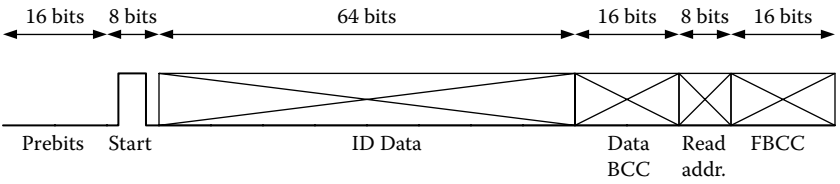

FIGURE 7.21
Return link for a multipage transponder.

After transmitting the pre-bits and eight bits that specify the start sequence, the transponder sends the 80 bits stored in its memory. The 64 first bits are the data bits, while the following 16 bits are the block check code (BCC) used to ensure the integrity of the data. These are followed by the stop and end bits. In order to be ready for a new activation, the transponder finishes the process by discharging its internal capacitor at the end of the transmission. The same protocol is used for rewritable transponders. Figure 7.21 shows the return link when accessing a multipage transponder.

In this case, following the BCC data, the transponder transmits the read address. This consists of a 2-bit status field that provides information about the function that that transponder has executed and a 6-bit page field that provides information about the page that was affected by the execution. The data format ends with reading the frame block check character (FBCC).

7.3 Transponder Operating Modes

7.3.1 Transponders Operating in the LF and HF Bands

After the transponders are initialized, they can enter into two different states, *interrogator talks first* (ITF) or *public mode* or *electronic surveillance*, depending on the status of their operating mode flags. In ITF mode, the data stream received through modulation from the interrogator

© 2011 by Taylor and Francis Group, LLC

undergoes different verifications. If they all result in a valid status, the transponder is synchronized with the data stream. At that point, the transponder is ready for communication. This communication always starts with a forward message, which is a message from the interrogator to the transponder. This communication method is used in multitransponder applications due to its anticollision capabilities. In this mode of operation, the transponder can be in any of the following states: *power down*, *ready*, *selected*, or *quiet*.

When the transponder is not able to harvest enough energy from the surrounding electromagnetic field to energize its internal chip, it enters power down state. The transponder can also enter the ready state after having received a reset command. The transponder enters the selected mode after having received an explicit command with its own serial number from the interrogator. It is possible to set several transponders into the ready state by sending a specific command containing a matching partial identification number. It is necessary to set a transponder into the selected mode before being able to access it. The quit state is entered after a selected state after the interrogator selects another transponder or receives a specific command to enter this state.

Public mode communications start with the SOF pattern, which is followed by continuously streaming the data from the user memory. As shown in Figure 7.22, the first bit being sent is bit 31 from data block 0. When the transponder reaches its final data block, it starts transmitting data block 0 again. This process terminates when the electromagnetic field that energizes the transponder is turned off or when the transponder receives the appropriate command from the interrogator.

Electronic surveillance mode is a particular operating mode in which the transponders are attached to specific retail articles. By programming all bits in block 0 of the user memory to *0*, the transponder is set to an *unpaid state*. After the article has been purchased, the cash register sets the bits of block 0 to *1*, thus entering the *paid state*. Additional security can be achieved by protecting the bits of block 0 with a write password. If a transponder in the *unpaid state* enters the electromagnetic field generated by the interrogator located at the doors of the store, it will modulate the field. Consequently, the presence of a transponder marked in the *unpaid state* will be detected by the

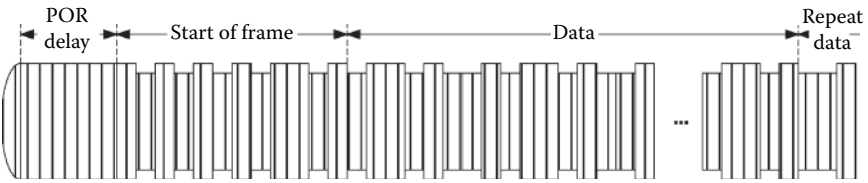

FIGURE 7.22
Initial sequence for the public mode.

© 2011 by Taylor and Francis Group, LLC

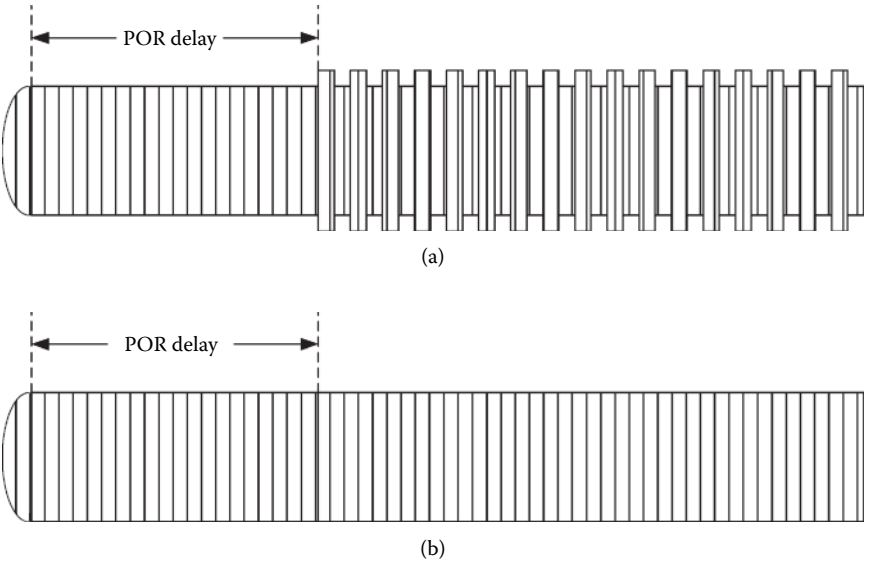

FIGURE 7.23
Signals from the transponder in electronic surveillance mode: (a) article unpaid, and (b) article paid.

interrogator, triggering the appropriate alarms. Conversely, a transponder marked as being in the *paid state* will not alter the electromagnetic field and will be transparent to the interrogator. Figure 7.23 shows the signals for these two cases.

Figure 7.24 shows the relationships between the different states for the transponders depending on their operational mode.

7.3.2 Transponders Operating in the UHF Bands

The possible states for the transponders manufactured by Atmel® operating in the UHF band are RF Field OFF, RF Field ON, Start, Mute, Observe, Ready, Active, and Isolated. These states and the paths between them are shown in Figure 7.25 and discussed here.

- The initial state is the *RF Field Off* state. Here, the transponder is not able to operate because there is no external radiofrequency field for which it can draw power. The transponder is able to store some configuration information for about 8 seconds after the field has ceased. After this time, the contents of these registers become undefined.
- When the transponder enters a region with an existing radiofrequency field whose magnitude allows the transponder to power

© 2011 by Taylor and Francis Group, LLC

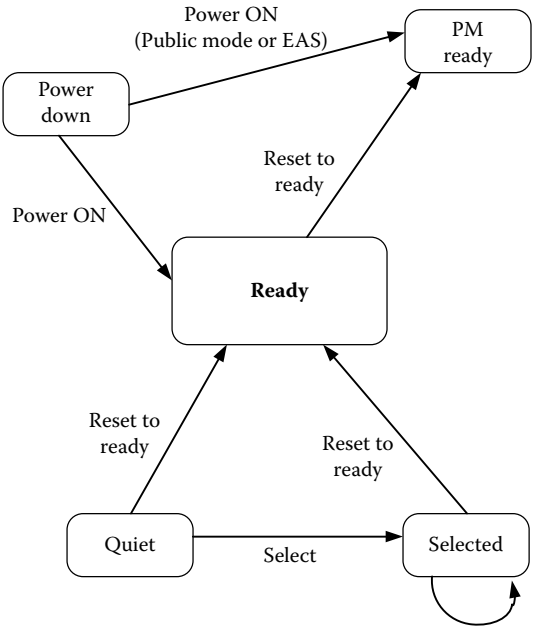

FIGURE 7.24
Different transponder states.

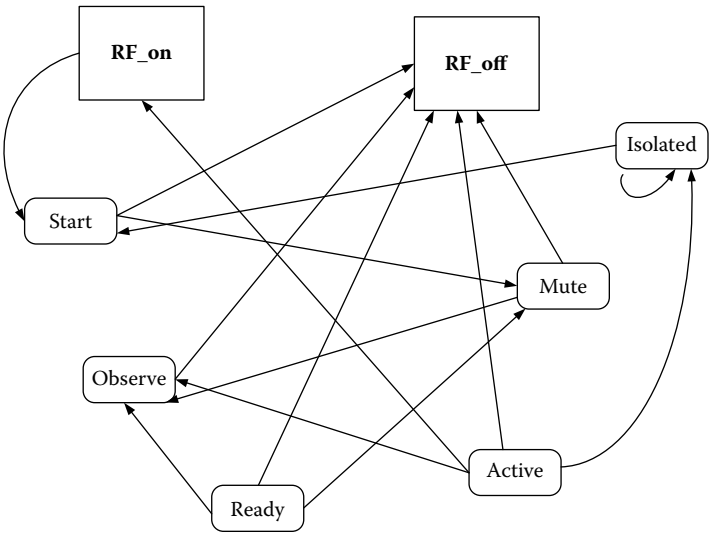

FIGURE 7.25
Operational states for UHF transponders.

© 2011 by Taylor and Francis Group, LLC

its internal circuitry, this generates a power on reset. This is the *RF Field On* state. After the POR has occurred, the internal oscillator in the transponder is switched on. It is important to note that for this process to occur, the frequency of the external radiofrequency field must match the resonant frequency of the transponder's antenna and associated circuitry. Once this process has finished, the transponder moves into the *Start* state.

- In the *Start* state, the transponder refreshes the contents of the status registers and reads their configuration from its memory, enabling or disabling its trigger function. After this process, the transponder is able to detect the modulation ticks that signify information being sent from the interrogator. From this state, the transponder can move to the *Mute* state or to the *Observe* state.
- In the *Mute* state, the transponder cannot respond to operations such as programming, arbitration, or backscattering data. The transponder leaves the *Mute* state after some of its internal configuration registers have been modified.
- The *Observe* state allows the transponder to become synchronous with the interrogator for performing operations such as programming. To become synchronous the transponder checks that the forward header received from the interrogator is valid, that the command received is within the list of known commands, and that its CRC is also valid. If all these checks are passed successfully, the transponder moves to the *Ready* state.
- During the *Ready* state, the transponder receives the parameters associated with the type of commands sent by the interrogator. If any of the parameters are false, the transponder enters the *Mute* state. Otherwise, the transponder enters the *Active* state.
- In the *Active* state, the transponder is able to execute the command sent by the interrogator after receiving and checking the rest of the forward frame. If there are any errors in the information sent after the header frame, the transponder moves into an *Isolated* state or *Mute* state depending on the type of errors received. If the information sent in the forward frame is correct, the transponder executes the command. Once the transponder has finished the execution it moves back into the *Ready* state. Figure 7.26 shows with more detail the processes that occur during the *Active* state.
- The first step in this process is to verify the length of the received stream. If this is correct, the transponder checks for the validity of the position of the end-of-transmission frame. Depending on the result of this check, the transponder knows if the anticollision procedure has been activated in order to select that specific transponder. If this is the case, the transponder will enter the appropriate

© 2011 by Taylor and Francis Group, LLC

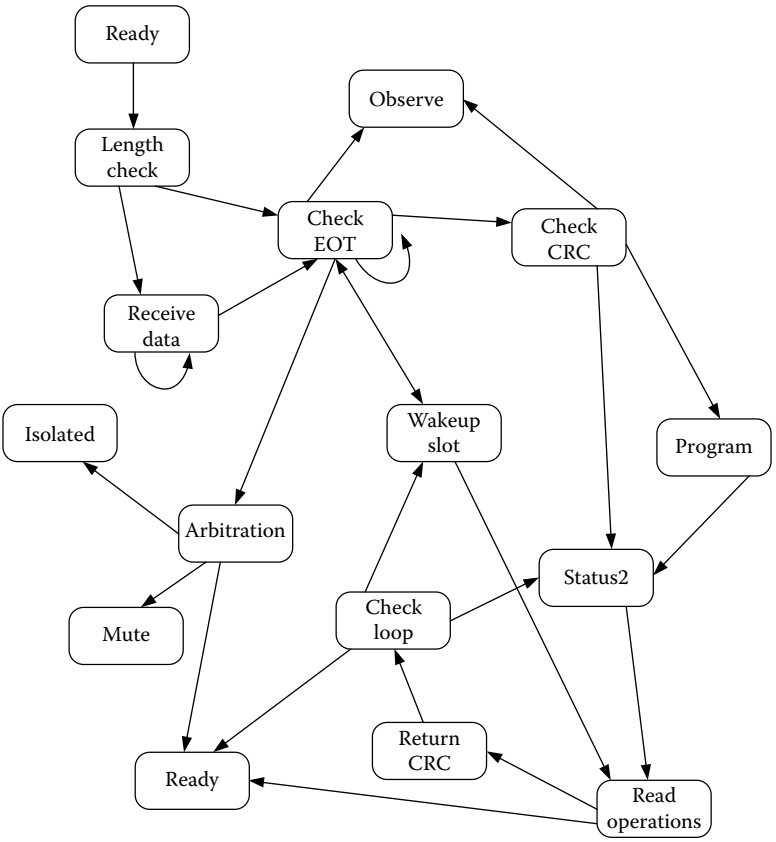

FIGURE 7.26
Processes during the active state of transponders.

anticollision and arbitration procedures. The transponder can also enter into receiving wakeup commands or other types of commands sent by the interrogator.

- In the *Isolated* state, the transponder is isolated and waits for either a POR or reset command to leave this state.

7.4 Arbitration for Transponders

7.4.1 Principles of Arbitration

When there is more than one transponder immersed in the electromagnetic field generated by an interrogator, it is necessary to develop and establish a

© 2011 by Taylor and Francis Group, LLC

procedure to select a single transponder or a specific group of transponders for carrying out specific functions. Alternatively, it can also be necessary to isolate a specific transponder or a group of transponders so they do not disturb communications. In some applications it may also be interesting to know whether there are transponders in the field or not. All these functions require the use of arbitration procedures. The two main types of arbitration procedures are *deterministic arbitration procedures* and time-slot based procedures, also known as *aloha procedures*.

Deterministic procedures are based on a *tree-walking function* in which the interrogator acting as the control node uses the individual IDs of transponders to select one or a group of them. The interrogator starts by polling all the transponders in the field. If there is more than one, their responses will collide and the interrogator will not receive the message. Therefore, in the next step, the interrogator polls only a specific subgroup of transponders based on their IDs. If the responses also collide, the interrogator reduces the population by polling only a specific subgroup from the previous subgroup. This process is repeated until the interrogator receives a response from a single transponder.

Aloha procedures are controlled by slot commands. After the transponders are turned on, they calculate random values for as long as they are powered. Once the transponder has received a slot command, it creates a random number from its generator, which points to a slot number in the chip. After receiving a start command, the transponders transmit their information to the reader during the first slop. If the random number matches the first slot number, it calculates a new one during this slot. When the random number matches the slot number controlled by the interrogator, that transponder becomes active. This allows the transponder to communicate with the interrogator. If the numbers do not match, the transponder enters a mute state and therefore does not respond to any commands. When the transponder receives a new slot command, it calculates if it is supposed to be active or mute.

7.4.2 Principles of Anticollision

The aim of anticollision procedures is to detect and identify the transponders that are present within the range of the electromagnetic field generated by the interrogator. While the implementation of specific anticollision procedures may vary between manufacturer and models, the principles of anticollision are common to all of them. For transponders manufactured by Atmel®, the communication with a single transponder or a group of transponders is controlled by the interrogator. The arbitration is initiated by the interrogator issuing a command for the transponders to transmit their identification numbers. The command can be tailored to the transponders that the interrogator expects to be in its area of influence. If the interrogator does not know anything about the transponders that are expected to be, the command is general and the detection encompasses all transponders. Otherwise,

© 2011 by Taylor and Francis Group, LLC

the command can use parameters such as a partial transponder identification number that will cause only transponders with partially matching IDs to respond to the command.

After the interrogator receives responses from the transponders, it scans their ID number from the most significant to the least significant bits. Each time slot corresponds to a specific bit position in the ID number. Because all transponders respond simultaneously with their modulated signal, their responses will be superimposed on one another. Therefore, because of the modulation being used, a damped signal overwrites a nondamped signal. With this, a logical *1* prevails over a logical *0*. Consequently, the transponders with these ID numbers are removed from the process. When the interrogator detects a logical *1*, it responds by broadcasting a gap in the radiofrequency field. The detection of a logical *0* does not originate any response from the interrogator. The gap in the field that is created as a response to the logical *0* is monitored by the transponders in the field and deduces, by comparing their ID number to the gap that was just broadcasted, if that specific transponder should continue in the current anticollision loop or eliminate itself from it. The transponders that are eliminated are muted and return to the ready state, in which they will remain until the interrogator initiates a new anticollision loop.

The transponders that have not been eliminated remain in the current loop as long as the final bit of the identification number has not been reached yet, and the process repeats itself. By the time the last bit has been interrogated, there will be a single transponder active as all the other transponders will have been eliminated through the previous steps. At this point, the interrogator is able to identify the associated ID for that specific transponder, and the transponder enters into the Selected state. Now, the transponder can establish direct communication with the interrogator and can be read or written. The transponder remains in the Selected state until the interrogator starts a new anticollision loop.

The MCRF450 family of transponders manufactured by Microchip Technology also supports anticollision. Their algorithm is based on time division multiplexing the transponder responses in which each transponder is only allowed to communicate with the interrogator during its time slot. This algorithm contains four control loops: Detection, Processing, Sleeping, and Reactivation.

The control of these loops is done by five commands as well as the transponder internal flag bits. The commands that control the anticollision loops are as follows:

- *Fast read request (FRR).* With an internal flag set, the transponder will respond only to an FRR command. An FFR command consists of five timed gap pulses, as shown in Figure 7.27, in which the period of the gap contains specific information. There are a total of nine possible pulse positions allowed in this protocol.

© 2011 by Taylor and Francis Group, LLC

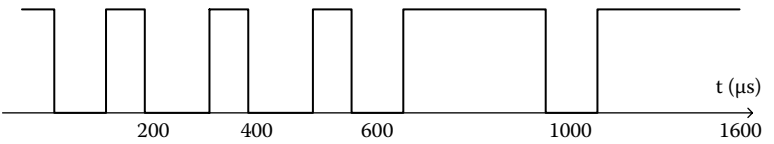

FIGURE 7.27
Structure of a fast read request (FRR).

- *Fast read bypass (FRB).* This command is used in the reactivation loop. Upon reception of this command, the transponder responds with a block of data. The structure of this command is similar to the FRR command, with the difference being in the period of the gaps.
- *Matching code 1 (MC1).* This command is used with the transponder and does not require any further processing. The command consists of time calibration pulses and pulse position modulation (PPM) signals. Upon the reception of this command, a transponder in the detection loops enters the sleeping loop.
- *Matching code 2 (MC2).* When a transponder in the detection loop receives this command, it enters the processing loop. The structure of this command is similar to that of MC1.
- *End process (EP).* This command causes a transponder in the processing loop to exit it and enter the sleeping loop.

Transponders can enter the detection loop by waiting for an FFR command or by transmitting a fast read (FR) response without waiting for a command. The first operation mode is called *interrogator talks first* (ITF), while the second operation mode is called *tag talks first* (TTF). The read and write operations are carried out during the processing loop. Only transponders with a special flag set in this loop respond to write or read operations. The sleeping loop is used to keep all processed devices in a silent condition in which they do not respond to external commands. The reactivation loop is used as an intermediate step by the interrogator to set transponders into different loops depending on the command that is transmitted to transponders in this loop.

7.4.3 Deterministic Anticollision Procedures

Deterministic anticollision procedures are based on the transponder backscattering the information to the interrogator only if the result of a compare condition is true. The compare condition is set up by the interrogator while broadcasting a specific command. Deterministic anticollision procedures are also called tree-based procedures. The interrogator sends a series of queries, each one with a prefix that is part of the transponder's ID code. Only those transponders with matching IDs respond to the interrogator's query. If there is more than one transponder with matching partial IDs, these transponders respond at the same time

© 2011 by Taylor and Francis Group, LLC

RF — Test and Measurement Homepage

Topics 1998 - 2005

- SWL Page
- RF Preamps
- QRPHB Software
- Popcorn DC Receiver Mainframe
- 40 M Popcorn Superhet Receiver
- Broadband Transformer Topics
- Diplexer Topics
- Ugly Construction
- Wee Willy 75 M DSB Transceiver
- W7ZOI JFET Biasing Tutorial
- EMRFD Review
- Tapped Cap Impedance Transformation
- More Active Antenna Experiments
- Fun with LEDs
- SWL Receiving Antenna Experiments

Topics 2006 - 2009

- Experiments with JFET Biasing
- TRF Receiver for WWV
- MF and HF SWL Receiving Antenna
- MF and HF Receive Antenna Splitter
- MF TRF Receiver
- Junk Box Low Pass NDB Filter
- More NDB Ideas and Circuits
- Low Pass Audio Filter Experiments
- TRF WWV Receiver for 5 MHz
- Complementary-Symmetry Amplifier Biasing Basics
- Low Power Audio Amp Experiments
- Two Bravo Receiver Experiments
- ICOM IC-7200 Review
- Electronic Hobbyist Circuits
- Output of a Diode Ring Mixer in an Oscilloscope

Topics 2010 - 2011

- Low Noise Crystal Oscillators
- Crystal Parameter Checker Supplement
- Hobbyist Circuits 2010
- RF Workbench Page 1
- RF Workbench Page 2
- AF Transistor Input Z Experiments
- RF Workbench Page 3
- Misc RF Experiments 2011
- Hobby and Fun 2011
- QRP Modules 2011
- Receiver Band-pass Filters
- RF Workbench Page 4
- VFO-2011
- VHF Butler Oscillator

Topics 2012 - 2014

- VHF to the Max !
- HF Ragbag
- RF Workbench Page 5
- VHF-FM
- Sundry Experiments 2012-13
- VHF - Veronica
- RF Workbench Page 6
- HF Embarcadero
- Caitlyn 310 : UHF Beginnings

Make it — then measure it!

RF — Test and Measurement

Frequently Asked Questions

1. How to you make your schematics?

I hand draw my schematics using the Paint Program that ships with all Microsoft Windows(tm) operating systems.

I strive to make schematics as clear and as small in file size as possible.The Windows Clipboard is used extensively to copy and paste the desired components from previous schematics to new schematics — very few new components are ever drawn; rather they are recycled from schematic to schematic. My system allows me to paste color 3-D labels and small photographic bitmaps into schematics.

The raw 24-bit bitmap drawings are compressed to 16-bit png files. Prior to May 17, 2010, bitmaps were compressed as 8-bit gif files. An example drafted circuit using the Windows 7 Paint program follows.

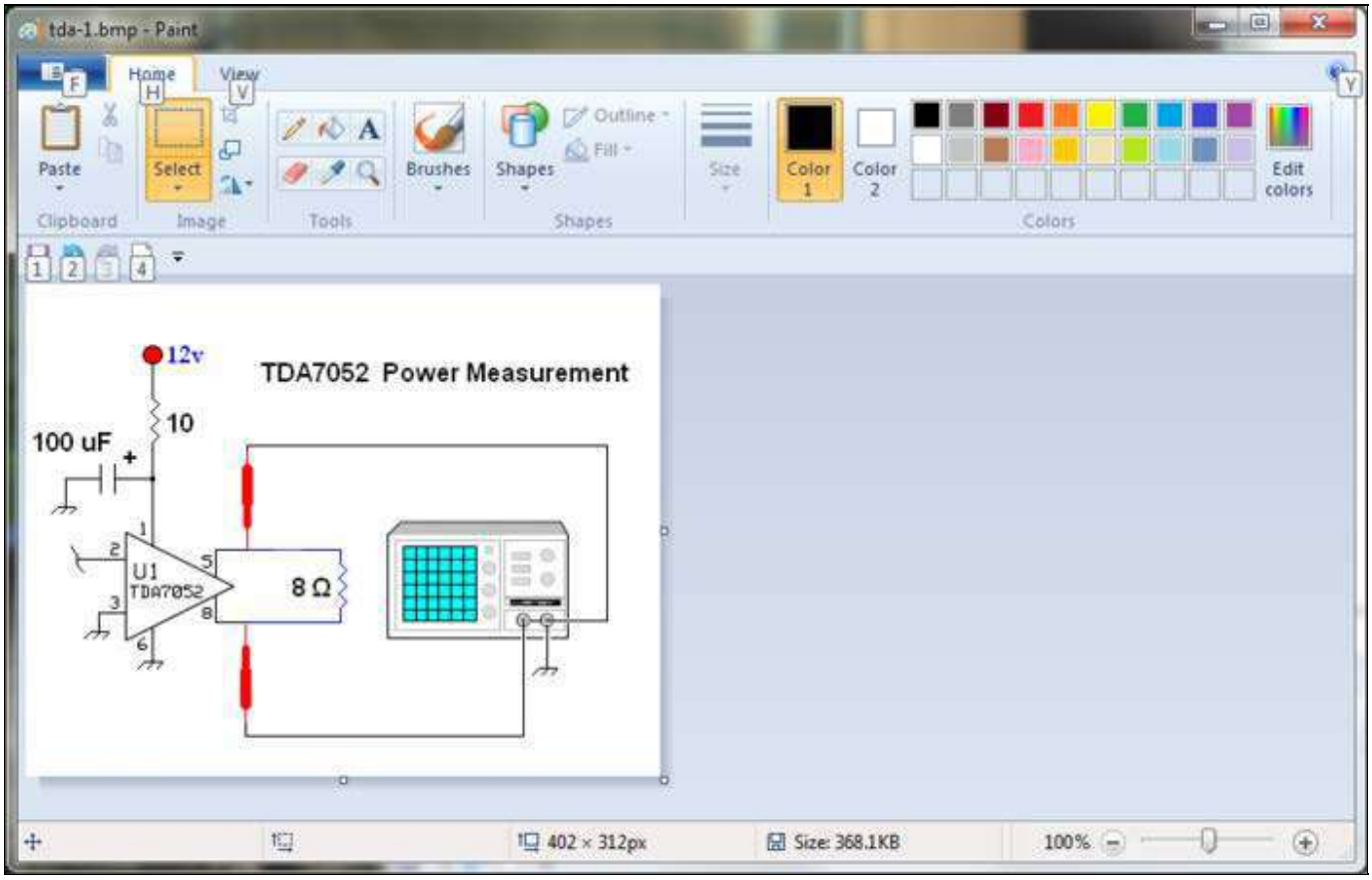

At least 25 people have sent or recommended software for making schematics. Thank you for this kind gesture, but I prefer my current method and after 15 years — make schematics quickly.

2. How come you don't supply parts lists? Other people do.

The answer is simple; lack of time. It takes considerable time and effort to put up a new web page and also to maintain a large web site. I save time by leaving the parts list up to the builder. In addition, this site is about experimentation and using what parts you have on hand.

3. Why didn't you answer my email?

I answer all legitimate emails as soon as possible. Our POP3 server gets an average of 2016 spam emails per month (December 2013 data), however, our software removes 99.27% of these and I never see them. Occasionally, legitimate emails are filtered in error and I apologize. I've received as many as 83 legitimate emails in a single day so can get behind. Please keep emailing — when readers stop emailing, I'll know the site has fallen totally obsolete [it may already be obsolete] and delete it.

Our mail server software logs and analyzes the network information of all spammers and may automatically filter and/or block their addresses or even their entire ISPs at the router level. Analysis indicates that 90% of our SPAM comes from just 3 countries and if you happen to live in one of these countries, the filtering will be especially sensitive.

This sounds dogmatic and unfriendly, however, until you've set up a domain and must handle ++ spam emails, endure and then develop router control software and other strategies to handle DDoS attacks and so forth, your completely naive about the 'dark side' of running a homebrew web server. Massive amounts of bandwidth might be otherwise wasted by allowing unwanted server use unless we actively counter these activities to keep the site running well for legitimate hobbyists. Not to mention all the wasted time. Further:

The 3 host web servers, the power, the server software, the security apps, the internet bandwidth etc.are owned or purchased by my family, and as you know, nothing is free. Despite many offers by companies to place ads on my pages, I've kept the site advertisment free and running pops.net costs us a few thousand dollars each year. We ask you to please respect our site for the sake of the experimenters who visit.

Pops.net server rack in our warehouse.

While I appreciate that some people might want to email invite me onto their social networks, I do not have time to participate. All email traffic from or involving social networks see this page for a list is deleted automatically by our POP3 server control software.

I **never** buy or sell parts via email, nor exchange hyperlinks. Never. I do give free parts to those in need though.

All email with the .info domain is blocked.

The number of people selling kits has jumped up by ~4 dB in the past 5 years. Increasingly, builders who need help with kits were emailing me for support. I rarely build kits and my knowledge regarding kit building is nearly 0. Please contact your kit seller for help.

You may wish to enquire with the kit seller about their online support polices and promptness prior to purchase. Additionally you might try the "support" email address provided and see if and how promptly they reply. Most of the popular kit sellers (AADE, Kits and Parts, etc.) provide excellent support to their customers. Like anything else online; buyer beware.

4. How come you didn't link to my web site - I linked to yours?

A big thanks to the folks who link to this web site! The QRP/SWL HomeBuilder site focus is content, not web links. Making a lot of links means spending time testing for and tracking down dead links - the so called "link rot". Time spent on the web site is time away from the electronics work bench. In addition, it is not logistically possible to reciprocate in kind, as hundreds of web sites and blogs have linked this site.

5. I see the word "popcorn" used a lot on this site- what's this all about?

Popcorn connotes the essential theme of the web site; simple, frugal, without fuss and over use of technical jargon, or complex math and engineering techniques. The QRP/SWL HomeBuilder web site is referred to as the popcorn site by many. The site targets hobbyists. The emphasis is fun. The hope is that it will attract new people to electronic design, measurement and experimentation. Hopefully, this site stimulates interest in QRP homebrew electronics.

Soon after I began building electronic circuits, my teachers and the popular electronic-related media of the day pushed me towards etched, printed circuit boards. I complied and this killed my passion for electronics. For me, habitually stuffing circuit boards lacks creativity and freedom.

Later, I discovered people were building guitar and bass amps using point to point wiring techniques with terminal strips and partial circuit boards. I became interested in building and repairing guitar amps and this passion continues today. In 1992, the discovery of 2 QST articles changed everything *for me (complete reference provided):* The Ugly Weekender: parts 1 and 2 by Roger Hayward, KA7EXM and Wes Hayward, W7ZOI; published in QST for August 1981 and June 1992. This was my first exposure to Ugly Construction and it was immediately adopted as the defacto standard bread boarding method in my electronics work shop. In fairness, etched circuit boards are a great tool, but not essential for the experimenter.
After working with Ugly Construction over time, considerable progress was made in understanding RF circuits and one output was the launch of this web site in 1998.

Currently, little has changed, I continue to prefer scratch-homebrew rather than kit-homebrew electronics. My interest in Short Wave radio and analog electronics has grown considerably. For me, electronic circuits hold a certain mystique which arouses my curiosity to learn, enjoy and share. As a lay person, this web site has facilitated meeting some awesome people through email from all continents and it has been a privilege to learn from them, my mentors, book and web authors and often enough; from my mistakes.

5. What do you mean by a 5K1 or 3K3 resistor value?

For E24 or 5% tolerance resistors 5K1 = 5.1K, 3K3 = 3.3K and so on. For E96 or 1% resistors 31.6K is written as 31.6K. All resistors are 1/4 watt unless otherwise specified.

6. How do you measure audio amp output power?

Please see Figure 4 on this web page. Any amp when cranked, outputs much greater power than when it is providing a clean sine wave. The quoted power for any audio power amp on this web site is the maximum average power it will give before the pure sine wave becomes distorted.

7. I noticed a new web page appears and then it is edited for 1-2 weeks. When is the web page completed?

When a new web page is added, it takes a week or so to find and change some of the grammar and spelling errors. Sometimes new ideas or feedback will cause me to further edit a web page at any point in time. This whole web site is a work in progress. The last date any given web page was edited is posted on the bottom of the web page.

8. Do you buy or sell stuff?

No and no. I receive numerous emails from people asking me to sell them stuff. I do not sell anything - no parts, books, coffee cups, ball caps, tee-shirts, ad space — nothing. I do not buy parts in commercial-quantity volumes and have no need to make contracts for obtaining any electronic components. Every week, Asian companies email to ask about buying their parts — please note, my answer is *always* the same: no thank you.

9. Questions and concerns about printing and printability

Each year, a few readers email to complain how poorly the web pages print. This is true and I apologize.

Some people prefer pdf files for easy printing. I have resisted going to pdf format for 3 main reasons:

1. The web site audience is international and many are using web translators. PDF files are 8-bit graphic image files and do not translate.
2. More and more readers are using mobile computer devices and pdf files are a pain for them.
3. We should all print less often to save resources

As an experimenter, I dislike crammed, small-size schematics and feel they should be drawn for *maximum* clarity. Therefore, my schematics tend to have a lot of white space and color contrast. I try to make them no wider than 700 pixels, although sometimes it's impossible to do this. Big schematics are *not* printer friendly. The only practical solution is to click on and open them in a separate browser window for easier sizing and printing.

I also feature big photos which burn up a lot of printer paper. Project photos are important to me; they provide a more intimate glimpse into the bench work and promote the real purpose of the site — building stuff.

A potential printing solution for Microsoft Explorer 8 users; Click

10. I have noticed in your CMOS logic photographs, you don't always ground unused input gates. Isn't this bad?

Proper CMOS logic practice mandates the grounding of all unused input gates. In prototypes and experiments, I don't always do this as I generally want to re-use the IC in other experiments. This is a cost saving measure. When you build a lot of stuff, it can get expensive and recycling parts makes sense. In keeper circuits or critical prototypes, unused input gates are directly soldered to the copper clad board. This also anchors the IC very well.

11. What is the proper URL of the home page?

http://www.qrp.pops.net

The following pre-2006 URL was decommissioned August 6, 2010: http://www.qrp.pops.net/default.htm

12. What are the QRPHB Design Centers and Professor Ivanenko character about?

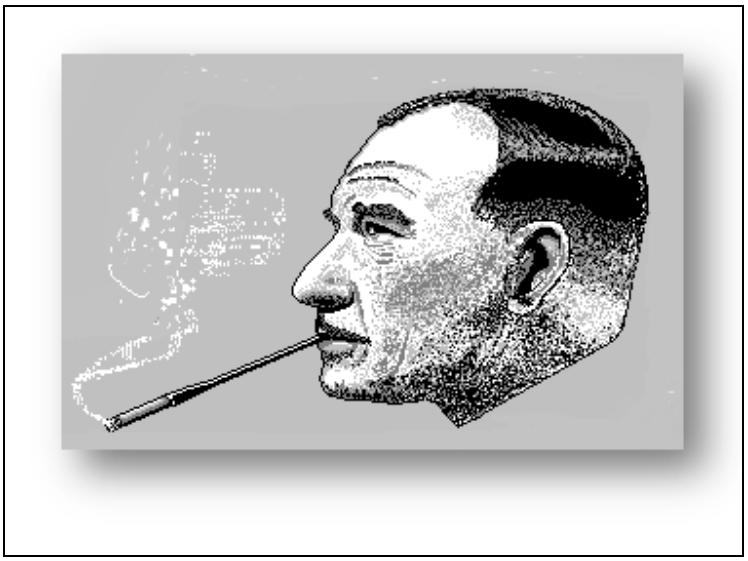

This web site is about design and not just providing circuits to copy; I'm hopeful that the QRPHB Design Center concept initiated in 2011 will invigorate the site. Design Centers are the presentation of simple, but useful algorithms for amateur builders to advance their skills on the bench.

Professor Vasily Ivanenko ( ), a *fictitious* retired Russian physics professor wants to share his knowledge and give back to society. He signifies each Design Center. Professor Ivanenko was drawn for me by Rod Adams in 1996 using the Paint program that ships with Windows (the same app I make my schematics with). Rod did all of the other original bitmap art for this website including the coil guy and junk box pictures. This character was inspired by one of my favorite photographers: Irving Penn — this photograph, which is all over the web.

A new character; Dr. Natasha Petrovna appeared in late Summer 2012.

The professors are just a good bit of fun — add intrigue, characters on whom to focus and a means of identifying Design Centers. Electronics with just math and physics bores us all. Adding splash, color, clear photographs and characters such as the coil guy or the Professors boosts the site's appeal and provides a creative outlet for me.

13. Why did you kill your blog?

Time mostly. *My* blog wasted *yours* and my time. I carefully analyzed my personal yield from blogs in 2012 to 2013 — for the most part, blogs just entertain + share trivia, or rehash someone elses idea(s), or 'innocently' attract you in hope to sell stuff — and sometimes, just fulfill the author's need for attention. I don't seek, nor have time for entertainment or spectacle within my RF hobby and I certainly don't wish to waste *your* time. Each to his own, I suppose.

My analysis showed that unfortunately, blogs rarely boosted my understanding of electronic design or measurement practices. My ardent focus is to learn + improve and then pay some of this knowledge forward on a web site. Of course, everything in context — many exceptional people blog. For example, Dave AA7EE, or Jason, NT7S.

Most of the RF design and measurement people I follow keep old fashion web sites and provide generous email support. Design and measurement web sites, plus reputable and/or peer-reviewed industry and hobbist books, journals and multimedia work best for me.

Further, great elmers don't just publicly hang-out on blogs, or web server groups, or publish Utube videos — some just check their emails and when asked — give wonderful support without fanfare. Hats off to these humble folks. Thank you!

14. What oscilloscope should I buy?

Yikes — a tough question I get nearly every month. Please do your research. My best answer is buy the best 'scope you can afford. Are you a casual experimenter, or sit in your lab a lot? I prefer DSO's , however, made due with a old boat- anchor CRT for my first 10 years. The Rigol 1052/1152 seem popular entry-level choices due to their cost versus performance ratio. On the other hand, view this video to see how much Rigol DSO technology has changed.

I owned and sold my 1052 to a builder in Michigan — a worthy choice like many other 'scopes. IMHO, the FFT and math functions on the 1052 and 1152 suffer due to low memory depth and clock jitter.

Even if you only work at HF, a bandwidth 5X higher than your main frequencies of interest works better for showing harmonics. Again, I advise people to simply buy the best 'scope they can afford since it will form the heart of your test bench.

15. I'm a beginner — what toroids should I buy?

Opinions will vary, but here's what I recommend. Buy any quantity you wish, but sometimes minimum quantities apply and shipping to some countries costs dearly, so I tend to order enough parts to last me for awhile.

A basic HF toroid starter kit might look like:

Quantity	Part#	Type
10-25	FT37-43	ferrite
10-25	T50-6	powdered iron

Above that, perhaps add these toroids.....

10-25	T68-6	powdered iron
10-25	T37-2	powdered iron
10-25	T50-2	powdered iron
10-25	FT50-61	ferrite

That's about it -- These will build most things RF on a HF beginner bench

QRP — Log: Updates To Permanent Content

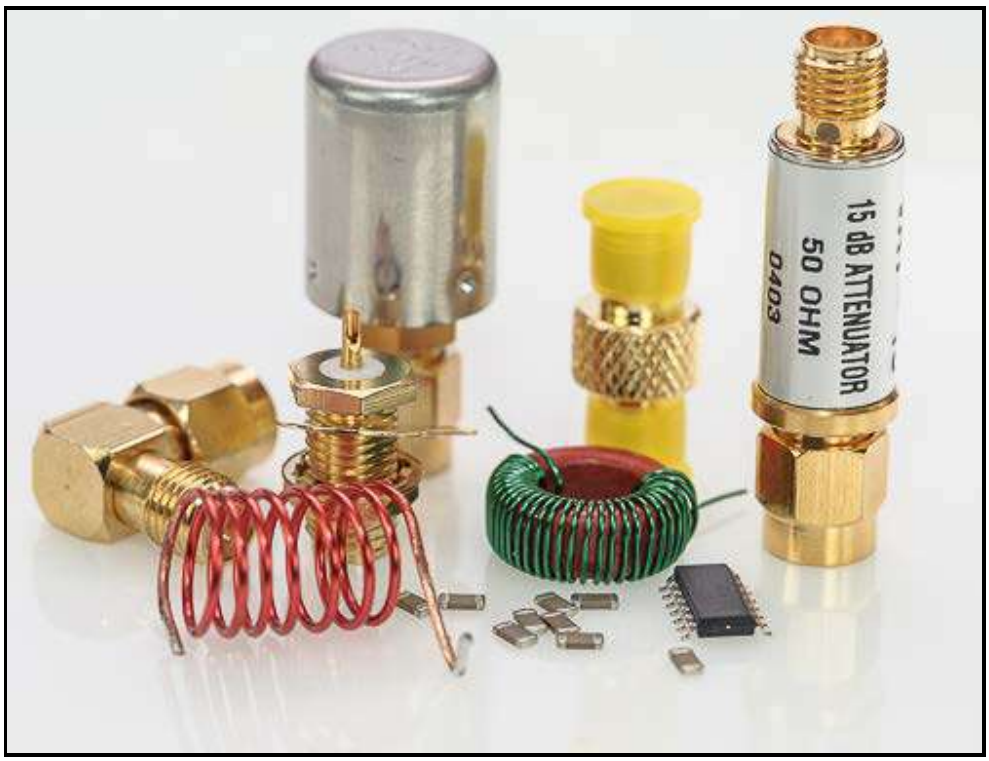

Oct 5, 2014 --- The end of QRPHB? Expect the Qrp site to go down each day for 1-4 hours. As I wrote before, we're losing an average of 10% of the outgoing packets and this peaks as high as 40% when many people are accessing the site. See an example graph below.

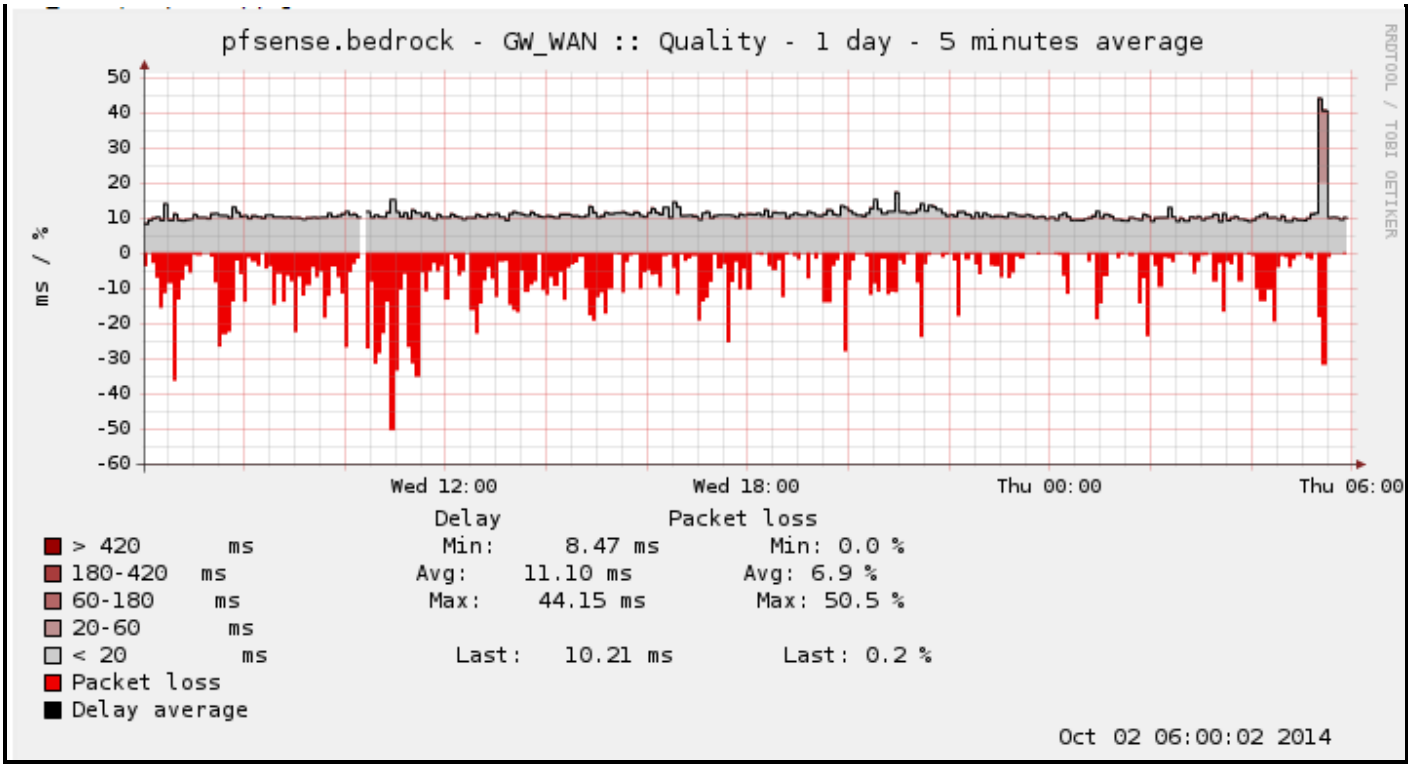

On Oct 2, 1 of our ISP's techs came and tested our WAN -- "it's better than most" he said. Hopefully they can do something to boost the performance on their side. Wave bought out all the local competition and we're stuck with them [this is happening everywhere]. Click for 1 of the many links writing about the emerging internet cable company monopoly.

You'd think that in 2014 we could properly host a web site like we've done since 1998? To boot, Stuart is paying for a high bandwidth business account and getting less than 1% of the promised bandwidth. We chatted today and will wait patiently for Wave to improve our outflow - but only for so long.

If Wave can't or won't boost performance, I am leaning towards taking this web site down as opposed to moving it -- it's been a good run. QRPHB creates a lot of work and I could get way more done without the web site hassles. So, 2014 might be it for me. If so, thanks for coming here all these years and best of luck with your experiments!

--- Sep. 19 --- Wave Broadband, our Internet provider suffered major problems recently and I shut the site down for 4 days rather than have it limp along pathetically. Well the Wave saga *continues*: the site loads slowly and pictures are missing etc.

Our email server remains working even when the main site is down. You can always email me if the site is not working for you -- or if you have a comment or question.

Vistor volume rose this Summer so we added a better router that provides bit by bit data performance collection and new features to help throughput. At minimum user bandwidth, a unique visitor hits the site every ~0.7 minutes. I'll start formal bench experiments on October 3 --- to kick off the sites' 16th season.

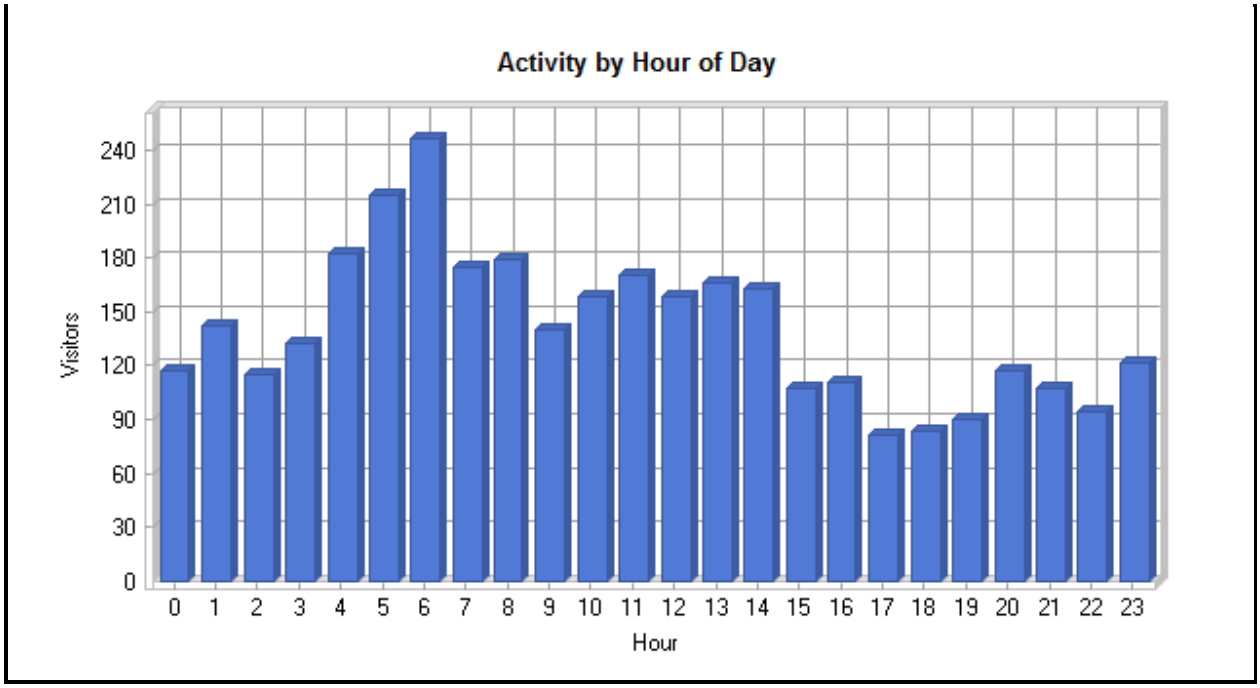

August 31, 2014 — Kit to upgrade my HP frequency counter to 3 GHz added as Section 5 on Caitlyn 310 — UHF Beginnings.

August 18, 2014 — QRP-POS Data on the Sundry Web Page. Look at the end of Section 8: Popcorn AF Amps For Receivers — Reprise. This new, all-discrete AF stage will go into the Funster Line receiver and ranks as 1 of my best in terms of power and headroom.

August 12, 2014 — Funster Line: a QRP 40M band CW trans-receiver added to HF Embarcadero web page as Menu item 4. Click here for Funster. Only the transmitter is presented for now.

June 18, 2014 — I tweaked the page now called About... on the top level menu. Also, on this web page, I added a new essay for 2014 just under the essay for 2010. I'm off the bench until Fall, but hope to add a little content on rainy days or such. I'm about 2 years behind in presenting some of my experiments.

May 22 and 26, 2014 — New Supplemental Web Page for VHF-FM launched. This page and another supplement will house some new receivers over time. The new supplement is linked on the original VHF-FM web page in section number 4.

May 5, 2014 — Section 7: NE612 Mixer Diddy added to VHF Veronica

April 14, 2014 — Completion of Return Loss Bridge Experiments [added Bridge #4] on Caitlyn 310.

April 7, 2014 — Return loss and VCO experiments added to Caitlyn 310.

March 7, 2014 — Section 3 added to VHF-FM. A DC Converter for VCOs. **March 25** QRP-POSDATA for March 2014 Poor Hams Scalar Network Analyzer (PHSNA) added to Section 1 of Sundry.

February 14, 2014 — Caitlyn 310 — New repository web page for my venture into UHF. Click. Surprisingly, the site averages ~ 3000 unique visitors every 24 hours. Click for the Feb 25 tally

January 15, 2014 — The FAQ was often missed and therefore moved to the top level menu + editted/augmented.

January 4, 2014 — A follow-on version of the K3NHI QEX power meter added to RF Workbench 5 as section 6.

December 15, 2013 — I added Section 3 to HF Embarcadero. VXO and VCXO Notes. I significantly updated the VFO-2011 web page on Dec 17, 2013.

November 7, 2013 — Section 6 added to VHF — Véronique. 1 photo added to the end of the Ugly Construction page. Severe Fall weather

conditions took down the server for ~1 hour today.

November 1, 2013 — I added Section 2 to HF Embarcadero. A vestigal set of notes regarding my attempts to update the Popcorn Superhet receiver.

October 31, 2013 — Section 5 added to VHF — Véronique.

October 27, 2013 — VHF-FM re-formatted and Section 2 added. I imagine this page will disinterest many.

October 18, 2013 — 3 rarely accessed web pages removed from drop down menu, but not deleted from the server. New QRP-Posdata added to HF-Ragbag (near the end). Section 3 edited and Section 4 added to VHF — Véronique.

October 11, 2013 — Build Season 15 begins [I bench experiment Oct to May]. I added HF Embarcadero to hold all my HF and perhaps AF experiments this season. I'll also add content to VHF FM, VHF — Véronique and RF Workbench 6 over the next 12 months. Thanks.

September 9, 2013 — Blog deleted.

August 8, 2013 — Section 2 of RF Workbench 6 added. Measuring PA collector V and I to calculate efficiency. On August 16 — I added a new essay on the Ugly Construction page called Is Ugly Construction Less Reproducible than Manhattan?

June 25, 2013 — I started RF Workbench 6. It will take 1 year to complete

April 14, 2013 — I added Section 3: 50 Ω MMIC Bench Amplifer to the VHF 2013 Veronica web page.

March 31, 2013 — I started a new content page called Pin Outs

March 25, 2013 — Section 9: an essay about the 1981 Progressive Receiver, plus the final section — 10: Miscellaneous Pictures and Figures added to Sundry 2012-13

March 18, 2013 — Section 8. Popcorn AF Amplifier for Receivers — Reprise added to Sundry 2012-13

March 10, 2013 — I added a new VHF content page for 2013: VHF-2013 - Veronica

February 16, 2012 — I added Section **7** -- A Journey Above HF -- to the Sundry Experiments 2012-13 web page.

February 14, 2012 — I added Section **6** -- Non-Mechanical Iambic Paddle -- to the Sundry 2012-13 web page.

February 1, 2013 — A seperate QRP—POSDATA added to RF Workbench 4. Now QRP— POSDATA 1, 2 and 3.

December 15, 2012 — I added Section 4 to Sundry Experiments 2012 - 2013 . A PLL circuit from EMRFD.

January 5, 2013 — I added Section 5 to Sundry Experiments 2012 - 2013 . A simple AF feedback amp. An essay concerning L-C meters was also added on RF Workbench 5. Section **5.**

December 22, 2012 — I deleted the web page ***Tuning VFOs with a PN Junction*** since some of the experiments were poor quality and performed back in 1998 when I was more ignorant than now. I've learned much since then and my new VCOs from the past 1-2 years reflect this knowledge. The ***Selected QRP Reading list*** and ***Cascode 7 Receiver*** web pages were also wiped.

December 15, 2012 — I added Section 4 to Sundry Experiments 2012 - 2013 . A PLL circuit from EMRFD.

December 3, 2012 — I added Section 3 to Sundry Experiments 2012 - 2013 . Interview with Jason from Etherkit

November 13, 2012 — QRP — Posdata added to the VHF to the Max web page. Section 5: Z-Comm VCO.

November 1, 2012 — Sundry Experiments 2012 - 2013 web page added.
QRP — PosData added to Section 2 of **Power Meter Calibrators** on RF Workbench 5 and updated again on Nov 22, 2012.

October 16, 2012 — VHF FM web page added. Already, it has spawned a first supplemental web page

Sept 24, 2012 — QRP — Posdata added to the end of the HF Ragbag web page. I added a bypass and decouple network for HF to lower VHF.

August 17, 2012 — QRP — Posdata #2 added to bottom of the Receiver Band-pass Filters web page.

August 6, 2012 — Section 5: **Some Experiments with RF Bypass Capacitors** added to the HF Ragbag web page. Also a new QRP — Posdata added to the bottom of the Crystal Parameter Checker web page.

August 1, 2012 — QRP — Posdata added to the Receiver Band-pass Filters web page.

July 12, 2012 — I added a corrected schematic on the Wee Willy page: Wayne. M0WAY — 14 MHz PA under August 25, 2011. Also, added a new essay on **Microphonics in DC Receivers**. See Section 4 on the HF Ragbag Page

June 23, 2012 — RF Workbench 5 added. Click here.

May 31, 2012 — Galina discovered that I neglected to publish the proper version of the Hobby and Fun 2011 page and corrected my error. A fine-tuneable Wien Bridge Oscillator idea from Ken Kuhn now appears at the page bottom.

April 21, 2012 — I heavily edited RF Workbench 1 and 2.

April 13, 2012 — Web site purge. I removed RF Filters, VFO 1998, QRP Workshop Ideas, Miscellaneous Schematics and Photos, Base-biased VFO, Funster Transceiver, Miscellaneous Circuits and Ideas 2005 and Crystal Oscillator Offsets. **Reason:** substandard.

April 6, 2012 — 50 MHz Receiver Pre-amp and Filter added to VHF to the Max web page .Section 4.

March 26, 2012 — HF Ragbag web page added to top-level menu. Non-VHF experiment repository for 2012.

March 19, 2012 — VHF to the Max web page added to top-level menu. 50 MHz VCO experiments added to this page in Section 3.

March 14, 2012 — EMRFD review edited.

February 29, 2012 — Minor edits to the Audio Transistor Input Impedance Experiments web page. Also, I updated the calculation of the common emiiter amplifier base input resistance using the better formula: **Rin = (B+1)*(re + RE')** [while ignoring REB]. This is my favorite web page on the site.

February 26, 2012 — QRP— Posdata added to the bottom of the 2nd NDB web page

February 17, 2012 — I introduced a new miscellaneous VHF page: VHF to the Max — I'll slowly add stuff over 2012. Major editing done to the Broadband Transformer web page.

February 4, 2012 — RF Workbench 1 and 2 significantly edited. 2 new photos added.

January 28, 2012 — QRP — Posdata added to Crystal Parameter Checker web page and to QRP Modules 2011 under 7 MHz VCO Experiments on this web page. I re-wrote the temperature compensation section of the VFO-2011 web page and added 3 photographs.

January 3, 2012 — Web site change: I update web essays with an "epilogue section". In 2012 and on, they will be called QRP — Posdata (Spanish for post-script or epilogue). Posdata #2 added to the RF Workbench 4 web page.

December 17, 2011 — The Butler Did It ! - First VHF Experiments 2011 web page added. A 50 MHz frequency doubler added Dec 26, 2011.

Nov 12, 2011 — Our server went down for 16 hours. Both AC power and cable Internet to the warehouse failed after a rain storm and wind gusts knocked down some trees that severed the hydro and cable wires. Expect more weather-related down time as Winter approaches.

Oct 15, 2011 — VFO-2011 added.

Oct 2, 2011 — RF Workbench Page 4 added. On **Oct 17, 2011** I added an epilogue.

Sept 20, 2011 — Double Stacked Toroid VFO 2008 web page pulled off. It was substandard and some of the material will re-emerge on a VFO 2011 page this Winter.

Sept 19, 2011 — I updated the SWL essay since it was 6 years old and much has changed with respect to Internet radio. Over time I have received ++ emails expressing different views. I am more a SWL than a Ham and offer just 1 opinion and live by a "each to his own" mantra. Context is everything - this is a radio electronic experimenters site that recognizes SWL'ers are important members of the radio community. Click. Wee Willy web page updated again!

Sept 12, 2011 — Design Center concerning popcorn receiver band-pass filters added. Click.

Aug 26, 2011 — Minor update at the end of Wee Willy DSB transceiver. ***New Junk Box Blog format***. Change is good.

July 30, 2011 — New web page QRP Modules listed on the main menu. Currently under construction.

March 31, 2011 — 2 photos added to the Ugly Construction web page

March 19, 2011 — New content; Hobby and Fun 2011 . I'll slowly add more stuff over the year.

Feb 12, 2011 — New content. Miscellaneous RF Experiments 2011

Dec 29, 2010 — New content. RF Workbench Page 3

Dec 12, 2010 — Final additions to the the 2010 Hobbyist Page added — these concern matching FETs, BJTS and diodes.

Nov 10, 2010 — Some editing and 2 photos added to RF Workbench page 2.

Oct 9, 2010 — This October marks the 12th season of experiments for the site. I have 4 partially completed web pages on the go — pure craziness. I decided to finish them 1 at a time and then add them sequentially. Today, a new web page was added and is 1 of 2 supplements to a future main QRP audio page: Audio Transistor Input Impedance Experiments. The first new "permanent" content since March 2010.

Oct 7, 2010 —The Junk box page lay out was simplified: Accommodating the various modern Web devices plus screen resolutions proved difficult with the old html code. Although less impressive, the new format updates quickly and looks the same on every computer.

Aug 15, 2010 — The cable supplying the Internet connection failed. The site went down for 25 hours. Expect more shut downs over the next couple of days as we resolve any remaining problems.

August 6, 2010 — I decommissioned the historic home page URL http://www.qrp.pops.net/default.htm. This page was a html hard-coded parallel version of the the *correct* home page URL http://www.qrp.pops.net. It was just too much work to continue to update the old (pre-2006) home page in addition to the proper home page.

June 28, 2010 — Web subtitle change : **Amateur Radio Electronic Design** to shorten the name and reflect the site's main purpose.

Effective May 17, 2010 — Schematics now use the 16-bit png format. I have abandoned the 8-bit gif format

May and June 2010: The pops.net net control crew rest up for the next big wind storm. The servers lost power for many hours on May 4 and June 12 due to bad weather. Severe storms arising from the Pacific Ocean threaten our AC power lines each Spring.

March 2010

Wide Range L-C Oscillator added to Hobbyist 2010 page. Link **March 7**

JavaScript Applet **K** added to the QRP Tools page **March 11**

RF Workbench Page 2 added. Link **March 15**

February 2010

JavaScript Applet **J** added to the QRP Tools page **Feb 6**

Editing of the Low Noise Crystal Oscillator web page **Feb 22**

RF Workbench Page 1 added. Link **Feb 18**

January 2010

Experiment #6 added to the Hobbyist page **Jan 2**

New content Low Noise Crystal Oscillator **Jan 10**

2 photos added to the bottom of the Ugly Construction web page. **Jan 12**

1 photo added to the Broadband Transformers page **Jan 12**

New content Hobbyist Page 2010 **Jan 13**

New content: Supplement to JavaScript Applet G which is located on the QRP Tools page **Jan 11**

Additions to the Low Noise Crystal Osc page: the DSO versus CRO essay, plus 5 MHz crystal oscillator added **Jan 31**

JavaScript Applets H and I added to the QRP Tools web page **Jan 31**

December 2009

It has been brought to my attention that the email replies I am sending are not compatible with some of the latest email software such as Thunderbird etc. The reason was that I was using a homebrew email program written over 10 years ago. It is now obsolete. A new email platform is now in place along with a completely **new email address**. Consult the email web page for more information. **Dec 30**

Experiment #5 added to the Hobbyist page FAQ updated and edited. **Dec 30**

Experiment #4 added to the Hobbyist page **Dec 26**

Experiment #3 added to the Hobbyist page **Dec 23**

What does the output of a diode ring mixer look like in your oscilloscope? This has become a FAQ. The question is answered in a contribution by Wes, W7ZOI. Big thanks to Wes for this content. **Dec 22**

I am very pleased to present the **Mike, KL7R Memorial Receiver Experiments**. Click here **Dec 19**

New bulleted list format added to this page to improve readability **Dec 19**

A minor addition was added to the bottom of the Ugly Construction web page. Flux pen photo and text. **Dec 19**

Minor updates to the VFO 2008 "Stacked Toroids" web page under **Epilogue - December 19, 2009**

Update to JavaScript applet **Item E: Calculate Cut off Frequency for an RC Low Pass Filter**. Now has a capacitor range from 0.1 nF to 1500 nF. QRP tools page. **Dec 19**

Editing plus a photo added to the broadband transformer page. This page was improved to support an upcoming project. **Dec 17**

Drafting errors on this schematic corrected (fuse position+ negative rail LED polarity). From this web page. Thanks to Paul, K0EET and Tom for the good eyes and their emails. **Dec 16**

VFO Experiments 2009 updated again; 3 images added. Supplemental web page added and updated **Dec 13**

New JavaScript applet added to QRP Tools page; **Item F: dBm calculator. Dec 12**

Nov 22-27, 2009

1 Hertz Precision Time Base added to the Hobbyist Page.
VFO Experiments 2009 added
The top level menu item "Java Tools" was renamed **QRP Tools.** This menu provides a link to my Webmaster's page and some basic JavaScript applets. Some new material will appear on the Junk Box page during this time.

Nov 20, 2009

Finally; Fall-Winter experiments begin. A small update on the VFO 2008 web page under A 3.5 MHz VFO for Diode Ring Mixers was added.

The RF Preamp page was updated with some content that was first presented on the Junk Box web page. I have received a lot of email about these amps and decided to permanently add them to the site.

The W7ZOI file linked on this page is now in pdf format.

Nov 1, 2009

The Ugly Construction web page was augmented and re-written. 2 new photos were added. This term actually came from Wes and Roger Hayward.

A new Electronic Hobbyist page was added to the drop down 2009 menu.

Oct 25, 2009

Some small updates to the Junk Box page were made. I don't ever think I have been so excited about upcoming Fall and Winter experiments as there are a number of cool, new ideas in my notebook. Extra work and travelling have kept me off the bench, but this will cease in mid November. After that, it's back to the work bench. The Fall-Winter experiments will include some HAM, SWL, general electronics and tube guitar amp experiments. Thanks for your feedback and ideas!

Oct 19, 2009

RSS feed. Click on the **orange RSS icon** above to establish a feed. I will only show 1 item; the latest addition of major new content to the site. Additions to the Junk Box page will occasionally be counted as "new content" and will be included on the feed.

Can anyone guess what brand of beer is in the tool box ? Yes.... its

Oct 12, 2009

Fall weather has come to Western North America! Thanks to Cor, PA3COR for debugging the JavaScript code on this page. Apps number D and E now work in Firefox. Rediscover the fun and learning of scratch homebrew electronics!

QRP SWL HOMEBUILDER

RF — Test and Measurement

About My Web Site

Welcome Friends!

Introduction

Welcome to the QRP and SWL Homebuilder web site. I write about my experiments with relatively simple and primitive electronic circuits.

Avoiding excessive algebra and obscure parts, I emphasize and show fundamental bench practices.

Through real experiments I examine topics to challenge and intrigue amateur designers — providing examples and describing ways to plan, problem solve, breadboard and measure your circuits.

As amateur experimenters we ought to advance in our hobby; not just perform cookbook electronics. Designing and improving your circuits requires considerable knowledge and effort. Fortunately, others selflessly share their ideas to teach us.

In time, you may recognize your electronics workbench as your greatest teacher. Bench experiments involve us thinking about and measuring our circuits so we know what's happening instead of relying too much on folklore, guessing and copying others. Designing and/or simulating circuits with software can enhance your learning but does not obviate the need to spend time in the trenches with meters, wires and solder.

People often learn skills by modeling others. We need sound examples of how other builders work and think to inform our own designs — inspired, creative and active learning driven by experience and reflection.

At some level, our bench experiences are stories of growth and realization sparked by going and doing. For example, why did the designer choose a particular resistor value? You try different resistor values while measuring the results and increase your knowledge. Collecting schematics, kit building or just thinking do not provide as intimate a learning experience as soldering your ideas on a bare copper board. Talking, tweeting or day dreaming about design is not the same as *doing it*.

Russian novelist Fyodor Dostoyevsky describes the contrast between real life and passivism; "love in action is a harsh and dreadful thing compared to love in dreams", The Brothers Karamazov, Братья Карамазовы. Dare to dream, but better yet, dare to innovate — to design and build *your own* circuits. You may start by just modifying a favorite circuit or scaling a stage to another frequency. We need more innovators and less imitators to grow and sustain our great hobby.

Electronic design produces more than a completed circuit. On the bench, even joy is experiential – a moment of discovery (or several discrete moments) yields more pleasure than stuffing a circuit board or operating a piece of gear. Creativity trumps process every time!

I hope this site demonstrates my passion for building basic, "popcorn" circuits and sharing ideas. Please remember I am just a lay person experimenter and not an electrical engineer.

Regards, Todd, VE7BPO

Essay for 2010

Building or buying test equipment and acquiring a good reference library are important to your experiments. Spurred by the realization that sound bench measurement practices are at the heart of good design, test equipment receives greater focus in 2010 and on.

A reference library is vital to our electronic experiments; good examples lead to better experiments. Poor circuits are everywhere and some builders can't tell a good design from a bad one. Minimalism and simplicity aren't excuses for sloppy design when your goal is to learn. Collecting and sharing well designed circuits helps us avoid wasting time and experiencing frustration. Circuits with attributes like well defined input or output impedances, low noise or harmonic distortion are desirable to fuel experimentation. Look for better quality circuit examples in 2010 and on.

The Internet is changing how we read and write. The prevalence of small portable web devices such as iPhones, ever increasing numbers of web sites and blogs, and the use of search engines create fierce competition among sites. Modern sites attract your attention with varied visual, aural and textural media and unfortunately, hype and pseudo-journalism. Narrative writing is more skimmed than read. Brief is in — bullets, subtitles, lists and graphics replace long lines of narrative prose which no one seems to have time for anymore.

Have you noticed the changes on this website? New content still contains lots of narrative writing, but assumes an active voice, with emphasis on brevity, clarity and speaking directly to you, the reader. Sharing mostly obsolete, analog 1970's-style circuits, QRP/SWL HomeBuilder attracts a tiny, niche audience. I believe the success of this website depends on providing good and diverse content — not Tags, RS feeds, adopting net-speak, or self promotion. You be the judge.

Essay for 2014

The Internet of Everything?

Bucking the trend, my contribution to amateur RF homebrew remains informational and not social. Why?

Social media information represents a Pandora's Box of good science and opinion, mediocre thought, or trash potentially created and/or disseminated by anyone who's connected. We accept that much of our social media content doesn't come from the best or brightest — some people are just plain interesting, or express themselves vigorously, seem like-minded, or touch our hearts.

Some builders, like me, seek objectivity and not just "likes" and "follows" based on sentiment and spectacle. While a few radio builders may prefer to join hands and sing Kumbaya, or pat themselves and others on the back simply because their breadboard actually works, a trifling of us care more about how and why our circuits work. We *like* measures and measurement tools and *follow* science, experiments and the works of those who shine brightly.

What's wrong with plain information, unfettered discovery, experimental rigor, objectivity and rational, kind thought?

It's not that these characteristics don't attribute social web clients — they do, but the negative impacts of social media worry me a little. A brief list of concerns: loss of privacy, the threat of wasting time while really just isolating ourselves from our real friends + family. The numbing exposure to the Internet of Ads and Spam. Still too, bubbling up like purulent sores come the charlatans, the misinformation peddlers, the opinion spammers, and those who anonymously leave stinging sarcasm, or outright hatred [hostile online comments that attack people, or divert a healthy flow of ideas].

Running a low-tech web site with nearly 0 commercials suits me better.

SEO — Search Engine Optimization

I've read that Google analyses your web site content, the number and quality of the sites that link to your pages, their search engine clicks and so forth. In part, Google seems to rank a site based on how relevant and authoritative they believe it is. Some people specifically employ SEO techniques to gather in more traffic.
To my surprise, each year, tens of thousands come to this site via search engines like Google. I don't think my material seems too relevant or authoritative. I've made no effort at SEO, so I conclude that you, my readers have more to do with the site's success than anything I've ever done.

Thank you.

Hope Invigorates

Invigorated by the excellent work either emailed to me by experimenters such as Michel F6FEO, or Dick, N4HAY; or posted on blogs or Community sites like Yahoo, I feel hopeful about the future of our hobby in 2014. The PHSNA Yahoo group leaders, the recent work of Jason, NT7S, Steve VE7SL and many others show that *amateur design* experiments still have a pulse + respirations.
The aforementioned get my vote for their MOF like behavior: a strong blend of creativity, tradition and quality.

Looking Ahead — Future Site Content

Most of my new receiver work involves quadrature and in-phase mixers fed with (2) local oscillators; 1 output shifted 90 degrees from the other — essentially, EMRFD Chapter 9. Even my Funster [a personal, lowbrow trans-receiver I drag onto hill and dale] now contains phasing receiver circuitry to reduce the opposite sideband by 20 dB along with further low-pass filtering. I hope to add some Funster content to HF Embarcadero in Winter 2014. Like many of you, the 1 resource I lack the most is time.
While I'm thrilled with the notion of a receiver appliance that contains just an antenna, LNA, ADC and some sort of "wonderfall" display or speaker, I'm still smitten by analog design with hardware. Still, the I-Q mixer will offer a nice transition into SDR should I ever wish to spend my free time writing C# and not melting solder.

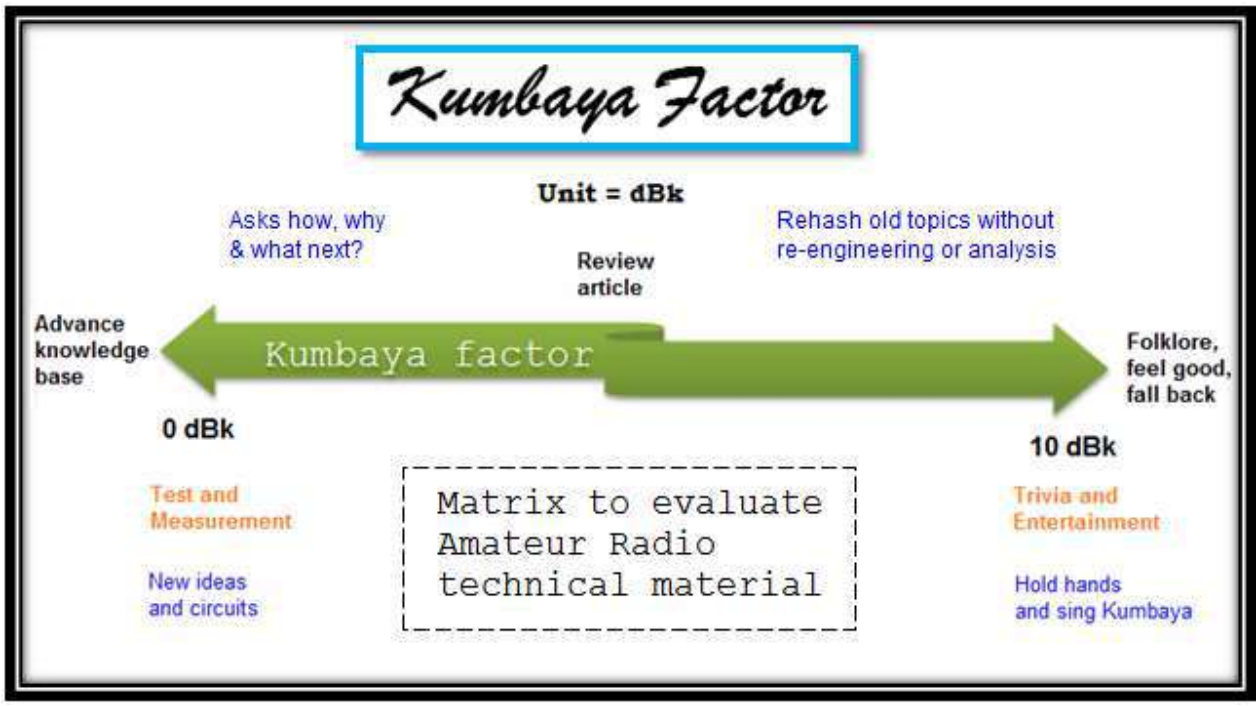

Best to you!

Miscellaneous

My special thanks to Wes Hayward, W7ZOI for his generous support and elmering over many years.

EMRFD is the main reference of my site

All permanant content circuits were built and tested. Schematics are drafted as carefully as possible. Please accept that bench and/or drafting errors may occur. No liability arising from the application, use, or misuse of these projects that results in direct or indirect damage or loss is assumed.

Full price is paid for all parts used and no monies are or were received for promoting any products or companies on this web site. Any ads, hyperlinks or mention of commercial products or companies is out of courtesy only.

"Until you build and measure it, you don't know what you don't know";
Rick Campbell, KK7B; VHF Open Sources — Design of Low Power High-Stability Low Phase Noise Single Frequency VHF Sources with High Spectral Purity; 2008

Information Regarding the Compression of Schematics

I see many electronics web authors compressing black and white schematics as jpg files. This results in distortion of the schematic. Schematics are best compressed using the 8-bit, lossless LZW algorithm which means converting the file to a png, gif, or even pdf format. The files sizes will typically be smaller than .jpg compression, have no distortion and can be edited easily.

RAC is the National Amateur Radio Society of Canada

For my web page concerning support of the **Radio Amateurs of Canada**, please click here

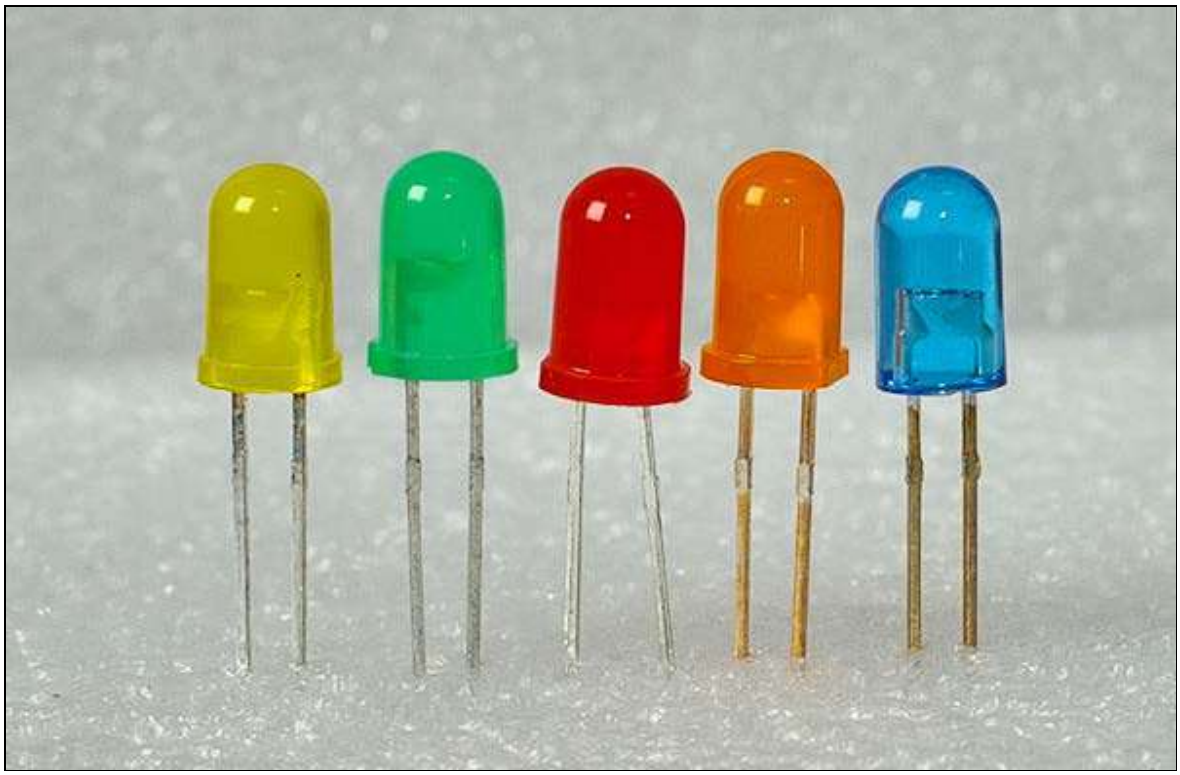

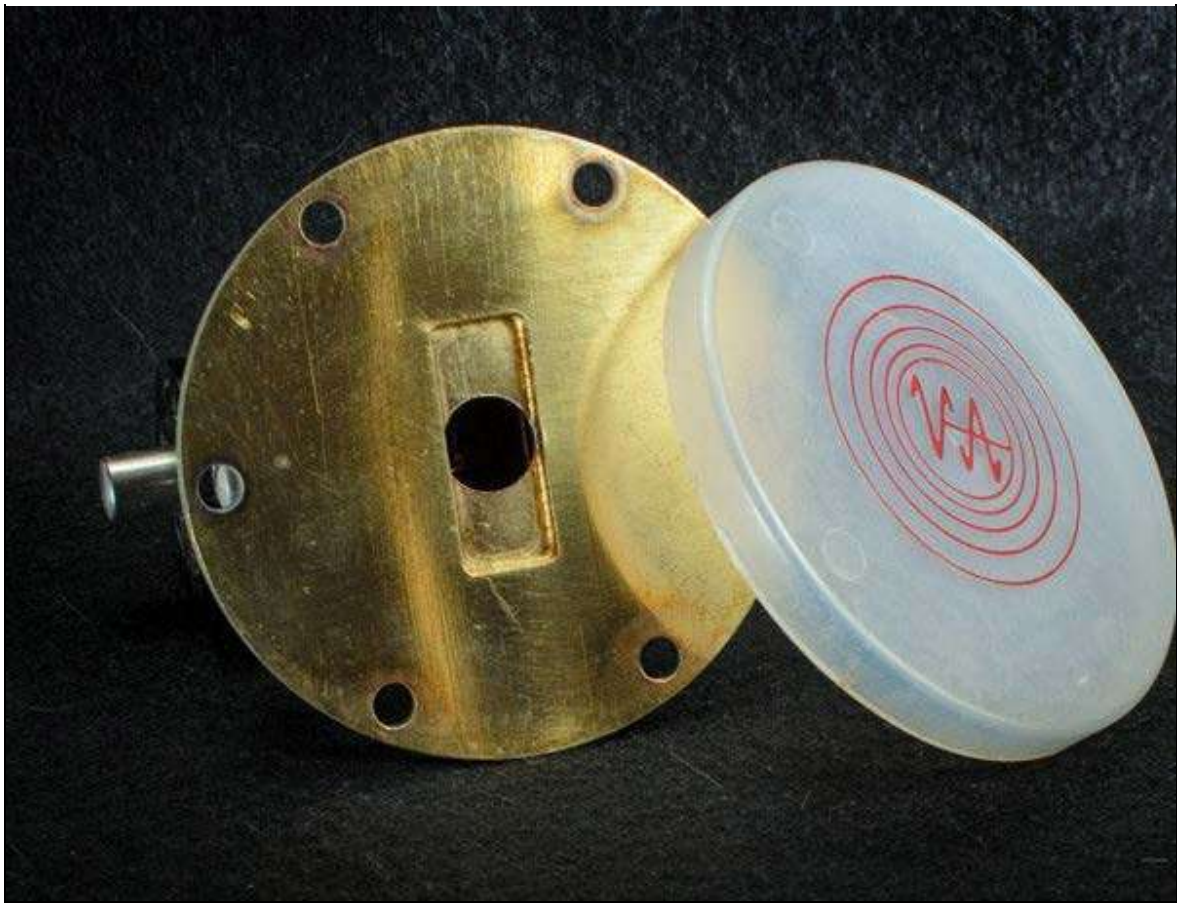

The hand drawn image bitmaps on this web site (logo etc.) are by Rod Adams. All website photographs were taken by VE7BPO except as indicated.

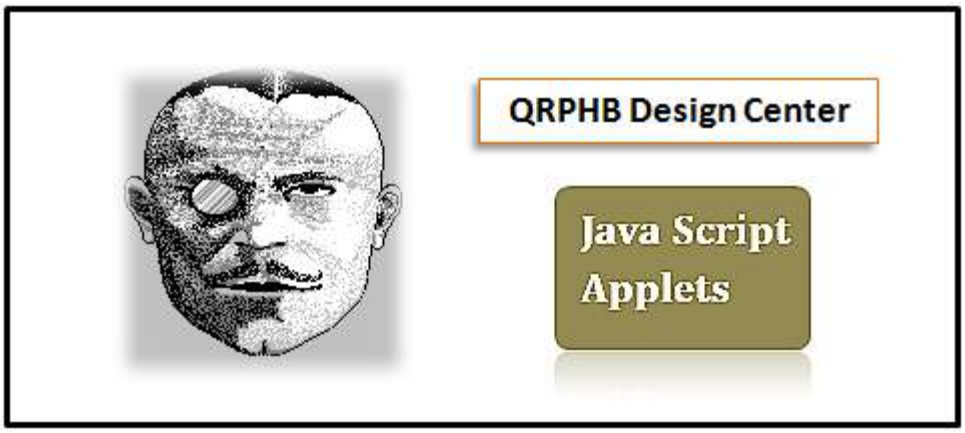

1. Click for the old QRP HomeBuilder Graphics page. Click for my Pin Outs page. Click for my Homepage

---

2. Some simple tools written in JavaScript for the QRP/SWL HomeBuilder:
`Minimal input error checking`

A. Calculate DC Voltage Divider Bias

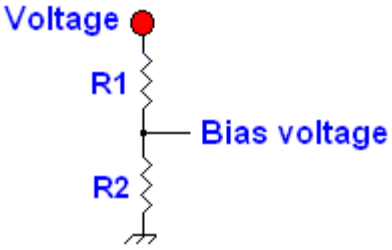

Enter Voltage: Enter R1: Enter R2: Bias voltage =

B. Calculate Inductive Reactance

Enter Inductance in uH: Enter Freq in MHz: XL (ohms) =

C. Calculate DC Current for a Current Mirror

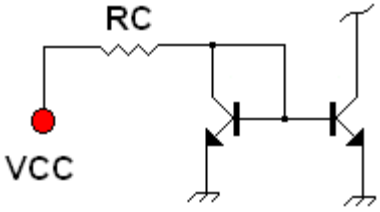

Enter VCC: Enter RC in ohms Current (mA) =

D. Calculate # of Turns To Obtain a Desired Inductance on a Ferrite Torroid

Enter Inductance in millihenries: Select Core: FT37-43 Turns =

The *AL for this ferrite core is* =

E. Calculate Cut off Frequency for an RC Low Pass Filter

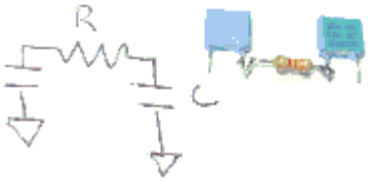

Enter resistor value in ohms: Select capacitor values in uF: 0.01 3 dB down frequency (Hertz) =

F. Calculate Power in dBm and mW from Peak to Peak Voltage

Enter measured peak-to-peak voltage into a 50 ohm load: dBm, mW

Application Note: This web site follows the EMRFD standard for dBm power measurement. dBm = the power delivered into a 50 Ohm resistive load which is temporarily substituted at that point in the signal chain.

G. Calculate Lm and Cm For a Crystal using the G3UUR Method

Enter frequency in **MHz** written on crystal (series resonant frequency):

Enter measured frequency in **MHz** with switch open: Enter measured frequency in **MHz** with switch thrown:

Enter crystal capacitance in **pF**: Enter open switch circuit capacitance in **pF**:

Cm = femto Farads , **Lm** = Henries

Supplemental web page for this applet: Crystal filter measurement and adjustment Link

---

H. Calculate Decibel Power Gain or Loss from 2 Peak-peak Voltages

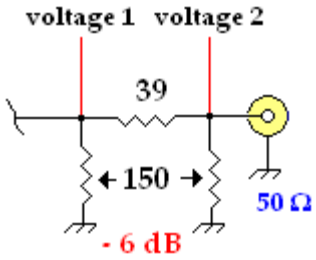

Enter voltage 1: Enter voltage 2 dB gain or loss =

I. Calculate Decibel Power Gain or Loss from Input and Output power

Enter input power in watts: Enter output power in watts dB gain or loss =

J. Calculate dBm and mW from RMS Voltage (50 ohms)

Enter RMS voltage dBm mW

K. Calculate Return Loss and VSWR (50 Ohms Detector)

Enter the detector signal in pk-pk volts when the unknown port is terminated in an open circuit: Enter the detector signal in pk-pk volts when the unknown port is terminated in the unknown impedance:

Return loss = dB, VSWR=1:

Measurements per Figure 7.41 EMRFD. Schematic here

L. Calculate Power from the DC Output of an AD8307 Meter

1. Linear calibration steps:

Enter measured DVM voltage at -10 dBm: Enter measured DVM voltage at -20 dBm:

2. Calculate power in dBm from DVM voltage:

Enter measured DVM voltage: Power =

M. L-C-C Tee Network

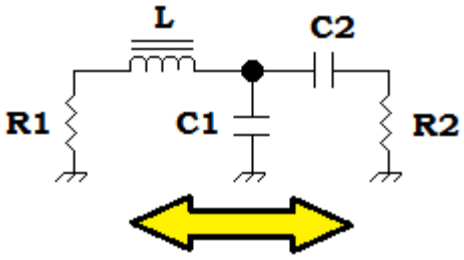

Enter **frequency** in MHz:

Enter **R1** in Ω: Enter **R2** in Ω: *R1 must be < R2, but the network is bi-directional*

Enter Q: *Perhaps start with 2-5*

C1 = pF, C2 = pF, L = uH

N. Parallel Resistor Values (2-4 resistors)

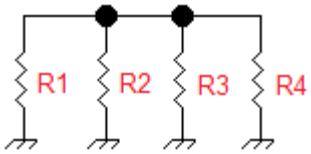

Enter R1: Enter R2 Enter R3: Enter R4:

R = ohms

O. LCR -- a Reactance Calculator In beta -- do not use !

Mode: L C to Reactance Inductance: uH Enter frequency in MHz

This page last updated: September 21, 2013

RF — Test and Measurement

Short Wave Listening коротковолновое радио

Introduction to Short and Medium Wave Radio Listening

Short wave radio listening was a childhood passion and I enjoy being an SWL just as much today and log at least 800 hours of SWL per year. There seems to be many web pages devoted to construction of radio equipment for the amateur radio experimenter but relatively few for the shortwave radio devotee. I decided to expand this web site to include projects for the SWL Homebuilder in 2005.

My favorite bands are 49 meters (5.9 - 6.2 MHz) at night-time and 19 meters (15.1-15.8 MHz) during the daylight hours. I also listen to medium wave DX around 1400 - 1600 KHz.

Why Listen to Analog Short Wave Radio?

Is analog short wave radio dead? I think not.

No doubt, short wave radio has passed its prime and is slowly dying, however, it's still fun and/or relevant to some.

World band radio: Almost 1/2 of the world's population lives on $2.00 *USD* or less per day. The Internet (the main alternative to shortwave radio) poses a luxury to many poor people living in lower-income countries — experienced travelers or those who support people in developing countries will understand this statement. In some countries now, ranking in the middle class just means you have a full-time job. In addition, oppressive governmental regimes may limit foreign media and Internet access: LW, MW and SW radio can break through obstacles such as natural or man-made disasters, borders, poverty and censorship.

For SWL hobbyists, analog shortwave radio entertains, informs and best of all, provides opportunities to analyze propagation and experiment with real radio topics including static, solar flares, QRN, antennas, grounding, baluns, coax, and wire. SWLing poses an adventure — it's unpredictable, challenging and increasingly difficult as stations decrease and QRN increases. I've built many antennas and even some noise cancelling circuits just to pull in a few Dx stations. The sport of SWL lies in making DX contacts: a theme shared with Ham radio.

What About Internet Radio?

Radio by definition is the transmission and reception of electromagnetic waves of **radio frequency**; but perhaps blue-tooth or Wi-Fi reception from a hot spot qualifies as *radio* in the modern era? Just as peanuts aren't nuts, Internet server or webcasted radio is not RF broadcasted radio. I think Internet radio is great, but fundamentally a very different medium from that enjoyed by SWL fans

Internet radio involves a radio player decoding a stream of compressed bits fed from a Internet radio station or virtual receiver. In some cases, the material originates from a real radio station that also broadcasts an AM or FM signal. For example, you can tune FM station Rooskie Radio "Русское Радио" in much of Slavik Europe or play them on a computer device anywhere you can get an Internet connection.

For lovers of foreign content, listening to Internet radio makes sense; providing convenience, a good signal when bandwidth is high and 24 hour per day listening on 1 IP address. Internet radio offers a much cheaper way for content providers to beam their news and music services around the globe — we've seen numerous large broadcast radio services such as the BBC World Service reduce or drop analog SW and add Internet radio, satellite and digital SW transmissions for their customers.

The exciting growth of independent and niche Internet radio stations increases personal freedom of choice and provides opportunities for unique

interest providers and consumers to find each. Media streaming companies and manufacturers of Internet radio *players* and their worldwide distributors benefit too.

This technology is a far cry from tuning the SW bands with a homebrew or commercial radio frequency *receiver* and a length of wire slung in a tree. Perhaps, the greatest advantages of Internet radio are that you don't have to get up early, or stay up late to pull in some rare Dx, nor do you need any radio skills or special equipment — perfect for the majority of listeners. But we're SWL radio hobbyists: people who listen for both content and because we love radio propagation and gear.

There is nothing wrong with Internet radio, or any of the modern data streaming techniques however, SWL aficionados driven by skill, the thrill of Dx and love of their experimental hobby share a special bond that Internet radio doesn't give them.

Assembling a station The most important component in your radio shack is your antenna. Don't hesitate to safely experiment with the many antenna designs available on the world wide web. Your sure to find a commercial unit or home brew antenna design that suits your real estate and budget.

Your next task is to find a receiver. It is difficult to recommend any one receiver because there are so many excellent commercial receivers to choose from. If you are thinking about purchasing a used receiver, you might consider checking eBay to find a receiver or to learn the going price for used gear. The ultimate SWL experience in my opinion is to build and operate a receiver on at least 1 band.

Favorite SWL and SWL-related Web Sites

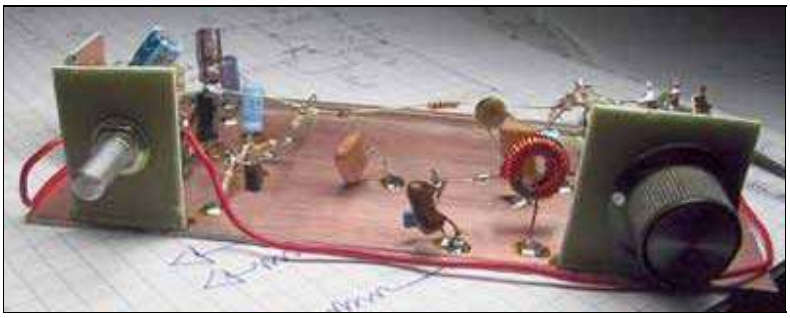

Wikipedia-Shortwave Bands A good description of the bands and their general propagation.

Canada's SWL-DXer website Hard core Canadian web site dedicated to SWL. Thanks gentlemen!

http://www.bobsamerica.com/swl

http://www.dxing.info/

Doug's Shortwave Radio Page

AA6V's SWL Links

Method for soldering a PL-259 to RG-213 or RG-8

Digital Modes For SWL Fans

PSK31

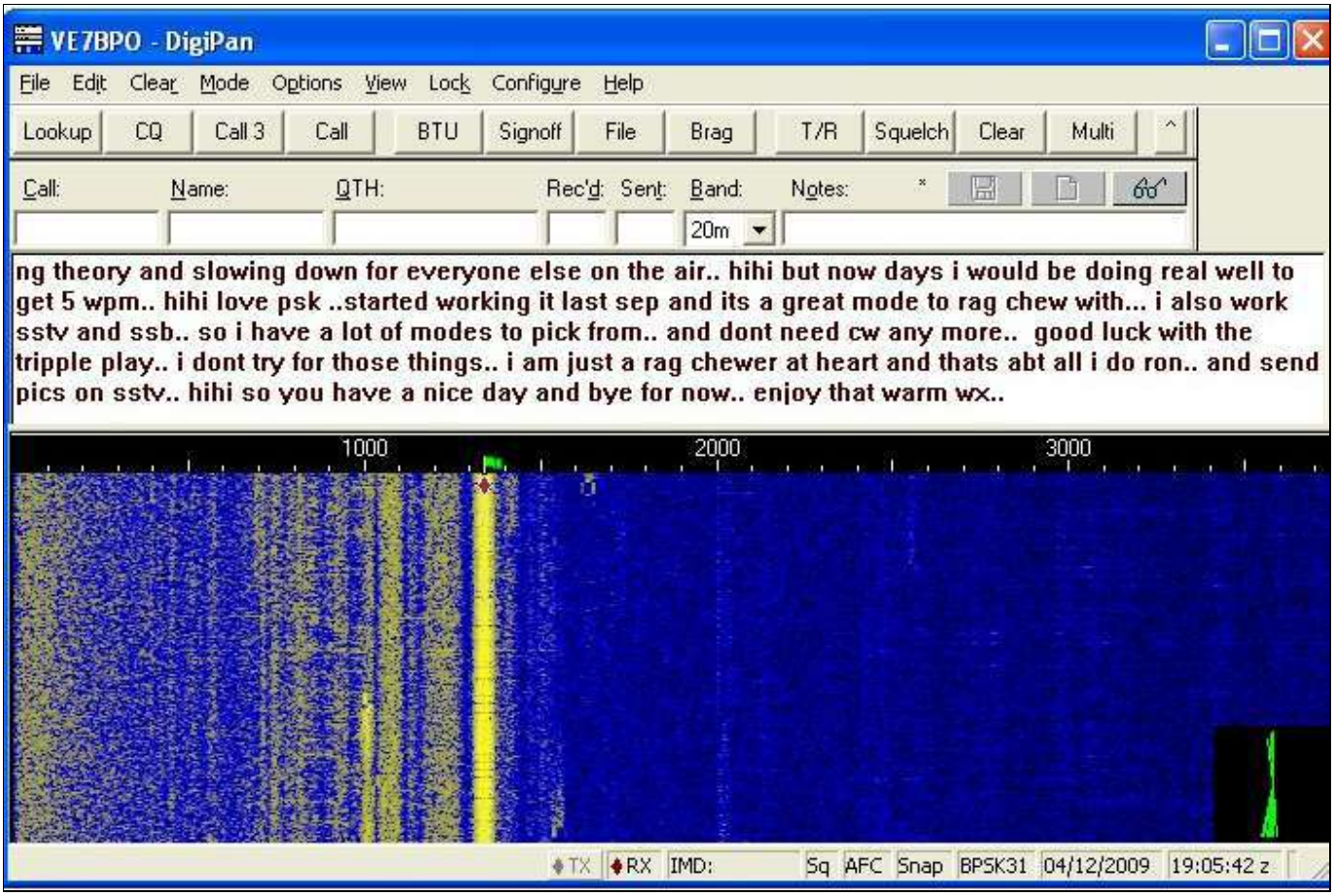

There are a number of good sites about this relatively new HAM mode. All that you minimally need is a receiver dialed in at 14.070 USB (or another

PSK31 frequency), a microphone hooked to your computer sound card and some free software. The software (DigiPan 2.0) is available at http://www.digipan.net/ .
I use a USB interfaced microphone and place it about 2 cm from my receiver speaker. If HAMs are operating; you should hear some warbles and see some waterfalls on your screen. Click on one of the waterfalls to begin receiving the text. I knew nothing about this mode, but was up and running in 15 minutes.

Additional Short Wave and Medium Wave Receiver Photos

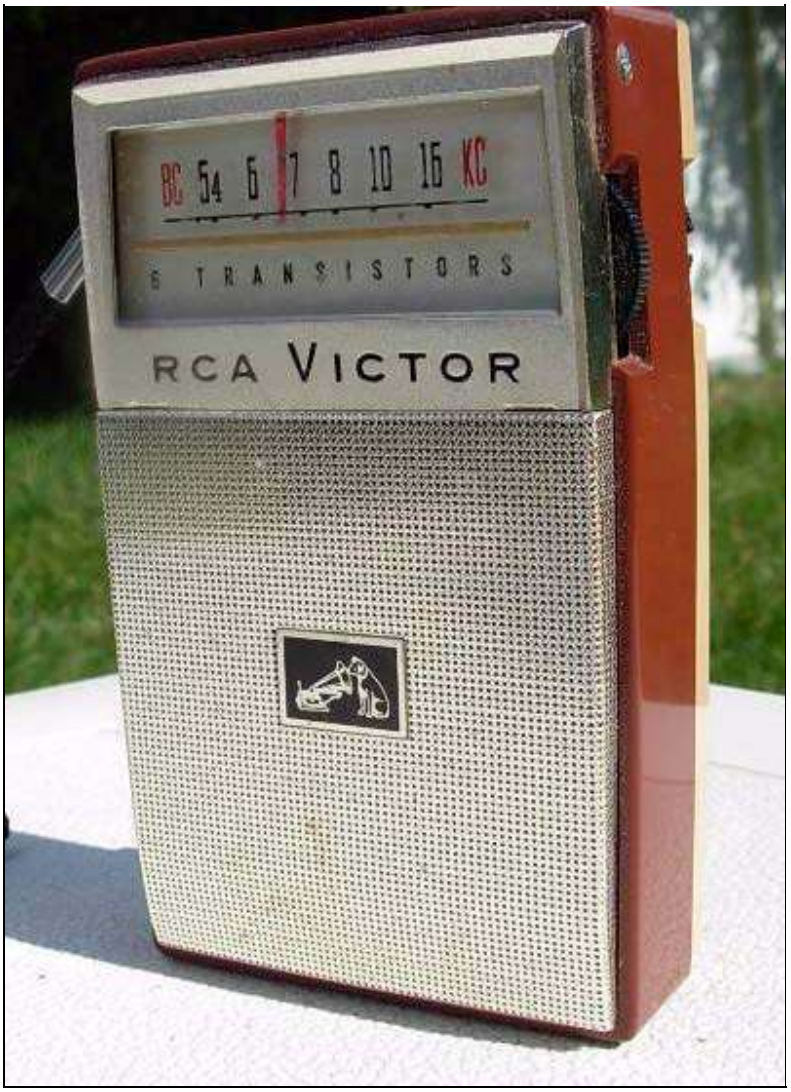
BC 54 6 7 8 10 15 KC
6 TRANSISTORS
RCA VICTOR

RCA VICTOR
SISTOR
DIO
MODEL 6P-626
RCA VICTOR
RCA VICTOR

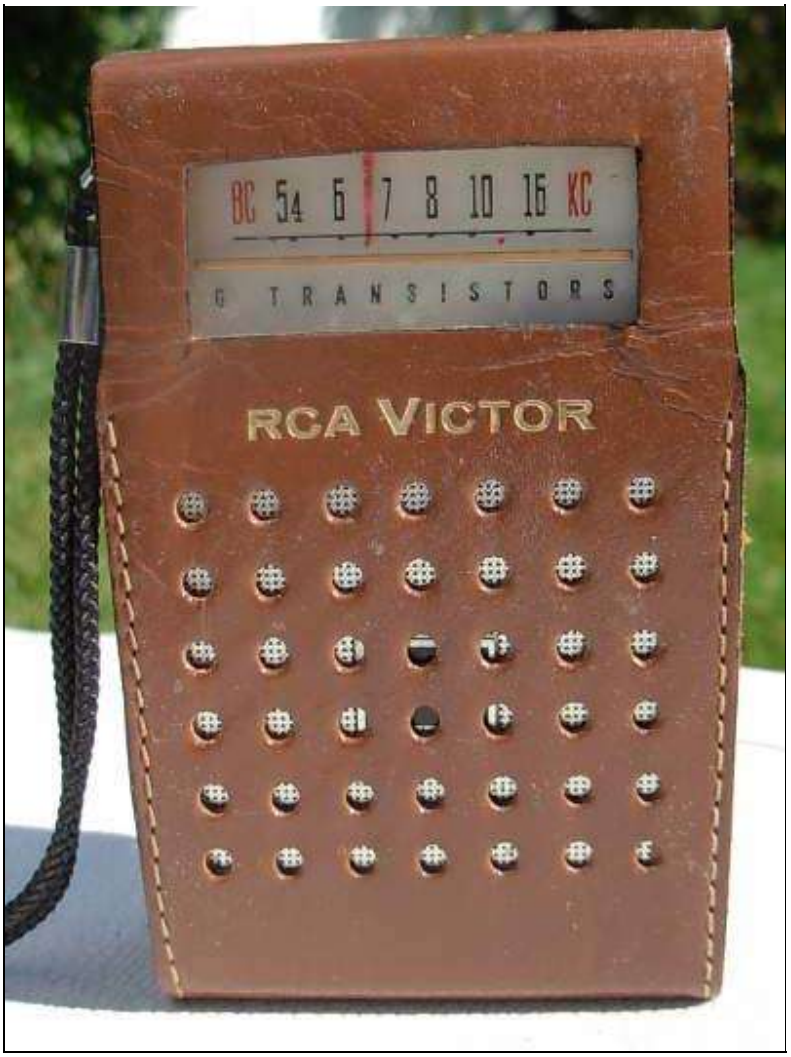
BC 54 6 7 8 10 16 KC
TRANSISTORS
RCA VICTOR

RF Preamps

W1FB 6M RF Preamp

Discussion:

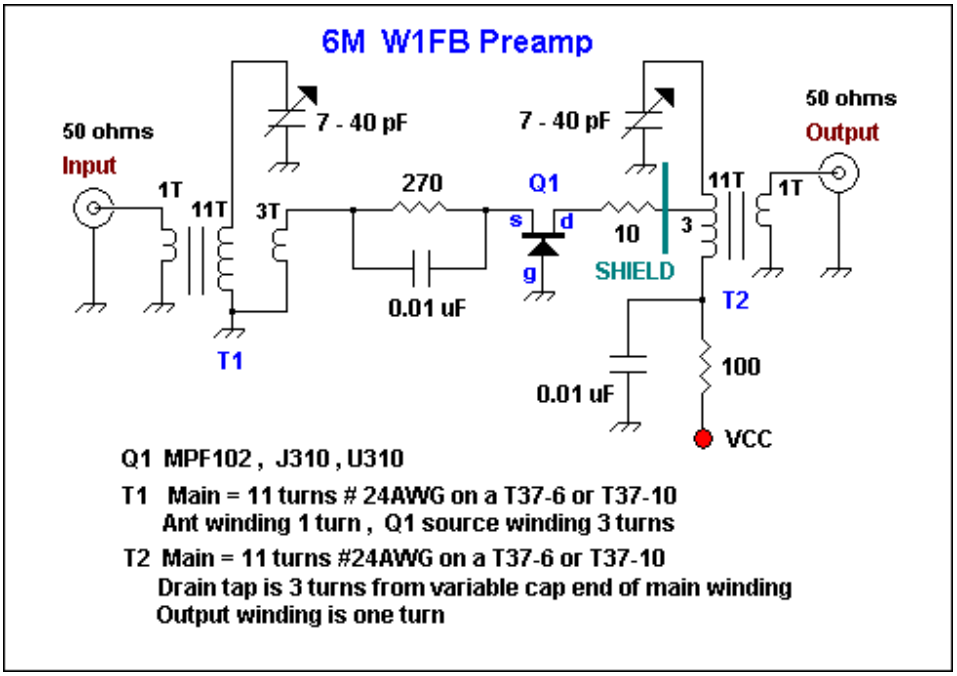

Here is a schematic sent to me by W1FB many years ago. It is very similar to a 6M two-stage preamp that he published in QST in the mid eighties. Doug really favored the grounded gate FET for narrow band preamps. His published work is replete with examples of them on just about every band. I built that amp and remember getting about 10 dB gain, which is all that I wanted for the 6M direct conversion receiver using a diode ring detector that I was building. The great feature of the amp is that it combines a band pass filter and preamp in one. I lost the original schematic that Doug sent me but was delighted to see that I made a bitmapped drawing of it on a floppy disk that was recently re-discovered when we were moving an old desk. The shield shown in the schematic was a small piece of grounded ,double sided PC board in which, I made a small chamfered hole in to pass the lead going to the T2 tap. The shield, along with very short component leads will help minimize parasitic oscillations. The T2 tap is 3 turns down from the end of the T2 main winding that connects to the variable capacitor. Doug specified T37-10 cores for the inductors, but I substituted T37-6 cores and used the same number of windings as specified for the T37-10 core inductors. It worked fine.

VE7GC Popcorn RF Preamp

Discussion:

Here is an easy RF preamp by Dick Pattinson, VE7GC. It uses a single tuned circuit at the front end and can connect directly to a mixer or product detector in a simple receiver project. Note how Dick provided adjustable RF gain control for this circuit in his Wee Willy project on this website. If you can not find Tak Lee green 10.7 MHz IF coils, probably any other brand of 10.7 MHz slug tuned IF transformer would work. The Mouser catalog number is 421F123 . If your 10.7 MHz IF coil has a built in capacitor at the base , remove it. A fixed inductor may also be wound using a powdered iron torroid core and then all or a portion of the C1 capacity would be made variable. The input impedance is 50 ohms and the output impedance is low due to the Q2 emitter follower stage.

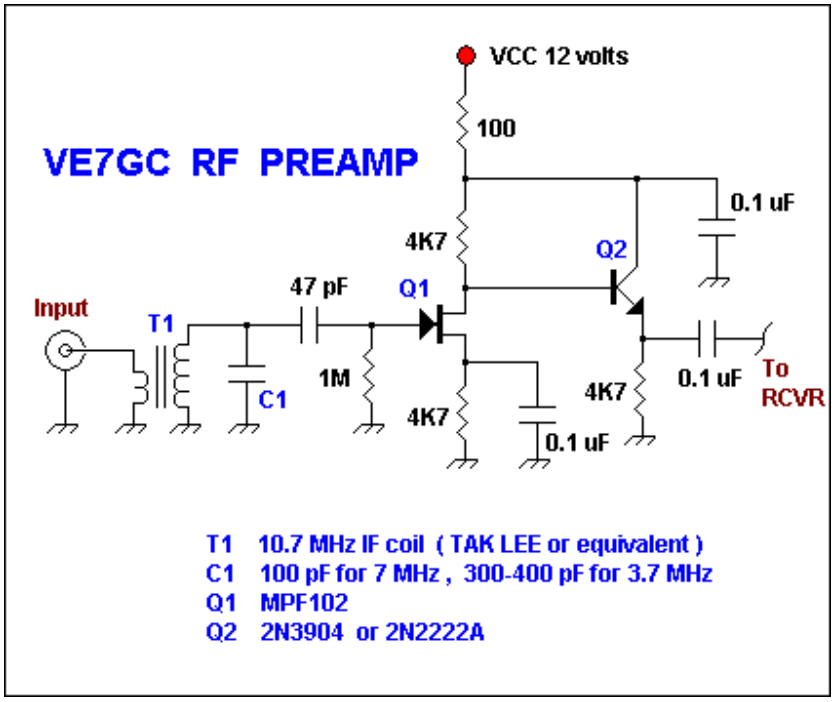

A Low Noise, High Dynamic Range Broadband RF Amp

Discussion:

This schematic is a version of a circuit developed and patented by David Norton and Allen Podell in June 1974. This variation was described by Joe Reisert, W1JR in the now defunct Ham Radio Magazine. The Norton design uses transformer coupling to achieve "noiseless negative feedback" and is really outstanding.
A great article utilizing and augmenting on this technique receivers is by Jacob Makhinson, N6NWP in QST magazine for Feb 1993 with "A High Dynamic Range MF/HF Receiver Front End". Makhinson arranged 2 in push-pull to obtain excellent results. Obtain a back-issue of QST for closer study. **Note** that the fore mentioned Feb QST article has the coil phasing wrong and the correct phasing can be seen at this web site from QST for July 1996. There is also information about Norton feedback RF amplifiers in EMFRD.

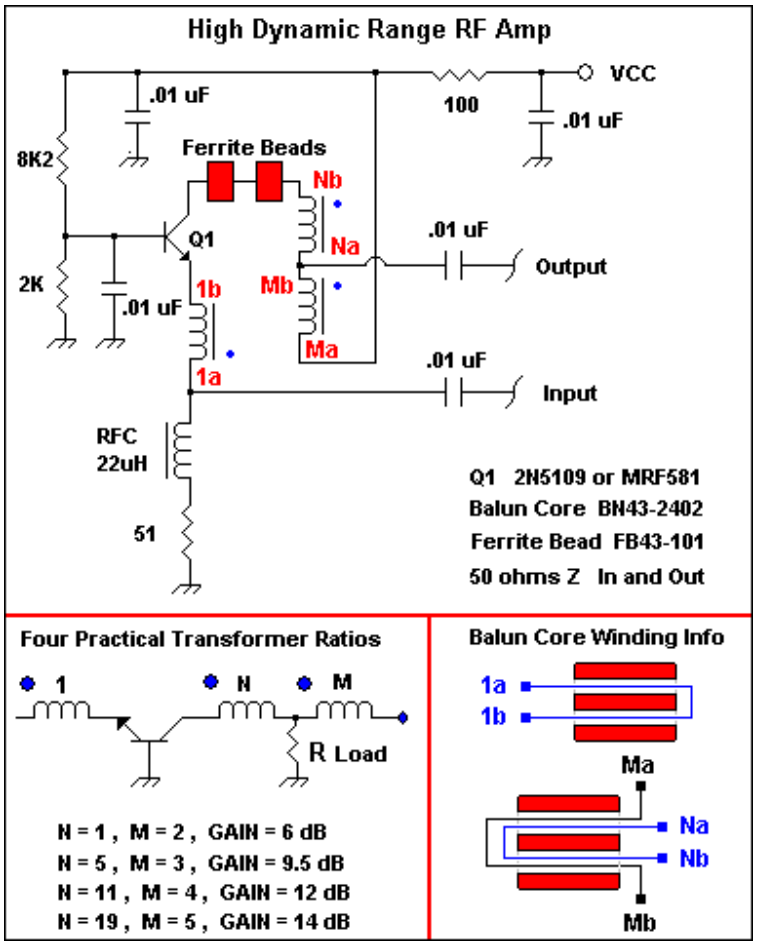

If you are building a contest-grade receiver and need a good RF preamp and/or post mixer amplifier, the Norton type is quite suitable. An amp built using a 2N5109 can have a noise figure in the 2.5 - 3dB range. I have also built them with 2N3866, MRF517, MRF581 and a 2N5179 although the last transistor would be a somewhat poorer choice. This schematic with a 2N5109 is good from 1.8 to 150 MHz with a 1.2:1 VSWR or less according to Joe Reisert. I have even put one in a friends CB radio and he was delighted.

Winding and Construction Hints

Making the Norton amps requires some planning to keep all component leads as short as possible. The transistor leads and any connecting components should be trimmed as short as practical to promote stability. Sketch the component layout on a piece of paper and modify it until you are satisfied you have designed a good layout. The ferrite beads on the transistor collector aid in stability and should be used to preserve the noise figure by squashing any oscillations should they develop. The 22 uH choke can be the little epoxy coated units that are color coded and look somewhat like resistors. Do not use a choke less than 22 uH.

Before winding, the builder must first decide how much gain is needed from the amp. For an RF preamp, the stage should have gain equal to or greater than the passive stages after it. Also there will be losses in the transformer, so the theoretical gain of the Norton amp maybe 1 dB off and will need to be factored in. For the purposes of discussion, a 9.5 dB amp is desired , so N = 5 and M = 3. The first step is to mark one side of the core with a dab of liquid paper, paint or a small piece of tape. This will allow you to keep track of the transformer later. To mark, hold the core so

that both channels are parallel to the floor, one on top of the other. Apply your dab of paint to the top of the core and use the marked top to denote the A windings. 1a, Ma and Na will all start from the top channel in the balun core. Using 32 AWG wire for all three windings, start with winding 1 and wind the single turn from point 1a to 1b. Cut off the leads so they are shorter than 5 centimeters (2 inches). Next, wind Ma to Mb three complete turns through the binocular core and trim the leads if needed. Tie a small knot in the wire at both ends. This will clearly mark this M winding. Both windings should look like the diagram under the schematic. 1a to 1b are on the left of the balun core and winding Ma to Mb are on the right side of the core. Mb has a distinguishing knot at the tip of both wire ends. Ma starts from the top of the core which you have marked with a dab of paint or something. Finally, wind Na to Nb five complete turns through the core in the same direction as the previous winding M. Strip wires Na and Mb (Mb has the knot), twist together and solder. Scrape the enamel off the leads **very** gently with a sharp hobbyist knife.

Insert the transformer in your circuit and cut the leads to their proper length and then solder away. It maybe preferable to pre-strip the leads on winding 1 as it is hard to strip the enamel off a fine wire that has only one turn and it may accidentally pull out of the core. If it does, just re-insert it into the balun core on the correct side. Once you have soldered Na and Mb you can always identify the windings later because you have marked the top of the balun core which denotes the A windings. Try and make your windings gently tight as if there is too much slack you may have difficulty getting the last few windings thru the core channels. A 14 dB gain amp maybe **impossible** to wind with 32 AWG wire, it may best to use 34 AWG for that amplifier. I have never built one for greater than 12 dB. The transformers are a bit tedious to wind, however persevere and the results will be well worth it. For HF, you can substitute 0.1 uF caps for the 0.01 caps shown if you like.

Toroidal Inductor Norton Amp Experiments

Discussion:

The amp shown in the schematic to the right uses a ferrite torroid for the transformer and has ~10 dB gain. Winding 1 turn of wire over the cold end as shown in the schematic is tricky. Try to keep this link as short as possible. A ferrite bead or a 22-51 ohm resistor on the transistor collector is desirable. You can try increasing the turns (1:21:5 etc) to experimentally obtain more gain from this amp. The torroid version is a valid option for builders who do not have balun (binocular) core ferrites in their junk box. Toroidal inductors are certainly easier to wind then binocular core versions.

In 2007, I built several Norton "noiseless feedback" RF amps using FT50-43 and FT37-43 ferrite torroids. These are outstanding and I recommend using them in projects. The input and output Z is 50 ohms. The overall BJT topology is reminiscent of a common base amp. I have some basic information concerning this amp on this web page . They are straight forward to build. The biggest problem is the phasing of the single turn link. Get it wrong and your amp can turn into an oscillator.

Figure 1

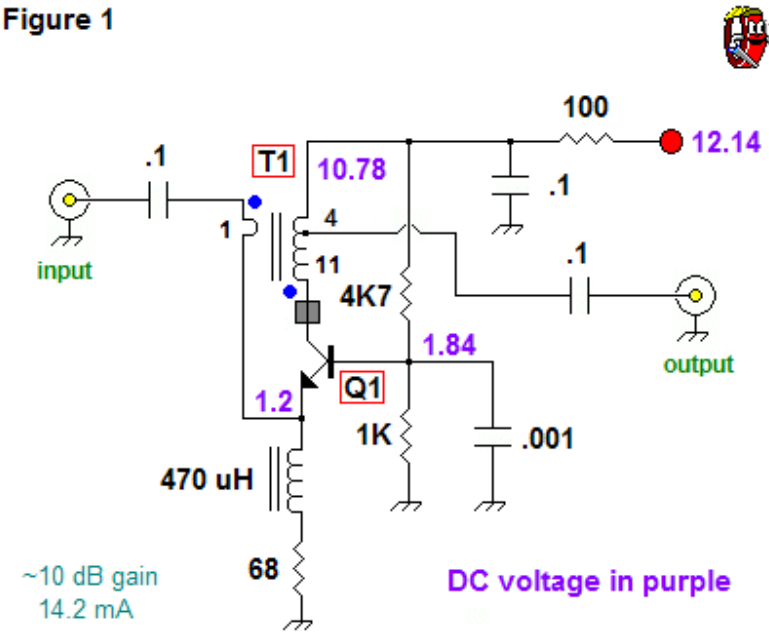

Q1 = 2N5109 or NTE 123 etc
T1 = Secondary: 15 turns with a tap a 4 turns from the cold end.
Primary: 1 link over cold end
T1: use FT50-43 or FT37-43 ferrite

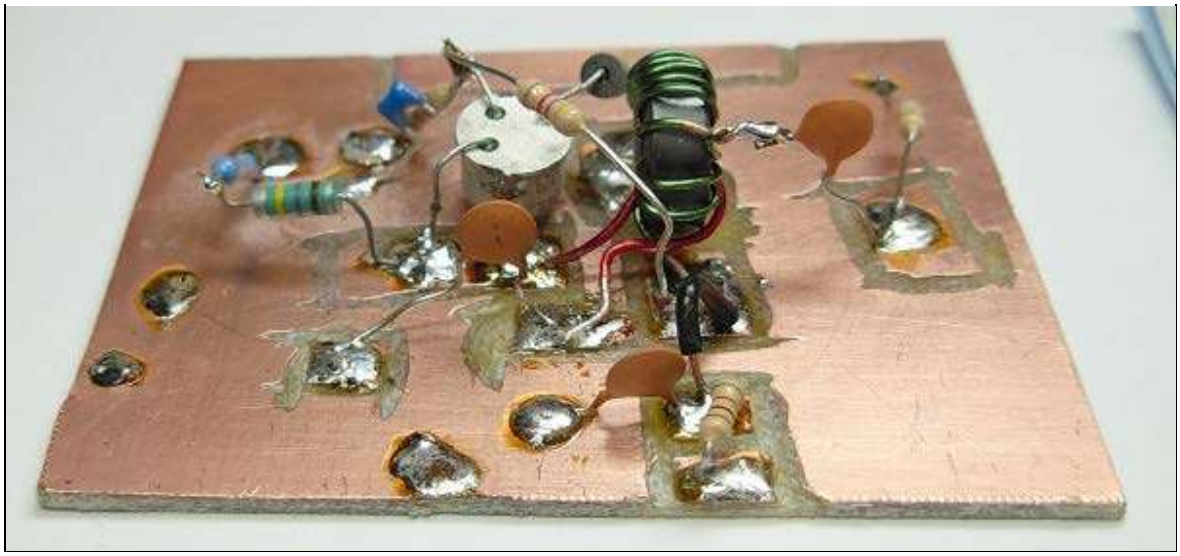

Shown above. The breadboard of Figure 1.

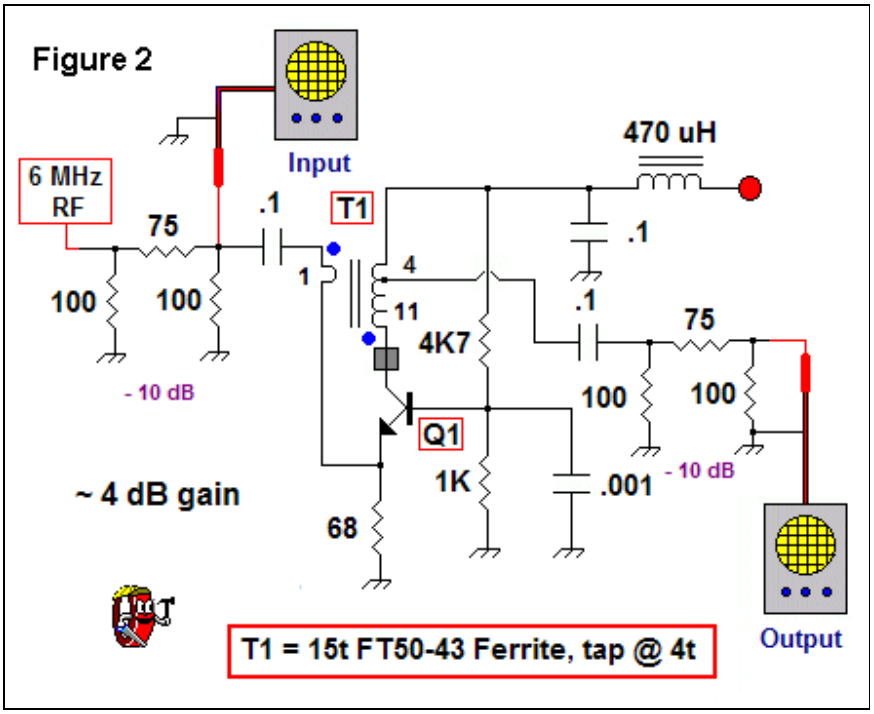

Shown above is the Figure 1 amp above (labeled Figure 2) with a 50 ohm -10 dB pad on the input and output, so gain is low. I used these pads to evaluate the amp in a number of experiments. I never got around to writing up these experiments on the web site and likely never will. I wish I had more time as my notebooks are full of unpublished experiments that would be great content for this web site.

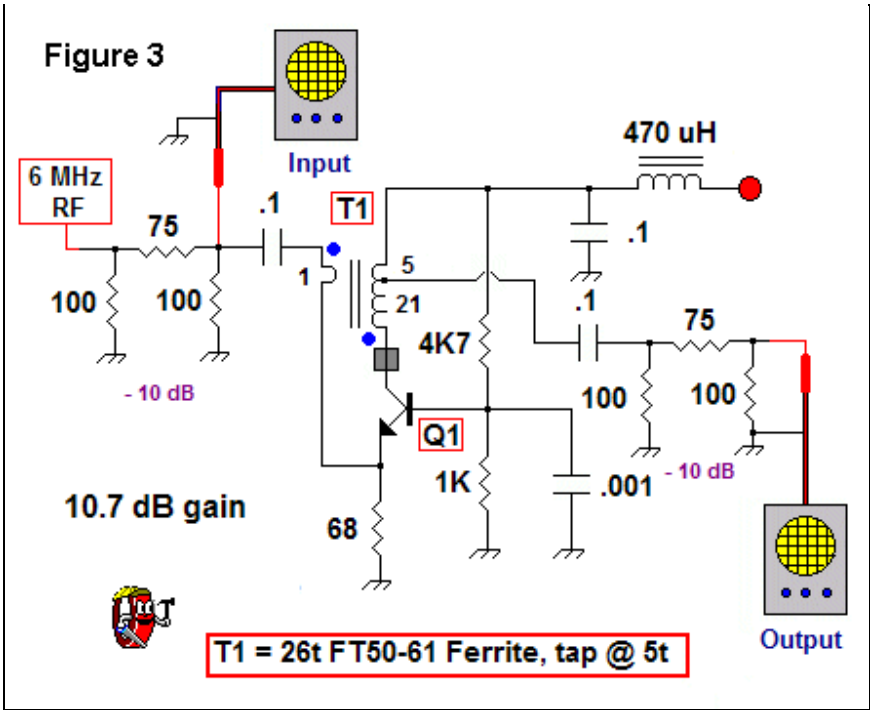

The amp above (labeled Figure 3) is a hot one; 10.7 dB gain even with 10 dB of attenuation. You can leave off the input pad and decrease the output pad to -6dB if you want or require a wide band, low noise RF amp with lots of guts. Most builders use binocular ferrite cores for the inductor, but torroids work fine for many applications.

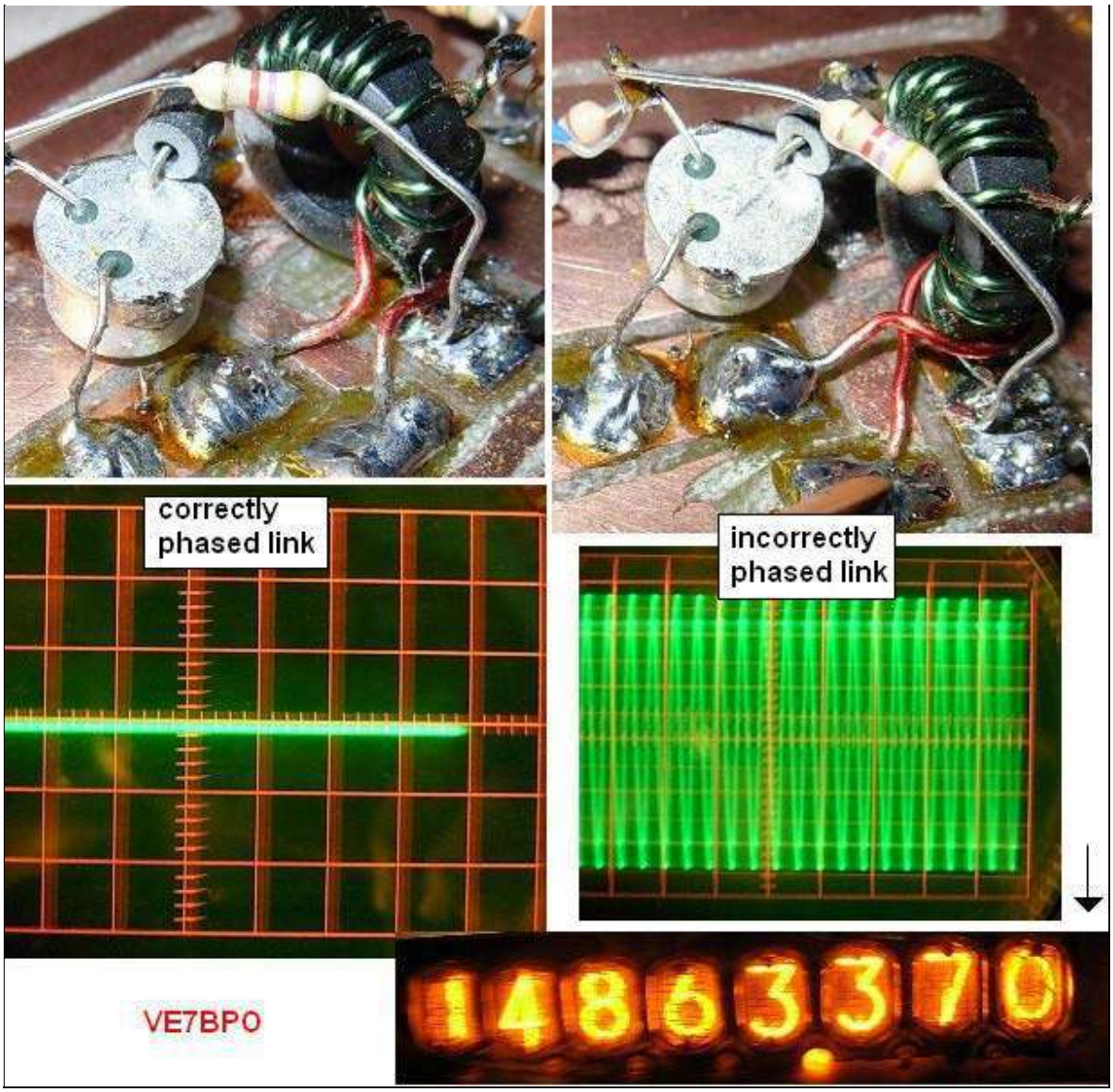

Shown above is a photograph of 1 of the experiments from 2007. The one turn link from the Norton amplifiers just above is shown phased correctly and then phased incorrectly. Note the oscillation in the "badly wired" amp at 14.86 MHz. I routinely check all of my noiseless RF amps using the oscilloscope. Occasionally, I will put a shunt coil and cap (from input to ground) on the input to "exaggerate" any oscillations. This has proven to be a useful technique for testing if the phasing of the one turn link was done correctly.

RF preamp for the 40 Meter band with 3 tuned filters

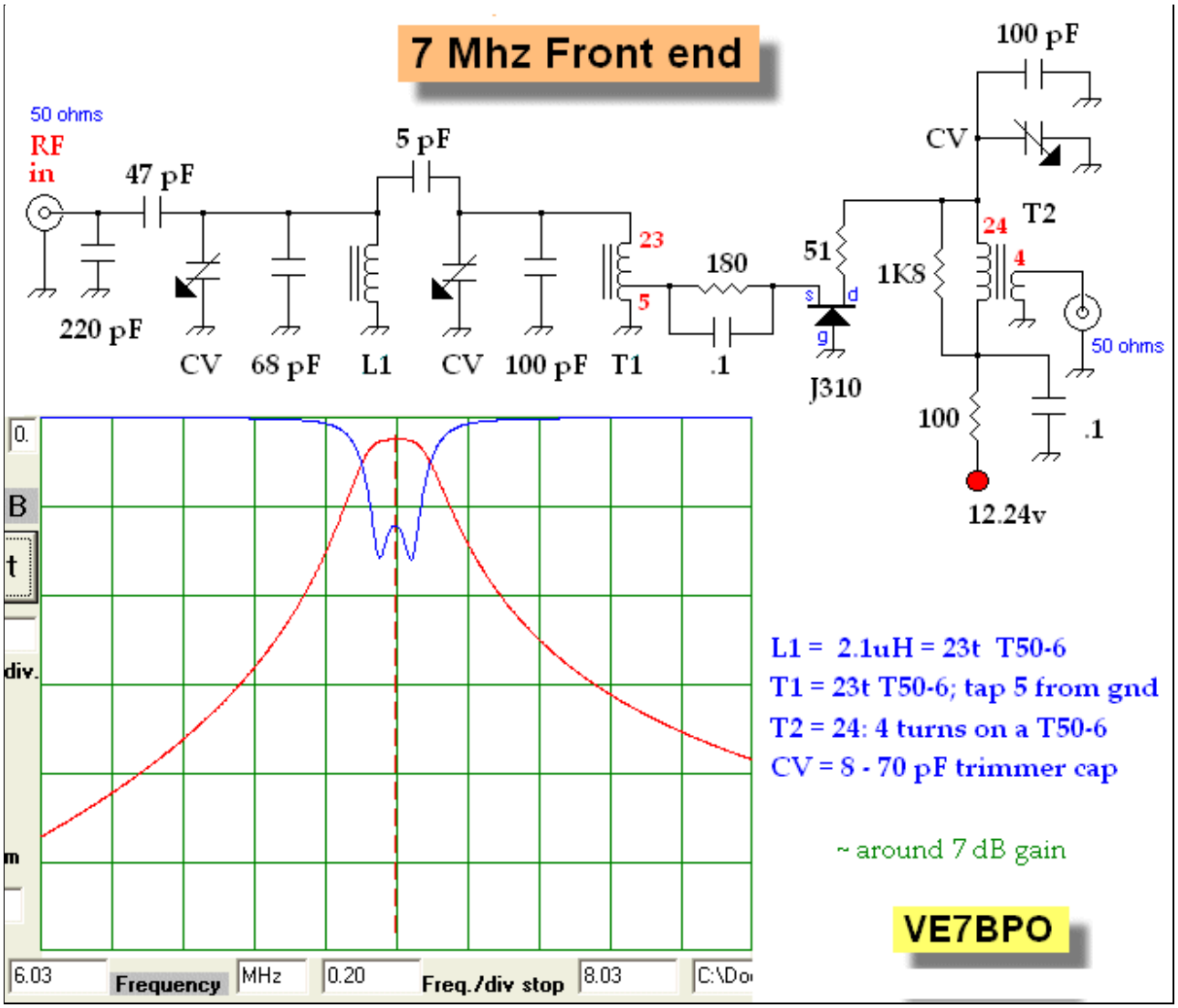

An experimenter's 40 Meter band front end for CW. This has a double-tuned filter and a low gain, lower noise RF amp. Great circuit for isolation of a product detector or mixer in a popcorn receiver.

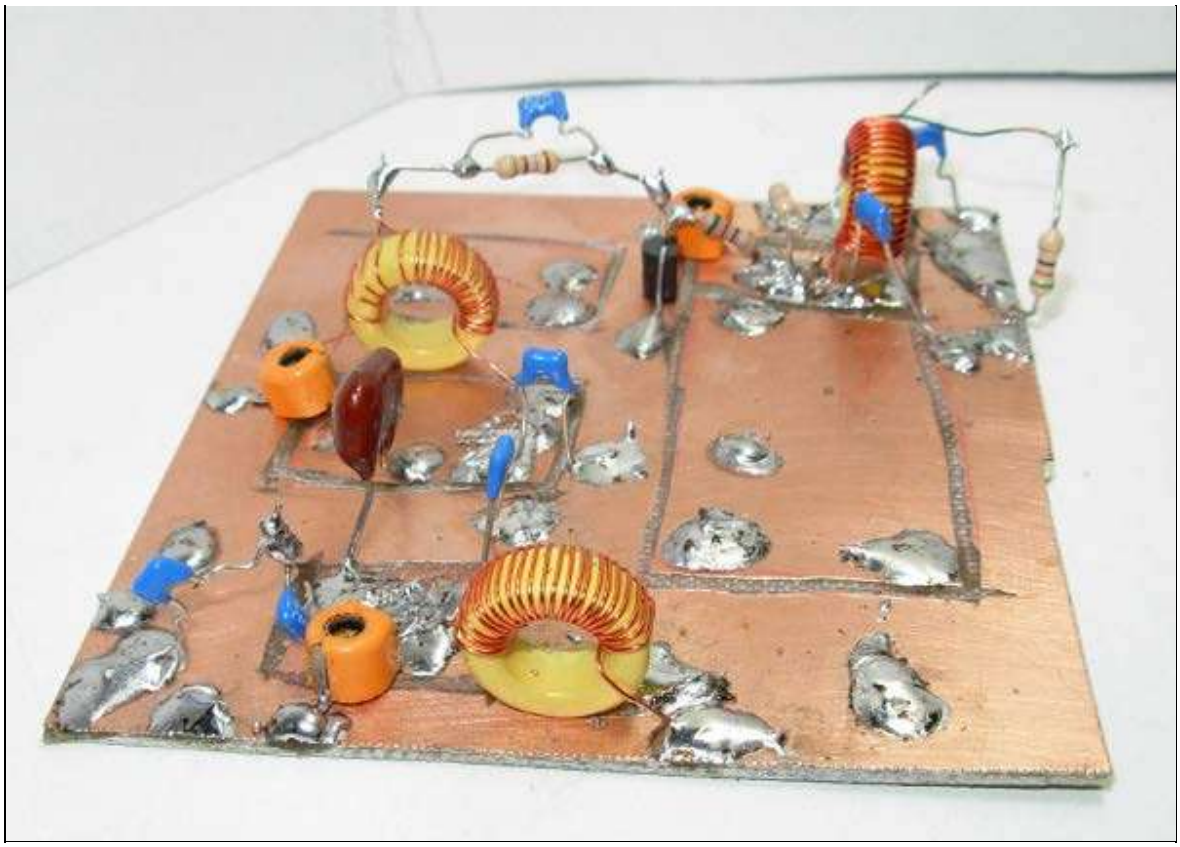

A photograph of the above 40 meter band front end, double-tuned filter plus tuned common gate RF amplifier. Input and output Z is 50 ohms.

Amateur and Short Wave Radio Electronics Experimenter's Web Site

QRP HomeBuilder Software

Disclaimer:

THE QRP HOMEBUILDER SOFTWARE OFFERED HEREIN ("THE SOFTWARE") DOES NOT COME WITH ANY WARRANTY, EXPRESS OR IMPLIED. IF YOU MAKE USE OF THE SOFTWARE, PLEASE BE AWARE THAT YOU DO SO AT YOUR OWN RISK. NEITHER THE AUTHORS OF THE SOFTWARE AT JENNA DESIGN NOR ANY OTHER PARTY WILL ACCEPT RESPONSIBILITY FOR ANY OCURRING OR UNFORESEEN CONSEQUENCES OR DAMAGES THAT ARISE AS A RESULT OF THE USE OR MISUSE OF THE SOFTWARE.

Technical Info and Distribution

The QRP HomeBuilder applications are written in C++ for speed and compactness. Apps will specified as GUI (graphical user interface) or 32-bit console based (DOS look). Anyone may display or distribute these applications via website or diskette providing that they do not charge for the program(s). I know longer have a C++ compiler and no future work on these applications is anticipated.

QRP - RELATED APPLICATIONS FOR DOWNLOADING

CoilBuilder_99

CoilBuilder_99 is a powdered iron inductor winding application. Enter desired inductance, select core size and mix and press the Calculate button to determine the correct number of windings for your inductor. Data is also given showing, core color, permeability, frequency range, AL value and maximum number of turns versus wire guage for the chosen core size. Encompasses 12 different core sizes and 8 different mixes of powdered iron. Calculated results can be stored on a disk file or printed out.

Style: GUI, File size: 90K, zipped, 44K.

Bug Fixes: Some missing AL values for # 7 material added April 24/99. K6WHP's superior version is linked below.

Current Version is: 4 / 24 / 1999

Download the CB99.zip file

PI Filter Designer

PI Filter Designer is a simple 3 element 50 ohm input and output impedance pi filter designing application. This program allows the user to design simple lowpass filters by selecting from a variety of standard capacitor values either empirically or to suit what you have on hand. The filter 3 dB cutoff frequency and required L1 inductance are automatically calculated and displayed. In addition, the user may select an additional capacitor value to put in parallel with both caps C1 and C2. In this app XL = XC = 50 ohms impedance. No other impedances can be calculated with this program.

Style: GUI, File size: 47K, zipped, 22K.

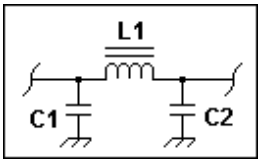

Current Version is: 1 / 14 / 1999

Download the pifilter.zip file

CapCoder

CapCoder gives the capacitance in microfarads, nanofarads and picofarads and tolerance of any capacitor code entered into its input section. Example : 104J. This app uses numeric spin-buttons and a combo box so that no typing is required for data entry.

Style: GUI, File size: 48K, zipped, 22K.

Bug Fixes : A nanofarad conversion error was corrected July 2, 1999.

Current Version is: 07 / 02 / 1999

Download the capcoder.zip file

Resistor Coder

Resistor Coder gives the resistance in ohms of any resistor color code entered into its input section. Four or five band resistors can be accommodated by this program. This app uses drop-down combo boxes so that no typing is required for data entry. Results may be saved to a disk file or directly printed.

Style: GUI, File size: 58K, zipped, 27K.

Current Version is: 1 / 16 / 1999

Download the resistor coder.zip file

Ferrite

Ferrite is used to calculate the number of turns required on toroidal ferrite cores to achieve the desired millihenry-value inductance. 15 different ferrite toroids are included in this application. This program will calculate the winding data for an inductance range of 0.001 to 27 millihenries.

Style: Console, File size: 64K, zipped, 31K.

Bug Fixes: Thanks to PA3CKR for the bug report; fixed Jan 19/99.

Current Version is: 1 / 19 / 1999

Download the ferrite.zip file

Universal Diplexer

Universal Diplexer calculates the inductance and capacitance values for a Bridge-Tee diplexer based upon a chosen superhet receiver intermediate frequency. The diplexer is the Joe Reisert, W1JR popularized design discussed under Diplexer Topics on this web site. The user inputs an IF and presses the Calculate button to have the capacitor and inductor values given in pF and uH respectively. The diplexer schematic is included in the application. Note that the this is for the Q = 1 version of the Bridge-Tee Diplexer.

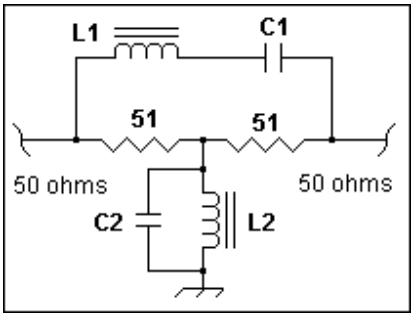

Style: GUI, File size: 49K, zipped, 22K.

Current Version is: 1 / 19 / 1999

Download the diplexer.zip file

HF Dipole

A very basic program for calculating the length of each leg of a 1/2 wave wire dipole antenna. Program good for 1 - 500 MHz, although intended for MF - HF useage. This app does nothing more than the standard 468/freq (MHz) type calculations. It was written for DOS many years ago and ported to Windows. The output shows the 1/2 wavelength and 1/4 wavelength design wire length in feet and meters. This app is probably of no help to experienced antenna designers.

Style: GUI, File size: 46K, zipped, 22K.

Update : Minor improvements made Feb 9, 1999

Current Version is: 2 / 9 / 1999

Download the hf_dipole.zip file

Resonator

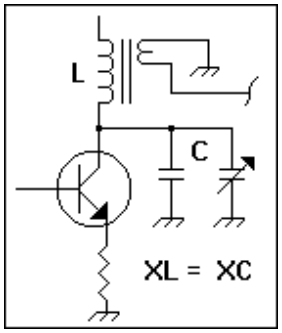

This application calculates the inductor and capacitor values for the tank circuit of a simple bipolar transistor RF amp. The basic schematic is shown above. Enter the center frequency plus the inductive/capacitive reactance you desire and press the Calculate button to calculate the necessary inductance and capacitance for L and C respectively.

Style: GUI, File size: 50K, zipped, 21K.

Current Version is: 1 / 23 / 1999

Download the resonator.zip file

NPN DC-BIAS

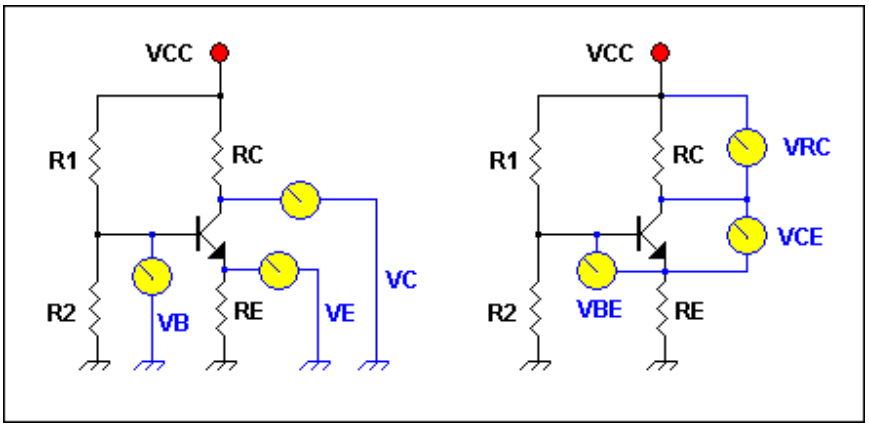

This application calculates the various voltages and currents of a simple voltage divider bias NPN bipolar transistor amp. The following is calculated: IB, IC, IE, VE, VB, VC, VCE and detection of Saturation or Cutoff. The user can alter the VCC, VBE, transistor beta and any of four resistor values R1, R2, RC and RE by picking the transistor value from a standard-value resistor table or manually entering the value. The schematic illustrates some of the voltage measuring points on the transistor schematic. *This app is in final BETA.*

Style: GUI, File size: 73K, zipped, 32K.

Current Version is: 16 / 04 / 1999

Download the nbias.zip file

Popcorn Direct Conversion Main Frame

Discussion:

Note: if you click on a schematic, a larger version will appear in a new web browser window.

Shown to the right is the schematic to a low cost popcorn direct conversion receiver main frame. To complete the receiver, a front end band pass filter and a VFO with an output power of 7 dBm is required. This is indeed a frugal project using 4 cheap transistors, an RC low pass filter and an LM386N for output power to a pair of low-impedance headphones. The builder also has a choice of 5 diplexers and an optional mute circuit. This receiver is easily built using Ugly Construction and can be built in 3-4 hours with a bit of luck.

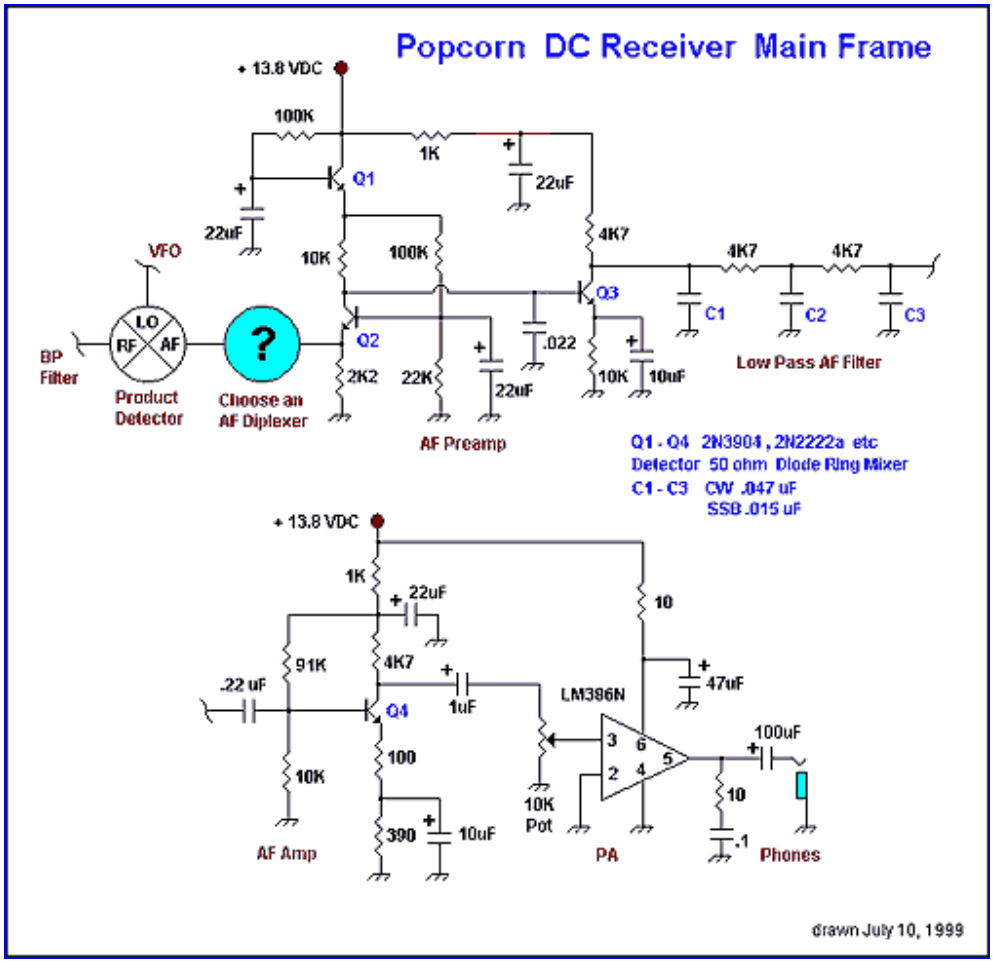

Product Detector and Diplexers

The 50 ohm diode ring product detector can be commercial units such as the Mini-Circuits SBL1 or TUF-1 or homebrewed 50 ohm impedance units. Five simple "diplexers" are shown in the lower "Adjuncts" schematic for you to choose from. The one you choose will depend on available parts, cost and your requirements in a popcorn receiver such as this. These diplexers are mostly of the low pass filter variety and provide a ~50 ohm termination to the diode ring mixer and some matching to preserve the product detector dynamic range. I realize that except for (A) and (D) these audio frequency filters are not truly diplexers and will not provide DC to daylight matching. The intent of this web site is not high performance-high cost

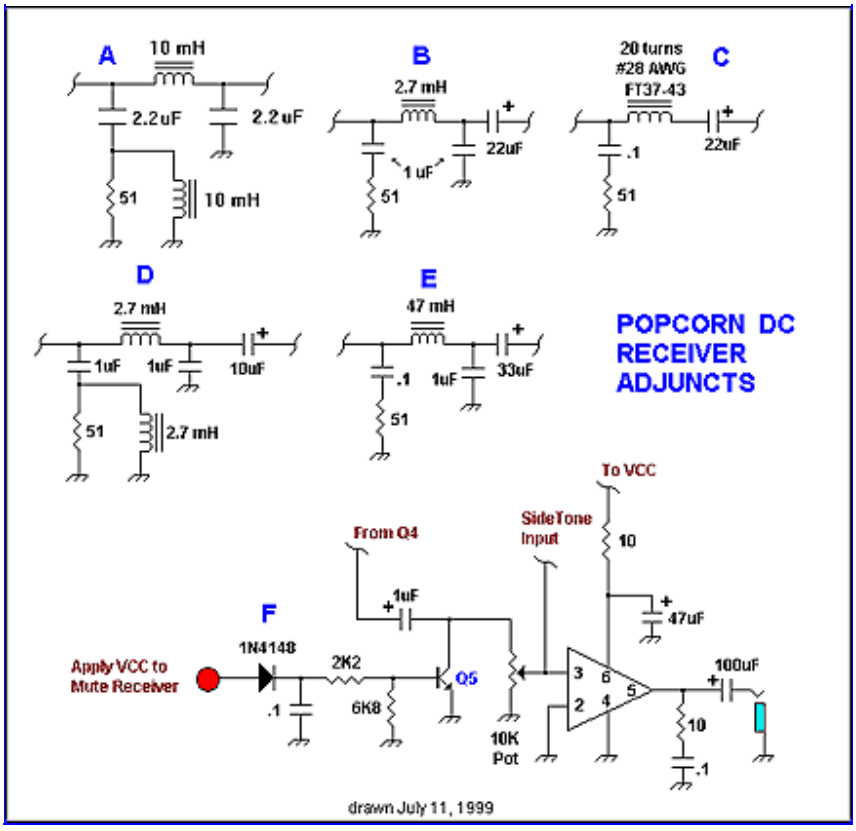

design and please do not confuse it as such. Note that electrolytic capacitors that bypass to ground such as the 1 uF caps must be non-polarized or bipolar for best results.

The (A) diplexer is by W7ZOI and is described on the Diplexer Web Page on this site.

The (B) and (D) diplexers are my designs and the (D) diplexer is the (B) diplexer with out the high pass component.

The (B) diplexer shown has a 3000 hertz 2 pole high pass/2 pole low pass design. This 2nd order filter provides reasonable overall matching Capacitors are standard-value, non-polar electrolytic types.

The (C) diplexer is a very basic, but very practical choice for this receiver.

The (E) diplexer is one that I used in one of my first DC receivers and the 47 millihenry inductor is a standard value unit sold by Mouser Electronics and others.

Another diplexer choice for this receiver might be the unit described by Rick Campbell, KK7B in his Binaural I-Q receiver project published in the March 1999 issue of QST.

Update May 15, 2009

There was confusion regarding the 2.7 to 47 mH inductors mentioned on this web page. I originally wound just the 2.7 mH inductor on a ferrite, but not the others. This is not a great idea as losses are high. For millihenries-value inductors, commercial parts should be purchased. A good brand to consider might be Epcos. Sorry for causing confusion.

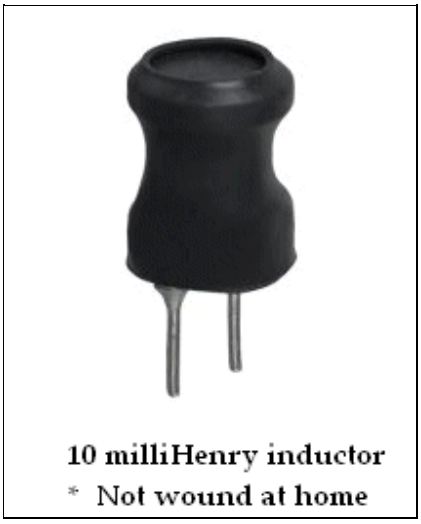

AF Preamps

The AF preamp section follows that of the Ugly Weekender Receiver designed by Wes Hayward, W7ZOI. I tried many other configurations

and came to the conclusion that these two simple but elegant stages give a winning combination of low noise, good gain, low parts count, low hum and good AM broadcast band rejection. The Q1 transistor decouples the receiver preamp very well and no hum was detected in the headphones providing a well filtered DC power supply was used. The Q2 grounded base amp provides a low impedance termination of the product detector and diplexer stages. Q2 and Q3 are direct coupled and provide lots of gain to drive the succeeding low pass filter without it adding a huge abundance of noise to the signal. The bypass capacitor (0.022 uF) is essential to bypass any broadcast AM detected in the Q1 stage to ground. Other values of capacitors maybe tried, but do not omit this critical part.

Low Pass Filter

I cannot handle listening to a DC receiver on a crowded band without some low pass filtering. The high pitch heterodynes effect my concentration and give me a headache. Nevertheless, it is neat to temporarily listen to an unfiltered DC receiver; to hear the pure and wonderful signals possible by beating RF directly into audio. I prefer low pass to band pass filters at audio and have used many combinations of active filters using discrete components and op-amps, as well as passive designs using AF inductors to build wave filters. This receiver uses none of these devices, however they could be easily substituted for the filter shown. Connected to Q3 is a simple, cheap RC low pass filter based upon the design criteria given on the Discrete Component RC Audio Filters web page on this web site. The cutoff values you calculate will be ballpark and values of 0.047 uF for CW and 0.015 uF for SSB were chosen, but other values could just as easily been used and please do not hesitate to experiment with the caps and/or the resistors to suit the parts you have on hand. For the capacitors in the low pass filters, avoid using ceramic disk type caps if you want the best possible performance. Polyester, polypropylene, polystyrene or polyester film type are all suitable, however, ceramic caps will work if you are really going junk box/low cost.

I attempted to make a wave file to demonstrate the low pass filter. I came right off the headphone jack into the input of the of my 16-bit PC sound card via a step up audio transformer and the results were a little disappointing. Sixty-cycle hum and distortion of loud stations were added by the sound card. The sound file is big (636 KB) and is a digital recording of me tuning through a 30 meter pile-up using the lowest sample rate and frequency possible on my computer. The low sample rate/frequency also degraded the sound somewhat as well, but I decided to put it on the page, warts and all. The DX station was a VK2 and sure did cause a lot of excitement on 30 meters that night around sunset on the left coast. Actually the wave file demonstrates how good the receiver sensitivity and AM radio immunity is. In addition, the low receiver background noise is also very apparent underneath the constant 60 cycle hum. The 60 cycle hum and clipping of loud CW signals is not heard in the headphones and is a soundcard manifestation. Perhaps the best method would be to come of Q4 and go right into the sound card with a smaller line-in signal voltage. Download the popdc wave file

---

AF Driver and Final Amp

Connected to the input and output of the Q4 stage are small value capacitors to provide some high pass filtering for the receiver amplifier chain. Some emitter degeneration is used on Q4 to provide a better termination of the preceding RC low pass filter. The receiver amplifier chain has a lot of gain and when the 10K pot is turned to minimal resistance (cranked) , the LM386N can be driven into distortion. You may want to limit the maximum gain with a series resistor connected to the 10K pot after building and testing this receiver.

The final AF amp is the perennial LM386N, a low cost, easy to use AF amp. Turn it upside down and solder pins 2 and 4 right to your copper ground plane to anchor this part. It can easily be configured to drive a small speaker.

An optional mute circuit is shown in the "Adjuncts" schematic and is labeled (F). This circuit is a simple transistor switch which grounds the output from Q4 and mutes the receiver audio. This circuit switches rapidly and there are no annoying pops or clicks to be heard in the headphones when it is switched. Apply the VCC to the diode as shown to mute the receiver during transmit if the receiver is used in conjunction with a transmitter. Q5 in the mute circuit can be a 2N3904 or 2N2222a or substitute.

In addition, a suggested side tone input to the LM386N is shown. I have started to use simple one section RC filters on the output of my side tone oscillators to smooth the waveform into a more pleasing audio tone.

Conclusion:

This popcorn receiver can be made very inexpensively and has good sensitivity and a reasonable noise level and selectivity. I tested this main frame on 30 and 40 meters and really enjoyed it. This receiver main frame could be combined with an inexpensive VFO using tuning diodes to keep cost down and the popcorn factor up. Although it does not use tuning diodes, a 40 Meter band VFO schematic has been placed on the VFO page.

Here is a YouTube Link using the receiver with a different front end filter and VFO. This is not my radio or video.

A blog post from Peter AK6L --- it's good to see builders moving beyond kits.

---

40 Meter Popcorn Superhet Receiver

Discussion:

Note: if you click on a schematic, a larger version will appear in a new web browser window.

To the right is the schematic for a no-frills, relatively low-cost CW superhet receiver with a 4.00 MHz Intermediate frequency. There is no AGC or RF gain control, however this receiver has good large signal handling capability. This receiver uses just 6 bipolar transistors and an op amp for reasonable volume into headphones. Much of the ideas/design of the various stages must be credited to Wes Hayward as I borrowed heavily from his previous work and through ideas obtained by discussion. If one were to homebrew the diode ring mixers, indeed this would be a very low cost receiver giving reasonable performance which outperforms any NE602 based superhet receivers that I have built or listened to. Below the main schematic is a diplexer diagram that allows the builder to choose from one of two RF and AF diplexers used to terminate the diode ring mixers.

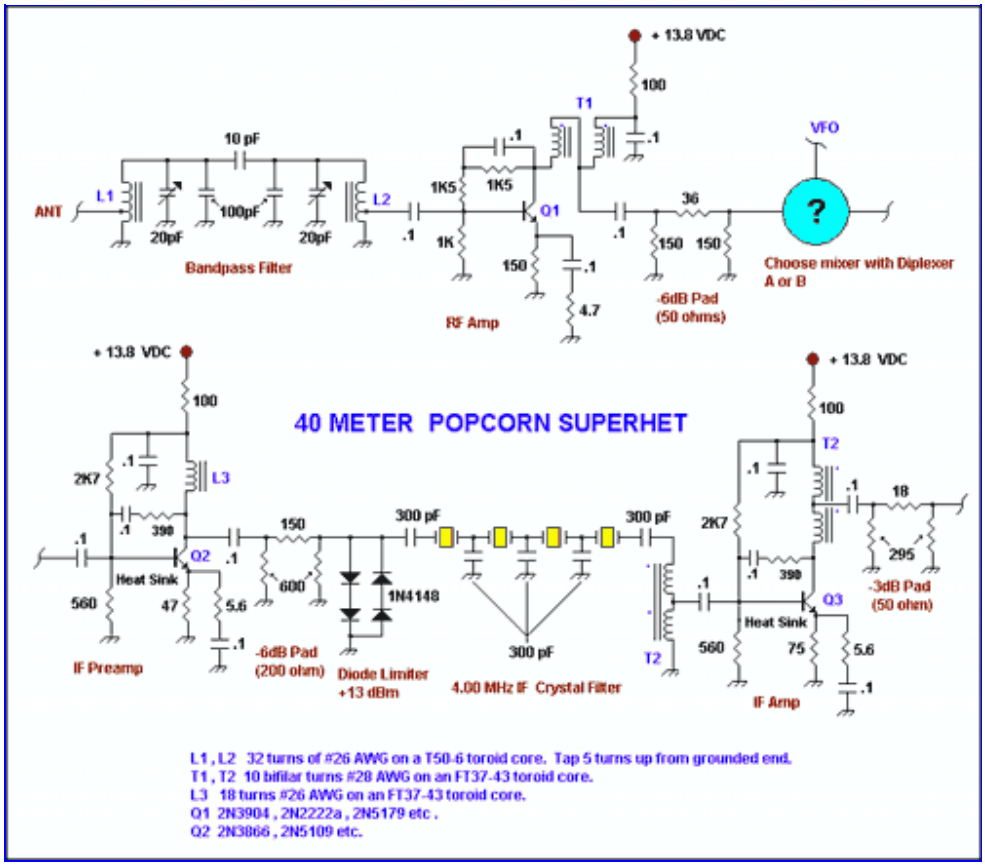

Band pass Filter and RF Preamp

From the 50 ohm receiver antenna jack, first off is a double-tuned band pass filter which was designed by Rick Campbell, KK7B and works very well. The trimmer caps can be the 5 - 20 pF units sold by Digi-key and Mouser. The fixed-value caps in my prototype were inexpensive monolithic ceramic capacitors purchased from Digi-key. Rick used an NP0 ceramic for the 10 pF coupling cap plus silver-mica type for the 100 pF caps in his original design. For possible lower insertion loss, the probable best/cheapest way would be to use all NPO ceramics for the fixed value caps in this filter.

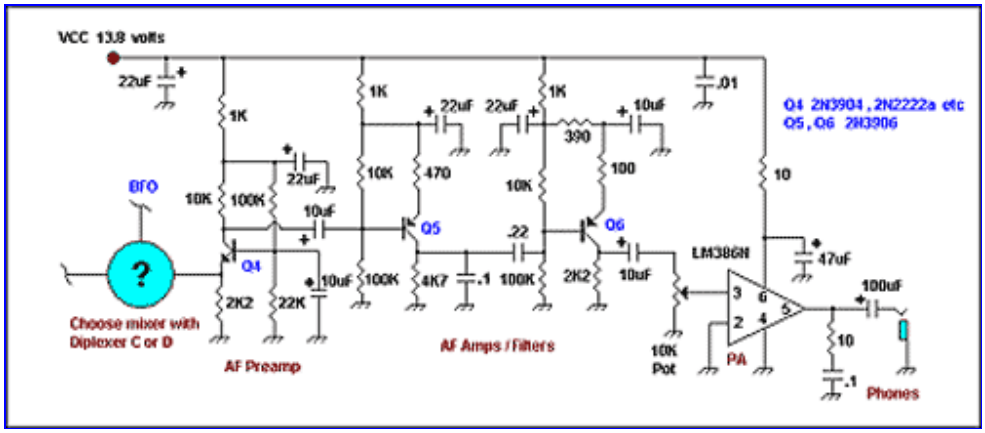

The RF amp is my favorite popcorn RF amp ; a 50 ohm feedback amp. A grounded-gate JFET amp was tried in its place and was also found to be quite suitable and does not require the -6dB pi attenuator that follows the feedback amp as shown in the schematic. The feedback amp's 50 ohm input impedance properly terminates the band pass filter. The -6 dB attenuator pad following the amp to helps provide a 50 ohm input impedance for the mixer and to reduce stage gain which aids in preserving the signal to noise ratio of the receiver. If a builder wants a little more sensitivity, the pi attenuation pad could be reduced to -3 dB however this may effect the receiver dynamic range. The transformer T1 is one of 2 broadband transmission line transformers in this receiver. It transforms the 200 ohm collector impedance to 50 ohms for the succeeding stage.

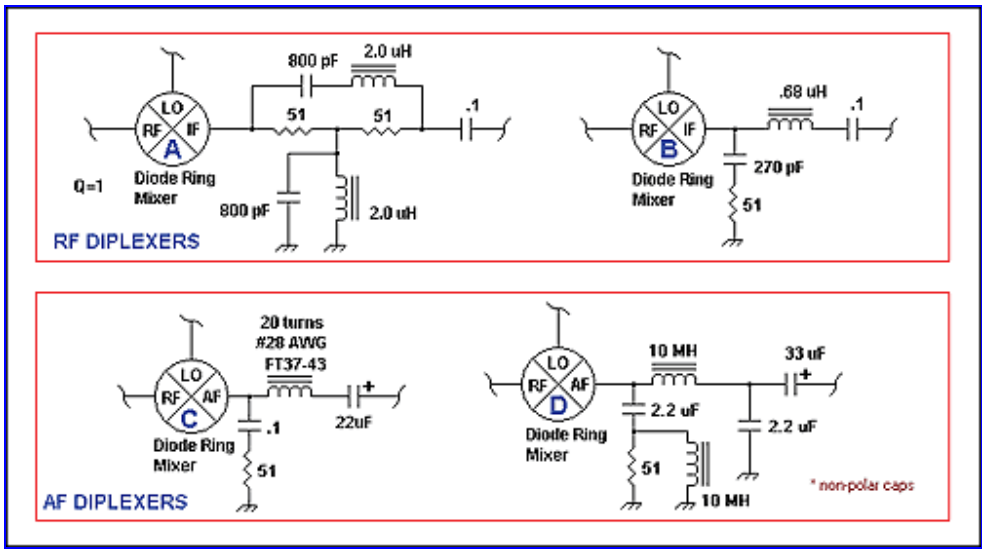

Mixer and Diplexer

A 50 ohm diode ring mixer (7dBm) such as the Mini Circuits SBL-1 or TUF-1 or homebrew are all suitable. Following the mixer is an RF diplexer of your choice. The more complex Brifge-Tee (Q = 1)diplexer (A) is an excellent design, however maybe overkill in a popcorn superhet such as this. For the (A) diplexer, to get the necessary 800 pF for the capacitors, simply parallel a 470 with a 330 pF or a 120 pF with a 680 pf capacitor. The inductors at 2.0 uH are wound on powdered-iron torroids. You can use # 26 AWG wire and it requires 22 turns on a T37-2 core or 20 turns on a T50-2 core. In addition, you can use a #6 material torroid to wind the inductors. This diplexer is described elsewhere on this web site.

The simpler (B) diplexer uses a ~3 times the IF frequency that I have seen this basic design in many textbooks and articles and provides reasonable matching with a 50 ohm inductive and capacitive reactance. The cutoff frequency chosen was 11.78 MHz as this allows the use of a standard value capacitor (270pF). To wind the 0.68 uH inductor use 13 turns on a T37-2 torroid or 12 turns on a T50-2 powdered iron torroid core. You can easily use 24 - 26 AWG wire for the inductor.

IF Preamp , Crystal Filter and IF Amplifier

Except for the inductors, the IF preamp and IF amp are identical and both warrant a small clip-on heat sink as they draw reasonable current. The standing current maybe increased or reduced by changing the 47 and 75 ohm resistors connected to the Q2 and Q3 emitter respectively. Factors such as available power supply current versus dynamic range requirements may come into play. One may want to stand more current in the IF preamp and less current in the IF amp. For example, the 75 ohm resistor on the Q3 emitter could be increased considerably and/or the 5.6 ohm degeneration resistor could be increased as well if less stage current draw is wanted. The 2N3866 transistor is usually a cheaper way to go for these amps than the 2N5109, but the choice is up to you as you may have something available in your junk box. The 200 ohm -6dB pad following the IF preamp should not be omitted as it helps prevents the stage from seeing reactance's created ahead by the crystal filter. The four diodes form a 13dB limiter to protect the crystal filter should a catastrophically large signal be present in the receiver's front end. They maybe omitted. A -3dB 50 ohm resistive pad terminates the IF amp and helps establish a 50 ohm input impedance for the product detector ahead. **Click here** for more on the IF preamp.

This receiver has a narrow IF Cohn Crystal filter. Bandwidth is ~ 405 hertz, which unfortunately makes tuning quite sharp however this filter is very nice for crowded band conditions. The IF filter crystals should be closely matched in frequency to prevent unwanted ripple in the pass band. Generally, you have to buy 10 and then if you have a frequency counter, use the receiver BFO stage to test your crystals for matching. Pick the closest 4 crystals and use them in your filter. It does not matter if the crystals have series or 20 pF load capacitance, but it does matter that they are matched in frequency within 40 hertz of one another or better for this receiver. For my prototype receiver, I purchased ten 20 pF load capacitance 4 MHz crystals and luckily found 4 that matched each other within 9 hertz! For those builders who do not have a frequency counter, some QRP parts retailers sell matched sets of crystals. It is important to note that the BFO should be set on the high side of the IF frequency as simple crystal ladder filters have a steeper upper passband than lower pass band.

The crystal filter is terminated by the 4:1 transmission line transformer and then 50 ohm impedance of the IF amplifier. The -3dB pad following the IF feedback amplifier helps to terminate the crystal filter by helping ensure a 50 ohm IF amp input impedance and should not be omitted. Place a 75 and a 220 ohm resistor in series to get the required 295 ohm resistance on each leg of the pi attenuator.

Many may balk at just one stage of IF amplification, but since there is no AGC and this is a CW receiver, it works well. A feedback amp is once again used to provide correct input and output impedances for stages connected to the IF amp. Following the IF amp is another attenuator set for -3dB and then a 50 ohm diode ring mixer.

Product Detector, AF Diplexer and Audio Amplifiers

The mixer/detector can be SBL-1 or TUF-1 types or homebrew if you want to reduce costs further as the mixers are the single most expensive components in this receiver.

Again a choice of diplexers is required. The (C) AF diplexer is very simplistic but very practical if you are trying to keep costs low. The (D) diplexer is designed by W7ZOI and is from the Diplexer Web Page on this site.

Following the diplexer, a grounded base audio amp provides a 50 ohm termination to the product detector. AF gain and some AF filtering are provided by Q5 and Q6 which together attenuate frequencies less than 72 hertz and greater than 638 hertz. This amplifier pair are described on the discrete AF filters web page on this web site. Keep your leads short on all the AF transistors.

The final AF amp is the perennial LM386N, a low cost, easy to use AF amp. Turn it upside down and solder pins 2 and 4 right to your copper ground plane to anchor this part. There are a number of low-noise alternatives to the LM386 available which are generally more expensive but would be quite suitable. Discrete component AF amps can also be used, but a popcorn part such as the LM386N maybe cheaper and easier.

VFO and BFO

VFO schematic

BFO schematic

Alternate version of this receiver

Construction Ideas

When constructing any project, build in small modules and test each one separately. For instance, the AF amp should be built first and then tested by injecting a very low-level audio frequency tone into that stage and listening for output in your headphones. Every QRP workbench should have a simple AF tone oscillator from a schematic similar to the ones used for keying side tones in CW transmitters. The encased oscillator should have to a 100K or so potentiometer connected to the output to vary the output signal amplitude. Generally use maximum resistance on the 100K pot to start with and reduce this resistance slowly as the in-test amplified oscillator output could be very loud!. After testing the AF amp, build the 3rd AF preamp stage including the 10K panel mounted pot so you can vary the gain going into the AF amp. Now inject the AF oscillator output into the input on the pot and vary the 10K pot to ensure that the stage you built is working. It should be a lot louder now and should go up and down in volume with the 10K pot. Finally build the remaining preamp stage and once again test the circuit with your AF oscillator. The output into the phones should be painfully loud now when cranked up! The next stage to build would be the BFO. If you do not have a scope, peak the tuned circuit by watching the S meter on a radio receiver located nearby. Ensure that you put a load on the output winding of the BFO such as 47 ohm resistor to ground. A small piece of wire can be used as an antenna if the BFO signal is too weak to activate the S meter on your receiver. Once peaked, you can now use the BFO to match your IF crystals. To use the BFO to match your crystals, use a small wire to bypass or disconnect the 60 pF variable capacitor that is used to connect the crystal to ground. In other words, the bottom lead of the crystal is connected to ground with a short piece of wire. This makes testing your crystals a little more scientific as the variable capacitor cannot influence the crystal frequency during testing. You can also use the BFO in conjunction with a scope or voltage probe to test the various RF amps in the receiver. I do this all the time with my scope. Proceed with this build a stage, test a stage method and you should be rewarded with a functional end product.

KK4RF's version of the 40 Meter Band Popcorn Superhet

Marty, KK4RF emailed me and described his version of the popcorn superhet from this web page and contributed some great info and photos of his receiver. Of note is Marty's use of Radio Shack IC boards for mounting the components for each stage other than the VFO circuit. This is yet another variation from ugly construction that I have also used which works extremely well. Marty built the VFO using pure ugly construction and I was glad to hear that he is enjoying good frequency stability even with the lid off the VFO enclosure.

He built the receiver into an old Heathkit HW-12 single-bander case from the 1960's and it is a very attractive receiver to say the least. He found an old National Velvet Vernier Drive at the Virginia Beach Hamfest this year and used it to tune the VFO. Don't you love Hamfests! For the BFO he used an BFO circuit with a 4 mHz crystal from a different receiver project (a project that never quite worked.) He built a small power supply and located it along with the BFO under the chassis.

I like Marty's generous use of ground plane and neat stage layout. He reports good selectivity with his IF filter and apparently built four superhets that did not work before building this popcorn version. This is more a testimony to Marty's perservance to home building than to this receiver design in my opinion. I won't tell you how many rig failures I have personally incurred, as it would take a long time! Many thanks to Marty, KK4RF for the feedback and great pictures.

Broadband Transformers plus Diode Ring Mixers

Discussion

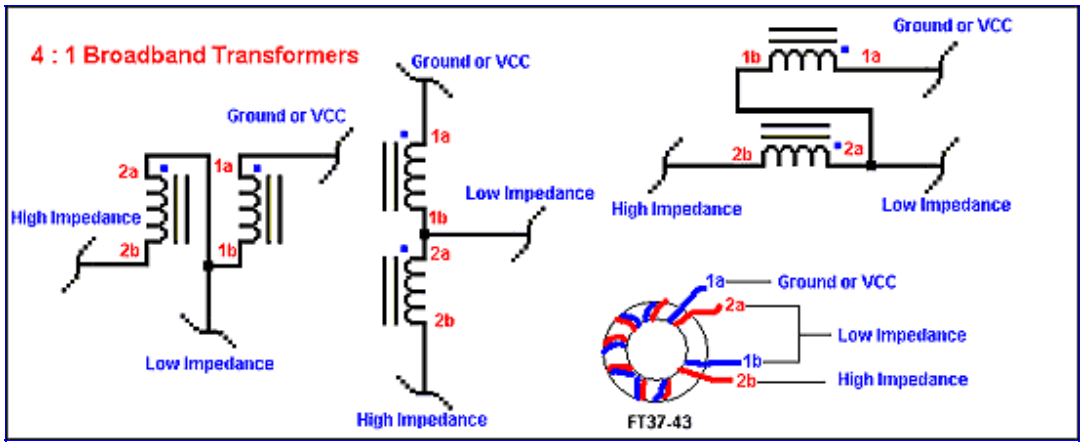

There are 2 basic types of broadband transformers used in most QRP work — conventional and transmission line style. Both types may be wound on ferrite toroids, pot cores or rods, however, I only discuss the toroidal transformers we employ to give a 4:1 impedance transformation.

I use these transmission line transformers on many projects on the QRP / SWL HomeBuilder web site. For MF and HF uses, a ferrite core permeability of 850-900 is generally required and the FT37-43 ferrite core proves suitable. Shown above are 3 equivalent schematics of the 4:1 transmission line transformer. You'll probably find that the center drawing easiest to conceptualize, however, with closer examination, all 3 schematics are the same and transform signals from unbalanced 50 Ω impedance up to 200 Ω unbalanced impedance or visa-versa.

The high impedance is 200 Ω and the low impedance is 50 Ω in all cases. It is important to know that these transformers are symmetrical and the points labeled Ground or VCC can be switched with the point labeled High Impedance. *Click on the schematic to enlarge it.*

Winding the 4:1 Transformers

Wire Twisting

Transmission line transformers are wound with bifilar (2 wires — generally twisted together). Winding these transformers is very easy. All you need are two ~18 cm (7 inch) pieces of #28 AWG enamel coated wire and an FT37-43 ferrite toroidal core.

A shop vise, a ruler, plus a brace and bit hand drill may aid your construction — I bought my brace and bit drill at a garage sale for 2 dollars. You need to twist the 2 pieces of wire together to get ~3-4 twists per cm (8-10 twists per inch) in the wire. To do this, loosely twist the wires at one end and place these twisted ends in a bench vise. Next, place the free wire ends together in your brace and bit drill chuck (no drill bit) and tighten up the chuck so that the wires are held securely.

Try to keep wire length and tension equal. Start turning your drill to twist the wires together and every once and a while measure how many twists per cm with a ruler. When you get to 3-4 twists per cm (8-10 twists per inch) you're done and then may trim the excess leads with a wire cutter in preparation for final winding and soldering.

At VHF, I often use just 3 or 4 total turns on an FT23-43 toroid with a piece of wire just a few cm long. I place the 2 wires in the vise and twist them using a pair of pliers held parallel to the wire.

Transmission line transformers will also work if the wires are untwisted. 3-4 twists per cm only serves as a non-criticial guide. Never wind your simple 4:1 transformers with bare wire.

A brace and bit hand drill plus a vise provides a good way to twist your wires.

Final Wiring and Soldering

Leaving a 2.5 cm (1 inch) lead, wind ten complete loops through the toroidal core leaving a small gap between the start and finish leads.

Untwist the leads a little so that you have 4 separate wires. One set of these wires wires will be called winding #1 and the other winding #2. You need to identify them and further break them into 1a, 1b and 2a and 2b. Generally I regard the the top two windings as (A) and the the bottom two wires (B), however, use whatever system works best for you. Strip off the enamel at the tips of all four leads and then get your ohmmeter or better yet, a beeping continuity tester.

Start on one of the top (A) wires by connecting the ohmmeter or continuity beeper to it and then touch one of the bottom wires and then the other bottom wire. Whatever bottom wire (B) shows continuity with your top wire should be marked along with the source top (A) wire with paint, liquid paper, tape, or whatever you like.

I prefer to wind 2 different colored wires if possible.

Designate the marked wire pair winding number 1. You may also want to test for a short circuit — there should be no connection between wire set 1 and wire set 2 at all. So now you have 2 wires sets, winding set 1 is marked and winding set 2 is unmarked. The top two wires are arbitrarily labeled A and the bottom two wires are labeled B . Refer to the schematic above for clarification. Connect 1b to 2a and twist them together and then solder. Your done!

It's really easy to make these things don't you think?.

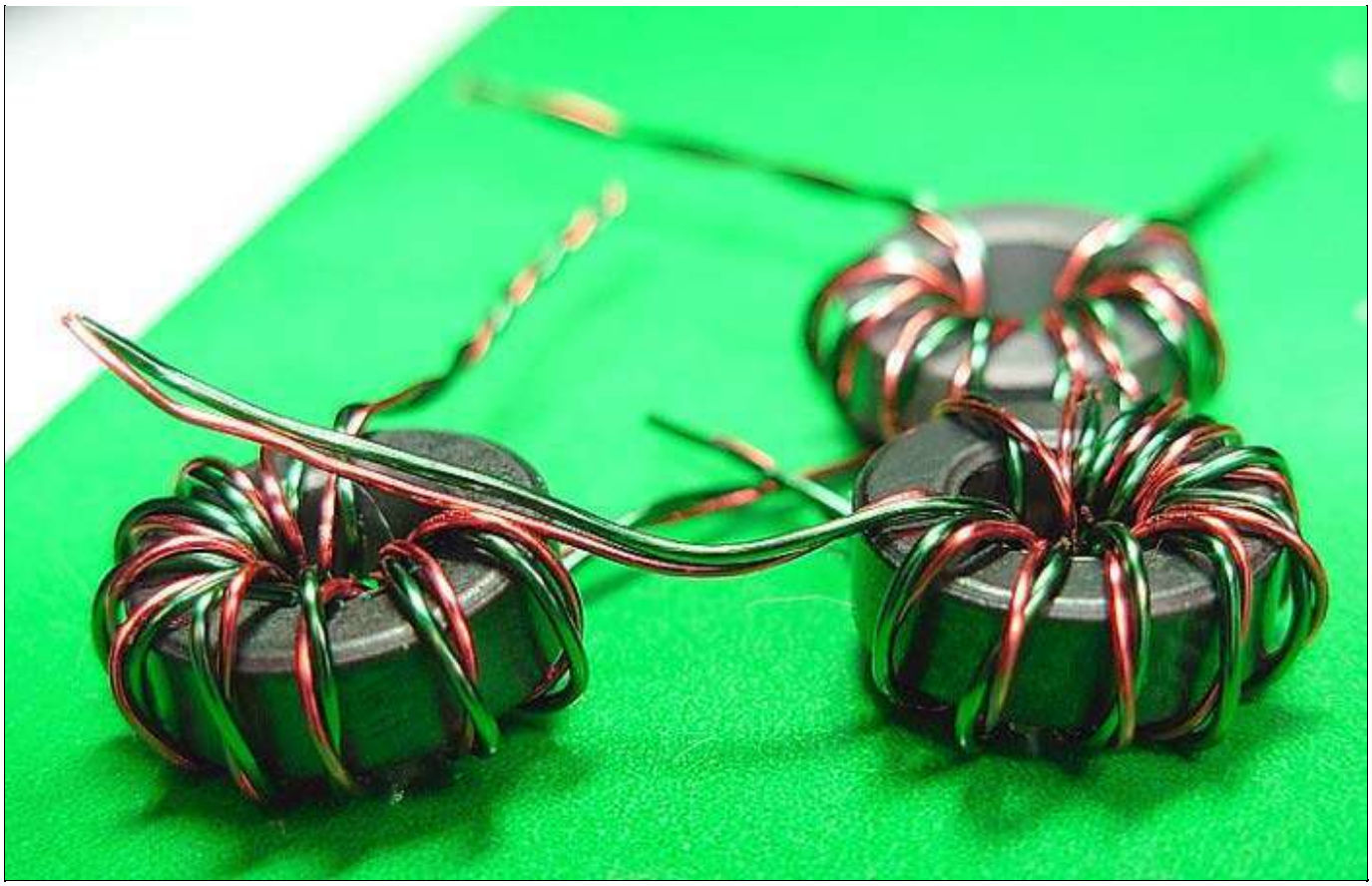

A trio of bifilar transformers wound on FT37-43 ferrite toroids. 2 colors of wire reduces errors and speeds up construction. Consider making up 5 at a time, so you have them on hand and do not have to interrupt your experiments.

Homebuilding Diode Ring Mixers

Discussion:

Easy to make, homebuilt diode ring mixers give a low-cost alternative to commercial diode ring mixers. A double-balanced diode ring mixer has 2 unbalanced to balanced transformers and a diode ring. The impedances at the three ports is 50 Ω. The transformers are wound with #28 AWG enamel coated wire on a FT37-43 ferrite toroidal core using a trifilar (3 wire) technique.

The wire twisting and winding technique is done as described above for the bifilar transformers. The connections 2b and 3a are twisted together and soldered. Again you will have to develop a technique to help you distinguish the wires from 1 another. *Click on the schematic to enlarge*

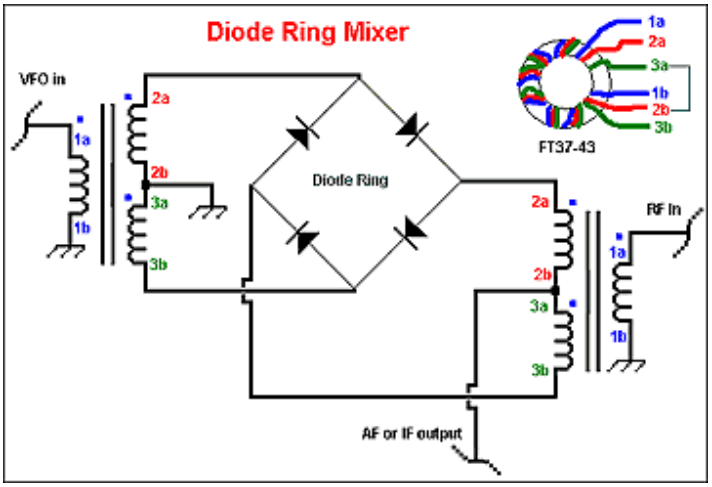

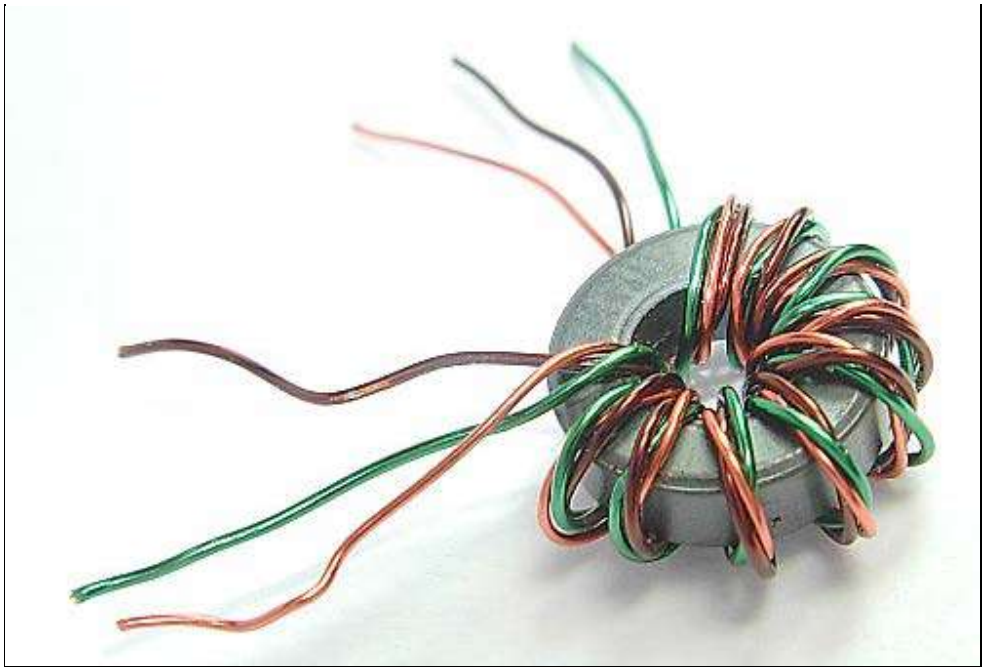

A trifilar transformer wound using 3 colors of wire on an FT37-43 toroid

A sample of the enamel coated copper wire collection I wind inductors and transformers with. In stock are wire gauges from 18 to 34. Like everything else, this collection started small and grew over time. Be vigilant for bargains and when you find a good price, purchase a whole bunch as it does not go bad. The Belden wire (orange spool ends) is over 40 years old and the enamel insulation remains perfect.

Diode Matching for Mixers

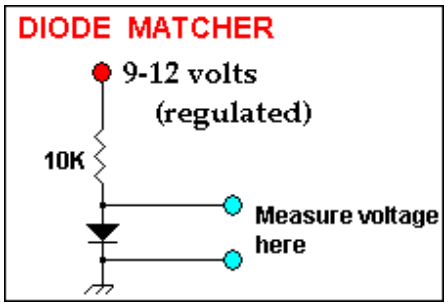

Discussion

For optimal results Schottky or Hot-Carrier diodes should be used. However, common diodes such as the 1N914, 1N4148 or 1N4454 are all quite suitable and are much cheaper. The four ring diodes should be matched to help mixer balance and thus carrier suppression. At MF and HF the most critical matching required is the forward voltage drop across the diode and this is easily performed with a sensitive voltmeter.

Set your voltmeter on the 2 volt scale to give you 3 decimal places for matching the voltage drops. Try and find 4 diodes close to one another. In addition, best results maybe obtained if all the diodes are the same type (i.e. all 1N4148) and if they are all from the same manufacturer. Look above for easy schematic to match your diodes with a voltmeter. Give the diode under test at least 20 seconds to warm up and stabilize before taking your voltage measurement.

Diplexers Topics

Introduction

My original web page on diplexers was rather incomplete and received some criticism from electronic engineers albeit the focus of this web site is "popcorn" designs. Wes Hayward, W7ZOI provided me some excellent schematics, analysis and simulations for diplexers which terminate doubly balanced mixers and these are presented below. After this section, the W1JR Bridge-Tee RF Diplexer from the original QRP HomeBuilder diplexer web page is presented along with new commentary and simulations by W7ZOI.

The final section presents a practical diplexer for terminating a product detector. All graphical images labeled as Figures 1-24 are copyright and property of W7ZOI and may not be presented elsewhere. Updated September 23, 2000.

W7ZOI Diplexer Notes

The usual amplifier is a two-port circuit. That is, it has an input port consisting of two terminals and an output consisting of two more. One terminal (ground) can be shared between the ports. Many filters are also two-port networks, including most of the ladders networks we use so often. Many other networks have three or even more ports. A common example is a mixer, which has three ports. Another example of a three port network is a diplexer. This linear network is usually designed around two port filters where one end of two different filters are paralleled to form an input port. This is illustrated as Figure 1. The purpose of a diplexer is usually to force a frequency constant impedance to occur at the input port, even though we usually only use one of the two output ports for signals. The simplest form of diplexer uses a pair of 1 element filters, a low pass and a high pass. This is shown in Figure 2.

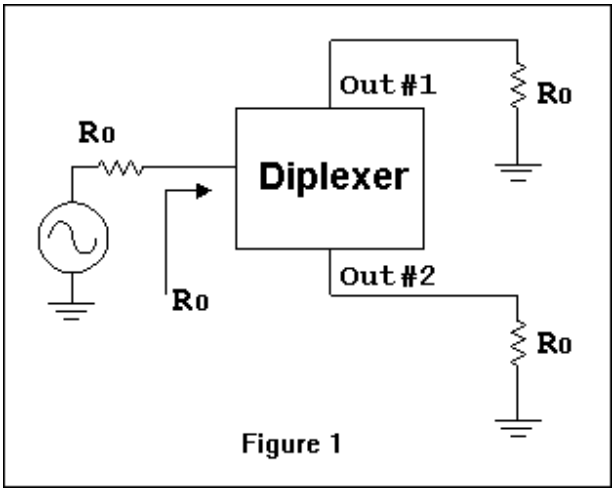

Figure 1

Where the

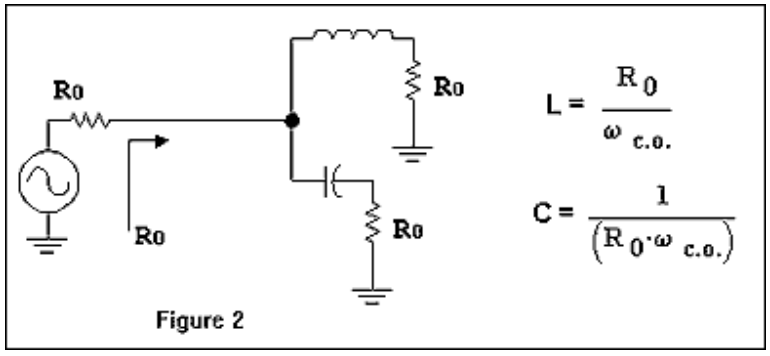

Figure 2

equations give the L and C that provide a perfect match. The angular frequency is called the cross-over. A familiar example is the cross over used in audio systems. The network that splits signals is a diplexer. Here is an example where both outputs are used. Another form of diplexer is the band pass/band-stop combination. This is shown in Figure 3:

Let's now consider further some examples, some that work and some that don't work as well. First, let's look at an audio diplexer that follows a product detector in a DC receiver. The load of interest is the first audio stage, which has a 50 Ohm input resistance. The diplexer offered is Figure 4. Note that this is not the combination of filters. It just looks like a low pass with an extra resistor. The response of this circuit is shown in Figure 5. The transmitted signal never gets

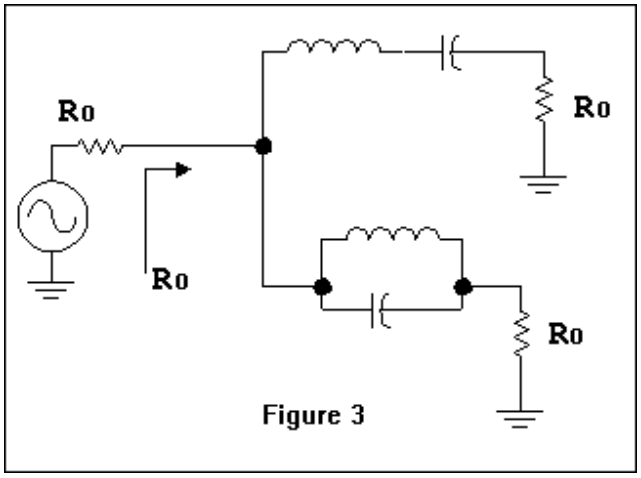

Figure 3

up to the desired 1 volt in the low pass passband while the impedance match, represented by reflection coefficient, never gets down to the desired zero. The response is just that of a lossy low pass filter.

In 2012; Click on many of the diplexer images to see the original sized version

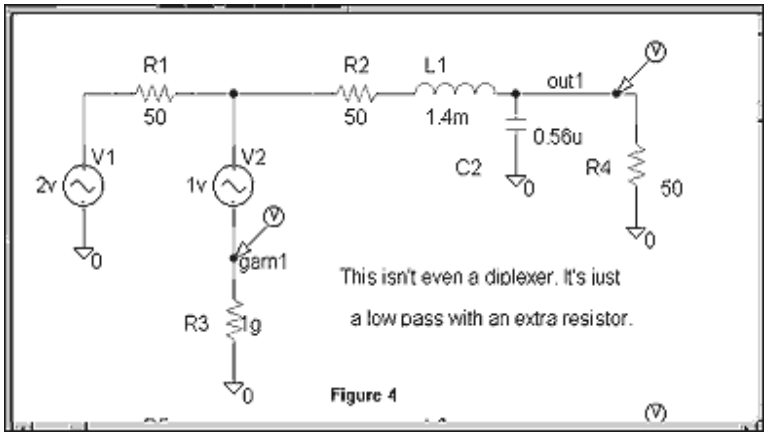

Figure 4

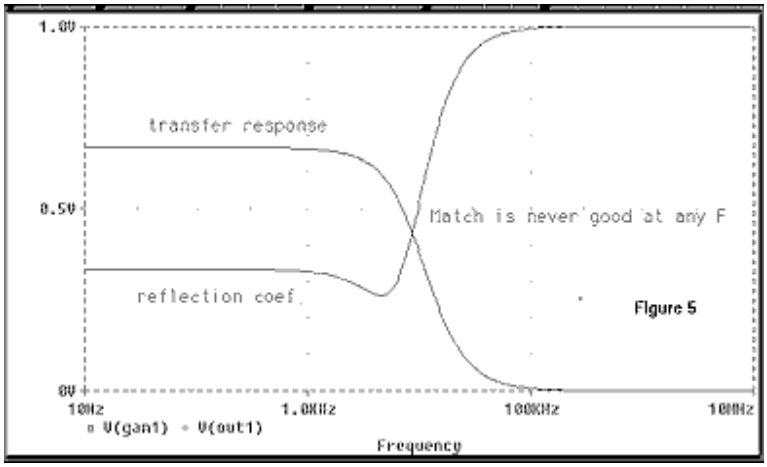

Figure 5

The normal filter circuit without the extra resistor is Figure 6. The corresponding output response is shown in Figure 7. Note that the transmitted signal is now up at 1 while the reflection is down to zero, both within the passband. Transmission goes to zero while reflection is 1 in the stopband.

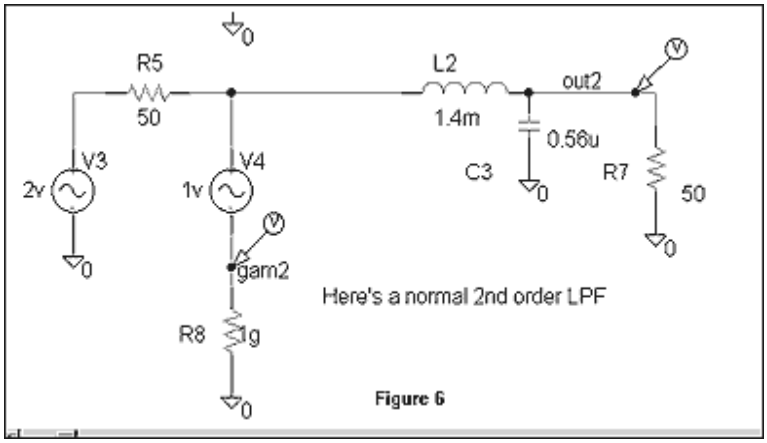

Figure 6

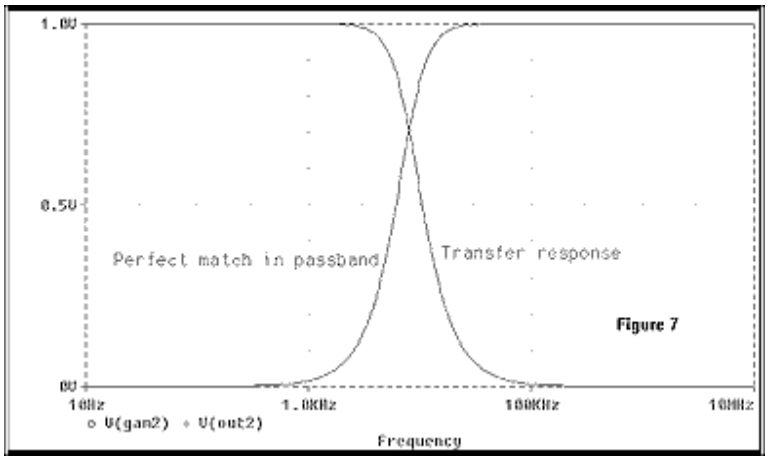

Figure 7

Now let's use the low pass and put a high pass with it to try to form a diplexer. This is shown in Figure 8 where we now have just guessed at component values. The response, shown in Figure 9, has high pass and low pass outputs that we might expect. The match is good at the frequency extremes, but is only so-so in the transition band.

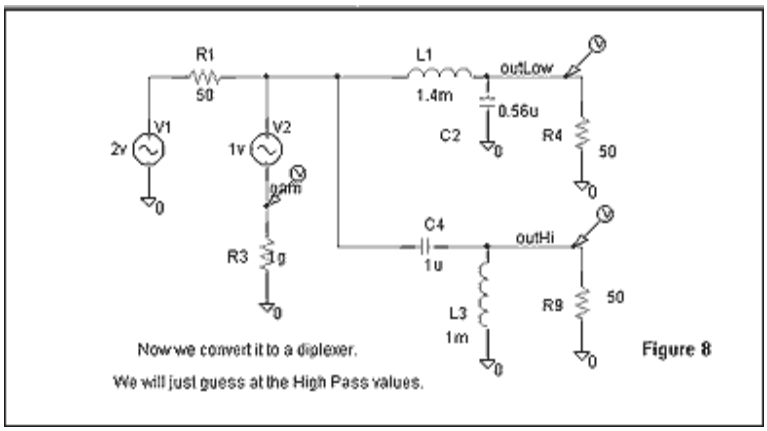

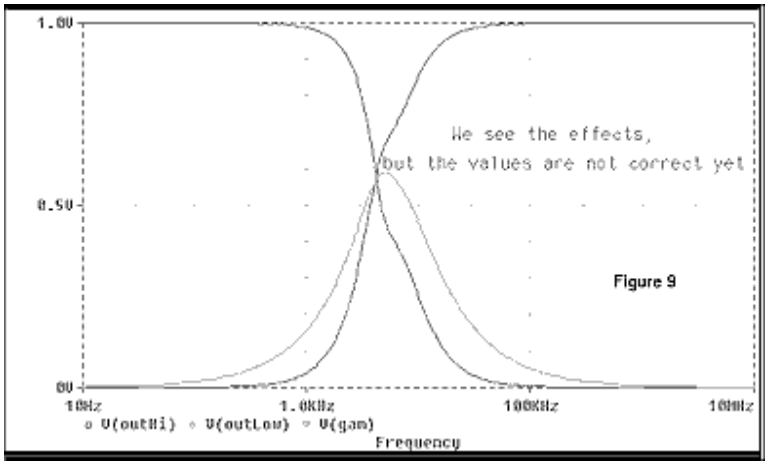

Let's now look at a carefully designed pair of two element filters. The circuit is Figure 10 an is a final example. The corresponding response is Figure 11. It is hard to see, for the response merges in with the baseline. However, the reflection is zero and it is zero everywhere. This filter was designed for a 1 kHz crossover, so it can be scaled to other frequencies with ease.

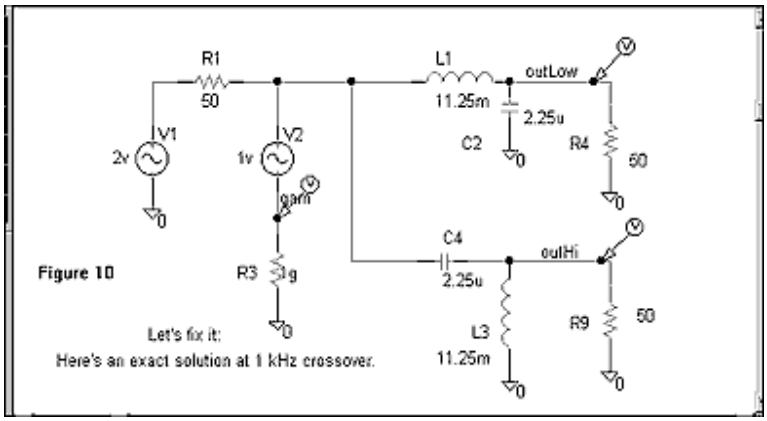

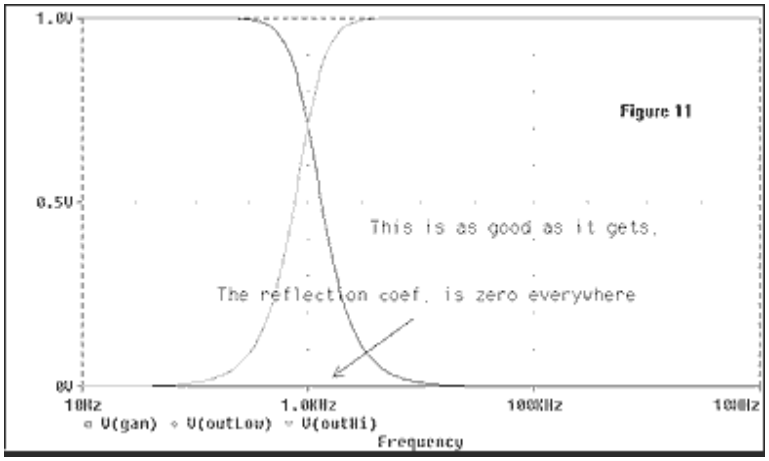

Figure 12 is another final audio example. This circuit is very similar to the one used in the past by Roy Lewallen, W7EL, although the inductor was smaller at 100 uH in his Optimized rig. The response of this diplexer is shown in Figure 13. This is not perfect, but it is probably quite a good performer in typical receiver situations.

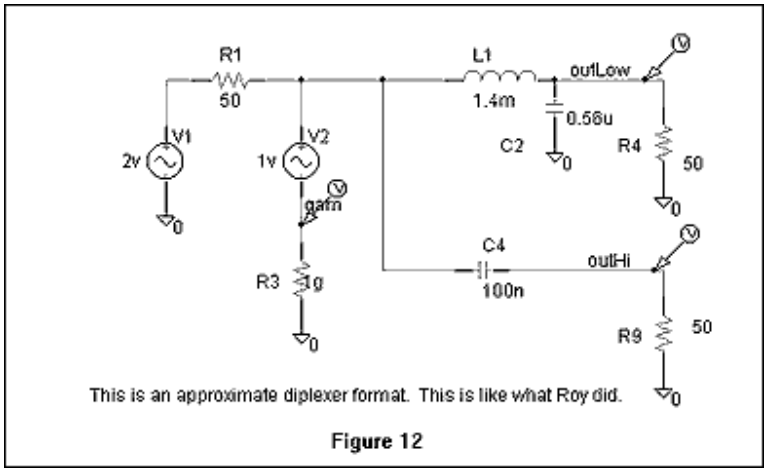

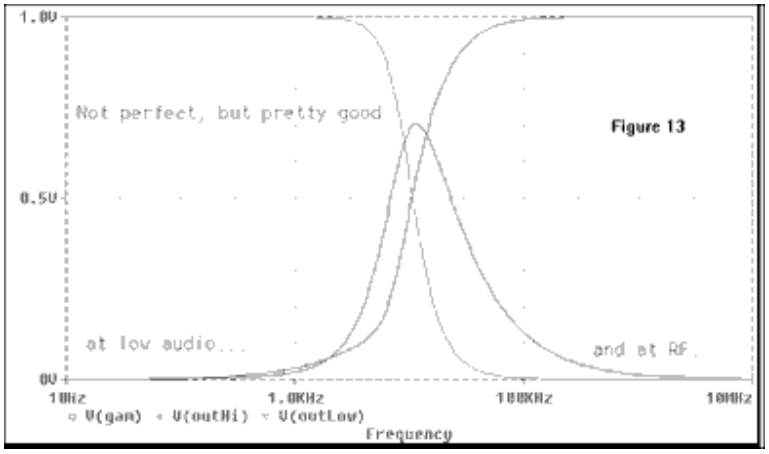

Finally, here's a higher frequency example. 5th order low pass and high pass filters are combined. The filters have a cross over at about 150 MHz. Note that there is a slight reflection in the transition band. This is probably just the result of our having rounded some values in the design process. Figures 14 and 15. An outstanding reference on this is Nic Hamilton, G4TXG, "Improving Direct Conversion Receiver Design," Radio

Communications, April 1991.

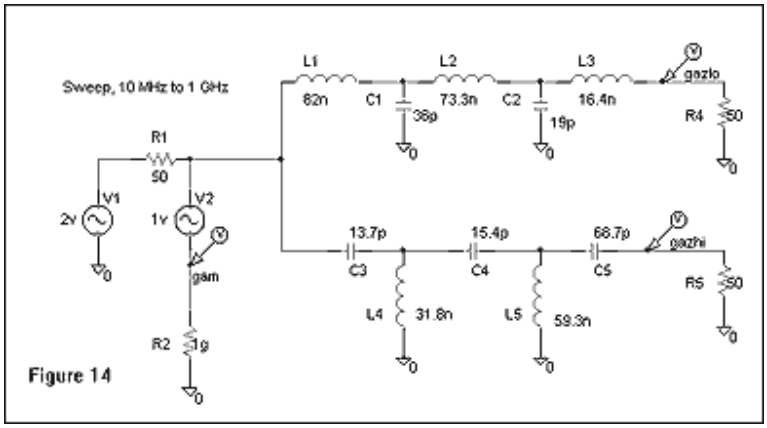

Figure 14

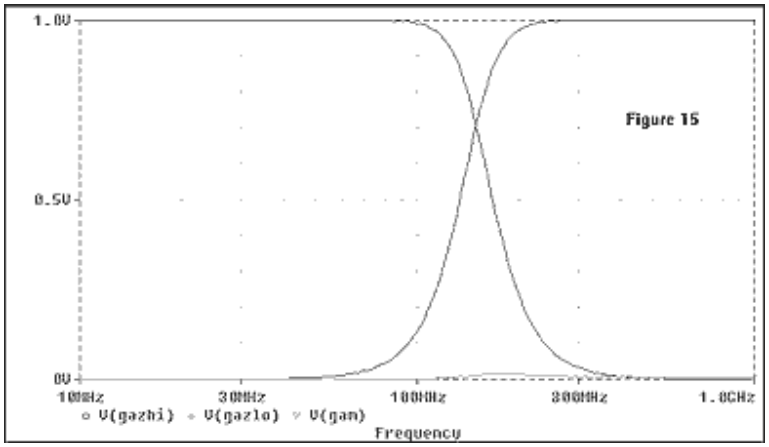

Figure 15

Bridge-Tee RF Diplexer

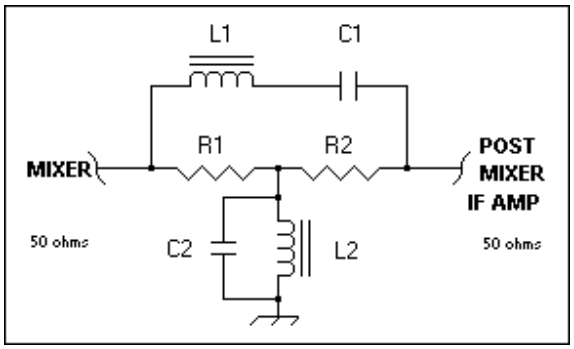

This is an excellent bandstop/bandpass diplexer popularized by Joe Reisert W1JR. This easy to build diplexer has a low parts count and is easily built using Ugly Construction. Resistors R1 and R2 present a 50 ohm impedance to the mixer output and a 50 ohm impedance to the input of the post mixer amplifier. The IF frequency is passed through the diplexer while out of passband RF is given a low impedance path to ground. The capacitance for C1 is generally built up by substituting the nearest standard value capacitor or by placing 2 or more capacitors in parallel with each other to achieve the desired value. The same procedure is then repeated for the C2 capacitance. For more strenuous purposes, a portion of C1 and C2 or the inductors L1 and L2 can be variable and adjusted on the bench. The inductors can easily wound on powdered-iron toroid cores. I have used T50-2 or T50-6 type toroids with good results. The Q of the inductors is 1.

It is possible to design a more generalized form of this diplexer with a higher loaded Q in the resonators. The diplexer shown and used in the program has a Q of 1. This was used by W1JR in his VHF/UHF World Column in the now defunct HAM Radio Magazine for March and November 1984. It was also more recently used by Jacob Makhinson, N6NWP in his A High-Dynamic Range MF/HF Receiver Front End in QST for February 1993. The actual formulae for this diplexer is far more complex than the simplified formula shown below or used in the program, but both provide a very good approximation for the Q = 1 version as used by W1JR and N6NWP. If you wanted Q=10, the series tuned circuit would use L that is 10 times as high with C to resonate. The parallel tuned circuit would then use C that was 10 times higher with L to resonate.

A supplemental web page with some hard-core mathematics for this diplexer can be found on the Diplexer Supplemental Page.

Simplified Formulae (Q = 1):

R1 and R2 are always 51 ohm resistors.

Inductors L1 and L2 -> 50 / (6.283 * frequency in Megahertz)

Capacitors C1 and C2 -> 1 / (6.283 * 50 * frequency in Hertz)

Example 1: For a 9 Mhz IF , L1 and L2 = 0.88 microhenrys and C1 and C2 = 350 picofarads

Example 2: For a 4.92 MHz IF , L1 and L2 = 1.62 microhenries and C1 and C2 = 647 picofarads

I wrote a simple program to do the math for the Q = 1 version. Download the Bridge-Tee RF Diplexer Diplexer Program

---

Comments and analysis by W7ZOI

This is a double ended version of the first order bandpass/bandstop design presented earlier. But it's a good one, within the constraints of what it can do. The first is the simulation schematic for the diplexer, which is better termed a Bridge-Tee Diplexer. (There are bridge Tee filters and attenuators too.) That figure is entitled Figure 16.

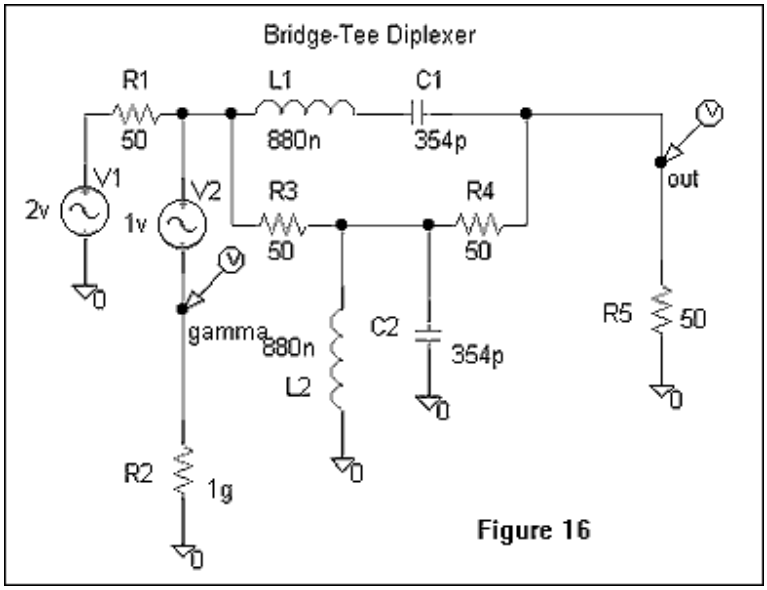

Figure 16

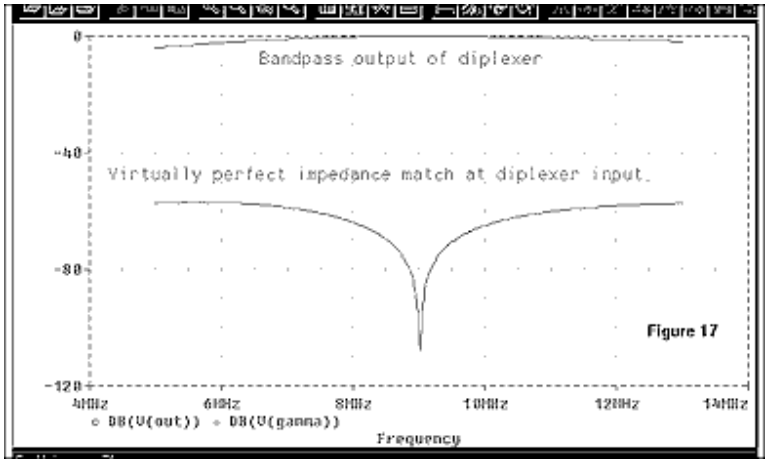

Figure 17

The response for this circuit is shown in Figure 17. This is extremely good. The through response is very flat owing to the low Q of the series tuned circuit. But even better is the match. It is very good. Indeed, it would have been perfect except for slight roundoff errors that occurred as we designed the networks.

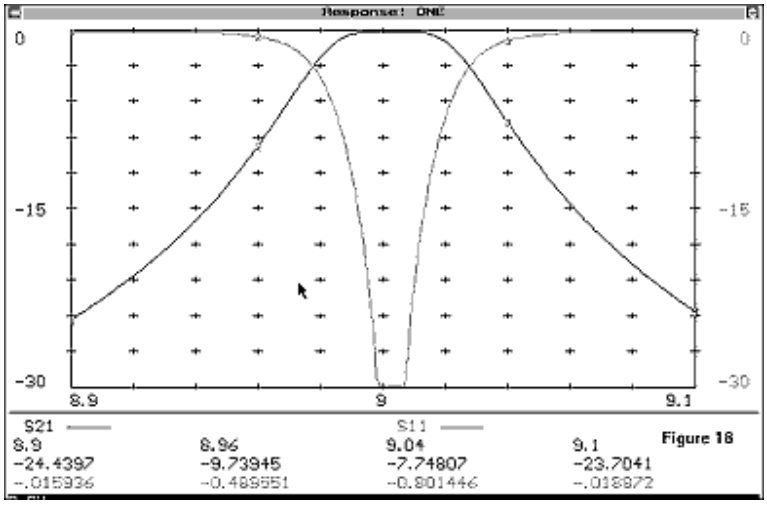

Figure 18

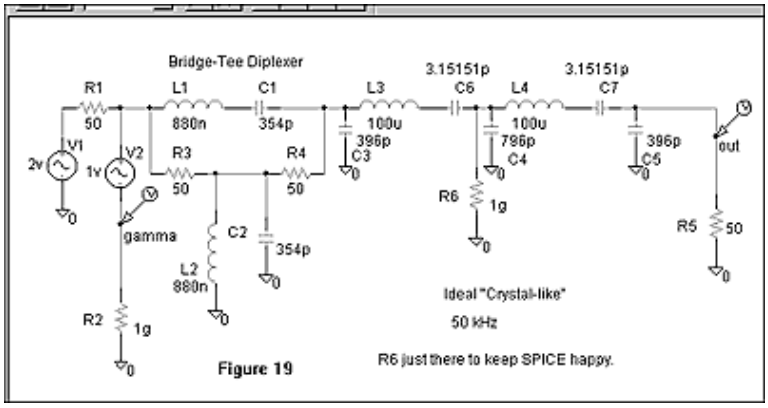

Figure 19

This kind of thing works fine if you really have a perfect match following the diplexer. But what if you don't. There are some places where they do not do the job that some folks think they will do. For example, a diplexer WILL NOT cause the impedance to be flat if it is followed by a filter. The diplexer must still be properly terminated at both output ports. In Todd's usual applications, he is worried about providing a good mixer termination for a product detector. The audio amp that he uses will usually have a common base first stage and that will present a good wideband load to the diplexer, so he is okay. But other folks have placed a diplexer after a switching mode mixer that then drives a narrow filter. The diplexer then does little good. To illustrate this situation, I designed a "crystal like" two pole LC bandpass filter with a 50 kHz bandwidth. This represents the general case where we try to put a diplexer between a mixer and a filter. The filter response by itself is shown in Figure 18. The schematic for the diplexer and following filter is in Figure 19.

The response for the combination is in Figure 20. Here we see a passband response that is fine; it's just the repeat of the filter response we already saw. However, the input impedance looking into the diplexer, the impedance that would be seen by a mixer, is terrible. The return loss is 0 dB at all frequencies except where we get within the passband of the filter.

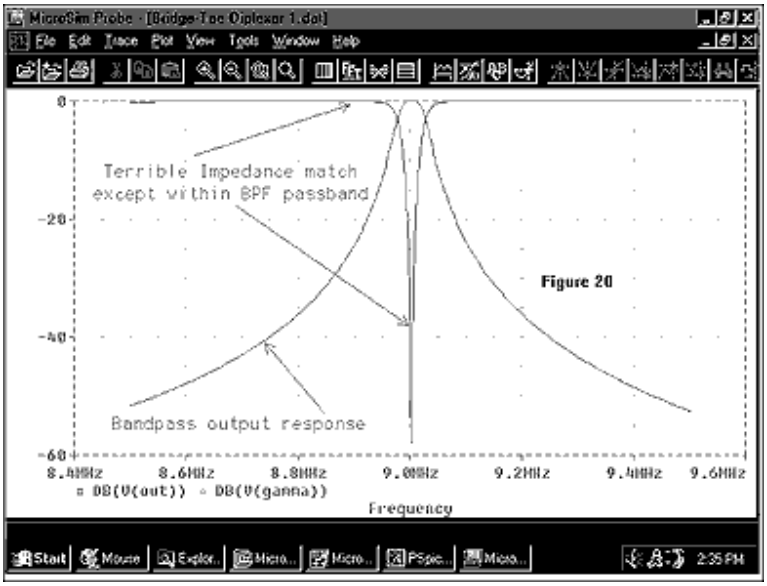

Practical Diplexer for Popcorn Receivers

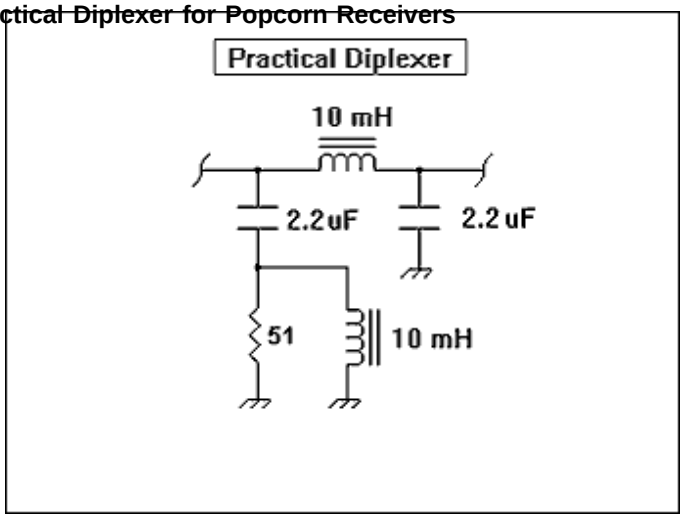

Building a diplexer to follow a product detector is not a cheap endeavor. Audio inductors and capacitors such as metalized polyester film types are not common in many builder's junk boxes. I really like the design shown in Figure 10 and wished to use it because it uses just 2 inductors and capacitors which is in keeping with the popcorn nature of this website. The main difficulty is that the inductors and capacitors are not standard value types and series connecting components to achieve the desired values would add to both the cost and size of the finished product.

Obviously, it will not likely match from DC to daylight. That is not the intention of this simple design or this web site in general. I asked Wes to place just 2 standard value capacitors and inductors in the Figure 10 diplexer design and see what happens.

Here was his response to my request:
OK, here are some "practical values." Note that things don't really change that much. We start with 11.x mH and 2.25 uF. Change the inductor to 10 mH and get Figure 21. Then change the cap to 2.2 uF and see almost no change in Figure 22.

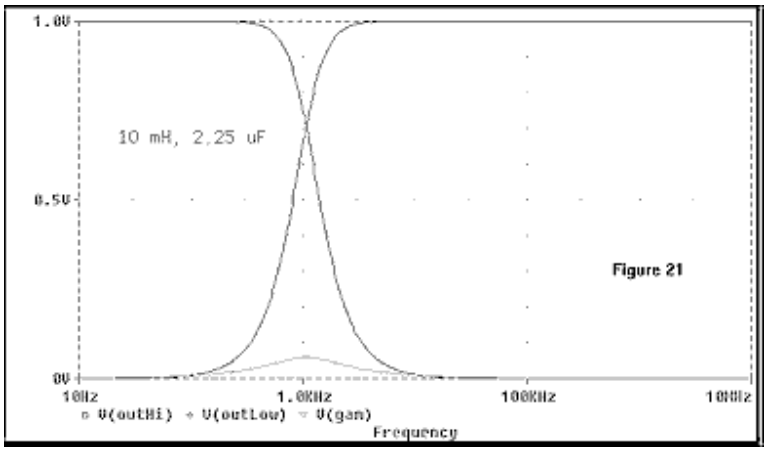

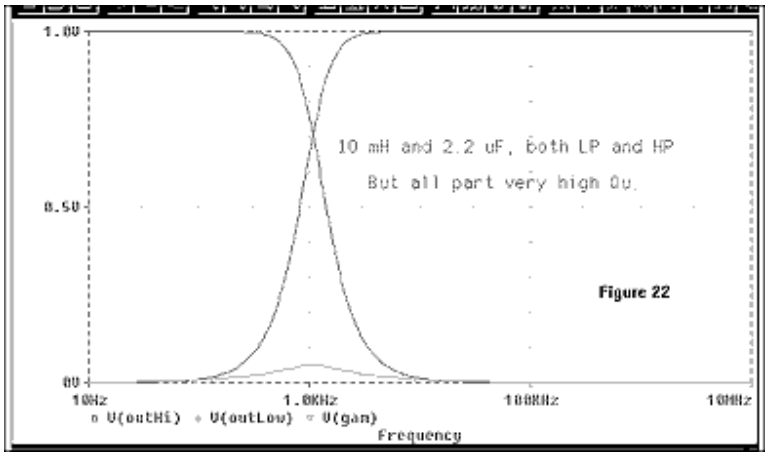

But now move into the world of even greater reality and acknowledge that many of the inductors we use at audio are very low Q. Change Qu of L to 10 at 1 kHz, so I put 6.3 Ohms in series with each L to get Figure 23. And do the same thing, but with a dB scale, for Figure 24. Note that we can see the difficulties, but things are still pretty good. We see some loss (about 1 dB) in the low pass path and less than perfect match. But the match is still very good. 20 dB is about 1.1:1 vswr, much better than 99.9% of the hams can really measure. (A 10 dB match is about 2:1.) Hope this is what you were after....Wes

It was and I will use this "practical" diplexer in my next popcorn DC receiver project. Note that the practical diplexer input and output impedance is 50 ohms and the 2.2 uF caps should not be polarized capacitors such as regular electrolytic types which have a positive and negative polarity.

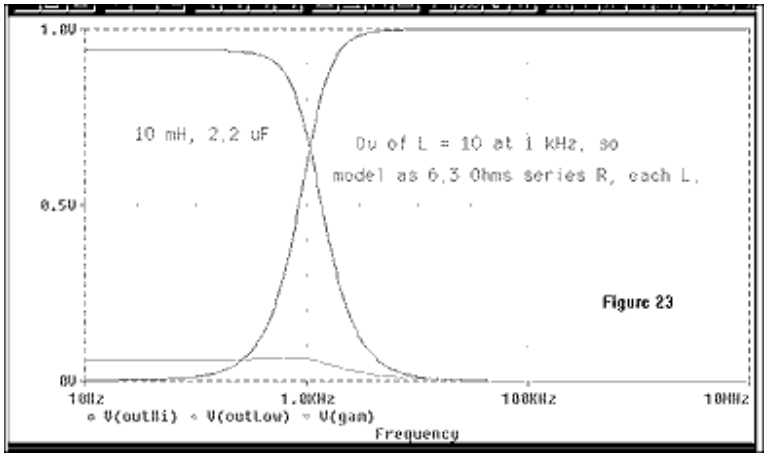

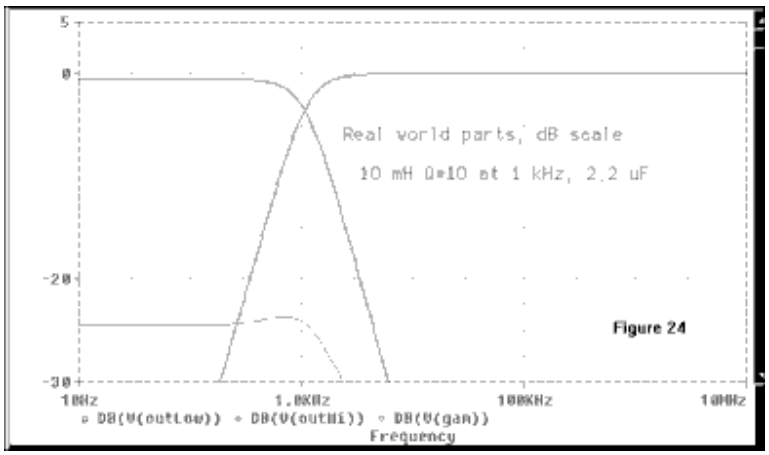

Many thanks to Wes Hayward, W7ZOI for his work on this page.

A version of this web page in Russian Cyrillic

Ugly Construction

Discussion

We enjoy many ways to build electronic circuits. For example, you might breadboard on a perforated circuit board, an etched PC board, a sheet of copper clad board, or even a piece of copper wire. In the hay day of tube electronics, builders used terminal strips and point-to-point wiring within the project chassis. I mostly breadboard using Ugly Construction.

Ugly Construction, "dead bug", or "ground-plane construction" involves building circuits on top of a double or single-sided copper clad board (copper side up for single-sided board). The copper ground-plane provides a low impedance ground and mechanically supports the parts soldered to it. Component leads requiring grounding are soldered *directly* to the copper surface, while the ungrounded leads of these parts anchor any ungrounded parts connected to them. Isolated sections called stand-offs hold other ungrounded or remotely located parts.

Example stand-offs include high value resistors (10 Megohm or greater), terminal strips, or small copper islands glued onto or cut into the copper ground-plane. Parts such as transistors, IC's or commercial diode ring mixers are generally flipped upside down and anchored by their grounded lead(s). Metal encased parts such as crystals can be grounded by a short wire or directly soldered upside down to the copper board.

DC voltage wires, or decoupling resistors may be supported by soldering 1 lead of a bypass capacitor to the ground plane while the other lead holds the DC voltage carrying part up off the copper board a short distance. I mostly use grounded caps for stand-offs and not 10M resistors.

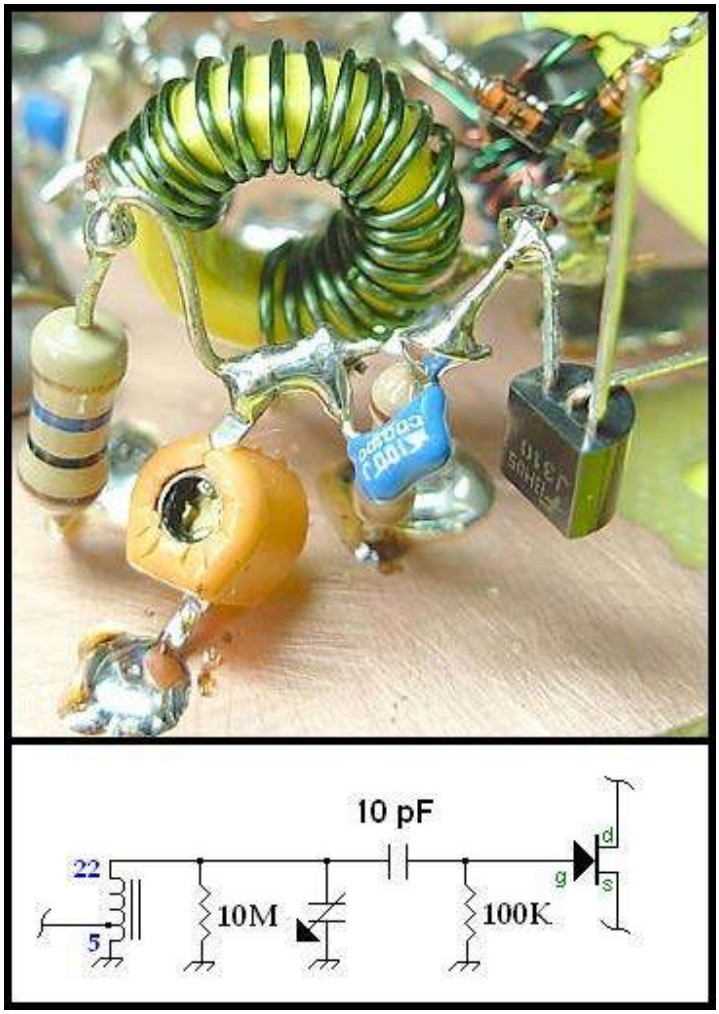

Shown above — a 10 Megohm, half-watt, stand-off resistor anchors the "hot" inductor terminal plus supports the ungrounded trimmer capacitor terminal. The coil's 24 gauge wire provides additional mechanical stability. The signal loss from adding the 10M resistor was about 0.1 volts peak to peak in 1 experiment.

Ugly Construction allows the experimenter total control over the design of a project and in my opinion, its greatest strength is *speed*. Ugly Construction yields rapid and flexible bread boarding — very appealing for prodigious home builders.

The Origin of the Term "Ugly Construction"

Roger Hayward, KA7EXM and Wes Hayward, W7ZOI coined the term "Ugly Construction" while writing the "Ugly Weekender" published in the August 1981 issue of QST. I asked Wes about this in 2009. The term was a takeoff from the 1958 book entitled The Ugly American by William Lederer and Eugene Burdick.

A big part of the learning of the QST article was Ugly Construction! The term and the bread boarding technique emphasized the fact that there is no correlation between the "prettiness" of a construction project and the way it works. According to Wes, the goal had a couple of corollaries. "First, people like myself who do NOT have the knack for doing pretty projects can still build successful radios. Second, is that we all need to look at our projects after the fact to discover what it is that really makes them work well. In the case of the Ugly Weekender, the thing that makes it fly is that there is a wonderful ground plane with that PC board material".

Indeed, this transceiver functions very well; especially after you temperature compensate the VFO. Wes also built versions for the 30 and 80 meter bands. I have versions on 15, 40 and 80 meters. The transmitter portion is a true QRP classic; both as a Ham radio transmitter and because it promoted "ugly" ground-plane or dead bug bread boarding techniques to the scratch homebrew community.

Classic Ugly Construction

This term emerged in Spring 2010 and describes the archetype popularized by Roger and Wes Hayward. All ungrounded leads not anchored to other parts are attached to the copper ground-plane via high ohm resistors — *no* glued pads or islands cut in the copper board.

In-situ comparisons of a 10 megohm resistor versus islands cut into the ground plane and glued-on Manhattan-style pads demonstrated that the resistor had the lowest capacitance; around 1 pF versus 4 pF or greater for the pads or islands. Click for a high resolution transmitter chain built

with 100% Classic Ugly Construction. Click for a crystal oscillator.

Above — *Classic* Ugly Construction using a high ohm stand-off resistor. The top of the 10 megohm resistor is the VCC connection point. It feeds a 150 ohm / 47 uF decoupling network connected to a transistor collector resistor. Bypass capacitors also serve as stand-offs and I prefer thick lead (100 volt or greater) caps for stand-off duty.

Above — The original Ugly Weekender. Photograph used by permission of Roger, KA7EXM.

Above — The original Ugly Weekender. Now this is *Classic* Ugly Construction. Please refrain from building this transceiver and adding modern notions such as a PIC microcontroller keyer — that's just wrong!

Photograph used by permission of Roger, KA7EXM.

Ugly Construction Variants

The most popular Ugly Construction variant is called Manhattan style. Manhattan or "paddy board" construction uses small square or round pads cut or stamped from PC board that are glued copper side up onto a large copper clad board also placed copper side up. The small pads or "islands" serve to anchor ungrounded components. Components soldered to the pads such as transistors or ICs are generally not positioned upside down like in Classic Ugly Construction. Many Manhattan style builders use IC sockets as well. These hobbyists sometimes build beautiful looking layouts — Manhattan is a wonderful bread boarding technique. Google for more information. The best Manhattan construction and copper board chassis bashing I've seen comes from Dave, AA7EE. Click for a blog describing his version of the WBR regenerative receiver. *Linked with the permission of Dave, AA7EE.*

Another interesting variant is used by Dick Pattinson, VE7GC. The circuit board is placed copper side up and holes are drilled and countersunk so that the holes are isolated from the ground plane. Ungrounded components are connected underneath the main board through the countersunk holes. There are many such variations. Each Ugly Construction variant has advantages and disadvantages.

On this website, stand-offs are created by cutting a few lines into the copper board with a small, motorized hobbyist cutting tool; with high megohm value resistors, and occasionally by a small Manhattan style pad or 2. Manhattan pads are great for supporting components needing solid anchoring such as a trimmer capacitor or potentiometer.

Classic Ugly Construction dominates circuits breadboarded after May 2010.

The motor tool may also be used to grind off the copper underneath where VFO toroidal inductors will lie, so that the inductor Q is not effected by the being glued onto a copper surface. In audio projects, I may also grind off the copper around the copper board mounting bolts so that they are isolated from the chassis and do not provide multiple grounds and create the potential for ground loops.

Is Ugly Construction Less Reproducible than Manhattan?

I've received well over 1000 emails about Ugly Construction since launching the site in 1998. Some feel that circuits made with Manhattan pads are more reproducible than Classic Ugly Construction builds. This might be true, but to my knowledge nobody has performed a comparison trial.

The important question is why would this happen? I've read/heard opinions that the stray L and C from the long component leads associated with Ugly Construction might wreck circuit reproducibility, but respectfully disagree from DC to HF. In microwave breadboards, we fabricate lumped element inductors and capacitors (*i.e. precisely dimensioned Manhattan pads*) right into the PC board — Manhattan pads glued all around a breadboard may potentially exhibit much more stray L and C than a few component leads in an Ugly build. Also, wise Ugly builders keep their lead lengths short where it counts: for example, RF bypass + ground and at the input/output of a BJT or FET that offers gain into UHF.

I conjecture human error probably inflicts more problems for Ugly Construction builders — Manhattan building, with its slower pace might trigger less mistakes by newbies. Still, too, Manhattan builders tend to make prettier, squared and aligned circuits and it's easier to spot trouble — plus they look nicer in photographs and some builders carefully document and photograph their builds for others to admire and strictly copy. I've see Manhattan build photos where every resistor tolerance band pointed in the same direction — wow! I think it might be difficult to put such a 'work of art' into an RF-tight metal box for much-sought isolation.

Further, in Ugly Construction — upside down parts might wreak havoc on the "spatially challenged" builder. Who knows? I'm comforted knowing that kit sellers who provide a screened printed circuit board with explicit instructions, still must provide major email support to mitigate build errors. To err in an ugly fashion is human?

Whatever variant of construction you choose, it's sure to be a winner!

Further Discussion

Wire

Non-stranded (solid core) copper wire such as the 22 AWG 3-color package sold by Radio Shack seems a good choice for hook up wire. With non-stranded wire, you do not have to worry about little stay wire hairs causing shorts and it's easier to wrap around components leads. I use red for wires that carry positive voltage, green for grounding and black for wires that carry AC signals short distances. In addition, RG-174 or shielded wire is used to carry AC signals for distances greater than 10 cm, and for connecting stages requiring 50 ohm input or output impedances such as diode ring mixers or low-pass filters.

Your Health

Please consider the following safety comments:

For regular soldering, ensure ventilation of your room — flux fumes can be harmful. Open your shop window and/or use a small fan to improve fresh air intake;

Whenever possible, perform high wattage soldering outdoors;

When grinding paths on copper clad boards, wear a small particulate respirator, gloves, plus ear and eye protection and most importantly; **do it outside** for yours and your family's health;

Wash your hands after soldering and handling freshly cut, fiberglass dust laden copper clad boards.

Soldering Irons

For soldering copper clad boards together, AC grounds on tube guitar amp chassis and performing antenna work, I currently use a Weller SP 80L (80 watt) soldering iron. It is heavy and unwieldy, so you have to be very careful when its plugged in. These high wattage soldering irons produce lots of smoke.

Shown above is an 80 watt "heat torch". My main soldering irons are typically in the 30-35 watt range. Consider keeping at least 1 back up soldering iron, as you never know when a soldering iron is going to burn up. My current 35 watt iron is shown below. These Weller irons have a built in lamp which lights when they are plugged in; a very nice feature. I also keep a small stock of new soldering iron tips.

Copper Clad Board

Some builders ask about sources for copper clad board. I personally use boards made by MG Chemicals as they have dealers in my city and are reasonably priced and good quality. Try the search words **copper clad board** plus **your country name** in your favorite web search engine. A few links follow, but as I have only used boards sold locally, I can't comment about the online companies.

MG Chemicals Worldwide distributer index

Electronic Goldmine Online store

Circuit Specialists Online store

Miscellaneous

Shown below is a schematic and the Ugly Constructed version of it.

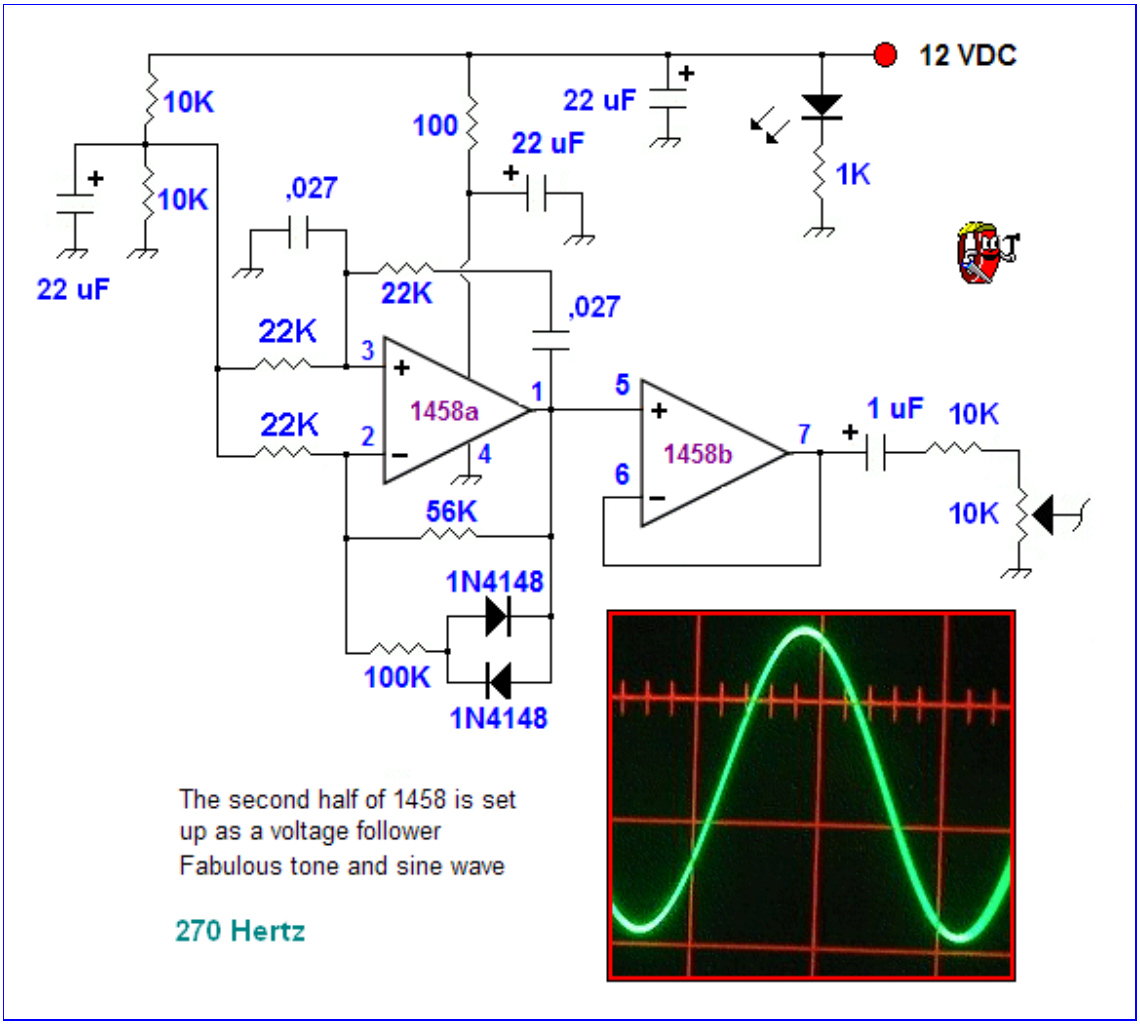

Above. The schematic of an adapted sine wave audio frequency oscillator taken with permission from EMRFD , Figure 12.4. EMRFD is the main reference for this web site. The original schematic author was Wes, W7ZOI

Above. I built this circuit from start to scope in about 25 minutes. This was a scrap, pre-used board with a positive voltage path and a potentiometer holder already on it When miniaturization is not your goal, construction is much easier and faster. I re-use parts and boards to save money. You may remove entire stages from 1 board and solder them onto another.

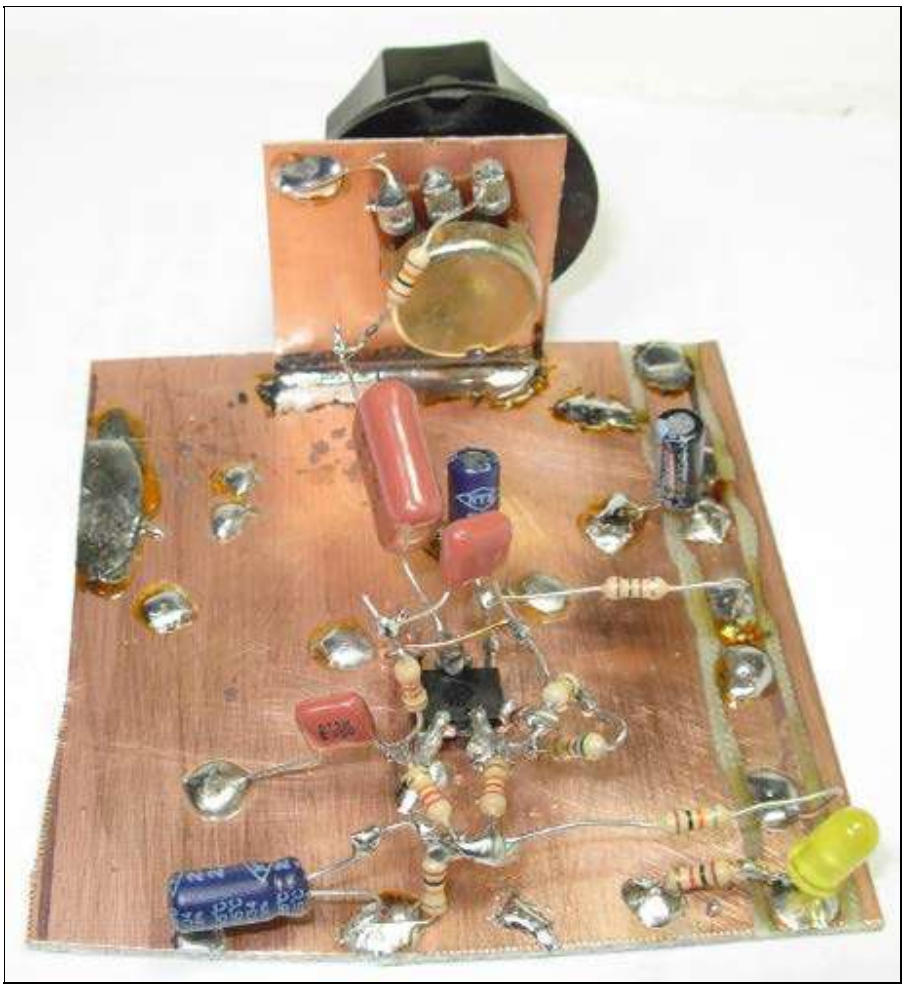

Above. Note how the 10K output potentiometer holder is soldered to the main copper clad board. The grounded 10K resistor is used to anchor the 22K resistors connected to IC pins 2 and 3 and can be seen in the foreground.

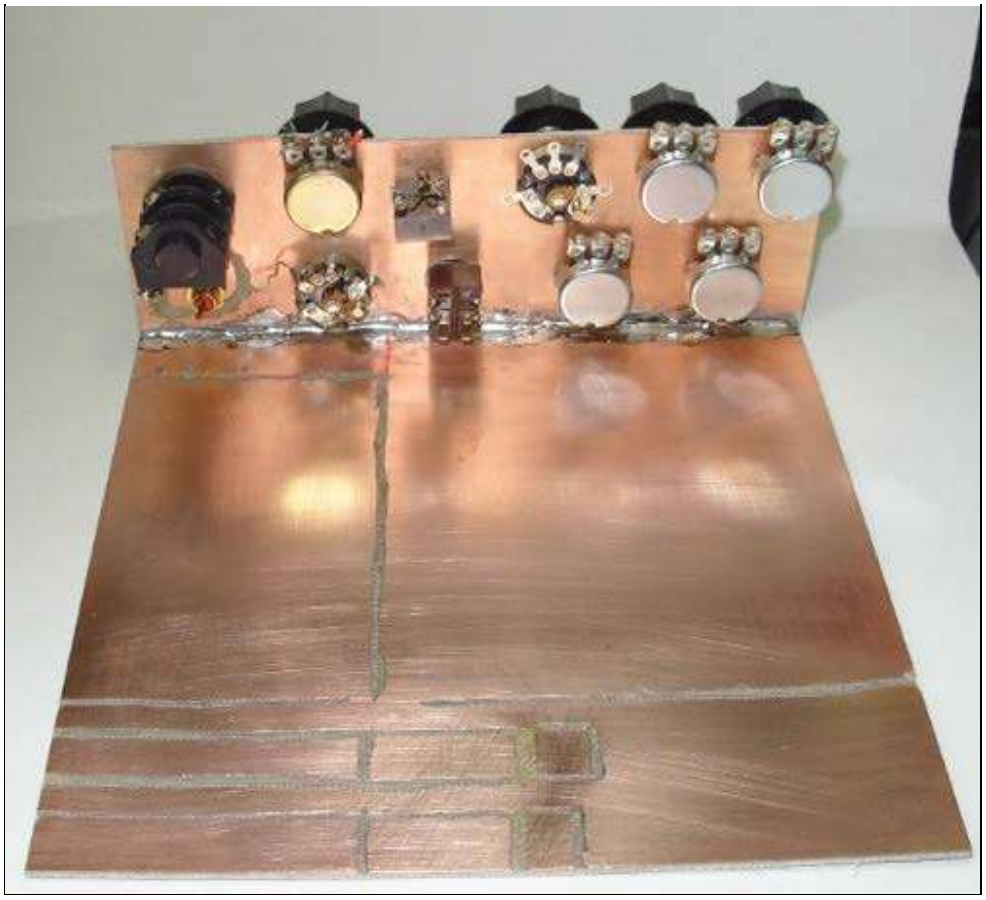

Shown above is another project. Entire control panels can be built from copper clad board for prototype circuits. In this board are numerous cut paths, 7 potentiometers, 3 jacks and a switch. Do not build an LC VFO over double sided copper clad board; lest it become "a capacitor" and affect your frequency stability.

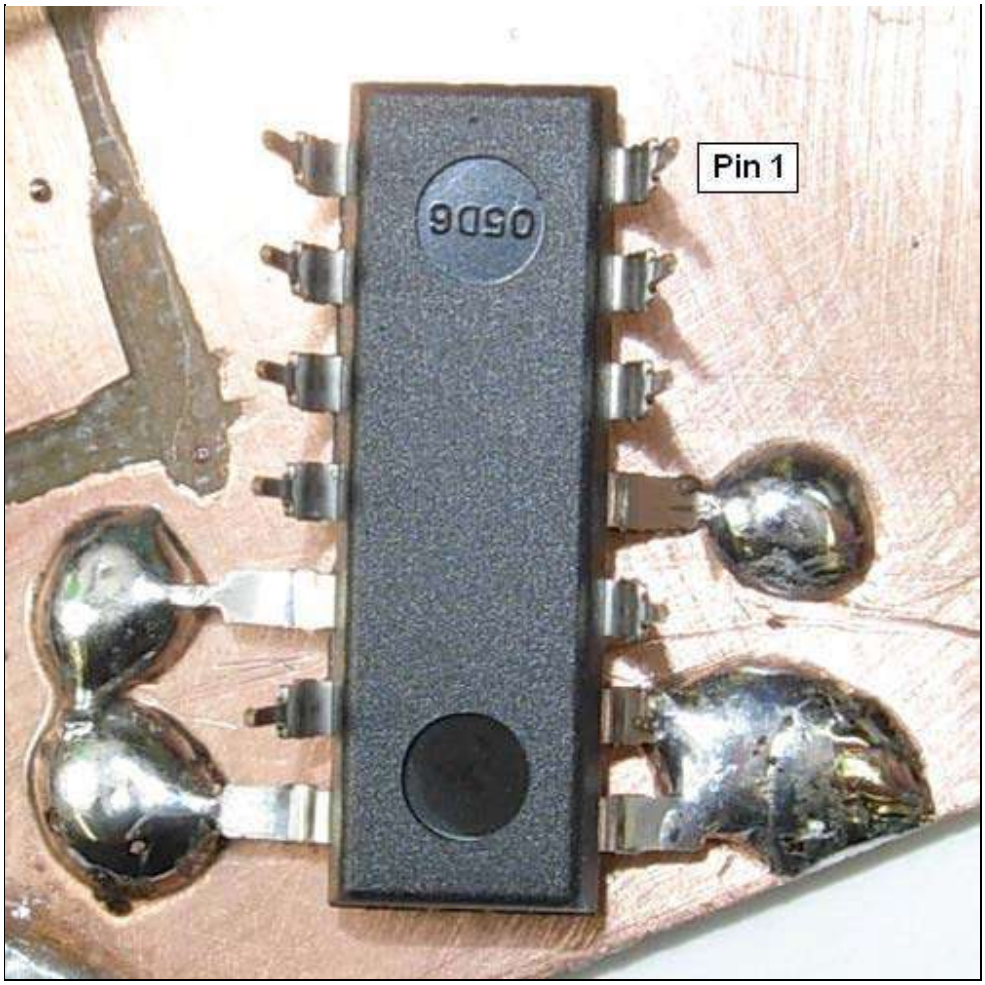

Shown above is a CD4013B D Flip-Flop soldered "dead bug" style. Pins 4, 6,7, 8 and 10 are grounded to the copper surface; well anchoring this part. Using proper static precautions, I have never had a CMOS device failure using Ugly Construction and also save the price of an IC socket.

Above — a method to anchor op-amps using a split (negative and positive) power supply. Pins 4 and 8 are soldered to the copper board via a 10 megohm resistor. A 0.1 uF ceramic bypass capacitor is also connected to these pins. The resistor leads were left a little long to allow easy connection of the power supply wires. I write each pin's polarity on the board to avoid wiring mistakes.

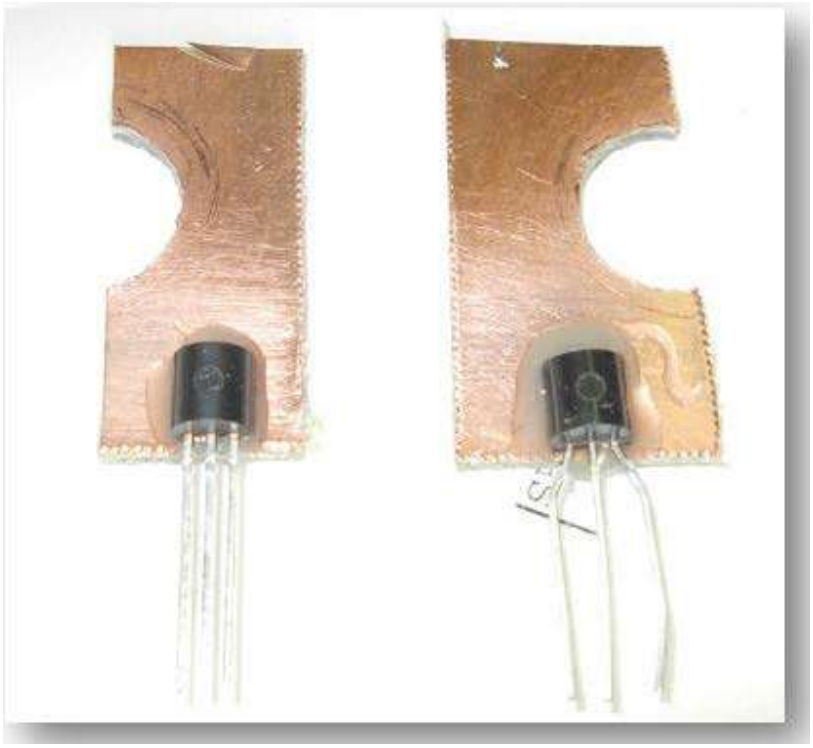

Shown above is another use for copper clad board; heat sinks. In this case, 2 scraps are epoxy glued to 2N3904 and 2N3906 transistors.

A flux pen like this one from MG chemicals is a handy item for the QRP workshop. They are great for applying liquid flux to allow easy and precise soldering of SMT components. Also sometimes when adding components to ground in already built up circuit boards, it can be difficult to get your soldering iron down at a low angle for proper heat transfer. Some flux can help solder a part to the copper ground plane in these situations.

Shown above are the basic tools used to cut copper clad board. A felt pen marker, small square and a set of straight aviation shears. If you press one end of the copper board into the side of your bench and keep pressure on the handle of the aviation shears with your thigh, it is possible to make long, straight cuts. The board will flex and move out of the way as you cut. Your leg provides the force to advance the aviation shears.

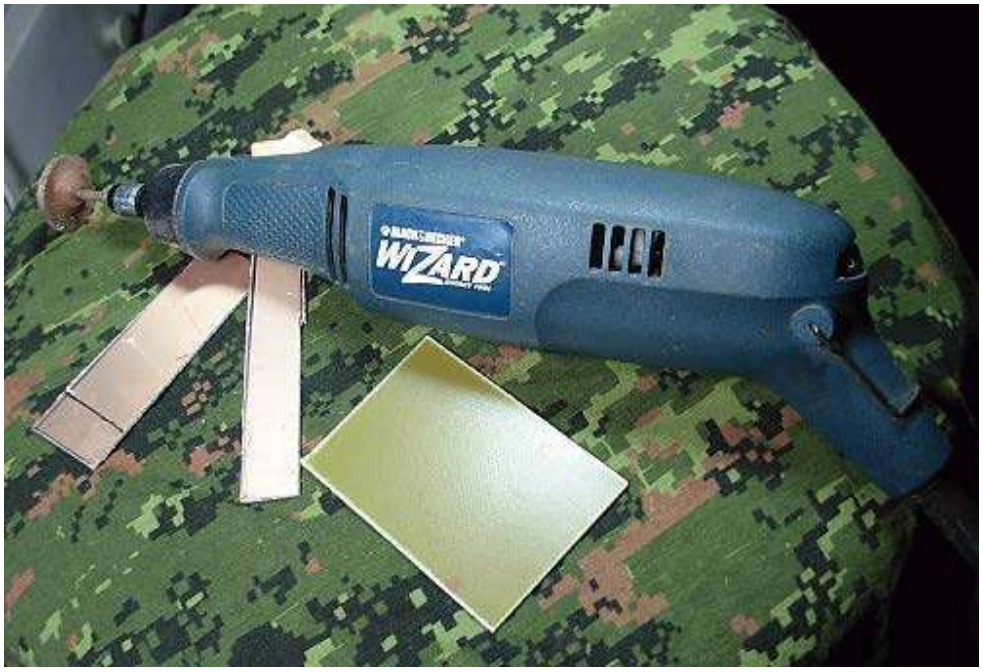

The motorized grinding/cutting tool used to carve out small pathways in copper clad board.

Steel wool used to clean up copper clad board before construction. A box like this will last for years.

For 15 years, I've used this 9 mm cutter to scrape the enamel insulation off the magnet wire wound on toroidal inductors.

VE7GC Wee Willy 75 Meter DSB Transceiver Project

Introduction

I meet a lot of interesting amateur radio enthusiasts online and on the air. Among them is Dick Pattinson, VE7GC who was first licensed in 1934. When Dick isn't sailing he builds and operates his homebrew QRP gear to hams around the west coast of Canada and the U.S.

Presented is a double sideband transceiver that Dick calls "Wee Willy". This rig has a low parts count and is easily built using non-etched PC board techniques. Dick even makes his own radio case using copper clad PC board for the front and back panels and cardboard for the rest of the case. The set itself is in a case 1 1/4 by 2 1/4 by 5 1/2 inches. There is a separate container which holds a 6 volt rechargeable battery and speaker. The speaker/battery case is about 2 1/2 inches cubed and is not shown.

The circuits are built in three sections on the circuit board, namely TX, RX, and VFO. An electret condenser microphone is on front panel along with T/R switch, volume and frequency adjust. The back panel has the antenna jack, power input cord and the speaker jack. The battery pack has a 100 uF capacitor to across the power leads for additional filtering and is shown in the VFO schematic.

The text that follows is clipboard pastings from email that Dick sent me with some additional comments and expansions by me. Dick's project exemplifies practicality and innovation and with that is a major contribution for the QRPHB site.

Construction Methods

Dick's electronic construction method is quite fascinating and represents yet another derivation of ugly construction. The electronic wiring is done on single sided PC board, copper side up. Small holes are drilled through the PC board material to allow component leads to pass through them. Then the holes carrying active leads are chamfered (countersunk) with a larger drill bit which is not run all the way through the PC board. This leaves an ground-insulated side to the hole and prevents a component lead short circuit. The copper being topside allows both convenient and short component grounding. The Wee Willy parts layout is extremely neat and compact. Dick, presumably through practice has great skill with this technique and I plan to try it in the future.

The project case is constructed from 1/16th inch cardboard which is cut and bent to fit the electronic PC board. Once cut, the outer surface and edges at the front are covered with tissue paper or Kleenex (tm) type tissues soaked in white glue. The applied tissue paper and glue is allowed to dry and then additional coats are added to build up a body. Alternately, the cardboard case can be coated with lots of glue and the covering material imbedded in the glue. The air bubbles are pressed out and extra glue is added where necessary. When enough material has been added to cover up and strengthen the case joints and the glue is perfectly dry, the case is painted with Rust Coat Enamel available at hardware stores. The end result is a glossy, durable finish which looks very sharp.

Transmitter

This transmitter uses an electret condenser microphone (Dick used an Archer 270-90). The mic is built right into the front panel of the chassis and this of course guarantees short mic leads. A 741 op amp is used as a speech amplifier which in turn drives the balanced modulator a Signetics NE602 doubly balanced mixer. The input and output impedance of the NE602 mixer is around 1500 ohms.

To adjust the transmitter, set the bias control on the VN10 stage to ground and tweak L1 to resonance using an RF probe or scope on the VN10 input. The input signal must be audio, spoken into the front panel microphone to get the DSB. Once L1 is tuned, connect a 50 ohm load to the antenna with some sort of RF indicator (such as a RF power meter) and advance the bias control to give a watt or so output. Then speaking into the microphone should result in a DSB signal suitable for communicating on QRP! No audio input should result in no RF output. The supplied voltage should be kept at 6 volts, remembering that NE602's cannot stand voltage greater than 9 volts. With suitable voltage control such as a 6.8 volt zener diode on these chips, one could use higher input voltage with a corresponding RF output.

There is another way of setting the bias on the VN10. After aligning L1, with a ammeter in the six volt supply line, advance the bias control until

the input current increases about 10 mA (with no modulation). If you do not have an FT37-77 ferrite core, substitute 10 bifilar turns on a FT37-43 ferrite core for the T1 transformer

.

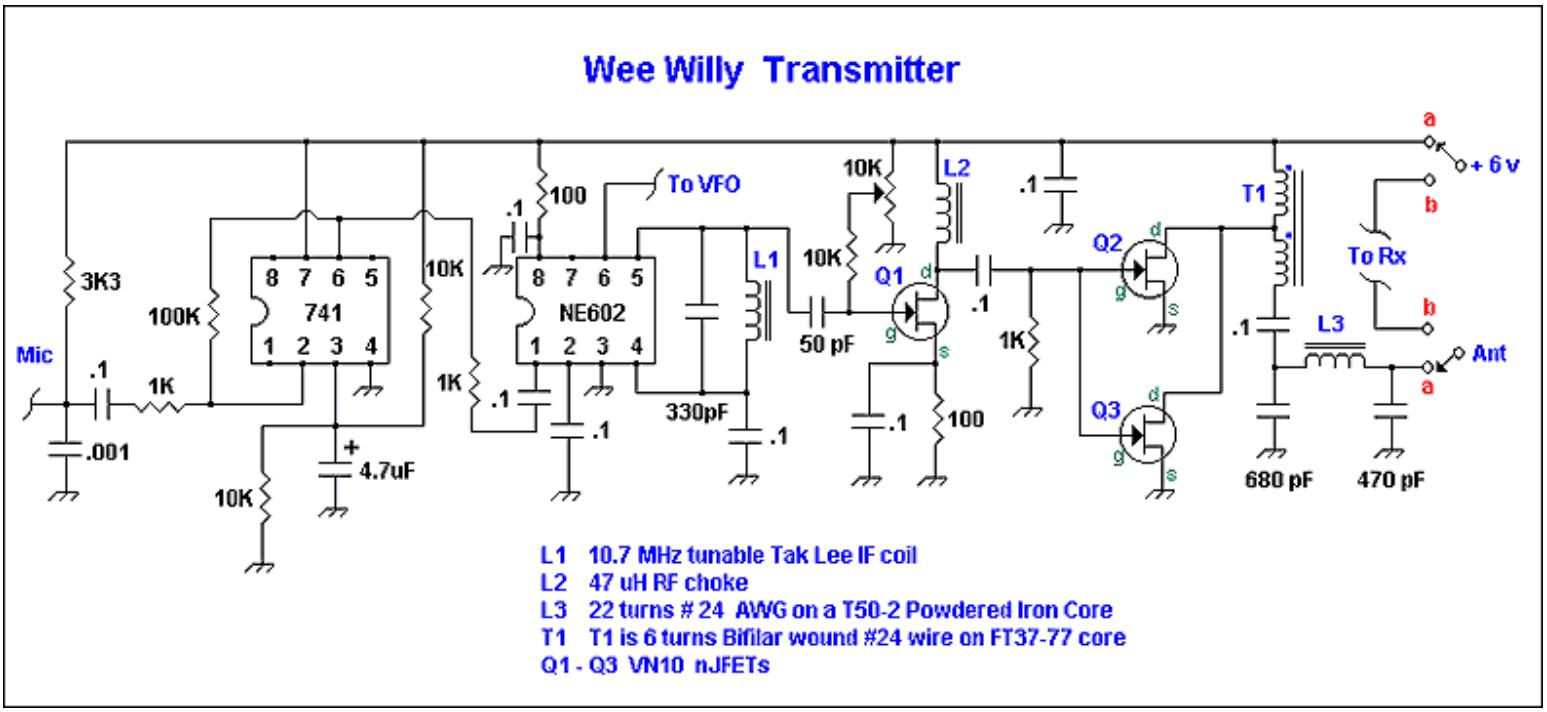

Receiver

The receiver is a direct conversion type with a manual RF gain control in the form of a 5K potentiometer. Listening to a weak signal on the desired frequency the RF stage and the mixer core (T1 and T2) adjustments are made until you hear the loudest possible signal, keeping the input test signal as low as possible. When the receiver is connected to a doublet antenna there is no lack of incoming signal, which can be controlled by the front panel RF gain control.

The antenna and 6 volt supply is switched manually from TX to RX mode and back by a front panel mounted switch. If you can not find Tak Lee green 10.7 MHz IF coils, probably any other brand of 10.7 MHz slug tuned IF transformer would work. The Mouser catalog number 421F123 would work well and in another 80 meter project I used it with a 470 pF capacitor instead of the 330 pF cap shown. I would start with Dick's 330 pf cap and if it will not tune to resonance sharply, slightly increase the cap value up to see if a bit more capacity is required to resonate it on the desired 75 Meter frequency. Note that the secondary coil on the L1 transformer in the transmitter schematic is unused. If your 10.7 MHz IF coil has a built in capacitor at the base, remove it.

During receive, the standby drain current at 6.0 volts was 24 mA and on loud signals it rose to 100 mA. If this is too much, probably the easiest thing to do would be to put in a series resistor from positive to the LM386 to limit the drain current. To get output on the speaker it is a matter of how loud you want it for the drain you draw. If earphone only reception is okay, then the drain could be reduced considerably.

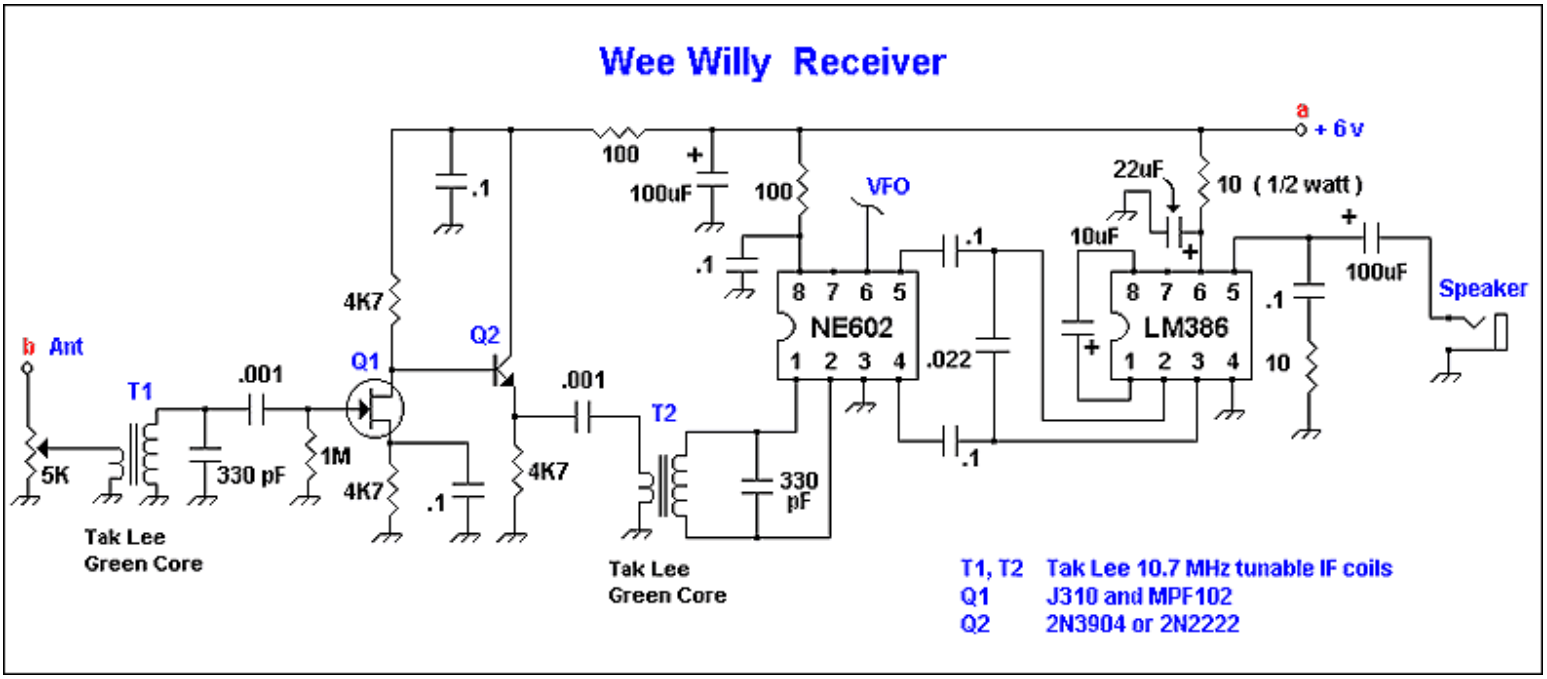

VFO

Dick's diagram indicate that this VFO was based upon a design presented in SPRAT for summer 1995. The main inductor L1 is wound with #32 AWG wire on a 1/4 inch slug-tuned coil former. This coil would have an XL somewhere between 250 - 310 ohms, so if you cannot find a coil former as described , you could easily wind one on a powdered iron toroid and make a portion of the C1 capacity variable for adjustment. A suggested alternate inductor is 53 turns of #26 AWG on a T68-6 core powdered iron core.

Dick suggests checking an old television to find suitable coil formers such as the one he used. It would probably be best to distribute the 120 pF C1 capacity among 3-4 capacitors to enhance stability. These caps should be NP0 ceramic for best results with frequency stability.

Dick's oscillator uses the slug tuned core to put VFO frequency close in frequency to where you want to operate and the variable resistor tuner on the front panel allows adjustment around the incoming signal to get the correct pitch. The desired band-edge is easily set by adjusting the slug while listening to the VFO frequency as audio on another receiver that has a frequency readout or directly with a frequency counter.

The L2 150 uH RF choke can be a simple epoxy unit which resembles a resistor. The D1 variable capacitance diode is a BB104 which has ~ 35 pF capacitance on each side. These are available at Dan's Small Parts and Kits whose URL is in the Links section of the site info web page. Experimentation with other tuning diodes could produce a practical alternative to the specified D1 part.

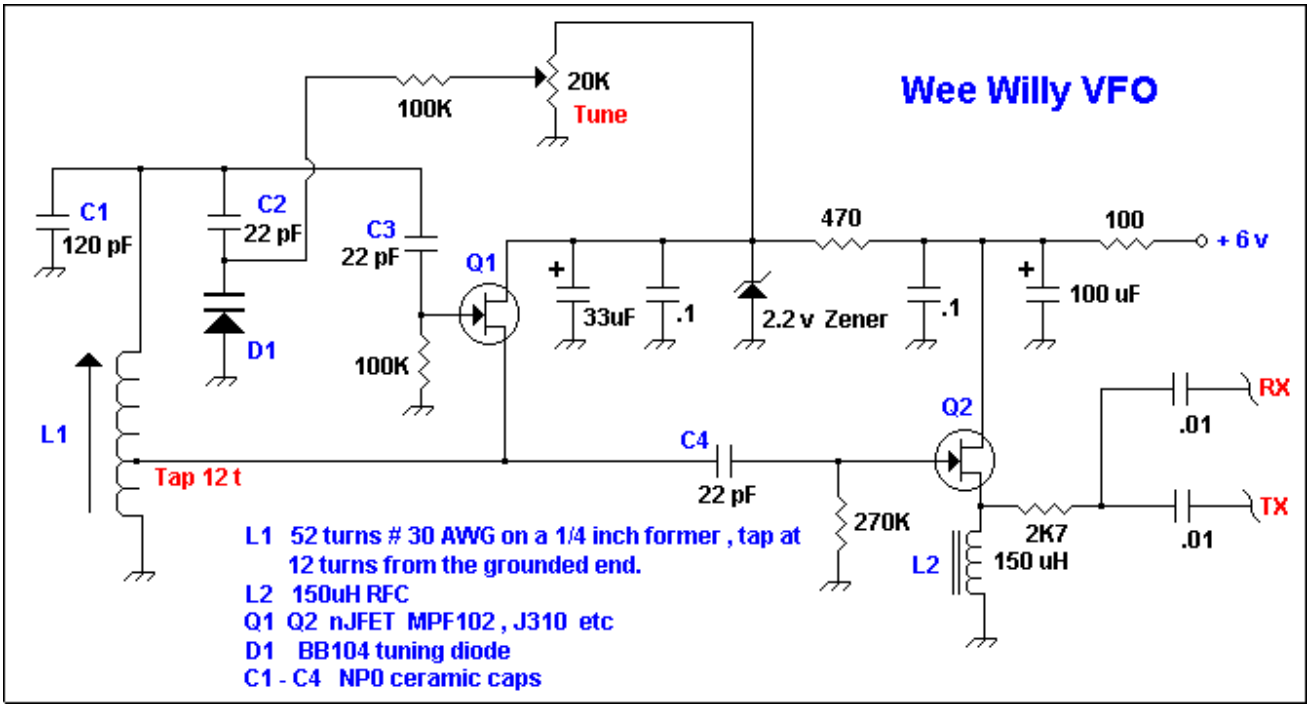

Operating Wee Willy

Dick sent me Willy in the mail and the first available moment I fired the little rig up and spanned the VFO which tuned from ~ 3721 to 3738 KHz. I then proceeded to tune 3729, the frequency of BCEN, our SSB provincial public service net and on my first break was able to check in with one call sign repeat to the net control station. The band conditions were noisy and most signals were S8 or lower, however Wee Willy's 1.5 watts P.E.P. were able to check me in with my folded Marconi antenna. I later changed the L1 slug and worked some stations higher up the band. My audio reports were favorible and no one knew I was running DSB. This is a fun radio and it looks cute to boot!

When transmitting, I had to be careful to keep my hand away from the VFO compartment to prevent pulling the VFO frequency with the capacitance change from my hand. The VFO has reasonable long term frequency stability and copying CW stations with the receiver was possible without frequent tuning readjustments.

The following are some digital photos of Wee Willy taken by VE7ZAC.

Move your mouse over the images for a larger version.

From left to right the electret mic, TX/RX switch, RF gain control and VFO tuning control. The number 375 is Dick's project identification number. He has given me many schematics of his projects and each has a unique number and case color. For the non-Canadians, the large coin on top of Willy is our "Loonie" a 1 dollar coin. The large 2 color coin in front of the rig is our "Toonie" a 2 dollar coin.

The hole on the left of this rear panel shot is for adjusting the L1 slug for the VFO. From wherever on the band the VFO is set a front panel tuning range of about 17 KHz was possible. Also shown are the speaker jack , BNC antenna connection and DC power leads.

Wee Willy with the cover off.

These top view shots clearly shows the 3 distinct compartments. From left to right the TX , RX and VFO sections. The VFO has a PC board seperator for shielding. Dick's construction method is well illustrated with this photo. The IC's are in sockets. The 3 VN10s have a small tab on the top. There are no heat sinks on the VN10 finals and they do require any for a 6 volt supply voltage. The rear panel jacks and VFO inductor are all mounted in PC board material.

Here is a bottom shot showing the connecting wiring through the chamfered PC board holes. Many thanks to Dick Pattinson, VE7GC for allowing me to present one of his projects.

Wee Wee Willy by NM8T

NM8T Builds Wee Wee Willy

Steve White, NM8T emailed me a few weeks ago that he was building Wee Willy and was not getting the expected output power. I forwarded his email to Dick and they problem solved the issue. It turns out that the V10KM's were the culprit.

Here are their final two emails:

Steve: I think you have found a solution to your problem. I did not know that VN10's are different. I bought mine in 1994 from a radio parts supplier and they are marked VN10KM F324A1. Have fun with your new rig and let us know how you are doing with it. 73, Dick

Dick, I have completed my little rig and have had a blast with it so far. My first CQ yielded me 3 contacts in Pittsburg, Pa. My friend across town gave me a 20 over S9 report. The three hams in Pa. were astounded that I had only 1.5 watt PEP. I had to use 12 volts and used small 5 volt regulators to feed the NE602's. This works very well. I even used a little homebrew tuner with it and got my swr flat. I am going to take the little rig to Dayton Hamvention next year. I go every year and take a little project each year to show everyone. I hope it is ok to call my little rig Wee Wee Willy, since it is a little smaller than your version. I want to thank you for your help in getting this rig completed and also thank Todd for his help in getting me in contact with you. Your little rig is very neat and right up my alley for a QRP rig. I look forward to working you someday on QRP. I'm 47yrs. old on the 24th of this month. I have a whole room full of QRP rigs such as HW-7, HW-8, HW-9, Argonaut 509, 515, Powermite PM-3a. Have built a Cascade, LCK, Spider, MXM, Keyers, Tuners, and all kind of other projects. I love QRP and hope to build many more soon. The Wee Willy is one of my favorite rigs. Here are some pictures for you and Todd. Thanks and Hpe CU Agn. 73's NM8T (No more 8 Tracks) Steve White - Fayetteville, WV

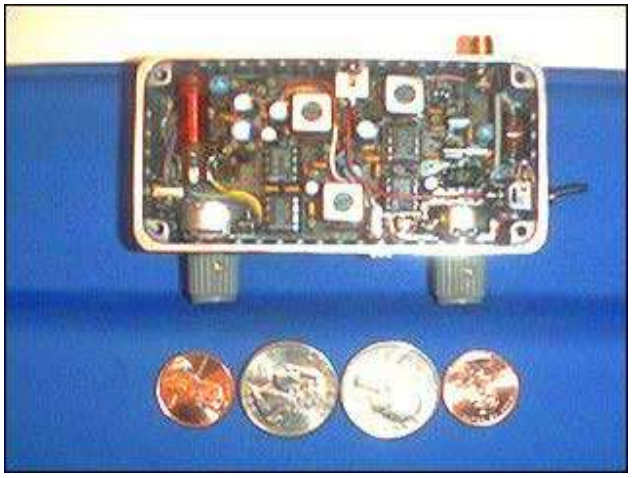

My special thanks to Steve White and Dick Pattinson.

Countless builders have constructed the Wee Willy on several bands. Here are 2 more examples. Paul, KE7HR Link1 and Link 2. The finals even made it into the the BITX17 transceiver. Allan Yates published some good work on the final amp.

I've also tweaked Dick's design, but decided to leave his little rig and this web page alone out of respect to him. It's always easier to improve rather than actually *design* something. I'll never better the experiences I had operating and documenting his transceiver.

Update February 15, 2011

I lost touch with Dick and decided to call him on Feb 10, 2011. He's 95 years old and no longer building. Sadly, his wife Christina died 2 years ago. She was a beautiful person and a gifted painter. Dick remains astonished that Wee Willy - Project 375 QRP Radiophone has been built by at least 50 people (that I know about) world wide, the subject of blogs and the basis/inspiration for numerous radio projects. I met Dick on 80 meters and my wife and I once visited his residence and spent 2 glorious, days on Saltspring Island with he and his wife.

Dick sent me the radio and documentation on Aug 13, 1998. He was a hardcore builder and a professional electronics technician who, for a time, flew his float plane to service equipment in the Gulf Islands of British Columbia. Dick keeps many binders full of his carefully numbered and well documented projects. He gave me a few sheets for my reference library as a gift. Dick's work inspired me early on and I cherish the time I had Wee Willy in my radio shack - blown away by DSB, QRP and such a novel little radio.

Dick asked me to send his greetings to all QRP Homebuilders everywhere.

More Updates

Aug 25, 2011

Hi. Been viewing your web site for a while, lot of great information for builders. I thought i would let you know that I built the "Wee Willy", it works great, so good that I decided to try building one for 20m. I built the 20m version with a 14.318 crystal instead of a VFO ideal for my local net, also changed the PA circuit using IRF510 giving me 2.5W output, the transistor can run 5W, but it does get rather hot, I must say that the quality of the transmitted audio is amazing, everyone comments how good it is and some do not believe it is home-brew!!! I have put a few CQ calls out with a simple dipole and made contacts into Belgium, Netherlands, Finland and Saudi Arabia. Many thanks again for putting the Wee Willy on your website, it has opened my eyes to how well you get get out with QRP power.

Regards Wayne. M0WAY. Click for Wayne's fabulous Wee Willy bread board.

Sept 19, 2011

Wayne, M0WAY wrote again,

I built another Wee Willy and put it into a box, but with a few extra bits:

A new VFO was added that runs 14.190 – 14.350 MHz (an 11 MHz crystal oscillator + a 3.2 MHz VFO + a band-pass filter) I got the power up to 4W, however the audio was a little over powered from the extra RF, so I had to reduce the audio gain and added an antenna switching circuit, after I burnt out my receive circuit with the 4W output.

Here's Wayne's PA (from the NE602 on ** updated July 12, 2012 **) Click for a photo of his latest incarnation. Thanks again!

Oct 19, 2011

Mark, WA4JAT built a "0 cost" Wee Willy from 100% junk box parts including a CB radio transistor for the final. Click and click. Mark tunes the VFO using an air variable capacitor mounted in the former Heath Kit signal tracer project chassis. The cable running out of the front is the microphone coax with an electret mic at the end. Employing large size VFO, Rx and Tx boards facilitate easy future modifications. Awesome work Mark!

JFET BIASING TUTORIAL BY W7ZOI

This tutorial is copyright © 2000-2001 by Wes Hayward, W7ZOI.

JFET Biasing and an Amplifier Design W7ZOI, 30Dec00.

Junction Field Effect Transistors (JFETs) are generally no more difficult to bias than a bipolar transistor. In many ways they behave essentially like a classic triode vacuum tube. The current flowing between FET drain and source is controlled by the gate-to-source voltage, V_{GS}. (This is the voltage you would measure with a voltmeter connected between the gate and the source.)

The Fig. 1 schematic defines the parameters we use to describe the DC behavior of a JFET. The 100 Ohm resistor is added to preserve UHF stability during measurements. The gate voltage, V, is then varied while measuring drain current. The results are then plotted, as shown in Fig. 1. The FET is characterized by the simple quadratic equation below the schematic with the two FET related parameters of I_{DSS} and V_p. I_{DSS} is the drain current when the gate is short circuited to the source. The pinchoff voltage, V_p, is V_{GS} when the drain current is essentially zero. The example in Fig. 1 has I_{DSS}=20 mA and V_p=-4 volts. Source and drain current are identical in the JFET.

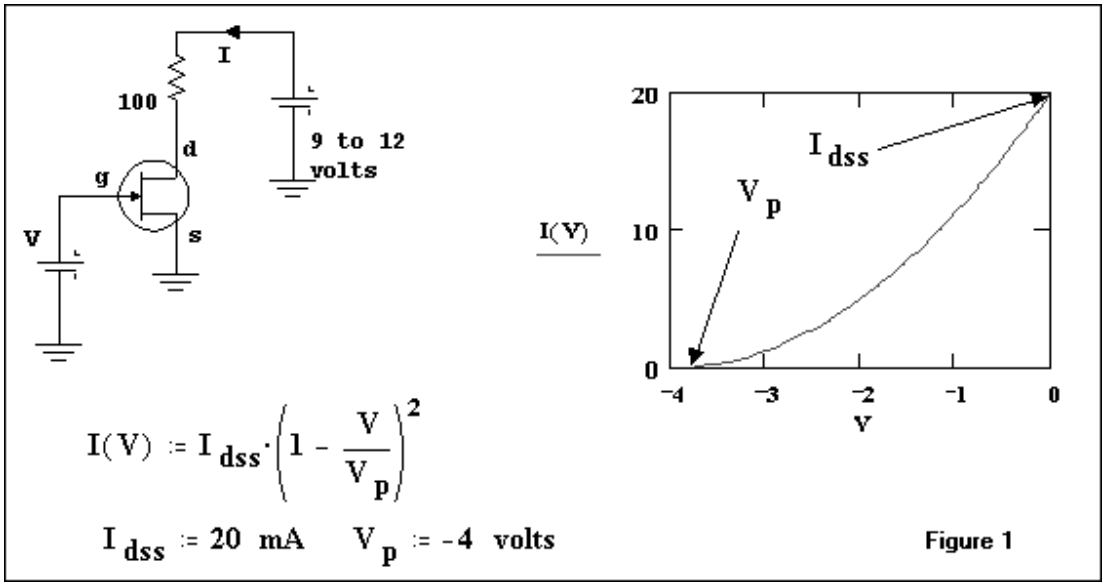

Figure 1

Basic behavior of an N-Channel depletion mode JFET.
The numbers shown basically illustrate the ideas.

The experimenter wishing to use a JFET in a circuit will most often use the method called "self biasing" where a resistor is placed in the source lead. The gate is grounded. The FET current also flows in the resistor. The current generates a voltage drop that elevates the source voltage above that of the gate, which is the same as biasing the gate negative with respect to the source. This establishes a drain current less than I_{DSS}.

Drain voltage is not critical so long as it is a few volts greater than the source.

The resistor value for a desired bias is calculated with Equation 1 if I_{DSS} and V_P are known. But these parameters are rarely well specified. For example, the popular J310 is characterized only by ranges: I_{DSS} is 24 to 60 mA and V_P is -2 to -6.5 volts.

$$R_s := \frac{V_p}{I_D} \cdot \left(\sqrt{\frac{I_D}{I_{dss}}} - 1\right) \qquad \text{Eq.1}$$

I_{DSS} and V_P are easily measured for a specific FET with the circuit shown in Fig. 2. The circuit is built with a variety of source resistor values and the source voltage is then measured for each with a high impedance voltmeter. The pinchoff voltage will then be the negative of the source voltage when R_S is a large value such as 100K. Grounding the source through a current meter generates a direct reading of I_{DSS}. This brief measurement will provide enough data to allow biasing.

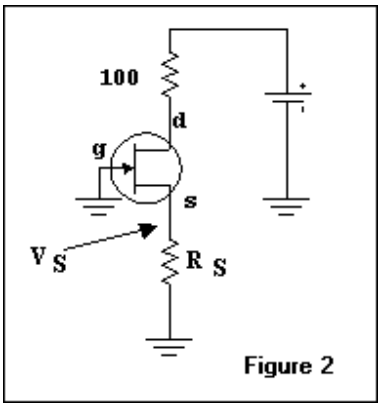

Circuit used to determine FET DC parameters.

This experiment was performed with a junk box 2N5454, producing the parameters I_{DSS}=11 mA and V_P=-2.8 volts. The current equation from Fig. 1 is plotted in Fig. 3 with these parameters. Additional points were measured producing points close to the curve.

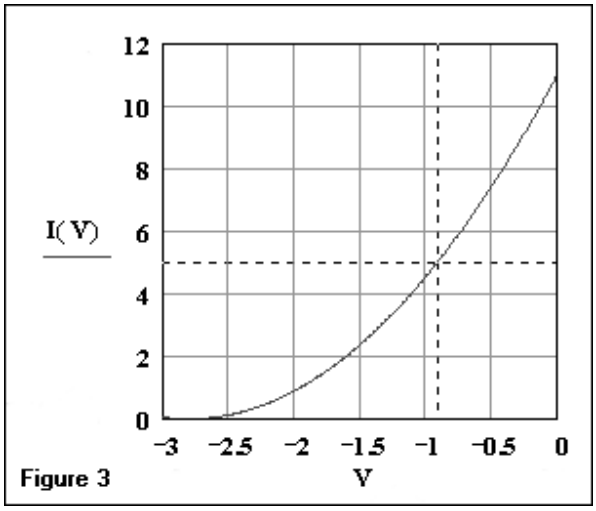

Data and smooth curve for a 2N5454 we measured.
This FET has a pinch off of -2.8 volts and a IDSS of 11 mA.

This exercise SHOULD be done with virtually every FET that the experimenter uses. It is not enough to obtain data for a given FET type, although if a group of parts are available from one manufacturing batch, moderate uniformity might be expected.

We mentioned the J310 earlier with an I_{DSS} spread from 24 to 60 mA. That 2.5:1 span range is one of the better of commonly available parts. The historically popular MPF-102 has a 10:1 spread in I_{DSS} (2 to 20 mA) with V_P extending from -0.5 to -7.5 volts! Clearly, this part should be used only with extreme care. It's a good RF part, but one MPF-102 may not resemble the next.

Assume the FET we summarized in Fig. 3 was to be used in an amplifier and that we wished to bias the FET for 5 mA. The 5 mA point can be picked on the graph and matches V_{GS} of approximately -0.9 volt. 0.9 volt drop from 5 mA matches a resistor of 180 Ohms. Application of Eq. 1 produces 182 Ohms. Crosshairs indicating the 5 mA point are included in Fig. 3.

Once a FET has been biased, it can be used in a small-signal amplifier. The significant gain parameter is the transconductance, given by Eq. 2. Transconductance is the drain signal current flowing for each volt of signal applied to the gate. Note that g_M depends upon the bias current. The g_M value given in data sheets corresponds to operation at I_{dss}.

$$g_m = 2 \cdot \frac{I_{dss}}{V_p} \cdot \left(1 - \frac{V_{GS}}{V_p}\right) \qquad \text{Eq.2}$$

$I_{dss} := .011 \quad V_p := -2.8 \quad V_{GS} := -0.9$

$$g_m := 2 \cdot \frac{I_{dss}}{V_p} \cdot \left(1 - \frac{V_{GS}}{V_p}\right) \qquad g_m = -5.33163 \cdot 10^{-3}$$

Figure 4

Data used to produce transconductance for the FET used in our sample amplifier.

Evaluation of g_M from Eq. 2 for our 5 mA bias produces the data in Fig. 4.

Consider the amplifier shown in Fig. 5. We will use this as an output buffer for an oscillator. Assume that we have tapped a signal from the oscillator tank where a voltage of 1 volt peak-to-peak is available. When this is applied to the FET gate, a current of 5.33 mA pk-pk will flow. The transformer uses a 15 turn drain winding and a 3 turn output link on a FT37-43 ferrite toroid. This turns ratio transforms the 50 Ohm load to appear as 1250 Ohms in the drain line. A current of 5.3 mA pk-pk flowing here produces a voltage of 6.25 V pk-pk. The no-signal drain voltage will be about 11 volts, so positive and negative 3 volt excursions will not cause voltage limiting. The current will vary from the 5 mA DC value down to nearly 3 mA (still well above zero) and up to nearly 8 mA, still below I_{dss}. The signal at the 50 Ohm load is reduced by the transformer to 1.33 V pk-pk. This is about +6 dBm, enough power to drive a diode ring mixer. This simple circuit is a low noise, efficient, and very useful amplifier.

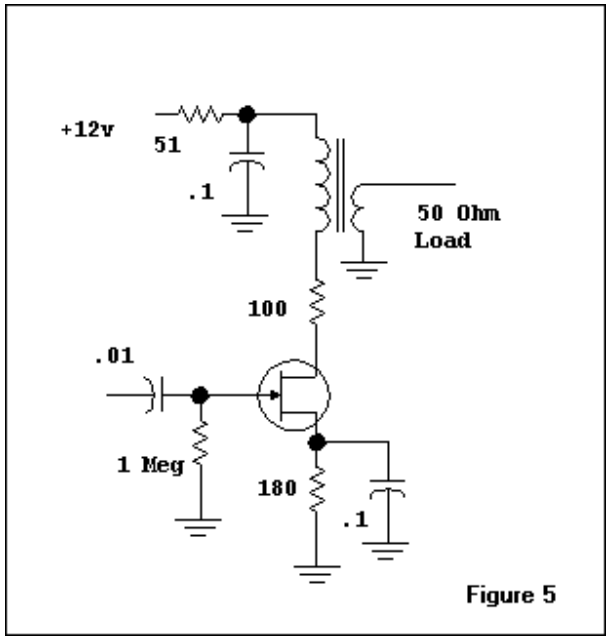

Figure 5

Common source amplifier biased for 5 mA drain current.

Figure 6 shows a FET amplifier that uses "long tail" biasing. A negative power supply is now used, forcing the biasing resistor to behave like a constant current source. This method can accommodate a wide range of FETs of a given type if the bias is set up for $I_d<I_{dss}$-min.

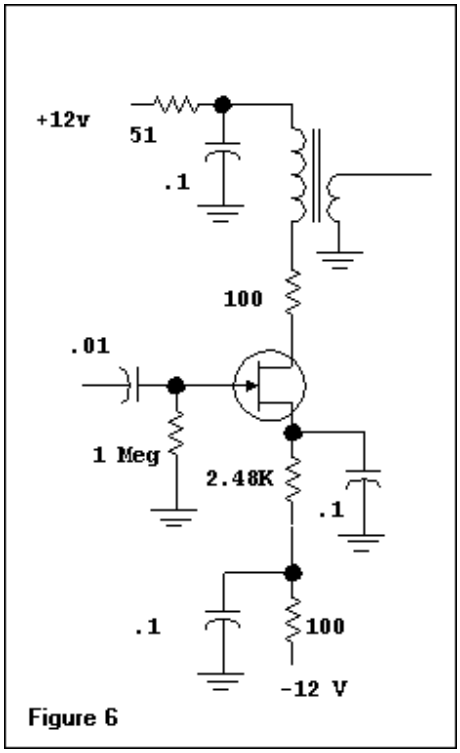

Figure 6

Amplifier with "long tail" biasing. This amplifier is biased for 5 mA and is identical in performance to that of Figure 5, but does not require the careful device characterization.

RF — Test and Measurement

EMRFD Review

Experimental Methods in RF Design

First published by the ARRL in 2003, EMRFD serves as the main QRP/SWL Homebuilder site reference.

Written by Wes Hayward, W7ZOI, Rick Campbell, KK7B and Bob Larkin, W7PUA, EMRFD is the follow-on to the 1977 ARRL publication, Solid State Design For The Radio Amateur (SSD).

A treasure trove of narrative and tabled information, schematics, references and photographs adorn this lengthy (512 page) book that comes with a data CD filled with software and key reference papers. With the included CD, EMRFD is about twice the size of the original SSD.

Wes and crew emphasize fundamental radio equipment design and bench testing rather than providing the usual catalog of circuits to just casually copy and not carefully examine.

Since we amateur builders own varied skills, abilities and test equipment, some sections may intimidate readers, while others may inspire and drive your bench practices to a higher level of competence and joy. The heart of RF design lies in measurement and reason: EMRFD emphasizes this and in doing so alienates some readers.

For some, homebrew radio electronics and kit building are synonymous — plenty of kits are sold to builders who chose to build someone else's design, rather than capture their own ideas on a scrap of copper board, or at least, to modify their equipment to suit their needs. EMRFD may appeal to builders who enjoy learning about RF *design*, or want more innovative and creative bench experiences — 1 stage at a time.

Although stressing that *build and measure* = a proven way to improve in this hobby, Wes and team share other pearls including bread boarding techniques, parts lay out, hot parts and pitfalls to avoid.

The first chapter is simply called Getting Started. On page 8, Wes shares his first simple receiver design — this page starts your breadboarding in haste! EMRFD features information and designs for all levels of experimenters, although basic electronics knowledge and some experience are needed to get the most out of its content.

Replete with sidebar examples about measuring or calculating data for common circuits, EMRFD also offers general purpose stages including a universal monoband superhet receiver front end or AF chain instead of less versatile, single- application circuits. The design information feels vibrant and flexible and some of the material is original, or presented in a way that adds to the existing amateur radio knowledge base. For example, new front-end mute circuits, or the cascode JFET mixer and RF amplifier.

Wes also shares some new ideas for RF and IF amplifiers ranging from simple to state-of-the-art. This book has something for everyone — I prefer to describe EMRFD's influence on our hobby in simple action verbs such as: improve, innovate, inspire, explore and transform.

Software:

The Microsoft Windows programs run on everything up to and including Windows 7. While a few programs are new, others represent updates of the historic W7ZOI Ladpac applications. Upon mastery of the Ladpac program suite, you'll generate the needed stages to boost *your* designs.

For example you can design complex double or triple tuned band-pass filters for your projects without any math — the software gives you the series capacitor values so you need not worry about putting links on your inductors to match input or output impedances.

EMRFD = the **must have** reference book for your homebrew workshop.

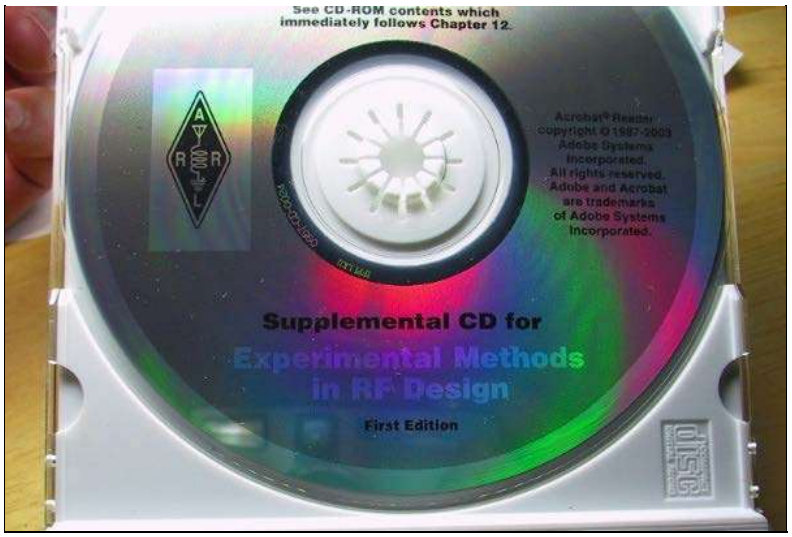

ARRL EMRFD web link

Link to the W7ZOI errata page for EMRFD

Tapped Capacitor Impedance Transformation in LC Bandpass Filters

copyright © Wes Hayward, W7ZOI, April 30, 2003.

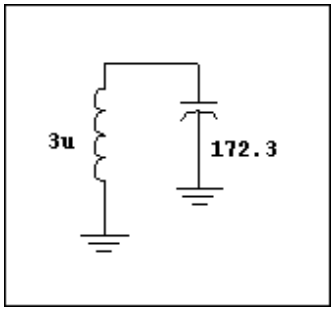

We often use a pair of capacitors to match impedances at the termination ends of LC bandpass filters. The circuit consists of a shunt capacitor at the termination followed by a series capacitor connecting to the high Z end of a parallel tuned circuit. Some readers have asked about how the capacitors are picked. Although there is considerable flexibility in some of the choices, it is not empirical as some have guessed. A simplified double tuned circuit design sequence is presented in the sidebar on page 3.14 of EMRFD and this is the beginning of the analysis used in the programs DTC.exe and TTC.exe contained on the EMRFD CD. I'll not go into too much detail here, for it's in EMRFD, beginning on page 3.8, and in chapter 3 of IRFD. Here is what happens in the programs:

Bandpass filter design begins with an almost arbitrary choice of inductor. We pick 3 uH for a 7 MHz double tuned bandpass filter that we will use to illustrate the ideas. This L resonates at 7 MHz with 172.3 pF.

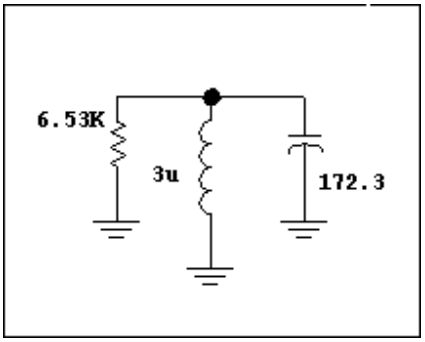

A bandwidth and center frequency are picked for the filter. This establishes a filter Q. The Q of an end section is then determined by the desired filter shape (Butterworth, etc)Let's say we want to do a 7 MHz center frequency Butterworth filter with BW=0.2 MHz. Filter Q is then 35=7/0.2. QE will then be 35x(root(2))= 49.5. The QE value in the sidebar (p3.14) includes the effect of finite inductor Q. Assume a lossless inductor for this example.

So what does this mean? It means that the end tuned circuit, when not coupled to the rest of the filter, needs to be set up to have a Q of 49.5. This is experimentally significant. (ref: QST, Dec, 1991). The reactance at 7 MHz of our 3 uH inductor is X=131.9 Ohms, so we need to load each end with a resistance R=QX=6.53K-Ohm.

What this means is that we would realize our double tuned bandpass filter with center frequency of 7 MHz and bandwidth of 200 kHz if we terminated a simple double tuned circuit in 6.5K at each end. The filter is shown below where we have used additional equations (EMRFD p 3.14) to calculate the coupling and tuning capacitors.

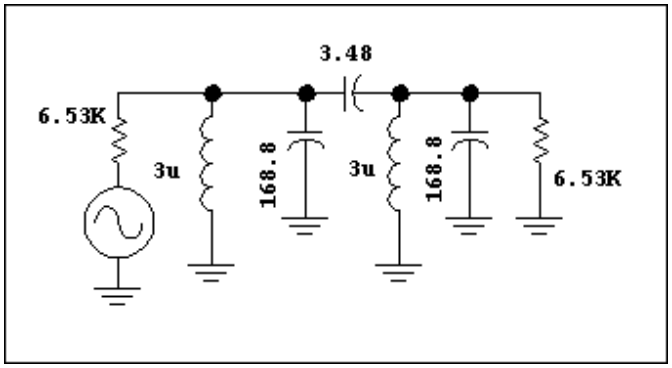

This is a useable filter design, for it will generate the desired shape and bandwidth. But, it is not very practical; it does not fit in our low impedance world.

The filter can be redesigned. One classic, but usually impractical solution is to scale the filter to lower impedance levels. For example, if we dropped L from 3 uH to 23 nH, we could directly load our filter with 50 Ohms and get the required end section Q. But this is not at all practical. First, it's difficult to build inductors with L this small and still have reasonable Q at 7 MHz. Second, the parasitic inductance of the rather large (high C) capacitors that we would attach to this inductor would begin to compare to 23 nH. A better re-design would use transformation circuits, schemes that will let us use a 50 Ohm termination (or whatever we need) and make it function as a 6.5K resistance when seen by the inductor.

One such scheme is a transformer. This could be realized with ferrite cores or with links inductors wound on the existing 3 microHenry parts. But link coupling with design precision is a challenge of it's own. Conventional two and three element transforming networks (L, pi, Tee) are also suitable.

The simplest transforming circuit uses a series capacitor. Let's do some analysis to see how this works:

We have arbitrarily picked a 10 pF capacitor to illustrate the idea. At 7 MHz, the reactance of a 10 pF capacitor is 2274 Ohms. Hence, the complex impedance of the 50 Ohm resistance and the series capacitor is Z=50-j2274. The impedance transformation behavior of this circuit is studied by transforming the series impedance to a parallel admittance. Recall that Y=1/Z. So Y=1/(50-j2274). The result is Y=(G+jB)=9.67E-6 + j4.4E-4. Of special importance is the resistive real part of the admittance.

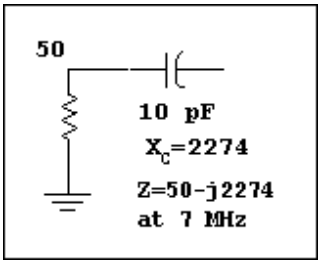

The 10 pF series capacitor in our example makes the 50 Ohm resistor look like a 103 K-Ohm resistor in parallel with a capacitor that is nearly 10 pF. The general case causes a R0 value resistor to look like a value of Rp with a series capacitor with reactance given by

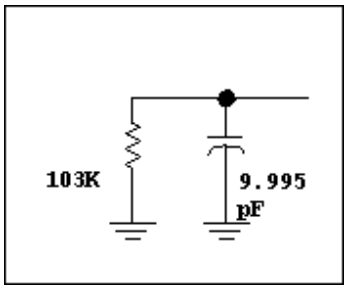

This equation is #3.1-5 from IRFD where it is derived.

$$X_C = \sqrt{R_p \cdot R_0 - R_0^2} \qquad \text{Eq. AA}$$

Our original example filter needed a parallel resistance, Rp, of 6.5K-Ohms, which is produced by a series capacitor with a reactance of 568 Ohms. This is a capacitor of 40 pF. Another version of our double tuned bandpass filter is then

Notice that the tuning capacitors, the elements across the inductor, have dropped as C is added at the ends.

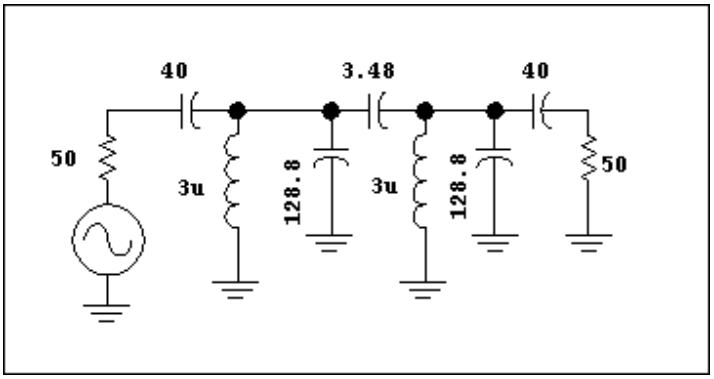

A capacitor in series with a resistance produces higher equivalent resistance. Consider a parallel combination. Here we pick a value of 200 pF as the parallel C and calculate the admittance. This is then converted to an impedance with Z=1/Y and the individual components are evaluated. This result is shown to the right.

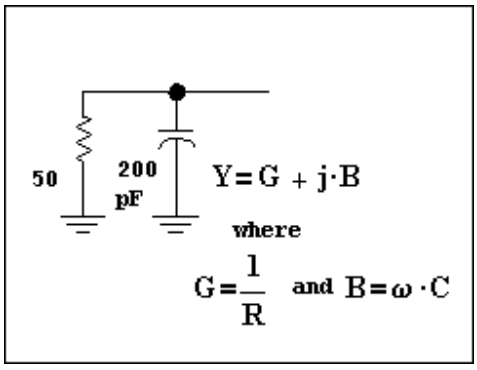

The parallel capacitor transforms the 50 Ohms to behave like a lower value. In this case, we obtain about 42 Ohms in series with a 1236 pF capacitor.

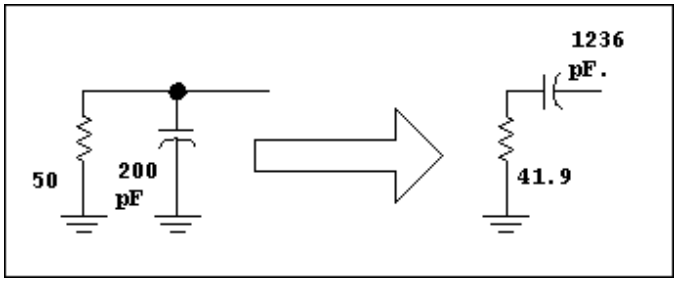

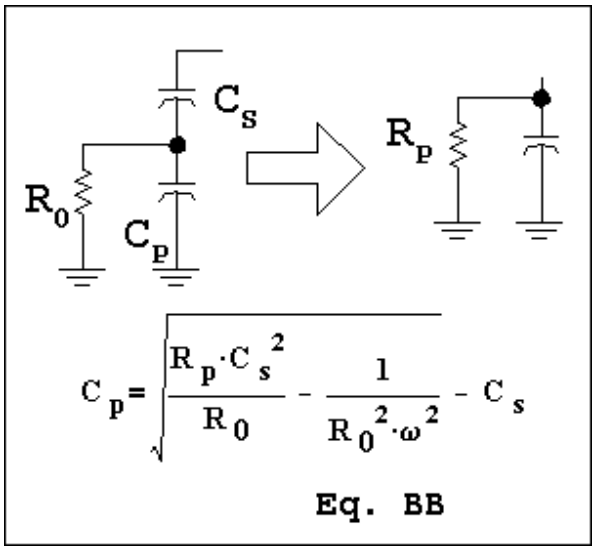

A series capacitor transforms a termination to “look like” a higher resistance while a parallel capacitor “transforms to” a lower R. Clearly, the combination of the two can generate about any result we need, realizing that they will also produce reactance that must be absorbed into the existing tuned circuits. The mathematics (now symbolic and not just number manipulation) is messy, but not difficult. A resistive termination R0 (50 Ohms or whatever) is paralleled by a capacitor Cp. The admittance is calculated and is converted to an impedance. The impedance of a series capacitor, Cs, is then added. The result is converted back to an admittance. The resistive real part is extracted and inverted to yield Rp. This expression is then solved to yield a design equation:

This is the equation used in the programs. A related expression provides the equivalent capacitance, needed to calculate the tuning capacitor for each resonator.

If we use the program with the center frequency and bandwidth presented earlier, we find that the minimum allowed series capacitance is 40 pF. If we then insert a value of 47 pF, we see that parallel 240 pF capacitors are needed to properly load the resonators. This variation is shown to the right. Circuits using the capacitor tap are practical, for they allow existing junk box parts to be used. The topology has little other utility, offering virtually the same response as a filter using only series capacitors for loading.

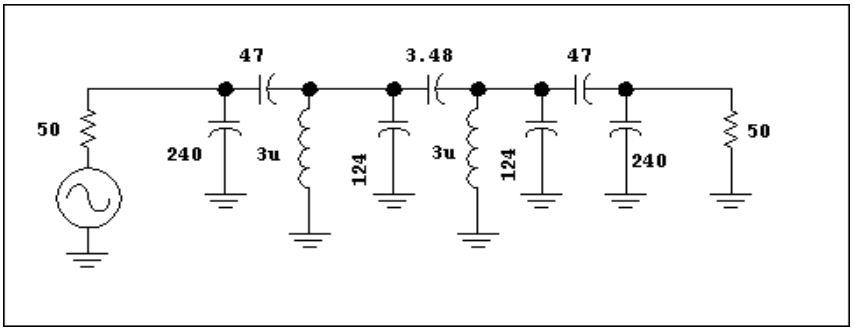

Useful link shared by Tim, KE7VYD on Feb 4, 2014. Click

More Active Antenna Experiments

Introduction

Many builders emailed me requesting a simple, broadband VPA (voltage probe antenna) design with more power gain than the common gate versions I have presented elsewhere on this web site. Connecting a whip antenna to a cascode JFET stage described by W7ZOI in Experimental Methods in RF Design is 1 method I considered.

I built the version shown in Figure 1 almost 2 years ago. This VPA. although more powerful, overloaded the front end of my test receiver with multiple RF signals. Clearly some tuning on the input was needed.

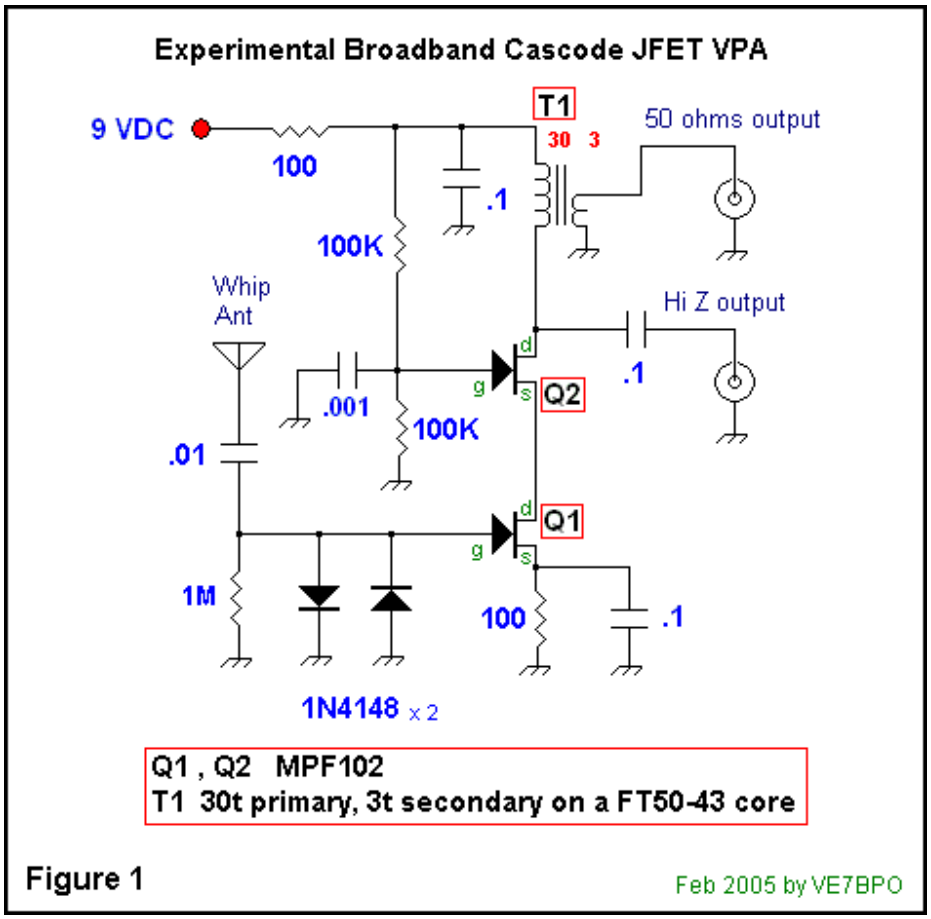

The Tuned Whip

Previous experimentation confirmed that it is easy to tune a short whip antenna by connecting it to the hot end of an L C (inductor and capacitor) tank circuit. The high impedance whip antenna was "matched" to a JFET RF amplifier by placing a high value (1 megohm or greater) on the JFET gate to ground. Although this method is practical, I desired a network to transform the output impedance of the tuned whip tank tank circuit to a known impedance. I do not possess the knowledge or mathematical skill to design such a network and asked Wes Hayward if he might consider doing this for me. My desired parameters for the network were 10.0 MHz, a 50 ohm output impedance and a 4 foot (122 cm) whip. Please refer to Wes' calculations and schematic in Figure 2 below. This math is difficult, however, a practical design for experimentation is provided.

Antenna Network. The antenna is a short whip at 10 MHz. We assume a length of 4 ft with a diameter of 0.25 inch. EZnec modeled this as 7.58 pF in parallel with 3.3 MegOhm. We assumed a perfect, ideal ground for a vertical with 48 antenna segments.

$R := 3.3 \cdot 10^{6}$ $A := 7.58 \cdot 10^{-12}$ $C_1 := 47 \cdot 10^{-12}$

$C_2 := 470 \cdot 10^{-12}$ $Z := 50$

$L := 3 \cdot 10^{-6}$ $Q_u := 200$

$f := 10$ F is in MHz.

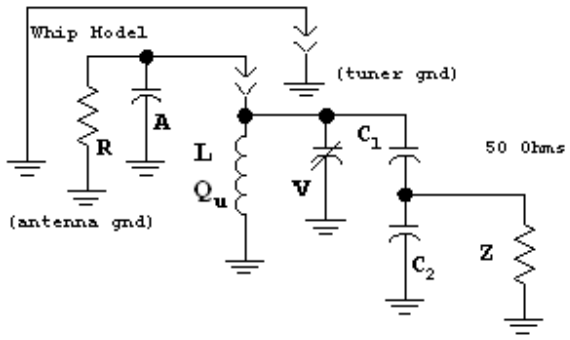

For given values of C1, C2, Z, A, R, L, Qu, we wish to calculate the value for V needed for tuning to the desired frequency (10 MHz) and the overall network Q.

$\omega := 2 \cdot 10^{6} \cdot \pi \cdot f$

"whiptune.gif"

$$R_Z := \frac{Z^2 \cdot \omega^2 \cdot C_1^2 + 2 \cdot Z^2 \cdot \omega^2 \cdot C_1 \cdot C_2 + \omega^2 \cdot C_2^2 \cdot Z^2 + 1}{\omega^2 \cdot C_1^2 \cdot Z} \qquad R_Z = 8.343 \times 10^{3}$$

$$C_Z := C_1 \cdot \frac{\left(1 + Z^2 \cdot \omega^2 \cdot C_1 \cdot C_2 + \omega^2 \cdot C_2^2 \cdot Z^2\right)}{\left(Z^2 \cdot \omega^2 \cdot C_1^2 + 2 \cdot Z^2 \cdot \omega^2 \cdot C_1 \cdot C_2 + \omega^2 \cdot C_2^2 \cdot Z^2 + 1\right)} \qquad C_Z = 4.39 \times 10^{-11}$$

The inductor resonates at f with Cnet, obtained with the usual resonance condition.

$$C_{net} := \frac{1}{\omega^2 \cdot L}$$

We must now subtract the C of the whip plus that from the load to get the variable needed to tune.

$C_V := C_{net} - C_Z - A$

Note: If CV is negative, we must reduce L or C1 to get a postive value.

$C_V = 3.295 \times 10^{-11}$

The net resistance across the inductor is the parallel combination of RZ, R(antenna), and the R related to Qu, Rp=QuωL.

$$G_{net} := \frac{1}{R_Z} + \frac{1}{R} + \frac{1}{Q_u \cdot \omega \cdot L} \qquad R_{net} := \frac{1}{G_{net}} \qquad R_{net} = 6.817 \times 10^{3}$$

The net Q is given as $Q_{net} := \frac{R_{net}}{\omega \cdot L}$ $Q_{net} = 36.167$

Figure 2

By W7ZOI Feb 27, 2005

Common Gate Amplifier Version

I built the circuit shown in Figure 3 and Figure 4 and tested it on a medium grade SWL receiver (Realistic DX 300), rather than an expensive Amateur Radio receiver. I required this active antenna for experimenting with a 10 MHz WWV superheterodyne receiver I am designing. For practical analysis, VE7TW and I did listening tests with a commercially made 4 foot telescopic whip antenna that is fitted to a standard PL-259 connector (Figure 5) and his deluxe multi-band commercial SWL antenna up a 25 foot tower.

The Figure 3 VPA was very quiet
and pulled in WWV much better

than the plain 4 foot whip of Figure 5, however, received station signal strength was quite weak when compared to the outside antenna. Our conclusion was that considering the significant losses of the 4 foot whip antenna it was connected to, the common gate RF amp does not likely have enough voltage gain to please most builders. This amp did present a low impedance to the whip network and no spurious oscillation were measured on the bench. Do not omit the 22 ohm or similar value resistor in the drain of the FET. It is used to to push the UHF parasitic oscillation tendency into the ground. Such oscillations will trash your receiver mixer intermodulation performance.

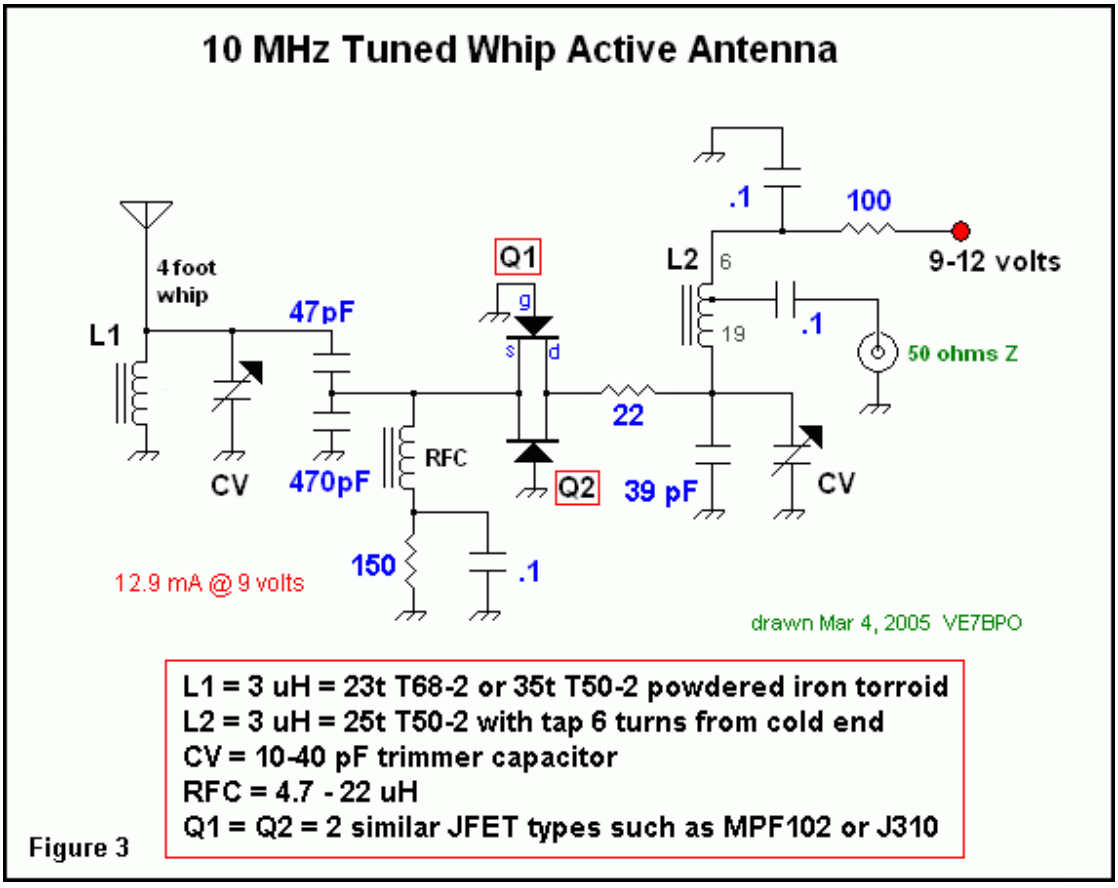

Figure 3

The 150 ohm source resistor can be increased in value and/or 1 of the JFETs removed if you wish to reduce the current draw on a 9 volt battery. It might be better to substitute 1 better JFET such as the J310 rather than use the "popcorn" MPF102 as shown. This VPA may be practical for a receiver that has an existing broadband RF preamplifier. The tap on L2 was found experimentally and the output impedance is probably higher than 50 ohms, but is likely a reasonable low impedance match to most receiver front ends. A broadband transformer for L2 might also be a good choice.

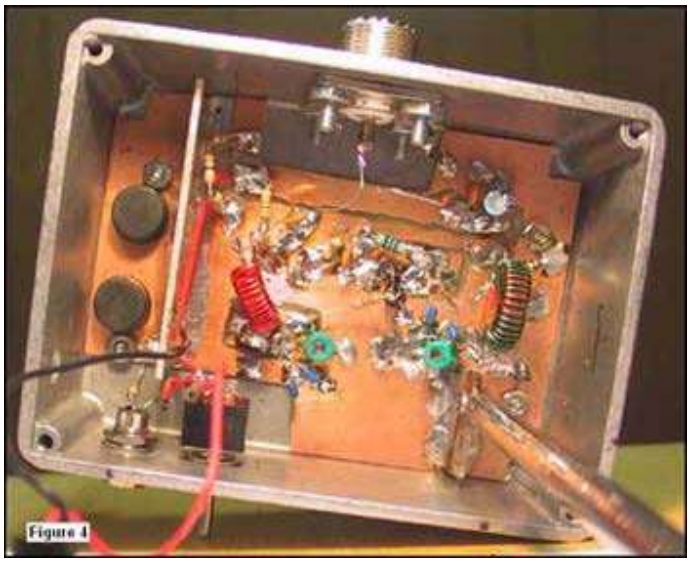

Figure 4 above: For the whip network, it is critical that you use a inductor that has an unloaded Q of 200 or above. Practically speaking, this means you cannot use a fixed value inductor such as an epoxy coated or molded RF choke. Use a powdered iron torroid instead. In my test VPA designs, for L1, I used a T68-2 core wound with (the green) 22 gauge enamel coated wire to get as high an unloaded Q as possible. If you use the T50-2 core, use 24 gauge wire if possible. Higher Q = lower losses.

Figure 5 above: This is a 4 foot whip antenna factory connected to a PL-259 that came with the Realistic DX300. It presents a very high impedance to the test receiver front end and probably wasn't a good choice to compare the VPA designs to.

Cascode JFET Amplifier Version

It was decided to use a cascode JFET amplifier to obtain more power gain. The whip network was changed to try to match the 10K input of the JFET amplifier shown in Figure 6. The whip network capacitor values (150 and 33 pF) were calculated to the best of my ability. This amplifier was tested in the same manner as the Figure 3 design. It worked very well. The WWV signal that morning was not very strong and could not even be heard with the plain 4 foot whip. The signal strength of the tuned whip was just below that of the outside antenna. The outside antenna was much quieter however and had less fading. The tuned whip antenna was quite noisy in comparison. The high gain RF amp brought up the strength of the environmental noise sources in the house. The RF gain of the receiver was reduced to compensate for the added noise.

Another problem was noted with this and other tuned drain versions of the cascode JFET amplifier; instability.

Recently, I connected a tuned drain version of the Figure 1 VPA to a receiver that contained a tuned input stage and was able to measure oscillations in the VPA with my scope. The FET drain tank and the tuned input amp seemed to be interacting.

A "swamping" resistor was placed across the VPA drain tank circuit. I had to use a resistor value of less than 1200 ohms to eliminate this instability. This greatly reduced the gain and selectivity advantage of a tuned output and I realized that output tuning may be impractical for many reasons. Some SWL builders use regenerative receivers and such a problem would be disastrous. I sent the Figure 6 schematic to Wes Hayward and he suggested using a broad or wide band amplifier as shown in Figure 8.

Instability can also occur in broadband output versions and a swamping resistor is still necessary but is used mostly to force an output impedance so that a transformer can be designed.

All of the cascode JFET amplifiers shown have fixed bias on Q2. Variable gain is possible by changing the bias voltage on Q2 with a voltage divider and/or modifying the amplifier circuit to give a greater range of bias controlled voltage gain. Please refer to EMRFD page 6.17 for information regarding this. A switchable resistor attenuator might also be practical for some builders.

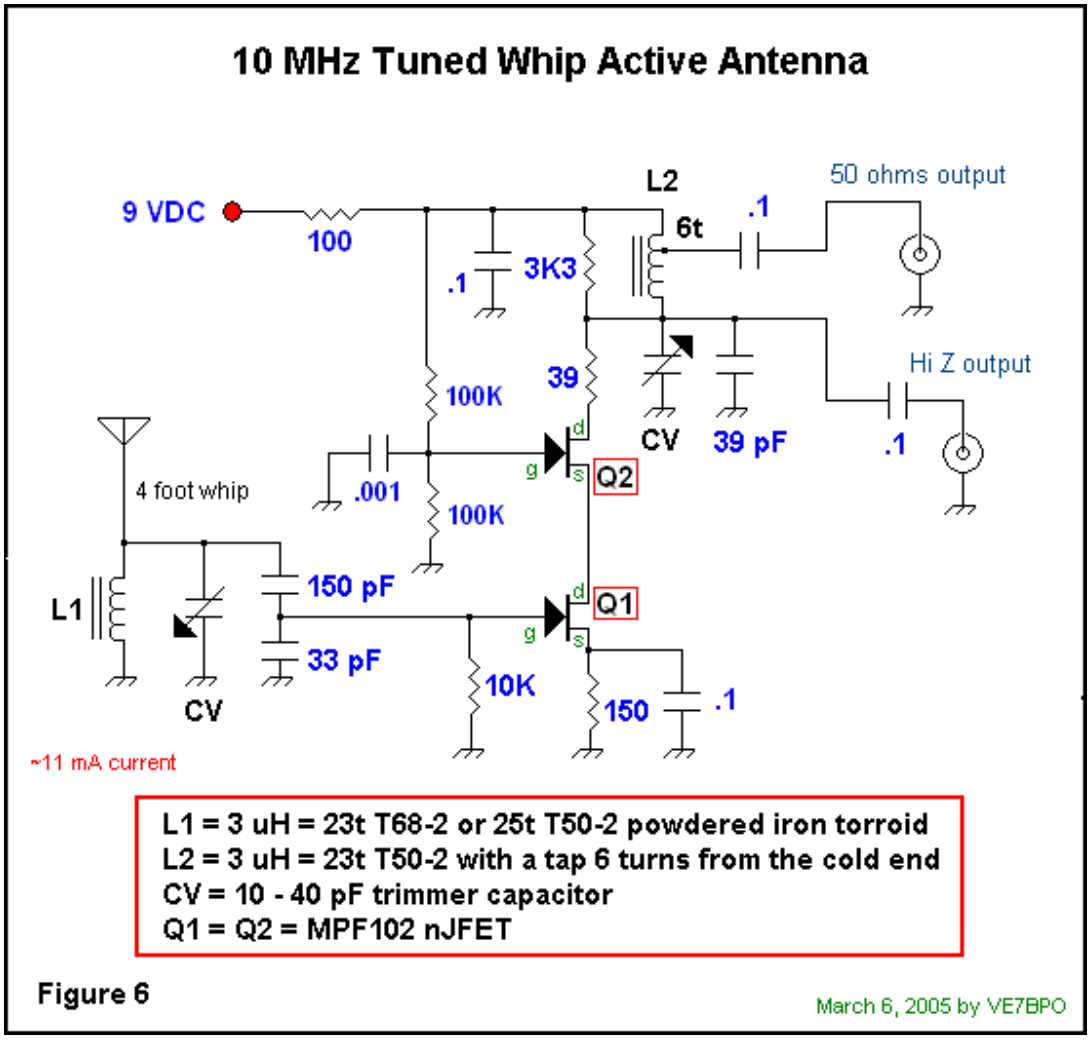

Figure 6 above: The tuned whip network is connected to a cascode JFET amplifier. A dual gate MOSFET would also be a great choice. I have many on hand, but chose the cascode JFET topology because many builders no longer have access to these devices or prefer not to use the more available surface mount types. They are also more expensive.

Figure 7 to the right: Detail of the tapped L2 inductor should you decide to experiment with a tuned drain version or need one for another project. Wind your coil and leave an extra long loop for your wire tap. Cut the tapped loop at the midpoint and use a small piece of folded ~150 grit sandpaper to remove the enamel from each of the 2 wires. Twist the now bare wires together and lightly solder them. Cut the end wires to the required length and use the sandpaper to remove the enamel. A method to strip enamel off wire is a frequently asked question for me and sandpaper works

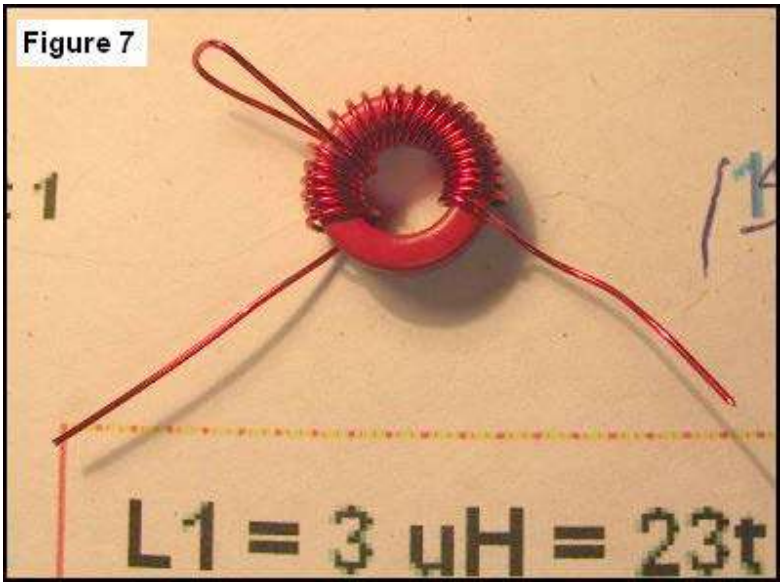

well.

Broadband Output Version

Figure 8: The broadband version W7ZOI suggested to try building. I modified the output transformer in the Figure 6 project and tested it with Tom, VE7TW. We really liked it. By adjusting the network trimmer capacitor, I was also able to tune the 30 meter Amateur radio band as well. For 30 meter band use, I peaked the tank circuit at 10.125 MHz by listening to receiver noise with a home brew direct conversion receiver and was suitably impressed.

This is the active antenna design I wll use for my future projects where strong voltage gain is required. If your receiver has a higher impedance such as 500 ohms, you might try using a couple more links on the output transformer secondary winding.

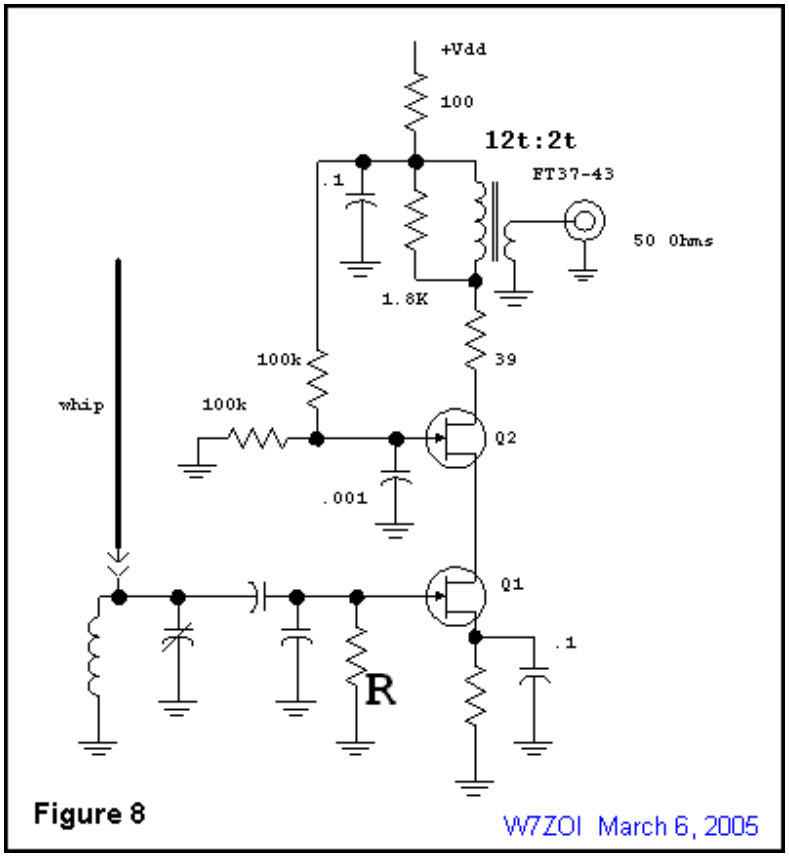

Tuning a Whip To Other Frequencies

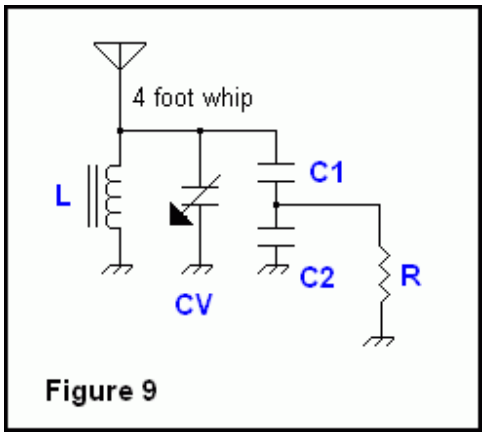

The ability to calculate the network values for different frequencies may prove difficult for those who lack software and/or math skills. To that end, a table follows which has some radio frequency bands and some suggested starting values for the Figure 9 parameters. Please note these are calculated and are suggested starting points based upon my limited understanding of radio electronics. Experimentation is the best method to find what component values will work for you.

Emails regarding the component values used in actual experiments is greatly welcomed.

The **R** value is the input impedance of your RF amplifier. In the case of the cascode JFET amp, it is the Q1 gate resistor.

Note that the actual circuit CV value is typically much lower than the suggested (calculated) CV value from the chart. CV is used to **resonate** the tank. CV is dependent on several factors including the capacitance of the whip antenna, your RF amplifier input capacitance , your circuit layout, component lead lengths and variations in the powdered iron core and C1 and C2 capacitors values. Expect that your whip antenna will exhibit between 8 and 15 pF of capacitance. You need to subtract this from the suggested (calculated) CV value from the Figure 10 table.

Wes, W7ZOI told me that the whip antenna capacitance will remain constant as you change frequency providing you are below 1/4 wavelength for a given frequency. Here is a good web site applet to calculate wire or whip 1/4 or 1/2 wave lengths per frequency: http://www.csgnetwork.com/antennagenericfreqlencalc.html.

The actual circuit CV might include a trimmer capacitor plus a parallel fixed value capacitor.

How to find the correct trimmer capacitor for any tuned circuit you wish to resonate

I suggest you chose a circuit CV value by placing a variable trimmer capacitor in your circuit that when set to minimum will be below half or more than the calculated CV value. Then peak the whip tank circuit using a test oscillator and scope or RF probe or by just using receiver noise. Now temporarily add a 5-10 pF capacitor in parallel with trimmer capacitor. Just barely solder it in place or even just hold it in place without touching the leads. If the output increases, you were under the correct circuit CV value. Add more capacitance and check again. Repeat until you are satisfied with your chosen circuit CV value.

If after adding the initial 5-10 pF capacitor, the output decreases, try peaking the tank again to see if you can restore the signal strength you had before you added the temporary capacitor. If after peaking, the signal strength is down, you now have too much capacitance and can remove the temporary capacitor.

You just might also have too much capacitance. You might try a smaller variable cap or reduce the value of any fixed capacitors in parallel with your trimmer to make sure your minimum capacitance is not too high to properly resonate the input tank circuit.

The point is you need to be able to tell if you have too little or too much capacitance for CV and by going under and over you can tell if you are truly resonating the tank when you adjust the trimmer capacitor. Experimentation will tell you.

Another option is to put in a front panel adjusted variable capacitor. Front panel switchable inductors might also allow other bands to be tuned with 1 tuned whip network.

Moving your body as you adjust the trimmer capacitor can change the tuning, so please keep this in mind.

Figure 10 above. Picking an inductor value for the whip network can be tricky and sometimes trial and error is required. This table may be used to find starting values for the Figure 9 network. Below 41 meters, I suggest trying a lowered RF amp input impedance as shown to allow practical component values. Most of these calculations have not been tested.

Tuned Whip Suggested Starting Values

Band	Freq (MHz)	CV (pF)	C1 (pF)	C2 (pF)	L (uH)	R (ohms)
120M	2.3-2.5	270	150	22	15	2K2
90M	3.2-3.4	165	150	10	12.6	4K7
75M	3.9-4.0	115	150	33	11	4K7
49M	4.75-5.060	83	47	22	11	4K7
41M	7.10-7.60	75	150	18	5.1	10K
31M	9.2-9.9	73	150	22	3	10K
25M	11.6-12.2	58	47	18	2.5	10K
22M	13.57-13.87	34	100	47	2	10K
19M	15.1-15.8	32	47	33	2	10K
16M	17.48-17.9	38	33	27	1.5	10K
13M	21.45-21.85	19	27	39	1.5	10K
11M	25.6-26.1	26	18	36	1	10K
10M	26.965-27.41	22	18	39	1	10K
Some Amateur QRP Frequencies						
80M	3.56	185	150	5	10	4K7
40M	7.04	85	220	10	5.1	10K
20M	14.06	56	22	10	2	10K
17M	18.069	36	33	27	1.5	10K
15M	21.06	22	27	39	1.5	10K
15M	21.06	27	18	39	.8	10K
15M	21.06	48	33	10	1.0	22K
10M	28.06	19	18	47	1	10K
10M	28.06	29	15	33	0.8	10K

Figure 10

I think an indoor active antenna for 74 meters or below might just be a noise generator.

I chose a frequency mid band for any given SWL band on the chart. The bandwidth of the input network is wide enough so this should be suitable to cover a good portion of the band.

Building An Active Antenna

To build this active antenna, chose the input tank network values from the Figure 10 chart or from your own calculations and then use them in the Figure 6 circuit. The Q1 source resistor can practically be from 100 to 390 ohms depending on how long you need your 9 volt battery to last. Increasing this resistor value will reduce the amplifier power gain. Try different values and see for yourself!

Some Practical Examples: 40 and 41 Meter Band

An active antenna that would provide coverage of the entire 40 meter Amateur Radio and 41 meter Shortwave band was designed. A varactor diode was used as the tuning element. The tuning voltage to the varactor was controlled by a 10K potentiometer which also had an integral switch. The finished VPA is shown in Figures 11 and 12.

Figure 11

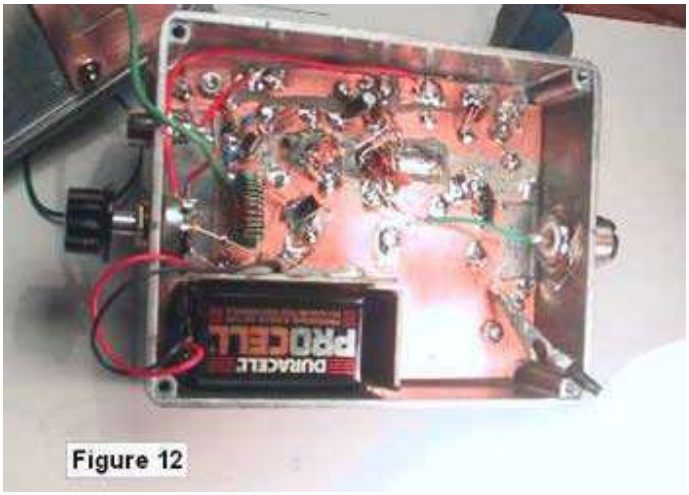

Figure 12

Figure 13 below: A hotter JFET, the J310 was used in this VPA. In the test receiver, I was able to peak a signal from ~ 6.90 to 7.60 MHz. Tuning is very sharp but peaking is easily performed by turning the potentiometer gently back and forth while listening to receiver noise or a station. It might have been better to use a smaller value zener diode as when the 9 volt battery fades below 7.5 VDC, the zener diode will not conduct and the voltage regulation will fail. Having said that, this "hotter" VPA is intended for use with an external power supply as current draw at 9 and 12 volts is 19 mA and 28.9 mA respectively.

I tried using this VPA as the antenna for the Cascode 7 receiver shown elsewhere on this web site. When the VPA was peaked at the receiver tuning frequency, loud oscillations occurred. The receiver and the VPA were about 1 meter apart. I had to turn on the -10 dB attenuator and detune the VPA for the oscillations to stop. Moving my hand near the whip antenna varied the oscillations. The high gain, tuned circuits of the Cascode 7 receiver are not a good choice for an active antenna.

Future receivers projects will have a integral VPA and clearly the front end of these receivers will have to be designed carefully. A low cost Grundig receiver was also overloaded with this VPA.

This VPA worked well with other receivers which did not have a tuned, high gain preamp.

Figure 14: From the chart, the MV209 exhibits about 44 pF (guessing) when 0 volts are

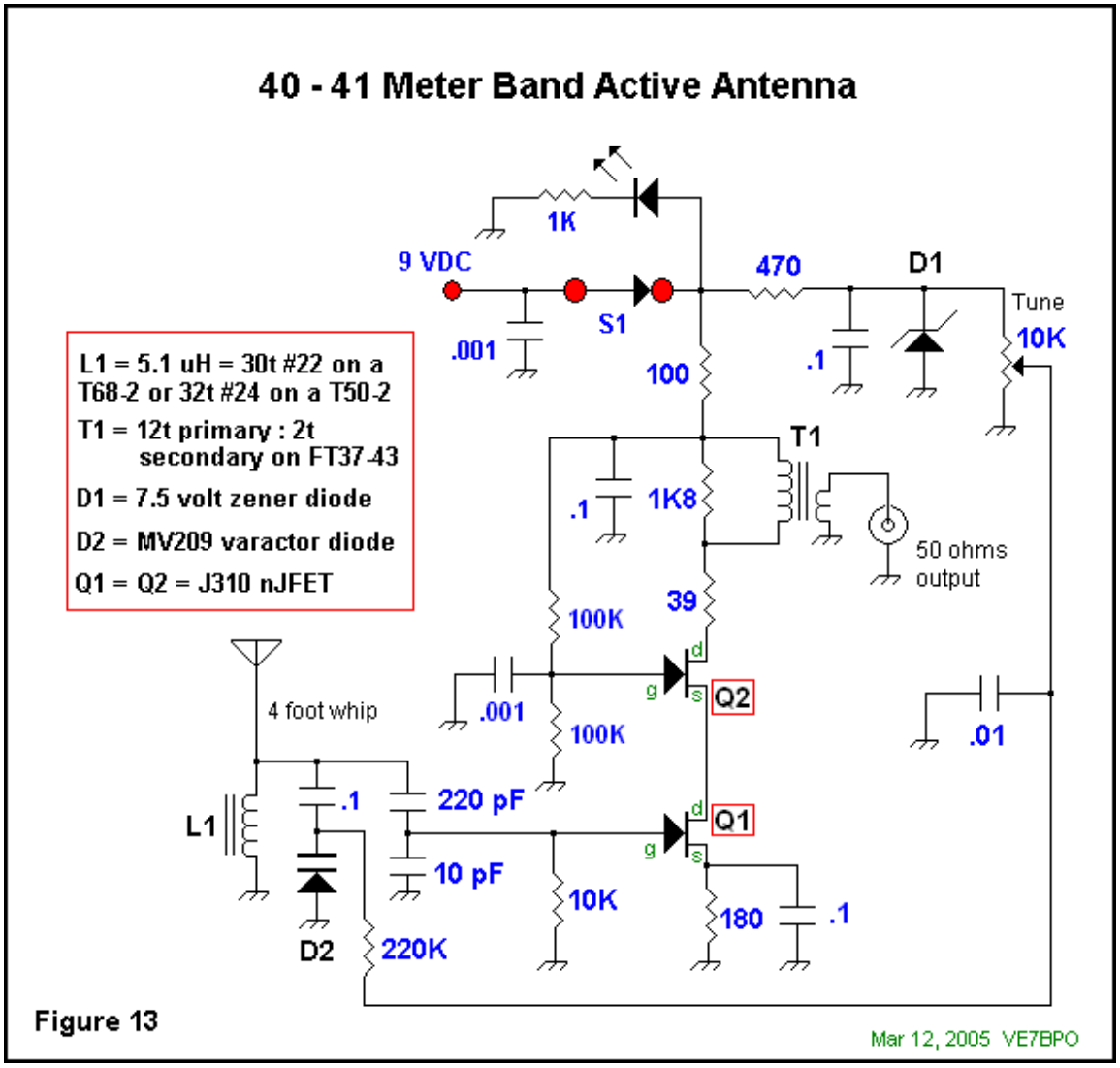

Figure 13

applied to it.

The VPA was built and tested before the tuning diode components were added. A 7.039 MHz crystal oscillator with a piece of wire for an antenna was used as an RF source. The T2 secondary was connected to ground via a 47 ohm load resistor.

A 47 pF fixed capacitor was lightly soldered in parallel with L1 and the voltage was measured with an oscilloscope. A 10 pF capacitor was then carefully held across L1 and the voltage increased by 0.25 volts. A 22 pF capacitor was then tried and the voltage decreased much below that of just the 47 pF capacitor. The nearest standard value I had on hand above 47 pF was 56 pF. The 47 pF capacitor was removed and replaced with the 56 pF one. I tried holding a 5 pF capacitor in parallel with the 56 pF and the measured voltage decreased. I had experimentally determined that to resonate L1 at 7.039 MHz I needed between 47 and 56 pF for the CV value. This range should be close enough to resonate the tank at 7.0 MHz as well.

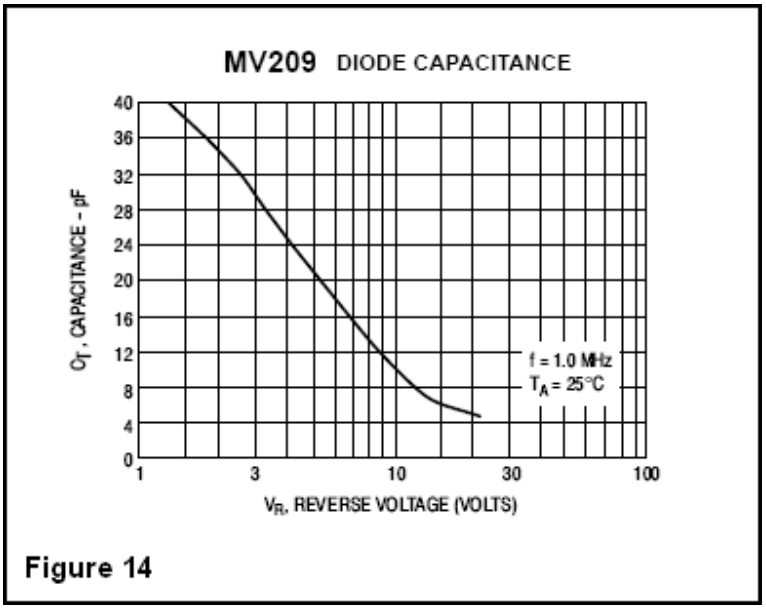

Figure 14

I then chose a varactor diode. The MV209 would be perfect for my project based upon the Figure 14 chart. I anticipated that I might have to place a small trimmer capacitor in parallel with the varactor to resonate the tank at the my lowest design frequency which was 7.0 MHz. As it turned out, in addition to the varactor capacitance, the voltage control circuit added additional capacitance and I actually needed 0.30 volts (measured between the 10K pot and the 220K resistor) to resonate the whip at 7.039 MHz. This was perfect; I did not need a trimmer capacitor! At 0 volts to the varactor diode, my whip resonated ~ 6.90 MHz.

---

5 MHz WWV Cascode Bipolar Amplifier

I wanted to build a non-FET version as shown in Figure 15. The tuned whip tank was originally resonated with a 5 - 40 pF trimmer capacitor. I unsoldered this trimmer capacitor and measured it with a meter; it was 27 pF. A 27 pF fixed value capacitor was soldered in and tested. The circuit was resonant at 4.98 MHz. This was close enough for me and also the 3 high Q fixed value capacitors provided a very narrow 6 dB bandwidth along with the inductor. The output impedance value of the tuned whip is around 200 ohms to match the Q1 bipolar amp input impedance.

Listening tests indicated that this circuit probably had too much gain at 5 MHz. It might be favorable to lower the Q1 emitter current to 7 mA or so by raising the Q1 emitter resistor or decreasing the Q1 bias voltage. Also, a series feedback, degenerative resistor on the Q1 emitter might be considered. This active antenna was comparable to the outdoor reference aerial for signal strength, however, predictably was much noisier.

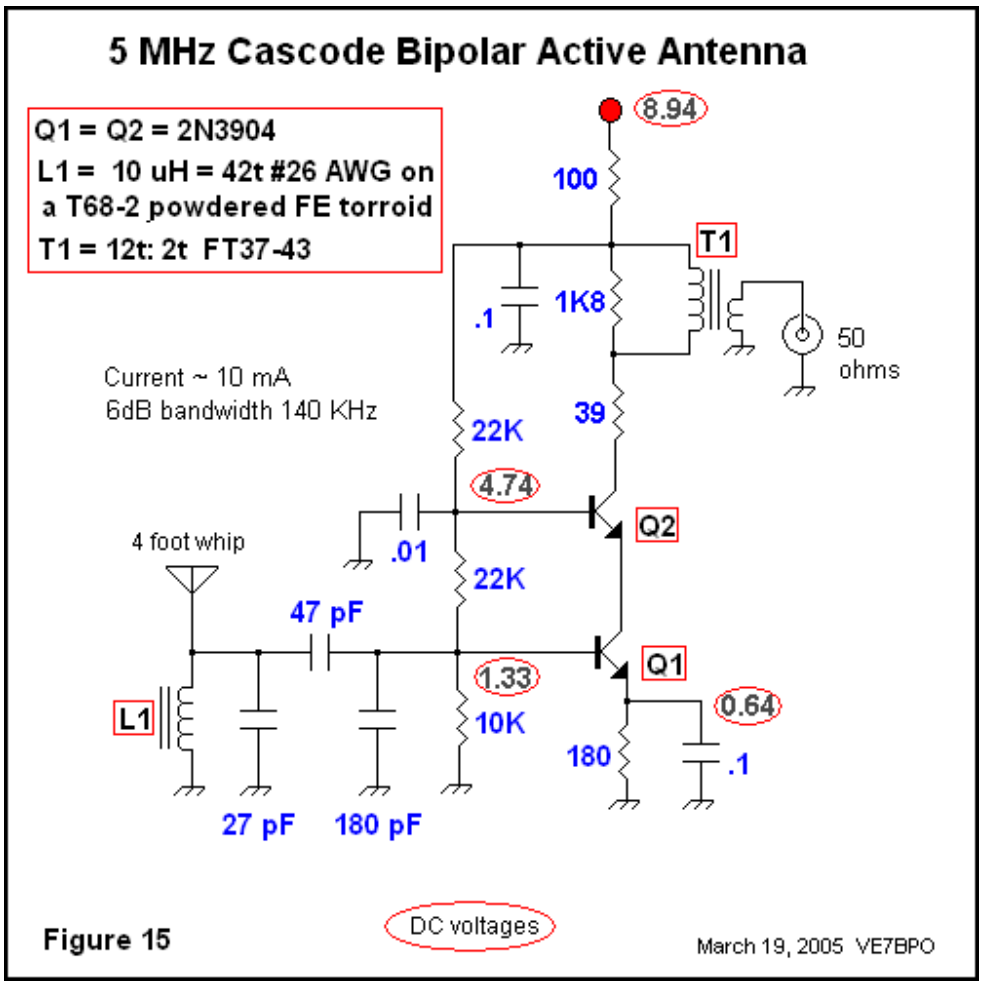

Final Comments

I found that using lower Q trimmer and fixed value capacitors undesirably increased the tuned whip bandwidth presumably by lowering the resonant circuit Q. The inductor unloaded Q was the dominant factor however. The worst case scenario was a tuned whip built with junk-quality parts which had a -6 dB bandwidth of ~390 KHz.

I also learned that you should expect high gain amplifiers to oscillate and specifically design to reduce or suppress this tendency.

The 2005 Active Antenna experiments were fun and provided many learning opportunities. An active antenna is a perfect weekend project. There is no substitute to learning by building and testing electronic circuits with your own hands.

My sincere thanks to all of the friends who helped me with these experiments.

Experiments by Other Builders

What follows are some VPA experiments by others that were sent to me by email. I seek your feedback and photographs to help improve this web site and also to gain motivation to add more new content.

Joe, K9LY
Hi, Todd :

Attached are some photos of a voltage probe amplifier that I built using ideas from your excellent website. I use a TenTec 1254 receiver in the car and listen to some shortwave broadcasts during the daily commute to and from work. The antenna is a 4-foot whip that screws into the trunk-lip mount shown. The amplifier is held to the bottom of the trunk lid by a magnet and has survived for several weeks without falling off.

The amplifier is tuned by a varicap diode and covers approx. 9-14 MHz. The tuning voltage comes from a potentiometer that I added to the front panel of the receiver.

I decided to use the 2N3904 cascode amplifier because I liked the idea of using the most common transistor possible. The LC-tuned input is nice because the antenna whip is held at chassis ground potential, which should help prevent damage to the amp caused by static buildup.

The TenTec 1254 Receiver. http://radio.tentec.com/kits/Receiver

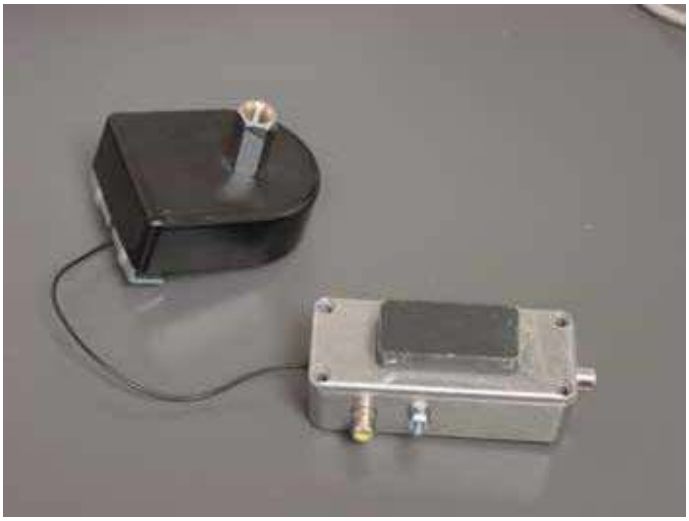

Above left: Inside Joe's trunk lid SWL Active antenna. Great ugly construction in a sturdy Hammond chassis.
Above right: Joe's remotely tuned SWL active (or voltage probe) antenna amp and whip holder. Thanks Joe!

Fun with LEDs

Introduction

This summer I built several LED projects including sequential LED chasers (sequentially left to right) and also "Nite-Rider" style which go (sequentially left-right-left-right-etc). Many more LED schematics can be found on the World Wide Web via a Google search. LED projects are great fun for both HAM's and SWL's alike. They are also a lot of fun for children to experiment with. Currently, I am experimenting with PIC microcontrollers to perform LED "tricks".

I also built several very bright LED flashlights which run on a single 1.5 volt battery. For ultra-bright LED flashlight schematics, check out Dick Cappel's excellent and very informative web site. He has a number of LED driver circuits and other great schematics and theory. To wind the inductor for these LED flashlights, I had good success using an FT-37-43 ferrite torroid core. I used at least 40 turns of wire which is generally center tapped.

LED Chasers

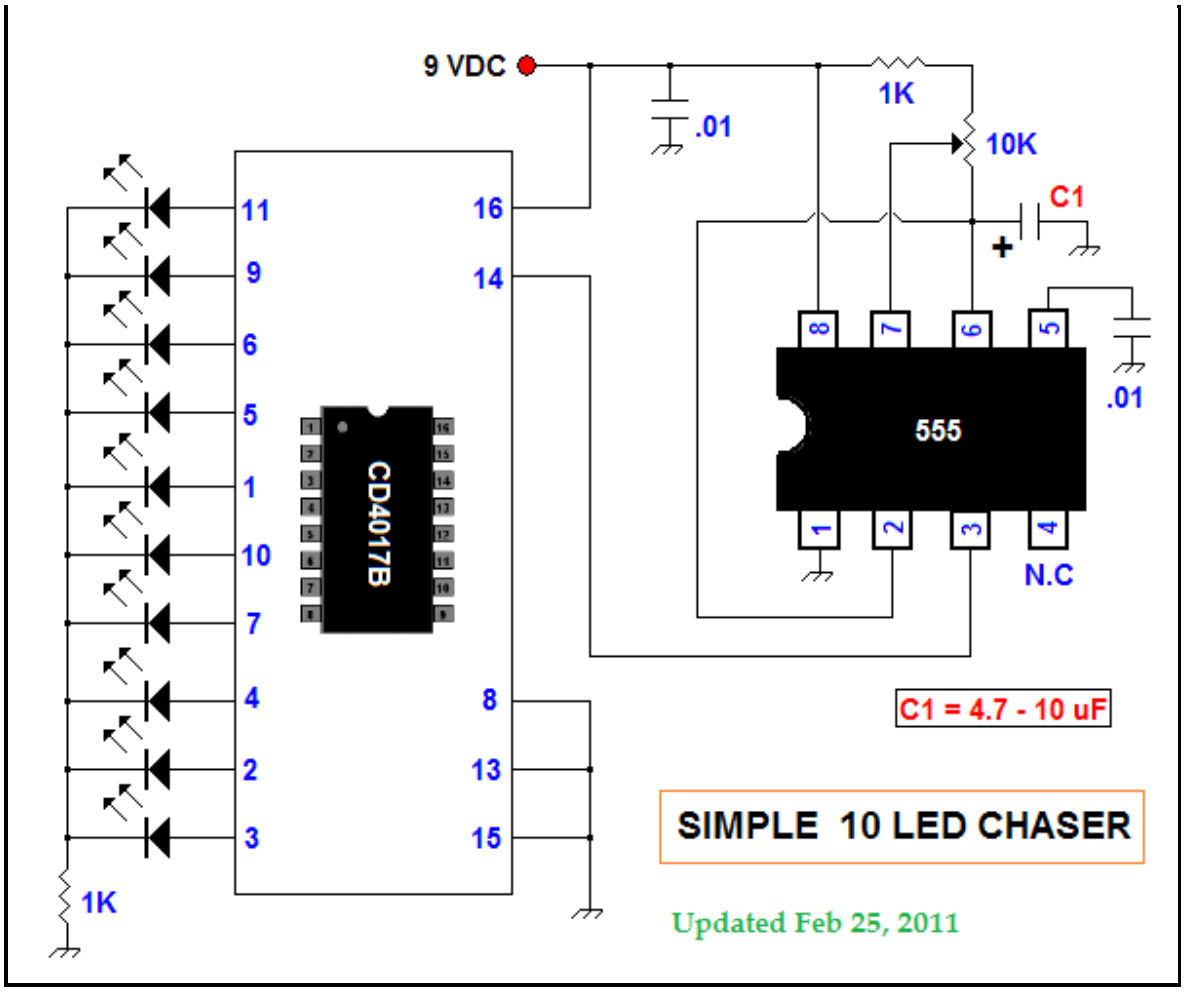

Above. This is the schematic for a ***very*** basic 10 LED chaser I built. I prefer my "chasers" to run slower than most and chose a 10 uF capacitor for C1. The 10K pot can reduce the flash speed from not moving to whatever minimum time constant is possible with the C1 value you choose. Don't bother with ultra-bright LEDs for these "chaser" projects as cheaper, lower millicandela (mcd) LEDS work fine. I favor blue and green LEDS. The 4017 decade counter is a fabulous part and can be driven to flash a row of LEDs with a 555 timer chip or a discrete BJT multivibrator.

Update Feb 25, 2011: Many "experts" have emailed, or flamed me on web forums to say this circuit can't possibly work. I really hope these unhappy men cultivate enough humility to study and understand the 555 and more importantly; to reap some of the happiness and joy that comes from being positive and helpful to others. Since 2005, greater than 300 builders have emailed to say this simple circuit works and they want to learn more about electronics.

My intent was to have the least number of parts to flash some LEDs. Some new builders become overwhelmed when the parts count is high — I once shared this fear and relate. You'll see a number of different bias circuits for the 555. Many builders run the reset pin; **Pin 4** high (connected to the 9 volt battery) and as a rule, this is a good thing to do, but it's not necessary for the circuit to work. Pin 7 is an open collector output to ground — its primary purpose is to discharge the capacitor.

It's important for the DC voltage in the pot wiper to not become too close to the + 9 volt rail or VCC (This happens when when the pot is rotated so that maximal DC voltage appears on pin 7), as pin 7 would draw excessive current. In my original schematic I left out a series resistor from VCC to the pot to eliminate this problem. After some thought, I added a 1K resistor on Feb 25, 2011, although this limits the rate somewhat. I run the pot on my circuit about mid-range and it hasn't been re-adjusted (or turned off) since 2005.

Also, the rotated pot wiper shouldn't get within a couple of hundred ohms of the capacitor as that too would cause excessive current spikes into pin 7. Generally, I prefer not to have much current on the wiper of a pot or, at least, try to keep the current small. Often, you can use a pot to set the desired timer speed and then remove, measure and substitute 2 standard value fixed resistors. A better way is to use math and calculate the resistor values, but this involves math and some people want nothing to do with equations.

This circuit is meant to provide a minimalist working circuit, but doesn't provide a great example of 555 design. Happily, for those wanting to learn more, countless great 555 tutorials may be found on the web. One of my 555 favorite sites is that managed by fellow Canadian Rob Paisley. Increasingly, I am exchanging electronics-related emails with model railroad enthusiasts across the globe and many of them know of Rob's wonderful web site.

Matthew Ritchie built and posted a nice version of the LED Chaser on YouTube. A reader sent in this breadboard photo.

By far, the coolest device incorporating the LED chaser lies within a sculpture called Cyanic by Seattle-area artist Allet. Click for his web site. Cyanic may be found on the New Sculpture Build section on his web site. You have to start the Quick Time video manually with a mouse click. I love Allett's work and his lastest light sculpture exemplifies how the Internet can unite creative people with a positive attitude.

A 10 LED sequential flasher in a blue Hammond chassis. The schematic is shown above.

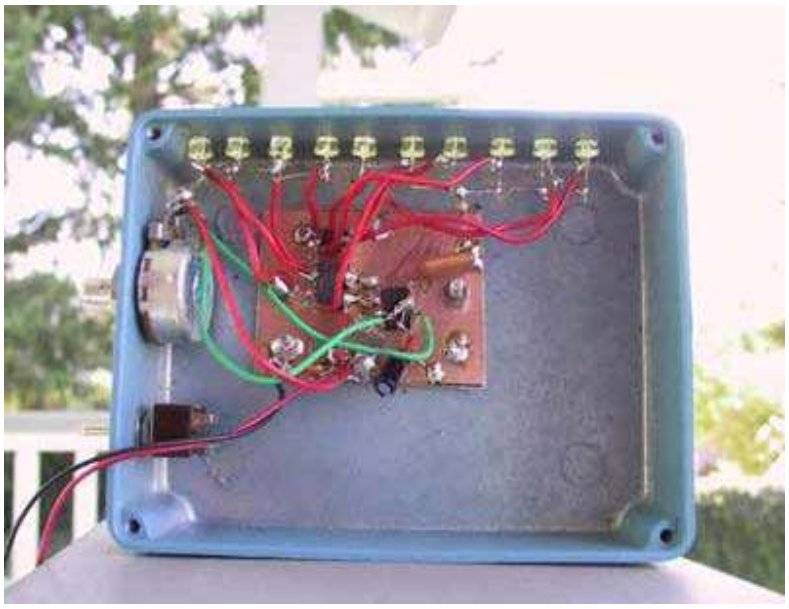

An RC oscillator designed for a 3 volt LED chaser. It oscillates quite slowly so the LED chaser it triggers will not be overly distracting. Some RC oscillator design details are discussed later. This oscillator triggered a 4017 decade counter instead of the 555 timer chip shown in the "Simple 10 LED Chaser" schematic. There are many links describing the theory of the 2 transistor astable multivibrator on the World Wide Web. I also have some information on this web page.

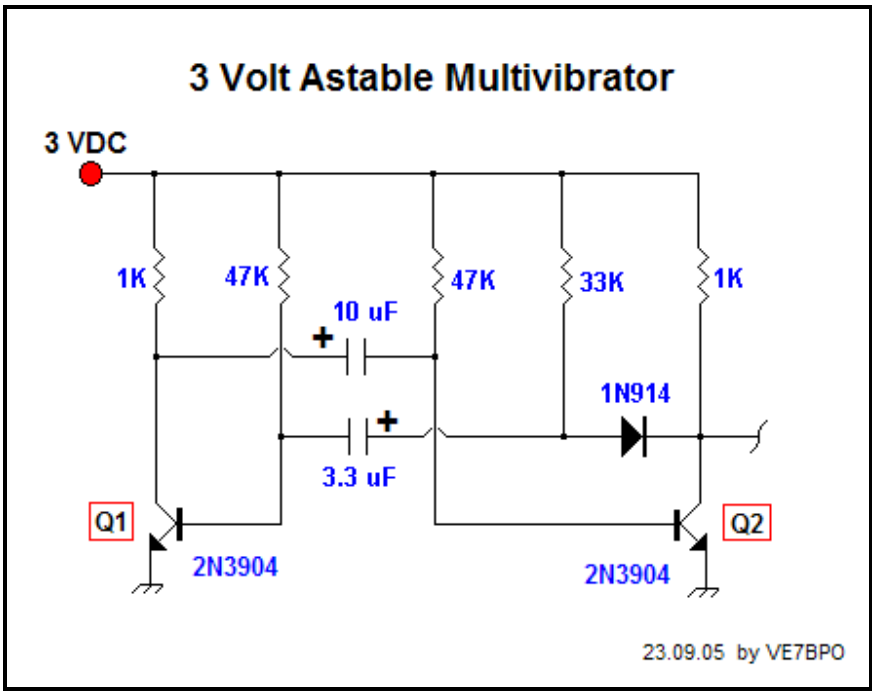

Above . This is a tiny 3 volt chaser which uses an LED bar instead of discrete LEDs. It draws 3.8 mA peak current on pulses. It uses the optimized BJT astable multivibrator shown directly above which fires at ~120 cycles per minute (slowly). The 3 volt battery pack is hidden behind it and should last several months. Soldering the LED bar was not an easy task. The plastic Hammond case measures 2.46 by 1.38 inches (6.25 by 3.5 cm).

A schematic to allow the 4017 decade counter to sequentially flash 6 LEDS left-right-left-right-etc. Connect your favorite square wave oscillator to pin 14. I built 4 of these using various oscillators and LED colors. You might consider using lower DC voltages and if so, may adjust the 1K current limiting resistor by using ohm's law. The 10 small signal diodes may be any appropriate type including the 1N914 or 1N4148. None of my 4 projects exceeded 6 mA peak current draw, so battery life is excellent. I increased the 1K resistor to 1K5 in my 4th project as I found the LED's that I used too bright.

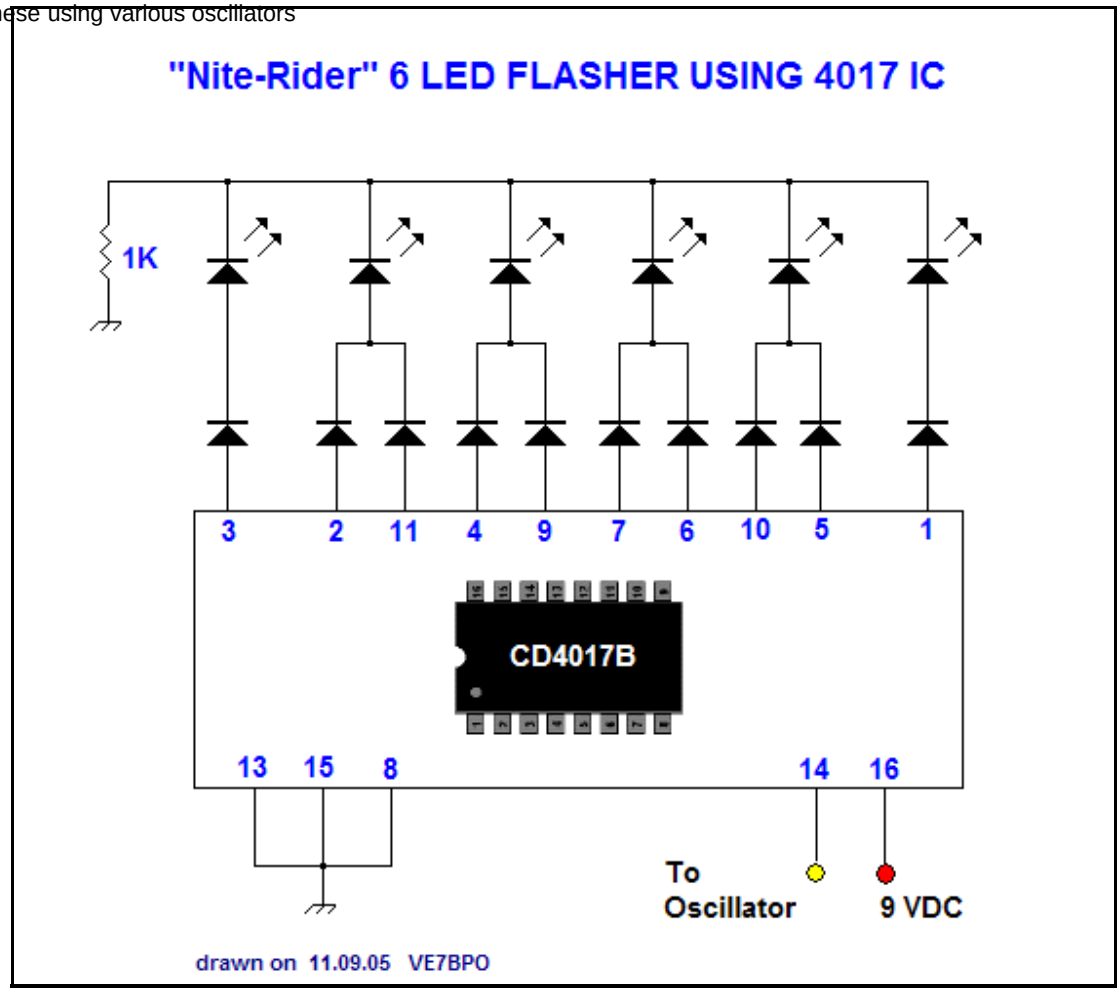

The prototype "nite-rider" project with messy wiring. The holes for the LEDs were bored with a hand drill and it shows! The discrete transistor multivibrator can be seen behind the 4017 IC.

One of the four "nite-rider"

project chassis I built. After completion, this one was given to the son of VE7KPB. When drilling in a plastic chassis, I learned it is best to use a drill press set to a lower speed.

Sequentially Off LED Pulser

This circuit uses a series of transistors with an RC pair to pulse a string of LEDs.

This the favorite LED experiment I performed this summer. This flasher circuit is different in that it turns **off** alternate LEDs for about 1 second in sequence. When you connect this circuit to the 9 volt battery, all of the transistors are usually placed in saturation and therefore all the LEDs are **on**. Closing the switch on the base terminal of Q1 for a moment initiates the correct pulse sequence. The pulse initiates in Q1 which turns off the LED connected to the Q1 collector for about 1

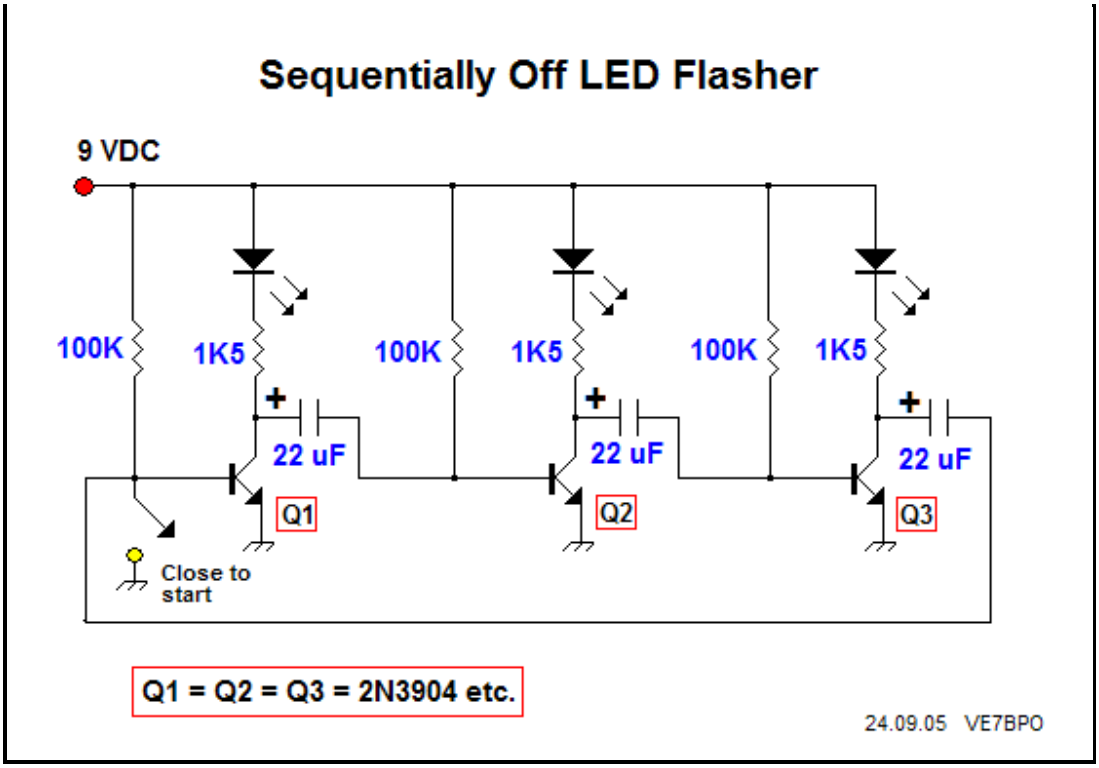

second. When Q1 turns back on (goes into saturation), Q2 turns off. When Q2 turns back on then Q3 turns off and so on. The circuit is a closed loop and many more stages may be added.

You can experiment with different base resistor and coupling capacitor values to vary the speed of the LED string or to create a sense of randomness by varying each transistor's RC stage separately. This is a fun circuit!

Youtube link (not mine).

The prototype 3 transistor version. I just used a piece of wire to ground the Q1 base terminal and establish the correct pulse sequence after powering it up. For the LEDs, transistors, resistors and capacitors you can use whatever appropriate parts that you happen to have on hand. Current draw is less than 10 mA with a fresh 9 volt battery. Decrease the 1K5 current limiting resistor to 1K or so if you want brighter LEDs at the expense of more current draw. Do not operate this circuit above 9 volts unless you connect diodes from the transistor emitters to ground to prevent emitter-base breakdown.

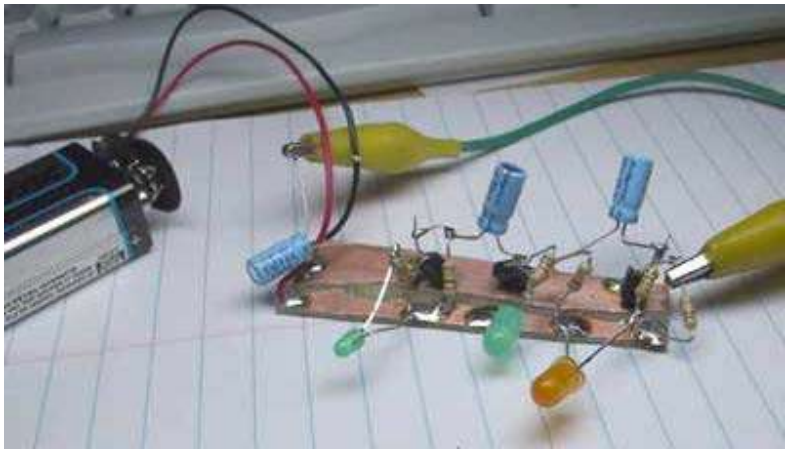

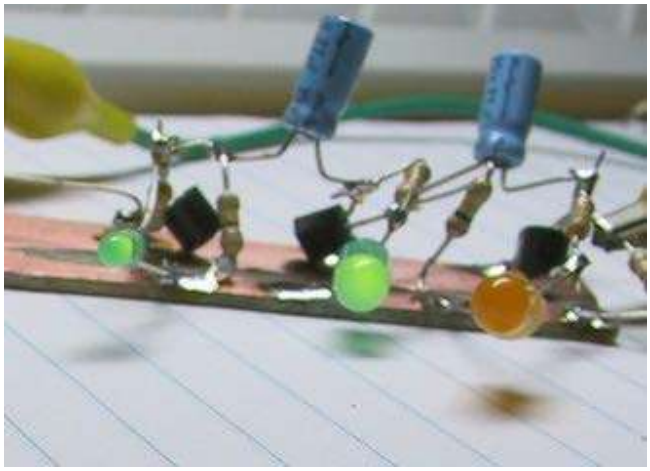

LED 1 and 2 are on and LED 3 is off at this moment in time.

Above and below photographs. This low current version has 9 LEDs connected in a chain and is powered by 3 volts. The 10th LED (extreme right hand side) is a flashing LED which is directly connected to the 3 volt supply and also uses a 1K current limiting resistor. Total peak current draw is only ~ 7 mA, yet it is still bright enough to see at night-time. The power supply is 2 D-cell batteries connected in series and then to the circuit by soldering wires directly onto the batteries with a 100 watt soldering iron.

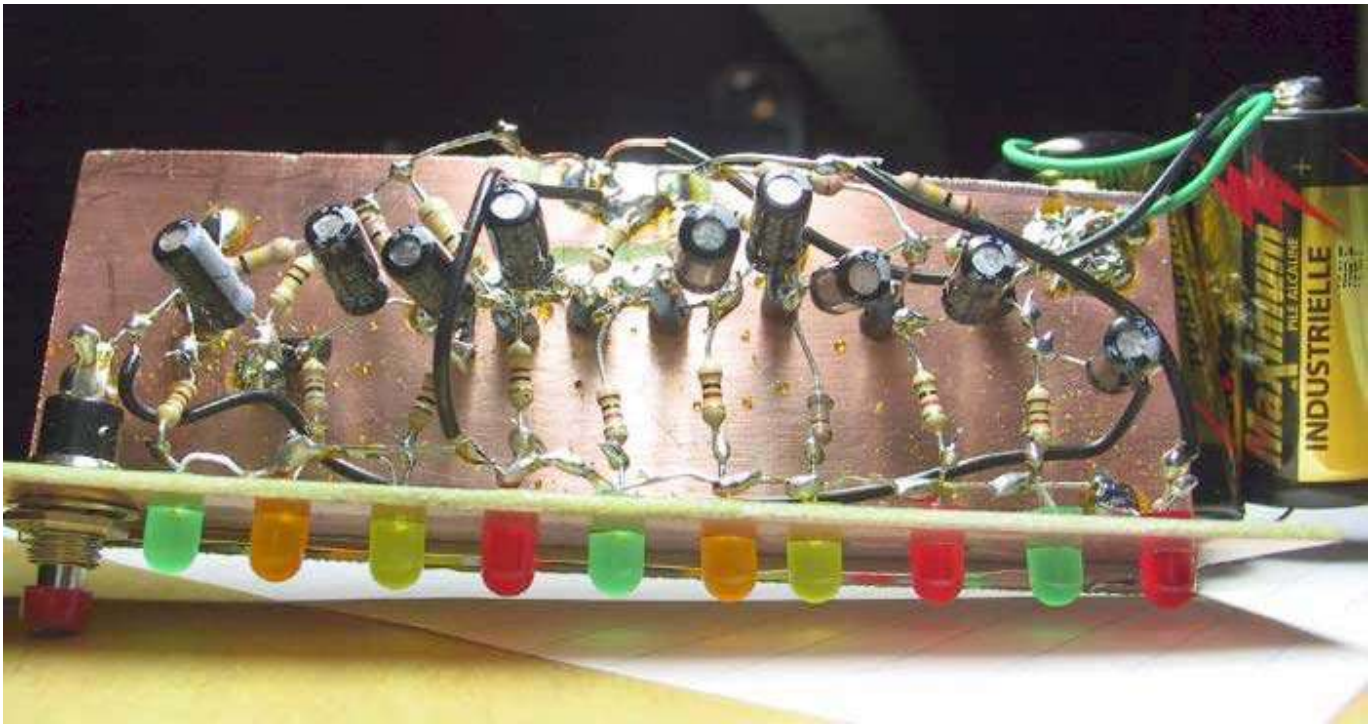

NoNot counting the 10th flashing LED, 5 of the 9 LEDs are on at any given moment. A sequential flash effect is noted (the state of each LED flip-flops and shifts over 1 position each flash). If you build this project with an even number of LEDs, the sequential effect is not seen. Half of the LEDS (spaced every other LED) are on and the other half are off at any moment. The same LEDs are lit or unlit each pulse. Thus the effect is more like a typical multivibrator LED flasher. This variable, even versus odd number of stages property makes the circuit quite versatile.

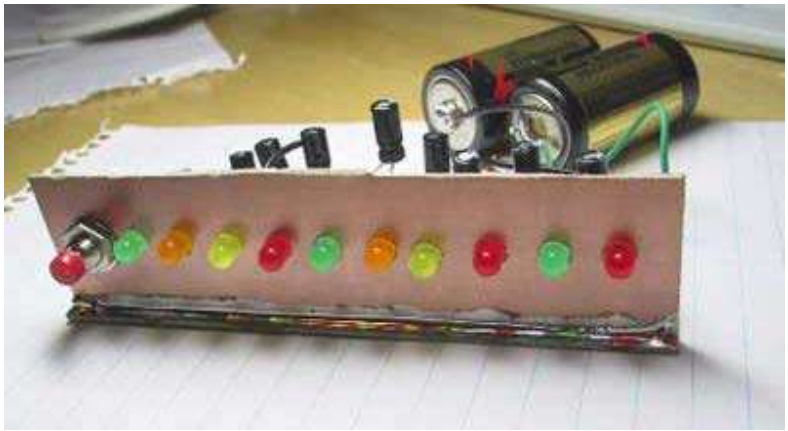

Conclusion

I hope that you have some fun experimenting with these and other circuits.

SWL Receiving Antenna Experiments

Introduction

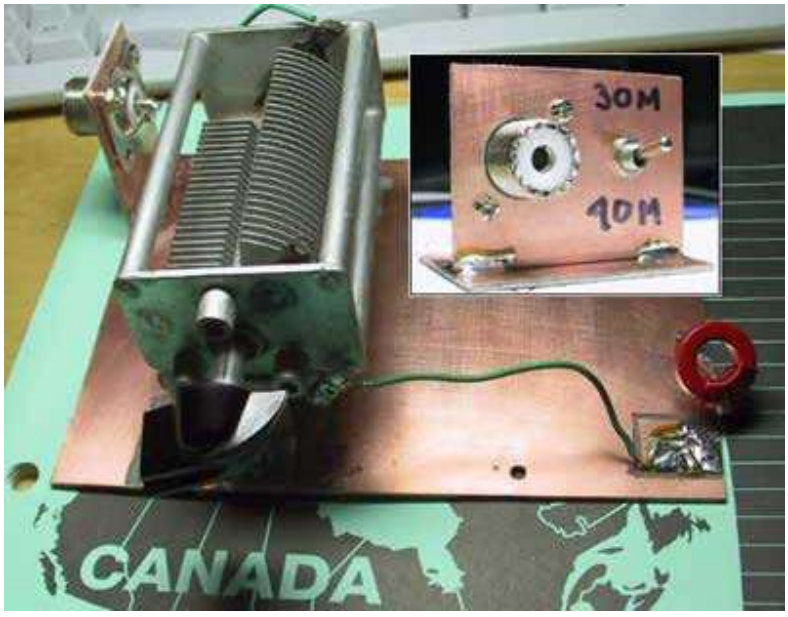

I have a lot to learn about SWL antennas. What follows are some brief experiments I performed in late October 2005. I have been experimenting with a half wavelength end-fed wire for use as a portable 40M band HAM transceiver (receive and transmit) antenna. This wire antenna is 67 feet long. End fed wires are very popular with those who pack a small portable transceiver when backpacking and camping. No feed line is required and the far end of the wire can be strung up using objects such as nearby trees or collapsible, portable poles. An elaborate ground system is not required. The return for the RF energy to ground might be grounding rod(s), short or long radial(s), or even just capacitively coupling to the local environment (including the operator!). Simple tuners are easily built to transform the high (thousands of ohms) wire impedance to the 50 ohms or so required by the transmitter.

I wanted to know if I could use this antenna as a tunable receive antenna for the the 30 and 31 Meter bands in addition to a tunable transmit/receiver antenna for my HAM radio work on 40 Meters. **What I verified is that tuning a multiband receive only antenna is not very practical.** When you tune a receive antenna you increase received noise and desired signals proportionally and therefore do not improve the signal to noise ratio in a meaningful way. Sometimes until you perform some experimentation, you don't really believe even good advice.

To the right: A computer simulation of a 40 Meter band end-fed Wire performed by W7ZOI on W7EL's EZnec program. The simulation was for 10.1 and 7.0 MHz with a 22 and 12 gauge wire. One 33 ft radial was used from the base of the 23.7 ft piece up 0.3 feet from the ground in this simulation. Z is impedance. Z and j are complex numbers used to represent the multi-dimensional quantities of the AC analysis of this antenna. In actual fact, j is an imaginary number. I suggest you might just ignore j unless your are well informed about impedance arithmetic.

Antenna Matching

A tuner can help match the impedance of the wire antenna and feed line (if used) to the input impedance of the receiver at a given frequency. This will result in more received signal and noise voltage to the receiver's input. HAM radio enthusiasts use antenna tuners to transform the impedance between the radio and the antenna tuner to 50 ohms to allow maximal output power from their transmitter. Non- amateur radio operators, can not use transmitters to

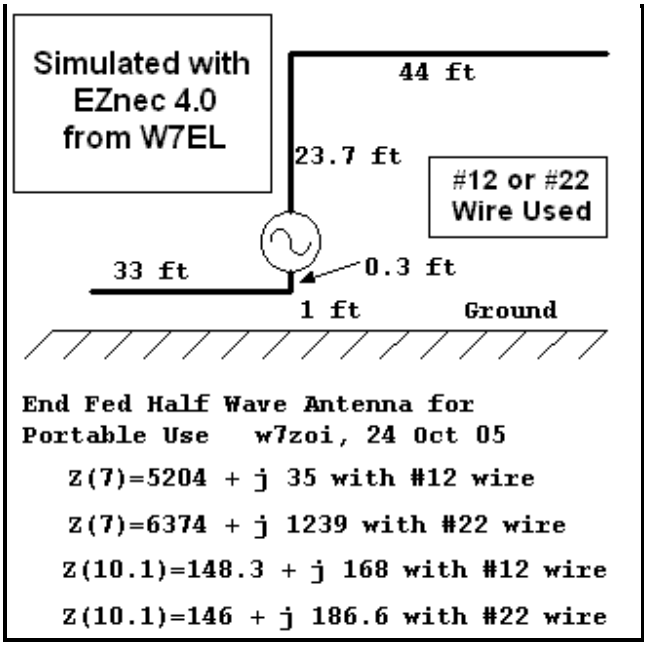

match their antennas. This leaves either using receiver noise, S-Meter or an antenna analyzer such as the MFJ259. I just used my ears and S-meter. All of the tuners presented work as transmitter tuners as well. Any network used for transmitter work must be able to handle the output power of the transmitter final amplifier.

The Wire Antenna Experiments

I tried 3 different antenna tuners to see if I could tune an 18 gauge wire on 40-41 and 30-31 meters. My wire went from my computer room in the basement out a hole in the wall and sloped at ~ 50 degrees up to a rope tied to a tree in my backyard. The tip of the antenna is about 50 feet (15 meters) high. A 10 gauge insulated ground wire also passes from the computer room outside under the back lawn. It is "earthed" to two, 2 meter copper grounding rods hammered into the ground. No direct connection to the house ground system and the outside antenna grounding system should be made as this may result in increased receiver noise.

Antenna Tuner 1

The schematic on the left below, is very popular with HAMS who use it to to tune monoband end-fed wires. It is very simple and works reasonably well. Although the capacitor was able to resonate the 35 turns inductor, the T1 turns ratio was wrong and reducing it to 28:3 was required to get the maximum receiver signal in my experiments on the 40 and 41 meter bands. The alternative was to shorten or lengthen the wire antenna which is not very practical as it meant repeatedly climbing a tree.

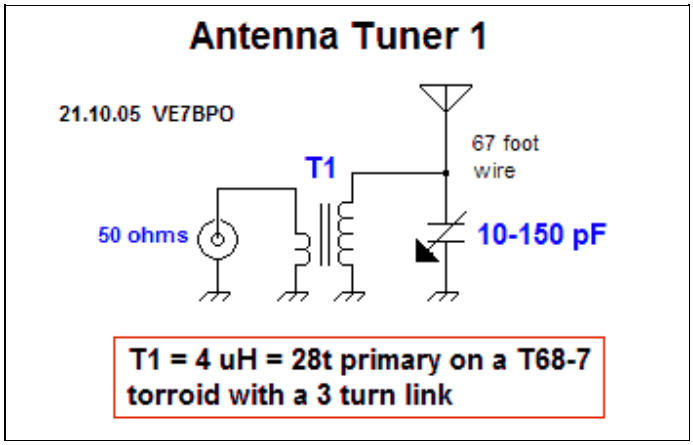

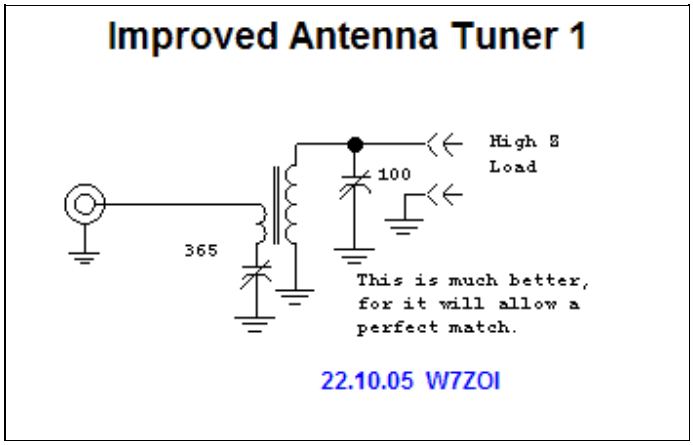

Above right: An improved version of the Antenna Tuner 1 schematic from W7ZOI. This tuner has 2 user "tweaking" adjustments much like most modern commercial antenna tuners (which typically also have a band changing adjustment).
I did not build this version.

In addition, this tuner would not tune the 67 foot wire on the 30 or 31 meters band. This was no surprise. When I turned the variable capacitor, I noticed some change in received signal, but not much. The signal strength was very poor and I could not hear much of anything.

Below. Two built up views of the Antenna Tuner 1 schematic. I soldered the antenna wire to the circuit in the isolated area connecting the inductor and capacitor. The outside antenna ground wire was soldered to the large copper ground plane.

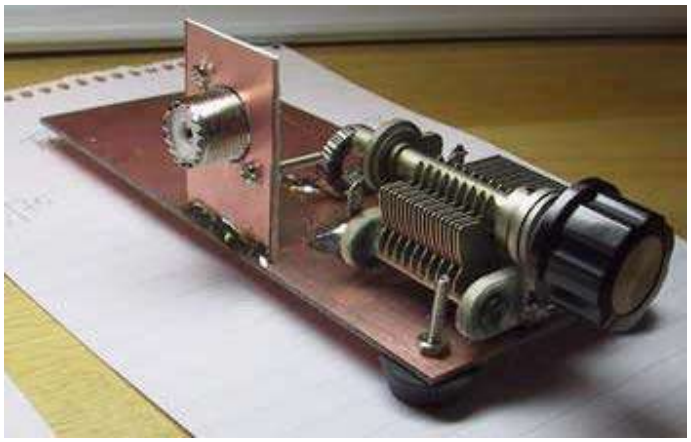

Antenna Tuner 2

This was the next tuner I built. Antenna tuner 2 tuned very sharply on the 40 and 41 Meter bands. It is designed to match a high impedance antenna, so it could not match the medium impedance (~150 ohms) wire to the 30 and 31 meter bands very well at all. Since ~ 150 ohms is fairly close to my receivers 50 ohm input impedance, I just connected the wire antenna directly to my receiver. The received noise and signals were then much stronger than those with the Antenna Tuner 2 network in the circuit on 30-31 meters.

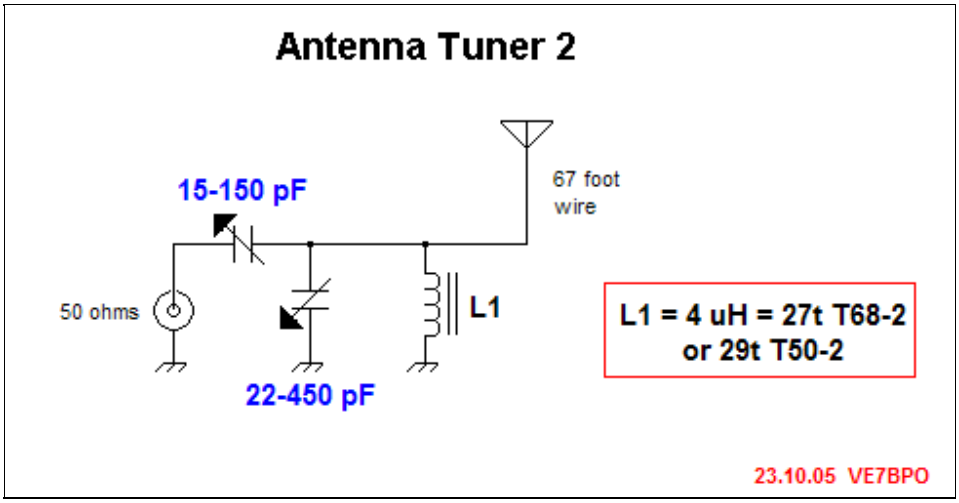

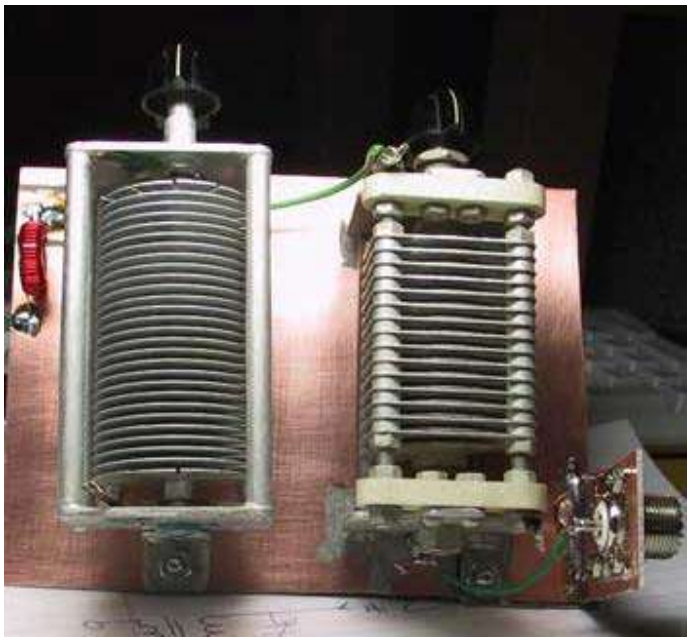

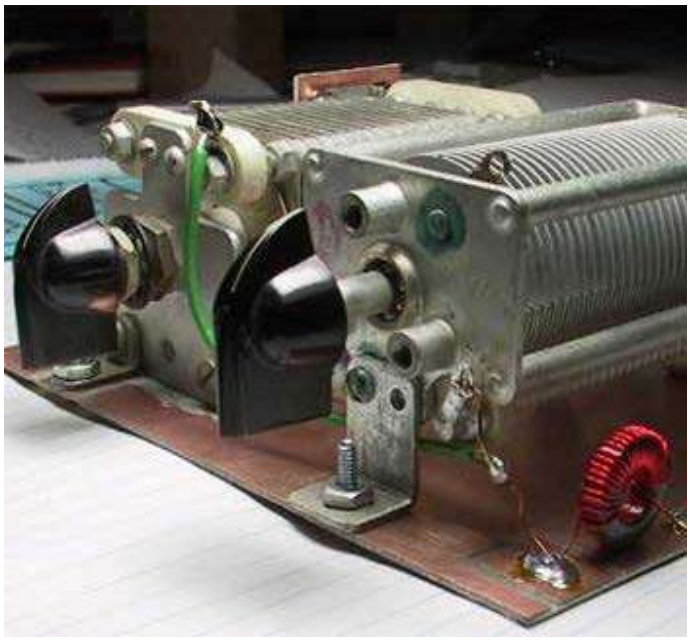

Above: Two constructed views of the Antenna Tuner 2 schematic. The variable capacitors were bought at a HAM festival in 1992 for 2 dollars each.

Antenna Tuner 3

The next antenna tuner topology I tried was the familiar L network. Circuit **A** is configured in a shunt L (inductor to ground) and series C (capacitor) and is a high pass L network. Circuit **B** is configured in a series L and shunt C and is a low pass L network.

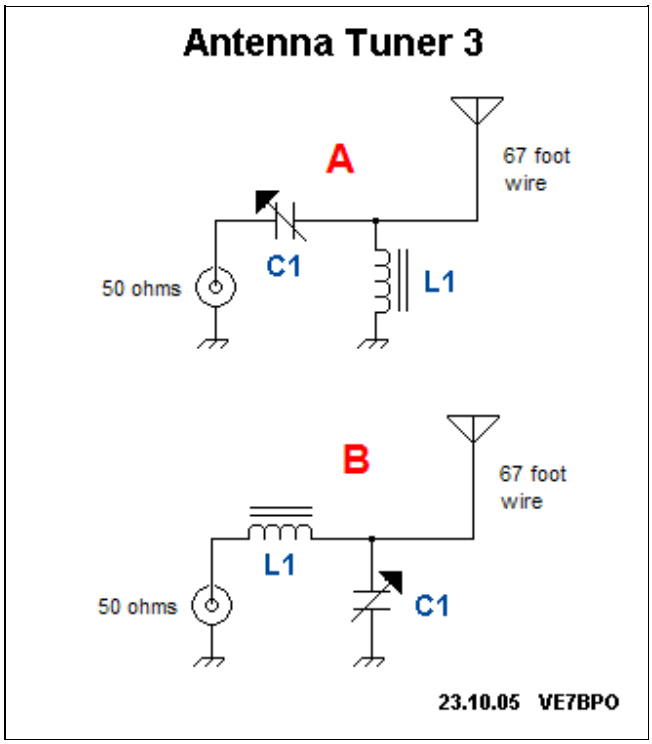

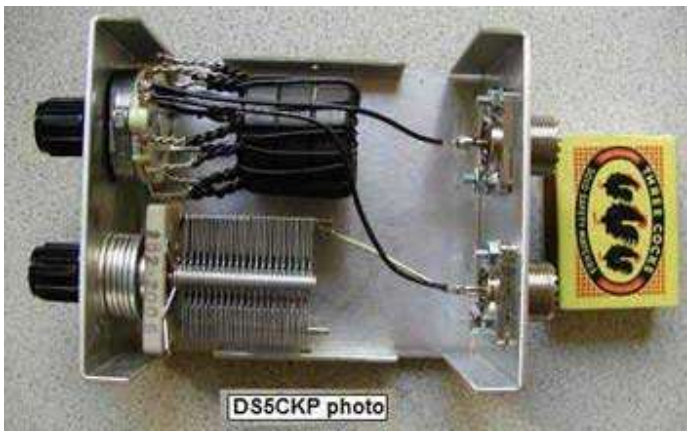

L networks (especially the low pass form) are very popular as random wire tuners. MFJ sells an excellent version as the model MFJ-16010. A photograph of this tuner is shown below right. The above left photograph was taken by **DS5CKP** who also sells a random wire antenna tuner at: http://user.chollian.net/~cyberline/ckptuner.htm

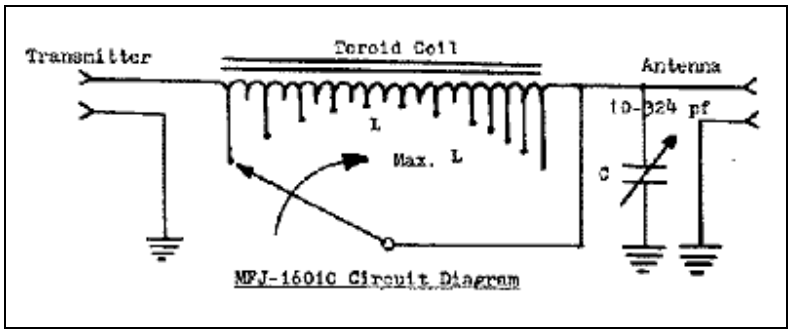

Above. MFJ web publishes their manual including the schematic for the MFJ-16010 random wire antenna tuner. The inductor is actually wound on 3 stacked (probably ferrite) cores which are tapped. The taps are connected to a front panel mounted 12 position switch. This allows coverage from 2-30 MHz. As a simple experiment, I tried stacking 2 and then 3 FT-50-61 ferrite cores and was able to get a wind range of inductances from the 6 taps I made on my test inductor.

Numerous examples of the L network antenna tuner can be found on the web and in print including the 2006 A.R.R.L. handbook. I decided to try the high pass L network topology to experiment with.

I built part **A** of the Antenna Tuner 3 schematic with shunt L and series C. On the 40-41 meter bands I tried 3 different inductors; 4 uH, 2.1 uH and 1.3 uH. I tuned the network to get the greatest receive noise and S meter reading and measured the variable capacitor value. At 7.30 MHz, the capacitance values were 86 pF, 141 pF and 182 pF respectively. Although non-critical, I settled on a 2.6 uH inductor (23 turns on a T50-2 powdered iron torroid) so I could use a junk-box 10-150 pF variable capacitor to resonate it. Later I decided just a trimmer capacitor might do. You need around 125 pF at 7.30 MHz to tune the network with a 2.6 uH inductor (to give you a ballpark C value to start with).

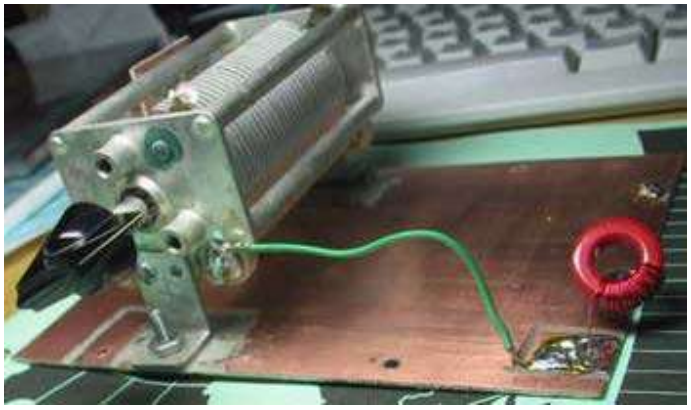

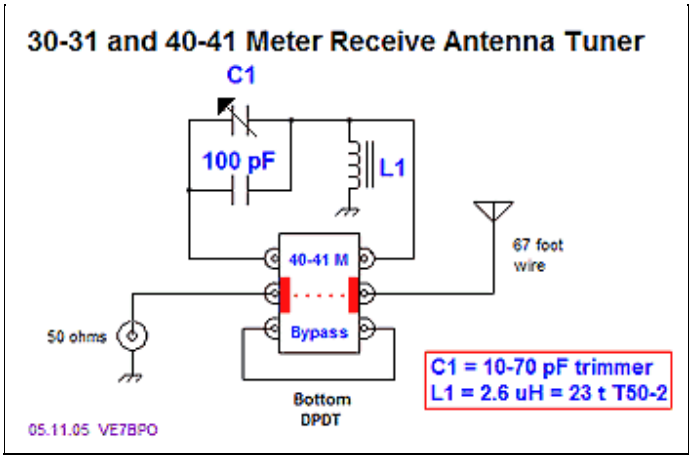

Schematic to the right: A very small receiver tuner that allowed the L network to be switched in and out of the antenna path was constructed. The L network is tuned on 40-41 meters via a small trimmer cap on top of the double pole, double throw switch. A small plastic alignment screw driver is used for signal peaking. An air variable capacitor would be much easier to tune as you move up and down these bands.

Below left: Front view. Technically, the switch label should indicate **40M** and **bypass** as the bypassed antenna could be used on any band.

Below right: Rear view The trimmer cap can be seen on top of the switch.

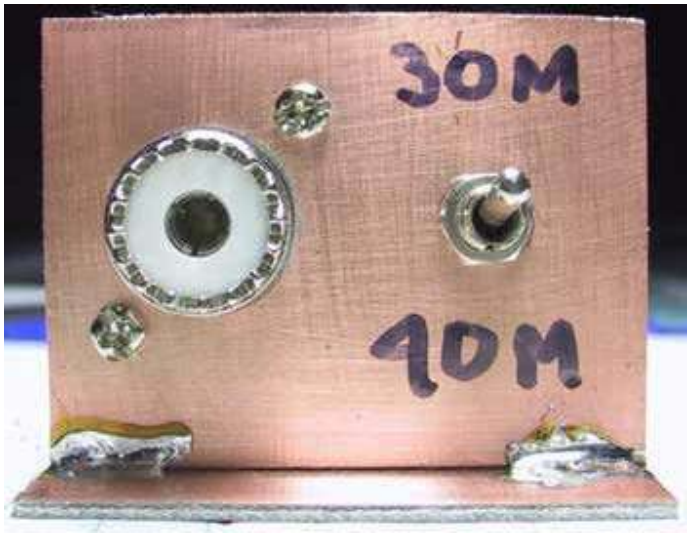

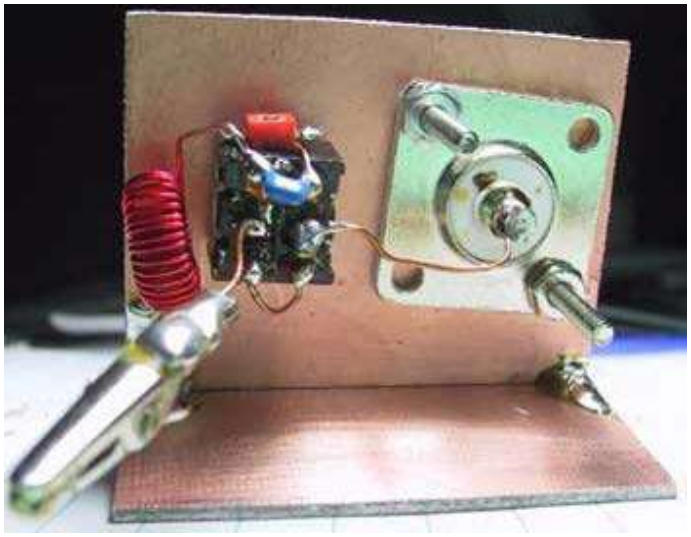

Below left: Side view, the antenna wire is held via an alligator clip. This allows me to unclip and ground the antenna when it is not in use. The antenna ground wire is soldered to the copper ground plane.

Below right: A T6-8 core wound with with 24 gauge wire. I used larger powered iron torroids to wind my inductors, however, they can also be wound on ferrite cores or be air-wound. The core size, wire gauge and type of inductor used can affect the selectivity and insertion loss of the tuner network, however for practical receiving purposes it is not a major concern.

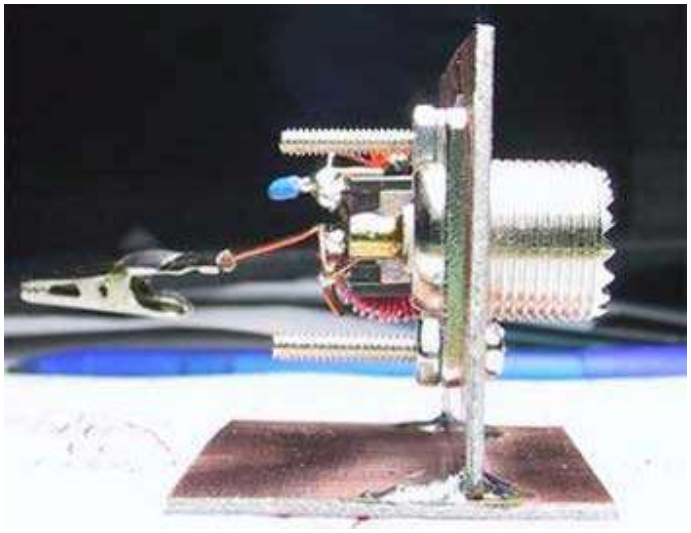

Conclusion

The final experiment allow me to easily switch between a matched and direct 67 foot wire antenna on 40 and 41 meters. I performed several listening tests and generally agree with those who say receive antenna tuners offer little to no improvement in signal readability. The only advantages I can think of for matching a receive antenna to a reasonably quiet and sensitive receiver are:

1. There may be some improvement in the receiver front end filter function as these filters are designed to have a specific input impedance.
2. Certain balanced mixers may function better with the correct impedance on their RF port.
3. The tuner itself (depending on design) may marginally improve the front end selectivity of the receiver it is connected to.

I do like the noise roar and louder signals with the matched antenna on 40 and 41 meters, although this is totally subjective. I think the reason for this is that as a HAM radio operator who always matches the antenna for any band I am on, I am used to louder signals and noise levels. I also spent most of my first 10 years of HAM radio operation on 80 and 160 meters which are relatively noisy bands and have been conditioned so that noise is "normal".

On 30-31 meters the bypassed antenna worked quite well and the L network can be switched in as an attenuator. Perhaps you might build up a tuner and try for yourself!

Although they are simple, low cost and easy to put up, it is likely unwise to use an end-fed wire without coaxial feed line as a receiving antenna. The ground wire is part of the antenna system and easily picks up household generated noise which will present to your receivers input. The time honored and easiest methods to reduce receiver noise are to get your antenna away from the house and other noise sources, use buried coaxial cable feed line to the house and directly earth ground the shield of the feed line with stakes. Antenna/ feed line "link coupling" by a transformer may also reduce noise (especially if the antenna system is balanced) and this topic begs further study.

Suggested Links

There are some fabulous web sites on the topic of SWL antennas and reducing receiver noise. I suggest these 5. Try a Google search for more.

http://www.dxing.info/equipment/

http://www.hard-core-dx.com/nordicdx/antenna/feed/feed1.html

http://www.aa5tb.com/efha.html

http://www.nyx.net/~dgrunber/

As usual, I learned a great deal from the process of experimenting. I look forward to spring when some more antenna experiments can be performed.

Experiments with JFET Biasing

The most common way of biasing a Junction Field Effect Transistor (JFET) is with a source resistor. This method, shown in Fig 1 below, has the advantage of offering negative feedback to stabilize the bias conditions. This is the same thing that happens when a bipolar transistor uses an emitter resistor. Self bias can be used as a method to evaluate a JFET to determine the critical parameters that describe it: Idss and Vp. These are discussed in Chapter 2 of **Experimental Methods in RF Design** and many other places.

The method used in our experiment is to set up the FET of interest in a test fixture with a power supply, bypass capacitor, resistors in the drain and gate to suppress parasitic oscillations, and a handful of extra resistors, R-test, that can be paralleled with an existing 100K source resistor. A digital volt meter (DVM) is the basis for the measurements. We begin by using the DVM to measure the resistance of our test resistors, for the values will be used in calculations. The DVM is then attached to the FET source to measure the DC voltage. The first value we measure is with no attached R-test. The measured value will be very close to the FET pinchoff voltage.

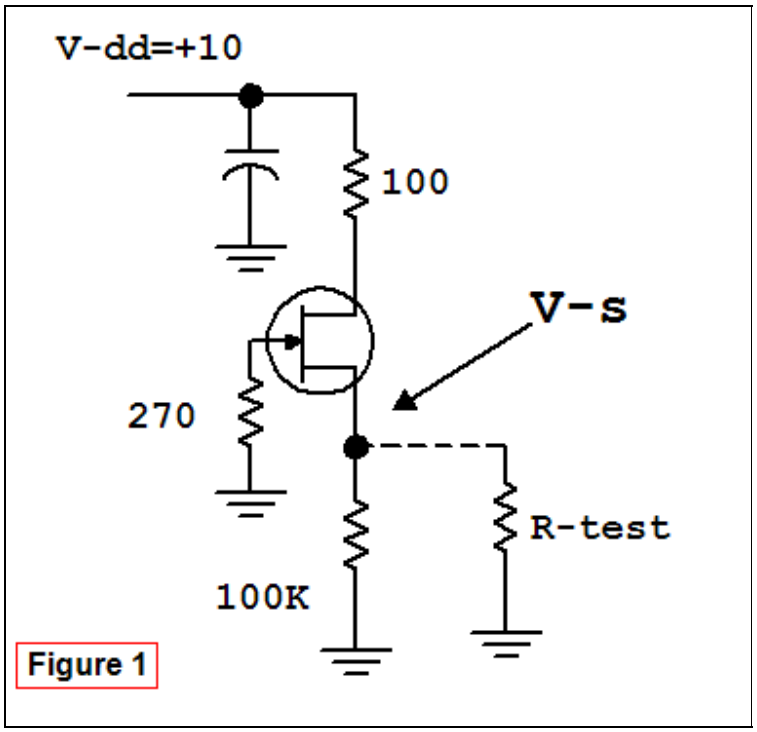

Figure 1

The measurements we will perform infer drain current as a function of gate to source voltage. The physics of the FET support the model that there is no gate current so long as the gate is not forward biased with regard to the source. Hence, the drain current equals that in the source. We will measure the source current by measuring the voltage drop across the source resistor. The gate is at ground potential, for there is no gate current, so the gate to source voltage is just the negative of the source to ground voltage.

The resistors that I pulled from my stock for some measurements were marked as 22, 39, 68, 100, 150, 300, 510, 680, 1K, 2K, 3.3K, 6.8K, and 10K Ohm. The measured values are shown in attached figures. A systematic pattern was noticed with all of the measured resistances under the marked value, suggesting an error in the calibration of my DVM, a Fluke Model 73. All resistors were 2% carbon film 0.25 Watt. However, when I measured a 499 Ohm, 1% metal film resistor, it came up exactly at 500 Ohms. The differences between the measured values and those marked on the part were small enough that I neglected the details and used measured values for calculations.

The first FET I examined was a 2N5454, a common JFET that I had in my junk box. The source voltage was 3.26 with nothing but the 100K for source bias. I started my measurements with the largest resistor, 10K. The voltage dropped to 2.90 and was stable. I merely held the resistor in place rather than soldering it. The resistor was kept in place long enough to get a stable reading that I could record in my lab notebook. All results were of the same character until I got to the 300 Ohm resistor. At that point I started to notice a slight heating effect. The source voltage was 1.523, but slowly dropped to 1.518 volts. This behavior continued through the lower value resistors. The 22 Ohms produced 264 mV on the source that then dropped to 256 mV.

Later I examined a J310 JFET. This is a much larger area part than the 2N5454 with an Idss that is about three times larger. With the 22 Ohms in the test fixture, V-source went to 701 mV, but settled at 652 mV. The drain current was then 32 mA. With a 10 volt power supply, there was nearly 200 mW dissipated in the FET. This is within ratings, but high enough to produce heating. Operation at higher voltages and at Idss would further tax the part. One must take care when doing these measurements to be sure that the source voltage is observed quickly.

Attached are the MathCad documents that I used to examine the data. A spread sheet such as Excel could be used, but I prefer the graphics of MathCad. The second page for the 2N5454 shows a graph for the observed data as well as a calculated one. The two FET parameters for the 2N5454 were varied to obtain a good correspondence between the two. The part had Idss=15 mA with Vp=-3.5 volts. This is similar to the popular MPF-102, but close to the high Idss extreme for that part.

The data presented for the J310 is more abbreviated with only two points shown. I picked the 22 Ohm and 1K source resistors. This still produced data that is very close to that obtained with many more data points.

My initial analysis suggested that we could characterize the FET by measuring the source voltage with 100K in place to approximately determine Vp, and to then short circuit the source through the mA scale on the DVM to obtain Idss. This is a reasonable start. However, the pinchoff will usually be a few percent more negative (for an N-channel depletion mode part). The long leads in the source also make me feel uncomfortable with regard to parasitic oscillations.

After the DC measurements were done, I thought it wise to look at the potential for oscillation. The J310 was in the test circuit at this time. The TO-92 J310s are parts that are well known for their propensity for oscillation, so I guessed that it would not be difficult to coax this one into such a mode. But this was not what I found. I eliminated the 100 Ohm drain resistor, but moved the FET close to the 0.1 uF bypass. This bypass is not a very good one for VHF and upward. No oscillation was seen. I then eliminated the gate resistor, replacing it with the normal gate lead. Still no oscillation. I eventually added a gate inductor and a parallel tuned circuit in the source. The source bias resistor had a RF choke in series with it. I finally saw a robust VHF oscillation, but nothing else up through 1.5 GHz.

Experiments with JFET Biasing, after correspondence with VE7BPO on 14Feb06. (See earlier Mathcad file "Jfet_bias1_ve7bpo.mcd) Measurements on 2N5454.

$n := 0..12$ **index for measurements and calculations. Vsn=measured source voltages.**

$$Rx_n := \begin{pmatrix} 21.6 \\ 38.6 \\ 66.9 \\ 98.3 \\ 149.4 \\ 298.3 \\ 508 \\ 671 \\ 998 \\ 1997 \\ 3270 \\ 6720 \\ 9810 \end{pmatrix}$$

<== Measured Rx values

R values paralleled with 100K ======>

$$Rp_n := \frac{1}{\left(\frac{1}{Rx_n} + \frac{1}{100400}\right)}$$

$Rp_n =$

	0
0	21.595
1	38.585
2	66.855
3	98.204
4	149.178
5	297.416
6	505.443
7	666.545
8	988.177
9	$1.958 \cdot 10^3$
10	$3.167 \cdot 10^3$
11	$6.298 \cdot 10^3$
12	$8.937 \cdot 10^3$

$$Vs_n := \begin{pmatrix} 0.264 \\ 0.429 \\ 0.654 \\ 0.85 \\ 1.09 \\ 1.523 \\ 1.845 \\ 2.001 \\ 2.203 \\ 2.492 \\ 2.652 \\ 2.82 \\ 2.90 \end{pmatrix}$$

$Vg_n := 0 - Vs_n$

$Vg_n =$

	0
0	-0.264
1	-0.429
2	-0.654
3	-0.85
4	-1.09
5	-1.523
6	-1.845
7	-2.001
8	-2.203
9	-2.492
10	-2.652
11	-2.82
12	-2.9

Use Mathcad "vectorize" operator.

$$Id_n := \frac{\overrightarrow{Vs_n}}{Rp_n} 1000$$

$Id_n =$

	0
0	12.225
1	11.118
2	9.782
3	8.655
4	7.307
5	5.121
6	3.65
7	3.002
8	2.229
9	1.273
10	0.837
11	0.448
12	0.325

Let pinchoff be $u_p := -3.5$ **and** $I_{dss} := 15$

$u := -3, -2.9 .. 0$

$$I(u) := I_{dss} \cdot \left(1 - \frac{u}{u_p}\right)^2$$

Try various values for pinchoff and Idss to get a reasonable match.

Blue is measured data while red shows calculated behavior.

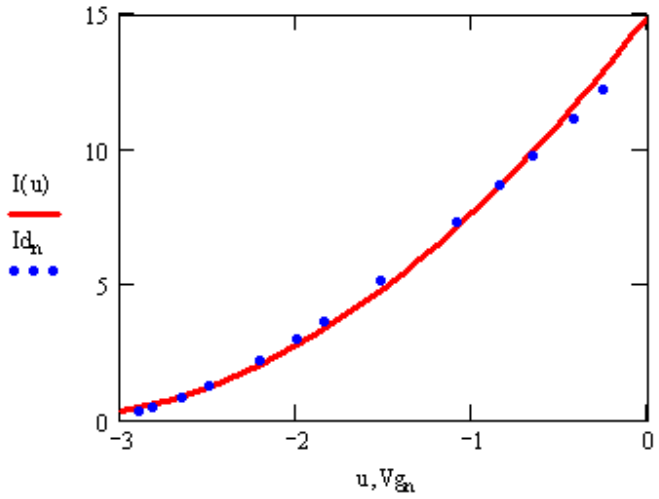

Experimental Note: During the measurements, I noticed a definite thermal change in Idss when dissipation was high. This occurred at higher currents, with low source bias resistors. The Vg values I used in my data were the first ones recorded with the DVM. The most extreme case was with the 22 Ohm source R. The source V started at 264 mV and went down to 256 mV. The effect was more dramatic with a larger part, a J310. That part, when operated with a 22 Ohm R, started with 701 mV and dropped to 652 mV.

Experiments with JFET Biasing, after correspondence with VE7BPO on 14Feb06. (See earlier Mathcad file "Jfet bias 18feb06.mcd) Measurements on J310.

Here we examine a minimal data set of just two points.

$n := 0..1$ **index for measurements and calculations.**

$Rx_n := \begin{pmatrix} 21.6 \\ 998 \end{pmatrix}$ **<== Measured Rx values.**

$Rp_n := \dfrac{1}{\left(\dfrac{1}{Rx_n} + \dfrac{1}{100400}\right)}$

Vsn=measured source voltages.

R values paralleled with 100K ======>

$Rp_n = \begin{pmatrix} 21.595 \\ 988.177 \end{pmatrix}$

$Vs_n := \begin{pmatrix} 0.701 \\ 2.97 \end{pmatrix}$ $Vg_n := 0 - Vs_n$

$Vg_n = \begin{pmatrix} -0.701 \\ -2.97 \end{pmatrix}$

Use Mathcad "vectorize" operator.

$Id_n := \dfrac{\overrightarrow{Vs_n}}{Rp_n} 1000$ $Id_n = \begin{pmatrix} 32.461 \\ 3.006 \end{pmatrix}$

Let pinchoff be $u_p := -4$ and $I_{dss} := 48$

$u := -4, -3.9..0$

$I(u) := I_{dss} \cdot \left(1 - \dfrac{u}{u_p}\right)^2$

Try various values for pinchoff and Idss to get a reasonable match.

Blue is data while red shows calculated behavior.

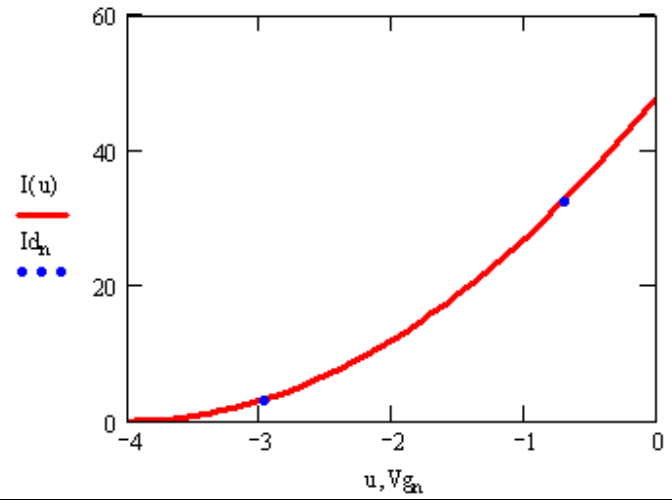

18 Feb, 2006 by W7ZOI

Many thanks to Wes, W7ZOI for this contribution.

10 MHz WWV Receiver Experiments

New feature: Click on a schematic to load it into a separate browser page for printing

Introduction

For nearly a year, I have been trying to develop a tuned radio frequency (TRF) 10 MHz, WWV, AM receiver. My initial RF stages were common emitter or common source stages with tuned input and output. Despite careful layout, parasitic oscillations plagued these designs and they were discarded. Later, I discovered that only tuning the input of RF stages reduced this tendency towards instability and still provided reasonable selectivity. Different detectors were also tried and evaluated.

A simple receiver that sounds great and is fun to build and experiment with follows. My special thanks to Wes, W7ZOI for performing many of the simulations and providing suggestions which kept me going.

WWV Audio Files from Sept 26, 2006

WWV File 1

WWV File 2

WWV File 3

The audio was digitally recorded using an electret condenser microphone held 3 cm away from the receiver speaker. The files were compressed using the WMA format.

Supplemental Web Page added June 29, 2007

Receiver Front End

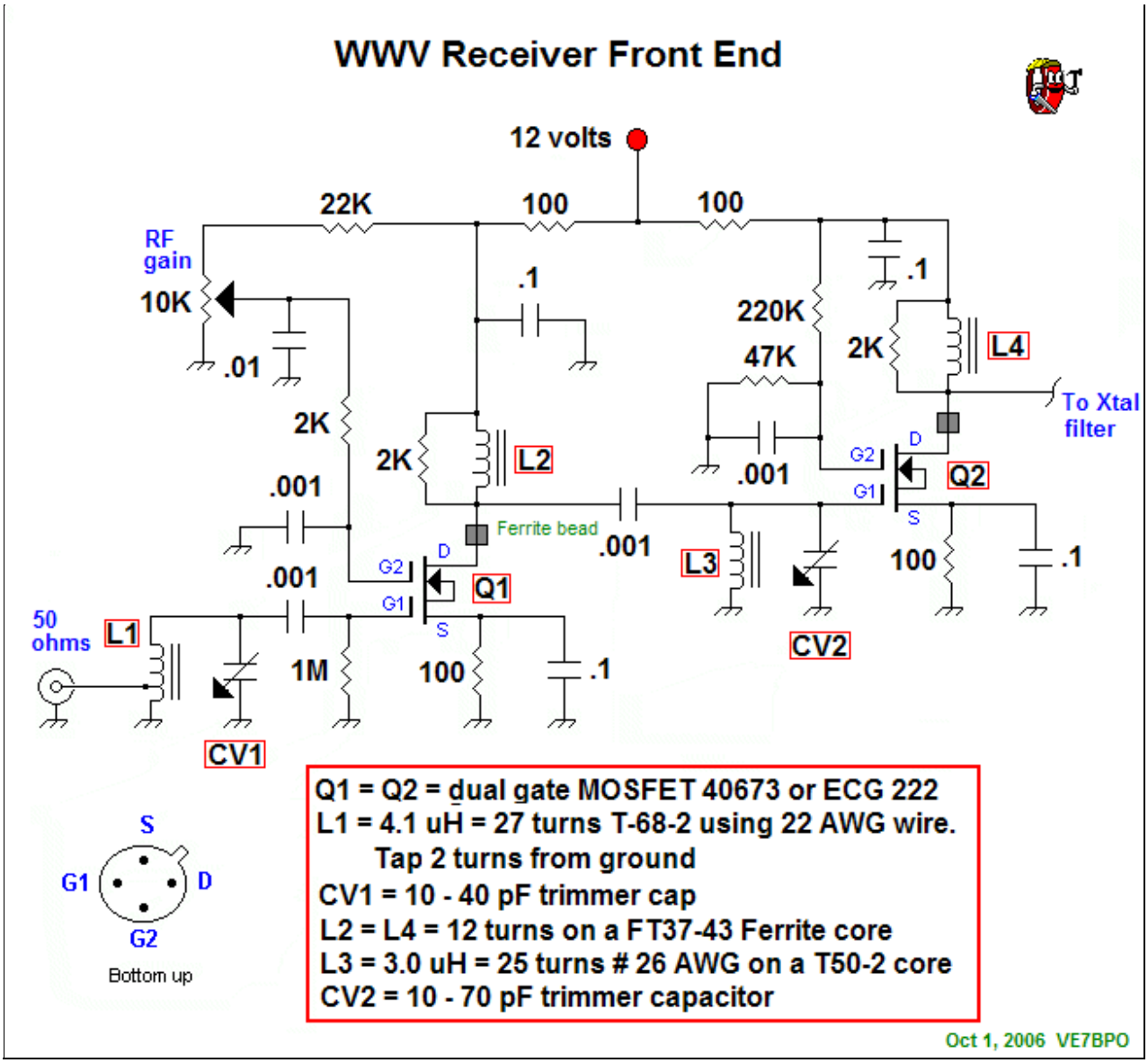

Above schematic. The receiver front end has just 1 single-pole filter. For even greater selectivity (but greater insertion loss), consider moving the L1 tap to 1 turn from ground. My receiver was connected to a 80 meter dipole via an antenna tuner. The antenna tuner provided additional selectivity. No local broadcast band (BCB) signals were heard when the chassis lid was tightened on. You may require additional RF high pass or band pass filtering in your location.

The RF gain control is very basic and only the first 1/3 of the 10K pot is used to go from minimal to maximal gain. Modifications to allow more precise variation in RF gain for dual gate MOSFETs or cascode JFETS are shown in EMRFD. The method shown works fine. For the most part, I keep it set to minimal gain. Using higher gain than necessary, increases receiver noise and may overdrive the detector.

TRF receivers require careful layout. A piece of wire greater than 2-3 cm between the stages may be enough to plague your receiver with local BCB interference depending on your layout and chassis integrity. For interstage connections that had greater than a 2 cm gap, shielded 50 ohm cable was used to prevent BCB interference.

Dual gate MOSFETs provide adequate gain and low noise. you might consider cascoding 2 JFETS for each RF stage if you cannot obtain them. titleernatively, bipolar feedback amplifiers may be used and examples are provided later on this web page.

XTal Filter and RF Amplifier

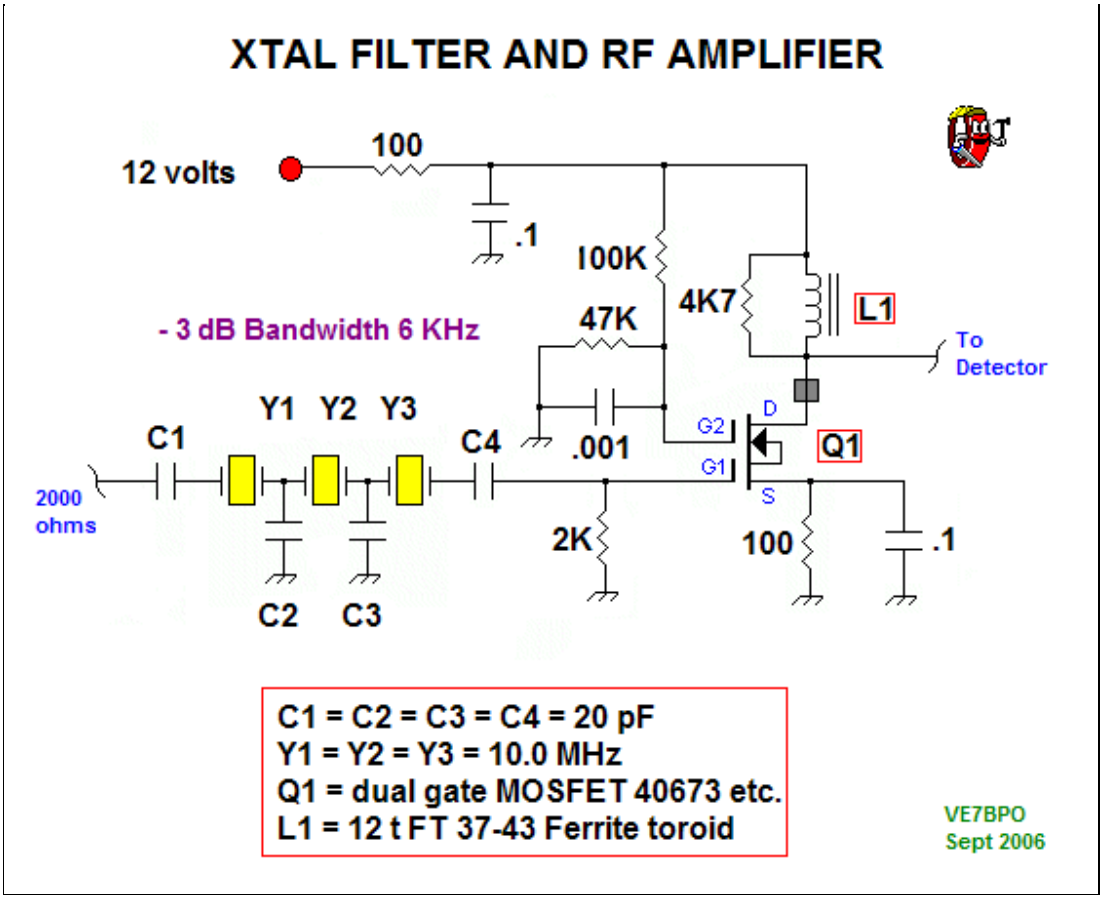

Schematic: The Q2 output impedance is 2000 ohms to match the input impedance of the Cohn crystal filter. This filter was designed by Wes, W7ZOI. Matched, computer grade, 10 MHz crystals were used. Choose 10 MHz crystals that are marked for a 20 pF or 32 pF load capacitance if possible. Using a 10 MHz crystal oscillator, find 3 that are closest to one another in frequency.

You may substitute 2K2 resistors instead of the specified 2K with a slight penalty in pass band shape.

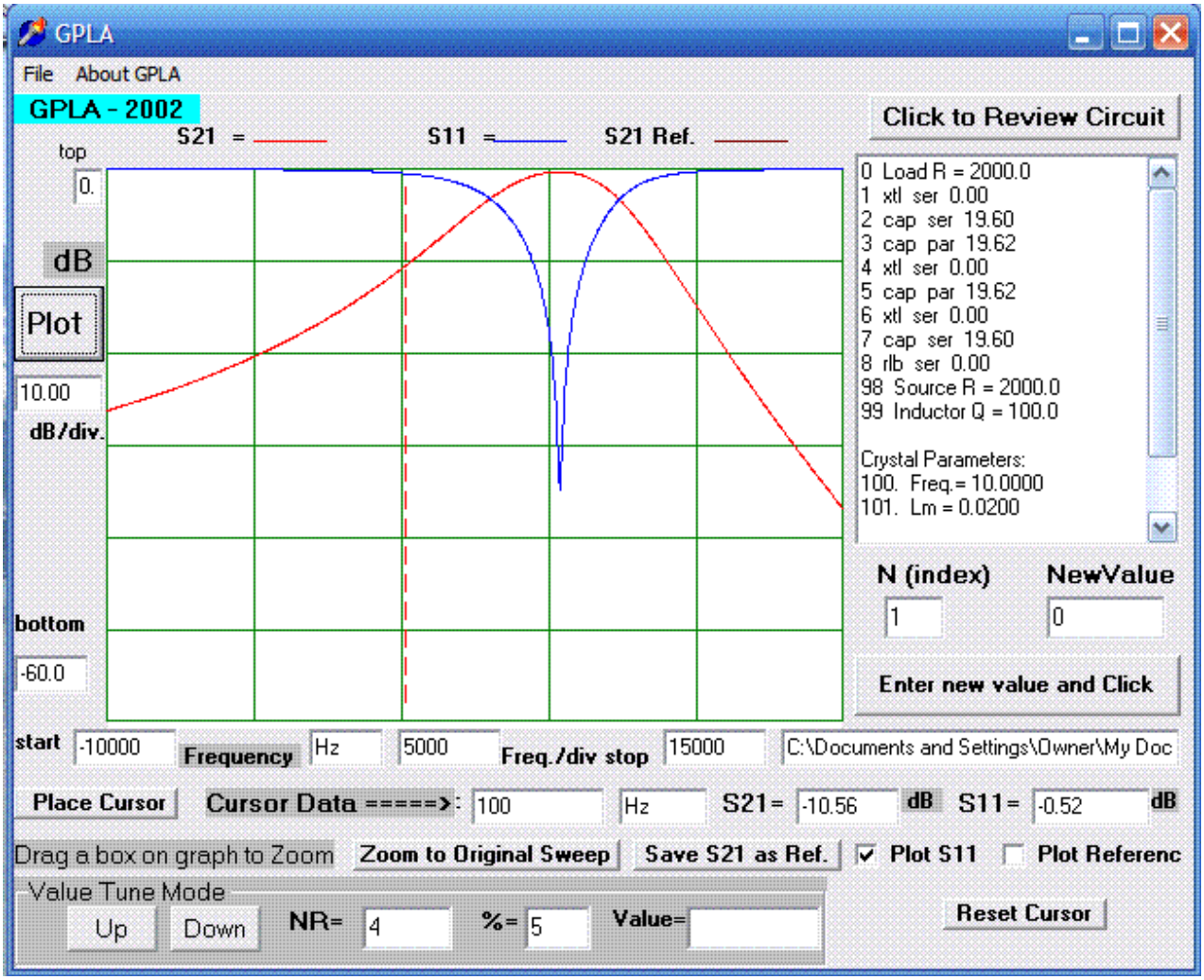

Above graphic. A simulation of the receiver crystal filter using GPLA, a program written by Wes, W7ZOI that comes with EMRFD. EMRFD is the major reference for this web site and I recommend that you add this book and companion software to your home library. The pass band is not symmetrical. It is mistuned for the lower pass band frequencies and would serve better as an upper sideband filter. Nevertheless, it works reasonably well and is simple to build and tolerant to component variation and match. At certain times, a very strong shortwave station at 9.985 MHz can be heard along with WWV. This usually occurs in the early evening when the WWV signal is not that strong at my location. For most of the day and night, whether WWV is present or not, very little interference has been detected.

Bypassing the crystal filter is an interesting experiment. As many as 5 stations were heard simultaneously and these varied as time passed. I heard Radio Vatican, Radio Habana and many other broadcasts during 1 evening. At one point I heard a station at 9.75 MHZ, WWV and a strong CW carrier at 10 .110 MHz!

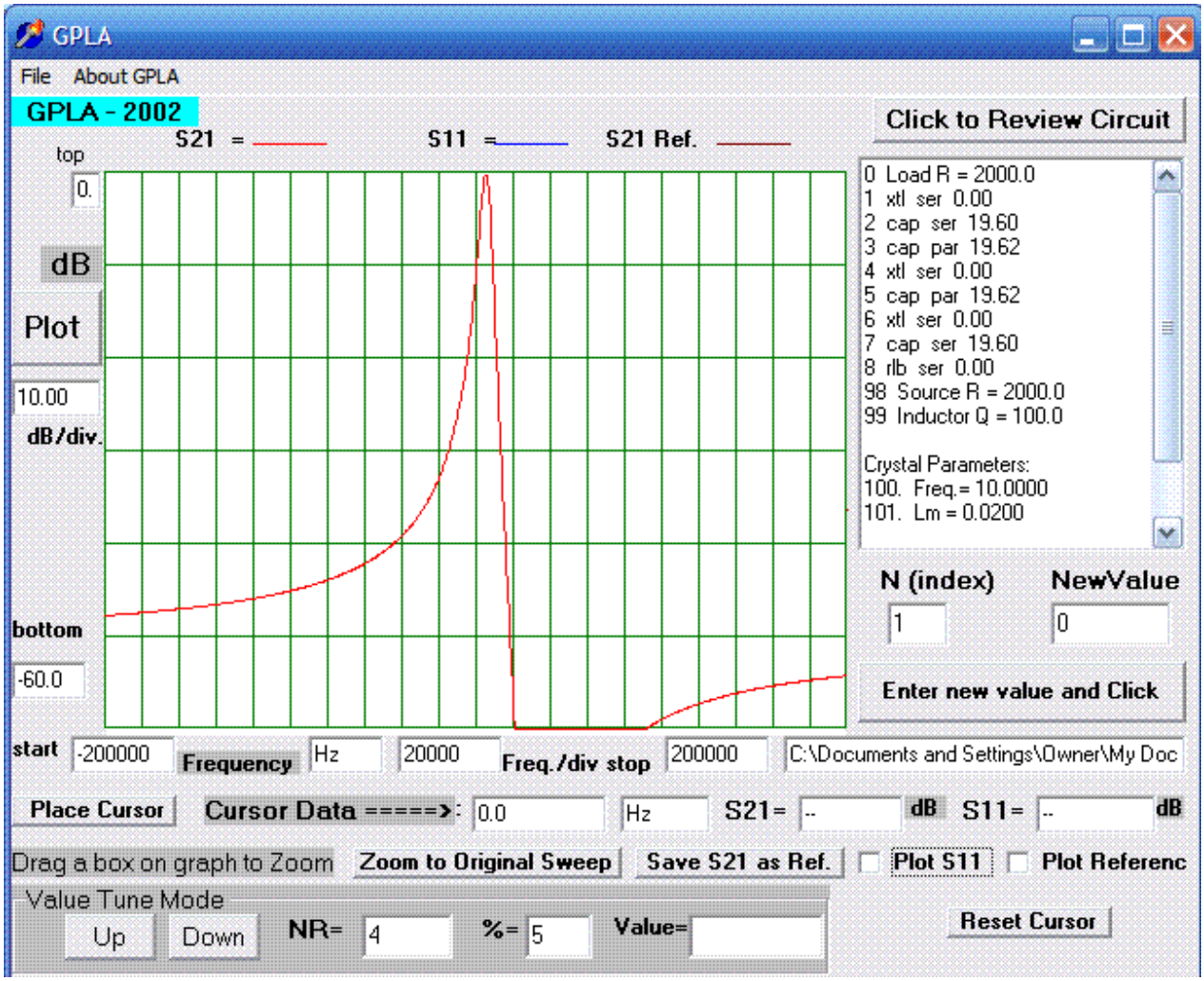

Above graphic. This is a sweep that goes from 200 kHz below to 200 kHz above 10 MHz to show the stop band response of this filter. This filter has a pretty decent response considering the low cost and effort involved.

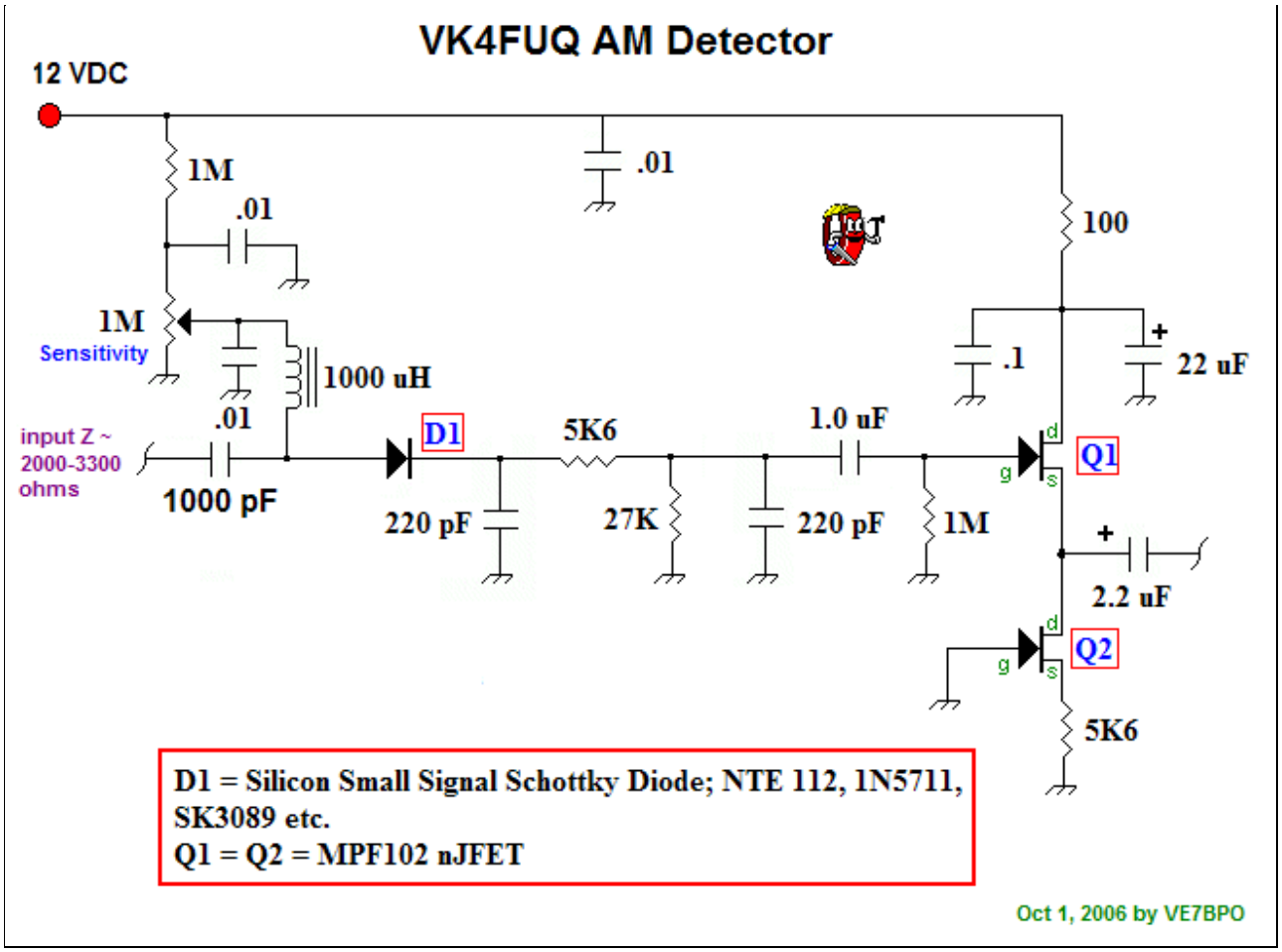

Above schematic. This detector is fabulous. It was designed by Felix Scerri, VK4FUQ. He has a web page explaining his high fidelity detectors at the Elliot Sound Products (ESP) site: http://sound.westhost.com/articles/am-radio.htm

The ESP web site is a personal favorite. Rod Elliot has one of the best do-it-yourself electronic web sites available. The main URL for his site is http://sound.westhost.com/index2.html

My sincere thanks to Rod and Felix for permission to present Felix's detector on this web page.

His improved AM detector has 3 positive advantages; it has high bandwidth, low distortion and incredible (and variable) sensitivity. I cannot get over how nice this detector sounds compared to others I have built and analyzed during weak and strong signal testing. The variable bias control allows the listener to adjust the bias to maintain detected audio fidelity even when the RF signal is weak.

This detector uses a UHF mixer diode often found in older television sets. Increasing the diode bias from O volts towards maximum causes three things to happen:

1. Increased sensitivity.
2. Increased audio high frequency response.
3. Slight increase in receiver noise.

When the WWV RF signal is weak, turning the bias off may result in the detected WWV signal disappearing. Increasing the bias will bring WWV back in. I generally run the bias control pot about 1/2 way and of course, higher as WWV fades out. I like the fidelity that the bias adds even when the WWV signal is strong. Note how the WWV audio quality continues to be high in fidelity as WWV fades out in this sound file.

Felix called for a 1 mH radio frequency choke. The largest I had in stock was a 1000 uH choke. I had to decouple it as shown to prevent oscillations from occurring in my receiver. For the 1 uF and 2.2 uF capacitors, I used polyester film types which sounded better than electrolytic capacitors.

Oct 13, 2006: Note. The 1000 pf input cap to the detector was omitted in error in the original schematic which is now correct.

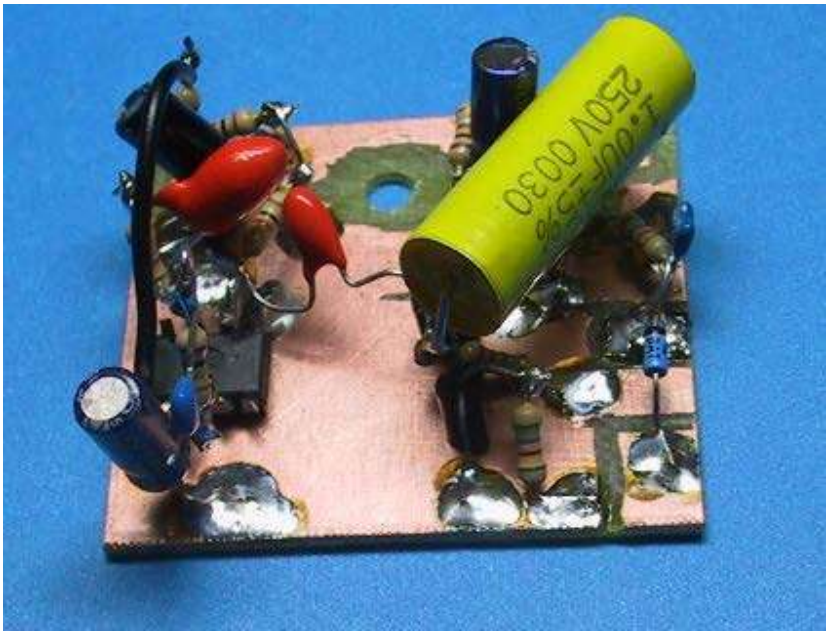

To the right: The detector board. On the left is an op amp preamp stage that was later disconnected as it was not needed. Note the copper is removed where the chassis mounting nut contacts the copper board. Both audio boards were isolated from chassis ground and star grounded to a single point. The speaker negative terminal was also directly connected to this point. There is no hum.

Audio Amplifier

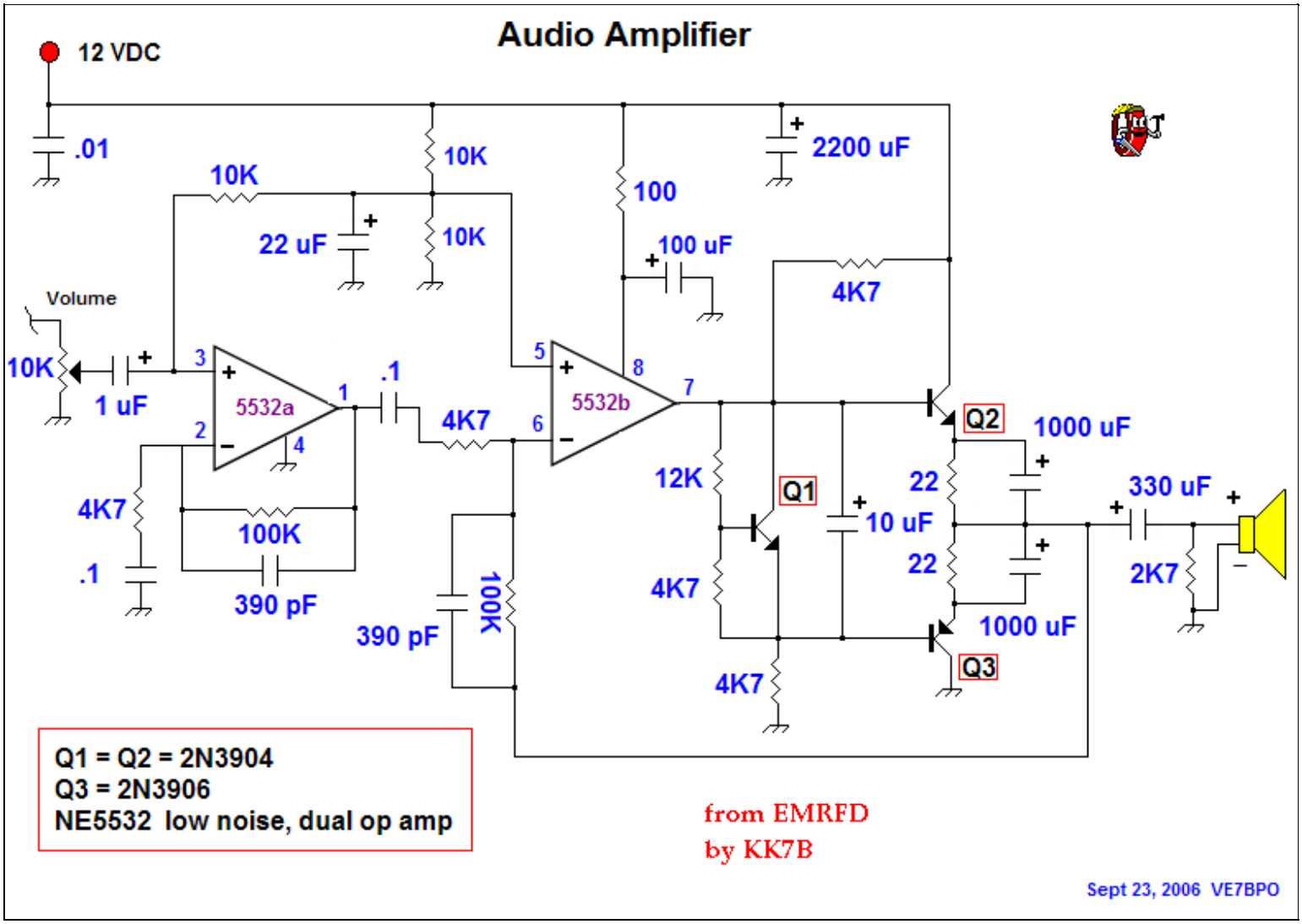

Above schematic. Rick, KK7B designed this low noise audio amplifier. It is from EMRFD. This superb AF amp greatly compliments the VK4FUQ detector. This is the best speaker audio amp under 1 watt I have ever used. Distortion is very low as long as it is not over-driven. I increased some capacitor values compared to the original schematic. Please refer to EMRFD for details on this stage. The chassis of this receiver greatly increases the low frequency response. On the 1 second pulses of WWV, the receiver "knocks" like a metronome. This does not occur when the

chassis lid is off.

WWV web site: http://tf.nist.gov/stations/wwv.html All the often subtle pulses and tones transmitted at various times during the hour can be heard with this receiver.

To the right: A bread board of the AF amp. This is the audio amp I shall use in future projects which contain a speaker. Kudos to KK7B.

Below 3 images: Different views of the TRF receiver. On the front from left to right are the bias "sensitivity" control, volume control with integral power switch and blue LED "power on" indicator.

On the rear from left to right are the 12 VDC input jack, an unused switch (was an -10 dB attenuator at 1 point), the RF gain control and a coaxial SO239 connection.

Further Experiments

What follows are some of the ideas and circuits tried over the past year.

Schematic to the right: A 10 MHz, double tuned RF band pass filter that may be used ahead of the receiver. Insertion loss is ~ 3 dB and this filter uses a 5 pF coupling capacitor which are not too difficult to find. Filters with bandwidths of 150 - 180 KHz were also tested.

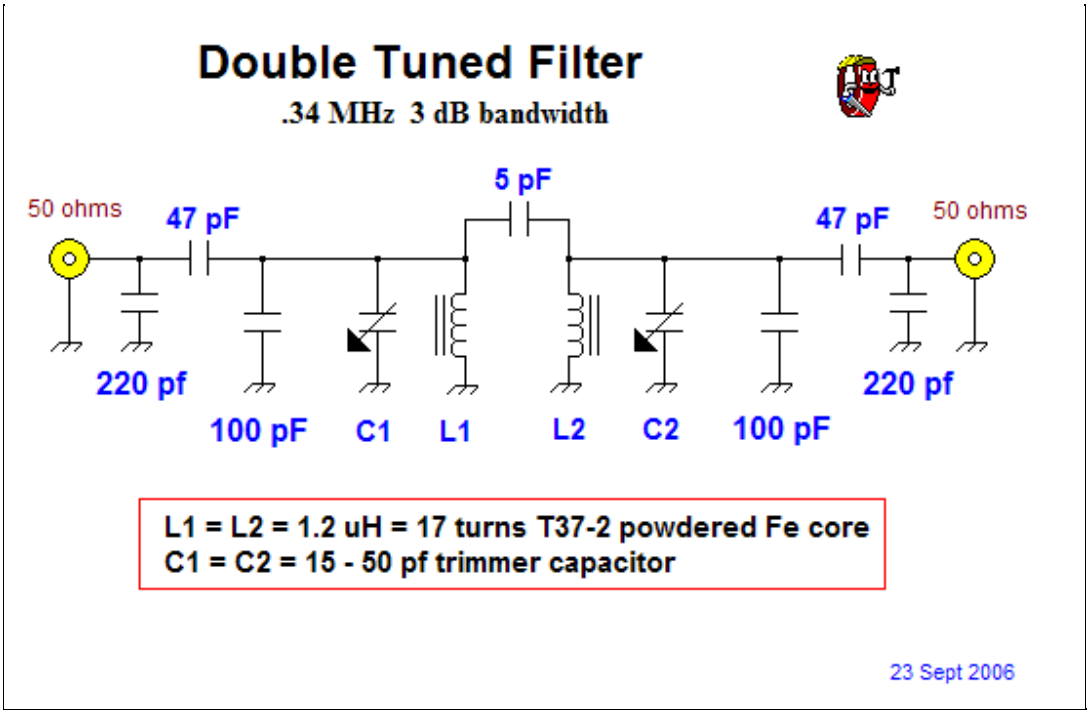

To the right: A GPLA simulation of the popcorn DTC shown above. titlehough a little mistuned, it is reasonable for a filter that uses common junk box values and has low insertion loss.

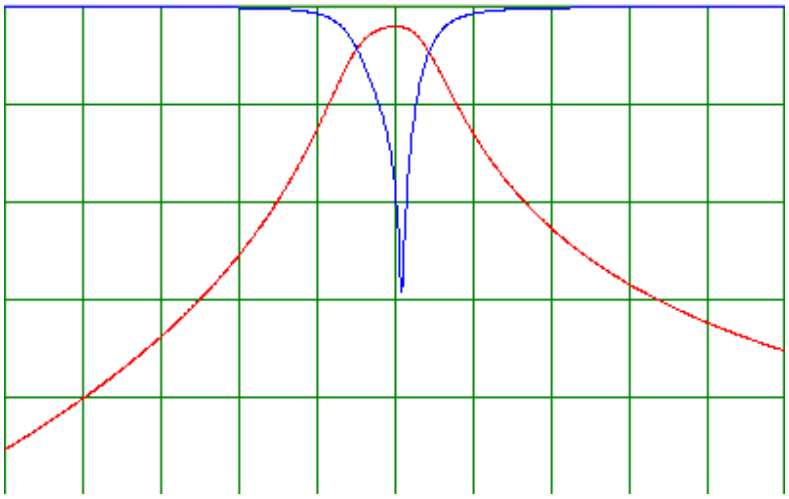

L-Match AM Detector

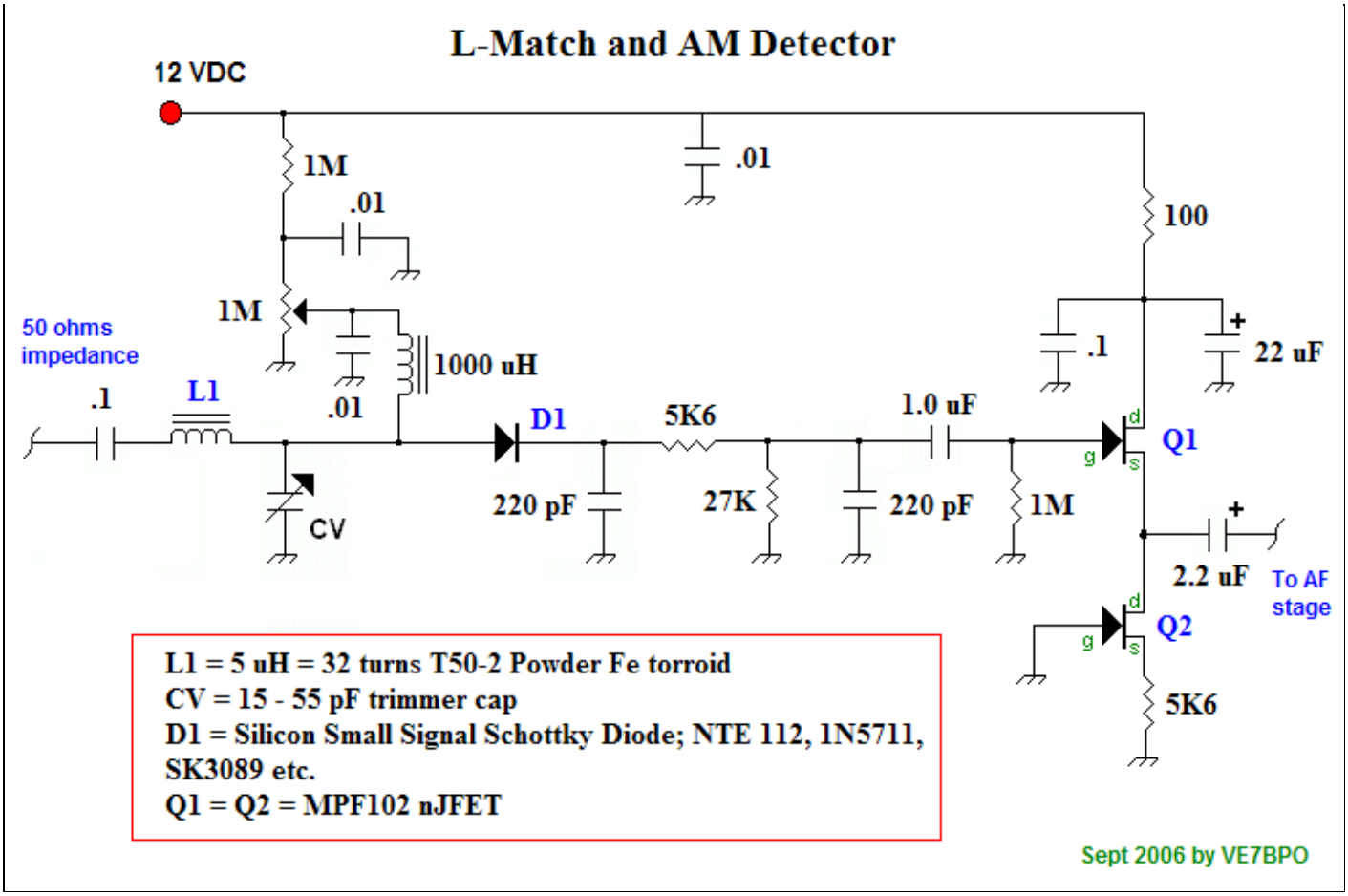

Above schematic. The VK4FUQ detector can also be used to follow a 50 ohm output impedance stage by using an L-match as shown. The L match tunes very sharply. I peaked the L-match with the bias at 0 volts.

The input impedance of the detector is related to the DC current flowing in the diode. This is established by the adjustable bias current or "sensitivity control". The input resistance will be 26/I, where I is the current in mA.

For example, if the current in the diode is 10 microamps (0.01 mA) the input Z is 2600 Ohms. I have found that any input Z value from 2000 to 5100 ohms worked well with this detector.

Image to the right: A photograph of the L-match connected to a - 6dB 50 ohm pad which terminated the 50 ohm feedback amplifier that drove the L-match.

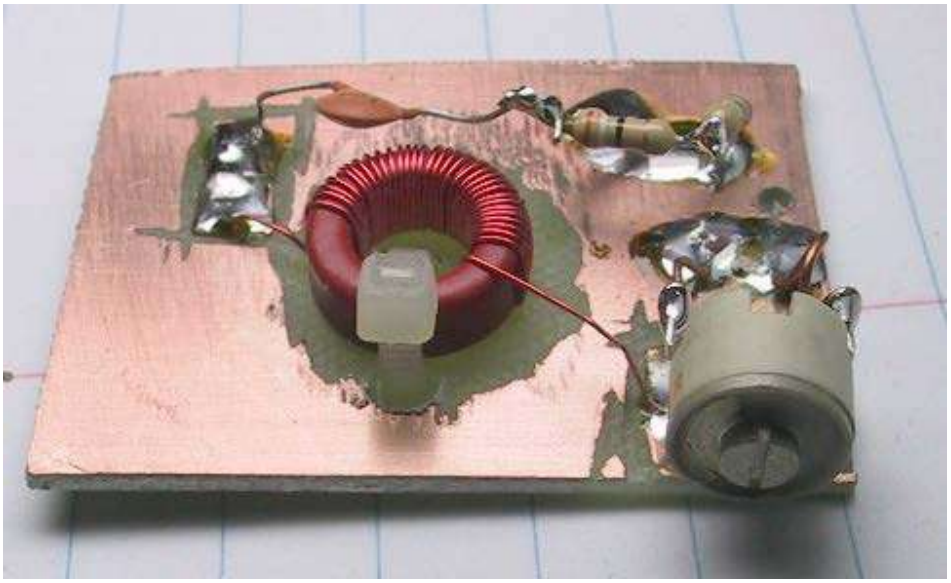

Feedback amplifiers

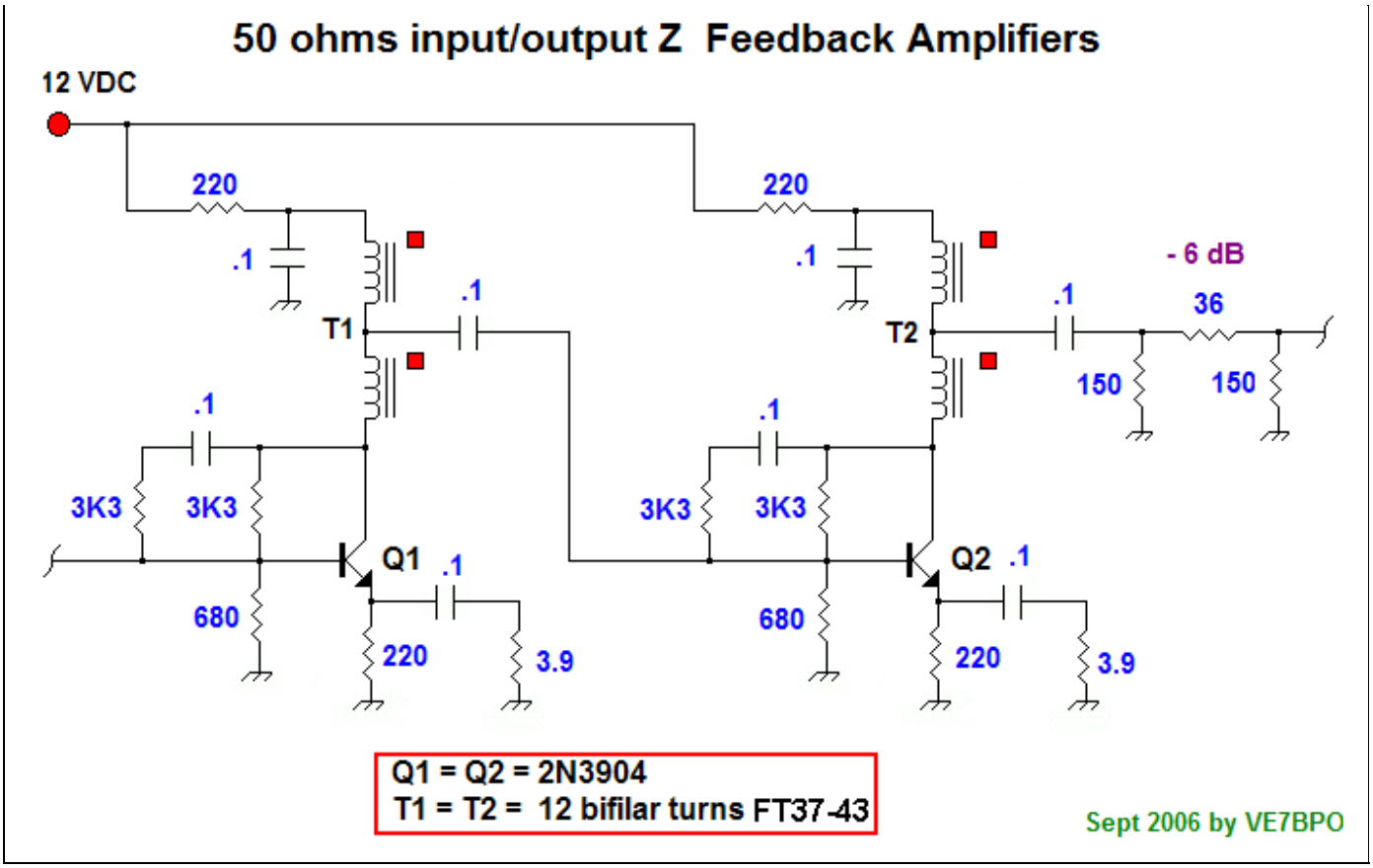

Above schematic. Feedback amplifiers may be used as RF amplifiers for a TRF receiver. This stage followed the crystal filter in one version of my TRF receiver. Stability was excellent. This feedback amplifier was designed by Wes, W7ZOI. It has ~ 20 dB gain and draws a little over 5 mA current.

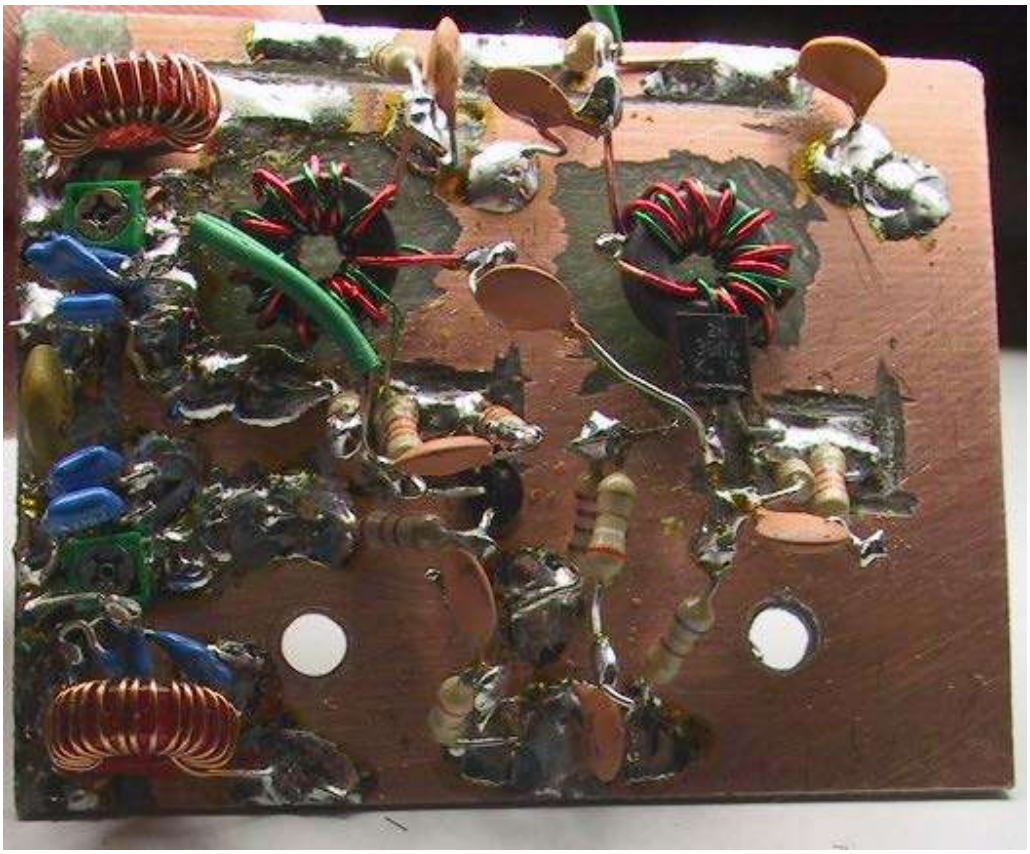

Above graphic. 2 feedback amplifiers are shown on this breadboard. The double tuned filter (DTC) shown earlier is also built on this board. In this version, the crystal filter was omitted and replaced with the DTC.

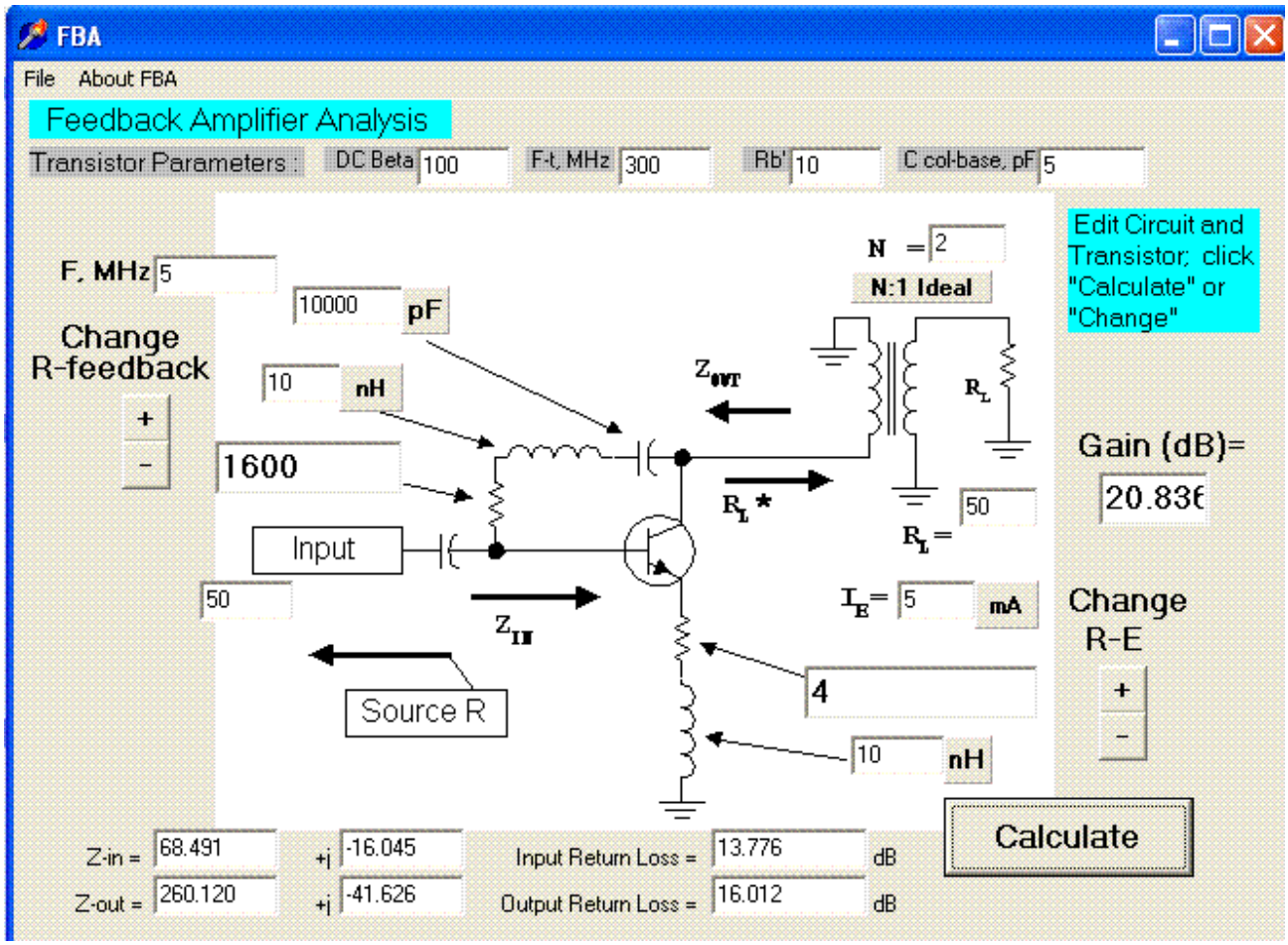

Above graphic. Using software that ships with EMRFD, W7ZOI designed the feedback amplifier used in this version of the receiver.

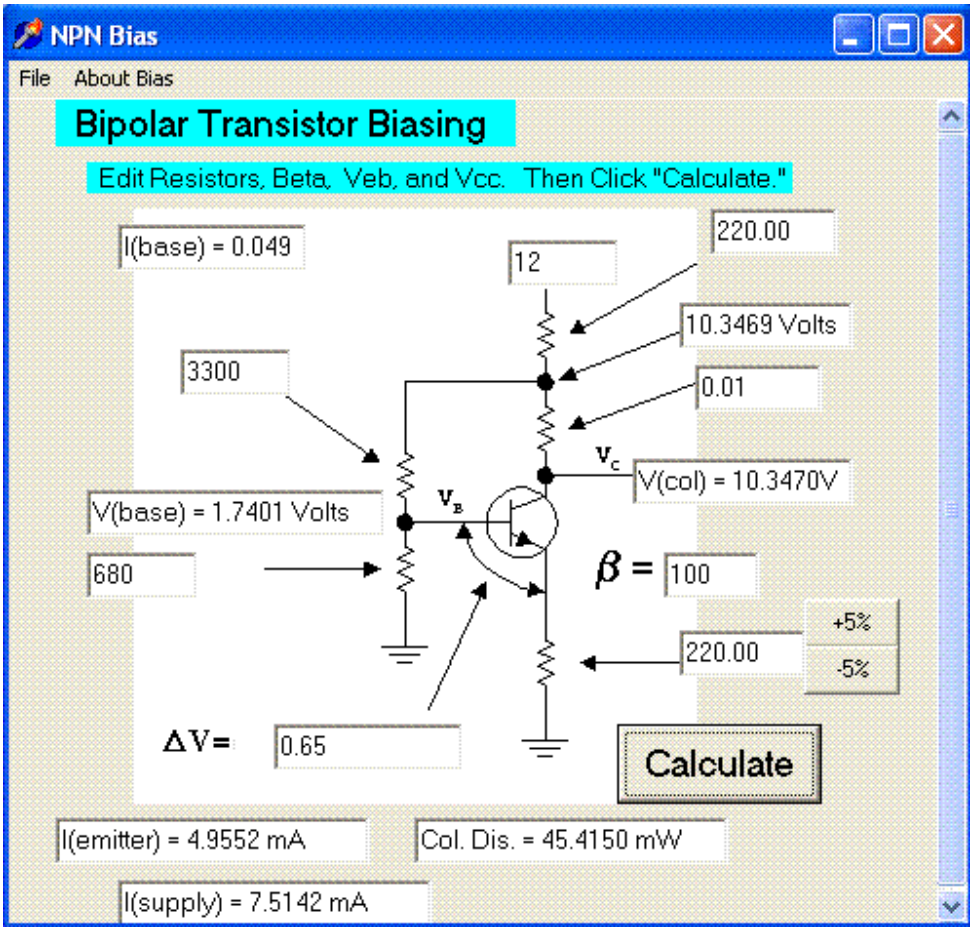

Above graphic. The feedback amplifier bias resistor values were also calculated using software written by W7ZOI and included with EMRFD.

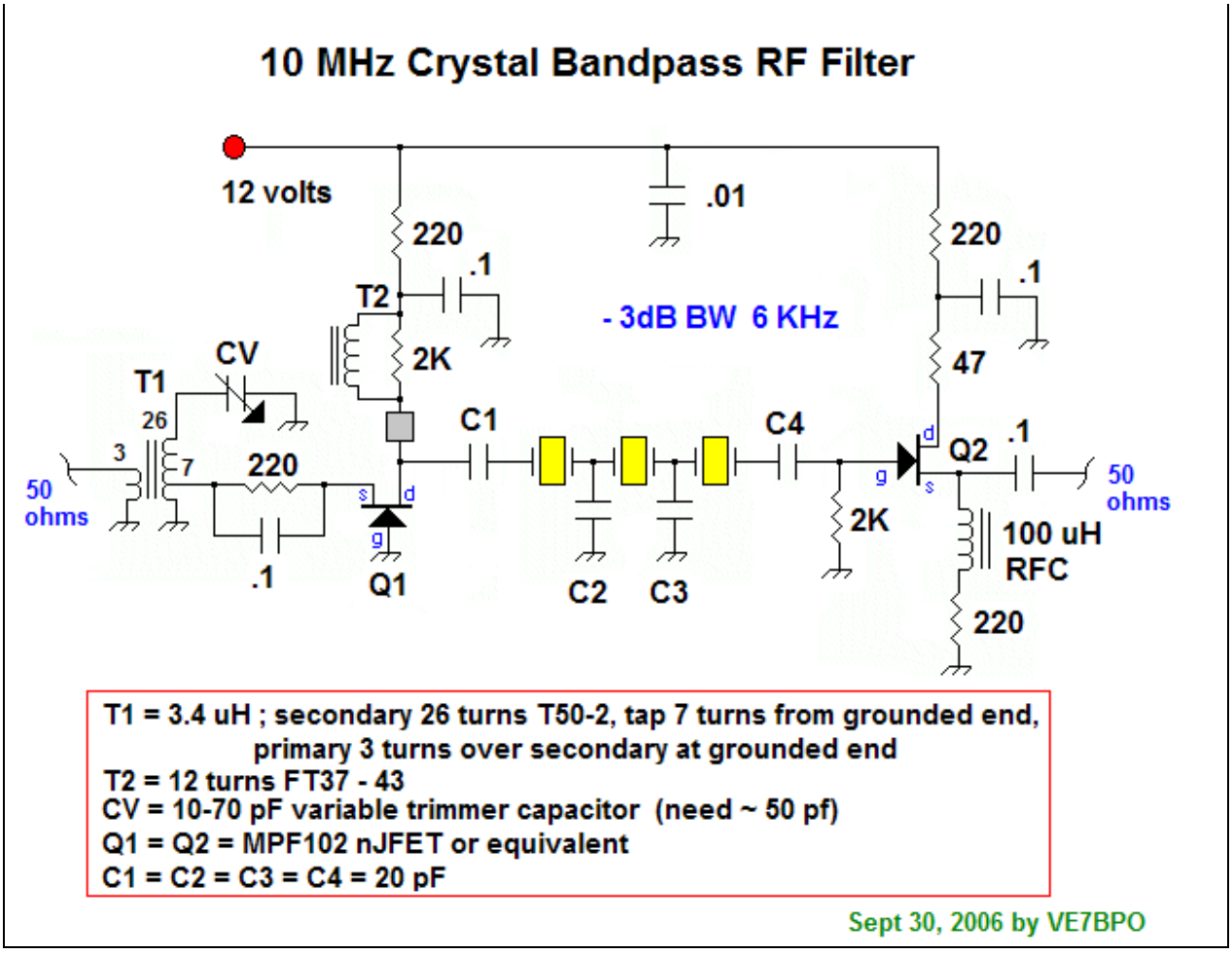

Above schematic. This circuit has the crystal filter matched to 50 ohms input and output stages using JFETs. The JFETs also serve to provide a little more gain. Careful layout is required to reduce BCB interference for all stages in a TRF receiver.

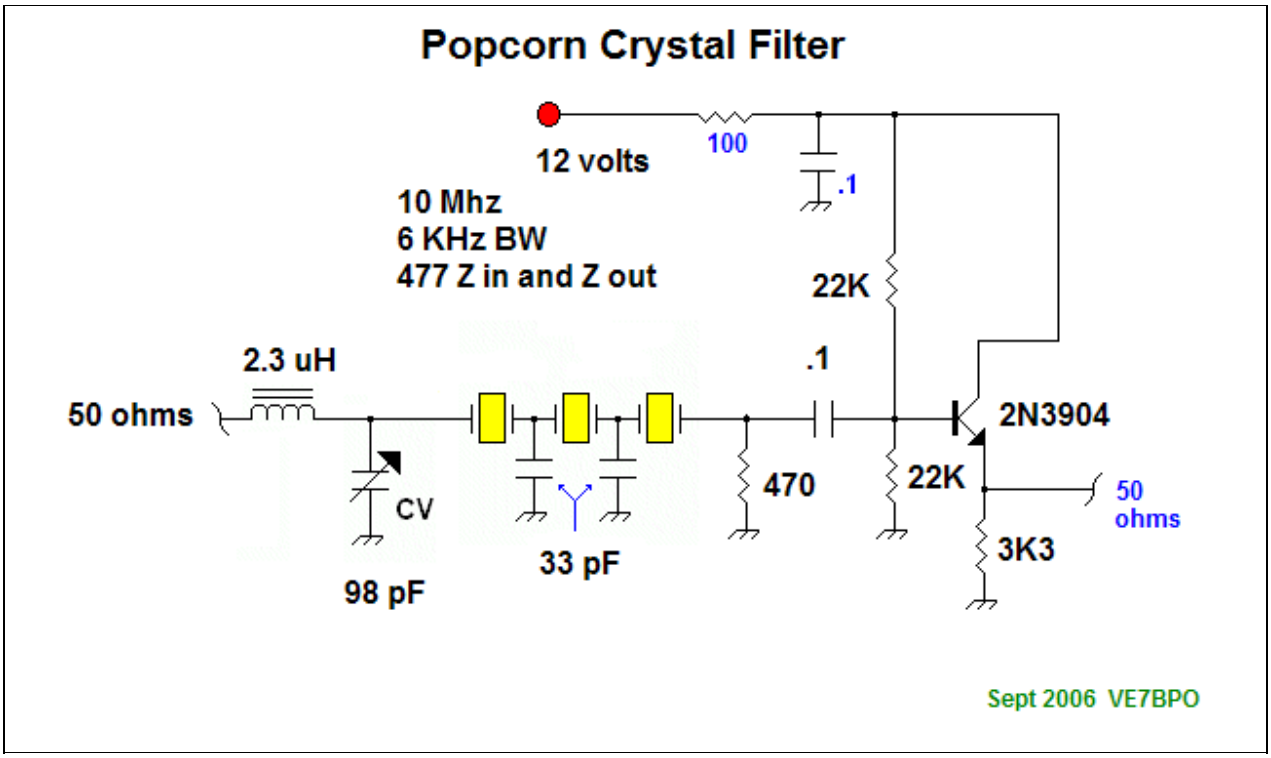

Above schematic. This is the original crystal filter that I designed. The input and output impedance is 477 ohms. The input was matched to the preceding 50 ohm stage using an L-network. A emitter follower is used to match the output to the 50 ohm stage which followed. Later, the emitter follower was replaced with the source follower (with a 470 ohm gate resistor) that is shown in the schematic directly above. The source follower

had greater immunity to BCB interference and provided a better termination for this filter. This popcorn filter worked well, titlehough occasionally there was another station in addition to WWV, in the pass band. This also happened with the filter used in the final version of this receiver.

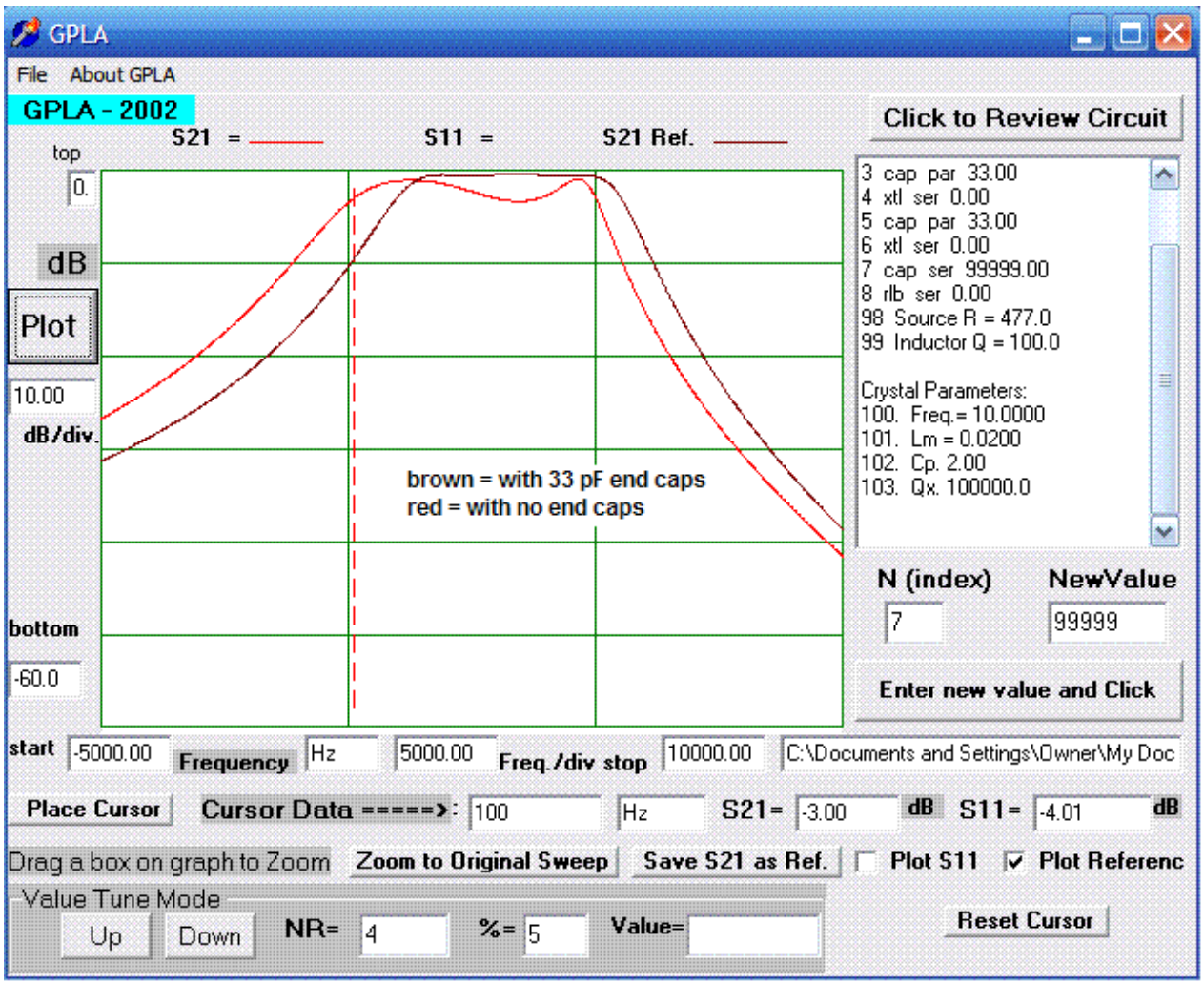

Above graphic. Here are GPLA simulations of the popcorn filter with and with out 33 pF series end capacitors which serve to tune the filter. The brown tracing illustrates that it is better to include a series 33 pF cap at each end of the "popcorn" crystal filter. I did not use this filter because the dual gate MOSFET RF amps used in the final version, have better gain driving or following the 2000 ohm filter designed by W7ZOI.

GPLA is a "must-have" program. You can "tune" filters with different or asymmetric input/output impedances.

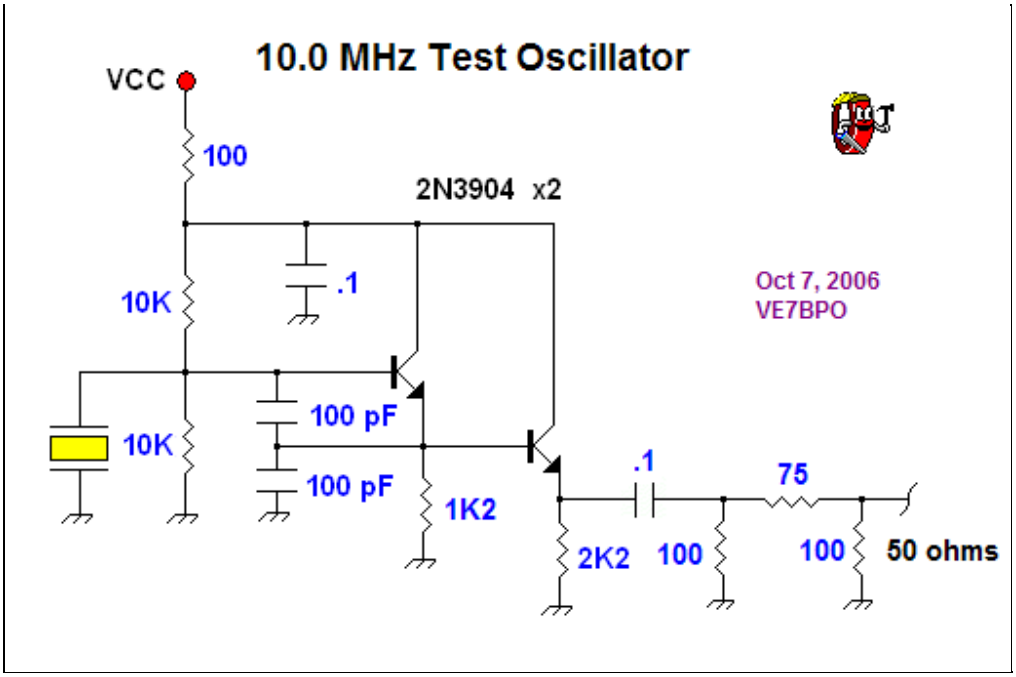

Above schematic. This 10.0 MHz crystal oscillator has a - 10 dB, 50 ohm pad on the output and was used to match the crystals, test the RF amps and align the filters used in these experiments.

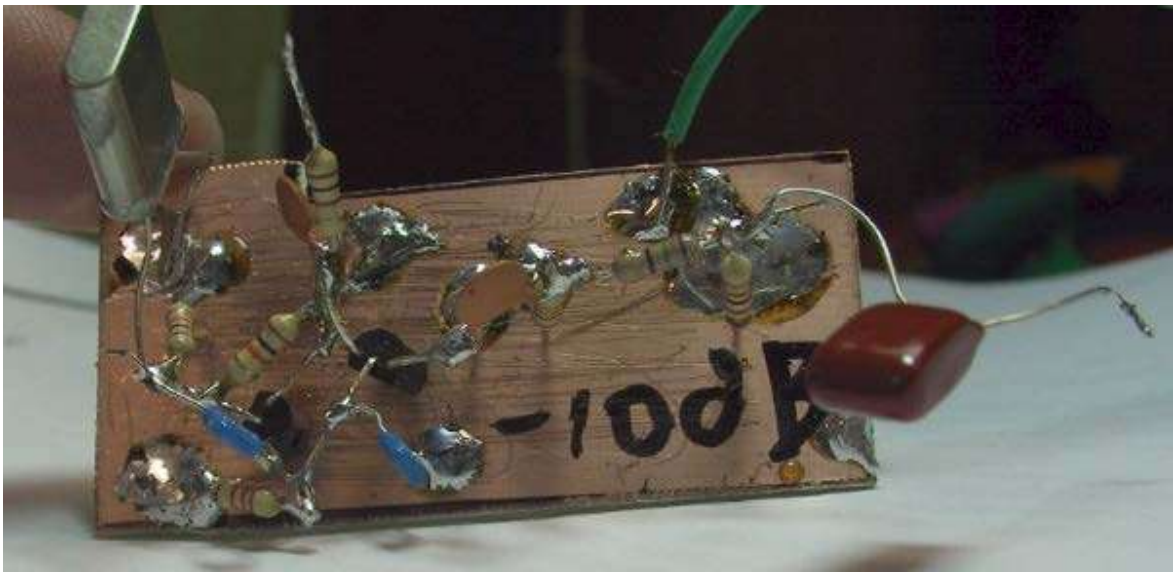

Above graphic. A breadboard of the test oscillator shown above.

Above graphic. Some of the bread boards developed during experimentation. My final receiver layout (and potentiometer positioning) is not optimal, however this is a prototype and I had no idea what the finished version would look like.

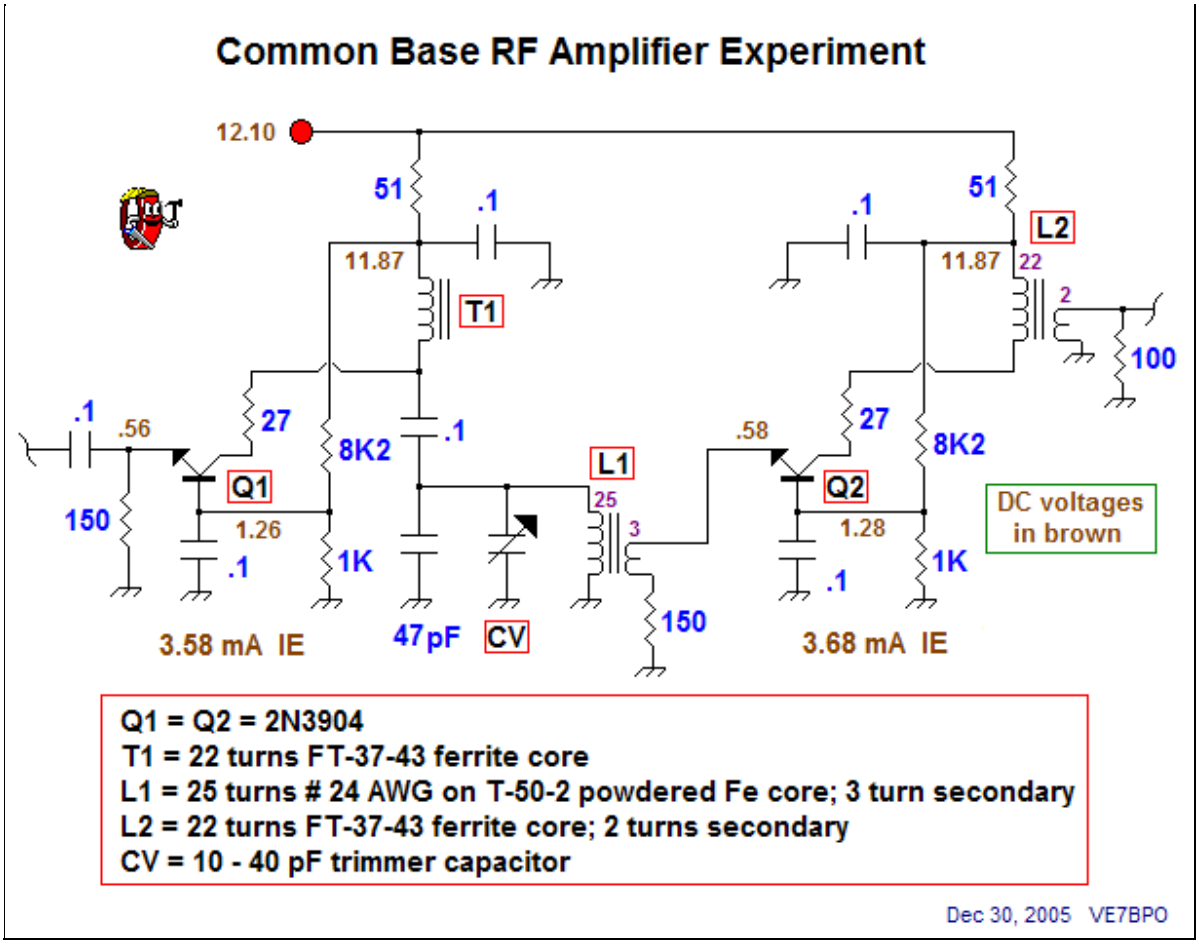

Above schematic. This is one RF amp that was built for this receiver. The turns ratios on L1 is too drastic to afford much gain.

Above graphic. I have been told many times that my breadboards are very ugly looking. This breadboard of the schematic directly above, shows that occasionally, I can build a nice looking circuit!

Conclusion

The highlights of these experiments were VK4FUQ's detector and KK7B's AF amplifier.

When constructing such a receiver, *build backwards*. Install the speaker and then build and test the AF amp. Test it by touching your finger to the input and listening for noise or BCB radio. Turn the 10K pot and verify that the noise increases or decreases appropriately. Perhaps test it using an AF oscillator.

If it works, you get immediate positive feedback and motivation to continue. If it does not work, you only have 1 stage to trouble shoot.

Next, build the detector. To test it, connect a piece of wire about 25 cm long between the RFC and the anode of the diode. You should then hear local BCB radio. Slowly turn the bias potentiometer from 0 to fully on. Notice how increasing the bias may bring in 2 or more stations compared to when it was at 0. Also notice how it changes the tone and sensitivity of the detector. Try shortening the "test antenna" and observing how sensitive this detector is with the bias increased.

If all went well, you now have an AM radio!

Next add in the Q3 RF amp and again test it using a short piece of wire. Then continue on until you arrive at the antenna connection for your receiver.

Best regards, VE7BPO

MF and HF Receiving Antenna

Introduction

My first shortwave antenna was a simple end-fed wire which started at my bedroom window and extended out horizontally to a tree which was 25 feet away from our house. The antenna feed line was a short piece of wire that connected to the near end of the antenna and entered the house through a small hole I made in my wooden window sill. This feed line was directly connected to my receiver's high impedance antenna input. My station ground was long piece of wire that was connected to a copper pipe located in the bathroom next door. While this antenna brought in "the world" to my bedroom, it was extremely noisy. Directly connecting your antenna feed line and house ground system to your receiver are not good RFI reduction practices. This web page will explore some experiments in trying to minimize the Radio Frequency Interference (RFI) arising from my local environment.

Indoor RFI sources are usually plentiful. Electrical appliances such as washing machines, televisions, DVD players, computers and electrical wiring may all emit RFI which your antenna, or directly connected house ground system may pick up and feed to your receiver. Certain indoor devices may be really strong RFI sources and will have to be eliminated or decoupled. Outside of your house are also potential sources of RFI. These may include such things as power transformers, electric fence and garage door openers. RFI location and reduction is out of scope for this web page, however a good place to learn more is the ARRL RFI book (out-of-print: search on Amazon). To find RFI sources in your home and neighborhood, try using a battery powered AM radio. At my QTH, I located a noisy VCR inside the house my Grundig S350. We rarely use this VCR and now just leave it unplugged until we actually need to operate it. I tuned the receiver to an empty frequency and found this VCR by trial and error. **Please note this web page is concerned with feeding a shortwave listening antenna and does not describe providing protection against lightning.** For web sites which covers lightening plus RF ground please refer to this offering from W8JI or eHam.net.
Protect your home and family from lightening !!

Outdoor MF and HF Antenna

The schematic to the left summarizes the outdoor VE7BPO MF and HF receiving antenna system for summer 2007. Although modest for a big city lot, this antenna seems to pull in the DX and is relatively free of RFI. This antenna was just a case of "putting as much wire in the sky as possible" and the dimensions are indicated for interest sake only. The 27 meter long horizontal section is supported between 2 trees at a height of about 14 meters high. The weight of the

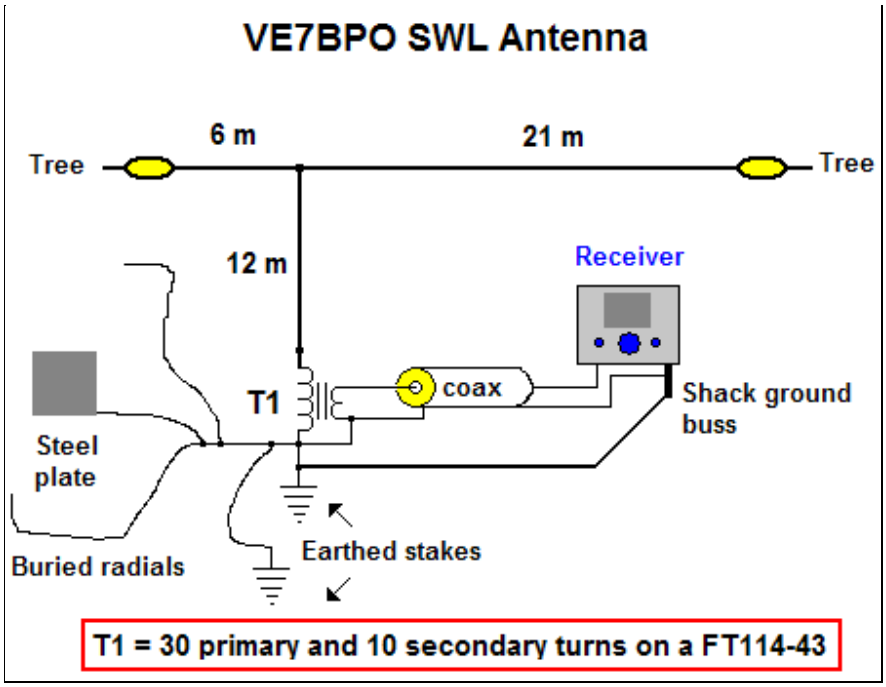

vertical element wire plus slack in the horizontal wire droop it to about 13 meters high in the center. The vertical section is soldered to the horizontal wire 6 meters from the nearest anchoring tree and runs straight down to the antenna feed point which is about 1 meter off the ground. The feed point is a piece of copper-clad PC board (with isolated sections created with a hobbyist motor tool) and is bolted to a long copper pipe which serves as the first station earth-grounding stake. A transformer (T1) configured as a UNUN **(unbalanced-to-unbalanced)** is used to interface the antenna with 50 ohm coax that runs through the house and into the radio shack. Some rudimentary experiments with the UNUN and the earth-grounding system were undertaken.

The methods I used to potentially lower unwanted RFI to my antenna system are as follows:

1. The receiver and power supply are independently connected to a single, central ground point (ground buss) in the radio shack.
2. 6-10 gauge wire is used for my ground system (not including the radials which are bare 12 gauge wire).
3. The ground wire connecting to my first earth stake to the station ground buss is just outside the shack window and is short as possible to provide a low impedance and low inductance path for MF and HF frequencies.
4. There is a second ground stake located 1 meter from the primary ground stake (I will add 2-4 more in time).
5. I have a large piece of steel buried underneath the soil tied in to my system as well as 3 bare copper radials. The radials are 3 - 7 meters in length.
6. New RG58/U coax was used as the feed line.
7. All wire splices in the grounding system are soldered and taped up. I used conductive grease (to prevent oxidation at the wire-stake interface) on any clamps connected to ground stakes. My ground stakes are ~ 2 meters long.
8. The earth grounding area soil is moist and peat-laden and is watered regularly.
9. I plan to maintain this ground system every 2 years.

4:1 UNUN

My antenna is almost an end-fed wire with both a vertical and horizontal section. I do not have the gear to measure the impedance versus frequency in the MF and HF bands. I do know that on some bands it may present an impedance of several thousand ohms and a transformer can smooth out the variation in impedance versus frequency so my receiver sees a relatively low impedance on most bands. The transformer also serves to help reduce RFI from my antenna system by eliminating unwanted common mode currents flowing on the outside of the coax braid. Grounding the antenna via the UNUN will also prevent static electricity from building up on the antenna. My first UNUN had a 4:1 impedance ratio. It is shown to the right. The antenna connects to point **A**. The ground stake connects to point **B.** Point **C** connects to the inner wire of the coax and point **D** is connected to the braid and also the grounding stake. I used 24 AWG wire and A FT114-43 ferrite core. You can clearly see there are 20 primary windings and 10 secondary windings loosely coupled. I chose the FT114-43 core because I had it on hand and the 24 gauge wire provides good mechanical support for the coil. I could have used an FT50-43 ferrite torroid as well with a smaller wire gauge. You can also use a bifilar transmission line type transformer. I was very happy with this UNUN and however it did not have as much signal strength as I expected on the 160 meter amateur band and below.

9:1 UNUN

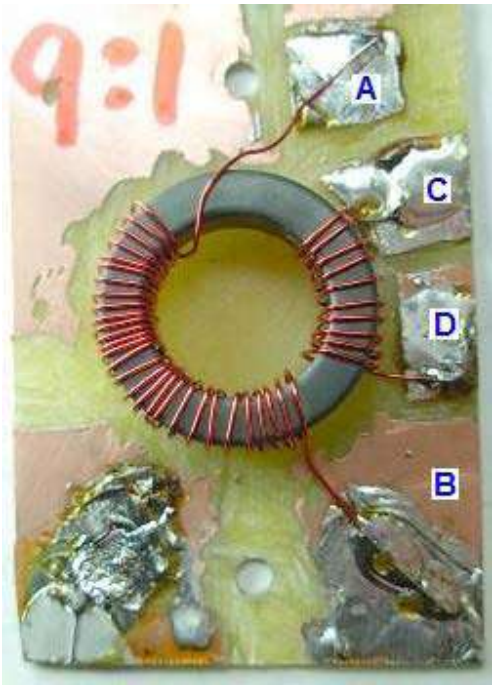

Next I tried a 9:1 impedance ratio UNUN. This an extremely popular impedance transformation ratio for end-fed or random wire SWL antennas. I wound 30 primary and 10 secondary turns on a FT114-43 ferrite torroid. The connection points are identical to those described in the above 4:1 UNUN. Remember that the impedance transformation ratio is the square of the actual turns ratio on your transformer; thus my 3:1 turns ratio is a 9:1 impedance ratio. Electrical engineers commonly use a rule when winding broadband transformers such as these. The inductive reactance (XL) of the smaller winding must be at least 4 times the load impedance at the lowest frequency that the transformer "looks" into. So for 50 ohm coax, the XL should be at least 200 ohms at 500 KHz which is the lowest frequency I intend to receive. The formula for XL is **XL = 6.28 X F X L**. Frequency (F) is in Hertz and L is the inductance in Henries.

At 500 KHz my inductor has an XL of 189 ohms which is almost perfect. I should have used 11 turns which is an XL of 229 ohms and strictly observes the 4X rule. Therefore my UNUN ideally should have used 33:11 turns on the FT114-43 torroid. If you use a FT50-43 torroid, use the same 33:11 turns ratio; this will provide 198 ohms XL at 500 KHz. For practical purposes, my 30:10 UNUN should work fine as I rarely tune frequencies less than 1000 KHz. I found this UNUN to have strong signals all the way down to MF and decided to use a 9:1 impedance ratio for my antenna system. Many experimenters and a few commercial UNUNs recommend the 9:1 impedance ratio for multiband end-fed or random wire antennas. Eventually I will encase it in a water and UV proof enclosure.

Conclusion

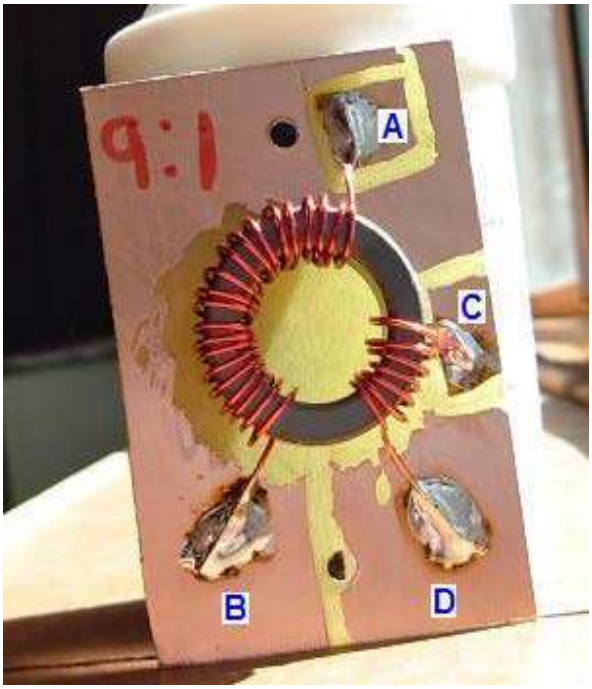

My experiments while constructing a reasonable quality MF and HF receiving antenna confirmed that using a UNUN, coax and a good RF ground system can reduce common mode RFI in my receivers.
I also tried temporarily connecting my ground system to a copper water pipe located in my shack while listening to WWV at 5 MHz and immediately the noise level rose 2 S-units on my receiver.
This pipe was clearly not grounded in my house where there is a mixture of plastic and copper water pipes. Additionally, my antenna wire and feed point is away from the house in a quiet area according to listening tests using a Grundig S350.

It is relatively easy to construct a UNUN on your bench using a ferrite torroid. Many builders have emailed me to say they do not feel comfortable winding torroids. Torroids are easy to use and by winding a couple and experiencing some success, your confidence working with them will surely improve. If you live in a part of the world where you can not easily obtain a suitable ferrite core, just email me and I may send you an FT50-43. You can also choose a ferrite with a different core permeability. Some builders use number 75 material. I used the FT114-43 because I get all my torroids from W8DIZ and just use what he has in stock for my projects. If you really do not want to construct a UNUN, commercial products are available on the web on sites such as http://www.arraysolutions.com/Products/baluns.htm.

I wish you good luck with your own antenna experiments and please be safe!

Some SWL Antenna Related Links

L.B. Cebik, W4RNL was a respected antenna expert. There is great information on his web pages

Build a Shortwave Antenna. A good overview of home brew multi-band antennas by N4UJW

MF and HF Receive Antenna Splitter

Introduction

As a radio experimenter, I have numerous MF and HF receivers to listen to but usually only 1 main outdoor antenna. Typically, this means that only my main radio receiver is connected to the outdoor antenna and my other receivers must use small indoor antennas with or without RF preamplifiers. I wanted to to permanently connect my main radio shack receiver and the receiver in the room directly above the shack to my main MF and HF antenna at the same time. The solution was to build a simple antenna splitter which allows the 2 radio receivers to connect to the single coaxial antenna feed line while preserving the correct impedance at all connection points. This project is based upon the splitter presented in EMRFD labeled Figure 3.81.

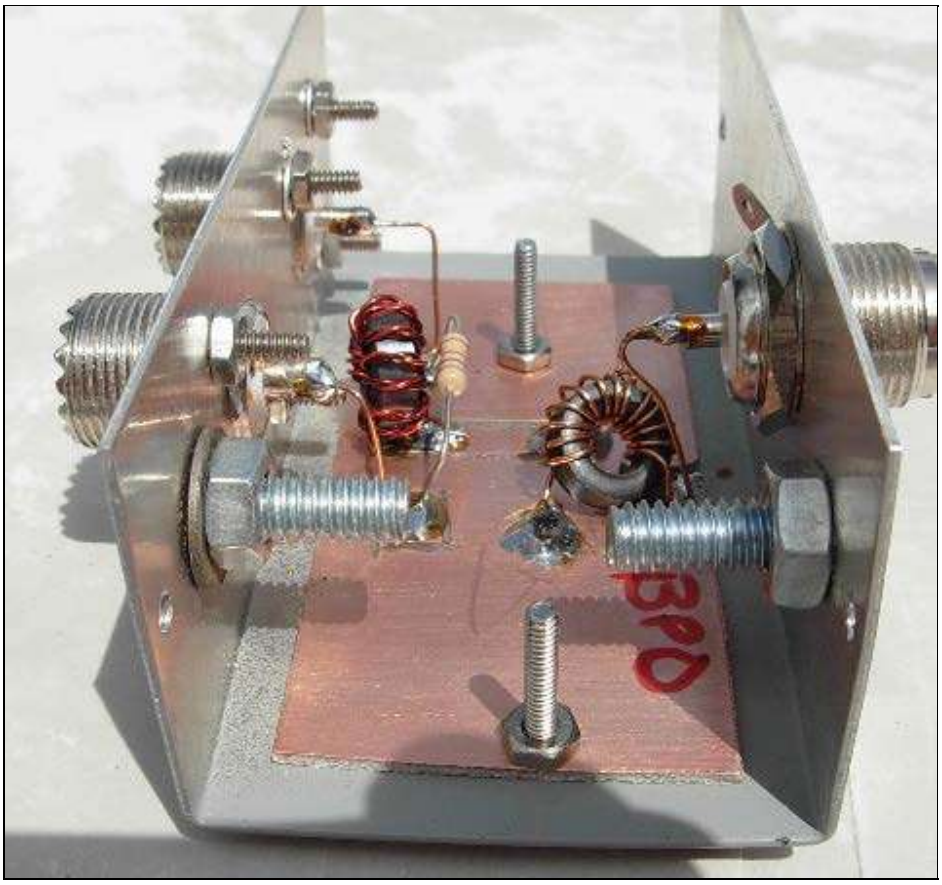

Each receiver and the antenna feed line have a 50 ohm characteristic impedance. This in-phase splitter is passive and has a loss of just over 3 dB. It is designed to operate from 500 KHz up to 30 MHz.

Please do not transmit through this device.

Project Schematic

The schematic to the left illustrates the entire splitter network from the antenna input to the input of the 2 receivers. T1 and T2 are broadband ferrite transformers with enough inductive reactance to tune down to the bottom of the broadcast band. If you only require a splitter for HF, then wind T1 with 10 total turns and a tap at 7 turns from the grounded end and T2 with just 10 bifilar windings. I used FT50-43 cores to allow the use of

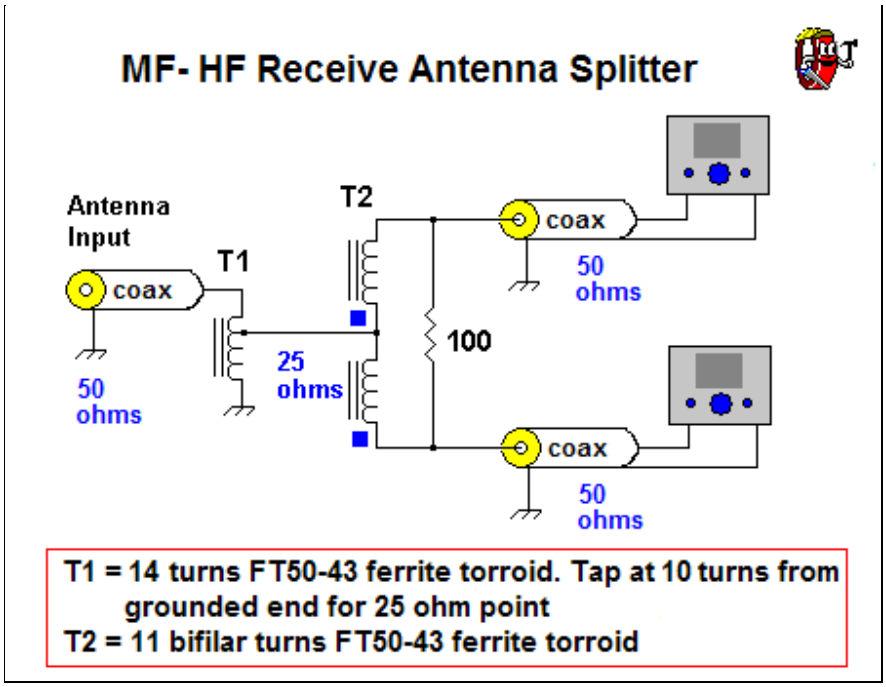

thicker gauge wire which provides reasonable securement of the coils without external anchors, and because bigger inductors are easier to photograph. The FT37-43 ferrite core would also be a good choice, especially if miniaturization is a design goal.

Circuit Building Details

The antenna splitter breadboard is shown to the right. I used 3 colors of 22 gauge enamel covered wire to make my inductors. T2 is the actual splitter network coil and is the lower transformer in the photograph. The 100 ohm resistor serves to isolate the 2 ports connected to the receivers and absorbs impedance mismatches which may present when one terminal is not properly terminated. Note that the characteristic impedance at the input of this 3 port network is only 25 ohms. You can choose to ignore this or use an additional network such as a broadband transformer or an L- match between your antenna coax and the splitter to match this 25 ohm impedance.

I chose to use T1 which is an autotransformer with a tap at approximately the 25 ohm point. The splitter network worked well during my tests. Having only 1 receiver versus 2 receivers connected made no difference to the signal strength due to the excellent output port isolation.

Note that Wes, W7ZOI uses this 3 port network network several times in EMRFD. One example is the Lichen transceiver while another is the 6M superhet receiver presented in Chapter 6. Consult EMRFD for further discussion of this and other multiple port networks.

T2 is a bifilar transformer. The 2 wires were twisted together by securing one end of the 2 wires in a vise and the other end of these 2 wires in the chuck of a brace and bit (manual) hand drill. I twisted the hand drill until I had 8 twists per inch on the 2 wires . I used 2 color wire for ease of construction, however, it is almost as easy to tell the windings from one another by using an ohm meter or audible continuity tester.

Chassis

To the right is the completed project showing the SO-239 connectors which are wired to the antenna splitter output ports. A chassis from an old project was recycled for this new project. The large bolts seen in some of the of the photos were used to fill in holes which had been drilled for the old project. This was done to provide improved RF shielding. The bolts also increased the weight of the chassis and help keep it from tipping over. Although it does not look as attractive as if I had used a brand new project chassis, considerable cost savings were realized. These little Hammond project boxes are getting very expensive. Also the

splitter is kept an the back of my main radio desk where it is out of sight anyway.

Update August 10, 2008 - Contribution by Dave, G4AON

This original network was designed for use in the MF to HF spectrum. Limiting this network is the input matching transformer T1 which negatively effects the T2 output port isolation; especially at 41 meters and higher. Testing by Dave, G4AON confirmed this. Dave designed, built and tested a trifilar wound, UNUN input matching transformer which provides a much flatter response for T2 port isolation from 0.1 to 52 MHz.

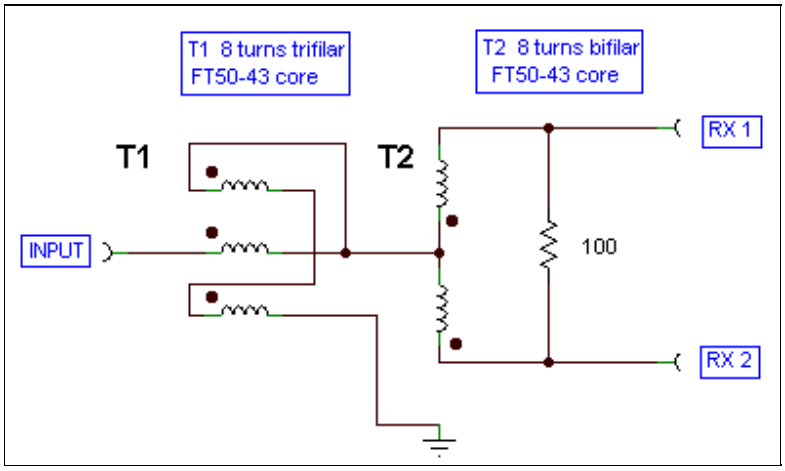

To the left you can see the G4AON input circuit for T1. In keeping with a design optimized for higher frequencies, less total turns are used on the transformers. His trifilar wound input transformer version is going to generate an impedance of (16/24)^2 x 50 = 22 Ohms at mid-band. My variation will generate (10/14)^2 * 50 = 25.5 ohms at mid-band. Using his version of T1 as opposed to my simple auto-transformer, Dave was able to provide better isolation of the output ports than the original design across a wider range of frequencies.

In the two popular, commercially sold RF splitters we have examined, the company did not even bother to match the input to the T2 transformer and some builders have written me to say they just omitted T1 and for their typical SWL listening this worked out fine for them. Increasing isolation across a wider frequency band and also matching the T2 input are issues that you the builder will have to consider. Certainly the lossy and often non-predictable #43 ferrite material is a factor which might affect your transformer performance. While a trifilar transformer is a little more difficult build for a novice as compared to an auto-transformer, this improved design might work very well at your QTH. Testing like Dave did is certainly the way to go and I greatly appreciate his contribution.

To the right are Dave's excellent bench measurements. He used a Marconi 2018 signal generator, a Racal 9301 RF millivoltmeter and a Bird load on the other port. Kudos to Dave for performing this experiment and contributing to the receive antenna splitter knowledge base.

Dave's web site.

Antenna splitter measurements		
Freq (MHz)	Port 1 & 2 loss(dB)	Port 1 – 2 isolation (dB)
0.1	-3	16
1	-3	31
2	-3	33
3.6	-3	32
4	-3	32
5	-3	30
6	-3	28
7	-3	28
10	-3	25
14	-3	23
18	-3	22
21	-3.5	21
24	-3.5	20
28	-3.5	19
52	-4	16

Conclusion

It is really awesome to be able to connect 2 receivers to the same outdoor antenna. The 3 port network and cabling to the additional receiver does not seem to increase receive noise levels from RFI in the house. Most likely this is due to the fact I am using shielded coax, a shielded project box and have a good RF ground system.

This is a simple project you can build in one evening.
I hope you receive some good DX! 73 es CUL, VE7BPO

Here is a link from F6AOJ

Additional Photos

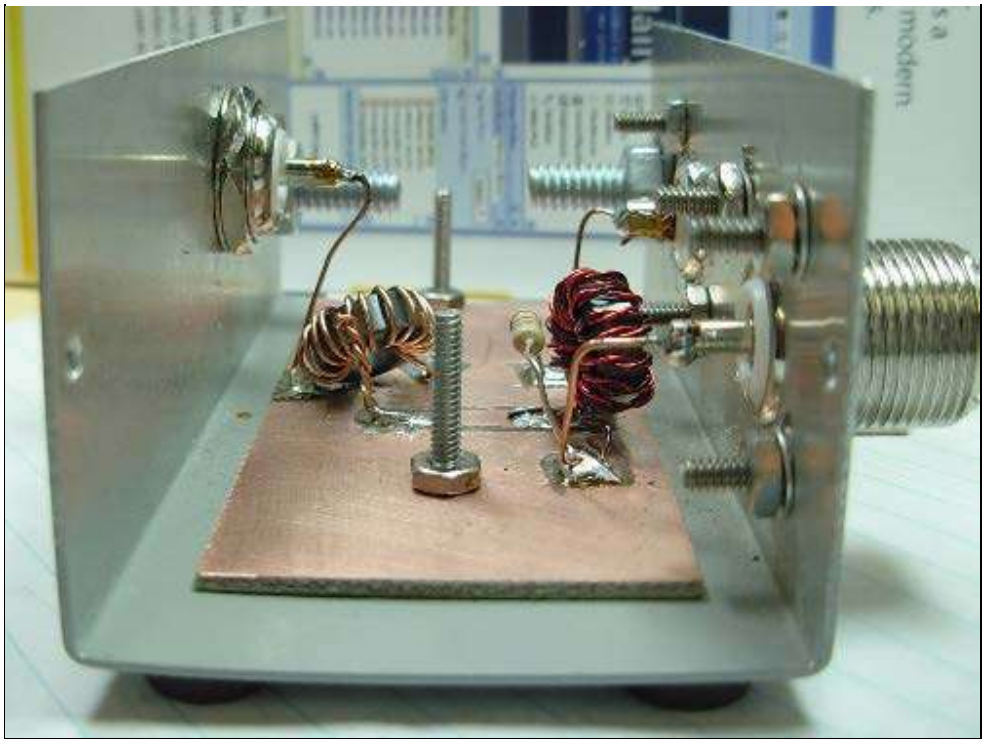

Medium Frequency TRF Receiver

Introduction

This series of experiments was initiated in 2006, stalled, and was finally completed 16 months later with the inspiration provided by work regarding zero power receivers web-published by Wes, W7ZOI in late summer 2007.

Described is a complete receiver, built and presented backwards from the audio stage to the antenna. The design goals were to build a Tuned Radio Frequency broadcast band receiver with one RF amplifier, a high performance detector and a simple, headphone-level audio stage.

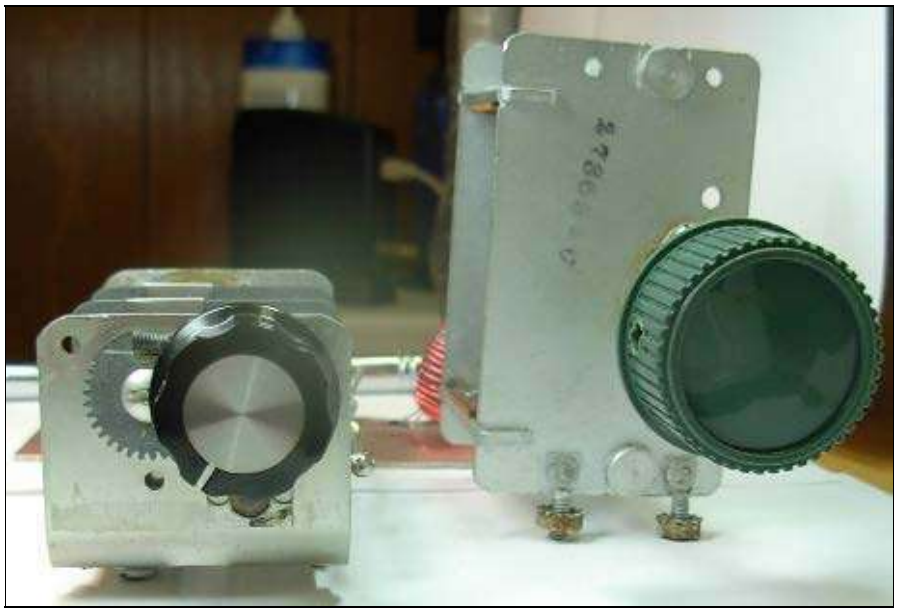

Receiver Block Diagram

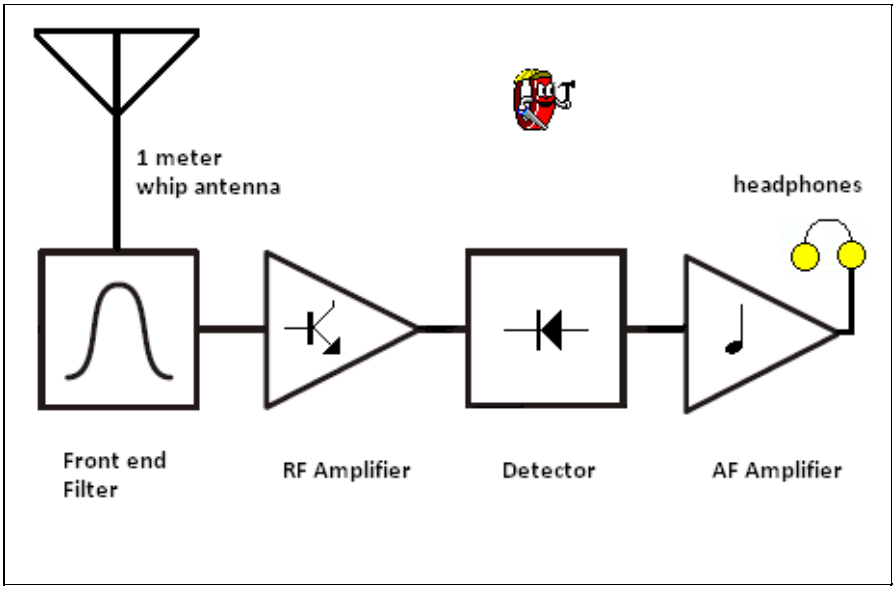

The receiver block diagram is shown to the left. The antenna is a ~ 1 meter long whip purchased from Radio Shack in the USA. A single cascode bipolar junction transistor amplifier boosts the RF voltage and drives an envelope detector which is terminated by a JFET source follower. The source follower connects to a 10K volume potentiometer which controls the AF signal voltage into a headphone-level audio amplifier. Like most of the projects on this site, the intention is to present some circuits and ideas for experimentation. This receiver is designed for local broadcast band AM radio reception, however, the various circuits could be used in or titleered for DX receivers as well.

A Supplemental Page can be found here

Audio Stage

The AF amplifier is a superb design by Rick, KK7B and is featured in many projects in EMRFD. This audio amplifier uses one 5532 op amp and has low noise and high gain. The 220 pF feedback capacitors can be increased to boost the low frequency response. I have built 6 or 7 versions of this stage and have used feedback capacitors up to 560 pF for this purpose. In the audio path, polyester film capacitors were used to try to improve the audio quality. Additionally, the value of the 15 uF capacitor connected to pin 2 is flexible. The quiescent current draw of this stage at 12.2 VDC is 12. 3 mA. Some builders may have to increase the 100 uF filter capacitor on the main 12.2 volt line to overcome motorboat oscillation. None occurred in my breadboard version. I suggest using this audio stage instead of the LM386 or discrete component final audio amplifiers in all projects which call for a headphone-level audio power amplifier on this web site.

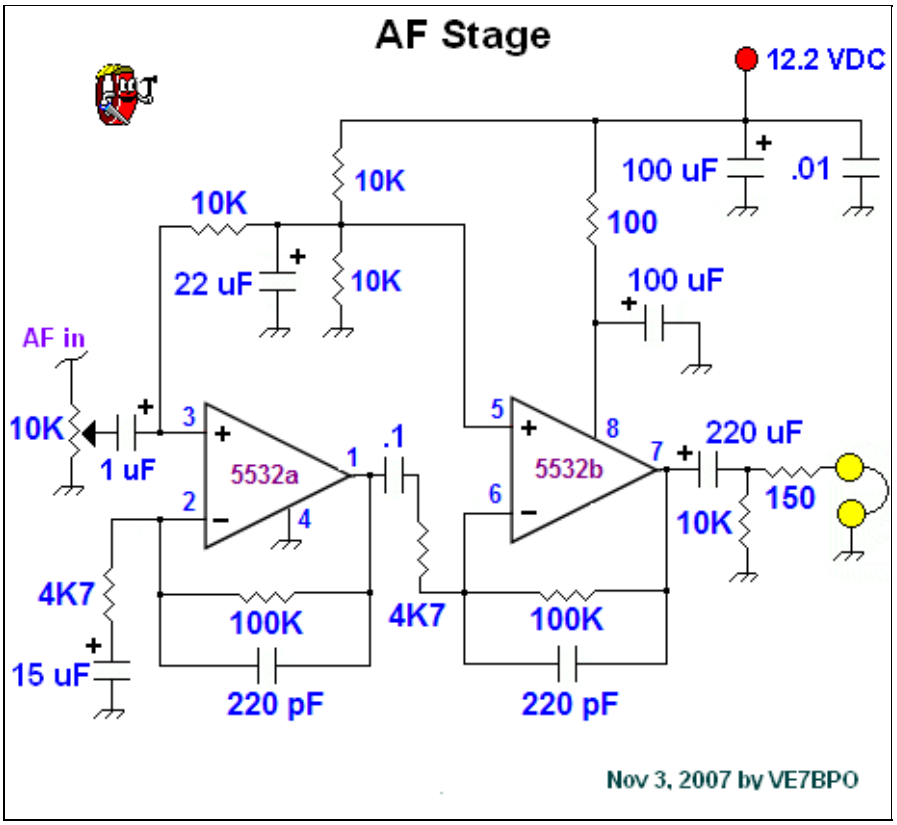

Close up of the KK7B audio amplifier breadboard from the 10K potentiometer to headphone jack

---

Cascode BJT RF Amplifier and High Performance Detector

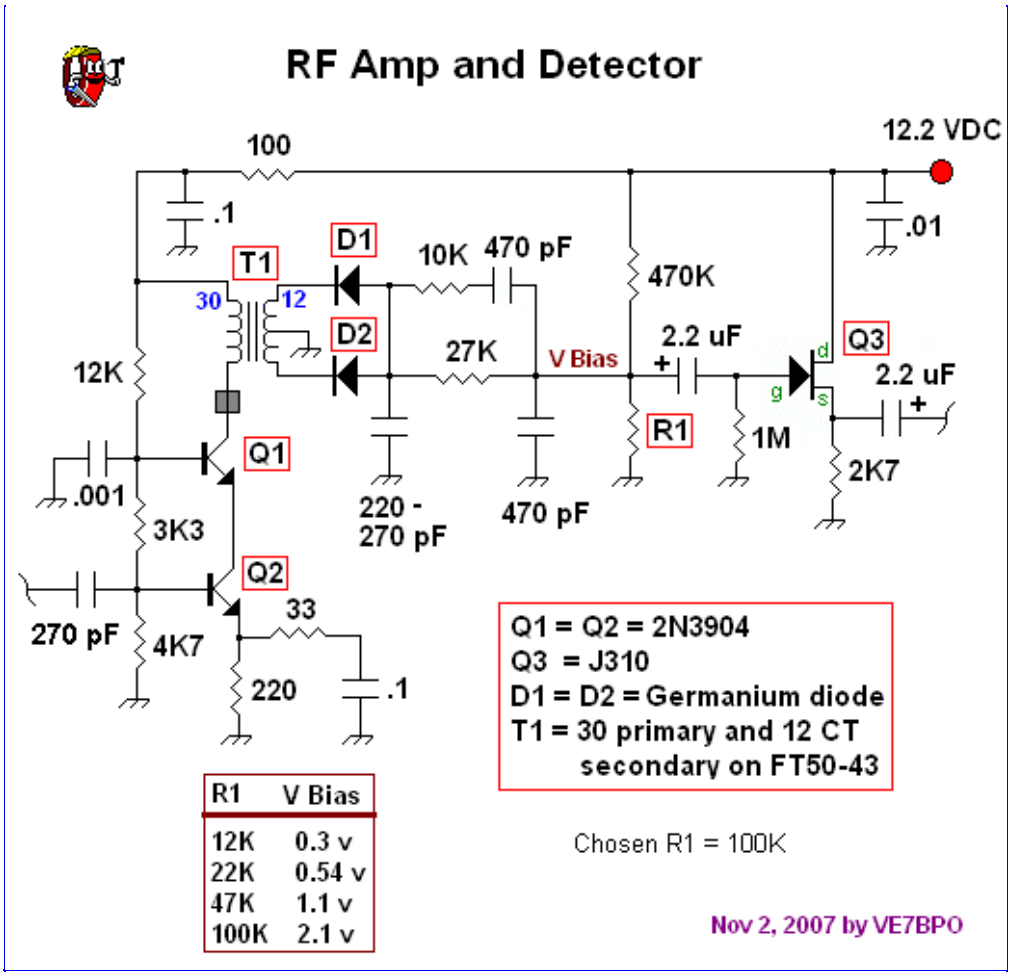

Above is the combined RF amplifier, detector and JFET source follower schematic.

Cascode BJT RF Amplifier

To the left is a simplified RF amp diagram taken from the schematic above indicating the measured DC voltages for reference purposes.

T1, the output transformer was wound on an FT-50-43 ferrite toroid. An FT37-43 would also be suitable. Number 28 gauge enamel coated magnet wire was used for the 30 turn primary and 26 gauge wire was wound over top to make the secondary 12 turn, center-tapped winding. The 26 gauge wire was used for the secondary winding because it provided good anchoring of the transformer by the center tapped ground connection.

You may consider substituting a 22 to 100 ohm resistor for the ferrite bead on Q1. It suppresses VHF oscillations.

Detector

To the right is a photograph of the detector from the Q1 transformer through to the JFET source follower. Schottky/hot carrier diodes or germanium diodes such as the 1N34A with a low forward voltage drop are strongly recommended. I have found there to be significant variation in

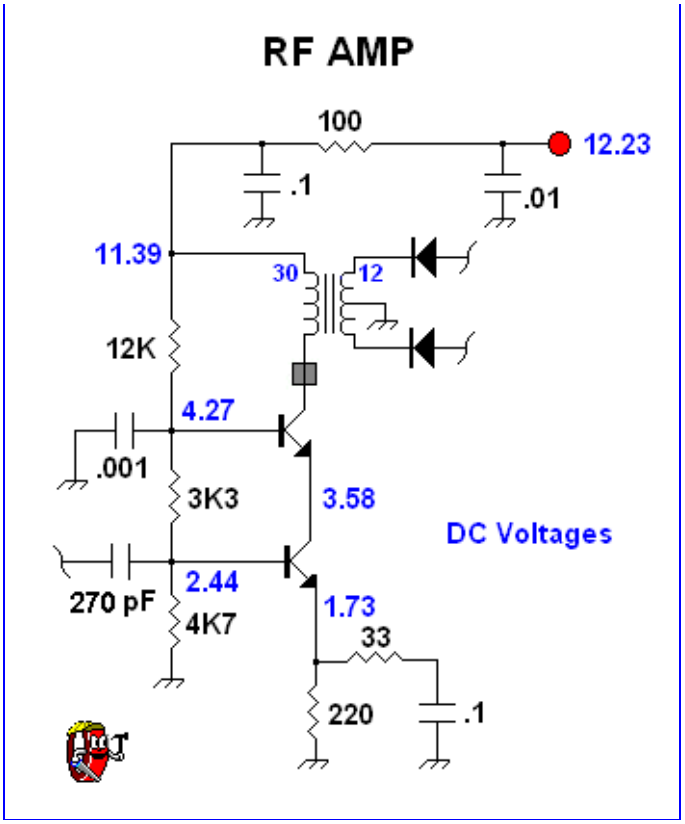

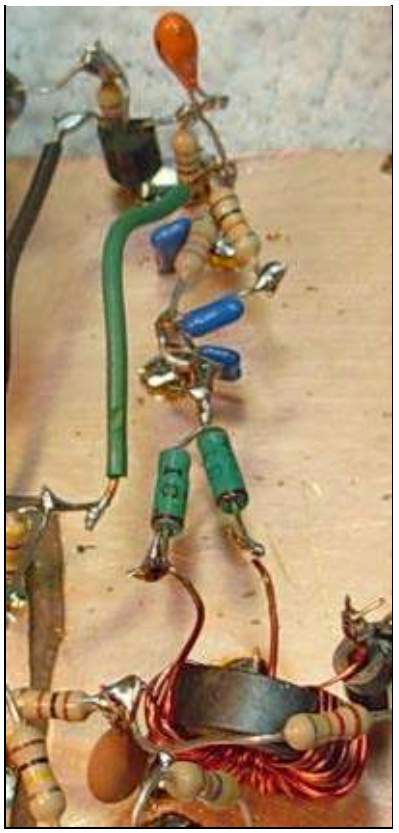

sensitivity between different types of these diodes. The 2 germanium diodes I used were matched as described on this web page. A number of detectors were built and tested for this receiver, however, the design shown had the best audio quality when compared to the others. The virtues of this detector include low noise, high bandwidth, high sensitivity and low distortion. although a little complex, this is a detector worthy of consideration in your AM receiver projects. The center-tapped Q2 transformer secondary and the 2 diodes provide full wave detection. This serves to reduce distortion somewhat and cancel even-order harmonics in the carrier signal. You may eliminate one of the diodes and convert the Q2 transformer secondary to a conventional, single link.

A 470K ohm resistor and R1 form a voltage divider that sets the detector bias voltage (V Bias). Some measured R1 values and corresponding bias voltages are shown in the schematic. I chose an R1 value of 100K for my final version. You may have to increase or decrease the R1 value to suit your local detector sensitivity requirements. You could also substitute a bias potentiometer for front panel adjustment of the receiver sensitivity. In this detector, changing the R1 value also changed the detector frequency response. I built a separate voltage divider with roughly the same V bias consisting of a 68K and a 15K resistor and swapped it for the 470K and 100K pair. Interestingly, the 470 K and 100K pair had better low frequency response and slightly higher sensitivity than the 68K and 15K voltage divider.
Diode detectors are best driven with a high impedance source and followed by a high impedance load. Q3, a simple JFET source follower provides a high impedance load. You might want to substitute a "popcorn" MPF102 for the high Idss J310 indicated in the schematic as a J310 is not really required here. If you substitute a MPF102, please increase the source resistor from 2K7 to 4K7 ohms.

Front-end Band Pass Filter and Antenna

In late summer 2007, Wes, W7ZOI conducted experiments with zero power receivers (crystal sets and such). He wound some inductors using ferrites with an unloaded Q of over 270 at MF! Please check out Wes' web site. His work with high Q ferrite inductors illustrates the importance of quantitative measurement and also provided the following revelation; we really do not have to resort to large, air core, Litz wire coils to build high-performance inductors at MF! The early prototype front end for this project was built using FT50-61 ferrite cores, however after Wes emailed me his work on zero power

receivers, I had to get some FT-114-61 ferrites for the front end of this receiver. The next day, I emailed Mark Laurain from Amidon Associates Inc and ordered some FT-114-61 ferrite toroids. The arrival of these ferrites prompted me to finish this project and put it up on the web.

The schematic on the right is the final band pass filter used for the front end. I initially tried using just L3 for the front end, but I was unable to just tune a single station. In my city, there are 2 powerful AM radio stations at 630 and 1150 KHz. With a single inductor, I could peak one of the stations, but the other could be heard in the background. Thus, the double-tuned band pass filter presented was designed and built. Now only one station can be detected with this circuit and tuning is sharp. Most builders would use a dual-ganged variable tuning capacitor, however, I elected to use 2 separate variable capacitors. Considerable flexibility with this circuit is possible. You will have to experiment to best determine your local sensitivity versus selectivity needs and to suit the variable capacitors you have available. Large AM receiver capacitors are getting hard to find. I obtained the 2 variable capacitors shown in the photographs below from 2 old receivers found in a second hand store. One of the receivers was a Marconi tube radio that was in poor condition. I paid $5.00 for both radios and harvested the 2 beautiful variable capacitors as well as some other parts such as knobs, switches and terminal strips. Never pass up on an old, derelict radio as a potential variable capacitor source!

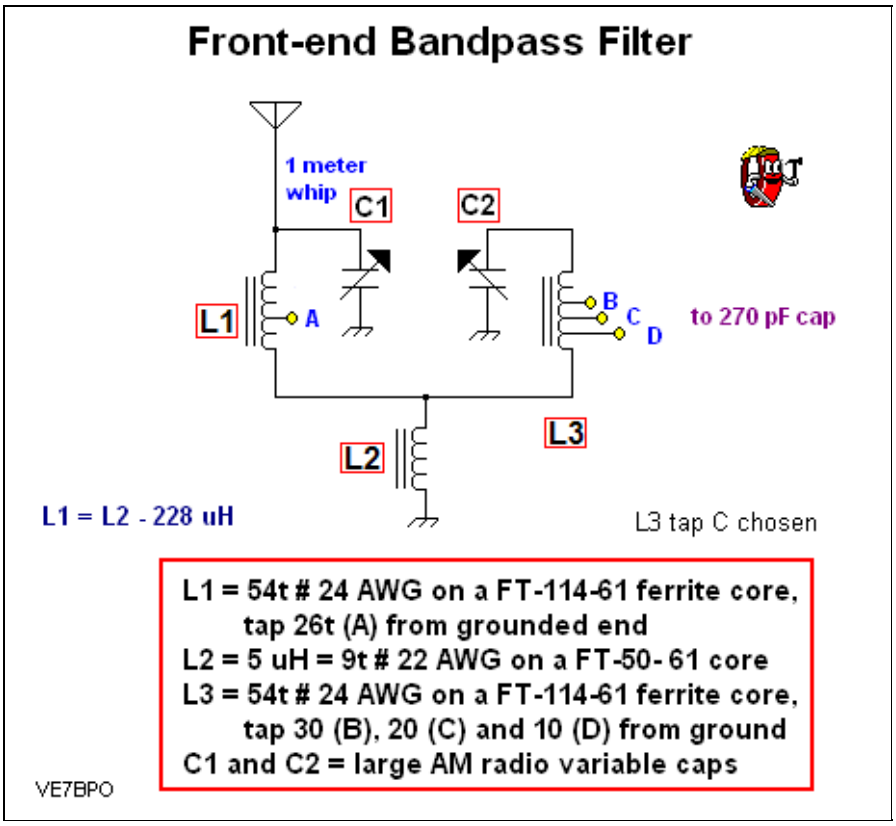

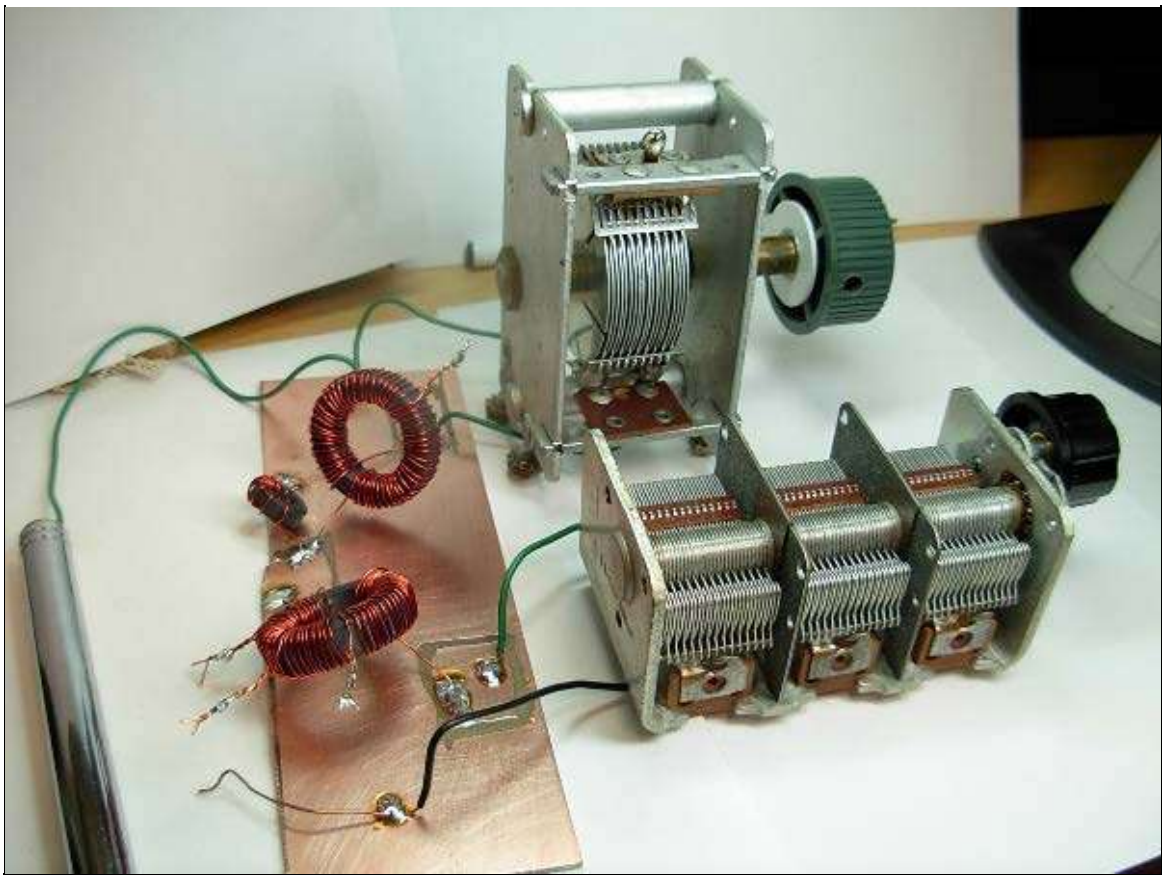

Shown above are 2 photographs of the band pass filter breadboards. The 2 variable capacitors had a variation of ~ 24 to 500 pF. There is considerable interplay between the 2 capacitors. For my QTH, it was better to peak C2 first and afterward to peak C1. Consider that L1 and L2 have a hot end and a grounded end. The antenna is connected to the the hot end of L1. Predictably, when substituting the L1 center tap as the antenna connection, the selectivity of the L1-C1 tank is increased and the sensitivity or received signal strength is reduced. This also occurs when testing the various tap points on L3 to feed the RF amplifier-detector stages. In the final circuit, I settled on Point C, 20 turns from ground. Using Point D, reduces sensitivity and increased selectivity. The opposite is true when using Point B. You the builder, have to determine which L1 and L3 connection points to use based on your own experiments and local factors. You may also change the receiver sensitivity by making changes such as increasing or decreasing the 270 pF coupling capacitor value, the emitter degeneration on Q2, or the detector bias.

Band pass Filter Analysis

It is impractical to sweep a BCB band filter using variable capacitors, so some analysis using GPLA, a program that ships with EMRFD was used to plot and better understand the double-tuned band pass filter response. A worst case inductor unloaded Q of 200 was used, but I imagine that the actual Q of L1 and L3 is much higher. For the source impedance, 100K ohm was used conjecturing that a short whip antenna at 1150 KHz would have a very high input impedance and not load down the L1 inductor. In reality, it is likely the antenna input impedance might be closer to 1 Megohm, however, I am using the worst case scenario. If the filter performs better than simulated - all is great! Higher source and load impedances and higher unloaded Q inductors would decrease the bandwidth of this filter which is desirable.
Note that I am concerned that L2 at 5 uH may may overcouple the 2 tank circuits. I did not see a double humped response on GPLA analysis, however, experimentation with L2 may be in order for the more astute homebuilder. You might consider lowering the L2 value to 3 or 4 uH and performing some testing. The load impedance for L3 was rather arbitrarily chosen. Considering that various taps on L3 may be used, the XC of the 270 pF coupling capacitor and the input impedance of the RF amplifier, I just chose 47K as the L3 load impedance. Below are 2 screen captures of GPLA plots. The top graph is the double tuned band pass filter and below it is the single tuned band pass filter consisting just of L3 and C3.
These graphs lead to 2 main conclusions:

1. The final band pass filter design appears to be reasonably sound.
2. We can understand why I could not tune in a single radio station with just L3 and C3 as the band pass filter; the filter skirts are not very steep and the second unwanted station was also amplified and detected.

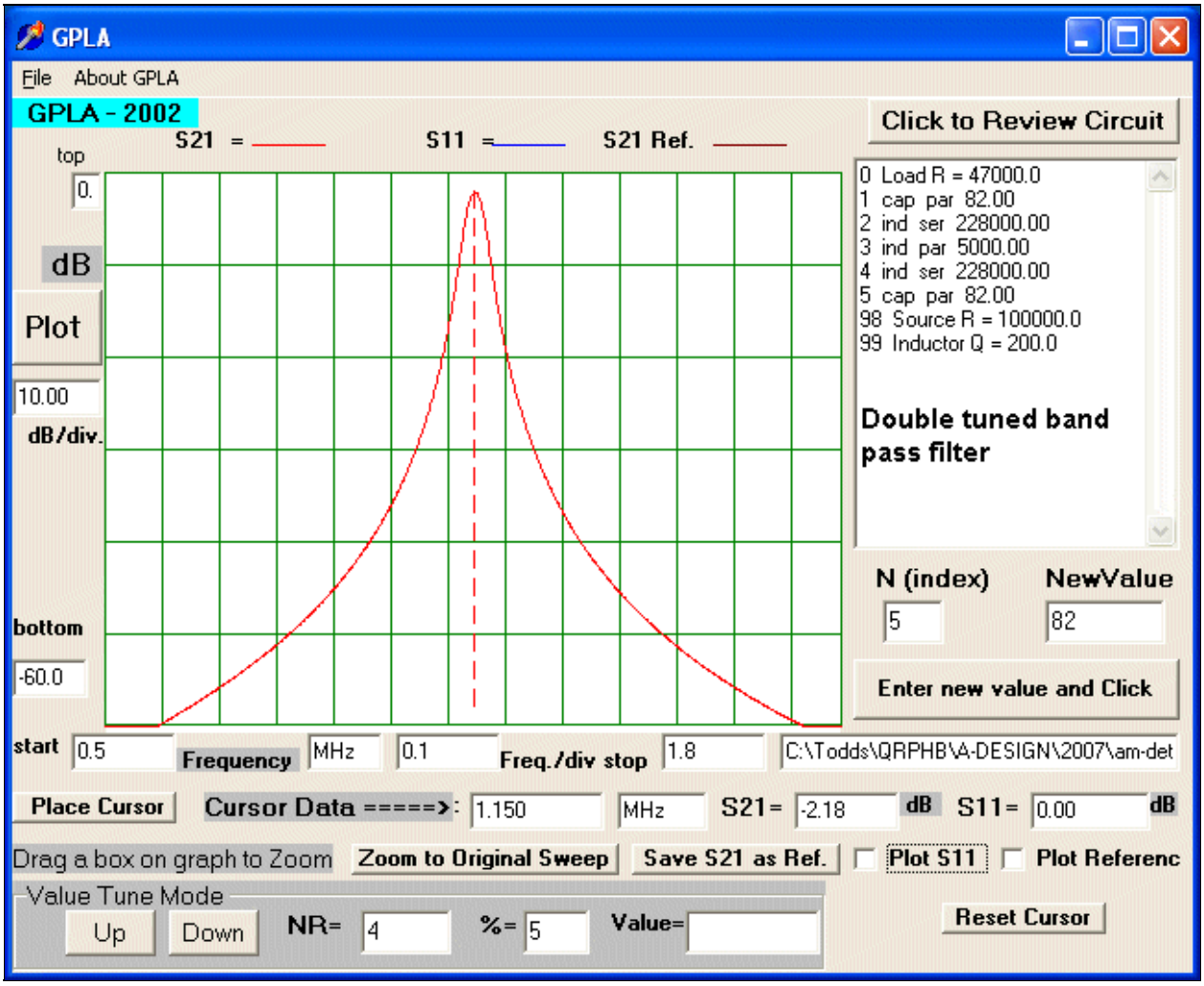

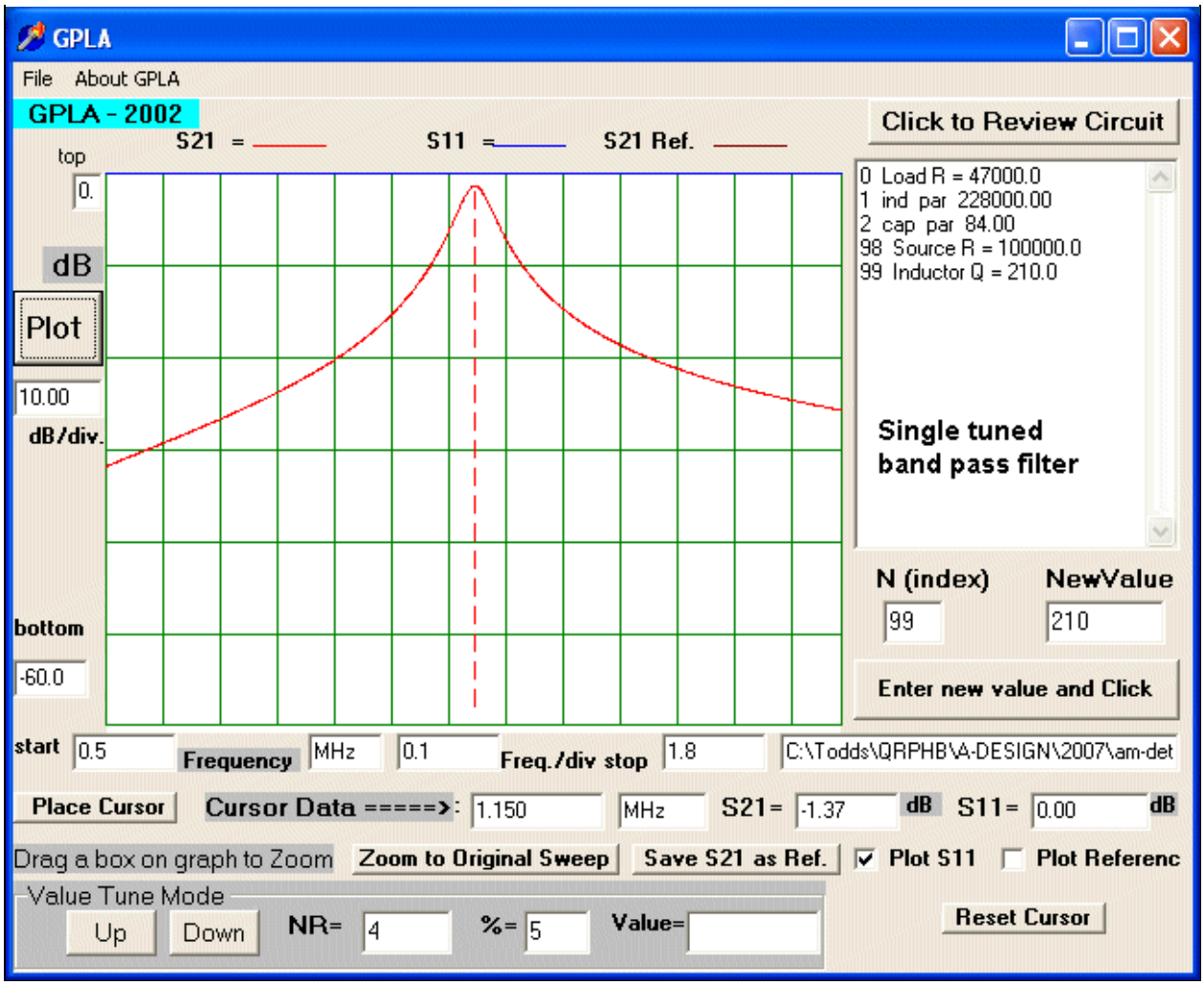

Varactor Tuned Front-end Filter

On November 11, 2007, I decided to investigate whether or not variable capacitance or varactor diodes could effectively replace the air variable capacitors in the band pass filter. In my parts cabinet were several MVAM -109 which is an obsolete but still readily available part. Another varactor, especially designed for tuning AM receivers is the 1SV149. This varactor is manufactured from Toshiba and is also appropriate.

While not comparable to the Q of 300 or greater of a good quality air variable capacitor, varactors are smaller, cheaper and can be easily ganged together so that only 1 potentiometer is required to tune the front-end filter. To the right is a photo of the varactor tuned front-end filter breadboard.

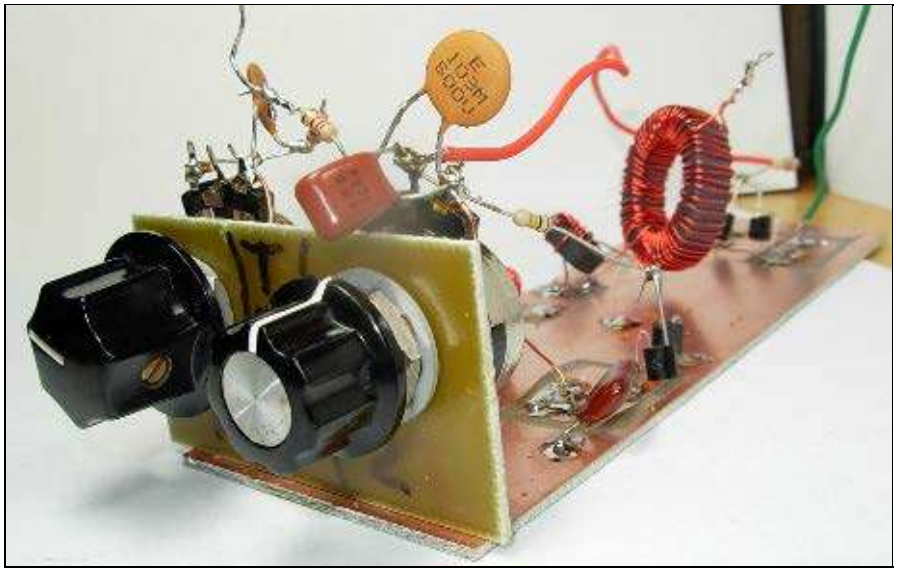

To the left is the schematic of the varactor tuned front-end band pass filter. The air variable capacitors were unsoldered from the original filter breadboard and a small board drilled and fitted with two 250K potentiometers was soldered to it.

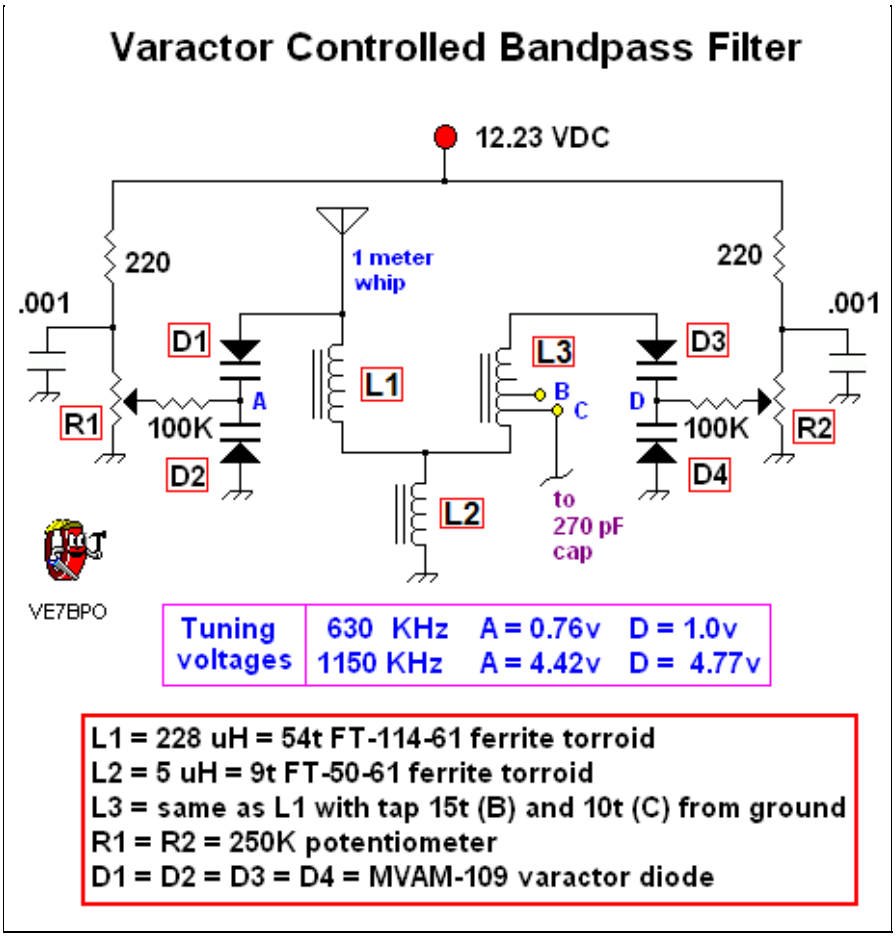

L3 was also modified to have taps at 10 and 15 turns from ground. I conjectured that since the varactor diodes have less Q than their air variable cousins, it would be wise to tap down on L3 to try and increase the selectivity of the L3 tank circuit. In the end, I used the tap at 10 turns from ground for my receiver as signal strength was still acceptably strong. You may choose to use the tap at 15 or some other point to suit your local selectivity/sensitivity requirements.

I was able to tune in single stations as I previously did with the air variable capacitors. Tuning is "touchy". Ten-turn pots would be a better choice, however, are not very frugal for such a project. You get used to tuning with conventional potentiometers after a few minutes or so. I measured the reverse voltages required to tune the 2 main local AM radio stations and they are tabled in the schematic. The L1 tank requires slightly more capacitance to resonate than the L3 tank. Thus it takes a little less applied reverse voltage to the varactor pair resonating the L1 tank compared to the varactor pair resonating the L3 tank .A side view photograph of the varactor breadboard is shown directly below. The component leads have been kept long so that I can recycle parts from experimental project to project as possible. This helps contain costs. Shorter lead lengths and proper lay out should be pursued in any final projects you build.

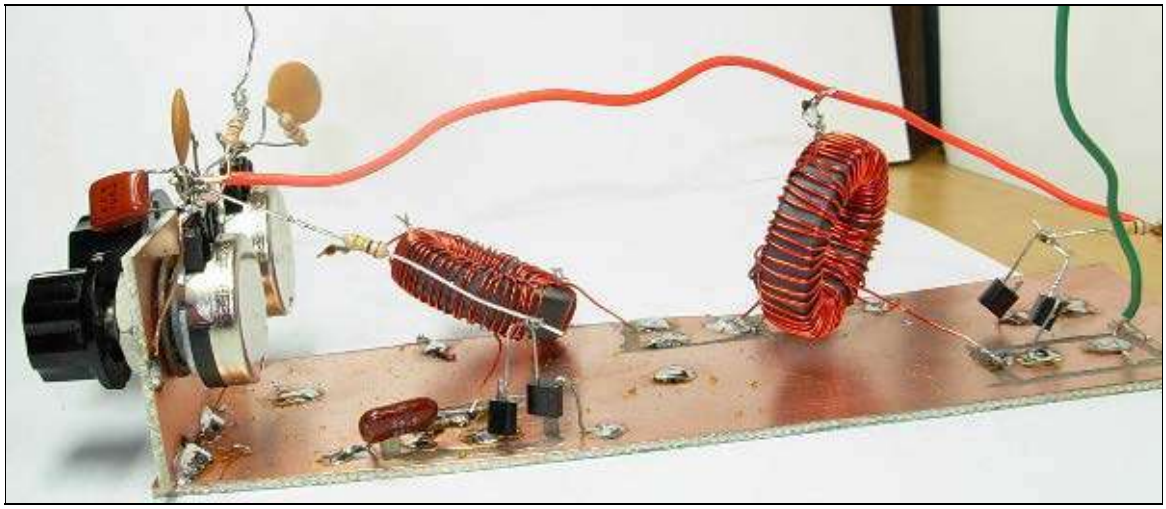

Single Varactor Tuned Front-end Filter

Tuning with a single potentiometer ganged to both varactors is easy to do after learning from the experiment above. All that is required is a method to compensate for the differences in capacitance between the the 2 LC tanks. I placed a high-Q (Q=300) variable trimmer capacitor in parallel with L1. By listening to the receive signal strength and tuning in one radio station using the potentiometer, I was able to peak CV for the strongest signal. I did this for both 650 and 1150 KHz and actually unsoldered CV and measured its value with a capacitance meter. The CV value was ~ 6 pF for both frequencies. I decided to replace CV with a fixed 5 pF silver mica capacitor and left it there in my final filter version. Your results will probably be different. I suggest just leaving CV

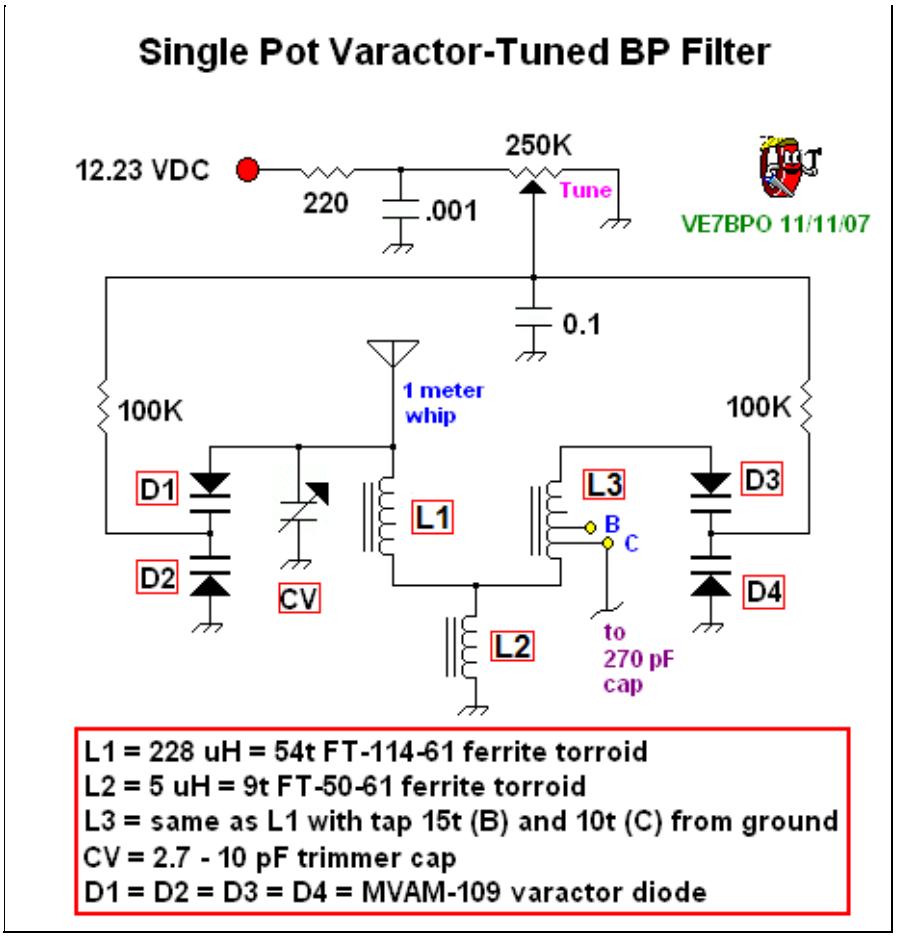

and using this trimmer cap to peak the signal once you have tuned a desired radio station with the main tuning potentiometer. An alternative to using CV is to vary L1. You could try compressing the number of L1 windings to allow tracking of the 2 LC tank circuits.

For the varactors, I used back-to-back VVC diodes as opposed to just a single varactor to resonate each tank. This was done in an effort preserve the highest varactor Q possible. The RF voltage of the AM RF signal may be high enough to forward bias a single varactor during a portion of the AC signal and degrade Q. This does not happen when back-to-back diodes are used. Almost all high-grade FM tuner schematics I have seen use back-to-back varactor diodes in their various ganged, tunable band pass filters. The major drawback of back-to-back diodes is your tuning range is reduced because you now have 2 capacitors in series. Experimentation may be required to achieve the BCB band-spread that you desire. You can add another pair of varactors in parallel or add some parallel fixed capacitance or even change the L1 and L3 inductance values for example.

This receiver tunes nicely and sounds fabulous. Last evening I was able to tune in 5 different AM stations, however, other than the local 2 radio stations, the others were quite faint. This is not bad considering this receiver has only 1 RF amp and a 1 meter long antenna. This band pass filter could be adapted as a pre-selector for AM radio reception. To match 50 ohms, lower L1 and L3 tap points could be chosen or a few links of wire may be wound around the inductors.

In the photograph below, you can see the 5 pF capacitor soldered in parallel with the MVAM-109 pair associated with L1. The antenna also connects to the ungrounded end of the 5 pF capacitor. Below in the last photograph; since only one potentiometer is used for tuning, a large knob was screwed on to the pot control shaft to make tuning a little easier. The solder-laden 220 ohm resistor is the connection point for the regulated 12.2 VDC. The 220 ohm resistor on the left has been cut from the 12.2 VDC connection point so 0 voltage goes to the left potentiometer.

Final Thoughts

I emailed Wes, W7ZOI and asked him why it is better to inductively couple a tuned circuit which use air variable tuning capacitors. Wes wrote his answer in the form of a complete web article entitled Coupling Methods in the Double Tuned Circuit. Big thanks Wes! From his summary, when the inductors used to resonate each tuned circuit are constant, and inductive coupling is used, the coupling of the resonators will remain constant as the variable capacitors are tuned across the band. Please download and study his web article for it not only discusses coupling in the double tuned circuit, but provides some insight into using his LadBuild and GPLA software from EMRFD.

Junk Box NDB Low Pass Filter

Introduction

With winter approaching, many HAM and SWL hobbyists find intrigue in tuning in NDB or **N**on-**D**irectional **B**eacons. Although the tunable NDB band depends on your location, in Canada it may be found in a band ranging from about 190 to 535 KHz. Canadian beacons either have just a carrier (no offset)or are tuned using the USB with about a 400 Hertz offset, however, different offset frequencies and certainly LSB are used when receiving DX from other countries.

Less than 10 Km away from my QTH is a 10 KW AM radio station at 1150 KHz. On my test receiver, the S-meter reads off the scale (> 60 dB over S-9) when tuned to this frequency. This local radio station causes spurious, second-order intermodulation products (direct mixing) that all but wipes out some weaker NDB stations that I am trying to tune in. Certainly, having a 500 Hertz crystal IF filter is useful, but attenuating this local QRM is also desirable and is the topic of this web page. Many general coverage receivers offer limited or in some cases no filtering of the NDB band, however an outboard filter is an easy project to build in one afternoon.

Update Oct 11, 2010: Here is a link to a version of this project built by Robert, K5TD

Project Schematic

To the left is the project schematic. It seems odd to build a low pass filter to reduce BCB interference (as usually a high pass filter is required for this purpose at HF) however for NDB, an aggressive low pass filter is required. For simplicity sake, a 7 element Chebychev low pass filter was chosen. Since it is easy to wind reasonably high-Q inductors for 10 uH and greater inductance using number 61 material on a ferrite torroid, the FT50-61 core was chosen for all of the inductors. Number 22 gauge wire was used for the coils to keep the unloaded Q as high as possible. The FT37-61 ferrite is also suitable, but will have less Q and require smaller gauge wire. Use 19 turns instead of 17 for the 20.2 uH and 21 turns instead of 19 for the 24.1 uH coil. Do not use number 43 material ferrite cores.

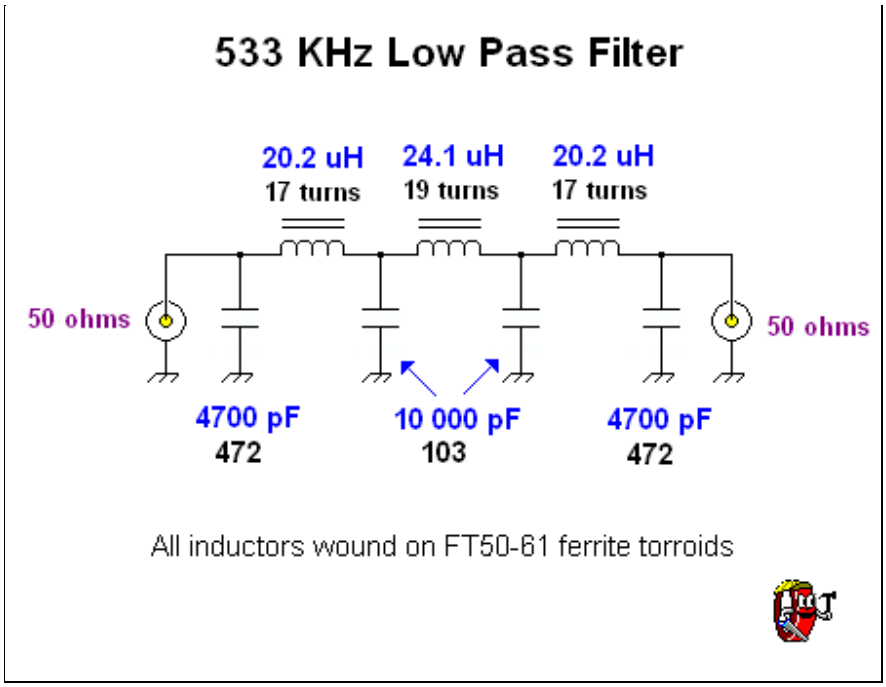

Components

I do not stock RF capacitors greater than 2200 pF, so junk box ceramic capacitors were used to build this filter. In fact, this design specifically uses more common, standard value capacitors to reduce cost and to not have to order in parts. Certainly, the astute builder could use higher quality capacitors or even large powdered iron torroids instead of the ferrite cores for inductors if higher performance is desired. Try to use high Q capacitors if you can find or are purchasing them. Poly or silver mica caps would be great choices. You can substitute a 5000 pF capacitor for the 4700 pF called for in the schematic.

To the right is a photograph of the components I used in the project breadboard.

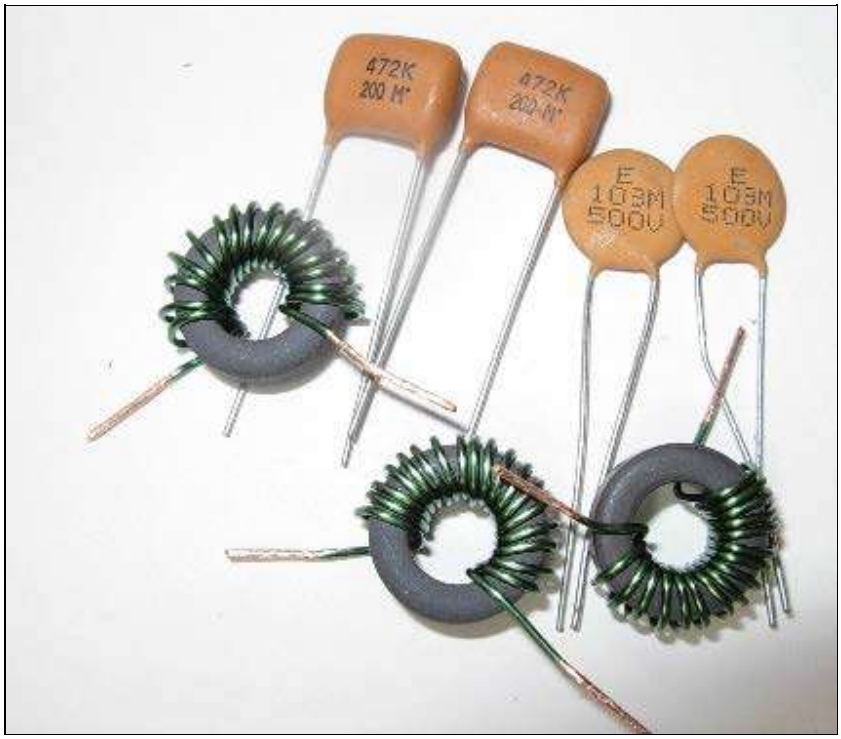

Breadboard

To the left is the completed project. Ugly construction as always, was used. The inductors were spaced at least 2.5 cm (1 inch) apart at right angles to try to minimize unwanted coupling.

GPLA Simulation

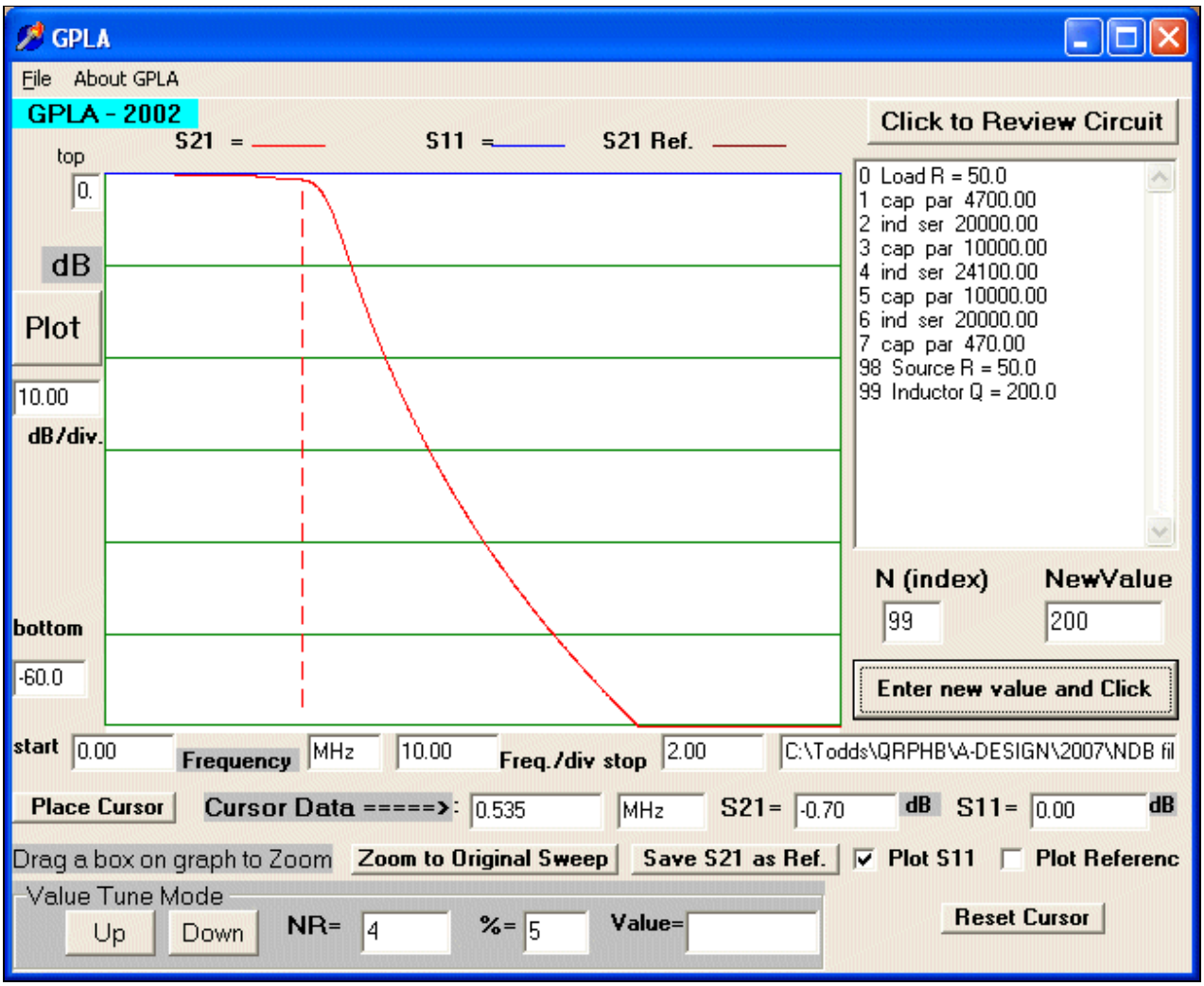

Above is the plot of the filter during simulation with GPLA. The simulation calculated an attenuation of ~46dB at 1150 KHz. At 1000 KHz the signal was 40 dB down, at 800 KHz it was ~24 dB down and at 630 KHz, the attenuation was only ~5.7 dB! Clearly this filter is not suitable if the offending BCB interference is from a station significantly less than 0.8 MHz. For my situation, this filter is acceptable. A 5 element Chebychev filter was also designed and plotted but was discarded as there was only 32 dB attenuation at 1150 KHz.
Since I wanted to tune as high as 535 KHz, the 533 KHz cutoff frequency was chosen. Additional work to help those with strong BCB interference at the lower BCB will be attempted in the future and presented on another web page.

Receiver Testing and Comments

Click on the picture to the left to hear the beacon YWB at 389 KHz with a 500 crystal hertz IF filter engaged on a borrowed Icom R-75 receiver. W7ZOI did some measurements on his R75 receiver S-meter using a signal generator and step attenuator. From S9 on up to 60 over, the steps were very accurate. However, below S9, correlation was poor. The built in attenuator is -20 dB when engaged. On my test receiver, I did some A/B testing with the filter in or out. For 1150 KHz (without the low pass filter) I had to engage the receiver's attenuator as without it, the S-meter reads off scale. With the attenuator engaged, the S-meter reads 50 dB over S-9 when tuned to 1150 KHz.

With the filter connected between the receiver and the feed line, (and the attenuator engaged) the S-meter read S-9.This is a drop of about 50 dB at 1150 KHz which means that this filter pretty much works as designed. I love the Icom R75 receiver; it is good value with it's many features in a compact package. Further testing was undertaken on other frequencies.

When listening to **WWV**; At 2.5 MHz, without the filter, the S-meter read S-9. With the filter inline, I could not hear WWV or see any S-meter reading. At 5 MHz without the filter, the S-meter read was at 20 dB over S-9. With the filter inline, I could still hear WWV very faintly, but the S-meter did not register. There was little noticeable attenuation at less than 700 KHz when using this filter.

Additional Photos and information

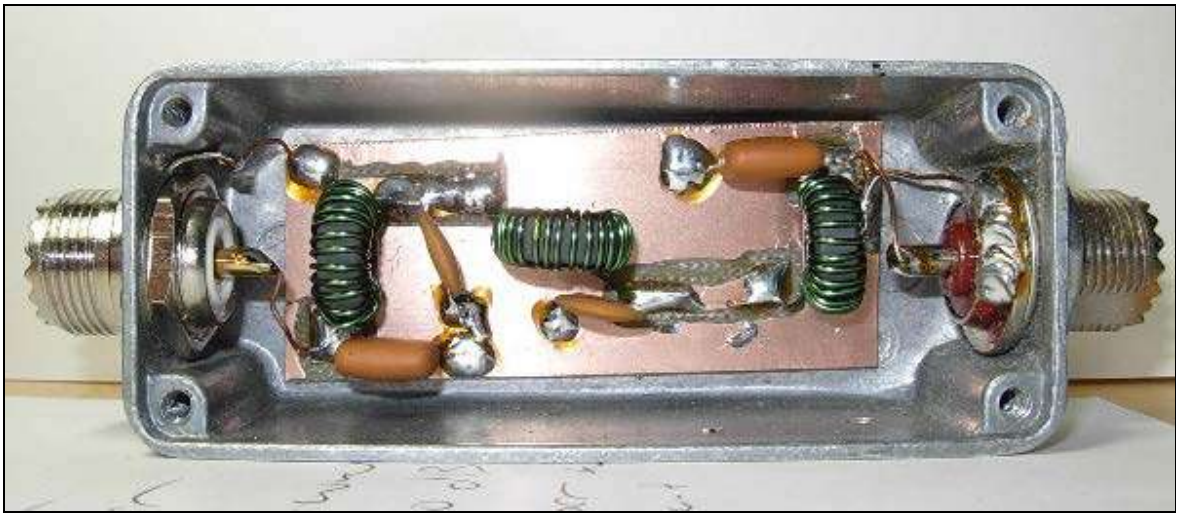

Shown above is the completed project in a Hammond die-cast case with SO-239 connectors at each end.

Shown above a photo of the Skookum beacon SX. It is on 389 KHz. This NDB is located in Skookumchuck BC, Canada

Links

My friend and fellow NDB enthusiast, Ken, VE7KPB has a posting on his web site showing some of the beacons he has logged from his QTH. Consider trying some of these frequencies from your own QTH to get used to finding beacons. Note you must temporarily allow pop ups to see his excellent log.

We recommend this non-directional beacon search and log utility program called WWSU from VE3GOP It must be registered and is a wonderful low cost tool.
I was near beacon L in Balti, Moldova (Балти, Молдова) in 2006. Below is a snippet from the VE3GOP program showing beacon L and also some nearby beacons. (Я изучаю русский язык). Приветствую Вас дорогие друзья!

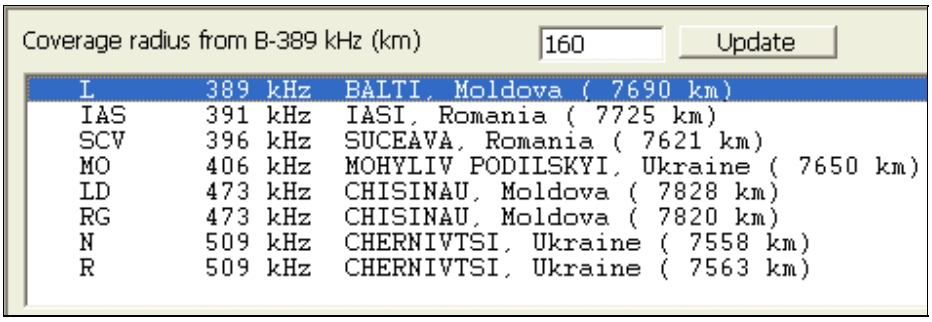

Martin Francis has an excellent NDB web site including the free program called NDB WEBLOG for a number of platforms

Some beacons may be located using this NavAid web site

Clint, KA7OEI has an informative web site regarding NDB listening including using digital computer processing to dig out weak signals. This is also a great overview site for newcomers to NDB.

Conclusion

To the right is the outcome when I connect my frequency counter directly to my antenna coax cable feed line. 1150 KHz is my nemesis frequency! Happily it can be tamed with a little filtering to allow NDB listening and logging.

To the right is the outcome with my SWL antenna coaxial feed line connected directly to the scope. The scope was on the 0.5 volts per cm scale, so the peak to peak voltage is 0.2 volts. In just about any high-gain audio amplifier I build, if I touch my finger to the input, I can hear AM 1150 loud and clear - no wonder!

Good luck with your own NDB adventures!

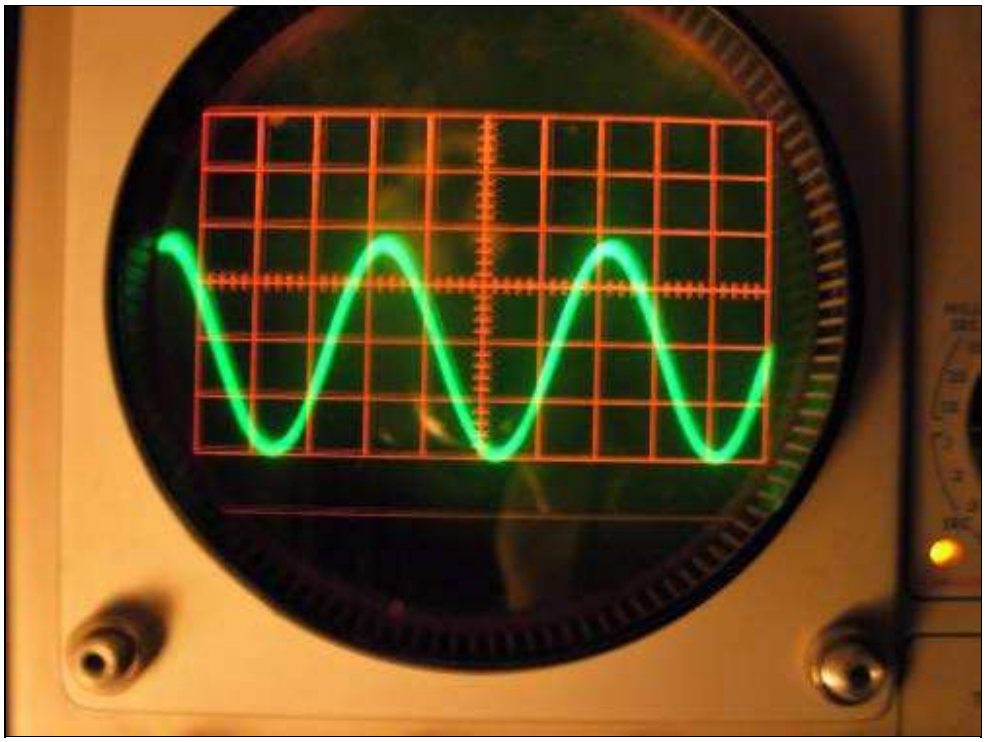

More NDB Information and Circuits

Introduction

Latest Update: December 3, 2012

This web page holds a collection of NDB-related ideas, experiences and hopefully will include some feedback from fellow NDB enthusiasts.

I devoted a new notebook to this topic and hopefully with inspiration from band listening and communicating/learning from others, I will fill it over time. New content will be added to the bottom of the existing material as QRP-Postadata

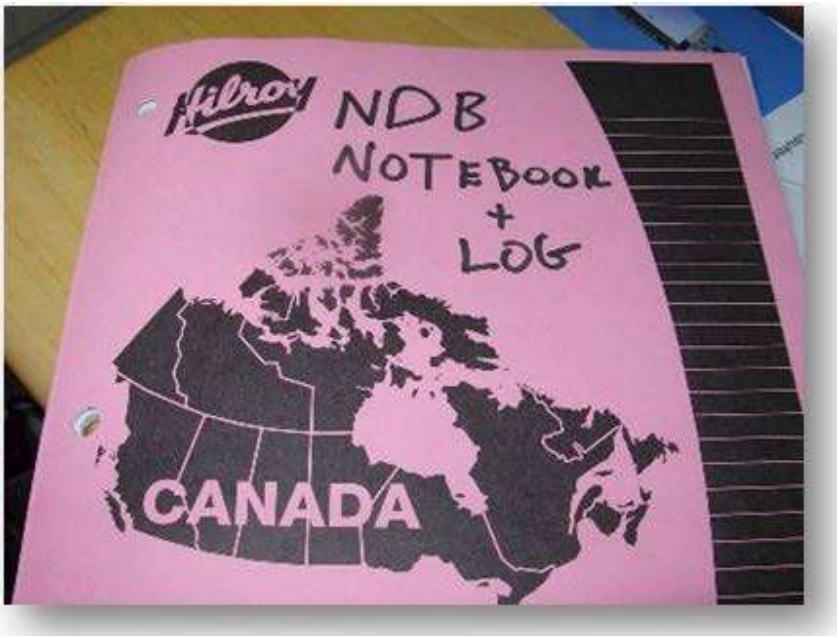

Improved NDB Chebyshev Low Pass Filter

A popcorn or "junk box" low pass filter was designed and presented on this web page. After discussion with VE7TW and testing a Realistic DX-300 and other receivers, it became apparent that even more attenuation of a strong local BCB station at 1150 KHz was desirable. In addition, there are other moderately strong AM radio stations from 630 to 800 KHz (especially at night time) which maybe causing mixer intermodulation distortion products. A fault of the junk box low pass filter is poor attenuation below 800 KHz and a better design was a prudent goal. Building on the learning obtained from the junk box filter experiments, an improved 7 element Chebyshev low pass filter was designed and is presented directly below. The 3 dB cut off of this filter is calculated to be 526 KHz. This is the filter that I now use for my home radio station. At my

nemesis frequency of 1150 KHz (where a powerful local radio station broadcasts), the attenuation is calculated to be 68 dB. It takes careful layout and a conductive chassis to realize this level of attenuation, but the effort is worth it. In very strong AM BCB locations, you might consider placing 2 such filters in series between your antenna and receiver if required.

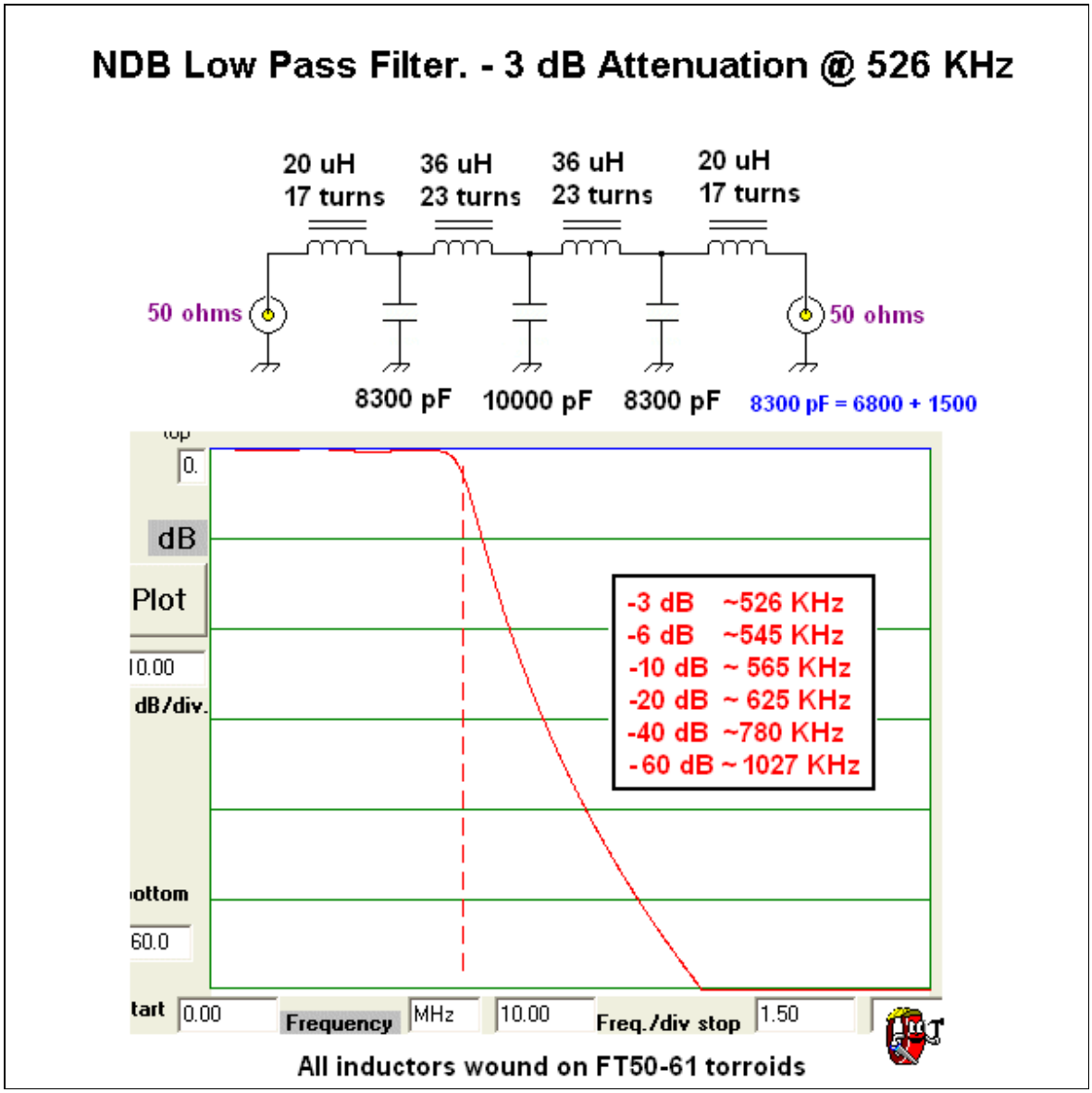

The schematic and simulation of the improved NDB low pass filter is shown above.

Non-directional Beacon Identification

It is interesting to visit nearby beacons. In the photograph to the right is XC which broadcasts at 242 KHz.

I have learned that it is very important to confirm the NDB stations your hear via a database or list. What you hear on the air should match the database/list for **both** call sign and frequency, else suspect that you may have copied it incorrectly. **RNA**, the definitive signal list for North and Central America plus Hawaii may be found here.

Three Questions

Steve Ratzlaff, AA7U is an experienced NDB DXer and has been listening to beacons since the mid-1980's.
I asked him the following 3 questions:

1. LF beacons do little more than send their station identification in Morse code, are mostly low power and generally might be perceived by some people as boring and low tech. Yet, on the World Wide Web, one finds numerous web sites, software, projects and commercial equipment all passionately dedicated to NDB listening. What's all this fuss about listening to beacons?

Steve: It's a hobby that requires quite a bit of skill and technical accomplishment to get the most from the equipment. Most folks have AC noise to deal with, which can be particularly bad at LF. Finding an antenna that works at LF and that can be used at your own location can be a major task; finding a radio that has decent LF sensitivity, or an LF converter to use with an existing radio--all these must be detitle with just to begin hearing anything at LF. I find it to be quite a challenge. If it were easy to receive LF beacons then I probably would have lost interest years ago! It's true that in recent years several software programs have become available that allow finding beacons somewhat easier--one simply looks for them on the computer screen and decodes the dots and dashes of the beacon being received. This is quite popular among beginners and veterans alike. But the traditional method of aurally listening for the morse code idents of beacons is probably used more often, though many are combining both aural and software techniques now.

2. Let's say I live in a small city lot or even an apartment. I have modest equipment and/or not a huge amount of cash to spend on gear for NDB listening. From the antenna through to the headphones, what are some basic recommendations you might give to a newcomer wanting to get started in NDB listening?

Steve: The radio must have decent sensitivity at LF, or else an LF converter must be used. Due to high local AC noise, any type of LF antenna used indoors will be a poor substitute to one that can be placed outdoors. A few portable radios cover the LF NDB frequency range that will work for hearing local beacons, though the radio may need to be used outside to get away from AC noise. The discontinued Sony 2010 was the standard for portable radios for reasonable LF performance. Newer radios like the Degen DE1103 have been found to work reasonably well at LF and can be bought for well under $100 by mail order from eBay sellers; or the more expensive Kaito 1103 version, which has a warranty, can be obtained from several distributors like Universal Shortwave. The much more expensive semi-portable Eton E1 works well at LF, but is more in

the price range of a tabletop radio. The Icom R75 is currently the best bargain in a tabletop radio that has very good LF sensitivity as well as 1 Hz tuning, which is an asset if a narrow external audio filter is used. I'm not too optimistic about what someone living in an apartment or high rise building might do to successfully receive LF beacons indoors. Often the AC noise level is too high to be able to use an indoor antenna. But some have been able to use loop antennas indoors for the stronger signals. An example of a top of the line commercial loop would be the Wellbrook ALA1530 or LFL1010. Unlike at shortwave frequencies, where simply tossing a wire out the window to a nearby tree or other support, or even running the wire around the room inside, will usually work fairly well, at LF a wire less than several hundred feet generally doesn't perform very well. It can be argued that an active whip antenna makes a very good LF antenna, and doesn't take up much room, but it must be used outdoors. And if there are strong AMBCB signals, then the active antenna, either loop or whip, must have very good overload resistance otherwise it can generate distortion of its own from the strong BCB signals.

3. What kind of distances are considered DX for NDB?

Steve: NDB DX is pretty much a relative thing. One just starting out might be thrilled to hear a beacon from the next town, or from the other side of his own state or province. As one improves his listening setup and gains experience, then usually DX goals also expand to try to hear beacons farther and farther away. NDB DXing generally is not a competitive hobby, unlike amateur radio with its various competitive "contests". Each person's listening setup, local noise level, etc. is usually very different from someone else's, even someone in the same town or general area. One person might live in the suburbs and have a lower noise level than his friend who lives right in town and has a much higher noise level. One might have room to put an antenna in a quiet spot; the other might be limited to much less. People who live near an ocean generally have a much better chance at hearing something exotic offshore than folks living far inland. Folks living in the central or eastern part of North America have many more beacons available to be heard than folks in western North America. But there are always a few beacons that are much stronger than most, and can be heard from long distances of 1000 miles or more, pretty much anywhere in North America at night. One example would be 206 GLS in Galveston, Texas, which runs around 2000 watts, has a large antenna, and is generally readily heard anywhere in North America at night--that beacon might be 1500 miles or more away, and might be considered real DX. However another 25 watt beacon from the same general area in Texas might be hard to hear only several hundred miles from that beacon. So "DX" is pretty much a relative term. Ndblist, an international email list devoted to beacons, is open to anyone with an interest in beacons--members post their loggings there. What might be a local beacon to someone might be DX to someone in a different part of the country. All levels of experience are welcome.

Thanks Steve.

NDB High Pass Filter

A high pass filter using standard value capacitors was designed using GPLA. although, such a filter would not help AC line noise and RFI generated in the house, I suspected my antenna was picking up local noise from below the NDB band. This filter was mounted inside a die-cast Hammond box with a SO-239 at each end. I used 22 gauge enamel covered wire for the inductors. A photo of the filter is shown to the right.
For the 0.01 uF caps, I used junk box ceramic capacitors with a 20% tolerance, however, I did measure a bunch and found 2 within 5% tolerance for my filter bread board.

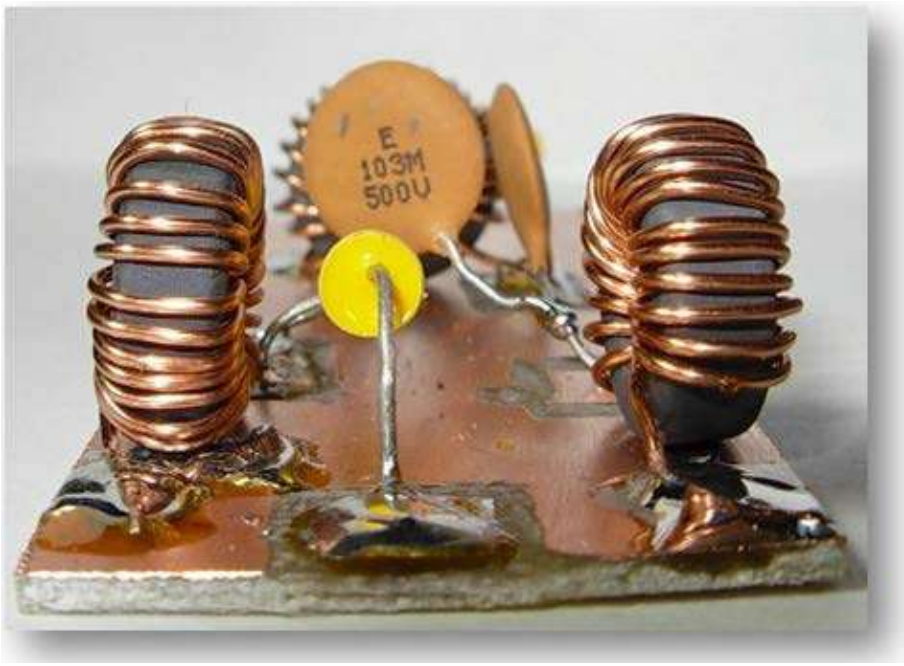

To the left is the filter schematic. This is an N = 7 Chebyshev high pass filter with a 3 dB cut off of 157 KHz. This cutoff frequency allowed the use of common, standard value capacitors and also even turns numbers to reach the desired inductance for the inductors when wound with FT50-61 ferrite cores.

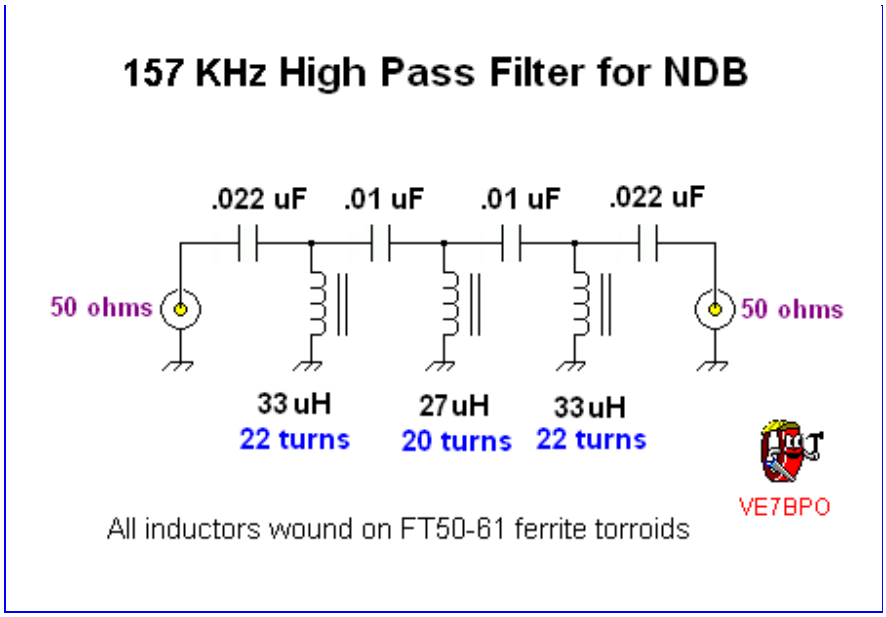

Use 5% tolerance, high Q caps such as polystyrene or NP0 ceramic and **not** junk box bypass-grade ceramic capacitors as possible. I used trashy ceramic caps for the 0.01 uF parts due to lack of better parts at the time of building and testing.

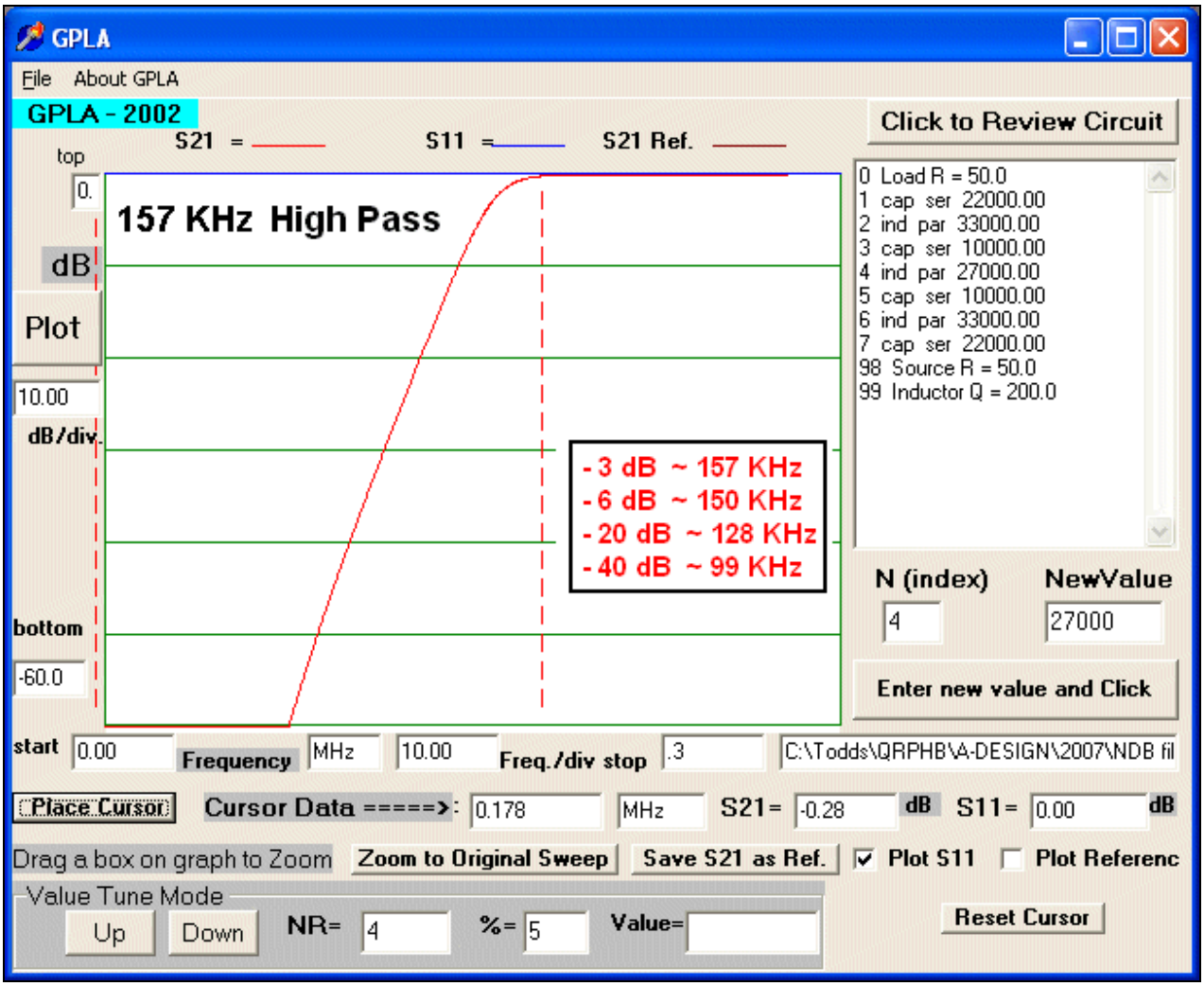

Above is the filter GPLA simulation. In particular, I have harsh noise from about 110 KHz on down. At 78 KHz, where this filter has a calculated attenuation of ~ 56 dB, I made an audio file of the band noise. This is in AM mode with the filter out for a few seconds and then in line. With the high pass filter in line, there is pronounced attenuation of the noise and my local 10 KW BCB station at 1150 KHz suddenly appears. Prior to this it was hidden by the harsh noise. At frequencies less than ~200 KHz (without my low pass filter) I can hear this BCB station intermittently as I tune around. I suspect that the R75 filtering down at 200 KHz and down is insufficient to stop this monster station.

At my QTH, using a high pass filter reduces some of the noise on the NDB band. At my location, a high pass plus a low pass filter in cascade between my antenna and my receiver results in less QRN and easier weak signal copying.

Long Wave Broadcast Radio Filter

I learned about LW Broadcast radio from Steve Ratzlaff. In particular, радио россий "Rah-deo RaSEE" (make sure you roll the R!) can occasionally be heard on the west coast and broadcasts at night-time using 500-1000 KW power. The frequencies he recommended to try were 153, 180, 189, and perhaps 171, 234 and 279 KHz. I have terrible problems with a local BCB radio station at 1150 KHZ that causes intermodulation distortion and/or blow-by detection at and below 200 KHz in addition to a terrible noise source at 78-120 KHz. Therefore, I built another cascade low pass/high pass filter and placed it in the same chassis as my regular NDB low pass/high pass combination filter for use when tuning LWBC and perhaps for when listening to frequencies less than 200 KHz.

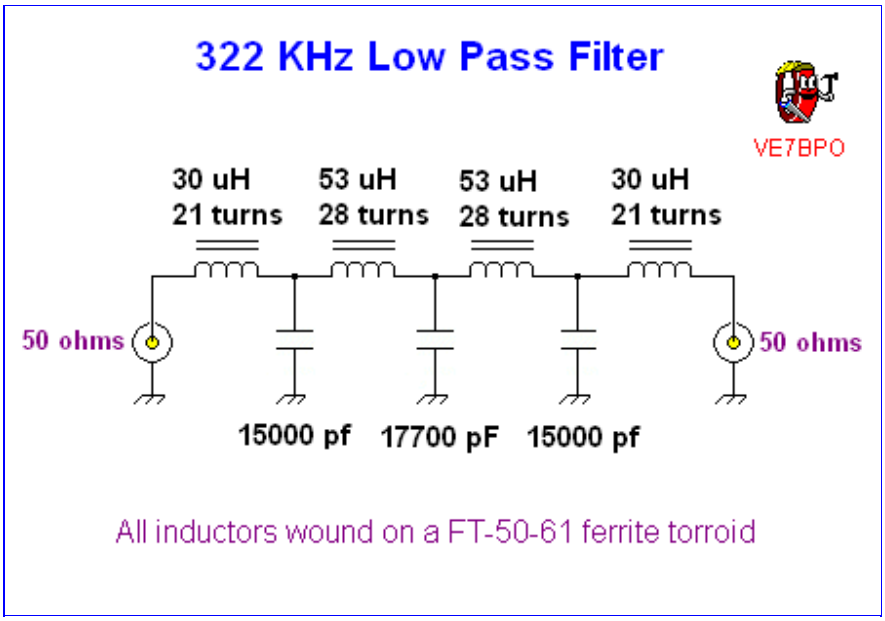

Above is. the schematic of the 322 KHz low pass filter. In the photograph above, you can see a 50 ohm pad at the input that was used only during testing. This filter offers a calculated attenuation of ~ 98 dB to my 1150 KHz interfering station. In reality it is not possible to achieve this level of attenuation, however, there is no detectable 1150 KHz signal interference with the filter in line which makes me happy. Click here to listen to the dramatic difference with regard to interference this filter makes at my QTH with my receiver tuned to 199 KHz. The receiver is set for wide band AM detection; first without the LWBC filter and then with the filter switched in. When the filter is switched in, the BCB interference disappears and a Canadian NDB (UAB @ 200 KHz can faintly be heard along with our cat meowing in the background. It is not possible to listen to LF without aggressive low pass/high pass filtering at my QTH.

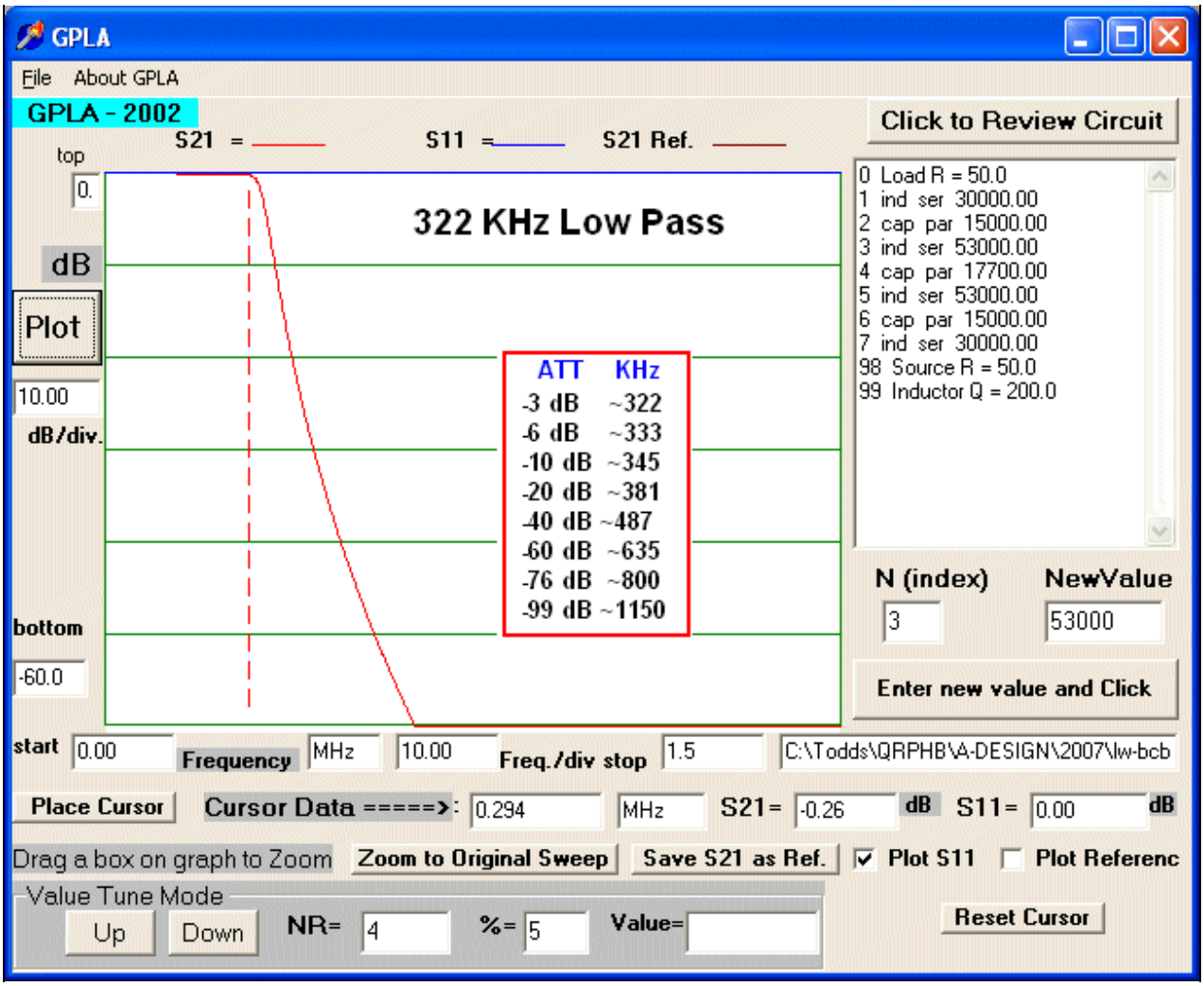

Above is the GPLA simulation of the LWBC low pass filter.

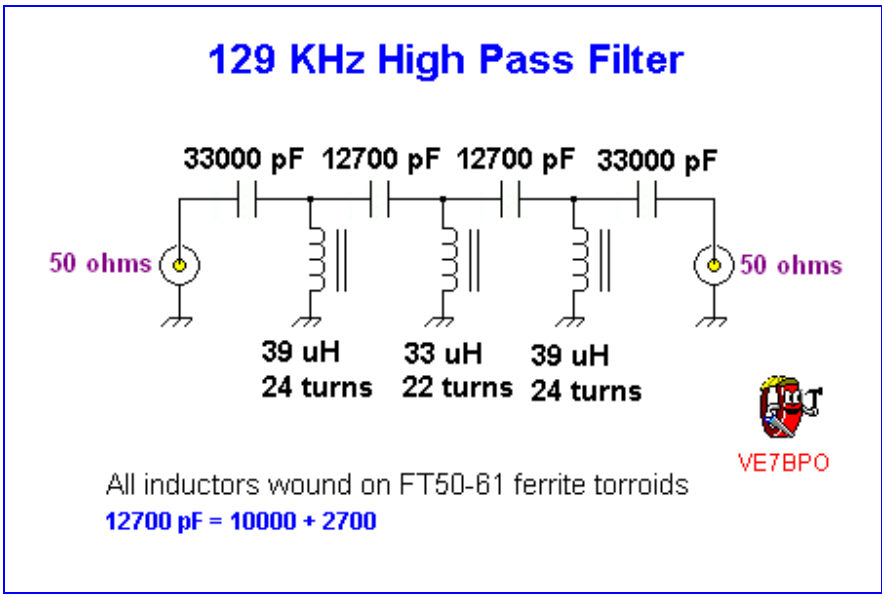

Above is the schematic of the 129 KHz LWBC high pass filter. In either of the 2 filters, capacitor values can be obtained using 1 or 2 standard value capacitors in parallel. The cutoff frequencies of both filters were chosen to allow using practical component values.

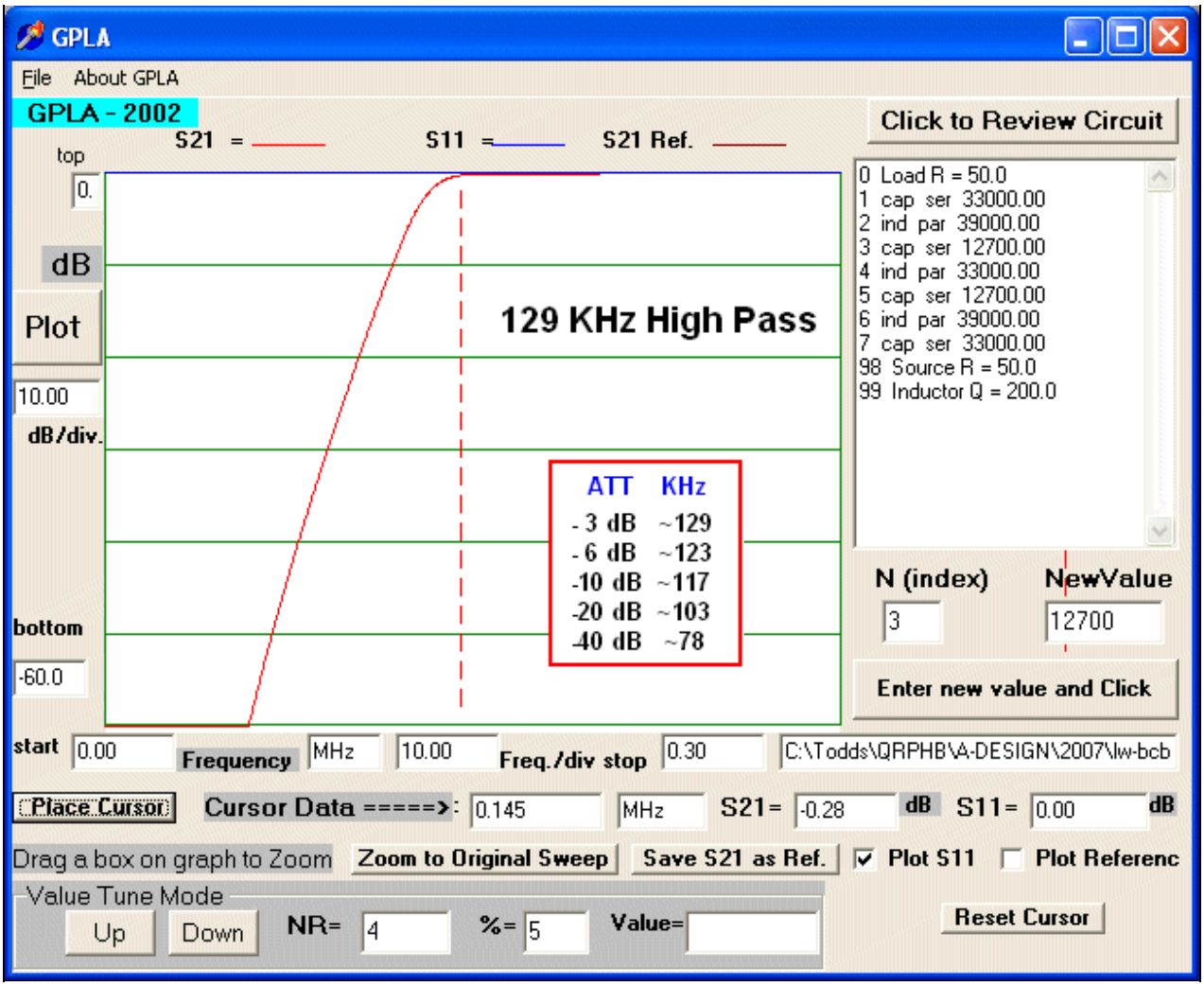

Above is the GPLA simulation of the LWBC high pass filter. The high pass filter might not be needed at your QTH. My LWBC filter has the low pass filter before the high pass filter. I.e. they are in series or cascaded.

Dual NDB and LWBC Filters

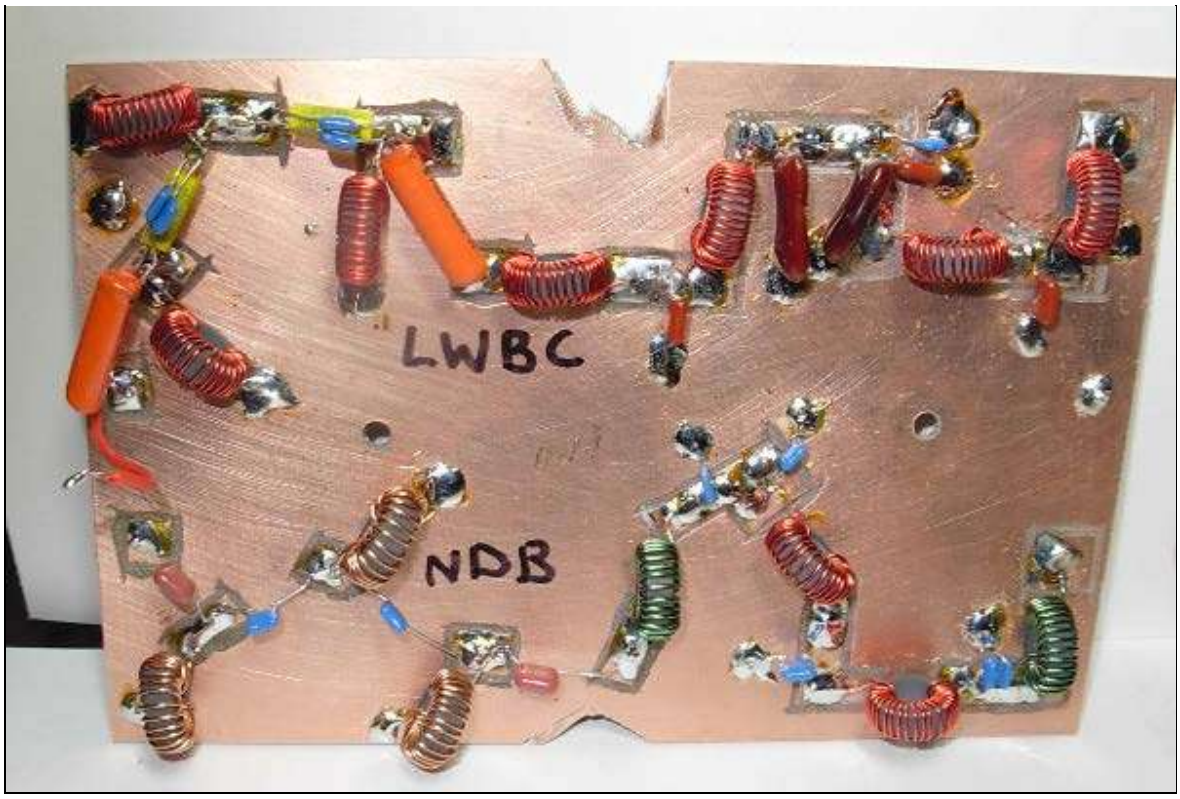

For use in my radio shack, I built LWBC and NDB filters inside 1 chassis with separate inputs and outputs. Some photos of this project are shown directly above and below. The NDB filter is the 526 KHz low pass filter in series with the 157 KHz high pass filter. The LWBC filter is the 322 KHz low pass filter in series with the 129 KHz high pass filter. High Q caps were used and the inductors were wound with either 22 or 24 gauge wire to obtain a relatively high unloaded Q. The large Hammond project case allowed reasonable spacing of the inductors and a nice long input to output layout.

Beacon XJ @326 KHz

Above is NDB XJ in Fort St. John, BC. Photo by VE7KPB in August 2008.

QRP — Posdata: NDB Low-pass Filter with Trap

An email from Rick, NU7Z spawned this 2012 addition.

Depending on their design, typical NDB low-pass filters provide less than 20 dB attenuation at 620 - 630 KHz, and if you hear a strong

station on this frequency — good luck!

Rick sought a filter with a trap at ~ 620 KHz — after mulling around, we encountered design problems with a trap frequency so close to the low-pass cut-off frequency and later asked Wes, W7ZOI if he might help design our filter.

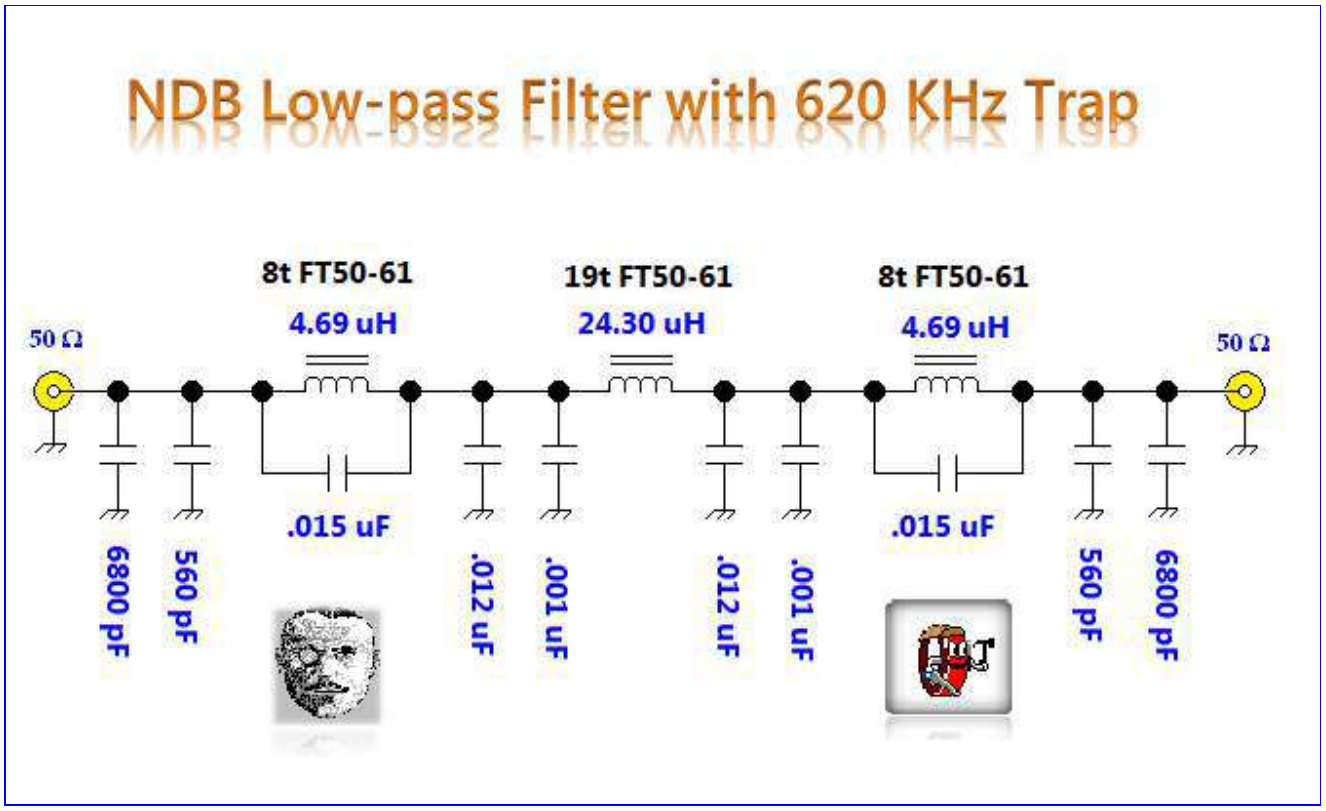

Above — My version of the Wes, W7ZOI designed NDB low-pass filter with a trap. **Red** filter below

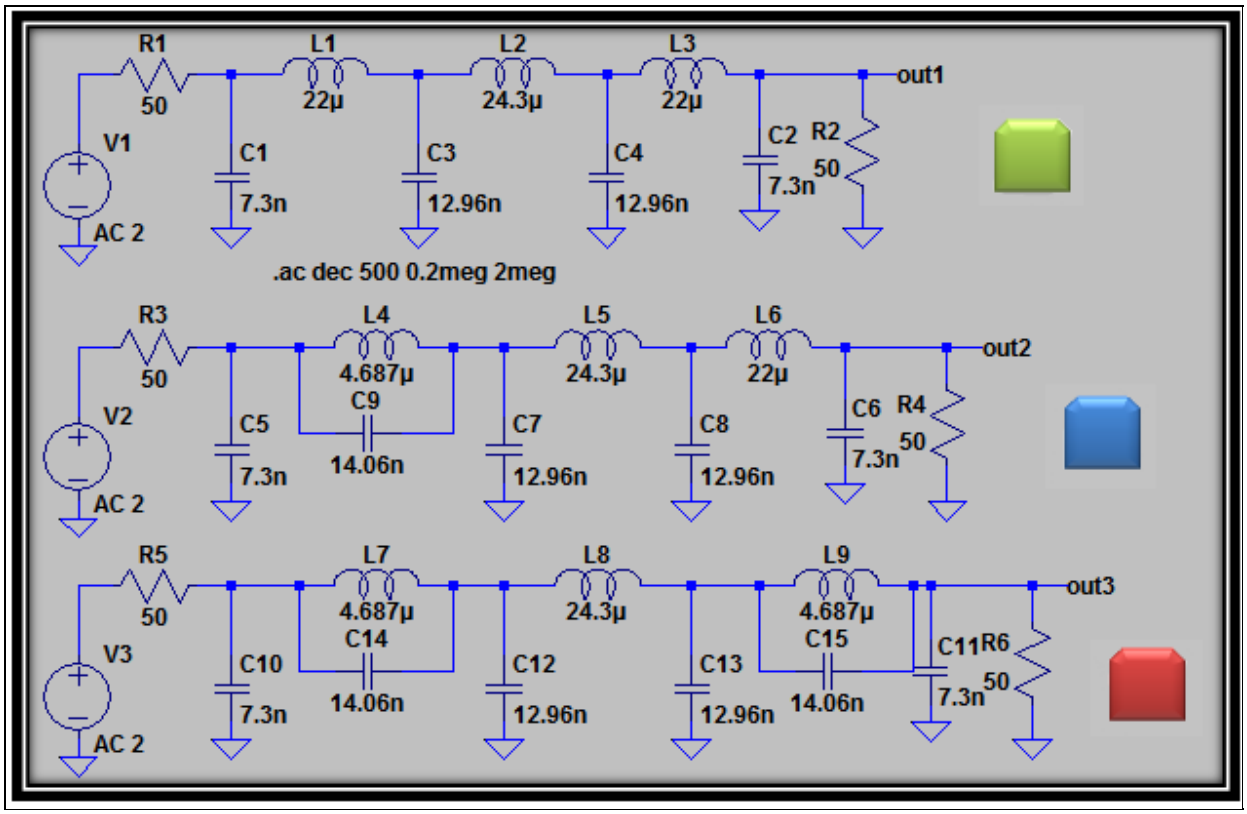

Above — A 7th order, 0.1 dB ripple **Chebyshev low-pass filter** with a 550 KHz cut-off filter evolved to include **1 trap**, and then **2 traps** at 620 KHz.

We learned that in simple situations, you may modify the elements of a low-pass filter so that the usual inductor is replaced by a parallel trap. See Wes' work in EMRFD Chapter 3; in particular, Figure 3.10.

Wes wrote he's employed this technique successfully before — for example, to add harmonic suppression to a simple output network for a QRP transmitter, although he hadn't added traps to higher order filters like the 1 we wanted. Click for a file containing the math contributed by Wes, W7ZOI.

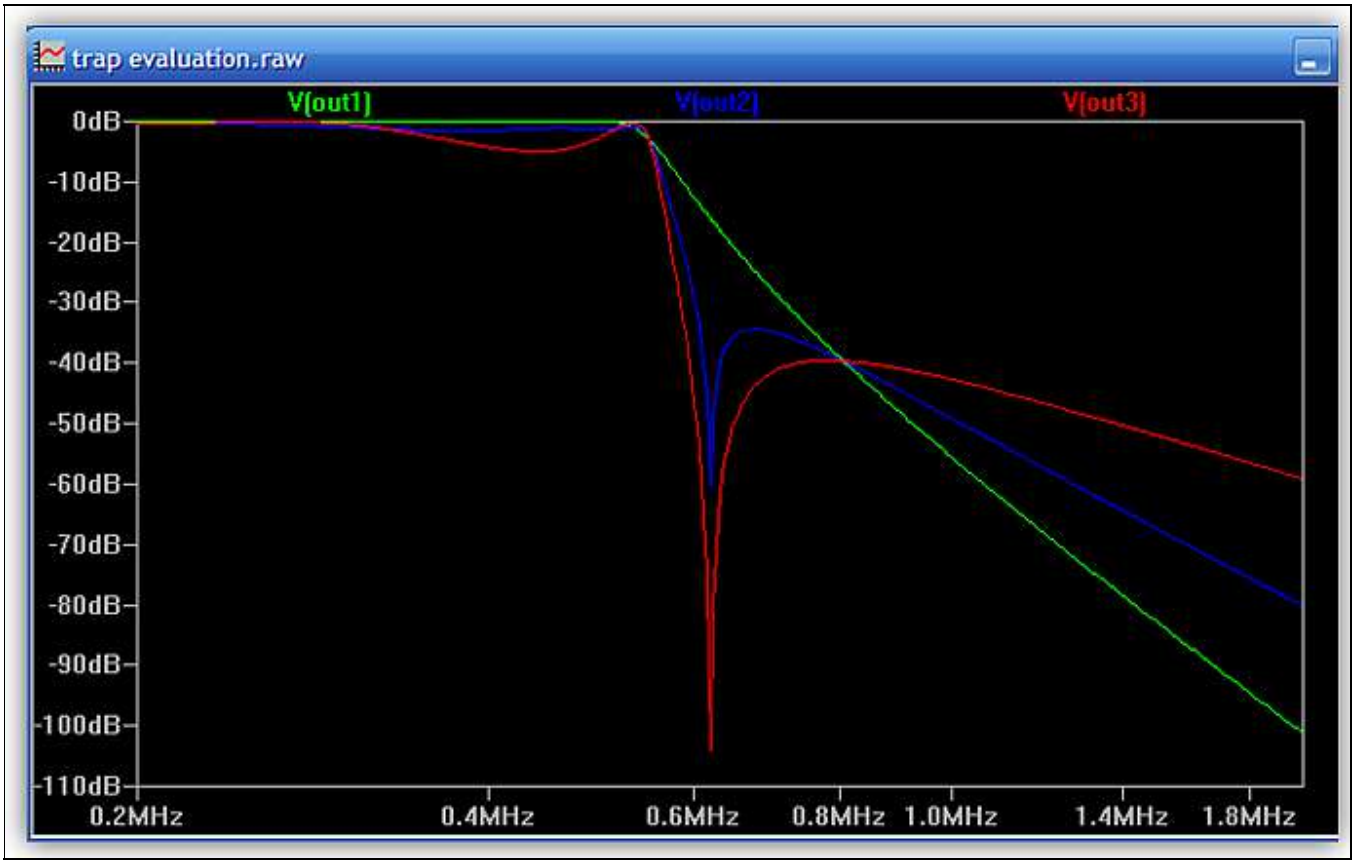

Above — The SPICE analysis of the 3 color-coded filters above. This design excludes the impact of finite L and C and the unloaded Q that could significantly affect function since the trap frequency is close to the low-pass cutoff frequency. These factors usually worsen the insertion loss near cutoff, but since we're using this filter in a noisy RF environment, filter misperformance should be tolerable.

In the future, Wes recommended designing an elliptical low-pass filter with software such as that distributed by AADE.

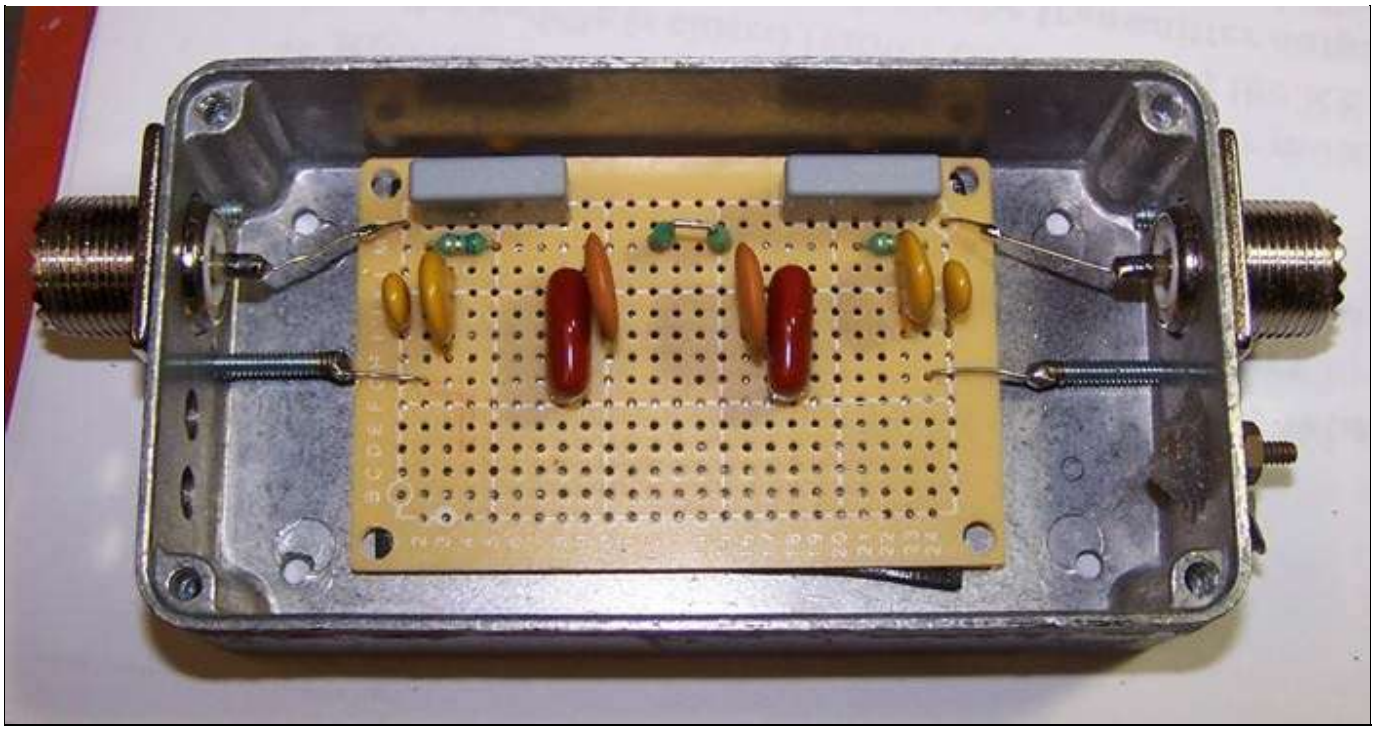

Above — A version of the filter built by Rick, NU7Z using epoxy-coated inductors for the L's. The insertion loss with these inductors = ~ 5 dB, although he runs a 40 dB receive preamp and can accommodate such losses.

Despite employing a loop receiving antenna, he could not listen around 500 KHz due to a loud, local broadcast station at 630 KHz. Inserting this filter reduced this 630 KHz signal from 40 dB over S-9 down to S-1 on his receiver S-meter.

Fantastic! Big thanks (большое спасибо) to Wes, W7ZOI.

---

440 Hertz Peaked Low Pass Audio Filter Experiments

Introduction

At audio frequencies, low pass filtering can go a long way to improving CW and beacon reception. It has a been a long time since I built one and therefore decided to experiment with some designs using the 5532 op amp. EMRFD has a great section on RC active audio filters starting at Chapter 3.5 and this is where I began. After some experimentation, I remembered a peaked low pass filter designed and published by Wes, W7ZOI in the 1970's. This filter became very popular in Russia after publication in a 1971 Russian Amateur Radio Journal. I asked Wes if he might design another low pass filter peaked for 440 Hertz, which is my favorite CW beat note frequency. This filter is intended for use as an out board headphone jack device for the Icom R75 or other receiver.

Base Project Schematic

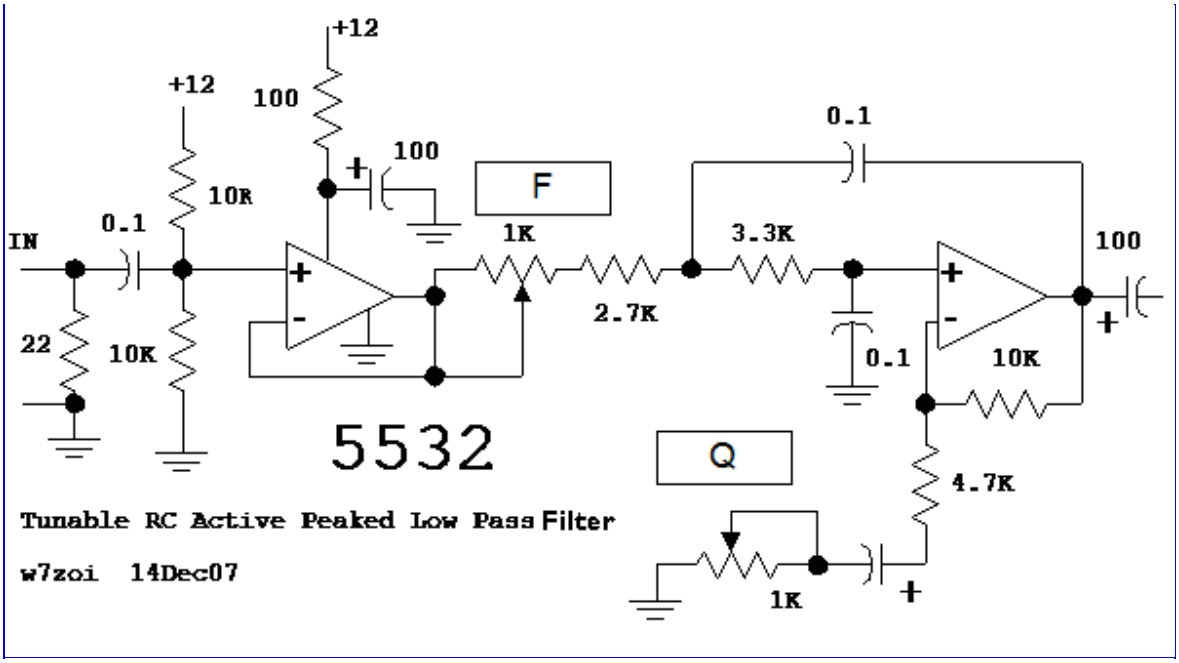

Above is the filter designed by Wes, W7ZOI. It has two 1K pots you can tweak; a subtle frequency control and a Q adjustment. It is theoretically possible to adjust the Q too strongly as to cause oscillation, although this did not happen with my bread board.

Schematic and Circuit Building Details

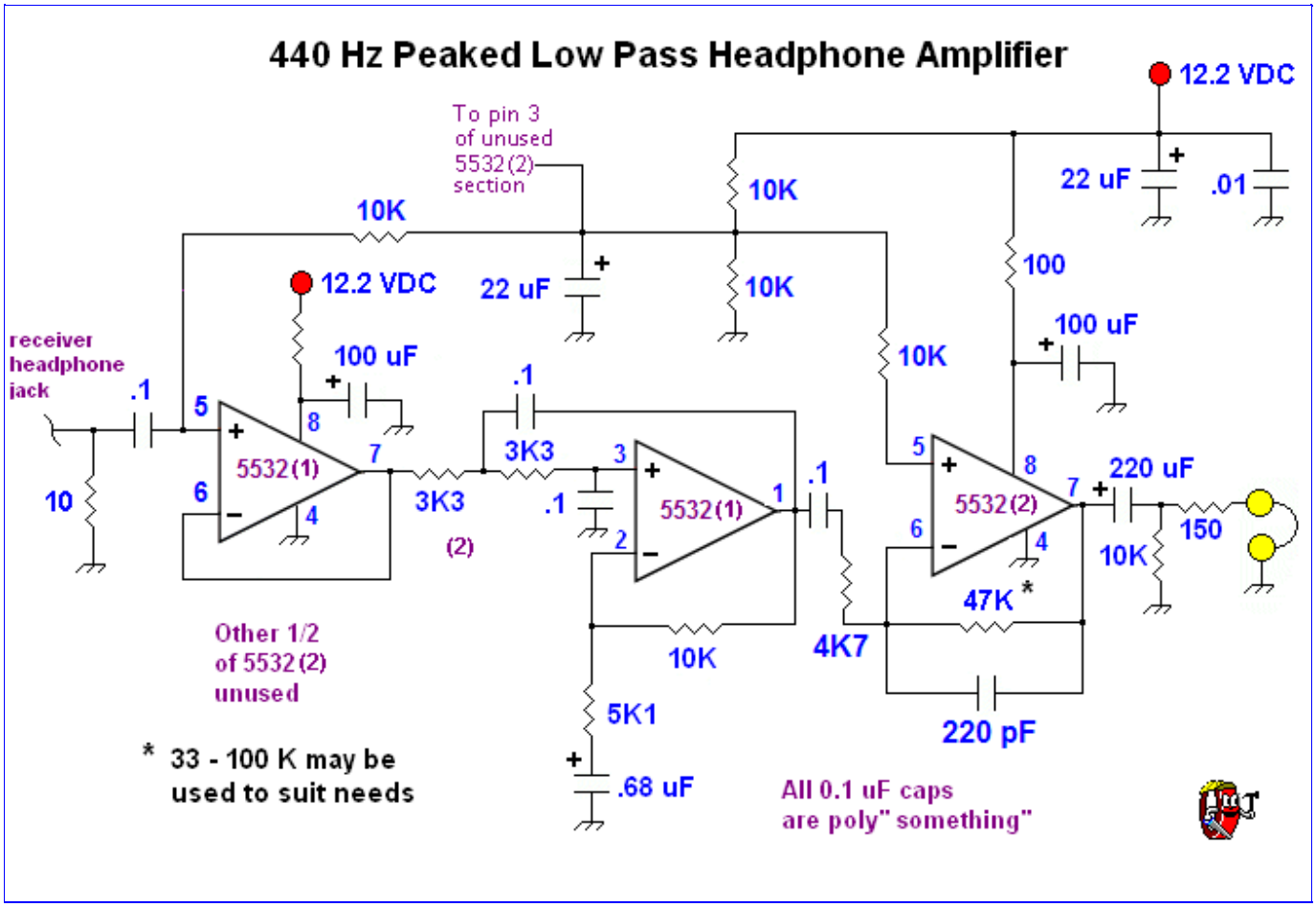

Above is the final filter design. My prototype filter had 2 variable pots and I disconnected and measured them after discovering my favorite setting

and then constructed the version shown above using fixed-value resistors instead of the potentiometers. If you like to tweak knobs, you might leave 1 or both of the pots in. The 0.68 uF cap can be raised as high as 4.7 uF if you have poly caps this large in capacitance value. although, it seems wasteful, I did not use one half of the second 5532 op amp. Feel free to add another pole of low pass filtering or something else to utilize this stage if you like. Pin 3 of the unused, second op amp 1/2 is connected to the 10K/10K voltage divider bias with a wire as indicated in the text.

This filter sounds the best when the R75 volume control is minimally turned on as I suspect some of the wide band noise heard is from the ICOM AF chain. More importantly, If the R75 audio gain control is turned too high, the filter will be overdriven and sound distorted This is especially true when using the 2.4 KHz wide SSB filter on the R75. The 10 ohm filter input resistor attenuates the receiver output and makes it more difficult to overdrive the audio filter. The 500 Hz filter at the 9 MHz Receiver IF has quite a bit of of loss and with this filter switched in, it is difficult to overdrive the audio filter. For best results, an audio filter should be placed just after the first AF preamp stage, however, using the headphone jack is the only option available for adding AF filtering in most commercial receivers I have used.
The second op amp stage is used to increase the headphone volume and the 47K feedback resistor can be adjusted to suit your needs. It is really important to experiment with the component values which will match your receiver and the IF filters and antenna you have. For example the input shunt resistor may be increased from 10 to 18-22 ohms if you always use a narrow IF filter during CW and beacon listening or received signals are low in volume. This is an experimenter's circuit, not a finished project. Overall, this circuit has low output volume and is really gentle on the ears in terms of noise and amplitude.

Project Breadboard and Samples

Shown to the right is a side photo of the experimental project. The big yellow Mallory polyester caps were used as I did not have any other desirable AF filtering caps in my parts stock. The day after, I built this filter, my parts order (including a big selection of polyester film audio caps) from Digi-Key arrived, however this is Murphy's law. These Mallorys are good quality capacitors- just a little large!

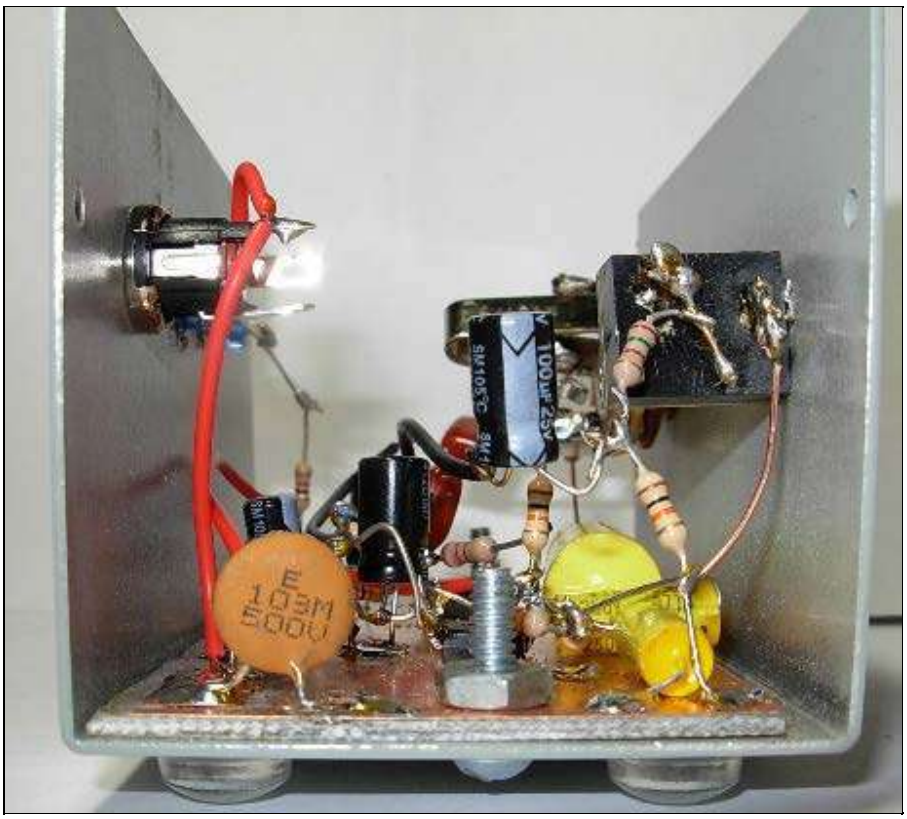

Low pass filters can really help reduce noise during reception. Two example audio files follow. These were heard in the NDB band using a 2.4 KHz SSB IF filter.
290 YYF
312 UNT
The occasional scratchy noises are me moving as I held the headphones around the microphone.

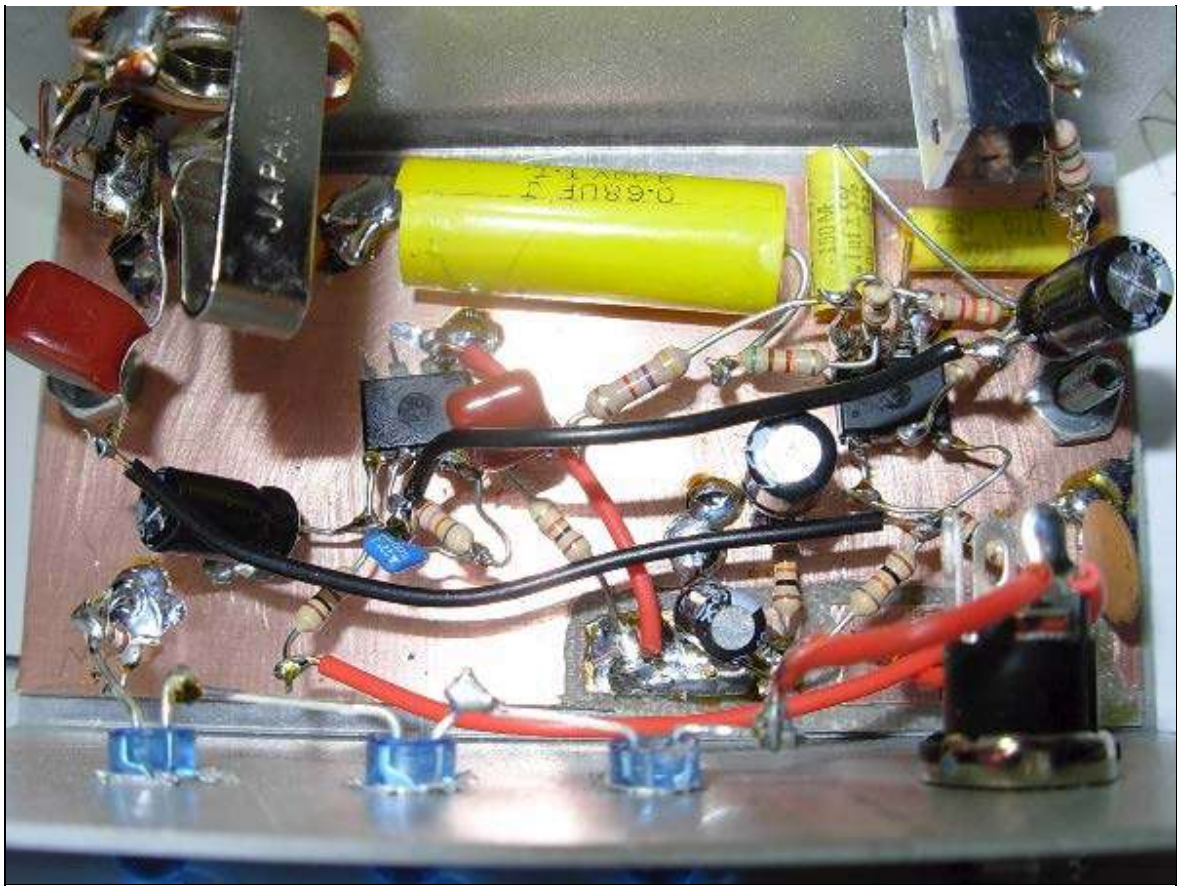

Above is the filter photographed from above. The 3 blue LEDs are used to light the lower row of buttons on the R75 as it is difficult to see them with a low level of light in the radio shack. No hum is heard with this filter. When you build AF amps or filters with the 5532, after soldering pin 4 to the copper ground plane, start out by connecting the components associated with pins 6 and 7 and then 1 and 2. I suggest this as placing components between adjacent pins is often the most difficult part of building when using ugly construction with op amps.
If by accident you make an unintentional solder bridge between 2 adjacent pins on an op amp, simply heat the 2 bridged pins up and gently drive a small screw driver between the pins. This should remove your unwanted solder bridge. The 5532 op amp is quiet and relatively inexpensive. In EMRFD, there are countless examples of how one can use them in a variety of applications.

Additional Information and Photographs

Above is a photo of the audio filter in action on the NDB band. The blue LED reflection can be seen on the receiver. For serious NDB and CW pile up work, narrow band pass audio filters are generally required. This simple audio filter experiment might be useful as a spring board for your own AF filter experiments and to learn the filter requirements of your own particular receiver.

Above is the filter photographed from the rear. The DC power cord has a built in RFI filter. For homebuilt projects, DC power cords can be obtain by cutting the power cord off old unwanted or broken "wall wart" power supplies. This provides you with a nice cord with a built-in plug. I collect old AC "wall wart" transformers for this purpose. This filter is powered by the main 12 volt DC supply on my radio bench.

Cascode Hybrid-Based WWV Receiver for 5 MHz

Introduction

This was my favorite project of 2007. When I web published the original TRF WWV receiver for 10 MHz in 2006, there were many complaints that I used hard-to-find dual-gate MOSFETs and also that the AF stage lacked the popcorn factor that this web site has become strongly associated with. In this experimental project, these 2 concerns are addressed.

The cascode JFET and BJT amplifier stage used in this receiver is based upon the amplifer described in the Hybrid Cascode IF Amplifier article which was published in QST for December 2007 and designed by W7ZOI and WA7MLH. This amplifier topology has many advantages including high gain + low noise, that it can function well at DC voltages less than 12 VDC and that the noise figure does not degrade when the BJT bias (and stage gain) is lowered during AGC action. Please read the QST article and also refer to the W7ZOI web site for more details on the IF amplifier and the cascode hybrid topology.

Receiver Block Diagram

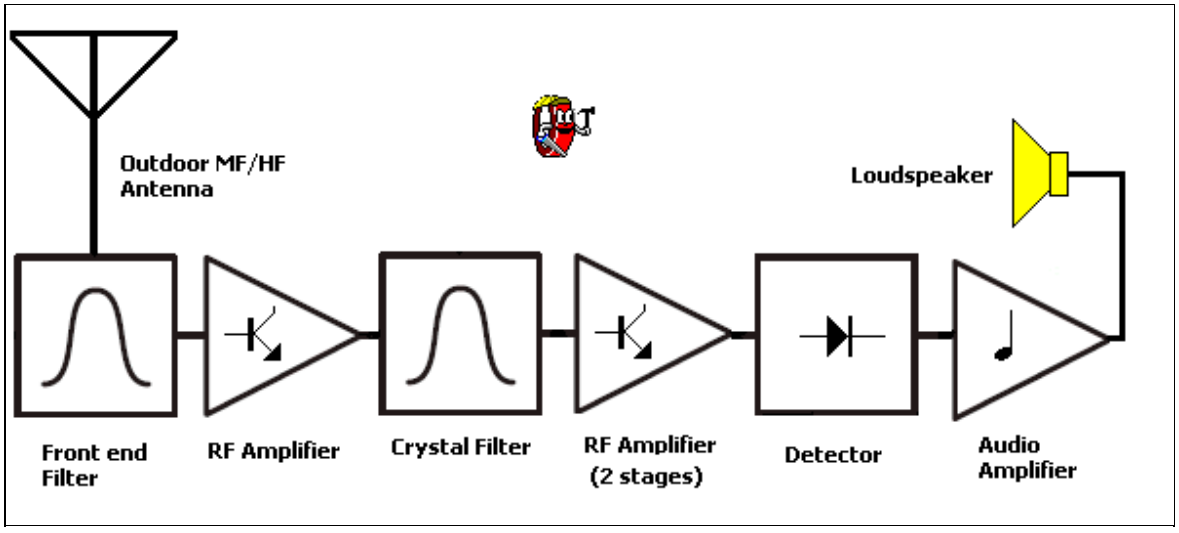

The receiver block diagram is shown above. To hear digitally recorded examples of this receiver, click here , here or here. No attempt was made

to make these files sound better than they really are- there is signal fading, room noise etc. A electret microphone was placed near the loud speaker to record these audio samples. *Note I am now compressing audio files in the mp3 format to allow listening by those who use Linux as their operating system.* **A supplemental web page** to this main web page is linked here

---

Receiver Front End: Band Pass Filter and First RF Amplifier

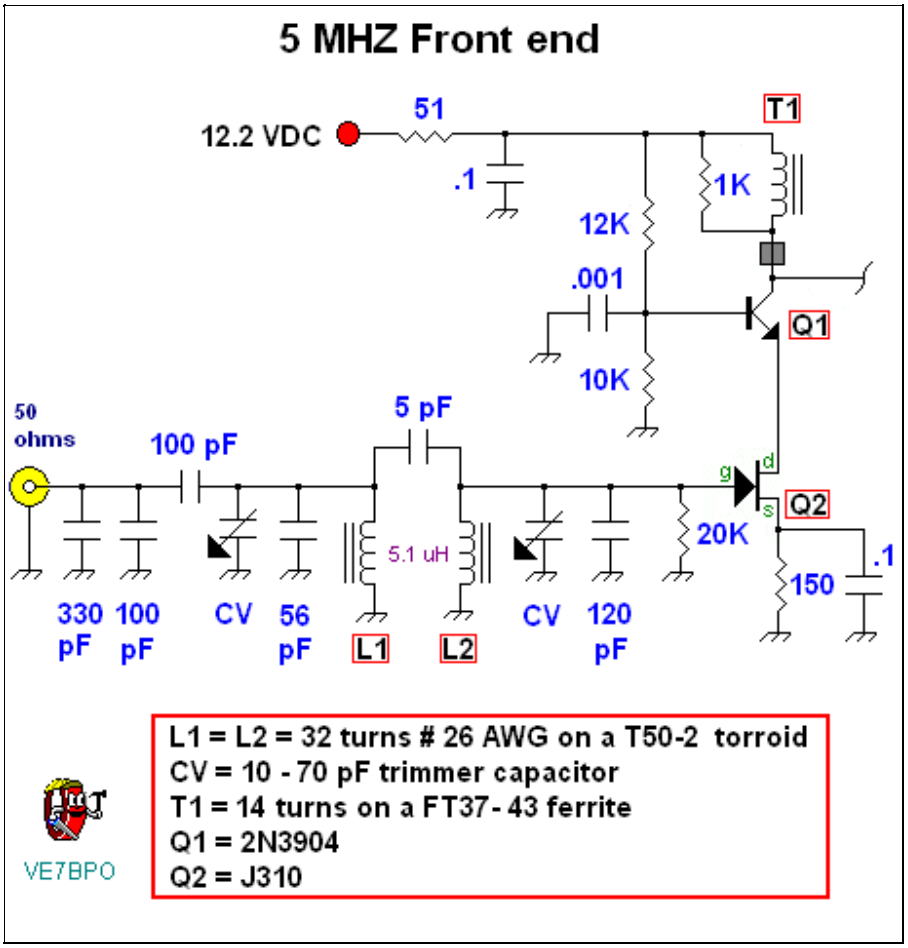

This receiver is meant to interface with a standard 50 ohm feed line. Testing was performed using my MF/HF antenna.
I built 3 separate bread boards of this receiver and tried varying the number of RF amps, using different detectors (as well as different detector followers) and eventually built and tested this basic receiver design for 5, 6 and 10 MHz. With respect to using the cascode hybrid amp (and probably any other amplifier type) **in a TRF receiver**, I learned 3 things:

1. Do not operate the RF amps at maximum gain. I built some very powerful amps with a Q2 source resistor of 47 ohms and over 6 volts bias on Q1. While powerful, this amp broke into oscillation and also consumed much current (nearly 20 ma).

2. Keep the RF stages at least 2-3 cm apart to reduce the chance of parasitic oscillations.

3. Keep the input band pass filter at least 2 cm from the Q1/Q2 amp or you might encounter some unwanted oscillations.

For the front end band pass filter, a reasonably narrow bandwidth was desired. When sweeping early filter designs using a signal generator and oscilloscope, a double humped response was noted. These filter designs used a 10 pF coupling capacitor. The coupling capacitor was then decreased to 5 pF. To obtain the required 5 pF, two 10 pF capacitors were placed in series as shown in the photograph directly to the right.

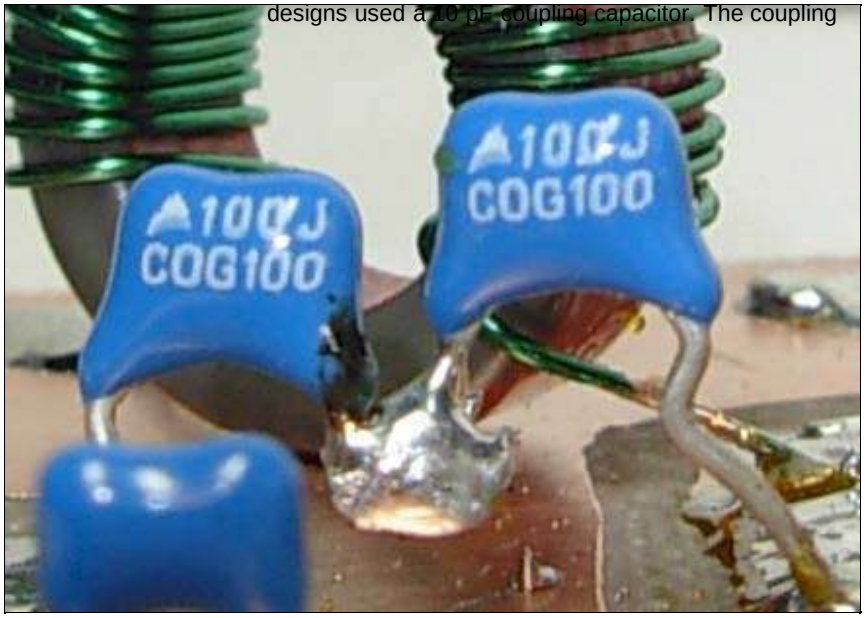

I struggled with this filter design because one end is terminated in the gate resistance of Q2 of the hybrid cascode amplifier and was not the standard 50 ohm impedance termination. My early filter designs suffered severe insertion loss or poor selectivity. I asked Wes, W7ZOI, for some instruction on solving my filter problems. I learned that this filter topology is referred to as a singly terminated, double tuned band pass filter. Wes designed the front end band pass filter for the 5 MHz receiver for us all to learn from and for this I am very grateful to him.

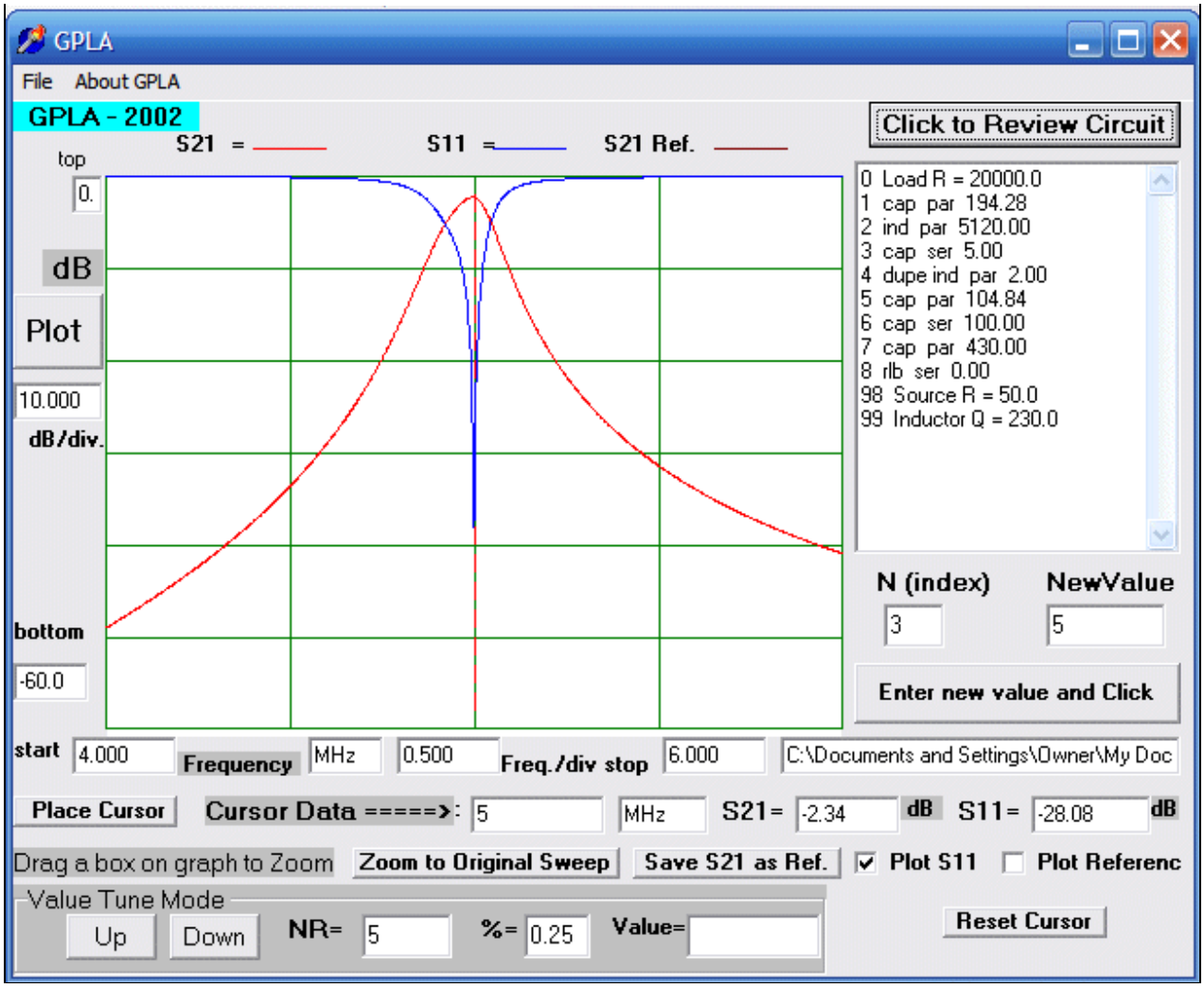

Above. A GPLA simulation of the singly terminated, double tuned filter designed by W7ZOI. A double tuned circuit is mandatory ahead of the WWV receiver as local BCB and other RF energy will be amplified by the first RF amp and may distort the WWV signal in the crystal filter or even might blow-by the crystal filter and be detected and heard in the speaker.

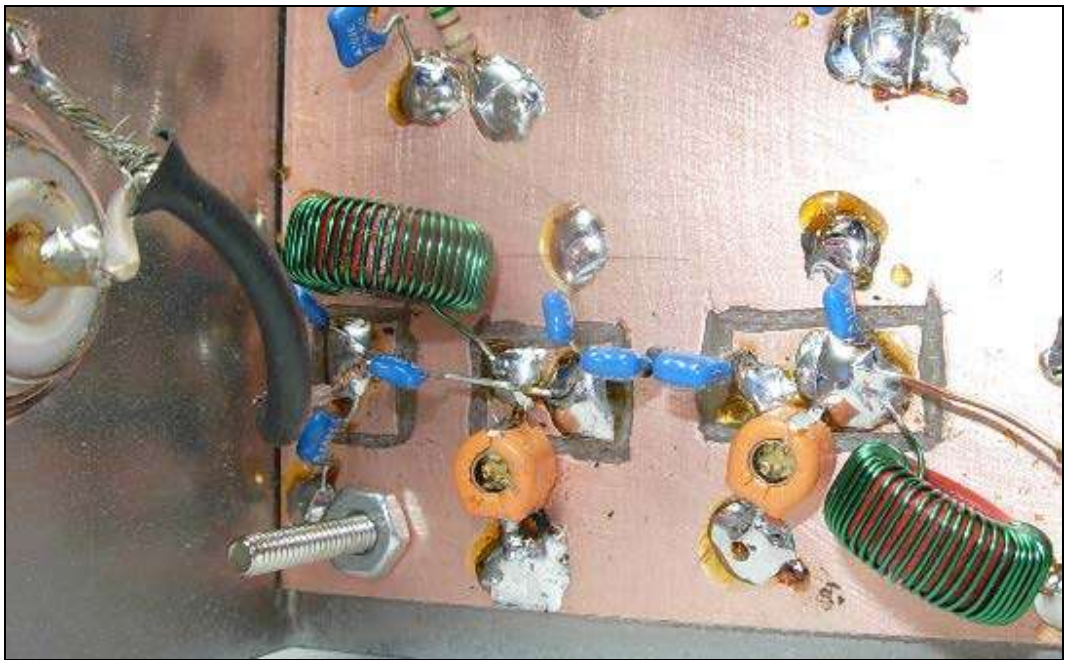

Directly above is a close up photograph of the input filter bread board. Filter tuning was done by ear (and screwdriver!) Simply tune the trimmer capacitors for the loudest audible WWV pulses in the speaker and you are set. If you can't locate a 20K gate resistor for Q2, a 22K resistor will work okay.

Crystal Filter and Second RF Amplifier Stage

In the schematic to the right is the crystal filter and second RF amplifier. The input impedance of the crystal filter is established by the 1K shunt resistor across the output transformer on Q1. The output impedance of the crystal filter is set by the 1K gate resistor of Q4. A filter input/output Z of 1000 ohms gave the best overall shape and bandwidth during my testing.

Developing this filter was difficult. My first batch of junk box crystals had a low motional inductance and with the filter I built I could hear stations ~400 KHz below and/or above the filter center frequency in addition to WWV. After giving up in frustration for nearly 2 months, a batch of 10 crystals were ordered from Digi-Key. These were microprocessor crystals; ones with 18 pF load capacitance in a HC49/U holder. The new filter was tweaked and tested and now provides single signal reception of WWV. Your own results may vary according to your crystal parameters. The Digi-Key part number is provided for reference purposes only.

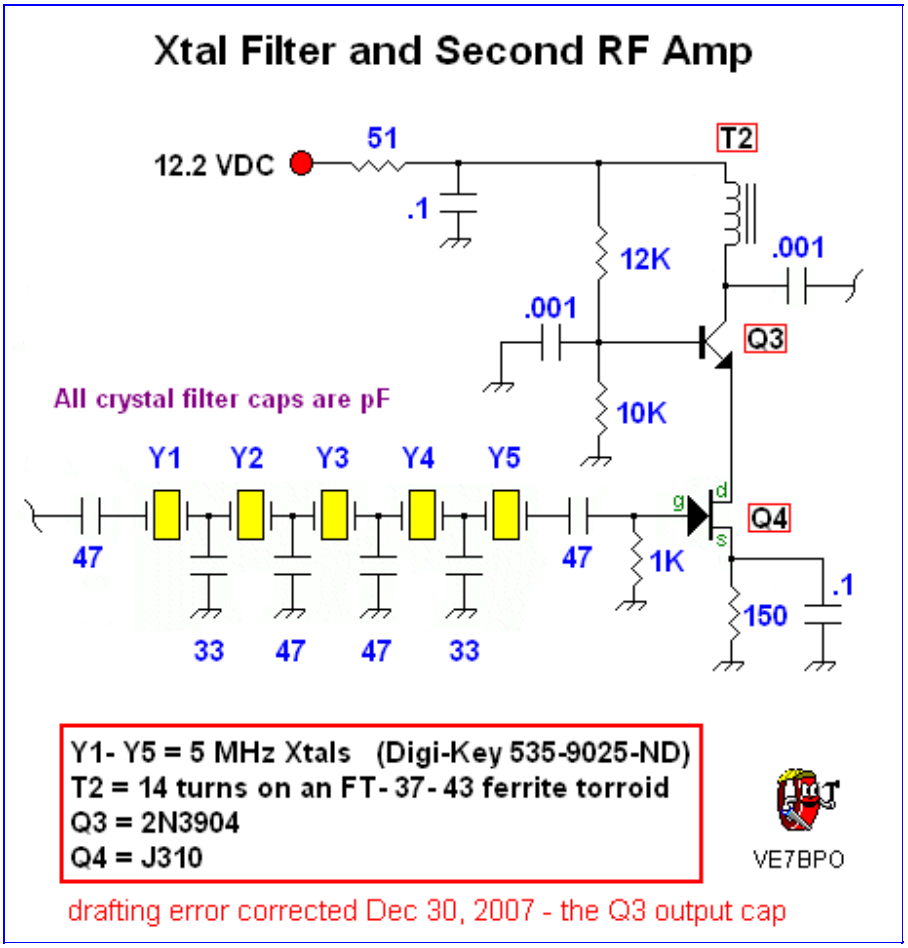

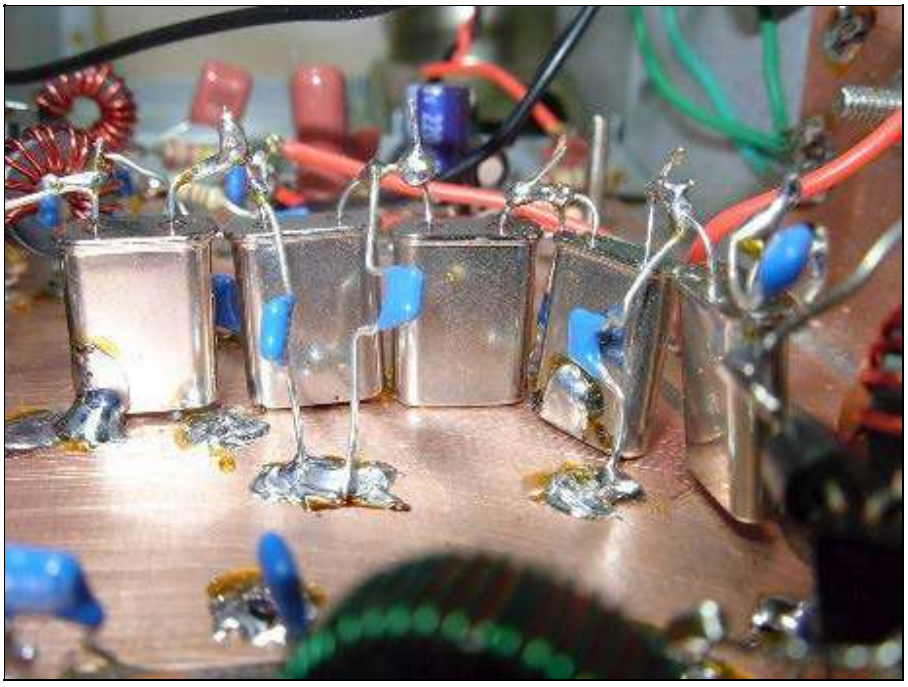

To the left is a close up photograph of the 5 MHz crystal filter. The crystals were turned upside down and the outer cases were directly soldered to the copper ground plane as you can easily see in the crystal to the left of the others. The rest of the crystals as well as one of the 47 pF tuning capacitors were soldered on the other side and solder points are hidden from view. The crystals were positioned to keep the output of Q1 away from the input of Q4. ***Stage lay out is very important in TRF receivers.*** I found stage layout to be far more important than keeping lead lengths short from my experimentation.

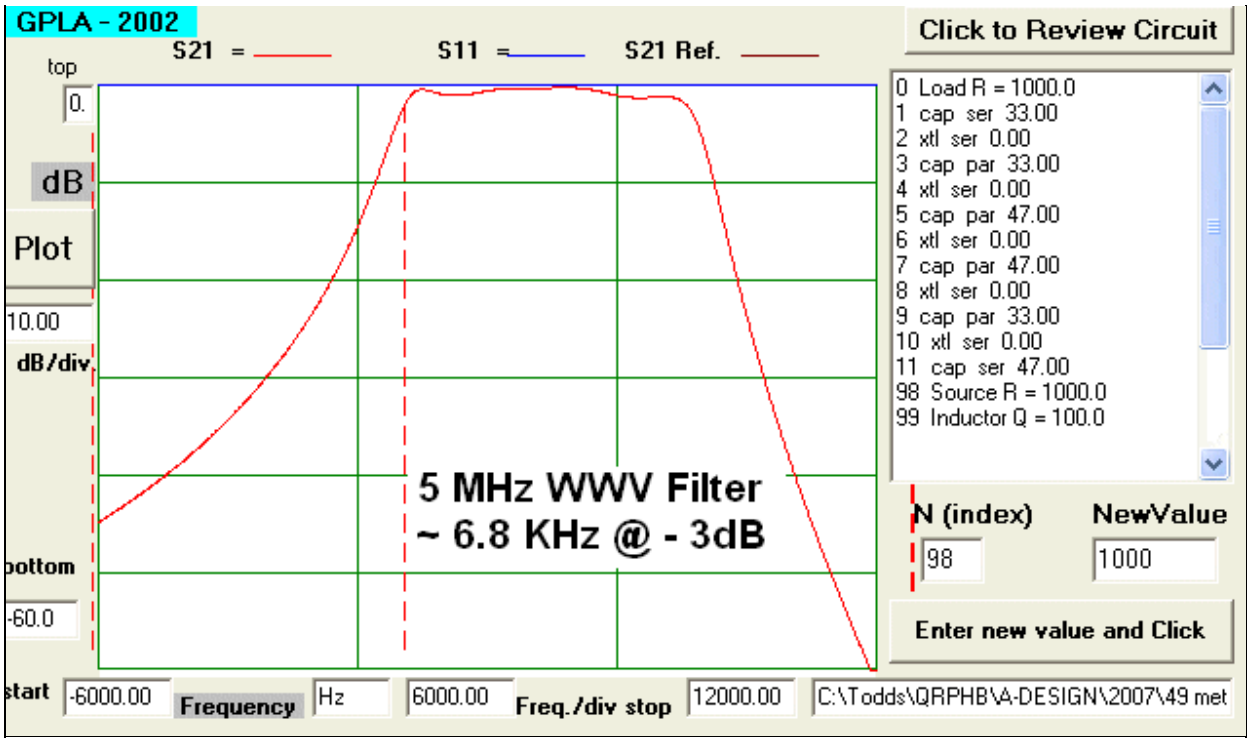

Directly above is the GPLA simulation of my crystal filter. The 5 MHz point is not centered exactly in the middle of the pass band, but a reasonable AM filter was built nonetheless. Crystal parameters, especially motional inductance and capacitance can make or break your filter. Motional inductance and capacitance describe the L and C values that make up the crystal's electrical LC model. Very large inductive and capacitive reactance values at the specified operating frequency give the crystal its extraordinarily high "quality factor" or "Q". For example, If the motional L is too low, your filter may not work as expected; providing single signal reception of WWV. The Lm was 0.02 and the Cp was 5 in the crystals which I used for my filter. In general, low Q crystals will give poor results. Oppositely, crystals with very high Q may give a lower then expected bandwidth and this may reduce AM receive fidelity. Experimentation is necessary.

Third RF Amplifier Stage and Detector

To the left is schematic of the final RF stage and the envelope detector. This RF stage has variable gain by means of a front-panel mounted 10K potentiometer which is used to vary the bias on Q5. The input Z of this stage is 100 K and is set by the Q6 gate resistor. The output of Q5 is AC coupled to a detector designed by Wes, W7ZOI. I performed considerable experimentation with basic diode detectors as well as detector source followers; some of which I sent to Wes for his consideration. He designed and emailed me back this simple, good sounding detector design which uses the gate voltage of Q7 to bias the germanium diode. Other types of diodes such as as hot carrier diodes will likely not have the output voltage of the Germanium type. Germanium diodes, when biased, had more noise and high frequency response in addition to higher output when compared to others I tried during my experiments. Diode detector guru, Felix, VK4FUQ advised me of an excellent diode he is now using called the BAT46. The audio samples of a local AM radio station using this diode and his other hi-fi lab equipment that he sent me are beyond fantastic.

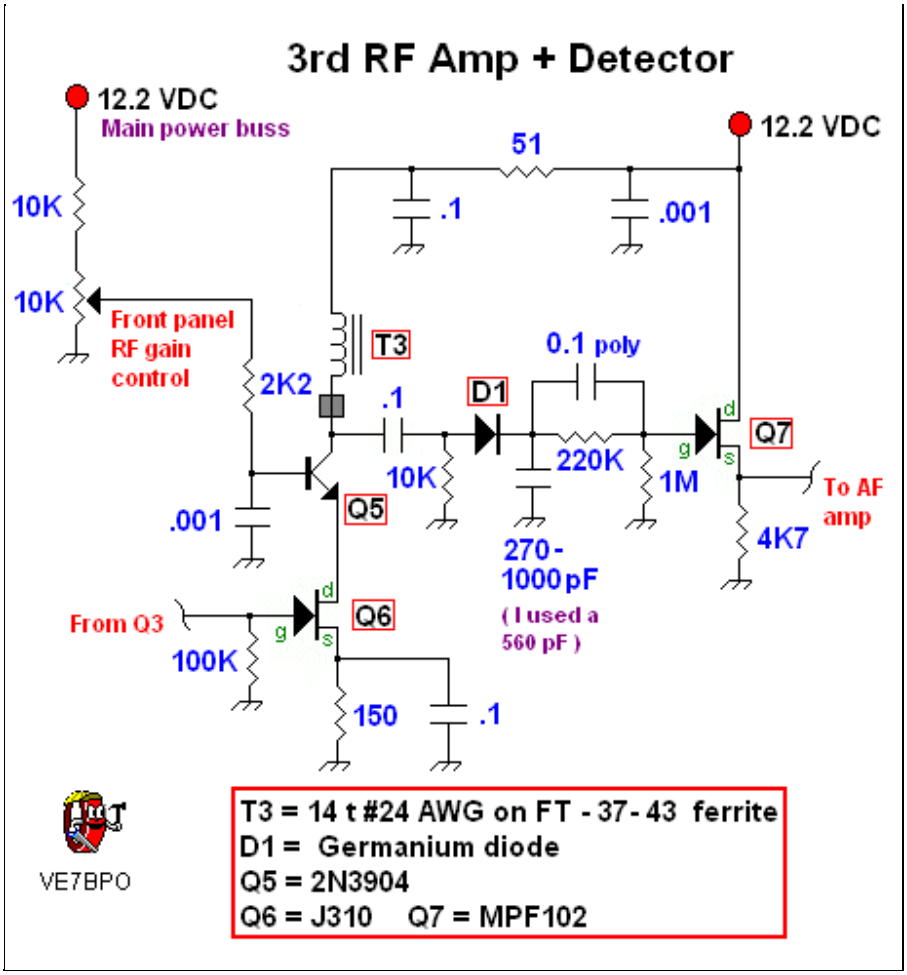

The photograph on the right is a close up of the enveloped detector designed by W7ZOI. The germanium diode was purchased from The Source in Canada (Radio Shack in the USA). The blue, partially hidden shunt capacitor is a multi-layer ceramic 560 pF cap. The other capacitors are metalized, polyester film types. Ensure correct diode polarity.

Audio Stage

To the left is the schematic of the audio stage. The very "popcorn" LM386 AF chip is used to please the audience who complained about my AF stages not having enough popcorn factor. A 4K7 resistor was inserted between pins 1 and 8 to reduce the gain somewhat. Thus, the LM386 is still being operated in the high gain mode but won't hurt your ears with loud noise and distortion. The 470 pF cap on pin 3 may be changed or eliminated. It is a simple low pass filter.

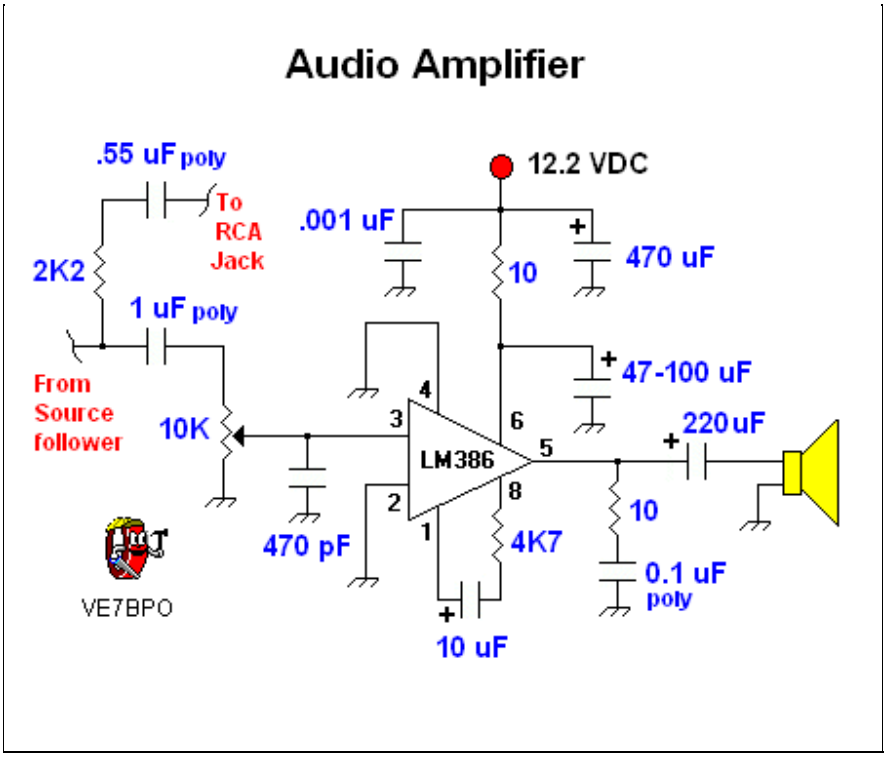

A secondary, audio output connects to a front panel mounted RCA phono jack. This allows me to use my lab grade (KK7B AF amp) and turn the audio off on the normal receiver AF amp.

The photograph to the right is a close up of the LM386-based audio stage. This is where I started. After drilling the chassis, wiring the speaker, installing the chassis potentiometers, making the main power buss and LED indicator, the AF stage was built on the main board. The main board was then temporarily soldered in and tested.

(Some connections were made via alligator clips such as the speaker wires). When the AF amp worked as expected, the main board was removed from the receiver chassis and the net stage was built. Up next were the detector and source follower. After bread boarding these, again the main board was laid in the chassis, wired, tested and then removed when all was functioning well. To test the detector I touched my finger to the input and heard local BCB radio. Following this, RF Amp #3 was added to the main board and again the main board was temporarily wired up and tested by touching the input of Q6 with my finger and observing that a local broadcast radio station increased/decreased in amplitude when the RF gain control was turned up and down. DC voltages were also measured and considered from project start to finish.
Actually, all you need to do is connect a band pass filter such as this to Q6 and the components after and you will have a nice TRF BCB AM radio. Each successive stage was built and tested, so when the receiver was finished, I already knew that it worked. I cannot emphasize enough how important it is to build your receiver backwards and test each stage as you go. There is strong temptation to start at the antenna connection and work until you get to the speaker, but please consider doing the opposite.
The bare copper wire in the photograph is the positive connection point for the speaker wire. It was trimmed somewhat during final assembly to reduce the possibility of it shorting.

Miscellaneous Photographs

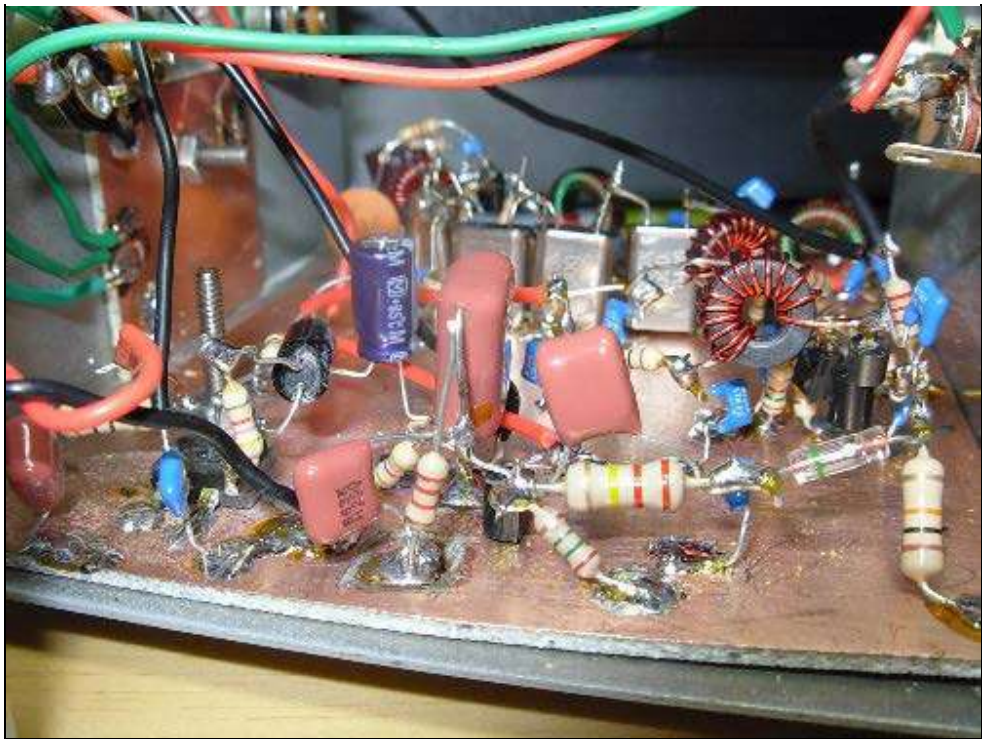

The photograph above shows some of the detail of the receiver main board from the right hand side which contains the detector, source follower and audio amp stages from right to left.

The photograph above shows a top view of the main chassis and also the chassis cover with the speaker bolted on and wired up.

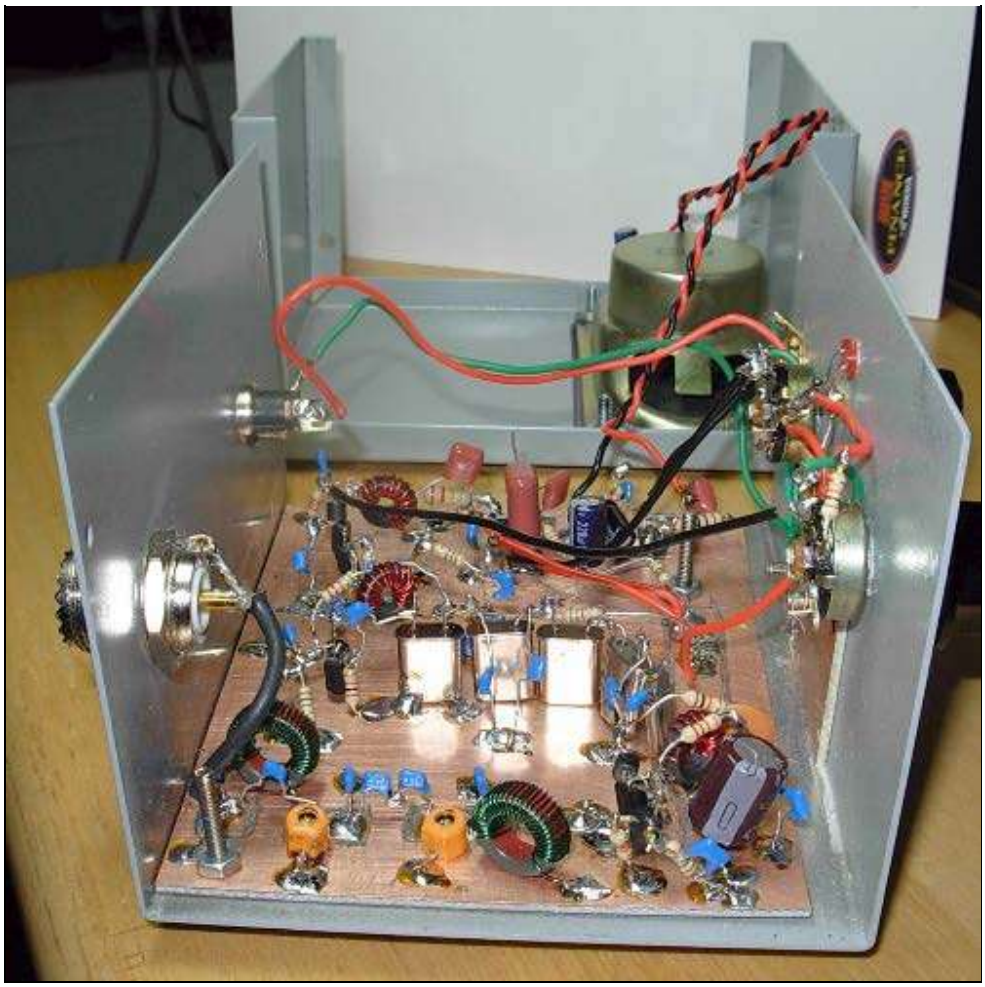

This wider angle photograph shows the main board from the left side. From left to right in the nearground are the SO-239 antenna connector, LC band pass filter and first RF amplifier.

The photograph above shows the speaker attached to the Hammond chassis top. Holes were drilled in the chassis lid with a drill press to allow the sound to pass through.

The photograph above shows the reverse view of the receiver chassis.

Complementary-Symmetry Amplifier Biasing Basics

Introduction

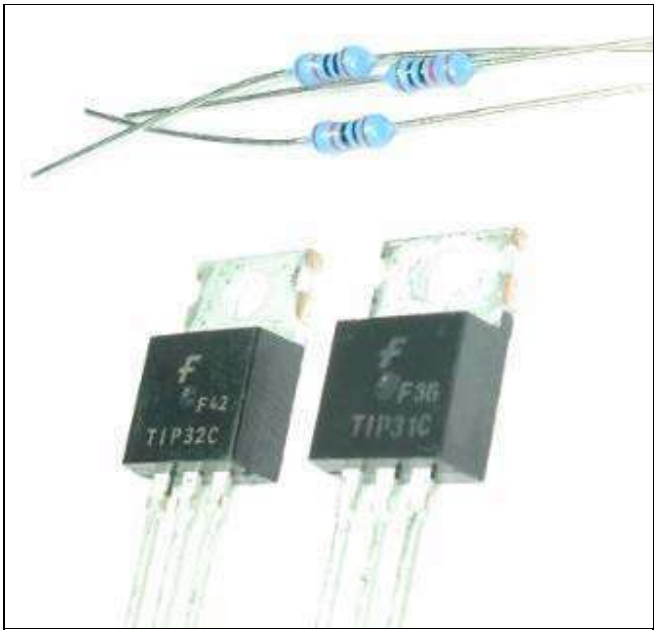

This page provides information concerning the biasing of Class-AB, complementary-symmetry audio amplifiers. These schematics should be considered theoretical, as design considerations such as thermal stability, negative feedback and component power ratings are minimized or excluded for sake of clarity.

The basic 2 transistor complementary-symmetry amplifier may be used as a simple low power AF amp or as a building block for a high powered stage such as a 50 watt guitar amplifier. It is important to understand how to properly bias your AF power amps to reduce distortion and to promote easy troubleshooting when problems arise. This web page describes the hows and whys of biasing in a progressive manner with minimal math.

Discussion

Figure 1

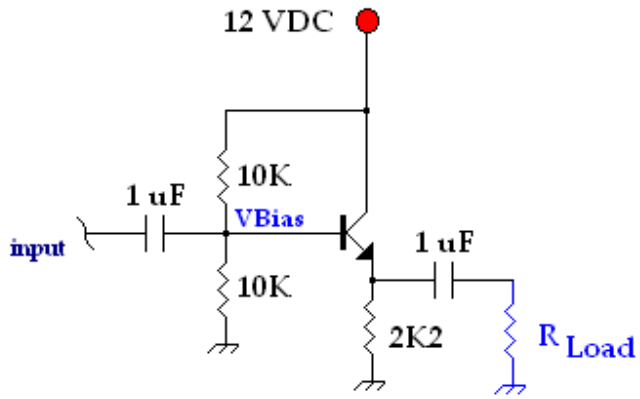

A review of the common collector amplifier (which is more commonly called the emitter follower) is a good place to start. We may refer to the complementary-symmetry transistor pair as complementary emitter followers since they are an NPN and PNP emitter follower connected in series. An emitter follower amp is shown in Figure 1. Its properties include:

- ✓ input on the base - output on the emitter
- ✓ high input impedance and low output impedance
- ✓ a voltage gain of 1
- ✓ good current and power gain

In an appropriate configuration, these qualities are perfect for driving a low impedance load such as an 8 ohm speaker with large output currents that are not provided by our typical transistor or op amp voltage amplifier stages. In many cases, we bias the emitter follower with a voltage divider network comprised of 2 identical value resistors. In Figure 1, the voltage divider consists of a series pair of 10K resistors and thus VBias = 6 volts. These 10K bias resistors will be used throughout this web page as the circuits evolve.

In Figure 2 is a pair of complementary emitter followers which have their

bases biased with our now familiar series connected 10K bias network for a VBias of 6 volts. When the power is turned on, output capacitor C2 charges through the NPN transistor until it reaches about 6 volts *(theoretical value used to keep things simple)*. When the voltage at point V Emitter reaches 6 volts, the NPN transistor goes into cutoff because VBias voltage now equals the V emitter voltage. Recall that the NPN transistor base must be positive with respect to the emitter for current to flow. Both the NPN and the PNP transistor are in cutoff. This is the amplifier's quiescent state *(assuming no signal is applied to the input via C1)* and is called Class B bias.

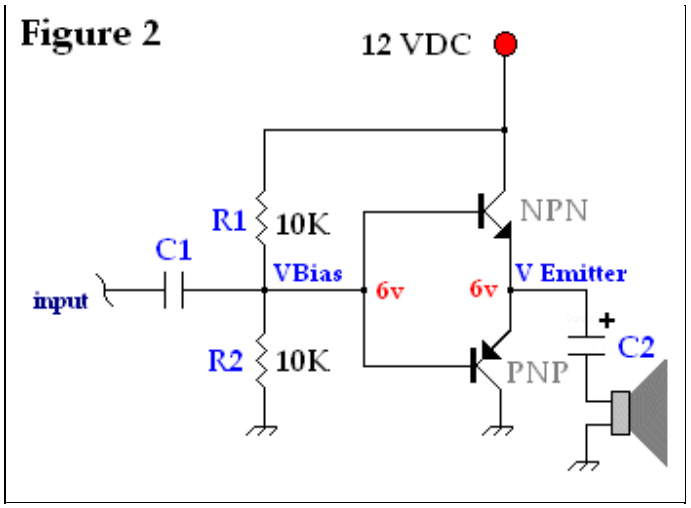

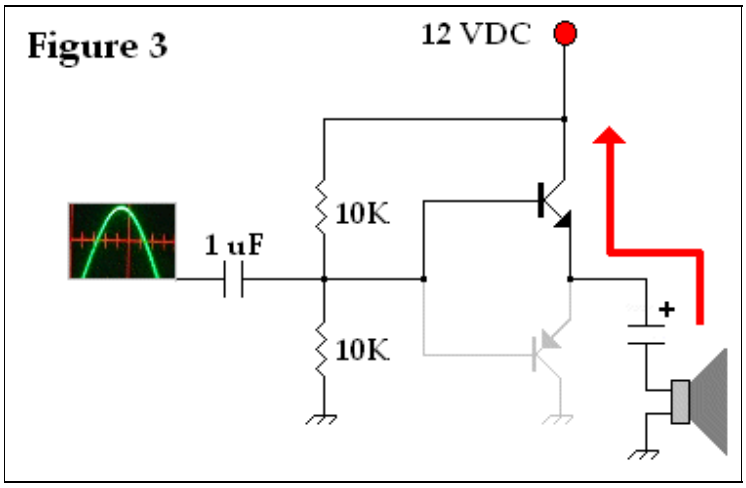

In Figure 3, a positive going signal is applied to the input capacitor. The NPN transistor becomes forward biased and turns ON. Current flows **through the NPN transistor** and charges capacitor C2 to a higher potential. The PNP transistor stays in cut off. The NPN transistor is an emitter follower connected to the speaker.

In Figure 4 a negative going signal the (negative half-cycle) is applied to the input. Q3 turns ON and discharges the output capacitor through the speaker as shown in **red.** The PNP transistor is an emitter follower connected to the speaker.

Thus the NPN and the PNP transistor conduct on alternate half cycles which causes AC current to flow through the speaker. The complementary emitter followers are said to be in push-pull operation.

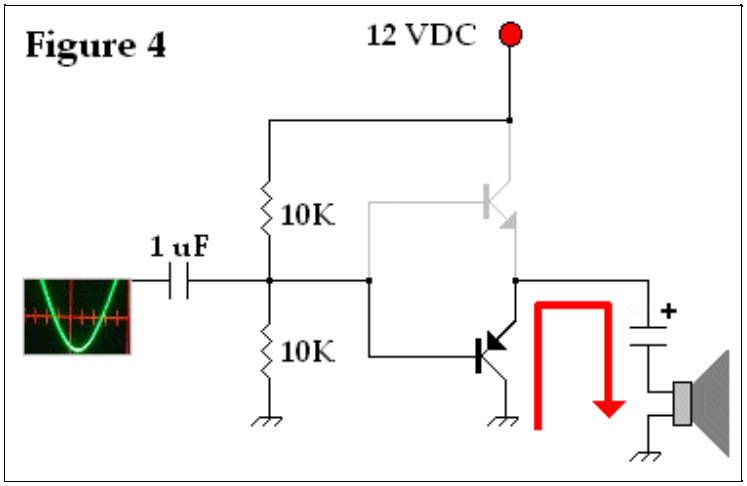

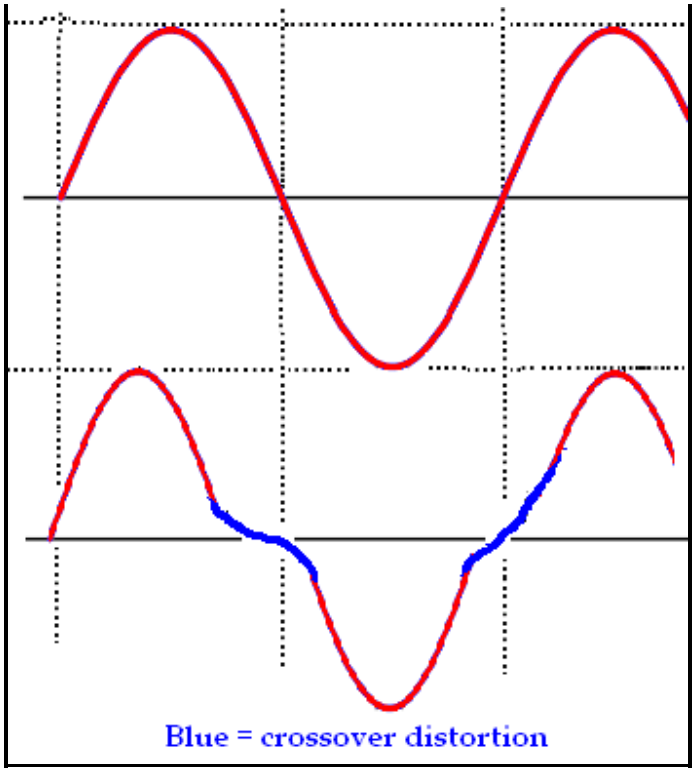

The circuit of Figure 2 has a significant problem; output signal distortion. Silicon transistors such as the 2N3904 and 2N3906 will not conduct until their bases are forward biased by somewhere around 0.7 volts. For the NPN transistor, this means that it will not conduct until the input signal has gone positive by about 0.7 volts. Oppositely, the PNP transistor will remain in cut off until the input signal goes negative by approximately 0.7 volts. As a result, there is a dead zone during the point in time when one transistor cuts OFF and the other turns ON. Shown above is a normal sinusoidal AC waveform in red and another with the distorted waveform of Figure 2 in red and blue. This distortion is called crossover distortion because it occurs at the zero crossing point of the AC waveform. This introduces odd-order harmonics into the output signal. Such is the drawback of the Class B amplifier.

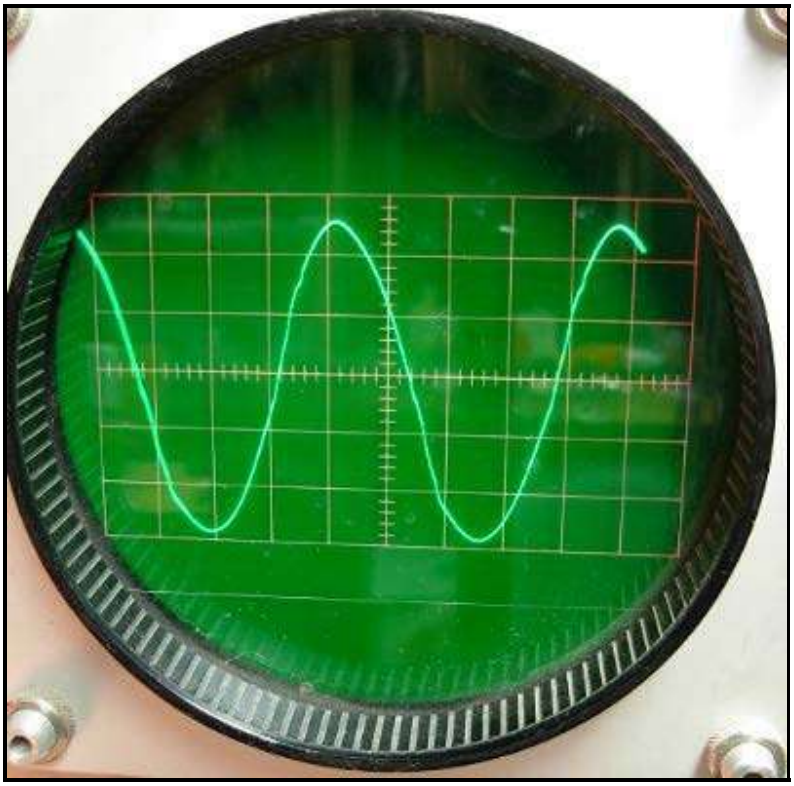

The above photograph shows crossover distortion in an under-biased power amp.

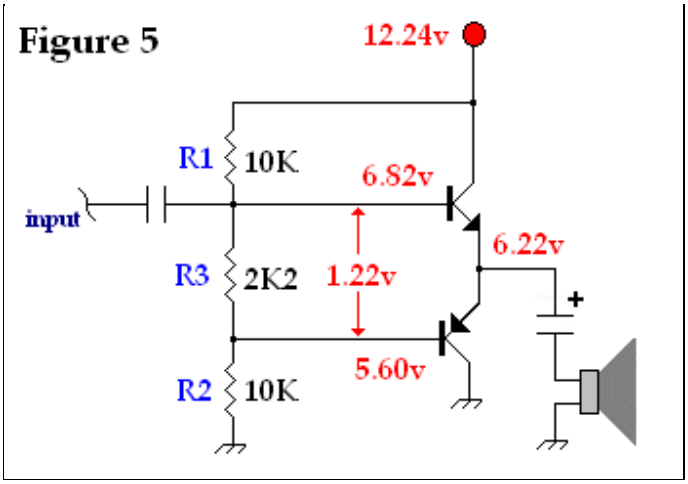

Figure 5 shows the principle technique used to reduce crossover distortion; both transistors are (slightly) forward biased almost to conduction in their quiescent state. As a result, any amplitude of positive or negative going signal will bias the appropriate transistor into conduction. An easy way to achieve this biasing is by adding 1 resistor to our 10K voltage divider network. In Figure 5 is a circuit I built, measured and listened to. R3, a 2K2 ohm resistor was placed in between R1 and R2, our usual 10K bias resistors. As a result , both transistors are forward biased.
That is: the base of the PNP transistor is negative with respect to its emitter and the the base of the NPN transistor is positive with respect to its emitter. As a rule of thumb, you need to drop at least 1 volt across R3. I chose a 2K2 resistor and it worked fine in my particular amp. The Figure 5 biasing topology is rarely used as it puts a series resistance on the PNP input among other problems; however, it exemplifies the basic principles of biasing our complimentary pair. With the forward bias on the transistor pair we now are in Class AB. The output capacitor serves to block the quiescent DC current from flowing through the speaker.

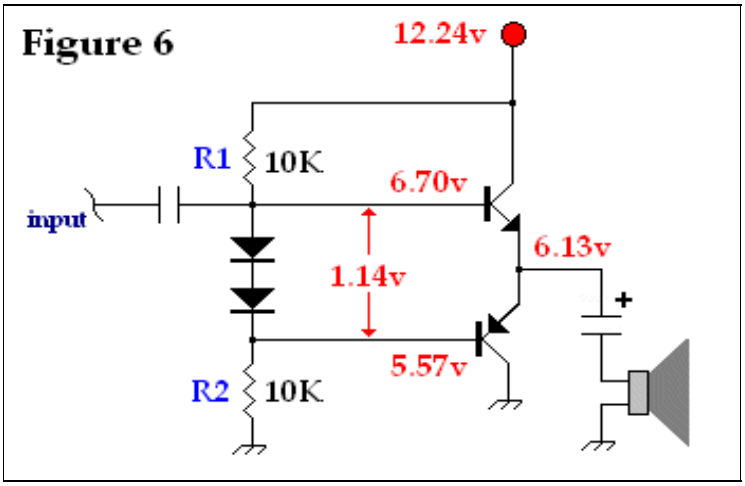

Figure 6 illustrates an improved biasing method over that of Figure 5 by using a pair of silicon diodes. You see this circuit used a lot by hobbyists. The voltage divider consists of 2 resistors and the 2 diodes. The 2 series connected diodes are connected in parallel to the NPN and PNP transistor base-emitter junctions which serves to keep the transistors turned on slightly. The net effect of the diode pair is the same as R3 in Figure 5. The voltage drop per diode was measured at 0.57 volts. The AC resistance of these 2 forward biased diodes is non-significant. There is major problem with the diode/resistor voltage divider; no way to adjust the diodes forward voltage drop. If each diode's forward threshold voltage is unequal to the base-emitter junction voltage of each transistor, either not enough forward bias is applied, or the 2 transistors may be turned on too much reducing efficiency and possibly cause excessive heating. Additionally, the pair of diodes lack the ability to provide temperature compensation when the transistors get hot.

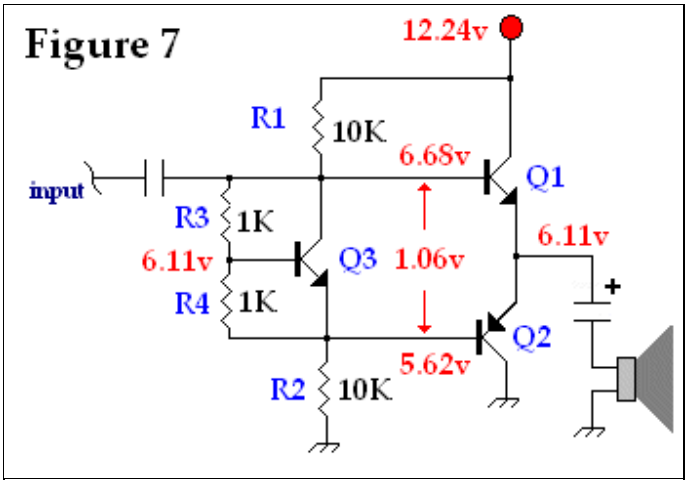

Figure 7 shows the best way to bias our complimentary pair. Our familiar 10K-10K voltage divider is kept, but a transistor Q3 with its own biasing resistors R3 and R4 are added. You might think of R3 and R4 as a voltage divider within a voltage divider. Q3 is referred to as an amplified diode or DC level shifter. It often receives local thermal feedback from the power follower output transistors. This usually involves mounting Q3 on the same heat sink as the finals. If the output transistors heat up, so does Q3 and this results in a a smaller voltage drop across Q3 which translates into less forward bias to Q1 and Q2. Within limits, Q3 with its own base-emitter junction provides variable forward bias for the output transistors.

Shown above is the breadboard of the Figure 6 circuit built on scrap of copper clad board. Transistors were 2N3904 and 2N3906 types, diodes were 1N4148. The capacitor and resistor to the right were a low pass filter (10 ohm and 0.1 uF) to stabilize the output. The unseen speaker was connected to the red and green wires.

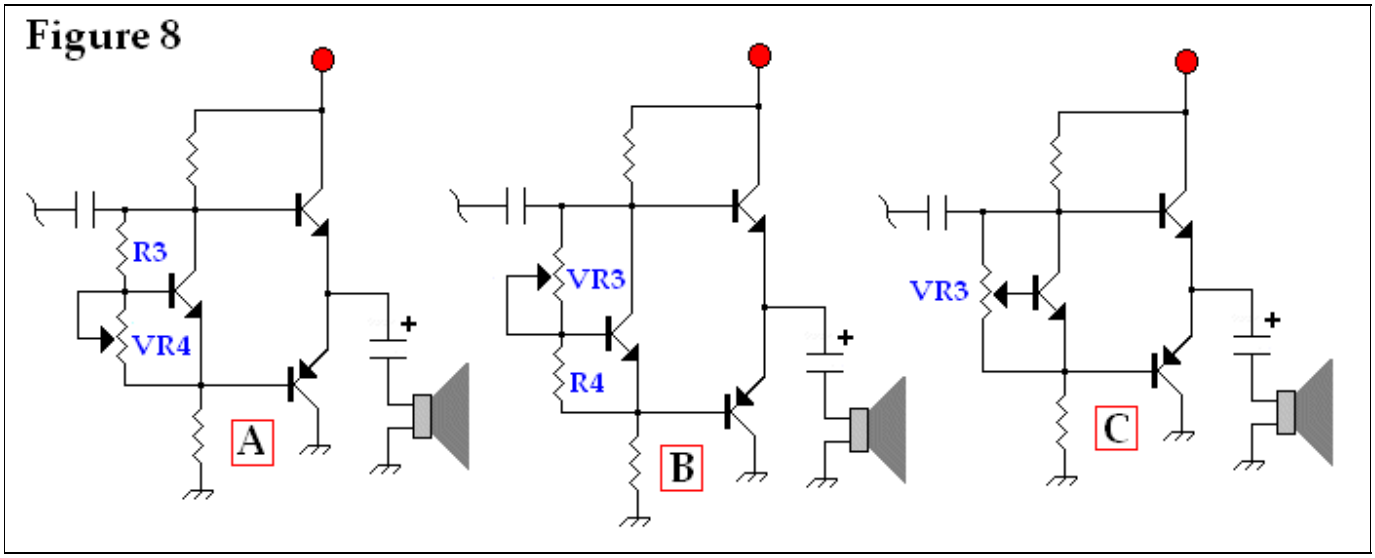

In practice, either R3 or R4 is often replaced with a trimmer potentiometer or a trimmer potentiometer is used instead of R3 and R4 and sometimes R3 and R4 are not of equal value. Shown above in Figure 8 are 3 variable bias topologies for Q3 that I have used. In some cases you will notice that the builder places a fixed value resistor or even a diode in series with the potentiometer in circuits like A or B. Using a potentiometer allows precise adjustment of the quiescent bias current and the ability to dial in the lowest crossover distortion possible. You can set the bias current using any combination of an oscilloscope and signal generator, a voltmeter, an ammeter or possibly try do it by ear when listening for and removing crossover distortion at low volume levels. The procedure I have read to adjust the bias by listening is as follows: Allow some low level signal through the amp so you can just hear it in the speaker. Turn the potentiometer from 1 extreme to another until crossover distortion is heard. Move the pot in the opposite direction until the crossover distortion disappears.
From my limited experience; in some amplifiers under 2 watts or so, you may not hear much of an audible change in crossover distortion when adjusting the bias control potentiometer, so the listening method is not useful in certain cases. It is worth mentioning, that crossover distortion sounds awful and you can usually hear it in amplifiers that are under biased.

Many builders just have a multimeter. In this case, measure the voltage drop across Q3 (the amplified diode) and ensure that is a least 1.1 volts and then slowly adjust the bias up or down from that point. Ultimately, you may have to just make the final bias setting by deciding what voltage drop across Q3 and/or what complementary pair quiescent current you want to establish. It is really not that difficult. *Whatever method you use,*

always re-check the Q3 voltage drop and amplifier bias current with no input signal to inform yourself of what is happening.
I am uncertain of the best method to measure the amplifier quiescent current, however I normally measure it using an ammeter connected in series with the emitter of the NPN transistor of the complementary pair.

Shown to the right and below are more images of what crossover distortion can look like in an under-biased power follower stage. The *right* output waveform also contains a little harmonic distortion, however that's a separate issue. I listened to this amp when connected to a speaker and music audio source; the audio had a noticeable "grungy" distorted sound. As mentioned, crossover distortion sounds terrible. The bias to the power followers (a complimentary pair of two 2N3906 and two 2N3904 transistors set up as Darlington emitter followers) was increased and the crossover distortion disappeared. A post bias adjustment audio listening test confirmed that the crossover distortion was gone.

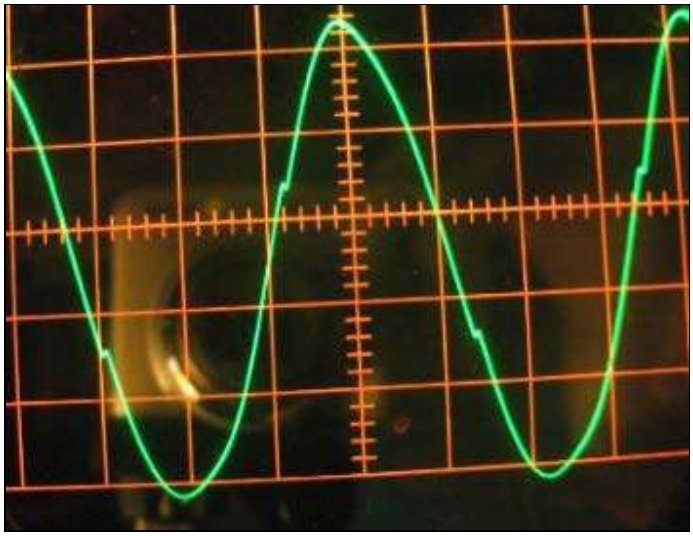

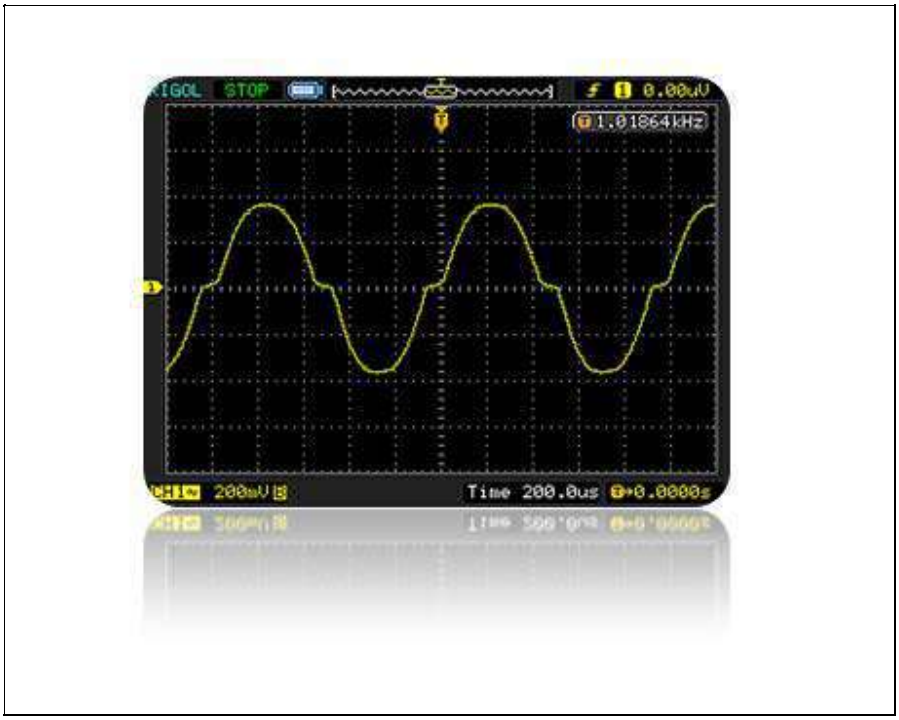

Click for a Russian language mp3 audio file. Vladimir (Volodya), a fellow builder in Ukraine, wanted an A - B comparison of Class AB versus Class B (cross-over distortion). In this audio file, I tweak a potentiometer biasing a pair of power followers to give contrast between the 2 amplifier classes. Under biased AF amps sound terrible in any language! The audio source was a cassette player. The speaker output was recorded, digitized and stuffed into the mp3 file.

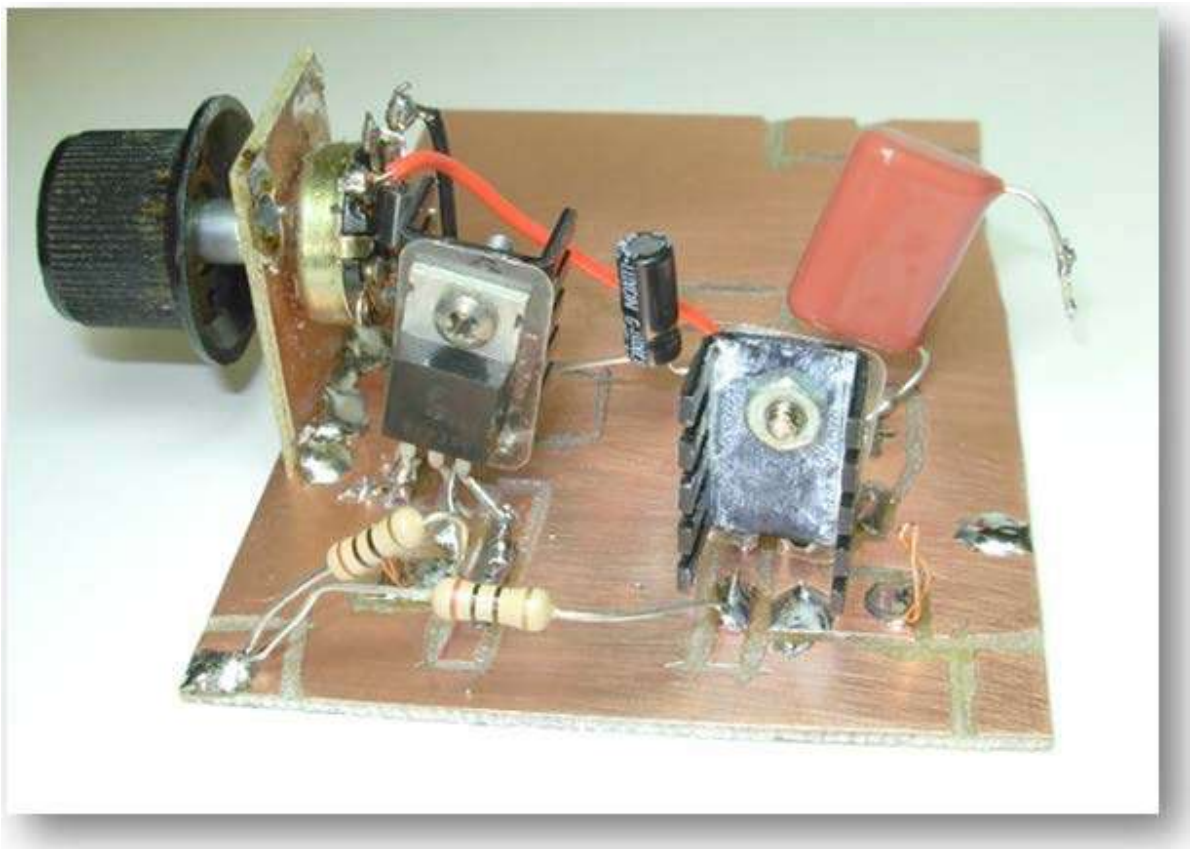

Shown above is a bread board of a complete amplifier utilizing a 10K pot to vary the bias on the amplified diode *(see Figure 8 c)*. With a 12.22 volt power supply, turning the potentiometer from one extreme to the other varied the current draw of the amplifier from about 0 to 95 mA. The average quiescent current draw of a properly biased **single complimentary pair** was somewhere between 5 and 10 mA in my bread boards.

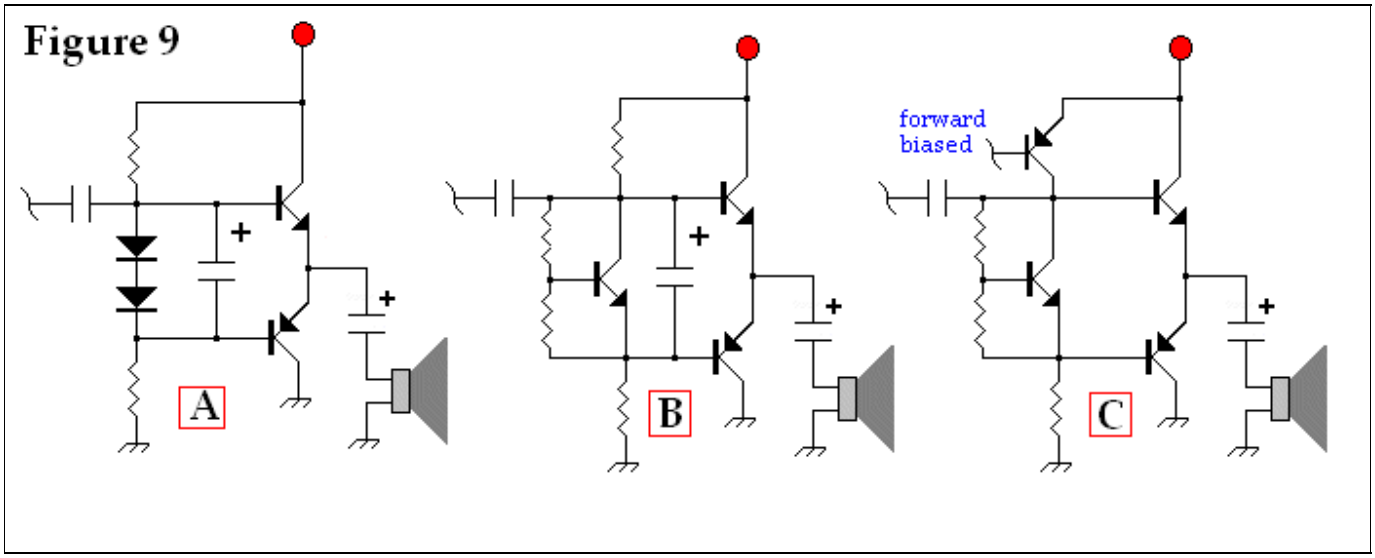

You may see a capacitor inserted between the output transistor bases as shown in Figure 9A and 9B. I have seen capacitor values from 4.7 uF to 100 uF used and the value is not critical, however, from my experiments, I have learned it is mandatory. This capacitor serves to keep the bias voltage constant as the AC signal swings up and down. Some engineers refer to the amplified diode an **NPN shifter bias amplifier** or a **level shifter**. Its function is to charge up the capacitor between the bases of the power follower NPN and PNP pair to a voltage difference that establishes the quiescent current.

In 9C, R1 has been replaced with a PNP transistor which is usually forward biased by another transistor. You may observe any number of variations of the basic biasing circuit presented in Figures 6 and 7, including 3 or more small signal diodes, 2 amplified diodes, current sources, feedback loops and more. although the techniques vary, the authors are still just biasing the complementary emitter followers to achieve low crossover distortion, stability and/or thermal tracking.

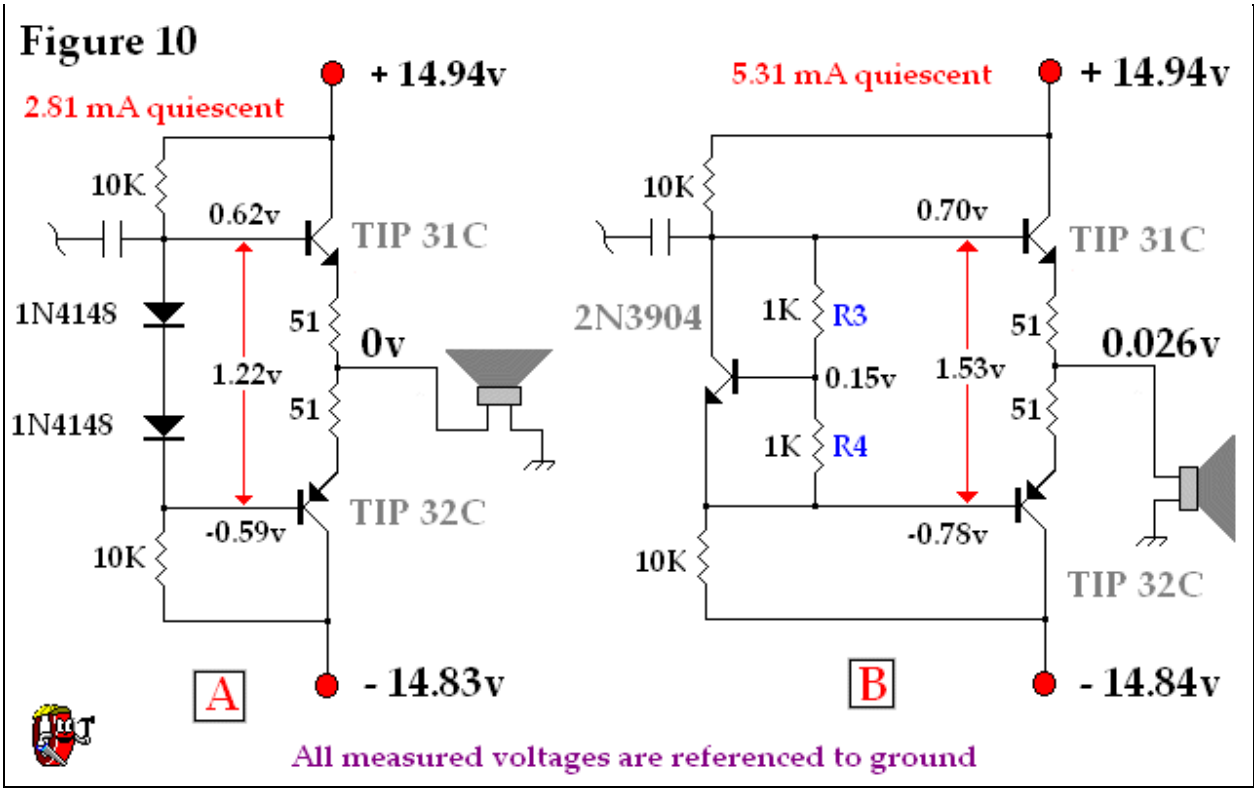

Shown above in Figure 10 are 2 amplifiers using a split power supply. The split power supply offers increased headroom due to a greater AC voltage swing as well as increases the available RMS output power without using super high AC power transformer secondary voltages. In addition, the split supply works well with op amps and if desired, enables you to reduce the number of coupling capacitors by allowing direct coupling of the preamp and speaker to the power amplifier. Coupling capacitors alter frequency response and perhaps may present phase shift issues. In some cases, we as builders use coupling capacitors to provide effects such as high pass filtering, however in Hi-Fi amps, enhanced low frequency response is usually desired; which necessitates the use of high value coupling caps in single power supply amplifiers. In split supply amps, the choice of using a coupling capacitor or not is available to you. In the Figure 10 a and b circuits above, the speaker is directly coupled to the complementary emitter followers output. Note that the voltage at this point is 0 or nearly 0 volts. For any given power supply voltage you chose (split or not), please ensure the amplifier components can handle the current and subsequent heat when a signal voltage is applied. This topic is out of scope. Build and measure...build and measure...

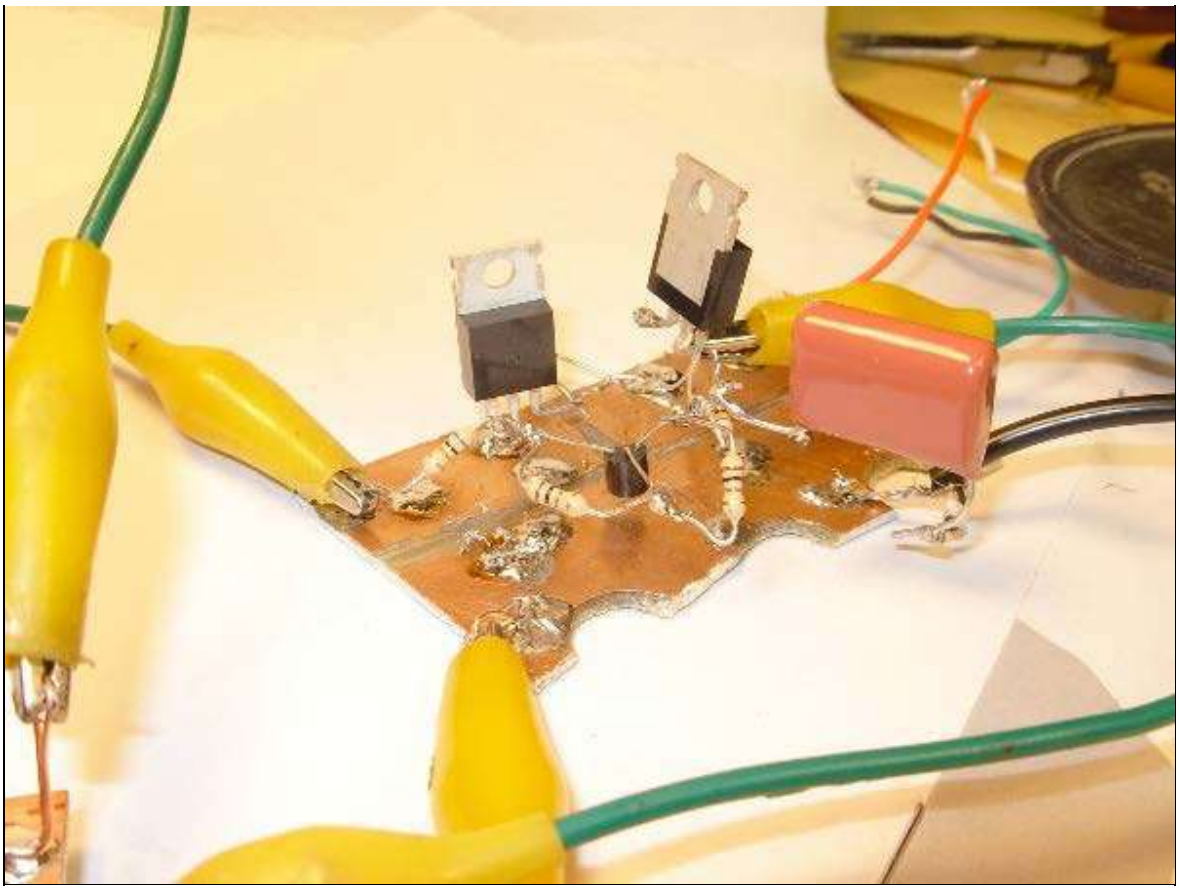

Shown above is a breadboard of the Figure 10b circuit. Additional experiments using even higher voltages were also performed, hence the moderate power TIP transistors were utilized. I burnt up four 2N3904/6 transistors performing many experiments with biasing over 3 nights. Some of the outputs of these experiments will be presented in future projects.

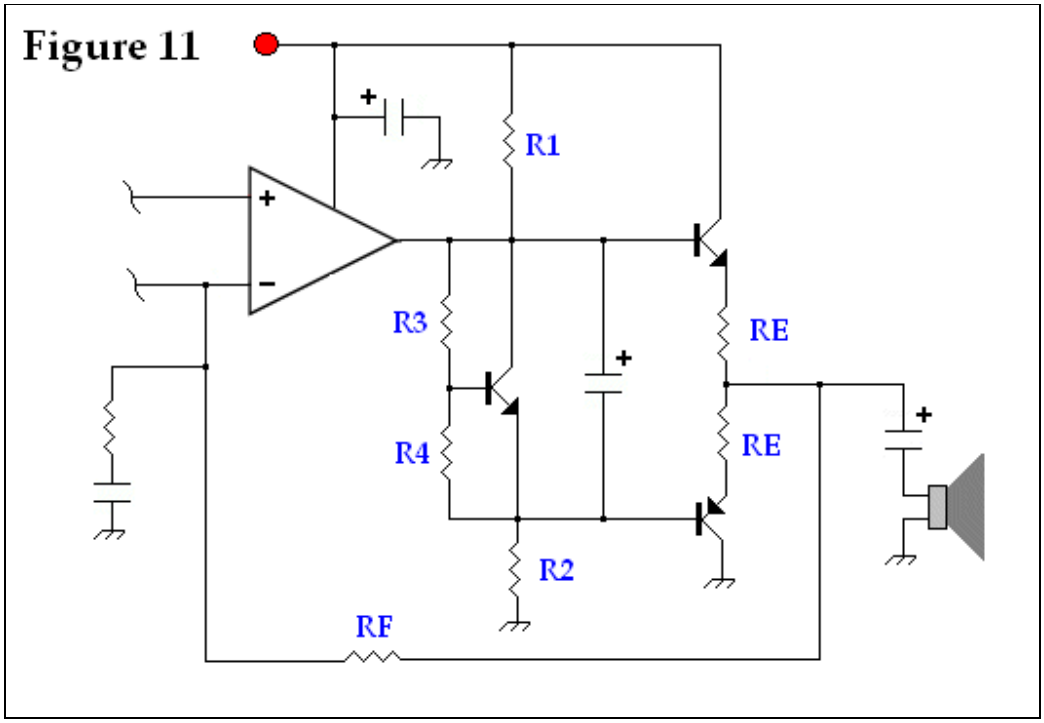

Shown above in Figure 11 is a complimentary emitter follower pair directly coupled to an op amp. The amplified diode and its biasing network is inside the op amp feedback loop. There are examples of this circuit in EMRFD and also on this web site. In single supply powered op amps, it is possible to omit R1. An example of this may be found in Figure 12.30 in EMRFD. Using a low noise op amp such as the NE5532 to drive your power followers can give outstanding results.

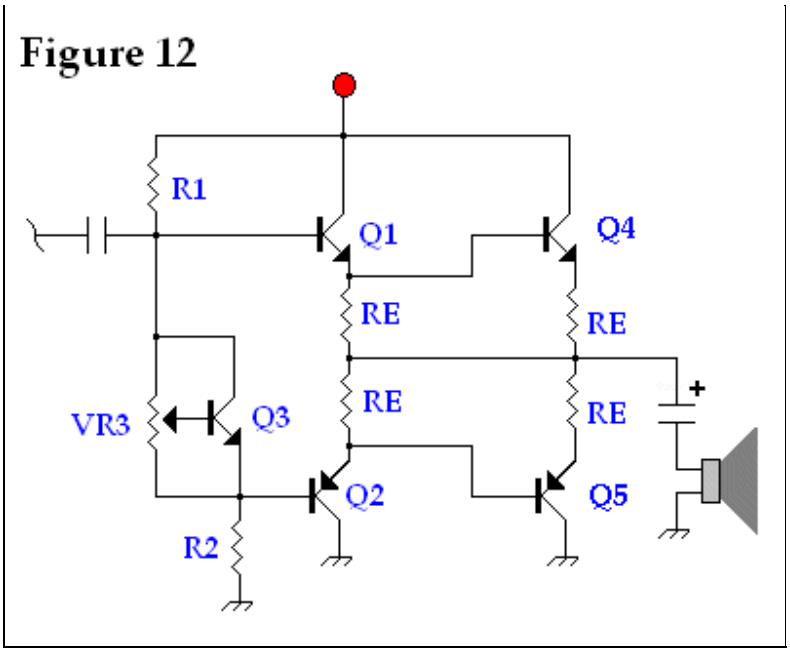

Shown above in Figure 12 is another theoretical power amp which illustrates the building block aspects of the simple stage we have been discussing. Q4 and Q5 are cascaded with Q1 and Q2 to build up the current (Darlington emitter followers). Such an amp could have several watts of output power depending on the supply voltage. The emitter resistors on Q4 and Q5 are often 0.47 to 1 ohm power resistors.

References

EMRFD Although Rick Campbell and Bob Larsen contributed chapters and circuits, the principal author is Wes Hayward. It amazes me that any human being could know so much about electronics and is so willing to share his knowledge. Respect.

Henderson, John. Electronic Devices Published in 1991 by Prentice Hall

Oleksy, Jerome E. Practical Solid-state Circuit Design Published 1974 by Howard W. Sams and Co.,Inc

Slone, Randy G. Understanding Electricity and Electronics Published 1996 by TAB Books-McGraw Hill

---

Low Power Audio Amp Experiments

Introduction

This web page contains some experiments on simple, low power, speaker output audio amplifiers. Presented are ideas, some measurements and examples of audio amplifiers which will likely sound better than the IC audio chips commonly seen in many receiver projects. This web page is a follow-on to this one and is a completely new area of experimentation for me. Audio amps were built using both split and positive power supplies. In all cases the complimentary power followers were driven by an op-amp. I tried building some power amps using discrete transistor differential amplifier stages with current sources as the driver, but the noise performance and simplicity of the NE5532 or NE5534 op-amp was superior.

Split or Bi-polar Power Supply Audio Amplifiers

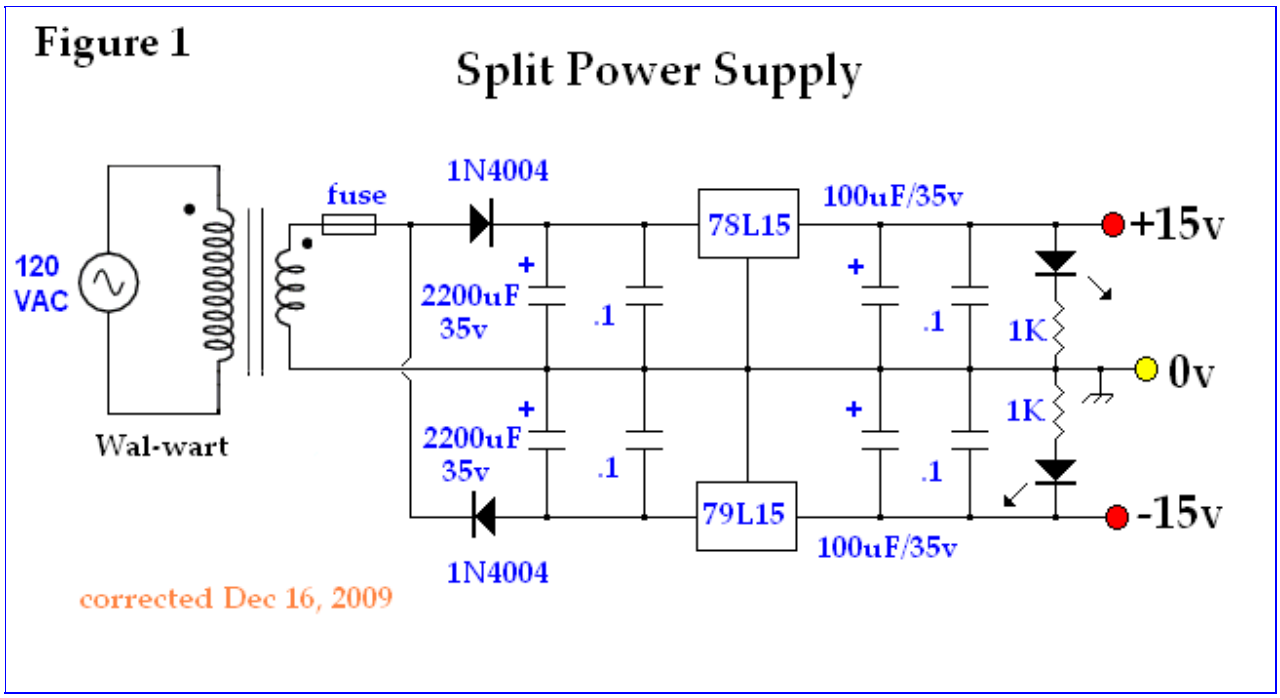

In order to build up some split power supply amplifiers, a basic power supply was constructed and the schematic is shown in Figure 1 above. I

found it was essential to regulate the voltage or hum would appear on the output. Choose a standard value fuse that is rated somewhere just above the maximum current you measure. I used 2 different AC output power transformers which were in the 18-24 volt, 375 mA to 1 amp range. The LEDS are strongly suggested. They inform you when there is power applied and their relative brightness will also often fall when higher current is being drawn on one side or the other. This alerted me to an accidental solder bridge to ground on more than 1 occasion.

The split power supply is shown in the photograph to the left. The retro Bakelite fuse holder is from an old tube audio amplifier. If you are wondering why the copper clad board is so large, the power supply is part of a future project. Some builders would use even greater value filter capacitors than those shown. Heat sinks on the voltage regulators are required for supplying DC to higher power amplifiers.

Rod Elliot Headphone Amp

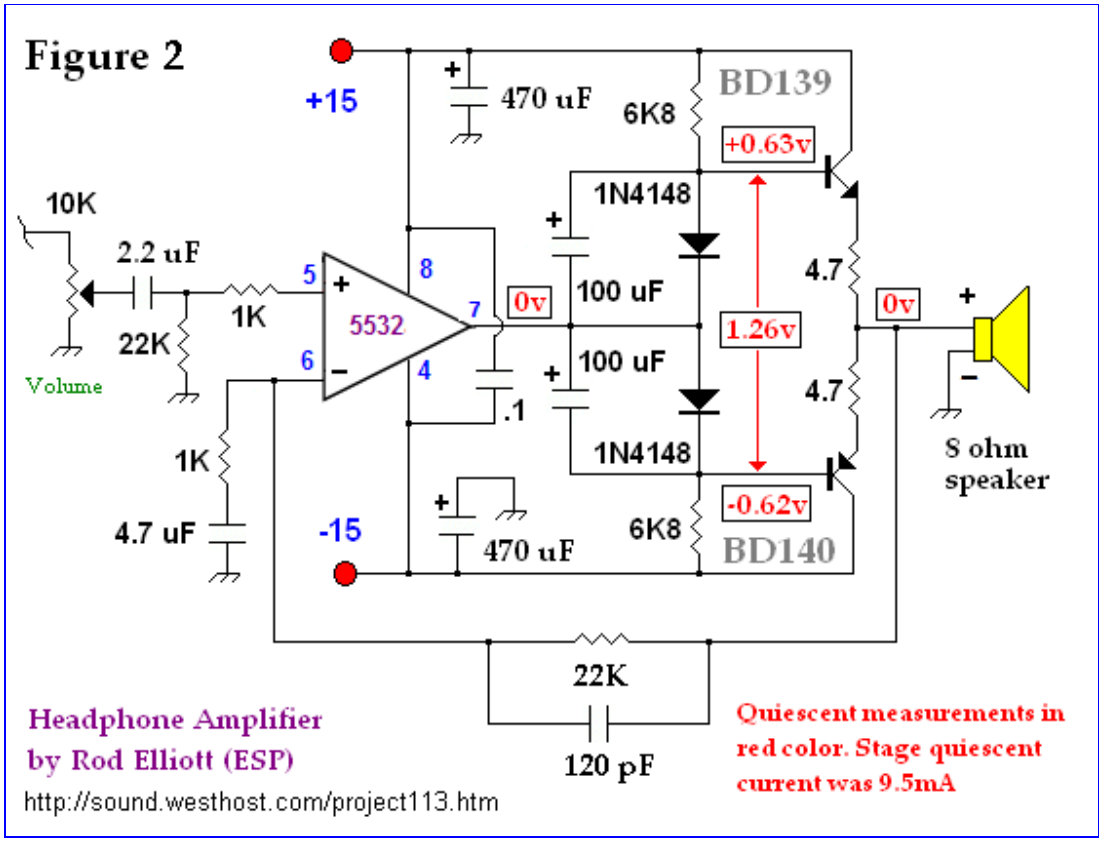

The first amp I built is shown in the Figure 2 schematic above. This amplifier was designed by Rod Elliot and is used with his permission. Rod's ESP web site is a virtual treasury of audio design information. If you are into understanding audio design, visiting his web site is strongly recommended. Rod sells printed circuit boards for all of his circuits if you prefer this building method . Note I have made some minor modifications to some part values. although primarily designed as a low distortion, high power, headphone amplifier, it drives an 8 ohm speaker very well. I was able to drive this amplifier as high as 0.68 watts average power with a pure sine wave output during analysis. Power measurement is discussed in the next section. Note that on this web page, I quote the entire stage quiescent current. Since the op-amp and the

2 (or more) power followers are a "package", it is a lot easier to just measure the current at the power supply lead(s) of the stage than unsolder and lift up a transistor lead. In this case, with no input single, the stage current was about 9.5 mA. I did check and about half the current is going to the op-amp with the other half to the transistor pair. This is a wonderful sounding amplifier and Rod has an entire web page devoted to it, so I will not comment further.

There are a variety of suitable transistor pairs for audio power amplifiers depending on the power output you are choosing. I stock just a few; BD139-140, TIP 41C-42C, NTE 128-129. The higher beta 2N3904-3906 or 2N4401-4403 pairs worked well in the low power, single power supply amplifiers shown on this web page. I also performed some higher output power experiments which required the TIP and BD transistors and these are not shown.

Above photograph. A breadboard of the Rod Elliot headphone amplifier. This early version had a temporary output capacitor. When first testing a new circuit that has a direct speaker output, it might be a good idea to temporarily use an output capacitor until you measure your voltages and current and feel your transistor temperatures. This will save your speaker if you made a big mistake and/or blow up the transistors when you first power it up.

Amplified Diode Biased Audio Amp

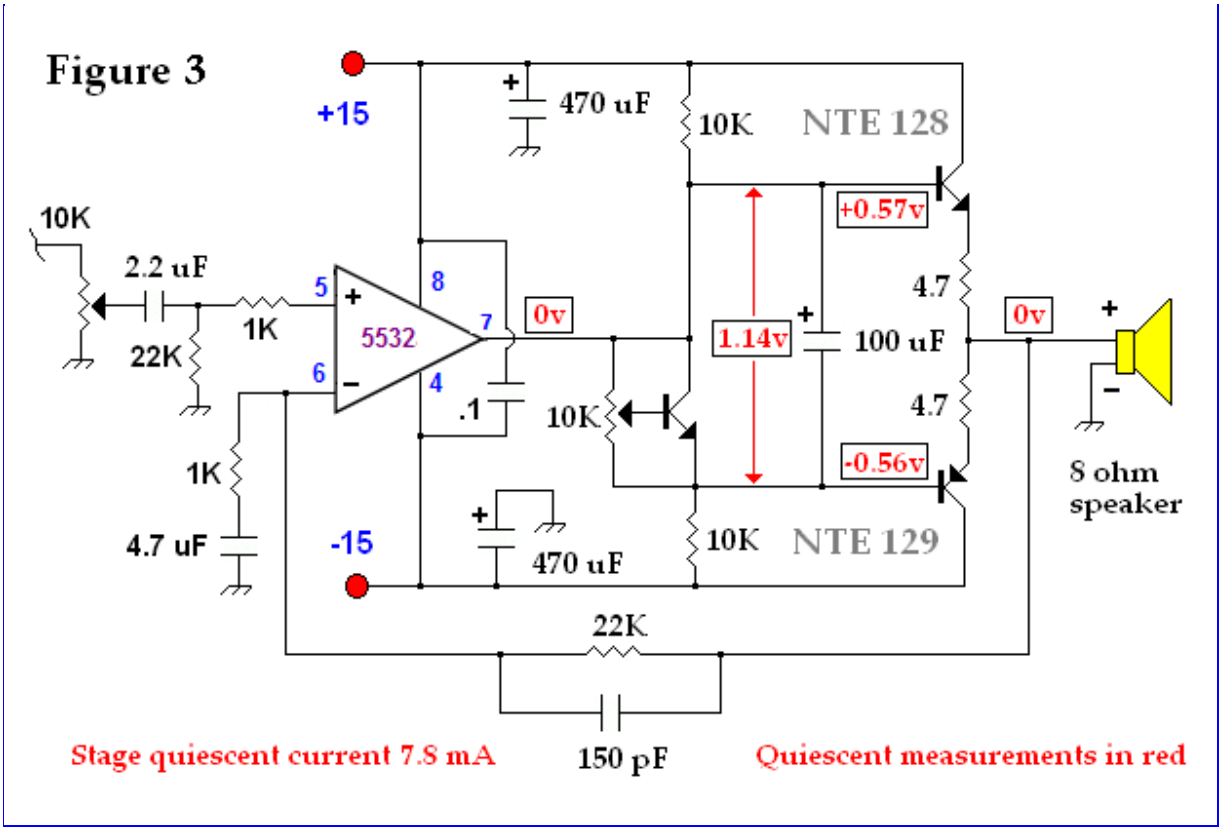

Above in Figure 3 is a split power supply audio amp using an "amplified diode" to control the bias. The bias transistor was wedged between one of the output transistors and a piece of copper clad board to allow thermal tracking. The 10K bias control resistor was a trimmer type suspended over the copper clad board in most of my bread boards. Usually, you just need to set and forget about this resistor after initial set up. I adjusted the bias by watching in my oscilloscope with a low level, 1 KHz sine wave connected to the input. I measured the various voltages and stage current at quiescent and have indicated these values in red for learning purposes. The bias current range was 7.2 to 154 mA when turning the 10K trimmer pot from 1 extreme to the other. The maximal clean output average power of this amp was 0.78 watts. I used press on heat sinks for the NTE128-129 pair and they ran quite warm to touch. These TO39 type packaged transistors are somewhat difficult to heat sink compared to the TIP/BD transistor packages where you can just bolt on a heat sink of any size that is required. Please remember that the metal tab on the TIP and BD transistors is connected to the collector terminal.

In the above photograph is my first bread board of the Figure 3 amplifier. This particular version had TIP transistors, a 4 ohm speaker and an 470 uF output capacitor. Note the full size 10K bias control potentiometer on the left hand side. This was purely a experimenter's bread board, but it sounded amazing when listening to music through it.

Harmonic Distortion and Measuring Output Power

Average Power Formula

Applies to a continuous sinusoidal tone into a purely resistive load

$$P = \frac{\text{Peak Voltage}^2}{2 \times \text{Load Resistance}}$$

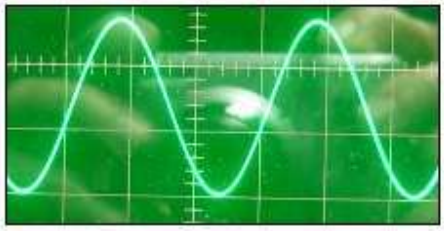

Figure 4

In Figure 4 is the formula used to calculate the average power of the circuits on this web page. For example if you measure 6 volts peak to peak on the oscilloscope, (3 volts peak voltage) and your resistive load is 8 ohms, the average power is 560 milliwatts. At any point in an AC waveform there is power and it may be reported using a variety of ways. Was it clean? distorted? a peak value? an RMS value? - often it is unclear.

To be clear, I measured the peak voltage on a pure, undistorted sine wave into an 8 ohm resistor. Stated power values are the mean sine wave power calculated with the formula shown. See this somewhat controversial link for details. You may not agree with my methodology, however, it allows you to compare the circuits on this web page. If you really must know the peak power, multiply the stated average sine wave power by 2. I will leave the power measurement and calculation debate up to scholars; as a lay-person, I need something simple.

The bench voltage measurement was as follows: The amplifier was connected to a 1 KHz pure sine wave generator and the 10K volume control pot was advanced just until any sign of distortion of the amplifier output sine wave appeared. Voltage measurement was taken at the point just before distortion occurred.

It is difficult to photograph a sine wave without a tripod. Motion, the angle, light reflection and jpeg graphic compression all wreck the perfect sine wave. In the Figure 4 graphic above is a typical 1 KHz output waveform from my power amplifiers (squeaky clean) at the amplifiers maximum average power level.

To the right is a photograph of my AF signal generator. This is an old, tube device but the output sine wave is beautiful. I did not perform spectrum analysis with a computer audio sound card program and will leave this up to audiophiles. These audio amps sound great; especially when compared to the IC audio power amps that many of us tend to use in our receivers.

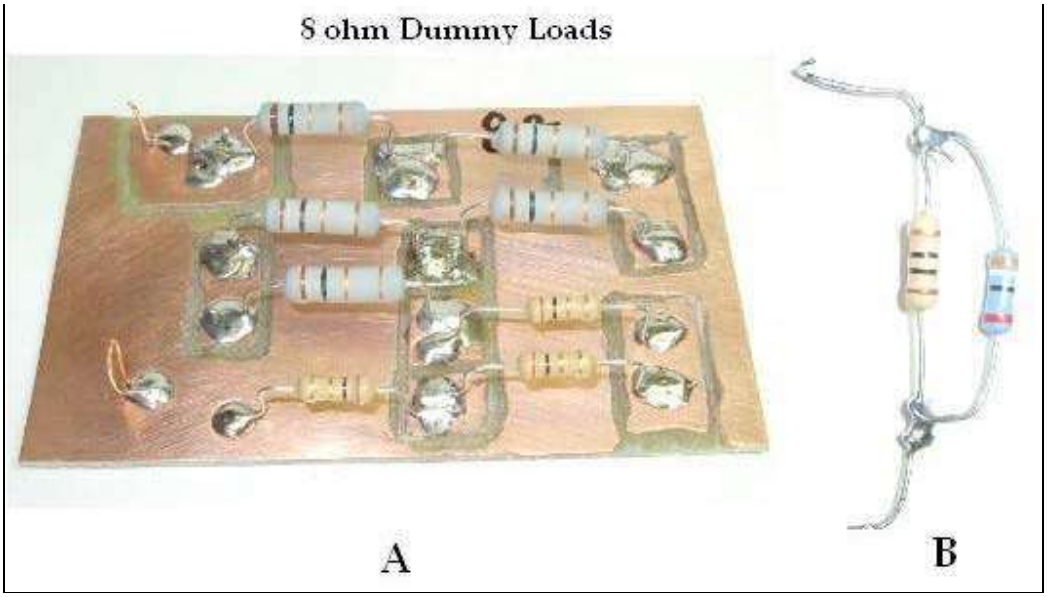

In the above photograph is **A**, an 8 x 1 ohm resistor load and **B**, an 8 ohm load made from parallel 1/2 watt 10 and 39 ohm resistors. In dummy load **A**, I used 5 two watt metal film resistors plus 3 half watt resistors. In the future, I will obtain 3 more 2 watt resistors and replace the 1/2 watt resistors for a 16 watt rating. For a quick resistive load, **B** is the way to go for most of the circuits on this web page.. You can make a 4 ohm load from parallel 4.7 and 27 ohm resistors. In truth, a single resistor or any combination of resistors adding up to the desired load R value will work.

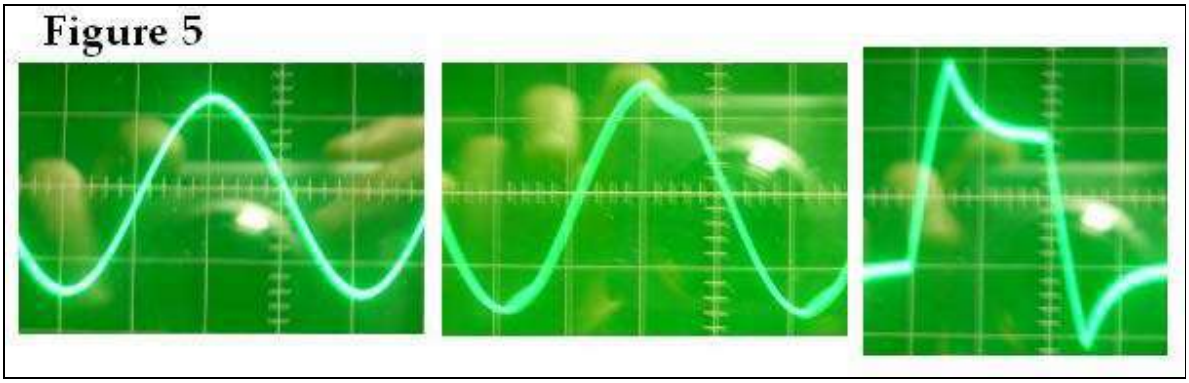

In Figure 5 above are some scope waveforms ranging from mildly distorted to full-on dirty.

Power Amplifier Concerns

Although the amplifiers on this page are 0.15-0.8 watts or so, they can consume relatively large current compared to the usual voltage amplifier circuits we build. Some potentially helpful tips to help keep away ground loops, oscillations and thermal run away are suggested as follows:

✓ Connect your negative speaker terminal directly to the AF power amp (do not use a common ground for the negative speaker terminal).
✓ Use big power supply line bypass capacitors (no 10 uF caps here)
✓ Keep your audio amplifier copper clad board separate from the rest of your circuit boards and star ground it to your main power supply ground point.
✓ Use heat sinks on your final transistors and voltage regulator(s) when you go for bigger power
✓ Watch your layout - keep the output away from the input etc.
✓ Watch your emitter resistor power ratings in "higher wattage" amplifiers. Burning resistors stink.

Single Power Supply Audio Power Amps

Since most 12 volt power supplies are actually closer to 14 volts; these experiments were performed with a typical radio bench DC power supply at 13.69 volts.. Figure 6, 7a and 7b represent evolving experiments aimed at obtaining greater output power.

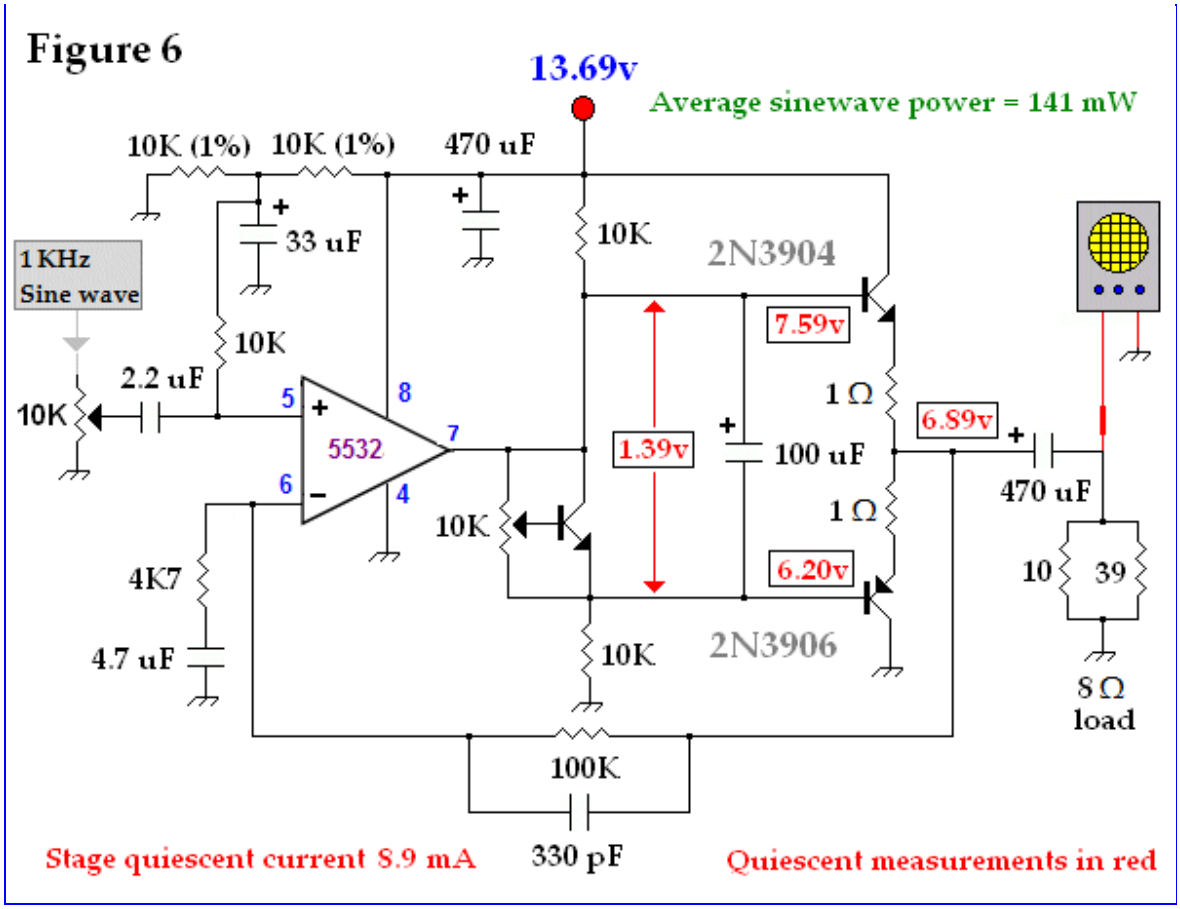

Shown above in Figure 6 is the fundamental design using one op-amp and 2 power followers. It is shown in an AC output power measurement configuration. The bias current range was about 5 to 100 mA when turning the 10K trimmer bias control pot from one extreme to the other. Maximal sine wave average output power was only 141 mW. Nevertheless, it might be loud enough for some receiver applications.
I connected this amplifier to a VCC of 15 volts. The maximal sine wave average output power was then 220 mW. In all of the single supply audio amps presented , increasing the VCC increased the maximal power output. Driving these amplifiers beyond a pure sine wave output power resulted in predictable harmonic distortion plus the re-emergence of crossover distortion in the output. This was an incredible learning; how could there be crossover distortion re-emerging in a amp that was properly biased to begin with? Increasing the bias current to the maximum level did not remove this crossover distortion. After emailing this question to Rick, KK7B and Wes, W7ZOI, and reading their replies, my best guess was that at some power level, the 5532 op-amp can not provide enough current to properly drive the complementary symmetry pair. The AC current in the output transistors may be limited by the base drive of the op-amp and they were no longer forward biased at the crossover point.

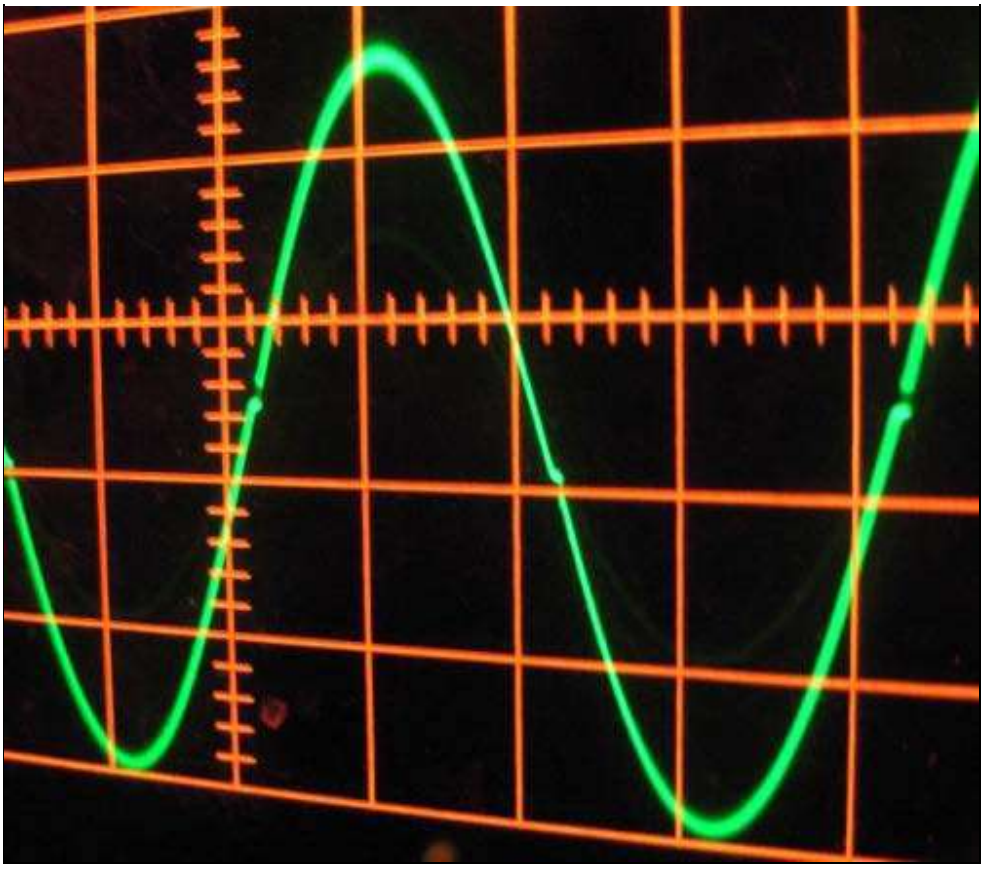

Above photograph. This is the Figure 6 amp driven past the point where the sine wave is pure. Note the crossover distortion blips on the sine wave. The base drive current for the power follower pair all comes from the op-amp. At this point there is likely not enough base drive to keep the base emitter junctions forward biased.

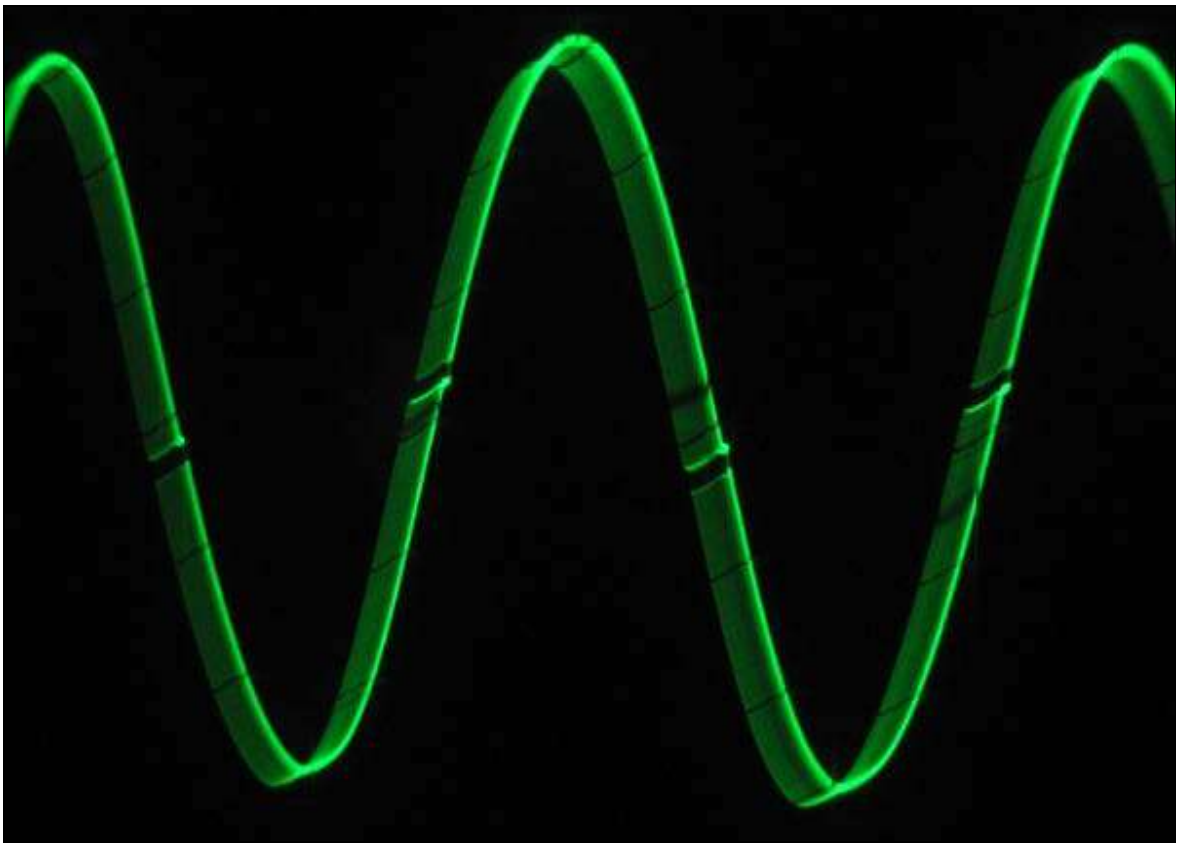

In the above photograph I blacked out the room and photographed the same scope waveform as above while shaking the camera from side to side. This adds some horizontal spreading of the signal and provided more information about what was happening as compared to a single,

clear oscilloscope trace.
I should mention that this crossover distortion blip occurred in all of the Figure 2 to 6 amps when they were driven past the point where a pure sine wave was seen. It is clear that maximal available power from a simple audio amplifier like this **(one NE5532 op-amp plus 2 power followers)** is constrained and thus its application is limited. Greater output power is possible using a split supply per Figures 2 and 3, however, a typical radio project has a 12 volt, single power supply. These basic amplifiers with a single power supply, may be very appropriate for projects such as a compact radio receivers or a code practice oscillator project, but not for applications where you require louder audio.

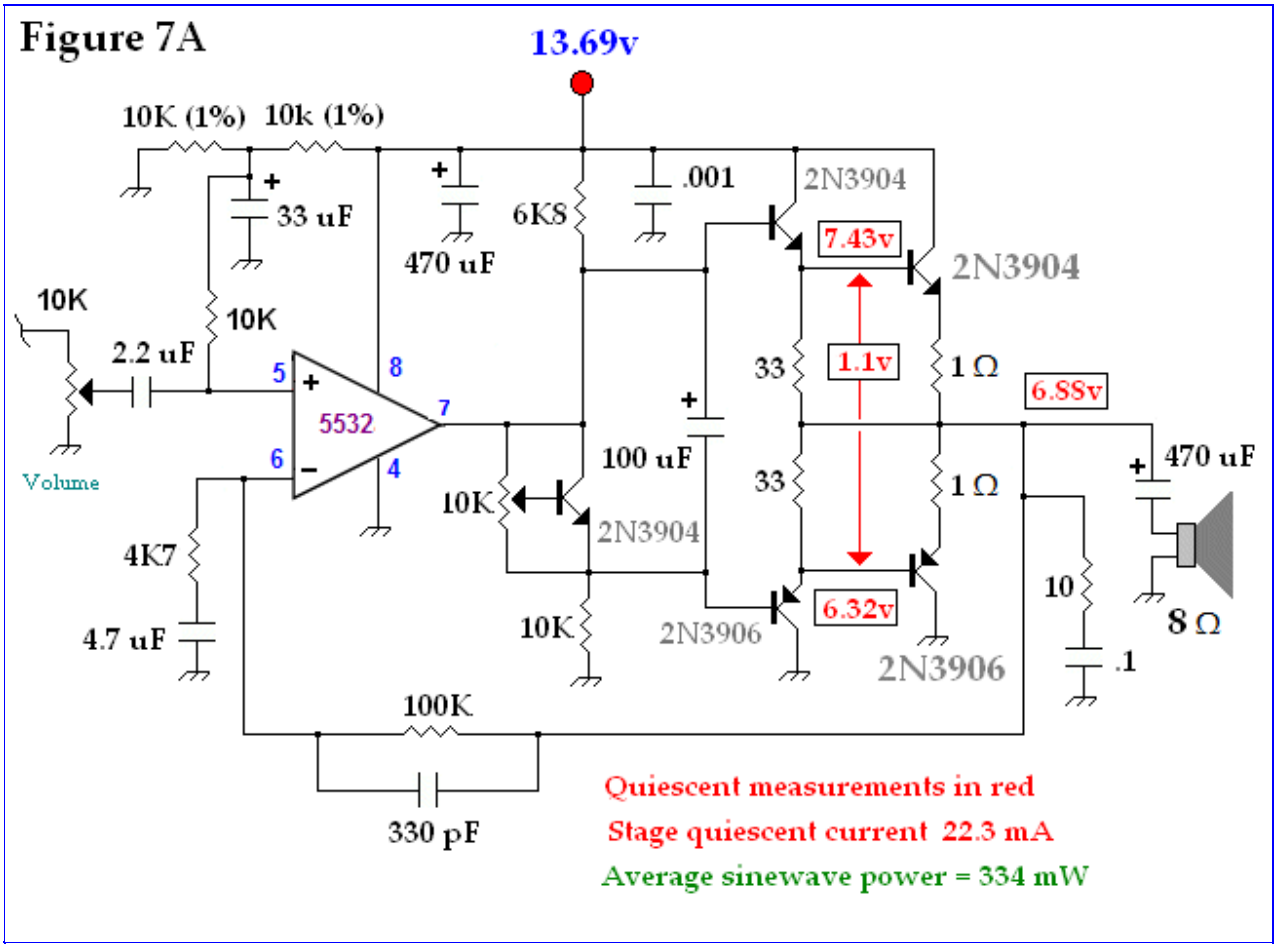

Shown above in Figure 7a is an easy method to get more output power from the Figure 6 amplifier; add another set of complimentary pair current amplifiers. I found 33-39 ohms to be a good emitter resistor value during my experiments. Many hi-fi amp builders will use greater emitter resistor values, however, a design goal was to get more output power from our 12 volt supply. Series emitter resistors are used to improve linearity and operating-point stability. I kept the final power follower pair emitter resistor values at 1 ohm to get maximal output power. An output 10 ohm + 0.1 uF low pass filter was used to help prevent oscillations in view of the low emitter resistor values on the finals.

Biasing

The top 10K bias resistor was lowered to 6K8 to facilitate "more linear" setting of the output transistor bias with the 10K trimmer potentiometer. It did not help much. Setting the bias is very delicate procedure and you must turn the screw driver very slowly. In my bread board, the optimal stage bias current was 22.3 mA but anything around 20 mA should be fine. If you do not have an oscilloscope, after ensuring that there is no input signal, connect an ammeter in series with the positive power supply lead. Turn the bias potentiometer with with the screwdriver until you get close to 22 mA. If you only have a voltmeter, the rule of thumb of 1.1 seems to work... Measure the voltage across the final 2N3904-2N3906 bases and ensure the difference is at least 1.1 volts while adjusting the 10K trimmer pot. Personally I do my biasing with an oscilloscope at at least 2 different frequencies on the signal generator, however the for mentioned methods will work okay. This is a popcorn stage and a popcorn web site after all!

For the lowest potential noise, consider using metal film type resistors in your audio amps and "polysomething" capacitors wherever AC signal is coupled to another component or ground, excluding the output capacitor.

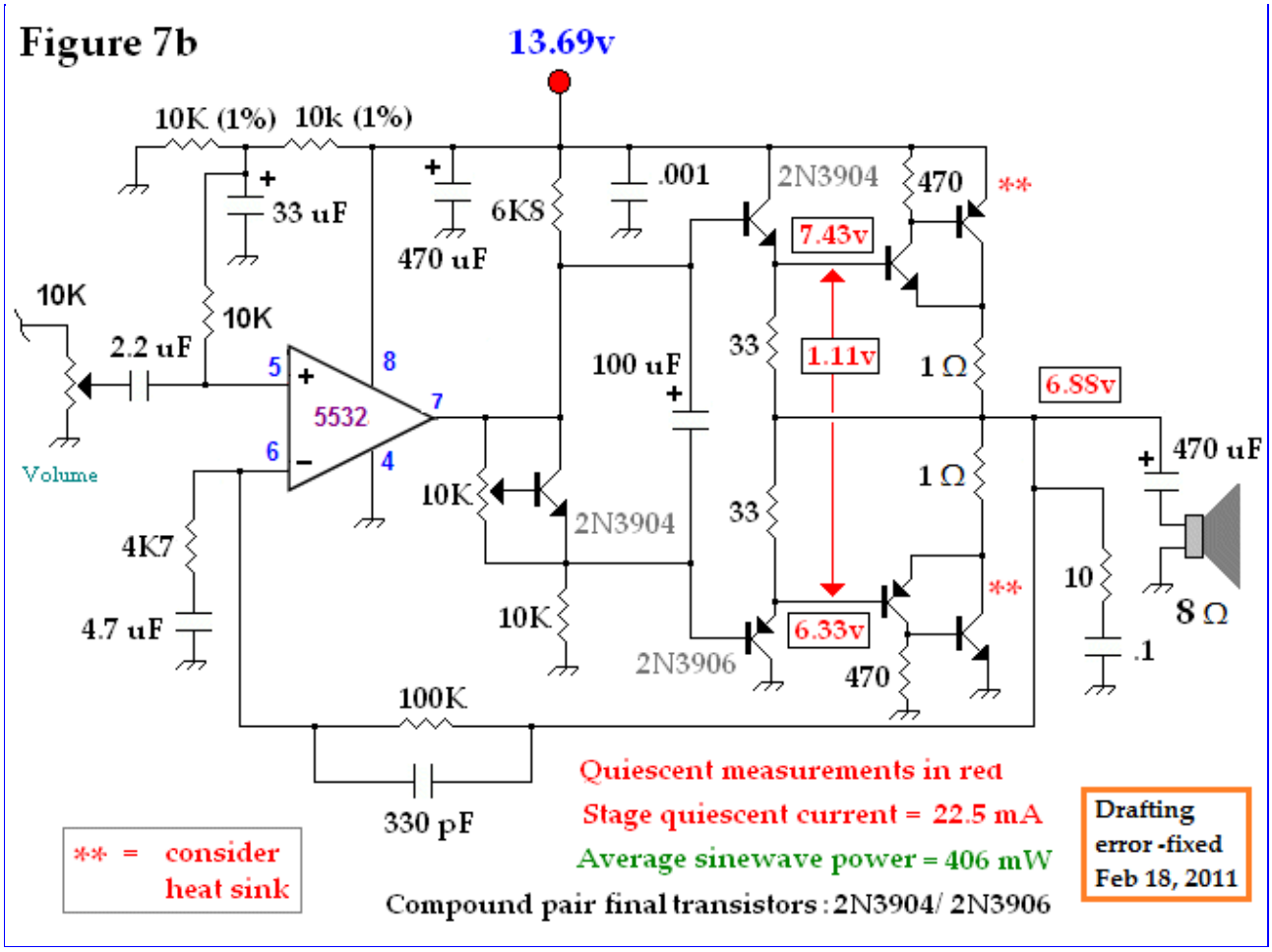

Further experiments to increase output power were frustrating. Finally a compound or Sziklai pair was trialed and increased the average power to over 400 mW as shown in Figure 7b . I used a small piece of copper clad board on the finals for a heat sink, although they really didn't get that warm. Ideally, the amplified diode should also be glued onto one of the heat sink boards for thermal tracking. This amplifier is now in a chassis as a bench reference audio amp for receiver testing.

In the above photograph is the Figure 7b prototype. I am using a new miniature potentiometer for my experiments that I bought from Digi-Key. The base has 2 leads which can be soldered right on the copper clad board for easy anchoring and removal after testing.

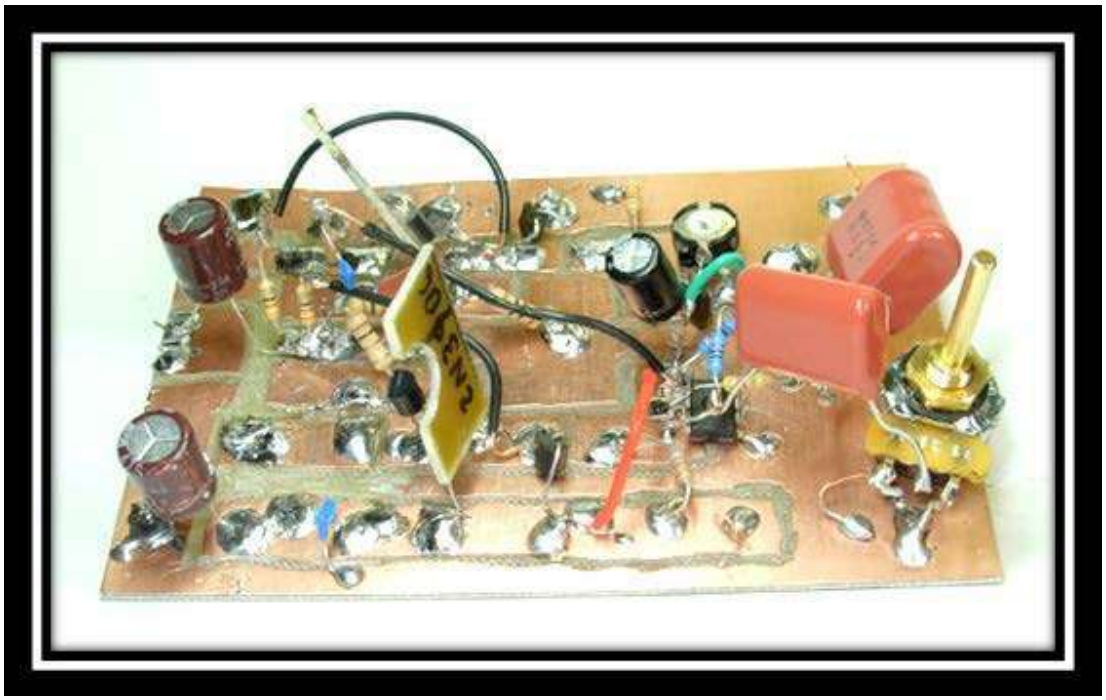

Another view of the bread board on which the Figure 6, 7a and 7b experiments were conducted.

KK7B Headroom Boosting Emitter Capacitors

We first learned about using large value emitter caps in audio amp complimentary pairs from EMRFD. Experimentation revealed that these capacitors do 2 things: **1.** Can increase the amplifier sine wave headroom and **2.**

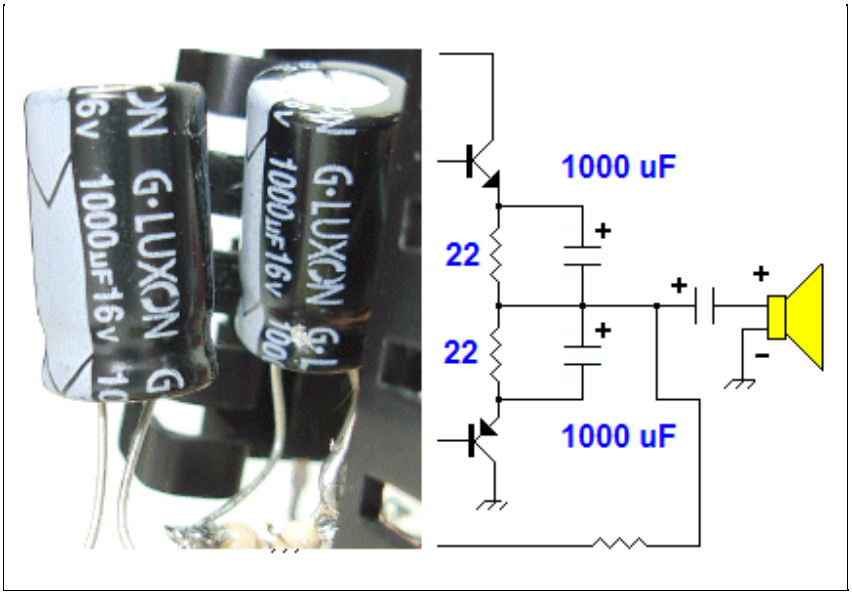

Add some low pass filtering. I learned from Rick, KK7B, that he designed his EMRFD amp to achieve low output power, low distortion and lower DC current drain. He desired a clean output audio amplifier for his R2 series of receivers without needing a lot of quiescent current or heat sinks on the 2N3904-2N3906 pair. The caps were added to make the amplifier think it had much lower emitter resistors at AC than the 22 ohm resistors he used in the EMRFD projects. When Rick made measurements and simulations of the amplifier, it was very stable, had low distortion and provided a very nice clean sound at all signal levels, from very weak signals in a few milliwatts of noise, to music driving the speaker. The result is outstanding and Rick's design was the catalyst for my own interest in audio amplifier experimentation.
I performed experiments with these capacitors and found that they increased my amplifier power and head room in some cases, and that the boost is indirectly proportional to the emitter resistor value. With 1 ohm output transistor emitter resistors the boost is generally not that significant. With 4.7 ohm or greater emitter resistors, they can make a big difference and you might consider trialing them for more power and headroom as appropriate. They can also add a nice, warm sound to your audio amp. Refer to EMRFD for numerous examples of this technique.

Popcorn Audio Amplifier

What follows is a popcorn or "poor man's" audio power amp using the 2N3904-2N3906 pair. To meet true popcorn criteria, all of the capacitors used in my breadboard were electrolytic and you can substitute different values from your own junk box. It would be better to use "polysomething" capacitors for the NE5532 pin 5 and 6 signal capacitors if you have them. I normally use a 1 uF to 4.7 uF poly-type capacitor in series with the 4K7 resistor on pin 6. The 270 pF feedback capacitor could be omitted or substituted with a higher or lower value to suit whatever high frequency roll off you desire.
The transistor glue-on heat sinks seen in the 1 bread board photograph are completely unnecessary. This BJT pair were used in other higher power experiments as well. The 22 uF capacitor between the transistor bases is essential from my experimentation. Without this capacitor, the amplifier headroom decreases and crossover distortion occurs. You can use the other half of the 5532 for a preamplifier or use a NE5534 instead. A 741 op-amp would be a horrible substitution. The NE5532 performance is breathtaking considering its low cost. 181 mW is surprisingly loud. All resistors are quarter watt rated. What a fun little amplifier! The schematic is Figure 8.

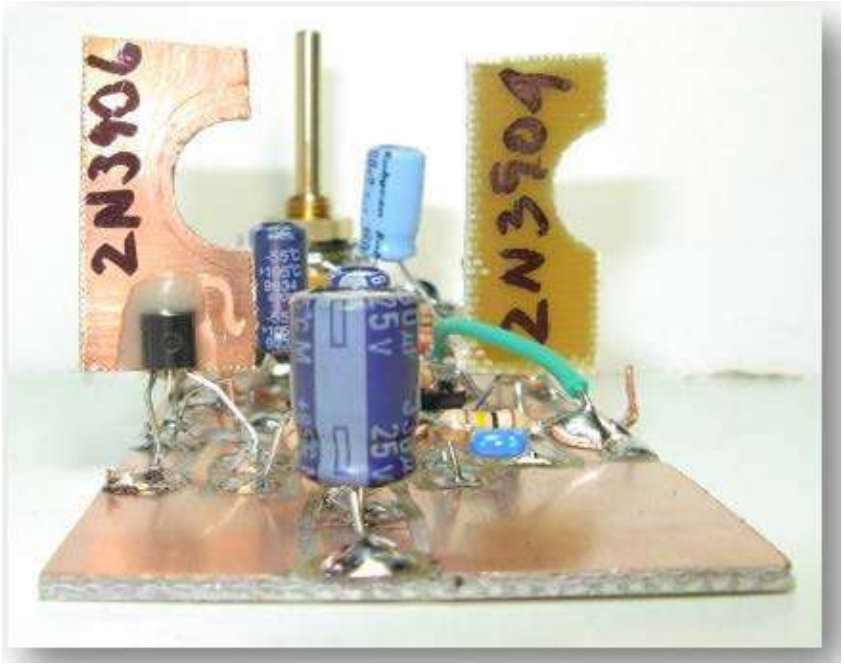

Figure 8

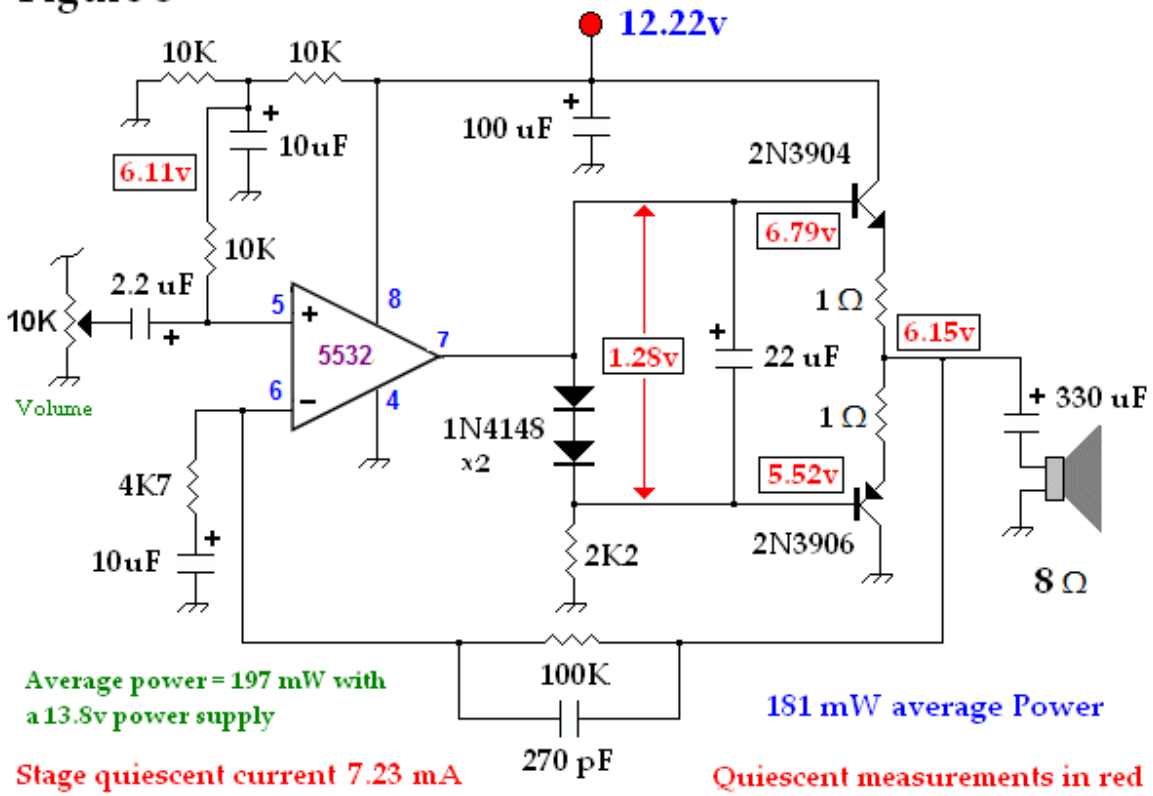
12.22v
10K
10K
10uF
6.11v
100 uF
2N3904
6.79v
10K
2.2 uF
10K
5532
1.28v
22 uF
1 Ω
6.15v
Volume
1N4148
x2
1 Ω
+ 330 uF
4K7
5.52v
10uF
2K2
2N3906
8 Ω
100K
Average power = 197 mW with
a 13.8v power supply
181 mW average Power
270 pF
Stage quiescent current 7.23 mA
Quiescent measurements in red

missing
10K pot

The bread board of the Figure 8 popcorn amplifier using transistors without heat sinks.

Additional Outputs

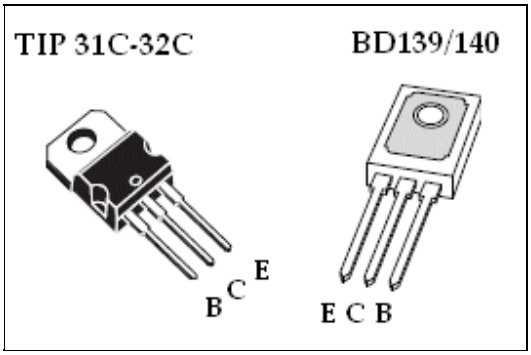

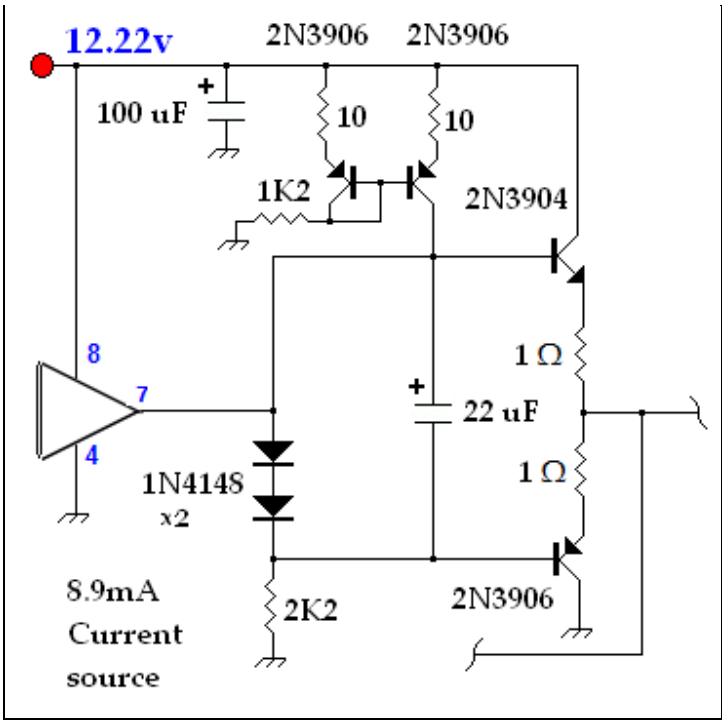

I tried putting a current source on the Figure 8 bias and it made no difference to the amplifier characteristics according to my simple oscilloscope, listening and DC analysis.

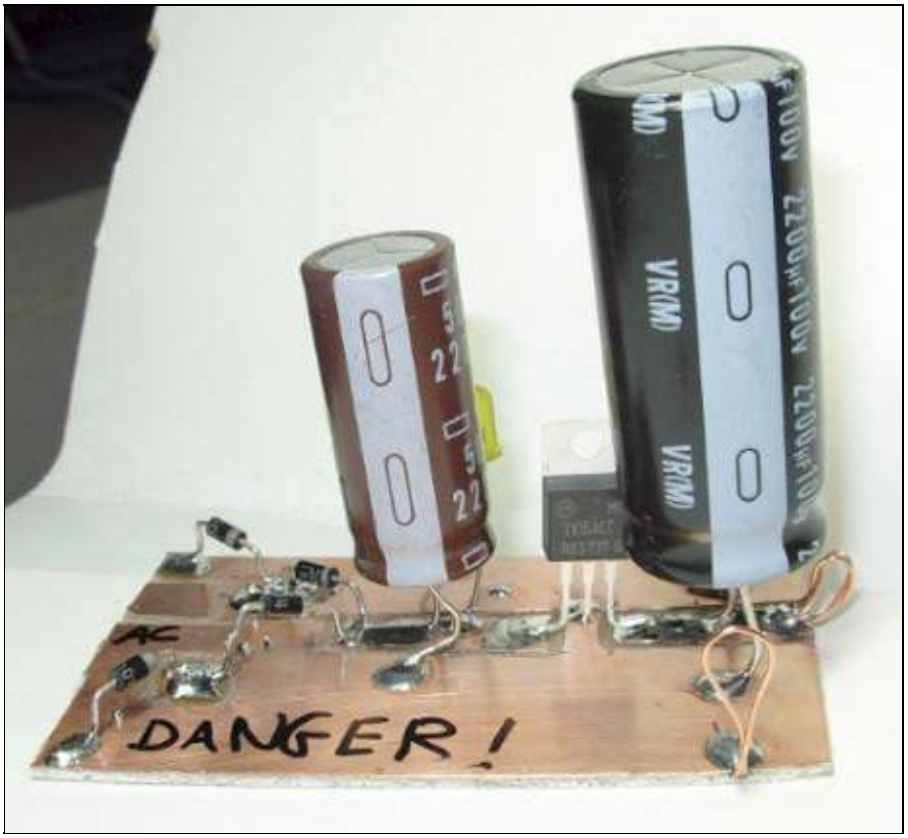

One of the full wave rectifier, voltage regulator and filter bread boards used in these experiments. I went as high as 24 VCC on some single supply amps I tested and was getting over 5 watts average output power

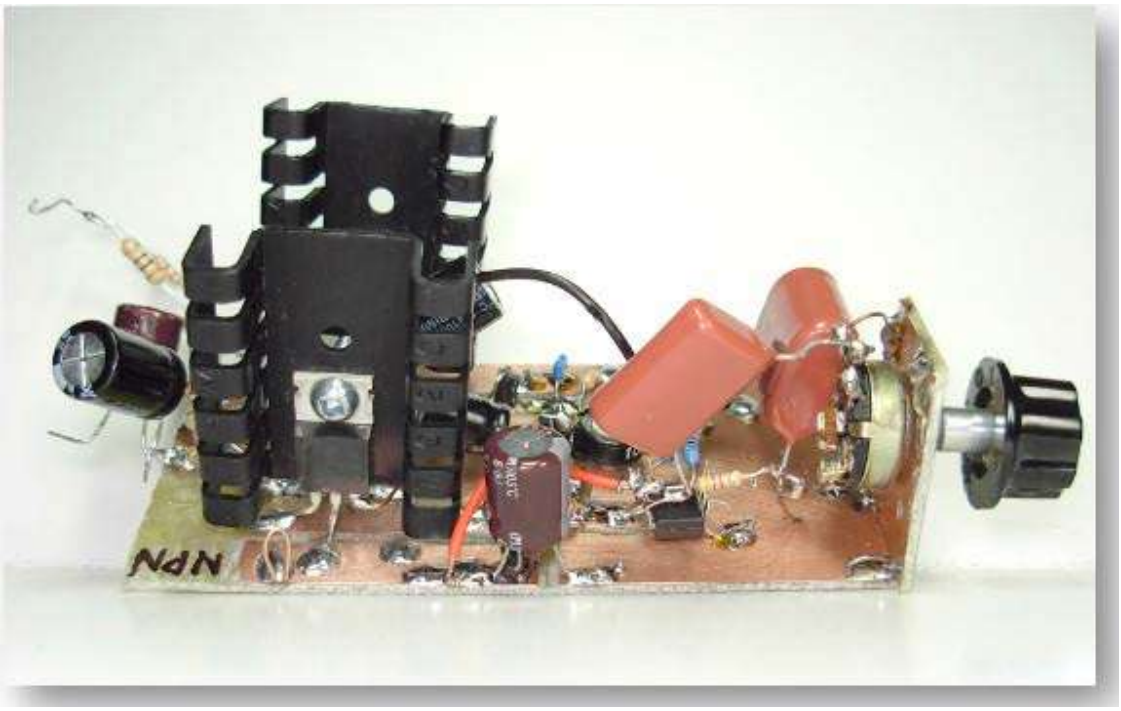
NPN

Two Bravo Receiver Experiments

Introduction

An experimental direct conversion receiver is presented. This 1990's style receiver was built to re-familiarize with DC receivers and try out a few new ideas. Design-on-the-bench bread boarding was used exclusively and was a pleasant way to both learn and pass time. Feedback has been received stating that that certain stages of previous receiver experiments were either too basic or too complex and thus a particular receiver was not built. This web site is as much a cookbook as anything. Kludge together whatever receiver stages you want; no project is meant to be set in stone. This receiver has a high popcorn factor with MPF102 and 2N3904s as the main semiconductors.

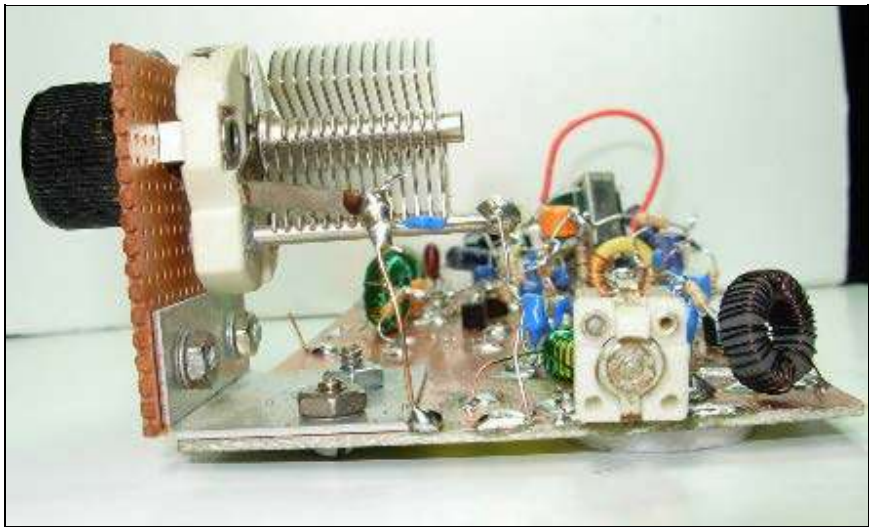

Variable Frequency Oscillator

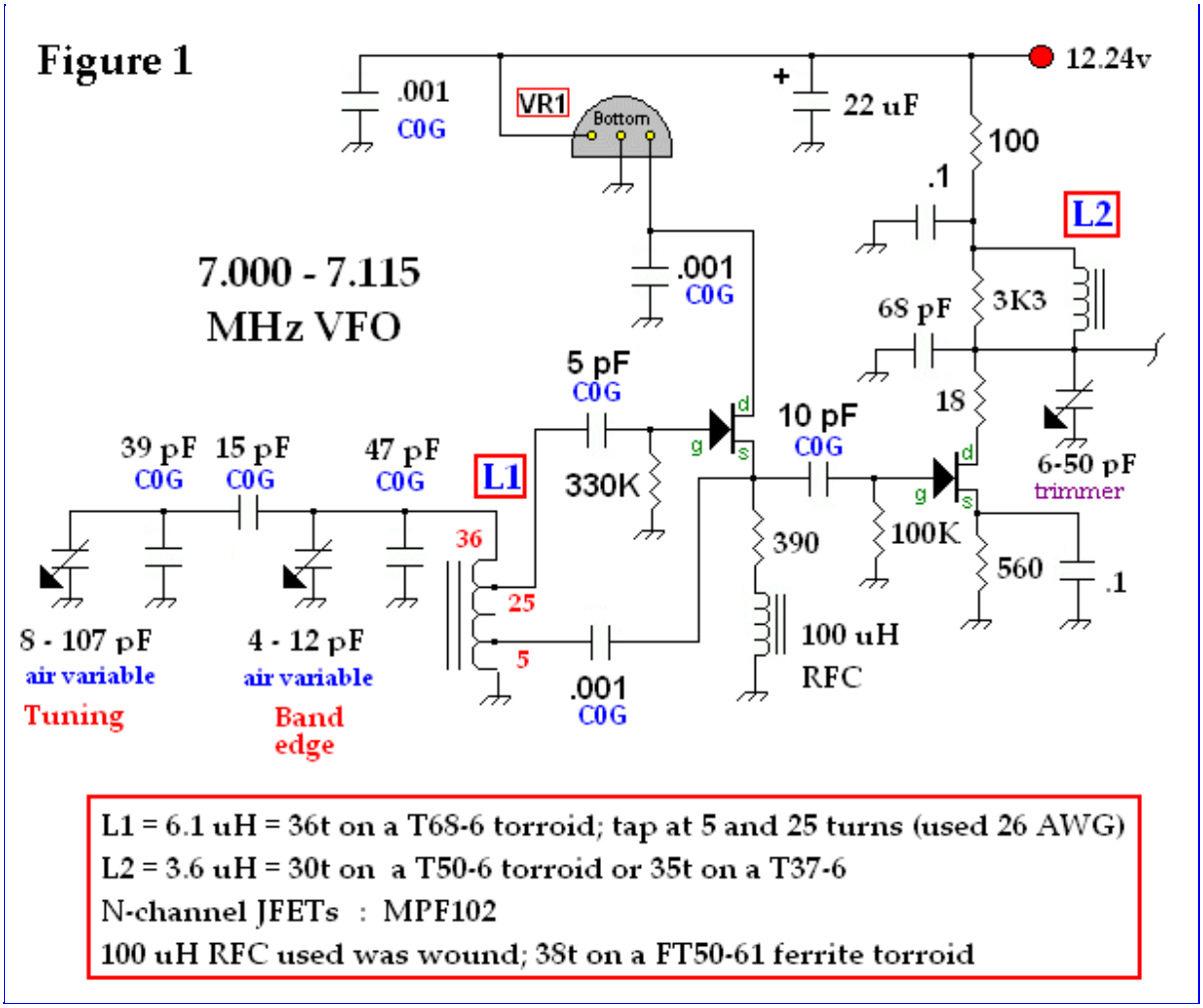

The first stage built was the VFO shown above in Figure 1. The oscillator portion is based upon Figure 4.15 from EMRFD. The VFO resonator tank is isolated from the JFET by tapping down as shown. This is an outstanding VFO topology. See this web page for a few more details and a coil tap calculator. I favor high L to C ratios in my RF tanks, although this does not affect the VFO function. The tapped inductor in this oscillator allows you to use a high RF voltage (low C + high L) while still keeping the FET gate AC voltage at a reasonable level. The buffer amp was designed for high output power and supplies nearly 5 volts peak to peak to the product detector local oscillator port. You can vary the output voltage by increasing or decreasing the 15 pF coupling capacitor for use in other projects.
To peak the L2 tank trimmer capacitor, use a scope, RF voltmeter, or temporarily connect a 10K (or greater value) resistor load to ground via a 10 - 47 pF output capacitor and adjust this capacitor while listening with a nearby CW receiver. (Use a short piece of wire as an antenna.) Additionally, you could also peak this trimmer cap while listening to a CW signal with the completed 2 Bravo receiver. It takes around 100 pF to resonate the L2 tank at 7.040 MHz in case you are wondering.

Since air variable capacitors were used for tuning and to set the band edge, Q is high and frequency stability is excellent. My 1 hour frequency drift was 50 Hertz uncovered. The high RF energy in the tank circuit results in low noise. The L1 taps also allow the use of a 5 pF gate coupling capacitor rather than the hard to locate 3.3 pF cap used in many example VFO schematics. With different buffer/amps as required, this is now my number 1 VFO topology and it is nothing short of stellar. Note that the 100 uH RFC can be wound with 15 turns on an FT37-43 ferrite torroid, or replaced with a fixed value choke.

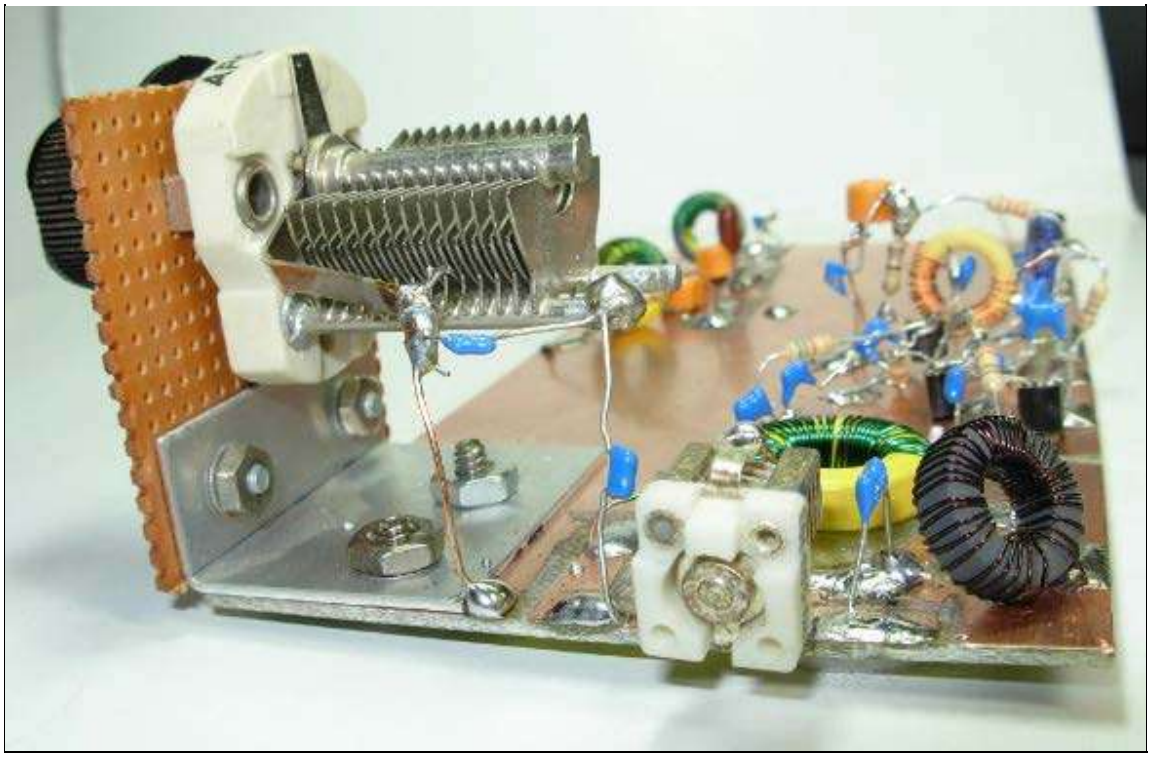

In the above photograph is the VFO bread board. I used 26 gauge wire for the inductor and took my time to make sure the wire was laying flat on the T68-6 torroidal core. You can pull the wire tighter if you wash your hands before winding.

Band pass Filter and Product Detector

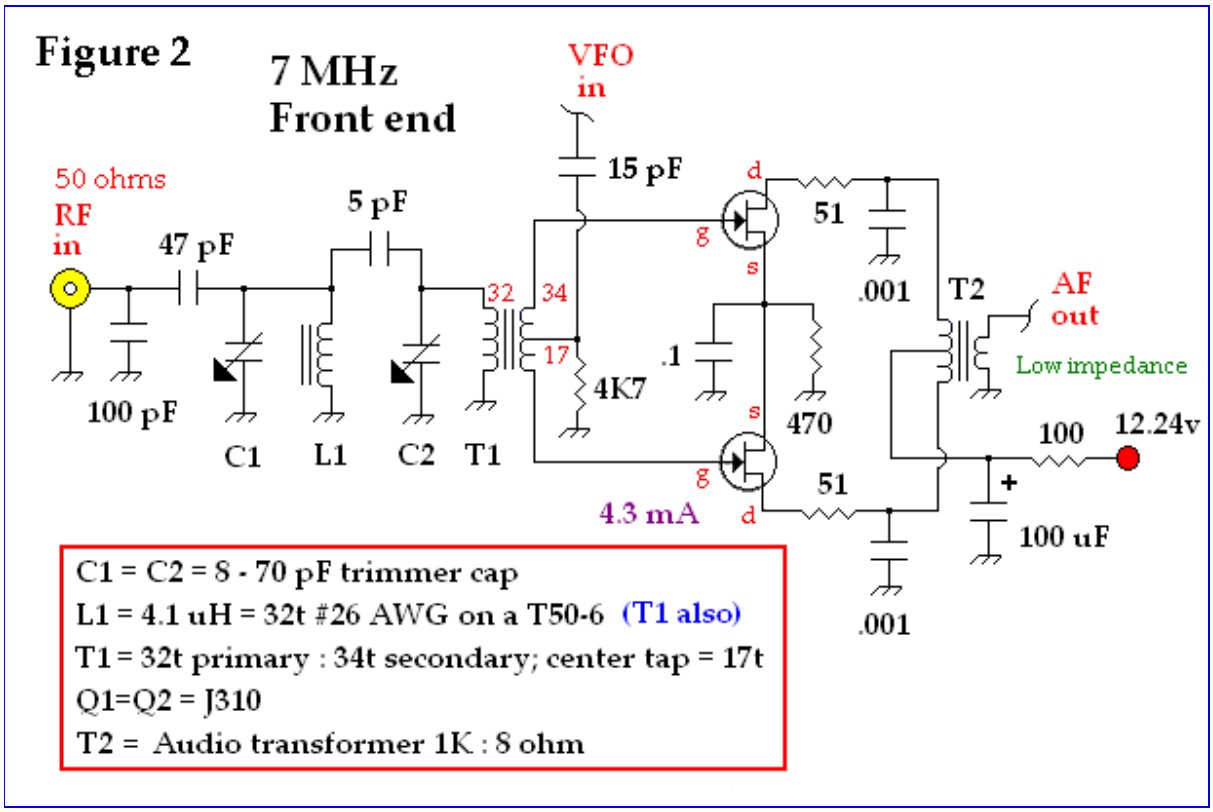

Please refer to Figure 2. The second stage constructed was the double tuned band pass filter. You will need about 50-54 pF to resonate L1 and T1 at 7.040 MHz. The C1 and C2 values chosen are thus perfect for tuning the 40 Meter CW band. I peaked my particular front end filter at a center frequency of 7.025 MHz using a 50 ohm output impedance RF generator and then did some fine tuning with an antenna connected after the receiver was constructed. You may also just tune C1 and C2 for maximum signal strength when listening to band noise and QSOs. Filter bandwidth is sufficient to cover the whole CW sub-band. No AM broadcast band radio was heard during several nights of testing.

The product detector is single balanced for improved port isolation and BCB rejection. Lay out your circuit to try to achieve symmetry. The schematic calls for J310s. I built the first prototype with MPF102 that were matched for Idss. To find two with the same Idss, I had to measure 16 transistors! This is too painful, and I recommend just using a pair of J310s. The words "matched" and "MPF102" should not be used in the same sentence! Ideally, your J310s should be matched, however, the process should not take as long as for MPF102 JFETS. The choice is yours to make. T1 is a little tricky to wind, however, your best effort should be good enough.
Some builders will be unhappy with using a audio transformer (T2), however, they are still in catalogs and online stores, or can be harvested from an old transistor radio. CB radio modulation transformers are also a possible source. A higher impedance audio transformer, will likely give even more conversion gain. Without the 51 ohm drain resistors, oscillations occurred in my bread board.

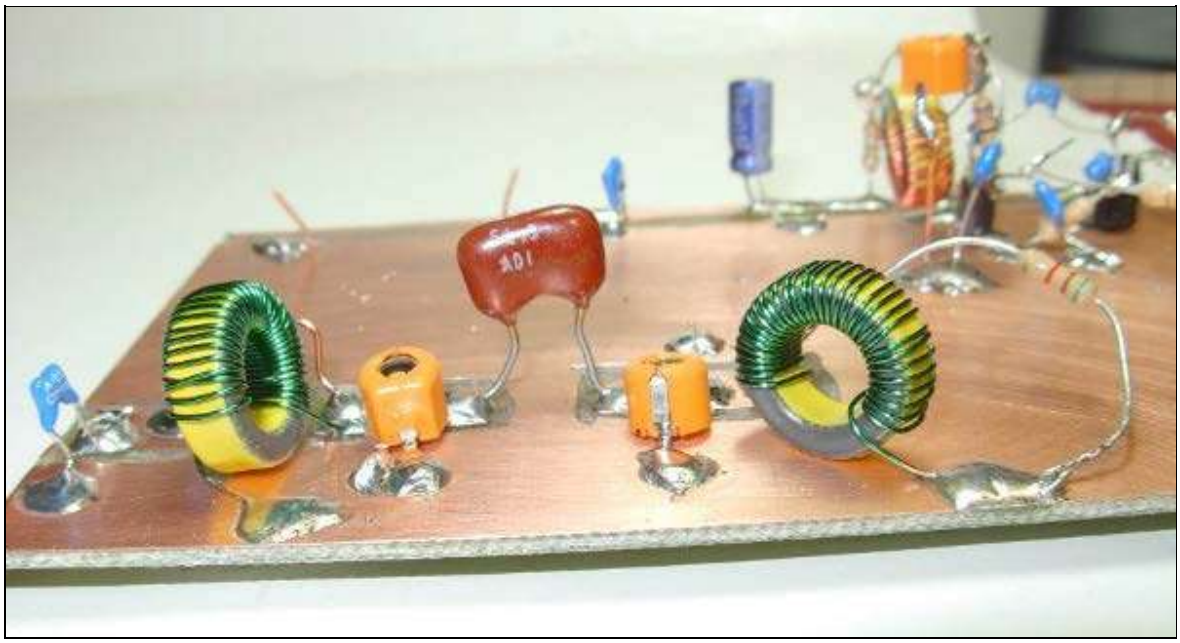

Above. A temporary 5K1 (5.1K) resistor was soldered across the second tank for testing when the front end filter was designed on my work bench.

Audio Pre-amplifier

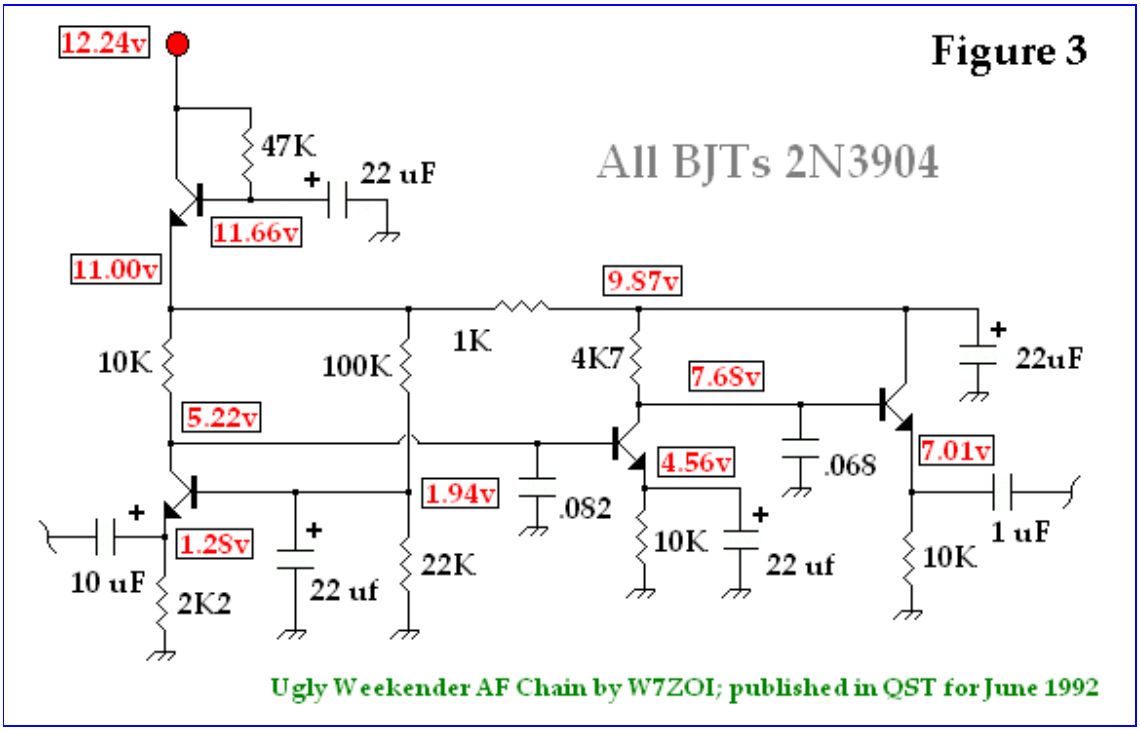

To match the low impedance winding of the audio transformer, a common base amp topology was chosen. I decided to use a favorite circuit; the

audio chain from the first amateur band receiver that I ever built -The Ugly Weekender. The final common emitter feedback amplifier from the original schematic was omitted as the 3 stages above provided enough voltage gain. The Figure 3 amplifier is worth studying. It is difficult to DC couple audio amplifier stages and not end up with your second and/or third stage in saturation. This example of good design by W7ZOI illustrates how to do it. The third stage, a common emitter amp is a level shifter and drops the DC voltage back down, although this stage is AC coupled to the volume potentiometer. For lower noise, you could AC couple the first common base amp to a 5532 op-amp, although, this would reduce the popcorn factor a bit. Do not expect ear blasting voltage gain from this humble circuit. It provides reasonable drive to the power amp stage.
The 0.82 and 0.68 uF capacitors shunt any detected RF energy to ground and also provide some low pass filtering. The original schematic called for 0.1 uF capacitors and which values work the best is yours to decide. Polyester film type capacitors were used in the bread board.

Photographed above is the Figure 3 bread board. You can also see the VFO buffer/amp and the audio transformer. I tried several AF preamplifiers, but preferred Figure 3 to all others.

Audio Power Amplifier

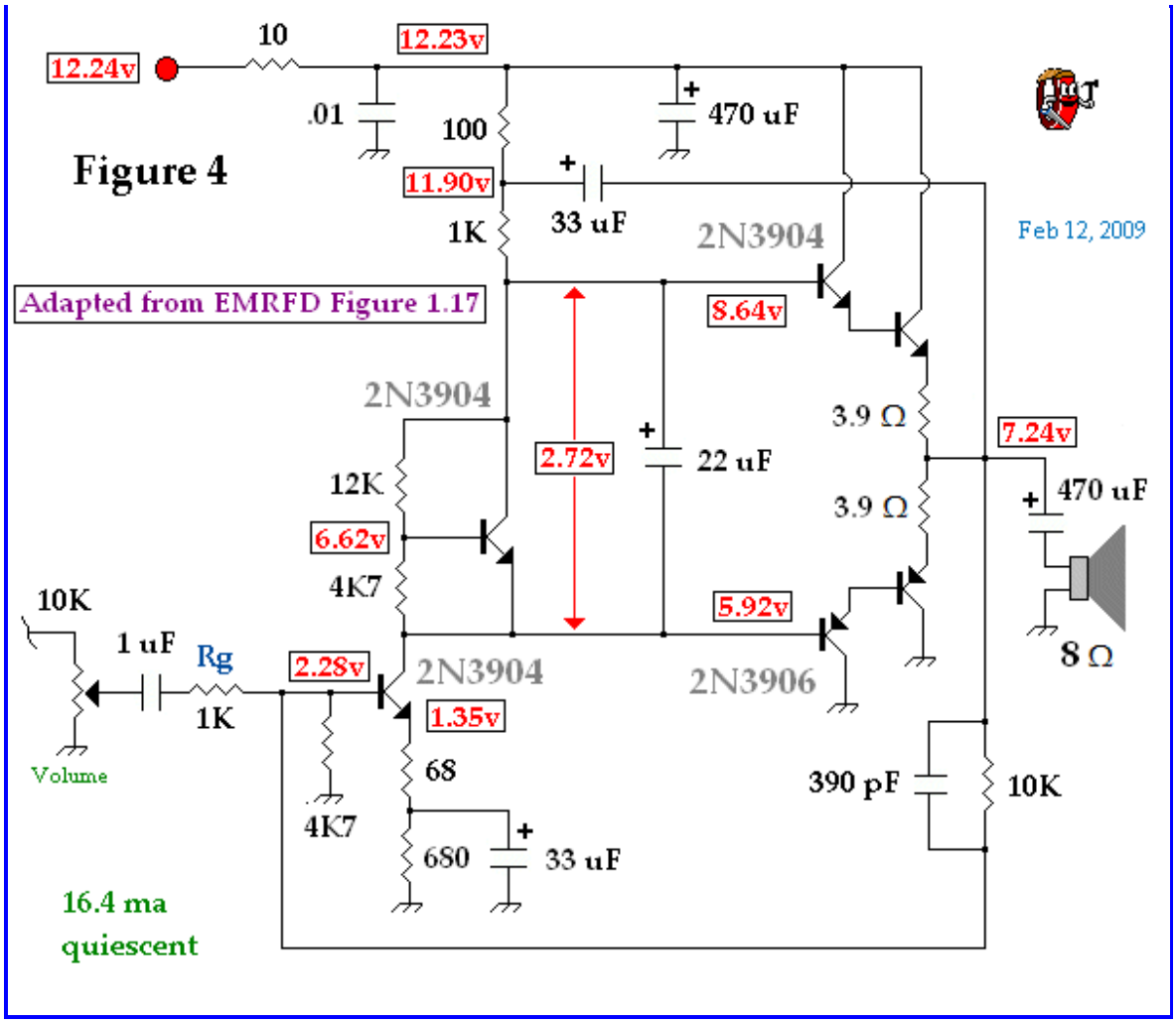

Figure 4 provided 3 nights of experimentation. The base circuit for this amplifier was Figure 1.17 from EMRFD. To increase power gain and reduce harmonic distortion, Darlington configured emitter follower pairs were employed. This worked, except the power followers were under biased and had serious crossover distortion. To remedy this, the amplified diode (level shifter) bias was increased until a sine wave was seen on the oscilloscope. This was achieved by replacing the 10K resistor (R6 in the original schematic) with a 4K7 ohm resistor. The next task was to try to increase the voltage gain. Rg in EMRFD Figure 1.17 called for a 3K3 resistor. Rg was dropped to 1K; this worked. The degenerative feedback on the common emitter amplifier of EMRFD Fig 1.17 was also dropped somewhat. Next some bootstrapping feedback was AC coupled to the collector of the main common emitter amplifier. Each of the 2 collector resistor values was changed around and the outcome was recorded. Ultimately the 100 ohm plus 1K ohm resistor series pair was chosen and provided a boost of 0.85 volts peak-to-peak clean voltage gain to the output waveform. The power follower emitter degeneration resistors were also decreased from 22 to 3.9 ohms. The result is a low distortion power amp with about 150 mW of clean average power output. This receiver is not super loud, but it is reasonably loud and the audio is bell clear. If you use this amplifier stage in other projects that have a higher gain pre-amplifier, I recommend keeping Rg at 3K3 ohms as this amplifier will likely exhibit lower distortion characteristics.

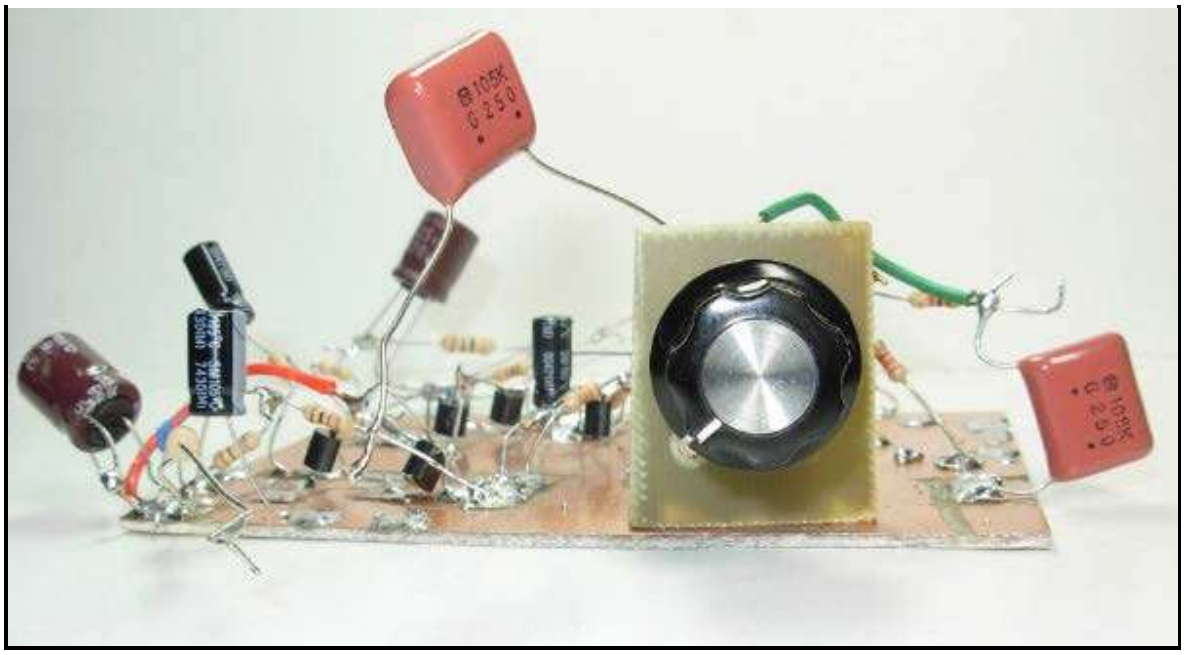

Shown above is the Figure 4 bread board. A 10 ohm resistor was used to decouple this stage. Without the resistor, audio oscillations at around 850 Hz manifested when the volume was greater than about half way up. The voltage drop across the 10 ohm resistor is trivial. You may have to increase this resistor value if you experience instability. Expect all amplifiers to oscillate and decouple them accordingly. The 390 pF feedback capacitor is required. The Figure 4 amplifier exhibits greater gain as frequency increases and in a direct conversion filter with no low pass filtering, this would be very harsh indeed. Feel free to experiment with the value of this feedback capacitor. Kudos to W7ZOI for the EMRFD Figure 1.17 schematic which serves as a great specimen to inform and challenge us experimenters. The original common emitter amplifier (Q1 in EMRFD Figure 1 .17) bias current is perfect and although I tried increasing and decreasing it, I returned to the originally specified bias resistor values.

Additional Outputs

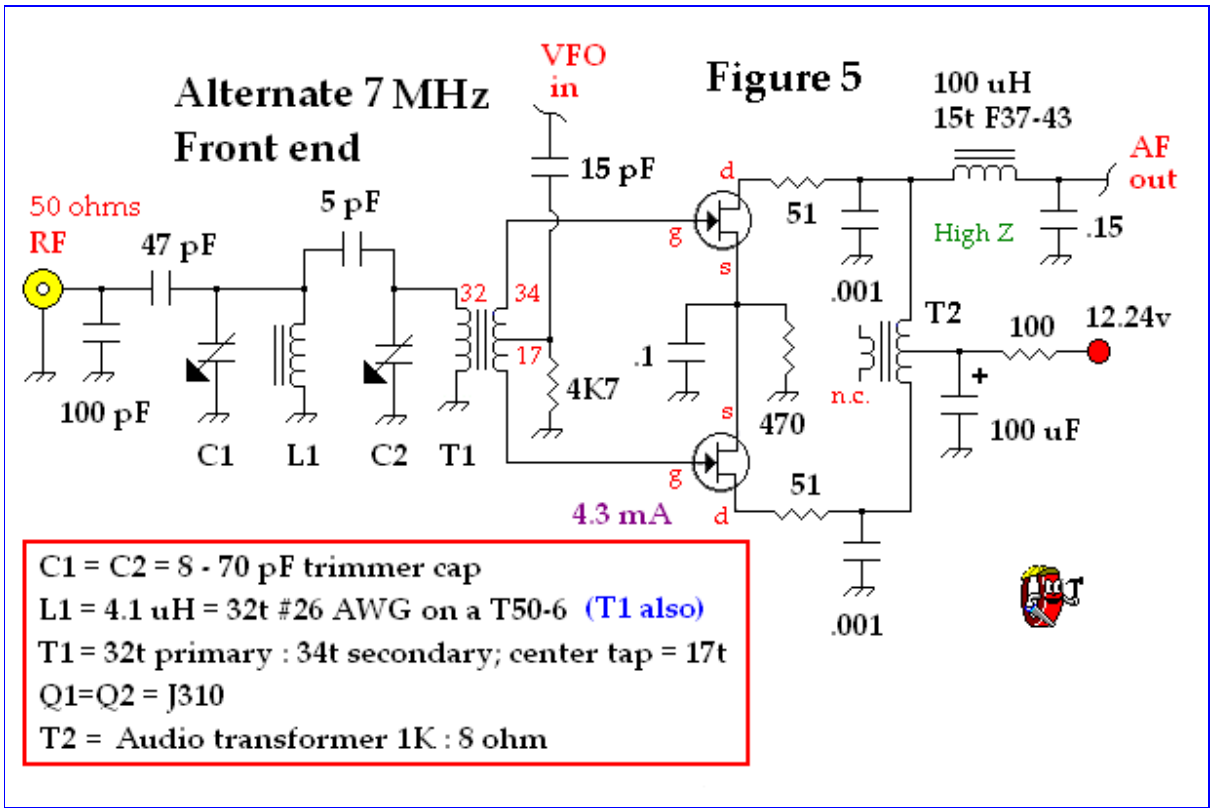

Figure 5 depicts the product detector with a high impedance output. From my experiments at least, it was better to use the low Z coil for improved product detector balance and audio voltage gain.

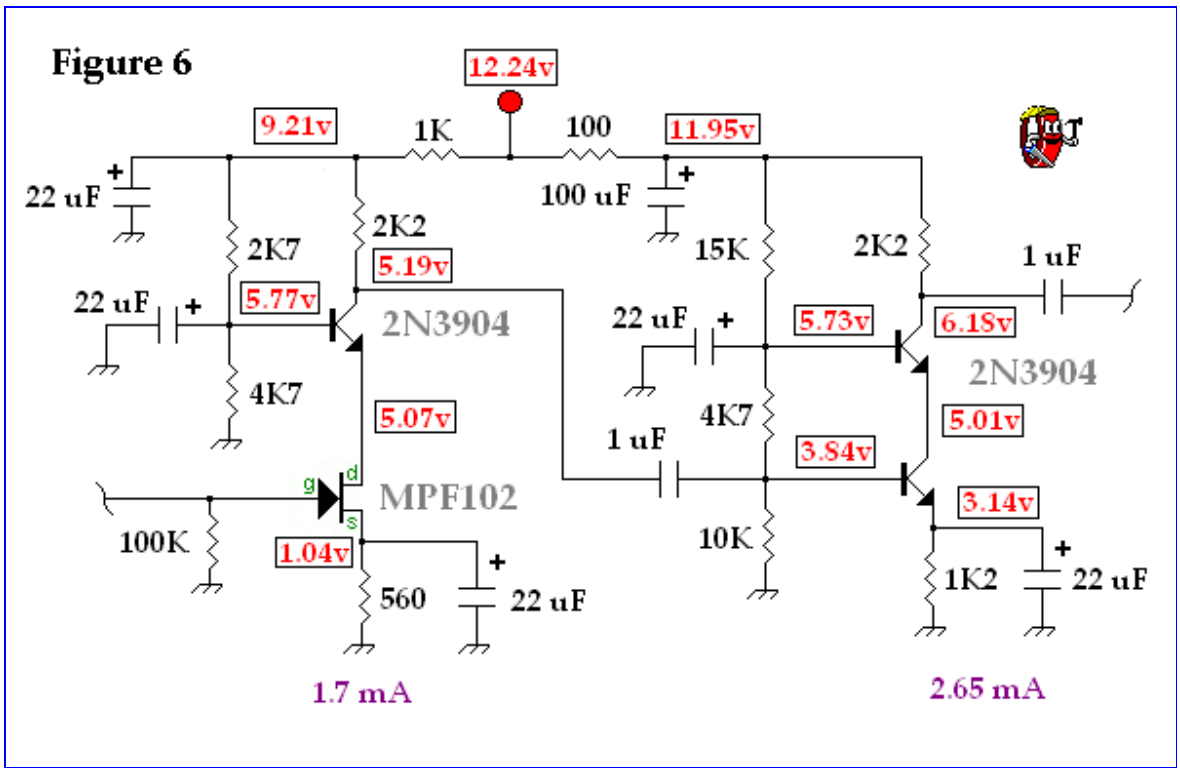

Figure 6: A high impedance input audio stage. The first stage is a hybrid cascode. The second stage is common emitter, common base cascode. Care was taken with transistor biasing to try to optimize distortion characteristics. Certainly, I am a total novice with such amplifiers and more time on the bench and also with computer simulation is required to better understand these amplifiers. At any rate, the schematics with DC voltages are posted for others to study and hopefully improve.

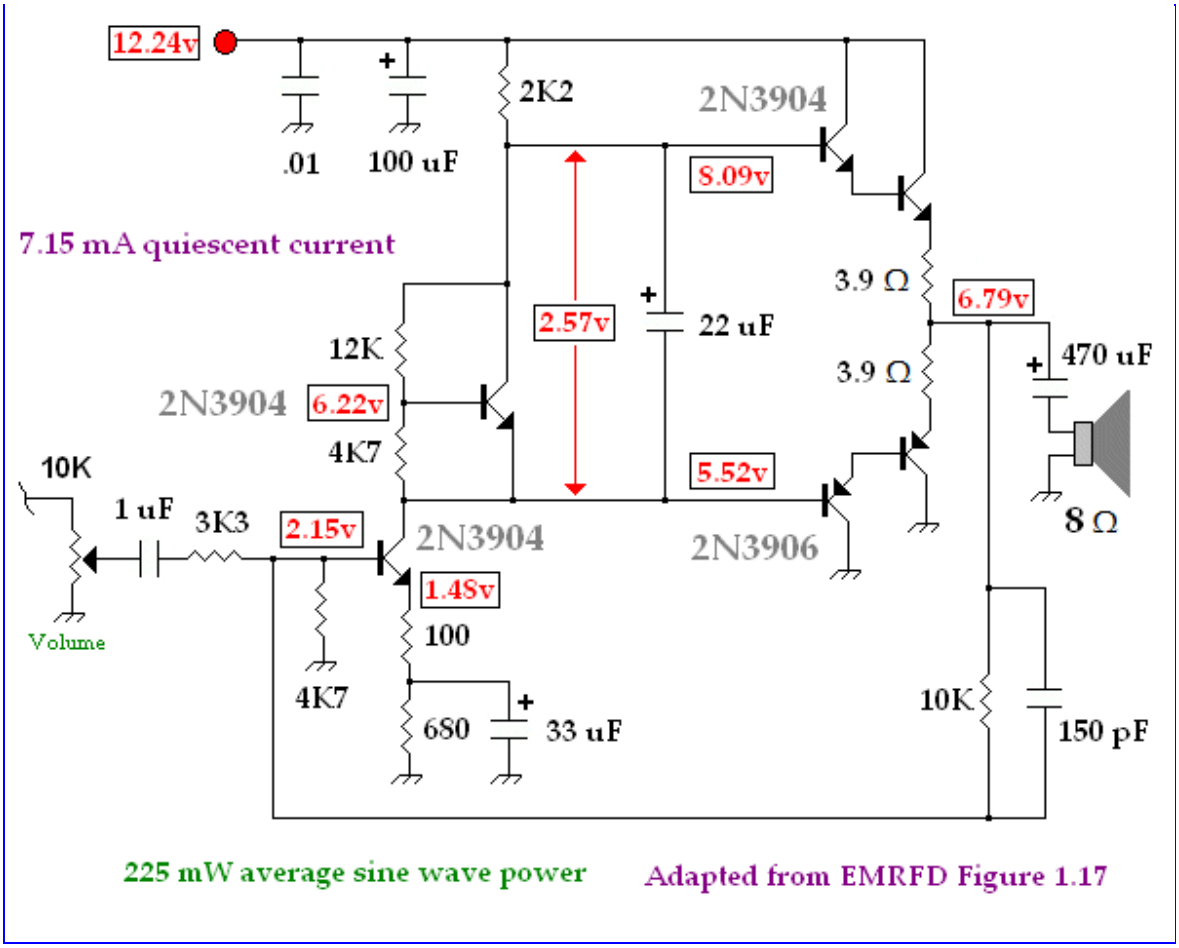

I have 3 adapted versions of the EMRFD Figure 1.17 amplifier in my note book. This is my favorite and has the greatest clean maximum average power output of all of the 3 versions. This power amplifier somewhat lacks sufficient voltage gain for the 2 Bravo receiver (with its relatively low gain audio pre-amplifier) and thus Figure 4 was chosen as the more suitable power amplifier. You could lower the 3K3 resistor to increase the voltage gain. This circuit begs experimentation.

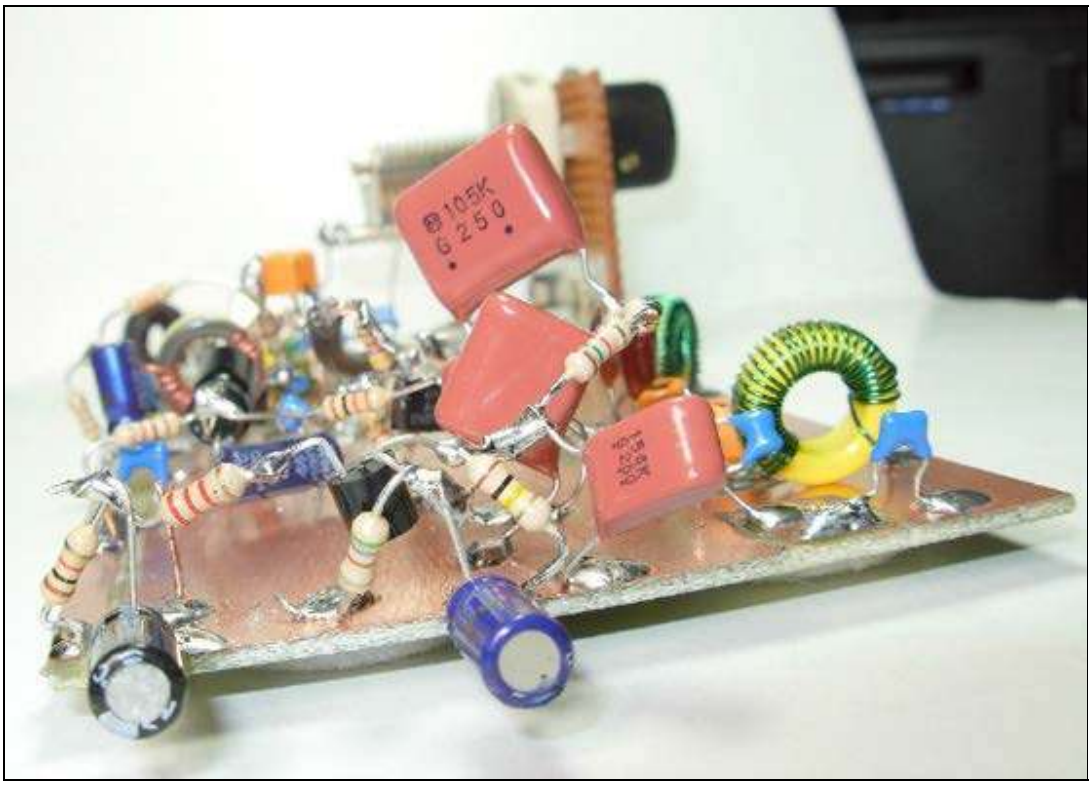

A couple of low pass RC audio filters were tried but later abandoned. One filter with its 1 uF AC coupling capacitors is shown in the photo above. It is quite an experience to hear an unfiltered direct conversion receiver. I love the purity. This is okay for an experimental or casual receiver, but not for a contest rig. Low pass filtering is definitely required in that context.

A different angle photo of the VFO bread board. My "build most of the project on 1 copper clad board" construction technique is not really suitable for "a keeper" receiver. VFOs should ideally be in a shielded box. Proper construction techniques and grounding ideas for DC receivers can be found in EMRFD, so they are not covered on this web page.

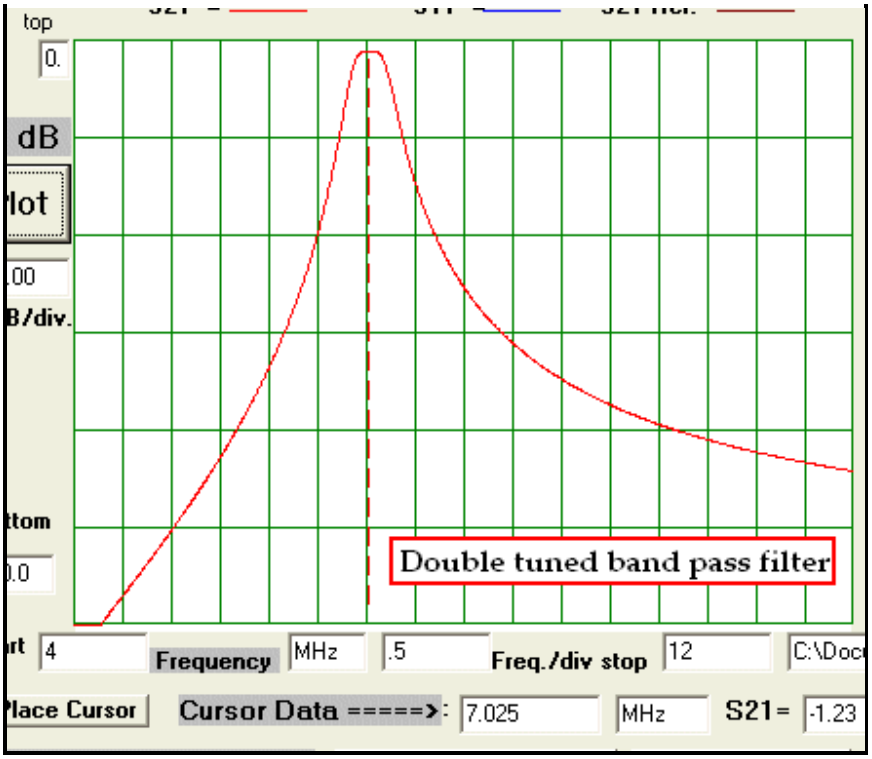

A GPLA simulation of the front end band pass filter centered at 7.025 MHz.

Amateur and Short Wave Radio Electronics Experimenter's Web Site

ICOM IC-7200 Listening Tests and Observations

Introduction

In Spring 2009, I evaluated and photographed the ICOM IC-7200 transceiver. For this web page, only its receiver was evaluated for HAM and SWL purposes by using my eyes and ears. For technical evaluation, please click on these assessments written by Adam, VA7OJ/AB4OJ or Peter, G3SJX . Additionally, eHam.net has a review web page to consult and the ARRL publication, QST for June 2009 has a review. With my modest camera and lighting equipment, it was difficult to well photograph this very dark colored transceiver indoors.

I like ICOM radio equipment and am therefore biased in my review. Please consider trying this and any other radio out before you purchase it. Our needs, expectations and budgets tend to be uniquely different. Like others, I would rather own the new ICOM IC-7600, Yaesu FT2000D or Elecraft K3, however, my budget does not allow this.

It appears that the target audience for this transceiver is as follows: portable or field/emergency communication usage and/or it is oriented towards entry level HAMs or perhaps those wishing a modern DSP-filtered back up rig. My review is from a SWL/HAM perspective.

General Thoughts

Although modern and stylish, this radio is very easy to use. The owners manual is well written with clear examples of how to perform the various setting changes. After reading the manual and and trying the radio buttons and knobs out, I pretty much mastered receive operation on my first night. The LCD display is small, however is reasonably adequate considering that this whole radio is compact. I believe some operators will have difficulty with this diminutive display. The S-meter is a little difficult to see. You can push a front panel button which announces the S-Meter reading, set frequency and mode in English or Japanese language if you can't quite see the display at an odd viewing angle.

The VFO knob has adjustable resolution and works well, however, it lacks that silky smooth/weighted feeling of many other radios including the R75 receiver. The ICOM engineers had there work cut out for them; include all the modern interference fighting features; place them in a small chassis; make it easy to use and come in on budget. They did it! This radio is full of useful interference management tools. One example is the (DSP) manual notch filter; it works superbly. There is no FM mode. I imagine by dropping FM mode capability , the designers were able to use the specified 6 KHz roofing filter at the second IF which has the potential to improve dynamic range at close-in signal spacing for some modes. When I started in Amateur Radio many years ago, roofing filters were never mentioned, but have become a huge marketing lever and seemingly a topic of much confusion.

DSP IF Filtering

The DSP IF filtering works very well. Does it function better than more traditional crystal IF filtering? Yes and no. It is a question of compromise for me. The greatest DSP attribute is that there are no expensive crystal filters to purchase. Additionally, you can customize the desired IF filter bandwidth (wide, medium and narrow) for each mode and also set a "hard" versus "soft" filter shape. The soft shape equates less ringing and potentially less listener fatigue than the hard setting. I have never liked listening to CW signals through stiff, 6-8 pole 250-500 Hz crystal filters on any receiver, so for me, adjustable DSP IF filtering is preferable. DSP IF filtering is not perfect as authors like Rob Sherwood, NC0B have presented, however, ICOM have a pretty good DSP platform out now and I am pretty sure their latest technology from the IC-7600/PRO 3 on down have also been used in this receiver. After all, you can always try to find an old Drake and order some crystal filters for it, or spend significantly more cash on a high-end transceiver if you need better performance.

Shown to the the left is a few front panel controls and the front firing speaker. This speaker is reasonably nice sounding. There seems to be less harmonic distortion and audio gain than the R75 receiver. The radio front panel controls are well thought out and seemed intuitive to use after reading the manual and/or just trying them out. The various hardware components such as potentiometers, rotary switches, microphone jack, PL-259 jack etc seem not to be of the highest quality. When you compare such components to that used in their older designs, there is

evidence of modern cost containment. I have seen many reviews describing this transceiver as rugged. Certainly the diecast frame is solid, and I hope the forementioned hardware is as well. There is only one antenna connection. I believe that any radio offering the 6 meter band should offer two SO239 antenna connections, however, this likely would have crowded the back panel layout and increased cost for the RF in/out switching.

The VFO knob (shown to the right) looks and feels a little cheap. Functionally, however, the knob spins very well and precise tuning is easy to perform. One of my first tasks was to input various the frequencies I use for both amateur and short wave listening into the (201 maximum) memory slots. This was very easy to do and each memory channel also stores the mode and filter setting.

AM Reception(R75 versus IC-7200)

The IC-7200 is a good short wave receiver. With a high quality external speaker connected, pleasant and warm sounding AM audio may be heard; however it is not Hi-Fi. That is; the IC-7200 is not an audiophile AM receiver. There is no synchronous AM detection and no 15 KHz wide IF filter for example. For AM reception, the user may choose from an 8000 to 800 Hz IF bandwidth in the 3 switchable filter settings. During testing, I set my wide filter setting to 8000 Hz, my medium setting to 6000 Hz and my narrow setting to 3000 Hz for AM reception. Of course these bandwidths can be further adjusted at any time. Local MW broadcast radio sounded great with an 8000 Hz IF bandwidth during testing. The various AM reception appropriate interference controls such as pass band tuning (PBT), automatic notch filter (ANF) and digital noise reduction are all configurable or adjustable and I found the ANF and digital noise reduction helpful when listening on the crowded 49 meter band during a rain storm.
I performed A/B comparisons with the IC-7200 and the R75 simultaneously hooked to the same antenna. For AM reception, they are comparable with the R75 having marginally better sounding (more Hi-Fi) audio. I had the R75 IF filter bandwidth set at 15 KHz and the IC-7200 IF bandwidth set at 8 KHz (both at their maximum IF bandwidth).

CW/SSB Reception (R75 versus IC-7200)

In CW mode, both were set to have a 500 Hertz IF bandwidth.(The R75 had the FL-100 model 500 Hertz crystal filter in its 9 MHz IF slot). The IC-7200 was quieter, clearer and less overloaded by adjacent stations during pile ups. There were occasionally weak signals I was able to copy on the IC-7200 that I could not even hear on the R75 due to noise. The IC-7200 is a joy to use on CW; really fantastic.
On SSB, I found both receivers fairly comparable, but the IC-7200 was better for pulling weak signals out of the noise as the noise floor was a little quieter and the audio a little more crisp. My wife also agreed with me in her "independent tests" of the CW and SSB reception. I am certain to catch flak because my subjective comments are based upon listening tests and not measurements. It is interesting to note that in almost every aspect of our lives, preferences are made using 1 or more of our 5 senses. From listening, observing and also reading the reviews of others, it seems ICOM has a hit with the IC-7200.

Mouse over the images below left to view a full size photograph

The IC-7200 in the sun.

Rear view of the transceiver.

Top angle view. There are ventilation holes at the top right hand side. You can just see the ventilation screen just next to the right top panel screw.

Reverse angle top view. The military look is attractive.

The IC-7200 and R75 side by side.

Another photograph of the 2 radios from the front angle for comparison. The LCD display size difference is quite obvious in this shot.

The receivers at a right angle. The IC-7200 is a glad update, although, I would likely not upgrade from the R75 to the IC-7200 just for receiving purposes. If I was considering choosing the IC-718 (transceiver version of the R75), the IC-7200 is worth the extra money. It is also an excellent transceiver consideration for an entry-level rig, for back up purposes. or for the budget-minded operator.

Conclusion

The IC-7200 is a serious choice for amateurs seeking a good, modern HF plus 6 Meter transceiver. It is more than adequate as an SWL receiver if you are an amateur radio operator plus SW listener like myself. Please try one out for yourself if you are considering this transceiver.

Amateur Radio Electronic Design

Electronic Hobbyist Circuits

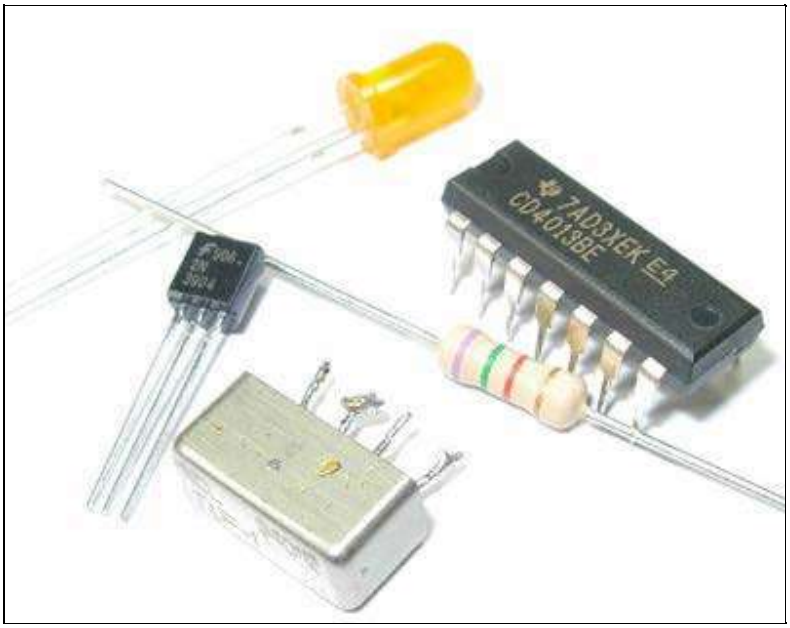

This page will house a collection of brief hobbyist experiments.

1. Pseudo-Random Number Generator

This circuit describes a simple, 6-bit random number pseudo-generator used to study binary counters and in particular, shift registers. Some very basic background information about binary counters and shift registers is provided. In reality there are dozens of different shift register topologies available and it can get quite complex. If you wish to find a good logic tutorial website, I strongly recommend Ken Bigelow's site as it has interactive diagrams. Flip-flops are also covered well on wikipedia and many other web sites.

Binary Counter: The circuit most often used as a counter is called a binary flip-flop. The basic flip-flop can be viewed as a toggle switch having either an ON or OFF position. This is the binary state 1 (HIGH) or 0 (LOW). Like the toggle switch, the binary flip-flop has 2 binary states 1 or 0. A binary flip flop counter counts in a sequence such as 0, 1, 0 ,1 etc. A straight binary counter can be built by using 1 or more flip-flops connected in a manner that the binary number stored in these flip-flops will represent the total number of trigger pulses received at the counter input.

Ring Counter: A ring counter has 2 or more flip-flops cascaded so that the output from one flip-flop becomes the input of the next flip-flop. The flip-flops are connected so that all of their outputs are at the binary state 0 except for one flip-flop. By pulsing the input of the ring counter, it will sequentially change the binary state of the succeeding flip-flop from binary 0 to binary 1. The flip-flop that contains the binary 1 indicates the count of this binary counter. The maximum number of pulses that can be counted by N flip-flops is N pulses.

Shift Register: A serial entry shift register is similar to a ring counter, except that the output flip-flop is not connected to the input flip-flop. Like the ring counter, the flip-flops are cascaded so that the output from one flip-flop becomes the input of the next flip-flop. All the set trigger and reset trigger inputs are tied together to form what is called a shift bus. Clock pulses are applied to the shift bus to cause the stored binary information to shift from left to right; one bit position per each received clock pulse. In Figure 2, this serial input/output + parallel output register has its 5th and 6th bits exclusive ORed to the serial input to form a pseudo-random sequencer, which is called a pseudo-random number generator by some.

The CMOS logic ICs used were one 4070 XOR (Exclusive OR) and three CD4013B D flip-flops. Junk box LEDs were used to observe the binary state of the clock and each of the 6 bits of the shift register.

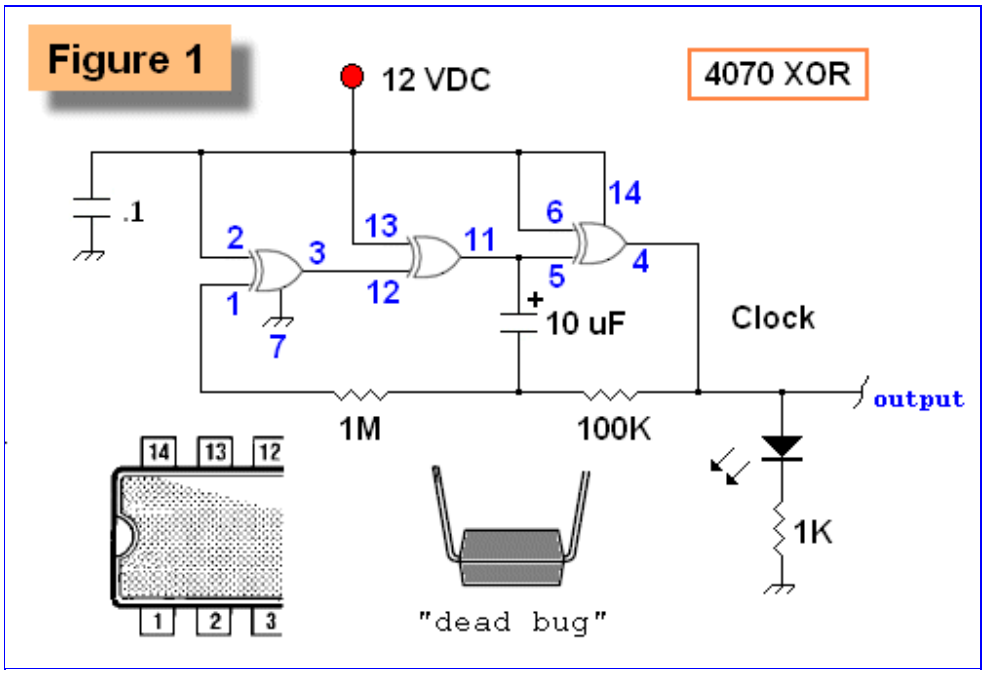

Since only one XOR gate is needed for the shift register, the remaining gates were configured to make the clock. These gates are essentially wired up as inverters to form an astable multivibrator with a frequency of about 0.45 Hertz or 27 pulses per minute. Shown above in Figure 1 is the clock schematic and the pin 1 marking for all of the digital ICs on this web page. The output LED is not mandatory, but will instantly tell you whether or not your clock is working. I built this whole circuit using Ugly Construction with the ICs flipped upside down in a "dead bug" fashion. You can increase the clock speed by decreasing the 100K resistor or the capacitor values. F Hertz = 1/ (2.2 * R * C) with R in ohms and C in farads. The slow clock speed was chosen to better observe the digital output of the shift register.

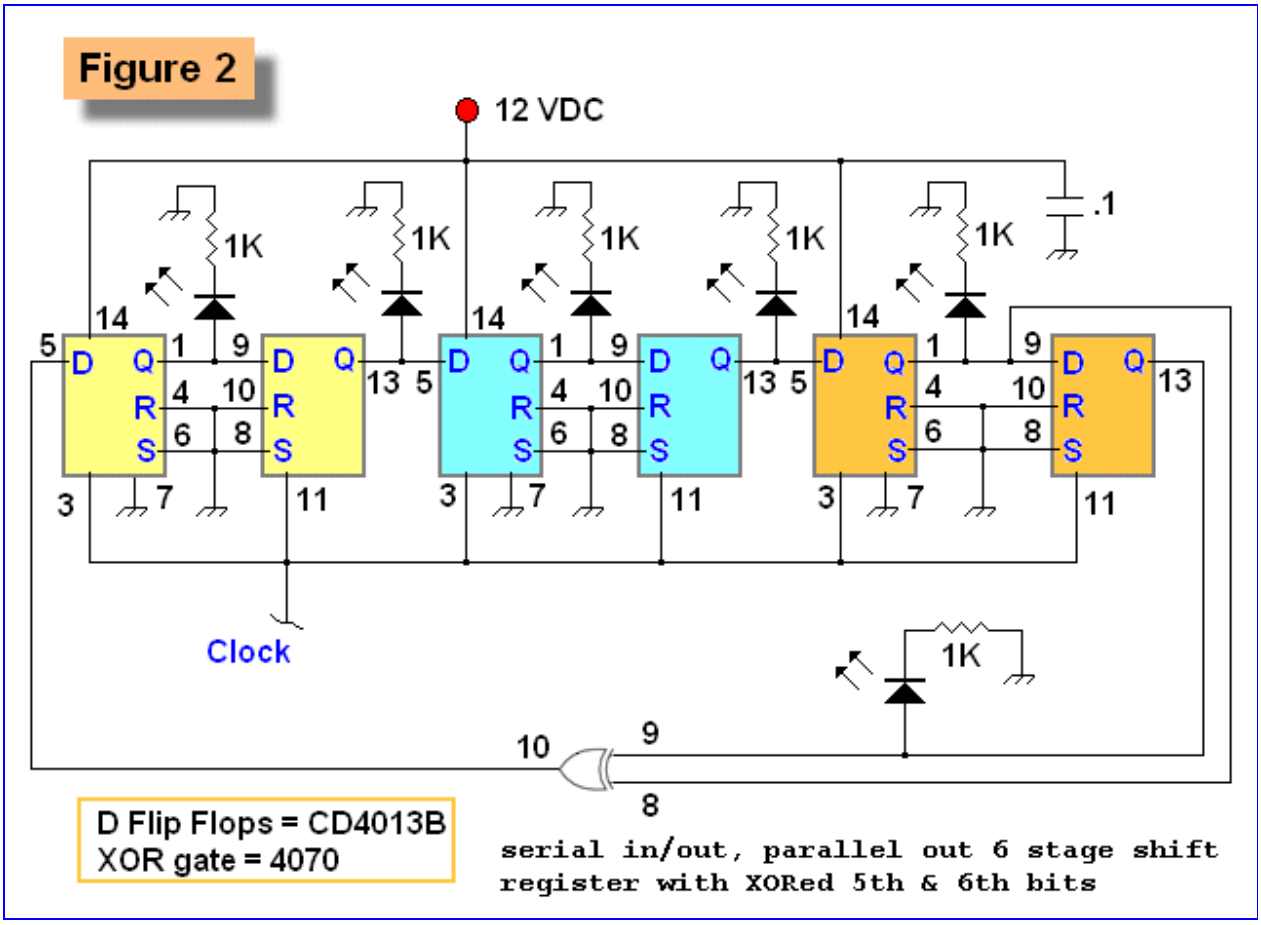

In Figure 2 is the shift register. Each 4013 was wired up as 2 cascaded flip-flops and connected to the clock. Power was applied and then a test lead was used to bring pin 5 of the first flip-flop HIGH (connected to 12 volts for 1-2 seconds) . Both flip-flop state monitor LEDS turned ON in sequence with subsequent clock pulses. Afterwards, pin 5 was set LOW (shorted to ground with a test lead for a couple of seconds) and each LED turned OFF in sequence with subsequent clock pulses. The remaining two 4013s were wired up and tested the the same way and then finally the last XOR gate was wired up.

To avoid error, frequent pin counting and a systematic approach is recommended. For example, for each 4013, I soldered the ground pins, wired the pin 14 VDD, connected the clock to pins 3 and 11, then wired up the pin 1 and pin 13 LEDs. Systematic construction techniques are something that you the experimenter can develop and perfect over time. This approach saves time and grief. On some projects, when you have a lot of pins wired up, tracing and repairing an early mistake can be difficult.

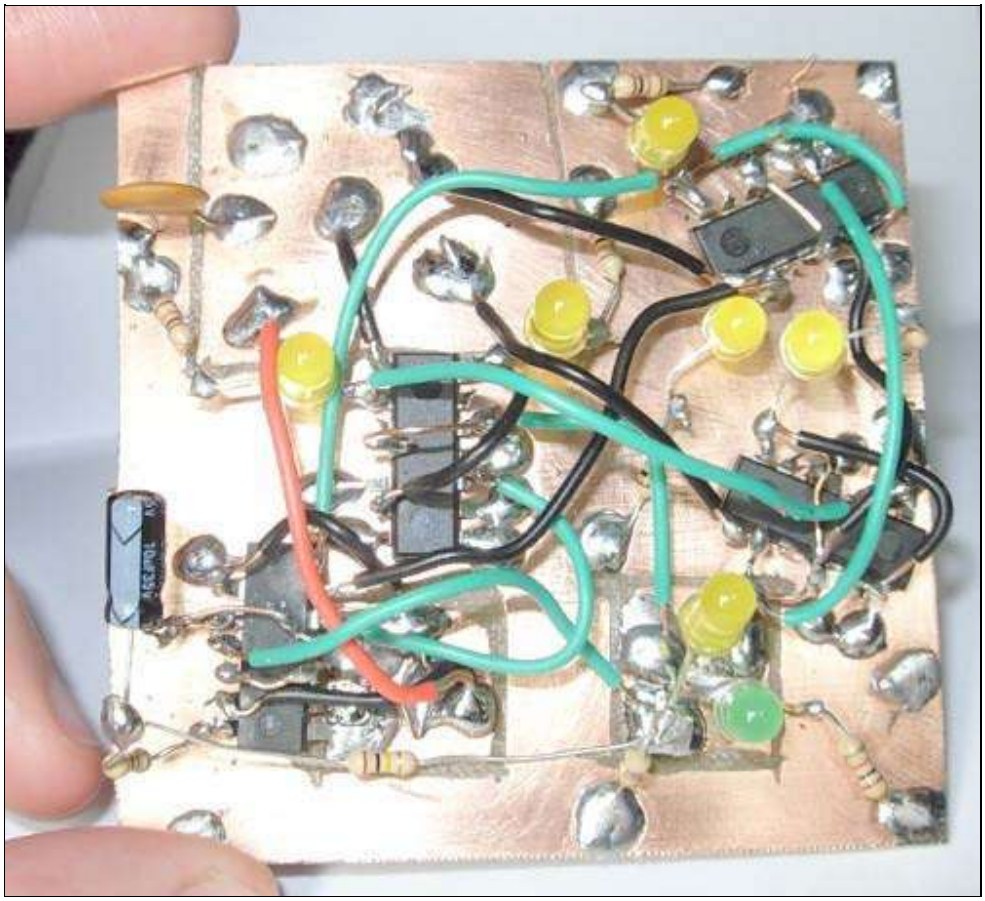

Shown above is a bread board of the entire pseudo-random number generator. I just built in on a scrap of board and did not lay it out so the LEDs were in a row, as I am not going to keep this project. The clock state monitor is the green colored LED. There are 63 possible states or combinations of the 6 bits (111000, 100110, 100101, 000101, 000001 etc.) State 000000 is disallowed and will hang up the shift register. If your clock LED is flashing and no shift register LEDs are lit, then "reset" by momentarily setting pin 5 of the first flip-flop HIGH (momentarily apply 12 volts). Long live the reset switch!

Pseudo-random numbers are now mostly generated by computer microprocessors controlled by software and have applications in cryptography, electronic music, security and many other applications. This "hardware" pseudo-random number generator experiment was really cool and if you want to randomly flash some LEDs, this could be the project to use!

If you are new to digital electronics; (like me) Welcome! Starting small with projects like this one will hopefully lead to increased confidence and problem solving skills for even bigger projects. You can also build the shift registers with J-K flip-flops, but it is more difficult and 4013s or other series D flip-flops are cheap as Борщ (borscht).

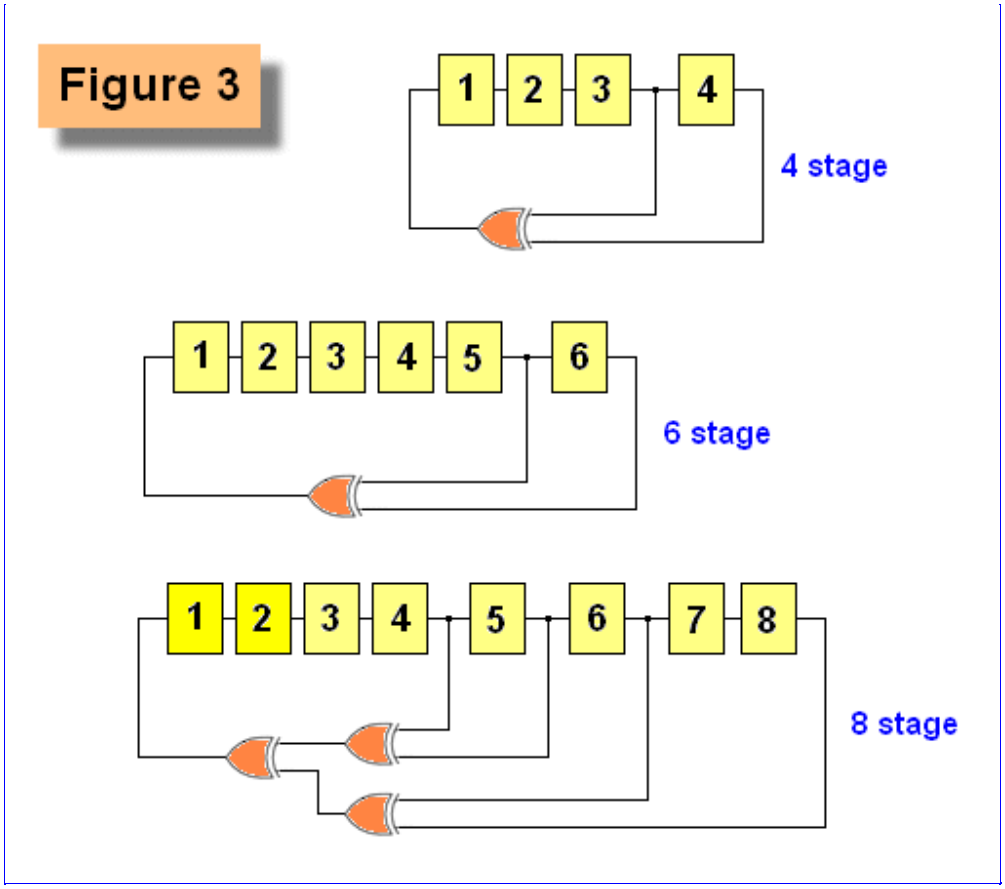

Shown above in Figure 3 is how to hook up the XOR gate(s) for 4, 6 and 8 stage pseudo-random number generators. The 6 stage shift-register is of course, Figure 2 above and is presented for reference purposes. The 8 stage version = 1 byte.

2. One Hertz Precision Time Base

Digital clocks are very interesting. In the past 6 months, 10 -15 RC clocks have been constructed and tested. RC oscillators in the KHz to Hertz range are surprisingly frequency stable. For many projects, a plain RC clock is adequate, however, like in radio design, a crystal controlled time reference is sometimes required. Two examples of projects requiring precision clocks are time of day clocks and frequency counters. Presented is a 1 Hertz clock built from two 4000 series CMOS Logic ICs. Here is a great 4000 series tutorial with pin outs and more.

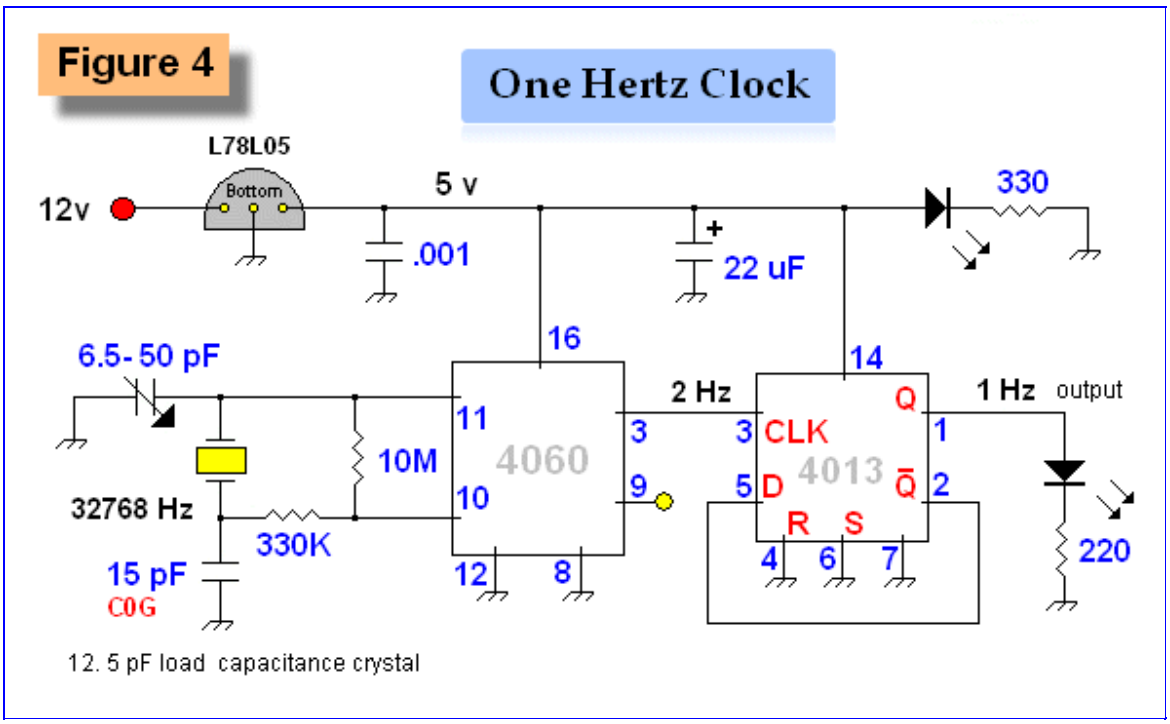

Shown above in Figure 4 is the complete schematic with an output LED for testing. In the past, the MM5369 17 Stage Oscillator/Divider was popular for hobbyist precision time bases, however, it has gone obsolete. The 4060 ripple counter is a good "modern" replacement, although a different crystal is required. A 32768 Hertz crystal was used and is divided 16384 times to provide a 2 Hz output. The 4060 then drives a 4013 D Flip-flop configured as a divide by 2 to provide a 1 Hz output frequency. Key parts references may be found on the Webmaster's page.

Shown above is the frequency and output waveform when a frequency counter and oscilloscope are (respectively) connected to pin 9 of the 4060 in Figure 4. The 6.5-50 pF trimmer pot is used for calibration. Originally, I used a trimmer cap instead of the fixed 15 pF capacitor shown between the 330K resistor and the crystal. After adjusting this trimmer capacitor for the best looking waveform, I removed the trimmer cap and measured it at 13 pF. I substituted the nearest standard value I had in my parts collection; 15 pF. It was interesting to measure the 4013 output frequency at 1 Hz.

A close up photo of the 4060 oscillator/divider breadboard. The 10M resistor used was a 1/2 watt rated R as I have dozens of these in my parts collection. You can see the tiny cylindrical crystal just above and left of the orange Murata trimmer capacitor. It is oriented horizontally. This is a useful time base for the QRP workshop.

3. 10000 and 5000 Hz Multivibrator Clock

It is fun to occasionally build circuits using discrete semiconductors rather than with ICs. A 5000 Hz digital clock was needed for an experiment. It

was decided to use multivibrators for the basic oscillator and a divide by 2.

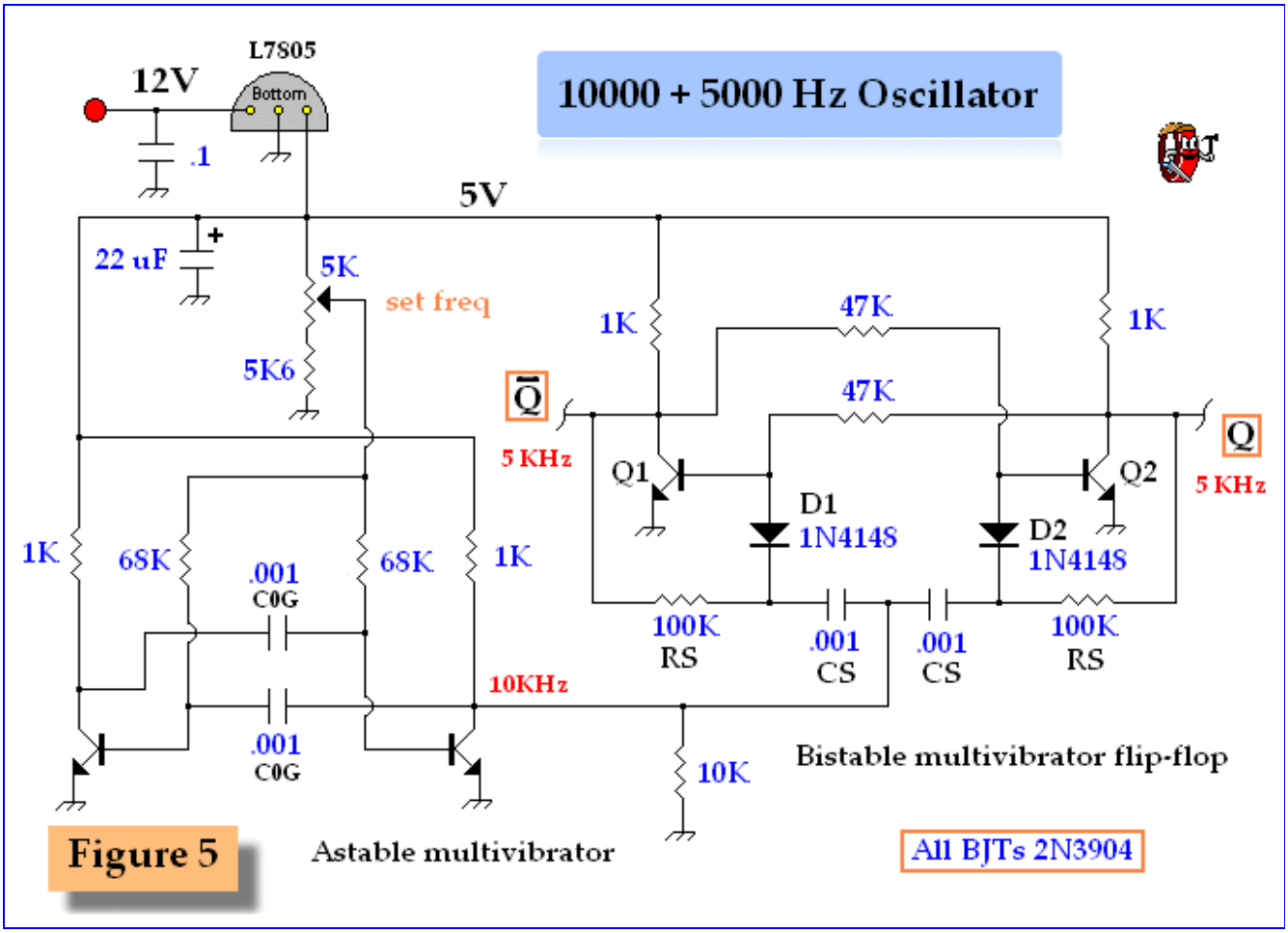

Figure 5 is the entire circuit. The tuning range of the astable multivibrator was about 7060-10650 Hz. The 5K pot was slowly adjusted until 10000 Hz was measured in a frequency counter. Following testing of the astable multivibrator, the flip flop was built and examined. Astable multivibrator function has been discussed previously on this web site.

Please refer to the bistable multivibrator. It is a one input circuit set up for toggle or flip-flop operation. Negative edge pulses applied between the two 0.001 capacitors will cause the binary state of Q1 and Q2 to change to the opposite state. The multivibrator circuit is made up of Q1, Q2 and the 47K and 1K base and collector resistors respectively. The other components D1, D2, the RS resistors and CS capacitors comprise a steering circuit to generate the proper response to the negative edge pulses. When a negative input pulse arrives, it is guided to the base terminal of the ON transistor, but prevented from reaching the base terminal of the OFF transistor.

In order to study this circuit at DC, I temporarily exchanged the 0.001 timing capacitors in the astable multivibrator with some 22 uF electrolytic caps to slow it down. Referring back to the bistable multivibrator, let us assume that Q1 is OFF and Q2 is ON. The collector voltage of Q1 is high (cut off). The collector voltage of Q2 is low (saturation). The Q1 collector is connected to the cathode of D1 by the 100K RS resistor. The cathode of D1 is reverse biased by the high Q1 collector voltage and also because its anode is held close to 0 volts by the 47K resistor connected to the collector terminal of Q2. It would take a very strong negative input pulse to forward bias D1 enough to reach the Q1 base terminal. The Q2 collector voltage is nearly 0 volts and therefore the D2 cathode has little to no reverse bias voltage via its RS. Thus, any small amplitude negative input pulse will cause D2 to become forward biased, reach the base of Q2 and drive Q2 OFF. Once Q2 switches off, in turn Q1 is toggled ON and its collector voltage goes low. The large reverse bias on D1 disappears. However, Q2 is now OFF and D2 will now be strongly reverse biased which will steer the next negative input pulse to the base of Q1. This is the basis of the circuit's negative edge flip-flop operation.

In another experiment, I changed the .001 C0G capacitors of the astable multivibrator to 470 pF. This gave a usable range of 22968 to 14832 Hertz (11484-7416 Hz at the Q1 and Q2 output) . Looking at the output of the flip-flop in the oscilloscope; at the higher frequency range, the flip-flop could not keep up and failed to divide by 2. I found experimentally that the time constant of each of the CS and RS components seemed to be the problem. When the CS capacitors were also decreased to 470 pF, the flip-flop worked properly.
As you increase the flip-flop operation frequency, speed up bypass capacitors might also be required across the 47K base resistors of Q1 and Q2 . A suggested starting value to try is 220 pF. Some builders also bypass the resistors in the RS steering circuit at higher frequencies, however, this is getting a little crazy. It is really important to look at the output waveform in the oscilloscope to ensure reasonable performance.

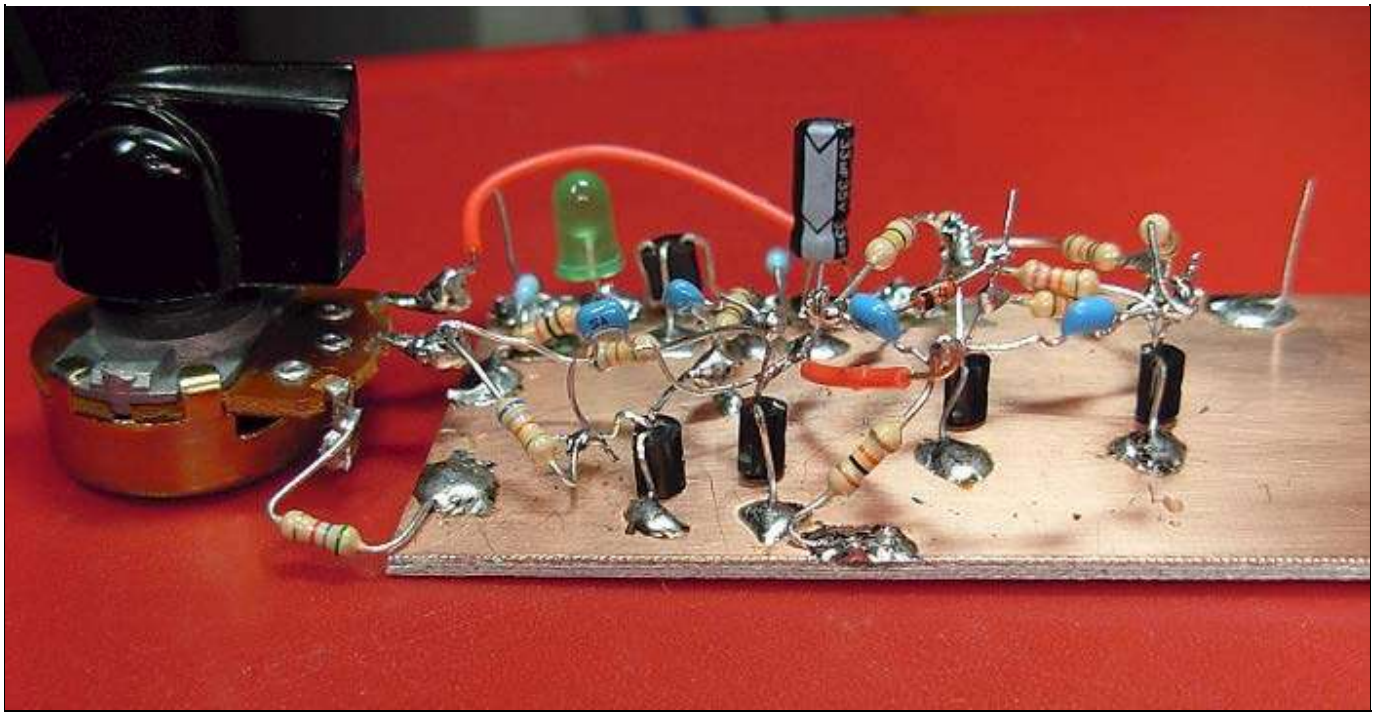

Shown above is the Figure 5 breadboard prototype.

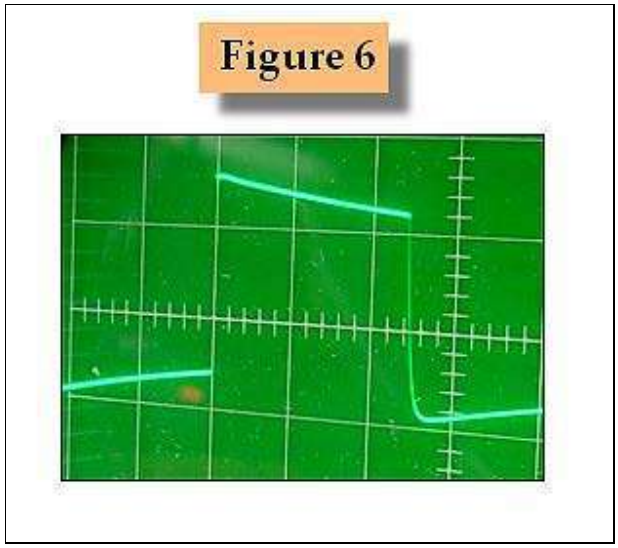

5 KHz output waveform of Q2

4. One KHz Digital and Analog Oscillator

A 1 KHz oscillator with 5 volt digital outputs 180 degrees apart and an analog output was sought. The frequency had to be near to, but not exactly 1000 Hertz. A major question to answer was how much low pass filtering is needed to remove the odd harmonics from digital circuits?

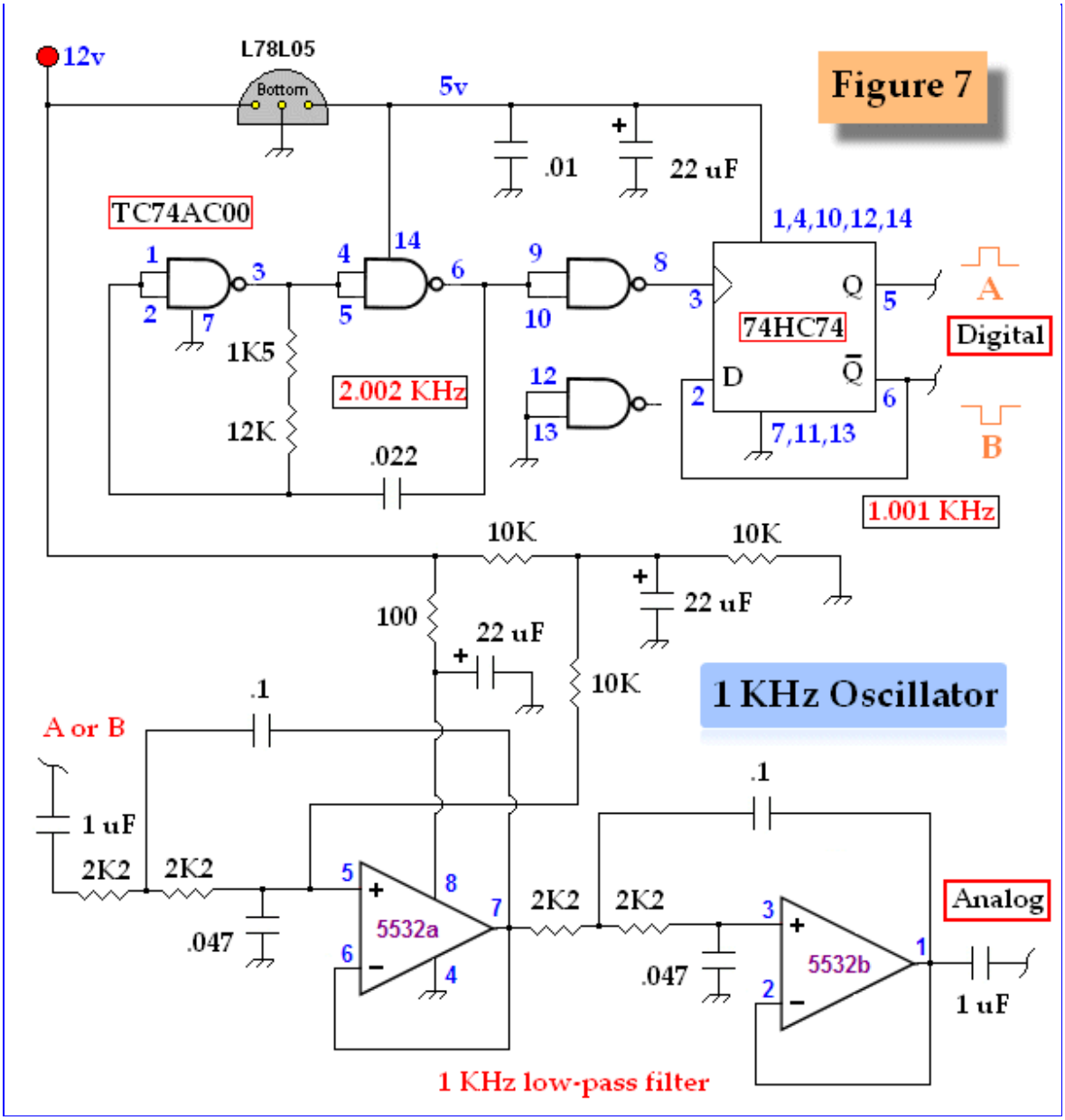

Figure 7 shows the complete schematic. NAND gates from a 74AC00 were wired as inverters and with the 13.5 K resistance and a 0.022 uF polyester capacitor, the frequency was 2002 Hertz. To improve the digital waveform and get the desired 2 outputs, a D flip-flop was used. The output frequency was 1001 Hertz. The digital part was completed!

For the analog filtering, active low-pass filters were tried, and in total 4 poles with a 1 KHz cuff off worked reasonably well. The filter uses the 5532 op-amp with common vales capacitors and resistors. Poly"something" caps were utilized.

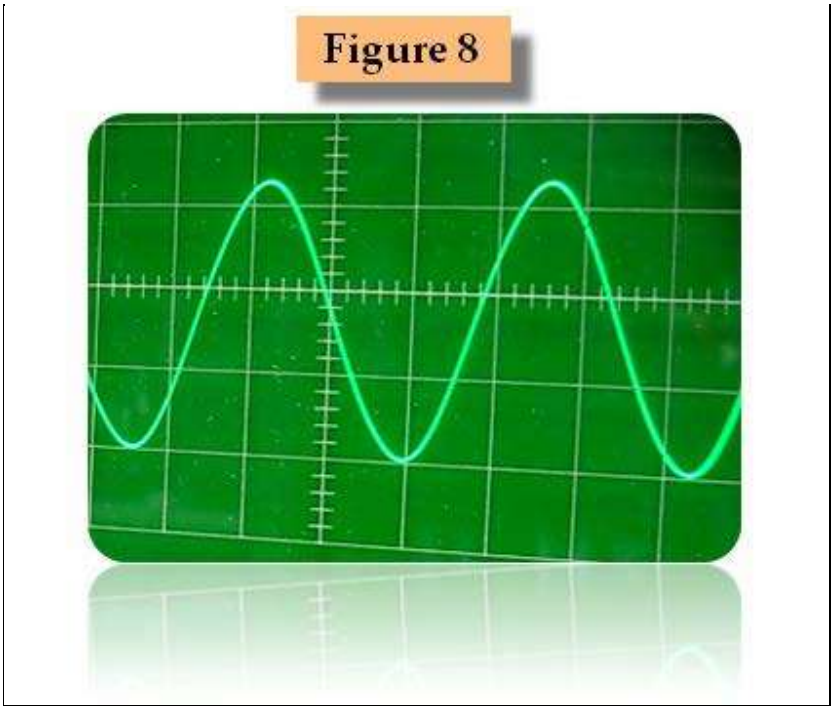

In Figure 8 is the output waveform of the low pass filter stages. A pretty nice sine wave was achieved and this oscillator could see duty for testing audio amplifiers. The scope was photographed at an angle to avoid the camera reflection and this distorts the sine waves a little.

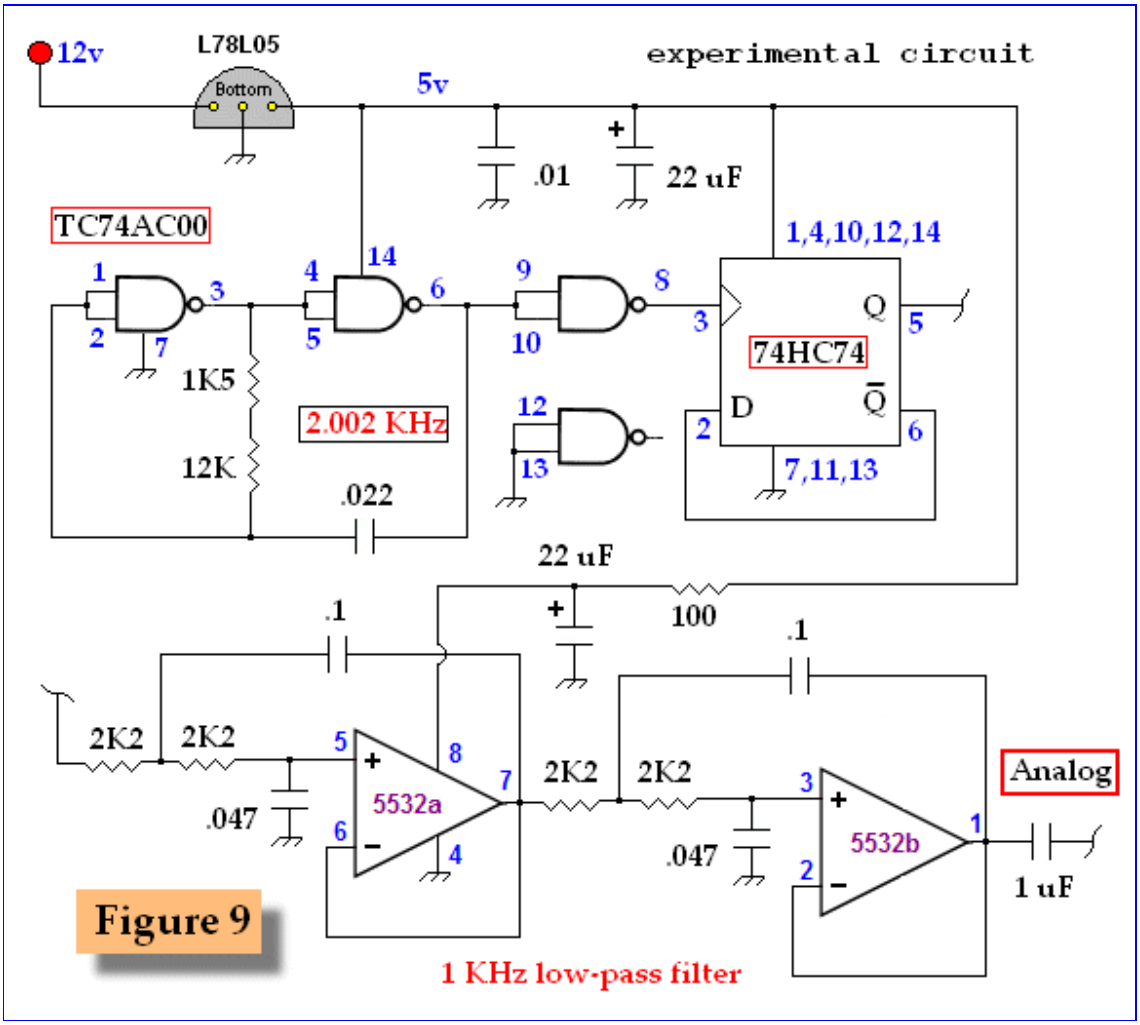

Figure 9 depicts an experiment with the op-amp biasing. If the op-amp is run at 5 volts VCC, the bias requirement is 1/2 VCC or 2.5 volts. The DC voltage at the output of the D flip-flop was 2.55 volts. The 2K2 resistor was connected directly to this output and this eliminated the VCC/2 resistor bias network and a coupling capacitor.

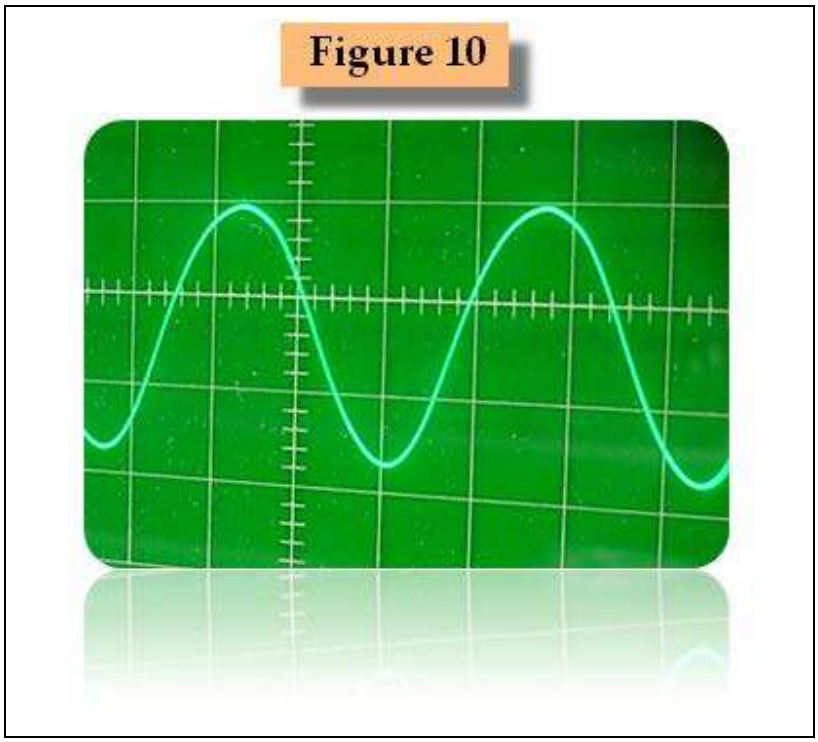

Figure 10 shows the output waveform of Figure 9. The AC waveform has harmonic distortion and thus the Figure 9 circuit will not be kept nor utilized.

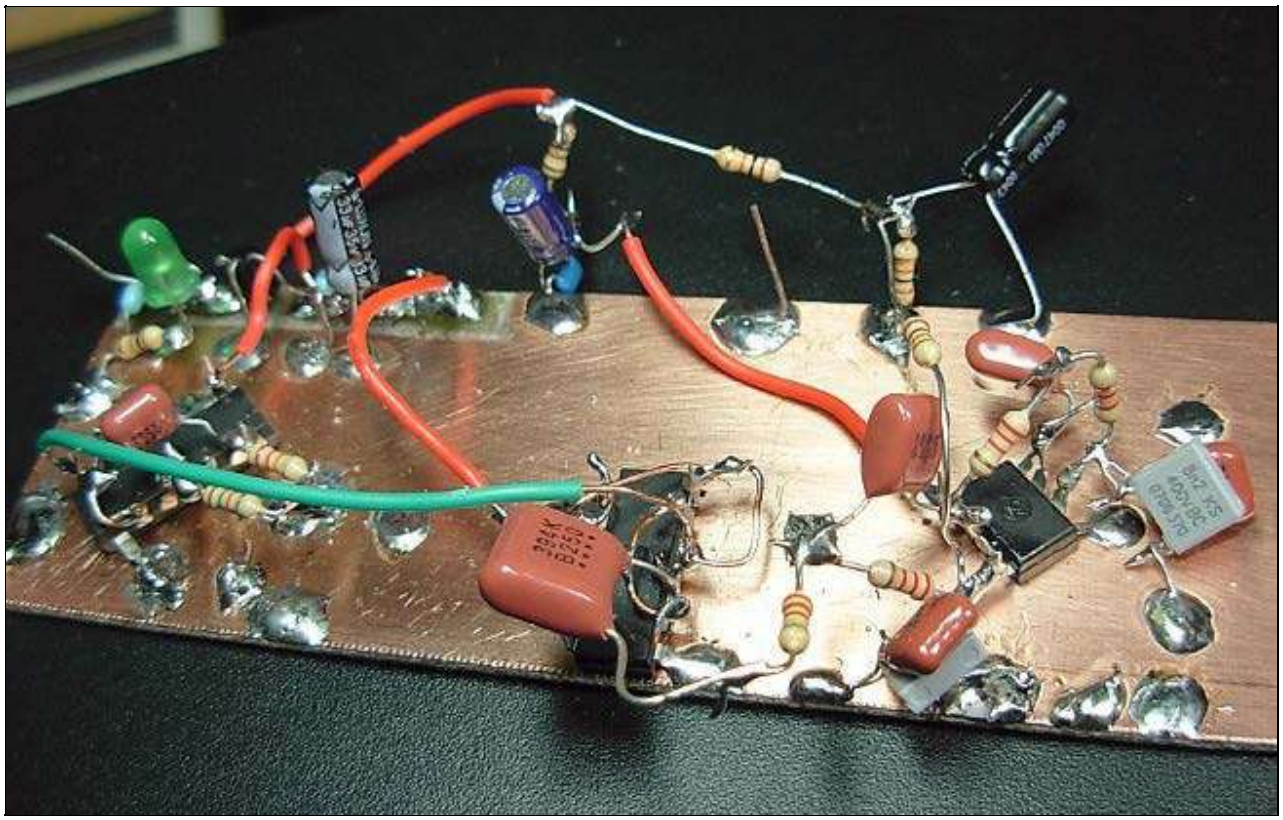

The Figure 7 breadboard. A 0.39 coupling capacitor (not 1 uF) was used between the D flip-flop and 5532a in this particular version. Unfortunately, no 0.047 uF caps were available for the low-pass filters and therefore a 0.039 plus a 0.0082 were placed in parallel for each of the .047 uF caps.

5. One KHz Low Distortion Signal Generator

Although I own a variable frequency wein bridge oscillator, it has been been set to 1 KHz for 2-3 years and is large and temperamental. It was decided to make a low distortion sine wave oscillator for just this one frequency. The circuit will be placed in a box along with another signal generator.

There are a number of ways to build signal generators using op amps. Countless example circuits may be found on the World Wide Web and some of them are really fantastic. Chose whichever method works best for you. Some might find my circuit to be overkill, but to each his own.

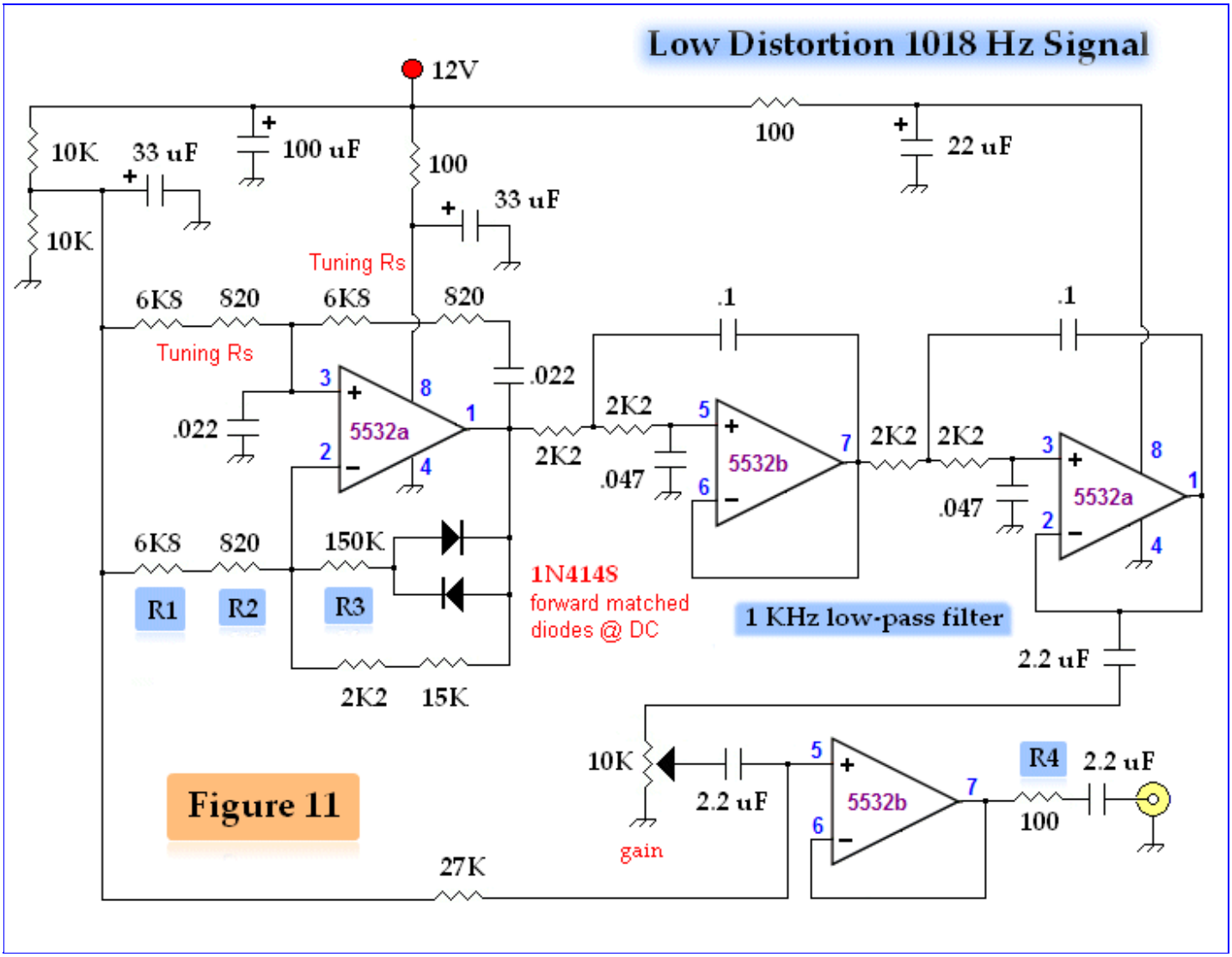

Figure 11 shows the entire circuit. The Wein bridge oscillator is from EMRFD and was designed by Wes, W7ZOI.

A 0.22 uF capacitor was chosen for the tuned circuits. Using resistors from my parts collection, 1018 Hz was the closest I could get to 1 KHz. This is the 6K8 + 820 ohms resistors labeled "tuning Rs". Other values were tried. For example, a single 6K8 gave 1142 Hz and a single 8K2 gave 939 Hz.

When the circuit was first built, I used a 10K on the VCC/2 bias point to pin 2 and a 22K feedback R from pin 1 back to pin 2. The sine wave had mild distortion. By experimentation, it was learned that the resistance from the VCC/2 bias point to pin 2 significantly affected the waveform purity. The 2K2+15K plus the R1 + R2 resistance values shown were determined by using a potentiometers rather than fixed resistors. Care was taken to adjust the feedback resistance from pin 1 back to pin 2 to keep away any overdrive distortion. I do not understand this, but even changing the 820 ohm R2 to 570 ohms, altered the sine wave purity.

The best looking sine wave came when the resistance from the VCC/2 bias point to pin 2 was the same as the tuning resistance; 6K8 plus 820 ohms. Later, the pin 1 to pin 2 feedback resistance was chosen for an unclipped; waveform with a reasonable output voltage using a potentiometer. The potentiometer was removed and measured at 17.1K, thus the 15K + 2K2 were soldered in. It was also discovered that by increasing R3 from 56K or 100K to 150K slightly improved the waveform.

The Figure 7 low-pass filter was connected to the main oscillator as shown. The final op-amp stage was used as a buffer between the low-pass filter and the gain control. R4 is used to set whatever output impedance you choose. Practically speaking, it could be any value between 47 and 620 ohms. Many AF oscillators have an output impedance of 600 ohms and 620 is the nearest E24 standard value. For my project, a 100 ohm

R4 was chosen. Output peak to peak voltage is 0.0 to 4.84v continuously.

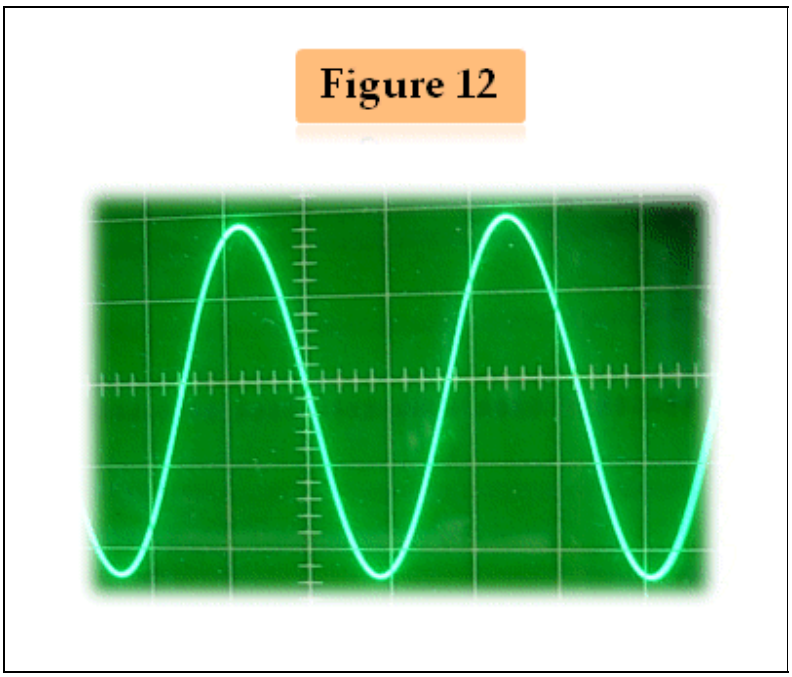

Here is the raw output of the basic Wien bridge oscillator. It is hard to photograph well, but it is stellar to say the least.

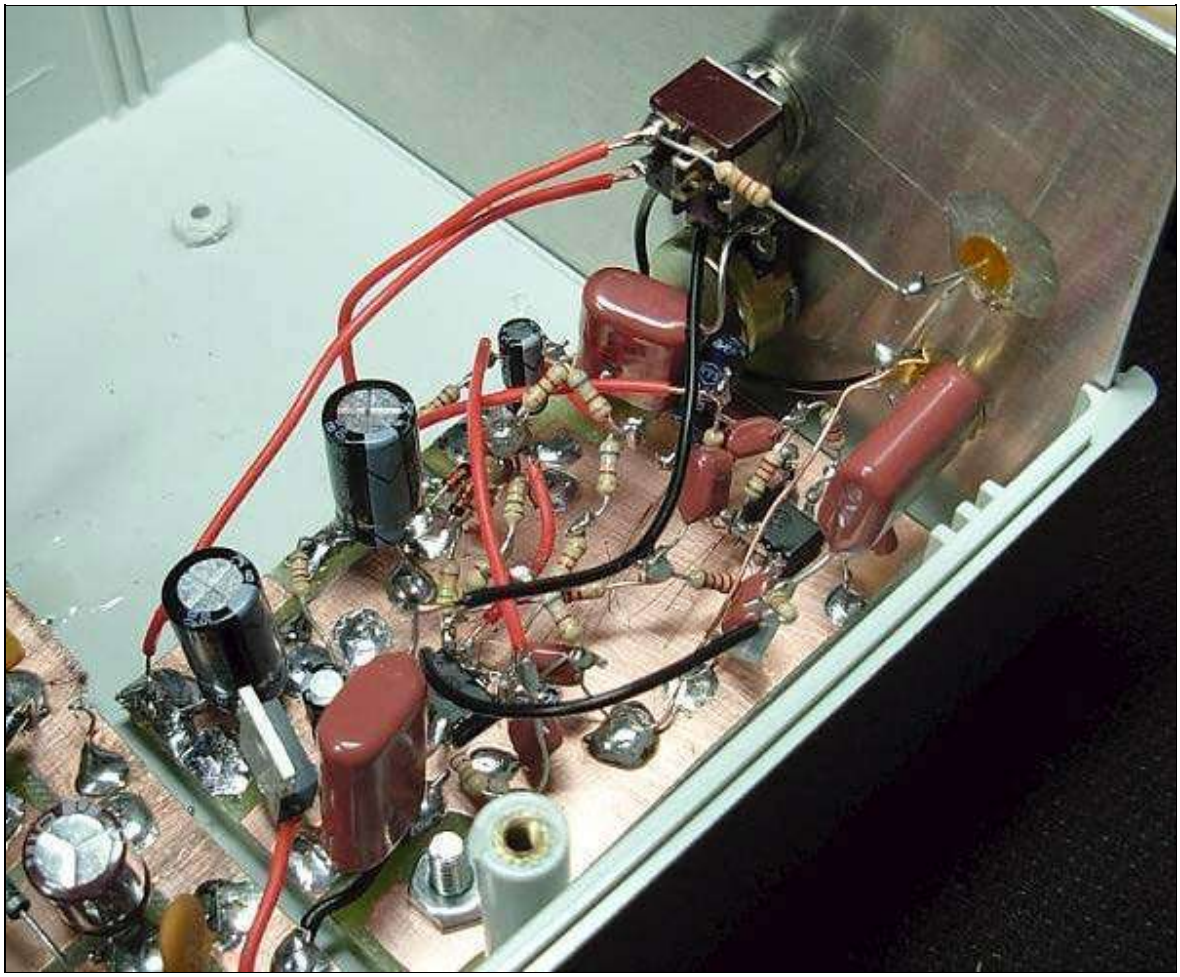

The Figure 11 breadboard mounted in a plastic Hammond chassis. The voltage regulator seen to the left of the bottom polyester cap is a 7812. This project has its own regulated power supply. Other view of Fig 11. Two 10 Megohm standoff resistors were used to help support all the resistors soldered to pins 1, 2 and 3 of the main oscillator.

A front view photo of the AF oscillator. A separate 7 plus 14 MHz oscillator circuit and controls will be placed on the right hand side of this box. The orange power ON indicator LED was epoxy glued into the chassis hole. Putting circuits in cabinets is one of the most expensive aspects of homebrew construction. One must be ever vigilant for bargain chassis boxes and hardware to keep costs down. Techniques such as gluing in the LED rather than purchasing a separate holder and recycling knobs and switches are also practiced for cost containment.

Figure 13

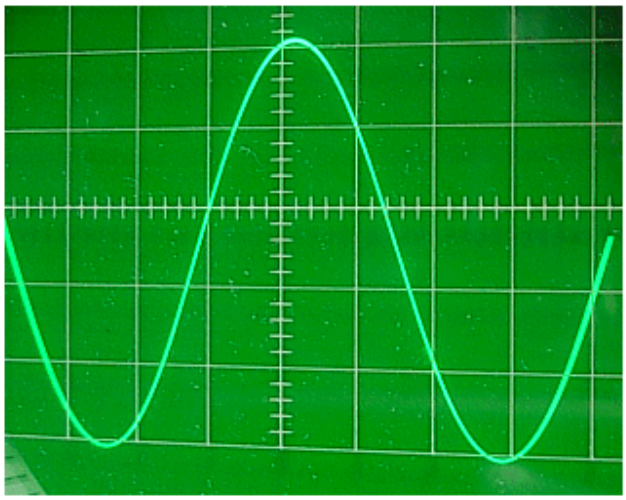

The output of Figure 11 is shown in Figure 13. This is the best sine wave seen ever on my scope. I looked at it closely and there is no change in line thickness or symmetry anywhere. It inverts with no change on the scope. Testing audio amplifiers will now be much more fun.

6. LM386 Power Experiments

The LM386 is an IC audio amp that has been used in thousands of hobbyist projects over the past 2 decades. By adding a capacitor +/- a resistor between pins 1 and 8, this device's internal gain can be changed from x20 to up to x200.

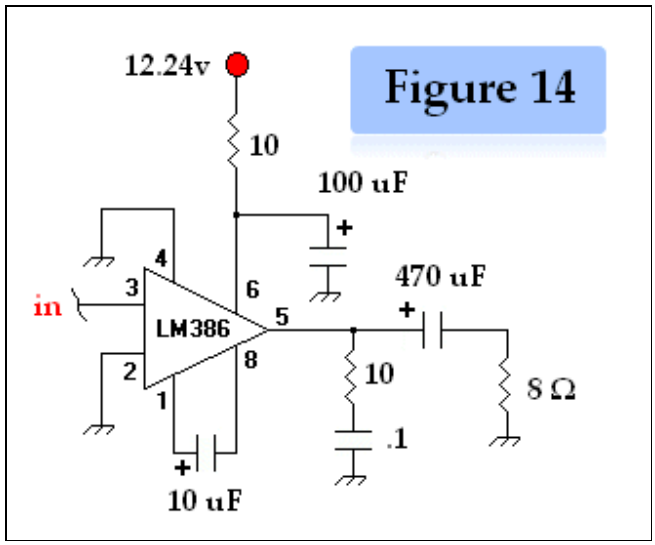

Test circuit schematic in Figure 14.

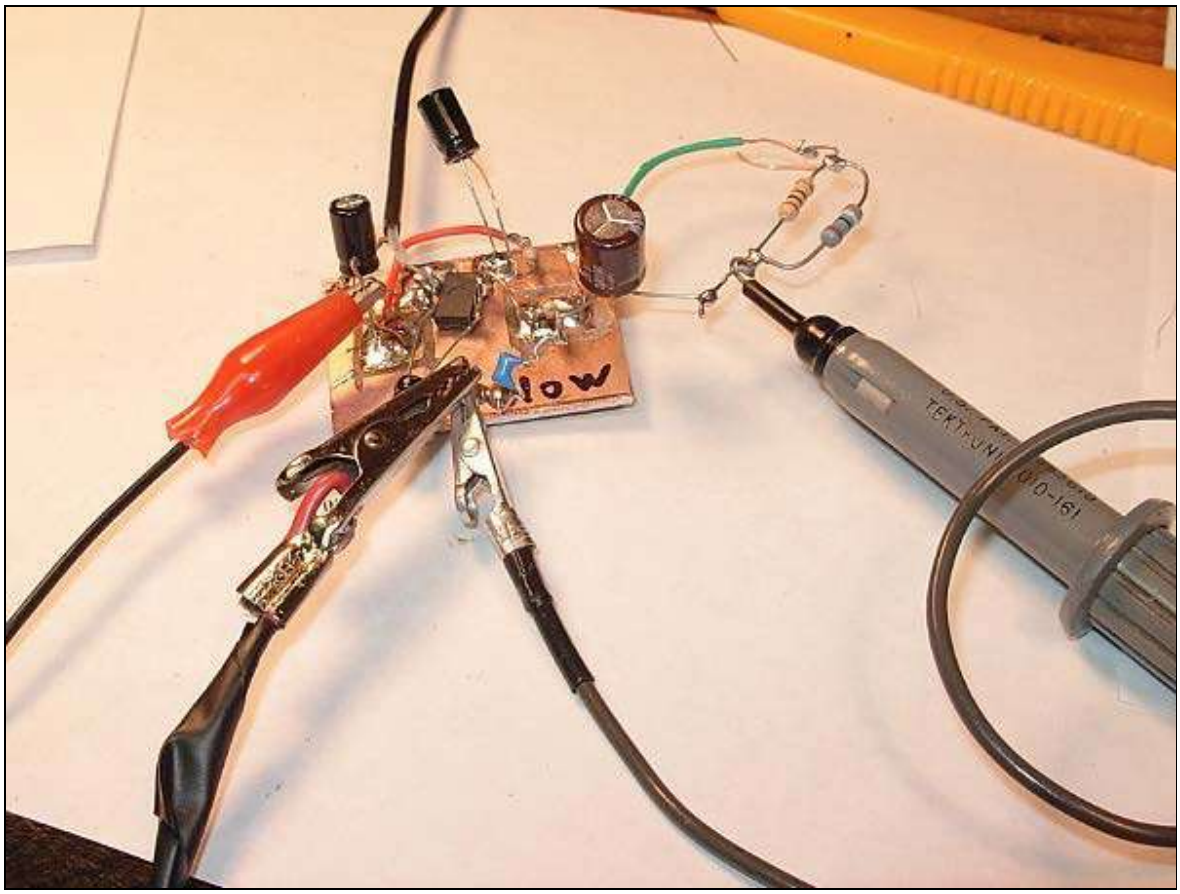

The experiment breadboard is shown above. A very standard configuration. The amplifier drove an 8 ohm, 1 watt resistive load.

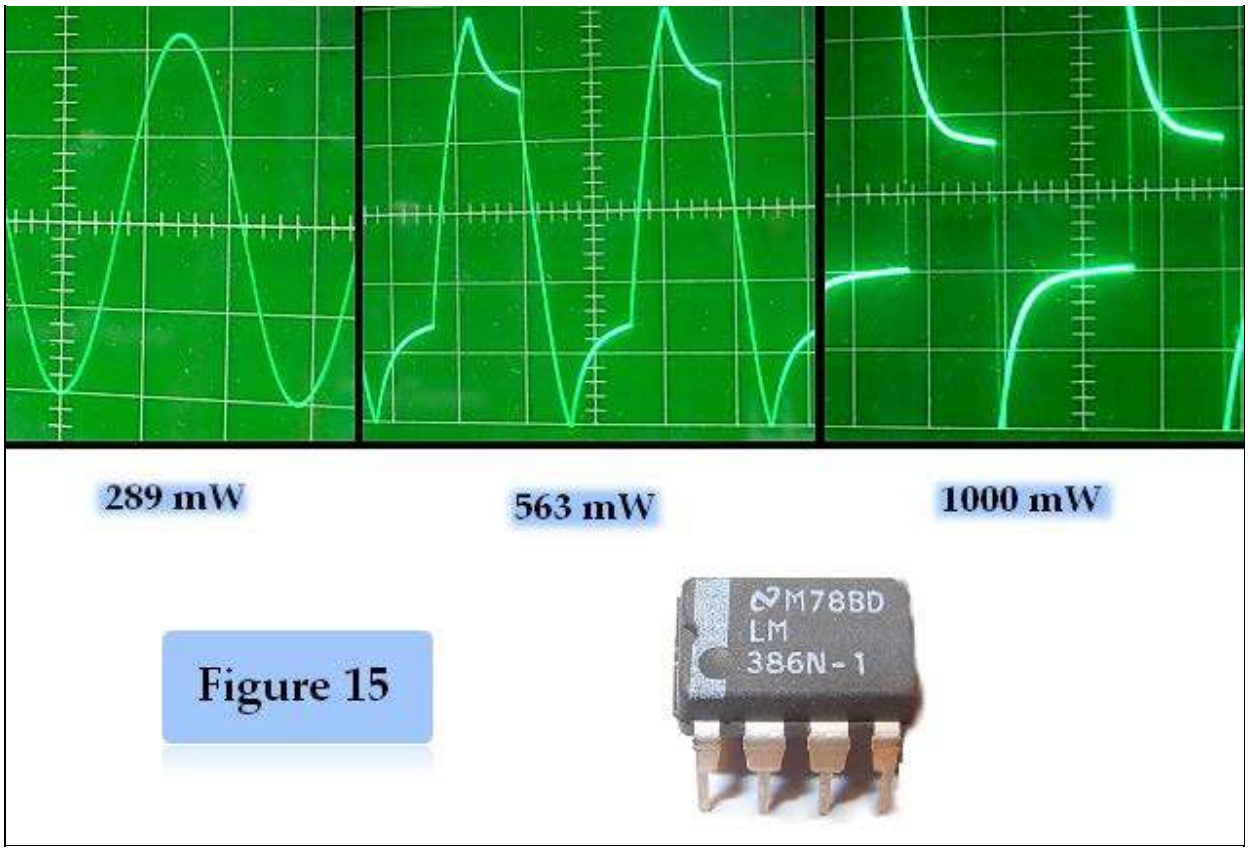

Figure 15

Over the years, I have noticed some kit sellers and project authors claiming that their LM386 based AF stages gave 1 or occasionally even 2 watts of output power into an 8 ohm speaker. This was confirmed on the bench. This device will output 1 watt into 8 ohms at 1018 Hertz with little problem. However, this is clearly 1 watt of square wave distortion.

The quiescent current of the LM386 was around 7 mA. The signal generator gain was increased until the first signs of distortion appeared. The gain was then backed off a little so a pure sine wave was observed in the oscilloscope. The current was ~ 155 mA and the measured power was 289 mW. Please refer to Figure 15 for the 289 mW sine wave. This was the clean signal power of the LM386 on my bench. The output waveforms at 563 mW and 1 watt are also shown. Extreme harmonic distortion occurred above 300 mW. This device will draw 240 mA or more when driven and clipping hard. It is not my intention to malign the LM386. It is a useful part, albeit a little dated. Its AF gain capability versus size is something to behold. Many builders have moved to the TDA7052 audio amplifier IC, or like myself, build their own low noise audio power amps.

The 12.24 volt DC supply and the 1018 Hz AF audio oscillator used in these experiments.

Time Domain Output from a Diode Ring Mixer

22 Dec 2009, w7zoi

Figure 1. Some available experimental modules.

Some folks wonder about the output that they should see on their oscilloscope when looking at the output from a diode ring mixer. There is no set, pat answer. The output
can change dramatically as levels, frequencies, and even terminations are changed. This complication is illustrated here with a few screen shots, taken with a Rigol DS1052E 50 MHz bandwidth digital storage oscilloscope. The experiments started with the following pile of modules. Your collection will probably differ.

Figure 2. The inside of the module containing a Mini-Circuits SBL-1 diode ring mixer. This is a standard part that is essentially generic.

The first experiment was to set up a pair of 10 MHz signal sources. One was from a homebrew generator, shown below.

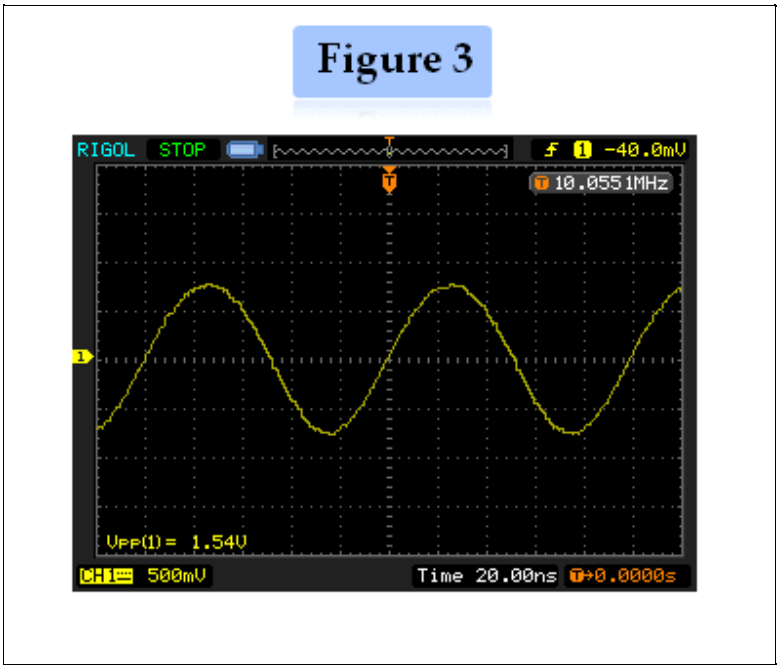

Figure 3. The 10 MHz signal from a homebrew signal source. The 1.54 volt peak to peak signal is applied to a 50 Ohm terminator at the oscilloscope. The delivered power is then +7.7 dBm.

This signal was filtered with a 14 MHz low pass circuit. This caused the amplitude to drop by 0.2 dB. The source was then attached to the LO (local oscillator) port of the SBL-1 mixer.

Figure 4

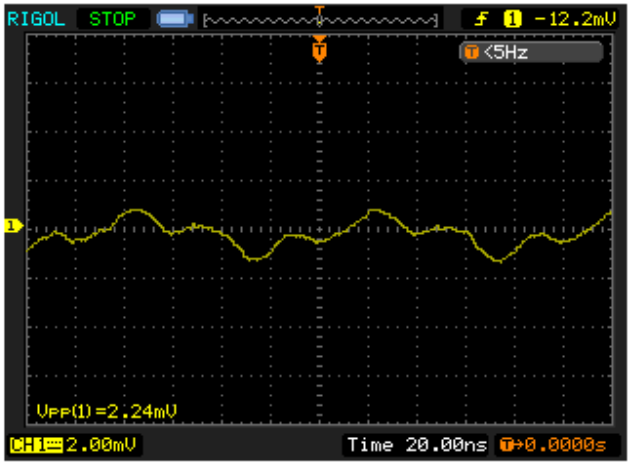

Figure 4. The IF output from the mixer when there is nothing attached to the RF port. Note the scope sensitivity of 2 mV/div.

Next, we attached a 50 Ohm terminator to the R mixer port.

Figure 5

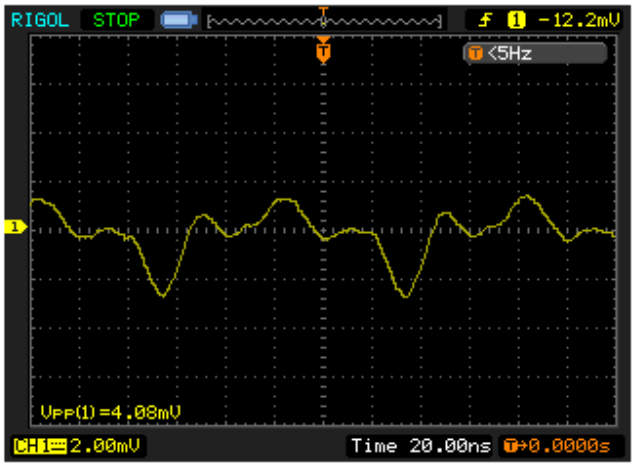

Figure 5. The IF output with LO drive, but without an R signal. But the R port is now terminated. This waveform, when compared with Fig 4, shows just how sensitive the mixer can be to termination.

In the next experiment, a -20 dBm signal was applied to the R port. The frequency was very close to the 10 MHz LO that is still present.

Figure 6

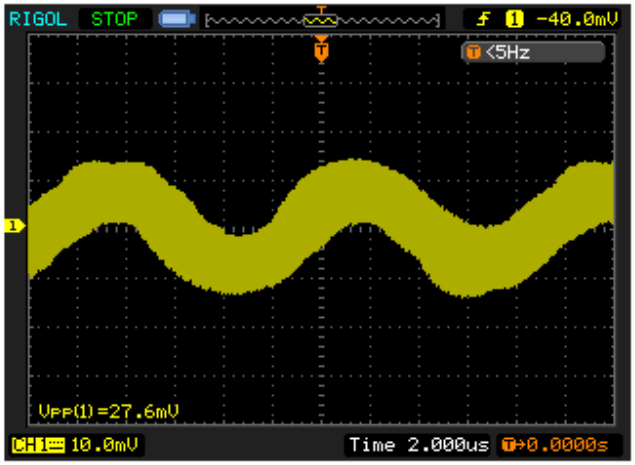

Fig 6. There are two dominant signals from the mixer. One is a low frequency at 100 kHz. But this is accompanied by a high frequency of about 20 MHz. These two outputs, a sum and difference frequency, are expected from any mixer.

A filter can isolate the two dominant outputs. This is shown below where a 500 kHz low pass filter is inserted in the line between the mixer and the oscilloscope. A 6 dB pad is between the mixer and the filter, for direct insertion would upset the termination of the mixer.

Figure 7

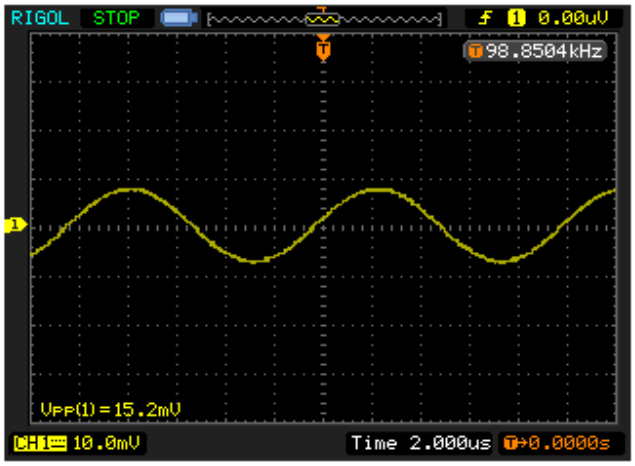

Figure 7. The output of about 100 kHz after a low pass filter is inserted in the mixer output.

The next experiments emulate a SSB transmitter. We start with a signal at 11.06 MHz with strength -20 dBm. (This is a common IF used in homebrew SSB transceivers such as the BITX-20.) This is applied to the mixer R port. The L port is driven with a +7 dBm signal at 3.19 MHz. The LO signal is low pass filtered to attenuate harmonics, a measure that is probably not necessary, but the filters were there. The IF output is shown below.

Figure 8

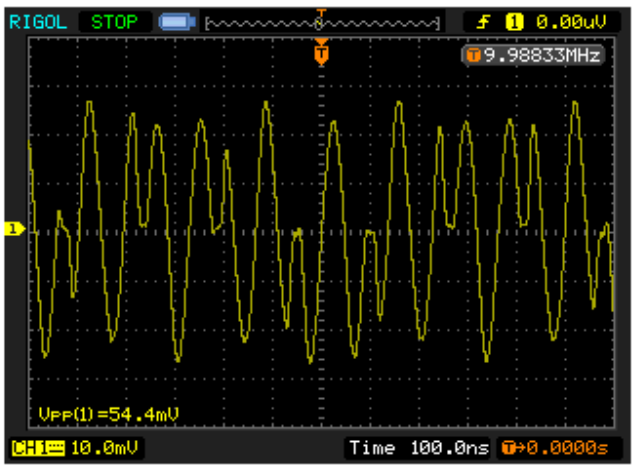

Figure 8. Time domain output of a SBL-1 set up as the “transmit” mixer in a SSB rig. This is far from the “perfect sine wave” that some folks tell us we should observe. This waveform contains many different frequency components. The counter output should not be interpreted to have any meaning. (I should have turned it off.)

The signal of Fig 8 can also be viewed with a spectrum analyzer. This is shown below. This measurement was taken with the August 1998 QST Spectrum Analyzer and not the FFT routine in the DSO. The Rigol scope has a nice display for an analyzer.

Figure 9

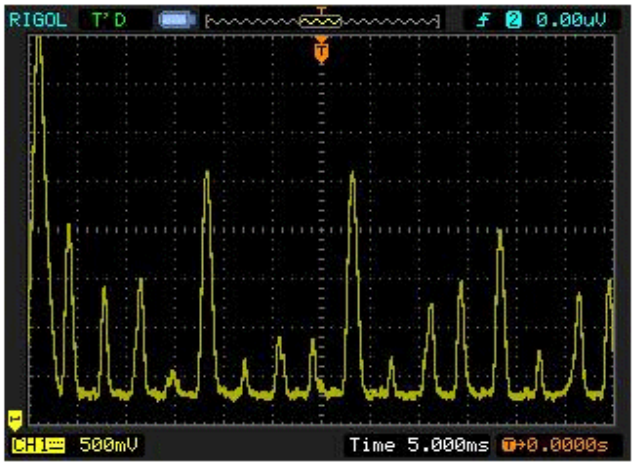

Figure 9. Spectrum of the signal shown in Fig 8. The largest signal on screen is that at the left, which is the spectrum analyzer zero spur. This is a spurious output that is typical of most SA systems. The desired signal at 11.06+3.19=14.25 MHz is just to the right of center. But the image is also present at the different frequency of 7.87 MHz at about 3 major divisions from the left edge.

Alas, I didn’t find a 14 MHz bandpass filter in the junk box. Such a filter would have allowed selection of the dominant 14 MHz component while attenuating all the rest of the junk shown. The many other signals are the result of harmonic mixing. That is, we observe IF outputs at N x FLO +/- M x FRF where N and M are integers. Some of these spurious outputs can be quite strong with diode ring mixers. They are best avoided with high frequency LO signals. In this case, a LO at 14.25+11.06=25.31 MHz would produce a much cleaner output spectrum. It is much easier to obtain LO stability with an oscillator built at 3.19 MHz.

Bottom Line

It is not reasonable to have a well defined, predictable time domain (i.e., normal oscilloscope) output from a mixer. The exact results depend upon too many variables. A spectrum analyzer can be used to garner much more information.

Low Noise Crystal Oscillators

Introduction

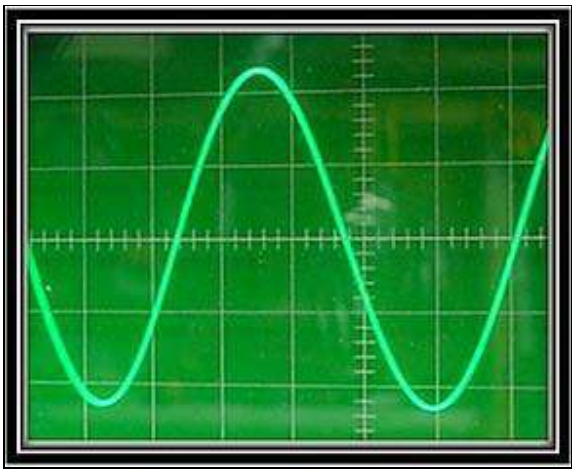

Some experiments were conducted to build a low noise crystal oscillator with 50 ohm output at 7 and 14 MHz for the test bench.

Some readers might wonder why build such an oscillator? Although a variable RF signal generator is an important bench tool, it is also nice to have a fixed frequency signal source on your favorite HAM band. This RF source can be connected to other 50 ohm modules such as band-pass filters, diode ring mixers or feedback amplifiers to conduct experiments at a whim. The project goal was a low noise oscillator with 2 outputs so it could drive a divide by 2 flip-flop for 40 meter band digital mixer work, or fundamental frequency use on the 20 and 40 meter bands.

Presented are some experiments carried out to realize this goal. Only some of the better experiments and circuits are shown. An additional circuit was added Jan 31, 2010.

First Steps

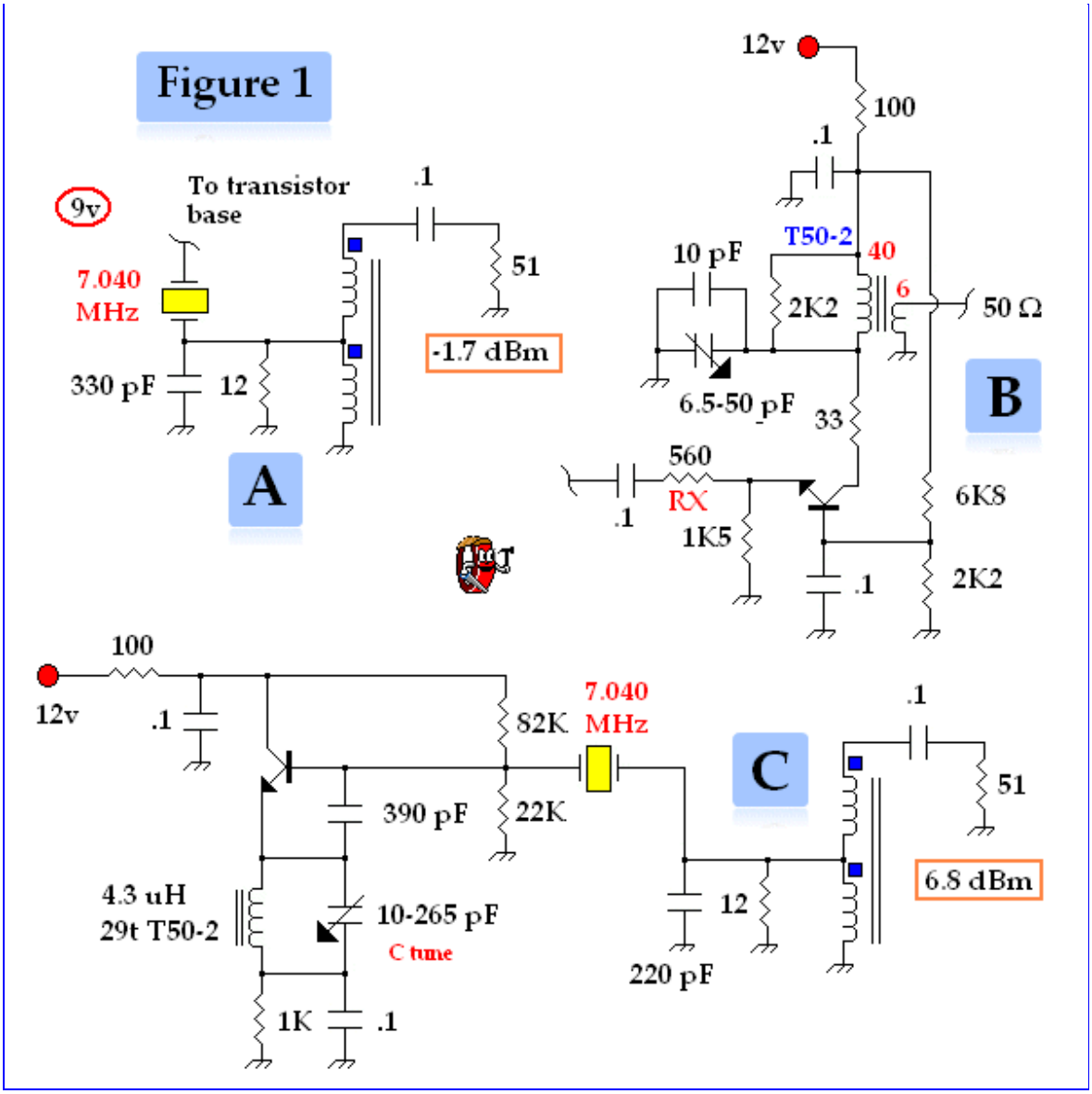

The 7.040 MHz crystal used is an AT cut, HC6-U holder part made locally by West Crystal. I reviewed the information concerning crystal oscillators in Chapter 4.5 of EMRFD and then started melting solder. The oscillator output was extracted as described in EMRFD Figure 4.24. The output is low distortion, low impedance and low gain. Like in most experiments, I built it, measured the DC voltages and then looked at the AC voltages in the oscilloscope.

In order to measure the output, a 51 ohm load was transformer coupled as shown in Figure 1a. I am uncertain if this was a good method for power measurement, however, it allowed comparison of the experimental circuits. As shown, the output with a 9 volt regulated power supply is low; -1.7 dBm. Still, a circuit like EMRFD Figure 4.24 can be used with a variety of crystal frequencies and has great utility.

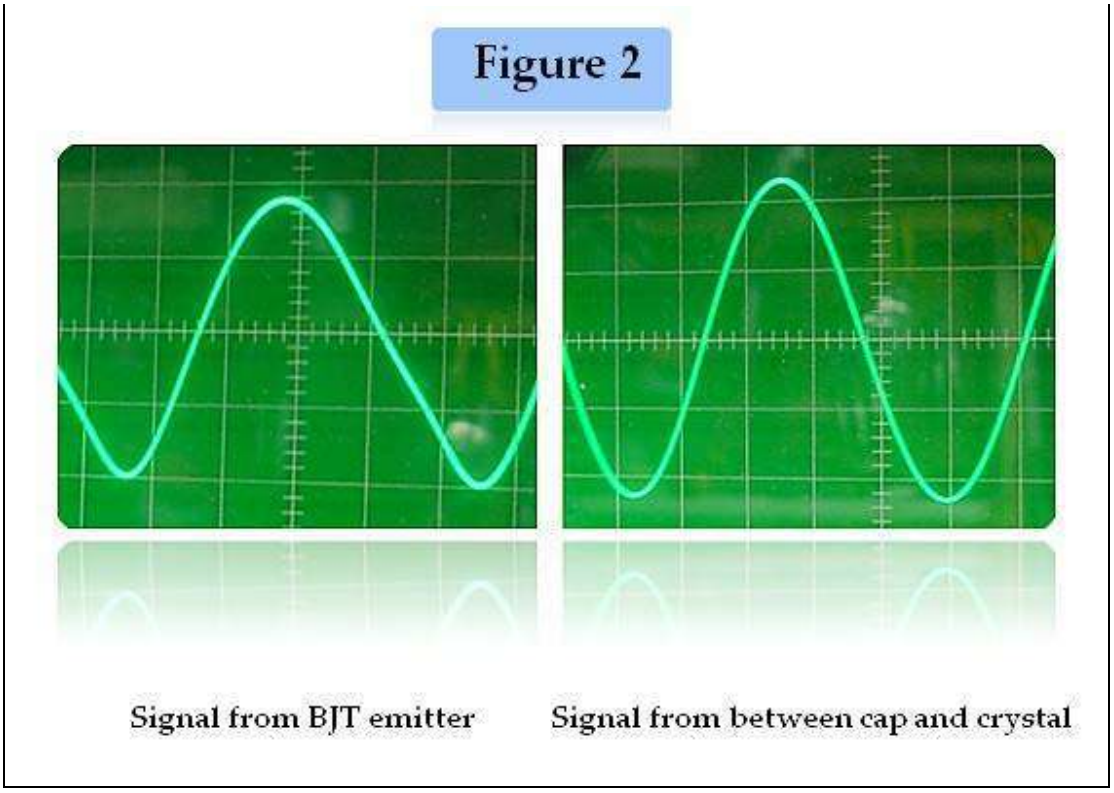

Figure 2 shows two output waveforms taken from my crystal oscillator. When a signal is taken from the emitter of the main oscillator transistor (what we typically do) harmonic distortion occurs as shown in the above left. Actually, the distorted waveform photo above left looks better than most do. Typically, they look like this. Many builders will just place a low pass filter on such an oscillator's output and be very satisfied with the harmonic content in their signal. Certainly this is a good, common and practical way to go. However, for some builders, the experimenter's journey is what counts. That is, the fun and learning occurs during designing/building/testing and not just operating home built gear.

When the output is taken from between the shunt capacitor and the crystal per Figure 1A, a much cleaner sine wave is available. The photo above right tells this story. The focus of all of the experiments on this web page is boosting this lower distortion, lower phase noise signal into something useful. To increase the base oscillator output voltage, the VCC was raised to 12 VDC and the BJT emitter circuit was tuned per Figure 1C. Resident on my work bench are a few potentiometers and a 10-254 pF air variable capacitor with short attached leads. These parts are inserted into test circuits to allow tweaking of R or C as desired. Once the desired tweaking is performed, the potentiometer or variable capacitor is removed and measured. The closest fixed value R or C is then substituted as appropriate. In this experiment, the highest output voltage occurred when the variable capacitor measured 181.7 pF. Thus in my version, 33 pF and 150 pF capacitors were placed in parallel and are shown later in Figure 3.

The Figure 1A output transformer circuit was again used and the power output was 6.8 dBm. Being tuned to 1 crystal frequency is the biggest drawback of the 1C circuit. Tuning a crystal oscillator as described earlier is easy to do however.

The next task was to design and build a buffer/amplifier. To match the low impedance of the Figure 1C crystal oscillator, a common base amp was built. The circuit was morphed over time, however, the initial design is shown as Figure 1B. It was interesting to note that a series resistor (RX) is required to keep the waveform pure. Any RX value less than 470 ohms compromised the sine wave purity. The 560 ohm R shown was perfect, however, as expected, attenuated the oscillator signal. In order to get a decent output voltage, the common base amp had to be run at 5 mA or greater current and ultimately collector tuning was added to try and realize an output voltage greater than 4 dBm.

Through experimentation I learned that adjusting Fig 1B's tuning, emitter current and RX value all could distort the output of the main oscillator at certain values or settings. Running high current also invites parasitic oscillations and soon it was realized that common base was perhaps not the best choice (at least for me) as another separate amplifier stage would be required to get a decent output voltage with or without an attenuator pad.. After trying a number of different buffer-amplifiers including a 50 ohm feedback amp, I chose a favorite circuit which I know has excellent gain plus back to front isolation and would not distort the oscillator waveform; a lightly coupled JFET amp.

---

7 MHz Circuit

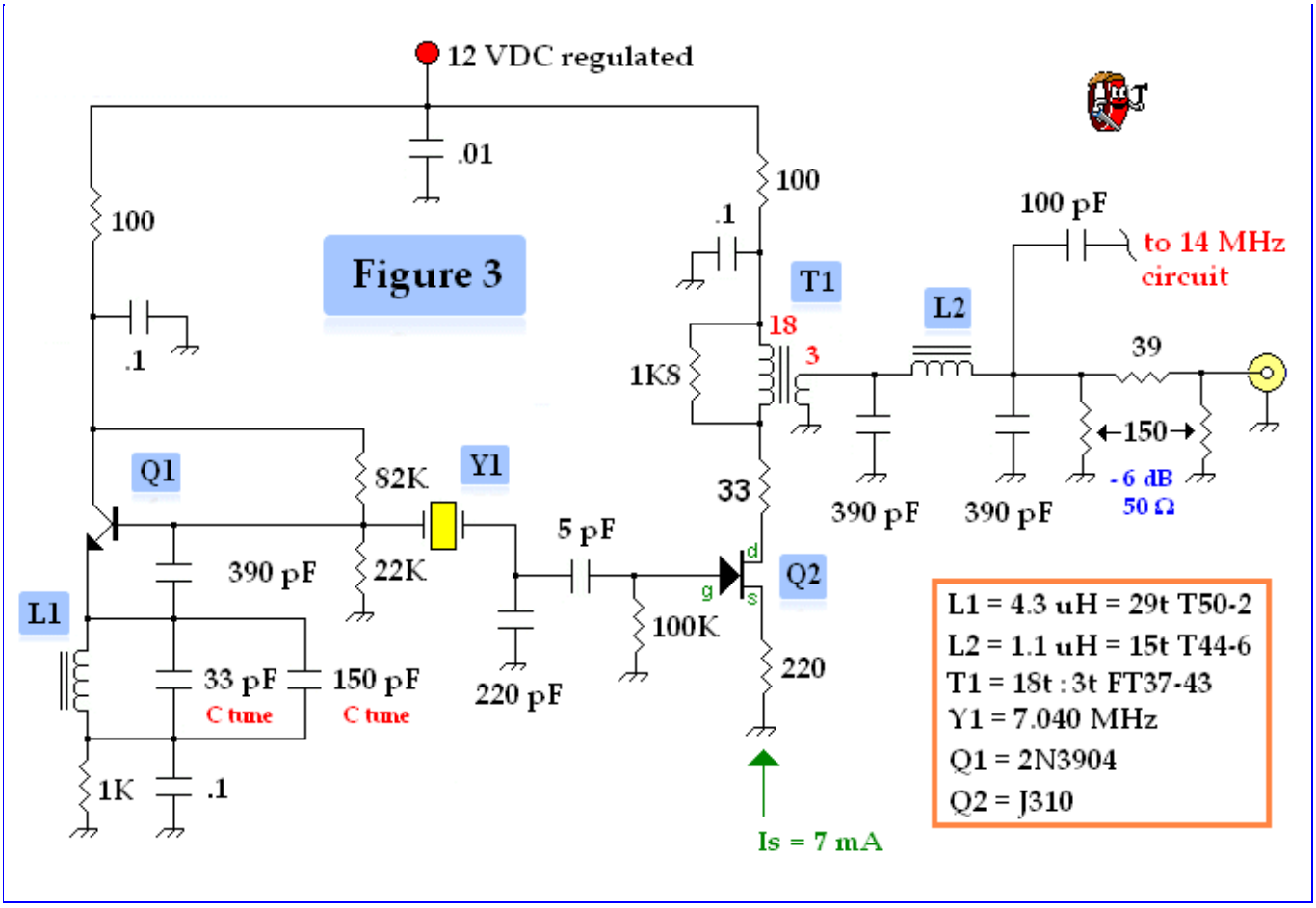

In Figure 3 is the complete schematic of the 7 MHz portion of the low distortion crystal oscillator. The output was 0.52 dBm. A 6 dB 50 ohm pad ensures a well-buffered 50 ohm termination. This aids in calculating gain or loss in circuits it drives. You could easily decrease this to a -3 or -4 dB pad. This reflects the wisdom handed down by our mentors who encourage building RF stages in 50 ohm impedance blocks. A Q2 source bypass capacitor was not placed as it increased harmonic distortion in the output signal. The output is filtered with a simple pi filter. The 100 pF coupling capacitor connect this circuit to Figure 6; the 14 MHz circuit.

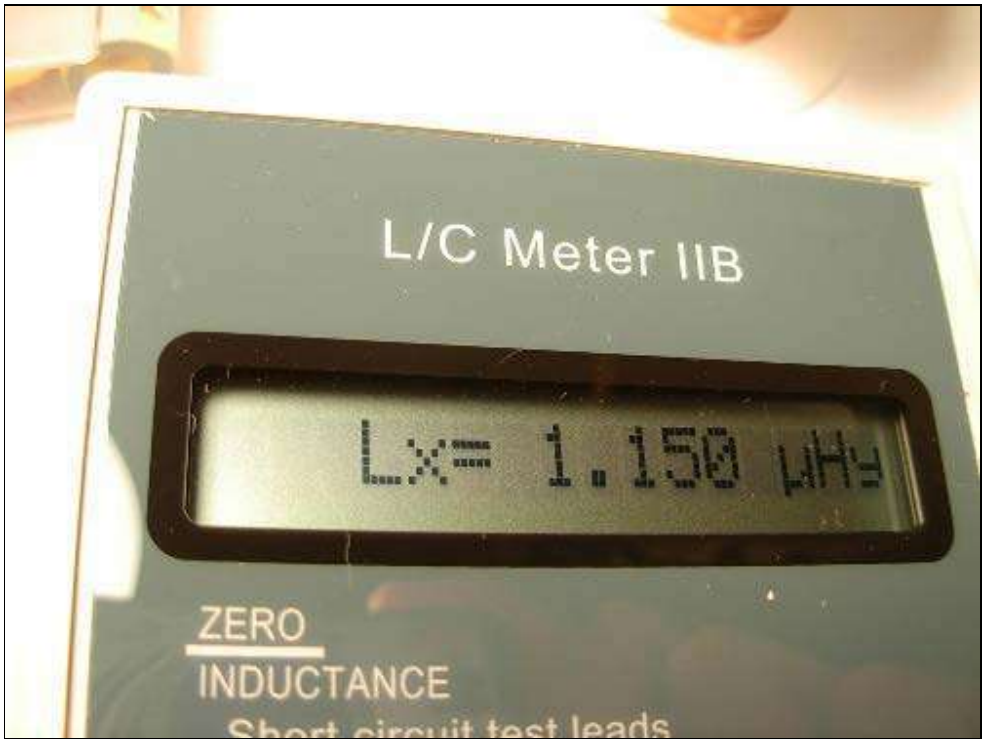

L2 was wound and measured. It is desirable (but not absolutely necessary) to perform measurement on powdered iron toroids to compensate for

variations in wire spacing and toroid permeability. I used a T44-6 core; use whatever appropriate powdered iron toroid you want.

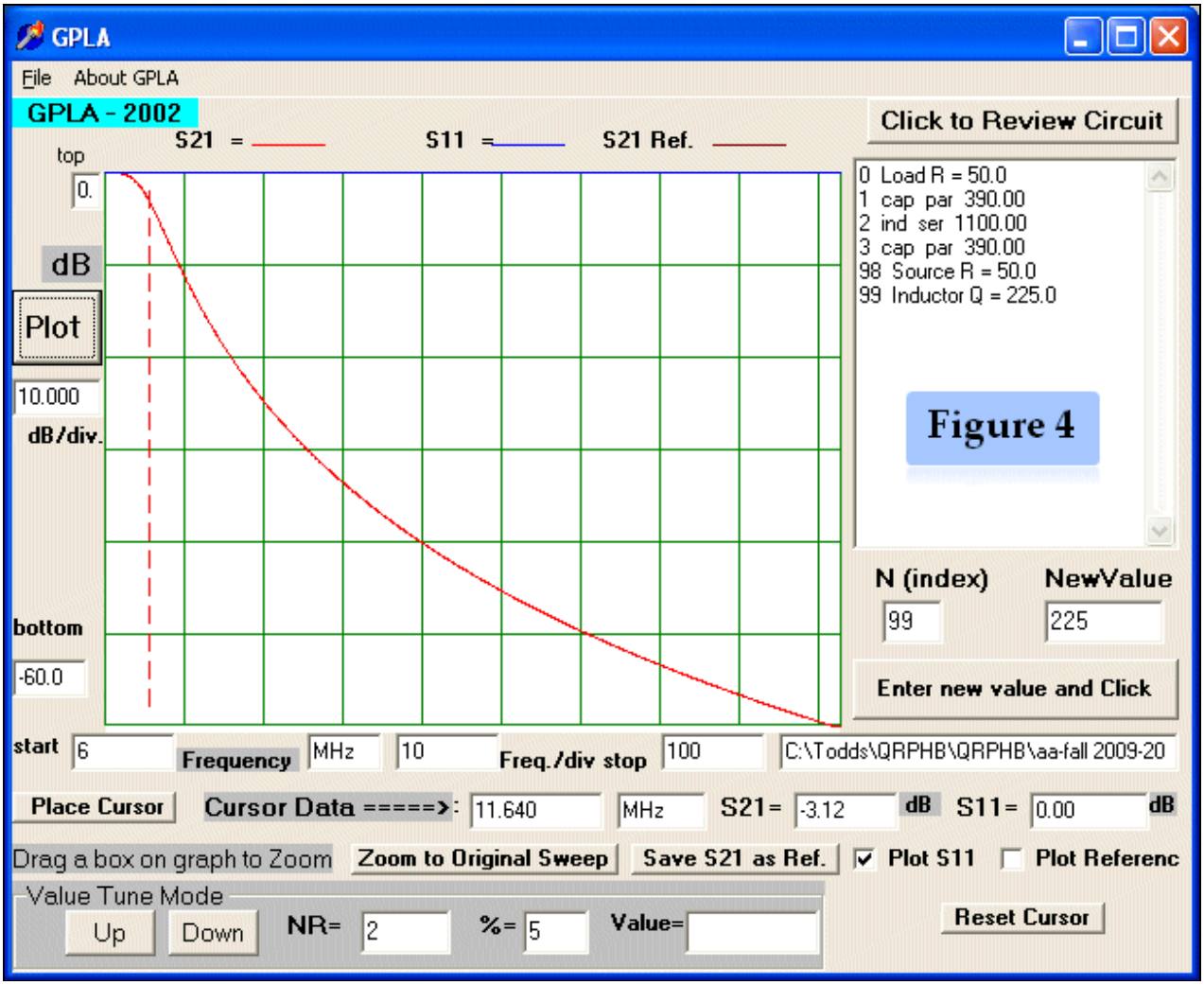

A GPLA analysis of the Pi low-pass filter is shown in Figure 4. The basic circuit was designed with PI Filter Designer on this page and tweaked in GPLA. You may wish to omit this filter or perhaps, design a better one yourself.

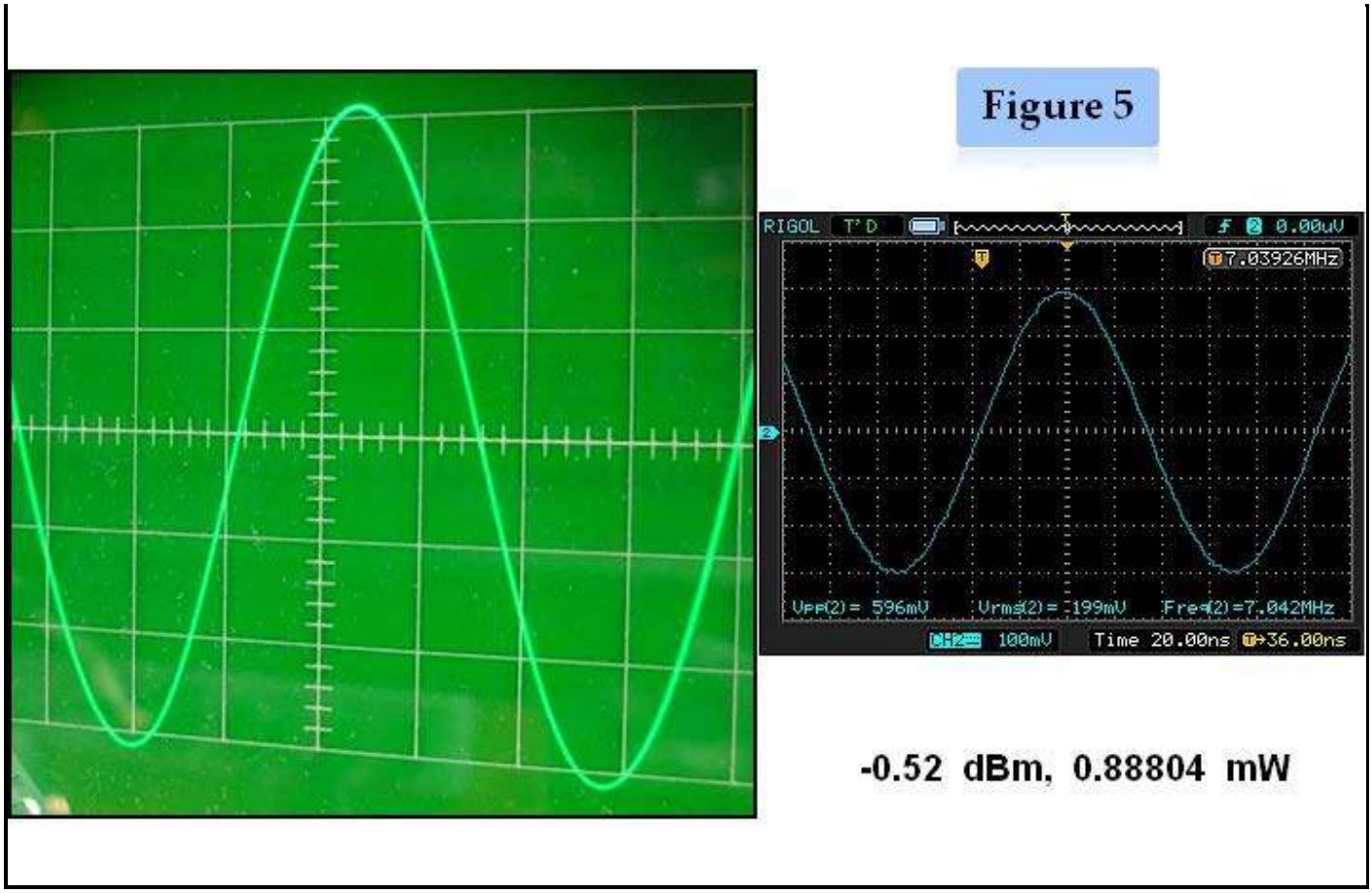

The 7 MHz output waveform on the Tektronix (left) and the Rigol oscilloscopes. On the Tek scope, the output power was 0.50 dBm and on the Rigol scope it was 0.52 dBm. The Rigol is an amazing oscilloscope, but only has 256 horizontal lines of resolution, therefore cannot replicate the stellar and beautiful waveform tracings of the ancient Tek scope. In reality, probably, no other modern scope can. I have received many positive comments about the old Tektronix oscilloscope waveforms. It is important to mention, that Rigol waveform viewing is not bad, just very different. The visual display is incredibly accurate and its triggering options, bandwidth, sampling rate and waveform display tools are fantastic. фантастический !

During these experiments, the 40 year old (plus) Tektronix scope was distorting frequencies greater than 10 MHz and breaking into oscillations. After 3 major repairs in 2009, the scope replaced with a Rigol DS1052E. Signal viewing will certainly different; that is for sure. The decision to move from a cathode ray oscilloscope (CRO) to a digital storage scope (DSO) was not taken lightly.

DSO versus CRO - some comments from the workbench

Choosing a CRO versus a DSO is an individualized process. It is your decision alone. Questions to ask yourself may include: What are my needs? What is my budget? Do I have weight and/or space constraints? Carefully weigh the advantages and disadvantages of each.

Proponents of CROs state that these scopes cannot generate artifacts, nor distort the signal. This of course is true as long as the scope bandwidth is adequate. Further, some people feel that aliasing or artifact generated in DSOs due to undersampling (taking too few samples of a waveform) is unacceptable. They may even feel that DSOs are not precision measurement instruments as a result. Limited horizontal screen resolution in DSOs is also a bugaboo for some experimenters and provides further evidence of DSO inferiority in the minds of these folks. These concerns are indeed valid; however, black and white thinking is a little out of fashion in a world more containing shades-of-gray.

The DSO takes a series of samples and stores them in memory. When sufficient samples are present, they are assembled and displayed. The sampling rate of a DSO is variable and depends on the time base setting used. Modern DSOs, like the Rigol, Tektronix Oscilloscopes and Agilent Oscilloscopes have better sampling rates and larger memories than their predecessors and hence aliasing is less of a problem than before; although in some measurement situations, undersampling can occur. One must always well consider and interpret whatever you are measuring and if you use a DSO, always keep undersampling in mind. When first using a DSO, you are on the bottom of a learning curve, however, with attentiveness and practice, one can learn to look for and possibly mitigate undersampling should it occur. In certain cases, a CRO will be superior to a DSO. In my discussions with others about Rigol signal viewing , only 1 significant "aliasing" problem has been noted by a builder when he tested a balanced modulator. The display did not give the expected result (was not filled in as expected) and a CRO was pulled out and the problem was verified. The builder knew there was a problem and could understand why it occurred. This builder also wrote that this was not so much a problem, as a reality of using a DSO.

Some techniques I have gleaned from the Internet about detecting aliasing may include the following:

Vary the time base over several ranges. Events occurring near the time base should be reproducible and if they are not, undersampling might be occurring.

As possible, use a single sweep and dot display. The 'dots' will indicate just where the scope took each sample. If the dots are far apart relative to the waveform timing, aliasing is a possibility.

Some techniques to minimize aliasing:

Choose linear interpolation when using math functions.

Use bandwidth limiting in low level measurements (The Rigol seems to automatically use B/W limiting in these situations).

Use trace averaging for low level measurements as possible.

The Rigol weighs 50 times less than my old scope and fits on a small shelf in my small workspace. As a hobbyist, it meets my needs and budget plus has some very cool features. Undersampling is considered and in some cases, such as low level measurement, an analog scope might be a better choice. Happily, a CRO is available to me if I really stress out over it. Signal viewing was taken for granted with my old scope. In some ways, this DSO has prompted me to dig deeper; to become more vigilant and thoughtful about signal measurement and display. If you have a spectrum analyzer, and use a DSO for signal viewing, the ability to perform slow sweeps while maintaining a perfect display is quite enjoyable. Again, please decide the CRO versus DSO issue for yourself (or maybe get a hybrid). The DSO is not a perfect solution to every signal viewing situation, but their constraints are quite livable considering their numerous modern features.

DSO's: “They are not your father’s oscilloscope”; that is certain!

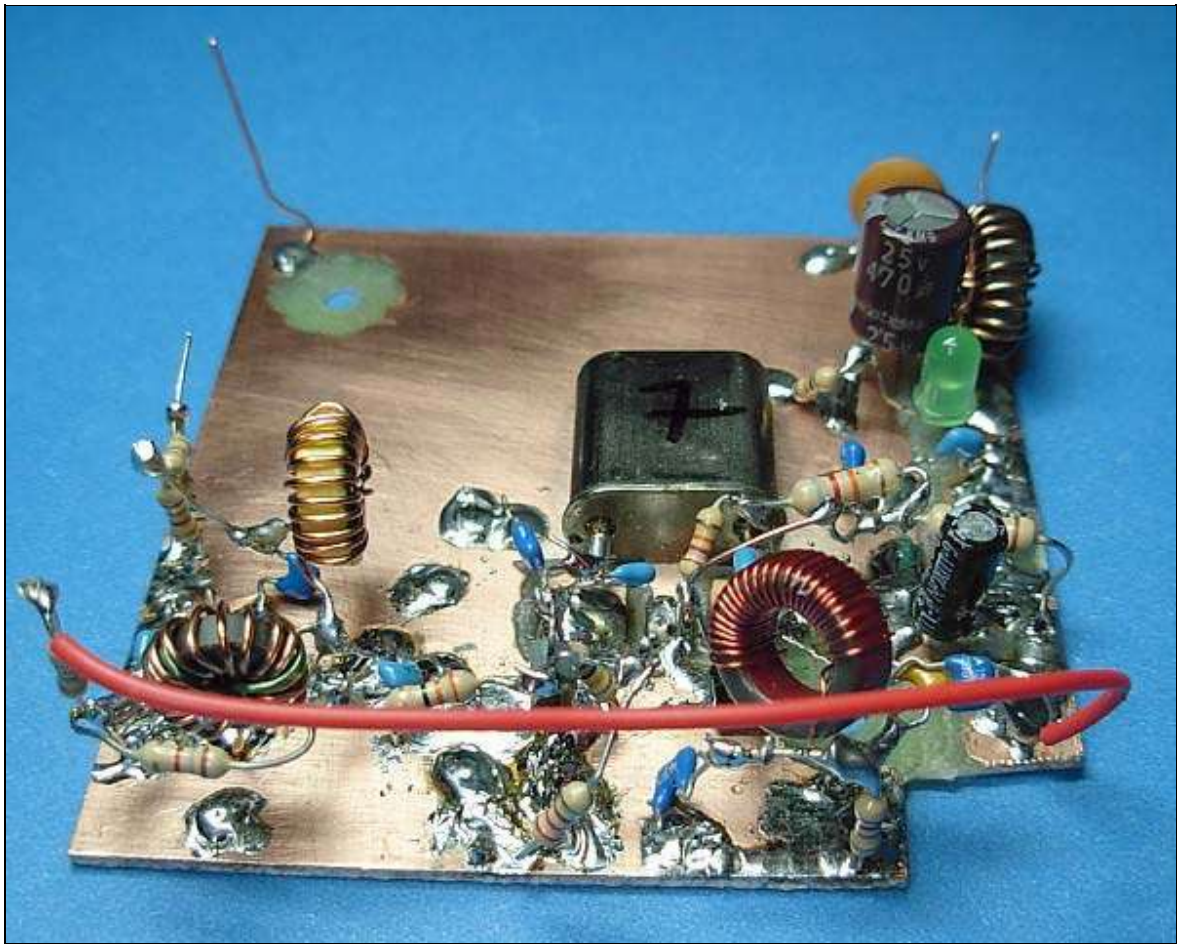

The Figure 3 breadboard. AWG 24 to 26 gauge wire was used in the various inductors and transformers to better secure or anchor these parts.

14 MHz Circuit

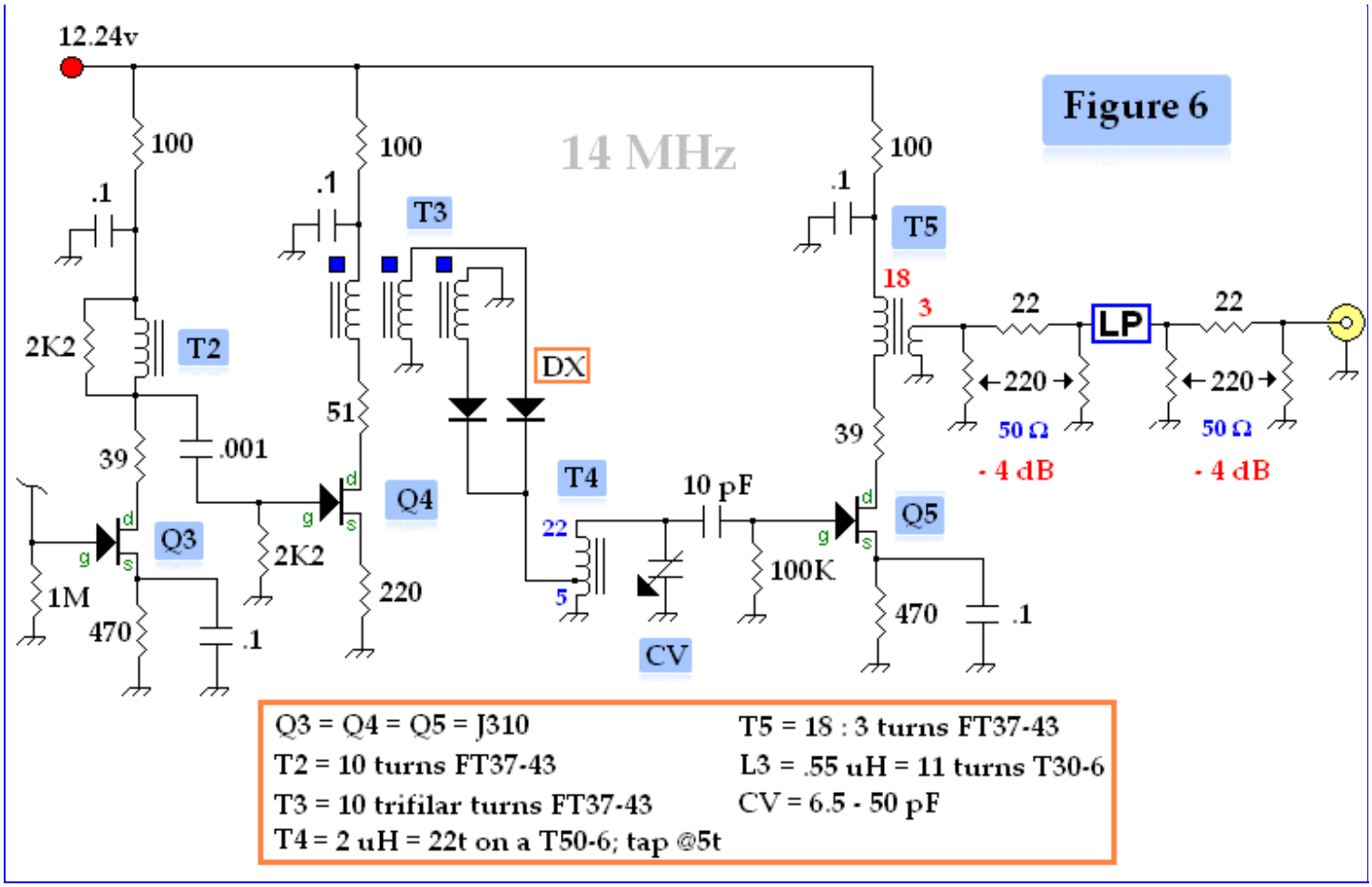

Figure 6 is the final schematic for the 14 MHz circuit as developed on the workbench. Your design might look very different than mine. In the first version of this circuit, there were only 2 JFET amplifiers and the resultant output voltage was too low (even without a 50 ohm attenuation pad). To compensate, I ran the source current of the JFETs above 15 mA, placed a source bypass capacitor on Q4 and also used a 1000 pF capacitor to couple the input to Figure 2. Some fairly bad harmonic distortion was measured at the output and it seemed crazy to run so much current. Therefore it was decided to run a third JFET amplifier and use only modest current in the trio of JFET amplifiers.

CV tunes very sharply and required some care when peaking the output voltage.

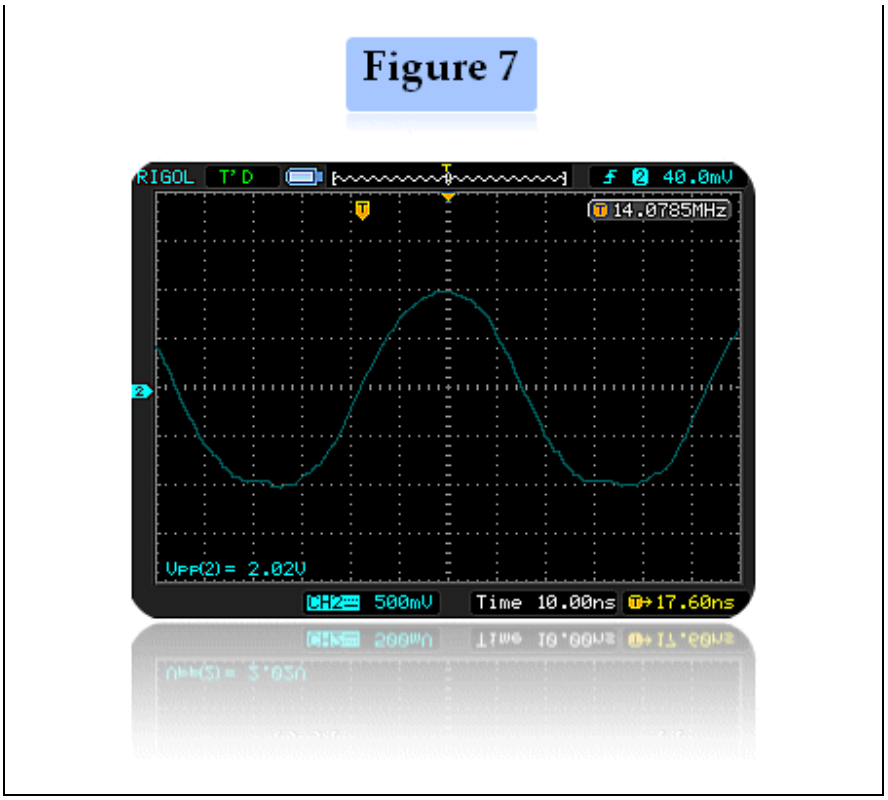

Figure 7 is a screen capture of the 14 MHz circuit output measured using a sensitive 50 ohm terminated oscilloscope. This was with no low-pass filtering. The output is distorted. Presumably this happened in the diode frequency doubler. This is not a low-distortion oscillator.

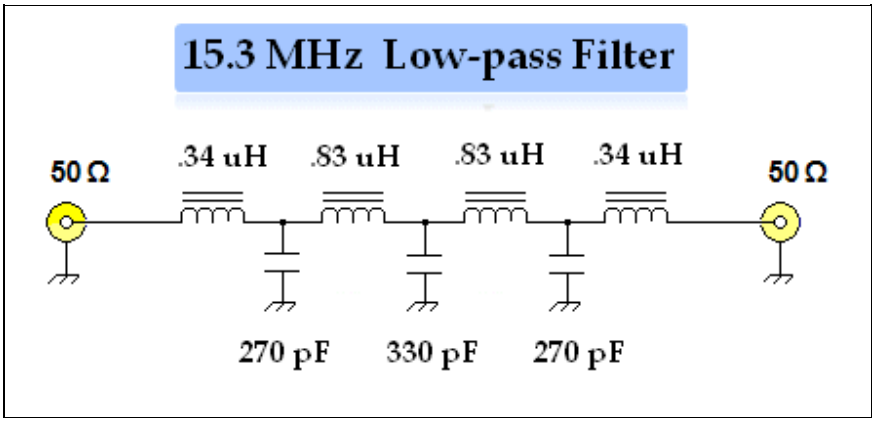

A N = 7 Chebyshev low-pass filter was inserted in Figure 6 at point LP. I checked with a spectrum analyzer and the 2nd harmonic was down 38 dB. There were no other measurable harmonics after that.

Figure 7b

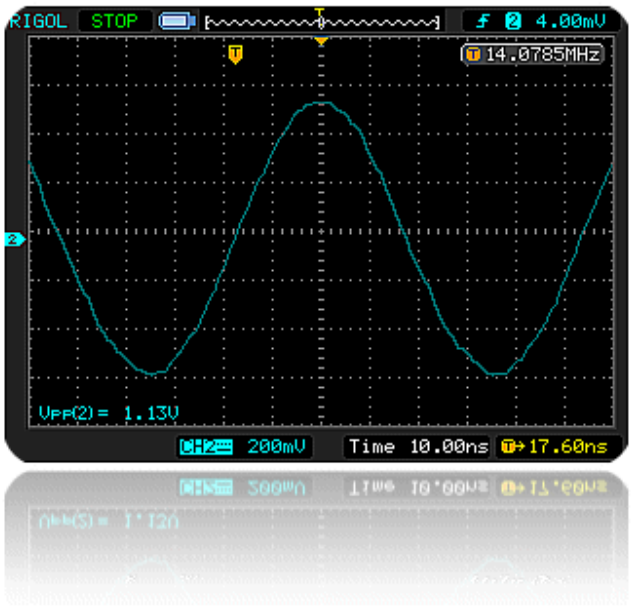

Figure 7b is a screen capture of the 14 MHz circuit output after the low-pass filter and final attenuator pad. Vpp on this graphic = peak to peak voltage = 1.13 volts. The output power is 5.04 dBm, or 3.19 mW . The Q4 and Q5 source resistors and the output attenuator pads are 2 areas of the circuit where you might easily change the output power. In the end, the circuit labeled Figure 6 was chosen. Your output voltage will probably vary, but can be easily adjusted as described.

A

Figure 8

B

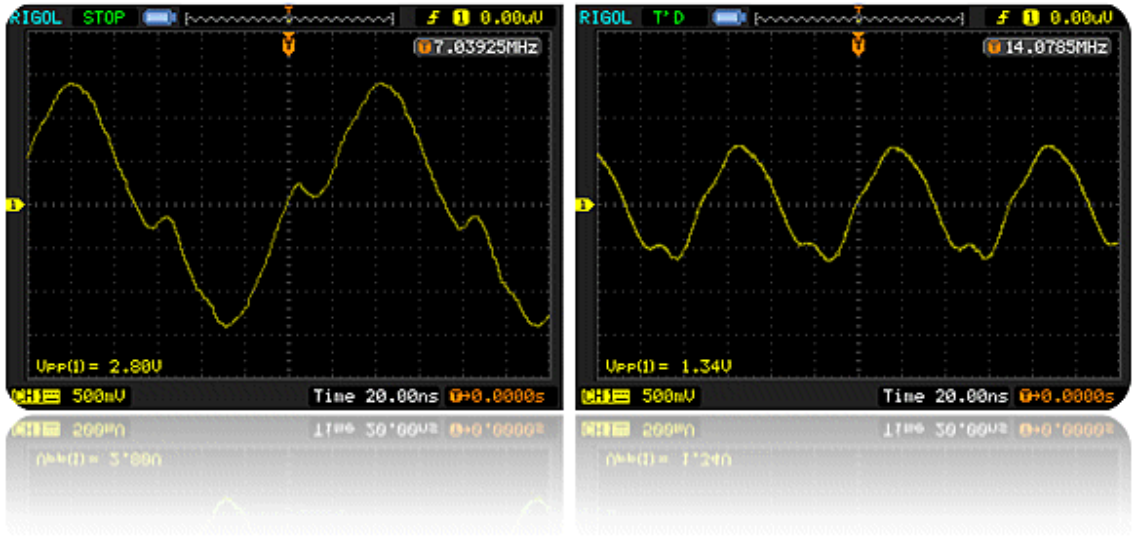

Figure 8 are Rigol digital screen captures. Figure 8A is a measurement taken from the anode at point DX from Figure 6. Figure 8B is a measurement taken at the cathode of DX and shows distortion caused by the diodes, reduced AC voltage and of course, frequency doubling.

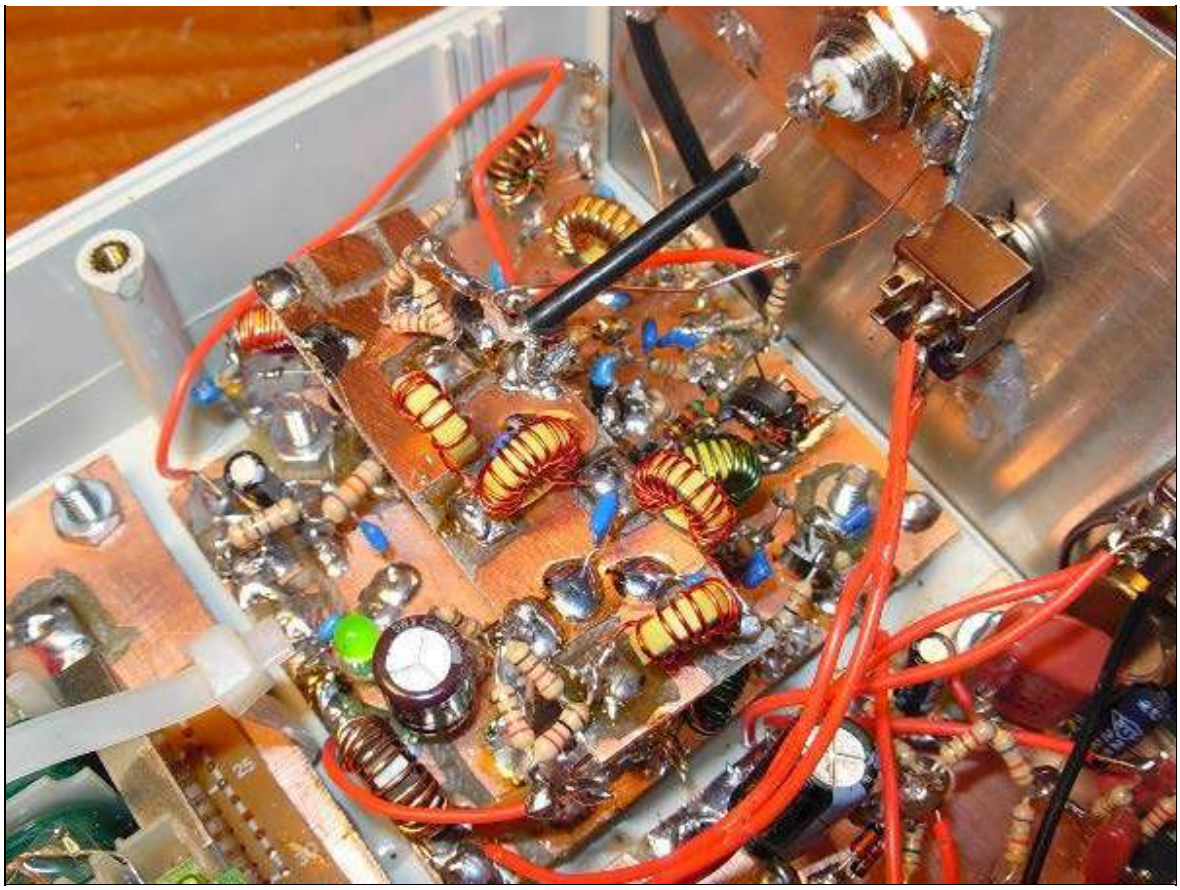

The 7 and 14 MHz circuits bread boarded and mounted in a chassis. The 7.039 MHz and 14.079 MHz outputs are connected to BNC jacks via RG-174 cable. The 15.3 MHz Chebyshev low-pass filter and -4 dB attenuator pads are on a raised Ugly Construction board. Some VCC decoupling parts are also on the bottom RF board.

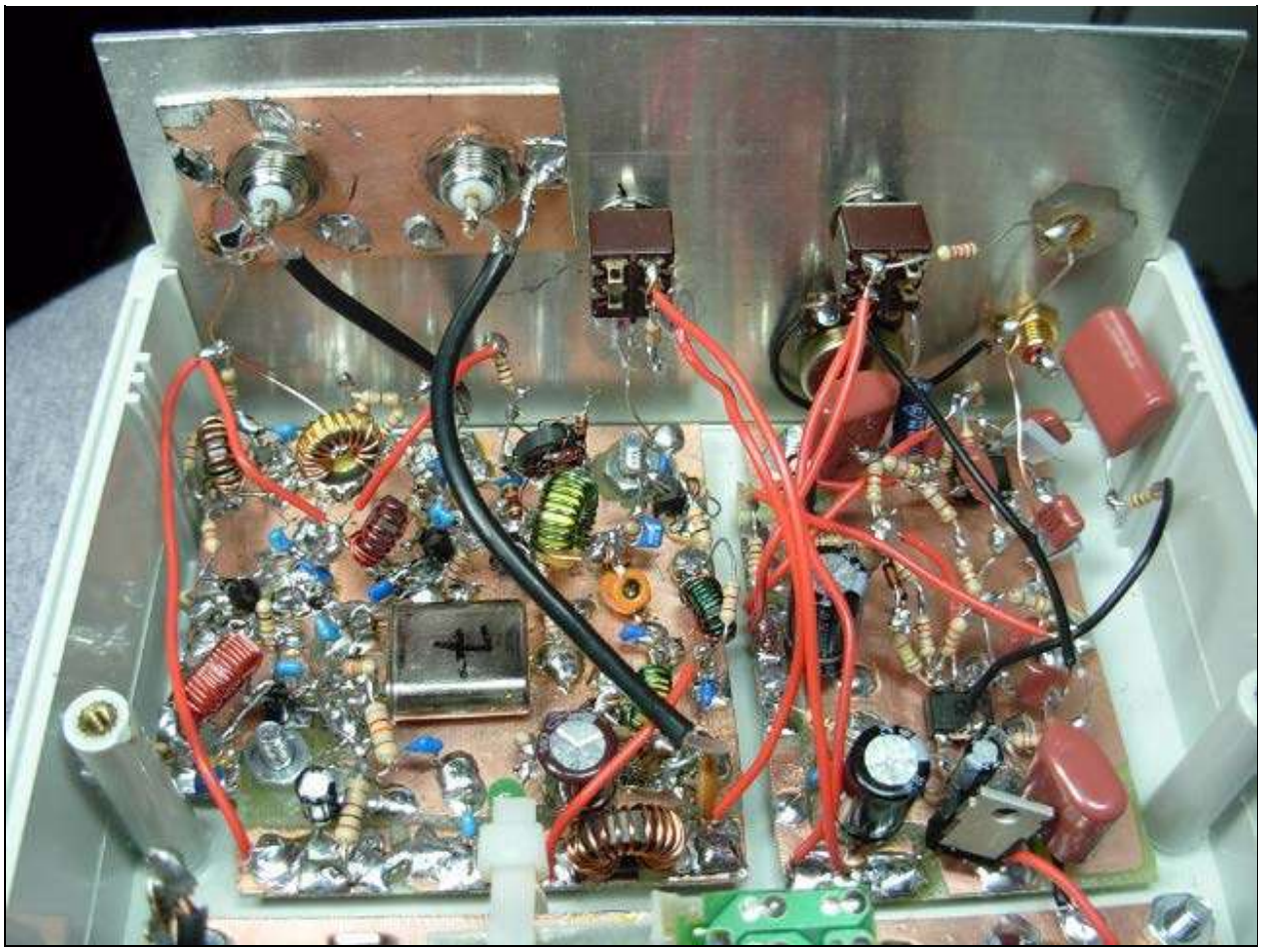

The 7 and14 MHz crystal oscillator board mounted in a project chassis along with a 1 KHz low noise oscillator This photo was a prototype version that did not have a Chebyshev low-pass filter after the 14 MHz stage.

Front view of the .001, 7 & 14 MHz oscillator. It is really fun to build your own test equipment.

Transformer Notes and Conclusion

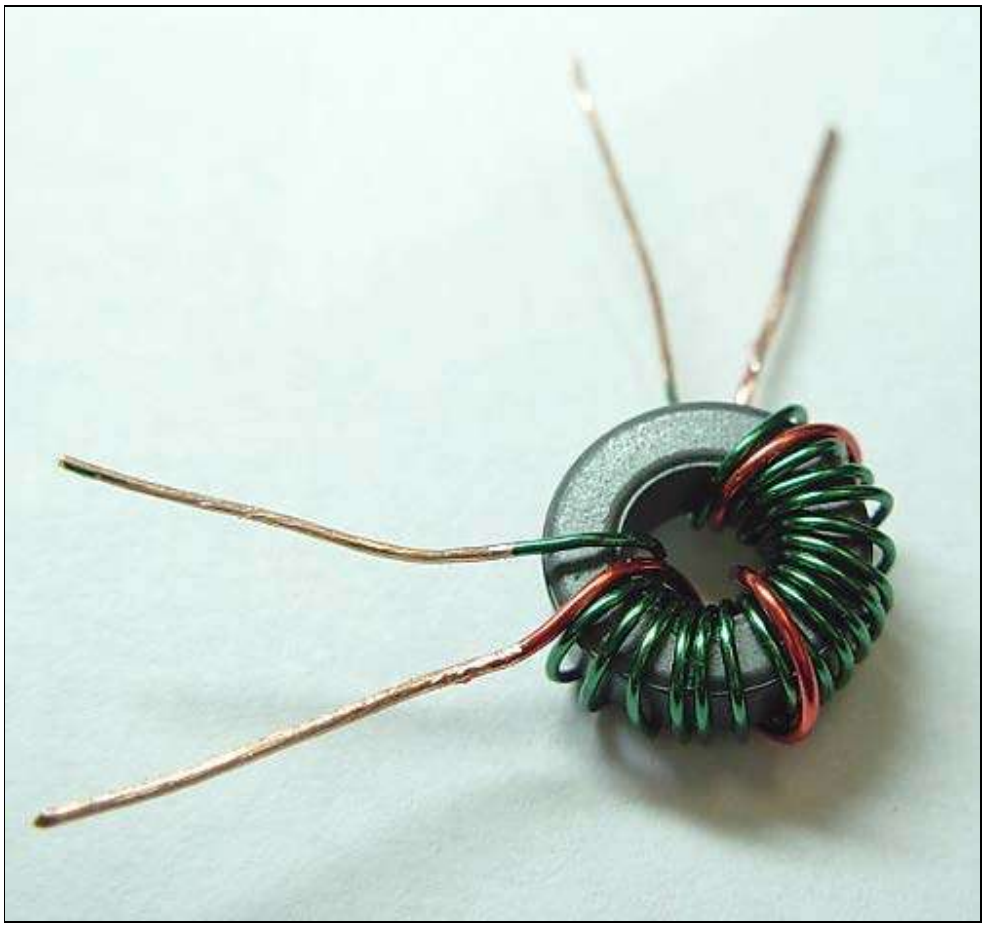

A photo of T5 from Figure 6. Some builders have emailed and stated they do not like to wind inductors/ transformers. I always ask them why? Often these builders were concerned with little details such as wire gauge and spacing, choosing the core size and which magnetic material to use. The Radio Amateur literature is replete with great tutorials on winding coils using toroids. Truly; the more toroids you wind, the easier it gets. Here are some simple points for beginners:

Powdered iron toroids are generally for tuned circuits. I.e. A capacitor and the inductor are tuned to a center frequency. Powdered irons containing the #2 and #6 material tend to tune sharply and have fairly high Q

Ferrites toroids are generally for use in broadband or wideband (untuned) applications. #43 material is relatively low Q and lossy as compared to the number #2 and #6 powdered iron toroids

Wind your inductors with enamel coated magnet wire. Popular gauges include 28, 26 and 24, but this is quite variable.

Minimally, you could get by with just #43 ferrite and #6 powdered iron toroids. For example, FT37-43 ferrites and T50-6 plus T68-6 powdered iron toroids could build a lot of inductors/transformers. In the photo above, I used #24 AWG wire for the 18 turns and #22 AWG wire for the 3-turn link. The 3 turn link is grounded on one end and well anchors the transformer. Thicker wire was chosen because Ugly Construction was used and the part is really anchored with the #22 AWG wire.

Conclusion

It took quite a lot of experimentation to reach the project goal. The experience was pleasant and comparing the old and new oscilloscopes was an added bonus. Perhaps, the circuits are overly complicated, however, they are critical signal generators for my workbench. Well designed signal generators have extensive RF-proof shielding to allow serious attenuation. These will have to do.

Addition - Jan 31, 2010 5 MHz JFET Low Noise Oscillator

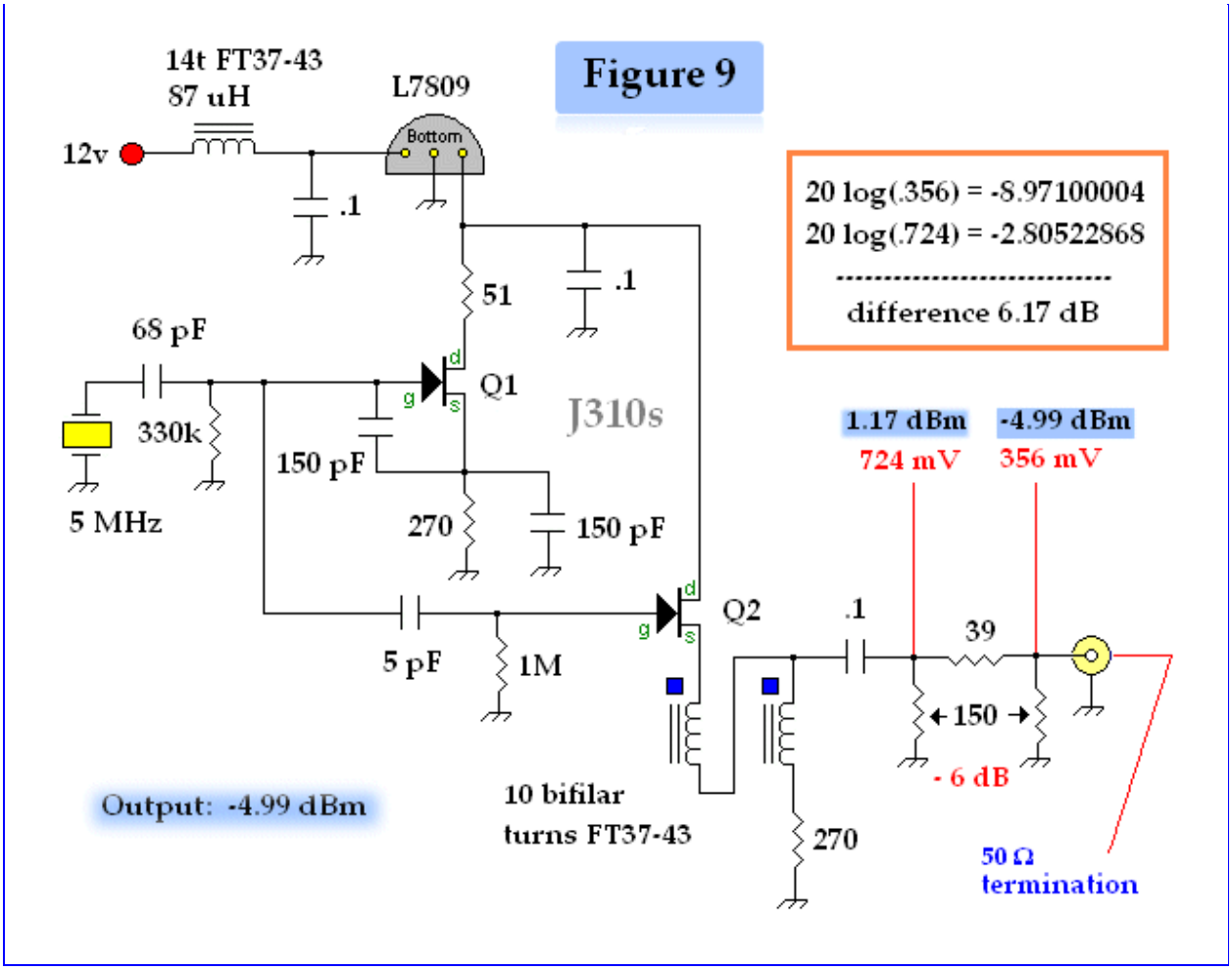

Another experimental low noise oscillator was built for 5 MHz. The desired output power was -5 dBm. The schematic and peak-peak output voltages and powers are shown in Figure 9. The 68 pF capacitor in series with the crystal was found experimentally by using a variable capacitor and measuring the output voltage and observing the scope waveform. When these appeared to be optimal, the trimmer capacitor was removed and measured at 67.17 pF. This circuit can easily be adjusted to give higher output power such as 7 dBm. To increase power, you may consider increasing the VCC to 12 volts, add a 0.1 uF source bypass capacitor in parallel with the 270 Ohm resistor of Q2 and/or adjust the pad attenuation. There are other circuit alterations to increase power, but the aforementioned are a good start.

It is important to measure your output voltages with a 50 ohm load connected to the device. Standard value resistors were used which throw off the value somewhat, but the actual attenuation of the pad is very close to the 6 dB attenuation expected. The math can be done with software such as Applets H and I on the QRP tools web page.

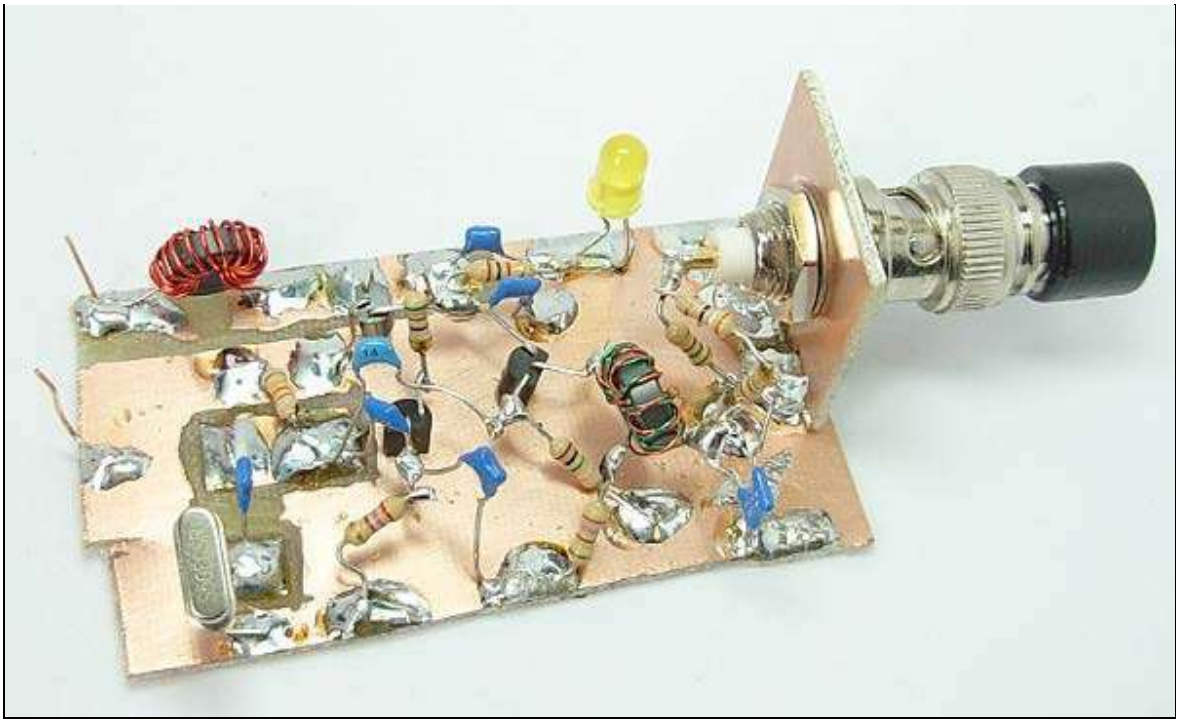

The breadboard of Figure 9 is shown above. The - 5 dBm output was required for some upcoming experiments and to study log and power measurements. The black BNC appliance is a 50 ohm load. These are very handy, but not a necessity. In most cases, a simple 51 ohm resistor to ground is the load.

Figure 10

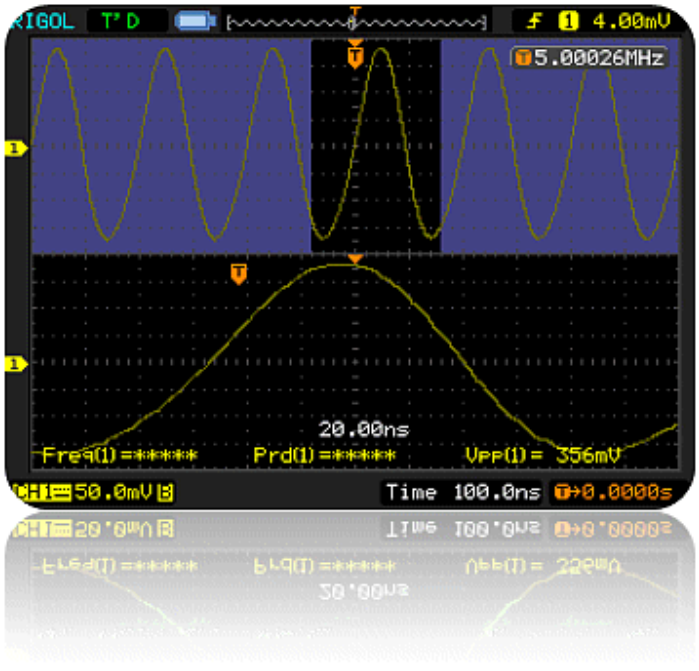

A screen capture from Figure 9 signal viewing maneuvers.

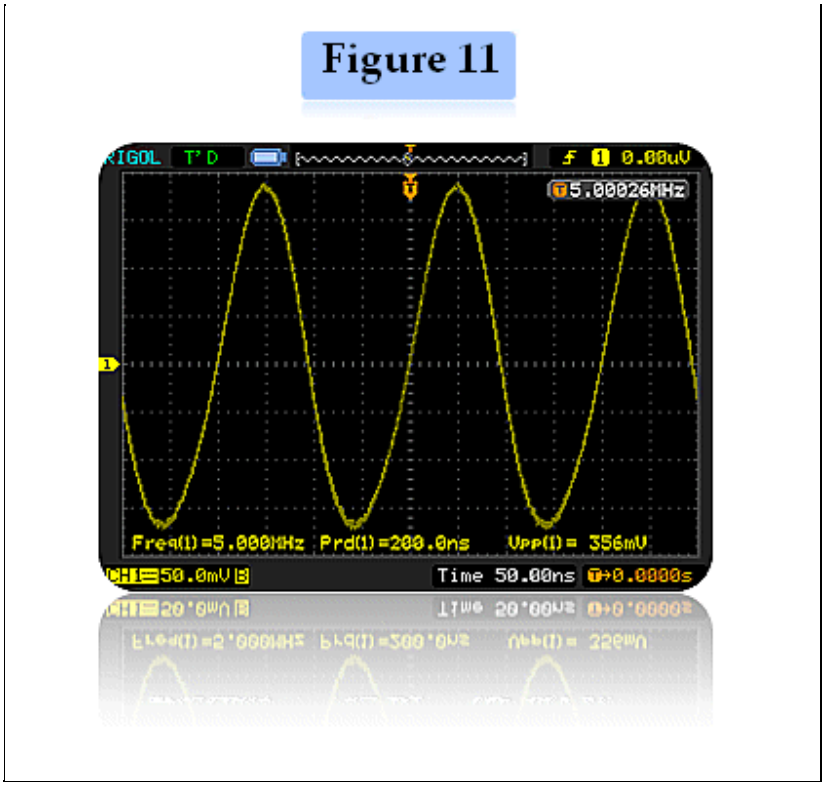

The output waveform looks good - even on a DSO!

Spectrum Analysis

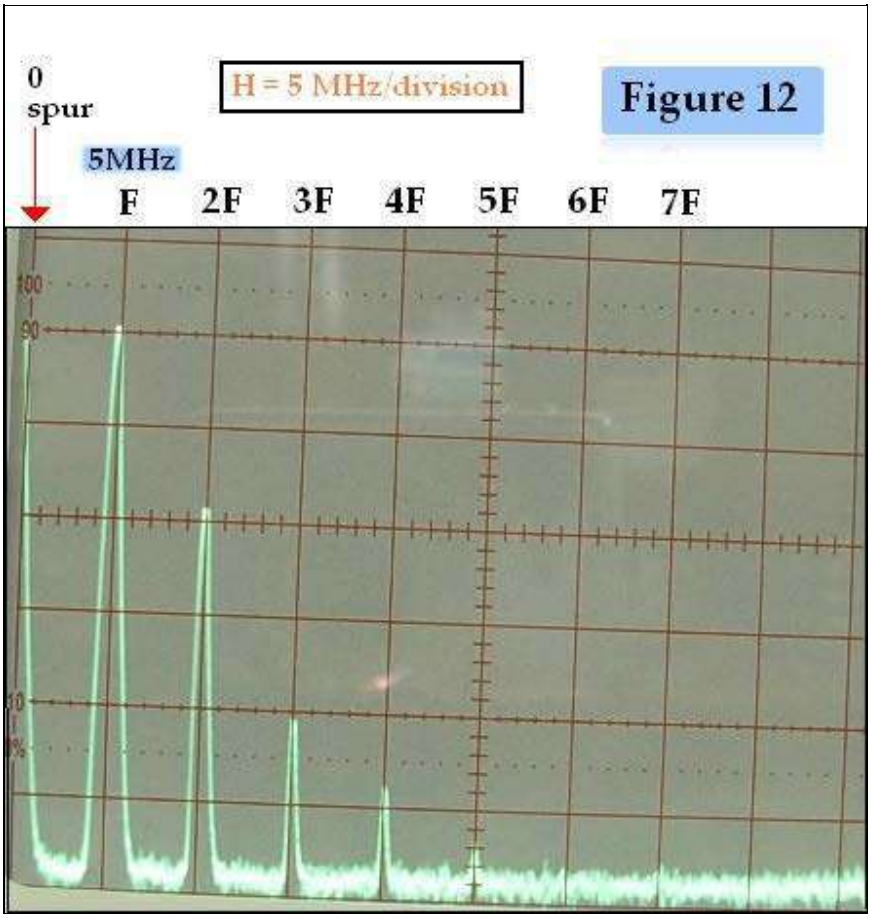

The output of the Figure 9 oscillator was further attenuated -19 dB for analysis in a spectrum analyzer. The -19 dB was chosen as this 50 ohm pad uses near standard resistor values and would well ensure a very safe signal level for the spectrum analyzer. The pad is shown in the Figure 14 schematic. The second harmonic (2F) is down about 20 dB from the fundamental. Each horizontal division is 5 MHz and each vertical division

is 10 dB. Compared to other more conventional oscillators that were checked in the spectrum analyzer, this oscillator has low harmonic content.

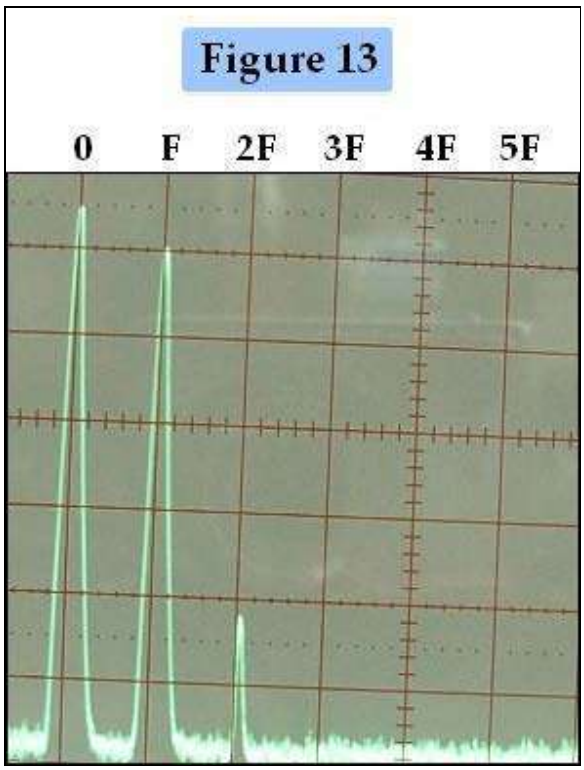

A N=5 or 5 element Chebyshev low-pass filter was placed after the Figure 9 oscillator and connected to the spectrum analyzer to see what happens. The 3 dB down frequency of this low-pass filter was 6.53 MHz. The second harmonic is now ~42 dB down. There are no measureable harmonics after 2F. It is really cool to "see" what a filter does to a signal.

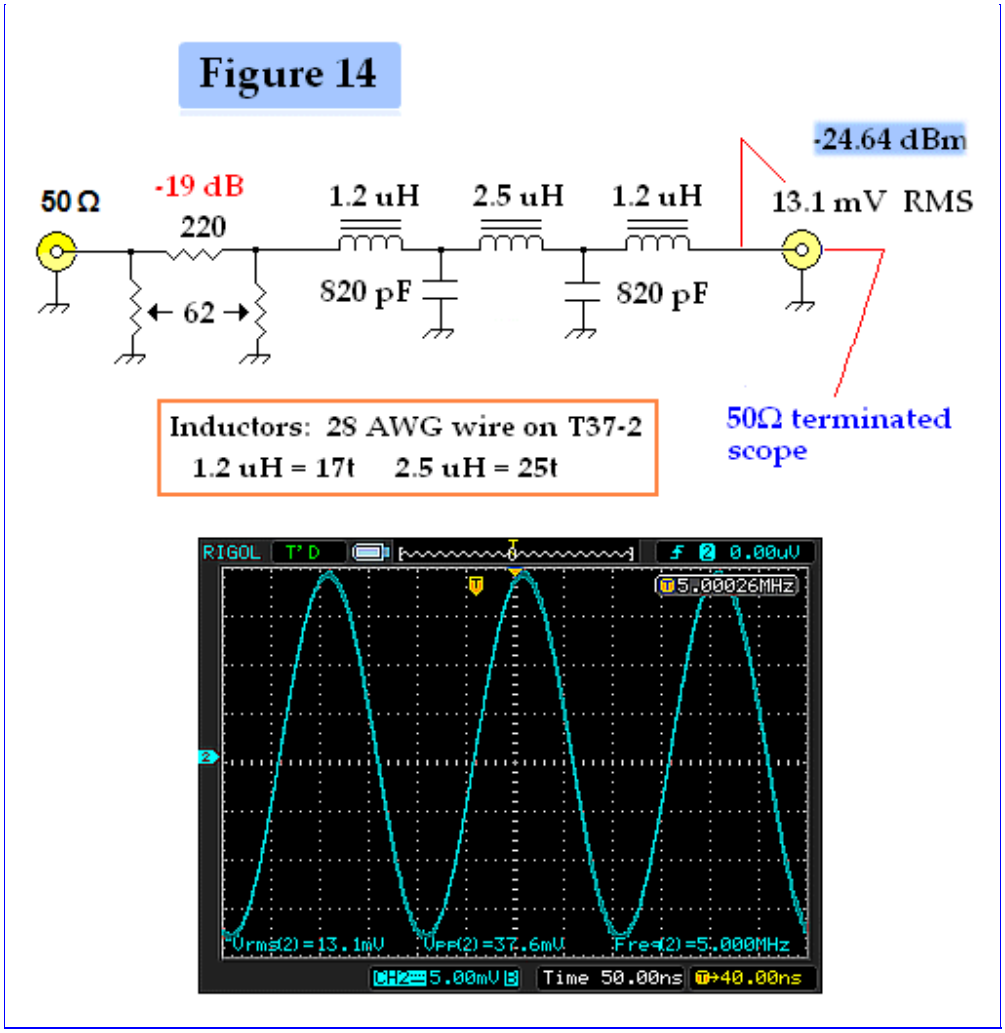

The schematic of the -19 dB attenuator pad and the low-pass filter is shown. To measure the output, the 10X probe was disconnected. The circuit was connected to the oscilloscope via 50 ohm coaxial cable and the scope input was terminated with 2 paralleled 100 ohm resistors. The 50 ohm scope termination technique will be discussed in a future web page addition. The RMS voltage values were inputted into Applet J on the QRP Tools page to calculate the output power. The RMS output was 0.131 volts which calculated to an output power of -24.6 dBm.

Crystal Parameter Checker

Introduction

This web page is a supplement to JavaScript Applet **G** on this web page. This software does the math using a simpified version of the method to determine motional inductance and capacitance developed by David, G3UUR. This is a very basic tutorial meant as an introductory guide for novice builders.

Shown in the photo above is 1 of my crystal parameter checkers. The schematic may be found in many places including EMRFD Figure 3.35 (See Errata) and on this pdf by Nick, WA5BDU. A power indicator LED has been added, but the circuit is the standard design. In this breadboard, the crystal being measured is tack soldered in.

Many builders just copy other builder's I.F. filter schematics, however, your crystal filters will perform better if your design is based upon the exact parameters of the crystals you have. For the simple design or optimization of a crystal filter, it is necessary to measure crystal parallel capacitance plus take other measurements to calculate motional inductance and capacitance. Determining your crystal parameters is not difficult if you have a capacitance meter, a frequency counter and some math skills. It is easiest to use a program to crunch the math; hence I wrote a stupid-simple JavaScript applet.

Designing filters is another story; it takes knowledge, practice and good software for this. Filter design theory has been extensively covered by Anatoly Zverev, Wes Hayward and others. The work of Nick, WA5BDU is also greatly appreciated. His presentations and references are excellent for those keen on learning more about filter design.

A four crystal 5.00 MHz SSB I.F. filter was desired. 20 crystals were on hand — they were from the same batch. The crystals were all placed in the above oscillator and their frequency was measured. The 4 crystals closest matching in frequency were set aside. The crystal parameters of these 4 were then determined. Typically these values are averaged and this average is used to design or tweak the filter using software.

---

1. Measure Capacitance

The procedure for determining the parameters of 1 crystal is described.

The first step is to measure the crystal capacitance (called parallel capacitance) using a capacitance meter.

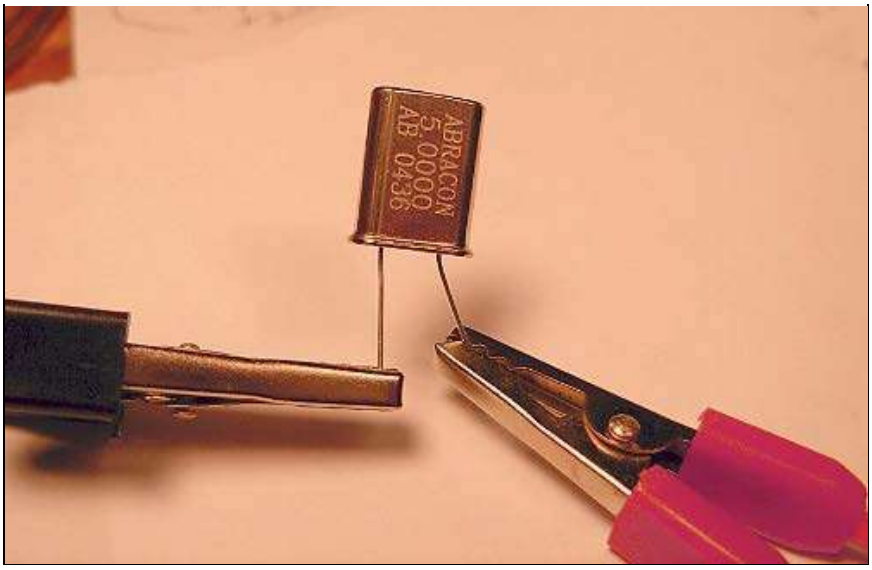

Measuring the crystal parallel capacitance

Parallel capacitance of the above 5.0 MHz crystal in an AADE LC meter

Next, measure the capacitance of the open switch plus the 33 pF fixed value cap wired in-situ. This will give you the total circuit capacitance of the open switch, the 33 pF fixed value capacitor, and any stray capacitance from your crystal holder, wires, etc. The switch itself plus stray wiring will be a few pF so the total should be around 36 to 40 pF or so. In my test oscillator, the result = 41.19 pF as shown. On my other crystal checker with a better switch, it's 36.9 pF.

In the calculation of crystal Lm and Cm, the parallel capacitance and the switch circuit capacitance will be summed.

---

2. Measure Frequencies

A crystal is put in the oscillator with the switch open. Record the frequency. Your counter must have resolution down to 1 Hertz. After recording this value, throw the switch and measure and record this frequency. You now have all the measured values required to calculate motional parameters and adjust or design a filter. Motional parameters are calculated in Applet G.

Frequency measured with the switch open = 4.999274 MHz

Frequency measured with the switch thrown = 4.998317 MHz

---

3. Do Math by Hand or with Software

G. Calculate Lm and Cm For a Crystal using the G3UUR Method

image

Enter frequency in MHz written on crystal (nominal frequency): 5.0

Enter measured frequency in MHz with switch open: 4.999274 Enter measured frequency in MHz with switch thrown: 4.998317

Enter crystal capacitance in pF: 4.65 Enter open switch circuit capacitance in pF: 41.19

Calculate Xtal Parameters Cm = 17.55 femto Farads , Lm = 0.0578 Henries

The applet **G** calculation of the crystal parameters using the above measured values

---

4. Example Filter Adjustment

It is assumed that most builders will use software to design or tweak their crystal filters. The only 2 programs tried *(to date)* include AADE Filter Design and the Ladpac software collection that supplements EMRFD. I am more familiar with the Ladpac programs written by Wes, W7ZOI. Only

these programs are demonstrated. Please read the instructional file Ladpac2008 Manual.pdf to understand these programs. *The Ladpac software bundle includes GPLA.*

The purpose of this tutorial is not to teach crystal filter design, but to describe a relatively simple method to tweak an existing design using your measured crystal parallel capacitance and its calculated motional inductance.

The first step is to digitally format your filter into a file that can be analyzed in GPLA. In my opinion, the easiest way to do this is to use the ladder circuit editor ladbuild02.exe or better yet, its update - ladbuild08.exe. The model filter follows:

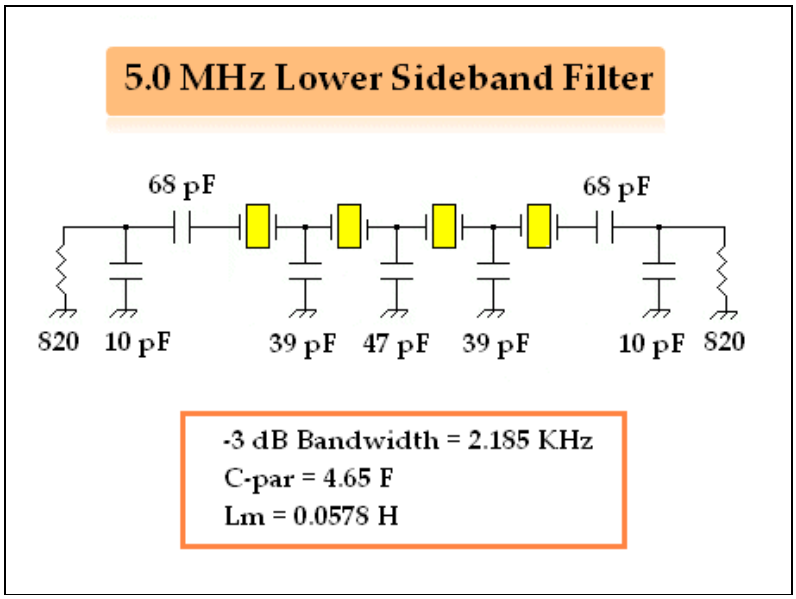

The model 5 MHz SSB filter

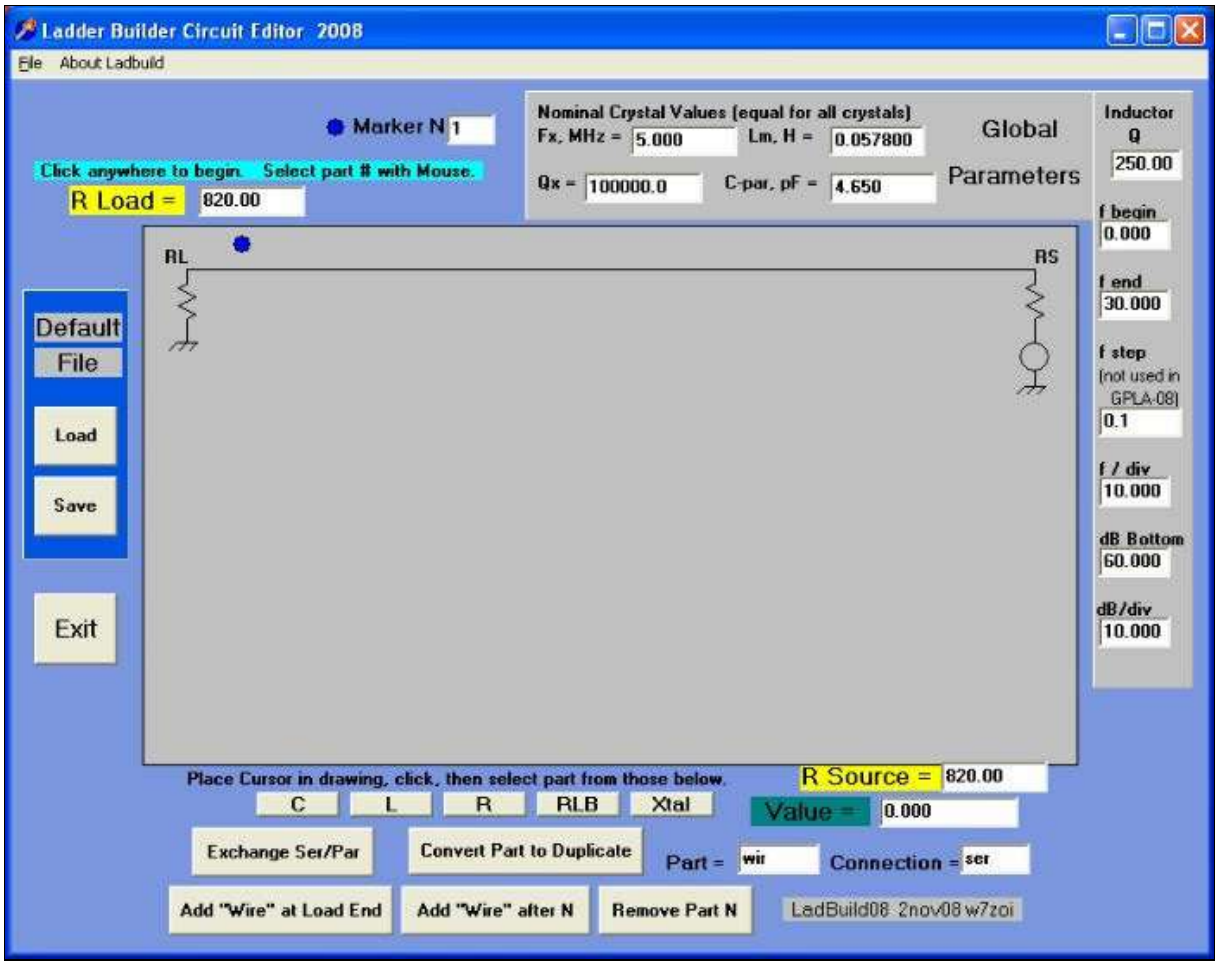

Clear any existing components and enter the termination R, C-par and Lm values. Qx is set at 100000

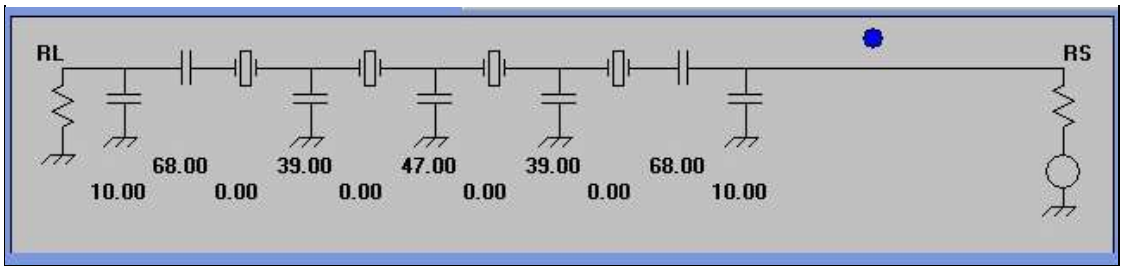

Build your filter within the editor. Save your work. Start up GPLA and load your newly saved filter.

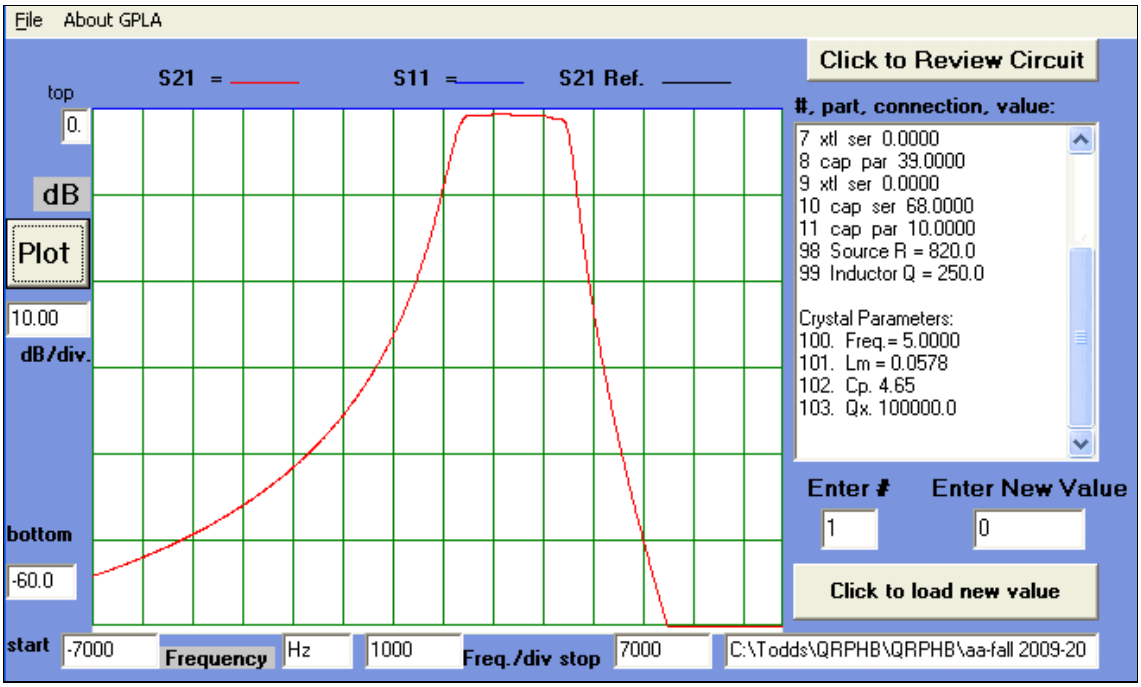

Set a sweep and **x** axis increment (-7000, 1000 and 7000 in this example). Push the Plot button

Let's say you wanted to use this filter design and have determined the average parameters of the 5.00 MHz crystals in your parts collection. Let's assume that for your crystals, C-par = 3.1 pF, and Lm = 0.098H. Input these values in GPLA.

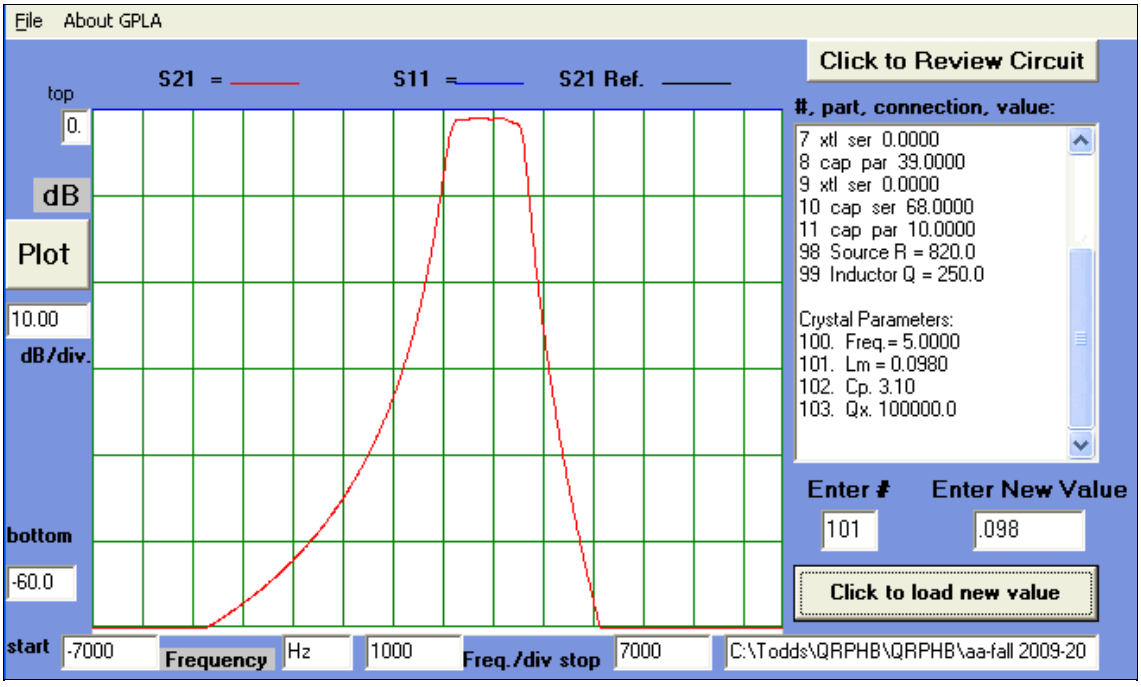

Look what happened to the crystal filter's bandwidth. Our - 3dB bandwidth is now somewhere around 1464 Hertz. This simple experiment illustrates how important it is to use the parameters of your crystals to obtain a desired filter response.

Experiment with the various functions in GPLA to learn how to use it. Set whatever reasonable sweep you want. This program is best learned by using it repeatedly.

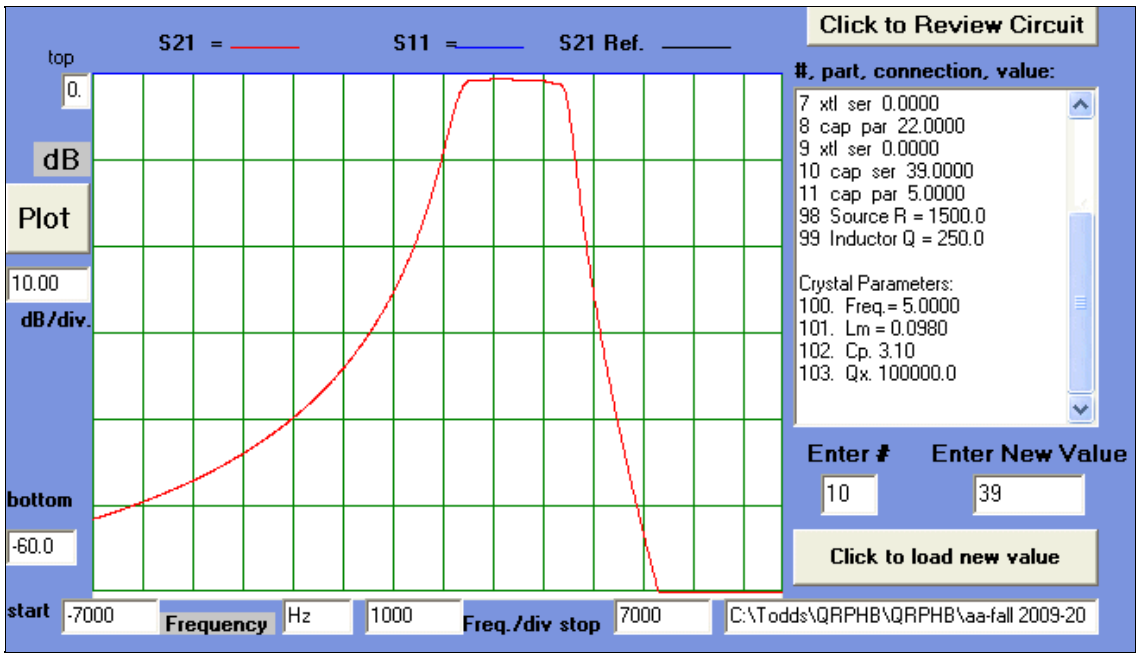

In the above screen capture, the above filter was tweaked to "re-establish" a -3dB bandwidth of ~2.172 KHz. All adjustment was performed entirely in GPLA by swapping capacitor values and observing the resultant waveform. When you get an overall pleasing bandwidth plus shape, but there is too much ripple at the top, generally you must increase the terminating R values. This is the brute-force, manual way to tune filters. For this method, you need not understand terminology such as as series resistance, MESH, K or Q values, Butterworth response, or Chebyshev with 0.1 dB of ripple.

Admittedly, at first, this method can be quite time consuming and tedious, however, with practice, you may be able to tweak a filter in only a few minutes. Clearly, the more you dig into understanding crystal filter design, the better your filters can be, however, getting overly complex can scare off builders who are new to this hobby. Note these filters use standard value capacitors and resistors; perfect for popcorn I.F. filters.

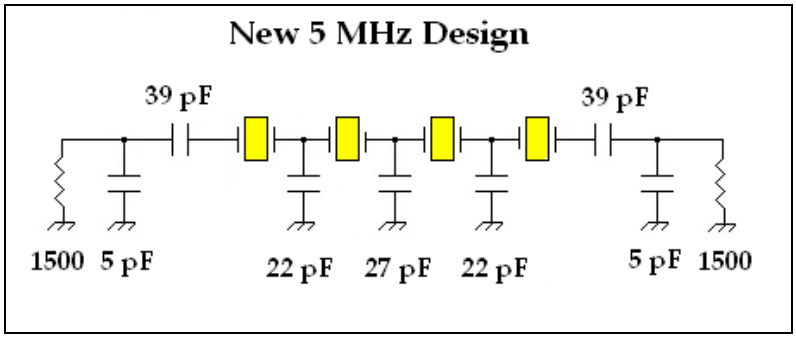

The original 5 MHz Model filter with updated C and R values using Lm = 0.098 and C-par = 3.1

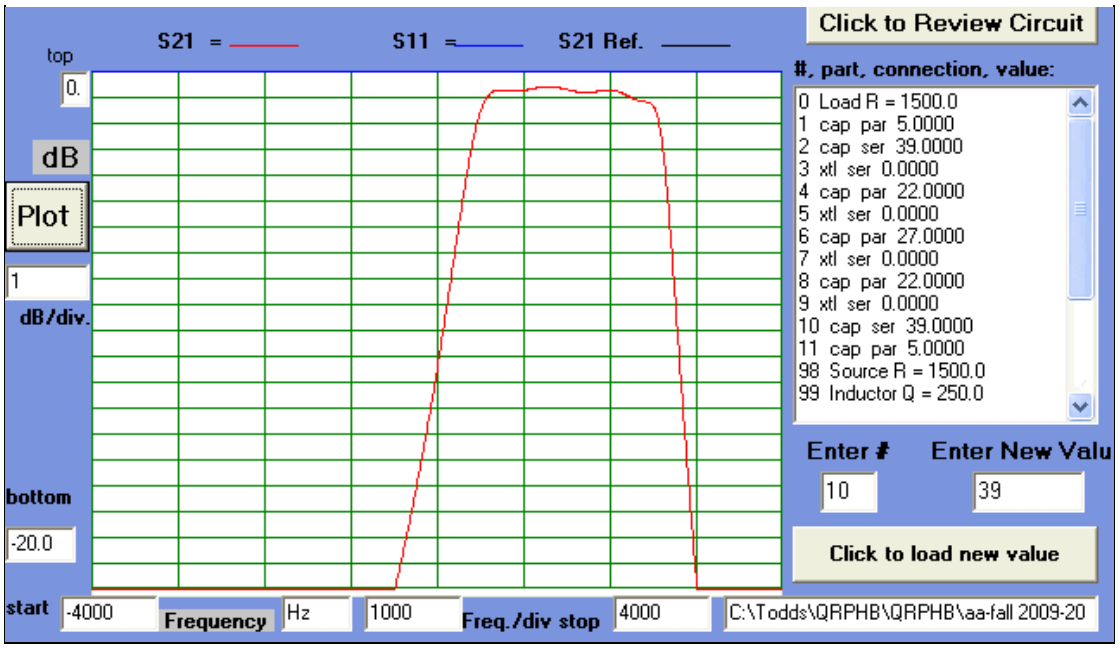

GPLA zoom of the **Y** axis showing the first 20 dB of attenuation.

---

5. The Model 5 MHz SSB filter Design

Although this page is not about crystal filter design, an example follows for reference purposes.

For designing filters, the application xlad08.exe is a good choice. The following 3 screen captures show the raw design process and GPLA analysis of the model 5 MHz Lower Sideband filter shown earlier with C-par = 4.65 pF and Lm = .0578. There are some great articles in print and on the Web to study if you want to learn about filter design. The Ladpac software from EMRFD is excellent. My special thanks to Wes, W7ZOI for answering my questions about his software. From this information, I was able to make this web page.

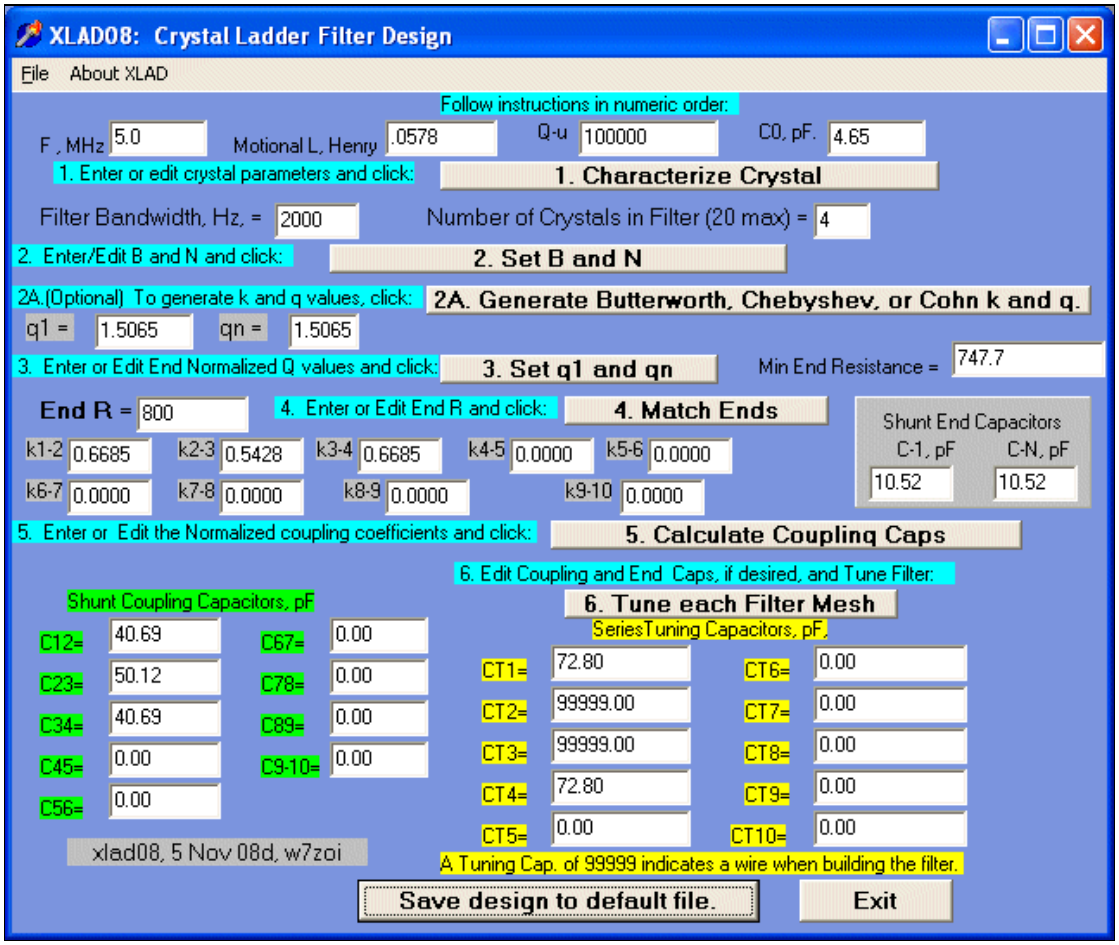

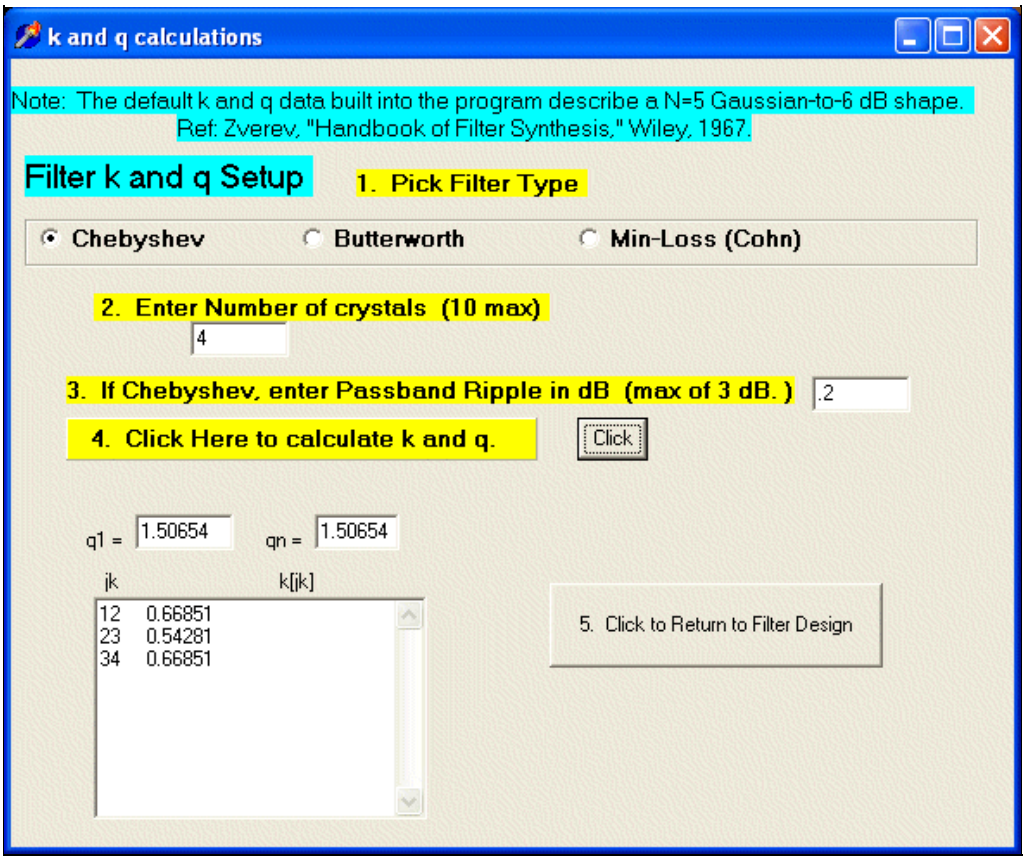

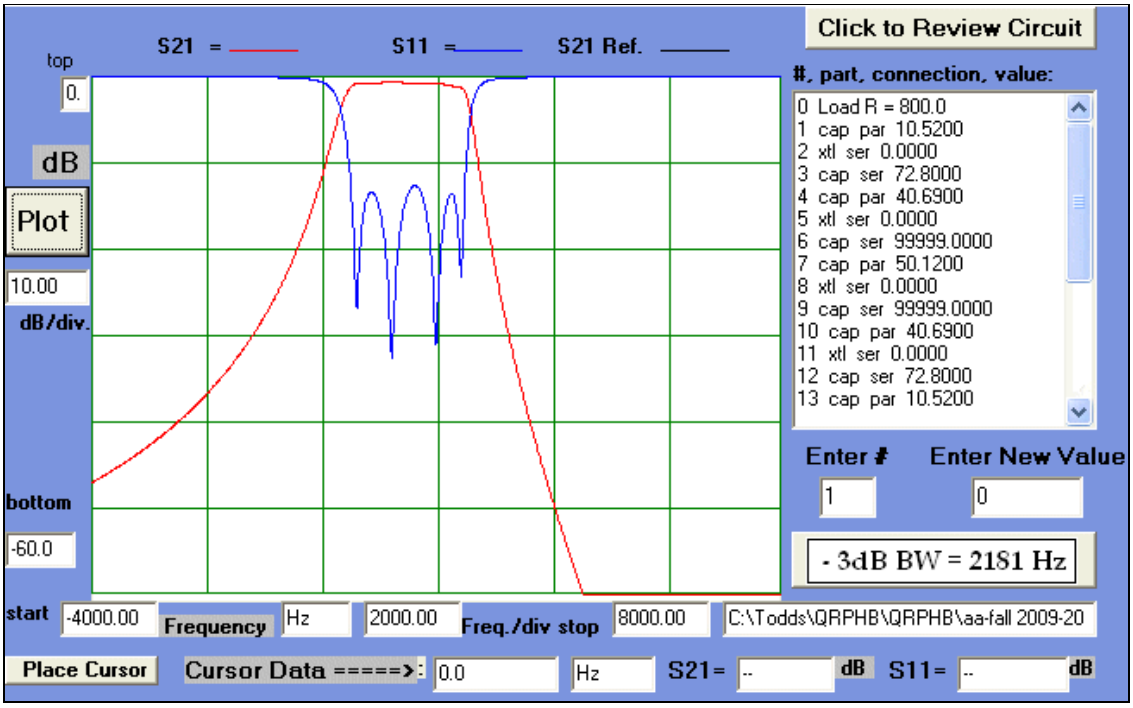

6. Conclusion

This web page presents a brief method to calculate crystal motional parameters and as required, to adjust crystal filter circuits to function optimally. This approach like my Java-script applet are simplistic to avoid the fear factor associated with crystal ladder design.

Listening tests are also valuable for assessing crystal filter function. Is the bandwidth as you expected? Does the filter ring excessively? Does it sound tinny? In the recent past, the crystal filters in 2 kit receivers/transceivers were tweaked as a favor to friends. *Please note, I have total respect for people who sell kits and appreciate the contribution they make to our hobby.*

The crystals of these Cohn type filters were removed and analyzed and the bandwidth was not as specified. In 1 case, the filter shape looked terrible in GPLA. Clearly, the kit sellers provided crystals which had markedly different parameters from those used by the original circuit designer. The I.F. filter capacitors were replaced with appropriate values and the R values were adjusted via either resistors and/or transformer

ratios and the improved filters sounded pleasant.

It is a real treat to listen to a receiver with a well designed crystal filter — sadly, I don't enjoy this experience that often.

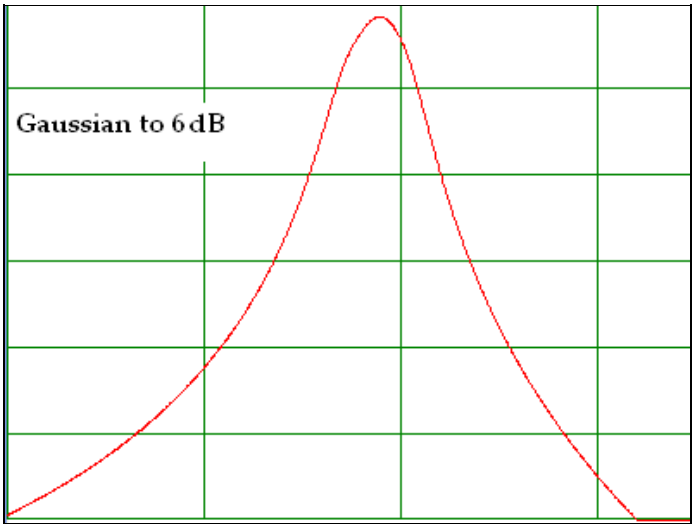

In my opinion, the best sounding CW crystal filter design is the Gaussian to 6 dB. Some operators would never use such a filter in a contest-grade receiver as the filter skirts are not steep enough for them. There are tricks to make the stop band better (more like a Chebyshev response, but without the ringing), however, this topic is out of scope.

I sincerely ask for your feedback on the G. JavaScript Applet. Does it work correctly? How could it be improved? Can you contribute better code? Thanks and 73.

QRP — Posdata for January 2012 — More on Crystal Ladder Design

Important to both superheterodyne receivers and single sideband transmitters, crystal ladder filter design lies juxtaposed as both a favorite and feared RF design topic. Newer builders may lack math skills, and/or become paralyzed by the terminology — or lack the ambition to learn or apply good bench practices. Even a cursory Internet search returns many fabulous files to read — witnessing a crystal ladder filter design article explosion.

The difficulty characterizing and building filters has progressively declined since the advent of the first handheld computers — improvements in personal computers and filter design software allows astute builders to pursue even complex xtal filter response shapes in 2012.

In QST for July 1987. Wes, W7ZOI wrote **Designing and Building Simple Crystal Filters**. This article promoted Cohn or Min-loss filters and its intent was to transcend the math and measurement associated with xtal ladder filters of the day and allow builders to just frequency match some crystals, and then go experiment.

In my estimation, this article proved revolutionary — soon after, builders around the globe, Elecraft, and other kit companies embraced this technique/topology and the rest is history. *(I call it the paper that launched a thousand kits).* If you're a new builder and feel overwhelmed by the material on or referenced by this web page, please consider first obtaining this article.

Learning about crystal ladder filter design is time well spent.

In 2011/2012 I explored the works of 3 builders who share their work via the web and/or journals.

Horst Steder, DJ6EV and Jack Hardcastle, G3JIR

The Steder and Hardcastle works emphasize that we need to measure/calculate crystal L and C parameters, plus the coupling and tuning capacitances (not just frequency). Through emails with Horst, DJ6EV, I learned many things, but 3 stand out:

1. It's better to design a good filter than fix a bad one.
2. Careful measurement of your crystal parameters plus software design and simulation = the best chance for getting your desired performance.
3. Deriving motional parameters from a 3 dB bandwidth measurement remains a great way to characterize multiple xtals. *In my opinion, the G3UUR method is the easiest way to characterize a small batch of xtals.*

Some of the earliest references to modern crystal ladder design I've found were written by Jack Hardcastle and published in RadCom and QST — I later confirmed this by reading work by Wes, W7ZOI and others. Hardcastle's and Haywards' work proved foundational for the experimenters that followed including David Gordon-Smith, Chris Trask, Jim Kortge and many others.

Steder and Hardcastle's combined experience assessing and/or documenting crystal ladder design spans decades.

Their QEX article **Crystal Ladder Filters for All** may be legally downloaded from the ARRL website here.

Program download URL: http://www.arrl.org/qexfiles (select 2010, "11x09_Steder_Hardcastle.zip")

The QEX article describes Steder's Microsoft Windows™ program, methods to derive motional parameters, plus cites many important references. The main program calculates practical lower-sideband crystal ladder filters based on the exact equations published by M. Dishal in 1965. Hardcastle transformed these equations into a computer useable form in 1983 and Steder incorporated these equations into a modern, easy-to-use and interactive application with nice graphing and table displays.

For simplicity, the program assumes lossless crystals, however, the calculated values can easily be transferred into another simulation program such as GPLA to add or refine parameters such as loss resistance.

The main "Dishal" application calculates filters with Butterworth, Chebychev and constant-k (Cohn) properties and the so-called "QER" filter type by G3UUR (a low ripple version of the Cohn filter). Further; sub-programs in the top-level menu calculate xtal parameters (by both the G3UUR and 3 dB method), plus L-C impedance matching and ladder termination networks. An extensive help file well explains the program.

Iacopo Giangrandi — Introduction to Crystal Ladder Filters

Link: http://www.giangrandi.ch/electronics/crystalfilters/xtalintro.html

Iacopo (Jack) uses a transmission measurement to infer the motional parameters — inserting a series capacitance and measuring the series resonant frequency shift was also described in 1998 by Rolf-Dieter Mergner, DJ9FG.

His web article/applications provides what is likely needed by most builders — simple filter synthesis while avoiding expensive test gear. His filters plots/figures are spectrum analyzer measurements that I really like. Although his program can generate aymmetrical filters that some builders might not be used to, the frequency domain plots indicate proper function.
Giangrandi's filter design programs appear to be based on Jack Hardcastle's work and possibly content published in a paper by Patrick Magnin, F6HYE and Bernard Borcard, F3BB in Radio REF for April 1990.

I encourage you to try all the methods and applications mentioned to discover what works best for you. Don't lose heart, for characterizing crystals with a vector network analyzer is also a time-consuming endeavor and simple often = best on the QRP Workbench.

QRP — Posdata for August 2012 — Measuring Crystal Q

Prior to July 26, 2012, I could not measure Xtal Q. Why? I tried to measure crystal Q with the shunt-series tuned method (essentially the crystal acts as a trap and a step attenuator is used to calculate the insertion loss the xtal exhibits when centered in the notch) but failed because I could not precisely set the frequency with my homebrew L-C oscillator.

You really need a DDS or a Si570 based signal generator and preferably a spectrum analyzer to exact the measurement with the "trap method". The DDS is critical, while the SA only preferable — a power meter, or a 50 ohm terminated 'scope can work as the detector if a low-pass filter is placed just after the xtal.

On July 26, 2012 Wes, W7ZOI developed a simplified method and wrote a pdf file called **Simplified Measurement of Crystal Q** after feedback from myself and John Larkin about Q measurement difficulties without a digital-based signal generator. Unfortunately, this pdf file is no longer offered for download by W7ZOI. His method works well and I'm glad that as of now, I can *completely* characterize any crystal I own.

I present an experiment showing how I measured the Q of a 10 MHz crystal applying the new method developed by Wes, W7ZOI.

The crystal is evaluated as a N=1 low-pass filter resonated by a shunt capacitor at each end. I stuck with Wes' suggestion to try 1000 pF at 9 to 10 MHz. For lower frequency xtals he recommended trying larger value shunt capacitors. Just experiment with the shunt capacitance — if you use too high a C for a given crystal, your xtal low-pass filter bandwidth might get too narrow to measure with an L-C based signal generator.

The following diagrams employ 2 programs from the Ladpac software that ship with EMRFD

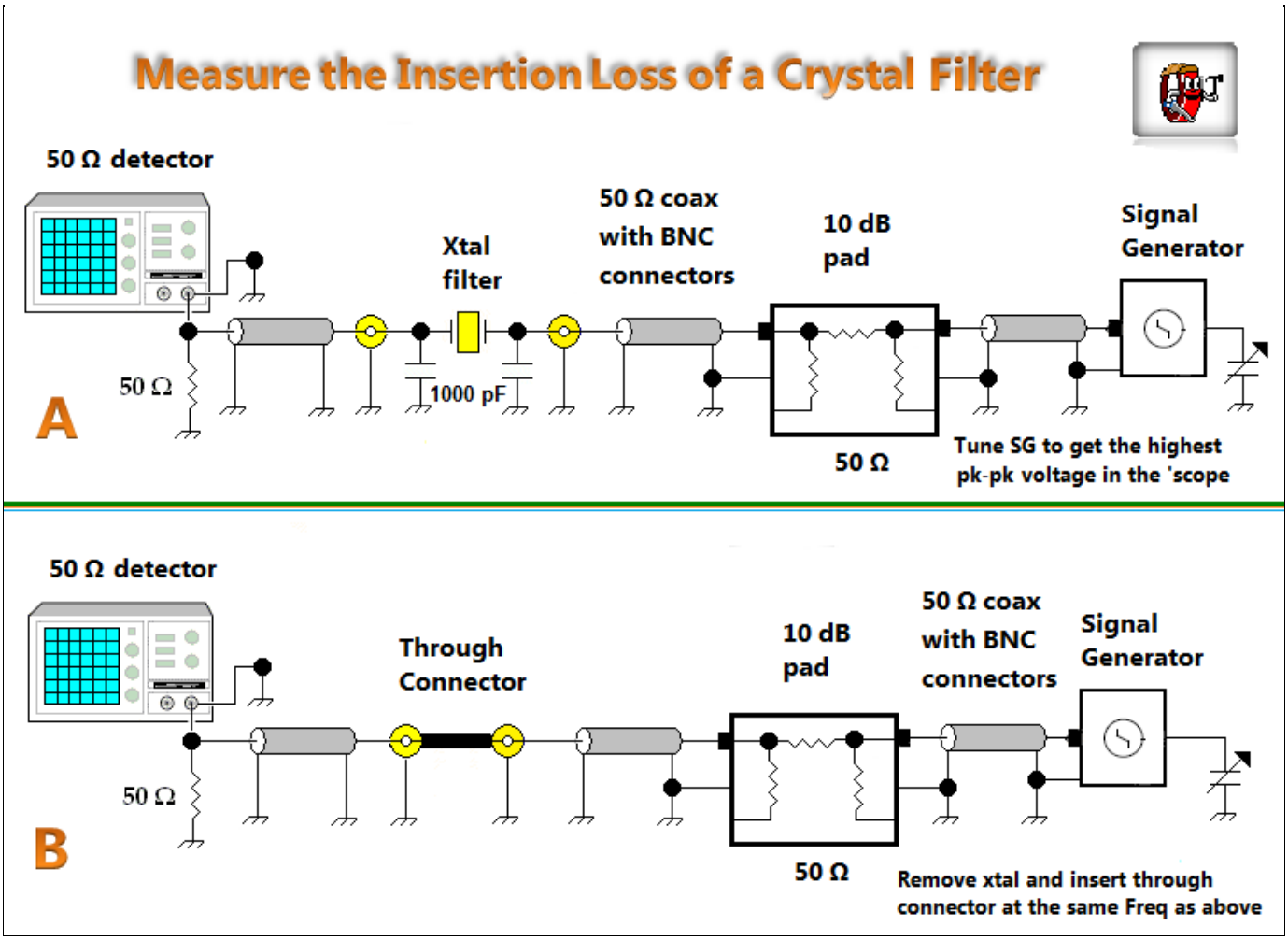

Above — Measurement of crystal filter insertion loss. In Part A, I carefully tuned my signal generator to get the highest peak-peak voltage in my 50 Ω terminated oscilloscope. I recorded this AC voltage as V Fil. In Part B, I removed the crystal filter board and replaced it with a BNC clad RF through-connector. I recorded this AC voltage as V Cal.

I discuss this standard method to measure the insertion loss or gain of a *device under test* in RF Workbench 2.

Even with the simplified method, you'll need a signal generator with good tuning resolution. My generator is shown on VFO 2011 as the 2.8-10.5 MHz Signal Generator. This is my version of the EMRFD Figure 7.27 generator.

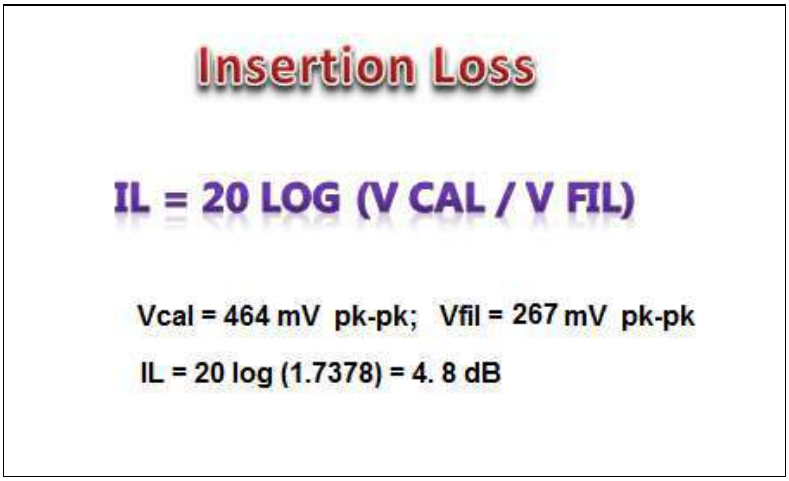

Above — The formula for insertion loss using peak-peak voltages. With my 10.0 MHz crystal, V Cal = 464 mV pk-pk and V Fil = 267 mV pk-pk. The insertion loss of my crystal = 4.8 dB.

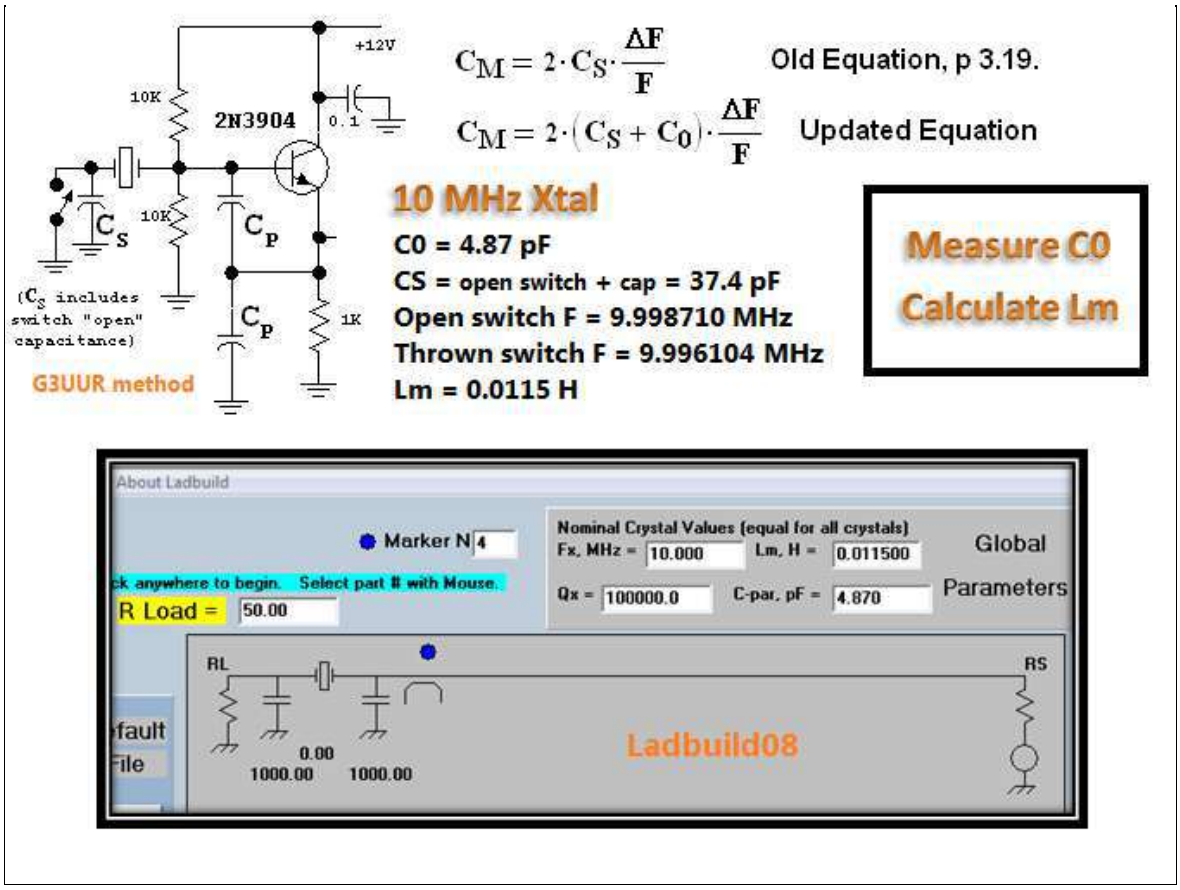

Above — First I measured C0 (C-par) and then with the G3UUR method, calculated the motional inductance of my xtal. Finally, I entered all the needed variables into Ladbuild08 to make a filter to analyze in GPLA.

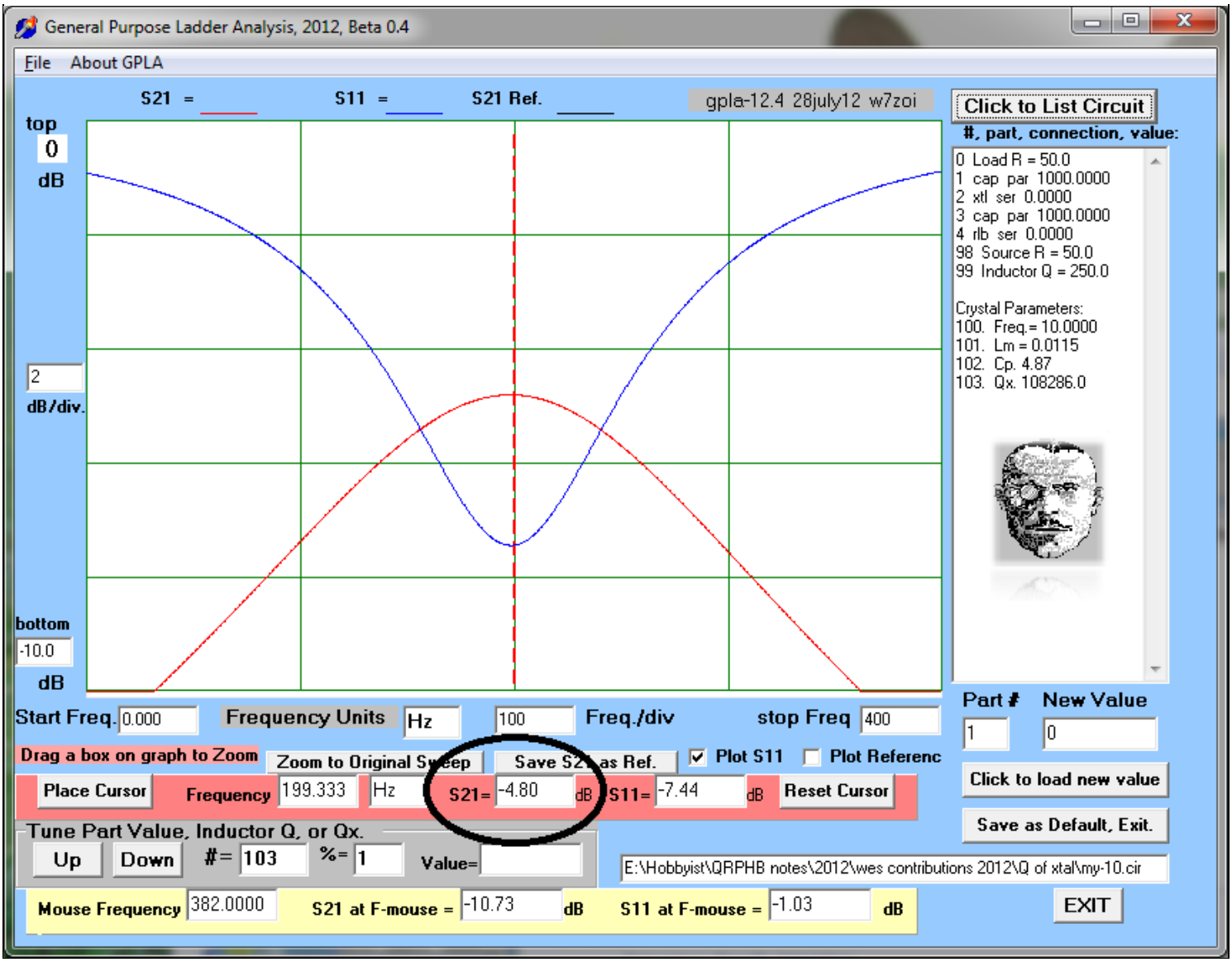

Above — With GPLA, I adjusted the value for *Qx* up or down until my *centered* S21 value indicated -4.8 dB (the insertion loss of my crystal determined earlier). My crystal Q = Qx = 108286.

Above — 10 MHz Crystal filter breadboard.

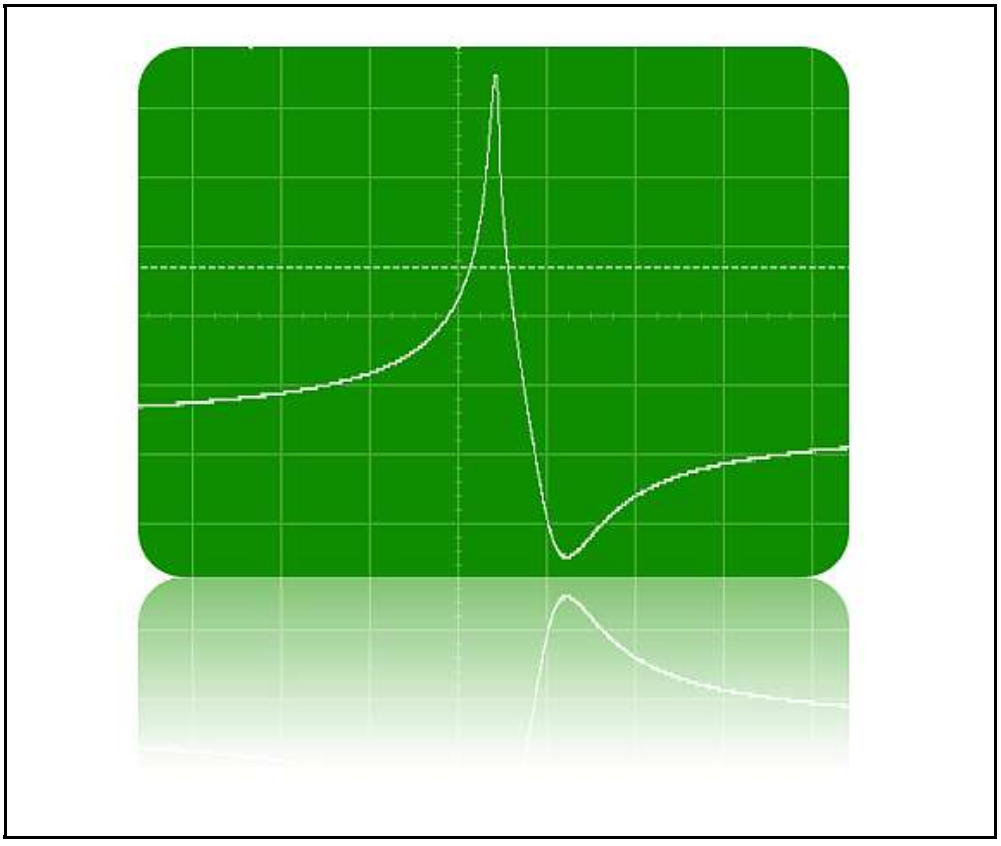

Above — A sweep of the 10 MHz Crystal filter used to determine the Crystal Q

Amateur Radio Electronic Design

Electronic Hobbyist Circuits 2010

This page houses a collection of brief hobbyist experiments.

1. LM380 Power Examination

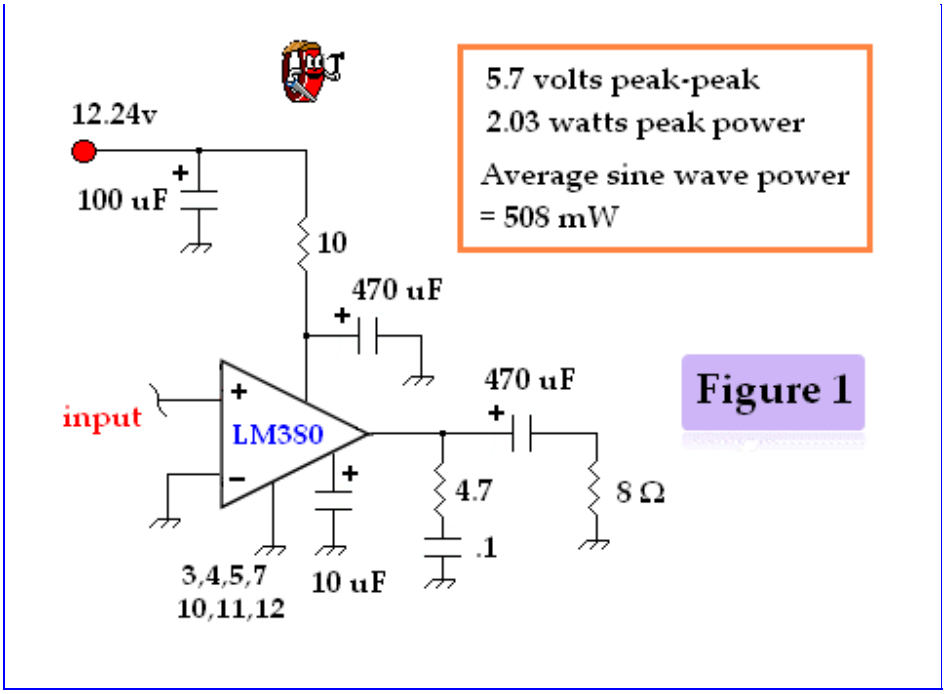

Figure 1 shows the test set up. This is a good part with an input impedance of 150kΩ. The gain is internally fixed at 34 dB. The average clean power was 508 mW. The test input frequency was 1018 Hertz.

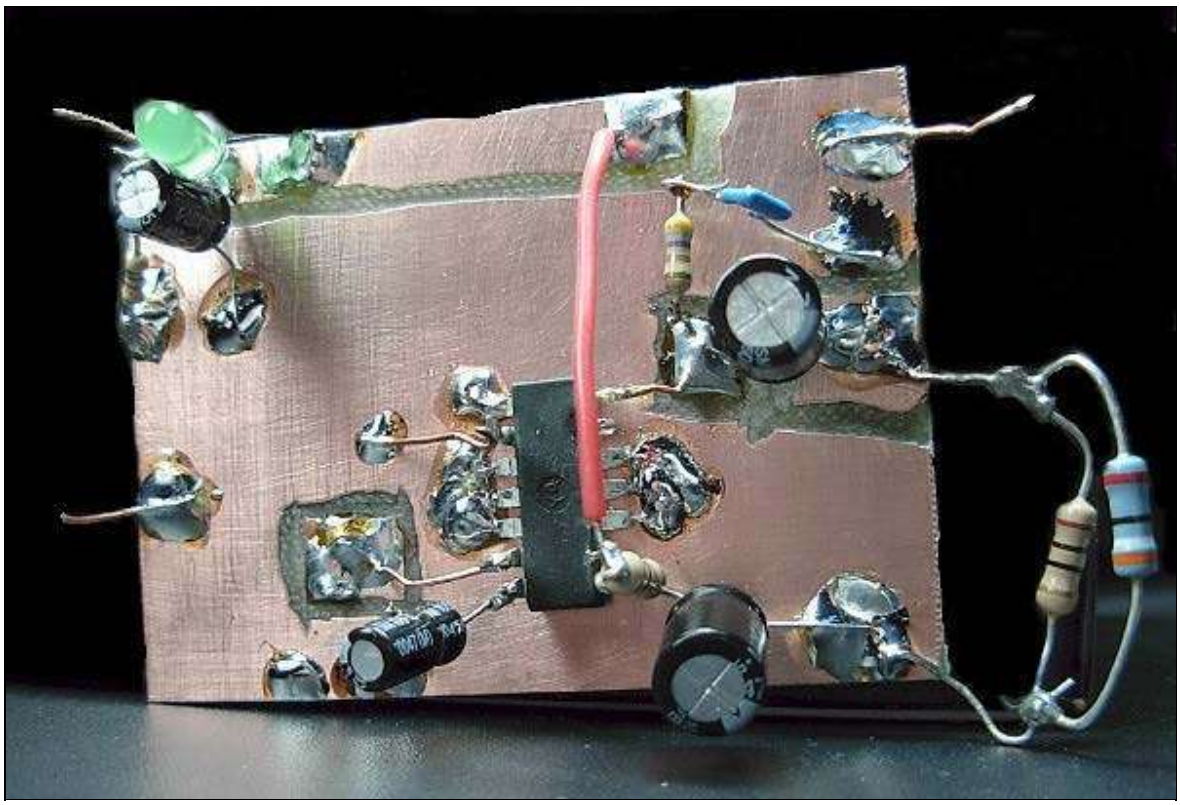

The breadboard of Figure 1 is shown above.

2. Wide Range L- C Oscillator

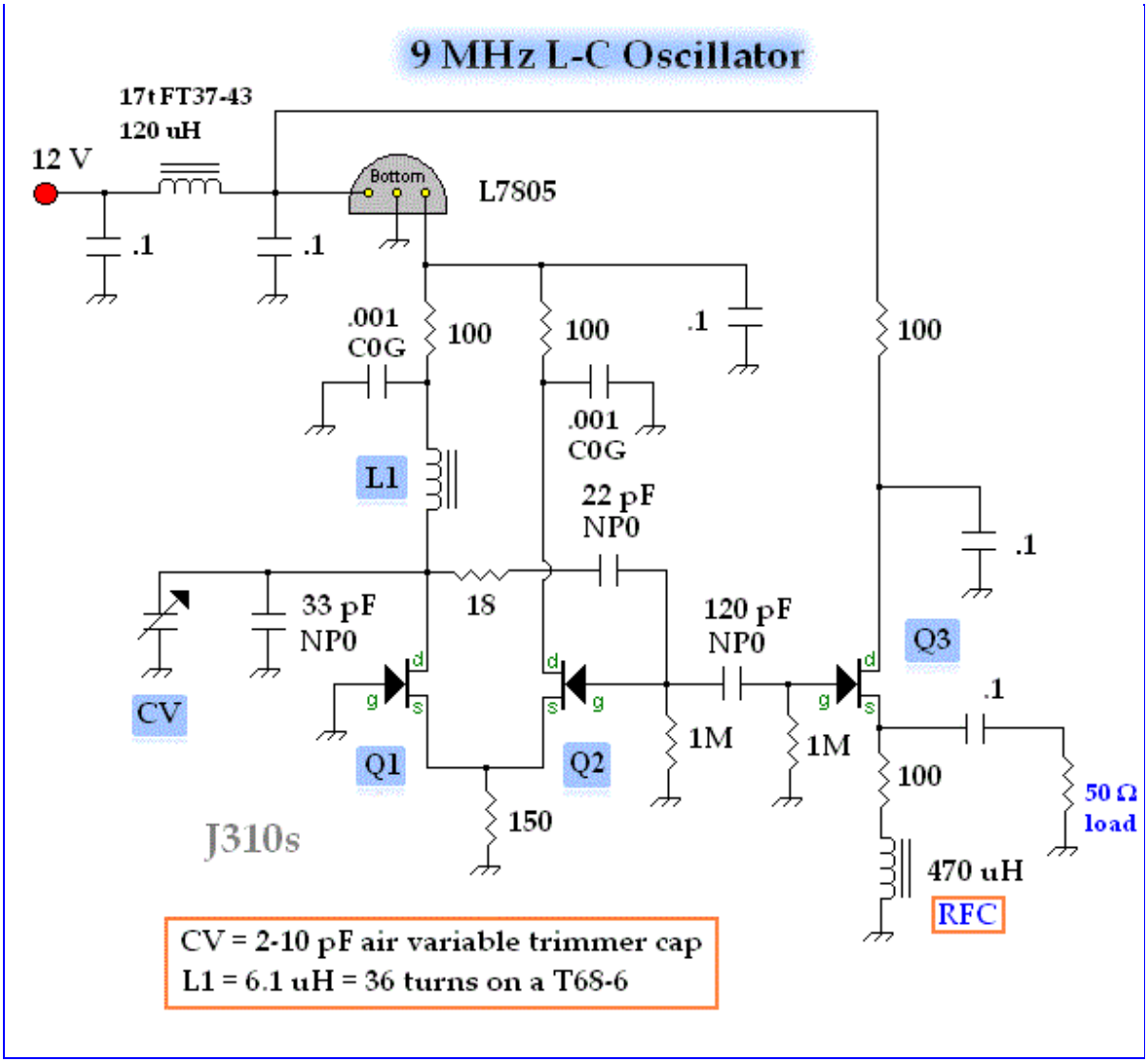

Shown above is a single frequency version of a VFO topology which allows a wide frequency range when additional switched inductors and/or capacitors plus a tuning variable capacitor are used. One good usage example would be a to use such a VFO to drive a bridge to make a wide range antenna analyzer. Q1 is essentially a common gate amplifier. The source is driven and the output is taken off the drain. This FET exhibits no signal phase shift. Q2 is a source follower that is AC coupled through that 22 pF capacitor The 18 ohm resistor is used to kill UHF parasitic oscillations. The Q2 follower also has no phase shift. Connecting the output of Q2 back to stage Q1 gives zero phase shift. The L-C tank will select the frequency where 0 phase shift is obtained. The tank will show phases other than 0 away from its resonance.

Q3 is an AC-coupled source follower to further buffer the VFO from its load. The RFC can be anything from your junk box, although it should likely be low Q. The low-pass decoupling filter on the the 12 volt supply path can also be anything reasonable. I wound mine using 17 turns on an FT37- 43 ferrite toroid. Its purpose is to keep RF from traveling down the 12 volts DC voltage wire to other parts of your circuit.

Any component connected to the L-C tank (at the Q1 drain, or the cold end of L1) can affect VFO tuning and drift. Temperature compensation will be necessary to achieve perfect stability. I use NP0 and C0G caps interchangeably. In the design shown, stability was good and the output had low measured distortion. This VFO will pretty much oscillate with any reasonable L and C values in the tank circuit. I found frequency stability was a little better with a higher L to C ratio. This is a great experimenter's circuit. One version built oscillated at 150 MHz.

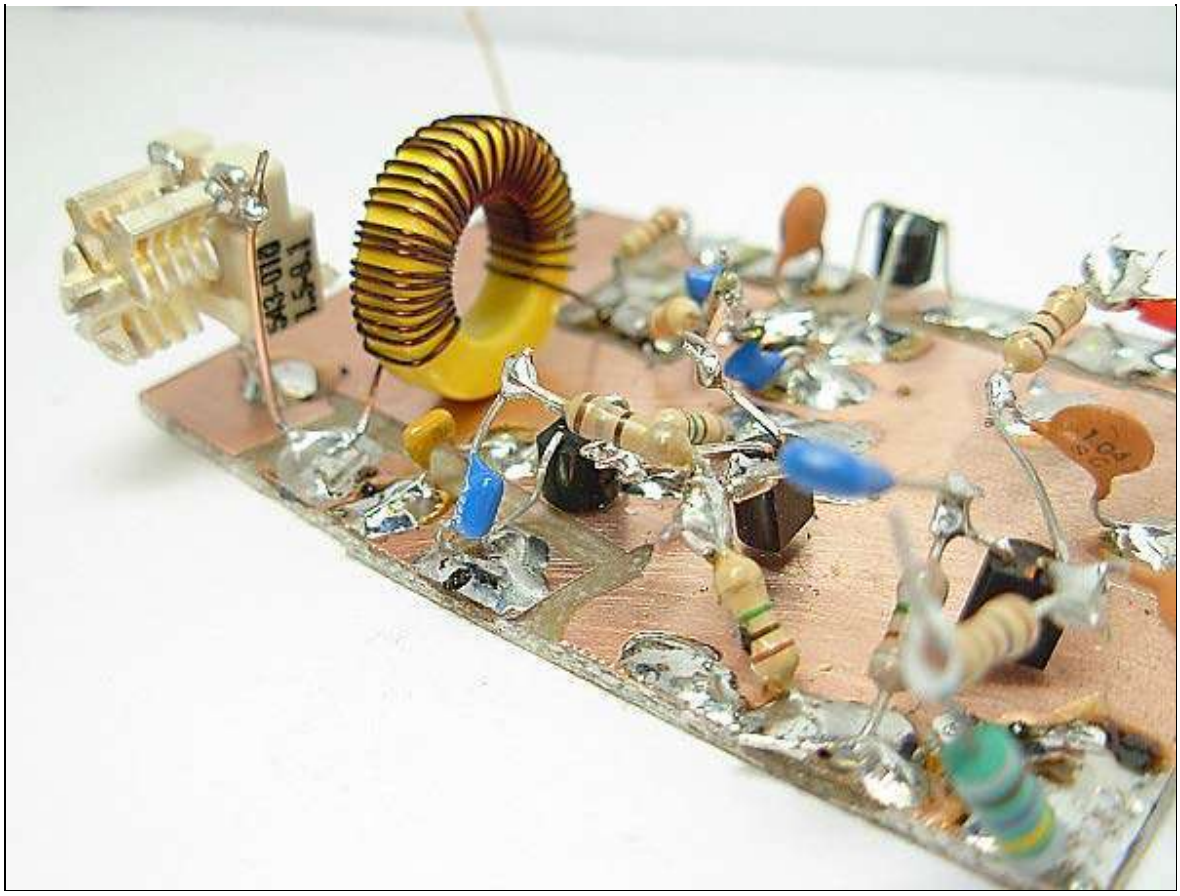

The breadboard of the above schematic. Pull the wire on your #6 powdered iron toroids tight to prevent air gaps between the toroid and the wire. Number 26 gauge wire was used on L1 as shown. High Q tank parts will garner the best results.

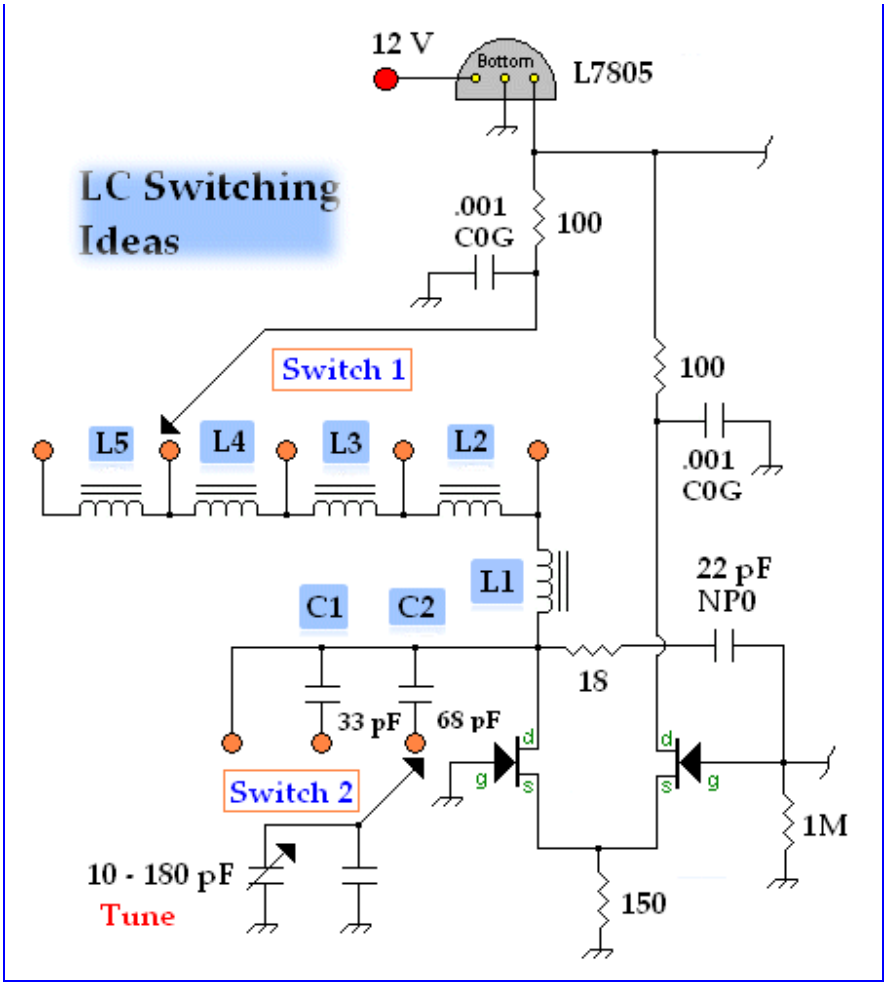

Some potential switching ideas are presented above. The builder is in total control of the tuning range and must calibrate the L and C values according to needs and the parts on hand. Output power will vary according to the L-C ratios and some designs include automatic signal amplitude leveling and/or RF gain controls.

3. FET Matching

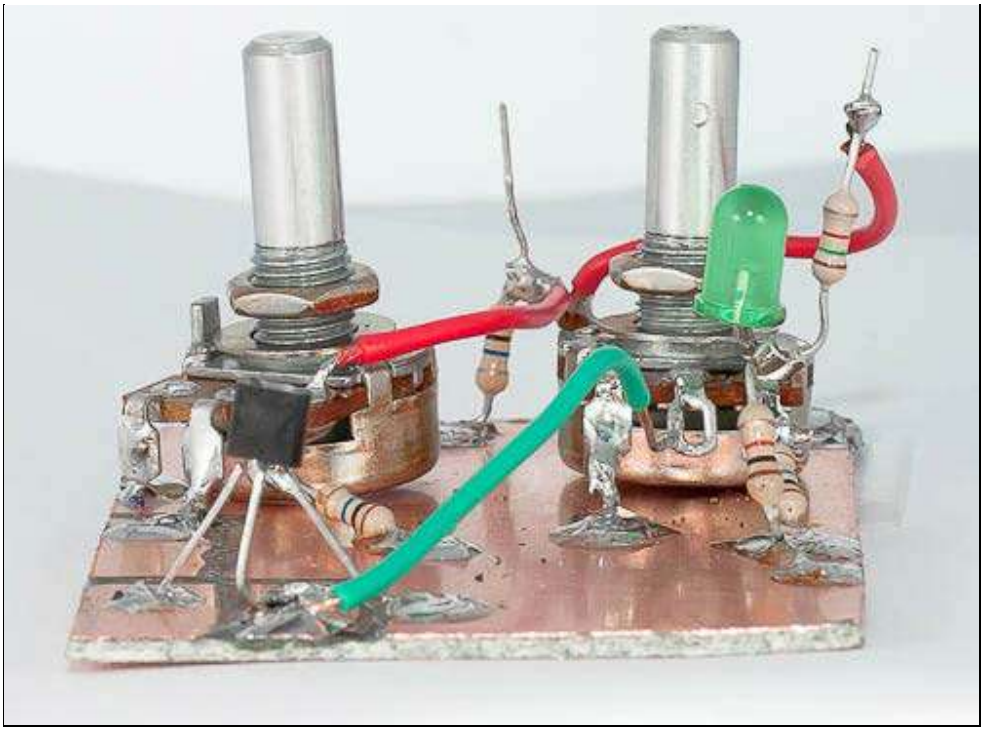

I find matching high IDSS FETs like the J310 to be a pain. I generally matched them for IDSS and occasionally for IDSS and VP. Observations that when the IDSS of 2 or more FETs match, their pinch-off voltage (VP) also matches, led me to not measure VP. In addition, the variability of VP measurements causes me distress. Click here for a tutorial if you don't understand the terms IDSS and VP.

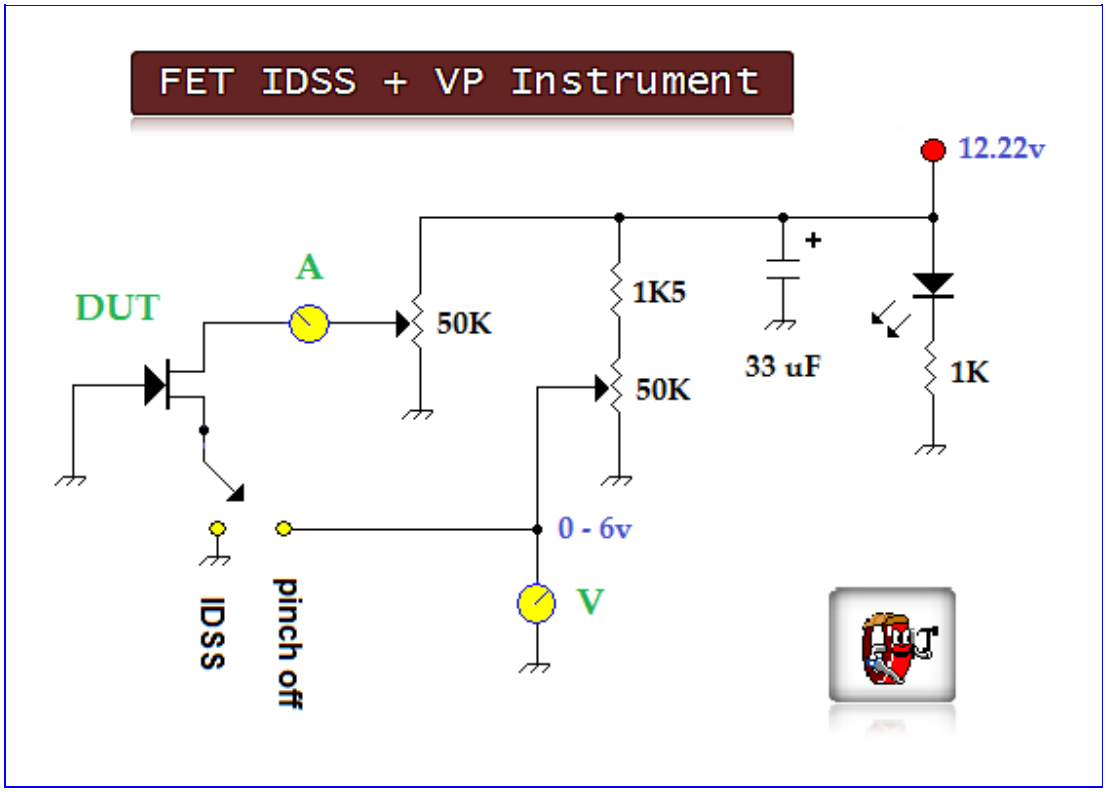

Above — The device I use to measure IDSS and VP. From Ken Kuhn's web site.

Conceptually IDSS and VP aren't difficult to understand — measuring them is another story. With the above device, first IDSS is measured; the final drain voltage potentiometer setting is left and then I measure VP. While measuring IDSS in high IDSS FETs, heating can occur and you may actually see current start to drop as you increase the drain voltage (negative temperature coefficient). On J310 specification sheets, the manufacturers state they pulse the current during measurement to prevent heating. While performing IDSS measurements, I am fearful of destroying the FET I am trying to characterize! Measuring VP is also problematic.

I have tried 3 methods to quantify VP:

Adjust the 0 - 6 volt supply until I think the current goes to 0. Serial measurements 1 day apart can vary by a variation of as much as 0.5 volts; it's quite subjective.

Adjust the 0 - 6 volt supply and measure the gate voltage that produces a drain current somewhere between 0.1 and 1 percent of IDSS and declare that to be VP.

Adjust the 0 - 6 volt supply so the ammeter reads ¼ IDSS and multiply this voltage by - 2.0. Refer to Ken Kuhn's site for details. Although reasonably accurate, the second order math is only a rough approximation — the real math is impossible to do by hand as it involves fractional exponents and these exponents and other factors vary as a function of the physical JFET geometry.

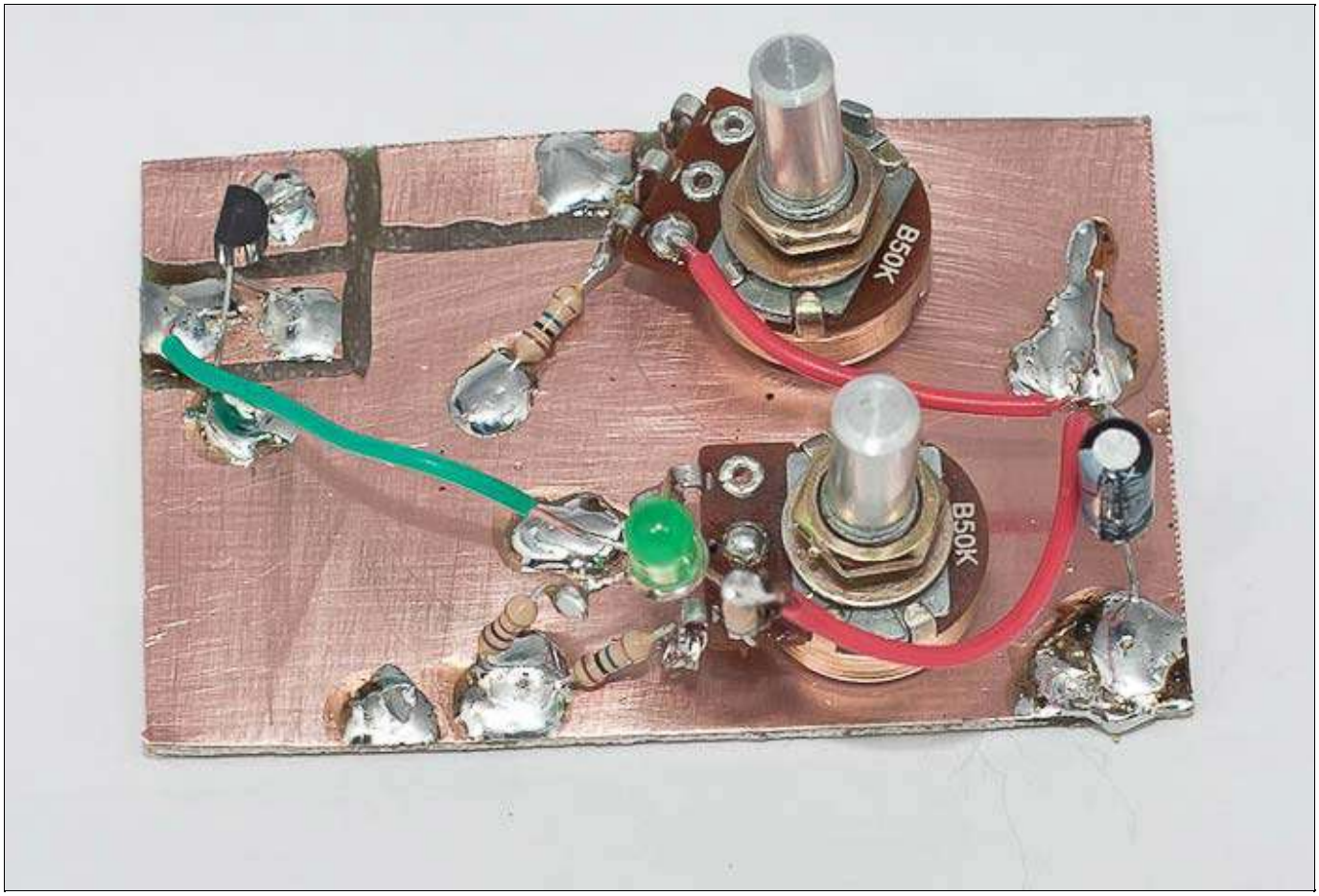

Above — The breadboard of the device I use to measure IDSS and VP. There is no actual switch, I either ground the green wire to the copper board, or tack solder it to the 0 - 6 volt potentiometer wiper. 10 megohm resistors plus the pot ground wire anchor each pot to the copper clad board.

All 3 methods to quantify VP frustrate me. There must be a way to match J310s or other FETs without characterizing them. I frequently collaborate with readers to problem solve and learn. A potential solution contributed by a supportive reader follows:

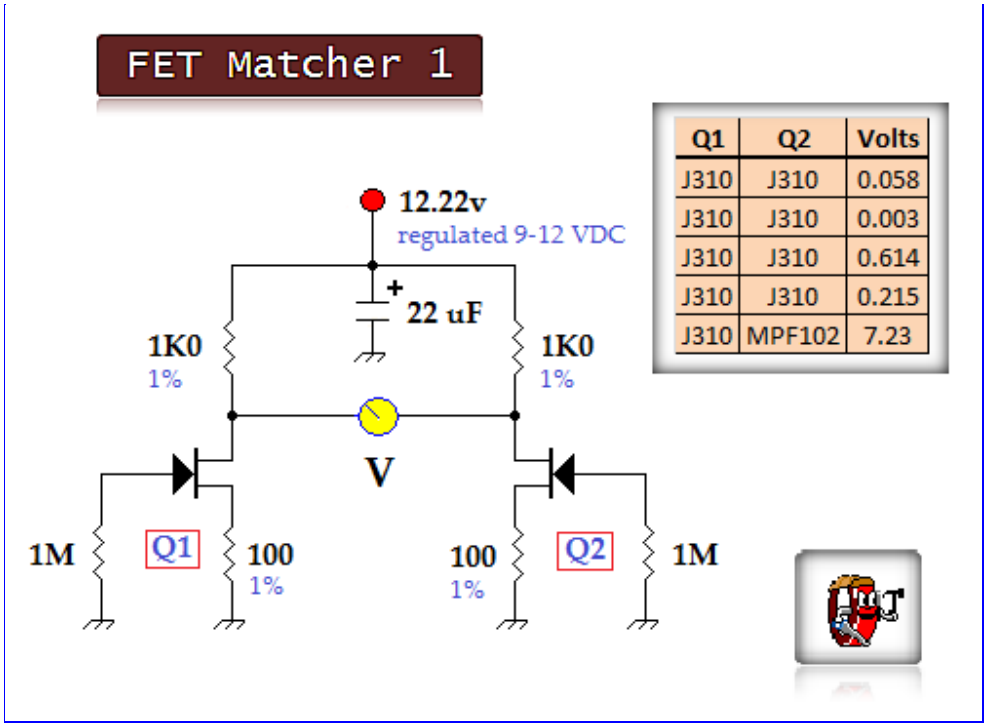

Q1	Q2	Volts
J310	J310	0.058
J310	J310	0.003
J310	J310	0.614
J310	J310	0.215
J310	MPF102	7.23

Above — A bridge is used to match a pair of JFETS. It's often best to match devices in a circuit that closely resembles the one that you intend to use them in. The differential output of each drain is measured by placing a DVM lead on each drain and recording the voltage. Generally, I stick a FET in the Q2 slot and put FETs from my parts bin in the Q1 slot to match it. The results of 5 different FET pairs are tabled above. A match <= 50 mV is probably acceptable and in 1 case, I found a match of 3 mV! You can match 1 FET with many using this device.

Note the poor match when an MPF102 and a J310 were tested. 1% tolerance resistors are recommended for the bridge.

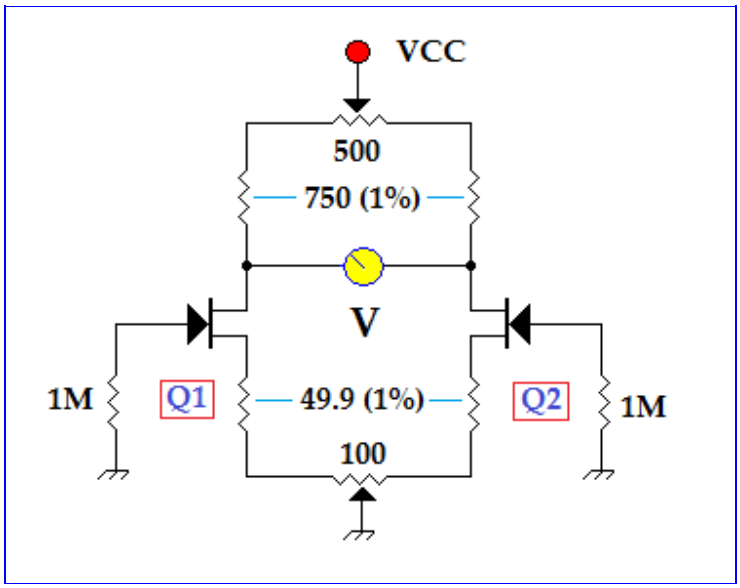

Above — A set and forget precision bridge using trimmers to establish a perfect DC match on both halves. If you don't have 1% parts, the trimmer resistors offer a solution. You can place a trimmer at either the drain or source end as shown and just use 5% resistors. Calibrate each half of the bridge with your ohm meter. I cover bridges on this web page if you need more information on them.

Above — A differential FET matcher breadboard. This version had a 9.1M gate resistor on Q1 by accident, although it made no difference to the experiment, as no DC gate current flows.

4. BJT and Diode Matching

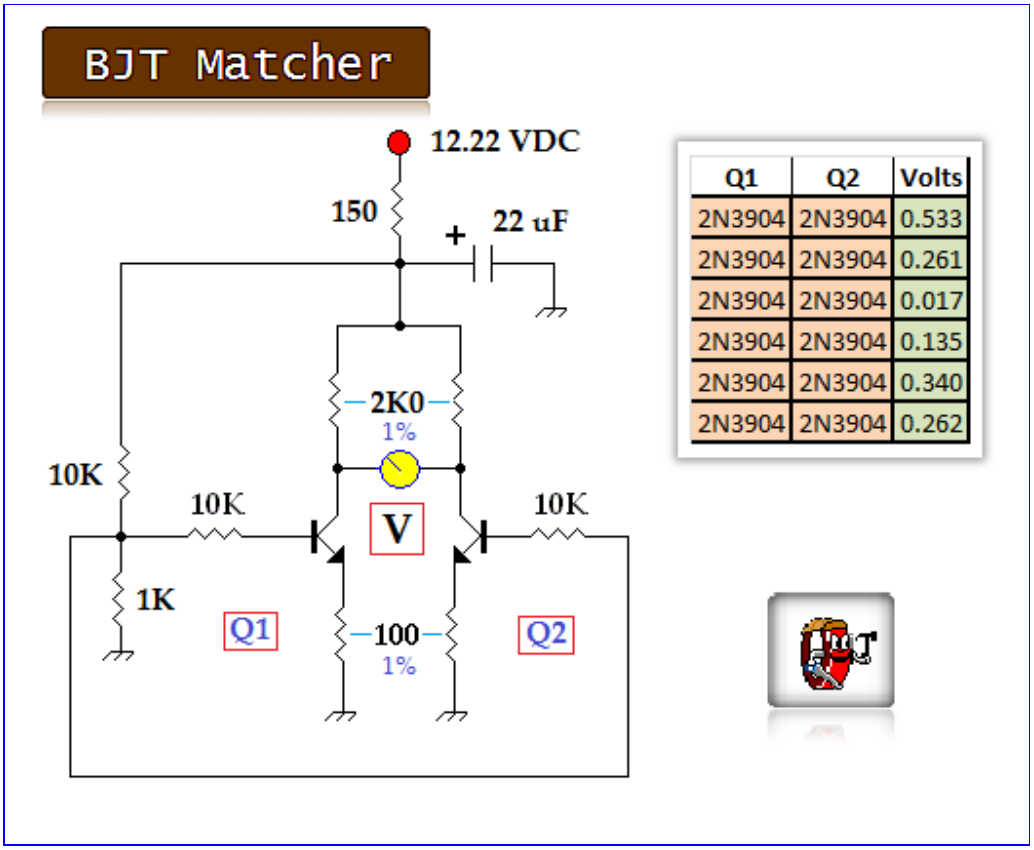

Q1	Q2	Volts
2N3904	2N3904	0.533
2N3904	2N3904	0.261
2N3904	2N3904	0.017
2N3904	2N3904	0.135
2N3904	2N3904	0.340
2N3904	2N3904	0.262

Above — Differential BFT matcher. Differential voltage matching works for bipolar junction transistors and diodes also. PN junctions are thermally sensitive — let them stabilize before testing. I measured 6 2N3904 transistors and the tabled results remind us why this transistor isn't the best choice for matched BJT circuits.

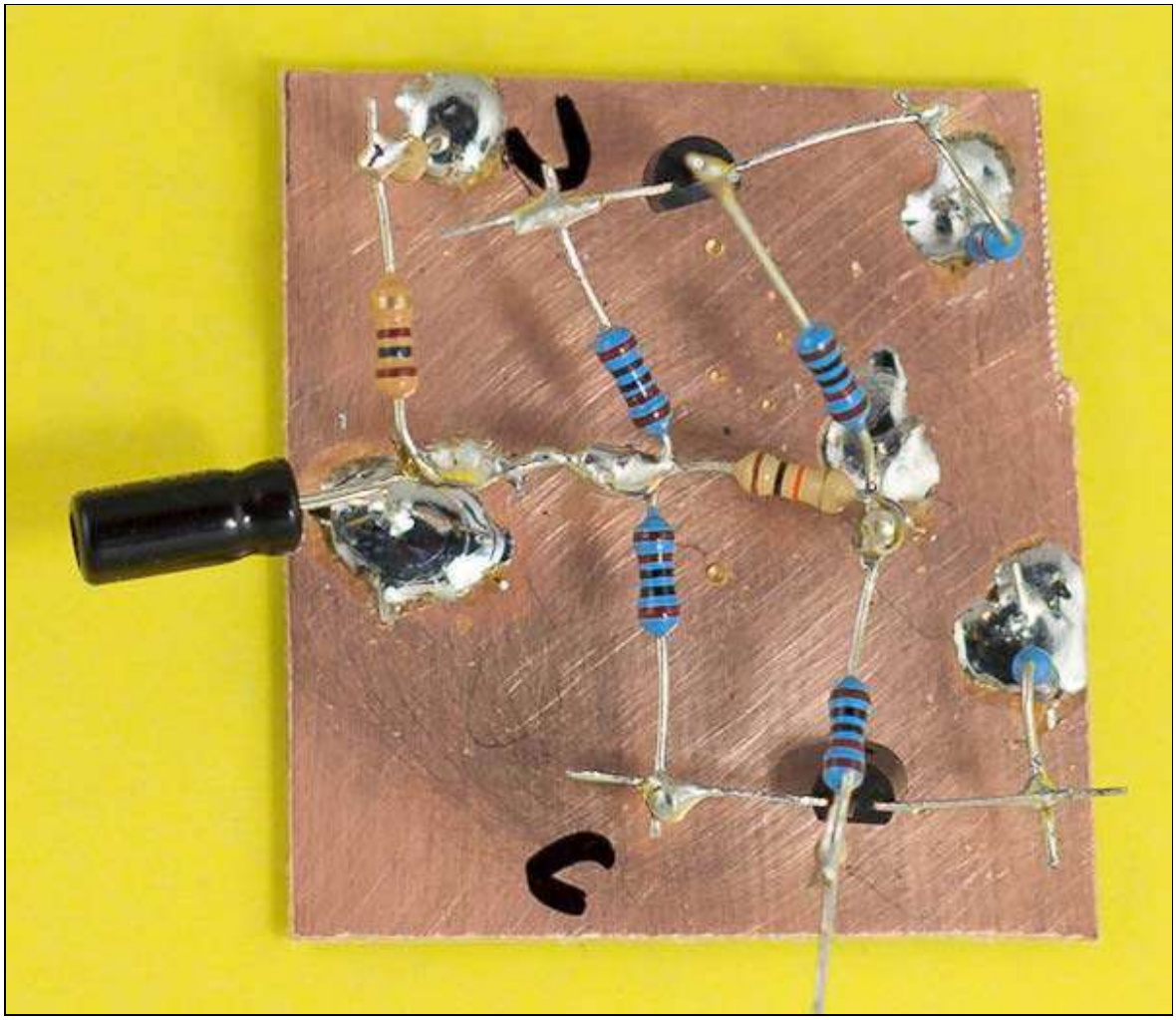

Above — The breadboard of the differential transistor matcher. Any reasonable resistor values will work fine, but don't run the current too high — my circuit has a nominal emitter current of 2.25 mA.

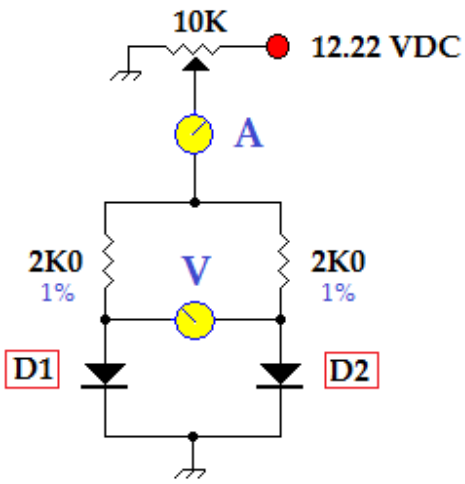

D1	D2	Millivolts
1N4148	1N4148	2.4
1N4148	1N4148	4.1
1N4148	1N4148	6.6
1N4148	1N4007	18.1
1N4148	Schottky	315
1N4148	Ge	169
1N4148	1N4148	6.8
1N4148	1N4148	4.9

Measurements with each diode current @ 77.3 µA

Above — The differential diode matcher. The 10K pot allows you to vary the current to suit your needs. The ammeter reads double the diode current. Considering only 1 diode; the current ranges from 0.01 to 5.82 mA. You can drop the 1% metal film 2K0 resistors down as low as 470 ohms or so if you need serious current. Tabled are some measurements performed with the 10K pot dialed to give 0.636v (77.3 uA per diode). This provided excellent sensitivity. Measurement was performed on my DVMs 200 mV scale. Builders might experiment with diode current to assess measurement sensitivity and linearity or even to match the diodes across a range of current values.

Clear glass passivated diodes can be affected by light — photons will pass through the glass and knock electrons through the barrier. Ensure each D.U.T is exposed to the same amount of ambient light. Some microwave detector diodes can be damaged with as little as 1 mA of current. Replace the 2K0 resistors with 10-15K resistors, or lower VCC to prevent damage .

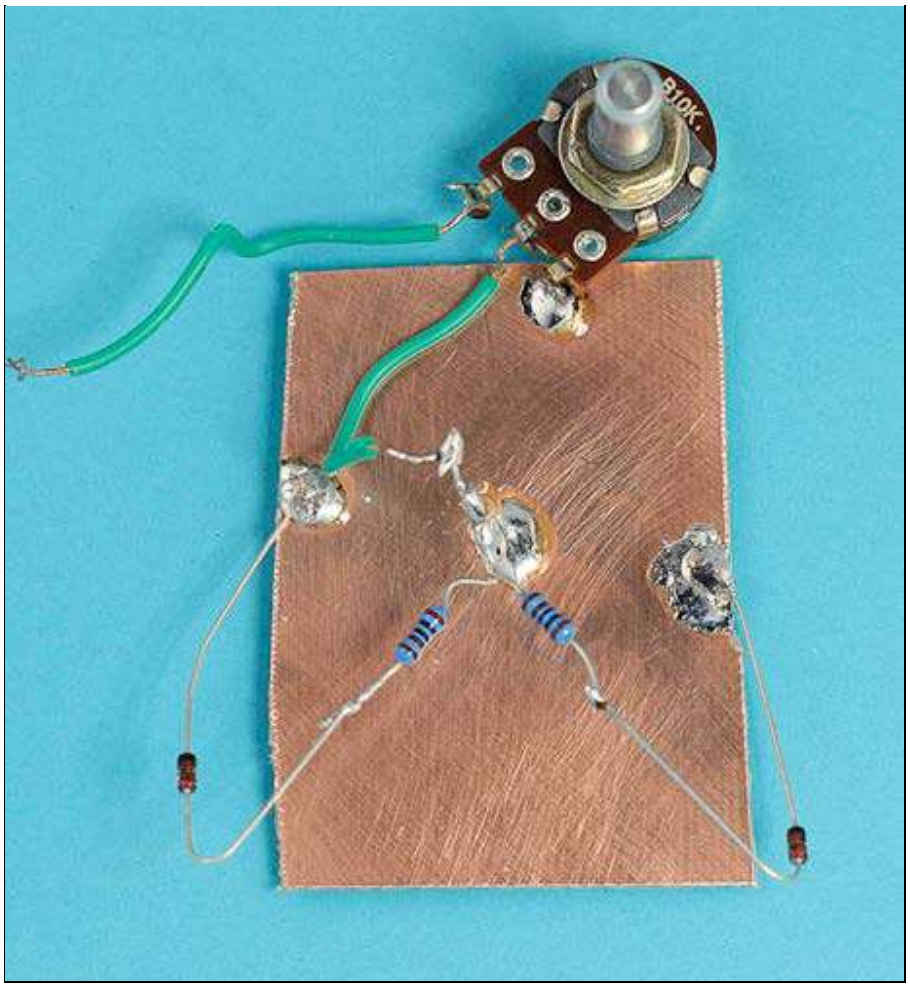

Above — Breadboard of the differential diode matcher. The 2K0 resistors are suspended by a vertically mounted 10M stand-off resistor.

5. Bipolar Junction Transistor Beta Tester

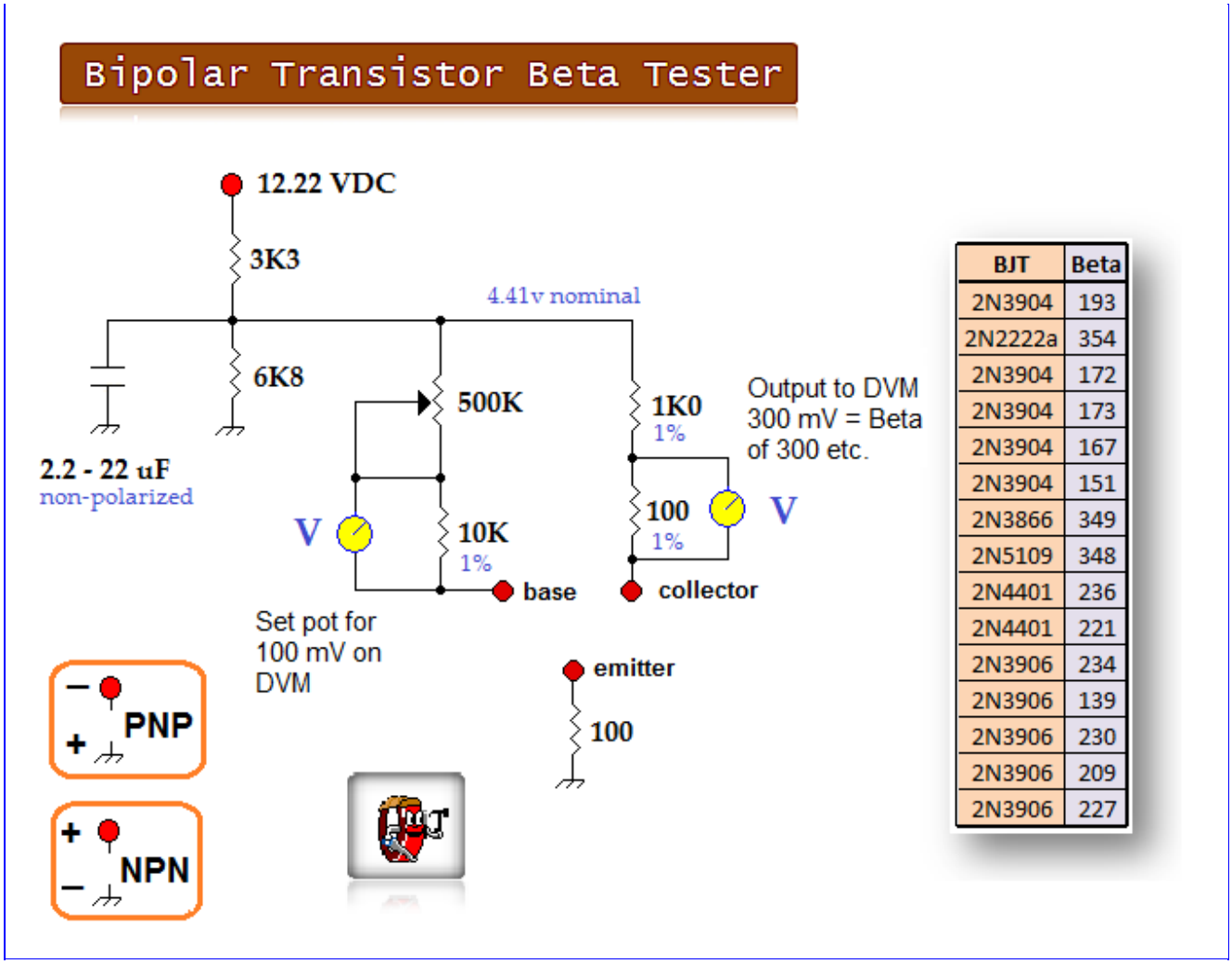

BJT	Beta
2N3904	193
2N2222a	354
2N3904	172
2N3904	173
2N3904	167
2N3904	151
2N3866	349
2N5109	348
2N4401	236
2N4401	221
2N3906	234
2N3906	139
2N3906	230
2N3906	209
2N3906	227

Above — Disappointed with the transistor beta testers in our common, low-cost digital multimeters, we did the logical thing; designed and built our own. This collaborative project was more an experiment with BJTs than anything else. It's about as simple a beta measurement device as you can make and still get good results. Preventing damage to our parts inventory underpins this design — the 100 Ω emitter resistor plus ~ 10 microamps of base bias keeps the IC low to help avoid smoke since most new small signal transistors have a beta of 100-400.

Ensure the correct polarity for PNP versus NPN transistors. The voltage divider targets 5 volts using a standard ~12 volt supply; I just used whatever resistors were handy and ended up with the 6K8 — 3K3 pair. VCC should be regulated. Perform the measurements with a single multimeter allowing time for stabilization.

To use: Set the potentiometer so that the voltage drop across the 10K resistor is 100 mV. Then move your DMM leads to the 100 Ω resistor and measure the beta. This device measures beta, the static gain at DC.

Measuring beta is a bit inexact since beta is affected by so many variables as follows:

- Beta tends to be low at low operating currents and rises and plateaus for medium currents and then falls at higher currents.
- Beta tends to increase with temperature.
- Beta is affected by the voltage between the collector and emitter -- this is a weak effect except when the voltage is very small.
- The beta can vary as the battery depletes in DMM beta testers.

Above — Breadboard of the QRP beta tester. We hope you have as much fun with this circuit as we did.

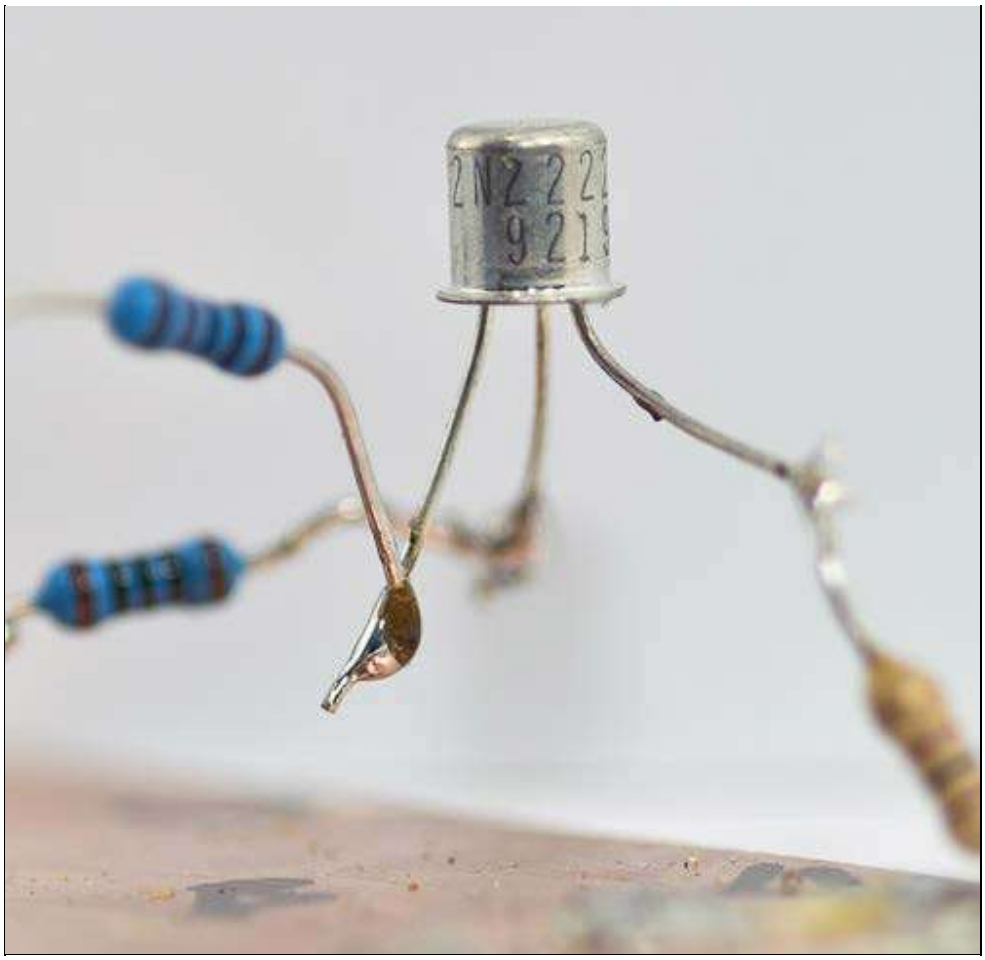

Above — Testing a 2N2222a. We found measuring transistors to be very instructive; comparing our results to specification sheets, handling the different BJTs, gaining experience — all part of the exciting world of bench electronics. Such circuits, although simple, are great for both learning and design.

6. FET Tester - VGS Measurement Tool

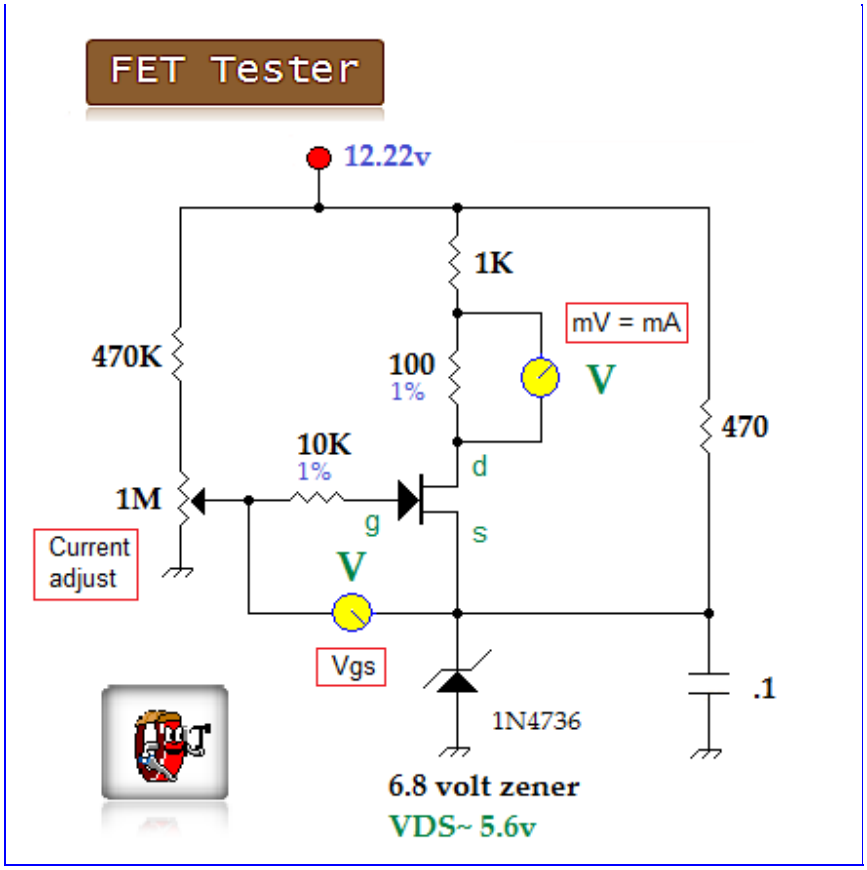

Above — A FET VGS Tester. The final collaborative output from late December 2010: a device to examine VGS. A zener diode value from 6 -7.5 volts or so should work okay. VDS should be greater than the nominal VP for greatest accuracy. The VDS using 7.5 volt zener diode was 4.85 volts. The range of VGS on my breadboard was roughly 6 to -6 VDC without the 470K range limiting resistor; it's up to you if you want to limit the VGS range.

Using the mV scale on your DVM, potentiometer adjust the current until the meter just reads 0. Then move your leads to the VGS test points to read the pinch-off voltage.

The 0 current point will only ever be close. The interesting issue with the 0 point as defined is it never goes to true zero — just zero enough — that point may be hidden if your meter scale truncates lower current measurements to zero. If you're able to repeatedly get consistent VP measurements with whatever method your using, then it's likely accurate.

We thought about measuring gate leakage current across the 10K gate resistor, but accurate measurement is impossible with this device. The gate leakage current is going to be in the low nanoampere region at the very highest unless the JFET is bad. The expected voltage across the 10K resistor would be a few 10s of microvolts. A better way to measure gate leakage is to use the 10M resistance of a DVM instead of this resistor. The DVM then acts as a current meter by measuring the voltage across the 10M resistance. A reading of 200 mV would mean a current of 20 nA.

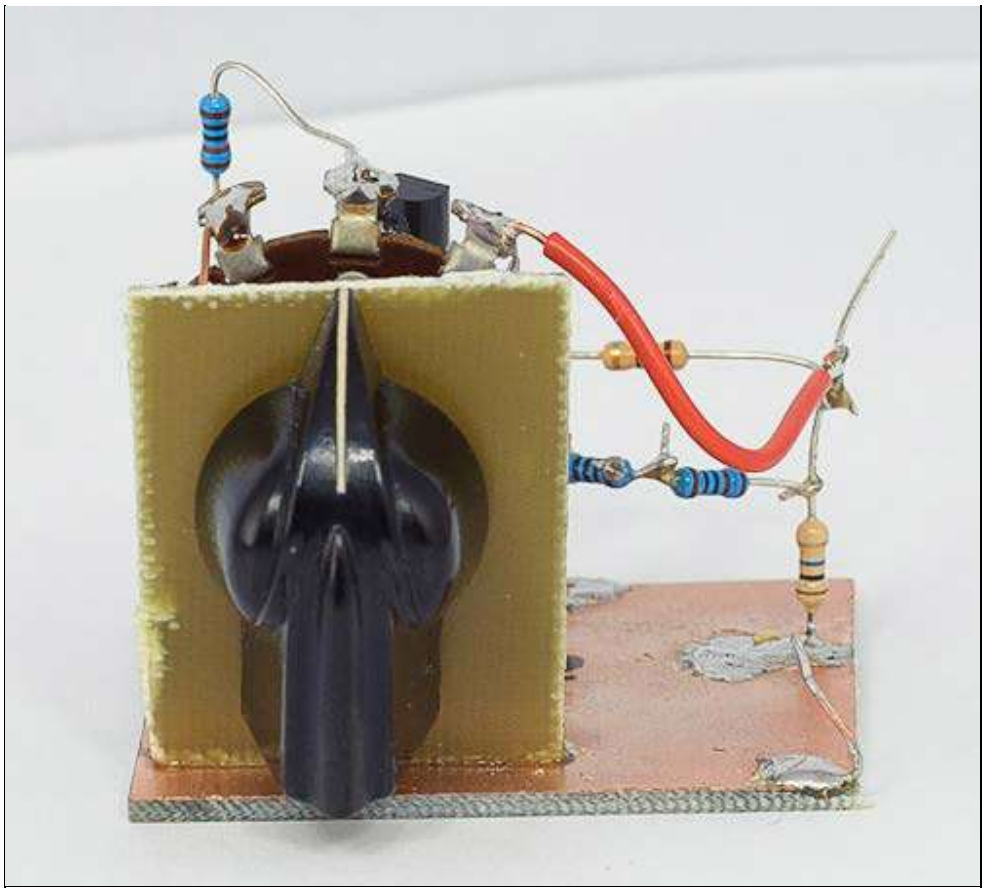

Above — Front view of the FET tester with a "chicken head" knob on the potentiometer.

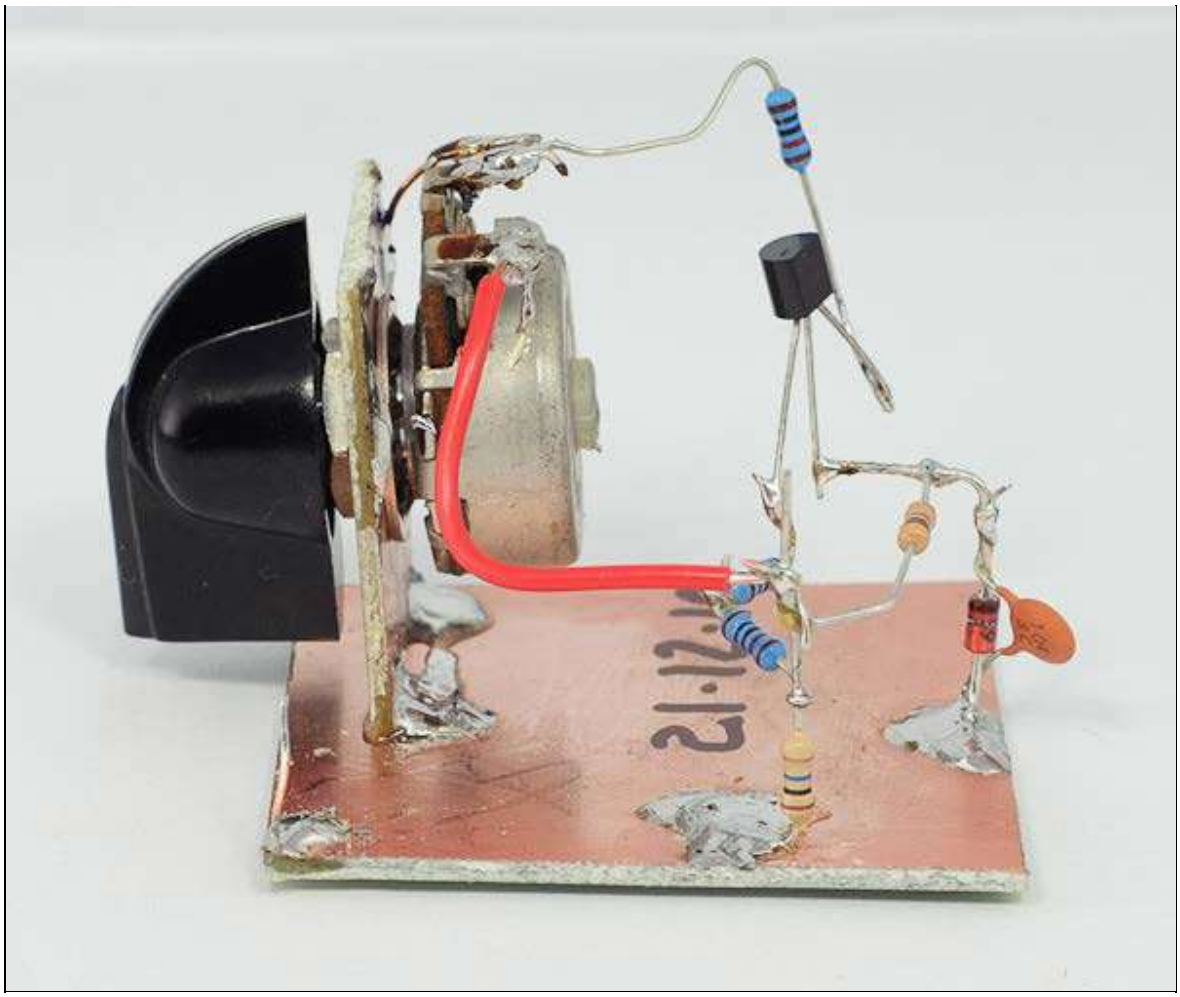

Above — Measuring a J310 with the FET tester prototype breadboard.

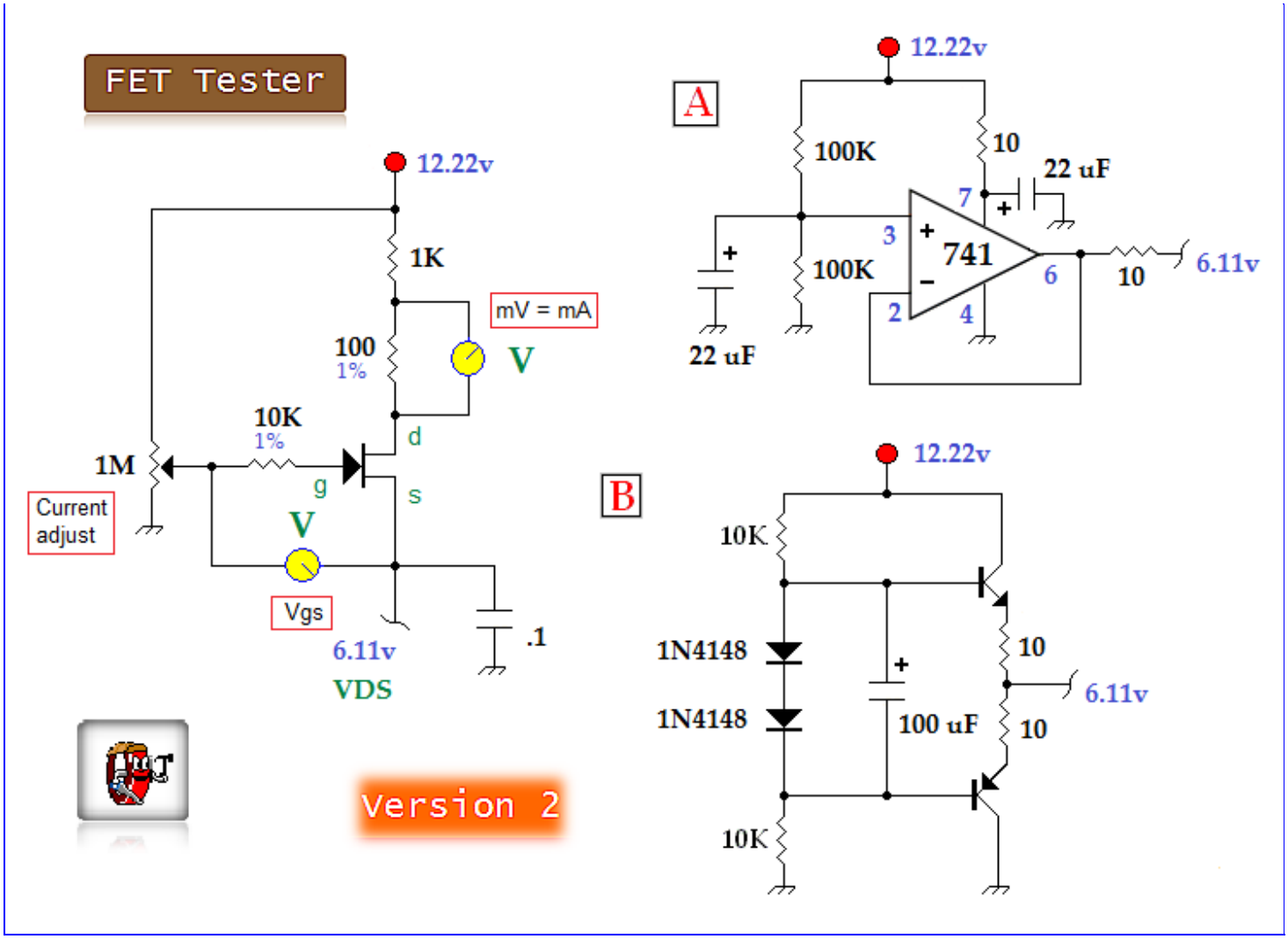

Above — Instead of a zener diode, low impedance VCC/2 splitters are shown as A and B; the zener diode is easier.

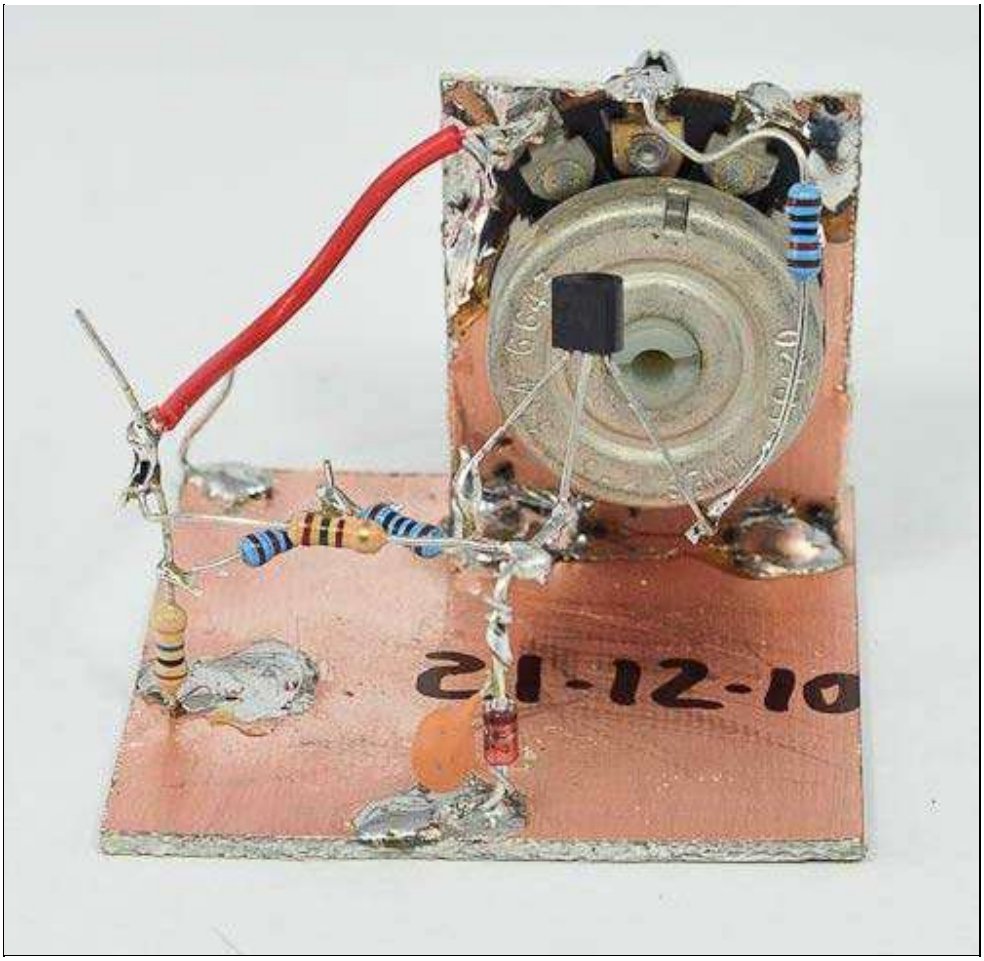

Above — Reverse view. I didn't bother with the 470K VGS range limiting resistor in my breadboard.

RF — Test and Measurement

RF Workbench Page 1

The first installment of a multi-part series exploring basic 50 Ω RF circuit measurement. This web series borrows heavily from the work of Wes, W7ZOI.

RF Workbench 1 shows a way to measure AC signals and quantify power. As circuit builders, knowing the power gain *or loss* in dB of stages like filters or amplifiers; or the absolute power in dBm of our RF signal sources dominates our bench work.

Ignite your bench measurement — Better measurement fidelity inspires confidence, creativity and fun!

Calculate Power Gain from your Oscilloscope Peak-Peak Voltage

An oscilloscope peak-to-peak voltage provides a popular way to determine power gain or absolute power.

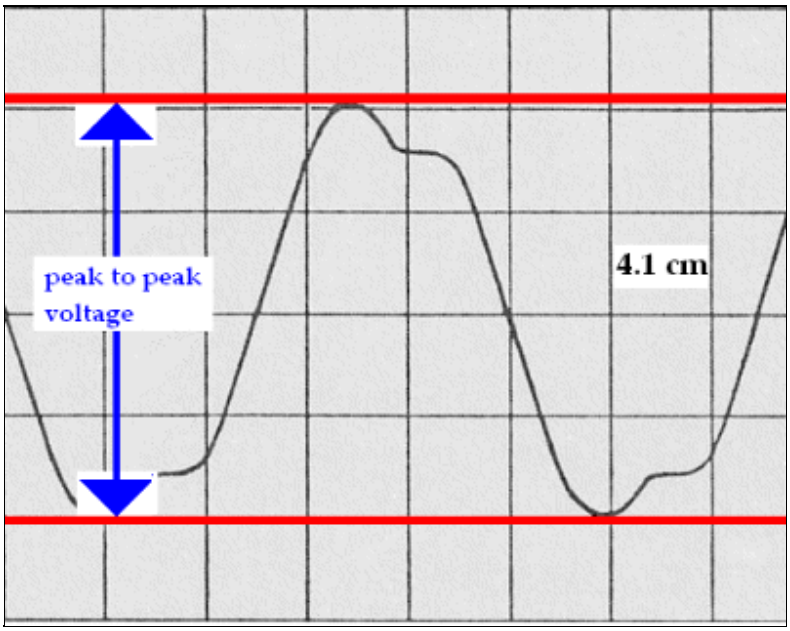

To calculate the power of a sinusoidal waveform, you measure its AC voltage. Assuming your 'scope is calibrated, the first step is to measure the amount of vertical deflection on the screen.

In the figure shown left, the vertical deflection = 4.1 cm. Multiply this measurement by the volts/cm setting of your scope. Lets assume your scope was set to 0.1 volts/cm. Thus the result = 0.41 volts. One final multiplication is required; you must multiply the resultant voltage by the attenuation ratio of the probe. In most cases, a 10X probe is used. Therefore, the measured peak-to-peak voltage is 0.41 x 10 = 4.1 volts. DSOs output numeric voltage readings in addition to that shown — a nice feature.

This signal exhibits a major problem; it's distorted. To calculate the power from peak-to-peak voltage, you require a sine wave. To obtain a sine wave, this distorted signal must be low-pass filtered. Let's examine this topic with some real experiments.

Signal Viewing versus Power Experiments

Measuring 'scope signals takes some skill to get accurate, reproducible results. Consider the following signals taken from an 8 MHz VFO.

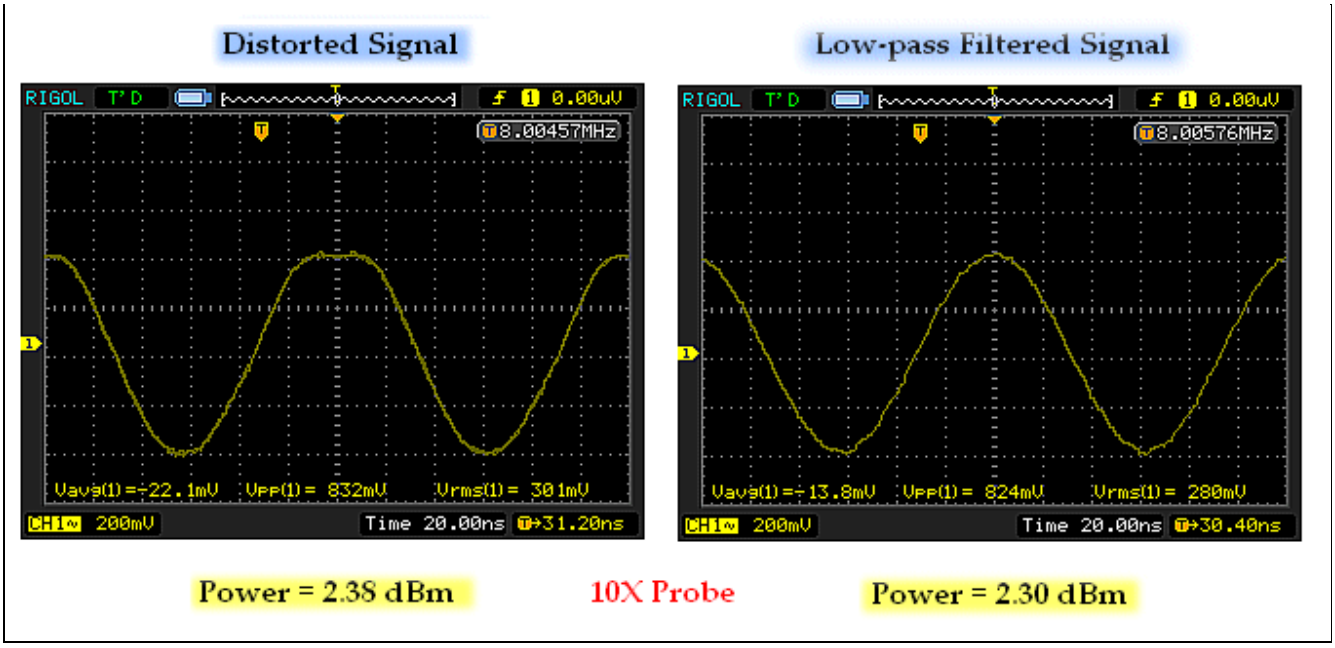

Examine the distorted signal on the left and compare it to same signal after low-pass filtering. I calculated the power in dBm from the peak-peak voltages (Vpp) shown as 832 mV and 824 mV: left to right respectively.

Only the sinusoidal power proves accurate. I'll discuss the formula to assess power soon.

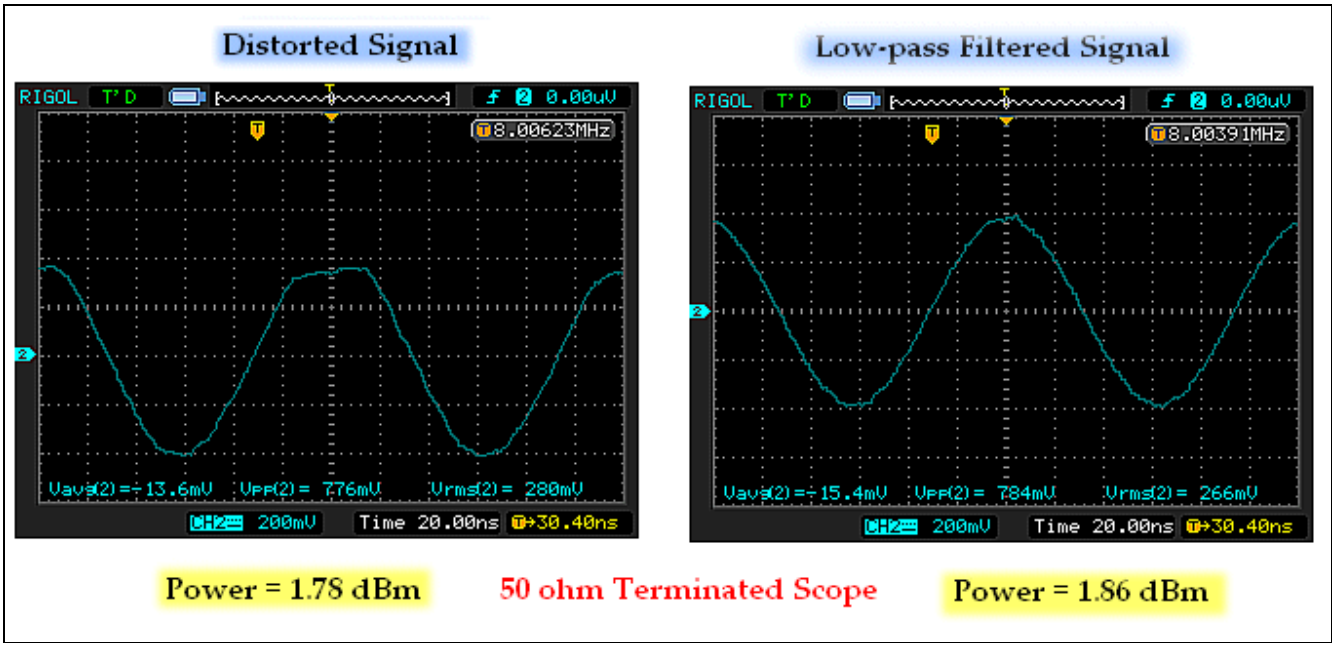

The same 8 MHz VFO examined with a 50 Ω terminated oscilloscope; a superb measurement technique that offers greater sensitivity. In all 4 cases shown, the vertical scale = 0.2 volts/cm.

To better compare the distorted and filtered signals, I attenuated the output of the VFO to allow safe examination with a spectrum analyzer. A spectrum analyzer graphs the power (in dBm) of all measured frequencies on its Y axis against a user defined frequency range on the X axis.

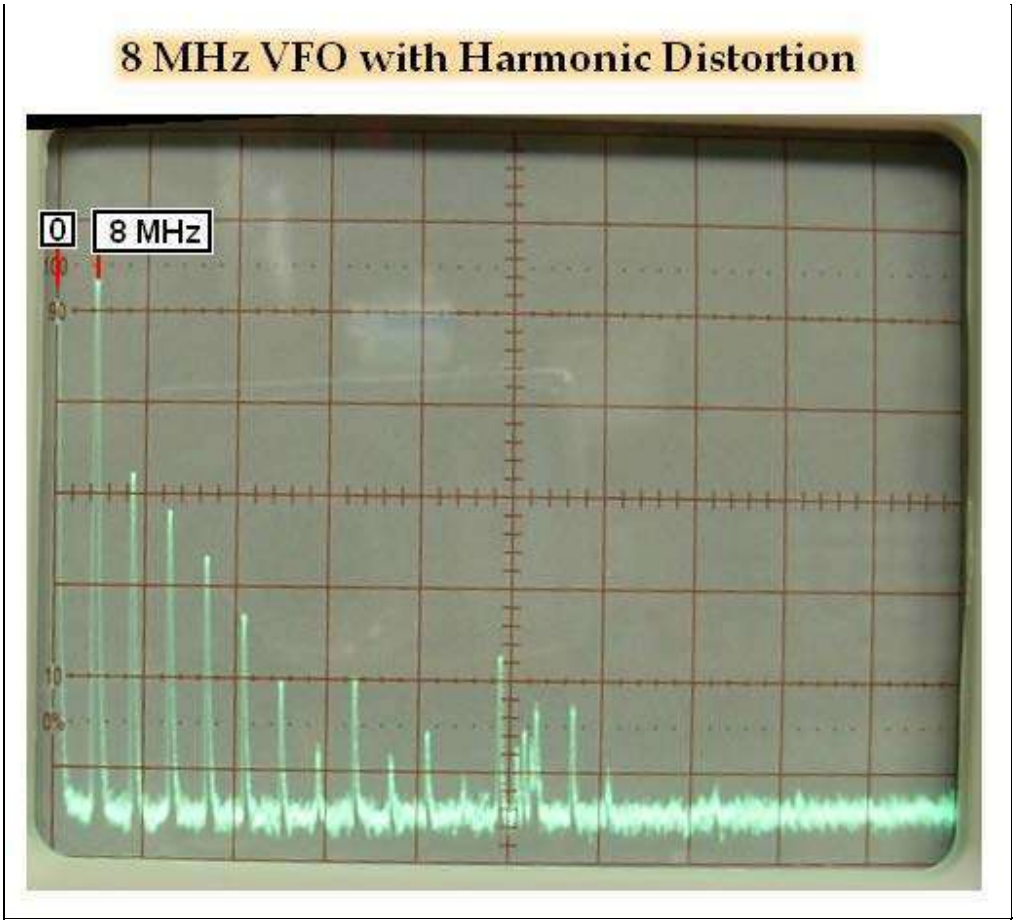

Spectral analysis of the distorted 8 MHz signal. The second harmonic (16 MHz) is about 22 dB down from the fundamental. The signal is rich in harmonics that causes error in the calculation of the output power. Each vertical square is 10 dB. Each horizontal square = 20 MHz. The harmonics go 2x fundamental, 3x fundamental, 4x fundamental and so on.

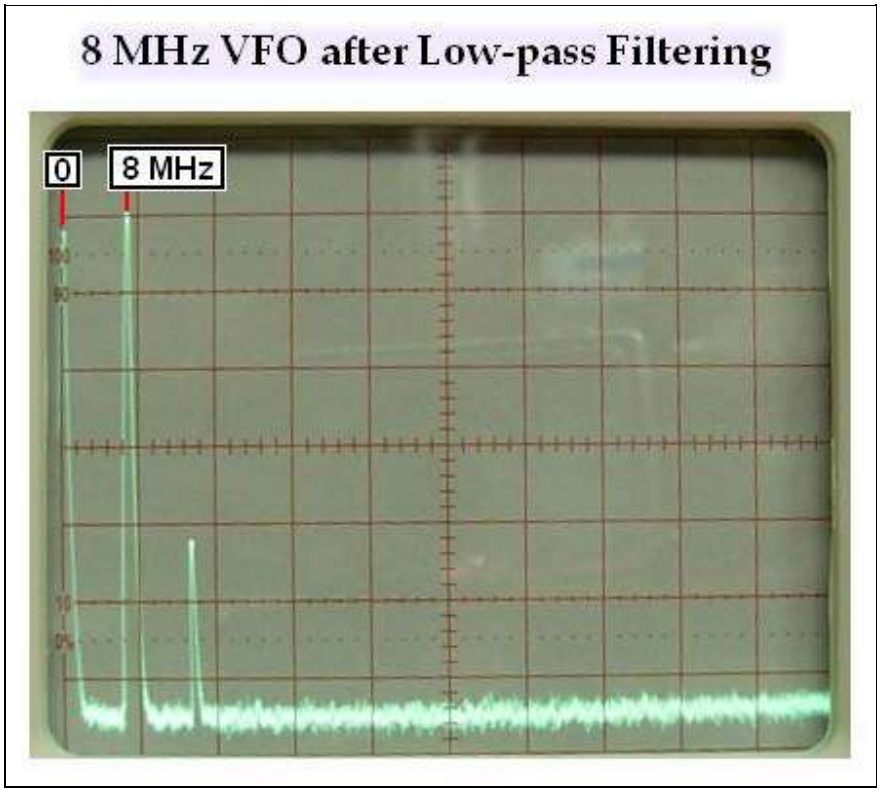

Spectral analysis of the 8 MHz VFO after passing through an N = 5 Chebyshev low-pass filter. The second harmonic now lies about 40 dB down from the 8 MHz carrier (-40 dBc) and the 3rd harmonic is almost down in the noise. Each horizontal square = 10 MHz.

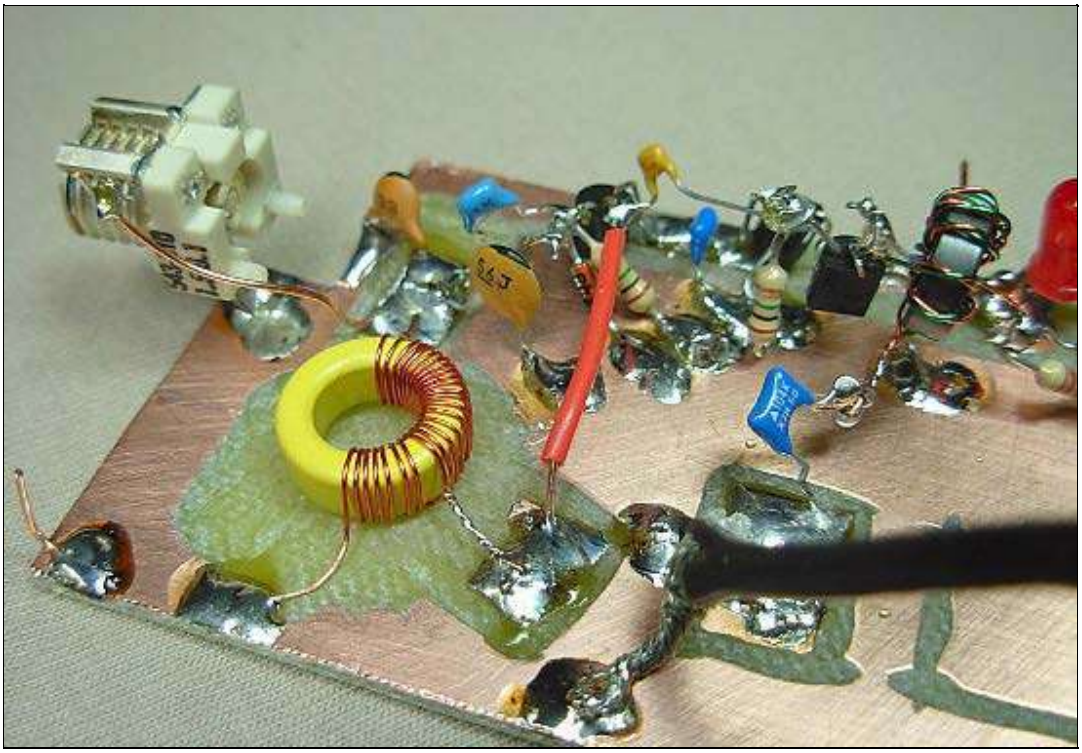

The breadboard of the 8 MHz oscillator oscillator from the above experiments. The output drove a BJT amp biased to give distortion and a 50 Ω output. I adjusted the frequency with the high Q air-variable trimmer capacitor seen to the left.

Low-pass Filter

Some builders wonder why I only employ sine wave signal generators on this web site. To calculate power, they require no low-pass filtering — now you know why. If you're calculating power from a distorted signal, a stiff low pass filter helps ensure measurement fidelity. All of my signal sources feature a 2nd harmonic response of at least -30 dBc, but -50 dBc is typical. To filter receiver front ends, signal generators, or mixer outputs, I keep several 7 element low-pass filter bench modules on hand that cover several 3 dB cut-off frequencies between 3 and 60 MHz.

Although, any old low-pass filters might work fine, Wes, W7ZOI suggests an N = 5 Chebyshev with 0.2 dB of ripple at about 1.2x the signal frequency as a starting point for designing a test-bench low-pass filter. If you don't know how to design low-pass filters choose a pre-designed filter from a filter table. For the experiments above, I selected a filter from an ARRL Handbook. See the schematic below:

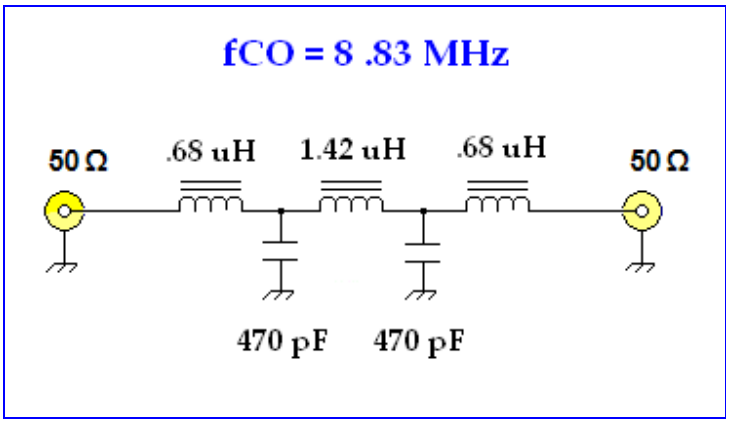

Calculating Power (dBm and mW) from Peak-to-Peak Voltage

To calculate the power from peak-peak voltage, the load impedance (Z) must be known. In RF design, the standardized impedance value = 50 Ω. For CATV and video, 75 Ω is common, and in audio and telecommunication design, a 600 Ω impedance dominates. Although we can technically employ any Z, this web site conforms to the 50 Ω RF impedance standard.

The SI unit of power is the watt. In radio, we might see the term dB used, however, dB is a decibel comparison between 2 signals and not an absolute value like the watt. On the bench, dBm serves as the most common and useful term — dBm is the measured power ratio in decibels

referenced to 1 milliwatt.

dBm represents an absolute power — so useful because both large and small signals are quantified with 1 number. Some important bullets follow:

- 0 dBm = 1 mW
- 3 dBm = ~2mW; so doubling the power from 0 dBm equals a 3 dB increase in power
- Increasing the power from 0 dBm to 10 dBm boosts power by 10 dB. The power is now 10X baseline or 10 mW
- 20 dBm = 100 mW
- -27 dBm means that the output has ~500 times less power than 1 milliwatt. -27 dBm = 0.002 mW or 2 microwatts

Hopefully over time, you' ll ingrain the concept of logarithmic power gain or loss (in dB) and power referenced to 1 mW (in dBm). This is bread and butter radio design information you must know.

50 Ω Measurement Virtues

You build a VFO, measure it with your 'scope; calculate the output power into a 49.9 Ω resistor and then record this power in dBm. Let's say it's 6 dBm. VFO output power = 6 dBm.

Next, you place a 6 dB attenuator pad on the VFO output. VFO output power now = 0 dBm.

Finally you connect a 10 dB gain RF amplifer to your VFO. Your VFO output now = 10 dBm. What a beautiful system ! ..... it really gets fun when we measure down at - 30 dBm and so forth.

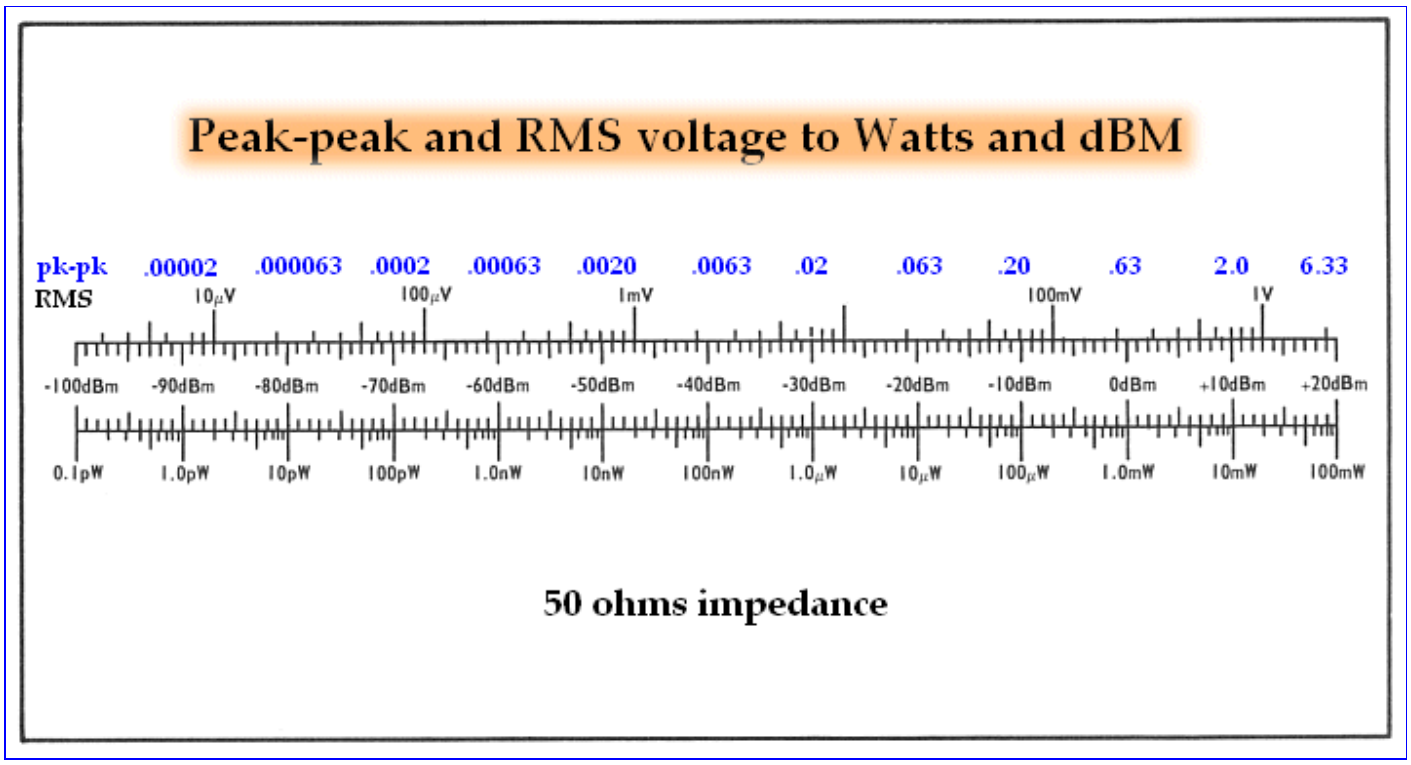

The chart above really helps you visualize the relationships of mW, AC voltages and dBm

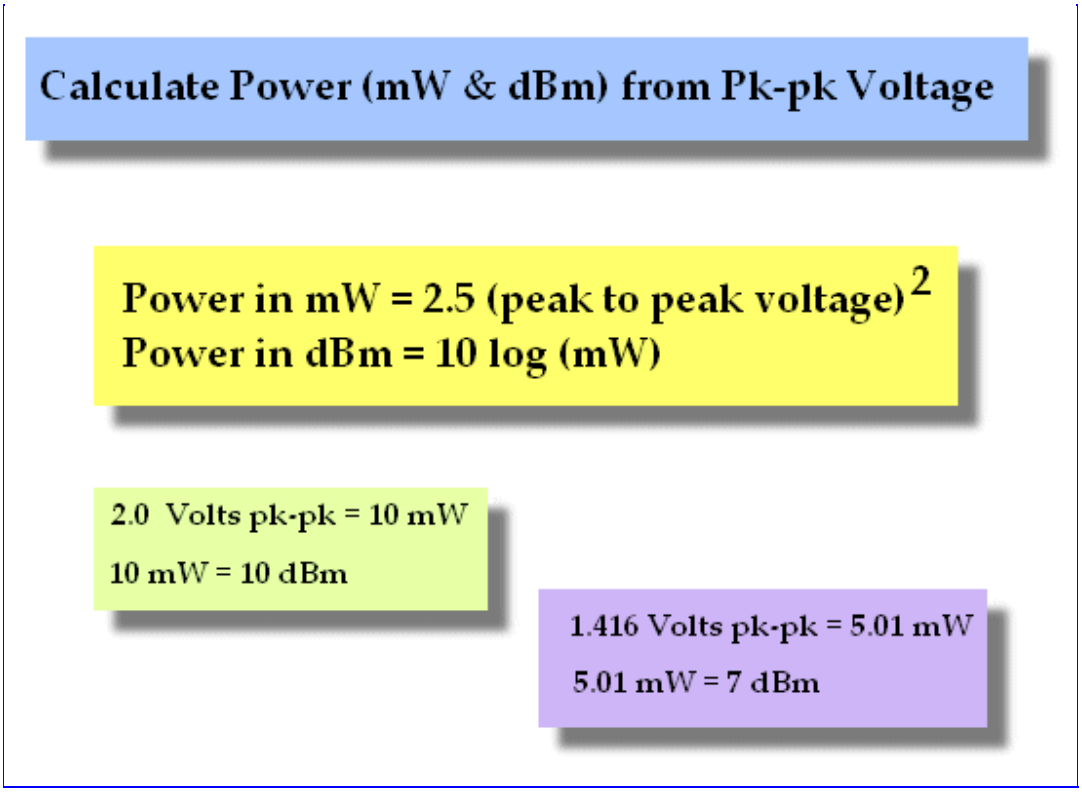

In order to get from peak-to-peak voltage to power, math is required. I show the formula above. You may elect to skip the math and calculate dBm or mW from peak-to-peak voltage with software. A number of programs are available; I wrote 1 here as Applet **F**.

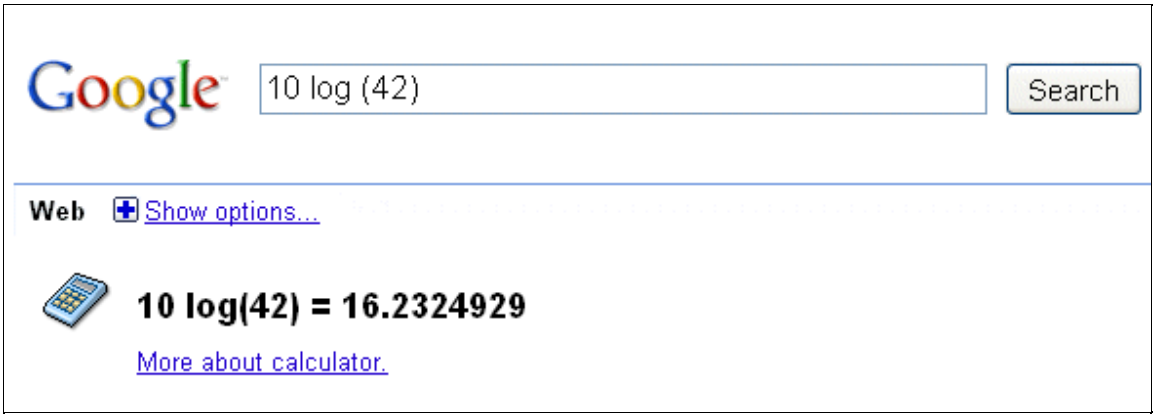

If you lack a scientific calculator, Google has math functions. Shown above = a logarithm calculation

In Search of 50 Ohms

How do I establish a 50 Ω output impedance in my RF amplifier? I get this question often.

From my experience, in **simple** amplifiers lacking negative feedback, a 50 Ω output impedance must be created by inserting a resistor somewhere in the circuit that forces a 50 Ω output impedance.

For example, we might use a 50 Ω collector resistor in a BJT amplifier (or a 50 Ω drain resistor in a JFET amplifier), or place a fixed resistor in parallel with the collector/drain transformer and use a secondary winding to establish the 50 Ω output impedance. Sometimes we'll place a series resistor (say from 22 to 51 ohms) on the output of an emitter or source follower to bring the low output impedance up to 50 Ω. These form basic explanations and usage examples may be found on many schematics on the QRP / SWL website.

We experimenters also employ negative **feedback** with or without output transformers to establish a 50 Ω input and/or output Z and I show many examples on this site.

The following diagram explores 1 method to get a 50 Ω output impedance in a simple amplifier. It doesn't matter if the transistor is a JFET or a BJT, the principle is the same. This diagram and tutorial are simplistic and meant to help novice builders learn to design their own amplifier stages. You may connect any resistor value across the output of a transformer to calculate power, however, this web site only considers 50 ohms.

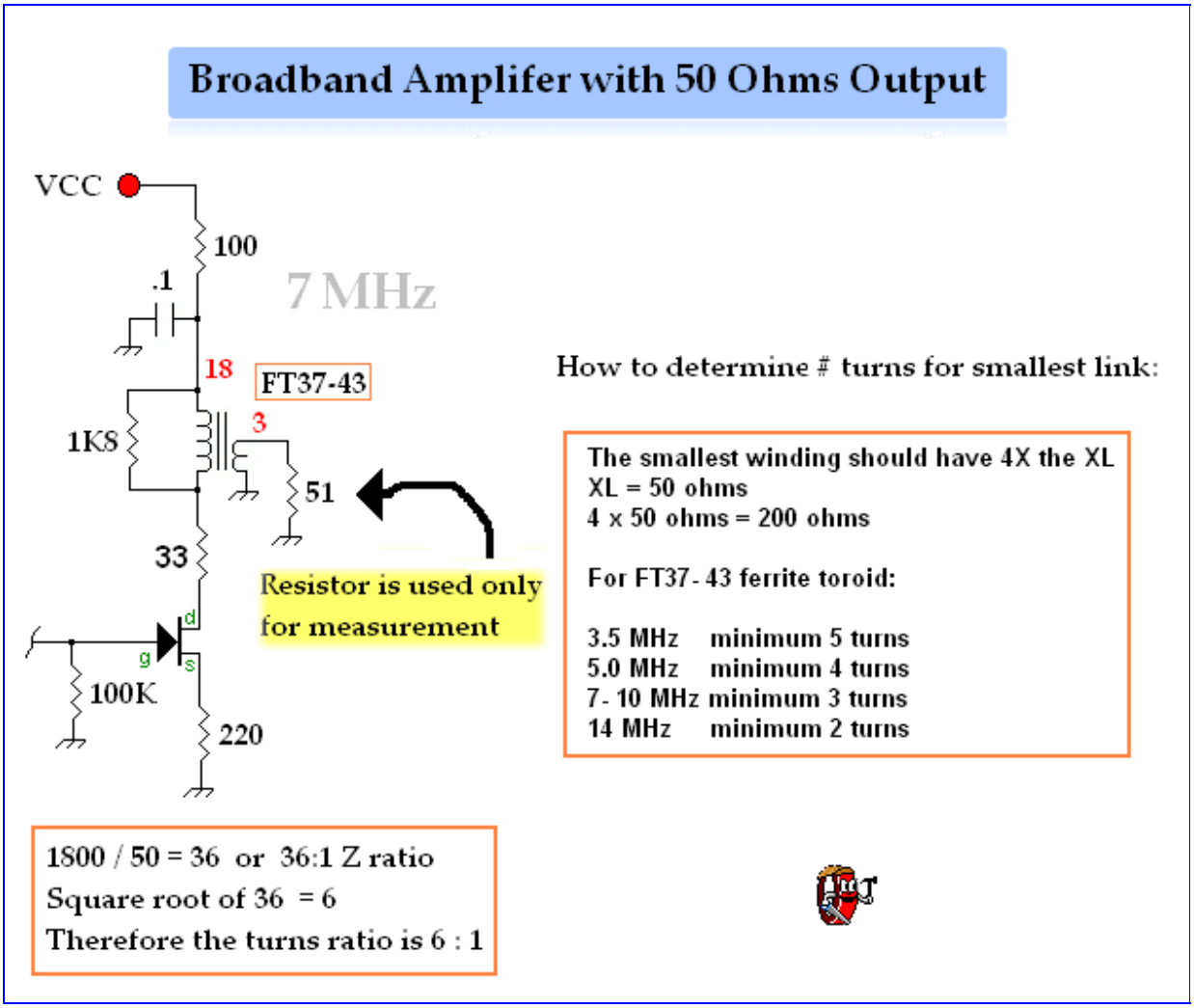

The above diagram describes a broadband (untuned) amplifier. I employed a FT37-43 ferrite toroid: a common part. Other ferrite toroids may be substituted, however the table depicting the minimum number of turns won't apply.

Consider the BJT amp shown. The transformer primary winding is shunted with a parallel 1800 Ω resistor. The 1K8 resistor "forces" a 1K8 ohm collector output resistance in the primary winding.

To transform the 1800 Ω primary impedance to 50 ohms; use a 3 turn secondary link. Calculate the primary to secondary turns ratio as follows:

1800 ohms divided by 50 ohms = 36. The impedance ratio = 36:1.
The turns ratio is the square root of the impedance ratio; thus the turns ratio is 6:1. The primary winding must have 6X the number of turns of the secondary winding. In the 3rd RF Workbench web page, you'll see that the above explanation pertains to the "ideal transformer", however, the concept is useful — especially to the target audience of this website.

New builders might ask — why not wind 6 turns for the primary winding and 1 turn for the secondary winding? We avoid this because the smaller or secondary winding should have have a minimum inductive reactance (XL) of 4X the impedance it is connected to. Thus for a 50 ohm circuit, the minimum XL = 200 Ω at the design frequency.

This design rule serves only as a rough guide. We employ the minimum 4X rule because employing an XL less than 4X may create unwanted signal losses and affect the smaller winding's impedance. The table to the right of the amplifier shows the minimum numbers of secondary turns for a few common frequencies with the FT37-43 ferrite toroid.

Thus for our 7 MHz amplifier, we need at least 3 secondary turns and multiply this number by the turns ratio to give a 18:3 turns ratio. You might also choose 24:4.

For ferrites other than the FT37-43, calculate the minimum number of turns with the XL= 2 pi * F*L formula and detemine L from the turns versus AL toroid data, or measure L with an inductance meter.

For AC measurement a 50 Ω purely resistive load should be temporarily connected between the output link and ground. This might be a 51 ohm resistor, a 49.9 ohm 1% metal film resistor, 2 parallel 100 ohm resistors, or some other "50 Ω" load. We measure peak-to-peak voltage across

the load and then calculate the power in dBm or mW. After measurement, the temporary 50 Ω load is removed and the circuit connected to the succeeding stage.

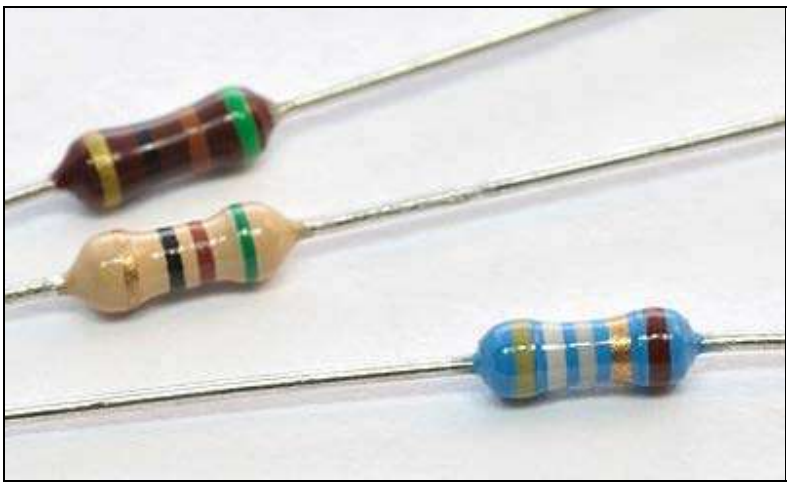

51 and 49.9 Ω resistors

We measure the peak-peak voltage across this 50 ohm resistor with a 10X 'scope probe; or alternately may connect the device output to a 50 Ω terminated scope to measure peak-peak voltage to calculate power.

I normally measure in a 50 Ω measurement environment and temporarily solder a BNC connector onto my breadboard and connect this port to a 50 Ω terminated scope with coax. After testing and voltage measurement, I remove the RF connector and then build and test the next stage.

Case Study

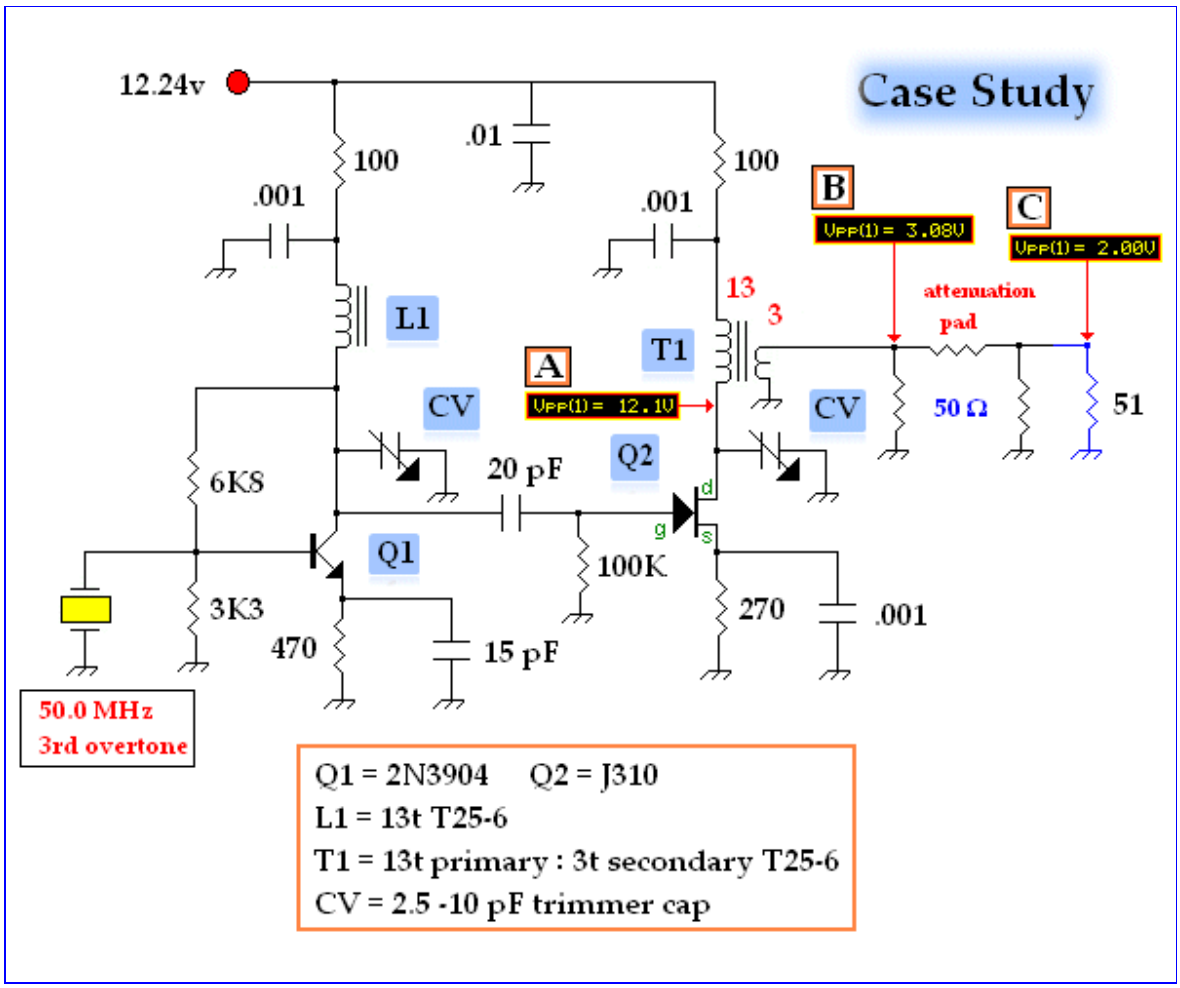

Pretend that you breadboarded the above circuit entitled "Case Study". This is a 50 MHz crystal oscillator and buffer. The crystal fundamental frequency = 16.7 MHz, but the L1 tank is tuned to its 3rd overtone; 50.0 MHz. You measure and record the peak-to-peak voltages at the points labeled A, B and C.

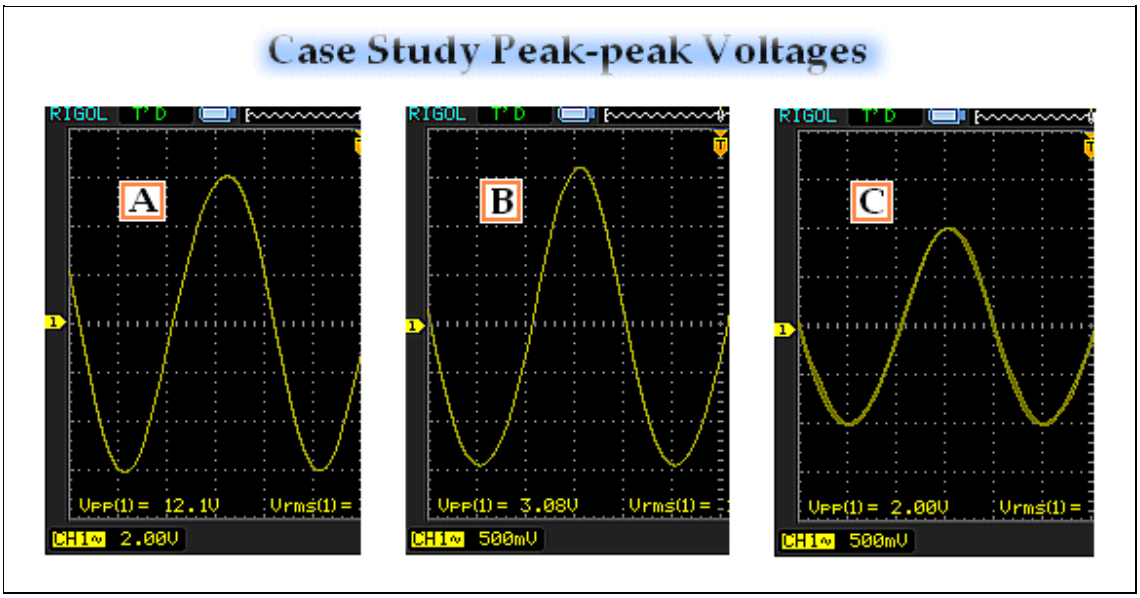

The peak-to-peak voltages are shown as Vpp. The vertical scale (volts/cm) is shown on the bottom of each figure.

Examine Point A. The AC voltage = 12.1 volts peak-peak. Compare this to the peak-peak voltage at Point B. Note the difference. Some builders emailed me after they measured similar differences on the primary and secondary transformer windings of their circuits with a 10X probe. These builders felt something must be wrong. All normal; you can expect the peak to peak voltage to roughly decrease (or increase) by the transformer turns ratio.

The 12.1 volts peak-peak decreased by a factor of 4.3 (13 / 3 turns ratio) which is 2.8 volts peak-peak. In our case, the measured secondary peak-peak voltage was 3.08 volts — in the ballpark. Please remember this serves as a **coarse** guide only. It helps you to know what to reasonably expect during signal viewing.

Peak-to-peak voltage changing in accordance with the transformer turns ratio represents a simplistic explanation describing the "ideal transformer". To understand real world transformer function, you must contemplate factors such as Ohm's law for AC, conservation of energy (this is what causes the voltage to drop while preserving power) and basic transformer behavior. These principles are explained in publications such as The ARRL Handbook for Radio Communications, or the RSGB Radio Communication Handbook. An old high school physics text book might prove a better reference.

Here are the case questions:

1. Calculate the power in dBm at point B
2. Calculate the power in dBm at point C
3. What is the attenuation in dB of the 50 ohms attenuation pad?
4. What is the output power in mW of this stage?

Click on this link for the answers and to see the actual resistor values of the attenuator pad.

Finally, placing a 10X probe at Point **A** will de-tune the L-C tank circuit somewhat and thus alter the AC voltage. In real-world building; to tune Q2, tweak the variable capacitor (CV) with your 10X probe connected to Point C.

The breadboard of the 50 MHz oscillator prototype.

Oscilloscope Probing

10X Oscilloscope Probe

Please refer to EMRFD Chapter 7 for great information about measuring power in RF circuits. The 10X oscilloscope probe is one of the most important measurement tools to have on your bench. There are countless web articles concerning the 10X probe, so I don't have much to add.

Take care of your 10X probe: don't solder components you've clipped your probe to; avoid setting heavy objects on the cable; store it carefully and inspect it frequently.

When do you use a 10X probe ? Measure with a 10X probe for in-situ ("in place", or "in circuit") voltage measurement and in situations where you can afford a 10X reduction in sensitivity. In low level measurements such as millivolt level measurements, the reduced sensitivity of a 10X probe may reduce or disallow accurate measurement. Additionally, the 20 pF or so capacitance of a 10X probe can detune resonant circuits; especially at VHF on up.

Close up of the Rigol oscilloscope probe 10X and 1X switch.

50 ohm Terminated Oscilloscope

At RF, we generally work with (or try to work with) circuits with 50 Ω impedances. If possible consider performing your measurements in a purely 50 ohm environment.

That is — instead of using a 10X probe, shunt the oscilloscope input port to ground through a 50 Ω resistor and connect your test circuit to the 'scope with 50 ohm impedance coaxial cable. On my 'scopes, I have Channel 1 set up for the 10X probe work and Channel 2 set up for a 50 ohm environment.

I asked Wes about the benefits of performing measurement in a 50 Ω environment. I learned the main advantage of a 50 ohm approach is a well defined port impedance. The second virtue; a 10X greater voltage sensitivity — the increased sensitivity for low level measurement amazes me. In some cases, small signals that I couldn't accurately measure with a 10X probe, gave an excellent scope tracing with more consistent voltage readings in a 50 Ω environment.

You also may enjoy improved signal viewing. For example, in a few cases I have observed harmonic distortion with a 50 ohm terminated scope unseen with a 10X probe I confirmed this distortion with a spectrum analyzer.

If you have never performed measurement in a 50 Ω environment, consider trying it out — you'll enjoy it. You may buy commercial 50 Ω feed-through devices that connect to your oscilloscope input, or homebrew your own, but try to keep the 50 ohm termination as close to the oscilloscope input as possible.

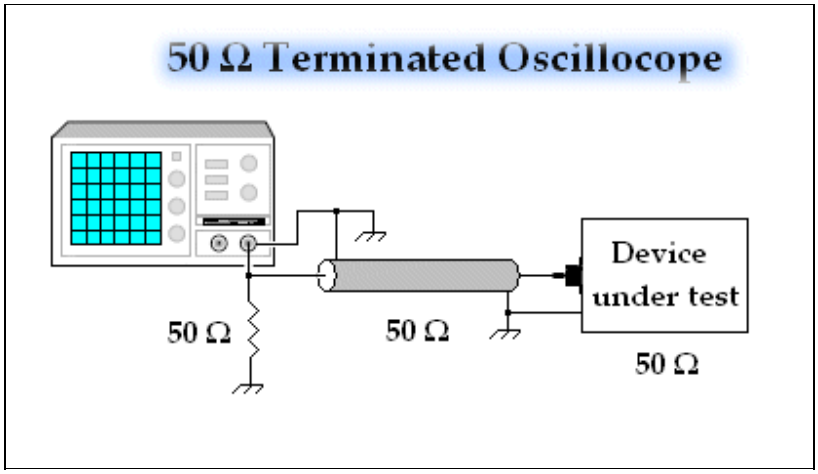

Establishing a 50 Ω impedance measuring environment. The oscilloscope input is terminated with a 50 Ω resistance and connected to a device with a 50 Ω output impedance via 50 Ω coaxial cable.

Try not to routinely connect a feed-through attenuator pad to your feedthrough 50 Ω 'scope terminator — error may arise.

My very first homebrew 50 Ω scope terminator module with 2 female connectors. I connected this module to my oscilloscope input via a commerical 9 cm long 50 Ω coaxial cable with a male connector on each end.

Two parallel 100 ohm resistors formed the 50 Ω load. Ideally, the 50 Ω shunt resistor should be right at the 'scope's female BNC jack — so this homebrew module shown fell short as a stalwart 50 Ω terminator. Inspired to move to a 50 Ω environment and lacking a male BNC connector, it did the job until my commercial version came by mail. You might find oscilloscope feedthrough terminators for sale at Ham festivals.

An ideal homebrew solution — place a male and female BNC connector in a small metal box very close together to allow a very short interconnecting wire. The box would hang off of the oscilloscope. Better still are commercial, shielded 50 Ω feed through terminators which thread right onto the oscilloscope's female BNC input jack.

Above — a commercial 50 Ω feed-through BNC terminator on my oscilloscope input.

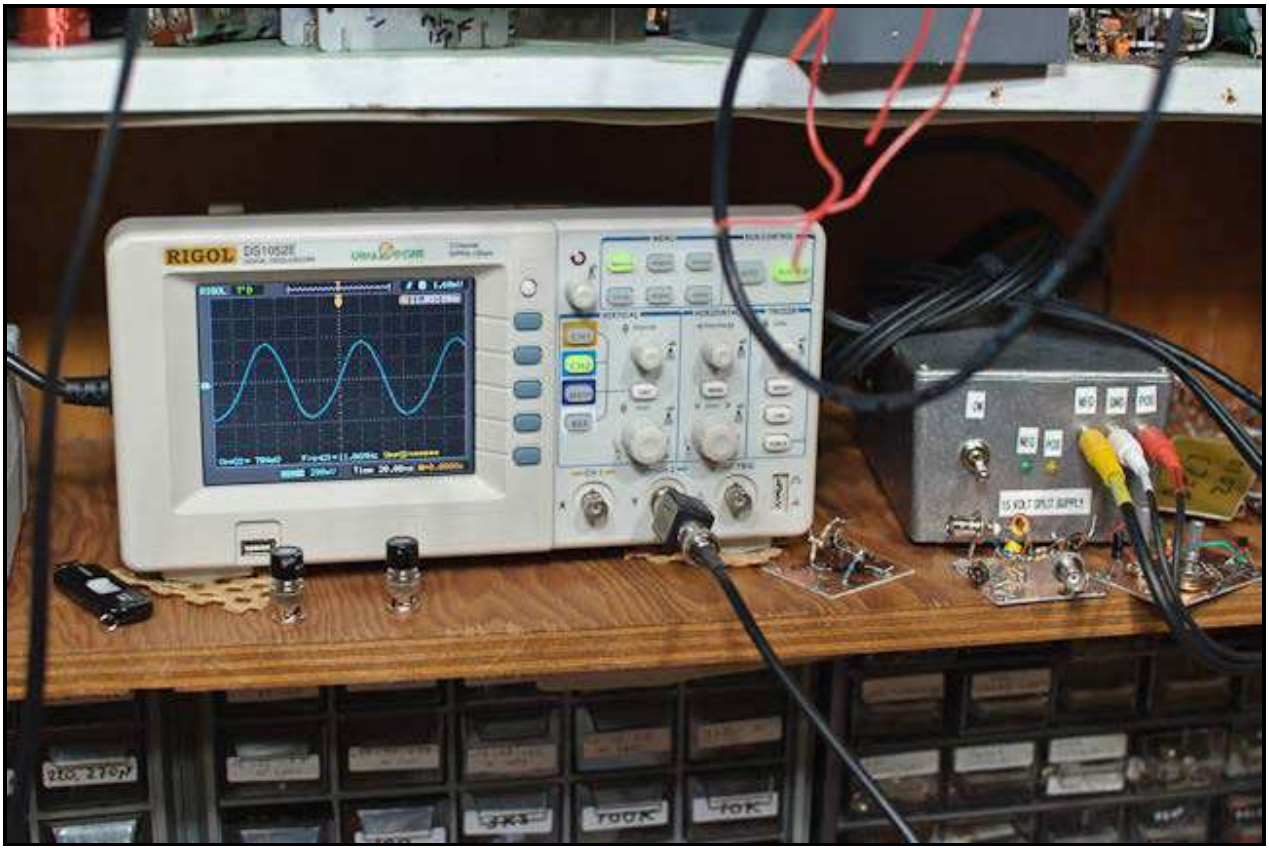

Above — Measuring in a 50 Ω environment. Bliss! Я люблю это.

RF Current Sampler

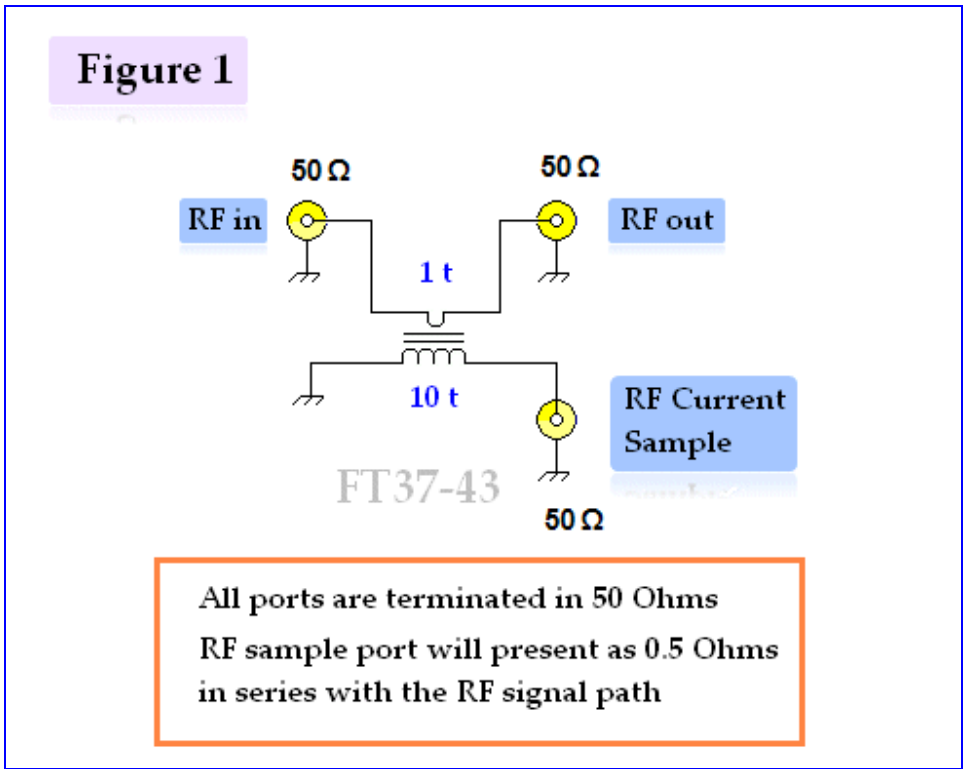

Figure 1 shows a basic circuit to sample RF current from a power stage such as a QRP transmitter. Many experimenters lack 50 Ω step attenuators rated to handle transmitter-level power. One basic solution is to sample the RF current of the power amplifier using a wideband step-

down transformer. Terminate the RF current sample port with a 50 Ω impedance device. This may include a spectrum analyzer, power meter, receiver with an attenuator, or a 50 Ω terminated oscilloscope.
A usage example = examining a transmitter's spectral purity with a spectrum analyzer. The output power at the sample port will drop by 20-22 dB. A 50 Ω impedance step attenuator can be used to further reduce this power level to whatever you want. For this chore, a typical experimenter's 1-2 watt step attenuator works, since it never "sees" the higher wattage transmitter power.

For example, a 5 watt amplifier 20 dB down is 0.05 watts or 50 mW at the RF current sampler port. 50 mW = 17 dBm. To examine this signal with a spectrum analyzer you may wish to decrease the power down to -27 dBm. The following chart shows the basic process.

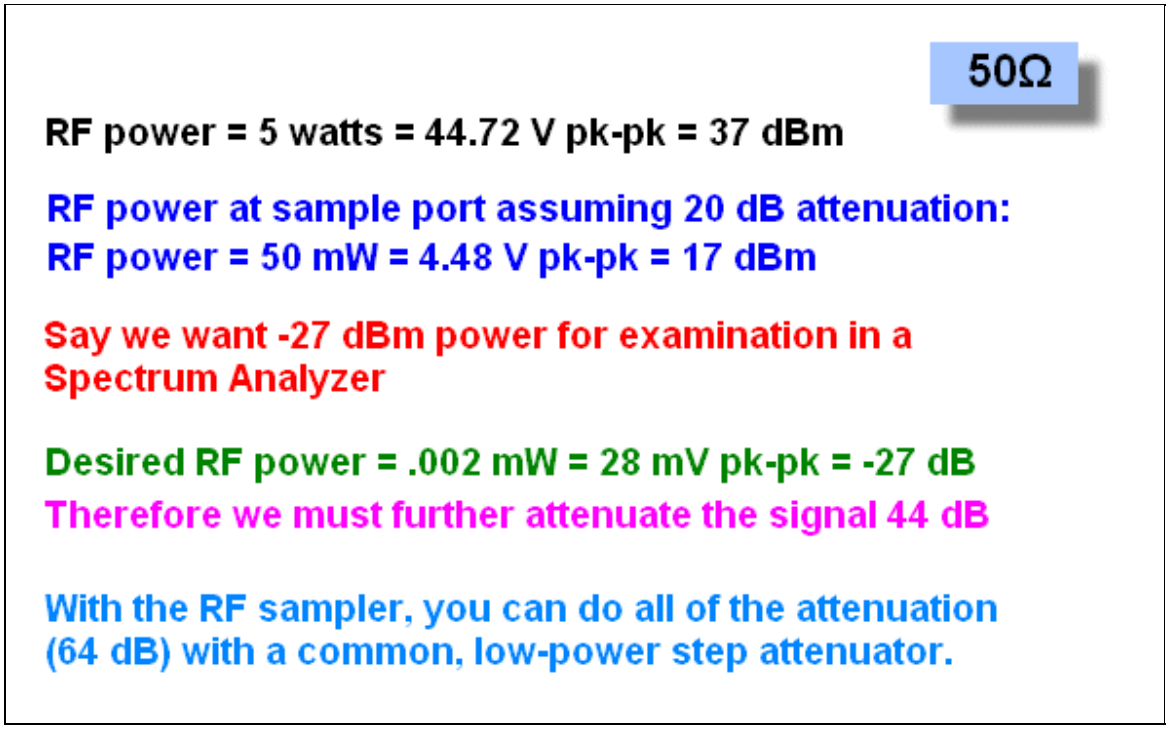

A Hammond chassis shields the RF current sampler used on my bench.

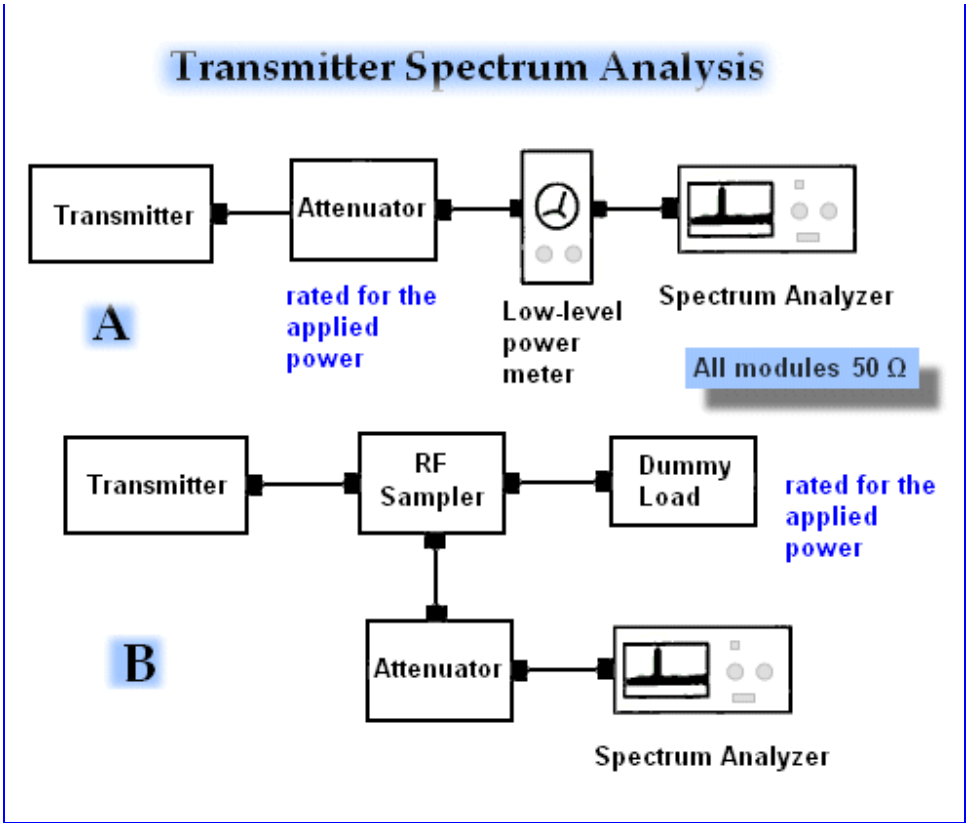

The above graphic illustrates 2 methods to examine the output of a transmitter in a spectrum analyzer. Method B is described above. The dummy load must handle the transmitter output power, however a 5 or 10 watt dummy load is easy to make. Method A requires a step-attenuator which can handle the transmitter output power. The low-level power meter promotes the need to quantify the output power before you connect anything to the output of the attenuator. This is also true for Method B.

Always measure the output power at the RF sample port with your oscilloscope or low-level power meter before hooking up any expensive low-level measurement device such as a spectrum analyzer! осторожно!

Miscellaneous Photos

Above — a 50 Ω BNC terminator. These are essential QRP work bench items and may be found on eBay for cheap.

Click for a photograph of 4 of my BNC RF port terminators: 27, 50, 75 and 100 ohms from left to right — useful to calibrate and test RF circuitry.

RF Workbench Page 2

Welcome to part 2 of a web series exploring basic RF measurement and bench practices. This installment builds on the information from the RF Workbench Page 1

I share introductory and practical content on attenuation, the return loss bridge, insertion loss or gain and spectrum analyzers. Consult EMRFD and use your favorite web search engine for more information.

The Attenuator Network

Like onions in your kitchen, the importance of attenuators can't be overstated. On the bench, attenuator pads go in nearly every test circuit to deliver correct power and/or help match port impedances.

Think of attenuators as passive networks that intentionally insert power loss between 2 components independent of frequency. For example: you might follow a 50 Ω signal source with an attenuator to decrease its power, increase its return loss, and/or buffer it from downstream impedance changes.

- Most attenuator networks have fixed input and output impedances.
- The input and output impedances may be the same, or different.
- Attenuation may be fixed or variable. Most often, we use simple, fixed resistive pads that function as voltage dividers.
- Express attenuation in dB.
- Attenuators increase return loss and reduce VSWR.
- Attenuators may function as buffers to isolate stages.
- All attenuators on this web site feature 50 Ω input and output ports.

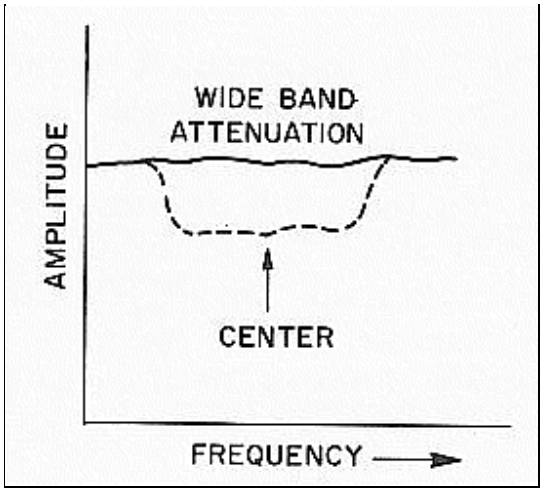

The desired response of an attenuator network. Practically speaking, device construction techniques including shielding will limit how high in frequency your attenuator will properly operate.

A pair of commercial 50 Ω input/output impedance step attenuators from the past. Occasionally, you'll find them for sale at Ham festivals or estate sales. Most work well for HF and perhaps even VHF work depending on their design and condition. Visually examine and test the attenuator before use.

How to Design and Build Attenuator Networks

To design attenuators with a 50 Ω input and output impedance, I recommend viewing a table. Click for a table.

After choosing the degree of precision; solder up 2 or 3 resistors and you're done. Nearest value 5% tolerance resistors offer reasonable precision for our popcorn circuits, but combining 1% and 5% tolerance resistors works too.

Choose low inductance resistor such as carbon film types and strive for short lead lengths. Well consider resistor power dissipation — for example, an 8 dB attenuator pad will dissipate 84% of the RF passed through it. I have seen attenuator pads that were exposed to high power and some or all of the resistors were burnt and turned to charcoal. Clearly the operator did not regard the power rating of the attenuator resistors. Refer to EMRFD Section 7.4 for practical information concerning attenuator design and power dissipation.

Three of the attenuator pads from my bench attenuator drawer. When using Ugly Construction or its variants, you can solder in, change, or remove attenuator pads at a whim. A small stock of these pads speeds up your work flow.

A 10 dB attenuator pad from my collection. This box uses two 100 Ω (5%) resistors and a 68 ohm (1%) resistor for the 96.2 and 71.2 ohm

resistances called for. I used the 1% tolerance part because all my 68 Ω resistors are metal film 1% tolerance 1/4 watt types. Perhaps, I'll pursue a closer match to the calculated resistor values 1 day, but this module works okay. You may also stick 2 seperate attenuators in the little Hammond box shown.

Two commercial BNC feed-through (in-line) attenuators. I use these *every* day and prefer them over homebrew R networks since they don't require a coaxial cable. I own many: two 6 dB, two 10 dB, one 3 dB and a 20 dB: all were purchased on eBay.

Two commercial SMA in-line attenuators for my VHF and UHF experiments: 6 and 15 dB. Click for a marker table with 4 data points derived from sweeping these 2 filters.

Step Attenuators

A step attenuator belongs on every serious RF workbench. They allow in-situ attenuation adjustment with a degree of precision as low as 1 dB. Step attenuators are nothing more than switched calibrated resistances and the switches can be SPDT, relays, rotary or digitally-controlled types. The quality and price of commercial attenuators varies widely. Experimenter concerns include the minimum attenuator insertion loss, power rating, return loss, noise from switch contacts and noise from the resistors themselves.

A homebrew step attenuator makes a great weekend project and almost every radio handbook contains 1. Web linked projects plus commercial kits may be found online — use your favorite search engine to find them.

Some homebuilders prefer 1% metal film resistors to keep resistor noise down. Stick your step attenuators in a metal, RF-proof box and insert quality interfaces such as BNC, N or SMA connectors. Your needs, budget and parts collection determine the outcome when you home build one.

Serebriakova Attenuator - Серебрякова аттенюатор (50 Ом)

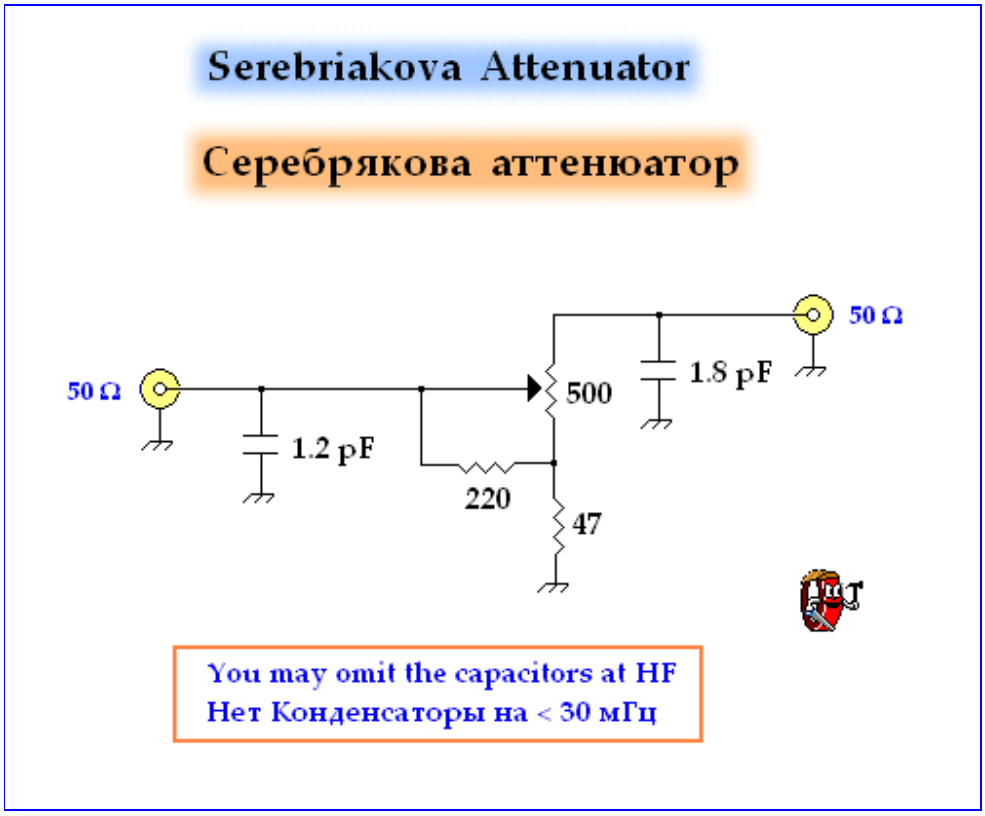

The Serebriakova; a simple, variable attenuator well suited for QRP homebuilding. Filled with gratitude to its Russian designer's family, I share this contribution with my readers. This attenuator network makes signals smaller or larger in a 50 ohm environment via a potentiometer. My analysis indicates acceptable performance considering its simplicity. The input match is close to 50 Ω across the range of the potentiometer. The output match across the potentiometer range is mediocre. Click here for a DC match analysis from Wes, W7ZOI. As shown, you wouldn't place this device on your main bench signal generator output as the output impedance diverges widely during amplitude adjustment.

Add fixed attenuator pads on the input and/or output to improve matching into 50 ohms. This circuit could serve in multiple applications including an RF gain control on a receiver front end, for bench measurement (when adapted) and for a low-level transmitter gain control. The Serebriakova attenuator may function up to 500 MHz in a carefully constructed, shielded box. The input and output capacitors may be omitted below 30 MHz. The attenuation varies a minimum of 20 dB when turning the potentiometer from CCW to CW. Click for a build by he yl.

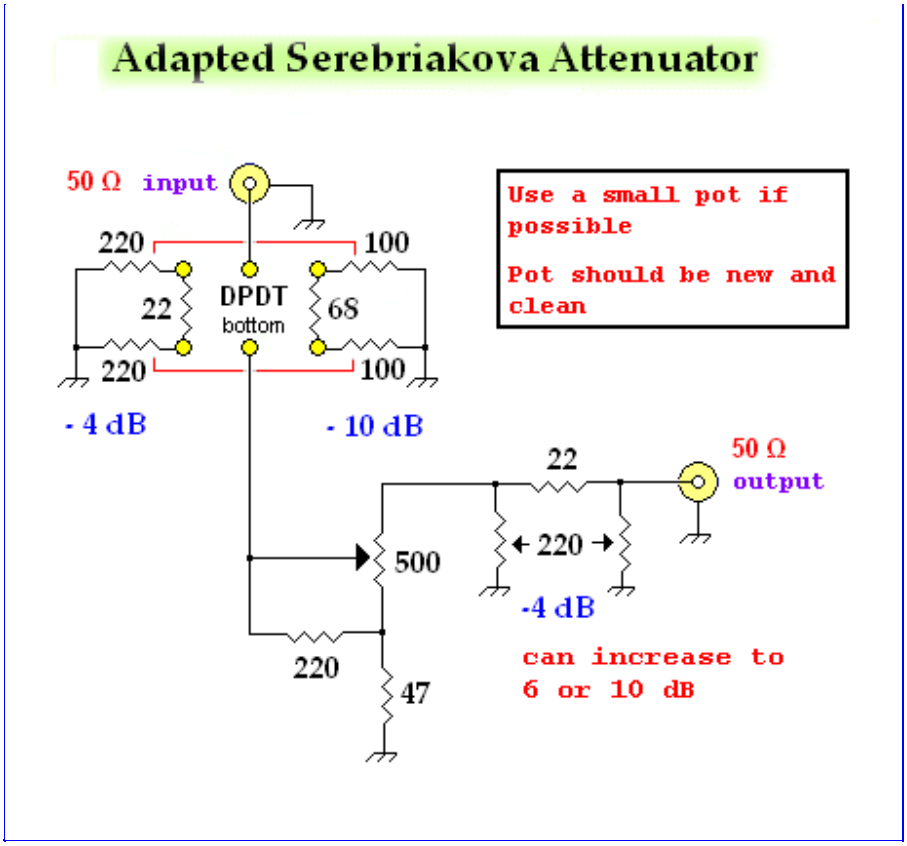

A variant of the Serebriakova attenuator is shown above. Input and output matching are enhanced by fixed attenuator pads. The input match into 50 ohms is fine. After testing, I learned that the fixed 4 dB output attenuator pad is likely too low to ensure a wide range output match into 50 ohms. A 6 or 10 dB output pad is preferable, however, if this is your only variable attenuator, the device would then only be usable for very low-level work. You can decide what value of input or output pads to use.

A new, clean and small size 500 ohm pot works best. Store your potentiometer collection in sealed plastic bags to keep out workshop and house dust.

Serebriakova Attenuator RL and VSWR @ 14 MHz			
Setting	Input -4 dB	Input -10 dB	Output
CCW	27.9 dB; 1: 1.08	30.6 dB; 1: 1.06	9.6 dB; 1: 2.00
Midrange	17.08 dB; 1 :1.30	25.2 dB; 1: 1.12	10.5 dB; 1: 1.85
CW	25.4 dB; 1: 1.11	30.8 dB; 1 :1.06	21.2 dB; 1: 1.19

Shown above are return loss (RL) and VSWR measurements performed on the adapted Serebriakova attenuator shown above. Clearly the input match is better than the output match. The output match did not significantly change when the attenuation switch was moved from 4 to 10 dB attenuation or back.

Based upon these values, it might be a better compromise to put a 3 to 4 dB pad on the input and a 10 dB attenuator pad on the output to ensure an output RL of at least 20 dB. Some might argue that the output RL should be higher. Perhaps, but the match is pretty good for such a simple circuit. Let's put it in perspective; a commercial signal generator that sells on the Internet for $450.00 U.S dollars was measured by a builder I know in the UK and he found a best case RL of 10 dB ! Jim later sold it and built a homebrew signal generator with a 35 dB return loss at all frequencies.

Fixed attenuator pads provide a good remedy for mismatched ports and I discuss why and how in the next section.

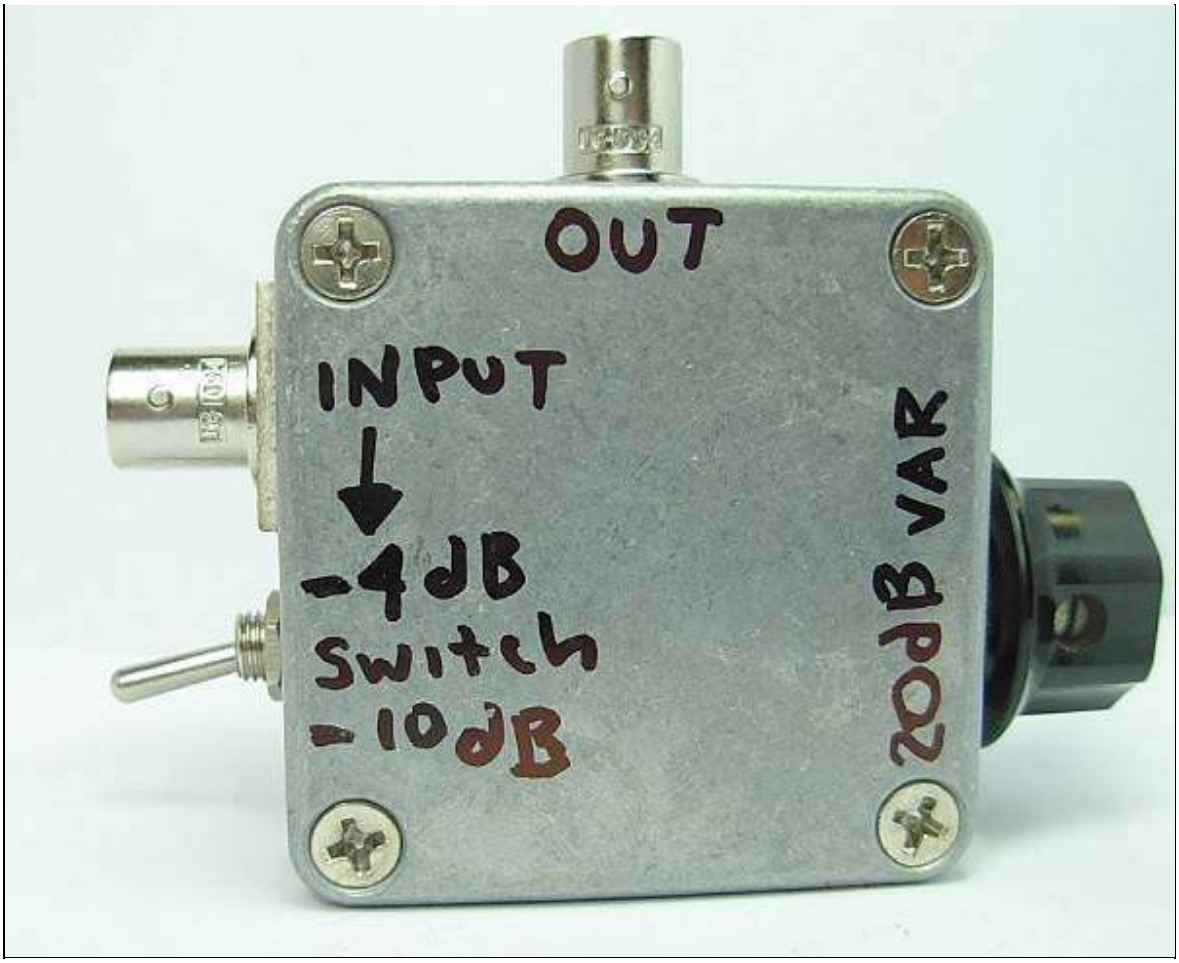

The shielded, adapted, Serebriakova attenuator. When home building your personal version, strive to make the AC connections as short as possible. The above device has nearly 23 dB of variable attenuation at 14 MHz. If you can't build, find, nor afford a precision step attenuator for your QRP workbench, this device may work okay for you.

Impedance Matching, Return Loss and VSWR

We radio folks build, buy and apply lots of gear with a stated *nominal 50 Ω input or output impedance*. In truth, a *pure* 50 Ω impedance occurs rarely and components in an RF system are frequently mismatched. Almost every Ham radio operator matches their antenna impedance to their feed line + radio to maximize transmitter output power — but radio and antenna system matching is often the only case where these Hams match their gear.

In contrast, we experimenters, tirelessly match our 50 ohm RF system components — this work flow avails our **modus operandi** on the bench**.** And so, we builders match the input and/or output ports of *all* our RF stages: signal generators, filters, splitters, antennas and so on. You can easily measure the impedance match of your RF components with a basic device based upon a Wheatstone bridge; the return loss bridge. First, let's discuss matching a little more:

On the RF Workbench, we talk about return loss, reflection coefficient and VSWR to quantify impedance matching. I only consider return loss and VSWR on this web site.

When 2 system components are impedance matched, maximal power transfers from 1 device to the other. If the impedances are different, RF power is reflected back to the signal source. This reduces the amount of power delivered to the load. Transmitted and reflected waves moving along a transmission line superimpose and cause standing or stationary waves. The greater the impedance mismatch between the 2 components, the larger the amplitude of the standing waves. Mathematical formulas compute how much power is lost due to mismatch. Consider reading a great tutorial on SWR, Return Loss, and Reflection Coefficient linked here by Wenzel Associates.

Return Loss

Return Loss = the difference between the outgoing incident power and the reflected power as a result of the mismatch between the the signal source and its load. Return loss is expressed in dB as a positive number on this web page. The higher the return loss, the better the impedance match. An ideal prefect match would have a RL of infinity; that is, no power is reflected back to the signal source and all of the incident power is delivered to the load. If a circuit has no load (open circuit), the RL is 0 dB — all of the power is reflected back to the signal source.

Other terms quantifying return loss are S11 and S22, however S11/S22 are the negative of return loss: RL = 20 dB or S11/S22 = -20 dB. We say S11 as S — one — one and S22 as S — two — two. I discuss these S-numbers, or Scattering Parameters elsewhere.

VSWR

Voltage standing wave ratio is another measure of how well the components in an RF network are impedance matched. Increasing the return loss lowers the VSWR and vice-versa. Most amateur radio enthusiasts are familiar with VSWR and often refer to it as "match" or "SWR". RL and VSWR can be derived mathematically from one other. VSWR = [10^(RL/20) + 1] / [10^(RL/20) - 1]. **Note X ^ Y means X raised to the power of Y therefore 2^3 = 2x2X2 = 8.**

Thus a RL of **10 dB** = 1: 1.92 VSWR and **20 dB** = 1:1.2 VSWR and **30 dB** = 1:1.07 VSWR

In EMRFD, Wes presents a return loss bridge as Figure 7.41. This circuit, shown below is easy to build and use.

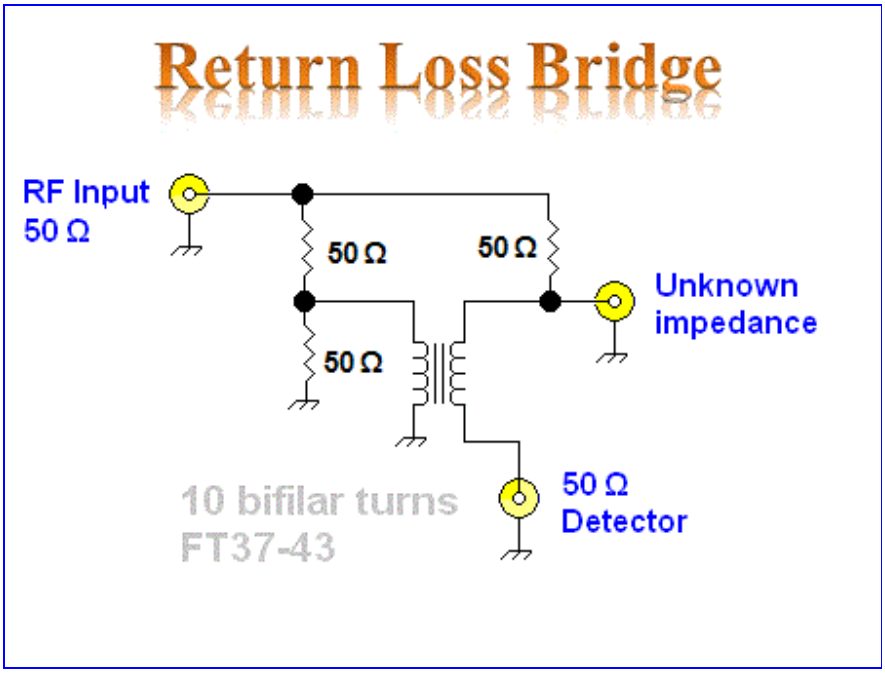

The 50 Ω impedance detector may include a spectrum analyzer, power meter, receiver with an attenuator, or a 50 Ω terminated oscilloscope. On my bench, a 50 ohm terminated scope is favored.

Let's measure the return loss of a 27 Ω resistor to learn how. The procedure with a 50 Ω terminated 'scope follows:

- Connect a 50 Ω output impedance signal generator to the bridge RF input port with 50 ohm coax;
- Connect a 50 ohm terminated oscilloscope to the detector port via 50 ohm coaxial cable;
- Record the peak-to-peak (open circuit) voltage with no load on the end of a short coax cable connected to the unknown Impedance port;
- Record the peak-to-peak voltage with "unknown" coaxial cable terminated with the 27 Ω resistor
- Calculate the power difference in dBm between these 2 peak-to-peak voltages.

Return loss = the difference in dB between these 2 values calculated by hand or with software. Please refer to the RF Workbench Page 1 for information how to calculate power. I wrote a JavaScript Applet that take these 2 peak-to-peak voltages and calculates RL and VSWR; its labeled **K** on this web page.

Before measuring the unknown RL of a circuit, we usually connect a 50 Ω terminator to the unknown impedance port and calculate the best possible return loss: we refer to this value as bridge directivity — the best possible match for that return loss bridge at that test frequency. I keep a permanent 50 Ω terminator + a barrel connector on my bench for this purpose.

Click for a photo of the gear I use for all RL measurement. *Best viewed at full resolution*

Lets run through the procedure to measure the return loss of a 27 Ω resistor again, but with added photographs and 'scope captures. I tested at 14.070 MHz.

Above — We'll measure the return loss of this device; a 27 Ω resistor soldered on a BNC connector. We call this a resistive terminator and I keep a small collection of 27 - 100 Ω terminators on-hand for calibration purposes.

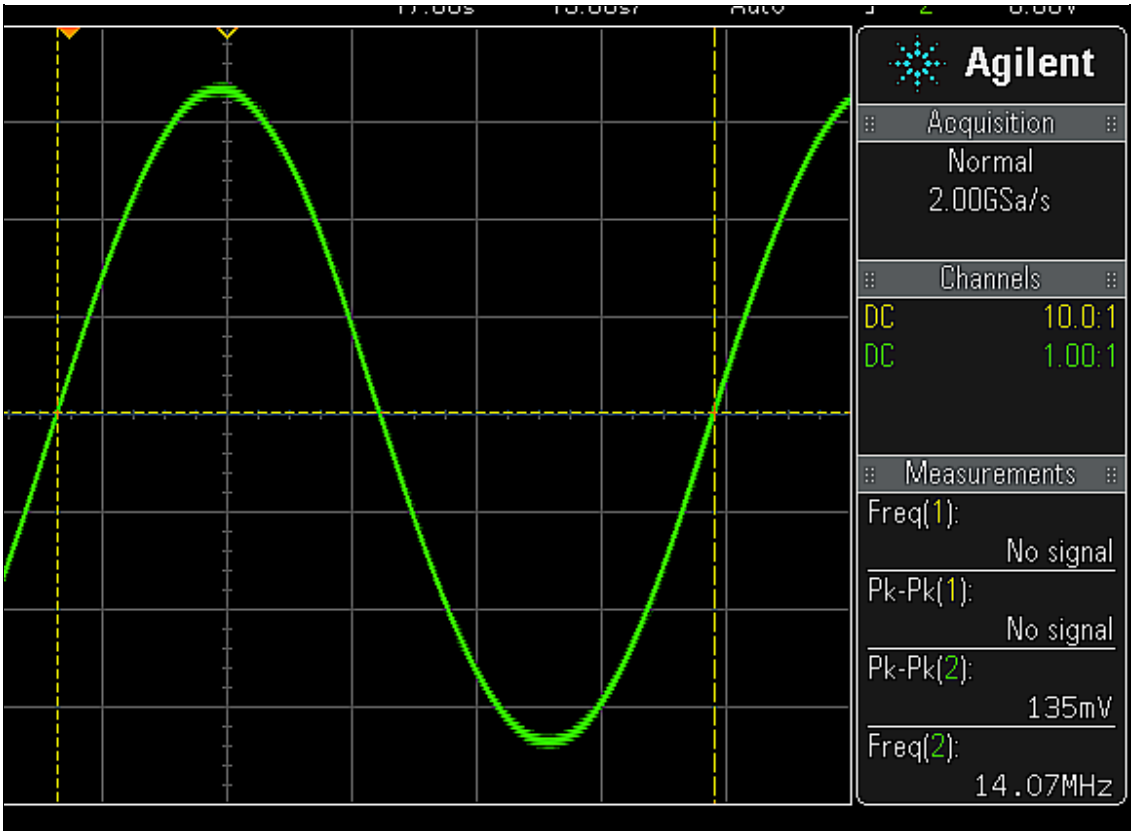

Shown above — The peak-peak voltage with a 14.07 MHz oscillator connected to the RF port; a 50 Ω terminated scope connected to the detector port; and a 20 cm — unterminated — 50 Ω cable connected to the unknown impedance port. **The open circuit measurement.**

Above — Next, I connected the 27 Ω terminator to the unknown impedance coaxial cable with a through-connector interface.

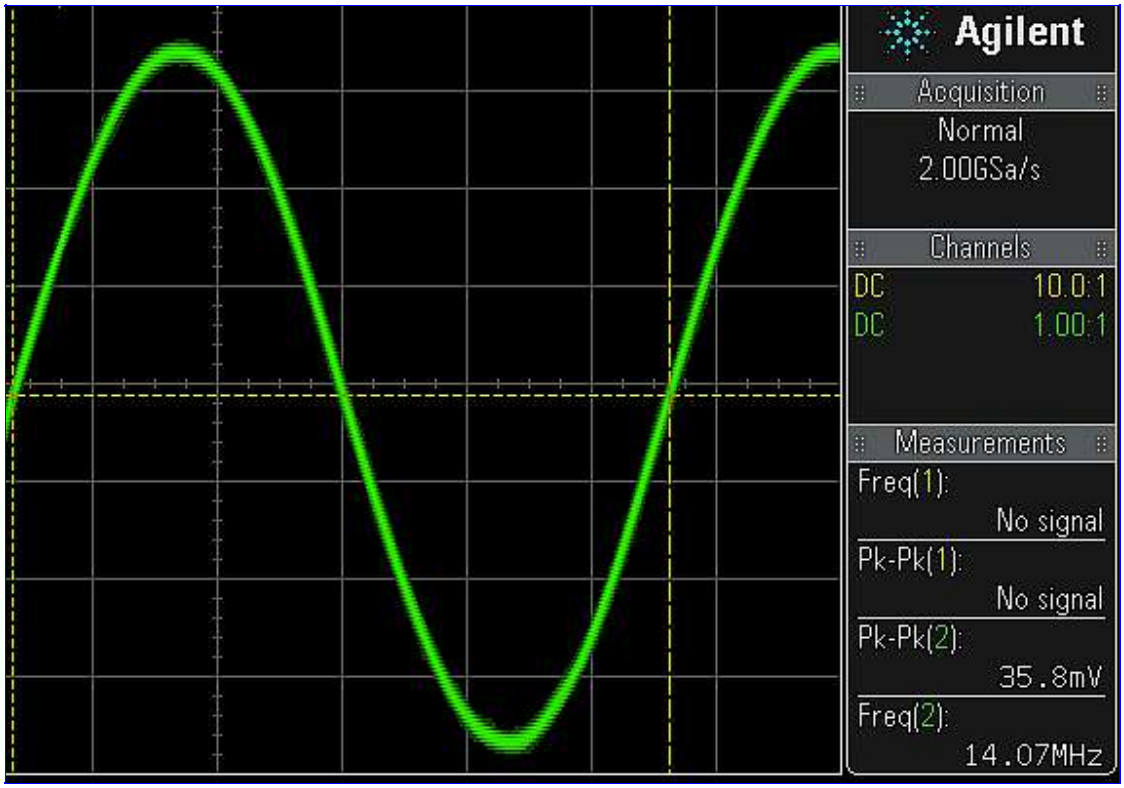

Shown above — The peak-peak voltage with a 14.07 MHz oscillator connected to the RF port; a 50 Ω terminated scope connected to the detector port; and a 27 Ω resistive terminator across the end of the unknown impedance cable**. The reflected signal from a 27 Ω resistor.**

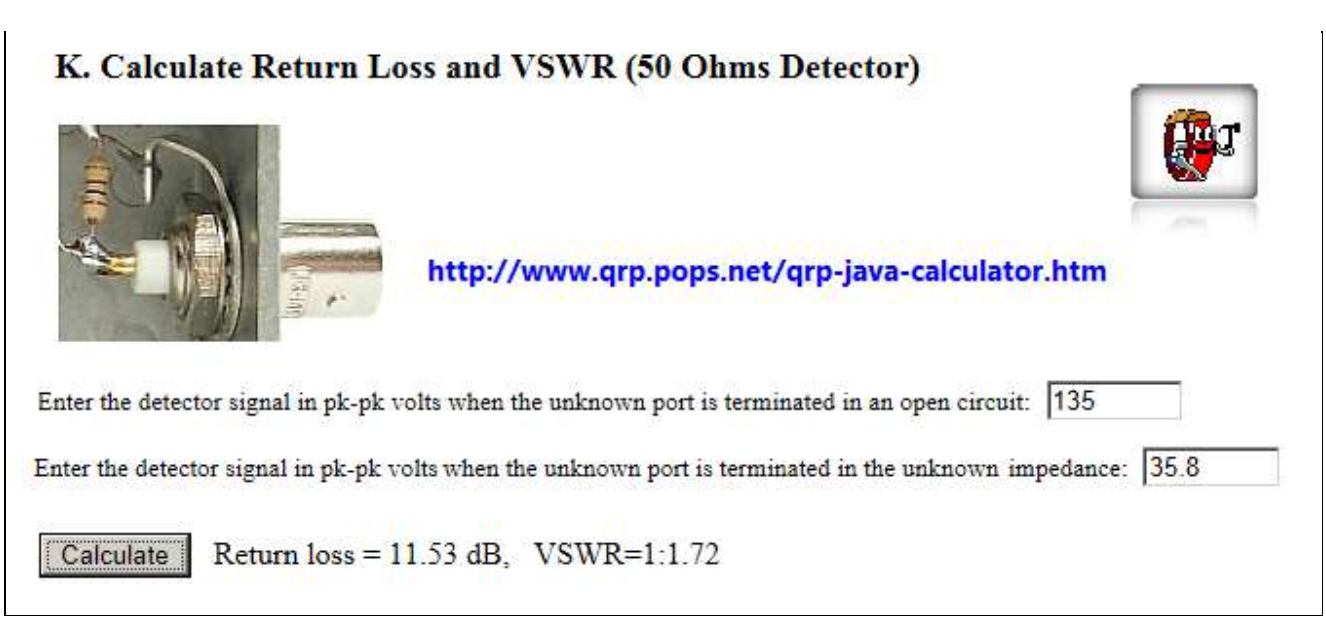

Shown above — Calculating the return loss and VSWR of the 27 Ω resistor with my JavaScript Applet **K**. mV versus volts peak-peak does not matter since we calculate a ratio of power.

Use the return loss measurement procedure depicted above to measure the return loss of any device you choose. If your D.U.T. has 2 ports, terminate the unmeasured port in 50 Ω. I show further RL measurment examples on RF Workbench 3.

I measured the return loss of some commercial gear in my shack and yard and will share 2 examples: 1) An expensive commercial transceiver I borrowed had an input port return loss of 15 dB (a 1.4:1 VSWR) The return loss of 15 dB indicates that the reflected wave power is 15 dB lower in power than the incident wave. 2) With a borrowed commercial bridge, my tuner-matched antenna revealed a return loss of ~60 dB.

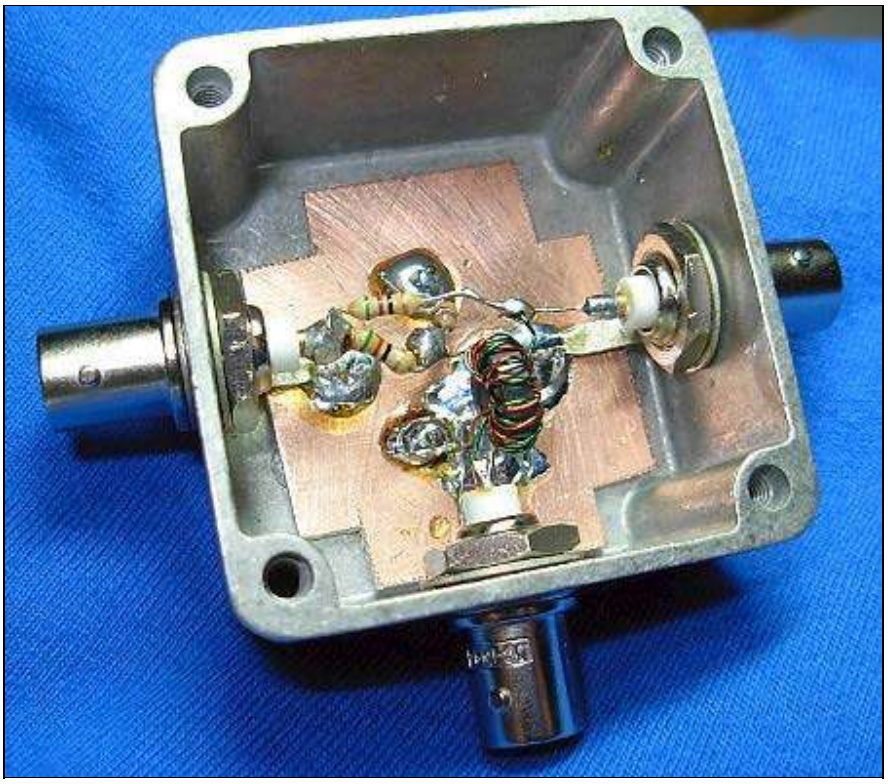

A RL bridge from my bench built with 51 Ω 5% tolerance resistors. I show a better RL bridge and some other experiments on RF Workbench 3.

Return Loss and the Attenuator Network (How Do Attenuator Pads Improve Component Matching?)

We routinely employ attenuator pads to increase return loss in a 50 Ω RF environment. For example, let's say you're testing a signal generator and measure a return loss of 6 dB. If you place a 10 dB attenuator pad after the signal generator, the return loss increases to 26 dB. If we used a 6 dB pad instead, the return loss would now = 18 dB. In both cases the return loss is increased by 2x the attenuator pad value. The doubling of return loss occurs because both the incident wave and reflected signals pass through the attenuator pad — that's how attenuator pads

improve matching.

Attenuator pads reduce power, but that is why somebody invented the RF amplifier.

What is the minimally acceptable return loss for a device such as a signal generator? No single answer exists. The minimum return loss depends on the context: are you making precision circuits or just tuning an antenna?

Precision Circuits:

For amateur experimenter bench circuits, aim for a return loss of at least 20 dB. This often means adding an attenuator pad to the ports of your signal generator, amplifier, or other device to get a minimum 20 dB return loss. For an electronic engineer, the minimal return loss is probably higher; maybe 30 dB or so. I have read conflicting opinions about this and for some people — me included — design overkill is normal.

Antenna tuning:

When tuning an antenna for full transmitter output power, the minimal return loss is around 14 dB (a VSWR of 1:1.5). If you measure an antenna system return loss of 14 dB or better, the match is fine. Many Hams will protest a 1:1.5 VSWR and ardently chase a 1:1 VSWR on every frequency with their antenna tuner.

A Method to Measure Insertion Loss or Gain

Often, we want to measure the gain of an amplifier, or the insertion loss of a filter, or attenuator pad. I show how to do this with a 50 Ω terminated scope:

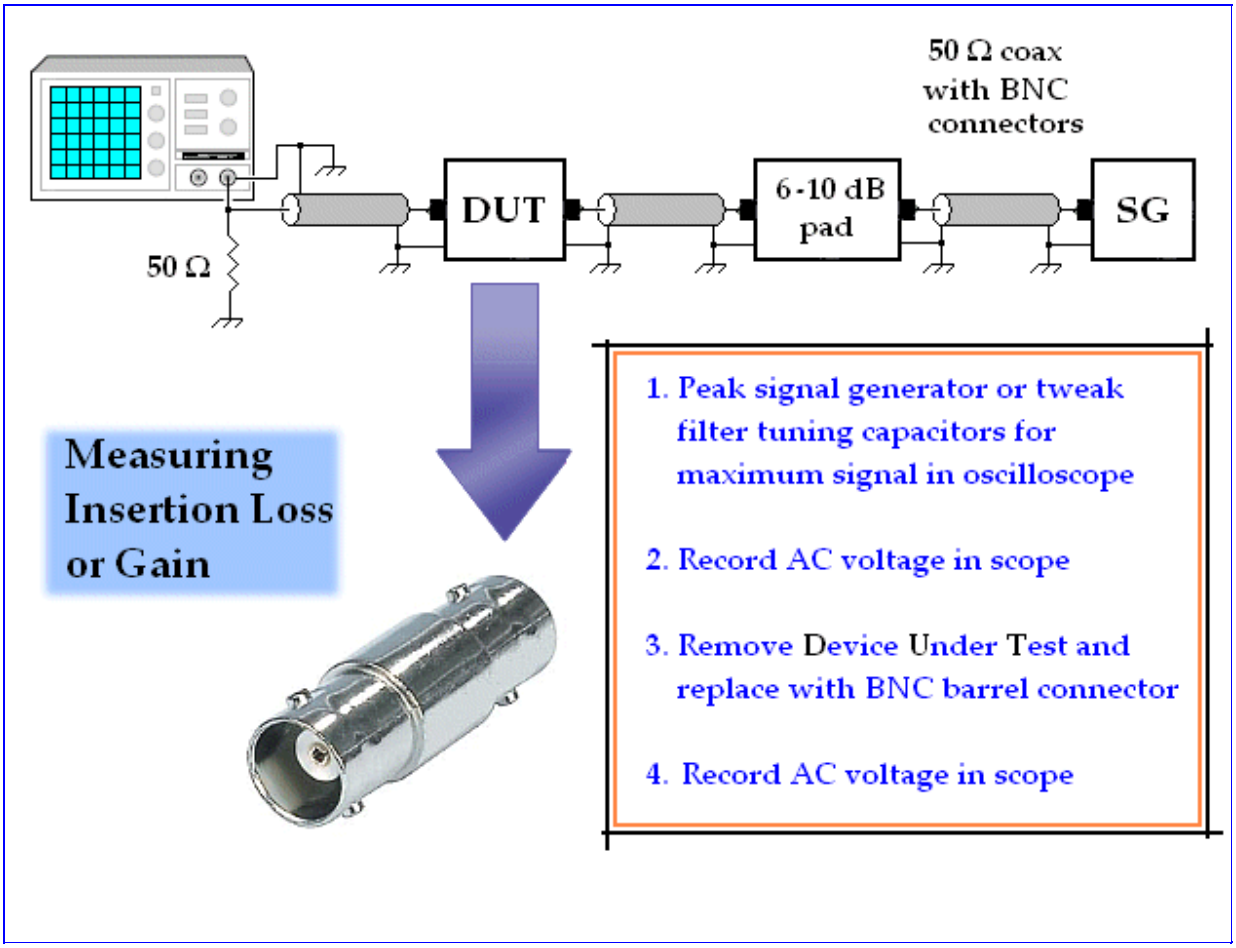

The circuit starts with a signal generator set to the frequency of interest. I show an attenuator pad in this diagram to stress that the signal generator output port must have a return loss >= 20 dB.

Connect the input of the 50 Ω **D**evice **U**nder **T**est to the generator output via 50 Ω coax

Connect the 50 Ω output of the D.U.T. to your 50 Ω terminated oscilloscope

Turn on the signal generator and if needed, peak the signal; In the case of a low-pass filter, the signal generator frequency control is tweaked to give a maximum pk-pk voltage in your 'scope. When evaluating a band-pass filter, tweak the filter trimmer capacitors for the maximum signal

at the desired center frequency. Signal peaking ensures that losses caused by the filters are not caused by the filter mistuning, or in the case of the low-pass filter, to allow for cutoff frequency deviation caused by component value variations. It may be necessary to increase the signal generator amplitude to view a good quality signal in your 'scope.

Record the peak-to-peak voltage.

Remove the DUT and replace it with a BNC through-connector and record this peak-to-peak voltage.

Calculate the power in dBm of the 2 recorded voltages — their difference equals the insertion loss or gain in dB. I wrote a JavaScript Applet to do this. Click and scroll to **H**

This awesome measurement technique controls the input and output impedance and uses the same coaxial cables with and without the D.U.T. for accuracy. Some builders might choose to terminate the D.U.T. with a 50 Ω resistor and measure with a 10X scope. The capacitance of the probe may alter measurement in some cases. As always, choose your measurement technique based upon whatever gear you own and how exacting your standards are.

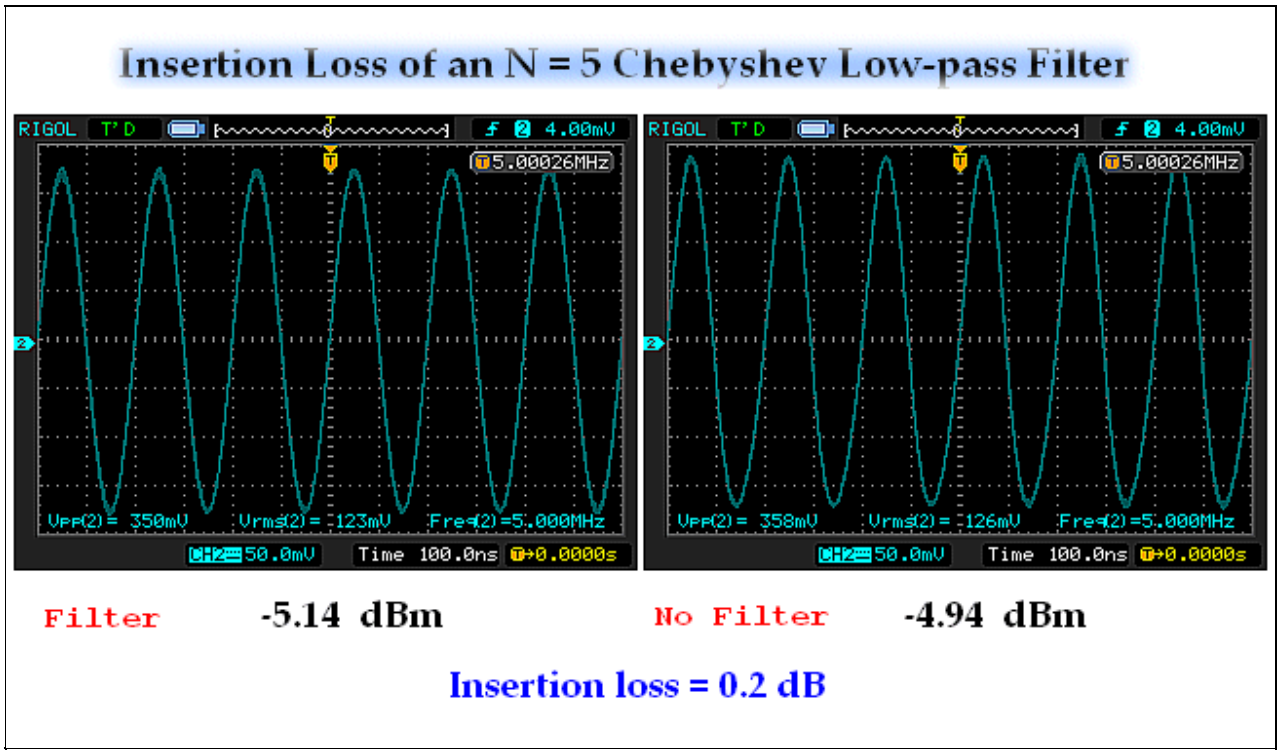

Spectrum Analyzers - Comments from the Workbench

Electronics professionals ruminate that spectrum analyzers are uncommon because experimenters perceive them as esoteric and difficult. My own opinion differs. Spectrum analyzers are relatively uncommon because of one reason - cost. I have watched prices on sites like eBay with amazement. The ads go something like this: 1.5 GHz spectrum analyzer for sale. Built in 1982. Ships in 2 pieces weighing over 22 kilograms. Minimum bid $1850.00. *And...sorry, I live in Florida, U.S.A. and in all likelihood, shipping these 2 heavy pieces is going to cost you a fortune. In the attached ad photos you can see lots of wear and tear, plus some screen burn-in on the display....* Guaranteed to turn on however!

Perhaps I exaggerate or even lampoon the perceived value of old boat anchor spectrum analyzers, but I have bought and sold cars for less money. Be prepared - spectrum analyzers are not cheap. They are however, very cool and open the door into a truly fascinating world. Frequency domain circuit measurement (spectrum analysis) addicts and intrigues. Homebuilding a spectrum analyzer is a serious option, but requires advanced building skills. Click and click for the W7ZOI/K7TAU project.

In recent times, the Rigol DSA-815 spectrum analyzer with tracking generator proved a game-changer to the bloated price of heavy, old and tired gear. Click for a Rigol datasheet. Signalhound also sells spectrum analyzers and tracking generators . A tracking generators *plus* spectrum analyzer allows you to sweep your device under test over a range of frequencies.

Prior to using a spectrum analyzer, I casually considered shielding stages or placing critical pieces in RF-proof boxes. Quickly I learned that RF in our home and community can and does get into your projects. p>

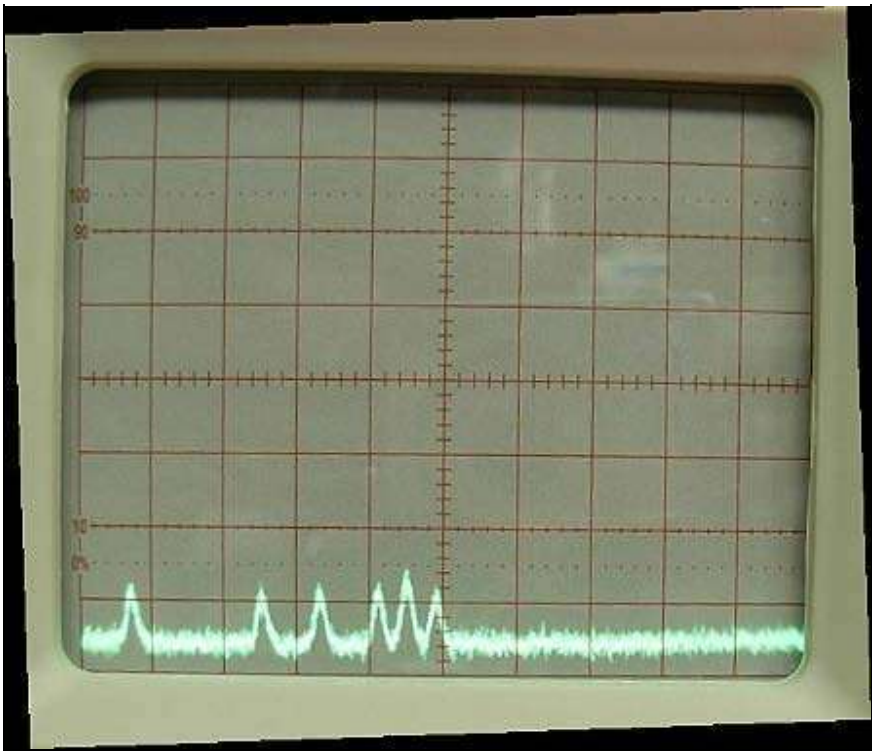

The center frequency of the display = ~150 MHz. The signal spikes appeared and disappeared after 4-9 seconds or so — after a little detective work with my scanner, I learned they were local police and ambulance FM radio conversations. I noticed this interference when I took the lid off a RF-tight band-pass filter — these signals arose in a 28 MHz superhet receiver !! While low in amplitude, experiences like this inform us to watch for lurking RFI.

I found numerous sources of RF in our home with a spectrum analyzer — the clothes washing machine during its spin cycle proved to be the worse RFI generator. RF-tight shielding with SMA, or BNC connectors and DC feed-through capacitors and aggressively decoupling and bypassing DC lines eliminated many of RFI problems during my experiments. I now better appreciate these anti-RFI techniques.

Spectrum Analyzer Calibrator

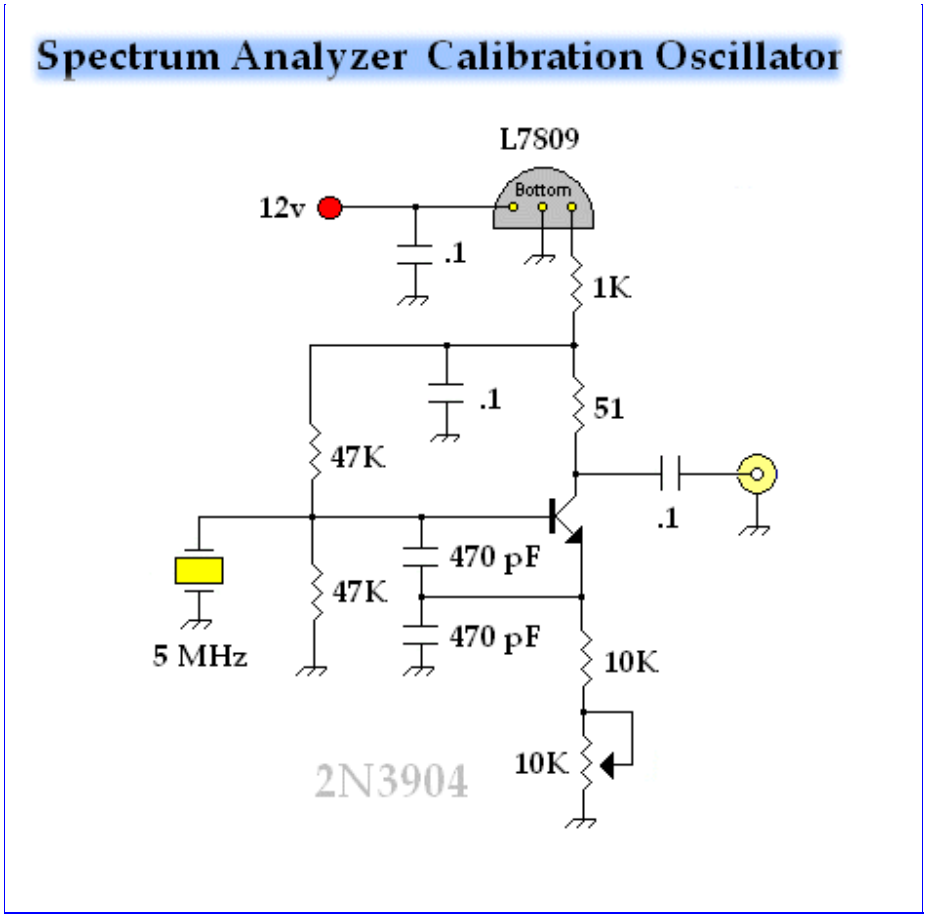

A harmonic rich, spectrum analyzer calibrator designed by Wes, W7ZOI and displayed with his permission. Adjust the 10K potentiometer to provide the output power needed to calibrate your spectrum analyzer. I set mine to -27 dBm. Be careful when connecting signal generators to your spectrum analyzer, since a higher than rated input power may destroy the mixer/front-end of your spectrum analyzer and cost you dearly.

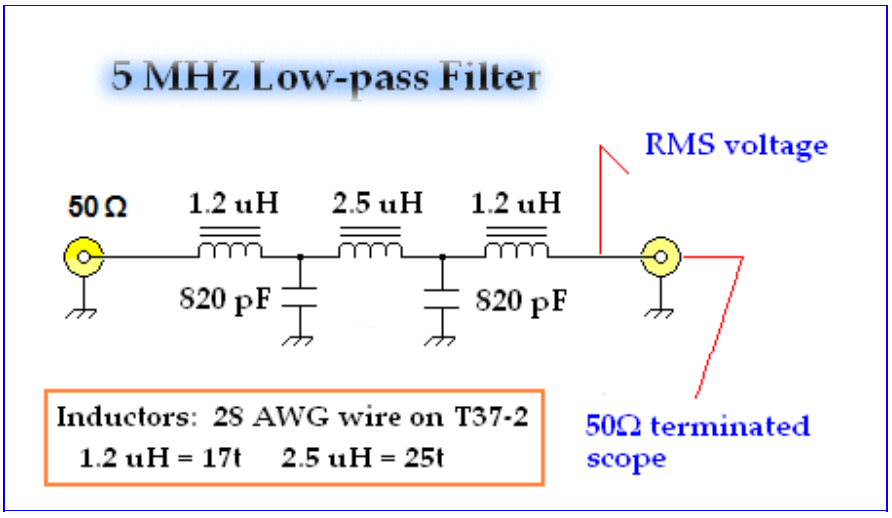

I used this filter to set the -27 dBm power needed to calibrate my spectrum analyzer.

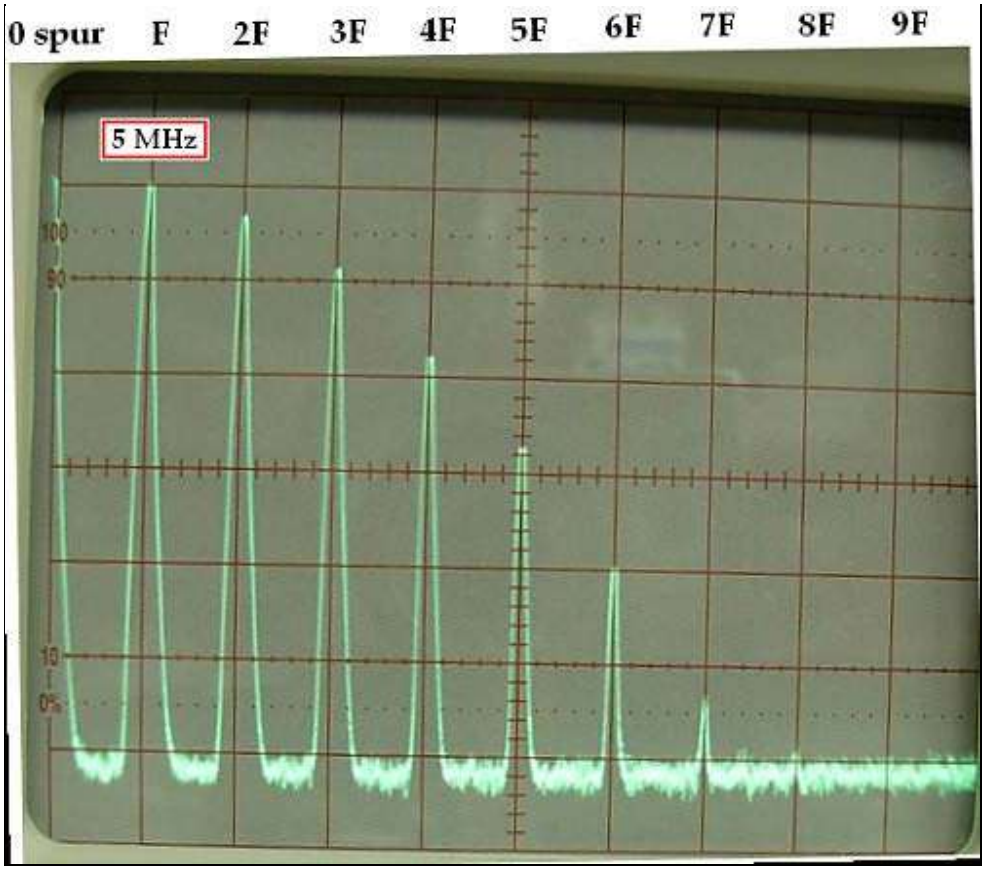

Spectrum analysis of the 5 MHz spectrum analyzer calibrator.

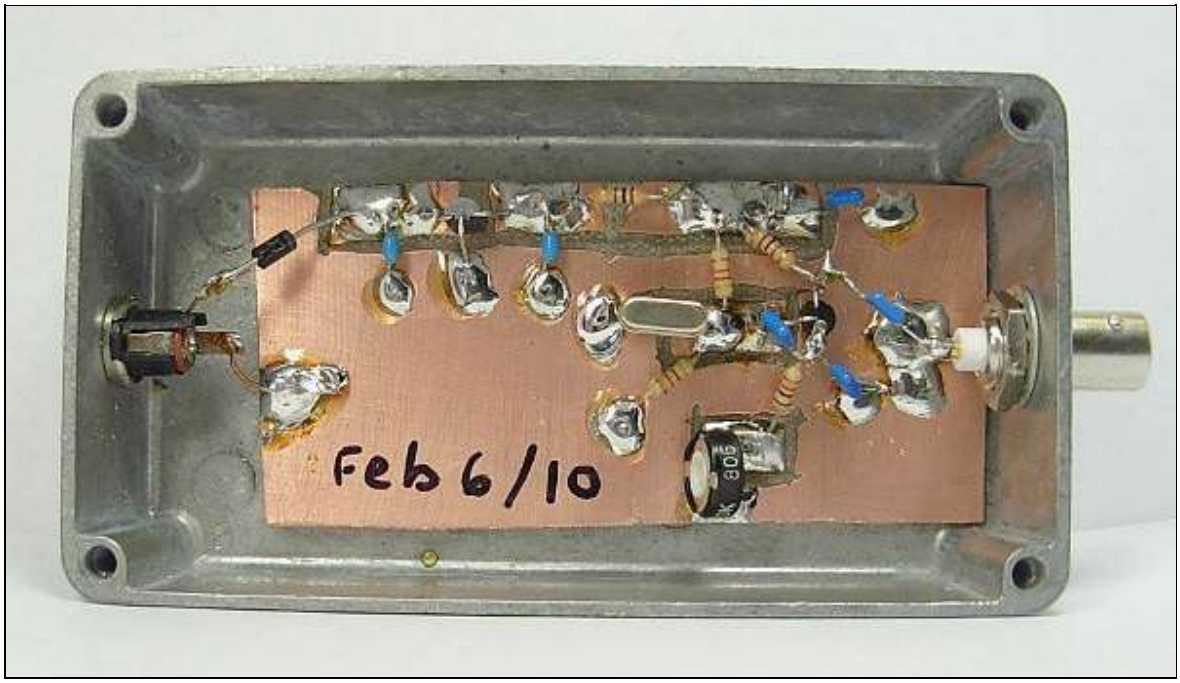

Breadboard of the 5 MHz spectrum analyzer calibrator.

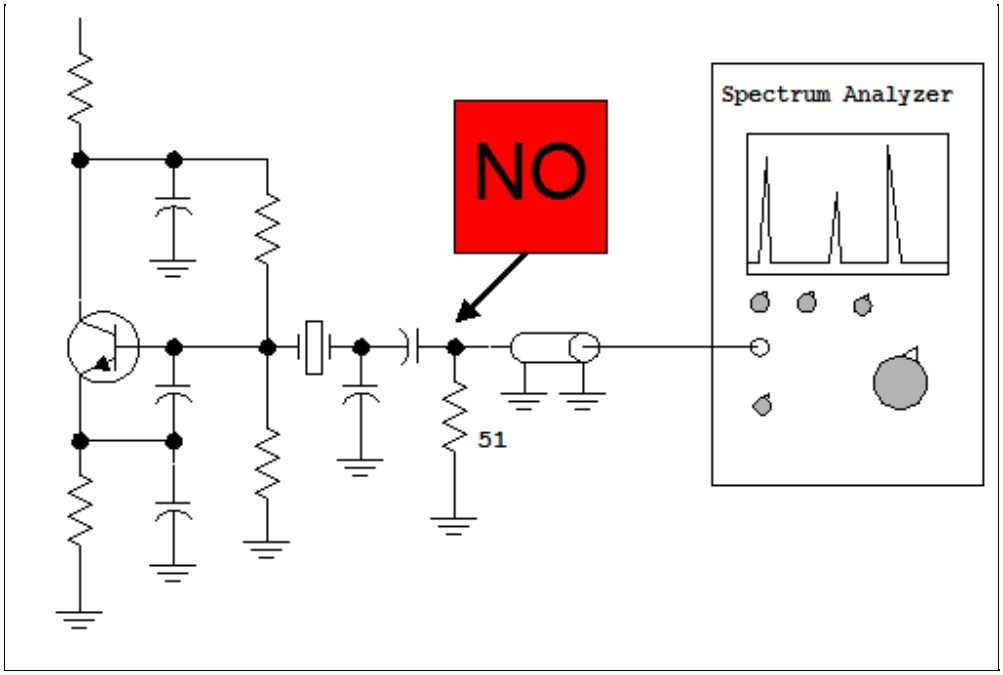

Don't use a "50 ohm" termination when measuring with a 50 Ω impedance spectrum analyzer.

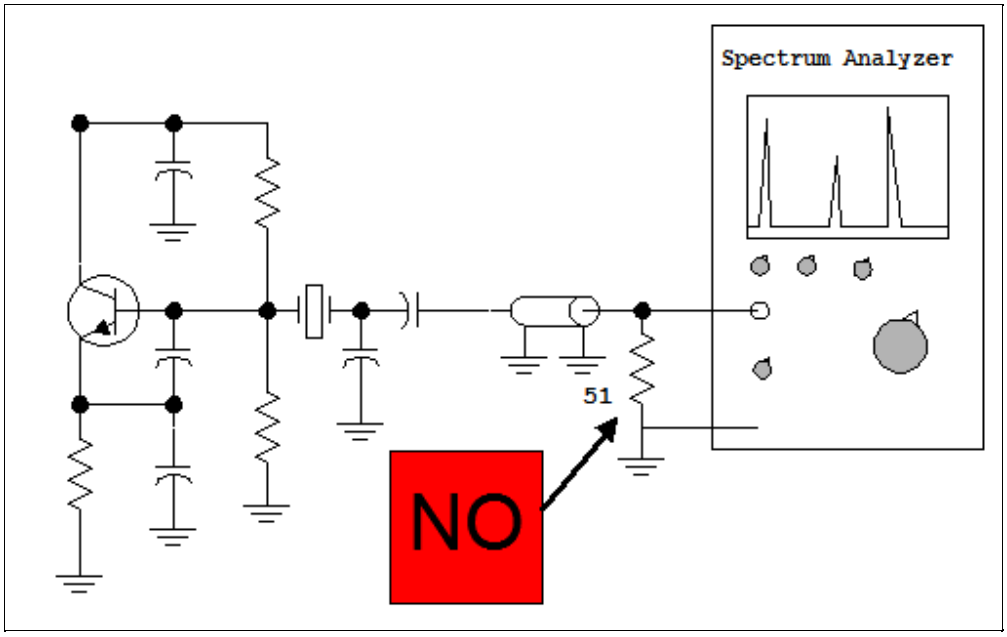

No resistor is required, as the the input impedance of the SA is 50 Ω.

Miscellaneous Photos and Notes

Some of the 50 Ω modules built during the RF Workbench page 1 and 2 experiments

1 3 6 9 30 dB
10 WATT LOAD

15542
HAT-6+
6 dB ATTENUATOR
50 OHM
15542
VAT-6
6 dB ATTENUATOR

Audio Transistor Input Impedance Experiments

Introduction

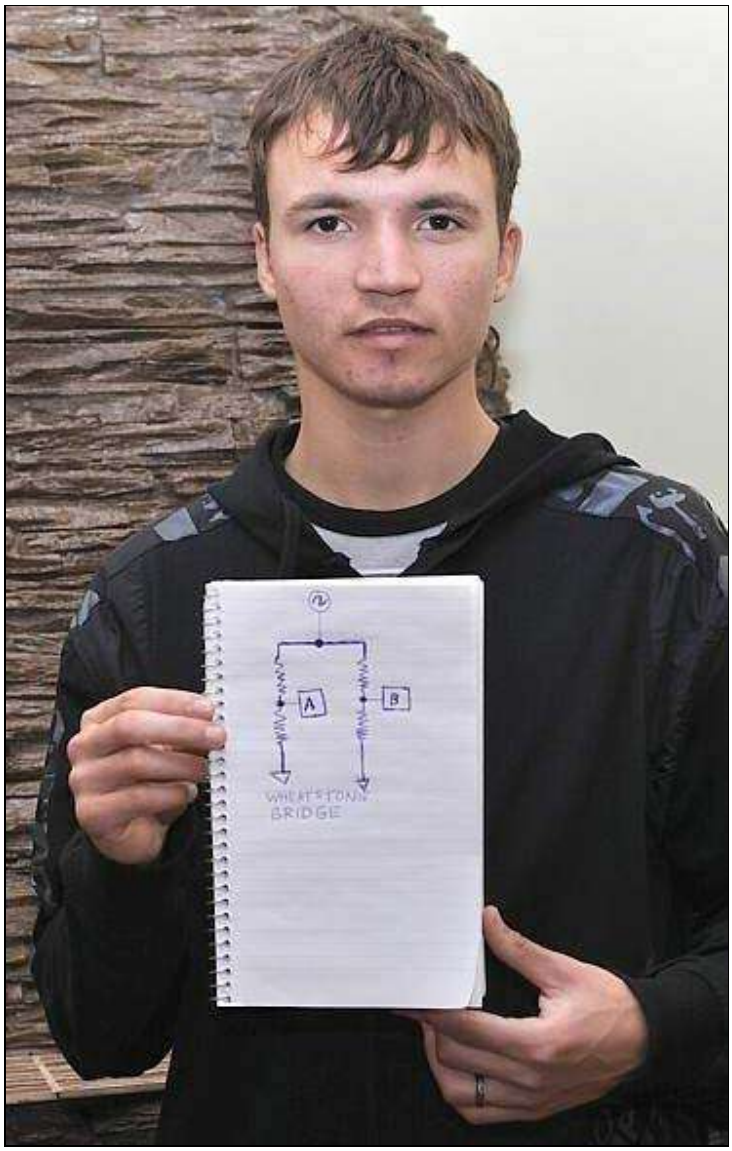

I examined audio transistor amplifier input impedance during Spring — Summer 2010 and generated enough content for a web page.

On this web page, I explore determining AF amplifier input impedance by using network theory and calculation, plus direct measurement with instruments containing a Wheatstone bridge. This content emphasizes learning through performing bench experiments and I hope it sparks your own experiments and research into impedance measurement test equipment and theory.

Many RF circuits require termination with stages containing a well defined input impedance. Consider, for example, amplifiers that follow L-C low-pass filters, diode ring mixers or crystal filters — a known impedance (usually 50 ohms) must terminate these stages to optimize return loss. A special case is the diode ring product detector; which must be followed by a 50 ohm input impedance audio amplifier. How do we design or assess a small-signal audio amplifier that has a 50 ohm input impedance? This question spawned every experiment on this web page — the content grew and evolved along with my understanding of this topic.

Audio transistor input impedance may be calculated with equations or software, however, doing the math or using or affording these programs might be problematic for some amateur builders. Additionally, component variances such as transistor Beta and different power supply voltages can causes significant differences between the theoretical and the actual input impedance realized. Further, amplifiers, such as a feedback pair that involve combinations of series or shunt feedback can be difficult to analyze accurately using equations during small or large signal analysis. It may be easier for experimenters to just measure and tweak amplifier components on the bench — the focus of this web page!

As an rank amateur, I have much to learn, and by no means am an expert in electronic design. If you see an error on this web site, disagree with my analysis, or have suggestions for improvement, please email them — I am an amateur hobbyist, who earns no money from this site, and who relies on the assistance of others to keep the content as accurate and vibrant as possible.

The topics:

Part 1: Some basic transistor network theory and how to calculate input Z

Part 2: 50 ohm input impedance Wheatstone bridge measurement

Part 3: Measuring unknown impedances

Part 4: Miscellaneous circuits, scans and photographs.

Notes:

Small signal analysis refers to modeling or examining an amplifier at a single operating point (its bias point) and applying linear equations which assess the amplifier with no signal applied. In small signal analysis, we assume that the signal is so small that transistor gain, capacitance and other factors are static.

Part 1: Some Basic Transistor Network Theory and How to Calculate Input Z

Some basic network theory plus methods to calculate the input impedance of common emitter and common base audio amplifiers.

Three basic small-signal transistor parameters include *beta,* emitter resistance *Re*, and bulk resistance *REB*.

Beta is the term used to designate the current gain of a common emitter circuit — it's the ratio of collector (output) current to base (input) current.

Small-signal emitter resistance; Re = 26 / IE ,or, 26 divided by the emitter current in millamperes. For example, an emitter bias current of 0.52 mA gives a small-signal emitter resistance of 50 ohms, or visa versa . Re is the resistance seen looking into the emitter whether the stage input is the transistor base or emitter terminal. Re is the dynamic resistance of the input junction due to carrier action.

REB represents the bulk resistance of the semiconductor not arising from contact resistance; in other words, it's the DC resistance of the base and emitter leads plus the pn junction. Typically REB = 2 to 6 ohms and is often ignored (your choice) when the current is low — say, for example, < 9 mA for a typical common-emitter voltage amplifier. In large power transistors or for switching operations, the typical REB value may vary. REB, in part, limits the maximal gain of a transistor.

The constant 26 used when calculating the dynamic resistance of a forward-biased PN junction is derived via calculus. Professor Kuhn's website link containing the math.

There is also a base spreading resistance generally known as 'rbb' that, in effect exists laterally across the transistor. A simple model puts rbb at about 100 ohms in series with the base and it's one of the causes of finite transistor frequency response. While interesting, rbb isn't discussed further.

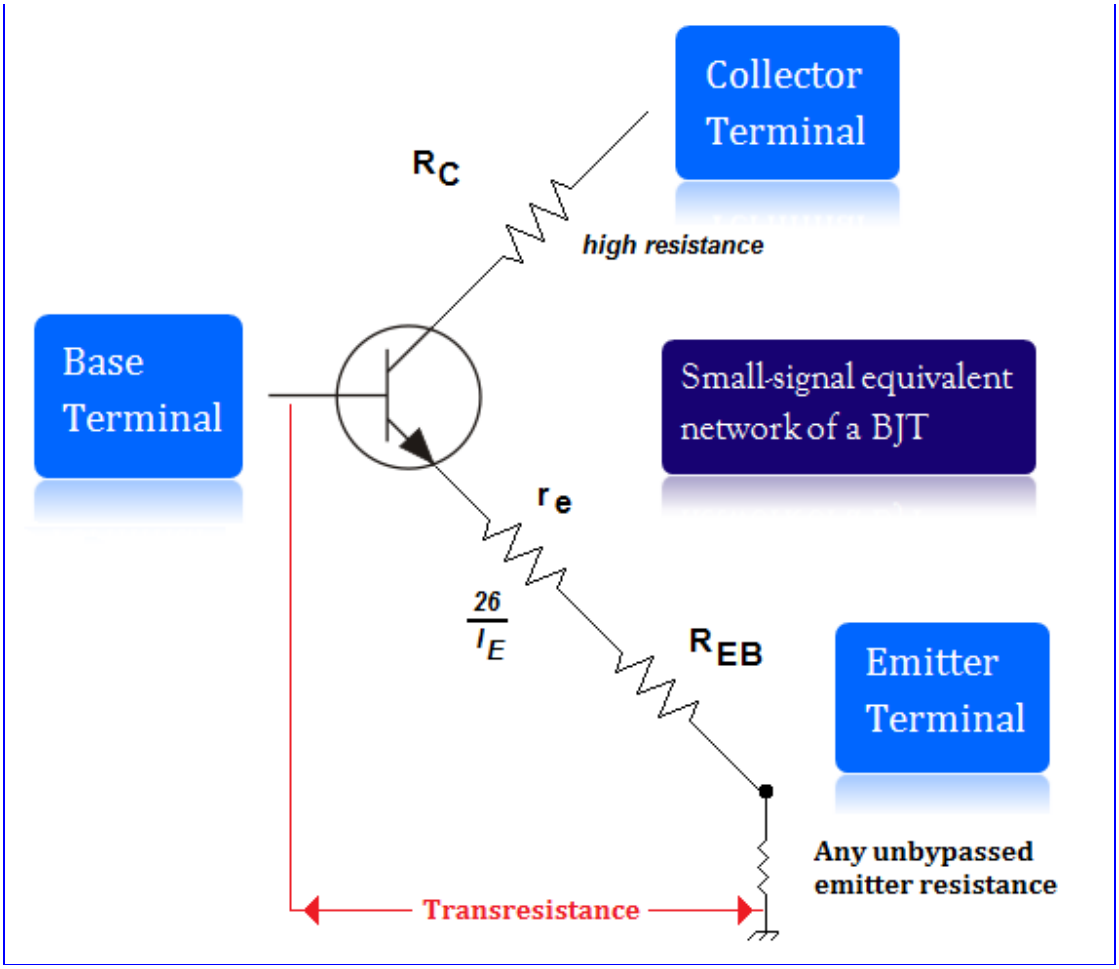

Above — the small-signal equivalent network of any transistor. re = 26/IE. Also, re + REB + any unbypassed external resistor may be termed the *Transresistance*, a DC ohmic value representing the total resistance of the emitter. The collector resistance RC is high because of its reverse bias. Collector resistance is not considered when calculating input impedance of simple AF transistor stages.

Calculating the input resistance of a common base stage

Calculating the input impedance of a common base amplifier is easy. Input impedance = 26/ emitter current (IE). You can either bench measure or calculate the emitter current using DC analysis. Click for the formula to calculate emitter current . A complete example follows:

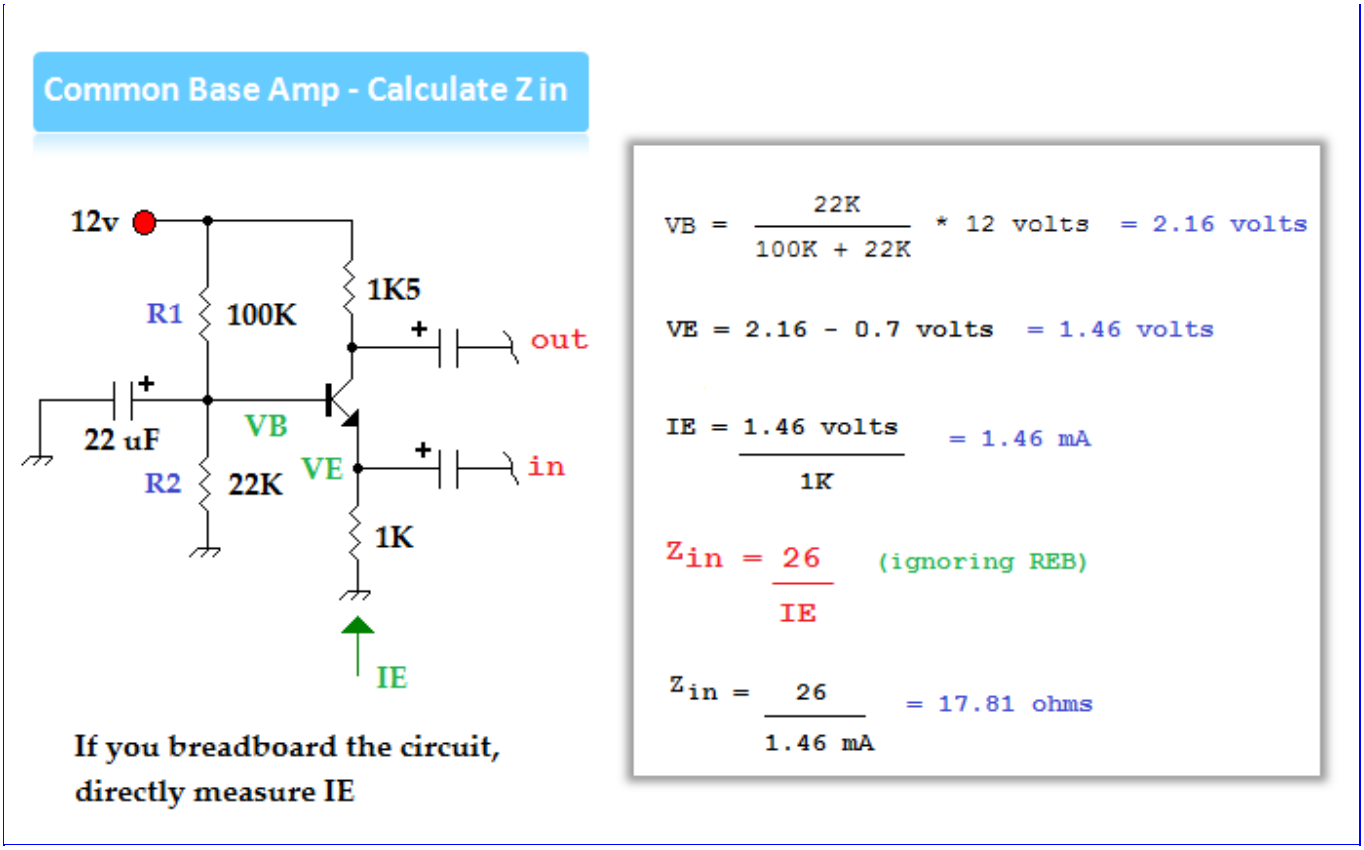

Above — An example common base amplifier and its input impedance calculation. In this example, emitter current is calculated using DC analysis. On the bench, it's better to un-ground the 1K emitter resistor and connect your ammeter between this resistor and ground to directly measure IE. REB was ignored and = 0.

Consider the 50 ohm input Z common base amplifier we often use after a diode ring product detector plus diplexer:

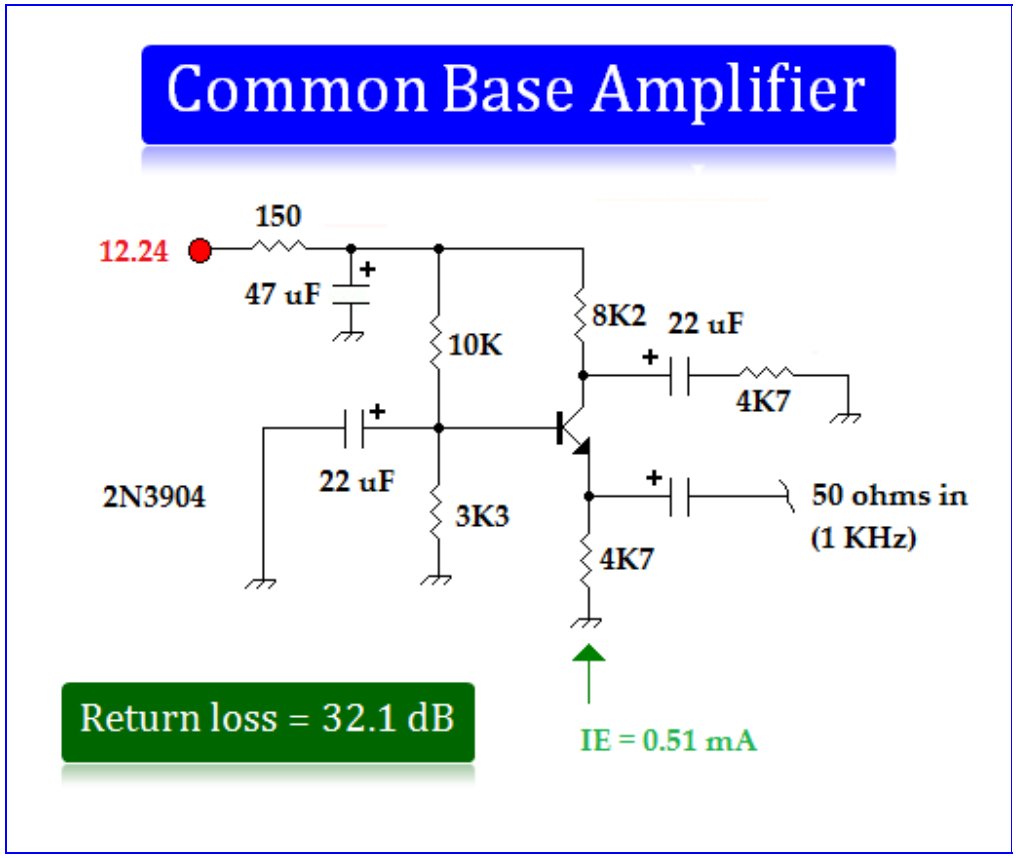

Above — A common base amplifier built for a direct conversion receiver in Spring 2010. This amplifier is shown in test setup for bench analysis

— with a DC decoupling network and an AC coupled 4K7 resistive load. The emitter current established using 5% tolerance resistors was 0.51 mA. Therefore, the calculated input Z is 26/0.51 = 51 ohms. The return loss of this amplifier as measured with the *active* 50 ohm Wheatstone bridge device described later on this web page was a spectacular 32.1 dB! If a different power supply voltage or biasing/emitter resistors were used, the IE would change and along with IE, the input impedance and return loss.

This amp illustrates that testing and tweaking AF amplifiers on the bench will garner the best results. If I just copy someone else's design; perhaps with a different DC voltage, or decoupling network and don't adjust the emitter current by tweaking the base biasing or emitter resistor resistors, the input impedance could differ significantly. Whenever you build a common base amplifier, measure its DC current and as necessary, tweak resistors to get the current needed for a perfect impedance match. It is good practice to measure all the DC voltages and emitter current on any amplifier you build — you will learn what is normal, what to expect and perhaps detect errors or parts failure(s).

Performing return loss measurement is also a fantastic way to ensure good matching to the 50 ohm impedance diode ring product detector that feeds this amplifier.

Calculating the input resistance of a common emitter stage

Calculating the input impedance of a common emitter amplifier is also straight forward, but not as easy as the common base amplifier.

In the **common base amplifier**, the emitter is the input element, therefore the input signal resistance is 26 / IE + REB. Often we ignore REB. If current of the common base amplifier is for example, 2 mA or so, then the 2-6 ohms of REB may be significant as 26 / 2 mA = 13 ohms. REB may be a factor because 2-6 ohms is a significant percentage of the total input resistance.

For a **common emitter amplifier**, the input resistance looking into the base is Beta (26/IE + REB + RE). Again REB is often ignored. We need to include any transistor DC biasing resistors which are also seen by the input signal as it moves through the transistor base. An example follows:

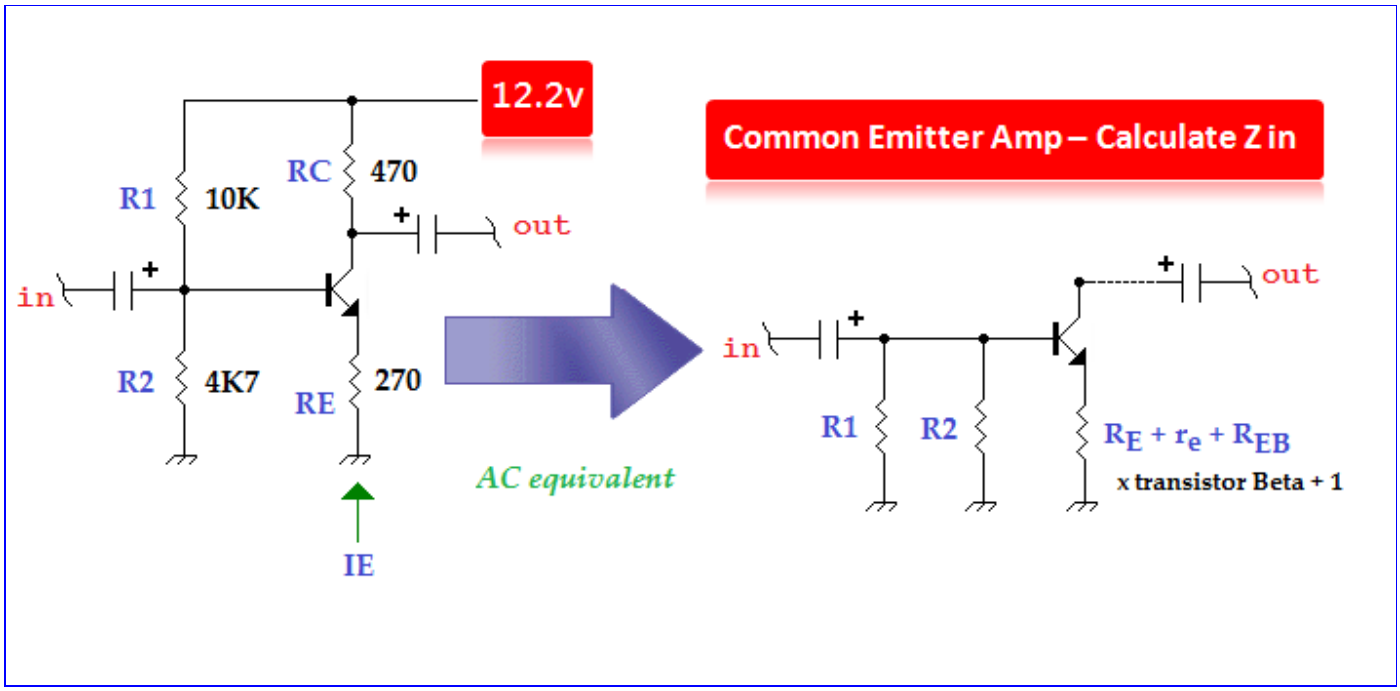

Above — An example common emitter amplifier re-drawn to illustrate how the input resistances combine to provide the AC input impedance. In this case, the 270 ohm emitter resistor RE is un-bypassed. R1, R2 and the components RE, re and REB are in parallel as the DC supply acts as a short to ground for the AC input signal. The components RE, re and REB (if used) must be multiplied by the transistor Beta value (+ 1) since the resistance looking into the base is Beta times that looking into the emitter.

Therefore: Rin = (B+1)*(re + REB + RE'). Normally we ignore REB so practically speaking Rin = (B+1)*(re + RE')

Common Emitter Amp – Calculate Z in

Beta = 100

$$V_{R2} = \frac{4K7}{4K7 + 10K} * 12 \text{ volts} = 3.84 \text{ volts}$$

$$V_{RE} = 3.84 - 0.7 \text{ volts} = 3.14 \text{ volts}$$

$$I_E = \frac{3.14 \text{ volts}}{270 \text{ ohms}} = 11.6 \text{ mA}$$

Calculate the base resistance R_b [ignore R_{EB}]

$$R_b = (\text{Beta} + 1) * (\frac{26}{IE} + R_{EB} + R_E)$$

$$R_b = 101 \ (2.24 + 270) = 27496.24 \text{ ohms}$$

$$Zin = \frac{1}{\frac{1}{R1} + \frac{1}{R2} + \frac{1}{Rb}}$$

$$Zin = \frac{1}{\frac{1}{10K} + \frac{1}{4K7} + \frac{1}{27496}} = 2.86 \text{ K}$$

Above — The math for the common emitter circuit shown directly above using DC analysis to calculate the current. On the bench, we just measure the emitter current (no need to calculate it). We assume IE = IC for a common emitter amplifier. REB = 0 (when ignored). If the 270 ohm resistor RE was bypassed with an electrolytic capacitor, the 270 ohm resistance would also = 0; and then Rb = Beta + 1 * (26/IE).

Conclusion

This theory explains how to calculate input impedance in 2 basic transistor AF amplifiers. Consult an electronics text for further explanation. Although the arithmetic is simple, quite frankly, it's a little boring. Let's go to the bench and have some fun. I was quite naive about measuring AF amplifier input impedance; however, my experiments yielded some knowledge and a strong appreciation for the Wheatstone bridge network. Onward...

Part 2: 50 ohm Input Impedance Wheatstone Bridge Measurement

Testing for a NULL or measuring the return loss of AF amplifiers with a 50 ohm input impedance.

Refer to the diagram on the right. Redrawn in a way more familiar to builders, the Wheatstone bridge network is just a pair of voltage dividers in parallel. We measure the difference in AC voltage between the ports labeled Out 1 and Out 2. The bridge is said to be balanced and produce NULL or 0 output when Out 1 and Out 2 are equal in voltage. Another description — when in perfect balance, the signal loss due to mismatch between the output ports is infinite. However, if this balance is disturbed by a mismatch between ports Out 1 and Out 2, an AC voltage appears and the return loss decreases in proportion to the mismatch (within limits and providing your

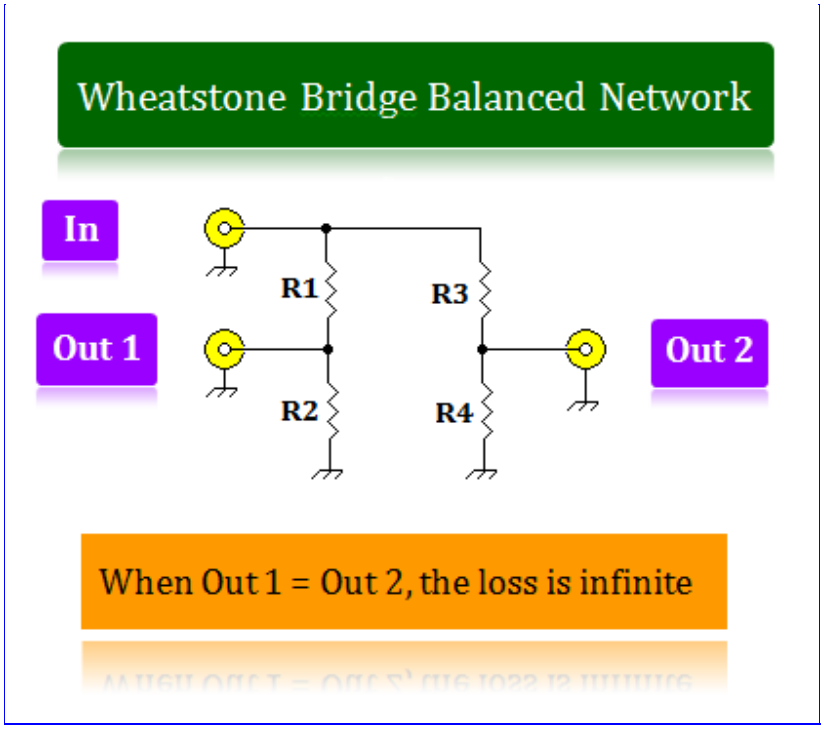

instrument can measure accurately).

Let's focus on some practical bench applications in the new millennia: On your bench, you might employ a Wheatstone bridge network to measure return loss (or VSWR) or to simply to detect a NULL indicating a close impedance match between 2 stages. Specific examples include tuning your feed line and antenna, checking the match between a signal generator and a filter, or measuring an audio amplifier input impedance. In my estimation, the Wheatstone bridge lies among the most important test circuits in the amateur designer's arsenal; worthy of study and experimentation.

Notes:

- The input signal can be AC or DC, but all discussion is confined to an AC signal source
- E96 (1%) metal film resistors were used in all Wheatstone bridges
- All bridges were tested at 1 KHz
- Ensure you do not overdrive your bridge; lest distortion occur! When a bridge is overdriven, you might cancel the fundamental frequency when balancing the bridge, but not the harmonics! Therefore, parasitic harmonics appear in the output that skew the the NULL or return loss values. I learned low pass filtering the amplified bridge output is really important.
- Any distortion in the bridge output means you must reduce your input signal drive level; however, this may reduce the accuracy of the RL measurements. There is no free lunch! You generally want just enough input signal to accurately measure the signal with the bridge at NULL.

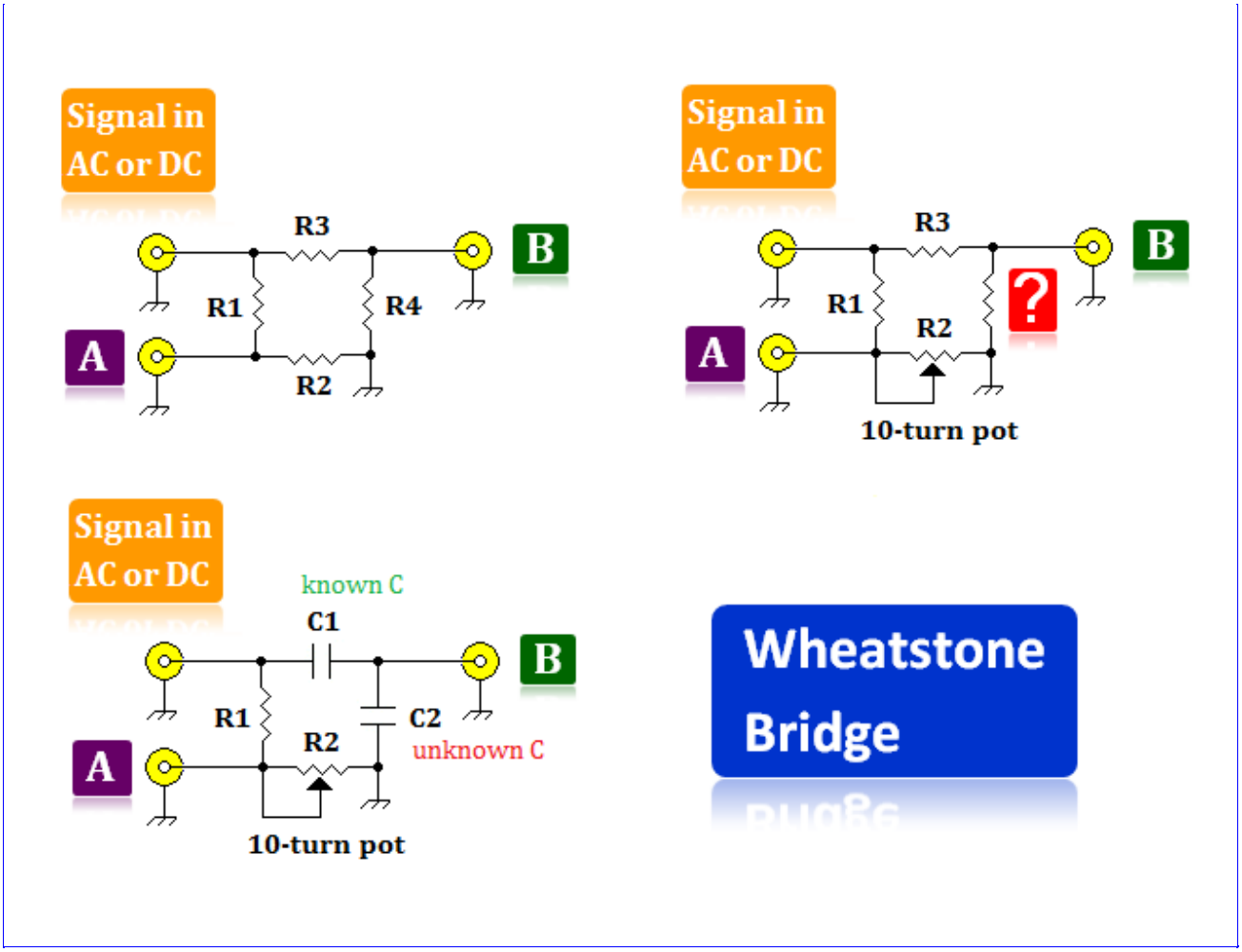

Comments from the Workbench

Above — an evolution of the 4 resistor bridge into a device to measure impedance and capacitance. In its classic form, each bridge leg is a resistor voltage divider with a detector connected across ports A and B. If ports A and B have equal voltages and R1 = R2, then R3 and R4 must also be equal; the bridge lies balanced or in a NULL state. If you remove R4 and measure an unknown resistance, the bridge will return to balance after adjusting pot R2 to equal the unknown resistance. In most cases, R2 is calibrated and the impedance is read directly off the potentiometer dial. Bridges can be arranged to measure unknown capacitance, inductance , frequency and other parameters by using precision 1% fixed components, calibrating the 10 turn pot to indicate the desired parameter, or for deriving the unknown value via equations.

Builders of lore used bridges to quantify many values on the bench. Although we have better ways to measure inductance and capacitance today, the Wheatstone bridge is still the *king* when it comes to simple measurement of network impedances; for example, QRP antenna tuners. Some builders use an LED to indicate bridge imbalance.

Building a passive instrument to measure the return loss of a 50 ohm input Z audio preamplifier.

Non-radio folks don't generally understand this — to properly terminate a diode ring mixer, 50 Ω impedance stages are needed. The inspiration driving *all* the experiments on this web page was to design a 50 ohm input impedance common emitter audio preamplifier to follow a diode ring mixer. I could have just used the familiar common-base amplifier popularized by Roy, W7EL, but of course, wouldn't learn anything. Somehow, I became drawn in by curiosity and generated enough content to fill a whole web page.

I decided to try and build some return loss bridges and test them by using known, fixed-value resistors as the unknown impedance. My first bridge, was an AF version of this RF return loss bridge using a junk box 600 ohm, 1:1 audio isolation transformer. It didn't work until I rearranged it as shown in the schematic below.

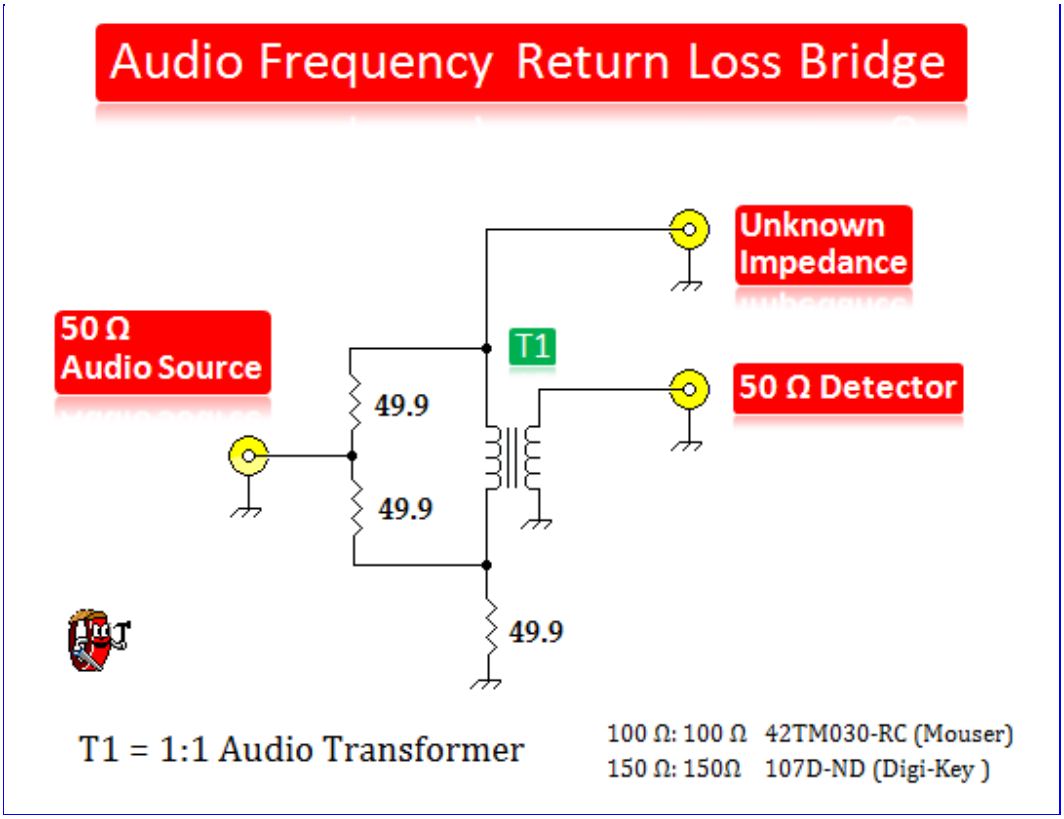

Above — A simple return loss bridge using an AF transformer and 50 ohm detector. Suitable detectors are described here in the section covering return loss bridges — I used a 50 ohm terminated scope. Using 20 log (peak-peak voltage) to crunch the 50 Ω AC voltage into dB, the bridge was measured at open circuit, plus with various fixed 5% tolerance resistors terminating the Unknown Z port. Using a junk box 600 ohm 1:1 AF transformer, my results initially seemed good, but upon analysis were fraught with error. Note the suggested transformers in the schematic.

Above — The very first AF return loss bridge built. Anchored to the ground plane with resistors, the transformer was a 600 ohm *junk box* special. Although I was able to achieve a deep NULL using a 49.9 ohm resistor, the return loss was 86 dB; not possible. Additionally, other fixed resistors gave return loss values more than 4-5 dB away from the proper value. Likely, my junk box transformer lacked sufficient inductance for 1 KHz. For testing your bridge, use a formula to inform you of what RL value to expect for a given fixed resistor.

Calculate the RL of a resistor in a 50 Ω bridge

$$V = \frac{(\text{Resistor value} - 50)}{(50 + \text{Resistor value})}$$

RL = -20 log (absolute value of V)

510 ohm resistor:

V = (510 - 50) / (50 + 510)
RL = -20 log | 0.82 |
RL = 1.72 dB

Above — The formula to calculate the expected return loss for a fixed resistor placed in the Unknown Impedance port on a Wheatstone bridge. Click for a table of Return Loss values for some non 50 ohm resistors. Your RL values, will rarely be exact, but should be close to the predicted value. A well functioning bridge should yield a return loss of > 40 dB using a 51 to 47 ohm resistor as the Unknown Impedance.

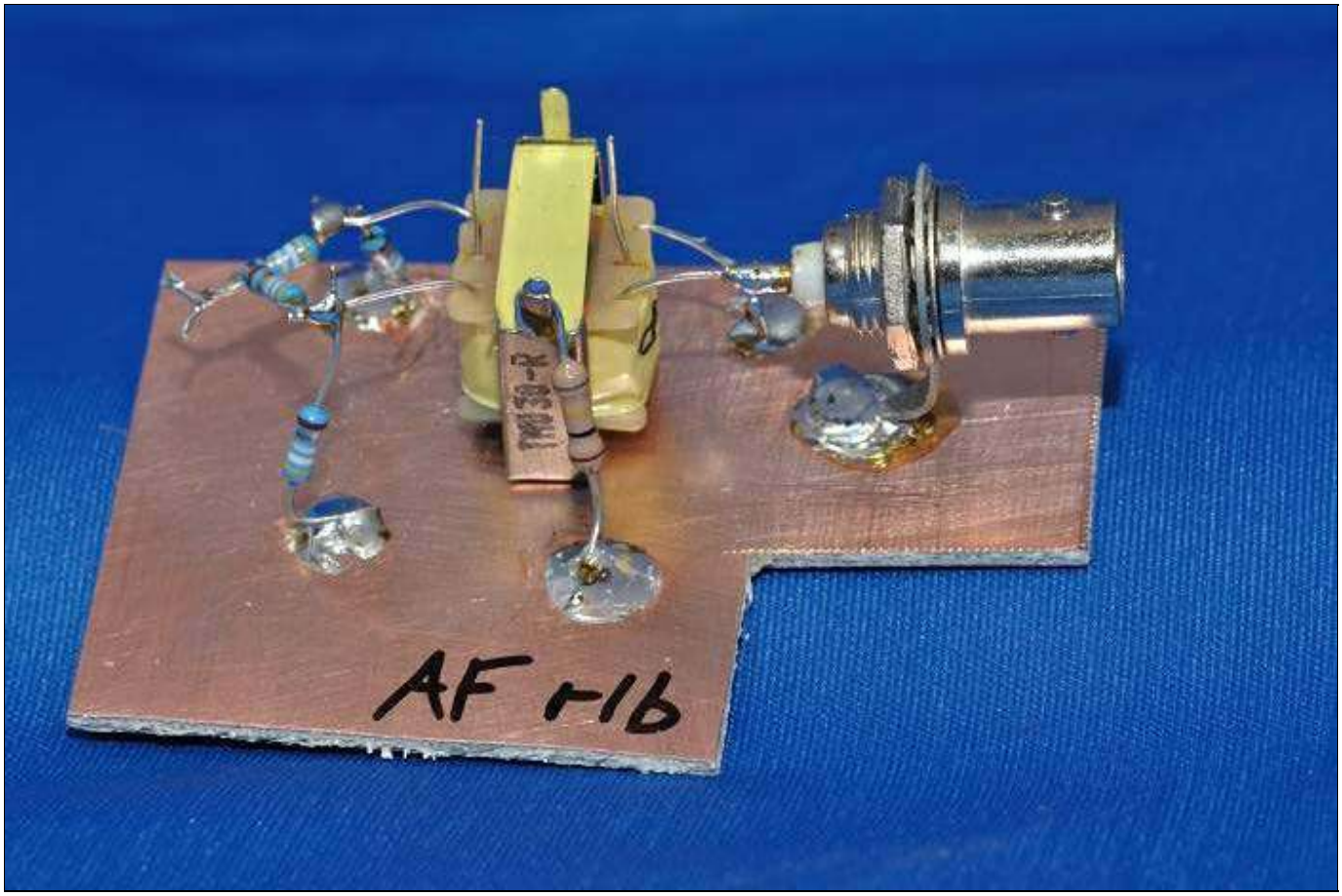

Above — A second bridge was built after obtaining a 100 Ω : 100 Ω AF transformer from Mouser Electronics. This transformer was ideal (each coil has ~ 1H in inductance!). Bench testing indicated good function. My results are tabled below:

Measurement of R L B	
Resistor Ω	Return Loss (dB)
10	3.35
22	7.47
27	9.74
33	12.39
39	16.23
49.9	56.73
62	16.54
75	12.82
100	9.15
220	3.95
510	1.63

Above — A table of the above 50 ohm Wheatstone bridge return loss measurements. These results are acceptable. The NULL with a 49.9 ohm resistor was incredibly sharp and garnered a RL of 56.73 dB. My AF source was a low noise 1 KHz, 50 ohm output impedance signal generator.

If you do not need return loss, and only require a NULL to indicate a match, a common 600 ohm transformer may work okay for you.

Building an active instrument to measure the return loss of a 50 ohm input Z audio preamplifier.

The results of my early experiments with a passive bridge were encouraging. Noting that most builders would have difficulty obtaining a 100 Ω : 100 Ω AF transformer, a version using op-amps was sought. My first 3 designs did not work properly and I became discouraged. Some guidance from Wes, W7ZOI allowed me to problem solve and experience success.

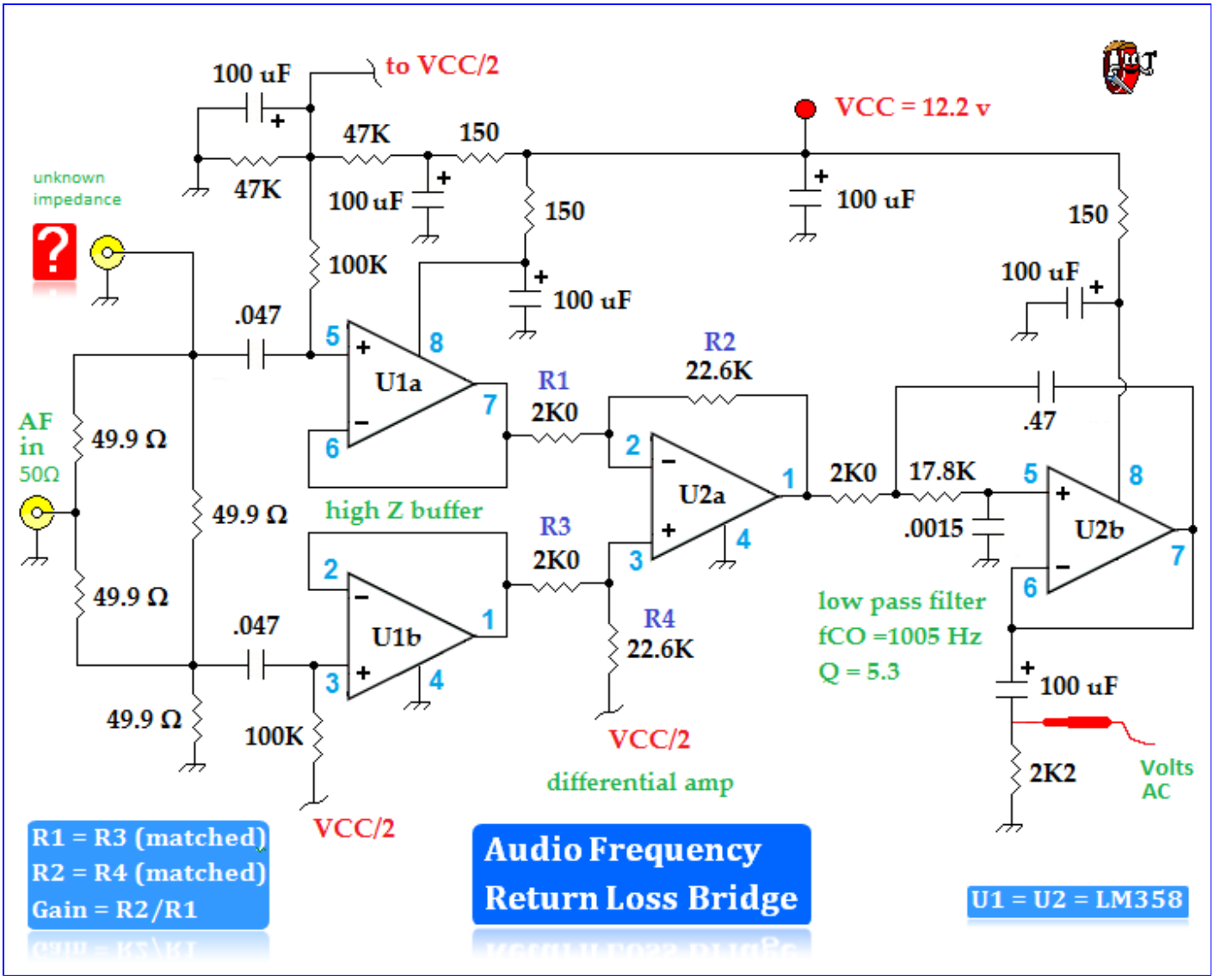

Above — Schematic of my active Wheatstone bridge, amplifier and low-pass filter for measuring the Return Loss of 50 ohm input impedance AF amplifiers. I built 3 copies of the above device; best results occurred when careful layout and planning were employed. Optimal performance occurred when encased in a metal box.

The bridge was built from 1% metal film resistors. 0.047 polyester film capacitors lightly couple the bridge to high impedance op-amp buffers labeled U1a + U1b. My experiments informed me that to minimize loading on the bridge is important. The LM358 is an excellent op-amp choice, but almost any other op-amp could be employed successfully. U2a is the differential amplifier and matching R1 + R3 and R2 + R4 with 1% tolerance resistors is critical; 5% resistors did not work well. The gain is non-critical — feel free to choose reasonable resistor ratios based upon the resistors you have in stock. The differential amp promotes the unfortunate side effect of amplifying both the desired AF source plus any common mode signals. Although common mode suppression is an important consideration when designing instrumentation amps, fortunately, performance is fine. A amplifier topology using a differential amp across the bridge was trialed, but functioned identically to the simpler differential amp shown. Consult a textbook for more information on Instrumentation amps. Much information was gleaned from Professor Ken Kuhn's web site.

The output is low-pass filtered by a single stage Sallen-Key low-pass filter with a peak frequency of 1 kHz and a Q of 5. This filter gain at 5 at 1 kHz is 0.328 at 2 kHz and 0.123 at 3 kHz. Thus, the second harmonic is reduced by a factor of (5/0.328) = 15.2 and the third harmonic is reduced by a factor of 40.6. **Do not omit a low pass filter**. I chose a 1 KHz cutoff, but experimentation indicated a low-pass cut-off frequency as high as 10 KHz may work okay if you plan to use the bridge at frequencies other than 1 KHz.

Power supply decoupling proved important. When less DC low-pass filtering (less than the 150 Ω plus the 100 uF capacitors shown) was employed, some low frequency audio noise appeared in the output.

I measured using a X1 oscilloscope probe on the output of U2b.

Above — A breadboard of the active Wheatstone bridge schematic located above. When tested with fixed value resistors, the RL @ 49.9 ohms was 55.4 dB and close to predicted value with other test resistors. This instrument will be put in a metal case and become a permanent part of my test equipment arsenal.

Part 3: Measuring Unknown Impedances

Building an instrument to measure the input impedance of an audio preamplifier using a NULL.

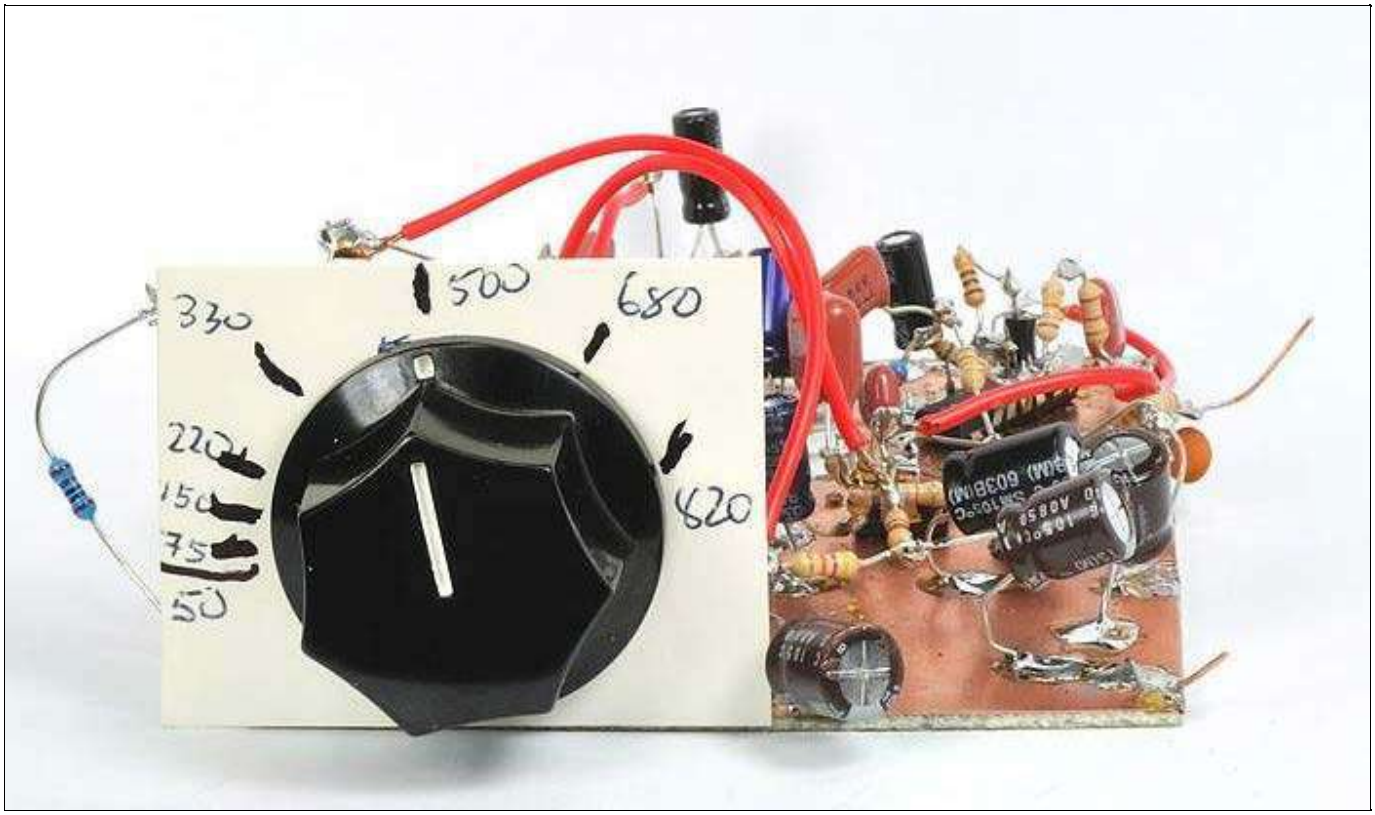

Above — One of several Wheatstone bridge circuits built in the Spring-Summer of 2010. In these bridges, the potentiometer was calibrated and the panel labeled using fixed resistances for calibration. One big challenge is range or resolution; dependent on the bridge resistor values and what impedance you are trying to measure. Greatest accuracy is associated with 5 or 10 turn potentiometers, but these are expensive. Often, I used standard, linear taper pots to save money during my experiments. Over 7 different bridges were built and tested. To save time, I didn't photograph many of my projects from the summer.

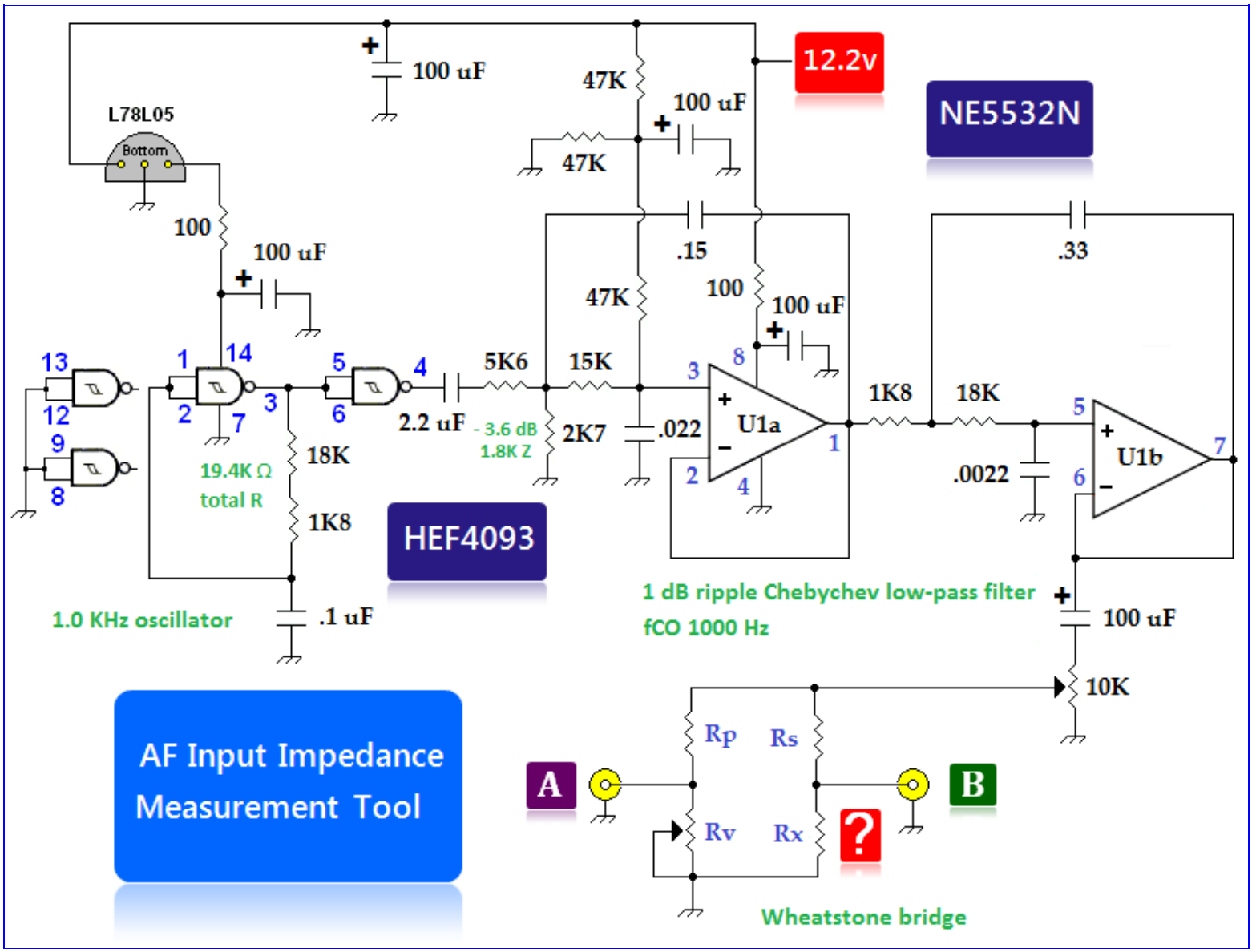

Above — A complete 1 KHz signal generator, low-pass filter and bridge circuit which became the prototype for most of my experiments in this section. Click for a high resolution photo of 1 of the breadboards during construction.

The 1 KHz signal generator is a digital oscillator built with 2 gates from a 4093. This excellent oscillator uses a single R + C network for tuning and requires a voltage regulator for frequency stability. The output signal is attenuated 3.6 dB and low-pass filtered by 4 poles of active filtering. A 10K pot controls the drive into the bridge circuit. The bridge outputs are labeled **A** and **B** and require buffering, amplification and low-pass filtering similar to the active bridge shown earlier. These functions and some comments on the bridge resistors come later.

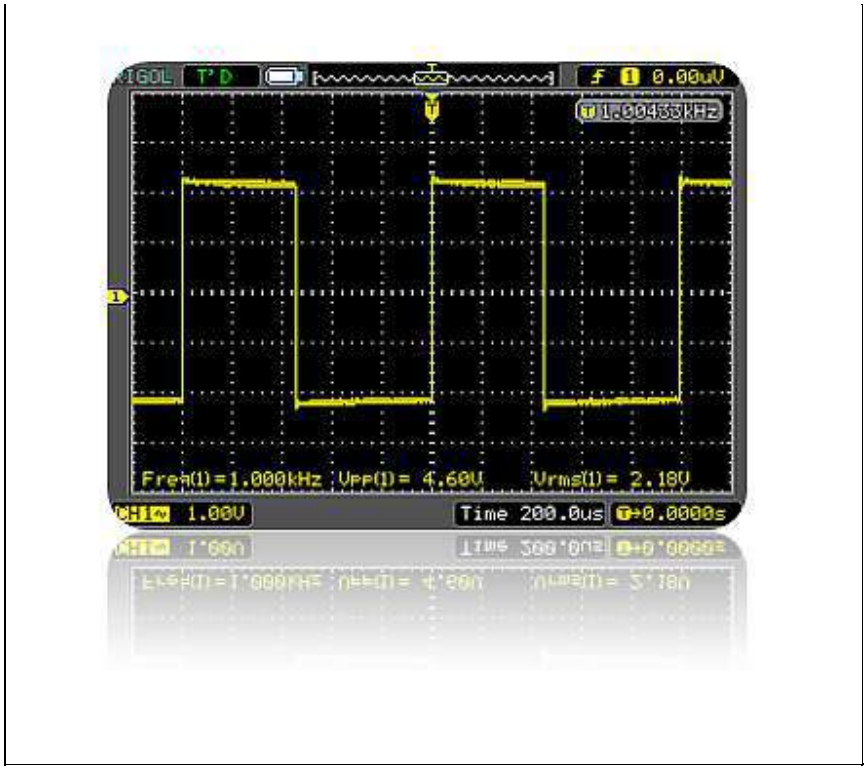

Above — The oscilloscope waveform from the digital 1 KHz oscillator. Digital clocks fascinate me and this was an untried design. Initially a CMOS 555 timer was considered, however, I own many 4000 series NAND Schmitt triggers and pressed 1 into service. Another good choice might be the 74HC132. The first NAND gate (inverter) contributes 180 degrees of phase shift, while the RC low-pass filter tank circuit digitally shifts the AC the other 180 degrees. Output noise is filtered by both the low-pass filter and the input Schmitt trigger dead band or hysteresis. The result is a fairly crisp square wave that may rival the 555.

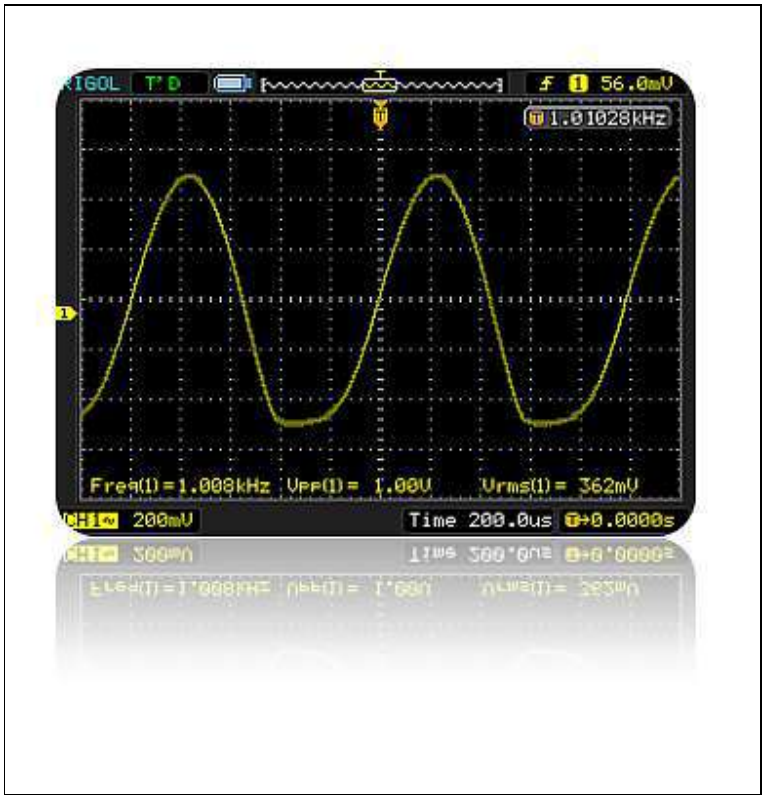

Above — The output of the 1 KHz low-pass filter. A sine wave is desirable, but not critical; suppression of energy in the range of 5-10 KHz, informed the filter design goal. At 8000 Hz, the attenuation is > 80 dB. All good.

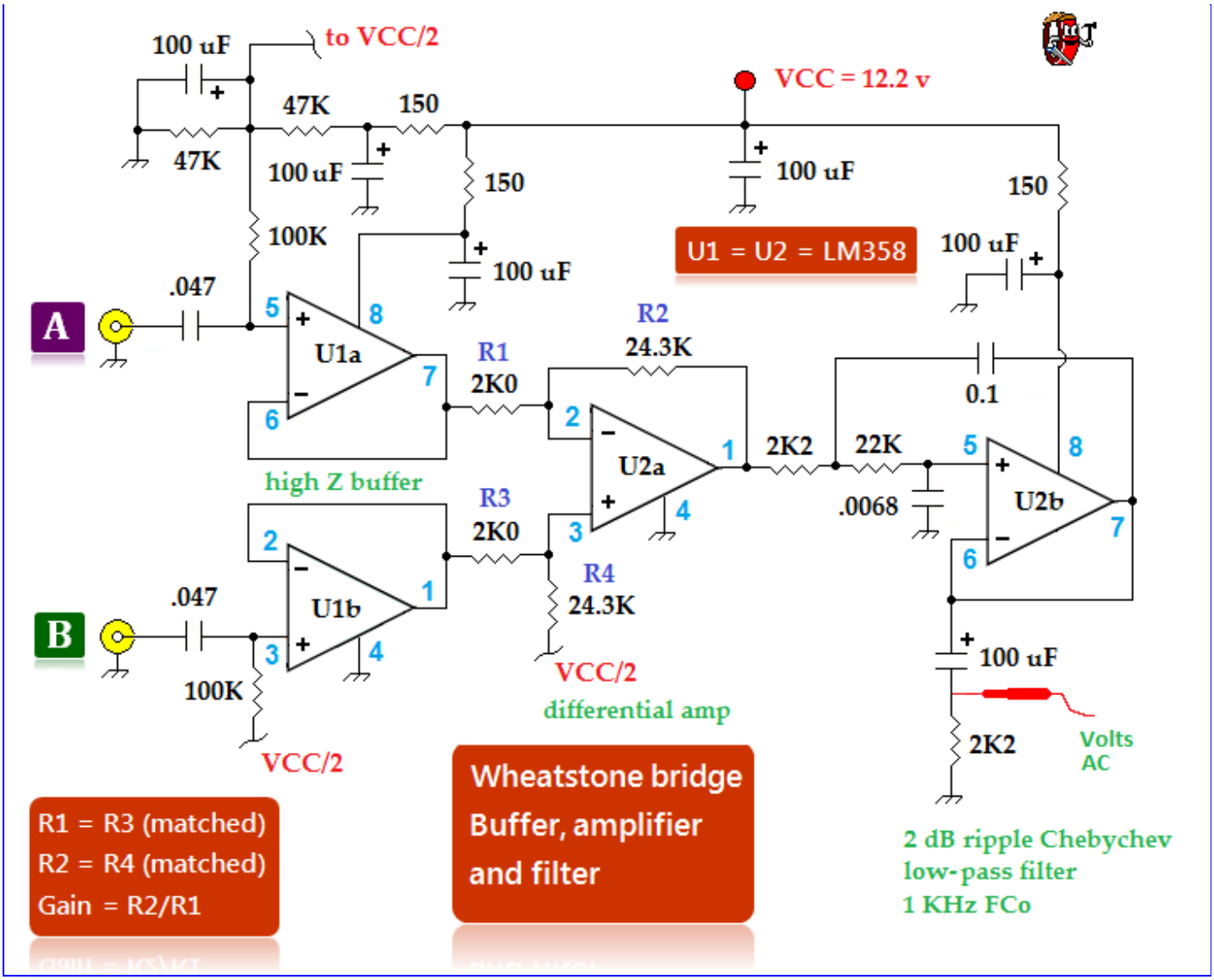

Above — The buffer, differential amplifier and low-pass filter employed during this series of experiments. Function is identical to the similar stage described earlier.

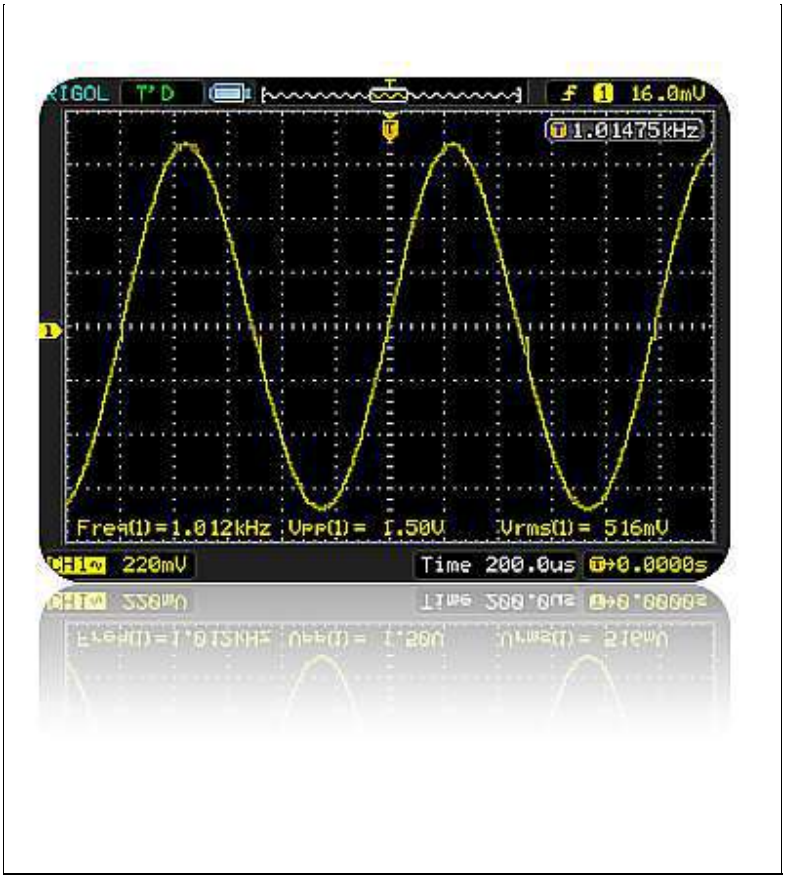

Above — The output of amplified and filtered Wheatstone bridge at open circuit (no resistance at the Unknown Impedance port).

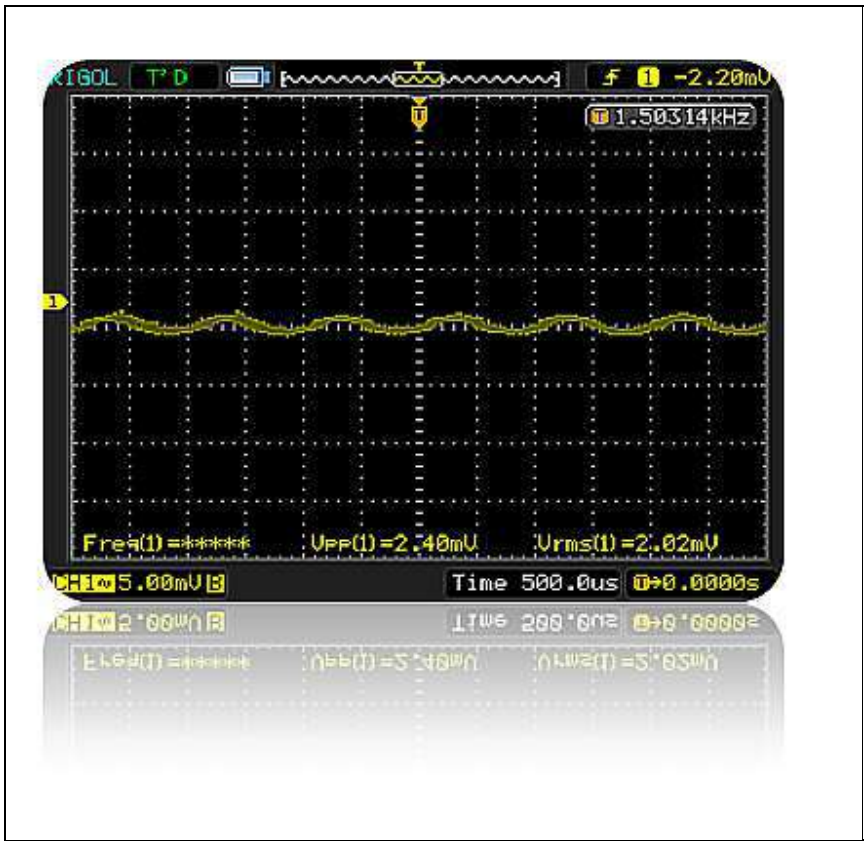

Above — the output of the amplified and filtered Wheatstone bridge at NULL (potentiometer setting balanced to match the resistance at the Unknown Impedance port. Below 2 mV, accuracy is lost.

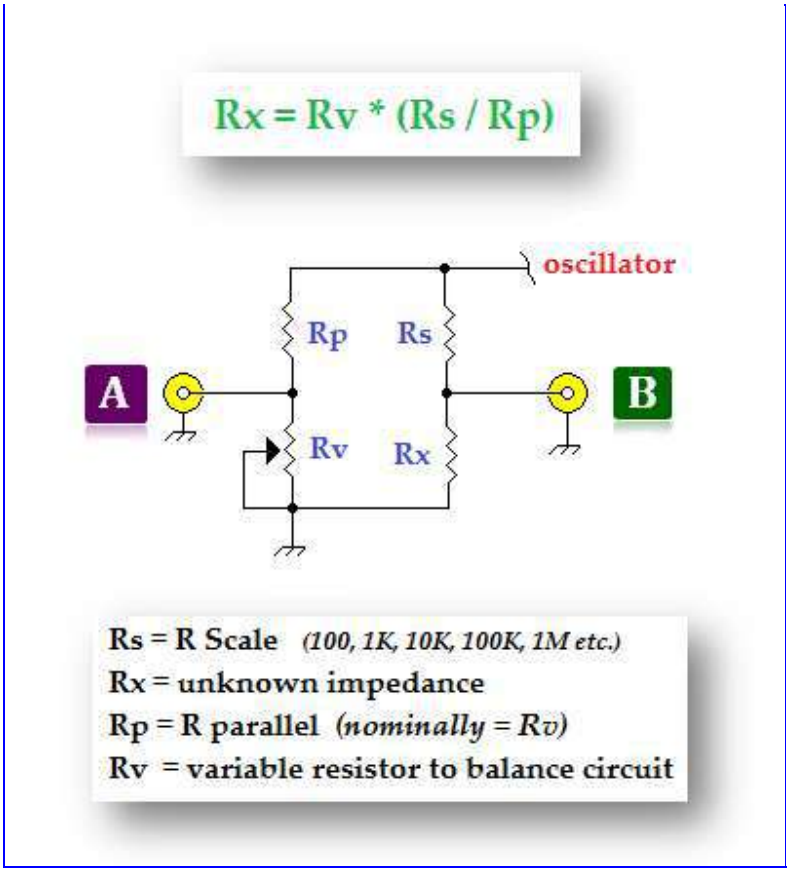

Above — The math behind the bridge. I found when R Variable (Rv) was the same resistance as the fixed resistor R parallel (Rp), reasonable resolution was possible. "Reasonable resolution" means your pot has a good range of rotation as you go from the lowest to highest measureable impedance. Generally, Rv has to be less than the maximal impedance you are trying to measure.

R Scale (Rs) can be switched in decades via a panel mount switch to cover a wide range of resistance with good resolution, or just be 1 or 2 values. It's your design call.

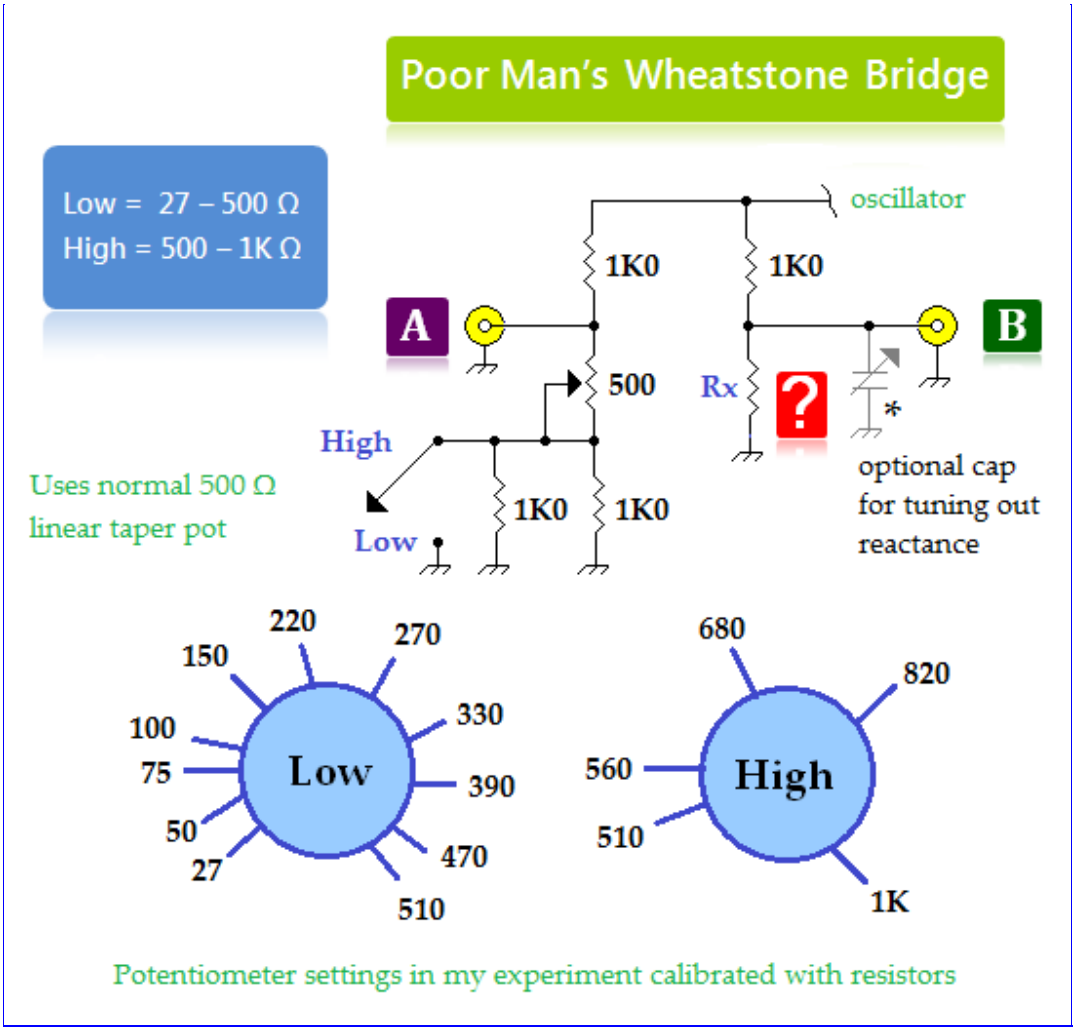

Above — My poor man's impedance measurement device that uses a common 500 ohm linear taper pot as the balancing resistor. In order to get good pot resolution, the desired range is switched. This bridge measures impedances at the Unknown Port from about 27 ohms up to 1K with decent resolution. The blue circles depict how I calibrated the front panel of my device using 2 colors. This device had an average return loss of 32.5 dB when a NULL was obtained.

Measuring resistors to calibrate a bridge is quite different from real-world measurement of reactive AF amplifier loads — if the unknown resistance has a large inductive or capacitive reactance, obtaining good bridge balance might prove difficult. Your bridge can *only* null the in-phase signal. An extension to the standard bridge involves adding a series or shunt capacitance (depending on the phase of the reactance) to the A or B port. This may allow you to null the reactive part and also provide the reactive impedance value as well. An outstanding reference may be located with your favorite search engine: Look for the manual for the **General Radio GR1650 Impedance Bridge.** I found a copy and the download was very slow, but worth it. This manual may be the greatest reference every published on the Wheatstone bridge and comprehensively covers tuning out the reactance of complex impedances amid a myriad of other topics.

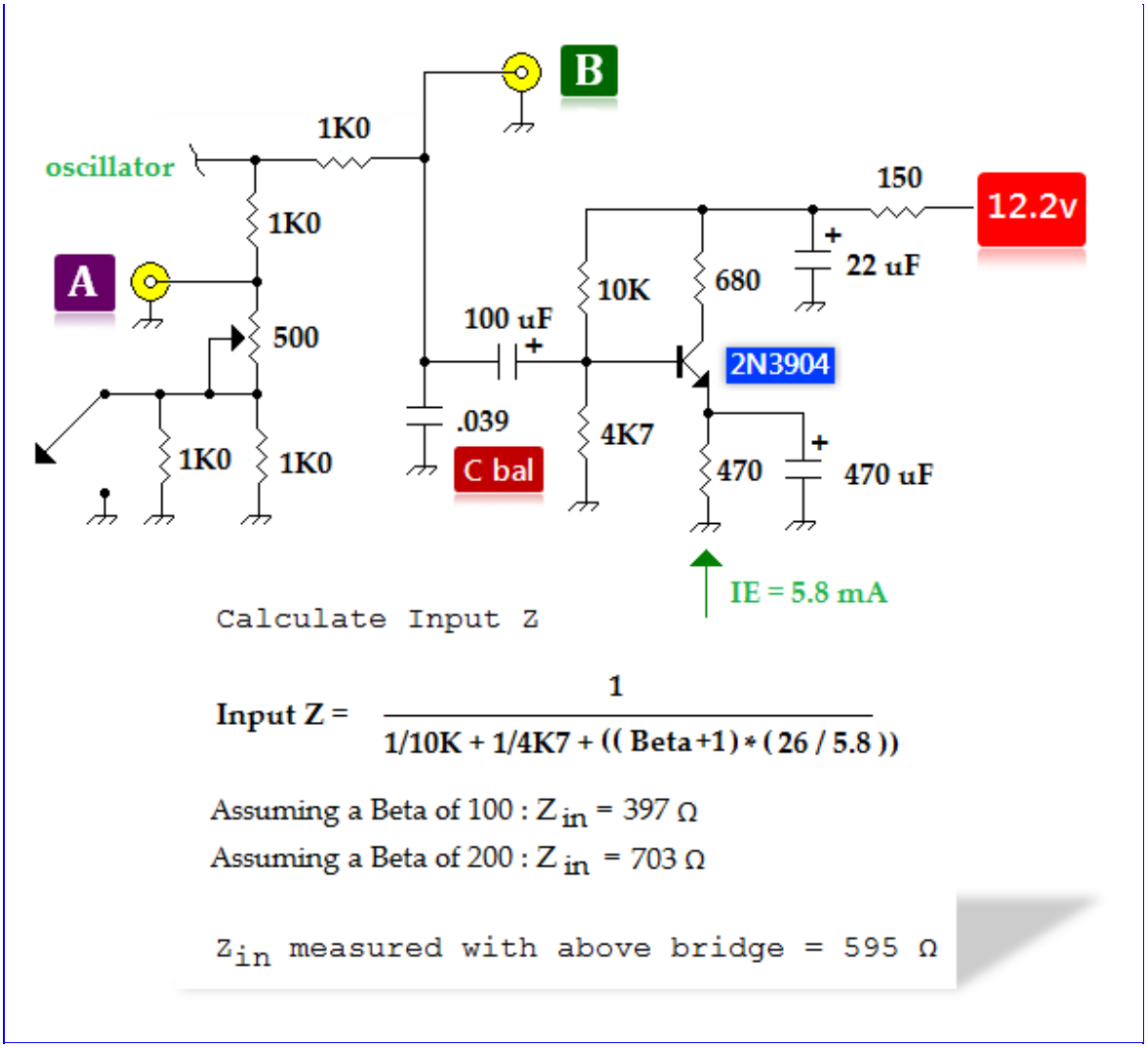

Above — The poor man's bridge measurement of a test AF amplifier on my bench. The reactive component of the amplifier input impedance was minimized using a 0.039 uF capacitor found experimentally. Of particular interest, is the difference between the *calculated* input Z and the *actual* input Z measured with the bridge.

The Beta of the 2N3904's in my collection ranges from about 100 to 225. Calculations with 2 different Beta values are shown (RE is *well* bypassed with a 470 uF capacitor, so, re = (Beta * 26/5.8 mA) . The measured input Z was 595 ohms. I confirmed this by removing the 0.039uF tuning capacitor, plus connecting a fixed 595 ohm resistance to the Unknown Impedance port. I then turned the potentiometer fully clockwise and adjusted it for a NULL. When the bridge was nulled, the potentiometer knob pointed at the same mark as when the amplifier was connected to this Unknown Impedance port.

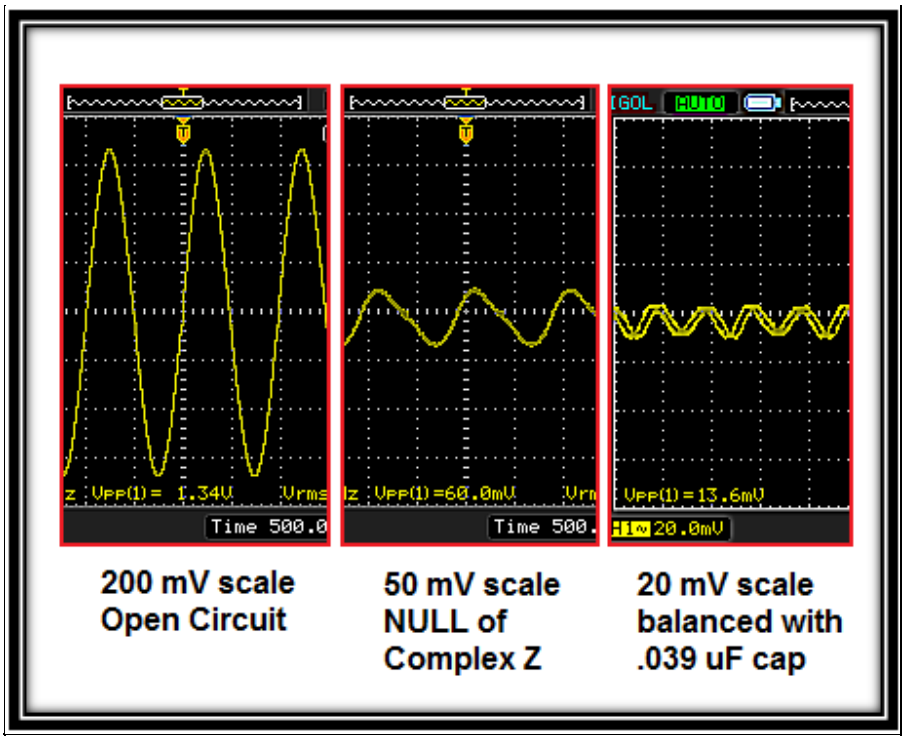

Above — The oscilloscope output waveform of the amplifier circuit shown above: open circuit, with the potentiometer balanced as well as possible and finally, the potentiometer balanced with the addition of a 0.039 uF capacitor attached to Port B. Although, I was able to get a NULL without the capactitor by just tweaking the potentiometer, slightly better precision was obtained after adding the 0.039 uF balancing capacitor.

Part 4: Miscellaneous Circuits, Scans and Photographs

Above — More accurate results will be obtained with a calibrated 10 turn potentiometer to balance your bridge. A local store sold me this precision 10-turn, 10K pot for about 11 dollars (still expensive for me). They normally sell for twice this price in Canada.

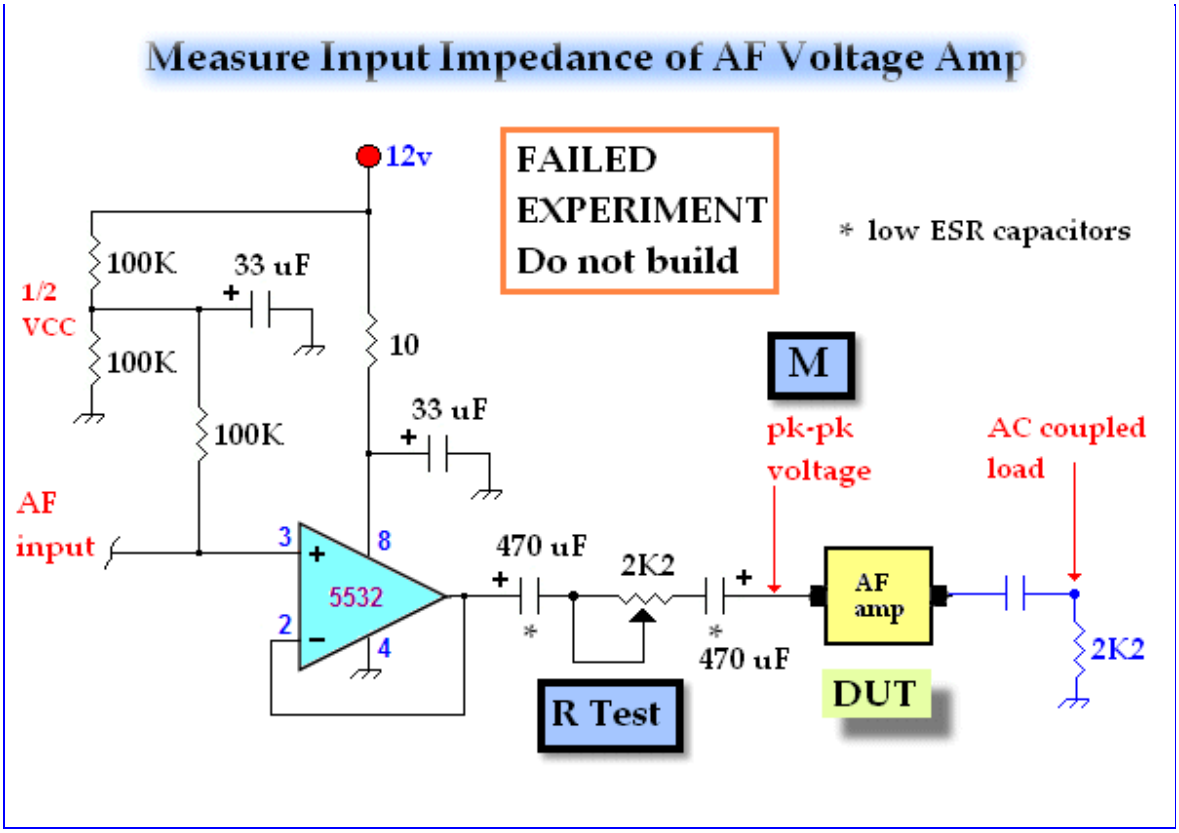

Above — My first input impedance measurement device that didn't work. It turns out my experiments were performed *incorrectly*, however, I'm glad because this failure spurred me to investigate bridge networks. The series resistance method *is* worth understanding and happily, Jeff, AD6MX described the correct procedure in a private email received December 2010. I quote him below:

"The series resistance method for input impedance should start with the variable resistor disconnected from the node to be measured. The open circuit voltage at the end of that resistor is measured (the resistor value doesn't affect the open circuit voltage since there's no current into an open circuit.)

Next the free end of the variable resistor is then connected to the input node and the resistor is finally adjusted for half the open circuit voltage at the same end of the resistor, at the input node being measured. What happens is the variable resistor and the node input impedance form a voltage divider, with equal arms or branches.

The value of the resistor when measured out of the circuit is the same as the input impedance at the measured input node. This scheme has some assumptions: the driving amplifier has negligible output impedance compared to the measured impedance, and the input impedance is purely resistive, with no reactance or V-I phase shift.

The phase shift condition may be checked by taking these 3 voltage measurements: across each branch of the divider separately, and also the driving source voltage (across both branches in series.) The sum of the separate branch voltages should match the source voltage when there is little phase shift.

This 3 voltage scheme is used in some antenna analyzers in order to measure phase shift. For checking for the resistive condition, it's not important the 3 voltage method has a sign ambiguity which needs an additional step to resolve. Your description seemed to suggest starting with zero series resistance, but you see that is not the same as the procedure above. The applied voltage needs to be small enough that the amplifier remains operating in its linear range during the measurement".

Thanks for this info Jeff!

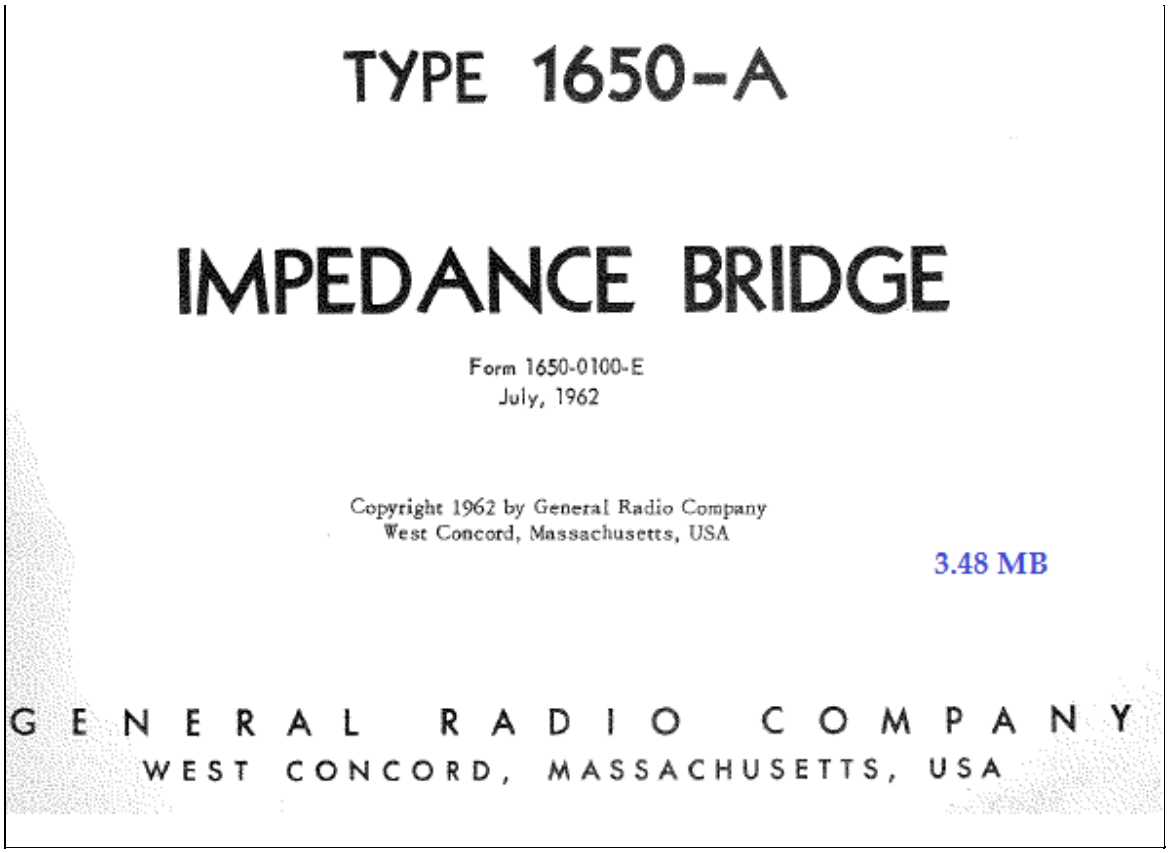

Above — A modified scan of General Radio's *über awesome* manual for the Type 1650-A Impedance Bridge.

RF Workbench Page 3

This web page is the third installment of a 6 part series that explores basic measurement of RF circuits.

Part 3, further examines Return Loss Bridges from a bench-practice viewpoint.

I borrow heavily from the work of Wes, W7ZOI per correspondence, direct contributions and from EMRFD.

I focus on measuring low-level, HF circuits with a return loss bridge — topics such as using the bridge for antenna matching are omitted and readily found on the web. This web page contains minimal text and just relies on simple diagrams and photographs to transfer ideas and knowledge. Information regarding wideband bridge network function may be found elsewhere on this and other web sites and in EMRFD.

More on Return Loss

Gear

Equipping for a 50 Ω measurement environment in 2010 greatly improved my design capacity. The 50 Ω terminated oscilloscope makes a sensitive and accurate detector for return loss measurement. Discussion about using a 50 Ω oscilloscope termination is on the RF Workbench 1 web page.

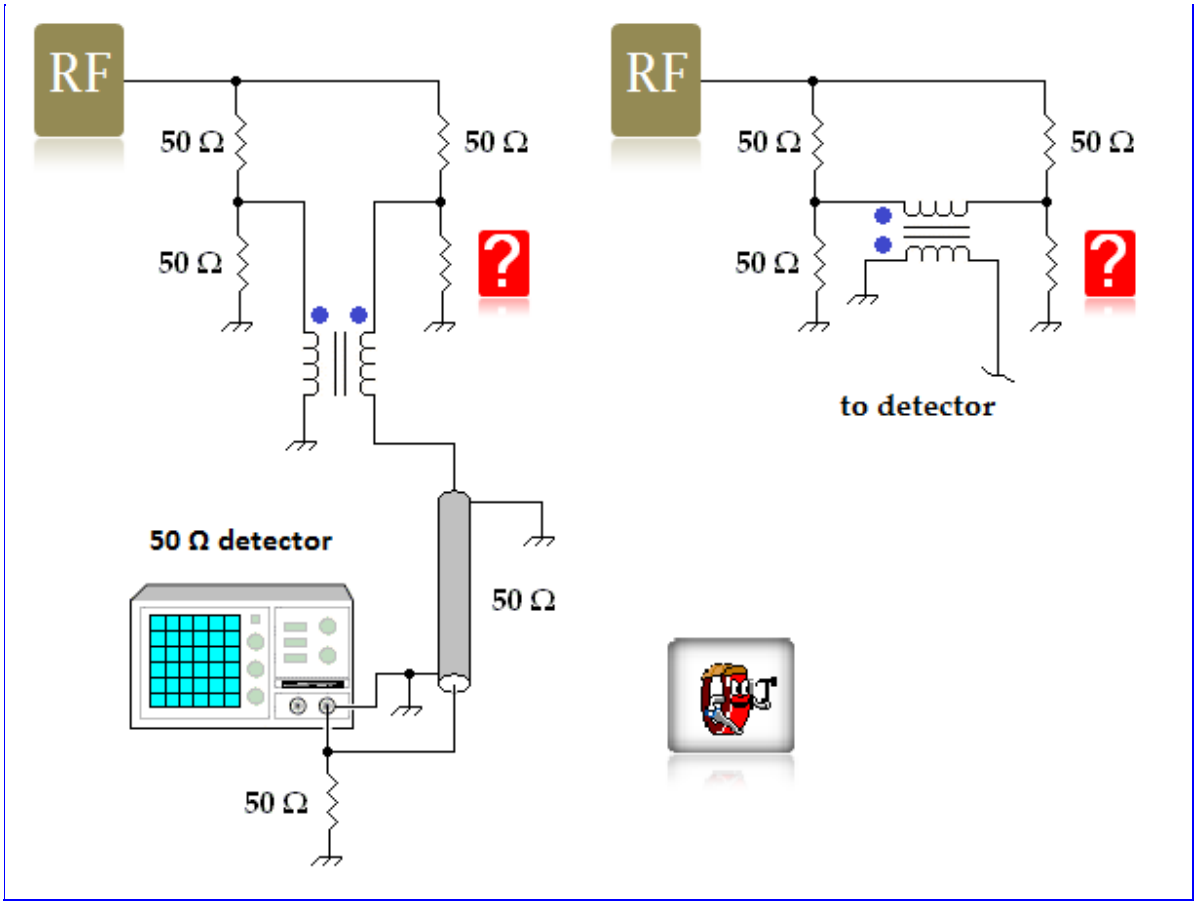

Above left — The RLB and measurement set up from EMRFD. Occasionally, you may see bridges using a different balun transformer wiring as shown to the right of this figure.

Above — All the needed parts to home build a return loss bridge. For some, the parts investment might seem substantial, but what hobby isn't expensive? If you consider the cost of commercially manufactured bridges, a homebrew solution seems a bargain. Recycled parts and a home-built chassis are inviting cost-containment techniques. See the web site of Jim, K8IQY for an example of a homebrew RLB chassis. Jim, a Manhattan style construction wizard, builds the nicest looking gear — he puts me to shame.

Above — A completed bridge. I used 1% tolerance 49.1 ohm resistors and an FT50-43 ferrite toroid for the bifilar wound transformer. Inductance = 38.4 uH. Many builders use the FT37-43 ferrite core. I prefer using 2 colors of enamel coated wire to avoid confusion when building stuff with transmission line style transformers and all I had in 2 colors was 24 gauge wire The bigger size ferrite toroid better accommodates the 24 gauge wire, plus photographs better.

Bridge directivity of the above RLB was 30 dB at 7 MHz, 34 dB at 14 MHz, 35.6 dB at 21 MHz, 42.1 dB at 50 MHz and 43.4 dB at 100 MHz.

If you build a circuit with a return loss close to 30 dB, it's a good day.

Above — The completed RF-tight bridge. Don't forget to label your network ports.

Measurement Technique

Measurement of an Amplifier Input Return Loss

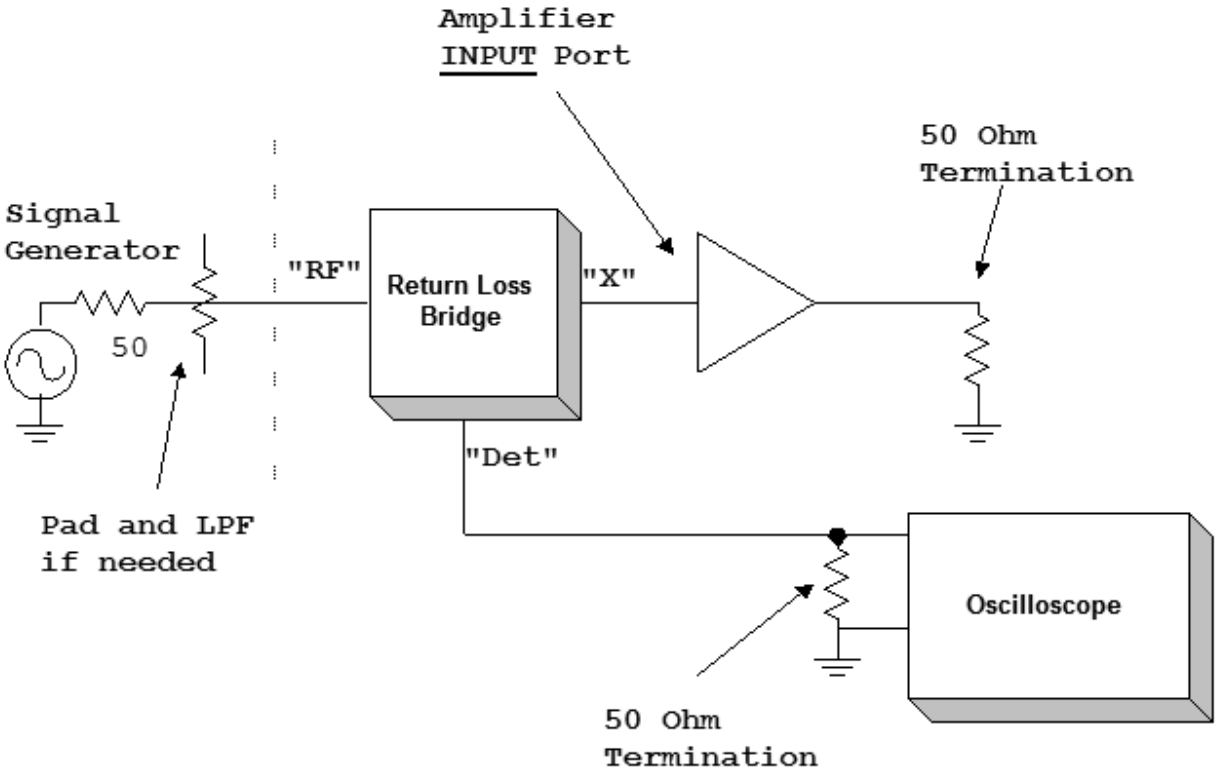

Measurement Procedure:

1. Terminate X port in an open circuit and note level. e.g.,250 mV pp at scope.
2. Attached a 50 Ohm load at X just to check the bridge. e.g., now see 5 mV pp.
3. Bridge directivity is 20Log(250/5)=34 dB. This is the best you can measure. Better numbers are meaningless.
4. Remove the 50 Ohm load. Attached the amplifier input and note level. e.g. 18 mV pp.
5. Amp Input RL is 20Log(250/18) =23 dB.

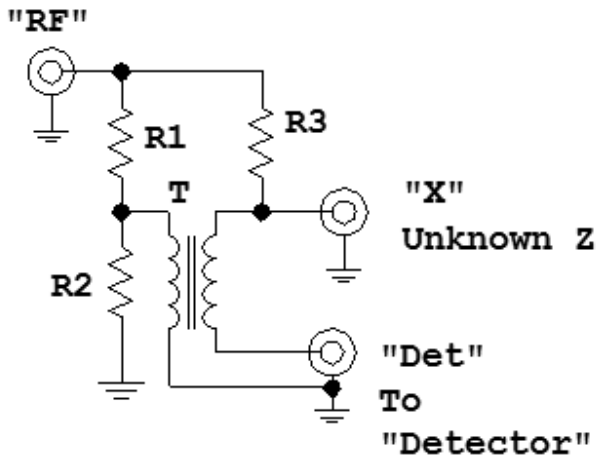

24Dec10
w7zoi

Above — Measure the return loss input of an amplifier. You'll need at least one 50 ohm BNC feed-through terminator on your bench to test amplifiers with wired-in BNC connectors (such as on this amp); else just solder a 47, 49.9 or 51 ohm resistor from the amplifier output to ground. The BNC connectors allow you to quickly and solderlessly interface components such as filters, attenuators, oscilloscopes or **50 Ω** signal generators.

A typical amp measurement work flow may go something like this: Measure gain using a signal generator and the 50 ohm terminated scope; add the bridge and measure input return loss; finally, flip the amplifier around and measure output return loss. All 3 functions can be performed in 2

— 5 minutes including time to drink coffee + perform calculations by computer or with a HP scientific calculator.

Measurement of an Amplifier Output Return Loss

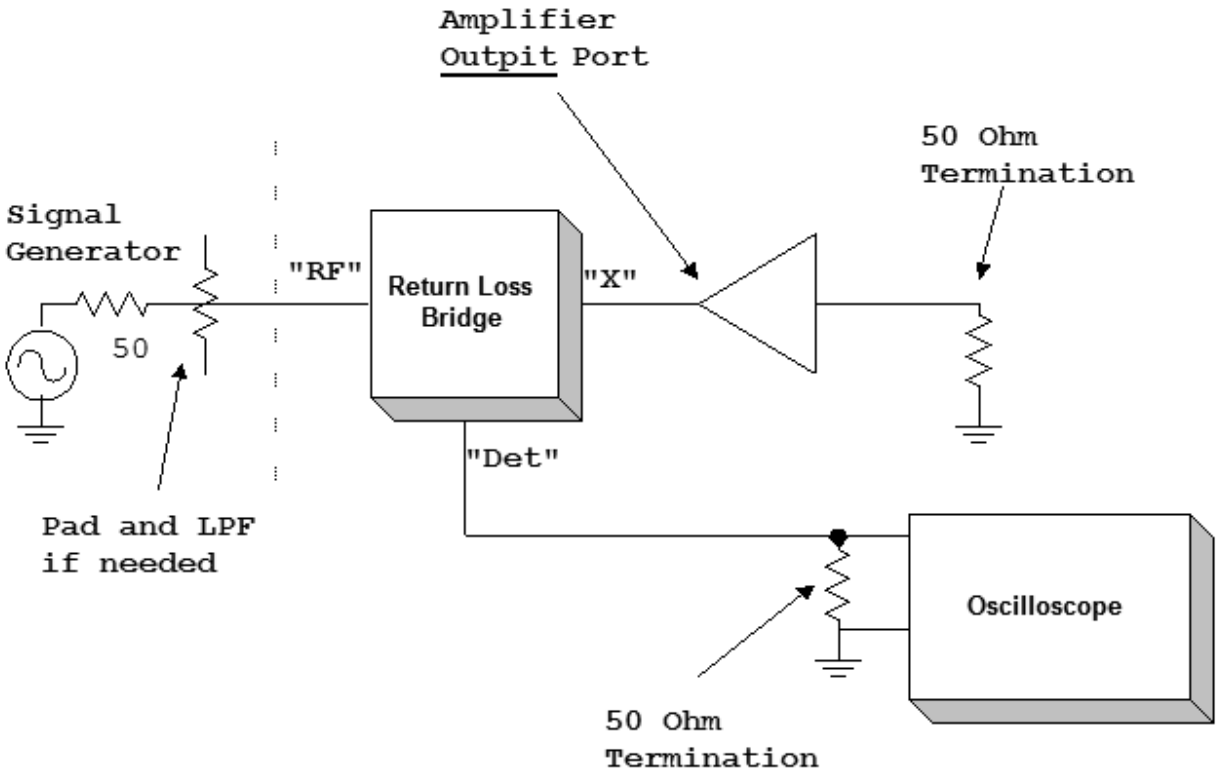

Measurement Procedure:

1. Terminate X port in an open circuit and note level. e.g.,250 mV pp at scope.

2. Attached a 50 Ohm load at X just to check the bridge. e.g., now see 5 mV pp.

3. Bridge *directivity* is 20Log(250/5)=34 dB. This is the best you can measure. Better numbers are meaningless.

4. Remove the 50 Ohm load. Attached the amplifier output and note level. e.g. 32 mV pp.

5. Amp Output RL is 20Log(250/32) =18 dB.

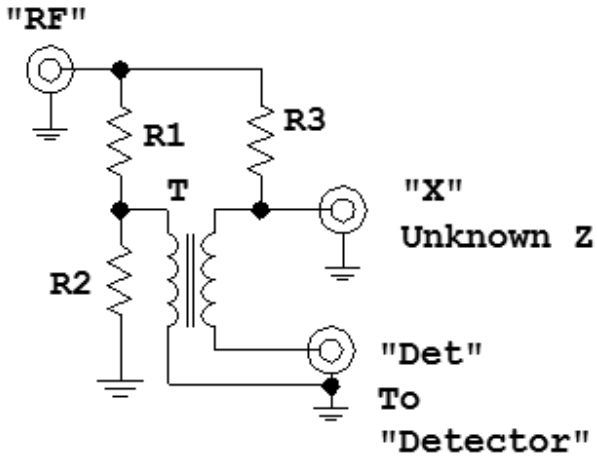

24Dec10
w7zoi

Above — Measure the return loss output of an amplifier. The above 2 procedural diagrams provided by Wes, W7ZOI. Many thanks to Wes. These figures are copyrighted © by Wes Hayward, 2010.

Your signal generator should have a return loss of at least 20 dB for greatest accuracy — all of my bench test generators have at least 30 dB of return loss. If you have a signal generator with a low impedance output and place a 10 dB attenuation pad on the output, you'll have at least 20 dB of return loss.

In the above figures, Wes gives an open circuit return loss of 250 mV; I set my signal generator output so the open return loss is somewhere between 170 and 250 mV; this allows you to accurately measure a really good 50 ohm return loss at >= 5 mV or so. Some people may have trouble going any lower than 5 mV due to scope accuracy. This is just something to consider.

Bench Exploration

For me at least, a special case of return loss measurement exists; measuring the return loss of a local oscillator. Since the oscillator under test must be *on* during measurement, it's emitting a signal at the same frequency as the bridge signal generator and interferes with measurement. If some 50 ohm attenuation is added to reduce the local oscillator under test output signal amplitude, this increases the return loss of the local oscillator under test. This is normally a good thing, however, we seek the **raw** output return loss or output impedance of the local oscillator under test.

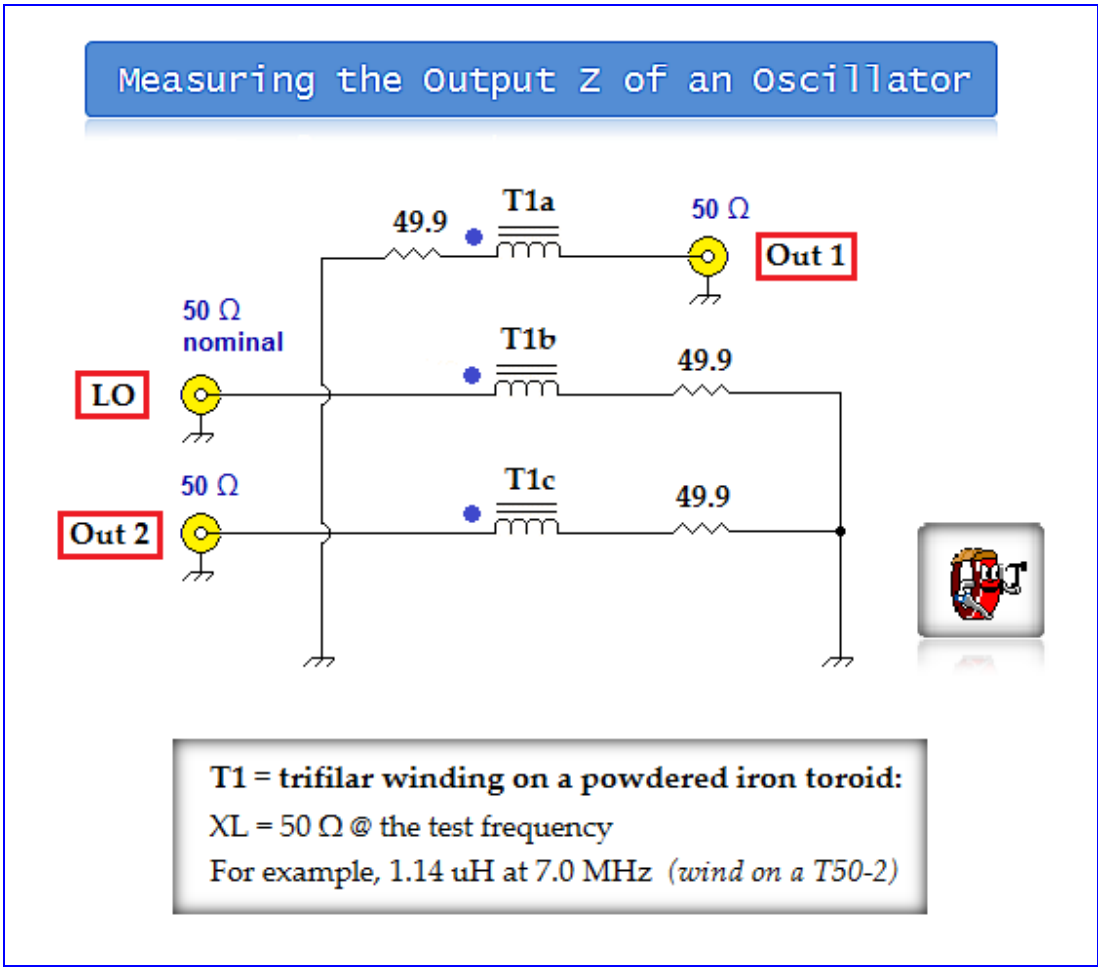

Above — An initial experiment that a builder from Michigan, USA and I first used to measure the output impedance of a local oscillator consistent with the breadth and scope of this web site. We wanted something simple and wished to avoid building a vector network analyzer or performing ugly algebra. I built a simple crystal oscillator for 7.0 MHz using an output transformer wound to give a low impedance output. The circuit was measured and calculated using the instrument above and the formula and procedure below.

The calculated output Z was 33.2 ohms. I build a standard value resistor 6 dB attenuator pad from this table. After fitting the pad, I re-measured and re-calculated the output impedance at 46.8 ohms. This seemed okay. I built a couple of oscillators for other frequencies and the output impedances were hundreds of ohms! — disappointing. Still, we were on the bench in a solution-focused mode and needed to try something else.

Formula

$$\text{LO output Z} = \left(\frac{\text{Out1} + \text{Out2}}{\text{Out1} - \text{Out2}} \right) \times 50$$

Make Out1 the larger pk-pk voltage

Out1 and Out2 are connected to 50 ohm terminated scope inputs, or 1 of them is connected to a 50 ohm terminated scope output, while the other is terminated with a 50 ohm resistor.

Above — The formula for calculating the output impedance with the *experimental* local oscillator output Z device.

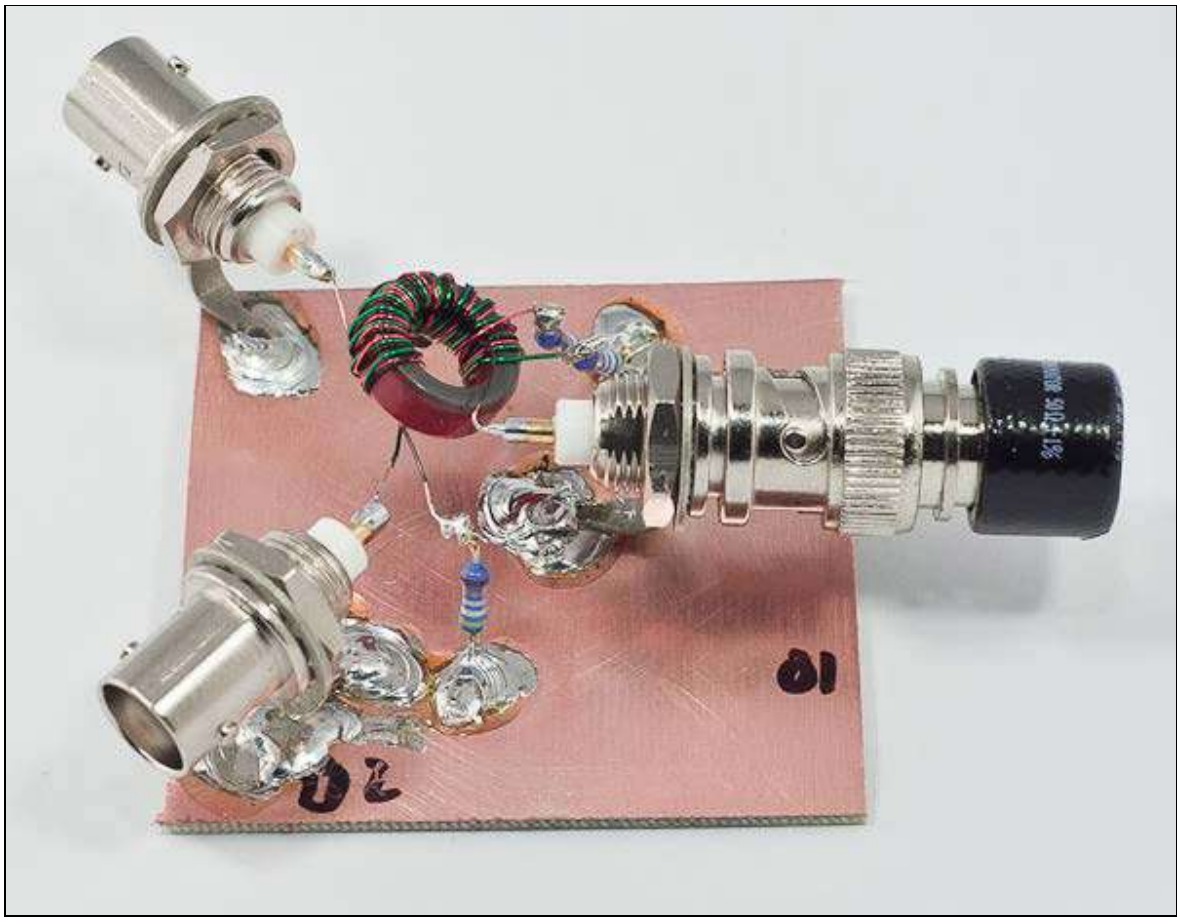

Above — Breadboard of the experimental L.O. output impedance bridge with a 50 ohm feed-through terminator on the Output 1 port. It failed to work as expected. Skillful adult problem solving goes something like this:

1. Identify the problem.
2. Brainstorm to generate some potential solutions.
3. Try out one of your ideas.
4. If that doesn't work, try another idea.
5. If none of your ideas work, wait a while, or ask an expert.

Well, we ran out of ideas and decided to ask experts for some more ideas; Professor Kuhn and Wes, W7ZOI.

I'll share their key messages. First, accurately measuring the output impedance of an RF oscillator can be difficult — measuring the return loss of a buffer amplifier is much easier. For this, some builders run the bridge signal generator on a slightly different frequency than the oscillator under test while using a spectrum analyzer as the 50 ohm RLB detector.

Another way is to short circuit the tank on the oscillator and measure the buffer output in the normal way — a popcorn solution indeed!

We tried calculating oscillator output impedance using different equations and 1 example is shown below. Failing to account for inductive and/or capacitive reactance plus resistance in the output circuit (including the transformer), plus upsetting the circuit during AC voltage measurement adds uncertainty to calculations — measurement seems more reliable.

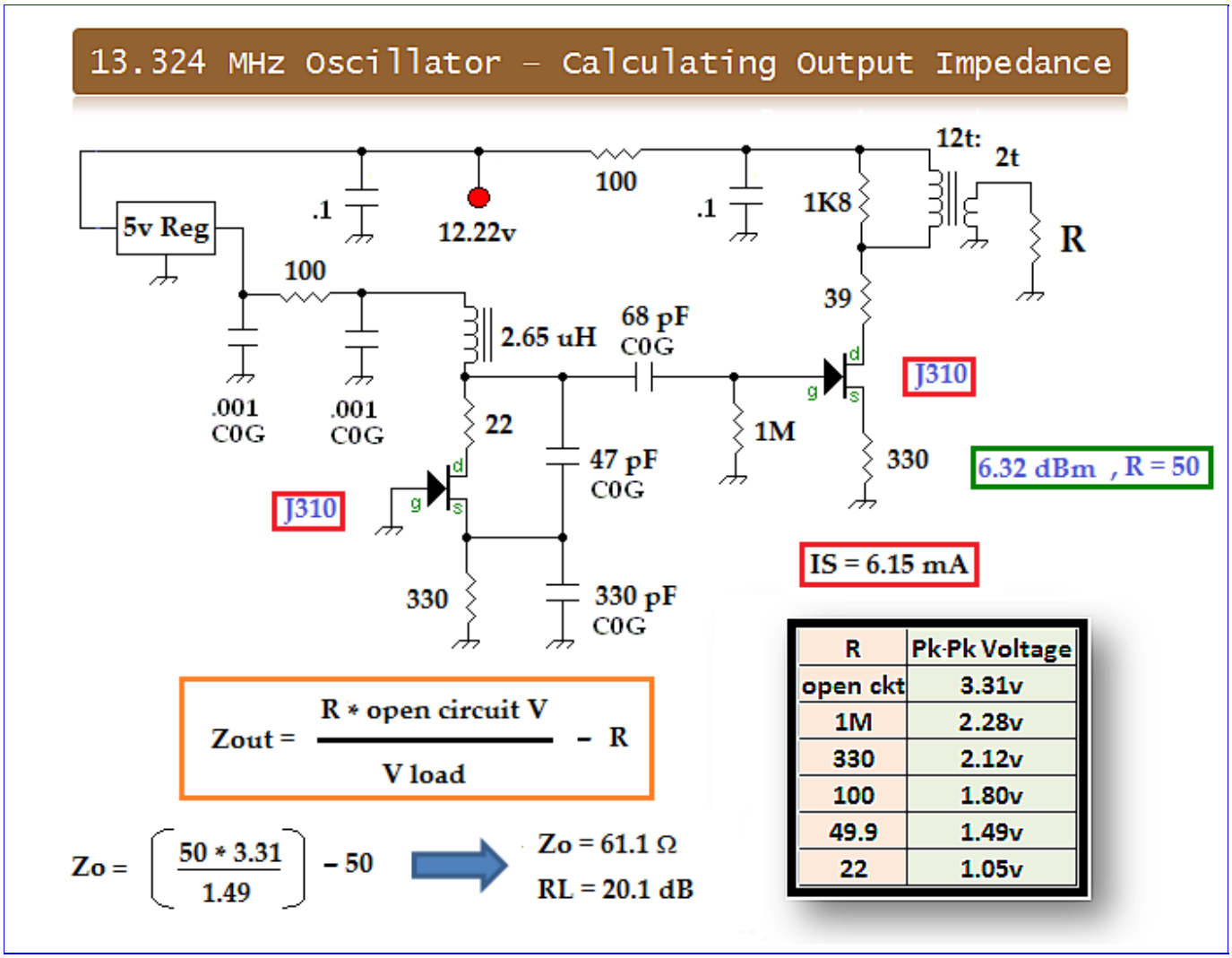

Above — One method of calculating output impedance. Running the output at open-circuit likely effects the oscillator by changing its load despite having the JFET buffer. Some builders use this equation for calculating the output impedance in their audio amplifiers. This amplifier **should** have a 50 ohm output impedance based upon the transformer turns ratio and the 1K8 resistor across transformer: 1800:50 ohms = a 36:1 impedance ratio and a 6:1 turns ratio.

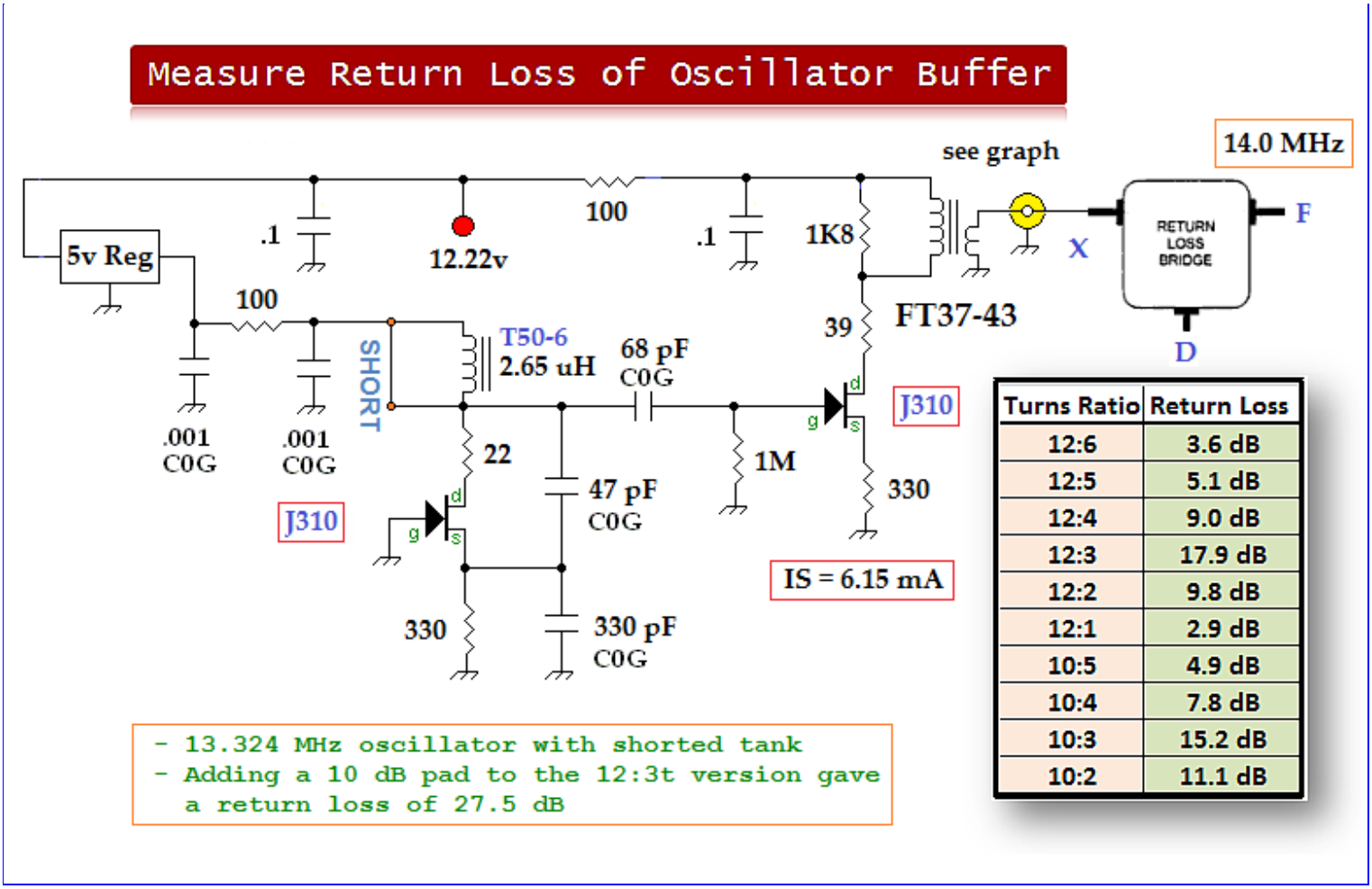

Turns Ratio	Return Loss
12:6	3.6 dB
12:5	5.1 dB
12:4	9.0 dB
12:3	17.9 dB
12:2	9.8 dB
12:1	2.9 dB
10:5	4.9 dB
10:4	7.8 dB
10:3	15.2 dB
10:2	11.1 dB

Above — A simple 13.3 MHz L-C oscillator was built and evaluated. After shorting the tank coil, return loss versus turns ratio was measured and tabled as shown. To my surprise, I observed the best match with a 4:1 turns ratio. This suggested that the transformer, wound on a ferrite FT37-43 toroid was exhibiting high resistance and far from the "ideal transformer". The inductance of my 12 turn transformer was 38.3 uH.

The initial secondary winding had 6 turns and then was reduced sequentially by 1 turn. After removing each turn, the 1/2 cm of increased wire length was cut off and the enamel scraped off of the new wire ending to ensure a short connection to the output jack. During measurement, unless the secondary transformer wires were kept tidy, a ~40 MHz oscillation occurred when the 1K8 resistor was disconnected. The 1K8 resistor prevented such oscillations and improved the return loss by 1-4 dB at the various turns ratios. Testing frequency was 14 MHz.

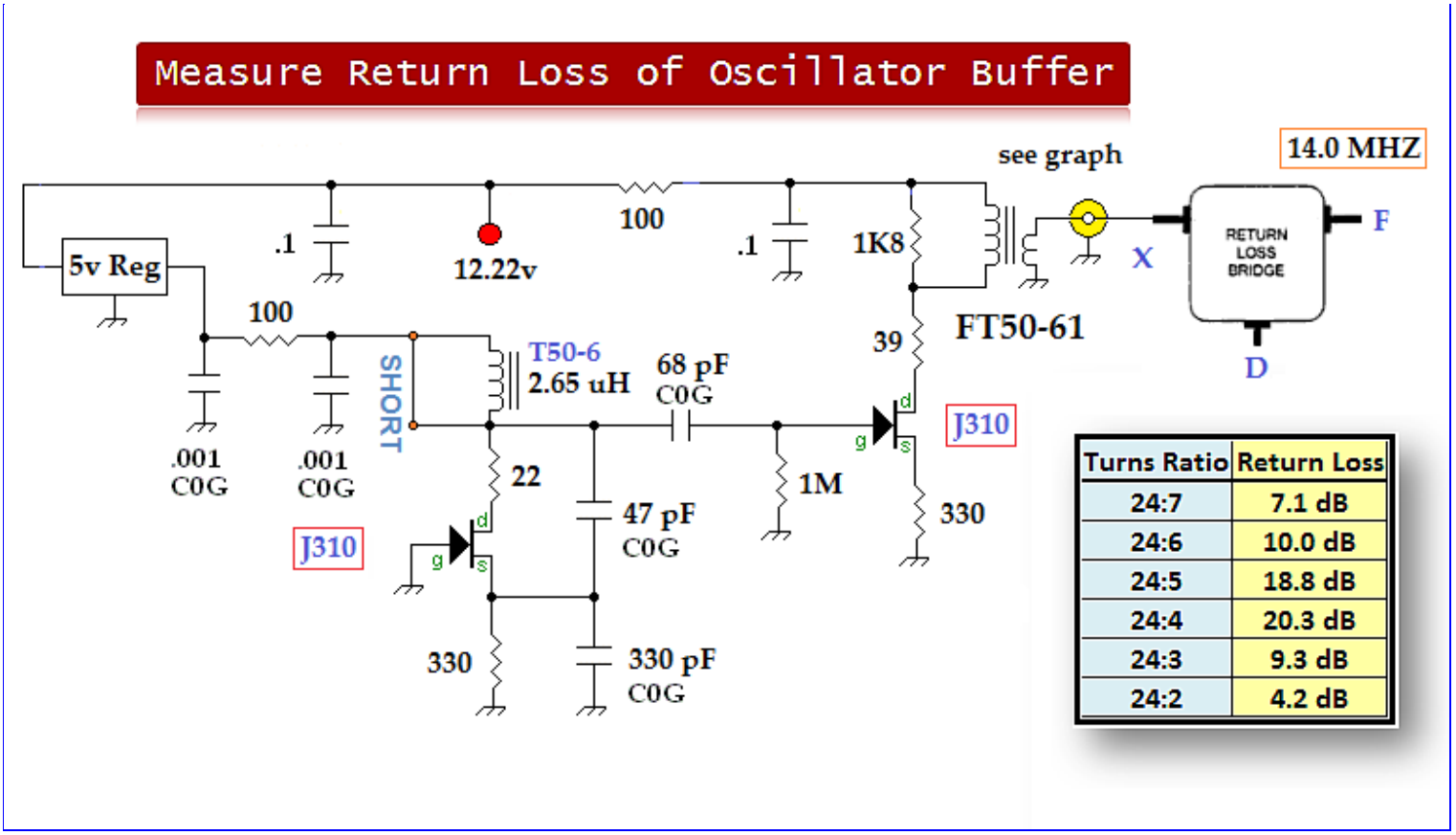

Above — The same circuit with a lower-loss, FT50-61 ferrite transformer. I could have used a FT37-61, but prefer the 50-61 as the bigger core allows the use of heavier wire which provides some robustness when performing intensive experiments. The inductance of 24 turns on a FT50-61 measured 36.2 uH. Although lower permeability ferrite toroids require more windings, this transformer is closer to the "ideal transformer" than that wound on a FT37-43 ferrite core — a 6:1 turns ratio gave the best return loss; the output Z is pretty close to 50 ohms.

The information garnered during these tests proved enlightening and reinforces why bench measurement provides the greatest way to learn about and optimize your circuits. I hope this simple web page on return loss measurement fuels your own experiments — the most important experiments will be those *you* do on *your* bench.

Miscellaneous Figures and Photos

Calculate Output Z of an Oscillator – Experiment 1

Measure the open circuit output amplitude of the oscillator and then add a load so that the loaded voltage dropped to something in the range of 50 to 75 percent of the open circuit voltage. Then use voltage divider theory to calculate the source resistance of the oscillator.

$$V_{loaded} = \frac{V_{unloaded} * R_{load}}{(R_{oscillator} + R_{load}}$$

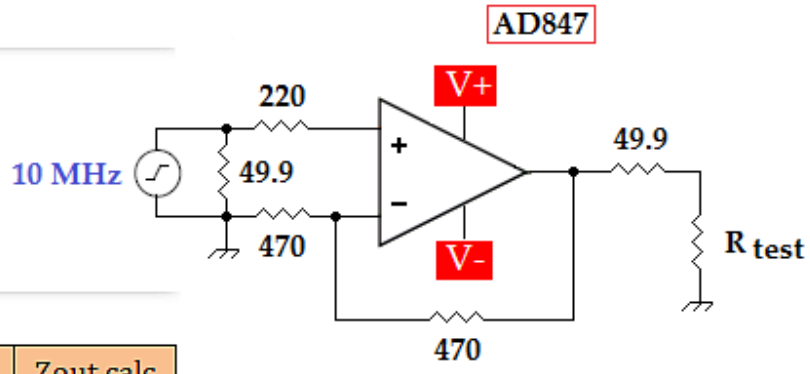

Rtest	Vout	Icalc	Pcalc	Zout calc
1000000	0.9999	9.999E-07	9.998E-07	
220	0.8148	0.0037	0.0030	49.9779
50	0.5003	0.0100	0.0050	49.9300
22	0.3056	0.0139	0.0042	49.9823

RF — Test and Measurement

Miscellaneous RF Topics 2011

Introduction

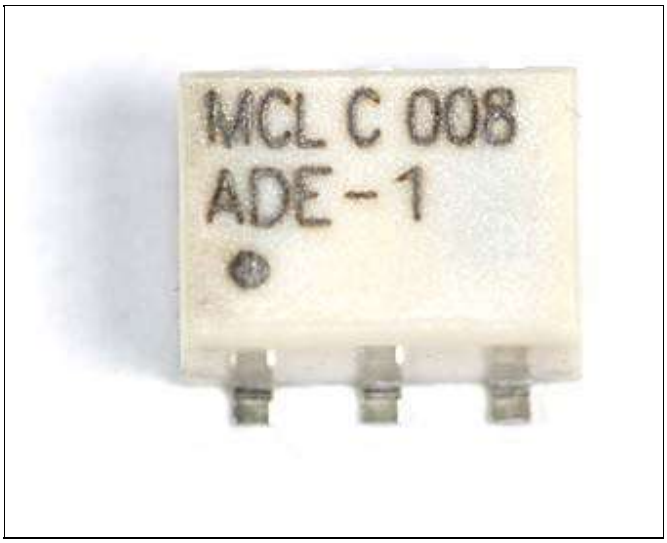

My basic goal for Fall and Winter 2010 was to fearlessly advance my RF design ability — pushing just beyond my comfort zone to impose the psychological stress that promotes focused learning. You may have experienced this in University or when working against a deadline. Cramming, "burning the midnight oil", or locked room brainstorming exemplify this approach.

These circuits feature carefully measured input and output impedances (nominal impedance = 50 Ω), plus voltage gain and DC current.

This web site spawns email with builders worldwide. Our interactions are varied; getting help, giving help — or just chat. On occasion, I design, build and/or test circuits to help struggling builders. After spending considerable time, I email them my work hoping it will help. Often enough, I never receive any acknowledgement from these readers — did the circuit work or did they appreciate I spent 1-2 hours researching their concern?. This is actually normal — we must constantly strive to overcome our innate, self-centered nature; lest it dominate our behavior. все нормальные.

To that point, I wish to gratefully acknowledge the people who support me in this hobby: Wes, Ken, Scott, Peter, Tom and the many others whose email advice and published and private work informs and inspires me.

Topics:

1. Transmit Mixer Experiments
2. Bipolar Transistor Feedback Amplifier Experiments
3. JFET Common Gate Transistor Amplifier Experiments

Navigation and Preamble:

This web page grew into a large monster — and includes a supplemental web page with numbered topics referenced in the text. I apologize for the navigation difficulties this web page poses. Equal time was spent experimenting with the circuit designs and circuit photography. I strive to provide a variety of bitmap and photographic image styles on this web site.

---

1. Transmit Mixer Experiments

Since I've never experimented with transmit mixers, I didn't appreciate how much time goes into their design. Consider, for example, the LO system from the project entitled A Monoband SSB/CW Transceiver in Chapter 6 of EMRFD. The mega low (about -20 dBm) output from a diode ring mixing a VFO and crystal oscillator is triple tuned band-pass filtered and then amplified to +8 dBm. Continuing on, the transmitter chain features more mixing, band-pass filtering and voltage amplification by a feedback amplifier chain boosting the signal to around 300 mW. The circuits needed to mix, filter and amplify this RF chain would challenge most amateur designers — me included.

Contrast this with a typical first transmitter built by a new builder. Likely your first scratch homebrew transmitter consisted of a crystal oscillator, a keyed Class A buffer/amplifier and perhaps a Class C final amplifier. No mixer was needed for we obtained a crystal cut on the frequency of

choice. Our focus was **power**— getting 0.25 to 1 watt into our antenna system! A good example was the Tuna Tin 2 transmitter by the late Doug DeMaw, W1FB that only used 2 stages. Although Doug wrote his 1976 article for Hams to build a transmitter from parts found at home, kitted versions are sold today.

Returning to transmit mixers — as amateur designers, we likely need to start on a small portion of the transmit chain and then after developing some competency, slowly extend our experiments all the way to the antenna port. In Fall 2010, I just examined some basic transmit mixing to get a feel for what's involved and what to expect. Mixing signals is a complex affair encompassing topics such as intercept point, conversion gain or loss, image noise suppression, noise figure, spurious/intermodulation products and port isolation. To keep things simple, only mixer port isolation and reducing spurious mixer products were examined.

Before beginning, I express the following concern: We experimenters, as stewards of the airwaves, must build exemplary transmitters with very low spurious outputs. I follow the example of Wes, W7ZOI and others — my transmit chains have spurious frequencies at least 50-60 dB down from the carrier (dBc). As a web author and radio amateur, I never want to directly or indirectly contribute to RFI and hope you agree.

Why Use a Transmit Mixer?

If you plan to design a superheterodyne based transceiver, you'll probably need to use a transmit mixer. Also mixing 2 frequencies permits using cheap microprocessors crystals to target a desired transmit frequency; separate crystal oscillators drive the RF and LO ports of the mixer. For added flexibility, the LO can be converted to a VFO once you have the basic design working well.

I purchased a bag of low cost crystals. By mixing 2 appropriate crystals, output on a Ham band is possible. For example, crystals at 2.048 + 5.0688 MHz = 7.117 MHz; 4.194 + 11.228 MHz = 7.034 MHz; and 3.932 + 11.046 MHz = 7.114 MHz. I frequently operate QRP on 40 Meters in the USA Novice band, so 7.114, or 7.117 MHz is okay. This helps CW operators avoid all the RTTY and QRM down in the traditional 40M band QRP frequency window.

Some Mixer Bullets

Mixers have 3 conventionally named ports; RF, LO (local oscillator) and IF (output).

The diode ring mixers presented are Level 7 mixers. Maximal LO power is 7 dBm.

Many builders limit the maximum RF power into a Level 7 diode ring transmit mixer RF port to between 0 to -3 dBm.

The term *isolation* refers to the amount of LO power that leaks into the RF or the IF ports.

Low-pass filtering the LO *can* significantly reduce harmonic products in a mixer

The top of the spectrum analyzer screen (always the top, and never the bottom) is called the reference level. That is the power at the top. If you have a signal generator with the output adjusted to be -27 dBm and pass this signal into the spectrum analyzer and adjust the attenuation in the analyzer to put that signal at the top of the screen, you then the reference level is -27 dBm. *(Pertains to examining a mixer output in a SA)*

Choosing a Mixer

A number of mixers were considered; passive, active, unbalanced, single-balanced and finally, double-balanced. The diode ring mixer is an obvious good choice commensurate with my goals of reducing spurs, LO feed through and achieving high port-to-port isolation. In future web pages, other mixers may be presented, however this page is focused on the diode ring mixer. Click for a file with a few scanned pages concerning mixers from my "ideas only" notebook from ~2002. I own over 30 notebooks now.

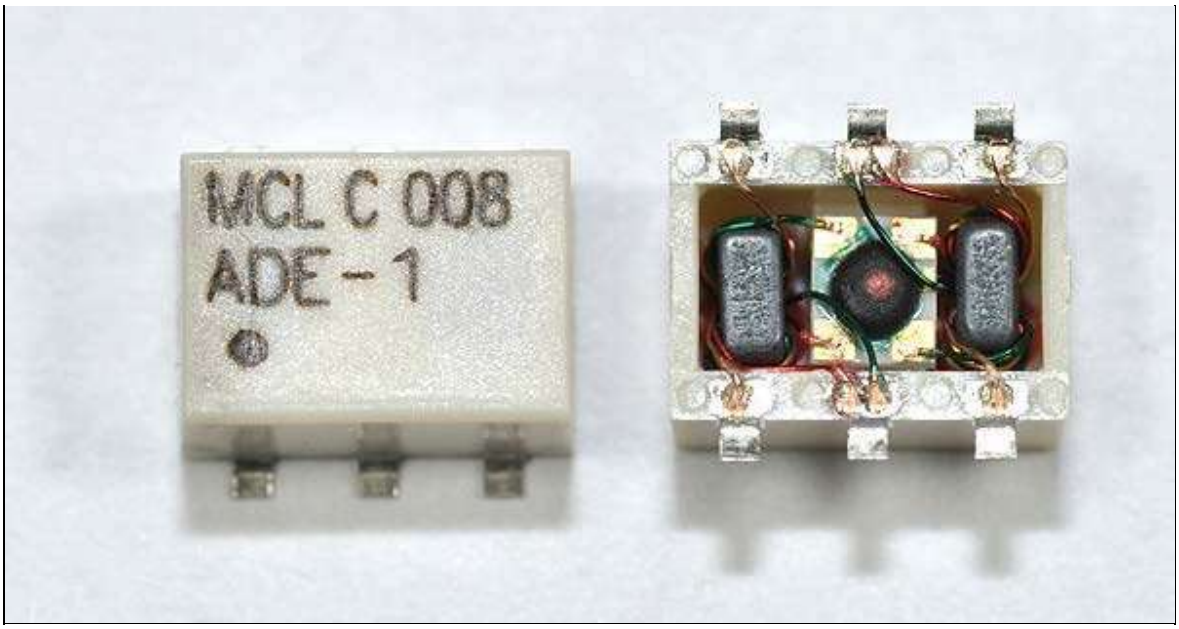

Above — ADE-1 diode ring mixers. We're using these now as they're cheaper than the SBL-1, TUFF-1 etc. hole-though versions. Although SMT parts, they can be flipped over and wired "normally" with a little effort, steady hands and good vision. Mini-Circuits will sell them in small quantities to Hams; email them and enquire. I feel the diode ring mixer has been misunderstood by some amateur builders — lore and misperceptions that the 7 dBm LO port drive, the need for 50 ohm port terminations, a ~ 5 dB insertion loss and cost make them undesirable. Their excellent performance and design challenges are reasons why we use them; "the journey — not the destination" stuff.

In receiver applications, some builders and kit sellers seem more focused on features such low-battery indicators, digital displays, miniaturization and cost containment than basic receiver performance. Certainly keeping cost down down deserves consideration, however, good mixer performance is king. You'll have to decide what's affordable and important and build accordingly.

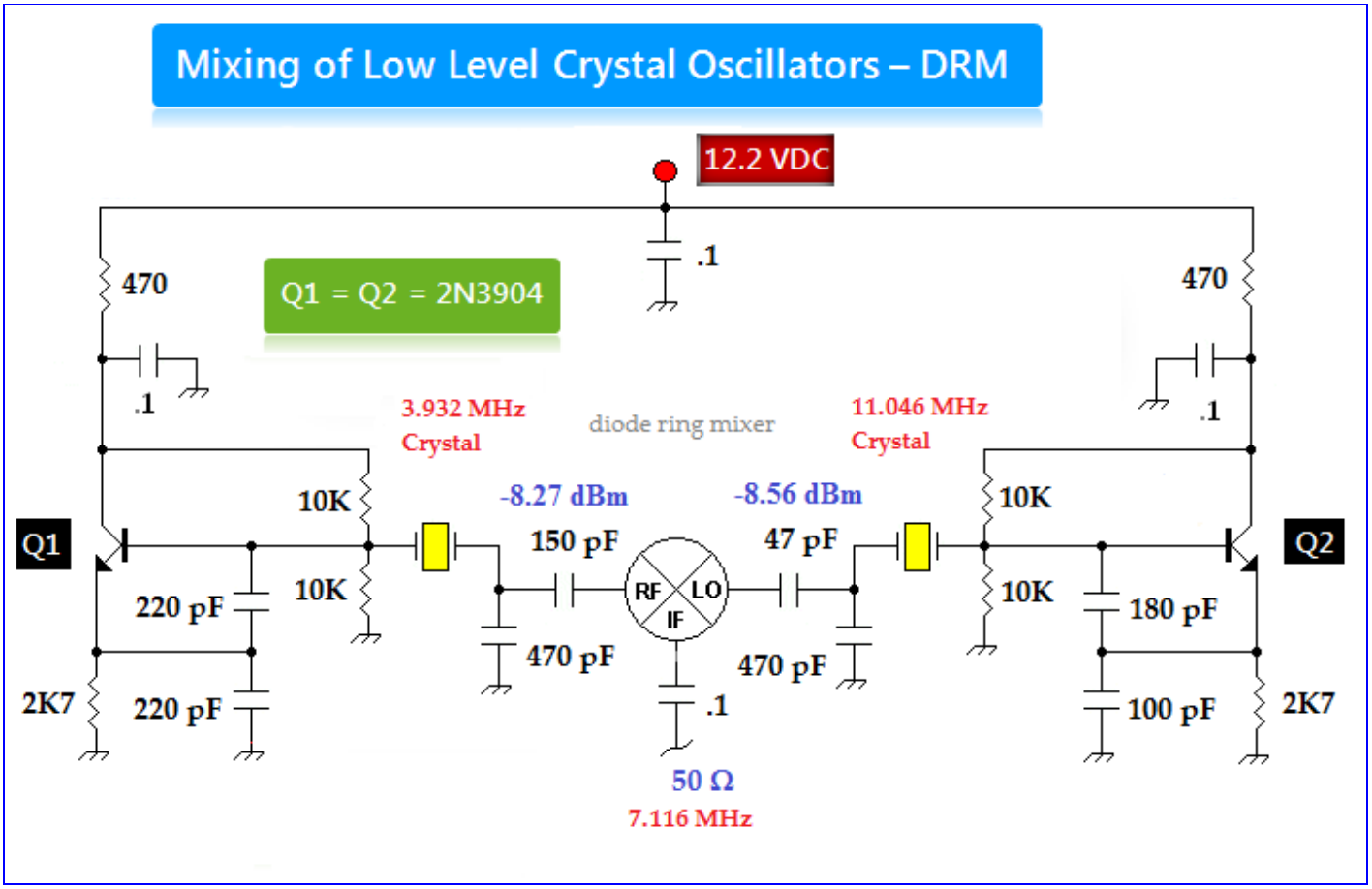

Above — My very first transmit mixer experiment. My hope was to build a transmit mixer possessing low spurious output to alleviate the need for stiff, post mixer band-pass filtering such as a triple tuned band-pass filter. Thus, low-level, low distortion output was taken from between each

crystal oscillators' shunt capacitor and crystal. The desired output frequency is ~7.114 MHz to build a transmitter for the 40 Meter Ham band.

The mixer output to 50 MHz looked like this in a Spectrum Analyzer. The dominant frequencies are the **sum** and the **difference**: 11.046 **+** 3.932 MHz = **14.98 MHz**; 11.046 **-** 3.932 MHz = **7.114 MHz**. The frequencies realized are *slightly* different since the oscillator output is shifted by crystal variances and from circuit capacitance.

In the experiments that follow, I built some circuits to filter and/or amplify the output of the *above* mixer circuit.

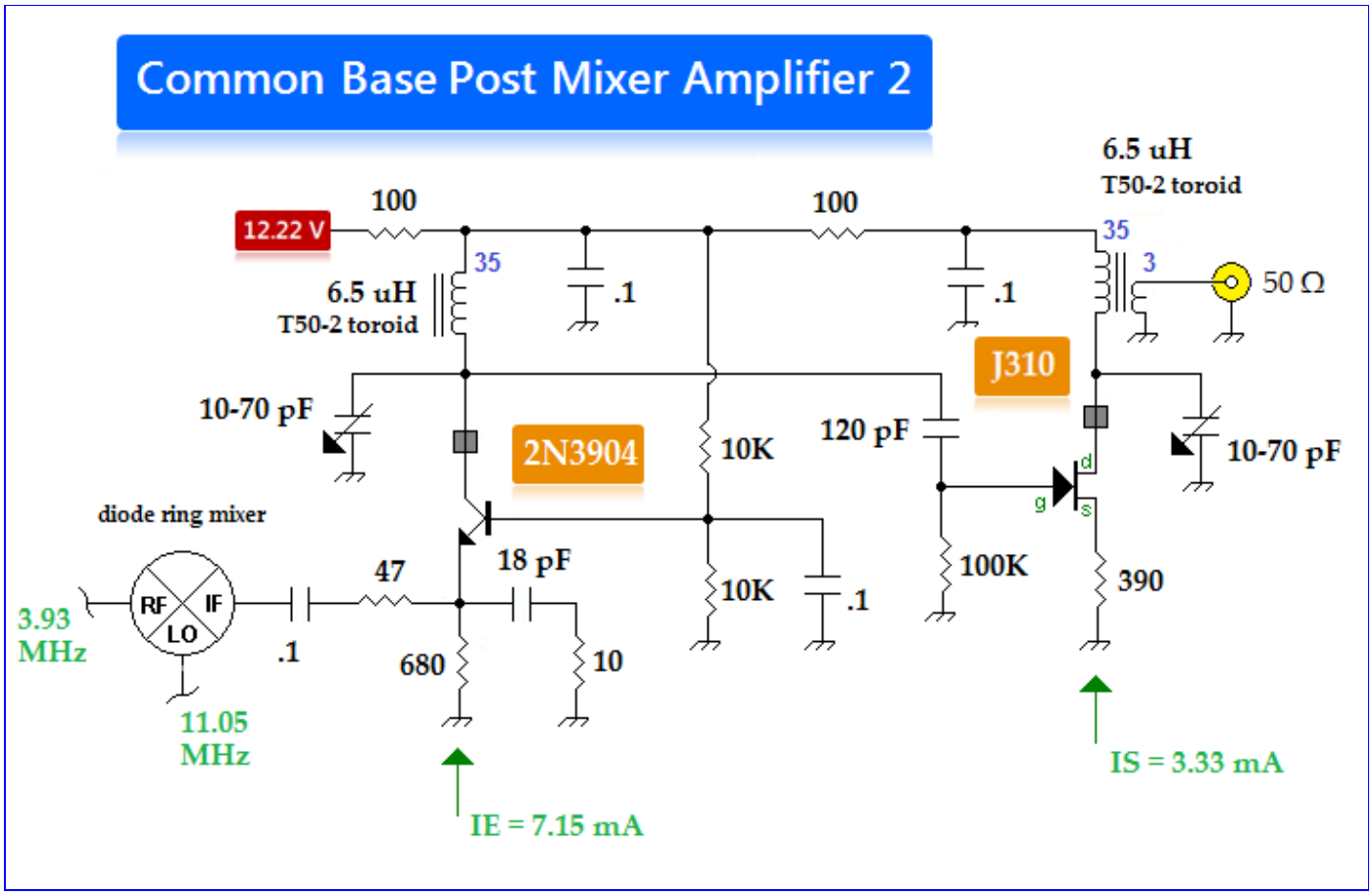

Above — The first post mixer amp; a common base input amplifier that's AC coupled to a common drain FET amp. I hoped that 2 tuned L-C tank circuits could substitute for a passive double or triple-tuned band-pass filter, plus provide some gain.

A broad-band, common base input amp was chosen to properly terminate the diode ring mixer and alleviate the need for a diplexer. A ~50 Ω input impedance is established by a 47 Ω series resistor since the 2N3904s input impedance is quite low due to the moderately high emitter current employed to boost gain and IMD performance.

This amplifier failed to reduce spurious output 50 dB down or greater — my design goal. Here are its scope and spectrum analyzer outputs; please observe that the unwanted 14.98 MHz signal is only 32 dB down from the desire IF of 7.114 MHz. An RC network consisting of a shunt 10 ohm resistor + an 18 pF cap provides additional low-pass filtering above 20 MHz. I attribute this simple filter to Dr. Ulrich Rohde as I have seen it in some of his post mixer, common base RF amplifier designs. Click for a brief supplement regarding his low-pass network ***(#2 RC Low-pass Network on the Supplemental Page)***

The amp design shown above was actually an improved version of this prototype. In the prototype amp, the mixer power at 14.98 MHz was only 23 dB down from the desired intermediate frequency of 7.114 MHz. You can't expect a single L-C tank to well filter a mixer output. Unfortunately, the 1K2 -12K resistor providing DC bias for the emitter follower lowers the Q of the common-base collector tank circuit. 12K is better than 1K2 in this regard. Poor performance sparked the design of the second common base amp shown above.

I use ferrite beads and 51 Ω resistors interchangeably on the collector/drains of amplifiers to snuff out UHF oscillations. According to my experiments, the resistors may work better. I purchased the ferrite beads from Diz. After the common base amplifiers shown above, I decided to try a tuned input + output common gate JFET amp:

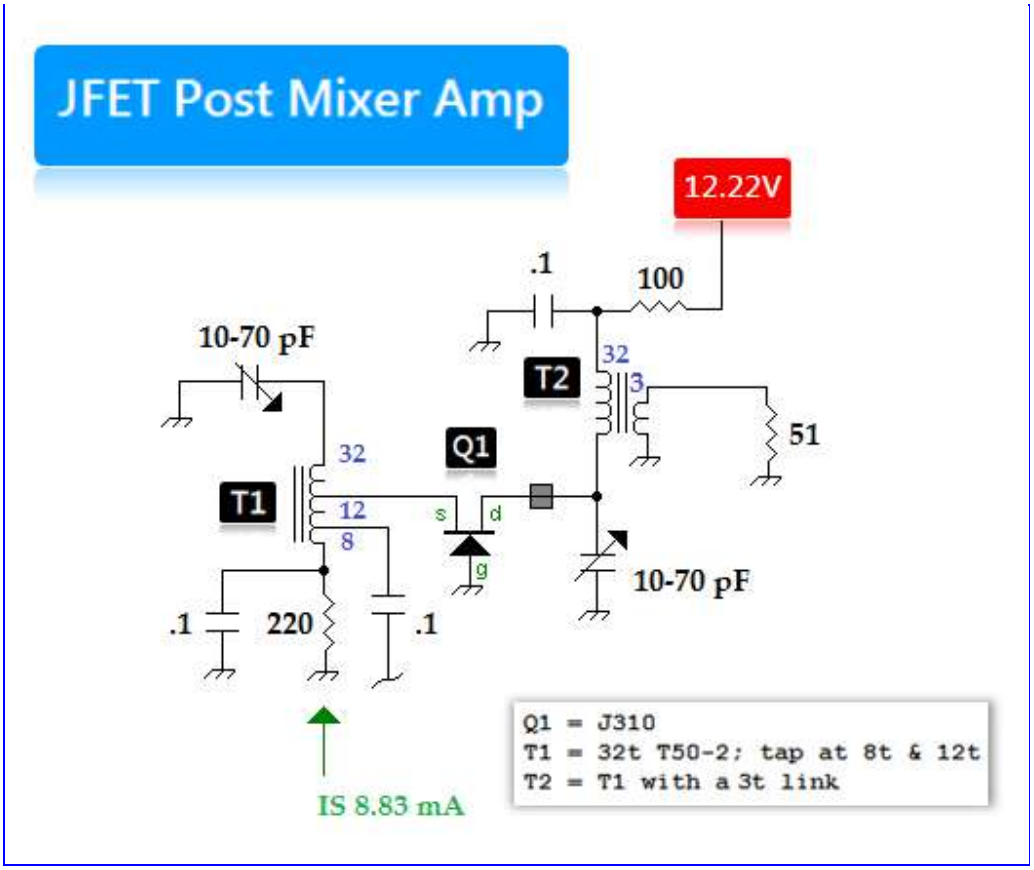

Above — A JFET common gate amp with tuned input and output built about 3 years ago. For spectrum analysis. I padded the amplifier output to provide a -28 dBm 7.116 MHz signal. The vertical resolution on the SA is the standard 10 dB/division. As shown, the 14.98 MHz signal is ~ 39 dB down; an improvement over the amplifiers shown previously. This narrow-band amplifier requires a diplexer. I wanted *better* filtering than that offered by amplified circuits with 2 tuned L-C circuits, so I halted this experiment and decided to try a triple tuned band-pass filter.

This JFET circuit experimentation spawned over 8 weeks of experiments concerning common-gate RF amps — some of them appear later.

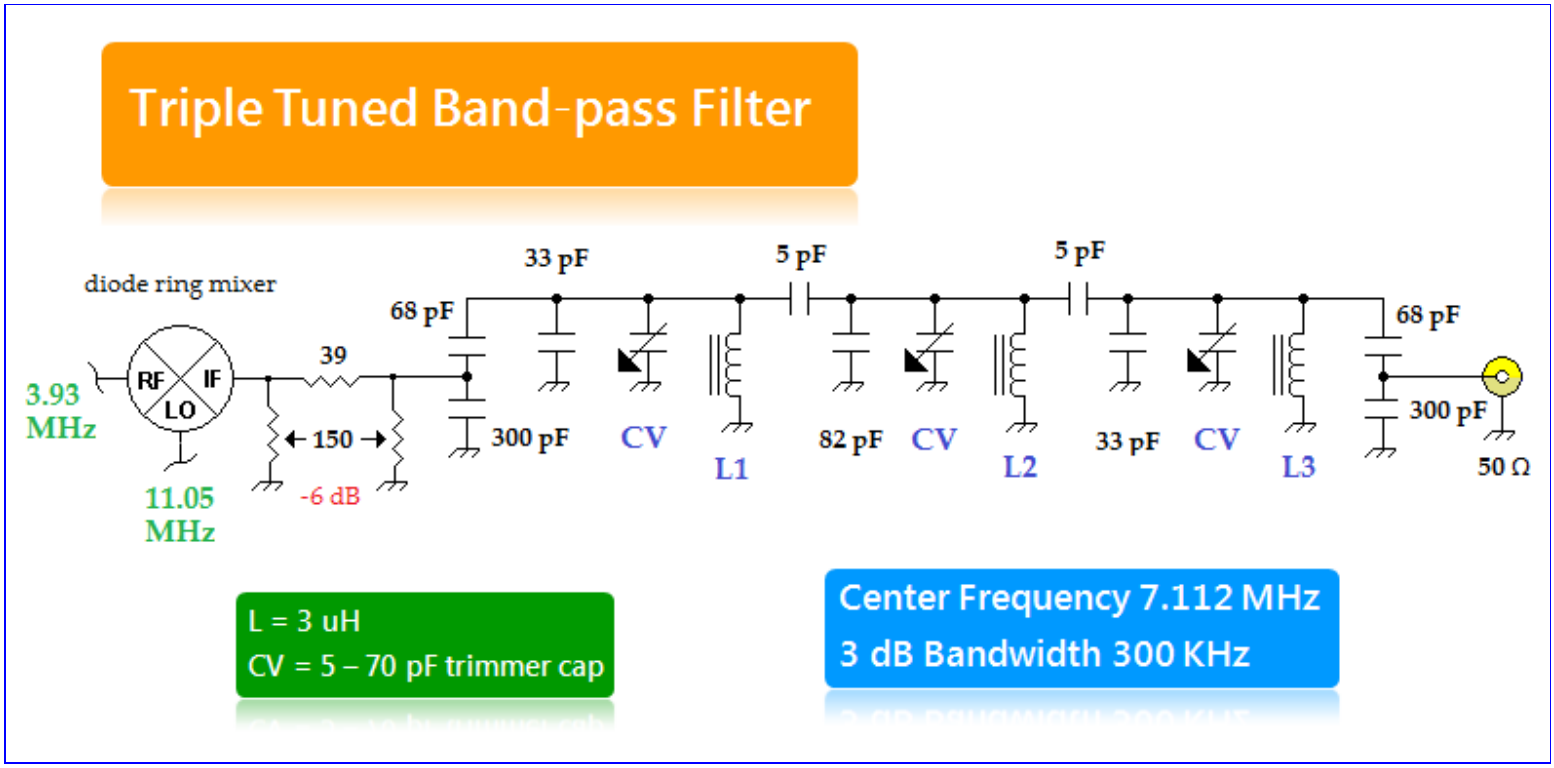

Above — A triple tuned band-pass filter designed with software from EMRFD called TTC-08. Click for the breadboard photo. The diode ring was connected to the filter input via a 6 dB attenuator pad using short leads. Click for analysis in GPLA. All inductors are 3.0 uH — 23 or 24 turns on

a T50-2 powdered iron toroid. I measured all the inductors and obtain the exact desired inductance by expanding or squishing the wire turns, or if necessary, adding (this means rewinding the entire coil) or removing a turn. If you lack an inductance meter, just winding the formula calculated number of turns will be close enough for most applications — I only got a good L- C meter in 2009 and somehow managed.

I learned that the ultimate way to peak a triple tuned filter is by tweaking the tuning capacitors while it's connected to a spectrum analyzer — what a thrill!

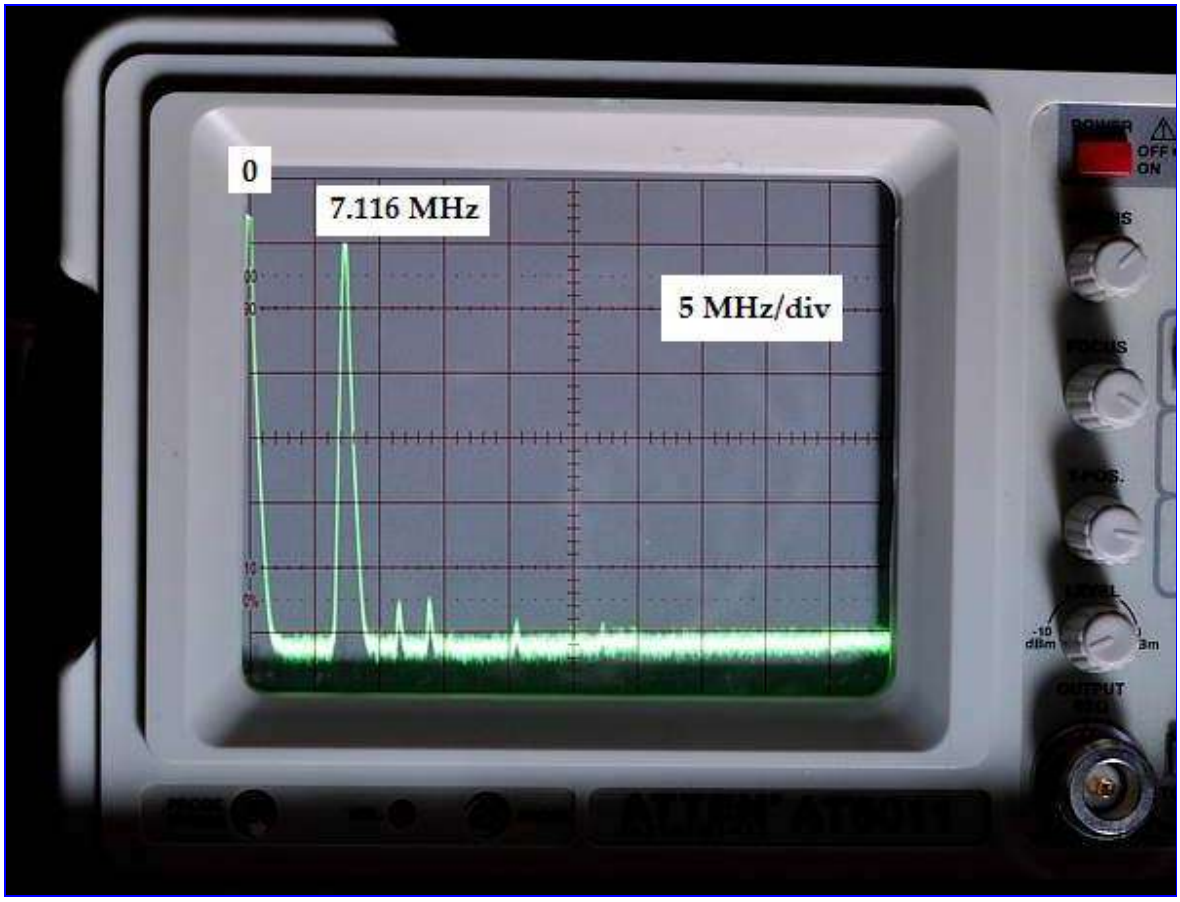

Above — While a little tedious to build and align, the triple tuned filter worked magnificently; the strongest spur is 54-55 dB down and the 14.98 MHz signal is gone. Insertion loss = 2.5 dB. This experiment provided a benchmark of what great post mixer filtering looks like. Post mixer filtering is an important topic worth studying further:

Why do we need filtering on a mixer output?

Let's examine mixer ports more closely. A port is just a pair of wires where signals are applied or removed. There are 2 kinds of mixer *outputs*: 1) the sum plus difference frequencies; 2) spurs.

Further, 2 kinds of spurs occur: One type is straight feed through where 1 signal from the 2 input ports makes it out to a 3rd port. Examples include LO feed through to the RF port, or LO feed through to the IF port.

The other type of spur is a mixing product such as a harmonic.

In general, the mixer output frequencies are numerically described by an equation:
IF (output) = N x L +/- M x R
N and M are both integers, 1, 2, 3, ... L = local oscillator frequency, R = radio frequency

A mixer is said to be balanced when you duplicate some of its functions and then combine them — usually with transformers. Consider, for example, the single diode mixer — they work, but the output contains ++ feed through and spurs. A mixer with 2 diodes or 2 FETs etc. can be much easier to use because the transformer combines the signals in a way that cancels some of the spurs and feed through. The double-balanced diode ring mixer uses four diodes and 2 transformers — producing even less feed through and harmonic output.

In a double-balanced diode ring mixer, the LO and RF ports are balanced and all ports of the mixer are isolated from each other. The double-balanced mixer greatly reduces, but does not stop all LO feed through at the RF and IF ports. A wideband match at 50 ohms is required to maintain mixer balance; hence you will often see attenuator pads on the LO, RF and *especially* the IF ports.

Let's focus on the IF port. Attenuator pads absorb any reflected mixer products and signals coming back into the IF port, thus increasing the

match to the IF port. You may have noticed some builders use a diplexer on the IF port. The diplexer presents a wideband match to all IF port frequencies — passing the desired sum or difference frequency and absorbing the unwanted mixer products reflected back into the IF port by subsequent stages.

Since the IF output contains the sum and difference of the LO + RF, LO feed though, and other spurious energy, band-pass filtering is required to launder the IF signal into something useful. Following a transmit mixer, we filter with an L-C band-pass filter — after a receive mixer, crystal band-pass filters dominate. If you choose an unbalanced mixer or single-balanced mixer, filtering becomes more difficult than with a double balanced mixer. Unbalanced mixers are usually reserved for situations where high performance is being sacrificed for cost containment and/or want of a low parts count. There is no free lunch — you either alleviate as many mixer products as you can at a low-level with good practices, or have to deal with them down your signal chain while sacrificing optimal mixer performance.

Double balanced mixers are sensitive to non-resistive IF port terminations. When improperly terminated, the 2 transmission-line transformers work poorly — any reflected power generates high voltage across the diodes and degrades mixer performance. According to Dr. Ulrich Rohde, some proper ways to terminate the mixer include using a diplexer followed by a wideband 50 Ω feedback amp, or a common-gate JFET amplifier. *(Reference 1)*

Improved Local and RF Oscillators

In the earlier experiment, I really should have the run the LO port at 7 dBm. In order to improve my experiments, new crystal oscillators were designed with emphasis on correct LO output power and low harmonic energy.

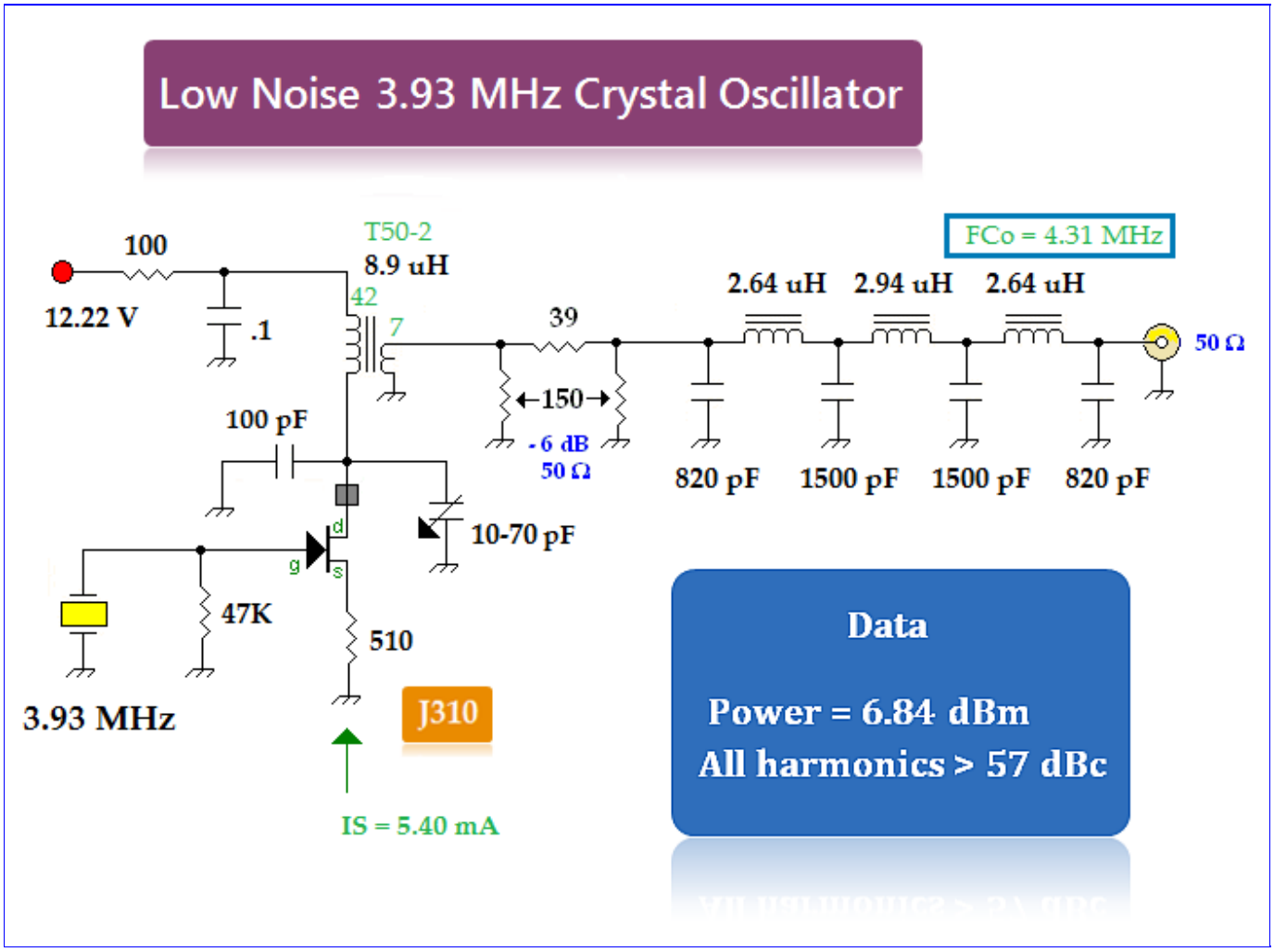

Above — The new LO; a 3.93 MHz crystal oscillator with stiff low-pass filtering. Admittedly, this 7 element Chebychev low-pass filter is overkill, however, I wanted to examine filtering and learn how much is required. On the bench — do whatever you like; even chasing crazy personal goals can be instructive and help you relate to information from texts and articles, or satisfy a whim. I can read something 100 times, but may not understand it well until I actually do it.

Above —The LO breadboard in close-up using a long focal length lens. Click for a wide angle photograph. The unsoldered end of the 100 Ω resistor in the close up photograph is where I connected the VCC.

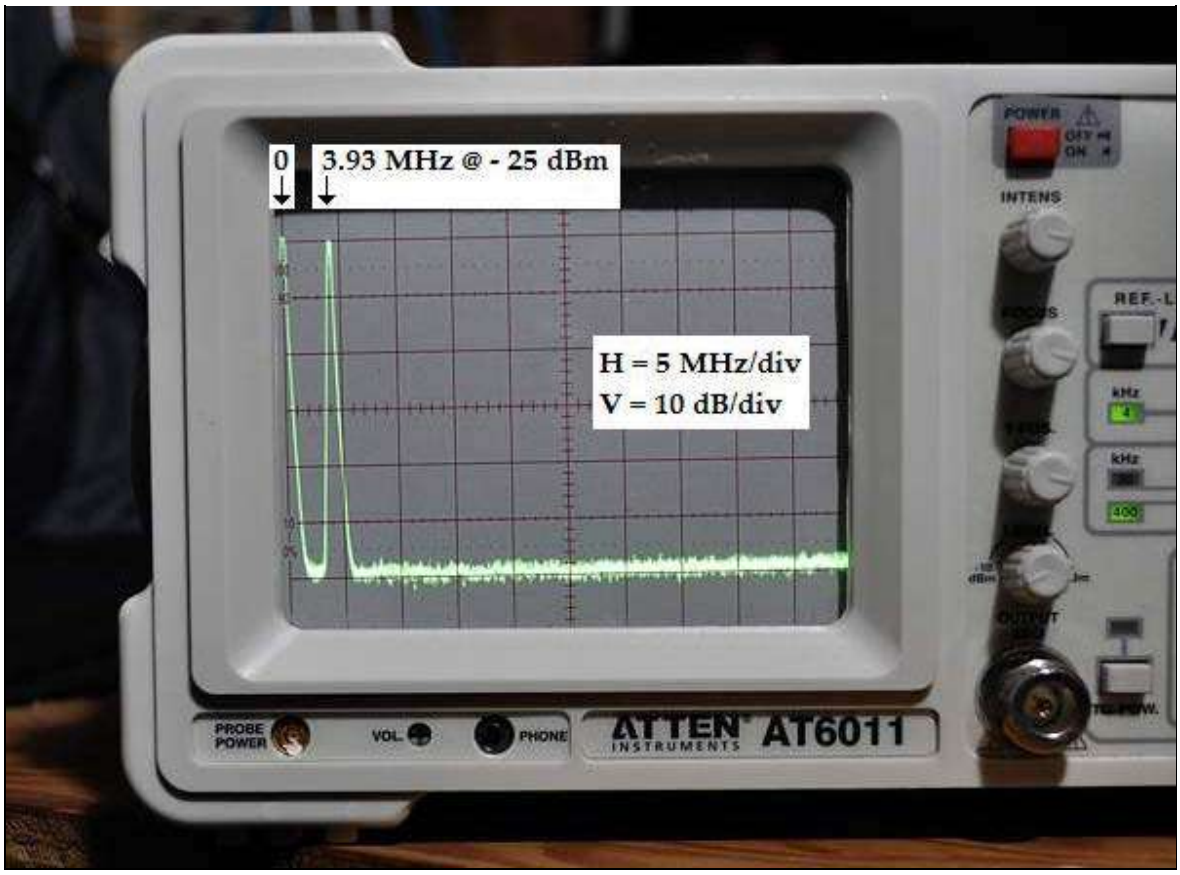

Above — Spectrum analysis of the well-filtered 3.93 MHz LO. Not surprising, no harmonic energy is seen.

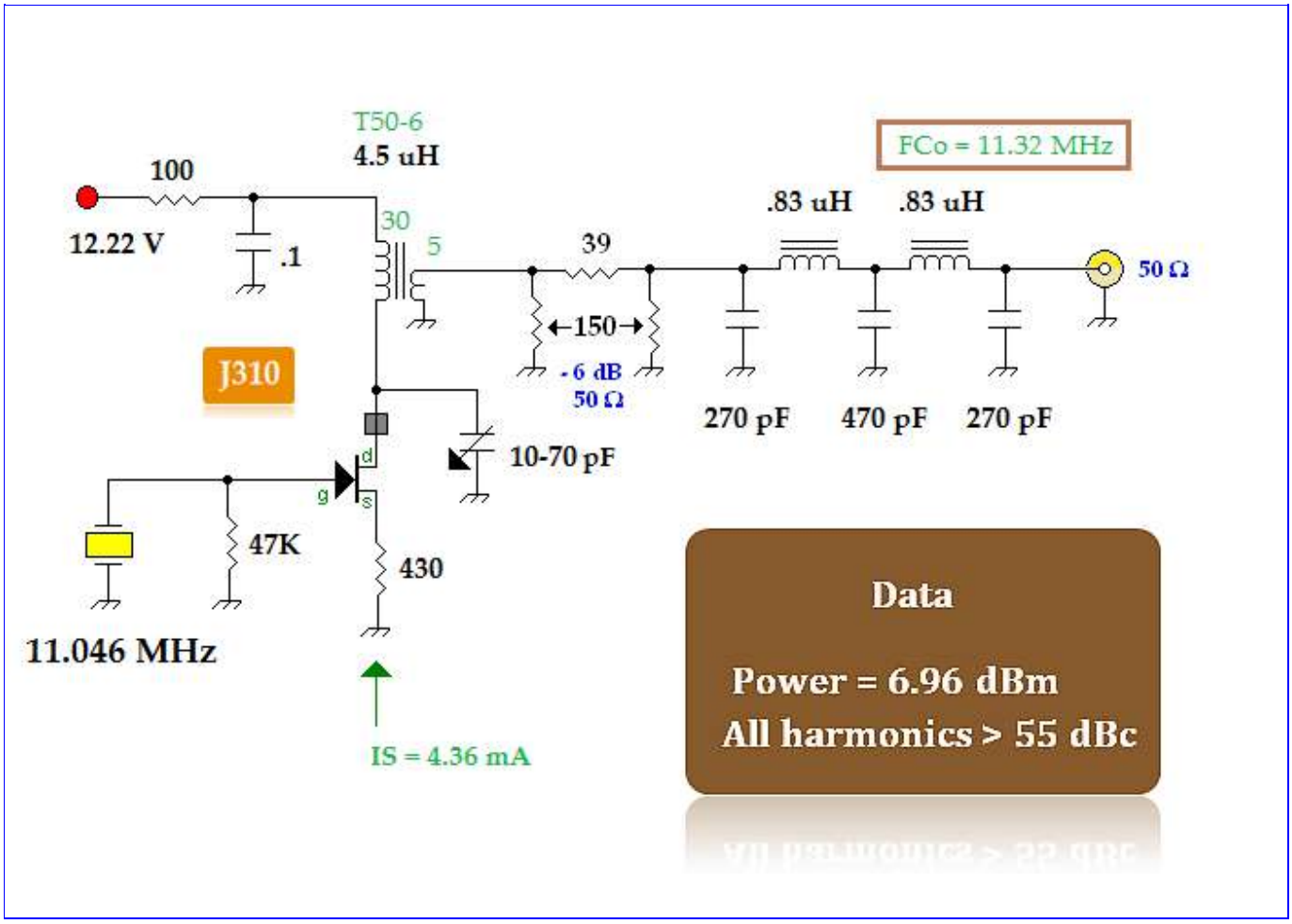

Above — The redesigned RF port oscillator. Clearly, the 7 element Chebychev low-pass filter isn't needed, so an N = 5 version was tried. Click for the spectrum analysis — again no harmonic energy was seen. In both the RF and LO signal generators, I tried to get as close to 7 dBm output power as possible.

To operate this oscillator at the desired RF port signal level; for example, between 0 and -10 dBm, you might just attenuate the output with a fixed pad or step attenuator. My conclusions echo the work of others experimenters; lowering the RF port down from 7 dBm to as low as - 10 dBm, lowered the amplitude of the spurious mixer products seen in the spectrum analyzer. Click for a sample. Refer to the QST Technical Correspondence citation in the references section for more information.

Above — The 2 re-designed oscillators wired up and connected to an SBL-1 mixer. I actually connected the attenuator pads after the low-pass filters as explained later.

Two different crystal oscillators were then built:

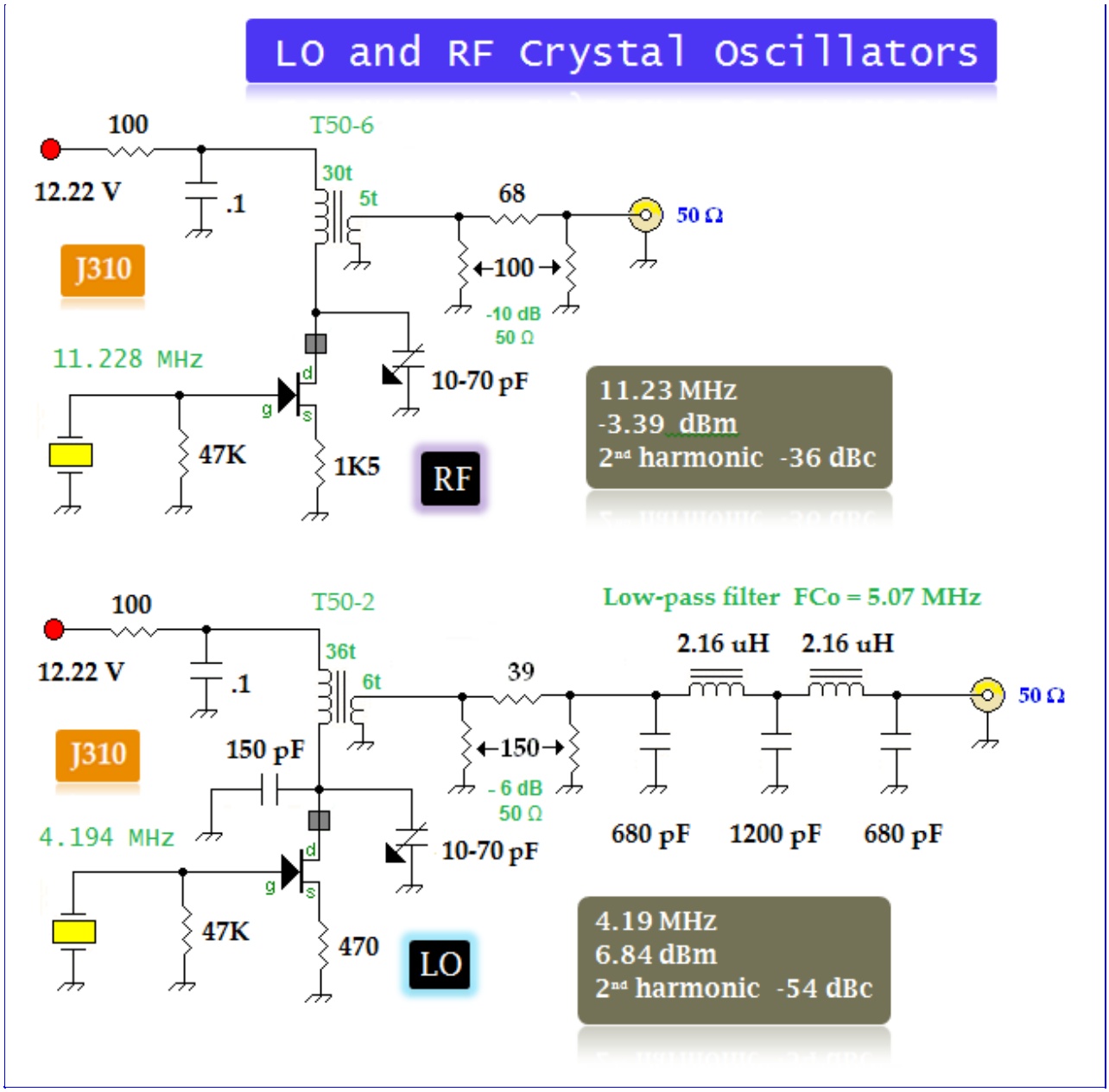

Above — Two different crystal oscillators targeting ~ 7.034 MHz were built. Click for the breadboard photo. You can see the crystal frequencies in this photograph. The RF port oscillator power was set to -3.39 dBm by choosing a low value JFET source resistor and attaching a 10 dB attenuator pad. Relatively low harmonic distortion prompted the exclusion of a low-pass filter on the RF oscillator. The LO output power was ~ 7 dBm.

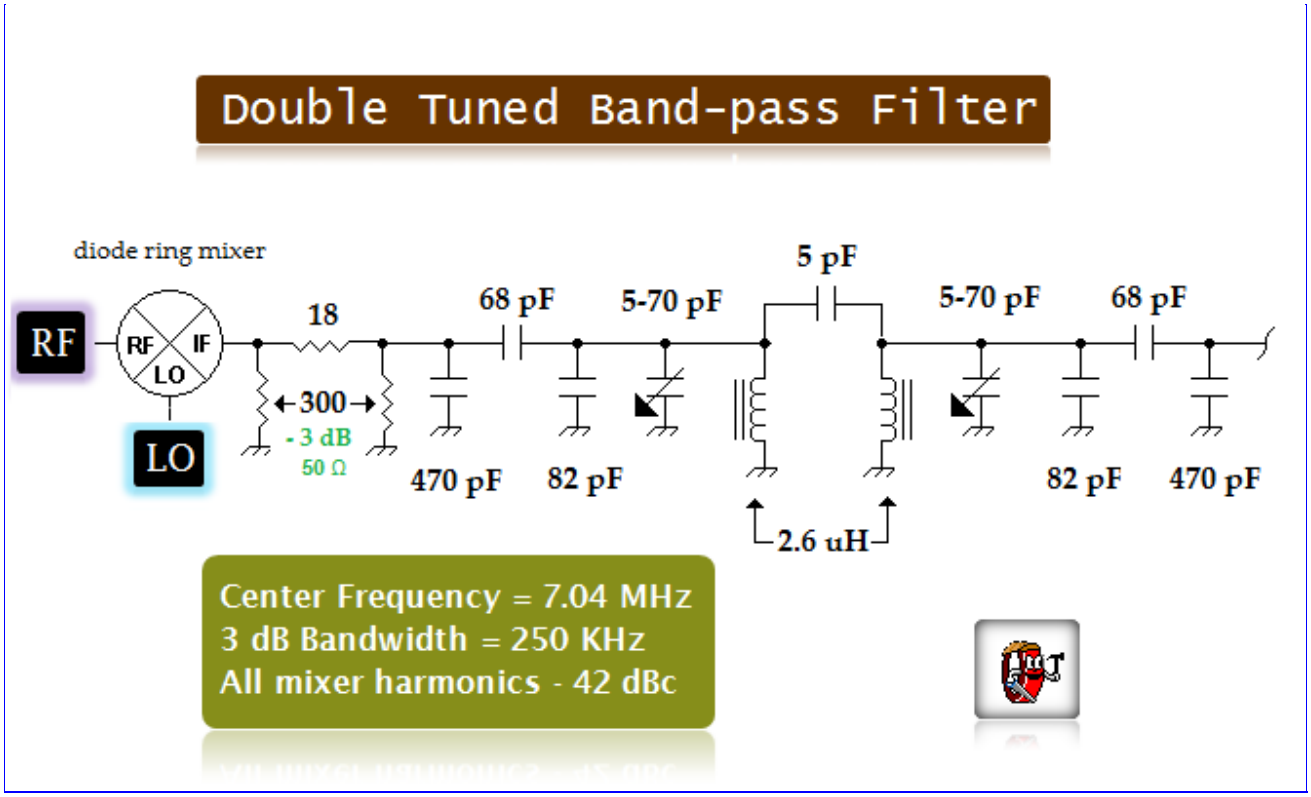

Above — The final experiment; placing a double tuned band-pass filter after the TUFF-1 diode ring mixer with the 2 latest crystal oscillators attached . This filter was in my junk box and I peaked it for the 7.034 MHz IF with a spectrum analyzer. The strongest spur was 42 dB down from the carrier — falling well short of the triple tuned band-pass filter presented before.

Clearly from all these experiments, a strong case for placing a triple tuned band-pass filter after a transmit mixer exists. If you use an unbalanced or single-balance mixer, a double balanced mixer might sufficiently not block feed through and spurious RF to keep your signal chain tidy. I enjoy studying the transmit chains of others to see how they filtered spurious and feed through RF. At the end of the day, as long as the output carrier spurs are low enough to meet your country's regulatory requirements, you're okay. Designing for low spurious emissions is an exciting challenge — one you'll miss if you don't try your hand with RF design.

A realization emerged following these experiments — I couldn't measure the return loss of the local oscillators! It technically could be done, but not by me. After 2 weeks of struggling, I engaged an American colleague with whom I occasionally build experimental circuits. After making some progress, we became stalled again. This time I asked Professor Ken Kuhn and Wes, W7ZOI for some ideas. Eventually a method to measure the RL of local oscillators came together along with enough material for another web page — RF Workbench 3.

When you do experiments, knowledge evolves as you go — for me, I learn mostly from making mistakes. I often think I should repeat most of my experiments over before presenting them, but this would consume too much time. However, footnotes can serve to steer readers for minor issues. If I had to re-build the crystal oscillators from Part 1, I'd build each crystal oscillator with a separate JFET buffer — then the return loss of the oscillator buffers could be measured as shown on RF Workbench 3 (with a shorted oscillator tank). Also, the pi attenuator pads on the crystal oscillators should follow the low-pass filters to garner the best output return loss. The good news is past experiments inform future experiments.

---

2. Bipolar Transistor Feedback Amplifier Experiments

I love making signals bigger — especially while preserving fidelity. It would be nice to become a reasonably competent amplifier designer — hopefully by studying sound schematics, applying software, building circuits and measuring evermore parameters this might occur. The mathematical equations of RF amplifier design seem quite daunting; they're the fodder of electrical engineers with their Hewlett Packard scientific calculators, SPICE software and GHz F-t transistors. With most things technical, as you try to advance, more questions than answers cross your mind; however, somehow this is normal and may actually signal progress.

Abundant amplifier references exist; for example, EMRDF Chapter 2: Feedback Amplifiers. This is essential reading and I won't repeat this information. Rather, I'll just share some ideas developed or reinforced on my bench. In the past, I've preferred amplifiers with narrow-band (tuned circuits) in an attempt to reduce distortion and maximize gain. Now after critically examining these tuned amps with scope and spectrum analyzer, I better appreciate the significant intrinsic feedback of RF transistors ***(the tendency to oscillate)*** and broadband designs are sought. Often you'll spend more time taming a tuned amplifier than building one.

This section focuses on return loss, bias techniques and achieving linear amplification — for example; finding ways to apply negative feedback,

match the input, or how to set the collector voltage. All my experiments and thoughts about RF amplifiers are from an amateur designers' perspective and I welcome your feedback. The first amplifier shown is a classic W7ZOI topology that I call the "Beaverton Special".

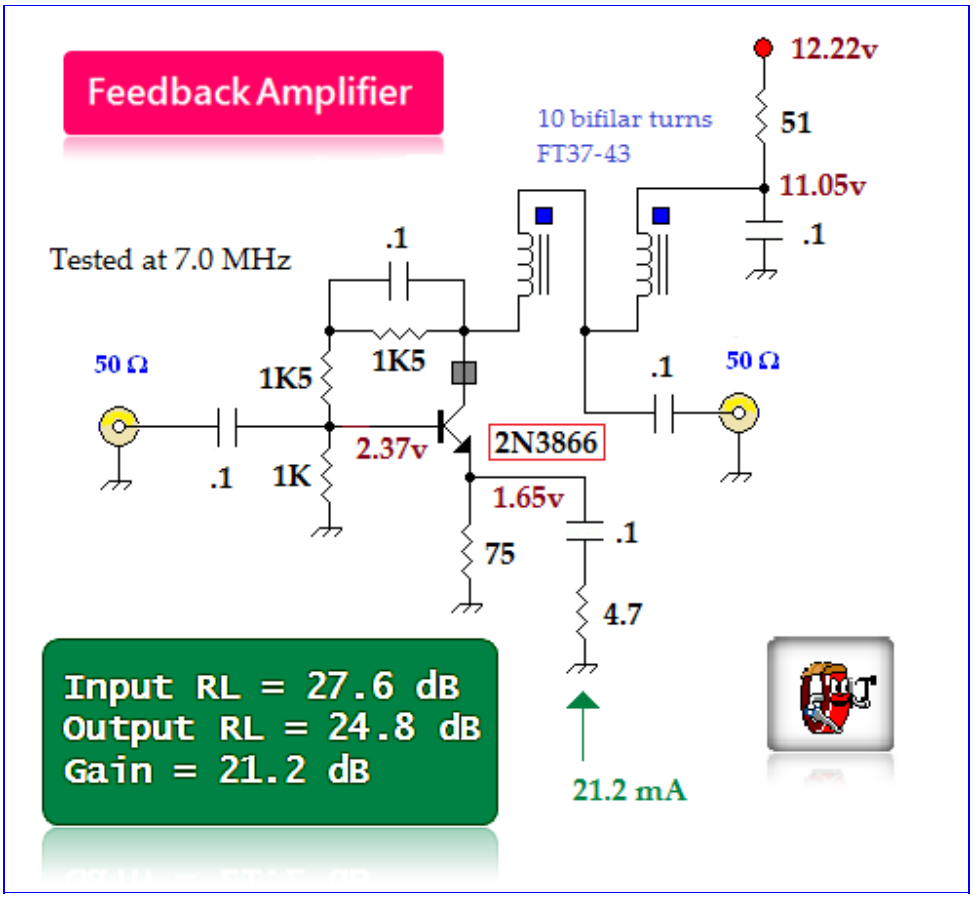

Above — A classic feedback amplifier popularized by Wes, W7ZOI in books like Solid State Design for the Radio Amateur and EMRFD. My respect for this humble design increased after building and testing 4 different versions to get a feel for amps with both shunt and series feedback. Of the 4 built, this particular version became my favorite — providing excellent input and output matching without crazy high emitter current. Employing a low noise / high F-t 2N3866 transistor is icing on the cake — an attempt to maximize impedance matching and performance using this standard, fits most transistors bias/feedback circuit. The humble 2N3904 also worked well in this slot. You don't need the ferrite collector bead with a 2N3904.

Other good experiments include trying different transistors and/or increasing the emitter current while being careful not to exceed the BJT's current rating (plus add heat sinking as required). You might also try the stage at different frequencies or perhaps sweep it to see at what frequency the gain starts to fall off.

Of the 4 BJT feedback amps shown in part 2, only this amp has a true broad-band input and output. What bothers me about broad-band linear amplifiers is that when you chain up 2 or more of them, signal fidelity generally degrades as it passes through each successive amp stage. Solutions include mopping things up with some low-pass filtering after the last stage, leaving it alone, or tuning the amplifiers (i.e. not using broadband stages).

The biggest caveat for feedback amps are variations in input and output impedance caused by source and load mismatches. For example, a 75 Ω resistor was connected to the output of the FBA above. The input return loss degraded to 16.8 dB. Further, the same 75 Ω load was removed and then connected to the input during output return loss measurement— this degraded the output RL to 23.4 dB. Clearly *load* mismatches upset return loss more than *source* mismatching. A 50 Ω attenuation pad should likely follow a feedback amp in situations where high input return loss are desired; for example, after a diode ring mixer.

Noticing a variation of the classis feedback topology in EMRFD Figure 6.140, I asked Wes, W7ZOI about it. It turns out there's another way to "skin the shunt feedback cat". The above RF amp uses a series connection of 2 feedback resistors (1K5 and 1K5 with a bypass cap across one 1K5). The result is a resistance at DC of 3K, but a resistance at RF of just 1K5. You could also use a 3K resistor directly from collector to base that is paralleled by a series connection of a 1K5 resistor plus a 0.1 uF capacitor. That network has the same impedance as my amp shown above. That is; the resistance would be 3K at DC, but 1K5 at RF.

This explanation fueled the next experiment — transistor amplifiers have 2 operating conditions; 1 at DC, the other at AC. Like a carpenter framing a house, you begin design by setting the DC bias — no small design task since bias concerns more than just establishing the base voltage and emitter current. For example, biasing may effect voltage gain, maximum signal handling capability, noise figure, impedance matching, class of operation, the operating point (sometimes called quiescent point or q-point), feedback and temperature stability. Biasing provides much to think about, however, a practical way to explore any topic is to chunk it into small, understandable pieces that become a stepping stone to advancement. Let's focus on biasing for temperature stability. The next amp uses the wrap-around PNP bias — an awesome technique.

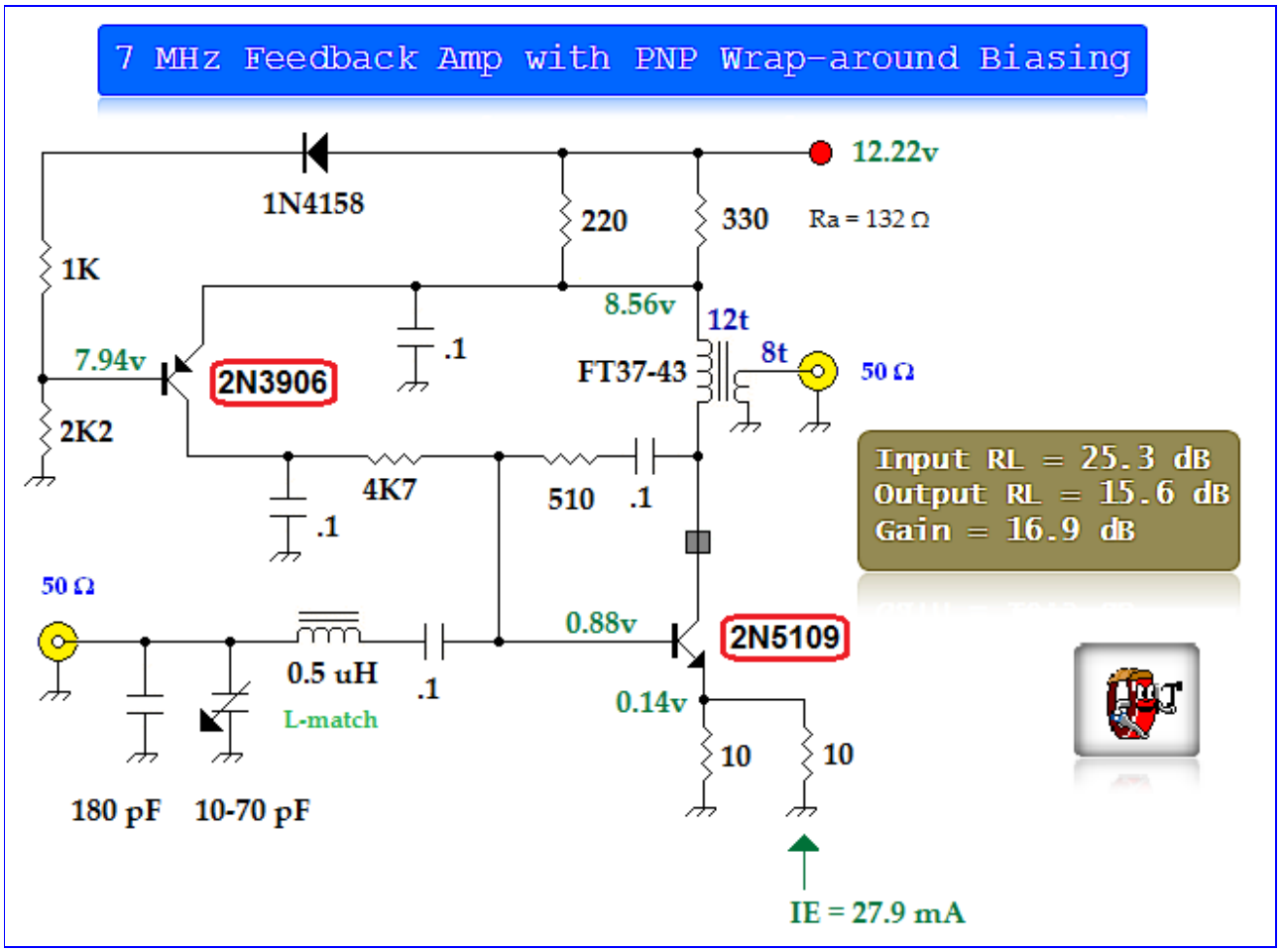

Above — A 7 MHz FBA using PNP wrap-around biasing. I learned about wrap-around biasing from Wes, W7ZOI and share a simple way for new builders to also learn this technique as the **#1 Design Center** on the supplemental web page. Click for a prototype breadboard photograph. This amplifier employs heavy shunt feedback from collector to base. Degenerative (series) feedback from the 2 parallel 10 ohm resistors also enhances temperature stability.
Expanded bias circuit temperature stability discussion follows amplifier number 4.

The wrap-around or feedback bias scheme is good because it's self stabilizing. The diode in the PNP bias network further ensures that the PNP bias remains constant with temperature changes. It really should be to glued to the NPN transistor (or its heat sink) to allow tracking of the NPN's

temperature variations. This bias circuit doesn't load the NPN base input impedance. Another great virtue is that the emitter of the amplifying transistor can be directly connected to ground allowing better performance at VHF and UHF.

Noise from the PNP will be amplified by the NPN, so the low-pass network formed by the 0.1 uF capacitor and 4K7 resistor is essential. In some related circuits, you may see an RF choke used instead of a resistor.

The actual 2N5109 input impedance is probably around 40 ohms — easy matching with an L-match network.

Amplifiers with an L-match tuned input shouldn't follow a diode ring mixer unless preceded with a diplexer since the narrow-band L-match tunes only 1 frequency. L-match networks can make an impedance bigger or smaller depending how they're oriented and also provide some low or high-pass filtering depending on the configuration. I design my L-networks on the bench using experience plus trial and error — a better way is to use software. I recommend the program called Zmat08.exe that is included on the CD that accompanies EMRFD. The software will get you close, however, bench tweaking is required since you're often matching a complex impedance, comprised in part, of stray reactance.

Setting up an L-Network for an Input Match

A suggested bench method for optimizing input Return Loss (RL) using an L-Match network.

Your task is find the "perfect" L and C values to get a RL of 20 dB or higher. Start by soldering in an inductor calculated from Zmat08.exe or according to your wisdom. Set up the amplifier for input return loss measurement. The first chore is to find the nominal target capacitance that provides the best match at the design frequency. I use a big range, air variable capacitor for this — with the input circuit connected to a return loss bridge, connect up and tune the big variable capacitor to give the greatest RL. Remove the variable capacitor, measure it, and then solder in an equivalent trimmer capacitor, and as required, fixed capacitor(s) so you can tune at least 25 pF above and below the target capacitance. Often, the target C will be close to whatever the software recommends. In amplifier 2, my C values are the 180 pF + a 10-70 pF trimmer.

Next, determine the optimal inductor. On my bench, I keep a variety of pre-wound #6; and #2 material powdered-iron toroid inductors and choose one close to the calculated or a self-chosen L value. I start with an inductor wound with 4-5 more turns than needed. After soldering it in, the RL is checked. Remove 1 or 2 turns, tweak the trimmer capacitor and again check the RL. If after removing 1 or 2 turns, the RL is going up, you've determined there was enough inductance to get the best RL. *(If the RL goes down, you probably didn't start with enough L to get the best possible RL).*

You can also also squeeze together or spread apart the toroid windings to vary inductance — the maximal inductance variation varies due to factors including wire gauge and total turns. Compressing the windings with thumb and forefinger *increases* the inductance and widening the gaps between windings *reduces* inductance on a toroid.

Assuming the RL increased after removing 1 or 2 turns, remove another turn, tweak the trimmer capacitor and check the return loss, and so on. Repeat until your return loss starts to decrease. Then add back a turn or 2 to find the absolute best match. *This procedure allows you to find the optimum inductance in-situ.* Once, you've figured out the best inductance, cut the inductor leads short, solder it in, tweak the trimmer capacitor, and then consider further tweaking the coil by expanding or squishing the windings on the toroid while looking at the RL in a bridge detector.

In summary, to get the best possible RL — design a prospective L-match with software, and then bench test to determine the optimal in-situ L and C by using values above and below the calculated L and C values while observing the results in a return loss bridge. This method seems tedious, but emphasizes that repeated bench practice and patience pays off. You can always just use the calculated L-network values and/or develop your own method to set them up.

Consider mitigating the stray inductance caused by the long lead that occurs after removing wire turns by cutting the lead and scraping off the enamel insulation every couple of turns or so. This is a gamble — If you cut the lead and need to add back a turn, you'll have to rewind the coil from scratch, or add in and solder another turn (messy). I'm often able to get a L-network RL of 22-26 dB using my method and feel it's worth the the time and effort.

When bench tweaking the L and C values, your actually looking at the peak-to-peak AC voltage with the amp input connected to the unknown port of the RL bridge. Tune for the lowest, stable peak-to-peak voltage. Test it against the open circuit peak-to-peak voltage to calculate the RL. Since the open circuit doesn't change, you know the return loss is improving when the peak-to-peak voltage of the amplifier under test is going *down*. I store the open circuit voltage in my scientific calculator and calculate the RL from time to time as I'm tweaking the L and C values. After awhile, the whole procedure becomes automatic and quick. Once you 're done and everything's tidy, measure the open circuit and connected amp peak-to-peak voltages and calculate RL a final time. This is your reportable return loss.

You can scale matching networks from other builder's schematics by calculating the XL and XL and then applying these reactances to your desired frequency. Bench tweaking is still required. I also hope the person whom I'm copying didn't make a bench or drafting error. Be discerning about whatever your find on the Internet "Misinformation Highway" — this site included. Although I'm no philosopher, I know at least 3 things about people. They: 1. are often biased; 2. can lie; and 3. can make errors.

Above —Some toroids and the *air variable capacitor* I sometimes use to **coarsely** bench tune L-C circuits to determine the "ballpark" tuning capacitance. This capacitor features built-in reduction drive and varies from 15pF to 428 pF. When using an external capacitor connected to your circuit with short copper wires, expect some signal distortion and watch out for hand and body caused capacitance variations. The connecting wires also have reactance which won't be there when you swap in a small trimmer cap plus any fixed value capacitors.

Next up is a common emitter amp using "noiseless" feedback - this means the AC feedback is achieved with transformers instead of "noisy" resistors.

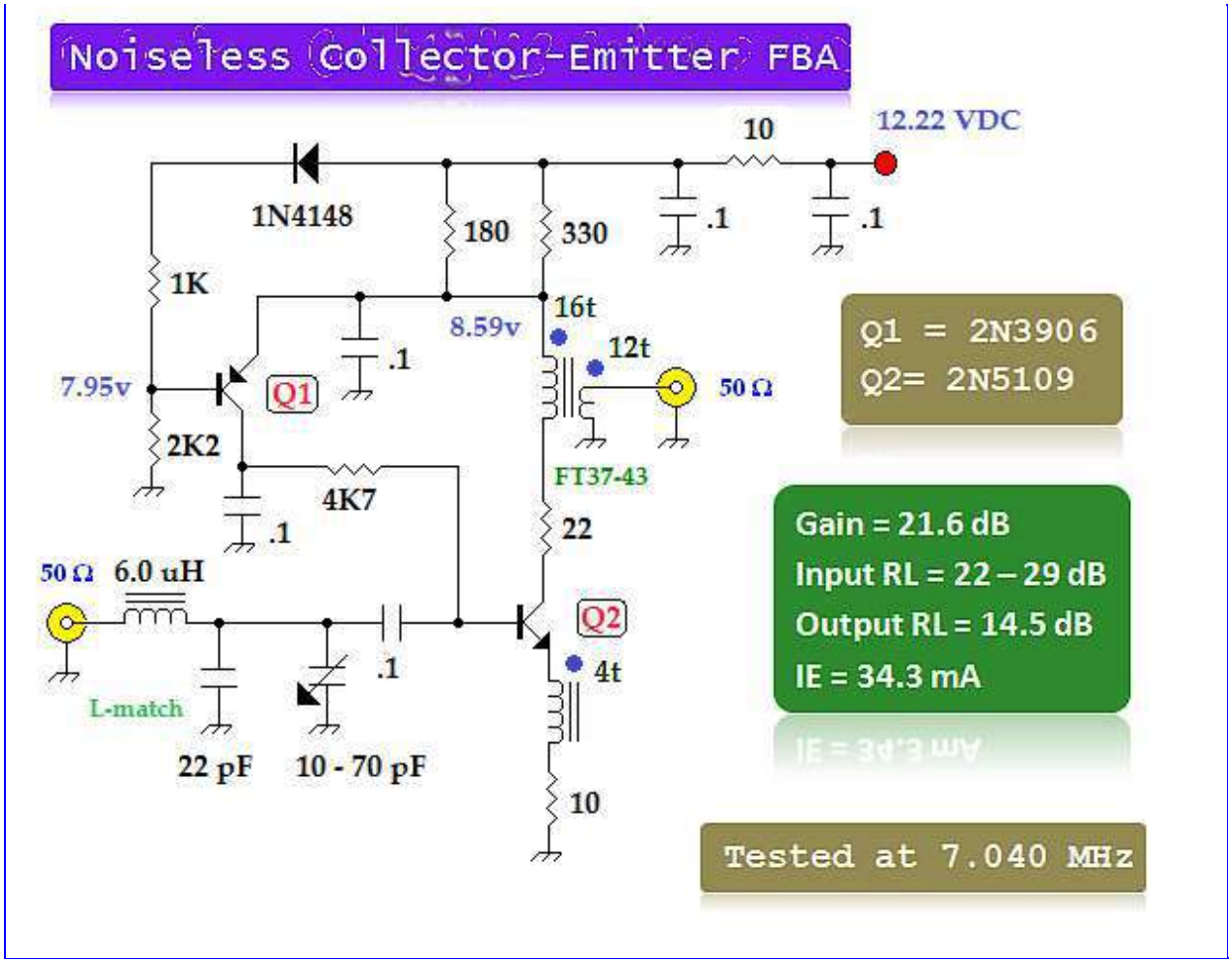

Above — Schematic of a 7 MHz collector-emitter "Griffiths" feedback amp. I ran substantial emitter current through this NPN. RC = 116.5 ohms — I paralleled 2 resistors for RC because I lack resistors between 100 and 150 ohms. The basic design is by Bruce Griffiths, who has a great web site. I thought I put up *big* schematics!

The input L-network was designed on the bench and provides a good input match peaked at 7.040 MHz — this pumped up the gain 3-4 dB. In my amp, a T50-2 powdered iron toroid inductor forms the L-match coil. Matching for the best possible input return loss is touchy and best done on the bench. For example, if the 6 uH inductor is decreased to 5.8 uH, the match could fall by 2-4 dB. With patience and careful tweaking return losses approaching 29 dB are possible, but likely too time consuming for most builders. The procedure as described earlier is pragmatic: connect a RL bridge to the input and adjust the L and C values until the lowest return loss is discovered. Even squishing or expanding the toroidal inductor windings can squeeze out a final dB or so of input matching.

Output matching proved interesting. Although I tried, the best output RL I could muster was 14.5 dB. Lowering the 10 Ω degeneration resistor or increasing the current could increase the output return loss. An output attenuator pad might be considered — a 3 - 6 dB pad would increase the output RL to over 20 dB.

All 3 output transformer windings were wound on a FT37-43 with care to keep the phasing correct. Amplifier gain is not dependent on collector current. For example, substituting an Ra of 180 ohms (clipping out the 330 Ω resistor) yielded a gain of 19.5 dB, an emitter current of ~ 20 mA and an output return loss of 12.6 dB, while the input match changed very little.

The oscillation snuffer 22 Ω collector resistor was 15 ohms in another version, however, parasitic oscillations were discovered at ~175 MHz and snuffed out by raising this resistor from 15 to 22 ohms. I sometimes go as high as 51 Ω; especially in JFET circuits.

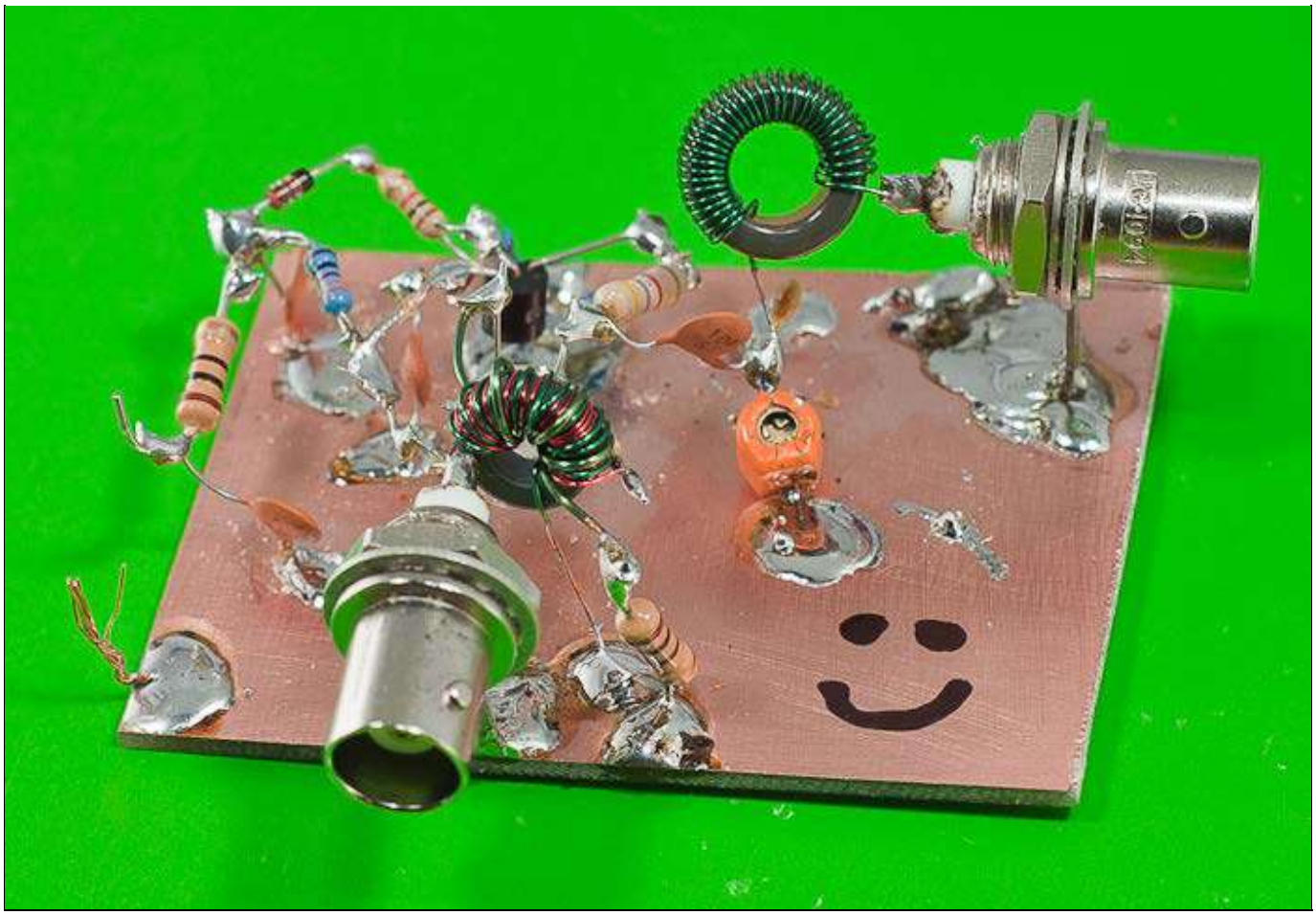

Above — The breadboard of the noiseless collector-emitter 7 MHz feedback amp. Click for a photo of another version. The hot "modern" replacement for the 2N5109 is this SMT part. I also like the BFG135 T/R BJT.

The final FBA experiments *below* use a standard voltage divider bias, tweaked for temperature compensation. The AC feedback is base to emitter — a rarely used topology in North America; although I'm not sure why.

4

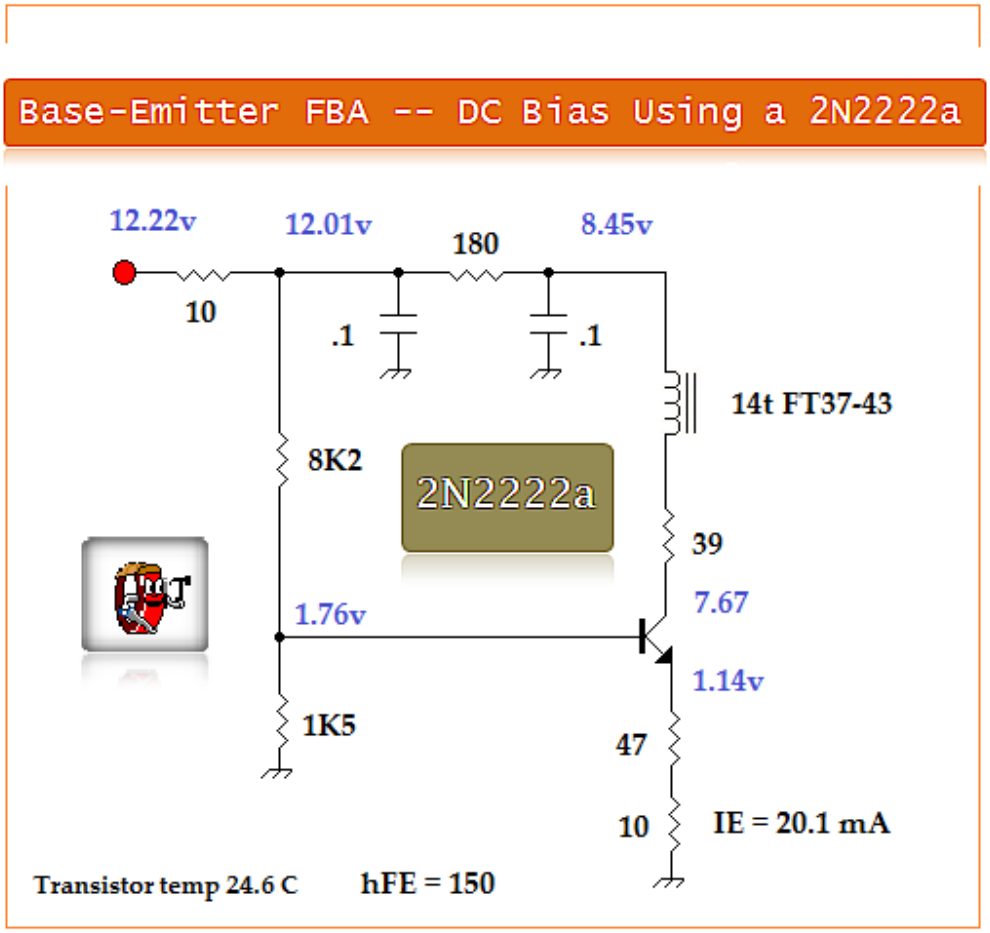

Above — The DC bias resistor values for a 2N2222a with a DC Beta or hFE of 150 and a emitter current of 20.1 mA. Almost every text author writes about voltage divider bias temperature stability, but some builders get bogged down in the details. Since the bipolar junction transistor is a voltage controlled device *(see section 4: QRP-POSDATA for an explanation)*, you must set up some DC voltages — I created a design center presenting an easy approach to design reasonably temperature stable BJT amps. See **#5 Design Center** on the supplemental web page. After getting the bias, the AC parts were added, and the completed schematic is shown below.

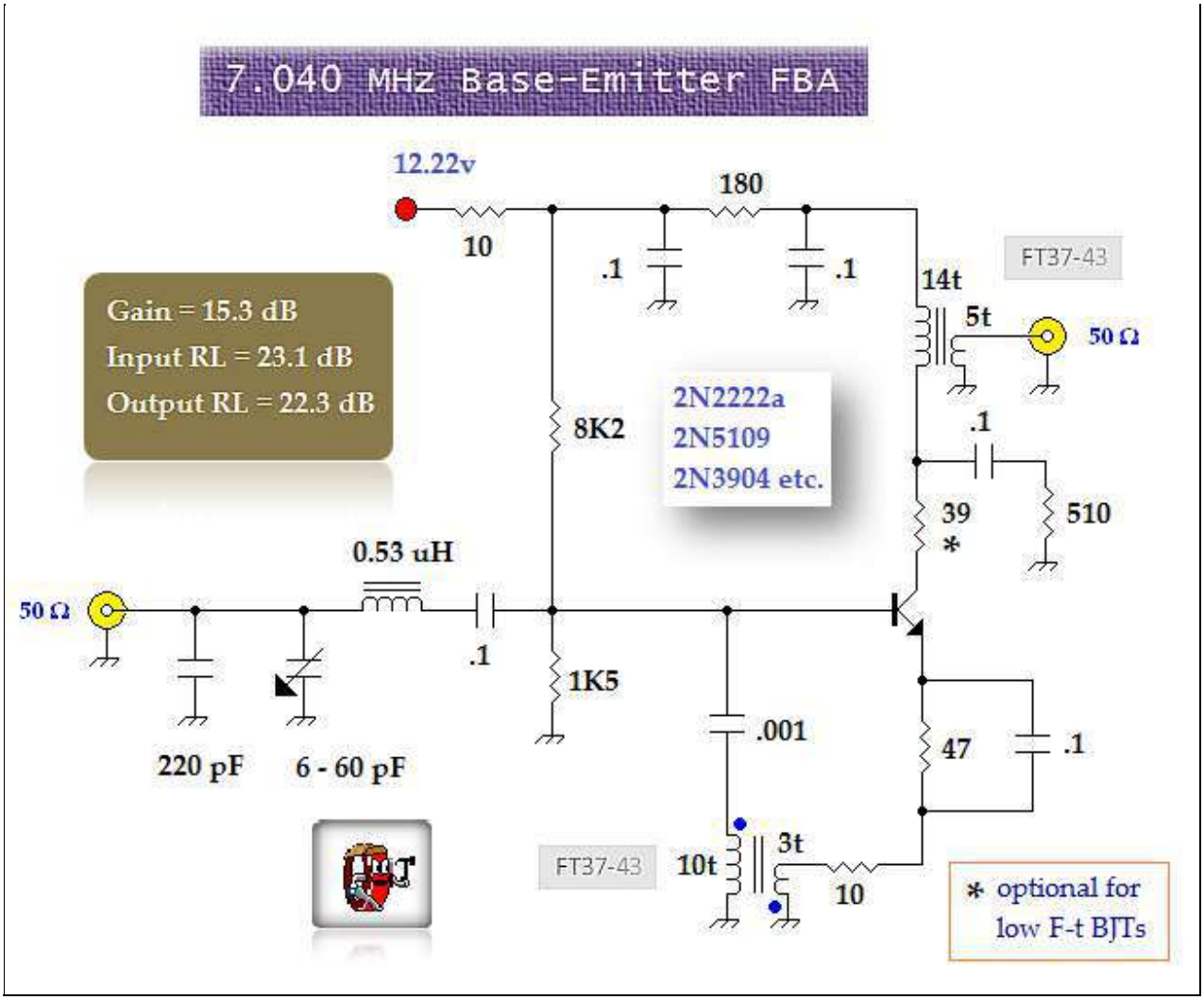

Above — A base-emitter feedback amp built Dec 21, 2010. I read about base-emitter feedback in Dr. Rohde's book *(Reference 1)*. He had some discussion, a small signal model and lots of difficult math, but no circuit examples. After searching on the web I found 1 example in the HBR-2000 transceiver; a project designed and built my respected Canadian colleague Marcus, VE7CA. Click for his web site. I decided to build my own design using a L-match to tune the input to 50 Ω.

The above amp was built around around a 2N2222a. The 39 ohm resistor is not really required with the 2N2222a. For high F-t transistors like the 2N3866, 2N5109 or microwave transistors, ferrite bead(s) or the resistor are *not* an option. Low F-t transistors like the 2N2222a or 2N3904 don't need the UHF oscillation snuffer resistor since they lack real gain at these frequencies. With the design center, you should be able to bias your own amp according to the emitter current you want — choose a BJT, measure or choose its hFE and then choose IE.

Missing from this web page is how to choose an operating point + discussion about DC load lines and related topics. I may tackle these topics on a future web page. I'm not sure anyone cares about this anymore.

The most difficult part was the output transformer. Lacking a base to collector connection, the collector impedance runs quite high and finding a good match into 50 Ω proved impossible — even with a shunt resistor across the primary coil. I saw a strategy in Marcus' amp; AC couple the collector to ground via a 510 Ω resistor. I did this. From then on, it was just trial and error to identify the optimum turns ratio for the collector transformer. An interesting experiment might be to figure out the turns ratio using a lower loss output transformer such as a FT-37-61.

The turns ratio of the various collector and drain transformers on most of these amplifier designs were determined by placing the amp in an output RL measurement setup and adding or removing secondary turns to get the highest possible RL. See the procedures for RL measurement on the RF Workbench pages.

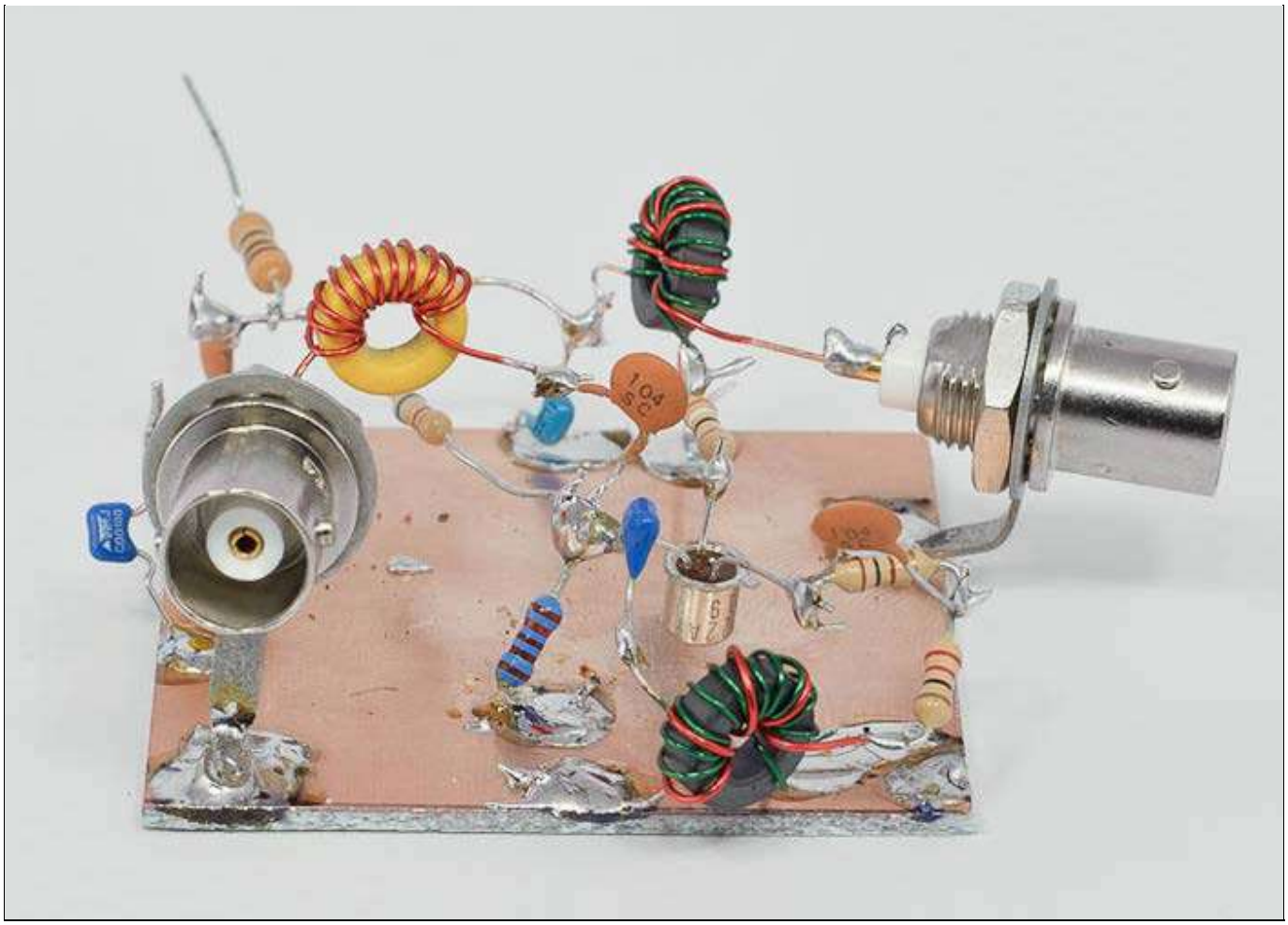

Above — The breadboard of the first version of the base-emitter FBA.

---

3. JFET Common Gate (CG)Transistor Amplifier Experiments

These experiments focus on setting up a desired input return loss and getting a reasonable output return loss in the CG amplifier. My expectation of an easy set of experiments proved wrong — assumptions never substitute for actually building and measuring.

I like motorcycles. The difference between riding a motorbike versus *driving* a car parallels learning on the bench versus learning by just simulating or calculating component "ideal" values on paper or computer. In the car you're isolated from wind, smells, temperature changes and subtle road traction and camber differences that you fully sense on the motorcycle. Bench experiments prove equally visceral and experiential — the sensory input from learning as you build and test circuits imprints deeply in your mind.

1

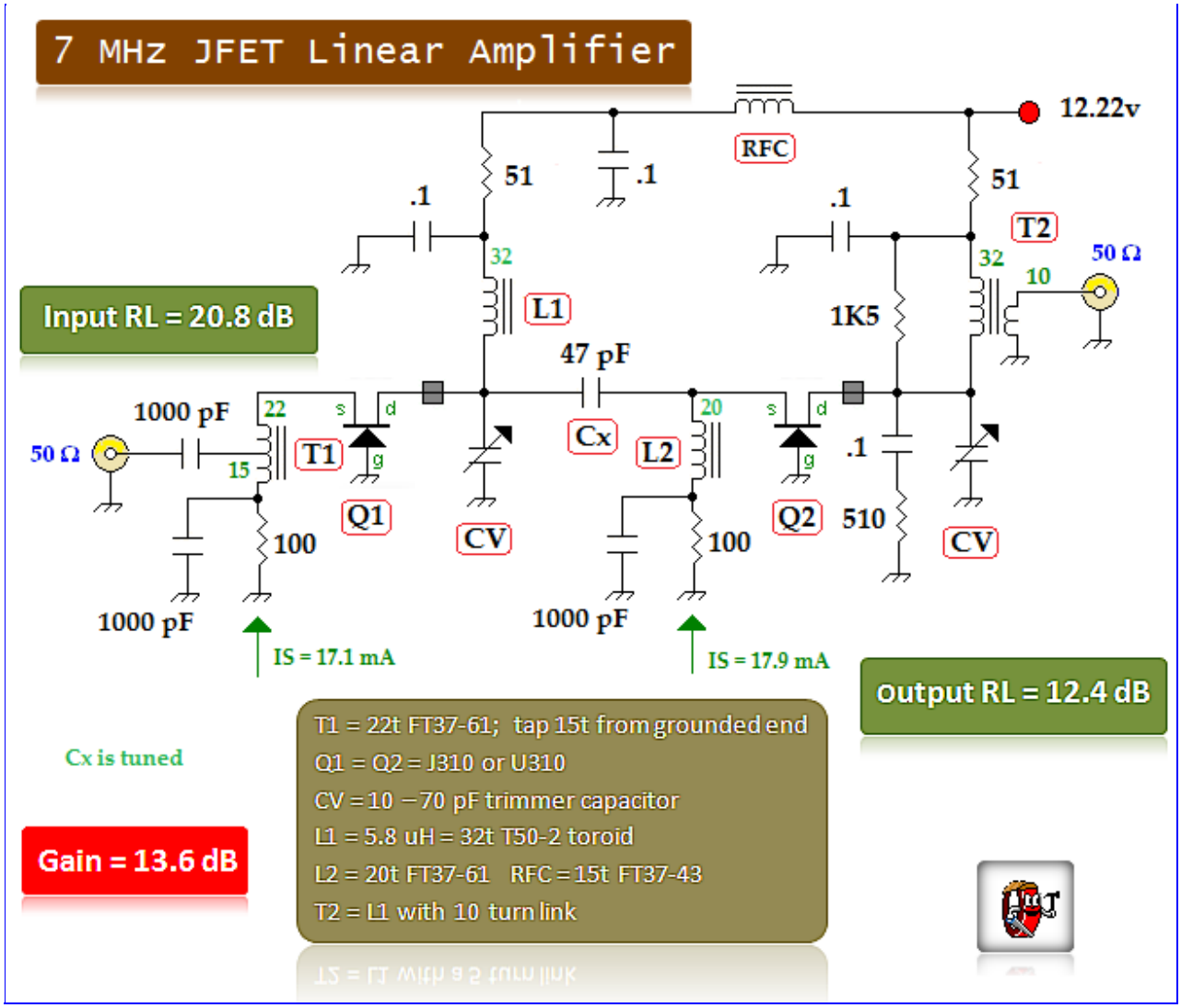

Above — A 7 MHz JFET "linear" amplifier built only for testing ideas — *do not build*. It went through several incarnations and prompted many experiments. The input return loss was deliberately set to 20.8 dB, although I set a RL from 10.0 - 28.6 dB during my experiments. Bypassing the JFET source resistor increases gain, but of course changes input RL.

The output transformer represents a terrible design, but shows the length I went to to try an obtain a decent output return loss. Working with this circuit, led me to abandon tuning the output transformer in situations where a high return loss was desired since the low value resistors required kill the tank Q significantly.

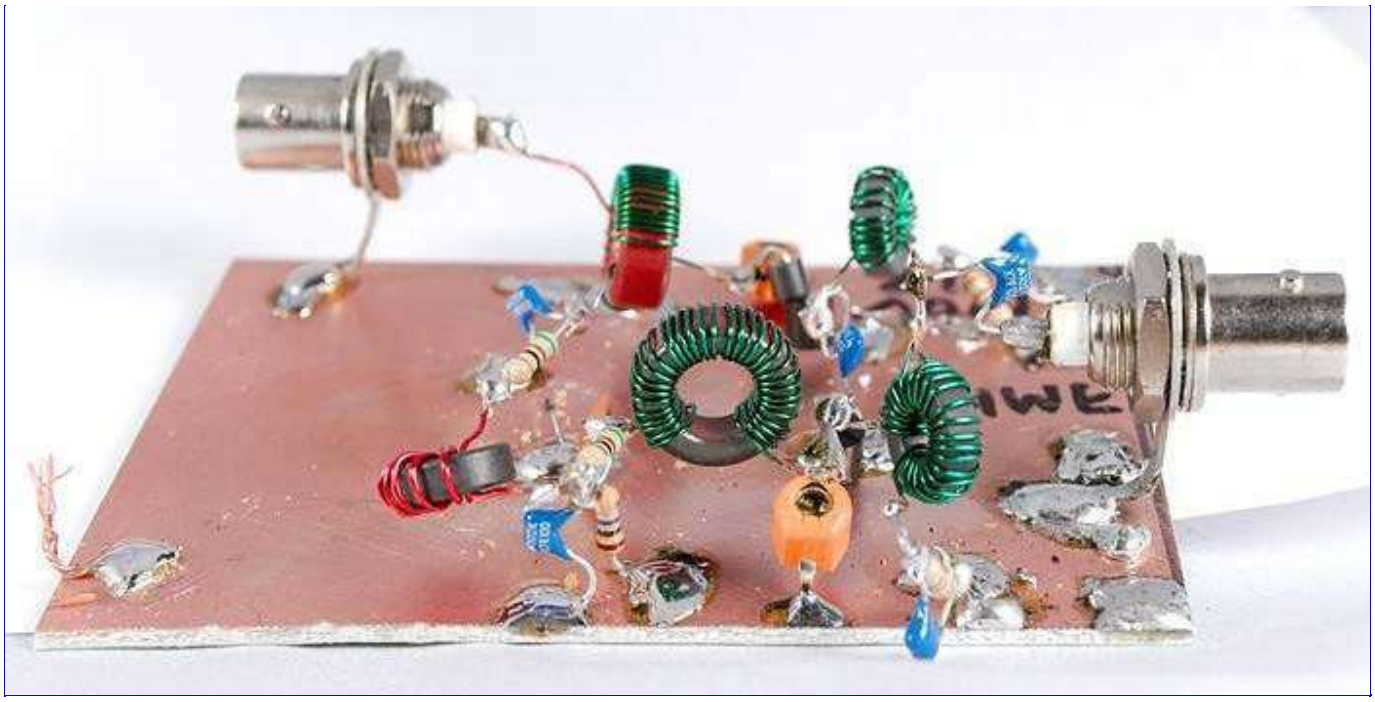

Above — Breadboard of 1 version of the prototype low-level JFET "linear" amplifiers for 7 MHz. Click Click . Cx is tuned with a variable cap and a nearest standard value substituted; in my case 46 pF was the measured value of the variable cap at point Cx.

Setting Input Impedance

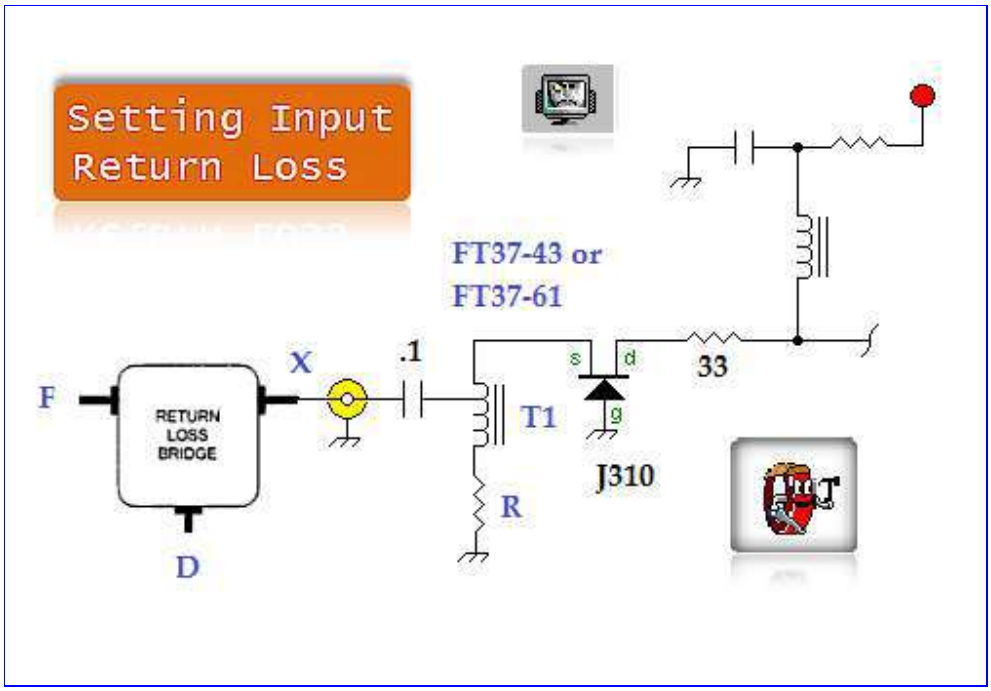

Above — The procedure used to set a desired CG amplifier input Return Loss. Numerous factors influence the input impedance and I discuss them in **#4 Some Factors Affecting Common-Gate Amplifier Input Impedance** on the supplemental web page. I keep some tapped inductors on my workbench such as this FT50-43 or these FT50-61 core inductors. To find the best return loss using such a coil, you can change tap points, remove windings and even wind more turns and solder the 1 end of your new windings to 1 end of the existing wire. Some builders omit inductor taps and manipulate the input return loss other ways as described in the supplemental article.

Normally we set the input match after establishing the output match since the output impedance dramatically affects the input impedance.

Further, you might notice that the tap point may vary between different JFETs. Most of my "real world" coils have at least 2 tap points and I choose the tap that gives the best return loss. More often than not, I bias for 14 - 18 mA and leave off the source bypass capacitor; it's your call.

The input return loss that gives the lowest noise figure is often chosen by engineers.

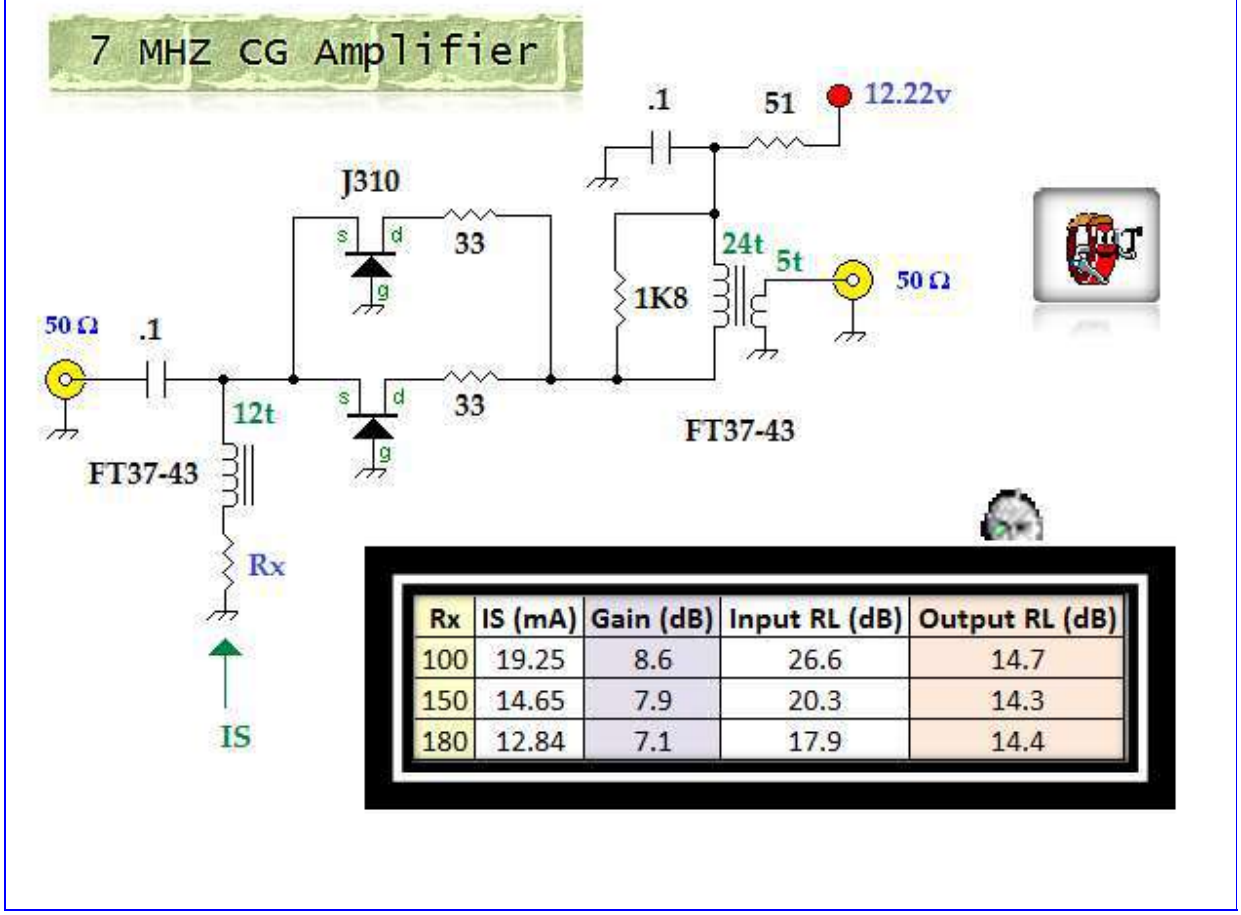

Rx	IS (mA)	Gain (dB)	Input RL (dB)	Output RL (dB)
100	19.25	8.6	26.6	14.7
150	14.65	7.9	20.3	14.3
180	12.84	7.1	17.9	14.4

Above — An experimental 7 MHz common gate amp designed to terminate a diode ring mixer. The best thing about using 2 JFETs is that you don't have to determine the tap point in the decoupling inductor (12 turns on a FT37-43 in this amplifier). I put up to 4 in parallel during my various experiments. It's faster to match just 2 JFETs, so 2 were favored.

The output RL wasn't great at ~ 14 dB, however is probably normal or better than most published amateur projects. I set the output match by adding a shunt 1K8 resistor across the primary winding and then finding the turns ratio to give the best output return loss. Without the resistor, the best output RL will be ~5 dB or worse. The resistor reduces power.

I learned that putting JFETs in parallel in a common gate amplifier reduced the output return loss in circuits using an output transformer like in the schematic above; this is unfortunate.

I wanted an output RL of 20 dB or greater — this is no small request; over a week was spent investigating transformer behavior and finding ways to improve output return loss when you really *want* to.

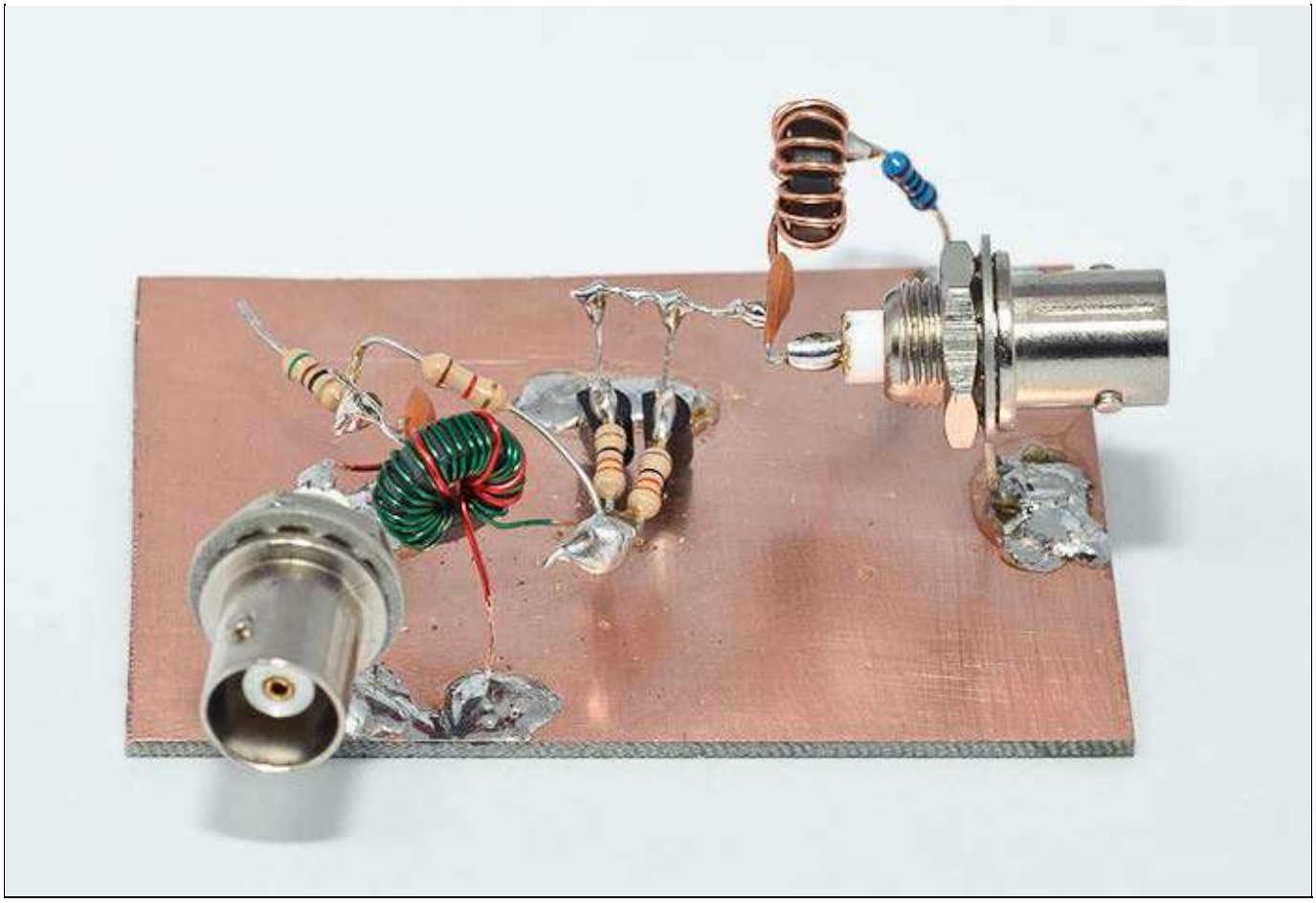

Above — The breadboard of the above 7 MHz CG amplifier.

Output Impedance Experiments

For some reason, I assumed that when using an arithmetically correct turns ratio, the output transformer will end up at 50 Ωs. For example, if I wish to transform 450 ohms to 50 ohms, I'd use a 9:1 impedance ratio (3:1 turns ratio) and get 50 ohms. Sadly, it isn't this simple — impedance transformation is complicated and whole books have been written about it. I'll share some of my experiments that might inform yours.

The first task was to built a simple jig to evaluate primary and secondary coupling, turns ratios and return loss.

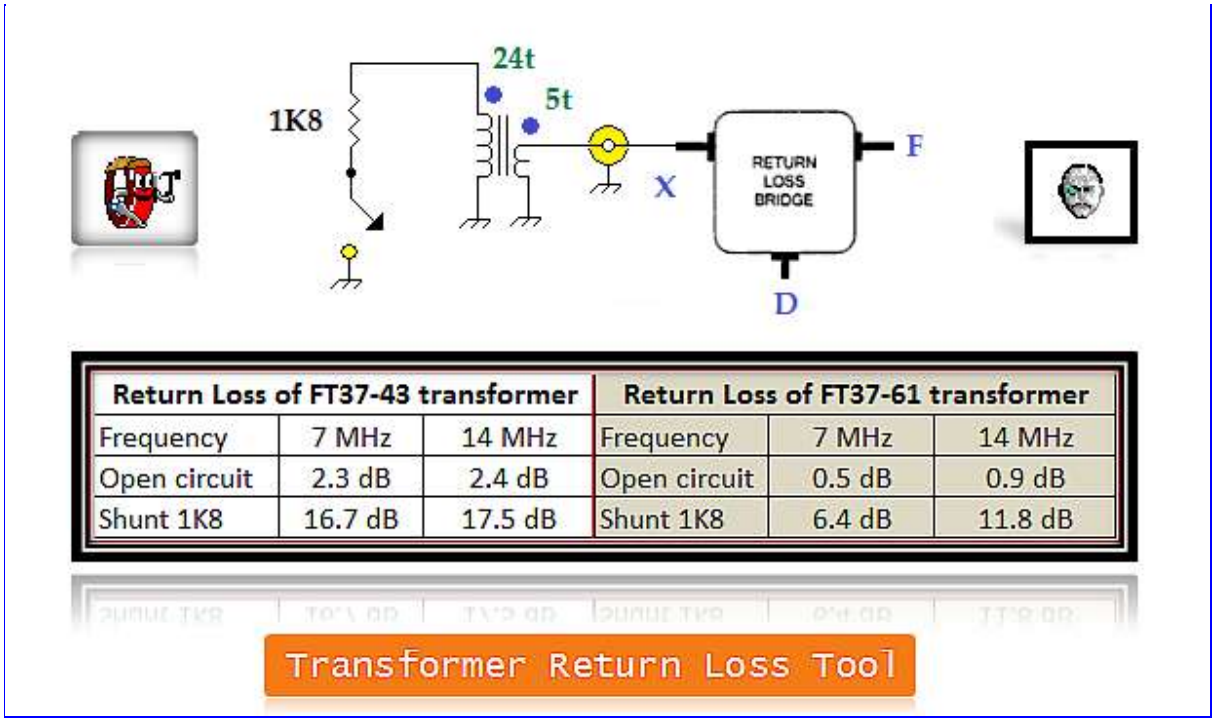

Return Loss of FT37-43 transformer			Return Loss of FT37-61 transformer		
Frequency	7 MHz	14 MHz	Frequency	7 MHz	14 MHz
Open circuit	2.3 dB	2.4 dB	Open circuit	0.5 dB	0.9 dB
Shunt 1K8	16.7 dB	17.5 dB	Shunt 1K8	6.4 dB	11.8 dB

Transformer Return Loss Tool

Above — The simple tool built to evaluate the return loss of a transformer out-of-circuit. In this case, I examined the 24t : 5t transformer of the 7 MHz CG amplifier shown earlier. The table shows the best possible return loss when the 1K8 resistor is across the primary coil. Additional experiments were completed and follow below.

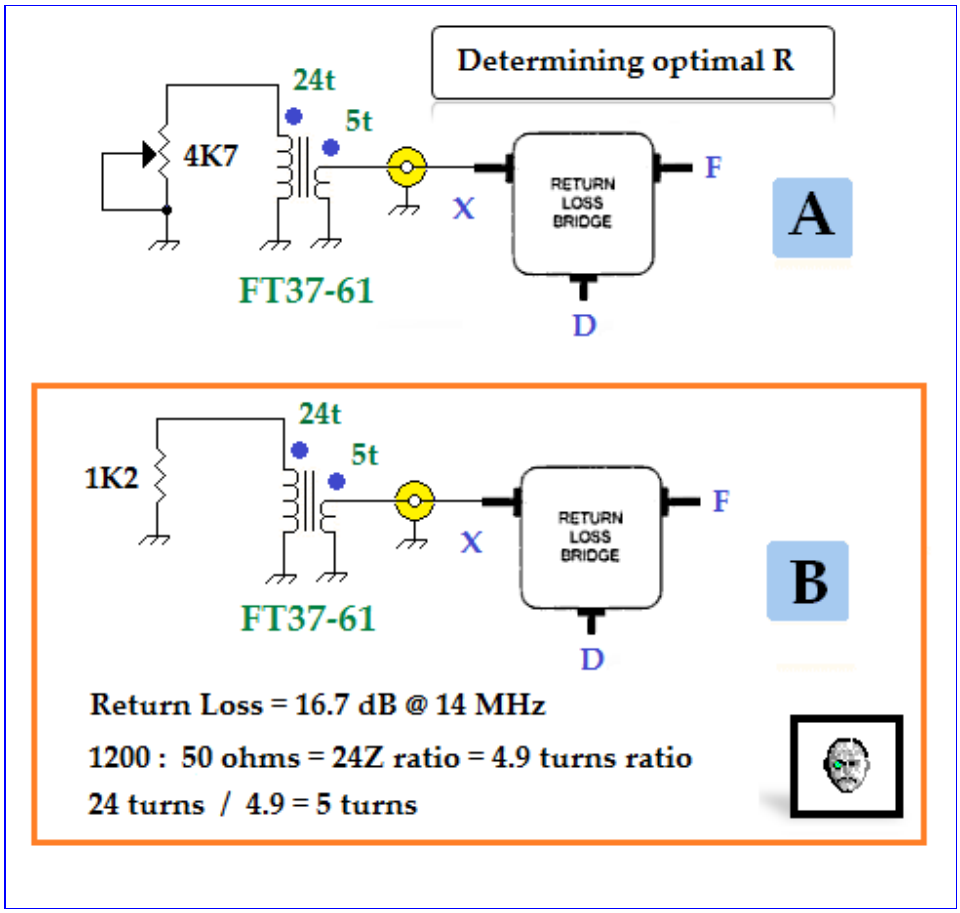

Above — An experiment to see if changing the shunt resistor can improve return loss; yes it can. The shunt resistor was a 4K7 potentiometer — Using the potentiometer, I was able to determine the optimal resistance needed to increase the return loss @ 14 MHz of the **FT37-61** ferrite-base 24t : 5t transformer. The pot was removed, measured and replaced with the nearest standard value; a 1K2 resistor. The best possible RL was 16.7 dB using a 1K2 shunt resistor. At 7 MHz, the FT37-61 didn't work well. Five turns on a FT37-61 based transformer doesn't have enough inductive reactance to get a good return loss.

Above — The transformer testing jig. I omitted the switch shown in the schematic above and just soldered the shunt resistor across the primary winding.

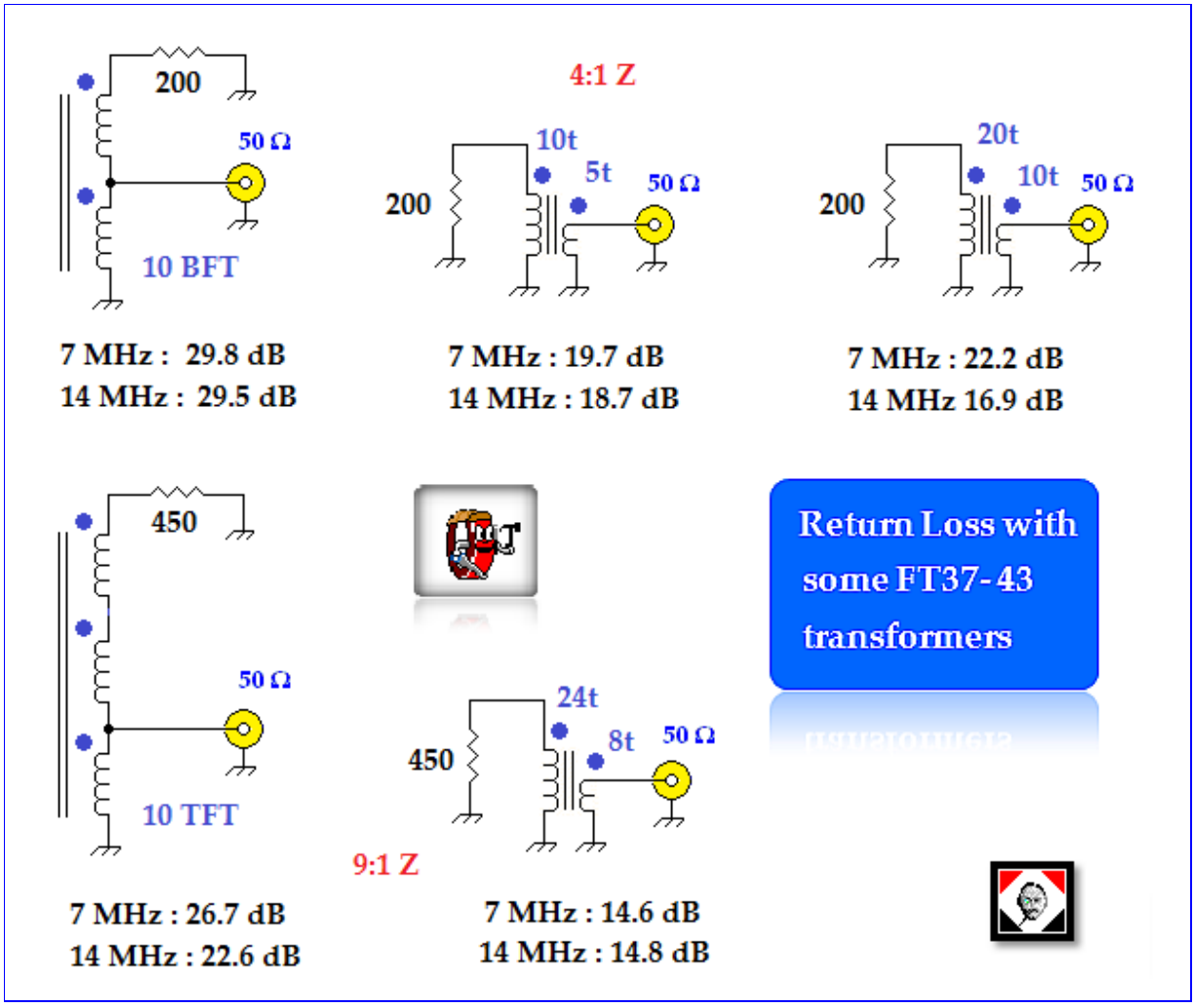

Above — Some of the outcomes using the transformer jig pictured above. While I basically understood that transformer efficiency tends to fall as

the turns ratio increases, I never thought this would also happen with return loss. By *no* means do these crude experiments constitute science, but the following themes emerged:

1. The better coupling of transmission line transformers (bifilar, trifilar etc.) translates into improved RL over conventionally wound transformers
2. Limiting the turns ratio to 3:1 or less generally improved the return loss. As the turns ratio moves above 3:1, the best possible return loss tends to decrease.
3. The smaller or secondary winding should have 4-10 times the inductive reactance of the impedance it's connected to. For a 50 ohms impedance this means a minimal XL of 200 - 500 ohms. I noticed a weak trend towards better return loss with higher XLs. This means that to use a FT37-61 at 7 MHz, the secondary winding should be 9 -14 turns or so.

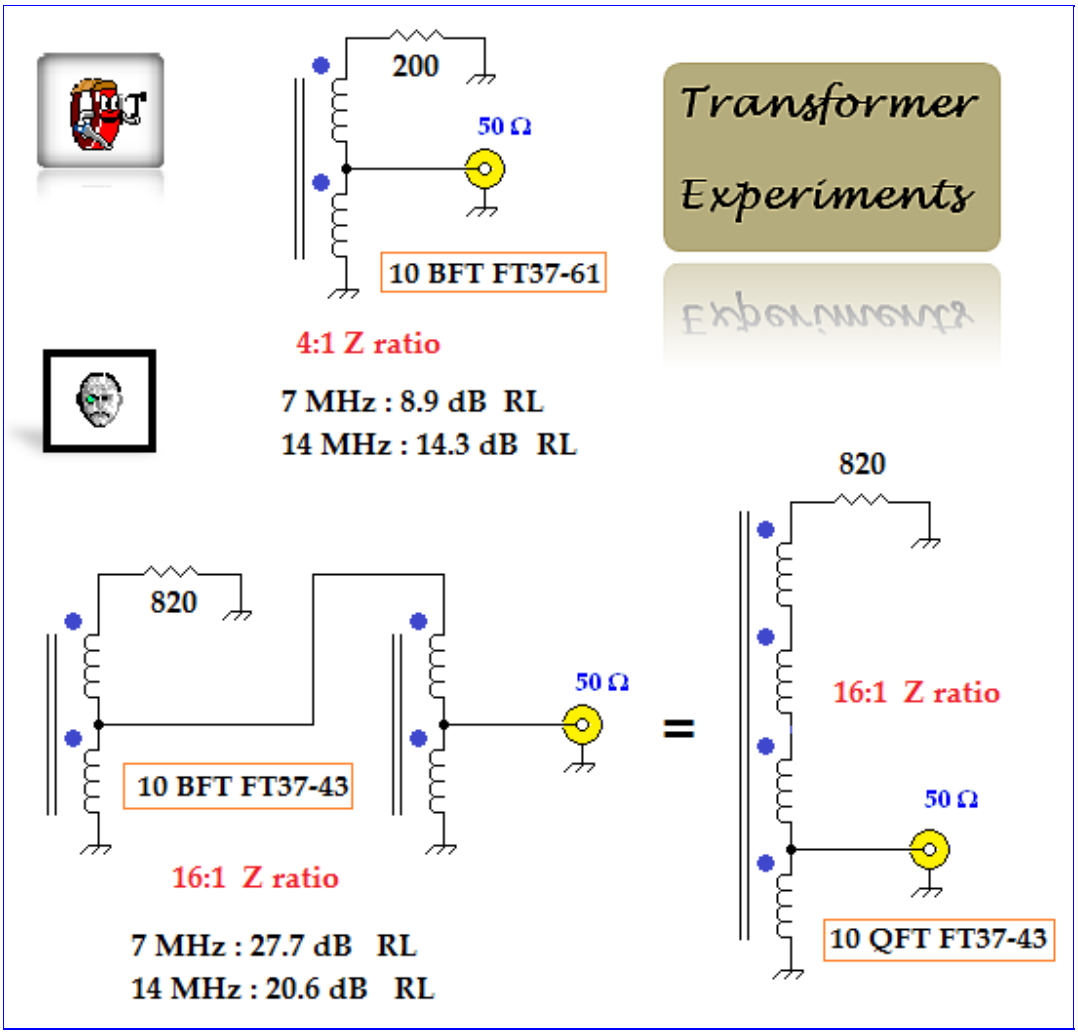

Above — Further transformer experiments. For a 4:1 impedance transformation at 7 and 14 MHz, a FT37-43 ferrite toroid gave a better out-of-circuit RL than the FT37-61 *The comparison transformer with a FT37-43 ferrite core was shown earlier*. It's possible to transform a big impedance such as 16:1 by cascading 2 bifilar transformers, or by using a quadrifilar transformer. I didn't build the quadrifilar transmission line transformer, but show it for completeness sake.

Of course, once you connect the transformers to a real circuit, things will change — still it's great to be able to examine transformer return loss in a controlled environment.

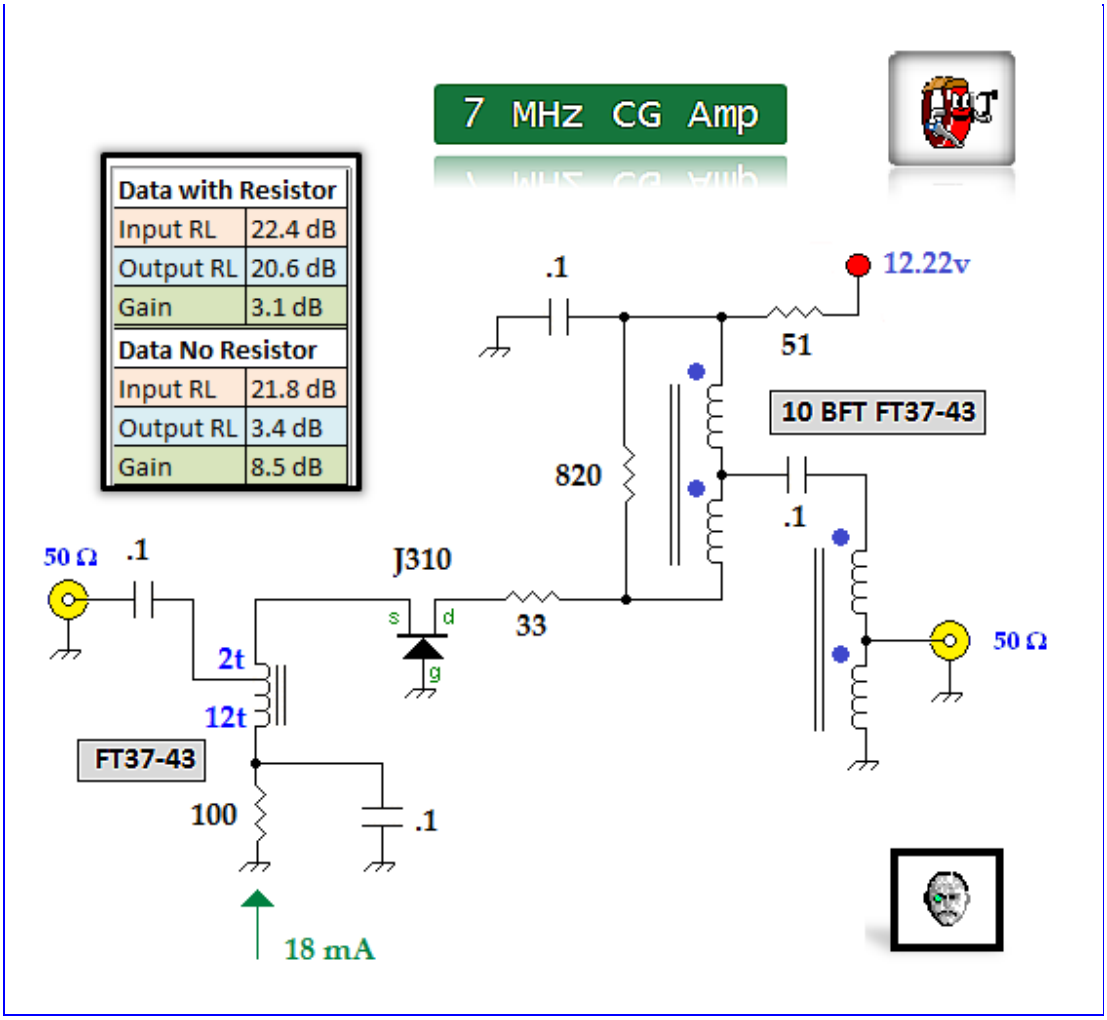

Above — a common gate amplifier experiment using 2 cascaded 4:1 Z transmission line transformers. Data with and without the 820 Ω resistor shows that while the resistor gives a great output RL; it eats a lot of power. In cases where I've seen cascaded transmission line transformers used, the resistor was omitted. The Ugly Weekender transmitter by Wes, W7ZOI provides a good example.

In many cases, it's prudent to sacrifice gain for return loss, however, when you see a builder (like the former me), put a 32:3 turns ratio on a 5 MHz amplifier output transformer and label the secondary windings **"50 Ω",** we'll know better.

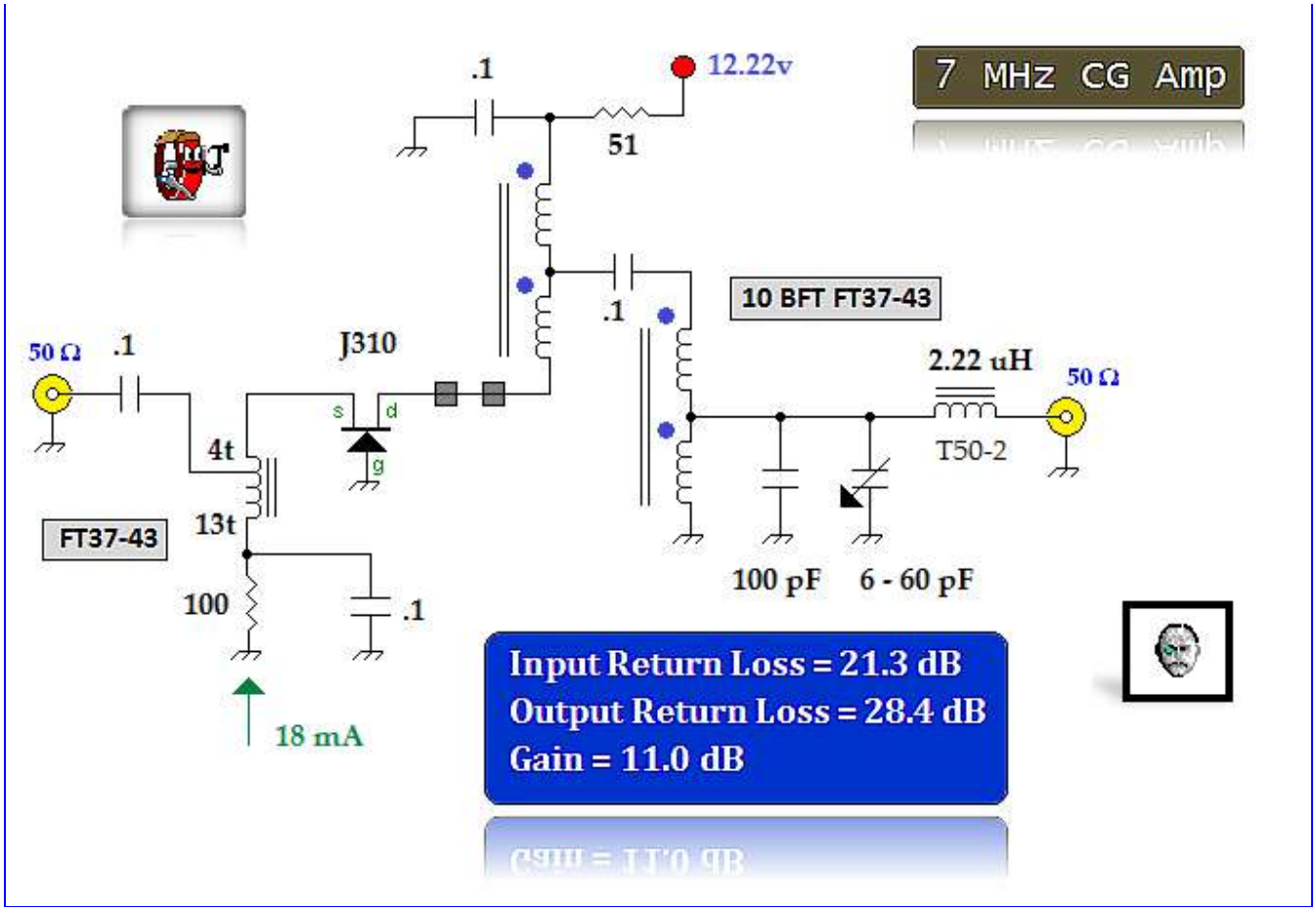

Above — An evolution of the amplifier above to get the best possible output RL. I omitted the 820 ohm resistor and matched the output with an L-network. The return loss on the output of the second transmission line transformer (measured before the L-match was added) was 3.4 dB.

The L-match values were *roughly* determined by using this chart (you can also do the math). According to the chart an *(output)* RL of 3.4 dB, is either 10 ohms or ~250 ohms or so. Ten ohms is unlikely, so I designed my L-match to match 250 to 50 ohms. This provided some starting values for the L and C parts and the rest was done on the bench using trial and error with an RL bridge. At the time, this was the highest output RL I'd ever achieved.

RF engineers use math to calculate impedance (they always do). I sent the schematic to Wes, W7ZOI for his analysis and summarize his return email comments as follows: At 7 MHz, the XL of the 2.22uH inductor is 97.6 Ω, therefore the impedance looking into that with 50 Ohms as the load is 50+j97.6. A complex inversion of this value gives a complex admittance that has a real part: 0.0041. Flipping that gives 240 Ω. The equivalent reactance is inductive with a value that would be tuned by a 184 pF capacitor; a bit more than you have there — so there is some reactance presented by the center tap of the second transformer. Neglecting these details, the L net generates about 240 Ohms. The two transformers then kick the Z up by 16 to 3856 Ohms.

I was pleased that my simple chart gave a value close to his calculation. Test it out — the chart may work okay for you.

The input match is over 20 dB and reasonable. More time could have been spent on the input autotransformer by tapping and such to increase the input RL, however, time is the 1 resource we all seem to lack.

The final amplifier experiments employ an L-match to set output return loss. When reading electrical engineering books you'll often see all sorts of matching networks on both the input and output of FETs and BJT amplifiers. The networks look simple, but in practice, aren't. They tune sharply, have a low bandwidth and in the case of the CG amp, harbor a big problem — tuning the output for the best output return loss, **dramatically** affects the *input* return loss and potentially, your return loss measurement by the reactance affecting the RF signal in your bridge.

When tuning the output, you're actually changing 2 complex impedances — this is not trivial.

Also if you're off by a few pF or tens of uH in your network C and L values respectively, you can wreak havoc with the measurements. At this point, I don't possess all the skills needed to tune both the output and the input network to a RL of 20 dB or greater; especially with a broadband input.

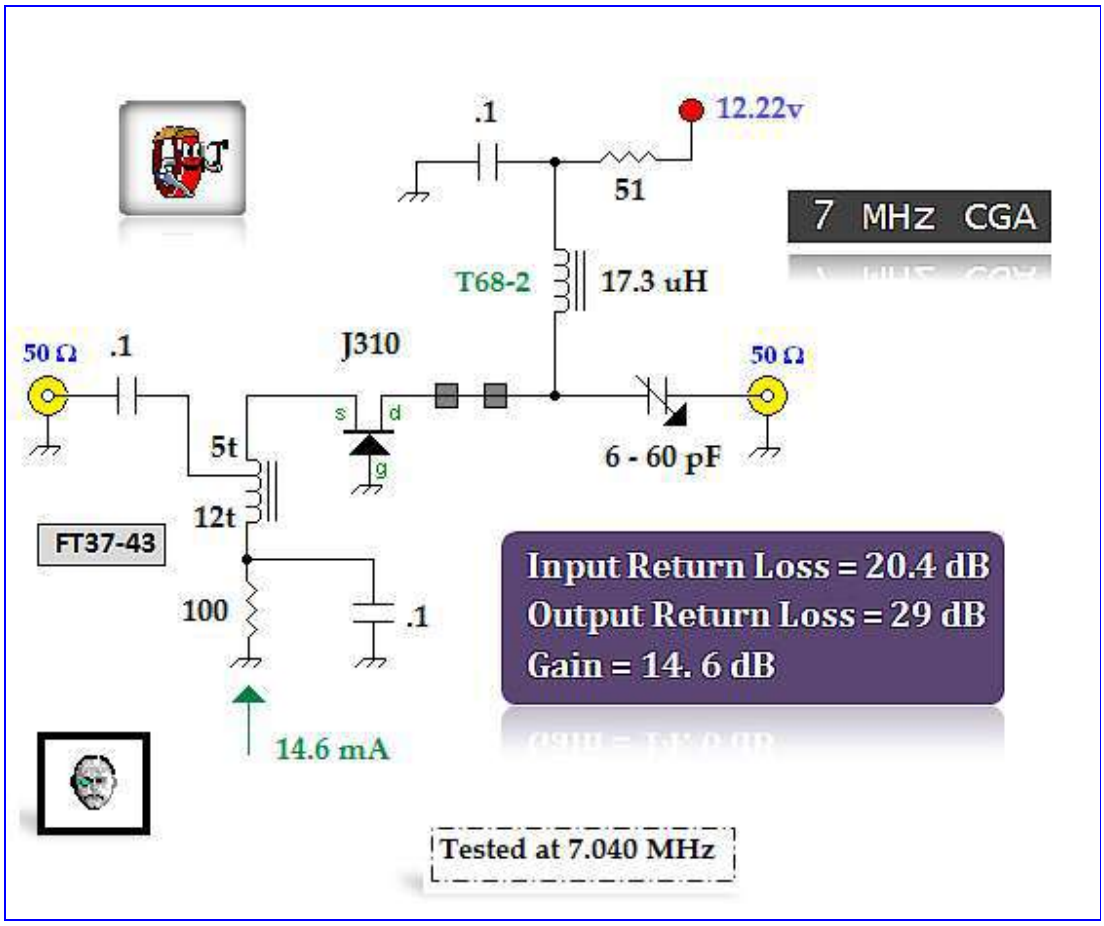

Above — A common gate amp employing a high-pass L-network to match the output. Miraculously after 2 hours of tweaking, I obtained a good input and output match; however this amp isn't reproducible. The inductor was wound on a T68-2 using 28 gauge wire — always a pain. Through trial and error, I learned that the output impedance of the drain was around 11800 ohms. Starting with 18.4 uH on theT68-2, I removed 2-3 turns at a time until a reasonably low return loss was obtained; then I removed 1 turn at a time. I went too far and had to add back a turn. I clipped the excess lead every second turn which made it tedious, but exacting. It seems that the L value is very critical – it would be nice to use a variable inductor to figure these things out. Compressing and expanding the windings also provided a simple way to vary inductance.

In several other circuits, the best possible input return loss was only 14 dB. Mistuning also caused oscillations to occur in one 14 MHz amp with an output network inductor of 7.4 uH. I also tried a 14 MHz amp with an L-match on both the input and output, however, was unable to match both the input and output due to the interplay between them.

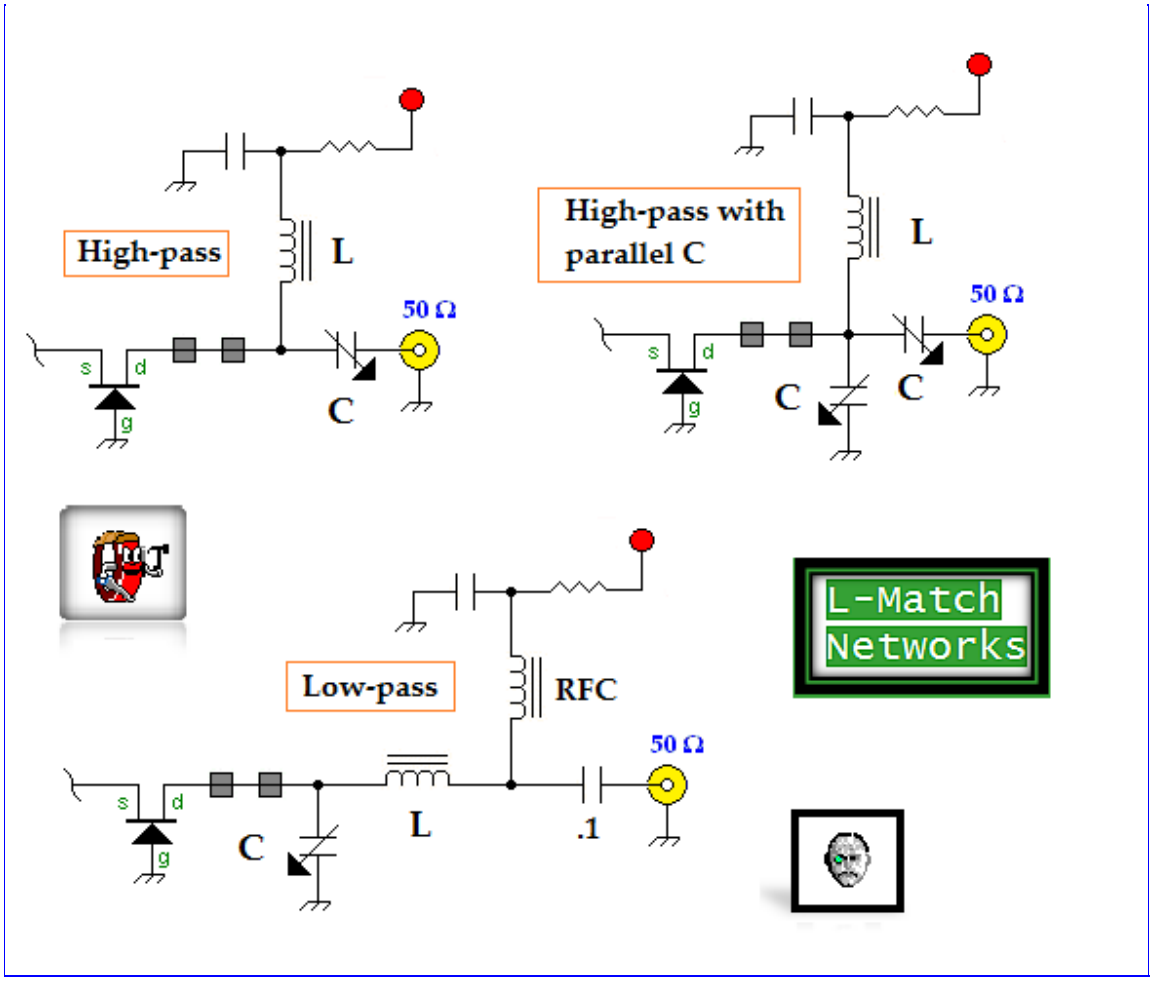

Above — Here are 3 possible L-network configurations for tuning a CG amplifier output. They can be used in other circuits and are worth studying. The L-match with 2 variable capacitors generally requires lower inductance than the others.

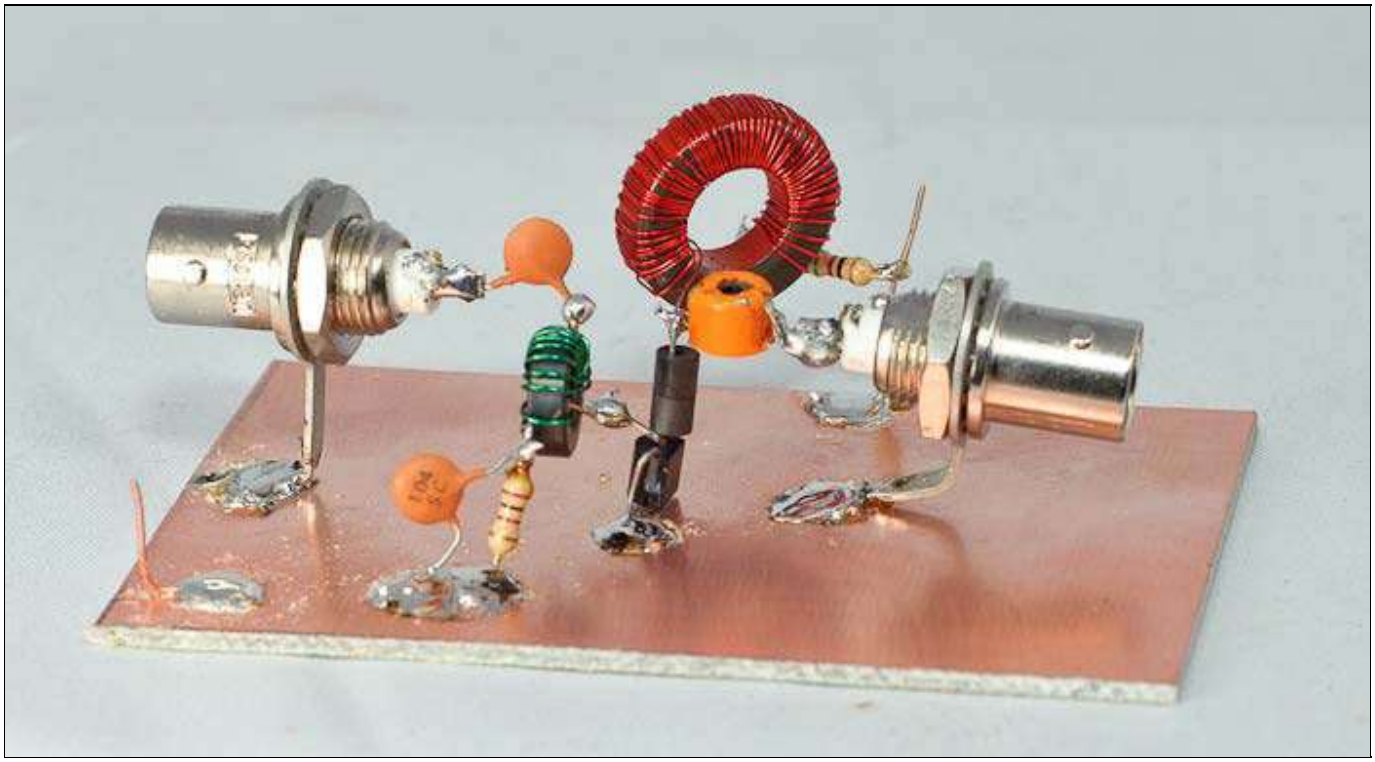

Above — A breadboard of 1 of the high-pass tuned CG amps. The gate lead on this transistor is too long — the inductance will likely cause UHF

oscillations. 2 ferrite beads were placed on the drain to mitigate these, but a better construction technique is recommended and shown below.

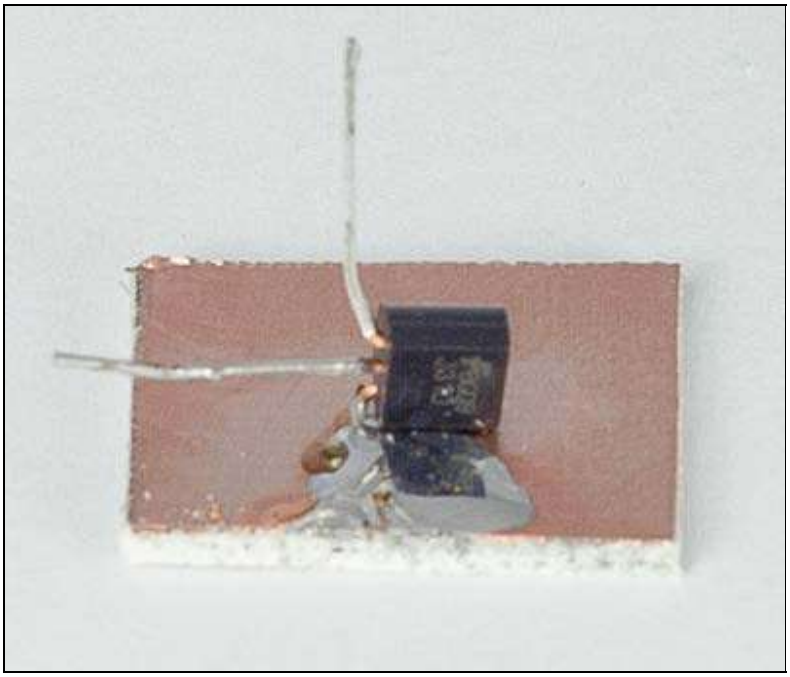

Above — the preferred way to ground the gate with the JFET on its side. The hole-through version of the U310 JFET has a metal case that is connected to the gate that makes it ideal for grounded gate amplifiers. Some suppliers only sell SMT versions of the U310 now.

---

4. QRP — Posdata for January 2013: Transistor Bias Model

This discussion concerns setting up the DC bias point for linear BJT operation.

Earlier I stated that a bipolar transistor is a voltage controlled device. A few readers thought I made a typo: something I frequently do, but not in this case, since I purposely made that statement. In reality, the argument could go either way since collector–emitter current is controlled by the base-emitter current (~a current controlled device) and by the base–emitter voltage (~a voltage controlled device).

Stated using the correct physical model, a transistor is a **current controlled current source**. With external circuitry we can manipulate this physical model into a voltage controlled current source, or a voltage controlled voltage source, or even a current controlled voltage source. Whether you model the transistor with current or voltage, the math tells the truth when properly examined.

Please view the following two 2N3904 SPICE models generated by Wes, W7ZOI for me many years ago when I began to learn small signal analysis using impedance and hybrid parameters, plus set out to learn ways to establish DC bias and temperature stability in BJTs.

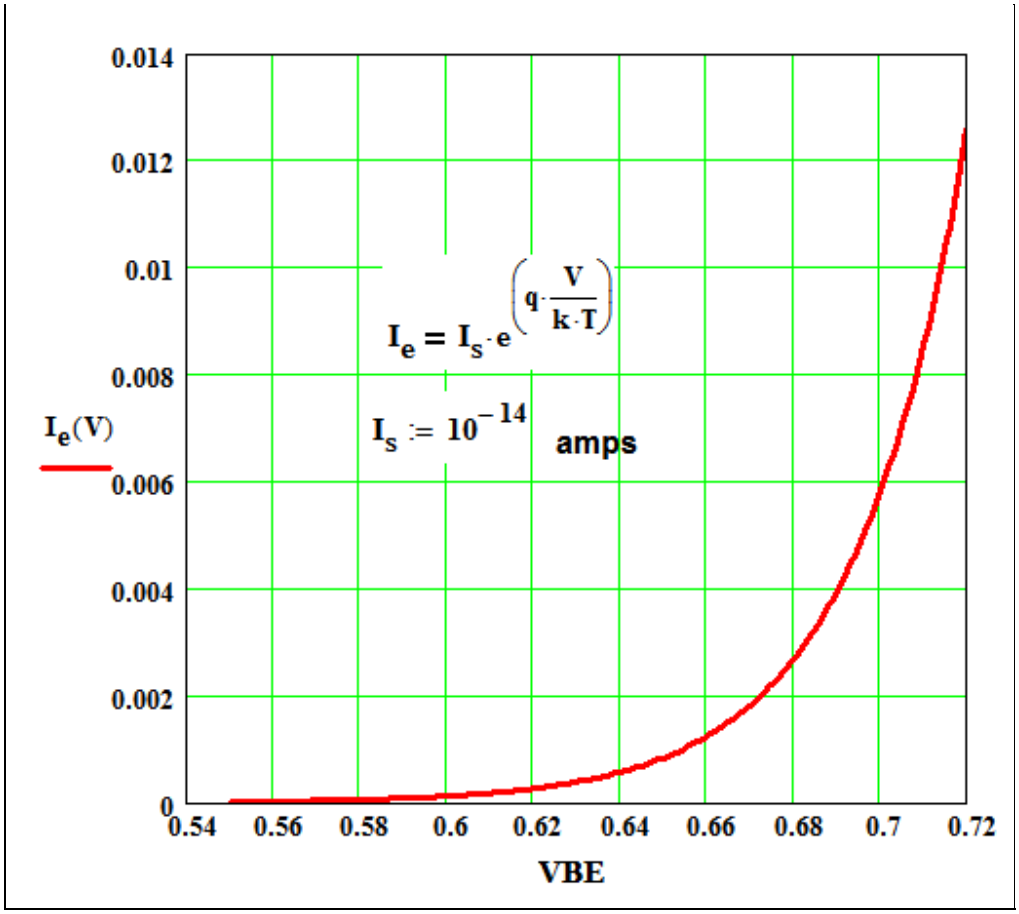

Above — the Y axis shows how changing base-emitter voltage or current changes the VBE. We tend to assume a VBE of 0.7, however, the math shows the truth. Whether we plot voltage or current for the Y axis data, the graph slope remains similar. The greater the applied DC voltage placed on the base-emitter port, the more current will flow.

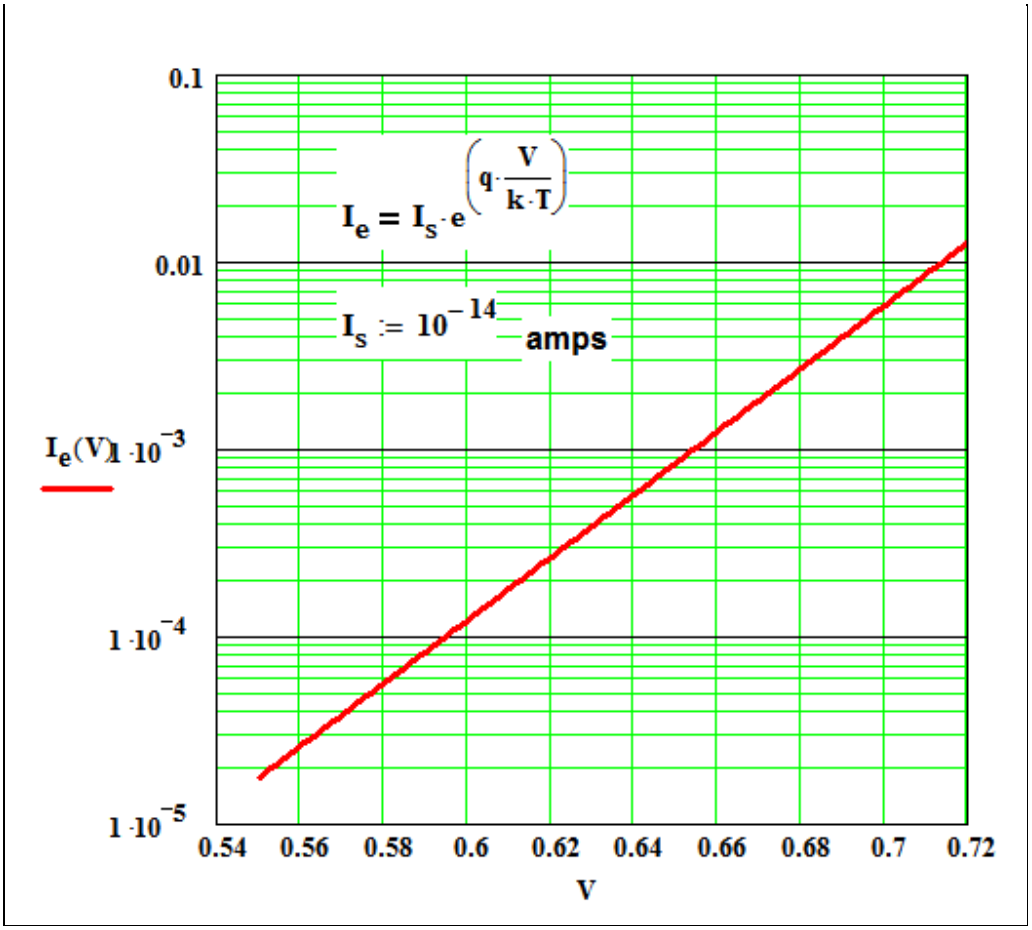

Above — Logarithimic base current plotted against VBE. If we want this current to increase, we need to put more DC voltage on the BE junction. On the bench, we may easily measure base voltage to confirm our calculations — measuring base current proves more difficult. Whether I'm setting up amplifer bias with voltage dividers, a current source, or even biasing it with a downstream AGC voltage, I prefer to think in terms of voltage control — although I get that V and I truly just coexist.

Current or voltage modelling — it's your choice and the math will guide you. Look for these equations on the Web, or in second hand bookstores. I've got 8 or 9 transistor theory books now and they're really timeless.

---

5. Miscellaneous Figures and Photographs

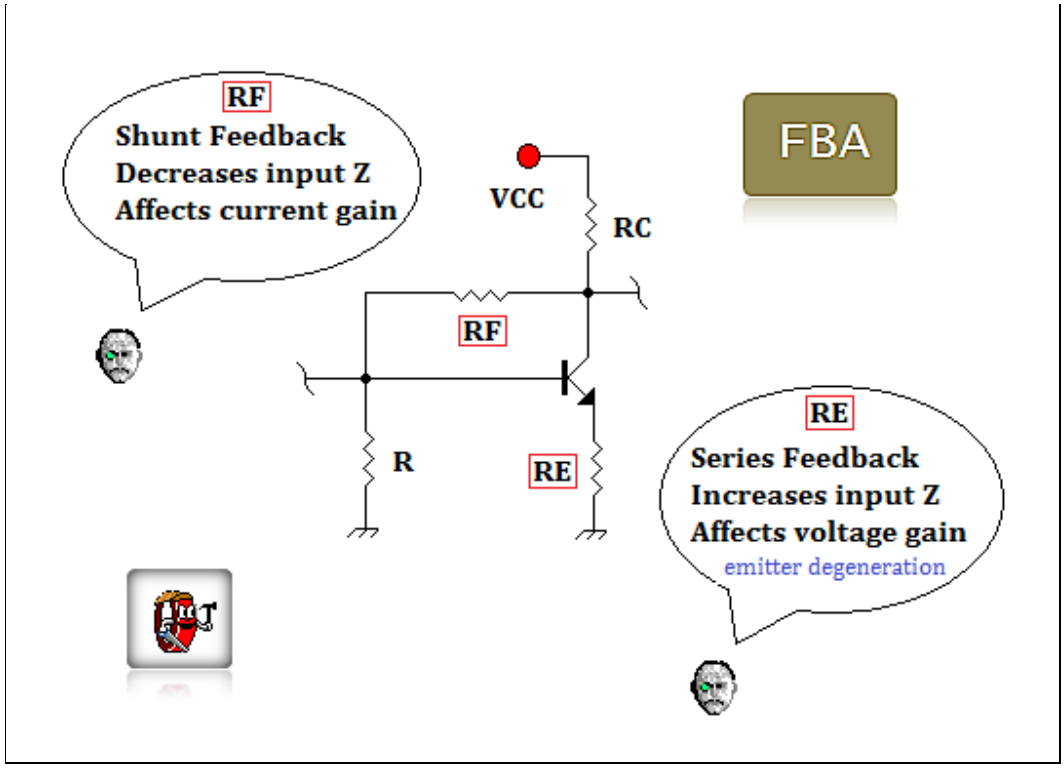
RF
Shunt Feedback
Decreases input Z
Affects current gain
FBA
VCC
RC
RF
R
RE
RE
Series Feedback
Increases input Z
Affects voltage gain
emitter degeneration

---

6. References

1. Communications Receivers - Principles & Design. Rohde, L.R and Bucher, T.T.N. 1988. McGraw-Hill.
2. Technical Correspondence QST Magazine (ARRL) Aug 1990. Hayward W.
3. Experimental Methods in RF Design (ARRL) 2003. Hayward W. Campbell R. Larkin B.
4. Microwave Handbook Vol 1. Components and Operating Techniques. 1989 RSGB.
5. Emails with Wes, W7ZOI and Professor Ken Kuhn, Winter 2010-2011 — Thanks! Никогда не забуд.

Hobby and Fun 2011

Introduction

Hobbies are supposed to be for recreation. Electronics should be fun, not stressful — heavy math, big parts counts and complexity are more likely to scare away experimenters than recruit them. This page avoids the measurement focus of my latest stuff and simply promotes fun and discovery.

You might be interested to know that my simple experiments/projects garner the most emails. Many wrote "I'm rediscovering electronics", or, "I want a simple and fun hobby". Hobby and fun are my goals too.

Simple Regenerative Receiver Experiments

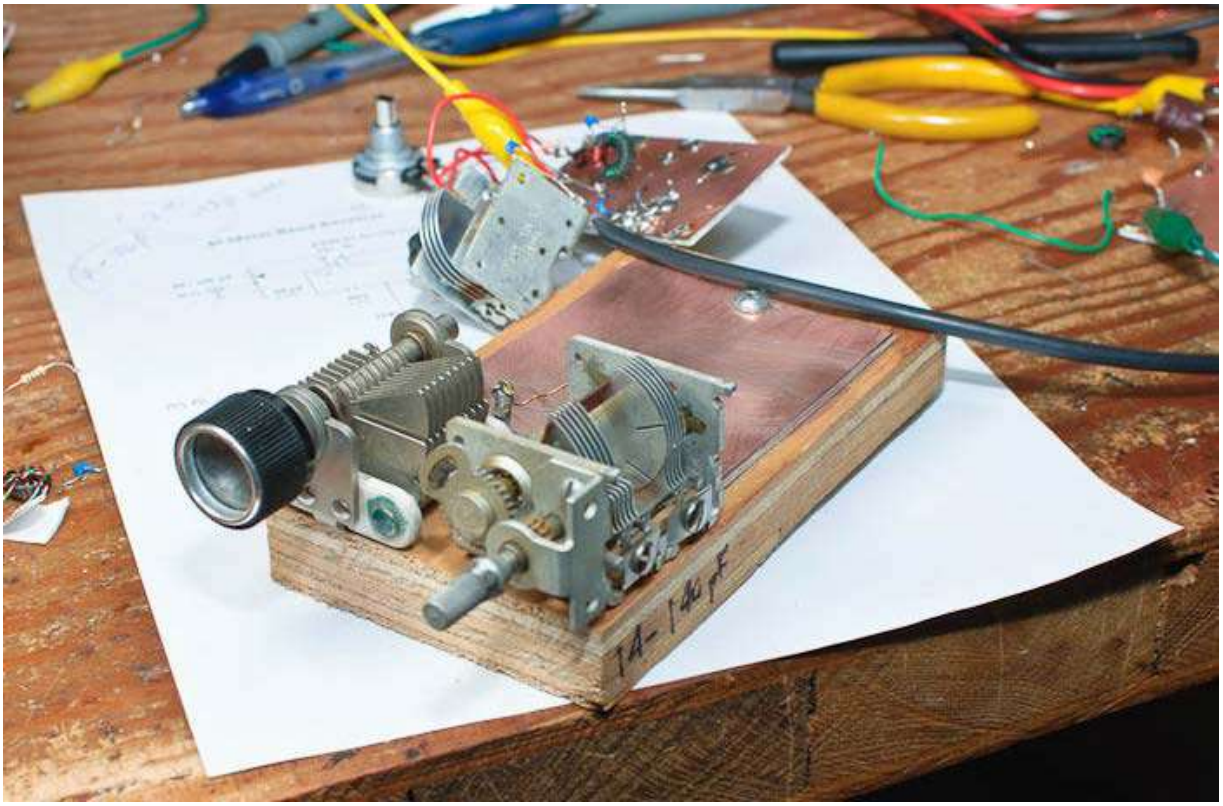

Above — 2 air variable capacitors and a copper clad board screwed onto a piece of wood for my bench musing. Regenerative receivers delight and amaze — some builders take them very seriously. I respect this, but to me; they should be as simple as possible. I wanted a 2 stage "genny" receiver for this page and present 2 different receivers; 1 is my design, the others is a JFET variant of a favorite W7ZOI circuit. Quoting Wes, W7ZOI "feedback your imagination".

Some builders place a simple common gate or a common base RF preamp on the input to boost gain and reduce antenna radiation of the RF oscillator, while others place an RF gain control on the input — usually a potentiometer; to prevent overloading the RF stage. I won't prescribe what to do — that's up to you. There are countless example of regenerative receivers on the web and you can many spend hours viewing them. Some of the most intriguing are those built by Russian speaking experimenters. Example link.

My circuit ideas are meant as fodder for your own experiments.

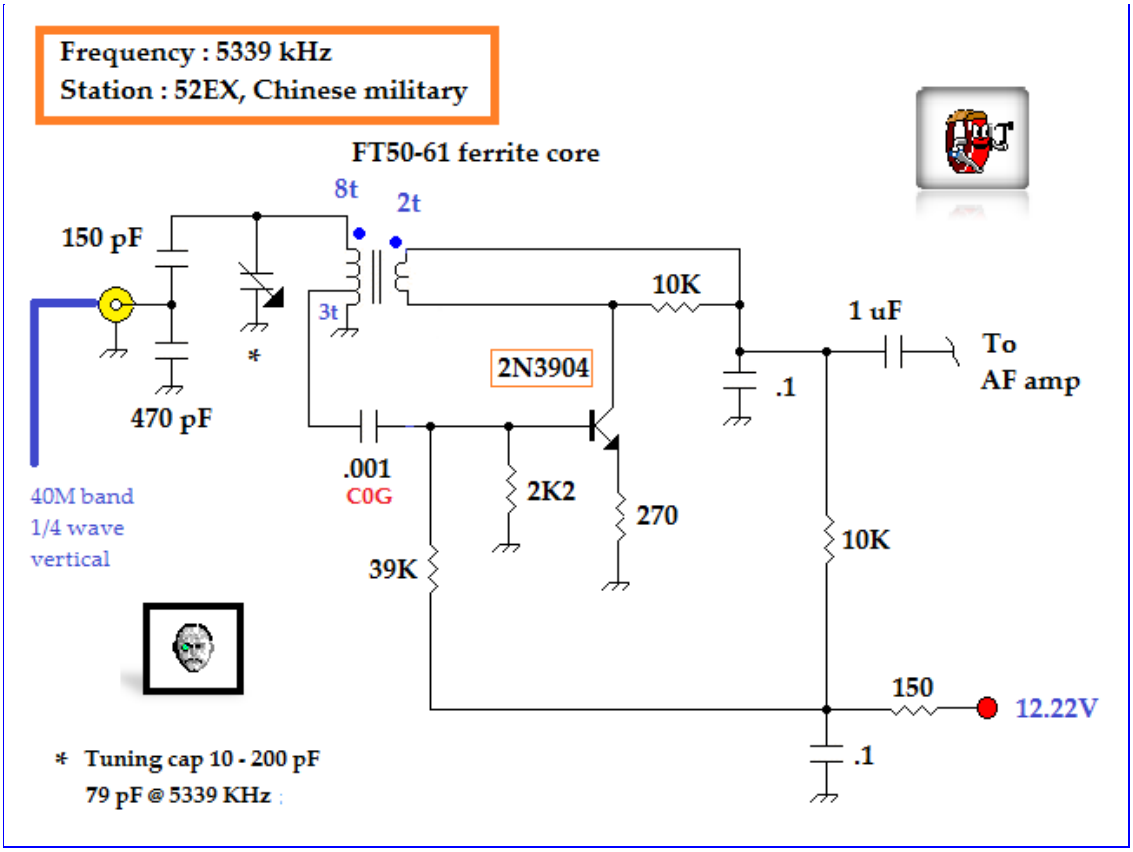

Above — An experimental, ultra-simple "CW" receiver. At 5339 KHz I hear strong Morse code each night. It's suggested to be from China, but I'm unsure. Connected to my 1/4 wave 40M band vertical - a simple matching network and trimmer tuning capacitor were fitted to the input. Here's some audio. I like the beat note of this receiver - it has no regeneration control and is fixed for CW. Minimalist circuits are fun — some hardcore regen builders might freak out; no voltage regulator (here's a version with that + a T68-6 inductor), no regeneration control (here's a version with that), a relatively low Q coil etc. I wanted to try my hand at design and not just copy someone else's receiver.

I call it the Stupid— Simple receiver and although it emits crisp, warm audio, some bench work is required to get the correct bias and appropriate amount of positive RF feedback — an experimenter's circuit that explores DC bias and AC feedback. The sort of thing a father can build with his son. We need more circuits fitting this profile.

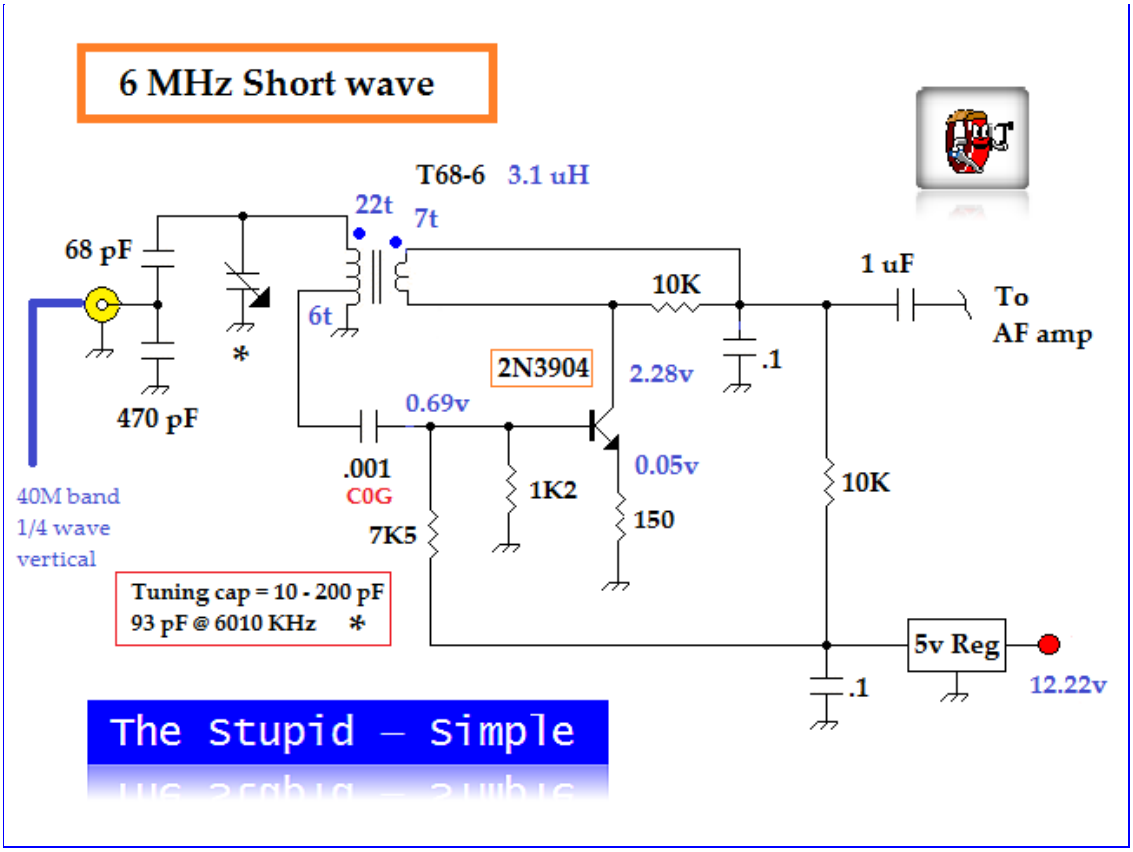

Above — The Stupid—Simple experimental receiver set up for ~6 - 7 MHz. 2011 marks the 50th anniversary of Radio Habana Cuba. We tune RHC at 6010 KHz, and as long as I've been listening to SW radio, I've tuned this station. Here are 3 sound bytes from around 6 MHz recorded from 2:30-2:40 GMT on Feb 28, 2011, including an old repeated episode of DX'ers Unlimited by Arnie Coro which had faded out by the time I located and turned on my audio recorder. Audio1 Audio2 Audio 3. The audio stage in these recording was a discrete transistor AF amp I designed, however, an LM386 was chosen for the final amp to keep the parts count and difficulty down. I got a little too close to the receiver a couple of times during the recording and made the open circuit breadboard squeal.

Arnie Coro talked about a "regenerodyne" receiver in Sound Byte *Audio3*. Very cool. Here's a link. Now this is radio!

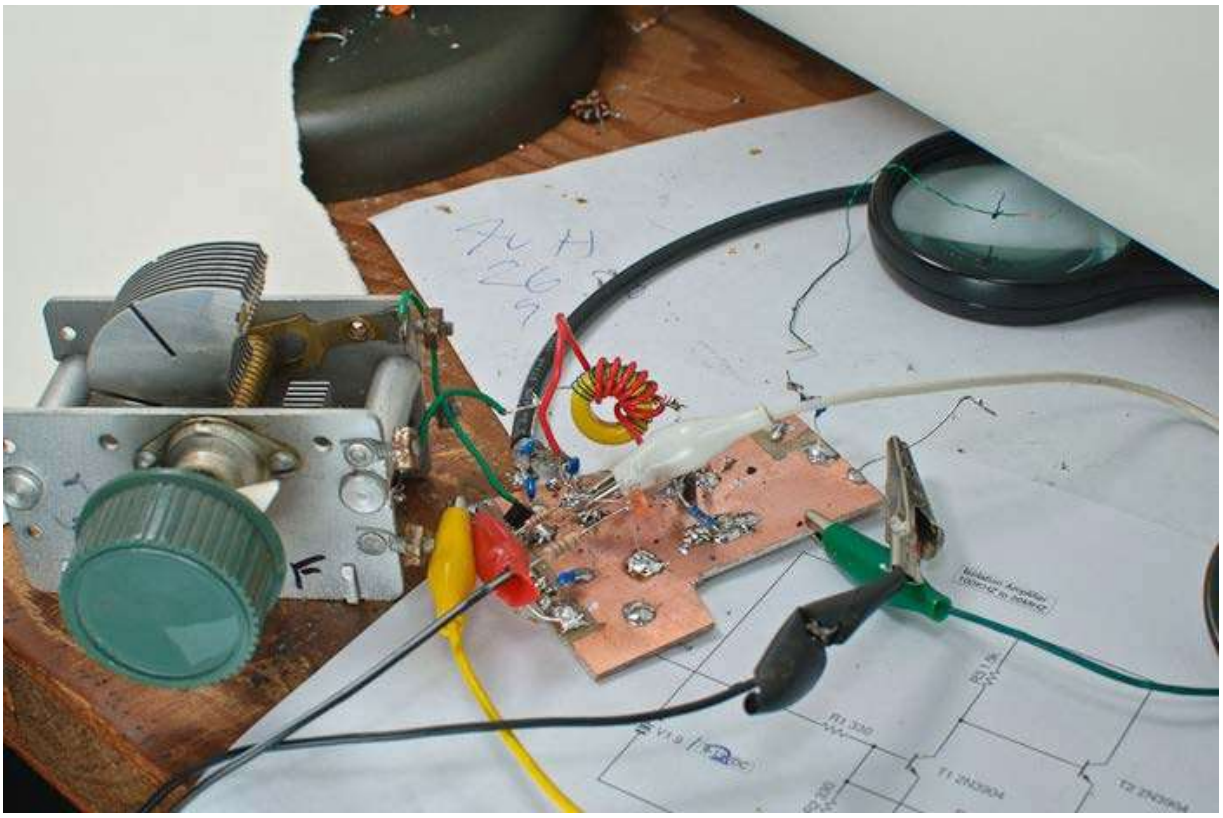

Above — The Stupid-Simple regenerative receiver breadboard for 6 MHz. You can see the T68-6 — the red secondary windings are wound in the same direction as the 22 turns of primary. I started with 9 turns and unwound a link and tested sequentially until I had the right amount of feedback for AM. I just used normal hook up wire for the secondary winding. The white colored cable goes to the audio amp. This is a prototype experimental layout — a regenerative receiver should have short connections around the tank circuit and be in metal box for best results.

On some stations, my little 1 RF + 1 AF stage receiver sounded better than my superheterodyne receivers. The 2N3904 is just barely turned on — I determined that a base bias of 0.66-0.69v provided maximal sensitivity. The 150 ohm emitter resistor can be a 500 ohm pot and used to fine tune the regeneration. 150 ohms gave the best compromise gain and feedback + current for the 2N3904.

Audio Amplifier

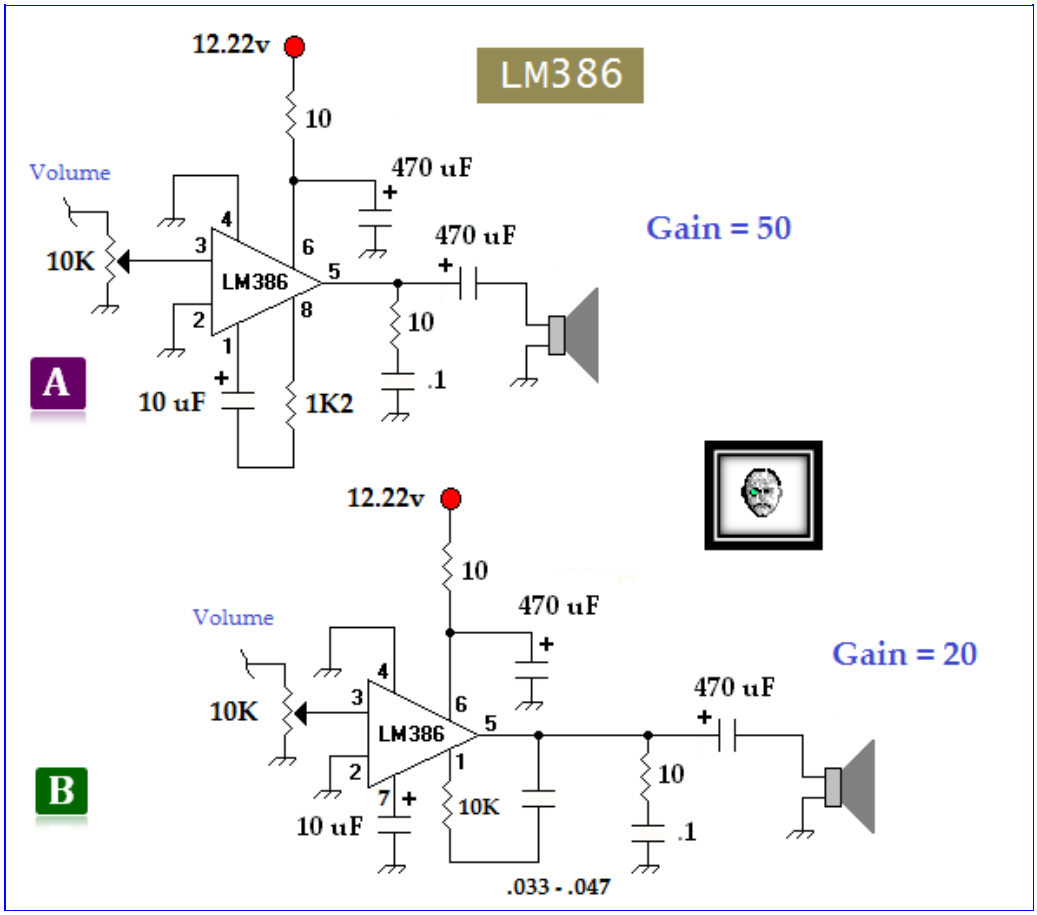

Above — I chose an LM386-N for my AF power amplifier. The LM386 exhibits less peak signal distortion when run in the low-power (X20) gain mode and a higher VCC such as 12 volts. My receiver used the schematic denoted B — a 10K and 0.033 to 0.047 uF RC network is used to reduce the amplifier high frequency response. Click for a sound byte of me tuning around 6 MHz with a 10K + 0.047 uF RC network between pins 1 and 5. Figure B is my favorite way to use the LM386 and comes right off the National Semiconductor LM386 data sheet. Look for this data sheet with your favorite search engine.

Because I have a big antenna, Figure B provides adequate volume to a speaker. Connecting pins 1 and 8 via a 10 uF capacitor bypasses some emitter resistance and gives X200 gain. A resistor in series with the capacitor pin 1 and 8 will reduce the gain. Figure A shows a gain = 50 configuration. You'll have to choose the LM386 set gain to suit your particular regenerative receiver, however, the greater the gain setting, the greater the chance of distortion, unwanted noise and audio feedback.

I generally build my audio power amps around op amps or discrete transistors, but the LM386 exalts this web page's theme. Distortion in all these small power amplifiers is dependent on input signal amplitude as much as anything else.

LM386 Motorboaters

Expect AF feedback motorboating via your DC power lines as you increase the AF gain pot in *many* LM386 circuits. If this happens, try better bypass and decoupling on the LM386 power line: 100 to 470 µF shunt bypass on the DC line + a 10-22 series decoupling resistor, plus 100 - 470 µF shunt bypass on pin 6. Click for 1 example. ypically 470 µF bypass is required if you suffer 60 hertz hum. You may model your simple RC filter with application E on the javascript applet page to see the 3 dB cut off frequency of your particular DC line low-pass filter.

Stupid—Simple Notes

The Stupid—Simple circuit really needs the adjustable 10K regeneration control if you wish to tune both AM and CW. The number of turns on the feedback winding varies with factors including transistor beta, how you wind the primary and secondary windings (greatly affects the coupling between the primary and secondary windings) and whether you want AM, or CW reception — or both. Experiment with the number of turns to figure it out.

You can try "matching" the tank circuit to your antenna by decreasing the 470 pF cap to as low as 68 pF. This will affect the tuning capacitor range. For an air variable tuning capacitor, use anything you can find. Consider connecting fixed parallel and/or series capacitors to reach or limit the desired capacitance. Many good examples are published on the web.

Some builders float the tuning capacitor across the inductor so the cap is ungrounded. The stator (body) of the capacitor should be connected to the circuit ground to help minimize the effects of hand capacitance. A grounded metal case further helps.

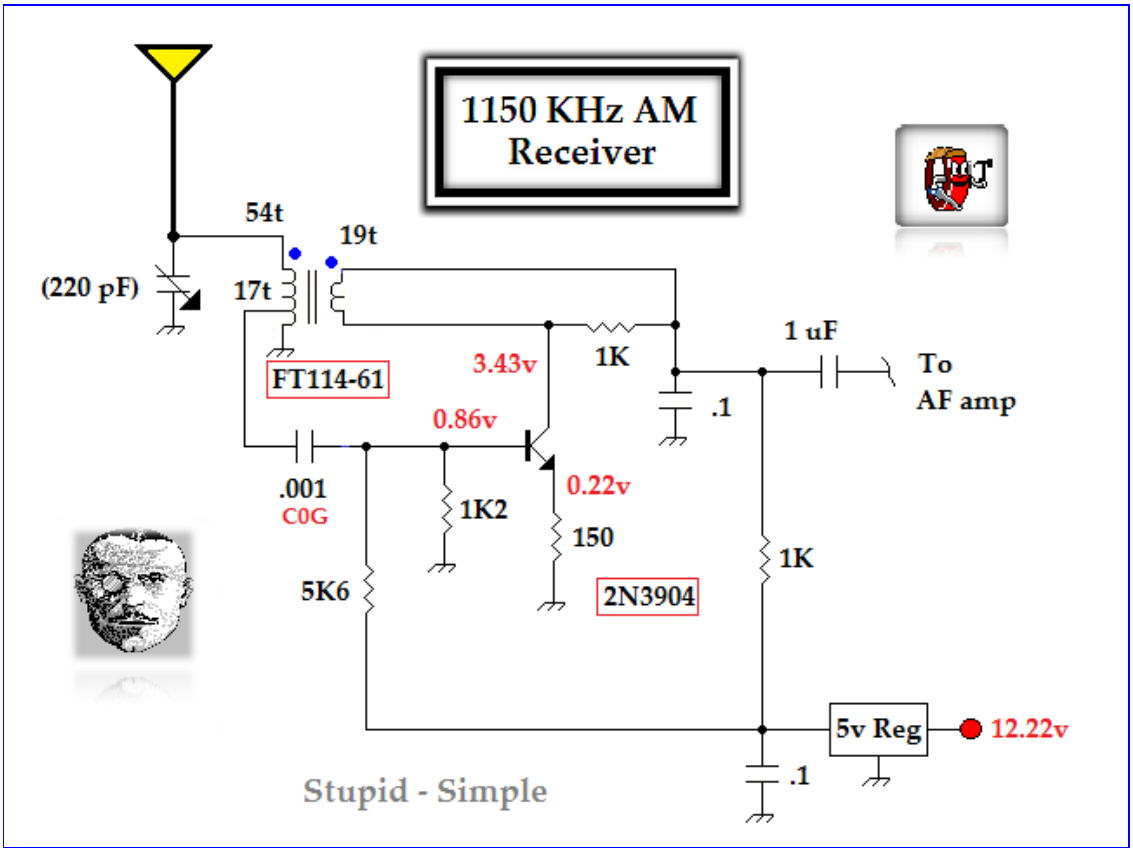

Above — My popcorn regenerative design "The Stupid-Simple" set up for broadcast band radio at 1150 KHz.

A reader from Brazil enquired about putting the Simple Stupid on MW. I had some time for a couple of experiments but only wanted 1 frequency — 1150 KHz, the local 10 KW sports radio station. Using 28 gauge wire, I wound 54 turns (about 230 uH) on a A FT-114-61. Most builders won't have this toroid, however ferrite rods from AM radios are plentiful and a great substitute.

This design relaxed the regeneration to improve audio quality (no whining or hissing). The bias and feedback loop were wound for the best sounding audio. For example, at the bias shown, if you increased the 19 turn link to 21 turns, the bass response increases; decreasing to 17 turns reduces the bass response.

As a result of lowered positive feedback, the selectivity is down, however, a variable capacitor is needed to peak the station. After peak tuning, I removed and measured the air variable cap at ~ 200 pF and then substituted a 220 pF fixed capacitor to simplify things.

For audio, I used a bench AF power amp into a speaker. It sounds nice for 1 transistor. Audio sample

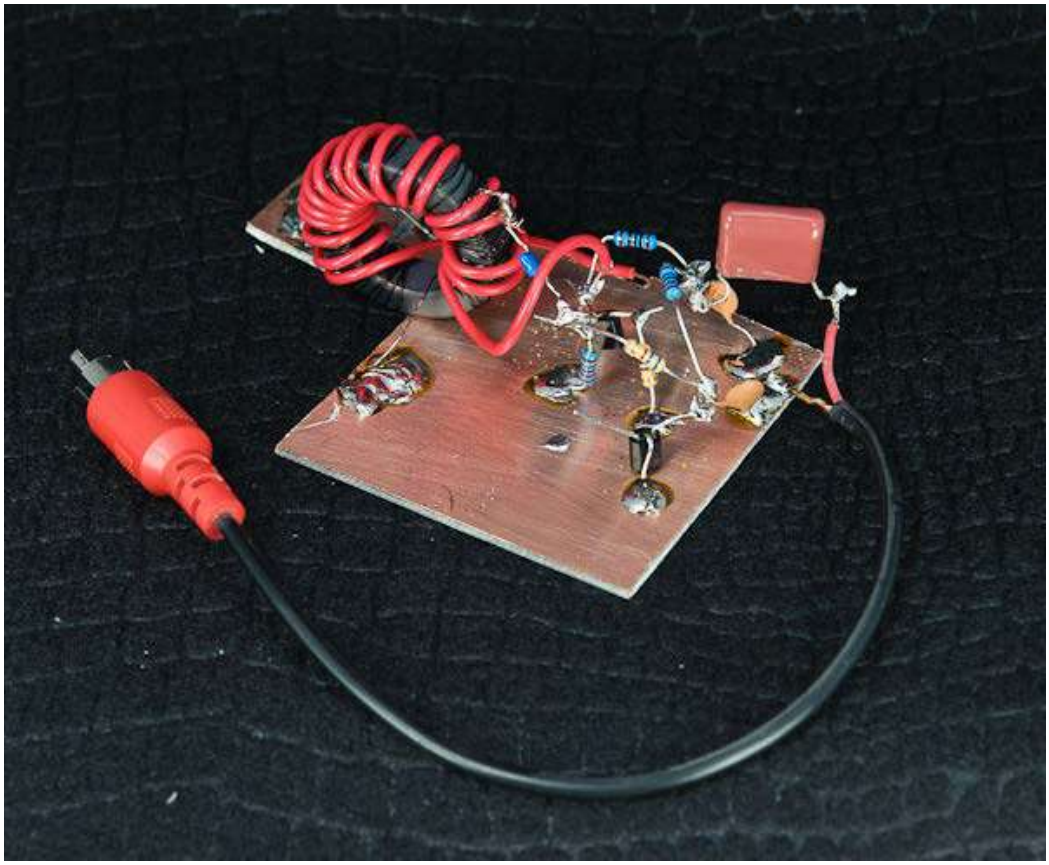

Above — The breadboard of the 1 channel receiver for my workshop - I'll use it to keep track of the Canadian Football League statistics. My test antenna was a long piece of outside wire. Red hook-up wire forms the 19 turn feedback winding.

For cities with multiple AM stations (AM stations are dying out in Canada), you'll have to add more regeneration and probably move to a better design. This radio is simple, but not extraordinary.

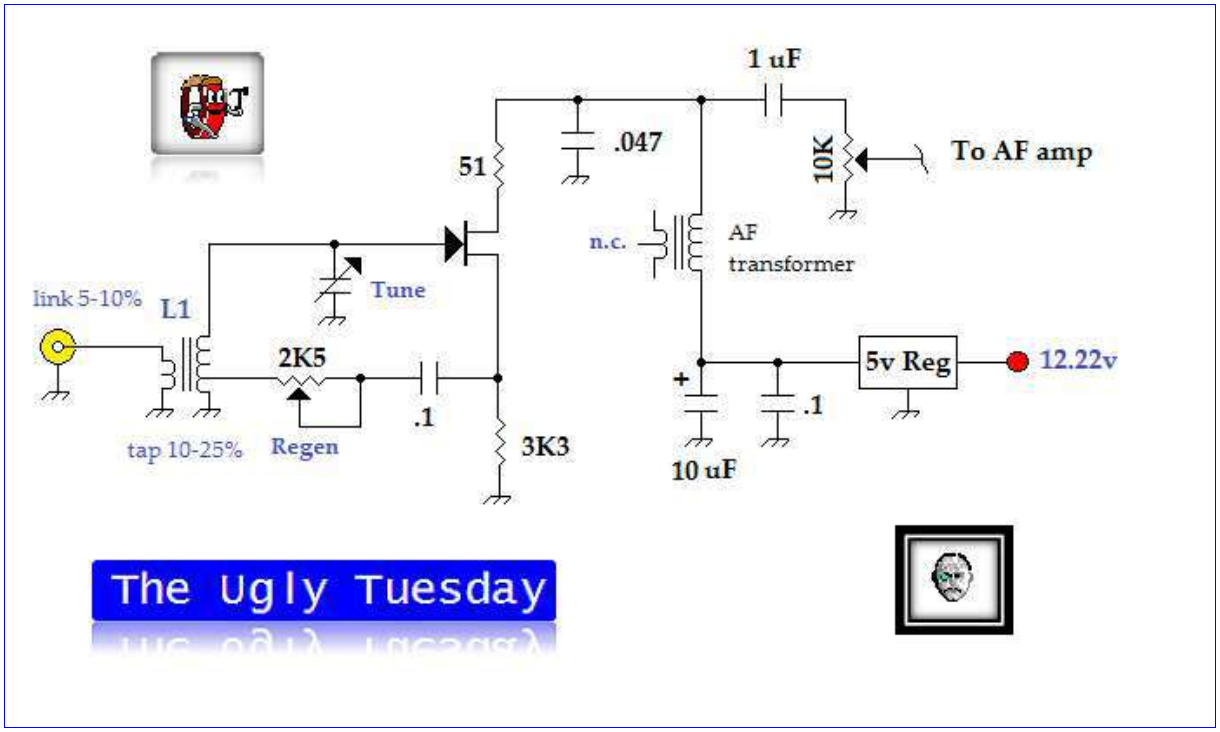

Above — Another regenerative design that tuned AM, SSB and CW from 5-11 MHz with different toroid coils wound on a T50-6. It's based on a favorite design by Wes, W7ZOI. I suggest tapping L1 at 10 - 25% of the total number of turns. The secondary link for the antenna connection depends on the impedance of the antenna, but 5 - 10% of the total number of L1 primary turns worked well at my QTH. Please experiment with the secondary link to determine the optimal coupling to your antenna. My L1 inductance ranged from 1.5 to 5.6 uH. You may have to add a fixed capacitor in parallel with your air variable capacitor when using low inductance coils such as 1.5 uH.

The 51 ohm resistor suppresses UHF parasitic oscillations. The AF transformer is a transistor radio output (1000 : 8 ohm) junk box special and serves as an RF choke. I tried various AF transformers harvested from old transistor radios in this slot and they all worked fine. Nothing's really critical on this receiver — that's why I like it. Truly junk box radio.

Simple Active Antenna Experiments

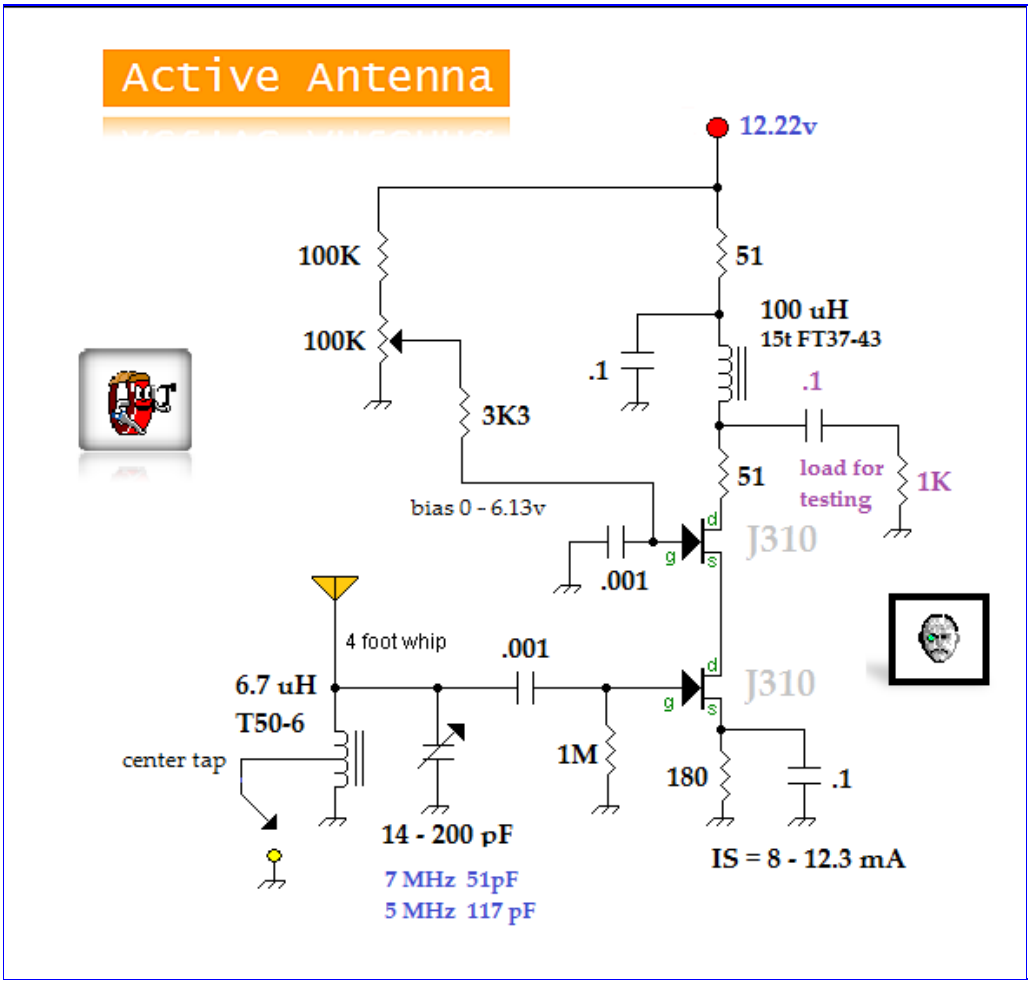

Above — A voltage probe or active antenna using a telescopic whip. It's been awhile since I built one in keeping with a minimalistic circuit theme. I tested this VPA from 5 to 14 MHz. The center tap on the coil allows the peaking at ~10 MHz and higher. The L value is non-critical; choose a value that will work with your tuning variable capacitor or varactor. The L - C values can be *roughly* determined from a chart like this, or just do the math (XL = XC at the desired frequency). Account for stray inductance. If you wish to perform return loss measurements on this circuit, you'll have to short the 6.7 uH inductor as the whip antenna can tune in RF from the RF signal generator used for the return loss bridge.

Without the 1K load, the circuit will oscillate. I thought about some ways to match the output transformer to a regenerative receiver tank circuit. The 100 uH drain choke could be replaced by a (bifilar) 2:1 transmission line transformer or two. Transformer experiments this Winter clearly illustrated the superior coupling of transmission line transformers and mandates using them over conventional transformers whenever possible.

Using a conventional transformer with a shunt resistor across the transformer would also work, but the resistor reduces gain. I built and tested this output circuit with an 8:1 transformation using two 2:1 transmission line transformers. The output impedance at the JFET drain is somewhere around 4300-4500 ohms at 7-14 MHz. The transformed output impedance is somewhere around 250-330 ohms at 7- 14 MHz. Connecting the VPA output to a tap in the regenerative main tuning inductor might work — being careful not to load down the regenerative tank coil.

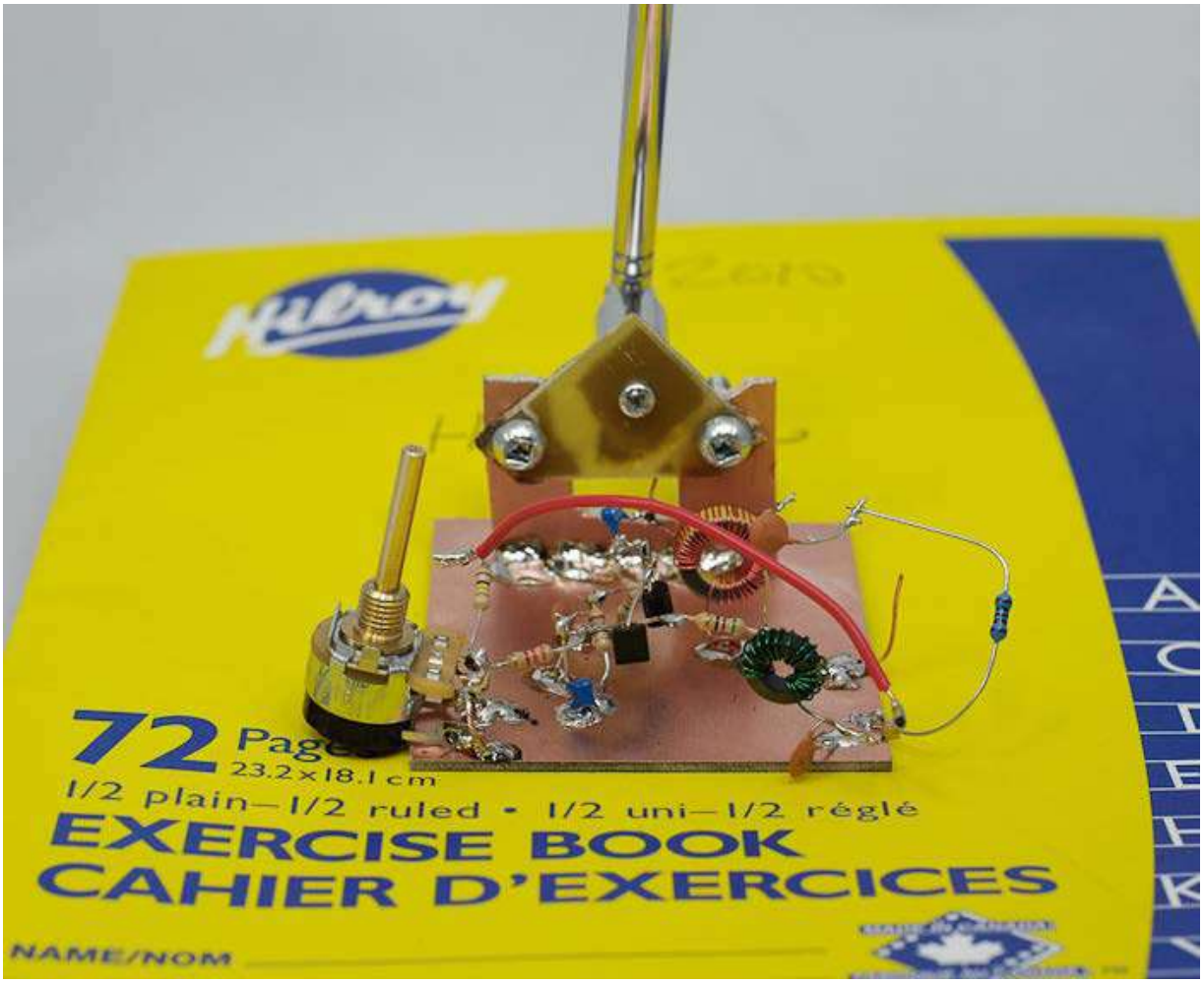

Above — The VPA breadboard on my latest notebook. The 100K pot sets the stage gain. While simple, it works okay.

Above — the VPA built March 12, 2011 (the 14-200 pF air variable cap is not shown). It took about 45 minutes to design, build and test it. The 1K load used for testing is the blue resistor to the extreme right.

Low-pass Filter for 21 MHz

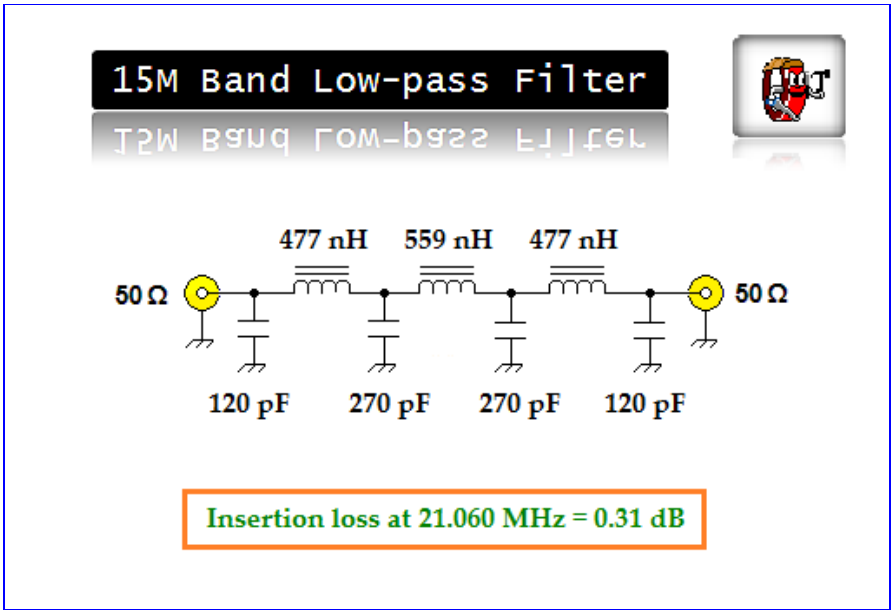

Above — A 7 element Chebyshev low-pass filter for the 15 Meters Ham band (fCo = 25.03 MHz to allow the use of standard value capacitors). A builder requested a band-pass filter design for his 15M band receiver. In order to accurately test my design, I decided to make a permanent, low-pass filter module to follow my signal generator. 15 Meters is a favorite Ham band, so I'm certain to use it in the future.

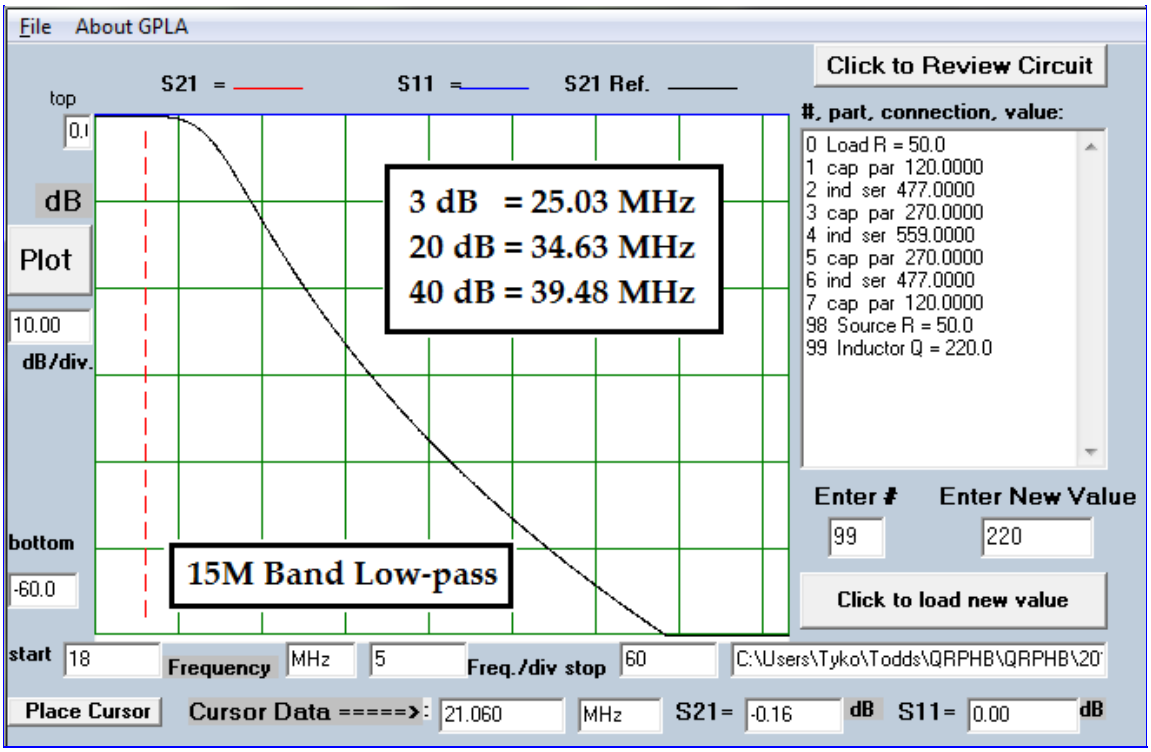

Above — A GPLA plot of the filter. The frequency cut-off at -3, -20 and -40 dB are shown. Perhaps this filter is overkill, but I had all the parts on hand and love a serious low-pass filter. Click for the bread board photo.

Fine-Tuneable 1 KHz Wein Bridge Oscillator

In 2010, I wanted a fine-tuneable Wien bridge oscillator to drive a notch filter in an AF distortion analyzer. Ken Kuhn drew me up a schematic on his coffee break and emailed it the same morning.

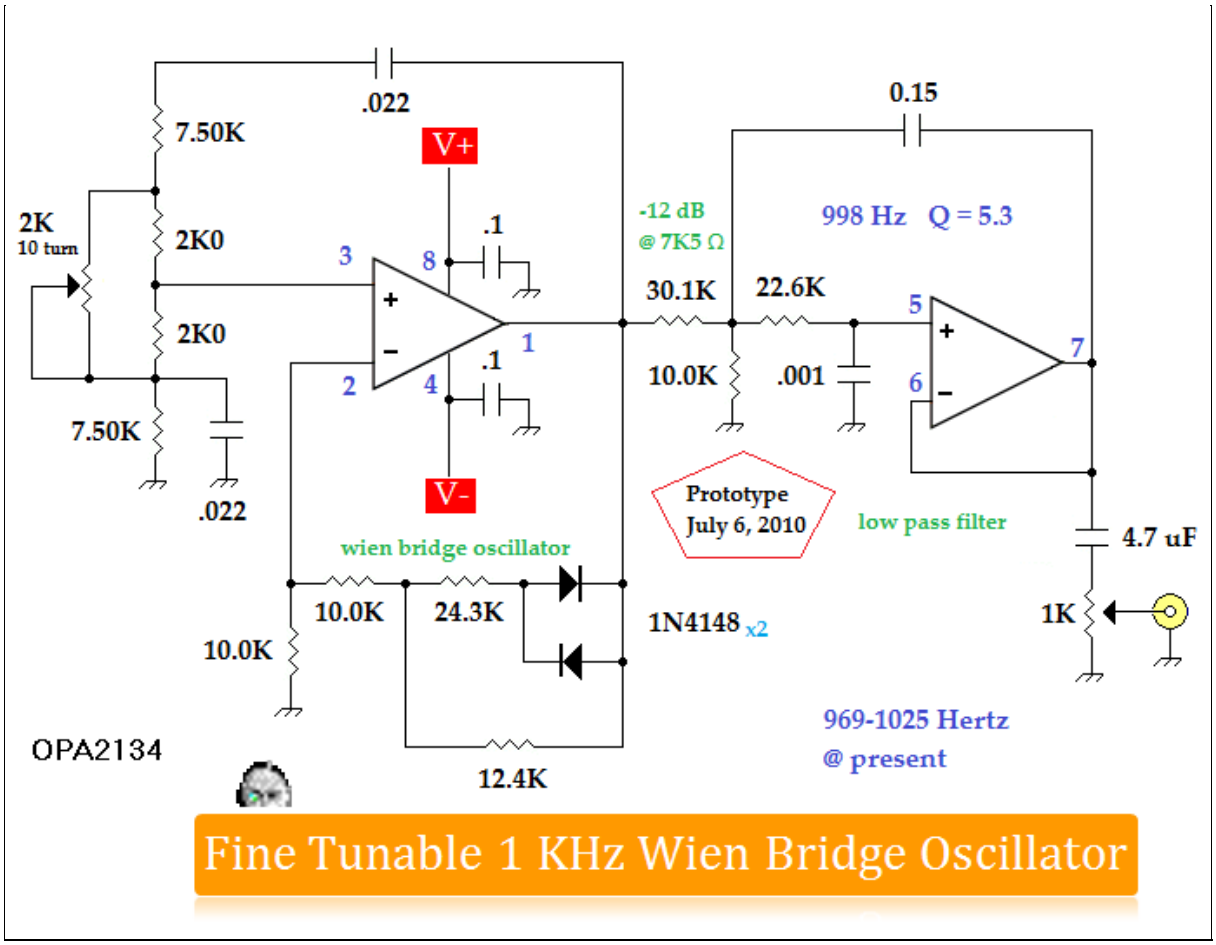

I applied anti-parallel diodes instead of the classic incandescent bulb for amplitude stabalization in the feedback loop; probably a mistake leading to higher distortion. Ken's fine-tuning circuit works perfectly. I matched the 7K5 + 2K0 + 0.22 uF components on each filter half. 1% parts go in this circuit.

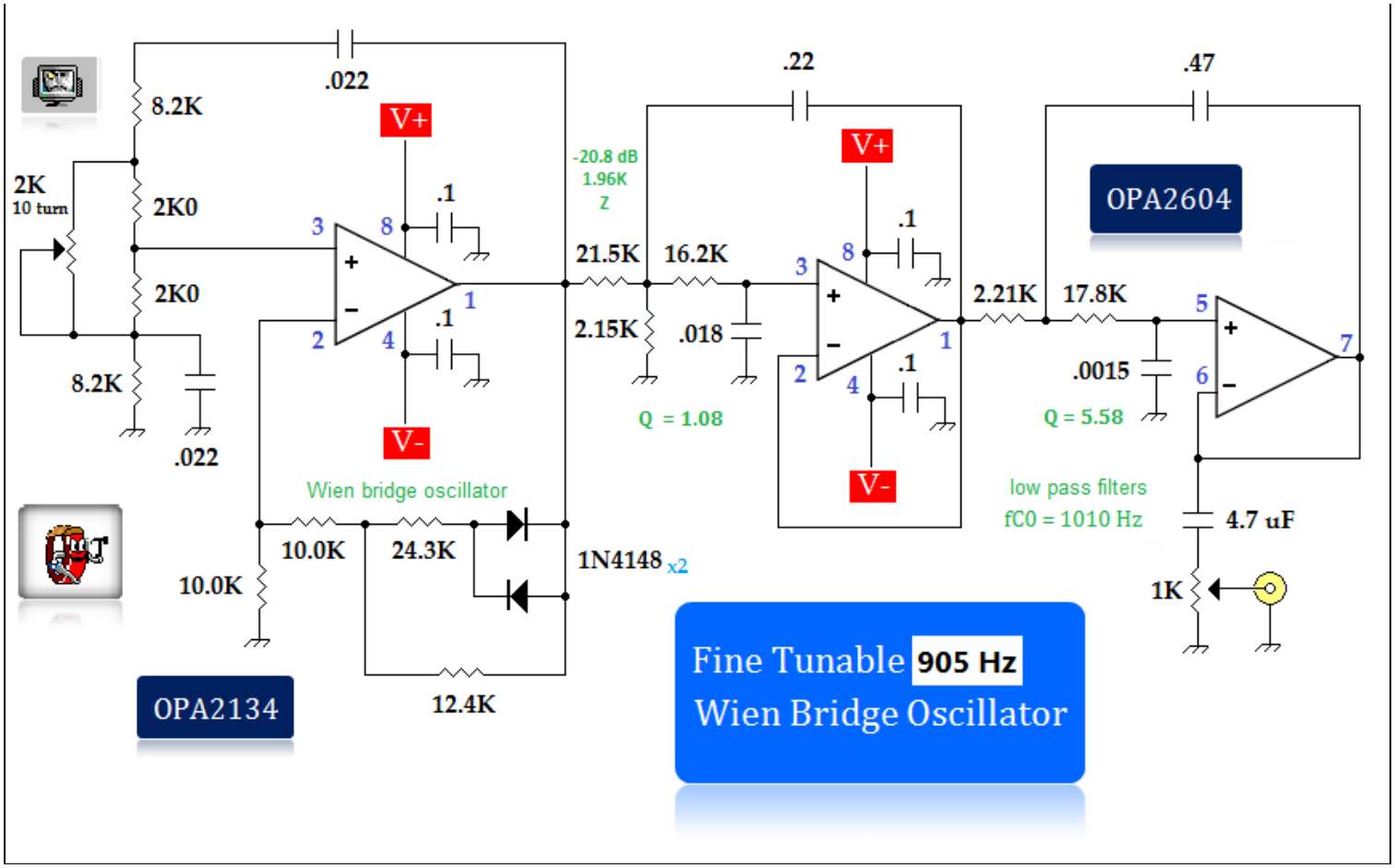

A version for 905 Hertz built with crazy expensive op-amps. I chose 905 Hz to match my notch filter frequency.

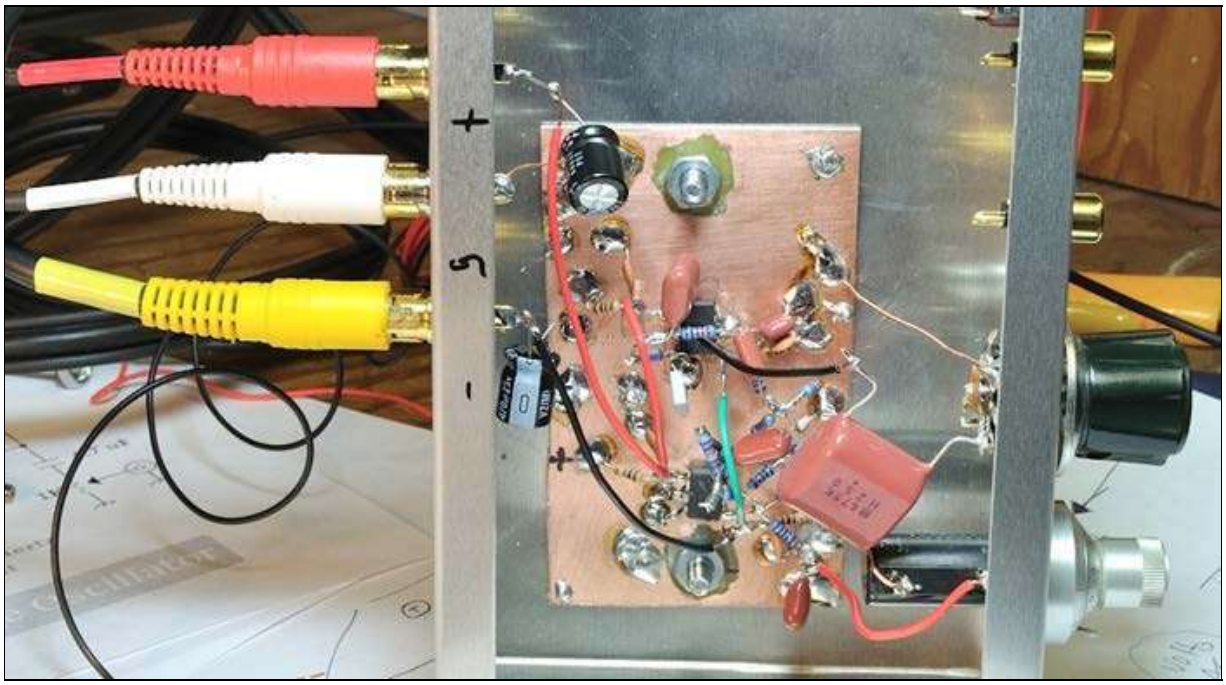

My breadboard.

QRP Modules 2011

Introduction

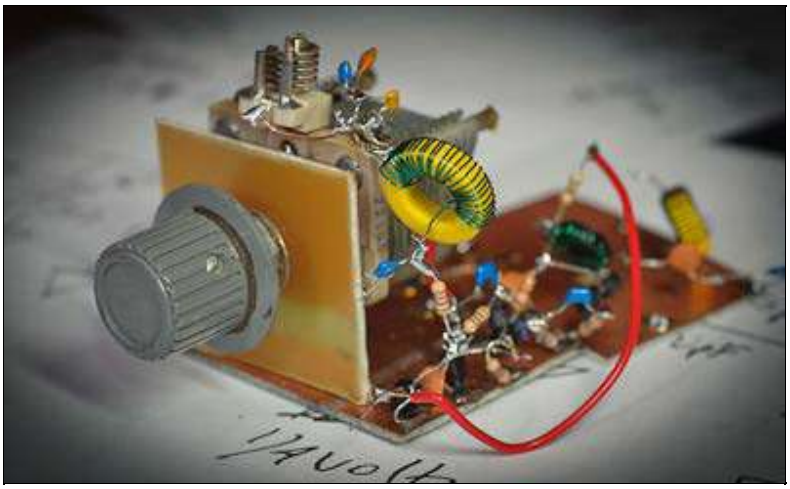

As experimenters, we rebuild core circuits over time. I decided to increase my collection of stock modular circuits to avoid re-inventing the wheel. This web page serves as a module repository for the website.

Since our needs differ, I've shared these circuits more for interest sake and really not as schematics to copy. All modules were carefully built and tested.

1 great virtue of the metal encased module is strong shielding. RF modules use a 50 ohm port impedance and BNC connectors. RCA jacks interface the AF modules.

40 Meter Band-pass Filter

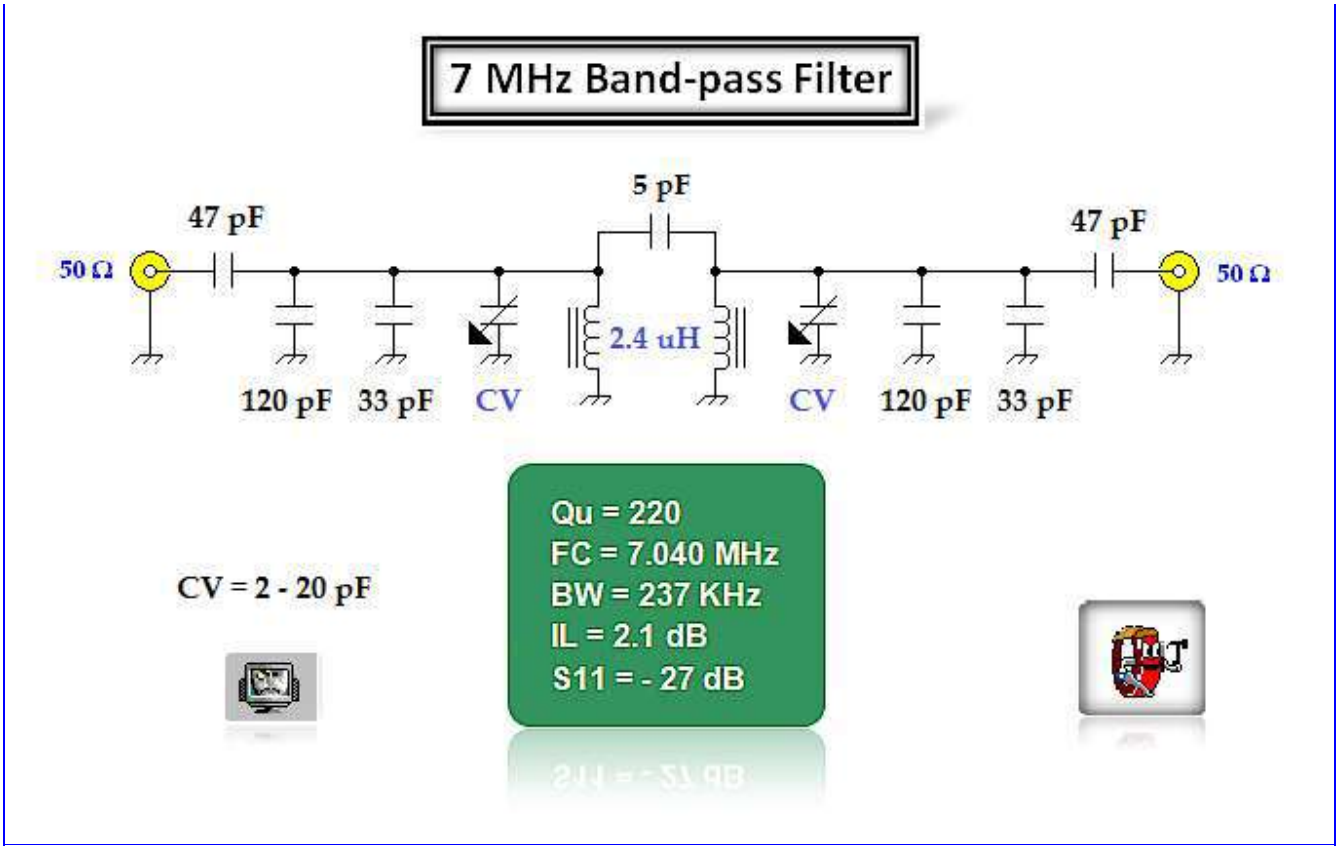

Above — A 40 Meter Ham band double-tuned band-pass filter. I designed this circuit using 2 programs that came with EMRFD and describe the process on this web page. The 2.4 uH measured coils were wound using #22 AWG wire on T68-6 powdered iron toroids and all fixed caps were ceramic C0G type. I centered my filter at 7.040 MHz. You should be able to peak it anywhere on the 40 Meter CW sub-band by tweaking the variable capacitors.

I peaked the trimmer capacitor while looking at the peak-to-peak voltage on a 50 ohm terminated oscilloscope. The filter input was connected to a 7.040 MHz signal generator with a 30 dB return loss, low harmonics (-55 dBc) and 50 ohm cables.

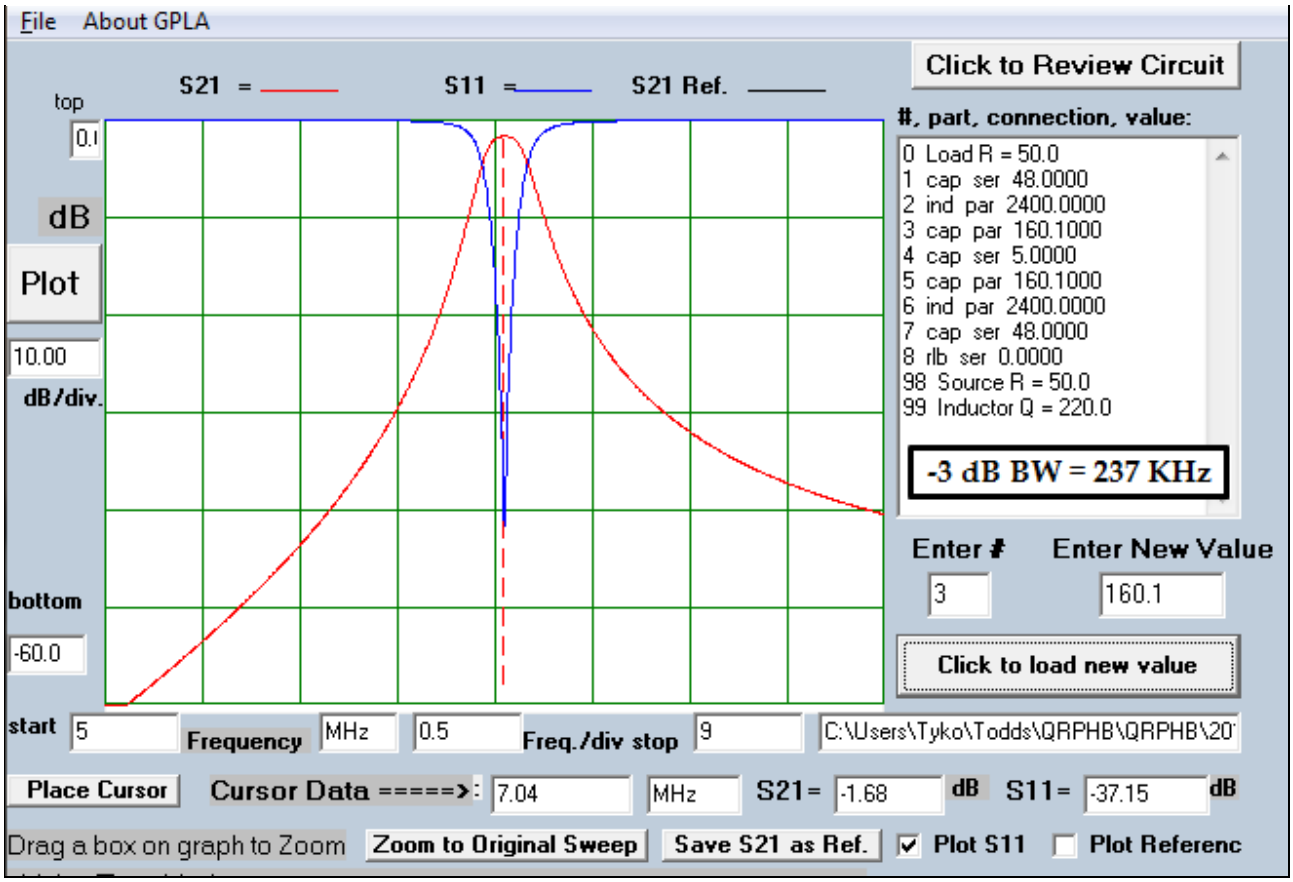

Above — A simulation of my filter design in in GPLA08. The calculated IL was 1.68 dB, I measured the IL at 2.1 dB The calculated return loss or S11 was 37.2 dB; I measured 27 dB. A good filter.

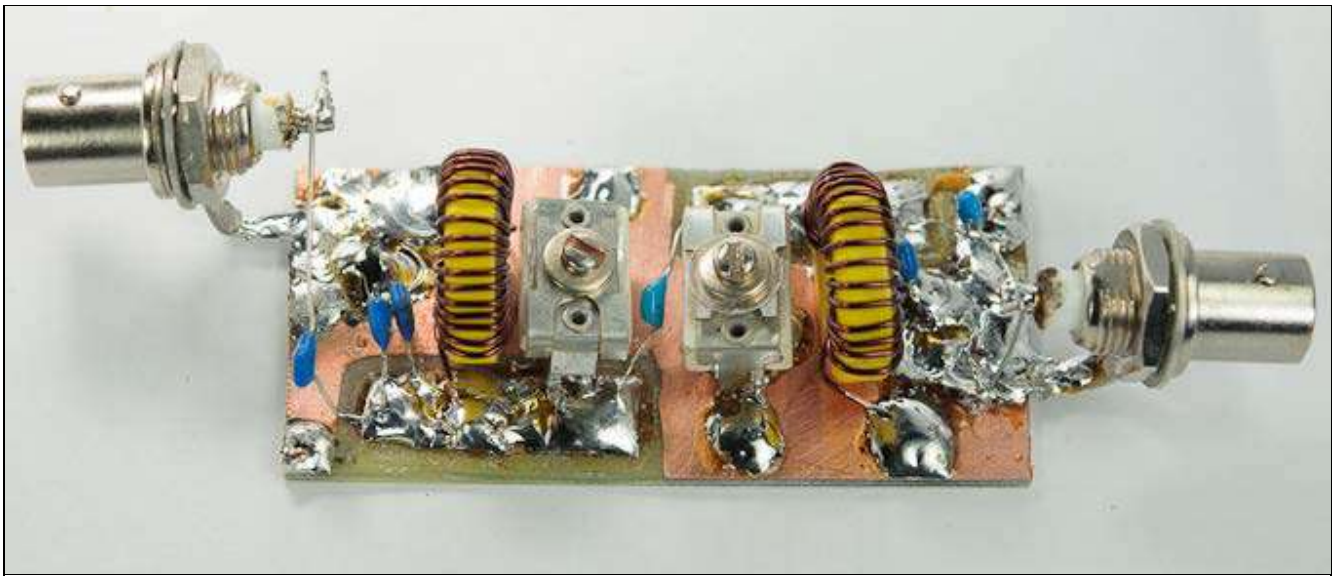

Above — the 40 meter double tuned band-pass filter breadboard with temporary BNC connectors and series caps. Since this filter will serve as my main front-end filter for all future 40M band receiver bench design, I blinged out and put in big toroids and high Q, air-variable trimmer capacitors. While I could have just use a single 150 pF tank capacitor and a wide range trimmer cap such as common, ceramic 10-70 pF, the small range, high Q trimmer capacitors offer better performance and fine tuning.

Click for a spectrum analyzer +tracking generator sweep where the center frequency = 7.040 MHz. Graticules: Horizontal = 1 MHz per division, Vertical = 10 dB per division. You can see why it tunes so sharply.

After testing the bread-board, I removed the temporary BNC connectors and series caps, I stuck it in a Hammond box and wired in permanent, short leaded 47 pF capacitors. Final testing in the sealed box varied minimally from the open bread board. This board looks especially ugly because it held a previous filter and contained lots of remnant solder.

Broadband Feedback Amp

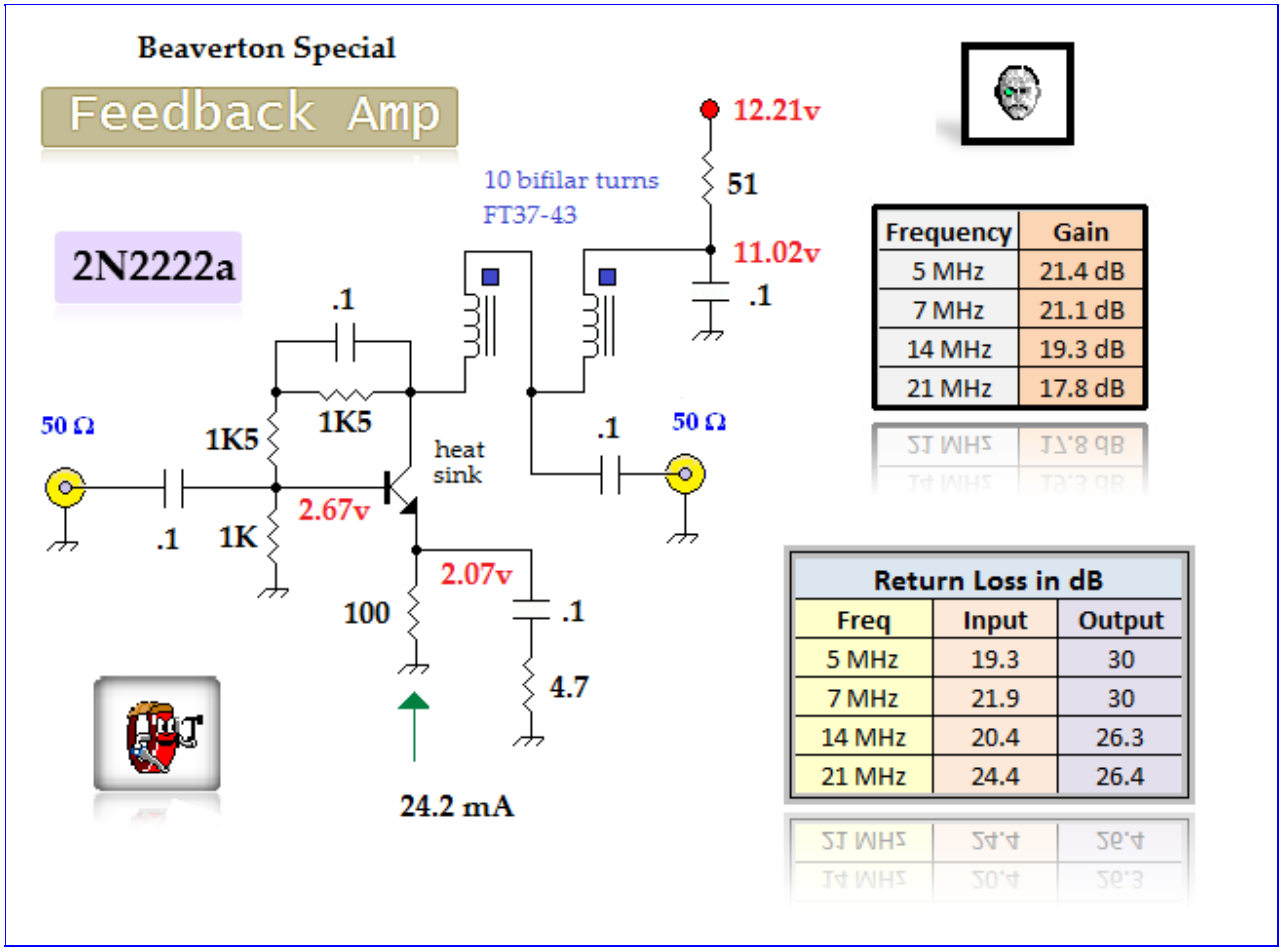

Above — A "Beaverton Special" feedback amp with analysis. As experimenters, we often need a go-to, broadband 50 ohms input and output RF amplifier. This is it!

Popularized by Wes, W7ZOI and Doug DeMaw, W1FB, this amp has stood the test of time and fits perfectly into the 50 ohm module concept. A bevy of transistors were tried — a 2N4401, 2N5179, 2N3904, 2N3866 or 2N5109 all worked fine. For the greatest return loss and signal handling possible, current over 21 mA is required and thus a 2N3904 isn't the best choice. Collector current = heat, so heat sink the BJT as appropriate.

I found that a 2N2222a biased with over 22 mA emitter current gave a stellar output return loss and low distortion. Within reason, for different transistors, keep the bias and feedback resistors constant and change the emitter resistor (100 ohms in my amp) to set the current you want or need.

Many builders follow this amp with an attenuator pad to preserve the input return loss.

Diode Ring Mixer

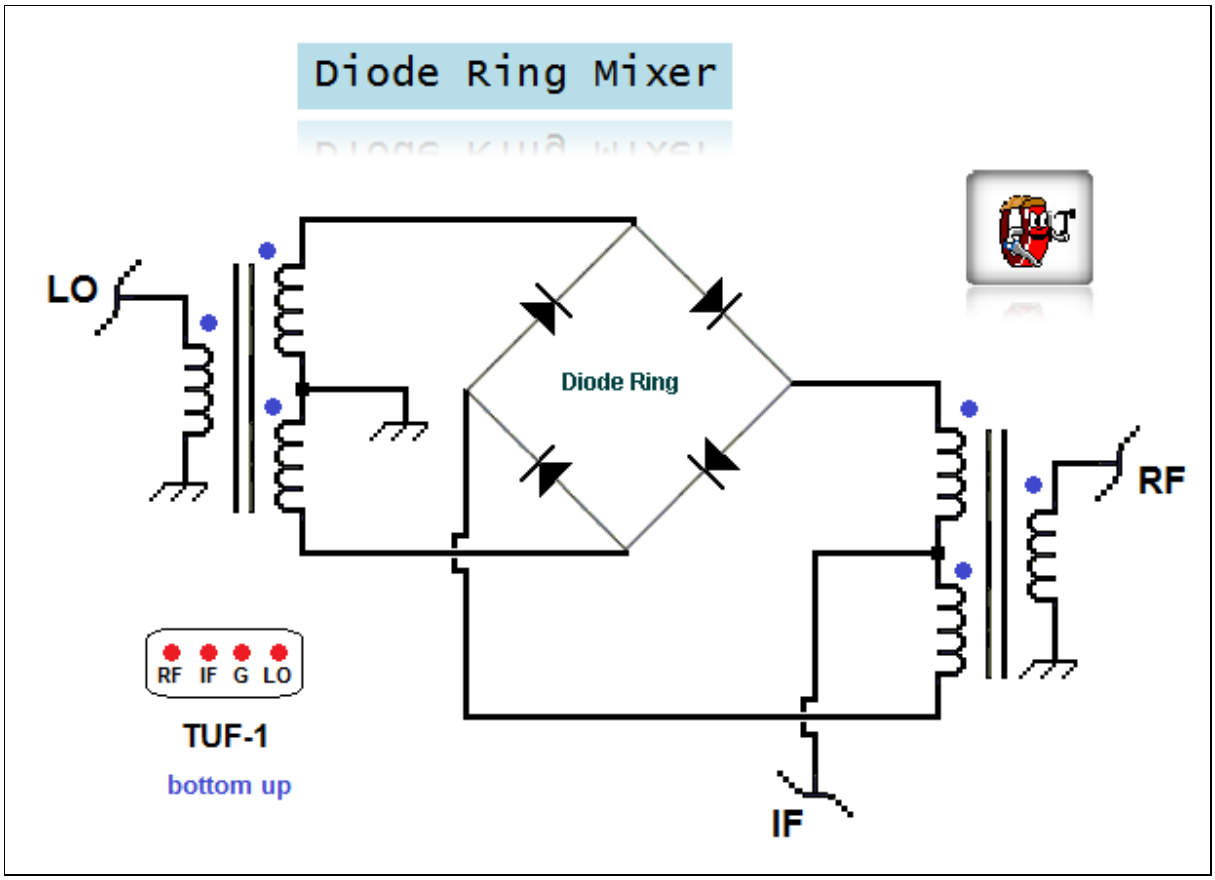

Above — A Minicircuits TUF-1 diode ring mixer was used in standard configuration. 7 dBm LO drive.

Above — The DRM module. It's hard to photograph inside a solder laden chassis. Connections are short.

Popcorn Audio Frequency Power Amplifiers

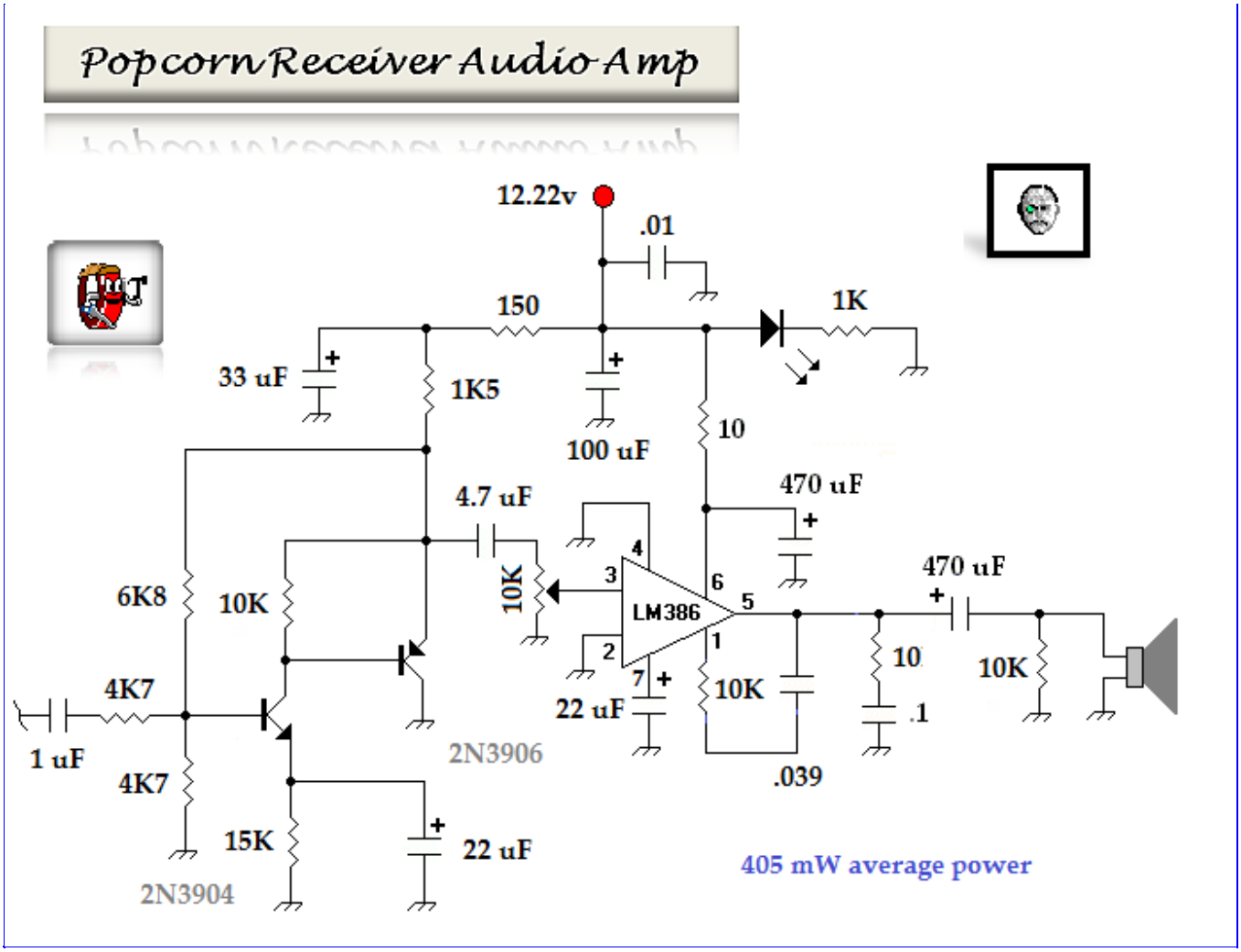

Above — Popcorn receiver audio power amp. I wanted a simple audio stage for testing popcorn receivers (to follow a high output impedance preamp device). Completing this module means never having to build such an amp again. The voltage gain is provided by BJTs to keep the noise down, but the popcorn factor up. The preamp impressed me with its strong signal handling capacity via feedback and careful biasing. The NPN is center biased so that when its intentionally distorted during testing, the positive and negative halves of the AC waveform distort equally — it provides a nice, big, AC voltage swing. An LM386 in X20 gain mode with some bass boosting comprises a reasonable power amp section. The 10K resistor on the output discharges the 470 uF cap when no speaker is connected to avoid a loud pop. The 4K7 series input R can be lowered, or omitted for more sensitivity.

Some builders might employ the LM386 in a higher gain mode at the expense of fidelity, or just wire up a TDA7052. I think in popcorn circuits, what really matters is that you understand what you're doing and try to *design* rather than just copy the "usual circuits".

Above — The popcorn AF amp in a clear blue chassis. Phono jacks provided a connection for the input and output — they 're inexpensive and readily available. The DC supply is connected to uninsulated banana jacks on the rear; it's well decoupled (resistor) + bypassed (capacitor) to help stop parasitic AF feedback. This amp is pretty quiet, considering its junk box legacy.

Above — The project with the top cover removed. The board is secured by the ground wires connecting it to the pot, jacks and DC voltage posts. The input is on the right.

I like a relatively simple, lower gain AF amp on the bench for receiver development. You can use such an amp to decide on how much overall AF gain is needed, how you'll distribute it, and not have to deal with unwanted AF feedback.

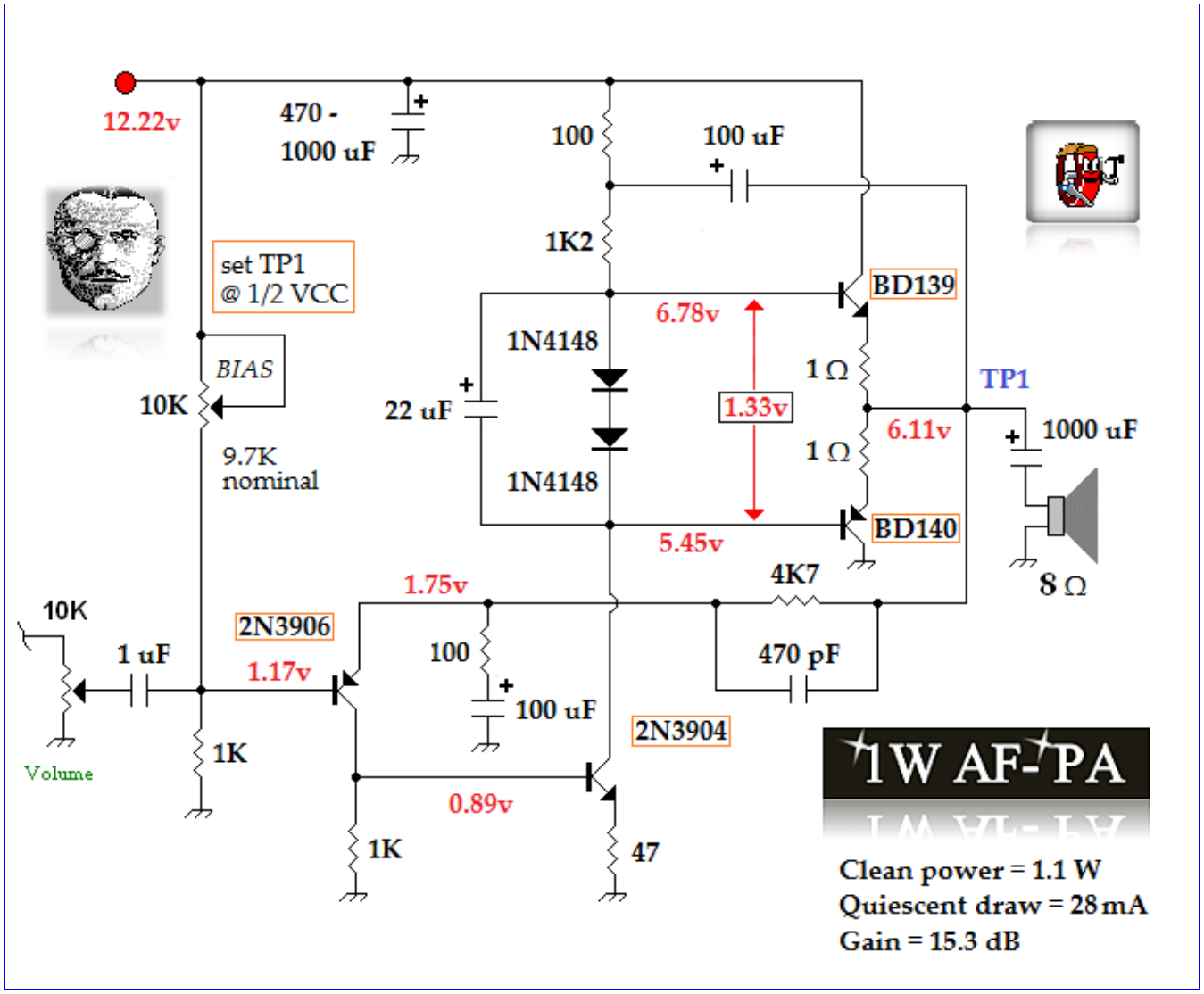

Above — 1 watt popcorn audio power amplifier. Built around the BD139/140 complimentary pair - I achieved a clean I KHz sine wave at 1.1 Watts power after testing + tweaking my prototype design. I chose the familiar series diode pair to bias the power followers into Class A/B; an amplified diode (transistor level shifter) might be a better choice.

Bootstrapping the 2N3904 voltage amp pumps up the clean signal power capacity. The 2N3906 establishes the bias for the 2N3904 and the BD139-140 pair. Set the 10K bias pot so that the DC voltage at TP1 is 1/2 of the VCC. During testing, the AC voltage was centered perfectly between the DC rails and when pushed into clipping, the positive and negative AC waveform distorted nearly equally. Quiescent current = 28 mA ; not meant for a field-portable receiver.

Click for a photo of my breadboard. Copper clad board serves as heat sinks for the power followers. The BD139 and BD140 make great complimentary transistors for audio frequency power amplifiers. With an Ft of 190 MHz, the BD139 can work okay as a driver or even the final in modest power QRP transmitters.

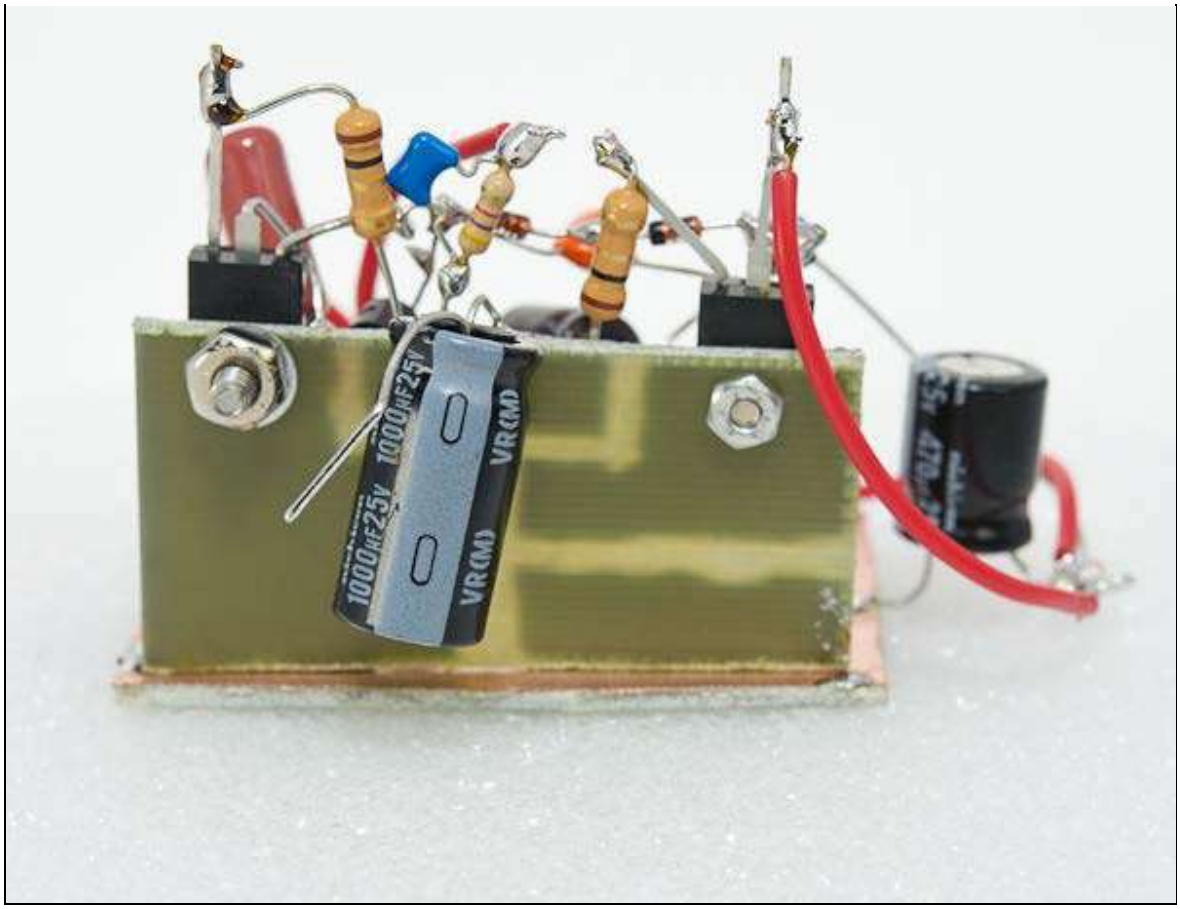

Above — 1 watt Audio PA (reverse view).

Pop DC2 — Popcorn Direct Conversion Receiver Main Frame

These circuits update the Popcorn DC receiver from 1998 and includes all components from the product detector through to the speaker, minus the VFO and band-pass filter.

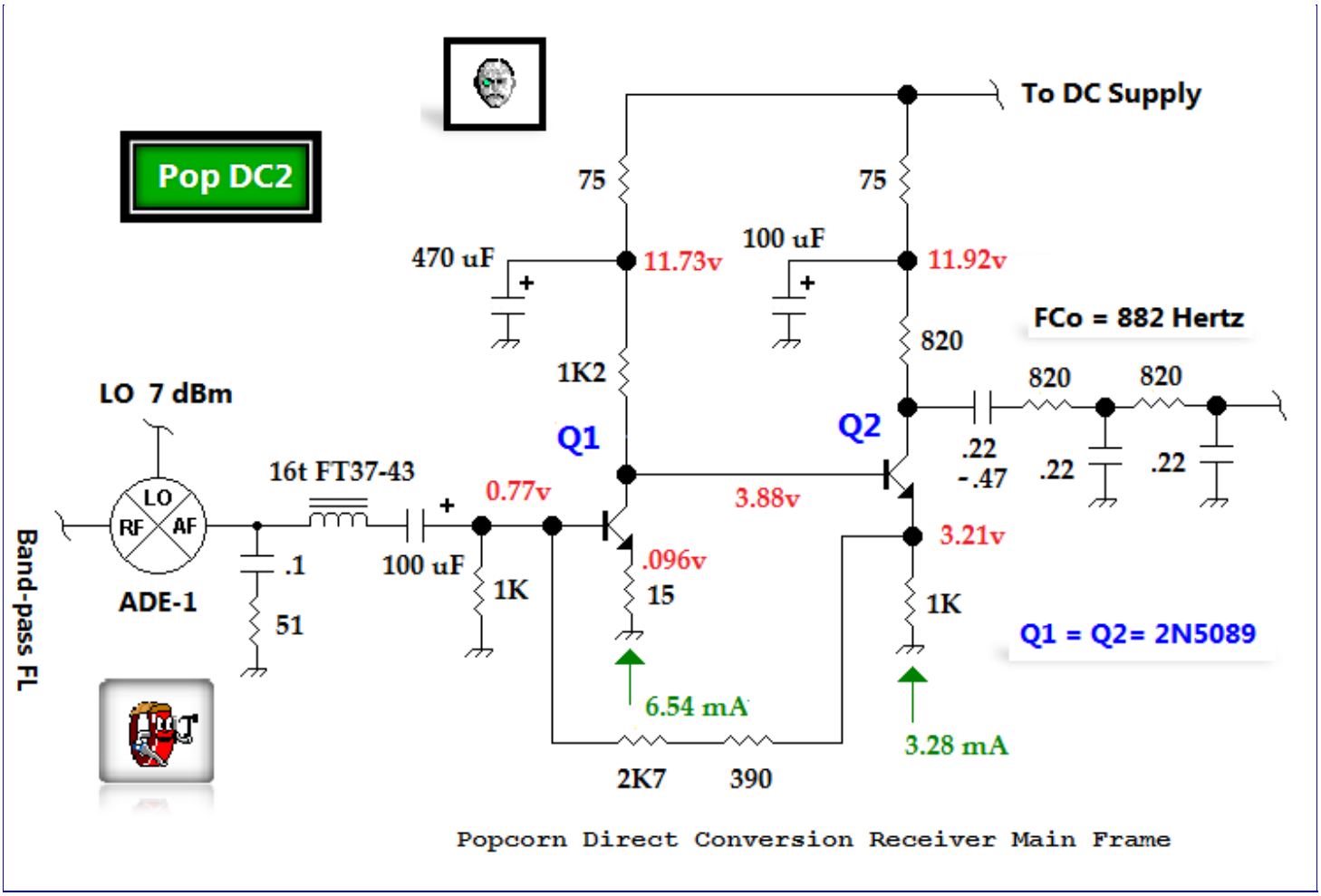

Above — The mixer and first audio preamplifier The 0.22 uF to 0.47uF cap connecting Q2's collector to the low-pass filter network exerts a high-pass response to remove low frequency noise and potentially any hum. I heard no hum, although a 470 uF filter capacitor on Q1 helps ensure that. Increase the 100 uF filter capacitor filtering Q2 if you hear hum or motor boating. The diode ring mixer exhibits AF that's hard to beat — very dynamic, vibrant and lively. I enjoyed the low microphonics with the double balance + a return loss of over 25 dB on all of 3 of its ports. Alternate photo.

I've read negative comments about my use of "those big filter capacitors" — 1 thing radiophiles can learn from audiophiles is that to adequately decouple and bypass means we need to stop fooling around with the usual 22 - 47 uF capacitors and *really* bypass. Viewing well designed AF amplifiers informs us so; these designers *really* filter their amplifiers from the DC supply. You can always increase the decoupling resistor value to allow use of a smaller capacitor value, however, we only have a single power supply at around 12 VDC, and I dislike giving up too much of it for DC filtering purposes. Do what ever amuses you.

Click for some analysis of the preamp. The MPSA18 went obsolete in 2011, so I chose the low-noise 2N5089 for Q1 and Q2.

The Popcorn DC2 receiver keeps the format of the earlier version; discrete transistors for all but the power amp and R-C low-pass filtering. The filter still allows you to listen to SSB, as there aren't many poles and the cutoff is nearly 900 Hertz —it just removes the ice-pick in the ear often heard in unfiltered DC receivers. You can change the capacitor values for a different cutoff frequency. Applet E performs this function.

Second Preamplifier Stage with TDA7052 final

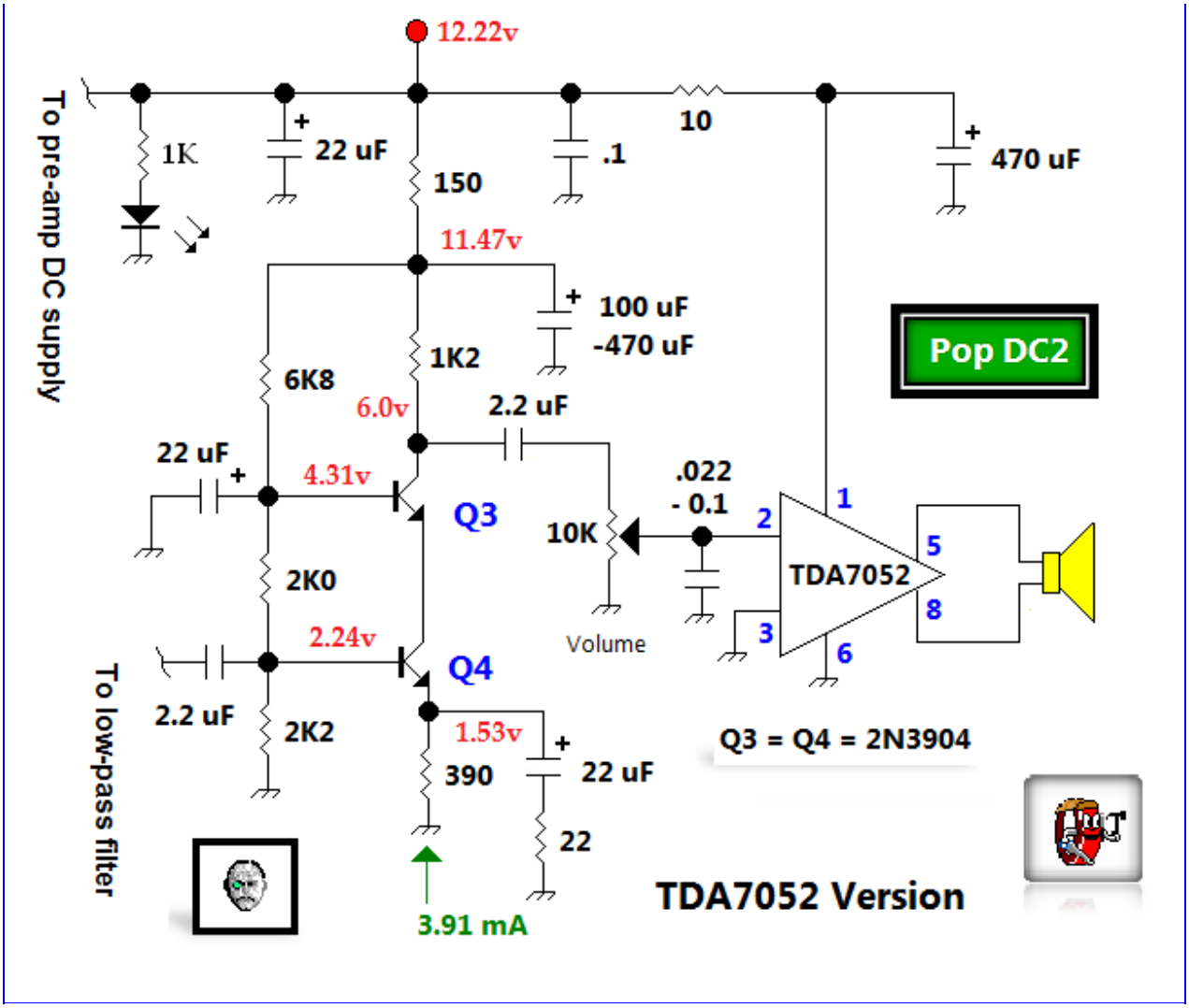

Above — The 2nd pre-amp and AF power amp. Experimenting with a number of audio stages, I decided on this cascode common emitter / common base amp biased to provide temperature stability, high gain, low distortion + proper termination of the low-pass filter. (The input Return Loss = 19 dB in my 820 ohm bridge set up). Increase the 100 uF filter capacitor on Q3 up to as high as 470 uF if you hear motor boating (low frequency thumping). This stage is prone to feedback since it's directly connected to the power amp. Photograph.

The simple and effective TDA bridged amp has a fixed gain of 40, so this receiver isn't crazy loud, however, it sounds okay. The bypass capacitor on Pin 2 filters hash noise and *can* remove some of the high frequency din from off frequency stations. Experiment to find the best value for your ears; even 0.015 uF might be your preference. I chose a 0.047 uF for my final version.

The 2 uF coupling caps between the power amp and Q3 can be lowered or raised to suit your parts collection. All the audio path coupling or bypass capacitors were "polysomething" types in my bread boards.

This is a base station receiver since the quiescent current draw listening to noise = 37 mA.

For low parts count or beginner's receivers, IC audio power amps make sense; 1 chip and you're done. Consider, for example, the TDA7052 — 2 bridged amplifiers supply reasonable power and headroom in an 8 pin DIP package. A good, but imperfect part. Depending on your goals and abilities, the limitations of the 7052's fixed 40 dB gain and/or the inability to drive grounded loads or insert additional feedback networks may constrain your designs.

Sound Bytes on 40 Meters:

I recorded these sound bytes prior to adding a 0.047 uF bypass capacitor to pin 2 of the 7052 chip and increasing the coupling cap on Q2 from 0.22 to 0.47 uF.

For a control — An ICOM superheterodyne receiver with digital IF filtering set to wide (2.2 KHz) was recorded immediately after recording the Pop DC2 receiver (although I pressed the middle (900 Hz) and narrow (600 Hz) filter selection briefly, but they made the noise worse), The antenna is a 1/4 wave vertical in a city lot with noisy conditions. I don't believe in artificially making my stuff sound better than real, and present warts-and-all audio files. I compressed these files heavily so you'll hear the noise phase shifting a little. Normally with this antenna, a "quiet" QRN level is S9; it doesn't bother me. Icom

Pop DC2 — I was tuning through a pile up to hear how the receiver copes with all the signals (twice as many with a DC receiver!)

Pop DC2 — More QRN, QSB and pile ups.

SSB - After this, I changed the .22 coupling cap between Q2 and the R-C filter .47 uF to add a little more bottom end.

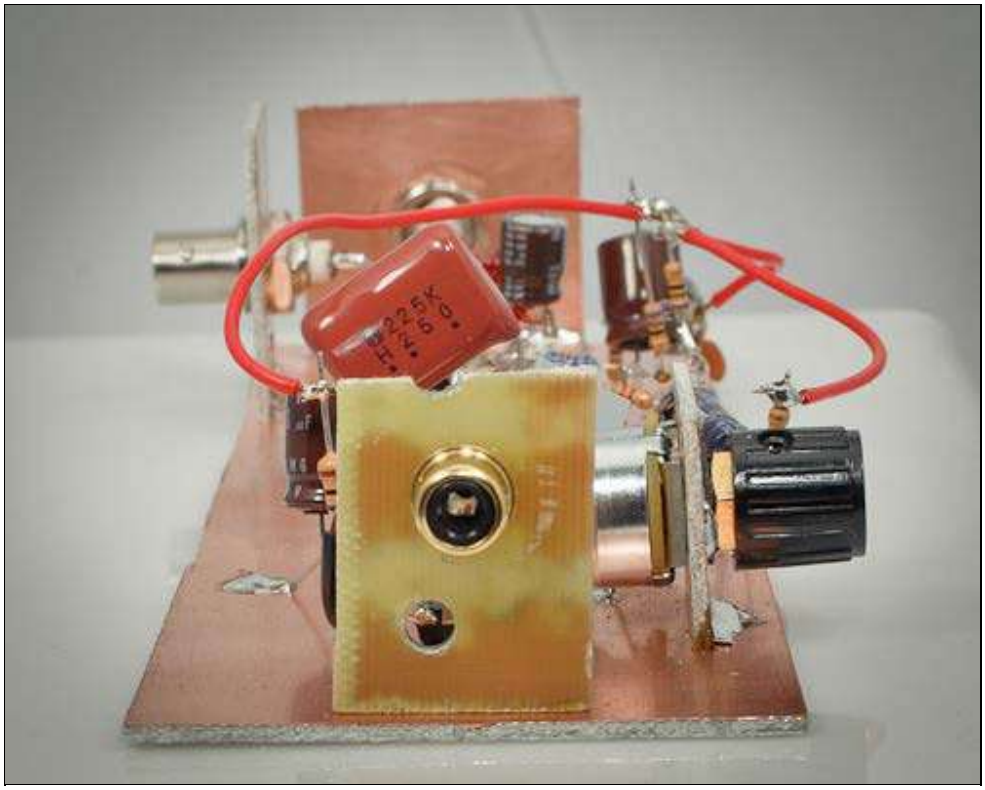

Above — Speaker terminal (an RCA jack isolated from ground on the TDA7052 version). Volume pot at right.

Second Preamplifier Stage with LM386 final

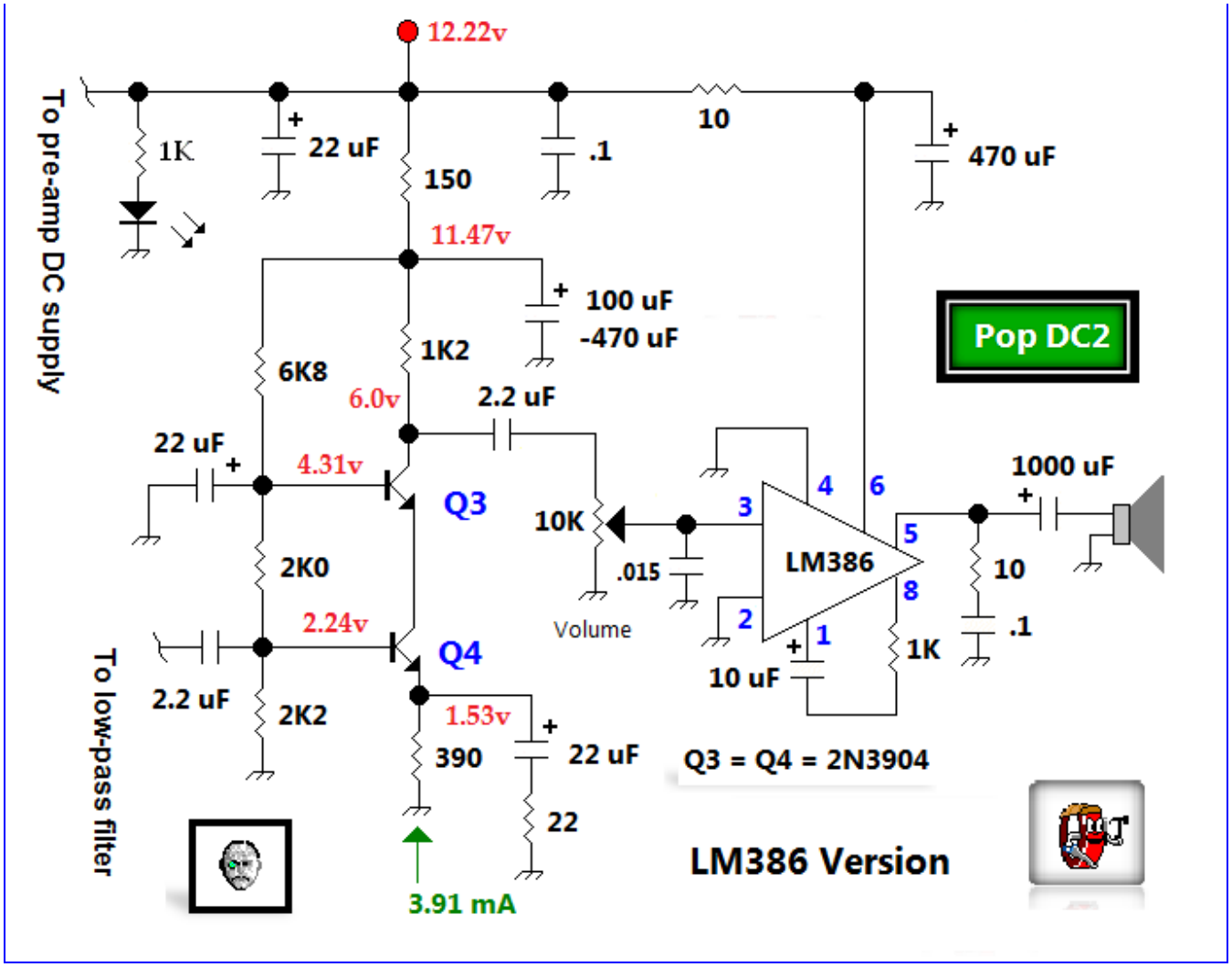

Above — The 2nd preamp and final with an LM386 set for just under a gain of 50. Click for a Canadian SSB sound byte.

Alternate Final Amp Stage that connects to the Q3 volume potentiometer

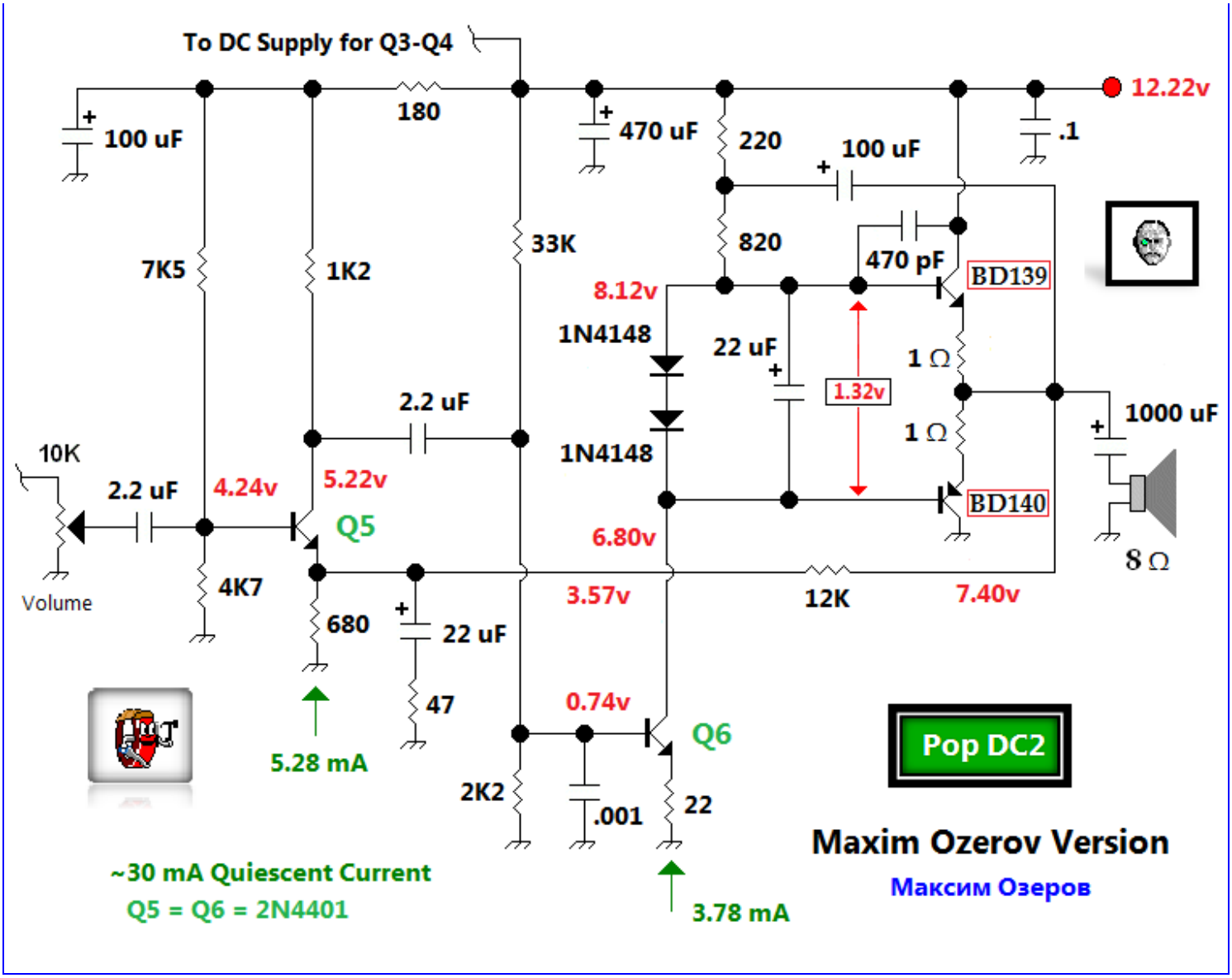

Above — A reader called Maxim Ozerov requested a discrete semiconductor version of the power amp after I posted the 7052 version on my blog. Placing 2 voltage amps inside the negative feedback loop proved challenging, since I'm no expert and learn on the bench. The gain = ~42 and the maximum pure sine wave power before clipping begins to occur = ~625 mW. This amp is louder and sounds warmer than the 7052 version.

2N3904s work fine for Q5 and Q6, but I found that the 2N4401 had a consistently higher DC beta and this helps ensure the bias and collector resistors shown will provide the widest possible, pure AC signal swing.

This amp replaces the earlier IC power amps (connects to 10K volume pot after Q2, however a 2.2 uF coupling cap is required after the volume potentiometer). If you need more **voltage** gain, increase the value of the 12K negative feedback resistor. Above 75K, the gain will approach 50 and *greatly* increase the possibility of distortion.

My dummy load for development and testing = three 1/2 watt resistors in parallel: 75, 82 and 10 ohms.

Certainly you can craft better - louder - quieter audio stages with low noise op-amps, however, my readers write that they enjoy building up discrete transistor designs, and for popcorn receivers; I do too.

Sound bytes from November 1, 2011

40 Meters - QRN is lower tonight. Some audio from a lineout tape deck (no tone controls nor equalization). I have only 2 cassette tapes, This one is Russian language from 1983 - the 1 strong accented syllable generates good peaks for AF listening tests. Audio recorded from an 8 ohm, 18 cm (7 inch) speaker mounted in a wooden frame with no back. Speaker choice and cabinets are critical and often overlooked; again we may look to audiophiles for guidance

Click for some 50 ohm AF preamplifier experiments cut from this page.

7 MHz VCO Experiments

As RF designers and builders, we rely on signal generators for nearly every experiment. I sought a reliable 7 MHz voltage controlled oscillator and built 1 after some effort. I'll describe and critique a VCO I rapidly designed for a reader and then present a better VCO with some design ideas.

7 MHz VCO Experiments: A rapidly developed Popcorn 7 MHz VCO

A reader needed a 7 MHz VCO in a hurry (3 hours); he only had 1 MVAM109 varactor and wanted to cover the bottom 60 KHz of the 40 Meter Ham band using a linear taper 10K potentiometer for tuning. He planned to use a dual-gate MOSFET cascode buffer (good choice), so I didn't have to bother with a buffer.

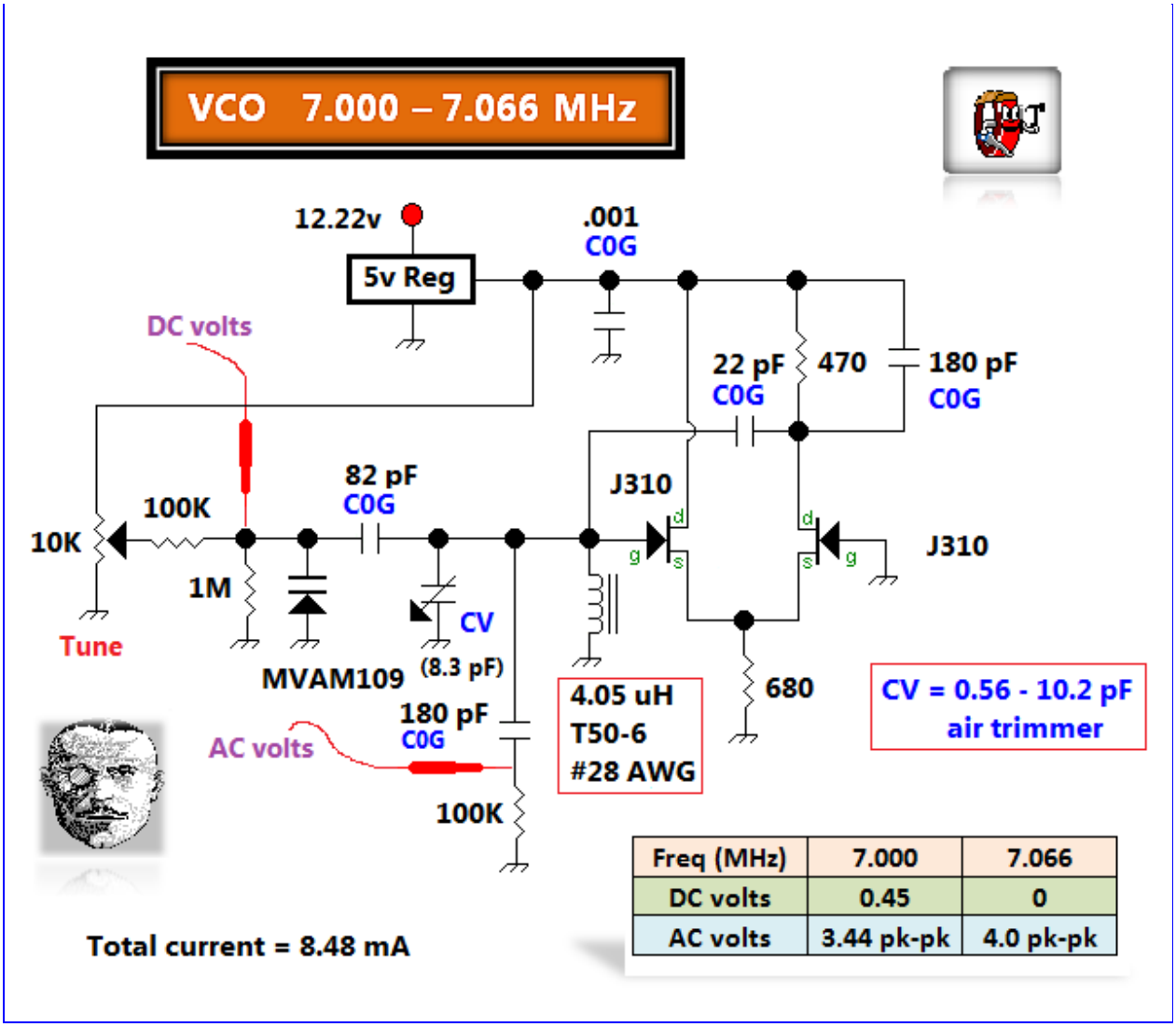

Above — The VCO with a 100K resistor as the temporary buffer. He'll use a 100K resistor on G1 of the 2-gate MOSFET buffer. With a Q of 150 at 1 MHz; high noise level and a hyper-abrupt capacitance-versus-voltage curve designed for tuning AM radios, the MVAM109 varactor ranks poorly. The C of my MVAM109 with no reverse DC voltage was 725 pF.

Still, this VCO tuned in a linear fashion, showed a nice sinusoidal output and proved frequency stable. I wanted the AC voltage at the varactor anode at under 1 volt pk-pk (it was 752 mV) to help reduce forward conduction during the positive AC voltage swing. I was bad and ran the tuning DC voltage from 0 to 0.45 volts which greatly increases the potential for forward conduction in a varactor. To mitigate this somewhat, an 82 pF couples the varactor to the tank and drops the AC voltage and reactance seen by the varactor.

In VCOs on the web and print, you'll often see builders connect their varactor to a high Z, and high AC voltage point in the VFO tank; whoa!

At HF, if a varactor is forward biased by the positive half of the AC signal, varactor leakage current and voltage-source loading increases momentarily and lowers Q + broadens tuning. Further, serious harmonic energy and phase noise might be generated as the varactor is biased positive and negative alternately. You can sometimes see distortion in your scope during experiments with extreme AC voltage swings across the varactor. The varactor coupling capacitor should be as low as possible.

Balanced varactor tuning (anode to anode) provides another way to reduce AC signal effects at the cost of reduced maximum capacitance since the 2 varactors are in series. With back-to-back varactors, as the AC signal swings, the varactors are driven into high and low capacitance alternately, but the net capacitance remains constant. Thus applied reverse DC voltage sets the varactor capacitance rather than AC signal amplitude.

The reader for whom I made this impromptu circuit can lower the AC tank voltage by decreasing the VCC or increasing the 680 ohm source resistor after installing the buffer and tweaking things for a 7 dBm output voltage. This topology suffers from an amplitude versus frequency issue — at 7.0 MHz, the output = 3.44 volts pk-pk and at 7.066 MHz the output rises to 4.0 volts pk-pk.

Stuck with an MVAM109 constraint and 3 hours to design/build a VCO, I share this circuit as a raw experiment; not an example of good design because it is not. I took the signal off the gate to derive the best sine wave; this requires a lightly coupled, high impedance buffer with strong reverse isolation to prevent the pulling of the VCO frequency by downstream changes.

A lower L + higher C in the tank, and/or a higher Q varactor could turn this VCO into something reasonable. Popcorn versus high performance? You choose!

7 MHz VCO Experiments: A Suitable 7 MHz VCO

PART 1: Introduction

During my Fall 2011 VCO experiments I studied books including EMRFD and built versions of EMRFD Figures 4.33 and 4.34. Figure 4.33 is a common-base Colpitt's Oscillator using a hyperabrupt varactor. On Q1, the 33 ohm resistor in series with the 0.1 uF cap "de-Q" the 2N3904 to reduce UHF oscillations. Wes also employs current limiting with a 1K5 emitter resistor.

The temperature drift compensation circuit involving a temperature sensitive reference diode + op-amp fascinated me — astute temperature compensation design. I built and tested the whole circuit; the VCO has some amplitude versus frequency and phase noise issues, but it's okay for general use and *great* for varied environments. After tackling Figure 4.33, I built and tested the JFET Colpitts oscillator in Figure 4.34 and share my experiences developing this VCO with an alternate buffer.

These circuits are not cookie-cutter / carbon-copy: they show raw design ideas from the bench.

PART 2: The Voltage Controlled Oscillator

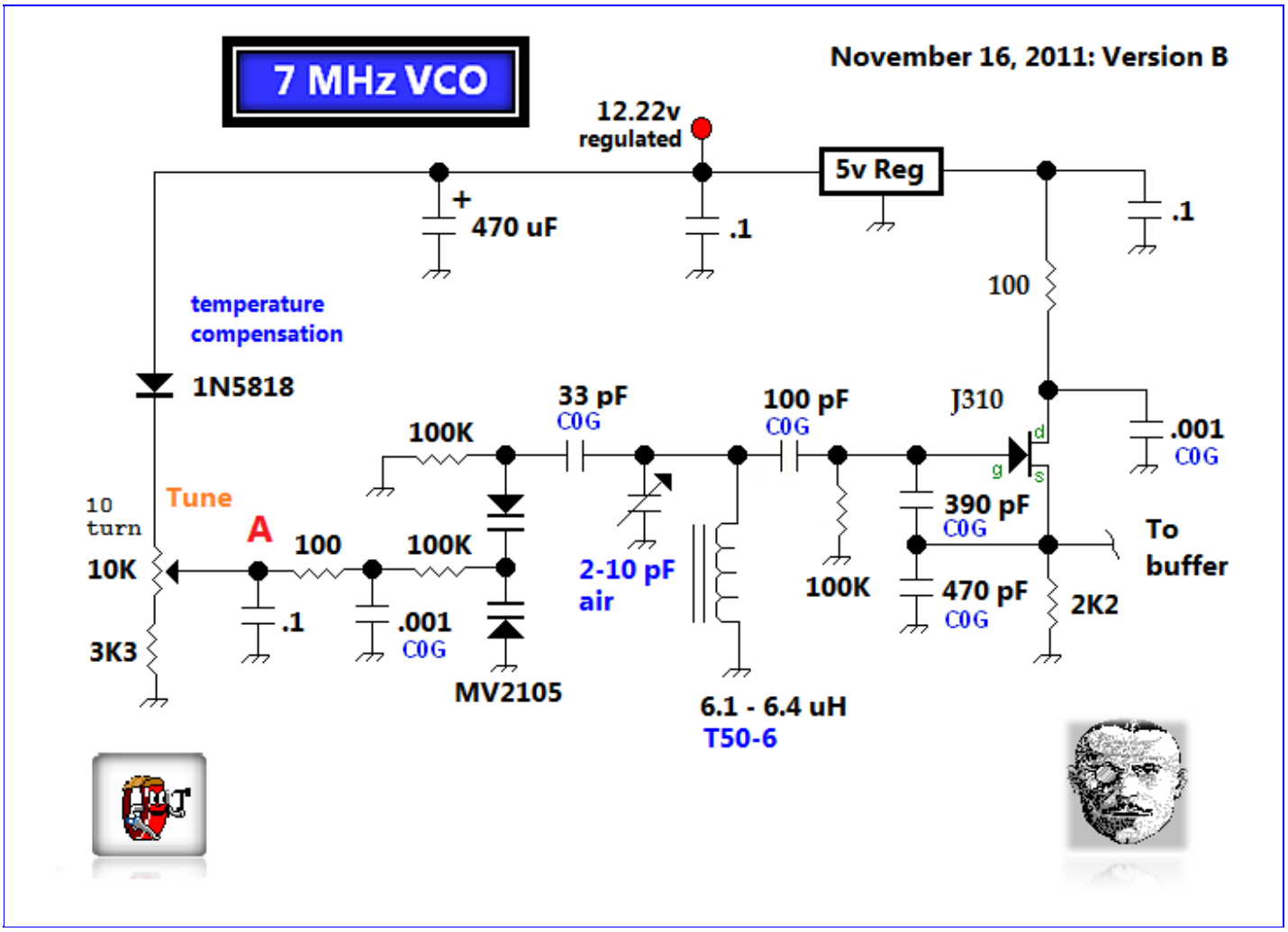

Above — A JFET Colpitts VCO picked after after trying 5 different topologies. This VCO is my version of EMRFD Figure 4.34; originally designed by Wes, W7ZOI.

This JFET Colpitts oscillator exhibits a flat output versus frequency, low noise, scales easily to other frequencies and accomodates a wide variety of varactors. For example, you may scale it to other frequencies by changing the L and tweaking the "Colpitt's capacitors" up or down as needed.

I employed a small air variable trimmer capacitor to set the lower band edge and this meant experimenting with the inductor to find 1 that allowed me to set the band edge with such a small trimmer capacitor. I built 2 versions; in 1 the required L= 6.09 uH and in the other, L= 6.4 uH. It would

be much easier to use a trimmer cap with a larger capacitance range as it makes chosing the inductor less exacting.

With the trimmer shown set to half its range, I started with a 6.6 uH coil and remove 1 turn at a time until the output in a counter was close to 7.00 MHz. After permanently fixing the inductor, I tweaked the trimmer cap so the lower band edge was 7.000 MHz with the chassis lid on.

To further drop phase noise, you could reduce the 33 pF coupling cap, add another pair of anti-parallel varactors, run a higher C to L ratio, or perhaps decrease the source resistor to increase the current limiting. Also low resistance, high Q, SMT varactors would help lower phase noise — SOD parts are tiny, but test your hand steadiness and vision.

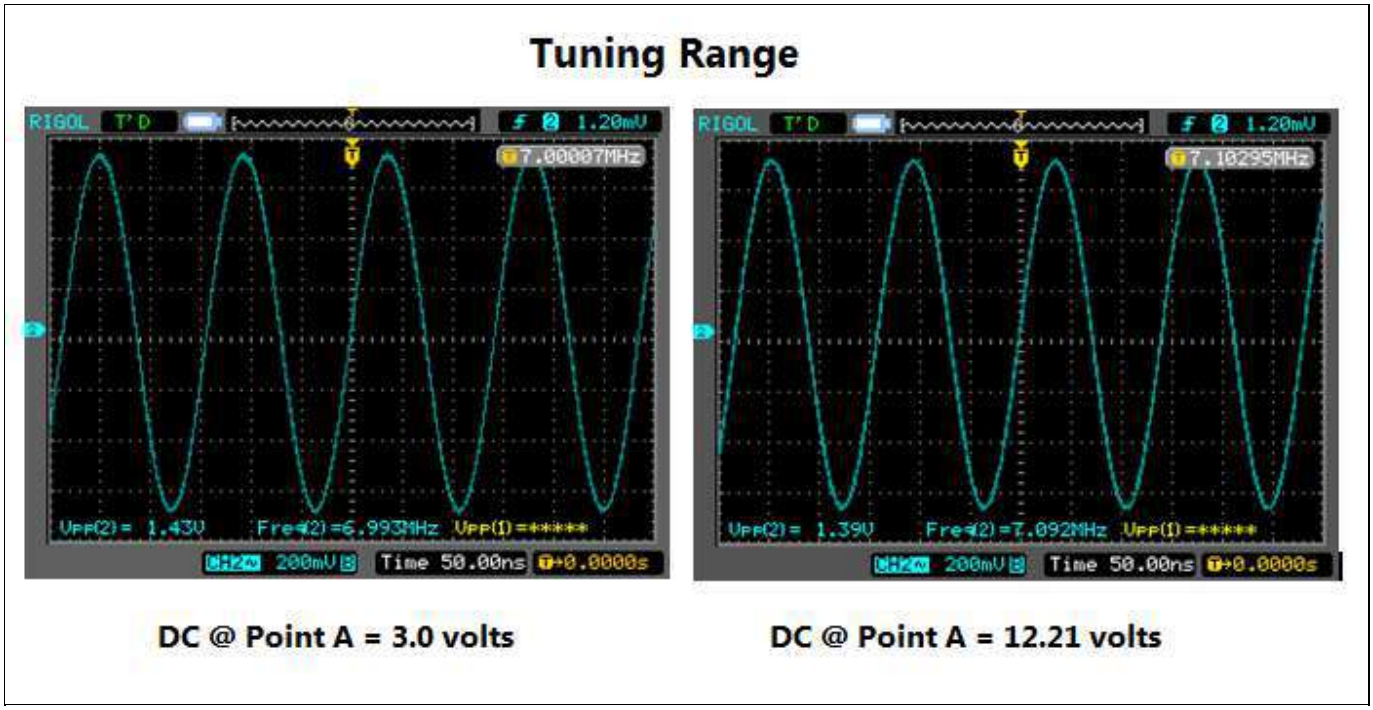

Above — When tuning from the minimum frequency and tuning voltage (7.0 MHz / 3.0 VDC) to the maximum tuning voltage and frequency (7.103 MHz / 12.21 VDC) the signal amplitude only changes 0.04 volts peak-peak.

I kept a minimum of 3.0 VDC on the varactors at the minumum frequency to provide reasonably linear tuning, keep the applied reverse voltage away from 0, and improve temperature stability. All were bench determined and are not factors you can generalize to all VCO circuits. Change the minimum DC voltage on your VCO control by adjusting the resistor on the grounded end of the pot; 3K3 in my case.

Click for a moderate resolution photograph of the VCO and buffer prior to adding the temperature compensation parts.

PART 3: The Buffer/Amplifer

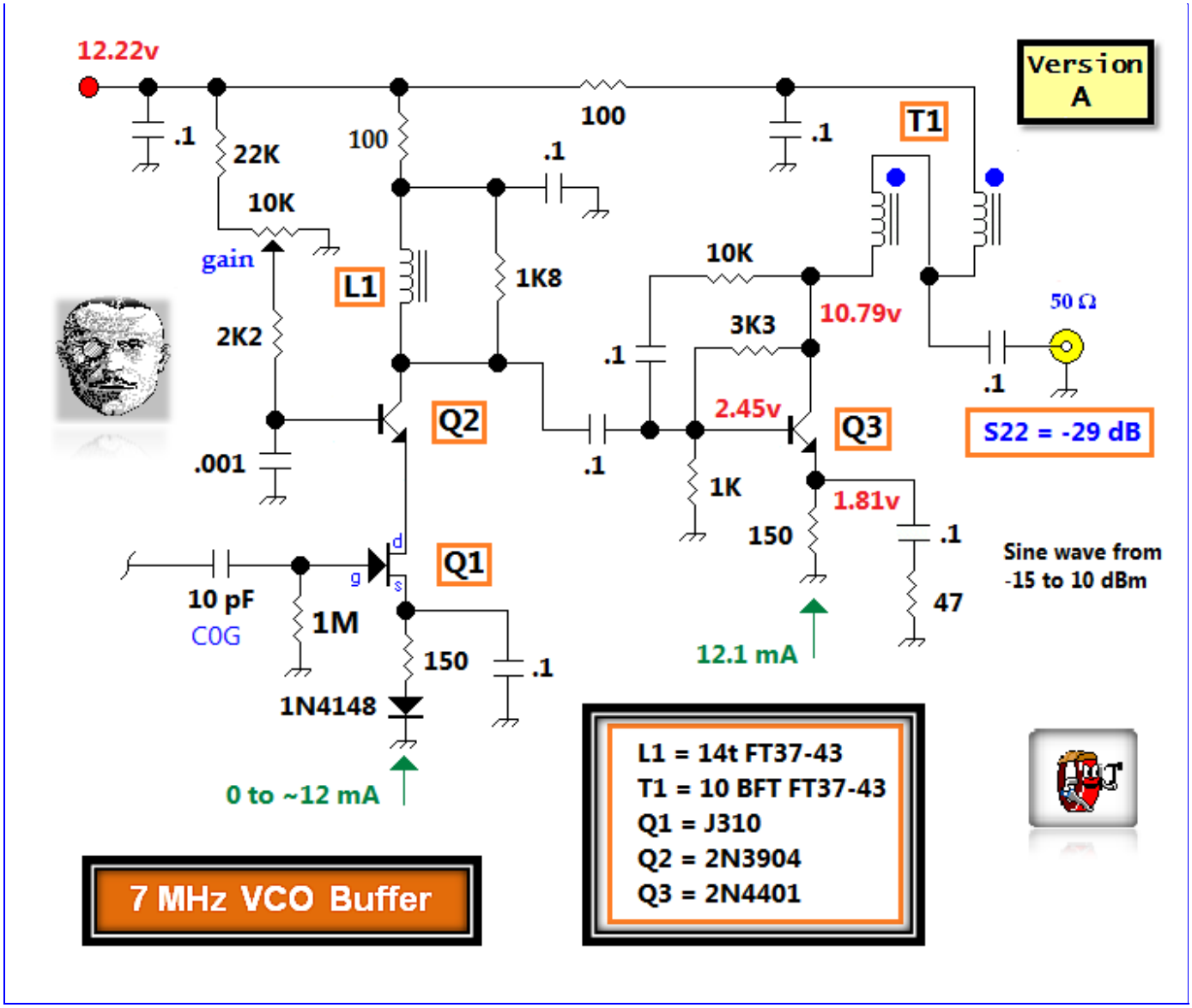

Above — The Q1-Q2 hybrid-cascode amp gives strong reverse isolation (nearly 70 dB) and front panel gain control. You could also employ a dual gate MOSFET or JFET cascode with either fixed bias, front panel control, or a trimmer resistor to adjust the bias on Q2

I enjoyed designing the Q3 final amp amp and matching its input impedance to the output Z of Q2. One way to establish a fixed + known output impedance in order to to get a strong return loss without tuned circuits/networks is to feedback some signal from the collector to the base. The difficulty lies in finding how much negative feedback to apply, while still DC biasing the amplifier for good temperature stability. I set up a crude experiment to determine the Scattering Parameter S22. The goal is to set up a good Q3 output return loss using feedback + matching the Q3 input impedance by tweaking the inductor resistor across L1 and adjusting Q3's emitter degeneration.

The return loss in my first prototype without any attenuator pad = 29 dB; some of this was pure luck.

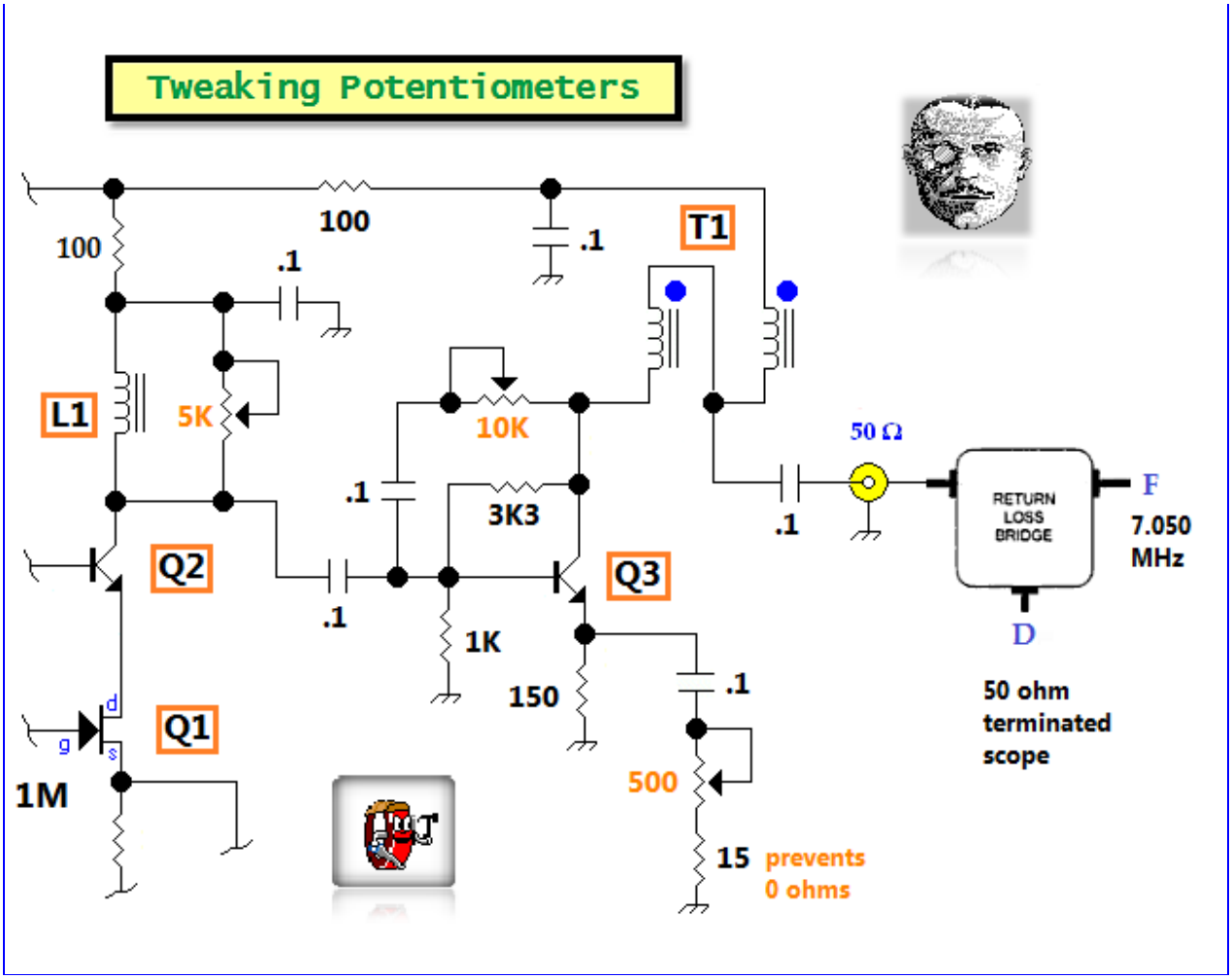

Above — Q2 and Q3 with 3 variable **orange colored** resistors in-situ and a Return-Loss bridge connected to the output. The potentiometers are tweaked while watching the detected output in an oscillocope. Adjust all the pots for the lowest peak-peak voltage and then carefully remove each pot and measure its resistance with an ohm meter. Replace all 3 pots with the nearest equivalent standard value resistor. Then measure and calculate the return loss (negative of S22). Watch the Q3 emitter resistance — too little R might bring distortion.

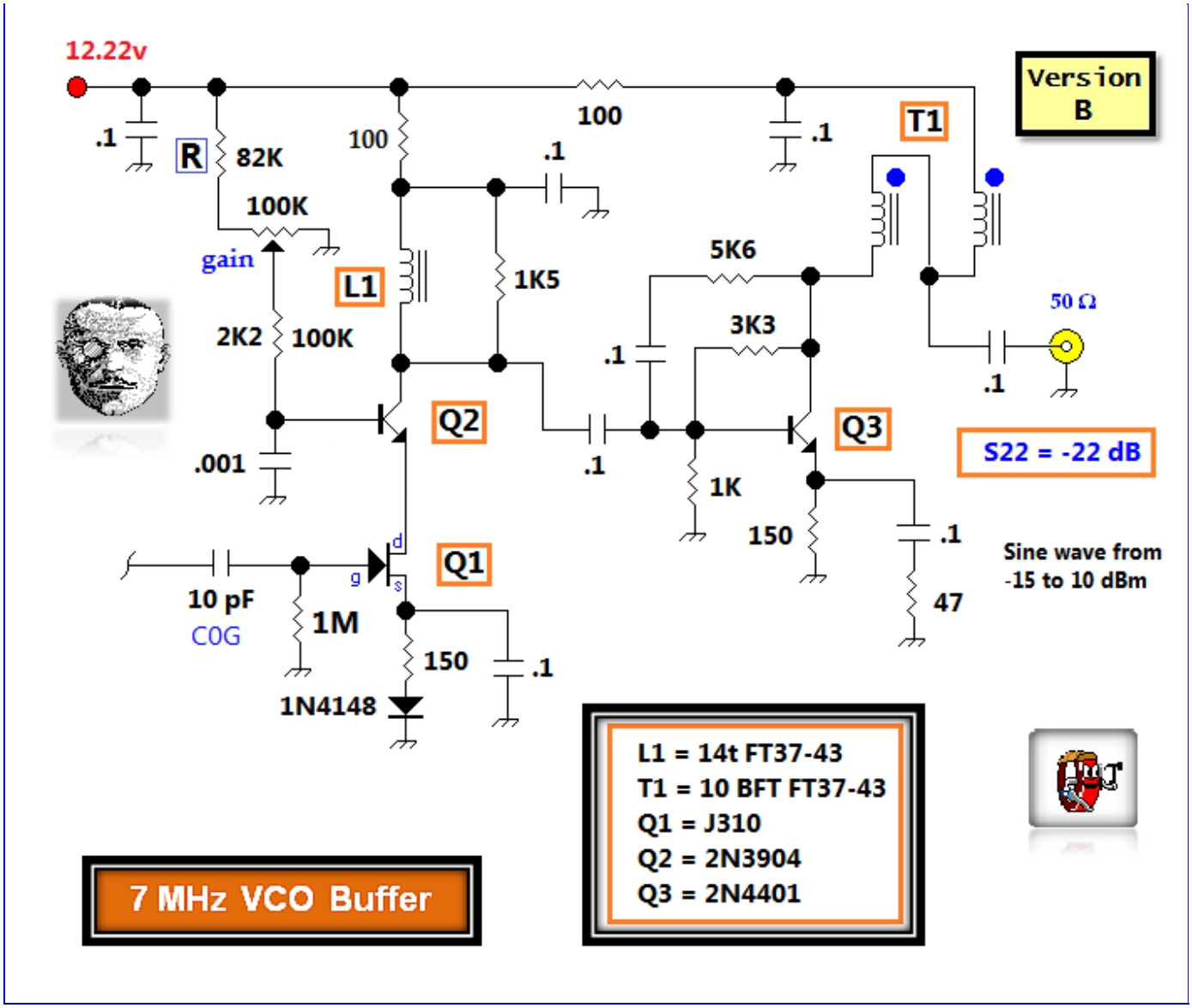

Above — A seperate buffer built with 100% different parts that required different AC feedback plus shunt resistor across L1. The parts in this circuit weren't as hot as Version A, and the maximum output voltage was only 1.8 volts pk-pk. In order to get the AC output voltage to just above 2 volts, I had to tweak the resistor labelled **R**.

To keep the heat and current down in the final amp, I decided to keep the maximum clean output to 2 volts peak-peak (= 10 mW = 10 dBm) with an emitter current of ~ 12 mA. If you want higher clean output than 10 dBm, you'll have to run more Q3 emitter current and maybe choose a different BJT, plus apply a heat sink.

When cranked to maximum DC voltage, the Q2 gain pot allows a peak output AC voltage of ~2.2 volts pk-pk into 50 ohms and distortion is evident. At or below 2 volts pk-pk all is well — I'll use this VCO mostly from 0 to 7 dBm.

Since the circuits uses 2 BJTs and a JFET and many 5% tolerance resistors , the Q3 output will vary according to your parts. Tweak the resistor labelled **R** to provide a maximum AC signal just over 2 volts peak-peak into 50 ohms. This translates to around 3.8-5.5 volts DC bias for Q2 with your gain pot cranked fully clockwise.

Return loss variations. You probably noticed the return loss in Version B = 23 dB, while Version A = 29 dB.

Version B originally had the 1K8 shunt resistor across L1 and the 10K + 0.1 uF AC feedback arm just like version A and I measured a return loss of 22 dB. I stuck in 2 tweaking potentiometers (did not bother tweaking the the emitter series feedback element). After pot tweaking, the best return loss I could obtain with 5% tolerance resistors was 23 dB and this probably represents what the average builder will obtain. An S22 of - 22 to -23 dB works fine for the QRP work bench.

If you don't plan to do any potentiometer tweaking, I recommend building circuit A since it has a little more gain due to the slightly higher shunt resistor, and also I built 3 versions of Version A with an S22 of -22 dB or higher.

PART 4: Temperature Compensation

Before temperature compensation, my VCO slowly drifted down in frequency and was unusable.

If you look through the Ham Radio VFO/VCO literature, you will see that many builders use polystyrene caps as the Colpitt's capacitors, and/or in parallel with other NP0/C0G tuning capacitors. Negative temperature compensation caps like an N750, or the polystyrene types temperature compensated the oscillator. Negative temperature co-efficient caps are hard to obtain for many builders; especially in small quantities, however, they are worth their weight in gold.

Diode Compensation

Stabilize your VCO as much as possible with compensating capacitors and by following prudent temperature stability techniques before adding diode compensation. *See the VFO 2011 web page and EMRFD.* Temperature compensation is best performed in a homebrew oven (see EMRFD) and normally takes an incredible amount of time and patience.

Temperature compensating diodes are far from static — a diodes temperature co-efficient is dynamic and may vary with current and also unfortunately, with temperature and even while tuning your VCO !

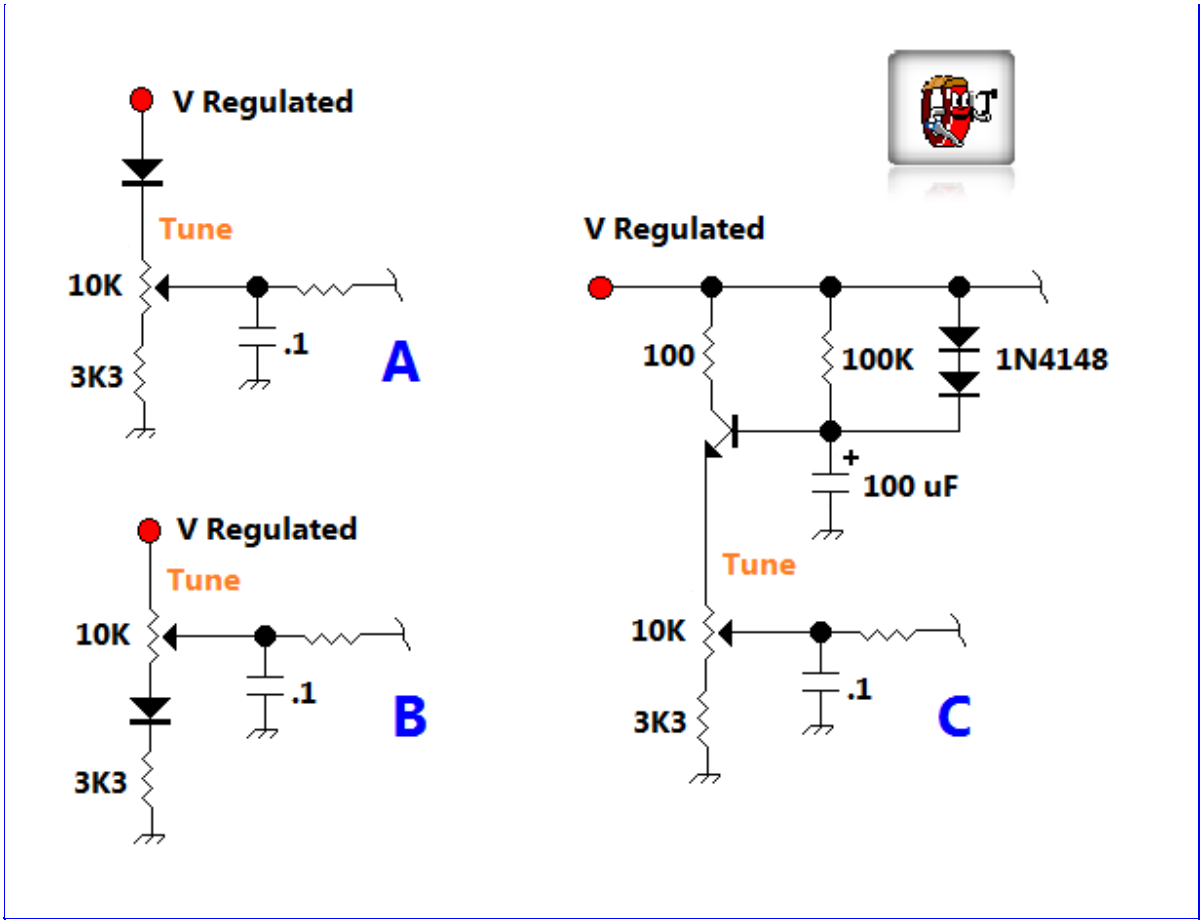

Above — Simplistic diode temperature compensensation schemes.

The late, great, Doug DeMaw advocated sticking a 2N3904 or 2N2222a (wired as a diode) between the control potentiometer and the varactor decoupling network since the forward biased P-N junction exhibits a negative temperature co-efficient and should stop the decrease in frequency. It can help, however, as you tune and swing the control DC voltage from minimum to maximum the forward bias on the diode increases and the diode temperature coefficient decreases.

I've never had success using a transistor in this way; the BJT caused the VCO frequency to increase in an erratic manner that varied along with the DC control voltage. When watching drift in a frequency counter set to sample every second or so, a stable design will slowly change frequency in 1 or occasionallly 2 Hertz increments — some people call this "linear drift". if you see your VCO dropping down frequency in 10 - 20 Hertz jumps per second, you'll have a bad time temperature compensating.

I experimented with the above 3 designs that keep a constant current on the diode. Figures A and B work. I tried both and confirmed that a given diode compensated slightly differently when in circuit A or B. This gives you a bit of a tweaking room for your chosen compensation diode. I tried Figure C, but it had too much negative temperature coefficient and sent the VCO drifting upward about 1-2 Hertz each second.

I settled on circuit A and then tried some diodes: the initial best was a grubby old Germanium from my junk box. The best choice turned out to be a Schottky barrier rectifier (1N5818). I connected the VCO to a receiver and could listen to CW QSOs without groaning. My VCO now drifted up in linear, 1 Hertz hops at about 105 Hz per hour. It took a long time to tack solder in and wait 10 or 15 minutes for each diode to stablize before I finally settled on the 1N5818.

The better solution is to choose a suitable diode and vary its current to tweak the temperature compensation. Wes did this in EMRFD Figure 4.33.

Advanced designs may use a reference voltage + a temperature dependent voltage that is applied to op-amps in a proportional way to temperature compensate the DC control voltage. Then, too, some builders ovenize their VCO container to maintain a very stable environmental temperature.

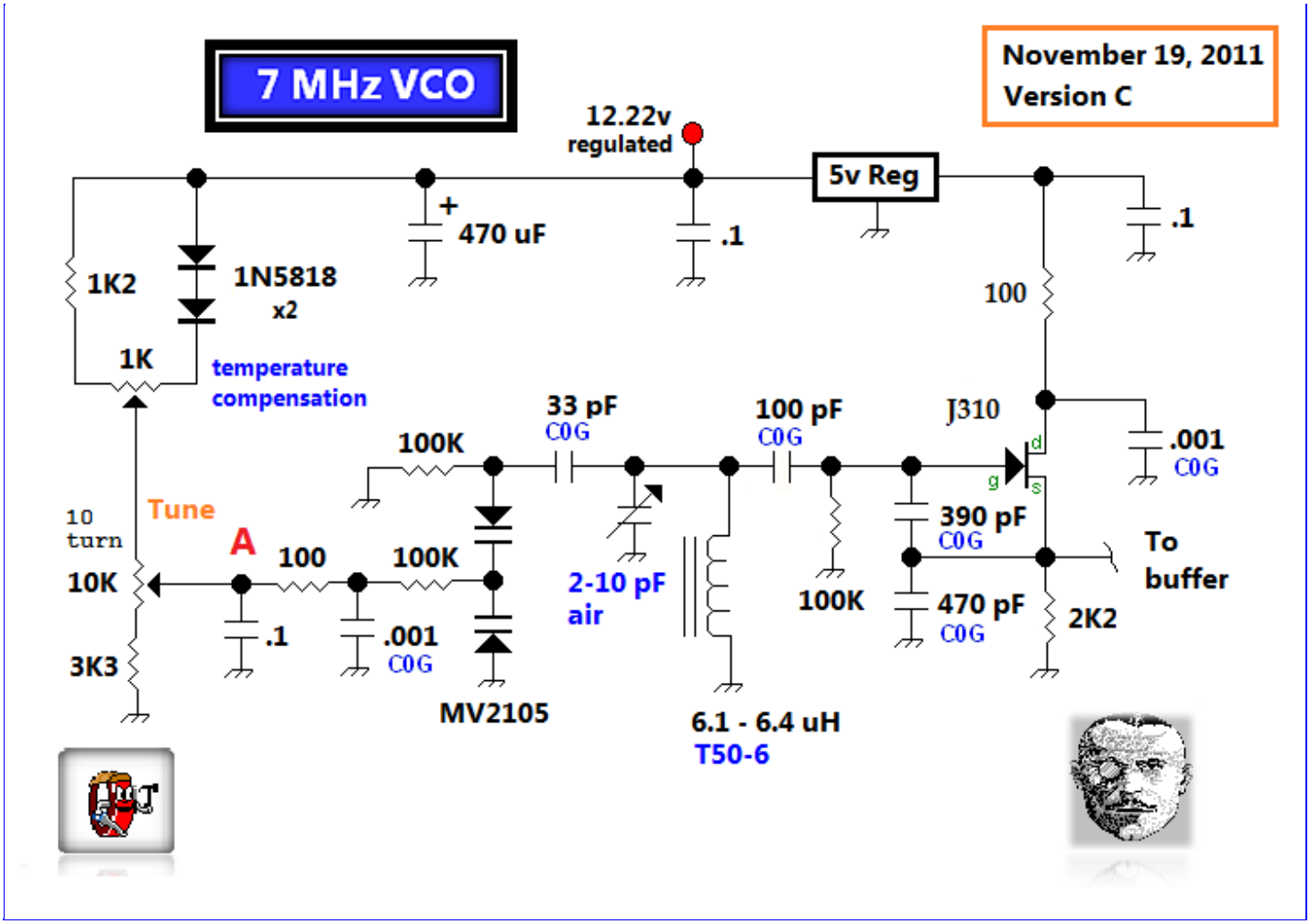

Above — A simple and elegant diode compensation scheme proposed by Ken Kuhn. Basically, it lets you tweak the degree of compensation to what is really needed rather than accept what you get from a diode. Adding more diodes will increase the effect — but the 1.2 K resistor should be increased accordingly to roughly match the overall voltage drop of the diodes. Hopefully there is a point on the 1K potentiometer where temperature compensation can be very good at a tuning point of interest. The diodes should be located to thermally match the rest of the oscillator circuitry.

Set the band edge *after* finding the sweet spot on the 1K potentiometer since it will affect the tuning frequency. This experimental circuit cannot be casually copied and it took a while to converge to the desired operating point on the 1K potentiometer. Generally you start with the 1K pot towards the 1.2 K resistor and then adjust for the best stability after warm-up. Then repeat and adjust as necessary over time.

Temperature compensatiing an oscillator like this is a challenge as all parts have some temperature drift and it takes a lot of measurements (and often, some dumb luck) to determine the overall compensation curve that is needed.

My 1 hour drift up in frequency is now ~ 60 Hertz per hour at various tuning frequencies across the tuning range. I stuck with the 1N5818 diode, and probably should have tried other diodes and also changed the 1K2 resistor to observe any effects, however, I have spent an inordinate amount of time on this circuit and leave it to others, or future bench work to improve. *See QRP — Posdata below.*

Above — Version C of the VCO. When I built the first versions, I drilled a hole to accomodate a third potentiometer, but filled it with a LED holder that was temperature sealed with epoxy glue. The 1K pot *jus*t fit into my chassis.

QRP— Posdata for January 2012

In late 2011, I shopped on eBay to build up a small quantity of 10 - 270 pF polystyrene, plus some 56 pF N750 ceramic temperature compensation capacitors. After 2 simple, but time-consuming experiments, I temperature stablized my 7 MHz VCO frequency drift to under 10 Hz per hour in the relatively constant temperature of our basement.

I didn't feel like re-doing the whole resonator circuit and thus focused on the tank to FET coupling capacitor. Placing a N750 capacitor in parallel with a fixed NP0/C0G cap to make 100 pF resulted in over-compensation and no amount of tweaking on the "adjustable diode" circuit worked. A few hours late, I swapped in a 100 pF polystyrene capacitor and after further hours of waiting and tweaking, I nailed the frequency stability sought.

An oven provides the best way to temperature compensate, however, whether you choose the oven method, or the bench method like I did, great patience is required to see if a change to your TC circuitry works or not.

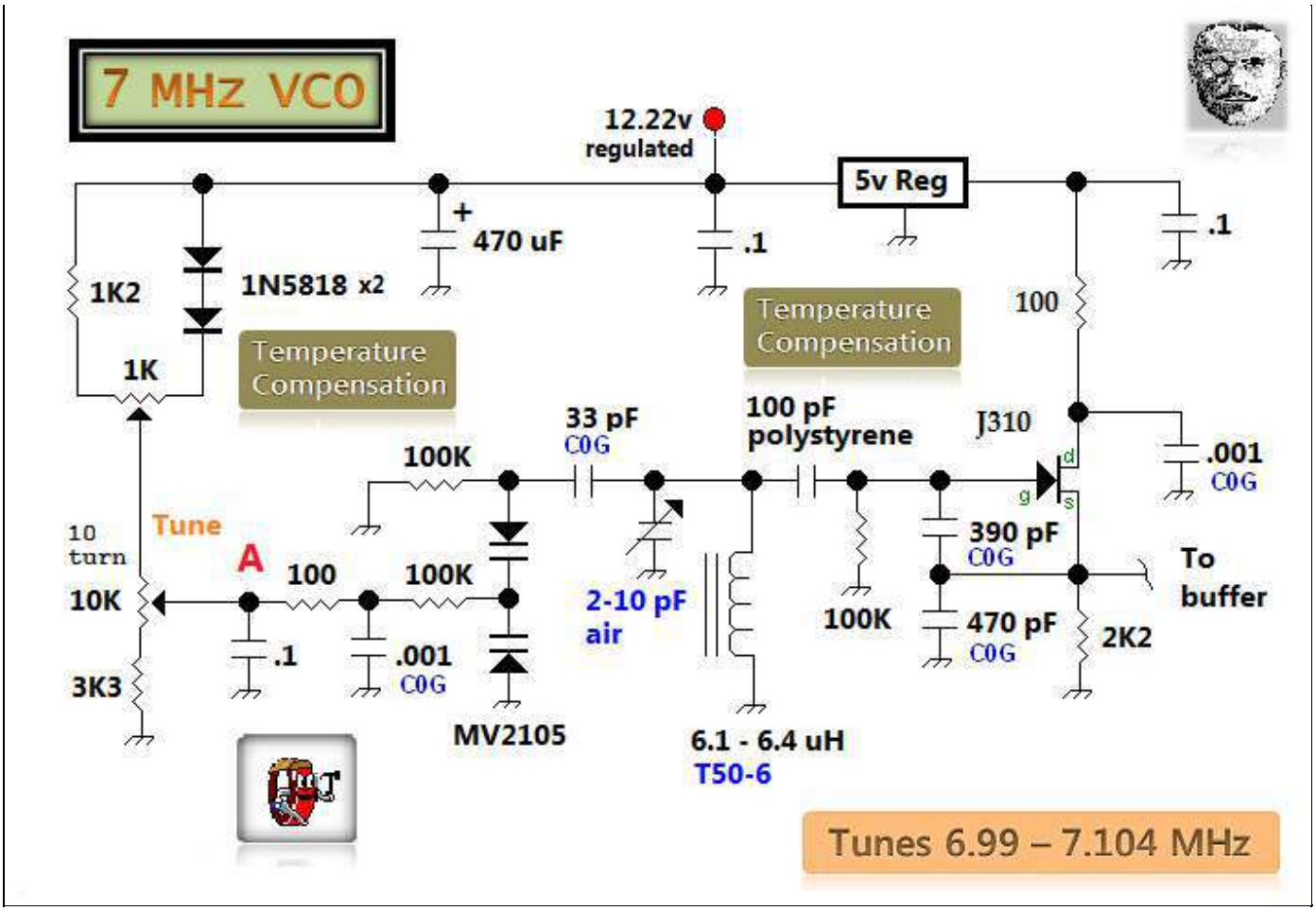

Above — Final version of the 7 MHz VCO. I changed the 100 pF capacitor coupling the JFET to the resonator circuitry from C0G to polystyrene and slowly tweaked the 1K temperature compensation pot to find the point of convergence.

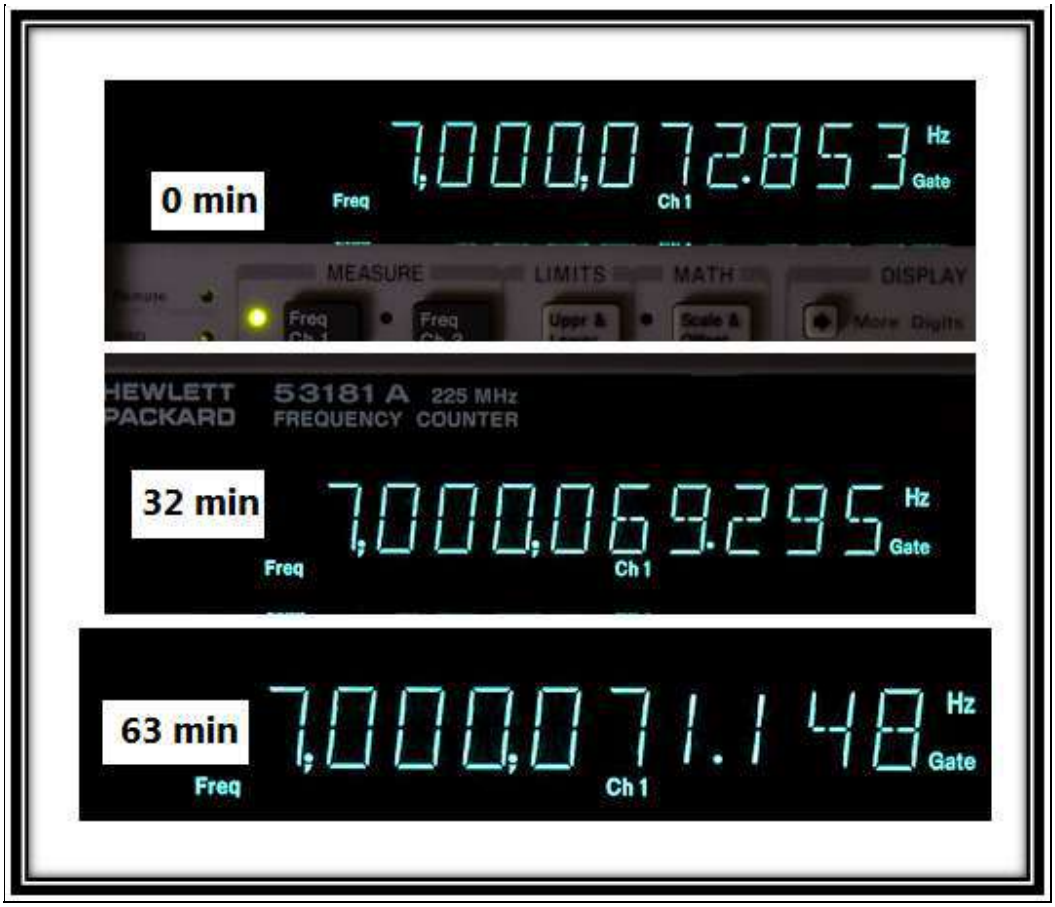

Above — The ~1 hour drift after a 30 minute warmup period for the 7 MHz VCO. Love this.

Above — My new temperature compensation capacitor parts drawer. I'll keep an eye out for further bargain temperature compensation parts on eBay and at Ham Radio festivals.

Fearless Leader and Hero Храбрый вождь и герой

Above — Professor Vasily Ivanenko ( ), fearless leader (ТЫ МОЙ ГЕРОЙ)

He's my hero because he's humble, fallible, well-intentioned and moral. Professor Ivanenko lives for learning — fame is filler — hollow and distracting. His current *ego* lags his voltage by 90 degrees. Is he part inductor / part human?

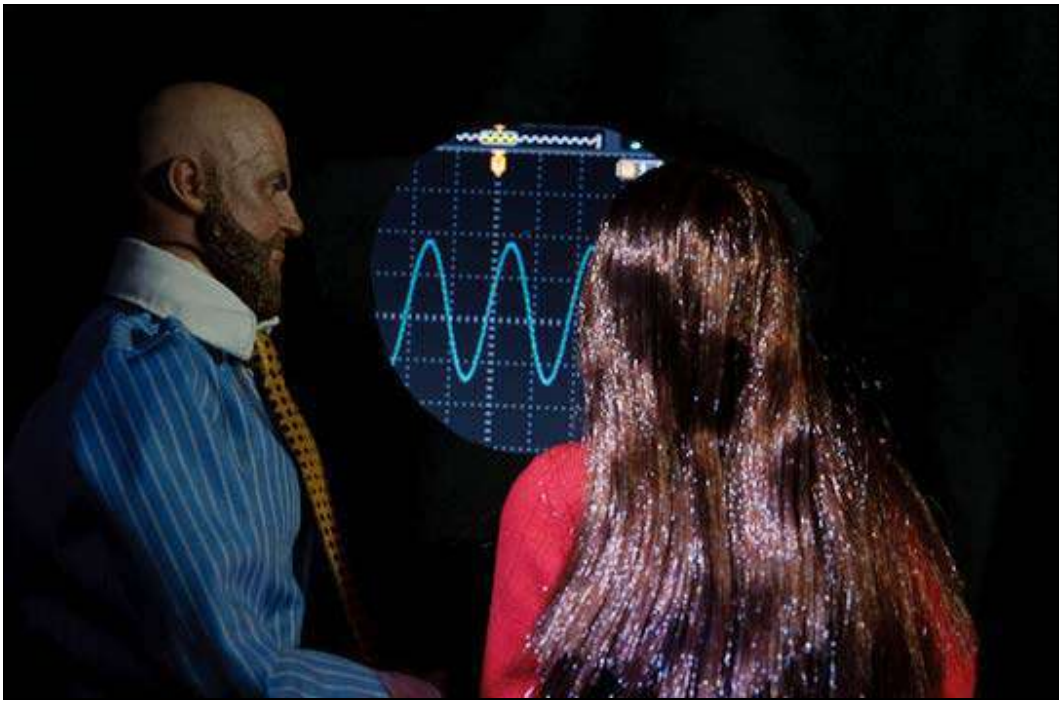

Miscellaneous Photos and circuits

Above — 3 types of adapters. A BNC male to SMA female, a BNC male to PL-259, and a BNC female to S0-239 allow the RF modules to be connected to a variety of equipment.

Click

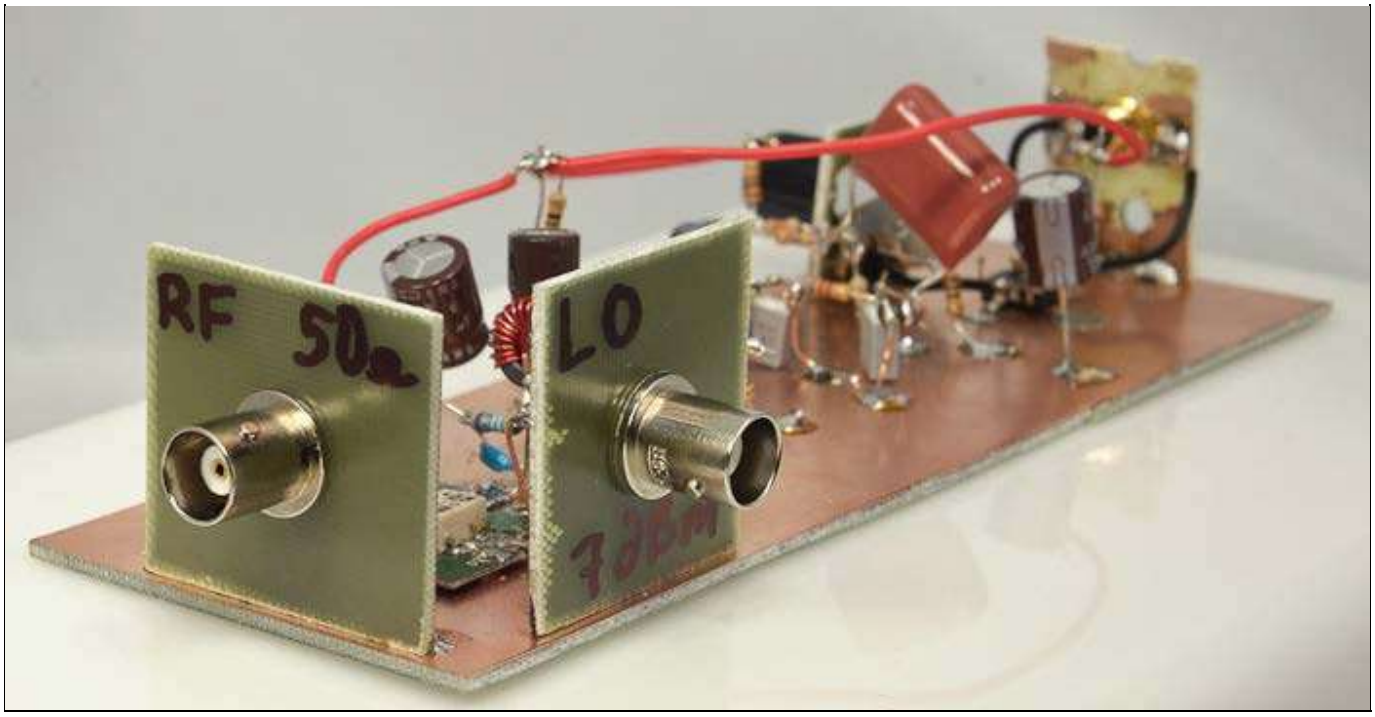
RF 50Ω
LO
7dBm

Double Tuned Receiver Band-pass Filter Design Center

This web page is for builders who own EMRFD. Assisted by 4 of the Ladpac programs from the EMRFD compact disk, and the information presented in EMRFD Chapter 3, I share some experiments building popcorn receiver band-pass filters. Prior to diving into this material, please read the help file ***Ladpac2008 Manual.pdf*** and a file on the EMRFD compact disk called The Double Tuned Circuit: An Experimenter's tutorial by Wes, W7ZOI.

Preface

Derived from experiments, my web content reflects the efforts of a lay-person, hobby-level designer — I make mistakes. I say this not to make excuses or avoid accountability, but to share the truth. My hope is that my experiments inform yours and we all improve over time. I correct reported mistakes and rely on your eyes to see them.

Arduous and requiring good math skills, filter design is out of reach for many builders. Software changes this and learning to apply computer programs in real-world situations is part of our hobby. This web page shares some bench experiences, plus my thoughts about using some programs written by Wes, W7ZOI. I present suggestions and examples based more on empiricism and from reading about band-pass filter design than scientific methodology.

From email regarding my VFO and RF Workbench pages, I have become aware that I've lead many builders to think that a perfect sine wave and a high return loss are "must have" bench outcomes. This is false. A clean sine wave proves useful for accurate measurement, but is not a *de rigueur* bench outcome. A desire for high return loss reflects my own personal *obsession*; in simple QRP rigs, this may represent folly. Please don't overestimate the importance of return loss from my bias; decide for yourself.

Part 1: Experiments with 2 coupled L-C tanks.

Goal: A 15 Meter band band-pass filter with an insertion loss < 4 dB and a return loss of >= 20 dB.

Software: Ladbuild08 and GPLA08.

The simplest band-pass filter is an L-C tank. To get a decent stop band we generally couple 2 or 3 tanks together with series capacitor(s). Other filter topologies were ignored. In Part 1, I just connected up a couple of tanks on the bench without the use of software. Some attempts at impedance matching via transformer links were also trialed.

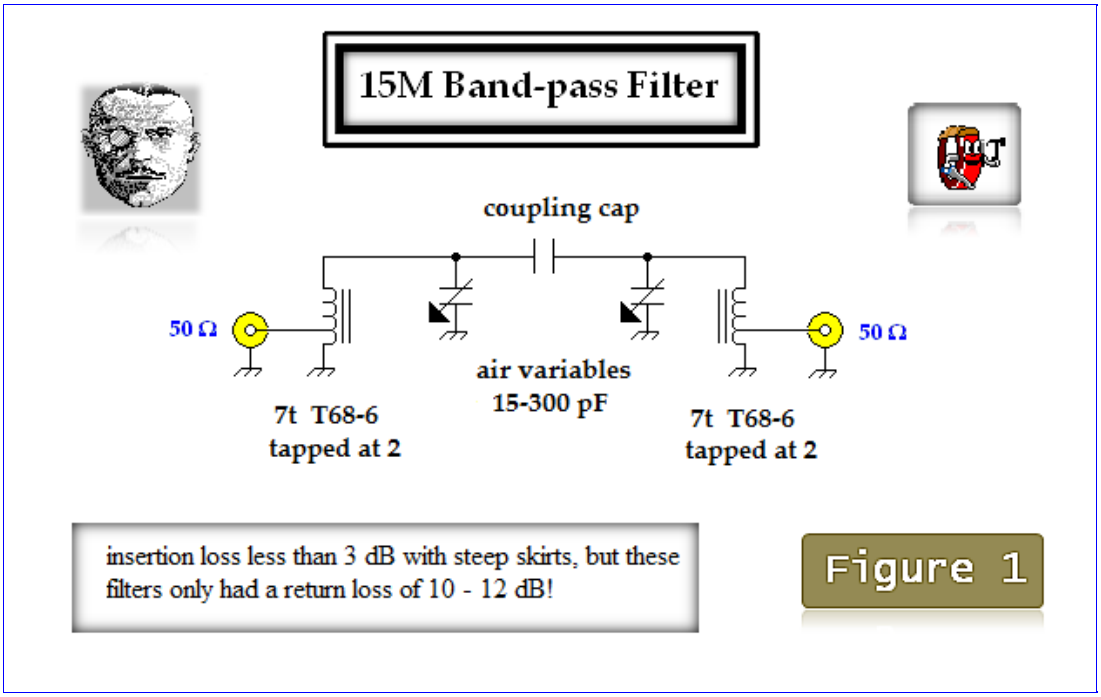

Above — I built a 5 component filter for the base experiment. Inductors = 7 turns of #22 AWG on a T68-6; tapped at 2 turns from ground. The inductors turns were expanded or compressed until L= 300 nH. Tuning capacitors = large 15 to 300 pF air variable capacitors. Coupling capacitors trialed = 2 pF, 3.3 pF, 5 pF, and 7.5 pF.

After soldering in a coupling capacitor, each tank (also called resonator) was tuned to resonance by looking at the peak-peak output voltage in a 50 ohm terminated oscilloscope. After tuning, I measured insertion and return loss and then swept each filter with a tracking generator + spectrum analyzer. On the bench I determined that the greatest return loss occurred with 2 transformer taps from ground; the result — a dismal 10-12 dB.

What effect does changing the coupling capacitor have?

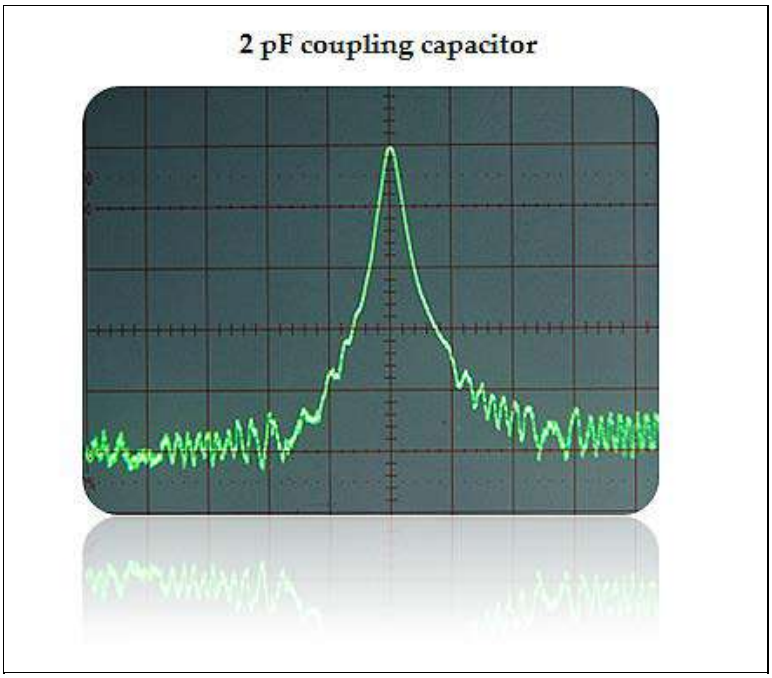

Above — A spectrum analyzer + tracking generator sweep of the filter response with a 2 pF coupling capacitor between the inductors. Graticules = 2 MHz per horizontal division and 10 dB per vertical division. Click on this zoom to better see the - 3 dB bandwidth. The sweep revealed a sharp peak response with steep skirts and a 3 dB down BW of ~220 KHz or so. Some of the noise arose from the big air variable caps connected to each tank with short hook up wires, plus no shielding.

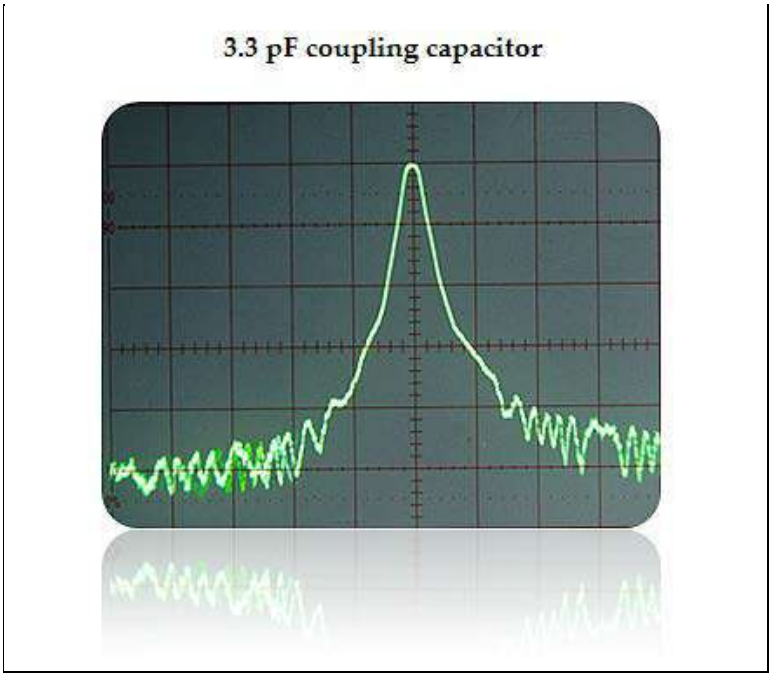

Above — The SA + TG sweep with a 3.3 pF coupling capacitor. The peak isn't as sharp, but still looks good. As shown, increasing the coupling capacitor value increases the 3 dB filter bandwidth with all other components equal.

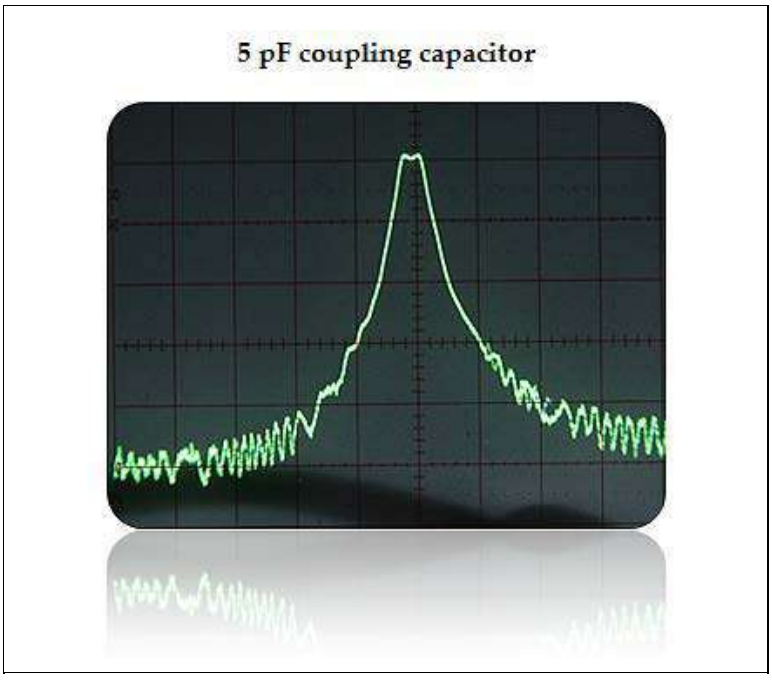

Above — With a 5 pF coupling capacitor, a double humped response appeared. The bandwidth further increases.

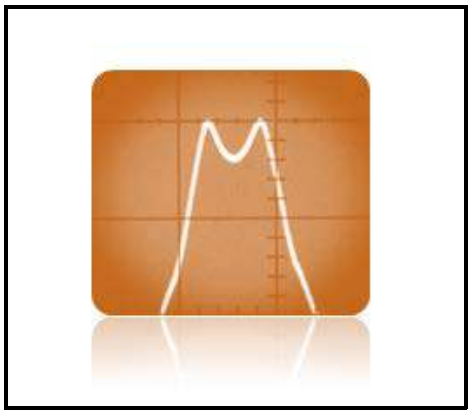

Above — A zoom of the double humped filter response employing a 7.5 pF coupling capacitor. Imagine the difficulty tuning this band-pass filter in a receiver by listening to band noise. Tuning in either peak skews the filter bandwidth. Additionally, the 3dB bandwidth now = ~ 1.6 MHz — Not a good filter!

Optimizing Return Loss

Despite trying, I could not obtain a better return loss than 10 -12 dB by changing the tap point on the 7 turn inductors. In part this was due to limited potential autotransformer ratios on a 7 turn coil. I emailed Wes, W7ZOI and he sent this file. I learned that adding a series capacitor to each end will tune the filter to 50 ohms impedance. What capacitor value should we use?

The answer can be found purely experimentally, or with Ladbuild08 to make a digital file of your filter and GPLA08 to analyze it.

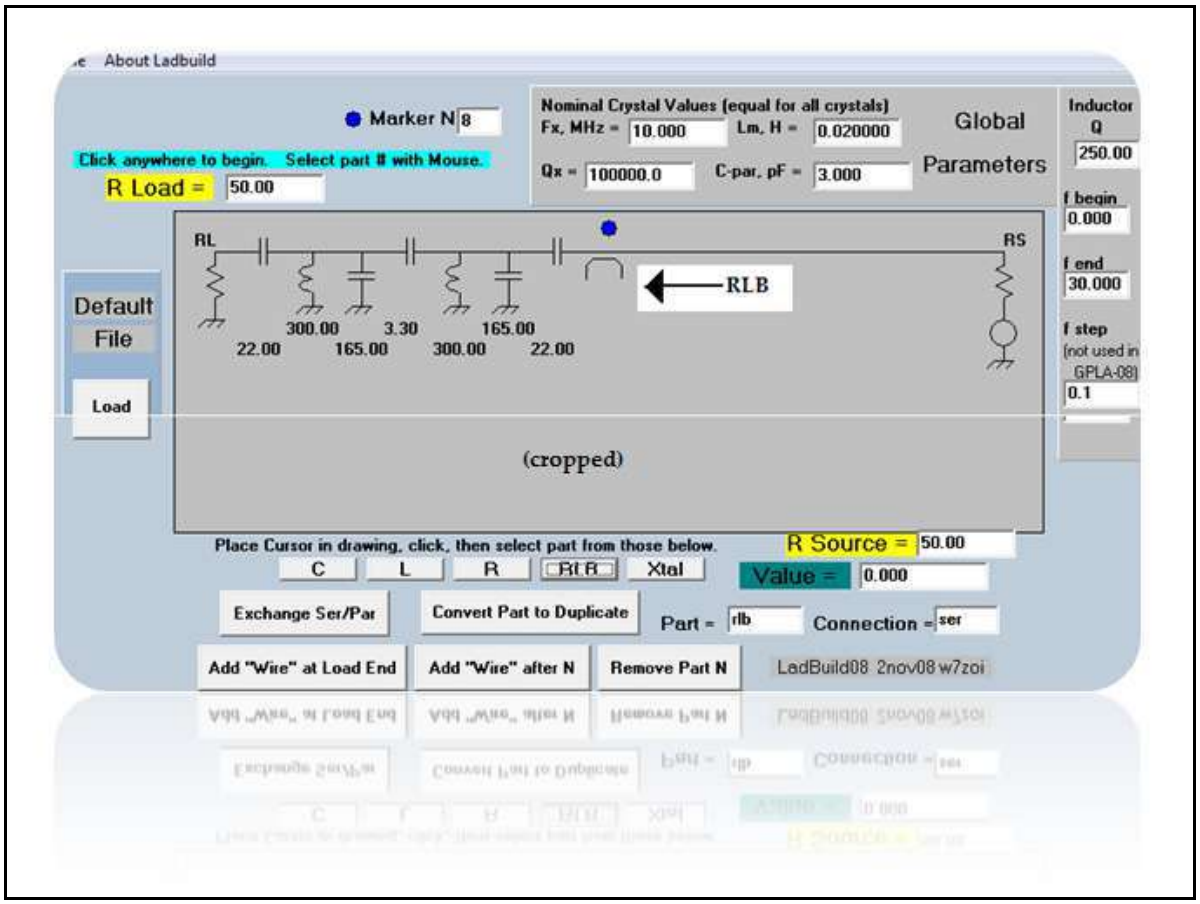

Above — I "built up" my Figure 1 filter in Ladbuild08 with a 3.3 pF coupling capacitor. Initially I guessed at the values for the series end capacitors and knew my tuning capacitor were ~ 165 pF because I removed and measured them from the peaked filter from Figure 1 and added a few pF for stray capacitance. Any of these values can be changed in GPLA, so educated guessing is okay.

For size 50 to 68 toroidal inductors, many builders choose a Qu value from 200 - 250 with # 6 material. Qu affects insertion loss and to some extent, return loss. Click for a tutorial from Wes', W7ZOI site and consult EMRFD for more information.
In order for GPLA08 to display an S11 plot (return loss), a return loss bridge (RLB) must be added as shown. Also check the **Plot S11** check box in GPLA08.

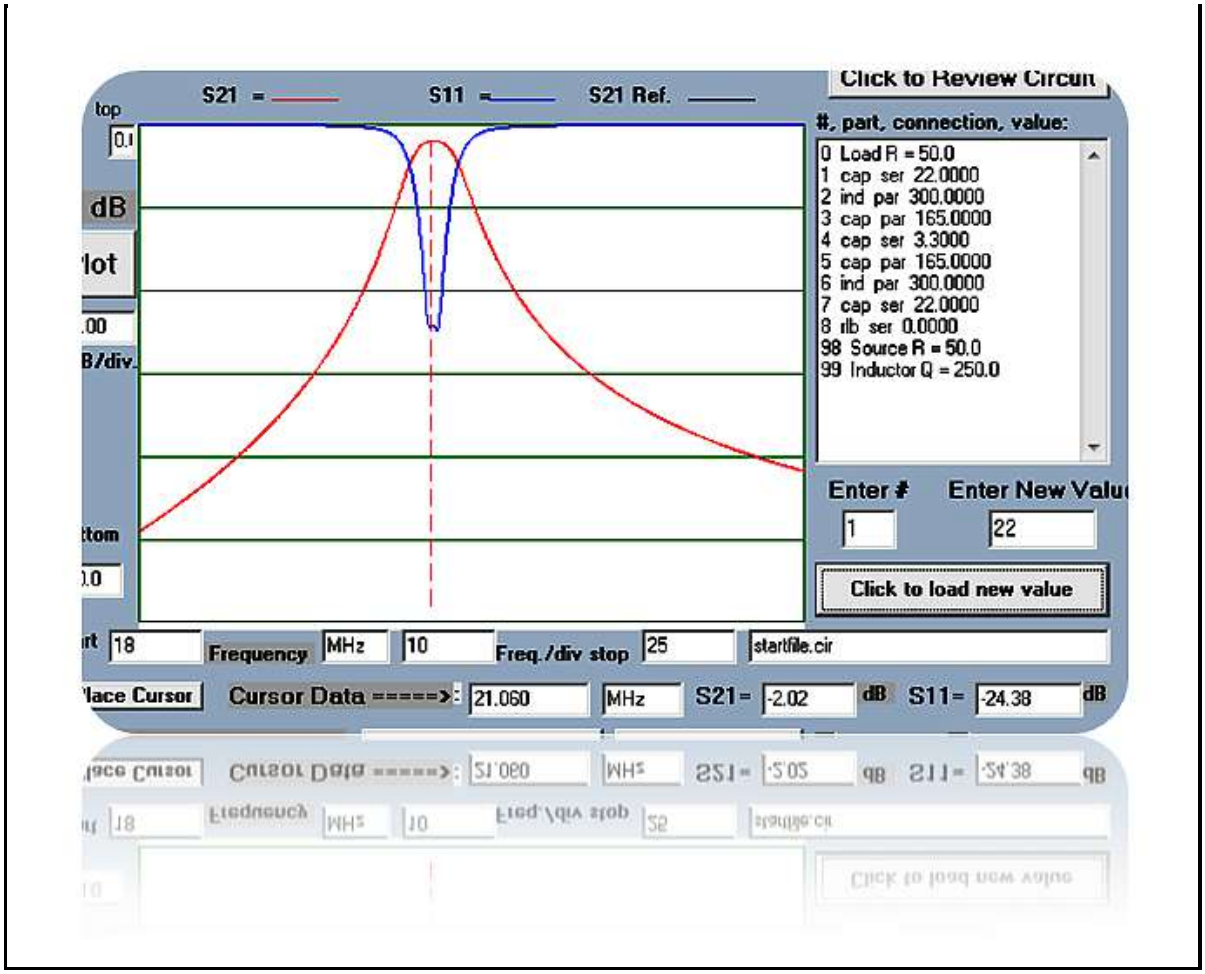

Above — The GPLA 08 filter simulation of the filter "built" with Ladbuild08 above.

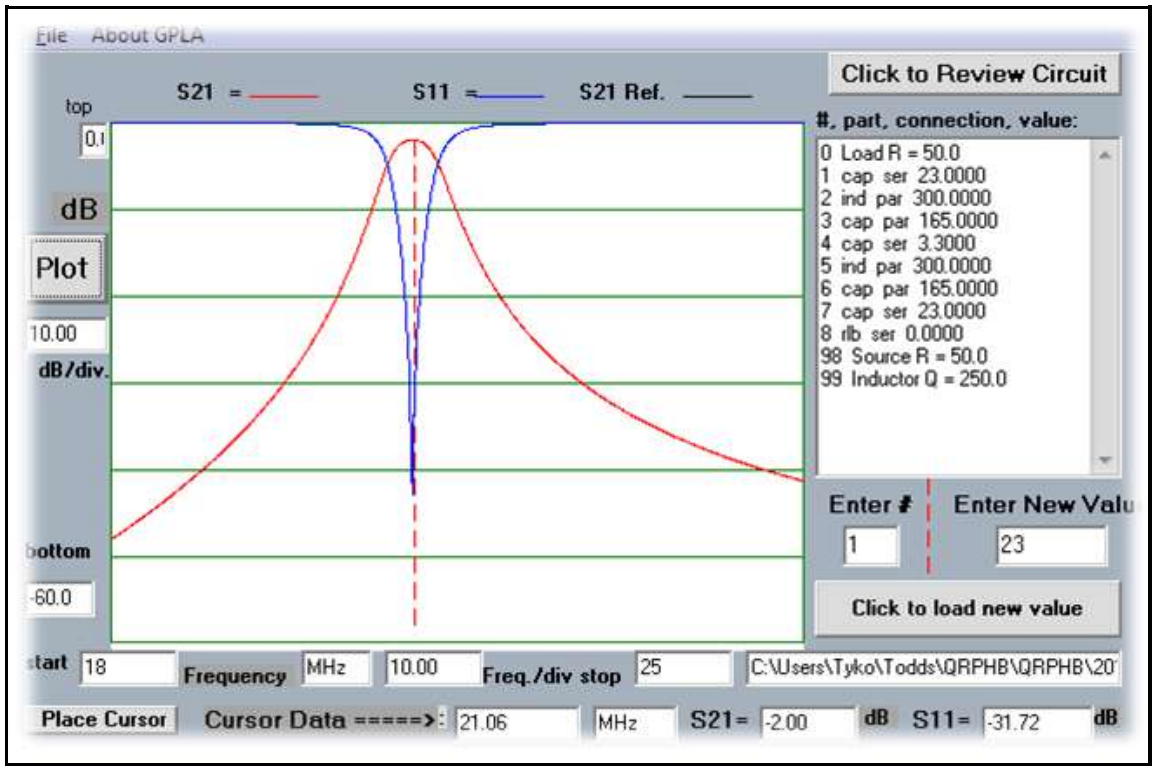

Above — In this filter simulation, I tweaked the end capacitors (parts #1 and #7) from 22 to 23 pF and watched the return loss (S11) improve by 7.34 dB — if wanted, you can optimize the end capacitor values to improve the match into 50 ohms. To re-establish the center frequency, slight retuning of parallel capacitors #3 and 6 is required when changing the series end capacitors; although I specifically didn't change them for this example.

Increasing the 2 end capacitors to increase S11 renders an option only; you don't have to go for the best S11 in your filters. Increasing the series end capacitors to bump up return loss tends to increase the 3 dB bandwidth and reduce insertion loss.

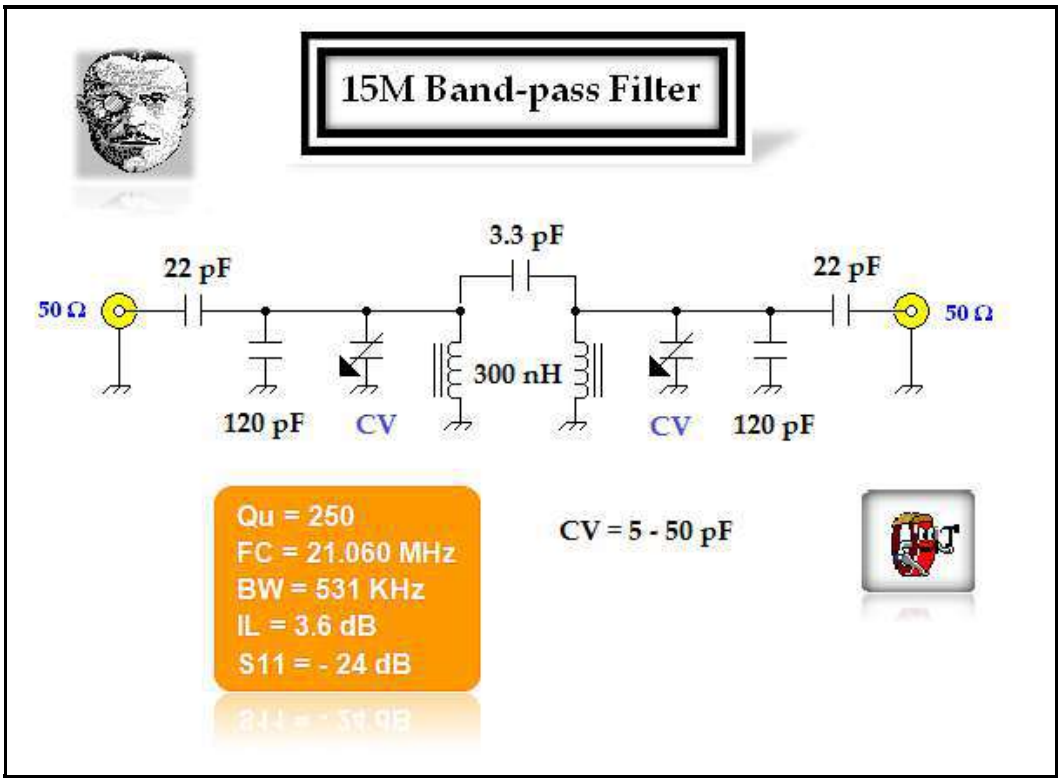

Above — I built and measured the filter with 22 pF end capacitors since these are common, standard values. In another experiment, a 1 pF cap was soldered in parallel with each series capacitor and the return loss increased by about 4 dB. Click for a bench photo of an alternate version of the above filter. Clearly, GPLA08 simulation furnishes us popcorn builders with a starting point to make top-notch band-pass filters.

Click for another simulation of a filter employing a 2 pF coupling capacitor, with the end capacitors tweaked for the best S11. *S-11 is just the negative of the return loss.* I would certainly use this filter in the front end of a popcorn direct conversion receiver.

An easier way to design your band-pass filters involves using DTC08 to design a raw filter and GPLA08 to substitute in standard value capacitors and tweak your filter. That's part 2. The material presented in this section supports the discussion in Part 2 and 3.

Part 2: Band-pass Filter Design using DTC08

Prior to using these Ladpac programs, some numbered design points and a preamble follow.

More than anything else, our parts collection dictates what filter parameters we choose and end up with. For example, if you want filters with a low bandwidth such as 150 KHz and under, you'll require inductors and capacitors that provide really high Q, or you might suffer from punishing insertion loss.

The following are general starting points only — *your* needs, parts and abilities drive *your* filter design. Example variances include: if a low noise amplifier follows a filter, a higher insertion loss might be okay; a high return loss is not always required for a low noise figure; especially in popcorn receivers. Also, it's a viable choice to trade off insertion loss for steep skirts in some filters.

1. A reasonable 3 dB bandwidth = 100 to 500 KHz, but this depends on the purpose of the filter.
Numerous considerations challenge us. Will this be a whole band (CW + SSB) filter, or a CW only filter? As a CW op who uses simple equipment, I tend to design moderate bandwidth (200-300 KHz) CW-only filters. If you need CW + SSB, then a bandwidth of 350 KHz or greater might suit you. It's really up to you.

Other factors affecting bandwidth choice include whether the filter drives a superheterodyne or a direct conversion receiver. In superheterodyne receivers, your intermediate frequency informs your filter bandwidth choice. Consider the following 2 diagrams:

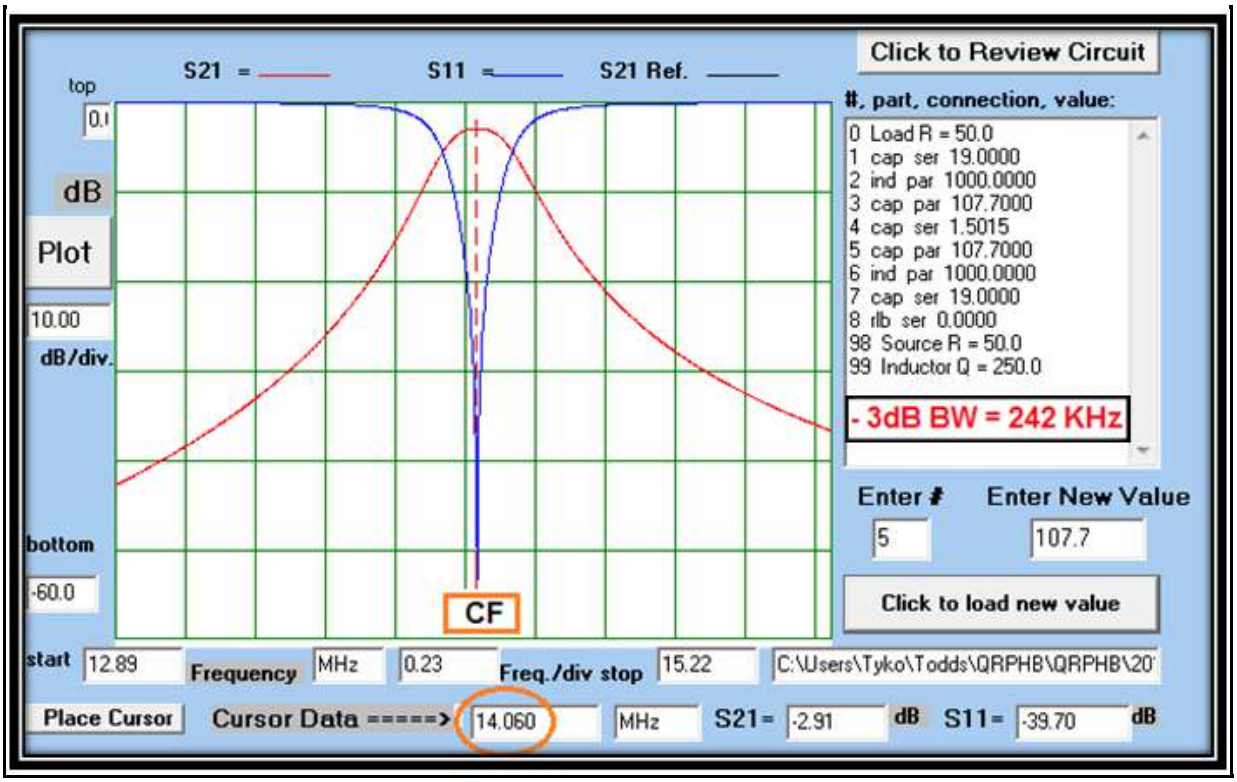

Above — Using DTC08 and GPLA08, I designed an example filter for the front end of a 14 MHz superheterodyne receiver with an 11 MHz IF. BW = 242 KHz. CF = 14.060 MHz; a frequency some QRP operators favor.

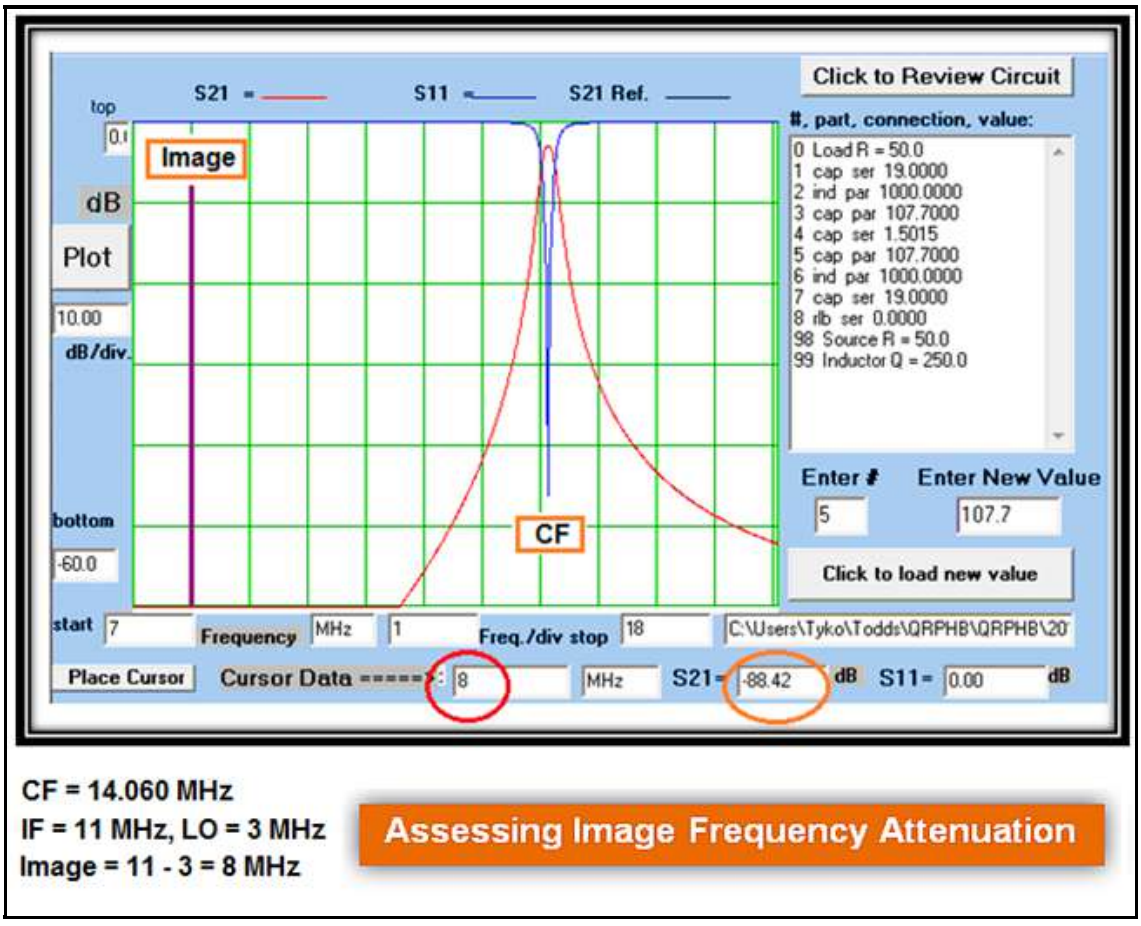

Above — Assessing filter attenuation at the image frequency using GPLA08. *To keep the arithmetic simple, I employed a frequency of 14 MHz for the image frequency calculation.* As shown, the simulated attenuation of my 8 MHz image frequency is 88.42 dB. Since I personally target an image frequency suppression of 60-70 dB; at 88 dB, if I wanted, I could increase the bandwidth of this filter for broader coverage and reduced insertion loss.

How much image frequency rejection is needed for superheterodyne receivers? I'm uncertain, for I have seen competent authors choose between 50 and 100 dB. I feel a good target = 60 - 70 dB, and 50 dB is the bare minimum. To realize image attenuation above 50 dB, shielding is usually required.

Three or more L-C tank band-pass filters may be required when your image frequency is close to the IF frequency. Choose both your intermediate frequency and your bandwidth wisely.

2. After selecting your bandwidth, *tweak the inductance* and only if necessary, make minor adjustments to your set 3 dB bandwidth to give standard, or near-standard value coupling capacitors that you *own.* Obviously, you can place fixed capacitors in series or parallel, or even couple your resonators with a variable capacitor.

3. I favor size 50 to 80 powdered iron toroids with number 2, 6, or 10 material for a reasonably high Qu.

4. I aim for an insertion loss of of 3-4 dB; especially above the 40 Meter band; *consider the variances discussed earlier*

5. I aim for a return loss of at least 20 dB; *consider the variances discussed earlier*

6. If you can, measure your bread boarded filter bandwidth to confirm or improve the GLPA simulation. Insertion and return loss are easily measured — see EMRFD and the RF Workbench web pages on this site for methods.

I provide no graphic tutorial of DTC08; however, some work flow suggestions follow:

Open up DTC08, choose your center frequency, Qu, inductance and bandwidth and then press the **Calculate** button. Adjust the L until you get close to a standard value coupling capacitor from your parts bin. If required, you may also tweak the bandwidth value to get the needed coupling capacitor. It's wise to change the L before BW since changes in inductance don't cause too many complications within limits.

Name and save your filter to a specific file system directory or folder; or simply save it as the default file.

Open GPLA08 and load your recently saved filter file. Press the **Plot** button and then the **Click to Review Circuit** button. In some cases, you will have to type the CF in the *Cursor Data* text box and press **Plot** to set the cursor at your center frequency.

Change the coupling capacitor(s) to a standard value using the **Enter New Value** data entry controls.

Adjust the series end coupling capacitors to standard values. and if S11 is an issue for you, tweak them up and down while observing S11. Re-establish your center frequency by tweaking the parallel tank tuning capacitors and then re-plot to ensure the CF is lined up with the center of the plot.

In Part 3, I provide 3 filter design examples. Your own filter designs will be the most important examples to study.

Part 3: Band-pass Filter Examples

Example 1: An 80 Meter Band Filter

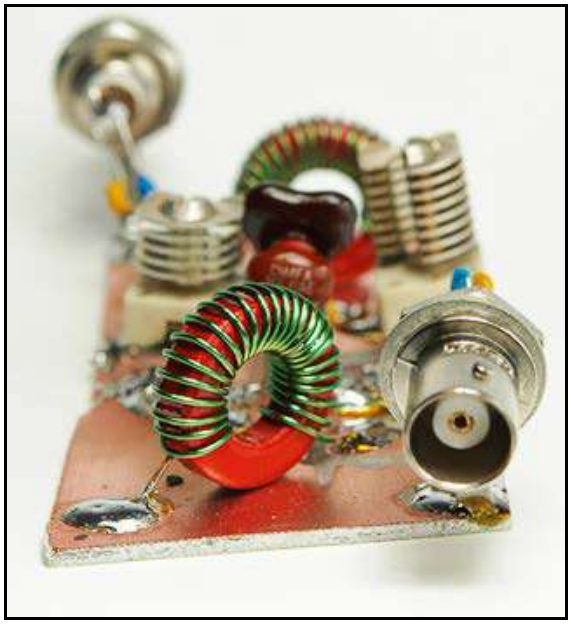

Above — Breadboard photograph of the 80M filter. This example filter may hit home for you — I like listening to CW at and below the 3560 KHz QRP calling frequency, however, another local Ham likes to talk on 75 meters SSB at or above 3790 KHz. This situation calls for a narrow band-pass filter. With my filter, the attenuation at 3790 KHz = ~ 24 dB; had I built a wide bandwidth filter, for example, 350 KHz BW; the attenuation at 3790 KHz, would only be ~4 dB. Perhaps a 3 resonator filter with even steeper skirts would be better?

I'll show the design process from start to test.

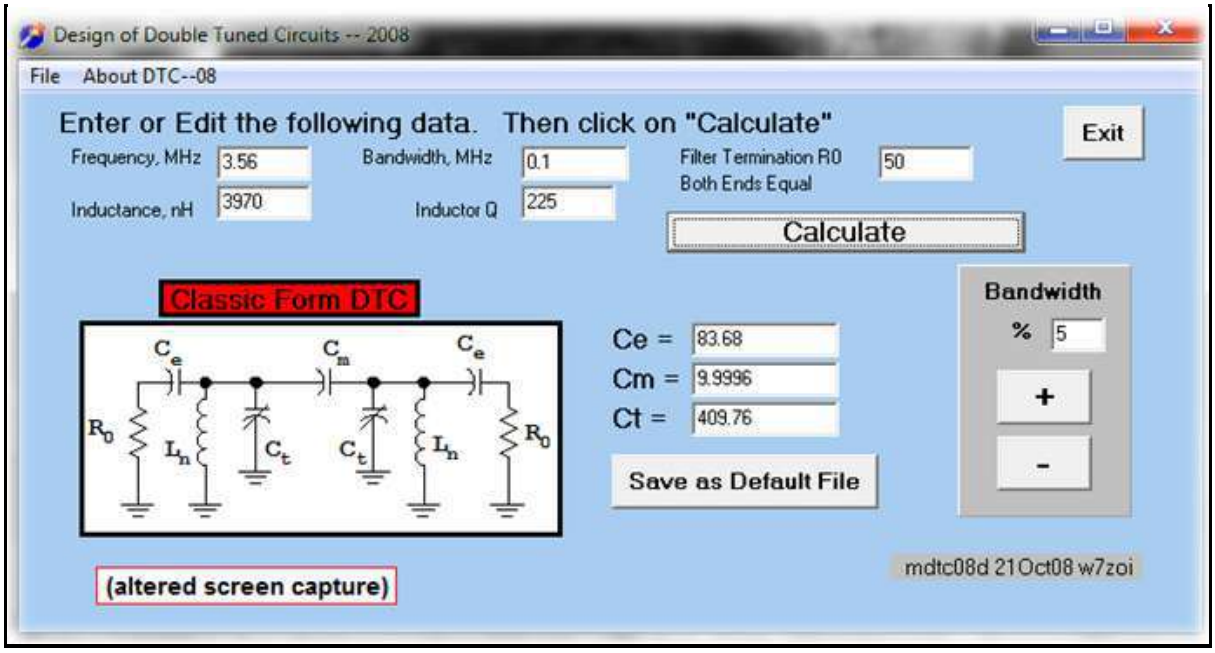

Above — The basic DTC08 data entry fields were populated. I chose a 100 KHz bandwidth and tried different L values until Cm = 10 pF, since I have a whole drawer of 10 pF capacitors. I believed my Inductor Q would be at least 225 and wound 25 turns of #22 AWG on a T68-2 toroid and expanded or contracted the windings until I measured 3970 nanohenries. In reality, we should measure the inductor Q and in future I will, however, my sense is that few builders do.

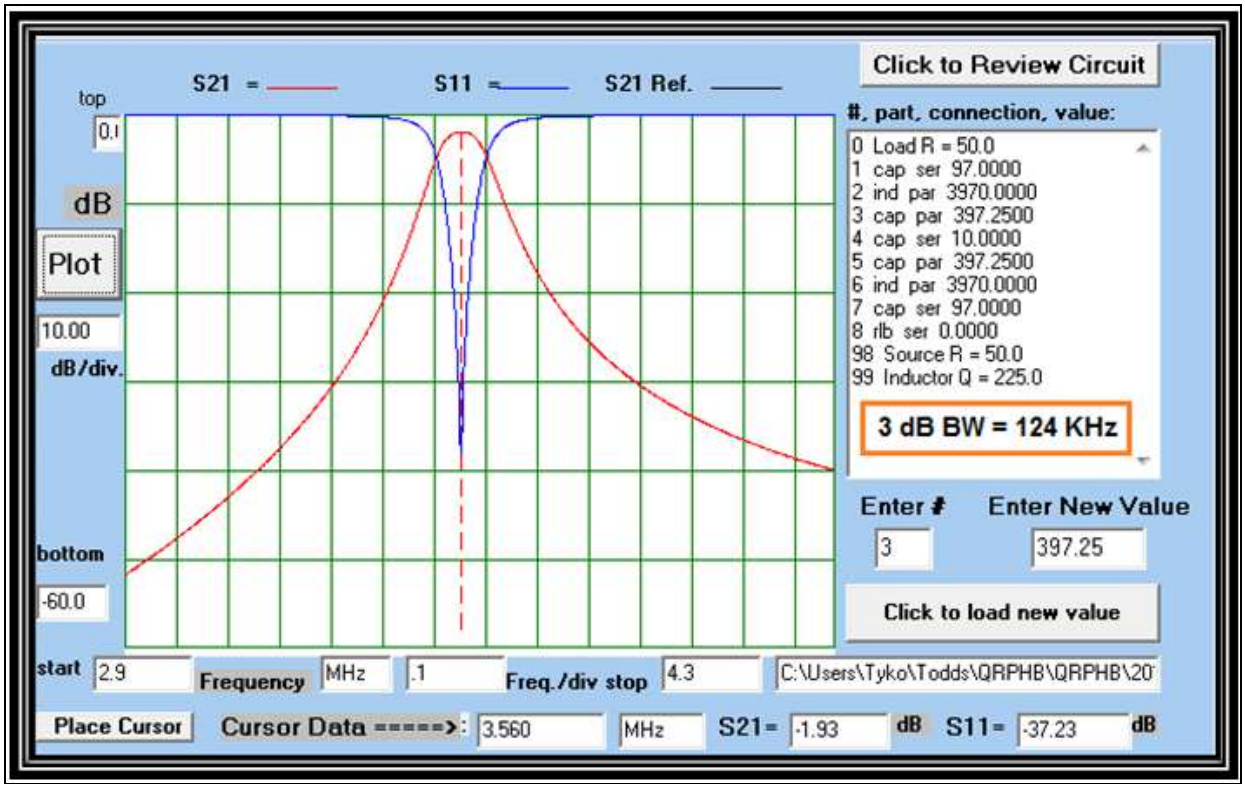

Above — After saving my filter, I opened it up in GPLA08 as above. I replaced #4 with a standard 10.0 pF value, and started tweaking the end caps; parts #1 and #7 to gain a better S11 per my obsession with return loss. Retuning #3 and #7 re-establishes the center frequency and allows the S21 and S11 values to be interpreted. I settled on this filter and headed for the bench.

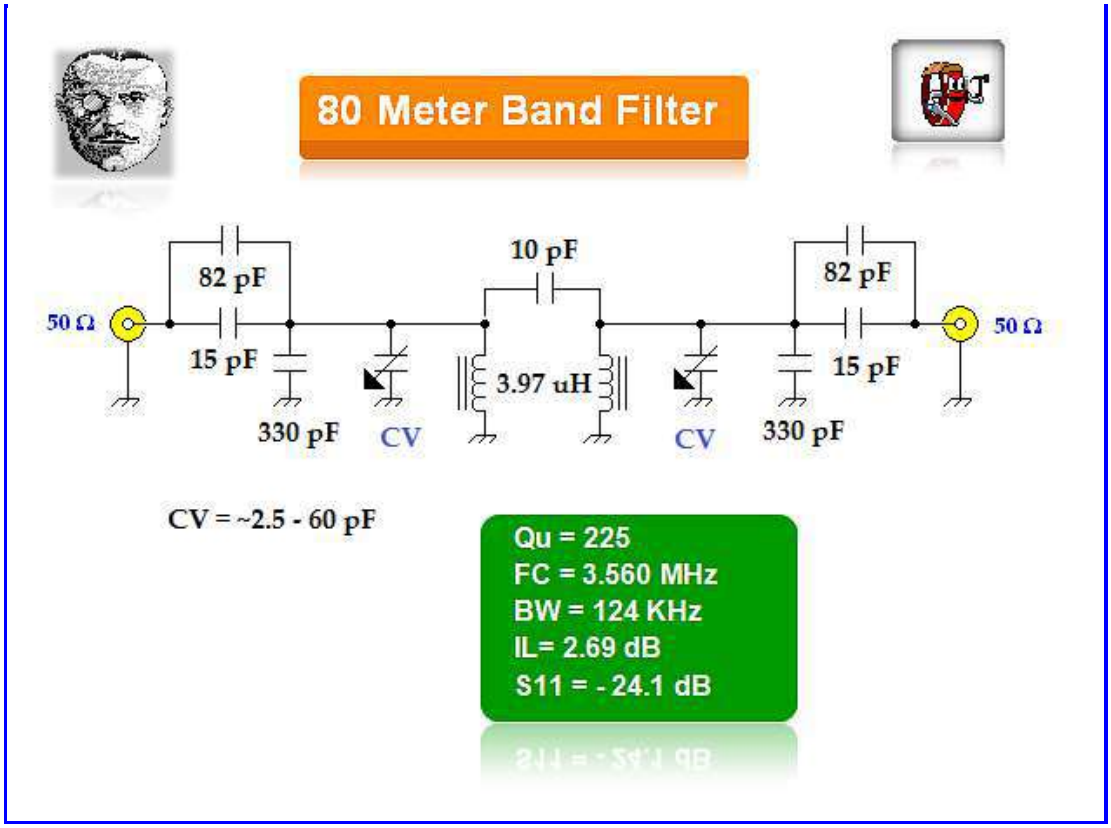

Above — Schematic and analysis of the breadboard. Click for another photograph. In reality, I bench determined the exact capacitance needed to tune each tank at 3.56 MHz with 2 large air variable capacitors that I removed and measured after peaking the filter. For each tank, I try to get just below this value with fixed value capacitors and add a small (2.5 - 22 pF, or so) air variable trimmer capacitor for peaking.

You need to test with capacitance under and over that required to ensure you properly tuned each L-C tank to resonance. Your parts collection, stray capacitance, mistakes or inductance variations in the toroids necessitate custom tuning of your tanks on the bench. I give capacitance values that should work, but it's up to you to ensure resonance of each tank. I find narrow BW filters require a steady hand to tune.

After peaking the tank in your oscilloscope, record the peak-to-peak voltage. Remove the filter and connect your signal generator to your scope with an RF barrel connector and again record the peak to peak voltage. The difference between the 2 is your insertion loss. You can calculate IL with Applet H on this page . Next, perform return loss measurements. If you can, determine the true 3 dB bandwidth of your filter by sweeping it with SA plus a generator. My filter 3 dB BW = 124 KHz.

Example 2: 20 Meter Band Superheterodyne Receiver Filter

A fictitious builder wants a superheterodyne receiver that covers 14.0 - 14.350. His IF = 2 MHz. The local oscillator = 12 MHz. The image frequency = (12 - 2) = 10 MHz. He centers his filter at 14.020 MHz. In this simulation-only example, we'll go from 1 resonator to 3.

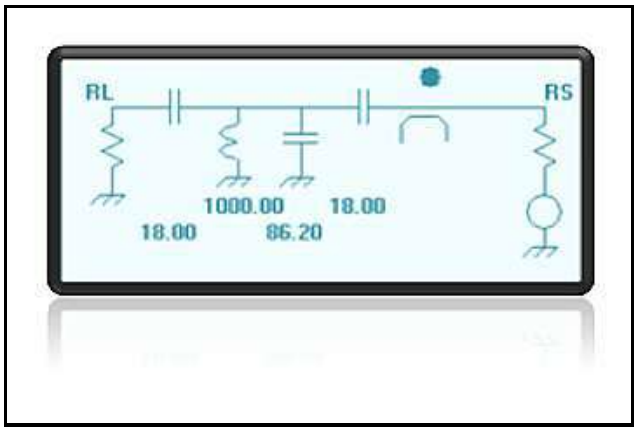

Above — A single resonator with series matching capacitors "built up" in Ladbuild08.

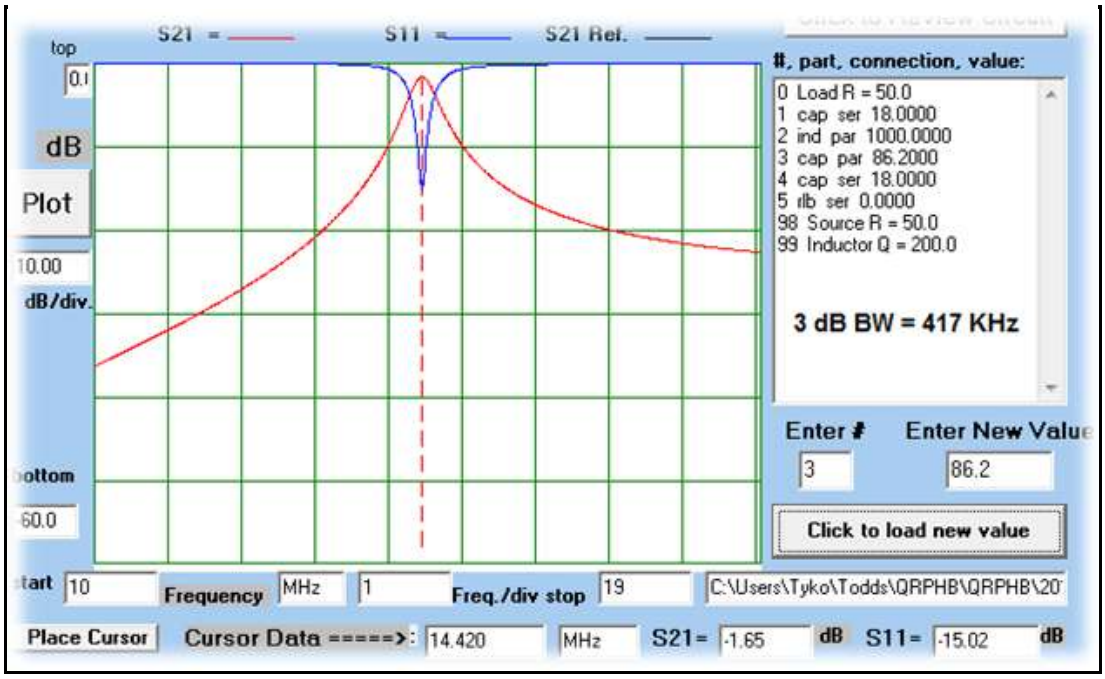

Above — The GPLA08 plot of the single tank filter. The bandwidth = 417 KHz. Increasing the end capacitors to 22 pF to try to increase return loss increases the 3 dB bandwidth as shown here, so we better stick with the original design.
In GPLA simulations with a perfectly centered filter, S21 = the insertion loss and S11 is negative of the return loss.

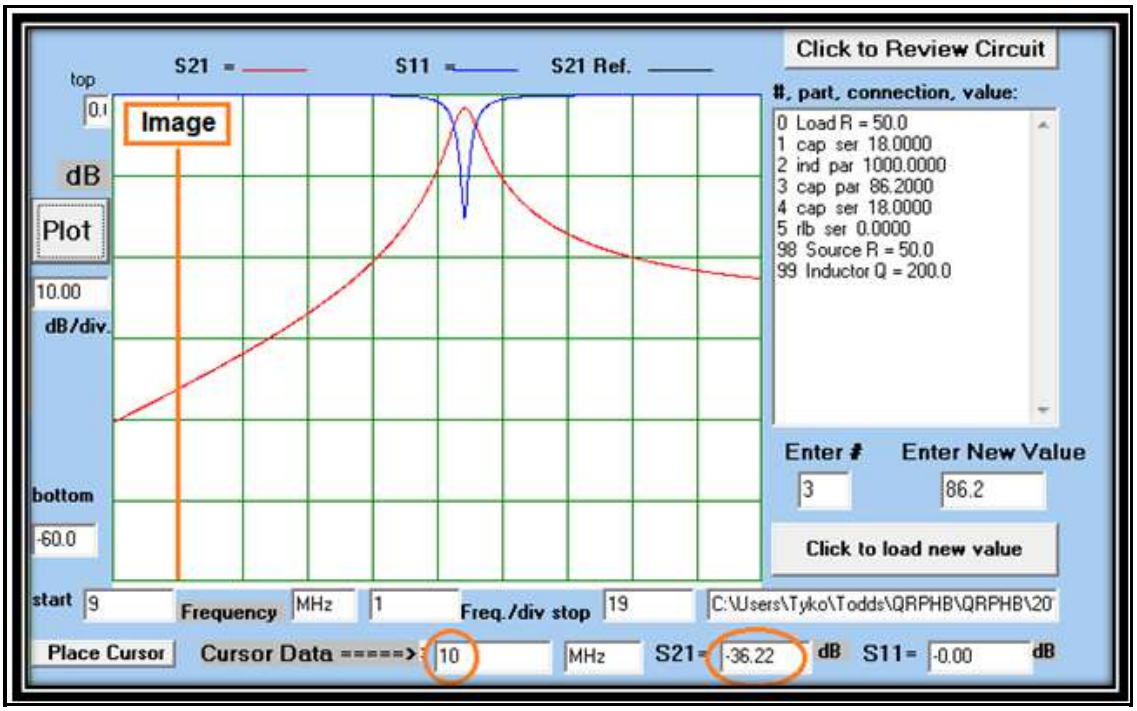

Above — Assessing image frequency attenuation in GPLA08; this sucks — only 36.2 dB down. We need to add a tank.

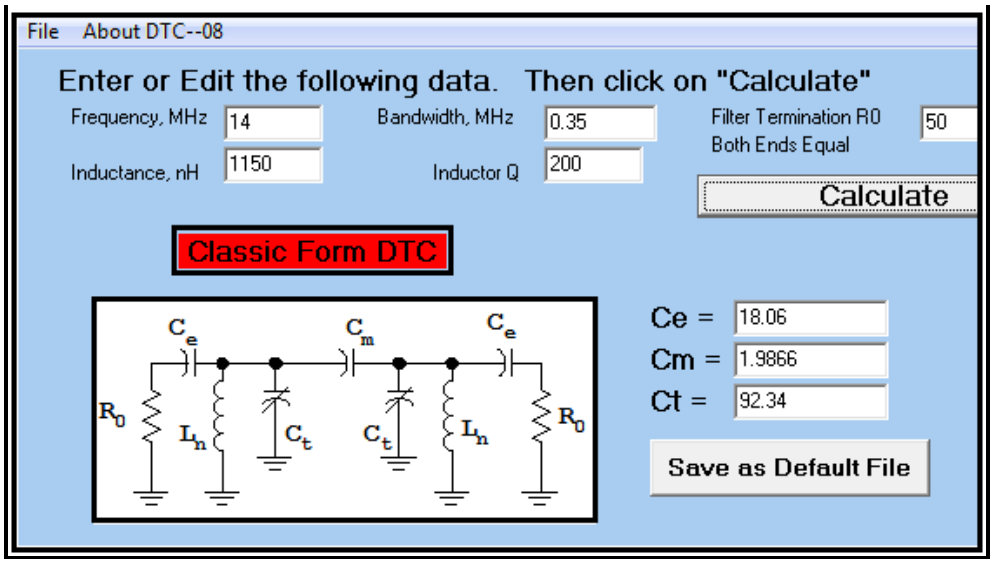

Above — Building up a filter in DTC08, I increased the L from 1000 to 1150 nH to give a Cm near to a standard value.

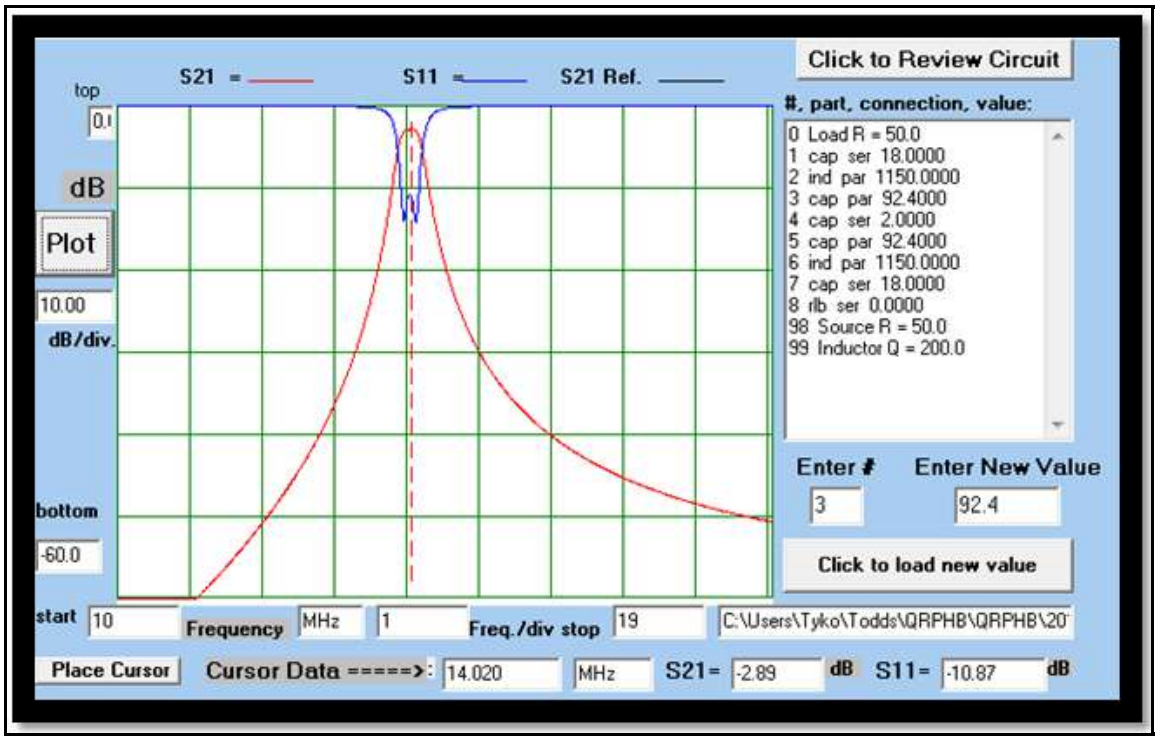

Above — The GPLA08 plot of the double tuned filter. I set #4 to 2 pF and #1 and #7 to 18 pF (nearest standard values). #3 and #5 were slightly tweaked to center the filter. The simulated IL is only up 1.24 dB from the single resonator version. You are probably wondering why I didn't design the filter for a CF = 14.020 MHz in DTC08 above to keep consistency. I probably should have, but wanted to illustrate the versatility of GPLA08 to center filters "on the fly".

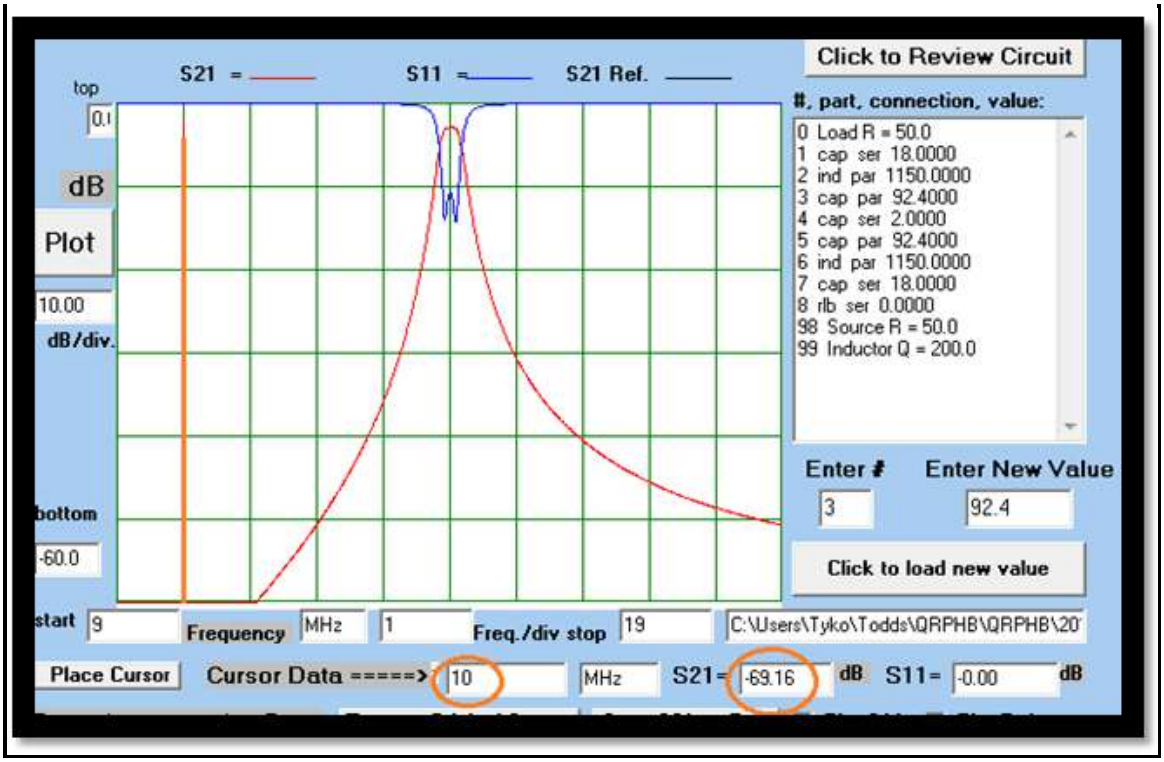

Above — Assessment of the 10 MHz image — now it's 69.2 dB down. Although this filter will work well for his particular receiver specifications, this fastidious builder wants even greater image attenuation and decides to add a third resonator!

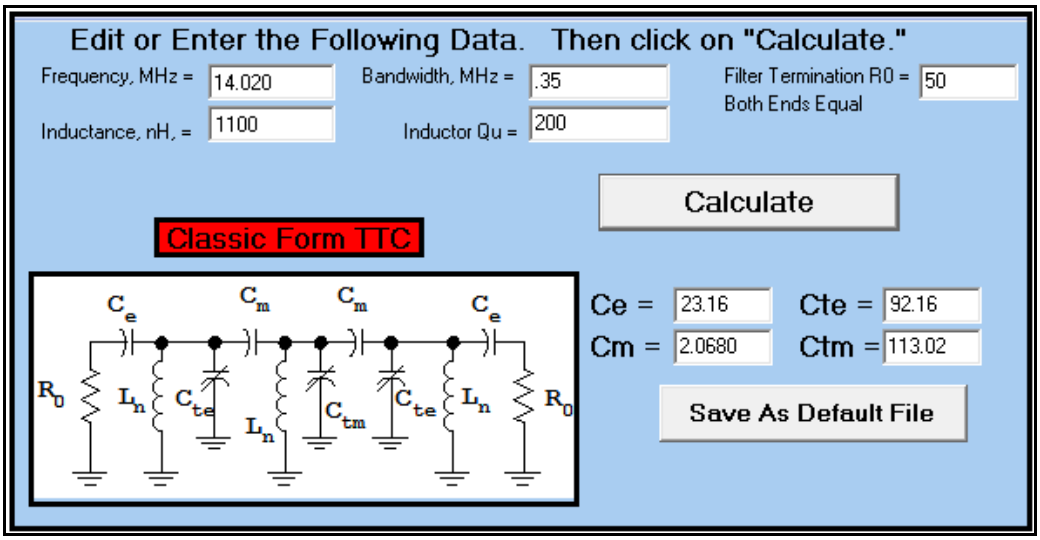

Above — Building up a filter in TTC08, I chose an L of 1100 nH to give a Cm close to a standard value.

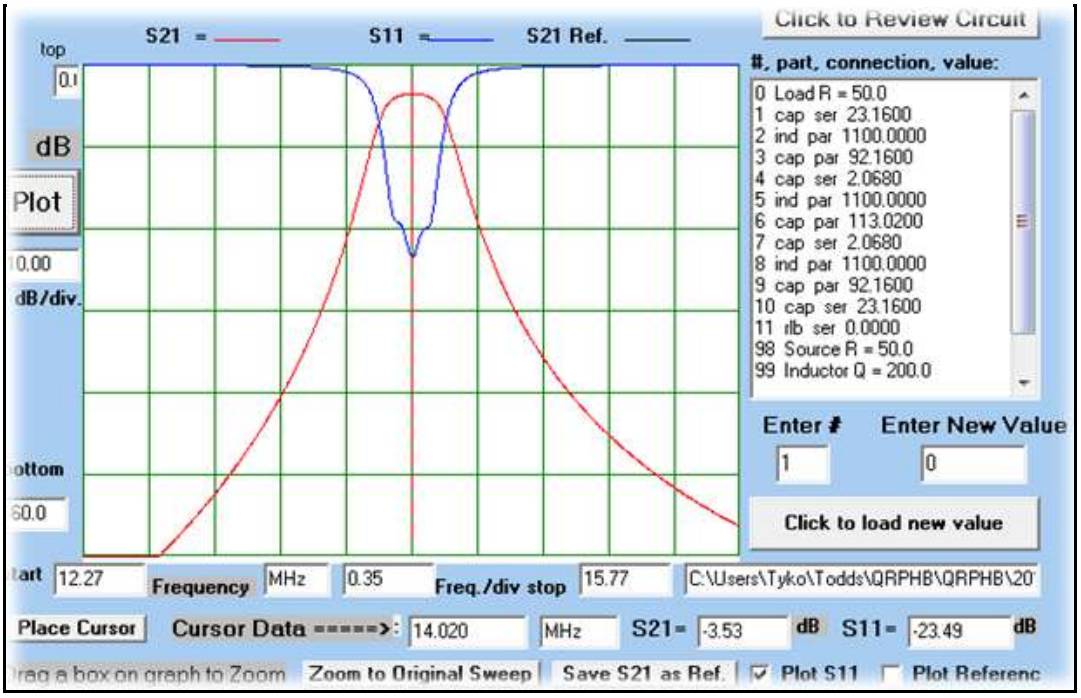

Above — The GPLA plot of the 3 tank filter. I performed no parts tweaking — it's up to you from here on in. The simulated IL remains quite reasonable.

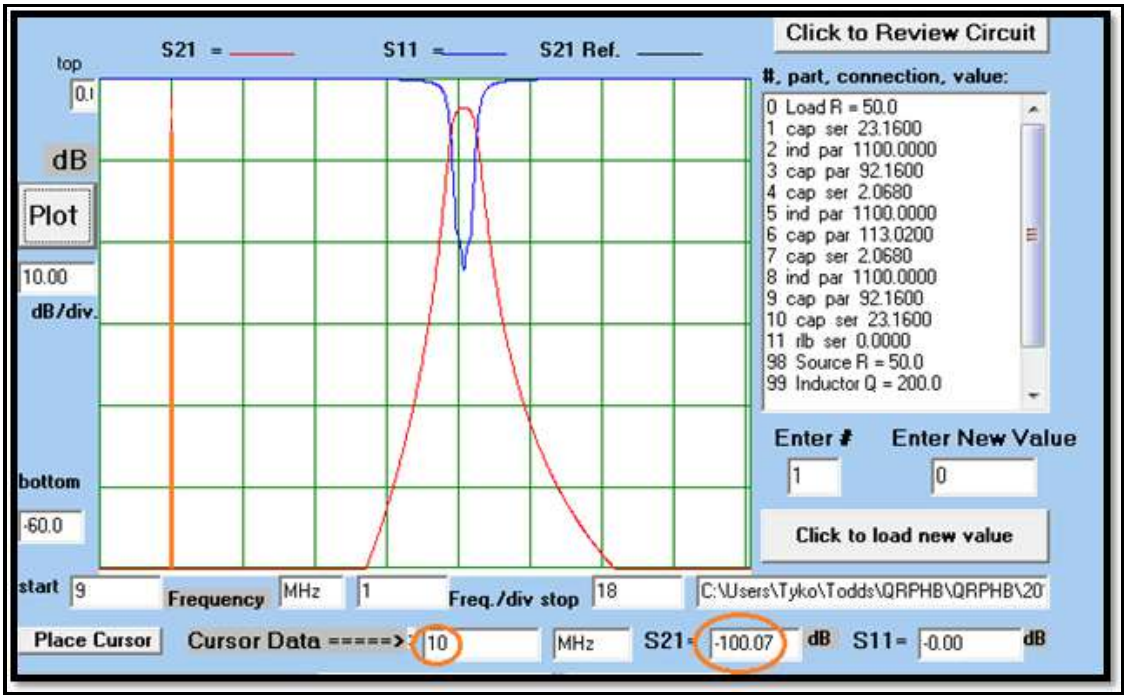

Above — The GPLA08 assessment of the 10 MHz image frequency. Now 100 dB down!

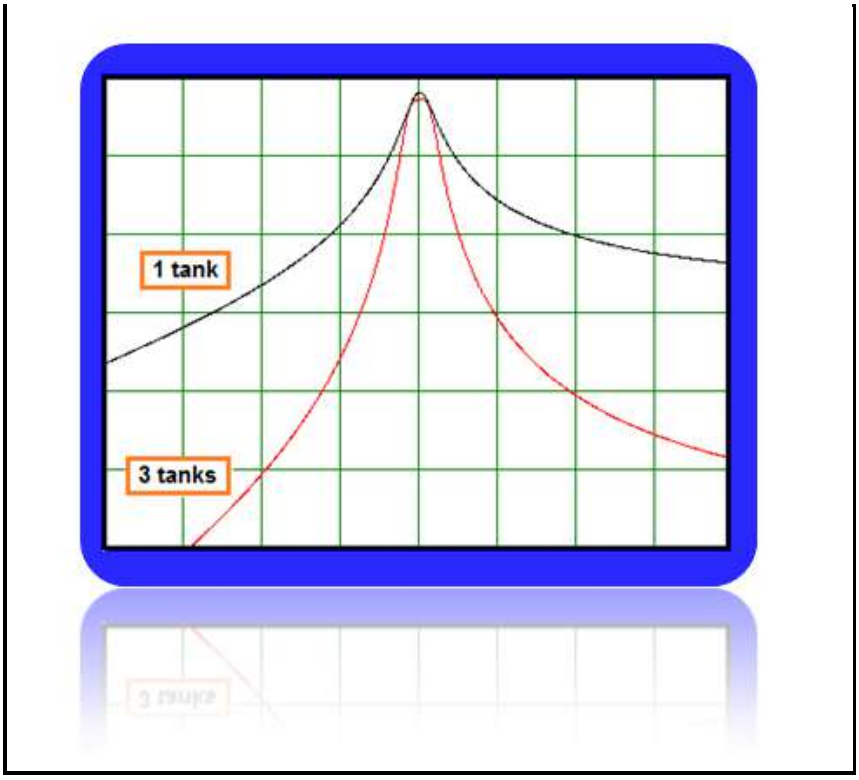

Above — The 1 tank and 3 tank filters superimposed to show the skirt action. The 3 dB bandwidth is the same!

Example 3: A 20 Meter Band-pass Filter for a Builder from Argentina

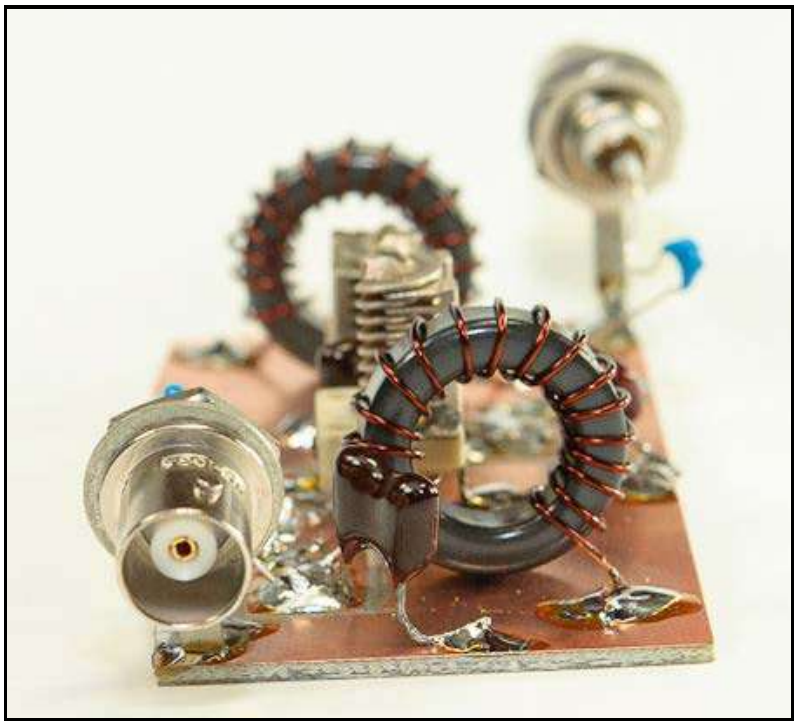

Above — An Argentinean builder emailed that he wanted a band-pass filter optimized for 14.070-14.095 MHz RTTY but also usable for the CW sub-band and lower SSB frequencies. He wanted a center frequency in the RRTY sub-band and I chose 14.079 MHz. Tuning this filter to a center frequency as low as 7.030 MHz for CW should be possible with the variable capacitor value shown, but as mentioned, you really need to do this carefully on your bench. I employed T80-10 toroids and scrunched or expanded the 16 turns of # 22 AWG wire until they measured exactly 1000 nH.

The best return loss will only occur when your filter is perfectly tuned to the test frequency, so tune carefully.

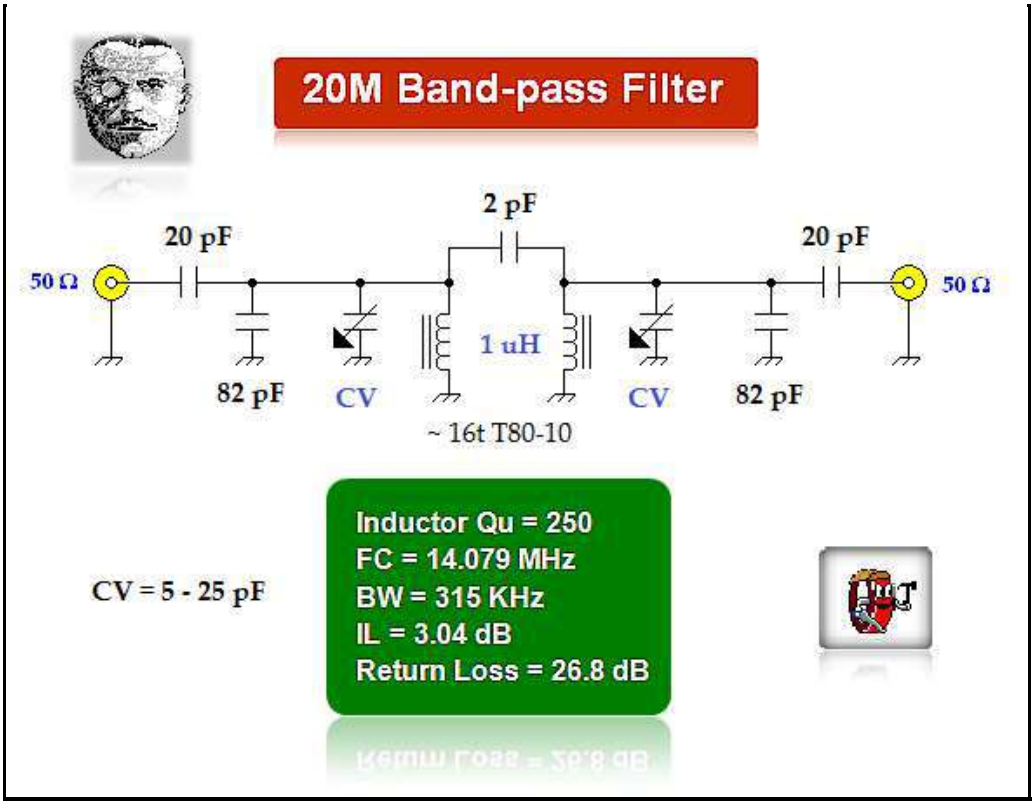

Above — The schematic + bench analysis for the 20 Meter band double tuned band-pass filter. My original design called for 22 pF series end capacitors to get a decent return loss. After building and measuring the circuit, the results were disappointing: insertion loss = 3.7 dB and a return loss = 17 dB. I wanted a better S11 and IL, so I decreased the end capacitors to 20 pF and savored the measured data shown in the schematic.

Simulating this tweaked design in GPLA08 unveiled a lower return loss than the original design simulation with 22 pF end capacitors; exactly opposite to my bench observations.

Bench work reveals the truth — The filter *you* get is dependent on factors such as parts types + tolerances, stray reactance, layout, test gear and any bench errors. For example, I don't know the Qu of my 1 uH inductors, but suspect that the Qu is greater than the 250 specified. Also my intended - 3 dB bandwidth was 350 KHz, yet my filter = 315 KHz; in part, because I lowered the series end capacitors, but also due to other fore mentioned factors.

Many popcorn builders can't easily measure their filter bandwidth. Does it really matter? Probably not, however, the big realization for me is that unless you measure, you won't actually know your data like insertion loss, return loss, or bandwidth — simulations are great, but don't obliterate the need for bench testing as possible.

Consider this; with the SPICE program you can design a circuit with a 2N3904 and run 400 mA of current through it — the transistor won't smoke 1 bit ! Project outcomes depend on understanding and employing best practices, experience and measurement on the bench. Finding best practices proves difficult in a day and time when general scientific literacy, the number of expert mentors and interest in analog electronics are all waning.

Click for another photo of the filter. On my actual filter, I used high Q, air variable trimmer caps that only had a capacitance variation of 15 pF or so. I soldered in fixed capacitors to get close to the capacitance needed to tune each tank. If possible, I think its better use smaller value trimmer caps because they permit finer tuning. The air variable trimmer offers high Q plus you can see when the capacitor is fully meshed (maximum C). This signals that you need to add more fixed capacitance to that tank for peaking.

Conclusion

To repeat; our parts collection dictates our band-pass filter outcomes. Size 50 to 68 #6 material toroids will work fine for most HF frequencies above 3 MHz. Don't stress out too much if your insertion or return loss is a little higher than you wanted; in all likelihood your filter will work fine and you'll be glad you didn't just copy some else's design and rob yourself of the design experience.

I am hopeful, this web page will inspire a few builders to experiment with band-pass filters for their receivers and other applications. My sincere thanks to Wes, W7ZOI for his guidance with filter design.

QRP — Posdata for August 2012 — NE612 Mixer Band-pass Filters

I designed some band-pass filters for NE612 based front-ends with LadBuild and GPLA and show my 75 Meter band filter design figures below. I'm not a fan of employing an NE612 as a receiver mixer since it easily overloads and spews harmonics when mixing strong input signals. The 1K

'RF gain' pot found in many receivers, or the more conventional switchable attenuator pad prove essential when receiving 'booming' signals with a NE602/NE612 mixer in your front-end.

Still, for field-portable tranceivers/receivers, the NE612 mixer keeps the current and radio size down nicely.

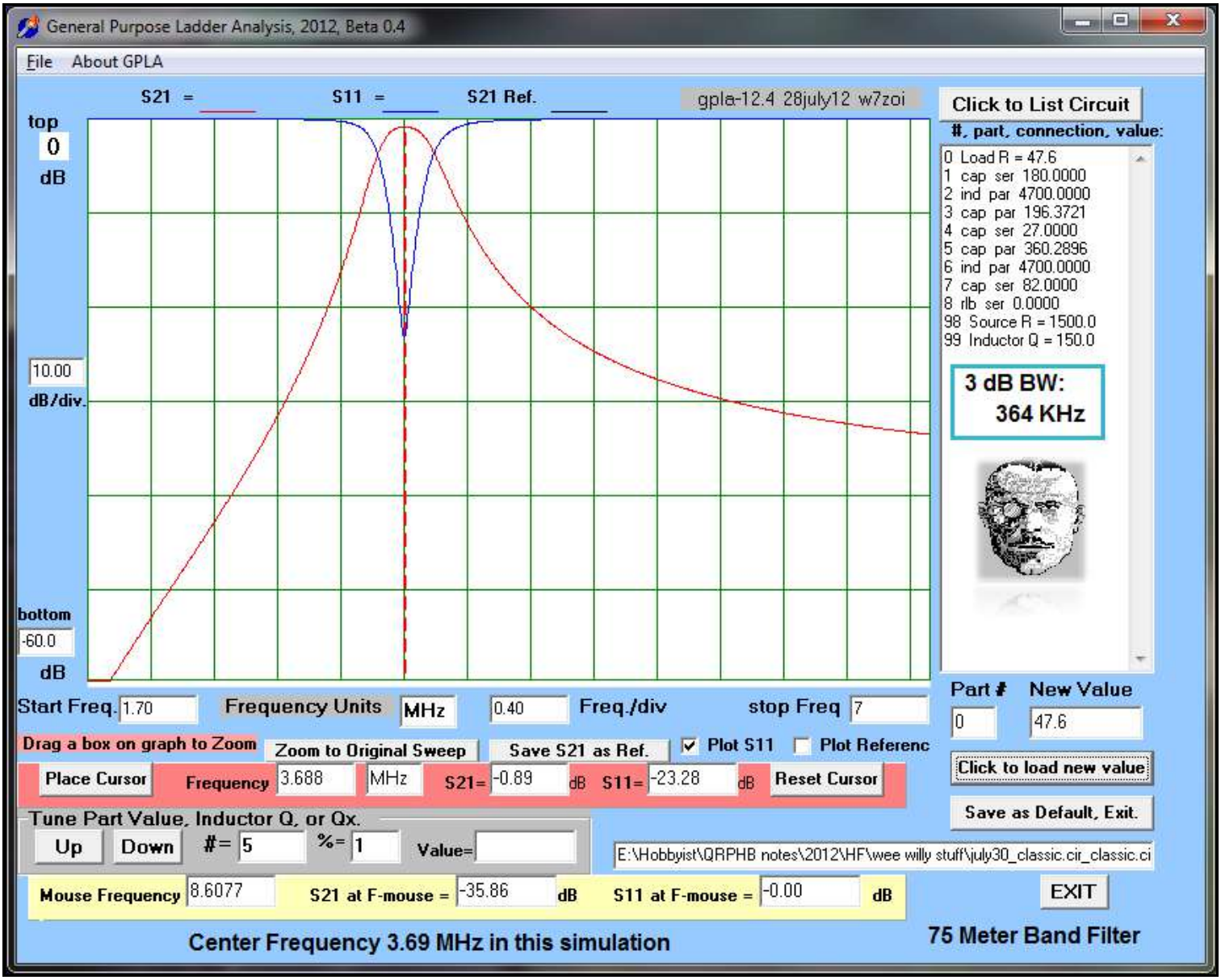

Above — My filter centered at 3.69 MHz. I set the 3 dB bandwidth higher than my usual 200-300 KHz so I could tune a good chunk of the 80-75M band without losing too much signal.

To establish some starting L and C values, I built a classic form filter in DTC08 with a 50 Ω input and output impedance centered at 3.69 MHz. After some tweaking, I settled on L = 4700 nH, Ce = 148 pF, coupling capacitor Cm = 27 pF and about 220 pF (Ct) to resonate each tank.

Next I changed the termination R's to 1500 Ω in DTC08 to simulate the right half of the filter matched into the 1K5 input impedance of an NE612. This gave me some Ct and Ce values to start with. I started Ladbuild 08 and built up a schematic.

In a seperate experiment, I determined that the resonator Qu of a 3.7 MHz L-C tank with an L of 4700 nH wound on a T50-2 core, was ~150.

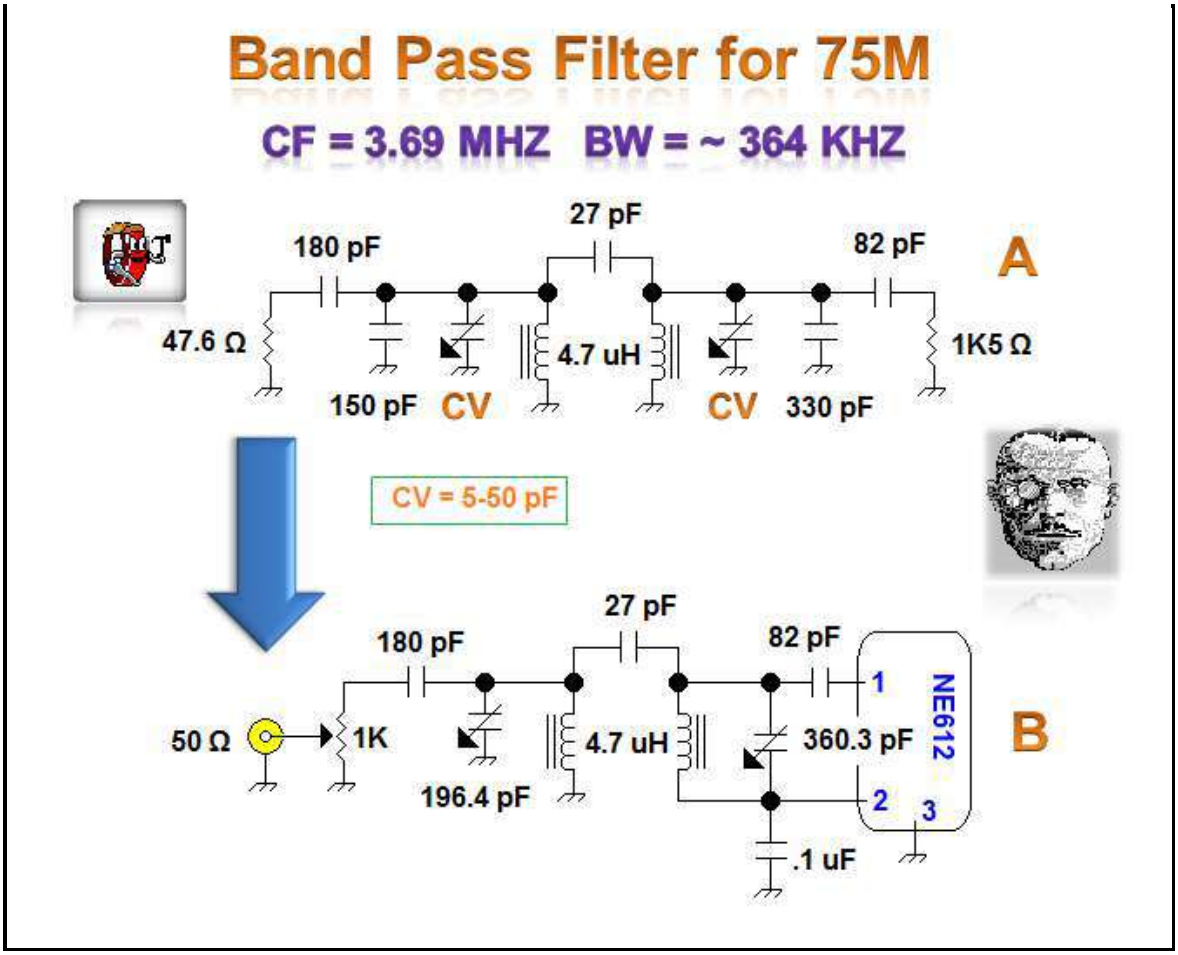

Above — The completed schematic. My filter exhibits an attenuation of ~70 dB at the top of the AM radio broadcast band (1500 KHz) providing I shield it in an RF-tight box. I took the 47.6 Ω input Z from the 1K pot and my 50 Ω antenna in parallel. An input Z of 50 Ω would work just as well in simulation and on-bench.

In Part A, I show a possible way to resonate each tank with 1 fixed C and a trimmer capacitor. In Part B, I omitted this detail and just show the calculated C needed for resonance as a variable capacitance.

To make this filter with GPLA, I tweaked the capacitor values to nearest standard value parts and tuned the filter with the GPLA Tune Part Value controls while looking at the waveform and my 3 dB bandwidth. I love tweaking values in GPLA and over the years have designed several hundred RF filters for readers.
The rubber hits the road on the bench however! You can get an E.E. degree without melting solder in this day and time — but only bench measurements tell the truth.

Please tune each tank carefully like I mentioned earlier... For example, say a tank needs 180 pF for resonance, *but you don't know this*. You solder in a 100 pF cap and a 5-50 pF *enclosed* ceramic trimmer capacitor into the L-C tank. While watching the 'scope this tank will "peak" since the tank will exhibit its highest peak-peak voltage when the trimmer cap is set to 50 pF and fall off as you decrease the C of the trimmer. You might think you peaked the tank, however you' re actually under by 30 pF!

While leaving the trimmer set to maximum C (peak-peak voltage) in this theoretical example, if you tack solder in another 10 pF cap your 'scope will show an even greater pk-pk voltage. , If you remove this 10 pF cap and then place in a 27 pF cap, the pk-pk voltage will go even higher since you're almost at the target 180 pF. If you removed the 27 pF cap and tack soldered in a 47 pF cap, the pk-pk voltage in the 'scope will go down since your now at 197 pF. Thus you know that resonance is somewhere between 177 and 197 pF.

Of course you could decrease the trimmer cap C and stil use the 47 pF cap, however, my description isn't a prescription to follow, just some things to think about. Sometimes I remove a trimmer cap and measure it to ensure the cap is not set to maximum C; that would tell me I need to add more fixed capacitor(s) to the tank. Air variable trimmer caps give visual indication since maximum C occurs with maximum mesh. Unfortunately they are rare and expensive.

On my bench I keep a pair of small 12 to 400 pF air variable caps and temporarily solder them into my tanks. After peaking, I remove and measure them — then I have a good idea of what capacitance is needed to resonate the tank at my test frequency.

It's all an experiment.

Click for another low loss, well matched example: CF = 5.17 MHz, 3 dB BW = 196 KHz. 50 ohm version. NE612 final version.

QRP — Posdata for August 2012 — More NE612 Receive Mixer Band-pass Filter Experiments

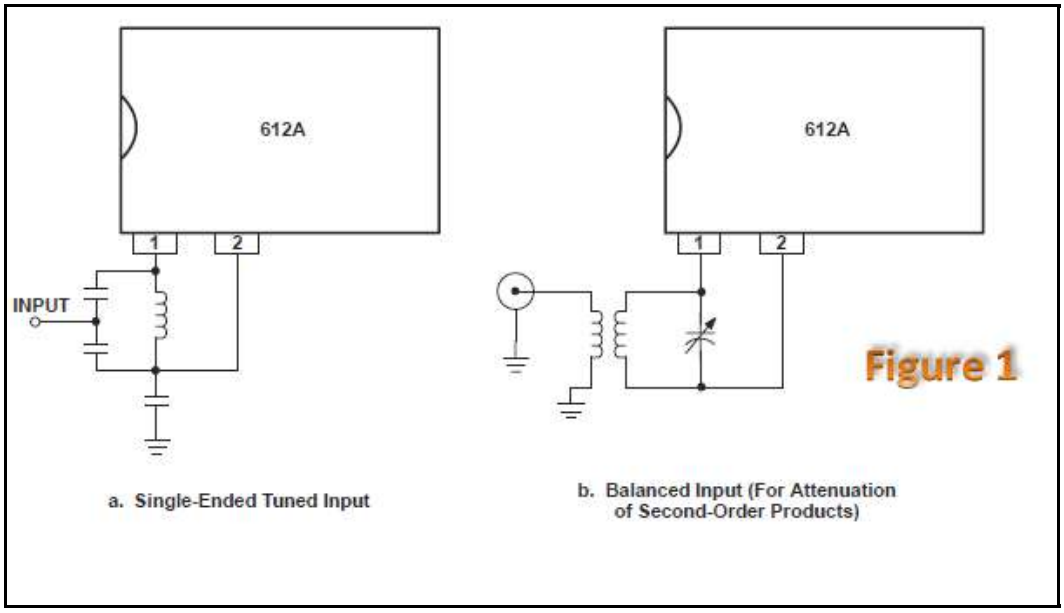

Above — NE612 input circuits. The NE612 datasheet specifies a 3 pF input capacitance + a 1K5 input resistance.

If you look around the Web, many builders just run a single tank for band-pass filtering. While okay for novelty-grade rigs, the poor filter stopband may unleash some ugly problems in the mixer and on down the receiver chain.

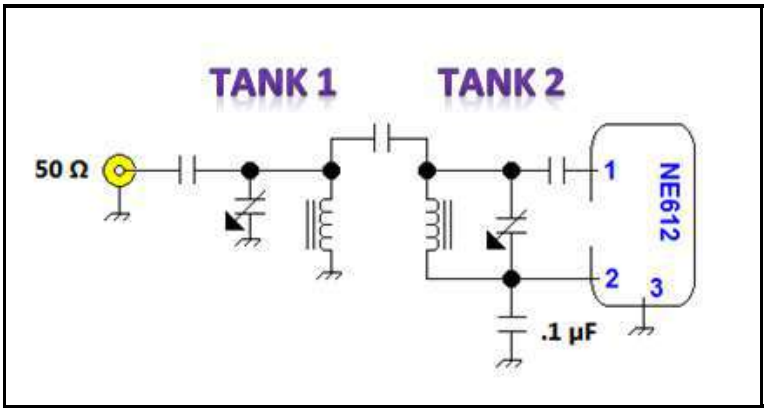

Above — A double tuned circuit with the L-C tanks named 1 and 2 and a series capacitor to match Tank 2 to the NE612.

Most builders match Tank 1 into its 50 Ω source with a capacitor divider, or a matching transformer. For Tank 2, some enthusiasts just connect the Tank 2 coil directly to pin 1 as shown in Figure 1a. Without the matching series capacitor, unfortunate side effects may arise...

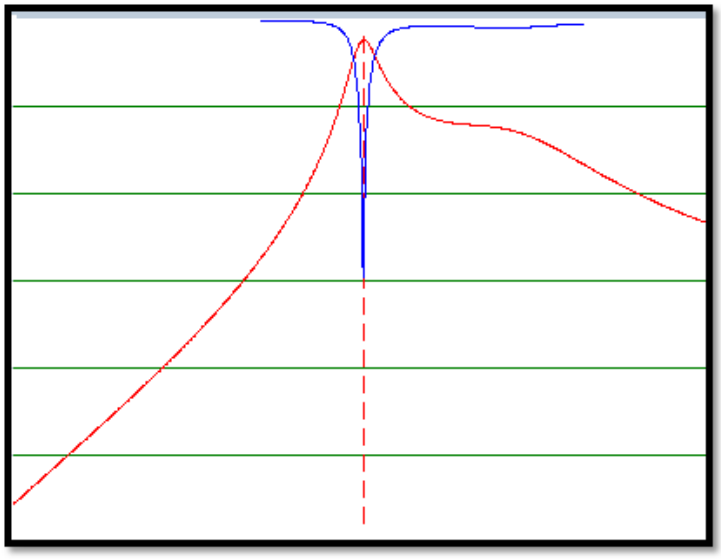

Above — The low-pass skirt of a double-tuned filter may attenuate higher frequencies poorly when no series capacitor (or other network)

matches Tank 2 to the NE612 input. I perfectly matched Tank 1 to its 50 Ω source just connected Tank 2 to a 1500 Ω resistive load in this simulation. I wonder how bad things get in the real world when a complex impedance is involved?

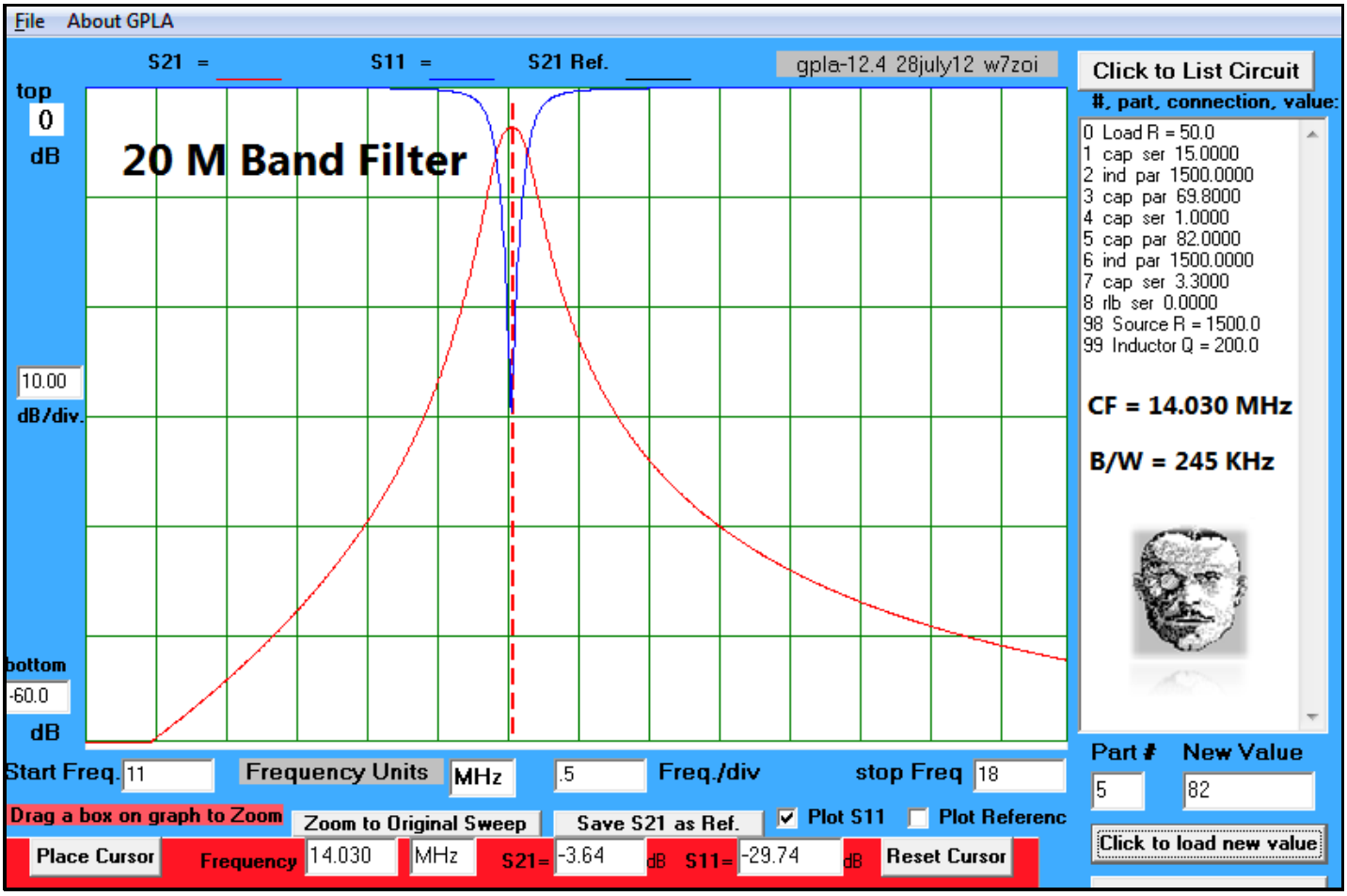

Above — I designed a filter for a 20 Meter band CW receiver centered at 14.030 MHz with DTC and GPLA. The design 3 dB bandwidth = 245 KHz. NE612 filter design was discussed in QRP — Posdata 1.

I then breadboarded the filter with T68-6 inductors, but common lower Qu ceramic trimmer capacitors.

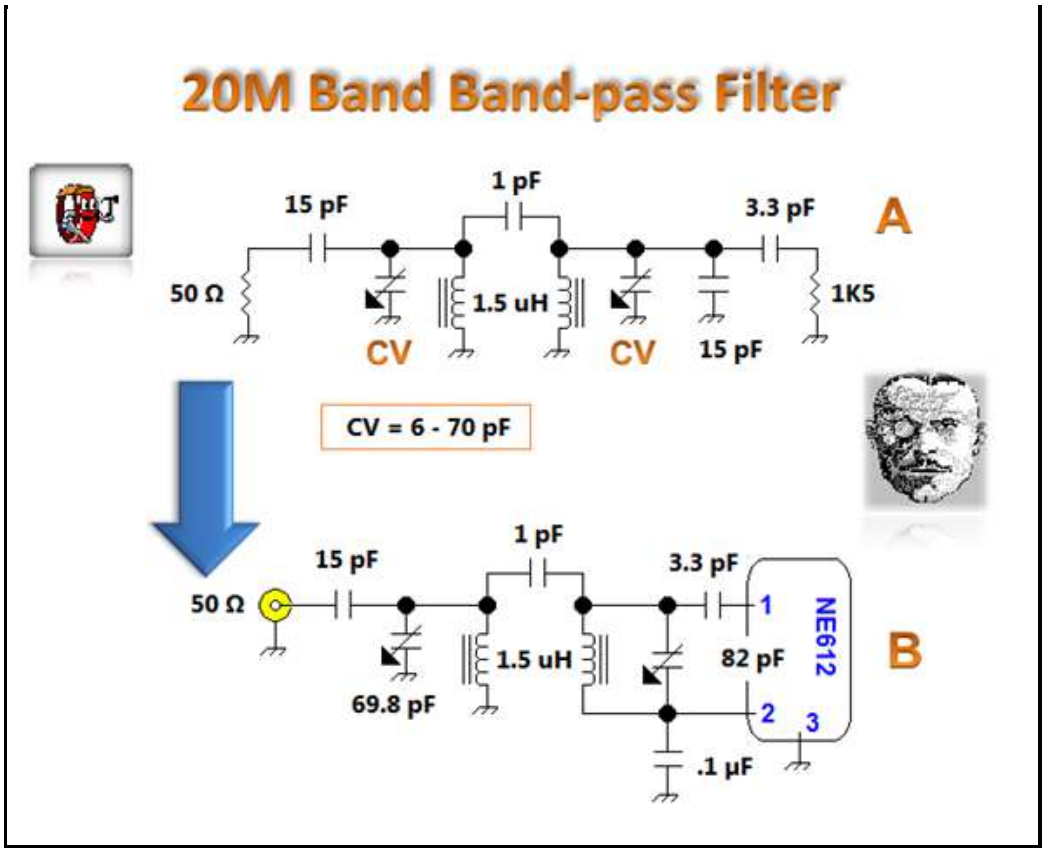

Above — The DTC/GPLA filter design with Tank 2 evolved to provide single-ended input for the NE612.

I wanted to test 2 questions:

1. Does the 0.1 µF coupling cap connected to the cold end of Tank 2 and Pin 2 change the bandwidth or filter skirt shape?
2. Will the 3.3 pF cap really match the NE612?

I expect that worldwide, the NE612 input impedance may vary slightly from part to part; different breadboards will exhibit different reactances and that although the datasheet specifies 1500 Ω , we may be dealing with a complex impedance that varies with the aforementioned factors plus perhaps, input frequency. I simply want a good filter with clean skirts.

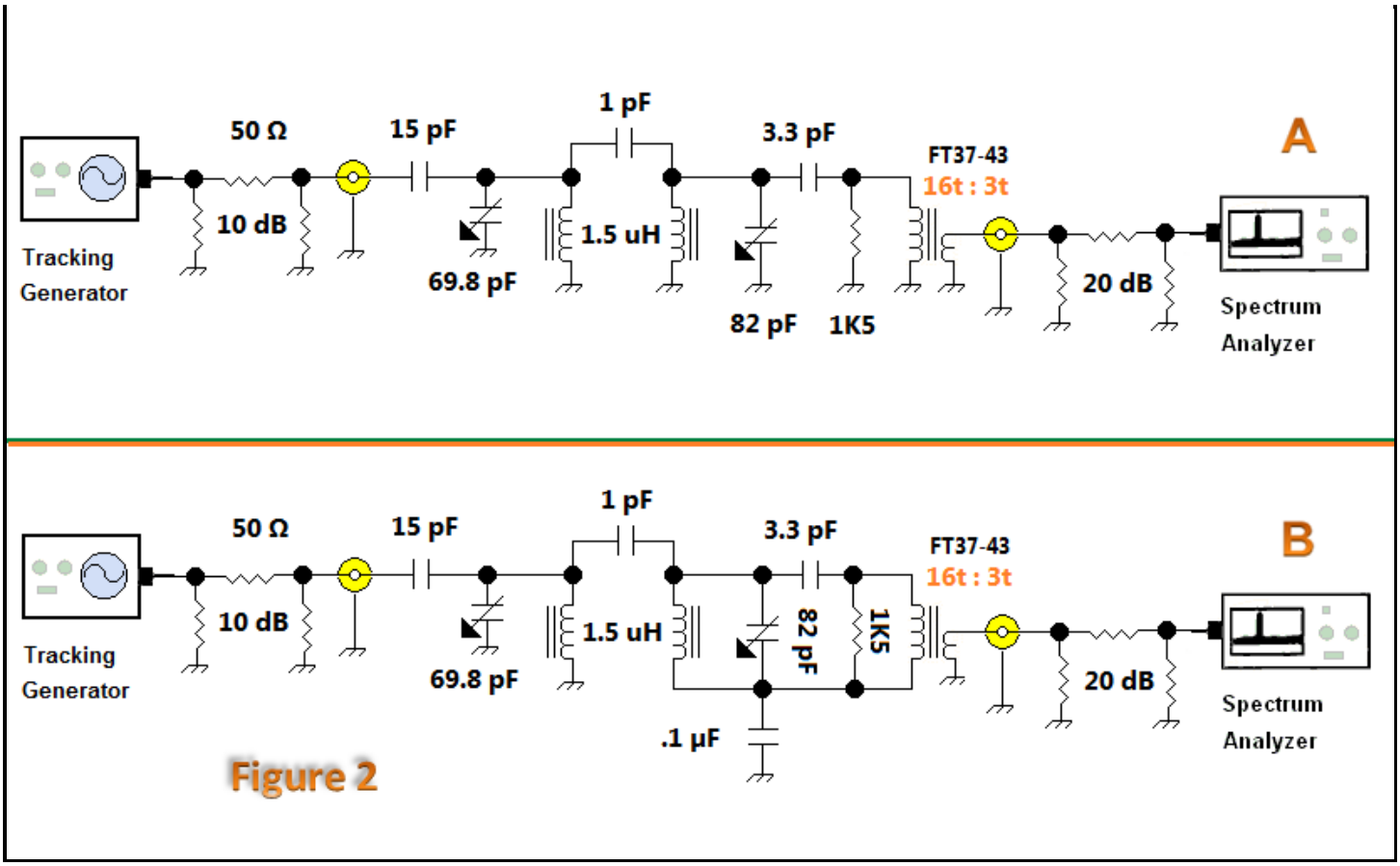

Above — Experiment #1. I compared spectrum analysis of circuit A with B. I built and measured A and then cut away some copper to isolate the copper board grounding the Tank B parts. This "island" was AC coupled to the rest of the ground plane with a short leaded 0.1 µF ceramic capacitor.

I saw no significant difference between Circuit A and B — it appears the 0.1 µF capacitor does not affect the filter parameters to any extent.

To simulate a NE612, I soldered a 1K5 Ω 5% resistor across Tank 2. Tank 2 was transformer coupled to the 50 Ω Z required for spectrum analysis. A 20 dB pad ensured a strong return loss and a safe input amplitude for the SA.

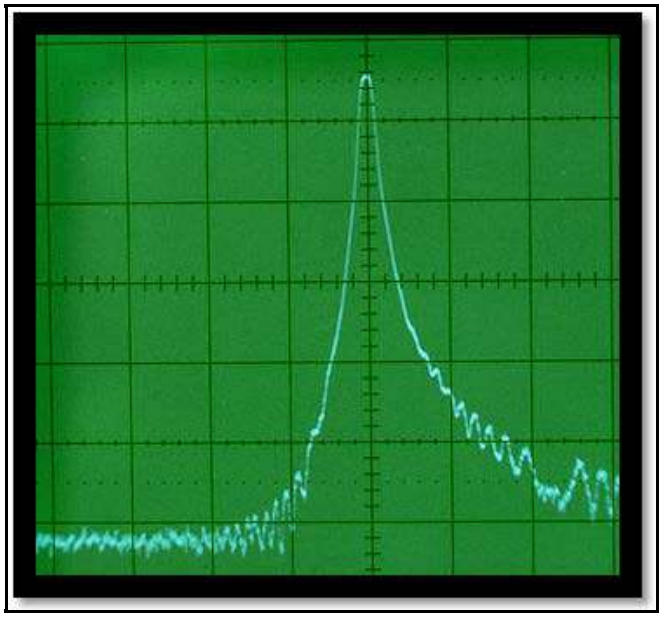

Above — Spectrum analysis of Figure 2A or B. I saw flat topping of the waveform – almost double humping with a higher than wanted 3 dB bandwidth; this bothered me. Fixing this problem was Experiment #2.

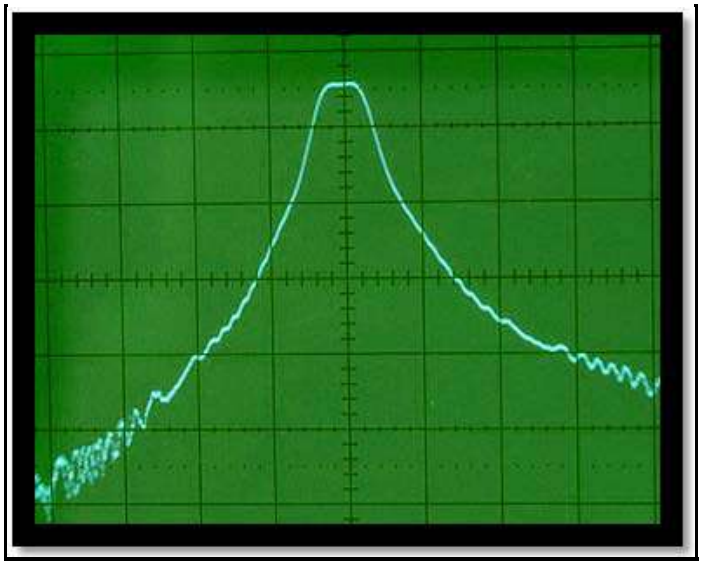

Above — A zoom of the poor coupling of Figure 2A or B. From my experience building filters, I suspected a termination resistance mismatch in Tank 2 ; exactly what I was trying to avoid!

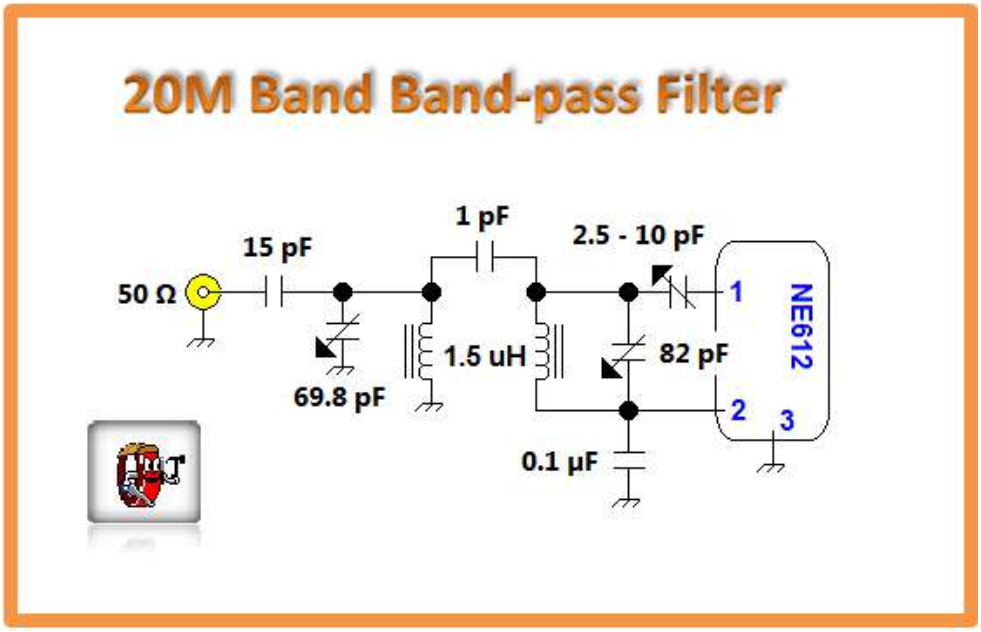

Above — I swapped a trimmer capacitor for the series 3.3 pF fixed cap in Tank 2. Then I reconnected the circuit into my test set up.

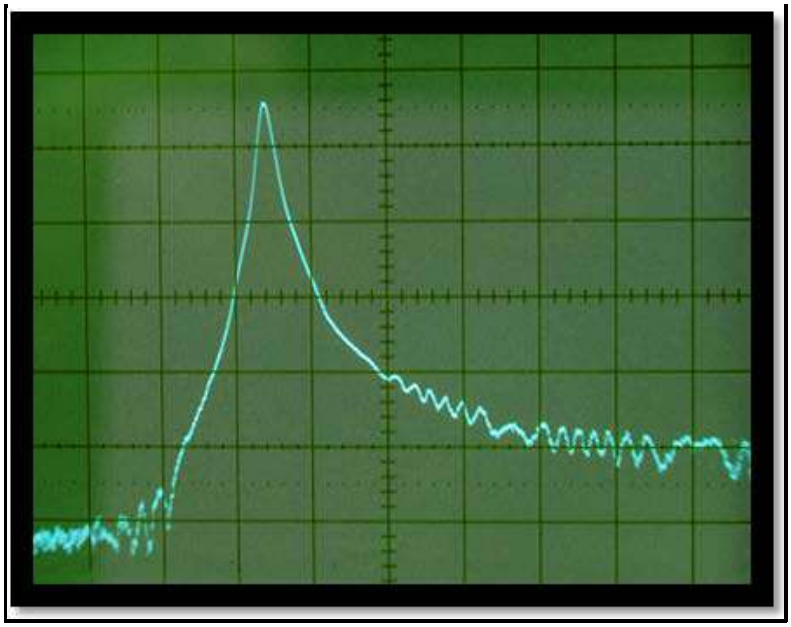

Above — A photo of my TG + SA measurement after tweaking the newly added trimmer capacitor and peaking each tank. I shifted the SA screen center over so the tracing could be seen without all the hash marks in the center. Wonderful.

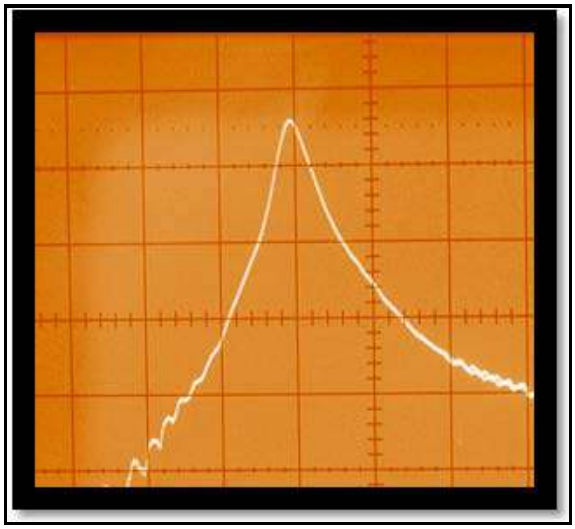

Above — A zoom of the now matched Tank 2. Due to the bench-altered Tank 2 match, my low-Q variable capacitors and other factors, the 3 dB bandwidth now is just over 300 KHz.

I'm not sure if these experiments reflect what actually happens with a NE612 input band-pass filter, however, I plan to match my second tank with a series trimmer capacitor in future NE602/NE612 work. I also want to explore balanced input.

RF — Test and Measurement

RF Workbench Page 4

The 4th installment of a QRP/SWL HomeBuilder series exploring *basic* RF measurement

Part 4 describes a method to calculate reverse isolation in the **50 Ω environment** after converting measured peak-to-peak AC voltages to dBm. I tested 2 common amps at ~7 MHz to show the concepts and calculations.

In this series, I gratefully borrow from the work of Wes, W7ZOI per correspondence, direct contributions and from EMRFD.

Tools Needed

1. 50 Ω terminated scope (or a spectrum analyzer) and a 50 Ω signal generator
2. 50 Ω RF cables with RF connectors (such as short cables with female BNC connectors)
3. 6 dB 50 Ω attenuator pad; plus an adjustable attenuator if you use a fixed output signal generator.
4. BNC through-response connector(s)

Procedure

1. Measure the amplifier forward power gain. This is S21.
2. Measure amplifier reverse power gain. This is S12. Like S11, express S12 as a negative value.
3. Reverse isolation using dB values = S21 - S12.

Step 1 : Measure the forward power gain

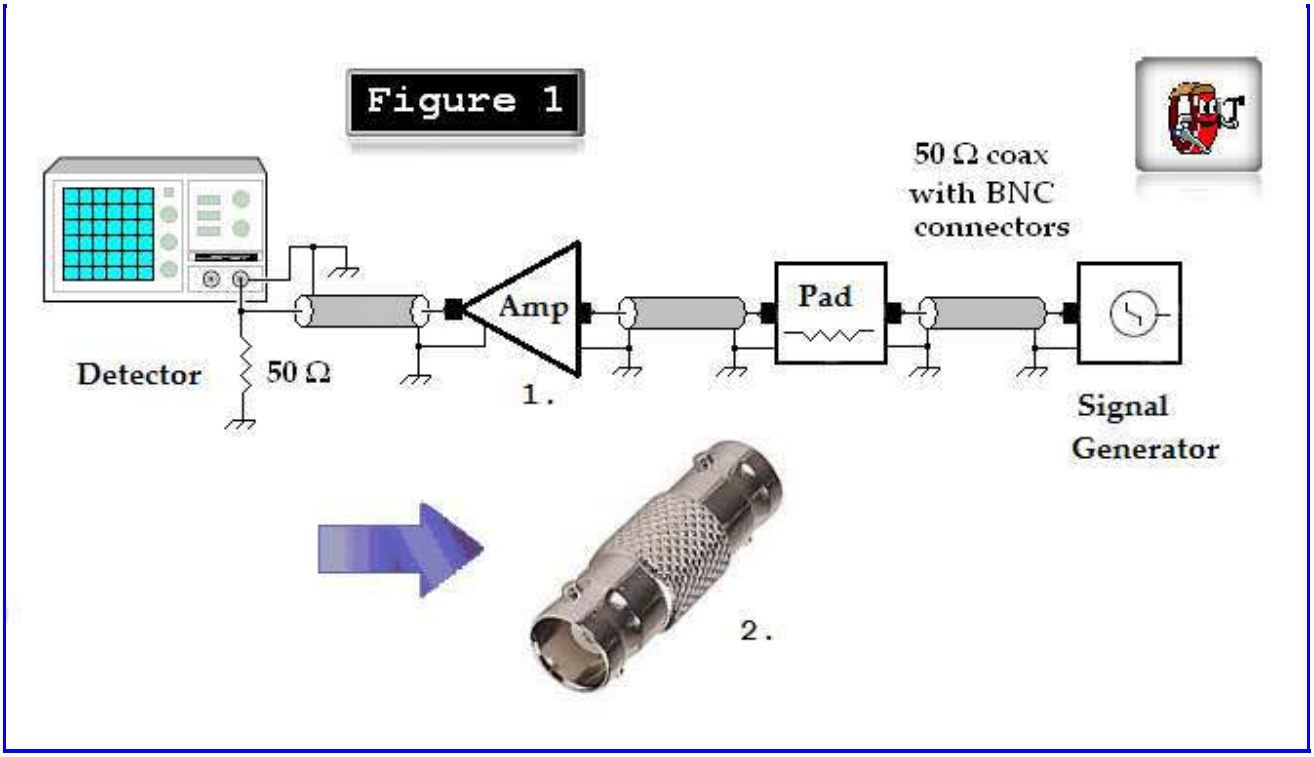

Figure 1 shows how to measure forward gain in a 50 Ω environment — **1**. Convert the measured AC voltage to dBm, **2**. Disconnect the amplifier, insert a through-response connector and convert this measured AC voltage to dBm. The difference between the 2 values = S21. Applet H will do these calculations from the peak-peak voltages. *The attenuation pad following the signal generator in Figures 1 and 2 signify that the signal generators have a 50 ohm output impedance and is optional.*

Choose a signal generator level that ensures the output of your amplifier is linear while providing a good signal to noise ratio for measurement. With an oscilloscope, I generally test amplifiers with an input power of between 0 and -11 dBm; although choose whatever level that works for you consistent with linear amplification.

After measuring the forward gain of your amp, a good way to test for linearity is to add a fixed 6 dB pad between your signal generator and your amplifier to drop the applied signal by half. *[A 6dB pad drops the peak-peak voltage by 1/2 . A 3 dB pad drops the power in dBm by 1/2]*. The power gain should be equal or nearly equal to the measured dB value obtained before you added the 6 dB pad. If they vary significantly, you are likely driving the amp too hard and causing some non-linear output products. S21 = complex *linear* gain.

Step 2 : Measure the reverse power gain

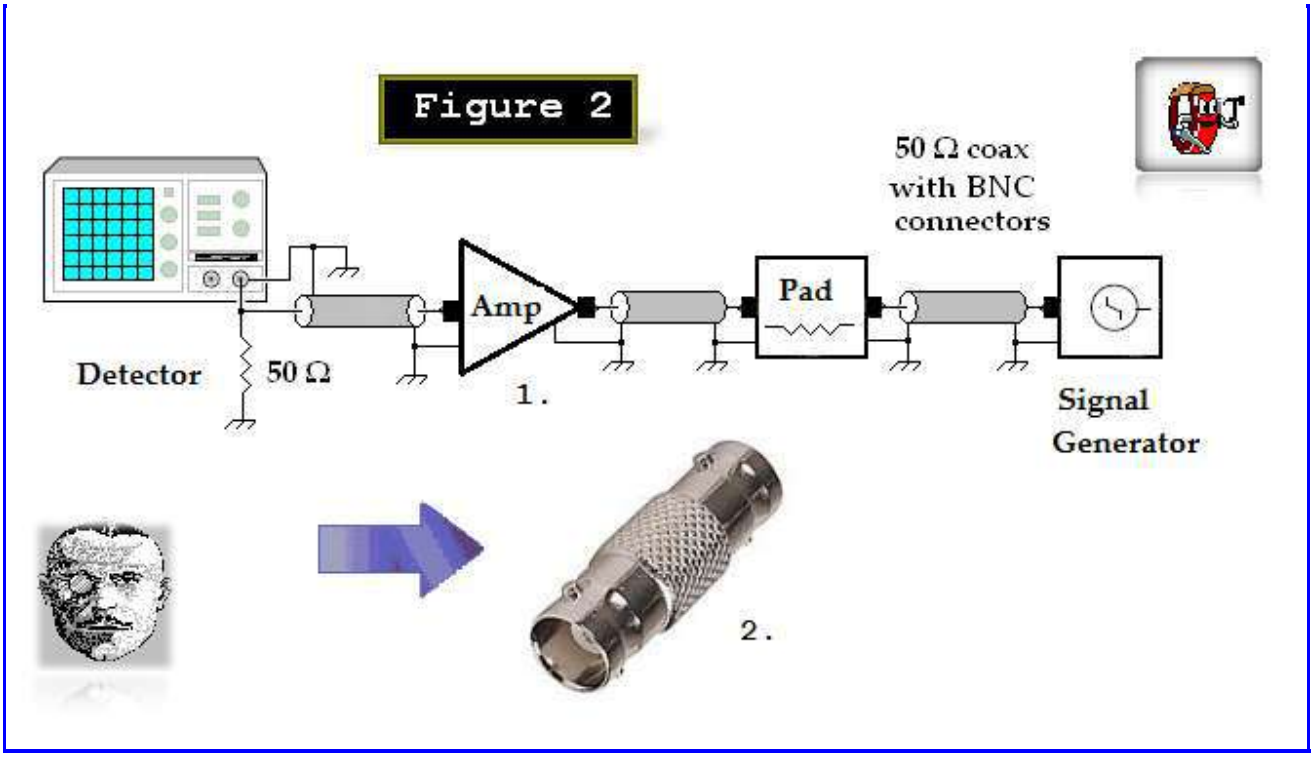

Figure 2 shows how to measure reverse gain in a 50 Ω environment — **1**. Convert the measured AC voltage to dBm, **2**. Disconnect the amplifier, insert a through-response connector and convert this measured AC voltage to dBm. The difference = S12. Ensure that you employ the same drive level used to measure the forward gain.

Measuring reverse gain may be tough. When the amplifier under test requires a low drive level and/or has strong reverse isolation, you may not have enough signal to accurately measure with your oscilloscope. The tool of choice for low reverse voltage measurment is a spectrum analyzer (SA) — a narrow band SA may be required to distinguish the weak signal from random noise with low signal voltages.

Summary

A **practical** bench work flow goes something like:

1. Measure the through-response peak-peak voltage.
2. Measure and record the peak-peak AC voltage while driving the amplifier input port (forward gain set-up).
3. Reverse the amp so you're driving the output port and then measure the peak-peak AC voltage (reverse gain set-up).
4. Calculate S21 and S12.
5. Calculate reverse isolation.

Example 1: Feedback amplifier

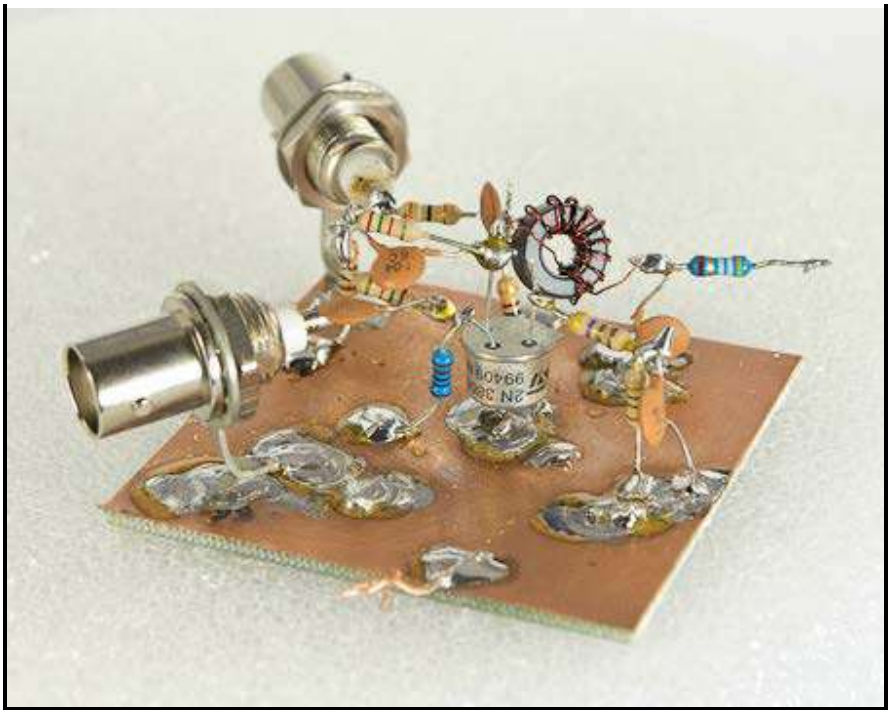

In the first example, I measure the reverse isolation of a Beaverton Special feedback amp. The schematic is shown below. Tested with a 7.039 MHz signal generator possessing a return loss of 30 dB.

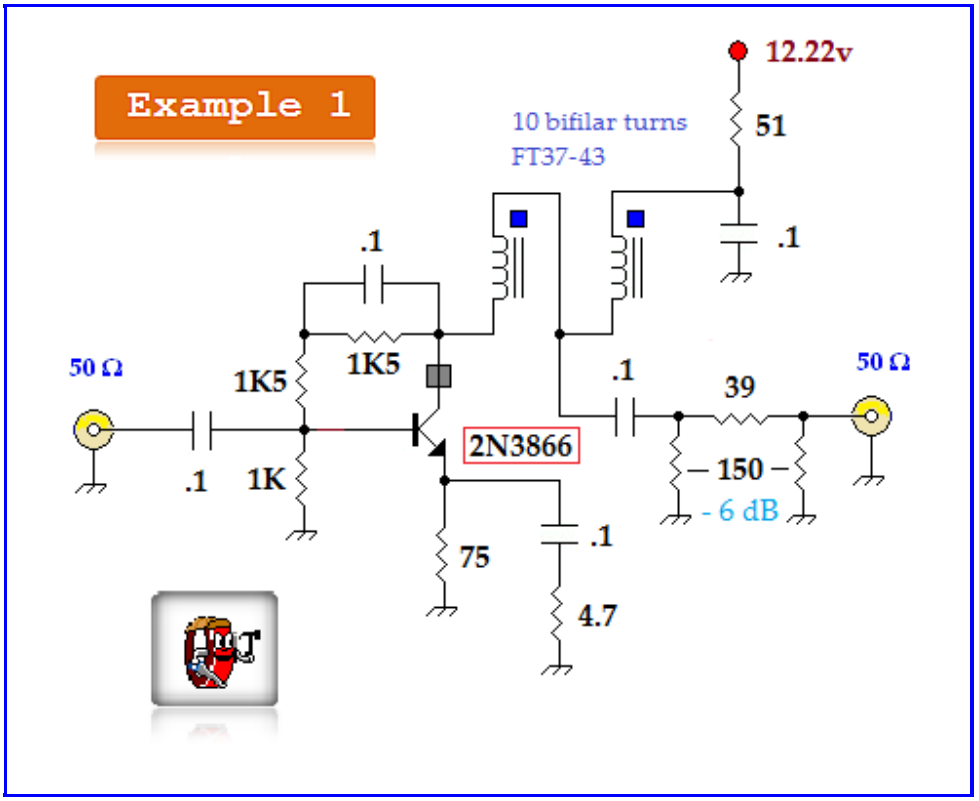

50 ohm Voltage Measurements:

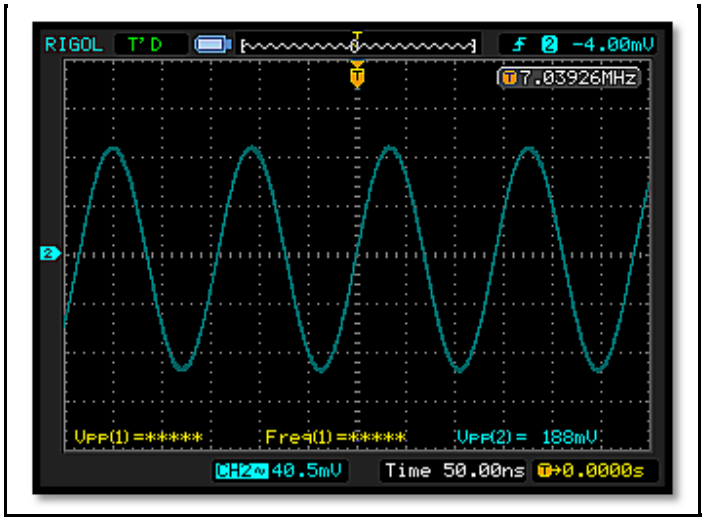

Above — AC voltage with a through-response connector in-situ: 188 mV pk-pk

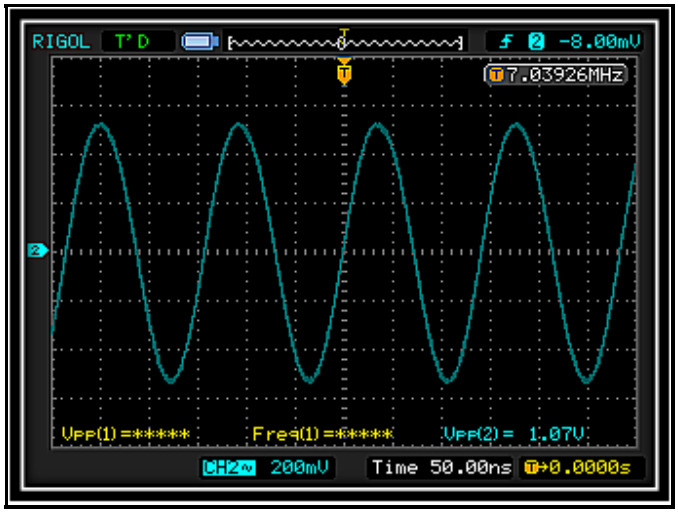

Above — AC voltage with forward gain set-up: 1.07 V pk-pk

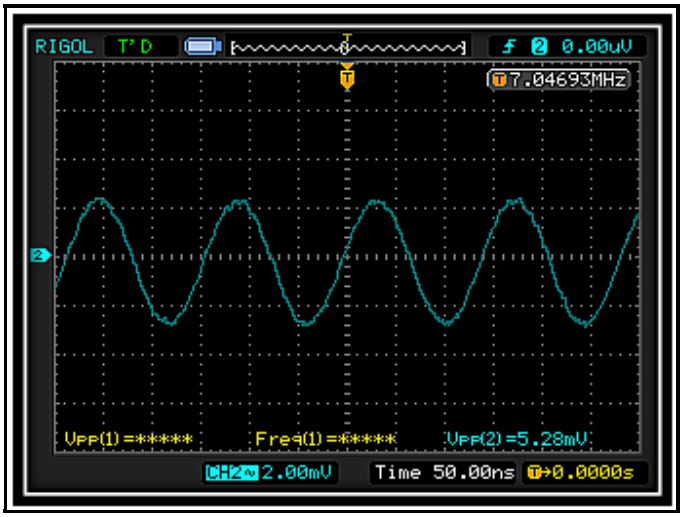

Above — AC voltage with reverse gain set-up: 5.28 mV pk-pk.

S21 = 15.1 dB. S12 = -31 dB. I tested my driven amp's linearity by adding a scrap, standard value 6 dB pad in between the signal generator and the amplifier — the S21 was 15.2 dB with the pad and 15.1 dB without the added 6 dB pad. It's linear.

Reverse Isolation Calculation

R.I. = S21 - S12
R.I. = 15.1 dB - -31.03 dB
R.I. = 46.13 dB

Example 2: Common Base Amplifier

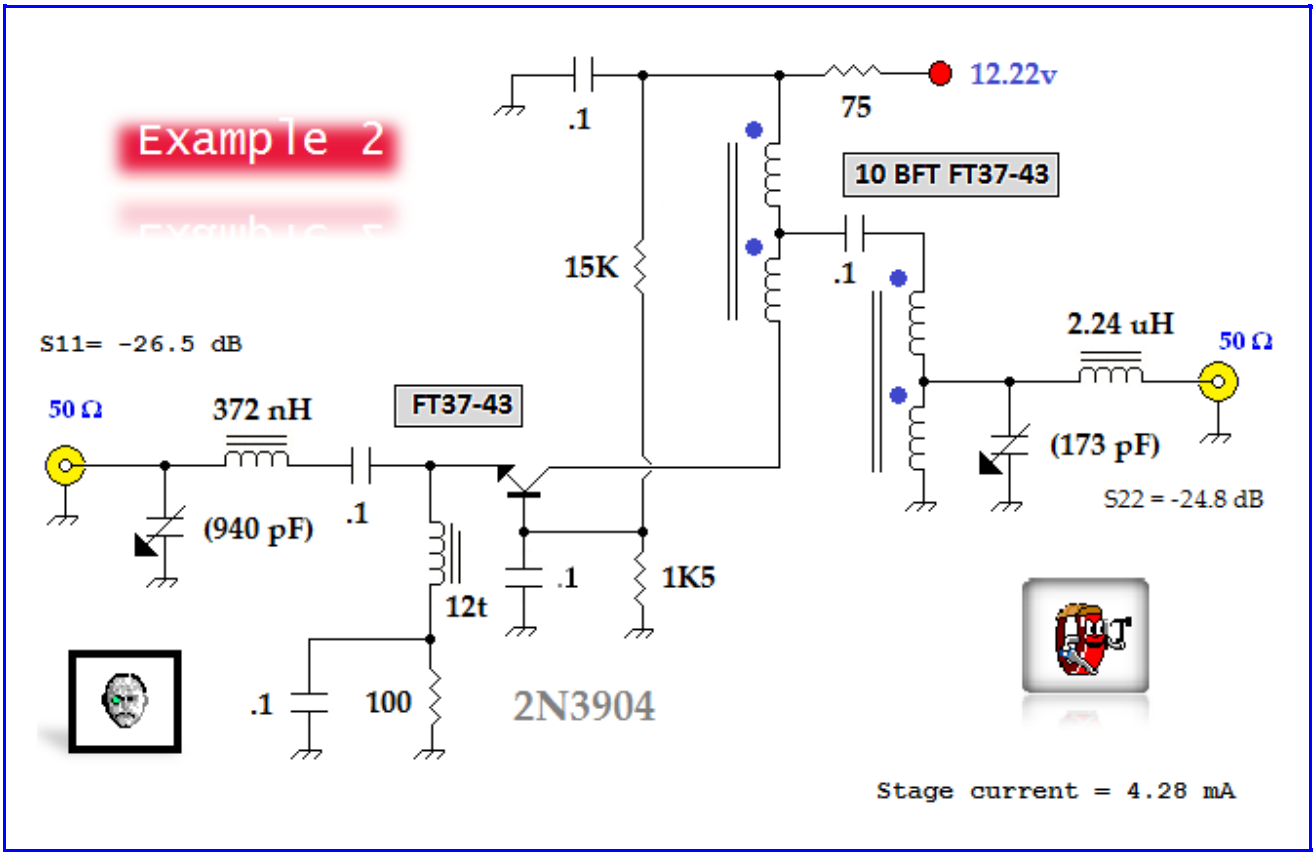

Above — A common base amp employing L- networks for a strong return loss in and out at 7.039 MHz. S11 and S22 = the negative of return loss.

Through connector voltage = 192 mV peak-peak.

S21 = (1.88 volts peak-peak AC voltage) = 19.82 dB.

S12 = (1.68 mV peak-peak AC voltage) = -41.16 dB.

Reverse isolation at 7.039 MHz = (S21 - S12) = 61.42 dB

I confirmed the linearity of my S21 using the aforementioned 6 dB attenuator pad — I couldn't increase my signal generator output level above the indicated -10.35 dBm, since gain compression emerged in the common base amplifier (reduced AC voltage was measured).

My reverse AC voltage was under 2 mV; about the threshold where my oscilloscope waveform becomes rather ugly and sits in the noise. Clearly, the limitations of measuring reverse isolation with an oscilloscope must be factored. Still, you got to love 60 dB + of reverse isolation in a popcorn circuit.

1 local professional EE told me if you can measure it with a 'scope, you don't have spectacular reverse isolation - no doubt, a spectrum analyzer

pumps up the measurement quality in circuits with high reverse isolation, but more amateur designers have 'scopes than spectrum analyzers, so just do your best.

Involving Scattering Parameters as possible on your workbench can only lead to circuit improvement. You can't better your outcomes if you can't or don't measure them — applying and more importantly, understanding test equipment is just 1 component of our hobby. A hobby unto itself; test equipment activity complements amateur radio design. I have met test equipment focused builders who make radio gear just as an excuse to apply their test gear!

Improved bench practices are the corollary of striving to learn more about measurement techniques and increasing our collection of measurement devices.

QRP — Posdata 1: Hycas Amplifier

I love the hybrid cascode (hycas) as a general purpose RF amplifier. What's not to love about a using a common source FET followed by a common base bipolar amp? I attempted to measure the reverse isolation of a version just using an oscilloscope.

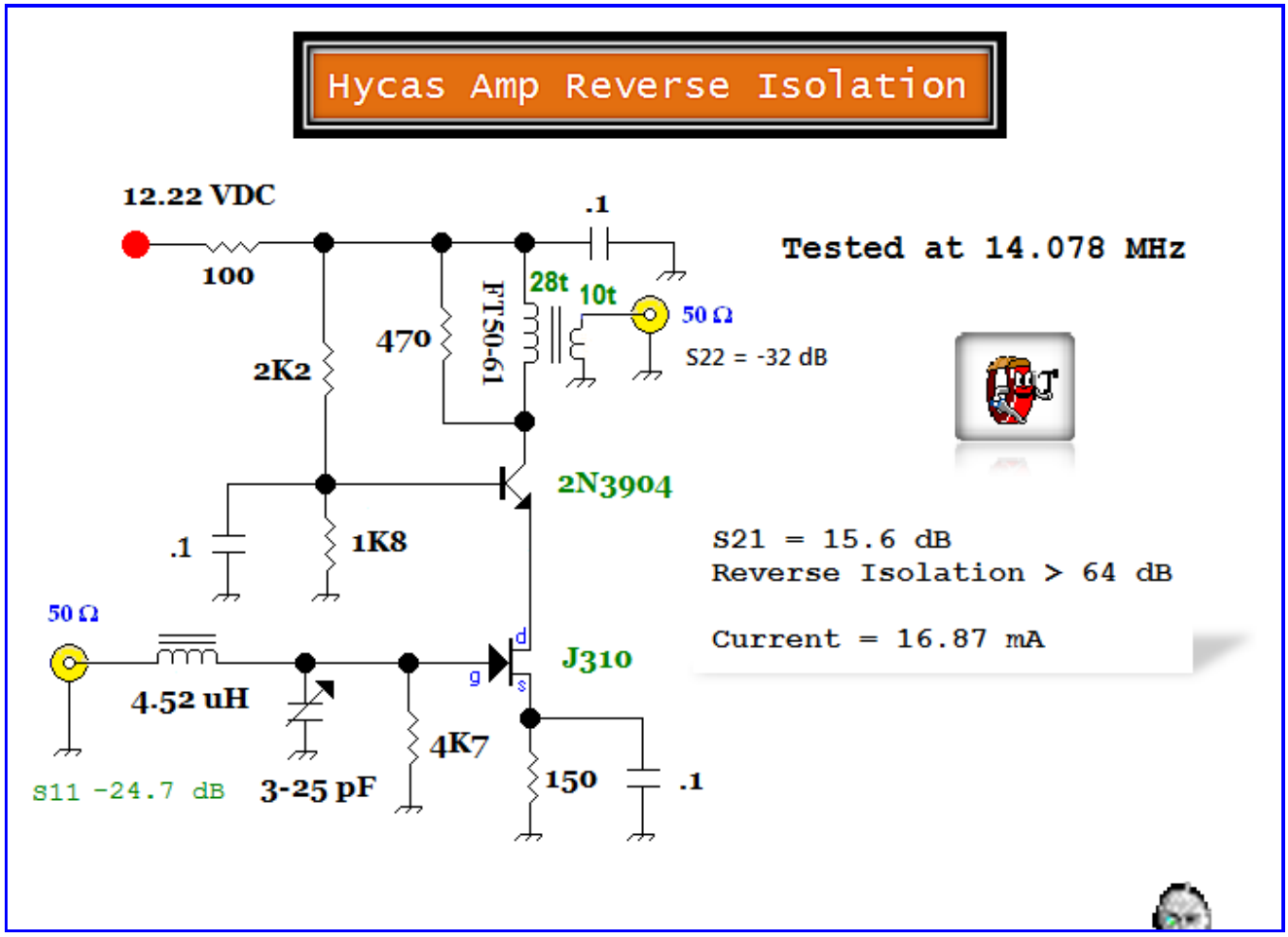

Above — A hycas amp set up for high return loss on both ends at 14.078 MHz. Too much current may cause gain compression and harmonic distortion, so please test your hycas amps for both. I tested using a signal generator with a 30 dB return loss driving a 50 Ω terminated oscilloscope. Since the hycas amp contain a high impedance input JFET and a common base amp, the reverse isolation should be reasonably high, or at least as good as a common base amplifier.

My testing failed — The reverse isolation was too high to measure with an oscilloscope. Using proper bench techniques (linear amplification + honest scope reporting), I determined the highest reverse isolation I could measure = 64 dB. In fact, injecting a whopping signal of 1.08 volts peak-peak into the hycas output port only gave an S12 of 1.84 mV — whoa!

The problem is such a strong signal (1.08 volts peak-peak) at the input port results in severe limiting and distortion; so valid reverse isolation measurement isn't possible. Even a 350 mV peak-peak signal may give some gain compression during S21 measurement depending on your matching. Thus, I can only accurately say that the reverse isolation of my hycas amp is greater than 64 dB.

Strong reverse isolation is 1 reason I favor hycas amps as VFO buffers. They make pretty good I.F. amps also.

The hycas IF amp system by Wes, W7ZOI and Jeff, WA7MLH offers amazing performance and features an excellent JFET bias scheme. I built 1 in 2008 — amazing design.

QRP — Posdata 2: Doesn't S12 = Reverse Isolation?

Many web sites, books and people report that reverse isolation = S12, yet above, I depart from this argument. In truth, I think reverse isolation equals S12, but reverse isolation may also equal S21 - S12.

I'll let you decide what to do, but explain why I enjoy the latter.

S12 is a negative value.

I prefer to turn that negative value into a positive 1 — RF Workbench 4 concerns measuring and applying amplifiers with the goal of high reverse isolation and not just measuring S12.

The main purpose to quantify amplifer reverse isolation is to strive to *improve reverse isolation* and an amplifier is but 1 component in our 50 Ω block. I believe in a creative, systems approach; open minded and positive (pun intended).

The whole RF Workbench series attempts to present 50 Ω bench measurements in a vibrant way devoid of excessive + boring engineer-style content that could blank the eyes of the budding Hams/SWLs designers that visit my site. I imagine this web site bores more advanced RF designers *to tears*.

Our goal is to obtain high reverse isolation while applying a 50 Ω systems approach.

Break away from strict + "stodgy" math-driven methods to fuel creative thought and experimentation.

I posit that an appropriate figure of merit in a well designed isolation amplifier is the difference between S21 and S12; and therefore, the term reverse isolation can be more than just S12.

Ham/SWL component-level experimentation by commoners like me is ~~slowly~~ dying and being replaced by a new generation of skilled, code writing experimenters. Although, some builders just copy other people's code and then apply it to kitted hardware. Reverse isolation impacts both our analog and digital designs.

Please consider this example:

I'm switching a level 7 diode ring mixer with 12 MHz and per normal, create lots of internal harmonic energy. With my spectrum analyzer connected to the mixer RF port I measure my 12 MHz LO signal at 50 dB below a +7 dBm signal, or -43 dBm. That's a 50 over S9 signal — very high amplitude in context!

I require strong LO isolation in my circuit and thus stick in a 50 Ω input/output amplifier. I measure this amp: S21 = 15 dB and S12 = -31 dB.

So, the signal at the amplifier input is -43 dBm plus -31 dB = -74 dBm. But, alas, -74 dBm isn't good enough me — I want to use that amplifier to elicit greater isolation. However, I don't want any gain in my system, so I insert a 15 dB attenuator pad after the amplifier. For this pad, both S12 and S21 = -15 dB. For my amp, the net cascade is S21 = 0 and S12 = -46 dB.
Since S21 = 0, the block has 0 impact on the signal amplitude applied to the mixer, but the signal at the input of my isolation amplifier is -43 dBm plus - 46 dB, or -89 dBm. This isolation I like — it also illustrates a systems approach that gets you thinking about measurement in your own 50 Ω blocks.

The figure of merit for making a good isolation amplifier is now the difference between S21 and S12. If you want, go ahead and just use S12 for reverse isolation, but you'll probably measure S21 plus S12 anyway and that's what this web page is about! Onward.

QRP — Posdata 3

Comments From the Workbench

I'm no amateur electonics expert — I'd like to be one, but this is a tough field; RF and AF *design* is quite scientific, under-resourced and a bit overwhelming. How do we experimenters advance and stay motivated? Reading works by professionals like Chris Trask, N7ZWY, Bob Larkin, W7PUA, Doug Self, Rod Elliott and others may highlight our lack of knowledge and scientific methodology — a realization which can distress and demotivate us lay-designers. To a degree, this is irrational thinking; personal growth is always about hard work, problem solving and overcoming barriers.

Unlike the white belted Karate student, who studies and practices under the guidance of a master to attain black belt skill level, most amateur designers, excluding electrical engineering students, can't access good teachers. As a lay-person, with few face-to-face mentors (nobody in

Canada), I try to learn by experimenting and incorporating whatever knowledge, advice or schematics I can find. Fortunately, some Electrical Engineers give me advice by email and in turn I'm able to share this information via experiments on QRP / SWL HomeBuilder.

Our dusty, analog hobby fades palpably — the number of analog electronics gurus dwindles each decade and modern electronics embraces miniature circuitry often involving digital ICs controlled by lines of code.

Current electronics hobbyist magazines rightfully focus on topics that are contemporary or important to their advertisers; for example, promoting mixed-signal ICs, DSP, microcontrollers and the kits they describe and then sell for income. Nuts and Volts is 1 example. Both analog RF and AF design increasingly lies in the hands of a small group of specialists, enthusiasts and students.

Yet, we *persevere*. Sharing our knowledge, circuits, experiences and references on the Internet helps sustain our small global community. That's the site purpose— sharing the (warts and all) experiments + basic information of a lay-person.

The Emitter Choke in Common Base RF Amps

This web page covers reverse isolation — a really important topic. 2 principle amplifiers we employ for strong reverse isolation are the common base BJT and common gate JFET alone or in cascode with other amplifier topologies.

Some comments regarding using a radio frequency choke in the common base amplifier follow.

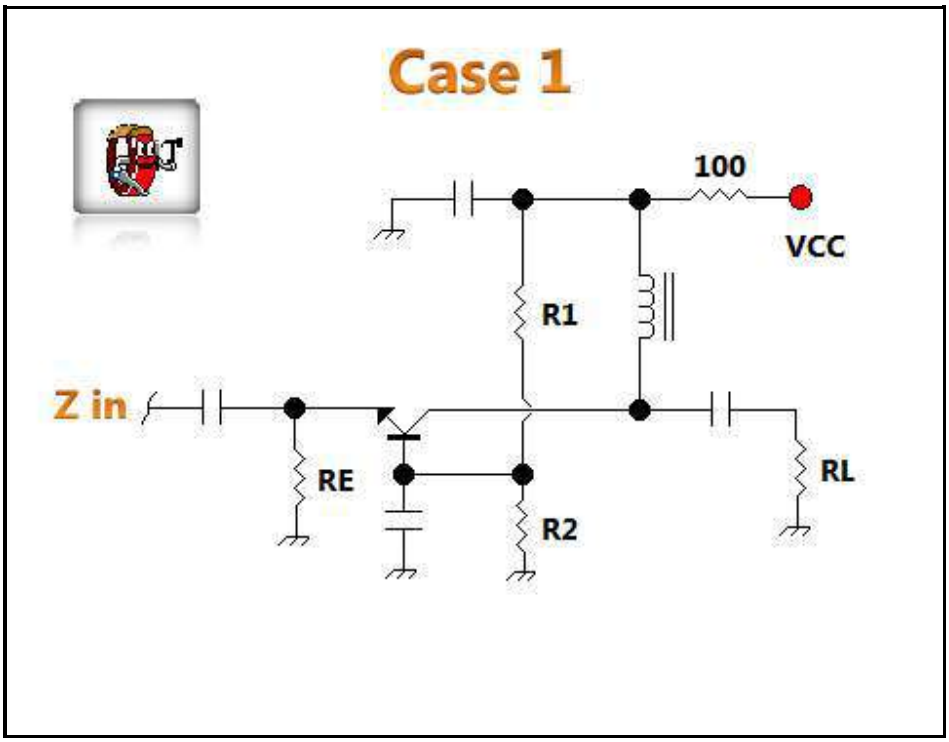

Above — Case 1: Emitter resistor only.

Apart from providing DC bias along with R1 and R2, emitter resistor RE plays another important role. Despending on its value, a portion of the input AC signal may pass through RE to ground instead of going through the transistor — degrading signal amplitude and noise figure. To minimize this, the resistor value should be many times (~10X or more) than the input impedance of the amplifier.

Although we might bias a common base amp to give an input Z of 50 Ω, often we'll choose a much lower input Z to get higher voltage gain. Input Z = 26 / Ie where Ie = mA; so if you bias for 5 mA, you are looking at an input Z of ~5 Ohms. In that case, a low value bias resistor such as 100 Ω won't shunt much of the input signal to ground, nor will it likely contribute much noise.

For most common base RF amps, a correctly chosen emitter resistor is all that's needed to decouple the AC signal and using an emitter choke proves hard to justify. However, it's important to understand how to apply an emitter choke since the basic principle also extends to the common gate JFET amplifer and other circuits.

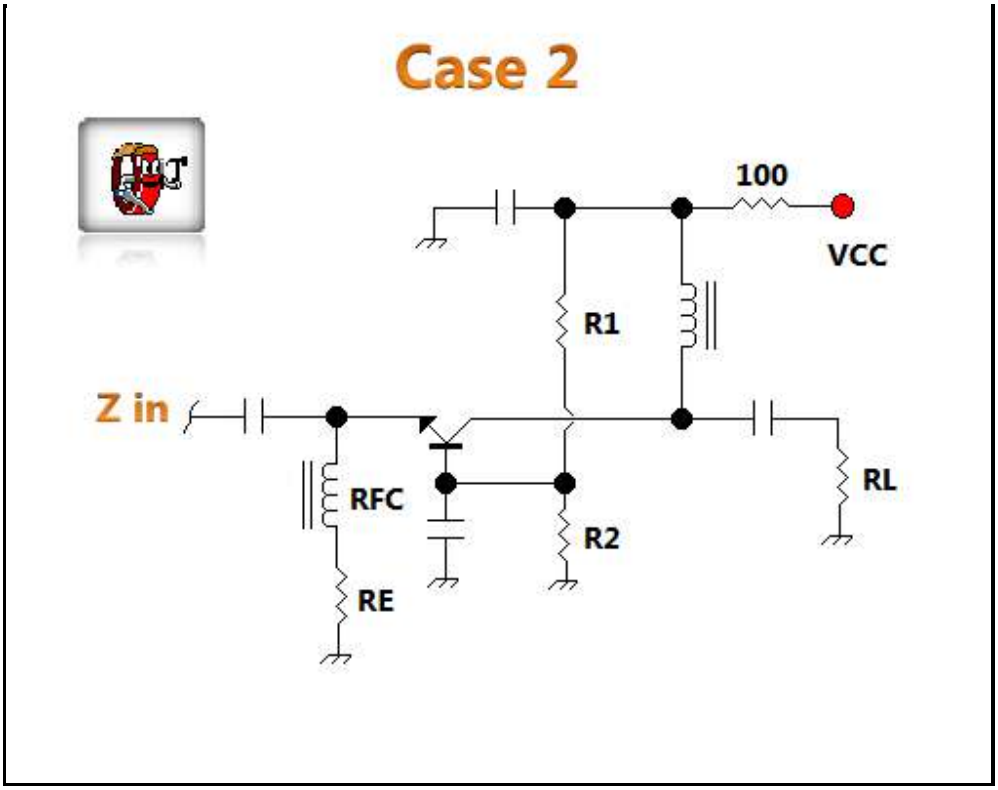

Above — Case 2: Emitter resistor plus a choke.

The choke's main purpose is to block or choke RF from passing to ground. The ideal choke would present infinite impedance to AC signals, plus 0 resistance to DC voltage. In reality, "ideal" = fantasy electronics and you can simply estimate a choke's inductive reactance using the classic formula (XL =2*PI * Freq * L).

Using a coil (and not just a resistor) is generally better for decoupling — although how much better might be debatable. If the inductive reactance (XL) of the coil is significantly higher than the input impedance of the transistor, then all of the input signal power goes to the transistor.

By convention, a minimum choke XL should be at least 3 times the input resistance, however, the self-resonant frequency of the coil must be significantly higher than the applied frequency. Thus, an ideal range of inductive reactance exists, and too little or too much can degrade performance. Many builders target an XL around 10 times higher than the transistor input impedance at the lowest operating frequency.

Example: For a common base amp biased for an input Z of 50 ohms, the minimum inductive reactance (XL) for the choke = 500 ohms. To calculate the inductance of an emitter choke for this amp at 50 MHz, we re-arrange the formula to solve for L.

L = XL / 2* Pi * F
L minimum = 1.59 uH.
Winding the choke on a ferrite core, or possibly a bead for VHF often means less turns, less winding capacitance and a higher self-resonant frequency.

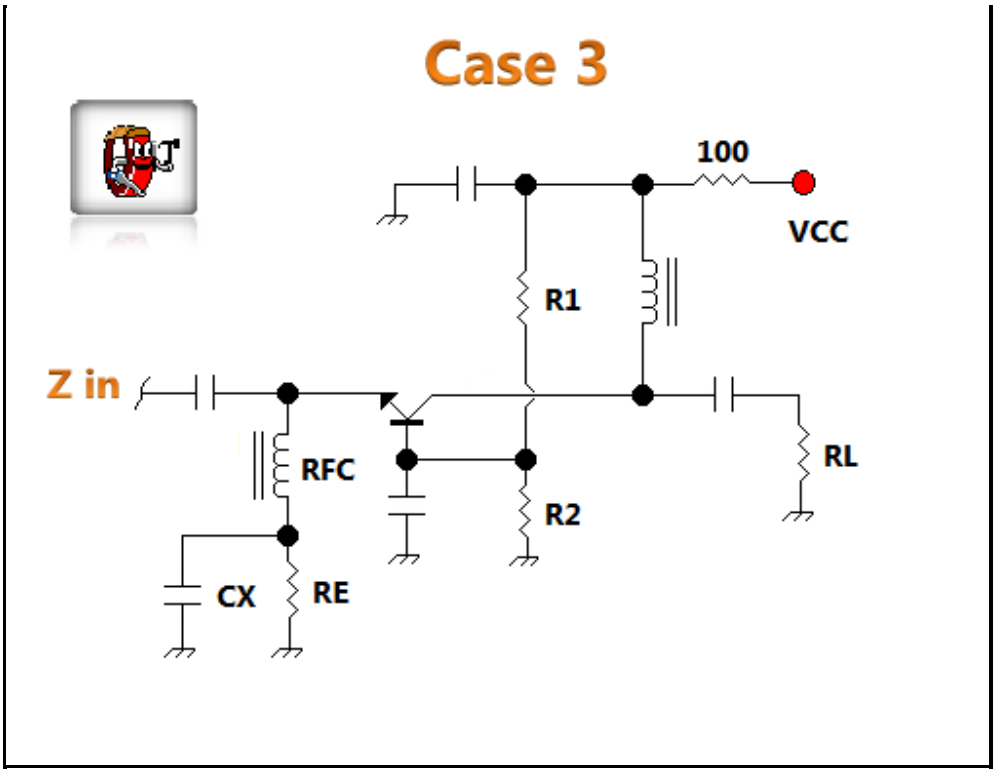

Above — Case 3: Bypassed emitter resistor plus choke.

The primary purpose of the capacitor across RE is to filter resistor noise — but that is only an issue well below the frequency of interest and it should not be relevant at high frequencies where the choke reactance is significant. There may be some useful effect if the self-resonant frequency of the capacitor Cx is above the frequency of interest.

You can only use bypass capacitor **Cx** when a choke is implemented.

A 0.1 uF may be useless at high frequency. In error, I've used this value previously on the site; after 14 years of experimenting, I've learned a lot from my design mistakes.

The case of the common gate JFET amplifier

This discussion also informs common gate JFET amplifer design. The JFET source requires signal decoupling similar to the emitter of the bipolar transistor discussed above.

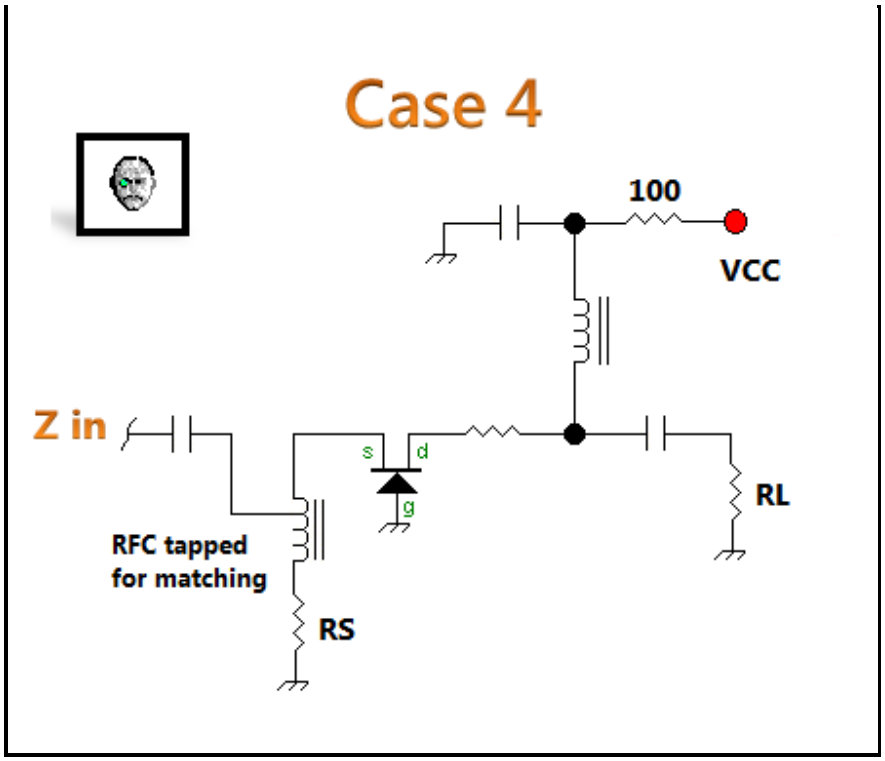

Above — Case 4: A choke plus source resistor will commonly be the "go to" design. Things get a bit more complicated with some, but not all JFET circuits — engineers often match the JFET input for a low noise figure rather than just the "correct" input impedance.

A good example follows: We might place a common gate JFET amp after a diode ring mixer because of the wideband load it presents to the mixer's RF port. The best noise match may occur with a hypothetical input Z of ~70 Ω (this argument represents an advanced topic).

After measuring the JFET pinchoff voltage and Idss, you would likely find that a source bias resistor of ~100 Ohms would be needed. This R value is so close to the JFET input Z that signal losses to ground would occur — demanding a choke for signal amplitude preservation, plus impedance and noise figure control.

VFO - 2011

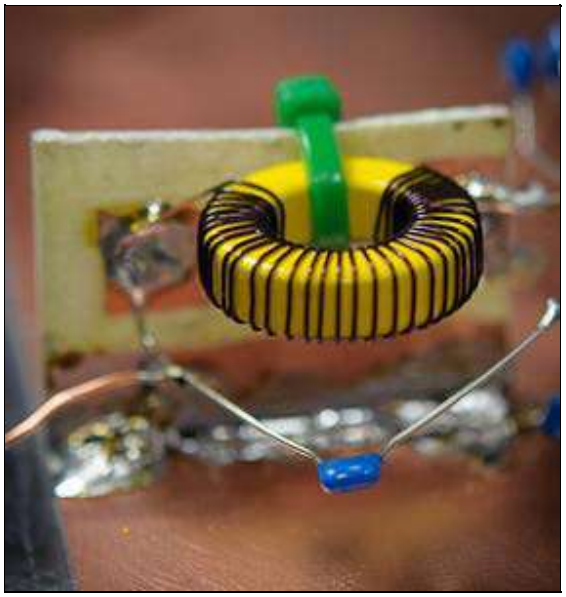

Building VFOs in 2011 might seem an irrelevant exercise given the move to and evolution of digital signal generators laden with bells and whistles like memories and audio or video frequency displays.

A successful L-C VFO requires skill, patience and some good parts to pull off — else, a "drift monster" may result. Despite their limitations, it's possible to build L-C VFOs with low frequency drift, distortion and phase noise; our typical VFO performance markers. L-C VFOs don't require programming skills or equipment to encode a microprocessor — making them a good choice for people who don't build or can't afford kit oscillators. Most of all, they kindle creativity, problem solving and pride when your oscillator actually works as planned. Junk box radio; my passion.

This material reflects lots of empiricism; not pure science. It's really *your* VFO design odyssey; a chance to think creatively and critically to sort out what works and what's folly.
Countless web pages discuss VFO design and I encourage you to search for and read them. Wes' EMRFD oscillator and temperature compensation notes = essential reading. Only your first 25 VFOs will prove difficult — it gets easier after that.

VFO 2011 Topics:

1. Frequency Stability Notes
2. Vackar VFO Experiments
3. HF Signal Generator
4. Miscellaneous Bits

1. Frequency Stability Notes

Building an oscillator that stays on frequency purports our greatest challenge and goal in L-C VFO design. Since drifting VFOs pose a source of frustration, I cover some topics that may help your VFO stay on frequency — do they help?

What is good drift parameter?

I'm uncertain, for after warm-up, I've measured kits that drifted 50-150 Hertz per hour, built L-C VFOs that drifted under 20 Hz per hour and every once and a while, build a drift monster VFO that sweeps upward at 2 - 8 hertz per minute! Likely under 20 Hertz per hour after warm up = a gold standard to compare against. You should be able to listen to a 10-20 minute QSO with no re-tuning, however, this assumes the transmitting stations are locked on frequency.

1. Unloaded Q and Frequency Stability

The number 1 reason to employ high resonator Q in oscillators is to obtain low phase noise. Secondly, the very steep phase slope through high Q resonance minimizes the effect of amplifier phase shifts caused by temperature changes and this in turn, minimizes any amplifier-induced frequency instability.

Long term frequency stability is chiefly dependent on the temperature, environmental and age stability of the resonator components regardless of Q.

I often see designs featuring high Q inductors wound on powdered iron toroids complimented with trashy, low Q variable and/or fixed capacitors, If you design for a high Q tank to minimize phase noise, consider using a high Q coil plus appropriately temperature stable, high Q capacitors.

2. Temperature Stable Inductors

Knowing that I'm venturing into a topic of great debate and lore, the inductor is 1/2 of the VFO resonator and thus a major source of temperature drift in L-C VFOs. Since MF and some HF VFO designs *may* preclude using the *inherently more temperature stable air wound inductor*, powdered iron toroids dominate our evermore compact designs. Many builders choose #6 material, although the lower temperature coefficient of #7 material theoretically should be better — however, my experiments have failed to measure a significant difference between these 2.

Some builders prefer size 68 inductors, for the bigger core is less affected by heating than smaller size toroids. My experience suggests that providing the VFO amplifier current is kept low, both size 50 and 68 are both suitable and the inductance needed should inform the core size.

I used to think that heavier gauge wire created greater frequency stability than smaller gauge wire until Wes, W7ZOI, woke me up. As it turns out, smaller gauge wire is often better for thermal stability because smaller gauge wire lies closer against the toroid core. Winding stiffer, heavier gauge wire creates more air gaps than smaller gauge wire and air gaps expand and contract during temperature changes. Smaller gauge wire will have a reduced Q, but it won't be as significantly lower as you might guess. As possible, I prefer tightly wound number 28 wire. 26 gauge wire tends to be my maximum size wire for VFO coils, however I suggest you make your own conclusions.

Wash your hands before winding and use both hands to actively move both the toroid and wire for tight turns. Take your time, ensure steady wire pressure and avoid kinking your wire. Taps increase the likelihood for air gaps — mitigate this by stripping the 2 tap forming wires as close to the toroid as possible and twist them into 1 wire right down tightly to the toroid edge to reduce any air gap.

The thermal stability characteristics of wire can be mitigated somewhat by annealing the wire with temperature cycling or by dunking it in boiling water. Roy, W7EL first reported annealing coils in 1980 and this has been confirmed during experiments by builders using temperature controlled ovens. I don't boil my coils any more.

3. Double Stacked Toroids

I noticed a new trend in VFO design is to stack 2 powdered iron toroid inductors. This allows the builder to double the inductance per number of windings over a single toroidal inductor. In an L-C VFO, the goal of these builders possibly is to reduce heating effects, increase unloaded Q, or perhaps to reduce core magnet flux density. For me the goal is far simpler, I just want to make compact, large L value inductors for 3 MHz and less.

Above — A T68-6 hamburger. The two T68-6 cores were epoxy glued together and compressed lightly in a vice for several hours. One of the initial tests I performed was to see if boiling the stacked coil affected the epoxy glue. The glue was not effected by annealing wire on a stacked coil with 5 or even 10 minutes of boiling in water. As mentioned, I stopped boiling my VFO inductors as tightly winding them with 26 gauge wire seems to work well.

I hold concern that stacked toroids may create more wire-air gaps when compared to a single toroid and stay with 1 toroid as possible. In compact antenna tuners and other non VFO projects, this isn't an issue.

4. VFO Tank Capacitors

We choose VFO tank capacitors to avoid temperature change caused frequency drift, or to counter drift during our temperature compensation process.

Many authors have published guidelines for long term temperature stability. It's important to consider these guidelines, but also try whatever works. I believe the following arguments are accurate based upon my experiments:

1. Multiple NP0 or C0G (0 temperature-compensation) tank caps: Most builders minimally use 4 or more C0G or NPO capacitors to reduce heating effects and to average out temperature coefficient variations.

2. No VFO tank capacitors from online surplus parts stores; buy new stock from known and reputable manufacturers. Grab bags and musty, old, surplus parts can obviate good design.

3. Trimmer and tuning caps need to be temperature stable. Air variable capacitors = my favorite, as possible.

4. Varactor, or diode tuning generally = more drift and a greater need for temperature compensation.

5. Employ short, stiff capacitor leads. I use 100 volt or higher voltage C0G tank caps as they tend to have thicker leads that stay put — perfect for Ugly, Manhattan, or Chuck Adam's MUPPET construction.

5. Temperature Compensation

The goal of temperature compensation is to cancel the tendency of the VFO to drift in 1 direction — easier said than done + very time consuming. A web search for VFO temperature compensation will yield many good write-ups. I feel it's partly art, partly luck and partly science. Your net VFO temperature coefficient can be affected by so many variables, so no 1 recipe will ensure a low drift VFO. Experiment, allow a lot of time to assess your changes and be patient — you'll figure it out.

The simplest way to test for drift involves watching a frequency counter, but if you don't have one, you might use a commercial, frequency stable (synthesized) receiver set in the SSB/CW mode. I use both. Experienced builders often employ an oven to test their temperature compensation at different, controlled temperatures. Wes, W7ZOI employs a styrofoam cooler housing a light bulb heat source controlled by a Variac. See EMRFD for more details and a photograph.

In 2011, I decided to build up a supply of temperature compensation capacitors and keep them in their own parts bin.

Above — "Tempco caps". A parts drawer containing polystyrene capacitors from 10 to 270 pF plus some 56 pF ceramic N750 capacitors for negative temperature compensation. I purchased these capacitors on eBay.

For capacitors other than NP0 (which use 0 instead of a ppm value), the temperature coefficient = **P** for positive and **N** for negative, followed by a 3-digit value specifying ppm/°C. For example, N220 is - 200 ppm/°C. and P100 is +100 ppm/°C.

I use NP0 and C0G ceramic capacitors interchangeably for both tuning and RF bypassing the VFO tank resonator. For C0G/NP0 *temperature compensation bypass*, I normally apply 0.01 or 0.001 µF caps, however, the more expensive 0.1 µF COG ceramic capacitors are still sold if you need C0G/NP0 bypass <= 7 MHz.

If your VFO is drifting upward you might insert 1 or more positive coefficient capacitor(s). If your VFO drifts downward, then try using negative coefficient value(s). Sometimes just 1 capacitor will do the job.

Since I don't stock any positive coefficient capacitors for positive coefficient compensation, I might try a adding a silver mica capacitor. ***Caution*** silver mica capacitors are extremely non-predictable and can't be universally recommended in temperature compensation schemes. You might also try swapping out 1 or more of your main tank NP0 or C0G capacitors in case they are bad; sometimes it gets frustrating. I provide some temperature compensation examples on the QRP Modules 2011 web page in the 7 MHz VCO section.

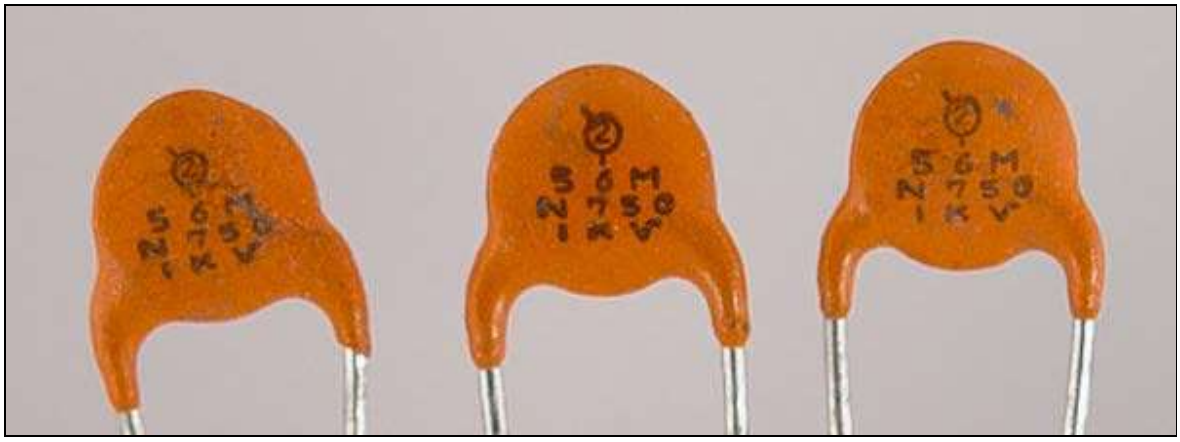

Above — 56 pF N750 ceramic capacitors rated at 1KV

6. Mechanical Rigidity

Movement of your VFO tank parts may lead to frequency instability. For example,

1. Well secure your single-sided only copper board. I use at least 4 number 8 bolts — 4-40 hardware is too light. Boards can warp over time if not lashed down properly. Aggressively bolt down any variable capacitors. No tank parts should move.

2. Anchor your inductor so it cannot budge: nylon bolts, zap-straps, glue - whatever.

3. Consider placing the VFO in a strong chassis with rubber feet.

4. Buss wires should be made from thicker gauge, well anchored wire.

7. Miscellaneous Points

1. Regulate the VFO amplifier DC voltage and wideband filter it. Voltage regulators require RF and often AF bypass to attenuate any noise or ripple riding on the DC.

> A decoupling resistor with a bypass cap on either side will widen your DC supply filtering bandwidth and deserves strong consideration. A poorly filtered DC supply can easily transmit the VFO tank energy to other stages along your DC lines and also may allow noise on the DC supply to modulate your VFO and increase phase noise.

2. You should have the buffer + a load resistor connected to your VFO when testing. **Do your temperature stability work after the buffer is built and the VFO is in its case.**

3.Stick your VFOs in an air tight, RF tight case to minimize air temperature changes and RF leakage respectively. Sometimes a VFO will drift once in a case because any radiated buffer amplifier heat will warm up the inside of the chassis. This usually levels off after warm up.

4. Modern voltage regulators may significantly reduce noise compared to a zener diode regulator. Specific low noise and low temperature coefficient voltage regulators are available, but maybe overkill for you. Whatever you use — filter it well —
The Micrel MIC5209-5.0BS in SOT223 sits in a couple of my reference oscillators.

5. JFET Gate clamping diodes may increase phase noise, but not prohibitively so in most popcorn designs.

6. When winding toroid inductors, wind 2 extra turns. When finished, unwind the first 2 turns since they are usually loosely wound and prime culprits for air gaps.

7. Since magnet wire comes off small spools, wire has a natural curve or radius — ensure you wind your coils according to the natural curve of the wire.

8. The need to secure powdered iron windings with dope, wax, goop, etc. is over-emphasized and usually unnecessary.

---

2. Vackar VFO Experiments

Some builders proclaim the Vackar as the "King of VFOs". I built a couple and became impressed by the low distortion and less than 5 Hertz per hour long-term drift achieved in my 2 designs. Inspired by work from Iulian, YO3DAC entitled Very Low Phase Noise Vackar VFO for HF Transceivers *(link and reference used by permission of Iulian)*, I crafted my version from his notes and schematic.

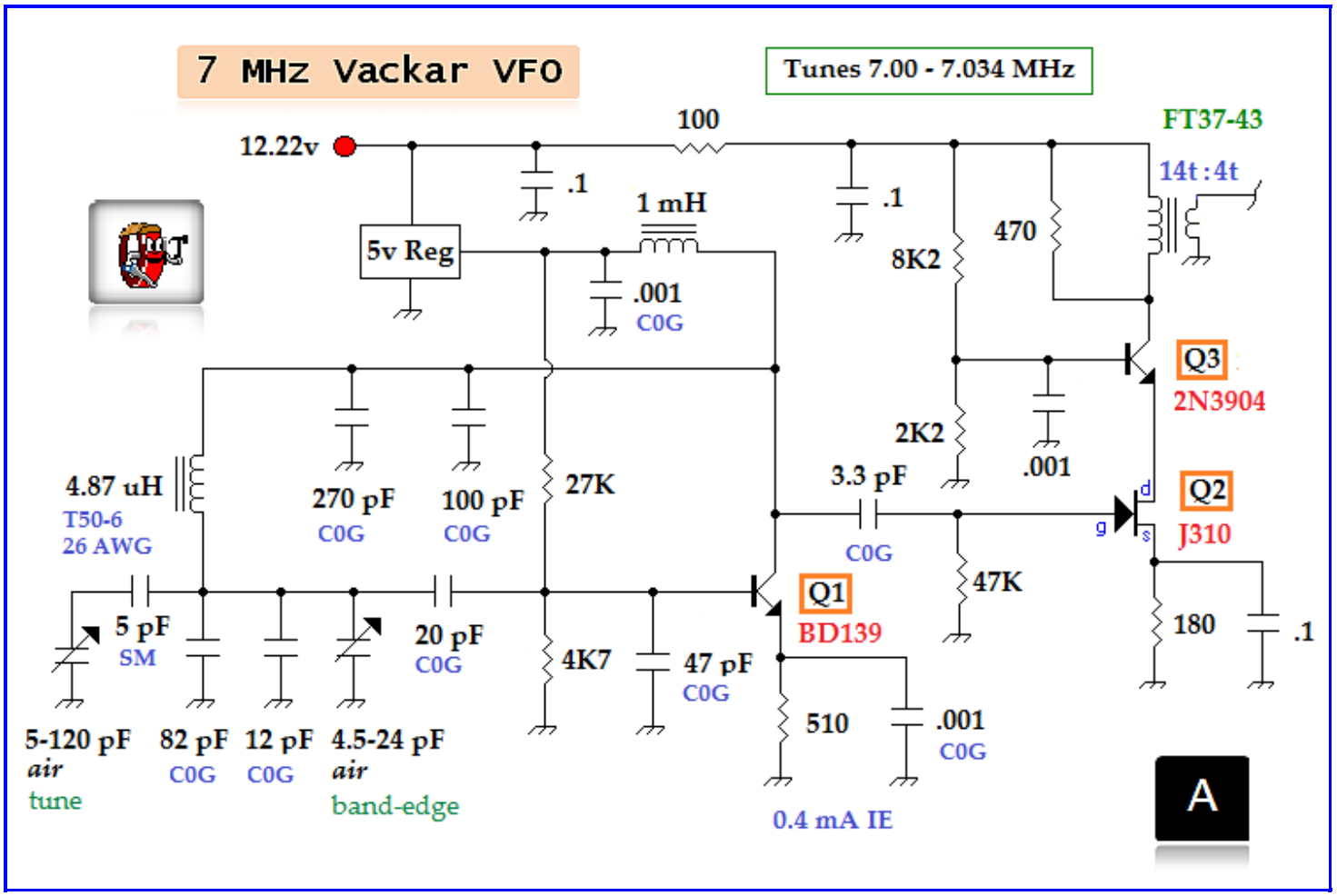

Above — Schematic of the Vackar VFO employing a BD139 — a large area transistor, to reduce 1/f noise. Iulian shared many design pearls in his paper and I won't repeat them. I ran Q1 with 0.4 mA emitter current to reduce heating and flicker noise. It's difficult to measure flicker noise, so no objective comments can be made.

I limited the tuning range to 34 KHz since the tuning capacitor lacked reduction gear and I was born with fumble fingers. As a CW operator - you'll find me down at the bottom of the band away from the RRTY anyhow. Increasing the 5 pF cap coupling the tuning capacitor to the tank increases the tuning range as expected.

Temperature compensating my VFO with the 5 pF silver mica capacitor proved a gamble since SM caps are unpredictable and often best avoided. In *my* VFO, it worked perfectly, however. This circuit is difficult to replicate and *not recommended* for new builders. Temperature compensation provided the sublime frequency stability.

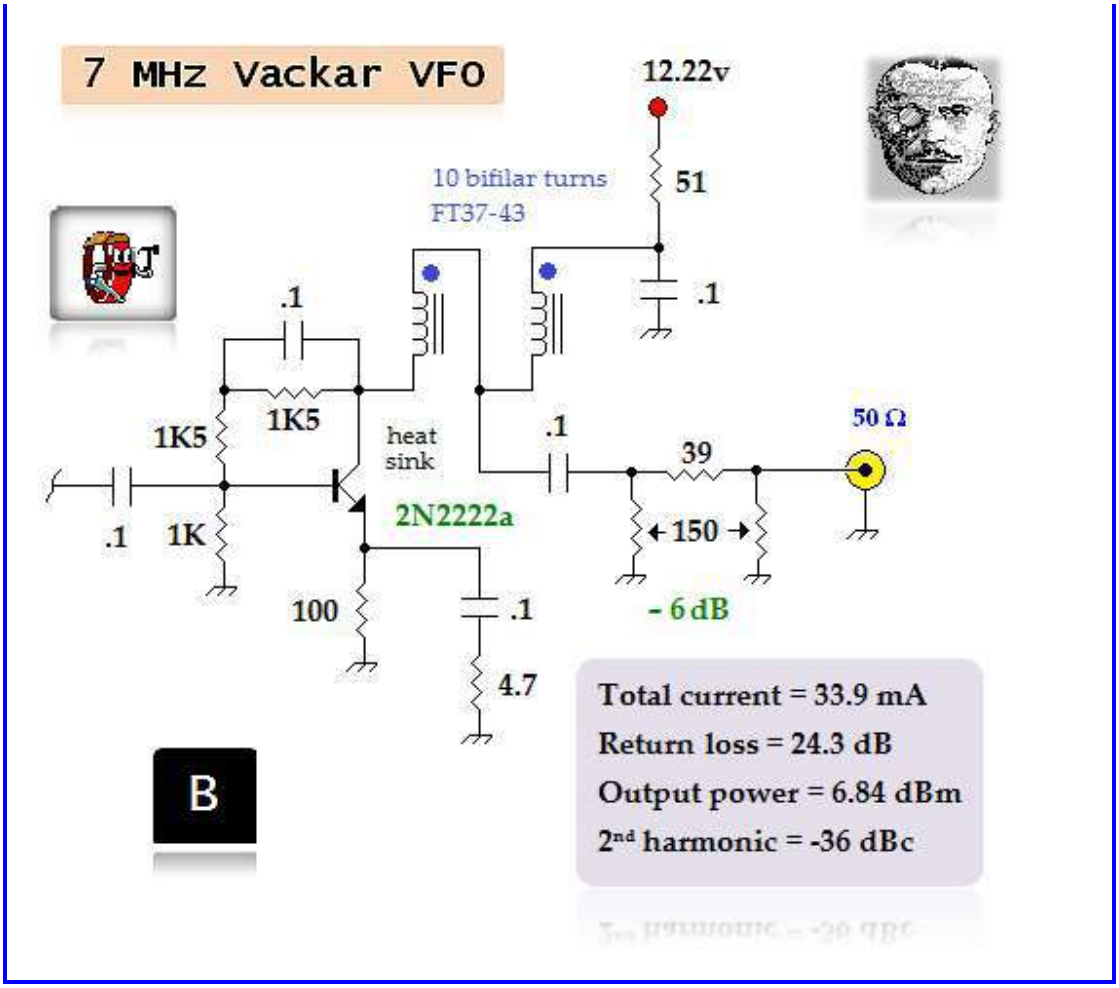

Above — The final amp and measured output data. Measuring the 2nd harmonic 36 dB down without any tuned circuit or low-pass filter rocked. I ran nearly 22 mA of emitter current to bump up the return loss and spectral purity. A 2N5109 or 2N3866 would likely do a better job with less current. Total current = the entire VFO current. I glued a drilled copper penny on the 2N2222 to dissipate heat.

A photo of my version of a Vackar VFO. My design goals included low phase noise, low distortion, a return loss over 20 dB, good reverse isolation and ~7 dBm output power. I believe all VFOs are experimental; you build to suit whatever tuning capacitor or varactors you have, plus design around constraints such as total current, tuning range and other personal criteria.

Unlike harmonic distortion, oscillator phase noise, being close to the oscillation frequency, cannot be removed by filtering nor limiting — you must design for low phase noise. Modern digital VFOs are well harmonically filtered, and any phase noise depends on the DDS clock employed, so check the DDS specifications carefully if you go the DDS VFO route.

I'll be the first to state I'm no expert with VFOs, however, likely the only way to become expert is to build many and learn from your mistakes.

Above — A 7 MHz Vackar VFO with the lid off

Sound Test?

Although this technique raises the ire of some builders, I test my VFOs in a nearby receiver. The VFO output was terminated with a 51 ohm resistor that was also attached to my frequency counter via alligator clips and wire. I tuned a nearby CW superheterodyne receiver to 7.00 MHz with the audio beat note centered in its 600 hertz wide I.F. filter and watched the counter plus listened to the receiver.

Click for a 1 minute 32 second audio file of the result (it stayed perfectly on frequency for ~5 hours of testing before I got a bad headache from listening to it and shut it off). *You can initially hear a station in the back ground despite only having a 45 cm piece of wire as the receiver antenna.* The VFO slowly drifts down to 6999996 Hz and then slowly back up to 7000000 Hz. You can hear the signal amplitude decrease as the VFO drifts down. So it doesn't stay perfectly on frequency, but slowly cycles up and down a few hertz. This VFO is my lab temperature stability benchmark for an L-C VFO.

A badly drifting VFO will move out of the test receiver I.F. pass band and sound like a Theremin as it does. Testing in a receiver; places the VFO in the exact circumstance it will be used — beating RF to mix to another frequency; in this case, base band audio.

The temperature stability and compensation of any VFO schematic are rarely reproducible since there are just too many variables. Try your best to get the drift out of your VFO using low temperature coefficient capacitors (NP0/C0G) and then after that, temperature compensate. Even today, I occasionally build a drift monster VFO and become frustrated. VFO design is not for the faint of heart and it's no wonder that many builders make a VXO, or cave in and build or buy a DDS signal generator.

---

3. HF Signal Generator

Above — I built a general purpose ~2.8 to 10.8 MHz signal generator (SG) for my lab in 2011. The first VFO topology tested was the Vackar. In my version, while employing a 100K ohm resistor as the buffer, the VFO only tuned from about 4 to 8 MHz and suffered from *extreme* amplitude variation as I changed the frequency across its range. For sweeping filters or measuring Q, a signal leveling circuit would be needed as normally we like our SG output to be flat across its frequency range. I later changed to a Hartley VFO because of its flatter output and the wider available frequency range with any given resonator.

This initial Vackar VFO experiment wasn't a total waste as I learned a way to accurately sweep a **D**evice **U**nder **T**est with an unlevel amplitude SG. Measure the peak-peak voltages of the DUT with a signal generator and an oscilloscope in the same manner we measure insertion loss or gain in a 50 ohm system: Measure the peak-to-peak voltage with the DUT in line; disconnect the DUT, insert a barrel connector and then re-measure.

The dBm difference between the 2 becomes the dB value to plot for *that* frequency. To a sweep a filter, say for example, a band-pass filter, find the center frequency and then sweep below and above that CF while plotting the dB versus frequency.
This "in and thorough" measurement described takes time, but resolves any frequency versus amplitude issues and can be used to test signal generators. We tend to ignore things like cable loss versus frequency and scope or spectrum analyzer ripple.

Still, it will be easier to just use a Hartley VFO where our sweeps are assumed to be level due to the flatness of the amplitude versus frequency for **small excursions** such as 3 dB band-pass filter sweeps. Do not expect amplitude flatness over wide excursions however — this requires additional circuitry.

To reduce noise and boost fidelity, this SG runs modest current and was not designed for battery use.

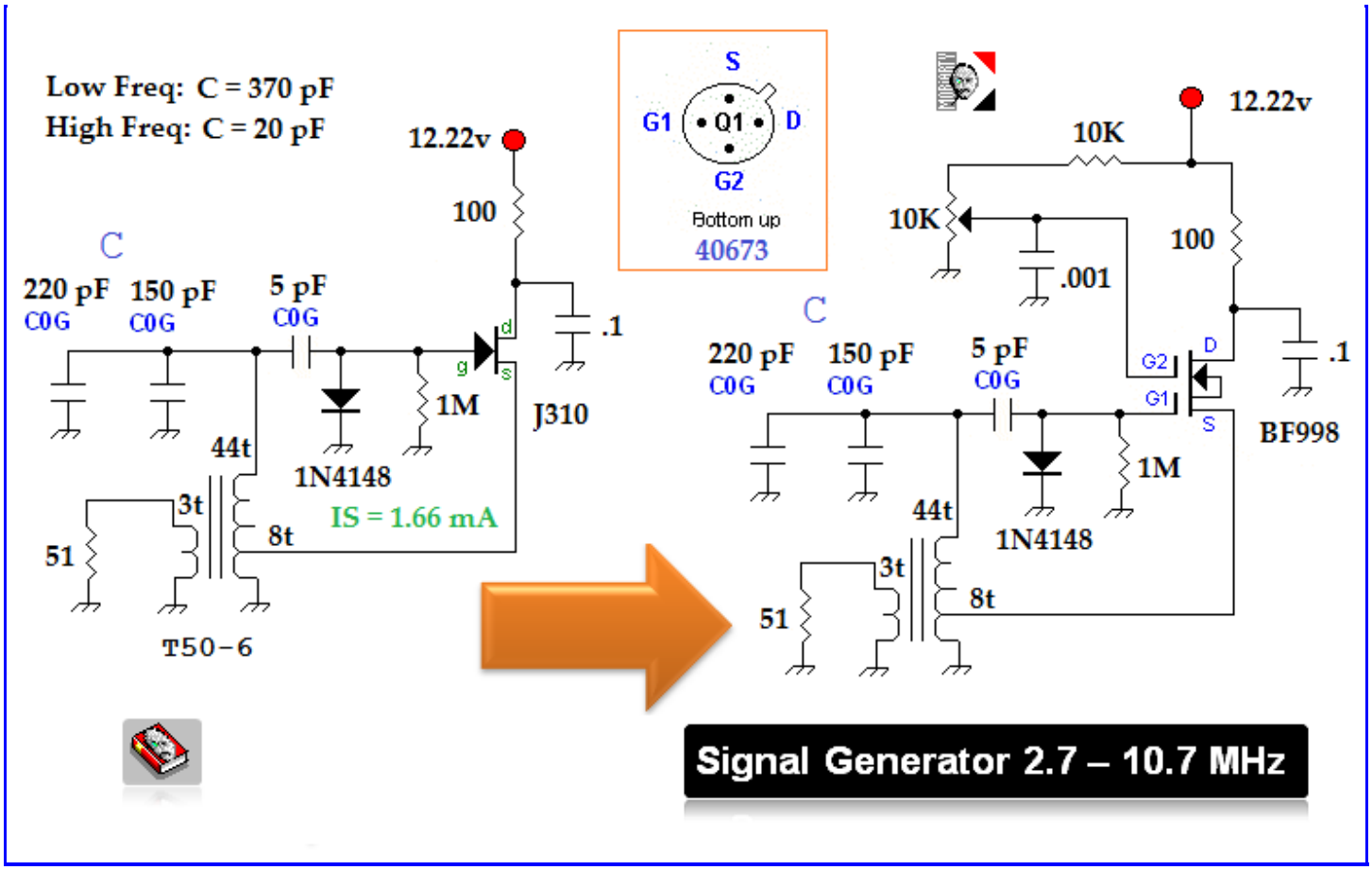

Above — My Hartley VFO is morphed into a double-gate MOSFET VFO; this was a mistake and I make lots of them.

When venturing out, it's often best to confirm a proven design is working before morphing it to something untried. Shown above left is the Hartley oscillator from EMRFD Chapter 7 sans buffer. Fixed "tuning" capacitors; either 20 pF (not shown) or 370 pF (150 pF + 220 pF) represent the intended high and low frequency swing of my air variable tuning capacitors.

I wanted a variable amplitude VFO and thus replaced the JFET with a double-gate MOSFET using a simple variable voltage divider to control gate 2. I showed this to Wes, W7ZOI and he informed me that the flicker noise of MOSFETs precludes their use in oscillators. I have always wondered why I've never seen MOSFET VFOs in any radio literature.

Above — My project chassis fitted with hardware. I employed 2 air variable tuning capacitors — the fine tuning capacitor ranges 13.6 to 27.5 pF,

features built in 6:1 reduction gear and was purchased from Doug DeMaw many years ago. I secured the main copper board with 6 number 8 bolts. Rubber feet provide a stable, shock resistant base for the sheet metal box.

Final Build

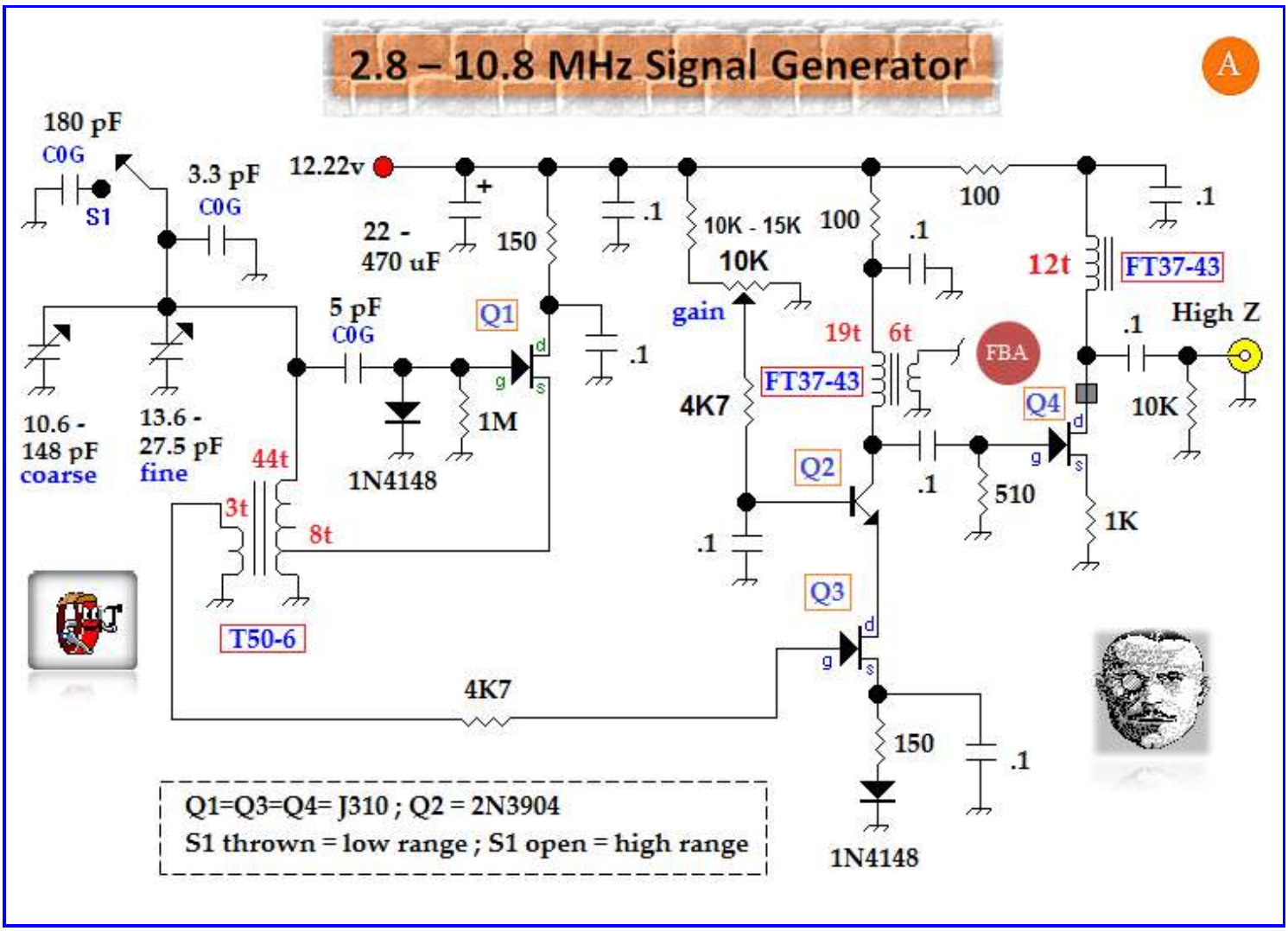

Above — Oscillator + buffer schematics of the latest version of my signal generator. I spent 1 evening playing with VFO designs and settled on the simple Hartley from EMRFD, Figure 7 .27. The 3 turn link provided lower distortion than coupling the oscillator to its buffer by the JFET source or gate.

Regulated 12.2 VDC powers the oscillator; avoiding the typical 5-9 VDC voltage regulator we normally use. A 22 to 470 µF cap should be employed to filter any voltage regulator noise from our DC supply. Mine has a 470 µF capacitor.

1 hour drift lies under 40 Hertz when averaged from 15 different frequency points between minimum and maximum. The Q2/Q3, Q4 and Q5 transformer inductances were optimized to allow good signal and/or matching performance in the ~ 2.5 to 10.8 MHz frequency range.

A hybrid cascode (hycas) buffer with variable base bias on Q2 forms the amplitude control for both the high impedance and low impedance outputs. The 510 ohm gate resistance on Q4 terminates the hycas amplifier and sets up a known output impedance to drive the 50 ohm feedback amp. I measured a greater than 22 dB return loss on the output of the 19:6 turn transformer from 4 to 14 MHz — indicating it drives the feedback amp reasonably well.

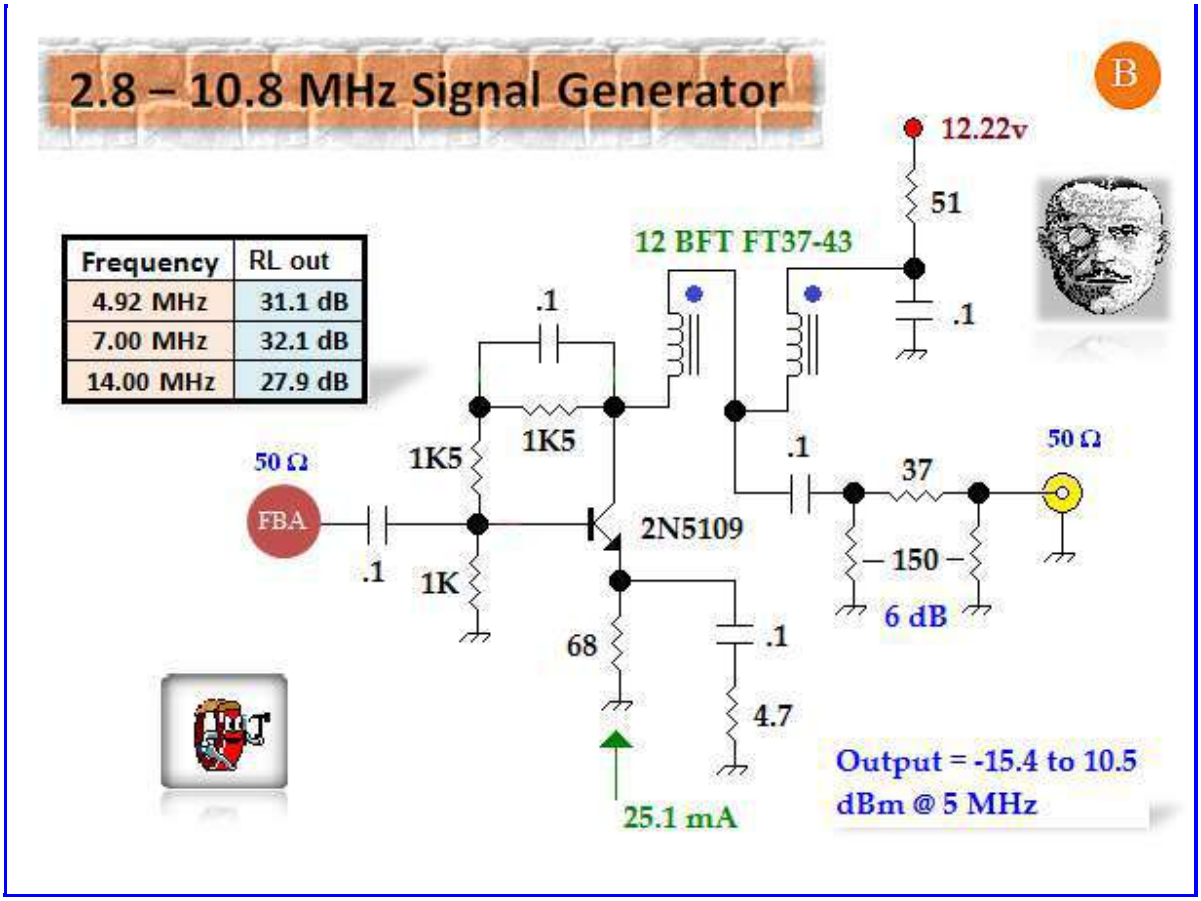

Frequency	RL out
4.92 MHz	31.1 dB
7.00 MHz	32.1 dB
14.00 MHz	27.9 dB

Above — The 50 ohm impedance feedback amp. Running 25.1 mA current allowed a clean sine wave output up to 2.12 volts-peak to peak into a 50 Ω terminated oscilloscope, plus an output return loss of over 30 dB across the SG tuning range. 3 tabled output return loss measurements are shown; including an out-of-range 14 MHz measurement.

Two series resistors made up the 37 ohm "resistor" depicted in the 6 dB pad, although a 39 Ω resistor would work fine.

At low output amplitudes, I typically stick an external 6, 10 or 20 dB attenuator on the output since the hycas amp can distort the signal a little when the gain control is set to a really low bias voltage on Q2. Then I fine tune the output power with the gain control.

Above — A "lid off" front panel photograph. Click or click for other photos. I'm now using miniature pots with a shaft diameter of 3.18mm. The potentiometer shaft lacks a knob and I'll purchase some on my next parts order.

Above — The completed signal generator.

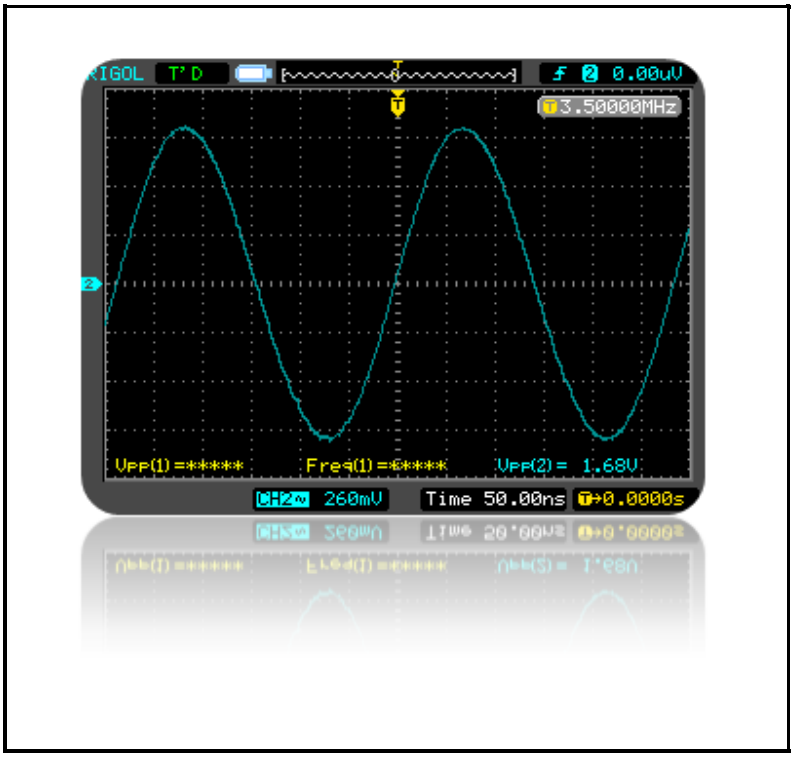

Above — Signal generator output at 3.5 MHz.

I appreciate that the VFO tank would be difficult to replicate since the 2 air variable capacitors are unique, however this is true of most VFOs. Wes wrote some great notes in EMRFD Chapter 7 regarding copying signal generators and the versatility of the Hartley VFO. I hope this project furnishes some ideas that spawn you to build something better than I did. *(I've received over 350 related emails since posting this page in 2011*

and many readers have built really great VFOs — Way To Go !)

QRP — PosData for December 17, 2013

I slightly boosted the tuning range from 2.8 to 10.8 MHz by dropping the 5 pF resonator capacitor to 3.3 pF in October 2013. The schematics now reflect this changes plus clarify 1-2 stumbling blocks readers had. For example: my use of a 100K gain pot plus a 150K maximum voltage limiting for the Q2 bias. My build still has these, however, I altered the schematic to show a common 10K gain pot, plus a fixed 10 to 15K resistor used to limit the Q2 bias to between 5 and 6 VDC maximum.

In reality, any reasonable pot and resistor will do since they function as simple voltage dividers. With a 12 volt supply, we don't want to drive the Q2 bias with more than ~ 5 to 6 VDC since this will just distort the AC signal as the hycas stage saturates. Measuring with a voltmeter, solder either a 10K, 12K, or 15K resistor to limit the maximum Q2 bias with the 10K potentiometer turned fully clockwise.

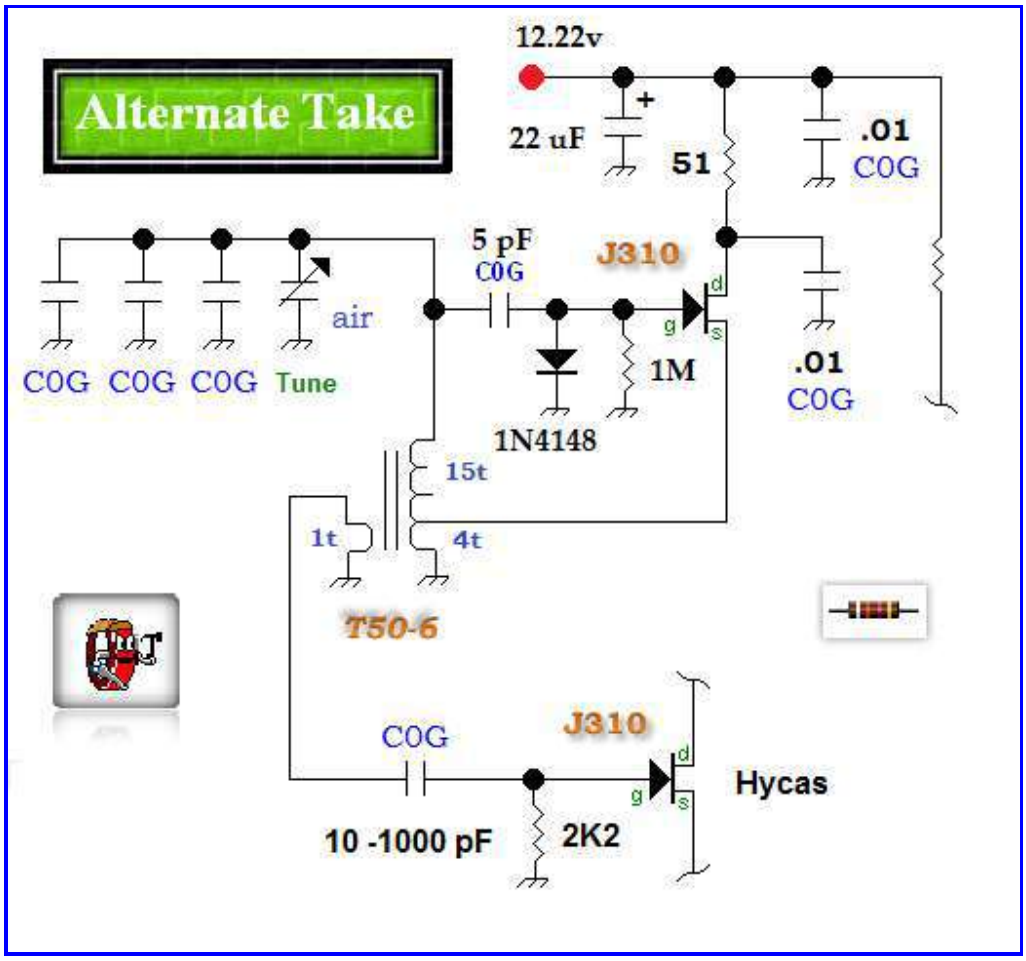

Above — Alternate way to couple the Hartley oscillator to the hycas buffer. Ground the JFET gate with a shunt resistor and lightly AC couple the JFET gate to the Hartley secondary coil with a series capacitor. You choose the capacitor value to limit the signal amplitude as needed. Our main goals are to lightly couple the Hartley tank to its buffer and avoid overdriving the hycas stage. Numerous examples of this "Alternate Take" circuit may be found on the QRP / SWL HomeBuilder web site.

---

4. Miscellaneous Bits

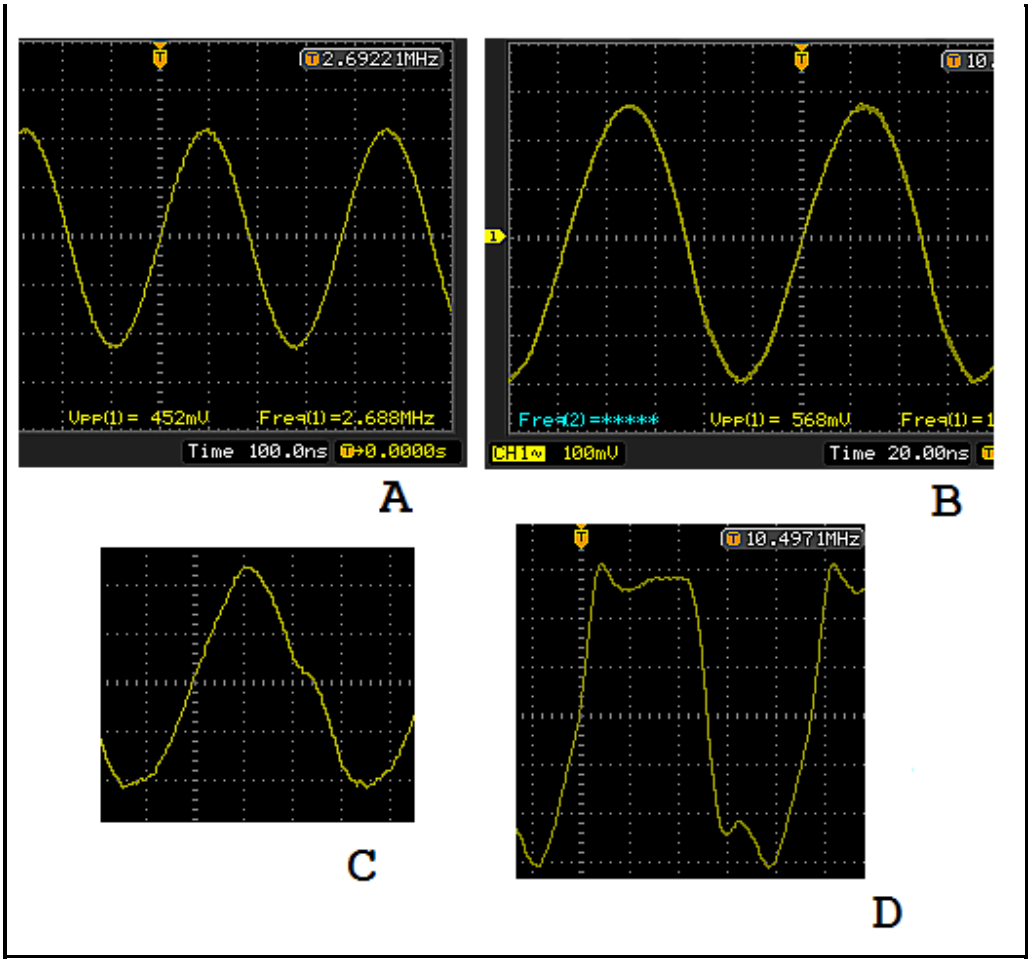

Above — Scope traces of an unbuffered Hartley oscillator with a X10 scope probe across a 51 ohm resistor across the 3 turn link. The unbuffered Hartley sine wave isn't harmonic free, but cleans up when properly buffered with a higher impedance amplifier. Figure A = the lowest frequency (2.7 MHz) — the distortion increased with frequency (Figure B was measured at 10.5 MHz). Figure C illustrates how slightly stronger output coupling with a 6 turn link trashes the output waveform — the strategy of using 2-3 links over the center of the main inductor works well.

Figure D is the 6 link coupled Figure C oscillator with the gate clamping diode removed; yikes! I spent 4 hours studying what different current, voltages, coupling and so forth do to the Harley oscillator. I recommend the Hartley topology because it's simple, always starts and versatile.

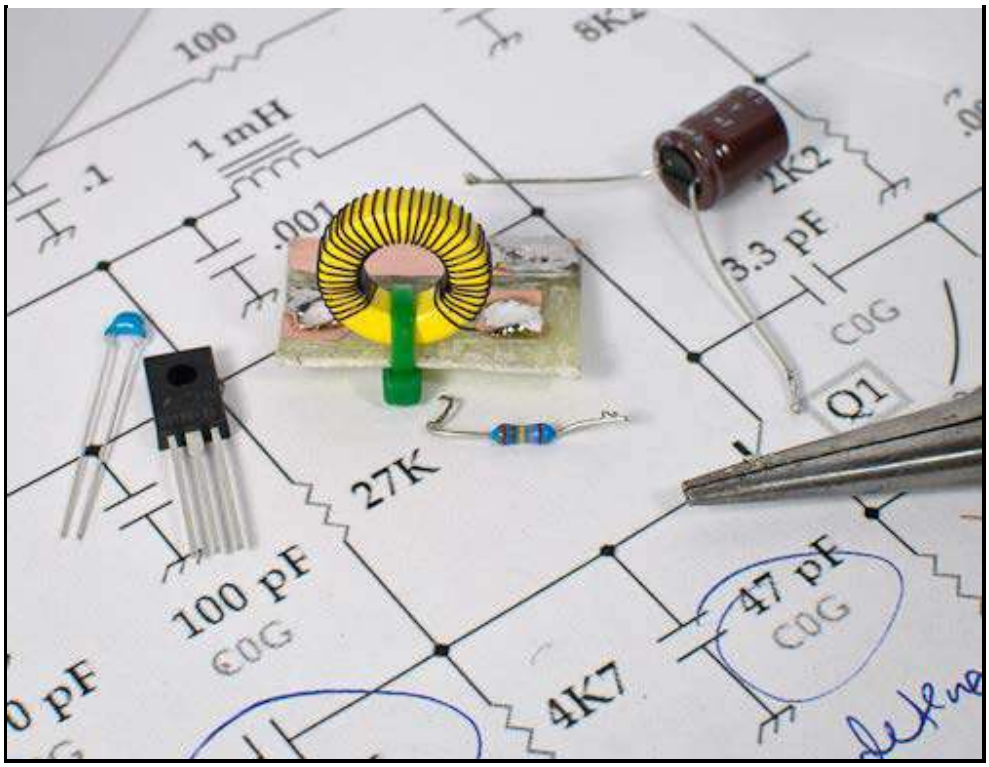

Above — In my various signal generator experiments, I zap strapped the toroid to a small piece of thick copper board that was later soldered to the main board. The L seems robustly secured.

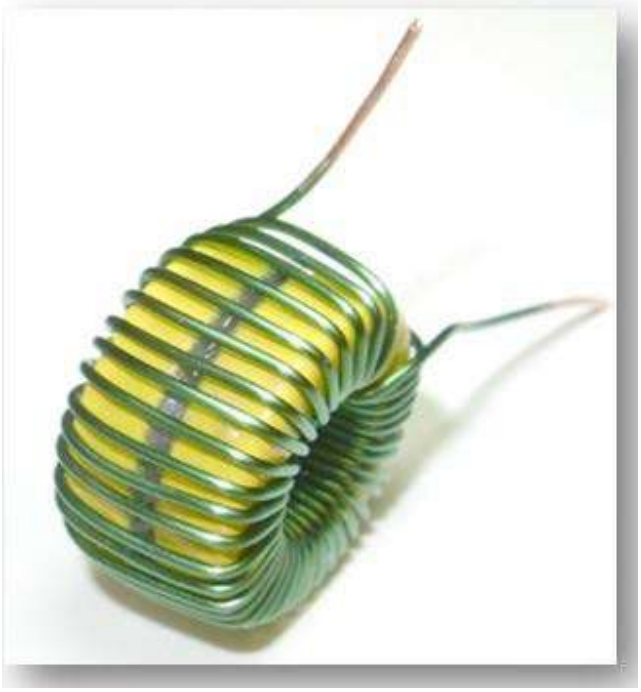

Above — A stacked toroid from the deleted VFO-2008 web page. I incorporated some of the information from the VFO-2008 page into this web page

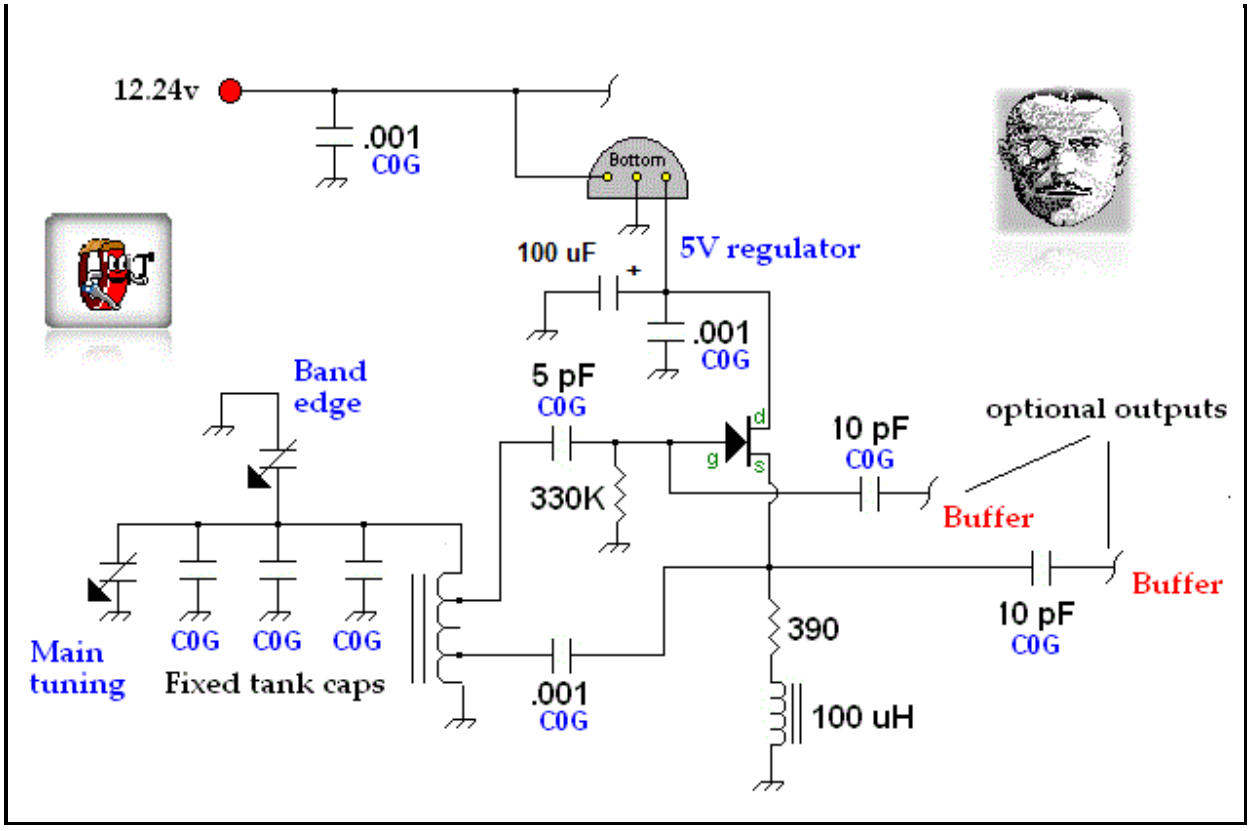

Above — In order of preference, 3 ways to couple a Hartley oscillator to its buffer. From now on, I'll couple with a 1-3 turn link since it gave a lower distortion signal than with source or gate coupling. This figure omits the gate clamping diode seen earlier— tapping the inductor as shown keepings the FET gate AC voltage at a reasonable level when not using a gate clamping diode. Some builders leave off the gate clamp diode that clips positive signal peaks for lower phase noise. The diode acts as an AGC and offers benefit. Reverse biasing this diode was suggested by Dr. Ulrich Rohde: see — Key Components of Modern Receiver Design - Part 2: Dr. Ulrich Rohde, KA2WEU , QST for June 1994.

A formula to use for the inductor taps: Divide the total turns by 1.45 to get the first tap and by 7.25 to get the second tap (near ground link).

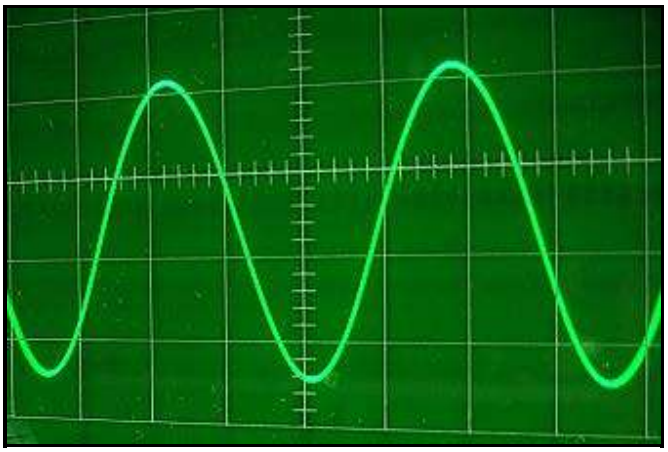

Enjoy your VFO experiments.

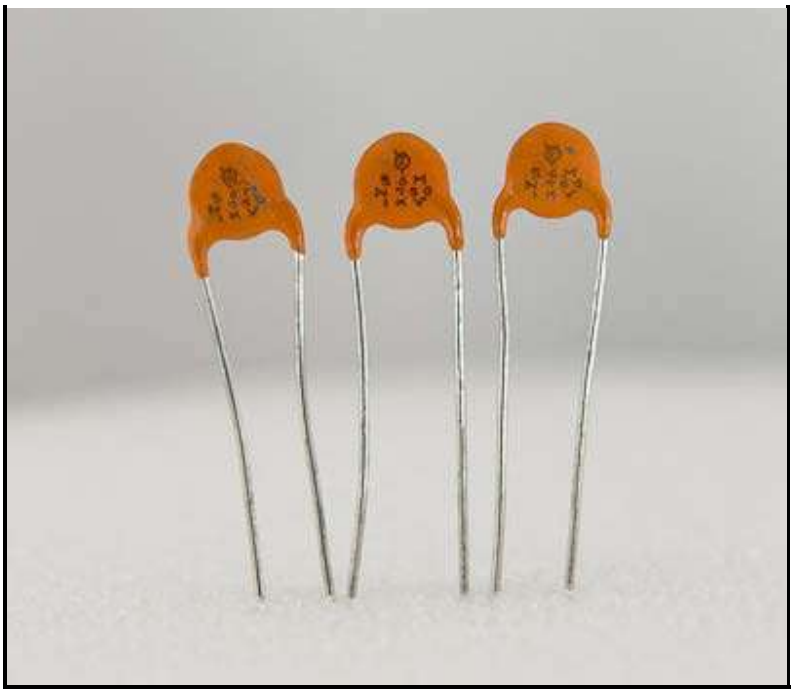

ON
HI-Z
50 OHM
GAIN
HI

The Butler Did It ! - First VHF Experiments 2011

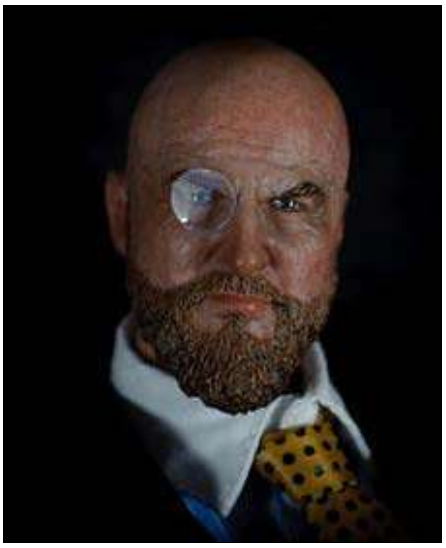

Venturing into VHF, I felt like a beginner with no experience or confidence — however, the excitement and allure of new parts and circuits kept me going.

After performing a literature review, talking to some colleagues and renovating my QRP work bench, my first tasks involved buying some VHF parts + exploring the Butler crystal oscillator. Specifically, I'll cover my experiences with the common base version of the Butler oscillator.

Like HF, the VHF knowledge base contains ever-present lore. Consider the Butler oscillator — I have read arguments stating that the emitter follower version of the Butler oscillattor is vastly superior to the common base version because the latter is prone to UHF and other spurs. These comments seem to have originated from a good book entitled Crystal Oscillator Circuits. *Revised Edition* by Robert J. Matthys published in 1992 by the Krieger Publishing Company.

While examining the schematics of professional/world class gear using a Butler, the common base version clearly dominates. Spectrum analysis and other measurements indicate that when common UHF oscillation management techniques are applied, common base Butler crystal oscillators work well.

Suppressing UHF oscillations with ferrite beads (and small value resistors), feedback, neutralization, limiting gain, etcetera are routine practices for us experimenters applying active devices that have strong gain into UHF on up. This is vanilla, or matter-of-fact construction for us; no worries. While fun and often convenient, lore ultimately stifles our progress.

Increasingly, I'm adopting the philosophy of Bob, K3NHI; "TMITK" — to measure is to know. Consider, too, you have to know what to measure and possess the required gear.

For BJTS, I purchased PN5179, MPSH10, 2SC3355, BF199, 2SC3357-RE, 2N5109/2N3866 and NE46134. The PNP part = MPSH81.

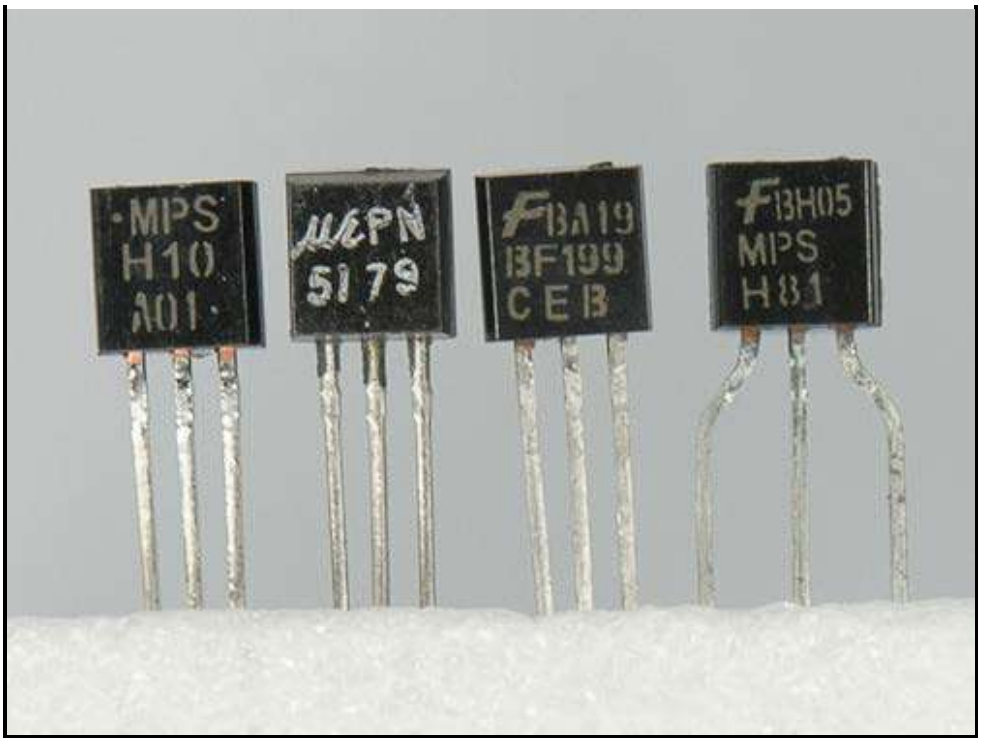

For JFETs, the J310 in TO-92 and SMT will remain my workhorse FET part along with a couple of other *low noise* JFETs and 2-gate MOSFETs. At VHF, the noise figure in a receiver chain is established by the first amplifier so a low noise preamp ranks important.

A collection of 100 volt NP0 capacitors ranging from 1 pF to 22 pF were added along with some chip and SMT caps as low as 0.5 pF. You might need a few air trimmer capacitors with a minimum capacitance ~ 2 pf — I applied 2 - 20 pF trimmer capacitors in most of the circuits that follow.

---

1. Experiments with a Butler Oscillator with a 23.3 MHz Fundamental Crystal

Fundamental Frequency

Long ago, I pulled a crystal marked 70.00000 MHz from a Drake Transmitter. I keep a fundamental oscillator based upon EMRFD Figure 4.23 on hand and verifed the fundamental frrequency at 23.3 MHz.

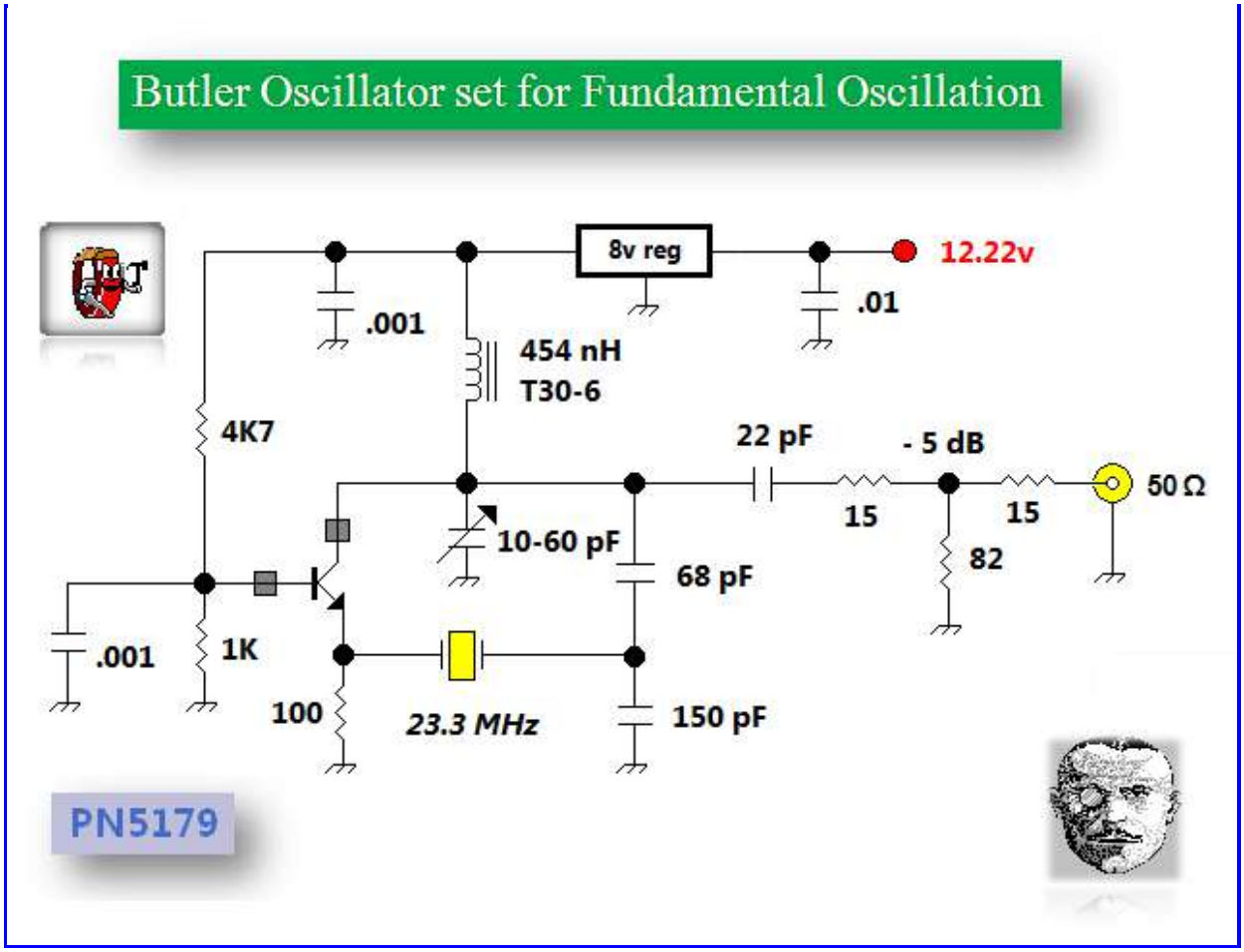

Above — A Butler oscillator arranged for output at the fundamental crystal frequency. While commonly arranged as an overtone oscillator, the Butler is a good oscillator for any application. Consider, for example, EMRFD Figure 7.32. Wes applied the Butler at a 14 MHz fundamental because he wanted the lowest phase noise and IMD prone signal source possible. Tellingly, his buffer circuitry also conforms to this high standard.

My initial waveform looked distorted and prompted a solution. My experience yields that the L value needs to be adjusted for the best looking waveform in the Butler circuit. The inductor wire, wrapped around a T30-6 toroid was either scrunched to increase the inductance, or expanded to decrease the L while re-peaking the trimmer cap. Eventually, with patience, a beautiful sine wave emerged on my 'scope. I removed and measured the L with an ADE inductance meter. Consider all of my reported inductance values as nominal — gentle expansion or contraction of the inductor coils might be required to get an agreeable sine wave.

Click for the oscillocope tracing at 23.3 MHz.

The Butler at Overtone Frequencies

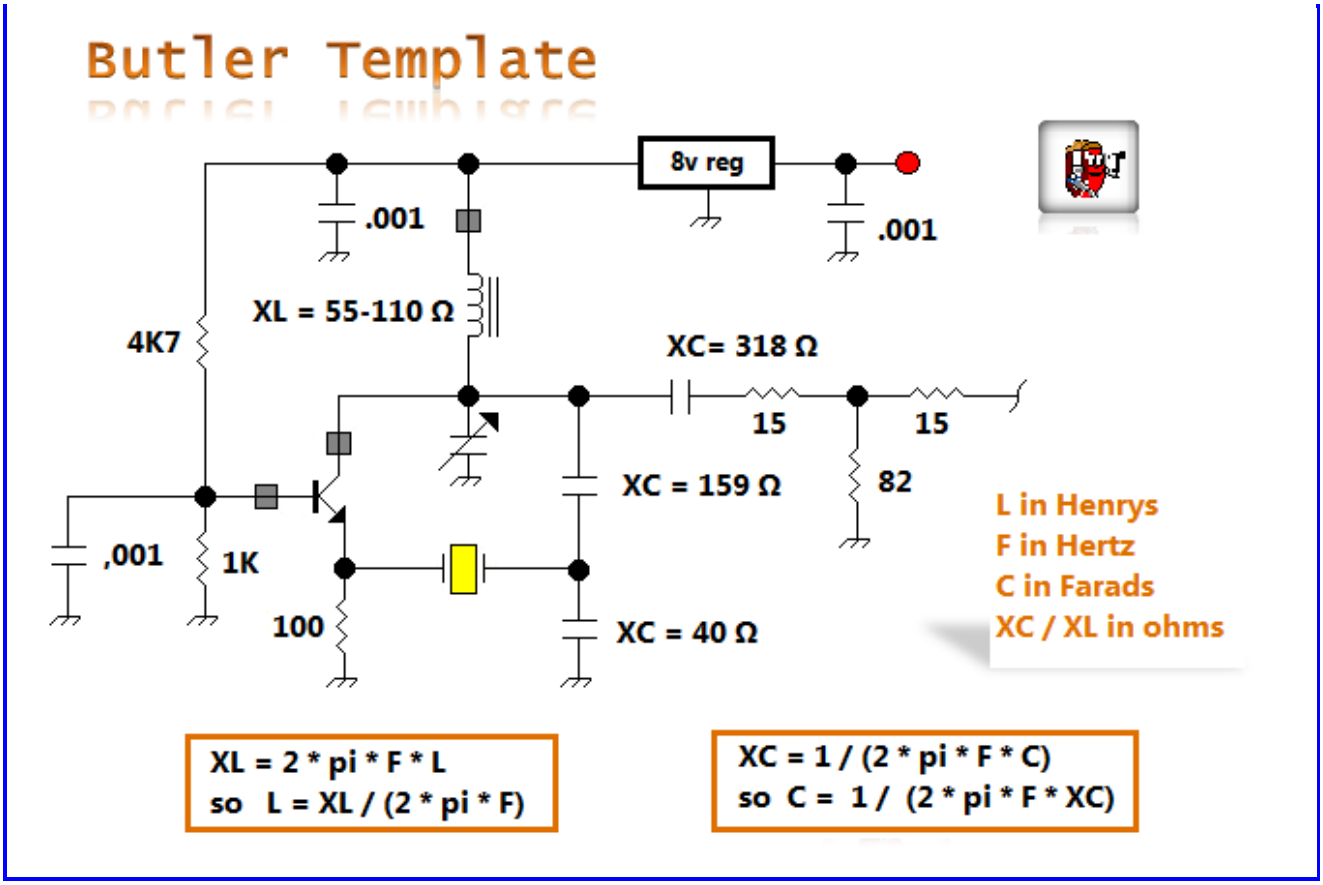

Above — A template (of sorts) for calculating Butler capacitor and coil values. The concept, rather than the absolute value matters most. I examined some well-designed Butler oscillators from professional equipment and determined their average XL and XC values. From the reactances shown, calculate the L and C values for the overtone frequency of interest with the 2 formulas in orange boxes. *Remember these XL or XC values just serve as starting values for experiments.*

For example : At 50 MHz with an XL of 108 Ω : L = 108 Ω / (6.28 * 50000000 Hz) = 0.000000344 H or 344 nH.

Fine tuning of the capacitor and inductor values might be required since factors including buffer input resistance +/- reactances, the overtone frequency and/or your breadboard layout may affect your Butler oscilator function.

In the experiments from the 3rd to 9th overtone frequency, the L = an air inductor wound with 21 to 22 AWG wire on a bolt.

Third Overtone Frequency

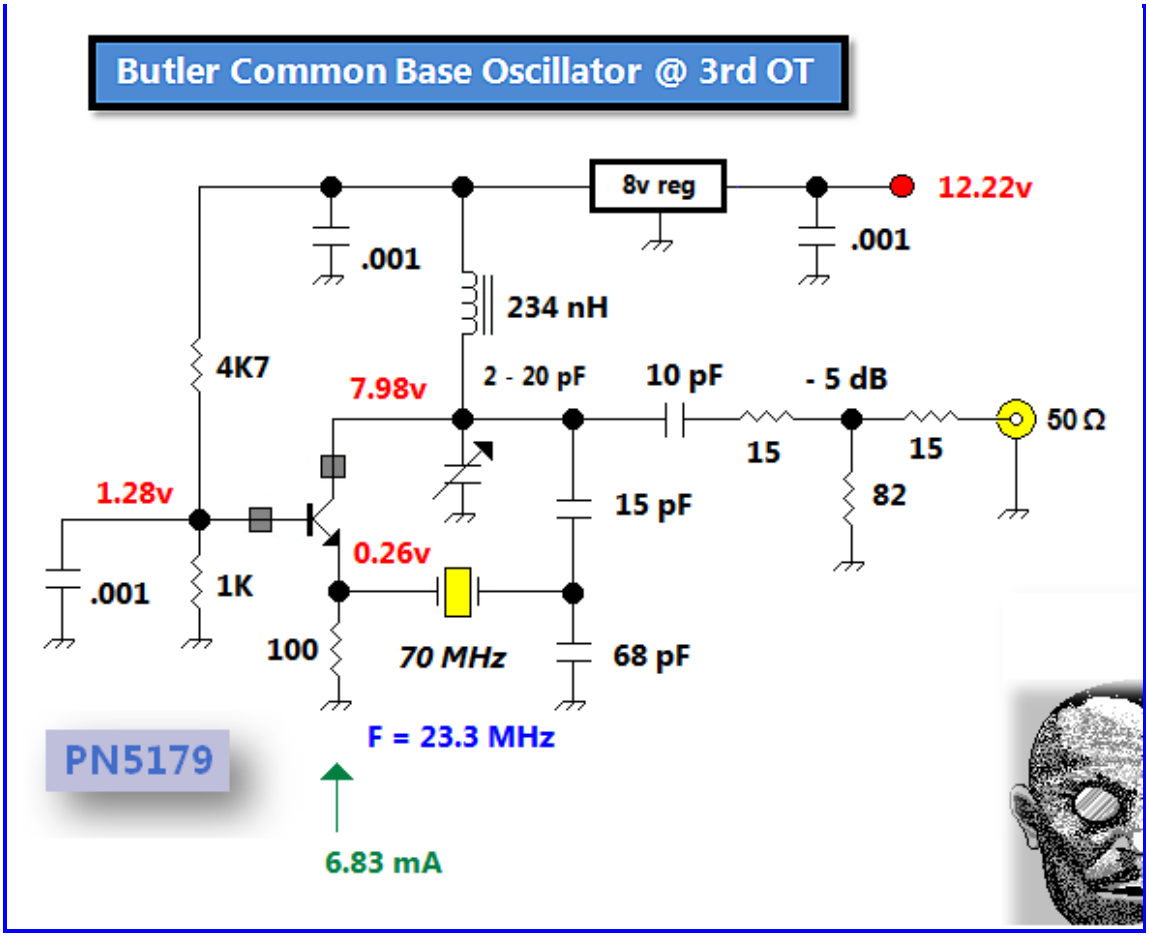

Above — The Butler oscillator now arranged for output at the third overtone. Click and click for the 'scope outputs at the third crystal overtone. The first scope tracing was slightly mistuned. Once again, the inductor had to be gently squished or contracted to obtain a pristine sine wave.

Fifth Overtone Frequency

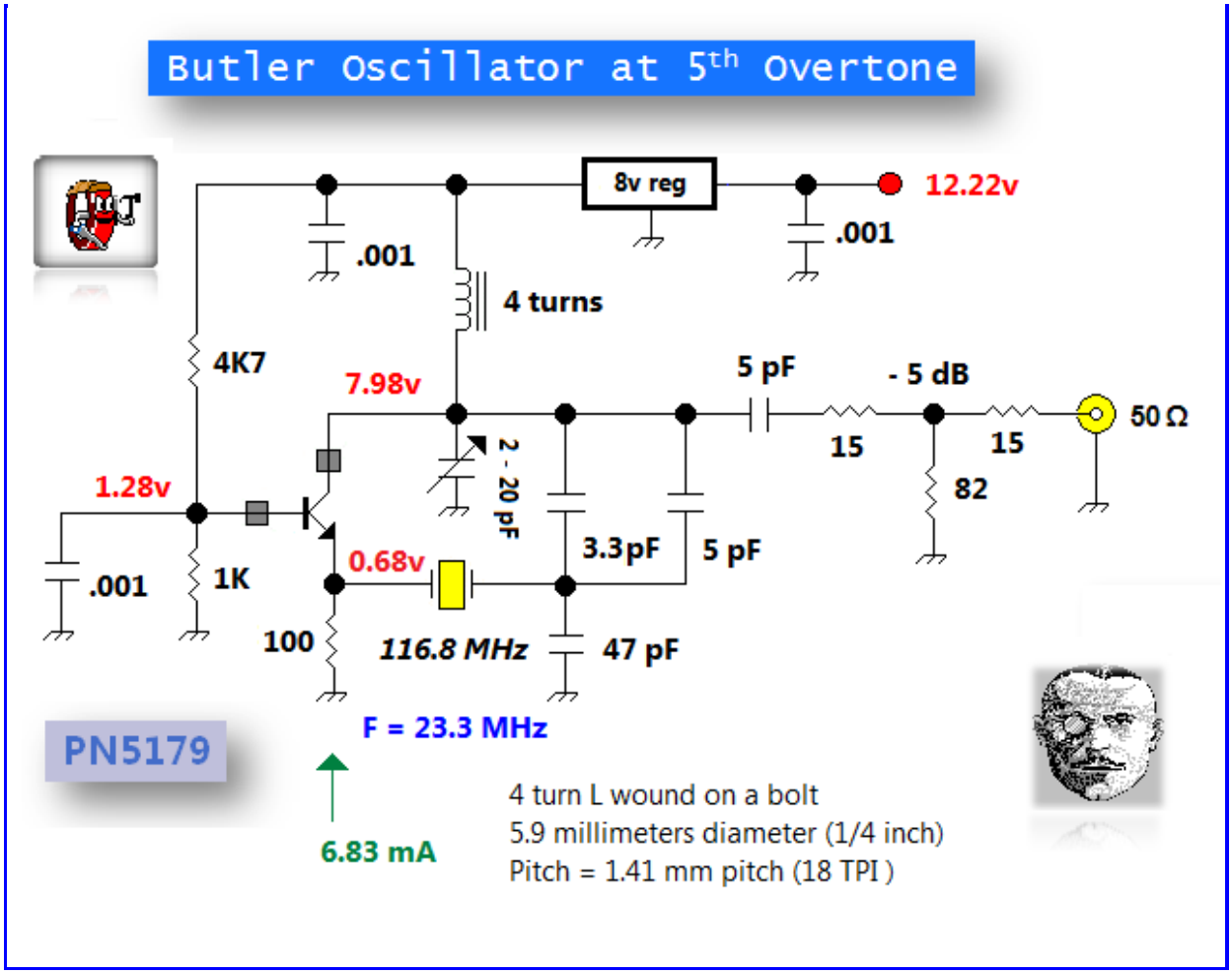

Above — The Butler oscillator at the 23.3 Mhz crystal's 5th overtone. Here's the 'scope tracing and an Ugly Construction photograph. The output = 7 dBm — very cool.

Some authors directly connect the attenuated output to the Local Oscillator port of a diode ring mixer. The signal is adjusted to the desired 7 dBm power by tweaking the 50 Ω pad attenuation, and/or the NPN's current. A good example = Single-Conversion Microwave SSB/CW Transceivers by Rick Campbell in QST for May, 1993.

The circuit above was measured with a 50 Ω terminated oscilloscope however, I also tested it with a 10X probe attached to termination resistors from 51 to 1 Meg ohms. When changing the 51 ohm termination resistor to a higher value such as as 47K, a previously working Butler may stop oscillating. The buffer input impedance and capacitance greatly affected the oscillator in my experiments.

When I wired up a Butler, 1 of 3 things happened: it did not oscillate, it gave a distorted output waveform, or it wowed me with a nice sine wave. Tuning the L-C tank is critical + finicky and may test your patience.

Adding an Inductor Across the Crystal

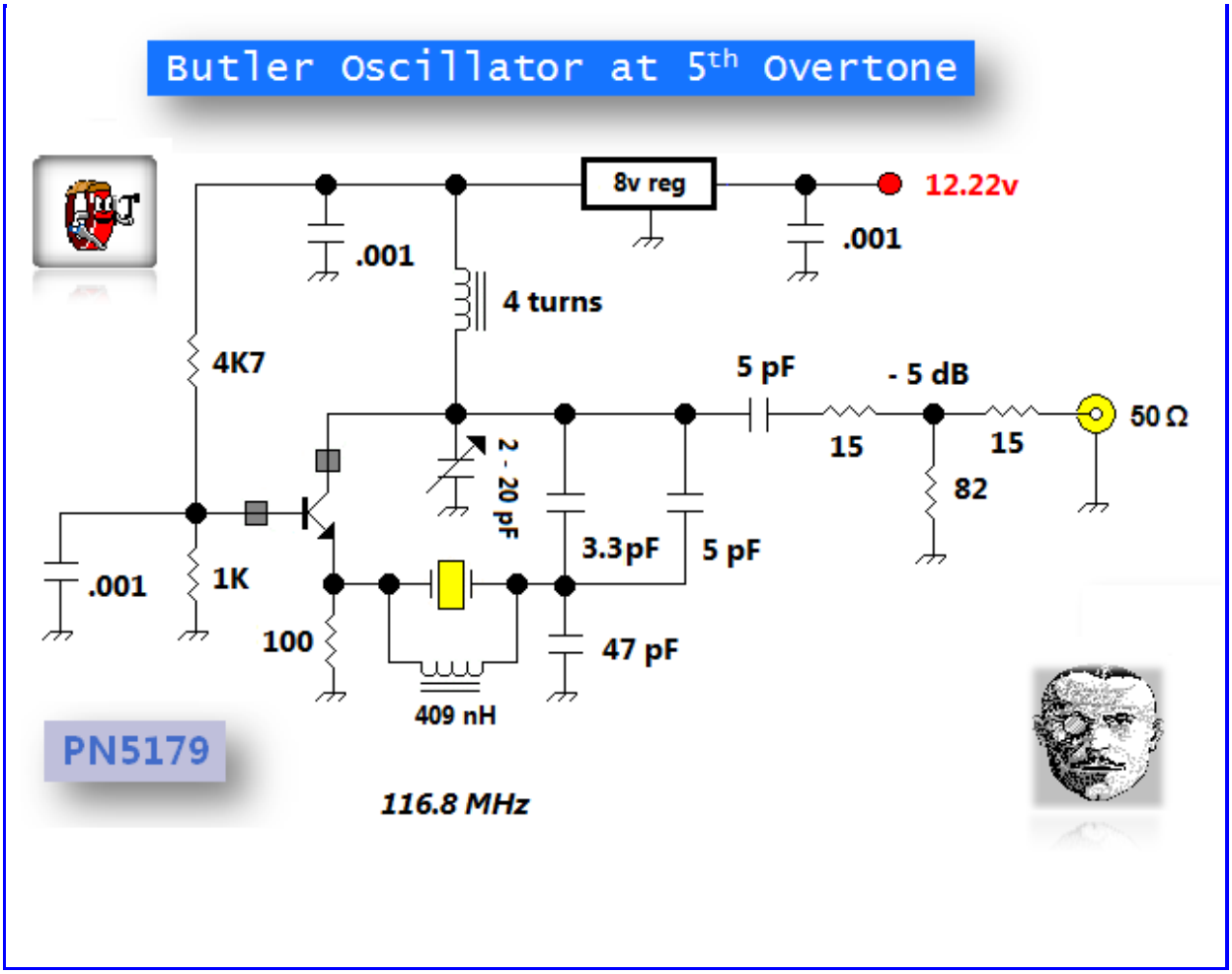

Above — The 5th overtone Butler with an inductor in parallel with the crystal

Above — My 116.8 MHz oscillator breadboard with an inductor wound on a T50-6 with wide spacing to allow scrunching and expanding of the windings across the crystal. I roughly determined my L should be ~ 400 nH and wound this on a # 6 toroid. While observing the output in my scope, I scrunched and then expanded its windings and adjusted the trimmer capacitor. The goal was to find a clean signal that snuffed out immediately when the trimmer cap was tuned off resonance. After finding the optimal L, I later removed and measured the coil. There is very little "wiggle room" — the oscillator tunes up and then dies very sharply as you tweak the trimmer cap. No sidebands were observed.

The inductor across the crystal is optional — some suggest it might only be needed above ~ 70 MHz.

At frequencies above ~70 MHz, the parallel capacitance of the xtal (C par) approaches the internal series resistance of the xtal and this provides an alternate path around the crystal for the signal and may short-circuit the crystal. The parallel inductor resonates with the crystal's parallel capacitance and tunes it out, so the crystal remains unbypassed.

Our teacher, Wes, W7ZOI published a document covering the Butler parallel crystal inductor here.

Simply put — the inductor allows clean tuning and output. That is, when you tune the trimmer to one side or another, the oscillator just dies and doesn't produce the sidebands that are shown in Wes' web article.

Since many of us choose computer, or other surplus crystals, a high C par + low Q crystal might give you tuning woes depending on your overtone frequency. In this case, adding the L to your circuit may improve tuning and ward off any unwanted sidebands.

With my particular crystal the parallel inductor is not needed, however, I can report that even slight mistuning just snuffed out my oscillator with the added inductor.

Seventh and Ninth Overtone Frequency

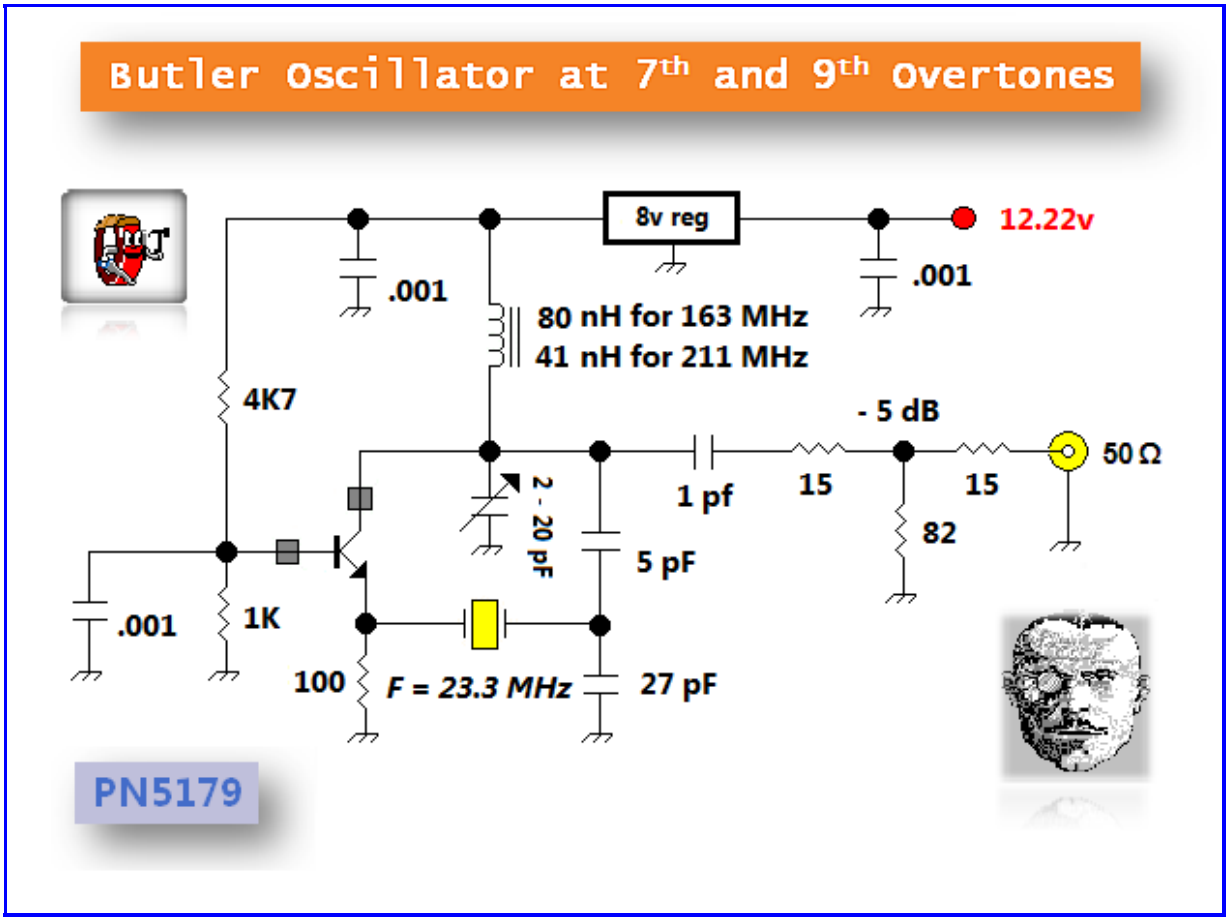

Above — I decided to take the Butler up to the 7th and 9th overtones. The 1 pF coupling capacitor proved the most critical part; for example, if I raised it to 5 pF, the oscillator would not tune above the 5th overtone. I wound the inductors on bolts and then compressed or stretched the links to get the perfect inductance. At these frequencies, stray inductance becomes quite significant and my coils were 1 to 1.5 turns less than indicated on

a spreadsheet coil inductance calculator. Click for the seventh overtone 'scope shot. Click for the ninth OT 'scope tracing.

I'm confident that if my 'scope bandwidth was higher, I could have resonated the 11th overtone.

---

2. Butler Oscillator-based 50 MHz Signal Generator

Lacking a 6 Meter band signal generator, I decided to build a 1 frequency device employing a Butler oscillator. Some may laugh at a 1 frequency signal generator — I won't since I'll use it to design and align amplifers, filters, a new 6 Meter band VCO and measure scattering parameters. Besides, you can double, triple, VXO or mix single frequency generators with another variable oscillator — this web site has roots in humble, simple test equipment.

In my bag, I found a crystal labelled 50.0000 MHz and measured its fundamental at 16.67 MHz in a simple Colpitt's oscillator — perfect . Design goals included variable amplitude, strong reverse isolation + reasonable shielding and return loss. Since, I lack another 6 Meter band signal generator I could not measure return loss, however, choosing proven circuits + a terminal attenuator pad will help.

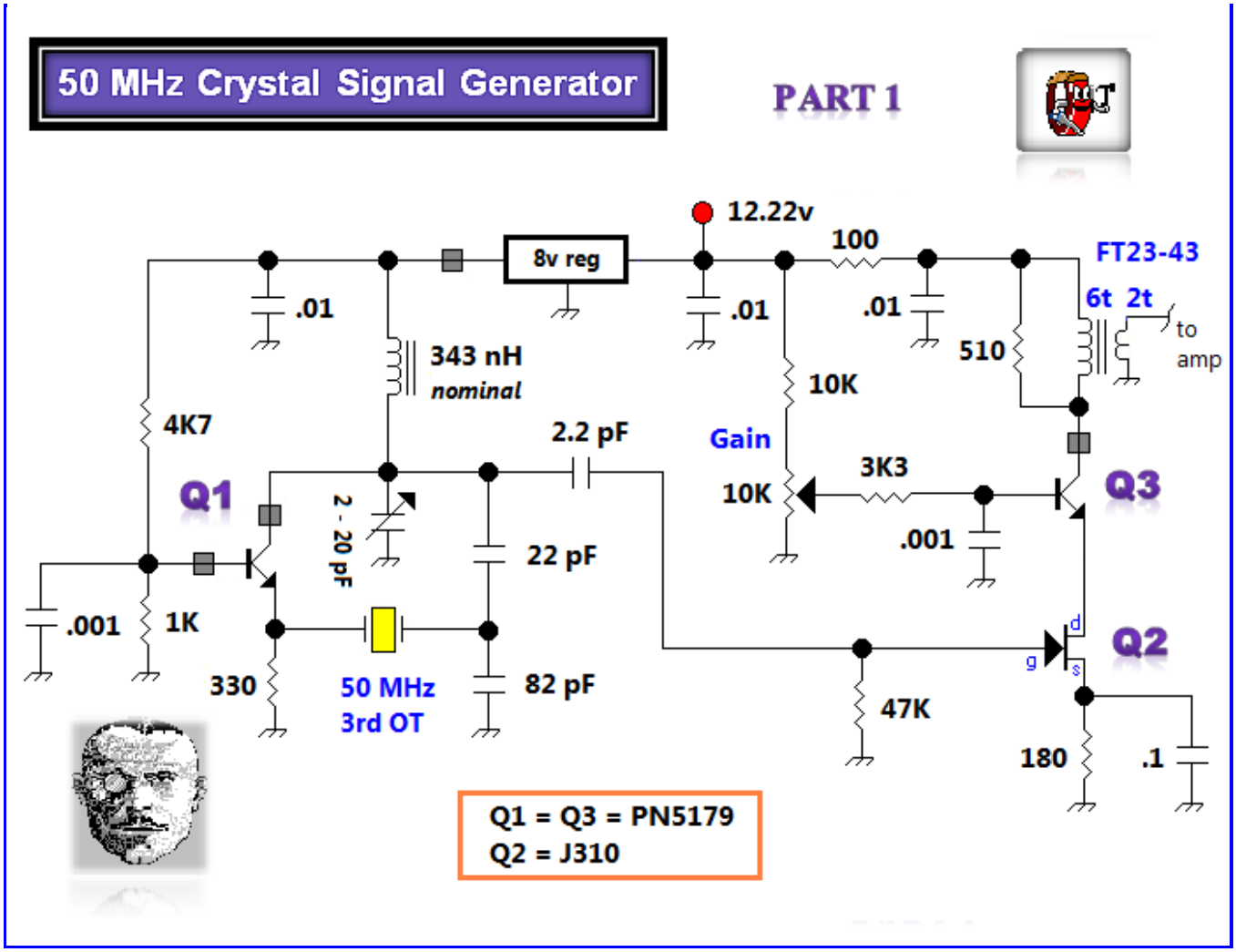

Above — Butler oscillator + hycas buffer. The 22 pF cap in the Butler was originally 15 pF, but when tested with various coils, oscillations proved a litle sluggish, so the 22 pF was substituted. I experimented with the coil, but ran out of time, so I wound a few turns of wire on a T50-10 toroid and soldered it in. After some careful manipulation of the windings, a glorious sine wave arose. I removed the L, measured it at 343 nH and then re-soldered it in place. An air coil or other size 6 or 10 powdered iron inductor should work fine.

Click for a moderate resolution photograph of the entire project.

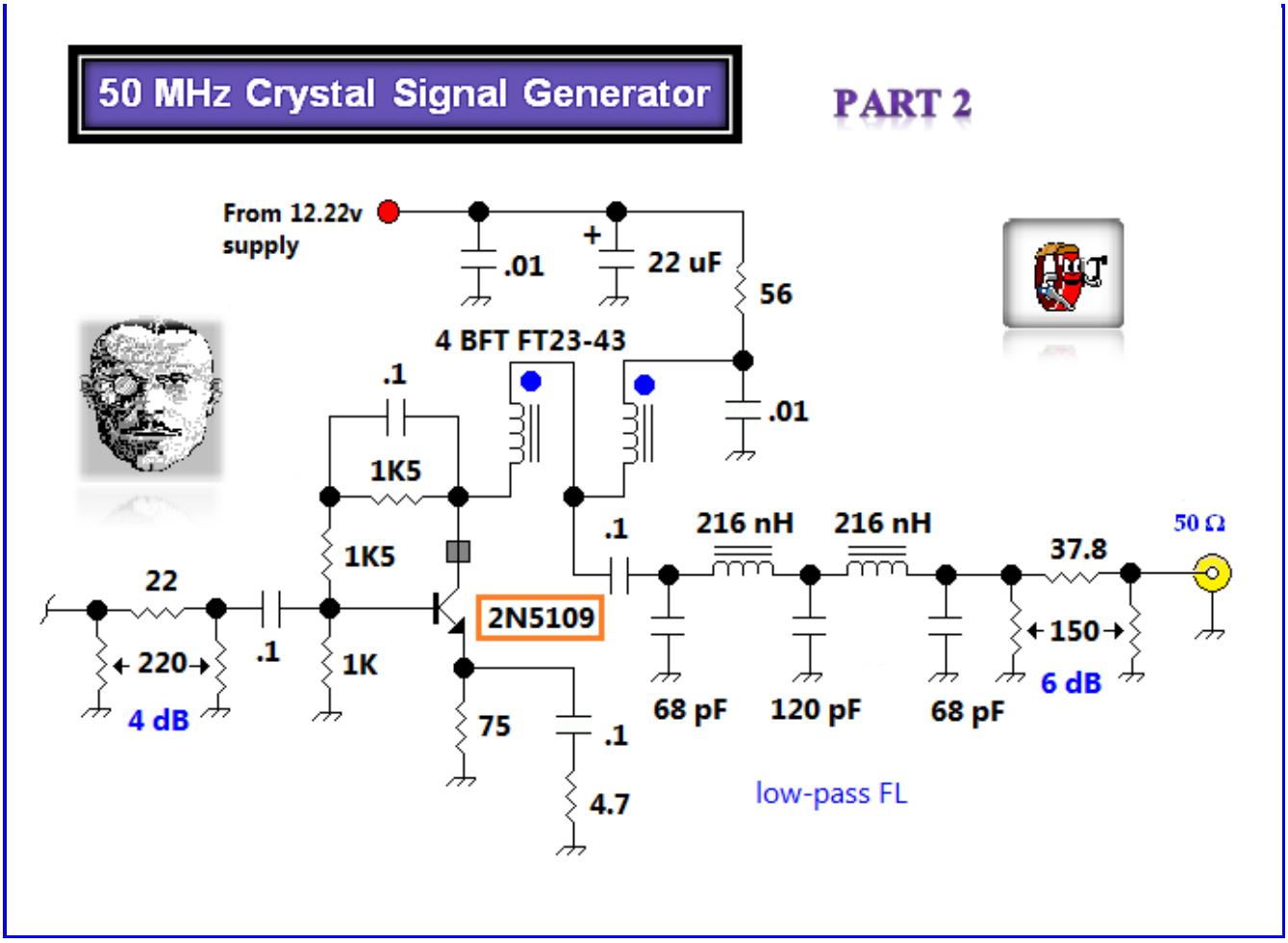

Above — The final amplifier and low-pass filter. The maximum output of the Q2/Q3 amp is hot and can overdrive the 2N5109, therefore a 4 dB pad was added. This pad also improves the input return loss of the 2N5109. An alternate technique might be to further reduce the maximal DC bias voltage into the Q3 base and remove the 4 dB pad.

Click for the minimum and maximum output voltage waveforms from my 'scope

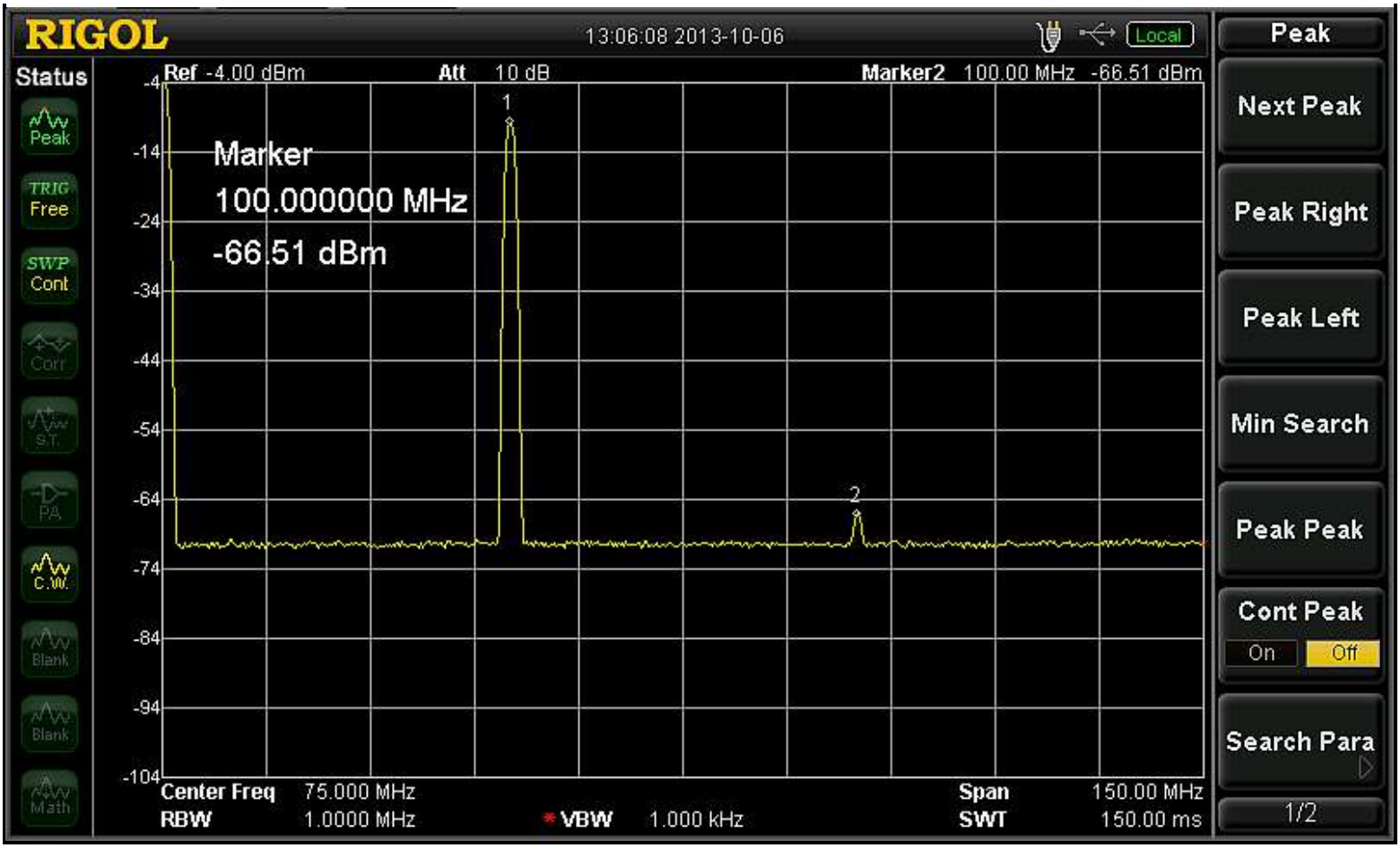

Above — Spectrum analysis with the generator output at -10 dBm. I placed Marker # 2 on the 2nd harmonic peak (100 MHz) and measured the power. The low-pass filter only attenuates the 2nd harmonic by ~ 25 dB, however, with the nice sine wave from the Butler, the 2nd harmonic measured -66.51 dBm = -56.51 dBc.

The 37.8 resistance indicated in the pad = 2 resistors in series. Many just use a 37 or 39 Ω R.

I look forward to advancing my VHF skills with this little signal generator.

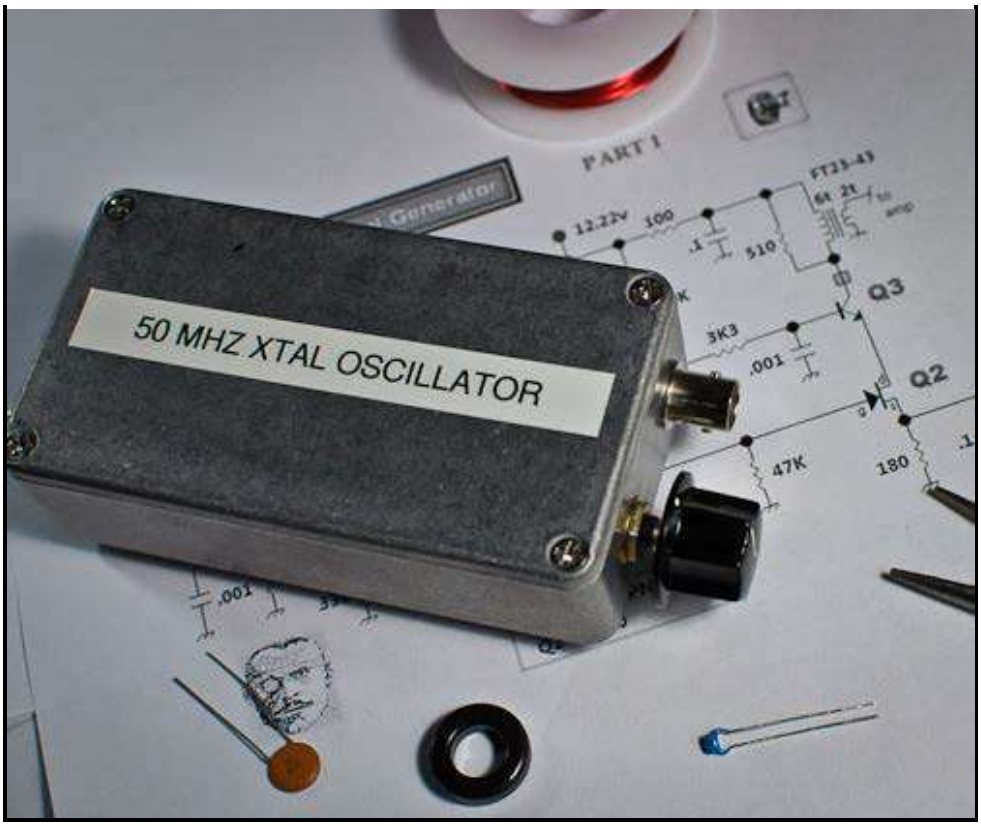

---

3. Doubler for the 50 MHz Signal Generator

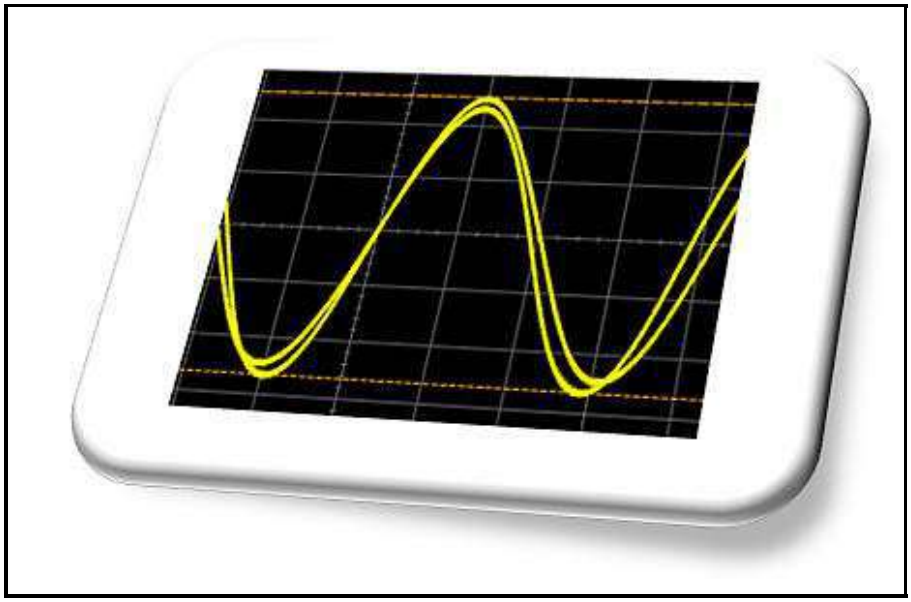

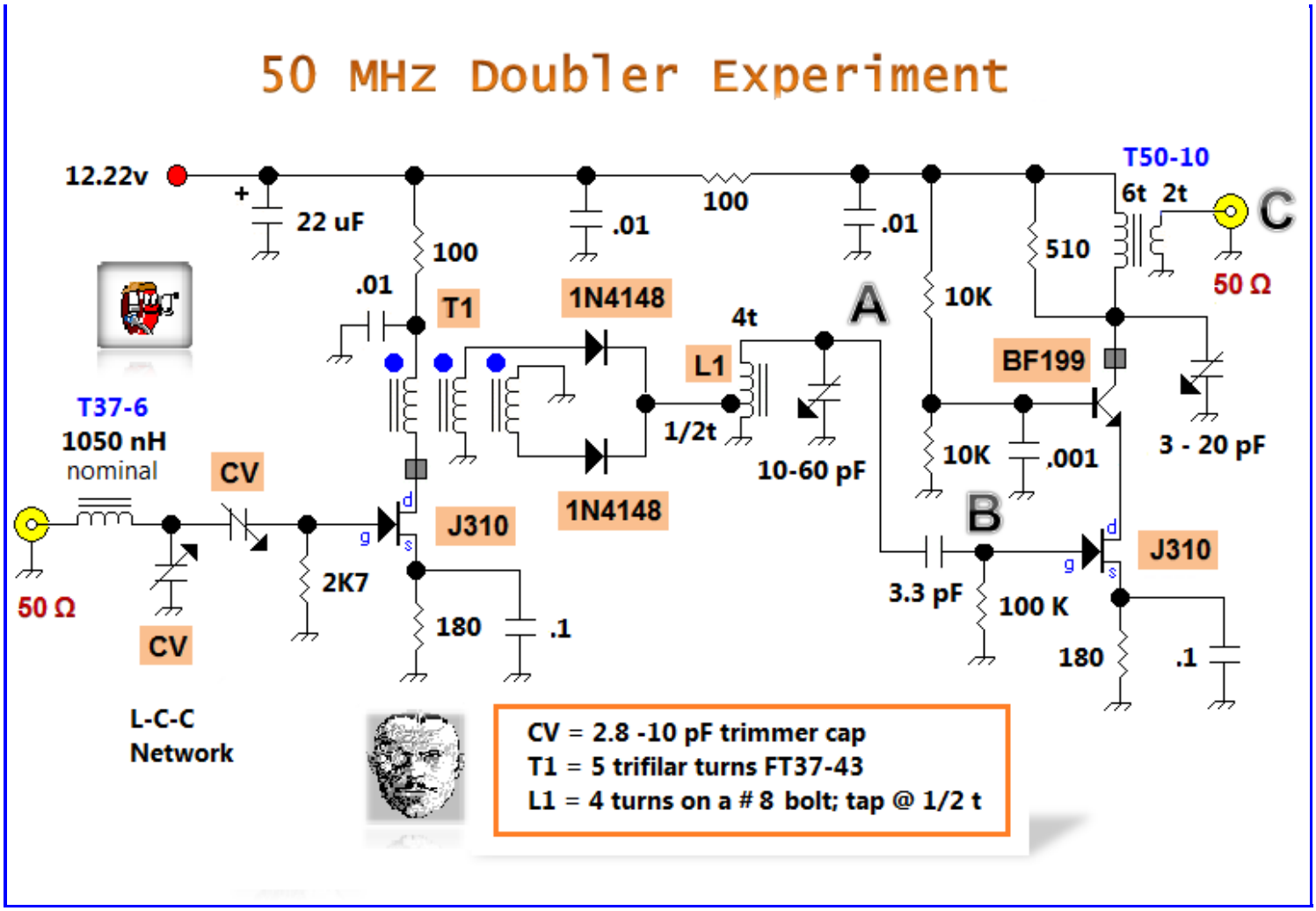

Above — An experimental frequency doubler for the Butler Oscillator-based 50 MHz Signal Generator shown above.

After trying a few circuits, I settled on a simple full-wave doubler featuring matched 1N4148 diodes driven by a JFET amplifier. Chapter 3 of Solid State Design for the Radio Amateur by Hayward and DeMaw for the ARRL = my key reference. Matched diodes (and a little luck), may suppress the 50 MHz signal up to 60 dB so only a single-tuned circuit follows the diodes.

The first JFET amp drives the diodes to improve harmonics + output voltage — an L-C-C Tee network matches the 2K7 Ω input to the 50 MHz signal generator output. I designed this matching network on the bench with the 2 diodes disconnected to avoid distortion during signal measurements. Using a 10X probe, I peaked the capactors for the greatest signal amplitude after finding the optimal L by educated trial and error. The inductor wound on a T37-6 was scrunched a little to further peak the L-C-C network.

I wound L1 with bare copper 26 AWG wire on a #8 bolt with coarse threads. To make enough space to solder on the 1/2 turn tap, I stretched the last turn with the other 3 turns still on the bolt to prevent stretching these coils. Click for a 'scope tracing at Point A. My 10X scope probe has ~ 15 pF capacitance and this affected the tuning — you can see some harmonics in the signal. With the 10X probe at Point B, I was nearly able to turn the circuit to 100.0 mHz, but still the 10:1 probe upsets the circuit somewhat.

This L - C tank tunes sharply and best with a non-conductive screw driver. I final tuned the L1 tank when the hycas amp was completed and connected to a 50 Ω terminated 'scope — eliminating the earlier tuning problems caused by the 10X probe. It seems that VHF requires more thought and care than HF when tuning resonators (tanks).

Point C is the maximum output (10.34 dBm) into a 50 ohm terminated 'scope. The 100.0 MHz signal is okay, but some builders might want to add low-pass filtering +/- an attenuator pad; or perhaps drive another feedback amp?

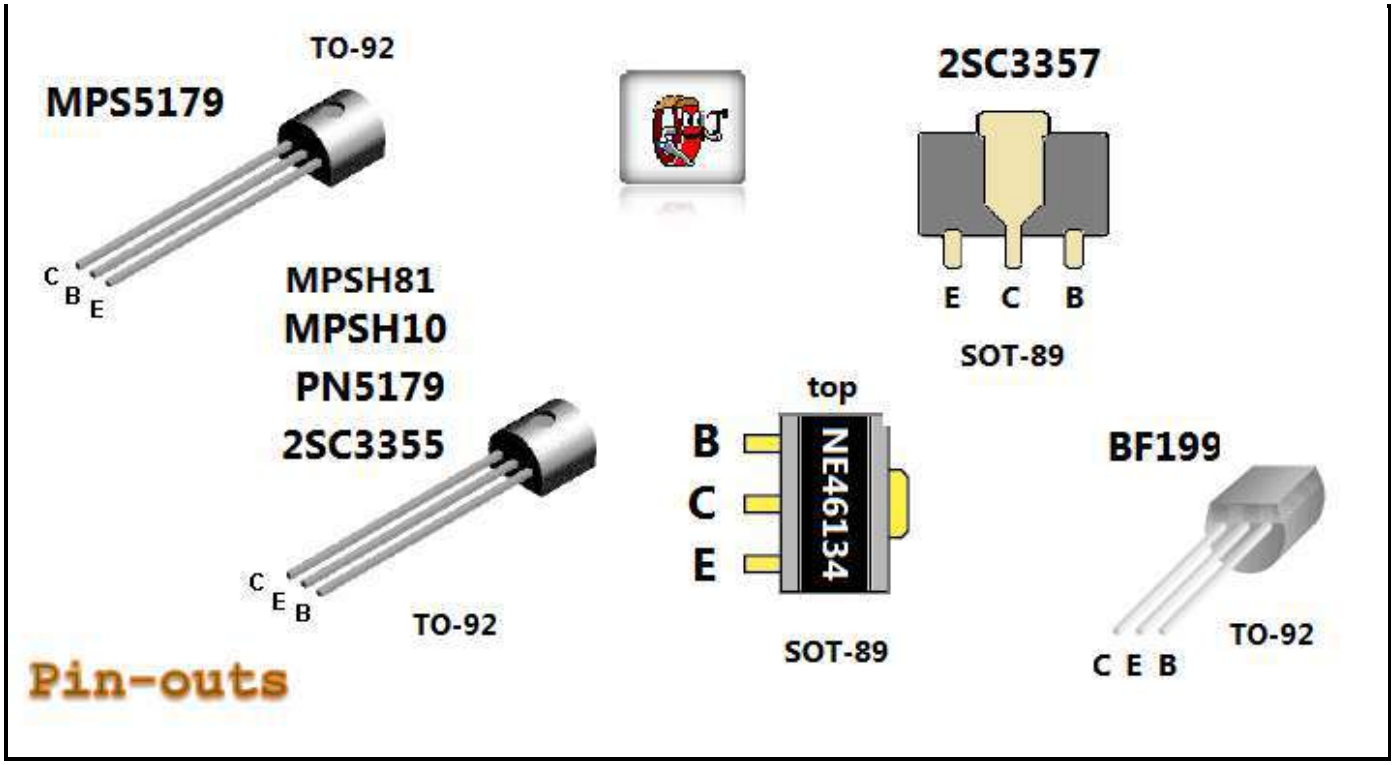
TO-92
MPS5179
C B E
2SC3357
E C B
SOT-89
MPSH81
MPSH10
PN5179
2SC3355
C E B
TO-92
top
B
C
E
NE46134
SOT-89
BF199
TO-92
C E B
Pin-outs

VHF to the Max — Miscellaneous 2012 Experiments

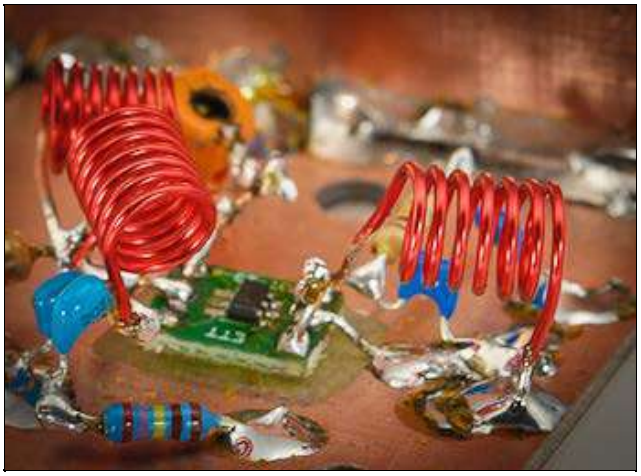

As a VHF newcomer, I need to make lots of circuits, measurements, mistakes and maybe — I might advance. My literature review revealed a big gap between popular, "for-fun", novelty-grade projects and the blinged-out circuits such as ultra low-noise LNA's featuring GaAs, MESFET, and pHEMT devices. Where do we find the middle ground projects? Likely on our own RF work benches.

Numerous questions arose — Will Ugly Constuction work? Do I have the right test gear? Am I measuring the proper things? What about noise figure? All a bit overwhelming — but even improbable discoveries began as simple questions and observations. We solve far more difficult problems each day.

I'm learning that whether your a beginner, or a master, bench fundamentals rank supreme. Want to avoid oscillations in your high fT BJT VHF amplifier? Work towards high reverse isolation, strong S11 and S22, careful layout and employ techniques that suppress instability — nothing earth shattering huh? I'm told that acquiring the needed skills takes time and practice.

In early Winter 2011-2012, I built some VHF signal generators, amplifiers and a lots of junk. This web page documents a few of these experiments.

Section 1. Early MAX2606 VCO experiments
Section 2: A 2-band signal generator based upon the MAX2606 VCO
Section 3: 50 MHz VCO
Section 4: 50 MHz Receiver Pre-amp and Filter
Section 5: QRP — POSDATA: Z-Communications VCO Experiments

Section 1. Early MAX2606 Experiments

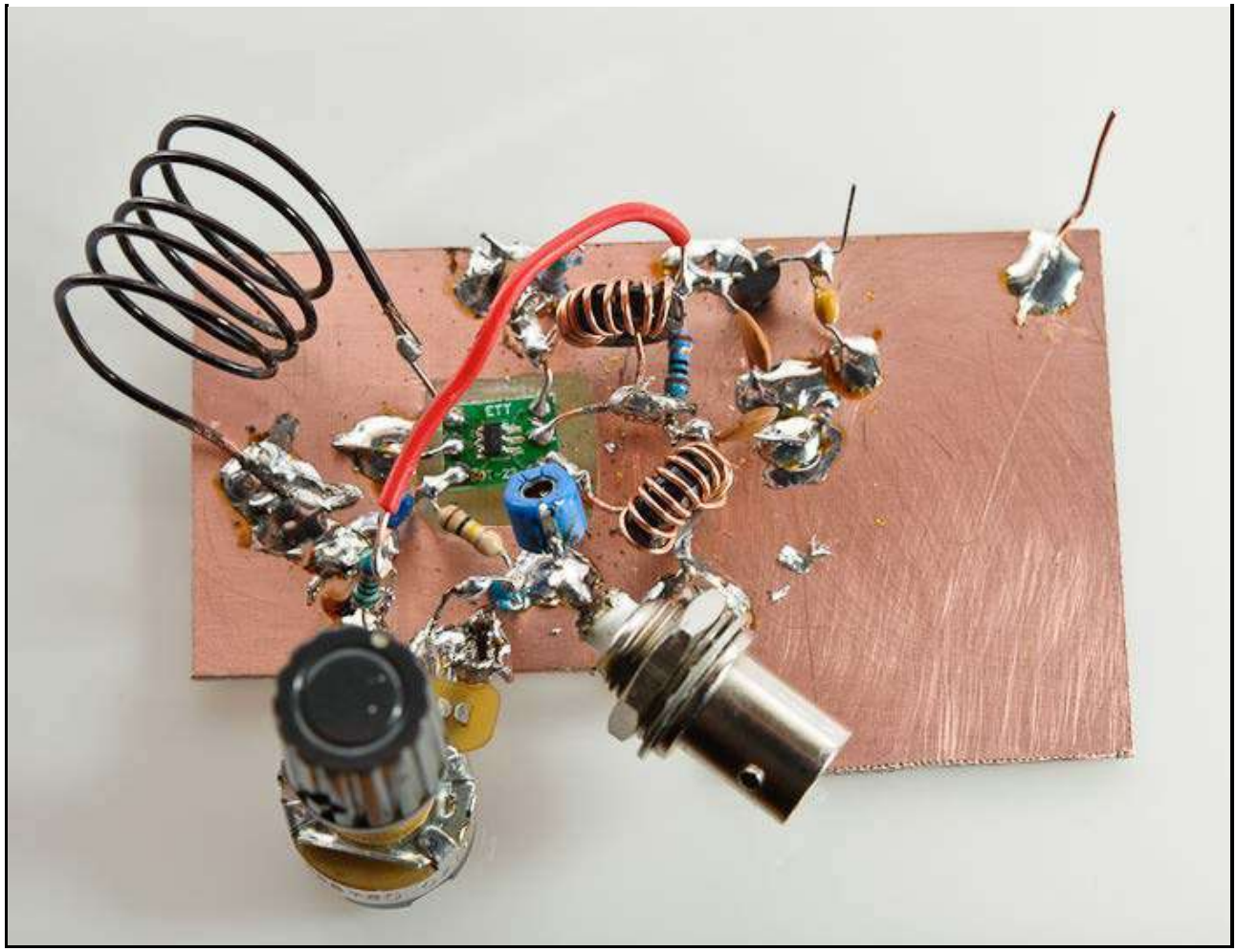

Above — My first of many MAX2606 VCO Experimental breadboards.

Maxim makes a series of cool SOT23-6 VCOs ranging from 45 to 650 MHz. Wanting a VCO to cover from ~100 to 106 MHz, I just had to try this chip. The datasheet provided all the online information I could find; save for a few homebrew, flea-powered FM transmitter projects that proved unhelpful.

After soldering the IC on a breakout (prototype) board using about 20X magnification, the proto-board was dropped onto a copper clad board with some of the copper ground away.

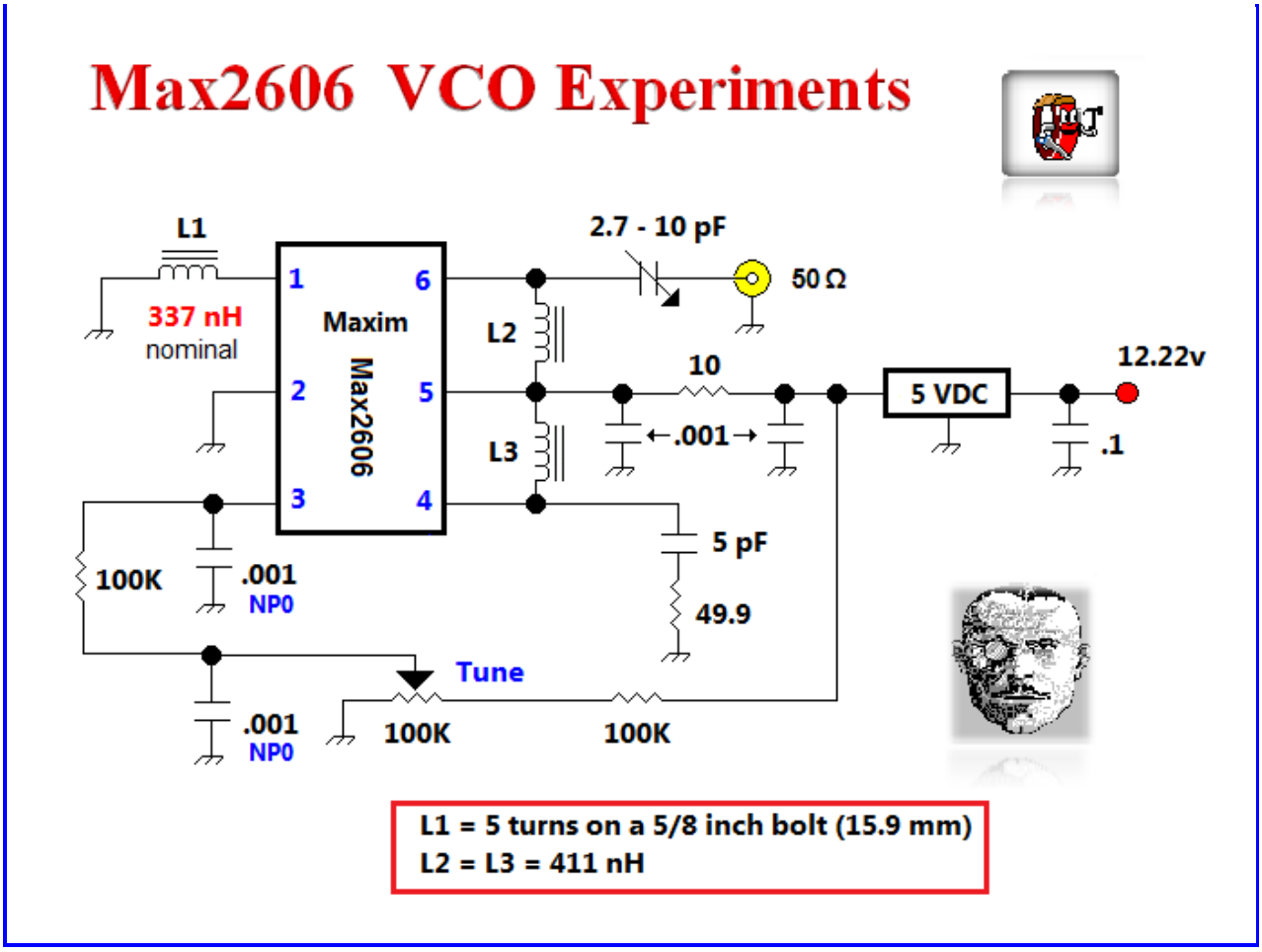

Above — My first MAX2606 VCO experiment. A coil lying on the workbench was soldered in as L1. I stretched it a little to set the lower band edge. Going from CCW to CW on the 100K tuning pot, I measured from 86.3 — 106.3 MHz. I'll write about L1 a little later, for making a good output network consumed my initial experiments.

The Maxim datasheet shows a simple output network consisting of 2 pull-up resistors with a maximum R of 1K. All the online FM transmitter designs I saw used 1K pull-up resistors and made no attempt at matching or even employing inductors in place of the resistors. I applied two 560 ohm pull-up resistors in place of L2 and L3 and the output looked distorted and low in amplitude. Click for a 50 Ω terminated 'scope tracing and click for a tracing with a 10X probe connected to a 10K load resistor. Unacceptable for even us scratch-builder RF experimenters.

Wanting to match the output into a 50 Ω load with high-pass L-network instead of just resistors, I calculated that an L of 250 to 800 nH, plus a capacitor from 2 to 10 pF might work, however, as a VHF newbie, my hopes weren't high. I went for a single-ended output and not knowing what to do, terminated the unused port with an AC-coupled 49.9 Ω resistor.

Choosing a 100 MHz test frequency (where I own a doubled 50 MHz xtal oscillator), I removed L1 to snuff the oscillator and measured an output return loss of ~ 17 dB with L2 = L3 = 298 nH and the variable cap set to 7.3 pF (I removed it and measured it). It took about 1 hour of trying different L values to get this return loss. I also learned that the L value and L to C ratio of L2 and its series capacitor greatly affects the purity of the output waveform.

Like all L-networks, the L and C *must* be correct to obtain a strong, clean output. Since C is variable, I tried various inductor values and further fine-tuned them by scrunching or expanding the L2 windings. *Compress or expand the L2 windings + trim the variable capacitor to peak the L-network at your desired frequency.*

From my experiments, the L3 inductance should be close to L2 for the best output voltage and symmetry, however, don't bother scrunching or expanding L3 because this won't greatly affect the output signal as long as the L3 inductance is close to L2.

Click or click for some 'scope captures of poorly matched output L-networks — low gain and/or distortion appeared with mistuning.

Click for the output where L2 = L3 = 298 nH. I had the tuning set to 100.6 MHz for this screen capture, however, you can see the nice waveform and strong peak-peak voltage when compared to the pull-up resistor only versions.

The problem with a high Q L- network = low bandwidth. I wound L2 and L3 on T37-10 powdered iron toroids and later tried T37-6 toroids. The higher Q of the number 10 material seemed to translate into higher output voltage, but narrower bandwidth over the number 6 material toroidal inductors. Alternate breadboard. When tuning the MAX2606, signal amplitude changes with tuning frequency and a single L-network peaked somewhere near the middle of the tuning range further worsens this amplitude issue.

The *unbuffered* VCO waveform distorts somewhat as you move farther away from the peak L-network frequency. After trial and error, I settled in a compromise of L2 = L3 = 411 nH. This gave the best overall signal purity + amplitude from about 98 to 106 MHz with a set peak at ~ 102 MHz. Tuning below 98 MHz tended to really distort the waveform. Click for the *unbuffered* minimum and maximum frequency 'scope tracings.

Placing an attenuator pad plus a buffer amp after the VCO dramatically reduced this distortion in my experiments, assuming the L-network components are correct and tuned.

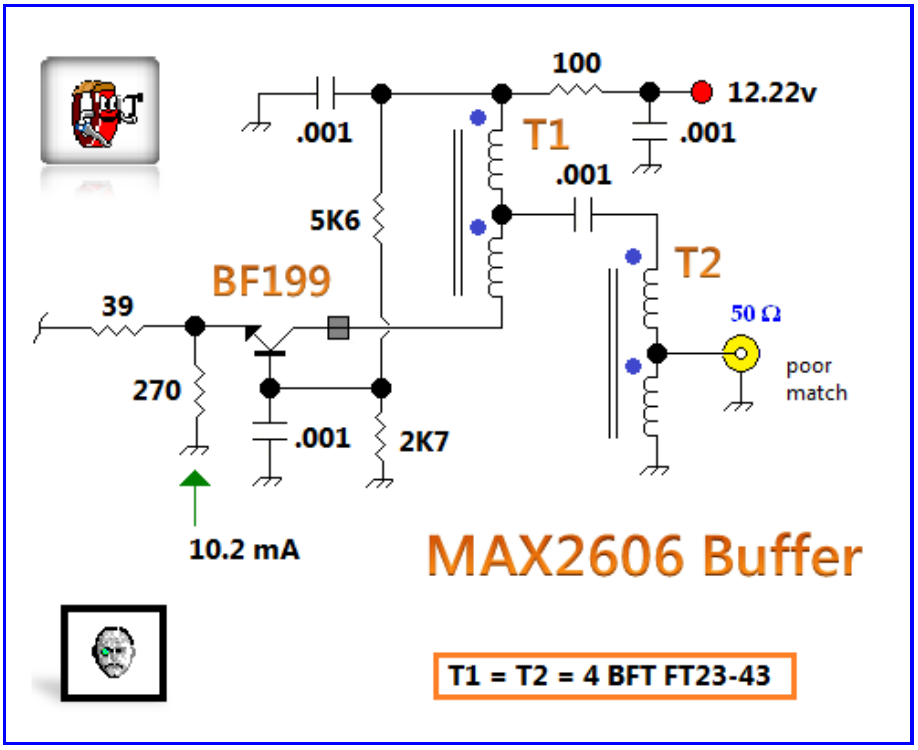

Above — A trial buffer first connected to output of the VCO schematic above. Two series-connected 2 transmission line transformers dropped the output impedance down for examination in my 50 Ω terminated scope — unfortunately the output return loss was poor (less than 10 Ω). Unlike the common base stage in a hybrid cascode amp, varying the bias to adjust gain worked poorly and lower applied bias caused distortion. I found it preferable to just fix the bias to get the greatest voltage gain + lowest harmonic distortion.

This buffer was discarded since the return loss was too low for my needs.

Testing a Hybrid-Cascode Buffer

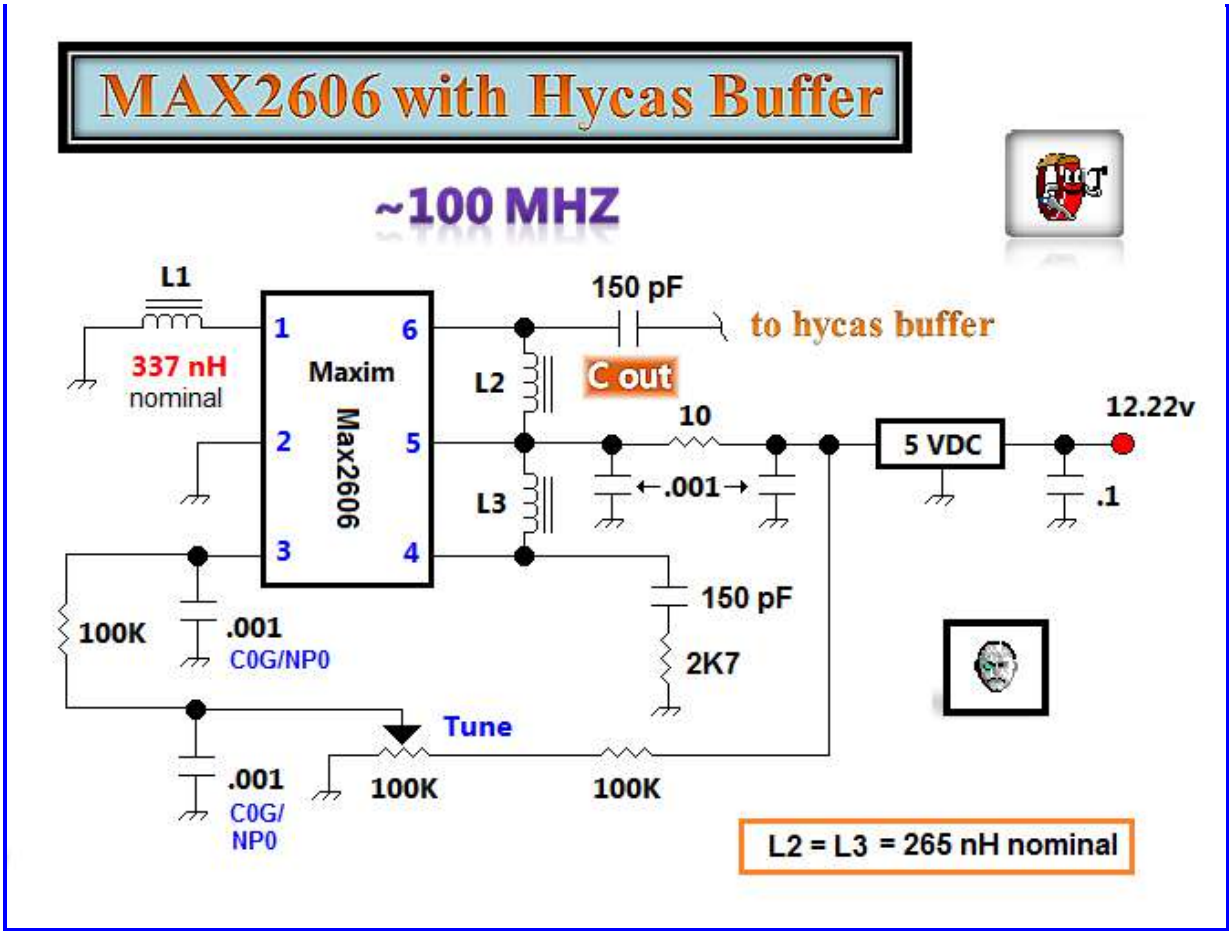

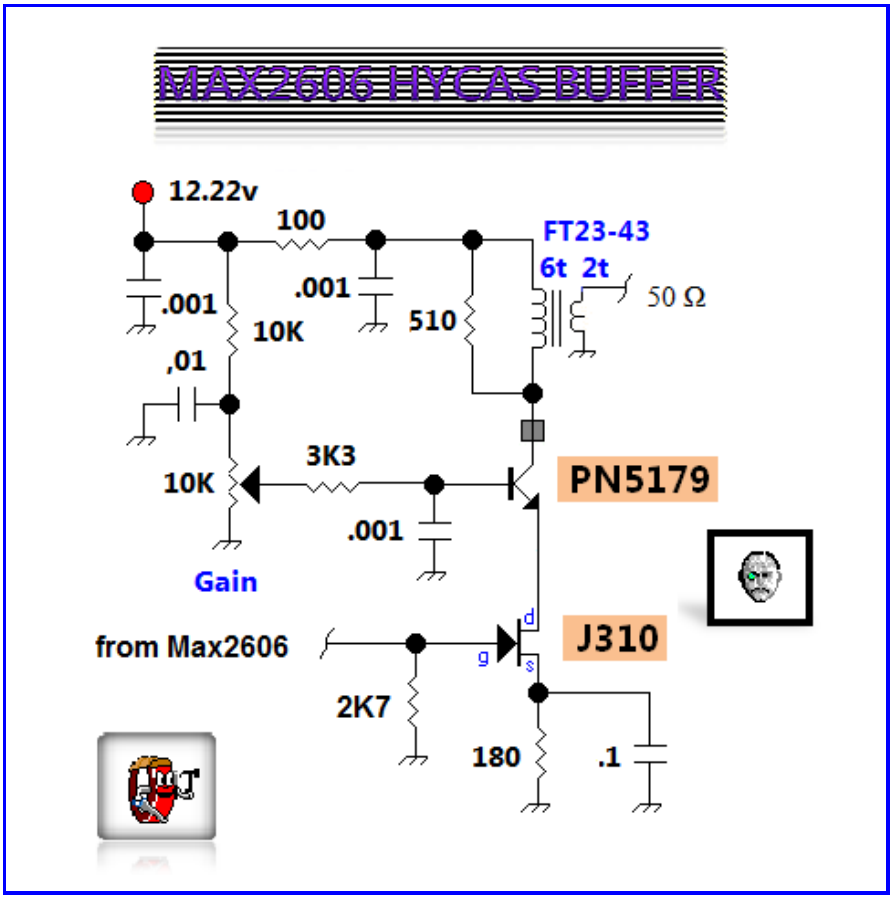

Above — MAX2606 VCO into a hybrid cascode buffer at ~ 100 MHz. I also tried a buffer with a cascode of PN5179 transistors, however, the input Z of the buffer changed when adjusting the gain potentiometer and wrecked the input matching, so I stuck with the hycas buffer shown

above.

L1 and L2 = ~ 265 nH wound on T37-10 toroids. To peak the L-match at ~102 MHz, I originally placed a 100 pF in parallel with a 10 - 70 pF trimmer cap for *C out*. After tuning, I removed, then measured these 2 caps to discover that *C out* = ~150 pF; so I just substituted a 150 pF capacitor. The L1 windings were expanded a little to re-peak the output network — expanding the coils raises fCo, while compressing the windings lowers the cut-off frequency. I don't recommend omitting a trimmer capacitor unless your confident with your measurements.

Click for the maximum power 'scope tracing of the hycas amp with the L-match peaked at 102.2 MHz (3.44 dbM)

Once again, I terminated the secondary output of the MAX2606 with an load resistance equal to the main output with an approximately equivalent fixed-value capactor — I'm not sure if it's needed, but it works okay and I stuck with it.

Up at ~ 144 MHz

Click for another experiment with the fore mentioned MAX2606 into the hycas buffer shown above at ~ 144 MHz. I peaked the L-match for 142.2 MHz and the output power = a surprising 7 dBm. The output is a clean sine wave from 135 to 169 MHz, although the signal amplitude varies widely. I also peaked it at ~144 MHz. I wound L1 - L3 with #21 AWG on a #10 bolt. Photo 1 Photo 2.

Let's build something useful with the MAX2606 based upon the experiments thus far...

Section 2. A 2-band Signal Generator Based Upon the MAX2606 VCO

Above — My dual VCO based on the MAX2606. This general-purpose signal generator will start my VHF circuit development in these 2 frequency bands. The importance of owning good signal generators can't be overstated — while not engineer grade, this box features a clean sine wave, strong output return loss and 1 KHz or better tuning resolution.

The center ON-OFF-ON toggle switch only turns on 1 oscillator at a time. The top 2 (ten-turn) tuning potentiometers lack knobs *(I'll get some later)* and the black knobs below them are attached to *unused* potentiometers. Initially, I planned to employ front panel gain control and drilled holes and fitted 10K pots in the chassis — I later decided to control the output power with outboard variable attenuators and skipped front panel power control for simplicity sake. Click for a side view of the unfinished project. Click for an early photo of the VCO **A** breadboard — I attached a shield to the copper clad board to help isolate the 2 VCOs.

I chose the frequency band **A** (138.5 - 172 MHz) to include the Ham 2 meter band + local commercial/service VHF segment and band **B** (98.919 - 109.06 MHz) to capture the FM broadcast band above 98 MHz.

Band A: 138.5 - 172 MHz

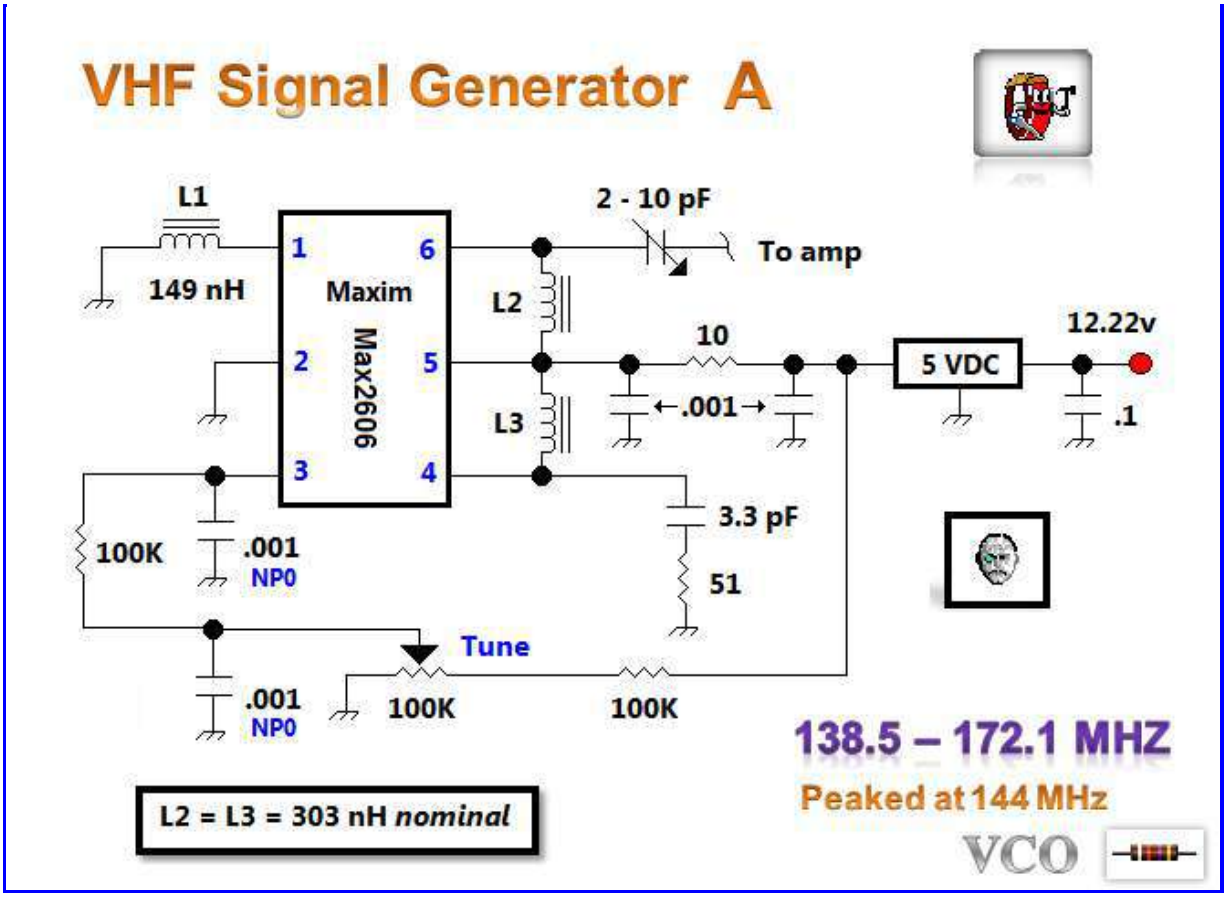

Above — The VCO schematic **A**. An L-match peaks the output at 144 MHz into 50 Ω. The beauty of this circuit = simplicity; just 2 active devices give low distortion and a strong output return loss (S22) on the 2 Meter Ham band.

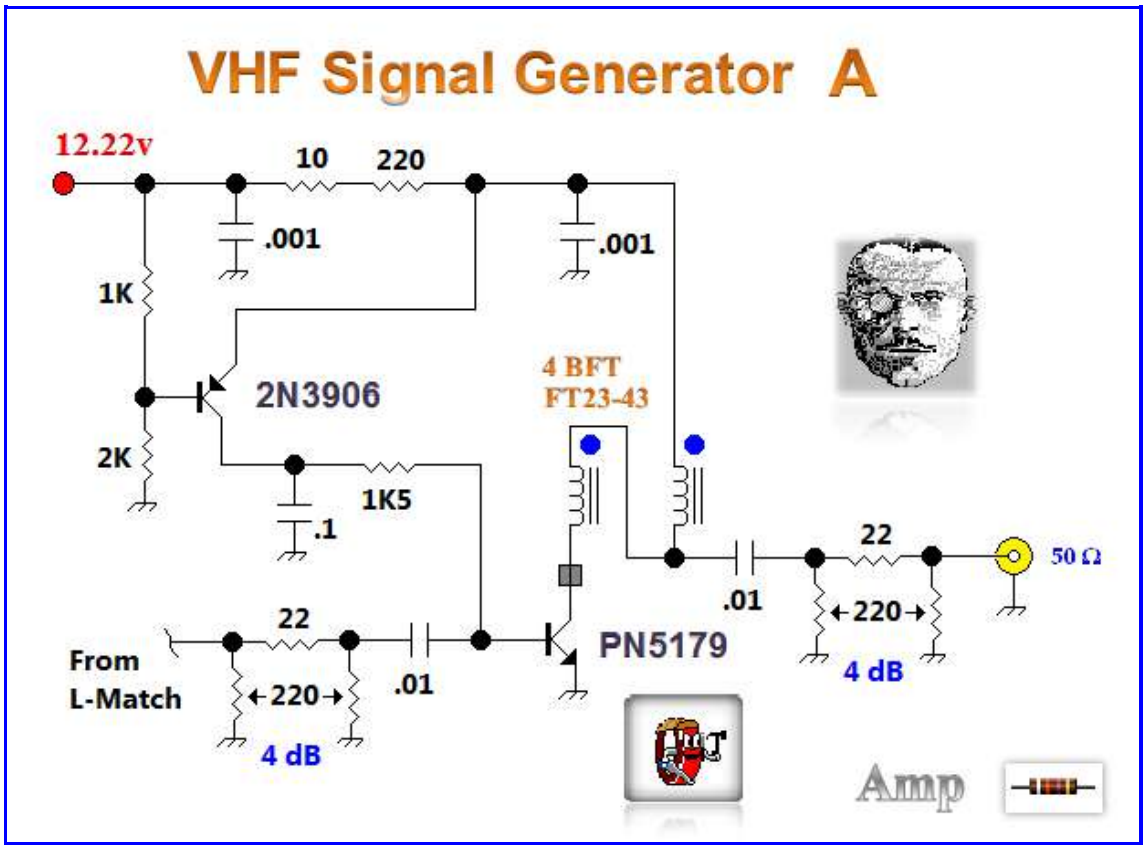

Above — The output amplifier for VCO "A". Click for a schematic with some analysis at 144 MHz (the frequency I'll use the most). I spent a lot of time trying to develop a 50 Ω output Z voltage amp up at ~ 144 MHz. My attempts to employ shunt and series feedback gave generally poor results — stray reactances plague the standard FBA designs that work great under ~70 MHz.

Since the MAX2606 has an output L-Match, getting a high output return was my only goal — grounding the PN5179 emitter, employing a 4:1 transmission line transformer and biasing for ~15 mA emitter current did the trick. A 4 dB pad on the NPN input further establishes a strong S22 (output return loss).

As possible, I attach additional 50 Ω outboard attenuators on my signal generators, however, the S22 on the stock generator should be okay across the VCO range due to the two 4 dB pads.

I measured the S11 on a prototype NPN amplifier by using the MAX2606 VCO shown to drive a MMIC with a 16 dB 50 Ω attenuator pad on the output and connecting it to the RF port of my return loss bridge. Thus, the actual VCO helped me design the final amplifier which buffers it in my final build. I kept the PN5179 and all other leads short as possible.

The output power looks like a sine wave when tuned from CCW to CW: With the 10-turn tuning potentiometer set to CCW [138.5 MHz], the output power ranges from -1.9 dBm; hits a peak of 0 dBm at 144 MHz and then gradually drops to -11.2 dBm at CW [172.1 MHz].

I moved away from the hycas buffer amp to simply my design and increase reproducibility. A MMIC might also work well, however the high current drain, potential for instability and biasing considerations introduce new problems — a simple wrap around PNP-biased NPN amplifier works okay. Sometimes the best solution = the simplest.

Band B: 98.919 - 109.06 MHz

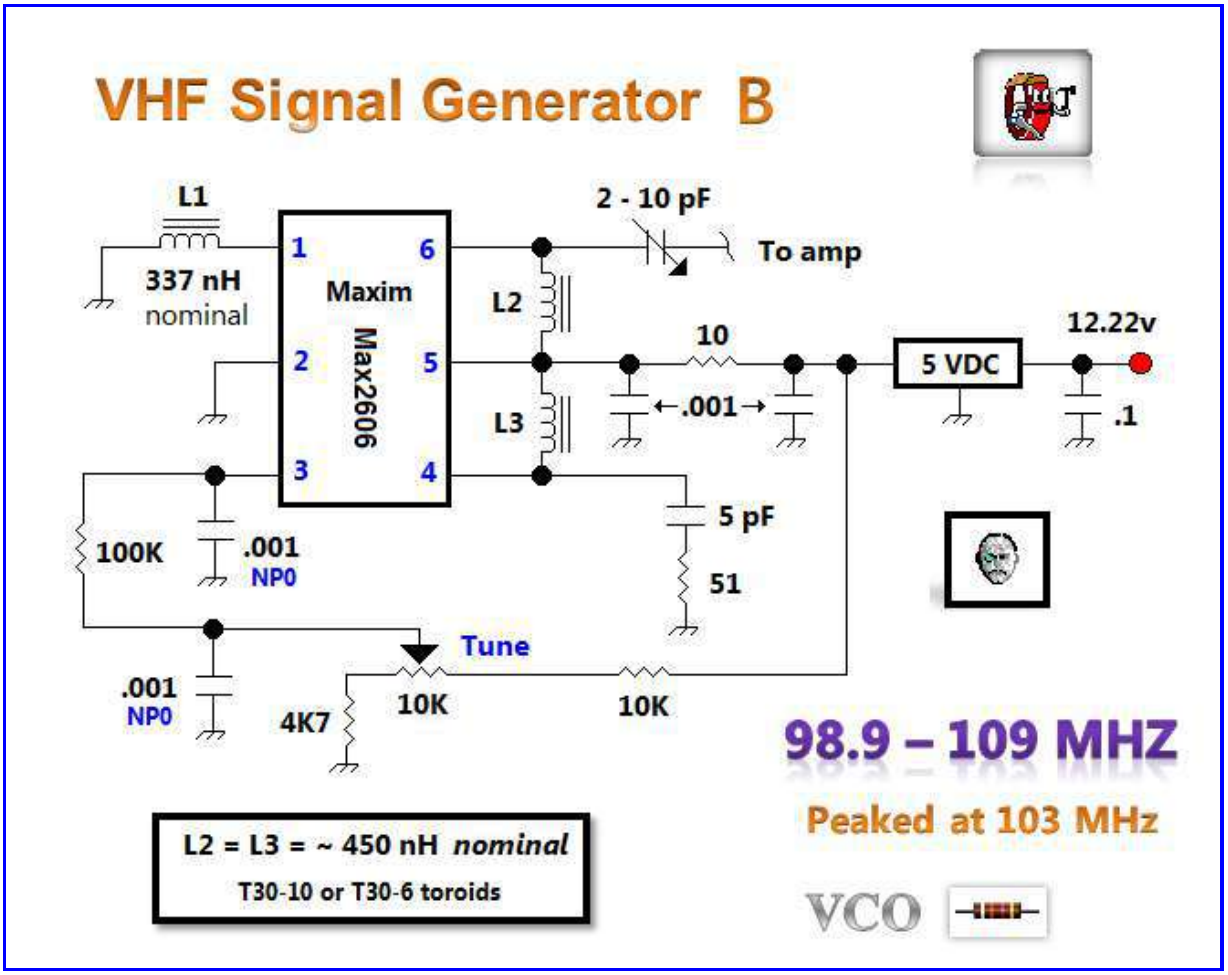

Above — The VCO schematic **B**. An L-match peaks the output at 103 Mhz, although compressing or expanding L2 and tweaking the 2 -10 pF capacitor can peak the L-network anywhere in the tuning range. I limited the tuning range by adding a 4K7 R to the tuning pot to enable better matching and fine tuning.

In all cases L1 = an air inductor wound on a coarsely threaded bolt using 20 or 21 guage enamel-coated magnet wire for mechanical stability. I set the lower band edge of the VCO by setting the tuning pot to CCW and compressing or expanding the L1 inductor to get the frequency shown.

For L1, I found that excessively long leads can create unwanted oscillations and my coils are just a few mm above the copper board. Some builders properly mount their coils in a upright "smokestack" fashion and/or well away from the nearby metallic chassis or copper PCB to minimize Q losses + inductance changes. My coils lie well away from the metal chassis walls.

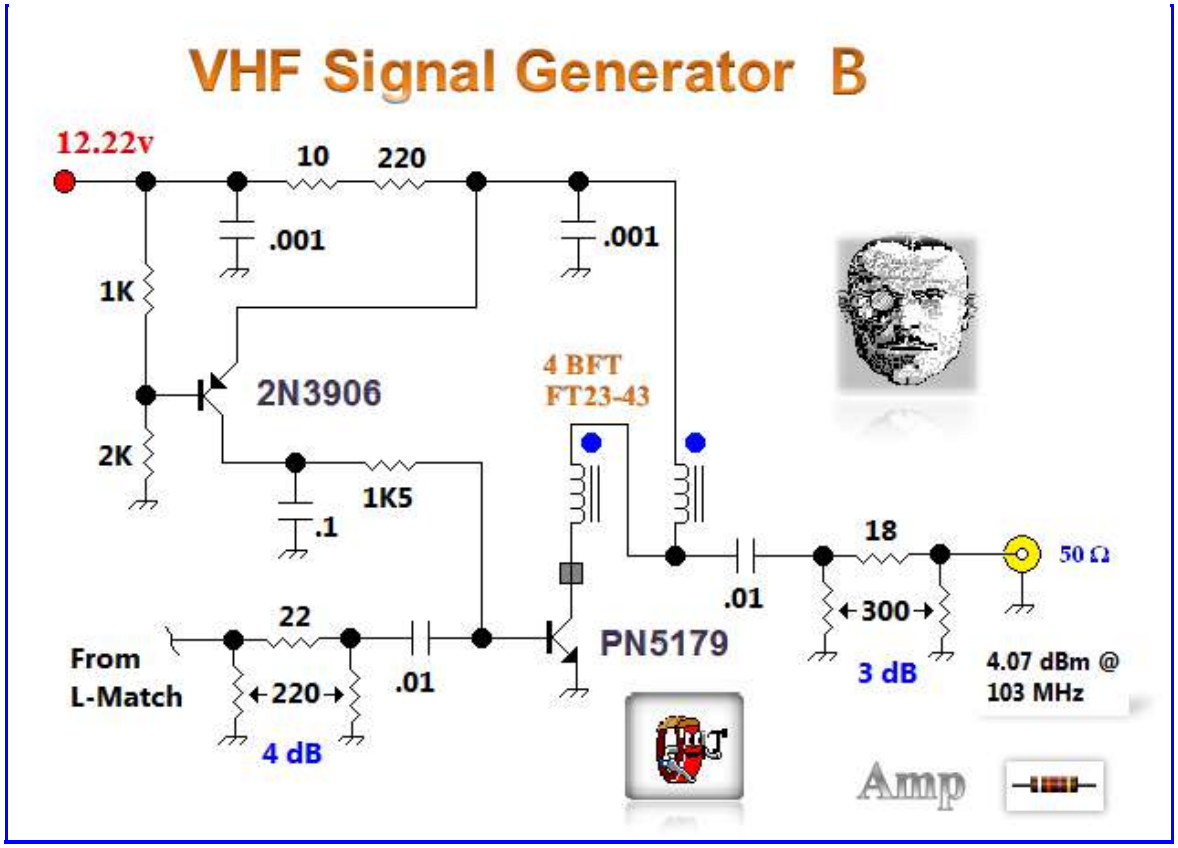

Above — The VCO **B** buffer/amplifier schematic. A clean sine wave appears across the entire tuning range — output return loss tuning from minimum to maximum was > 21 dB before I added the 3 dB pad.

Click for a photo of the completed, partially labelled project during the final tune up with all the boards bolted in.

Section 3. 50 MHz VCO

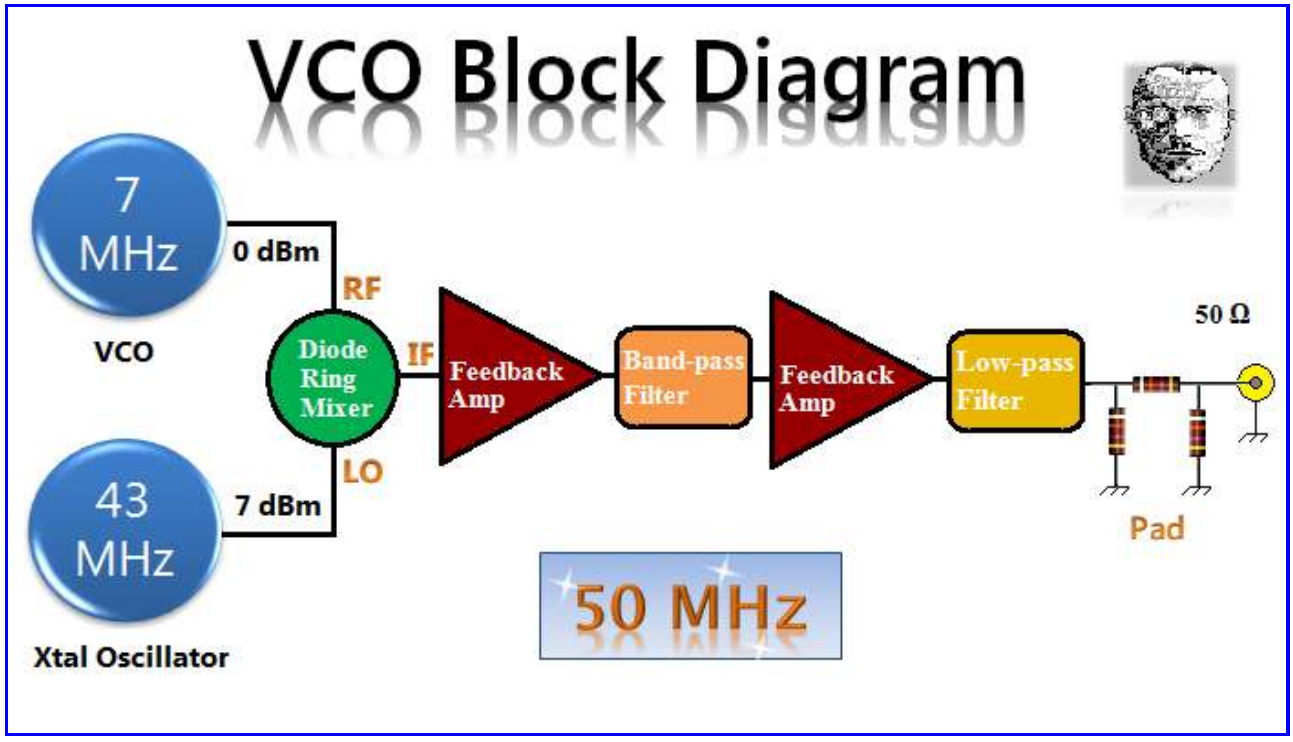

Above — Block diagram of the 50 MHz VCO I designed and built in February-March 2012. Click for a photo.

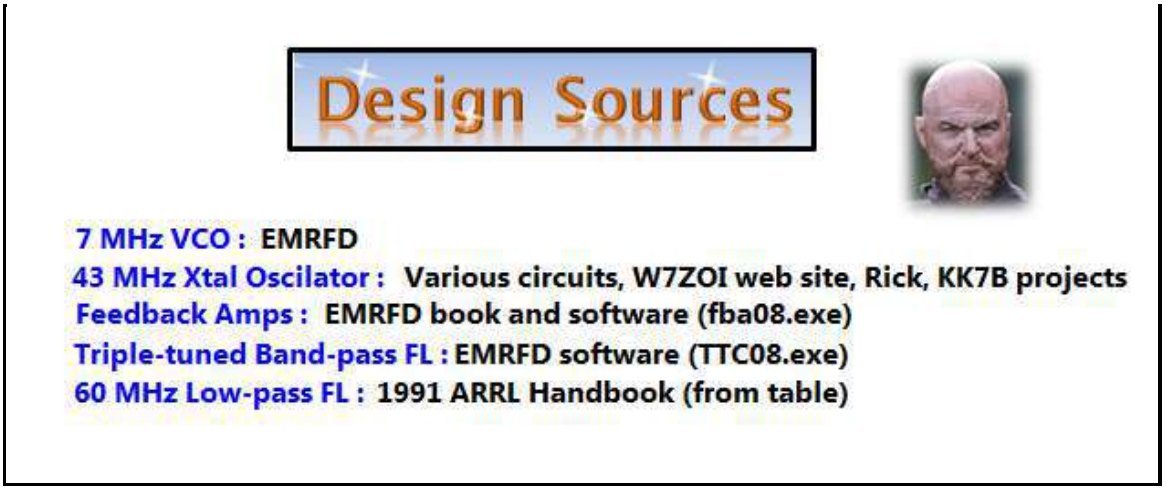

Above — Like most of you, I'm just an amateur designer who relies on others for example circuits, design procedures and inspiration. These cited references plus hard work drove my experiments. This project succeeds the Miscellaneous RF Experiments web page from 2011 — QRP SWL HomeBuilder evolves as I do.

7 MHz VCO + Buffer Amplifier [0 dBM output power]

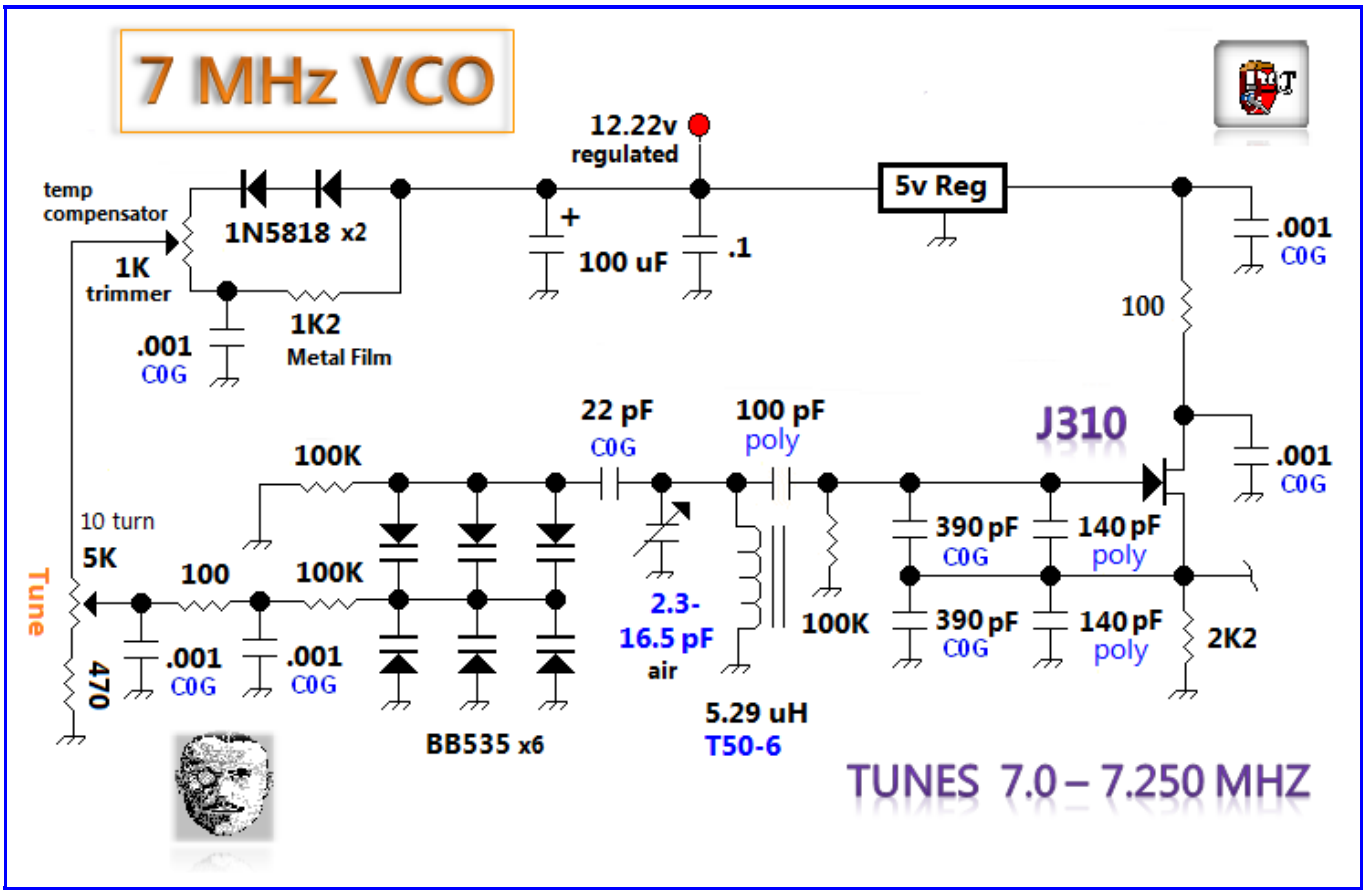

Above — 7 MHz Colpitts VCO schematic.

This VCO tunes ~7.00 to 7.250 MHz, although a wider tuning range occurs if you allow the tuning diodes to drop to 0 VDC with the 5K tuning pot cranked CCW. A 470 ohm resistor keeps about 1 VDC on the varactors at the lowest tuning frequency/applied reverse DC voltage.

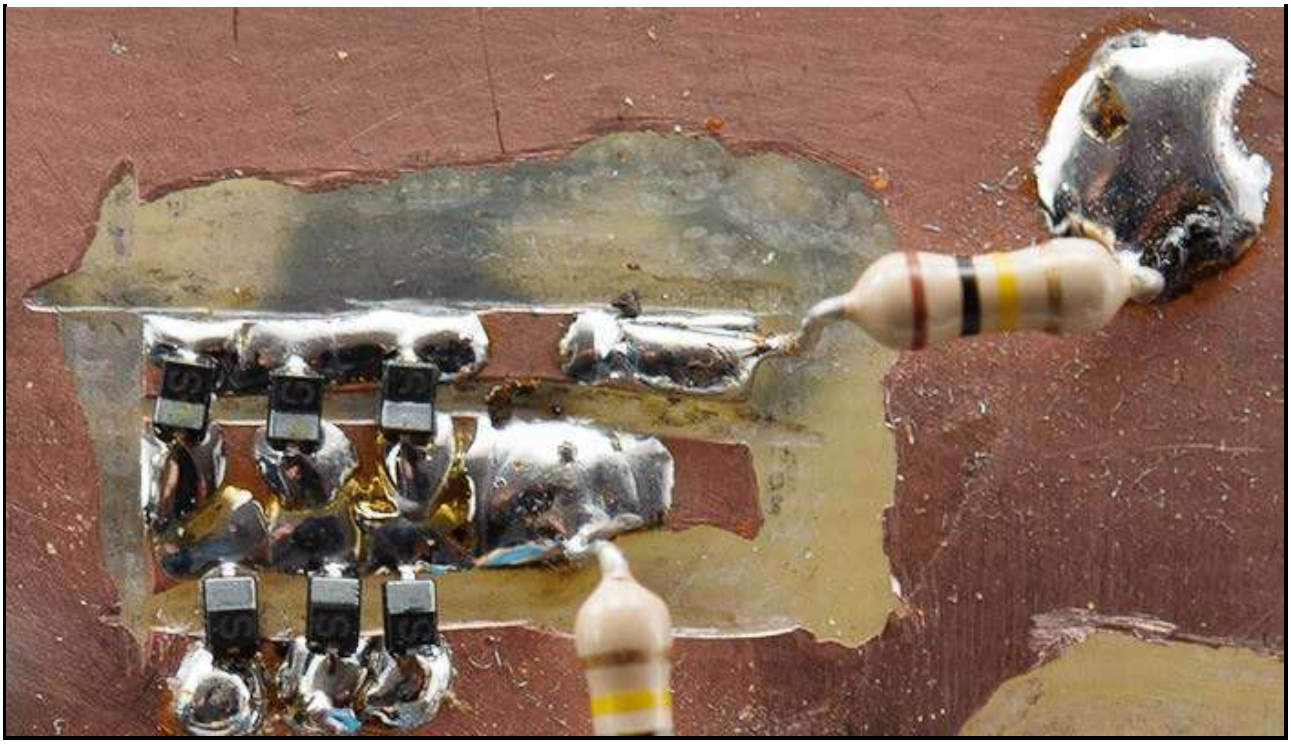

Above — A macro photograph of the six BB535 varactors soldered on the VCO breadboard. With 0 applied reverse DC voltage, their total C = 43.5 pF. I left room for up to 4 more diodes, but didn't need them.

Macro photography provides an excellent way to inspect SMT parts — apart from all the fiberglass dust on the board, no shorts or other problems arose when soldering. Next to pF-value chip capacitors, these SMD varactors proved the most difficult surface-mount parts I've breadboarded to-date. Using clear tape, I tape my SMT parts to the PC board when soldering. With tape, you can still make tiny device placement adjustments with a pick or tweezers and yet the device holds steady enough to solder. I recently obtained a microscope for SMT work, although didn't need it for these diodes.

Striving for lower phase noise meant properly applying high Q tank parts — I soldered in 3 pairs of high-grade BB535 varactors and arranged them anti-parallel to avoid forward conduction + even harmonics. I also limited the AC voltage swing they "see" by connecting them to the L with a 22 pF capacitor. Tight windings of #28 gauge magnet wire on a T50-6 toroid formed the inductor. 4 number 8 bolts anchor the 7 MHz VCO board to the chassis and prevent board warp + movement.

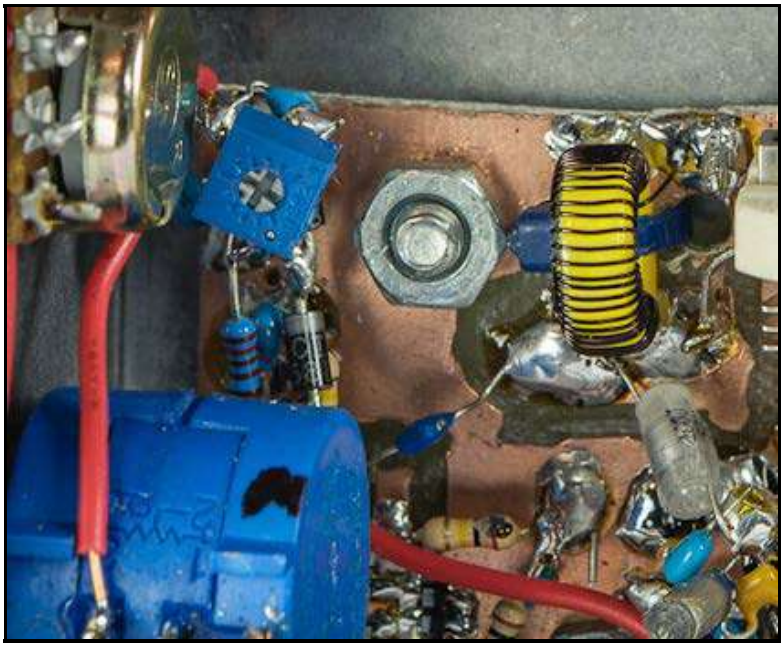

Above — a view of the square blue 1K temperature compensation (tempco) trimmer potentiometer.

To aid temperature compensation, I included 3 polystyrene capacitors in the base VCO — the tempco circuitry represents about 16 hours of work from December 2011. Click or click for photos of the bread board before the tempco parts were soldered on — the temporatry BNC connector lies in the background was removed after testing.

With care and patience my lid-on 1 hour temperature drift = ~10 Hz. My temperature compensation strategy worked because I took the time to measure and then determine how to cancel temperature drift in this 1 circuit — your results will vary and *experimentation* remains the key to temperature compensating VCOs and VFOs.

See EMRFD, and the VFO-2011 + QRP Modules 2011 web pages for more tempco information.

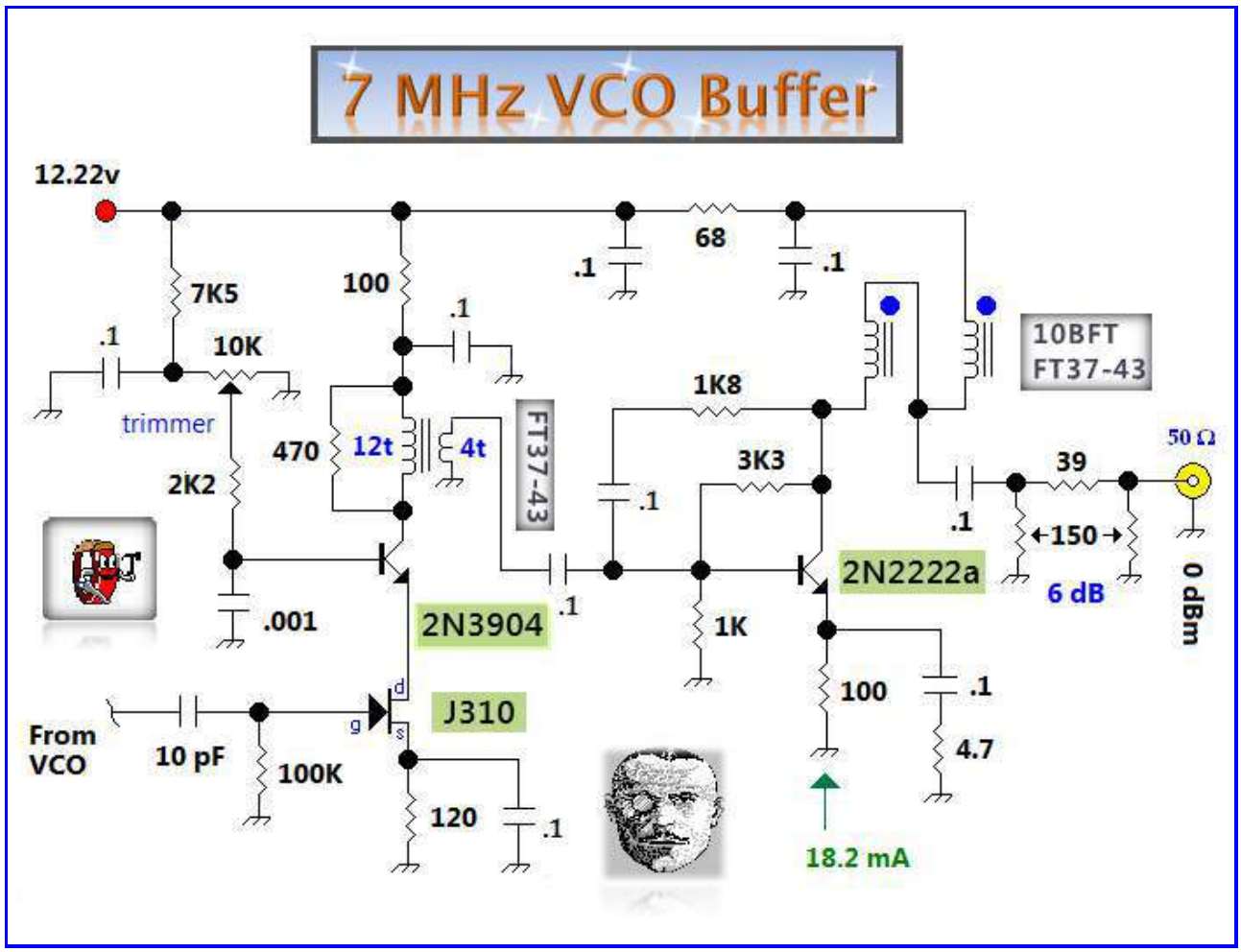

Above — 7 MHz VCO buffer/amplifier. I adjusted the 10K trimmer pot on the hycas buffer for exactly 0 dBm drive. Even before adding the 6 dB attenuator pad, the output return loss = 23.8 dB @ 7.0 MHz.

Originally, I wanted a VCO output of 7 dBm and applied ~18 mA emitter current in the final amp to preserve signal fidelity and eliminate the need for a low-pass filter. This buffer works great up to an output power of ~10 dBm: above 10 dBm or so, distortion occurs and you'll need to add a low-pass filter.

Adjust the hycas trimmer pot for whatever output power you seek, but If you're ever using this buffer for 7 -10 dBm output power, drop the 6 dB attenuator pad to 3 dB. This drops the drive level to maintain low harmonic distortion (2nd harmonic down > 35 dBc).

43 MHz Butler Xtal Oscillator [6.4 dBm output power]

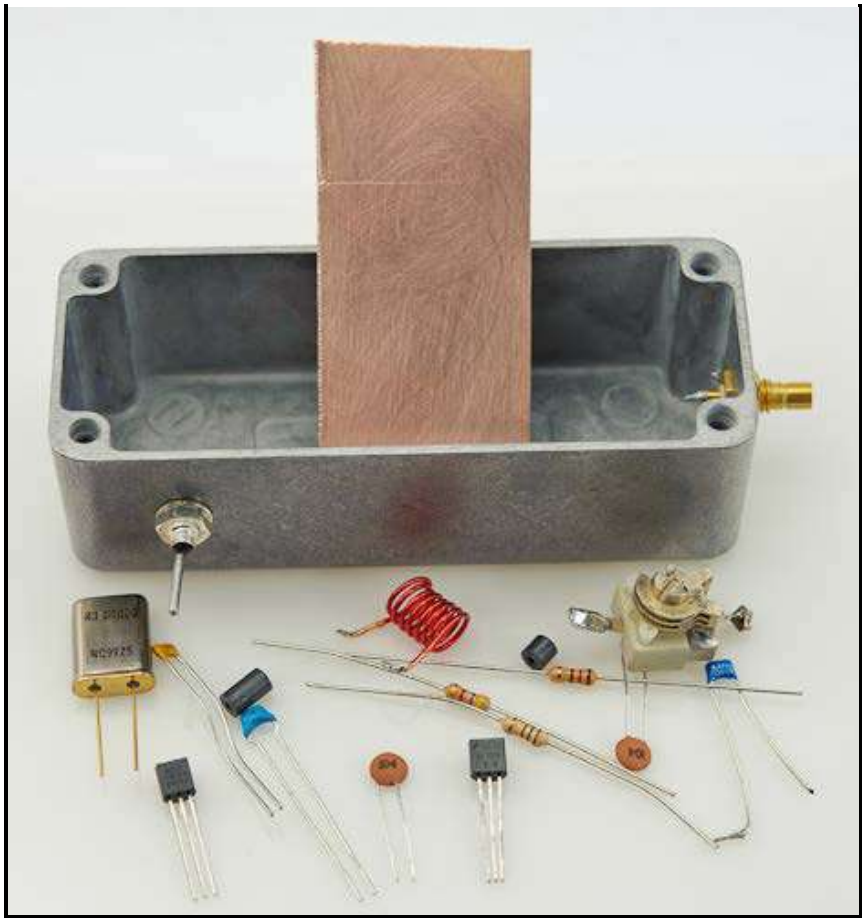

Above — Some Butler crystal oscillator parts prior to the build. Since this Butler will go inside a box containing a VCO and some high gain amplifiers, it would be foolish to not stick it in an RF-tight box. On the Hammond chassis above, you'll notice a feedthrough capacitor for the 12 VDC and an gold colored SMA connector for the output.

Since the required L = over 400 nH, I opted for a toroidal inductor wound on a T30-10 instead of the air coil shown in the photo.

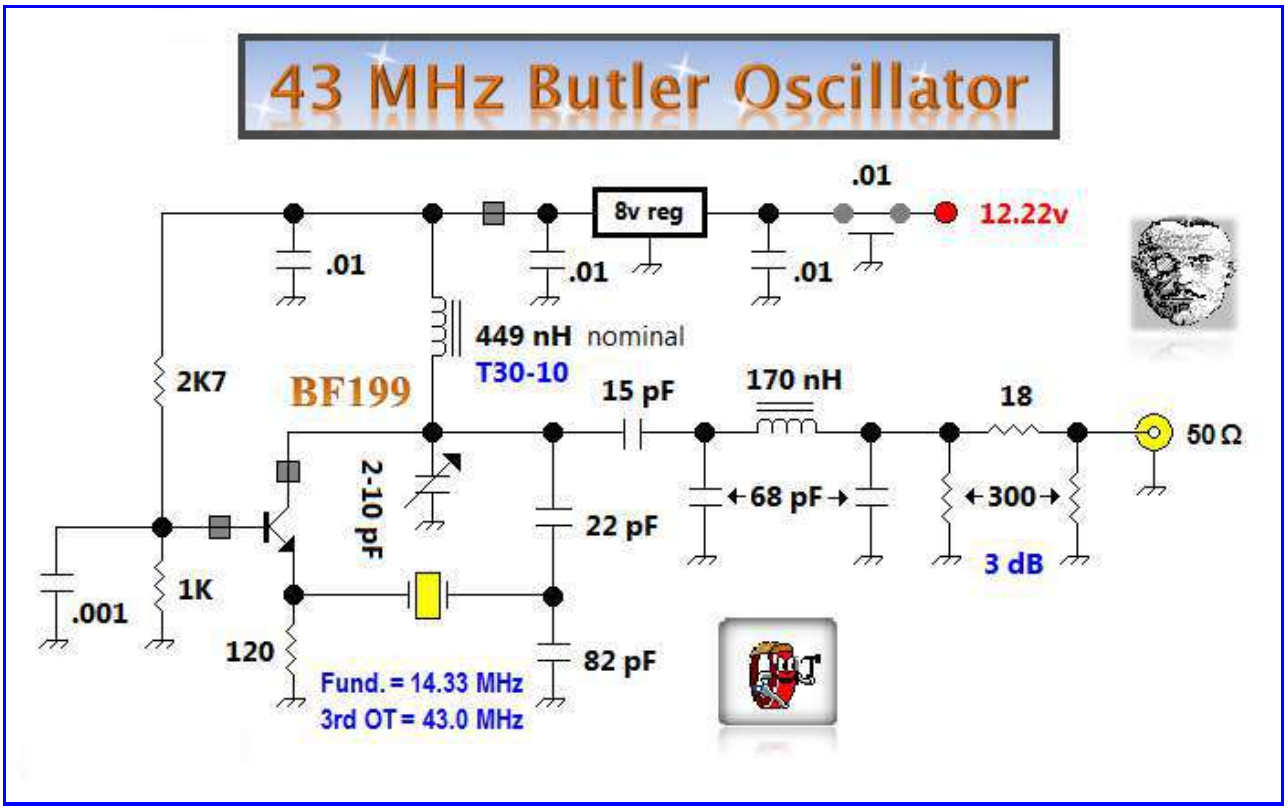

Above — 43 MHz Butler overtone oscillator schematic. The highest power I could muster = 6.4 dBm (close enough to 7 dBM).

This Butler looks good on FFT. Click, Click or click for 3 'scope captures. Despite trying to milk maximal power, the 2nd harmonic is over 40 dBc down. Click for a snap shot of the completed oscillator.

Above — The original Butler oscillator before adding the pi low-pass filter. The bolt (seen at top right) will also pass through the outer VCO chassis to hold this sub-chassis in place. Click for a bigger photograph.

Post-Mixer Amplifer and Triple-Tuned Filter

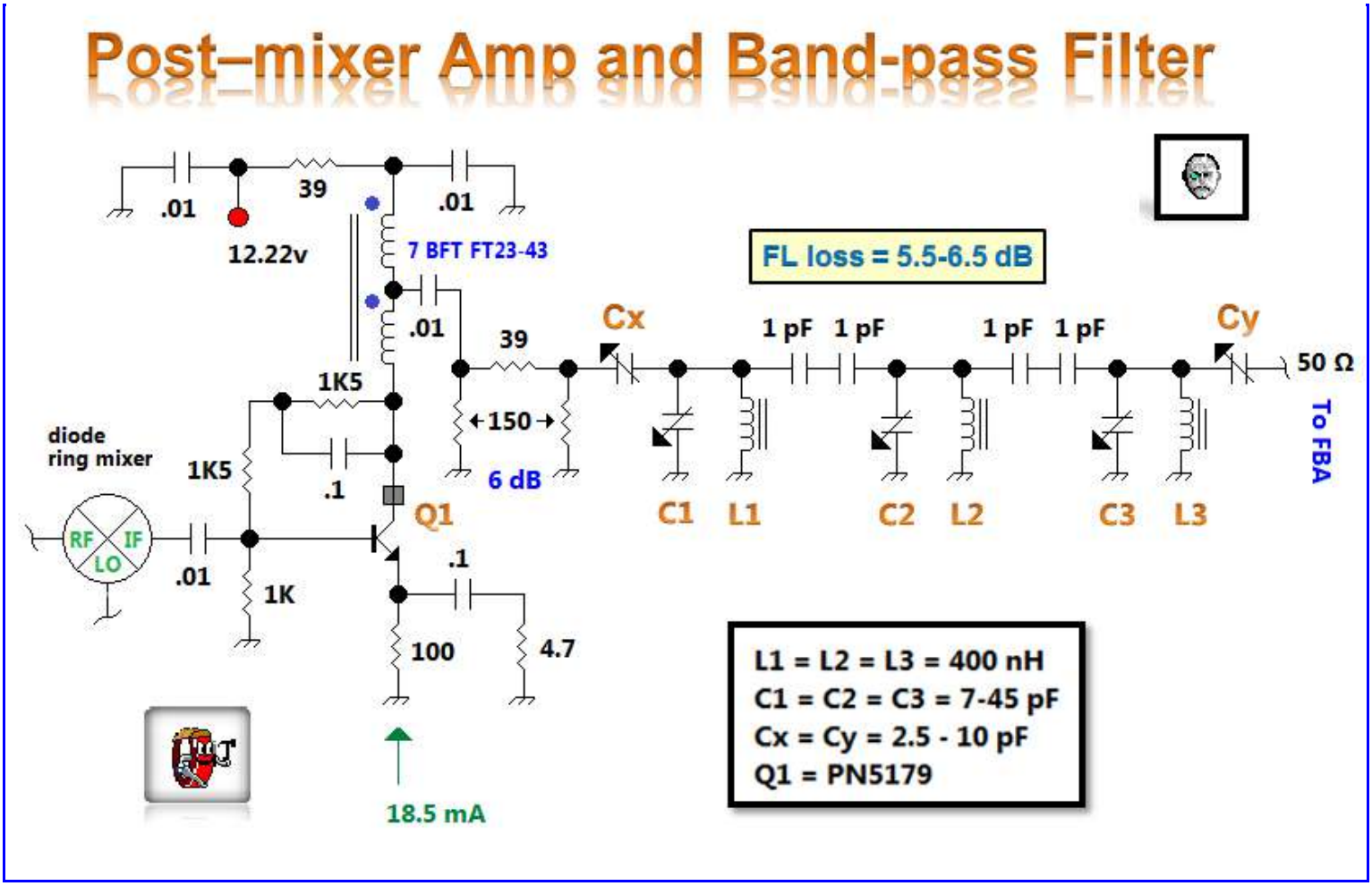

Above — Schematic of the diode ring mixer, Q1 feedback amp and the triple-tuned filter. *I used a MCL SBL-1 mixer*. L1 - L3 were wound on T30-10 toroids. I bought my #10 and some #12 toroids from the great folks at Debco Electronics.

The post-mixer feedback amp data at 50.0 MHz (isolated from the mixer and pad + filter) : Emitter current = 18.5 mA, S21 =18 dB, S11 = -24.4 dB, S22 = - 21.5 dB. *(S21 = power gain; S11 = negative of the input return loss; S22 = negative of the output return loss).*

The 6 dB pad helps absorb signal reflections from the filter caused from stray reactance plus capacitance variations caused by coupling the 2 tanks with only 0.5 pF (2 series 1 pF capacitors with a +/- 0.25 pF tolerance!)

Preliminary filter alignment: Peak your filter however you want — but here's how I peaked my filter with a crystal controlled 50.0 MHz signal generator connected via a temporary BNC connector tack soldered onto the copper board and wired to the Q1 input. Terminate the filter with a ~50 Ω resistor, or a temporary BNC connector plugged with a 50 Ω resistive terminator.

Connect the signal generator to Q1 and peak C1, C2 and C3 (in that order) using a 10X 'scope probe. It's better measure with your probe at point C2 when tuning C1 since this reduces mistuning caused by probe capacitance — measure at point C3 when tuning C2 etc.

Then peak C3, Cx and Cy with the probe touching the terminating 50 Ω resistor. *It easier to perform the first tune-up with a 10X probe going sequentially from C1 to C3 since these peaking capacitors tune pin sharp.*

After the preliminary tune-up, if possible, connect a temporary BNC connector to the output and re-peak all the caps with a 50 Ω terminated scope; this boosts sensitivity and eliminates 'scope probe capacitance.

Perform pentultimate 50.0 Mhz alignment after you add the post-filter amp, low-pass filter and the 3 dB pad. Capacitor Cy critically sets the output return loss of Q2 and when properly matched, establishes a 50 Ω termination for the triple-tuned band-pass filter.

You can also match Cx by connecting a return loss bridge to the input of Q1 and terminating the RF chain with a 50 Ω resistor, although tuning Cx only changes the input S11 a little. In 1 experiment, I replaced Cx with 6 pF and it worked okay.

I wonder how I ever managed before making a return loss bridge: the workhorse of the QRP workbench.

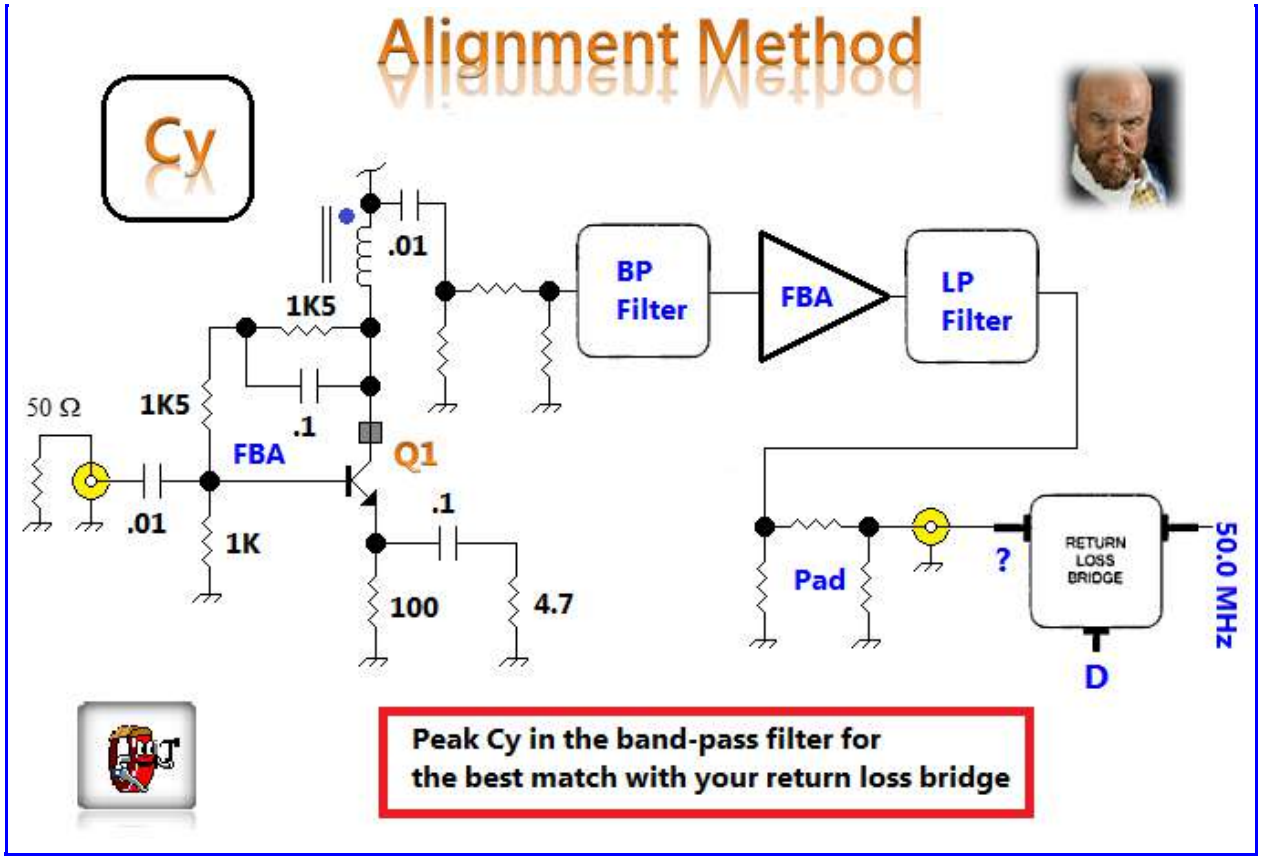

Above — Schematic depicting how to tune up Cy.

Tuning Cy matches the band-pass filter output to the Q2 input impedance — it's fascinating to examine the interdependence of these 50 Ω stages. After setting Cy, I connected the 50 MHz signal generator to the Q1 input and a 50 Ω terminated 'scope to the output and re-peaked Cx, C1, C2 and C3 — finally I tweaked Cy 1 last time with the whole stage in a return loss measurement set-up.

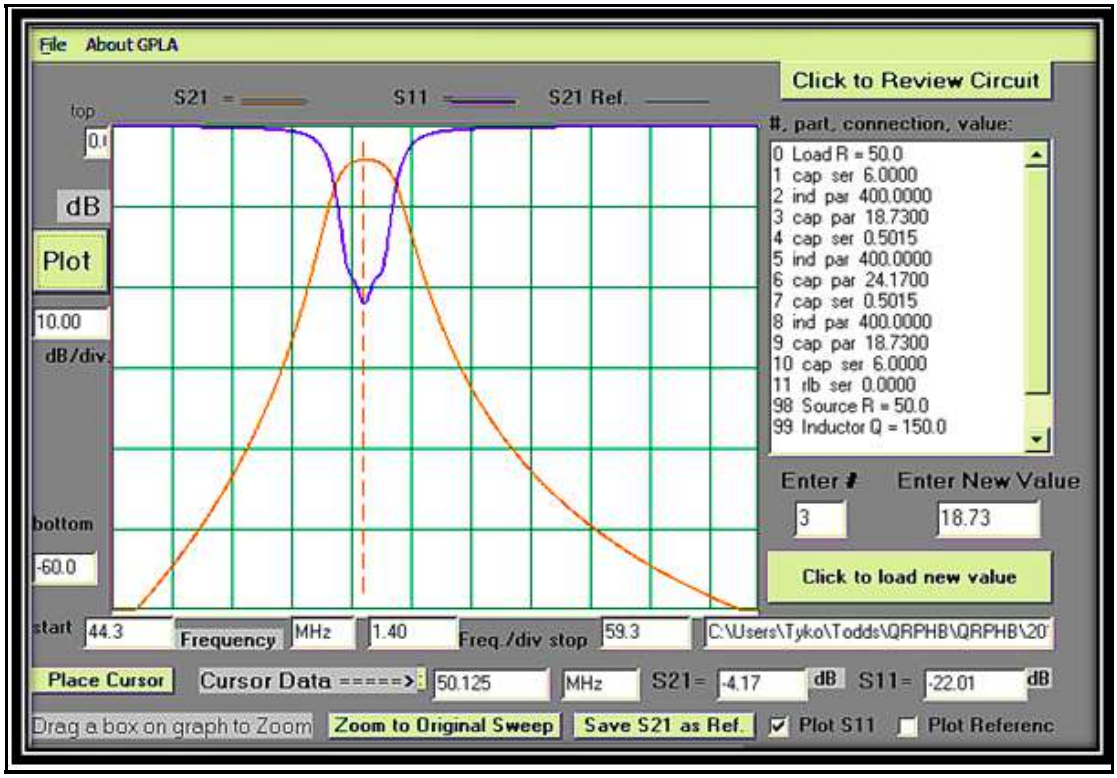

Above — A GPLA simulation of the triple-tuned band-pass filter. CF = 50.125 MHz. I substituted 6 pF (the nominal value) for the 2 series end capacitors in my simulation. отлично!

Post-filter Feedback Amplifer, Low-pass Filter and Pad

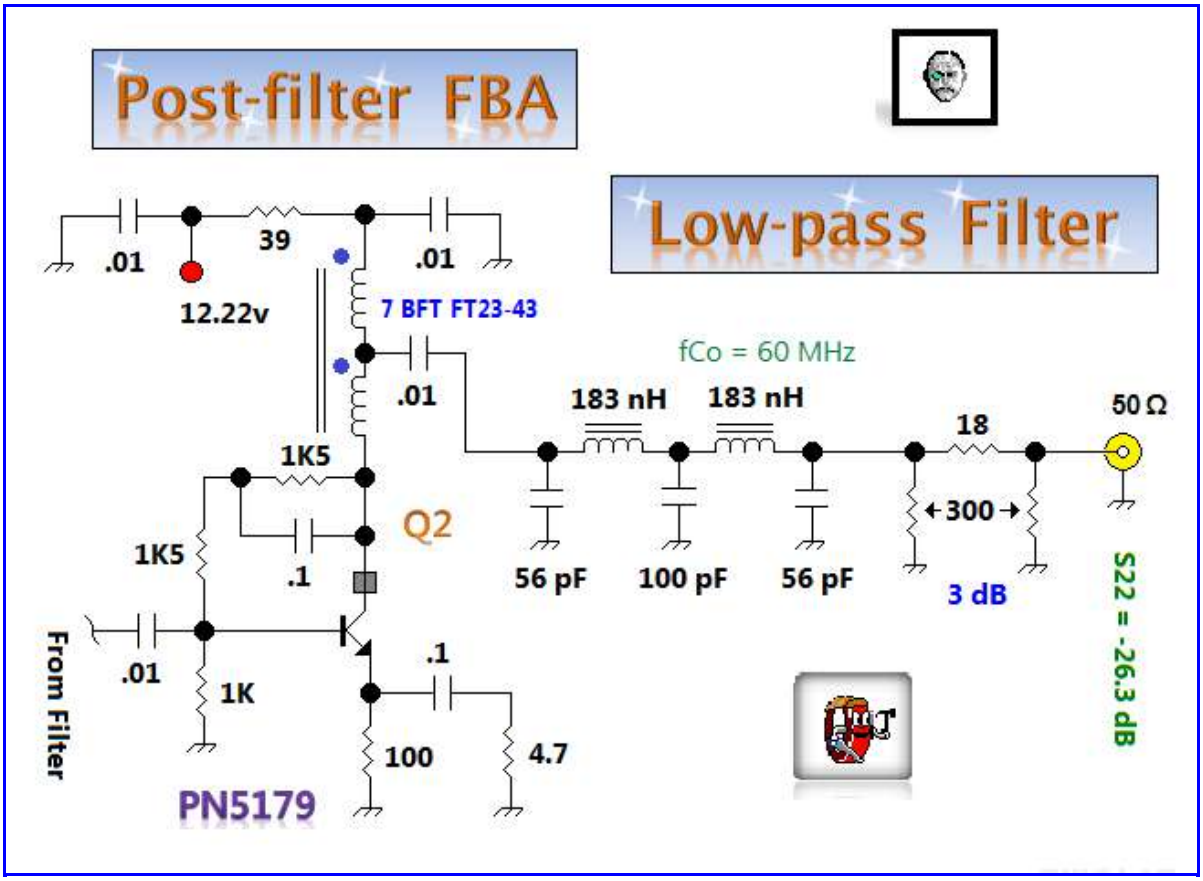

Above — Q2, the post filter feedback amp (FBA), an N=5 Chebyshev low-pass filter plus a 3 dB pad.

For Q2, I copied Q1 to deliver a strong input and output return loss. In many circuits employing cascaded FBAs, you increase emitter current in each successive FBA to reduce distortion, however, increasing emitter current affects both the input and output impedance and may trash your amplifier's S11 and S22.

I spent days studying, simulating + bench testing different amplifier designs in the Q2 slot — I generated enough material for another web page and plan to show this work in an update to my Popcorn superhet receiver some day.

It's possible to overdrive Q2 depending on your amplifer power and stage matching. If so, you might consider placing a 3-4 dB pad after the band-pass filter. Some might opt for a 7 element low-pass filter; experiment — as always.

Low-pass filter inductors = turns on T30-10 toroids, although #6 material toroids, or air coils will work fine.

Outputs

After bolting down the boards, wiring the DC and RF and confirming it worked, I finalized alignment. Using a frequency counter, I tuned the VCO to 50.125 MHz (the half-way point) and peaked C1, C2, C3 for the maximum peak-peak voltage into my 50 Ω terminated 'scope.

Click for the output at 50.125 MHz — 10.09 dBm. I normally hang an outboard 50 Ω attenuator on the output of my signal generators and keep 3 dB, 6 dB, 10 dB and 20 dB BNC-connected pads handy. With a 3 dB pad, the output power = 6.84 dBm — perfect for switching Level 7 diode ring mixers. Click for the 'scope shot with a 3 dB pad applied.

Click or click for an FFT of the output signal. The second harmonic is > 50 dB down. What fun!

The "vestigial" RF gain control shown on the chassis remains unused; wastage.

Miscellaneous Photos and Figures

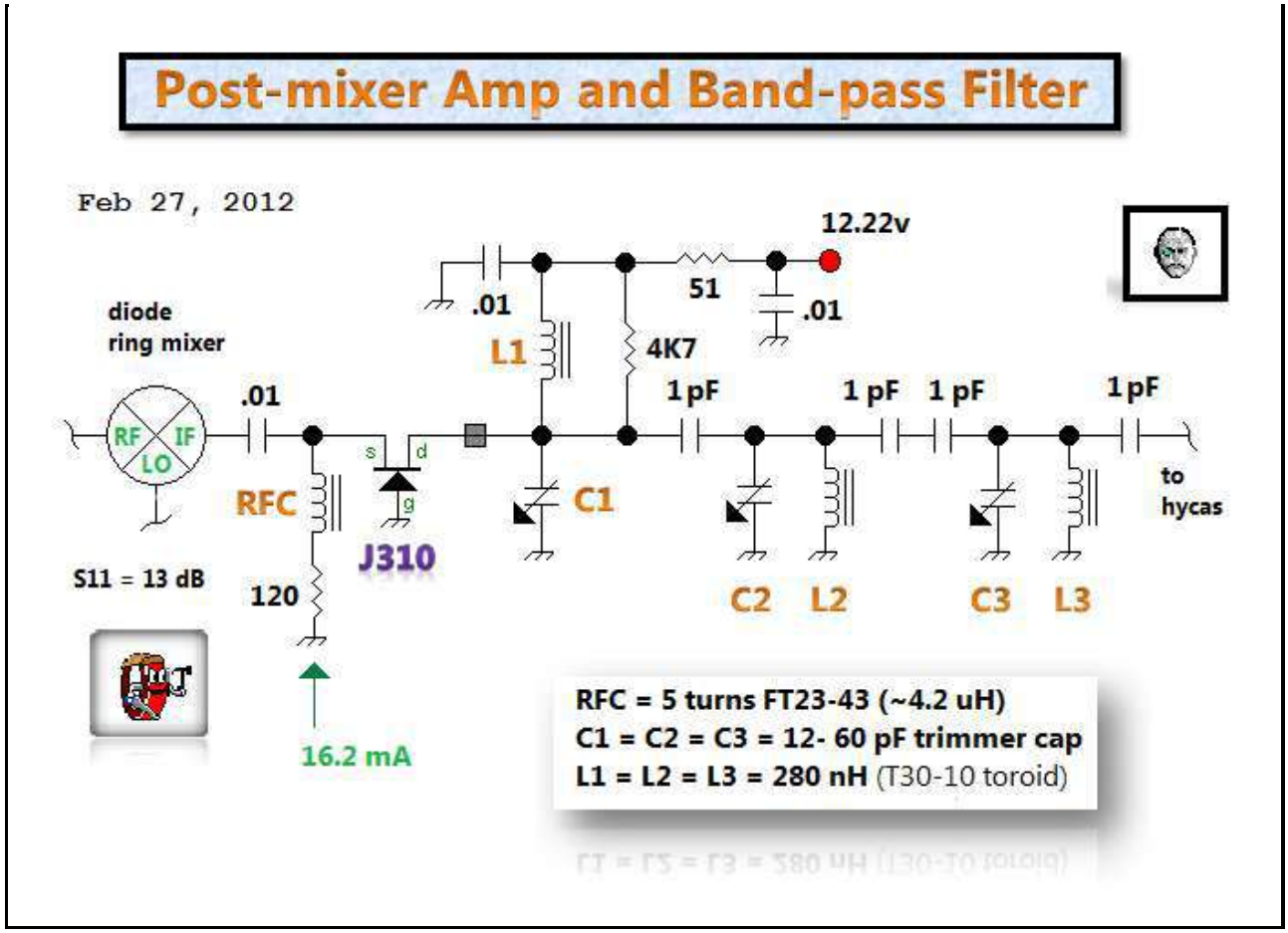

Above — A **failed** experimental JFET post-mixer amp with tuned output driving a double-tuned filter.

Click for a GPLA simulation of the double-tuned filter. The common gate JFET amp provides a great way to terminate a diode ring and obviates the need for a diplexer network. Click for a breadboard photo of the above stage.

The amplifier input match @ 50 MHz is only ~ 13 dB, however, we're not interested in a narrow band match — the tuned output network makes strong input matching at 50 MHz impossible *(for me at least)* without additional L and C (narrow band components that we don't want!). I tried a few tapped inductor schemes, however, at VHF, adding turns added significant capacitance and things got ugly fast.

The common gate JFET amp/filter goof-up shattered my expectations. The 4K7 input/output impedance drove instability through unwanted coupling between the inductors. I learned my lesson: at or above 50 MHz, *stick to 50 Ω stages* for stability.

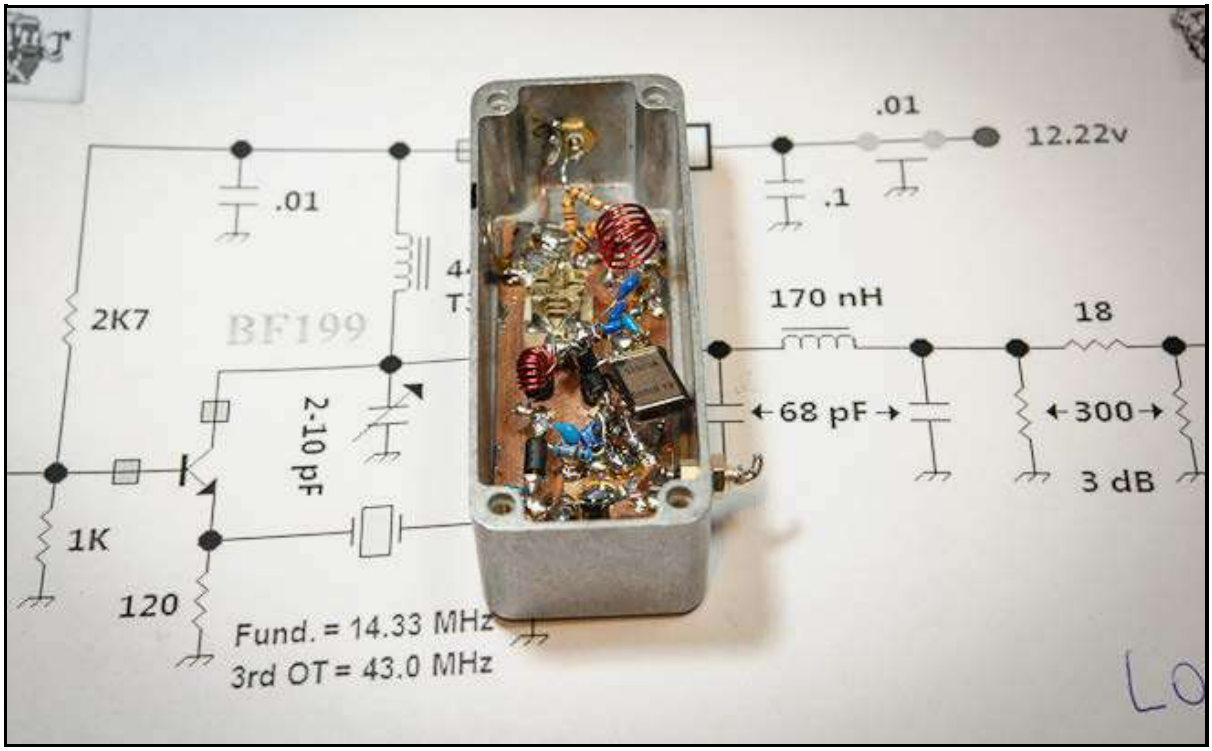

Section 4. 50 MHz Receiver Pre-amp and Filter

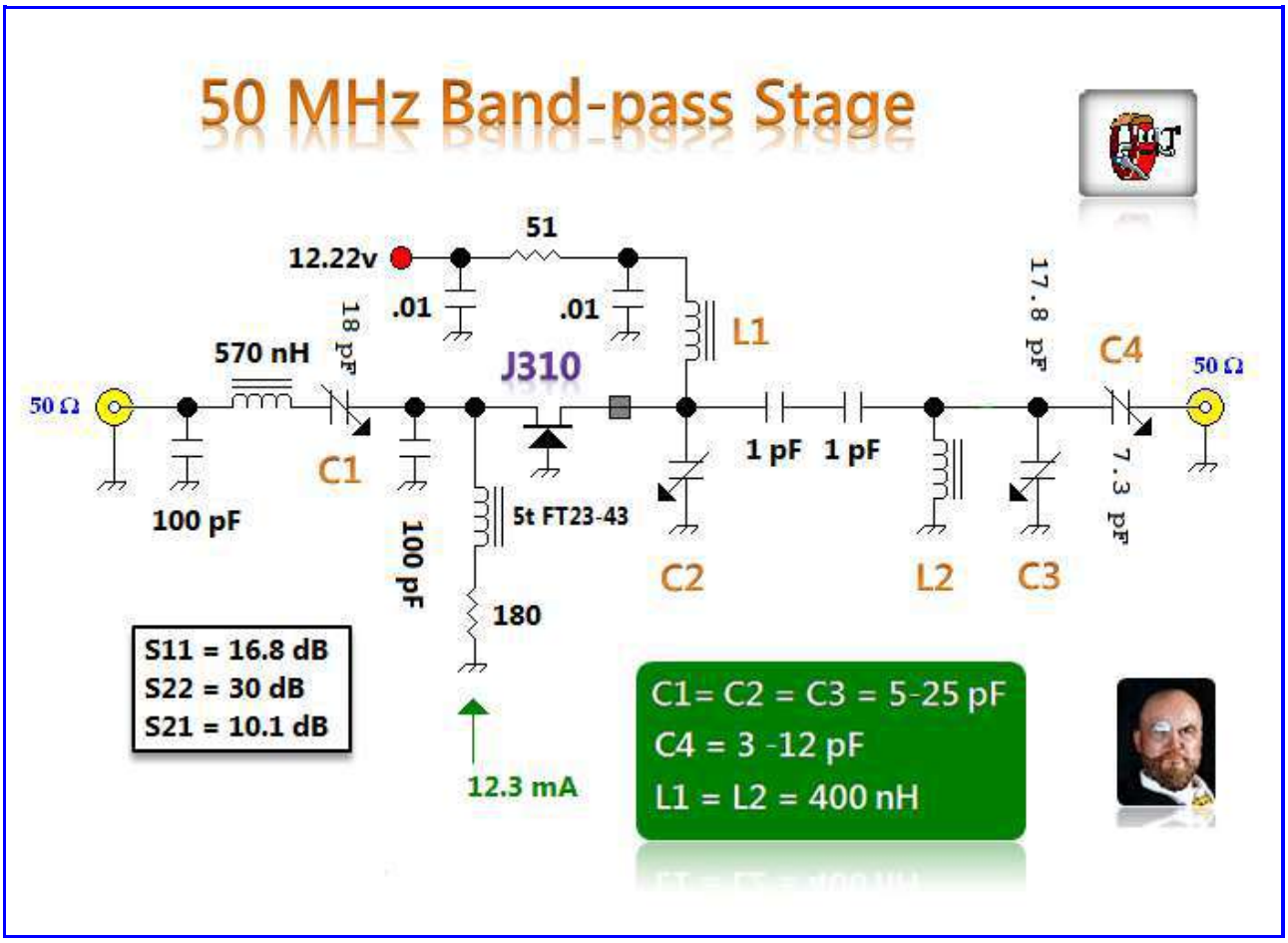

Above — A 50 MHz receiver front end filter with embedded common gate amplifer.

Inspired by the General Purpose Monoband Receiver Front End from Figure 6.69 in EMRFD, I applied inductive and capacitive reactance modeling, DTC08, Ladbuild08 and GPLA08 from the EMRFD ladpac series and built a 50 MHz equivalent.

Connect an antenna to the input and a 50 Ω impedance mixer to the output.

I tested the stage at 50.0 MHz and wound my inductors on T30-10 toroids, although #6 material cores would work okay. You'll find all the measurement techniques in my RF Workbench series 1-4 available though the top-level menu.

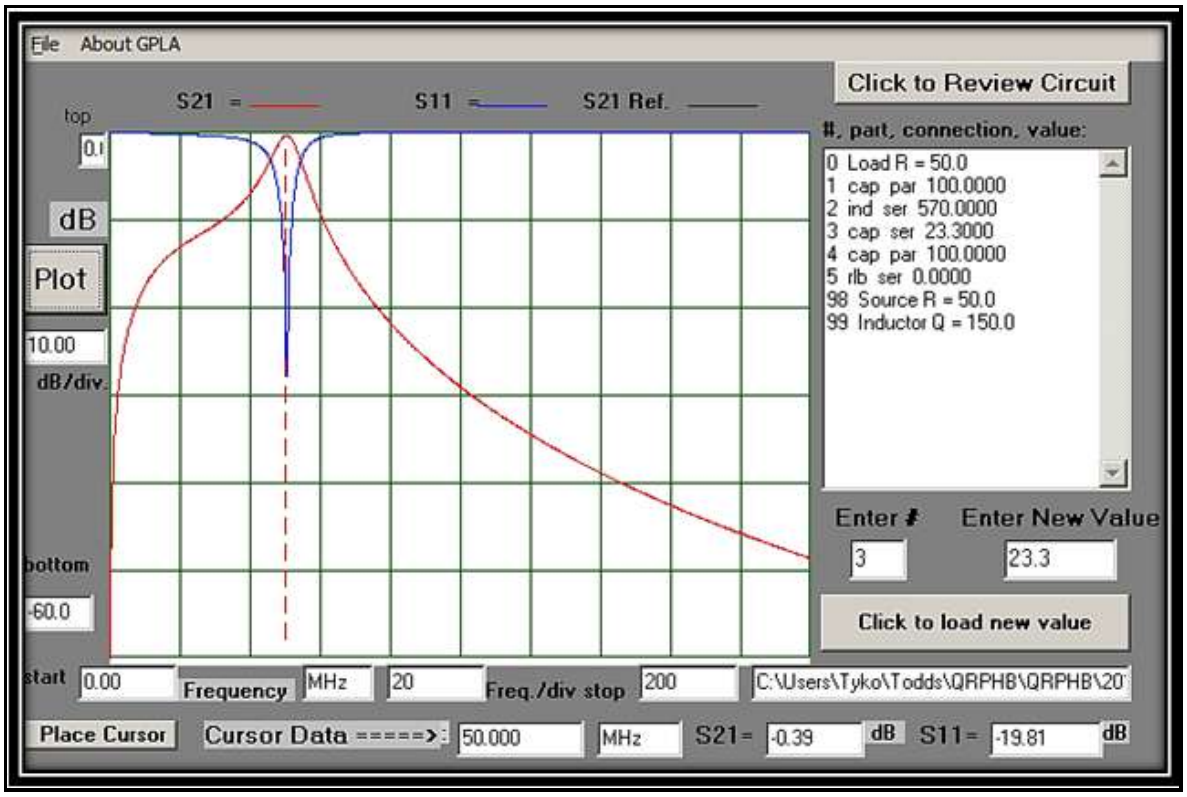

Above — GPLA simulation of the peaked low-pass filter "built" in Ladbuild08.

Wes often employs a peaked low-pass filter and after studying his work, I can see why — way better attenuation than a simple 3 element low-pass filter. The FM broadcast band runs from about 87.5 to 108 MHz and in Russia, they call it "YKB" (Ультракороткие волны) or ultra-shortwave. At 87.5 MHz, attenuation = 25 dB; pretty good for such a simple filter. At 144 MHz, filter attenuation rises to ~ 40 dB.

This peaked low-pass filter acts as a preselector for the JFET amp that follows it. *Please read the text describing Figure 6.69 in EMRFD for some great notes by Wes.*

In the simulation above, a 50.0 MHz peak response occurred with C1 at 23.3 pF, while in my real circuit, the capacitor was set to ~ 18 pF. Stray L and C + the input Z of the JFET amp caused this variance, but assuredly; GPLA gets you close.

To peak the low-pass filter, I connected a return loss bridge to the input port and tweaked C1 for the lowest possible peak-peak voltage (tuned for the the best return loss which = 16.8 dB in my circuit). *You may also compress or expand the 540 nH inductor to aid tweaking.*

Since common gate amplifiers often exhibit a lower noise figure with a slight mismatch, an S11 of -16.8 dB works fine .I wish I had the gear to set the input match for the lowest possible noise figure — perhaps 1 day I will.

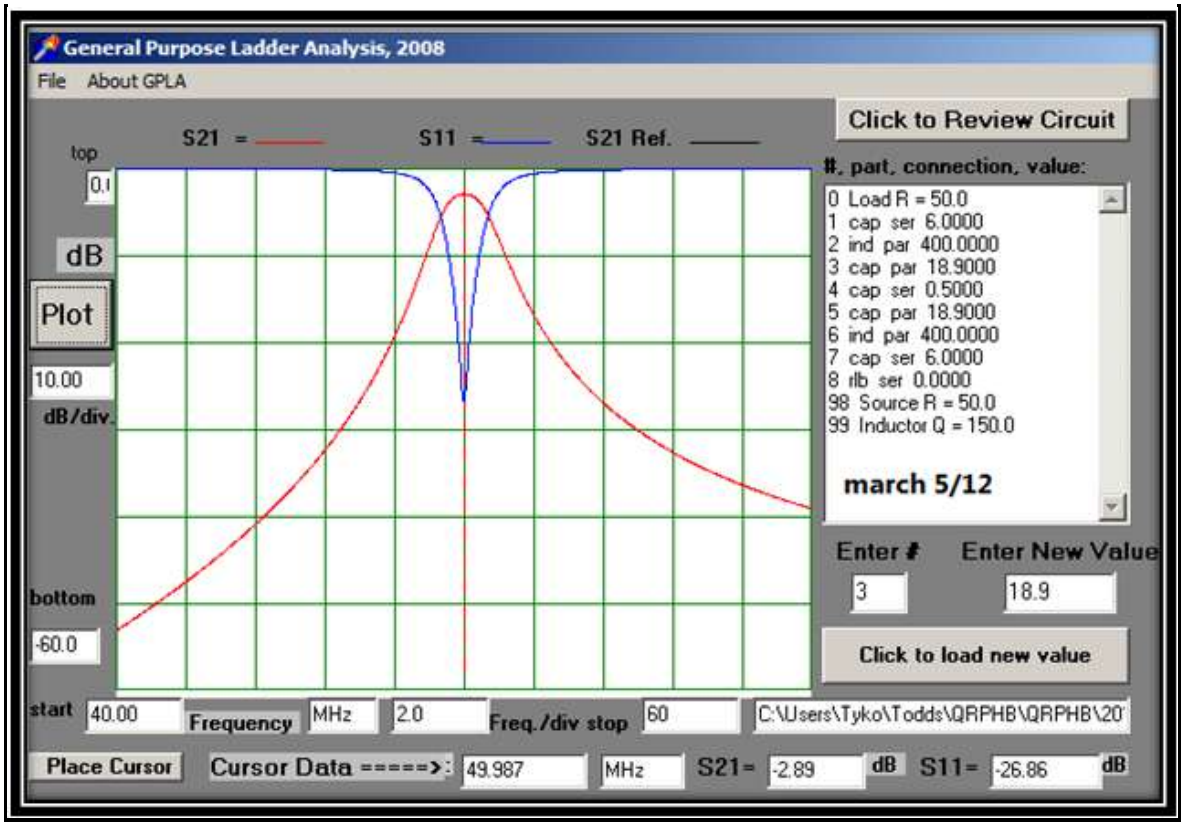

Above — A GPLA simulation of the 50 MHz double tuned band-pass filter "built" in DTC08. The bandwidth = ~1.8 MHz and varies slightly with the tuning of C4.

I peaked both C2 and C3 with a 50 Ω signal generator and a 50 Ω terminated scope connected to the input and output ports respectively.

Next, I connected my return loss bridge to the output and tweaked C3 and C4 for the lowest peak-peak voltage — the best return loss — and since you tweak 2 capacitors, a strong output return loss delights you.

Finally, I measured the peak-peak voltage with the amp in-line, and after removed the amp and reconnected the 50 Ω cables with a through-connector. Inputting the 2 pk-pk voltages into Applet H on the Design Center web page gave a gain *or S21* of 10.1 dB. I repeated all of the steps above a couple more times to ensure I had set C2, C3 and C4 perfectly.

I found tuning the resonators difficult due to the sharp tuning and wide capacitance range of C1-C3. Assuming your tanks are peaked, the best amplifier gain correlated to the highest input and output port return loss. Have I stressed the importance of a return loss bridge enough?

10.1 dB gain should be enough gain for listening to terrestrial 6 Meter band signals with my 5 element Yagi antenna.

Above — A photo of my protoype 50 MHz pre-amp breadboard. In my "keeper" version, I'll swap in a U310 JFET and bias it for ~15 mA.

Section 5. QRP — POSDATA: Z-Communications VCO Experiment

Looking on eBay, sellers list numerous VCOs, although most are surface mount and go well above VHF. My favorite VCO comes from Mini-Circuits Labs: the POS series. Click for an example: the POS-75. These "plug- in" VCOs come in same package as the SBL-1 mixer and are likely obsolete, but still for sale. If you're building a frequency synthesizer with low phase noise requirements, MCL VCOs seem hard to beat. You can still order them from MCL, but the high product and shipping costs might alarm you.

I've looked for cheaper alternatives and the Z-Comm VCO raises 1 possibility. Last year, I purchased a V149MEM1 device for 5 dollars including shipping. Some experiments follow:

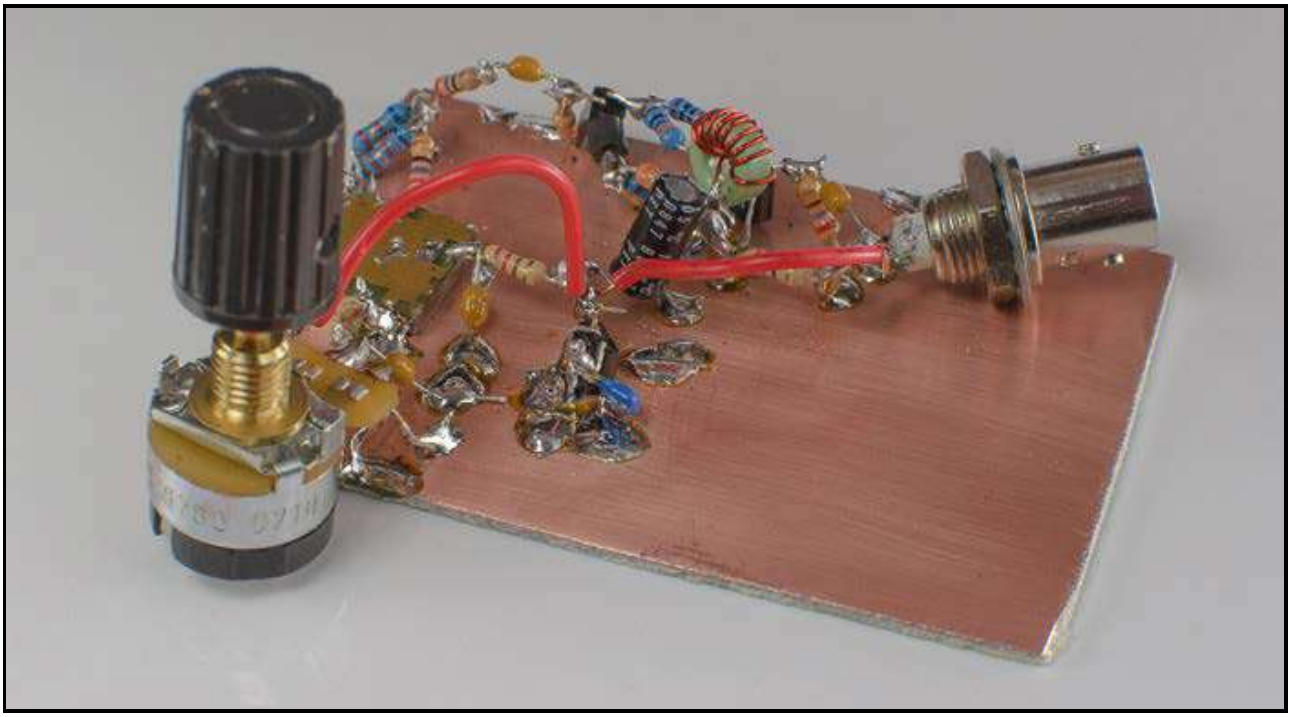

Above — My first breadboard. Lacking the MINI-16 receptable, like with MCL POS VCOs: I turned it upside down and soldered the metal case to my ground plane. If I were to keep this circuit. I wound solder all 4 sides to the copper clad board, plus run some copper de-soldering brade from the bottom to the ground plane, or even cut a square hole and flush mounted the VCO on is back.

While mounting it upside down deviates from the recommendations found on the Z-Comm mounting datasheet, I fiigured that for VHF at least, it might work okay. We desire low inductance grounding, but creativity might allow dead bug construction techniques to work.

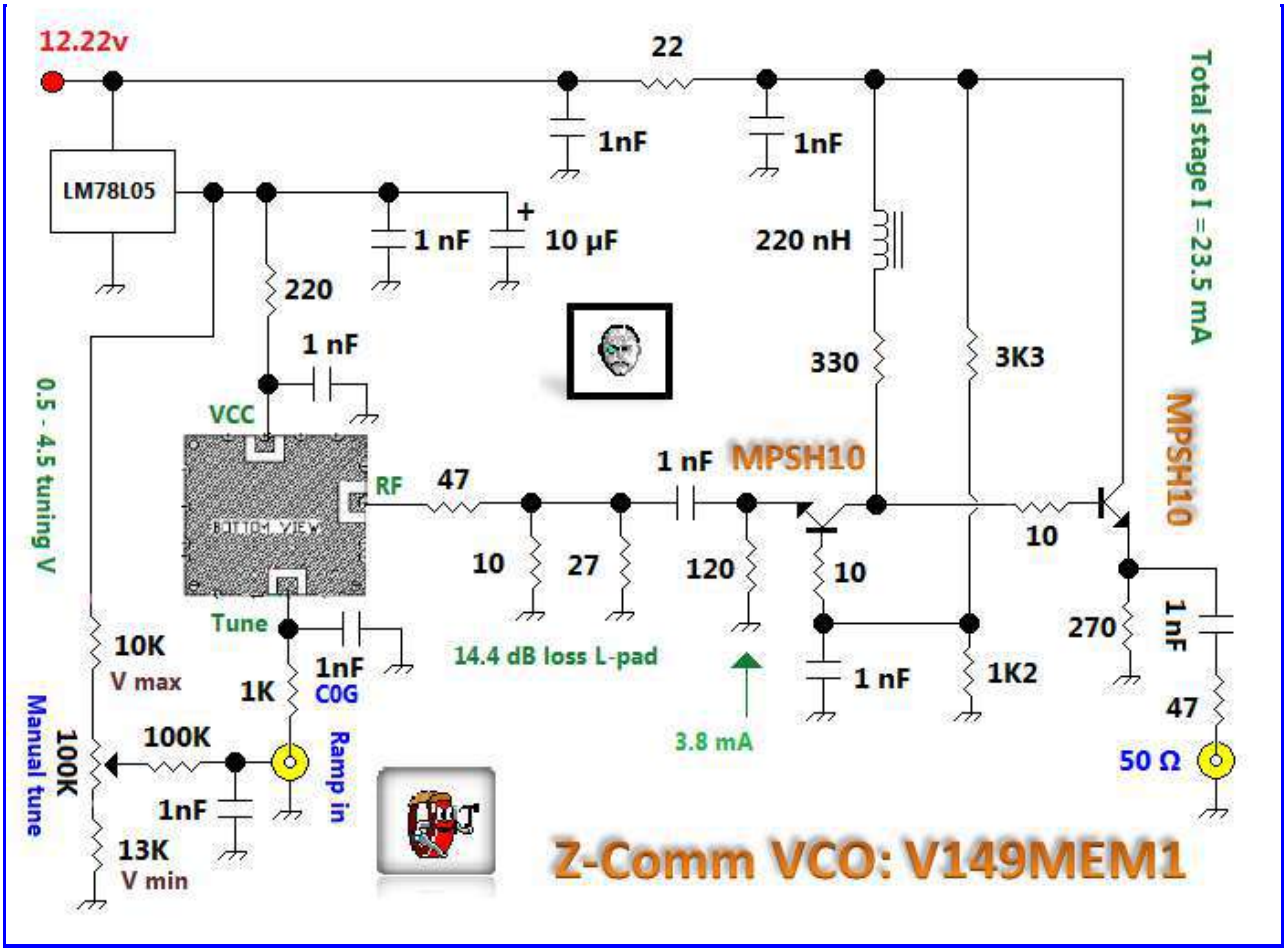

Above — My complete VCO. The Z-comm VCOs require at least a 10 dB pad on the output to keep port return loss high. Without a pad, you might see something like this plus boost the phase noise. In my circuit, I applied a resistor L-network with ~ 14.3 dB loss to pad the output and provide a match into a common base amp with an input impedance of ~ 6.8 Ω.

The 2-stage buffer is the brainchild of Bob, K3NHI and I love it. This buffer features a common base stage driving a emitter follower yielding high bandwidth and great reverse isolation. Normally, at VHF, the buffer is followed by more such stage(s), or a MMIC. The 220 nH inductor wound on a T30-12 toroid improves the high frequency response of the common base amplifer — experiment with this L to suit whatever VCO you wish to buffer. The gain of the 2 amp buffer is typically around 9 dB and the return loss at the input and output ports lies under 11 dB, so apply attenuator pads to boost S11/S22 as required.

Click for the scope tracing at 0.5 VDC tuning voltage. Click for the 4.5 VDC tuning voltage 'scope tracing. The harmonic distortion at the lowest tuning voltage = ~ -19 dBc and decreases to -28 dBc at the highest tuning voltage; better than specified. Notice that power decreases as frequency increases. All the commercial VCOs I tested do this. A higher fT amp like the PN5179 or other BJT might be a better choice to offset the power change versus frequency *contribution* of the buffer/amp.

For a sweep circuit, I would mix this VCO with another low level, single frequency VCO with its current controlled by a downstream leveling circut to derive a flat amplitude over the range of the VCO. I plan to try the Z- Comm V150S015 in such an arrangement to make a 70 - 150 MHz VCO for sweeping.

Please refer to the datasheet for the pin out on the Z-Comm VCO: I chose the pinout shown in the schematic to make an efficient drawing. The two 10 Ω resistors in the buffer/amp snub UHF oscillations first measured by Bob and confirmed by me. Ferrite beads might work as alternates.

Section 6. Miscellaneous Photos

VHF SIGNAL GENERATOR
138-172 MHz
98-109 MHz
50Ω
ON
OFF
ON
50Ω

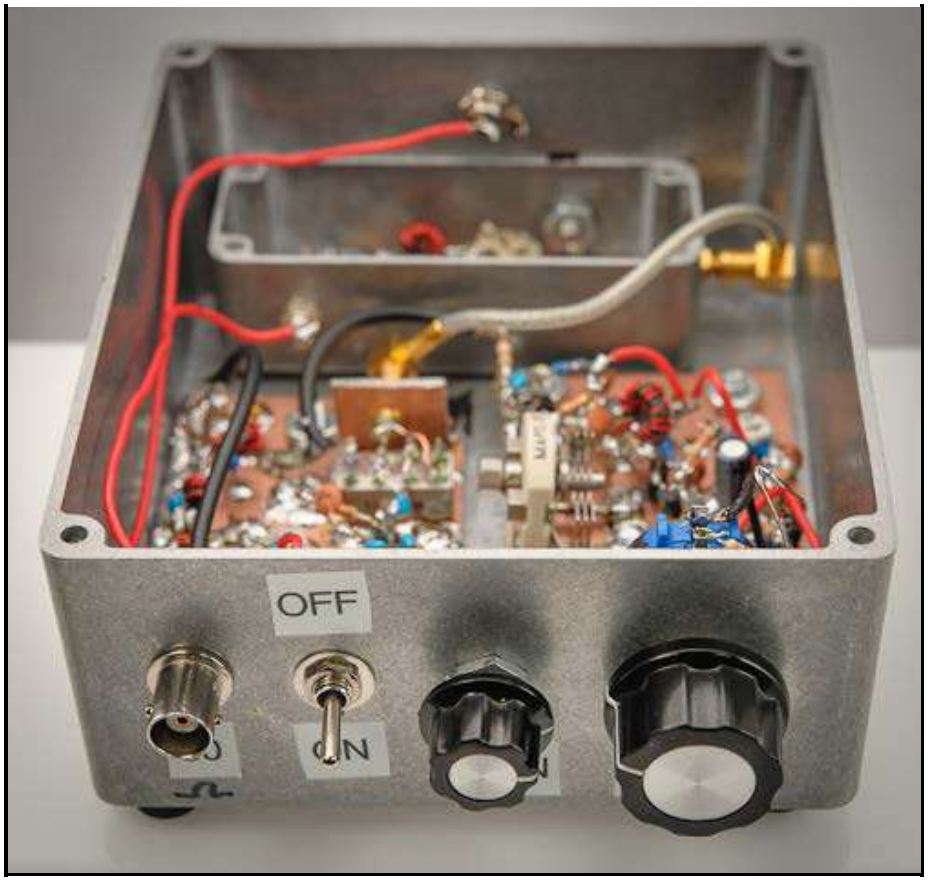
OFF
ON

TERMINATOR

HF Ragbag

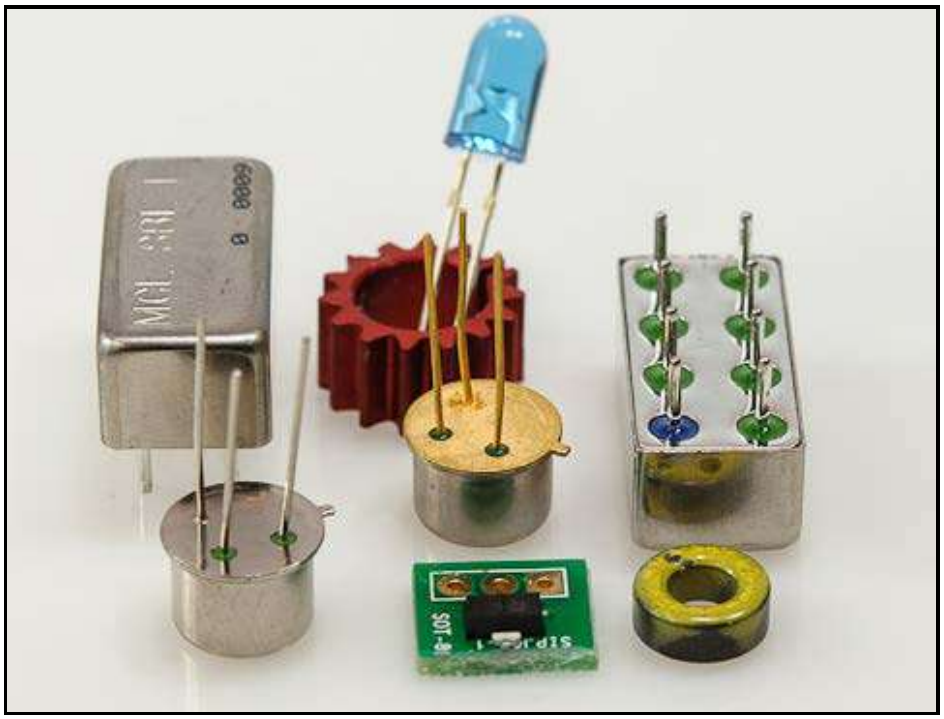

It's easier to present short topics on catch-all web pages — HF Ragbag shows some 2012 non-VHF experiments in no particular order. I also share thoughts on circuit building and writing: we can think and work better.

1. Comments from the Workbench - The Need for Clarity

On Building

In 2012, I boosted my circuit and writing quality to improve your experence: a genuine, return-to-basics approach in amateur, component-level electronic design. As possible, RF circuits will feature 50 Ω input and output ports — totally adopting a 50 Ω environment — for I'm convinced this is the best way to go. The 50 Ω building and measuring standard offers much: an easy-to-interface modular approach; 10 dB improved sensitivity over a 10X 'scope probe and if wanted, measurement with commercial or homebrew test equipment such as a spectrum analyzer, network analyzer or RF power meter.

Like many, I started out by collecting and copying circuits with little emphasis on true understanding. I wanted a completed circuit — quickly as possible — failing to develop my design skills. Without design skills honed by studying and properly measuring our circuits, we bide in hit-and-miss electronics — a frustrating repetition of trial and error, over and over again. We ought to adopt the attitude and thinking of engineers while keeping our design work —including the math — fun. However, embracing scratch-homebrew electronics with the overall goal of trying to understand each stage takes effort. "There is no substitute for hard work" wrote Thomas A. Edison. Scratch homebrew involves reading, simulating, collecting parts, mastering new techniques and building or buying test equipment.

This is more than knack, an abused noun that often means "hack". Our key tasks: to measure, analyze and understand the circuits we copy or create takes patience and practice. Dissecting circuits to understand their function means to hypothesize and reflect — to apply science on

paper, with software, and finally, through careful bench experiments. Often we lack the math skills or test equipment to fully investigate some aspects of our circuits, but try our best: measure what we can measure, seek help and grow. I hope this site shows our hobby can be less about making stuff and more about the rewards of actual design: an authentic, personal journey to get better at something you love.

I've never been much of a kit builder; it's too much like Max Klein's Paint by Number for my tastes. But kits dominate HF QRP homebrew and may offer a cost effective way to make gear; especially test gear. Stuffing parts in a printed circuit board won't teach you much about design, but might get your feet wet. Some people remain perfectly happy building kits or madly copying circuits — all the power to you! Do whatever you want. One day you might awaken, but don't worry; I won't try to goad, or convince you.

My favorite builders include people over 50 who suffer the often crippling symptoms of 'appliance apathy' — an epiphany reminds them why they first got into radio: homebrew experiences. Maybe a crystal radio set, or a simple superhet receiver they breadboarded long ago. *Then they come back full circle*; like a loop antenna. Oh-boy — "Bob" rediscovered his radio roots and needs to unleash his creativity and passion to learn and improve. I write for people like Bob. Heck; I am Bob.

On Writing

You'll notice improved narrative writing too: I prefer to read and write crisp statements in short sentences and paragraphs. Brief, yet descriptive text accompanied by ample white space, clear headings and bulleted lists invites you to read on. Plain language writing — simple, clear, writing that is easy to read and understand — signals a refreshing move away from the turgid, word-filled claptrap I learned in grade school. Making your prose easier to read requires greater effort writing and re-writing. My first..to...fourth drafts always suck.

Passive verbs, or nouns and adjectives that function as verbs with no clear subject confuses readers and boosts wordiness: I employ active verbs to invigorate my writing — active verbs connote me or some else performing an activity you can visualize or feel. Actions that may inspire, persuade, or even vex you! Ours' is an emotional hobby.

RF electronics contains rich amounts of jargon. Of course, we must learn some jargon to communicate our ideas as hobbyists, but writing jargon to impress, or to place yourself above others lacks humility and alienates people. Do you know anyone who likes being talked down to? The first step towards becoming humble is to admit you're not humble and then work on it — and I'm working on it.

Although I enjoy writing about electronic experiments, I'm not sure it's worthwhile — Does anyone actually design circuits anymore? Well, back to my 1970's-style analog experiments...

---

2. Magnitude Only Scattering-Parameters

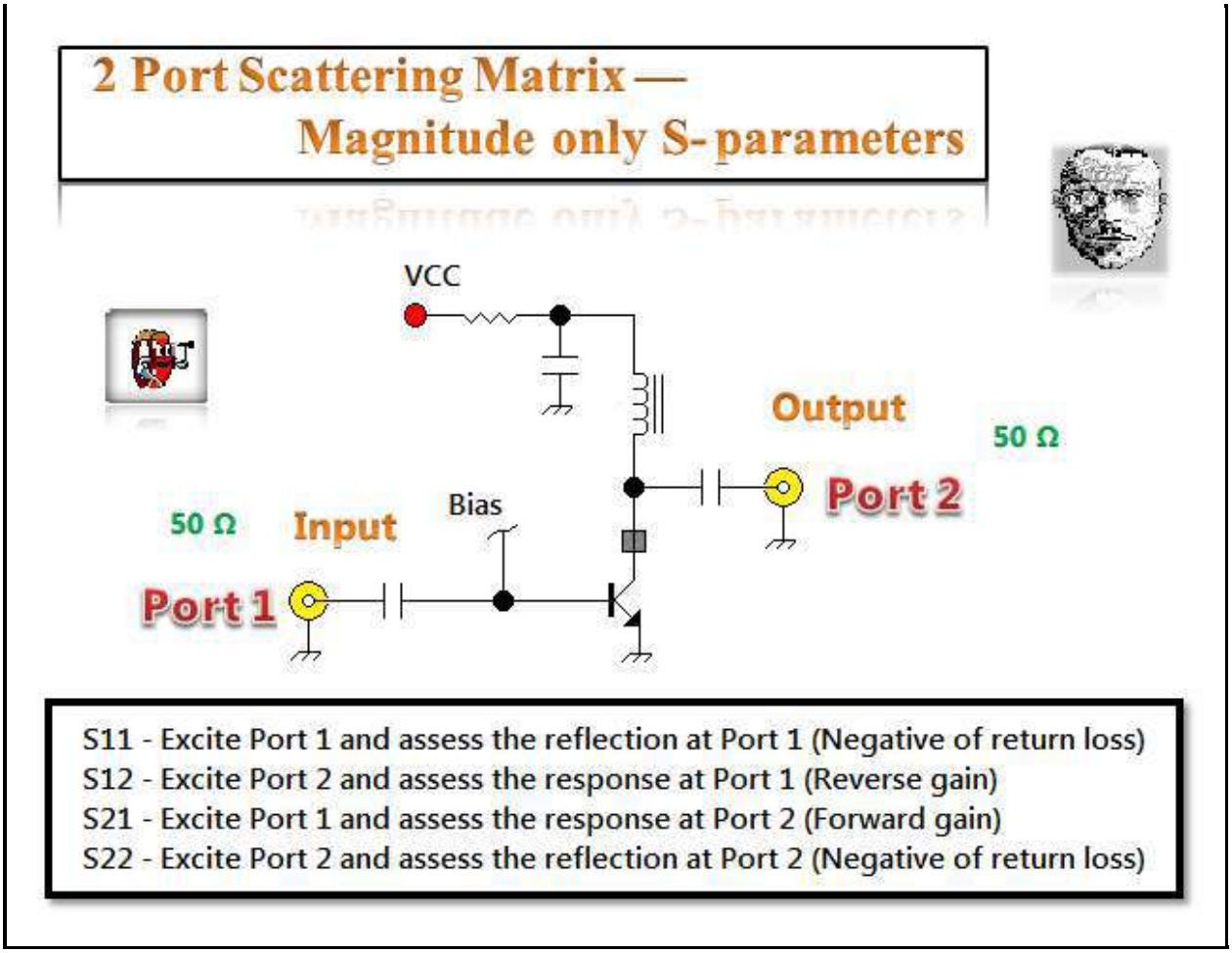

Above — A simple model describing the S-parameters displayed on QRP / SWL HomeBuilder in a Class A amplifer with 50 Ω ports.

S-Parameters

Any device with 2 connectors may be modelled at AC for a specified frequency with just 4 scattering parameters: forward gain, reverse gain + input and output impedance (match or VSWR).

S-parameters address voltage ratios: comparing the amplitude of different signals at the 2 ports. For example, S21 is the magnitude of forward gain and equals the ratio of output voltage to input voltage.

S-parameters are vectors; a mathematical quantity that may be visualized as an arrow anchored at 1 end that pivots around its base. The length of the arrow represents magnitude while the angle it makes with another vector or its base line decribes its phase in degrees. In addition to phase and magnitude, S-parameters allow analysis of gain, stability, complex impedance (resistance + reactance), admittance and other vector quantities.

Measure S-parameters with all ports terminated in a 50 Ω impedance.

Some of us worry only about the gain, losses or "match" in our 50 Ω circuits and could care less how the signal phase changes as it passes through our amplifiers or attenuators. I express only S-parameter magnitude in logarithmic form (dB) and take this *Über simplified* approach because builders can easily measure S11, S12, S21 and S22 on a 50 Ω test bench with a small staple of bench accessories + a 50 Ω 'scope or detector.

Topics like matrix theory, vector math, the "jay" operator, converting S-parameters into other matrices, Smith charts etc. may turn *off* the average amateur designer. You advanced readers, may raise your 2 port network skills by visiting better web sites + reading books, simulating with SPICE, or better yet, measuring your port parameters with a vector network analyzer.

---

3. More on Feedback Amplifiers (FBA)

Many builders (myself included) copy feedback amps rather than design their own. By tweaking the emitter current, shunt and series feedback while measuring S11 and S22, plus simulating with a program called FBA08.exe, I've learned it's possible to design good feedback amps FBA08

is 1 of the Ladpac programs that ships with EMRFD.

I wanted a FBA with ~35 mA emitter current for improved IMD and low distortion on strong signals. Such an amp might follow a diode ring mixer in a receiver I.F. chain.

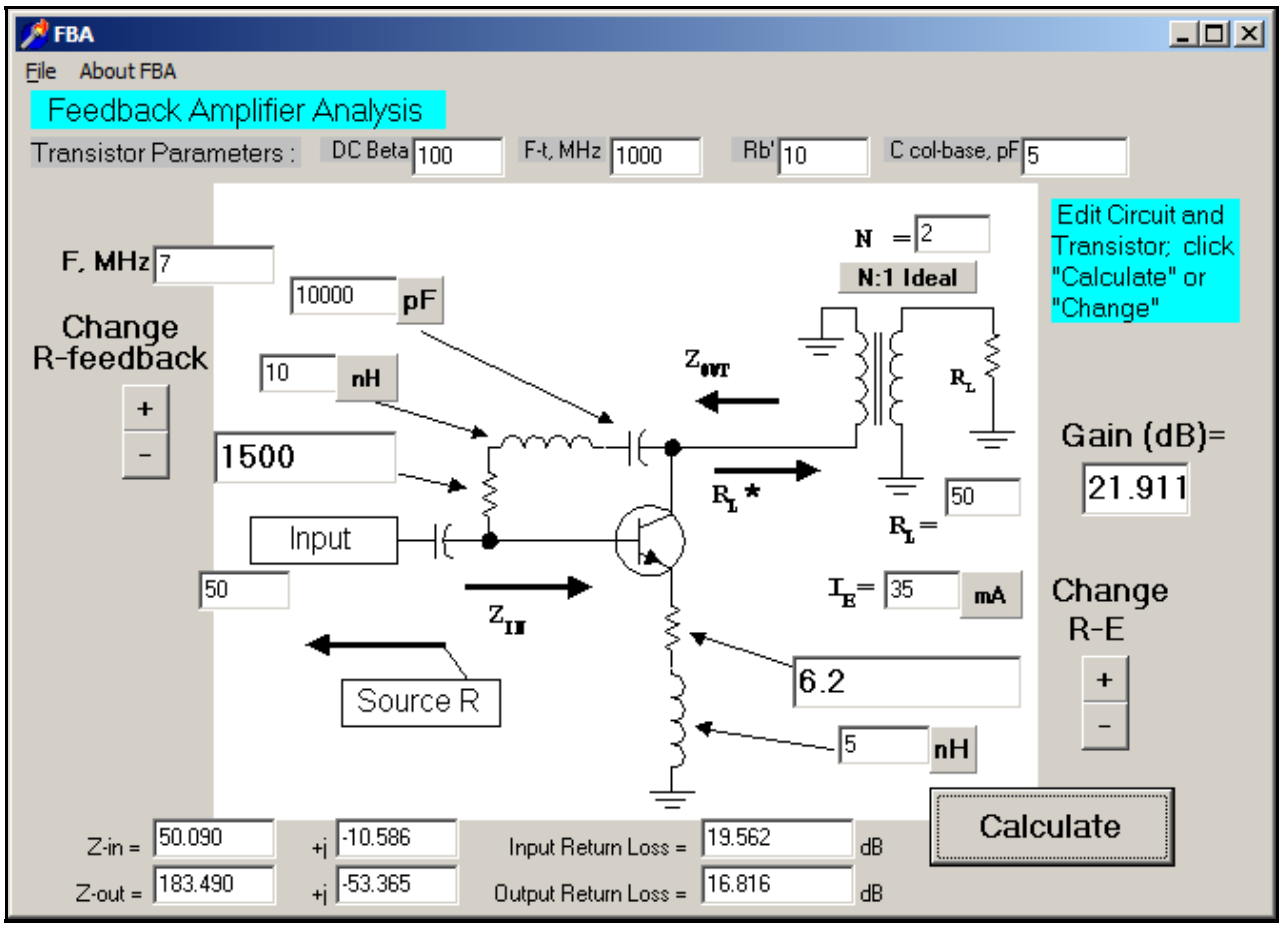

Above — My 7 MHz FBA set up. Wes, W7ZOI suggested using 5 nH as the default emitter inductance and 10 nH for the default collector to base inductance in FBA08. These represent stray inductances in your circuit breadboard. Emitter inductance affects the input impedance more.

Zin = input impedance. Zout = output impedance.

Explore this program to learn how changing the emitter resistor, feedback resistor and emitter current affect the input and output return loss.

Adjusting the transformer N and load values only affect the calculations for Zin because this app wasn't really designed to crunch output transformer Z ratios for Zout manipulation. The default output Z = 200 Ω and thus for the N parameter with a 50 Ω RL, RL is multiplied by N^2 to set the amplifer load impedance.

From FBA08 simulations: with an emitter current of 35 mA, my series feedback = 6.2 Ω and shunt feedback = 1500 Ω.

I chose a simple voltage divider bias network to set up the ~35 ma and ensure reasonable temperature stability.

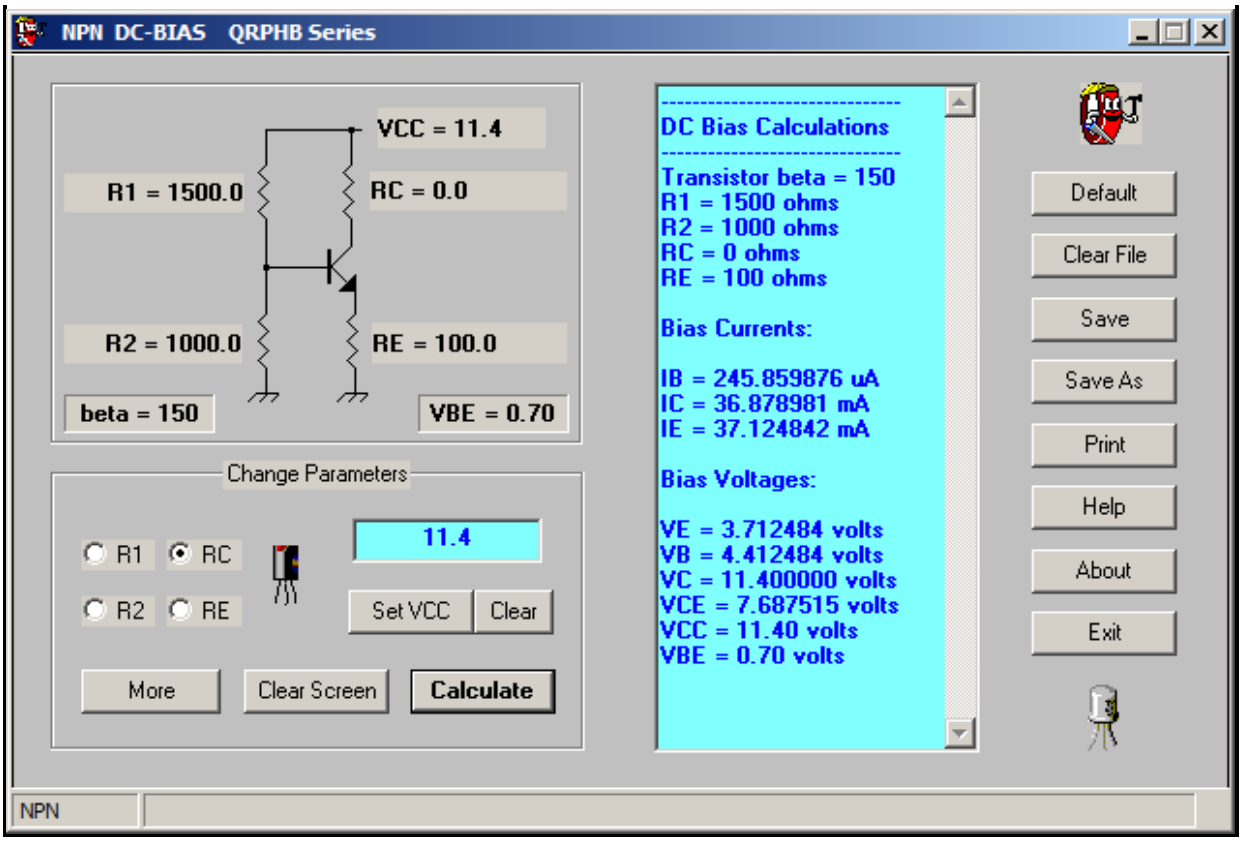

Above — Choosing the emitter and nearest standard value bias network resistors to set up ~ 35 mA emitter current with a program. Actual biasing requires you to set up the correct emitter current + establish reasonable temperature stability.

Click and scroll to #5 for some basic transistor biasing notes. While this supplement shows a simple method for stable bias networks, it probably understates that **Beta** bias stabiility is a function of the ratio of RB to RE, where RB = the 2 base resistors in parallel. The lower the ratio the better, but then more input power is lost in those resistors. A higher ratio reduces stability but wastes less input power — another trade off we must negotiate! See Ken Kuhn's web site for thorough, expert-level information on voltage divider biasing your BJT amplifiers.

I use NPN DC BIAS, a program I wrote, however, Wes included 1 in the Ladpac software called Biasnpn08.exe that's also good. Determine the VC for the program by first multiplying the value of your decoupling resistor by the emitter current in Amperes to learn the voltage drop across the R. Then, subtract that voltage drop from your power supply voltage: 12.22V - (.0371 A X 22 ohms) = 11.4 VDC.

Our software allows you to pick approximate base and emitter resistor values to set up a desired current in your amplifier breadboard, but you must still choose reasonable values for temperature stability. Tweak them as needed, or choose some other bias method such as a current source. Let's move to the bench...

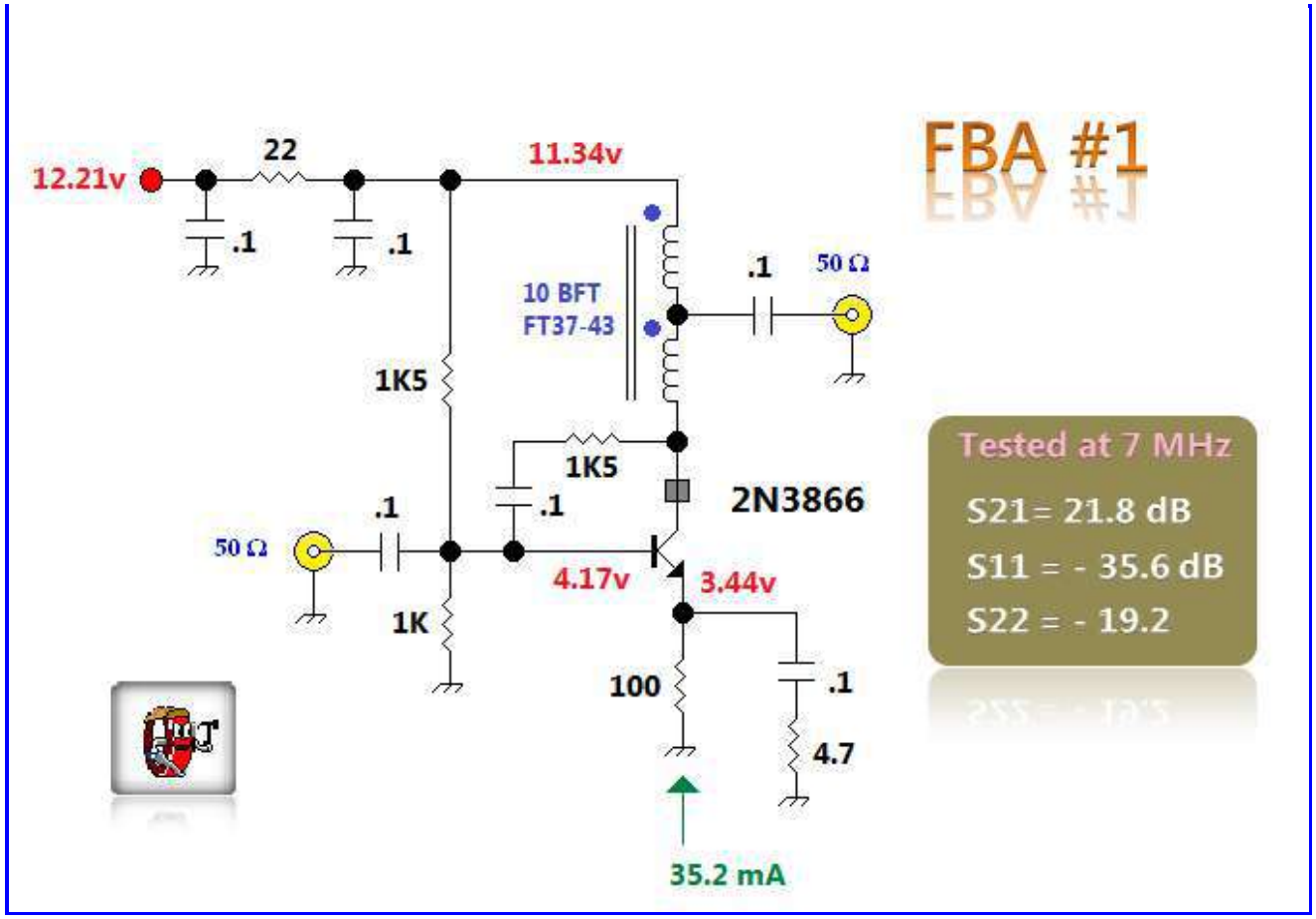

Above — My 7 MHz FBA with some measured S-parameters. On the bench, I lowered the 6.2 Ω series resistor to 4.7 Ω because the voltage divider bias network also affected Z in. I tried 3.3, 4.7 and 5.7 Ω resistors for series feedback and settled on 4.7 Ω since an S11 of -35.6 dB wins the prize!

The S22 of -19.2 dB bettered the value predicted by FBA and seems quite acceptable considering we normally follow a FBA with a 6 dB pad that raises the output return loss another 12 dB. FBA08 gets you close, however, only bench experiments will realize the amplifer you want, and sometimes, a decent S11 and/or S22 may elude you.

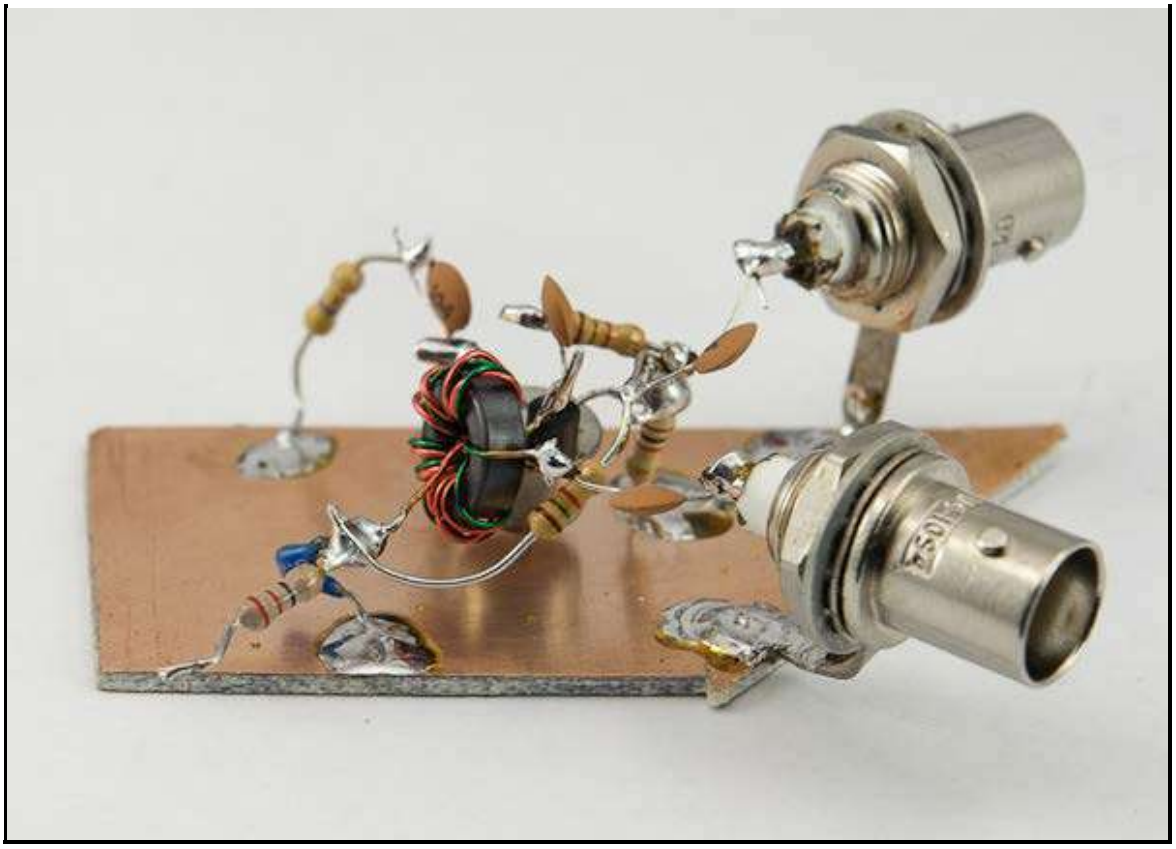

Above — A photo of the 35 mA feedback amp built on scrap of copper clad board.

Parallel Transistor Feedback Amp

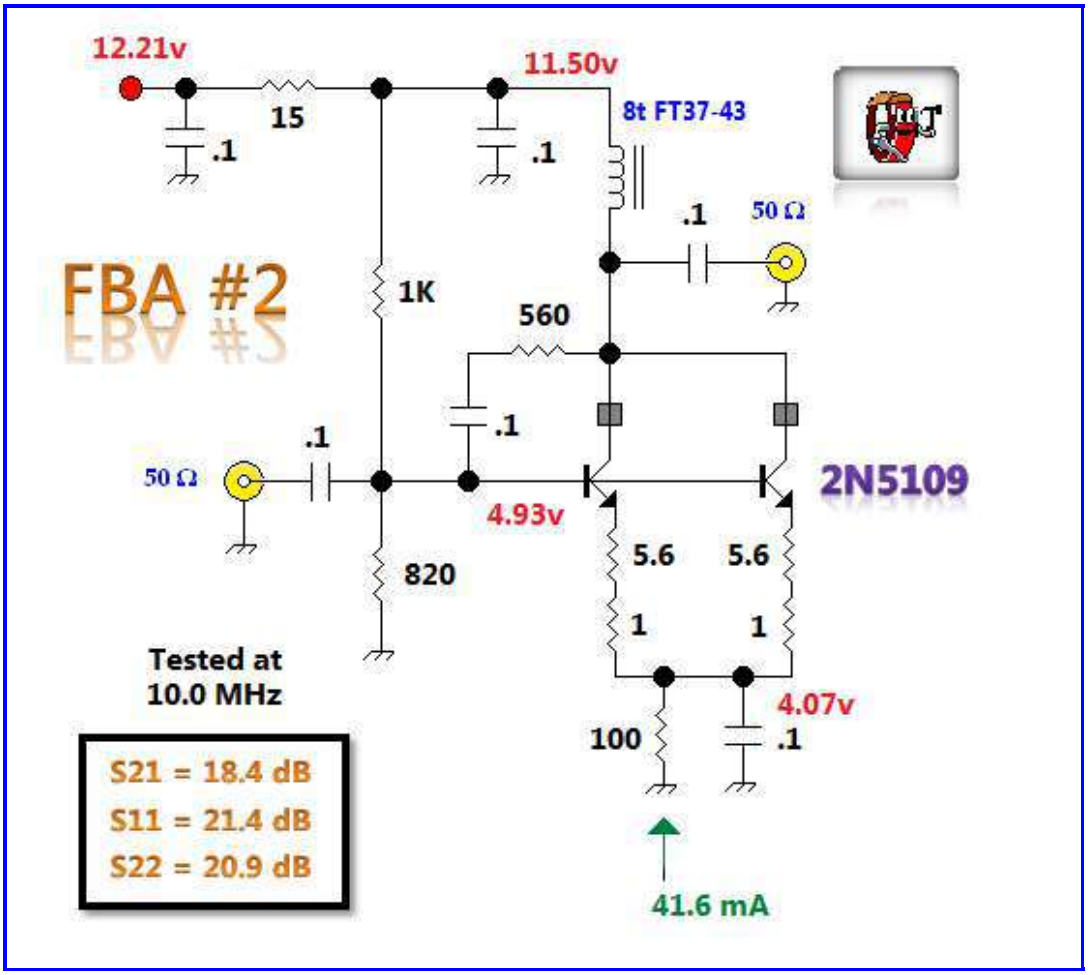

Above — A feedback amp with two 2N5109 transistors wired in parallel. Click for a photograph of this prototype. I lacked 6.8 Ω resistors and placed 1 Ω + 5.6 Ω to make the needed R for a strong S11.

Originally, I built FBA #2 with a 4:1 Z transmission line transformer, but measurements of S22 disppointed me. Later, a L wound with 8 turns around an FT37-43 ferrite toroid drove an S22 of 24 dB, but S11 was only 18.5 dB.

With the amp set up to measure return loss on the input port, I placed a 500 Ω potentiometer in series with a 100 Ω resistor between the collector and base terminals and tweaked the pot to obtain the lowest peak-peak voltage in my 'scope (lowest return loss). After, I removed the pot and measured its resistance at 572 Ω. Finally, I soldered in a 560 Ω resistor and re-checked S11. Perfect. With my goal of at least 20 dB for S11 and S22 obtained, I powered down my bench and took some photos.

Wes, W7ZOI displayed parallel transistor FBAs in EMRFD and other works and recently I noticed Lyle, KK7P employed a parallel NE46134 FBA as a post-mixer amplifer in the Elecraft K3.

Wes wired 2 parallel 2N3904s to avoid using an expensive medium power BJT like the 2N5109. Doing so splits the heat between 2 devices, but does not deliver better IMD performance beyond what is offered by increasing the emitter current. In a typical FBA bias setup, you may measure as much as 10 volts between the collector and emitter terminals and with a supply of 12 VDC + a standing current of 20 mA, the collector dissipation = ~200 mW. This is about maximum for a TO-92 device likes a 2N3904, but only half of maximal dissipation for 2 in parallel.

Then, too, the K3 applies 2 parallel medium power BJTs get power dissipation with an SMT transistor. For strong IMD performance, Lyle and crew are throwing 80 mA or so into the pair — hard to do with SMT parts, so they overcome heat and power dissipation issues with 2 devices. Cool (literally).

Heat sink BJTs when you crank up the emitter current.

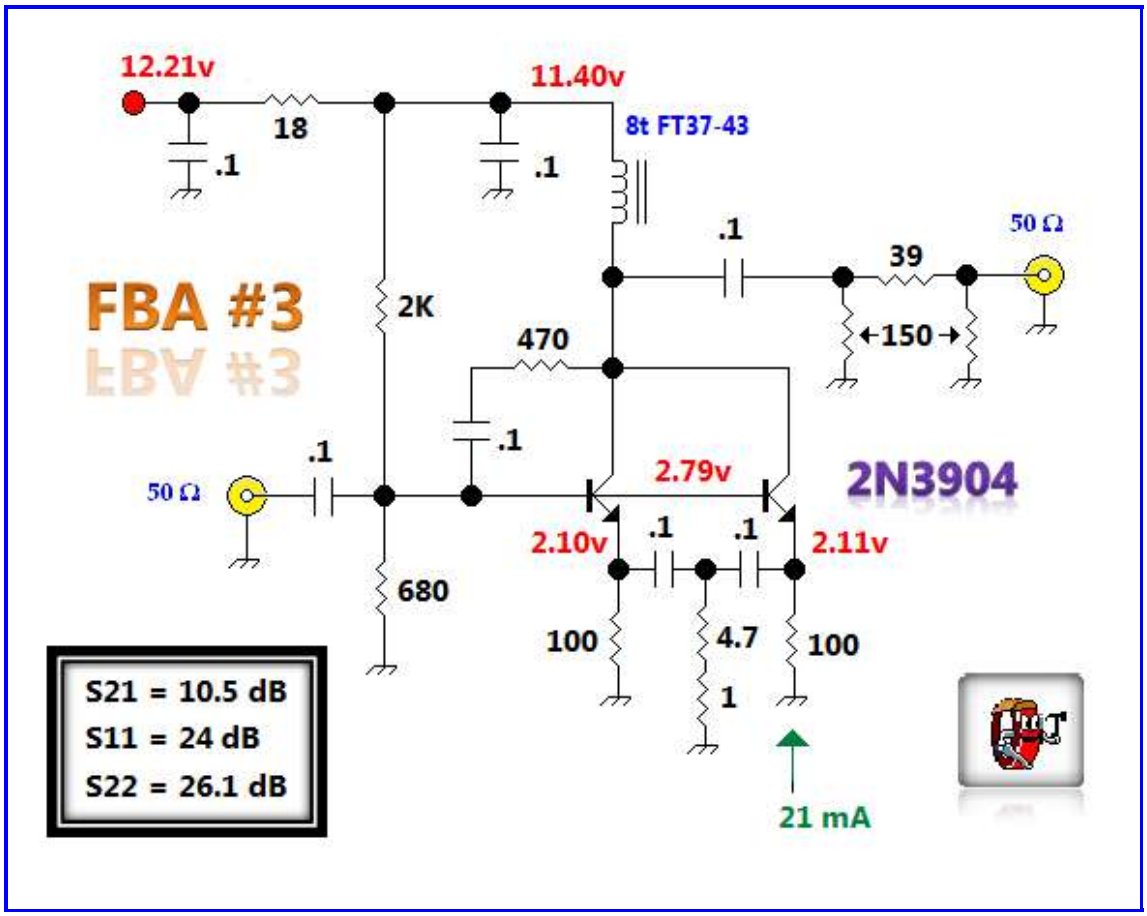

Above — An attempted 2N3904-based parallel feedback amp. Each BJT draws ~21 mA emitter current. Without the 6 dB output pad, the output return loss = 14 dB — I *failed* to realize both a strong (raw) S11 and S22.

The power gain including the 6 dB pad = 10.5 dB. I'll discard this design since it's substandard — without failures, victory may taste bland.

For bench designers, making a parallel FBA where both the raw S11 and S21 are > 20 dB is difficult and bench failures may either frusturate you, or enhance your resolve to succeed. With success, great satisfaction arises and I'm addicted to that feeling.

An FBA bench triumph means you managed to establish the perfect combination of series + shunt feedback, emitter current and the correct

output transformer ratio for *that* transistor plus its biasing circuitry — no small task.

A well matched amplifier = a thing of beauty! The fetching trio of high S11, S22 and S21 rewards your efforts and boosts your confidence to experiment further. And so it goes...

Sadly, only a fraction of hobbyists create and evaluate their own circuits.

---

4. Microphonics in Direct Conversion Receivers

LO = local oscillator or VFO. DC Receiver = direct conversion receiver.

Microphonics are induced electrical responses that arise from a mechanical vibration on the DC receiver chassis or circuitry. The audio amp, acting like a transducer, makes a clicking, or popping noise when you do things like tap the chassis, or unplug components — the disturbance throws out a burst of DC voltage that's amplifed by the AF chain and pops the speaker.

We may read or hear inexperienced builders tell us to expect microphonics in our DC receivers — *de trop* folklore strikes again! As a student of EMRFD and those wise designers who live in and around Beaverton, Oregon, I share some of their best tips to decrease microphonics in your DC receiver projects. " Keep Your LO From Radiating to the Outside World and Keep Unwanted RF from the Outside World Getting Into Your Receiver" seems the appropos title for the bulleted notes that follow:

Read EMRFD pages 8.7 to 8.11 and then build or apply the presented examples. Wisdom is experiential; it comes by doing, not just reading. It's no accident that Chapter 8 author Rick, KK7B mentions microphonics and hum in the same section. I've never read more thorough notes regarding DC receiver nuances anywhere; for example, did you consider that an ungrounded air variable capacitor shaft poking outside the LO box will radiate LO signal per Figure 8.18 ? I didn't in my early days.

Stick your LO in a RF-tight enclosure with RF-grade connectors and coax to patch the AC signal to the product detector. Bypass RF with feedthrough capacitors on any DC voltage lines that pass through the LO chassis wall. Many enthusiasts have only operated kitted or homebrew DC receivers where the LO and receiver guts lie on the same circuit board — this *ensures* microphonics. Wes and Roger built the historic Ugly Weekender VFO, transmitter and receiver in seperate boxes — resulting in low microphonics and no pulling of the VFO when keying the transmitter. Nothing in that 2 part QST series was done by accident. Read these articles to "go to school".

Reciprocally important; keep unwanted outside world RF from getting inside your DC receiver! Apply resistors plus capacitors, or inductors plus capacitors to decouple and bypass RF from moving along on your DC voltage lines, key line, microphone cables etc.

Keep product detector port-to-port isolation high. Typically, we employ double balanced mixers to obtain high port-to-port isolation. I cover mixer balance on this page . For diode ring mixers, measure the return loss of the circuits that you connect to the product detector LO, RF and AF ports — I aim for 20 dB or greater return loss on my LO output, RF output and AF amp input circuits to help preserve the product detector balance and keep port isolation as high as possible. Along with 50 Ω amplifers, attach attenuator pads, AF diplexers, or whatever to help increase port return loss as required.

LO-RF port isolation: Consider a common gate amp with an output matching network to get a high output return loss (S22). The common gate amp provides strong reverse isolation without adding much noise.

Avoid end-fed wire antennas where there is a strong antenna field right next to your radio.

I favor sturdy chassis/cabinets with rubber feet. Homebrew copper clad board or die-cast aluminum cabinets may work best as joints and screwed connections won't corrode. *This is a weak recommendation.*

Double the LO frequency or apply a heterodyne VFO. Often microphonics arise in the VFO tank. EMRFD cover this well. If the VFO operates at a significantly different frequency than any of the signals reaching the balanced mixer, leaked LO won't cause as much havoc as when a LO tank is tuned to the mixer RF port frequency.

Despite proper techniques, RF can exit via the antenna port and make its back into our rig through power supply cables (often modulated by our house AC electricity). In some cases, we require special power supply decoupling to decrease hum and microphonics. We might need to add a common mode choke (+/- capacitors) for common mode noise suppression in addition to the usual differential mode choke(s) and capacitors. In my main shack power supply, I run a common-mode choke plus I soldered a 0.01 uF capacitor across each bridge rectifier diode to bypass RF.

Some radio operators just run battery power supplies.

Above — Feedthrough capacitors. I prefer hole mount over solder mount parts, however, quality feedthrough capacitors of any kind tend to be expensive. As a hobbyist, I'm constantly searching for bargains and when I find 1, I'll purchase a bunch to meet my current and future needs.

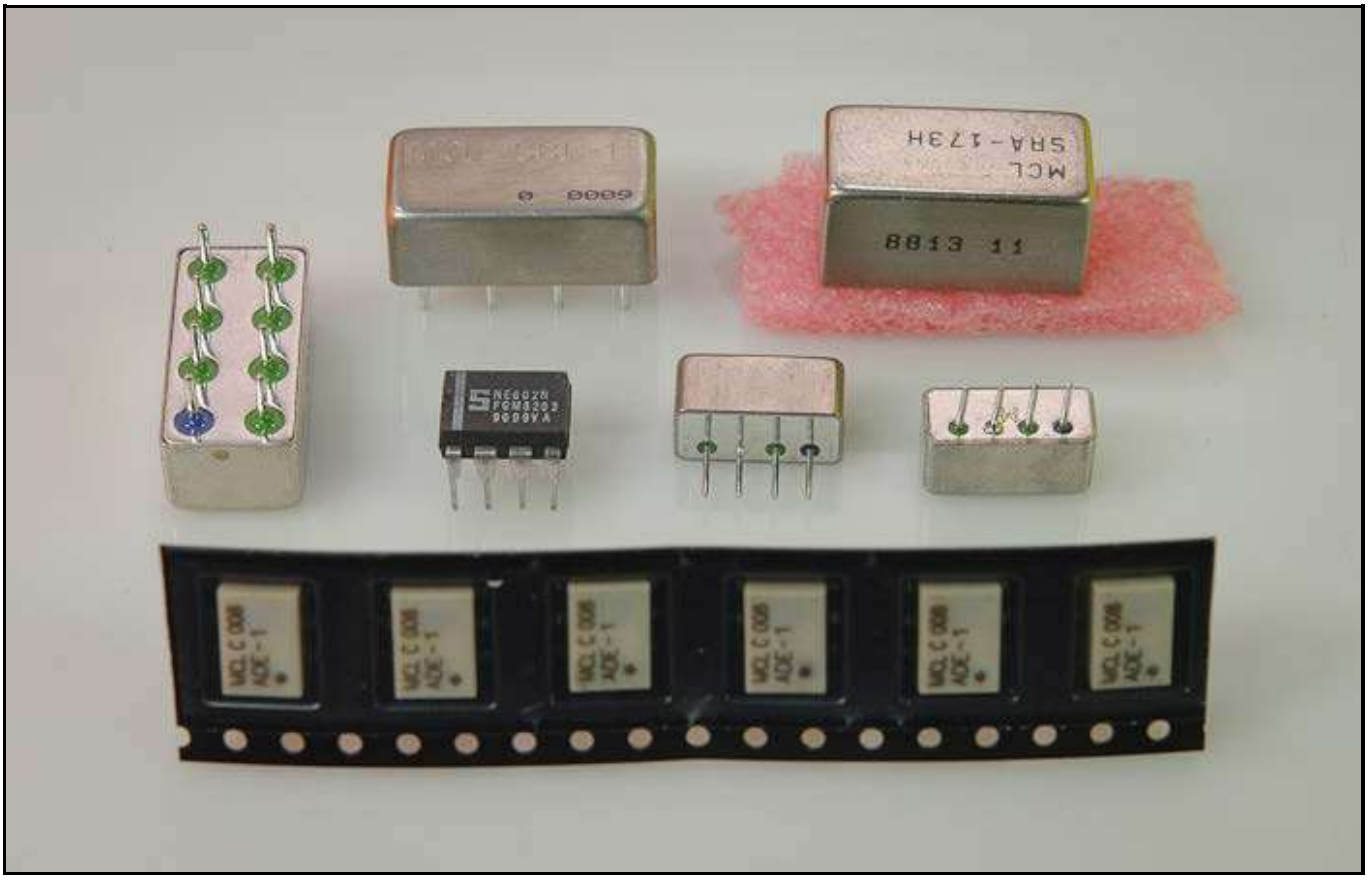

Above — Some double balanced mixers from my collection: ADE-1, NE602, TUF-1, TUF-2, SBL-1 and a SRA-173H; a MiniCircuit Lab's Level 17 diode ring mixer.

You owe it to yourself to listen to a DC receiver designed and built to reduce microphonics — music to our ears.

---

5. Some Experiments with RF Bypass Capacitors

Introduction

Bypass implies a low impedance path to ground for RF at 1 or more frequencies. After reading EMRFD pages 2.28 - 2.31, I decided to explore this subject for the first time. My bench measurements from Spring 2012 punctuated how little I knew about RF bypass and I share these notes as something for me and others to build on.

In these experiments, I

1. observed the self resonant frequency of MuRata RPE Series, 50v, 5% capacitors with X7R temp compensation at 0.1, 0.01 and 0.001 µF.

2. examined a wire short, plus 1 and then 2 Johanson Dielectric 0.01µF, 50v, X7R, size 1206 chip capacitors.

3. tested a 0.1 µF RF cap plus a parallel 2.2 µF electrolytic capacitor to look at parallel resonance side effects.

4. attempted to reduce the Q of some parallel capacitors to reduce unwanted high impedance peaks.

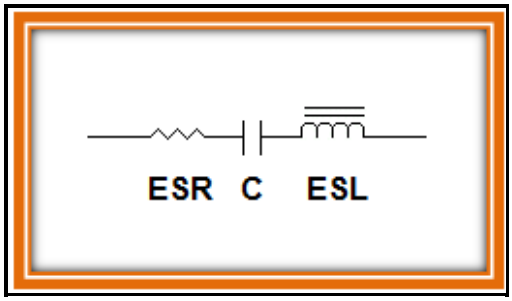

Above — The frequency dependent components of a capacitor are shown in this capacitor equivalent circuit schematic; essentially an RLC network. Engineers use mathematical formulae to describe the components of a capacitor along with reactance and with this math, you might derive an unknown variable from available data so it's worth diving into on your own.

ESR or equivalent series resistance = the sum of all of a capacitors' resistive components. Expressed in ohms, ESR acts like a resistor in series with the capacitor. Normally we desire capacitors with an ESR as low as possible. Consider reading the capacitor datasheets for those your stock and/or searching for information regarding low ESR capacitors on the Internet.

ESL refers to the equivalent series inductance; the sum of all the capacitor's inductive components. This includes lead length in hole-through parts.

In a given capacitor, the series resonant frequency is the frequency where the inductive reactance from the ESL = the capacitive reactance, but since the 2 reactances are 180 degrees opposite in phase, they cancel to drop the impedance to 0 and the capacitor acts like a resistor at its ESR.

The series inductance of a capacitor may be determined using a network analyzer and unfortunately this in unattainable by most average builders. When designing RF bypass with network analysis, we strive for a low impedance over a wide frequency range, although small ripples typically occur.

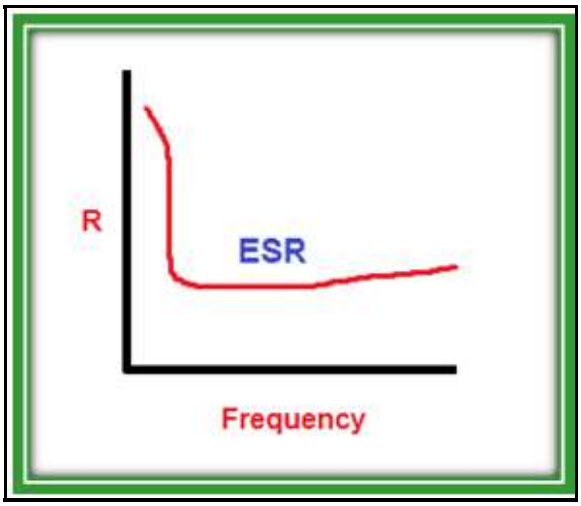

Above — A plot of equivalent series inductance. ESR tends to increase with frequency.

Methods

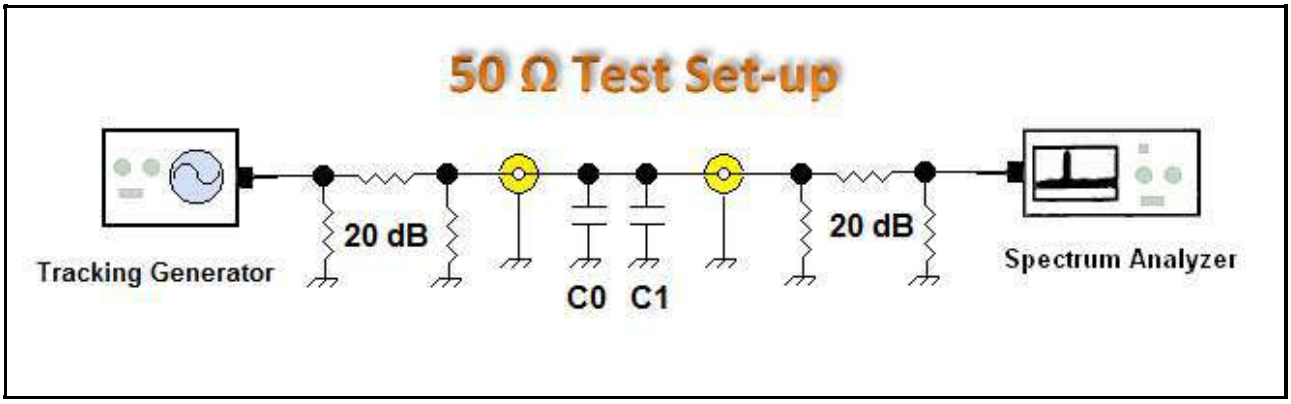

Above — My test set up. I performed all analysis with a tracking generator plus spectrum analyzer. The 50 Ω system used short coax patch cables fitted with BNC connectors with 20 dB attenuator pads before and after the capacitors under test. The capacitors shown as C0 and C1 were soldered on a copper board with short leads and BNC connectors. C1 is omitted when evaluating only 1 capacitor.

You may also perform capacitor self resonant frequency testing with a vector network analyzer, a signal generator plus a 50 Ω terminated scope, or with a sweep generator ramp-driving the oscilloscope X input while simultaneously driving a VCO with logarithmic output to the Y oscilloscope input. SPICE simulations may also yield insight.

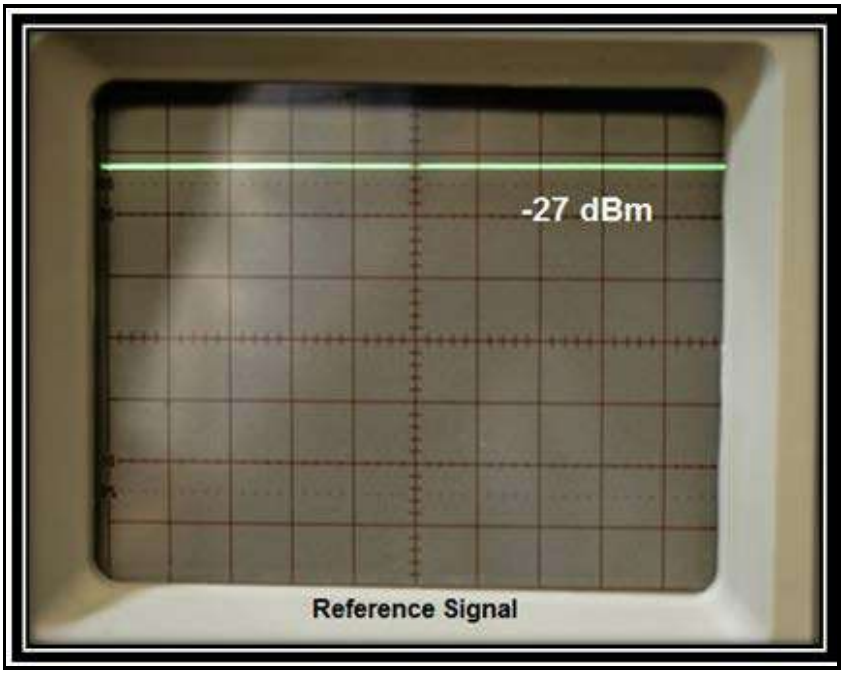

Above — The -27 dBm reference with a through-connector between my 2 coax patch cables (C0 + C1 board removed).
To save time I shot these SA photos handheld and prefer a slower shutter to capture a nice CRT tracing, so some of the photos show a little hand jitter.

Single Shunt Capacitors

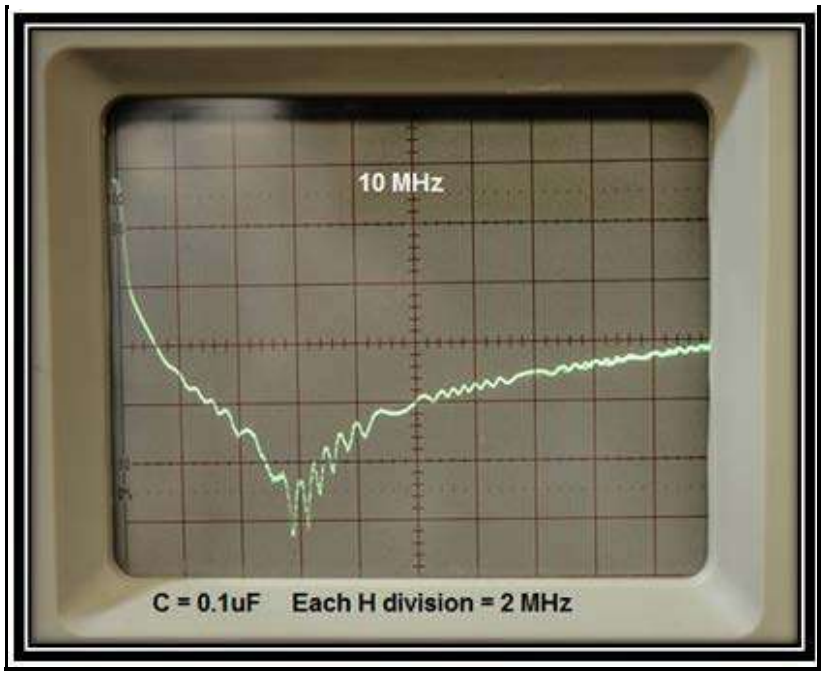

Above — C0 = 0.1 µF. I view the capacitor like a trap. At almost 5.8 MHz lies the peak attenuation, or lowest impedance — this is C0's self resonant frequency. The peak bypass frequency lies ~ 60 dB down. At 20 MHz, the attenuation is only ~ 30 dB.

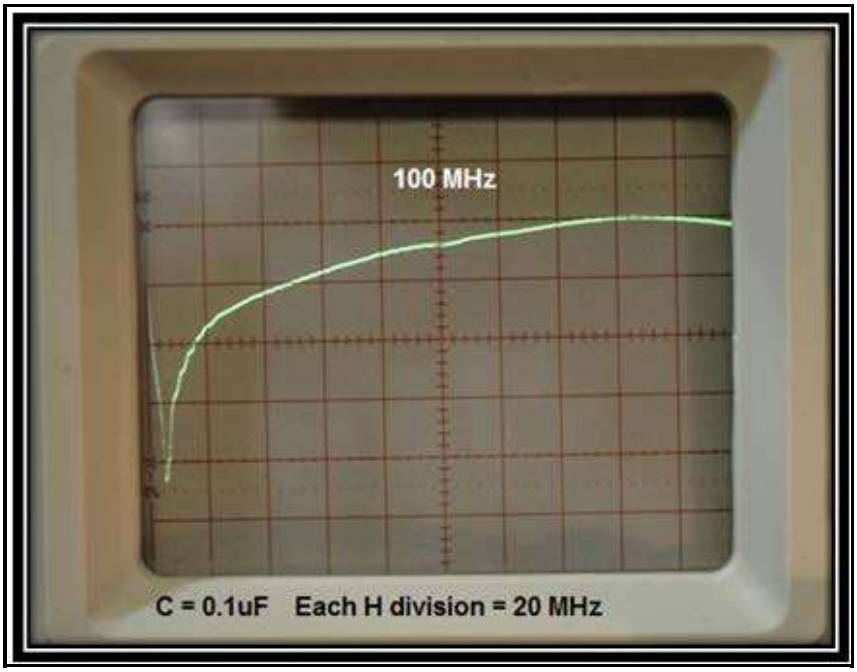

Above — Another shot of the 0.1 µF bypass cap with a 200 MHz span. At 50 MHz, the reference signal lies only ~ 17 dB down. At 100 MHz, the attenuation is only ~ 11 dB — this hardly qualifies as “bypass” much above the self resonant frequency. Above the self resonant frequency, a capacitor's XL affects impedance more than the ESR and XC of the capacitor.

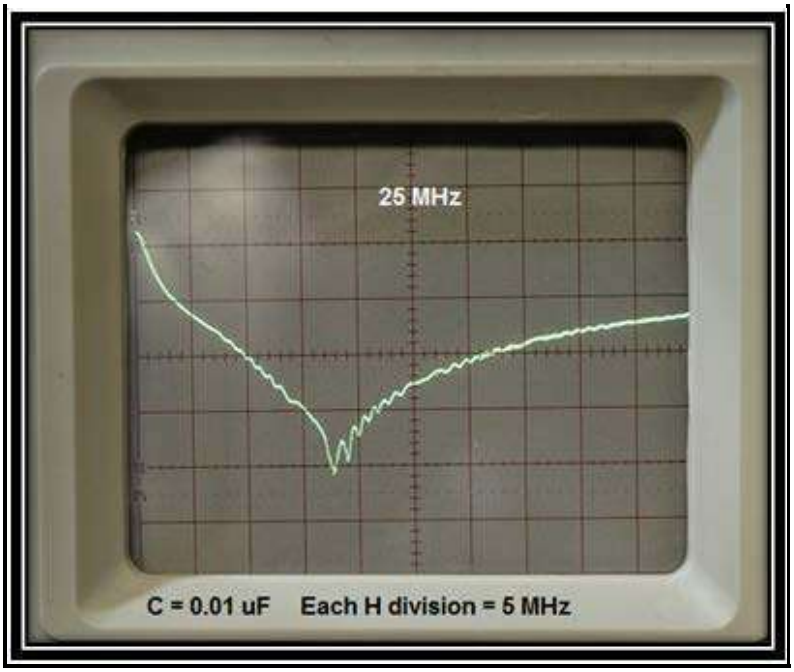

Above — C0 = 0.01 µF. The peak bypass frequency (capacitor self resonant frequency) is centered at 17.5 MHz and is ~ 50 dB down; not as deep as with the 0.1 µf cap. At 50 MHz, the attenuation is ~ 21 dB.

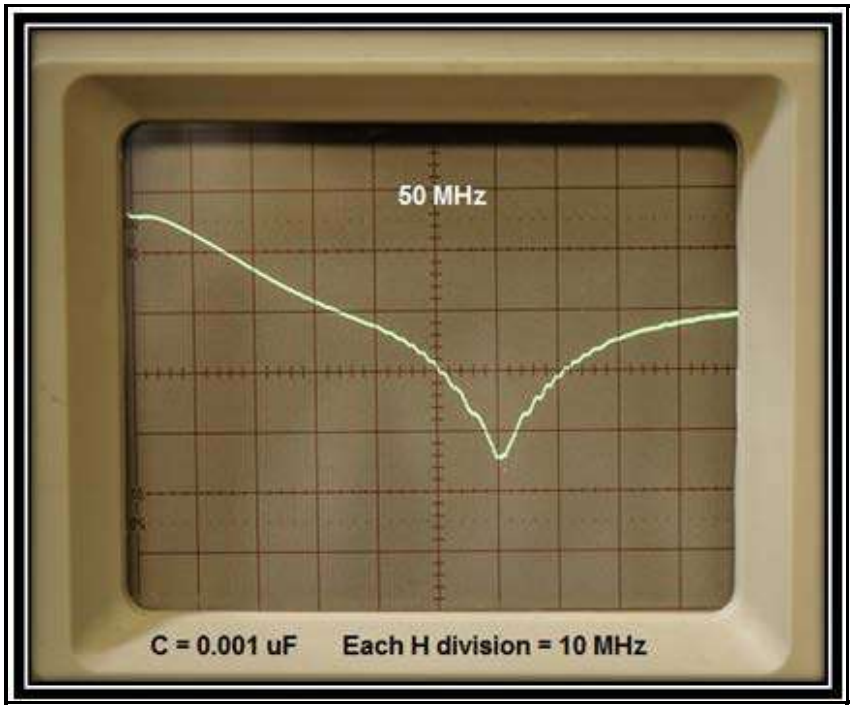

Above — C0 = 0.001. The response is peaked at 62 MHz with an attenuation of ~42 dB. At 100 MHz, the signal is 17 dB down. Again, the peak attenuation looks diminished compared to that of the 0.1 µF and the 0.01µF caps.

Capacitors in Parallel

Now I placed 2 caps in parallel (C0 + C1) as some builders do to try and garner a wider attenuation bandwidth.

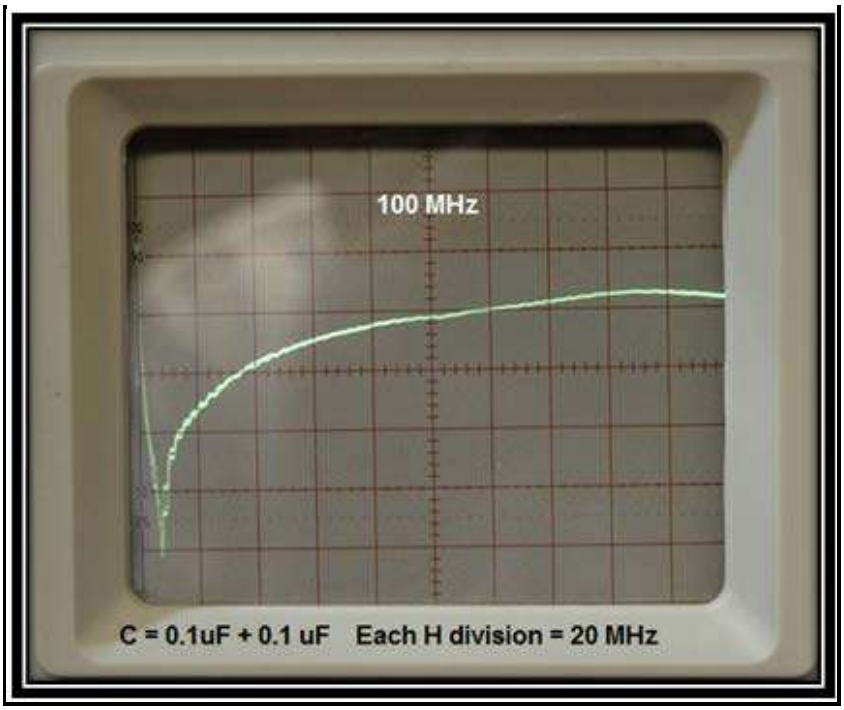

Above — C0 = 0.1 µF + C1 = 0.1 µF. The peak attenuation = 60 dB at 8 MHz; up 2 MHz from that of the single 0.1 µf capacitor. At 100 MHz, attenuation = ~ 19 dB — better than a single 0.1 µF but still low.

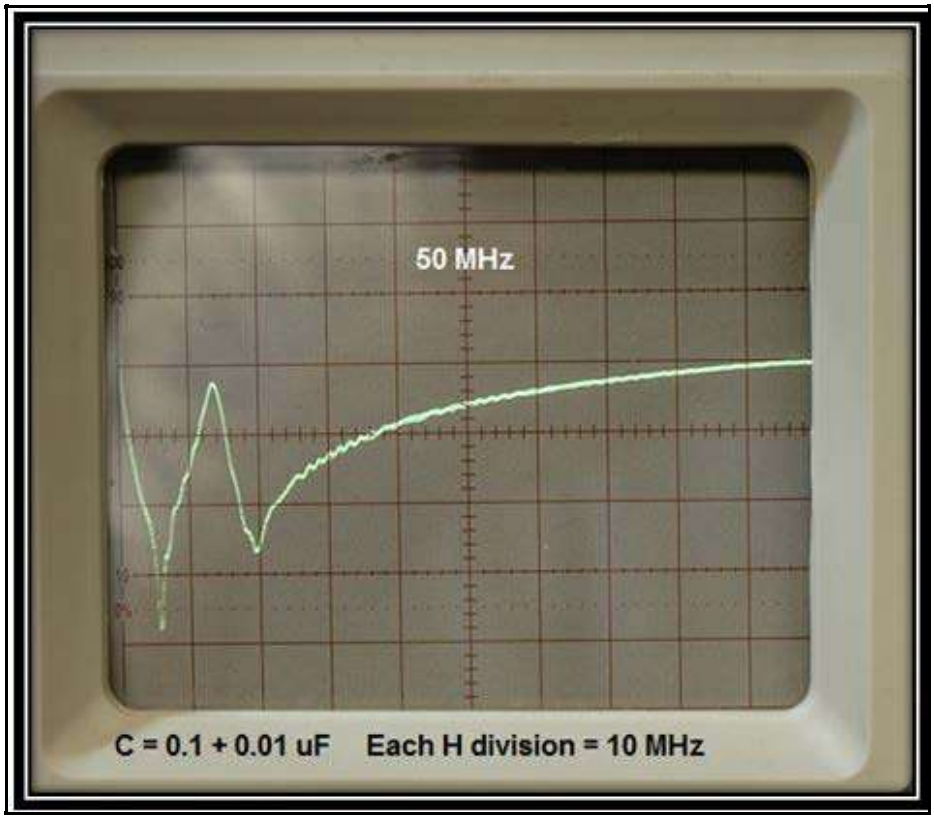

Above — C0 = 0.1 µF + C1 = 0.01 µF. Yikes! With the 2 different cap values, we get an unfortunate high impedance blip peaking at 13 MHz. Each capacitor exerts its self resonant frequency, but in between these self resonant frequencies, lies a disaster.
When placed in parallel, the inductance of 1 capacitor resonates with the capacitance of the other to form a parallel resonance — leading to a high impedance — that blocks RF bypass and peaks at a specific frequency.

But wait. Things can get worse:

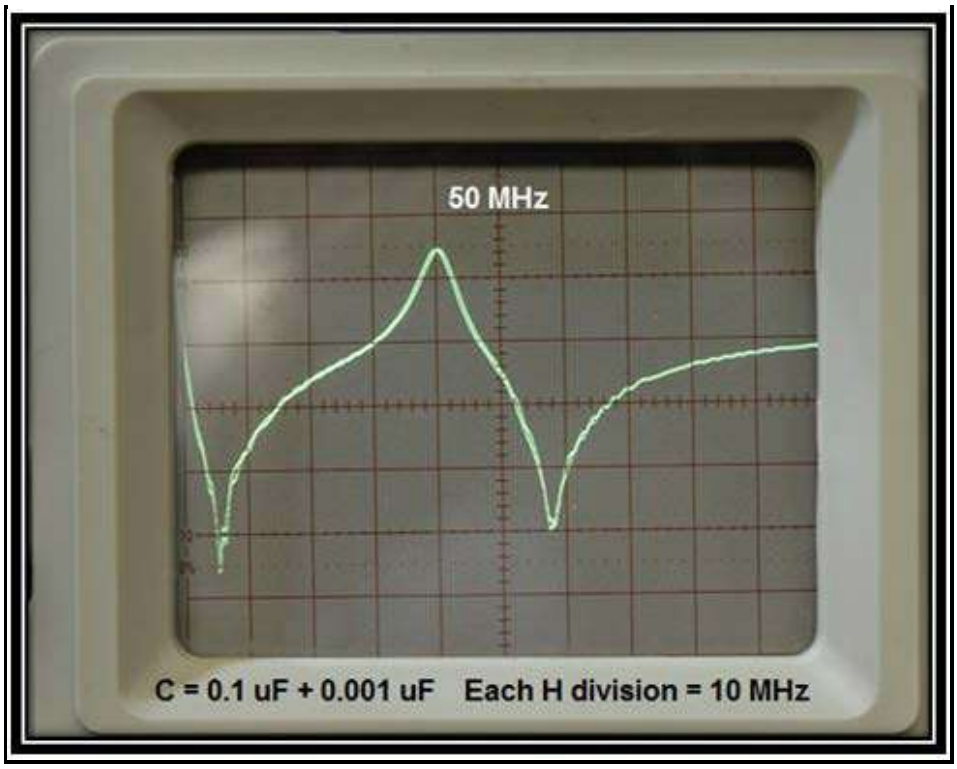

Above — C0 = 0.1 µF + C1 = 0.001 µF. The wide value variance between these 2 capacitors creates a huge, high impedance spike where the attenuation is only about 6 dB at 40 MHz. Catastrophic bypass indeed. катастрофа.

A 7 mm Length of Copper Wire

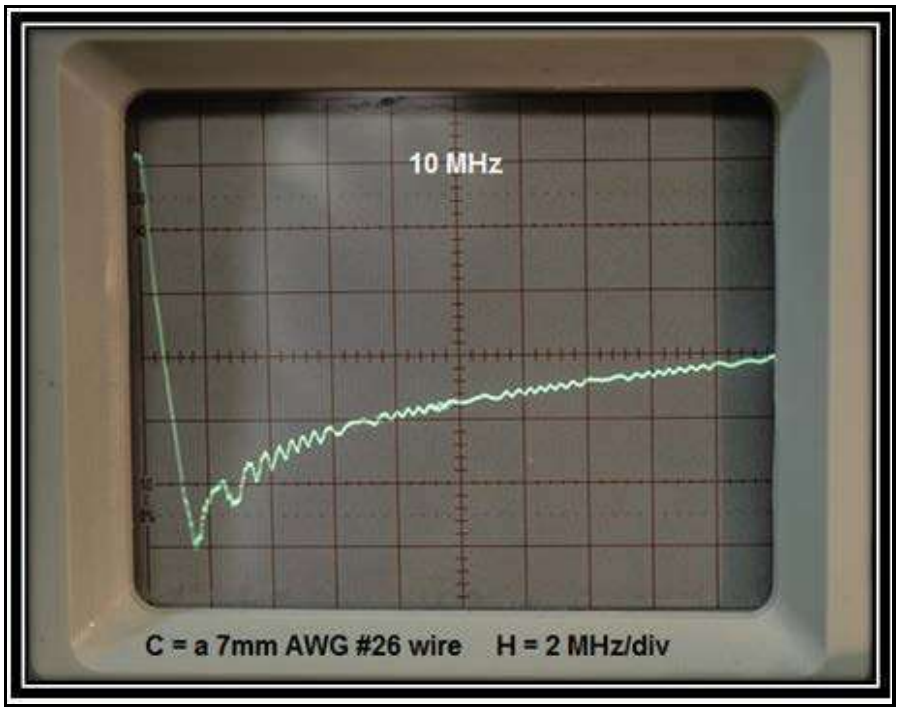

Above — A 7 mm piece of 26 gauge copper wire was shorted to ground instead of C0. This wire measured at ~7 nH of inductance and I saw that attenuation decreases with frequency from 62 dB at 8 MHz to ~33 dB at 20 MHz. Even a short piece of wire doesn't exhibit a flat, wideband bypass.

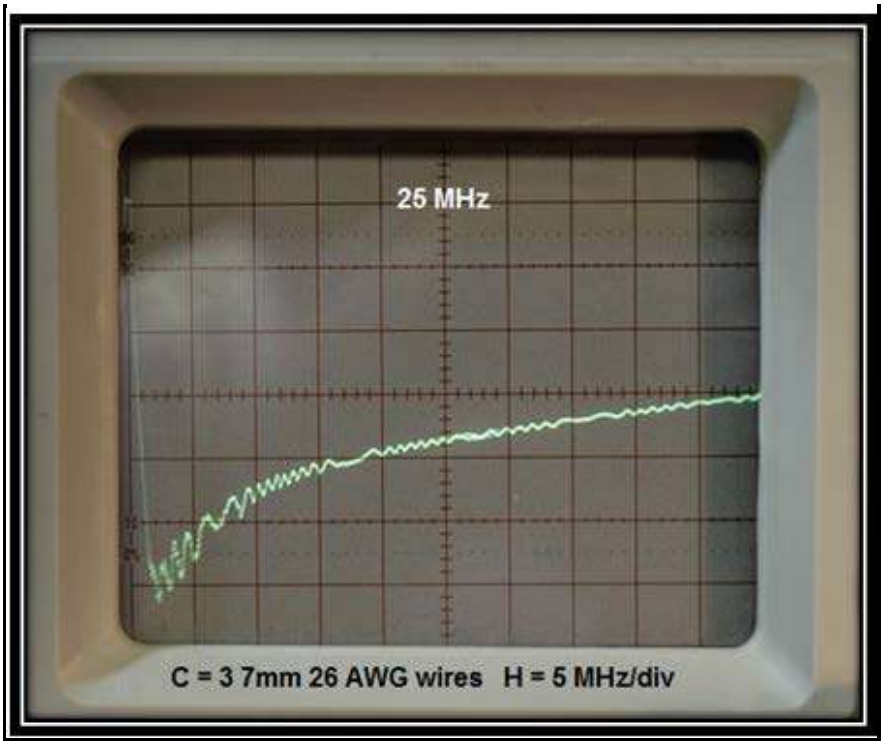

Above — This spectrum analysis shows three 7 mm wires shunted to ground – not much different than 1 wire.

0.01 µF Chip Capacitor(s)

Above — The magnified copper board that I tested one or two 0.01 µF chip capacitors. You can see 1 capacitor soldered in.

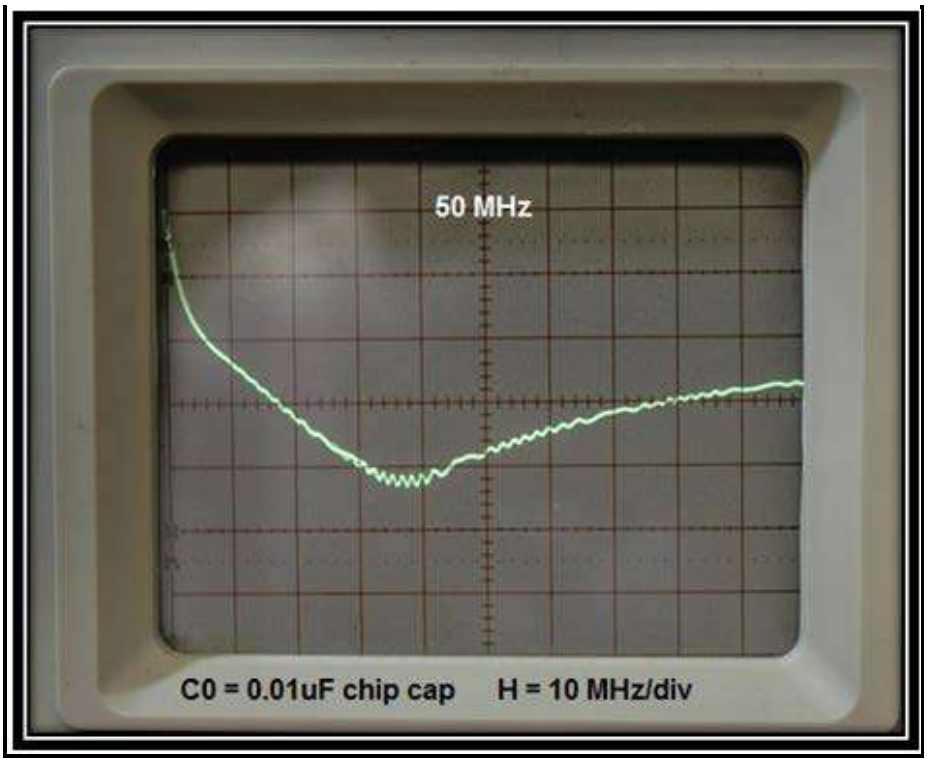

Above — C0 = 0.01 µF SMT cap. The SMT parts exhibited a peak attenuation of 45 dB at ~37 MHz. The attenuation dip lacks the sharp peak of the hole-through 0.01 µF cap shown eariler and exhibits a somewhat wider bandwidth. The self resonant frequency of the chip capacitor is 5 MHz higher than the particular hole-through capacitor I measured. Click for a side by side photo.

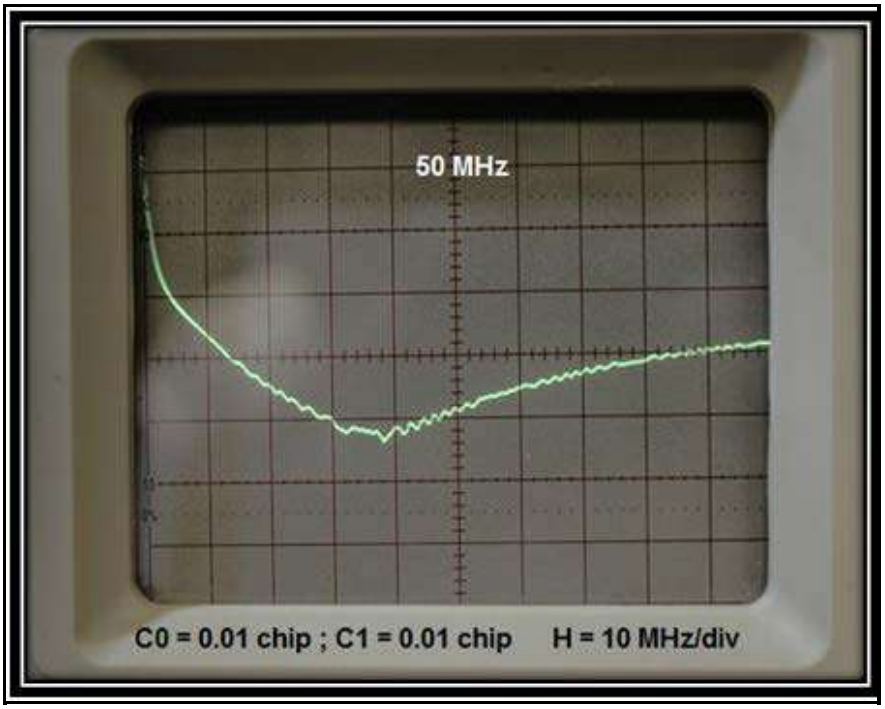

Above — C0 = 0.01 µF + C1 = 0.01 µF. The SMT parts exhibited a peak attenuation of 45 dB at ~37 MHz; similar to the single 0.01 µ F chip cap, but with a few more dB attenuation between 10 and 20 MHz.

0.1 µF Ceramic + a 2.2 µF Electrolytic Capacitor

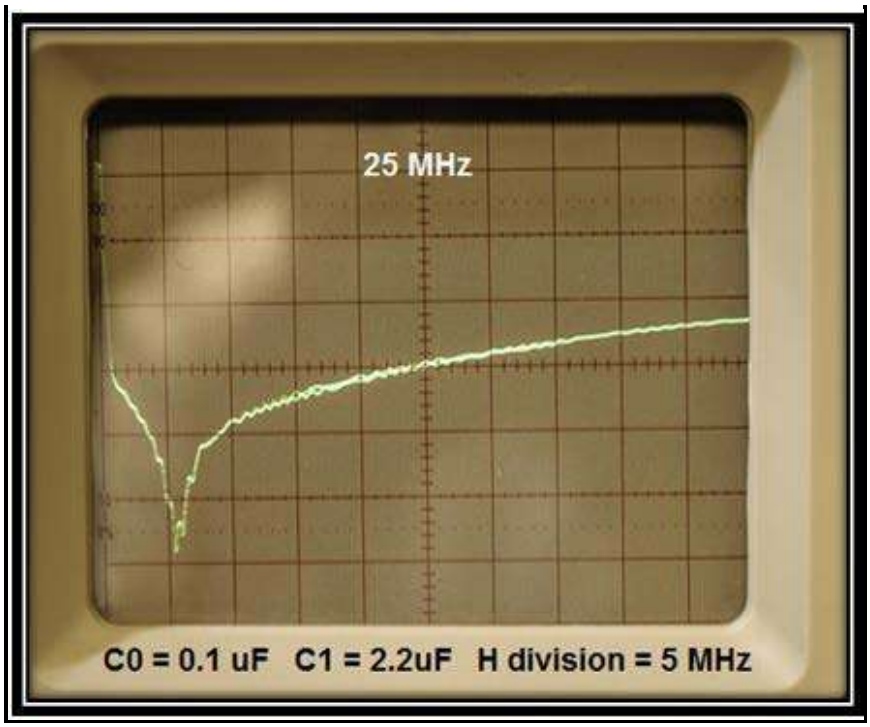

Above — C0 = 0.1 µF and C1 = 2.2 µF. The low Q 2.2 µF C1 electrolytic cap did not create the a parallel resonance with C0. Shaky photo — sorry. I also tested a 10 and 22 µF cap in parallel with C0 and saw no disturbance caused by a parallel resonance between a big AF capacitor and C0 (an RF value cap) with my RF spectrum analyzer.

Some additional experiments applying a low Q *A*F capacitor plus a ceramic *RF* capacitor for wideband bypass yielded some interesting results and I'll present these in a future project.

Capacitors in Parallel with a Series Resistor to Lower Q

In previous experiments, placing 2 RF capacitors in parallel led to the formation of a peaked high impedance blip between the low impedance peaks set by the self-resonant frequency of the 2 capacitors. If multiple capacitors are soldered in parallel, the series inductance of each capacitor will resonate with the capacitance of the next smaller C value.

One solution is to put a resistance in series with all but 1 of the parallel capacitors so that the Q of resonance formed by this capacitor's series inductance and the capacitance of the next smaller capacitor is low. If capacitors exhibited 0 inductance then putting capacitors in parallel would be fine, however, since capacitors exhibit inductance, a parallel resonant frequency may occur with capacitors in parallel.

I found applying a series resistance to lower Q may flatten the impedance versus frequency response of the bypass network, but didn't decrease the impedance at any 1 frequency. Optimal bypassing or achieving the lowest impedance over a wide frequency range presents a complex topic that might even challenge some engineers.

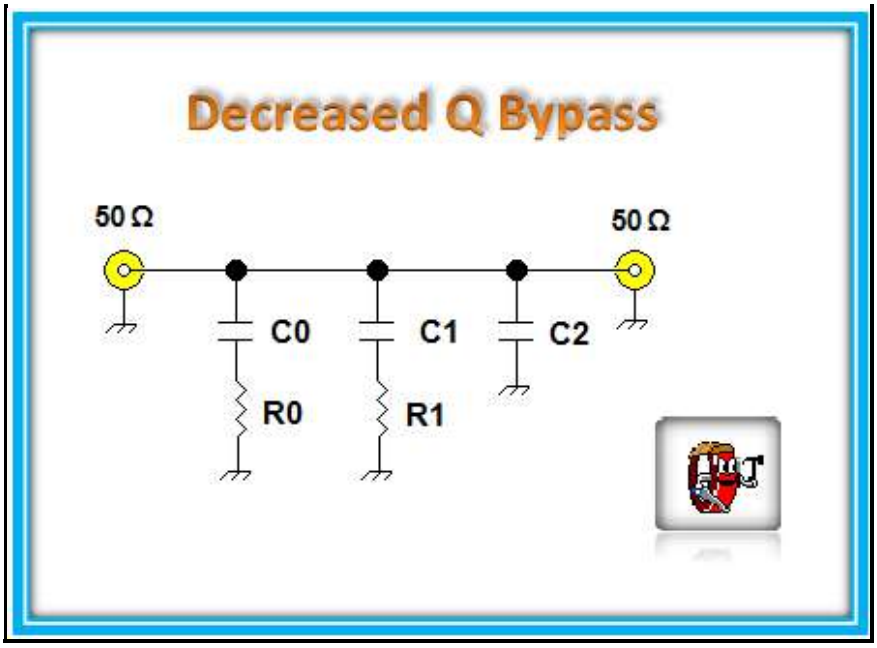

Above — A method to exact wideband bypass.

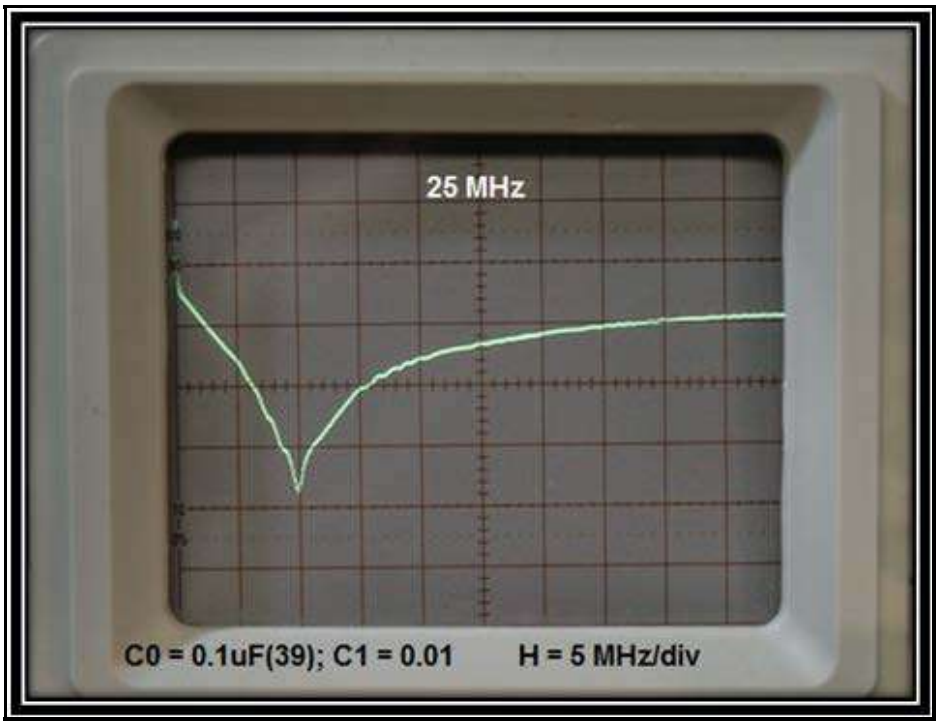

Above — My first try with C0 = 0.1 µF, R0 = 39 Ω and C1 = 0.01 µF. I arbitrarily placed the 39 Ω resistor in the R0 slot and saw that the high impedance peak seen earlier disappeared. This gave me the confidence to try 3 capacitors. I had no idea what R value to use and really just wanted to see what happens.

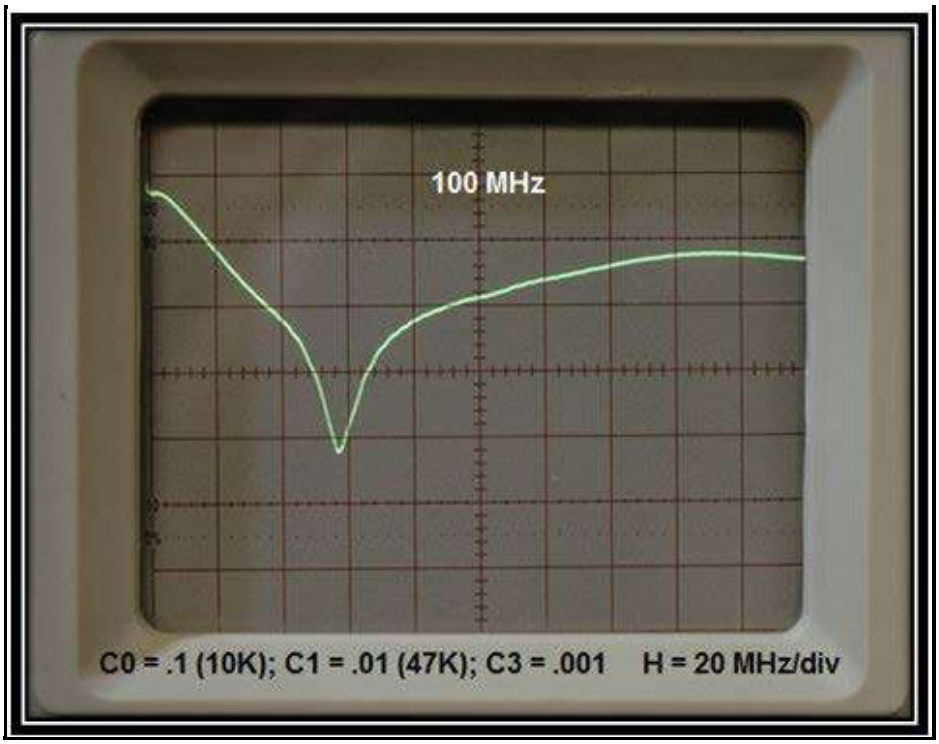

Above — The spectrograph with C0 = 0.1 µF, R0 = 10K, C1 = 0.01 µF, R1 = 47K and C3 = 0.001 µF.

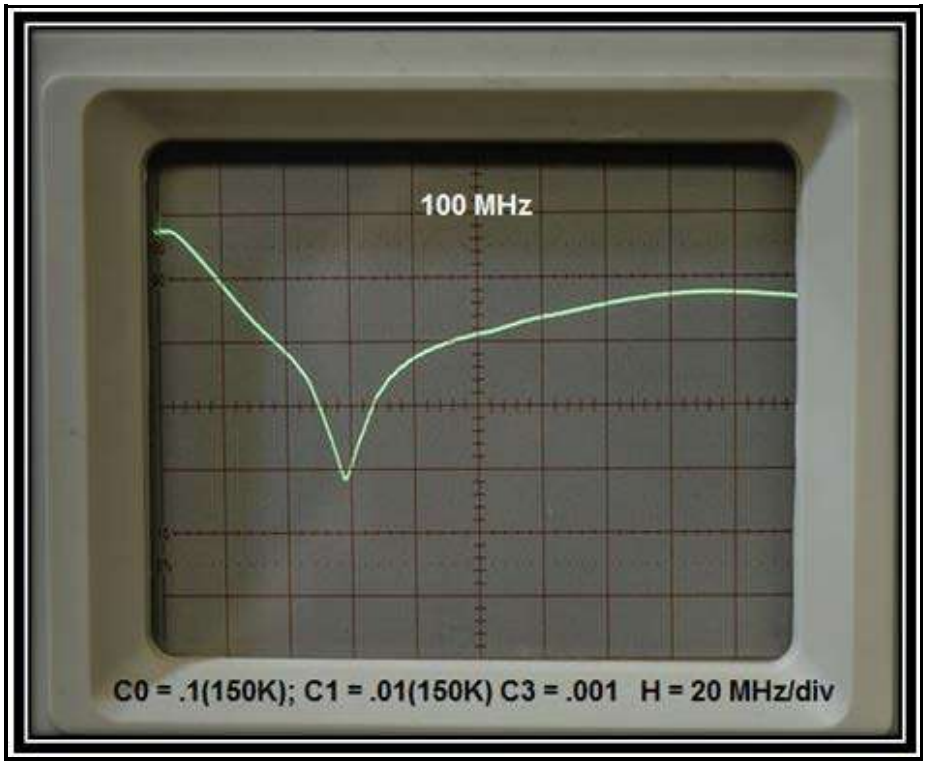

Above — C0 = 0.1 µF, R0 = 10K, C1 = 0.01 µF, R1 = 47K and C3 = 0.001 µF. Again, no high impedance peak response; the self resonant frequency is close to that measured with a single 0.001 uF earlier, however, the peak bypass frequency moved from to 57 MHz from 62 MHz. Changing the resistor values moved the self-resonant frequency and the peak attenuation value a little, but I fell kilometers short of setting a wide band bypass. My approach lacks any real science and I need to step it up.

I hope to learn what capacitor values and types, plus R values to apply. This sounds like a job for simulation as well as further on-bench experiments? After writing this material, I learned that Ken Kuhn wrote an Excel spreadsheet to examine the net impedance of up to 3 capacitors in parallel Click to download.

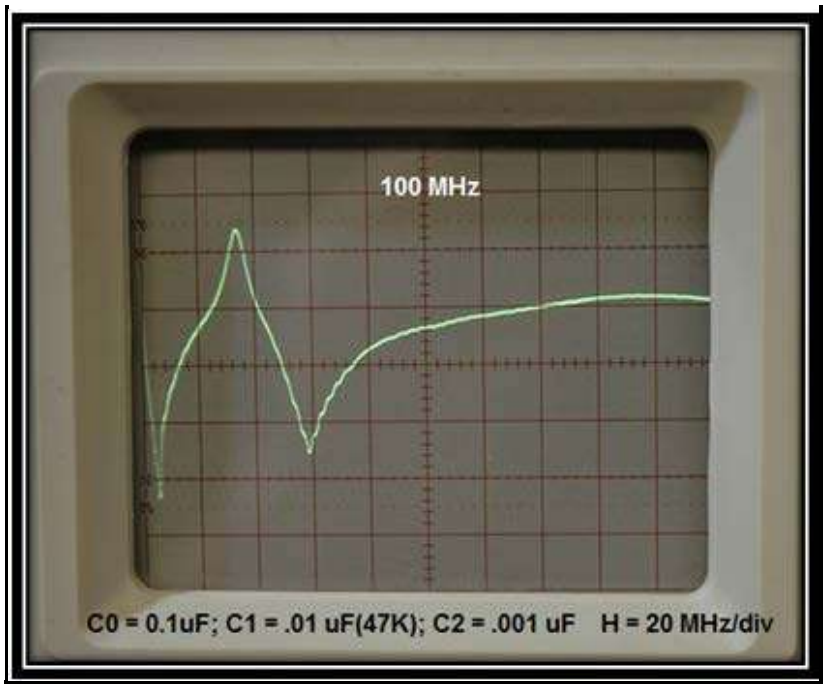

Above — Just as a gag, I removed R0 from capacitor C0 in 1 circuit and then hooked up the board. The high impedance peak re-emerged.

A Commerical Example

I found a wideband MMIC employing (R1 + C1 and C2) as part of a bypass strategy. Cick for the datasheet excerpt. Note the size of the SMD capacitors; 0603 — tiny caps! My experiments showed some high gain MMICs require careful low inductance grounding and correct part choices or crippling oscillations and other bypass issues might arise.

My Learnings

When we think bypass, we really should think frequency dependent attenuation. The bypass cap is actually a network where impedance versus frequency varies significantly. At its self resonant frequency, a capacitor will exhibit the lowest possible impedance making a single capacitor a relatively narrow-band bypass device. Intuitively, we might want to choose a capacitor with a series resonant frequency at the frequency we wish to bypass, however, if we require a wideband bypass, the need to evaluate our bypass capacitor(s) increases.

In short, above the series resonant frequency of a capacitor, its bypass is basically useless and we should likely ensure that the self-resonant frequency of the particular capacitor we're using is above the highest frequency to be bypassed.

Bypassing with 2 or more unmatched RF caps will lead to an attenuation gap with peak(s) determined by the parallel resonance of these capacitors. Going above a 10:1 capacitor ratio, for example, greater than a 0.1 and a 0.01 µf, may cause a **severe** gap in attenuation at the parallel resonant frequency generated by the 2 capacitors.

Mine and work from more reputable authors clearly shows we should avoid applying parallel **RF** bypass capacitors of *different* values unless we apply a Q-reducing resistor to the capacitor(s) in parallel with a given RF bypass capacitor. Please read EMRFD page 2.3 for more information and watch out for abundant folklore concerning RF bypass.

The need for measurement and analysis challenges us; in some cases, you may realize good attenuation in the radio band of interest, while poorly bypassing the frequencies above it and compromise an otherwise good design.

Capacitor lead length may affect self-resonance at RF.

Future Work

It would be awesome to learn more about getting a wide-band bypass. I want to order some low or ultra-low ESR caps and measure them. My MuRata RPE Series caps specify low inductance; low is relative — how low is low? Should we apply chip capacitors for bypass in our critical circuits such as low noise VHF amps or MMICs?. Am I fussing about nothing? Lots of questions that folklore just won't answer.

Per EMRFD page 2.3, bypass is only half the equation — we need to *decouple* + bypass to filter RF from moving along our DC lines and so forth.

---

6. Some Experiments with Chokes plus Decouple and Bypass Filters

Introduction

SRF = self resonant frequency; XL = inductive reactance; XC = capacitive reactance. L = inductor; C = capacitor; R = resistor.

Like the capacitor, inductors are networks with R, L and C and possess a SRF. R, L and C may vary with factors including the number of windings, frequency, or whether the L is wound on a ferromagnetic material, or air wound.

Considering R, L and C:

at frequencies below the SRF, XL dominates;
at frequencies above the SRF XC dominates;
at the SRF, the magnitude of XL and XC are equal but 180 degrees out of phase leaving resistance to dominate.

I encourage you to learn more by visiting the fabulous web site of David, G3YNH.

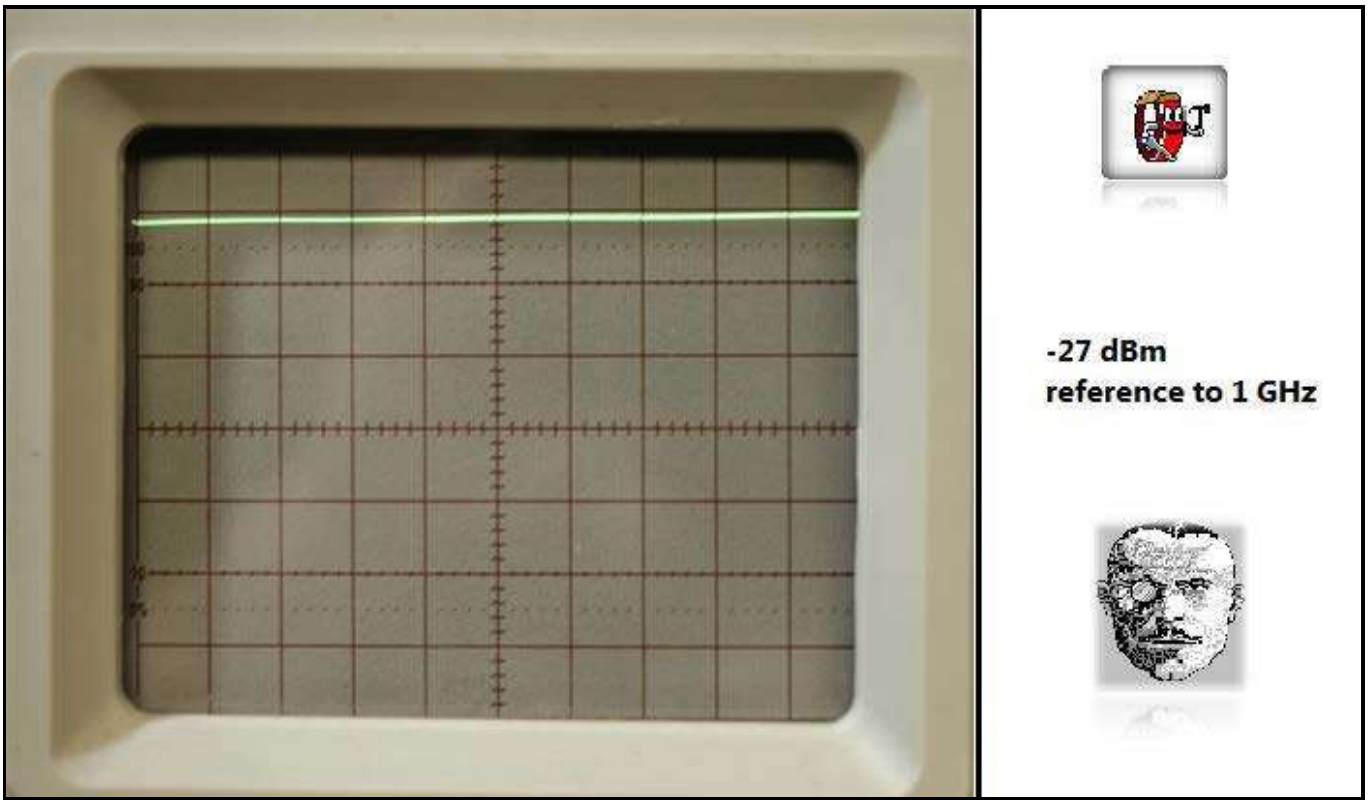

Above — Reference signal at -27 dBm. I used the exact test method shown in Section 5.

For those unaware, the spectrum analyzer screen is divided into 10 by 10 graticules. Each vertical division represent a 10 dB change; read down from the reference -27 dBm to measure the attenuation of the reference signal in dB. Horizontal divisions represent frequency; start at 0 on the left hand side and increment as specified on each figure.

A Few Inductors

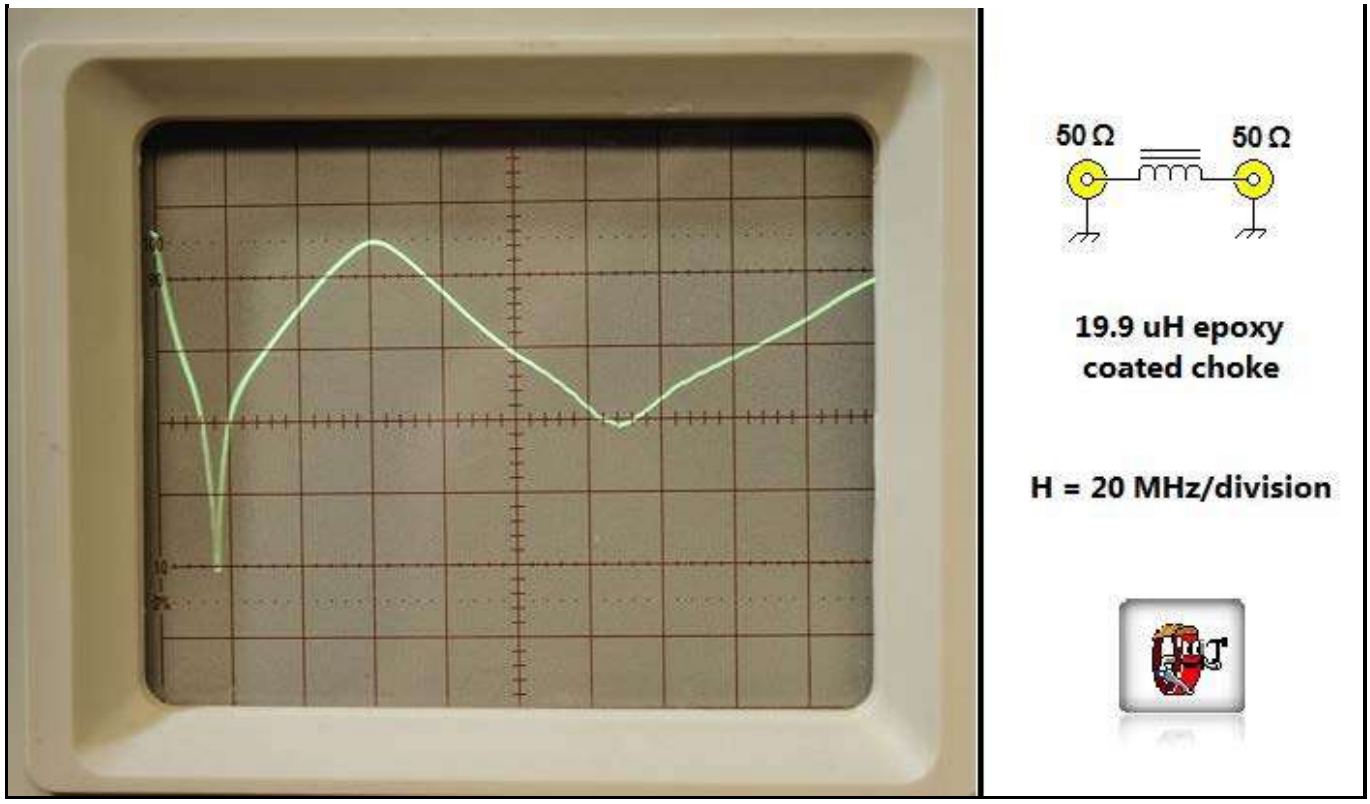

Above — A 19.9 uH epoxy coated choke that exhibits a primary SRF at 18 MHz and a second, smaller SRF at ~128 MHz. This wretched L gave me grief at 63 MHz. After measurement, I tossed it in the garbage can.

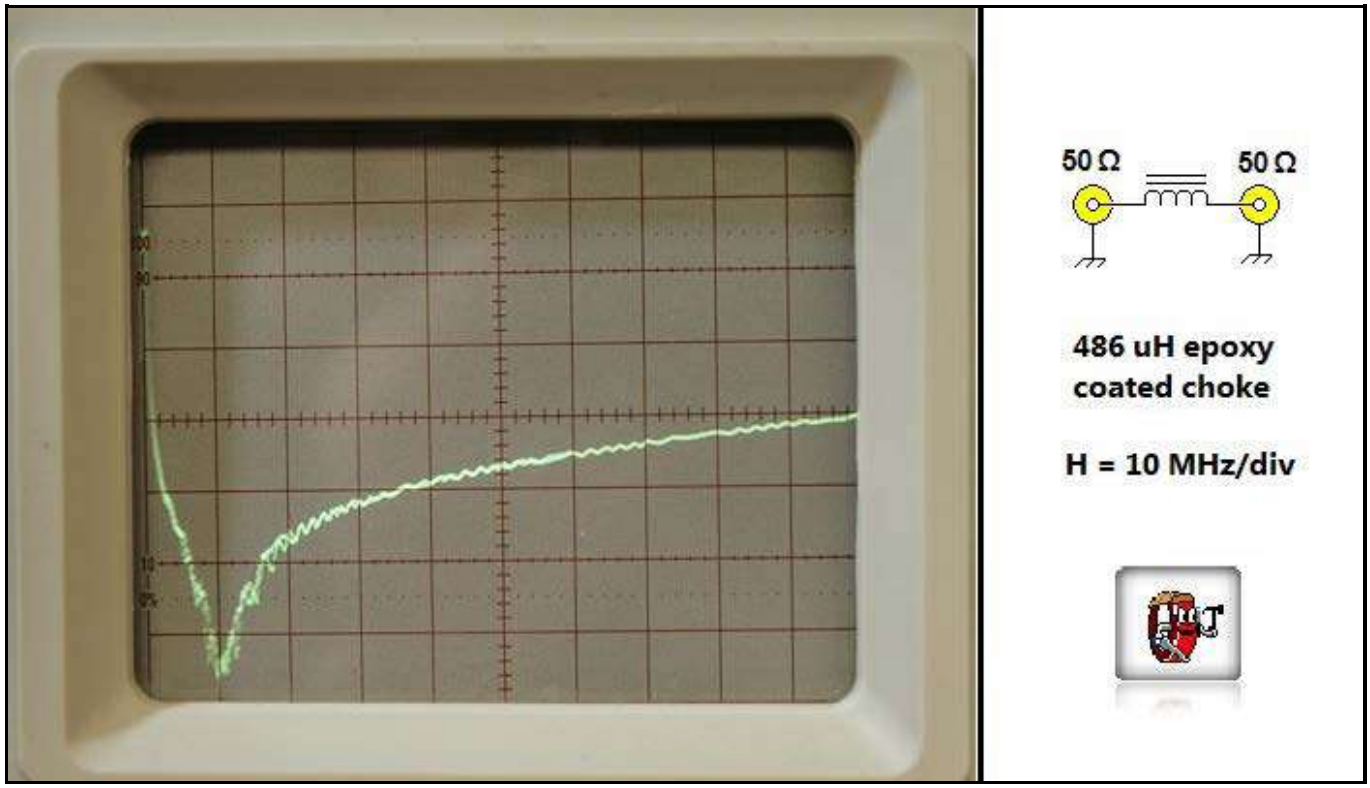

Above — A large, junk box choke with an SRF at about 10 MHz.

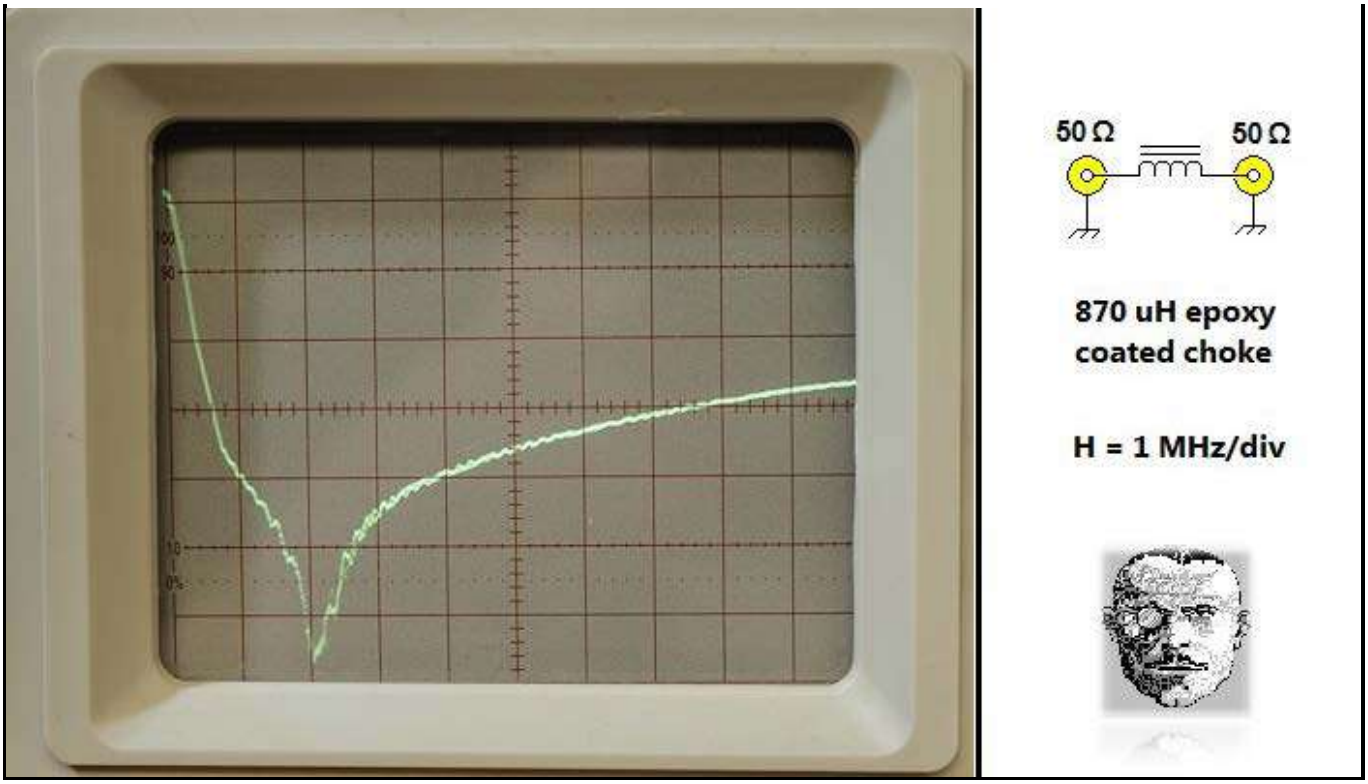

Above — I rarely use these big chokes: 870 µH with a SRF at about 2 MHz.

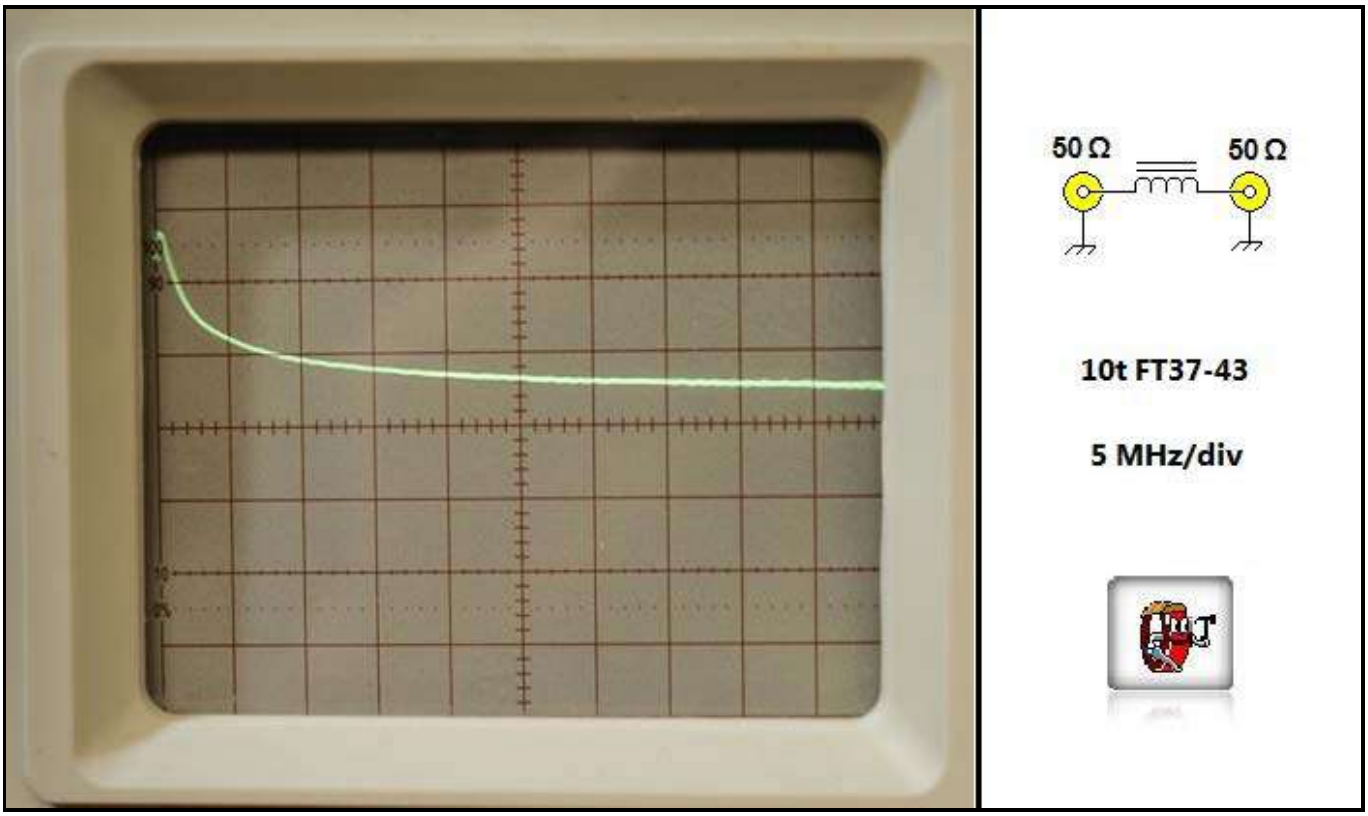

Above — A common L on our benches — 10 turns of #26 AWG on a FT37-43 ferrite toroid.

I couldn't measure the SRF with any span on my spectrum analyzer. I expect that a parasitic capacitance lies in parallel with the inductance, but the #43 material, with its low Q and high losses blankets the usual deep notch we see when the L exhibits a higher Qu.

10 Turns on a FT37- 43 with a Bypass Capacitor Shunting Each End

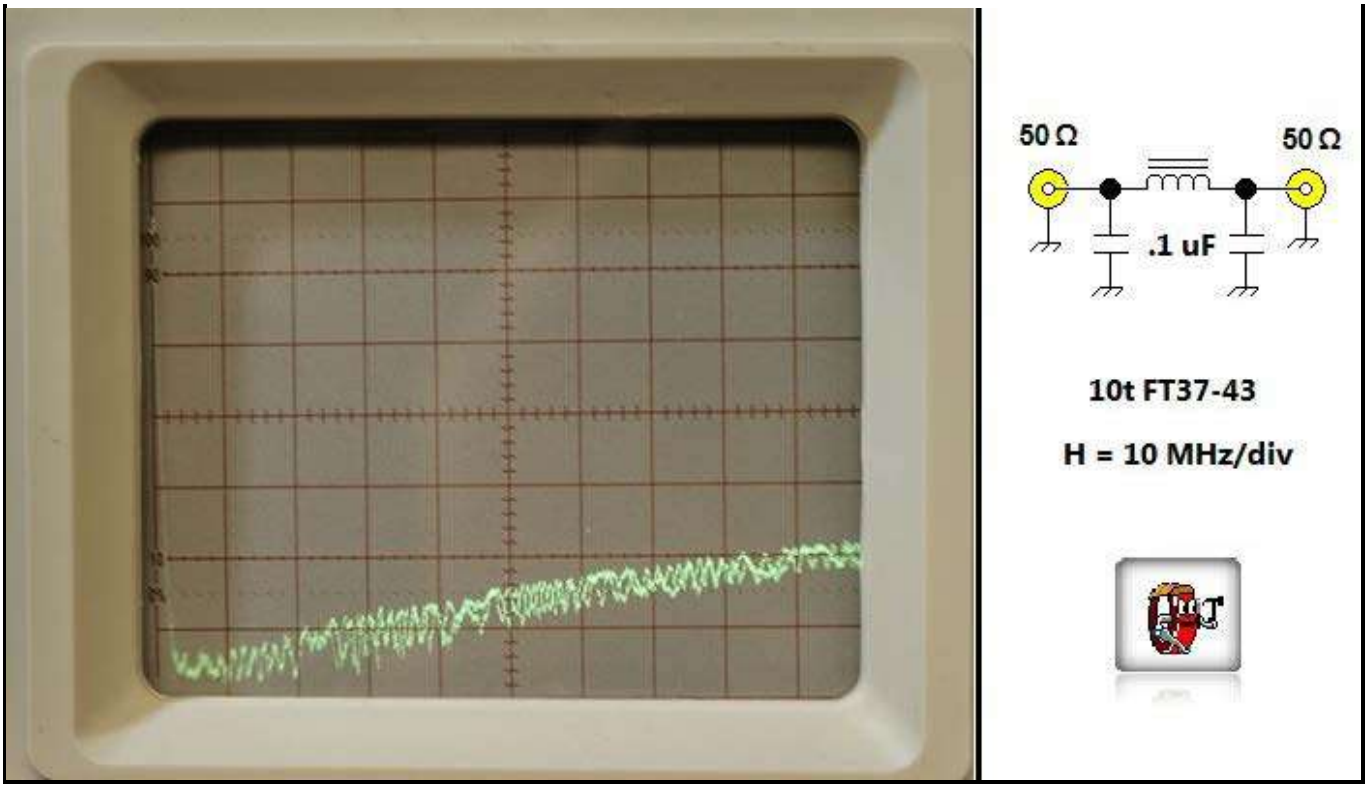

Above — Look at the big difference after adding shunt capacitors to a 10 turn FT37-43! Even at 100 MHz the attenuation lies nearly 50 dB down. Now I understand why Wes says **decouple plus bypass** when filtering our DC lines and so forth.

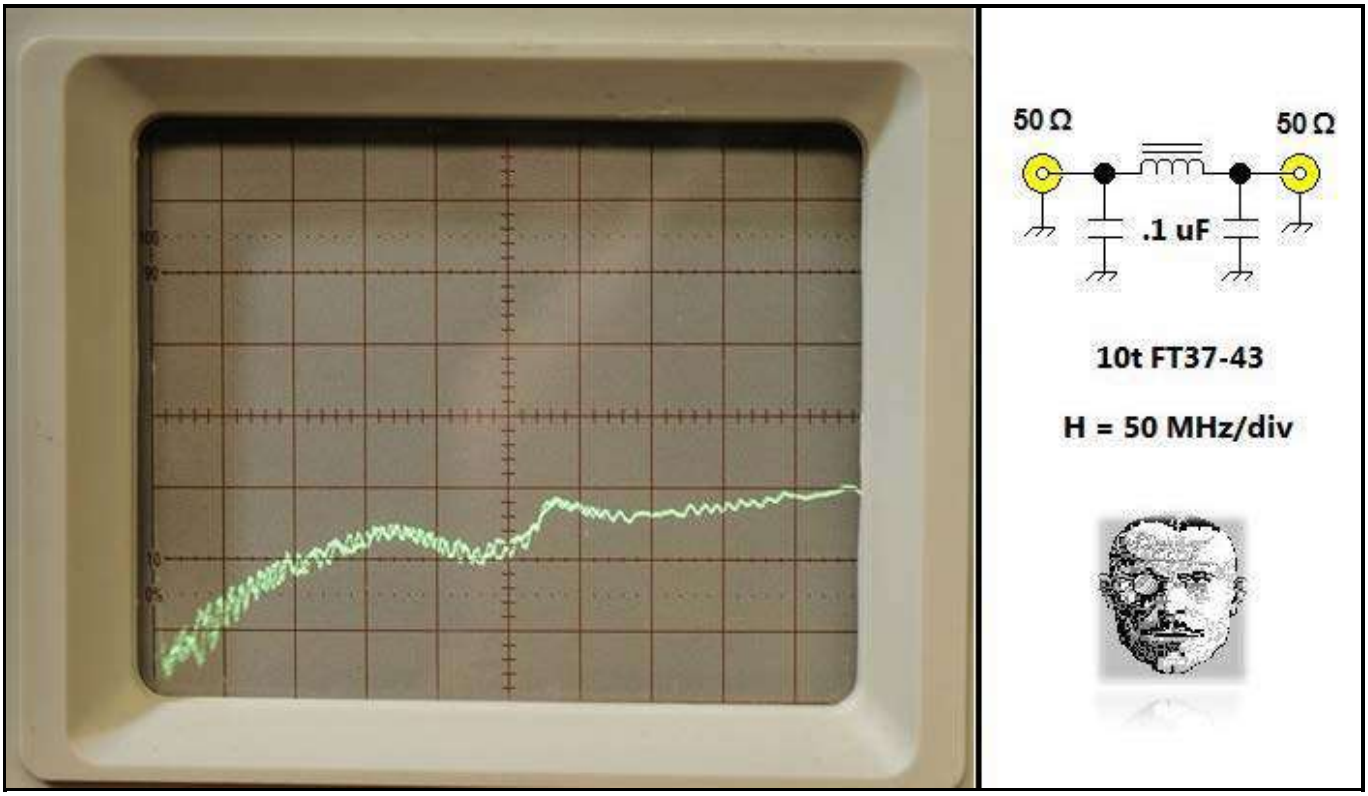

Above — The 10 turn FT37-43 coil with 0.1 µF shunt caps measured out to 500 MHz. Pardon the camera shake; I took all the photos hand held to save time.

A Resistor with a Bypass Capacitor Shunting Each End

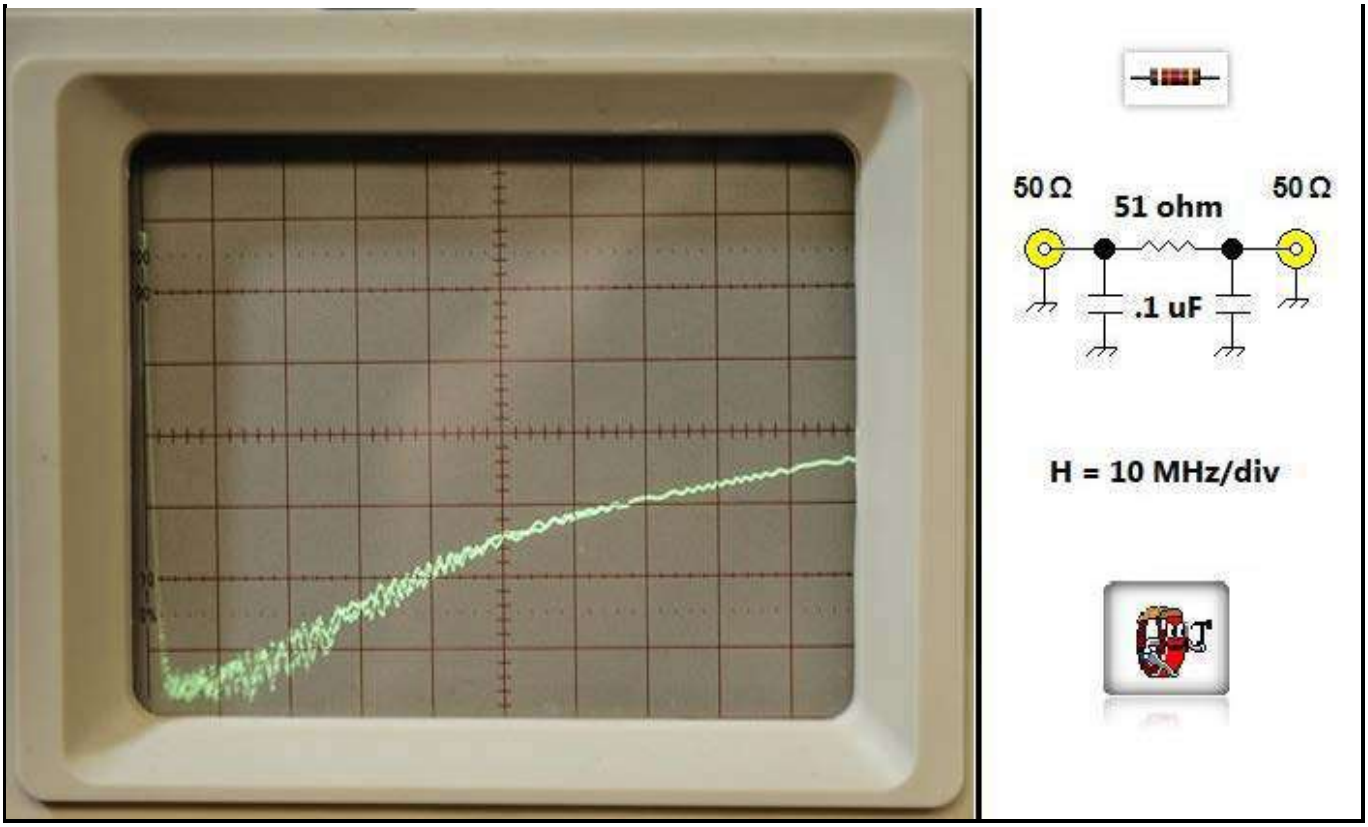

Above — A 51 Ω resistor bypassed with 0.1 µF capacitors at each end spanned out to 100 MHz. Even at 30 MHz, the attenuation looks stellar.

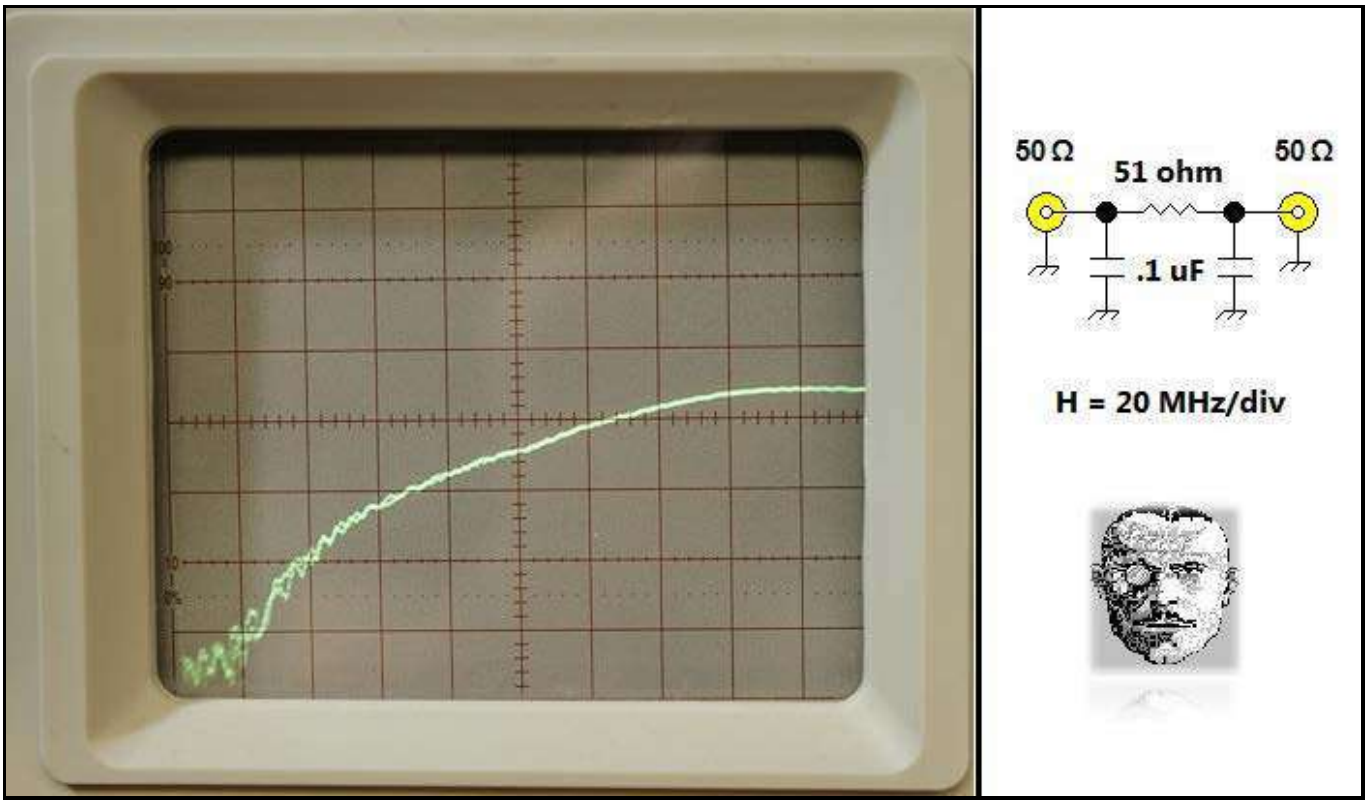

Above — The 0.1 µF bypassed 51 Ω resistor out to 200 MHz. I often use a 51 Ω decoupling resistor with appropriate capacitor values in active circuits that draw from 10 - 18 mA.

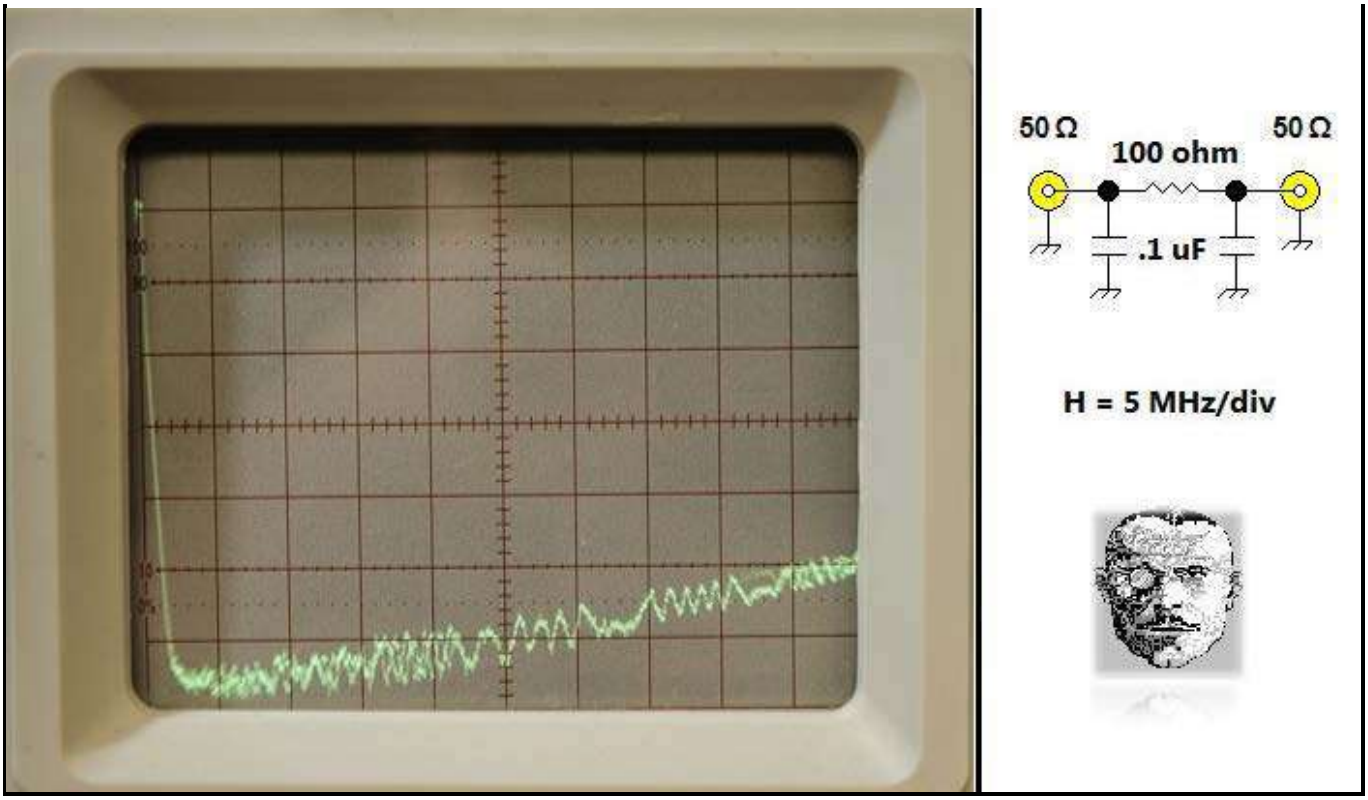

Above — The "bench standard"; a 100 Ω R with a shunt 0.1 µF at each end. We use this all the time. Even at 25 MHz, the attenuation looks around 55 dB down.

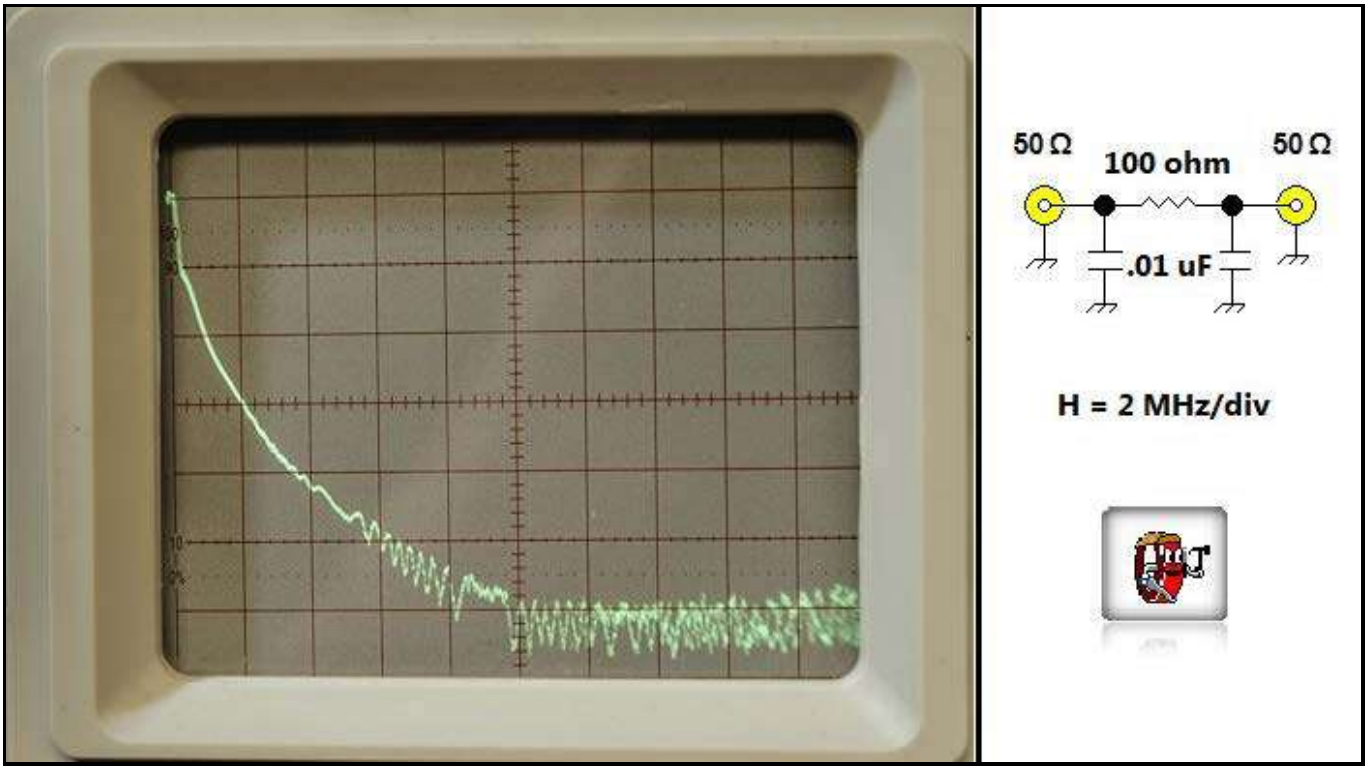

Above — The 100 Ω R with the shunt capacitors decreased to 0.01µF. At 6 MHz, we're about 50 dB down. From 10 to 20 MHz, the attenuation is about as high as I can measure.

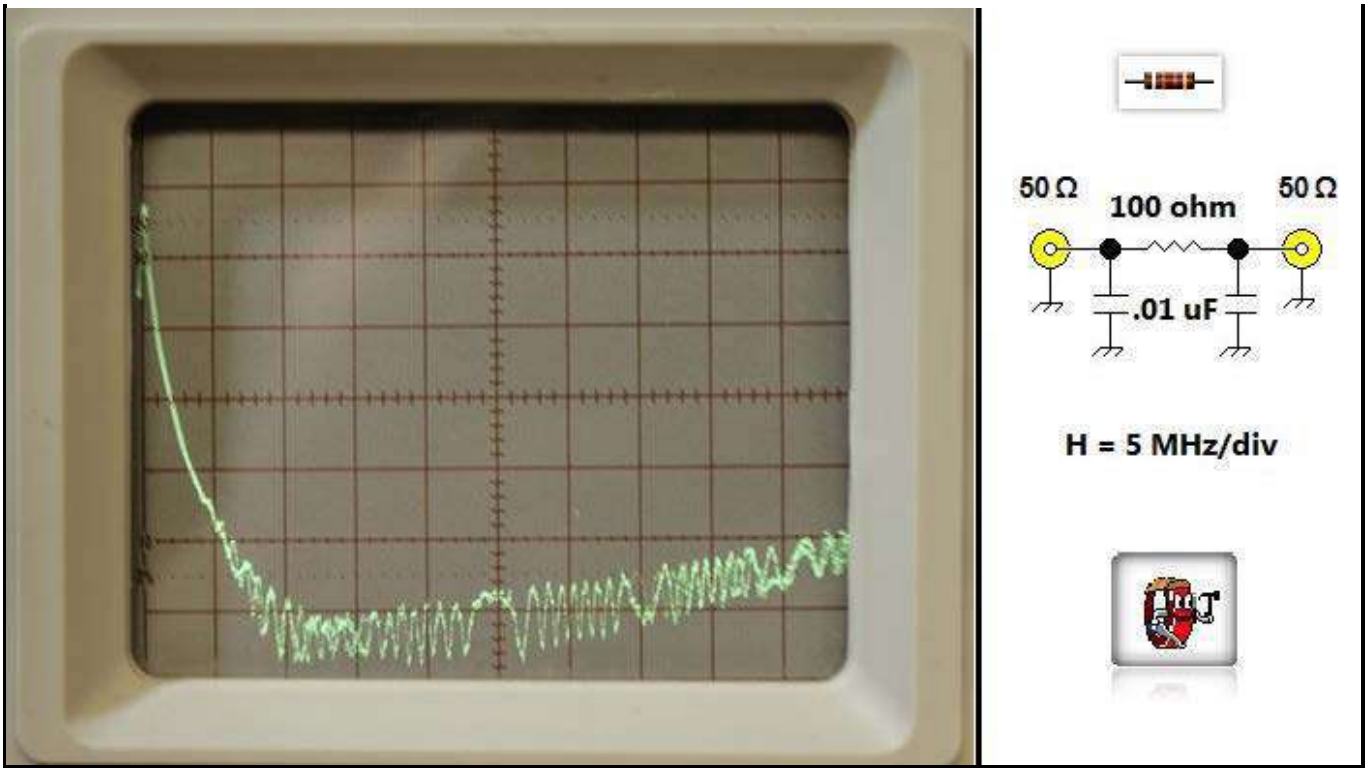

Above — 100 Ω R plus 0.01 µF caps out to 50 MHz. I've used this combination of R and C for filtering at 50 MHz a lot.

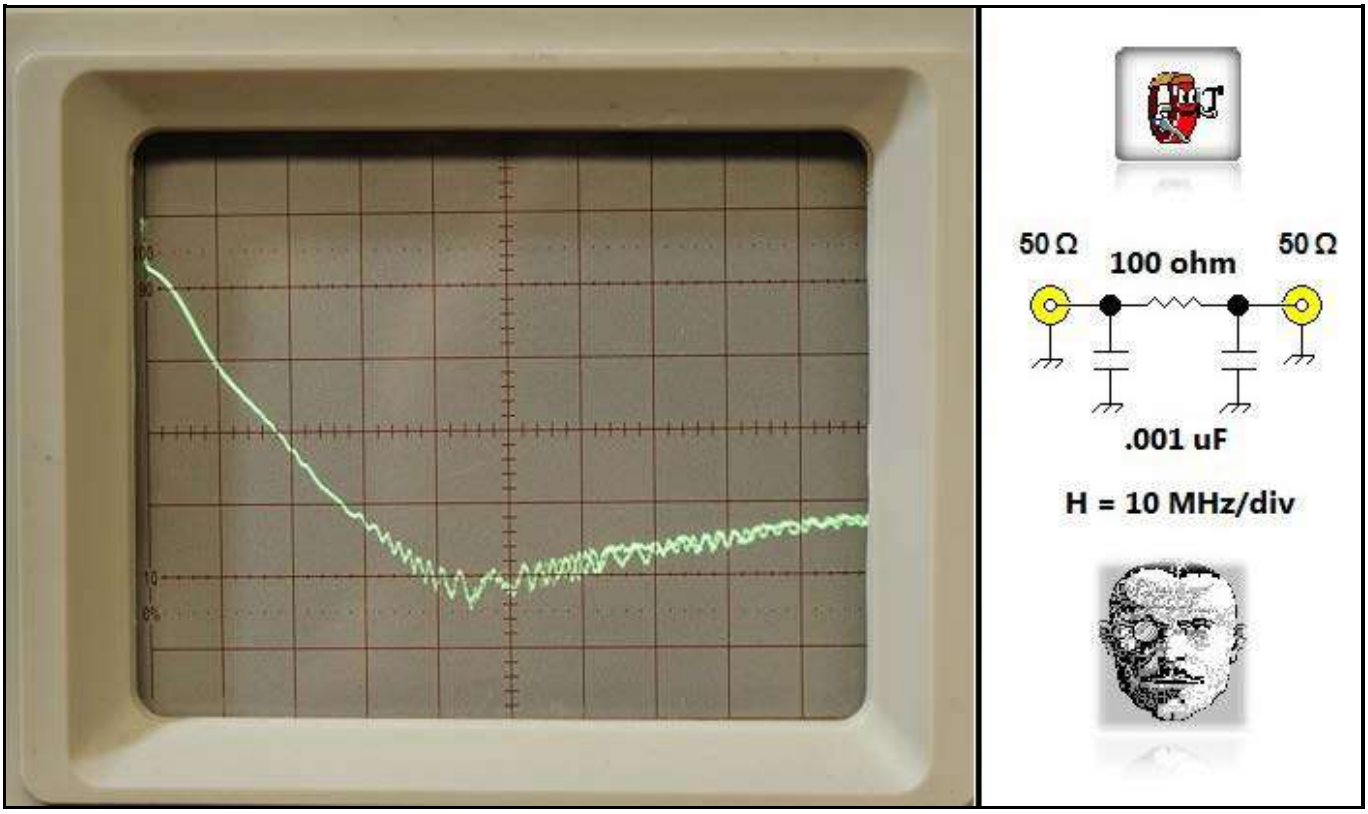

Above — 100 Ω R plus 0.001 µF capacitors out to 100 MHz. In my particular circuit, the attenuation at 50 MHz equals that of the 100 R + 0.01 µF C low-pass filter shown directly above.

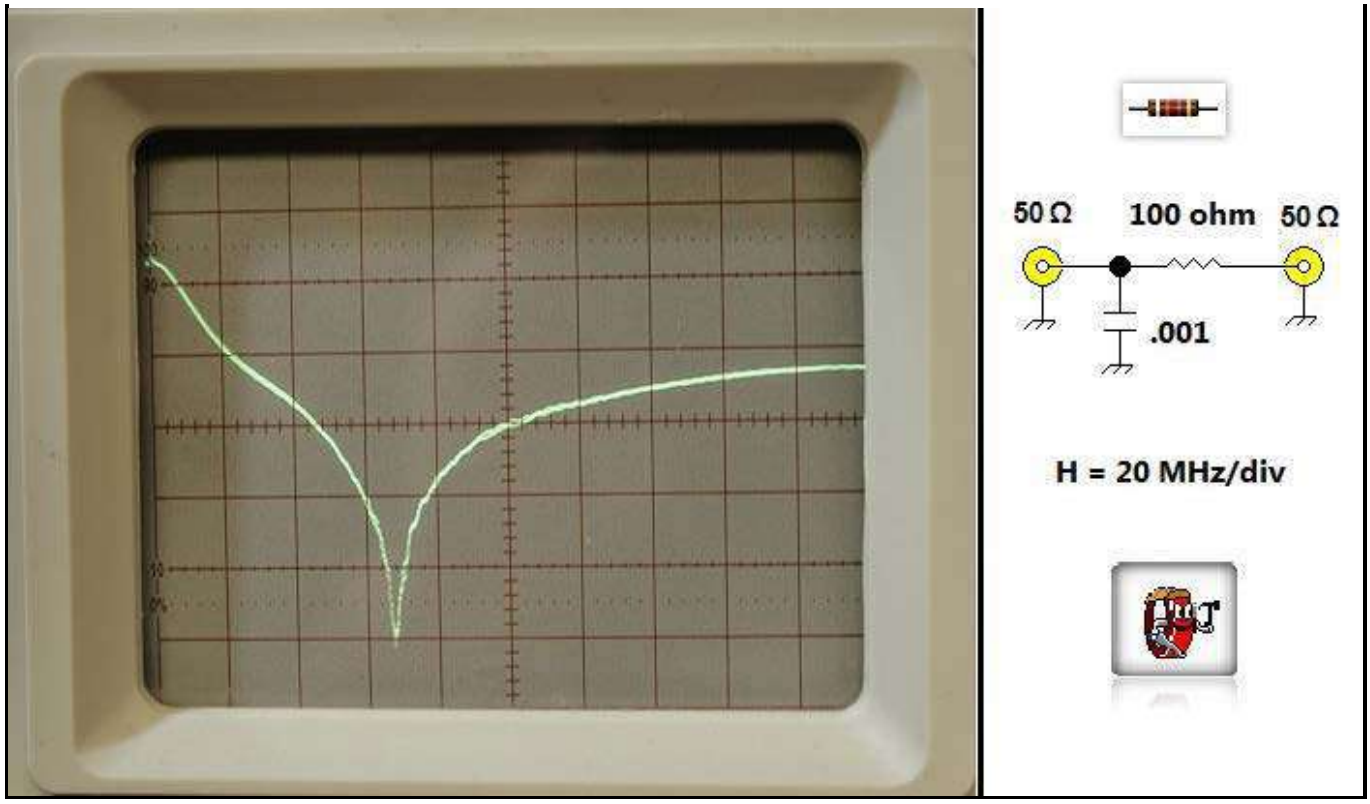

Above — A 100 Ω R plus a single 0.001 µF capacitor. If you leave off 1 capacitor, a serious notch appears at ~ 68 MHz. If you flip the filter around so the bypass cap is on the right hand side, the tracing appears the same. This problem occurred with all the filters tested in all experiments. As possible, solder a suitable bypass capacitor on *both* sides of the R or L.

I encourage you to experiment with the SRF of coils and wideband decouple + bypass filters on your own.

QRP Posdata for Oct 2013 — SRF of some common bypass capacitors

Capacitor	Notch Freq
0.1 µF	6.56 MHz
0.01µF	22.68 MHz
0.001 µF	69.62 MHz
0.0022 µF	53.2 MHz
680 pF	87.34 MHz
470 pF	88.17 MHz
220 pF	154.58 MHz
100 pF	222.91 MHz

* Self resonant frequencies of some common bypass capacitors covering ~ 6.6 to 220 MHz

* Use table to inform bypass cap versus frequency choices

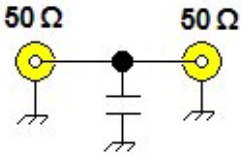

Tested as shown to left in calibrated TG + SA using instrument grade 9 cm SMA cables and connectors.

* The deepest notch [-64.32 dBm] occurred with the 0.1 µF cap and decreased progressively with capacitance

* Caps tested = muRata RPE series monolithic ceramic with C0G temp compensation. Different brands, types, etc. of caps may change results significantly

* Leads short as possible with the SMA connectors soldered right on the ground plane

Above — A reference table showing the self resonant frequency of several comon value bypass capacitors in my parts collection. For example, if

I'm making a 21 MHz circuit, the best bypass capacitor choice from the table above = 0.01 µF. If possible, sweep the capacitors in your own collection to determine their SRF; or whether they're even suitable.

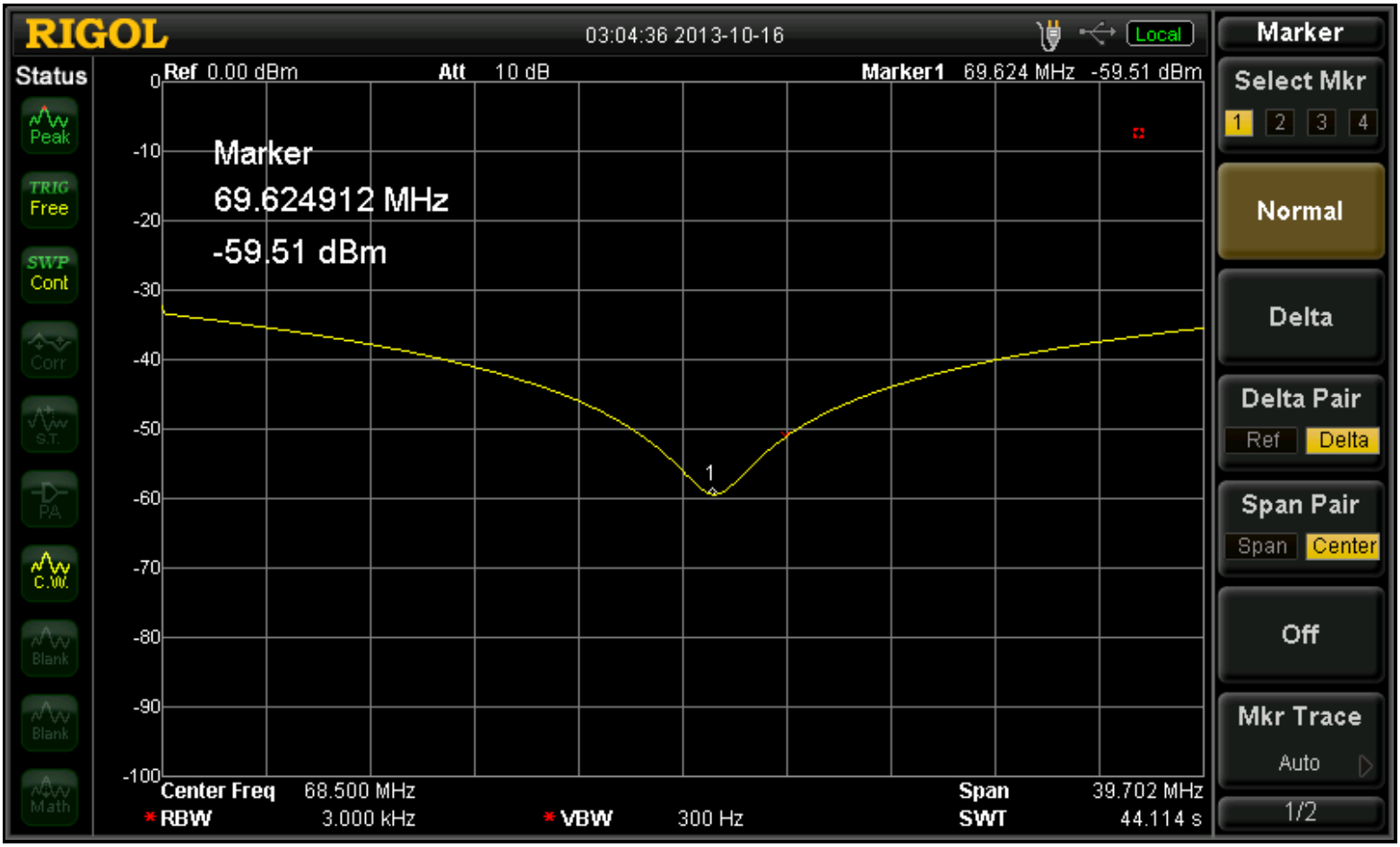

Above — The close-in sweep of the 0.001 µF capacitor tabled above.

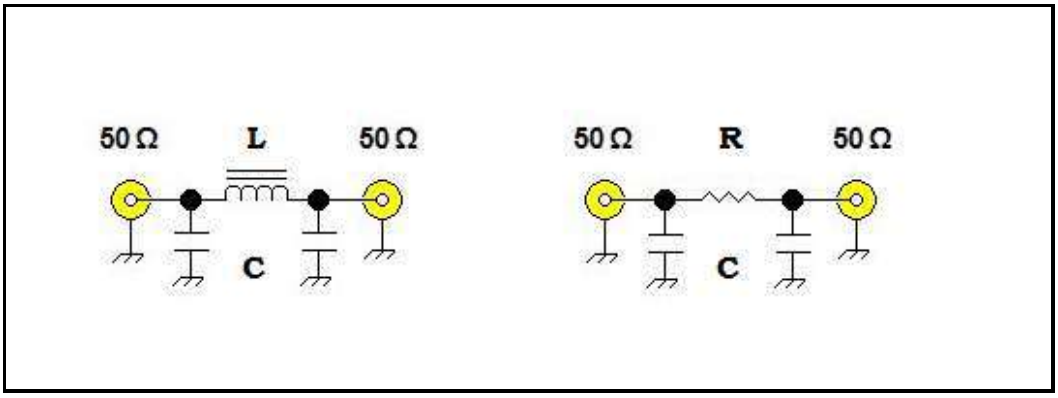

Above — As possible, stick 2 of your bypass cap values in a pi filter network with a series decoupling L or R to derive wideband filtration. For example, to filter your DC power lines.

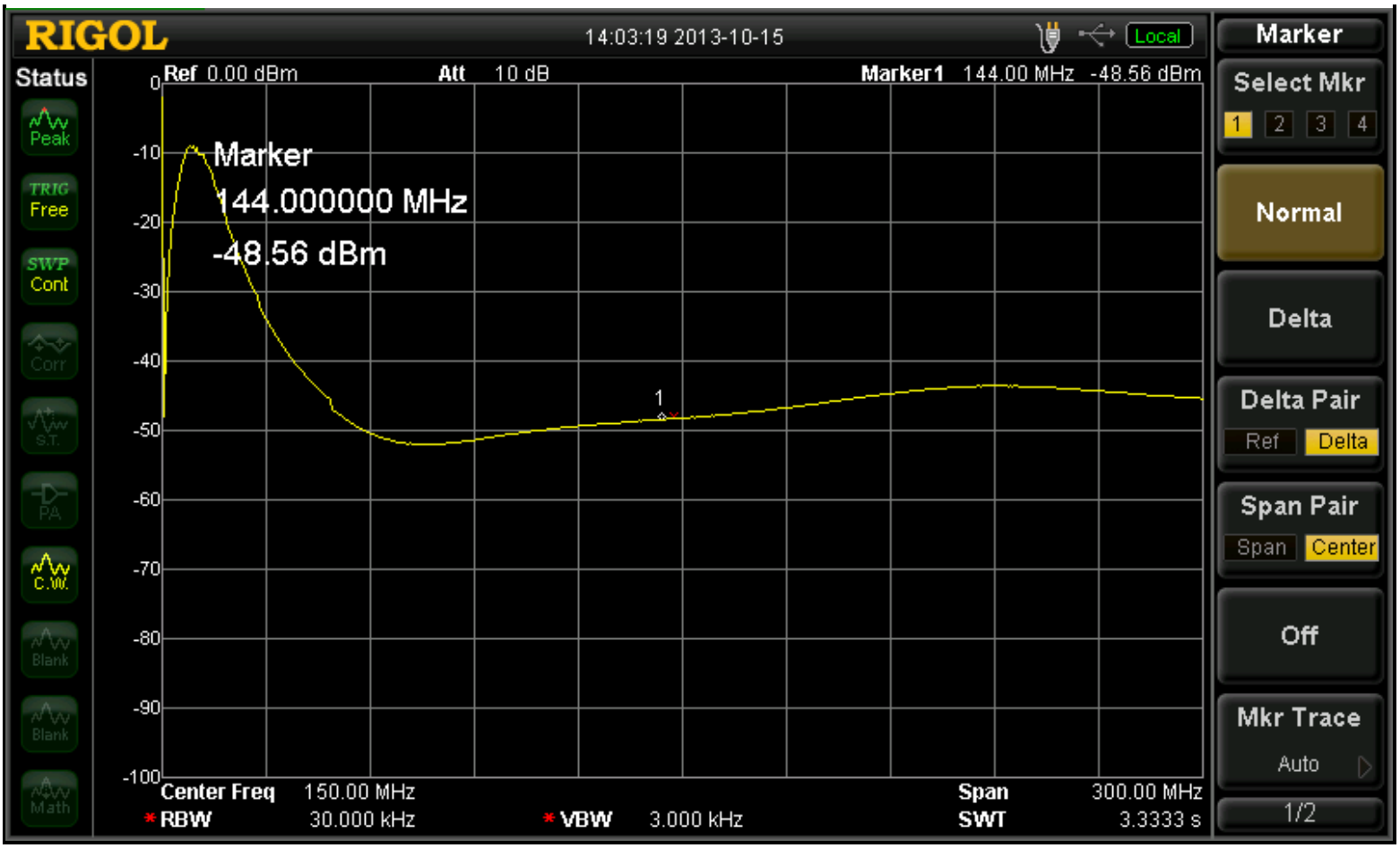

Above — A 300 MHz sweep of a pi filter [220 pF + 1.2 µH + 220 pF] for the DC supply line of a 150 MHz oscillator. The SRF peak lies at 76.69 MHz, but this filter works okay out to about 200 MHz. I placed a marker at 144 MHz and could use this filter for the 2M band as well.

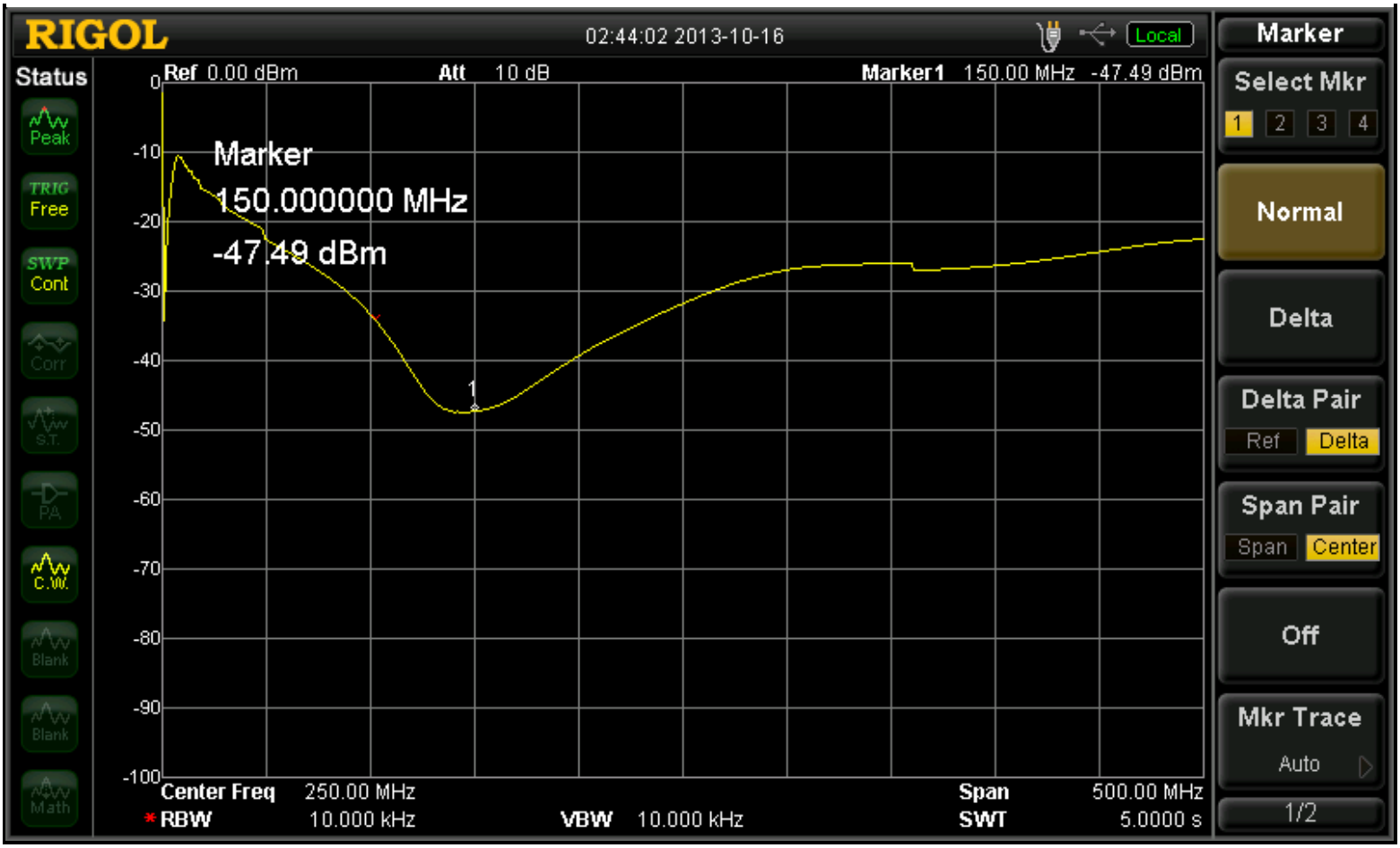

Above — The network described above, except I replaced the 1.2 µH L with a size 0805 10 Ω resistor [220 pF + 10R + 220 pF] and swept to 500 MHz. I set Marker 1 on 150 MHz; the frequency of the oscillator I wanted to DC powerline filter. The resistor gives a bit more filter bandwidth around 150 MHz. A 51 or 100 Ω resistor will further increase the bandwidth while decreasing the attenuation depth somewhat. Although resistors incur a DC voltage drop, they avoid the potential of an unwanted SRF in your filter arising from a renegade inductor— and so, a resistor may pose a better choice for pi filtering DC lines and so forth. It's your call.

At HF and lower VHF, I've found a hole-through capacitor may sometimes filter better than a "garden variety" SMT counterpart. Click for a graphic that shows this. Presumably, the SMT cap exhibited a lower Q than the equivalent hole-though part. At some frequency above 200 MHz, the lead inductance of the hole-through capactor may cause the opposite effect.

Further, on the VHF — Véronique web page, Section 6: I swept 3 capacitors including an ultra-high Q SMT part.

RF — Test and Measurement

RF Workbench Page 5

Welcome to part 5 of a web series exploring basic RF measurement and bench practices. This installment builds on the information from RF Workbench Parts 1 - 4.

In RFWB #5 I share a hodge-podge of thoughts and circuits concerning power measurement on the beginner-level RF workbench. Consult EMRFD for more support. Big thanks to my mentors: Wes, W7ZOI. Bob, K3NHI and John, K5IRK for their support as I advance to the basics.

Power Measurement Empowers You

Before embracing the 50 Ω RF environment, I misjudged the need to quantify small signal power — now I get that we measure lots of low-level signals on the 50 Ω RF workbench. Whether you're driving a mixer RF port with -30 dBm to reduce spurs, or tweaking an amplifer-under-test to exact the best S21, low-level RF power measurement is fundamental to fruitful RF design.

1 way to measure low-level RF power includes building a log linear RF power meter (PM) based on the Analog Devices AD8307. The basic circuit I show posits that most of you measure from MF to HF and don't need a PM that reads flat into UHF and further; a simple, 2 chip circuit might even prompt you to actually build a barebones PM for your QRP workbench.

Search for and download the Analog Devices AD8307 Revision D datasheet — it's definitely worth a read. Kudos to the design team that brought us a truly milestone device for low-cost power measurement.

Analog Devices offers a whole family of log-amps at different frequency ranges — for example, the AD8311 Log Amp/Detector covers from ~100 MHz to 2500 MHz. A sister product, the AD8302 2.7 GHz RF / IF Gain Phase Detector looks amazing.

---

1. A Barebones RF Power Meter

Lacks the usual input frequency compensation network needed to keep power measurement flat over several hundred MHz — since most input compensate by attenuating HF, this simple version offers stronger sensitivity at HF than usual.

Good from MF up to about 100 MHz.

4.5v B+ to eliminate power supply decoupling issues and to give greater battery life than a 9v battery.

Minimum input power about -70 dBm. Maximum input power +15 dBm. Requires a metal box.

Big thanks to Wes, W7ZOI for letting me present his simple RF power meter. I found *numerous* AD8307-based RF power meter designs in periodicals and on the web and the writers devised simple to elaborate input compensation networks to establish a flat response out to 500 MHz — involving parts such as nH-level inductors, chip resistors and capacitors. This PM goes the opposite direction; a plain circuit for you builders who measure under 100 MHz; particularly at HF.

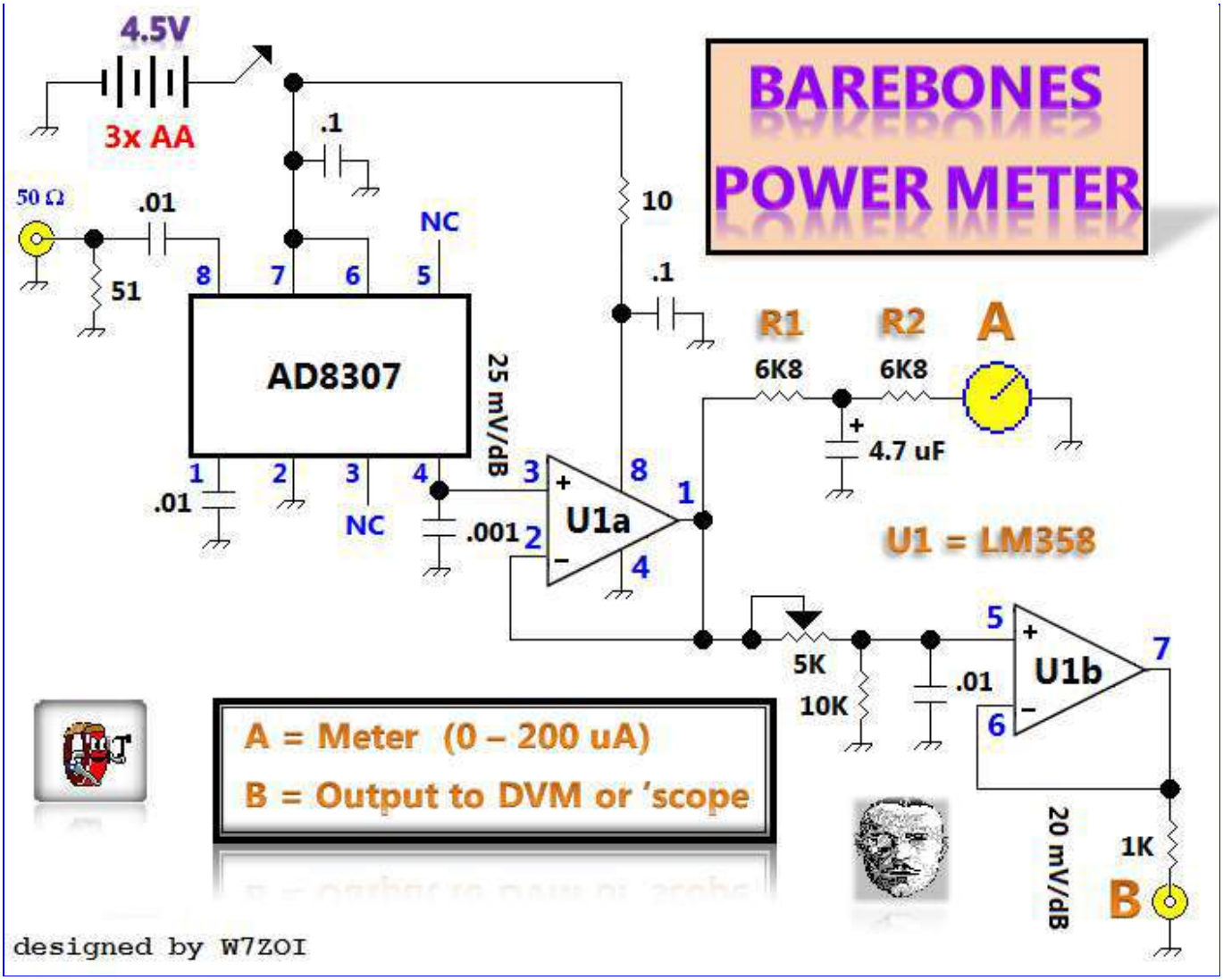

Above — the complete Barebones PM schematic. Presented with the permission of Wes, W7ZOI.

AD8307 Input Pin 8: Some Graphs and Notes:

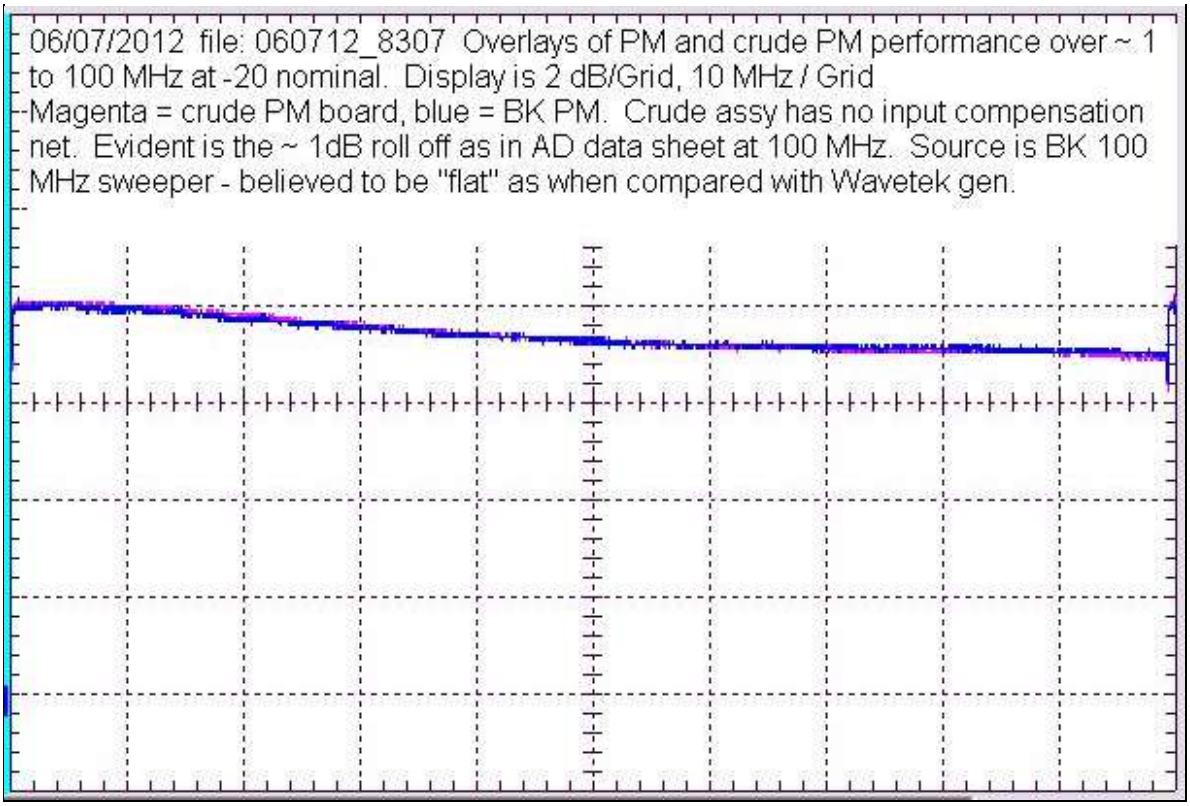

Above — The lack of input compensation might raise a few eyebrows! A sweep of the Barebones PM by Bob, K3NHI shows a reasonably flat response out to 100 MHz that's comparible to some of the 0-100 MHz range of wider sweeps in the published compensated circuits I've read.

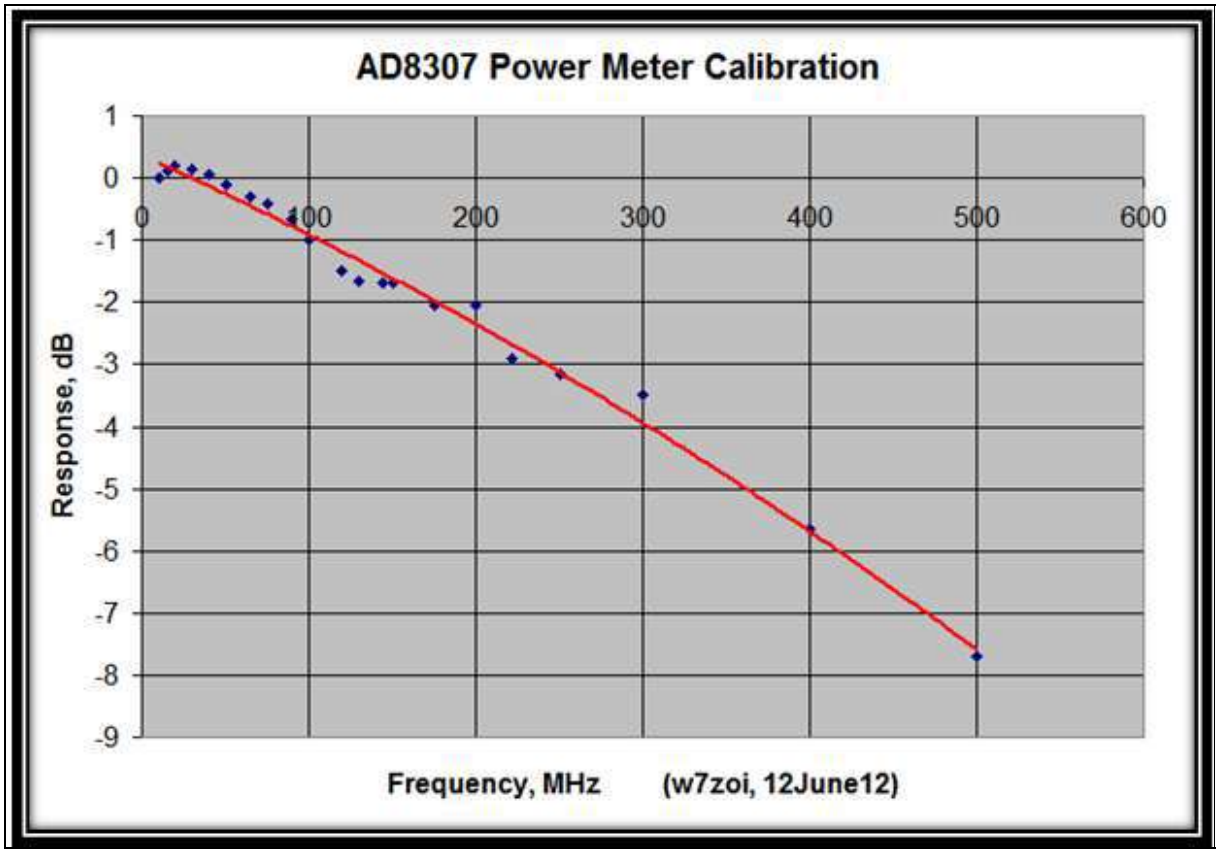

Above — A different Barebones PM plot from Wes, W7ZOI that goes out 500 MHz. For HF work, this power meter proves adequate for QRP HomeBuilders. By all means, add some input compensation if you want to — good circuit examples abound. For example, EMRFD Figure 7.13, or Bob Kopski's — An Advanced VHF Wattmeter referenced in Section 5.

AD8307 specifications allow a typical +/- 0.3 dBm "ripple" in the input to output transfer characteristic. Bob, K3NHI verified this ripple in his lab.

Therefore; depending on the position of a signal in the transfer curve, a move between 2 different power levels may yield as much as 0.6 db peak difference error. Figure 8 of the Rev D datasheet shows this. Figure 24 plus associated text tells why this occurs: the transfer characteristic is a chunk or segmented realization of a log transfer characteristic. It's really good — just not perfect.

If you consider the cost of thermal sensor power meters from Agilent, Techtronix, or even the Mini-Circuits PWR-6GHS, the AD8307 seems a bargain.

Measuring U1a Pin 1 With a Panel Meter

The first output at Pin 1 drives nearly any junkbox DC panel meter you might own The schematic specifies a 0-200 uA movement, however a 1 mA meter movement also works by tweaking R1 and R2 to establish the correct current. In the circuit shown the R = 13.6K. This R establishes the current required to drive the 200 uA meter Wes used in his design — nothing more. A wide variety of panel meters work because the drive current comes from an op-amp. Don't order an expensive panel meter just because you want to employ a 100 or 200 uA model — choose your meter because it affords good needle movement and resolution to allow accurate power measurement.

Although elementary for some, the following diagram shows you how to measure the maximum current for your meter: 100 uA, 200 uA, etc.

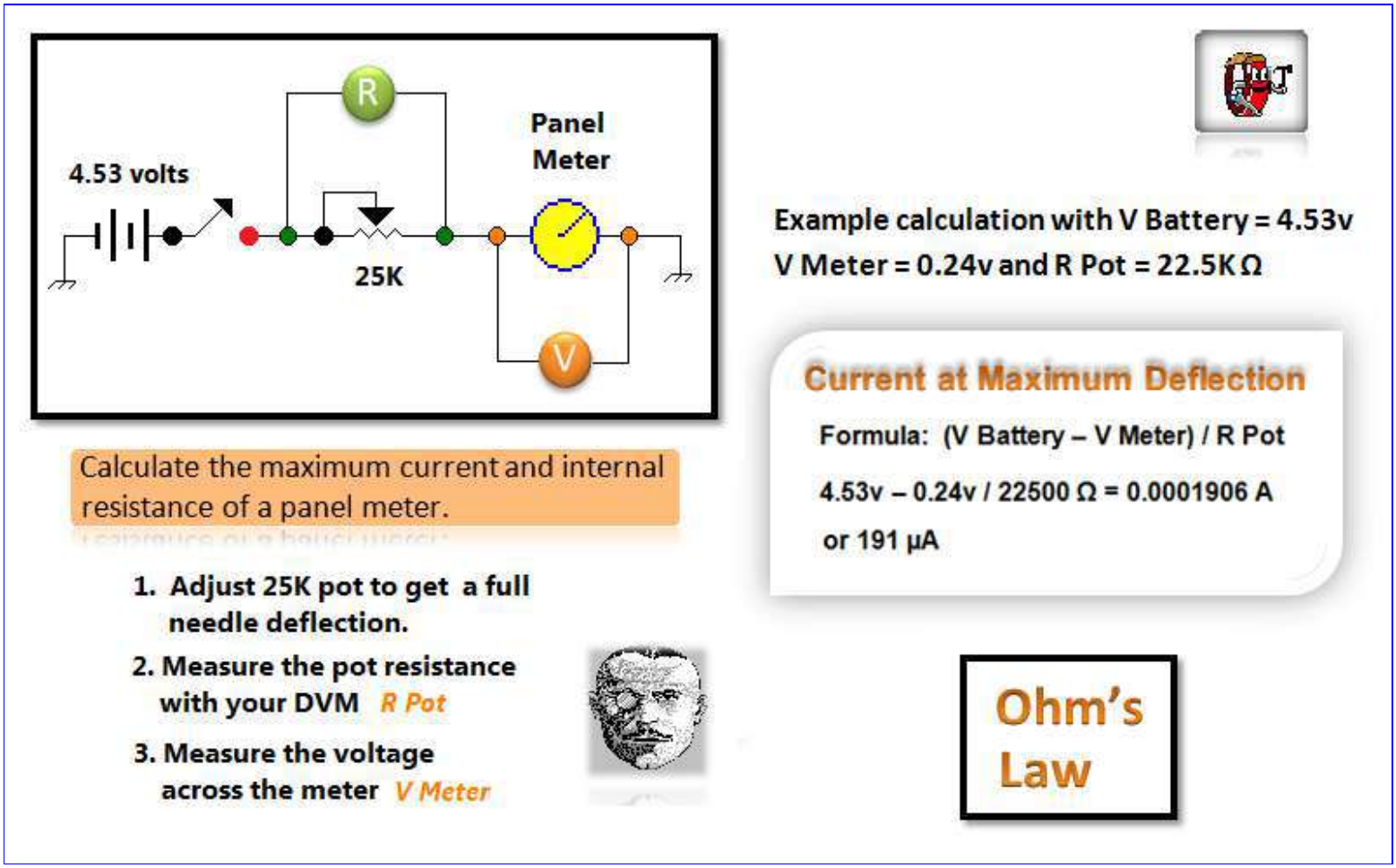

Above — In my shoebox sat 4 different panel meters. I measured 1 meter and show the math above — a 191 µA meter.

Above — An antique 1 mA panel meter driven with 1 mA to achieve full deflection.

Meter resolution presents the biggest problem for junkbox panel meters and if you look around the web, you'll see some great examples how builders calibrated and/or marked the scale on their AD8307 circuit panel meters.

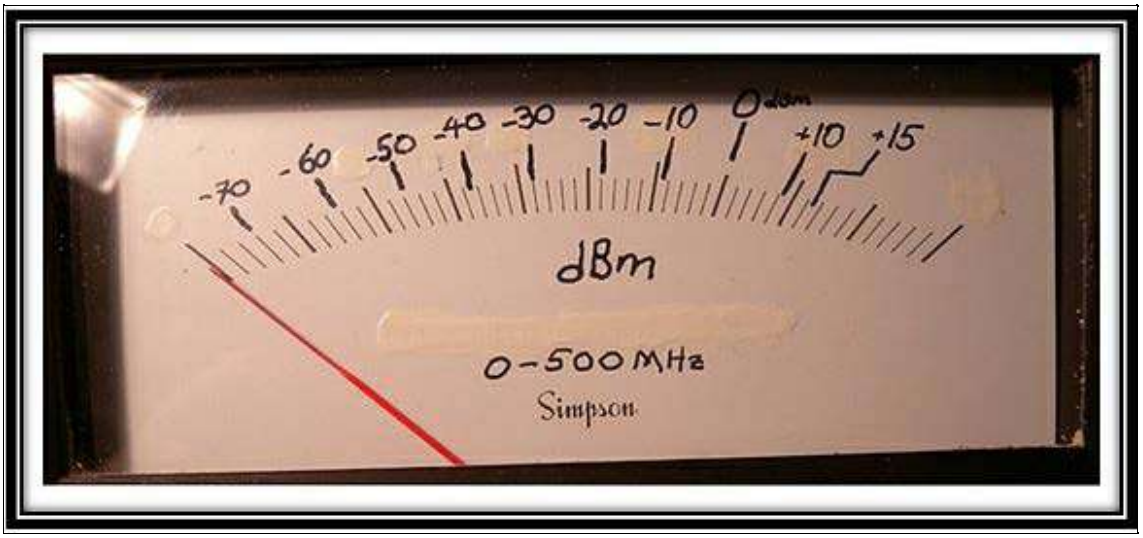

Above — Panel meter markings on my friend Peter's power meter.

I personally like my panel meters to read about 75% of full deflection at 7 dBm, but it's really your choice. Adjust R1 and/or R2 up or down to give the desired amount of meter deflection for whatever panel meter you own.

You may apply Ohm's law to figure out the maximum in-situ current for any panel meter. In the schematic the total R is 13.6K, so when you apply +10 dBm applied to the power meter input, the current in the panel meter will be 2.0v /13.6K = 147 uA. The maximum 200 uA will occur with a Pin 1 voltage of 2.72v. The op-amp won't go all the way to the positive rail, but If it did go all the way to 4.5v, you would hurl 331 uA into the panel meter. This exceeds the meter's uppermost scale, but likely won't destroy it.

The 4.7 uF cap can be any small uF capacitor value and low-pass filters the DC to smooth out the meter movement. I used a 10 uF in my breadboard.

I normally view the panel meter to tune resonant circuits and observe trends; but not to precisely measure power — it's often more accurate to quantify power readings at Port B since this eliminates panel meter resolution issues.

How to Measure Power at Port B

We measure the DC voltage at port B and use equations or graphs to translate this voltage into an actual power reading after reference calibration. U1a and U1b are unity-gain voltage followers to buffer the AD8307 output. U1B features a 5K potentiometer in series with a 10K

shunt resistor to form a voltage divider that changes the 25 mV/dB AD8307 output to 20 dB/mV. Tweak the 5K pot to calibrate to get as close to 20 dB/mV as possible, although since the LM358 buffers just pass on the DC voltage changes of the AD8307, the pot does not technically alter log linearity.

Wes published some essential notes on his web site. On page 8, you find his formula to convert a measured DC voltage into dBm. I wrote a program that incorporates his formula: Applet L on my Design Center web page; except that it takes calibration power at -10 dBm and -20 dBm.

Let's run through 1 example:

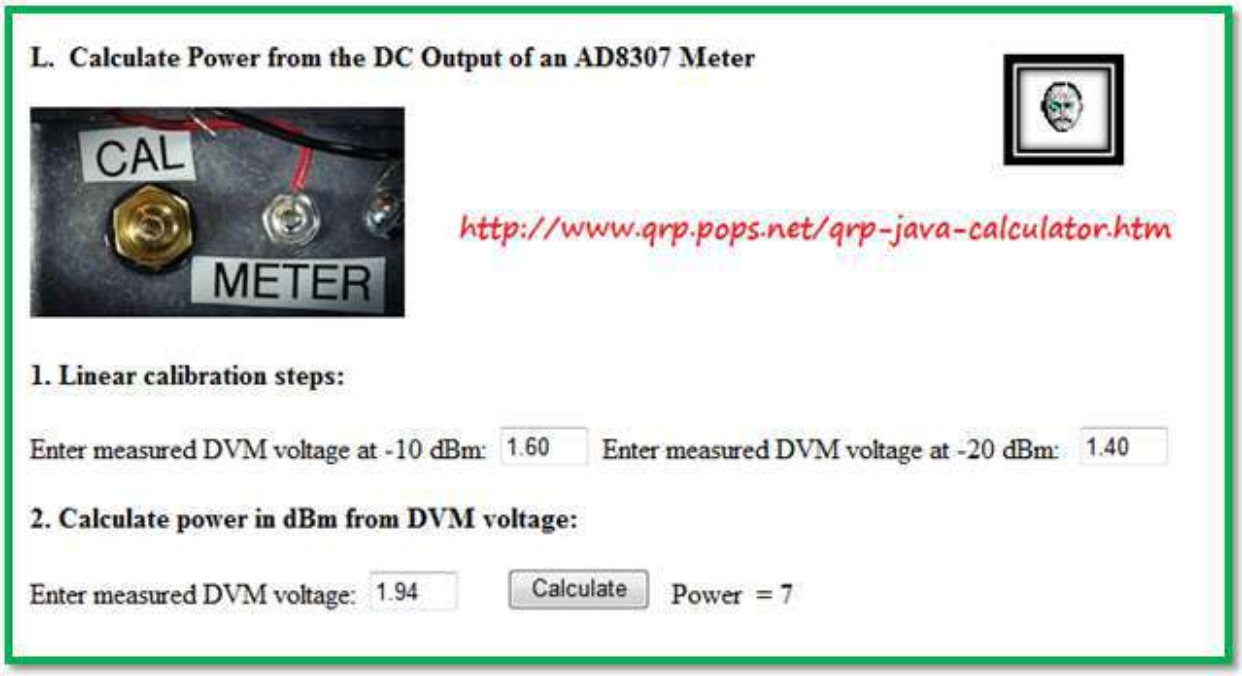

Above — A screen capture of JavaScript Applet L. I calibrated my instrument by connecting a 10.0 MHz sine wave calibrator to the 50 Ω input port of my PM. At -10 dBm input power, my Port B reading was 1.6 VDC; at -20 dBm, I measured 1.4v at Port B. These 2 points establish the log linearity per Wes' notes. After this calibration, I measured the output power of a 4 MHz sine wave VFO that I designed to run at 7 dBm output power to drive the LO port of a diode ring mixer. Port B read 1.94 volts and when I entered this into Applet L and pushed <<Calculate>>, the VFO output power was indeed 7 dBm. More on this later...

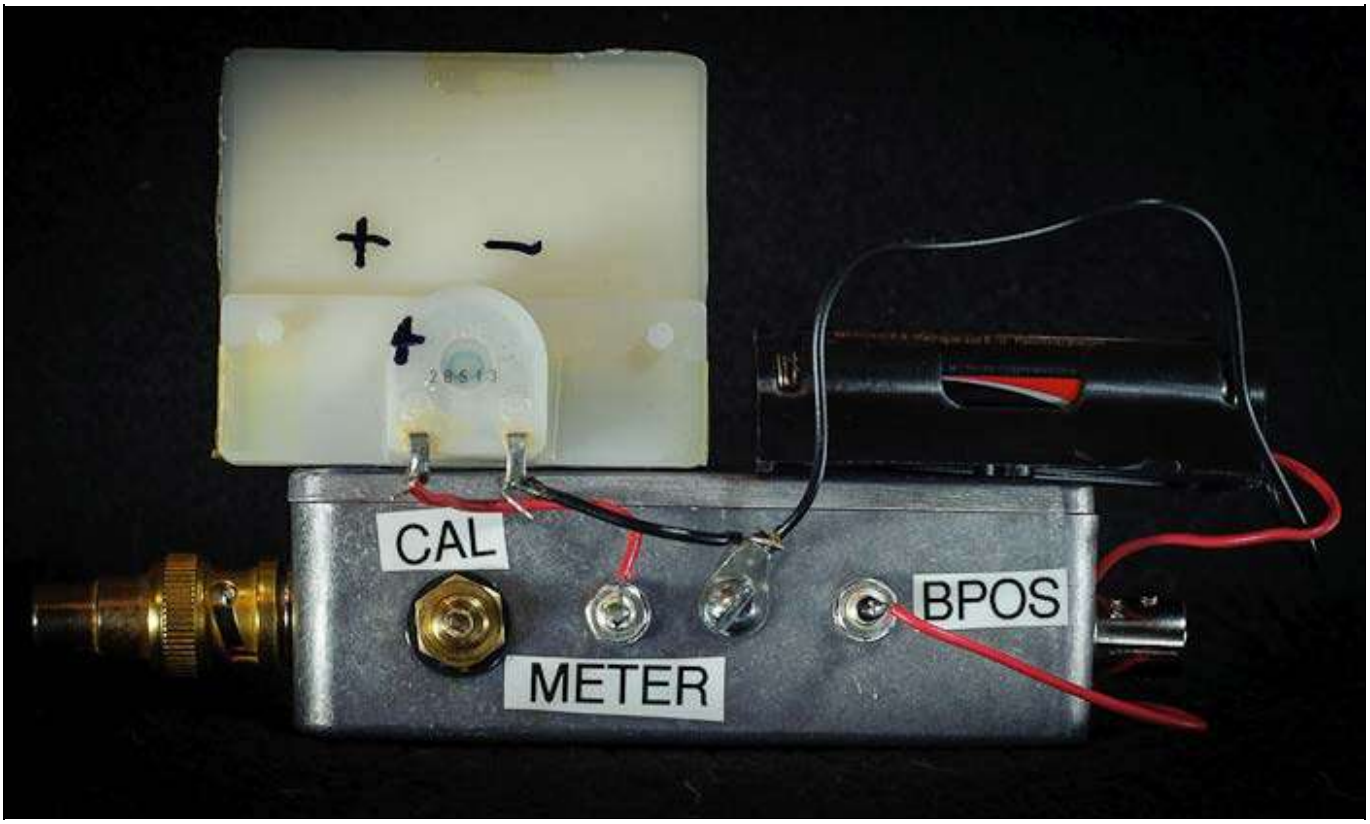

Above — My prototype RF-tight breadboard of the Barebones PM. I ran my 'trademark' die case box, BNC RF input and Port B connectors, a common ground lug and feedthrough capacitors for the B+ and panel meter connections. I placed a BNC to RCA adaptor on Port B to allow the insertion of a standard-type positive DVM probe. A black alligator clip terminates the distal end of the negative probe on all my DVMs. I just clip it onto the ground lug.

Above — A view of my breadboard showing my 100 uA panel meter and the 4.5v battery pack. I raised R2 in the original schematic up to 8K2 to set my preferred needle movement in this 100 uA panel meter. A meter with linear markings might be better?

Some Further AD8307 Notes

After power up, you'll notice a DC output voltage around 0.22v or so with no input signal; this arises from wideband noise caused by resistors and

amplifiers in the AD8307— all normal.

If possible, verify a 25 mV per dB power change with a manual sweep using a sine wave signal generator on the input and a DVM to AD8307 Pin 4. If you don't have the test gear to perform this function check, no problem.

The AD8307 input resistance = 1100 Ω , so we must place a resistor in parallel with the input to establish 50 Ω. Many builders just shunt a short-leaded 51 Ω resistor from input to ground like Wes did, however, you might also see builders place a 1% tolerance 53.2 Ω R in that slot to derive an input Z of 49.9 Ω. I did this in another "blinged-out", frequency compensated AD8307 meter I built for future UHF circuit experiments.

With 20 and/or 40 dB taps, attenuator pads and some 50 Ω cables, a Barebones AD8307 PM can measure everything HF you might build or buy for your *QRP* workbench. I posit that a simple AD8307 power meter may form the heart of a basic, first QRP workbench. Lacking a oscilloscope when I started in radio electronics, I measured RF with a germanium diode RF probe and a DVM — I would have enjoyed a simple log power meter plus a basic calibrator, however, the AD8307 did not exist back then.

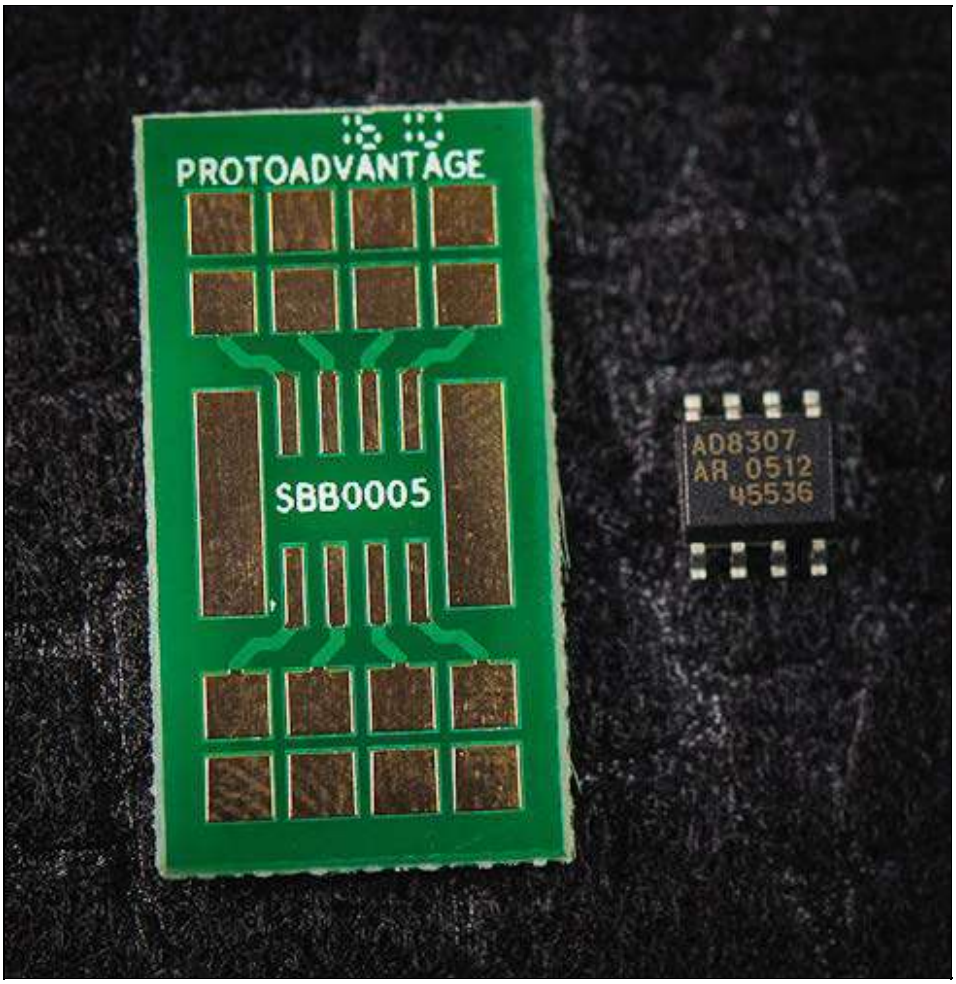

Above — Some builders lament because an AD8307 (in DIP) costs around $10.00. I bid for and bought the AR version chip shown above for $4.42 USD. The above green Proto Advantage breakout board cost $1.00. To compare; some people spend $5.00 for a boutique coffee in Canada — it's all good.

The SMD packaged AD8307AR may offer better performance above 100 MHz with its lower lead inductance.

QRP — PosData for Dec 3, 2013

Realize your bench acumen — adapt and build some test equipment to suit *your* needs. Steve, VK2SJA crafted a version of the AD8307 PM. Click for his beautiful box featuring a 1mA meter movement. Aided by the Tonne software "Meter" program and the AD8307 datasheet, his ranks among the best I've seen. Kudos Steve.

---

2. Power Meter Calibrators

1. CMOS Clock Oscillator RF Calibrator @ -10 dBm

Bob, K3NHI designed a 10.0 MHz reference oscillator for -10 dBm that might help equip the beginner bench. This CMOS signal source does not

need an AC power reference to calibrate it — just a DVM to make a DC measurement and your good to go!

In addition to calibrating an AD8307-based PM, you might use this -10 dBm reference to calibrate other gear including homebrew sine wave signal generators; that's what I'll do later.

Above — The recommended CMOS clock oscillator for the CMOS RF calibrator. Digi-Key part # CTX772-ND. Data sheet.
If you substitute another CMOS clock, it must swing nearly rail-to-rail for accuracy. Bob intended this calibrator for those who lack the bench instruments needed to precisely calibrate RF devices since only a DVM is needed for calibration. This generator also offers a range of calibrated harmonics as Bob described in his January-February QEX article A Simple RF Power Calibrator — great when you want to examine a spectrum analyzer over a limited span.

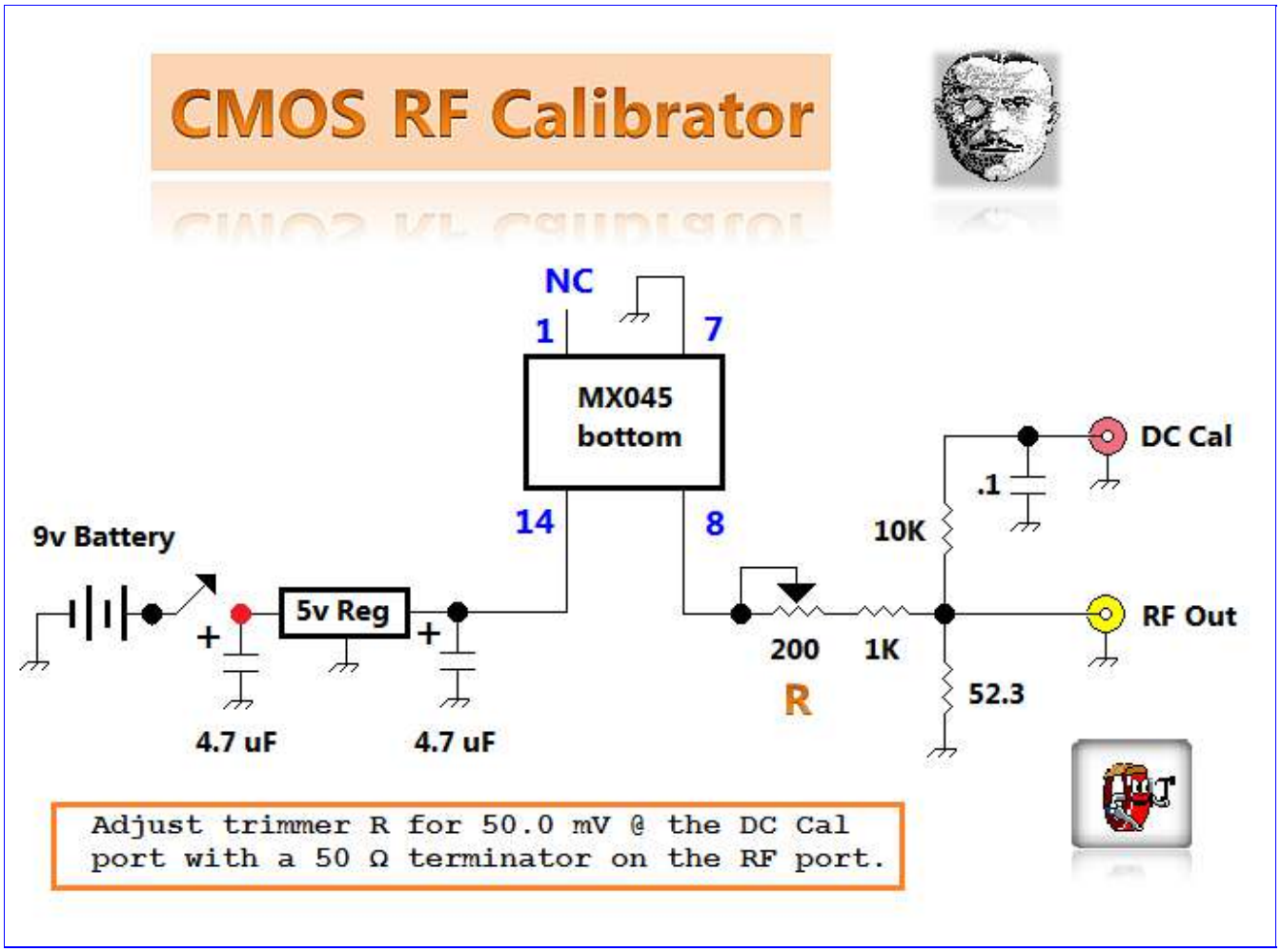

Above — My version of the K3NHI CMOS signal source (presented with the permission of Bob, K3NHI). The 52.3 Ω resistor is a standard 1% part and I bought 5 for all my AD8307 projects and this little signal generator. In my first version, the trimmer resistor was 500 Ω and worked okay, but the 200 Ω trimmer improved calibration. I ordered 10 Bourns 200 Ω and 10 Bourns 500 Ω trimmers on eBay for a few dollars and after studying Bob's published work and applying his influences to my own, I now love to precisely calibrate or bias circuits with a 200 or 500 Ω trimmer R as appropriate.

QRP — PosData for November 22, 2012

If required, you may substitute a 49.9 to 51 Ω resistor for the 52.3 Ω specified.

Per Bob's QEX 2010 Tech Notes and his emails specifically about calibrating the AD8307 with a CMOS *square wave*: Modern AD8307 chips are better calibrated with a -10 dBM square wave. To test log linearity after CMOS signal generator calibration, apply a sine wave signal generator to your power meter and adjust its output to get the same power meter DC output voltage as with the CMOS generator. Then insert attenuator pads on the now calibrated sine wave generator to assess the mV/dB change with different power levels.

Bob's original CMOS calibrator outputted - 20 dBm, however, he updated it to output -10 dBm in 2010 as reported in his QEX 2010 Tech Notes.

Some readers have asked why calibrate the AD8307 at 10 MHz? Calibrate at whatever frequency you want, or more than one. However, at 10 MHz, the AD8307 exhibits its best log performance compared to other frequencies. Click or click for datasheet graphs.

Above — The DVM calibration port reading (2 volt scale) from my CMOS clock calibrator after calibration. That was easy!

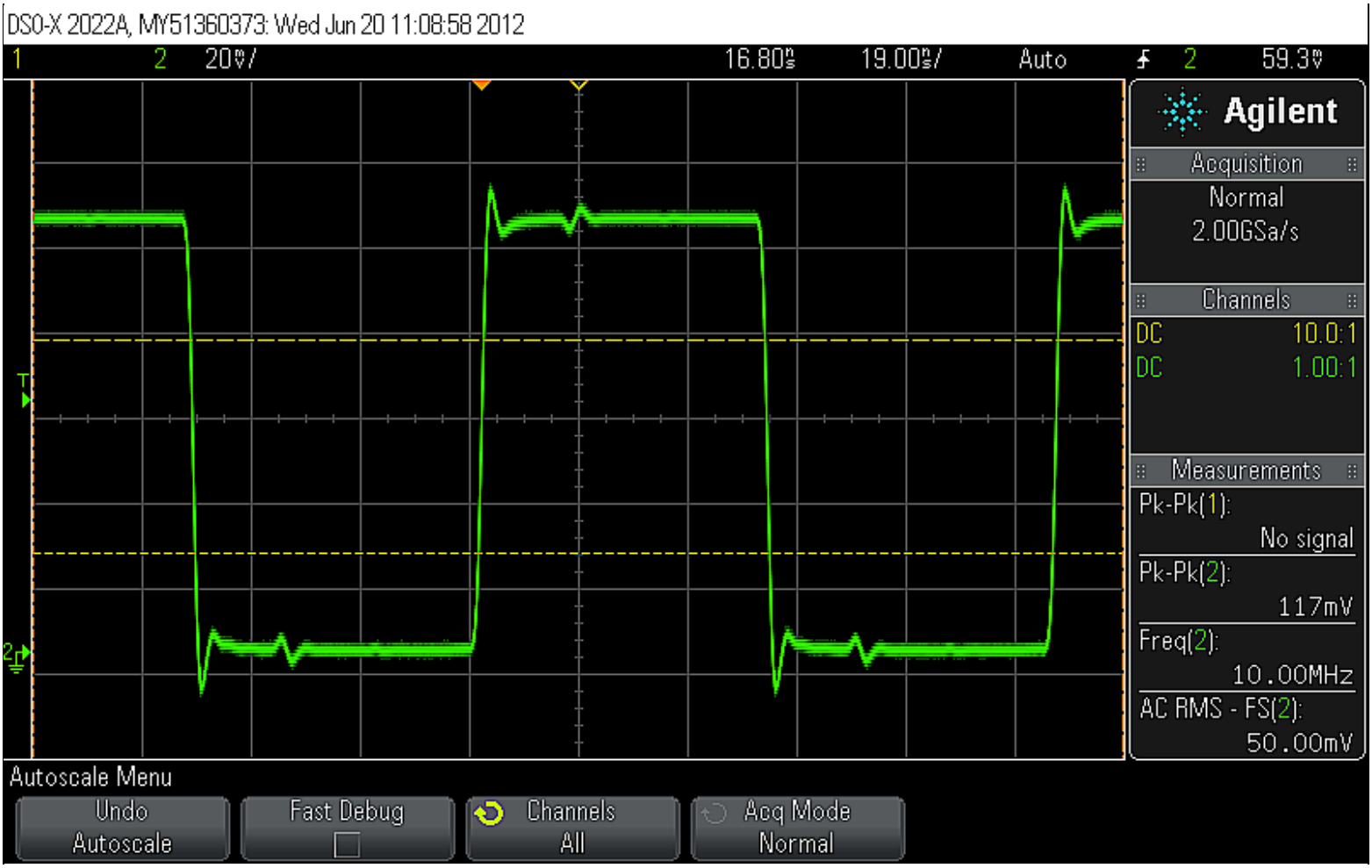

Above — The calibrated CMOS clock RF calibrator in my 50 Ω terminated scope.

Above — The breadboard of my version of the K3HNI CMOS -10 dBm RF calibrator. For best results, stick it in a shielded box. When correctly calibrated, it outputs -10 dBm on an AD8307 PM, -14 dBm on a spectrum analyzer and -13 dBm on a conventional, thermal-sensor power meter.

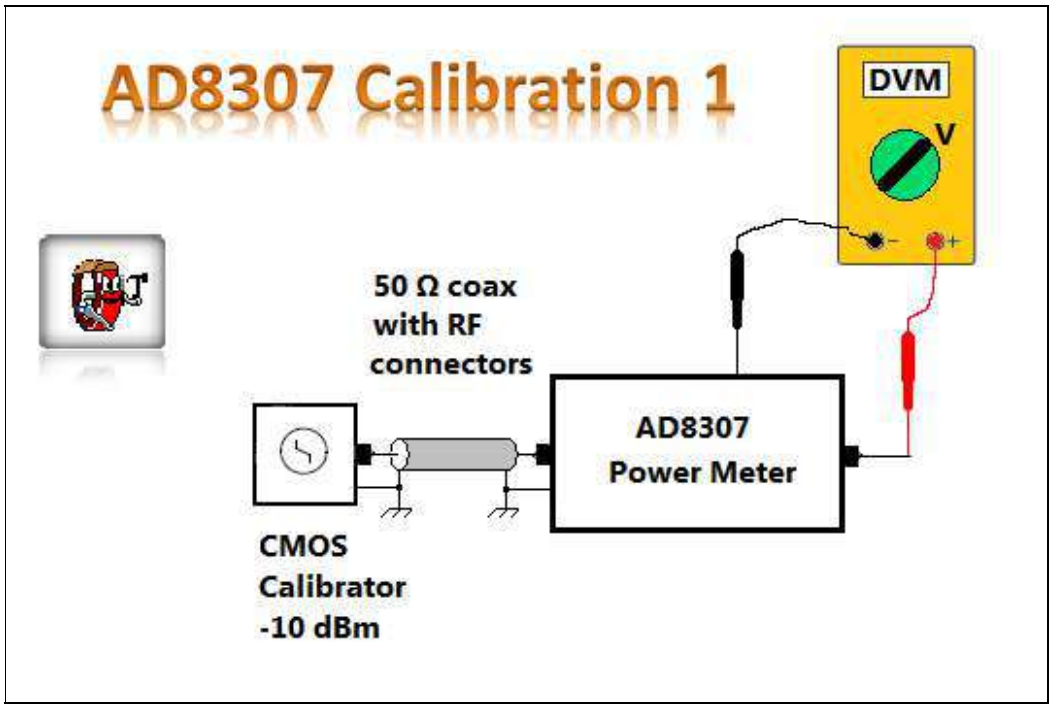

Above — The procedure for calibrating an AD8307 PM with the -10 dBm square wave CMOS signal source.

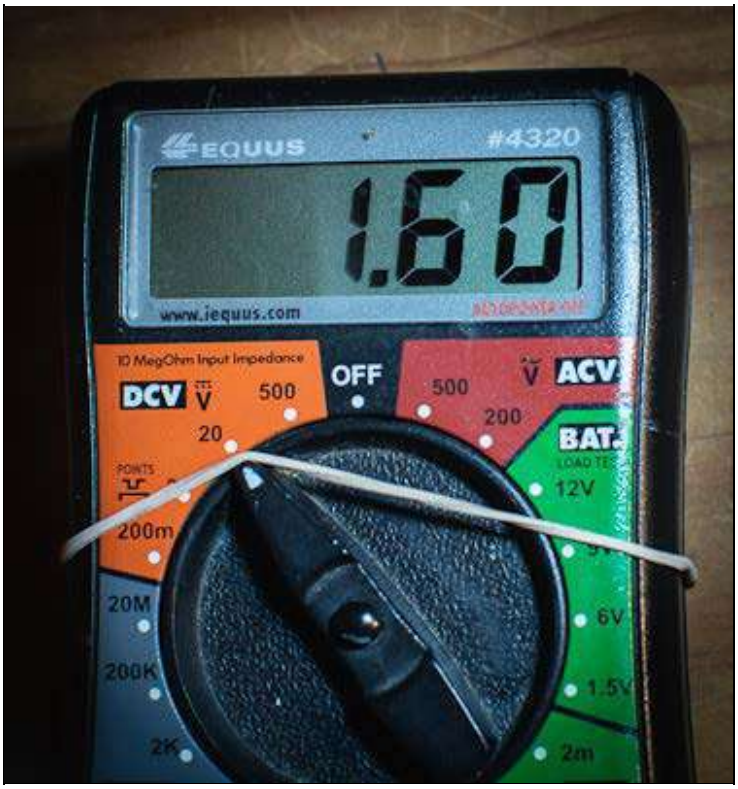

Above — When I connected the calibrated CMOS clock RF calibrator to my build of the Barebones PM, I measured 1.60v with my DVM; ***the -10 dBm reference voltage.*** Since the log-linear power changes 20 mV/dB; for my calibration reference voltage: 1.40v = -20 dBm, 1.20v = -30 dBm, 2.0v = 10 dBm etc.

Remember that the Barebones PM runs on a battery pack and over time the B+ will change. *Each time* I measure power with the meter I first calibrate it to establish the -10 dBm reference voltage.

Here's a simple formula that only works for 20 mV/dB @ my particular 1.60v calibration voltage, but gives you the general idea:

Power in dBm = 50 x (V - 1.8)

So if I measure 1.94v: 50 x (1.94 - 1.8) = 7 dBm.

2. Sine Wave Oscillator for Calibration @ -10 dBm and -20 dBm.

You may also calibrate your AD8307 PM with a calibrated sine wave signal generator. Advanced builders who own the gear needed to measure RF power tend to use a sine wave for calibration.

It's easy to calibrate the AD8307 with a sine wave signal source. Normally we calibrate our sine wave signal generators with instruments such as a 50 Ω terminated 'scope, a spectrum analyzer, a calibrated power meter, or a 49.9 to 51 Ω terminating resistor plus a 10X probe etc., but if you lack these instruments, your stuck.

No problem. You may calibrate any appropriate sine wave oscillator at -10 dBm with your Barebones PM and the CMOS RF Calibrator shown earlier. Let's examine the procedure:

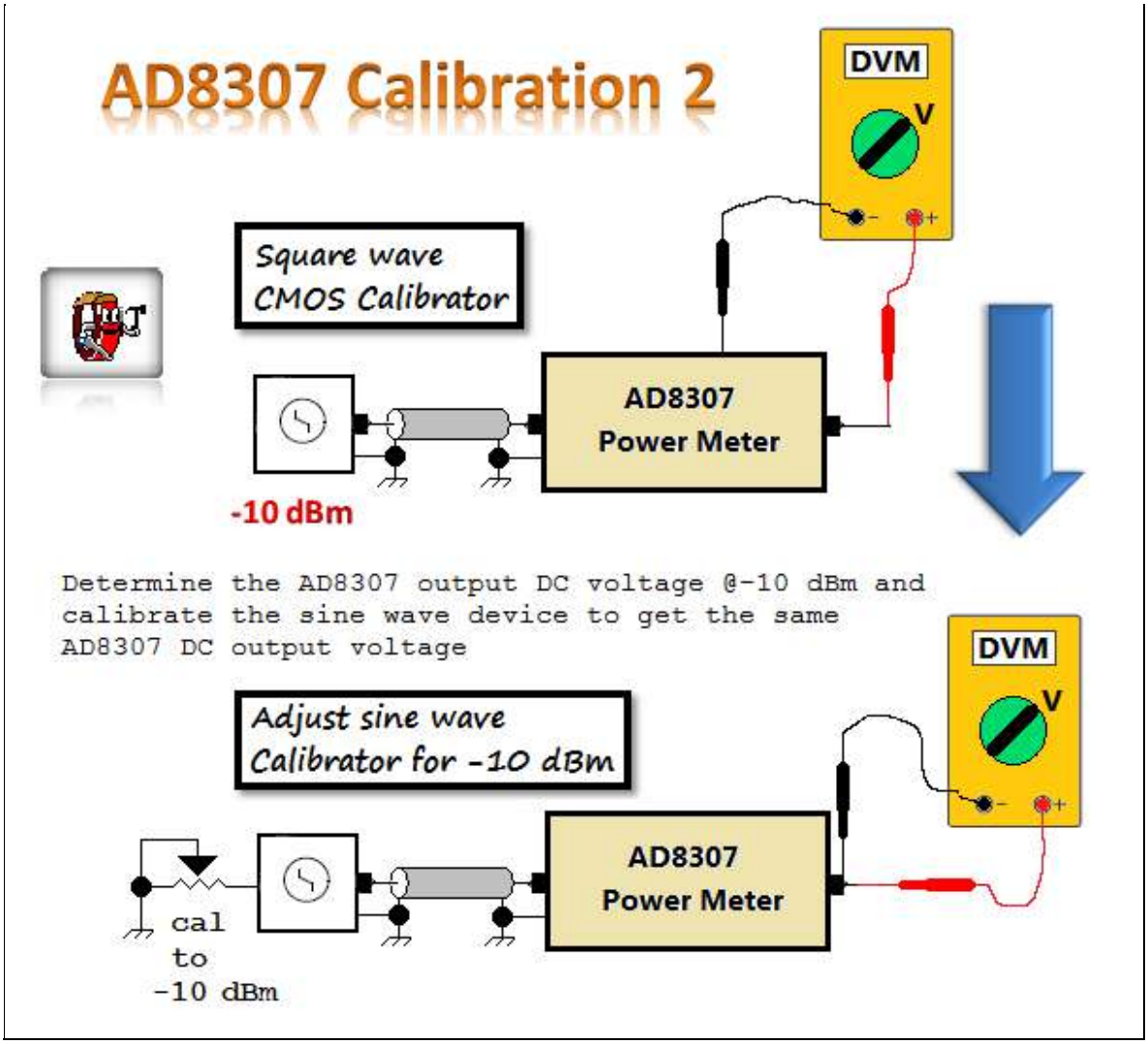

Calibrate the AD8307 PM with the CMOS square wave reference and record the DC voltage at the output of Port B. Connect up your sine wave generator and adjust its output until you get the same Port B DC voltage as the reference CMOS RF signal generator — your sine wave oscillator should now be calibrated to -10 dBm.

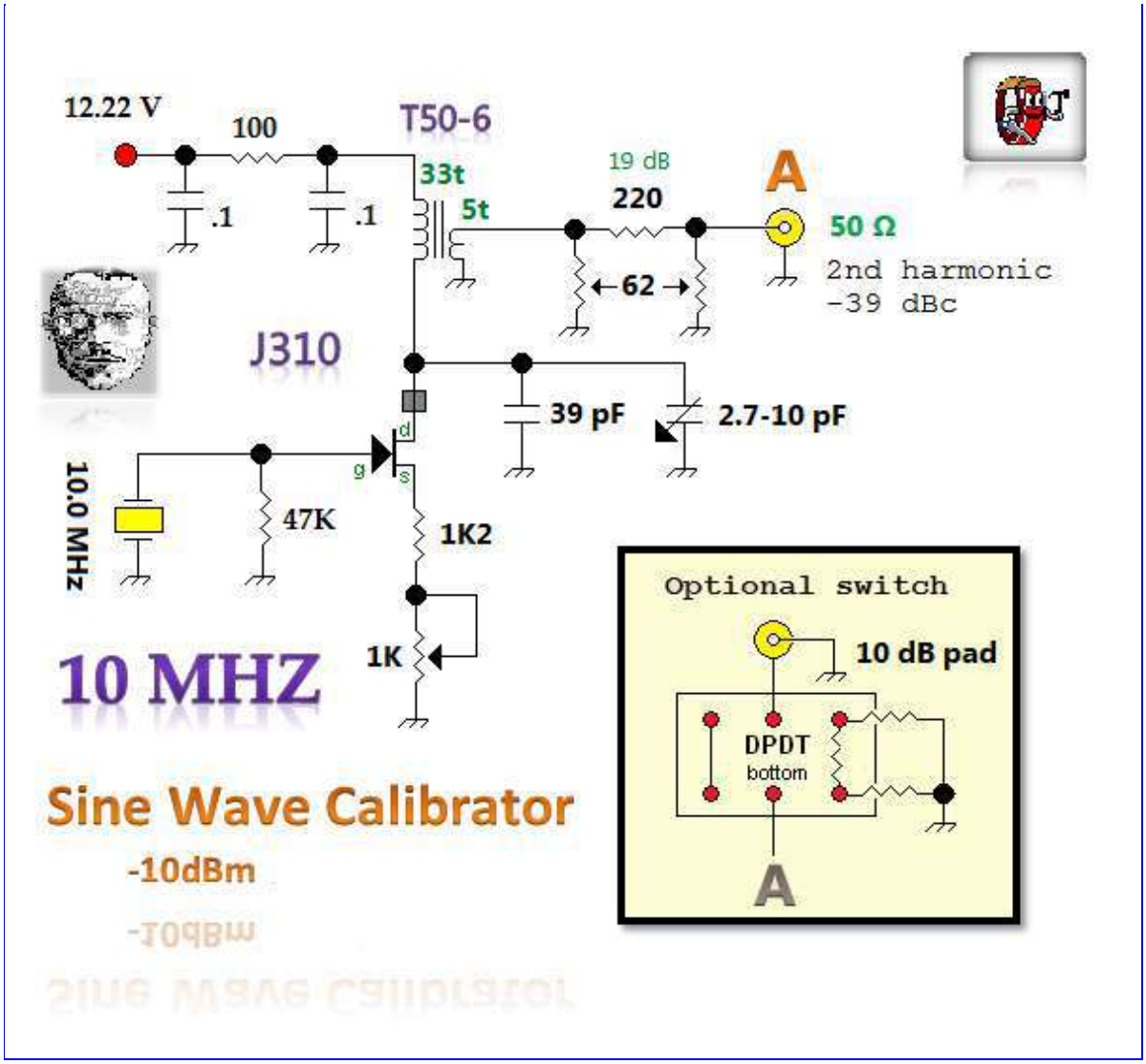

Above — I designed this simple 10.0 MHz sine wave calibrator to evaluate Bob's CMOS square wave RF calibrator and serve as an example sine wave reference oscillator. When running a regulated VCC of at least 12v and the *tank is perfectly* tuned, low distortion arises. I measured the second harmonic @ 39 dBc down. The L with 33 turns = 4.43 uH.

The initial tuning procedure goes like this:

1. Terminate the output with a 50 Ω resistor terminator, or a 50 Ω terminated 'scope, or your AD8307 PM.
2. Connect an ammeter between the VCC node and the regulated power supply.
3. Adjust the emitter trimmer R so that the circuit draws around 2.7 mA — then disconnect the ammeter leads.
4. Adjust the trimmer cap for the highest pk-pk voltage (and/or or best looking waveform) in the 'scope, or highest power in the AD8307 PM. *Nominal total C to resonate my particular circuit was ~ 45 pF.*

If not already done, connect the tuned-up sine wave signal source to a AD8307 PM. Adjust the trimmer potentiometer so the Port B DC voltage = the reference voltage measured during your CMOS RF generator power meter calibration. Your sine wave signal source is now calibrated to -10 dBm.

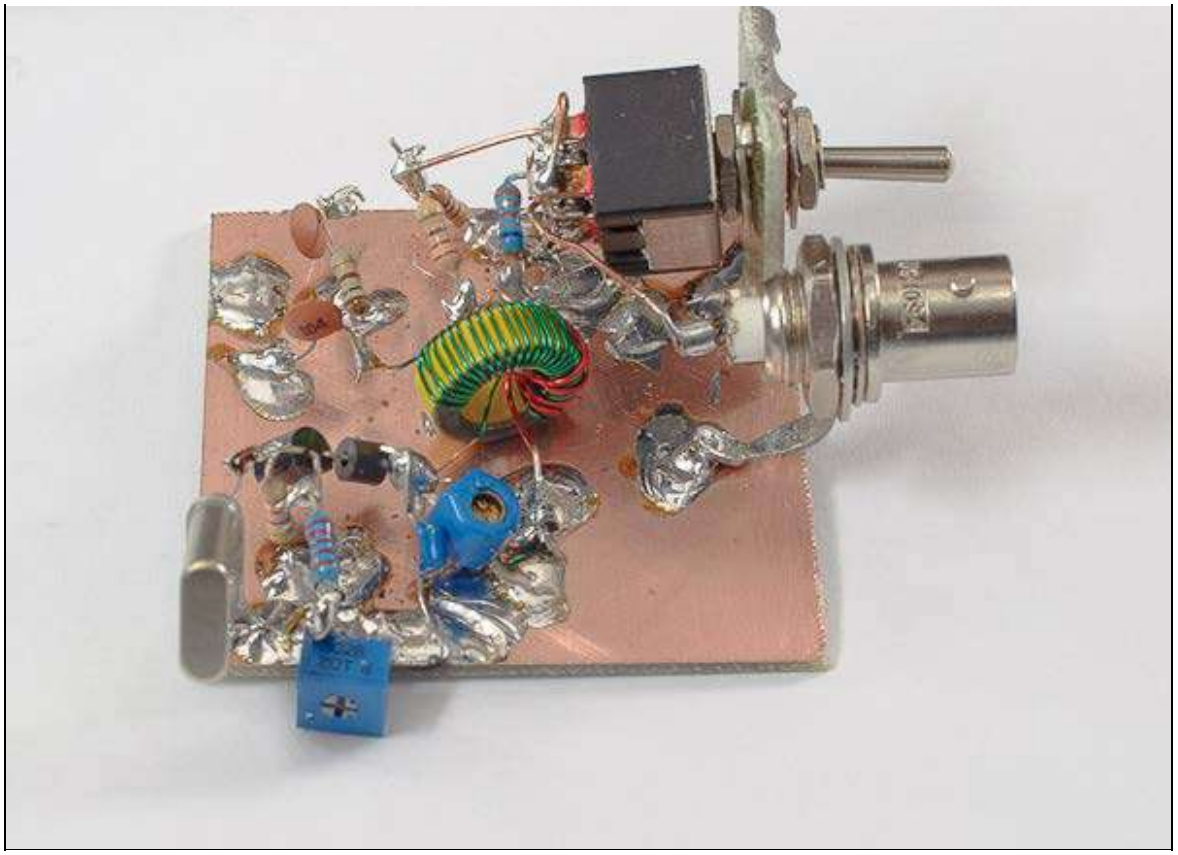

Above — The breadboard of my 10 MHz sine wave signal source. I included the optional switched 10 dB attenuator shown on the schematic inset. In the end I decided to just stick a removable **10 dB** pad like this 6 dB pad in-line for my -20 dBm measurement.

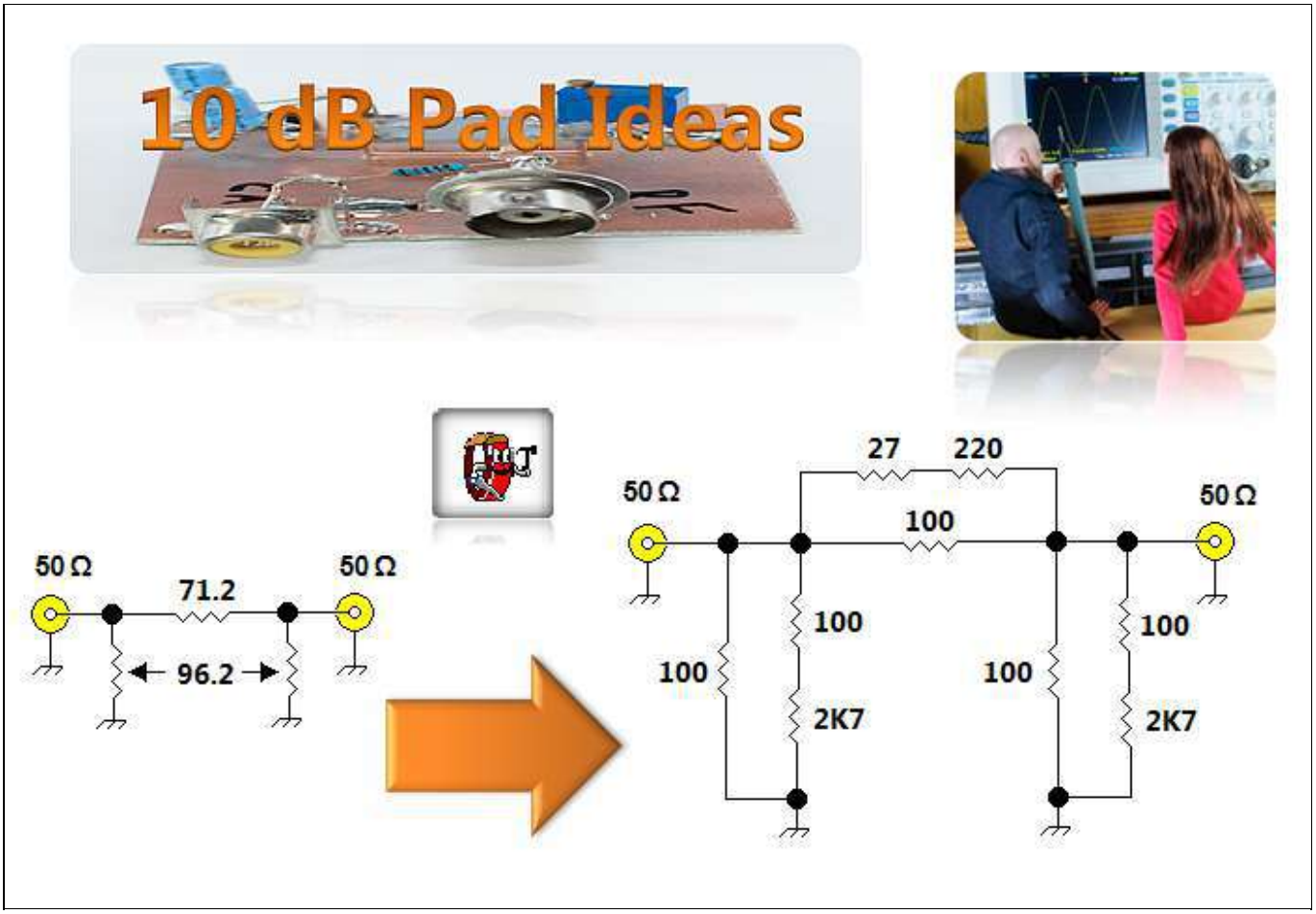

Above — Craft accurate attenuator pads with parallel + series resistors and some creative energy. Lacking the proper 1% parts, I hand selected some 5% resistors among the values shown to the right and built a pad that *precisely* gave a 10 dB power drop at 50 Ω.

Now let's check the calibration of this little sinusoidal RF generator...

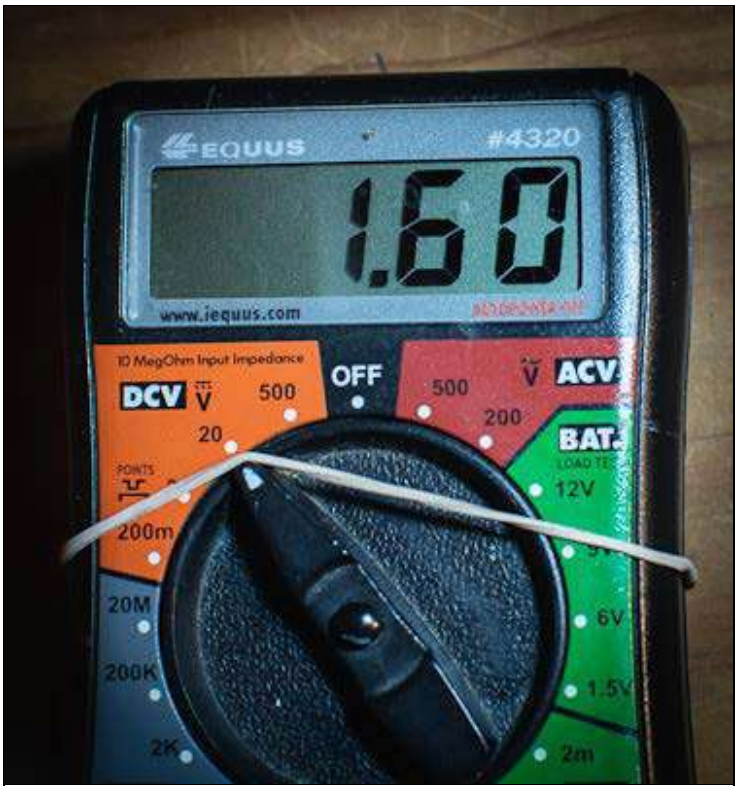

Above — When connected to the Barebones PM, I calibrated the output power of the sine wave generator by tweaking the trimmer pot to give an output of 1.60v; the same Port B voltage yielded by the CMOS RF calibrator.

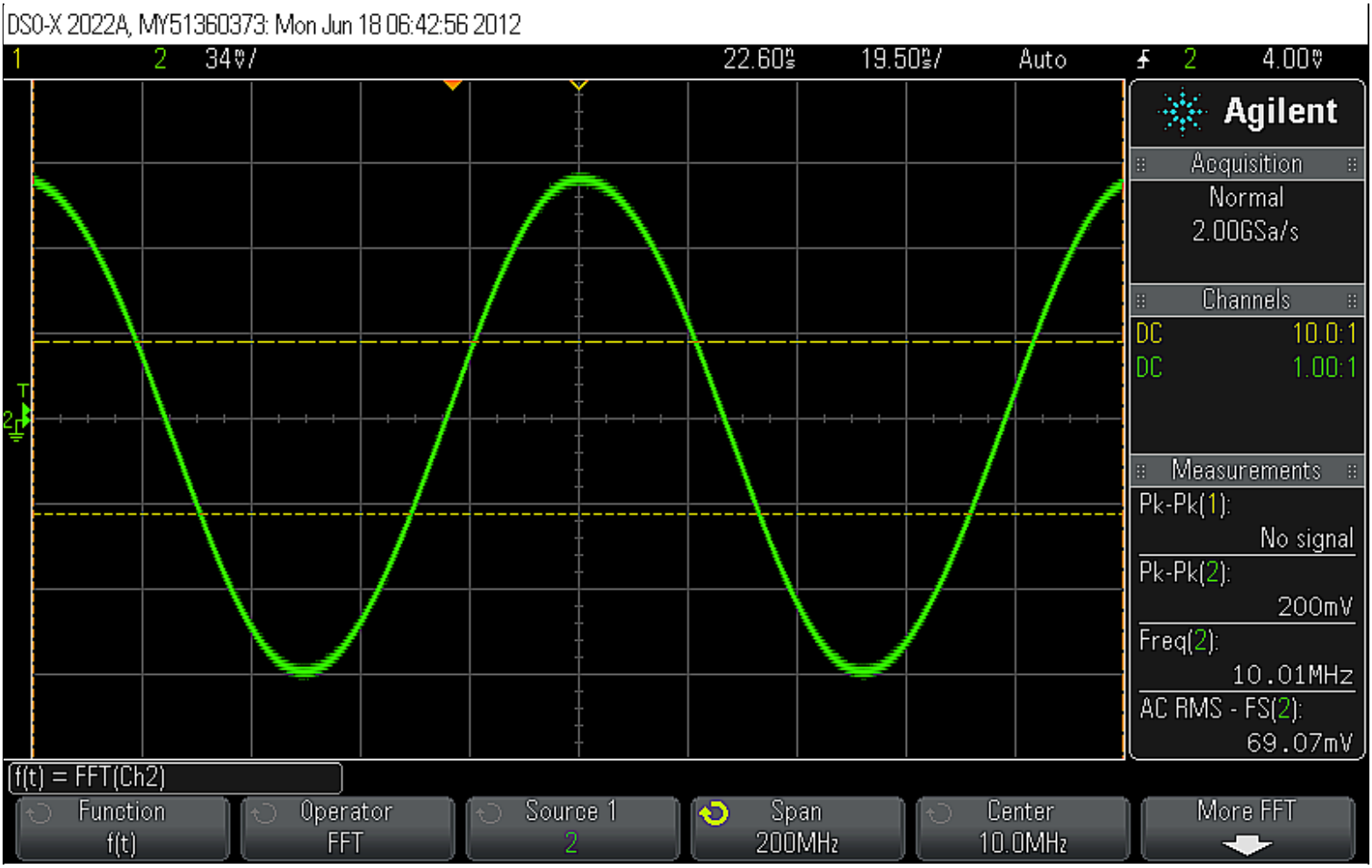

Above — The 50 Ω terminated 'scope verification of my calibrated 10 MHz sine wave signal source: 200 mV pk-pk = -10 dBm. Wow, thanks for this Bob!

Above — The Port B voltage when a 10 dB attenuator pad was connected to the calibrated -10 dBm sine wave signal source: Measured power = -20 dBm. Notice the 20 mV/dB power drop — right on specification.

Refer to the section titled **<How to Measure Power at Port B>** Recall Wes' calculation needed 2 points to set the log linearity. I chose -10 dBm and -20 dBm instead of 0 dBm and -10 dBm so the CMOS RF calibrator could be used to calibrate any sine wave signal generators on hand.

The -10 dBm calibration reference power serves as 1 of the calibration points in Applet L while we derive the other by adding a 10 dB attenuator pad to a *sine wave* signal source output port. ***Don't connect an attenuator pad to the CMOS square wave calibrator —*** error in the AD8307 arises. Why? Analog Devices mysteriously changed the AD8307 at some point after 2004 and altered its crest factor — this disallows us performing log linearity calibration with a square wave.

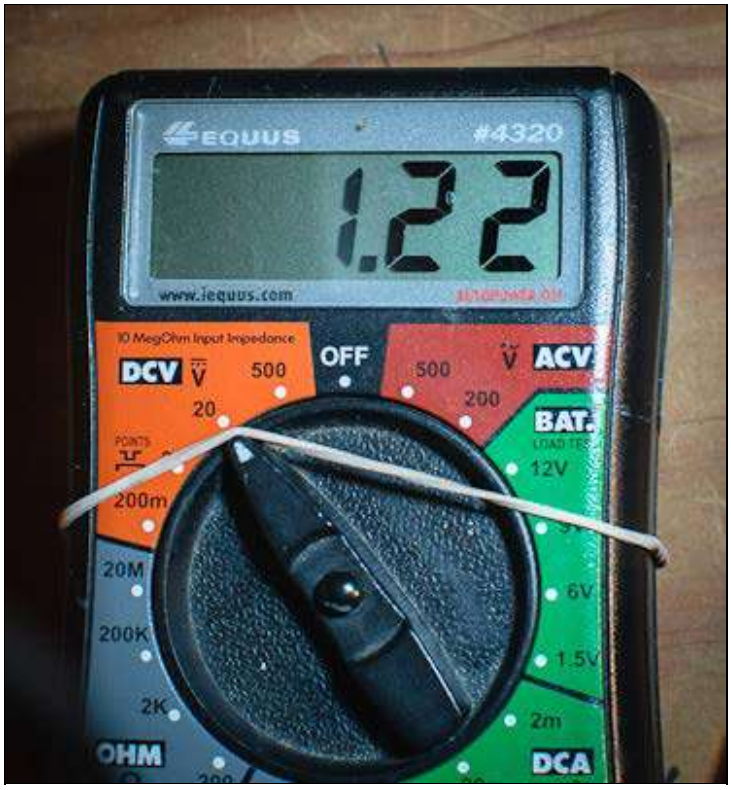

Above — A 20 dB pad connected to the -10 dBm sine wave signal source yielded 1.22v at Port B in the Barebones PM. See the power calculation with Applet L below:

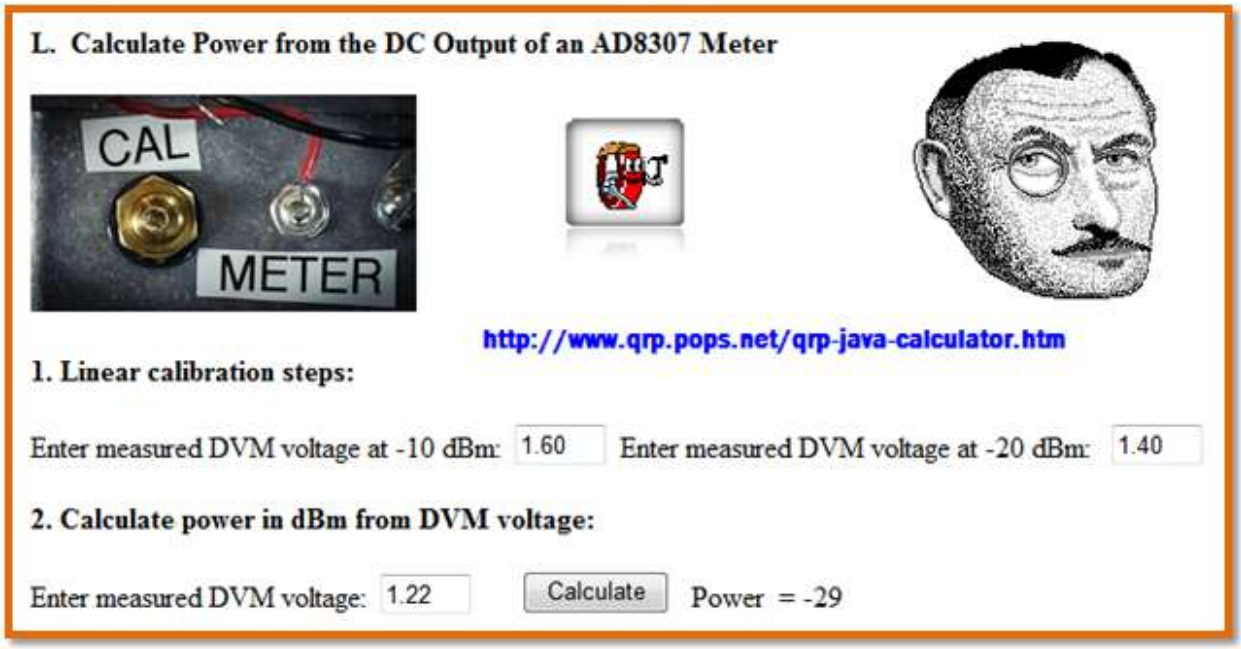

Above — The calculation of the output power with a 20 dB attenuator pad on the sine wave signal source output. We're off by 1 dB since it should have calculated a power of -30 dBm. Could this be error caused by my attenuator circuit, or non-linearity by the AD8307 PM, or a bit of both? We have to live with such problems. Still, the Barebones power meter seems quite impressive for a simple circuit that I scratch built and calibrated in about 25 minutes.

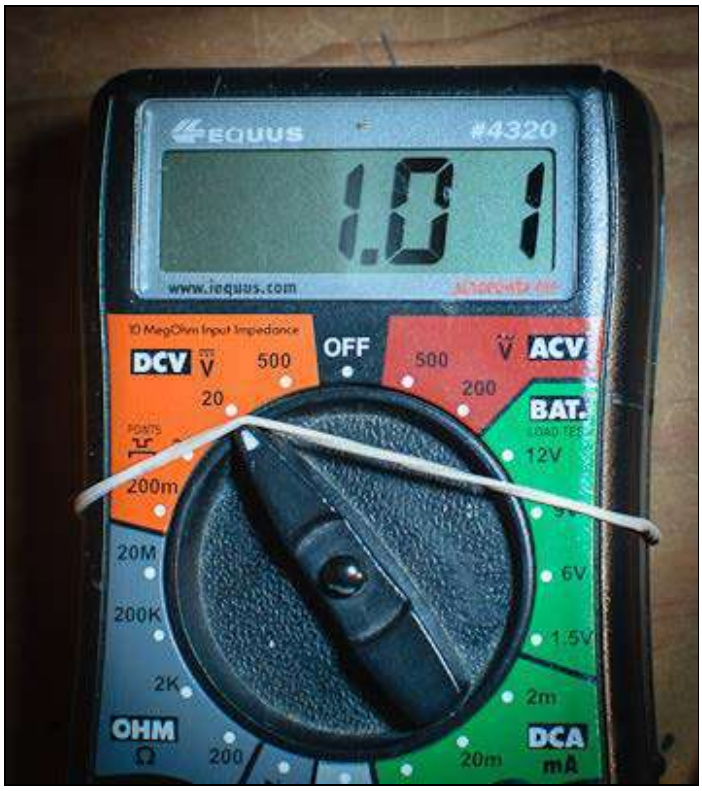

Above — The Barebones PM DC output voltage with a 30 dB attenuator pad on the output of my -10 dBm, 10 MHz sine wave signal generator: Measured power = -39.5 dBm. Again; a very good — but not perfect power meter.

A Barebones power meter allows builders with modest equipment to measure power, gain/loss, and with a return loss bridge, return loss at HF. I wish I owned this little gem back when I started out.

Richard, "Dick", N4HAY, posted some great notes on his blog. I recommend following his blog since he really digs deep and likes math — thanks Dick!

Best!

---

3. A Basic RF Workbench

Since January 2012, a handful of readers asked what I consider a good basic *RF* work bench. Again, I'm just an amateur hobbyist, so my opinion might show my ignorance.

A stand-alone 50 MHz oscilloscope with at least one 10X probe. *More bandwidth if you plan to work above 50 MHz*

If no oscillocope, an AD8307-based power meter *The modern version of the diode RF probe*.

3-4 50 Ω coaxial cables with BNC connectors; a 50 Ω scope feed-through terminator, *1-2* 50 Ω BNC port terminators, a though-connector and some BNC connectors to solder onto temporary circuit boards or mount in a chassis.

A homebrew return loss bridge.

3, 6, 10 and 20 dB BNC connector equipped attenuator pads, or a step attenuator.

Signal generator(s) that cover most of HF; +/- VHF signal generators described in the next section.

AADE L/C Meter IIB. Click

12 volt regulated power supply good for at least 1 amp.

Digital multimeter. *I use 2 and keep 1 set up for current measurement only.*

Frequency counter: homebrew or commercial. *I ran a 40 year old, ovenized, accurate HP counter until 2012.*

With these devices, as possible, you can work in a modular, 50 Ω environment and measure gain or loss in dB, return loss in dB and absolute power in dBm. Starting small and expanding your bench around 50 Ω input and output impedance devices will provide a lifetime of challenge and excitement in RF design.

Later, the big toys can follow: spectrum analyzers, VNAs, commercial signal generators and other lab quality stuff.

Equipping an RF bench presents quite a financial burden. I started small and slowly added pieces over time. Many pieces such as my L/C Meter IIB were gifts for holidays or my birthday. Other pieces were old, inexpensive equipment that I restored and calibrated.

Above — RF tools of the trade. We're RF experimenters! As scratch homebrew builders, gear like BNC, SMA and through-connectors, 50 Ω terminators and inline attenuators lie scattered on our benches; our fodder. Alternate photo.

---

4. VHF Signal Generators

Having only started at VHF in November 2011, my knowledge suffers, however, a search for accessible, affordable, good quality VHF signal generators disheartened me. Ten year old or newer signal generators covering the VHF band work up to several GHz and cost a small fortune.

Lamenting old timers often recommend the vaccum tube HP-608 series that covered ~10-480 MHz. These heavy, glowing beasts sometimes come up in estate sales or on eBay for $200-400.

Then, too, the HP8640 series seems attractive, however, they are full of decaying parts. Ken Kuhn and others restore old HP gear as a hobby and this direction certainly gives us a valid option.

I've investigated 1 or 2 new, low-cost, commercial signal generators that work into VHF, but they failed to excite me; especially after I downloaded the schematics and sat in disbelief over their poor design.

Some minimum commercial signal requirements might include stable, linear tuning, a metal chassis, 50 Ω output with a return loss greater than 20 dB and low harmonic distortion at all frequencies. Like the rest of our lives, our budget usually determines what we buy.

I decided to build my own VHF signal generators and document them on this web site. I've learned that home building signal generators between 50 and 200 MHz requires skill and care, but can be done.

What about digital clocks?

At VHF, DDS spurs get extreme as you get closer to the maximum clock frequency .

The Si570 looks intriguing, however, still requires an MCU + components, I haven't read any lab quality evaluations of the Si570 as part of a engineer-grade VHF-UHF signal generator and if you know better, please email me.

---

5. L - C Meters

If you search for opinions about which L/C meter to get, you'll find an abundance of super write-ups including those that cover measuring with Kelvin probes, SMD tweezers; or statements suggesting that if you really need maximum accuracy, purchase a VNA. I encourage you to research this yourself and find the best L/C meter for *your* bench. Here are my 2 cents worth of opinion and please remember — I'm often wrong.

I use an AADE L/C IIB meter to test inductors and capacitors for HF and even some VHF work. Yes, the AADE L/C IIB doesn't measure large-value electrolytic caps and so forth, however, considering the cost versus performance — it's accurate enough for the popcorn RF workbench.

The AADE L/C meter uses the method described by William Carver, W7AAZ in an article called The LC Tester published in Communications Quarterly, Winter 2003 . EMRFD page 7.12 briefly examines Bill's circuit and shows his original oscillator along with an extended range Colpitts oscillator designed by Wes. For brevity sake, I'll just discuss inductance measurement with Carver-style meters. With care, an inductance resolution of 5 - 20 nH might be realized with such a device.

We normally don't consider that our inductor is actually a network with L, a parallel C and losses that might be modelled as R in series with the L, or a R in parallel with the C depending on our model. The inductor also exhibits a self-resonant frequency and for our design purposes, we usually *ignore* all these details and just consider it a "pure L". My L/C meter's oscillator runs from a few tens to a few hundred KHz and generally lies below the self-resonant frequency of the inductors I measure with it. I've learned by sweeping/analyzing my completed filters, that as long as you avoid the coil's SRF, *the low frequency* Carver-style meter proves a stalwart inductance meter for most HF and some VHF applications.

Often, we popcorn builders want to make a filter, an oscillator, or a pi, or L match and we apply software or tables to calculate the L and C values needed to resonate our filter tank(s) or matching networks, or to synthesize a low-pass filter. These math-driven programs/tables assume the *pure* "pixie dust" L described eariler — disregarding the stray C and R. So getting all worked up about whether our coil is 4.50 or 4.59 microHenries seems moot.

Further, we man-handle our inductors [changing the inductance somewhat] into a breadboard laden with 5% (or greater tolerance) capacitors, copper board pads/paths that exhibit C, active devices and so forth. Then, too, we connect these resonators, or filters to other blocks with sometimes reactive ports, plus or minus shielding. Despite all these variables, miraculously, we make the filter with our "measured" L work!

As we move up in frequency, the effects of stray L effect magnify and at some point our filter networks may behave poorly.

For band-pass filters with Carver-style device measured inductors, we need only adjust each trimmer capacitor to get the highest possible peak-peak voltage, or RF power with our filter between a signal generator and a 50 Ω terminated scope, power meter *respectively*, or whatever. After sweeping these peaked filters, rarely do I need to compress/expand, or add or remove windings to tweak the L get the desired filter response when the filter input and output ports are well matched.

In the case of single frequency matching networks like the L-match, we might need to tweak up or down the L to derive strong port matching. In all cases, our software and the L/C meter can get us into the ballpark, but in-situ bench measurement with other instruments will garner the home run.

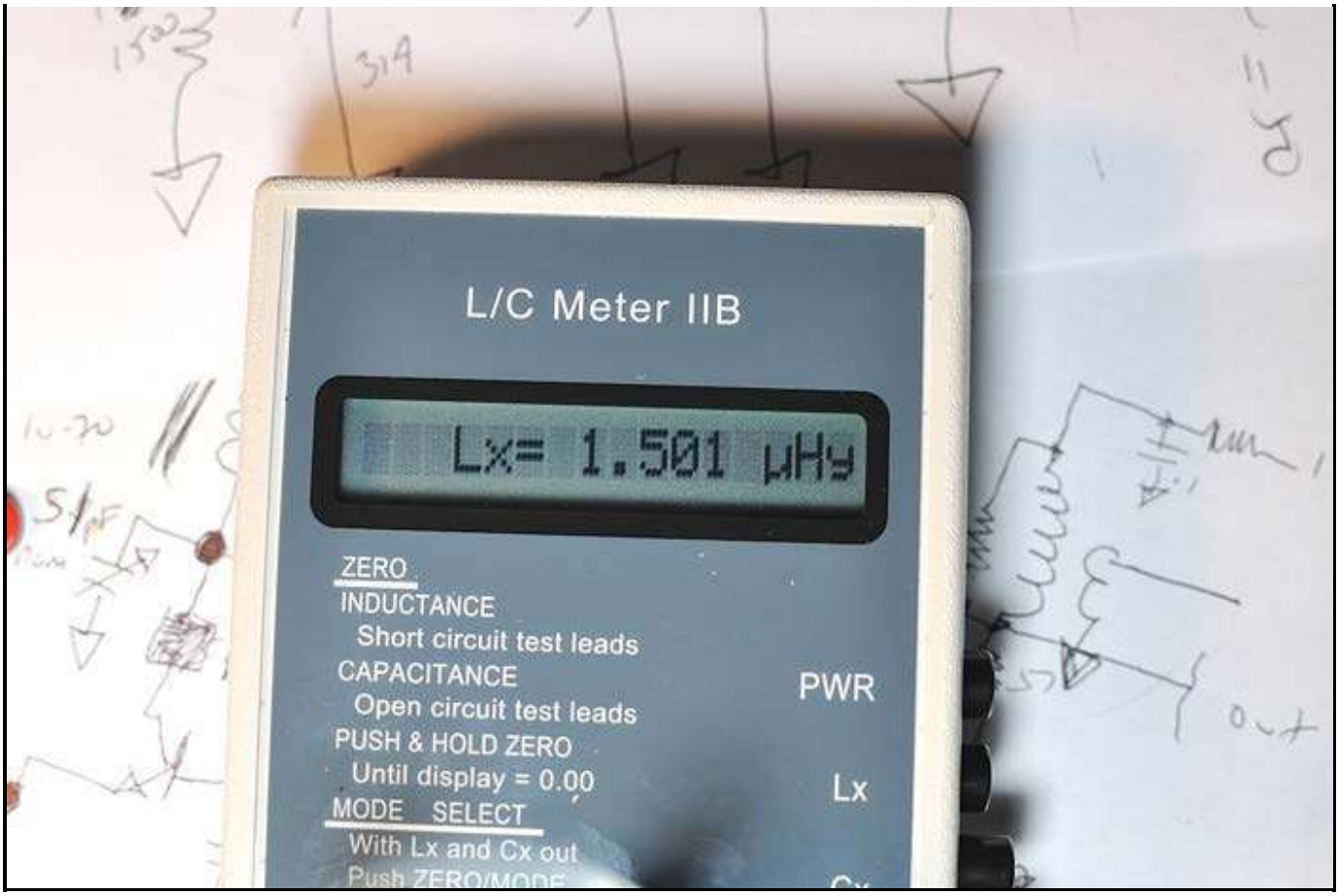

---

6. Bob, K3NHI — RF Power Meter Follow-on

Bob built a follow-on detector and power meter to his 2002 QEX power meter *[Reference 3 in Section 7].* Bob gave me the green light to share his creation on my site. Thanks awfully Bob!

Click for the schematic in pdf format. Per typical K3NHI fashion, it's laden with trimmer pots allowing precise calibration — Bob's stuff contains loads of tweaks and wiggles! The new PM offers more flexibility + features including bigger battery supplies that won't quickly die when you fail to turn it off. He also included a means to measure battery voltage on the analog meter. Click for a photo showing the batteries. Low noise, high-speed, rail to rail, CMOS op-amps for IC1 and IC3, allow you to capture PEP during sideband transmitter measurement with appropriate attenuation.

The TS922 op-amp might be hard to find in DIP since that package went obsolete, however, it's available in SMD. If you can't get any TS922, likely other modern, high speed, rail to rail, CMOS op-amps will work fine — consult datasheets to ensure you meet or beat the TS922's performance for IC1 and IC3. Some of the latest design op-amps offer truly sublime specifications and evoke joy in our breadboards.

Bob critically *isolated* the entire RF sub assembly **outlined in green on the schematic** with metal shielding and feed through capacitors for the B+ and DC output. This helps ensure stable and accurate AC voltage measurement. Click or click or click for more of Bob's photographs.

---

7. References

[1] Roger Hayward, KA7EXM — A PIC-based HF/VHF Power Meter, QEX May/June 2005

[2] Wes Hayward, W7ZOI, Bob Larkin, W7PUA, Simple RF-Power Measurement, QST, June 2001

[3] Bob Kopski, K3NHI — An Advanced VHF Wattmeter, QEX, May/June 2002.

[4] Bob Kopski, K3NHI — A Simple Enhancement for the Advanced VHF Wattmeter, QEX, Sept/Oct 2003.

[5] Bob Kopski, K3NHI — A Simple RF Power Calibrator, QEX, Jan/Feb 2004 **+** Tech Notes article, QEX, May/June 2010.

RF — Test and Measurement

VHF FM

Yes - I could purchase a FM radio-in-an IC for $2.00 and be done in 35 minutes, but what would I learn?

Repository for FM superhet receiver experiments conducted from 2012 to 2014.

1. 10.7 MHz IF Filter Experiments
2. A Basic Colpitts VCO
3. DC-DC Converter for VCOs
4. Supplemental Page #1 - it's time to make some receivers
5. Miscellaneous Photos or Figures

---

1. 10.7 MHz IF Filter Experiments

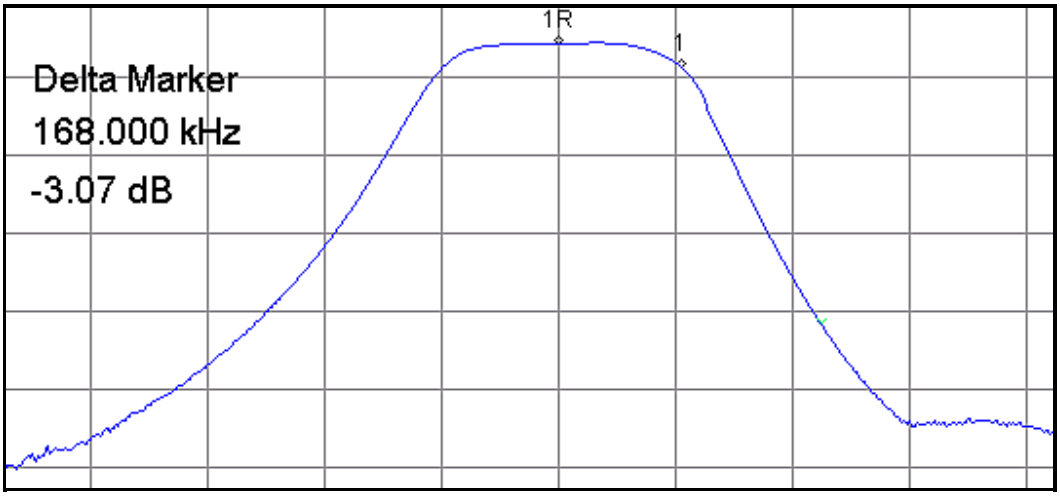

As a FM receiver design newbie, I read about and experimented with some 10.7 MHz IF filters to learn common practices, what's available and which measurements might help me to reach my goals. Over time, I've collected a variety of crystal and ceramic filters for hopeful future work. Click for 2 exotic examples. IF filters might be purchased at Ham festivals, surplus electronic parts stored and/or online. Prior to paying for a

filter, I've found it useful to politely request a sweep of the filter, or, better yet, perform this task myself. To sweep a filter in your lab, you'll need a tool such as a spectrum analyzer with tracking generator, a VNA, or some other analog/digital sweep system.

I'll homebrew some crystal filters for narrow band FM in future installments — I ordered some 20 MHz xtals.

Sometimes a filter in your junkbox will state the IF and perhaps the 3 or 6 dB bandwidth, but not the input/output port termination impedance. How do we determine this impedance? I've learned we can figure this out by testing differerent termination resistors with this simple test jig:

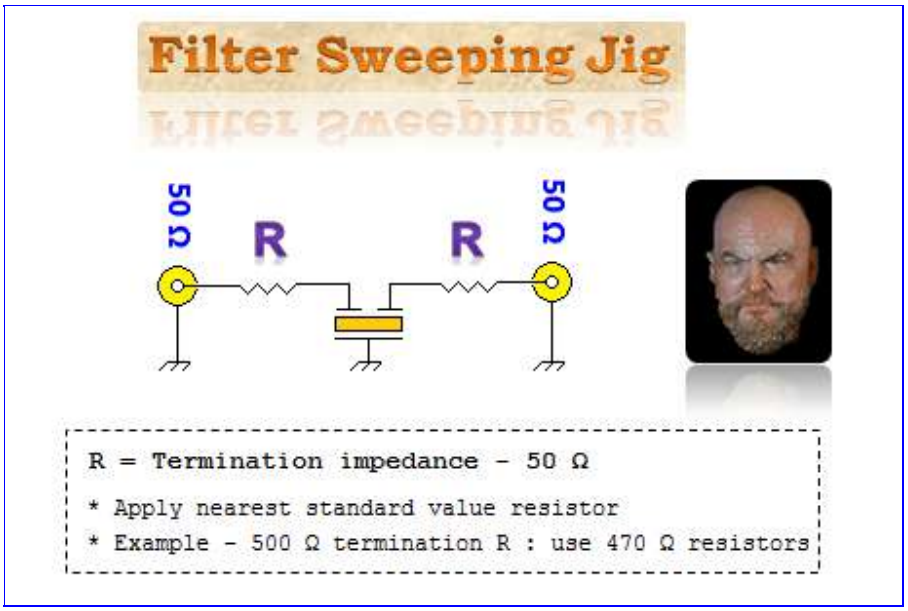

Above — A simple crystal or ceramic IF filter sweeping jig. Since the series resistors attenuate the signal, losses occur; but the shape should look clean with minimal ripple. Normally, we builders will also place (or switch in) 50 Ω attenuator pads on both the signal source and detector within our sweep system to buffer impedance mismatch. Comparisons of this simple jig with more precise and complicated matching methods suggest that for many filter sweeps, it might work fine.

Above — My test jig with a Murata ceramic filter soldered in-situ. Keep the resistors *close* to the board. I've pretty much moved to SMA connectors in my lab: they're cheaper than BNC, plus we can buy a wide variety of quality 50 Ω patch cables donning various connectors for low cost. For example, a 30 cm cable with a male BNC and SMA connector on either end.

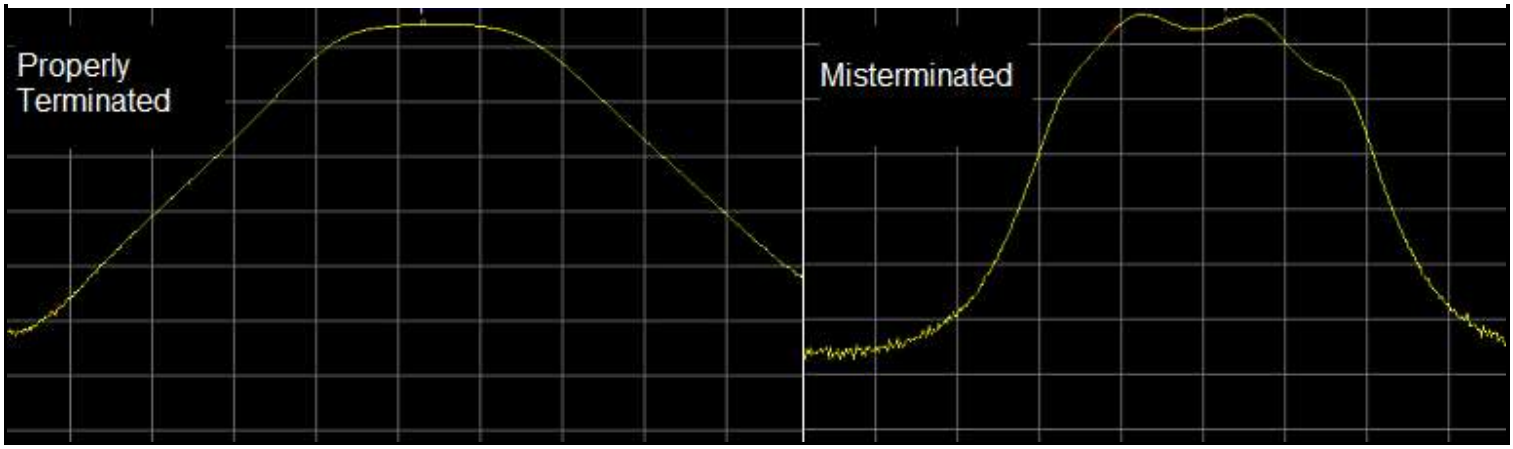

Above — A poor termination may result in improper bandwidth and ripple — easy to spot in this trace. Click for a trace from a 'gone bad' instrumentation crystal filter: 10.7 MHz @ 30 KHz with 2200 Ω Z in/out. Not really usable with ~ 10 dB ripple.

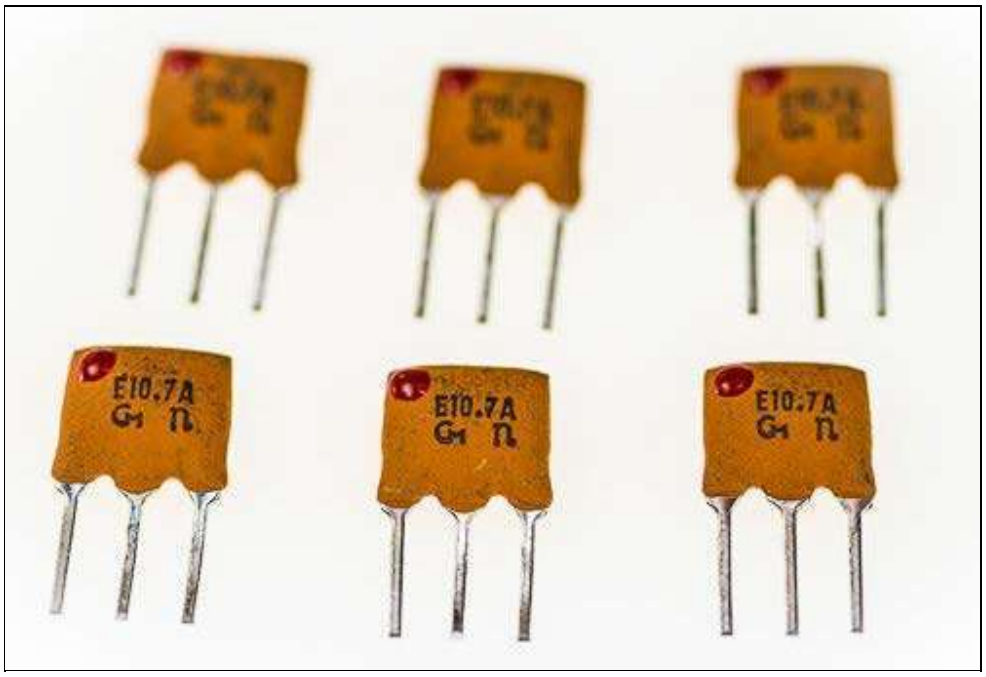

Above — Older 280 KHz Murata 10.7 MHz IF filters purchased long ago. Low cost = their main attraction, although they too will suffer total obsolescence and a price increase.

I bought some newer, lower insertion loss ceramic filters in the following bandwidths: 280 KHz, 230 KHz, 150 KHz, 25 KHz and 20 KHz. Check their datasheet — most Murata ceramic filters require a 330 Ω termination (preferably resistive) and I keep a filter sweeper jig with 270 Ω resistors as a regular bench tool. 280 KHz was a popular WBFM filter bandwidth in many older high-end FM receivers including my 1980's T-85 Yamaha receiver; my benchmark FM receiver.

Many of us hopeful FM builders, smitten by modern digital gear, fail to recognize the fantastic design achievements made by FM receiver engineers back in the day. All those air-variable, ganged band-pass preamp stages, low noise amplifers and often incredibly complicated and great sounding FM multiplex circuits just blow me away. Perhaps I'm a hopeless analog nostalgic? My T-85 sports 5 ceramic filters [280 KHz and 230 KHz B/W Muratas] and the narrow filters are listener switchable for narrow band Dx.

Ways to Match These Filters with Amplifers

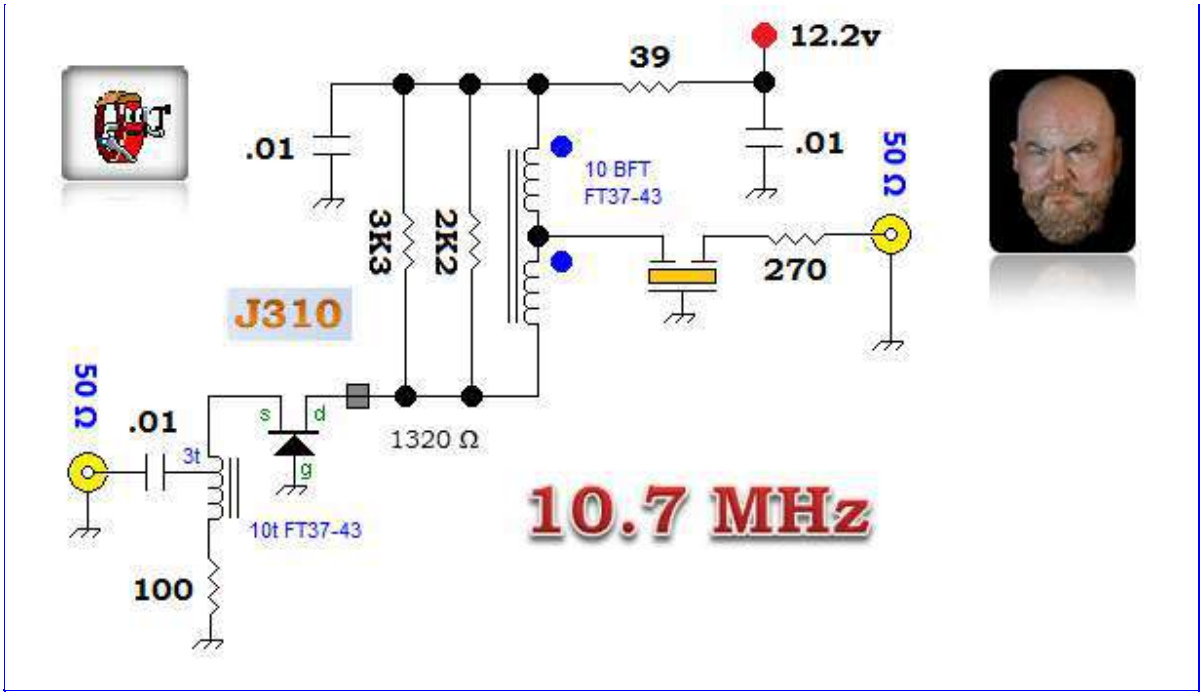

Above — A common gate JFET amplifer drives a 330 Ω ceramic filter. I placed 2 resistors in parallel to get the needed shunt R of 1320; my 2 resistors measured 1316 Ω. The bifilar transmission line transformer provides the 330 Ω Z to drive the filter. Details of the JFET amp come in a later schematic, but the input return loss at 10.7 MHz = 23 dB. I swept this circuit and it looked similar to the tracing with the same ceramic filter in my 270 Ω filter sweeping jig. This particular filter exhibited 6.4 dB of insertion loss.

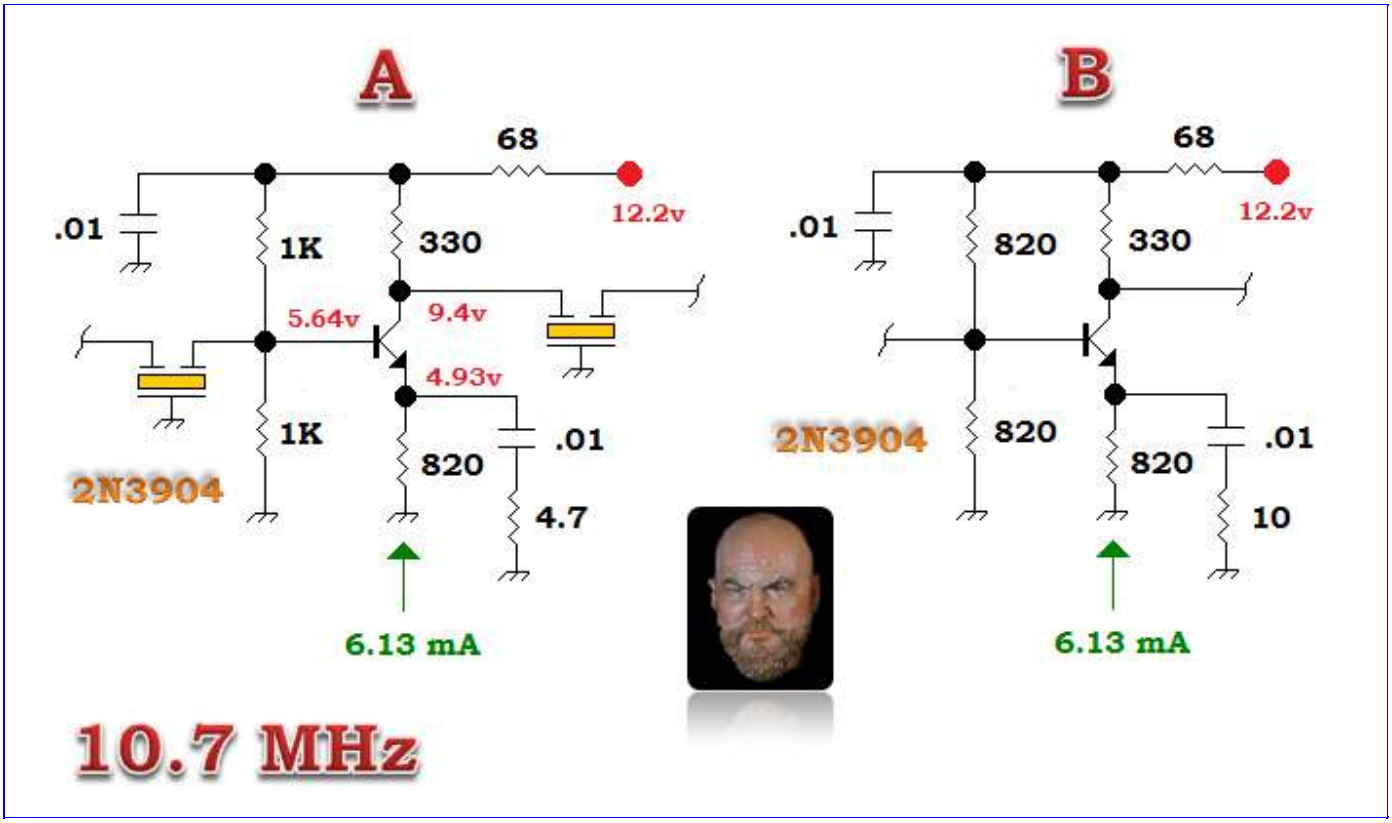

Above — 2 versions of a BJT amp with a 330 Ω input and output impedance. If you read schematics of good FM receivers, often the designers drive the filter with a 330 Ω collector resistor. Click for an example. By keeping the bias and degeneration resistors low and the current moderate, an amplifer with 330 Ω input Z is easy to design [although the input Z will vary with Beta].

I felt surprised that version **A** exhibited a voltage gain of 11.7 despite those low bias and collector resistors. You can stick a filter on either side as shown. Murata recommends a buffer amp between cascaded ceramic filters and you'll see this often in FM receiver schematics from the 1980s or so. Resistors provide wideband termination. Version B is the same amp with a little more degeneration to lower the gain and serves as a design example. I've got the procedure documented here under '*Calculating the input resistance of a common emitter stage'.*

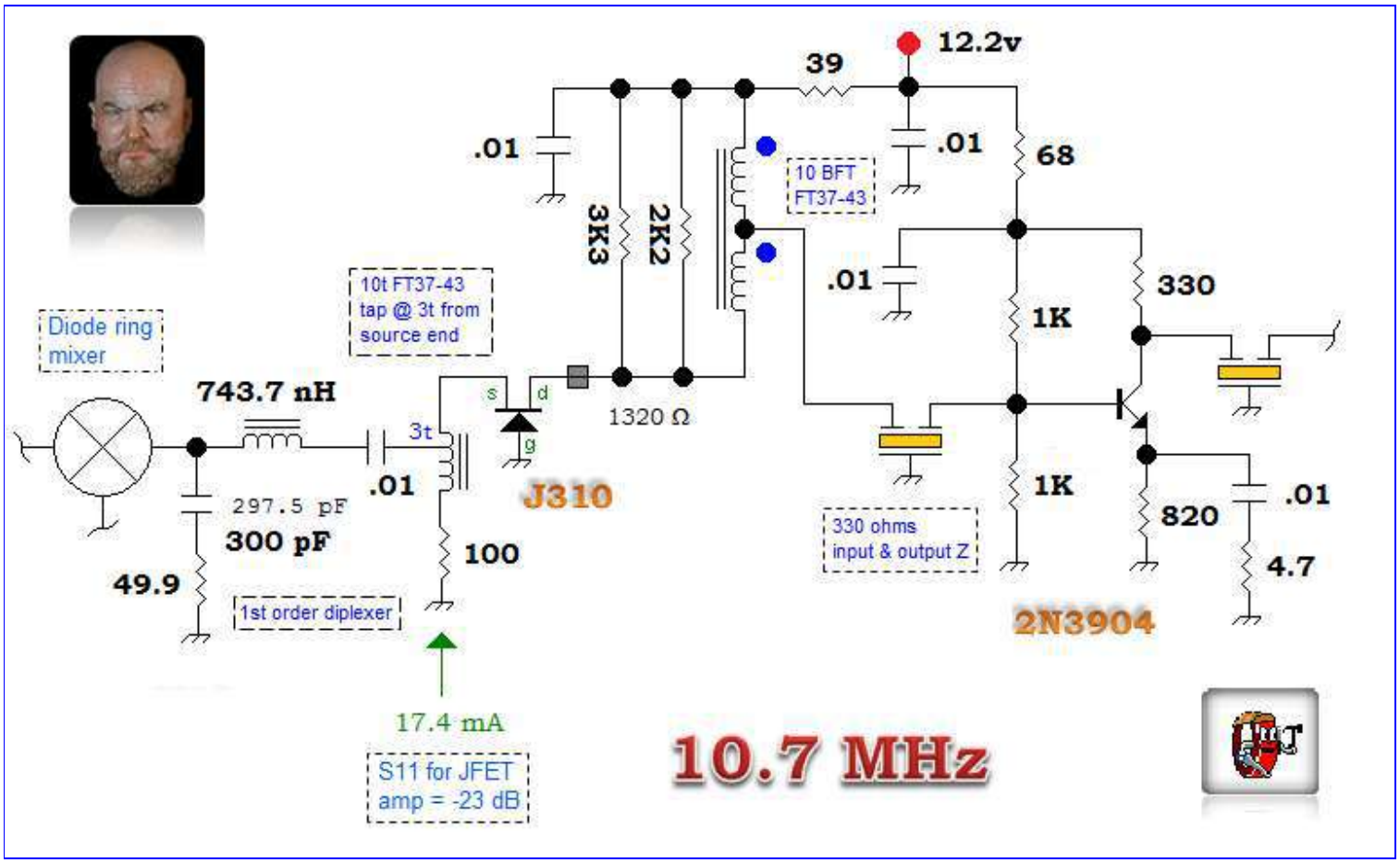

Above — An IF block using the designs shown earlier. I terminated this stage with a 270 Ω resistor and of course removed the mixer and diplexer. 2 sweeps lie below. I'm tempted to tune the JFET drain and couple the transformer with a few links as needed to get a 4:1 impedance ratio. Anyhow — food for thought.

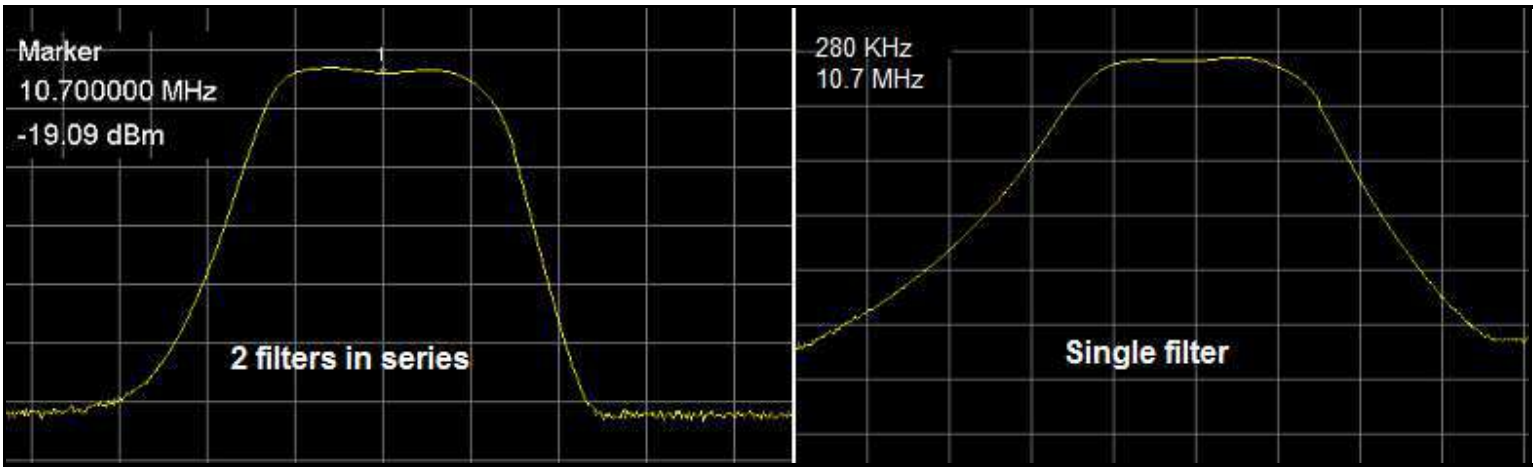

Above — A sweep of the IF block shown above left sans the mixer + diplexer (*two* 280 KHz ceramic filters). On the right lies the trace of the common gate amp driving a *single* 280 KHz filter with its output terminated with a 270 resistor. The advantages of 2 cascaded filters seems apparent, although the slight downward dimple at the center frequency might represent some capacitive loading at the output of the common gate amplifier.

I built a number of other amplifers and swept all of them Click or click for 2 early examples that use active devices instead of series matching resistors on the output. In these circuits, R Term was changed and then the circuit was sweeped. The tracings looked good.

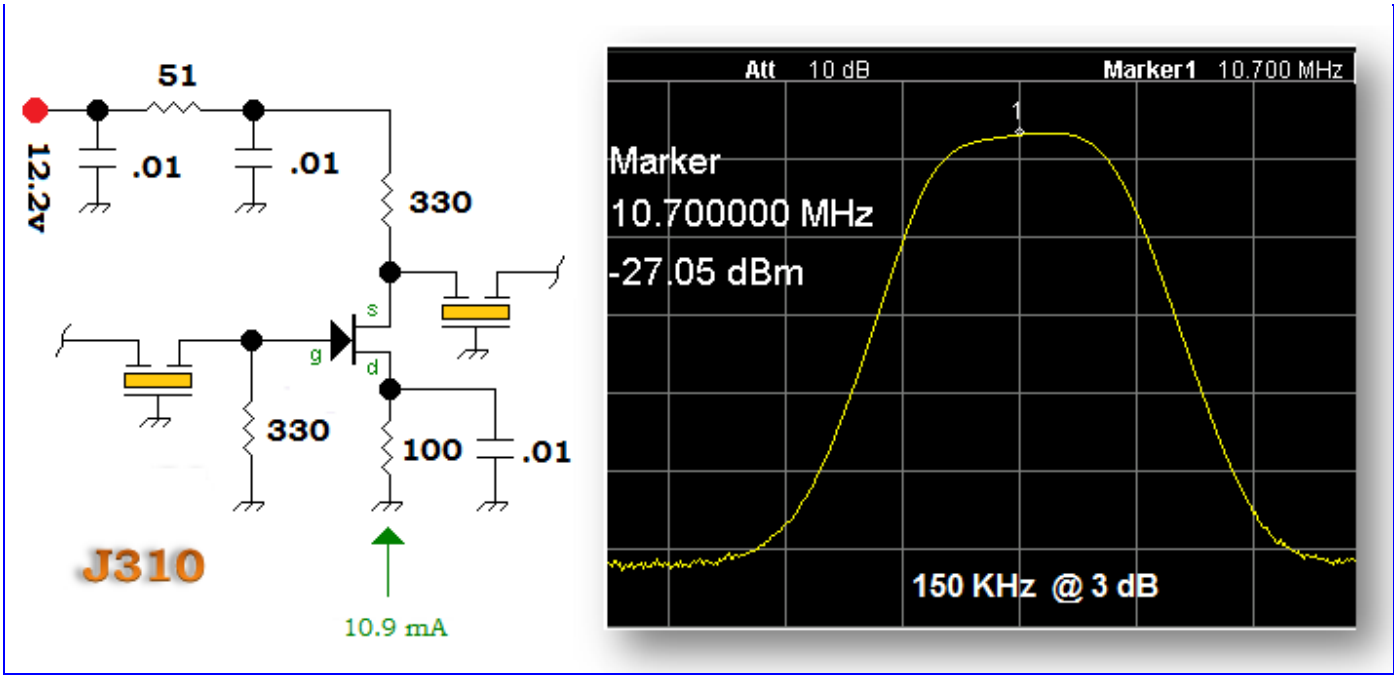

Above — I built Brian, K6STI's nJFET IF amp. He used it to offset the losses associated with 2 ceramic filters. Click for Brian's fabulous website. I placed 150 KHz 3dB BW filters before and after a J310 and swept — my circuit exhibited a 2 dB net loss which seems quite reasonable.

The 330 input resistor is a load/termination on the input filter and will dissipate some energy and lower the AC input voltage to the gate compared to the usual high Z input resistors we apply in our JFET common source amps — from open circuit to full termination would incur a 6 dB voltage drop. Still, for simplicity versus performance, Brian's circuit looks hard to beat.

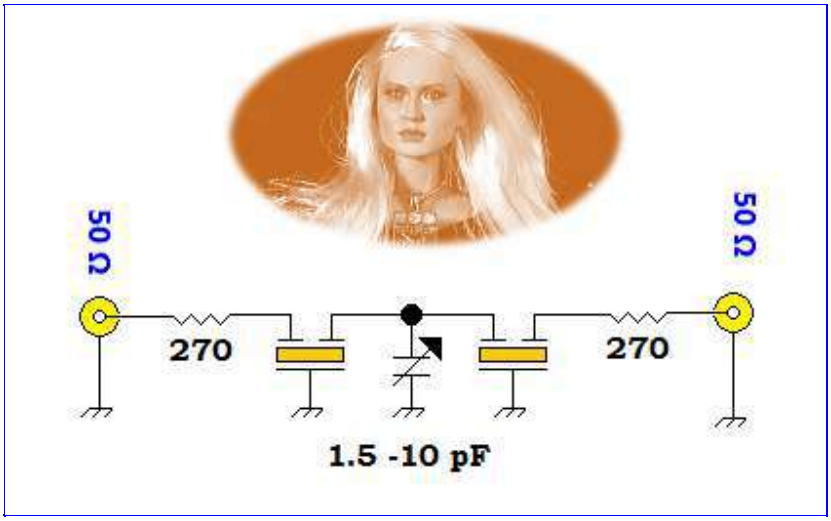

Above — 2 ceramic filters in series. I added a small trimmer between the pair in hopes to mitigate any filter skirt distress or ripple. Click for a tracing with and without the trimmer capacitor. You might experiment with the filter coupling and the filter block termination impedances to better their skirts and passband The losses of the above filter block may reach 12-14 dB.

If you don't have a sweep system, I was able to crudely test the amplifers + filters with my 10.7 MHz signal generator and a DSO.

Resistance Bridge

If you go with a BJT IF amplifer, it's possible to measure the input impedance with a bridge and tweak the emitter current and/or degeneration resistor to get very close to a 330 Ω Zin. I keep a drawer with through-hole resistors rated between 1 and 10 Ω for tweaking my emitter resistor values to change series feedback in my common emitter amps.

I first designed a simple 330 Ω bridge for measurement with my DVM. It worked, but the null lacked the depth and resolution we need. Later I improved the sensitivity by adding another coil and changing to a 'scope or SA detector, but after building EMRFD Figure 7.36, I abandoned my bridge. Figure 7.36 just blew me away. The null of a 330 resistor was only a few 10s of microvolts during calibration.

I placed a small 500 Ω pot in parallel with a 120 Ω resistor for the variable resistance. After some basic testing, I calibrated it with a 330 Ω

resistor; adjusting the pot for the deepest null and just left it there for testing my 330 Ω IF amps @ 10.7 MHz.

I plan to make Figure 7.36 for VHF and maybe UHF with chip caps plus a small screwdriver adjustable trimmer pot [to get the lowest possible L] calibrate it and make it a part of my test bench arsenal. After getting a null, we measure the pot's resistance with an ohm meter to learn the impedance at the ? port

Considering that our predecessors measured just about everything RF with a bridge, this little circuit suddenly become relevant. A series L and C "add-on" circuit shown as Figure 7.39 may be placed in series with the ? port and device under test to deepen the null in the face of reactance. Bridge circuits form the very essence of RF measurement. Yes Bobby, we can measure impedance without a VNA.

---

2. A Basic Colpitts VCO

Above — My completed Colpitts VCO. *I installed the unlabelled, left-sided pot in case a potentiometer is required for future AFC circuitry changes. It's not hooked up.*

I reviewed some 1970's FM receiver schematics to learn that before PLL-locked VCOs dominated, often Colpitts VCOs were locked onto a strong frequency with Automatic Frequency Control (AFC). Local oscillators tanks often employed a inductor plus an air variable capacitor that tuned from ~77 to 119 MHz with a varactor for AFC. All the tuning and front-end filter air variable capacitors were ganged together and I'm sure alignment took some skill.

Some VCOs tuned with varactor(s) instead of an air variable cap — this is what I wish to do. Varactor tuned VCOs usually suffer more thermal drift than air variable capacitor versions.

AFC compensates for VCO thermal drift by a seperate varactor with its control voltage line DC coupled to the FM detector through an R-C low-pass filter. Any difference between the VCO frequency and the desired FM frequency produces a proportional DC voltage. The DC control voltage changes the oscillator to the desired frequency by re-tuning the AFC varactor within this feedback loop, albeit over a limited range. AFC is unsuitable for weak signal DXing, since it may pull the receiver onto a strong adjacent signal. Many 1970's FM receivers supplied an AFC defeat switch.

I remember 1 old FM receiver in my parent's home that stayed locked on 1 frequency for years thanks to AFC.

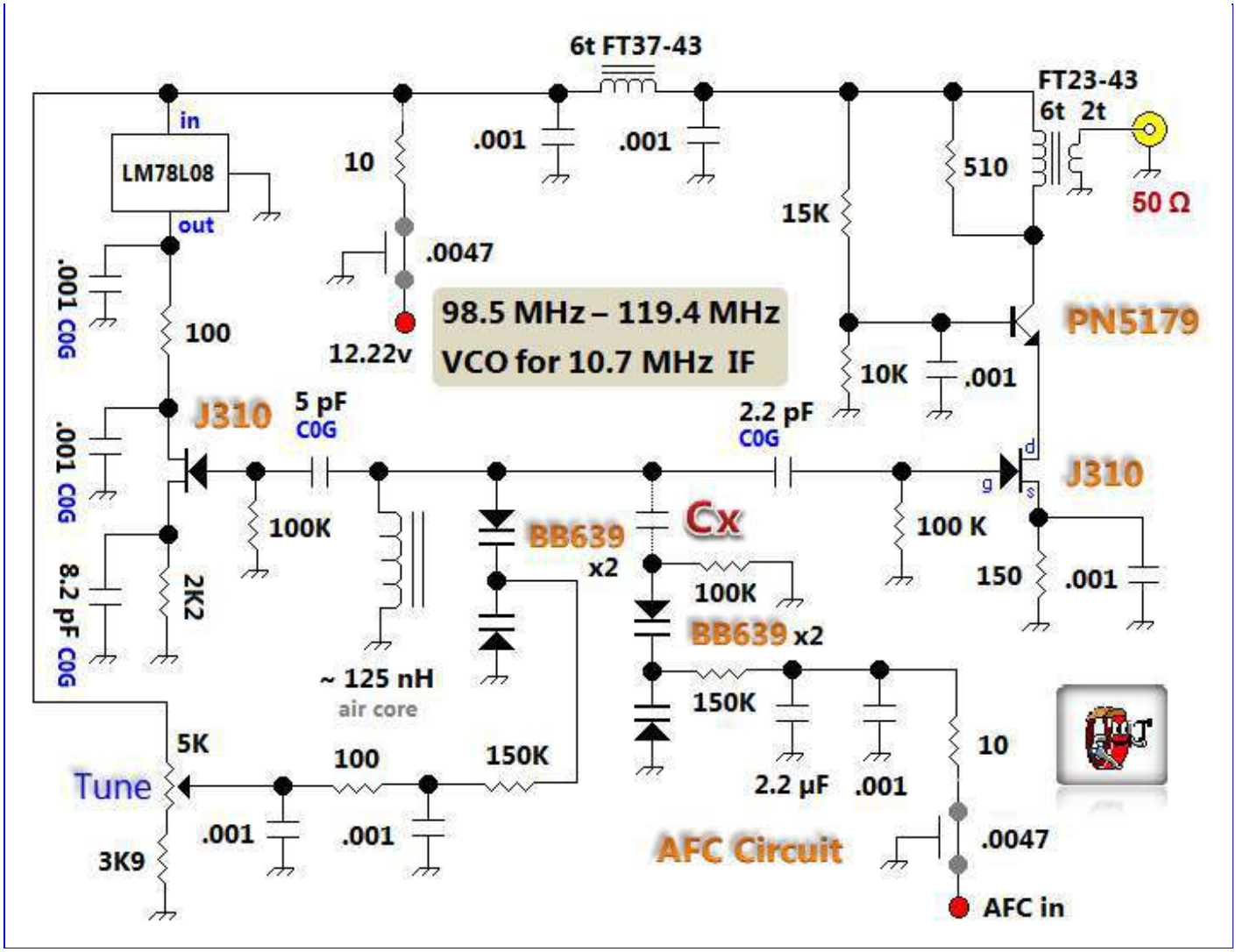

Above — The schematic of my version of a JFET Colpitts VCO (with AFC) that lacks the standard gate to source feedback capacitor; the intrinsic capacitance from the J310 gate to source provides the feedback needed for oscillation.The 8.2 pF bypass cap was determined on the bench — too little, or too much C decreases output voltage, or snuffs out the oscillator.

I just couldn't bring myself to make a VCO with a BJT, since on my bench at least, they suffer more thermal drift than JFET-based oscillators. I built with a mixture of SMT and hole-through capacitors and resistors. The anti-parallel arranged hyperabrupt varactors were found on eBay. Click for a rear photo of the project chassis. The gold colored jack is an SMA connector.

I bench designed this VCO and it took many hours to find the correct amount of L and C for the resonator to give a low distortion, sine wave output across the ~21 MHz tuning range. This meant soldering in and removing these tank components frequently. Click for the lowest frequency output. Click for the highest.

In the example local oscillators I reviewed, the engineers made no attempt to level off the signal that normally increases in AC voltage as you increase frequency. I also ignored levelling. Presumably the designers didn't worry with leveling the oscillator output in their superhet receiver as long as the output voltage sufficiently drove the mixer into complete switching. Levelling would add cost and complexity. This isn't a lab grade RF signal generator — that's for sure.

At present, the AFC varactor pair is disconnected since I won't know how strongly to couple it with Cx until I have a working detector. Also I will need to experiment to determine the best R-C time constant for the low-pass filter; likely the 2.2 uF capacitor will need an increase in value.

With the 3K9 Ω resistor under the 5K tuning pot, I keep at least 5 VDC on the tuning varactors or the VCO would stop running as I tuned the pot towards CCW. The coil = about 3 turns of 16 gauge wire on a 5/8 inch bolt. (Despite Canada going metric in ~1975, they still sell nuts and bolts in inches at our hardware stores). The stiff wire prevents the inductor from turning into a "microphonic" spring when the VCO is bumped. Click for a photo. The nominal L = ~ 125 nH, although I bent and manipulated the coil so it sat attached to the copper clad board with no tension and then squished or expanded the turns to establish my lower band edge.

In many FM receivers, either a single or balanced dual-gate MOSFET mixer was driven by a high impedance buffer/amplifer. If I mix with a 2-gate MOSFET, I'll insert a common gate JFET amplifier on the IF strip to boost the LO output impedance and AC voltage.

The feedthrough capacitors are 0.0047 µF - they were on sale so I bought them. To prevent a parasitic high impedance when placed in parallel with my standard 0.001 µF bypass caps, I placed a series 10 Ω resistor.

I enjoyed this crazy design; trying to replicate a relic, but popular local oscillator idea from decades ago. Let's hope I did it justice. Perhaps future VHF stuff on the FM and even 2 meter band will involve an Si570 and PIC, Arduino or other microcontroller? This simple VCO will do for now. My greatest passion lies in designing and building the front end.

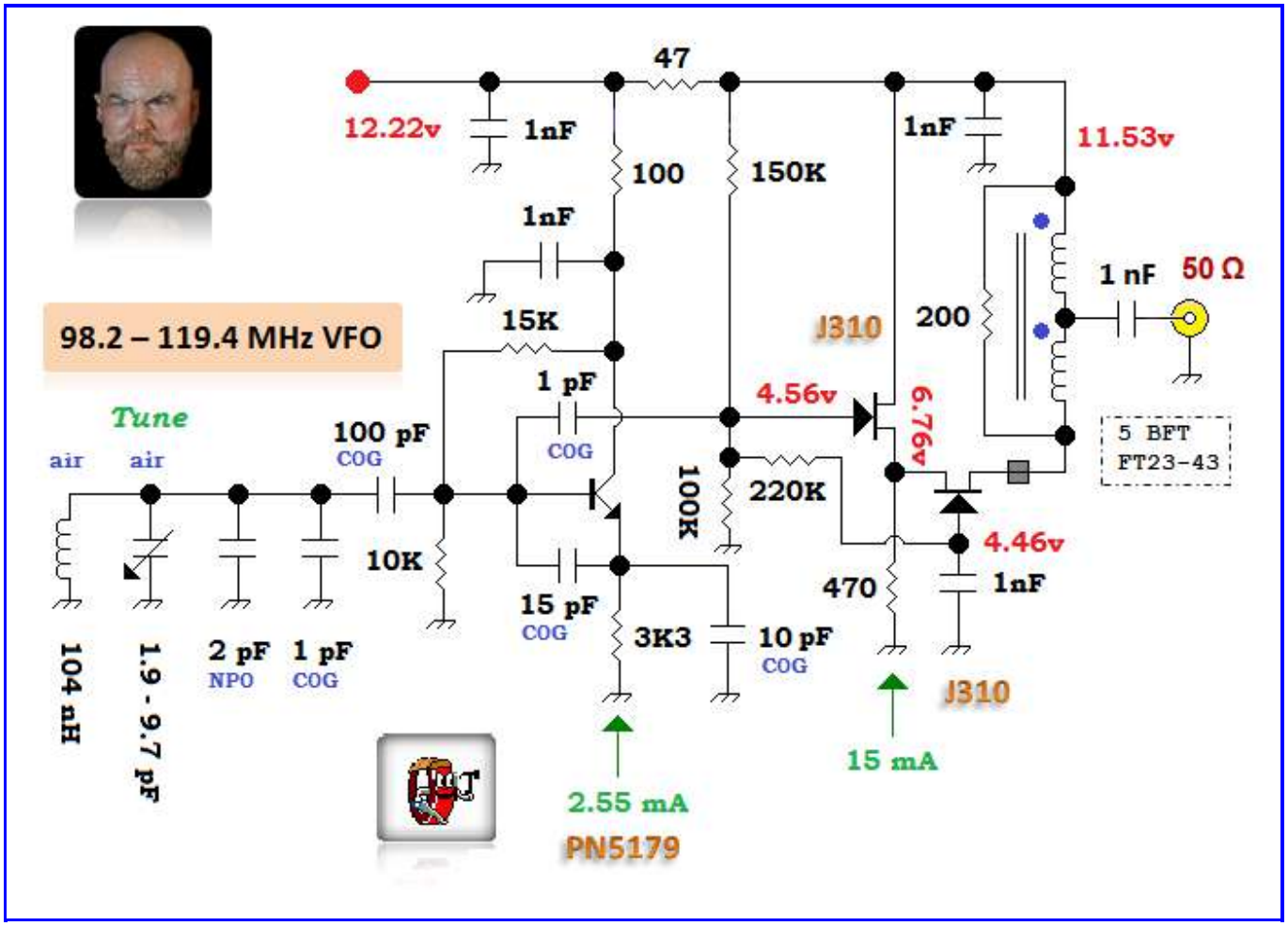

Above — A well-buffered, bench-module, high-side VFO I sometimes use for broadcast FM band mixing into a 10.7 MHz IF. The output at 98.5 MHz = -5.35 dBm, perfect for switching Gilbert cell mixers with a little padding or amplitude tweaking. Click for the output of the Colpitts only with a 10X probe @ 120 MHz. With care, you can see the second harmonic in the 'scope tracing — click for the SA tracing that shows the 2nd harmonic 27.5 dB down from the carrier. Click for a 'scope tracing with my MMIC bench module amplifier from VHF Veronica connected; the amp exerts some low-pass filtering that cleans up the signal somewhat.

---

3. DC-DC Converter for VCOs

Until now, I ran a maximum reverse DC voltage of ~12 volts in my varactors. For wider VCO or L-C filter tuning, builders may chose 28 volt varactors such as the BB535 or BB149A and boost the 12v supply up to 28v with a DC-DC converter. Some build inductorless converters pulsed from 555 timers, or use CMOS voltage converters like the CL7662, or Si7661 to make a doubler. As an RF constructor, I like working with coils and built the following circuit:

Above — Bench module: 28v DC to DC converter. While containing no tuning control pot, my build places the zener diode regulator control potentiometer on the front panel to allow fast-tweaking of the output voltage from ~21-30 VDC depending on the load. Click for the breadboard photo.

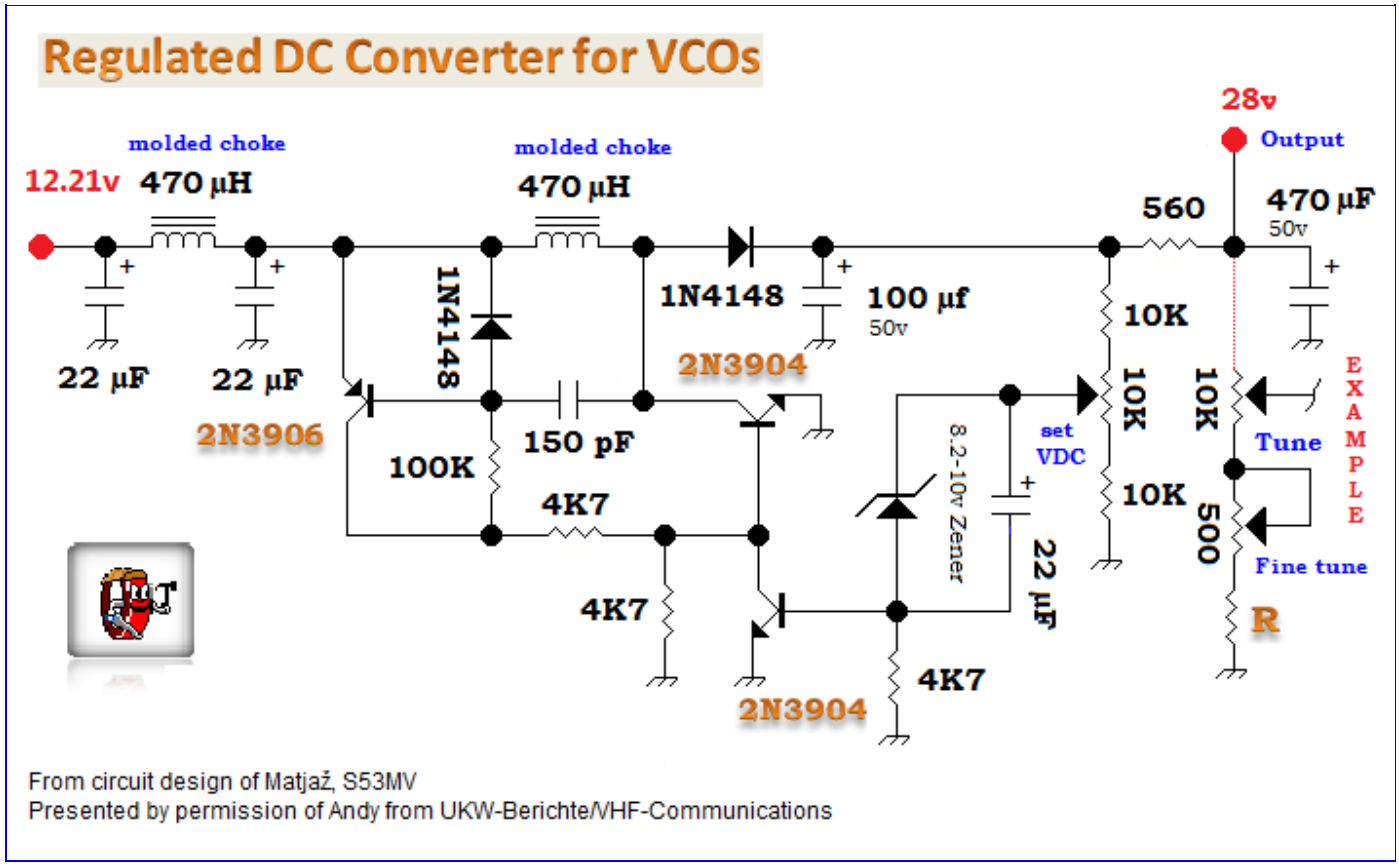

Above — My regulated 28v converter for varactor tuning adapted from a design by Matjaž, S53MV. I pulled this circuit from his *amazing* 2-part article with circuits that span from 11 GHz RF to DC. *See the reference articles below*. I filtered heavily and at switch-on, my circuit draws ~ 50 mA, but then drops to ~ 11 mA after the capacitors charge. The 10K *[set VDC]* trimmer pot allows you to dial in your desired output voltage and thus this converter may work over a wide range of DC power supply voltages.

The tuning control(s) might be a single potentiometer, or even seperate pots for tuning 2 different VCOs. In the above schematic, I show 1 possible tuning scheme: a 10K coarse tuning in series with a 500 Ω fine tuning potentiometer. R keeps some minimal reverse DC on the varactor(s) and is optional. Again, my bench module DC converter omits any tuning controls — these are built into the circuit containing the varactor diode(s).

The oscillator frequency varies slightly with the set output voltage. Click for a screen capture at ~32 VAC with a 10X probe placed on the PNP emitter. In another test, with no load, I watched the coil's magnetic field collapse and ring in this cool 'scope capture. This is why I love deep memory DSOs so much.

Above — Andy, G8ATD who owns VHF Communications magazine granted me permission to show the DC converter circuit. His magazine archives provide a treasure trove of useful circuits from VHF to Microwave and it's clear Andy passionately spent lots of time publishing the magazine until 2013, plus scanning and organizing the archived material.
Although VHF, UHF and microwave focused, much of the concepts and learning can also enrich your HF exploits.

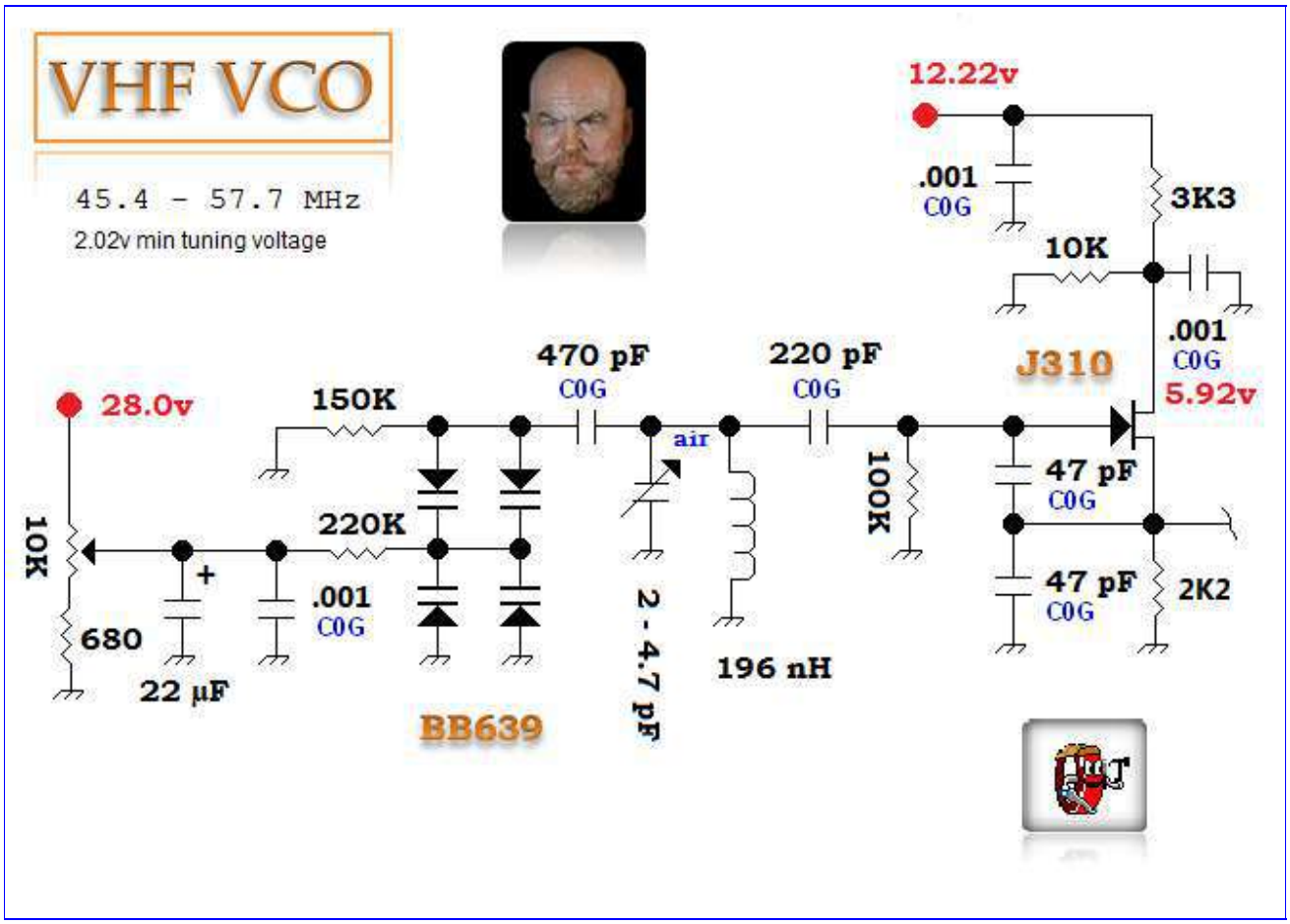

Above — A "quicky" VCO thrown together to test the DC-converter. Click and click for the output with the tuning pot set to fully CCW and then

CW. The 680 R keeps about 2 volts on the varactors with the tuning pot set to CCW.

In the reference articles cited above, you'll find 2 HF-VHF Hartley VFO designs that tune over a 20 MHz span thanks to 28 volt varactors and careful design. In yet another UHF circuit, a 1 octave tuning span is realized with the author's specially designed VCO. Truly hardcore design from a great teacher — I crave exposure to the work of such authors.

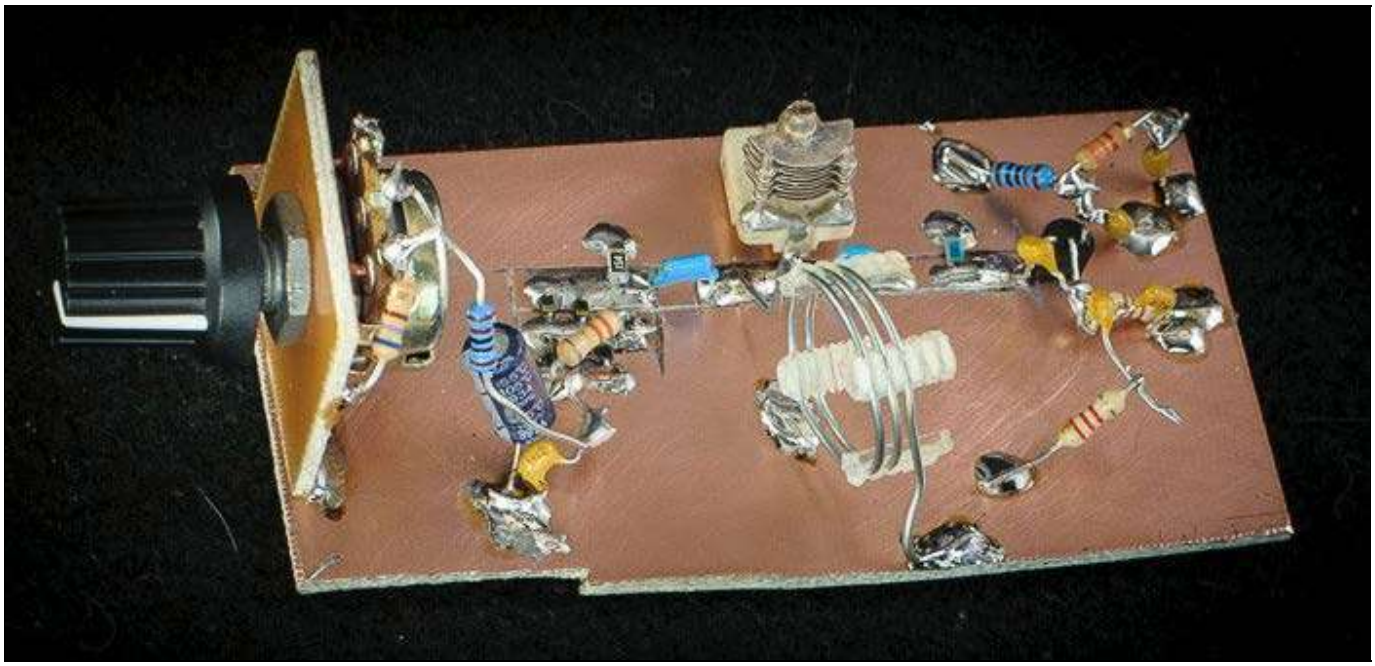

Above — A photo of my "quicky" VHF VCO. 73!

---

4. Supplemental Web Page #1

Click for the first supplemental web page.

---

5. Miscellaneous Photos or Figures

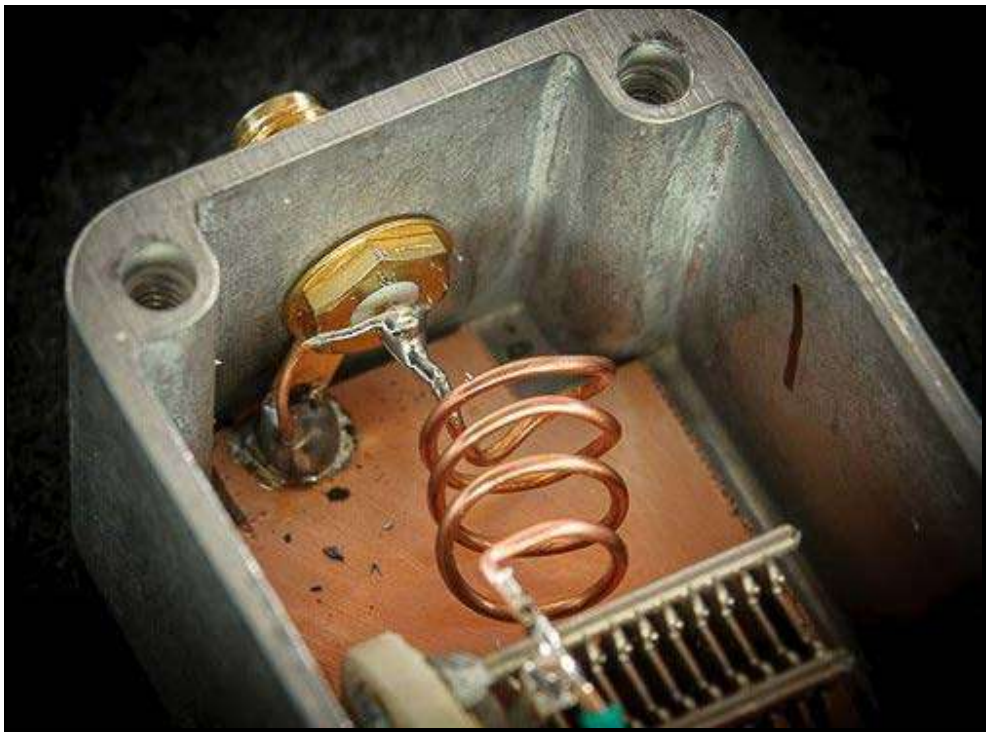

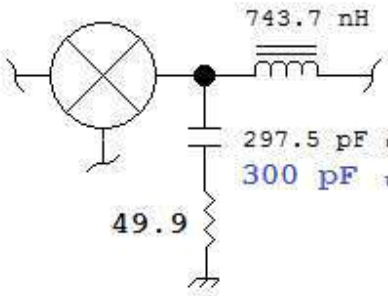

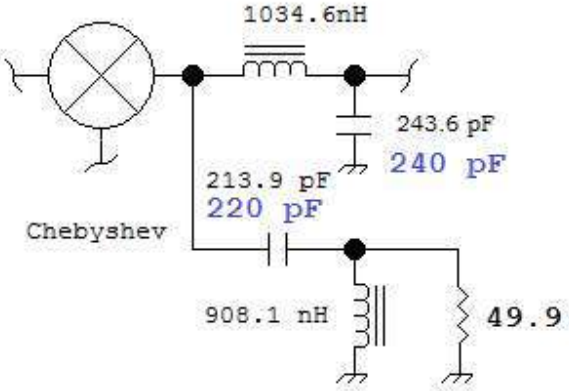

1st order

10.7 MHz IF Diplexer

2nd order

Oct 19, 2013

VE7BPO

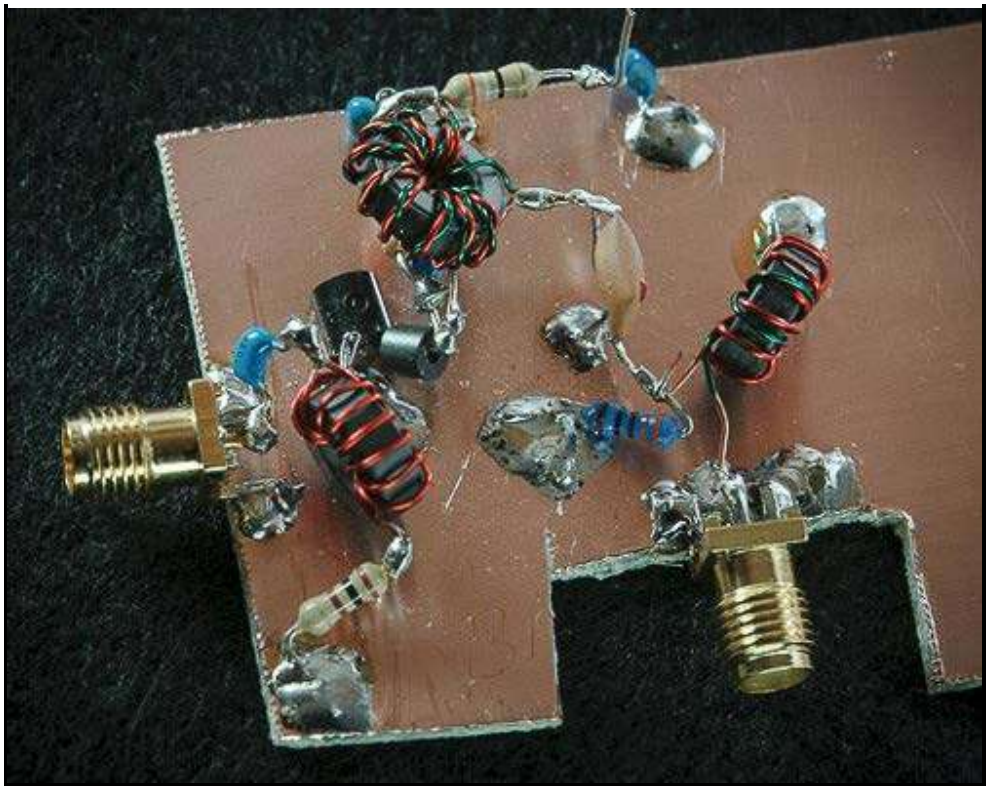

Sundry Experiments 2012 - 2013

This page shows some of my better non-VHF experiments for 2012-2013.

Although VHF and UHF excite me greatly, It's always fun to build at HF, or even AF.

Section 1: I explain why you might see sweeps that look like oscilloscope tracings on QRPHB: they're devices swept with equipment designed by Bob, K3NHI. Bob's work simply amazes me — full-on, creative precocity.

Section 2: An LM1875 AF power amplifer test.

Section 3: Three Questions with Jason, NT7S.

Section 4: EMRFD Experiments — A 1-on-1 Tracking or Offset Phase-locked Loop.

Section 5: Boot-strapped Popcorn AF Feedback Pair.

Section 6: Non-Mechanical Iambic Paddle.

Section 7: A Journey Above HF.

Section 8: Popcorn AF Amplifier — Reprise

Section 9: The Progressive Receiver by John, K5IRK and Wes, W7ZOI

Section 10: Miscellaneous Pictures and Figures

1. Analog Sweep System

Today, advanced experimenters might build a network analyzer/sweeper incorporating a microcontroller, a DDS, or Si570 based frequency synthesizer, plus the needed analog RF circuitry. I went another direction: the Bob Kopski, K3NHI sweep system — all analog, no lines of code and probably 4X the bench work. I show some photos, traces and text in hope it might inspire you to pursue your own sweep system — digital-based or otherwise.

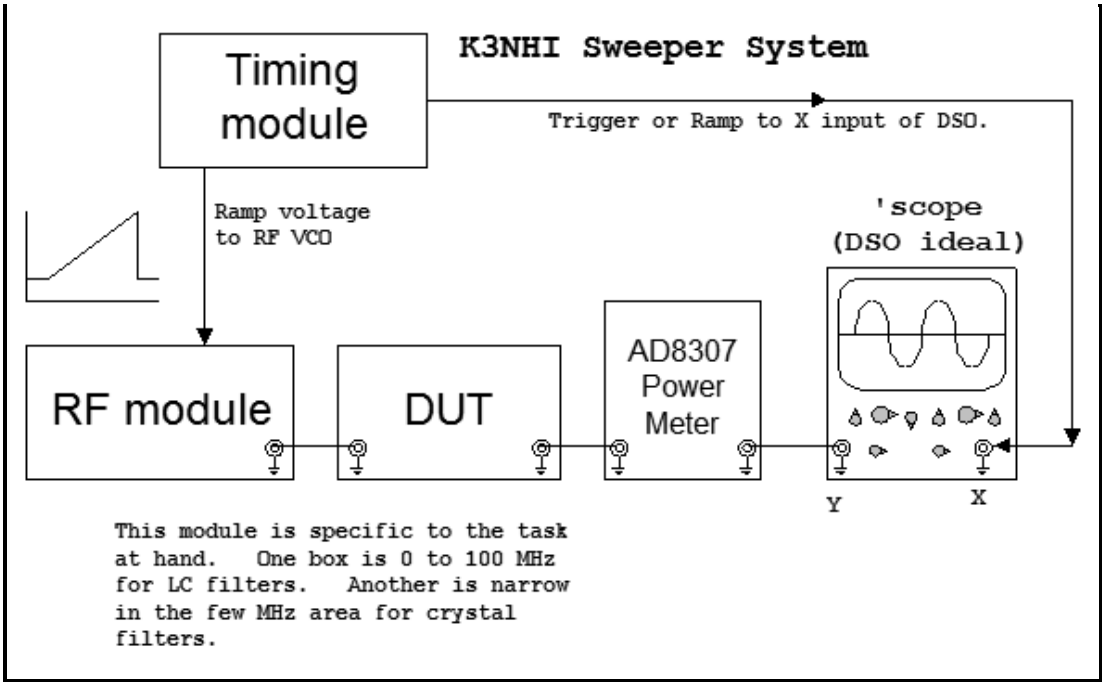

Above — The K3NHI Sweep System macro diagram drawn by Wes. The resultant trace looks like the output of a tracking generator plus spectrum analyzer. What I like most is that I'm measuring with my "tough" 'scope and need not worry about input power and so forth like we do with expensive RF test gear. I simply love measuring signals with my oscilloscope. Testing circuits with Bob's sweep system compels me to treasure component-level analog design and renews my passion afresh.

Above — 3 components of my K3NHI sweep system. Click for a higher resolution photo. To date, I've made the Utility Sweep Generator (time base) *on the bottom*, a 1-118 MHz VCO with clean and level output *top left*, an AD8307 power meter optimized for sweeps *top right* and a crystal filter VCO *shown later*.

Building Bob's Utility Sweep Generator proved difficult. Although technically just a ramp generator, this 1 is calibrated, provides high isolation between the X and Y channels and will sweep *anything*. The power supply has 8 different regulated DC voltages including ~ - 3V. I may use it as the time base for a spectrum analyzer project 1 day.
Bob gave me permission to post the schematics: One Two Three IC1-5 is an LM324 op-amp. Doc 1 Doc 2

Email me for some build notes.

Click, click, or click for photos of the 1- 118 MHz VCO. Click for the schematics. One Two

I show a bare-bones AD8307-based Power Meter (PM) on the **RF Workbench 5** web page, however, to augment the PM for sweeping, I added input compensation, plus some tweaks from Bob's QEX articles: Bob Kopski, K3NHI — An Advanced VHF Wattmeter, QEX, May/June 2002 *and* Bob Kopski, K3NHI — A Simple Enhancement for the Advanced VHF Wattmeter, QEX, Sept/Oct 2003.

I strongly recommend you build Bob's power meter (referenced above) if you're contemplating a power meter build.

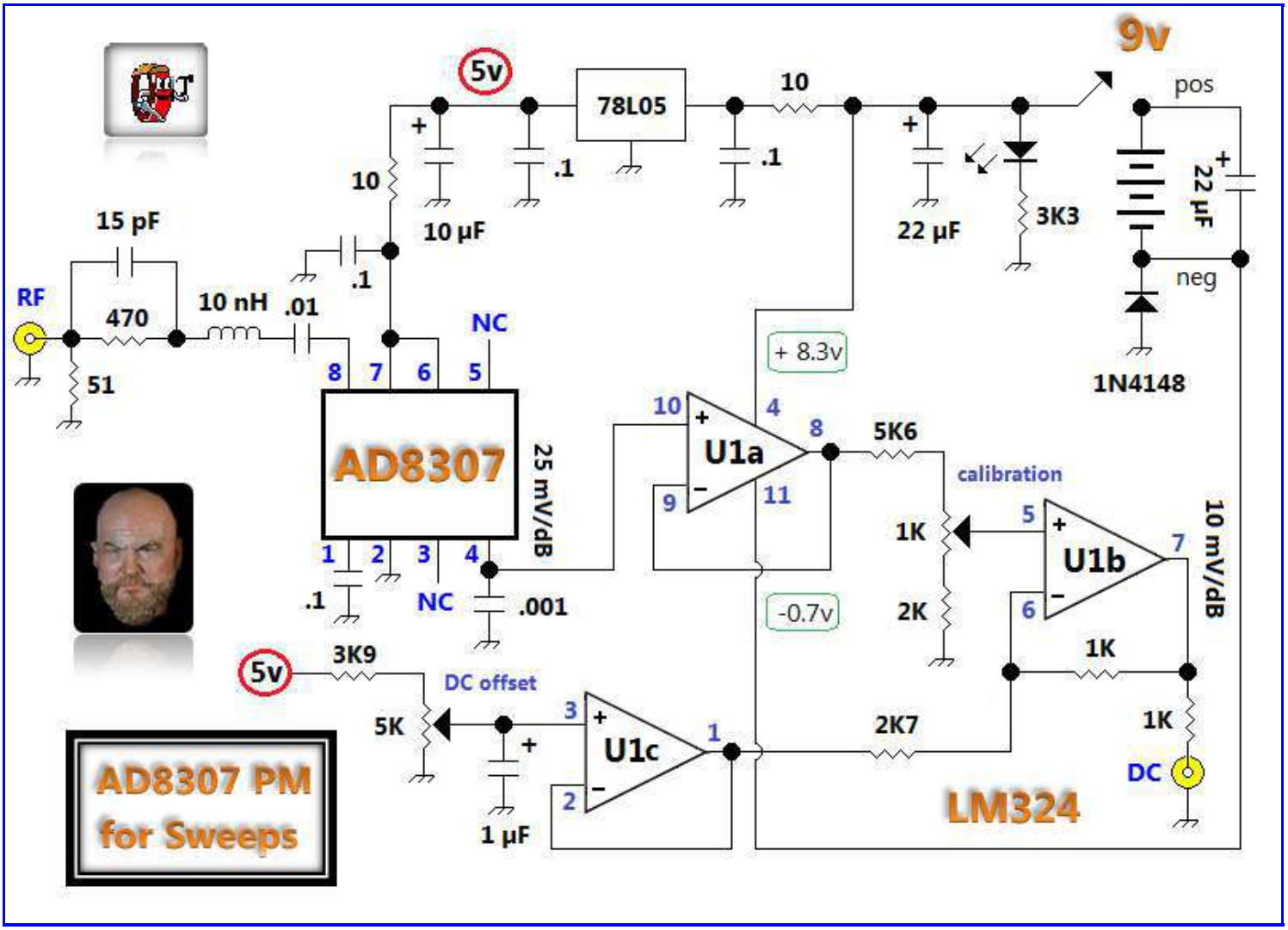

Above — My AD8307-based power meter. Click for a photo of an early version lacking the level shifter. The level shifter, or DC offset control allows precise Y axis control to enable a resolution up to 1mV/dB when set up properly in the DSO. With this resolution, it's possible to see filter ripple.

Above — The K3NHI sweep system in action. This photo shows the power meter with the (later) added DC offset control. Using the offset control potentiometer, I'm able to examine the top of a signal peak at 1 dB per division with various spans.

Above — I swept a 7 MHz band-pass filter bench module.

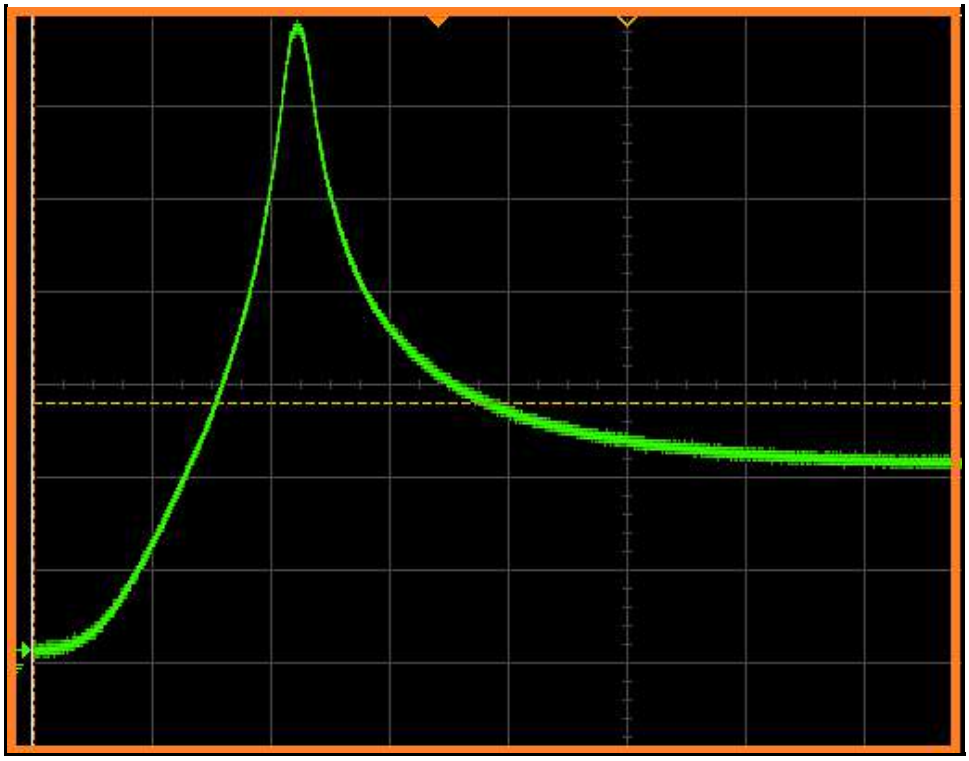

Above — A sweep of the above 7 MHz band-pass filter. At the time I was still learning system calibration and remember feeling blissful that I made such a cool sweep system.

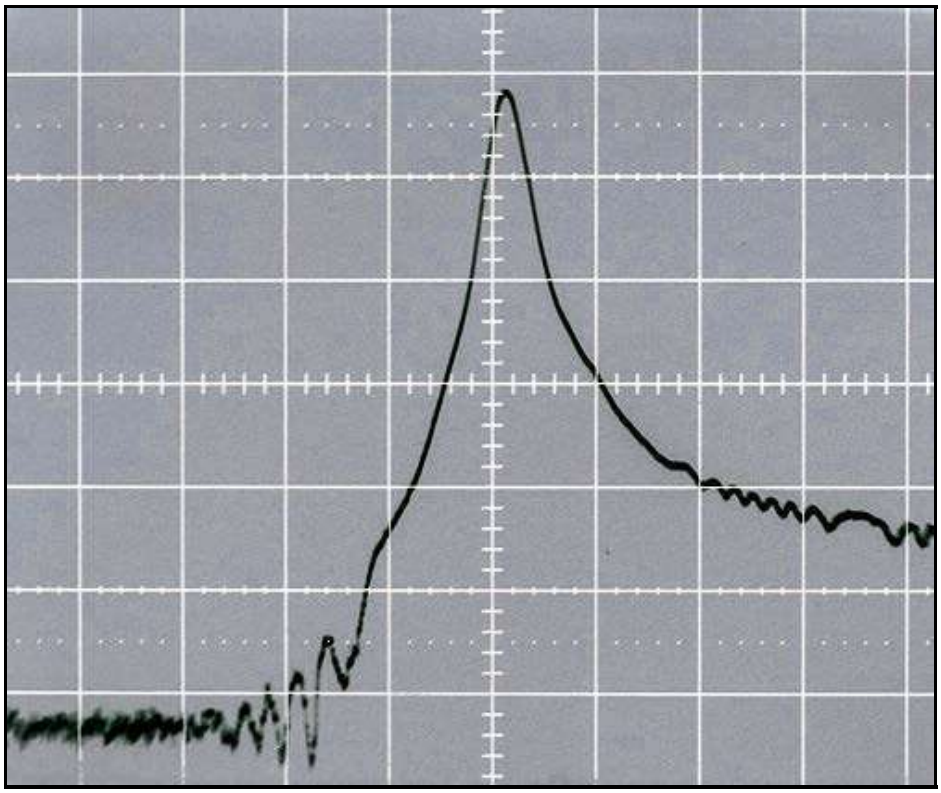

Above — A sweep of the 7 MHz band-pass filter with a tracking generator plus spectrum analyzer for comparison. The span differed from that used with the K3NHI sweep system, however, I'm sure I'll get better with the K3NHI system over time.

Above — My build of the K3NHI *Hartley* VCO for sweeping crystal filters. I ordered a 4 mm tuning knob for the 10-turn "Manual Tune" potentiometer used to help center the sweep in my 'scope. This 10-turn pot, a DIP switch with C's and a secondary L, plus two MV209 varactors allow narrow resolution sweeps (< 5 Hz nominal) within a ~2.5 - 18 MHz range.

I monitor the sweep frequency on a counter via the VCO monitor port and all the tweaks on this VCO and the Utility Sweep Generator allow easy filter centering. Click for a breadboard of the VCO with the first buffer and a temporary BNC connector for testing. Click for the whole project. The secondary wideband buffer provides strong signal fidelity, reverse isolation and output return loss (22.3 dB) — it draws 61 mA. Click for the VCO schematic courtesy of Bob, K3NHI. Click for a side-by-side of a xtal filter as measured with Bob's sweep system plus an N2PK VNA.

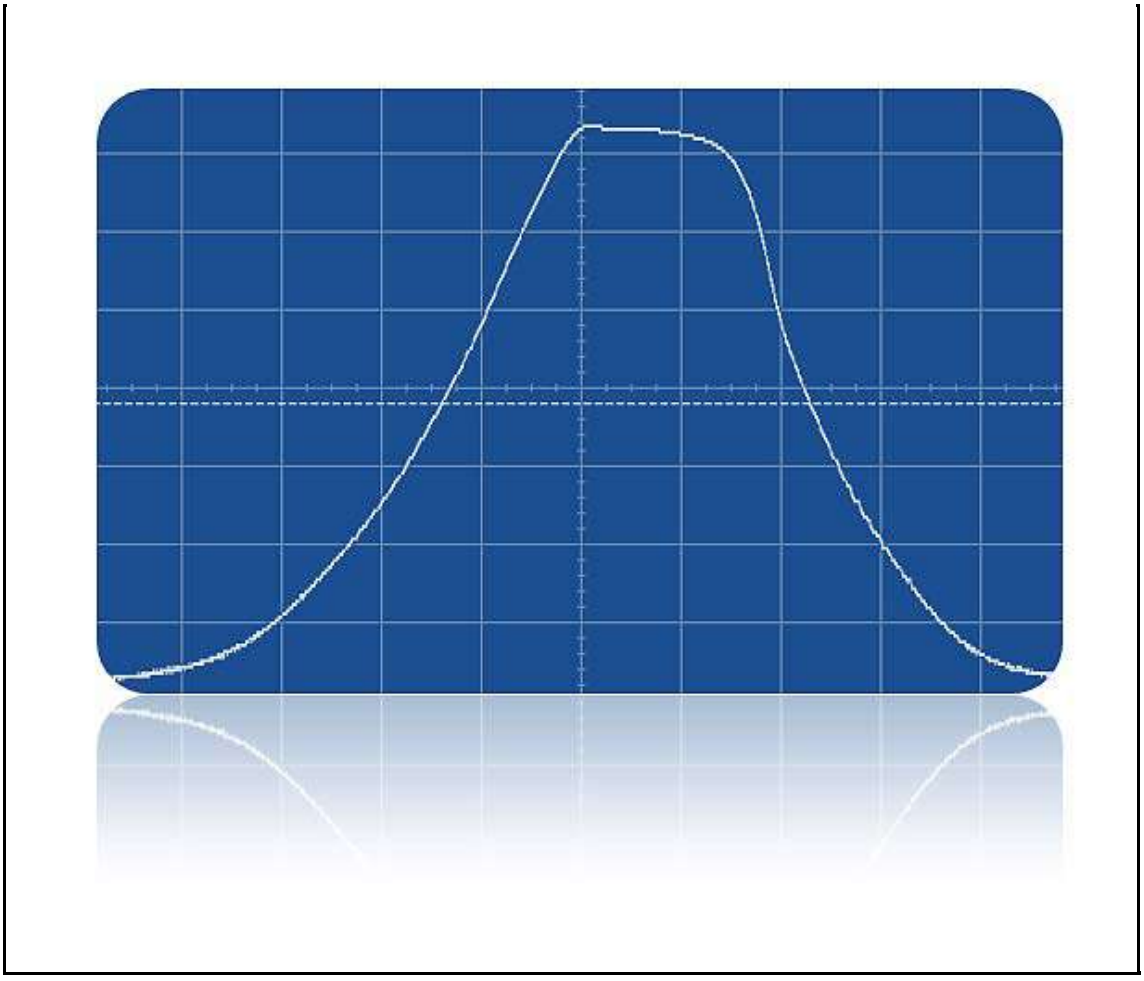

Above — I made and then swept a simple ~500 Hertz wide 4.9152 MHz Cohn or Min-Loss filter using 4 crystals.

So now, if you see sweeps on the site that look like oscilloscope tracings, you'll understand how they were created. I've learned so much from Bob's work and his mentorship last Spring. John, K5IRK coached me also.

QRP-POSDATA for October 2013

3 builders incorporated Bob's sweep system circuitry into projects including a receiver, a spectrum analyzer and the following build of the Utility Sweep Generator (USG) by Jay: Jay built some PC boards to simplify the wiring challenge this USG presents. Click 1 Click 2 Click 3. Great stuff — thanks for sharing.

QRP-POSDATA for March 2014 — Poor Hams Scalar Network Analyzer (PHSNA) —

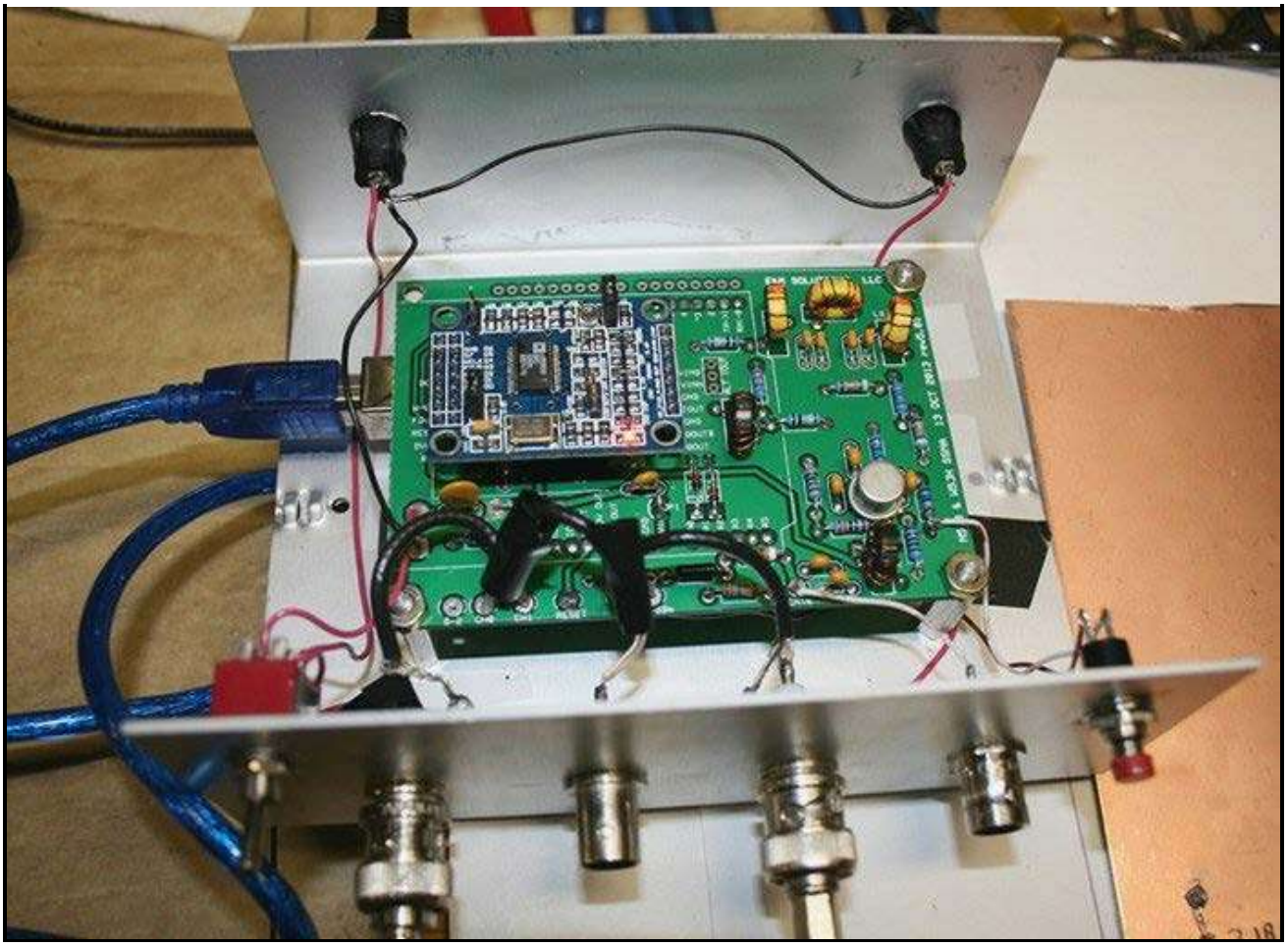

Above — The PHSNA built by Mikey, WB8ICN.

Jerry W5JH, along with Jim, N5IB and Nick, WA5BDU developed this low-cost sweeper/ lab toolkit.

The Poor Hams Scalar Network Analyzer consists of an Arduino UNO R3, plus an AD9850, or AD9851 DDS, a W7ZOI/W7PUA Power Meter and a MS Windows OS based computer. Builders can scan and plot L-C filters, crystal filters, RF amplifiers and such — much like Bob's sweep system — or an HF tracking generator + spectrum analyzer. The PHSNA also measures crystal parameters with little fuss. Connect a return loss bridge to easily sweep return loss measures of the input or output ports of filters, amplifiers, antennas and more. The total cost to build the PHSNA is approximately $50-60 USD.

Mikey graciously sent me some photographs of his PHSNA build. Complete system in his lab with the chassis lids removed for these photos. Monitor photo showing menu choices. Power meter. Mikey's jig to examine crystals with a 12.5 Ω termination. Once you own a calibrated sweep system, you'll wonder how you ever managed without 1.

Thanks again to Mikey for the photos. I built and tested the return loss bridge using the PCB from the PHSNA Yahoo group. Click for a 613 KB pdf file of my build. Nick, WA5BDU web site.

Hats off to Jerry and crew for this open-system project! A Yahoo group called PHSNA serves as the communications hub and houses superb, detailed documentation. You need to join Yahoo to access this group. Then search for PHNSA and while your at it, also sign onto the EMRFD group.

---

2. LM1875 Audio Power Amplifier

I tested the LM1875 AF power amplifer because its specifications look great: 20 watts into a 4Ω or 8Ω load on ±25V supplies and a TO-220 package for easy heat sinking. Of course, for this web site, I tested it with a typical radio experimenter bench power supply; a single-supply at ~ 12 VDC.

This is probably not a great part for Ugly Construction and I *attempted* to return the load ground, the output Zobel RC filter network, feedback loop and input grounds to a central grounding point through separate paths cut paths into my copper board. A better breadboard method might include the so called "star grounding".

I saw RF oscillations on the 'scope and removed them by soldering a 0.001µF bypass capacitor across the input. A 470 pF bypass capacitor did not work well enough. The datasheet describes specific causes and cures for RF oscillations and I've learned they must be heeded. I once found

similar problems with an LM380.

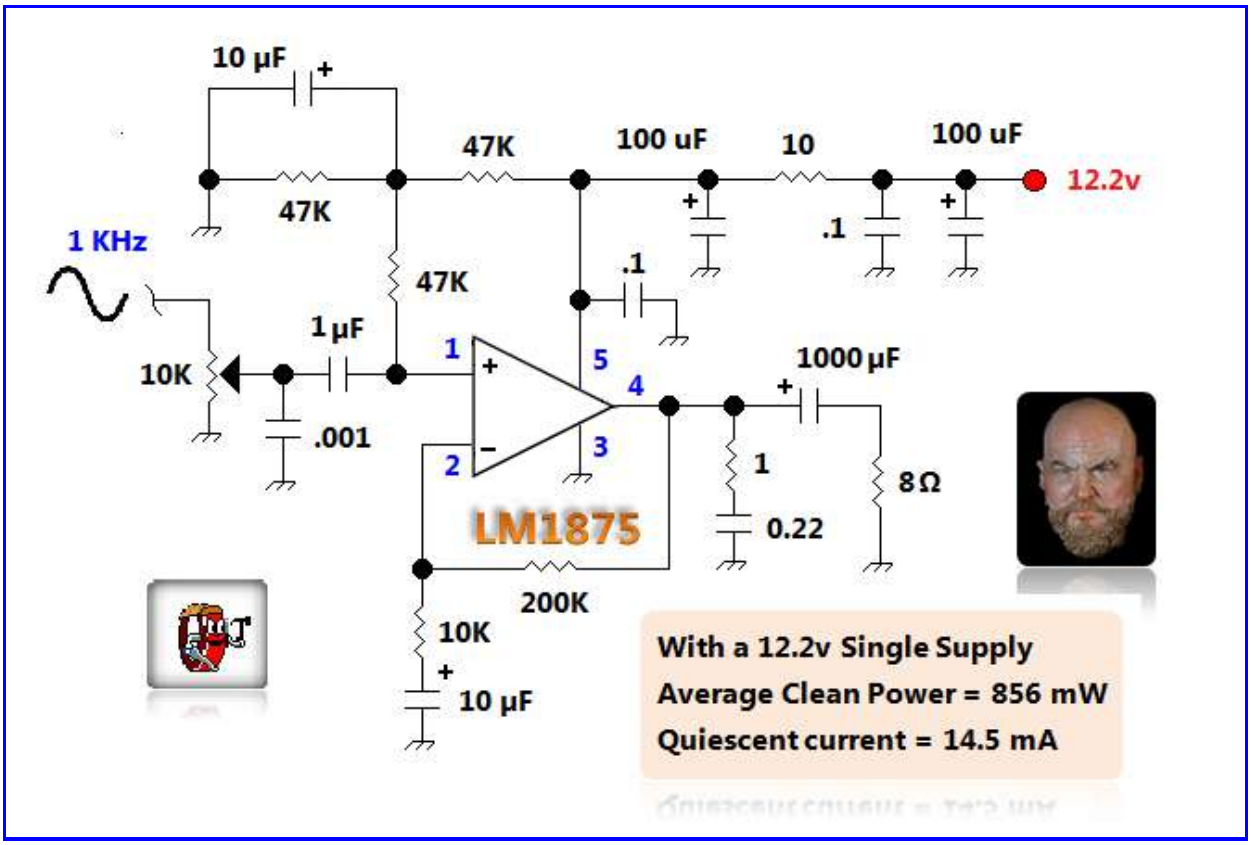

Above — The LM1875 in the ~suggested datasheet, single-supply set up. This amplifer reminds me of setting up an op-amp. Unlike the LM380, within limits, you may choose the gain to suit your needs. As shown the gain = 25.6 dB. Dropping the feedback R to 100K dropped the gain down to 20.5 dB. For clean output power capacity; it blows away the LM380.

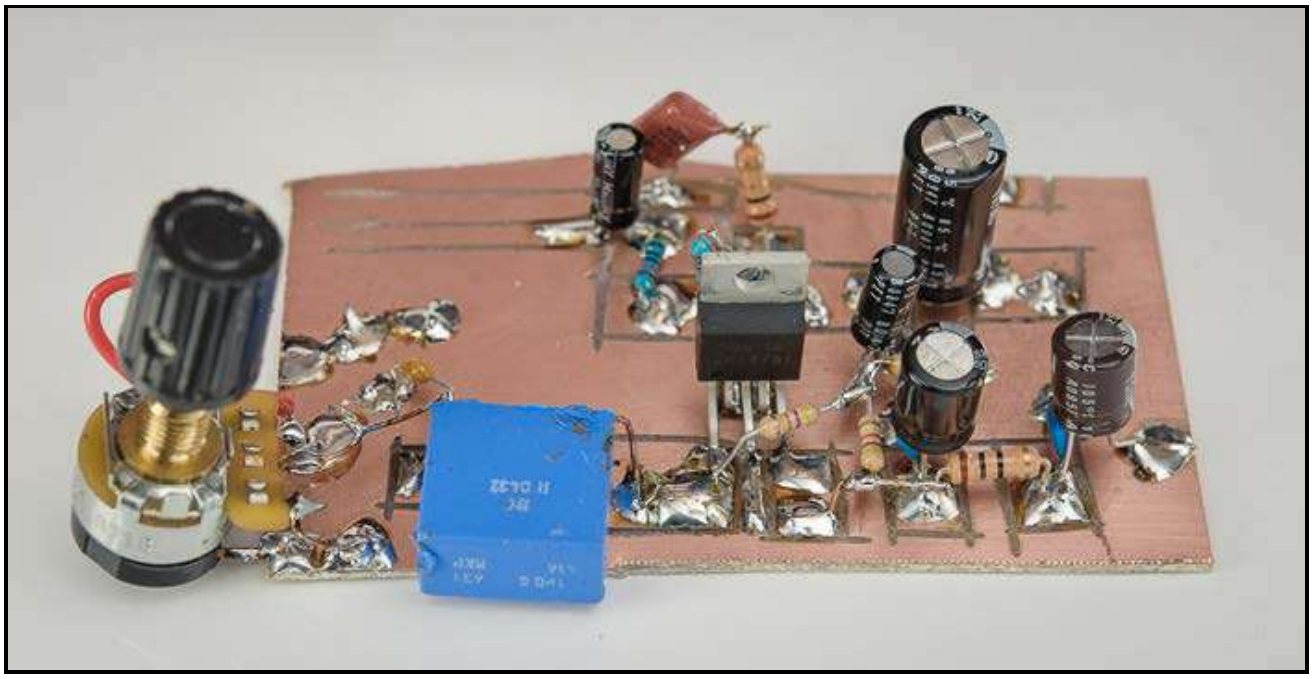

Above — My first LM1875 test breadboard. After the photo, I moved the 0.1 µF RF bypass cap right onto lead 5 — we should carefully RF bypass device power supply leads, but I got sloppy.

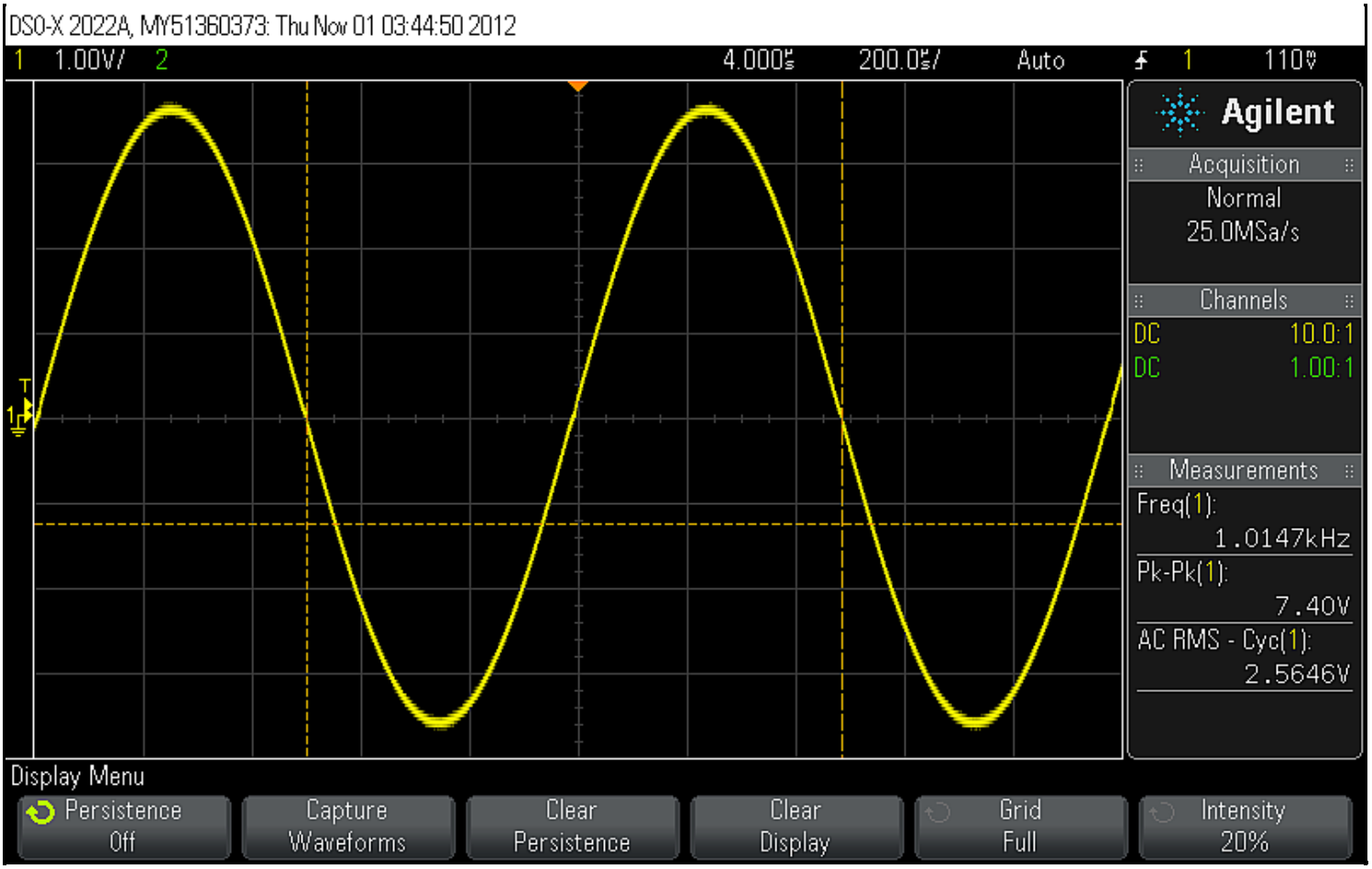

Above — At the maximum power before visible sine wave distortion appears; 856 mW. I listened to this amp while connected to a line-level tape player and an 8 Ω speaker load: very nice. I want to try it with a split +/-15 VDC supply and a star grounded breadboard since a 12v single-supply limits the output power so much. Still, at 12 volts single-supply, this IC yielded the highest clean, average output power of any AF Power chip I've tested: a worthy consideration for a high-grade receiver.

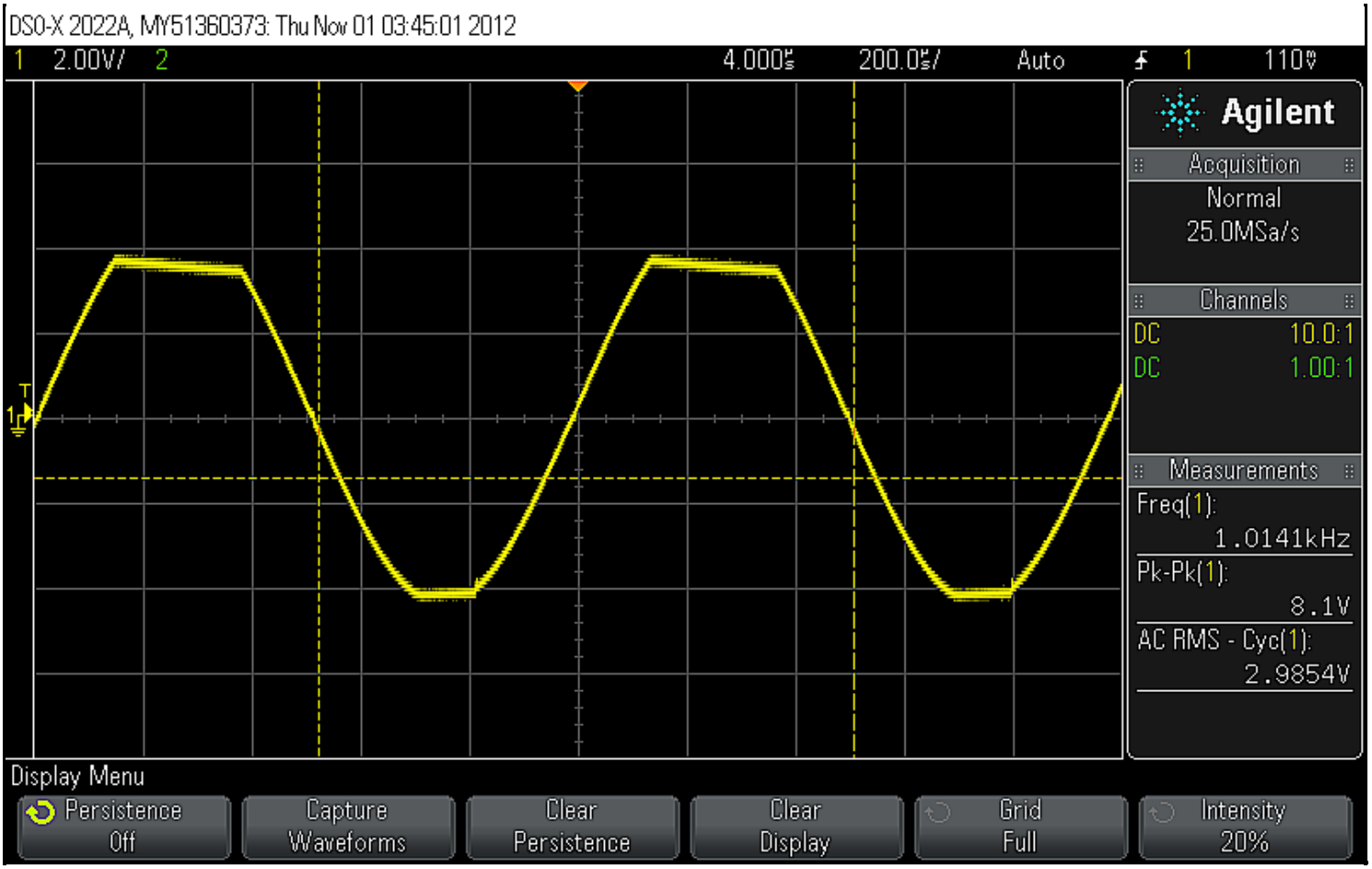

Above — 'Scope tracing; I advanced the 10K volume pot to drive the amp into clipping.

---

3. Interview — Three Questions with Jason, NT7S from Etherkit

I follow 2 English language amateur radio blogs — 1 is Ripples in the Ether by Jason, NT7S

Possessing a modern flare, Jason, the blogger, gently but resolutely challenges some of the cliquish, dogmatic thought and behavior that tarnishes amateur radio, or just blogs about fun stuff. He writes well — creating an emotional dialog that stimulates thought and reflection. We get a sense that he cares about our radio hobby and wants it to grow and improve.

Jason, the man behind Etherkit, champions a modern, open-source vision that I find both positive and refreshing.

1. Tell me about your decision to embrace the open source software philosophy for your hardware in a time where proprietary code, copyrights and patents still hold strong. How do Ham Radio equipment sellers benefit from code sharing?

I believe that the open sharing of knowledge has always been one of the cornerstones of our amateur radio community, going back to its earliest days. So the open source/open hardware ethos has always resonated with me in regard to our hobby. I started Etherkit with the intention of providing a small bit of income to my family and as a way to promote the idea of open hardware within the ham radio community at large. I have no illusions of becoming the next Elecraft, but I hope that I can build up a stable of affordable and fully-open ham radio kits that will be "hackable" and extensible for the motivated experimenter. I do this by providing the full source code for my microcontroller firmware, all of the PCB design files, Creative Commons licensed documentation, and programming ports for my products. I've already seen some neat examples of

customers extending my first product (the OpenBeacon MEPT kit) by doing things such as adding in WWVB time discipline and pairing it up with a Raspberry Pi for cheap automation. I hope that others will take my code or my circuits and re-purpose them in their own work, even if they don't buy my products.

I am not an open source zealot and do not begrudge the large majority of vendors who choose to keep their intellectual property closed. However, most of what us smaller companies do is not on the cutting edge of radio. We leverage the knowledge and works of those who came before us. Perhaps if I created something wholly-new that would be patent worthy, I would consider keeping it closed, but that's not the kind of products that I'm able to develop as a one-man operation. We do not copy the designs of others, but we do take concepts that are for the most part well-tested and come with new ways to implement them. Because of that, it's my personal opinion that I have a duty to keep my designs open.

In the open hardware world at-large, there is a discussion about whether open source hurts your own business prospects. There are still some debatable points in that discussion, but I think it has been shown that if you look at the entire balance, open hardware is a good thing for smaller companies. One of the largest concerns is that under most open source licenses, a competitor can just clone your hardware and undercut your sales. That is a genuine concern, but I think that products such as Arduino have shown that if you make a quality product, most folks will recognize that quality and stick with the original.

Even if others buy a clone of your hardware, in all likelihood, that may be strengthening your brand identity (as long as that vendor isn't stealing your name). Another concern is that a customer can just copy your product for themselves. To that, I say good!. Because of the work and costs involved (economy of scale), it's going to be time and/or money consuming to make that copy. It's probably cheaper and faster to just buy the kit. The reason you copy it for personal use is because you love working with the technology. Which is exactly what I want to encourage. You may lose a small bit of sales, but I think it gives you more name recognition in the end.

2. What's it like being a vendor at Dayton?

To be clear, I wasn't a vendor at Hamvention in 2012 (hopefully I will be there by 2014), but I was a vendor at Four Days In May at the Fairborn Holiday Inn. It was a wonderful experience to get to sit with the big names in the QRP world, selling my wares. I got the opportunity to meet tons of QRPers and build up some good relationships. Online sales are wonderful for the ultra-small operations such as myself, but nothing beats actually meeting your customers face-to-face, especially when you are at the world's most well-known QRP convention.

3. In industry, SMT parts are normal and hole-thru might better be called "hold-over"; what's your view on kitting products with SMT parts?

We've seen some SMT kits within the QRP world, but they still are more of an oddity than anything else. I understand the concerns that people have with SMT assembly, but I think that there is still a lot of trepidation that builders needn't have. It's my opinion that SMT construction with "larger" components such 1206 or 0805 is well within the capabilities of the average kit builder. I also believe that once you are comfortable with SMT construction, it is probably faster and more efficient than through-hole construction.

OpenBeacon is a through-hole product, but I have had a QRP CW rig in development for the last two years that is a SMT design. In beta testing, I've found that one of the biggest challenges in kitting is that I have to clearly identify each and every component. With a through-hole kit, you can just throw all of the resistors or all of the capacitors together because they are clearly marked. Not so with SMT. You have to have a system to keep each value separated from the others and marked with a value. SMT resistors and semiconductors have a laser-etched value, but it's nearly impossible to see by naked-eye, and SMT capacitors generally have no markings at all.

So I have had to compartmentalize each strip of components of the same value cut from a reel, and mark them with a sticker. That is pretty costly and time-consuming. I'm hoping to find ways to streamline this process so that I can release SMT kits without the large time investment that it currently takes.

---

4. EMRFD Experiments — A 1-on-1 Tracking Phase-locked Loop

I built the 1-on-1, or offset phase-locked loop circuitry described on EMRFD page 4.22 and share these schematics in faith you'll create your own. Rich with wisdom and reason, this section lies among the best topics from EMRFD. Please read Wes' notes since I won't repeat his narrative — only supply a few ideas and measurements. In the article closer, Wes suggests some modern parts to raise performance and I applied all of them with the exception of the 14 MHz VCO.

Rather than building the main VCO with divide by N circuitry to allow multiband use, I copied the original 14 MHz oscillator verbatim. Why? Well, I wanted to test this VCO: a design that wisely doesn't expose the varactor to high impedance or signal amplitude and thus avoids forward-biasing the single tuning diode. I've discussed this before on the QRP Modules 2011 web page under **7 MHz VCO Experiments**. Also, I really just wanted to learn about PLL circuitry. The Figure 1 macro schematic below illustrates this project.

In my circuit, a frequency stable 14 MHz VCO = **the goal**; the rest of the circuitry supports this.

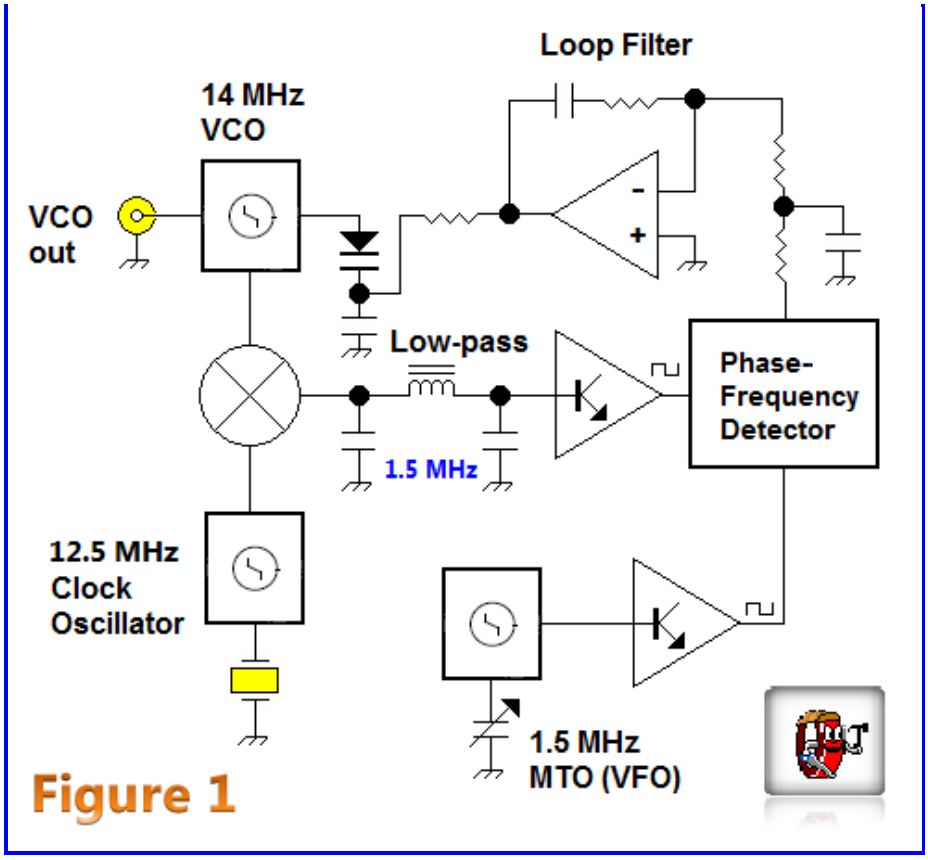

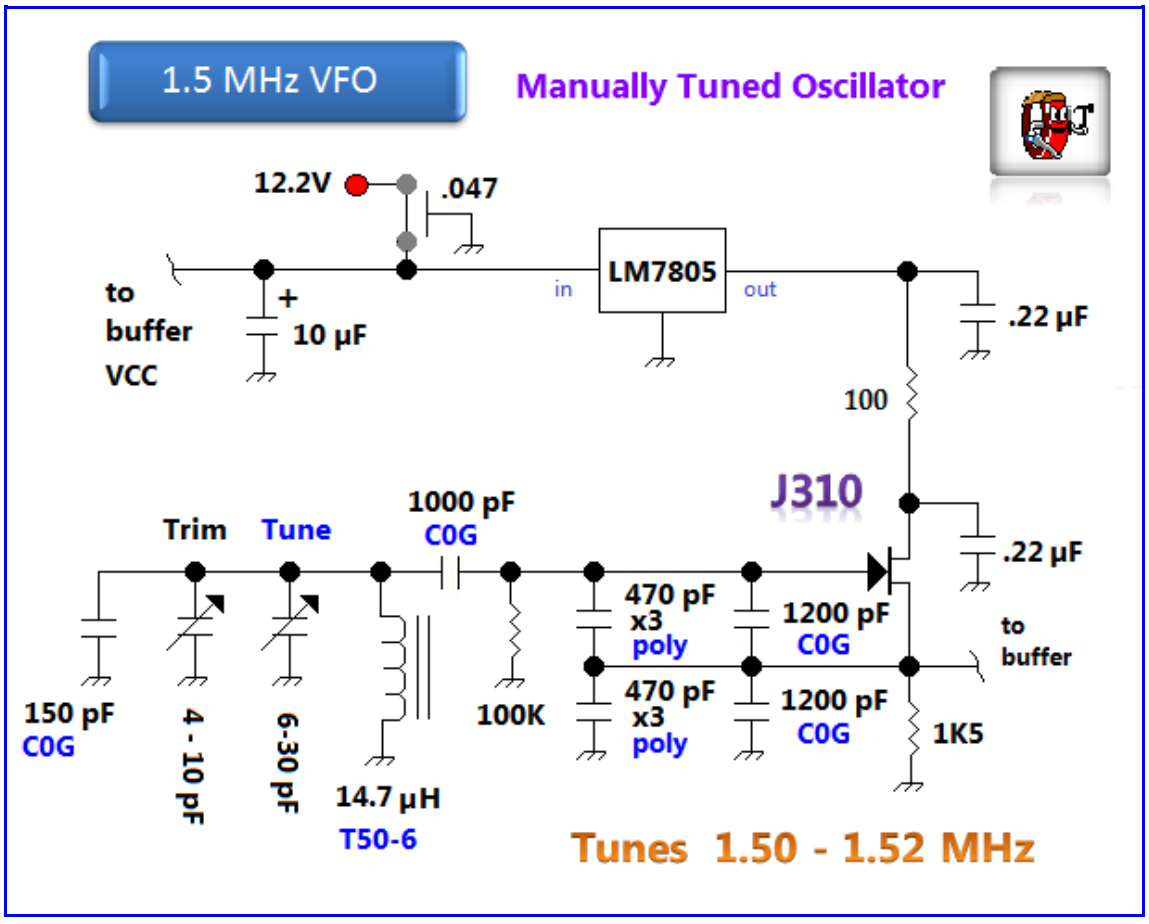

Above — The 1.5 MHz VFO. In his modern writing, Wes calls this the MTO, or Manually Tuned Oscillator *in the context of a tracking PLL.* I wound the L with # 30 AWG wire on a T50-6 toroid.

My MTO exhibits a low tuning range (only 1.50 to 1.52 MHz) since I built in a box with a small air-variable capacitor that swung only 24 pF and I ran the "Colpitts capacitors" at 2610 pF to keep phase noise low. This box normally holds a VHF oscillator and I just removed the main board and swapped in a 1.5 MHz equipped copper board. I won't keep this PLL and thus sticking the 1.5 MHz MTO in an existing oscillator chassis with a grounded tuning shaft and feedthrough capacitor helped save money and time.

Above — The built 1.5 MHz MTO. With temperature compensation from 6 stiff-leaded, 600 VDC, 470 pF polystyrene capacitors, my frequency drift measured between 3 and 4 hertz per hour upward at room temperature. Properly designed + built + temperature compensated L-C oscillators at 1.5 to 3.5 MHz may exhibit stellar temperature stability. See the VFO - 2011 web page for some tips.

Since this VFO was sublimely frequency stable, I didn't possess the guts to change up the L-C ratio to garner a wider tuning range from the small air-variable tuning capacitor. A 100 pF, or greater delta-F air-variable tuning capacitor would stretch the VFO (MTO) tuning range nicely.

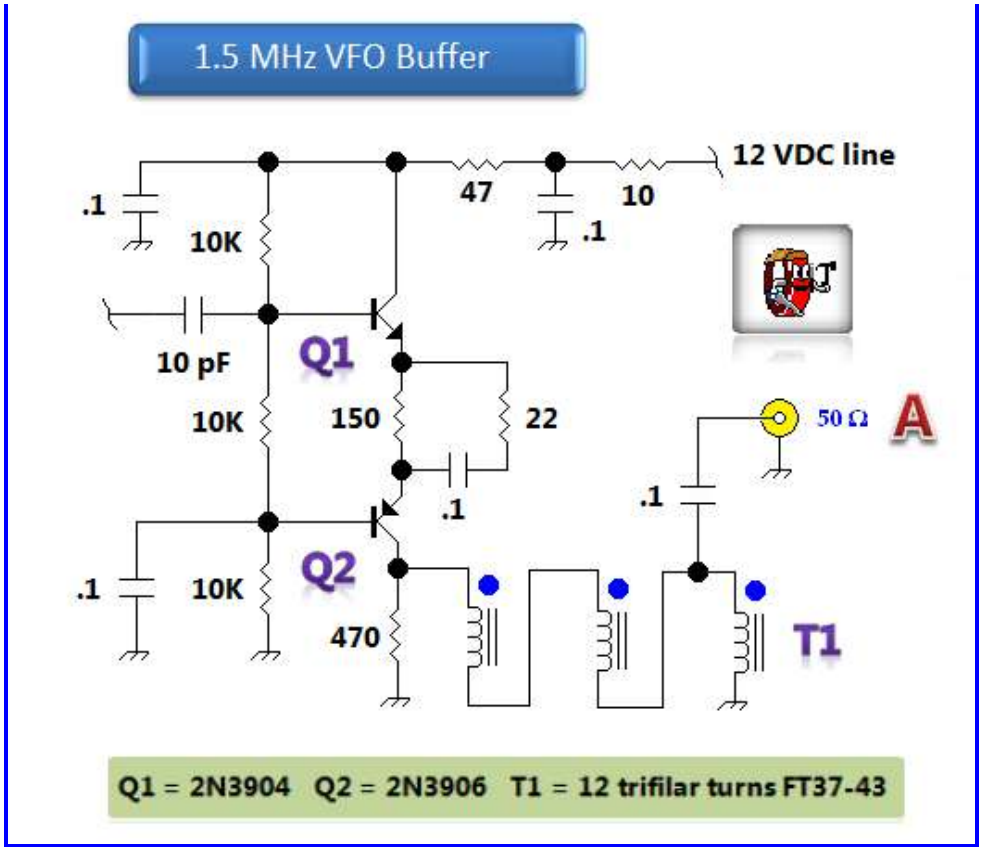

Above — I designed this buffer last year and it's my new favorite. Click for the original. A 10 pF C0G/NP0 capacitor lightly couples the MTO output to the high impedance of Q1, an emitter follower. Further, a common base amp provides gain and *essential* reverse isolation. You may adjust Q2 gain by changing the degenerative feedback offered by the 22 Ω resistor and 0.1 µF capacitor. For example, decreasing the R to 18 Ω may provide 7 dBm output for a diode ring mixer.

MTO output power = 6.71 dBm.

I transformed the 470 Ω collector resistor impedance to 50 Ω with a transmission line transformer. Even though part of the PLL circuitry involves logic gates, or is at DC; as possible, my circuits employ a 50 Ω input or output impedance to allow measurement with my 50 Ω modules and/or instruments, plus transmission via 50 Ω cables.

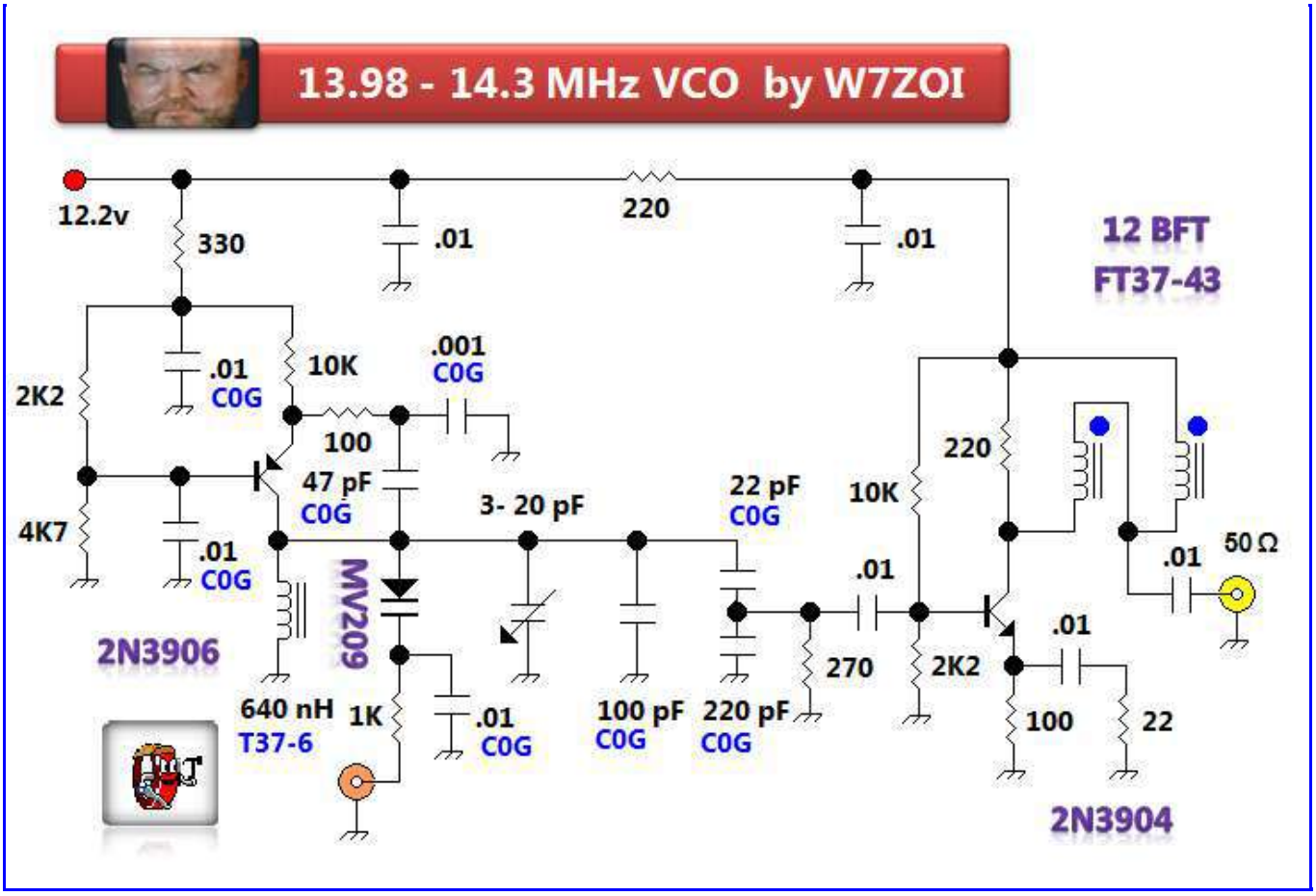

Above — The 13.98 to 14.3 MHz VCO by Wes, W7ZOI (Figure 4.43 in EMRFD). The connector in series with the 1K varactor resistor was an RCA type. Output power = 1.62 dBm. I employed a 3 - 20 pF air variable for the trimmer.

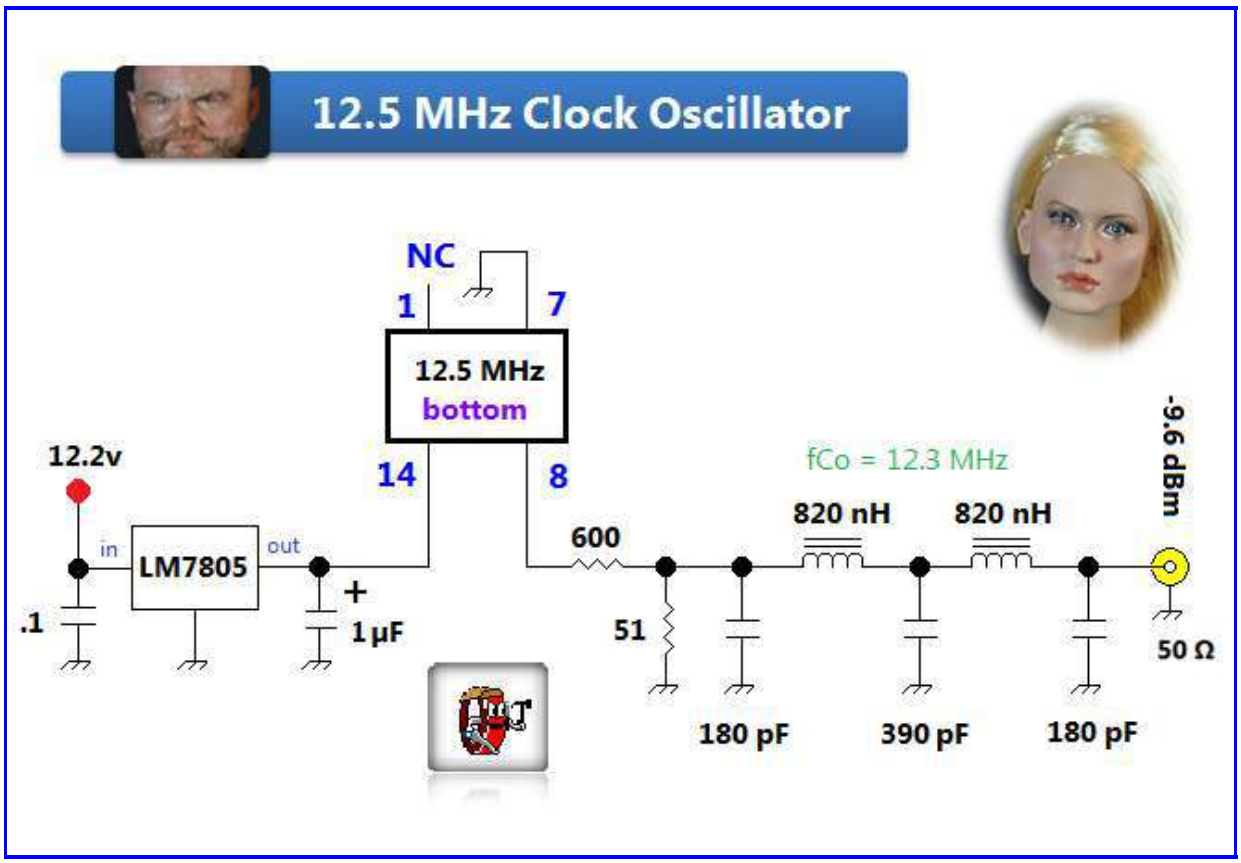

Above — In the original circuit, Wes built his 12.5 MHz crystal oscillator with a single 2N3904. Lacking a 12.5 MHz crystal, I built my xtal oscillator

from an old, junkbox 12.5 MHz clock oscillator. A resistor L- matching network drove a low-pass filter to scrub off harmonics, Click for the clean output 'scope tracing at 211 mV pk-pk in my first version. Later, some tweaks gave a final power of -9.6 dBm (208 mV pk-pk). Many authors switch their NE612 mixers with a peak-peak voltage of ~200-300 mV. An AC-coupled 51 Ω resistor on the NE612 pin 6 properly terminates the oscillator to establish the desired drive power and filtering.

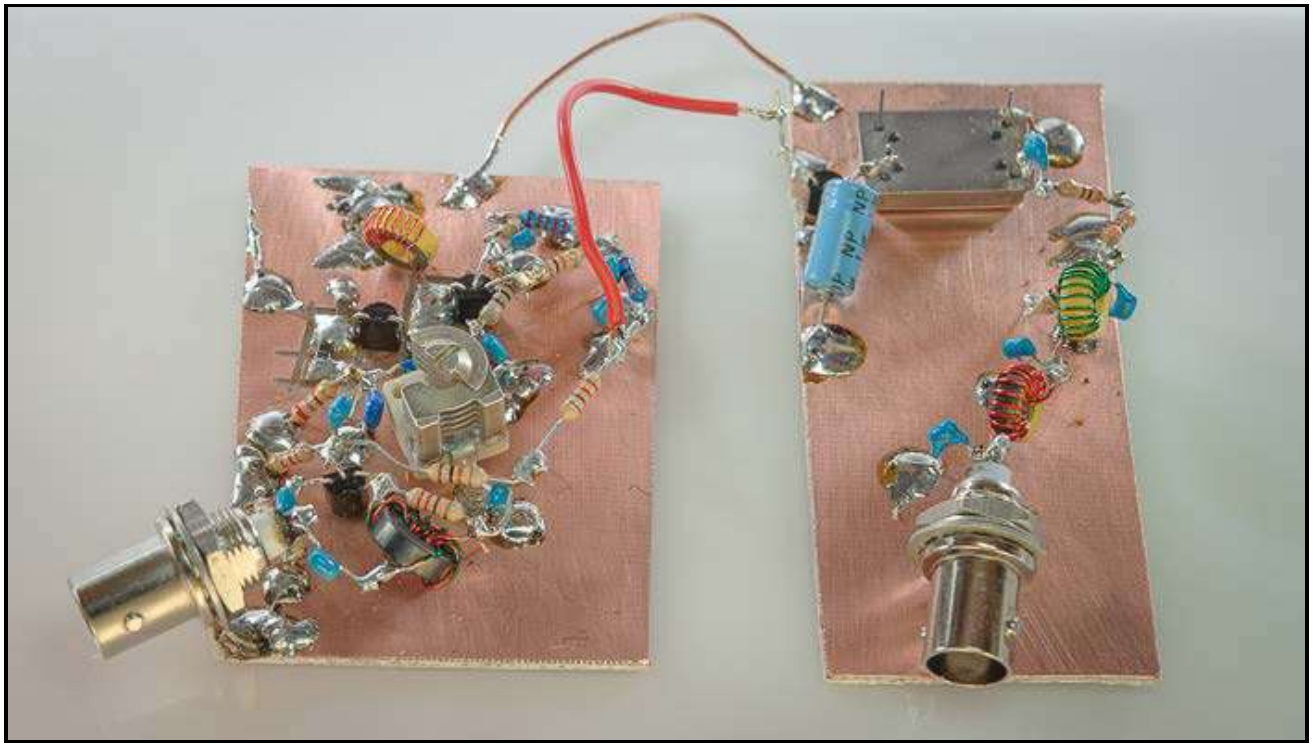

Above — Oscillator breadboards: 14 MHz VCO (left) and the 12.5 MHz clock oscillator (right).

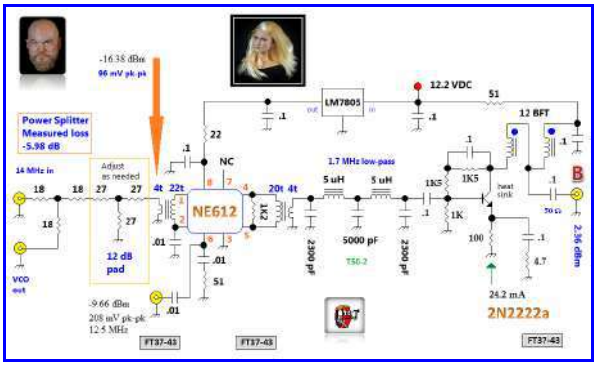

Above — Click to view the power splitter, mixer, low-pass filter and amplifier schematic. Click for an FFT of the clean 1.5 MHz output sine wave. At this point, the 14 MHz VCO has no DC voltage connected to its frequency compensation varactor. As shown, the mixer products are seriously attenuated by the simple, low-pass filter + keeping the mixer RF port signal amplitude low. The power splitter provides the input for the mixer and also the main output for the 14 MHz VCO. The main VCO output requires 50 Ω buffer/amplifer(s) to drive a receiver mixer, transmitter chain, or whatever.

I inserted the 12 dB attenuator pad to keep my mixer RF port signal low to drop the mixer products amplitude down; further losses occur in the transformer. You can change this pad to whatever is required. I belong to the camp of builders who drive their transmit mixers with low-level RF signals to avoid messy outputs at the IF port.

Click for a breadboard photo of my initial bench tests with the mixer board. A 50 Ω resistive terminator shunts the main VCO output port during this testing. I temporarily insert BNC connectors along my development breadboards to measure output signals with my 50 Ω terminated 'scope, spectrum analyzer, or power meters and *rarely* measure RF circuits with a 10X probe.

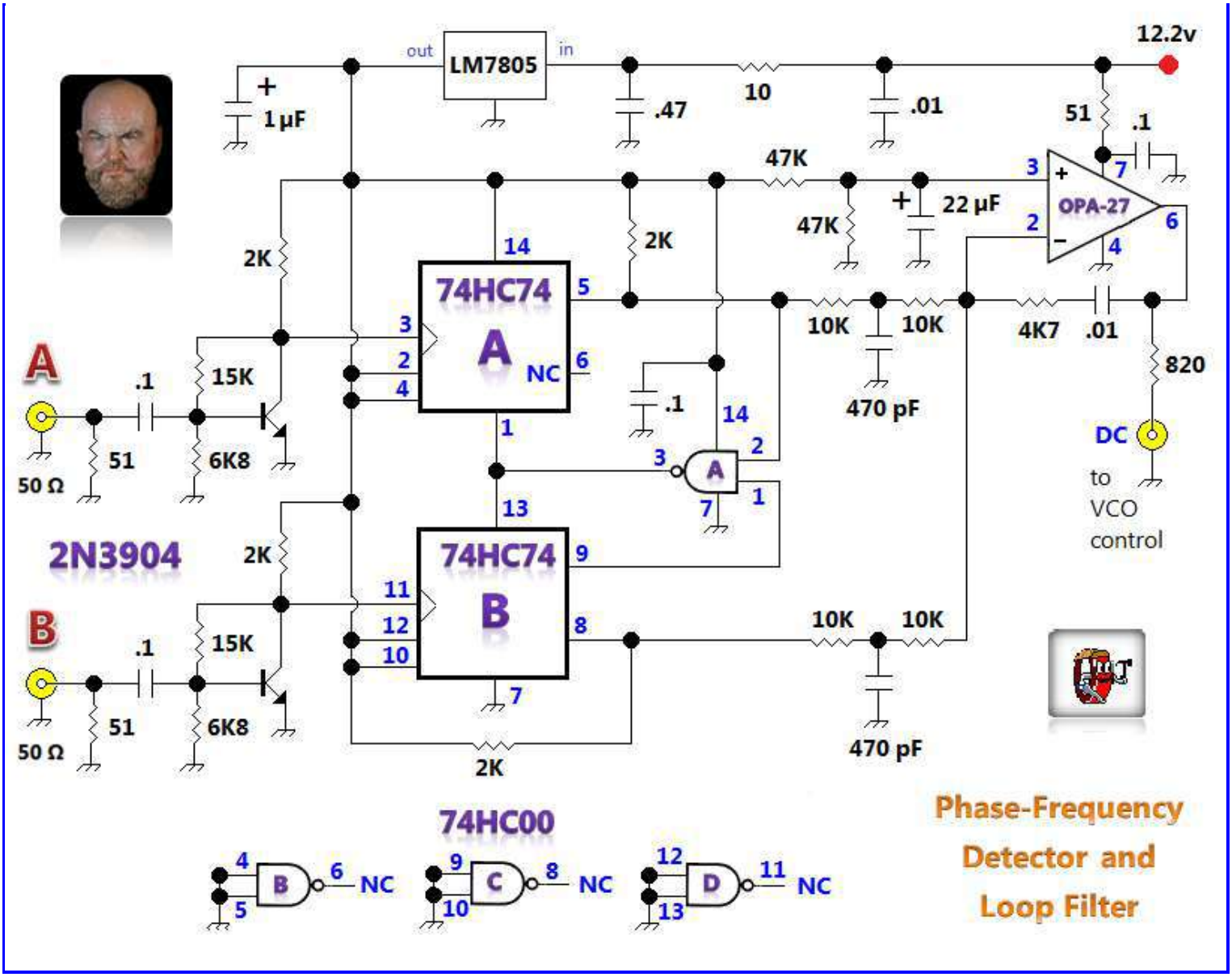

Above — Phase-frequency detector and loop filter schematic. 51 Ω resistors terminate each 1.5 MHz input and drive two 2N3904 switches per EMRFD Figure 4.41. The loop filter design from EMRFD works as described, however, if you make a loop filter for a different circuit, casual copying goes out the window. Engineers design their loop filters according to factors including the crossover frequency, VCO gain, the N-division for the loop, etcetera *with software.* Some people and companies offer such software on the Web.

My loop filter 0.01 µF cap was a 1% polyester capacitor, although Wes specs a 10% tolerance in EMRFD. No cheapo ceramic bypass caps here please.

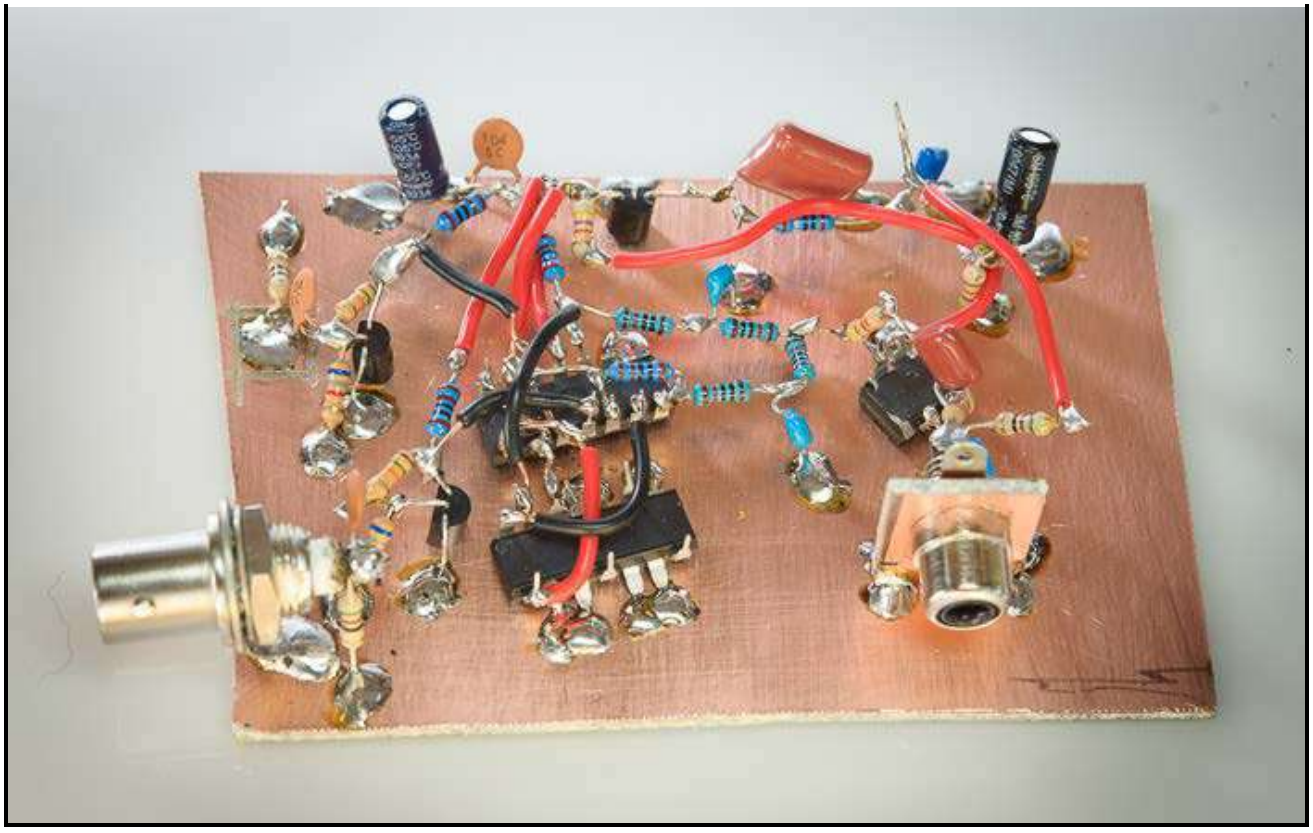

Above — Phase-frequency detector and loop filter breadboard. Click for a photo of the scattered, ugly, working boards on my workbench. Many prototypes look like this on our benches, however, sometimes, they work perfectly until we stick them in a box! Do you relate? Each oscillator belongs in its own metal box with strong bypass and decoupling networks (feedthrough caps reign supreme here) since the 3 oscillators might decide to party together and create havoc.

Above — My VCO frequency with the 1.5 MHz MTO set at full mesh. Since my MTO only tuned from 1.50 to 1.52 MHz, my VCO only tuned from

14.00 to 14.020 MHz, but that's easily fixed as I've stated. I'm very happy — it locked perfectly and my 14 MHz VCO stayed on frequency at the exact previously measured frequency drift of the 1.5 MHz MTO. When I connected the 14 MHz VCO to my counter without the PLL circuitry, it drifted willy-nilly.

Conclusion

The sense of awe and joy arising from locking a VCO on frequency won't be understood by many. The concepts and circuitry offers many possibilities. If the MTO and VCO exhibit low phase noise, short-term oscillator stability may be fantastic.

The 14 MHz VCO could be a 56 MHz VCO with sequential division by flip-flops to provide output at 28, 14 and 7 MHz with the 14 MHz portion going to the offset mixer. In EMRFD, Figure 4.44, Wes offers 14 and 7 MHz output by dividing the 14 MHz signal from the main power divider output port. The 7 MHz band is low-pass filtered to remove harmonic energy.

Wes extended this circuit by dividing the MTO by a hardware programmable frequency divider so that the difference from the mixer and low-pass filter is 170 kHz nominal. He uses this 'Almost Synthesizer' on the air for his QRP adventures.

While most builders will sensibly jump from an L-C VFO to a kit containing a programmed microcontroller plus a DDS or Si579, it's also fun to play with hardware to learn and ingrain synthesizer concepts + gain bench wisdom.

QRP — PosData for April 17, 2013

For a good read on the offset PLL, consider studying Wes' book **Introduction to Radio Frequency Design**, ARRL, 1994, page 320 and on. *This book is now out of print*. Wes ported the PLL active loop filter design program he wrote for IRFD from DOS to Windows in April 2013. Click and scroll for it. Thanks for this Wes!

---

5. Boot-strapped Popcorn AF Feedback Pair

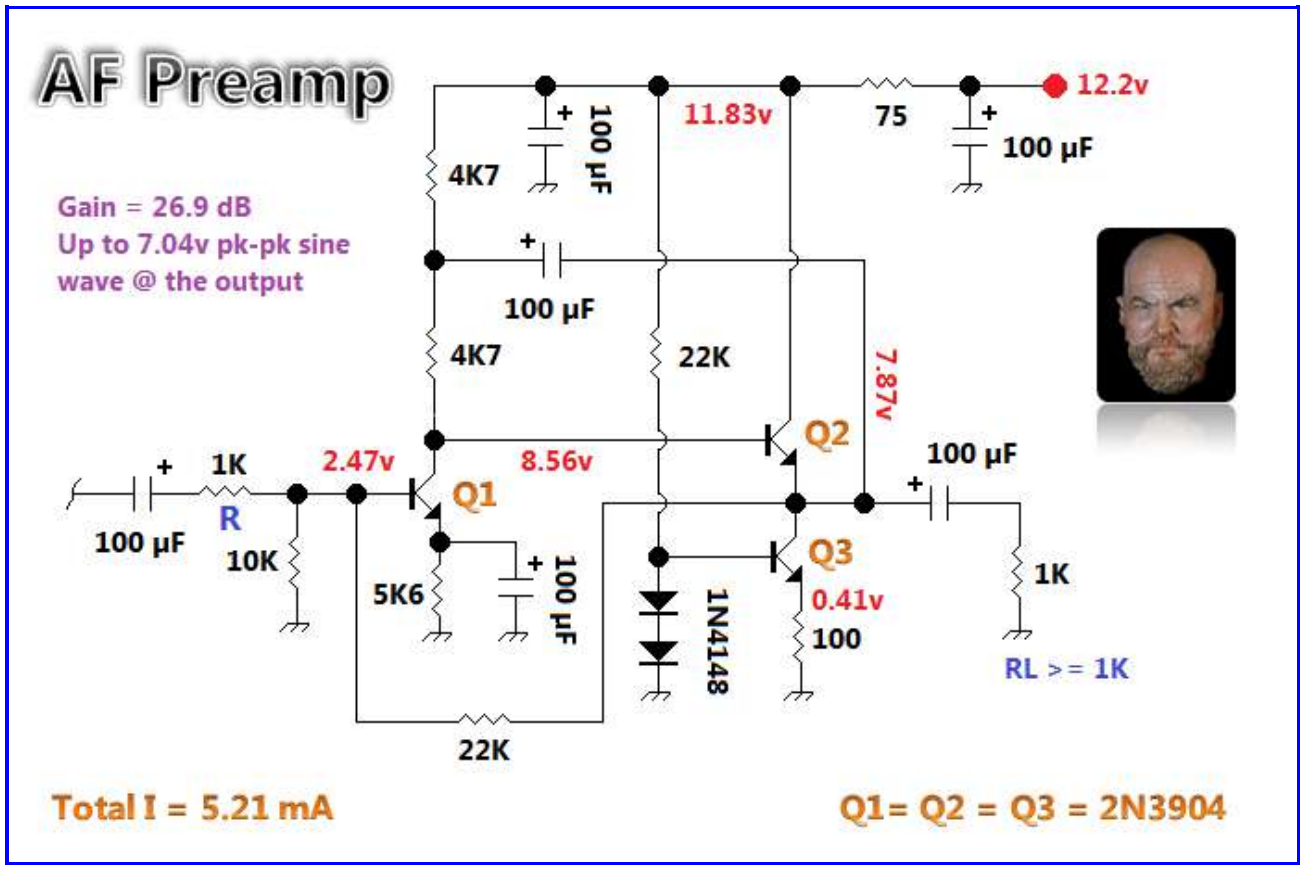

Above — I designed this AF stage for a builder from Indonesia; a popcorn AF shunt feedback amp based on the work of Douglass Self. Despite only drawing ~ 5 mA, this amp stayed clean until the output voltage exceeded 7.04 volts peak-peak on my test bench. Boot-strapping increases gain and lowers distortion in Q1.

Q2 buffers the Q1 voltage amp from external loading and increases gain.The Q3 current source boosts the load-handling capacity of the Q2 emitter follower. The input R can be raised to reduce sensitivity. The 1K output R could be a 5-10 K volume pot.

---

6. Non-Mechanical Iambic Paddle

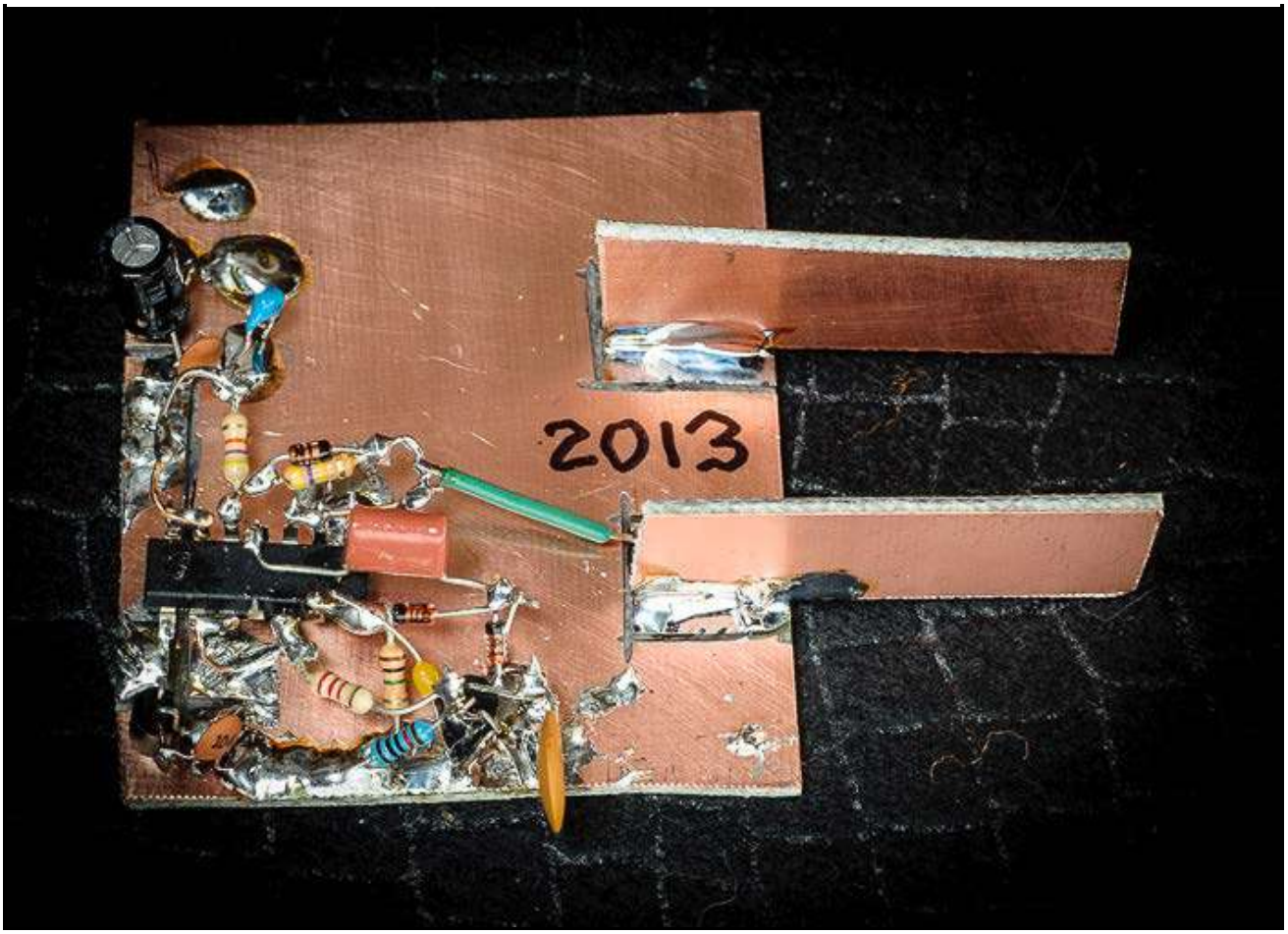

Above — The very ugly development proto-board of my half-done non-mechanical Iambic paddle. At some point I'll build the other half (the dah paddle switch) and press it into service. You might also use this circuit as a non-mechanical straight key.

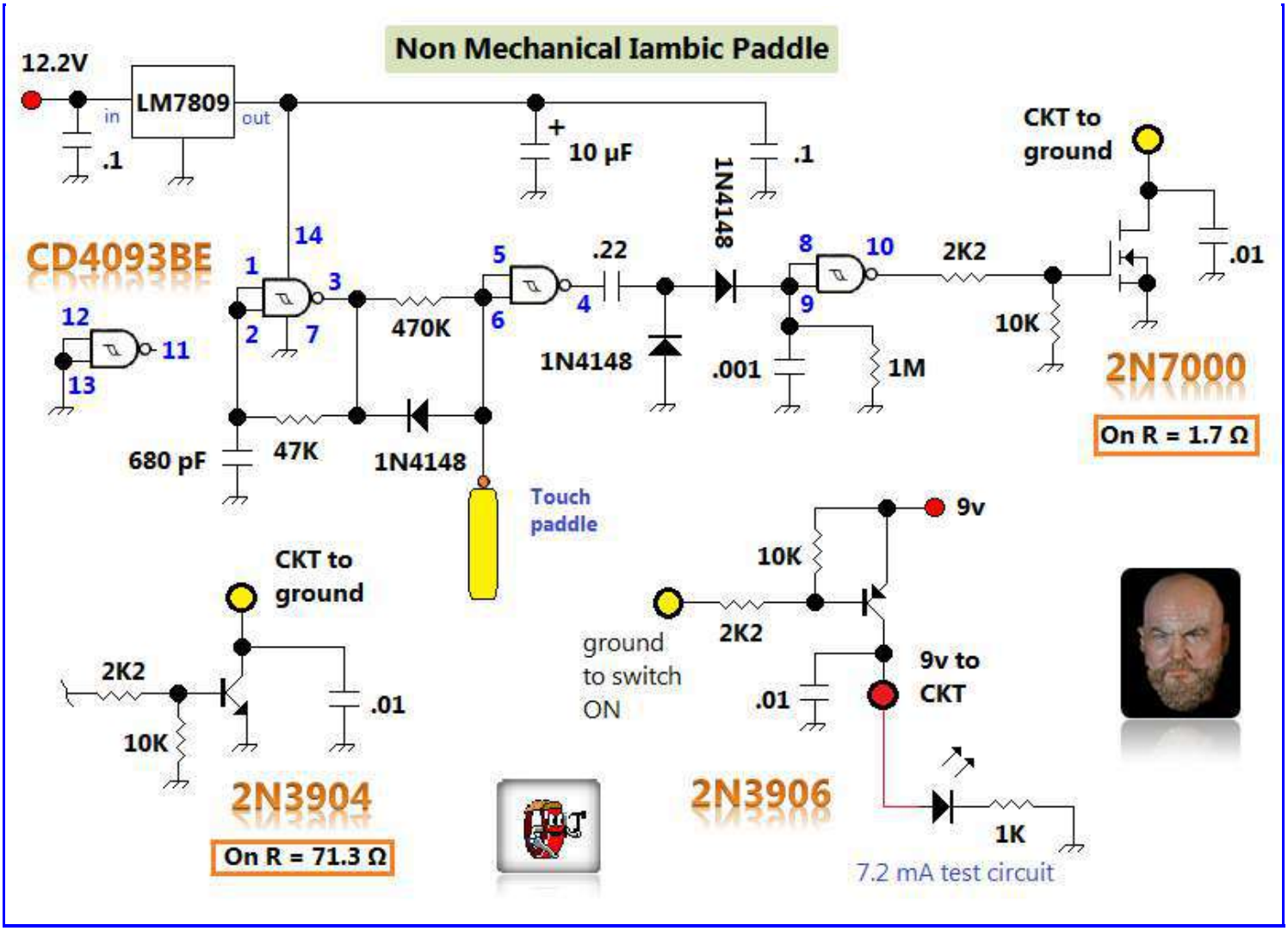

Above — The schematic for 1 of the paddle circuits. I compared the ON resistance of the BJT switch with the enhancement mode FET and the 2N7000 won: only the FET could key the continuity tester on my DVM.

You may extend this circuit with a 2N3906 switch for paddle-switched 9 volts (or whatever VCC you want). In the bottom right, I connected the PNP collector to an LED and flashed it for fun. The 0.01 µF capacitor on the switch drain or collector bypasses any RF to ground. With higher power RF, you may have to place a similar bypass cap in parallel with the shunt 10K resistor on the 2N3904/2N7000 base and gate respectively.

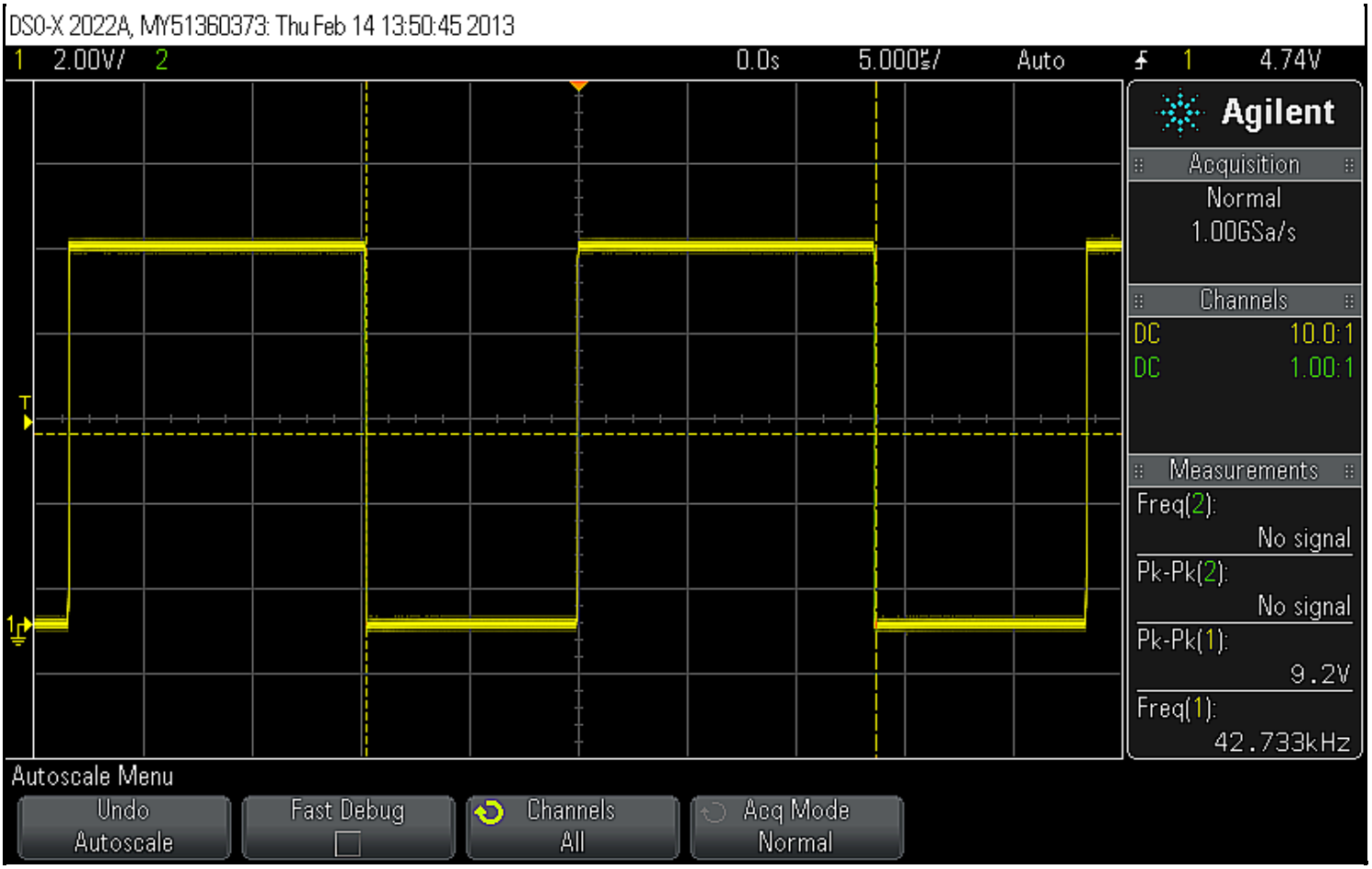

Above — A 'scope shot of the ~ 43 KHz oscillator generated in the first 4093 Schmitt trigger NAND gate.

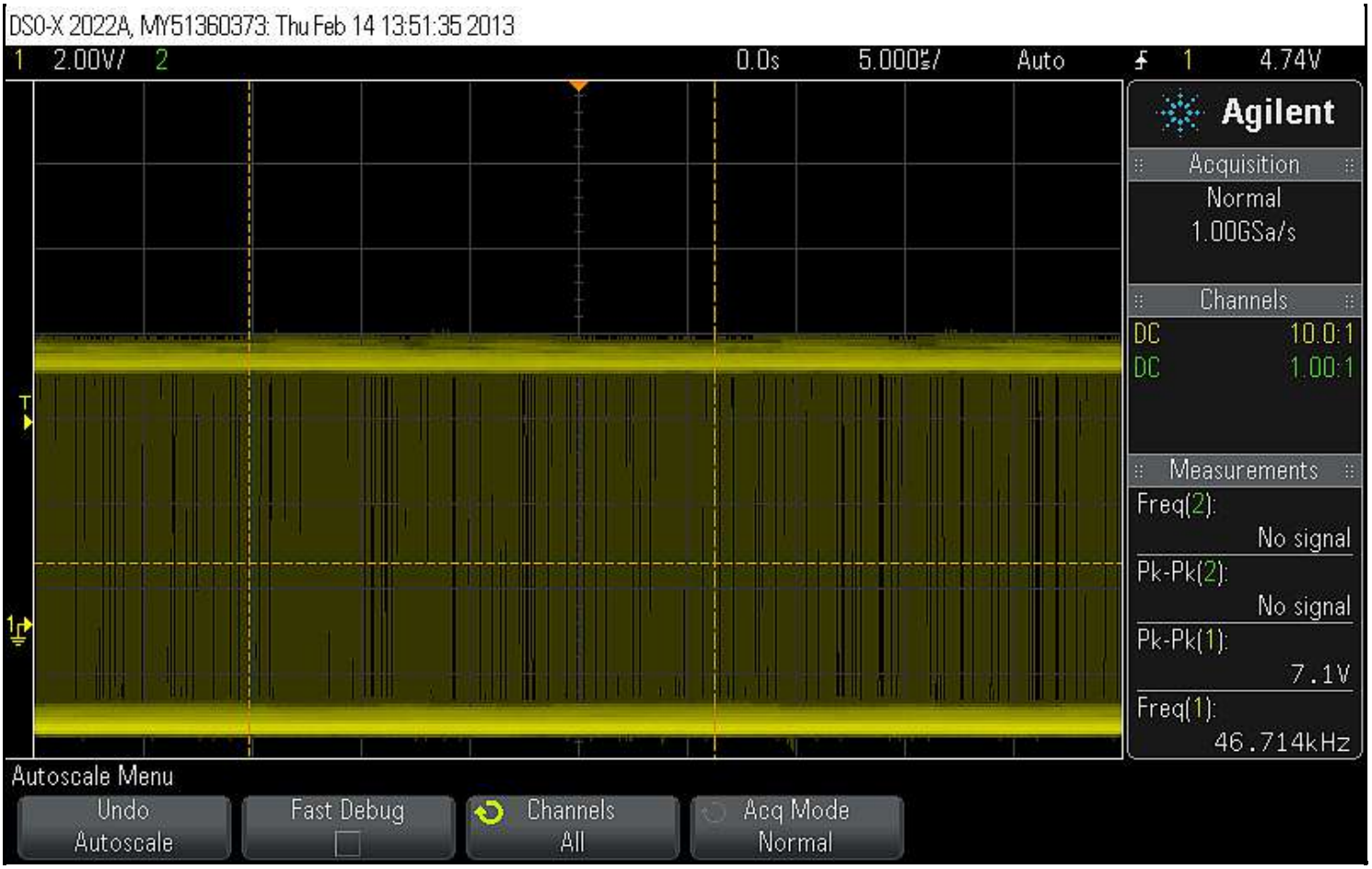

Above — Here's the disturbed oscillator output *just* after the paddle is touched: this stops the signal at pin 5 and 6 of gate 2 and kills the AC output at pin 4. The DC voltage across the 0.001 µF cap discharges through the 1 megohm resistor pushing pin 10 HIGH to turn on the 2N7000 (or the 2N3904). Normally, pin 10 is LOW since the rectified output of the undisturbed ~43 KHz oscillator goes to both pin 8 and 9.

A fun circuit for a Saturday afternoon...

---

7. A Journey Above HF

This project began as a 14 MHz low-noise amplifier build, but ended up with me learning more about SMT breadboard techniques and suppressing spurs. A short exploratory/descriptive account of my bench journey plus some photos follow.

Above — I'm slowly adding SMA connectors and pieces. Since modern consumer digital network engineers use them, they're abundant and often rated from DC to 18 GHz; more bandwidth than I'll ever need.

I'm also building with evermore SMT components and just love it. Through-hole (I prefer to say hole-through) stuff continues to disappear like lemonade on a hot August afternoon.

Above — The schematic of my version of Victor 4Z4ME's feedback amp (FBA) as tested at 14 MHz: he emailed me a paper and provided some online support. Click for another version from December 2012. Typical noiseless FBAs suffer from poor reverse isolation, however, Victor runs the collector to base feedback through an asymmetrical 3 dB power combiner/splitter that boosts port isolation, defines the gain, plus sets the input and output impedance.

Strong virtues of the asymmetrical power splitter — fully utilized in this design include a very low loss on the input side (the 1 turn side) and a much higher loss ont the feedback side that allows the feedback to defines the input impedance on one side while exerting a negligible impact on noise figure and dynamic range on the other side. Victor measured a noise figure of 1.5 dB using a MRF586 BJT. Thanks to Victor for the information and design.

For strong IMD properties, I ran 50.6 mA total stage current into a gorgeous, low-noise, NE46134 NPN transistor with a fT of 5.5 GHz. Using VHF-UHF techniques, I built with mostly SMT parts on 2–sided board using copper wire vias to connect the 2 copper surfaces. I discussed the wrap-around bias technique in 2011 as number 1.

Above — My prototype breadboard with dremel cut islands for soldering the size 1206 or 0805 SMT parts, plus a few hole-through items. Carving an island for the SOT89 transistor package proved difficult, but even I (a challenged dremelist) did it.

Woe to Oscillations: Like misplaced car keys, oscillations may remain hidden unless you search for them. Often, the only difference between a proper oscillator and a regular amplifier is we *want* the former to oscillate. To check for instability, we might use our high bandwidth scope, or a spectrum analyzer, but many will have to find spurious RF with basic, DC - HF bandwidth test equipment. In any case, just do your best. To some extent, unwanted oscillations are the *elephant in the room* that few talk about. Well, it's okay to think, talk and feel some emotions about them.

Sure enough, when I connected a 14 MHz signal to the amp's input and a 50 Ω terminated 'scope to the output to measure gain, my sine wave had 2 or 3 others on top of it. In the 4Z4ME amp, the PNP bias transistor can be a source of AF to HF oscillations.

Victor wrote: "The circuit has a low frequency amplifying loop that goes through both transistors. The PNP transistor does not invert the signal (it is a common base amplifier) and the RF transistor inverts so it is a loop with 180 degrees phase shift (negative feedback). The various decoupling and RF coupling capacitors in this loop add phase shift on this low frequency loop. If the accumulated phase shift adds to an additional 180 degrees and gain is larger than 1 you have oscillations. The simplest way to solve it is to make one of the capacitors very large so it will add only 90 degrees phase shift but it will drop the gain at the higher frequencies where the other capacitors start to add phase shift to be less than 1 so there are no conditions for low frequency oscillations. This technique is called "Dominant Pole". That's the reason that I suggested to connect a very large capacitor to the PNP transistor".

I found my oscillations disappeared with a 0.1 µF collector bypass cap on the PNP (Cx on my schematic). The 0.1 µF cap on the PNP collector was critical – a 0.22 µF failed to work, as did a .001 µF --- but a 0.1 µF held it stable. In another 2N2222a-based 4Z4ME amp with 0.01 µF input and output caps, it took a 10 µF capacitor on the PNP collector to snuff out some ~766 Hz oscillations.

We don't use a wrap-around PNP bias with our RF oscillators — that's asking for trouble.

I aso measured oscillations at ~ 372 MHz with my spectrum analyzer. A collector 10 Ω R killed these UHF oscillations and after that I saw no spurs from .001 to 1 GHz. (I should have made the dremel cut right close to the NPN collector for the 10 Ω resistor. I hoped there were no oscillations above 1 GHz because I can't measure them.

Finding oscillations:

Many builders lack a spectrum analyzer, let alone 1 that goes up into UHF bandwidth. I'll share a few tips I've learned on the bench that don't require expensive test gear:

A 10X scope probe on the drain or collector of an amp may sometimes reveal oscillations up to the maximum 'scope bandwidth — set your 'scope vertical scale for high sensitivity. This provides direct measurment of oscillations.

Indirect methods to infer unwanted oscillations also lie in our armatorium. I learned this trick from Wes: Place the circuit under test in your normal gain measurement set up with an oscilloscope. Then vary the DC power supply voltage slowly and smoothly — your measured 'scope voltage changes should also track slowly and smoothly. You may see an AC voltage jump as the amplifier goes into and out of oscillation with the DC power supply tweaking. After finding this oscillation caused AC voltage spike, you work to remedy it with a variety of means such as better bypassing, changing bias voltages, shielding and locating breadboard errors.

Sometimes if you put your finger near the active part while watching the bias voltage or current you may see the bias jump around *if* oscillations are present.

My final indirect oscillation busting technique: If you measure the specified/expected gain and return loss on the input/output port, this *may* signal your device is stable — I've noticed this with MMICs where I saw oscillations on my SA, stabilized them and *only then*, measured the expected S21, S11 and S22.

Sometimes, eliminating a hot part proves the best fix! In 2012, a new builder wrote to say that he soldered in a Mini-Circuits DC - 6GHz MMIC; the ERA-2SM in SOT-86 as a buffer for his 3.5 MHz VFO. Anyhow, in the photo were long leads plus no decoupling resistors etc. It sounds like the circuit behaved hyperreactively and *vibrat*ed in spasm. The cure was to eliminate the microwave part and put in a hycas amp built with a J310 + a 2N3904 — we encounter risk when plying the latest, hottest, super-high fT amplifiers sold on eBay with casual abandon.

Practice makes perfect. if you believe learning is experiential and build to learn, you'll learn to build.

Finally, as an amateur, I struggled to choose a SMT ferrite bead and after reviewing many datasheets and application notes I ordered a size 0805, 800 mA part with 120 ohms Z at 100 MHz and its peak impedance at 340 MHz. I'll let you know how that works out.

RF Bypass on our DC lines: As possible, we ought to provide a broadband RF bypass to provide a low impedance to RF from low frequency up to the maximum frequency wherever our FET, BJT, MMIC, etc. operates. For example, you can't just swap a higher gain BF998 (1 GHz) for a 40673 (VHF) dual-gate MOSFET and expect the same stability and bypass requirements can you? At the very least, I bypass G2 of the BF998 with a size 0805 0.01 or .001 µF SMT capacitor and the drain with RF bypass good for 1 GHz.

Wideband RF bypass may solve oscillation issues too.

I tried to apply a broadband bypass in my breadboard, although it gets extremely difficult to think about bypassing RF at > 1 GHz for the QRP homebuilder. Our hobby should include reflection and proper intention at the very least.

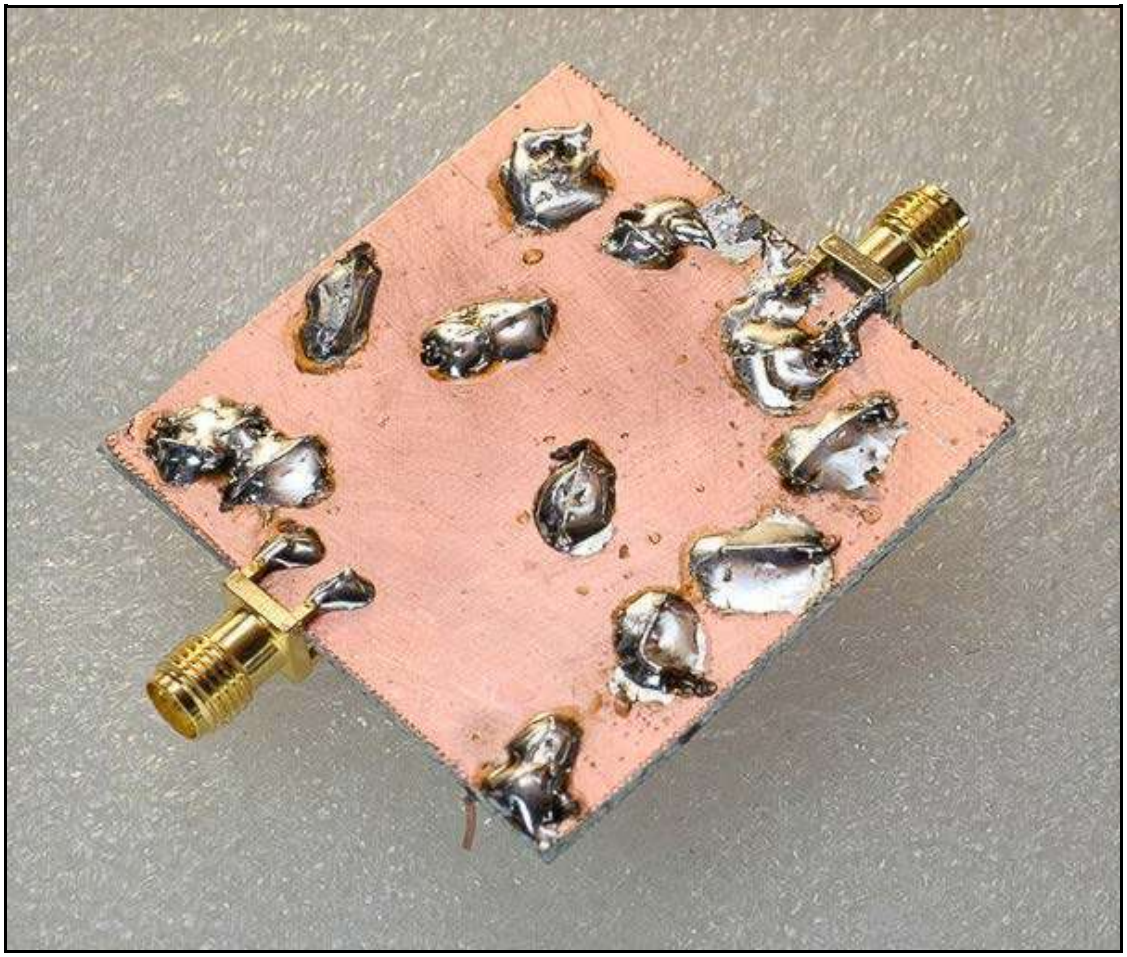

Above — A photo of the bottom of my breadboard showing the vias. I made mistakes: we should try to keep the via holes as close as possible

to all bypass caps, my 10 Ω collector snubber resistor, collector port, or whatever we need to put at RF ground. The vias connect circuit areas to the large area, low impedance ground plane to minimize inductance. We should also try to place bypass capacitors as physically close to the pins of whatever we're bypassing.

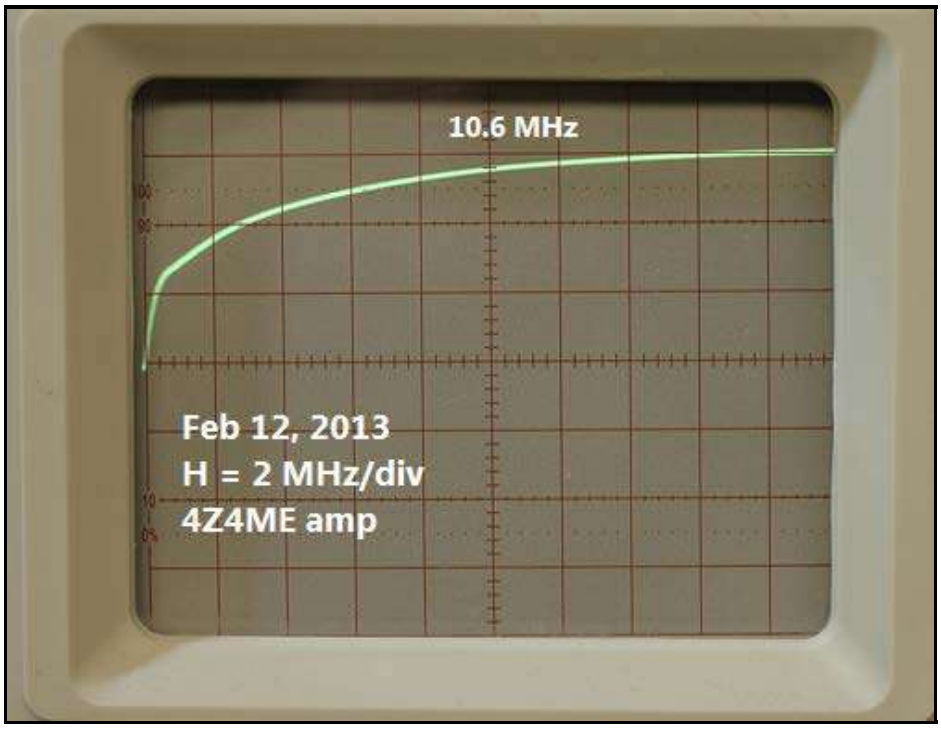

Above — A TG + SA sweep of the gain of my 4Z4ME NE46134 FBA from ~1 to 20.6 MHz. Each vertical quare denotes 10 dB. Each horizontal square = the value specified in the photo. In this case; 2 MHz per division. Maximum gain was ~16 dB.

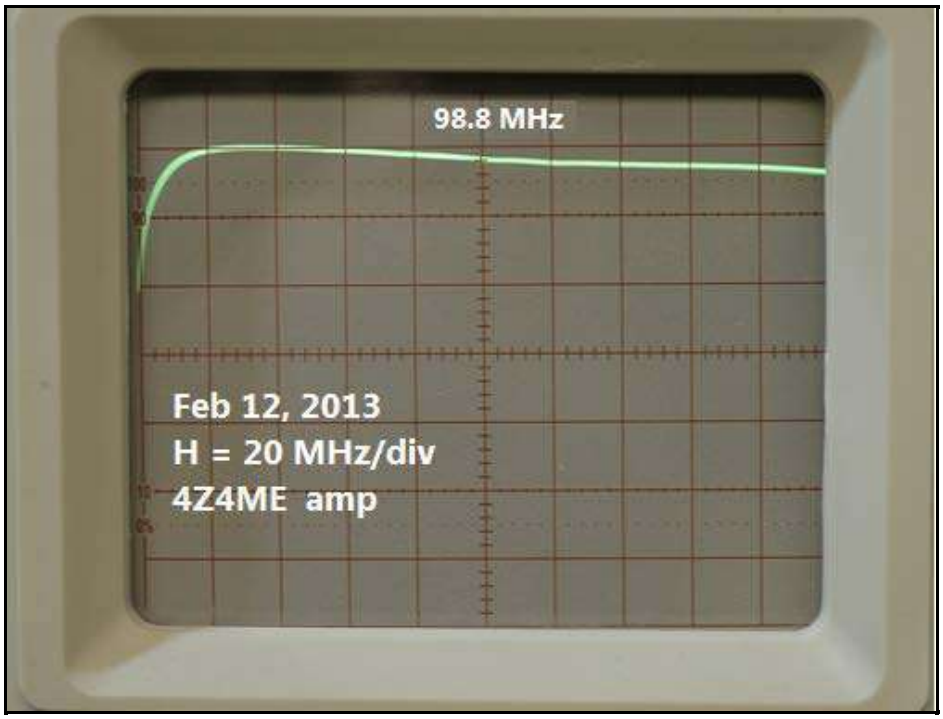

Above — A sweep from ~ 1 to 200 MHz. This would also make a good 6 meter band amplifer or ????.

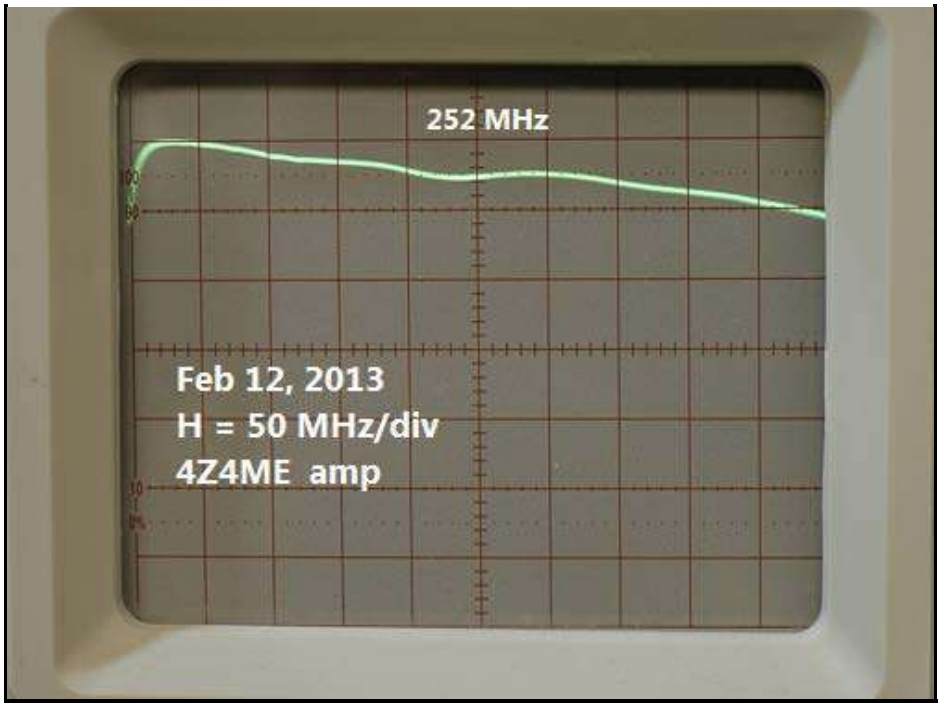

Above — A sweep from ~ 1 to 500 MHz.

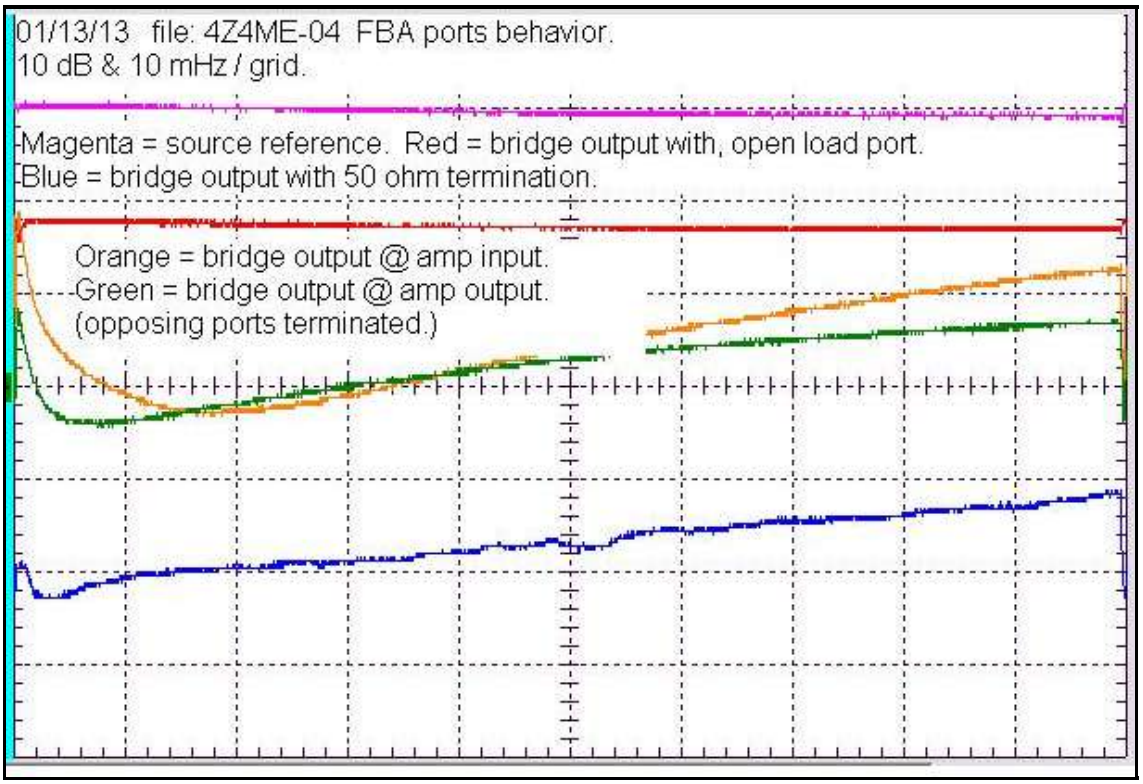

Above — Bob K3NHI made and swept a 2N5109 version of the 4Z4ME amp biased for ~47 mA emitter current. Here he swept return loss at the amp's input and output from about 1 to 100 MHz. The output return loss of my build was down, however, I didn't own many SMT resistors between 33 and 68 Ω. For example, if the output impedance at the collector is 10 Ω, then the series resistor should be 40 (39) Ω.

I've found that in my FBAs, changing the current and also the transistor type (2N5109 , 2N2222a etc.) also affects the input and output return loss. At HF, it's possible to measure RL with a simple bridge, so optimization is possible.

I learned a lot by building just 1 amplifer and discussing my findings by email with friends. Hopefully the next version I make will show improved understanding and skill.

---

8. Popcorn AF Amplifier for Receivers — Reprise

I've worked on a popcorn audio power amplifier (PA) since 2008 and offer my latest experiments. There's only so much you can do with a single-supply 12 volt AF power amp, but I enjoy improving my circuit.

My power measurement technique is shown as Figure 4 here. To enhance versatility, the following PA's may be coupled to whatever preamplifer you choose. In all cases, I drove the power amp stage with a 5532 op-amp voltage amplifer. The power followers were biased with a 2N3904 amplified diode (also called NPN shifter bias amplifier, or DC level shifter) rather than just a pair of series diodes, since this allows you to dial in just the right amount of bias as you watch the AC signal in your 'scope. I wrote a tutorial that explains how to bias complimentary-symmetry power followers in 2008: Click for the link.

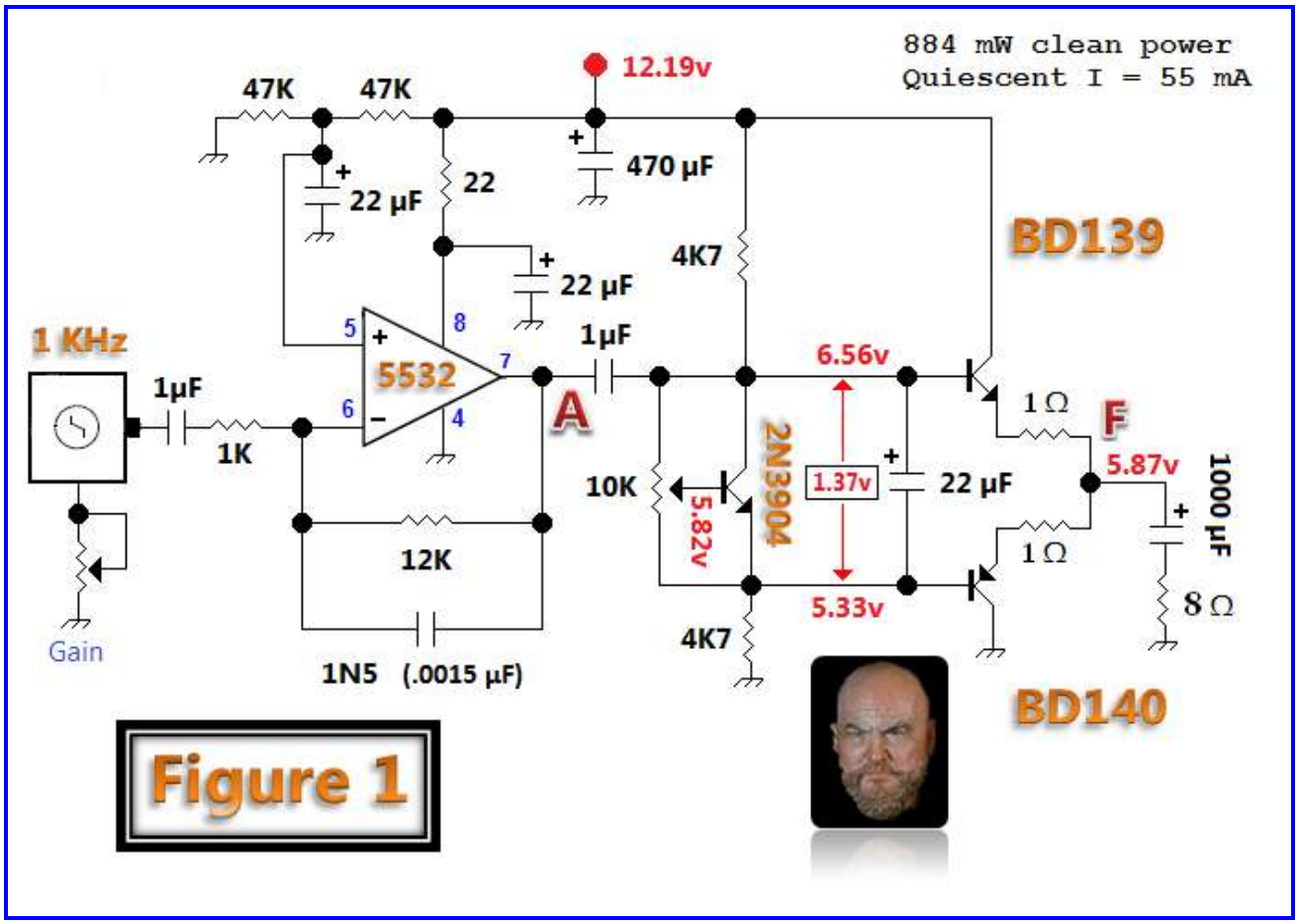

Above — Figure 1: A popcorn AF power amplifer in full bench *test* mode. Measure the AC with a 10X 'scope probe across the 8 Ω resistor and the DC voltage and current with a multimeter. A distortion analyzer proves useful, but not essential for popcorn circuitry. I also listened to each amplifer connected to a line-level cassette player and an 8 Ω, 15 cm speaker. A 4 Ω speaker doubles the maximal clean power, but I don't own any and stuck to 8 Ω.

Containing no negative feedback, the power amplifer stage runs from the red-colored designator points **A** to **F**. You can AC or DC couple point F to your preamplifer stage as required to apply negative feedback.
As mentioned, you can use the 5532 preamp shown with any reasonable gain (i.e. change the 12K resistor), or opt to replace it with your own design. A low output impedance amplifer best drives the power stage.

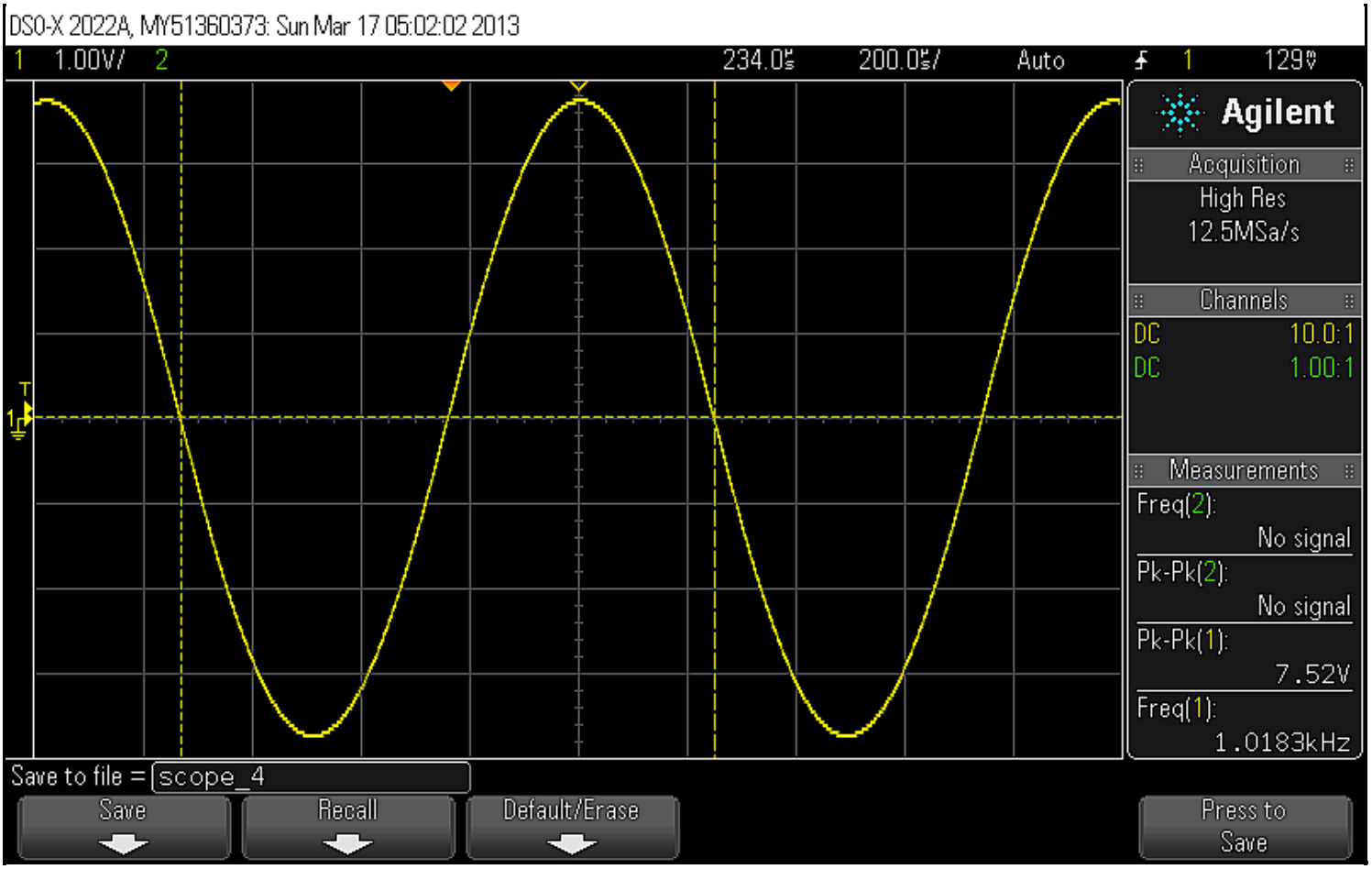

Above — The output of Figure 1 in my 'scope driven to the maximal pk-pk voltage just before distortion begins to appear. Obviously this task is somewhat subjective, however, allows comparison of the amps you build on your bench.

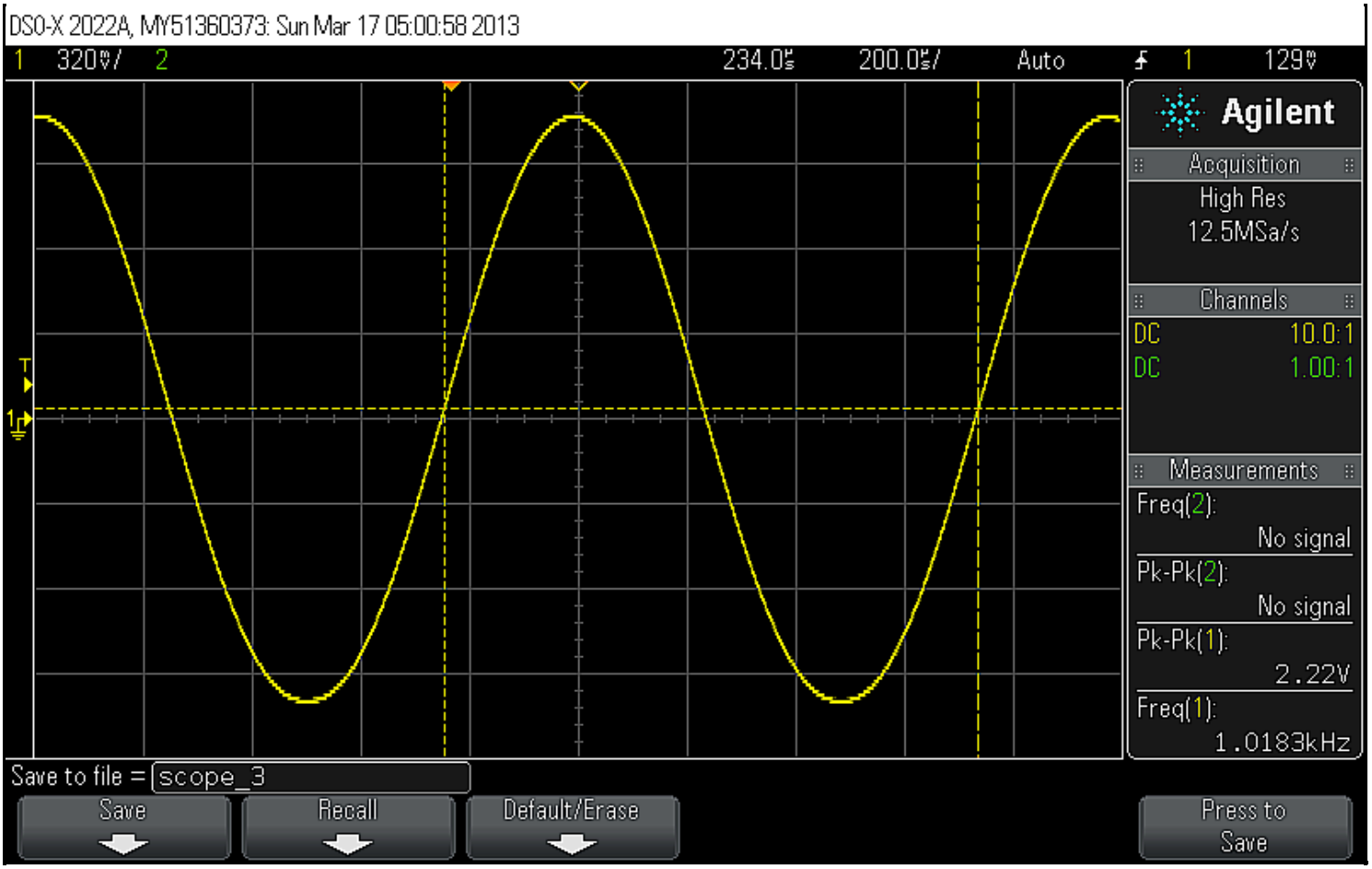

Above — A 'scope screen capture with the 22 µF level-shifter filter capacitor from Figure 1 removed. Look what happened; the maximum clean signal fell from 7.52v pk-pk to 2.22v pk-pk. That capacitor is essential to get the maximal possible headroom.

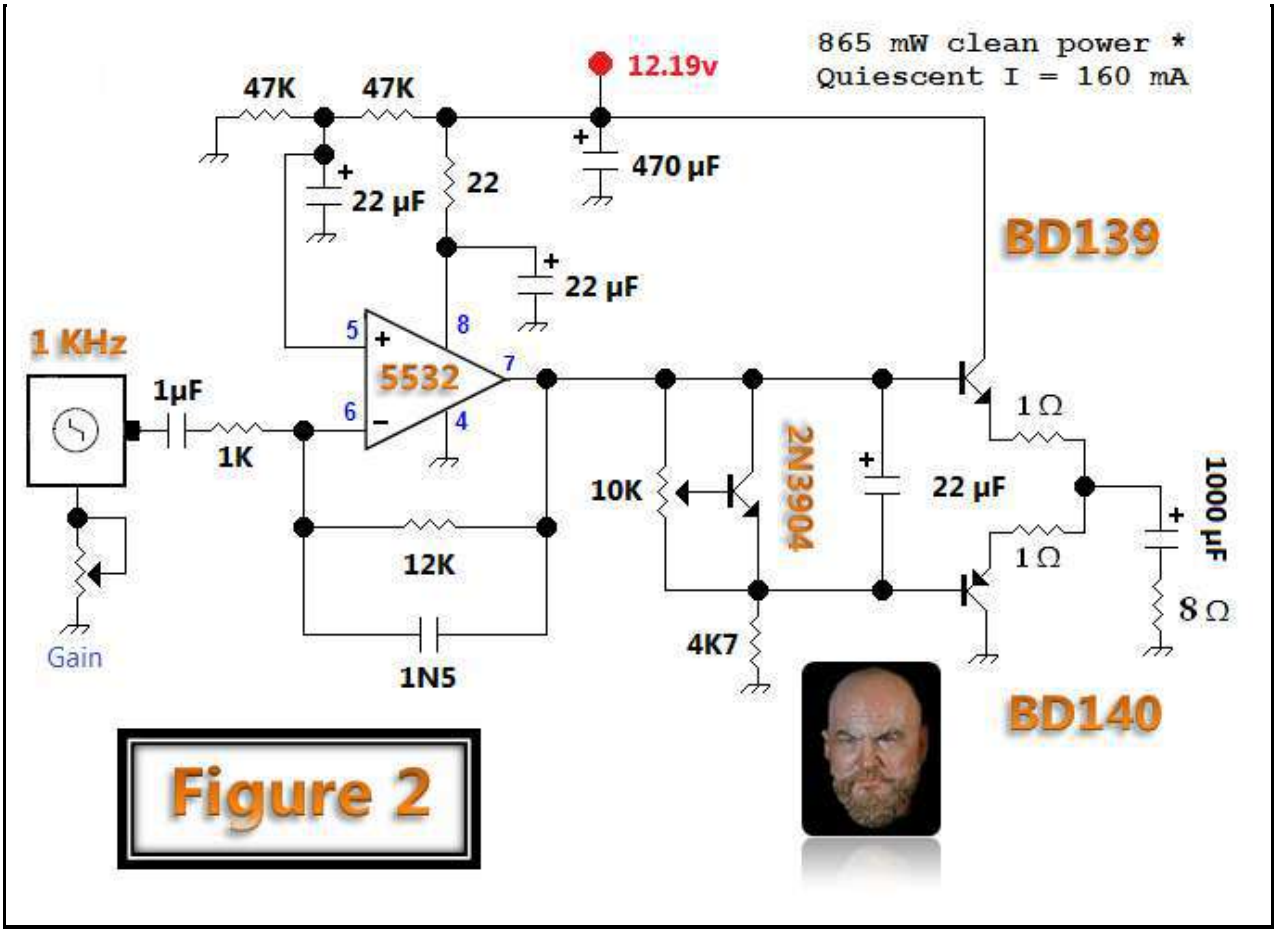

Above — Figure 2 is Figure 1 with the op-amp DC coupled to the level-shifter. I tested the circuit with and without the 4K7 resistor connecting the base of the 2N3904 to the DC supply: it didn't boost the amplifer headroom, nor reduced crossover distortion, so I removed that R.

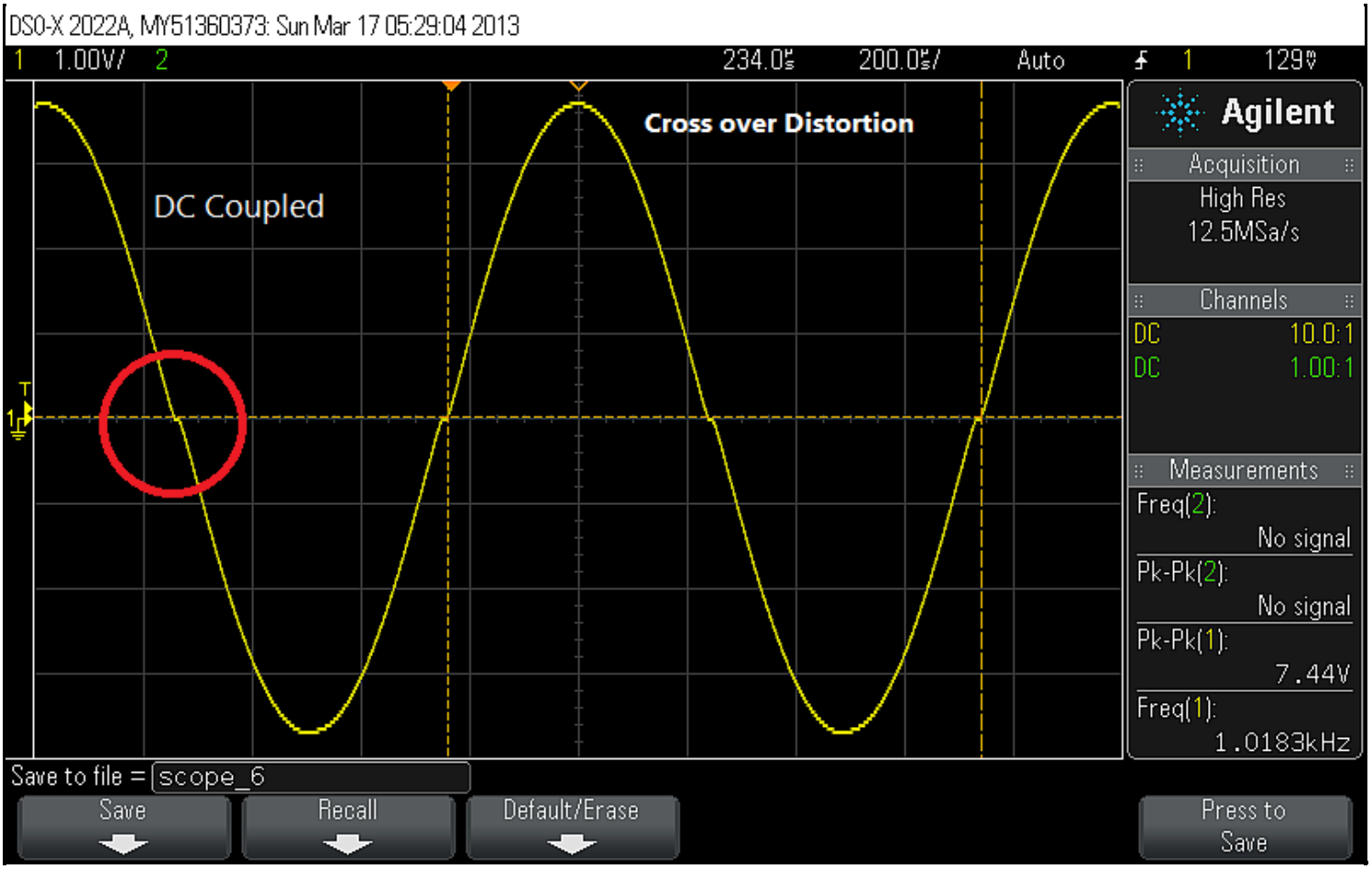

Above — The Figure 2 amplifer 'scope tracing. At *maximum power*, crossover distortion appeared and I've seen this before. Likely, there is not enough base drive to keep the power followers forward biased. By adjusting the level shifter, I almost removed the crossover distortion, but never eliminated it. This drove the quiescent current up to 160 mA. Yikes!

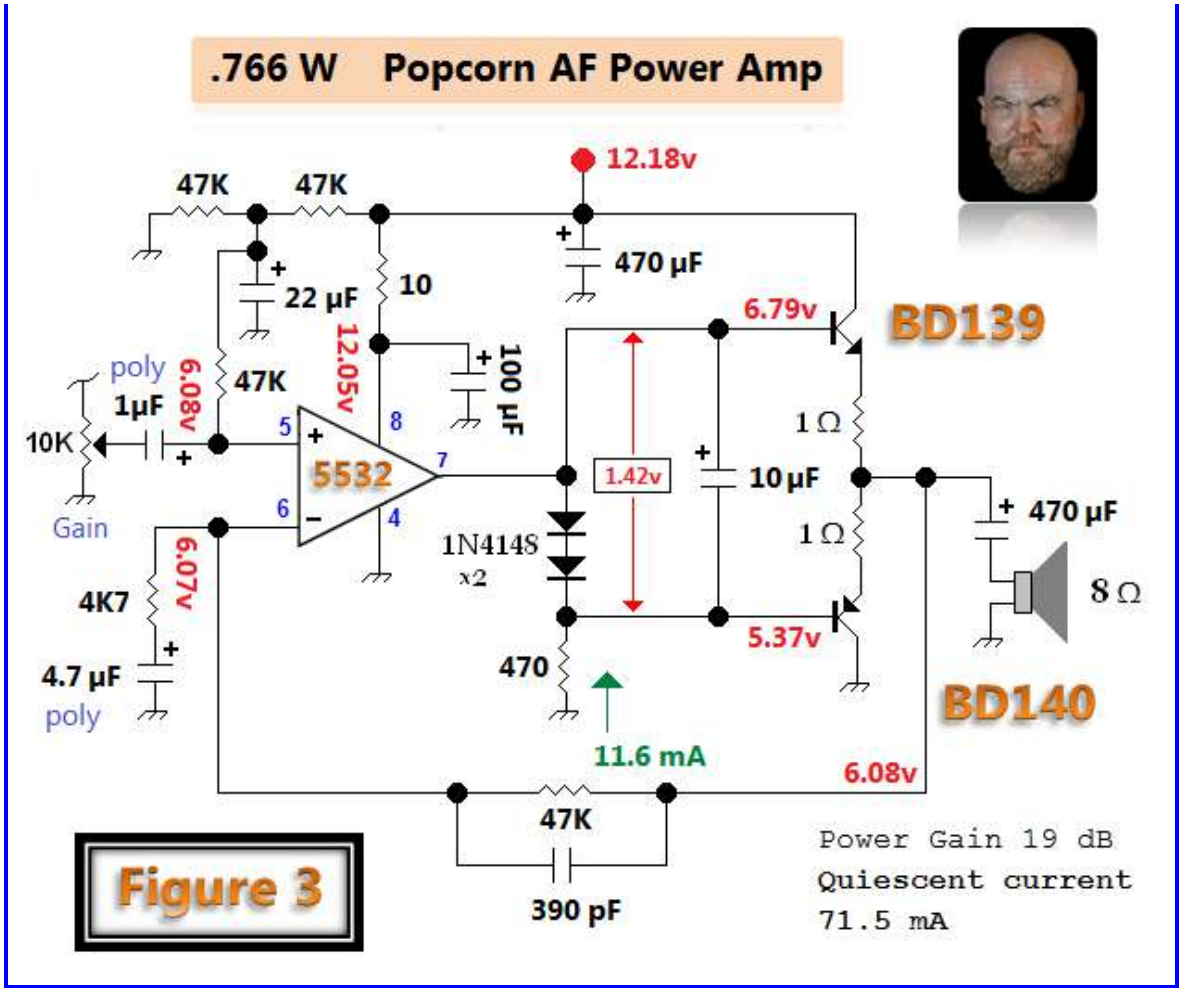

Above — A variation of Figure 2 employing diodes instead of an NPN level-shifter. To kill the cross-over distortion, I lowered the 4K7 resistor by a magnitude of 10. This gave a maximum clean power of 766 mW with a quiescent current of nearly 72 mA. Head room and quiescent current are inferior to the Figure 1 circuit.

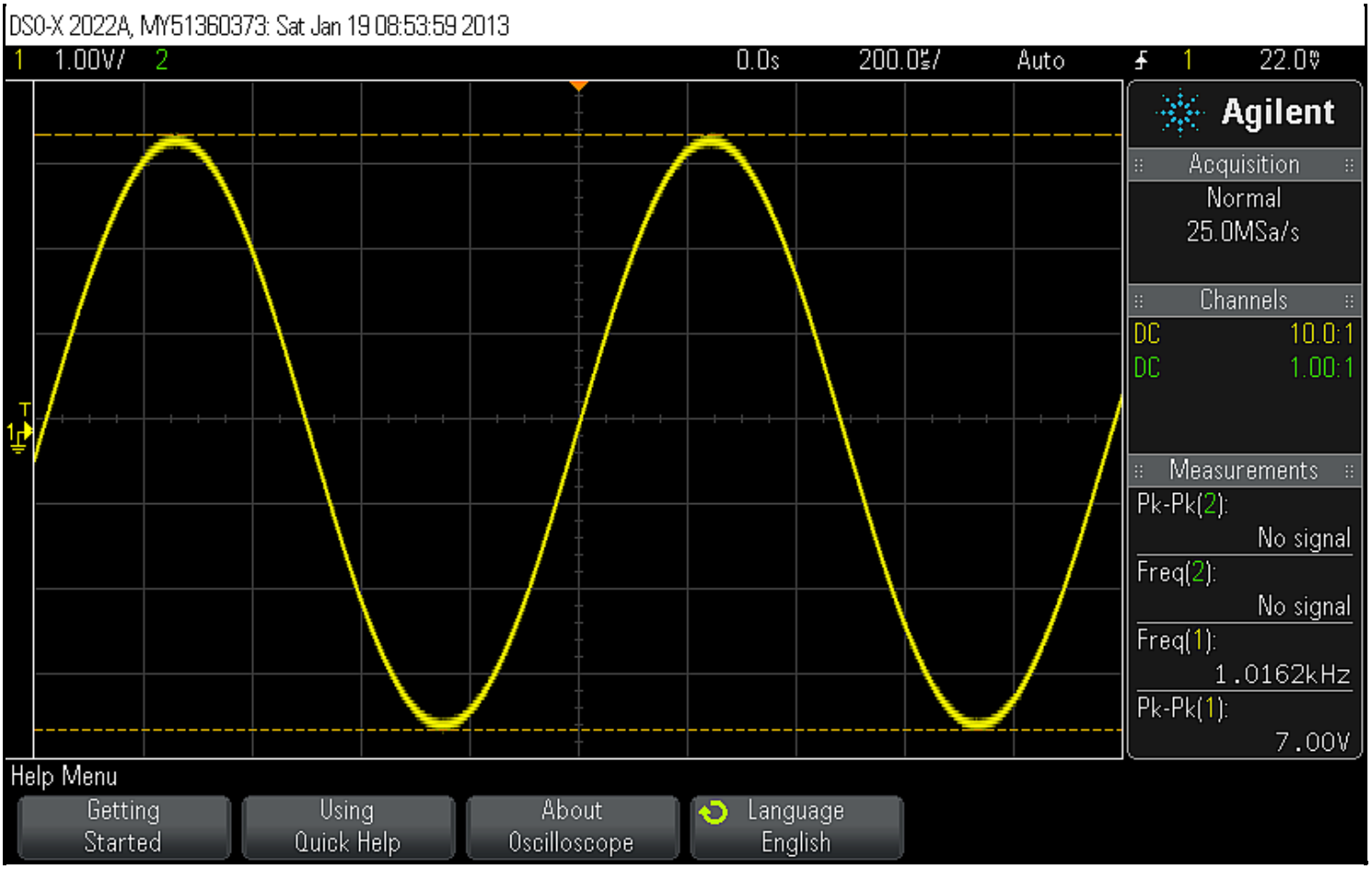

Above — The Figure 3 'scope tracing. Click for a 'scope tracing with the signal generator amplitude increased *slightly* to push this amp into clipping.

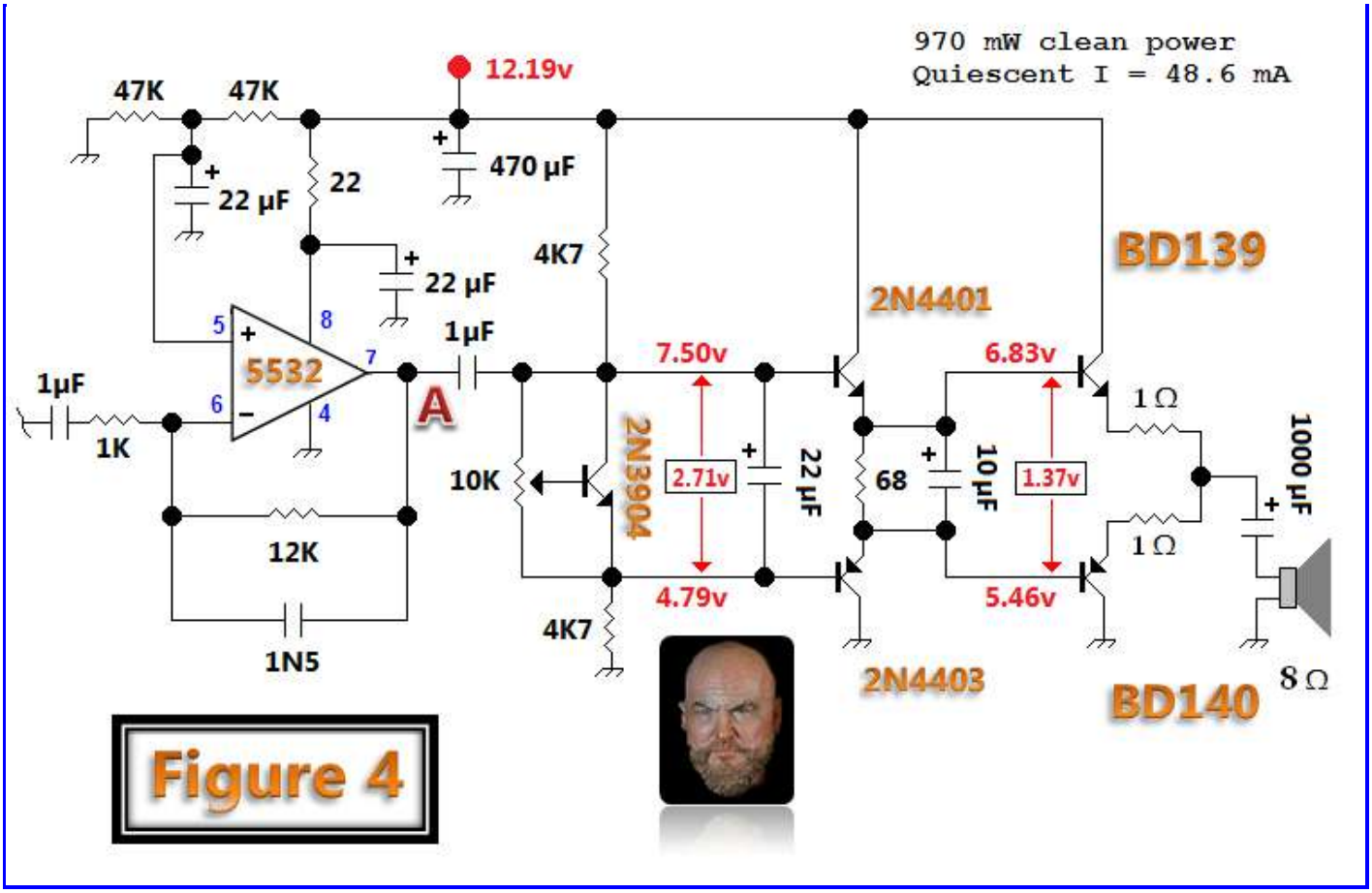

Above — Back to an AC coupled power amplifer like Figure 1. I added a set of intermediate followers built with a 2N4401/2N4403 pair. The clean output power now lies at 970 mW with a quiescent current under 50 mA. Adjusting the trimmer potentiometer on the level-shifter even a tiny amount may change the quiescent current dramatically.

I found a bias of 1.37v across the BD139/140 pair removed all trace of cross-over distortion at maximum clean signal power. Just tweak the 10K trimmer potentiometer while looking at your 'scope and decide what bias you prefer. I lower the bias until crossover distortion appears and slowly tweak it to find the sweet spot. Then measure the DC voltage across the power follower base terminals, plus the total stage quiescent current with the signal generator switched off. You might have to repeat this procedure a few times, since trimmer pot adjustment is quite sensitive.

Jerry, W5JH made a PC board. Click for front photo. Click for rear photo.

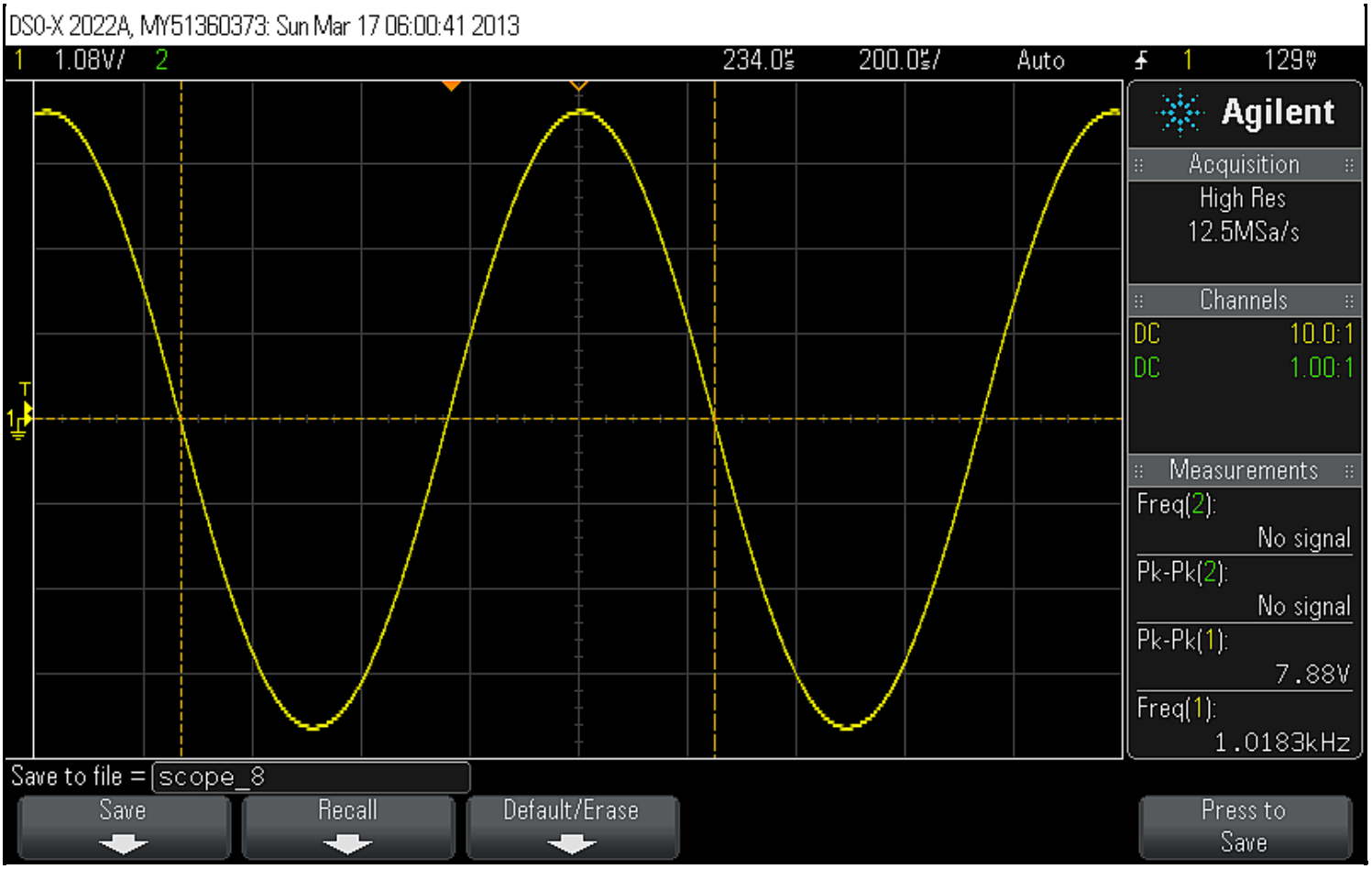

Above — The Figure 4 'scope tracing.

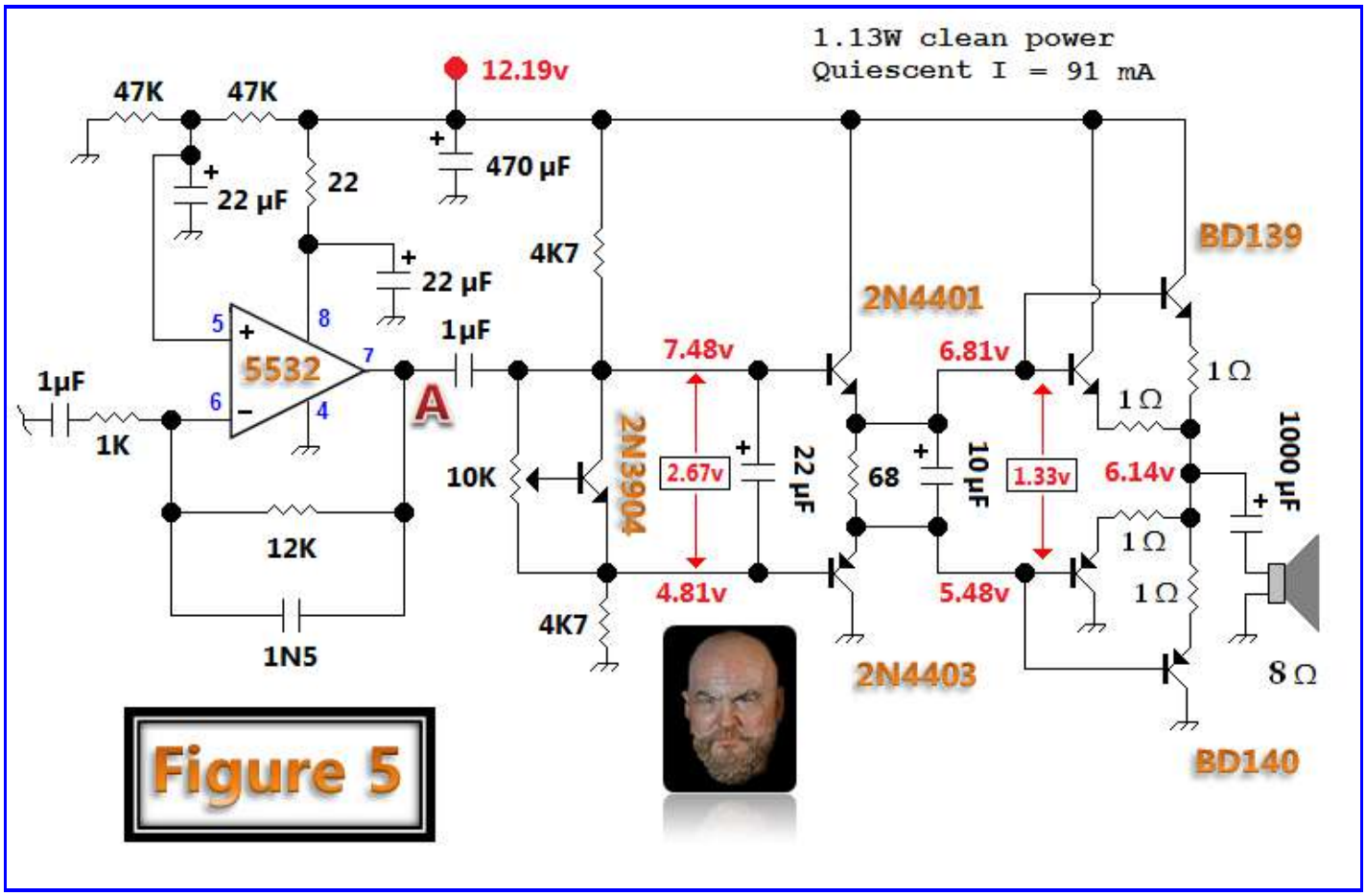

Above — I added another BD139/140 power follower pair in parallel. The boost in headroom over Figure 4 was small, but it was nice to break the 1 Watt barrier. This amp sounded great and blew away an LM386 set up for a gain of 20 — more headroom, less noise and boosted warmth.

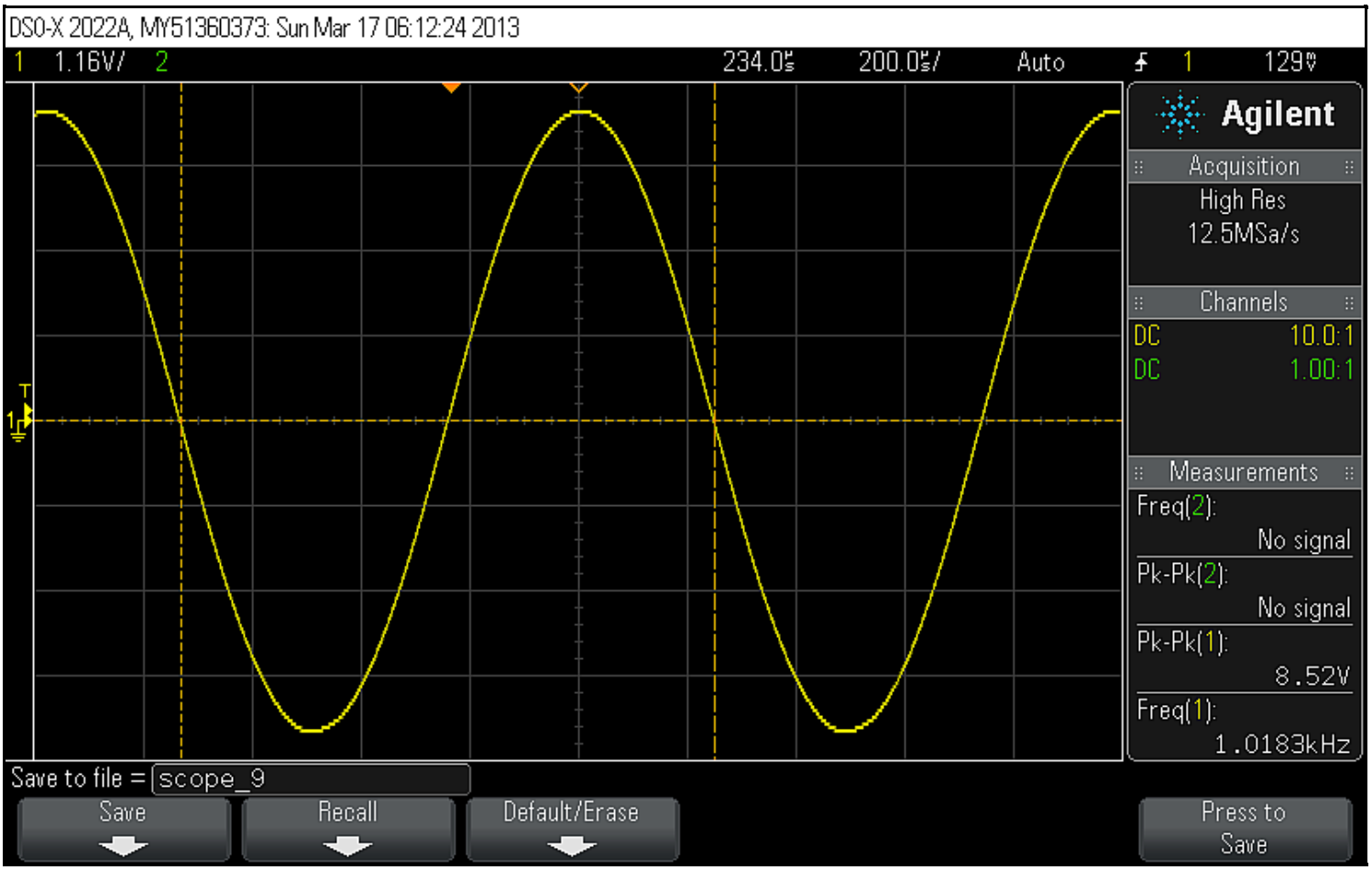

Above — The Figure 5 'scope tracing.

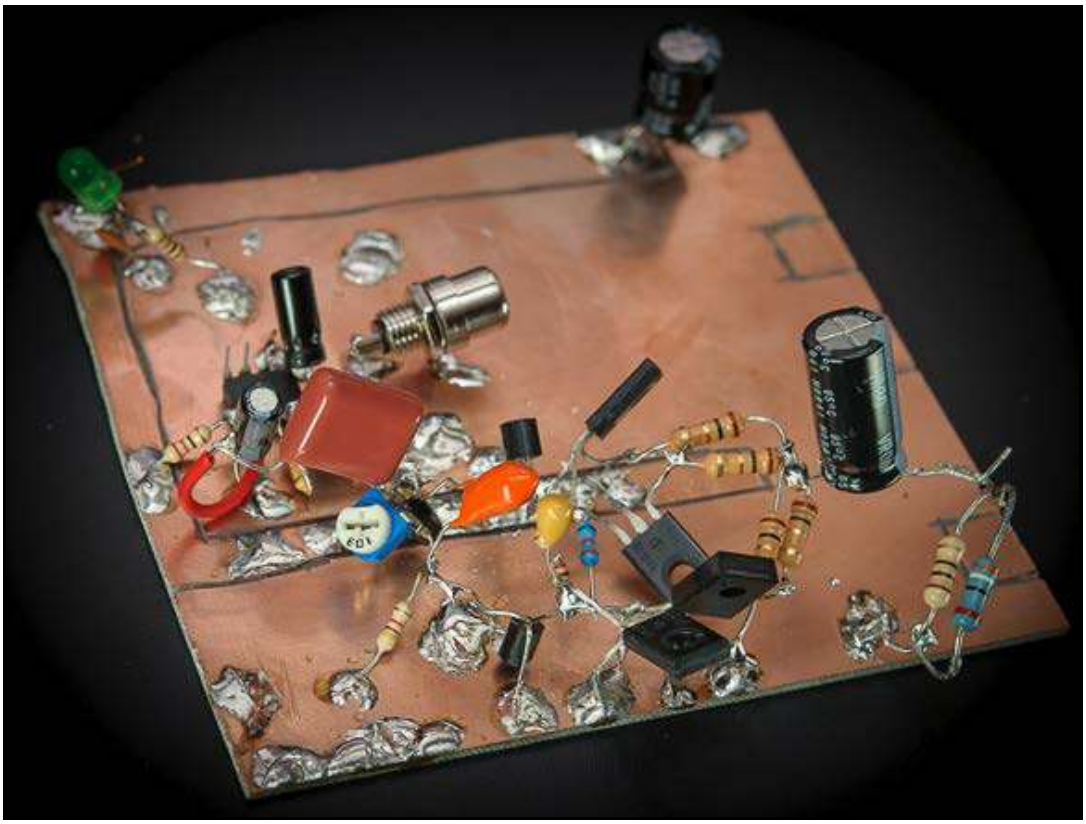

Above — The Figure 5 breadboard. I built all the AF power amps on this board. Signal caps <= to 1 µF were polyester film, while I employed 10 or 22 µF tantalum caps for the level shifters. Electrolytic caps work fine; especially for the level shifter capacitors. The green power indicator LED drew 10 mA and I subtracted this from the quiescent current measurements.

Depending on the AF gain of your receiver, you might wish to add the familiar Zobel filter; a 10 Ω R in series with 0.1 µF C from the positive end of the output capacitor to ground, or more AF bypassing/ decoupling to the circuitry.

No component values were critical — imbuing the spirit of homebrew radio, substitute parts and measure outcomes.

QRP — PosData for August 18, 2014

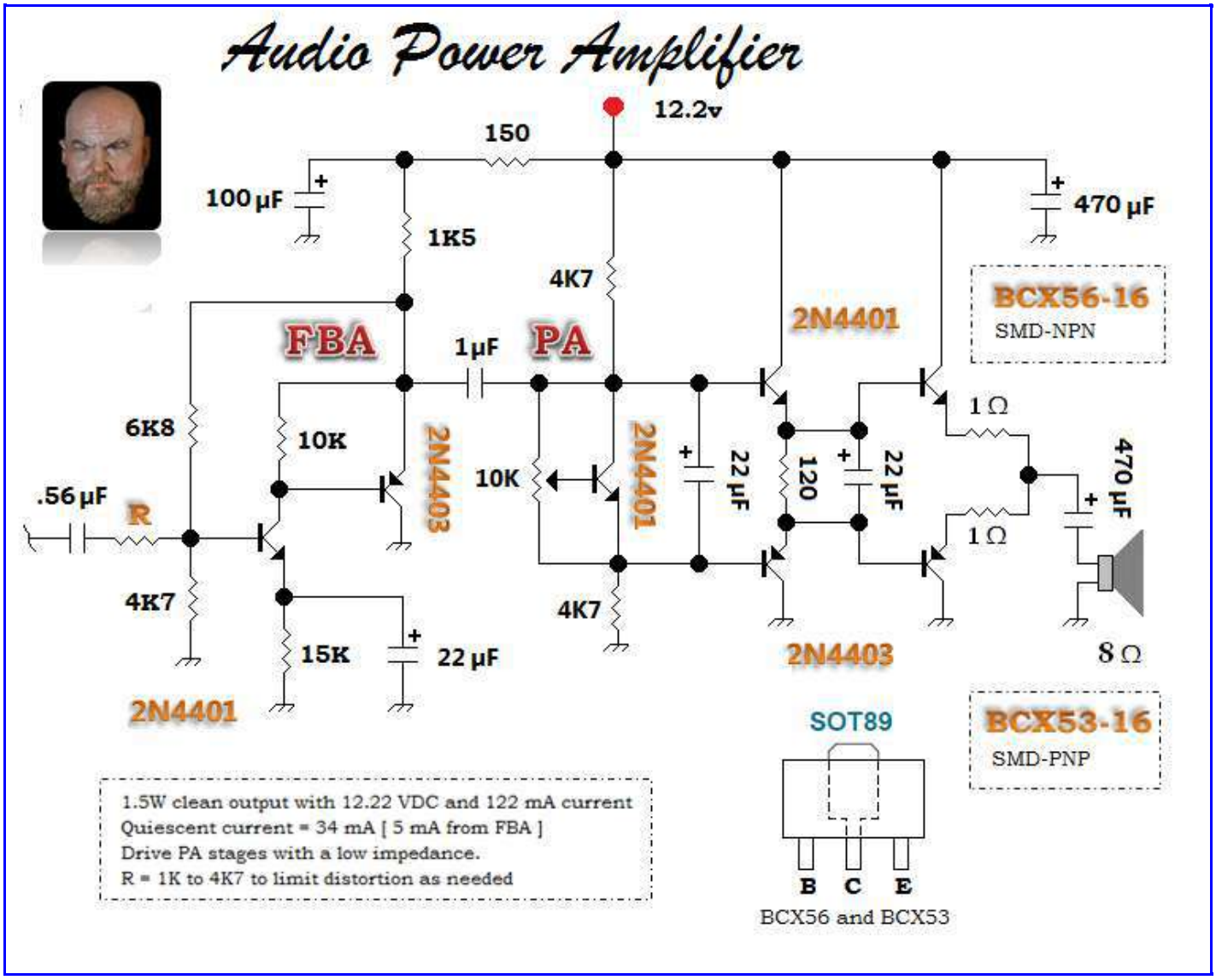

Above — I built a 100% discrete version of Figure 4 power amplifer with a 2N4401/2N4403 feedback voltage amp that drives the PA stage with a low impedance. Without a low impedance drive, the PA [all the components right of the 1 µF capacitor where you see **PA**] the headroom of the PA section falls down. Thus an op-amp or emitter follower drive works great.

I moved to SMD power transistors: the NXP BCX56 + BCX53. These give a little more output than the BD139/140, and take much less board room. I ran no heat sink other than 8 mm by 4 mm PC board traces for the collectors. A better choice might be the related BCP56 + BCP53 pair in SOT223 since the bigger package of this version better sinks heat.

I determined the optimum emitter resistor for the 2N4401/2N4403 followers = 120 Ω [not 68 Ω as shown in Figure 4]. This drops the the PA quiescent current in half and yields the same performance. If you build Figure 4, change to 120 Ω.

I meant Figure 4 and the QRP POS-Data amp as easy-to-make power amplifiers with a *little* gain. You will have to add voltage gain in some AF projects. For Figure 4, it's easy to change up the 12K resistor, or apply the other half of the 5532. Decouple and bypass better if you get motor boating or hum. 73 de VE7BPO

---

9. The Progressive Receiver by Wes, W7ZOI and John, K5IRK

When introduced in QST for November 1981, the Progressive Communications Receiver (PR) by Wes, W7ZOI and John, K5IRK set a dynamic range benchmark for dual-conversion homebrew receivers: 94 dB in CW mode. 31 years later, few other home-built radios have ever reached this benchmark.

The PR is a single conversion superheterodyne 80m receiver; or perhaps it's a direct conversion receiver with an extra mixer ahead of the product detector? It's both and that's the point. Further, Wes and John added other bands with another mixer, plus a crystal oscillator, RF filter +/- an RF amp for each band.

You'll see the PR listed as A High-Performance Communication Receiver in ARRL Handbooks from the early 90s or so. ARRL staffers built and enjoyed the PR in their test lab for many years.

After purchasing the 1991 ARRL Handbook and reading about this project, I slowly adopted and entrenched the PR's progressive (modular) approach. When I built and web published my 2 TRF WWV receivers with crystal IF filters, a couple of people wrote that I "grossly over-designed" them, however, other, more astute builders placed a mixer on the front end and turned their TRF into a multi-band superhet like I later did. These builders understood how progressive circuit building works — all PR inspired.

I hope my introduction renews your interest in the PR. Wes and John's article is thorough and complete — I can't add to it, however, I'll share my thoughts along with those from Wes and John all these decades later.

The IF Stage gain comes from 2 dual gate MOSFET amplifiers. The final MOSFET amp drives a BJT differential pair providing 9 MHz RF to the product detector at 50 Ω and signal for the AGC circuit. Wes recalls using a 3N211 in the original MOSFET slots since Doug DeMaw owned a pile of them and contributed some. In some areas, the 40673 was the dominant 2-gate MOSFET soldered by radio home builders back in the day.

An evolved version of the PR Intermediate Frequency stage appeared in EMRFD as Figure 6.50. Wes replaced the now hard-to-find and *expensive* leaded dual-gate dual gate MOSFET with a cascode of J310s. I built this stage and it performed well with my 12.2 VDC power supply.

Jeff, WA7MLH built the general purpose IF system and noticed if the power supply dropped below 12 VDC, the gain control and maximum gain fell off and he wrote to Wes about his findings. Wes later confirmed dysfunction with a lower DC supply. I asked him to recollect this time:

"…. Frankly I don't remember if I went immediately to computer simulations or if I built a single stage. I think I built. Anyway, Jeff was correct, depending upon the FETs that were used. Then I got to plowing into the details of the cascode, this time with SPICE. I was using PSPICE for some simulations, but was in the process of switching over to LT-SPICE. That makes no difference, for I used the same models in both.

Anyway, playing with a single stage showed that the mechanism for gain reduction was that when the voltage on the upper gate was reduced, it did nothing to the upper stage, but it compressed the supply on the lower FET. So far as signal goes, the upper part was nothing more than a common gate stage that passed whatever signal current was there in the drain of the lower part on into the source of the upper part.

But these were depletion mode FETs, the normal thing for most of the JFETs we use. As such, you have to get the gate down pretty low to get the source voltage low enough to be effective in reducing the gain of that lower FET. That's when it became clear that one could use other parts in the upper slot. An enhancement mode FET such as a MOSFET would work well. And just a common bipolar would do the job nicely too..." *Wes, W7ZOI per an email - January 2013.*

In QST for 2007, a refined version of the EMRFD Figure 6.50 IF stage appeared with a hybrid cascode amplifier instead of the cascode JFETs (and the 2 original dual gate MOSFETs of the PR). Further, Wes added a third amplifier to widen gain control. The hybrid cascade stage has since gone in 100s of receivers across the globe; ensuring the PR legacy lives on as the modernized hycas version.

Roger, KA7EXM sold kits of the hycas amp for years, however, these kits sold out. PC boards may still be available via his web site. Roger received permission to publish the QST hycas article online:

Above — The now *sold out* hycas IF System kit once offered by Roger, KA7EXM.

To underscore my love of the original PR IF amp, I built a version using SMT dual gate MOSFETs in 2013 and feel the SMT version might be perfect for builders who prefer to manually control IF gain in most situations, but want AGC control now and then. Versions built with the BF998 MOSFET may suffer parasitic ocillations at UHF and so meticulous attention to decoupling and bypassing out to UHF and in some cases double-sided copper board may be required to prevent unwanted ringing at UHF.

If you build the entire PR with the BF998, the VFO output runs about 10 dBm and requires attenuation. Again, please consider UHF oscillation precautions.

Wes and others have built both leaded and all-SMT versions of the hycas amplifer.

John, K5IRK Recalls

I wanted John's recollection of the PR design and build and received the following narrative in late March 2013:

"…One night in late 1979 I had telephoned Wes to chat about QRP and building rigs. During the conversation he told me he had a project and related QST article in mind and asked me if I wanted to participate. He was in the process of writing a book (IRFD) and didn't have much free time, so he needed some help. I told him yes. A few weeks later I received the first schematics and began to gather parts.

Recall that the project started as direct conversion receiver. But it then progressed (hence the title of the article) to a superhet. I choose to build my superhet with a SSB filter as I had already built Wes' CW Competition Grade RX from SSD. During the next year he sent me schematics and a few critical parts thru snail mail. (The Internet and e-mail would come later.) I would build the circuits and report the results back to him. As I recall, we only had about three phone conversations throughout the whole project.

The design was an iterative process. For example, the IF circuitry began with a single 40673, but grew to include two stages. Wes bread boarded this in a mono band version of the receiver at his end. An early audio derived AGC system was replaced by the IF derived circuit that appears in the article. The VFO was also designed twice, as were the Front end Filters and the BFO. More is said below about the design procedure.

I designed the circuit board layouts. The traces on my boards were drawn by hand and etched at home. I sent hand drawn sketches of each of the boards to Doug DeMaw; Circuit Boards Specialists (CBS) then created the commercial boards for those folks who wanted boards. I recall that we sent out layouts to any readers for a SASE. All of my boards were designed and built on double sided PC material with the exception of the VFO board and the Audio Filter boards. This can be seen in the photos. The boards eventually sold by CBS were single sided. All layouts and functionality were confirmed prior to publication.

The traditional design process for a homebrew ham receiver in 1980 started with schematic sketches based upon the intuition and experience of the designer. The total circuit would then be built. Measurements were merely things that were done afterward, something to characterize the result. The PR was different. Individual stages were designed, built, and measured. Negative feedback was used in the critical amplifiers to guarantee that the gains were high enough for reasonable noise figure, but low enough to preserve input intercept.

Only after the individual stages were operational, were they assembled to form a working receiver. Some stages were further modified during system assembly and evaluation. We had no computers available for circuit simulation, although the gain distribution was optimized with a hand calculator. The goal was not just a receiver that sounded good, but a box with good two tone dynamic range.

Once my receiver was completed, I sent it to Wes for MDS and DR measurements. A goal was to compare these measurements with those already done in Oregon. Roger (KA7EXM) took many (if not all) of the photos. Wes then forwarded the receiver to ARRL. They returned it to me when they were finished. Wes refined the article during the final months of the project before it was finally published. I received copies of his drafts, and then offered my feedback.

We had hoped that a "few" experimenters would enjoy building the receiver, but had no idea that it would be as successful as it was. We eventually learned why this occurred: First, the receiver held up well when it was measured at ARRL Headquarters, exceeding the performance of most of the appliances being evaluated at the time. This prompted some League staff members to build the receiver for their own use. This, in turn, prompted them to include it in the Handbook for several years.

My original receiver plays as well today as it did in the beginning. The electrolytic caps on the audio board have been replaced, for they were beginning to go south on me, but that's the only change. I do have a second version that is used for experiments..."

Some PR photos taken by John in March 2013

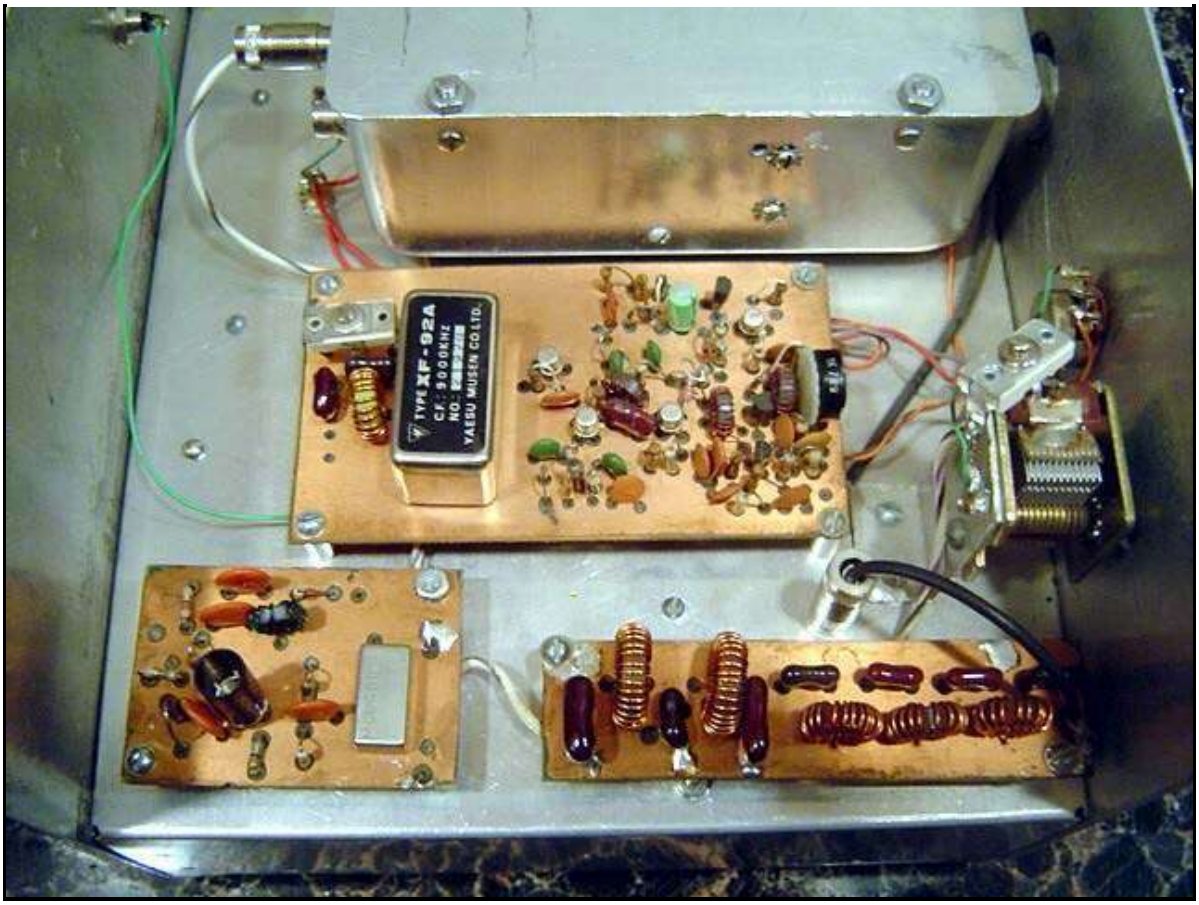

"...You will notice a couple of things different in these photos than in the photos in the article. First, tacked on to the Front Panel 365 pF variable cap is a mica trimmer cap.....this is of no significance as I was just messing with lowering the BW upper and lower frequencies to see what difference it would make....None is the answer..." *John, K5IRK.*

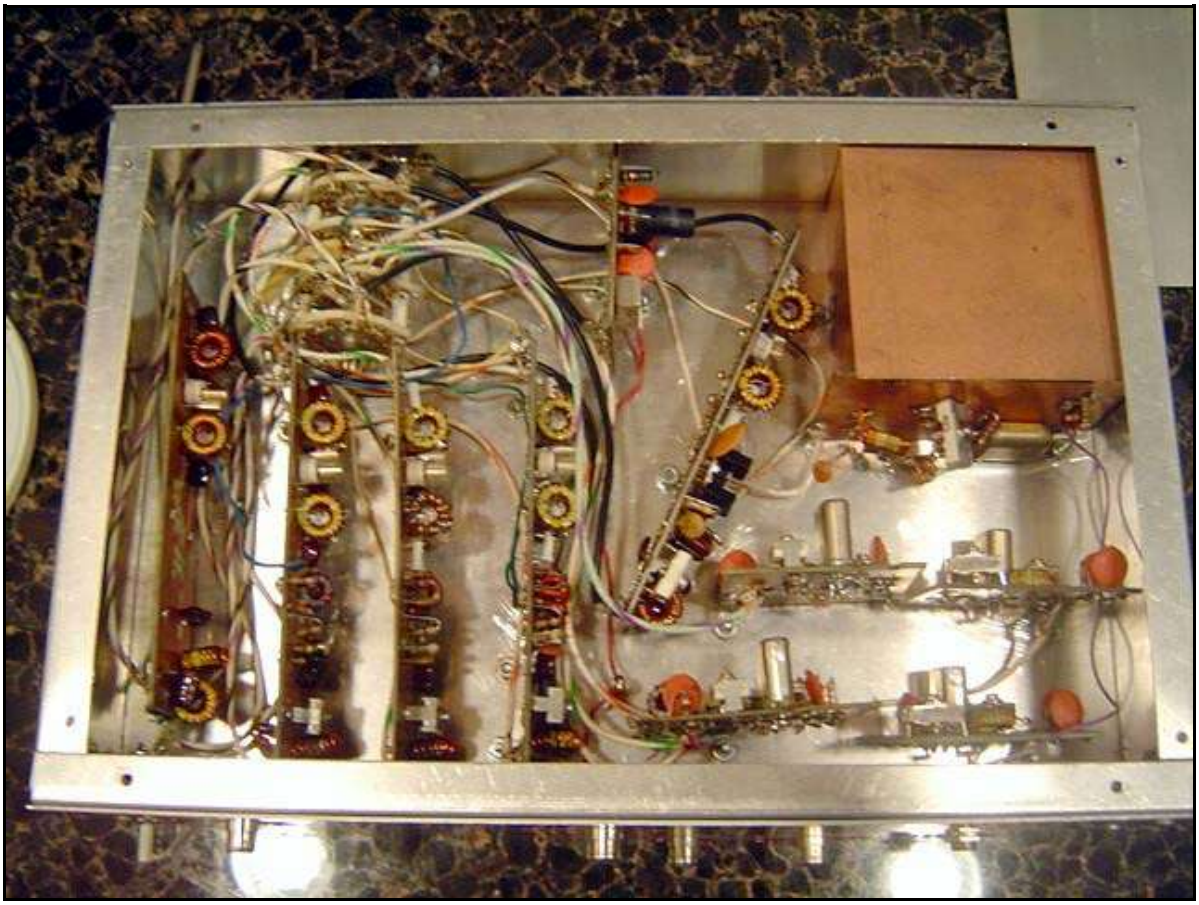

"...In the above photo you will see the addition of the 30 meter band to the RX with the diagonal front end filter board and the Xtal Oscillator attached to the BFO Box's wall that was added some years after the article was published…." *John, K5IRK.*

High-pass plus Peaked Low-pass Filter

If you know me, you know I love the peaked low-pass filter both at RF and AF. This adoration came from studying the PR and other work published and shared privately to me by Wes. *A good reference = The Peaked Lowpass: A Look at the ultraspherical filter by Wes for Ham Radio, June 1984.*

While the high-pass + peaked low-pass filter placed ahead of the second mixer in the PR wouldn't likely go in a modern W7ZOI design, its narrow-band LC filtration generates a roofing action when the receiver uses converters for bands other than 80 meters. The result is that much of the DR obtained in the single conversion version is retained in the dual conversion receivers.

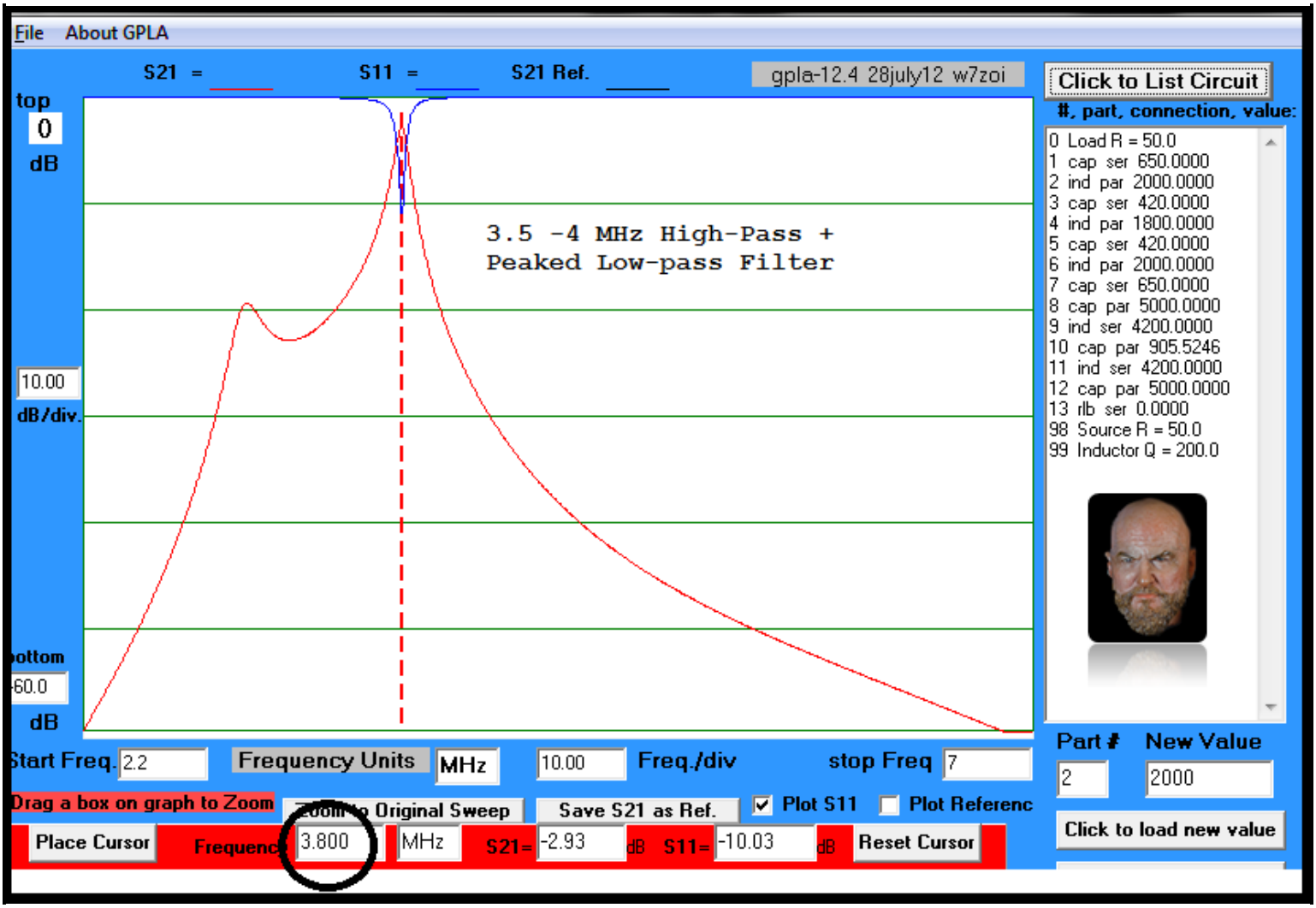

Above — A GPLA simulation of the front end high-pass/peaked low-pass filter centered for 3.8 MHz by tweaking capacitor #10 in the software. Click for another simulated filter that covers 3-4 MHz. Look at the sublime low and high-pass skirt action with a 3 dB bandwidth of 73 KHz. Love this!

Click for a screen shot of an entire 40 Meter band version shown with the low-pass filter section centered at 7.003 MHz. I also made 1 for WWV 10 MHz — by scaling the original version's XL and XC and tweaking with GPLA, you may build 1 for any HF band.

AF Amplifier

The post product detector AF chain sounds great. Many of us later replaced the Q5 mute switch with something quieter, however, even today — this AF block holds its own against most discrete component headphone-level circuits. I particularly love the crisp fidelity of the Class A feedback pair Q3 and Q4. Today, I would substitute a BD139 for Q4.

Wrap up

I could go on, but this web page is already too long. Studying + building stages from the PR; a receiver designed more than 3 decades ago, might raise your game today. Go team!

---

10. Miscellaneous Pictures and Figures

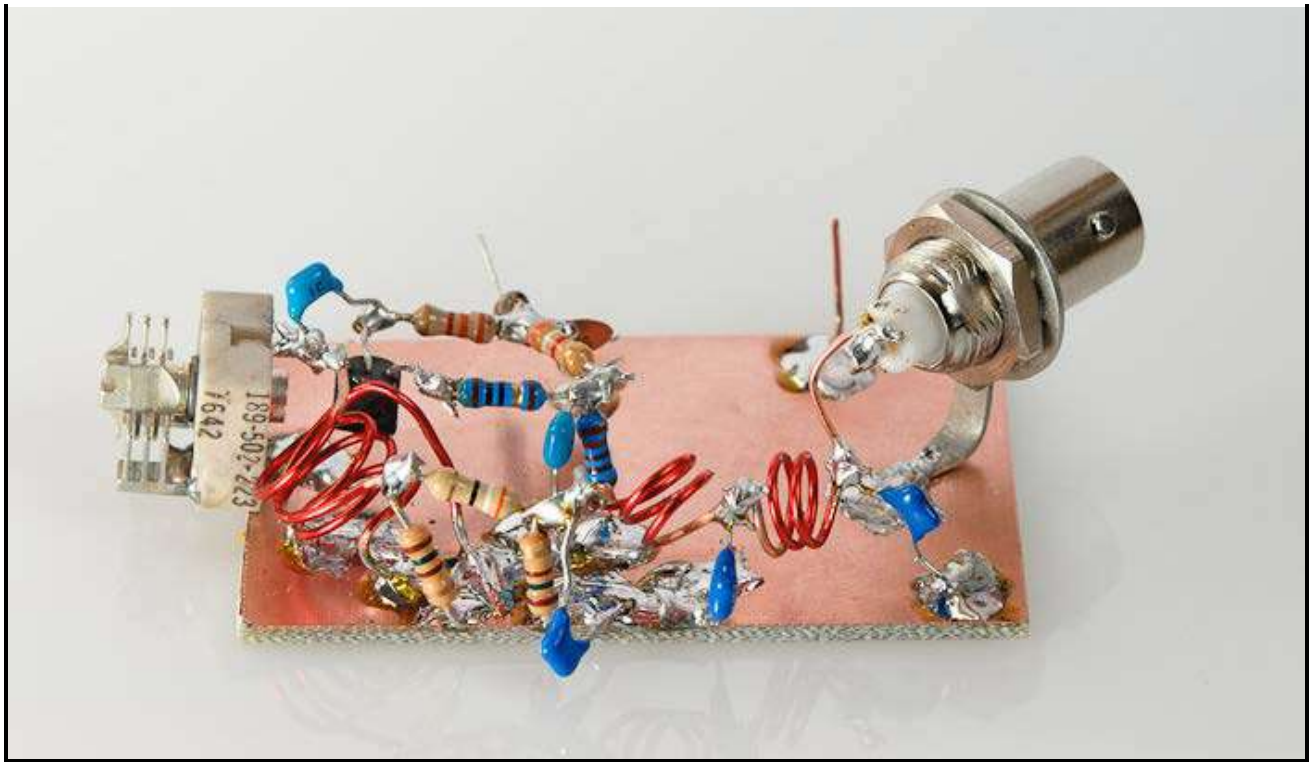

Above — I built a prototype 200 MHz oscillator with trailing low-pass filter before making the 210 MHz version placed in the 1-118 MHz VFO for the K3NHI sweep system. (Section 1). The secondary coil floats and may be positioned between any of the 4 primary links to change coupling and thus output power.

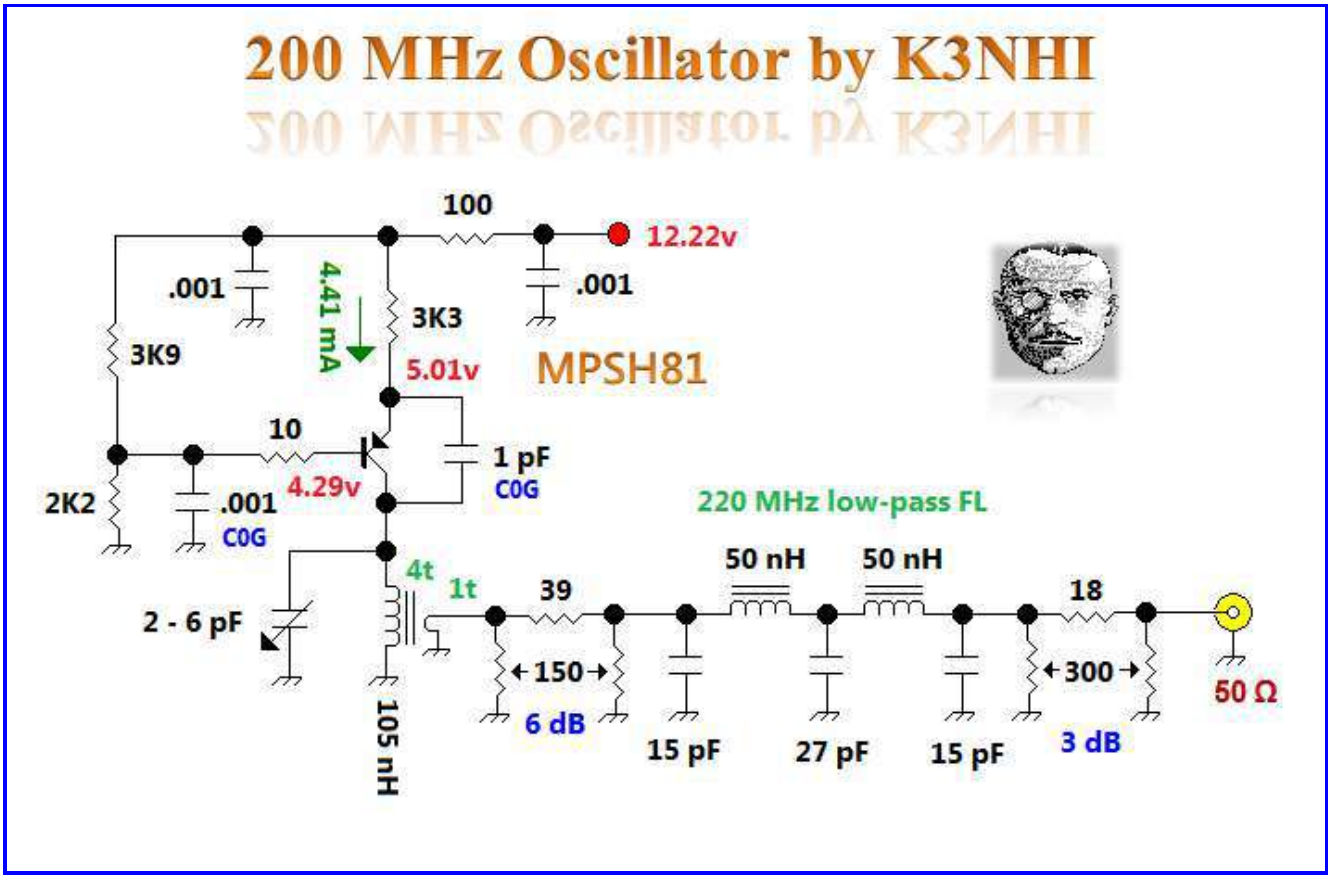

Above — The schematic of my 200 MHz local oscillator. Click for another version I designed that tuned from ~135-208 MHz.

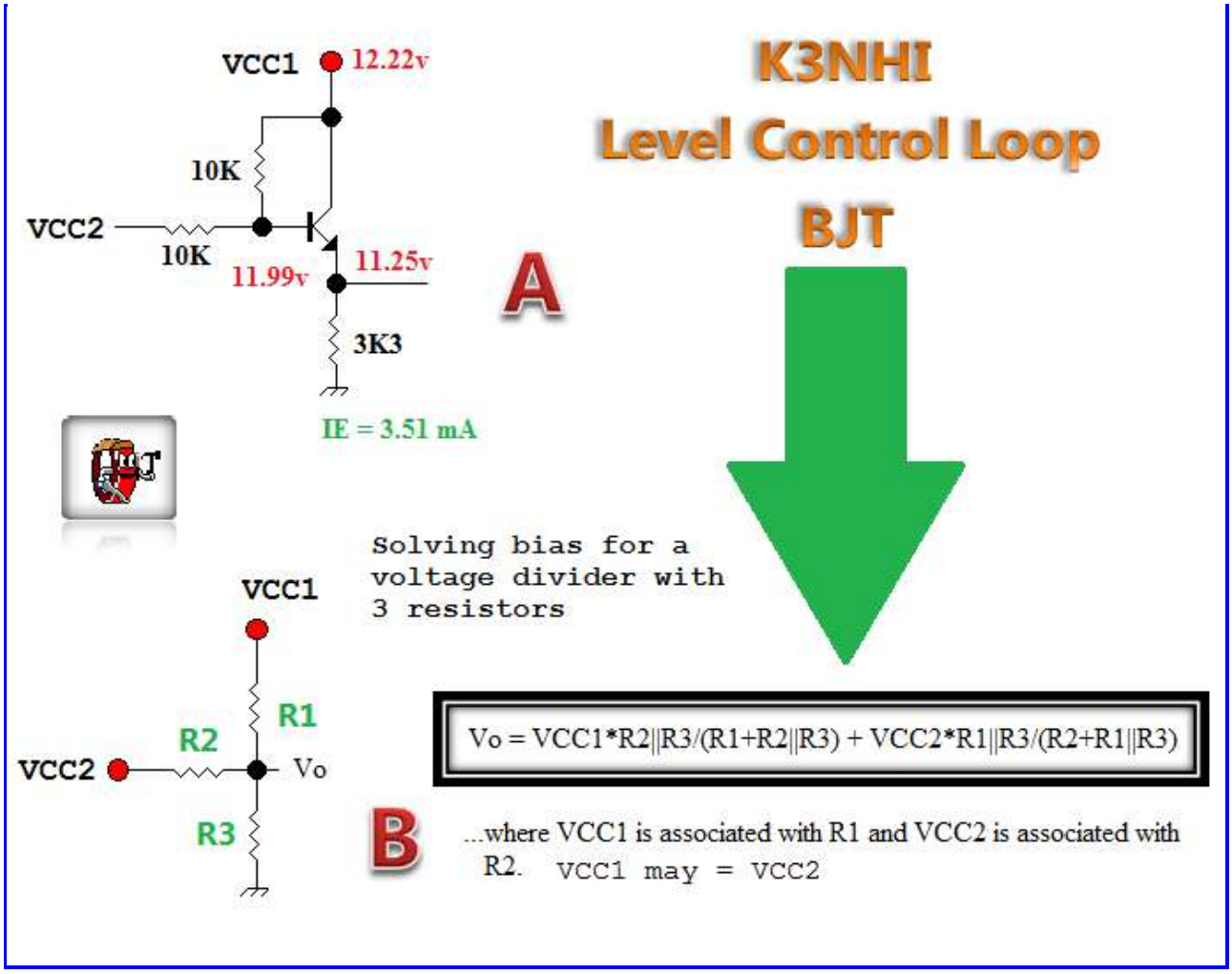

Above — In the K3NHI 1-118 MHZ VCO lies a fabulous leveling circuit that involves a CMOS rail-to-rail op-amp controlling a BJT level shifter. To understand the bias of this BJT, I made a breadboard (A) and then a simple model (B) and developed the equation shown that involves 3 bias resistors. Bias or Vo is determined by superposition. VCC1 and VCC2 may be equal or not. VCC2 comes from the op-amp. I also learned it's a good thing to surround myself with smart people.

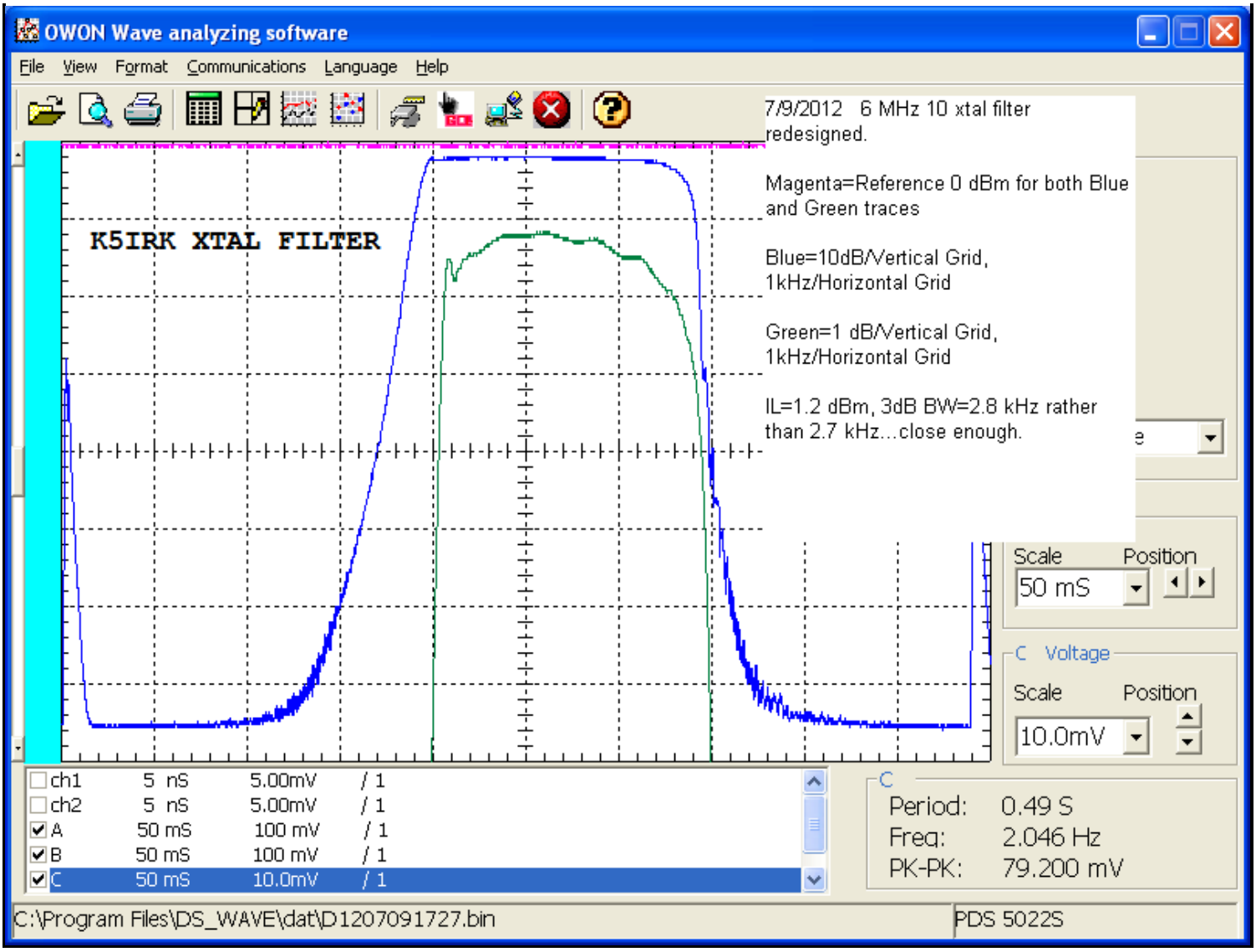

Above — John, K5IRQ designed and swept a 10 crystal SSB filter with an insertion loss of 1.2 dB in the K3NHI sweeper that I just had to show you. Click for his build up in Ladbuild08 and then GPLA08 from the EMRFD CD. Bob's xtal sweeper from Section 1 and Wes' software arm us experimenters with solid tools. Nothing can replace measurement and reason.

RF — Test and Measurement

VHF — Véronique

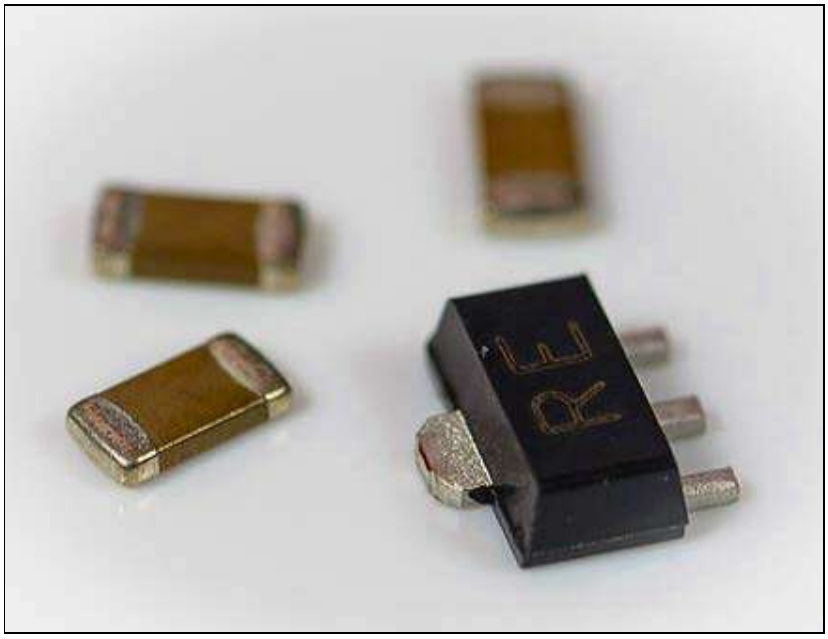

Repository for VHF experiments conducted in 2013 and 2014.

1. Ferrite beads
2. BFS17A transistor
3. 50 Ω MMIC Bench Amplifer
4. Breadboarding Double-Sided Copper Boards
5. Simple Preamp Filter
6. VHF Band-pass Filter Experiments
7. NE612 Mixer Diddy
8. Miscellaneous Photographs

1. Ferrite Beads

I toiled to choose an SMT ferrite bead for my junk box. Selecting suitable chip beads not only troubles us, but even some engineers I've read — which to choose? Chip beads act as high frequency resistors that present a low impedance to DC plus our desired RF signal while impeding and dissipating UHF through resistive losses caused by minute heating of the ferrite material from eddy currents. SMT beads are typically rated by their maximum current, resistance at DC, and the impedance they present at 100 MHz.

Since a ferrite bead's impedance is essentially resistive to parasitic UHF oscillations, I remembered that the model for a bead is actually an inductor paralleled by a resistor. It's the "resistor" we're after, for that's the extra load that tends to stabilize the amplifier. From past success in UHF supression with low-value (10-51 Ω) resistors, I chose my SMT bead to have a relatively low Z at 100 MHz. Consider, too, that many chip beads sold today serve as RFI suppressors for high speed digital lines where the Z at 100 MHz and maximum current lie well above my requirements.

I found a chip bead that appealed to me on eBay and bought 50: size 0805; 800 mA; with a Z at 100 MHz of 120 Ω.

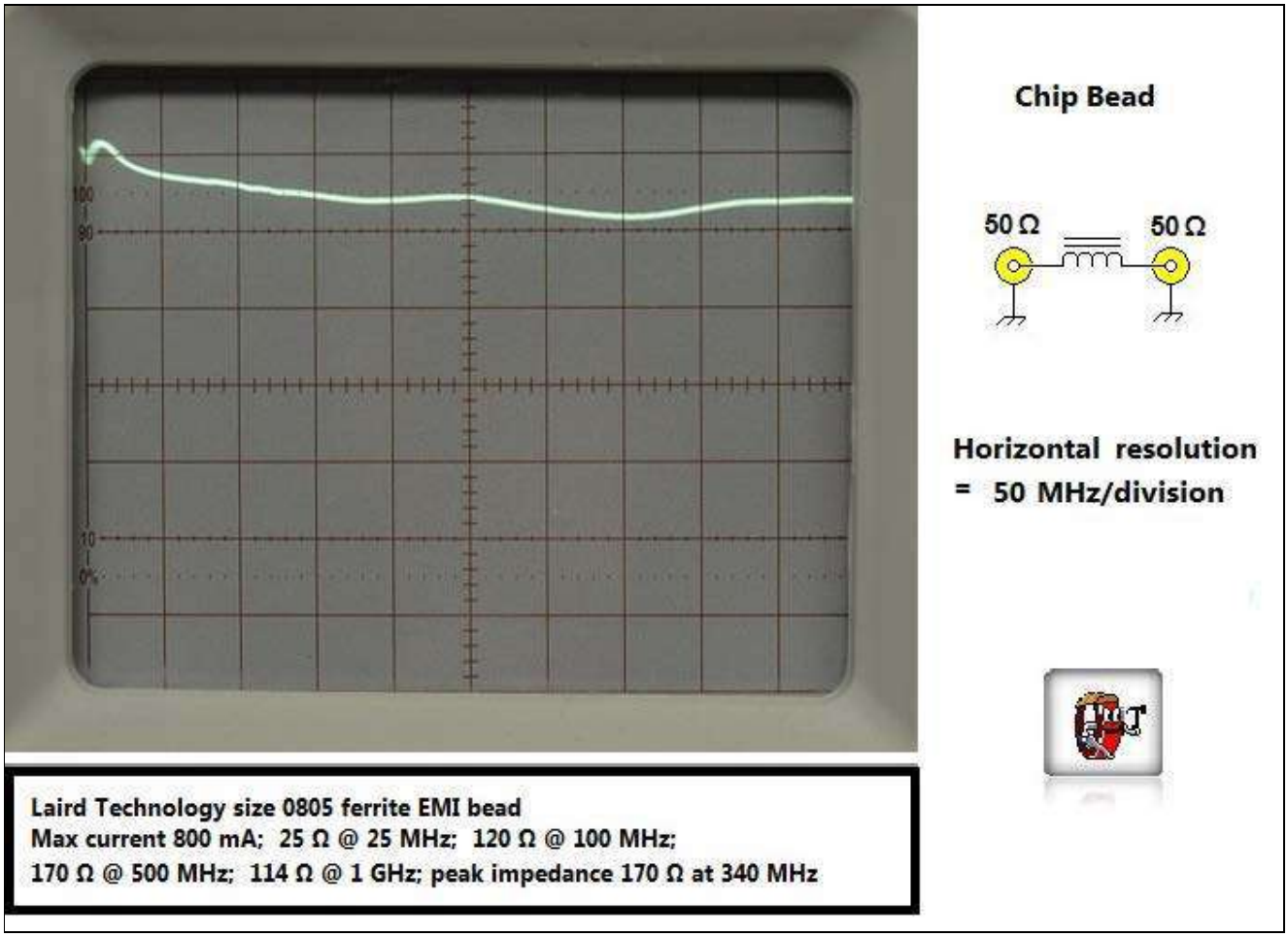

Above — A sweep of my bead from 1- 500 MHz. Sadly, I did not perfectly center the sweep at 250 MHz, but the peak impedance occurred close to the specified 340 MHz.

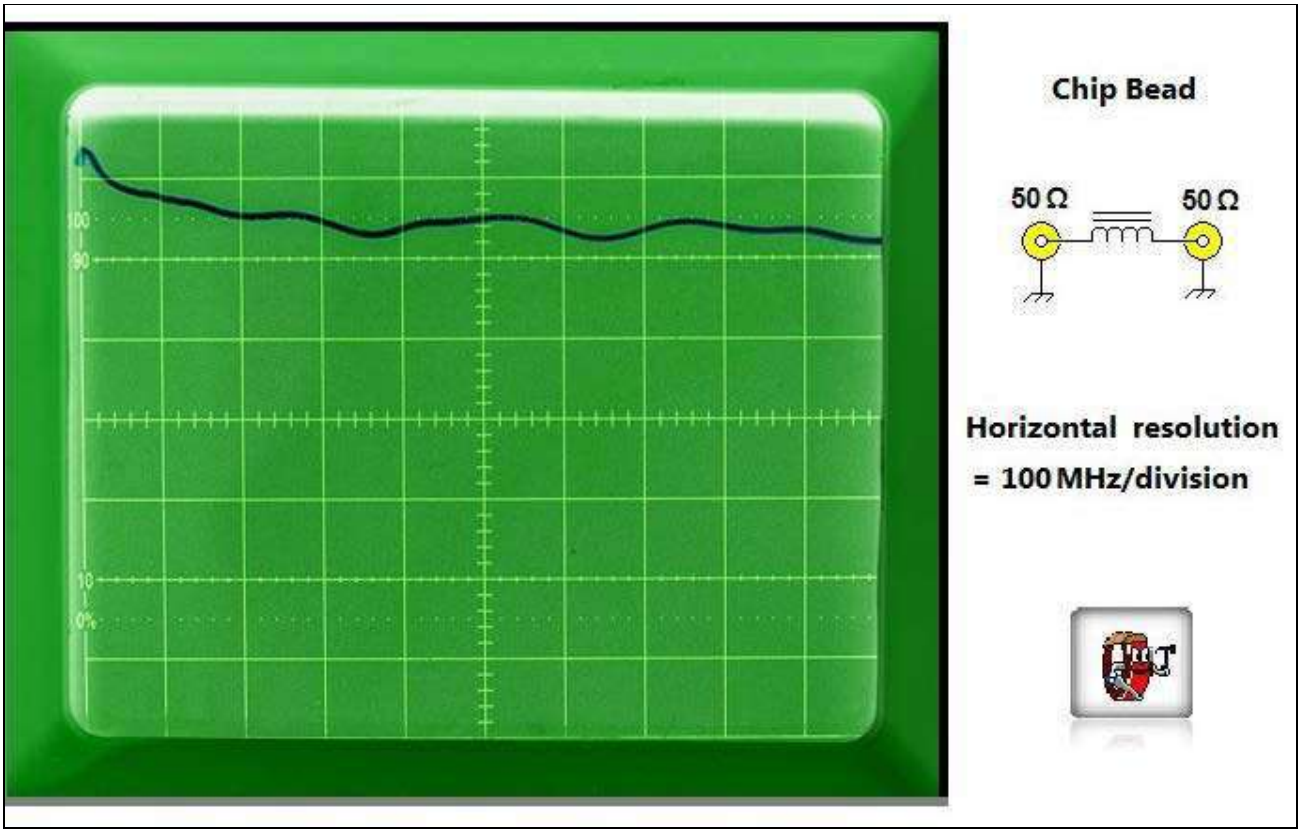

Above — I swept my Laird techlogies chip bead out to 1 GHz. Ultimately, I'll have to verify its function with in-situ experiments. For example, before and after chip bead analysis of a low noise amplifier that's oscillating at UHF.

FB43-101

If you sweep the floor under my QRP work bench, you'll find 2N3904s, J310s and a few FB-43-101s in the dust pan. In our hobby, FB-43-101s are common as fleas on a dog; many builders like to stick them on the drain, collector, or base/gate lead(s) of an active part to squash UHF oscillations. I've never seen a datasheet for this part and decided to sweep 1 for reference purposes.

2 sweeps of the FB-43-101 follow:

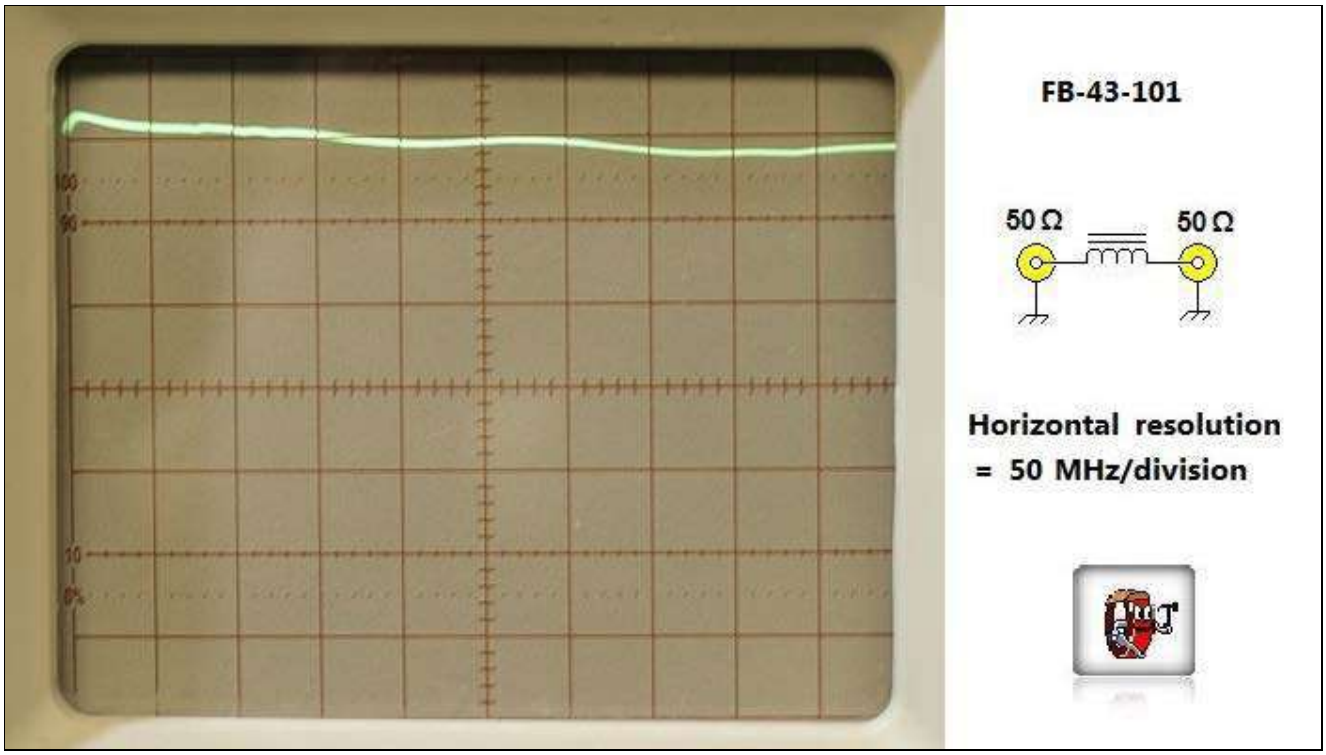

Above — A 1 - 500 MHz sweep of the FB-43-101 slide-on bead. This tracing shows very subtle attenuation that peaks between 400 and 450 MHz. Probably this minimal attenuation at UHF provides the reason we often need to put 2 on the drain or collector of our amplifiers?

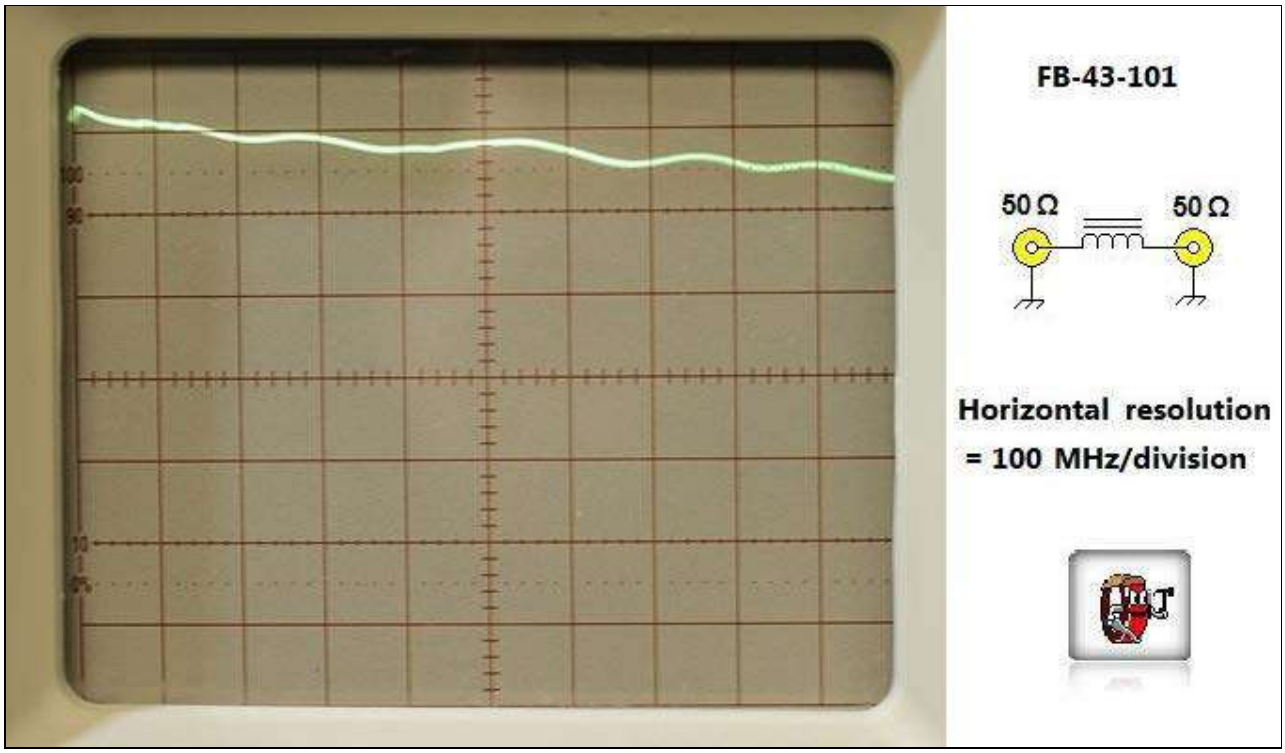

Above — A 1 - 1000 MHz sweep of the FB-43-101.

2. BFS17A Transistor

I sought a surface mount NPN transistor to supplant my leaded transistors such as the PN5179, BF199 or MPSH10. Serving as a general purpose transistors biased for ~5 to 20 mA collector current — they'll work as buffers + oscillators + as the BJT for hybrid-cascode amplifiers built with a SMT J310 on the bottom.

My requirements were SOT-23 (3 well *seperated* leads allow easily carved islands in a copper board with a dremel tool); an fT that's not too high to help reduce higher UHF oscillations; and a noise figure < 3. Other factors included price and availability. We enjoy many choices with such criteria, but I settled on the BFS17A. Click for the data sheet . In summary, it's a 2.8 GHz part with a NF of 2.5 dB at 800 MHz.

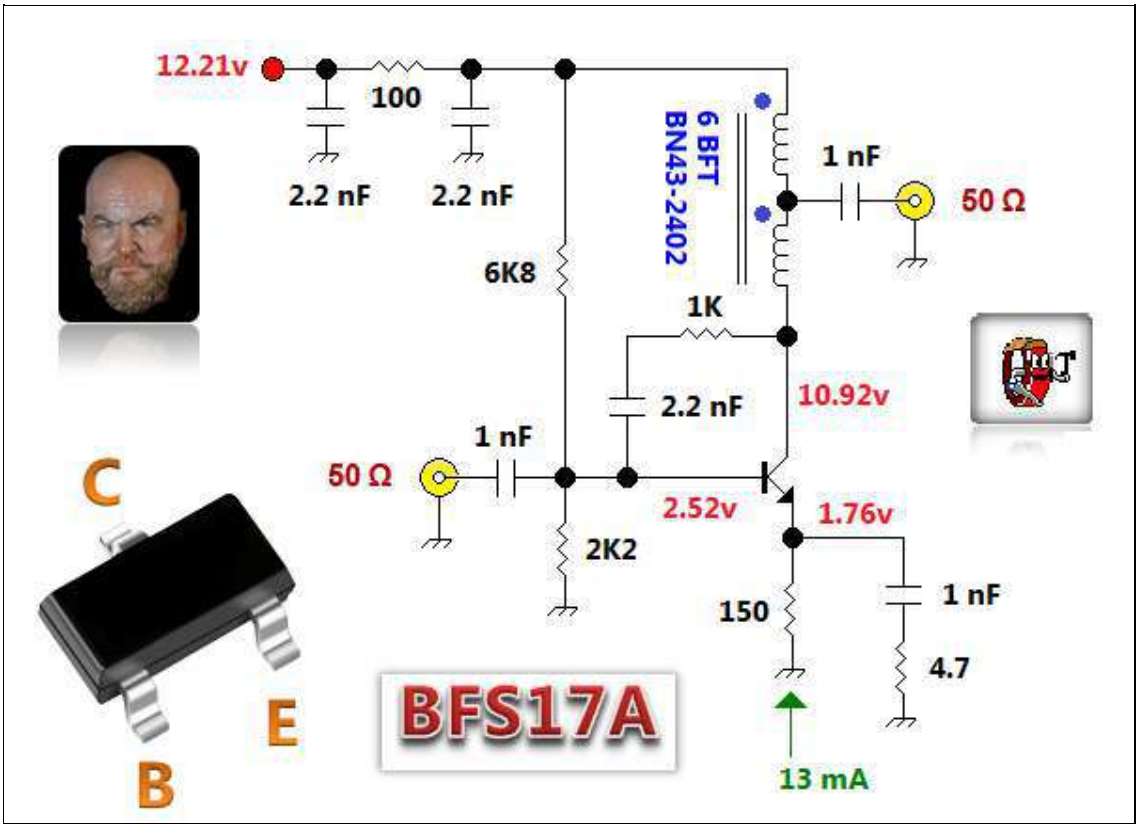

AAbove — My test schematic; a simple feedback amp with capacitors oriented to 50 MHz and above. A limited selection of SMT resistors constrained my experients, but the results seem okay. I strove for the best possible input and output return loss at 50 MHz. I wanted a emitter current of ~ 12 mA and got 13 mA with the bias resistors on-hand.

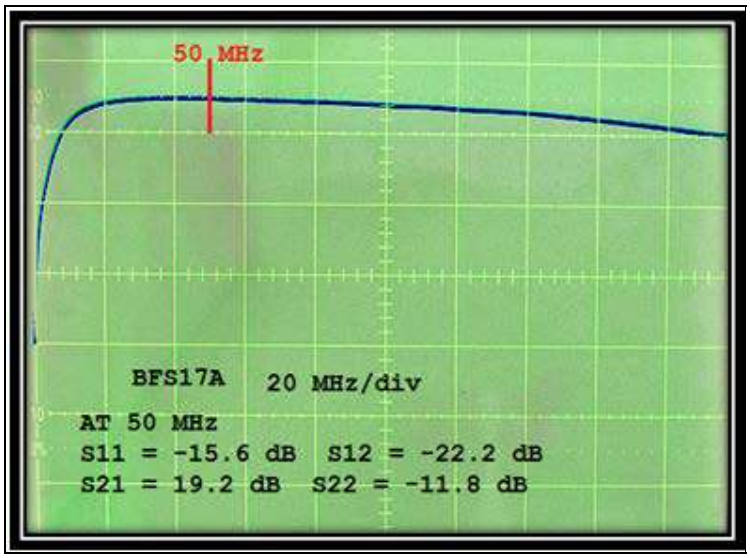

Above — A 200 MHz wide sweep of my breadboard with tracking generator + spectrum analyzer. Please view the various 2-port measurements

at 50 MHz in the lower half. Despite some input and output port mismatching, a gain of 19.2 dB was measured at 50 MHz.

I wound my output transformer within a BN43-2402 binocular ferrite, but ordered some #61 material equivalents for assessment at VHF.

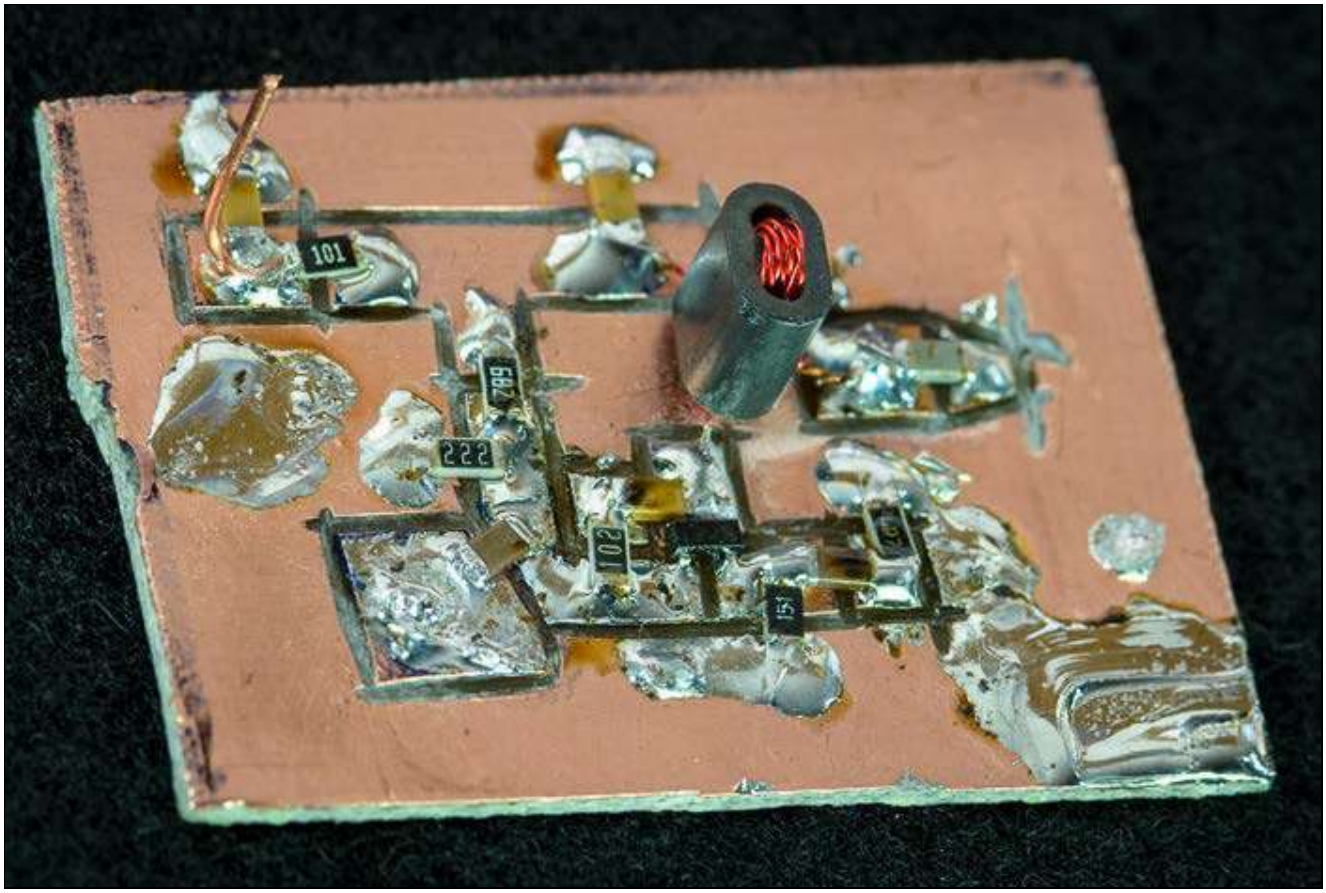

Above — My magnified breadboard looking messy after many parts substitutions from experiments to find the best possible S11 and S22. I removed the shiny RF connectors prior to photography since they often create blown highlights. Alternate image. Despite a limited RF bypass before and after the 100 Ω decoupling resistor + crude bread boarding, I measured no parasitic oscillations from 0.001 to 1 GHz — likely due to the heavy shunt feedback. I liked this transistor, found it easy to breadboard and ordered 100. You'll see the BFS17A in my experiments hereafter.

By all means, order whatever transistor *you* want. Past emailers wrote to say they enjoy reading how other experimenters think about and assess their parts such as RF beads or transistors.

Surface Mount Part Soldering

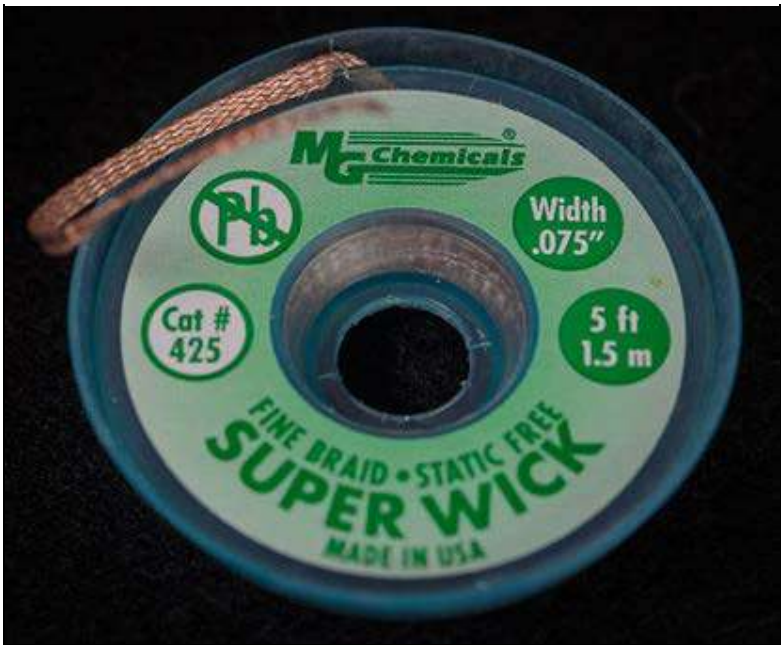

Above — Solder wick. On my SMT workbench, wick proves the most important tool period. A piece of desoldering wick can transform a monster mistake into a perfect circuit in under 2 seconds.

I've read many accounts of how builders anchor the parts they're soldering. We need to keep the SMT part flat on the board to avoid mechanical tension and poor solder joints — a system is required. For size 0805 and 1206 parts, I often just use my index finger fingernail to hold the part in place while I solder 1 lead with my other hand. After a few seconds of cooling, I solder the other lead and then usually touch up the first joint. For tricky formats like SOT-23, or SOT-143, I usually tape down the part while ensuring even pressure on all leads and just solder 1 lead. After cooling, I remove the tape and easily solder the other leads. Again, the intial lead may require some retouching.

SMT Size

Above — A 5X magnified roll of 50 BFS17A in SOT-23. Compact or what?

Above — BFS17A in SOT-23

---

3. 50 Ω MMIC Bench Amplifer

To boost low-level signals during experiments, every 50 Ω workbench needs a utility RF amp module. With strong wideband gain + RF port return loss (S11 and S22), MMICs make a good choice. Since I own 15 pieces, I built an amp around the MCL MAR-3, a modest gain + noise figure, 2 GHz plastic part in the Micro-X package. We enjoy a bevy of MMICS to choose from and as they increase in fT and gain, so does the need for solid, low inductance grounding techniques.

Above — The completed amplifer module in a Hammond box with an RCA jack for the DC voltage.

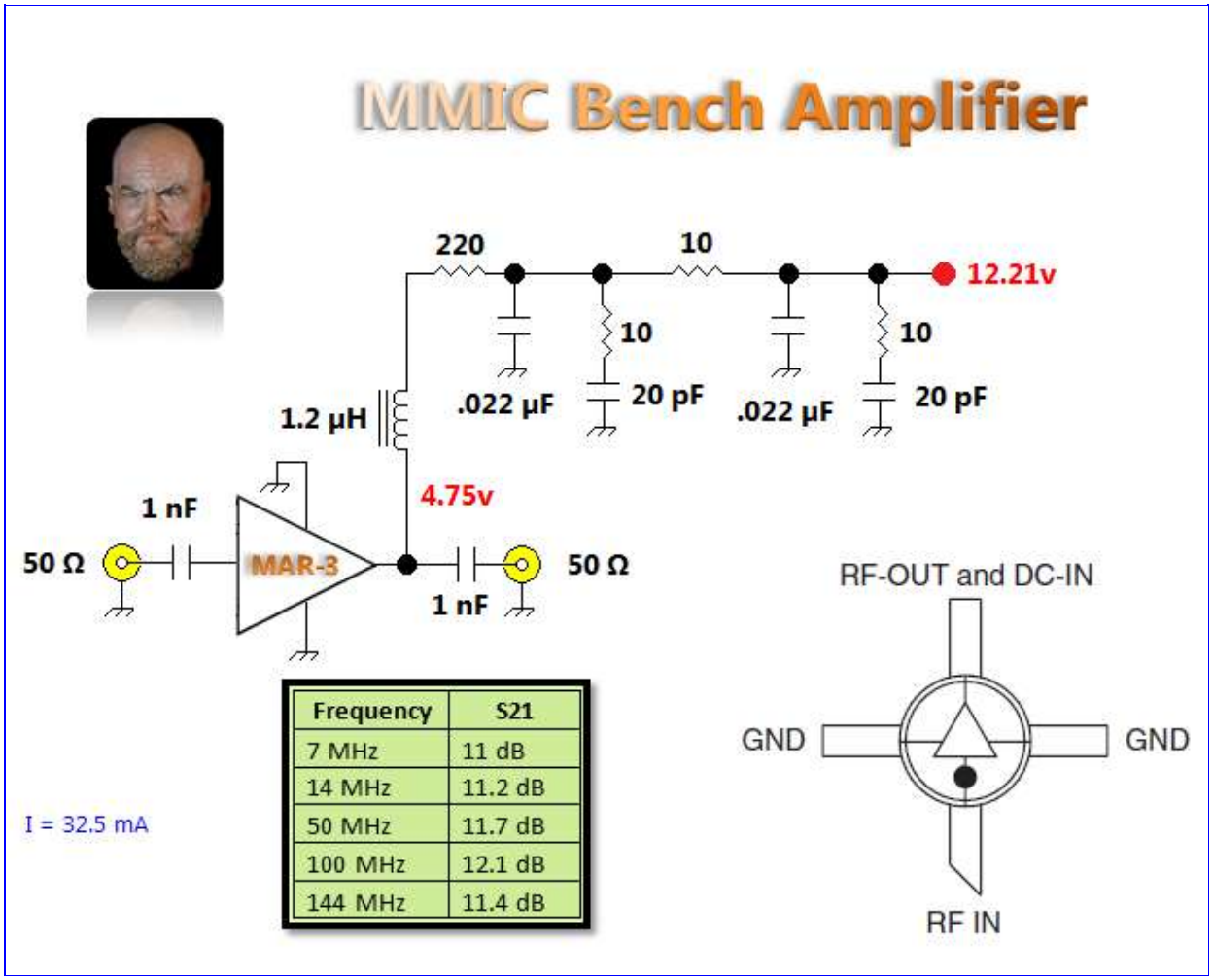

Frequency	S21
7 MHz	11 dB
14 MHz	11.2 dB
50 MHz	11.7 dB
100 MHz	12.1 dB
144 MHz	11.4 dB

Above — Schematic with a table showing gain versus frequency. I built all SMT (size 0805 mostly) except for *short* leaded 1 nF input and output coupling capacitors. I applied sturdy wideband DC filtering since I can't risk RF flowing on my DC lines during bench experiments. I measured no oscillations from 100 KHz to 1.5 GHz.

I chose a 1.2 µH SMT choke in an attempt to boost gain from ~66 to 150 MHz. Many builders leave off the choke, but some RF will flow through the 220 Ω bias resistor to ground and thus, to get maximum gain, a high impedance RFC might help. Recall this RFC should exert an inductive reactance of at least 500 Ω (>= 10 X the load impedance) at the lowest amplifer operating frequency; in my case this occurs at ~66 MHz. A better choice for the RFC might be 1.6 µH which exerts ~ 500 Ω at 50 MHz, but I just own size 0805 1.0 and 1.2 µH chip inductors.

My particular amp delivers ~10 to 12 dB gain from about 5 to 180 MHz. Since the coupling capacitor value determines the low frequency response, if you want a MMIC amp for mostly HF, try reducing your input coupling caps from 0.001 to 0.01 µF or so. You mighty increase the RFC to say 10 µH as well — that's why we don't just build kits; design to suit *your* needs.

The 220 Ω bias resistor should really be 200 Ω for a VCC of 12.2v, however, I had to substitute the 220 Ω R due to a low selection of SMT parts. This dropped the current and also my gain at 100 MHz = 0.4 dB less than that specified in the MAR-3 datasheet — no big deal.

I built the bread board on 2-sided FR4 copper clad board. I soldered thin copper foil around all 4 edges to adjoin the top and bottom copper surfaces. Around each MMIC ground lead, I drilled 4 via holes and soldered copper wire from top to bottom. 2 vias were positioned near every bypass capacitor and all along the input and output paths. 23 total via wires.

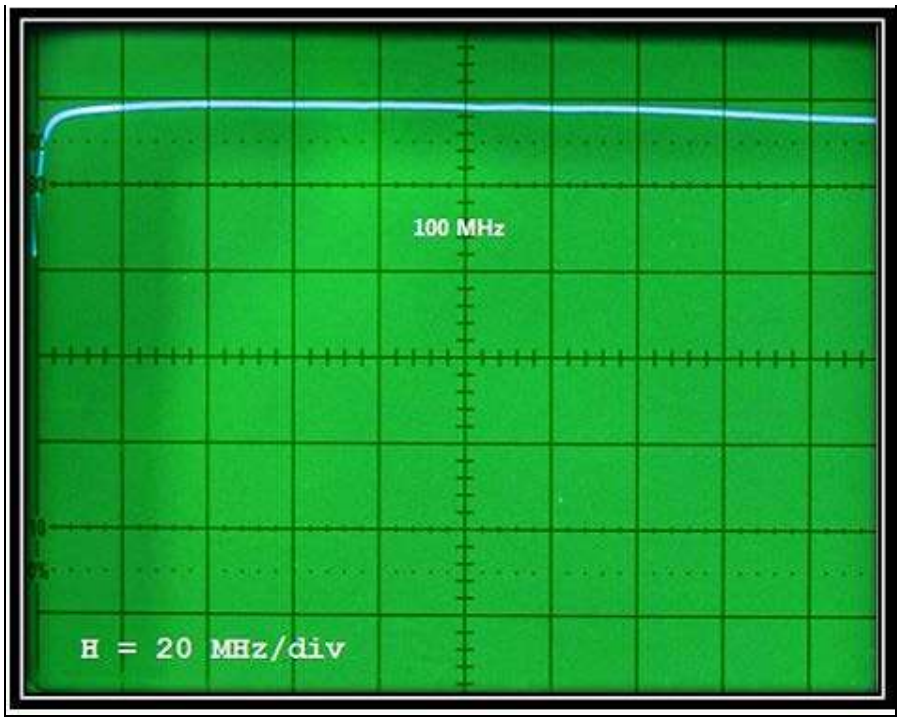

Above — Tracking generator plus spectrum analyzer sweep out to 200 MHz. Click for a sweep from 1 to 10 MHz showing a rapid fall off below 5 MHz. This little amp will serve me well for most HF and especially my VHF experiments. A UHF amplifier module is planned and all knowledge gained from VHF circuit building will flow forward.

Above — Part of a strip of MCL MAR-3 amplifiers.

Feedback Amps (FBAs)

MMICs like the MAR-3 use a Darlington feedback pair. Still, too, we shouldn't write-off discrete component FBAs wielding transformers + shunt and series feedback at VHF. These amps; staples of countless W7ZOI and W1FB projects since the 1970s; evolved commercially into GaAs FBAs built on a tiny wafer by companies like TriQuint Semiconductor.

In broadband amplifiers, negative feedback permits a wideband (flat) gain response, reduces input and output VSWR (S21 and S22) and controls performance changes from S-parameter and other variations from transistor to transistor. In 2013, I needed an amp chain with >=25 dB gain at 144-165 MHz [~150 MHz mostly] for low level stuff : -25 to -10 dBm input power. Inspired by Wes' 144 MHz CW/DSB transmitter FBA chain *(**SSD** -- Chapter 8 -- Figure 30 in Solid Stage Design for the Radio Amateur; ARRL published in 1986 and out of print)*; I cascaded 3 PN5179 BJTs as FBAs:

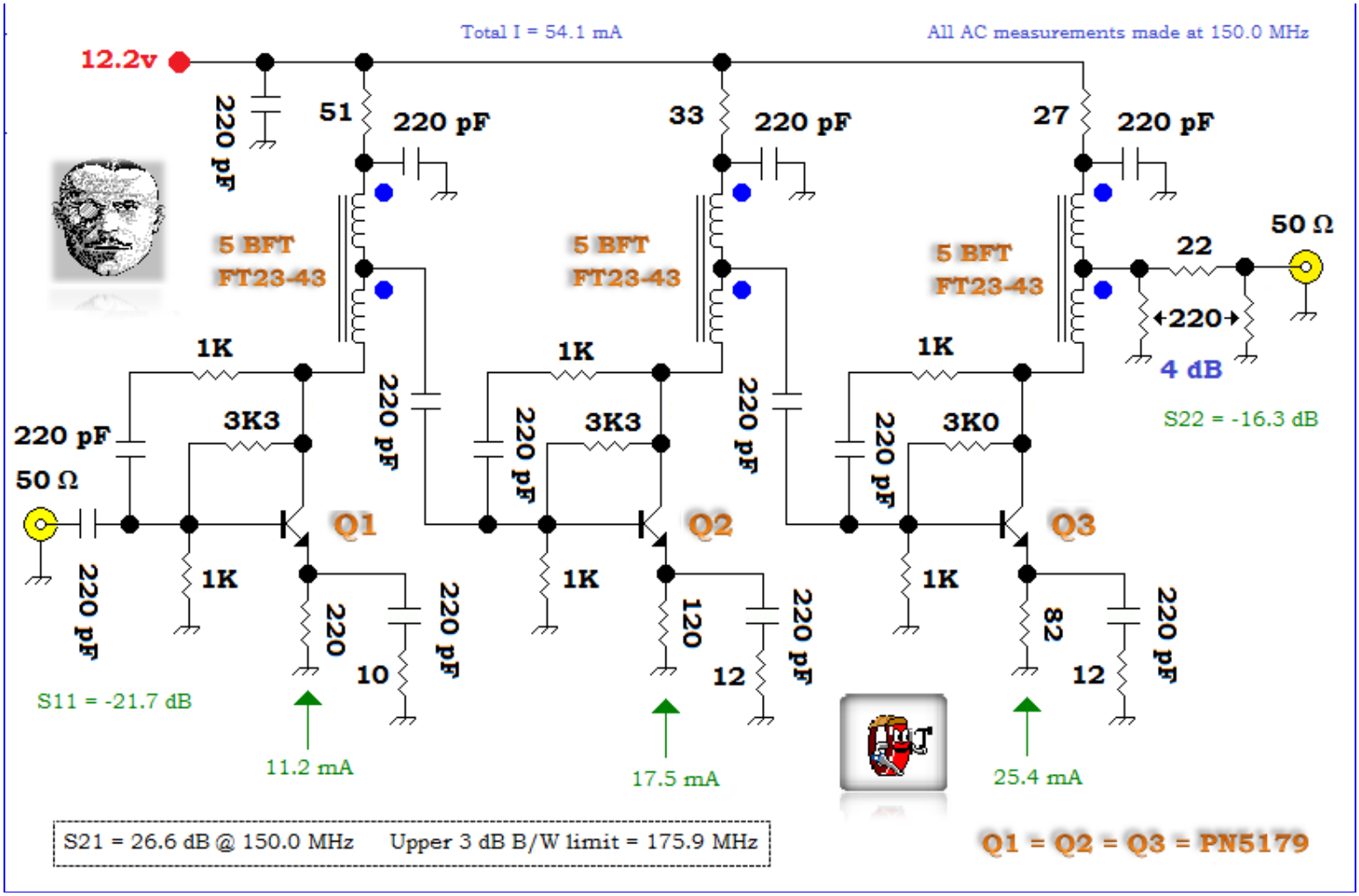

Above — My 150 MHz (design frequency) FBA module. Since the fT of the PN5179 = 900 to 2000 MHz @ a 100 MHz test frequency, gain drops steadily as we move up above 100 MHz. Centered at 150 MHz, my upper 3 dB drop off point was 175.9 MHz — thus this amp works okay from 144-165 MHz where I need it.

I built and tweaked each stage to derive the best S11 and S22 . *Click for a snapshot taken of my test of Q1 with a BNC connector attached to both ports — I did this for each stage.* It's a trade off since if you boost the emitter degeneration R, the S11 will improve but the gain decreases. Typical stage S11 = -18.5 dB and S22 = -17 dB. I progressively bumped up the current in each stage to reduce gain compression. I get ~12-13 dBm power out of the whole amplifer before compression/distortion occurs.

Securing the best S11 and S22 for each stages might seem silly, but invoked learning. The S11 and S22 of the *total amplifer* counts the most. An interesting thing happened to S22 – with a RF connector soldered right on the board without the pad, S22 = -23.8 dB. When I added the 4 dB pad and stuck it in the box and then ran a ~ 5mm copper wire to connect an SMA output jack, the S22 decreased to -16.3 dB! At 150 MHz — life differs from 7 MHz.

Placing the 4 dB pad between stage 2 and 3 will stabilize + enhance S22, gives a 4 dB higher 1 dB compression point and output intercept, which may make a FBA chain more useful for experiments like transmit driver applications. I can report I measured no oscillations out to 1.5 GHz and this amp works okay for my intended purpose with gain of 26.6 dB at 150 MHz.

I employed 220 pF caps because the plus the self resonant frequency of my 220 pF Murata caps = 154.6 MHz. Therefore, gain at lower HF is low.

Above — FBA breadboard photograph.

QRP — Posdata for October 27, 2013

I first learned radio electronics from SSD, EMRFD and the ARRL Handbook and still remember the joy when my copy of SSD arrived in 1990. Feedback amplifiers litter this book — and for good reason — they offer stable 50 Ω blocks for building up our RF signal. Wes' 144 MHz CW/DSB transmitter still intrigues me and inspired the circuit shown above.

I asked Wes if he kept that 2M transmitter, and if so, could he snap a couple of photos for me? Wes opened it up to see that the VXO and the frequency multiplier chain were missing. Click Click Click . Thanks to Wes, W7ZOI for the photos.

---

4. Breadboarding Double-Sided Copper Boards

Seeking a low inductance AC ground for some of my VHF and UHF FR-4 prototype breadboards, I join the top and bottom copper surfaces with solder wick along its 4 edges and copper wire vias in the main board area.

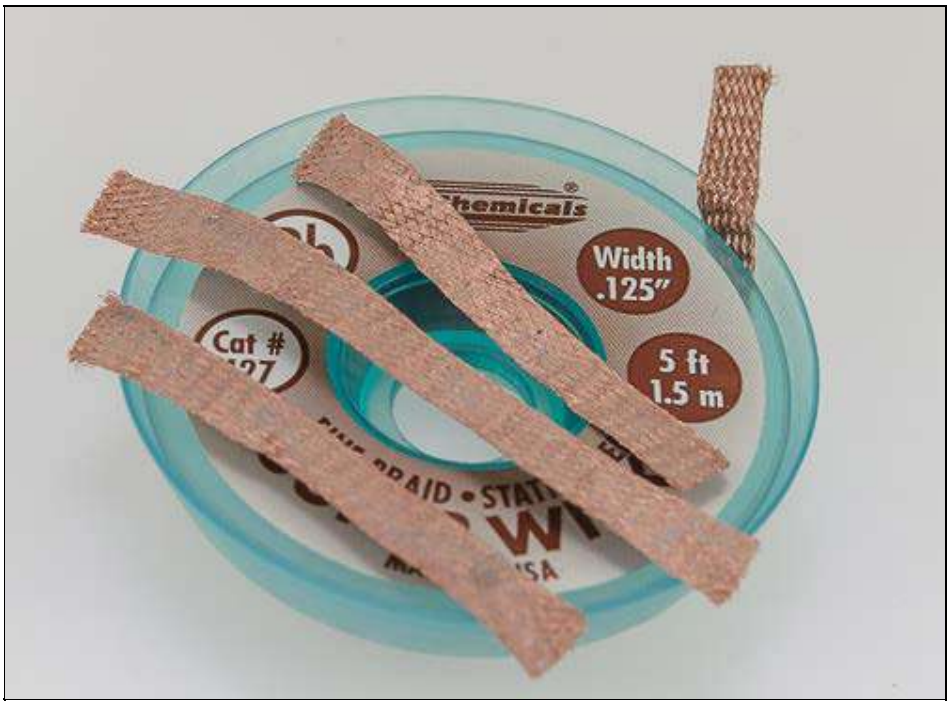

Above — A bench staple, solder wick, joins the 4 edges in true Ugy fashion. Many prefer copper foil for this task, but it's not cheap, nor readily available prompting a pragmatic approach. I take a hammer and pound the solder wick [0.125 inch minimum] so it becomes wider and thinner.

Above — Take a piece of wick and tack it in 2-4 places along the top surface of the copper board. The center solder shown above looks perfect — too much solder will flow into the wick and make a difficult bend job around the board edge. Tack just enough wick so you have enough left to go over the edge and to solder on other side of the copper board.

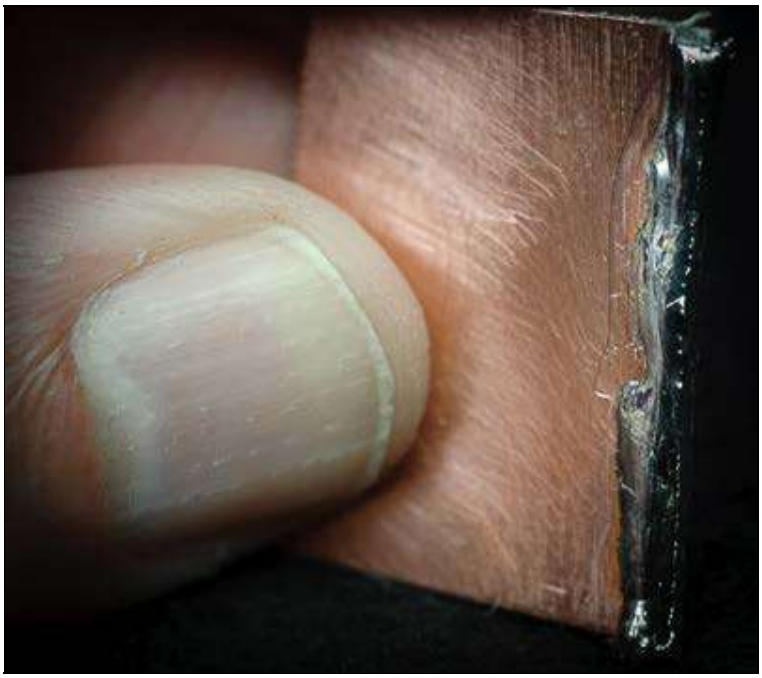

Above — With hand and/or pliers manipulate the wick around the other side to completely bridge the top to bottom. Finally, liberally solder the wick on both surfaces, move to the next board edge and repeat. Click for a rather messy UHF board with copper wick on 2 edges and numerous vias around a prescaler chip, some input + DC lines and a switch.

Above HF, most don't make pretty prototype boards to admire — rather, builders strive for good AC grounding and generally stick their board in a metal box for shielding and this hides the breadboard. No one's ever told me I make pretty circuits for any frequency and I'm okay with it.

Onto wire vias:

Above — Your drill chuck will need to accommodate small bits such as those shown above (3/64 inches = 1.2 mm) . I keep these and others that vary from 0.5 mm to 1.2 mm for making via holes.

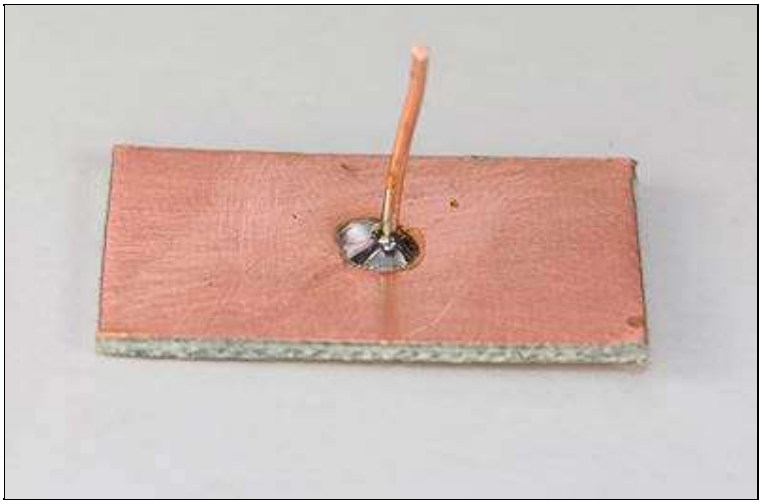

Above — Magnified via wire soldered at the top side. I found making a hole close to the same size of the via wire will hold the wire in place for rapid soldering. This wire is normally clipped flush at this point. Click for a photo of my flush cutters.

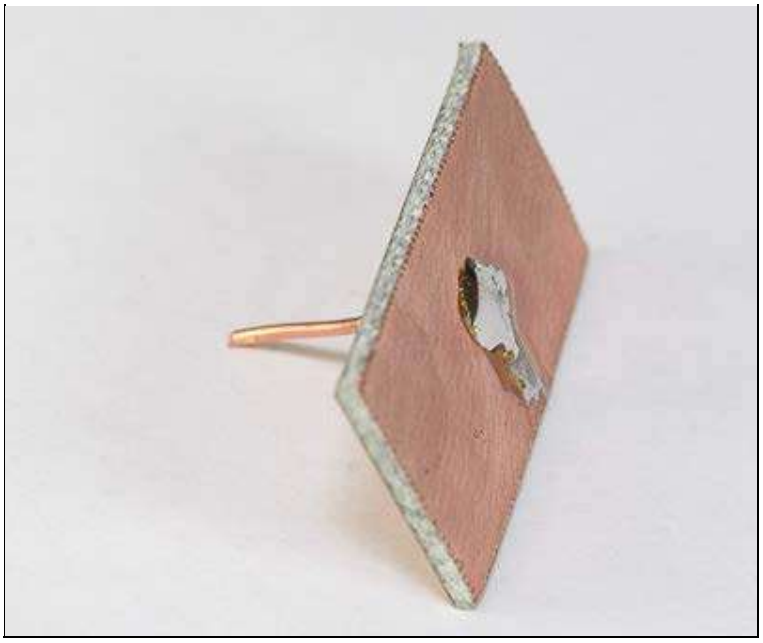

Above — The board shown above was flipped over to solder the bottom copper surface. I try to drill and solder in all vias prior to soldering active devices, since the board heat may damage some parts.

---

5. Simple Preamp Filter

Some RF filtering should proceed our receiver low noise amplifer (LNA) input — but what? Low-pass, high-pass, band-pass, 2 poles, many poles? Factors informing this decision might include our receive frequencies, QRM, selection of IF and thus our image stripping requirements, plus maximum tolerable signal loss before the LNA. We might not want image rejection from this filter since the post LNA filter can tackle this function.

I examined an input filter presented by Joe Reisert, W1JR in the November 1986 Ham Radio. Joe wrote a fantastic column called VHF/UHF World and his context was a high dynamic range 2M receive converter to a 28 MHz IF.

I'm uncertain how to classify this filter: it looks like a standard pi low-pass filter except the input and output series capacitors exert a high-pass skirt. Joe built his filter for 144 MHz. After "building" Joe's filter in Ladbuild08 I tweaked the filter in GPLA *[software from EMRFD]* to center it at our local NOAA weather channel: 162.55 MHz. Click for the GPLA plot.

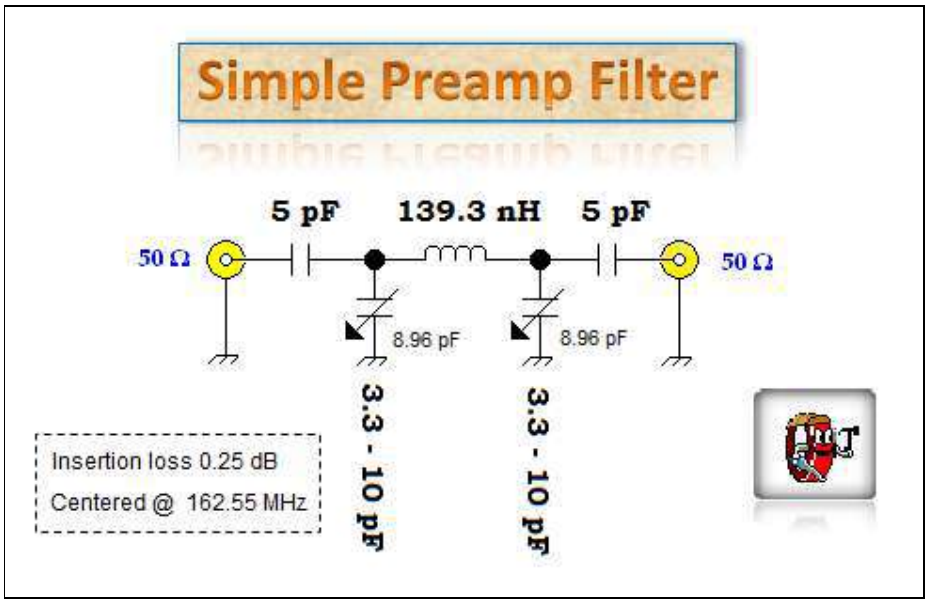

Above — Input filter schematic with values shown to center this rather symmetrical filter at 162.55 MHz. The half power (3 dB down) bandwidth = 18 MHz. You can easily scale it to other other frequencies — by tweaking the trimmer caps and perhaps squishing or expanding the inductor links some, this filter will tune widely including the 2 Meter Ham band. The IL blew me away (better than calculated) — the resonator Q was high due to the air wound L and Q >= 700 trimmer caps along with good port matching.

Click to view a larger photo of the breadboard. I wound the coil on a 3/8 inch diameter bolt but then spread the turns to get the L and length I wanted. Built on double-sided copper clad board, a few copper wire vias connect top to bottom. I joined the LC circuit to its ports with leaded 5 pF ceramic caps.

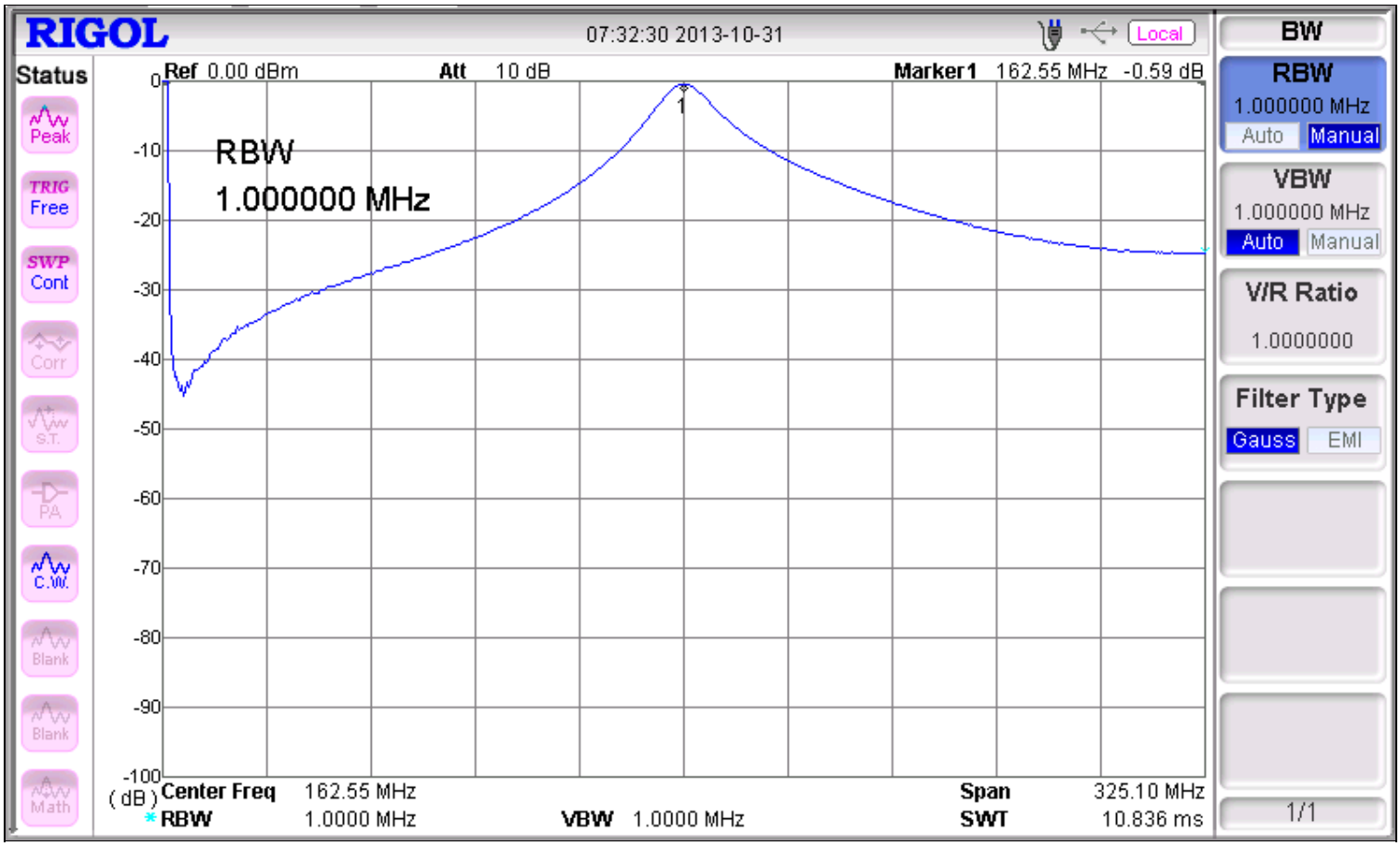

Above — Tracking generator plus spectrum analyzer sweep. Under sweep set up, I minutely squished or expanded the L and tweaked the caps to peak the filter at 162.55 MHz while obtaining the lowest insertion loss. Further, I had to tweak the trimmer capacitors to center the filter with the Hammond lid on since putting the lid on changed the center frequency slightly. A *TG equipped* spectrum analyzer proves the ultimate bench tool for VHF and UHF in my humble opinion.

Above — Zero calibration of my AADE L/C IIB meter. By sweeping numerous LC circuits after measuring the L with this tool, I've learned it's reasonably accurate with low inductance coils. I zero the meter prior to *each* measurement and zero calibrate it with the alligator clips butted end-to-end while gripping a small piece of copper wire. Try to keep the same relative alligator clip position during coil measurement. I'm uncertain if this is protocol, but it seems to work for me.

Thanks to Joe, W1JR for this circuit and the opportunity to learn more about component-level VHF design and construction.

---

6. VHF Band-pass Filter Experiments

Build Notes

1. All filters designed with the EMRFD ladpac programs DTC08, or TTC08 and then tweaked in GPLA.

2. Seeking a band-pass filter for my experiments with the local NOAA weather channel at 162.55 MHz, I designed, built and tested 3 filters. With a 10.7 MHz IF superhet receiver, the image frequency = 141.15 MHz.

3. My VHF sweep system = a tracking generator plus a spectrum analyzer.

Filter 1

To avoid the need for proper electromagnetic/electrostatic shielding, I kept my HF experimenter hat on and built my first filter with powdered iron toroids (T30-12) knowing I would pay a Qu penalty that may wreck filter insertion loss, bandwidth and port matching. I hoped that the passive electromagnetic shielding offered by toroidal inductors would reduce resonator coupling.

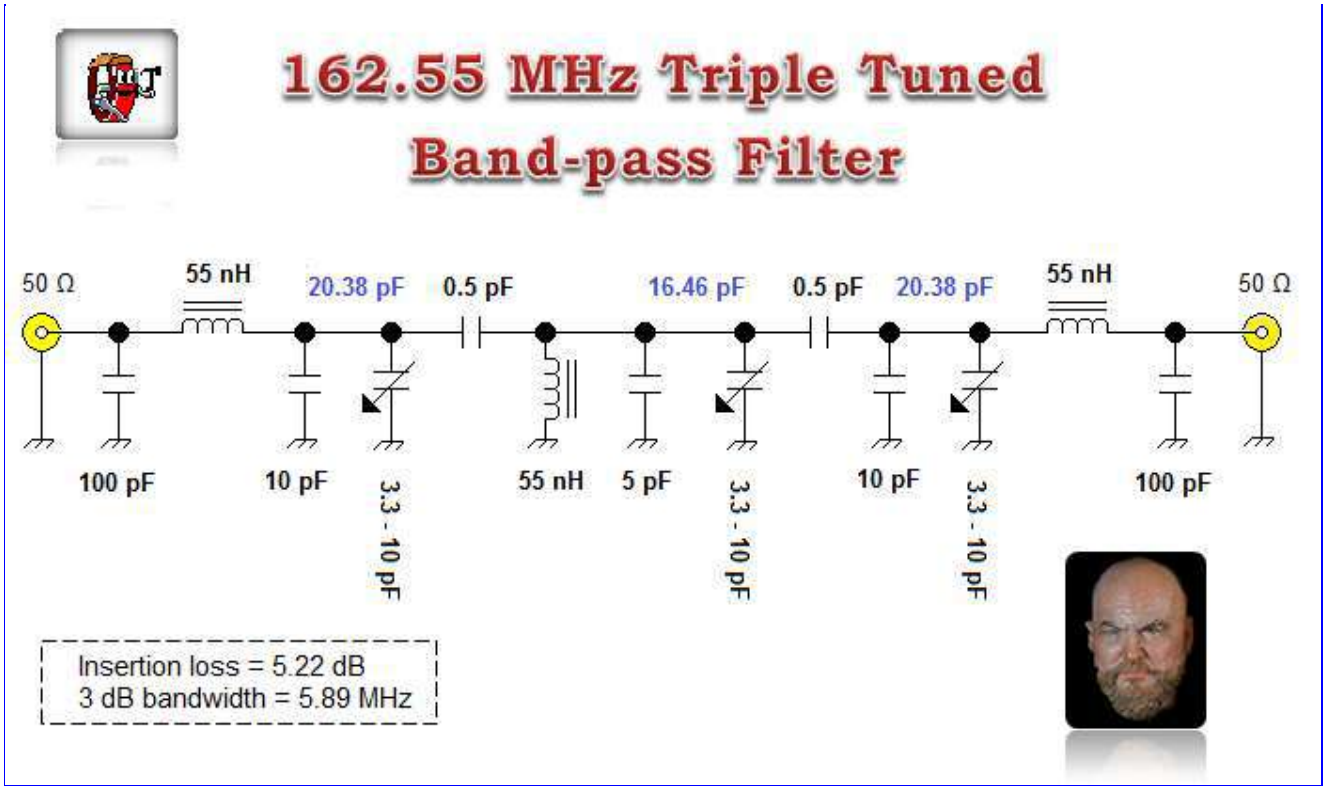

Above — Mixed-mode triple-tuned filter schematic. Click for the GPLA simulation. When we want to go up in frequency plus desire a narrow bandwidth, we face 2 options: reduce our inductance and/or coupling capacitor(s). This taxes our parts collection and breadboard skills since capacitors less than 1 pF are relatively uncommon and require SMD breadboard techniques. I adjusted my design bandwidth and inductance in TTC08.exe to allow the 0.5 pF capacitors plopped in my parts bin to work. For a change of pace, I chose a mixed-mode filter topology.

I strive to place a single high Q variable capacitor in my band-pass filter tanks, however, my Q = 700 SMD trimmers only ranged 3.3 to 10 pF so I stuck a leaded ceramic capactor in parallel with each trimmer.

Common SMD capacitors exhibit low to medium Q and I try to avoid them in my at HF band-pass filters: often I'll just solder a short leaded though-hole caps instead. I also applied this logic to my VHF filter, however, this might prove foolish at VHF since the self-resonant frequency of a given leaded cap is lower than that of an equivalent SMD cap and capacitor XL becomes more significant as we move up in frequency.

Click for a pdf file showing a simple experiment with 3 capacitors . I'll occasionally use ultra-high Q SMD caps in my future experiments based upon these results.

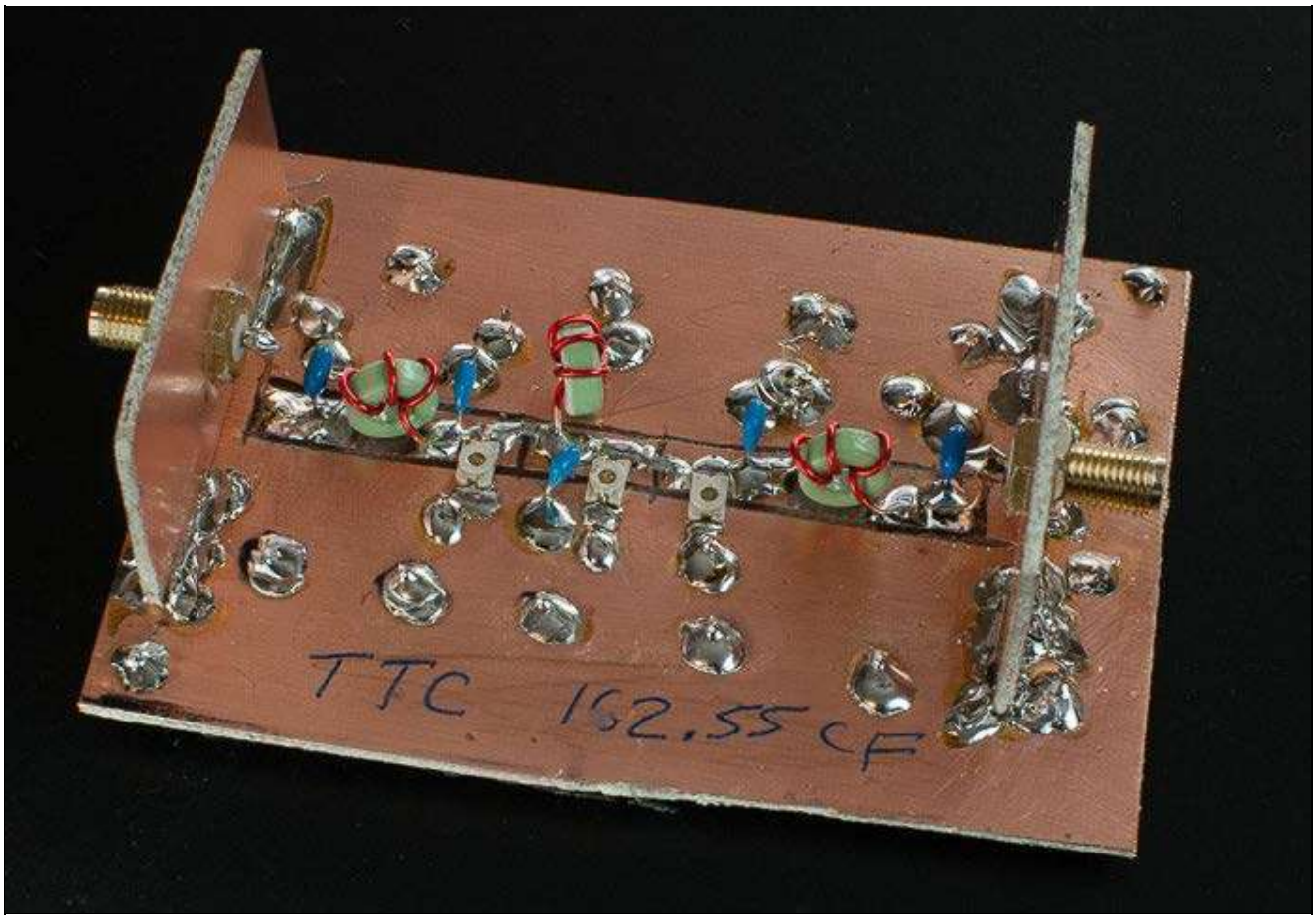

Above — My TTC breadboard. Click for a larger photo. Click for a bench sweep to view a feculent skirt peak in the filter spectogram. Some resonator coupling occurred despite spacing and placing the inductors at right angles. This circuit possessed 6 tweaks: the 3 trimmers and the 3 Ls — I just kept tweaking them until I got the best shape and lowest IL. That's 21 gauge wire on the toroids. My image frequency = 47.28 dB down. Since the sweep yielded such a wide discrepancy from my GPLA simulation, I discarded this filter and moved on to design #2.

Filter 2

Attempting to obtain a resonator Qu of at least 300-400, I moved to air core inductors wound with bare 22 gauge copper wire *plus* air-variable capacitors. Double-tuned classic topology. Without stout shielding, air wound inductors will couple and trash the stopband.

Above — Copper and brass sheets I bought for making filter boxes after Wes recommended using metal sheets or strips for shielding filters. In North America, builders can purchase a sheet metal hand brake plus a rotary cutter/shear for under $100 and make all sorts of boxes for radio gear. I'll equip my QRP workshop with such equipment over the next year. This was my first experience man-handling sheet metal or strips.

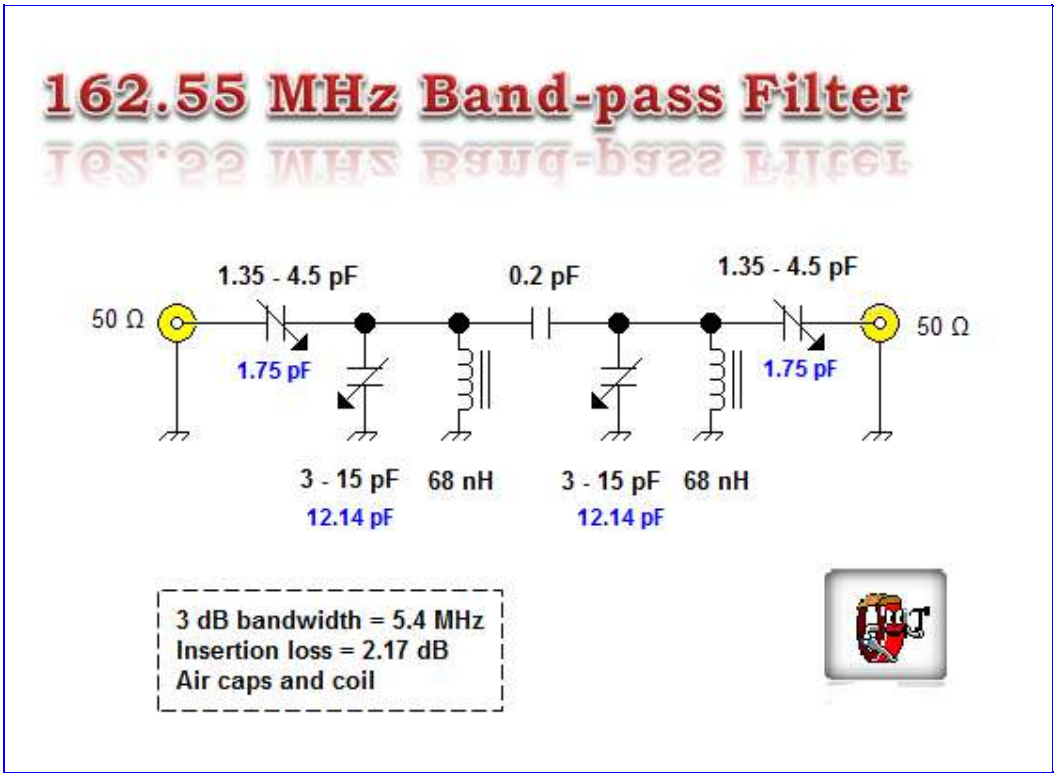

Above — Schematic diagram of Filter #2 with tabled IL and half-power bandwidth. Click to view a macro photograph of the filter. I soldered the brass box onto a double sided copper-clad FR4 bread board laden with some copper wire vias to enhance the ground plane. The 0.2 µF coupling cap = an ATC microwave cap.

Click and click for the sweeps. Notice the splendid skirt symmetry at the filter top and also the fantastic peak attenuation in the low-pass skirt

(~81 dB from the filter peak to the lowest point in the low-pass filter skirt). I'd never seen deeper attenuation on my bench before: quite gratifying. My double-tuned filter had essentially matched the 3 dB BW of triple-tuned filter #1 with less insertion loss.

Not all appeared perfect however; attenuation of frequencies above the passband looked so-so and I was unable to get a lower 3 dB bandwidth by manipulating L and C in each tank.

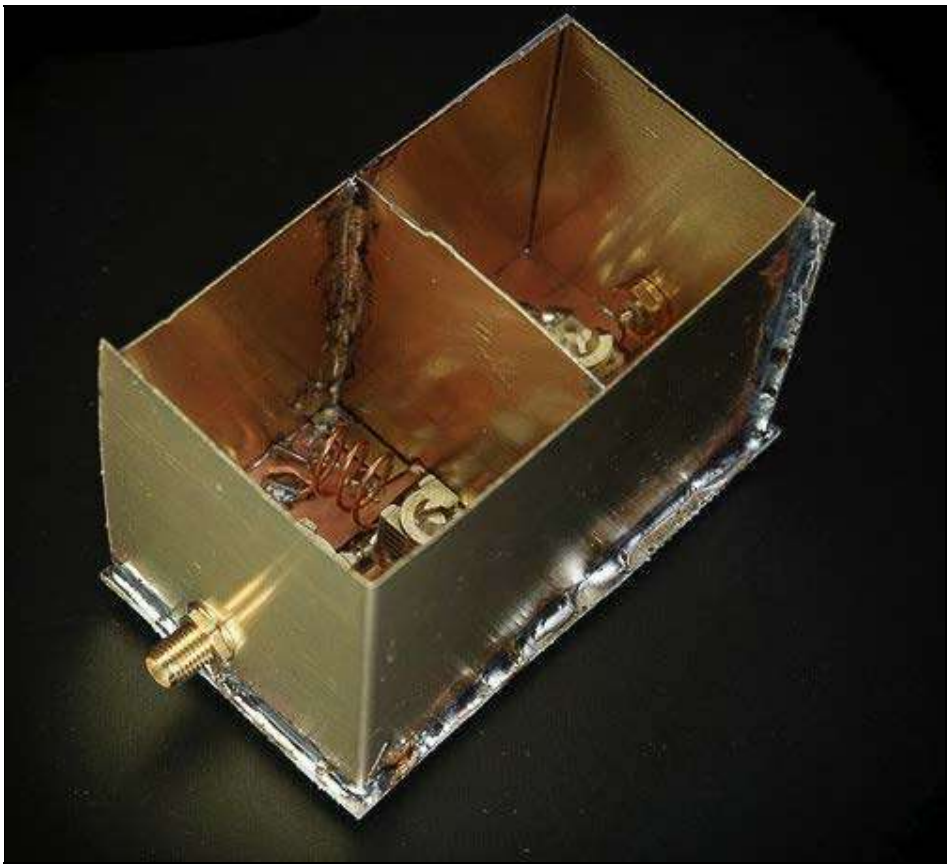

Above — My first ever brass box soldered on a 2-sided copper clad board: Filter #2. Lacking proper tools and also the knack for making beautiful chassis like Dave, AA7EE does, I just did my best. My only concern was getting tank isolation. I chiseled out a small cut in the center brass divider just high enough to clear the SMD 0.2 pF chip capacitor and center copper strip. Overlaps allowed soldering of brass walls After tweaking the L and C parts, I placed a brass lid on top during sweeps. Okay, onto filter # 3:

Filter 3

When coupling caps fall below 1 pF, some builders place their resonators in close proximity to couple the tanks, however, these usually involves slug-tuned powdered iron or ferrite inductors with a generally low Q. The coil consists of cup core and a threaded center core which combine to give a magnetic shield. A tin plated copper can surrounds the core for electrostatic shielding. I think after these experiments — placing each resonator in its own sealed box seems a better option.

I noticed another approach in The Double Tuned Circuit: An Experimenter's Tutorial in QST for December 1991 by Wes, W7ZOI. Wes drilled a hole in the tank compartment divider and passed a wire soldered to 1 tank through the hole and positioned it near the variable capacitor of the other resonator. We change coupling by adjusting this wire.

The wire may be thought of a "tweakable" capacitor, however, the key point is we need to couple energy from 1 resonator to the next; whether by wire, capacitor or inductor, proper resonator coupling will give the required skirt shape within the the limits imposed by Q and the matching to the 50 Ω ports. When establishing a filter passband, the end Q and resonator coupling pretty much dictate the outcome.

Filter #3 involved more mechanics than electronics. I made a U shaped box from a small sheet of copper.

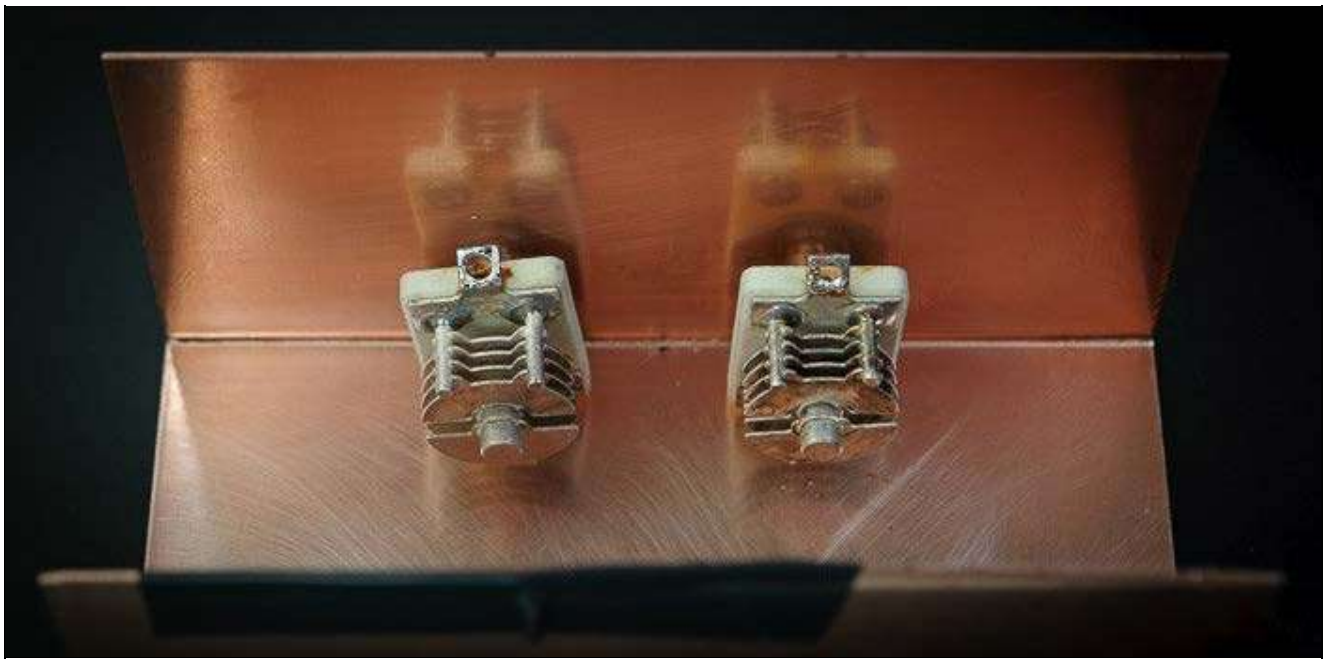

Above — My copper box drilled for the 2 air-variable tuning capacitors. I built the walls, top and divider from thinner gauge brass strips. Rosin flux aids soldering your metal sheets together — I soldered mine with a Weller 80 Watt iron and began with the center divider. Click for a side shot after completion.

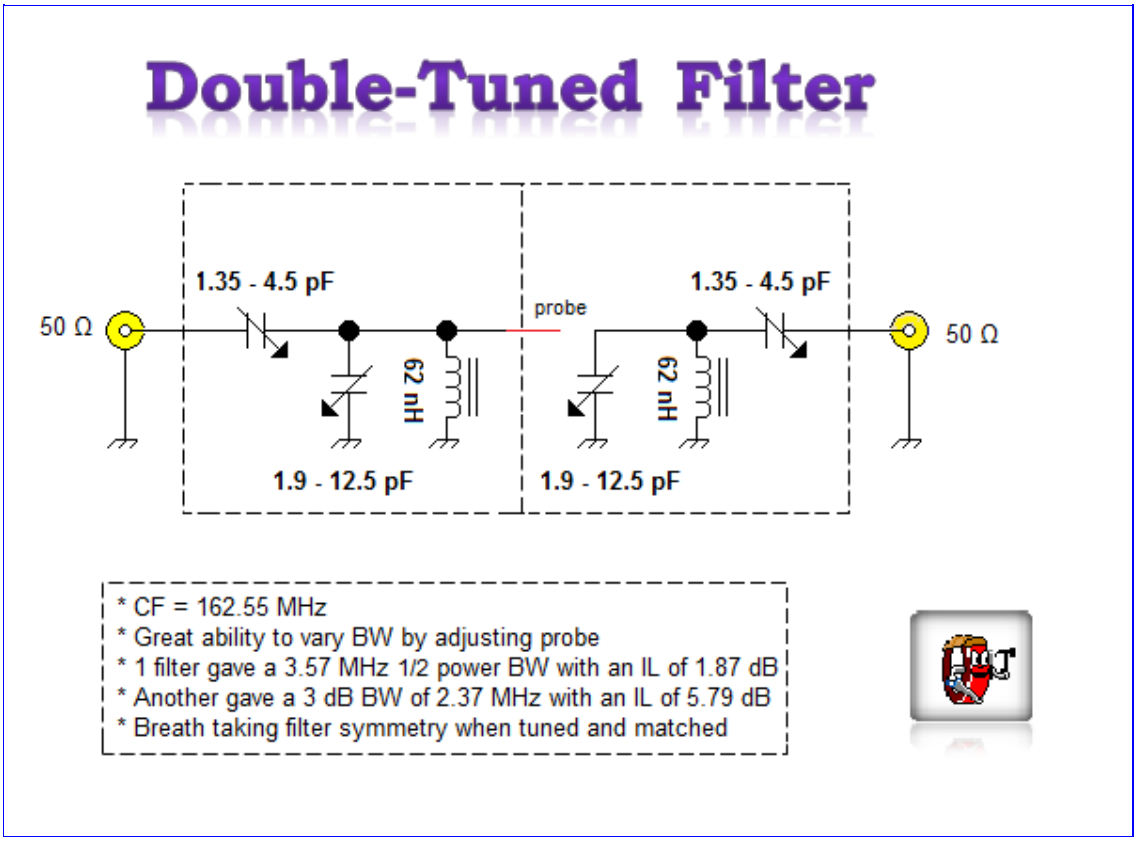

Above — My filter schematic with some tabled data. Click for a top off photograph where you can easily see the black wire probe. To change coupling, you change the wire length and/or its distance from the second tank capacitor. I really enjoyed moving the wire and watching the outcome on the screen. Per usual, I tweaked the coupling, Ls and end caps to derive many 3 dB bandwidths. In 1 arrangement with a 3 dB bandwidth of 3.57 MHz, the insertion loss was only 1.87 dB — I had evidently found a perfect ratio + combination of L and C yielding a low IL.

I'll increase the coil wire gauge in future experiments to lower solenoid resistance and try to garner even more Qu.

This is the *best* filter I've ever built. After peaking the tanks to 162.55 MHz, resonator adjustments weren't really needed. By moving the wire probe I saw that BW and IL change inversely. While tweaking the series caps and moving the probe, it felt like déjà vu from my experiences simulating these exact changes in GPLA over many years — except now they were alive and kicking. With some inductor manipulation (or as

needed, changing the inductors) this filter can be centered from ~140 to well over 200 MHz. A high-octane, dramatic and versatile filter indeed.

Click for a sweep where I moved the wire very close to the neighboring tank capactor and over coupled the filter.

Click for a screen shot of another sweep.

Conclusion

With new awareness that resonator coupling and other issues may *also* occur in HF band-pass filters, making these 3 filters surely boosted my future band-pass filter construction standards at any frequency. Over the years, builders have emailed me sweeps of HF band-pass filters (usually VNA sweeps) with also sorts of extra resonances +/- poor insertion loss. Since I'm just an amateur, often nimrod RF enthusiast, I won't pretend I possess all the knowledge to critique their filter woes.

However, photos of their HF filters usually look messy and rushed: opposite to our needs — eschewing important factors like symmetrical layouts, inductor spacing, a first-rate ground plane, larger gauge + well spaced wire wound on big as possible toroid cores Yikes, I better stop now lest I venture into filter folklore.

Today, designing a filter with software is merely half the battle — construction poses the harder task. Unsurprisingly, measurement and experimental methods will elevate your outcomes.

Filter analysis with a sweep system is the ultimate, however I built and then tested many band-pass filters with a frequency counter, a signal generator, a 'scope and a return loss bridge during the first 12 years of my RF life.

Assuming you have a filter that peaks and isn't overcoupled: to measure the 3 dB bandwidth, first peak the filter to resonance for the highest peak-peak voltage in your 'scope. Here's the rest of the procedure:

1. Multiply the peak-peak voltage of your centered filter by 0.707 and record this value.
2. Decrease the frequency of your RF generator until the scope shows the .707 value and record it as Frequency Low
3. Increase the RF generator frequency above the peak until you once again get 0.707 of your peak-peak measured voltage. Record this as Frequency High.
4. 3 dB bandwidth = Frequency High - Frequency Low.

You may also wish to measure the insertion and return loss as described in EMRFD, Radio Society Handbooks, or the RF Workbench series on this web site.

Whether you run superhet, low IF, SDR, or Zero IF (DC) receivers, or need to filter a transmit chain, well made band-pass filters just might boost your project performance. VHF poses additional challenges but offers great learning opportunities.

QRP — Posdata for Nov 12, 2013

A. Notes for Filter #2

Victor, 4Z4ME wrote to explain why the attenuation above the passband in Filter #2 looked mediocre. Filter topology and component values yielded the poor high-pass attenuation and not unwanted coupling as I originally shared.

Victor wrote: "The problem is that all the couplings are of one nature, in this case capacitive.
At very low frequencies the inductors short the signal to ground while the capacitors impedance gets higher so it is clear that the output signal goes to zero.

At high frequencies the inductors may be regarded as disconnected because their impedance get very high, however although the capacitors impedance get lower , you have them both at the series arms and at the parallel arms, so the signal gets to be attenuated by their impedance ratio and not get shorted to ground.

This can be shown in analytic calculation, or easier by simulation. See the attached file (LTSpice simulation). You can see that the filter (similar to your filter) gets closer to a finite attenuation at high frequencies, getting closer to the attenuation of a similar circuit with the inductors *removed*.

You can get better high frequency results by trading the center 0.2pF capacitor coupling to an inductive coupling. Remove the coupling capacitor and insert a wire through the center shield, ground its ends close to the main inductor. Shape the wire to a small loop near the grounded end of each of the resonator inductors to get small inductive coupling, and you get again a good BPF but with better high frequency attenuation. Instead of loops you can connect the coupling wire at a tap at the bottom of the main resonator inductors, close to the ground".

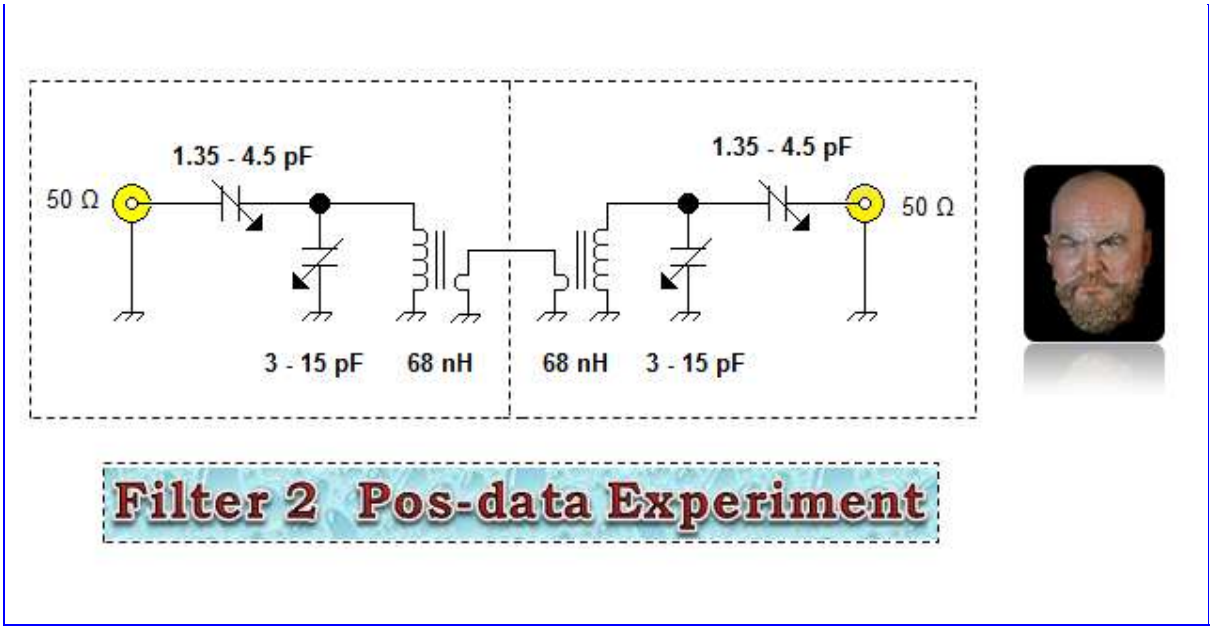

Above — Following Victor's suggestion, I inductively coupled the Filter #2 resonators with a wire looped near the grounded end of each tank inductor. Please view the schematic above. High-pass attenuation above the passband improved significantly. Click for a sweep out to ~ 511 MHz that shows the peak high-pass attenuation much closer to the low-pass skirt peak reponse.

At 2X center frequency (325.1 MHz) the high-pass skirt peak attenuation closed within 14 dB of the low-pass peak attenuation compared to the original Filter #2 response where the delta was around 30 dB. Further improvement occurs as we move above ~400 MHz. Big thanks to Victor for his support.

B. Sheet Metal Safety

A cut finger while working sheet metal prompted the following remarks: Jagged edges from cut sheet metal (especially brass stock it seems) may lead to deep cuts. Filing a burred edge with the metal clamped in a vice between some thicker metal stock with its raspy edge barely showing will reduce the "knife edge effect". When drilling, clamp the metal piece to your bench on a wooden backing board . If you jam your hand drill in an unclamped piece of metal it could spin and really gore you. Safety first.

---

7. NE612 Mixer Diddy

The Signetics NE612 and ilk enjoys wide use by the amateur radio community in novelty-grade Ham band receivers, or in somewhat better receivers laden with abounding front end filters + *stout,* switchable RF attenuators. Do you think of the NE612 as an ersatz receiver mixer? Some only consider them for the transmit mixer slot. Read this link why.

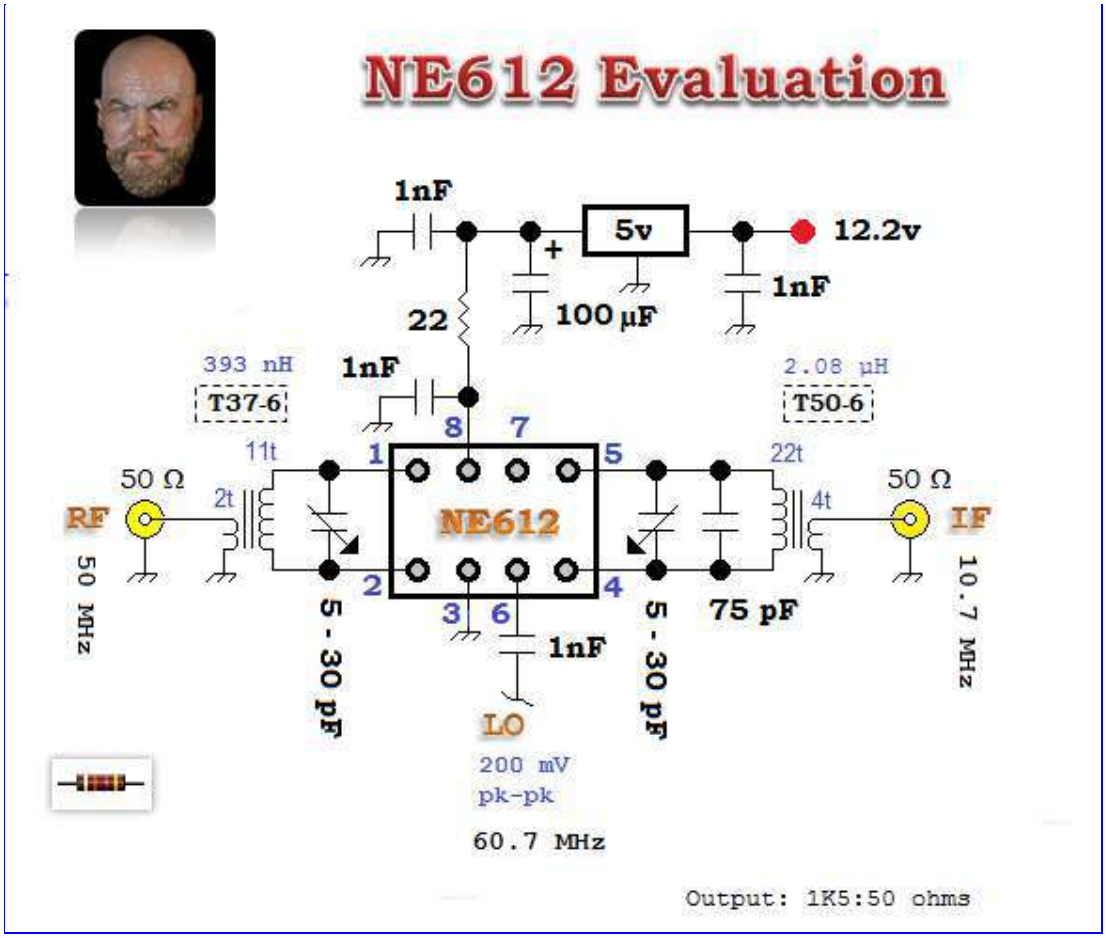

Above — My base schematic. I applied differential input to cancel 2nd order mixer products and balanced output to obtain maximum conversion gain. Click for the breadboard. Powdered iron toroids, Q = 1500 trimmers and a fixed C on the output formed the resonators. I chose a 10.7 MHz IF to drive low-cost ceramic filters in further (unshown) experiments. Normally, we don't bother tuning the input since our bandpass filter should launder the input signal sufficiently.

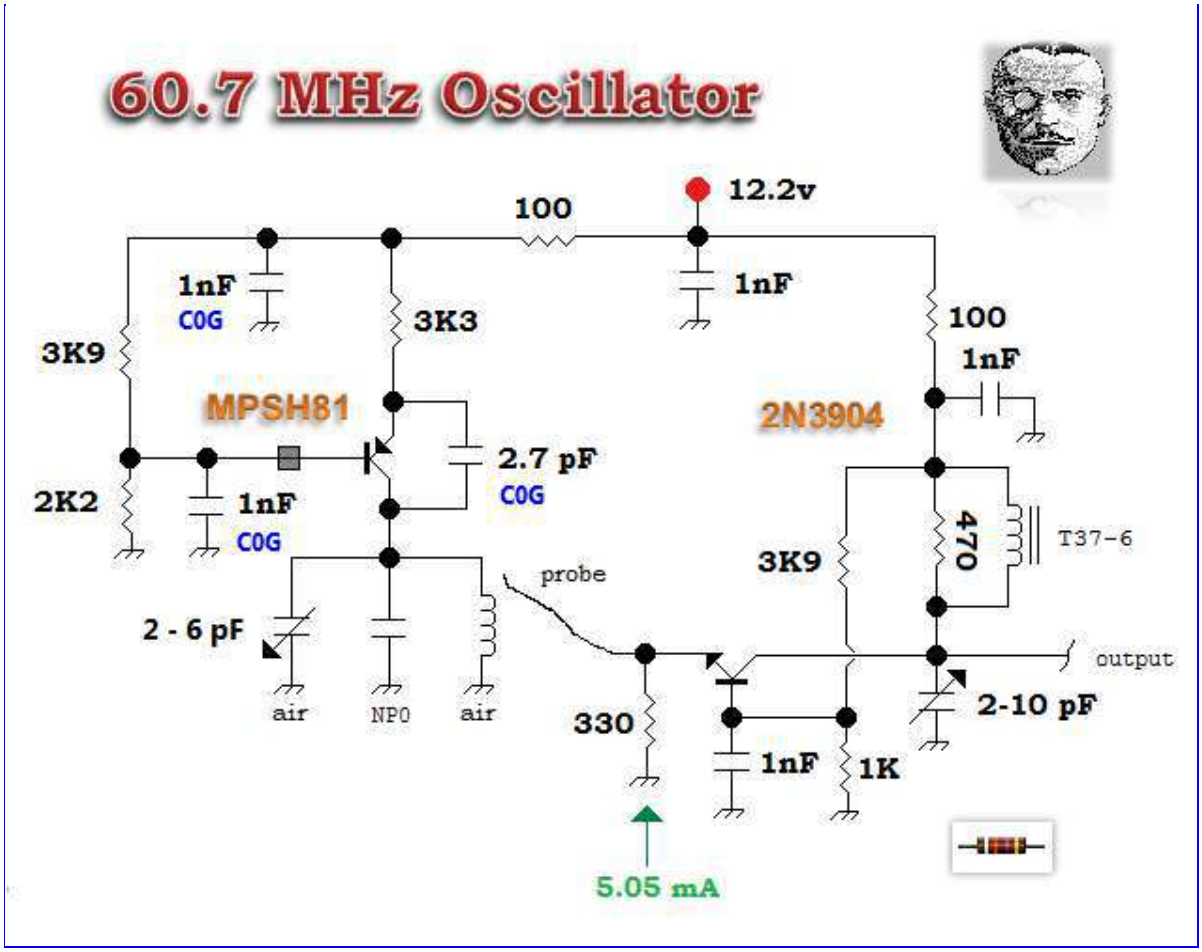

Above — My 'thrown together' 60.7 MHz local oscillator. A wire on the common base buffer amp input avoids the series R and C usually required and I moved the wire probe to set the output power between 180 and 250 mV peak-peak into a 1K resistor load.

Input power	IF	RF	LO	2RF	Gain
-35 dBm	-24.3 dBm	-68.71 dBm	-47.09 dBm	-68.14 dBm	10.7 dB
-30 dBm	-19.89 dBm	-63.68 dBm	-47.01 dBm	-58.29 dBm	10.11 dB
-25 dBm	-17.41 dBm	-60.07 dBm	-46.96 dBm	-50.06 dBm	7.59 dB
-20 dBm	-16.21 dBm	-55.62 dBm	-46.65 dBm	-45.06 dBm	3.79 dB
0 dBm	-13.27 dBm	-55.64 dBm	-45.99 dBm	-53.28 dBm	-13.27 dB

Above — A table showing the mixer input, IF, RF, LO, 2xRF [the worst spur] power readings, plus calculated conversion gain. This table echos the datasheet + work by others — input power >= -25 dBm drives this mixer into compression. The NE612 runs low current plus low voltage across the output transistors — thus the maximum output power is limited to somewhere between +2 dBm to +5 dBm from my experiments.

Even with -35 dBm input power, I measured a conversion gain much lower than the typical 14-18 dB enjoyed by others who applied differential output at ~ 50 MHz. Turns out, I goofed — each output transistor contains a 1K5 Ω resistor, so when wired differentially, the output Z = 3K. Back to the bench!

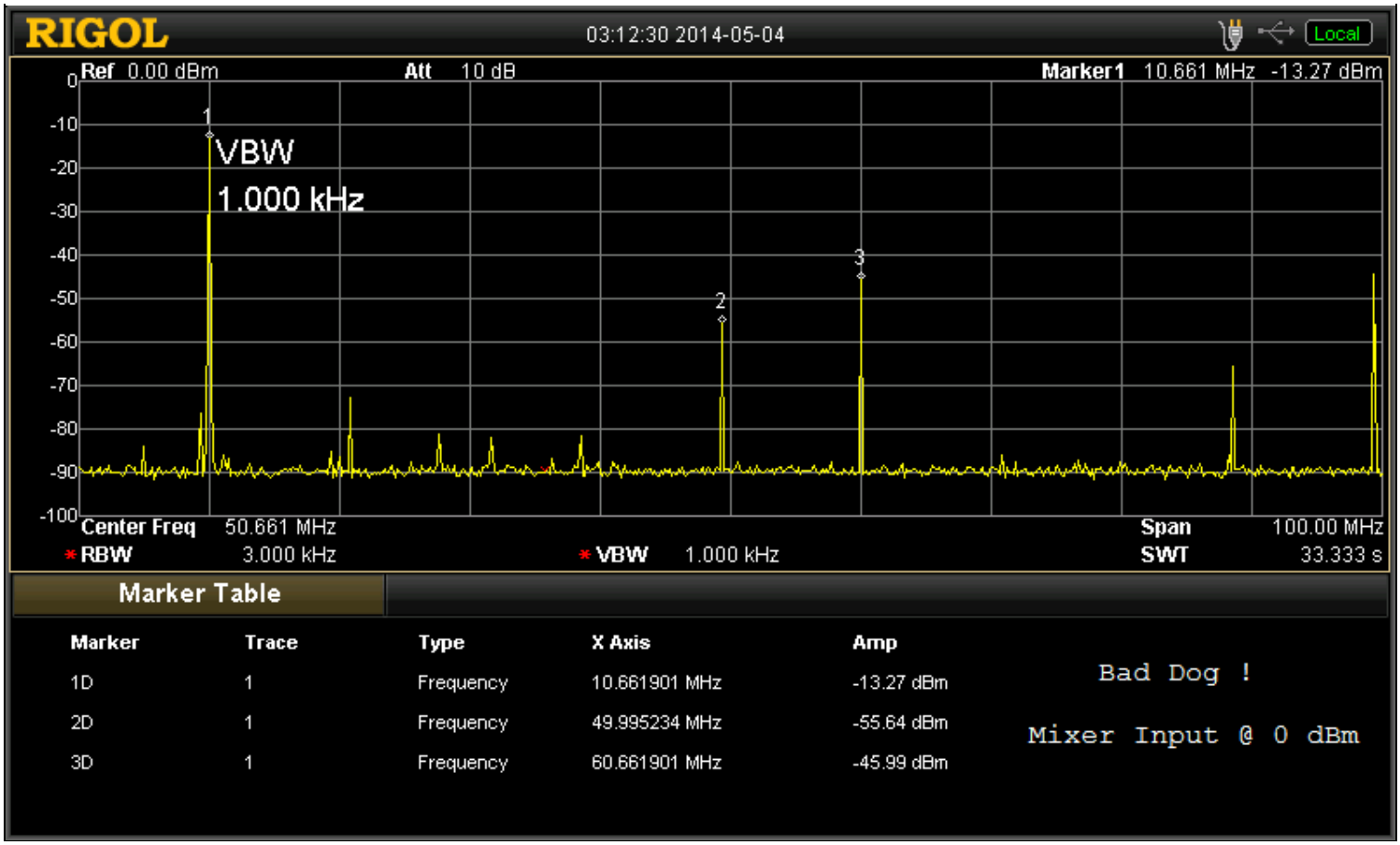

Above — SA of the mixer output with 0 dBm RF input. Something we would never do in real-life, but I wanted to see the spurs with such a drive: the spurious output actually looks great! The NE602, NE612, MC1496 and SO42P [all Gilbert cell mixers] output cleanly; especially when compared to diode-based mixers.

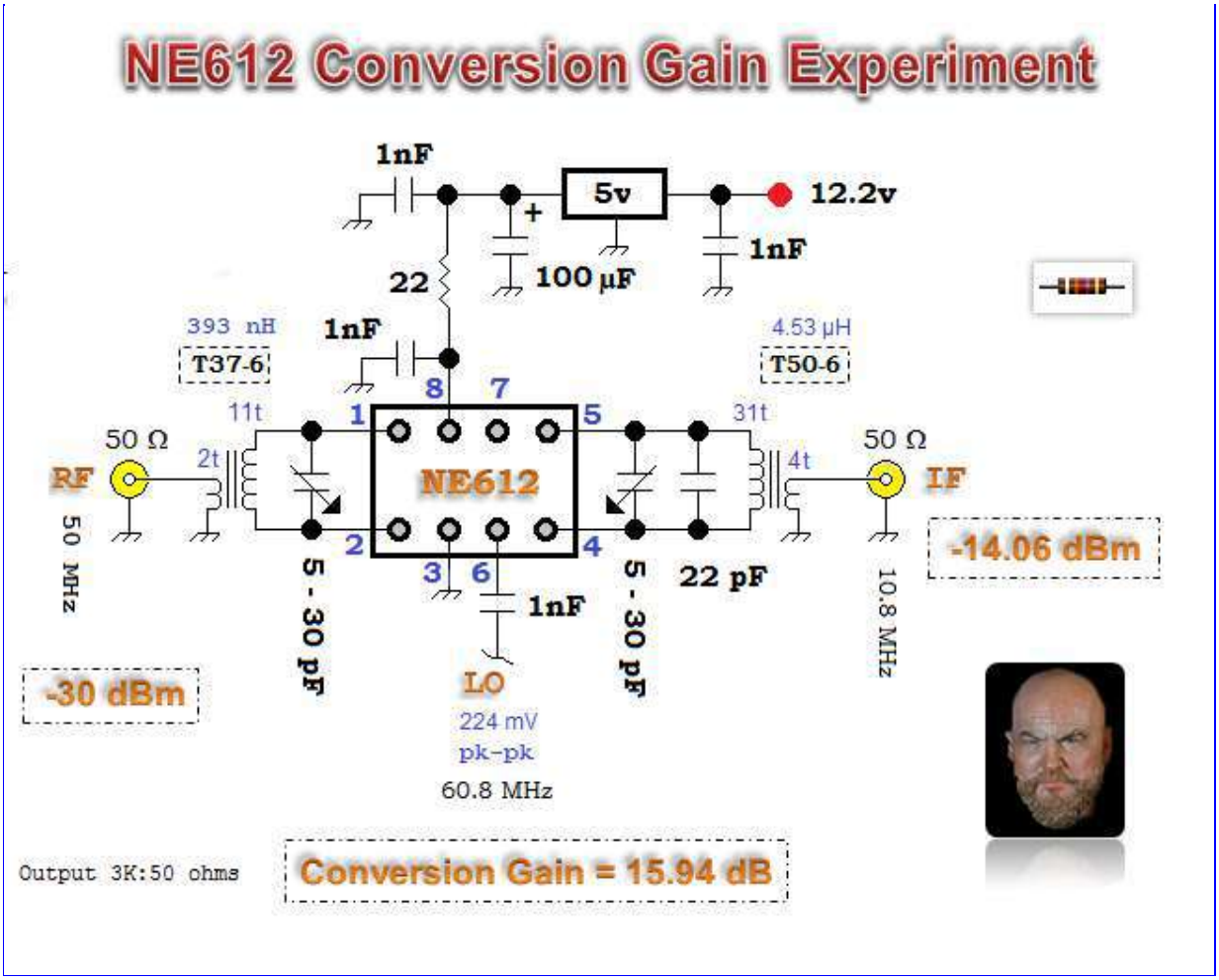

Above — My mixer with output Z corrected at 3K Ω. Wow, a conversion gain of 15.94 dB with -30 dBm drive. All good now. Click for the IF measurement on my SA. The LO had drifted up to 60.8 in this experiment, however, I left it and peaked the output resonator for maximum smoke. I also extracted another 0.5 to 0.8 dB gain by tweaking the LO drive. In my breadboard, a drive of 224 mV pk-pk gave the highest conversion gain.

Hereafter, I'll drive my NE612 transmit mixers with between -26 to -30 dBm on the RF port with differential input and output.

---

8. Miscellaneous Photographs

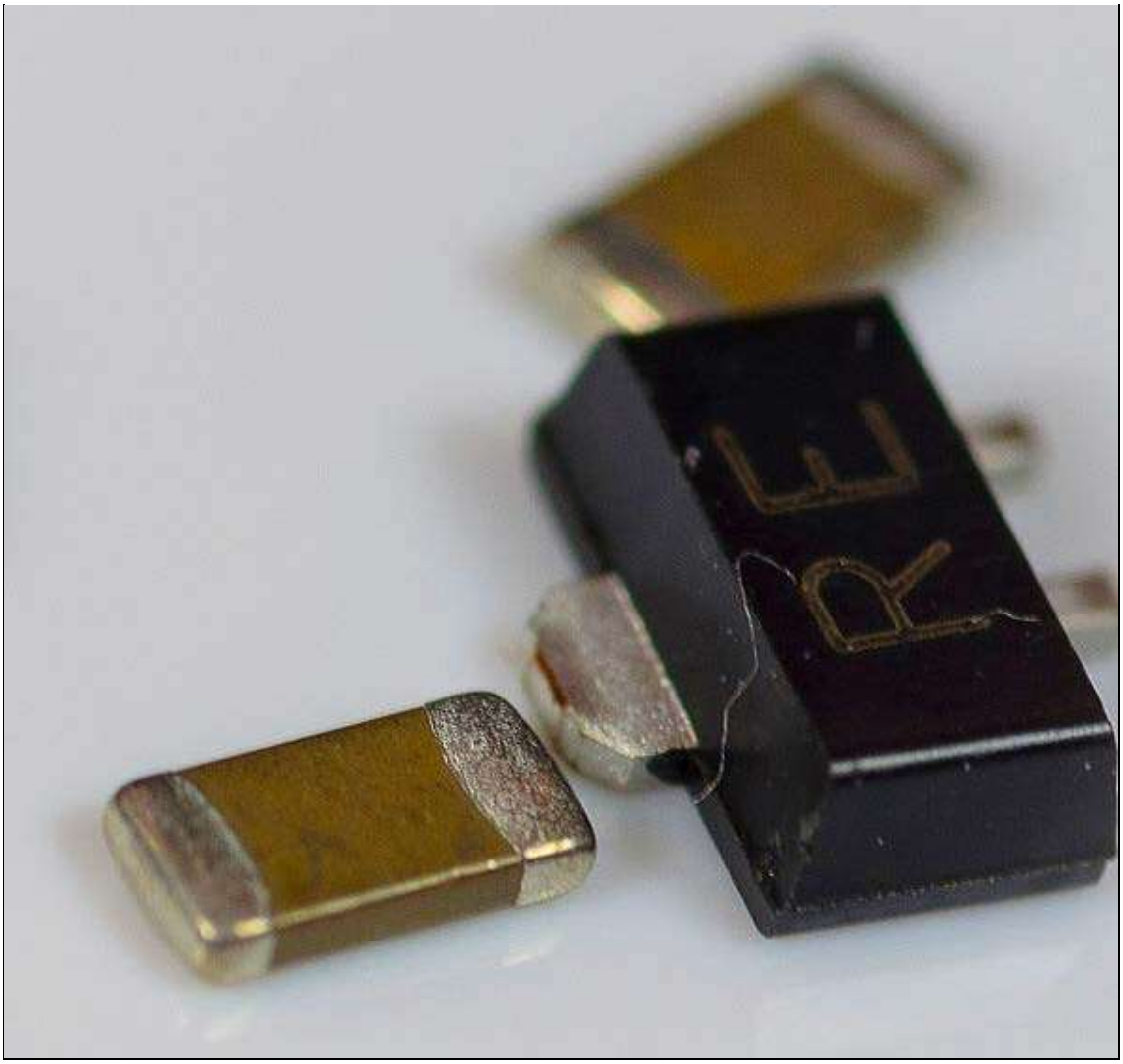

Above — Hair or lint in my SMT macro photo

Above — Instrument grade N-male to SMA female

Above — Instrument grade N-male to SMA female; gorgeous machine work.

RF Workbench Page 6 — QRP Transmitters

RF Workbench 6 explores some questions regarding basic transmitter power amplifer (PA) design. Since I write for both Ham and non-Ham readers, I feel badly that RF Workbench 6 excludes pure radio listeners; please consider getting your amateur radio licence to join the fun.

For Class A, AB and C transmitters in current source operation, radio builders knew most everything presented on this web page back in the 1980's — humbled and guileless, I've but a skosh of new ideas to further elevate this topic. Sometimes I feel bound in a creative straightjacket because puzzling design questions paralyze my understanding and progress. This web page explores a few transmitter questions born on my QRP work bench and I hope you'll relate and go design your own high-octane transmitters. As always, I hope to share insightful + actionable info for the DIY scratch builder; albeit from a lay-person perspective.

I borrow heavily from the work of Wes, W7ZOI per correspondence, direct contributions, from EMRFD and the references listed in Section 5. My sincere thanks to Wes for his support and inspiration.

Preface

You require an amateur radio operator licence to operate a radio transmitter and it's up to you to know and ensure your transmitter spurious emissions meet or beat the regulations in your country.

Although I measure my circuits with calibrated equipment, expect your measured voltage and current to differ from mine. **Why?** Variables may include your DC power supply voltage and current rating, dummy load resistance, stray L and C, cables and wire effects, bench errors, parasitic oscillations, temperature effects and parts tolerances.

I unabashedly declare my love for experiential learning: to build and measure, discover and develop — and best of all, to tune, tweak, and transform my RF power amps to unleash the "smoke" and power we all crave.

Contents

Section 1: 21.06 MHz Bipolar Transistor Transmitter in Class C: Dig out your old transistors and explore some Class C topics.

Section 2: PA Measurement with Examples: Measure collector V and I

Sections 3, 4: Incomplete and coming in 2013-14. I'll post any additions on the QRP Log -- Thanks

Section 5: I'll list all the references for this web page

Section 6: Photographs and Miscellany. I'm told at least ~~3~~ (now 4) people enjoy my photos.

Section 1: 21.06 MHz Bipolar Transistor Transmitter in Class C

Despite all the buzz about PA efficiency and the trend towards more efficient switched-mode power amplifiers, my email inbox fills with content regarding those Class A to C power amps. Consider too, most Hams, including QRP buffs, power their rigs with an AC connected DC supply that makes battery life moot. Perhaps our love of PAs in current source operation harkens from our historic tube days: do we simply enjoy making heat and wasting power? Like me, you might just love making and measuring bipolar transistor circuits.

A Class C power amplifer excited by a crystal oscillator offers both new and reawakening homebrewers the chance to make a simple but relatively powerful, 1 frequency transmitter with only 2 - 4 RF stages. Keying a Class-C PA embodies the Ham glory days: put some RF into the

sky with basic, analog circuitry.

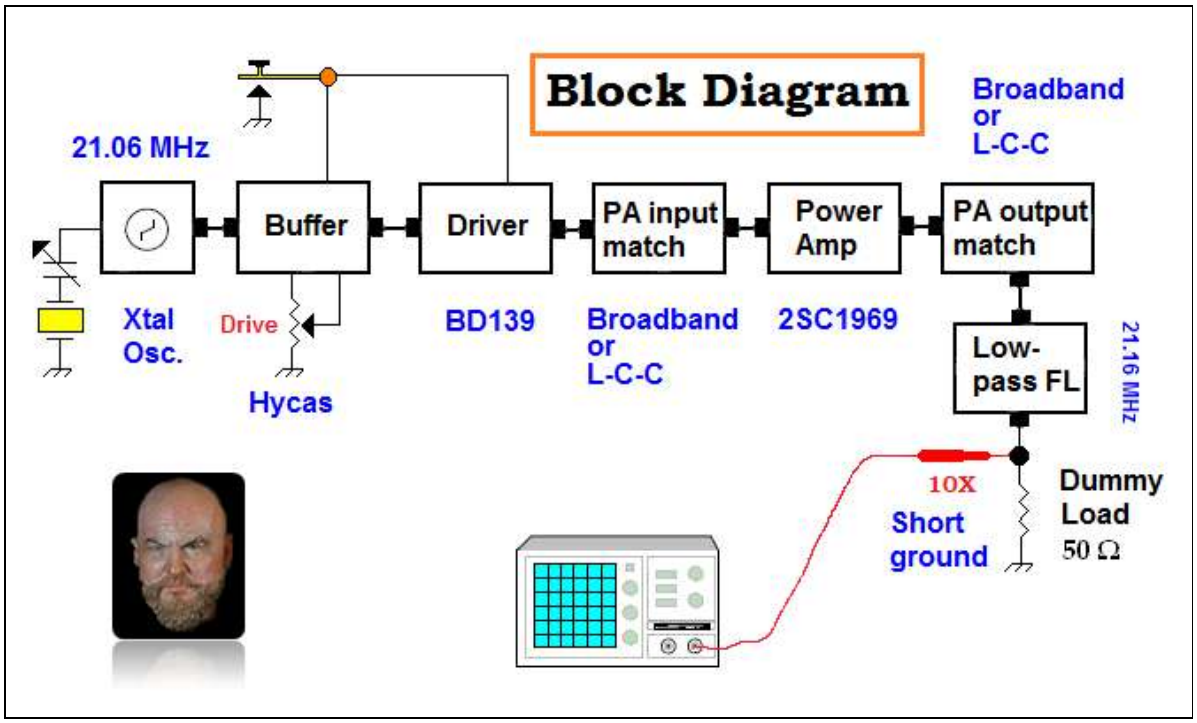

Above — The block diagram for all the experiments in Section 1. Each stage involving transistors was built and tested from left to right before making the next stage.

Crystal Oscillator, Keying Switch and Hycas Buffer Amplifer

As more a listener than a talker, I wanted a low-level crystal oscillator to keep my *key up* current draw low. In the class C power amplifers based on the above block diagram, I measured only 7.5 mA. *key up* and several hundred mA *key down*. I also wanted my back wave to be > 40 dB when I eventually converted the PA to Class AB during another set of experiments.

Design Question 1: What backwave should I strive for?

Backwave = the dB difference in output power between key up and down. Opinions differ and context may partly explain why. If you're working DX, backwave is less important than when your working nearby ops on 80 meters. From asking respected authors, experiments and operating, I feel 40 dB should be the minimal backwave to strive for. Operating Class C, your final(s) are turned off during key up and a >= 40 dB backwave proves an easy goal.

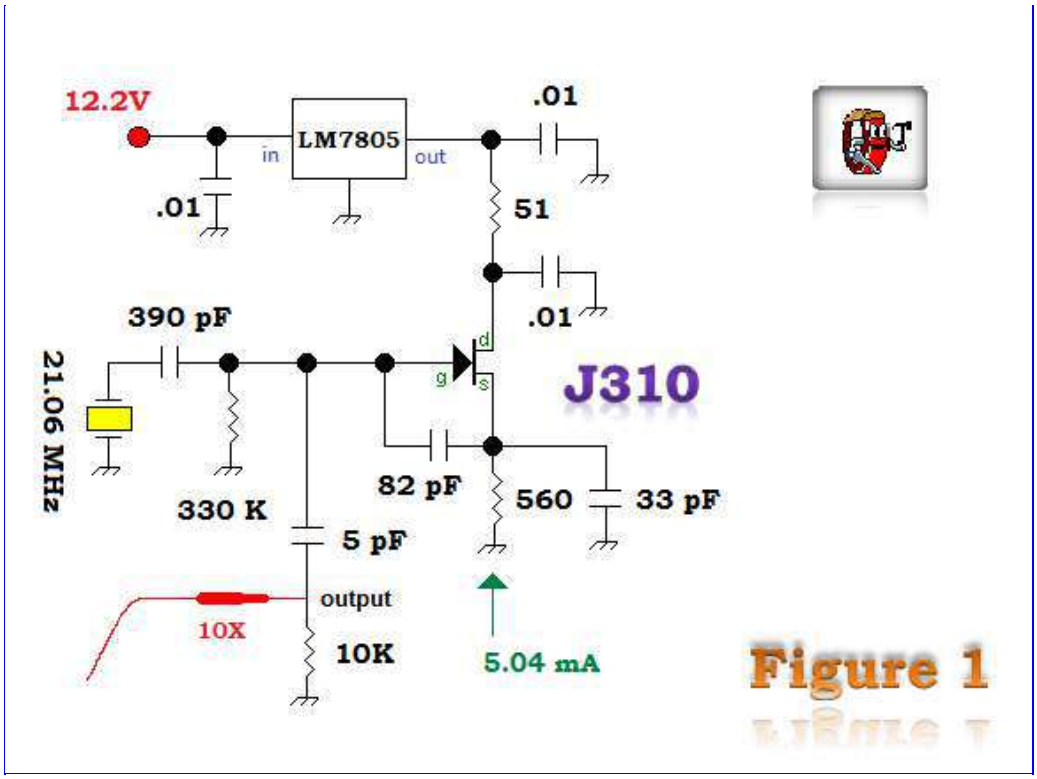

Above left — The 21.06 MHz crystal oscillator. Click for the output voltage into 10K Ω. Click for the FFT. Seeking low distortion and output power, I placed variable capacitors in the feedback and source slots and also played with the 560 Ω source resistor. While watching in my 'scope and tweaking , I chose the the lowest distortion signal under 1 Vpp. The variable capacitors were removed, measured and replaced with nearest standard 5% parts. The 10K load of Figure 1 corresponds to the gate resistor of the hycas amplifer input.

Above — Without the 390 pF capacitor, the crystal oscillator vibrated at 21.058 MHz.

Above — The crystal oscillator measured frequency after experimentally adding a 390 pF cap. Should I have tried a 470 pF capacitor and attemped to get 21.0600 MHz?
My oscillator looks unconventional and in some cases you might want 1 with higher output voltage. Check EMRFD and the other W7ZOI references in Section 5 for xtal oscillator design ideas.

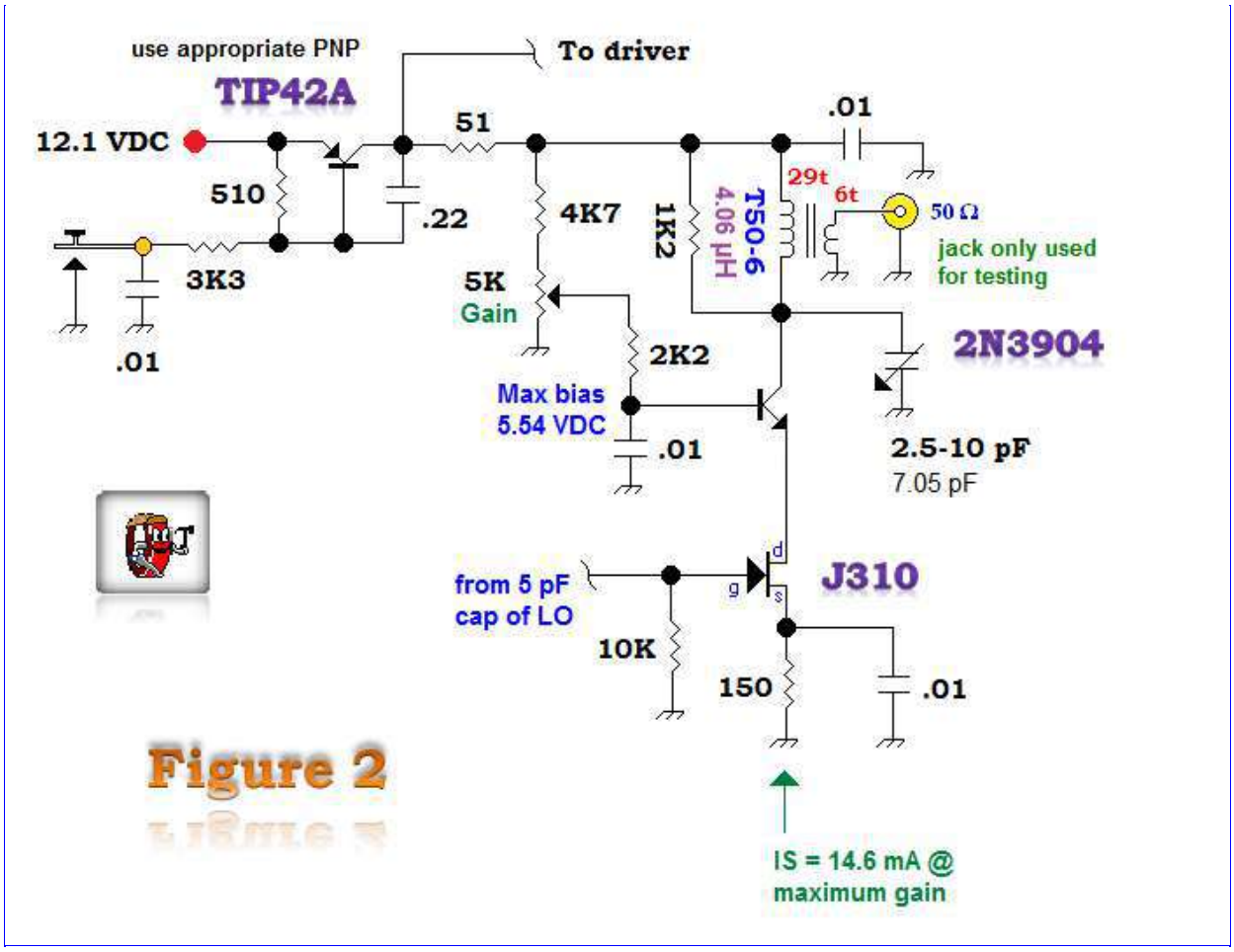

Above — Figure 2, the hybrid cascode buffer. I've never tuned, nor keyed a hybrid cascode amp before and it works well. Click for the oscilloscope output. Click for the FFT measured with a long wire grounded 10X probe. I applied a junkbox TIP42A switch lying on my bench since I keyed a number of *unshown* high current stages during my experiments. Only about 10% of my experiments ever make it onto the QRP/SWL HB web site. For the PNP switch, just use whatever can handle the *measured* current with key down: 2N3904, 2N4403, 2N2907, BD140, etc.,etc..

Yes dear reader, measure everything.

The Driver Amplifer

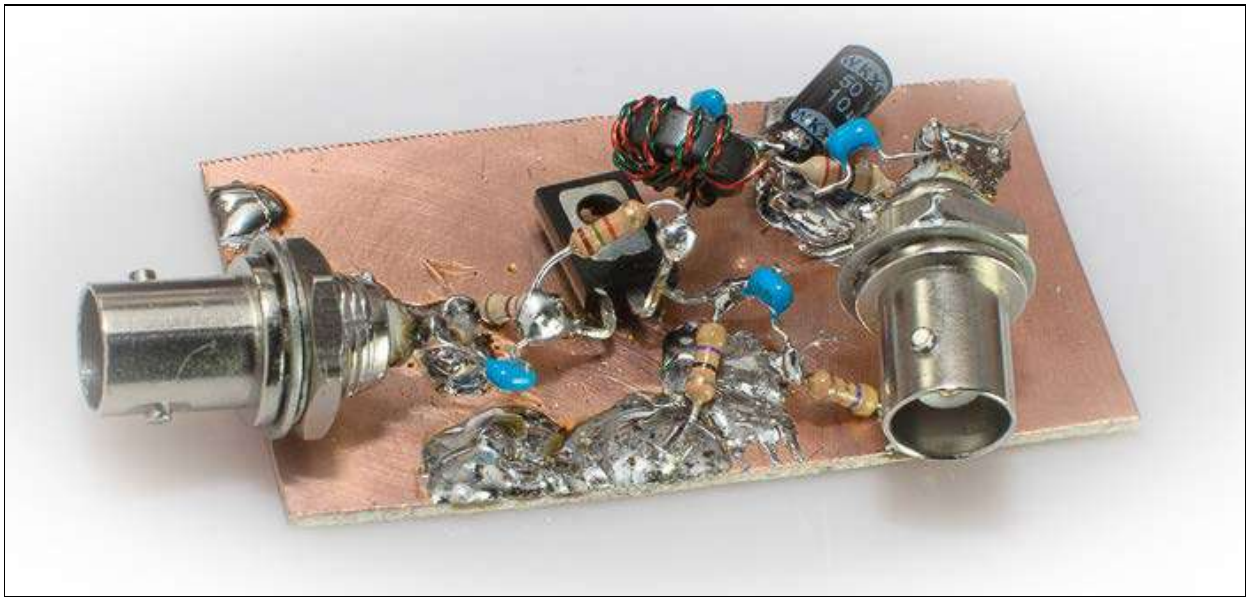

Above — A BD139 feedback amp breadboard. Click for the schematic. Wanting an output power of at least 22 dBm to drive my final, I built 3 varieties with both the BD139 and a 2N3866. Normally, for receiver amplifers, I focus on a strong input and output return loss and work hard to maintain linearity — but mostly keep the emitter current under 50 mA. At 21.06 MHz, the biggest *clean* signal I could muster with such a

broadband feedback amp was +16 to +18 dBm — well short of my goal. Click for a DSO screen shot of the 41.3 mA amp at 6.42 Vpp or ~20.13 dBm power; quite distorted.

I needed to try something else and saw the Figure 3 amplifier in some of Wes' work; wielding bold emitter current to boost signal handling and power.

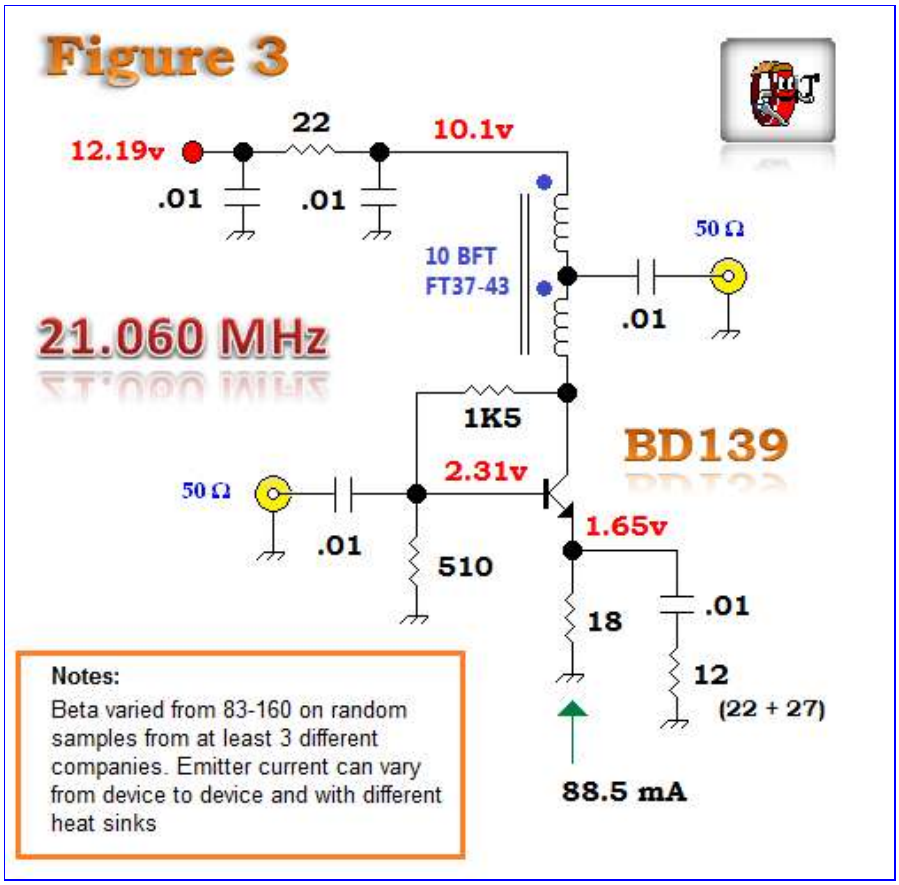

Above — The W7ZOI designed feedback amp used for a driver in all Section 1 power amp experiments. Love it! Many builders feel tempted to abandon series and/or shunt feedback and just "go for gain". My experiments suggest this approach often leads to instability within the driver circuit and possibly on down the RF chain. We should strive for linearity and stability; 2 big reasons we apply feedback. Flirt with a driver *lacking* feedback if you dare.

Click for the maximum output power attained by turning my hycas bias pot fully clockwise: 7.77 Vpp, or 21.79 dBm. You can see distortion, but since this stage will drive a Class-C transistor PA (i.e. it will switch "a diode" on and off and generate clipping), I decided it will work fine. A VHF-UHF transistor such as the 2N3866 or 2N5109 may yield as much as 3-4 dBm more power, however, you'll see more clipping at higher driver levels. I stuck with the BD139 and tried several pieces from at least 3 different manufacturers (The BD139 was made by at least 10 companies at 1 point). A Philips version purchased in 2008 yielded the 21.8 dBm, so I bolted it to a home built copper clad heat sink and soldered it in place.

Calculating Transistor Output Power Off the Bench

Design Question 2: How do I mathematically estimate my Class A amplifier output power?

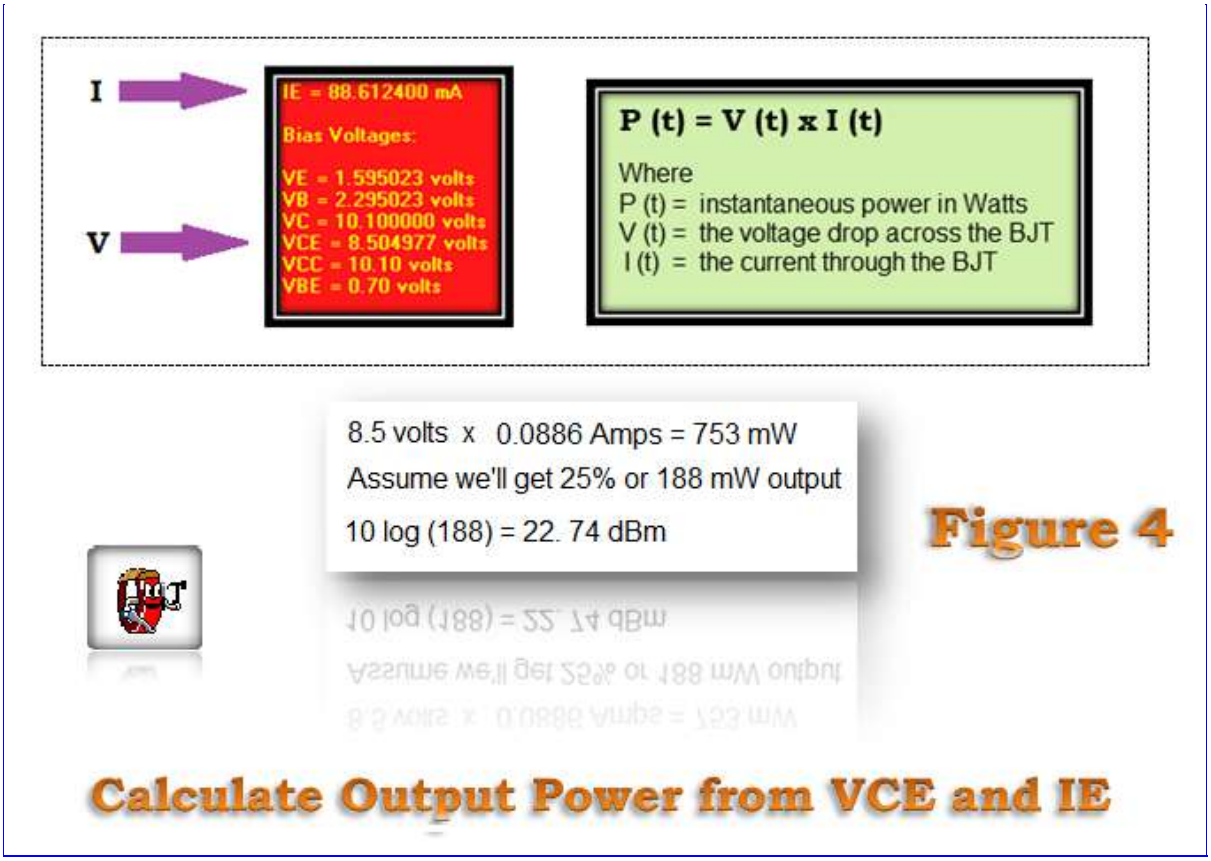

Above — Estimating output power from my Figure 3 amplifier. I measured a static DC Beta of 125 as shown in Section 5 on this page. Then I calculated VCE (the voltage across the transistor) and emitter current with my program NPN-DC Bias. Wes wrote a similar and likely better program called Biasnpn08.exe that's included on the EMRFD compact disk.
You may also measure your VCE and IE directly and improve the above calculation with measurements. I do this frequently.

Class A amps exhibit about 25% efficiency and also imagine that Figure 3 will bear some gain compression.

My measured power = 21.8 dBm — it amazes me how close a non-bench calculation using DC analysis can get to a AC bench measurement. The Figure 4 procedure is apparently a bread and butter RF design tool.

The Power Amplifer Input

Design Question 3: How do I match my driver output to the Class-C power amp input to maximize power?

This question provided a few nights of reading and experiments; time well spent. We have 2 main ways to match our driver output to the PA input: broadband or tuned. First, lets explore the problem theoretically:

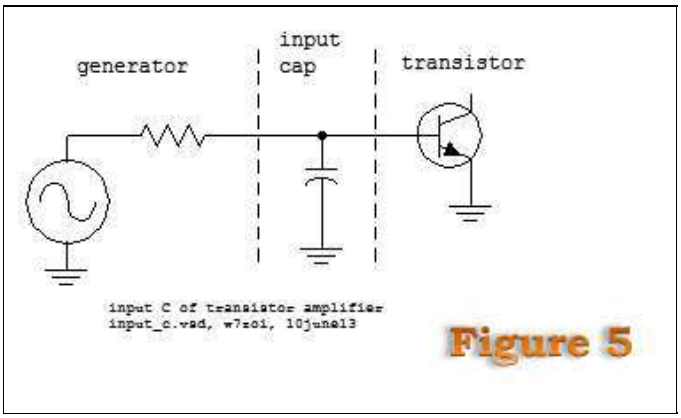

Above — A simple model sent by Wes: driving an amplifier with a power source. As amateur designers, simple models help us understand complex concepts.

A pure voltage source doesn't really exist. We don't apply a voltage to the base of the PA; rather, we apply a power source (our signal generator) — a signal voltage followed by a series impedance that's usually just a source resistance for a load. The power source + source impedance together *source* the load that includes the load capacitance represented as an input cap in Figure 5. You may wish to read about Thévenin's theorem and its dual, Norton's theorem to learn more about linear network analysis.

The load presents an impedance where the power is delivered and either dissipated in its resistance, or reflected back to the source when the load contains a reactance . At our PA input, this capacitive load reflects some of the signal back and induces a pole that corresponds to a "capacitor" time constant.

If you consider our power source, its source resistance, the PA input capacitance and just omit the effects of Q you'll see that the the voltage across the capacitor decreases as frequency increases. If you insert a 2:1 turns ratio transformer after the driver, you'll drop the AC voltage by 2 and its resistance by 4. For the same capacitance, the 3 dB cutoff frequency of this single pole filter increases. Also, the lower output impedance drops the driver amplifier voltage gain and may boost stability.

In short, we need a low driver source impedance since the Class C bipolar amplifier base-emitter junction has lots of capacitance To get current flowing into the PA base, we drop our driver output source impedance down *low*.

I thought — couldn't we just neutralize this capactance with an inductive output impedance? Thus our PA driver stage would drive a resistive load and everything would be "ducky". I consulted Wes, plus viewed some math and circuitry.

You can't effectively neutralize a bipolar transistor amplifier, since the capacitance isn't constant and behaves more like like a varactor diode rather than the C shown in Figure 5.. Even when forward biased, diode capacitance depends on the instantaneous voltage that appears across the diode. In contrast, 'FETs prove less troublesome and thus it's possible to achieve some neutralization with a 'FET amplifier. Please view the power stage from EMRFD Figure 11.14. Check out the push-pull pair of IRF511s. C5 and C6, at 22 pF each, are neutralizing capacitors.

In some cases, the capacitive reactance may be absorbed as part of a resonant circuit on the PA input. For example, a low-pass filter might soak up some of the C.

In all cases, our goal is drive in some power and switch the PA transistor solidly on and off (i.e. technically approaching class B but definitely class C because conduction will be less than 180 degrees) — a low output impedance can drive that input capacitance.

Driving final(s) with a very low output Z rings true even if your driving the latest (super-costly) ultra-low loss, high breakdown voltage, silicon GaN FETs to output >100 Watts at 1296 MHz in Class D, E, F, or Inverse Class F. Just get it done!

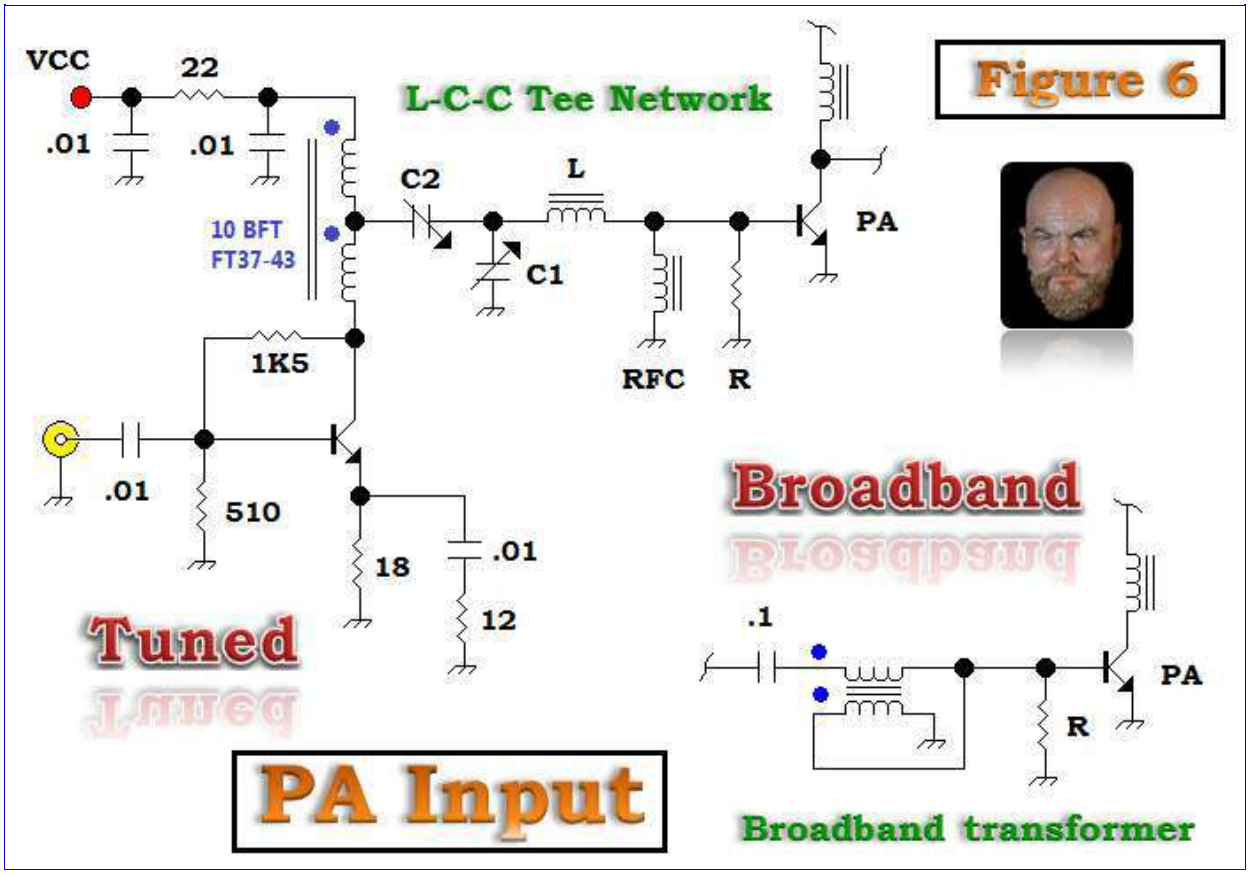

Above — Figure 6 shows 2 basic methods to drive the PA with a low impedance: single frequency network or broadband step-down transformer. I'll discuss both methods in detail later. Let's move away from theory and lighten things up for a couple of minutes.

Above — A short 10X probe ground lead boosts Tx measurement accuracy; in particular, for FFT analysis with your DSO. You can read or see **why** by searching the web for text and/or videos concerning oscilloscope probes.

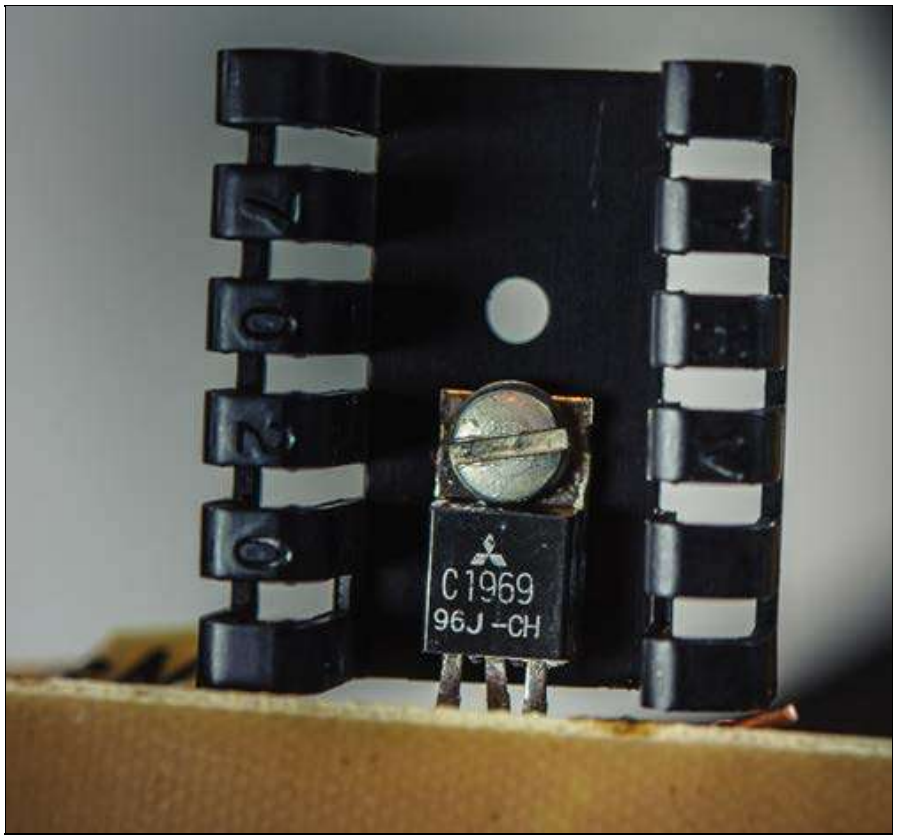

Above — The long gone 2SC1969 works great. Beware of counterfeits however.

Bipolar transistor selection troubles us since most of the 'old standbys' went obsolete way back when. I've been collecting dusty, old *QRP* driver and PA transistors for decades and my bag includes BD139, MJE181, 2SC2509, 2SC1969, 2SC2166, NTE123, 2N3053, 2N4037 and 2N2219A. For VHF, apart from the 2N5109/2N3866 standards, I've kept a few MRF607, 2SC1971 and 2N3553.

VHF/UHF transistors exhibit tremendous gain at lower HF, but they might oscillate without due care.

Some rules I've gleaned: The fT of a BJT should be at least 3-5 times the operating frequency; the VCEO should be at least double the VCC (more is better) ; don't exceed the maximum heat dissipation, nor maximum current. In short, read the datasheet. I won't cover heat sinking, nor gain compensation for multi-band amplifers on this web page; for it's been done by far better authors.

Lets make a basic Class C power amplifier based upon the RF blocks presented thus far.

Class C PA with Broadband Input and L-C-C Tuned Output

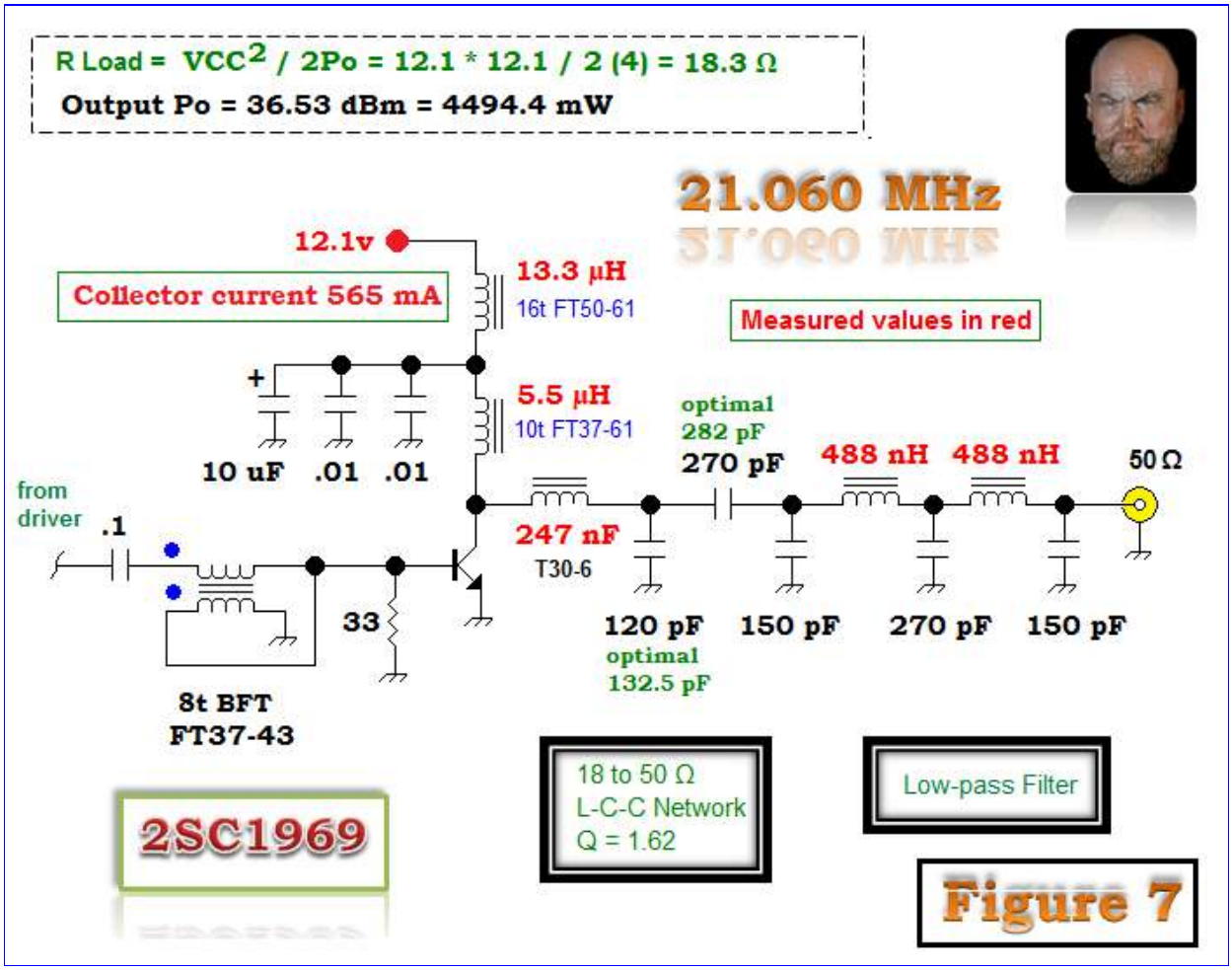

Above — Input matched PA via a broadband transformer (a bifilar wound transmission line transformer with a 4:1 Z ratio). A great example of this design includes the Figure 2 of Ugly Weekender transmitter by Wes. The 50 Ω output Z of the driver is transformed to 12.5 Ω. to drive the PA input. While a conventional link-coupled transformer works okay, the closer coupling of a twisted wire transmission line transformer often affords a better impedance transform and lower losses. You might experiment with a 9:1 Z transformer instead of the 4:1 shown. Click for a highly compressed photo of 1 of the full breadboards.

The 33 Ω resistor helps lower gain and stabilize the amp. I ran 33 to 100 Ω applying experimental methods. Read more about the PA base resistor and coil XL requirements in the text following Design Question 6.

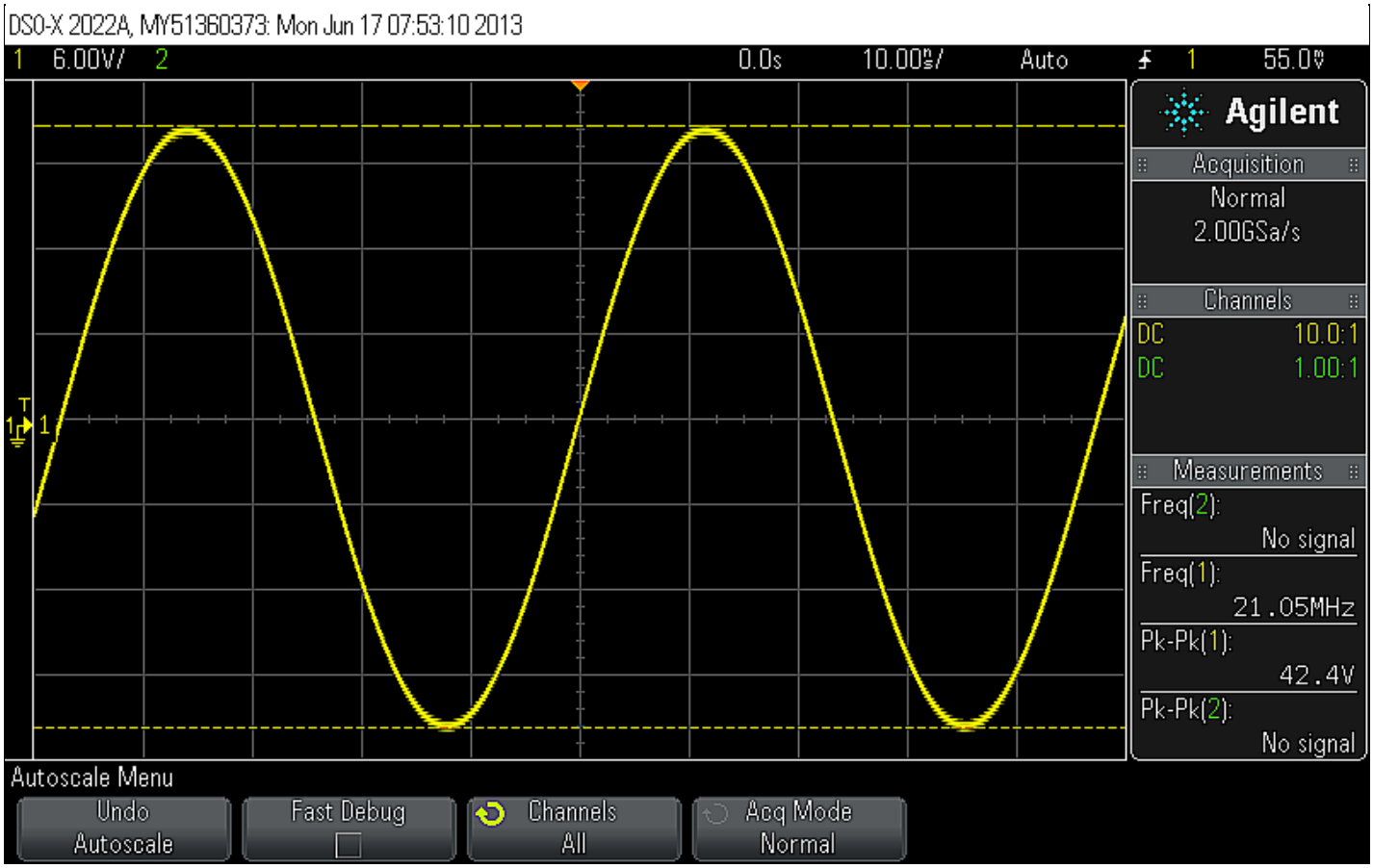

Above — The 'scope output from Figure 7. 42.4 Vpp = 36.53 dBm = 4.49 Watts.

L-C-C Output Matching Network

3 discussion points arise from Figure 7: [1] the output matching network. [2] the collector choke + decoupling circuitry, and [3] the low-pass filter. I'll discuss choosing a collector choke and decoupling in Section 2. We design our low-pass filters with tables or software; I used an old ARRL Radio Amateurs Handbook and then tweaked it in GPLA to get standard value capacitors. Click for a GPLA simulation of my filter. The L-C-C network also provides some low-pass filtering.

To calculate the collector output resistance, we use the formula R(load) = Vcc^2/ (2*Pout) as shown in Figure 7 for 4 Watts. For 1.5 Watts at 12 VDC --- R(load) = 12 * 12 / 2(1.5) = 48 Ω --- no output matching network is required; making 1.5 watts a popular transmitter power for new builders eager to learn about Class C.

Design Question 4: How do I make an L-C-C matching network?

Let's stick with 4W power and make an L-C-C Tee network for a 18 to 50 Ω transform. I prefer the L-C-C network over the L-network because you get 2 capacitors to tweak and I find it much easier to match a wide range of impedances compared to the L-network. Since we may pinch, or expand the inductor windings, in reality, the L-C-C gives you 2.5 possible tweaks.

Normally I wind the L on a number 6 powdered iron toroid with 26-28 gauge magnet wire in size T25, T30, T37, or T50. 26 gauge wire allows for good coil squishing and expansion with thumb and forefinger. For design cycle capacitors, I mostly solder in those horrible, low Q, orange, green, or red muRata trimmer caps such as the TZ03Z500F169B00. Although rare, ceramic-mica trimmers work well.

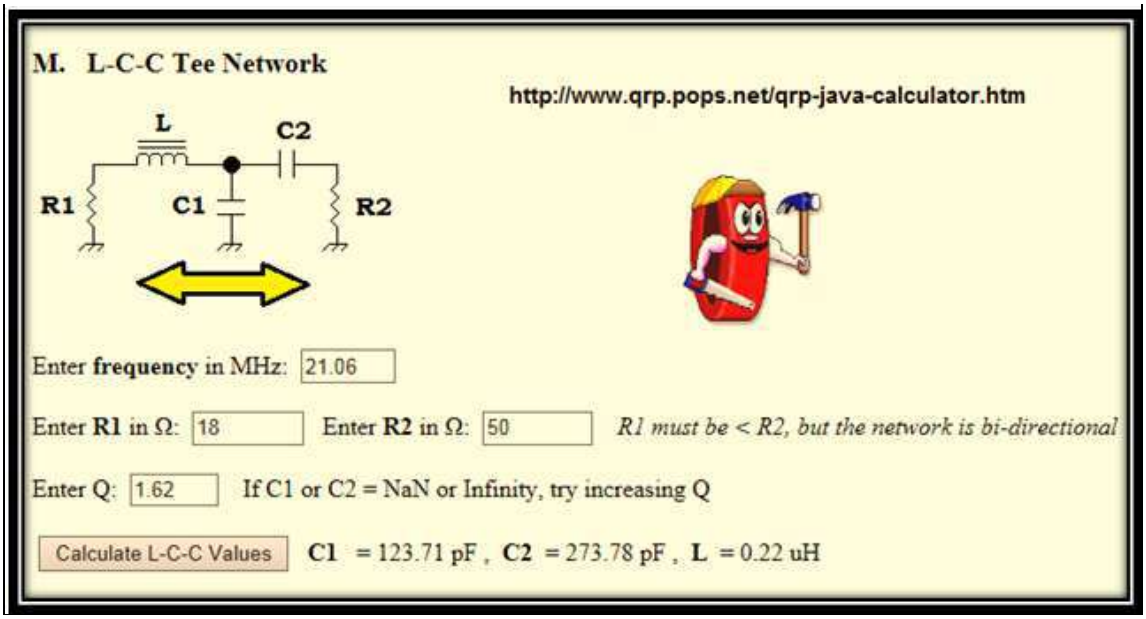

Above — To calculate L, C1 and C2 we may employ software to obtain starting L and C values. I recommend Wes' ZMAT08.exe, a Ladpac program that ships on the EMRFD CD. I wrote my own java-script applet with less prompting and error checking and put in on the Design Center web page as **M**. Note I used 18 Ω as the load resistance in my calculations.

During actual bench assessment of your network, output your PA to a 50 Ω dummy load rated for that power and preferably measure the peak to peak voltage with a short-grounded 10X probe.

For Figure 7, I wound and tack soldered in a measured L of about 230 nH and placed a 100 pF cap plus 6-50 pF trimmer for C1 and a 220 pF + 22 pF cap + 6-50 pF trimmer cap for C2. The tuning procedure goes like this:

Tune the capacitors for maxmum power. Try squishing the L, then re-tweak C1 and C2 and see what happens. Did the Vpp go up or down? We want it to go up, so if the Vpp went up you needed more L, and perhaps still need more. If you squish the coil again (or remove it, add 1-2 turns and then replace it) and the Vpp goes down, you increased the L too much and need to go back down. If the original Vpp goes up when you expand the coils, you had too much L and need to do the opposite procedure just described. Re-tweak C1 and C2 after every inductance change and calculate the power in dBm and/or watts on your bench.

Through trial and error you'll find the optimal L. If nothing works, suspect a bench error, or device failure. Occasionally, I add too much, or too little fixed C in parallel with the trimmer cap. Another time, my transistor was fried.

Once you've extracted the maximum power, remove the cap(s) that make up C1 and measure them. Do the same for C2. I replace C1 and C2 with the nearest equivalent standard value capacitor or (parallel capacitors) and then repeat the tuning procedure to find the optimal L for these 2 new capacitors. Normally, after optimizing the Vpp, I'll remove and measure L to confirm my L-C-C network design. You can use the L just removed or make a tidier version to permanently solder in.

Once you solder in the "keeper" L, you'll need to expand or compress the links a tad to peak your Vpp once again. Although it sounds like a chore, I love measuring a higher Vpp with each successful manipulation of the L-C-C network; it's quite a rush actually.

In the end, my optimal measured values were: L = 247 nH, C1 = 132.5 pF and C2 = 282 pF. In my final, I substituted C1 = 120 pF and C2 = 270 pF as shown in Figure 7. Although I designed for 4W, I squeezed out 4.49W with my L-C-C network.

Design Question 4: How do I choose my L-C-C matching network Q?

The easy answer is the degree of impedance transformation sets the minimum Q and thus choosing the best Q becomes the central question.

The theory regarding loaded versus unloaded Q + network losses and such may bog down many, but in context, a lower Q leads to a more efficient network with less loss. Low Q values also means we tweak larger value capacitors that minimize the effects of stray capacitance. In the collector output network of Figure 7, the Q of 1.62 gave more power than an earlier Q = 5 network. Further, during design, I sometimes slightly adjust the Q in software so I get closer to standard value caps for C1 and C2.

Don't be afraid to remove C2 and just make an L-network. Again, just experiment on your bench to gain confidence.

I tried making this circuit with a BD139 in the PA slot and managed to squeeze a mere 3.1 Watts power at 12.1 VDC. Others, such as Wes and Jason, NT7S delivered more power into 50 Ω at and even above 21 MHz with a BD139 PA.

Factors such as transistor specifications, frequency, VCC, and driver power may affect the output power. In the end, the 2SC1969, a final I harvested from an old Cobra CB more than 20 years ago delighted me. I constantly scrounge for old driver and PA transistors in my travels. Sadly, many old CB radios given to me over time suffered from fried finals.
You might try checking eBay, but watch out for fakes.

The BD139 grew to notoriety because it's widely available, cheap and generally does the job at or below ~28 MHz, depending on what output power your seek. I found wide variation in Beta (or hFE) and fT in the random batch I tested. Also remember we're hitting them with lots of current and they heat up and specs change. At 7 MHz, the BD139 works great. The BD139 reminds me of the MPF102 JFET; you never know what your going to get. The best I've tested were Fairchild BD139s and woefully, they're all gone.

Class C Power Amp with Broadband Input and L-C-C Tuned Output

Let's make a PA with an L-C-C Tee network tuned input: Figure 8.

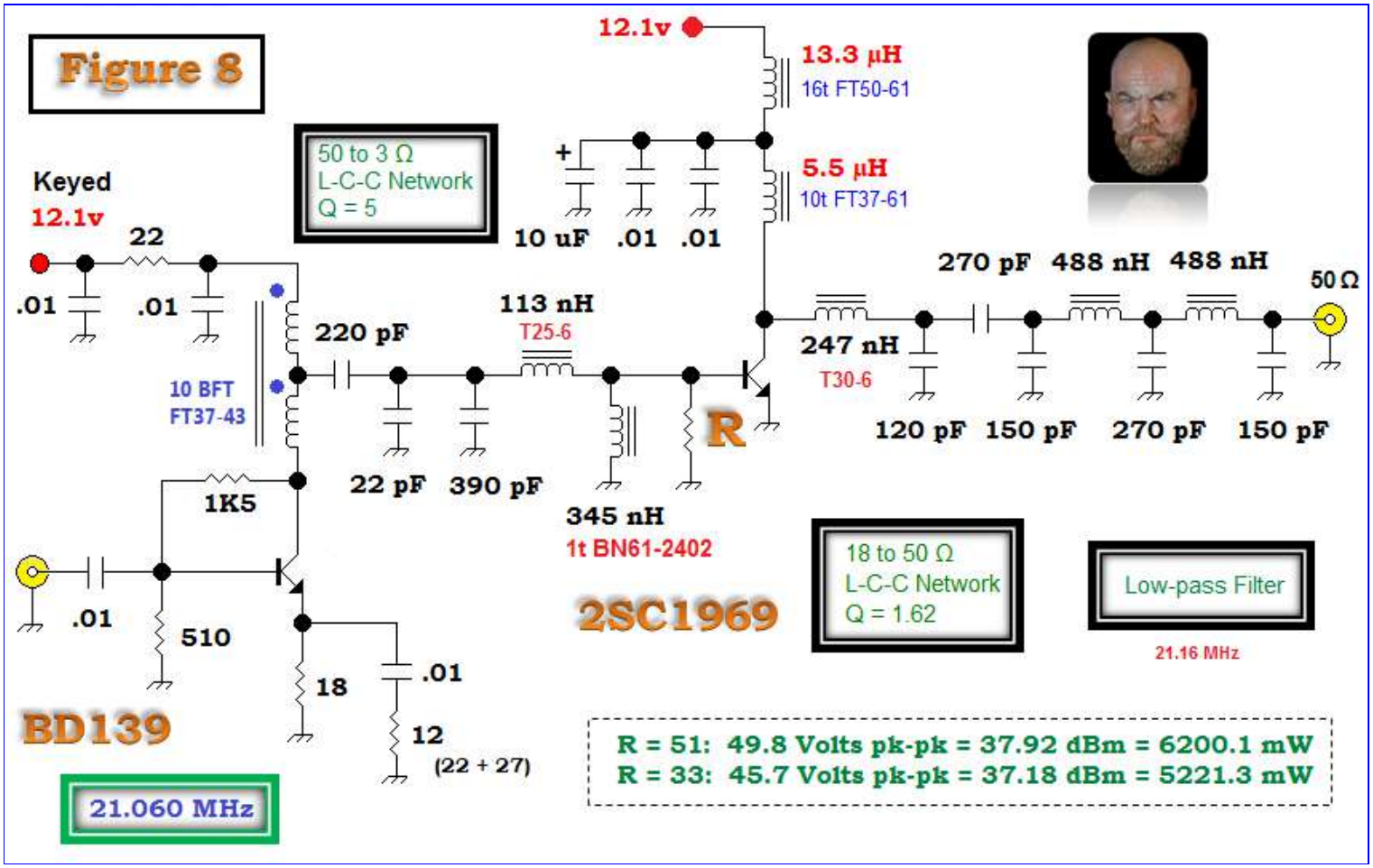

Above — Figure 8. The Figure 7 PA with a tuned input network smashed my world with 6.2W power. Click for the FFT showing the second harmonic down at least 55 dB. I later confirmed this with spectrum analysis.

Design Question 5: How do I choose my PA input impedance?

PA Input Impedance

Calculating the input Z of a transistor with 100's of mA emitter challenges us.The familiar calculations like Zin = (Beta +1) x 26 /I e (mA) don't work out perfectly since our transistor is hot and Beta changes, and in my case I'm way up in fT. I asked Wes and he suggested I assume an input Z of 3 Ω (with about 200 pF of parallel C). Thus , I chose a 50:3 Ω transform to design my L-C-C network.

From my experiments, bench tweaking an L-network, or L-C-C network will accommodate anything even close to 3 Ω input impedance — 3 Ω seems quite actionable. Tune your L-C-C network in the manner described for the PA output match. Since your transforming 50 Ω to 3 Ω, the minimum Q will rise.

Design Question 6: How do I choose my PA input choke and resistor when fed with an L-C-C network?

The RFC serves as a DC return path for the PA base just like in the transformer in the wideband version. We normally apply a rule that the minimum inductive reactance of a choke should be 10x the impedance it's connected to, so that's 30 Ω XL.
Since F = 21.06 MHz, the minimum choke value will be 30 Ω / 21.06 MHz x 6.28) = 227 nH. In order to keep the SRF up and for ease, I ran a single turn of 26 gauge wire through a BN61-2402 binocular core and measured 345 nH. Good enough. The # 61 mix will exhibit some Q. Likely # 43 material will work fine too.

The resistor labelled R serves to reduce the Q of *my* particular RFC, lowers gain and boosts stability. With R = 33 - 51 Ω, the amp held stable, but if I tried to increase R above 51 Ω spasm erupted. The resistor affected output power as shown in Figure 8. Again the resistor should minimally be about 10X the input Z or so. I tried an R of 10 Ω and the output power dropped down to a little under 3W as more of my driver output just flowed through the resistor to ground.

To conclude, I executed the time honored tradition of choosing parts and circuits to extract power from a crystal oscillator-driven analog RF amplifer chain. Much of this information extends to linear operation (Class A, AB) and general RF design. Have fun designing your own transmitters and as always, apply experimental methods!

Section 2: PA Measurement with Examples

In this section, I posted some PA measurement ideas + experiments and comments about PA collector chokes.

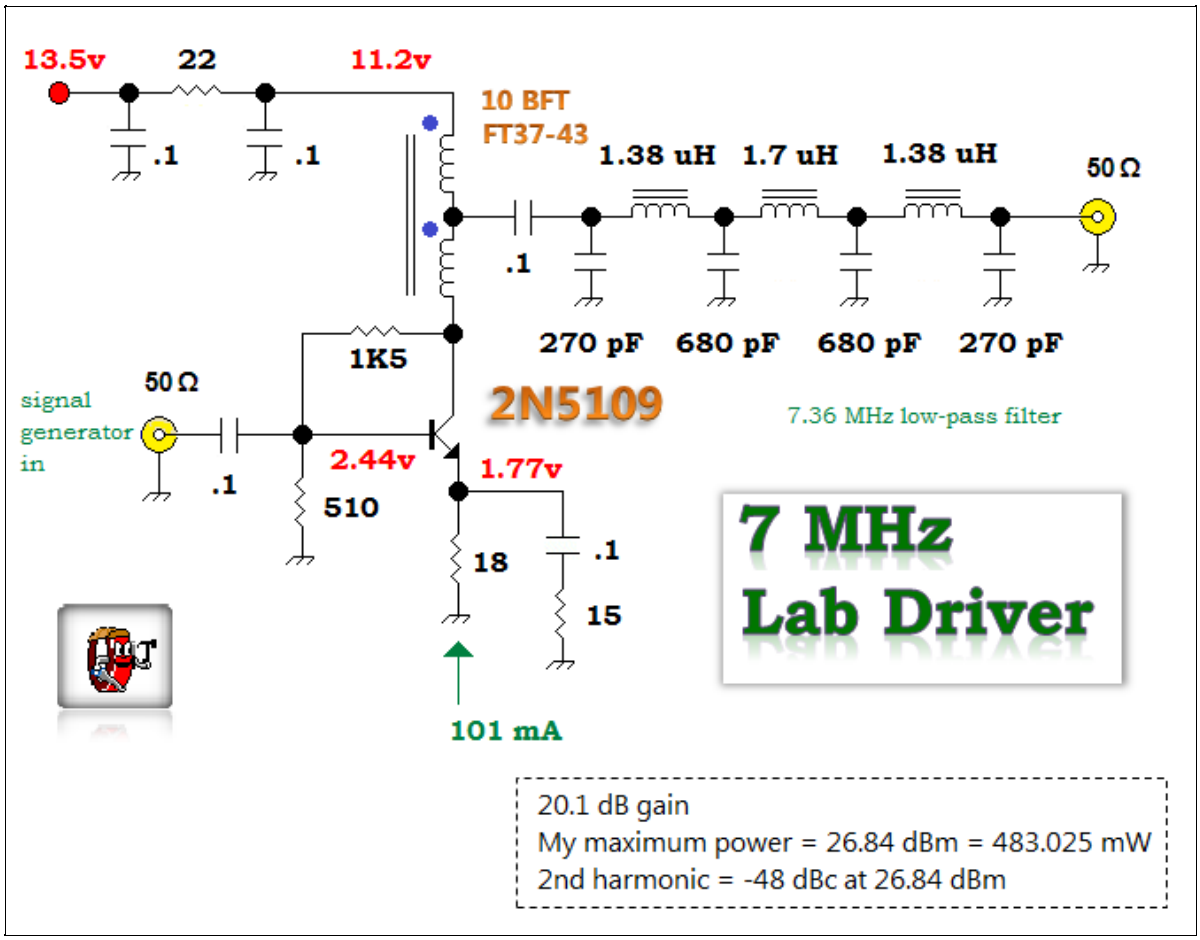

Above — To boost my signal generator output for driving *any* experimental PA up to about ~20W output, I built a high-current, sine wave driver. I excite this amplifer with my variable gain homebrew HF signal generator — in the version shown above, a 7 MHz low-pass filter is soldered on the amplifier breadboard. I'll stick this amp in a metal box sans filter and then apply the correct bench module low-pass filter via a BNC connector. Click for a photo of 3 of my HF low-pass filter bench modules.

Normally the low-pass filter output is pad attenuated to buffer and reduce the output voltage since it's rare I need up to 483 mW drive on the QRP workbench.

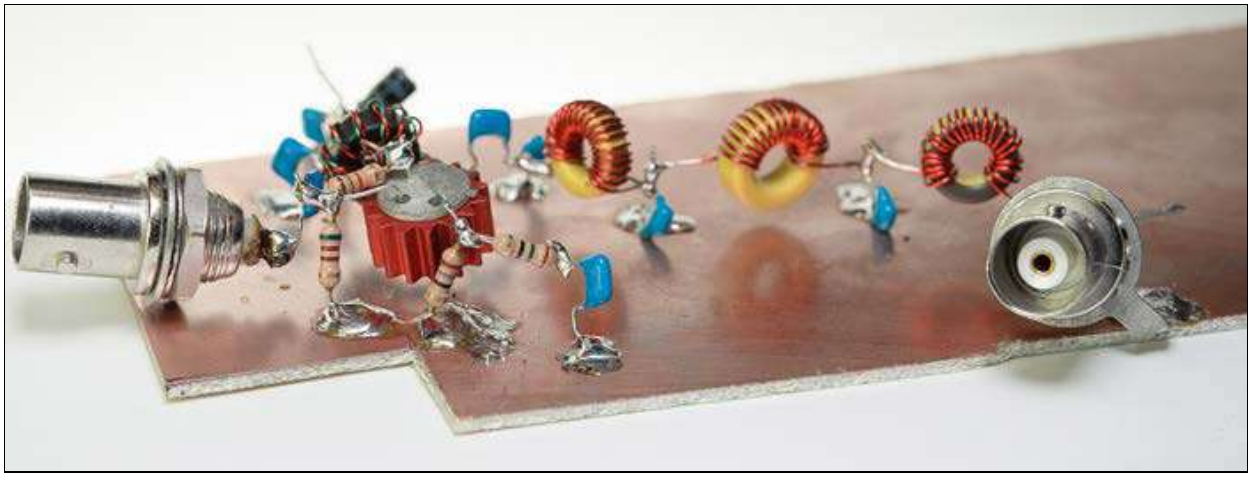

Above — A photo of the PA driver amplifer breadboard.

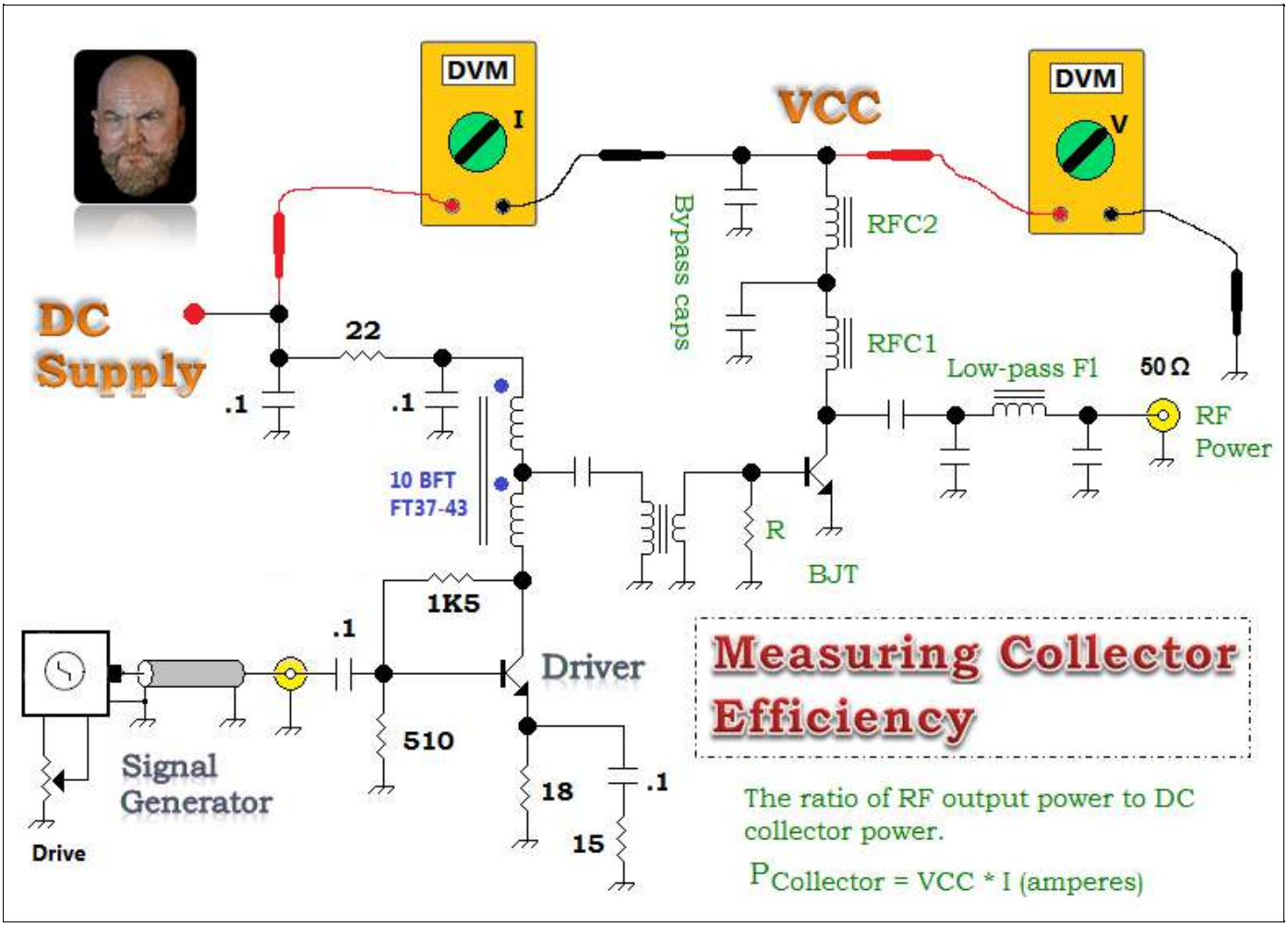

Above — A method to simultaneously measure collector **V** and **I** to calculate DC collector power. Two DVMs boost measurement fidelity since the current measuring ammeter's internal resistance will drop the DC supply ~ 0.2 to 0.5 volts depending on the device and current. Collector efficiency = RF output power / (V * I) .

This method provides a great excuse to purchase another multimeter.

Measure VCC where shown since the decoupling and bypass filters help prevent the AC signal from affecting the DC measurement. We only touch our 10X 'scope probe on the collector. Exert due care and wear eye protection in case you blow up the transistor and create shrapnel.

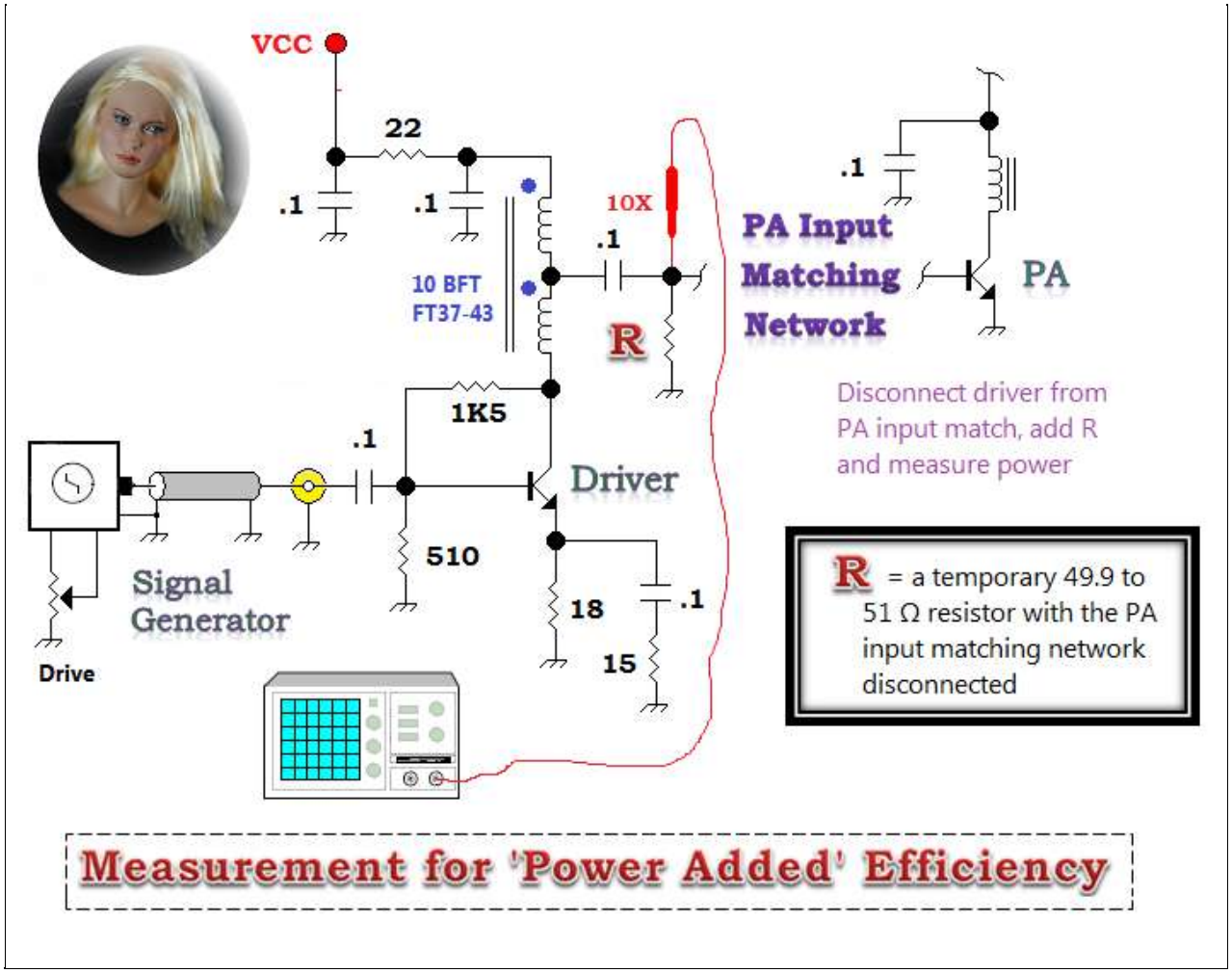

Above — Power Added Efficiency considers the base drive power in addition to the DC collector power. The formula = RF output power / (DC Power + RF drive power). Although uncommon, measuring drive power helps you to assess and compare both input matching and PA efficiency metrics.

At the very least — I like knowing my PA drive power and so employ driver amplifiers with 50 Ω output impedance to allow this power measurement. I often permanently solder a 49.9 or 51 Ω resistor to the breadboard ground plane and temporarily connect this R ; plus disconnect the input matching circuit to measure driver power when I've finished tweaking my collector to antenna port circuitry.

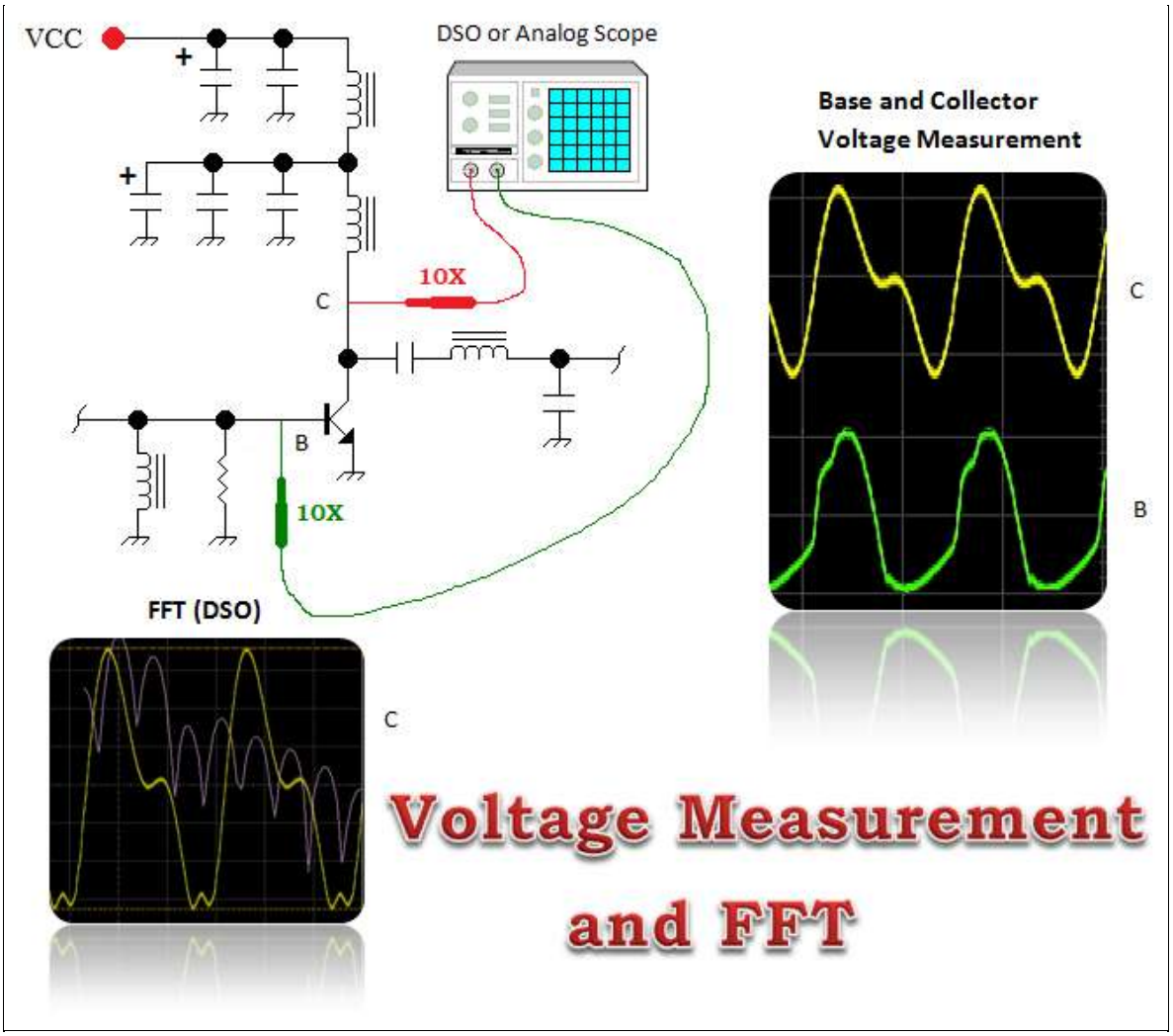

Above — Oscillocope measurements of the base and collector voltages. Most of us enjoy simultaneously running 2 channels on our 'scopes. With a good quality DSO, FFT analysis of the collector waveform may yield insight, however, this knowledge might also confound us since interpreting our measures is fully half of the task.

I often struggle to properly interpret measures. Some builders blog about or email me that they enjoy an innate gift at understanding electronic circuitry — I don't. I guess I lack the knack? For some of us, problems and complications block progress, but more often than not, we eventually cross the finish line.

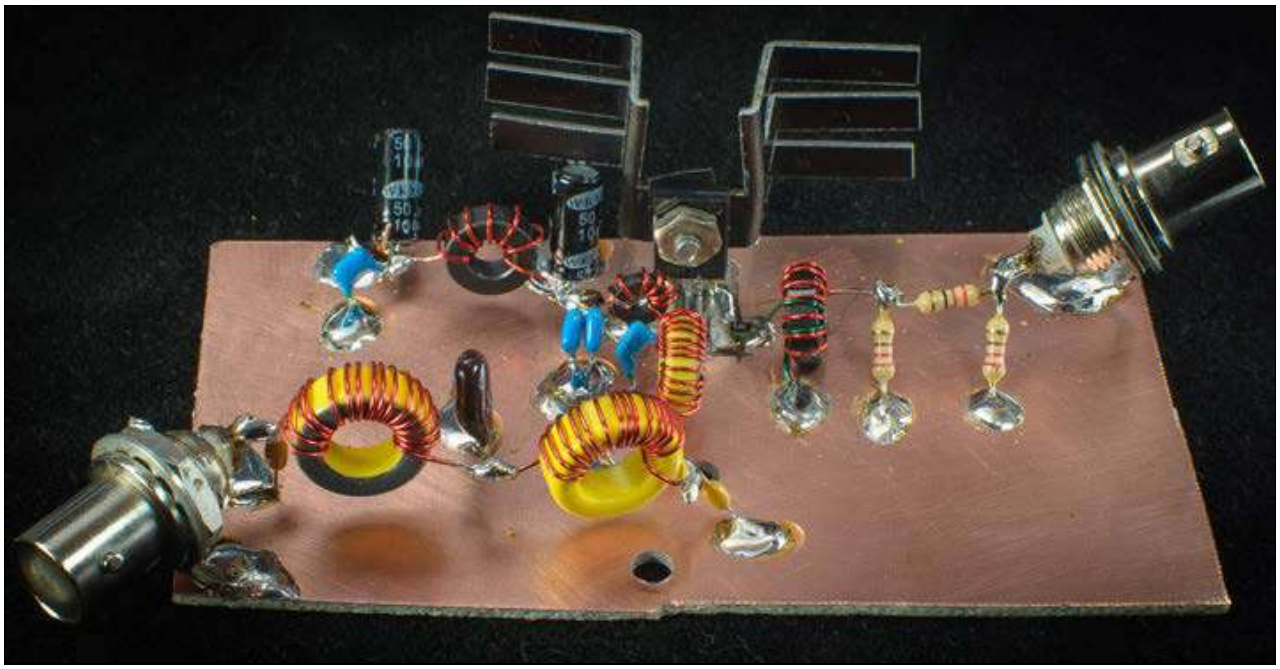

Above — 1.5 Watt, Class C breadboard used for the experiments that follow. I changed the collector choke (RFC1) and applied various filters to examine some of the measurement techniques aforementioned. Click for a bigger photo.

The Collector Choke

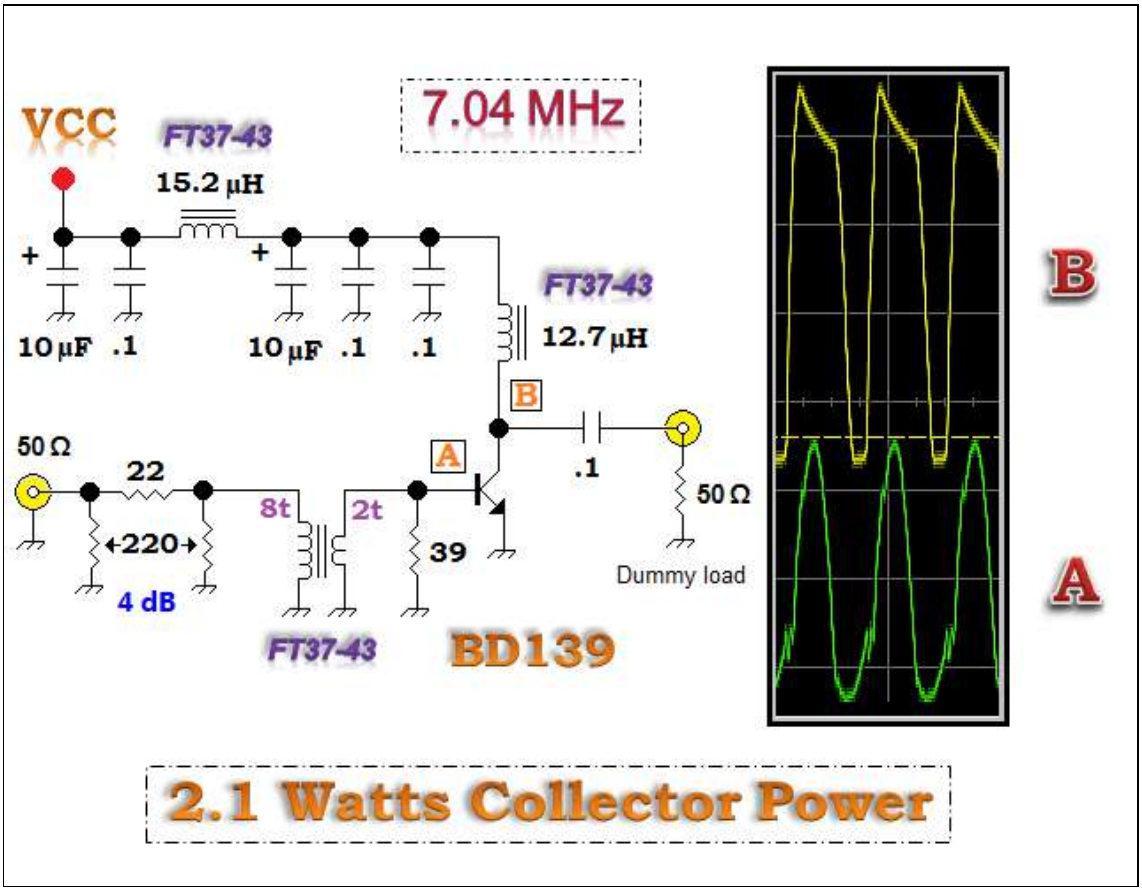

Above — A Class C amplifer with it's collector AC coupled to a 50 Ω resistor load. *No filter.*

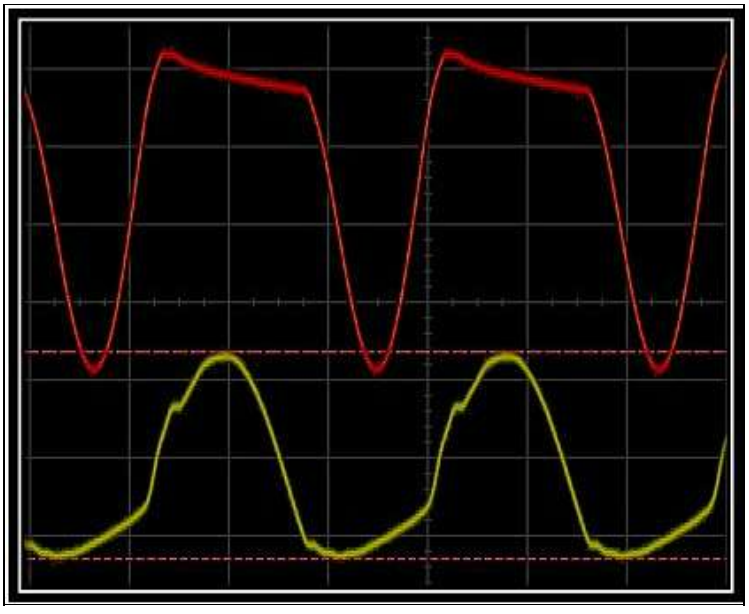

Above — Base and collector waveforms. The unfiltered collector waveform (top) rich in even and odd harmonics ~resembles a square wave. The maximum collector voltage occurs when the current is 0 and in concert, the maximum collector current flows where collector voltage falls to near 0. As the BJT shuts off, the collector circuit kicks and rings so that the DC collector voltage may rise as high as twice VCC.

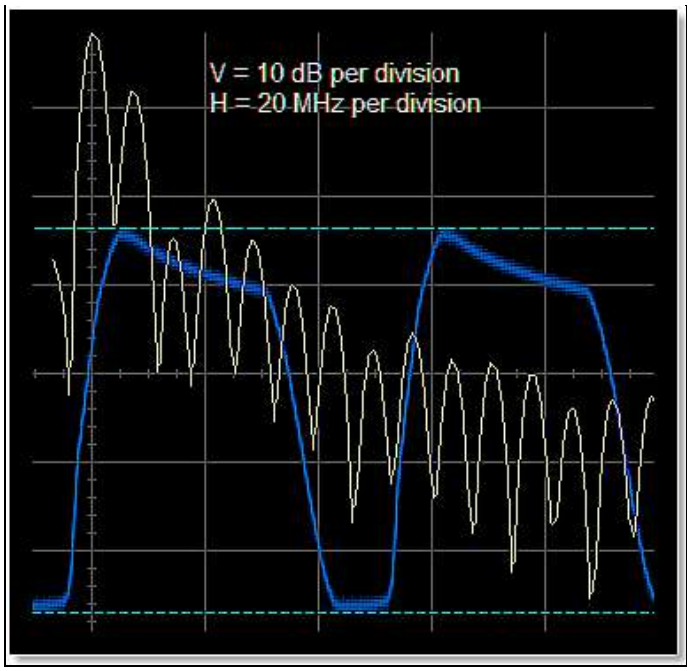

Above — An FFT of the unfiltered collector showing F1, F2, F3, F4, F5, etc. Distortion city!

The Collector Choke

I've read web pages suggesting we might boost PA efficiency by decreasing the collector choke inductance. While that's possible, in reality, it's not that simple. Experiments involving factors like collector load resistance, angle of conduction, RFC inductance/Q, matching networks, base drive configuration and output filtration are ripe with complicated math and theory that I struggle to understand — entire books and research papers explore these topics as author(s) configure their PA into Class D, E, etc. to boost efficiency. The published design work and PA devices out today are truly breath taking.

We should likely think of the BJT, collector current + voltage, the RFC, base drive and output networks as a system of parts that interact — changing 1 part might change collector current, impedance, efficiency, harmonics, etcetera. As such, the experiments that follow do not construe science; only some experiments by a neophyte to ponder and build on.

The ideal RFC passes only DC — i.e. exhibits infinite impedance to AC, but a short circuit to DC. The primary purpose of the choke is to block our high-power, distorted AC signal from flowing on our DC power lines. Some authors suggest that the minimum inductance for the inductor should be 5-10X the collector resistance and I'll leave that up to you. At HF, I wind my RFCs on #43 or #61 material ferrites while keeping the turns number low as I remember that the coil will exhibit a self resonant frequency that might cause problems if it lies near a frequency I need to filter.

1.5 Watt Amp with Three Different Collector Chokes

The 1.5 Watt obviates the need for a matching network since the collector load resistance = 48 Ω with a VCC of 12v. I rebelled and ran 13.5 V supply for a calculated 60.8 Ω collector load R. I probably should have this matched this collector load to 50 Ω at 13.5v, but wanted a "real world" amp without a matching network. At the very least, these amplifiers illustrate the PA measurement techniques shown above. I wound the RFC on a common FT37-43.

In all cases, I adjusted the base drive so that the sine wave PA output read ~24.5 Vpp while measuring collector V and I. I made DSO measures of the the base and collector voltage and collector FFTs, although forgot to save some of them as screen captures.

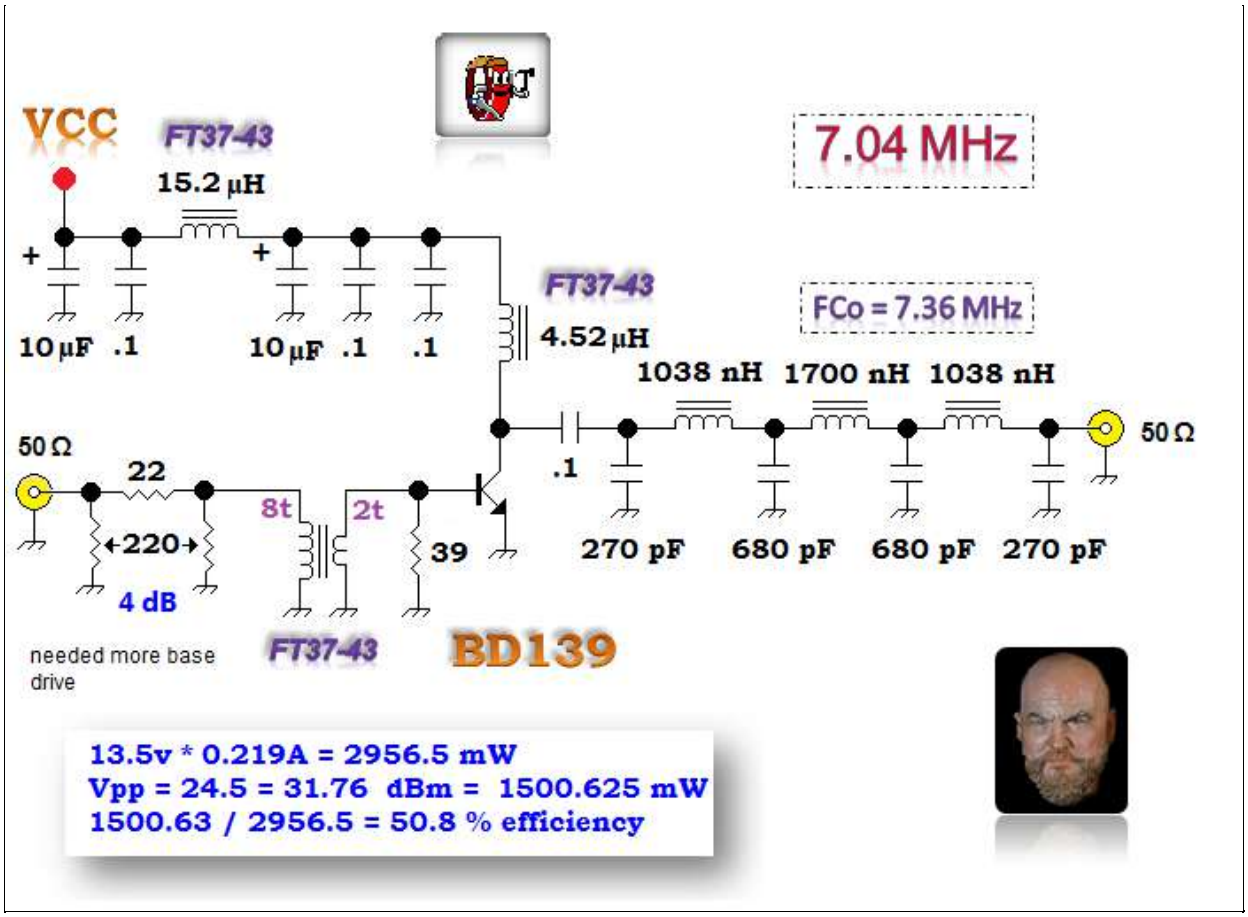

Above — The collector choke = 4.52 µH or an XL of ~ 200 Ω @ 7.040 MHz. My measurements indicate an efficiency of 50.8%. With a choke XL of only ~ 200 Ω, some of my collector AC might be flowing to ground through the bypass caps and that'll kill efficiency. Click for an FFT of the collector. This circuit required more base drive than the other 2.

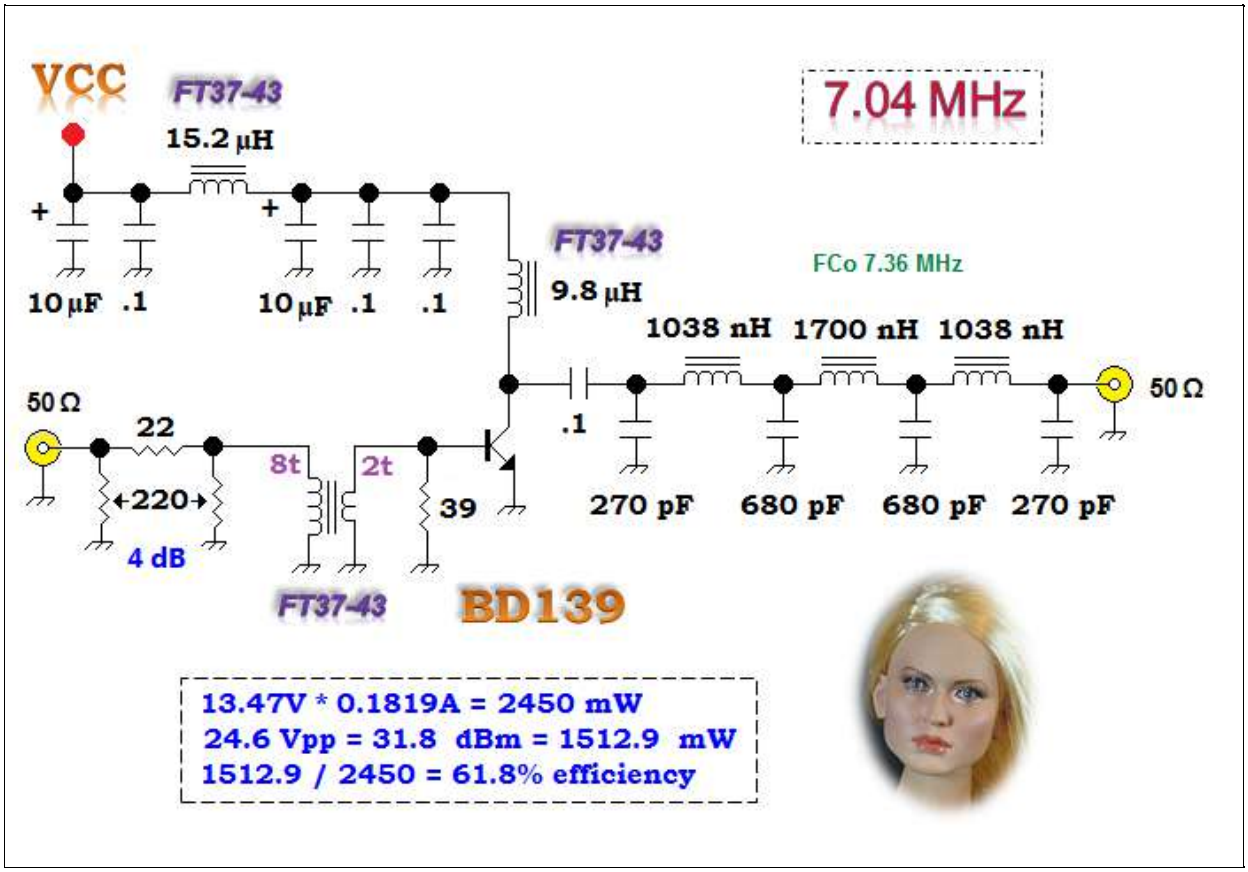

Above — The collector choke = 9.8 µH = an XL of ~ 434 Ω. Efficiency now 61.8%. Base and collector tracing. Collector FFT.

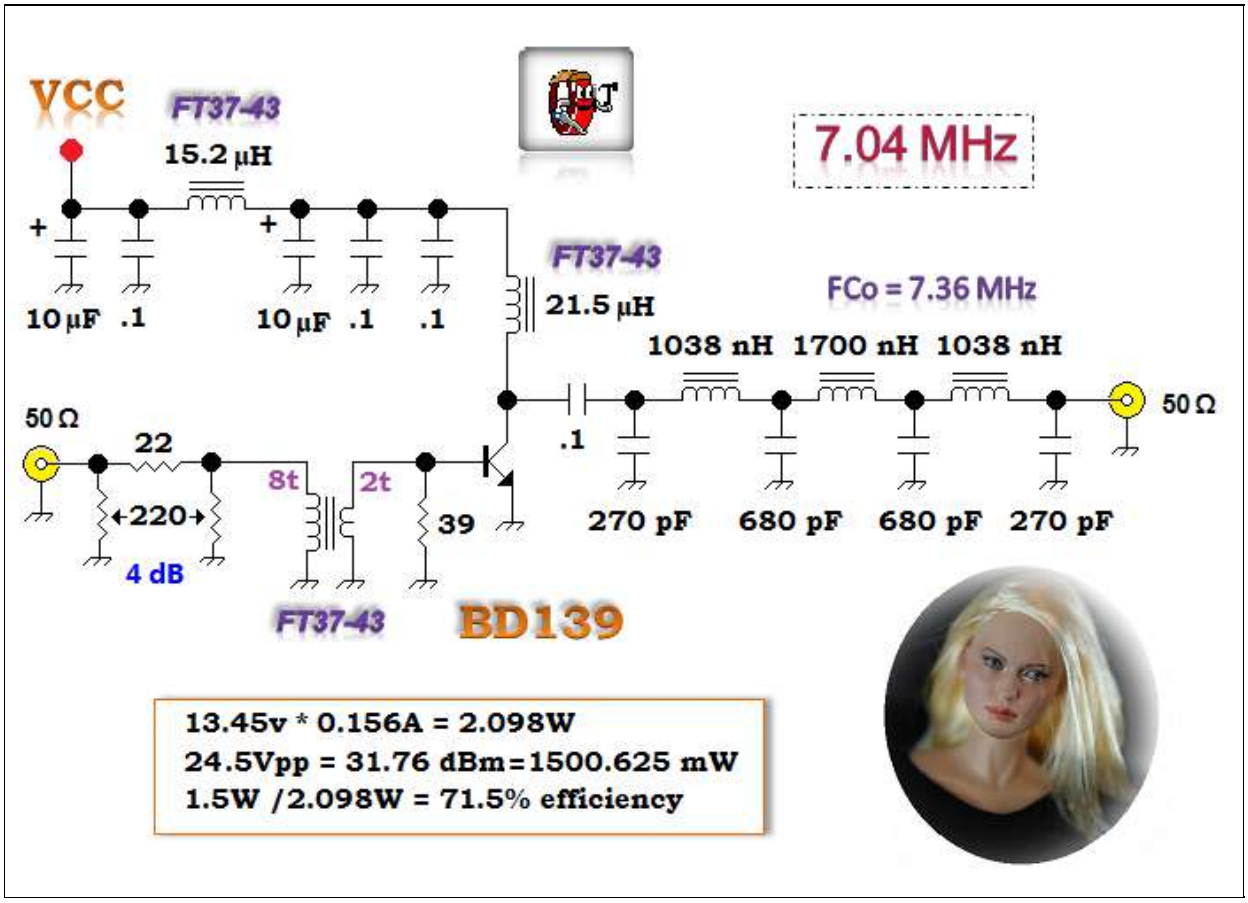

Above — The collector choke = 20.5 µH = an XL of ~ 951 Ω. 71.5% efficiency. Base + collector. Collector FFT. Sine wave FFT. To date, 71.5% is the best Class C efficiency I've measured.

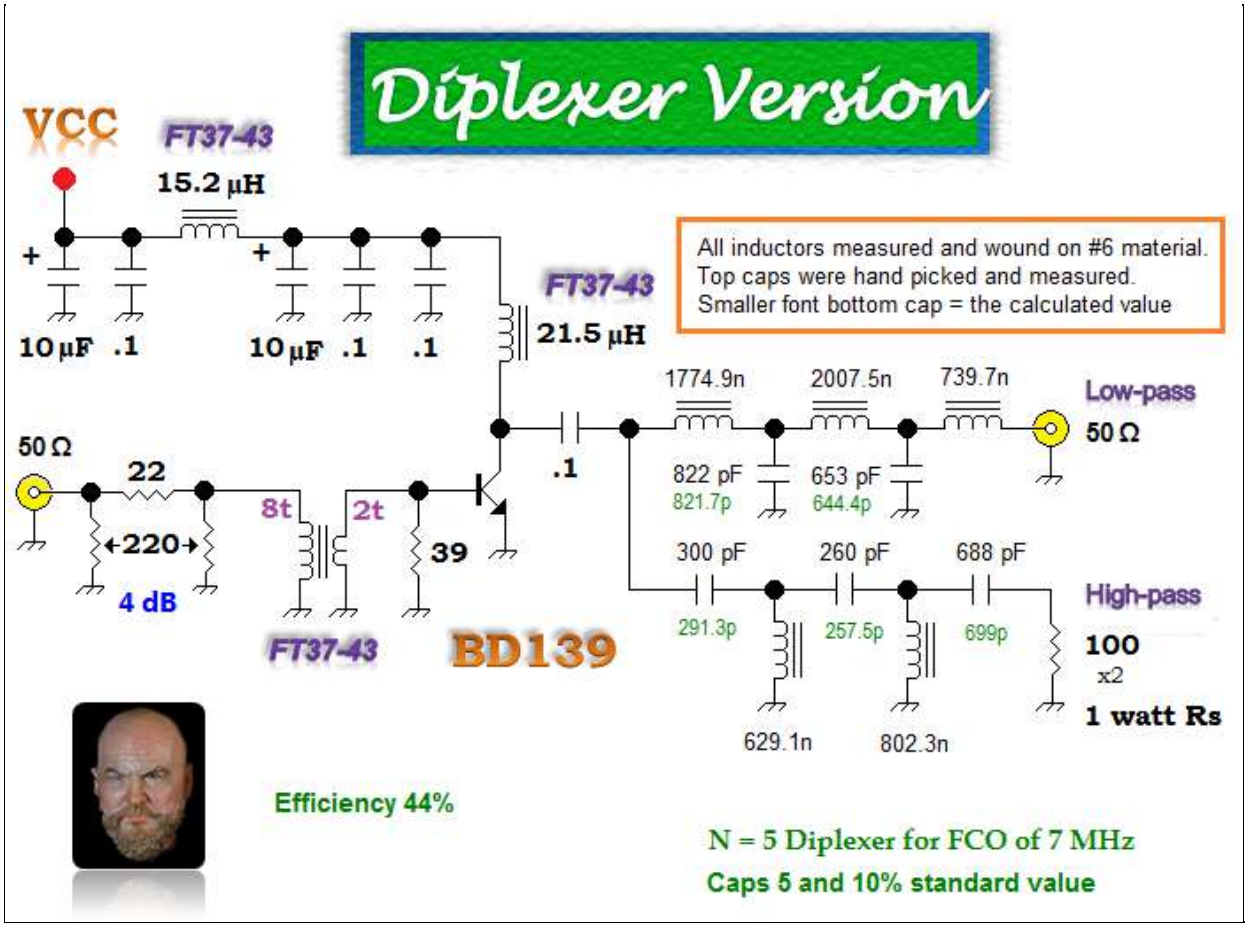

Above — A PA terminated in a N= 5 diplexer for 7 MHz. Click for the FFT of the collector. The collector waveform looks telling — resembling the 50 Ω resistor terminated version shown earlier. Unshown; I lowered the signal generator to 6.99 MHz and drove it to a sinusoidal 1825 mW to obtain a true 50 Ω collector load resistance plus get the greatest low-pass output signal and efficiency (44%) . Although diplexers will 50 Ω terminate the collector at all frequencies, they don't afford high collector efficiency.

Rogues Gallery

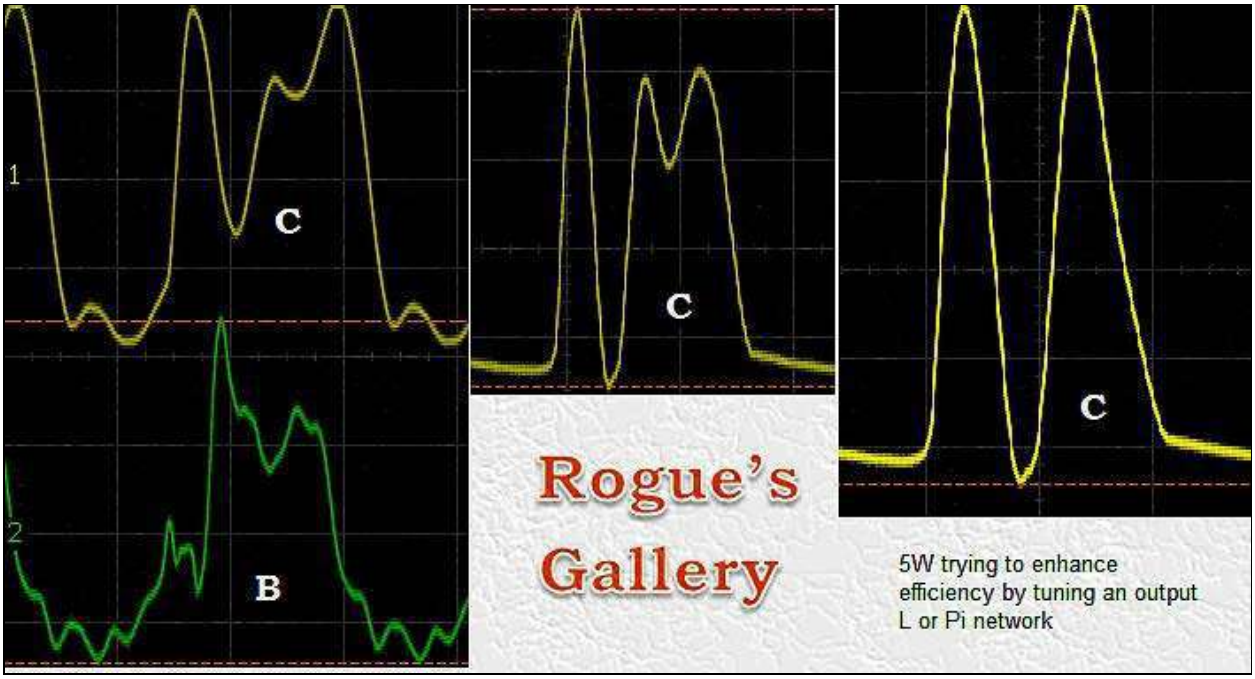

Above — Some 5W CW amplifier collector waveforms as I tried to boost efficiency by manipulating a matching network to drive up the ringing; all failures. These seemingly simple Class C PA's aren't so simple after all. Although failures — I felt thrilled by these experiments and vow to get better at it.

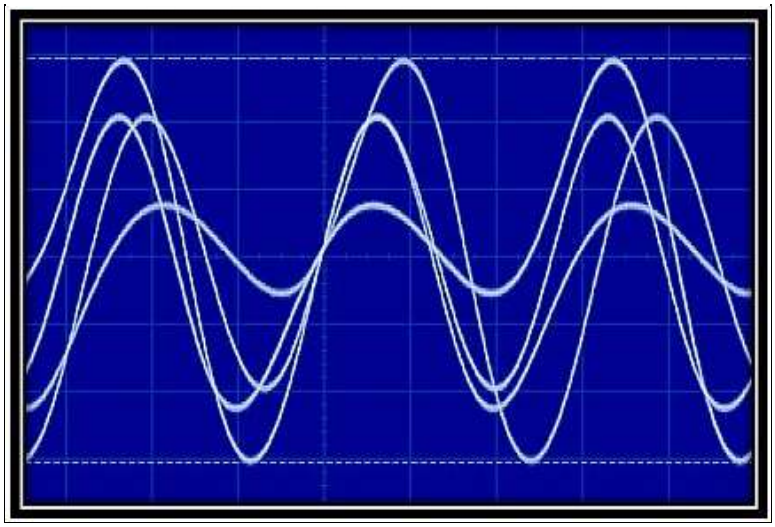

Above — A sine wave output of a very unstable PA.

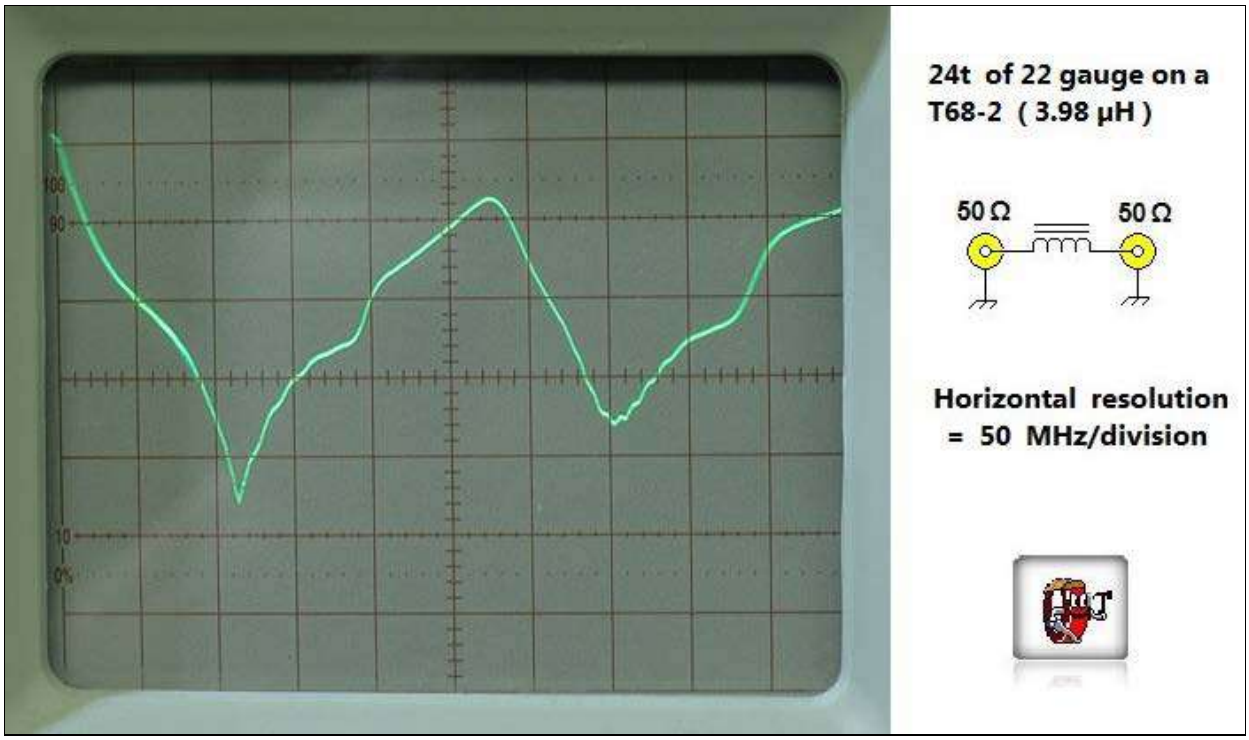

Above — To observe a renegade series resonant frequency, I wound a choke for a 21 MHz amplifer on a T68-2 powdered iron toroid: a casual 24 turns of wire. Sweeping it shows 2 SRFs at roughly 115 and 350 MHz. 2 SRFs jarred me.

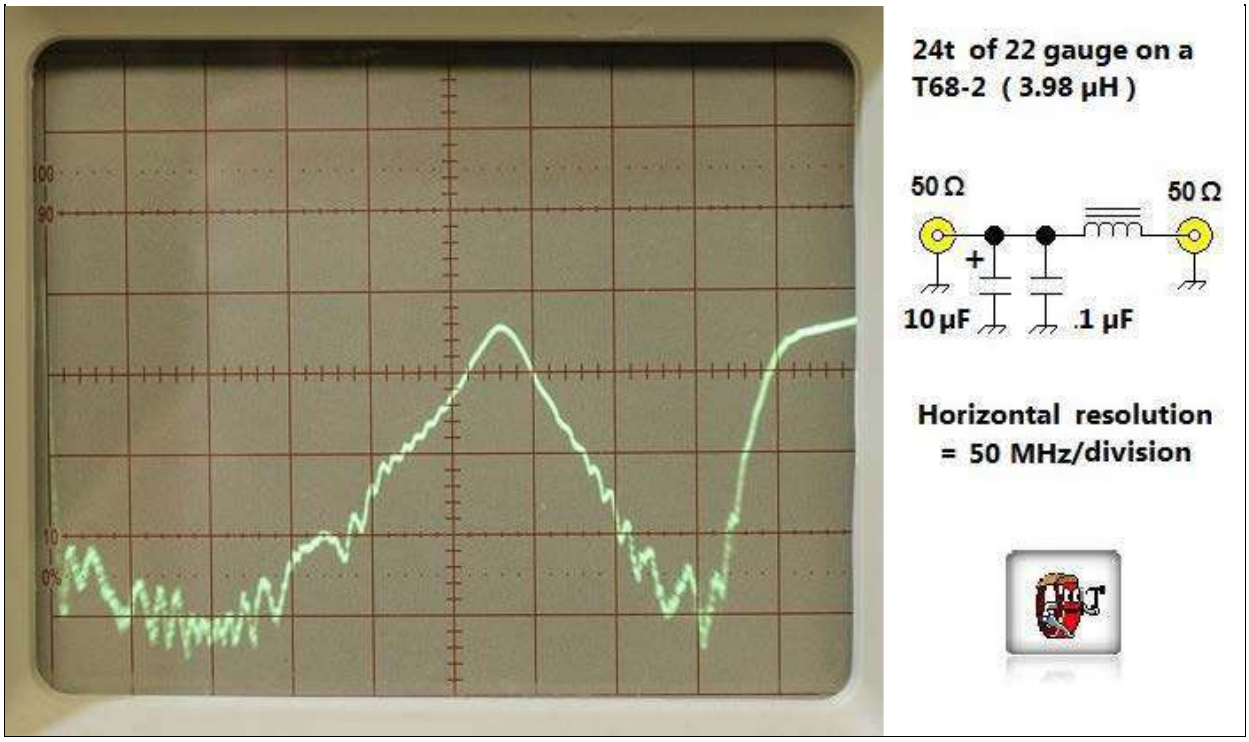

Above — I placed a couple of caps on the cold side like we normally do for our PA chokes. Likely I should have used a 0.01 µF cap instead of the 0.1 µF shown for 21 MHz, but the result would be the same: 2 SRFs remain and poor wideband bypass arises. We clearly need to consider SRF in our chokes and how it might affect our PA function and DC line filtering.

Conclusion to PA Measurement

With an oscilloscope and 2 DVMs you can easily explore boosting your Class C PA efficiency. I've seen precious little info on this topic in the amateur RF experimenter literature. 1 reputable reference = a section in EMRFD called **A Look at Some High Efficiency Amplifers**. For now, I'll temporize. Likely you'll advance faster than me, since I'm more a receiver guy and don't devote enough time to study transmitter design.

The math and concepts of efficient PA design within Class C - E flummox me. Most have just switched to driving FETs with a square wave built up from parallel inverters (high-speed logic gates in the now obsolete 74AC series) — but hopefully our experiments tweaking BJTs in Class C will carry us forward into other Tx modes.

Measuriing collector power with 2 DVMS while watching the sine wave output in your 'scope gives you incredible feedback: you can even observe thermal runaway. After purposely advancing the base drive to "heat up" a BJT, I saw the Vpp progressively drop in the 'scope, the DC voltmeter drop somewhat and then the DC current meter 'take off' : 400, 500, 890, 1200 mA and suddenly, poof, the BJT was on fire, exploded and flung 2 leads into the air. Normally, they just smoke and stink up your lab. I put a picture of a couple of blown BD139s in the photo section below. Expect to burn up some BJTs during experiments and please work safely.

Section 4: Class E Amplifier

This section unposted.

Section 5: References

1. Solid State Design for the Radio Amateur by Wes Hayward, W7ZOI and Doug DeMaw W1FB. American Radio Relay League 1986.

2. An Updated Universal QRP Transmitter by Wes Hayward, W7ZOI. American Radio Relay League: QST for April 2006.

3. Class E Amplifiers Part 1: Class E Basics. Dan Tayloe, N7VE / Ozarkcon Class E Presentation, 1994. *Search for it online*

4. The Handiman's Guide to MOSFET "Switched Mode" Amplifiers by Paul Harden, NA5N Part 1 Introduction to Class C,D,E and F. First Published in the journal "QRPp". Paul's Site

---

Section 6: Miscellaneous Figures and Photos

C3039
M0H4

2N3553
K0350
2N3553
K0350

2I D6000
WC9838

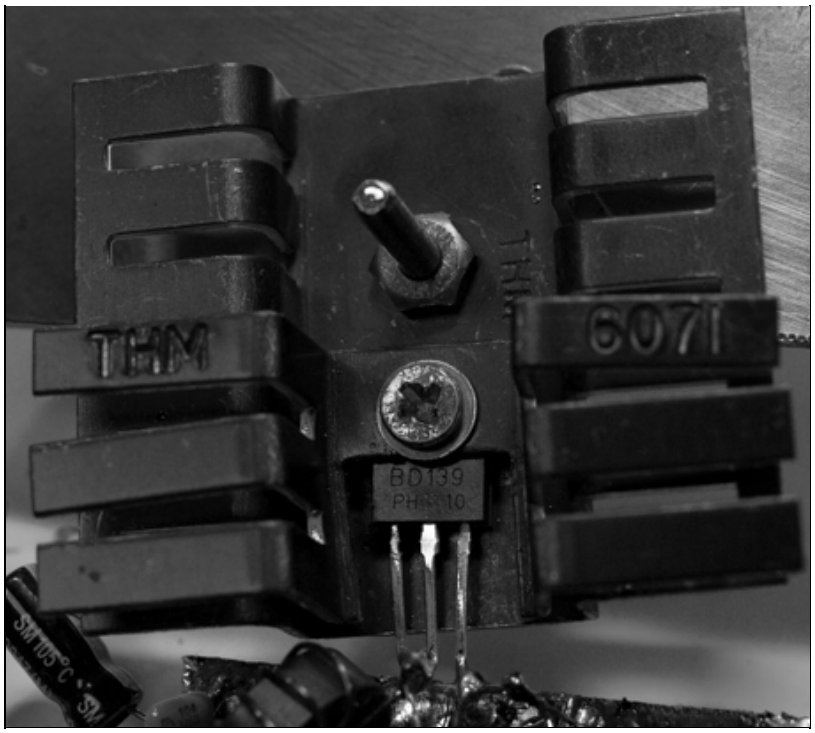
THM
6071
BD139

RF — Test and Measurement

HF - Embarcadero

Respository web page for HF experiments performed in Fall 2013 and Winter 2014.

1. IMD Oscillator Quest
2. Almost Popcorn Superhet — an older, variant and incomplete HF project added for sake of interest
3. VXO — VCXO Notes
4. Funster Line — A Simple 40M Band QRP Trans-receiver.
5. Miscellaneous Photos and Figures

---

1. IMD Oscillator Quest

To measure IMD and calculate IP3 in receivers and components, we need 2 oscillators that typically lie 20 KHz apart, although some apply other frequency spacings. We join these oscillators with a 6 dB (or 3 dB) hybrid combiner and often follow the combiner with an RF attenuator and/or low-pass filter before connecting to a DUT and detector. I sought an oscillator possessing low phase noise, low distortion, strong return loss + high reverse isolation and documented my experiments to fuel your own. Nestled half-way within the HF band, 14 MHz is a popular IMD oscillator frequency choice. I chose 14.0 MHz and 14.020 MHz for classic 20 KHz spacing.

Wes, W7ZOI well covers intercept measurements in EMRFD and in part, popularized receiver DR measurements with his QST article entitled Defining and Measuring Receiver Dynamic Range in QST for July 1975. Click for the article header only. After publishing his article, receiver DR testing by the major Ham transceiver manufacturers became standard.

If you own 2 crystals spaced 20 KHz apart, you're set. A Butler oscillator set up for vibration at the xtal fundamental frequency works well. See EMRFD Figure 7.32 for a great example — A Butler carefully biased to stand reasonable current for low phase noise with a low impedance in the Colpitt's tank. Wes placed a 100 Ω resistor on the link between base terminals of the differential pair. The low impedance and the bias levelling provides current limiting and prevents the oscillator BJT from going into saturation.

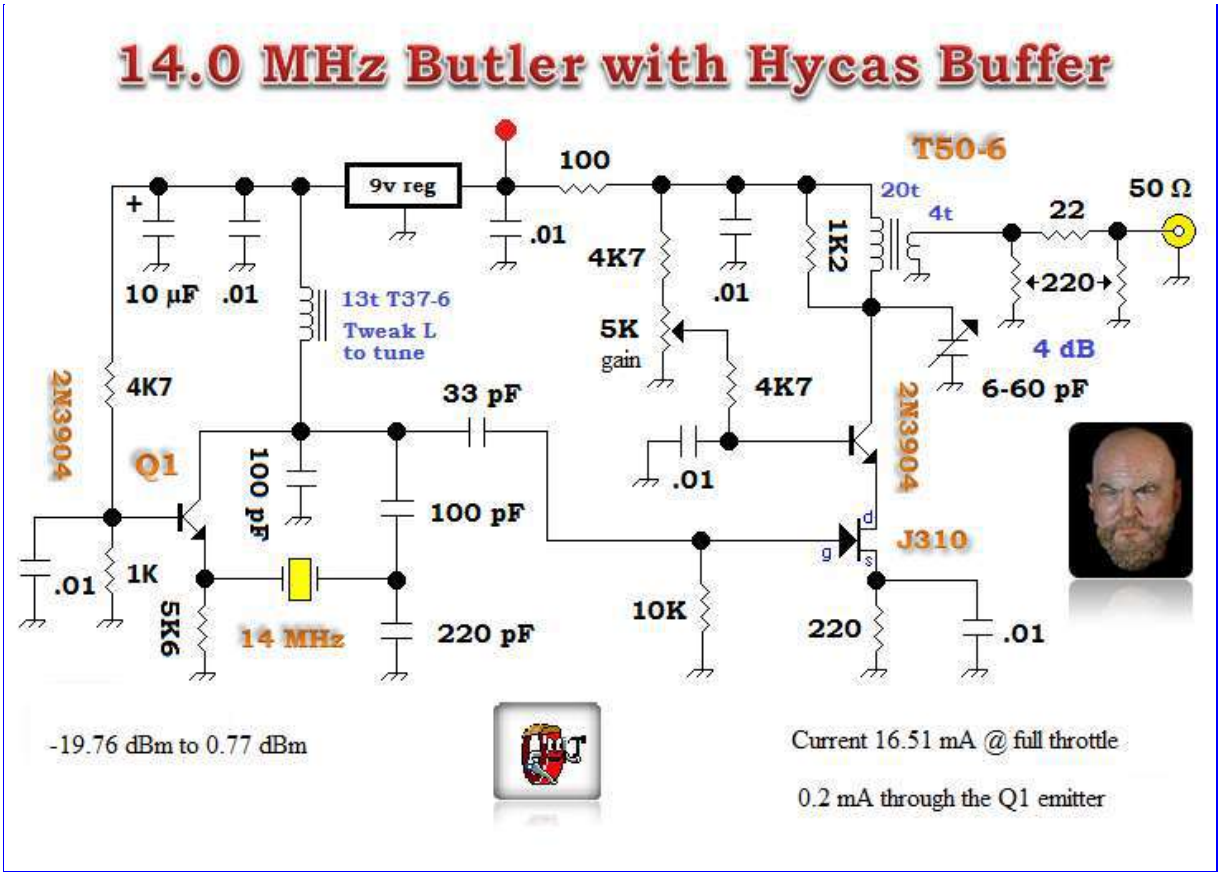

Above — A fundamental frequency Butler with hybrid-cascode (hycas) buffer I built for 14.0 MHz some years ago. Rather than tuning the oscillator tank with the usual low-Q trimmer capacitor, I designed for a fixed C of ~100 pF and thumb and finger tuned the tank to preserve the Q.

Alternately, a standard Colpitt's crystal oscillator with the crystal connected to ground via a shunt capacitor of >= 200 pF provides a great way to get a low phase noise, low distortion oscillator. Take the oscillator output from the junction of the xtal and shunt capacitor and ensure you lightly load this node. See EMRFD Figure 4.24 or my Low Noise Crystal Oscillator web page for examples.

A problem arose. I couldn't find 2 crystals 20 KHz apart, so running 2 fundamental Butler or Colpitts oscillators for IMD measurement seemed out of reach. A web search yielded 1 solution; pull the xtal oscillators to a desired spacing around 14 MHz and crystal filter the output to drop phase noise.

My next experiments mirrored the work of Christian, DL9NL on this web site. It appears he based his design on that of Stuart, KI6QP who authored A Precision Two-Tone RF Generator for IMD Measurements for QEX for April 1995. Stuart used crystals cut 20 KHz apart to make 2 Colpitt's oscillators running moderate current with output filtering by 1 xtal filter tuned to the oscillator frequency to reduce phase noise.

In his project, Christian, DL9NL wired up two 14.318 MHz microprocessor filters in a super VXO topology to cleverly move the xtals 5 or 20 KHz apart. He also output filtered his 2 oscillators with a xtal filter.

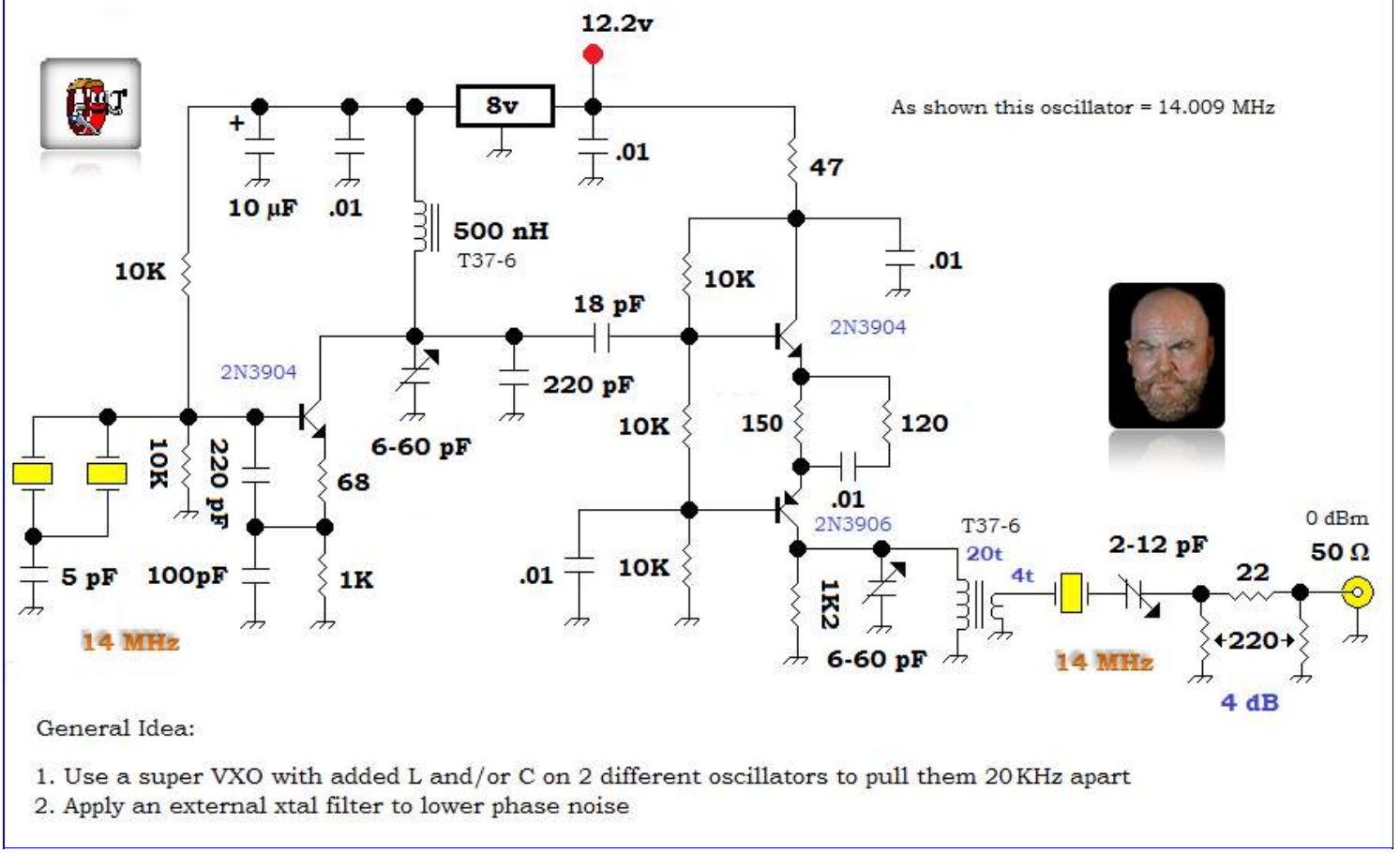

Above — 1 of my rudimentary experiments involving a super VXO plus output xtal filter. Not a great design. In this experiment, the 2 crystals were connected to ground via a 5 pF capacitor to yield 14.009 MHz. I learned that xtal frequency and xtal parameters determined the available frequency spread and output filter function.

After thought and the above bench work, and also because I need to make oscillators for IMD measurements at 50-100 MHz, I decided to go with an LC oscillator. They work fine for IMD measures with proper design and construction. For example, the signal generator shown in EMRFD Fig 7.27 sports a phase noise approaching -140 dBc/Hz @ a 10 kHz spacing; getting awfully close to the cherished vintage HP-8640B signal generator.

With LC oscillators, I learned that a metal enclosure with a feedthrough capacitor for the DC line proved important.Strong reverse isolation also ranks 'very important'. A case in point follows:

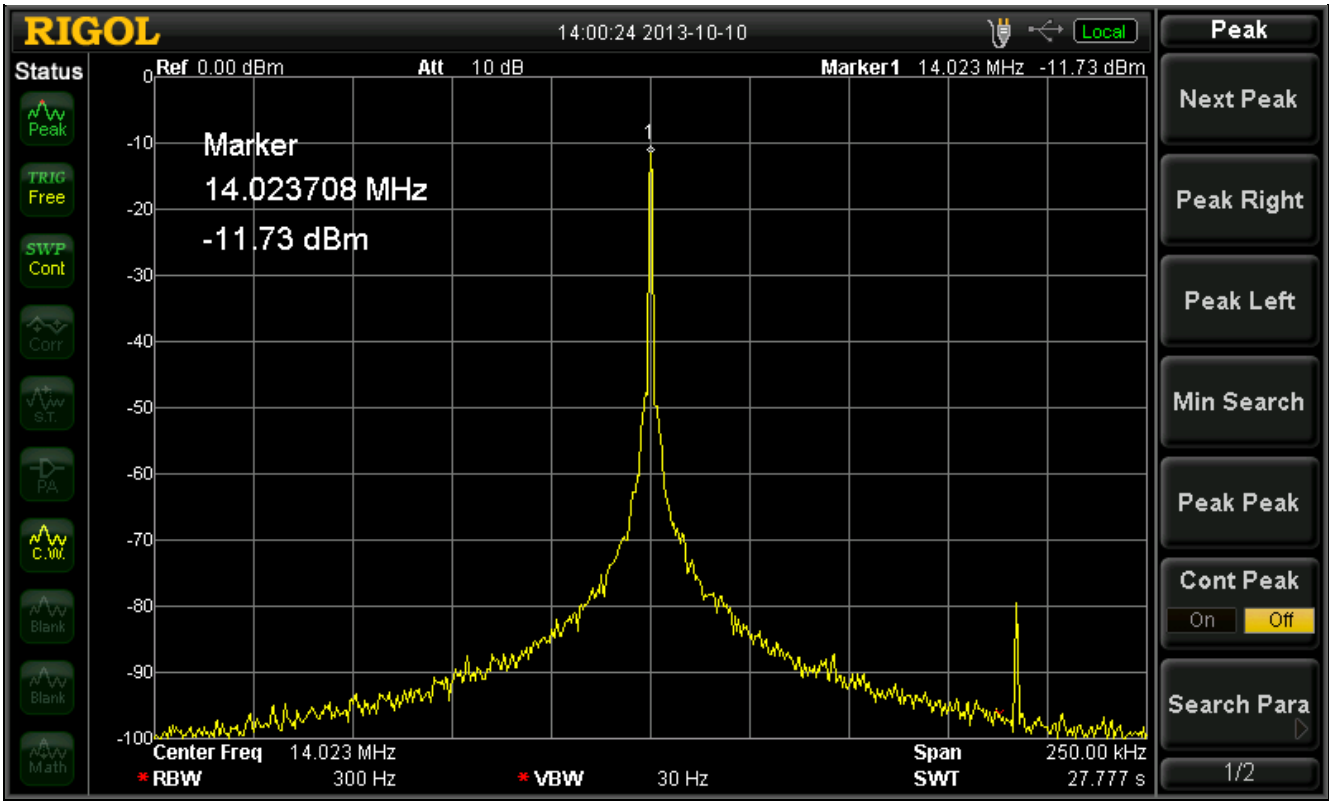

Above — A close-in spectrum analysis of 1 of my 14.02 MHz LC oscillators. Span = 250 KHz; RBW = 300 Hz and my video bandwidth = 30 Hz to "cut the grass". You can see a spur about 92 KHz right of center; a signal from my SA or environment is getting back into my VCO and low-level modulating it. Yikes! Another RF-tight LC oscillator with a common-base isolation amp showed no such spur.

Close in spectrum analysis may allow you to measure phase noise with your spectrum analyzer, however the wide-range, first oscillator of a Rigol spectrum analyzer operates in the range of 2- 4 GHz and is varactor tuned; as such, the best phase noise we can measure with it = -88 dBc/Hz @ 10 KHz spacing.

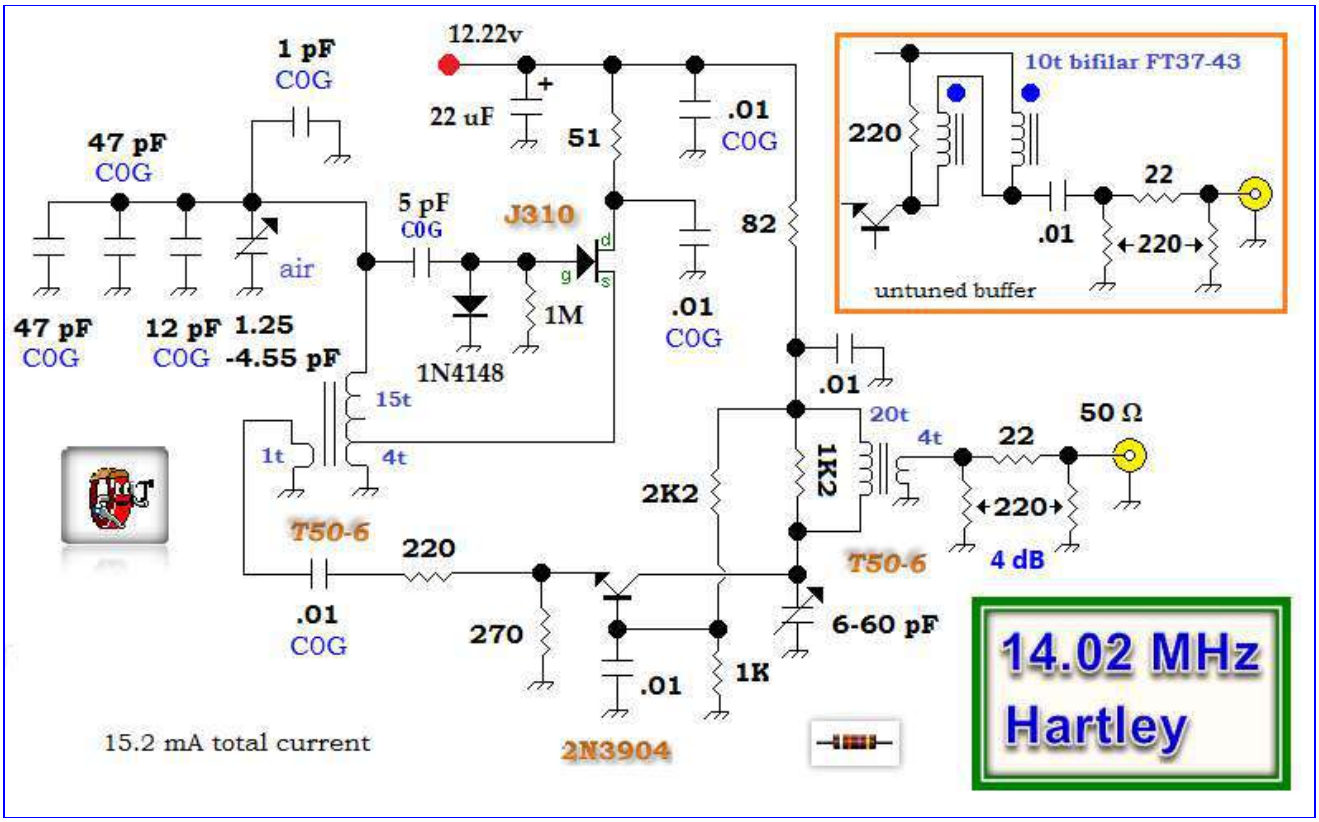

Above — 1 of my experiments: a Hartley with common-base buffer amp right out of EMRFD Figure 7.27 sans the final amp. I made 2 versions: 1 with a tuned buffer amp and another with a wideband output (see orange inset). The output power of the tuned amp and wideband amp = -6.7 dBm and -11.7 dBm respectively.

You may want to add a final amplifer — I've got a couple of amplifer modules if I need to get to 0 dBm or above. Prior to tweaking the lid-on frequency to 14.02 MHz, I measured the 2nd harmonic at 55 -dBC in the tuned output version— yay! Building with solid temperature drift techniques, the frequency drift in my counter went just a few hertz *up* over time. The Figure 7.27 oscillator remains a go-to circuit for us builders.

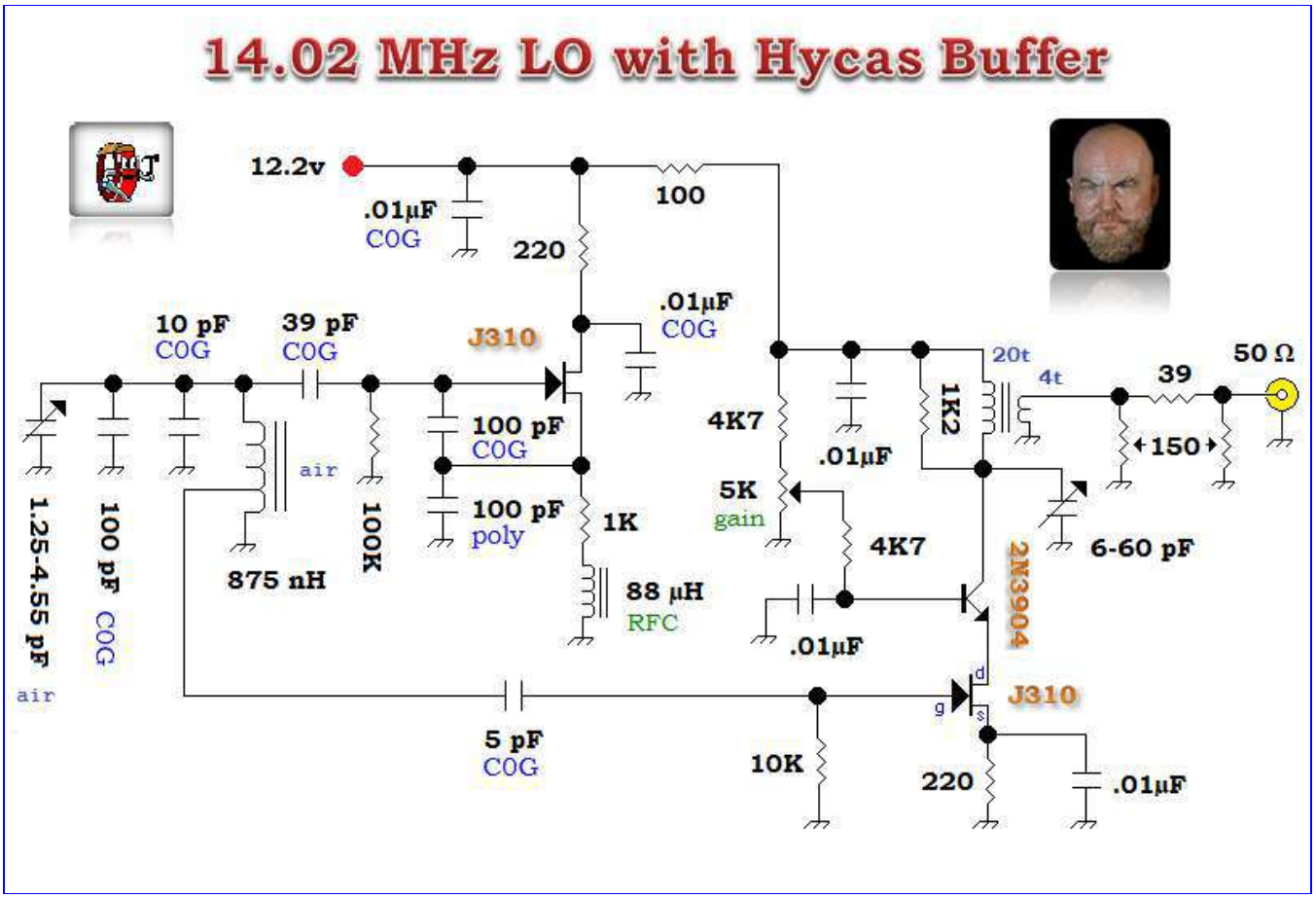

Above — A Colpitts with hycas buffer allowing variable power output. During measurement of IMD, the 2 oscillators need to exert the same amplitude, so only 1 needs to have variable output power. A wideband bench generator plus a 1 frequency oscillator like this might be all you need.

Above — A photo of the completed Colpitts LC oscillator. Running a phono jack for the DC input was a mistake. A feedthrough capacitor = the best choice. The epoxy glued air wound coil and air trimmer cap plus the regular temperature stability techniques and a 100 pF polystyrene

capacitor yielded a temperature drift under 40 Hertz per hour. 5 bolts anchor the copper clad board.

I connected the 5 pF coupling cap to the lowest turn on the air coil. Mounting an air coil (solenoid) in smokestack fashion over a copper board probably upsets its Qu, but it worked okay.

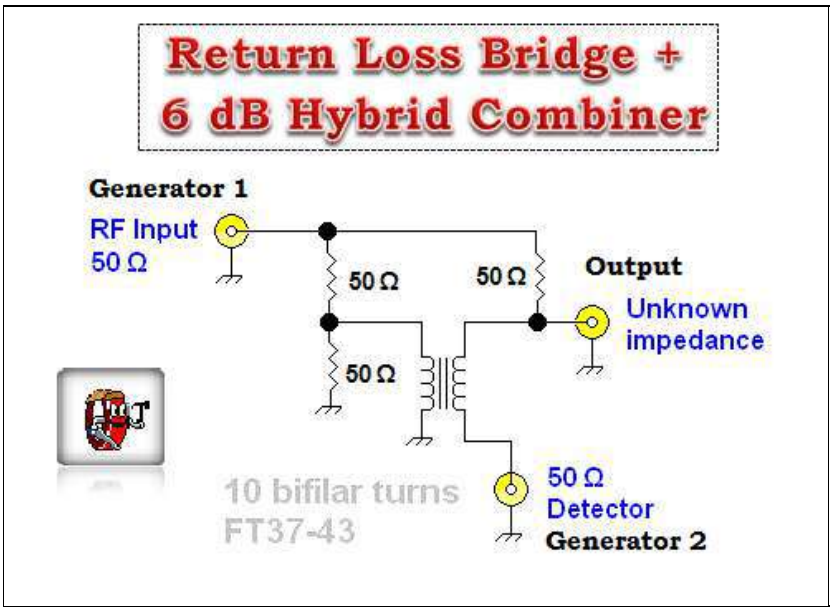

Above — Our old friend the Return Loss Bridge is also known as a 6 dB hybrid combiner and 1 serves double-duty on your QRP workbench as an isolator and a return loss bridge.

Phase Noise and Commercial Signal Generators

The worst of today's ham transceivers transmit a CW carrier with noise that is down by 117 dBc/Hz @ 10 kHz spacing. This is bad enough that if you had a Ham operating this rig 0.8 km away you would hear this noise, even with a perfect receiver. In a typical oscillator, the phase noise @ 100 kHz spacing lies ~20 dB lower than @ 10 kHz out to a noise floor that is around -140 dBm/Hz or better. The Elecraft K3 impresses us with phase noise at -138 dBc/Hz @ 10 KHz [Sherwood].

We either build, borrow or buy our signal generators. Second hand commercial products range from good old HP/Agilent gear or LC boxes once used by TV/FM receiver repairmen. The TV service equipment covers ~300 kHz to 150 MHz and tends to be inaccurate with a limited output amplitude range, while the vintage HP stuff often is heavy, decaying and crowds your bench.

Most of hobbyists can't afford nor justify spending $8-18k on boxes that go down to -127 dBm amplitude and -146 dBc phase noise at 1 GHz @ 20 kHz offset [Agilent N5181B MXG X-Series RF Analog Signal Generator]. These generators feature components like a YIG oscillator phase locked to an ovenized crystal reference. Professional, high-end gear.

Another choice = the Arbitrary/Function Generator or ARB that sell for a fraction of the cost of the aforementioned boxes. A few friends own them, in particular, products made by Rigol and GW Instek. These DDS generators range in frequency and price: higher price generally = better phase noise.
For example, the popular Rigol DG1022A phase noise = -108 dBc/Hz @ 10 KHz offset and the DG4162 = ≤-115 dBc/Hz @ 10 KHz offset; not good. Often ARBs will feature a host of modulation functions, sweeps, frequency counters and the 2 output channel models may offer I/Q outputs and the ability to perform 2-tone IMD tests. Search around the T Equipment website to read some equipment datasheets

My question to 2 informed EEs — Is the phase noise of a -115 dBc/Hz ARB *good enough* to reliably measure IMD? Their answer: yes, if you have a high end, modern spectrum analyzer with a minimum RBW of 100 Hz, deft analyzer skill and understand the measurement. Often us hobbyists have to make due with whatever test equipment we can build or buy.

You might just build a low noise oscillator with a crystal at 14.0 MHz and provide the other tone with your bench signal generator or some other combination of 2 devices. This is test equipment junkie fodder — band-of-brother's stuff. Thanks for reading.

---

2. Almost Popcorn Superhet

I published this rogue web page with hope you might find it interesting. It houses notes and photos for an incomplete update to my 1998 Popcorn 7 MHz, CW, superhet receiver.

Click for the Almost Superhet web page.

Click for the Almost Superhet Supplement page

---

3. VXO — VCXO Notes

VXOs and VCXOs provide a useful main or reference oscillator for HF and when multiplied, in VHF-UHF designs. Ignorant of such circuits, I executed some crude experiments to discover how they work and find ways to improve my designs. Increasingly clinical on my bench, I'm losing

patience with the radio mystique — although the limits of my lab equipment, brain power and bench skills humble and tumble me into deeper understanding why educated people might submit to electronics folklore and go in blind faith.

I'm not sure my bench work accomplished much, but if I can add 1 factoid to the RF enthusiast VXO knowledge base, then, I'll feel happy. I'm officially adopting **System D**; the slang term that originated in the French-speaking African continent and Caribbean Plate. In Down and Out in Paris and London, George Orwell called these System D practitioners "débrouillards" — low-level kitchen help, who achieve culinary success in the worst of circumstances. Television hero MacGyver practiced System D.

System D in the context of the QRP Homebuilder describes an effective, practical and resourceful builder who skillfully adapts to any situation and *gets it done*. System D builders don't just kludge together crap — these science-informed débrouillards innovate and shine. Sounds hopeful doesn't it?

Nearly all my bench adventures begin with a web search and the key word *VCXO* yielded many espléndido files + presentations by people and companies who passionately share their knowlege and experiences. Thanks to all!

Experiments

It started with an email from Paol — what's the S12 of the source follower in his 14 MHz VXO buffer amplifier? I built 1 for 10 MHz and tested it since I didn't know.

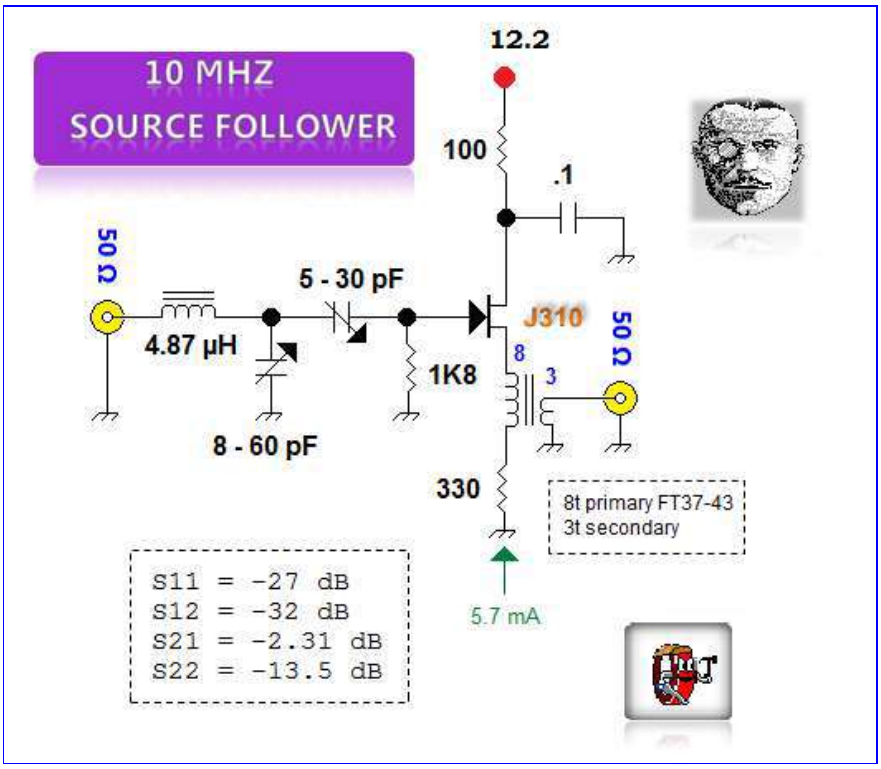

Above — Device Under Test. Paol copied a source follower he found on a web site (complete with an über kitsch 1 mH choke on the source). I tweaked the current and replaced that big, old MF choke with a tapped FT37-43 giving an output return loss of ~ 13.5 dB. Although mediocre, it's probably better than the match provided by the series resistor we typically stick between the JFET source and its 50 Ω load. Further, for my S12 measurement, I matched the input with a L-C-C network to get a strong return loss @ 27 dB. Measured with a spectrum analyzer, S12 = -32 dB; paltry reverse isolation. The matching networks incurred some losses but raised measurement fidelity.

-32 dB — not great, but okay if followed by another amp. For a diode ring mixer, I might couple it to a common base amp, or eliminate the source follower altogether and replace it with a hycas buffer amp. Paol drove a NE612 transmit mixer with his VXO + a source follower and it worked okay in his bare-bones TX. He AC-coupled a 51 Ω resistor to ground on pin 6 of the NE612 that well terminated the LP filter. Intrigued, I then helped him with his VXO.

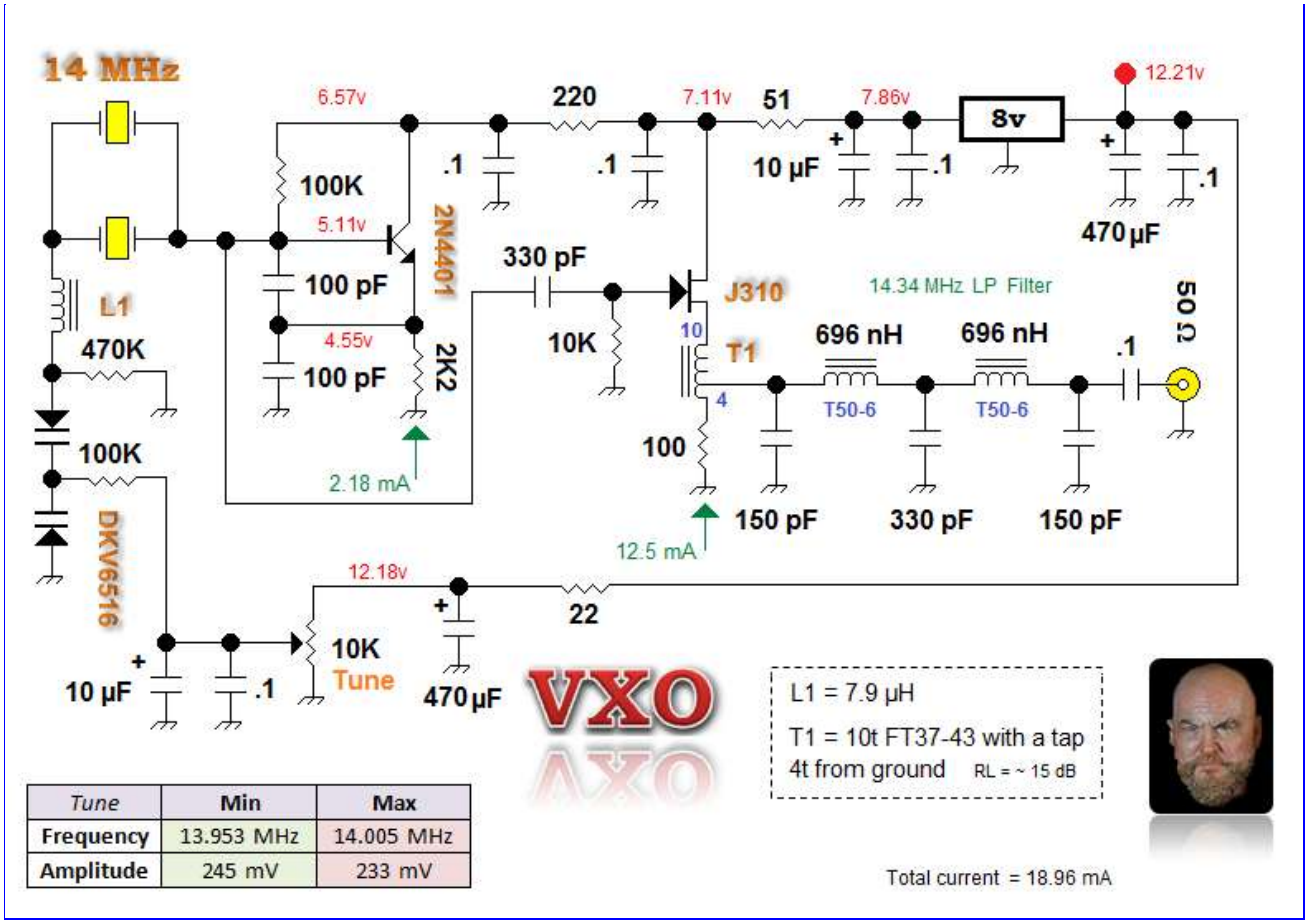

Tune	Min	Max
Frequency	13.953 MHz	14.005 MHz
Amplitude	245 mV	233 mV

Above — My first VXO experiment with varactors instead of an air variable cap that technically creates a voltage-controlled crystal oscillator (VCXO). The tabled values were measured with L1 wound on a FT50-61 ferrite toroid.

Paol had varactors but no air-variable capacitors. Both of us owned some Q = 200, DKV6516 silicon varactor diodes that with a reverse DC voltage of 2 to 10 volts give a nice tuning range of 18 to 140 pF for a single diode. We cheated and ran the reverse DC voltage from 0 to 12.2 volts, although later increased the 22 Ω R to limit the peak tuning voltage to 10v. Paol also put a fixed resistor on the cold end of his 10K tuning pot to keep a minimum 2 VDC on the varactors: I didn't bother, since my "this is only a test" breadboard will be dismantled and junked.

Above — DKV6516

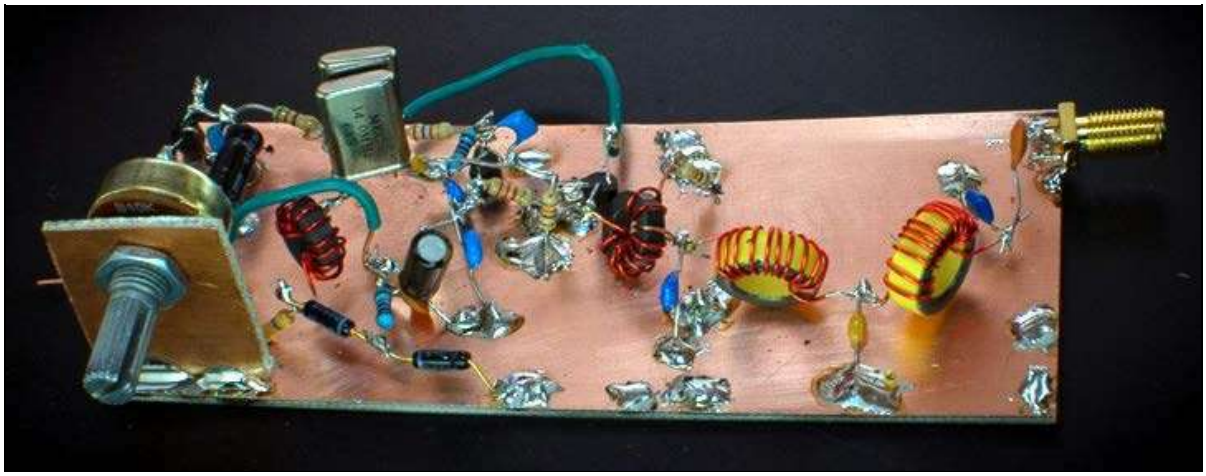

Above — VCXO breadboard. Paol and I each made a VCXO and he with 14.060 MHz crystals. Lacking these, I just used 2 junk box 14 MHz crystals with a measured Qu of ~80K. The tapped FT37-43 gave an output return loss of ~ 15 dB thus providing a reasonable match into a simple 50 Ω low-pass filter. Click for a sweep showing the 2nd harmonic suppression.

My initial build didn't contain the two noise filtering 470 µF caps on the 12 volt supply: I originally soldered a solitary 22 µF cap cap close to the 8 volt voltage regulator input. My 12.2 volts comes from a regulated DC supply. More on filtering noise later.

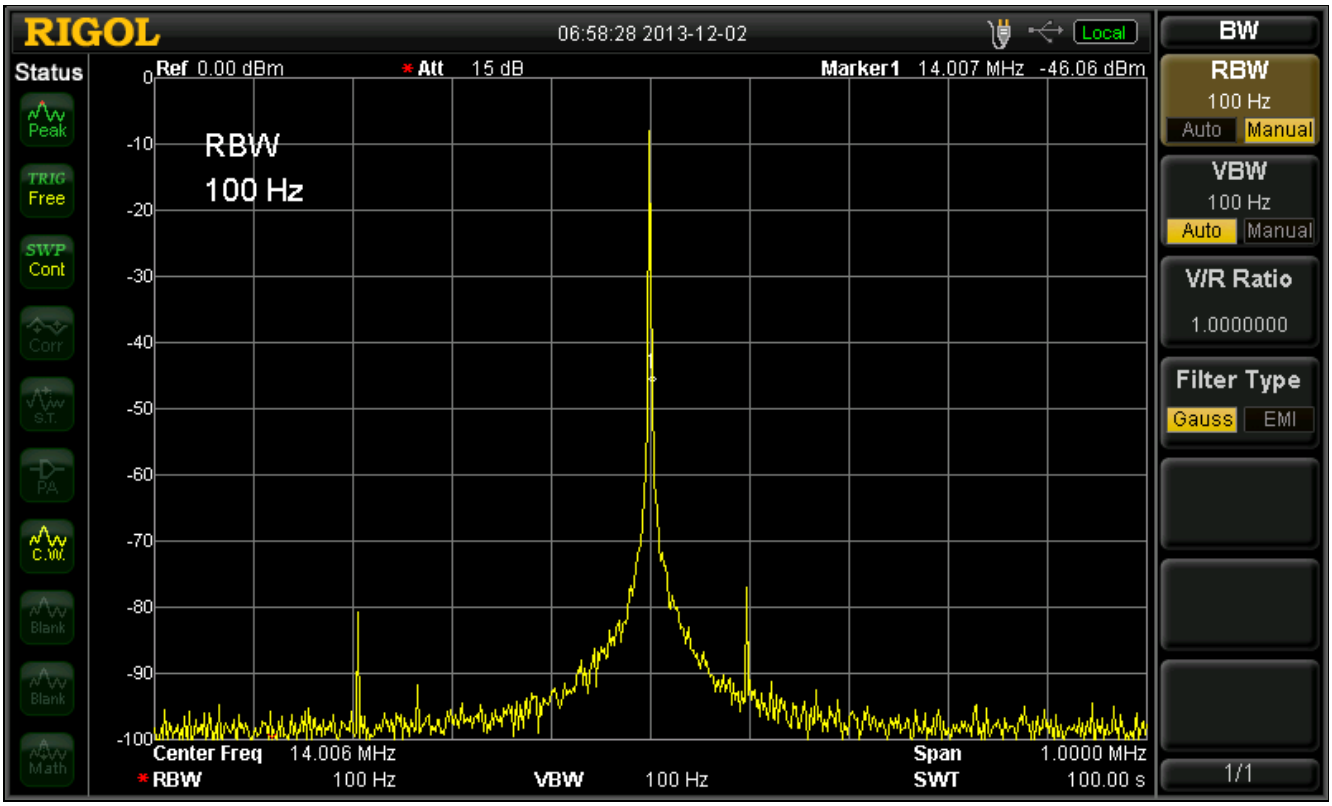

Above — My VCXO spectrogram showed 2 big spurs: 300 KHz down and 100 KHz up from center frequency (CF). I exchanged the varactors with an elegant, Q >= 1000 air variable, plus changed to a higher Q inductor, but could not get rid of these spikes. I assumed these spurs came from the crystals, or the BJT. Then, too, might they arise from my spectrum analyzer?

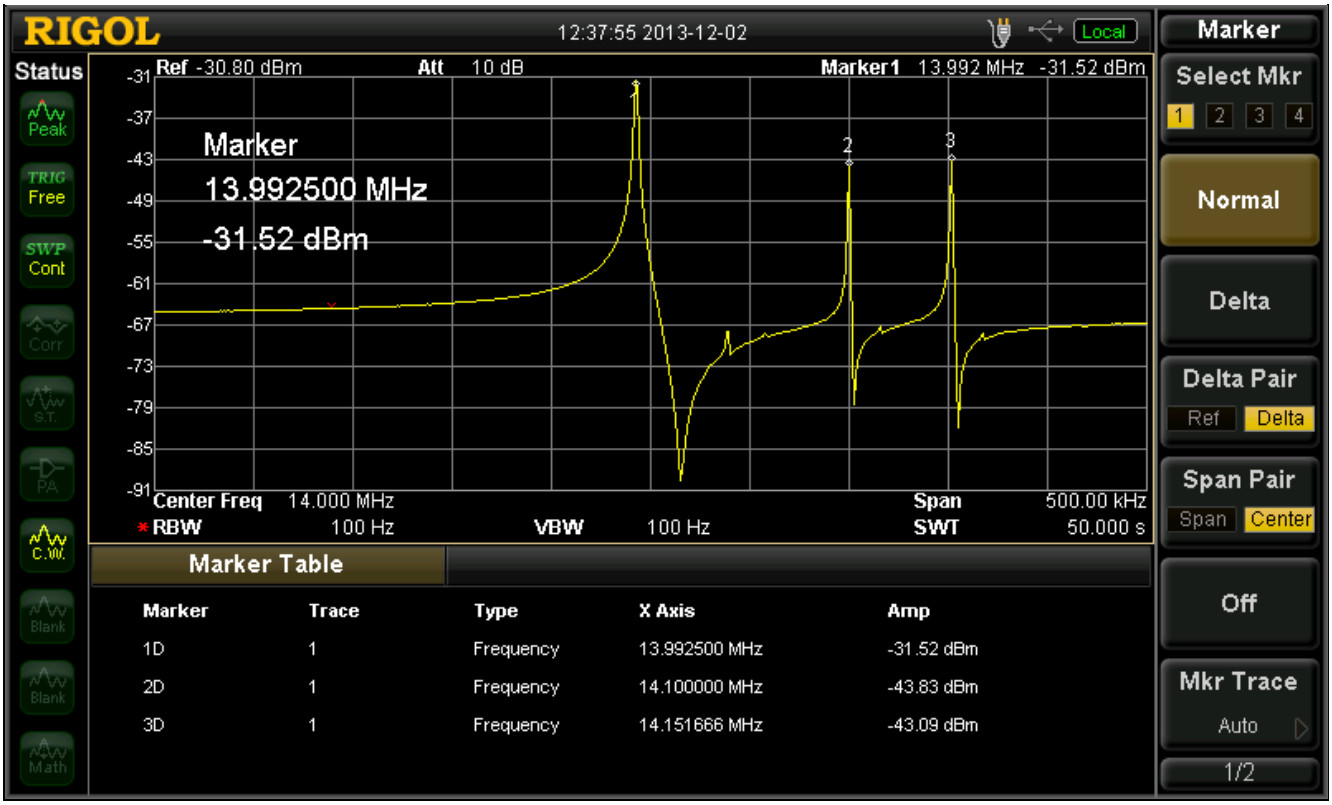

Above — 14 MHz crystal sweep spectogram. To find out why these spurs occurred, I swept 1 crystal at a time from my batch and saw spurs on all of them. However, after some reading, I discovered that the mere presence of a crystal spurious response doesn't signal causality since this is almost a normal happening. Wes, W7ZOI explains this on this web page. Crystals usually have a spurious response and from Wes, the spur is more often than not about 80 or 100 kHz above the main signal. This happens with fairly good crystals, less so with crappy, cheap crystals and even less often with good quality crystals. Since many of us buy computer-grade crystals from Mouser-Key, or online auction sites, who really knows what we're getting? 1 day I hope to test a Q = 1 million crystal — that will be fun.

However, renograde crystals could still be the cause. Sometimes when pulling a crystal(s), we're living on the edge — the main resonance is pulled so far that the circuit balks at the resonant frequency, or lies near the edge of such behavior and spurs start to show up. *Back to System D*. Simple substitution with 2 other crystals from another batch could tell me if these particular crystals were behaving poorly. It turns out, they were.

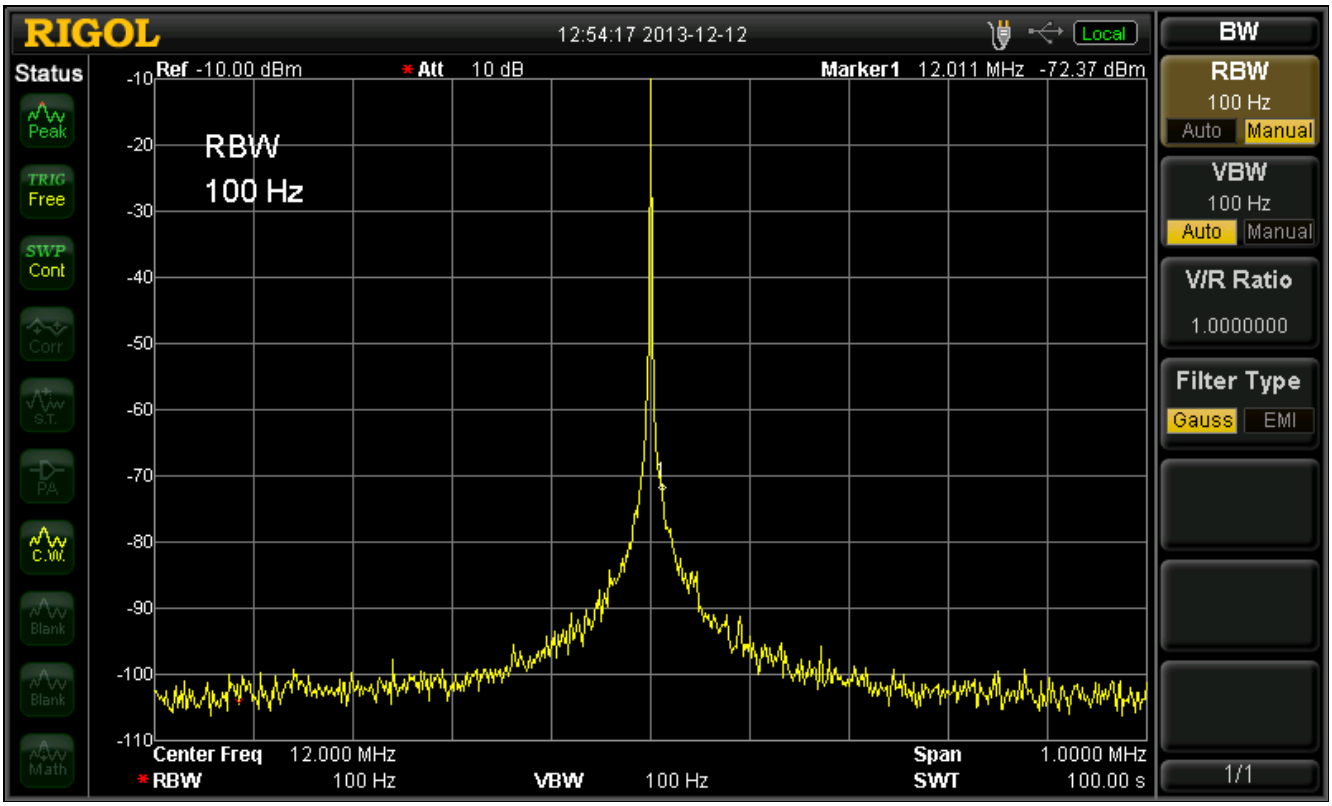

Above — Spectogram of the VCXO with 12 MHz crystals. I wanted to try other 14 MHz crystals, but didn't own any. My nearest value crystals were 12 MHz jobs with a Qu of 120K. Eh voila! No spurs — yay! Let's talk about noise:

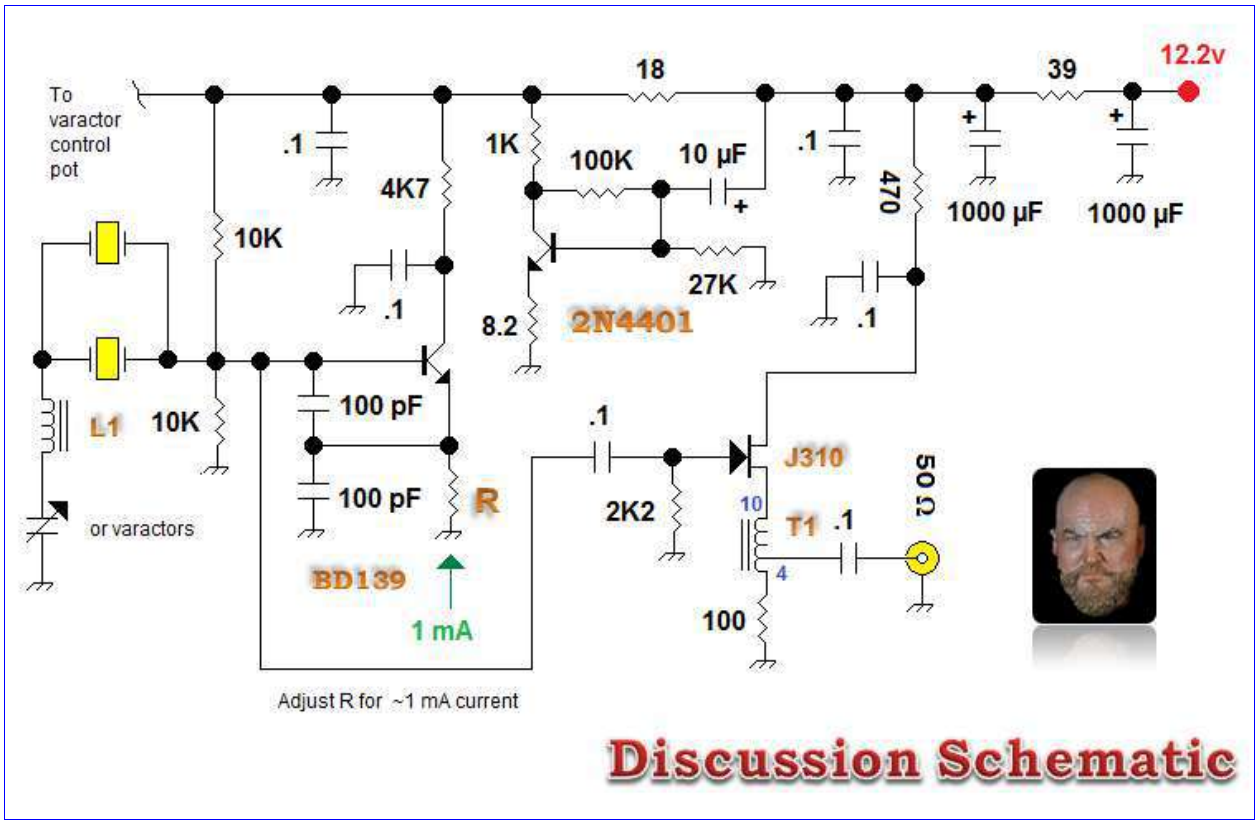

Above — Schematic for sideband noise discussion

System D design poses a real challenge with repect to noise. Measuring noise proves an advanced technique beyond the scope of this popcorn RF web site. We can't measure noise with our spectrum analyzer since the oscillator in the analyzer usually exhibits more noise than the VXO we want to test.

On page 4.12 of EMRFD version 1 is a small photo of 2 spectograms that show a clean crystal trace contrasted with a really bad oscillator trace. Baffled, because I could not replicate this experiment, I emailed Wes and asked him how he did it. Wes wrote we're able to see the noise in those traces because his SA featured a multiple pole, wideband filter with steep skirts that allows us to see the baseline noise close-in to the carrier. In contrast, most modern SAs feature synchronously tuned resonator type, or digital filters that produce a narrow peak with skirts that spread way out. The noise gets swept under the skirts.

By all means, advanced builders may apply notch filter techniques to measure oscillator sideband noise down low, however, a consideration for others might be to apply techniques proven to reduce noise and spurs — and just build the best oscillator possible plus measure what you can.

Some basic techniques to make a low-noise VCXO are well described elsewhere and may include: a high Q resonator, high Q varactors [with low series resistance], low power supply noise [including varactor tuning voltage], a low flicker noise amplifer, avoid overdriving the crystal and try to swing the highest AC voltage in the tank without reaching saturation and/or causing reverse breakdown in the varactor(s). Even the ratio of the Colpitts capacitors can affect phase noise, but without a method to measure phase noise, this gets esoteric. Some of these techniques also apply to VXOs.

Power Supply Noise

Bob, K3NHI and others have measured significant noise from the LM317 or related voltage regulators that we amateurs typically use. Power supply noise can FM our resonator and boost oscillator sideband noise. We may filter power supply noise with *large* value capacitors plus/minus series decoupling. See the work of Leif, SM5BSZ on this web page under the heading "The +12V supply is carefully decoupled like this". In addition, Charles Wenzel, published this web page.

I employed both techniques in my discussion schematic above. I went with the pi filter shown above 1000 µF - 39R - 1000 µF at the voltage input. A inductor might be used instead of the R if the voltage drop is too high for you. The Wenzel circuit fascinates me. The series resistor (18 Ω in my version) samples the current that flows into the oscillator. A voltage is then developed that is applied to the amplifier to generate a voltage that is out of phase with the noise current.

With good DC noise filtering I could measure small improvements in sideband noise in my SA despite only able to measure down to -88 dBc/Hertz at 10 KHz offset. In contrast, you rarely ever see even 1 electrolytic capacitor in the VXO schematics featured on many Ham radio builder sites.

Another trick is to avoid a regulator altogether. Since my DC supply already has a voltage regulator set to 12.2v, placing a second 5 to 8 volt regulator after it might just add another noise source.

Overdriving the Crystal

I heed the advice of Konstantinos, SV3ORA. He found that gently driving his crystal generated less noise and spurs compared to overdriving the crystal. Thus I adjusted my emitter resistor to about 1 mA current. For the schematic above, a typical emitter resistor starting value = 1K8. Just measure your emitter current.

I employed a large area, slower BJT, the BD139 to hopefully drop flicker noise. Expensive, super high Q crystals (Q = 500K to 1 million) may be driven with up to several mA of current, however, it's likely not so for the computer-grade xtals we typically use. I can't measure the outcome of these interventions, but System D thinking might just prevail.

Varactors

Varactors tend to be low Q and their Q deteriorates as we go up in frequency. I've seen very low phase noise VCXOs employing varactors, however, these were engineering marvels. Still, as a VHFer and hopeful UHF enthusiast, this is the direction I wish to go. We ideally need to keep some reverse DC voltage on the varactors at all times and not go to 0 — this also limits tuning range in our simple 12v supply radios. Read your datasheet. Air variable capacitors (a VXO) might be a better solution for your application.

How Does a VXO work?

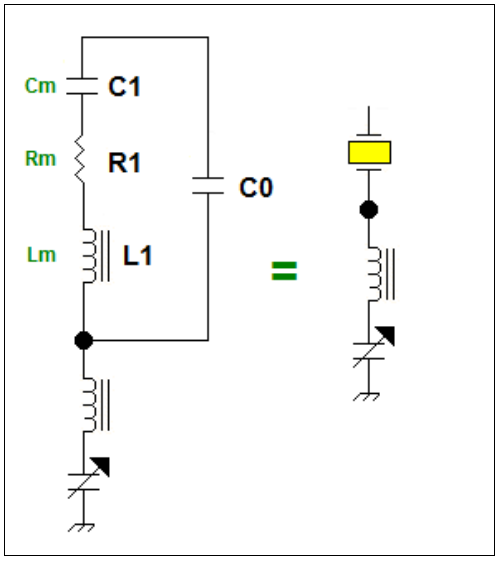

Above — The crystal equivalent electrical circuit has 2 arms: The impedance of the motional arm Zm lies in parallel with Zo, the impedance resulting from the parallel capacitance C0 (formed by the 2 crystal leads.) We measure and/or calculate these parameters when designing our crystal filters. In the above schematic I added the external L and C used to move the crystal's series resonant frequency around in our VXO, VCXO, or Super VXO circuits.

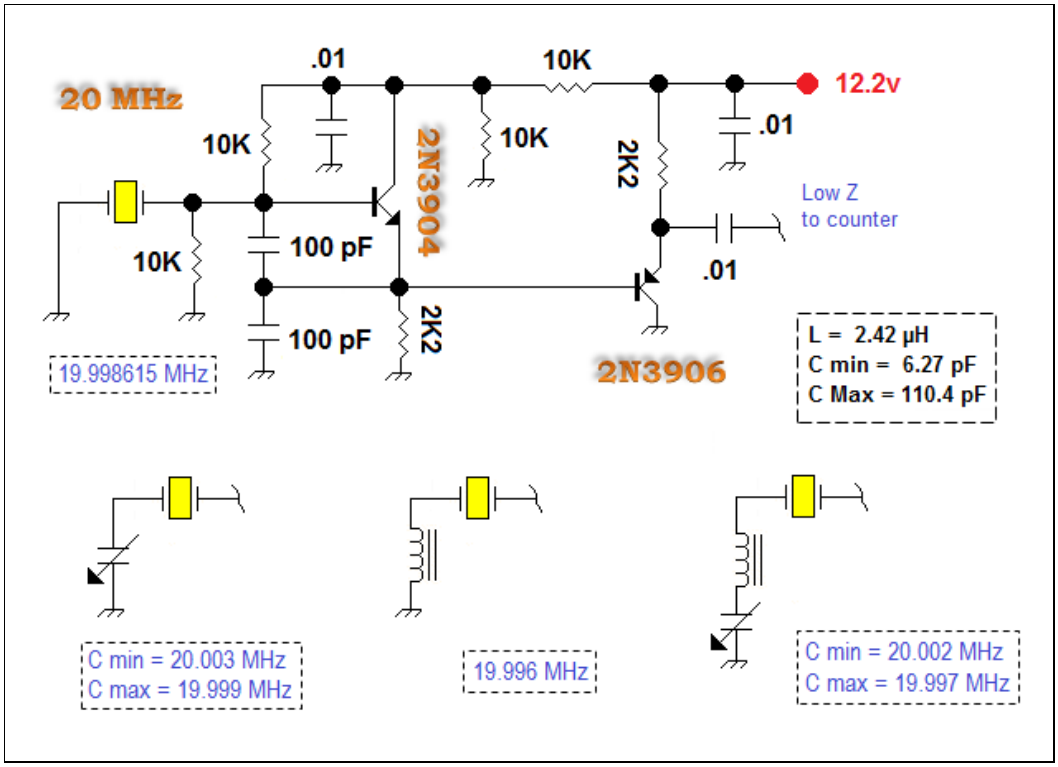

Above — I made some simple experiments to explain why we place both a L and C in series with the crystal and how it changes the crystal

frequency in our oscillator. From these experiments, some theory from EMRFD and wisdom from Ken Kuhn, I made the following simple conclusions:

Electrically a crystal looks like a large inductance in series with a small capacitance and in parallel with C0. An external inductor adds to the crystal's series inductance and *lowers* the resonant frequency.

The external variable capacitor adds in series with the crystal internal capacitance to lower the net capacitance and *raise* the resonant frequency.

The purpose of adding an external inductor is so that we can tune both lower and higher than the natural crystal frequency. In contrast, if we only apply an inductor, the oscillator frequency would always be lower and if we just apply a capacitor, the oscillator frequency would always be higher.

Since the external inductance has much lower Q than the effective internal inductance, it adds to noise and signal losses. The same goes for the external C.

As we raise the inductance ever higher to boost the delta F, at some point, the parallel C of the crystal resonates with this "too high" L and the series resonant frequency has nothing to do with the series resonance of the crystal. This kills the normally sublime frequency stability of a crystal-based oscillator.

Q of the VXO/VCXO Inductor

I experimented to learn that the Q of that L doesn't need to be that high to allow the frequency to be moved up or down by an air variable cap or varactor.

For example, if I wound a coil on a T68-2 and shunted it with a resistor no less than 1K8 — it worked fine (sometimes the frequency shift would even improve 2-3 KHz for a given L). A #61 ferrite toroid wound inductor also worked well and requires much less turns allowing thicker wire for mechanical stability. Also, the lower number of turns helps avoid significant SRFs. Temperature stability remains a question with the this and all ferrites.

An FT37-43 or FT50-43 ferrite inductor worked poorly – I measured high signal losses plus the maximum frequency swing dropped when compared to the same inductance value wound on a T-68-2, or FT-50-61. Avoid #43 ferrites in any resonator circuit unless you're purposely building a noisy oscillator for learning purposes.

Some guys use those little molded chokes with a Q of ~ 50 for the L and they also work well. Predictably, as I lowered the Q of the external L, or went from an air variable C to a varactor, signal losses increased resulting in lower signal output amplitude.

Decreasing resonator Q increases phase noise. For a popcorn radio, I'm not sure the change in phase noise would be a deal breaker in some homebrew projects, but as possible, I think it's wise to employ high Q resonator components: crystal, inductor and the variable capacitance. Thus I'll wind my VXO/VCXO inductors on powdered iron toroids hereafter.

Since a quartz crystal resonator is driven by the piezoelectric effect, fundamental plus overtone frequency modes (3/5/ 7/11) may be derived. I unbypassed the collector and placed a collector choke on it to examine the output with my 'scope. The waveform rung with many harmonics. Lots to learn.

Go débrouillards!

---

4. Funster Line — A Simple 40M Band QRP Trans-receiver

Click for the Funster transmittter notes.

---

5. Miscellaneous Photographs and Figures

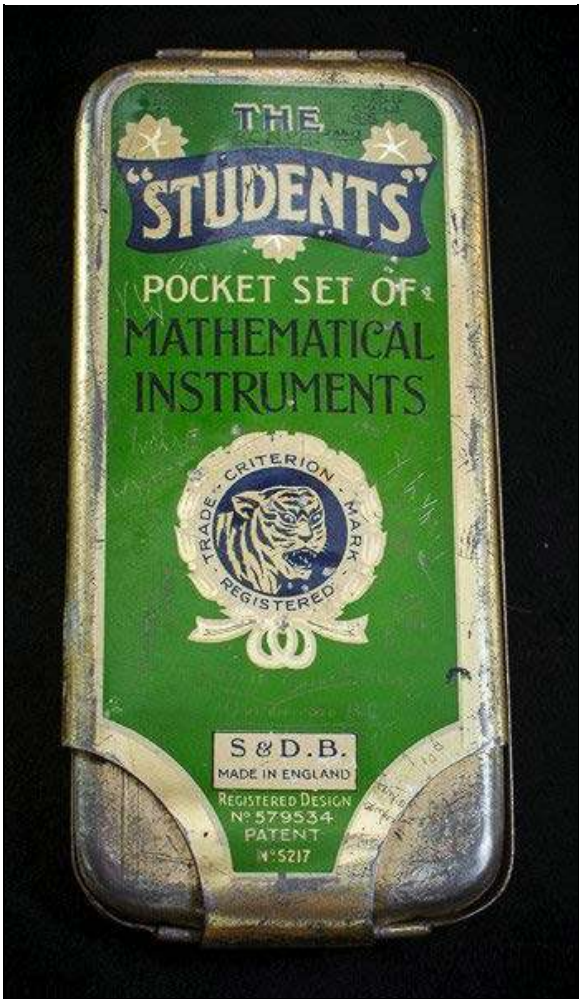

Above — My handed-down geometry set — purchased in 1938. Click for larger picture.

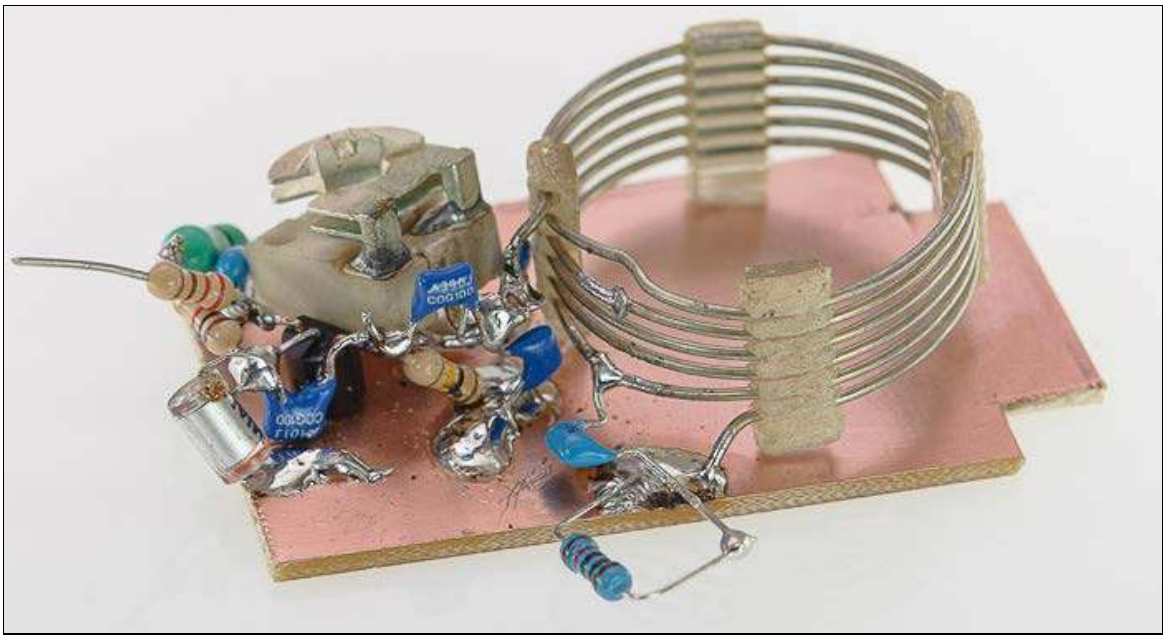

Above — My prototype Colpitts LC oscillator with only a 10K resistor as the load.

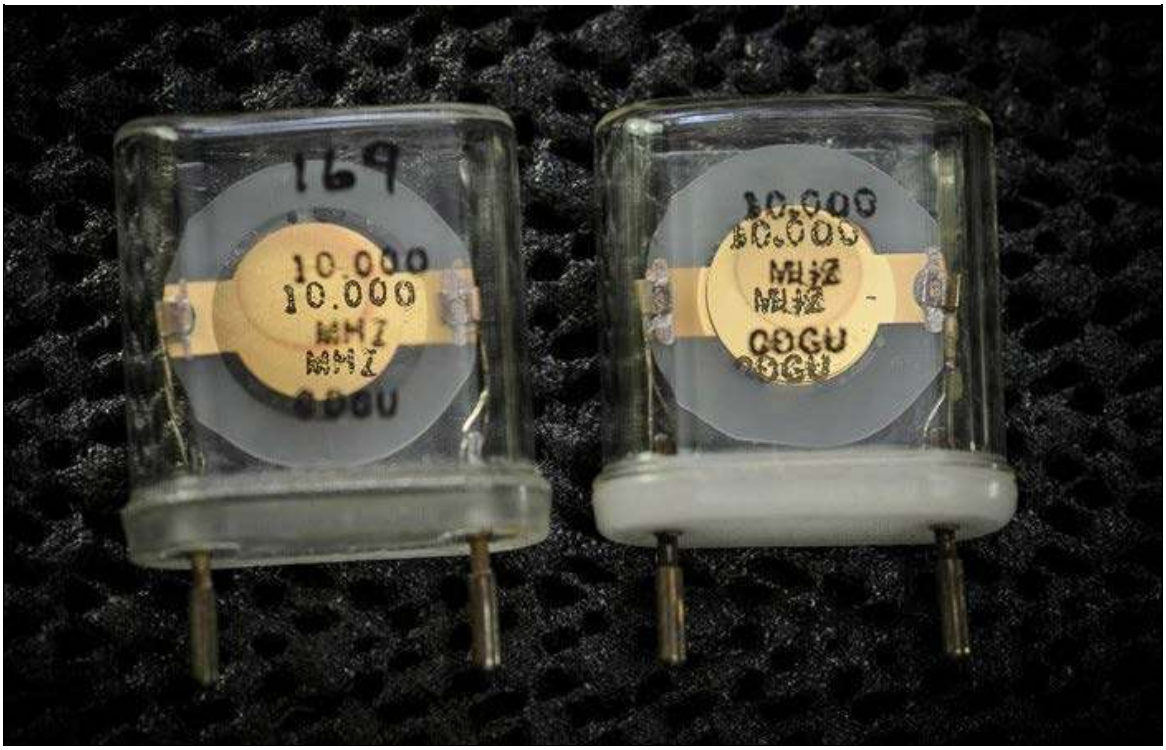

Above — Hi Q glass encased crystals. Click for another photo.

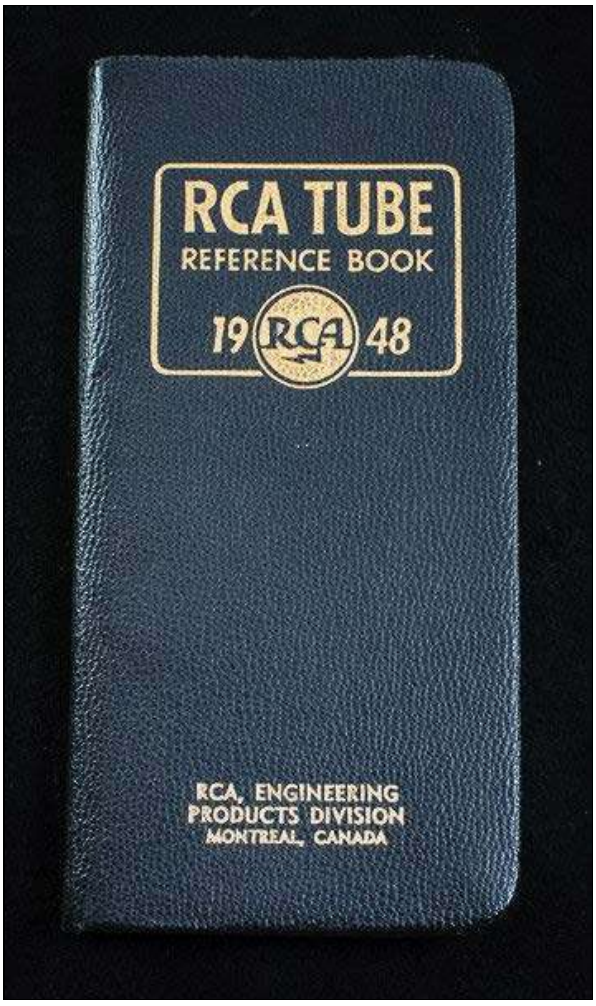

April 2014: New player on the scene — Bar Bar Kitty — chief science officer and QC consultant.

April 2014: Other new pet: Munchkin. Clear-spoken and direct — pet me, or feed me... and oh yah, Q2 is oscillating.

MP140
34M38B
OTS50331

Caitlyn 310 — UHF Beginnings

Respository web page for beginner UHF experiments in 2014-2015.

1. References
2. Transistors, RFCs, Capacitors and a 50 Ω Detector
3. Return Loss Bridge Experiments
4. VCO Experiments
5. Frequency Counter Kit

1. References

After a modest quest, I found an excellent microwave primer called Microwaves Made Simple. Principles and Applications by W. Stephen Cheung and Fred H. Levien. Published in 1985, the authors brilliantly teach the basics in plain language (no small task). My copy was printed in December 2013 by Artech House who print single copies of many classic texts on demand. Click for a photo of my book.

The ARRL published 2 UHF compendium books entitled: The ARRL UHF / Microwave Experimenters Manual [1990] and The ARRL UHF / Microwave Projects Manual [1994]. While out of print, used copies seem prevalent and might serve as good resources for builders who hunger for circuits and Ham-related UHF circuit building information. Click and click for photos.

Instrument companies provide continuing education and materials to educate & support their customers. With luck you'll find helpful free application notes and other tools. Two recent RF library additions include an Agilent CD containing all their current application notes and webcasts [my image is truncated and the CD includes applying SA's, 'scopes and signal generators], and this old Spectrum Analyzer Fundamentals booklet by Tek.

2. Transistors, RFCs, Capacitors and a 50 Ω Detector

I want to grasp circuits from 300 to 1296 MHz. This meant acquiring some UHF parts, making some bench tools and buying a 50 Ω detector to sweep and/or measure power in my UHF stages. Click for a snapshot of some of my parts cabinets.

BJTs

I'll employ the BFR93A, 2SC3356, and 2SC3583 as my mainstay NPN bipolars; at least to start with. Numerous transistors will work — price, availability, NF and shipping costs informed my choice. I'd also feel happy with MRF901, BFR92 and BFR96 NPNs and it's always fun reading datasheets. My PNP choice = BFT93 by NXP. Later on, I'll add in discrete GaASFET and other non-BJT species. Only 2 MMICs lie in the parts cabinet: MAR-3 and MGA-61563.

Radio Frequency Chokes (RFC)

Although, I'll also wind, or perhaps ply carefully dimensioned copper board traces to make RF chokes, I built up a stock of lower Q chip inductors in size 0805 and 0603. These include 8.2 nH, 33 nH, 68 nH, 220 nH, 330 nH, 470 nH and a few other values. For RFCs we need to consider L, tolerance, SRF, Q , maximum current and temperature stability — it's probably better to only buy clearly specified parts so you can study their datasheet to glean this information. I've swept nearly all my RFCs and recorded their SRF.

Choosing RFCs — SRF (series resonant frequency)

An RF choke exerts its greatest impedance at its SRF and in the case of a first-order RFC such as a single inductor, we should aim the SRF at or near the frequency we wish to attenuate the most. Consider a choke in the emitter lead of a BJT Colpitts oscillator with a frequency range from 375 to 400 MHz: The choke's ideal SRF should lie somewhere above 400 MHz. As possible, the SRF of a first-order RFC should exceed the operating frequency of the device it's choking.

In higher-order filter applications such as a C-L or C-L-C (pi filter) applications, engineers tend to target the choke's SRF to >= 10 times the operating frequency. Challenges such as limited inductor choices, needing to match stages, or coping with stray reactances will arise, however, as amateur UHFers, we just try our best to fit an RFC.

UHF Capacitors

I swept numerous size 0805 + some 0603 and 1206 capacitors in a microstrip line jig to determine their SRF. Math formulas enable us to calculate and plot attentuation, Q and ESR at self-resonance if we wish. Click for 1 example. Although we rarely apply capacitors at their SRF in practical circuits, considering Q, ESR and attenuation gets us thinking that capacitor SRF is a dynamic value that may vary widely with part size, capacitance and datasheet specified Q.

For instance, if you take a size 1206 capacitor, measure its SRF and then replace it with a same-value size 0805 capacitor, the SRF of these two caps might vary by as much as 200 MHz or more. Size does matter! Even the same value capactor by a different manufacturer may be a SRF game changer. Bob, K3NHI tells it correctly: to measure *is* to know.

Datasheet specified capacitor Q is usually measured at a low frequency like 1 MHz. Since Q decreases as frequency increases, a capacitor that specs a Q of 2500 at 1 MHz may only sport a Q of 87 at its SRF way up at 512 MHz. During sweeps, I measured a deeper attenuation notch and often a higher SRF for "very high Q" caps when compared to the common, low-medium Q, popcorn caps sold as mystery parts by online stores or auctions. I'm now hypervigilent about finding very high Q SMD capacitors for sale at a low price.

I wrote the SRF of all my SMD caps in my notebook and use this data to inform my capacitor choice for RF bypass and tuning. Click for a photo of 3 UHF parts drawers. I've pretty much gone to size 0805 caps to try and garner a higher SRF at VHF and UHF. Still, too, we might have to solder down 0603 parts up above 1 GHz. Yikes!

Did you notice that when you drop a 0805 part on the floor, you never ever find it again? Even a little cough can expunge a size 0603 part from your QRP workbench.

50 Ω Detector

From 0.5 - 200 MHz, my 50 Ω terminated input DSO forms the heart of my test bench. An analog, or digital storage oscillocope with a bandwidth >= 1 GHz, plus a suitable wideband probe costs dearly and for many, won't be an option. UHF bandwidth, thermistor-based 50 Ω power meters are also expensive and lack signal viewing.

Thus, a spectrum analyzer seems the best choice for the amateur UHF enthusiast. A spectrum analyzer with a built-in tracking generator adds serious value — giving us a MF-UHF sweep system with profound utility. One popular, modern TG + SA choice is the Rigol DSA-815. I'm fortunate to have access to gear that measures up to 3 GHz.

3. Return Loss Bridge Experiments (RLB)

I'd be lost without a return loss bridge at UHF. Directivity marks the touchstone of a return loss bridge — and up at UHF grabbing a minimum 20 dB directivity may pose quite a challenge. Experiments to find a bridge with good directivity from 250 to 1750 MHz follow:

Above — A macro photo of RLB#1: 1 of the 3 "string of pearls" type return loss bridge built this Winter. I tried different numbers, sizes and mixes of ferrites. This particular bridge had 3 and then 2 FT37-61 toroids as shown, although I did not shorten the RG-174 coax when reducing to 2 toroids. The 61 mix gave poor directivity and was abandoned.

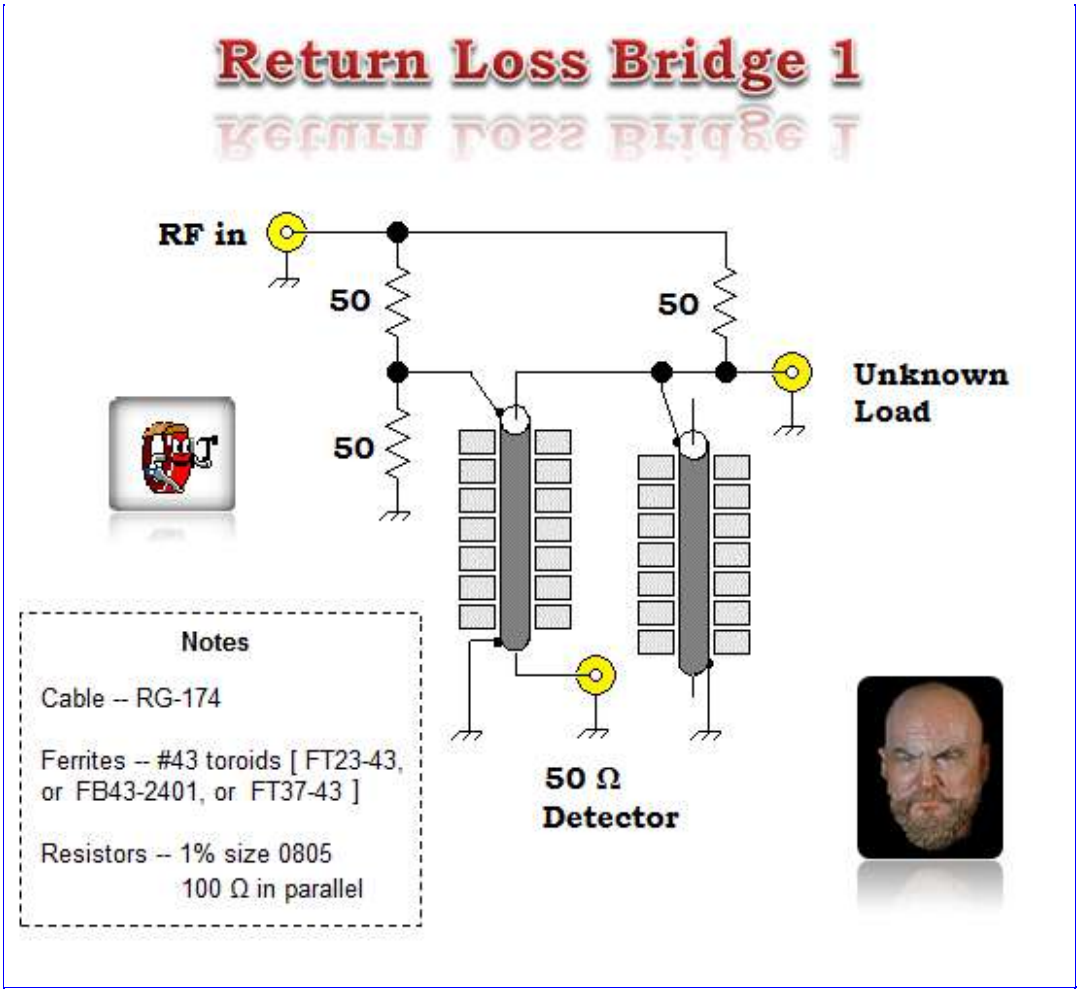

Above — Return loss bridge #1: the "string of pearls" variant. Several web sites feature great "string of pearls" RLB experiments for you to review and many place enough ferrite to extend from HF to UHF. I swept each of my builds in a Rigol tracking generator + spectrum analyzer with 4 frequency markers set. I made an open-circuit sweep [nothing on the unknown impedance port] followed by a sweep with a Mini-Circuits Labs DC - 18 GHz, 50 Ω load threaded on the unknown Z port. The difference between the open-circuit and 50 Ω measurement = the directivity at that frequency.

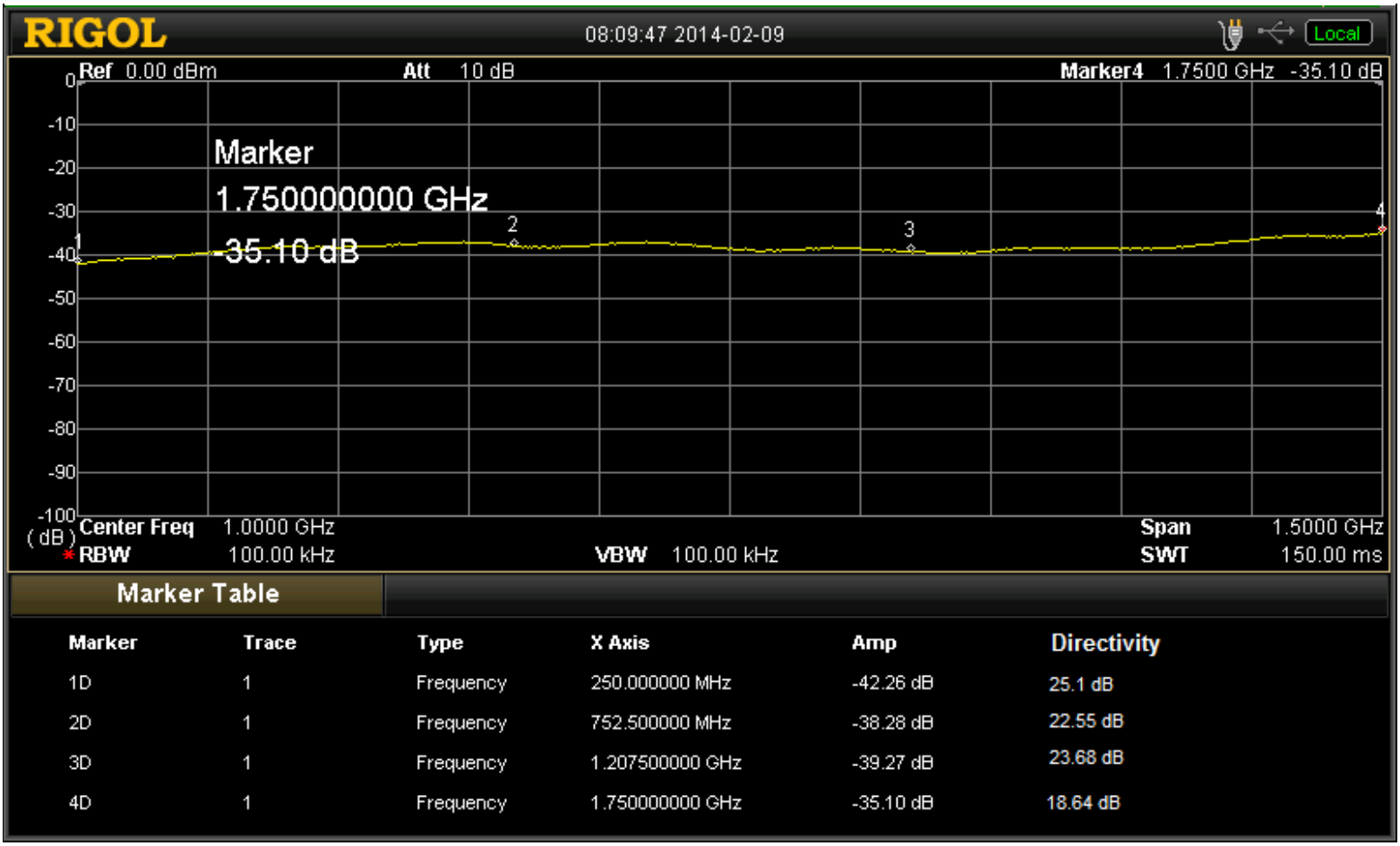

Above — The sweep of my best "string of pearls" bridge from 250 MHz to 1.75 GHz showing the directivity at 4 frequency points. Click for the open circuit sweep. I felt encouraged by this sweep with five FB43-2401 beads over each piece of coax cut just long enough to fit the beads. I built on 2-sided FR4 copper clad board with at least 6 via wires connecting the 2 copper surfaces.

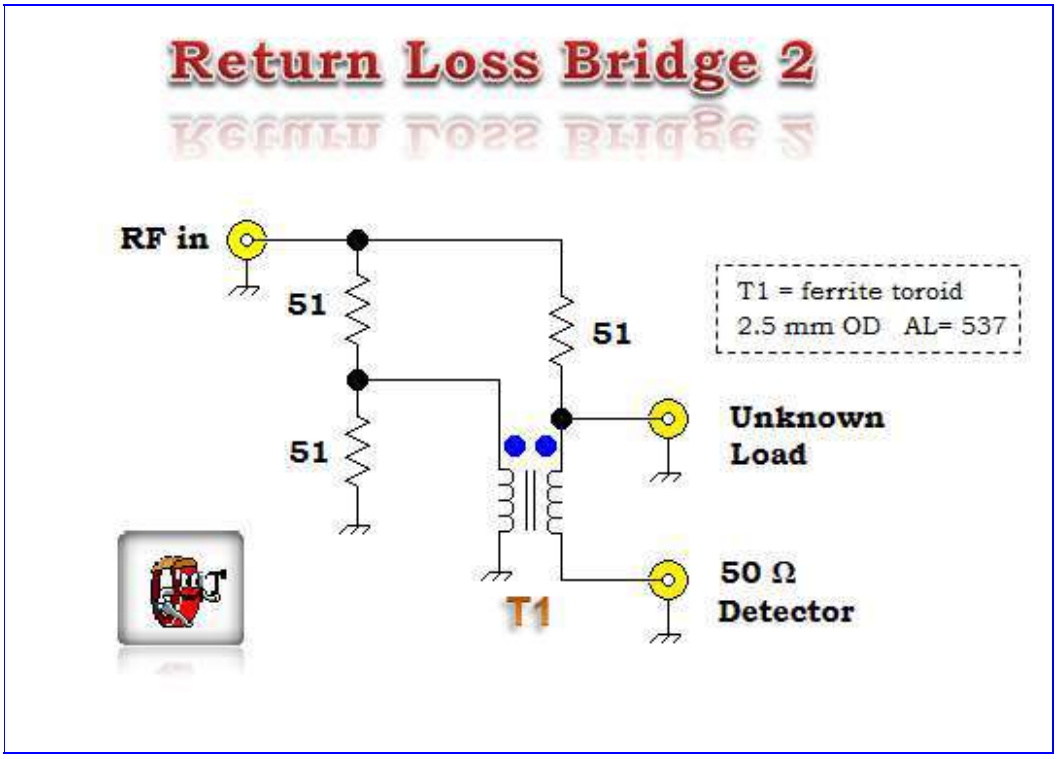

Above — Schematic of RLB #2: the bridge topology featured in EMRFD. T1 = 5 bifilar windings of 32 gauge wire wound on a *tiny* ferrite toroid boasting a strong AL. I pulled this ferrite from a blown up mixer removed from an old 1.5 GHz spectrum analyzer. I started with 5 toroids, but during winding, got spastic and dropped 2 of them on the floor and concluded that the SMD part gnome who lurks beneath my bench swallowed

them up, since I couldn't find them after an intensive search.

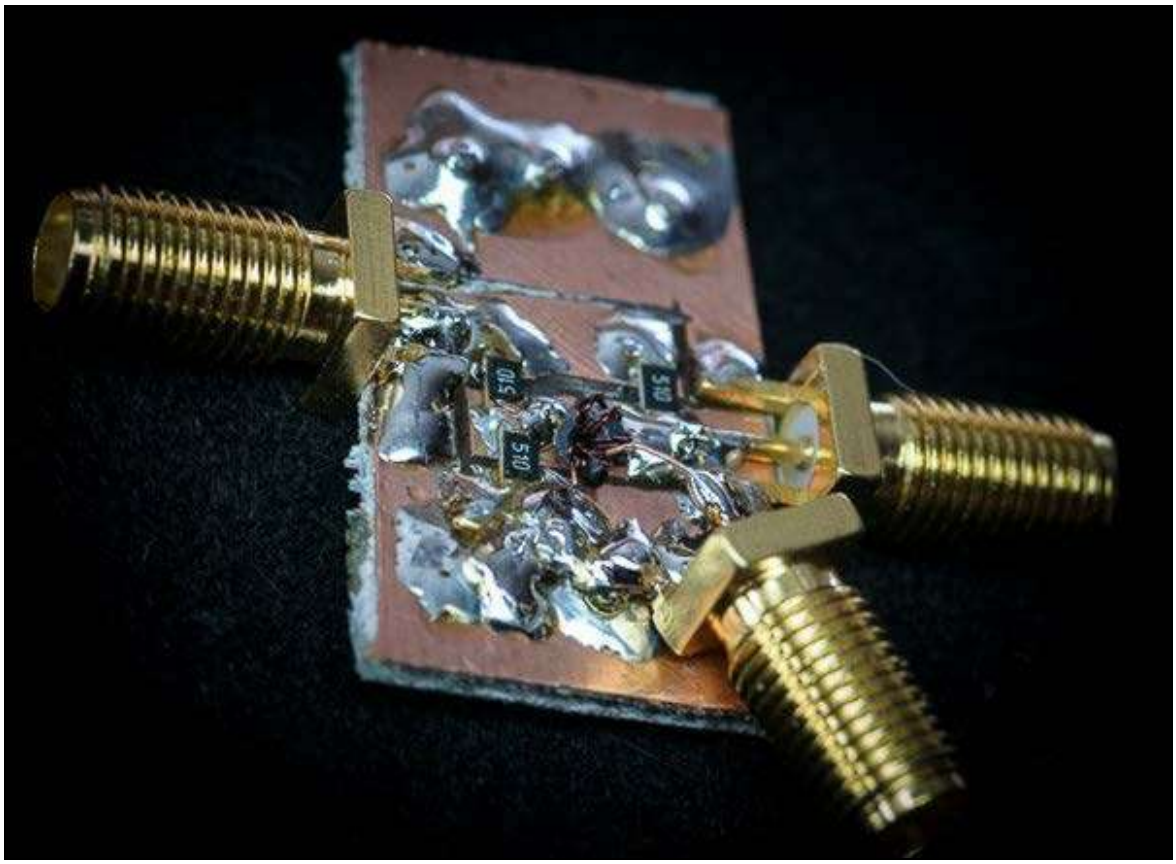

Above — Magnified return loss bridge #2 breadboard. Serious UHF enthusiast Paul Wade, W1GHz found that the smaller your breadboard, the better the UHF directivity in his bridge experiments: My findings support his. In RLB #2, I went with plain, size 1206, 5% resistors. I just ordered some size 0603 49.9 Ω 1% resistors for future experiments in my quest to make my ultimate UHF RLB.

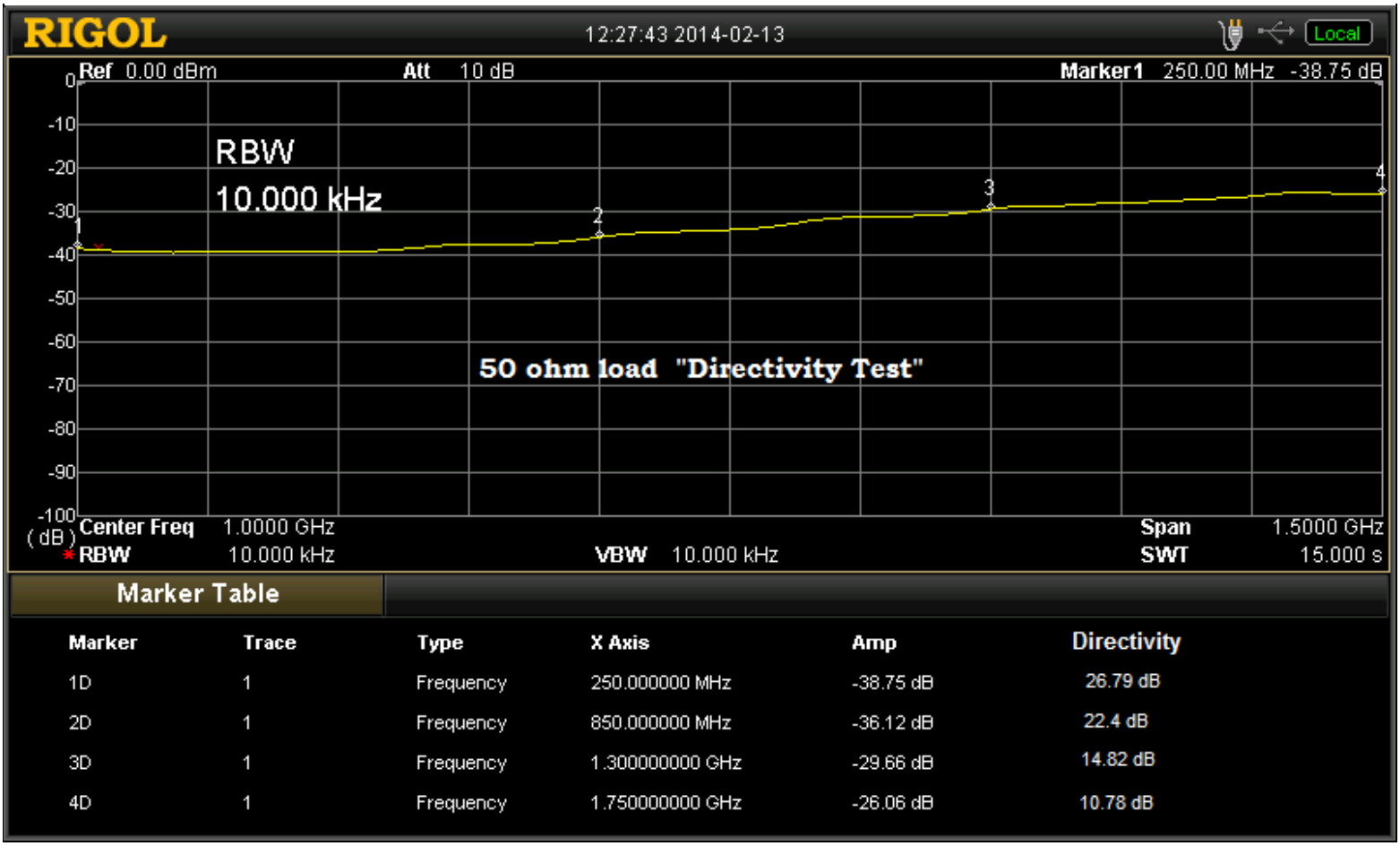

Above — The sweep of RLB #2 from 250 MHz to 1.75 GHz showing the directivity at 4 frequency points. Above ~900 MHz, directivity falls right off, so this bridge won't cut it for a serious UHF bench. I tried reducing T1 to 3 bifilar windings but this worsened the directivity. Click for a different sweep of RLB # 2 from 50 MHz to 1.5 GHz. Directivity = 27.5 dB at 50 MHz, so this bridge would work great for VHF. I imagine that SMD 49.9 Ω 1% resistors might boost directivity a little.

Of course, we're always impressed by the work of Kostas , SV3ORA.

Return Loss Bridge 3

Some experiments with the 3-bead RLB from Sam Wetterlin follow:

Above — My build of the Wetterlin 3-bead return loss bridge. This PC board was the only 1 left over from a 2006 joint project between the 4 Hams whose calls are etched on the PCB. Wes sent me this board and some of the parts and I'm grateful. My 3 dB pads = 294 Ω 1% resistors plus an 18 Ω 5% in size 0805. My 49.9 Ω 1% resistors = size 0603. The transformer = a Minicircuits Labs TC1-1-1-13M+. Click for the ferrite description. I used 24 gauge copper via wires to connect grounded nodes to the ground plane on the back of the PC board. I chose to permanently solder a 49.9 Ω resistor on the reference port.

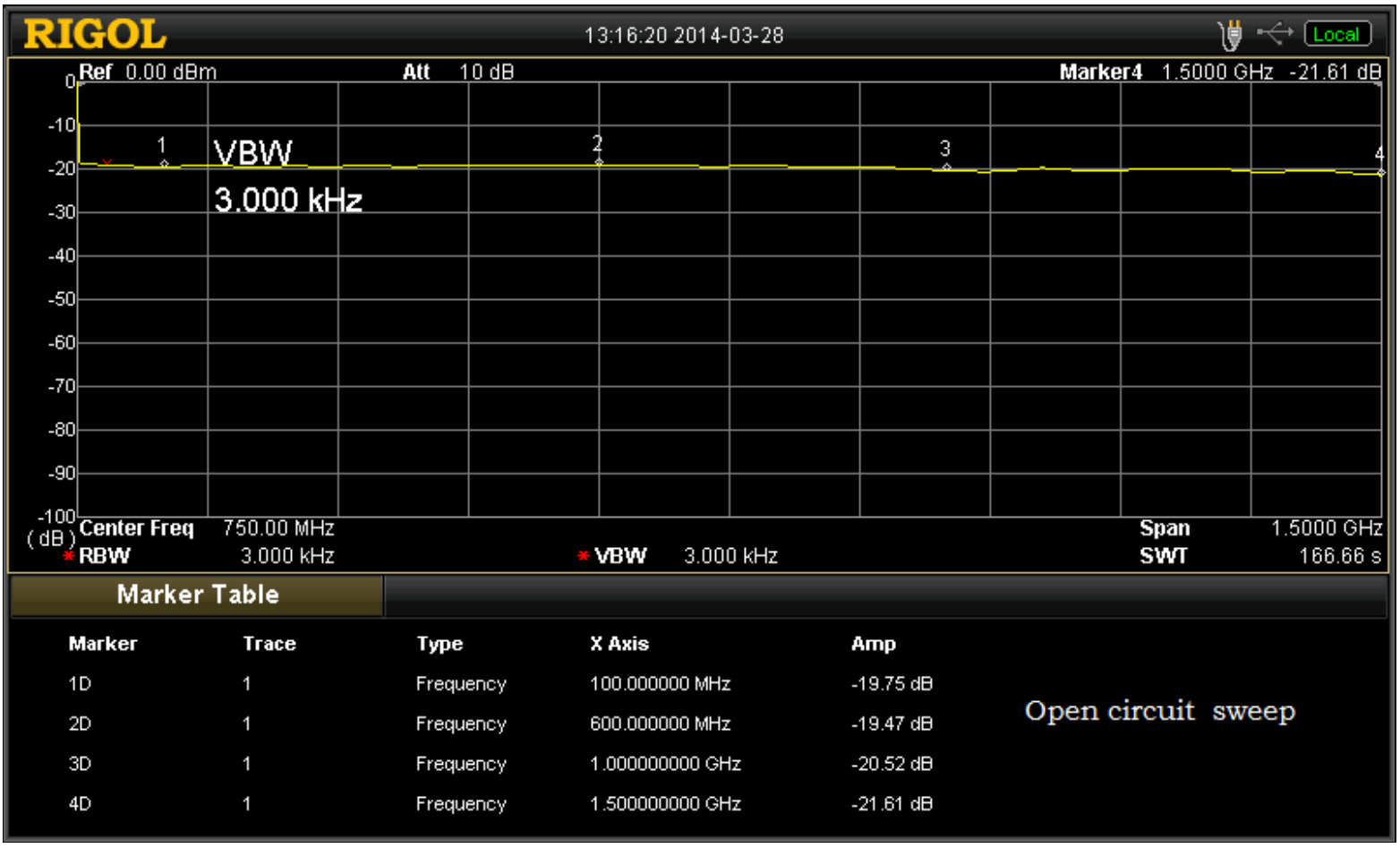

Above — Open circuit sweep with 4 markers set. Span = 1.5 GHz.

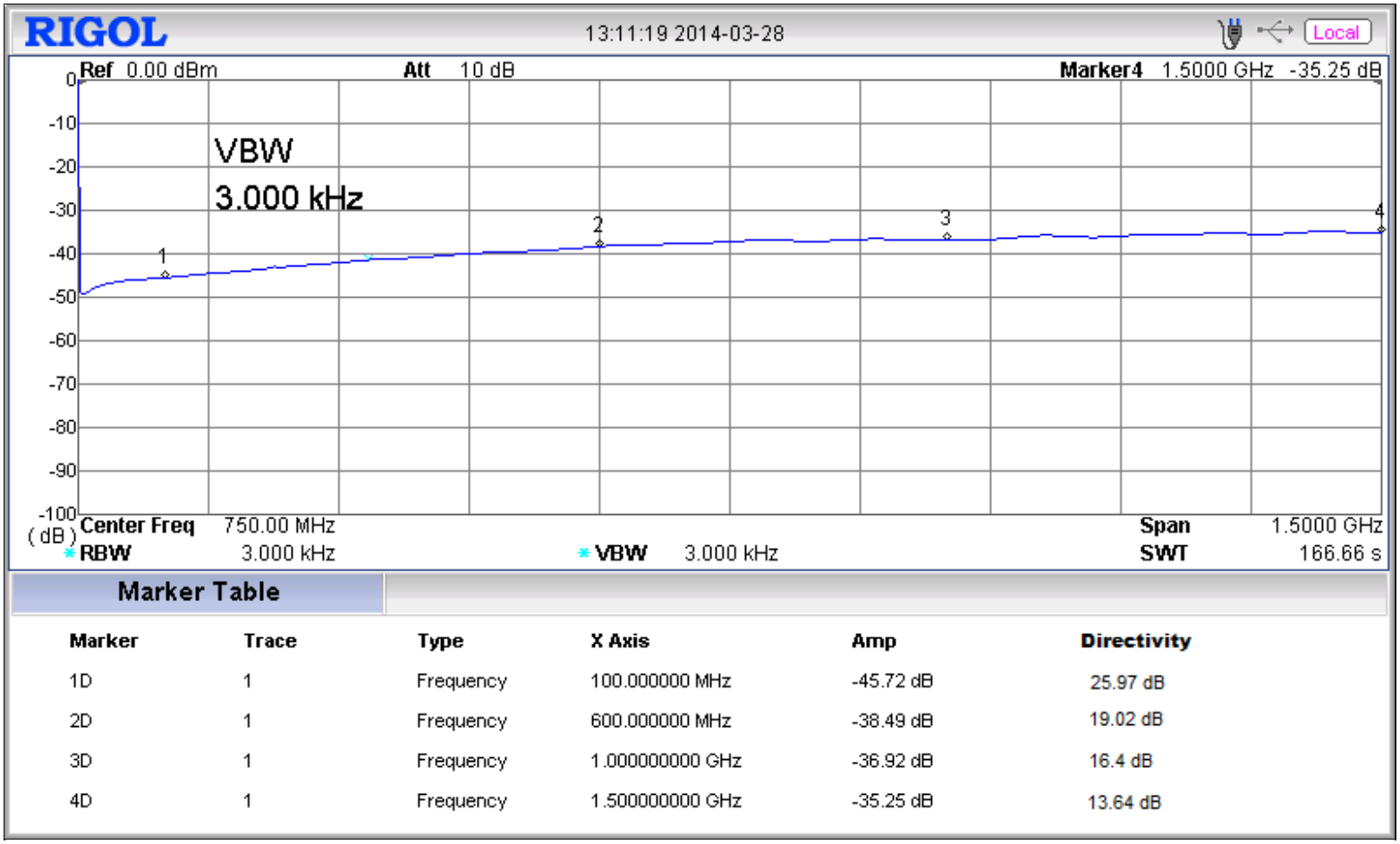

Marker Table

Marker	Trace	Type	X Axis	Amp	Directivity
1D	1	Frequency	100.000000 MHz	-45.72 dB	25.97 dB
2D	1	Frequency	600.000000 MHz	-38.49 dB	19.02 dB
3D	1	Frequency	1.000000000 GHz	-36.92 dB	16.4 dB
4D	1	Frequency	1.500000000 GHz	-35.25 dB	13.64 dB

Above — 50 ohm load termination sweep with calculated directivity. Click for the 50 Ω sweep where the span = 200 MHz. I was disappointed with the UHF directivity in *my* build.

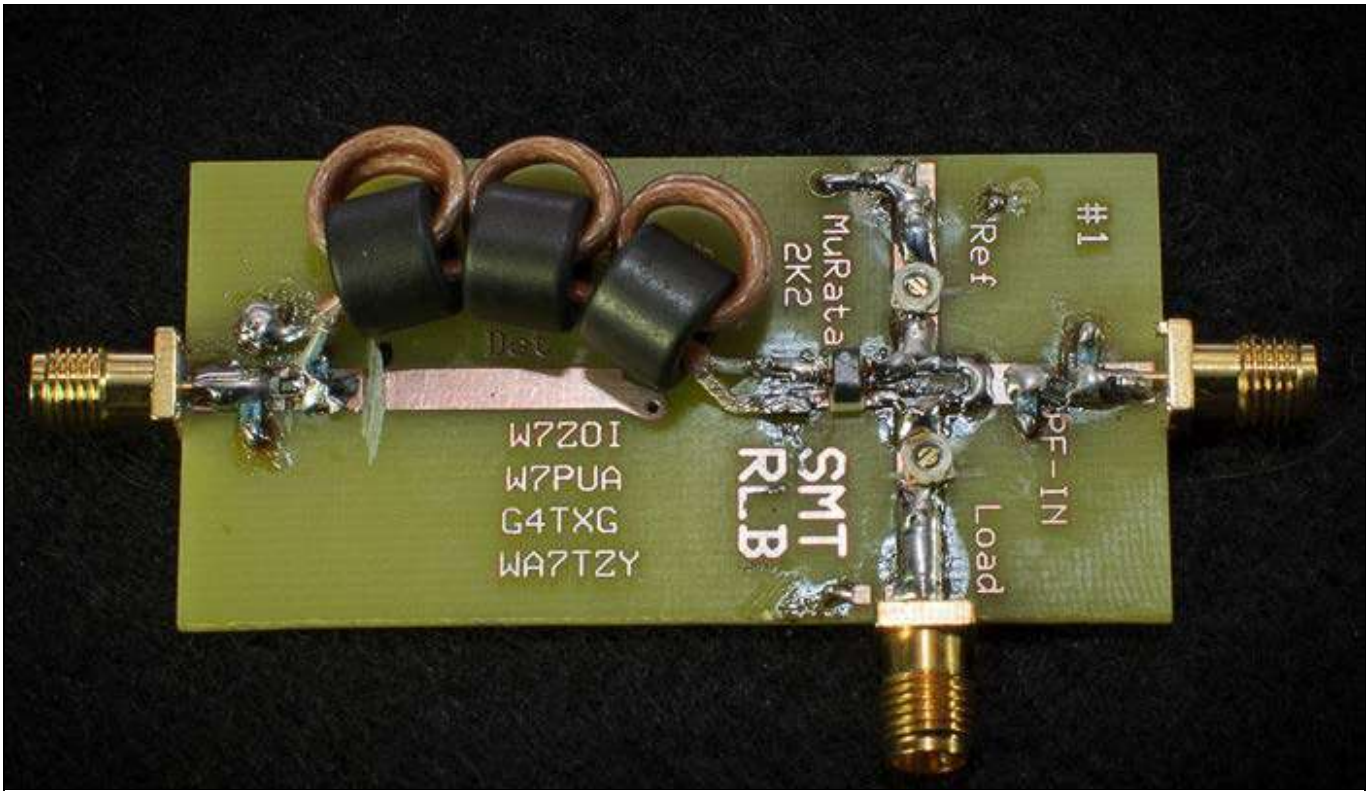

Above — The 3-bead RLB with added series trimmer capacitors on the load and reference ports. SMT trimmer caps = Voltronics JR300 5.5-30 pF with a Q of 1500. I tried both shunt and series caps to try and boost UHF directivity.

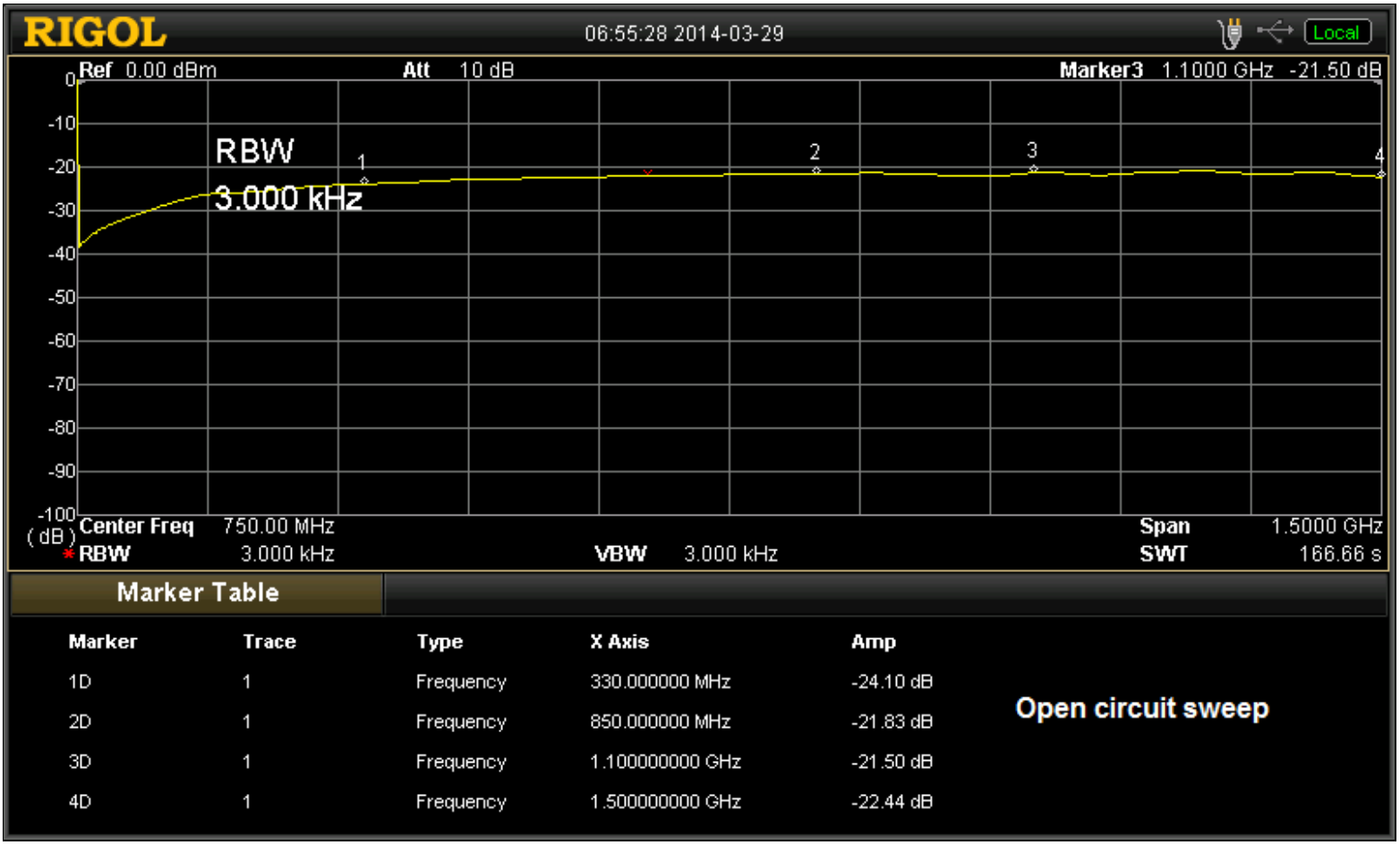

Above — Open circuit sweep of the 3-bead bridge with series capacitors on the load and reference ports.

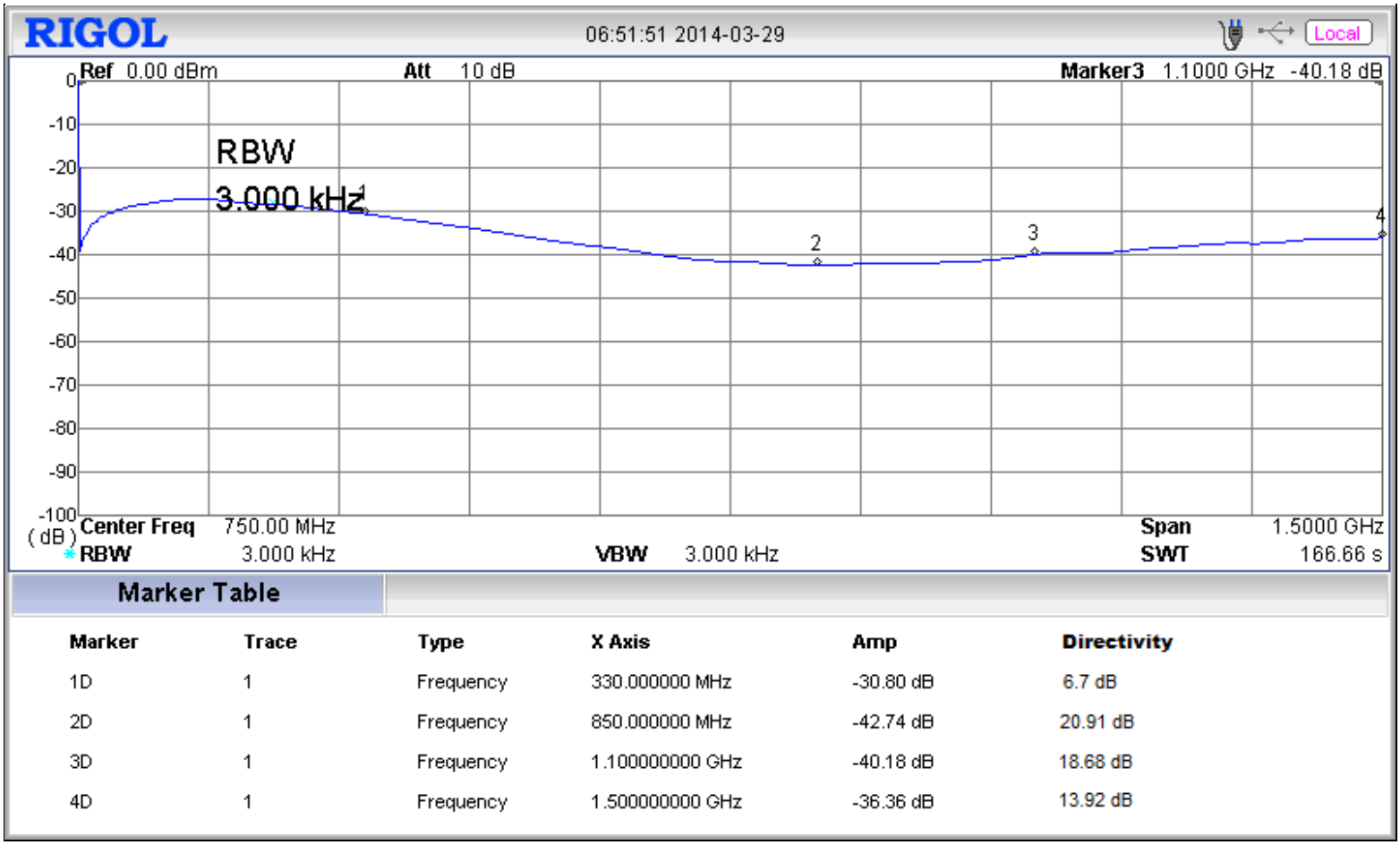

Above — 50 Ω load sweep. By carefully tweaking the 2 trimmer caps, I set the deepest NULL at ~ 850 MHz; although it's not as deep as I want. Low end directivity was compromised.

Return Loss Bridge 4

Since my bench experiments with the "string of pearls" (SOP) return loss bridge showed promise, I kept going and eventually built a version closer to my goal: A bridge for 300 MHz to 2 GHz with decent directivity.

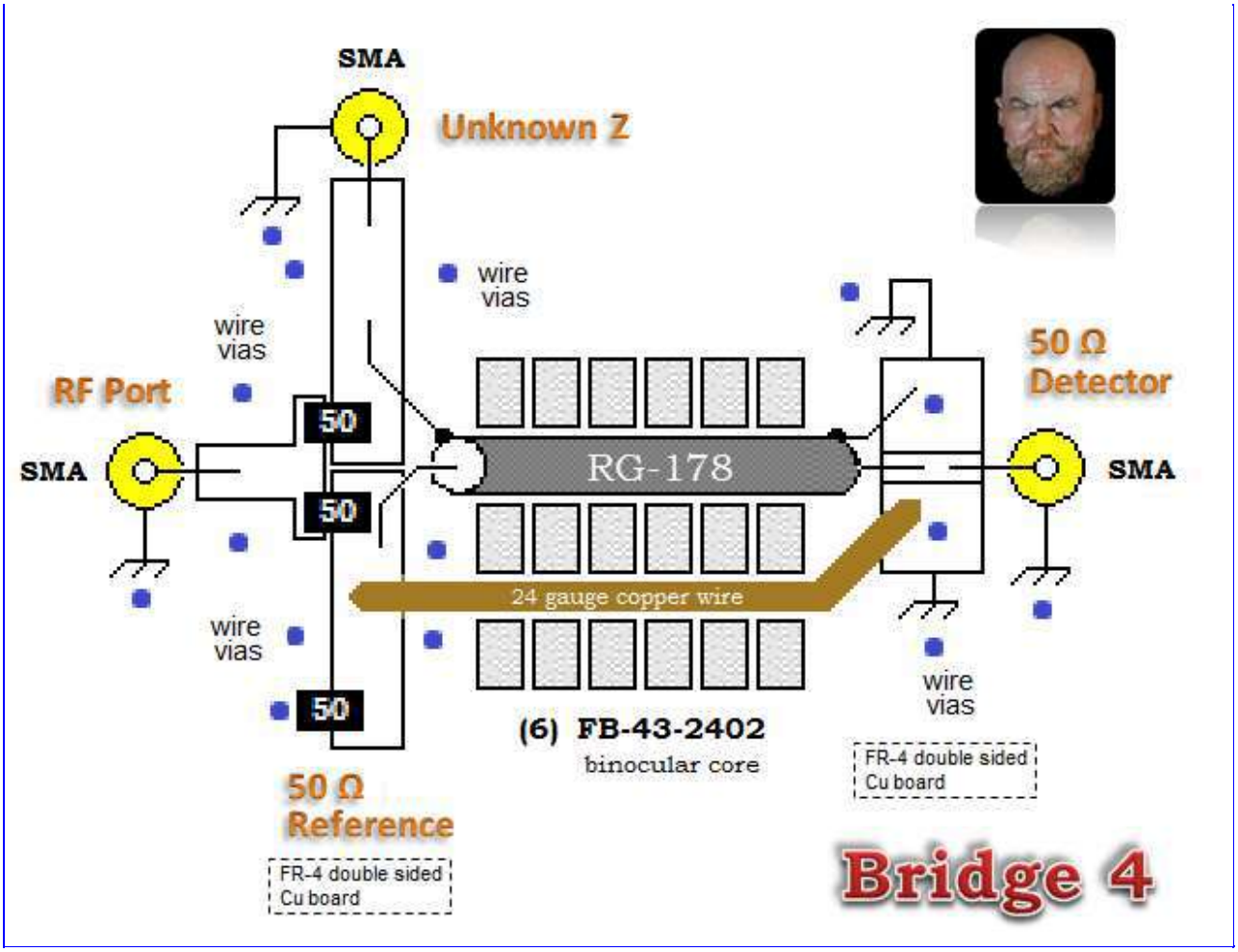

Above — My SOP build diagram of Bridge #4. I cut traces in 2-sided FR-4 Cu board to make the needed microstripline paths.The two 49.9 Ω 1% bridge resistors = size 0603, however, my reference port 49.9 Ω, 1% resistor was size 1206. The braid of the coax goes to the unknown impedance port and the center core to the reference port. Six FB-43-2402 binocular cores just passed the diameter of the RG-178 coax and binocular ferrites boosted balance compared to seperate beads in my experiments.

Rather than run coax through the remaining hole in the ferrite string, I just used a 24 gauge piece of Cu wire for balun symmetry. I left the green insulation on the wire to help keep it in place during soldering — I used the same wire spool to make the via wires.

Above — Breadboard photograph. Click for a larger photo. I soldered some thin brass sheet metal to electrically join the ground planes of the 2 carved boards [represents the normal RF-tight metal chassis we apply].The brass sheet boosted directivity 8 dB by improving balun function.

Comments by a prominent figure in our hobby ....."and the thing is 'ugly to the core'. Way to go."

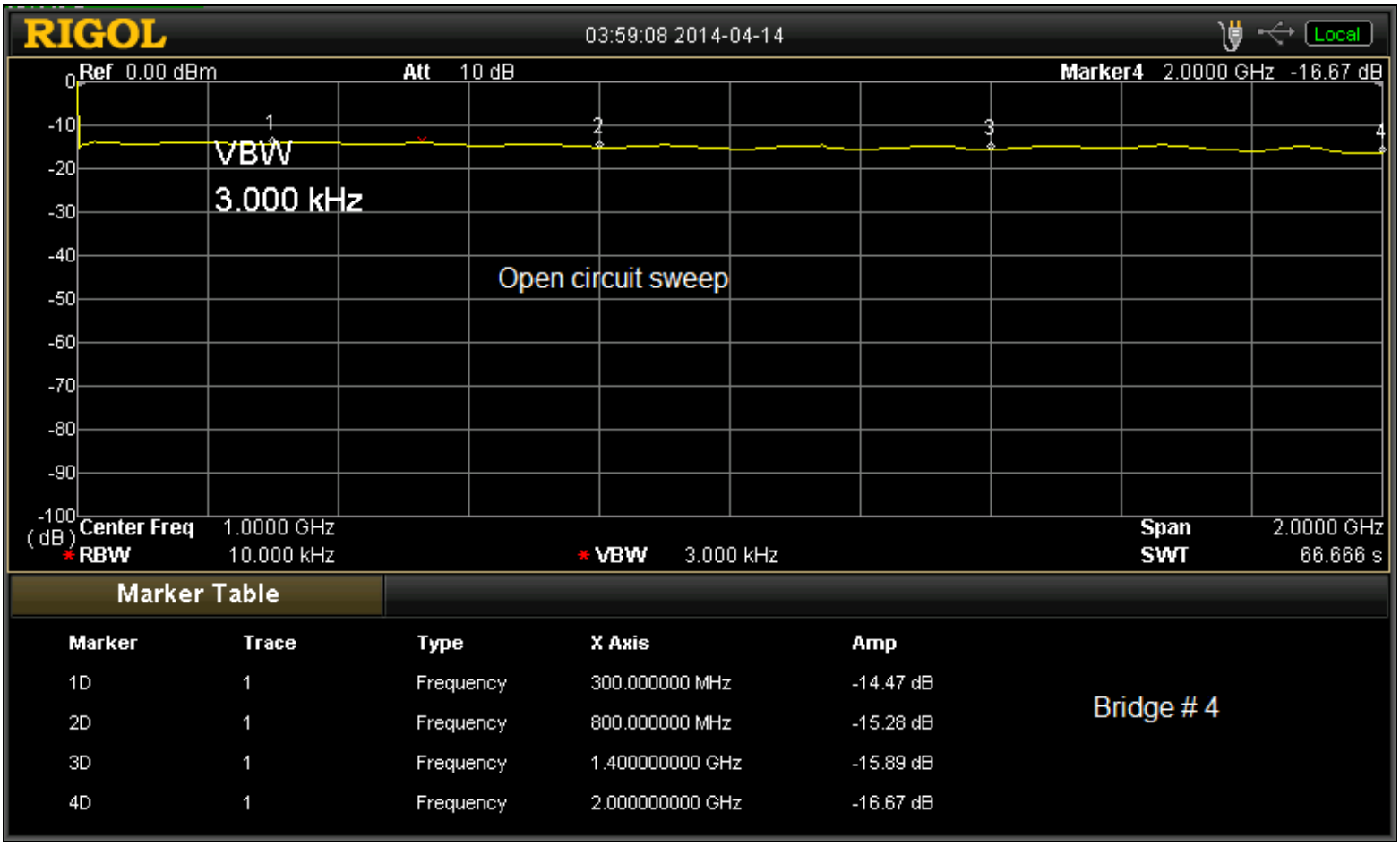

Above — Open circuit sweep with a 2 GHz span and center frequency of 1 GHz.

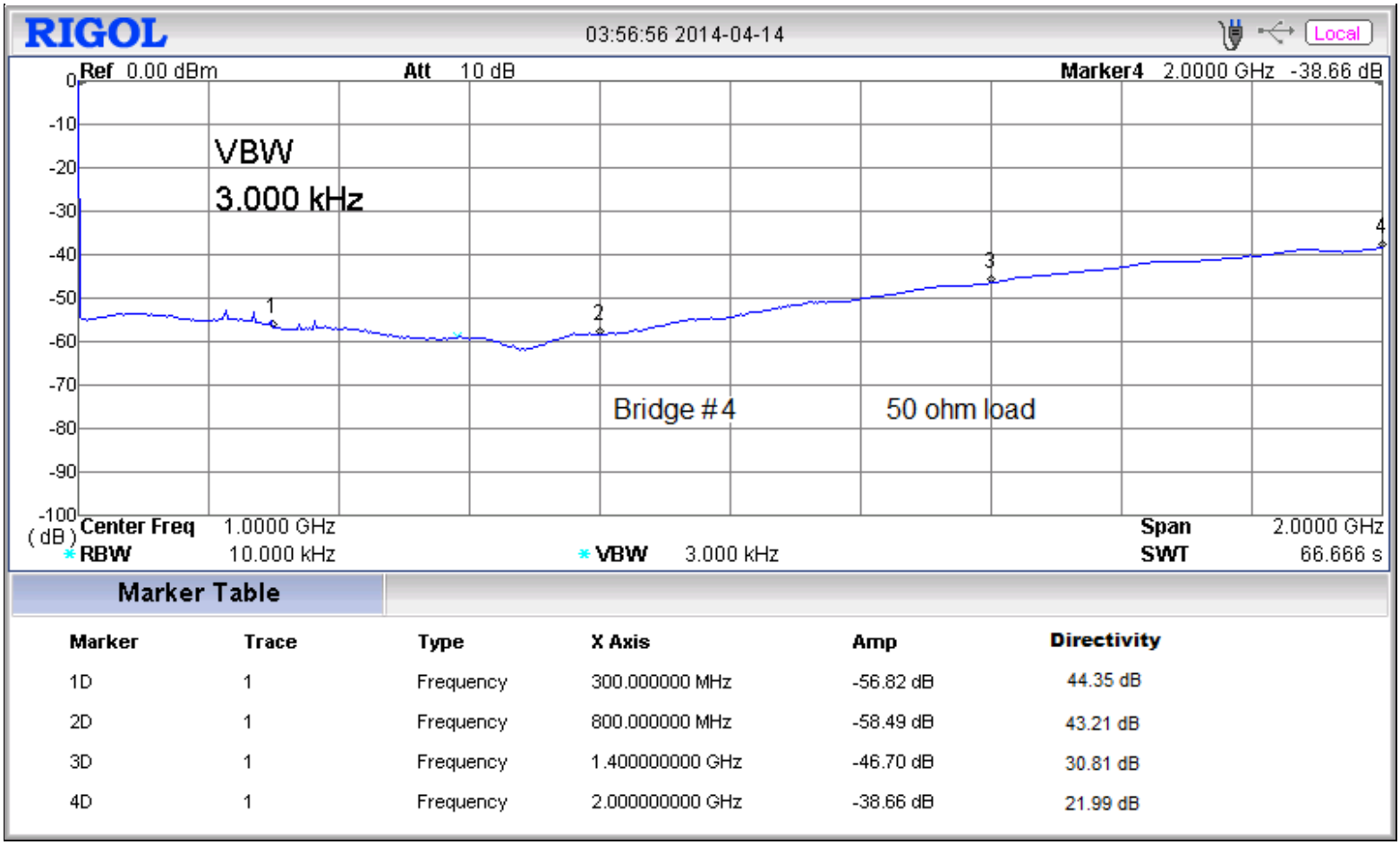

Above — Sweep with a 50 Ω load threaded on the unknown impedance port and 4 markers showing directivity at those 4 frequencies. Yay — this is much better! I wanted at least 30 dB directivity at 1296 MHz and got it.

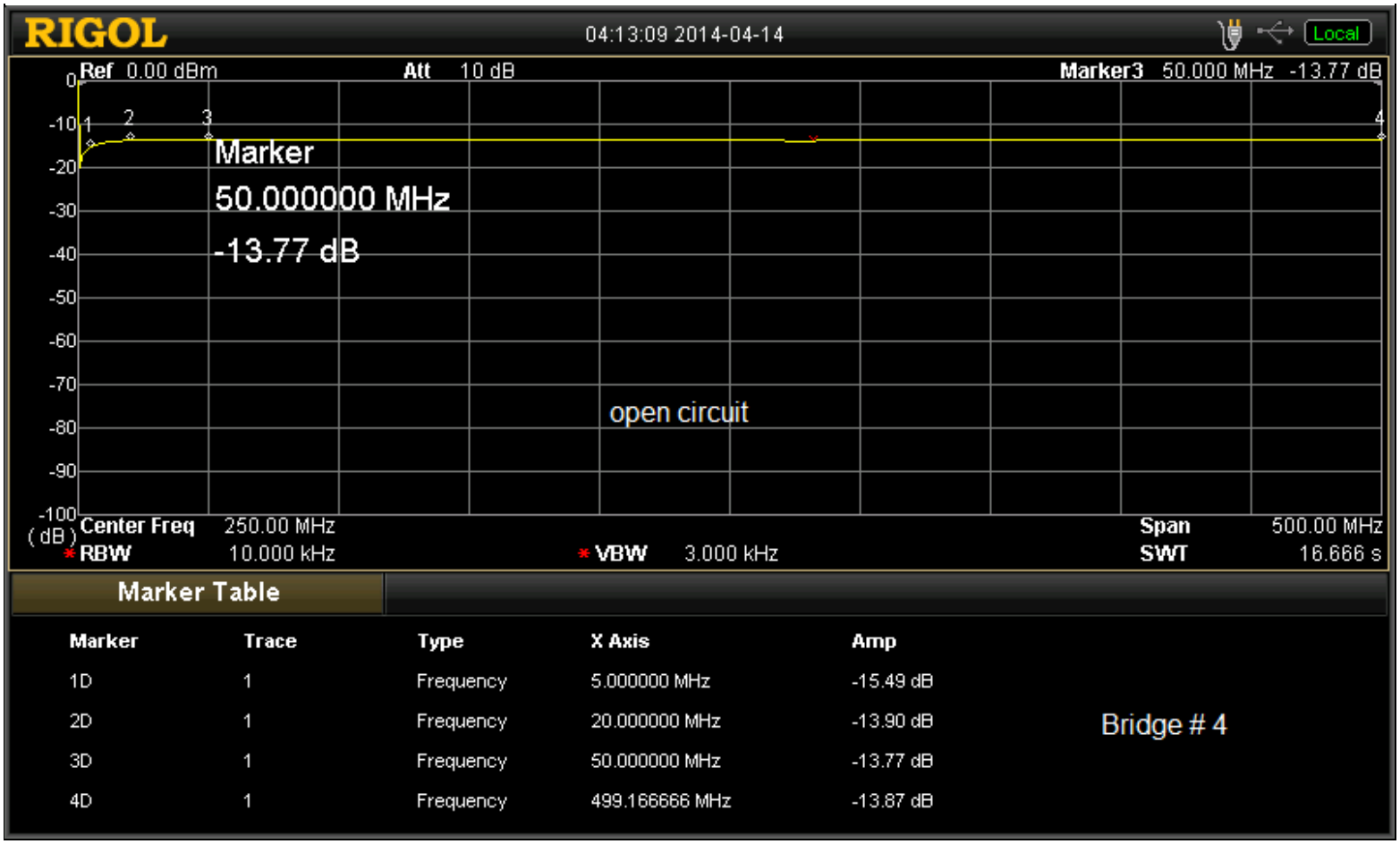

Above — Open circuit sweep with a 500 MHz span and center frequency of 250 MHz. I set 2 of the markers to evaluate the directivity at HF.

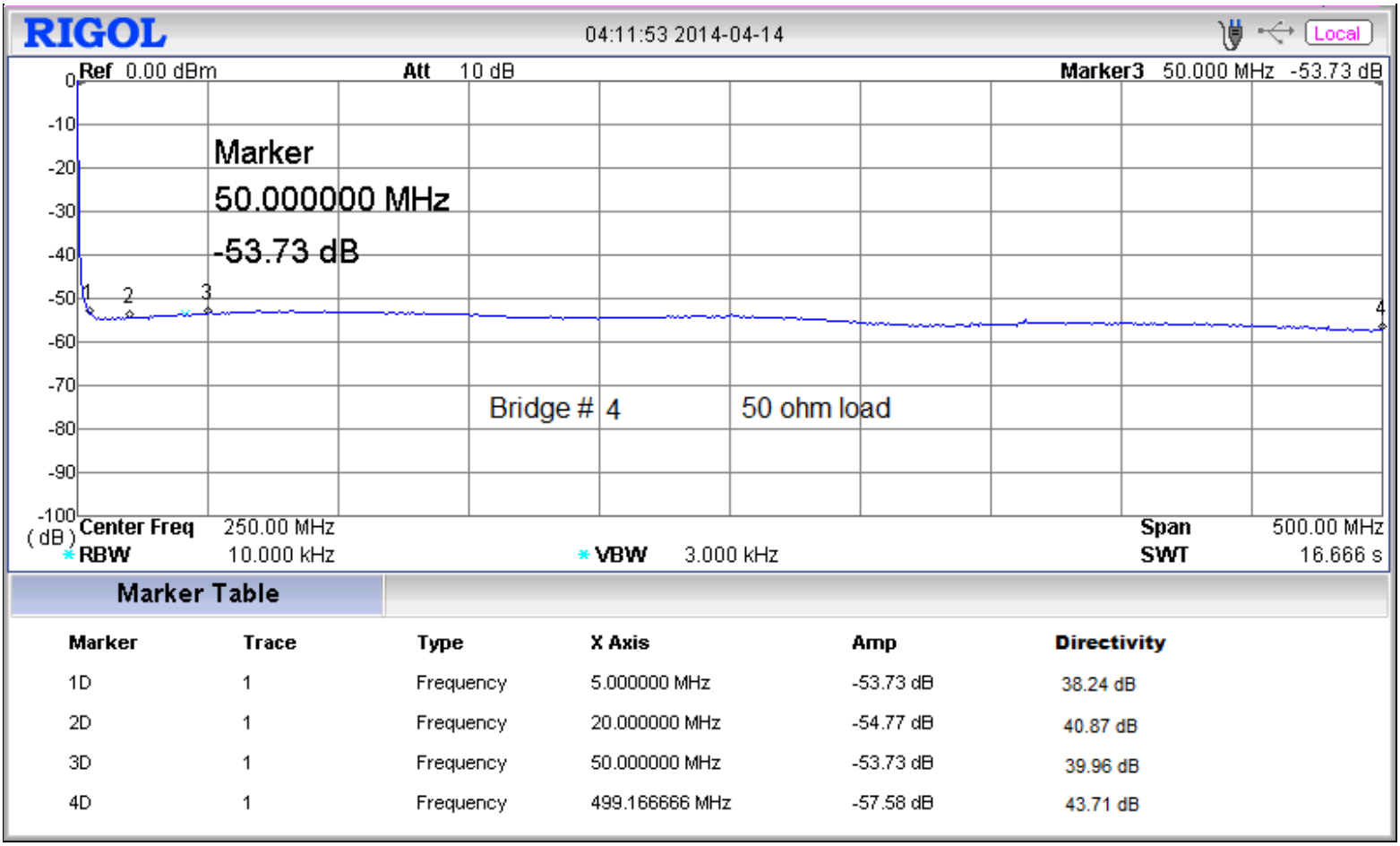

Above — 500 MHz sweep of Bridge #4 with a 50 load on the unknown impedance port. The directivity at HF surprised me. Although better suited for VHF-UHF, this bridge will work okay from 5 MHz to ~1.5 GHz.

---

4. VCO Experiments

Ask experimenters about homebrew RF oscillators and you might hear about a pleasing paradox — vexing and satisfying in the same breath! At UHF we usually make a VCO and keep it on frequency by phase/frequency locking to a xtal oscillator reference. I sought some wideband, free running VCOs in hopes I'd inch up the learning curve.

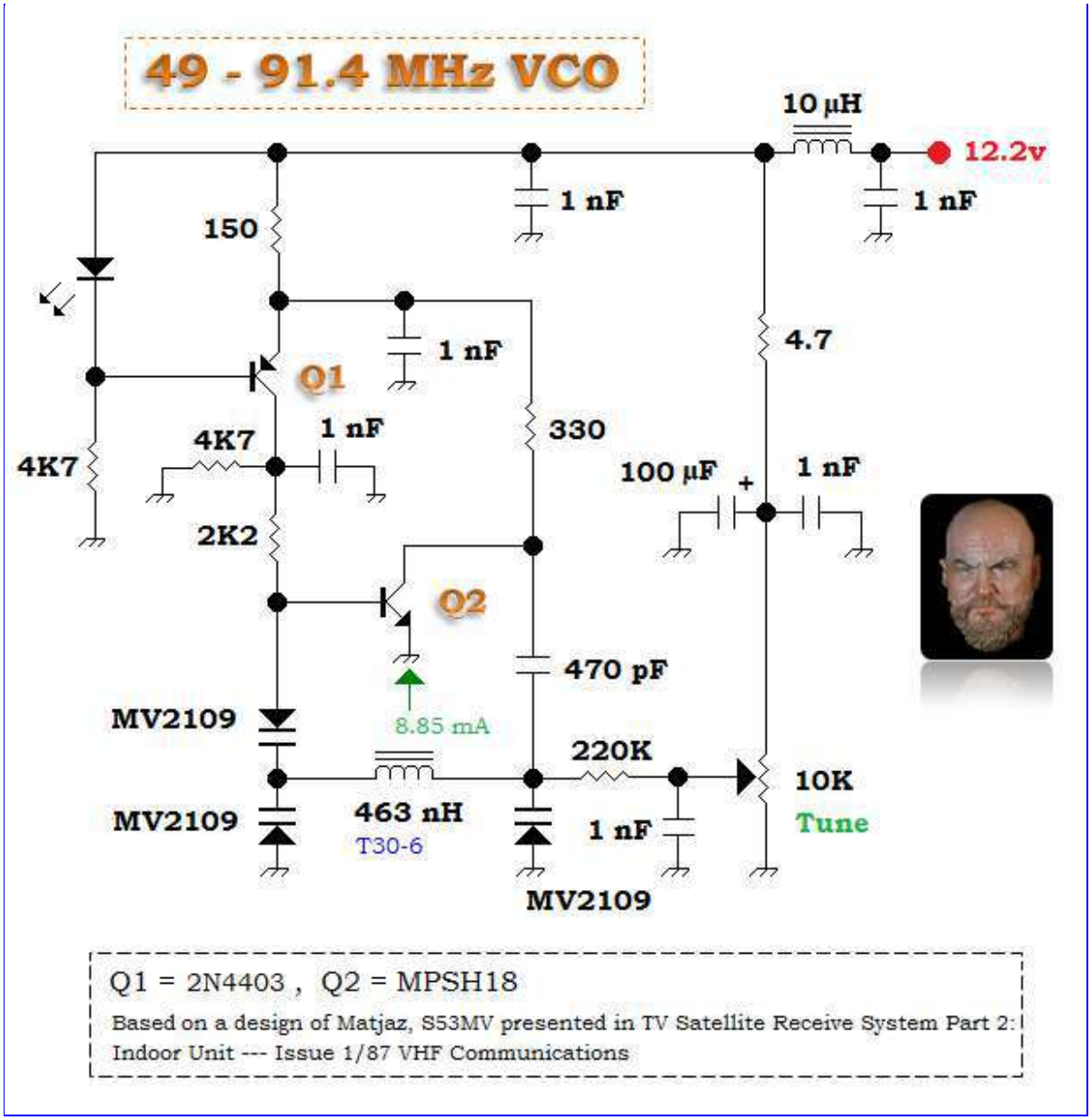

Above — My first attempt at a VCO circuit described by Matjaž, S53MV in a 2-part article published in VHF Communications magazine. The original circuit contained a tunable RF filter, mixer, buffer amplifer + more and I recommend you purchase the 2 articles for your own analysis. Shown with permission from Andy Barter of VHF Communications magazine, I ordered all issues from the 1980s which came on this DVD.

With 28v varactors, this VCO will tune 1 octave minimum.

To bench investigate this stunning common emitter Colpitts variant, I first built it at VHF using through-hole parts with a standard 12 volt tuning voltage that tuned from 49 to 91.4 MHz. The output came from 1 link around the 463 nH inductor terminated in a 1K resistor at the hot end + ground at the cold end to allow 10X probe measurement with my DSO.

Matjaž, S53MV describes his circuit function here. A variable C on the base in combination with the input capacitance of Q2 operates as a tuned impedance matching network and preserves a steep phase slope (which means you have higher Q) — a requirement for low phase noise. In essence, the inductor with a varactor at each end forms an adjustable pi-network to provide correct phase shift tracking.

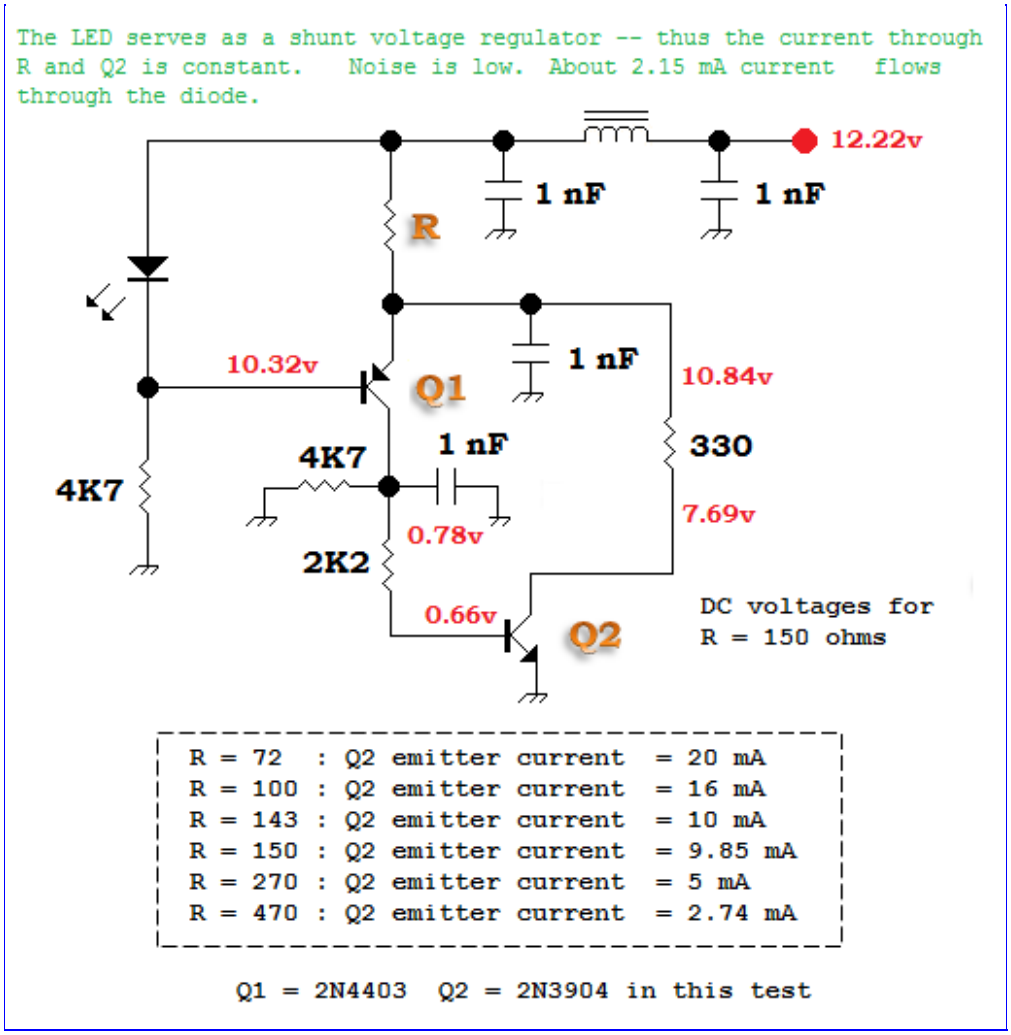

Above — I built the low-noise, temperature-stable, PNP current source using though-hole parts. R provides a convenient way to vary collector current, although changing the PNP base bias also works.

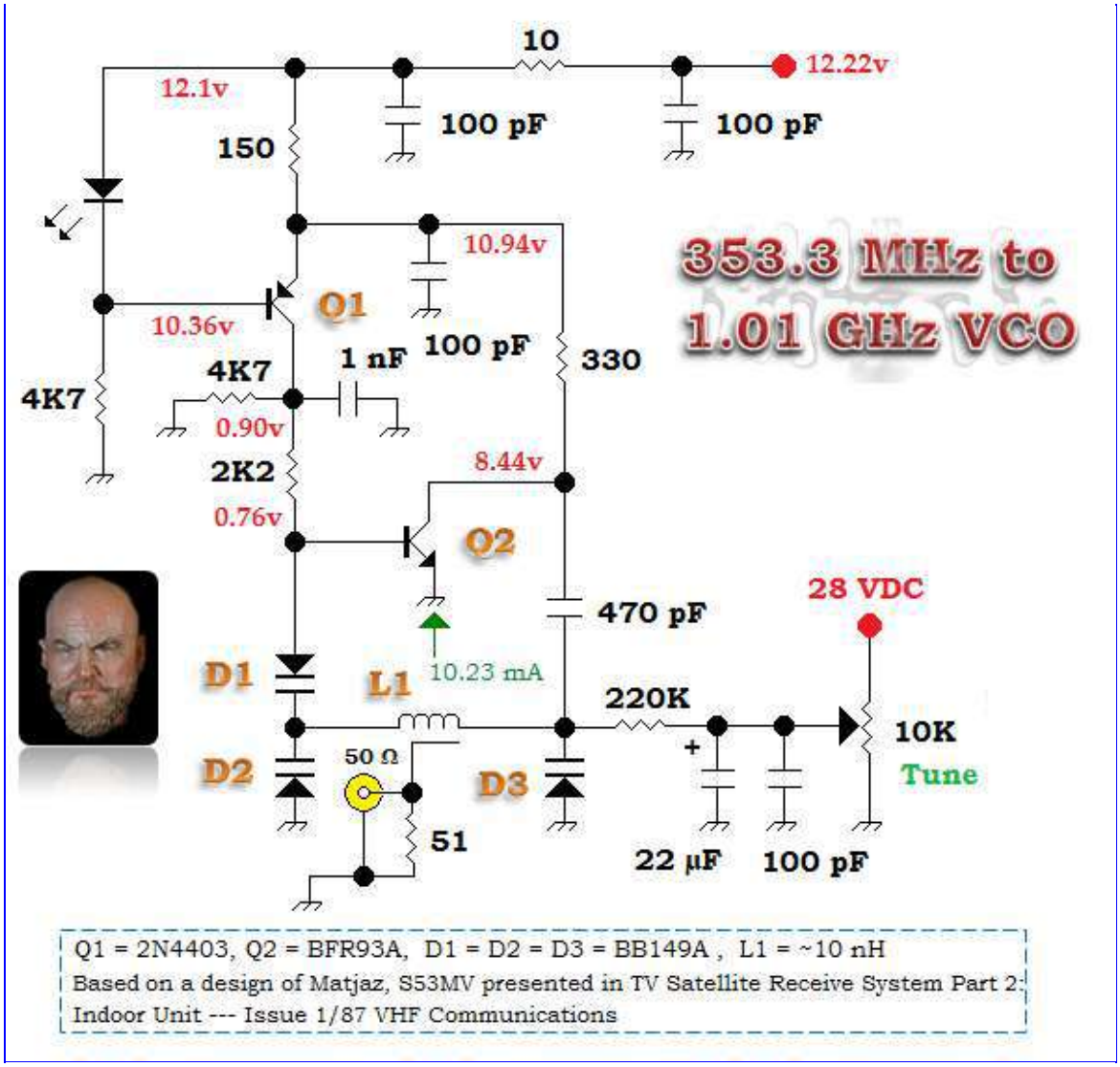

Above — My UHF VCO schematic. Click for the breadboard photo. A wire positioned near L1 provided the output into my spectrum analyzer. Click for a sweep with the reverse DC voltage set at 0v. Click for the a sweep with the tuning at 28v to establish the lowest possible varactor capacitance. Markers indicate the carrier frequency. As shown, a common emitter VCO exhibits rich harmonic energy and viewing the second harmonic at 2 GHz felt really cool in the 28v sweep. Not to worry — the tracking generator in the Rigol TG + SA units also exhibit strong harmonics and work fine for sweeping.

Click for a pdf file showing how I laid out my board. I cut traces on the top of 2-sided FR4 board and connected any grounded points on top to the bottom ground plane with a 24 gauge copper via wire. A 28v DC-DC Converter to supply the varactors lies on VHF-FM.

I varied L and even tried a 3 mm by 8 mm copper sheet metal inductor but this failed to oscillate. In the end, a single wire with ~10 nH inductance worked to give me the tuning span shown. L1's distance above the ground plane was determined by tuning the VCO for the smoothest transistion across its range. This circuit begs further experiments including Q2 current, L1 and the 470 pF fixed feedback capacitor.

---

5. Frequency Counter Kit

A sensitive UHF bandwidth frequency counter makes an important tool for the UHF homebrew experimenter. With a search engine, you'll find commercial and kit counters for sale along with DIY projects for builders handy with microcontrollers.

If you already own a decent counter, then a crude prescaler tool employing an IC like the MC12079 might work okay if you can tolerate or manage modulus division by 64, 128, or 256. The MC12079 requires an RF signal between -17 dBm to +3 dBm to count properly, so many builders place amplifier(s) along with anti-parallel clamping diodes before the digital IC. The Motorola datasheet shows a basic circuit to build off.

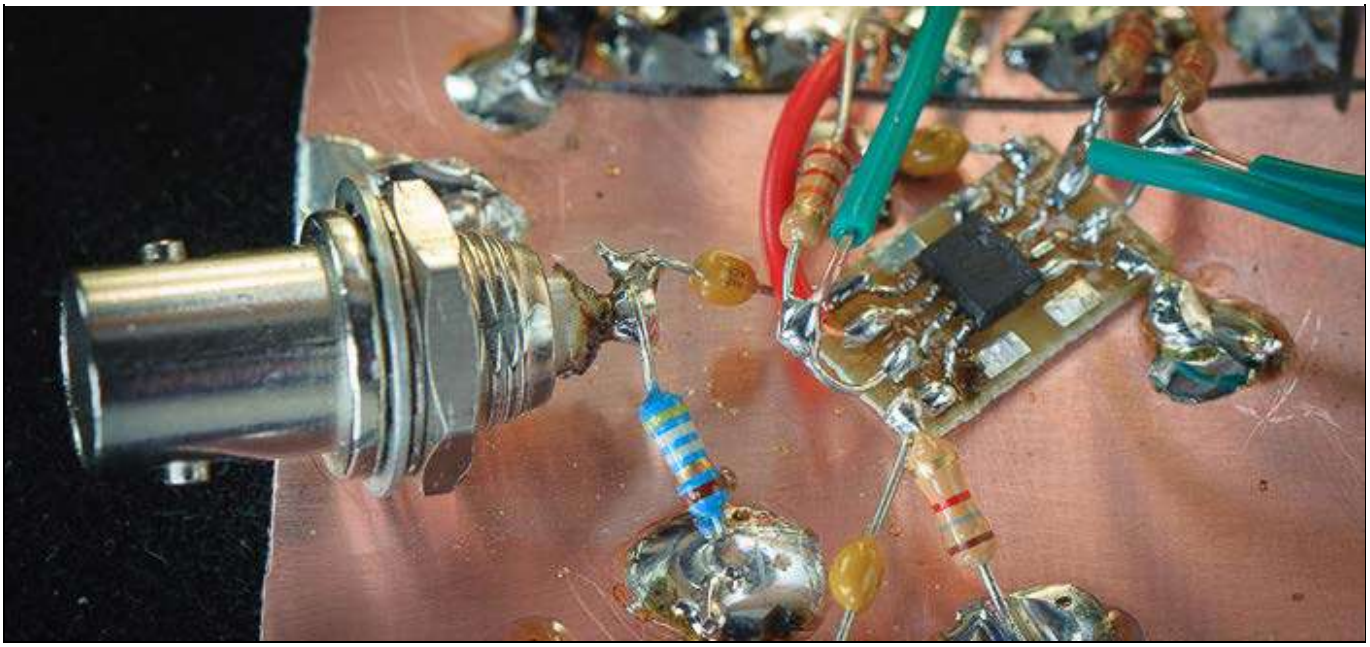

Above — My first UHF counter experiment involved the Motorola MC12079 and 12080 prescalers. Eventually I made a proper double-sided copper board device with anti-parallel diodes, a MMIC, the MC12079 and some 74AC series logic — it worked okay for casual use. The 2 big drawbacks were MC12079 self-oscillation with 0 applied input signal and having to remember to multiply measures by my set prescaler division integer. I sought a long-term solution.

A Solution Appears

In 2012 I bought a second-hand, calibrated HP 53131A with the optional A6 High Stability Timebase from an EE for ½ the going price at the time. 225 MHz bandwidth poses its only limitation; it even came with the original spiral bound manual.

This summer, Shahriar from TheSignalPath.com reviewed a Chinese kit to take the HP 53131A to 3 GHz with a clone of the original HP OPT30 Channel 2 kit. Based on his quantitative review and warm thoughts of using my sturdy HP counter at UHF, I got 1. Mine sold on eBay for $87 Canadian including shipping. Click for TheSignalPath.com video. Click for a larger photo of the kit I bought.

Above — My HP counter with the kit installed as Channel 2.

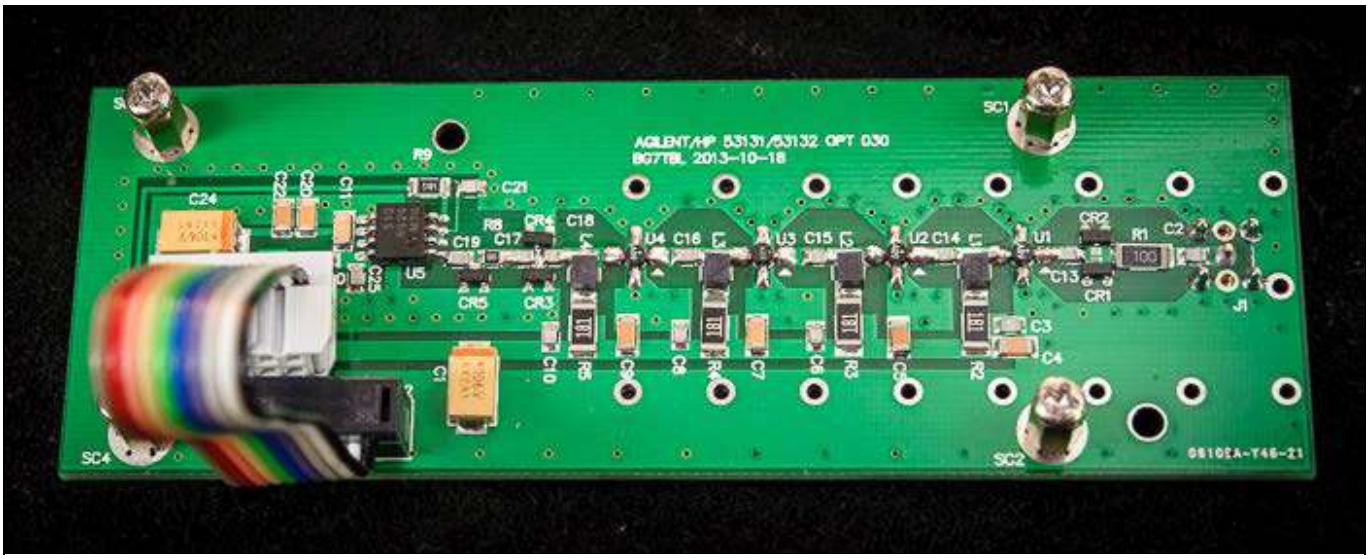

Above — Top of the circuit board. Anti-parallel diodes, 4 MMICS, passives and then even more anti-parallel diodes go before the prescaler chip.

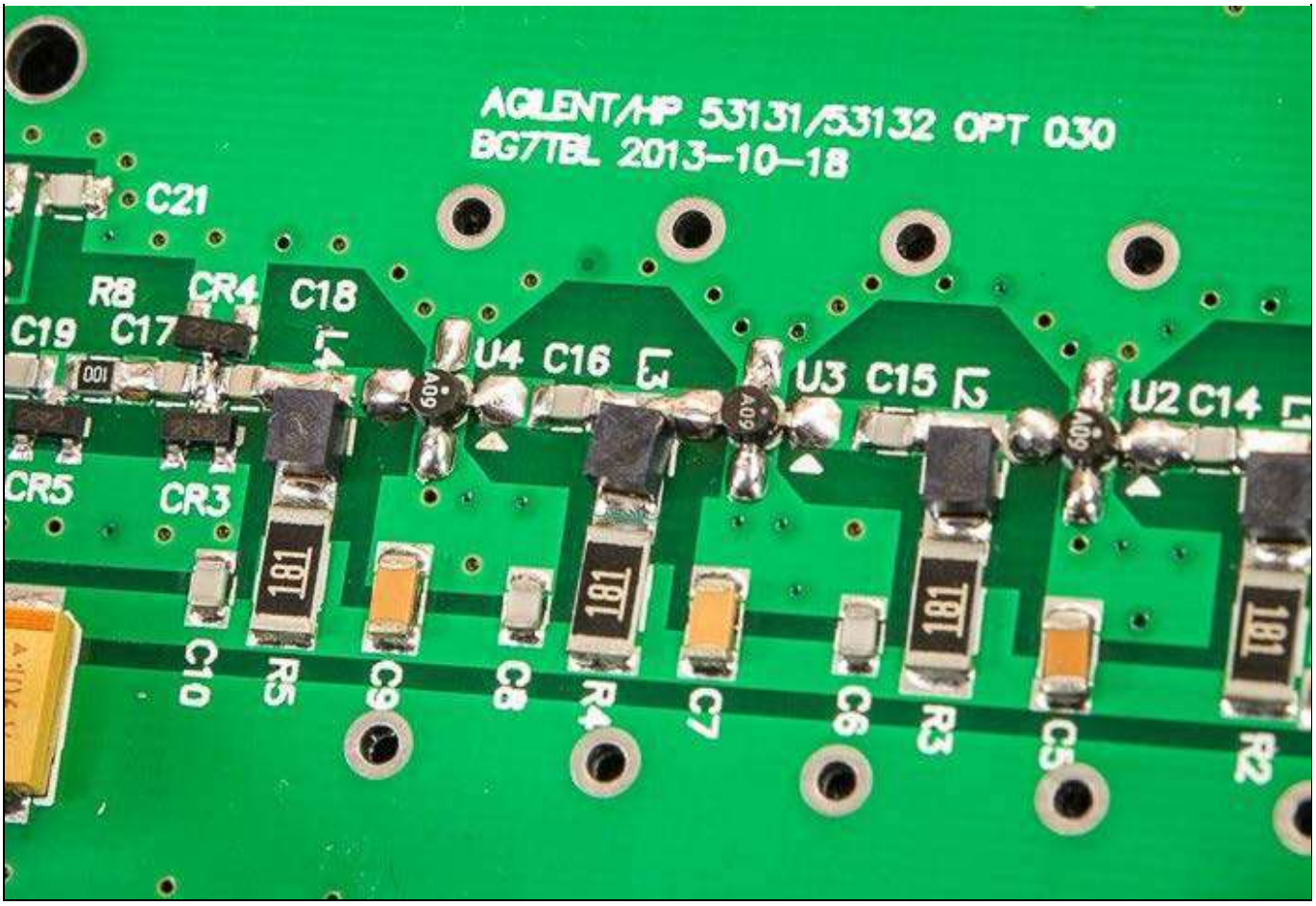

Above — Close up of SMD circuitry.

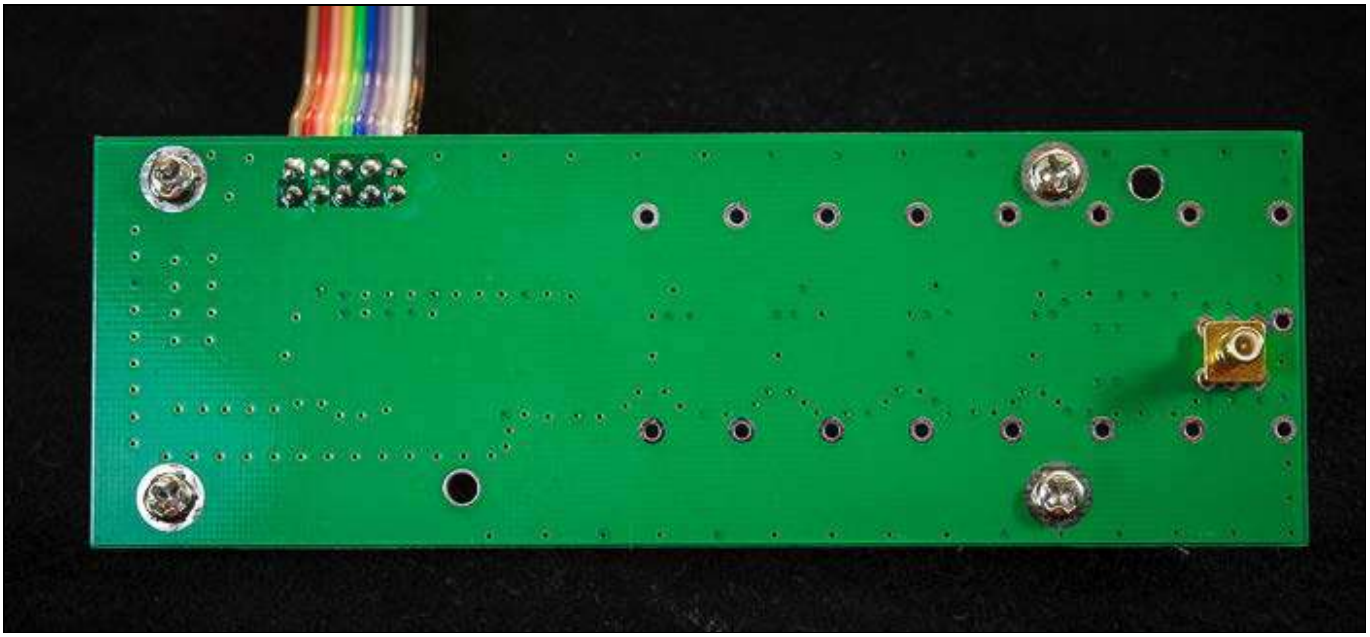

Above — Rear view of the circuit board showing stiching vias that join the top ground plane to the bottom ground plane along the signal path. My tests showed that it works okay to 3.1 GHz. Click for a picture of the installed board. I'm very happy with my HP counter's boosted bandwidth.

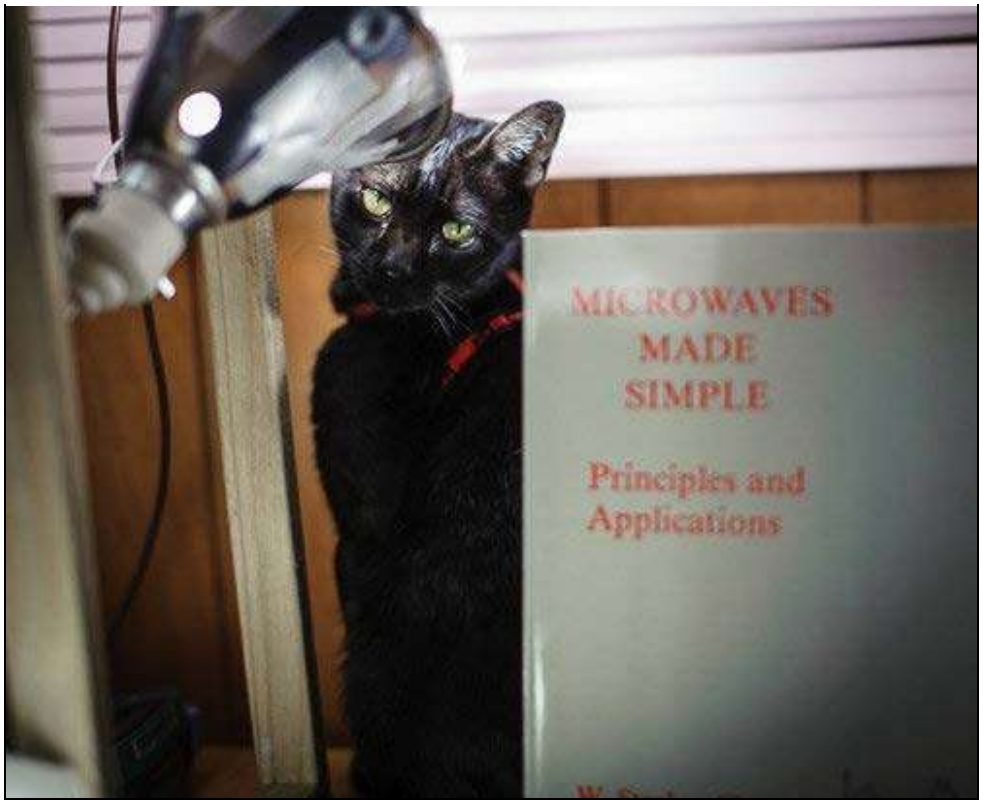
MICROWAVES
MADE
SIMPLE
Principles and
Applications

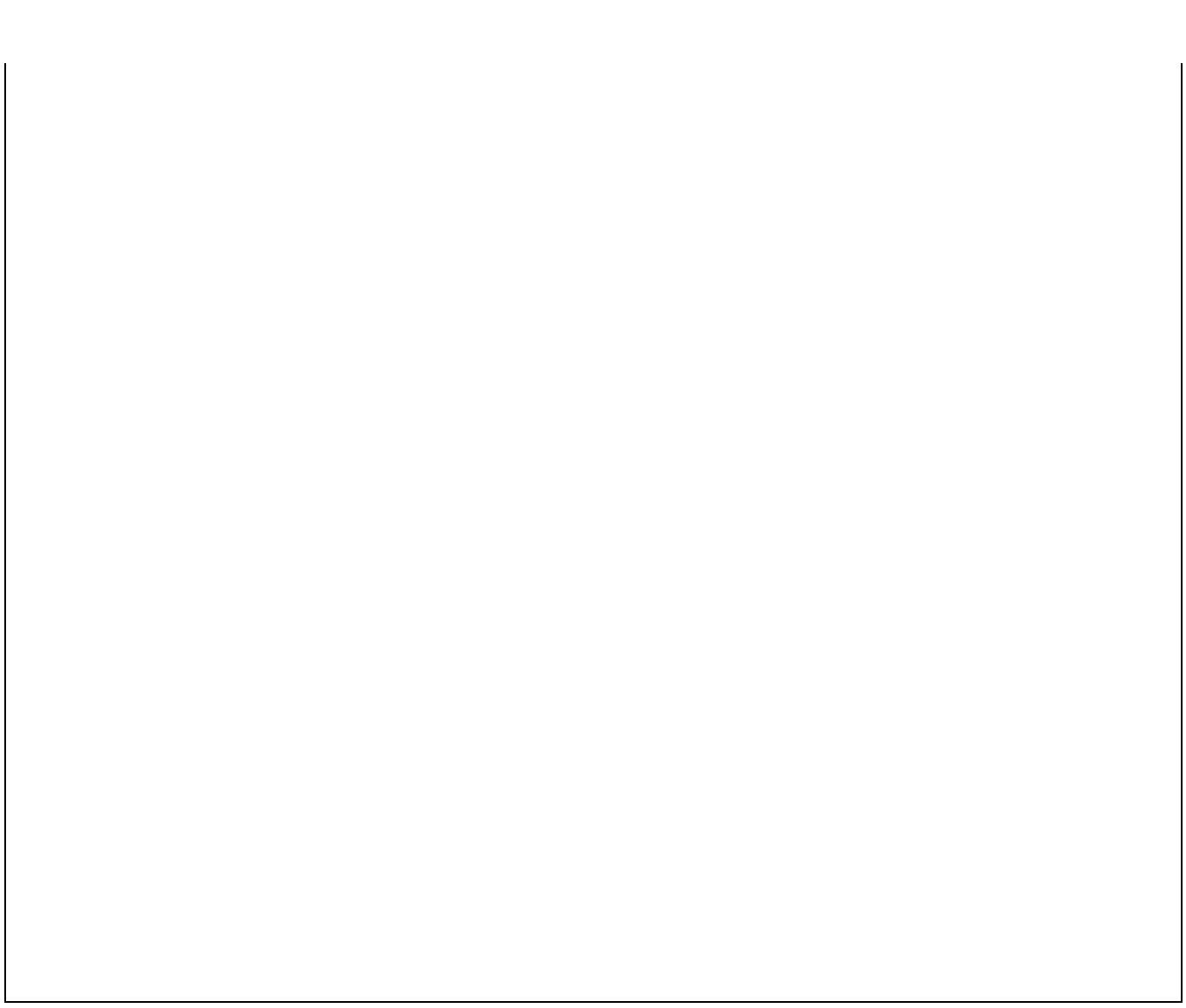

Funster Line — Transmitter

Menu Item 4 on the HF Embarcadero web page. Click here to go back.

The receiver will go on its own page and hopefully I'll complete and write it up this Fall.

1. Transmitter
2. References

Introduction

I began the Funster transceiver line in 1995 and show the 2014 version [now back to a CW trans-receiver on the 40M band]. Judging by reader feedback, plus analog scratch-homebrew threads in social networks, email lists and print, many of us feel a nostalgic pull towards old-school radio. Me too.

Now at version 8 — Funster shares my joy in making a simple, old-style radio with all discrete parts. In some ways, this radio set is a twisted version of Wes and Roger's Ugly Weekender from QST for August 1981.

1. Transmitter

Summary

Variable power: 128 to 3312 mW @ 13.6 VDC. Switchable 7.04 MHz xtal oscillator or external VFO input port. Solid state transmit/receive [T/R] circuit with PIN diode. External continuous and switched 12 VDC power jacks. Single-ended BJT Class C power amplifier with 67% efficiency.

Note: I state 12 VDC in my DC circuits, however, this nominal value might better be termed 12 -13.6 VDC.

Key up power current draw @ 13.6 VDC = 17 mA. Key down current @ 3W RF power with 13.6 VDC = 420 mA.

DC Circuitry

It's fun to march off the signal path and focus on DC circuitry — switching, regulating and filtering the DC voltage feeding our RF or AF stages with finesse. Trans-receivers contain DC, RF, AF and external patch cords that benefit from mindful DC line filtering + selective high-isolation amps in the signal path to prevent RF flowing where it's unwanted. You'll see heaps of decoupling with RF + AF bypass and a few strong

reverse-isolation amplifers in this radio set.

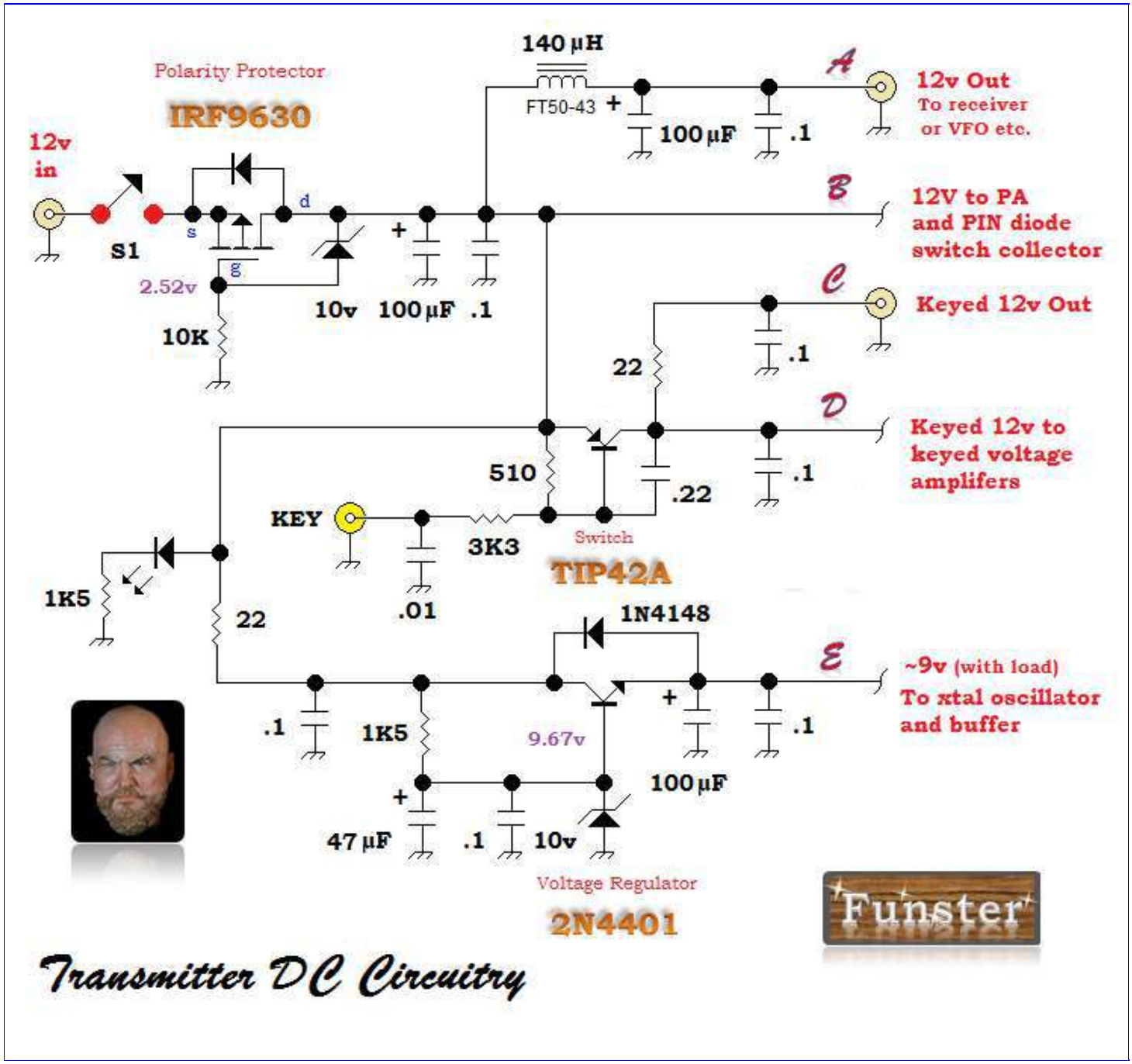

Above — The DC circuit board. Click for the breadboard photo. A reader sent me 2 IRF9630 power MOSFETS: avoiding the voltage drop of the usual single rectifier diode, I employed 1 as a reverse polarity protector. Another reader sent me a long strip of 2N4401 BJTs, so I ran them instead of the equally good 2N3904. Thanks for the parts guys!

A simple series voltage regulator with a zener diode reference supplies DC to the crystal oscillator and its buffer. The base-emitter voltage drop of the 2N4401 emitter follower lays in series with the load, so load current changes alter the regulator output voltage. Vout = Vzener - VBE : so the regulated voltage is roughly 9 VDC.

Oscillator Circuitry

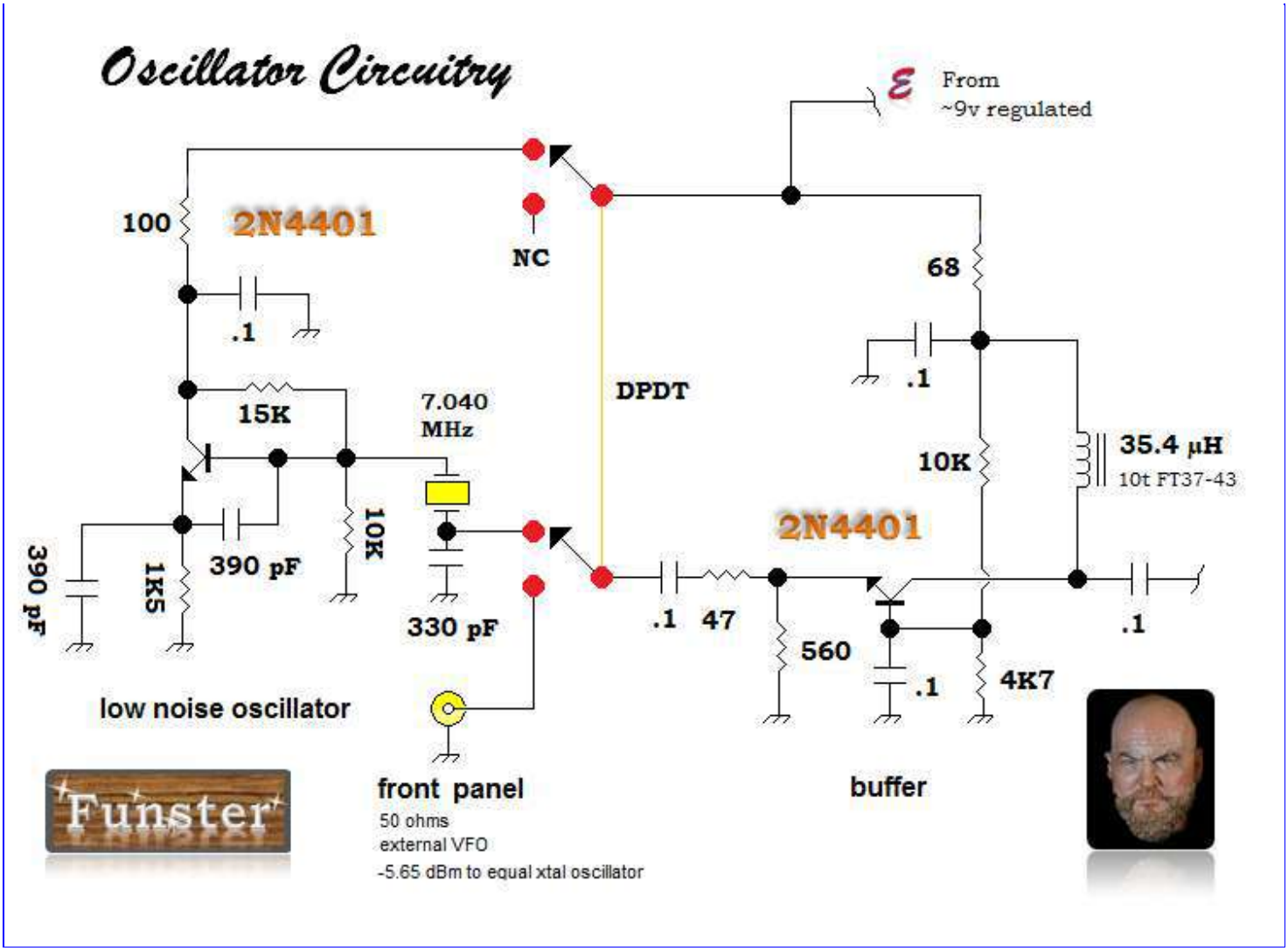

Above — Oscillator circuitry. I soldered my oscillator circuitry on the DC control board. Click for the breadboard. Click for a close-up of the old NorCal crystal supplied by NT7S — thanks Jason! To equilibrate to the xtal oscillator AC output voltage, the VFO input port should run about -5.65 dBm. I might stick a 6 dB attenuator pad on the front panel switch and use a 7 MHz VFO with 0 dBm output power.

Keyed Voltage Amps

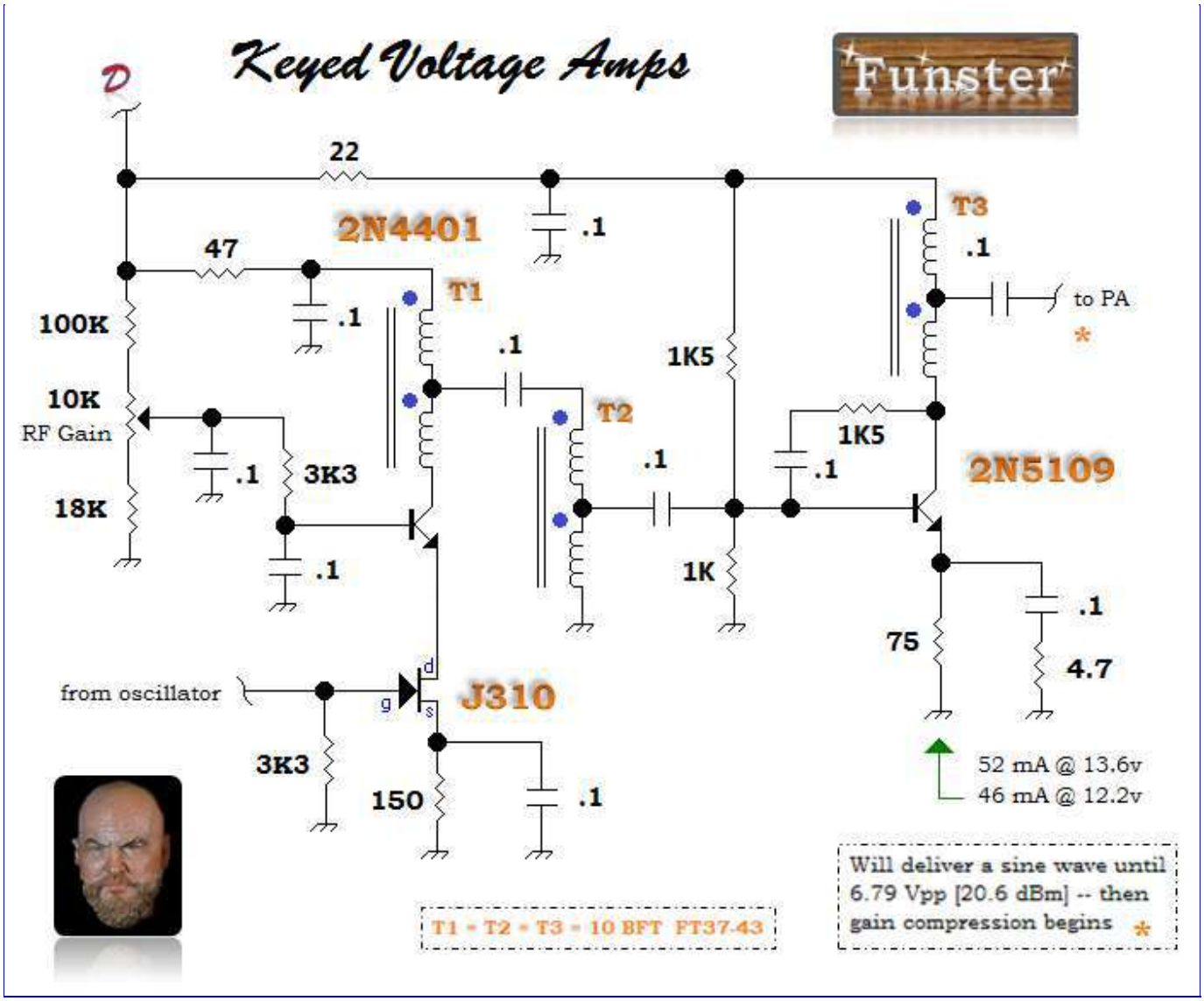

Above — The 2 keyed voltage amplifers. Click for a breadboard photograph. I set the value of the RF gain pot series resistors by placing a 100K pot before and after the 10K gain pot and tweaked them back and forth to find close to 3W maximum and 125 mW minimum RF power with the gain pot set @ CW and CCW respectively. The 100K pots were removed, measured and nearest standard value resistors substituted: 100K and 18K.

By carefully choosing the 75 Ω emitter resistor, the 2N5109 feedback amp output remains a sine wave at the drive levels needed for a PA output at 3 Watts. At 3 Watts PA output, the feedback amp output voltage = 5.91 volts pk-pk [19.4 dBm]. The emitter current shown will cleanly drive a PA for more power if desired. Boost it as needed.

Power Transistor and T/R Switching

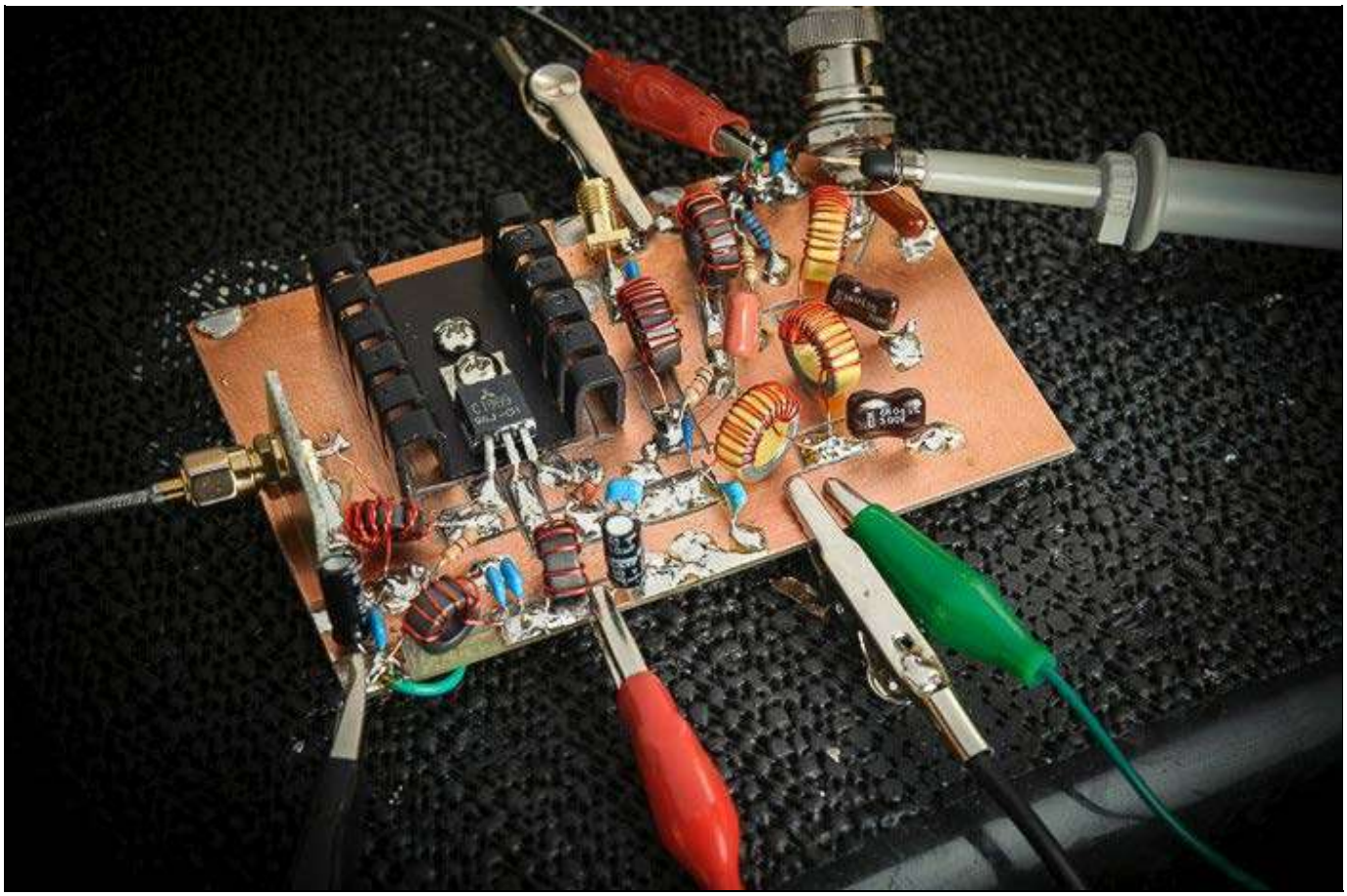

Above — Final testing the PA and T/R circuitry before installing it into the Hammond chassis. Click for a bigger photo of my test setup.

Three temporary RF connectors were soldered on this board for bench measurement. I connected the (SMA) receiver port to Channel 1 of my 50 Ω terminated 'scope to measure the RF not getting shunted to ground by the PIN diode. The SMA cable/connector to the far left is a temporary cable connected to the keyed voltage amp board output in the Tx chassis — thus I tested the PA stage with its own xtal oscillator and RF amplifers. The right-sided BNC RF port connects the PA low-pass filter to a 10W, 50 Ω dummy load via a 22 cm 50 Ω patch cable.

Further, I measured collector voltage + collector current with 2 DVMs and also PA output power in my oscillocope (DSO) Channel 2 with a 10X probe employing a tiny ground lead.

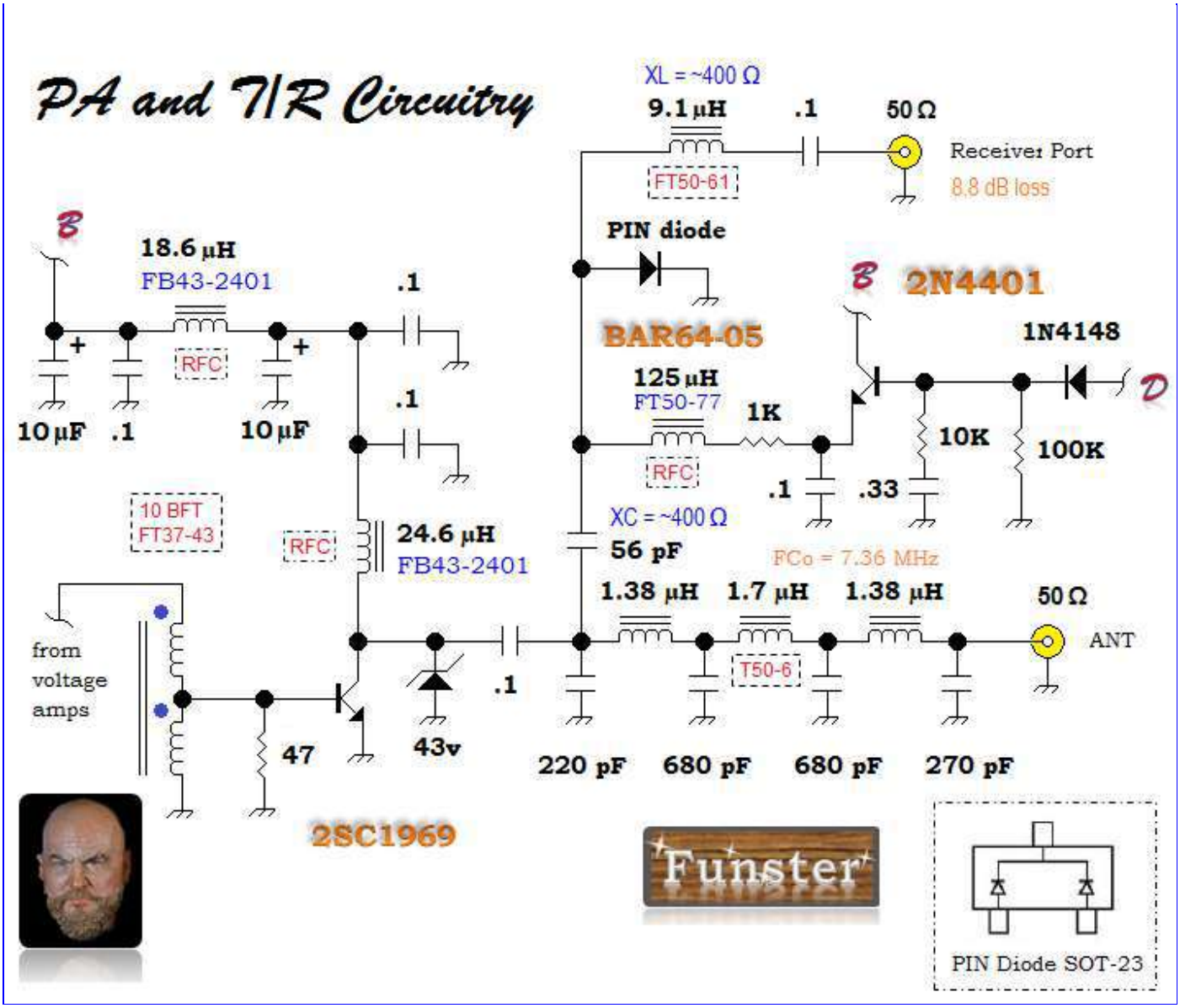

Above — PA and T/R circuitry schematic. Click for another breadboard photograph taken before the 2N4401 switch was added. Although we might run a BD139 or other cheap BJT for the final, I chose my favorite HF classic, the 2SC1969. This transistor will survive a high VSWR, however a 43 volt - 500 mW zener diode further protects it from such.

In 1 version with a 1:4 Z collector matching network and no zener diode, I measured 6.25W RF power after tweaking the 100K and 18K RF gain limiting resistors in the preceeding hycas voltage amp to drive the PA harder. At ~3W maximum power in my final experiment, the 2SC1969 barely warms up.

Collector Matching

After a number of experiments, I learned that from tens of mW up to ~ 3.3 Watts RF power, we may omit collector matching and still get reasonable efficiency if you run a collector choke >= 15 µH. Thus, I made the maximum power ~ close to 3W — easy peasy.

Ask QRP enthusiasts what QRP is all about and they might extol the thrill of exacting the most kilometers per Watt — in keeping with that spirit, I love turning down my Tx power and the Funster front panel RF gain control makes it a breeze.

The PA circuit is standard fodder. I wound the 24.6 µH and 18.6 µH RFCs on FB43-2401 ferrites [a single hole bead that looks like a fat FT37-43]. An FT37-43 or FT50-43 makes a great substitute.

PA Measures

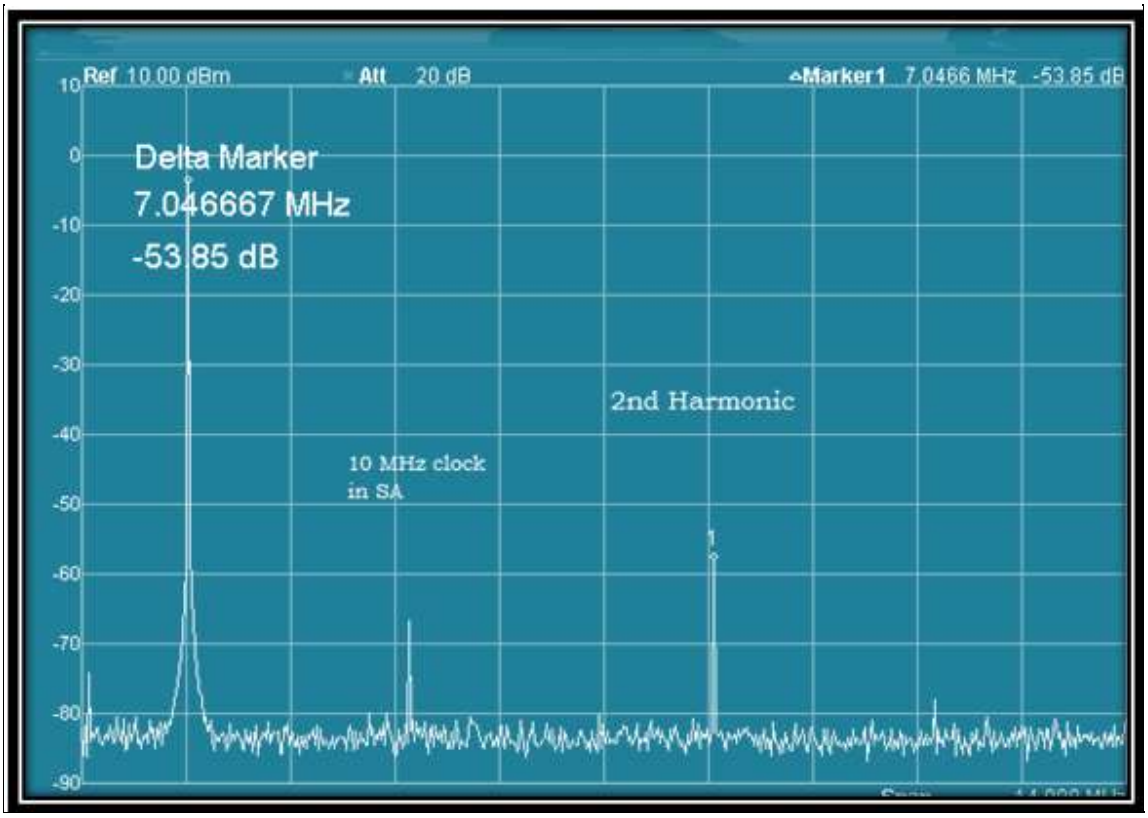

Above — Spectrum analysis of the Tx output. The 10 MHz clock signal from my spectrum analyzer lays between the fundamental and 2nd harmonic. The 2nd harmonic = -53.85 dBc @ 3W power output.

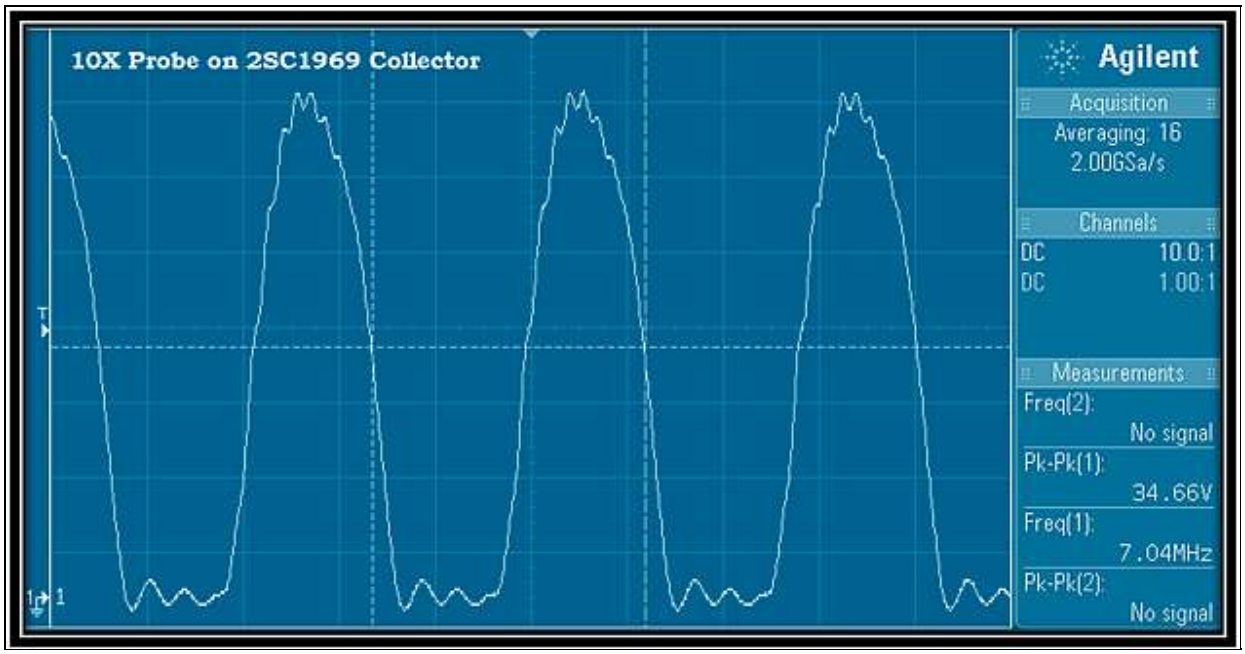

Above — PA collector waveform at 3W output measured with my DSO's 10X probe.

Above — Set your meters on stun! DC measures to calculate PA efficiency [See RF Workbench 6]: DC power = 13.58V x 0.331A = 4.49W. RF power = 3W. Efficiency = RF power / DC power = 3W / 4.49W = 66.8%.

T/R Discussion for Single Band Transceivers

Previous Funsters ran a simple QSK T/R circuit developed by Wes, W7ZOI in the early 1980s: a series X = 500 Ω resonator with anti-parallel diodes between the L and C. The series capacitor presents 500 Ω reactance to the 50 Ω transmit line so that only a small portion of the transmitter power flows to ground via the diodes and even less reaches the receiver input. In short, the 500 Ω capacitive reactance + clamping action of the anti-parallel diodes protect the receiver front end.

For 1 band, this simple circuit sizzles. Two potential concerns:

~6-9 dB loss of the receive signal making it better for lower HF, although I've seen builders add a receive preamp and use this T/R system on 12 and 10 meters. Since both band noise and signals get attenuated simultaneously, I've rarely had readability issues on 160-30 meters in my popcorn transceivers.

The anti-parallel diodes may cause IMD. The intercept for the 500 Ohm series reactances with shunt diodes is around +6 or +7 dBm. This might exert problems in a high performance receiver front end, but poses a non-issue with typical NE612 front ends. Many builders, including Wes, reduce IMD potential with 2 or 3 series diodes on each leg. Another solution includes running a PIN diode as the shunt element. That's what I did.

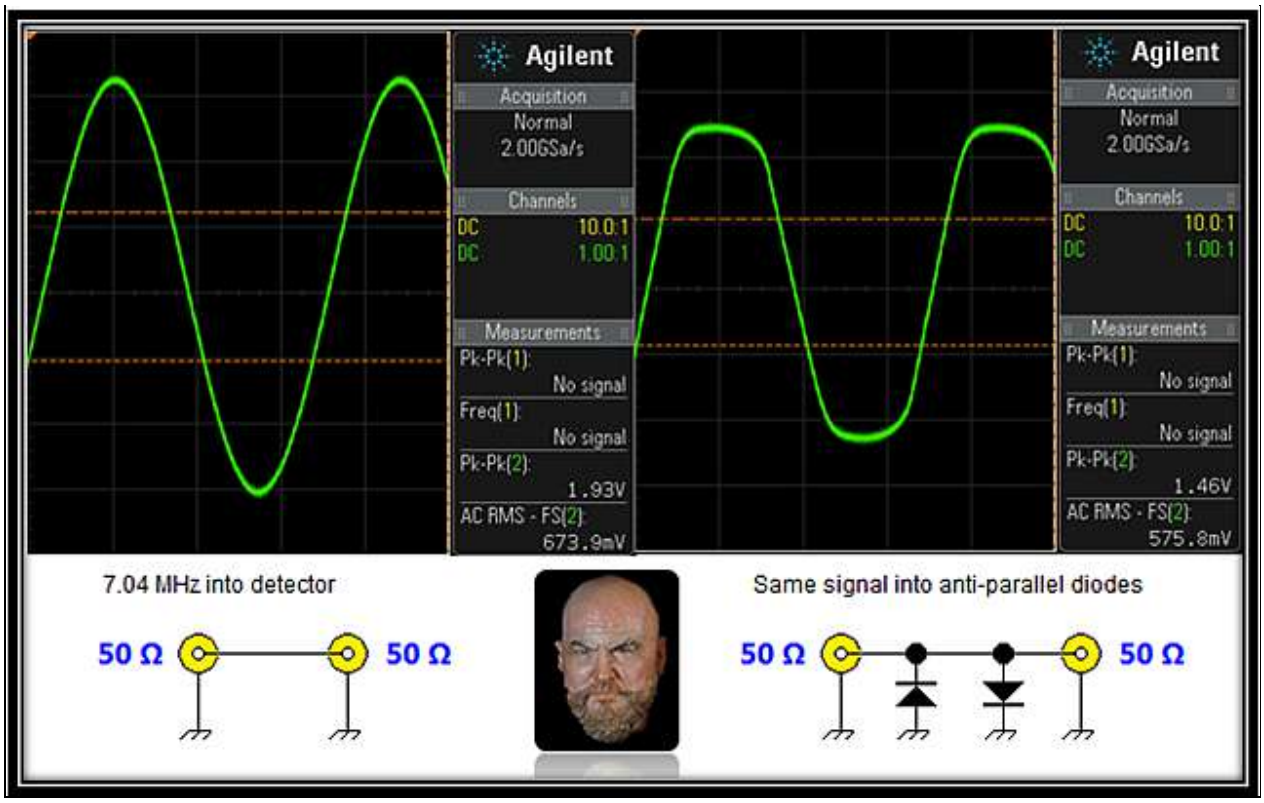

Above — The DSO tracing of an experiment showing the before and after effect of 2 anti-parallel diodes. The voltage across a silicon diode varies with the current going through it. Silicon diodes don't conduct much current until the voltage across them reaches a threshold [typically ~0.6 to 0.7 volts].

In situ, the forward threshold voltage of each diode limits the circuit voltage by clipping off AC voltage above its threshold. Clamping refers to the limiting of voltage in *2* directions using anti-parallel pair(s) of clipping diodes. For example, if a negative-going AC dips more than 1 diode drop below ground, the left hand diode will begin to conduct and clip off any voltage above its threshold. This, of course, describes the "ideal diode" — in real life, factors like switching speed, current-handling and temperature are all in play.

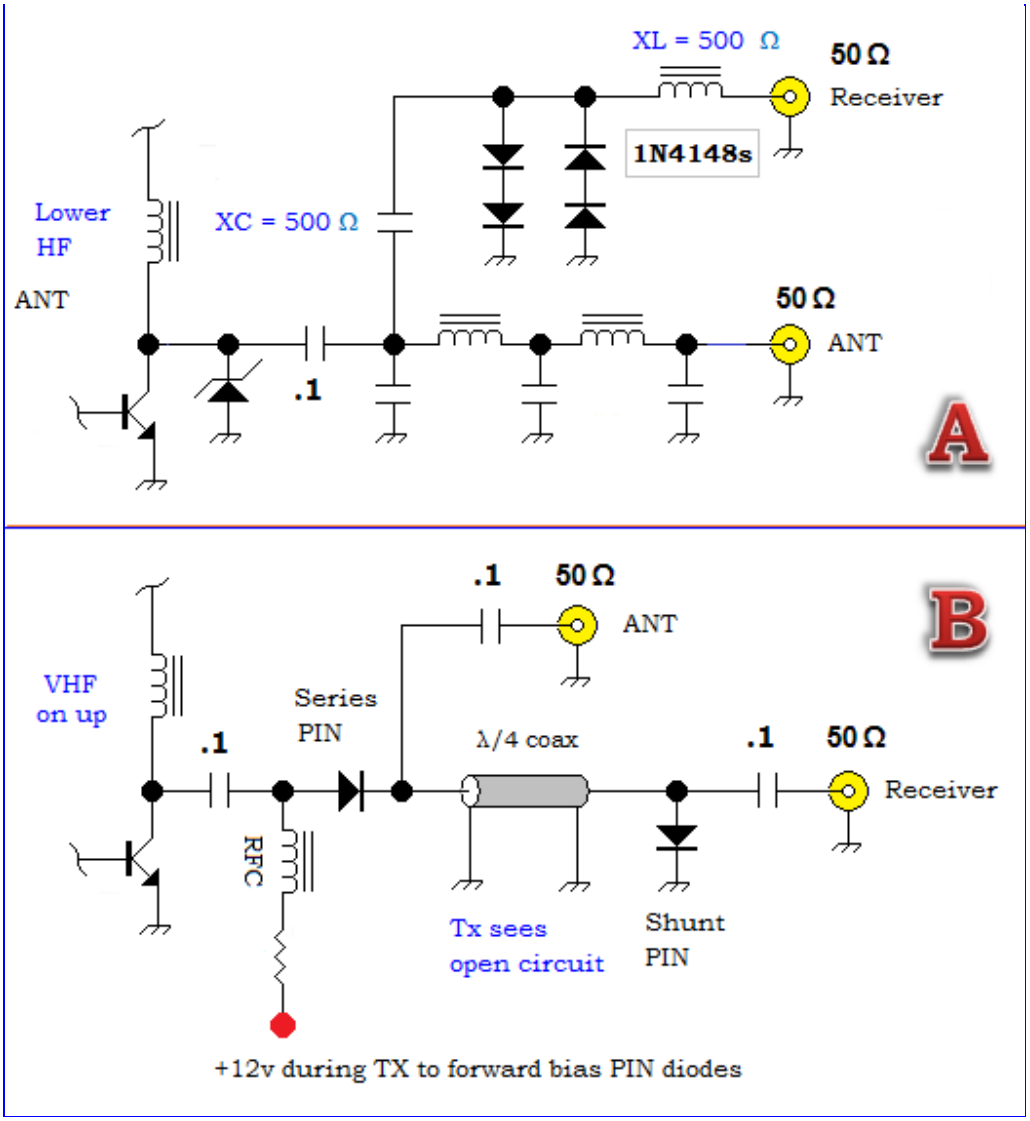

Above — 2 possible T/R schemes. Figure A shows the classic W7ZOI T/R system with 2 diodes per leg. See EMRFD Fig 2.112, for an example with 3 diodes per leg. For 1 band, it's often our go-to circuit.

Figure B shows a scheme well suited for VHF on up: Both PIN diodes get forward biased during transmit mode, however, a 1/4 wave transmission line lays between the series and shunt PIN diode. 1/4 wave transmission lines exert magic [actually it's pure physics that may be verified with a Smith chart]. When the shunt PIN diode gets biased *on* and grounds the receiver port end of the transmission line, the other end looks like an open circuit and thus power flows to the antenna port and not into the forward biased shunt PIN diode to ground. I hope to apply this system in future VHF and UHF projects and sadly, it's impracticable at HF.

Funster Version 8 T/R

As it happens, I seek experience with PIN diodes and therefore shunted a PIN diode instead of running anti-parallel diodes in the classic W7ZOI T/R scheme. This meant adding a transistor switch to quickly bias on the PIN diode @ *key down* and run a little hang time @ *key up*.

Please refer to the PA-T/R schematic. During key down, keyed 12 volts saturates the 2N4401 switch and 11 ma current biases *on* the PIN diode. At key up, the BJT switch's base voltage is held on by the 10K plus series 0.33 µF capacitor just long enough to allow the stored energy in the large PA collector choke to collapse — protecting the receiver.

Feel free to experiment with the timing capacitor value. Previously, Wes, W7ZOI suggested connecting the T/R receiver port to a 50 Ω teminated 'scope for general measurement and also for clocking up RC time constants in DC switching circuits. With a 2 channel 'scope you can monitor the receiver port switch function in 1 channel while watching the PA collector AC voltage in the other. Now that's experimenting! Click for a sample from my QRP workbench.

I chose an XC / XL of 400 Ω for the series L-C network. The 9.1 µH coil shouldn't be wound on a 43 material ferrite [the Qu is just too low]: a bigger powdered iron toroid like size 68, or even a 61 ferrite material toroid works okay from my experiments [Q's as high as 162 were measured on a FT50-61 @ 1 MHz in 2013]. Although this coil tunes coarsely, try tweaking the 9.1 µH inductor with thumb and forefinger during actual signal testing in a receiver.

I wound the 125 µH choke connected to the pin diode cathode on a 77 material ferrite toroid to get it done with just a few turns and avoid a self resonant frequency close to 7 MHz.

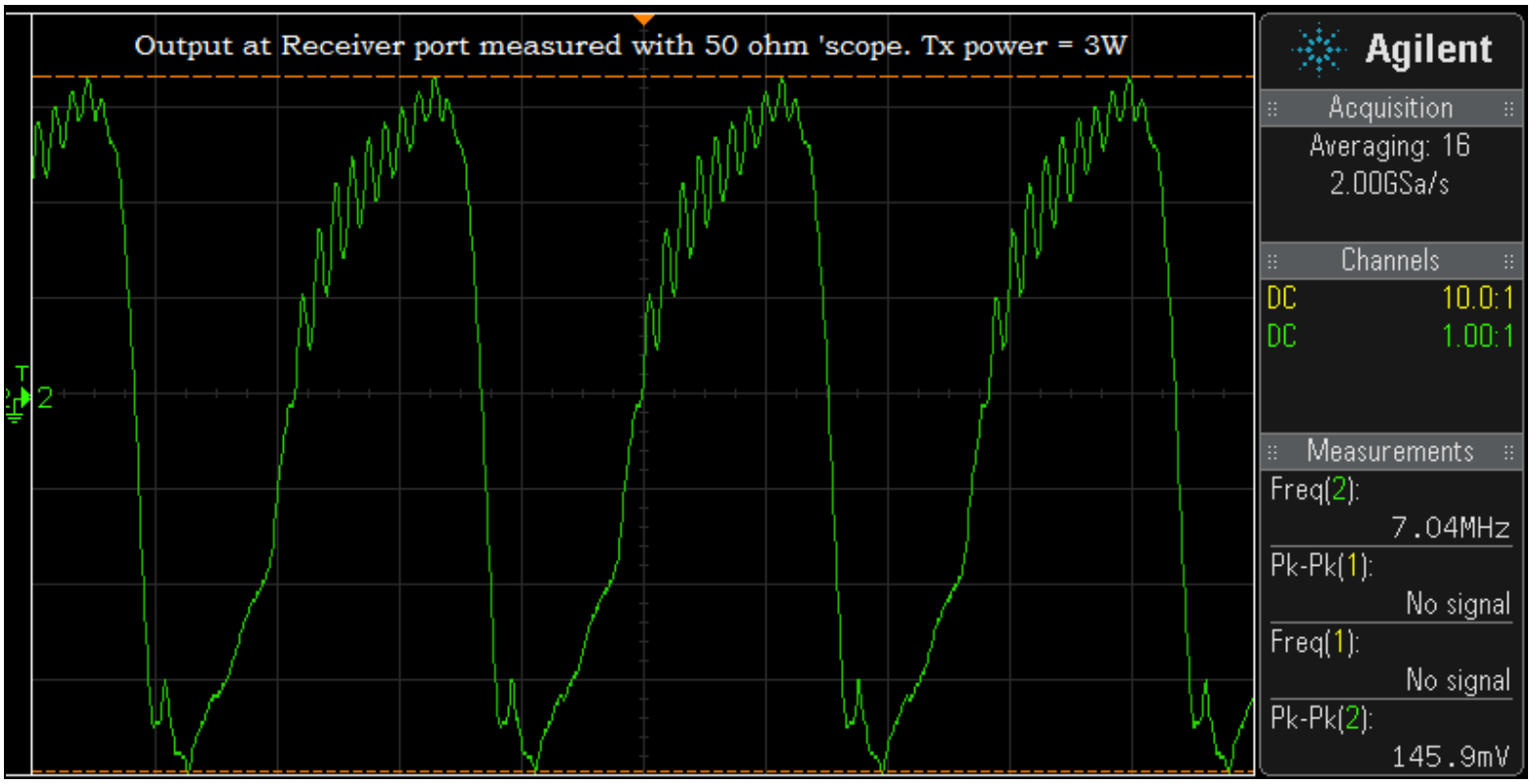

Above — 50 Ω terminated DSO measurement of the receiver port @ 3W transmitter power. Theoretically all power should shunt to ground through the PIN diode, however, the diode exhibits a little resistance and the series L-C circuit contains reactance, so isolation is never perfect.

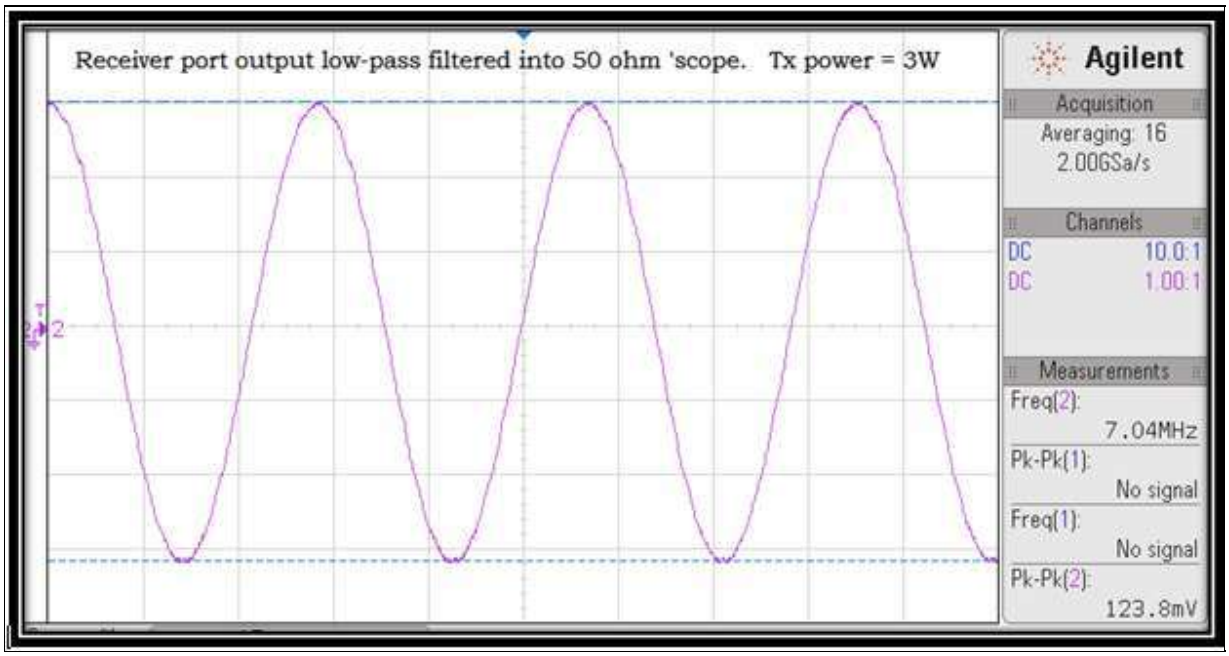

Above — A low-pass filtered measure of the receiver port while in transmit mode. The beauty of a 50 Ω measurement environment shines: I placed a 7.36 MHz-bench module low-pass filter between the receive port and my DSO to quantify the leaked power to the receiver port as -14.17 dBm when the transmitter delivers 3W. Safe for my receiver.

My sincere thanks to those who offered advice and feedback during the build of this transmitter.

Above — Funster in the field.

Above — Rear view of the Funster Tx.

2. References

T/R References

Perfecting a QSK System. QEX for Mar/Apr 2006. Markus, VE7CA. Click for pdf.

Electronic Switching and How it Works, QST for September 1984. Doug, W1FB

7 MHz receiver -- discussion begins on page 215 -- On page 214 in Fig 1 see the 33 pF input cap plus receiver protecting anti-parallel diodes. Also view the 555 timer and other T/R control circuitry in Figure 2 on page 215.

This receiver realizes the first-ever printed version of the W7ZOI T/R system described earlier. Solid State Design for the Radio Amateur. ARRL,1986 [out of print] by Wes, W7ZOI and Doug W1FB.

Transmit - Receive Antenna Switching. EMRFD. First published by the ARRL in 2003. Page 6.68.

Schematic for the 30-W, 7 MHz power amplifier. Figure 2.112 [page 2-42] EMRFD. Design by Wes, W7ZOI

VHF FM — Supplement 1

This page supplements VHF FM

1. 10.7 MHz IF Strip - with example broadcast band FM receiver
2. NOAA Receiver Experiments @ 162.55 MHz

---

1. 10.7 MHz IF Strip

I'm inexperienced with making FM receivers and lack confidence. I began with a utility module to allow basic assessment of the circuit gain required for different detectors, ceramic filter bandwidths, and more so — to get something working to boost my confidence.

The FM receiver 10.7 MHz IF standard began soon after World War 2 and 10.7 MHz still makes sense for the primitive radio builder — surplus IF filters still seem available in a variety of bandwidths. Although vexxing, if we suffer from receiver images at 10.7 MHz, we can always filter the input better, or jump up the IF and make a crystal filter for say 20 MHz. Above 20 MHz good, inexpensive, fundamental-mode crystals get hard to find.

Mixer

I chose a diode ring mixer; again. After trying other mixers such as balanced FETs, or an NE612 , I kept coming back to the diode ring. Partly I'm biased and partly it's from from measures like this one. Although the oscillators weren't perfectly set for a 10.7 MHz IF, the LO and RF signals are both > 40 dB down from the desired IF — love this.

Since I designed a 50 Ω bench module, the IF output contains a source follower to drive the IF port. In an actual "keeper" receiver, you probably wouldn't bother since you might just directly drive the detector, or perhaps another 330 Ω input/output IF amp before the detector.

Although I humbly build simple/primitive circuits, my design goal is never for a *low parts count* — each part serves its purpose. A low parts count ideology plus minimalism exploits the frugal and primitive homebrew nature of our brother hobbyists, however, often gets out of hand. Some builders just cite a low parts count *design goal* to rationalize a poor design. Worse yet, inexperienced minimalists often exclude vital parts such as DC supply decoupling and bypassing, temperature stablizing bias networks, or adequate band-pass filtering. To each his own. Please discern all you see or read in homebrew radio; we're builders, not lemmings.

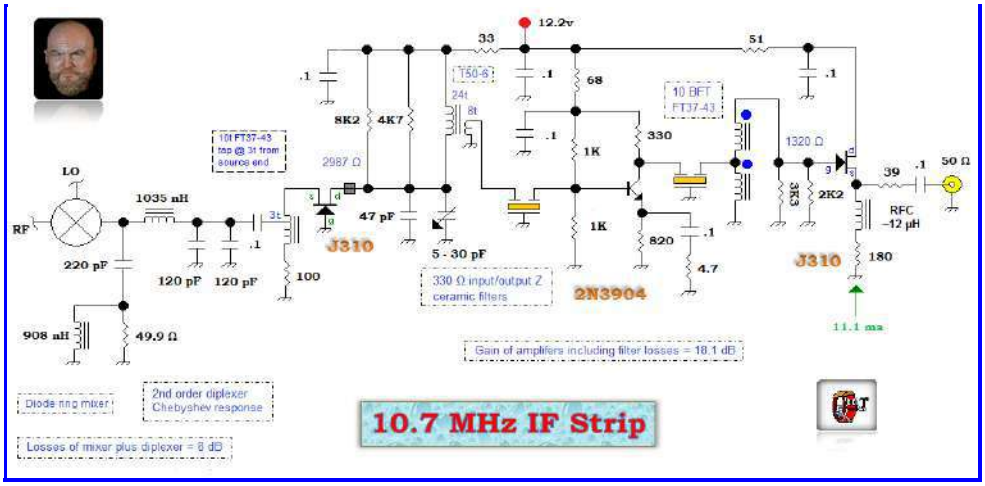

Above — Click on the IF strip schematic to view it. Most all the stages were discussed on VHF-FM. My net module gain = 10.1 dB. The 2 ceramic IF filters = 230 KHz Muratas with a measured average loss of 6.15 dB each.

Above — The boxed up circuit contains 3 SMA jacks. Click for a photo of the completed breadboard.

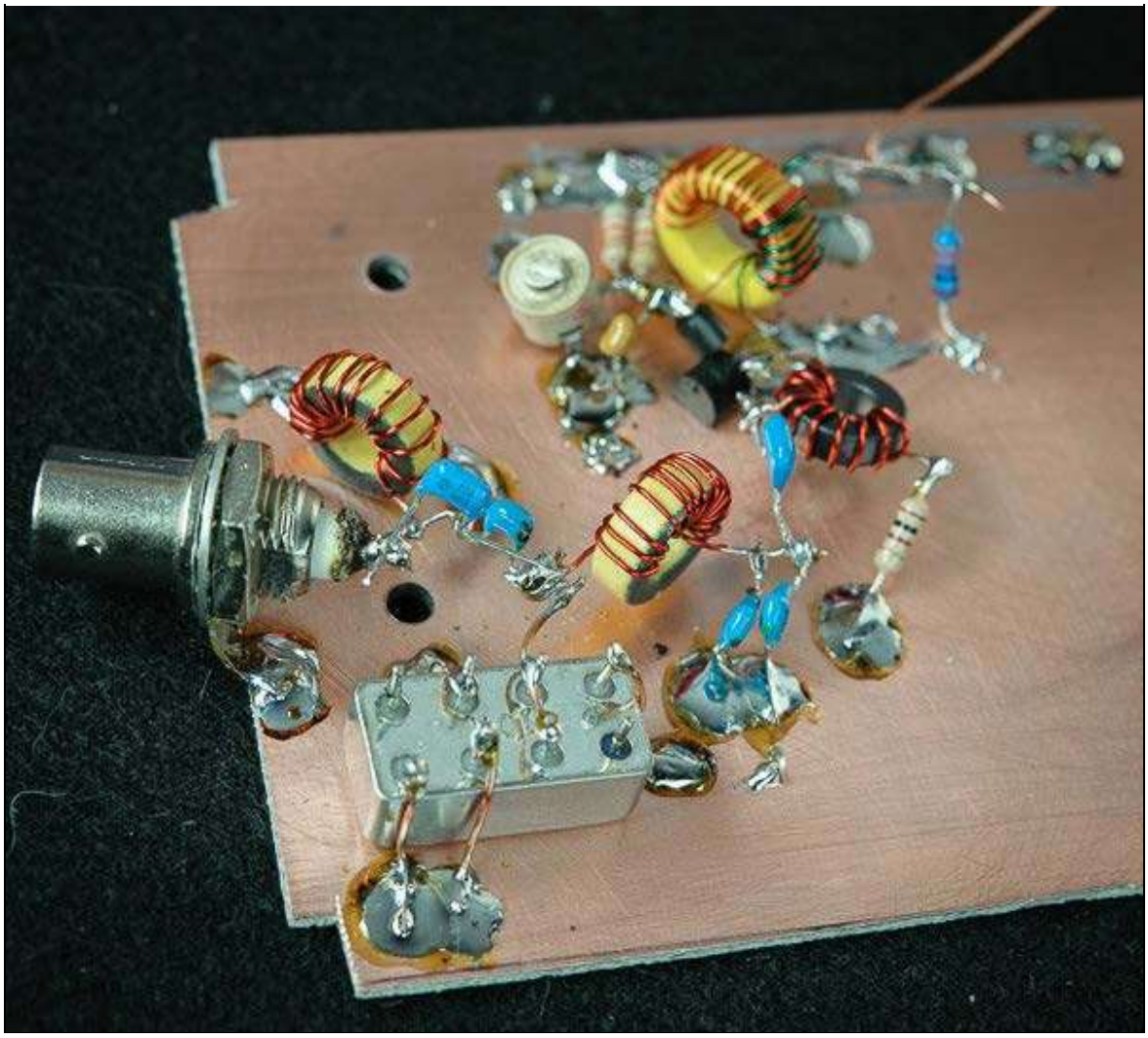

Above — A close up of the mixer, diplexer and JFET amp, although the SBL-1 mixer is disconnected. This board contains a temporary BNC jack to allow testing of the non-mixer parts such as JFET gain, diplexer loss, return loss, to confirm the tuning cap choice and also to look for any UHF oscillations eminating from the FET, a UHF part. Click to zoom in on the common gate amplifer with its gate lead soldered as close to the plastic case as possible.

Detector

I tried to homebrew my first IF amp +/- limiter and detectors , but felt unhappy with their performance, failures, circuit complexity and/or noise issues. Click click or click for 3 raw, miserable design examples from Winter 2014. Discouraged; after 2 months of lamenting, I opted for an IC detector subsystem. 3 relic part choices might include the CA3089, SA604A or LA1150.

In my case, the CA3089 suited me best and offers a lot: a double-balanced quadrature FM detector with limiter + IF ampifiers; squelch, AFC, AGC, AF preamp and the potential for high-fidelity FM reception. All that's required is an outboard detector resonator — easy to build with a powered iron toroid plus a fixed + trimmer cap.
Price + shipping varies widely, but last year, I got 5 shipped to me from Europe for $7.25 USD and these will make 5 receivers — not bad at all. What hobby isn't expensive?

I've even read that some builders used the CA3089 for an S-meter amplifer, although its logarithmic compliance is far from stellar. You'll need to download the CA3089 datasheet.

Let's build a receiver:

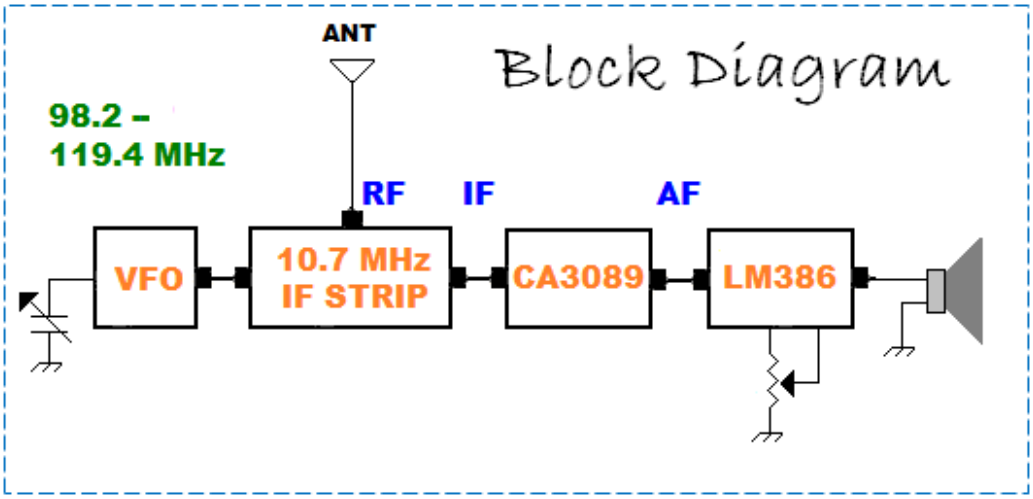

Above — The block diagram. The antenna = 1 meter piece of wire soldered to a SMA jack that was threaded into a brass sheet to fashion a crude ground plane. No LNA or input band-pass filtering was employed.

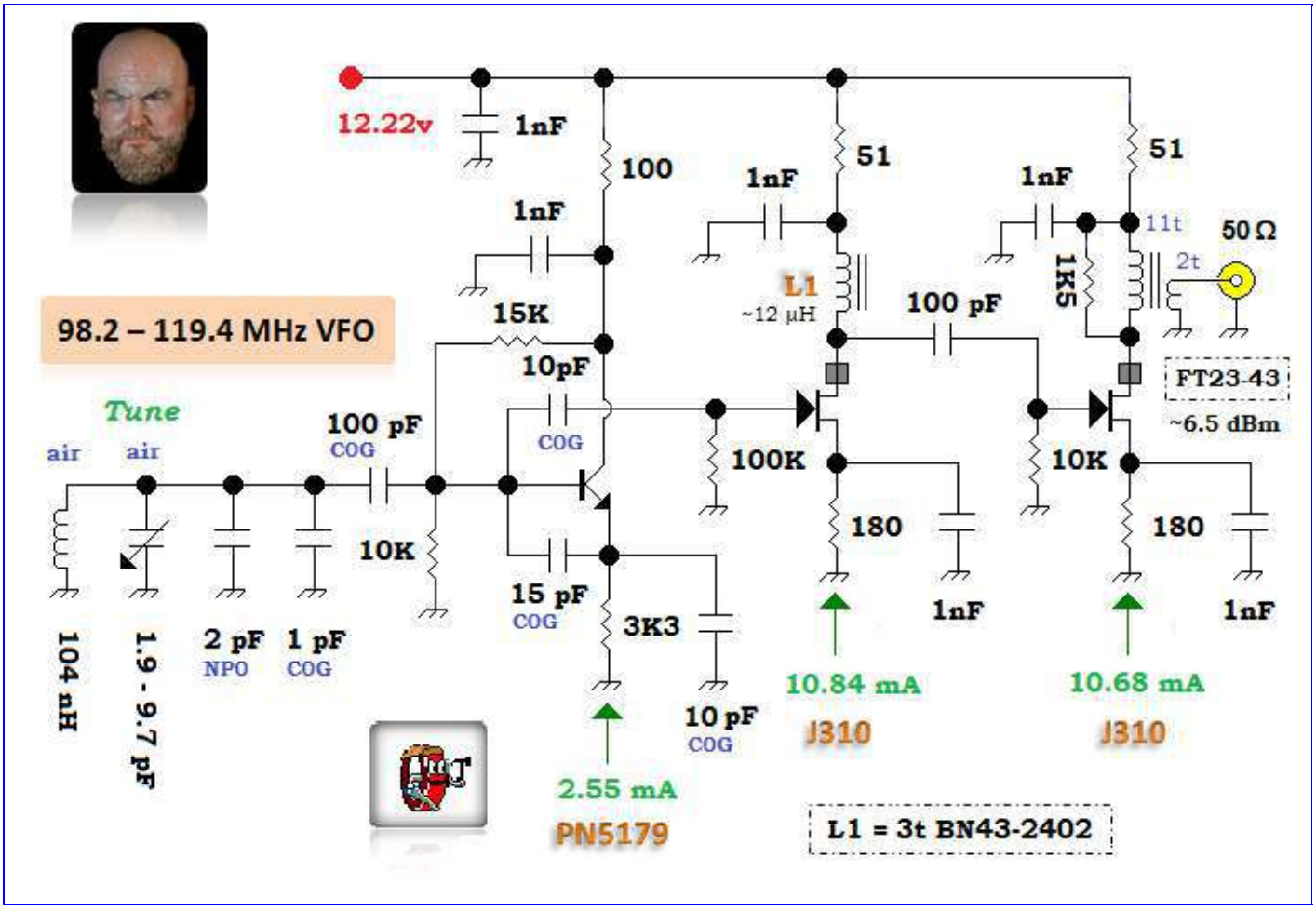

Above — The temperature compensated, free running VFO. Normally we should run a VCO-PLL, digital contraption, or a VFO/VCO with ALC feedback, but this thing worked fine to learn on.

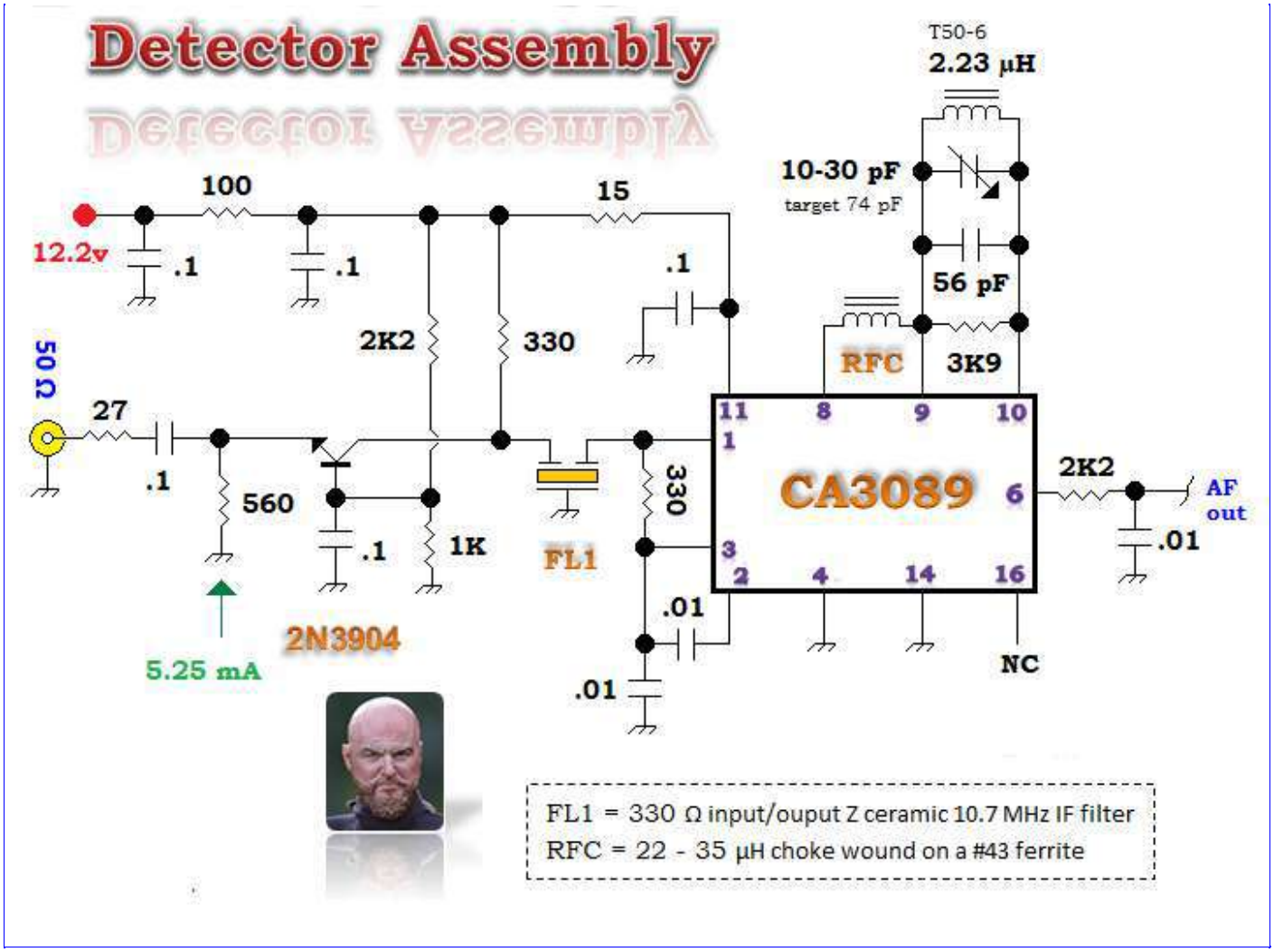

Above — The detector assembly. To match to the 50 Ω IF strip port, I employed a common base amp with a 330 Ω collector resistor driving a final 230 KHz wide "tail end or mop up" filter. In many designs you could simply drop this amp as the gain isn't really needed. On the other hand, the CA3089 contains a limiter and it won't hurt at all.

To make the detector coil, a small square island was carved on the copper clad board. The island was bisected so that pin 9 soldered to 1/2 the island and pin 10 to the other half. The 3K9 R, 56 pF C and a small, high Q SMT trimmer capacitor bridged the 2 islands. Finally, a 2.23 µH, T50-6 toroidal inductor was soldered across the 2 islands.

Tune a station and peak the trimmer cap for the most crisp sounding audio — it's set and forget. When driven with enough signal for full quieting, the CA3089 delivers very low distortion — the FM receiver in my truck sounds worse.

An RFC provides a DC short across pin 8 to 9 and keep ~5.5 VDC bias on the pin 9 transistor base. The minimum inductance should be 10X the detector coil. I wound my RFC with 6 turns on a BN43-2402 [35 µH] , but any old #43 ferrite wound choke >= 22 µH should work. For my chokes, I prefer a low # of turns on a binocular core to avoid any SRF issues.

Since the CA3089 contains a powerful audo preamplifer, only an AF power amplifer with low gain is required. I opted with the old LM386, but in future, better, "keeper rigs" I'll add an op-amp tone control stack driving a pair of power followers for good measure.

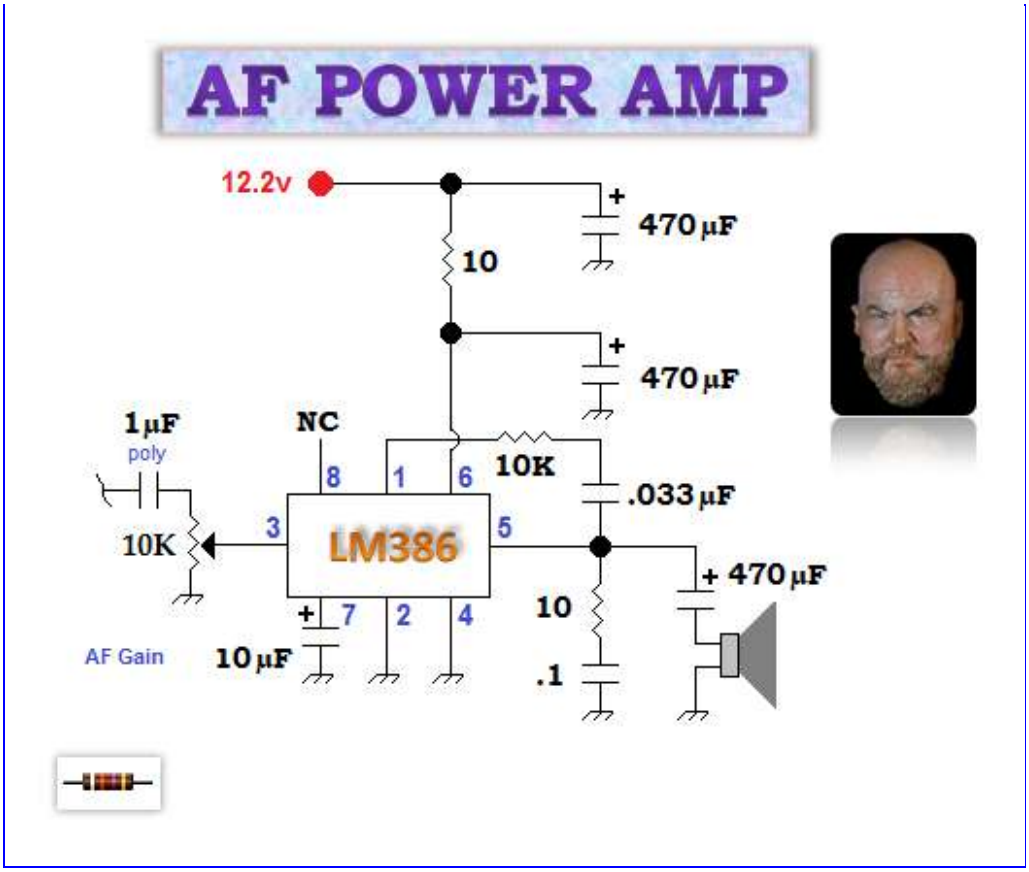

Above — Final audio power amp: an LM386 set for a voltage gain of 20 with some low-pass filtering and stout DC line filtering.

Click for a photo of the detector and LM386 assembly. Click for a better view of the outboard resonator and nearby RFC.

Outcomes

After connecting the VFO, antenna, IF strip, detector assemby, speaker and powering them up, loud FM radio blared through the loudspeaker. I tuned every local FM station with full quieting and felt surprised that despite no band-pass filtering, plus no RF preamp, it worked and sounded so well.

Further experiments showed that inserting as much as 15 dB attenuation between the IF stip and the detector assembly still kept full quieting on all the stronger stations. In some cities with multiple, strong FM stations, input band-pass filters will be needed. I'll cover that in a later installment.

I connected this VFO to the IF strip and tuned in my local NOAA weather station at 162.55 MHz. Click for a photo of the VFO built on a piece of bent copper sheet metal.

Future experiments may include changing ceramic filter bandwidth, trying different mixers, applying varactor-tuned input band-pass filters for strong FM environments and for FM Dxing. Finally, I'll design a low-noise preamp with a common gate JFET and/or a dual-gate MOSFET. Utimately, I hope to make a dedicated NOAA weather receiver, a broadcast FM Dx receiver and then some narrow band FM jobs for 2M or 6M. The future looks good.

Audio sample one : a few local stations [mostly recorded before I added the negative feedback on the LM386]
Audio sample two: a weak signal [our provincial Highway Report] that doesn't reach full quieting.

Thanks.

---

2. NOAA Receiver Experiments @ 162.55 MHz

I document some *raw* experiments and hopefully 1 day will make a good receiver for my local NOAA FM broadcast.

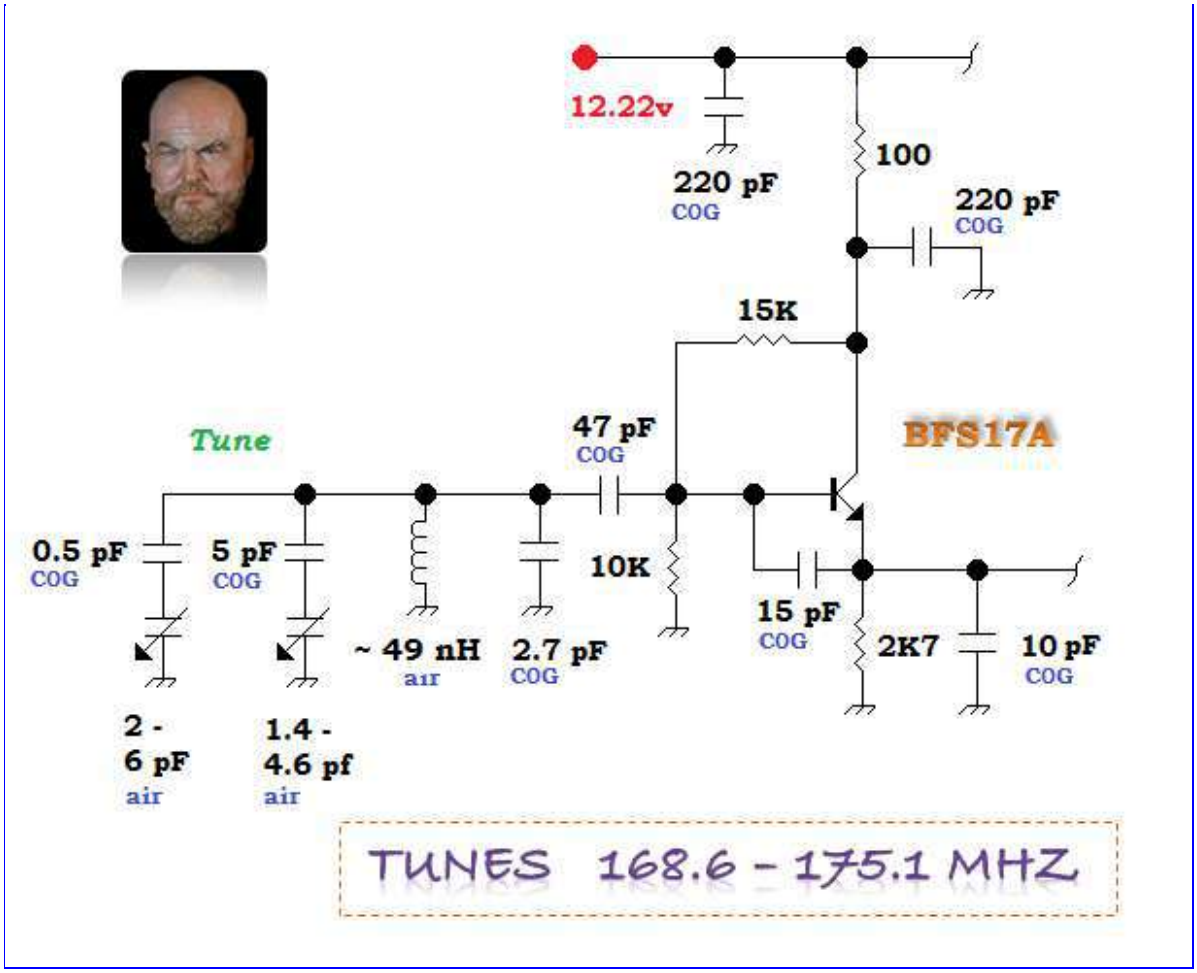

Above — I built a VFO for 173.25 MHz with fine tuning for my local, NOAA weather report receiver @ 162.55 MHz. The fine tuning 2- 6 pF variable capacitor in series with an ATX 0.5 pF chip cap resolves 10's of kilohertz to permit tuning narrow band signals. You'll especially need fine resolution tuning when applying ceramic IF filters <= 150 KHz.

Above — The 2 VFO air variable tuning capacitors. Click for the circuit breadboard with a tuned, common emitter buffer, that I'd rather not show [because it sucks]. I ran the VFO into a bench module to boost the power up between 5 and 10 dBm in my experiments.

Since @ VHF, my VFO went on 2-sided FR4 board with several wire vias joining the 2 surfaces. We normally avoid double sided boards for VFOs since doing so makes a low Q, potentially moisture absorbant, undefined temperature coefficient "capacitor" that may worsen temperature

drift. For bench learning and in particular, FM reception, temperature stability tested adequate and I can listen for hours without retuning.

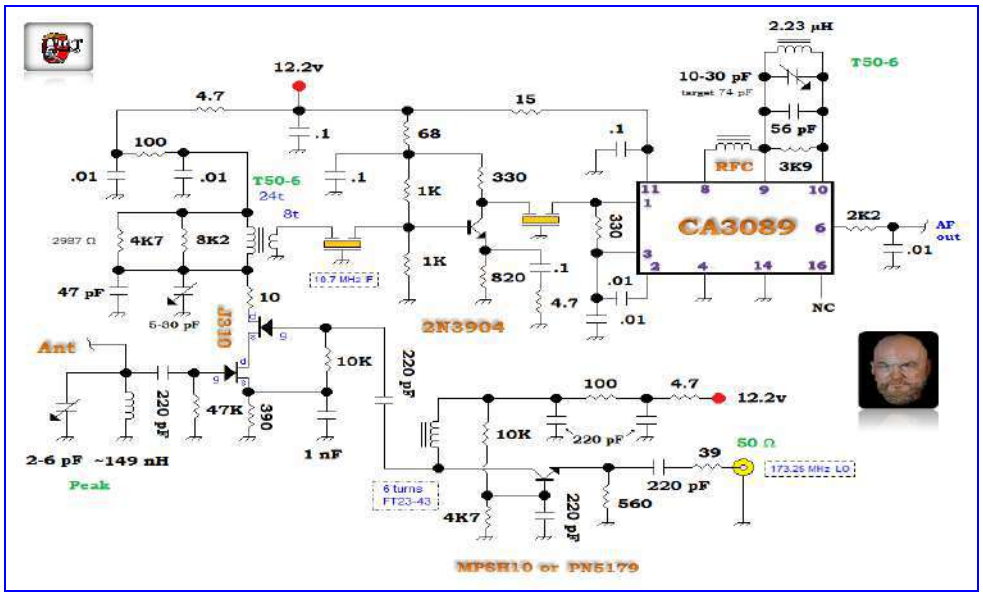

Above — The entire receiver with a cascode mixer from EMRFD. In experimenter's mode; I tried out many ideas. For example: different bandwidth IF filters [settled on 230 KHz] , 1 versus 2 ceramic filters, or eliminating the 2N3904 amp [2 better drove the CA3089]. One salient learning — IF filters may possess a wide variation in center frequency and thus if you have a sweeper, matching them might be useful. In this receiver topology, you don't need to match 230 KHz or 280 KHz ceramic filters; the mismatch became noticeable with a <= 150 KHz 3 dB filter bandwidth.

I boosted the VFO signal with a common base amp — I varied the power into this LO amplifier by applying different strength attenuator pads. Between 1.5 to 2 Vpp on the mixer gate gave a reasonable compromise of conversion gain, noise and easy-to-get VFO power. From EMRFD, maximum conversion gain occurs when driven with 5 Vpp.

This unbalanced mixer worked fine, however, without a metal case, I heard a little hum from my DC supply and noises from household appliances such as the clothes washer and fridge. This receiver suffered from microphonics as well. The AF amp was a LM386 set for gain = 50.

A simple LC resonator tuned the mixer RF input and proved essential. I tried different ways to couple a 25 cm long wire antenna such as tapping the coil and an L- network, however, my main antenna peeve was severe hand capacitance effects. Although this receiver does not require a preamp for RF gain, the isolation seems needed. If you put your hand near the telescopic whip antenna of my Realistic Pro 2020 scanner, no noise or RF disturbance arises.

From studying scanner and FM receiver schematics, most rigs contain a dual-gate MOSFET preamp for a low noise figure and high input isolation. These MOSFET amplifiers feature input and output tuning, although with slug-tuned inductor cans and the oh-so-typical varactors, the resonator Q runs low.

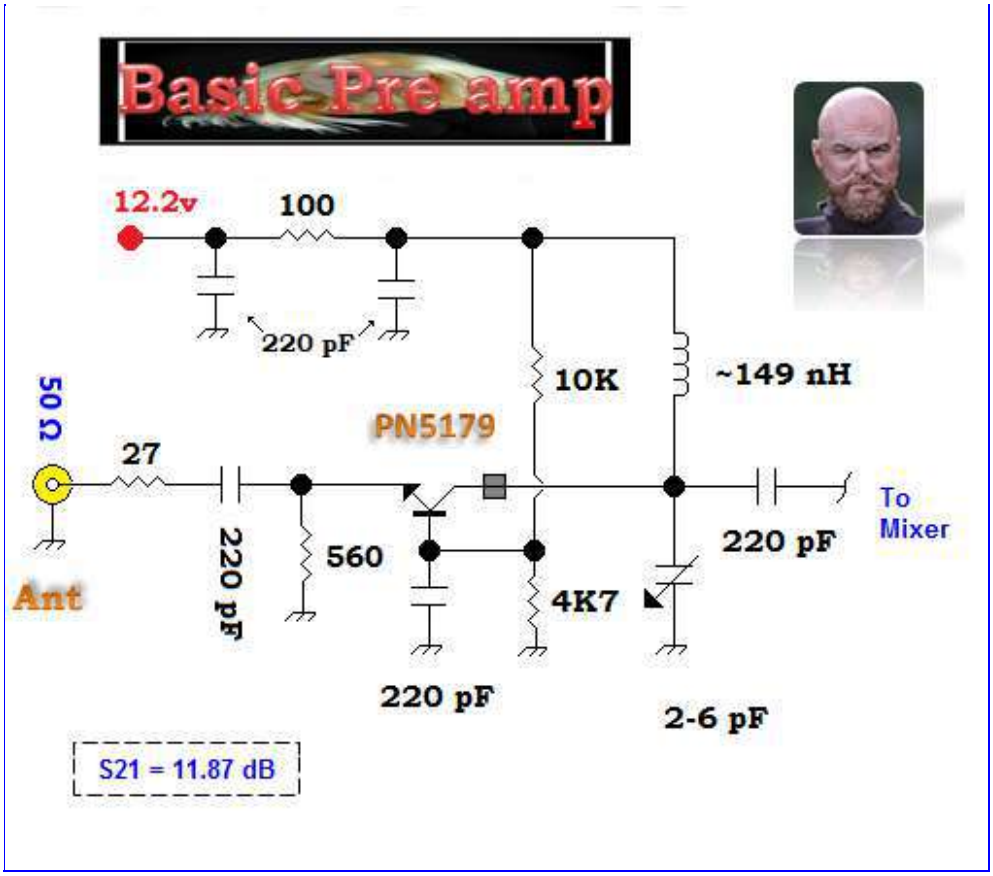

Above — I quickly built a tuned-output common base amp to study front end isolation. I removed the existing resonator and connected this to the JFET mixer gate. It eliminated antenna hand capacitance effects. Click for a sound byte of the receiver with this preamplifier and a 20 cm wire antenna attached to its input. [206 KB download]. I reckon some of my receiver problems arose from the mess of unshielded boards, modules and wire on my bench.

Tuned Input with a 2-Gate MOSFET [162.55 MHz]

A dual gate MOSFET preamp concluded this day's experiments. Tests of a simple input network follow:

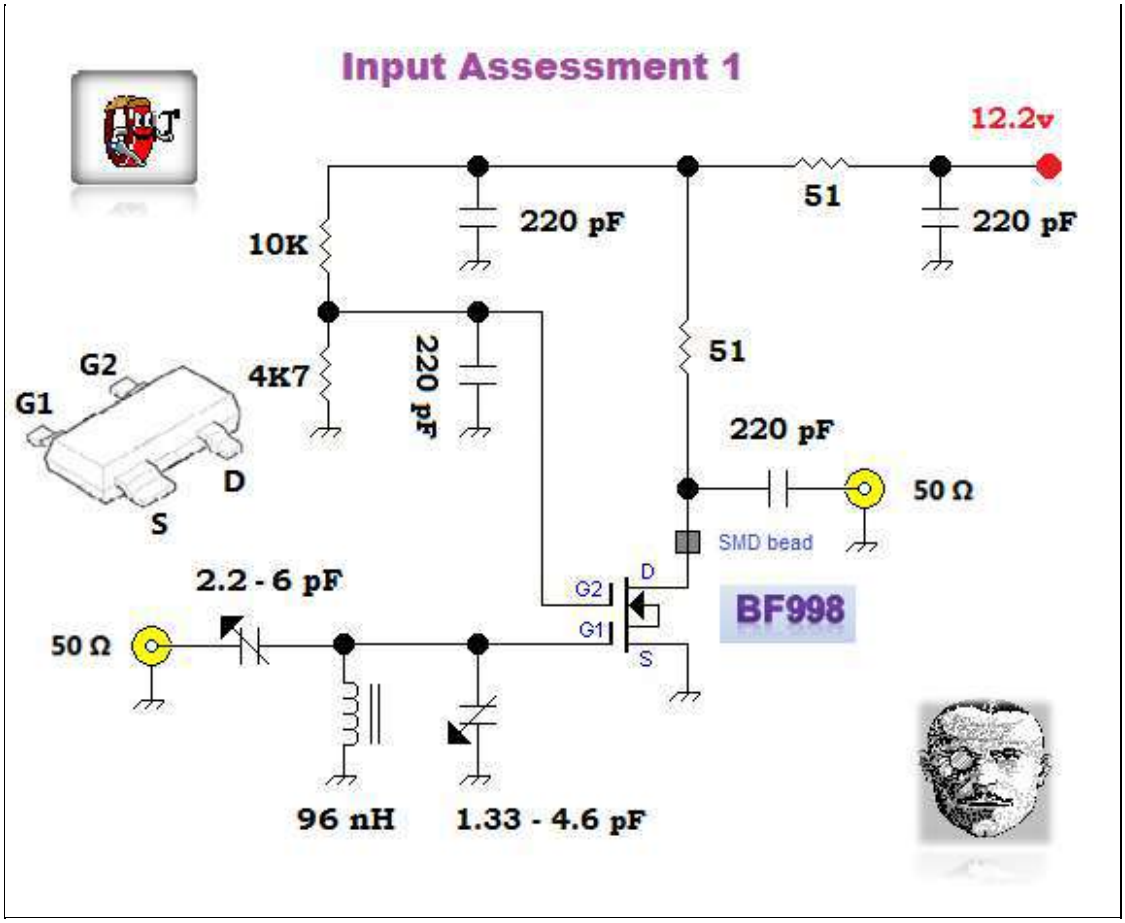

Above — Input Assessment 1. To examine the input without any output network effects, I loaded the BF998 drain with a 51 Ω resistor and matched the input parallel resonator for the greatest input return loss [-S21] by tweaking the series SMD trimmer capacitor. After setting the best input return loss [21 dB], I swept this amp.

The XL of the 96 nH air wound coil = 98 Ω and the XL and XC of this tank may be scaled to other frequencies by keeping the reactance values shown or choosing your own. For example; a coil for 50 MHz where XL = 98 Ω = ~312 nH. I discussed and swept the ferrite bead soldered on the FET drain in Section 1 of the VHF Veronica web page.

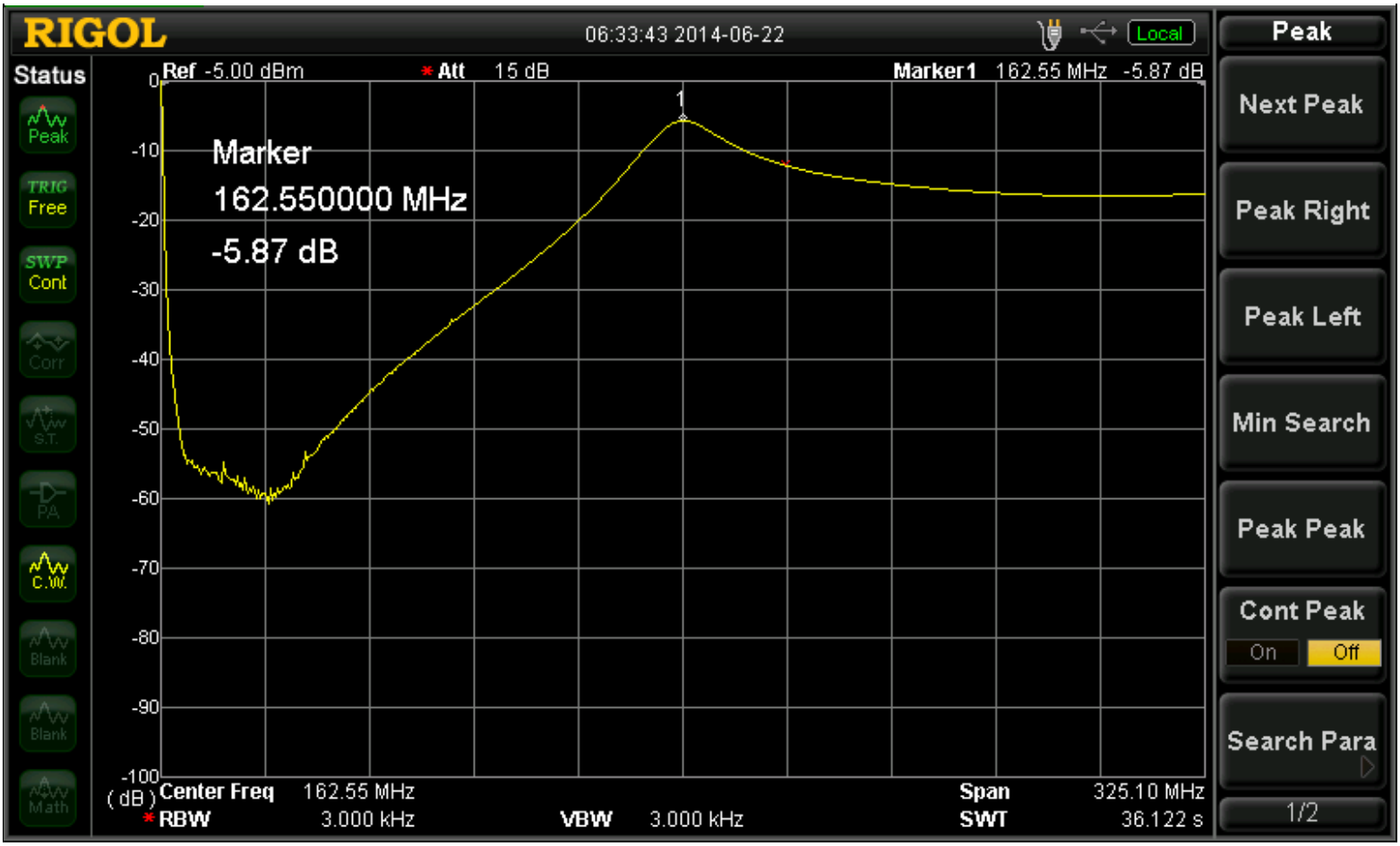

Above — A sweep of the Input Assessment 1 amplifer. Although easy peasy to adjust, series matching the resonator to its input load results in a slipshod right-hand [low-pass] skirt. Click for a screen shot showing the amp's 3 dB bandwidth.

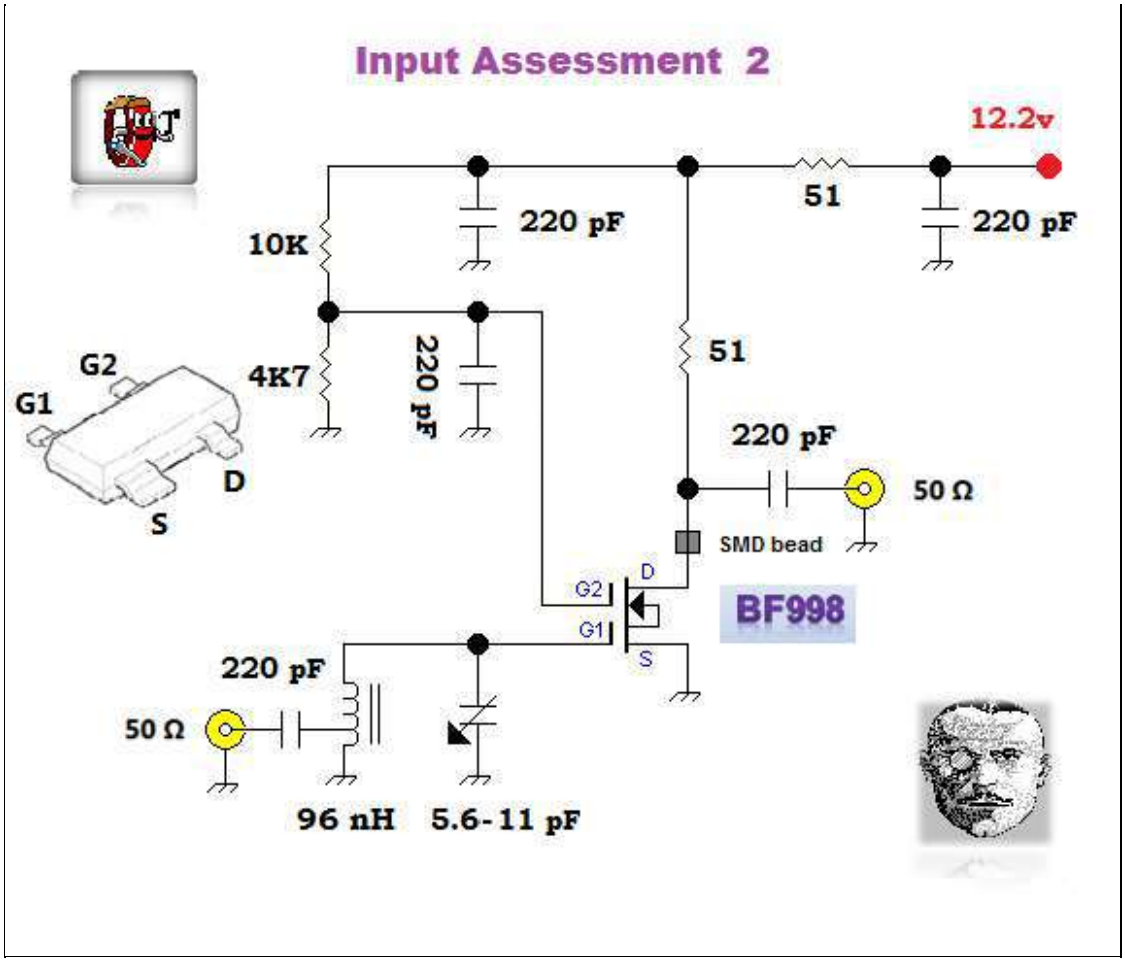

Above — Input Assessment 2. After measuring a poor low-pass skirt in Input Assessment # 1, I opted for the conventional tapped transformer to steepen the low-pass skirt response versus frequency. My sweeps *did* show a better low-pass skirt shape . Finally, I built a "real" amp and soldered in a broadband output network, tweaked the bias scheme + limited the VDD with a series 150 Ω resistor. A higher value input resonator trimmer cap is required for this amplifier versus that in Input Assessment # 1.

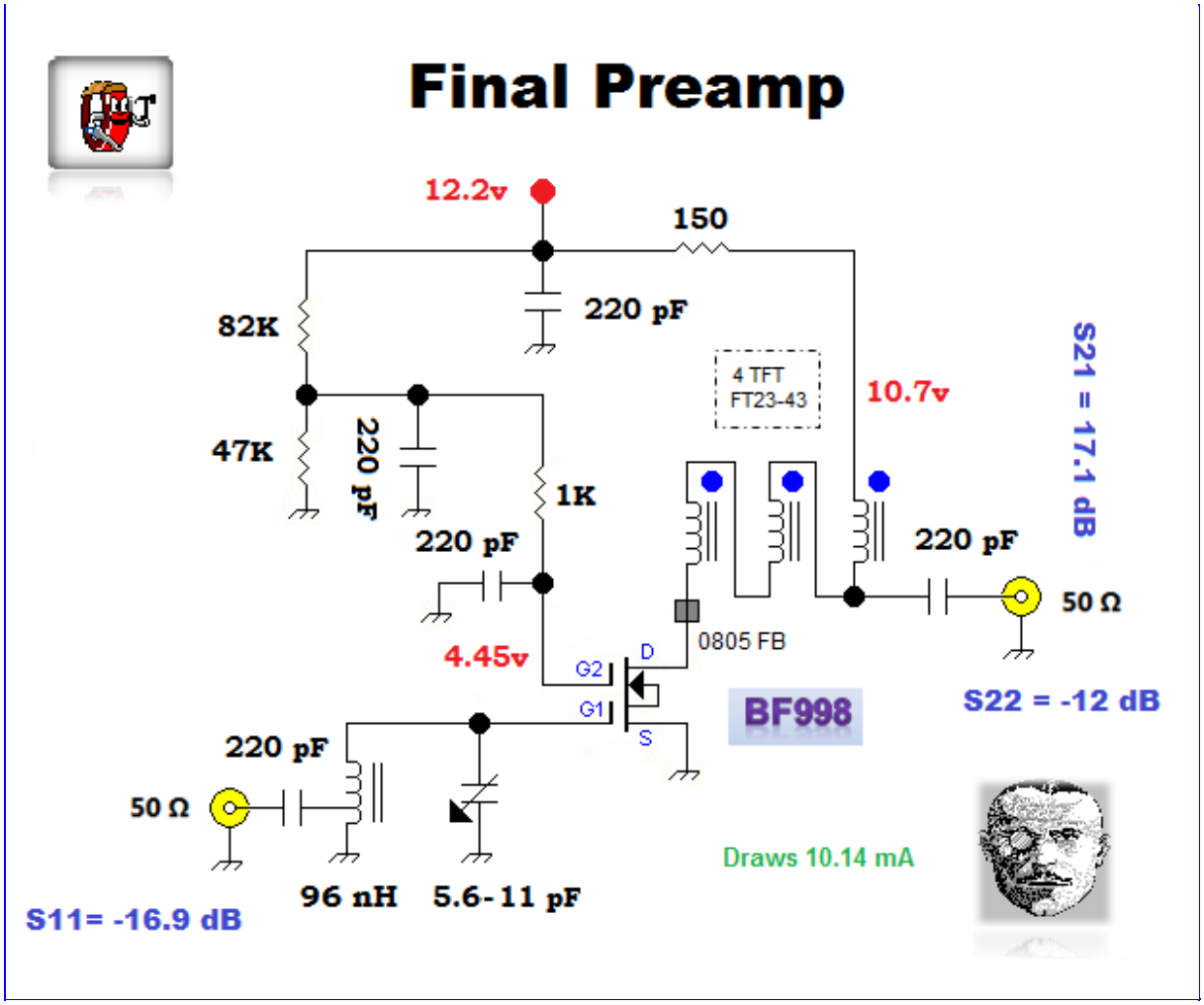

Above — The final 162.55 MHz preamp schematic + some measures. Click for a breadboard photo. Click for the gain measurement with a TG & SA. I measured the same S21 [within 0.3 dB] using my VHF signal generator plus my 50 Ω input DSO. I didn't push too hard with the gate bias or VDD, since neither maximal gain nor parasitic oscillations were sought. Click for a zoom of the filter peak response. Click for a wider sweep to see the right-hand skirt response.

Built on 2-sided FR4 with short cut paths to fit mostly size 0805 SMD parts, I placed via wires on every ground point and detected 0 unwanted oscillations from HF to 3 GHz.

A bare copper wire coil allows us to set the input impedance tap point anywhere along the wire — unlike the *integer only* tap points provided by magnetic toroid-based transformers. In LNA design, many builders set the input tap point for the lowest NF with the amp in noise figure test mode. Another vanilla flavored option is to set the tap with the amplifier input connected to a return loss bridge while adjusting the tap point for the best input return loss — that's what I did. My S11 = - 16.9 dB with my final tap around 1.2 turns of the total 7 links on my 96 nH coil.

The output transformer presents a poor match to 50 Ω with a S22 of just -12 dB. I plan to put a 4 dB pad after it for my NOAA receiver, so it's okay. Some might chase a better output return loss and also perhaps tune the output for better band-pass filtration.

Your FM receiver preamp might need better input filtration, however, if a simple design works, then simple rules! Have fun with *your own* experiments.

473
270
472

Pin Outs

Mini-Circuits Labs SBL-1 and TUF-1 diode ring mixers

...more later

Above — Normal set-up: **Ground** -- Pins 2, 5, 6 and 7. **LO** -- Pin 8, **IF** -- Pins 3 and 4, **RF** -- Pin 1

Above — **RF** -- Pin 1, I**F** -- Pin 2, **Ground** -- Pin 3, **LO** -- Pin 4.

VHF-FM Supplement — Amplifiers

Deleted October 26, 2013

Amateur Radio Electronic Design

KL7R Memorial Receiver Experiments

Introduction

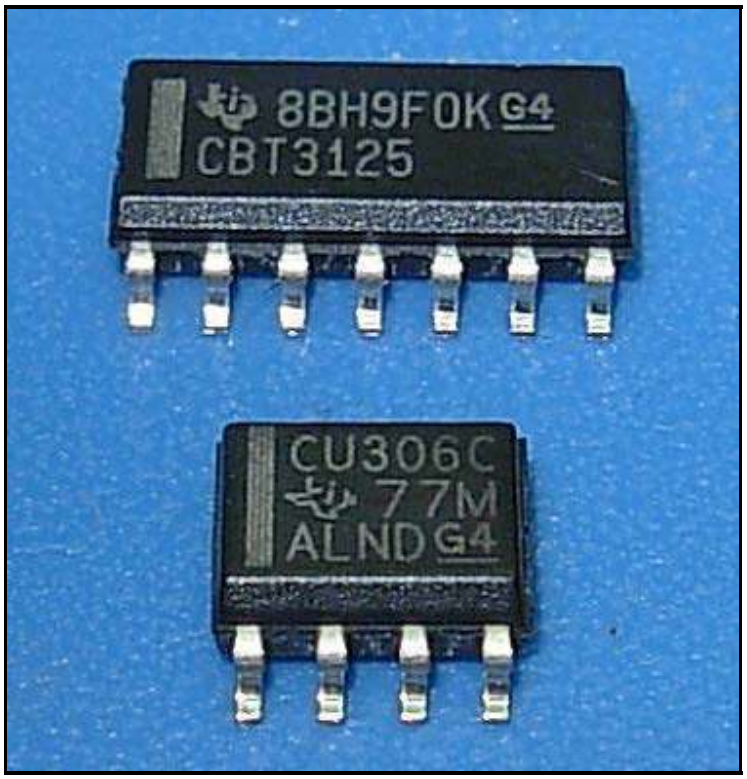

This web page is a memorial to Mike Caughran, KL7R, who died suddenly in January 2007. Mike was a passionate experimenter who was embraced by the homebrew radio electronics community. He was best known as the co-creator of and sidekick to Bill Meara, M0HBR on the podcast Solder Smoke. Mike was a hardcore science and technology buff. His knowledge of general science and curiosity about minimalist RF designs was amazing. I worked Mike on 40 and 80 meter CW and later by voice on eQSO. Mike was the first person to refer to this web site as the "popcorn site". He held an interest in digital circuits. In tribute to Mike, a series of receiver experiments which includes some digital circuits are presented. Mike Caughran will be remembered as a remarkable, kind and passionate homebuilder.

Navigation

There are 3 linked web pages associated with this KL7R tribute web page.

1. Mike's personal web page His own web page memorializes him best
2. Supplemental web page Additional schematics and photos which supplement this main web page
3. VFO web page Describes the VFOs used for these experiments

My special thanks to Wes, W7ZOI for his coaching and suggestions to improve many of the circuits on this web page. This web page borrows heavily from his designs as presented in EMRFD.

Receiver Description

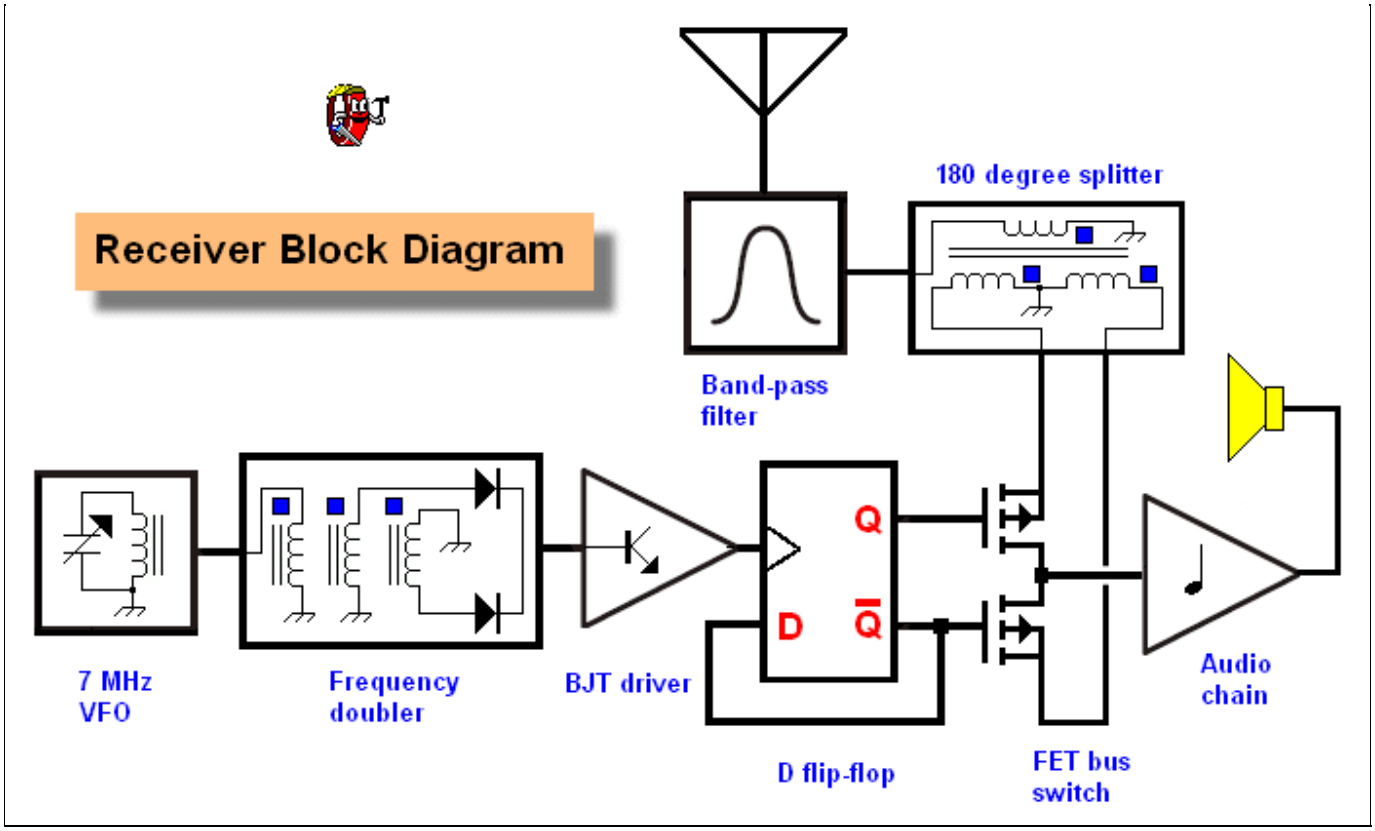

Shown above is the receiver block diagram. The KL7R memorial receiver depicted on this web page is the final output of many hours of experimentation. Most of the circuits or circuit ideas originated in EMRFD.
From our conversations, Mike was always challenging himself; experimenting, testing and pushing his knowledge threshold. The joy of discovery motivated him. Fired by his spirit of inquiry, I explored methods to build a receiver containing at least 1 digital circuit. On many days, I accomplished nothing. The circuits did not work and little to no progress was made. These were the difficult dry spells all experimenters must endure. Design and circuit failures can be very disheartening. I also wasted a lot of parts. However, I kept going and slowly successes occurred and my confidence rose. The end result was a little more knowledge and a cool, popcorn, direct conversion receiver which I hope will provide ideas and inspiration for your own experiments.

Double Tuned Band-pass Filter

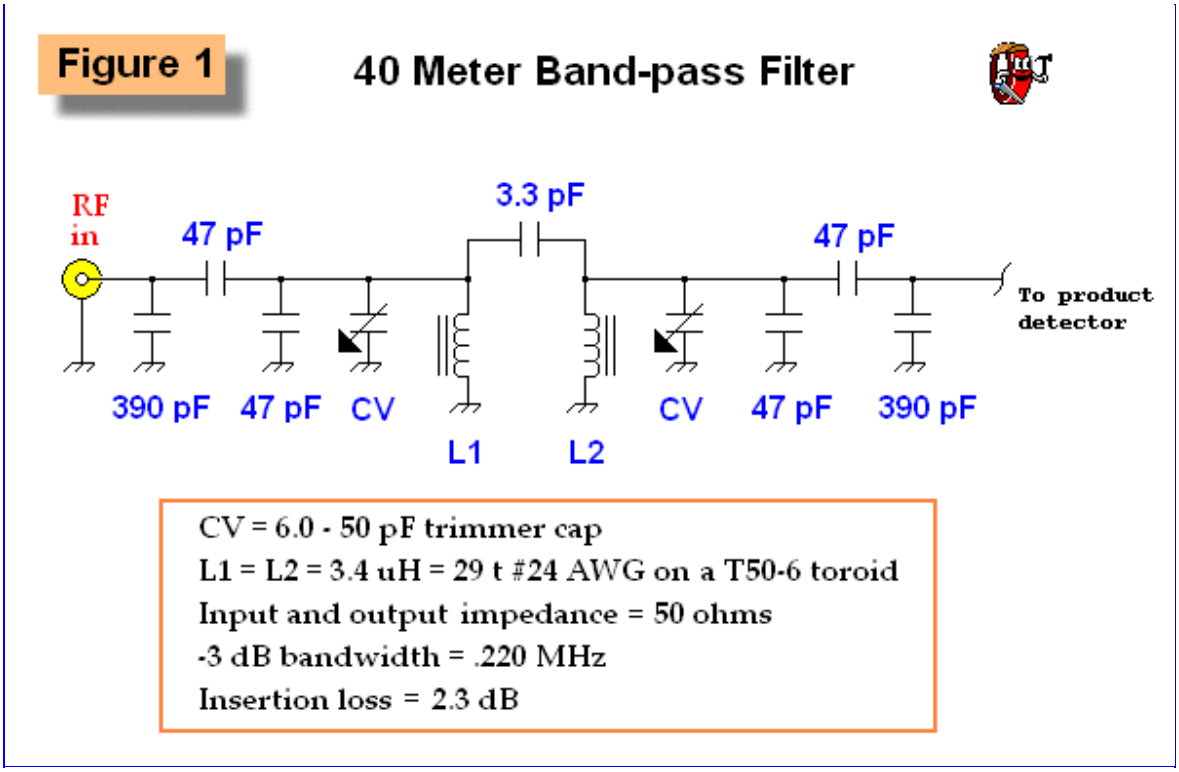

Figure 1 shows the front end band-pass filter. If you can't obtain a 3.3 pF coupling capacitor, try this other 7 MHz band-pass filter circuit or perhaps just design your own. See the Webmaster's page for information concerning many of the parts used on this web page.

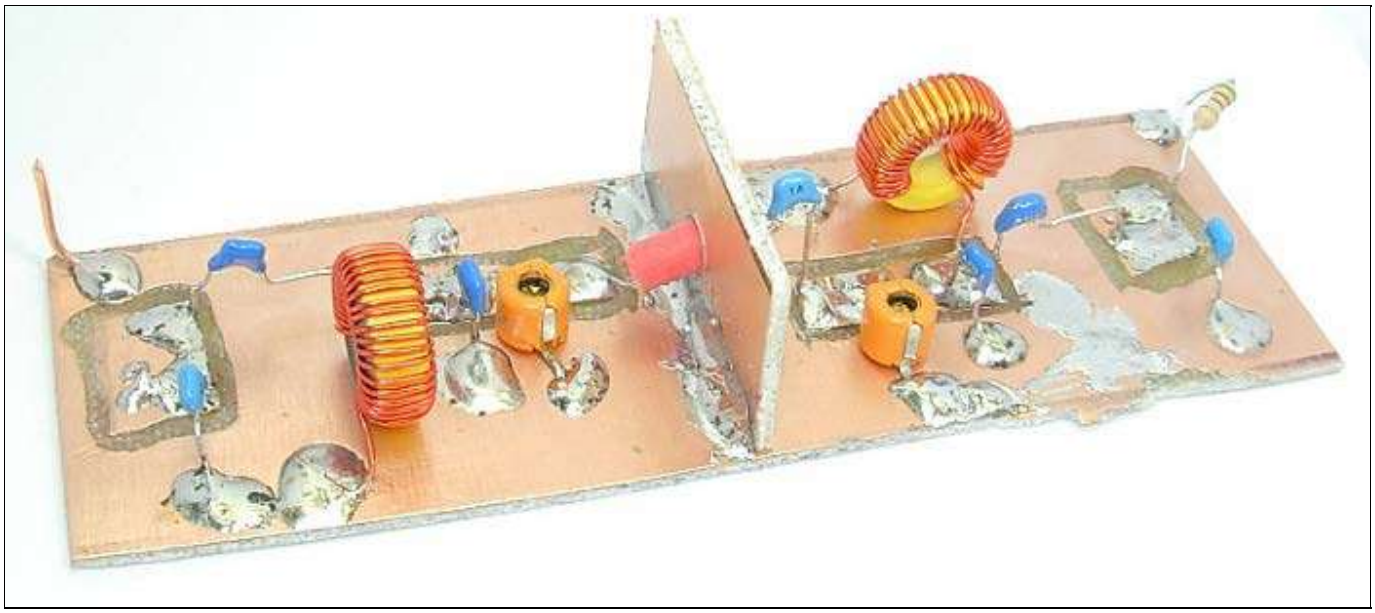

Shown above is a photograph of the Figure 1 breadboard. The inductors were spaced apart at right angles to reduce unwanted coupling. The copper clad board L-C tank divider is not necessary. The 51 ohm load resistor seen to the right was removed after testing.

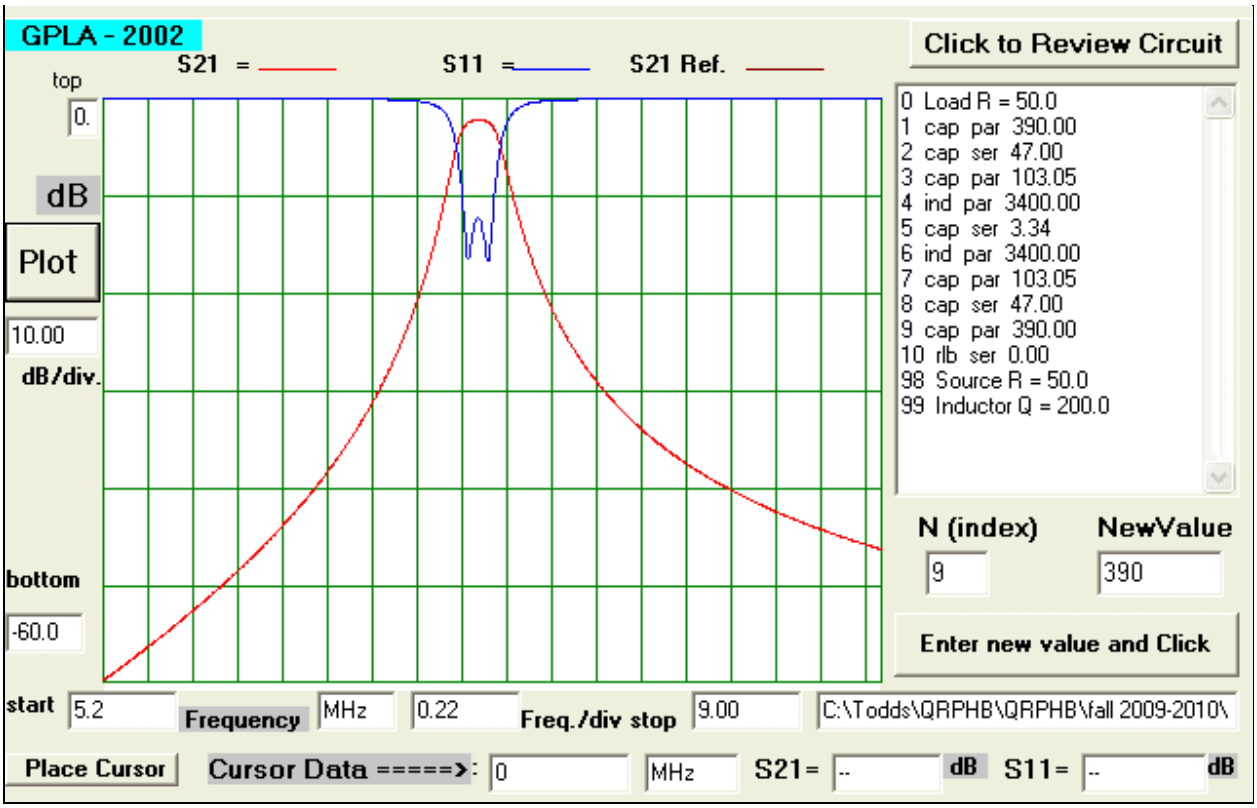

Shown above is a GLPA simulation of the Figure 1 band-pass filter. Хорошо.

Product Detector Experiments

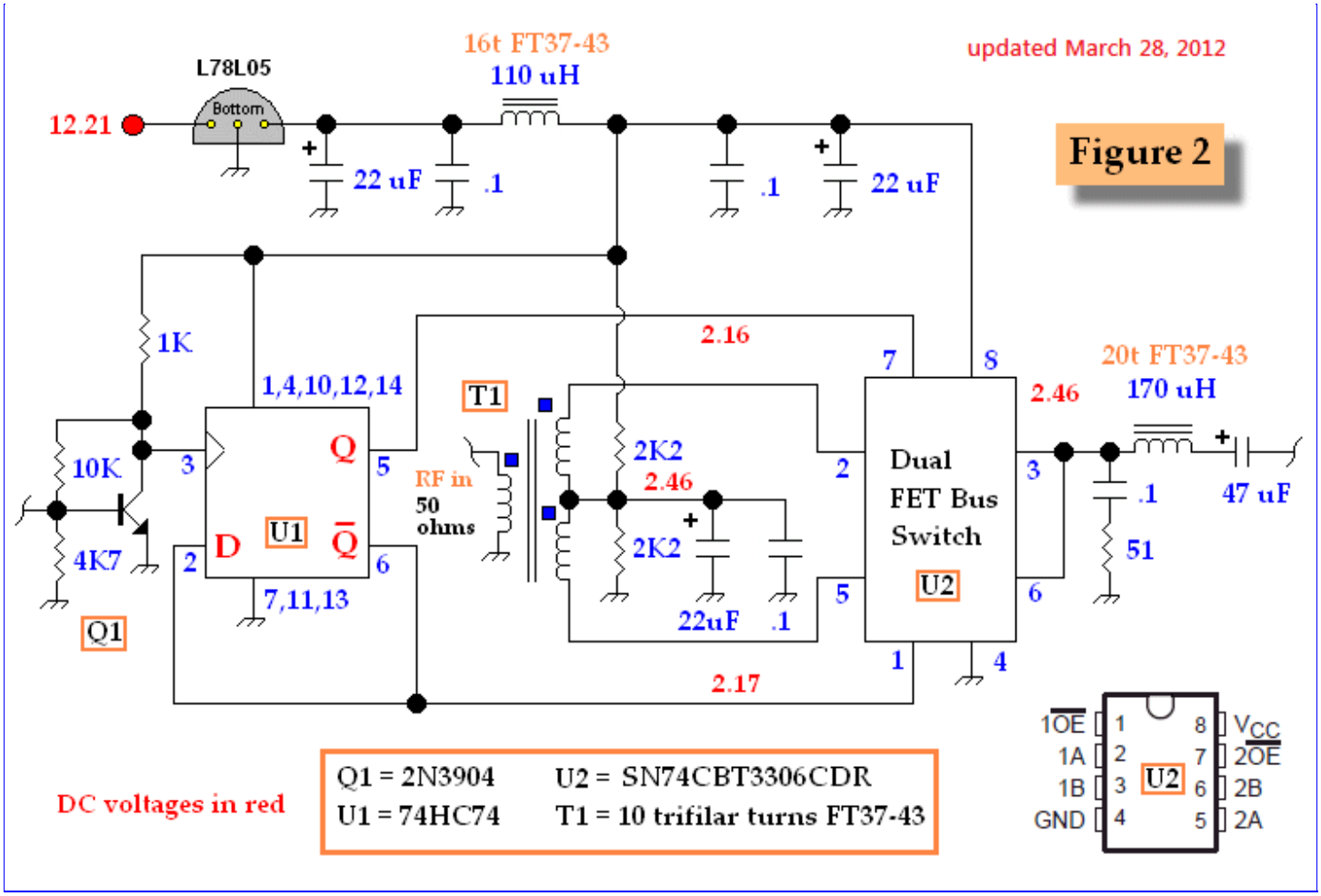

Shown above in Figure 2 is the BJT driver, D flip-flop and the CMOS switch product detector. The 14 MHz VFO connects to Q1 via a 0.1 uF coupling capacitor that is shown on the VFO schematic. A dual FET bus switch (CBT3306) serves as the product detector. The on-resistance of this switch is only around 3 ohms! If you are ambitious, you might try using a 14 pin SOIC switch such as the QUAD FET SN74CBT3125DR with 2 pairs of the 4 switches wired in parallel. I tried 3 different CMOS switches in the U2 slot. The other switches were the MAX4066CPD and a 74HC4053 (wired up appropriately using their datasheets). The insertion loss and performance of these 2 switches was disappointing. My bench standard for comparison was a 7 dBm diode ring mixer. Numerous experiments were performed. For example, I tried running the 4066 at 12 volts VCC to minimize its on-resistance and had to modify most of Figure 2 as well. Being new to digital, blending 5 volt and 12 volt logic IC required great effort to get it working properly. These experiments consumed the better part of 2 days. My conclusion was that if you are going to go to the trouble of make a CMOS switch work, you might as well use a part that has a low on-resistance. Hence, I have since abandoned using DIP IC CMOS switches (4053, 4052, 4066 etc.) as mixers and product detectors. They may still be a good choice in your own context.

The CBT3306 is outstanding and very similar to the diode ring mixer with respect to insertion loss and audio quality as a product detector. There are some other good CMOS switches you might try. I chose the CBT3306 because it was SOIC (the largest of the common SMT topologies), costs only 77 cents (Canadian dollars) and only has 8 pins to deal with. Pragmatism on the workbench is always good!

SMT versus VE7BPO

The difficulty with using the CBT3306 was that I had to learn about and equip for SMT. I ordered the switches and after their arrival, hesitated to do anything with them for 5 days. I managed to borrow a magnifier and bought a SOIC prototype board and some flux. Still, I seemed to be paralyzed with fear about soldering U2. I was stuck. For inspiration, I went back to Mike's web site and found this web page. Here Mike was working with a 18 pin SOIC chip and I was worried about a mere 8 pin IC! Part of the problem was my relatively poor eyesight. I learned this can be managed with a magnifying visor. I bought mine here , but only after U2 was soldered in. The borrowed table magnifier was okay, but constrained arm movement and reduced lighting. The visor seems to be a better choice.

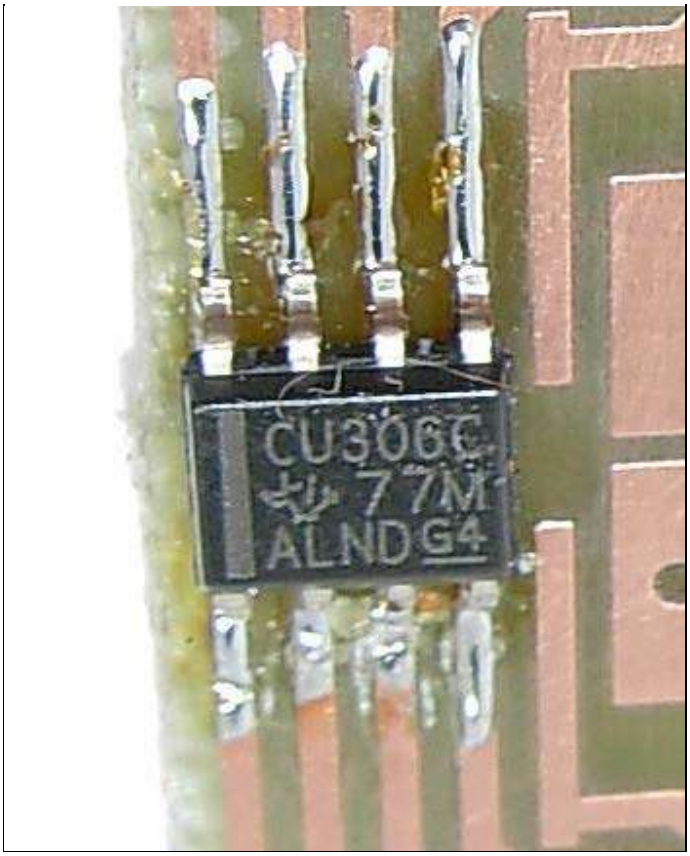

Shown above is the CBT3306 soldered on my prototype board. I put flux on the board traces and then tinned them. Following that, I lined up U2s leads on the traces and began soldering. The bottom pins (pins 1-4) did not go well, but they were soldered all the same. Following that, the soldering of pins 5-8 went very well. I was very happy; the SMT monster had been tamed! It was learned from Wes, W7ZOI that many builders use Surfboards for SOIC applications. I will get some for future SMT IC work. Using SMT parts in your Ugly Construction allows you to use parts which are unavailable otherwise. Increasingly, good old DIP ICs are disappearing from catalogs and some new parts are appearing as SMT only. It makes sense to jump in and use SMT parts when it is advantageous for spec reasons, or if miniaturization is required.

With some effort, the Figure 2 circuit could be morphed into Colin, G3SBI's H-mode mixer format. Not on this web site though! If you Google "H-mode mixer" , many good websites will be returned.

The product detector's baseband audio output is at the 47 uF capacitor which connects to Q1 of Figure 3. A simple 51 ohm, low pass network is used to terminate U2. This is from W7EL's An Optimized QRP Transceiver from QST for Aug 1980. I have some more information regarding AF termination circuits on this web page. You may wish to increase the 170 uH inductor value somewhat to get more low pass filtering. The product detector circuit is the number one potential source of hum and noise in this receiver. Take the time to plan your layout to minimize wire length and crossing and provide some physical symmetry. Decouple well.

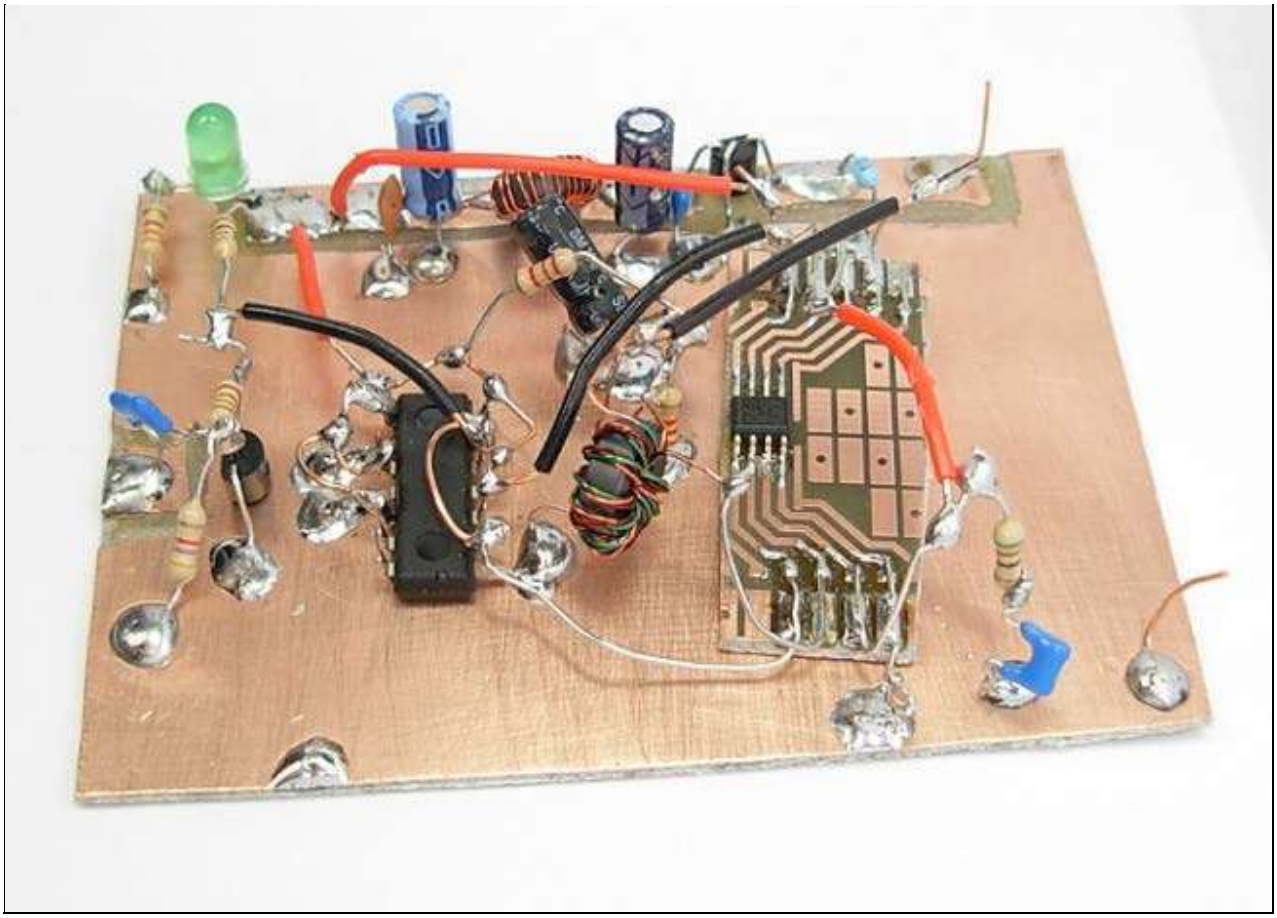

Shown above is the product detector. At this point, I had not decide how to terminate U2 and had soldered a shunt 0.1 uF cap and 51 ohm resistor to the switch output. U2 is dwarfed by the FT37-43 toroid; a part we normally think of as small in size.

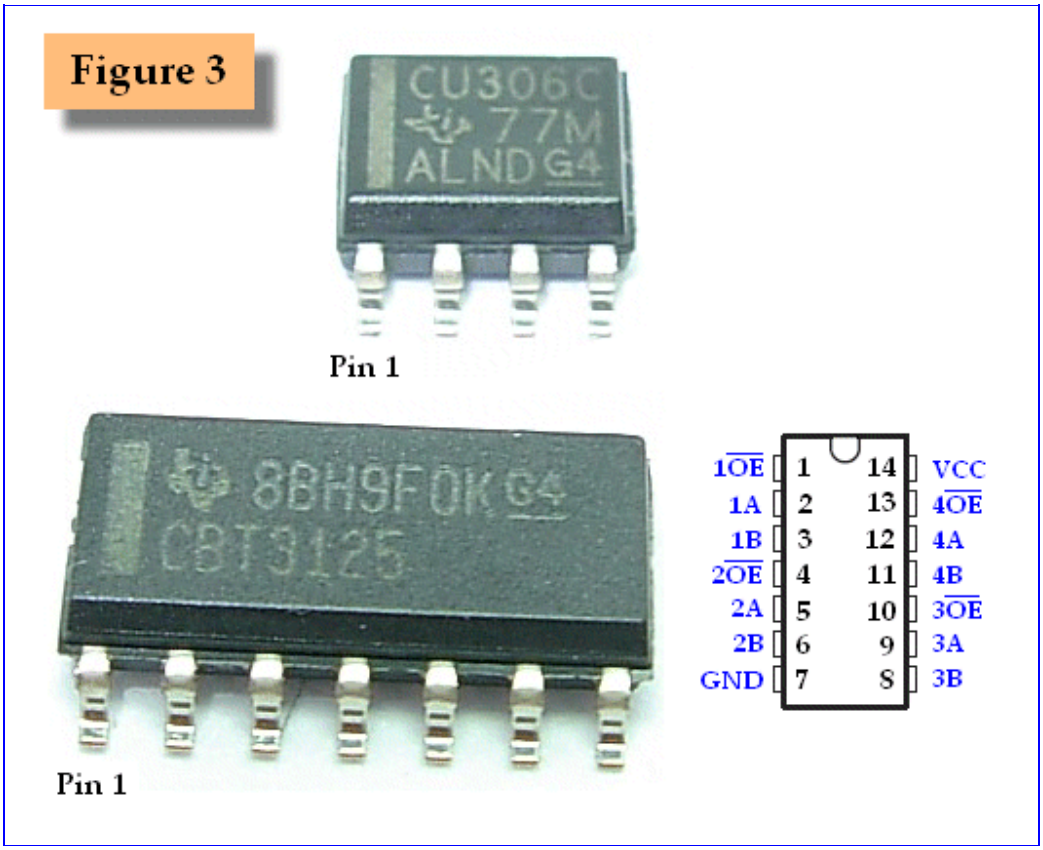

Figure 3. Photographs of the FET bus switches I have in my collection and the pin-out for the 14 pin CBT3125

A diode ring mixer was used as a reference mixer in the product detector experiments.

Audio Amplifier Chain

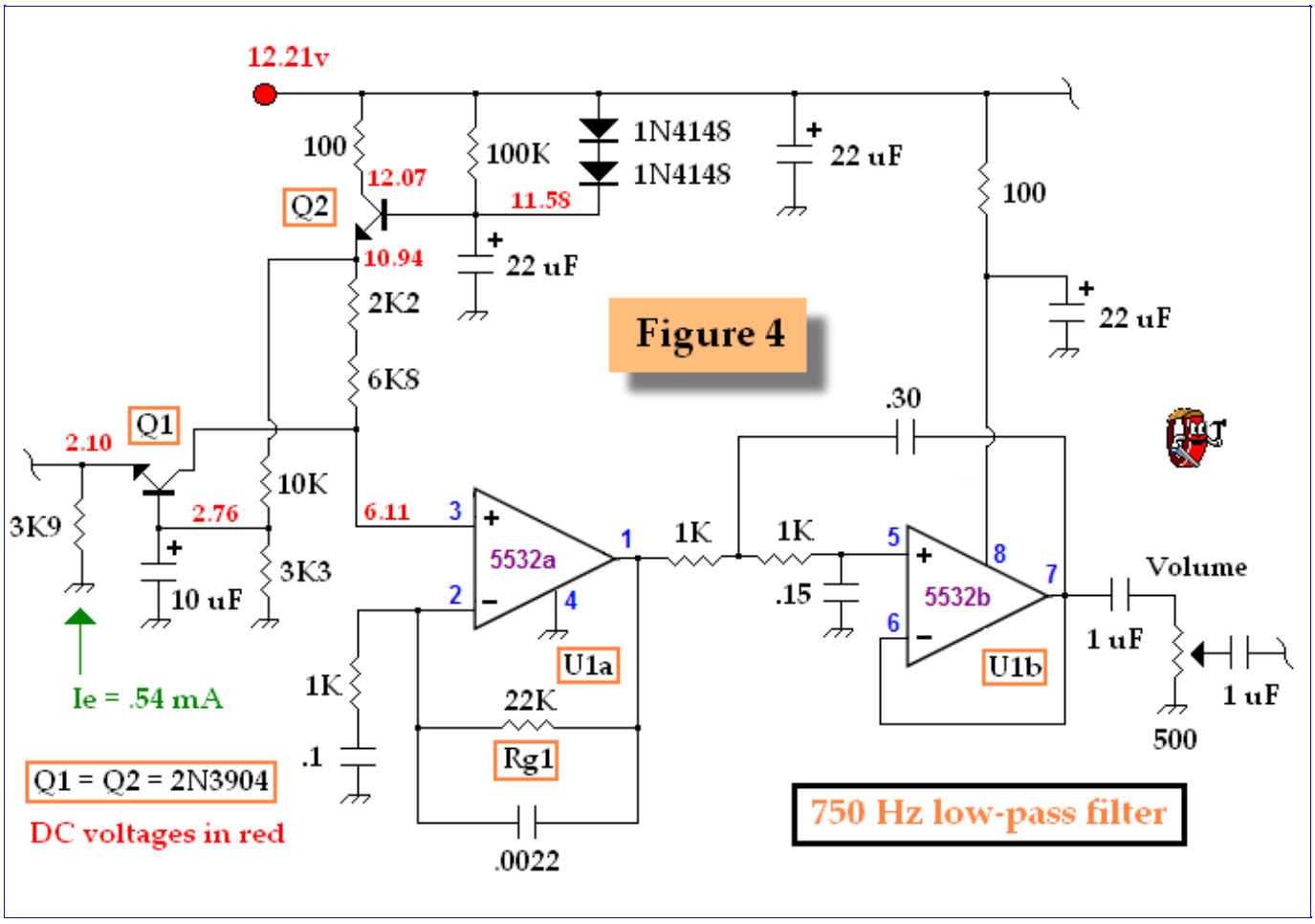

Shown in Figure 4 is the audio preamp and first low pass filter. Direct conversion receivers are all about audio. High performance DC receivers have become more common since Rick, KK7B unleashed his R1 on the world in 1992. High performance receivers are out of scope for this popcorn website, however, this design is welcome. The entire audio chain uses low-cost 5532 op amps, cheap BJTs, plus fairly common resistor and capacitor values. Poly"something" capacitors were used for all audio AC coupling and shunting capacitors of 4.7 uF or less.

For hum immunity, the familiar BJT capacitive multiplier popularized by Roy, W7EL was used at Q2. Using a high-end spectrum analyzer, Wes, W7ZOI demonstrated that this circuit can oscillate. He detected oscillations at UHF. Thus, Wes recommended using a 100 ohm snubber resistor on the Q2 collector to alleviate these parasitic oscillations. Additionally, 2 diodes were added in parallel to the 100K base resistor. This provides an instant-on feature for the audio preamp, as normally there is a time-constant delay when you switch on the receiver. I like this feature, but it is purely optional.

Q1 is a common base amp biased for 0.54 mA. Therefore, the input impedance is 26/0.54 or about 48 ohms. The 6K8 + 2K2 collector resistors were paralleled so that the quiescent collector voltage was close to 6.1 volts. You could also substitute a single 9K1 resistor, although this is an uncommon value. This voltage provides the approximate VCC/2 bias needed for U1a and U1b. Connecting the Q1 collector directly to the pin 3 op-amp input allows the exclusion of a coupling capacitor and the usual VCC/2 resistor network used to bias the 5532 op-amp from a single power supply. I borrowed this from EMRFD.

The gain of U1 is set by the resistor labeled Rg1. If after testing, the AF gain is too high (for example if this AF stage was used in a superheterodyne receiver), simply lower this resistor value. I chose a 22K ohm resistor to allow enough gain for weak signal listening. On louder stations, you will need to lower the volume control to prevent distortion in the stages that follow as overall, there is a lot of gain in this AF chain. Adjust the Rg1 value to suit your needs. If you use a switch such as a 4052 for U2, or your receive antenna is small, you may want to increase this resistor a little for more gain. This is an experimenter's receiver after all. The 0.0022 uF capacitor in the op-amp feedback loop provides a single pole of low pass filtering. I ran this capacitor as high as 0.0082 uF. This gave a theoretical 3 dB cutoff frequency of ~ 880 Hz, but the receiver lost its sizzle. Experimentally, I learned that using a 0.0022 uF feedback capacitor on both U1A and U2A dropped some of the high frequency noise while preserving some sparkle in the received audio.

The audio preamp chain is concluded with a 750 Hz low-pass filter. Resistor values were kept low to minimize noise. All the active low pass filters are low Q, Sallen-Key designs with a Butterworth response. They are stable, easily scalable and brain-dead simple. These filters are fatigueless due to their gentle cut off slope. I actually had a 0.30 uF capacitor in my parts collection, although it was a 600 volt rated part from my tube amp parts bag. You could use two 0.15 uF capacitor in parallel or just substitute a 0.33 uF capacitor. If you can't find a 500 ohm volume control potentiometer, swap in whatever you have, but try to keep the resistance low.

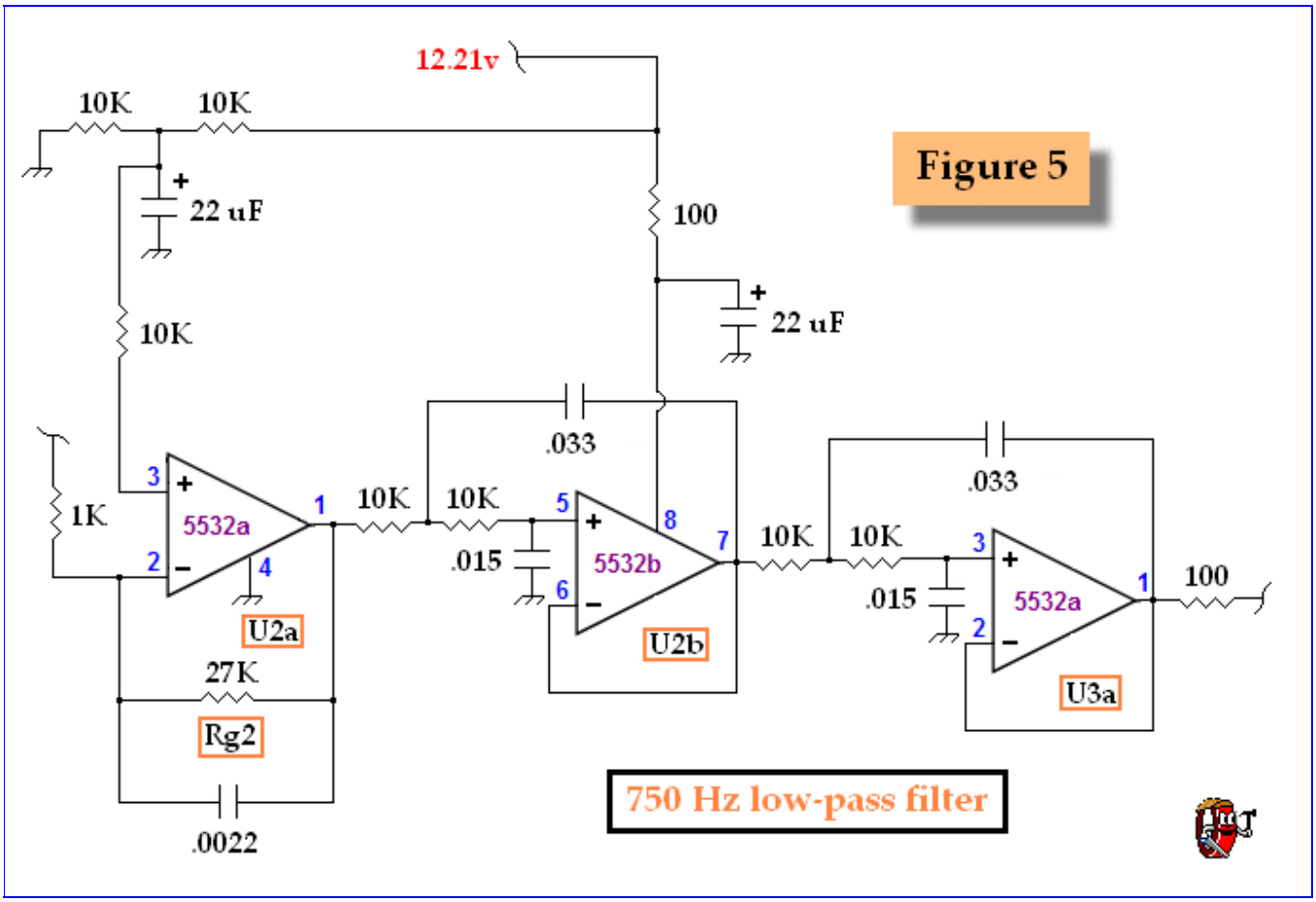

Figure 5

In Figure 5, the remaining preamplifier stage and low-pass filters are shown. Rg2 was chosen for the same reason as Rg1 in Figure 4. Please experiment with these values. The low pass filter stages are scaled up by a factor of 10 as resistance values are less critical at this point in the audio chain. You could use the same resistor and capacitor values used in the first low-pass filter or use the Figure 5 values for all of the low-pass filters. Very often, our parts collections dictate how we experimenters design and build circuits.

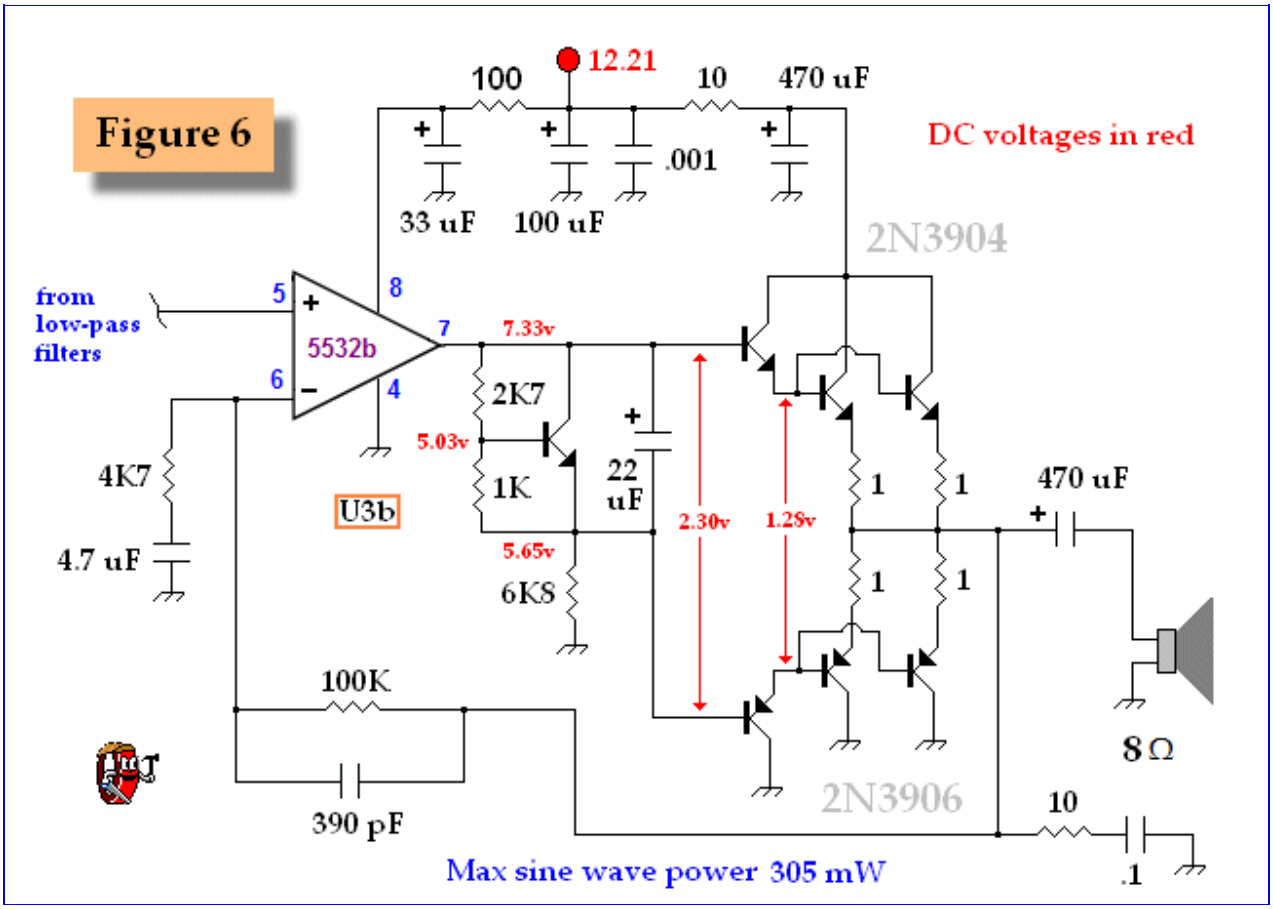

Figure 6 is the power amplifier schematic. Apart from field portable transceivers where headphones are used to save battery power, I exclusively listen to my receivers via a loudspeaker. This safely allows the exclusion of AGC circuits. You may have noticed that AGC circuits have not been presented on this web site. I rarely use them. The extensive VCC decoupling in Figure 6 is needed in this high gain AF chain. The 1 ohm emitter resistors in the finals invite instability, but were tamed with the 10 ohm / 0.1 uF low pass filter. My original design called for 2.2 ohm emitter resistors, but none were available. This final amplifier is moderately loud and very quiet. When it was first built (the AF chain was built backwards), you could not tell it was on when no signal was applied. With no antenna connected to this receiver and the volume on full, there is only a little noise. This is a good way to test a receiver AF chain for noise. Speaker choice is also important. Speakers of a greater power rating and size sound better; especially when mounted in a wooden cabinet.

Biasing power amps has been discussed extensively on this web site. Ensure you measure and record your quiescent DC voltages as shown in Figure 6. If you hear cross over distortion or the quiescent voltage between the bases of the paralleled final transistors is less than 1.25 volts, try decreasing the 6K8 resistor to 5K6 ohms.

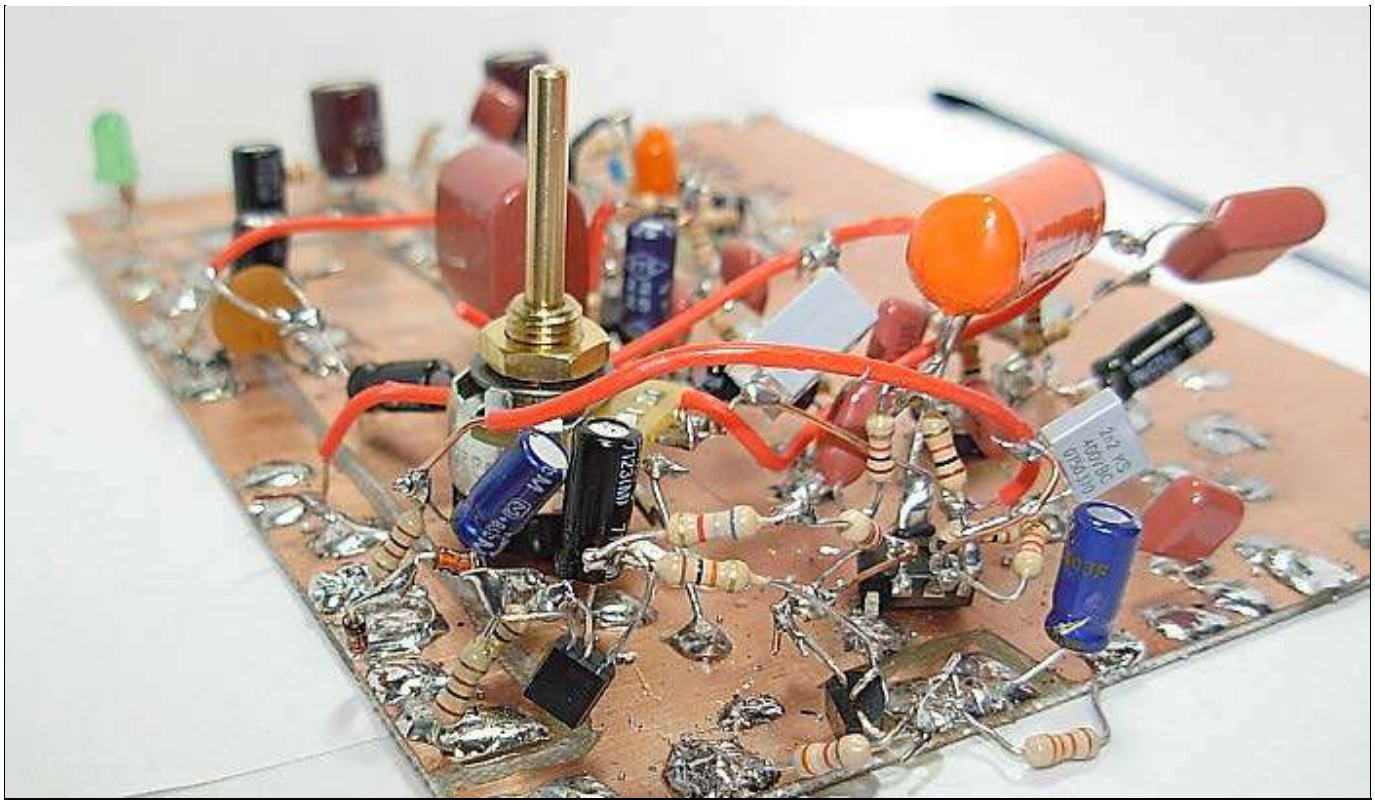

The final preamp breadboard is shown above. You can tell by all the grunge and the solder marks, that many different configurations were trialed. Despite looking haggard, the AF chain is quiet and does not hum nor detect broadcast radio.

Shown above is an early breadboard of Figure 6. In this version, the volume control was at the input and a voltage divider network was wired to pin 5 to provide VCC/2 bias. Testing with an audio signal generator, a tape player and other sources were performed. Later, the biasing resistors and the potentiometer were removed and the Figure 5 stage was added to the copper clad board and tested.

Final Thoughts

We are remembered best by those whom we affect. Certainly Mike's unique perspective and enthusiasm inspired me to dig deeper into this hobby. I asked Bill, M0HBR, for a quote to conclude this web page. Bill wrote this: "Just last week somebody was asking me for background info on Mike's DSB modification of the Heath HW-8... I think it is a real tribute to Mike that years after his passing, hams around the world are still talking about him fondly, still visiting his web site, still following his lead on homebrew radio projects. Certainly among the 3,000 + listeners of the SolderSmoke podcast, Mike is present in spirit every time a soldering iron is heated up." Thank you Bill.

My heartfelt regards to Mike's family.

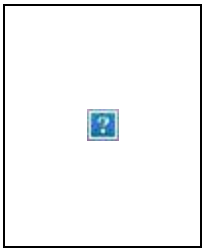

VFO Experiments 2009

Supplement to the VFO 2009 Web Page

This web page is a supplement to the VFO 2009 Web Page

Figure 10 Bipolar Transistor Notes

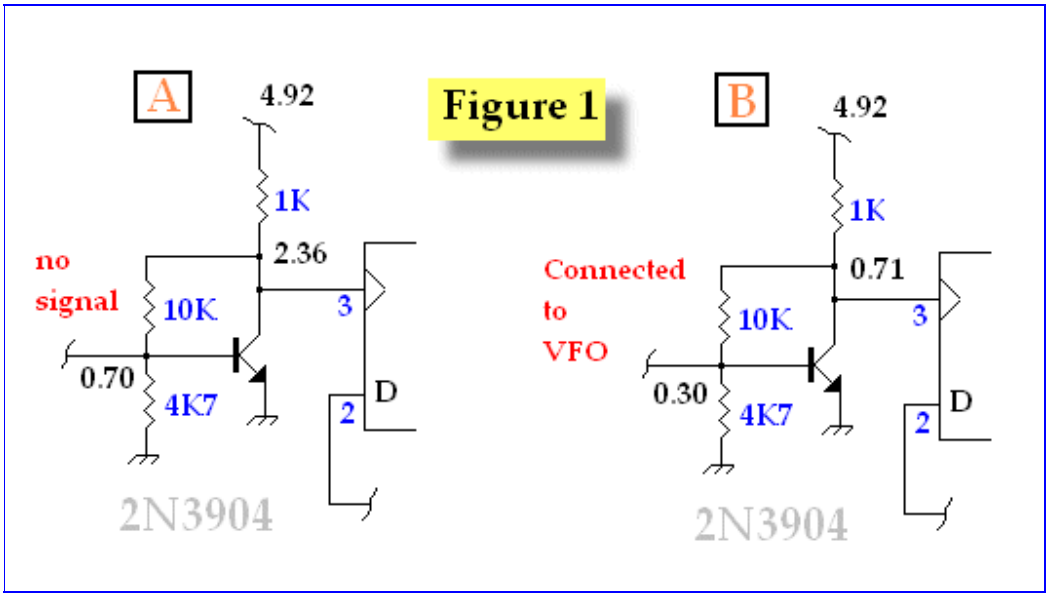

This circuit is from EMRFD and is an analog to digital interface for the VFO. I did not understand the circuit, so I asked Wes, W7ZOI to explain his design criteria and the basic circuit function. This transistor circuit is a driver. The purpose of this transistor driver is to positive edge trigger a D flip-flop. The paramount criterion was that the transistor collector has a quiescent bias voltage that fell between the minimal acceptable logic high and logic low DC voltages on the 74HC74 clock input. See this chart for details about this topic. The correct DC collector voltage is set via feedback from a voltage divider (in this case, a 10K and 4K7 resistor). The collector DC voltage (shown above in Figure 1A) was 2.36 and lies perfectly between the logic low and high state of the 74HC device that it drives.

This transistor circuit is also a high gain amplifier, however, its primary function is a driver. Refer to figure 1B. When connected to the VFO output, the base voltage drops to 0.30 volts. This is an average DC voltage because it fluctuates as the AC waveform swings up and down. More or less AC drive on the input will change this DC voltage.
When connected to the VFO output, the collector voltage dropped to 0.71 VDC. Again, this is just an average, as when the AC swings positive, the the collector voltage will drop down to saturation (where collector voltage is less than base voltage) and then increase towards the positive supply. It does not have to go into cutoff; just to 3.2 volts or so. It also does not have to go into saturation; just to below the 1.3 volts or so. Thus, the transistor remains between cutoff and saturation when appropriately driven with a sine wave.

Our VFO serves as the clock and data on the D flip-flop inputs are only transferred to the flip-flop's outputs on the positive edge of a clock pulse. Positive edge triggering means that the output only responds to the input changes when the clock signal transitions from logic low to logic high. What a fantastic little circuit! You can find additional information and some practical examples in EMRFD. My special thanks to Wes, W7ZOI for

helping me to better understand his design.

Positive Edge Triggering

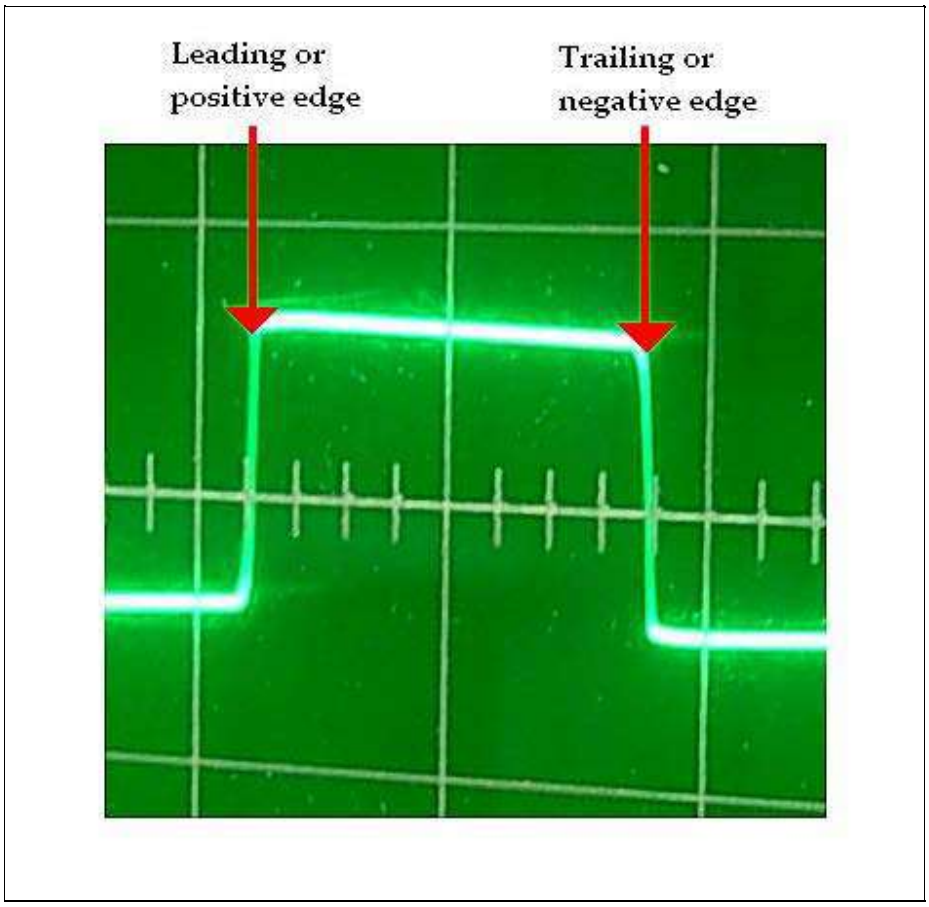

The triggering of a positive edge triggered flip flop is better understood viewing a graphic like above. The instant the waveform goes positive, the flip flop is triggered. It is easy to understand why a square wave is desirable for clean triggering.

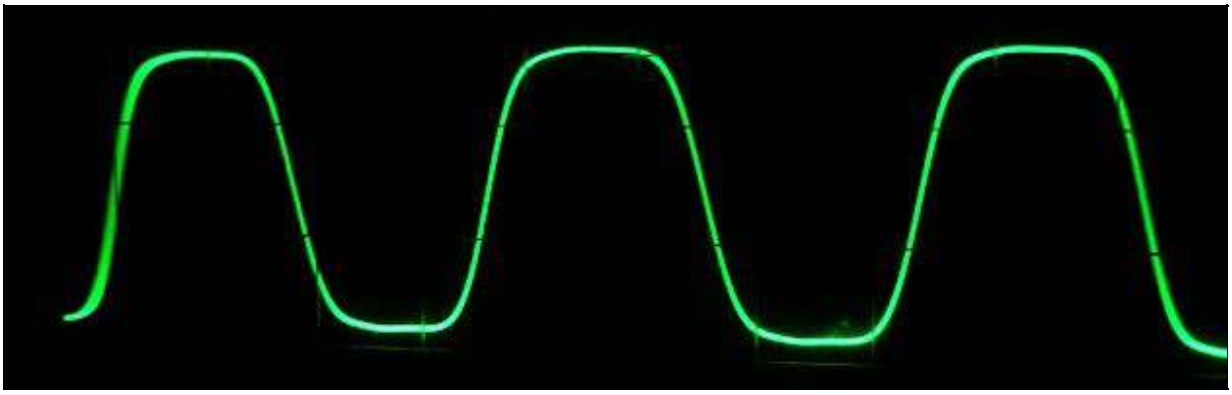

Amateur and Short Wave Radio Electronics Experimenter's Web Site

Radio Amateurs of Canada Support Page

Commentary for Canadian Radio Amateurs

A significant number of licensed Canadian amateur radio operators do not support their national amateur radio society: Radio Amateurs of Canada Typically support is by membership, but may also include volunteering time to perform the various functions required to run a large, non-profit organization. It has been demonstrated repeatedly, that a small percentage of people are doing most of the work in modern volunteer organizations.

Some thoughts concerning volunteerism

- Volunteerism is down in many sectors including service clubs, meal delivery programs, church groups, volunteer firefighters radio clubs, etc. etc.
- The population is aging and our current volunteers are retiring; Younger folks have so many distractions and things they can do today. We now live in a world with 200 plus TV channels! The spirit of volunteerism seems to be decreasing in the western world.
- There is some evidence that people who donate their cash to charities also tend to participate in groups, associations and organizations. Is this a characteristic or trait?
- People volunteer for causes they believe in. What do people believe in now? Is our culture too self-absorbed, individualistic and focused on our own personal agendas and pleasure?
- Economics. Are young to middle aged people less able to volunteer and contribute because they are spending more of their time working?

RAC Membership

If you haven't, please consider joining the RAC. I joined out of respect to the many RAC volunteers who have devoted their personal time and continue to toil to keep amateur radio viable in Canada. We cannot take our currently allocated radio frequency bands for granted. There are groups who for profit, want to apply technologies which will consume or interfere with the radio frequency bands we enjoy. Canadian amateur radio needs a strong, united voice to survive into the future.

Apathy and lack of awareness may significantly decrease the rights and privileges we enjoy as radio amateurs today. The least we can do is support our national amateur radio society. It would be even better if more of us contributed by volunteering our personal time towards our wonderful radio hobby and serving the RAC.

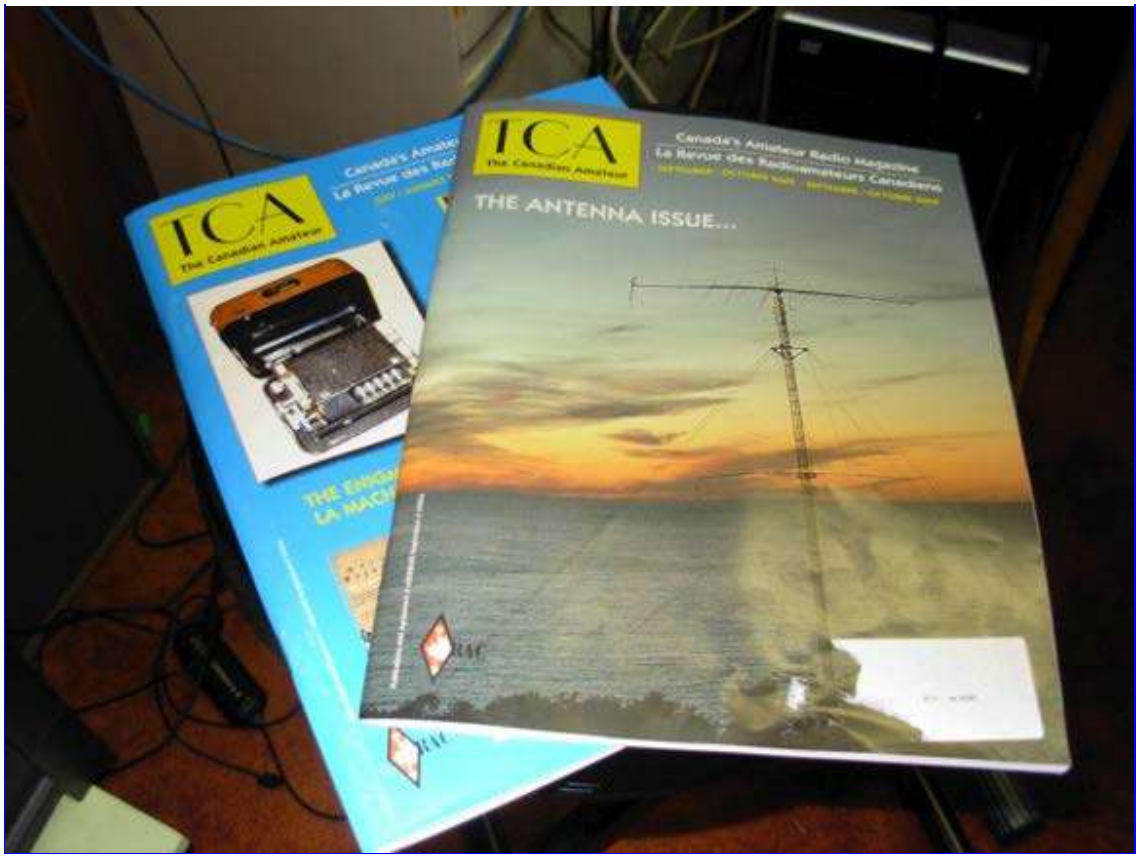

The RAC Journal The Canadian Amateur is an excellent resource. Sept-Oct 2009 marked the first ever antenna issue.

Old QRPHB Web site graphics...

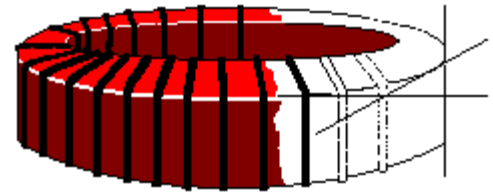

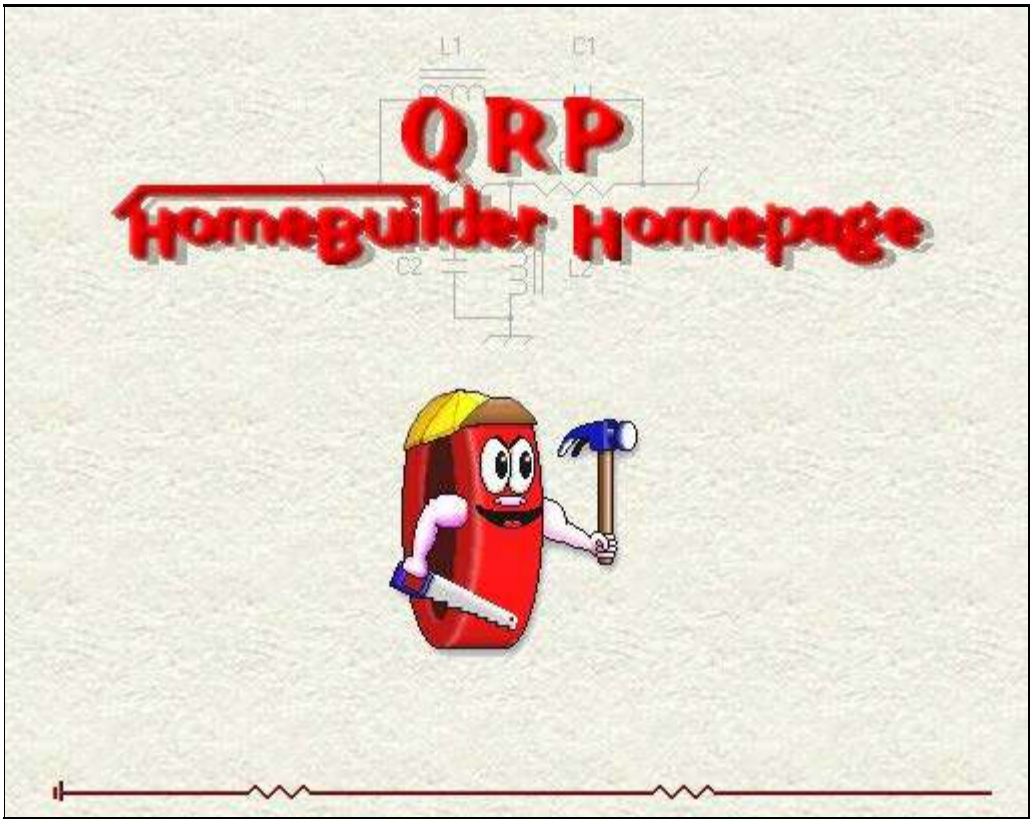
QRP
Homebuilder Homepage

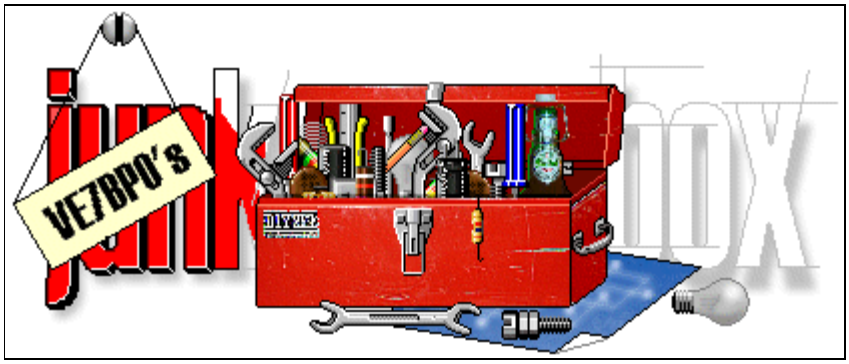
VE7BPU's

This page last updated: September 21, 2013

Info on the Popcorn Superhet RF Amp

Discussion

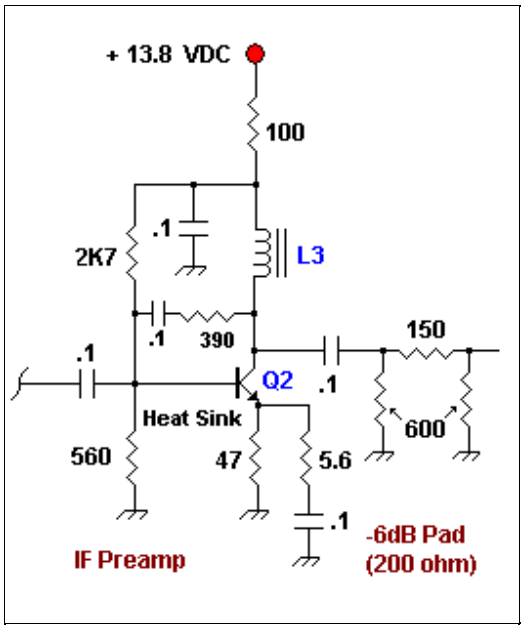

I have received a lot of emails regarding this RF amp from the popcorn superhet receiver. This amp was designed using a calculator and as it turns out, my input and output impedance was off by several ohms from the target 50 ohms input Z and 200 ohms output Z. Today we have computer programs to calculate the resistor values, so crunching the math is not a factor any more. This RF amp is preceded by a 50 ohm diplexer and followed by a 200 ohm pad, so it actually matches the preceding and following stages very well considering that it is clearly depicted to be a popcorn receiver. If I had to redesign this amp in 2008, I would use software to design a CE amp using "noiseless" Norton feedback, Still, this was a good sounding receiver at the time.
Probably the weakest section of this receiver is the audio preamp from Q5 on through to the LM386. I would likely never use these noisy stages in 2008-9. Instead I would use low noise op amps. This web site like my own abilities has grown over time. In the following section, I have paraphrased some writing from Wes, W7ZOI concerning the Q2 RF amp.

An Analysis by W7ZOI

The input impedance of a common emitter bipolar transistor amplifier is related to the standing current, the emitter degeneration resistance, the transistor beta, the F-t, and the operating frequency. Most of those details can be well modeled with the hybrid pi model. If you put quite a bit of emitter degeneration in such an amplifier, the gain drops while the input impedance increases. However, it is much less dependent upon beta and frequency. The emitter degeneration is one form of negative feedback. But now we introduce a second form of negative feedback by applying some of the collector voltage to a resistor that generates a current that is fed back to the base. This feedback tends to reduce gain just as does emitter degeneration. But it also tends to reduce input impedance. By playing a careful balancing act, you can design an amplifier that has a 50 Ohm input and output impedance with a reasonable amount of gain. This particular circuit has a gain of 21.7 dB at 10 MHz and an input return loss of 14 dB. The output return loss is even better at 18.6 dB. Z-in is 39-j14 while Z-out is 172-j34.

These are calculated values using that hybrid pi model. I have devoted a few pages to a discussion of this feedback amplifier topology in the ARRL 2003 book, Experimental Methods in RF Design. This was co-authored by KK7B and W7PUA. You can get the book on line from the ARRL. The book includes computer programs that will handle the design chores. One deals with bias issues while another does the RF design and analysis.

The RF amplifier under discussion may be found on this web page

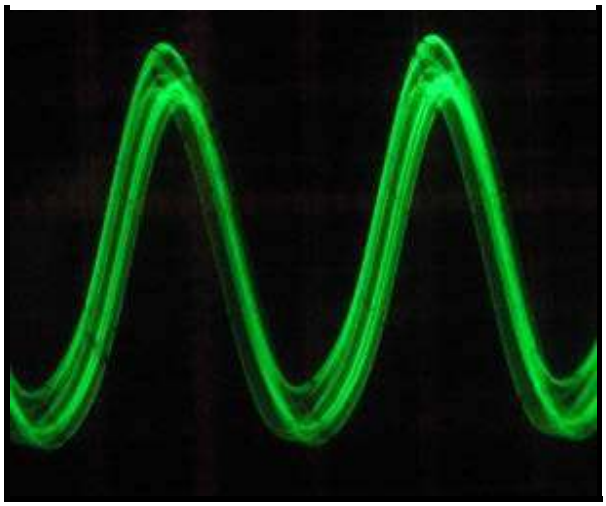

3 MHz VFO for 40M Popcorn Superhet Receivers

Discussion

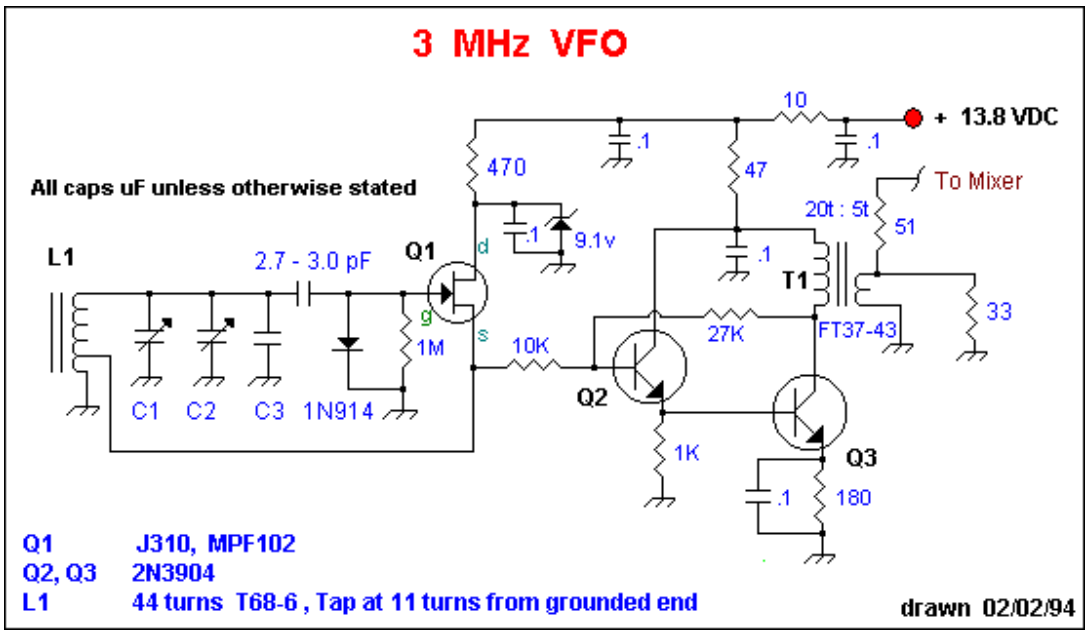

This VFO was first popularized by Roy Lewallen, W7EL and has been used in countless homebrew and commercially sold QRP rigs. For the 40 meter ugly super hets, you have a choice of a VFO frequency of 3 MHz or 11 MHz and I chose the former for this website. For L1, you can use the T68-6 as shown or redesign your own inductor using a T50-6 core. The T68-6 core allows the builder to wind the coil using # 24 AWG wire for enhanced Q and stability. The main tuning capacitor, C1 that was used had a built in reduction drive and went from 4 - 19 pF. If you use a tuning capacitor with a greater capacitance swing, you may have to connect it to the top of L1 via a small-value NP0 capacitor to reduce the tuning frequency range. This can be done using math or by just plain experimentation. C2 is a small ceramic air-variable trimmer from my junk box used to set the lower band edge of the VFO. It can be omitted if the user wants to go frugal and experimentally set the lowest frequency of the VFO using small-value ceramic NP0 caps. Air variable caps for C1 and C2 are mandatory for minimal drift VFO operation. C3 actually refers to 4 NP0 ceramic caps which were used to place the VFO on the correct frequency. Four caps were used to minimize heating and thus drift in the VFO. For the prototype VFO which tunes something ~ 3.00 to 3.67 MHz , I used the mentioned air-variable, four NP0 ceramic caps (20pF,100pF,5pF,100pF) and C2 the trimmer cap that went from 2 - 50 pF. These values should be used only as a guide for prospective builders as there are many variables at play. Following a 10 minute warm up period, the VF0 frequency stability is excellent. Again, keeps all component leads as short as possible. T1 is a broadband transformer wound by using 20 turns of # 26 AWG over a FT37-43 toroid core and then distributing 5 secondary turns spaced evenly over the primary windings. Do not omit the 33 ohm load resistor. The 2.7 to 3.0 pF coupling cap should also be of the NP0 ceramic type. Q1 can be the J310 (my favorite) , 2N4416 , MPF102 or other correct substitutes.

This VFO should be in a separate sealed, shielded box from the rest of the receiver

.

VFO Stability Hints

Numerous tips for enhancing VFO stability have been generated from Wes Hayward, W7ZOI, Roy Lewallen, W7EL, Doug DeMaw, W1FB and others. Here are a few summarized:

1. Use air wound or powdered-iron toroidal inductors made from number 6 material.
2. Use the heaviest gauge of wire possible to wind your inductor.
3. Anneal the inductor by boiling it in water for around 5 minutes after winding.
4. Use ugly construction above a SINGLE-SIDED copper side up ground plane.

5. Capacitors in the L-C circuit should be NP0 ceramic type.
6. Use air variable capacitors for tuning that have double bearings and no backlash.
7. The VFO should be operated at a lower regulated voltage.
8. Do not use cheap low-Q trimmer caps.
9. Completely encase the VFO to prevent RF leakage and to minimize environmental temperature changes.

---

4 MHz BFO for 40M Popcorn Superhet Receivers

Discussion

Shown is a 2 stage BFO for use with the Ugly 40 meter superhets with a 4.00 MHz IF. This is a design by W7ZOI which I have used from 3.5 to 9 MHz by only changing the crystal and the Q2 output coil and capacitor values to suit the frequency of choice. The output coil is 59 primary and 12 secondary windings on a T68-2 toroid core. You will need in the order of 79 pF to resonate this coil, thus a 68 pF plus a 5-20 pF variable works well. If you do not have a T68-2 core, a T50-2 could be used with 30 AWG wire which is a bit difficult so you could opt for an XL of 200 ohms which would be 40 primary and 8 secondary turns on a T50-2 core. You would need ~200 pF to resonate such a coil and the BFO would have reduced output power, but would still work okay. If you design your own tank, you probably should not use an XL/XC less than 190 ohms for the output stage at 4 MHz. Use a 5:1 turns ratio for primary to secondary windings.

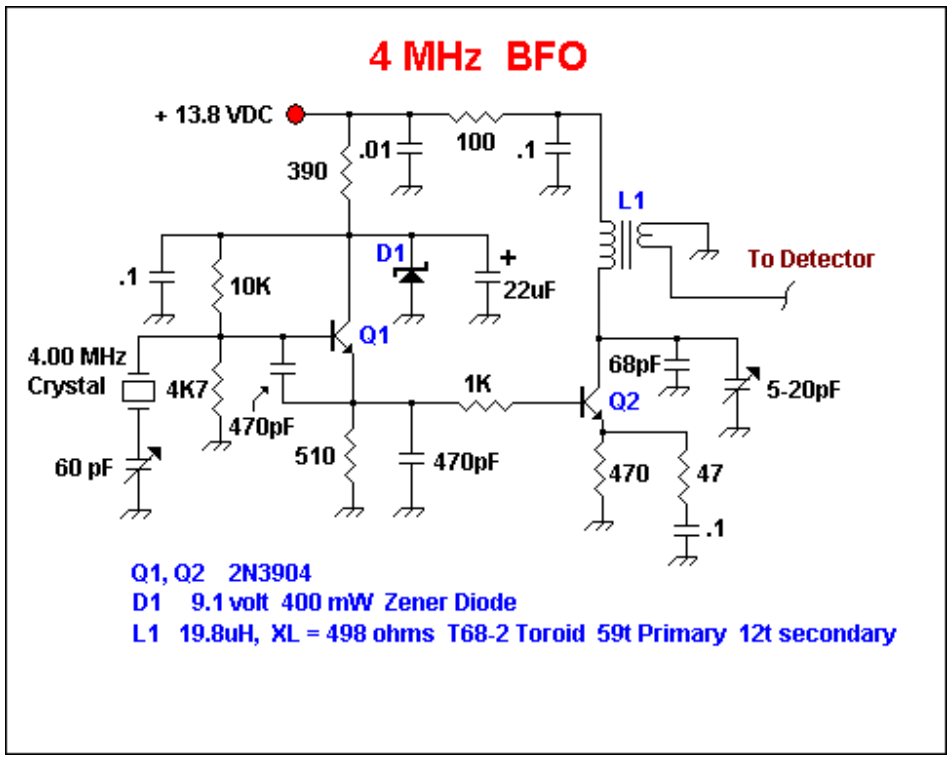

It

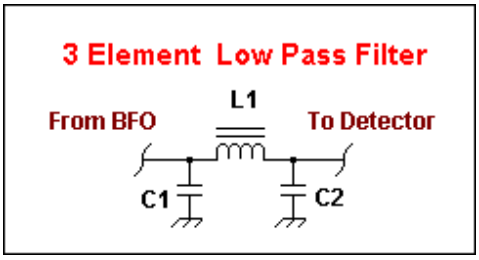

wouldn't hurt to follow the Popcorn Superhet BFO with a low pass filter. A simple pi-type 3 element filter is suitable. Since I had a couple of 470 pF caps left over, I made a low pass filter using a 6.8 MHz cutoff frequency with a 1.17 uH inductor. A 1.17 uH inductor using a T37-2 core requires 17 turns while on a T50-2 core requires 15 turns. Caps were inexpensive monolithic ceramics from Digi-Key. The filter is shown below, L1 = 1.17uH , C1 and C2 = 470 pF. If you want, you may use other cutoff frequencies to suit any junk box caps you have on hand and use an XL/XC of 50 ohms.

Construction

Keep component leads as short as possible to promote stability. Do not omit the zener diode D1. I thought of using a small ferrite bead on the base of Q2 and will try it on the next version of this BFO that I make. The BFO, if unstable can break into all sorts of weird AF sound effects that are very annoying. The BFO should ideally be in a shielded box, but many amateurs have good results by just placing the BFO strategically in the receiver chassis. When winding L1, make sure you wind the secondary coil so that the secondary's grounded end is on the cold side of the

primary coil that connects to the 100 ohm resistor and positive voltage. I just pick one end of the primary coil and close wind the secondary coil from this point in the same direction for the correct number of windings. Then the starting point of the secondary can be grounded and the other end connected to the detector or a low pass filter. After building the coil, temporarily place a 51 ohm resistor from the secondary output lead to ground. Then you can test and peak the tuning of the output tank into a load. Leave the resistor in place for all your testing work such as crystal matching or RF stage testing until you are ready to connect it to the product detector. The 60 pF variable cap connected between the crystal and ground is used to set the beat frequency of the BFO. Adjust it to get a good sounding beat note when listening to a station. You will notice that the beat frequency can be tuned roughly by just listening to 40 meter band noise in the headphones and then tweaked on an active QSO.

QRPHB Archive Schematics

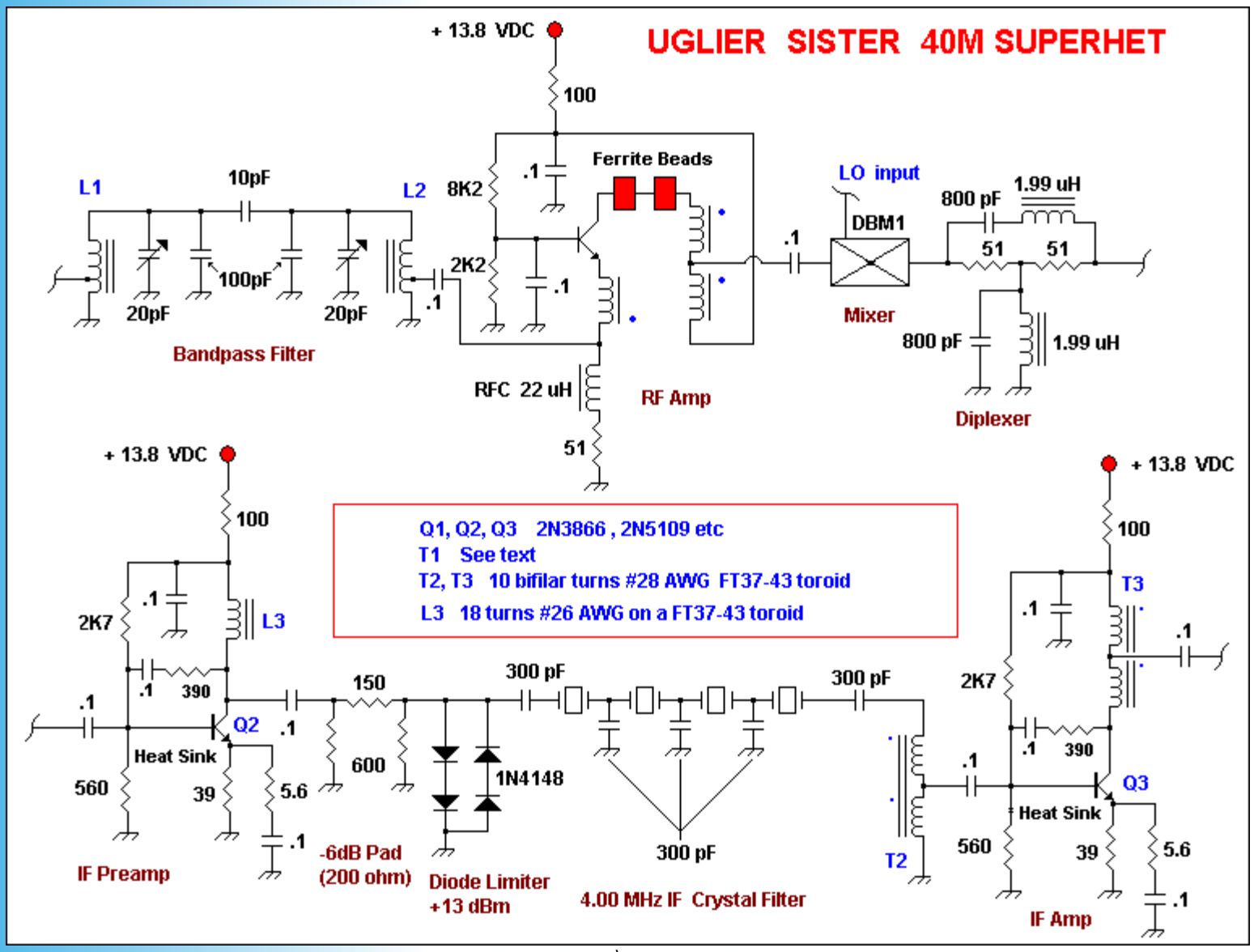

<\p>

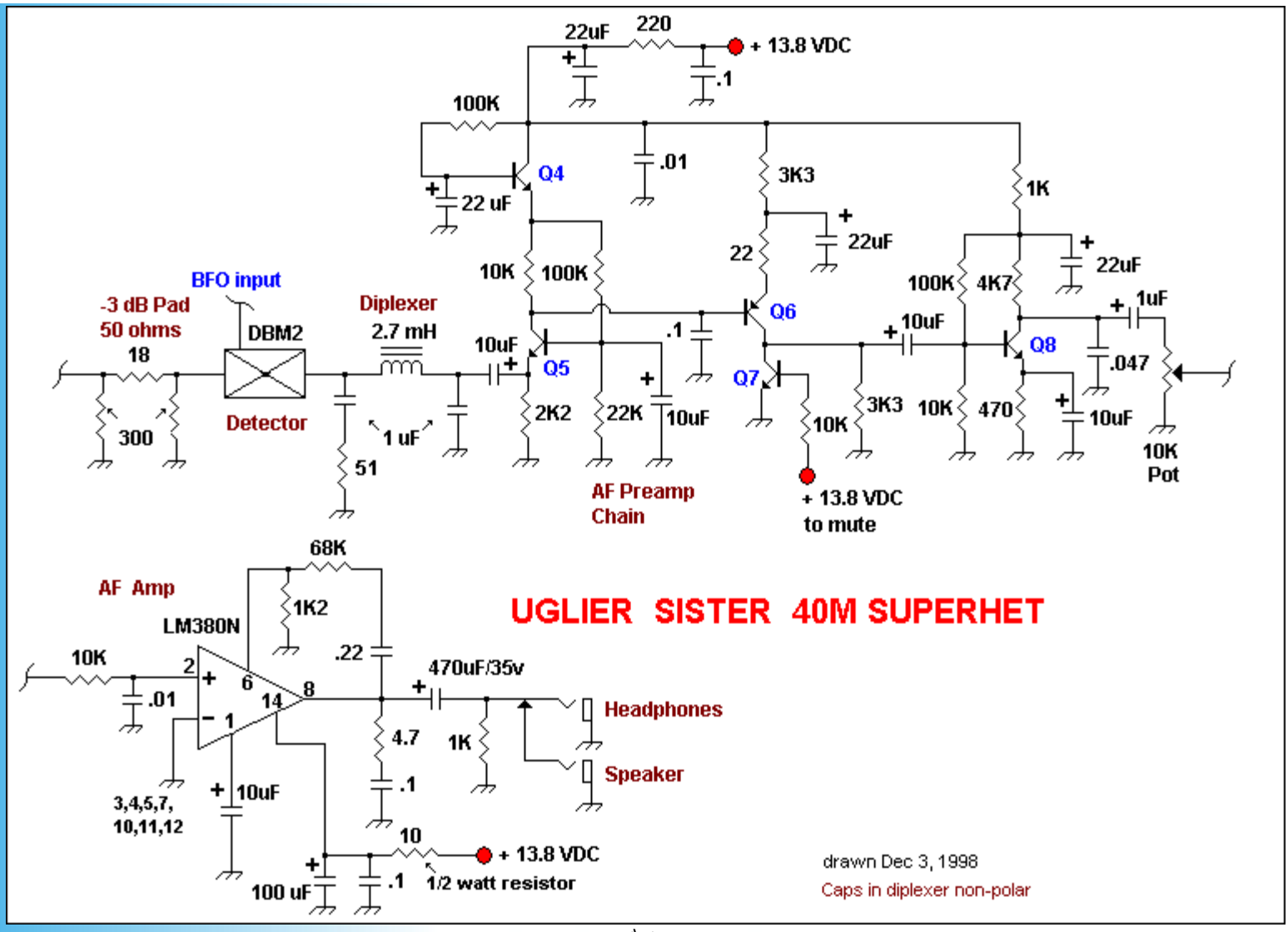

<\p>

Uglier Sister Superhet Receiver

This is a 40 M superhet that I built a few years ago. While I was happy with this receiver, it has been discontinued from the main listings on the QRPHB website. I have had a couple requests for this schematic, so I have created this archival web page.
I stood a lot of current in the IF preamp and main IF amplifiers, which is not really necessary, particularly in the case of the post-filter amp. Of course raising the emitter resistor values is easy to do in these amps if you do wish to lower the current. There also is no audio filtering in the AF preamp stages, which is something that I often use in better quality receivers that I build now.

VFO and BFO

VFO schematic
BFO schematic

Construction Information

Refer to this web page for details on the xtal filter, diplexer and construction information.

The Norton RF preamp is discussed on the RF Preamp web page.

Return to the QRP HomeBuilder Homepage

Diplexer Supplemental Page

More Information on the Bridge-Tee Diplexer

Introduction

No web page on the QRPHB web site has furnished more email and controversy than the Diplexer Web page. This page has received much work to improve its content and accuracy and the email received has been greatly appreciated. Presented is the detailed math and some information regarding the Bridge-Tee Diplexer by Helmut Strickner, VK4STR and Wes Hayward, W7ZOI.

VK4STR

The T-bridge diplexer math calculation (also known as the W1JR diplexer)

The formulae presented and used in the program for the Bridge-T Diplexer uses a Q of 1. Using a Q = 1 resonator is not optimal because we don't want a "broad peaking response" of the series LC resonator in the T-bridge diplexer. Our goal should be to only let the desired IF frequency pass and attenuate all other frequencies as much as possible by properly terminating them into 50 Ohms in the diplexer.

The optimal Q for HF frequencies is around 10, less for higher frequencies. The higher Q of the series resonator effectively increases the attenuation of undesired harmonic frequency components from the mixer IF-port, and the reflected products from the crystal back to the IF-port. The IM performance (IP3) of the receiver is improved.

The possible improvement in IP3 depends mainly on the following stages. The post-mixer amplifier following the diplexer has to handle huge impedance variations at the input of the crystal filter. Crystals do not absorb but reflect any products they cannot handle. These products are then reflected back to the IF-port of the mixer deteriorating the IM performance.

A low Q diplexer lets these reflections from the crystal pass unhindered and most mixers will react with degraded intermodulation performance. It is also important to note that a good termination insensitive post-mixer amplifier should follow the diplexer.

The best results for a high intercept (IP3) receiver can be obtained by choosing:

1. High level mixer
2. T-bridge diplexer with optimised Q (Q=10 for HF)
3. Termination insensitive post-mixer amplifier (see N6NWP - QEX July 1995)

I believe that the intermodulation performance of many receivers can be improved by some simple measures like a properly designed diplexer. The T-bridge diplexer from W1JR is the best one around, go for it.

A brief example of the calculation for a 10.7MHz diplexer follows in Figure 1. The value of K should be 10 for short wave and 2 to 4 for VHF (2 meter band). K is the ratio of L to C.

I hope that you can use this example to calculate the values for other diplexer frequencies.

To fully understand the basis of this calculation please refer to Meinke/Grundlach: "Taschenbuch der Hochfrequenztechnik", Springer-

$$K = \frac{1}{Z}\cdot\sqrt{\frac{L}{C}} \quad (K = 10) \qquad \omega_r = 67\,196\,000$$

$$L_1 = \frac{K\cdot Z}{\omega_r} = \frac{10\cdot 50}{2\cdot 3{,}14\cdot 10{,}7\cdot 10^6} =$$
$$= 7{,}44\cdot 10^{-6} \approx 7{,}5\ \mu H$$

$$C_1 = \frac{1}{\omega^2\cdot L_1} = \frac{1}{(2\cdot 3{,}14\cdot 10{,}7\cdot 10^6)^2\cdot 7{,}44\cdot 10^{-6}} =$$
$$= 29{,}7\cdot 10^{-12} \approx 30\ pf$$

$$L_2 = C_1\cdot Z^2 = 29{,}7\cdot 10^{-12}\cdot 50^2 =$$
$$= 7{,}42\cdot 10^{-8} \approx 74\ nH$$

$$C_2 = \frac{L_1}{Z^2} = \frac{7{,}44\cdot 10^{-6}}{50^2} =$$
$$= 2{,}97\cdot 10^{-9} \approx 3\ nF$$

Figure 1

73!
Helmut VK4STR

Verlag Berlin/Heidelberg. Page 127.

W7ZOI

Attached are some outputs from Mathcad, Version 7.0. The "proper" equations are derived, along with some other results. Feel free to put these on the web, although this is mathematics rather than the usual "formulas" and there might not be any interest in such stuff.

As it turns out, the formula that Todd presented in completely accurate for the case of Q=1. That is, both the series and parallel tuned circuits have inductors and capacitors with reactance of 50 Ohms. Evaluation then shows that S11=0 for all frequency, while S21 peaks broadly at the resonant frequency. If you pick a higher Q, the inductor in the series tuned circuit increases by Q and the capacitor in the parallel one increases by Q. Resonance is maintained in both. Again, you then get a perfect match at all frequencies and a S21 peak at resonance. But I don't know if this is what Joe had in his original work.

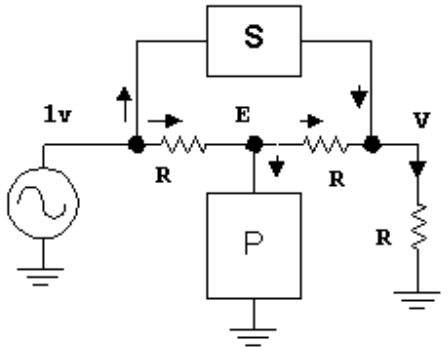

Shown is a general bridge T type network with series impedance S and parallel impedance P. We wish to find the input impedance seen by the generator. But to do this, we need to know the input current. The input voltage is set at 1, so Zin=1/Iin. To calculate this, we must know E and V. These are obtained with a nodal analysis.

We write the nodal equation at E :

$$\frac{(1-E)}{R}=\frac{E}{P}+\frac{(E-V)}{R}$$

We solve this for E:

$$\frac{(1-E)}{R}=\frac{E}{P}+\frac{(E-V)}{R}\ \text{solve},E\ \rightarrow\ \frac{-\left(\frac{1}{R}+\frac{1}{R}\cdot V\right)}{\left(\frac{-2}{R}-\frac{1}{P}\right)}$$

We now write the equation at V and solve it for E:

$$\frac{(1-V)}{S}+\frac{(E-V)}{R}=\frac{V}{R}\ \text{solve},E\ \rightarrow\ -\left(\frac{1}{S}-\frac{1}{S}\cdot V-\frac{2}{R}\cdot V\right)\cdot R$$

We now equate the two expressions for E to each other and solve that for V.

$$-\left(\frac{1}{S}-\frac{1}{S}\cdot V-\frac{2}{R}\cdot V\right)\cdot R=\frac{-\left(\frac{1}{R}+\frac{1}{R}\cdot V\right)}{\left(\frac{-2}{R}-\frac{1}{P}\right)}\ \text{solve},V\ \rightarrow\ \frac{-\left[\frac{-R}{S}+\frac{1}{\left[\left(\frac{-2}{R}-\frac{1}{P}\right)\cdot R\right]}\right]}{\left[\frac{R}{S}+2+\frac{1}{\left[\left(\frac{-2}{R}-\frac{1}{P}\right)\cdot R\right]}\right]}$$

which simplifies to $V=\dfrac{\left(2\cdot R\cdot P+R^2+P\cdot S\right)}{\left(2\cdot R\cdot P+R^2+3\cdot P\cdot S+2\cdot S\cdot R\right)}$

We now take one of the expressions for E and put V in it to obtain a complete solution.

$$E=\ 2\cdot P\cdot\frac{(R+S)}{\left(2\cdot R\cdot P+R^2+3\cdot P\cdot S+2\cdot S\cdot R\right)}$$

The next chore is to evaluate the input impedance, Zin. We get this by calculating the input current. The input voltage is set at 1, so Zin=1/ i-in.

$$\text{i in}=\ \frac{(1-V)}{S}+\frac{(1-E)}{R}\qquad \text{So } Z=\ \frac{1}{\left[\frac{(1-V)}{S}+\frac{(1-E)}{R}\right]}$$

which simplifies to $Z\text{ in}=\dfrac{-1}{(-R+R\cdot V-S+S\cdot E)}\cdot S\cdot R$

But to get a meaningful expression, we must sub V and E into this. When we do so, we get

Figure 2

$$Z\,in = \frac{\left(2\cdot R\cdot P + R^2 + 3\cdot P\cdot S + 2\cdot S\cdot R\right)}{\left(2\cdot R\cdot P + 3\cdot R^2 + P\cdot S + 2\cdot S\cdot R\right)}\cdot R$$

This is now a useful result. We can, for example, let S, P, and R be resistor values. We can then design bridge T attenuators. But let's continue with the analysis. Let's ask the question "What are the conditions that will provide an input impedance of R?" We merely set the Zin expression equal to R, and then solve that equation for S or P. We will solve for P.

$$\frac{\left(2\cdot R\cdot P + R^2 + 3\cdot P\cdot S + 2\cdot S\cdot R\right)}{\left(2\cdot R\cdot P + 3\cdot R^2 + P\cdot S + 2\cdot S\cdot R\right)}\cdot R = R \text{ solve, } P \rightarrow \frac{R^2}{S}$$

Hey, that's a cool result, and it's even rather simple. This is an expression for P in terms of S. If we use it for attenuators, it says that our pad is matched with these conditions. We can combine these results with the equation for V to get the attenuation. A couple of interesting matched pads are shown:

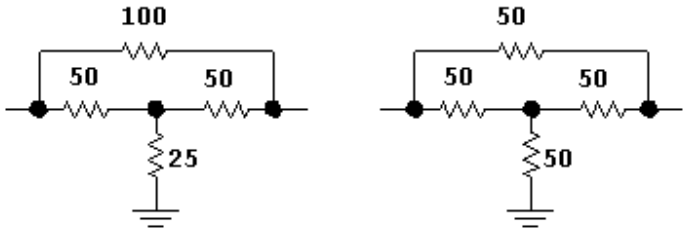

Figure 3

The expression for V was $\frac{\left(2\cdot R\cdot P + R^2 + P\cdot S\right)}{\left(2\cdot R\cdot P + R^2 + 3\cdot P\cdot S + 2\cdot S\cdot R\right)}$ But the conditions for a match were $P = \frac{R^2}{S}$ So, we put this in for P.

$$\frac{\left(2\cdot R\cdot P + R^2 + P\cdot S\right)}{\left(2\cdot R\cdot P + R^2 + 3\cdot P\cdot S + 2\cdot S\cdot R\right)} \text{ substitute, } P = \frac{R^2}{S} \rightarrow \frac{\left(2\cdot\frac{R^3}{S} + 2\cdot R^2\right)}{\left(2\cdot\frac{R^3}{S} + 4\cdot R^2 + 2\cdot S\cdot R\right)}$$

which simplifies to $V = \frac{R}{(R+S)}$ So the two pads have voltage outputs of 0.5 and 0.333 and the resulting attenuations are 6 and 9.54 dB.

But enough about the attenuators. Let's get back to the original question, that of the diplexer. The circuit of interest is one where the series network is a series tuned circuit while the parallel one is a parallel tuned circuit. But we want to know the conditions that will generate a perfect match. With such a circuit, it is clear that a match will exist at resonance so long as both circuits are resonant at the same frequency. The impedance of the series tuned circuit goes to zero while that of the parallel TC becomes infinite (neglecting loss.)

We write the susceptance (imaginary part of admittance) directly for the parallel tuned circuit as

$B_p = \omega \cdot C_p - \frac{1}{\omega \cdot L_p}$ But the reactance is the recipricol of this, $\frac{1}{\left(\omega \cdot C_p - \frac{1}{\omega \cdot L_p}\right)}$

which simplifies to become $\frac{1}{\left(\omega^2 \cdot L_p \cdot C_p - 1\right)} \cdot \omega \cdot L_p$

We know that this is resonant at the same frequency as the series tuned circuit with L and C.

So, $L \cdot C = L_p \cdot C_p$ and $L_p = \frac{L \cdot C}{C_p}$ We substitute these in the above expression:

$X_p = \frac{1}{\left[\omega^2 \cdot (L \cdot C) - 1\right]} \cdot \omega \cdot \frac{L \cdot C}{C_p}$ But earlier analysis showed us that this reactance was related to the series reactance:

$P = \frac{R^2}{S}$ with $S = \omega \cdot L - \frac{1}{\omega \cdot C}$ This lets us set up an equation that is then solved for Cp.

$\frac{1}{\left[\omega^2 \cdot (L \cdot C) - 1\right]} \cdot \omega \cdot \frac{L \cdot C}{C_p} = \frac{R^2}{\left(\omega \cdot L - \frac{1}{\omega \cdot C}\right)}$ solve, $C_p \rightarrow \frac{L}{R^2}$

This is a particularly simple, yet useful result

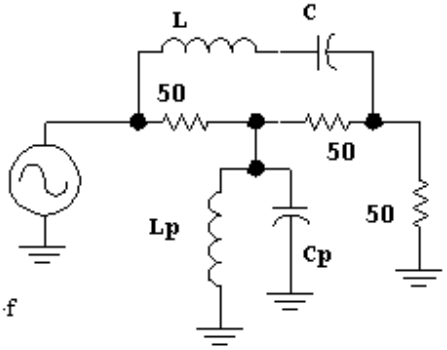

1) Pick a crossover frequency f, Hz. Then, $\omega = 2 \cdot \pi \cdot f$

2) Pick a series inductor L. Use one with a reactance of around 50 Ohms if you want a very broad response. Make it larger for narrower bandwidth.

3) Resonate the series L with a cap, $C = \frac{1}{\omega^2 \cdot L}$

4) Pick a parallel cap $C_p = \frac{L}{R^2}$

5) Resonate that cap with a parallel inductor $L_p = \frac{1}{\omega^2 \cdot C_p}$

Figure 4

This web page is copyrighted 1998-2005

Astable Multivibrator Projects

Discussion:

Astable or free-running multivibrators have been used in home-built amateur radio equipment for many years. The basic circuit is a two stage amplifier with AC-coupled feedback from output to input. One transistor stage is on (conducting current) while the other is off (not conducting current) until the stages switch conducting states repeatedly at a specific frequency. The oscillation frequency is set by the resistor and capacitor values connected to the base terminal of each stage. This RC network determines how long the transistor stays in the off position.

Presented are two projects which utilize astable multivibrators built using the ubiquitous 2N3904 BJT. The first project is a code practice audio-frequency oscillator while the second is a simple , no-frills electronic keyer for keying a transmitter. Either circuit would be a great first project to learn how to build circuits using Ugly Construction.

Code Practice Oscillator

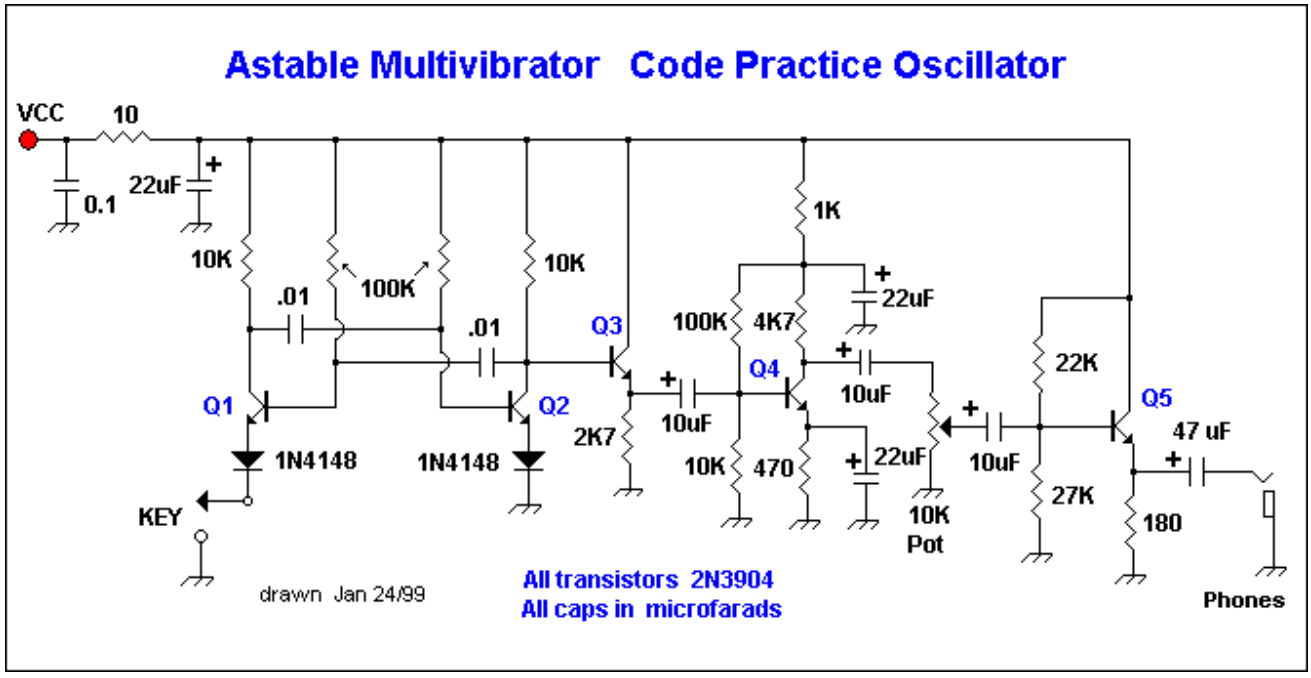

Above is the schematic for a simple Morse code practice oscillator. This circuit was originally built with 2N3904 transistors, however many different NPN transistors could be substituted as required.

Tracing the circuit from left to right first brings us to the multivibrator circuit which is composed of Q1 and Q2. The oscillation frequency of the multivibrator is ~ 700 hertz and is set by the RC network formed by the 100K resistor and the 0.01 uF capacitor connected to each transistor base terminal. The approximate time off for each transistor is given by the following formula:

[Time 0ff = 0.7 * R * C] with R in ohms and C in farads.

It maybe more practical to leave the resistance value fixed and vary the capacitor value to obtain a desired oscillation frequency. Rearranging the above formula allows this :

[Total Time Off = 1 / Frequency] with Total Time Off being the total number of seconds that both transistors are off and Frequency is in hertz.

Once the total time off is known, you must divide that answer by 2 as each transistor is off half of the total time off in this symmetrical circuit. Then you simply solve for the capacitor value:

[Time Half = Total Time Off / 2]
[Capacitor = Time Half / (0.7 * R)] with Capacitor answer in farads.

Lets run the numbers to solve for the capacitor values in the schematic;
R = 100K, desired frequency = 700 hertz.
Total Time Off = 1 / F ----> 1 / 700 = 0.00143 seconds.
Time Half = Total Time Off / 2 ----> 0.00143 / 2 = 0.00071 seconds.
Capacitor = Time Half / (0.7 * R) ----> 0.00071 / (0.7 * 100000) = 0.0000001 farads = 0.01 microfarads.

For 600 hertz, the capacitors would be 0.012 uF and for 400 hertz, 0.018 uF.

As you can see it is maybe necessary to adjust the base resistor value to achieve a specific oscillation frequency. The rule of thumb is that the base resistor should be ~ten times the value of the collector resistor assuming the base-bias resistor is connected to VCC as shown.

The output of the multivibrator is buffered by the high input impedance of an emitter follower Q3. This serves to prevent the oscillation frequency from changing when the output load is changed. The AF stage connected to the emitter-follower is a standard high gain common-emitter amp that has been used in many of the projects on this web site. As the multivibrator is buffered by 2 amplifier stages, good frequency stability is realized and frequency changes are negligible when turning the volume control pot. The final stage is a common-collector amplifier which can drive low impedance headphones with reasonable volume.

Code Practice Oscillator Project Notes

The voltage / time output waveform of the astable multivibrator is largely a square wave which some people find harsh. Many users prefer listening to a sine wave although that is beyond the scope of this web page. The multivibrator shown has real advantages in that, it is both dependable and tolerant with respect to parts substitutions. Keying the oscillator as shown practically guarantees that the multivibrator will start running each time you hit the key.

VCC can be 9 to 13.8 volts DC and the larger the voltage the greater the volume in the headphones. The B+ decoupling circuit at the top left can be omitted for battery operation or if you prefer not to bother with it. The basic multivibrator and emitter-follower circuit can be used in a transceiver as a sidetone for monitoring keying. A series resistor from the emitter-follower maybe necessary to attenuate/match the sidetone to the transceiver's AF amp.

If you desire speaker level output, the Q5 common-collector final can be omitted and the circuit shown below used. This circuit uses the LM386N and provides up to ~ 0.5 watts into an 8 ohm speaker. Connect the Figure 1 circuit as shown to the 10 uF coupling capacitor connected to the collector of Q4. Do not connect the 10 ohm half-watt resistor to the decoupled VCC shown in the schematic. The power supply to the LM386N AF amp should be directly connected to the VCC, not like the common-collector AF stage shown in the schematic to the right.

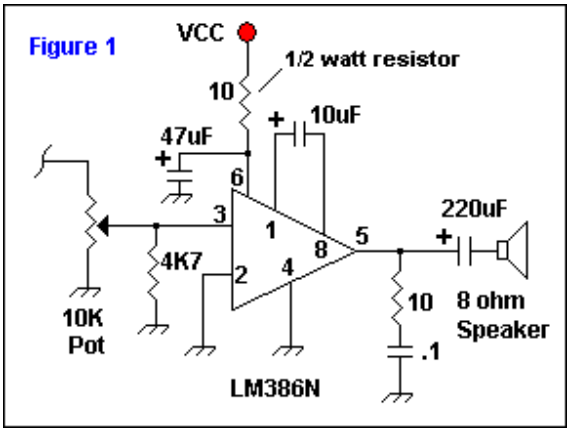

Simple Electronic Keyer

A simple keyer suitable for a popcorn QRP transmitter can be built around an astable multivibrator and an example of such is shown above. The basic design of this keyer is from notes, however the original author of the circuit is unknown. The notes were written in 1973 . I modernized the circuit, added a variable speed control and designed an additional output driver stage.

Keyer Operation

Keying this circuit generates either dits and spaces or dahs and spaces. When the keyer is idle, Q1 is on and Q2 and Q3 are switched off. When the user sends code, Q1 turns off and Q2 and Q3 switch on and in

turn key any device appropriately connected to the collector of Q3. The off-time of Q1 sets the on-time of Q2 and Q3. The off-time of Q2 and Q3 is set by the 22K Q2 base resistor. This off-time is the set time of the spaces and is constant.

The 68K resistor on the base of Q1 is about three times the resistance of the 22K base resistor on Q2 and consequently dahs are ~ three times the length in duration than dits. Spaces and dits are of the same length of time because when sending dits, the 68K base resistor is paralleled with the 33K resistor and effectively the resistance is ~22K ohms. If the optional relay driver transistor Q4 is used instead of Q3, the theory is the same, just substitute Q4 wherever you see Q3.

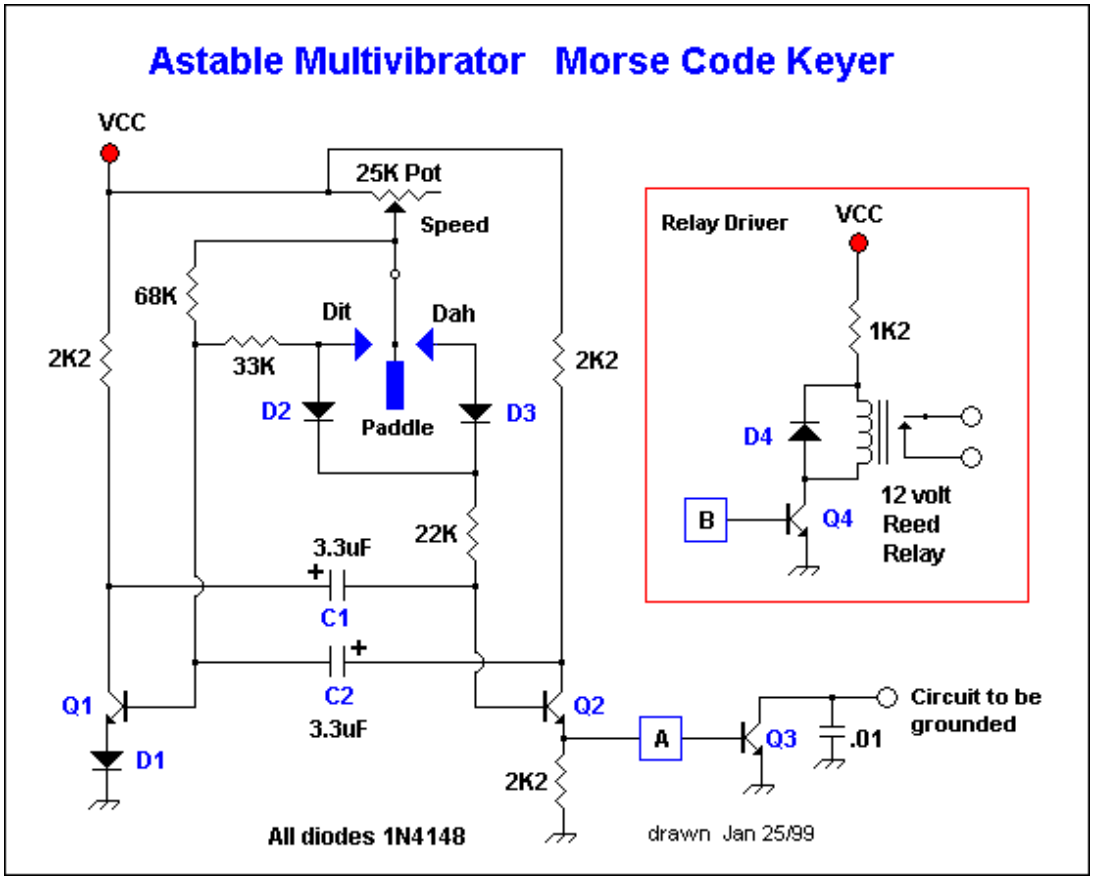

Keyer Speed

The keyer speed is very sensitive to the power supply voltage and any keyer speeds mentioned are ball-park values. Your results may vary depending on your VCC and component tolerances. If the 25K speed control pot is turned to minimum resistance, the actual power supply voltage will be present on both the paddle common and the top end of the 68K base resistor. This will be the maximum speed for the keyer. In fact, the speed control pot could be omitted if you want to economize and the keyer will run at the maximum speed as determined by C1 and C2. If you do not want the speed control feature, connect the paddle common and the 68K resistor to the VCC supply. Another alternative is to build a two speed keyer by using a switch to switch in or out a fixed resistor to vary the voltage instead of using a potentiometer. A trimmer resistor may also be used for "lid-off" speed adjustments.

Varying the base-bias voltage with a pot changes the charging rate on capacitors C1 and C2. Although, I experienced no problems be careful with some resistances/VCCs as the circuit may be unable to provide enough current to saturate the transistors when the base-bias voltage is at its minimum setting (pot set to maximum resistance). Smaller pots such as 10K can also be used with a more limited ability to reduce the keyer speed below the maximum rate.

To set the maximum rate for the keyer, it is necessary to vary the value of C1 and C2. For this circuit to function correctly, C1 must equal C2. An experiment was conducted with the 25K pot removed and the paddle common and the supply end of the 68K resistor connected to the main B+ terminal. VCC was measured at 13.8 volts. C1 = C2. The words per minute were counted for four different standard capacitance values and the results were as follows:

2.2 uF = 27 WPM
3.3 uF = 23 WPM
4.7 uF = 17 WPM
10 uF = 9 WPM

For this project, I settled with the 3.3 uF value, although personally, I use a 2.2 uF capacitor for C1 and C2. Sending speed can be reduced with the speed control pot or by increasing the time interval between characters and words. With 3.3 uf caps for C1 and C2, turning the 25K speed control pot to maximum resistance dropped the sending rate down to 12 words per minute. If you needed to slow down below 12 WPM, an amateur could send code using the Farnsworth method as mentioned above. At any rate this circuit allows you to determine the maximum speed rate by choosing the C1 and C2 capacitance value to suit your needs.

Q3, Q4 Output Stages

Two different output stages maybe used with this keyer and they will be referred to as the Q3 or Q4 stage.The Q3 stage is a simple transistor switch which will ground any component(s) connected to its collector when turned on during code sending. A variety of transistors maybe used here and care must be taken to ensure that you do not exceed the maximum dissipation of a given BJT.

The Q4 stage is a relay driver. The 12 volt relay used during bench testing was a Radio Shack reed relay that I had in my parts collection. Specifications were SPST 1A @ 125 VAC , 1050 ohms DC coil resistance, part number 275-233. My VCC was 13.8 volts so a 1K2 current limiting resistor was placed between the relay and supply voltage. The relay has suffered no harm despite significant torture but be careful when you are using a VCC greater than 12 volts. This resistance may be dropped down to 470 ohms or omitted if you are using lower voltages. Any relay with a DC coil resistance of 500 to 3000 ohms should work in this circuit.

I have never used this keyer with the Q4 relay driver for QRP operation as I prefer solid-state switching. The Q3 stage in turn can be connected to trigger a PNP transistor switch to supply DC voltage to a keyed transmitter driver and/or to pull a VFO to its offset frequency. A great example of PNP transistor switches can be found in The Ugly Weekender article by KA7EXM and W7ZOI. This article is referenced in the recommended reading list on this web site. Another bonus of the Q3 stage is that it draws less current than the Q4 stage.

Sending Code

If you are used to a deluxe iambic keyer, this keyer will take some getting used to. The dahs in particular can be problematic as they do not self-complete like they do on my station homebrew TTL iambic keyer. After some practice, however most people should be able to send some good morse code with it despite the lack of iambic luxury.

Miscellaneous

When you power up this keyer, it sends a dit. In one version of this keyer, used in a 40M transceiver, I had a 10K pot for the speed control with a built-in switch on the 10K pot to turn the keyer on or off during station setup.

The diodes D1 - D4 can be any common switching diode such as the 1N914. Q1 to Q4 can be any NPN transistor with a Beta greater than 50 such as the 2N3904 or 2N2222. In the test keyer, all BJT's were 2N3904.

For fun, I connected the multivibrator code practice oscillator to the keyer and gave the keyer a workout. They both work great together and are very complimentary. Have fun with astable multivibrators !

Update Oct 2007:

Giovanni, IW7EHC has posted a great web page on this schematic including PCB layout files in FidoCAD format

Check out his excellent Italian and English language web site

---

Supplemental Page for the 10 MHz WWV TRF receiver

I have received a tremendous amount of feedback regarding the 10 MHz WWV TRF receiver. Many builders have constructed their own versions and have improved it. This captures the spirit of the QRP/SWL Homebuilder web site; take an idea and evolve it into something better on the bench.

I will post some of the feedback as well as provide additional comments and images regarding the 10 MHz WWV project on this supplemental web page. Please continue to provide project feedback and help me to improve the QRP/SWL HomeBuilder web site.

Terry, K5HP
Hi Todd,

I have just finished (few days ago) your design for the 10 MHz WWV Receiver. I reduced you schematic diagrams to CirCad schematics, drug out the rat-net, positioned and connected everything, and etched the boards. I'll include a photo of the 4 finished boards. They are very roomy for extra tinkering. Except for two solder bridges on two very big pads on the tweeker capacitors in the front end, it all worked perfectly first try. Hmmm, I cannot say that for all my projects in the past. After repairing the two shorts to ground of the RF path, the front end then tuned and worked perfectly also.

I have not taken the project out to the Lab (barn) and put it on my Motorola Service monitor, but the input to the filter board is roughly 500 uV. It can easily hear WWV at this level with a decent antenna connected to the filter input when WWV is fairly strong at my location. Not bad, considering the mismatch at that location.

Have you or someone else tinkered with an AGC/AVC circuit? At one time I had a nice circuit using an National chip (don't remember the number) which is no longer available that was easy to build and easy to retro-fit into something. It was an AVC which they called an audio AGC.

When I built out the boards I placed proper credit to you and the other developers mentioned on the boards. Should you want my work product it's free for the asking. I'll be glad to send it to you. CirCad in ver 4 is a fairly

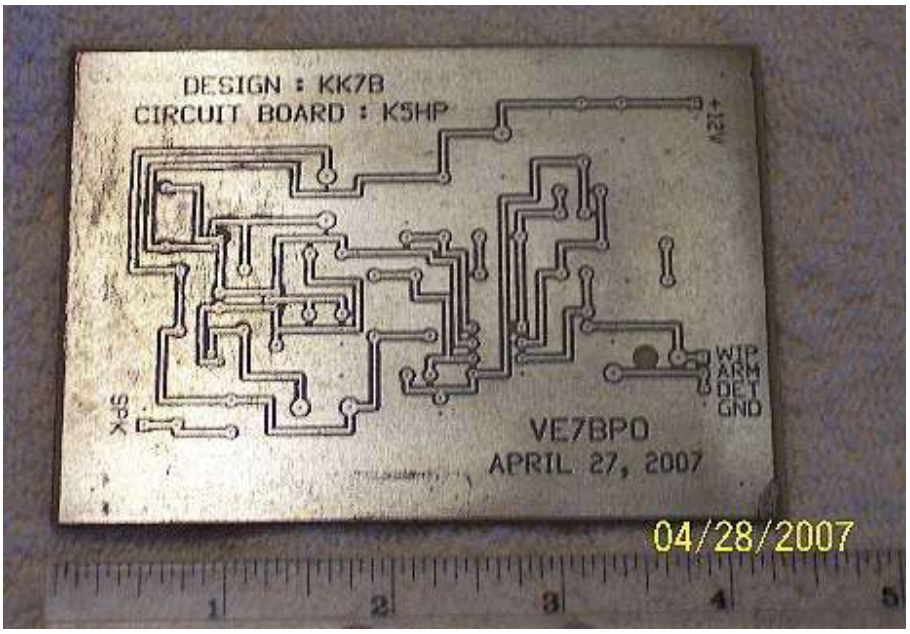

Above. Etched Audio amplifier PC board from K5HP.

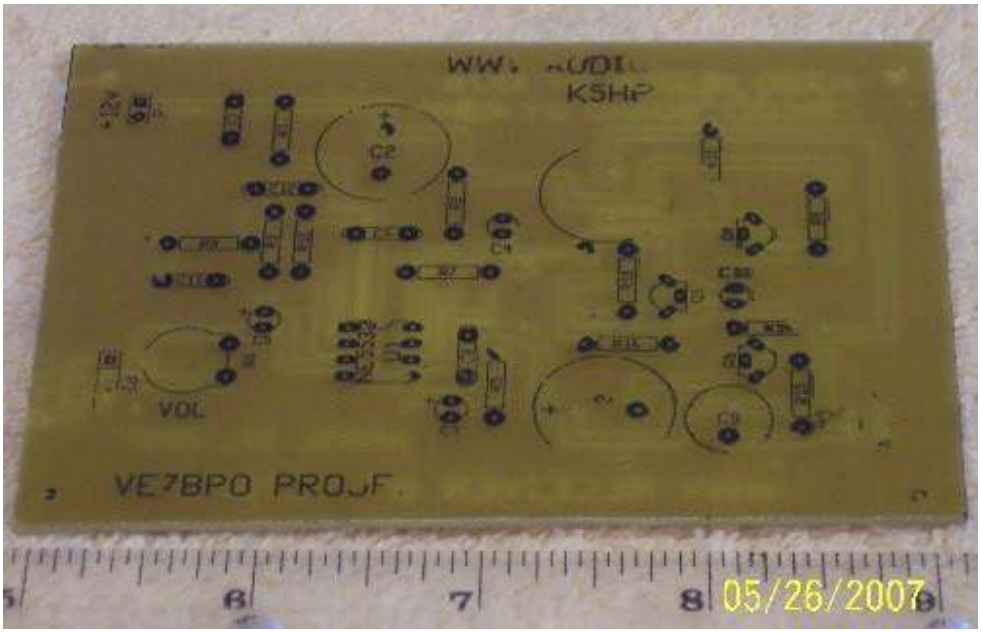

Above. Audio amplifier PC board overlay for parts placement from K5HP.

complete PCB cad program and it's free too. There is a version 5, but I have not tried it out yet.

My sincere congratulation for producing and error free web article. That is a heck of a more than you can say about many other projects in the past. Most of those in the past had errors a plenty, and some just did not flat work as described. Someone just thought they would as it turned out. Thanks for the fine article and I'll check your site over for more interesting thing to build or learn from. Best wishes and good luck.

Above. A layout of the 4 completed boards by K5HP.

"I use the CirCAD to produce the artwork, then take the laser printer output and bond the plastic toner onto the PCB. Works good most of the time. Sure easier than trying to do photo etch, and silk screening is pretty expensive. The bottom copper is viewed as you would look down onto the top of a circuit board, through to the copper side. The side you are seeing is bonded to the copper surface. Print one out, hold it up to a light source looking through non printed side and it becomes apparent."

Terry designed and built printed circuit boards. His photographs, etching and overlay files are all bundled together in convenient zipped files which can be downloaded below.

Download the front end zip file

Download the Crystal filter zip file

Download the Detector zip file

Download the AF amp zip file

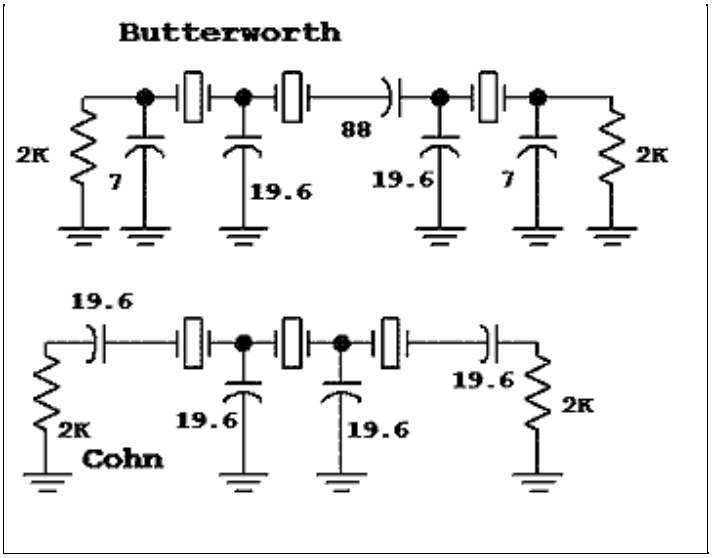

Above. Schematics diagrams of 10 MHz crystal filters by Wes, W7ZOI. I did not experiment with the Butterworth type filter.

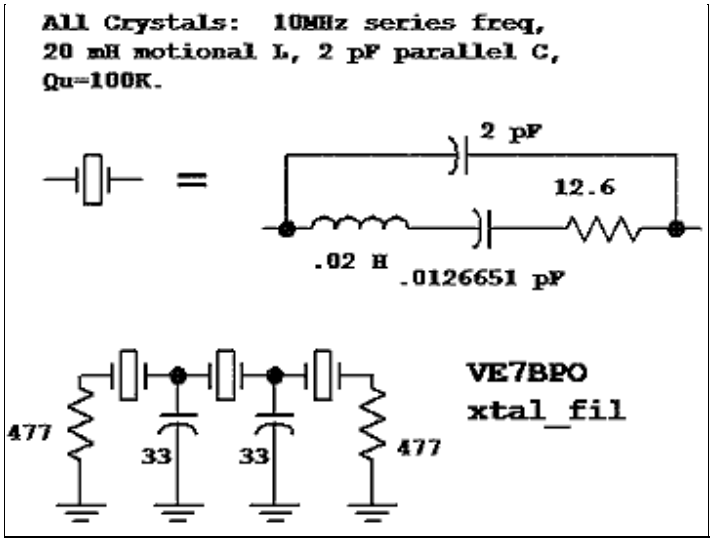

Above. Schematics diagrams by Wes, W7ZOI.
A schematic representation of the 10 MHz xtal is shown along with the "popcorn" 10 MHz xtal filter I designed.

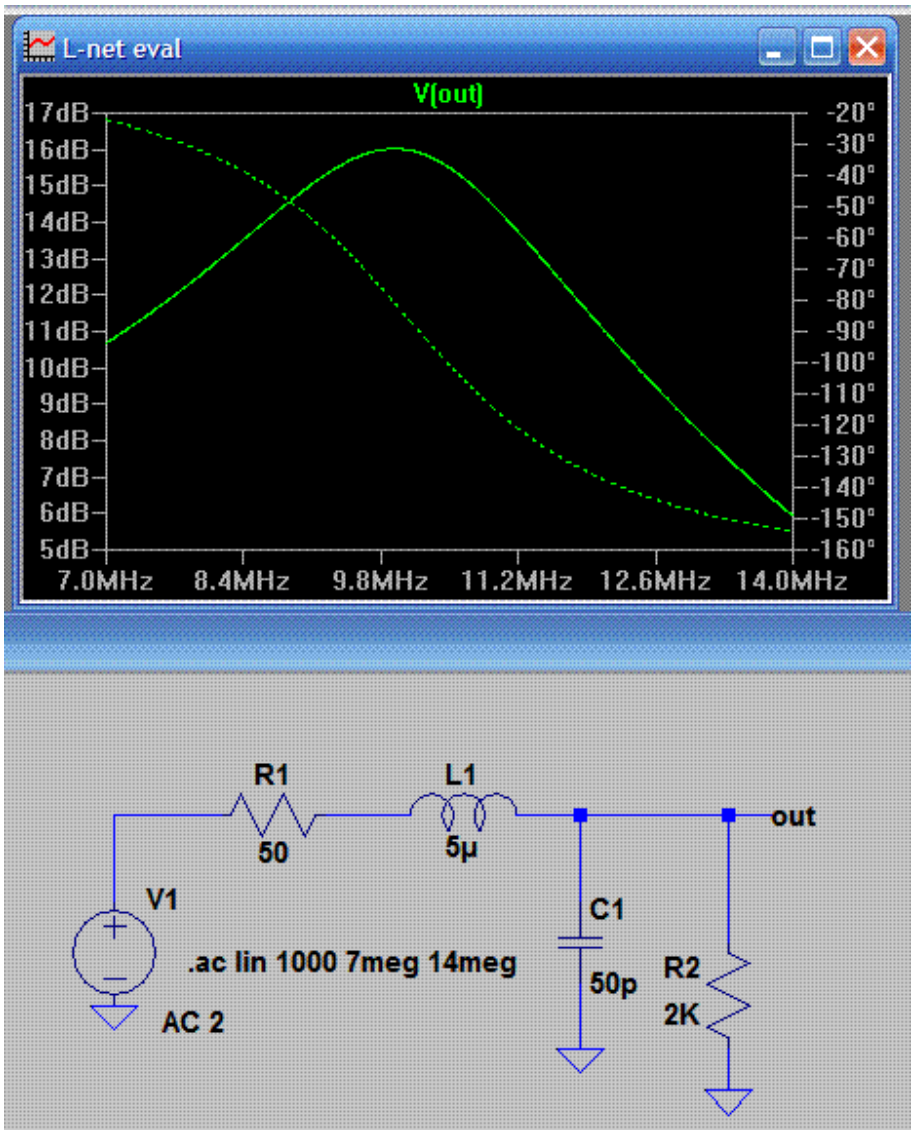

Above. A simulation of an L network depicted in the L-Match and AM Detector schematic for those interested in driving this detector with a 50 ohm output impedance.

Amateur and Short Wave Radio Electronics Experimenter's Web Site

MF TRF Receiver Supplemental Page

Click here to go to the main project web page This supplemental page is under construction

---

5532 Op amp Pin Out

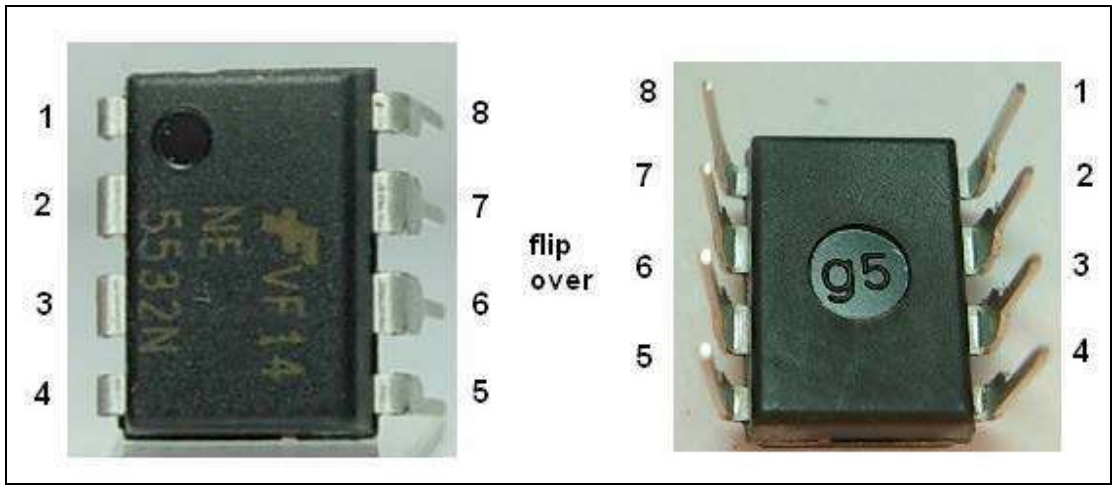

A Version of the Receiver Using Just L1 and C1 as the band pass filter

You can see a red LED and current limiting resistor in the photos. This is a power on indicator. The telescopic whip antenna can be seen in the lower photo.

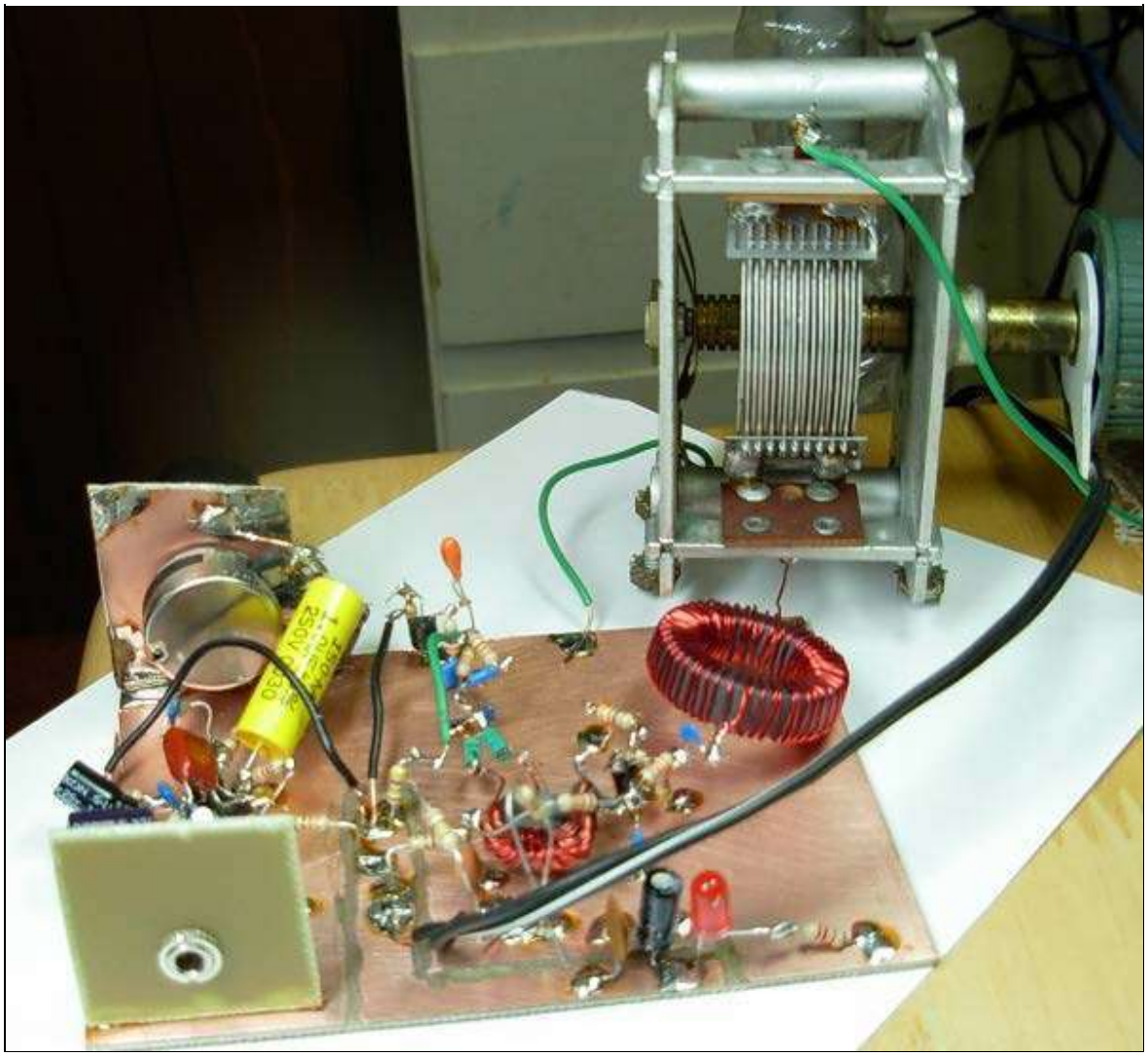

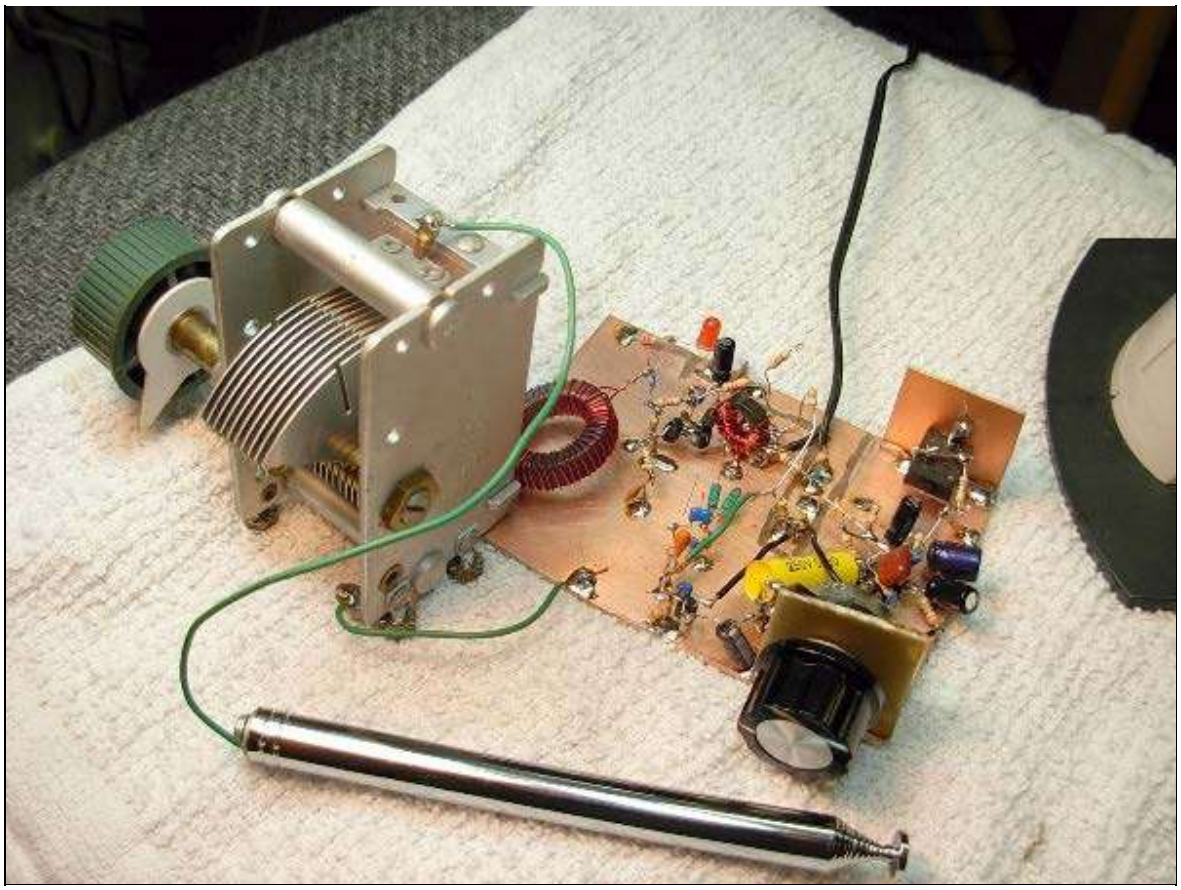

Early Versions of the Project Front End

In section A of the schematic below, a dual-ganged 365 pF air variable capacitor was used for tuning. CV, a small compensating capacitor may be required to adjust for the capacitive differences of the 2 L-C tanks in the front end filter. It may have to be placed on the L1 side of the filter (opposite to what is shown). A JFET source follower was used for Q1 but discarded because stage gain was insufficient with a short whip antenna.

In the version depicted as section B, two 12-110 pF air variable capacitors were used along with switchable 270 pF capacitors to provide 2 ranges of tuning. Although this worked, the switching mechanism was found to degrade selectivity somewhat. The JFET was reconfigured as a common source RF amp. This amp caused some distortion of the RF signal on stronger stations unless the gate resistor was lowered to 47K or less. Ultimately a cascode BJT RF amp was chosen for the project. A photograph of the section A breadboard is shown below the schematic.

Broadcast Radio Band Front End

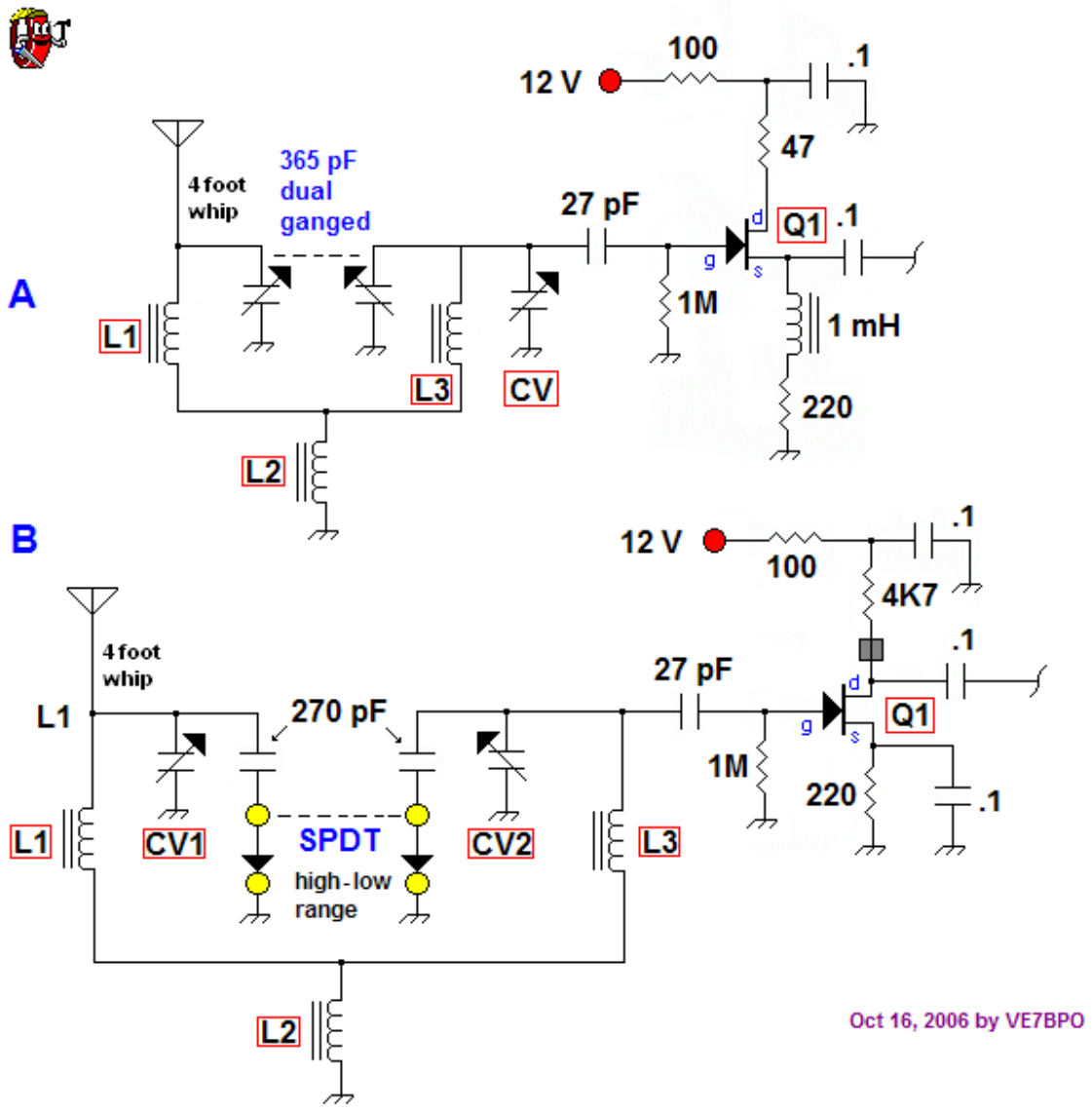

Oct 16, 2006 by VE7BPO

L1 = L3 = 200 uH or 55 turns #28 AWG on a FT50-61 ferrite core
L2 = ~ 5 uH = 9 turns #22 AWG on a FT50-61 ferrite core
CV = small value trimmer capacitor for tracking - 4.5 - 20 pF
CV1 = CV2 = 12 - 110 pF air variable capacitor
Q1 = nJFET; MPF102 or J310

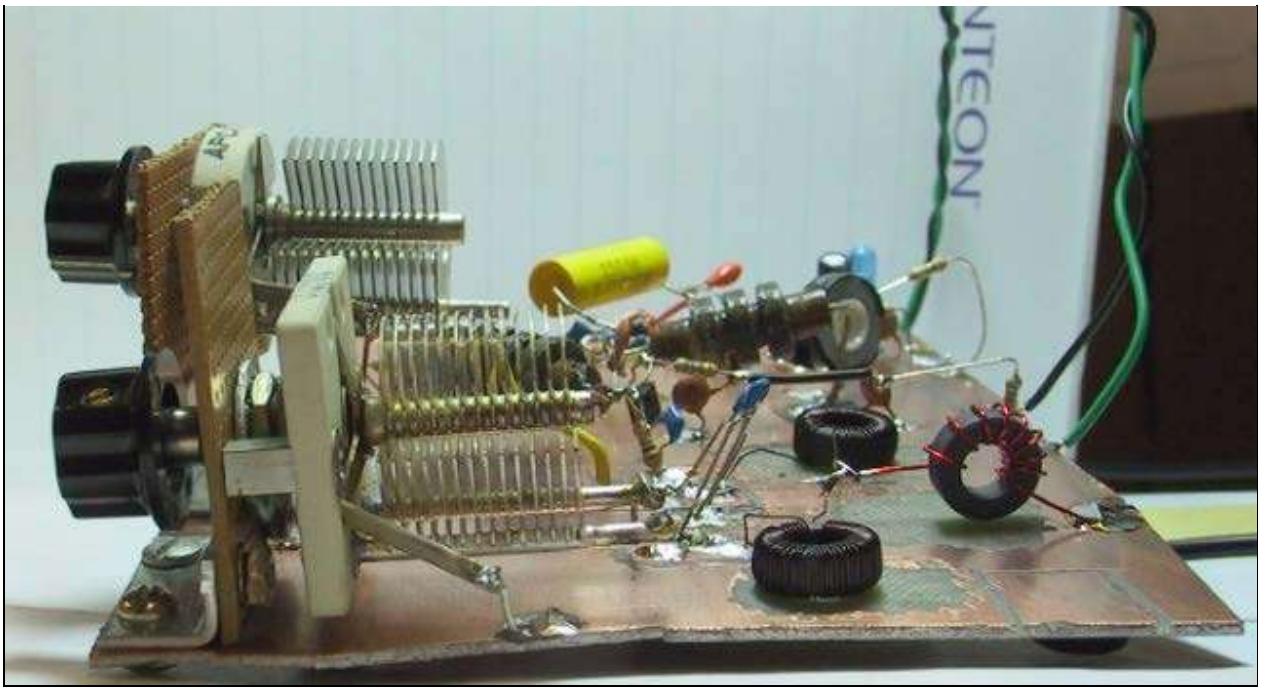

The inspirational detector schematic used for motivation to develop the full wave detector

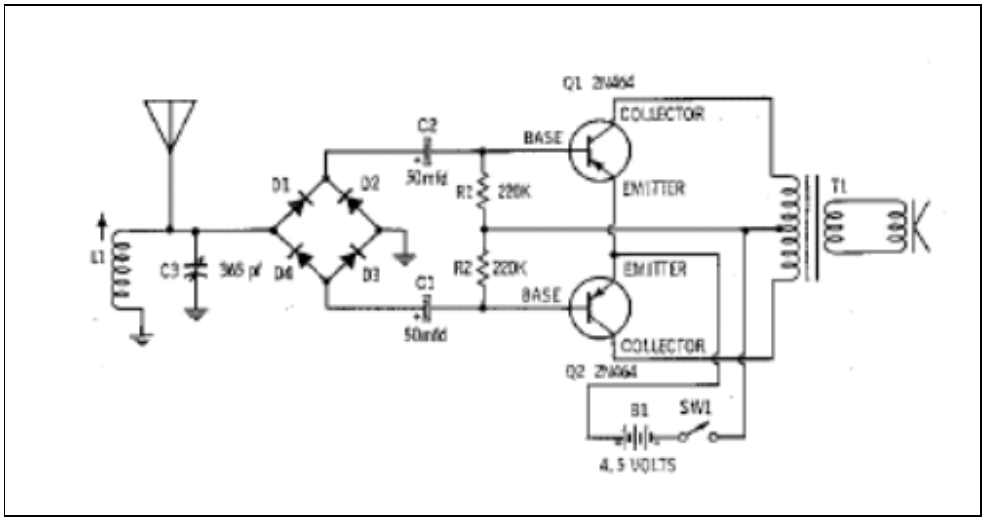

Varactor Tuned Front-end Band pass Filter

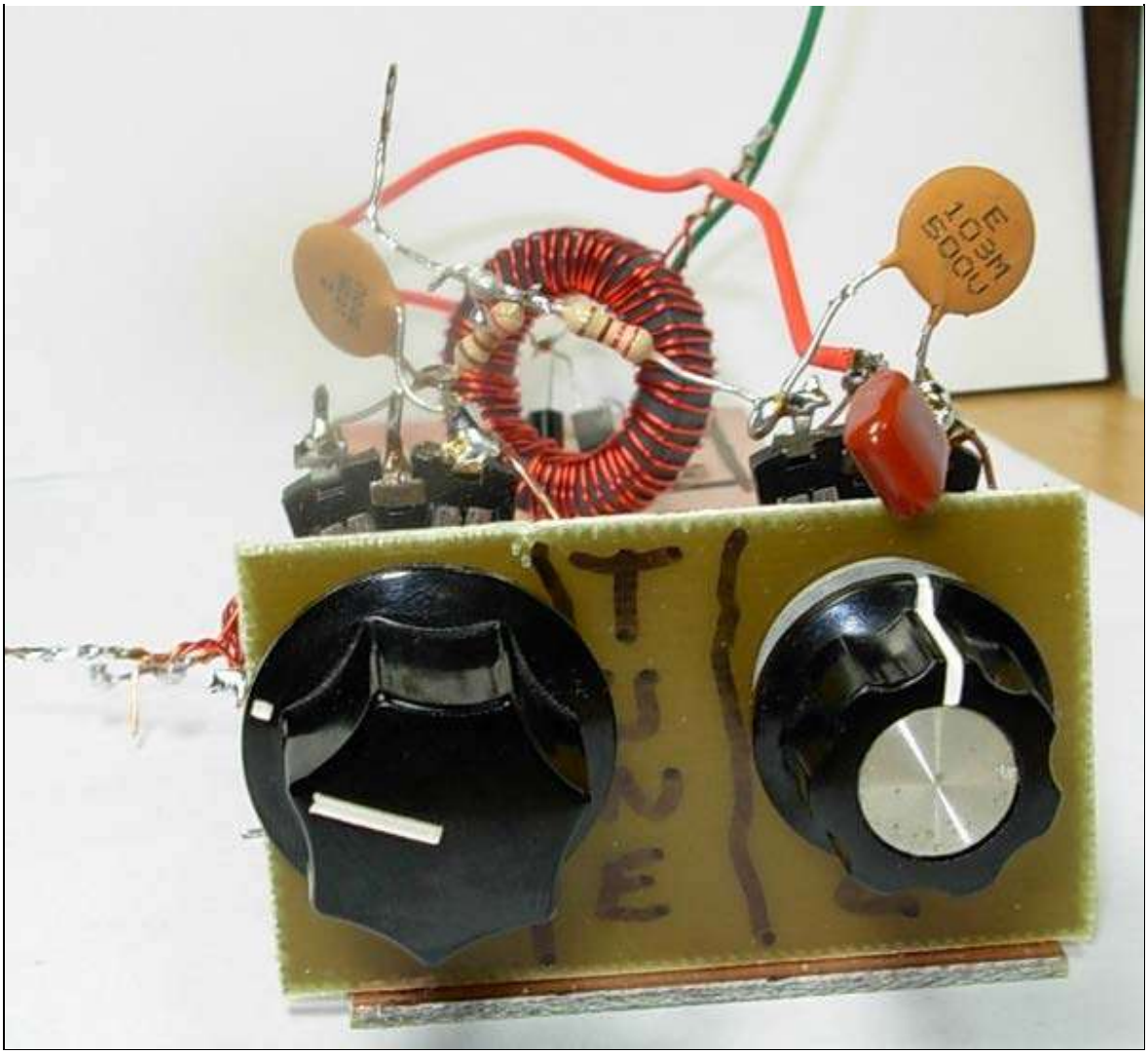

Above photo. The 2 potentiometer varactor controlled band pass filter.

Amateur and Short Wave Radio Electronics Experimenter's Web Site

Supplemental to the Cascode Hybrid 5 MHz WWV Receiver

DC Voltages of the Cascode Hybrid Amp

On the right is the basic hybrid cascode amplifier schematic. Note that the Q1 voltage divider bias has two 10K resistors as compared to the 12K and 10K combination used in the final project. A slightly lower Q1 bias voltage was ultimately chosen along with a 150 ohm Q2 source resistor to enhance stability. Early bread boards of this amplifier used a 47 - 100 ohms Q2 source resistor along with the slightly higher Q1 bias, but suffered from parasitic oscillations.

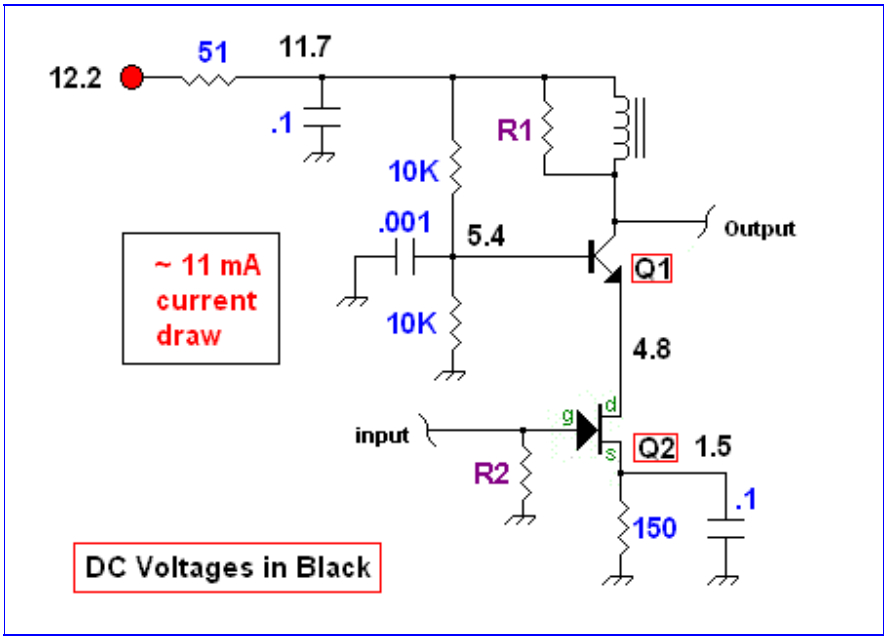

The DC voltages are rounded to 1 decimal point. These are ball park values for reference purposes. The typical stage current draw was around 11 mA. R1 sets the output impedance and is optional. R2 sets the input impedance. This amp is very versatile in that it can be used to match a wide variety of input and output impedances.

The **main 5 MHz WWV receiver web page** which this web page supplements is here.
Click here for a recording of 5 MHz WWV made with the Icom R-75 receiver using the 6 KHz AM filter and the stock speaker. You may wish to compare it to the recorded 5 MHz WWV receiver project audio files linked here , here and here.

10 MHz Components

For those who wish to experimentally develop a 10 MHz version, I have included some potential band pass and crystal filter schematics you may wish to consider. In addition, my preliminary experiments indicated that another RF amplifier stage might be necessary for 10 MHz WWV. During development of these band pass and crystal filters, 10 MHz WWV reception was very poor and due to lack of time and the poor conditions, further experimentation was abandoned.
To the left is a 10 MHz band pass filter schematic with a -3dB bandwidth of around 100 KHz.

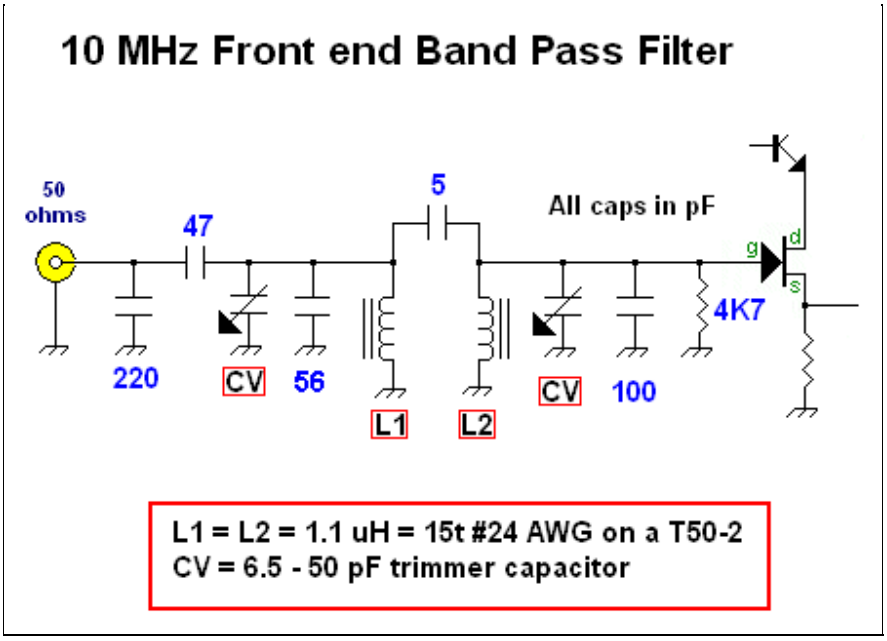

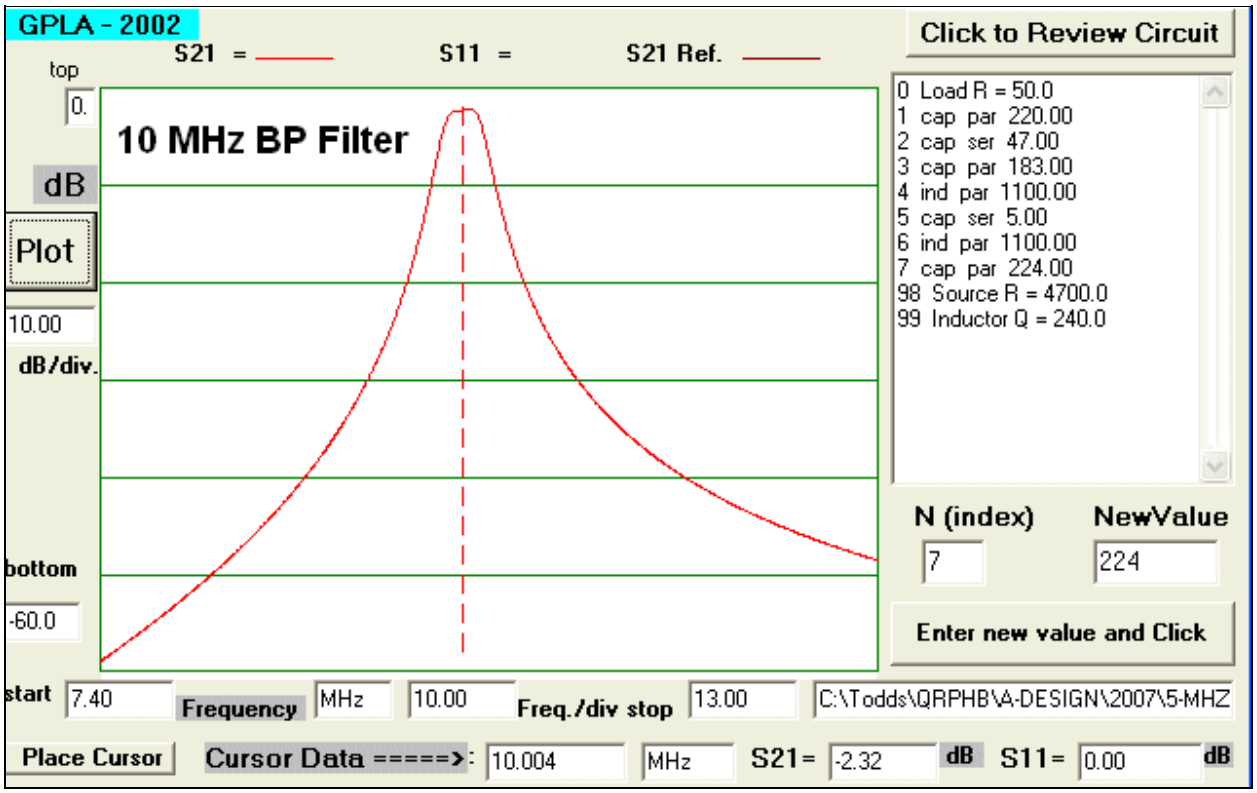

The GPLA simulation of the 10 MHz front end band pass filter. Tuning is very sharp with this filter.

To the left is a crystal filter design for 10 MHz. The realized bandwidth of these simple min-loss crystal filters is dependent on your crystal parameters.

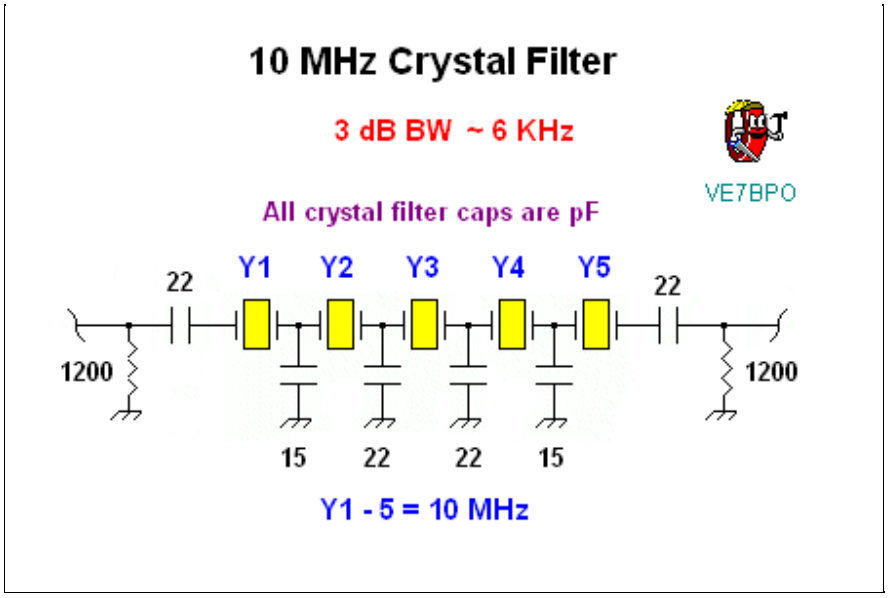

A photograph of the experimental 10 MHz crystal filter is shown to the right. Leads were kept long so that parts could be reused in future experiments.

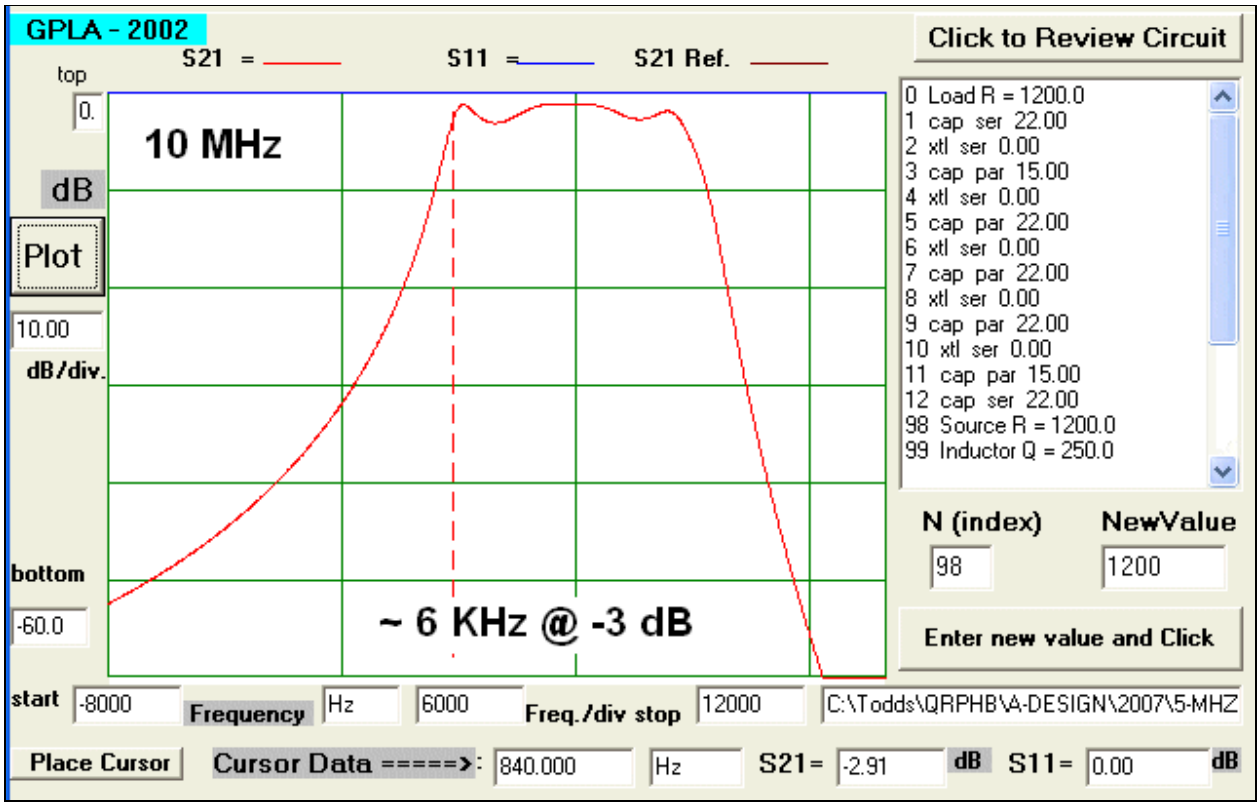

Above. The GPLA simulation of the 10 MHz crystal filter.

6 MHz Components

Since it is easy to find 6 MHz crystals and Radio Habana Cuba is on 6.0 MHz, band pass and crystal filters were designed for reference purposes. To the right is the front end, band pass filter schematic.

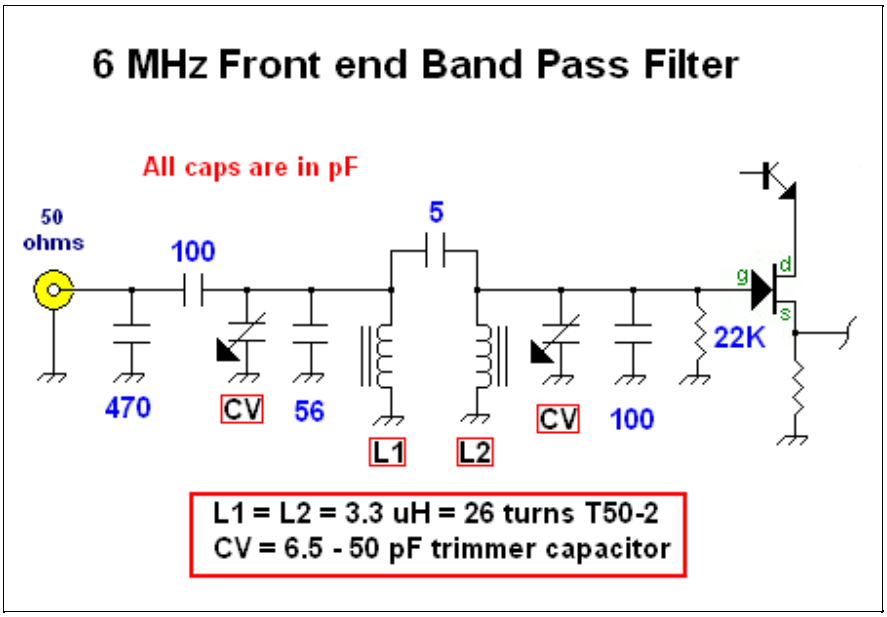

To the left is a potential crystal filter for 6 MHz AM reception. The bandwidth is ~ 5 KHz which is starting to get too narrow for some listeners, however, your crystal parameters will determine your filter's actual bandwidth.

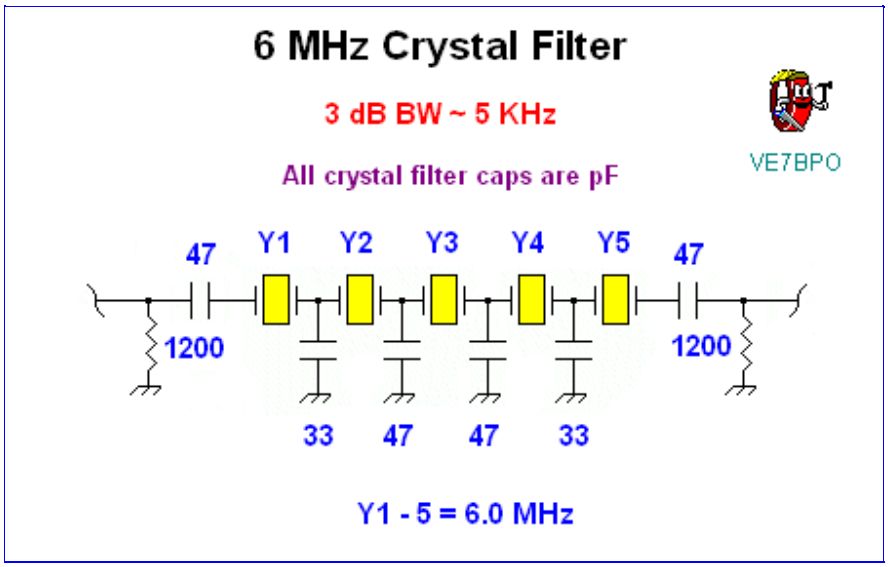

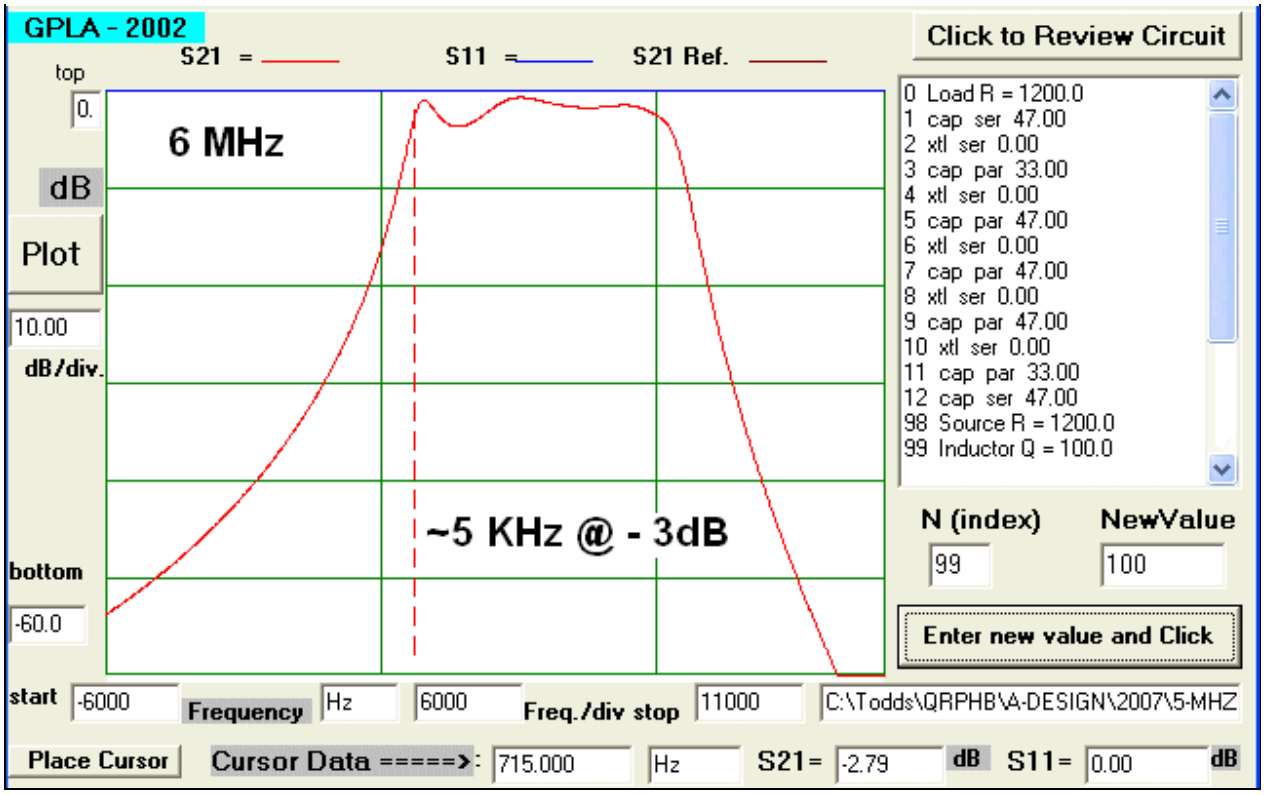

The GPLA simulation of the crystal filter using the parameters from the 6.0 MHz crystals I had in my parts collection.

VE7BPO Envelope Detector

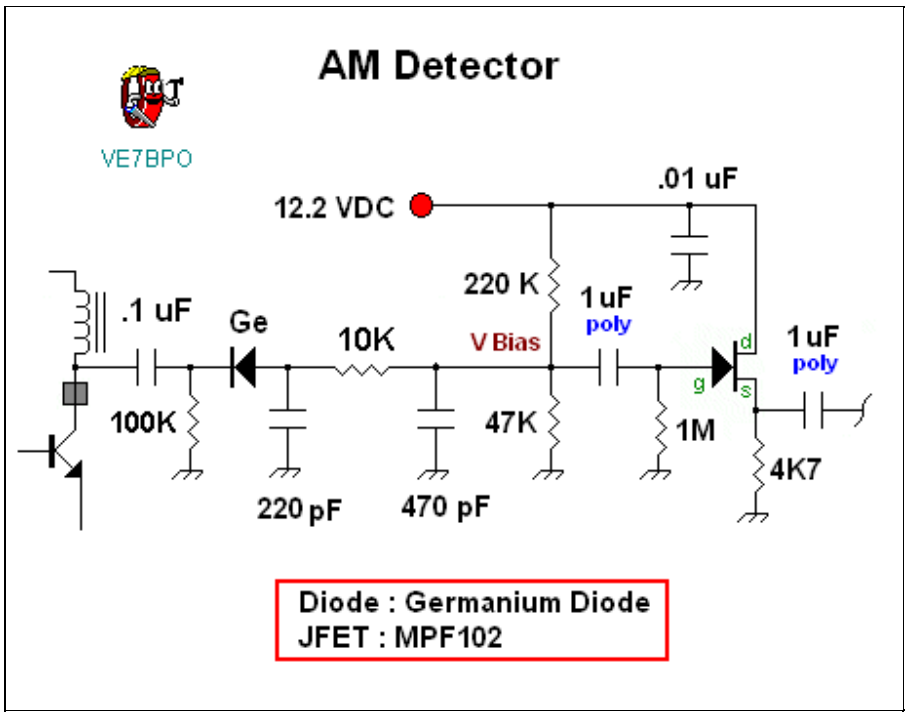

To the left is the schematic of another detector experimentally developed for the 5 MHz WWV receiver. The germanium diode has incredible sensitivity when biased, although noise tends to increase with applied DC voltage. This basic design also worked well with a hot carrier diodes, although had less sensitivity. V bias can be changed by adjusting the 220K, 47K and 100 K resistor values. Note diode polarity.

Miscellaneous Photos and Circuits

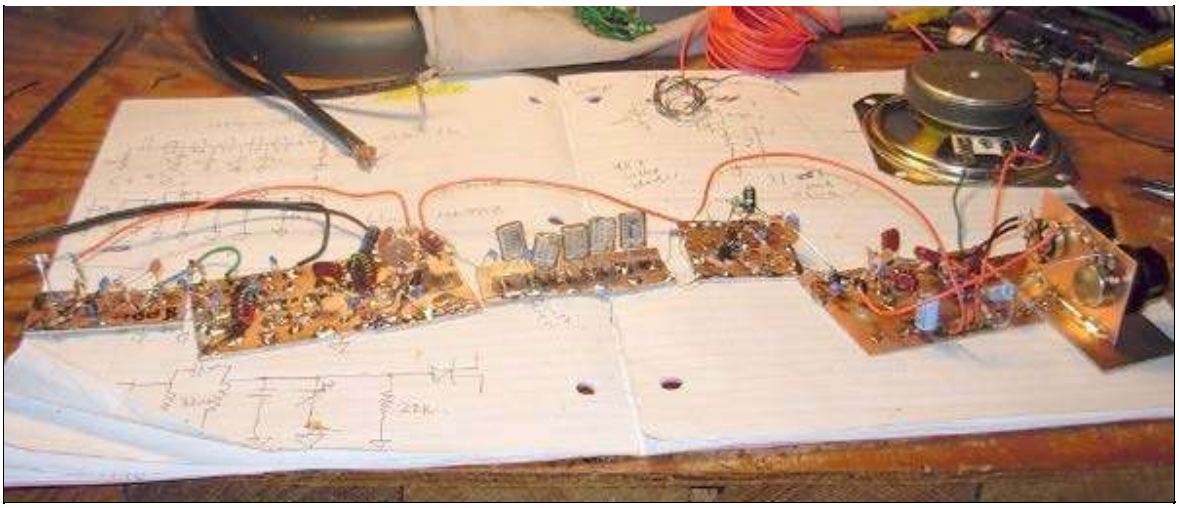

Above. A work bench version of the basic receiver bread board built in distinct stages from the antenna input to the speaker.

Above, A breadboard of the KK7B audio stage which is preferred to the LM386 stage used in the 5 MHz WWV receiver. The LM386 does take up less room and certainly increases the popcorn factor.

Above. The AF stage shown above in a chassis containing a speaker. This is my lab AF amp for testing receivers on my work bench.

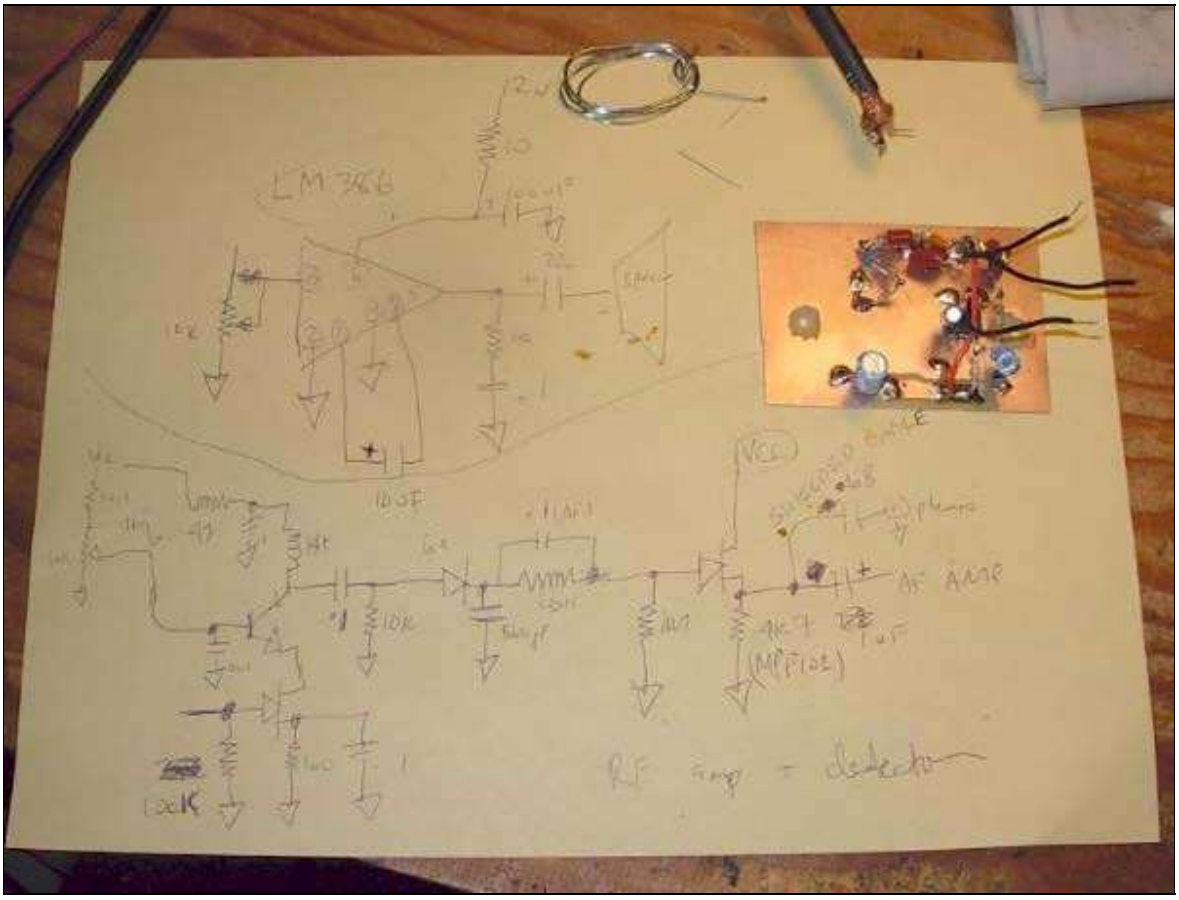

A work bench photo of the first version of the W7ZOI detector built in October 2007 is shown above.

RF — Test and Measurement

My Links

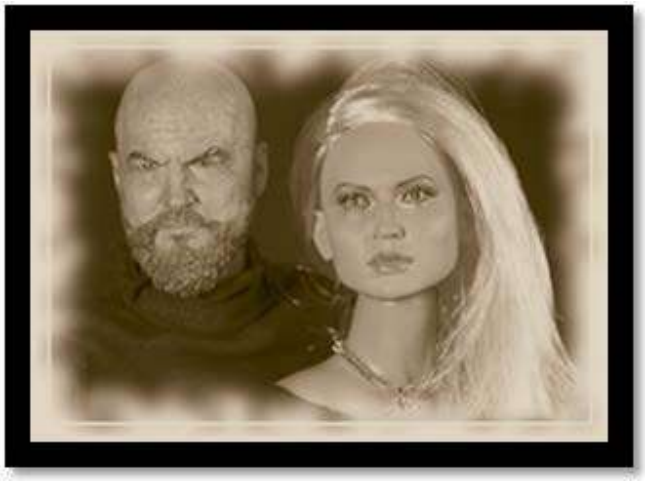

Greetings! I enter the QRPHB / SWL HomeBuilder site here and linked a few of my favorite tools, part suppliers and URLs I like and wish to remember. This page might feel intransigent.

In the following section called **Graphics**, I show the odd newer schematic or photo unpublished as permanent site content. A schematic might just represent my mistaken notion or whimsy: a sense of what's caught my fancy — not that my opinion is better than anyone elses.

Quick Navigator

Graphics

Russian giant sunflower — grew to over 3 meters tall

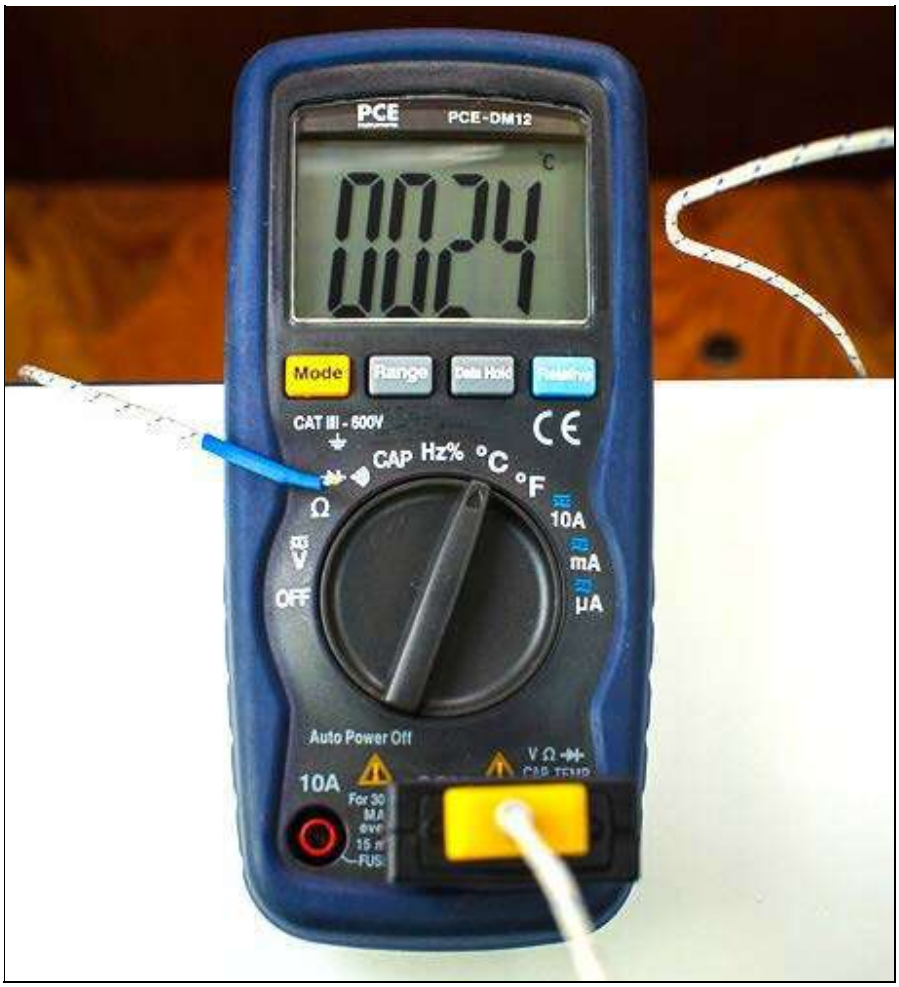

My gorgeous new PCE multimeter just in time for Season 16 experiments starting October 3. Click for another photo. Click for the PCE website — test equipment galore.

RF Transistor Data Spreadsheets

FET

BJT

Test Equipment

Test equipment

USA Rigol Dealer T Equipment

Online Tools and Publications

Standard resistor and cap values

Smith Chart information

Good inductive/capacitive reactance calculator other tools available

Resistive pad attenuator calculator

Ohm's Law 1 pager

VHF Communications website UKW-Berichte/VHF-Communications

The Signal Path EE video blog They review and show the DSA1030A SA + TG

Favorite Experimenters

Esteemed QRP homebrew mentor - Wes Hayward's, W7ZOI web site

Iulian, YOUDAC-VA3IUL Comprehensive design information and amazing circuits web site

Markus Hansen, VE7CA A venerable Room 19 Radio School graduate. He has authored for QST. See his receiver featured in QST for March 2006

Blog of fellow VE7-land experimenter Steve, VE7SL. Look for a link to Steve's web site on his blog

Professor Ken Kuhn's web site. Perhaps start on his site map. A treasure trove of useful information

Ripples in the Ether An always interesting blog from our friend Jason who runs Etherkit

SV3ORA's Site Friend Konstantinos from Greece. Design info galore. Check out his microwave links.

FM Tuner Site Vintage FM Tuner Information

Paul, KE7HR Caver website

Matjaž, S53MV Microwave and RF. My favorite microwave designer. See this page for some inspiration

Paul Wade, W1GHZ authors my favorite QST column *Microwavelengths* His site

Jacques, VE2AZX web site Retired EE with great ideas

Michigan QRP Club Publish *The 5 Watter* Quarterly

Website of Michel, **F6FEO** from France. F6FEO project pages: click and click

Roland, a retired EE who lives in France keeps this wonderful test equipment page

JF1OZL Mega site that first inspired me years ago. He once wrote me a letter - great guy

Brian, K6STI 88-108 MHz web site.

Leif, SM5BSZ Amazing work

KA7OEI Microwave Page web site

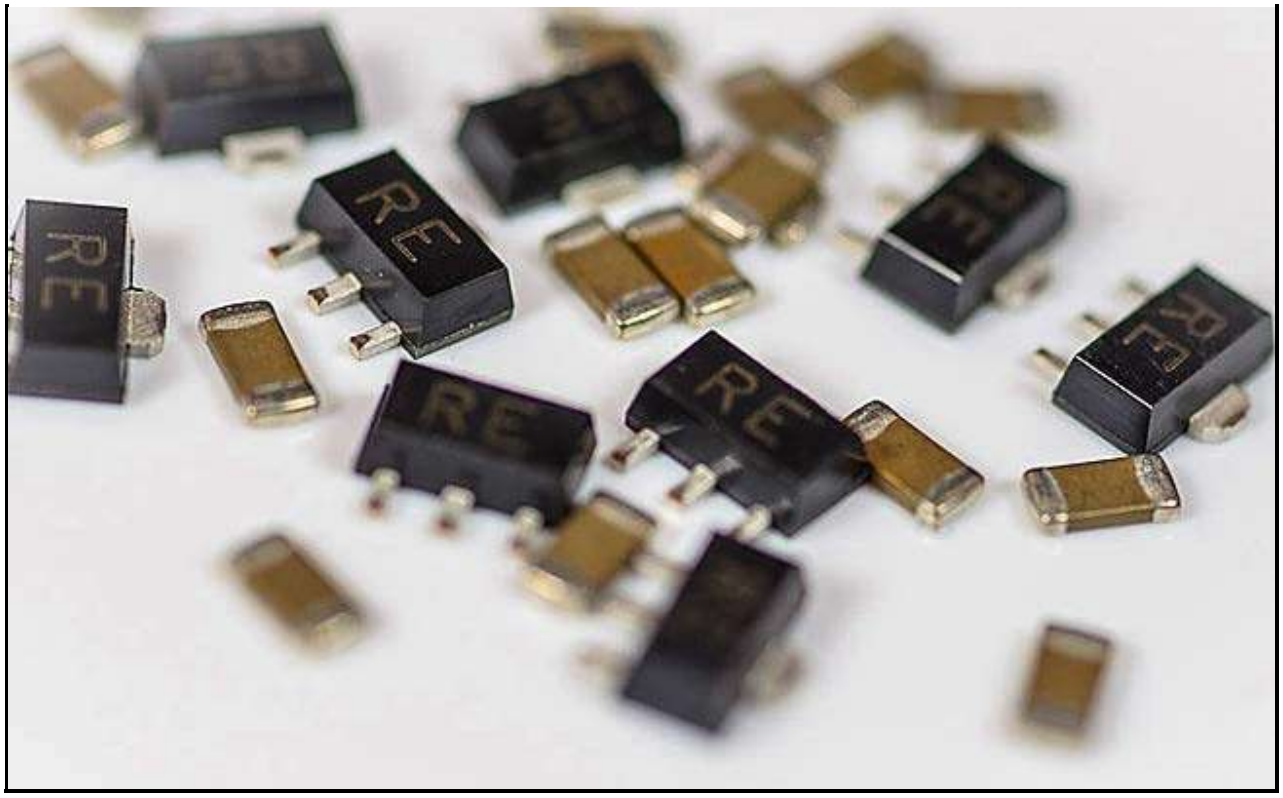
RE
RE
RE
RE
RE

Memorial Museum of the Leningrad Siege, St. Petersburg, Russia
Государственный музей обороны и блокады Ленинграда

VE7BP0 photos 2006

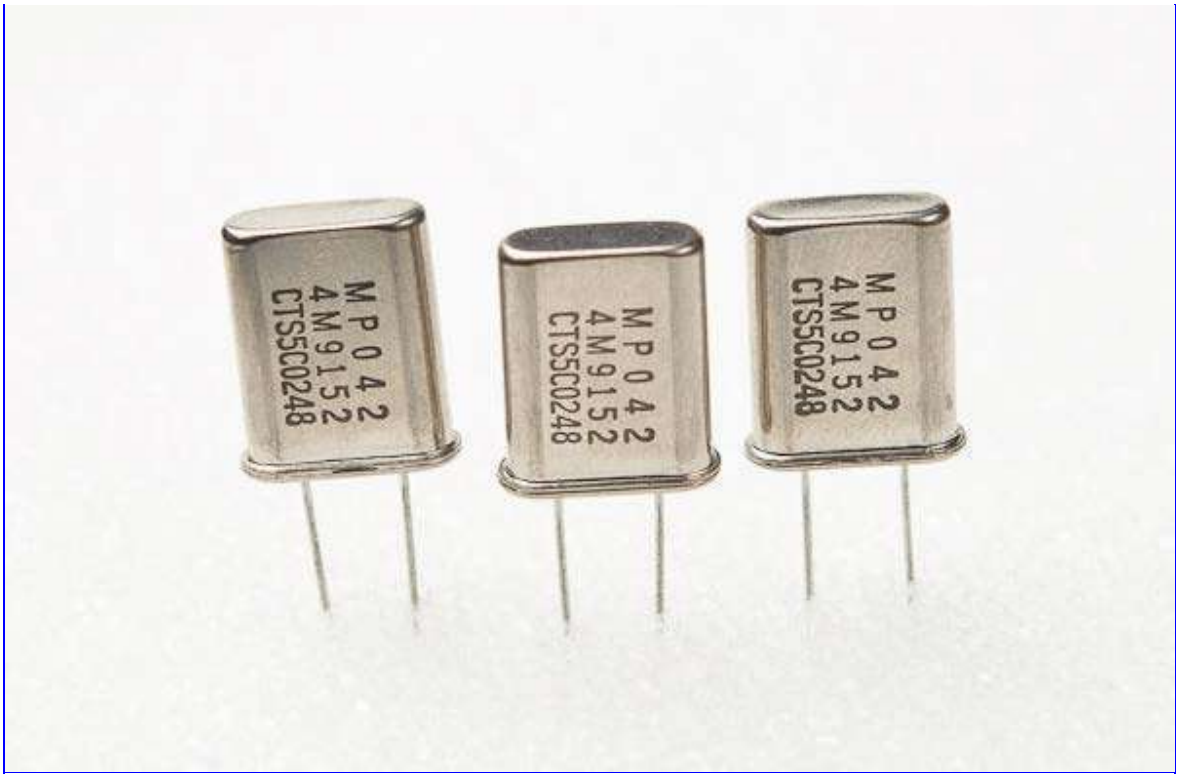
MP042
4M9152
CTS5C0248
MP042
4M9152
CTS5C0248
MP042
4M9152
CTS5C0248

RF Workbench Page 1 - Case Study Answers

This web page supplements RF Workbench Page 1

Answers:

1. Calculate the power in dBm at point B **= 13.75 dBm**
2. Calculate the power in dBm at point C **= 10 dBm**
3. What is the attenuation in dB of the 50 ohms attenuator pad? **= -3.75 dB**
4. What is the output power in mW of this stage? **= 10 mW**

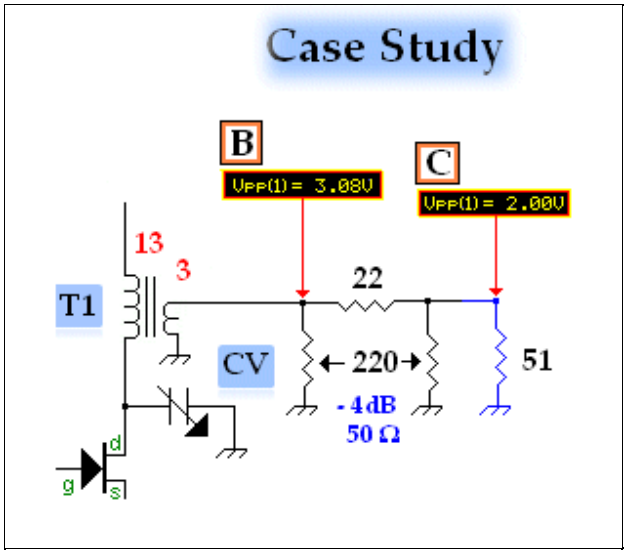

The design contained a "theoretical" - 4 dB, 50 Ω attenuator pad using standard value resistor substitutions

50 Ohms Attenuator Pads

This web page supplements RF Workbench Page 2

Table For Pi and T- type pads

Attenuation	Pi-type		T-Type	
dB	R parallel	R series	R series	R parallel
1	869.5	5.8	2.9	433.3
2	436.2	11.6	5.7	215.2
3	292.4	17.6	8.6	141.9
4	220.9	23.8	11.3	104.8
5	178.4	30.4	14	82.2
6	150.5	37.4	16.6	66.9
7	130.7	44.8	19.1	55.8
8	116.1	52.8	21.5	47.3
9	105	61.6	23.8	40.6
10	96.2	71.2	26	35.1
12	83.5	93.2	29.9	26.8
14	74.9	120.3	33.4	20.8
15	71.6	136.1	34.9	18.4
16	68.8	153.8	36.3	16.3
18	64.4	195.4	38.8	12.8
19	62.6	220	39.9	11.4
20	61.1	247.5	40.9	10.1
24	56.7	394.6	44	6.3
25	56	443.2	44.7	5.6

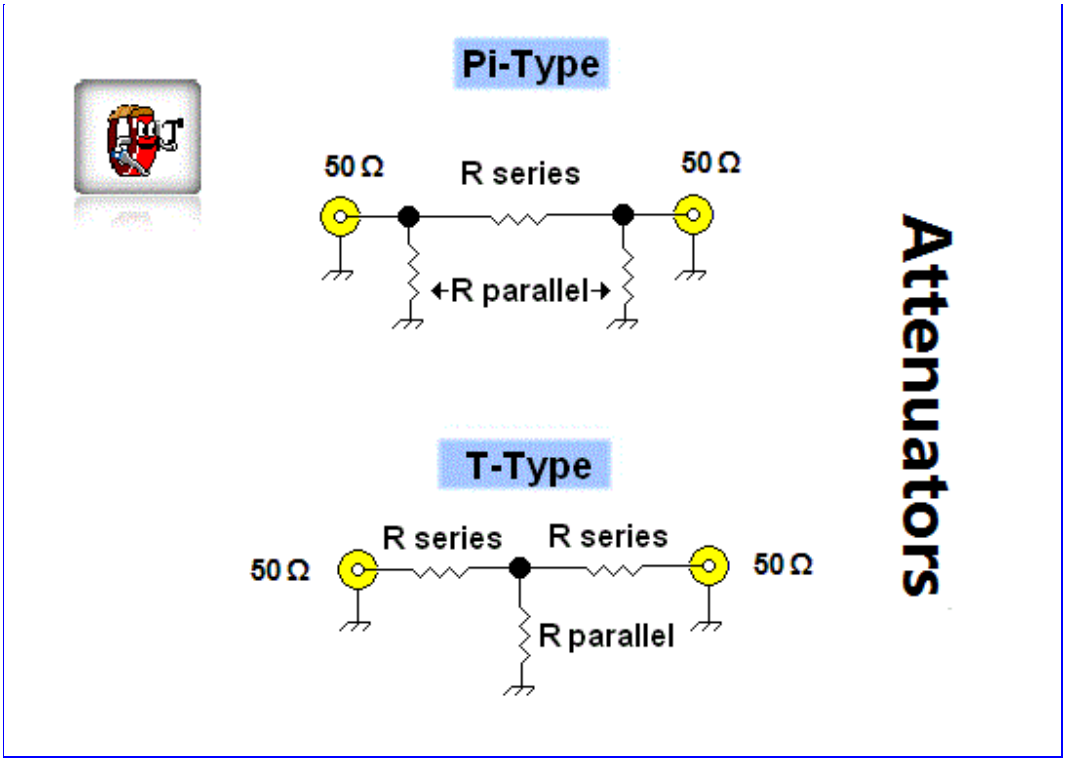

To build attenuator networks, we normally choose use nearest standard resistor values, or parallel/series 2 or more resistors from our resistor collection to approximate the tabled R. If you're building with 5% parts, consider measuring a few resistors with an ohmmeter to find the best match to the tabeled R.

Resistors in the 8 dB T-type or the 4, 14 and 19 dB Pi-type networks are close to 5% standard resistor values.

Expected Return Loss Table (50 ohm bridge)

This web page is a supplement to Transistor Input Impedance Experiments

Expected Return Loss in a 50 ohm Bridge	
Resistor (Ω)	Return Loss (dB)
10.00	3.52
15.00	5.38
22.00	8.20
27.00	10.50
33.00	13.77
39.00	18.16
47.00	30.19
62.00	19.40
68.00	16.33
75.00	13.98
82.00	12.31
100.00	9.54
120.00	7.71
150.00	6.02
170.00	5.26
200.00	4.43
220.00	4.02
270.00	3.25
330.00	2.65
390.00	2.20
470.00	1.86
510.00	1.71

Miscellaneous RF Topics 2011 Supplement

Introduction

This web page supplements the Miscellaneous RF Topics 2011 web page.

1. Design Center - Wrap Around Bias

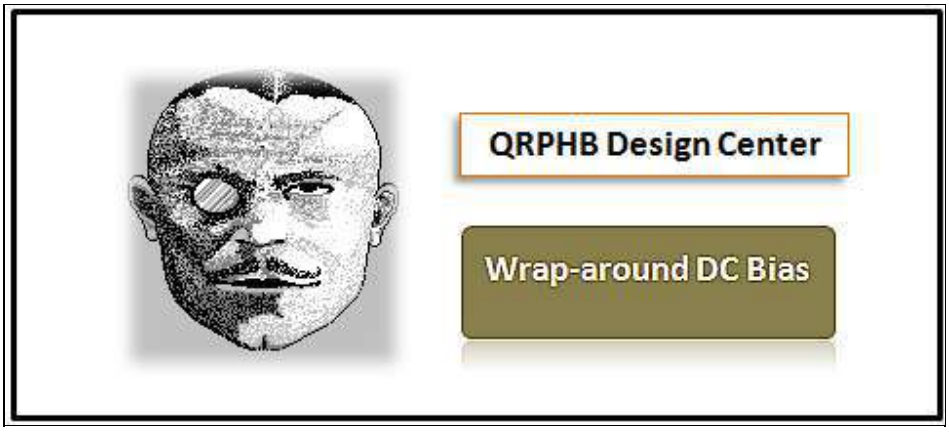

PNP Wrap-around Bias for an NPN RF Amp

There are entire books written on RF power amps. I don't pretend to be an expert and offer a simple approach to help move novice builders up the learning curve. Big thanks to Wes, W7ZOI for the theory and explanation for EMRFD Figure 2.16; the wrap-around PNP bias of an NPN transistor with grounded emitter. This bias circuit is fantastic and helps prevent you from burning up too many expensive medium power transistors such as the 2N3866 or 2N5109 during experiments and operation. From our emails, the following experiments were performed and information gleaned.

Since the NPN emitter terminal is grounded or near to ground on my web page examples, the current can really run high — Don't forget to use heat sinks and appropriately rated resistors on the NPN circuit when you really go for power.

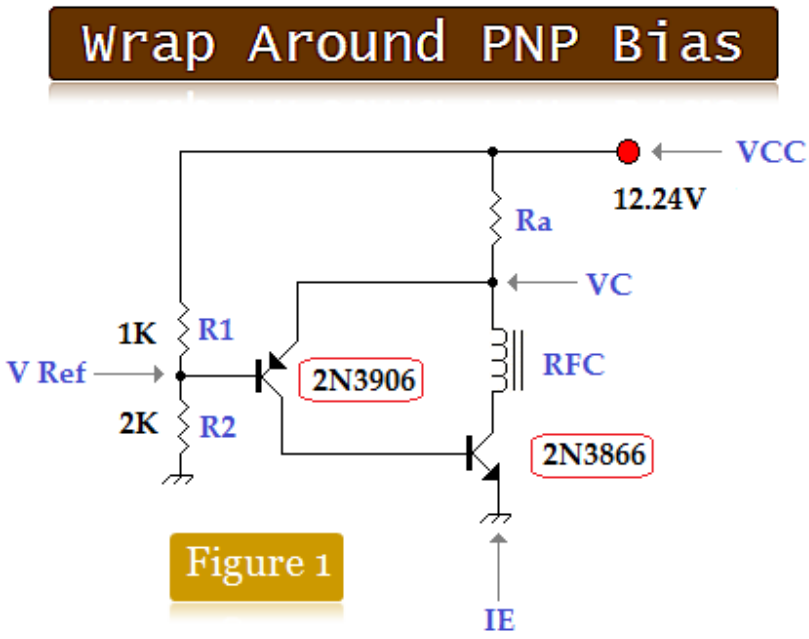

Desired IE	IE (mA)	VC (volts)	V ref (volts)	Ra (Ω)
19.0	19.83	8.62	8.15	180
42.0	43.51	8.31	8.15	82
105.0	108.50	8.22	8.15	33.3

Above — The schematic and data table from some biasing experiments. The normal decoupling parts were removed to isolate the biasing circuitry. All voltage and current values were measured. Another photo. A folded piece of paper is under the wire connecting the NPN emitter to the copper clad board. This is how I measure emitter current. The paper acts as an insulator and allows you to press hard with the ammeter probe to ensure good contact. After current measurement, the paper was discarded and the emitter soldered to the copper ground plane.

Biasing Procedure

Step 1: Choose a Target VC

Using collector resistor Ra, we want to drop about 2/3 of the power supply voltage across the NPN transistor. For a 12 volt supply or VCC, this is 8 volts VC. The formula is Target voltage = VCC x 0.66. Why choose 2/3 VCC instead of ½ VCC like we do for Class A audio amplifiers? In audio amps we just use a resistor as the load and the collector voltage can't go above the power supply unless we insert some reactances in the circuit. In simple AF voltage amps, the half VCC supply allows the greatest undistorted, peak-to-peak AC signal swing.

In RF power amps, a transformer or RFC lies on the collector terminal, so the instantaneous collector voltage (sum of the supply voltage plus the peak AC voltage) can go well above the supply voltage. If you have 8 volts on the collector, VC can easily rise to 16 volts or so on signal peaks. It's often prudent to choose a VC closer to VCC than the classic ½ VCC of audio amplifiers.

Hereafter, Target VC is referred to as **VRef**

Step 2: Choose R1 and R2 to bias the PNP @ VRef

Choose the PNP biasing transistors R1 and R2 so that the PNP bias = VRef. The formula follows:

$$VRef = \frac{VCC \times R2}{R1 + R2}$$

I wrote a Java Applet that does the math Applet A ; just plug in a VCC and play with the resistor values until you get your target VRef with the

resistors from your parts collection. Try to get a bias as close as possible to the targeted VRef, but don't stress out over it.

Step 3: Choose Ra to give (VRef + 0.6)

Ra = VCC – (VRef + 0.6) / desired current in amperes. Use or make up Ra with nearest standard resistor value(s) with an appropriate power rating. In a PNP, the emitter terminal is 0.6 VDC higher than the base, so need to we add that to VRef. The desired current is any reasonable current that you want to set up; for example 25 mA or 75 ma.

Example Calculation

I wanted a emitter current of 105 mA from the Figure 1 circuit. VCC = 12.24. Let's run through the steps.

Step 1: Choose a Target VC

Target voltage = 12.24v x 0.66 = 8.1 VDC -> Now called VRef

Step 2: Choose R1 and R2 to bias the PNP at VRef

I just plugged some resistor values into Java Applet A. R1 is normally lower than R2.

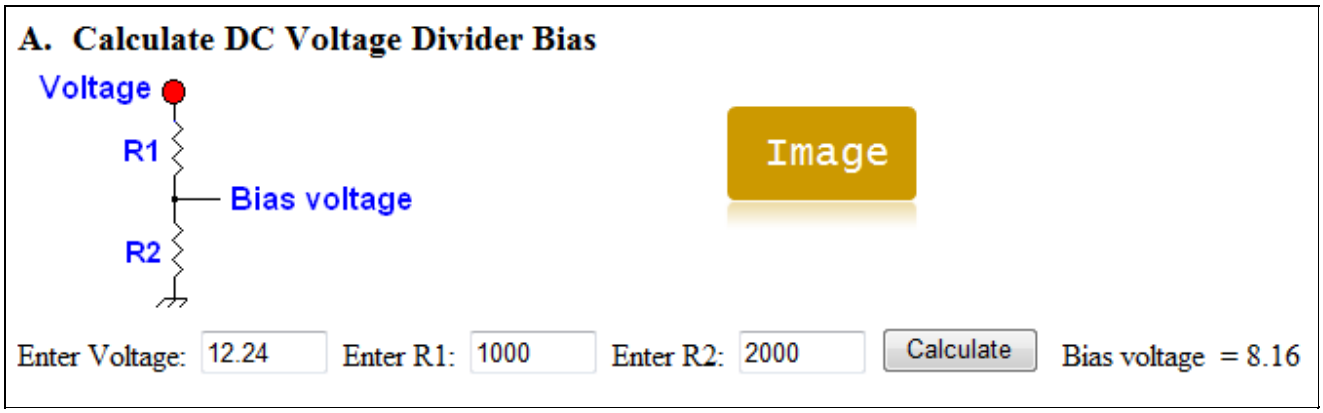

Above — A practical bias network. I have lots of 1 and 2K resistors. 8.16 v is close to my target VRef.

Step 3: Choose Ra to give (VRef + 0.6)

12.24v – (8.16v + 0.6v) / 0.105 A desired = 33.1 ohms. I put three 100 ohm ½ watt resistors in parallel for Ra. Click for lateral view photo showing the 3 resistors.

The exact measurements of this example and 2 other (19 and 42 mA) are tabled in Figure 1. I used an 82 ohm 1/2 watt resistor for Ra in the 42 mA version. The bench values closely approximate the calculated values. This circuit is quite instructive. In a real circuit (Figure 2) we add in the decoupling parts. Ra performs double duty as the decoupling resistor as well as the current regulator resistor.

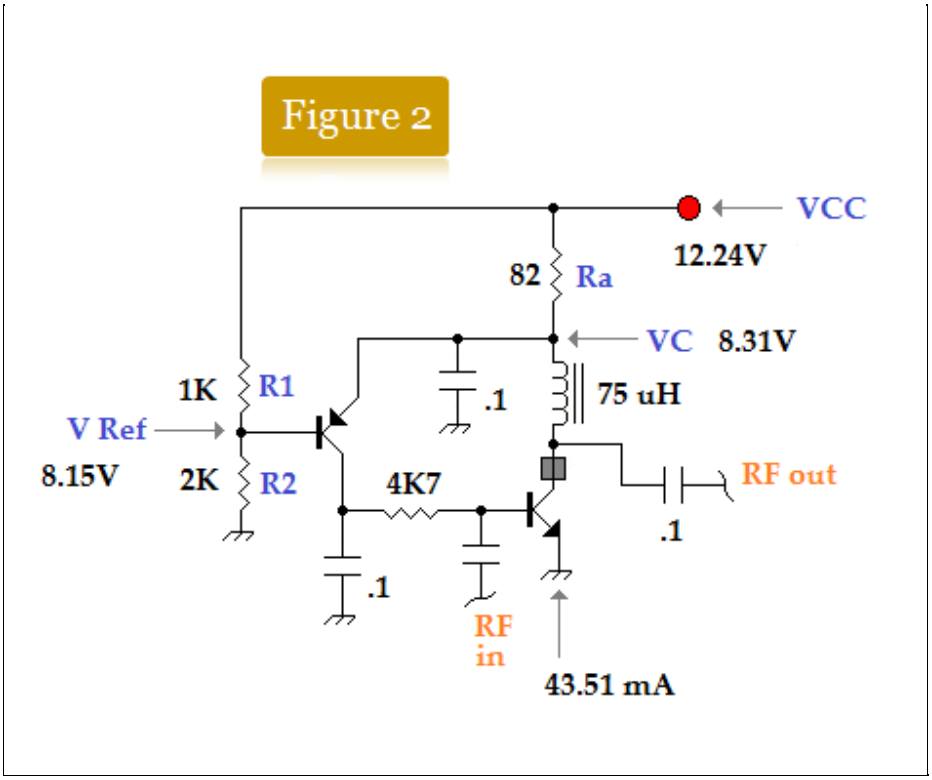

Above — A working version of the desired 42 mA medium power amp from Figure 1. Refer to EMRFD Chapter 2 for further information.

How does the PNP wrap-around bias loop work?

Using the sample conditions from Figure 2: VC = 8.16v calculated, Desired IE = 42 mA and VCC = 12.24v
The main decoupling/current limiting resistor Ra is established at 12.24v – (8.16v + 0.6v) / 0.042 mA = 82.9 Ohms.

No matter what, the PNP VRef = 8.16 volts. All of the desired conditions are established and the current is flowing in the NPN. Let's change these conditions and see what happens.

First, instead of 42 mA, assume that the NPN current drops to something less. Hence, there will not be as much of a drop across Ra. This will cause VC to increase. This is the voltage on the PNP emitter. When this voltage increases, there is more voltage between the base and the emitter of the PNP, which will make it draw **more** current. That current comes out of the PNP collector runs to the base of the NPN. This causes the NPN to draw more current (beta times) which increases its collector current and causes the collector voltage to drop because of the I x R drop in Ra. It drops until it reaches the 8.16 volt level.

Let's now assume the opposite. The NPN draw too much current, more than the desired 42 mA. This means that there is too much I x R drop in Ra and VC goes **below** 8.16 volts. This tends to turn the PNP off. The PNP collector current drops, so the NPN base current also drops, causing the NPN collector current to drop. This causes VC to again increase to reach 8.16 volts. Is this cool or what?

---

2. RC Low-pass Network

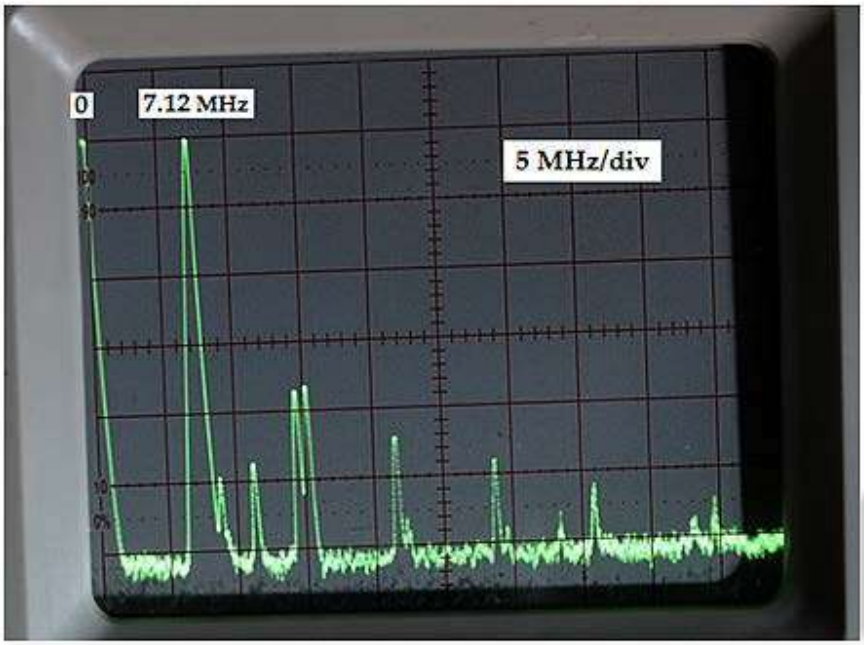

Above — Spectrum analysis without the RC low-pass filter.

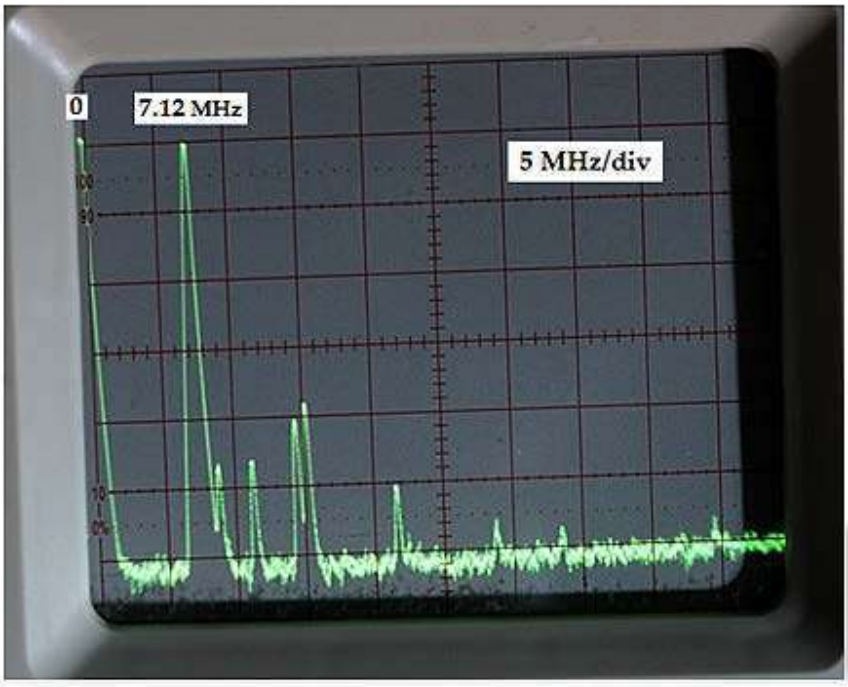

Above — Spectrum analysis with the RC filter in-situ. Above 20 MHz, the spurs are ~5-6 dB down.

3. Transistor Power Dissipation in the 2N3904

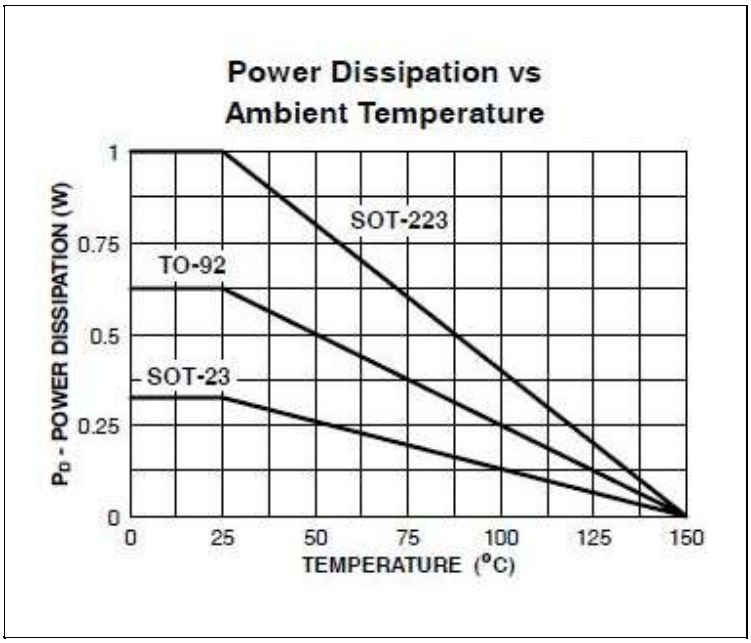

Above — Power Dissipation versus Temperature for the 2N3904 in 3 packages.

Power dissipation in the collector resistor

For example, VC (the voltage across the transistor) = 10 volts and the emitter current = 20 mA

P = I x E = .020 amps x 10 volts = 200 mW

Power dissipation in the emitter resistor

P = I x E = .020 amps x the measured emitter voltage

or P = I x I x R

For example, emitter current = 20 mA with a 5 ohm emitter resistor; P = .020 amps x .020 amps x 5 ohms = 2 mW

We assume IE = IC in the above examples. At 200 mW collector dissipation, the 2N3904 temperature temperature climbs to about 65 C. A metal can transistor such as 2N2222 has more surface area and better heat dissipation. A heat sink also improves heat dissipation. Temperature dissipation charts are referenced to ambient temperature which may be dependent on the air circulation around the transistor. If you plan on running 200 mW or so collector dissipation with a 2N3904, glue on a heat sink. A pinch of the finger and thumb, or a infrared thermometer are the most common popcorn ways to test for the need for more heat sinking, or a part with better power dissipation.

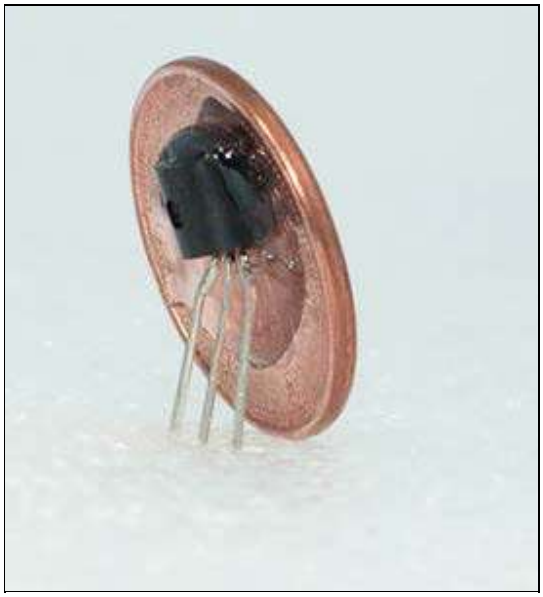

Above — I learned this from a Russian builder. 100 heat sinks for a dollar. Typically, a small blob of epoxy with the transistor positioned to the lower edge of the penny works best. I used too much epoxy and didn't wait for it to completely dry before taking this photograph — the penny slid down.

---

4. Some Factors Affecting Common-Gate Amplifier Input Impedance

A question arises: with all the devices and topologies available, why build a common-gate JFET RF amp in 2011 and on? For the J310 JFET at least: they're cheap, the input impedance is close to 50 ohms and wideband, the amp demonstrates good stability, signal handling capability and linear performance — all without running mega-current. Мне нравится. Many authors state the common-gate noise figure is inferior to that obtainable with the common-source topology, but for the popcorn builder, the common-gate noise figure is probably reasonable.

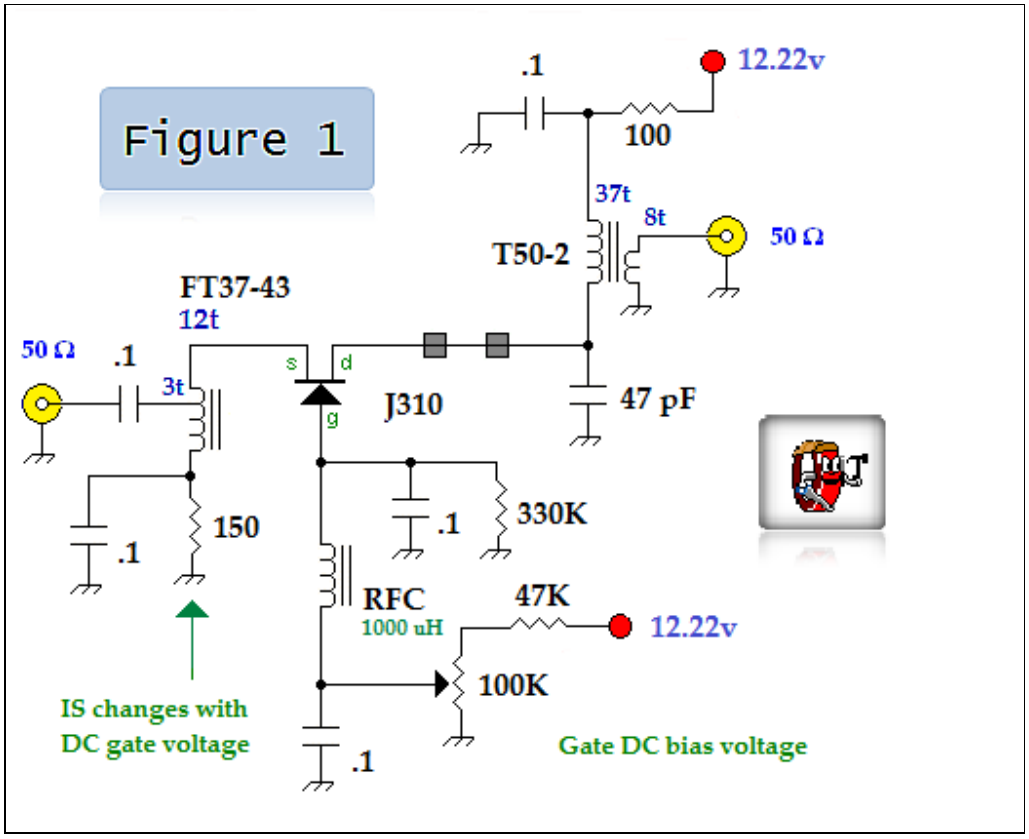

Above — A JFET gate biasing experiment. Here I applied 0-7 volts DC to the gate of a common-gate FET amp. The results proved interesting; see the graph below. The drain was tuned with a fixed 47 pF cap and manually "scrunch tuned" by pinching the T50-2 toroid with fingers and thumb. The input RFC serves to decouple the DC from the AC signal and the tap is used to improve the input impedance match.

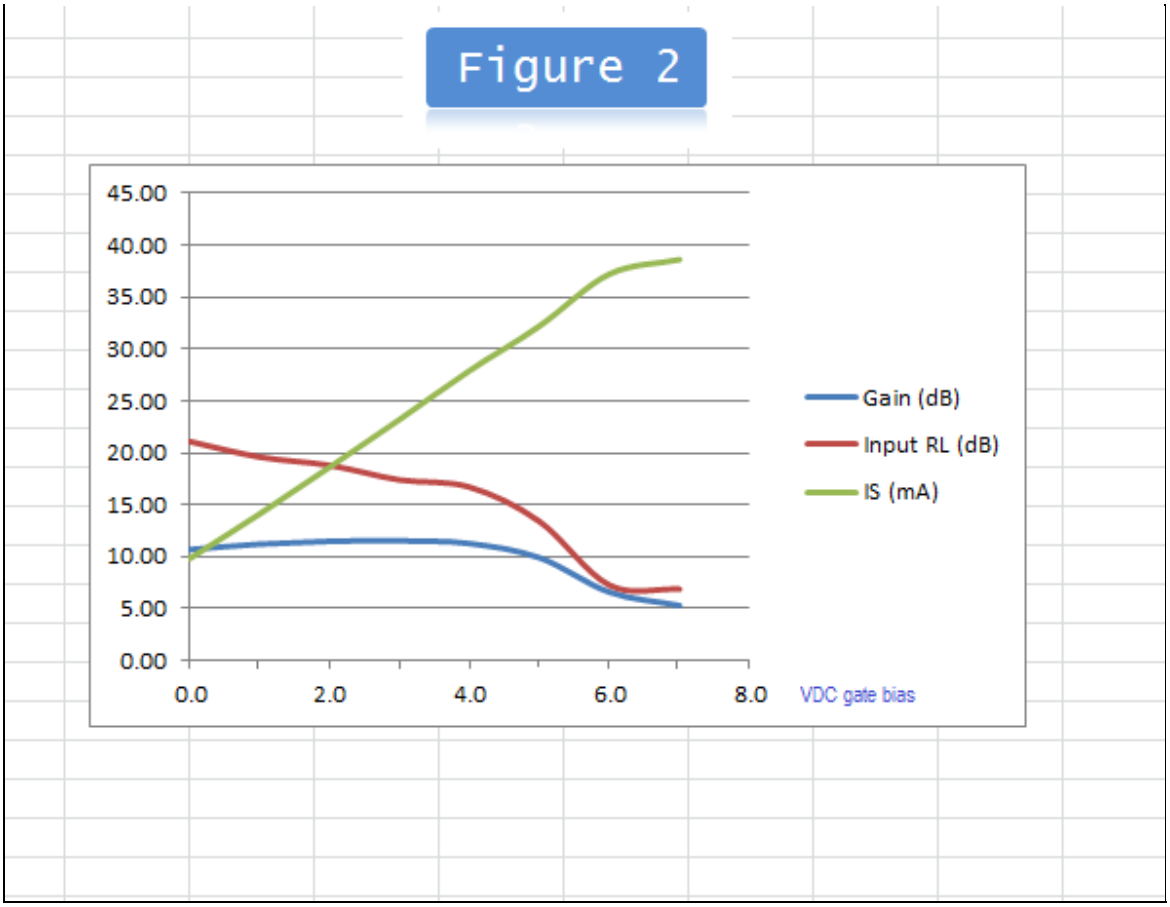

Above in Figure 2 — A graph of the DC gate voltage versus gain, input return loss and source current from Figure 1.

Increasing the DC gate voltage increases the source current as shown in the graph — ranging from 9.8 to 38.6 mA. From a DC gate voltage of 0 to about 4 volts, amplifier gain changes very little. Technically, the gain of this amplifier should increase along with drain current, however, the input resistance simultaneously goes down, creating greater voltage division loss at the input plus reduced return loss from impedance mismatch. This tends to cancel the increased gain as the plot shows.

The AC signal current injected into the FET comes out of the drain with power gain because that same current is now flowing into a higher impedance. The gain is dependent on the ratio of the impedance at the drain to that at the source. Click for a SPICE plot of DC gate voltage versus source current for 0 - 5 volts from Wes, W7ZOI.

From experiments, I learned that at least 6 things effect input return loss: the source resistor value, stacking or paralleling JFETS, the gate DC voltage(all which change current and/or transconductance), whether or not you bypass the source resistor, negative feedback and also the tap on the input RFC. Like other amps, the impedance of the device before and after the JFET amp can also change the input match, but those are external and normal considerations.

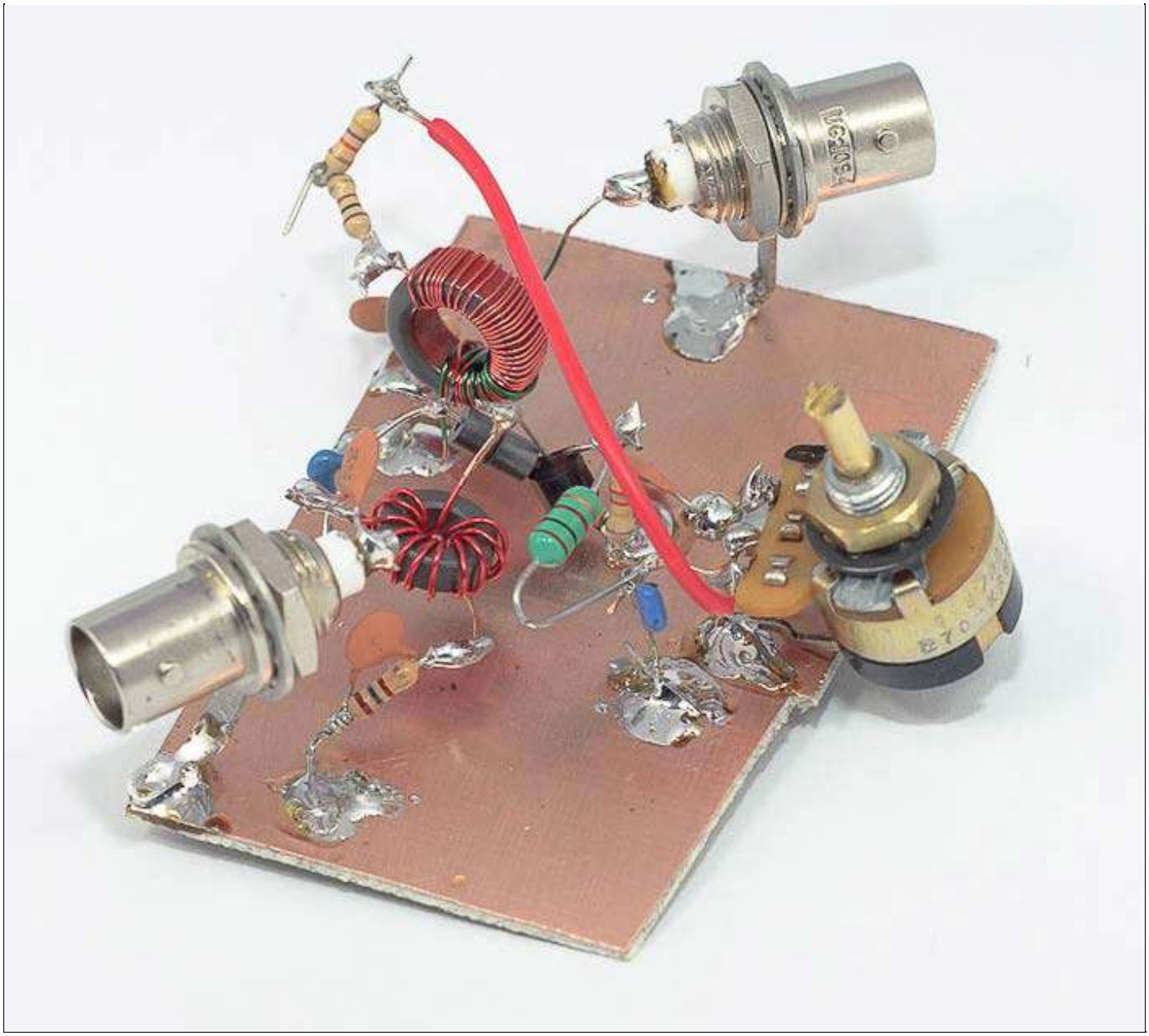

Above — Breadboard of the DC gate bias experiments of Figure1. Properly biased JFETs act like a current source where drain current is controlled by the gate-to-source DC voltage. The input impedance of the common gate amp is the reciprocal of the transconductance. Ken Kuhn posted some great JFET design notes in the yellow JFET section on his web site. EMRFD provides another essential reference for RF JFET design.

Noise Figure and the Common Gate Amplifier

Noise figure is important in low-level RF amplifiers such as a preamp or post-mixer amp because noise generated by these amplifiers contributes to the overall noise figure of a receiver. The input impedance an amp like the common-gate is considered an *active* impedance. Often, with active impedances, obtaining the maximum power transfer and lowest noise figure don't occur simultaneously. That is, the optimum input impedance match for gain is not the optimum input match for low noise performance. With pure resistances, the best noise figure possible is 3 dB; however, when using an active impedance, it's possible to achieve a noise figure less than 3 dB by applying negative feedback or other techniques to manipulate the JFET active input impedance and lower its voltage noise.

A stellar example by Bill, W7AAZI employs DC gate bias, noiseless negative feedback and paralleled JFETs to achieve a noise figure in the 1.2-1.5 dB range. This mind-boggling circuit is described in EMRFD as Figure 6.94. I wanted to explore this topic: can amateur builders design *common-gate* amplifiers for a lower noise figure? The answer is perhaps, however, unfortunately, there is no cookie-cutter approach.

Low noise amplifier design imposes an advanced topic and many builders lack the math skills and/or test equipment to design and generate results. Each design must be approached on a case-by-case basis, although similar fundamentals apply to all cases — using active impedance manipulation techniques and paralleling up JFETs while paying attention to all the resistances in a circuit — even loss resistance in the inductors. I learned from Professor Ken Kuhn that when amplifiers are paralleled the output signal power adds linearly, whereas the internal noise adds statistically (square root of the sum of the squares) and thus noise figure improves. In short, paralleling JFETs reduces voltage noise,

but only to a point, as input capacitance also increases which can degrade high frequency performance and noise figure. Ideally, the JFETs paralleled should be matched for IDSS and VP.

Further, all devices have a voltage noise specifications (in volts per root Hz) and a current noise specifications (in amperes per root Hz). The source impedance that produces the lowest noise is the ratio of the two — derived from Ohm's law. The input impedance of the device may be higher or lower; thus the optimum source impedance for low noise is not necessarily the optimum source impedance for maximum power transfer. It's unlikely that these two impedances differ widely, however, only careful bench measurements or closely copying proven designs will ensure the desired results.

---

5. Design Center - Temperature Stable Voltage Divider Bias

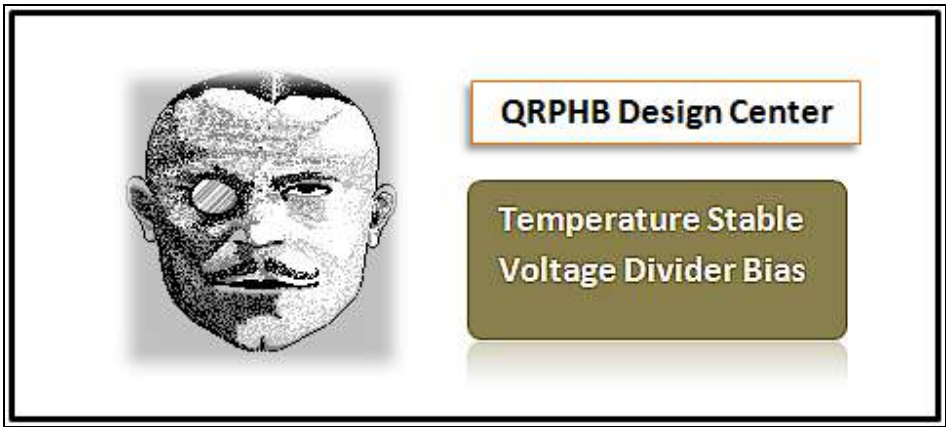

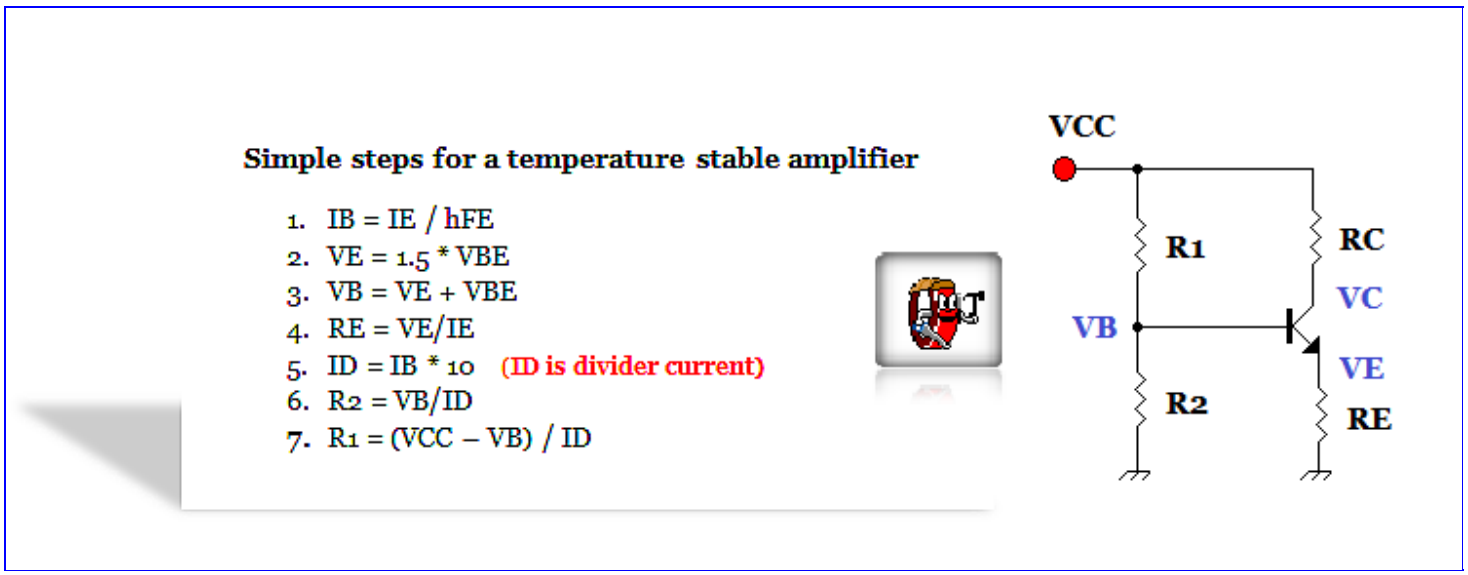

Above — A simple way to design a temperature stable BJT voltage divider bias. Assumes that IC = IE. You specify IE.

I sought to develop a simple way for builders to design a temperature stable BJT amp using voltage divider bias. It wasn't so easy. Here is the full math from Ken Kuhn. As shown, it gets complicated and over-the-head of the target readers of this web site.

My simple approach makes assumptions, and certainly an astute builder could improve my algorithm - I developed other formulae, however settled on this one because it well fits the scope of the QRP/SWL HB web site. Most engineers design their bias networks in SPICE and I recommend this.

To choose a Beta or hFE, you can measure the Beta or use the transistor datasheet Beta near to the emiiter current you intend to apply. Many builders debate this and even go as far to state that spec sheet Beta values are useless. This may be true, but you *have* to decide on some approach. Ultimately, you will build the amplifier and can tweak 1 or more of the bias resistor values to set your bias voltage (emitter current). Click for a snippet from a 2N3904 datasheet showing hFE at a range of currents.

Biasing BJTs is a great example of building to suit your design requirements. The average reader likely operates their radios at room temperature where a minimum temperature stability factor is needed. On the other hand, you may operate field portable, or use a crammed chassis where transistors heat threatens stability. As always, your design choices must fit your needs, parts and abilities.
The above 7-step method forms a simple **QRPHB Design Center** method to achieve a reasonable temperature stability factor at normal

operating temperatures. I considered 2 factors: VBE and Beta (hFE) changes.

VBE

We normally attribute the voltage difference from base to emitter (VBE) as 0.7 volts for silicon transistors. VBE changes inversely with temperature and at AF to HF, we mitigate VBE creep by applying an emitter resistor to increase the emitter voltage VE. The emitter resistor provides a feedback loop so as collector current starts to increase due to a rise in temperature, the voltage drop across RE also starts to increase. This voltage tends to reverse bias the base-emitter junction. The net effect is decreased collector current.

How do I choose an emitter resistor value for VBE bias stability asked the little grasshopper (novice)?

The VE value should typically be about 10 to 25% of VCC. VE recommendations really vary from author to author — some say VE should be at least 5X VBE while other authors suggest 2-4 volts as the minimum acceptable VE value for bias stability in typical AF-HF amplifiers. I use 1.5 * VBE (0.7) = a VE of 1.05 volts, but it's up to you. Since you know IE for your transistor, calculate the resistor RE to provide the target VE using ohm's law: RE = VE/IE.

At VHF on up, emitters are typically directly connected to ground since that path must have as near zero inductance as possible. In these amps, the bias is derived by a feedback circuit that controls the base current to stabilize the collector current at a specific level. Inductance in the emitter lead causes significant loss of gain at higher frequencies and also upsets the input impedance to the base. Similar effects occur in JFETs and even vacuum tubes. 10s of nH of inductance at 144 MHz represents a reactance of 10s of ohms. At UHF on up this becomes very serious — that's why construction methods are so critical for these builders.

In conclusion; to influence VBE stability against temperature changes and to some extent leakage current, at AF- HF, apply series feedback to a raise emitter voltage (VE). Accounting for variations arising from 5% tolerance parts, I chose a minimal VE of 1.05 volts (equation 2 of 7 in my "Simple Steps..." algorithm).

A tradeoff challenges us — increasing the emitter resistance, increases AC degeneration, lowers AC signal gain and raises the transistor input impedance. Bypassing all or part of the emitter resistance offsets these problems.

Beta

Beta variation arising from temperature changes must be mitigated. I briefly discuss the factors that change Beta in the bullets under the #5 Bipolar Junction Transistor Beta Tester on this page.

To design "beta independent amplifiers", the builder alters the resistance ratio RB/RE. Decreasing this ratio improves the Beta stability while decreasing the amplifier current gain. The ratio can be confusing, so the Design Center equations 5, 6 and 7 just make the current in the divider 10X the base current. It's simple — you're done. Feel free to choose whatever ratio you think is best. Good values for the RB/RE ratio lie in the 12 - 20 range.

Design Example

[hFE = 100, IC = 10 mA (0.01A), VCC = 11.22v, VBE = 0.7]

*I used a 100 ohm low-pass resistor; so VCC = 12.22v - (0.01 A * 100 ohms) = 11.22v*

1. IB = IE / hFE = .0001 A
2. VE = 1.5 * VBE = 1.05v
3. VB = VE + VBE = 1.75v
4. RE = VE/IE = 105 ohms **(Use 82 – 100)**
5. ID = IB * 10 = 0.001 A
6. R2 = VB/ID = 1750 ohms **(use IK8)**
7. R1 = (VCC – VB) / ID = 9470 ohms **(Use 10K)**

Above — A design example employing my "Simple steps for a temp stable amp" bias algorithm. My VCC = 12.22 volts, but, as always I decoupled and bypassed the VCC — in this case, I applied a 100 ohm /0.1 uF network. At 10 mA emitter current, the voltage drop across the 100 Ω resistor results in a VCC of 11.22 volts.

Big thanks to Wes, W7ZOI and Professor Ken Kuhn for helping me with my math problems and to better understand biasing concepts.

A friend made a Design Center spread sheet for MS Excel. In this application you enter the desired IC rather than IE.

---

50 Ohm Common Emitter Audio Preamp Experiments

Introduction

This page supplements the Pop DC2 Receiver Experiments from this web page.

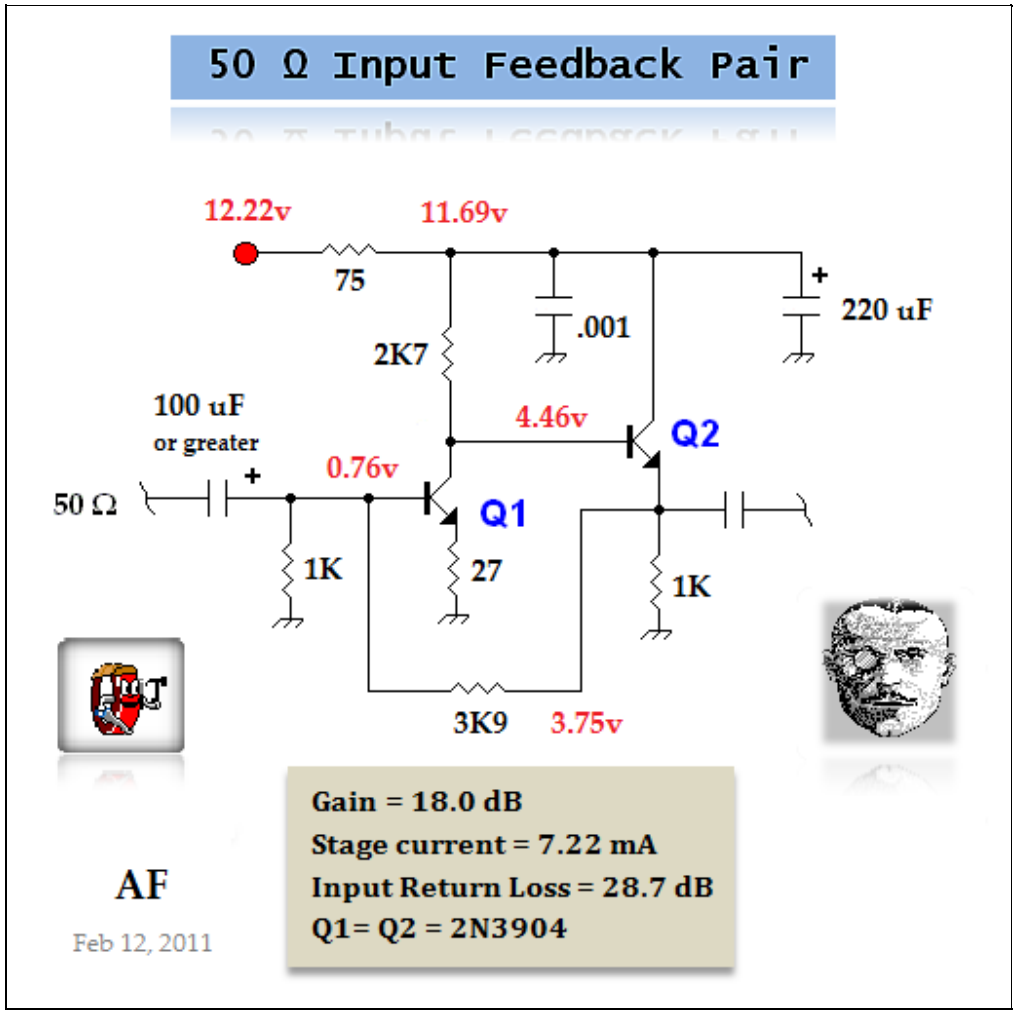

Above — A 50 ohm audio preamp to follow a diode ring product detector.

Many seek an alternative to the common base AF preamp that typically follows a diode ring product detector. Winter experiments yielded some possible ideas. The simplest is shown above.

Using all different parts, I built and measured another version to ensure reproducibility of the input return loss while just using standard 5% resistor values. The second amp proved similar: 18.4 dB gain, 7.27 mA stage current (3 .8 mA is consumed by the emitter follower), a return loss of 27.6 dB and a nice sine wave output. A 2K2 resistor AC coupled to the emitter follower provided a load. Note in the photo, I used 1% resistors

in some slots, but the values were standard 5% and not unusual values like 15.4 K etc.. The 3K9 feedback R is the most critical value — it's a 5% part.

About 1/4 of my resistor collection are 1% metal film, as I don't like stocking both 5% and 1% tolerances of the same R value. I envision this amp driving a 5532 amplifier/low-pass filter built with 5% resistors with the op-amp output connected to a 1-10K volume control potentiometer.

The amp above is pure popcorn fluff, yet represents over 8 hours of reading, calculations and bench discovery. In another version, I soldered in low noise transistors (MPSA18 for example) and 1% metal film resistors to try and drop the noise figure. Yet another stage had Q1 collector bootstrapping (3 layers of feedback). I'm not sure what I'll do with these experiments, however, at least 1 of these will end up on the module page as the update to the popcorn DC receiver mainframe.

Glenn, VE7DNL built a landmark common emitter preamp with parallel 2N4401s, shunt feedback and some 1% bias resistors. I built a version of his pre-amp without the diplexer. The input return loss in my version was only 5 dB — likely the diplexer network helps establish the input match. It appears Glenn's goal was low NF and the best match and noise figure don't always correlate. I matched Q2 and Q3 as well as I could since only 6 were available. An Hfe of 220 - 240 is not uncommon for the 2N4401 — a good part.

Here's a SPICE plot of the amp performed by Wes, W7ZOI. The two plots are S21 and S11. S21 is the forward gain in dB. S11 is the input reflection coefficient, which is just the negative of the return loss. At 1 kHz, the calculated gain = just under 42 dB and the input match = ~17 dB return loss.

To improve return loss in my breadboard, I need to tweek Q2 and Q3 bias (lower the 6.04K resistor), plus add some emitter degeneration. Emitter degeneration (series feedback) would worsen the noise figure. The 100 uF emitter caps offer some series feedback and capacitor values like 1000 uF are needed if "true" AF bypass is wanted.

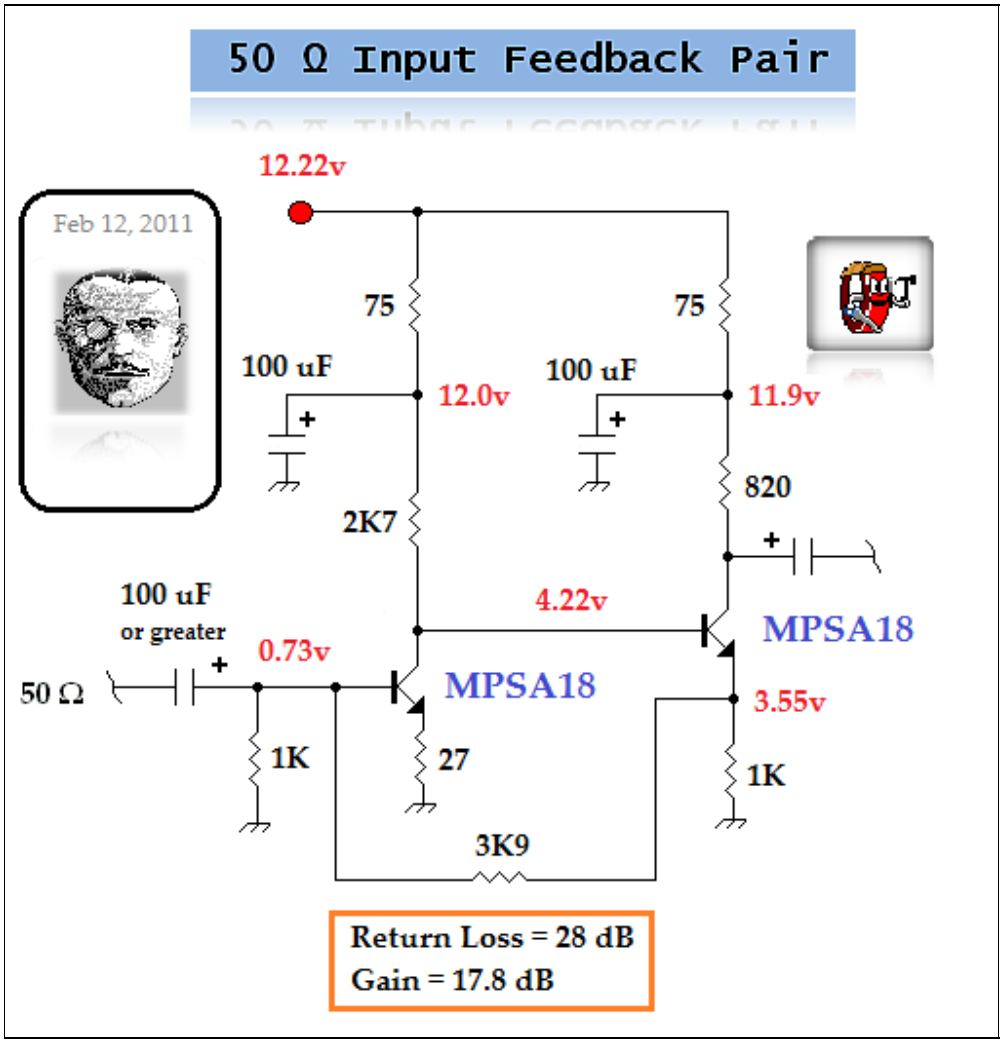

Above — Alternate experimental 50 ohm audio preamp to follow a diode ring product detector. The high impedance output enables small value output coupling capacitors for pseudo high-pass filtering. I simply added a collector resistor plus a decoupling network to Q2. The low noise MPSA18 BJT is a favorite and predictable part. The 2N3904, 2N4401 and others should work fine.

Don't even think about using an input capacitor less than 100 uF at 50 ohms — you'll trash the input Return Loss. I measured the highest Return

Loss with a 470 uF coupling capacitor, but the 100 uF cap shown worked almost as well.

I'm currently decreasing the (Q2) 1K emitter resistor with hopes of squeezing out a little more gain while trying to preserve strong signal handling capacity. I've found that heavy feedback is your friend.

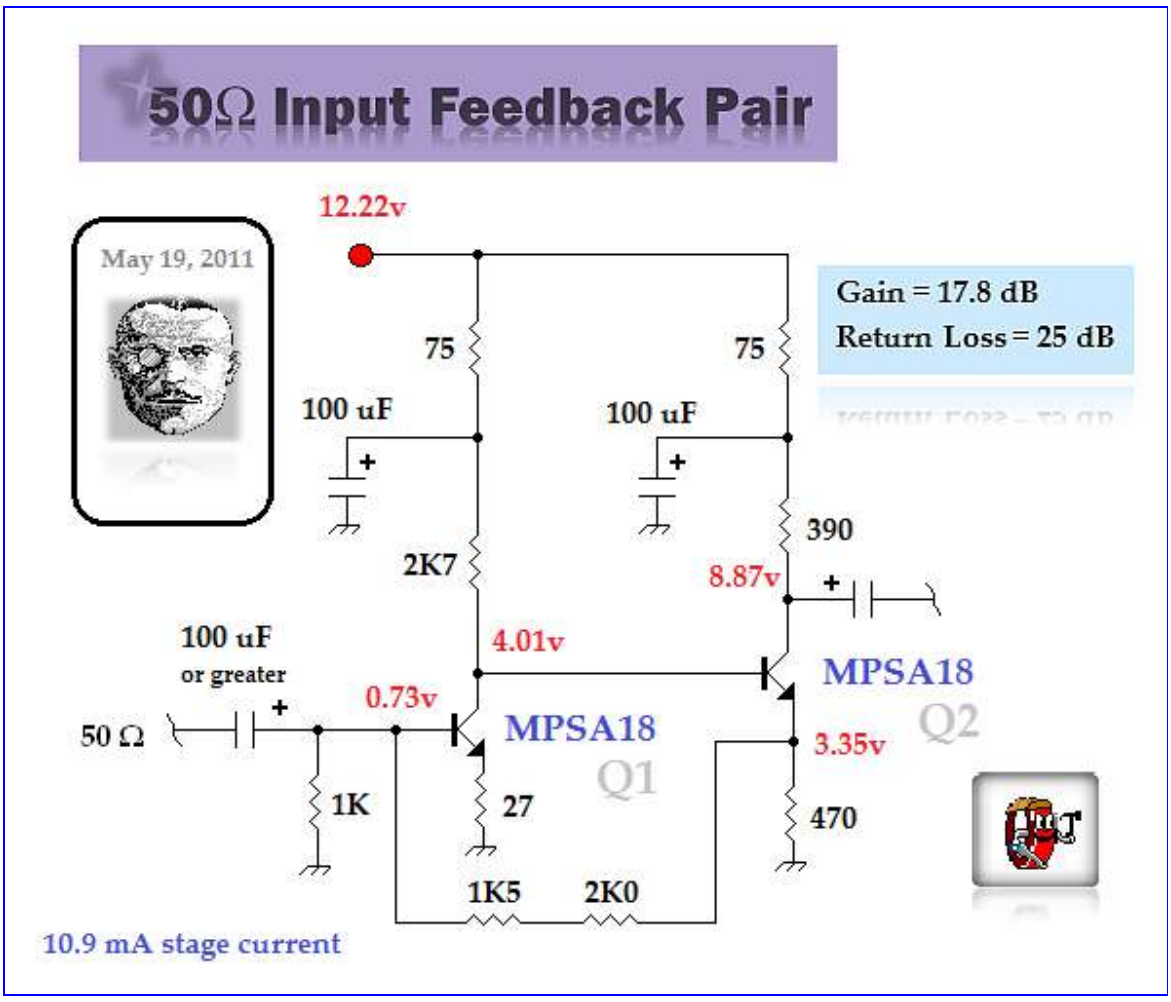

Above — Another version; trying to increase stage gain. The Q2 collector resistor dramatically affects clean signal handling — lowest distortion occurred with a 367 ohm collector resistance. I substituted a 390 ohm collector R. This dropped the gain a little, but increasing distortion over gain is never my goal.

During experiments, dropping the the Q2 emitter resistor below 470 ohms made the other biasing resistors more critical, decreased return loss and invited distortion. The best return loss occurred when critically biasing with 1% resistors — I'm avoiding that!

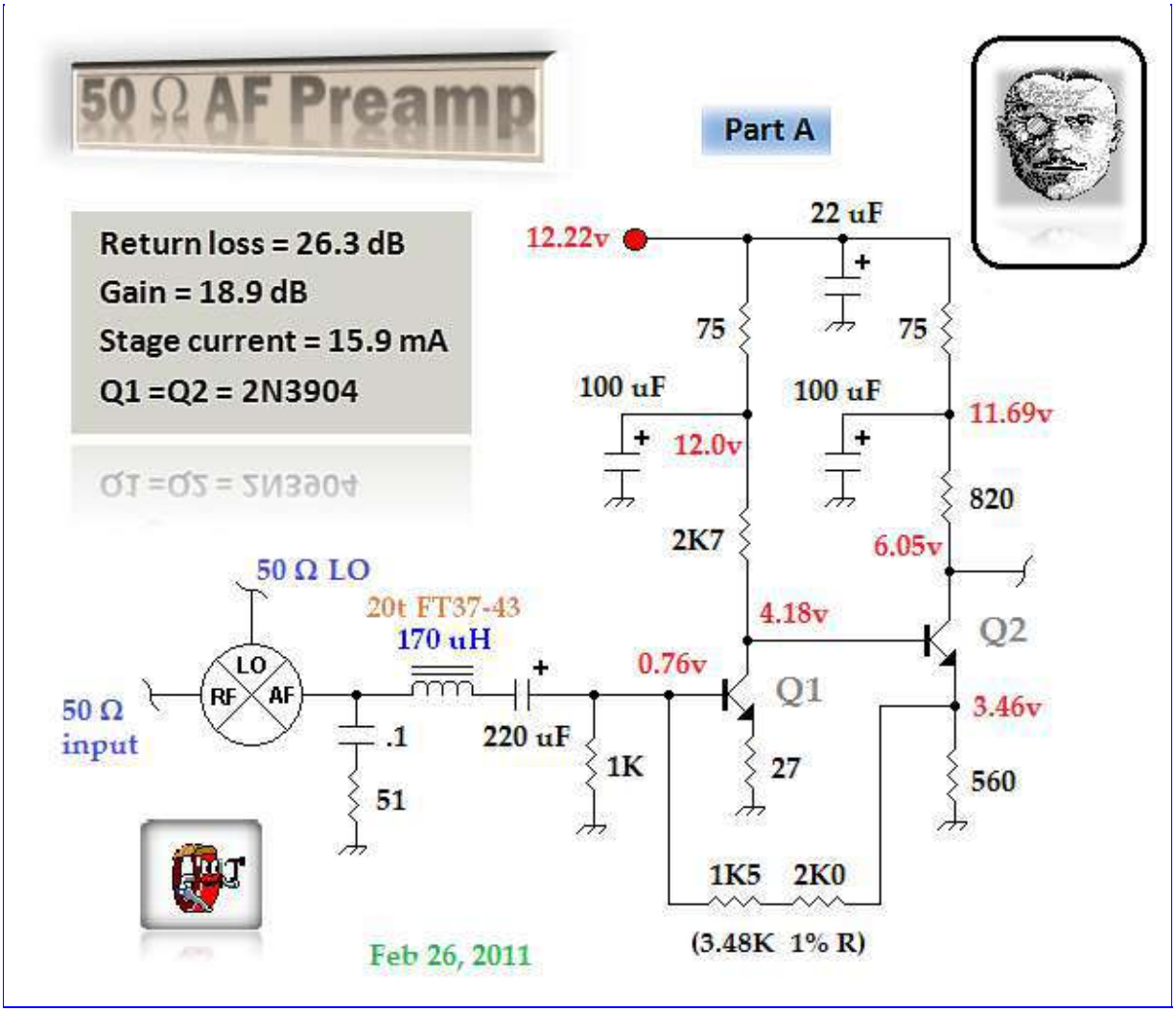

Above — Another popcorn part experiment from February. A low-pass network terminates a diode ring mixer and drives a 50 ohm input feedback pair arranged so the Q2 collector DC voltage is approximately 1/2 VCC — this provides the DC bias for a 5532 op-amp low-pass filter arranged in the Sallen-Key topology.

The Q2 collector voltage removes the need for a separate single supply op-amp bias network and an AC coupling cap. I didn't try this circuit in a receiver; arranging the feedback network and testing the possibility of such a design drove this experiment. A perfect 1/2 VCC Q2 collector voltage might be obtained with a standard 1% value 806 ohm R. I lack this part.

Almost Popcorn Superhet

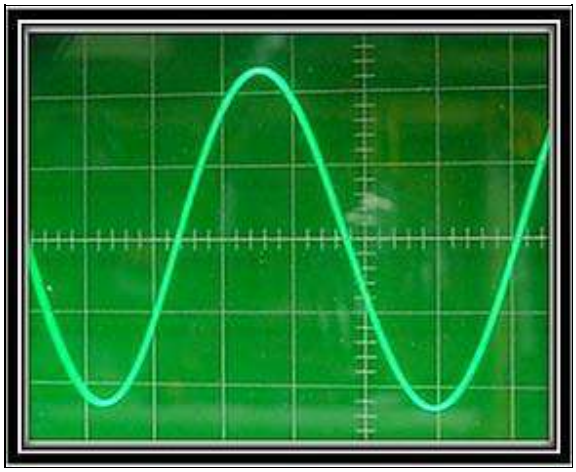

1. Receiver Concept and Macro Diagram

Not done.

Maybe a flight-of-fancy that never crosses the finish line? This page seems to repeatedly find the back burner; a good intention that never sees completion. Sadly this is normal for some of us builders — how many incomplete projects adorn your home and workshop? Still, this web page might fuel your *own* experiments.

For years, I've attempted to update my Popcorn Superhet from 1998 but always seem to lose interest from numerous distractions such as VHF and UHF experiments and other non-radio stuff. So here it is so far — raw and unrefined: more experiments from my analog-centric workbench. To clarify — I love the new digital radio stuff, but that's well covered on the net by numerous code writers and those bleeding edge, frontier-pioneer types. I prefer a 50 Ω lab with all the visceral enjoyment and learning it has to offer. To each his own.

This web page remains unlisted on the main top level menu — and for good reason.

Click for some supplemental lab notes.

2. N = 4, Gaussian-to-6 dB Crystal Ladder Filter

I frequency matched four 11.0592 crystals, characterized them and took an average of those crystal parameters plus some data from Zverev and inputted this into xlad08.exe, a program that ships with EMRFD.

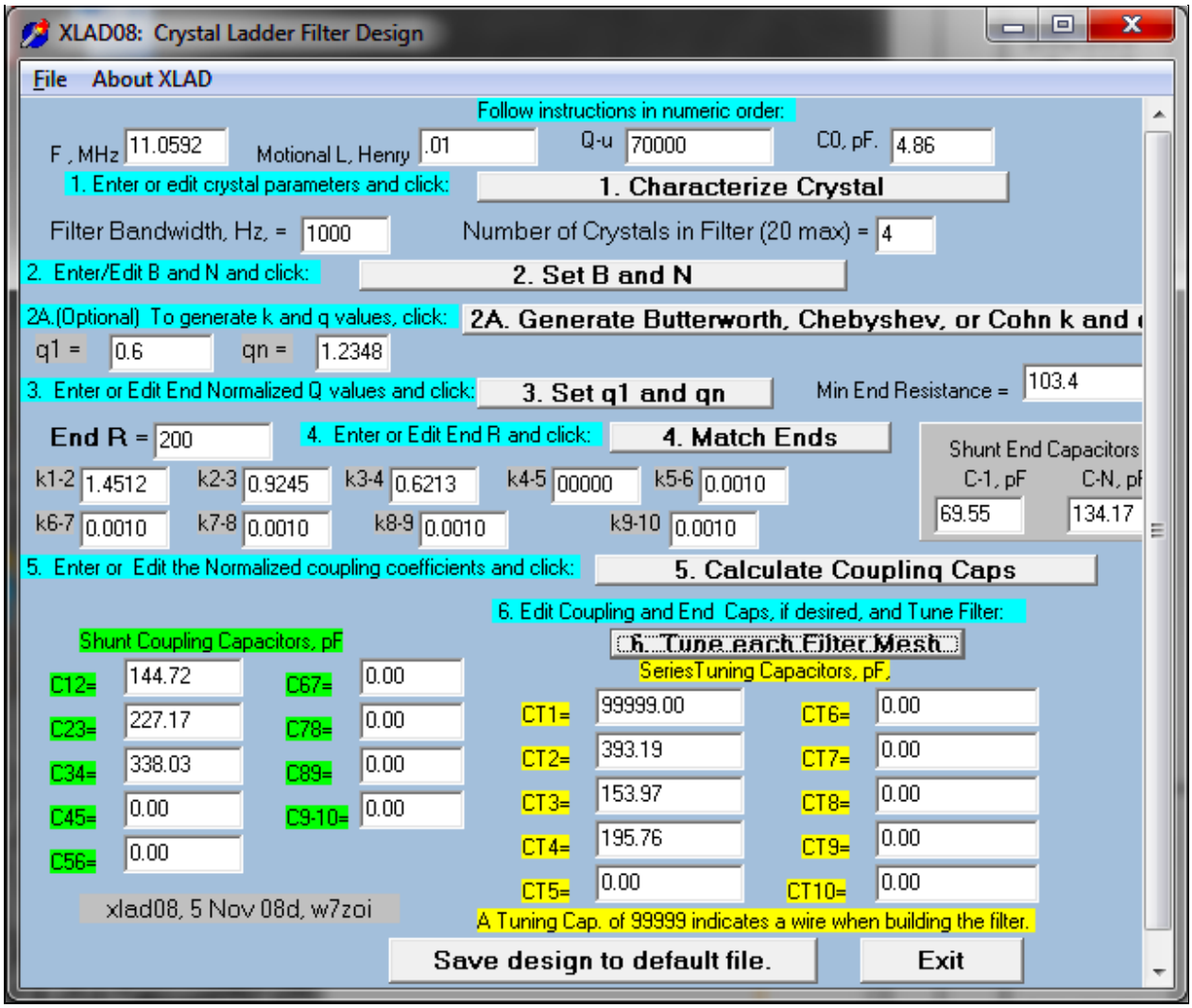

Above — Xlad08.exe screen shot.

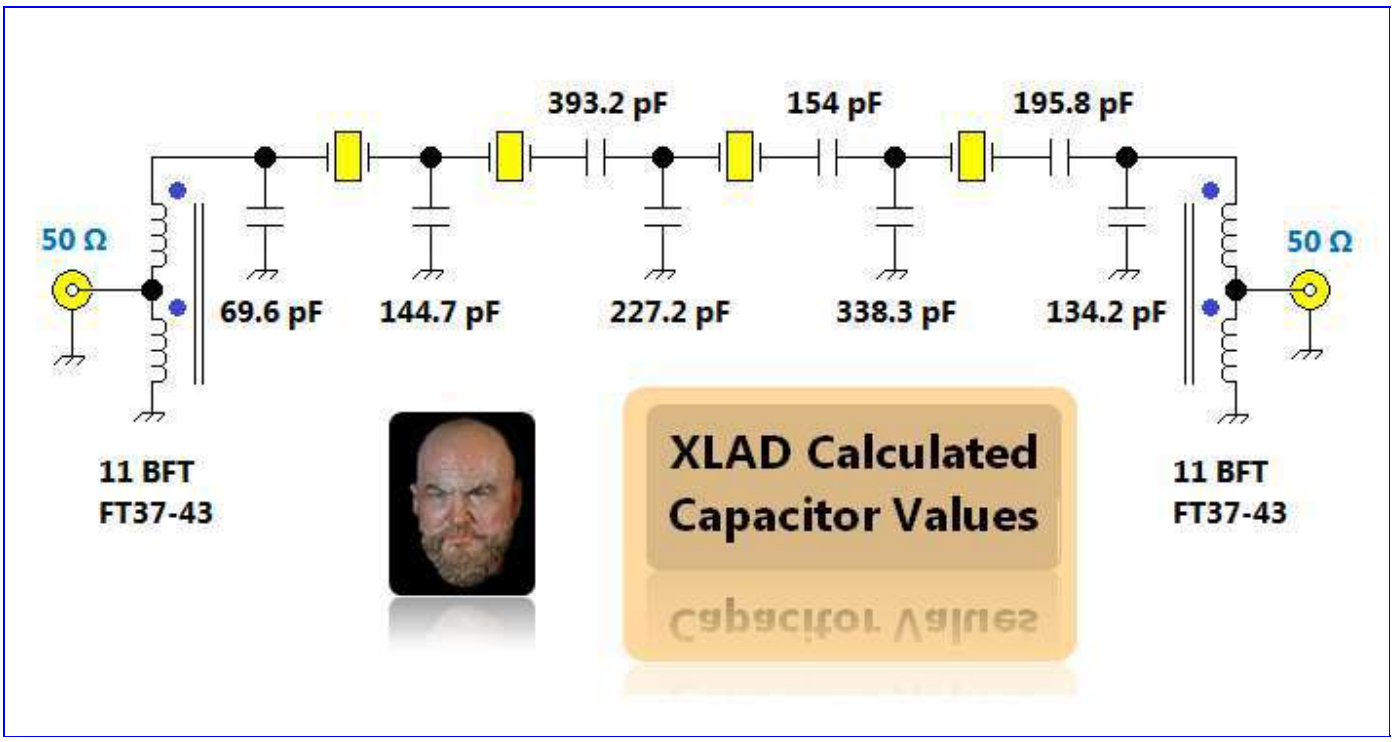

Above — The xlad filter expressed as a schematic. Click for a GPLA plot of the filter.

I built and hand tuned this crystal filter with my analog sweep system. Click for a photo of the optimized filter breadboard — I used 1 or 2 parallel capacitors to tune each capacitance to derive the best possible skirt shape. Click for a sweep of this optimized filter in my 'scope. 2 bifilar transmission line transformers provided the required 200 Ω port termination in my 50 Ω sweep system.

I sought a crystal filter based on the xlad08 calculated values using only 1 nearest standard value in each capacitor slot.

Transitional filters like the G-to-6 dB, are generally tolerant of part substitutions and thus I sought a filter with only 1 nearest 5% standard-value capacitor in *every* slot instead of 2 sticking 2 close in value parallel caps to make up the needed capacitance as needed.

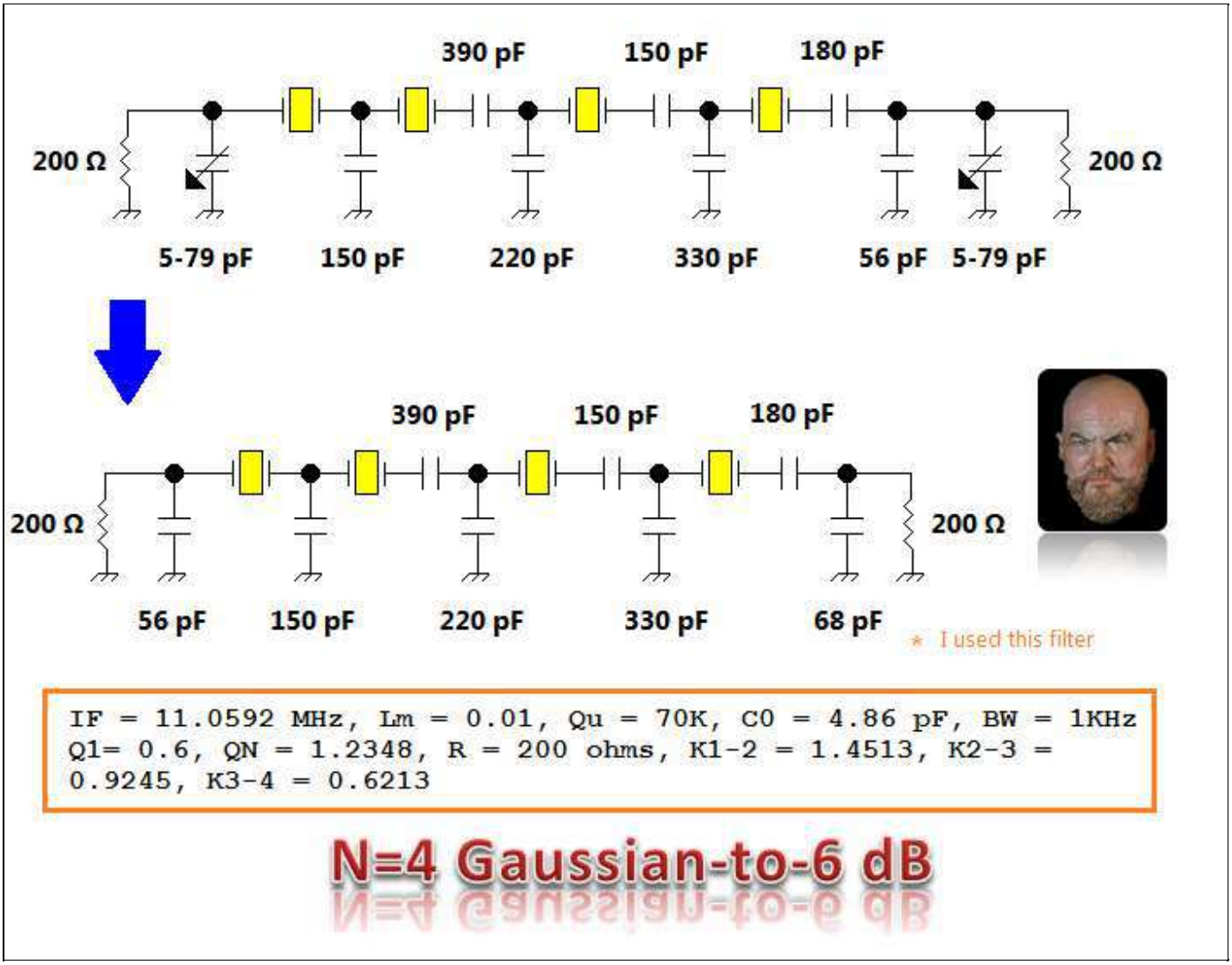

Above —The 2-step transition to a 1 capacitor, nearest standard value in each capacitor slot. In the top diagram, I placed a trimmer cap on each end to allow filter tweaking while looking at the swept filter in my 'scope. I've learned that adjusting the parallel cap nearest to each port a simple way to tweak a G-to-6 dB filter. After setting the best looking skirt, I removed and measured the end parallel capacitance and substituted the nearest standard fixed capacitor. Manipulating the capacitors values will change filter bandwidth and return loss.

You might compare the lower filter to the xlad calculated values to see how tolerant the circuit is.

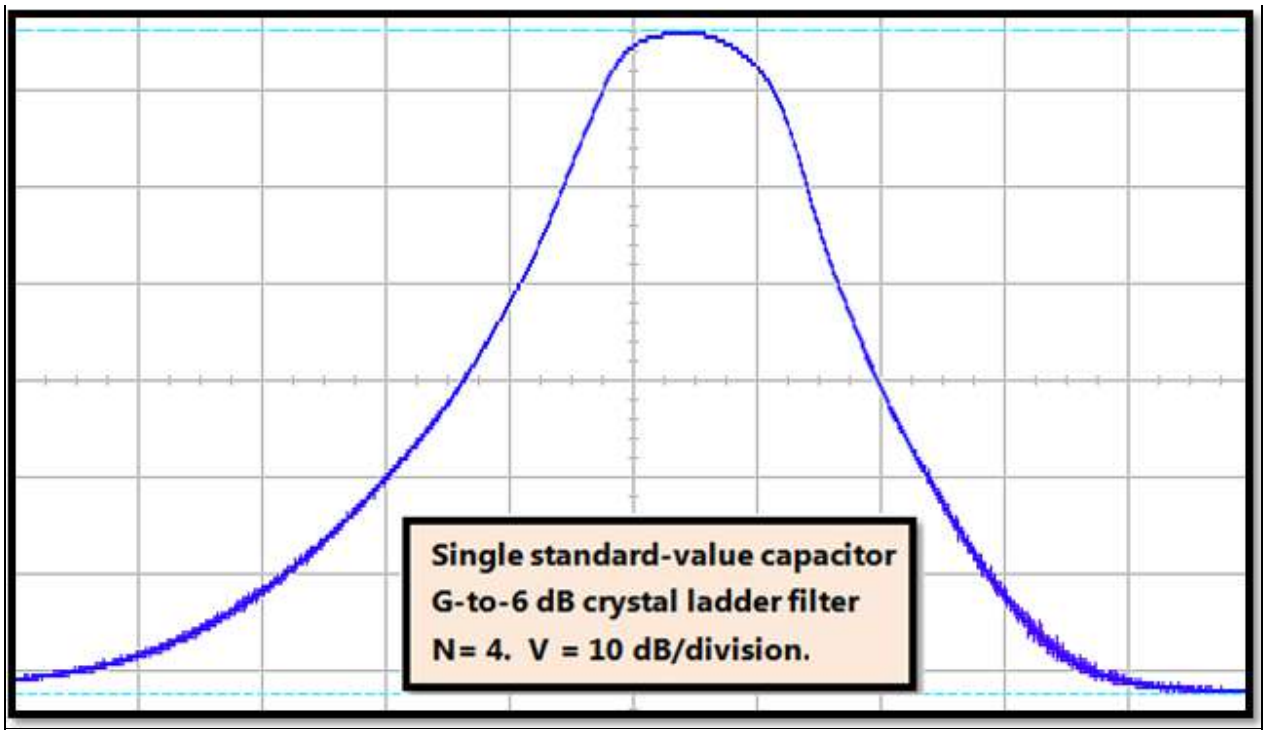

Above — A sweep of the single value capacitor version that's used in the Almost Popcorn receiver. While the 1 KHz filter skirt isn't perfect, it's reasonable. Click for the test bench breadboard. This particular filter measured 1/2 power bandwidth = 1227 KHz and the insertion loss was ~3.6 dB.

---

3. IF Amplifier

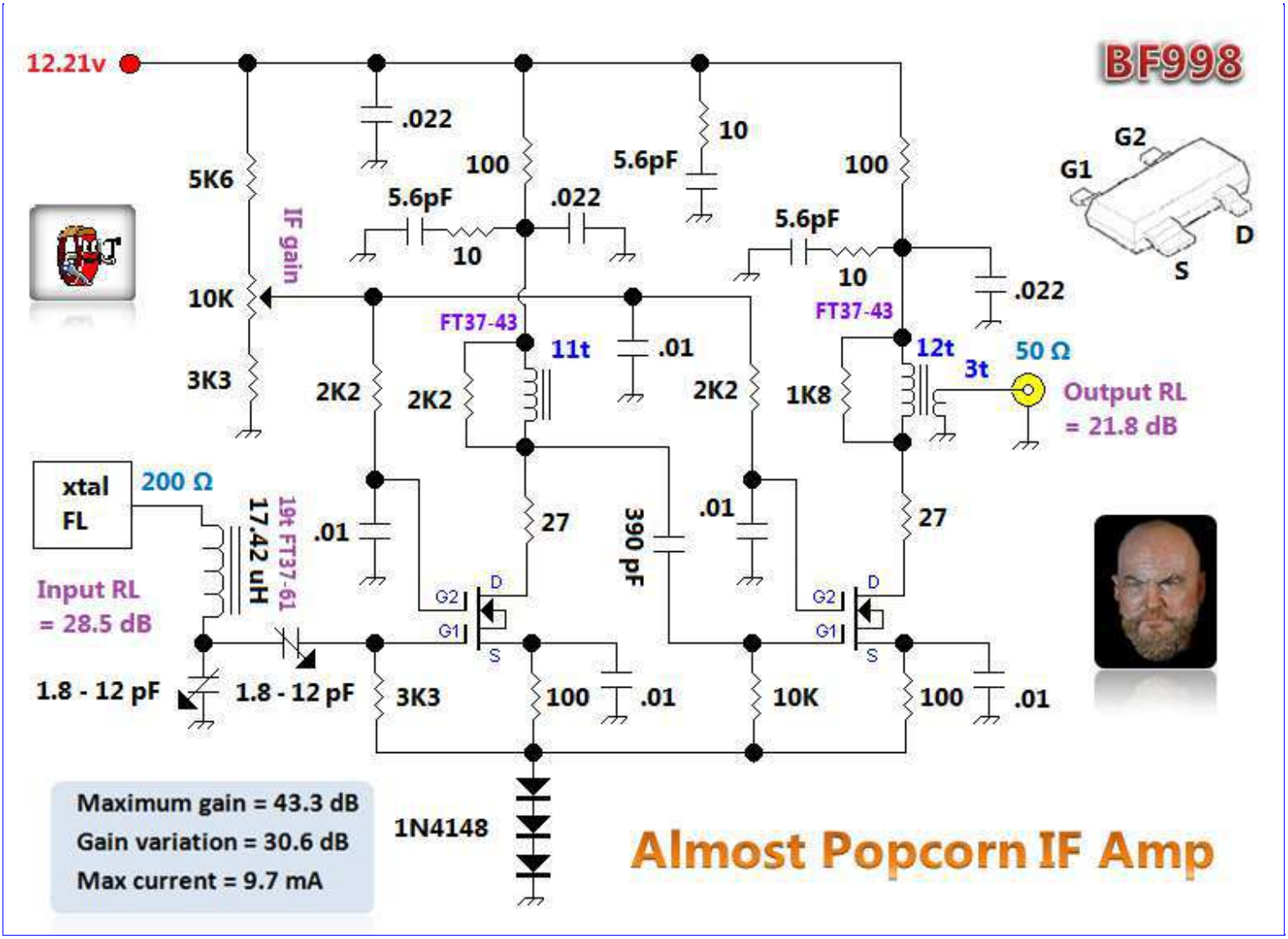

Above — Version 2 of a popcorn IF amplifer idea with BF998s. IF = 11.0572 MHz.

I have no use for AGC in my personal receivers since I listen through a speaker and *always* ride the RF gain control with my finger. Since the BF998 has gain into UHF, wideband decoupling + bypass SMT R-C networks filter each MOSFET in case of oscillations. Click and click for photos. This circuit will operate fine with just 0.022 µF bypass caps.

A network matches the 200 Ω xtal filter output impedance to the 3K3 input Z of the IF amp cascade. The L-C-C network has become a favorite matching weapon — 2 tweaks is often better than the 1 offered by a garden variety L-network. The product detector that follows this stage is a Level 7 diode ring mixer soldered onto the audio preamp board. This receiver will feature some modish circuits aimed at low noise + high fidelity but still stay "almost popcorn". Anyhow, that's my hope.

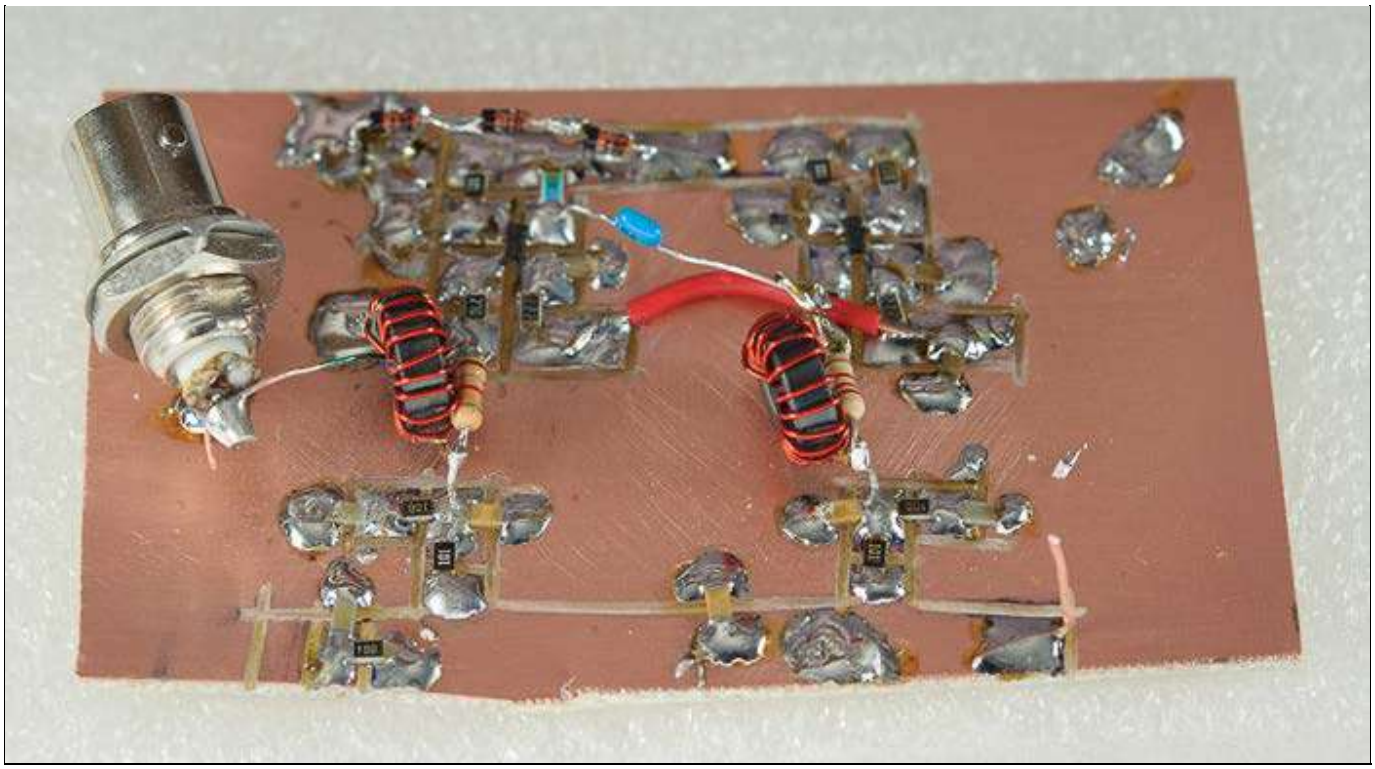

Above — A breadboard of the Popcorn IF amp sans the input network. I tested this stage using an oscillator with a 3K3 output impedance and liked what I saw. Click for a reverse angle view. After this build, I ordered some SMT versions of the 1N4148 diode. The BNC connector was only soldered on the board for testing purposes.

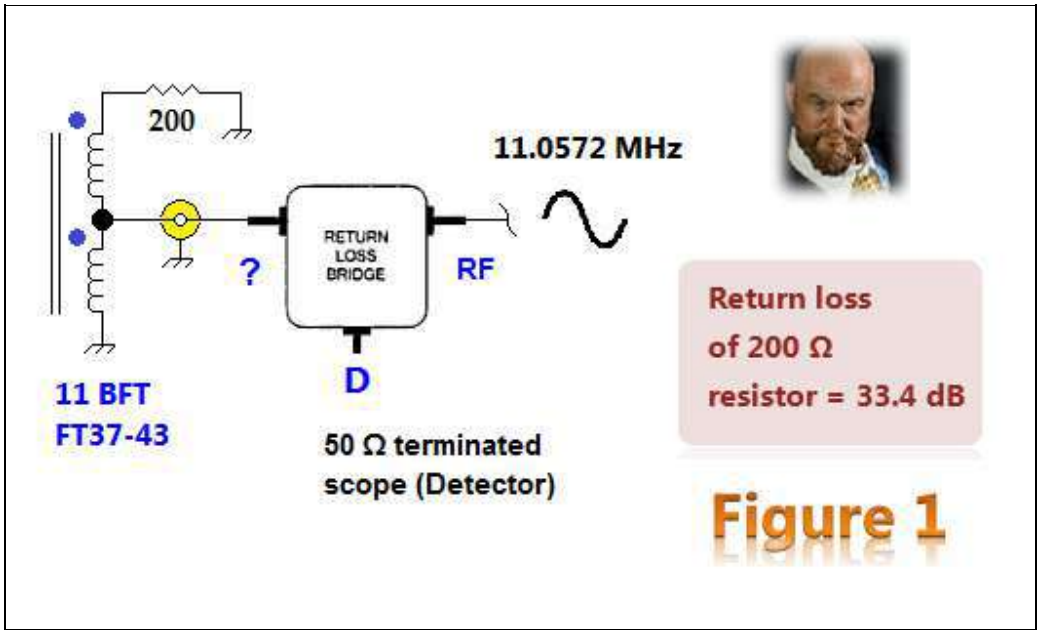

Above — Setting up to measure the return loss of the 200 Ω input Z of my popcorn IF amp. 1 difference between scratch homebrew and kit building is all the measurements you need to make to optimize your scratch receiver. A joie de vivre stems from our descriptive/exploratory analysis before and after making our breadboard. We just learn from mistakes and move forward to improve both our knowledge and gear.

I chose a 200 Ω input impedance for a reason — it's easy to apply a standard 50 Ω return loss bridge via a 4:1 transmission line transformer to establish the correct input impedance for the single frequency matching network.

From the set-up shown above, I found that with a 200 Ω resistor, my return loss at 11.057 MHz = 33.4 dB. This signals the very best we can achieve with our network: directivity. Click for a photo of the above experiment breadboarded on a scap of copper clad board.

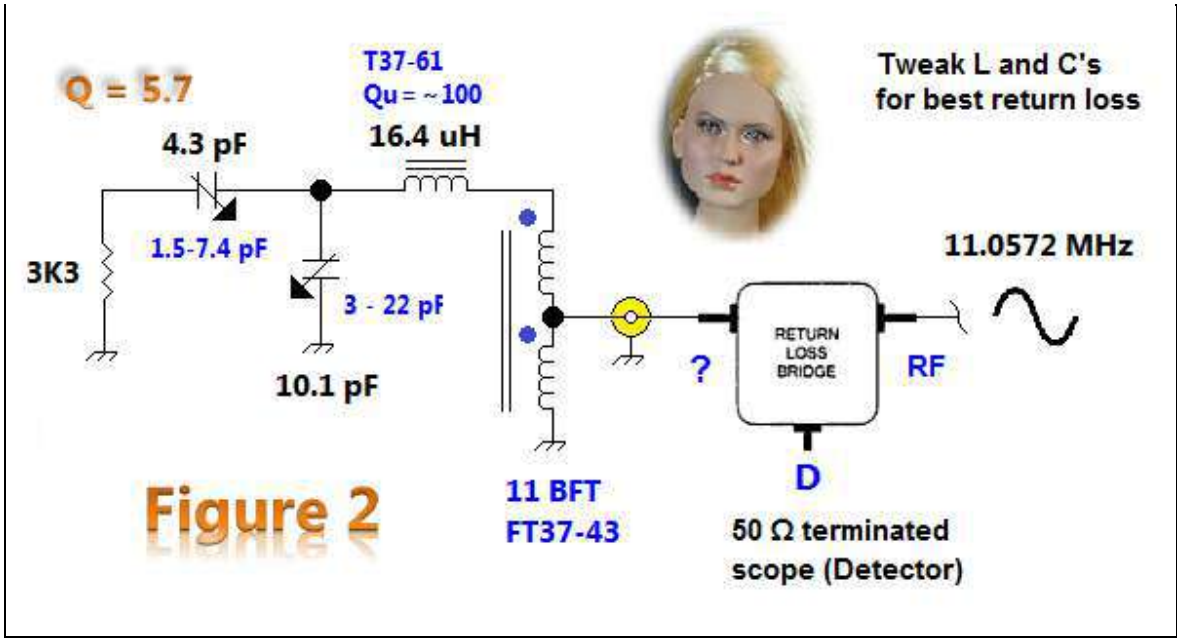

Above — The schematic of my 200 to 3K3 Ω matching network. I designed it with zmat08.exe, a program by Wes that I first used as a console app since the days of DOS. *Zmat08 program comes with EMRFD.* Click for a screen shot of from Zmat08.
The calculated values from Zmat08 only consider a pure resistance and not a complex impedance, so on-bench adjustments of the design L and C values are normally required and fun to do. Variable trimmer caps make tweaking the C easy.

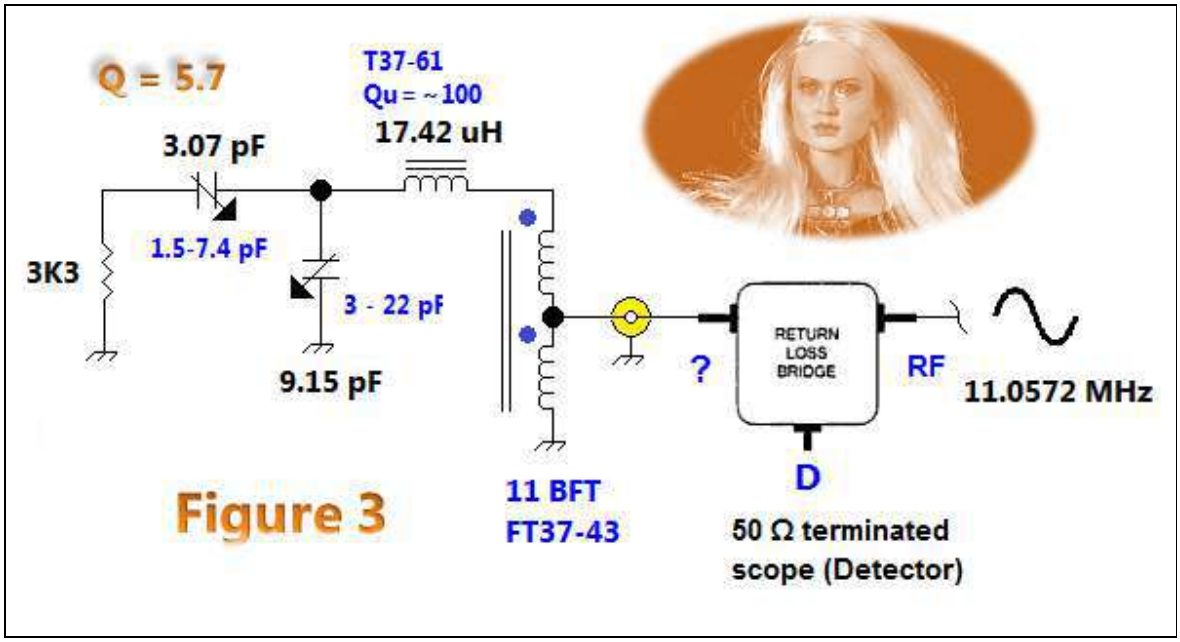

Above — The final— *measured* schematic — While watching the peak to peak voltage on my 50 Ω terminated scope, L and both capacitors were tweaked until I found the highest return loss. L is tweaked by scrunching or expanding turns, or adding/removing turns as needed: in this case, I added a turn and expanded the windings slightly. With the L-C-C match, a return loss greater than 25 dB may arise plying good bench practices — mine measured a lovely 29.2 dB. I removed and measured the inductor plus 2 capacitors to get the values shown **black** in Figure 3.

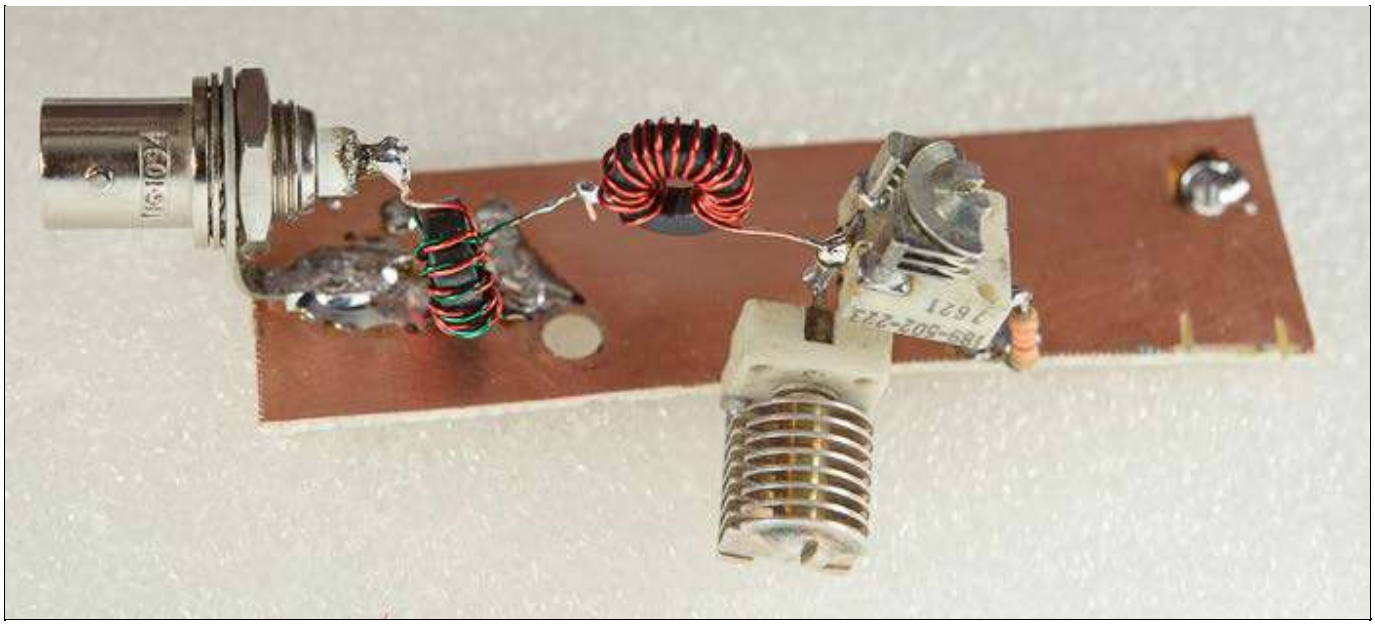

Above — A breadboard of the Figure 3 network before I experimented to find the best L (and shortened its leads).

After I making and tweaking the Figure 3 network, I took the coil along with 2 cheaper trimmer caps and added them to my IF amplifer breadboard. While measuring the return loss of the IF strip input, I had to expand a couple of links on the inductor, but after tweaking the L and the 2 trimmer caps, I measured a 28.5 dB return loss. This ensures my crystal filter will see close to a 200 Ω termination at the IF input. I love well matched stages!

Further, I made a L network and then a L-C-C network to match the output port, however, UHF oscillations erupted. I then went back to a simple broadband transformer and measured a RL of 21.8 dB with a 12:3 turns ratio. Done.

---

4. Mixer and Post-Mixer Amplifer

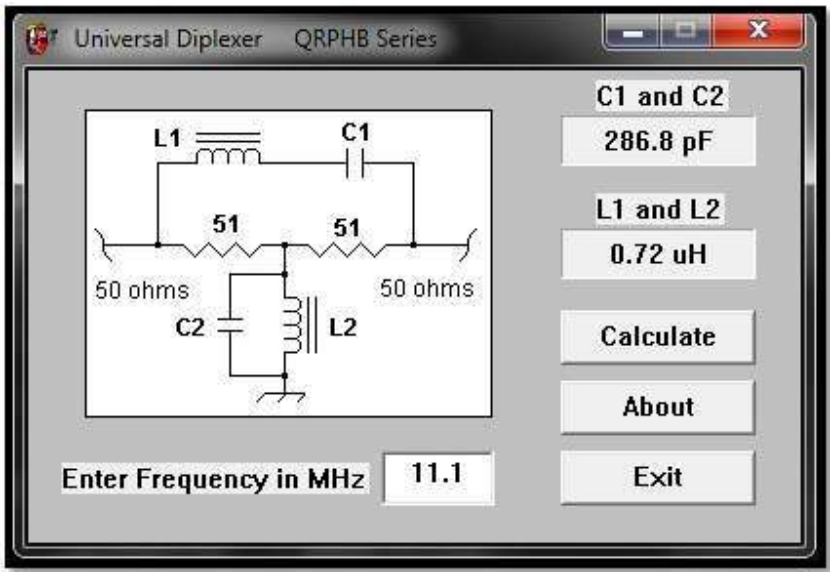

Above — I tested the W1JR (Joe Reisert) bridged-tee diplexer against another design used by Ten-Tek. I'll show the outcomes on the Almost Popcorn receiver page some day, but the W1JR better fullfills its purpose; termination from DC to daylight at the mixer IF port. I calculated the L and C values for a 11.0592 MHz IF with my Universal Diplexer application from many moons ago.

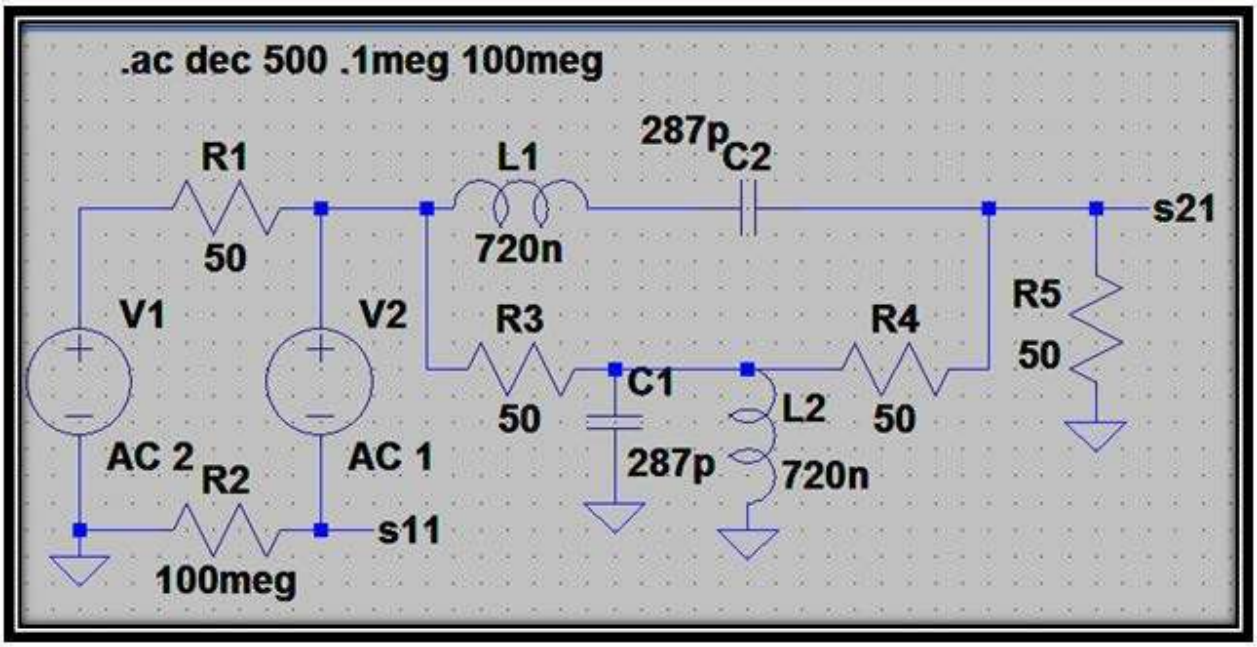

Above — SPICE provides a great way to assess a diplexer since you can plot both S21 and S11 against frequency.

Above — A fantastic match! Thanks Joe for the design and to **Wes, W7ZOI** for his help with diplexers and the SPICE plots through many years of related experiments. Since web publishing the diplexer page, at least 500 diplexer-related emails have come in. Human translated versions of the web page exist in at least 3 languages.

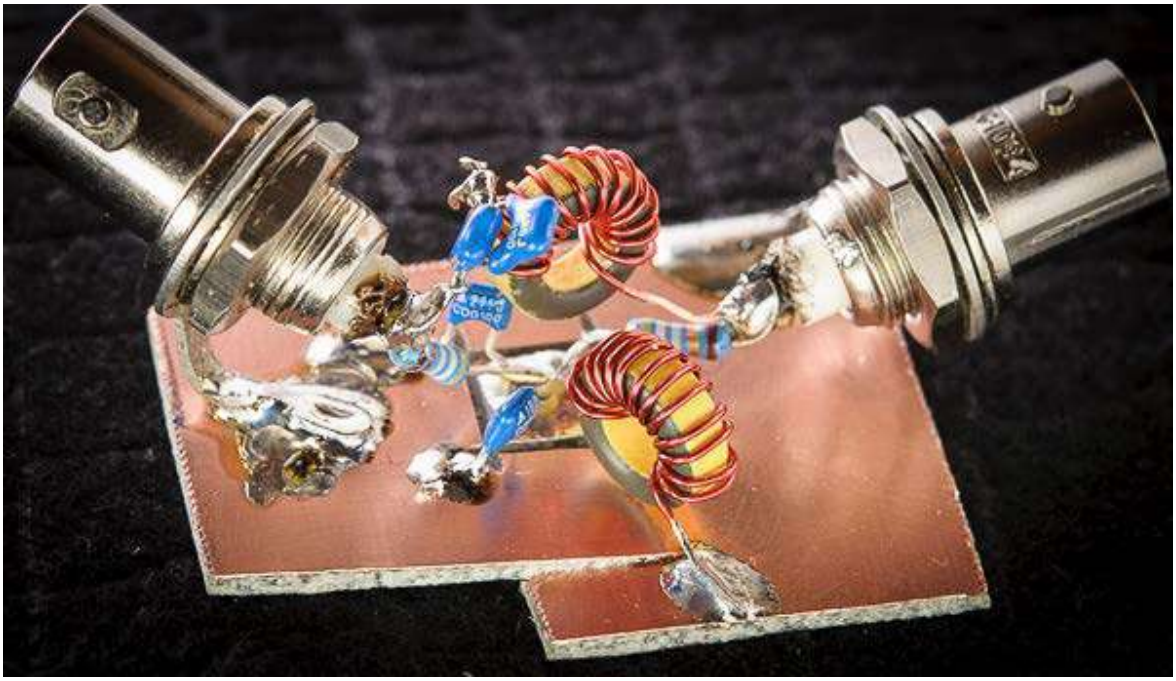

Above — The evaluation breadboard of my W1JR diplexer. Those are T30-6 toroids but they look huge in this photo.

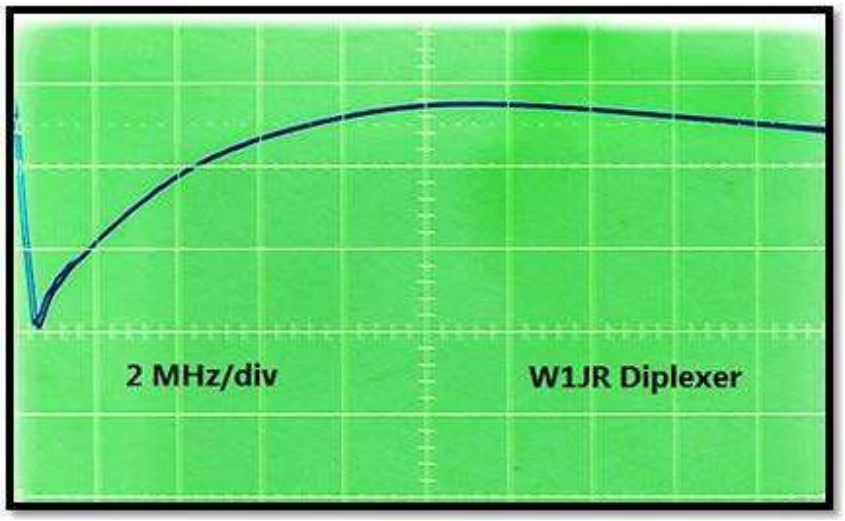

Above — Tracking generator plus spectrum analysis sweep. SPICE does a better of examining the high-pass side.

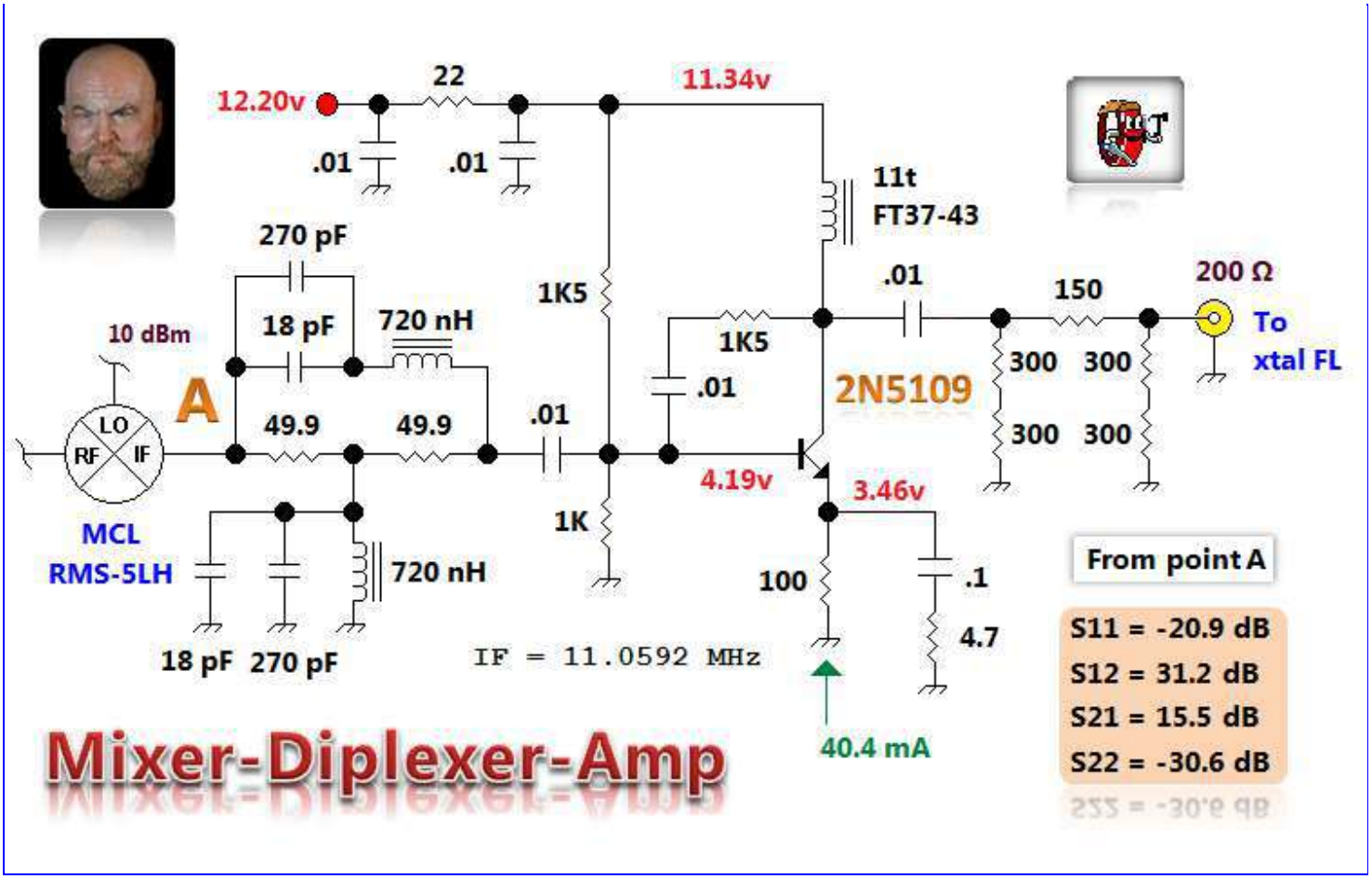

Above — A look at the diode ring mixer, diplexer and post-mixer amp from the latest version of my Almost Popcorn Receiver. I tested the diplexer and RF amp with pad as one unit (see the S-values).

It did not make sense to use a transmission line transformer to get 50 Ω on the amp collector and then use another transformer to build it back up to the needed 200 Ω impedance for the crystal filter, so I just employed a single choke driving a 200 Ω Z attenuator pad.
S parameters are 50 Ω values, thus S22 = the 200 Ω transformed into 50 Ω. After terminating the stages 200 Ω output with a 4:1 Z transmission line transformer, I tested it like any other 50 Ω circuit andmeasured S22 as -30.6 dB — my xtal filter input Z is well established.

Even with the 6 dB *(200 Ω)* attenuator pad and losses from the diplexer, the stage gain from point A = 15.5 dB. Click for to view a bigger picture of the breadboard. Losses from a diode ring mixer are typically 5 - 7 dB.

Above — Mixer and diplexer assembly. The RMS-5LH takes 10 dBm LO drive.

5. Product Detector and Post Product Detector AF Amplifer

I kept the diode ring for a product detector: an SBL-1 driven with a xtal oscillator (BFO).

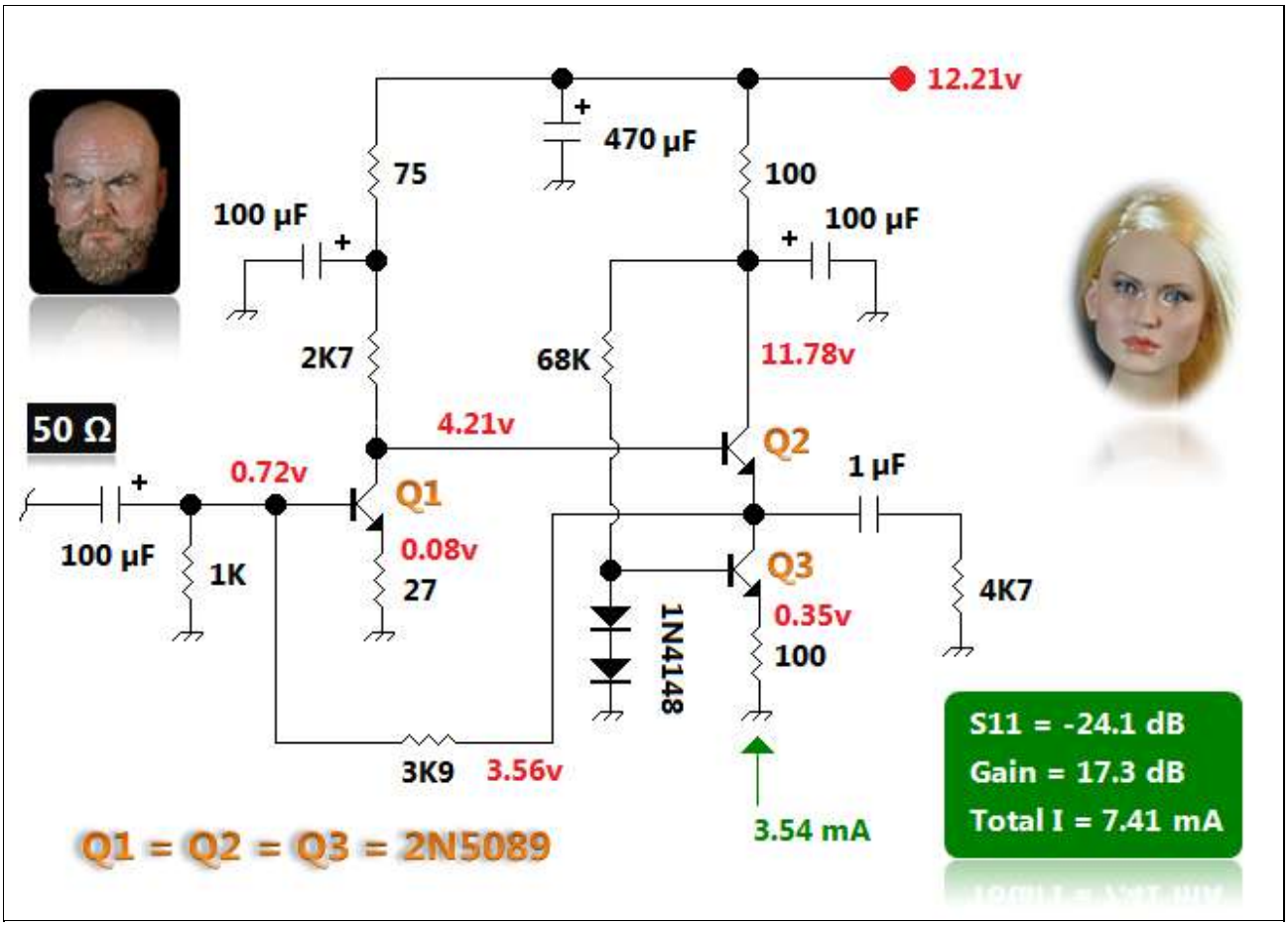

Above — My post-product detector amplifer: a common emitter/ emitter follower pair arranged for a 50 Ω input impedance with shunt and series feedback. Getting the biggest, clean sine wave in and out posed my only goal — the 3.54 mA current source on the follower helps that cause. The input Z tested quite insensitive to output load variations and the (S11) return loss = 24.1 dB.

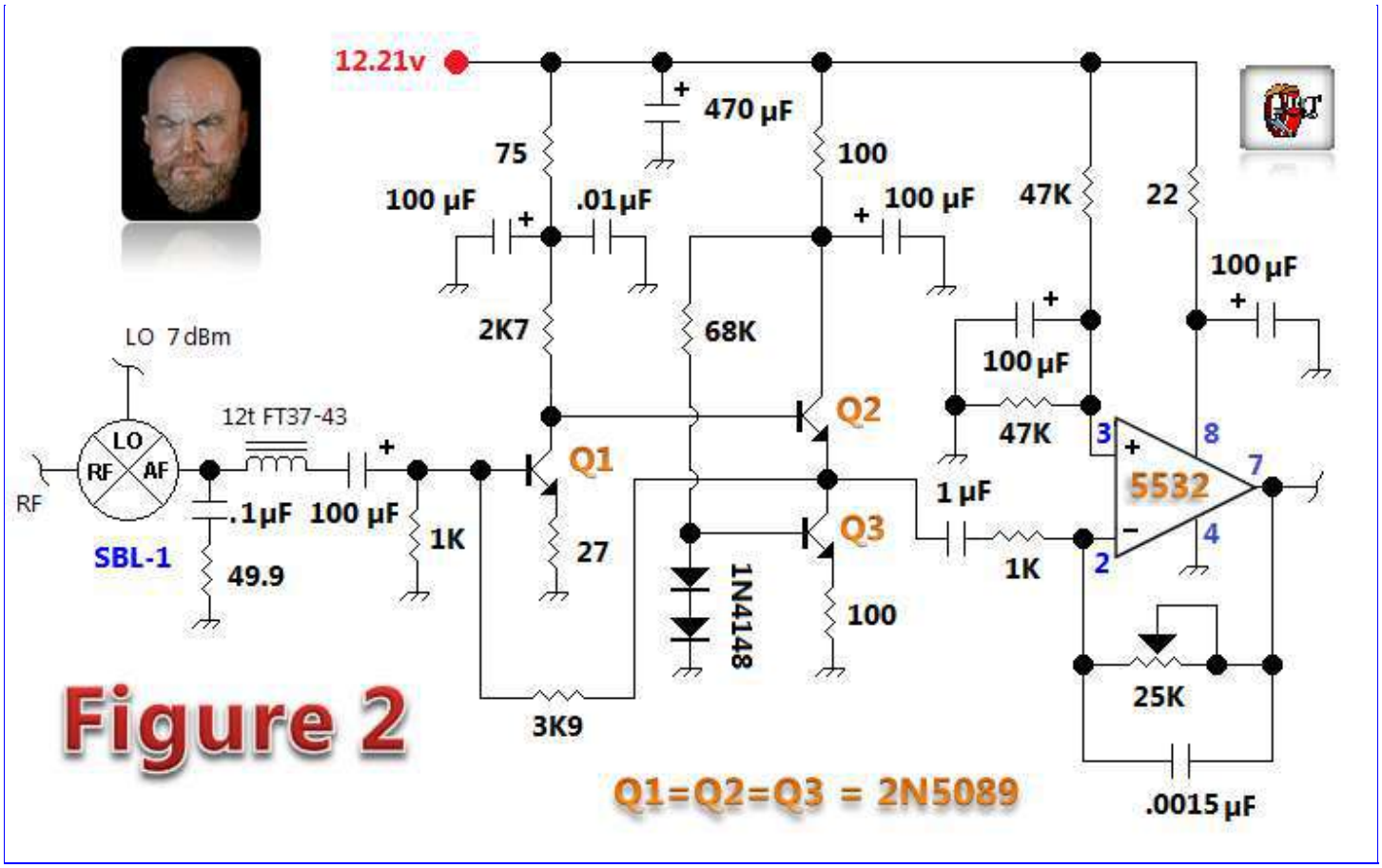

Above — The "Full Monty product detector to AF preamp". A MCL SBL-1 diode ring mixer drives the 50 Ω input Z feedback pair and finally a 5532 op-amp with adjustable gain. The 25K gain trimmer pot allows the builder to accommodate factors such as whether the stage is a DC receiver, or an RF-AF block for a superheterodyne receiver like in this radio. I'll set the gain as low as possible and hope to build up my AC voltage with active, gain producing low-pass filter op-amp stages.

The output t pin 7 is directly coupled to an op-amp AF filter. With software we can easily design a myriad of audio filters: band-pass, low-pass, high-pass, all-pass etc. I only run low-pass filters in this slot and even here we must decide whether to make our reponse Gaussian to 6 dB (or 12 dB), Bessel, Butterworth, or a Chebyshev with some degree of ripple. I'm testing out a few designs with an eye towards simplicity and 10% parts.

Spurred on by curiosity, with my ears as the main evaluation tool; I currently have a 5532 paper design to deliver 20 dB gain with a 500 Hz pass-band, Gaussian to 12 dB low-pass response. Click for schematic, I chose a 500 Hz cut off frequency since the skirt shape by definition is subtle and the Q low. This trick should better roll off the AF above 1 KHz a little faster without the ugly group delay associated with steeper filters employing more poles. We shall see!

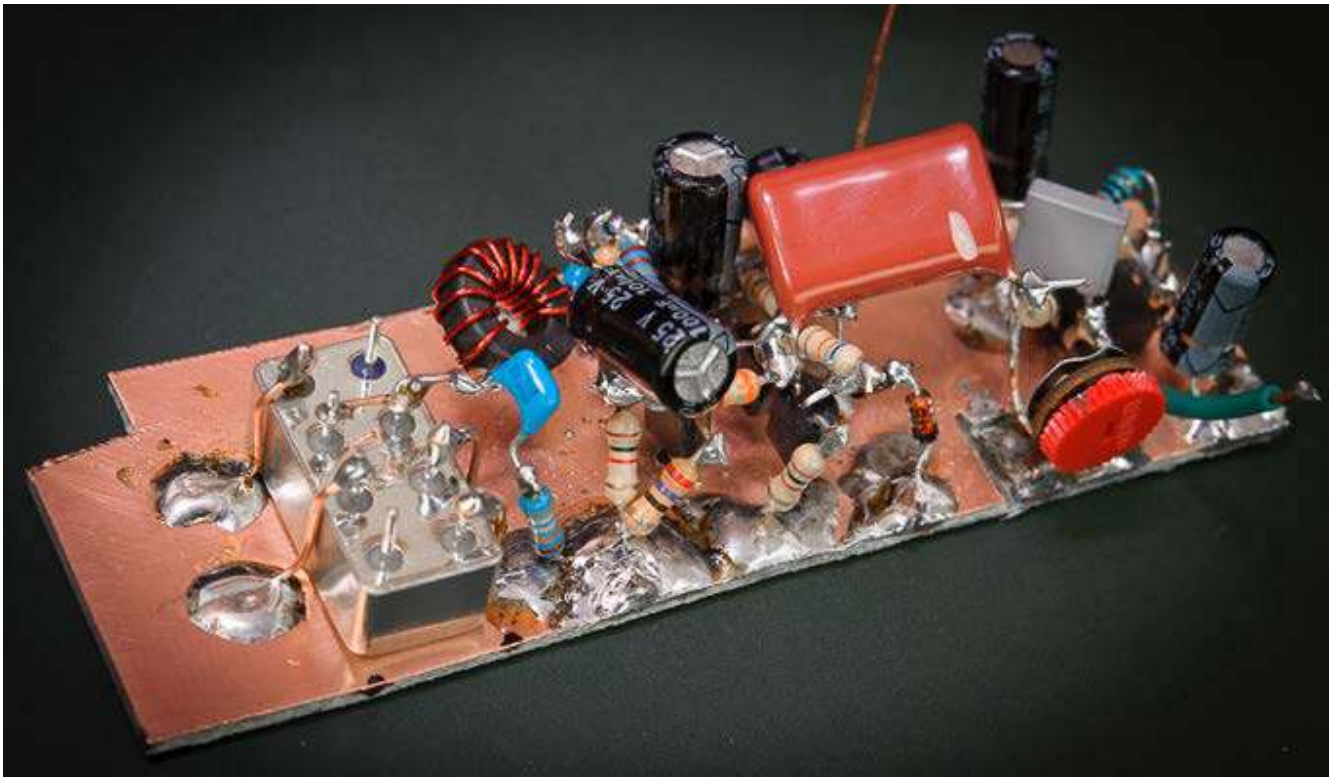

Above — The compact breadboard of Figure 2.

Audio filters and AF power amp are incomplete.....

Almost Popcorn Superhet — Supplemental Lab Notes

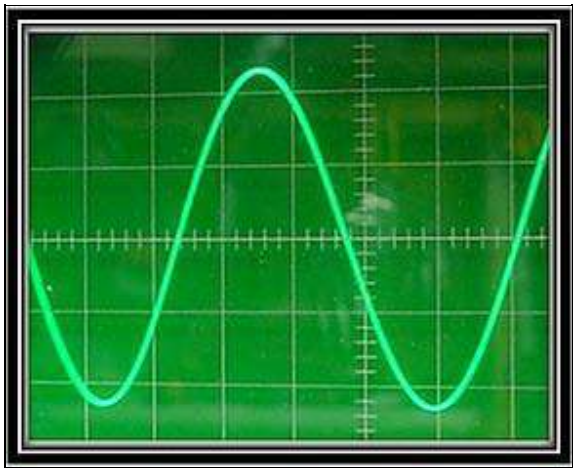

These lab notes supplement the Almost Popcorn Superhet Receiver Web page which has remained incomplete for greater than 10 years. I'm sorry for the rough writing and procrastination.

N = 3 Gaussian-to-6 dB Crystal Ladder Filter

I spent a pleasant Saturday afternoon designing, building and testing Gaussian-to-6 dB crystal filters. I inputted some xtal parameters + constants from Zverev into Xlad08.exe from EMRFD. Here's the N = 3 version

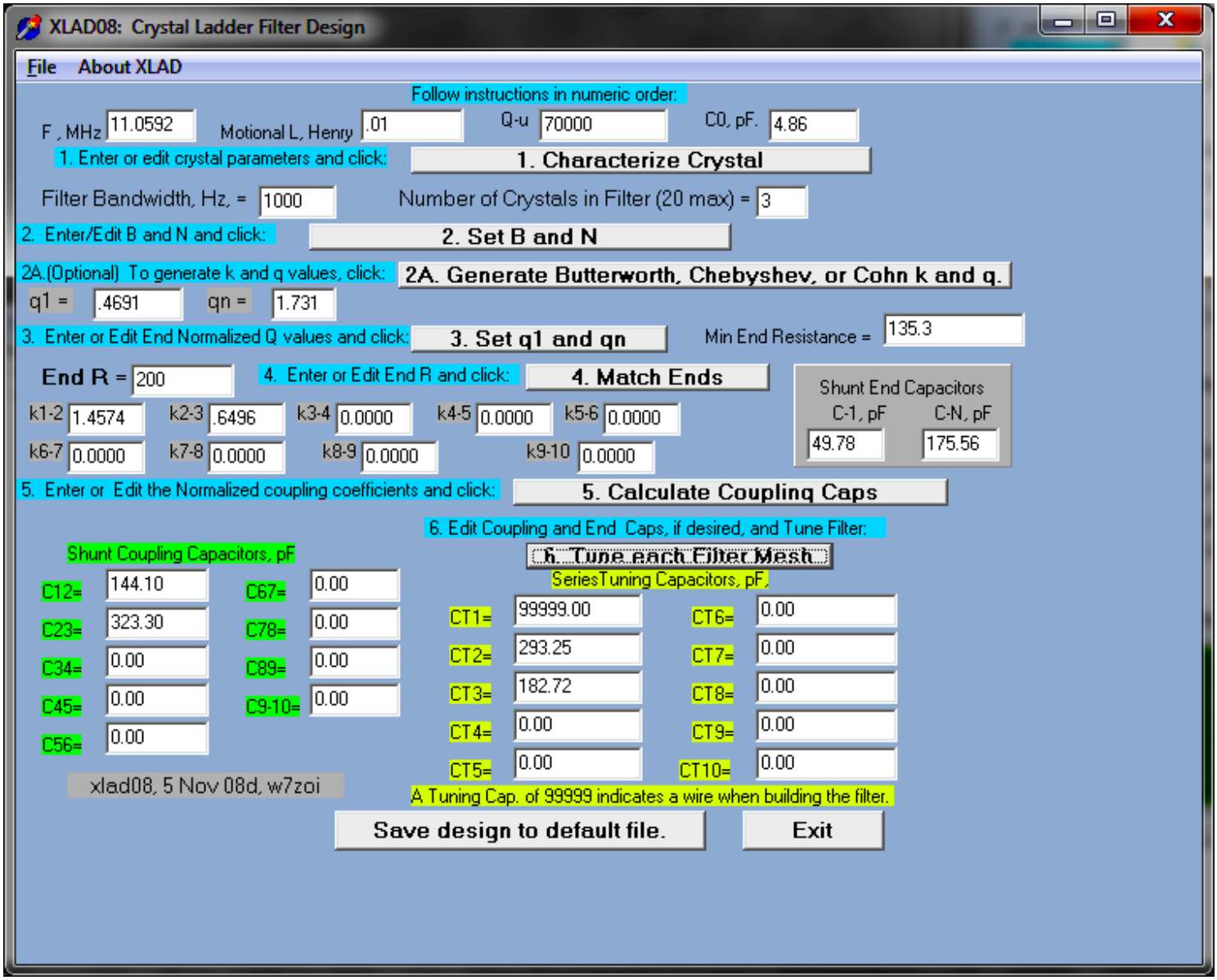

Above — A screen capture from Xlad. This app allows skilled builders to depart from the typical Cohn (Min-Loss) filter and tune filter poles to derive beautiful skirt shapes and low insertion loss if wanted. I'm not a great crystal filter designer, but I've seen work from friends who have a knack for it: imagine making a N= 8 to 10 crystal CW filter with just ~1 dB insertion loss like these builders! Click for the GPLA simulation.

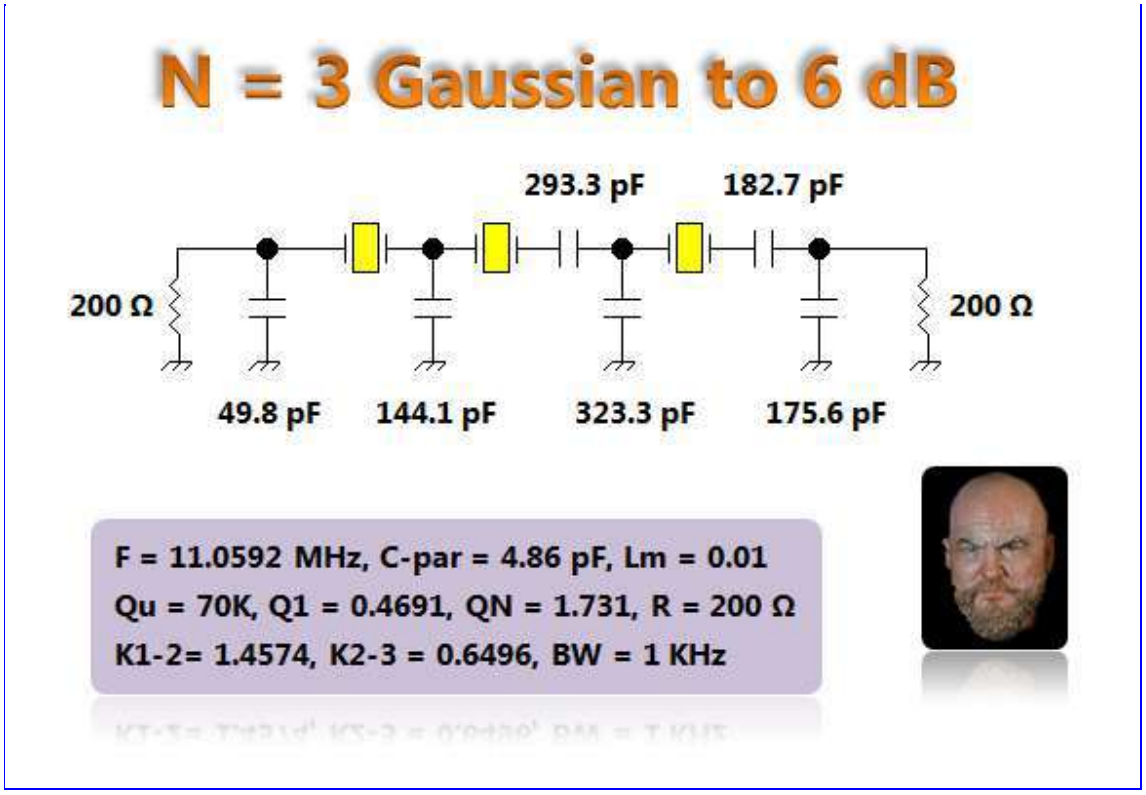

Above — Gaussian-to-6 dB xtal filer schematic where N = 3.

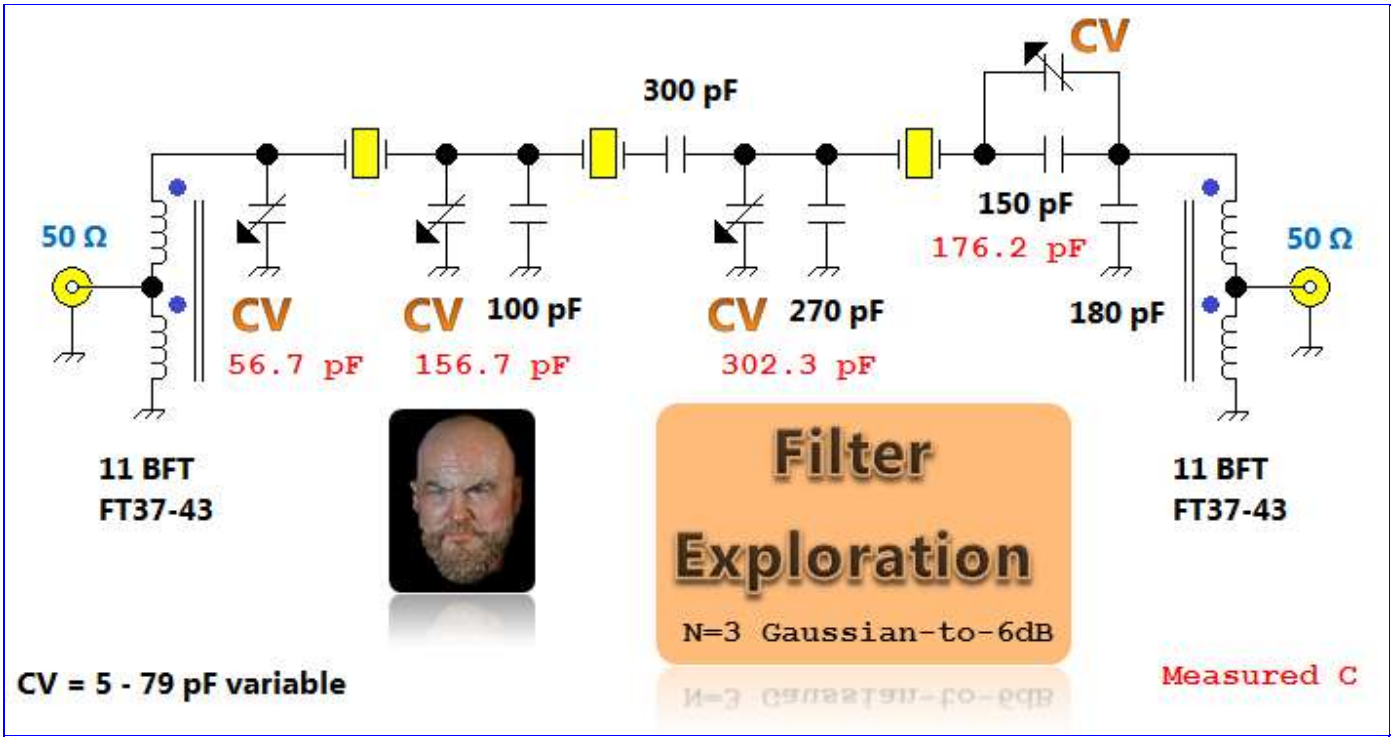

Above — Circuit to allow evaluation of the filter in my 50 Ω sweep system. Transmission transformers provide the needed 200 Ω filter termination. I inserted 4 trimmer caps to permit tweaking of the filter under test to establish the very best filter shape. With trimmer capacitor adjustment, I was able to trash the filter or peak it well. Click for 3 different swept bandwidths: Sweep-1 Sweep-2 Sweep-3.

After peaking, I removed *all* the caps and measured them as shown in **red font**. I'll replicate these values with nearest standard-value fixed capacitors. The trimmer caps nearest to the ports proved more sensistive compared to the 2 middle trimmers capacitors during tuning.

This might be the coolest thing I've ever done on my test bench.

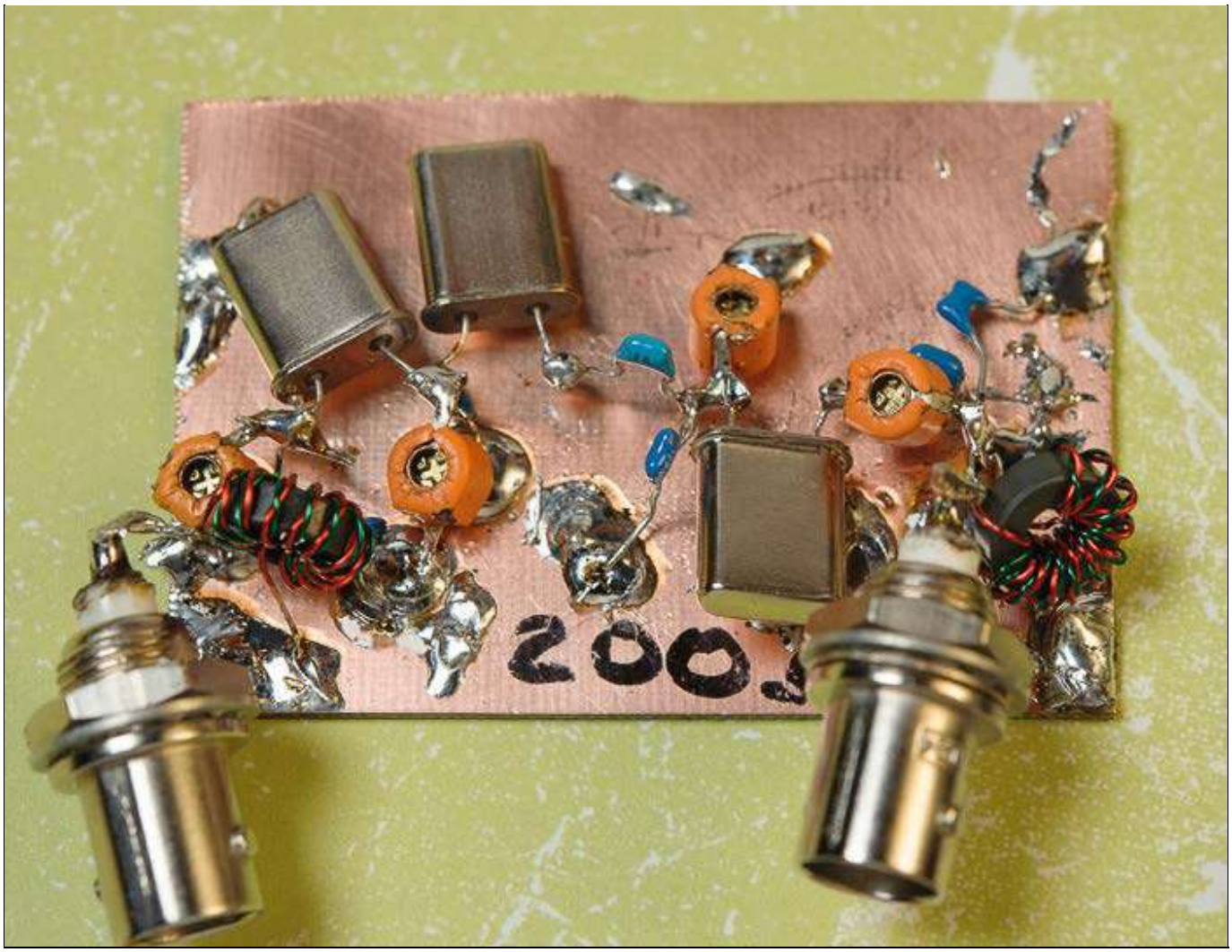

Above — My N = 3 filter breadboard. I left the capacitor leads long for re-use. I consume huge numbers of parts and recycle as possible to keep costs down.

Mixer and Post Mixer Amplifer Development

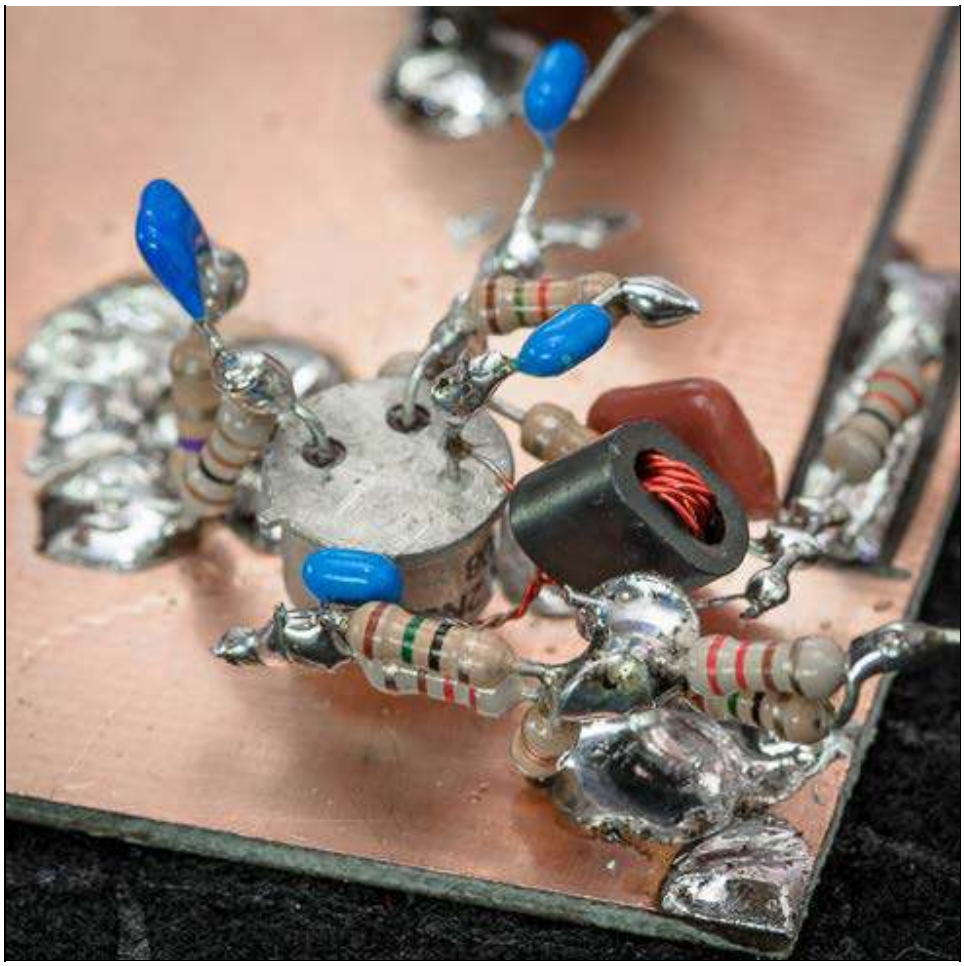

Above — Ugly breadboard shot with my ancient 105 mm lens for a change. It's a Beaverton Special feedback amp (FBA) biased for ~40 mA. For my post-mixer amp. If you need a stout RF amp, this one will do in a storm.

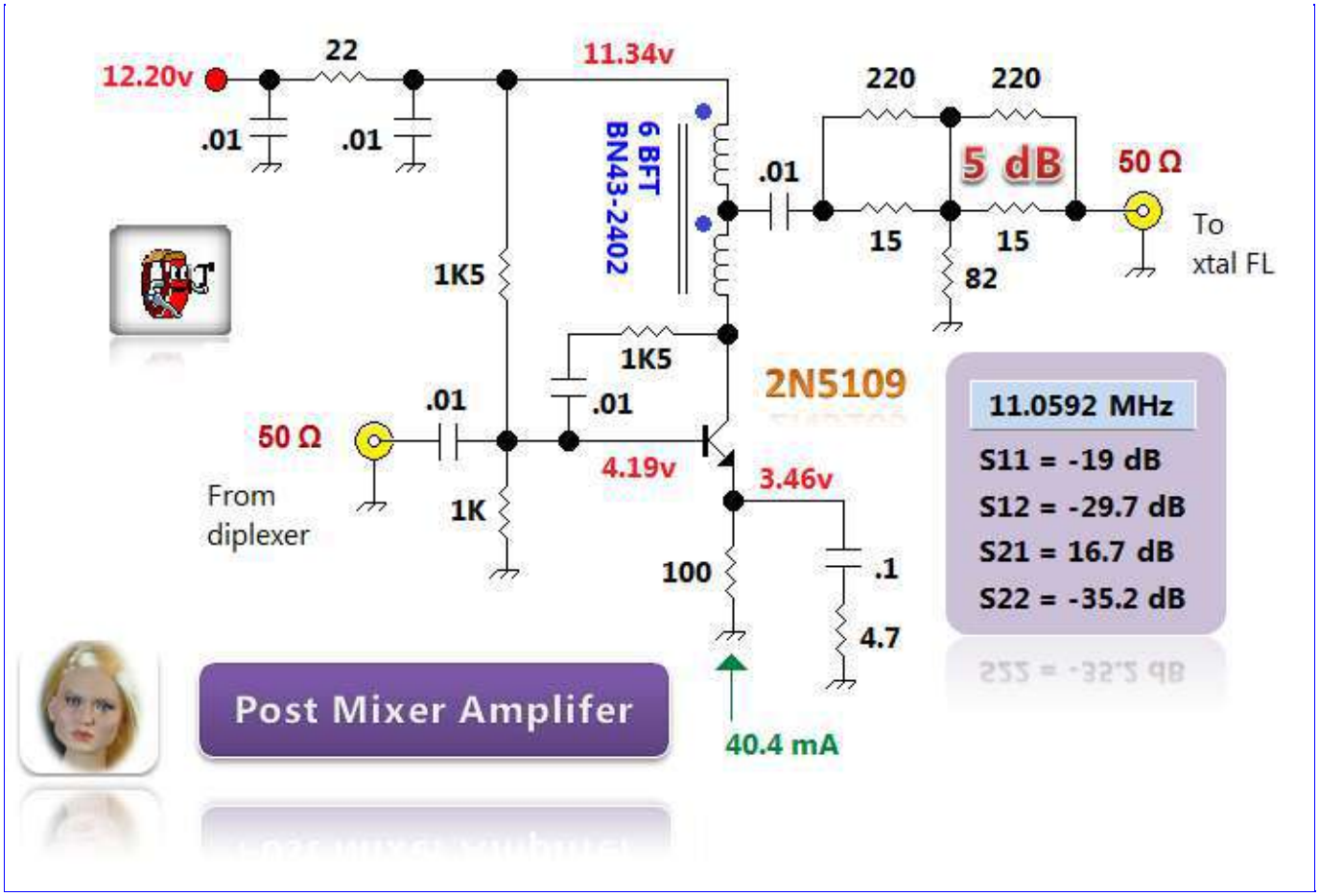

Above — The Beaverton Special feedback amp biased for ~40 mA with a 50 Ω output Z. The FBA with no 5 dB pad: S11 -18.5 dB; S12 -34.6 dB; S21 22.1 dB and S22 -31.8 dB. I love this FBA for its simplicity and well defined port impedance. My IF = 11.0592 MHz. Click for a discarded (but cool) photo.

To drive the 200 Ω input Z of my xtal filter I later converted the output to 200 Ω by changing the collector transformer and pad.

Frequency Synthesizers and Logic

I've spent a great deal of time reading about & playing with some HC series logic I bought in 2011-2012. I even purchased a few 74AC74, a D flip-flop you can clock up to 160 MHz or so. Most of my reading concerned frequency synthesizers: PLLs, dividers, prescalers, etc. Since most modern devices run a clock at GHz frequencies, the evolution of frequency synthesis technology from around the mid 1970's to now makes for a fascinating read.

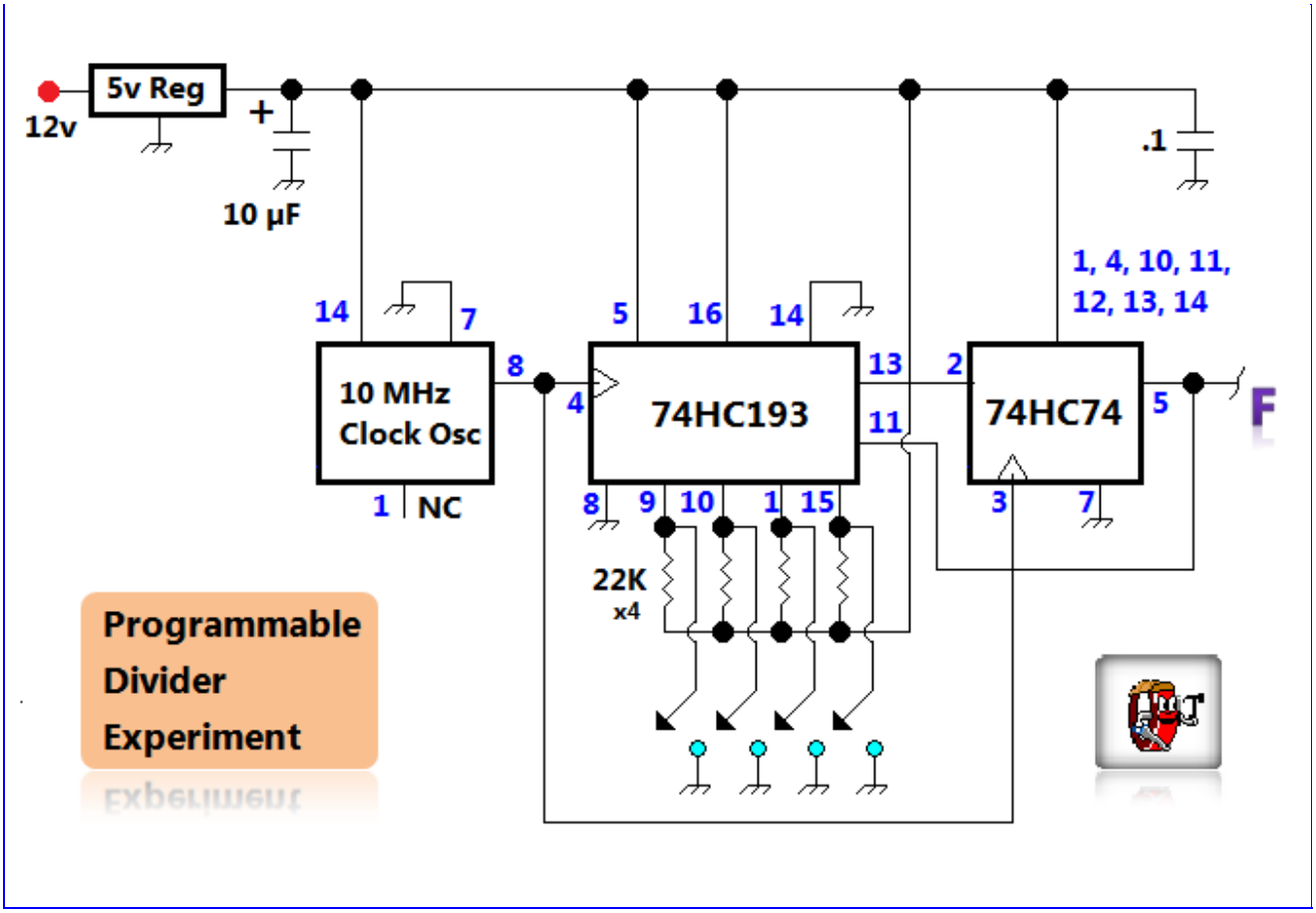

Above — Using a CMOS 10 MHz clock oscillator, I tested out a positive edge-triggered programmable frequency divider designed by Wes, W7ZOI in 2011. It works perfectly.

Switches	Frequency (KHz)	N
0000	0	0
0001	3333	3
0010	2500	4
0011	2000	5
0100	1666	6
0101	1429	7
0110	1250	8
0111	1111	9
1000	1000	10
1001	909	11
1010	833	12
1011	769	13
1100	714	14
1101	666	15
1110	625	16
1111	588.2	17

Programming Pin Sequence on 74HC193: 9, 10, 1, 15

Above — A test of all 16 combinations of the 4 programming switches with the 10,000 KHz input. I show the measured output frequency in KHz and the integer generated by dividing the output F into 10,000 KHz. You may leave pin 9 HIGH and just run it as a divide by 10 to 17 counter with 3 panel mounted programming switches — that's what I hope to do.

While working at Tektronixs, Wes designed the frequency synthesizer for the 492 Spectrum Analyzer; a portable SA that went to 21 GHz or so. His experiences informed the design of this simple, low-cost, edge-triggered divider.

Here, Wes applies the 74HC193 as a down counter where a number is loaded and then it count downs until zero is reached. The number gets boosted by 2 — 1 comes from the 74HC74 D flip-flop, while the other arises from the phasing of the signals. The 74HC74 makes the overall output coherent with its clock and avoids the flicker noise that otherwise might be generated in the long divider chain of the ripple counter.

The standard binary to decimal conversion is altered in this circuit.

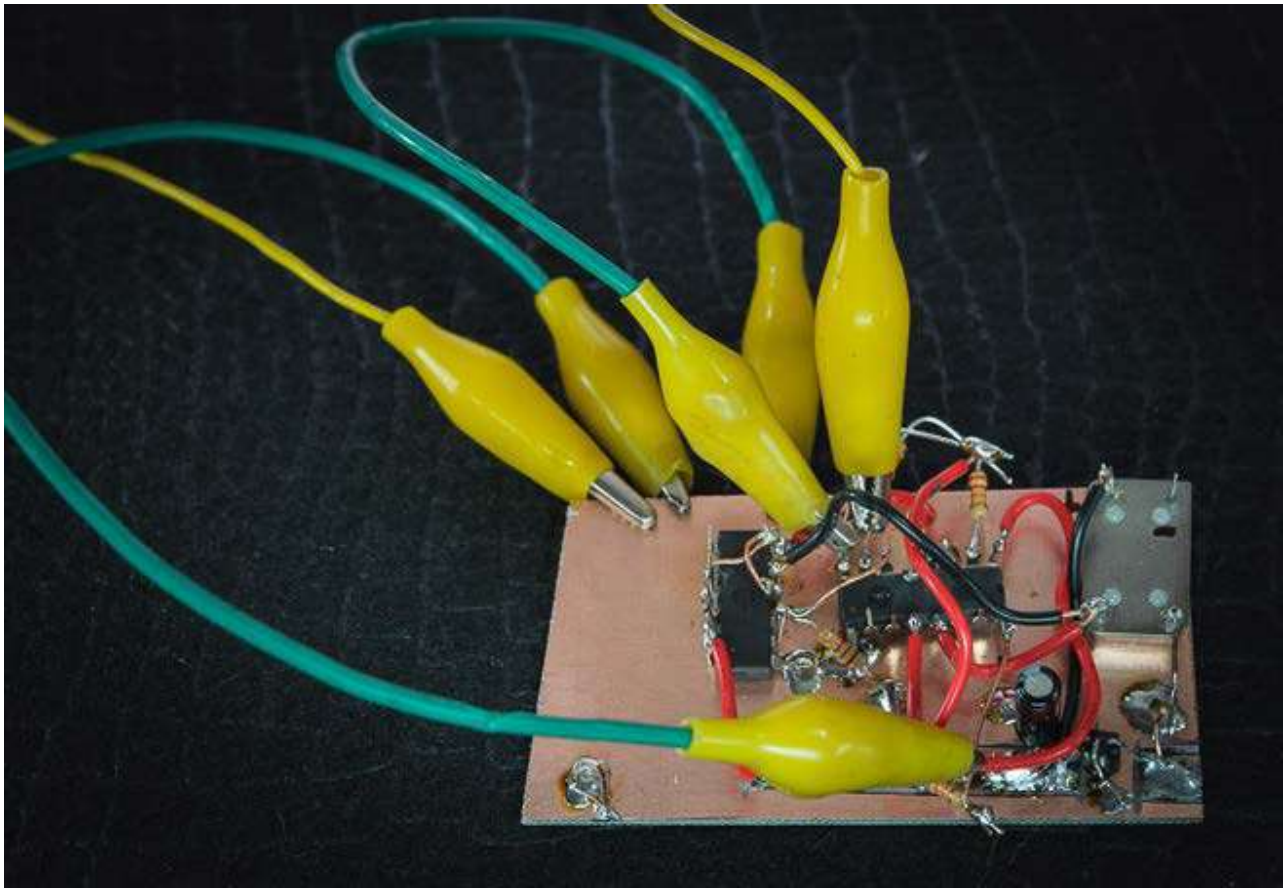

Above — My ugly breadboard. Instead of switches, I relied on bench jumpers to set a pin LOW.

Check out the standard binary switch combinations on this cool website: Math Is Fun. I also enjoyed their hexidecimal drum machine tool - Click. Actually, the whole web site looks great and I will recommend it to our friends with children and maybe even a few radio enthusiasts.

The Local Oscillator

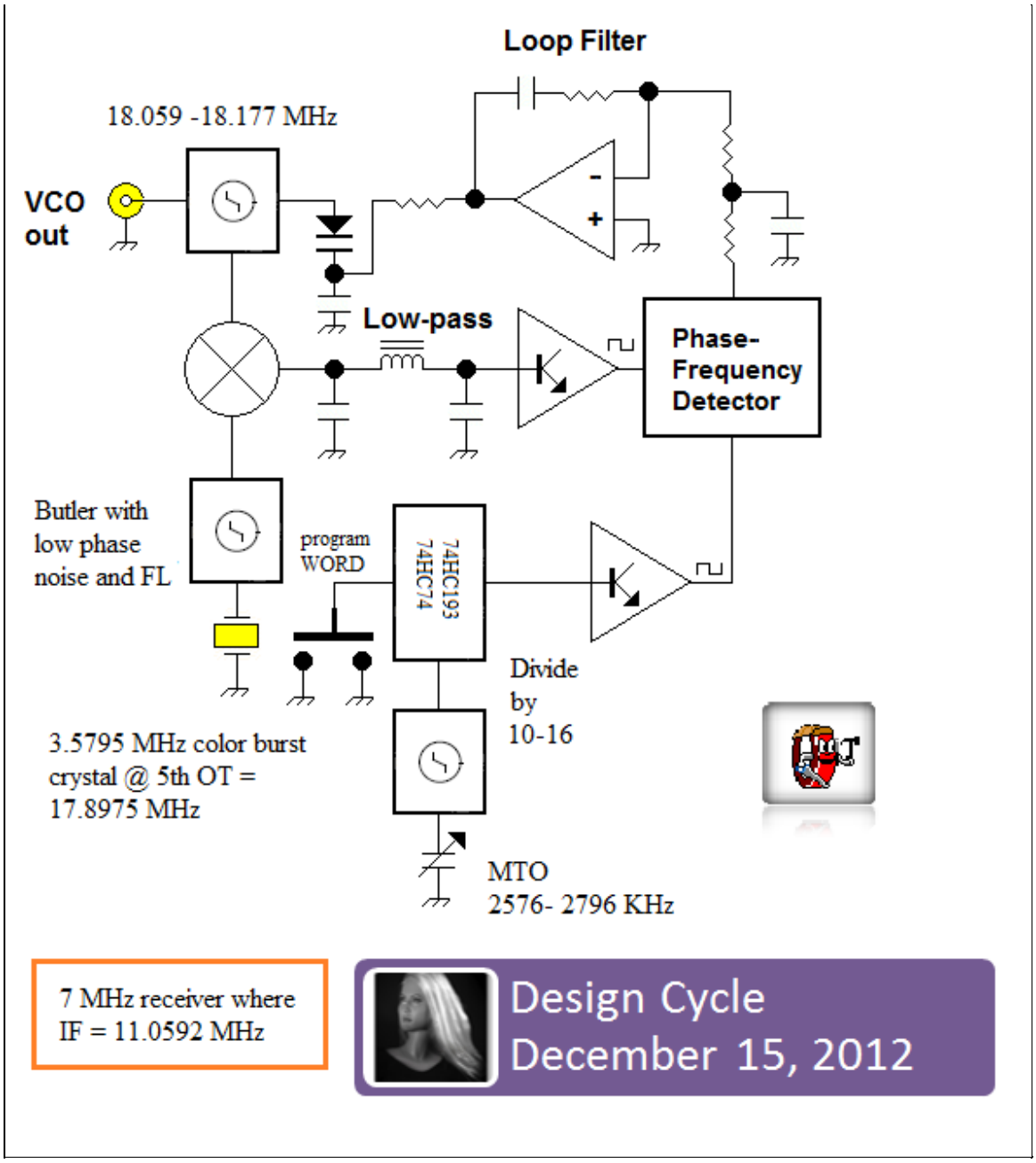

Above — An Almost Synthesizer based upon the design currently in use at W7ZOI.

I picked the MTO, xtal oscillator and VCO frequencies and will design the loop filter once I get the parts and a few small die-cast boxes on hand. The MTO division integer is low and quiet — plus this scheme enhances MTO frequency stability and spectral purity. A 4-bit ripple counter + flip flop perform the division where N = 10 - 16. I might go higher with N , but don't want to get too greedy. For CW, I'm generally in the bottom 20 KHz of the band anyway.

The MTO tunes about a 13-14 KHz range and the N gives 6 different tuning ranges (with some overlap) to span a total range of ~118 KHz. The 4-bit WORD is changed by 3 chassis-mount toggle switches and give a PLL reference of ~~175 to 280 KHz.

This almost synthesis seems a little crude in a time when people use microcontrollers to input a WORD into a chip with with the simple turn of a rotary controller, however this set-up fosters learning, huge fun, and when the oscillators plus loop filter are well designed; low phase noise and reciprocal mixing.

The Crystal Filter

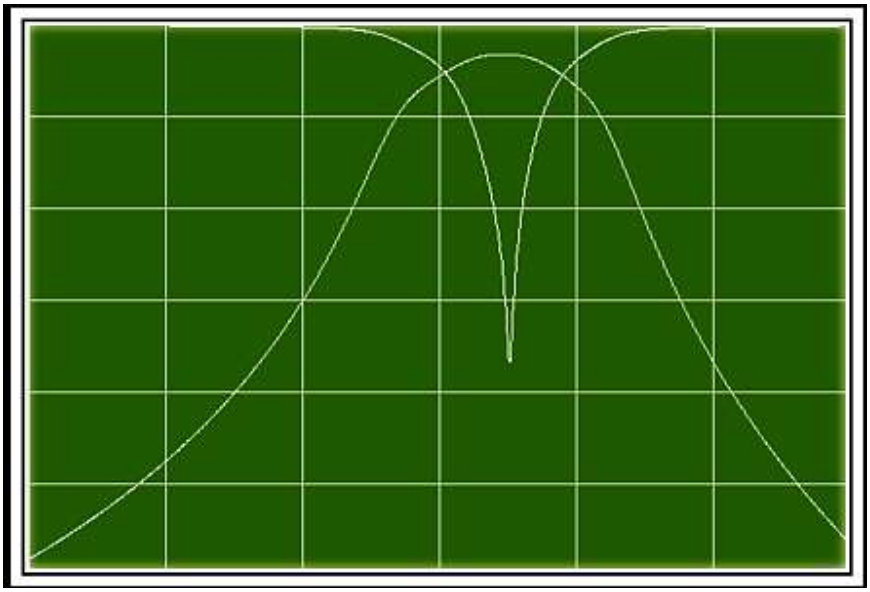

Above — A GPLA sweep of my 4 crystal filter where C parallel = 4.86 pF, Lm = .01 H, IF = 11.0572 MHz, BW = 1 KHz and R term = 200 ohms. This Gaussian to 6 dB filter design was chosen for speaker audio that sounds full + dynamic without the hollow ringing so often heard in homebrew receivers. I filter in my brain and first learned to copy CW across a room while listening to a speaker.

My code mentor Doug, could make coffee, walk around the room, talk to us and still 100% copy CW at 40 WPM. He taught us the ear to brain bandwidth is ~ 100 Hz when copying weak signal CW through a sideband crystal filter. To this day, I prefer listening through wider CW filters with brain band-pass filtering.

KL7R Memorial Supplemental Page

This web page is a supplement to the K7LR Memorial Receiver Experiments Web Page

Audio Preamplifier Focus

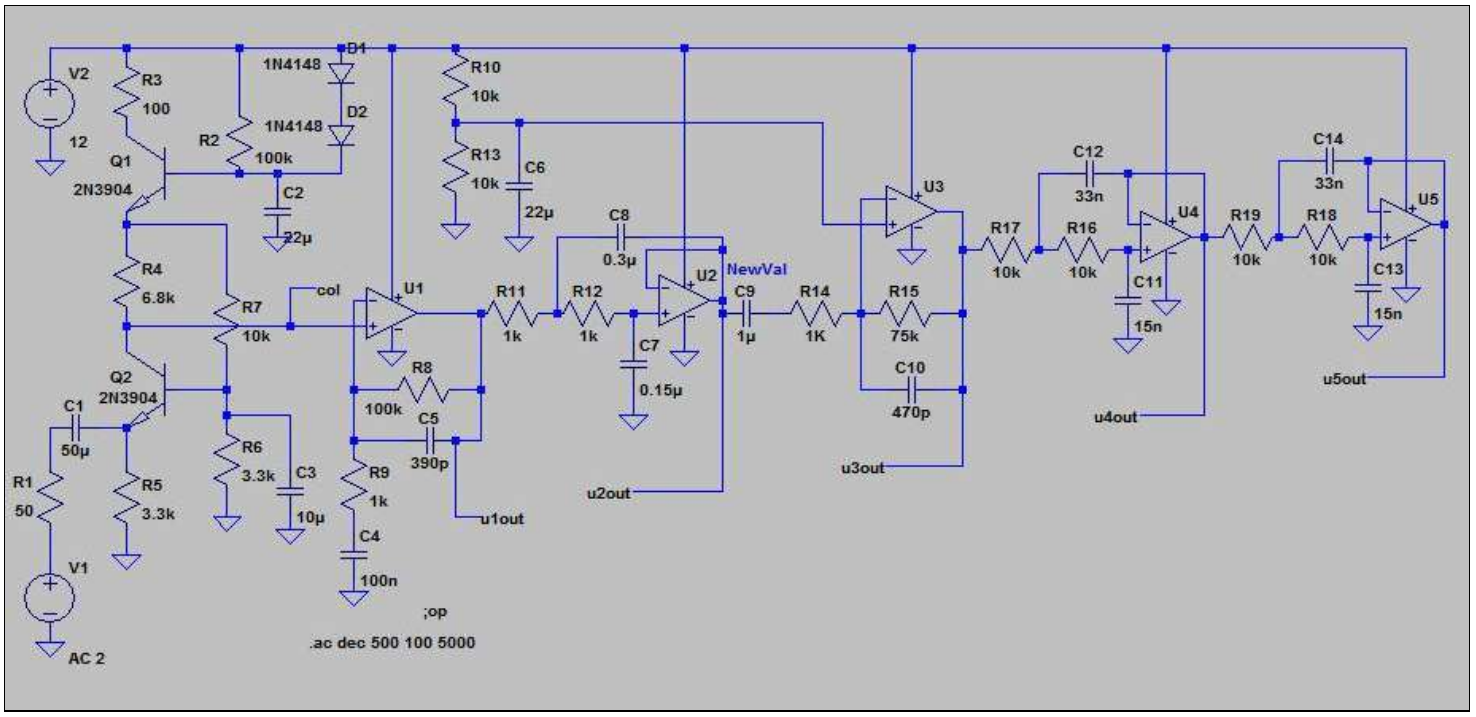

Shown above is a SPICE build of an earlier prototype of the audio preamp chain which was ultimately used in this receiver. This SPICE work was performed by Wes, W7ZOI. Note that at this point, I had 100K plus 390 pF feedback in U1 and a 75K plus 470 pF feedback resistors in the op-amp amplifiers (really massive gain). I spent 4-5 days trying different audio stages before settling on the circuits shown.

Shown above is the voltage versus frequency plot from a SPICE run of the schematic shown above. The gentle slope (decibels per octave) of the low pass filters can be seen. Certainly Chebychev filters with 1-2 dB of ripple would have provided steeper filtering, but the filters would have odd resistor values and be less easily modified or reproduced by popcorn builders. The V(u5out) shows a reasonable low pass response for the AF preamp.

Audio Power Amp

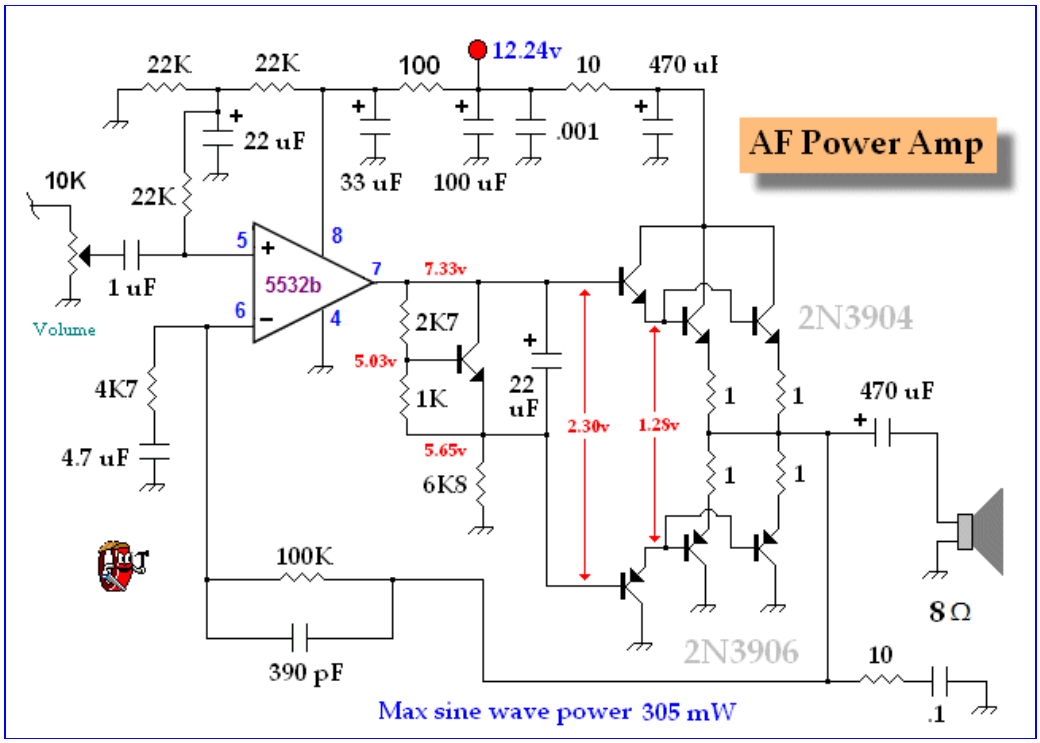

This schematic shows a stand-alone version of the audio power amp. If only 1/2 of the 5532 is used, connect pins 3 and 2 of the unused op-amp to the point where all the 22K resistors connect (VCC/2 bias point).

Product Detector Notes

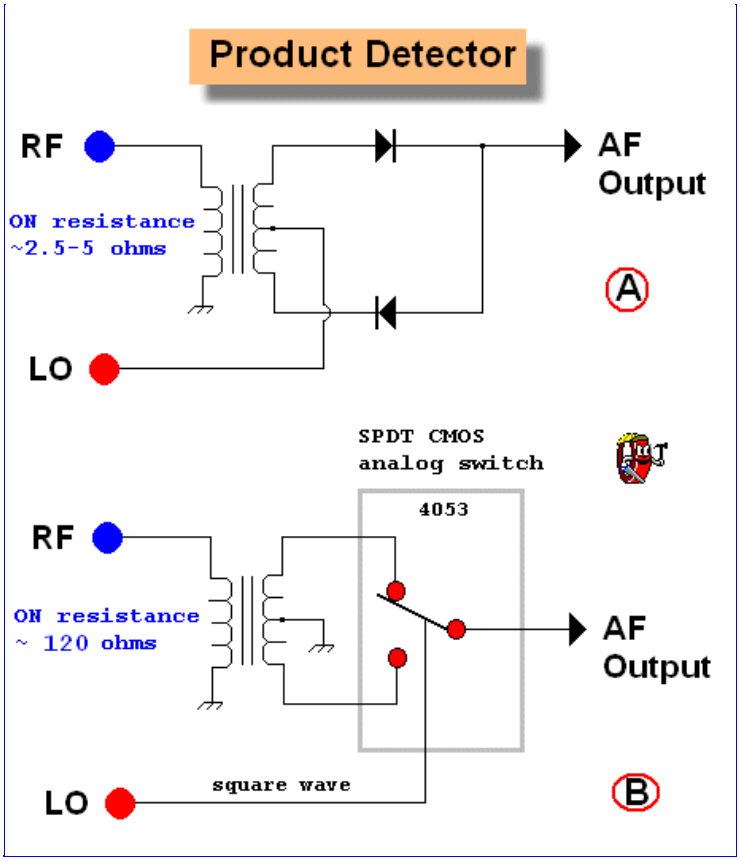

Shown above is the analogy between an SPDT CMOS switch and a single-ended, diode product detector. In both cases (A and B), the LO causes 1 diode (switch) to conduct, while the other is OFF. Then, on the other half cycle, the other diode (switch) conducts. If you wish to actually using the product detector/mixer depicted as "A" go with Figure 5.19B in EMRFD which has the LO applied to the transformer primary. As shown, "A" has poor LO to RF isolation, but it helps model the CMOS SPDT analog switch function. Function and performance are completely different topics... The on-resistance of the 4053 is much higher and thus performance is not identical.

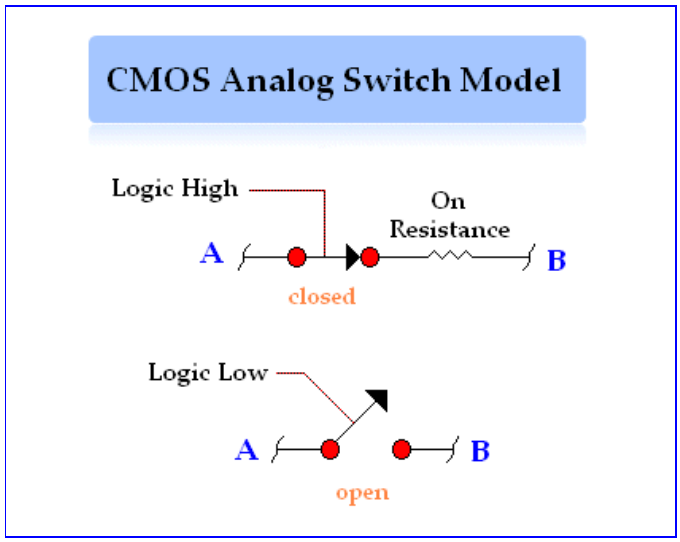

CMOS analog switch model. A or B are bidirectional and can be used interchangeably for the input or output. Ideally the on-resistance should be low to reduce propagation delay of digital signals plus resistance and perhaps distortion of analog signals. They can be used to switch digital bus data or analog signals. CMOS switches can replace mechanical reed switches in some low power circuits.

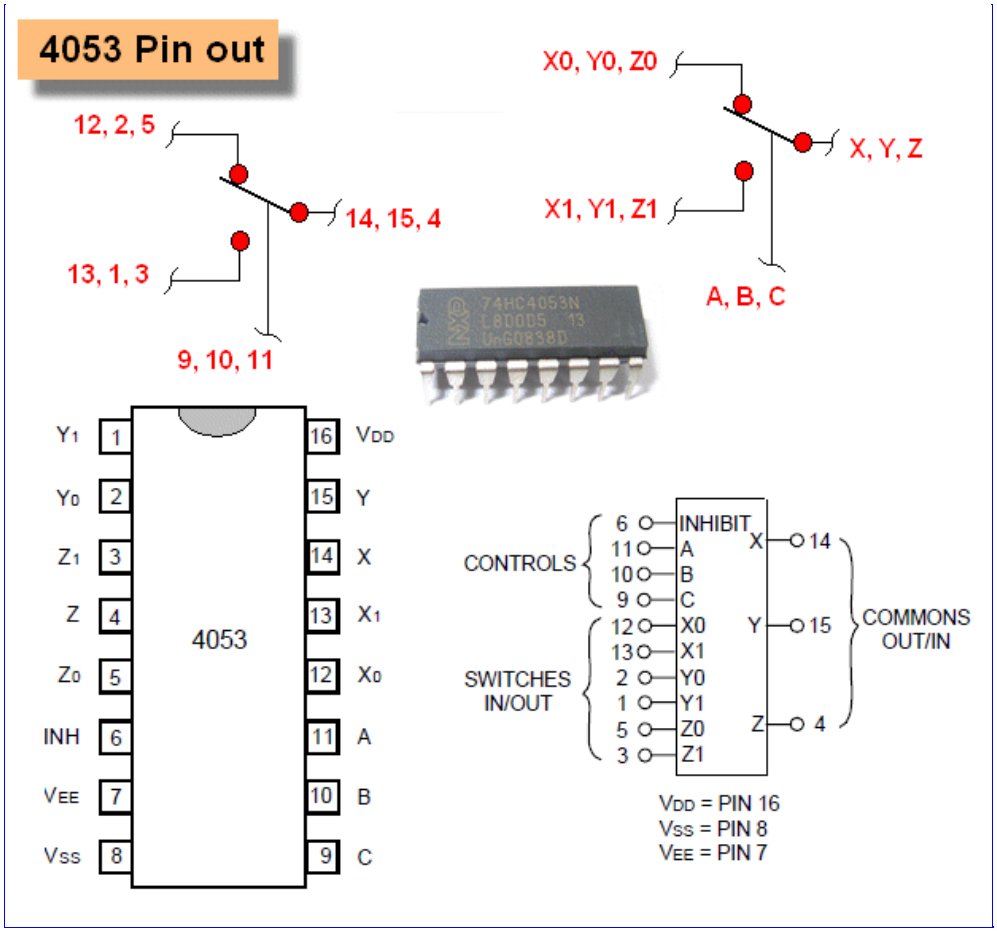

The CD4053BC is a triple 2-channel multiplexer having three separate digital control inputs; A, B, and C, and an inhibit input. Each control input selects one of a pair of channels which are connected in a single-pole double-throw configuration. A high on resistance makes the 4053 a compromise part for RF mixing. It might be perfectly okay for your design.

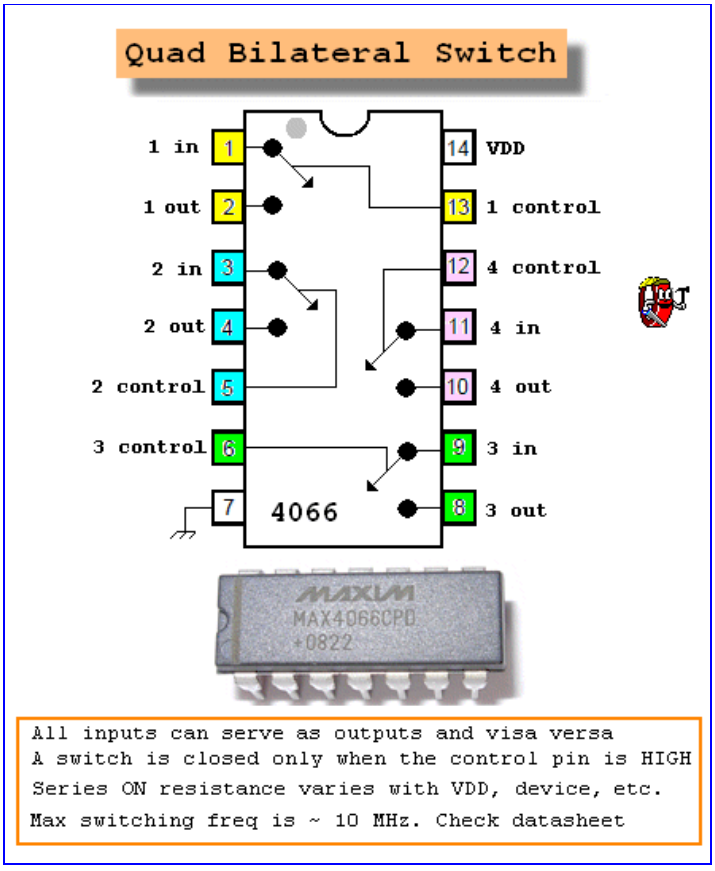

The 4066 is more easily understood when drawn in a semi-schematic. The on-resistance of this MAXIM version is better than the usual HC4066. About 45 ohms with a VCC of 12 or so.

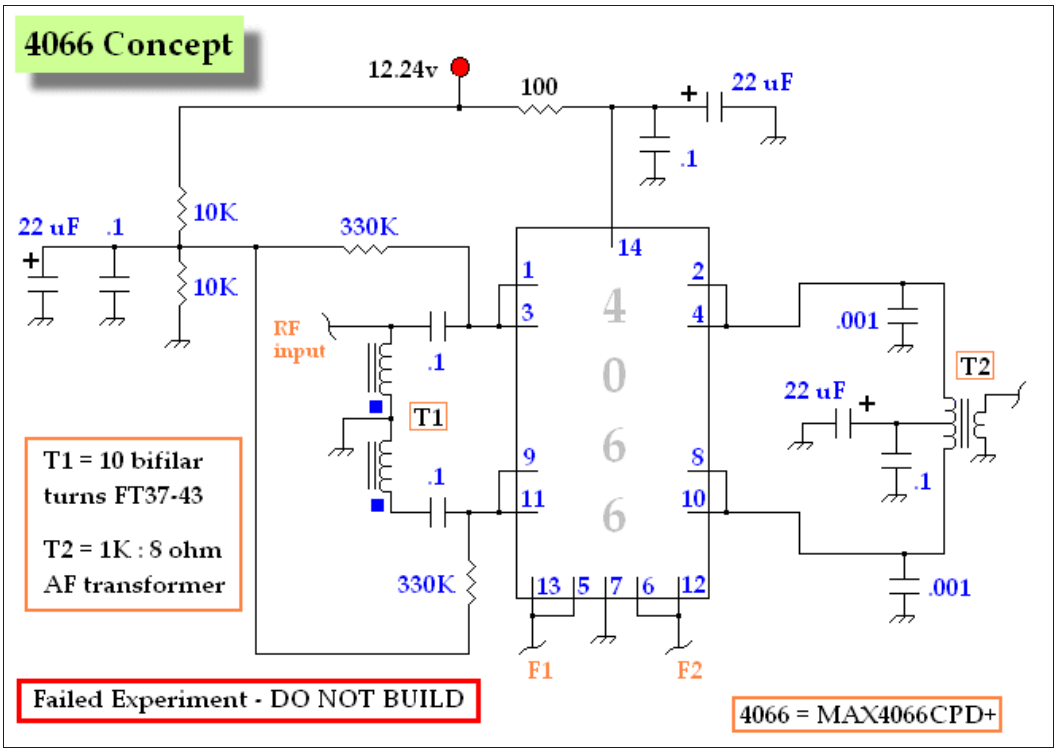

A 4066 experiment that was a total failure. It is both humbling and useful to show your failures and not just the good fruit. This circuit had hum, noise and low output. The input transformer was a bifilar type, which was really cool.

The breadboard of the 4066 Concept schematic shown above.

The DIP IC switches used as product detectors in the K7LR memorial receiver experiments.

My work bench during some final experiments for this project.

K7LR MEMORIAL RECEIVER VFOs

This web page is a supplement to the K7LR Memorial Receiver Experiments Web Page

14 MHz VFO Circuit

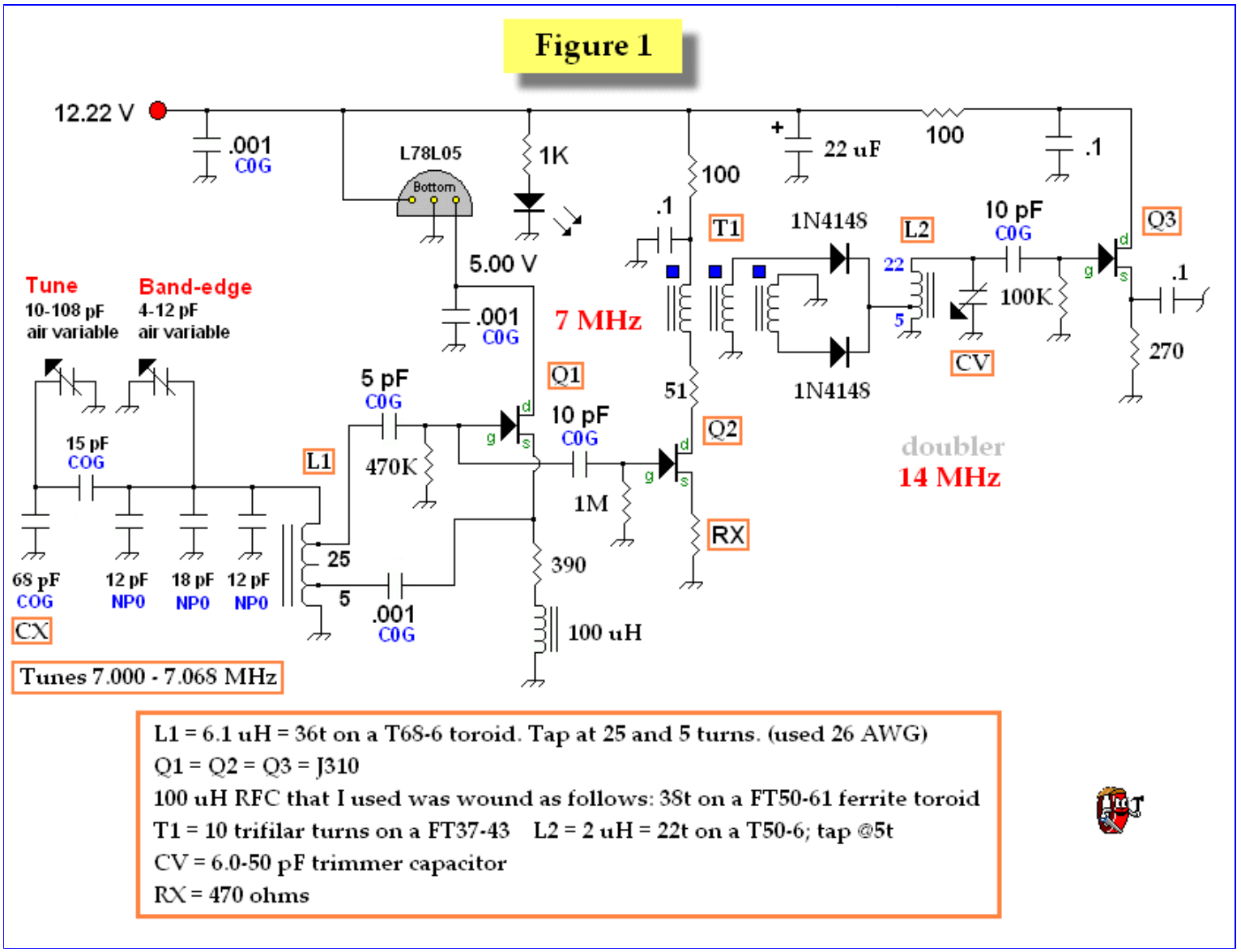

Figure 1 is the 14 MHz VFO used to switch (clock) the CMOS switch product detector. The tuning range can be easily changed by adjusting capacitor CX. As shown, the the tuning capacitor has a frequency range of about 68 Hz. If you decrease CX to 47 pF, the tuning range increases

to around 99 Hz. Increasing CX to 100 pF gave about a 40 Hz tuning range. When you use a larger tuning range, fine tuning can become difficult. A geared reduction dial is one possible solution. For simplicity, I prefer to just keep the tuning range low as reasonably possible and use a big knob on the main tuning variable capacitor. Even the 68 Hertz tuning range shown can prove difficult for fine tuning. As experimenters, we are continually problem solving. Choose the tuning range and/or methods which suit your personal needs.

The base 7 MHz oscillator is doubled since a D flip flop is used to clock the CMOS switch product detector. This oscillator has low harmonic content and this is important for suppressing the 7 MHz fundamental frequency and its harmonics in the frequency doubler. Some astute builders may even match the two diodes used in the doubler. Diode matching is discussed on this page. CV tunes very sharply and the output at Q3 is a clean sine wave. This in turn provides a well balanced square wave at each output of the D flip-flop. The Q3 output voltage was measured at -0.46 dBm (0.6 volts peak to peak into 50 ohms).

Choosing Capacitor Values

There are a number of ways to determine the capacitor values required to tune your VFO L-C tank circuit. It is pretty much essential to have a frequency counter and nice perhaps, to own a capacitance meter. Main tuning capacitors are typically harvested from an old radio or from the junk box. Its tuning range could be anywhere from 30 to 300 pF, or more. To limit the tuning range of this variable capacitor, normally you parallel a fixed-value capacitor and then series connect it to the top of L1 with a small, fixed-value capacitor. I performed this task entirely by trial an error using a frequency counter connected to the collector of Q2. Some fixed value NP0 or C0G capacitors plus a small trimmer capacitor are also required for tuning and to set the lower band edge respectively. Finding the right combination of capacitor values is painstaking, but with practice, gets easier. Once you have the basic capacitor values sorted out and your tuning range set, frequency stability experiments are then performed. This is known as VFO temperature compensation. Some times temperature compensation can be achieved by finding the right combination of NP0 and C0G capacitors. Additionally some negative or positive temperature coefficient capacitors may have to be soldered in and tested. Your final capacitor leads should be short as practically possible to reduce stray lead capacitance and for mechanical rigidity. Temperature compensation is discussed on this web page.

A 7 MHz VFO Circuit for Diode Ring Product Detectors

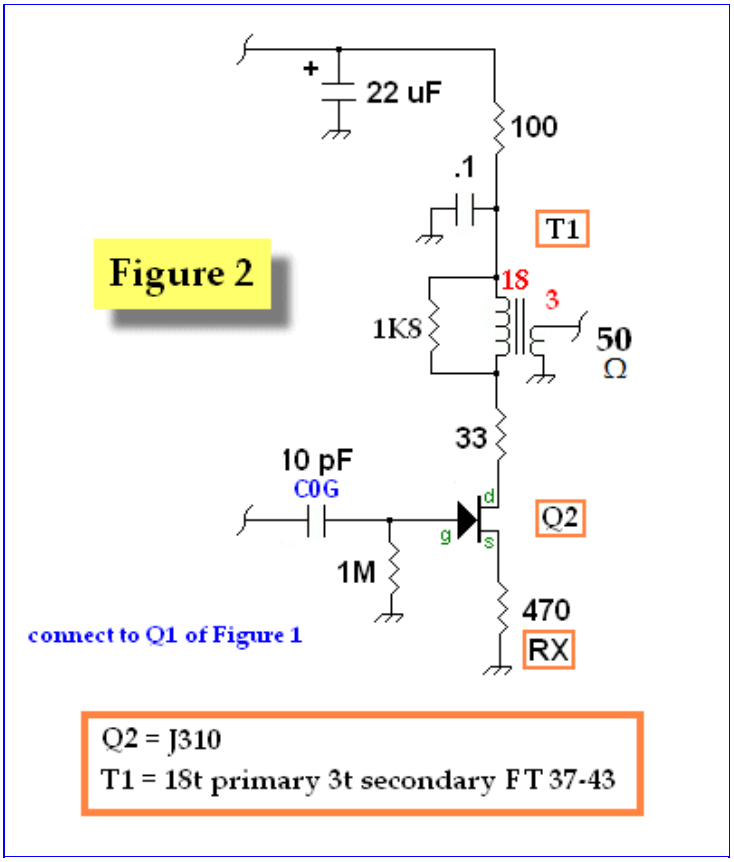

If you want to build a simpler version of the K7LR memorial receiver, a diode ring mixer may be substituted for the digital switch. The VFO requires modification as it will be run at 7 MHz. A different buffer is used and the Q2 to Q3 frequency doubler circuit is excluded. The diode ring product detector version is very nice. You could use a Mini-circuits TUF-1 , SBL-1 or alternate, or perhaps homebrew your own.

In Figure 2 is a VFO buffer configured to drive a 50 ohms input impedance, 7 dBm level, diode ring mixer. Change Rx to change the output voltage. With RX at 470 ohms, the output was somewhere around 5 dBm. This is useable for many situations. If you want exactly 7 dBm, the AC peak to peak voltage with a **51** ohm load resistor connected to the 3 turn link should be 1.43 volts. Adjust RX to achieve this voltage in your oscilloscope.

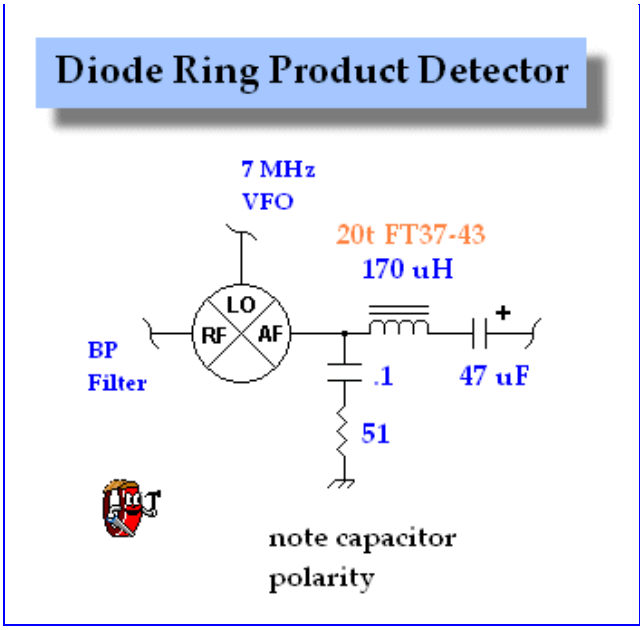

Note that if you build a diode ring product detector receiver version using the simple W7EL low pass termination network, the polarity of the 47 uF electrolytic capacitor will need to be changed as shown.

Key goals of this website include providing ideas, basic support and encouragement. I am delighted when builders make their own stuff and not copy my circuits. This is why we homebrew; to create, explore and share. Mike, K7LR did all of these very well.

Photography Links

Nikkor 50mm lenses

HENRI CARTIER-BRESSON - shot a lot with 50mm - video to watch over and over

The genius of photography -- BBC4 series about the history of photography

http://www.freestylephoto.biz

The Care and Feeding of Transmission Lines

Joel R. Hallas, W1ZR

A radio amateur's guide to understanding transmission lines

The Care and Feeding of Transmission Lines

Joel R. Hallas, W1ZR

A radio amateur's guide to understanding transmission lines

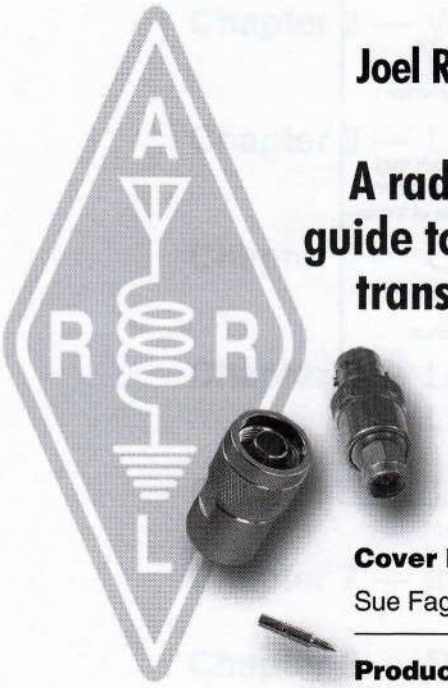

Cover Design:
Sue Fagan, KB1OKW

Production:
Michelle Bloom, WB1ENT
Jodi Morin, KA1JPA
David Pingree, N1NAS
Carol Michaud, KB1QAW

Copyright © 2012 by

The American Radio Relay League, Inc.

Copyright secured under the Pan-American Convention

All rights reserved. No part of this work may be reproduced in any form except by written permission of the publisher. All rights of translation are reserved.

Printed in USA

Quedan reservados todos los derechos

ISBN: 978-0-87259-478-4

First Edition
First Printing

Contents

Foreword

Chapter 1 — What is a Transmission Line and Why Do We Need One?

Chapter 2 — What Are the Types of Transmission Lines?

Chapter 3 — Let's Examine Coaxial Transmission Line

Chapter 4 — Other Types of Unbalanced Transmission Line

Chapter 5 — Let's Examine Balanced Transmission Line

Chapter 6 — Transmission Line Connectors

Chapter 7 — Installing Coaxial Connectors on Cable

Chapter 8 — Determining Which Line is Best Suited for a Particular Application

Chapter 9 — Application and Installation Notes

Index

Foreword

While radio equipment and antennas get most of the amateur's attention, arguably neither can amount to much unless interconnected by a transmission line. Unless the appropriate line type is selected and properly installed, the amateur is likely to be dissatisfied with the results no matter how heavily invested he or she is in what happens at each end of the line.

This book is intended to introduce readers with a basic understanding of radio equipment and antennas to the ins and outs of transmission lines. Subjects covered include an introduction to the various types of line available, detailed discussions of the key parameters of both coaxial cable and balanced line types as well as the types of connectors and how to install them. With that knowledge, we then go into how to select the best line for each application, then how to install the line in a real environment and make sure it will still work at peak efficiency after it has been in place for some time.

As with all ARRL books, you can check for updates and errata, if any, at **www.arrl.org/notes/**.

Chapter 1

What is a Transmission Line and Why Do We Need One?

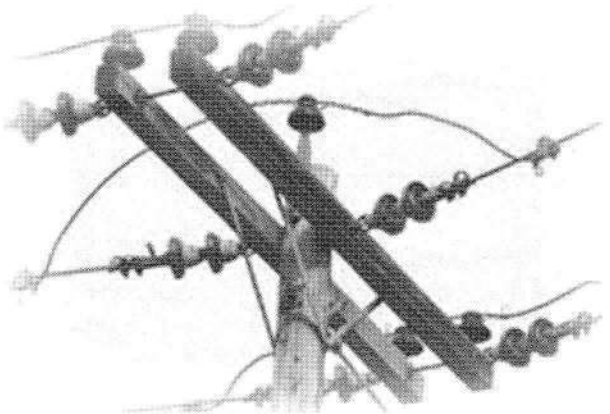

A transmission line is a kind of cable designed to convey power between physical locations. This kind of system is used for transmission of water, gas, sewage, electrical power, telephony signals and, in our case, radio frequency (RF) energy.

As with each of these applications, the desired results are the same: To convey the material or signal from one location to the other with minimal loss and with an output that includes all the characteristics of the input. While the ideal line is easy to imagine, real systems do not ever quite measure up.

In a pipe-based system, for example, material is lost through leaks in the pipe wall or at connectors. Friction of the fluid against the pipe wall results in a reduction of velocity and pressure over distance. Excessive pressure can result in a catastrophic rupture and loss of system functionality.

In a radio frequency transmission line, we have the same type of potential departures from an ideal transmission system, and some other issues that plumbers don't routinely worry about. The system functionality, however, is still very similar.

WHY DO WE NEED TRANSMISSION LINES?

We generally need a transmission line to carry RF between different parts of a radio system. **Figure 1.1** shows locations within a typical Amateur Radio station in which transmission lines would be appropriate. While not every amateur station includes all of these blocks, and some may have multiples of some blocks, the sketch is typical. Some larger pieces of equipment also have transmission lines within the unit for subassembly interconnections.

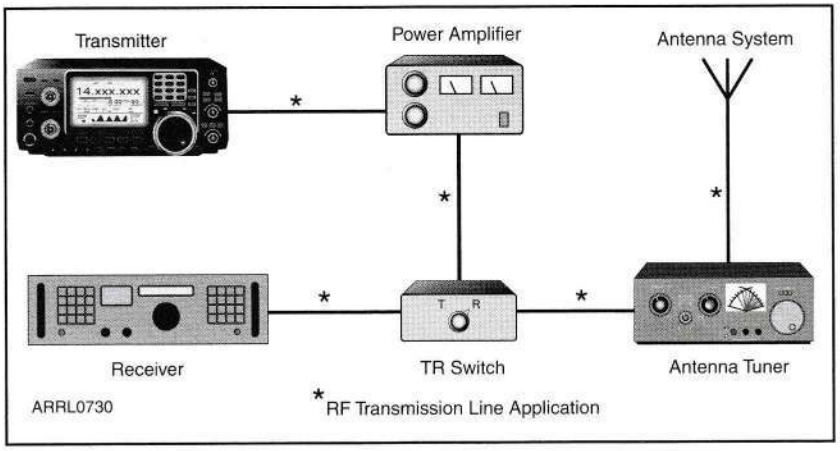

Figure 1.1 – Block diagram of a typical Amateur Radio station, showing places that would be appropriate applications for an RF transmission line.

While we may associate transmission lines with antenna connections, Figure 1.1 indicates that they have wider application. The short interequipment lines are sometimes referred to as *jumper cables*. Note that the dc power interconnections not shown between each piece of equipment and its power source could also be considered a kind of transmission line. Power transmission is a different topic beyond the scope of this book.

The reason transmission lines are used for these applications is that if other types of connection arrangement are used, we are likely to have radiation from the connecting wires. While the radiation does reduce the signal available at the end of the interconnection, it is usually more significant that the radiation will couple to other circuitry. This can result in a number of problems, including oscillation, transmitter lockup, and interference to reception of other systems such as computers.

BUT SOMETIMES WE DON'T NEED TRANSMISSION LINES

Actually, we don't always need a transmission line for a radio system. There are some cases in which all parts of a system are in a single location. In that case, no transmission lines are required. One example of such a system that I once worked with is shown in **Figure 1.2**. The problem was to accurately determine the reception pattern of a complex HF antenna array used as a part of a military over-the-horizon radar system. The solution was to monitor the receiver output as a helicopter rode in a circle around the array with a hanging center-fed dipole suspended below. A battery-powered low power transmitter was located at the center of the antenna and connected directly to each side of the antenna. A technician at the array center took azimuth data so we could tell the azimuth of the helicopter, while an onboard

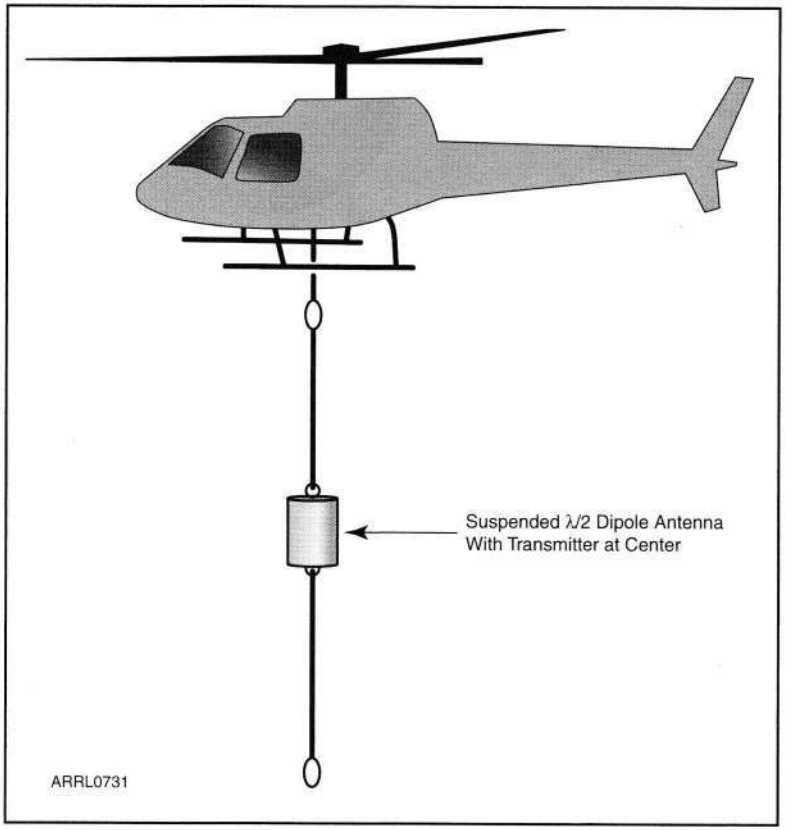

Figure 1.2 –
No RF transmission line required. This small battery-powered transmitter is located at the center of a directly fed dipole. The system was used to test the receive antenna pattern of a vertically polarized directive HF antenna array used in a military over-the-horizon radar.

navigation system was used to maintain a constant distance — worked like a charm!

Another more common application is found in some microwave systems. As we will discuss later, losses in transmission lines go up rapidly with frequency. Radio systems at microwave frequencies are usually designed to minimize transmission line length. Some have the actual microwave portion of the radio system located within the antenna structure. This is common in satellite TV receiver systems, as well as in microwave communication and radar systems. It is often more economical to have the interunit cabling carry the dc and intermediate frequency signals (on transmission lines, but with less loss because the signals are at lower frequencies) than to suffer the transmission line losses at microwave frequencies. **Figure 1.3** illustrates a typical configuration.

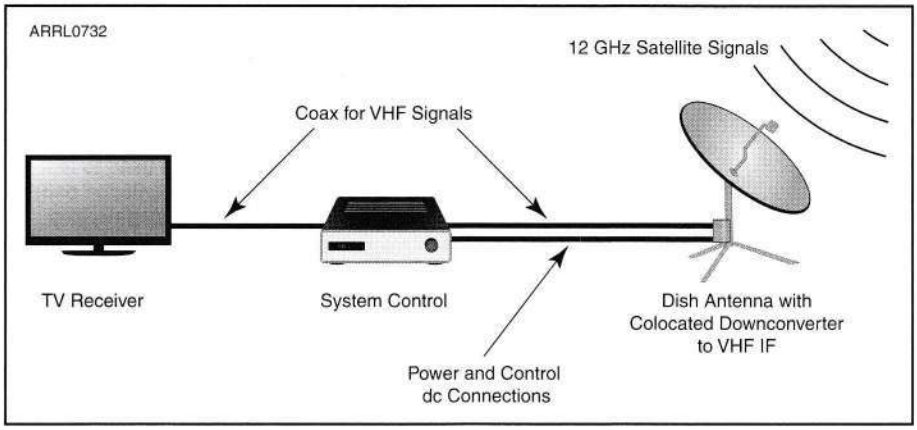

Figure 1.3 – In this simplified satellite TV receiver system, the microwave components are located directly at the antenna feed to avoid losses. A downconverter translates the desired channel information from the 12 GHz broadcast range down to a TV VHF channel, at which losses in the transmission line are more manageable.

A similar arrangement is used in many military radar systems. The rotating antenna with transmitter power amplifier and receive preamplifier can be located in one unstaffed vehicle while the signal processing equipment and sometimes the display systems are located in another at some distance. In this way, the operators and signal processing equipment are not part of the target for an antiradiation missile, especially popular as a counter to air defense radars.

Chapter 2

What Are the Types of Transmission Lines?

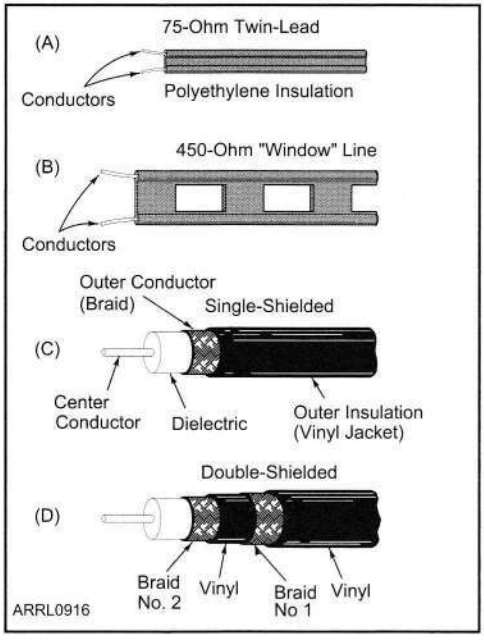

Examples of popular transmission lines.

Transmission lines come in multiple flavors, depending on the application. Here we will broadly categorize lines into their major types. We will also introduce some of the varieties within each category that we will discuss in greater detail in later chapters.

UNBALANCED TRANSMISSION LINE

Transmission lines in which the conductors are at different potentials with respect to ground are referred to as unbalanced transmission lines.

Coaxial Cable

Probably the most frequently encountered type of RF transmission line is coaxial cable. It is found connecting almost every television set to an antenna or to a cable service provider. The cable that cable service providers use is also coaxial cable, at least in the last part of the system, near the subscriber. Coaxial cable is one member of the class of unbalanced transmission lines.

Coaxial cable consists of two conductors, one surrounding the other in a concentric configuration as shown in **Figure 2.1**. In operation, if properly terminated and used, the RF field is contained within the space marked "dielectric" (an insulating material) between the two conductors. At the ends, the outer conductor, also called the *shield*, can be at ground potential. The inner conductor is at a potential above ground, thus the name "unbalanced."

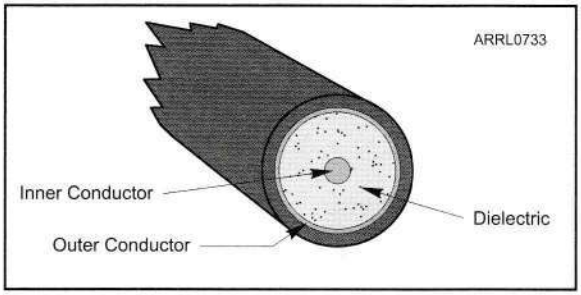

Figure 2.1 – The configuration of coaxial cable. The inner conductor is often wire, sometimes stranded for additional flexibility. Rigid cable may have a center conductor of solid wire or sometimes copper pipe. The outer conductor can be braided copper, wrapped tinfoil, or for rigid cable, copper or aluminum tubing. The lowest-loss rigid coax is made of copper tubing for both conductors with a dielectric mostly of air. Occasional ceramic spacers are employed to maintain the spacing. Other cables have a polyethylene dielectric, or sometimes a foamed poly that acts like something in between.

At RF frequencies, the phenomenon known as *skin effect* keeps the RF shield currents on the inside of the outer conductor. The outside of the outer conductor then acts almost as if it were a separate third conductor at ground potential along its length. This, along with the fact that the net field is within the cable, provides the effect of shielding the signals within the cable from the effect of any signals or other effects outside the cable. This is a major advantage of coaxial cable.

Within the class of coaxial cable ("coax" to its friends), there are a variety of subdistinctions:

◆ Characteristic impedance — The ratio of the conductor diameters and the properties of the dielectric determine the characteristic impedance, a topic that will get a chapter of its own.

◆ Cable diameter — The diameters together may scale up and down from less than ⅛ inch to many inches. The larger sizes are needed for high-power applications, and also have less loss than smaller-sized cable.

◆ Cable flexibility — There are both rigid and flexible coaxial cables, and some semi-rigid, or perhaps semi-flexible, a major factor in selection based on application. The rigid, and some semi-rigid, cables are usually made with a solid tube, rather than a woven outer conductor structure. Solid outer conductors result in coax with the potential for shielding properties closer to ideal than those with woven shields.

◆ Cable dielectric material — The properties of the material between the conductors, the dielectric, is the major factor in the cable loss at higher frequencies and also a factor in determining the cable characteristic impedance.

Unbalanced Microstrip Transmission Line

Imagine slitting the outer conductor along a length of coaxial transmission line and unfolding it so it lies flat. This is the essential configuration of microstrip transmission line. Its major application is found in intraequip-

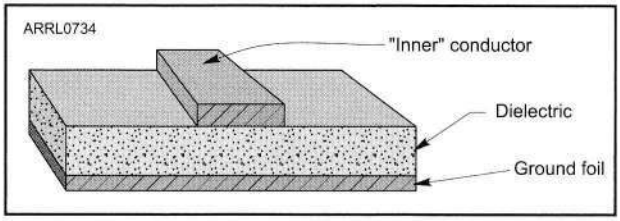

Figure 2.2 – Unbalanced microstrip line. A conductive microstrip left on one side of a piece of two-sided printed circuit board can be operated as an unbalanced transmission line with reference to the foil on the other side. While it acts a lot like coax in some ways, it does not share its shielding properties. In some implementations, a second board or layer of a multilayer board makes a sandwich with additional shielding. In all cases, the connections must be made close to the beginning and end of the conductors. With the sandwich configuration, the ground connection must be made to both ground planes near the location of the start and end of the conductive path.

ment wiring of assemblies made with double-sided printed circuit board. The line can be formed by etching away some of the conductor on one side of the board (see **Figure 2.2**) as part of the process of generating the rest of the wiring on the board.

While microstrip line is efficient from a manufacturing standpoint, it does not offer the shielding qualities of coaxial cable. The fields between the conductors will extend outward from the space between the conductors, requiring care in locating wiring for other parts of the circuit to avoid coupling between circuits. Of course, if coupling is a problem, small coaxial cable is well suited to PC board use, if not quite as easy to implement.

Single Wire Line

Before the days of radio, a single wire was used as a transmission medium for wire-line telegraph systems. The wire was fed against an earth/ground connection and was useful but very lossy. It is not particularly suited for RF systems since it will act more like an antenna, unless it is very close to a highly conductive ground. Think virtual microstrip line.

BALANCED LINE

A transmission line with two parallel conductors can be used as a balanced transmission system — meaning that each conductor is at the same magnitude of potential compared to ground but of opposite sign. This means that at a particular instant, if one wire is at +5 V, for example, the other will be at –5 V, with respect to some common level or ground reference.

Open-Wire Line

The earliest balanced transmission line was a pair of wires at a constant spacing insulated from ground (see chapter photo and **Figure 2.3**). Before the days of radio, and for some time thereafter, such a pair was used for each telephone circuit, making for very imposing utility poles with many cross Ts, almost blocking out the sun in large cities. Current telephone

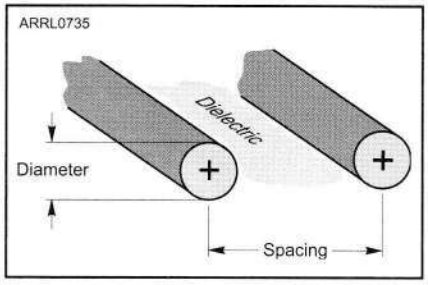

Figure 2.3 – Balanced transmission line. Just two wires, spaced a fixed distance and separated by a dielectric — air, or some other insulating material.

wiring uses insulated twisted pairs, bundled with others in large cables supporting multiple end-user customers. Once individual circuits reach a switching center, they are concentrated with switches and routed between centers on high-density fiber optic links.

Very early radio was conducted on low frequencies typically using large top-loaded monopole antennas fed directly from the transmitter.[1] As operating frequencies became higher, horizontal antennas could be high enough to be useful, and balanced antenna structures, such as a center-fed dipole, became popular. A natural way to interconnect the typical balanced output of the transmitter's tuned transformer to the center of a balanced antenna was to use balanced open-wire line (see **Figure 2.4**).

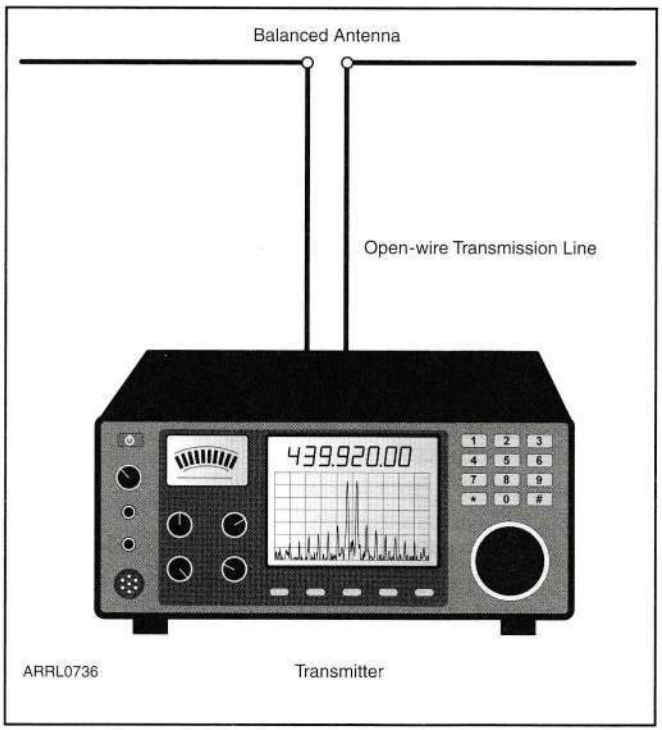

Figure 2.4 – An open-wire transmission line is a natural for interconnecting a balanced output transmitter and a balanced antenna.

The wires of open-wire line require some method to hold them at a relatively constant distance. In early telephone systems, this was accomplished by tying each wire to a glass insulator held to a cross T by a peg. In recent rural travel, I saw quite a few of these still in use on poles along railroad right-of-way, likely for signaling. Early radio transmission lines used paraffin-soaked wood dowels to position the wires. These gave way to glazed molded ceramic insulators made for the purpose. Current amateur practice is to use PVC plumbing pipe or acrylic plastic with slits to hold the wires (see **Figure 2.5**).[2]

Twinlead

After World War II, television started to become popular in the US. The signals were transmitted over the air using a portion of the VHF range. All antenna designs of the time were of balanced feed and used easily installed transmission line developed for TV applications.

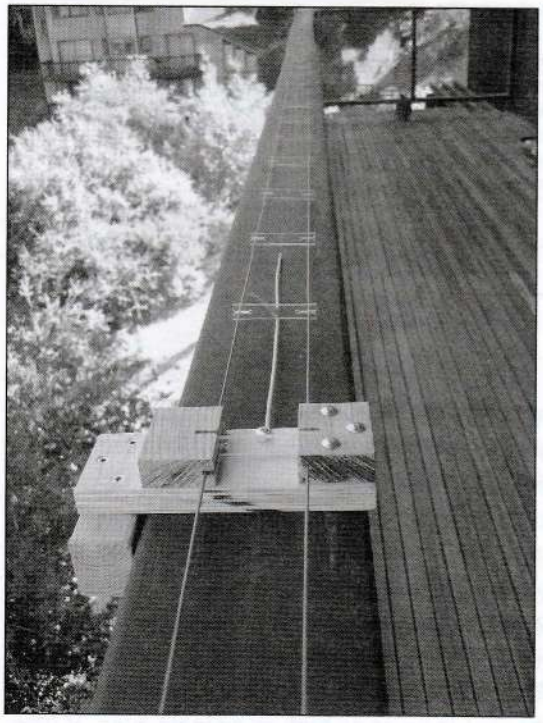

Figure 2.5 – The production line is in full swing as Barry Shackleford, W6YE, fabricates his own open-wire line. [BARRY SHACKLEFORD, W6YE]

The answer was called twinlead. It was a balanced transmission line made from a pair of stranded wires held about half an inch apart and enclosed in a polyethylene web that insulated each wire and filled the space in between with a flexible insulating material (as shown at the top of the chapter photo). This was the line of choice for this application, as well as some amateur antenna systems until it was displaced in TV service by coaxial cable.

Window Line

This derivative of twinlead is made for higher power and is often used in Amateur Radio transmitting applications. Window line is constructed similarly to twinlead, but has windows cut in the webbing along its length. The windows make the line act more like open-wire line in terms of attenuation, without having the complication of discrete insulators.

The wider spacing typically results in a higher characteristic impedance than regular twinlead.

Twisted Pair

A pair of wires twisted together can be used as a makeshift balanced transmission line. The characteristic impedance will be close to 100 Ω. This type of line is not often used for RF applications, although it can serve in a pinch. It is frequently encountered in telephone and local area network (LAN) wiring.

Shielded Twisted Pair

By enclosing a twisted pair in a shield, we can get some of the benefits of balanced line, along with the shielding effect of coax. Of course, we get the disadvantages of each as well, primarily the high attenuation of coax as compared to most balanced lines. The trade name for this cable is Twinax, and it has most recently been used in computer networking, but was once a choice for RF applications as well.

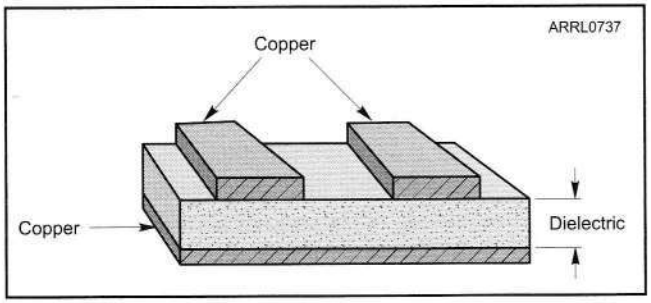

Figure 2.6 – Balanced microstrip line. This works the same way as unbalanced microstrip line, but the two conductors on one side act as a balanced pair.

Balanced Microstrip Line

A pair of etched conductors on PC board material can serve as a balanced line within equipment in the same way that microstrip can provide unbalanced connectivity (see **Figure 2.6**).

Parallel Coax Lines

Two similar coaxial cables of the same length can be operated as a balanced line if the balanced signals are connected to the inner conductors and the shields are tied together at both ends (see **Figure 2.7**). This is not a good choice for many applications of balanced line, since the attenuation is the same as for coax and the cost is twice as high as a single coax. It does work well for balanced line installations in which a small section of the line must be on the ground or in some environment that is unsuitable for open-wire line. Because the fields are entirely within the coax, the two lengths can be run separately as long as they are the same length and the shields at each end are connected together with short connections.

GUIDED WAVE STRUCTURES

UHF and especially microwave (UHF above 1000 MHz) signals are sometimes transported using a kind of mechanism different from a transmission line. The signal loss associated with coaxial cable at UHF and higher frequencies makes them unattractive for all but very short connection paths. A better alternative is to transmit the signals as electromagnetic waves propagating in space. An antenna could make such a transition, but suffers because the signal will spread spatially as it propagates. Instead, the waves are guided by propagating them within a different kind of medium.

The structures described below are a substitute for transmission lines. They are not frequently encountered in Amateur Radio, except when used by some microwave specialists. Beyond the short description below, they will not be covered in this book.

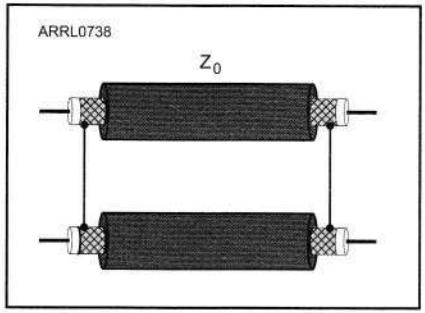

Figure 2.7 – Pair of coaxial cables used as a balanced transmission line. This is particularly useful as a short section of a balanced run to transit an area that is not appropriate for the fields surrounding open-wire line. The attenuation is as high as coax, so short sections are key. It is important that the shields are interconnected at both ends as shown. Since the shields are at reference potential in a balanced system, either may also be connected to structural ground, if appropriate.

Waveguide

The most common guided wave structure is a hollow metal tube called a waveguide. The waves are launched into the tube by an antenna-like probe, propagate within the tube, and are extracted by another probe at the far end. In order to carry the waves without significant attenuation, the guide needs to have a width of at least ½ wavelength and is often of rectangular cross-section. The size restriction limits the usefulness of the technology to the higher UHF frequencies, although I have seen waveguide in use in military radar installations at frequencies as low as 450 MHz — the waveguide tubes looked like very large heating ducts.

Single Wire Transmission Line

It is also possible to guide microwave energy along a wire. This method was originally called Goubau line (after its inventor), or G-line for short. The wire was surrounded by a special dielectric with the appropriate properties for slowing the wave in order to keep it traveling along the wire, rather than radiating as if it were an antenna. Special conical launchers are used at each end of the line, to and from coaxial transmission line. This type of line is easier to deploy in the field than waveguide since it can be rolled up, but it must be used in straight runs. G-line was part of a military microwave communications system that I encountered in the 1960s.

It was later found that waves of a different orientation could be launched onto an uninsulated wire and transmitted with low attenuation using a different configuration of launcher. This method is called E-line.

Notes

[1]J. Hallas, W1ZR, *Basic Antennas*. Available from your ARRL dealer or the ARRL Bookstore, ARRL order no. 9994. Telephone 860-594-0355, or toll-free in the US 888-277-5289; **www.arrl.org/shop**; **pubsales@arrl.org**.

[2]B. Shackleford, W6YE, "Custom Open-wire Line — It's a Snap," *QST*, Jul 2011, pp 33-36.

Chapter 3

Let's Examine Coaxial Transmission Line

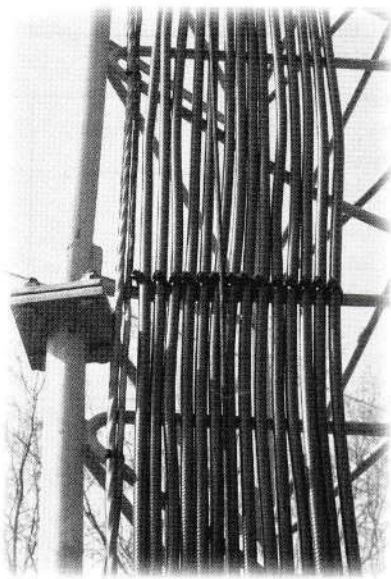

Coaxial cables going up one of the towers at W1AW, the ARRL Headquarters station. An advantage of coax is that the runs can be in close proximity to each other without interference.

Coax cable is the most commonly encountered type of transmission line. Coax is composed of two concentric conductors separated by a dielectric material (see **Figure 3.1**). While some types have an exposed outer conductor, the commonly encountered flexible cables and some rigid types are covered by a protective insulating jacket. Coax is found in many sizes for different applications, with the most common ranging from about 0.075 inches to a bit less than half an inch in diameter.

While individual conductors are occasionally connected directly to circuitry, most often within equipment, in most applications the cables are fitted with one of a number of special connectors on their ends. There are different series of connectors, some appropriate for higher frequencies, some waterproof, and some selected just because of the equipment to which they must connect.

EQUIVALENT CIRCUIT OF A COAXIAL TRANSMISSION LINE

Any two conductors separated by a dielectric will have electrical capacitance between the conductors. The capacitance is a function of the surface area of the conductors, the separation between them, and the dielectric constant of the insulation material between them. Coax cable has these properties, with capacitance created by the insulation between the inner surface of the outside conductor and the outer surface of the inside conductor. Any dielectric between the conductors will increase the capacitance compared

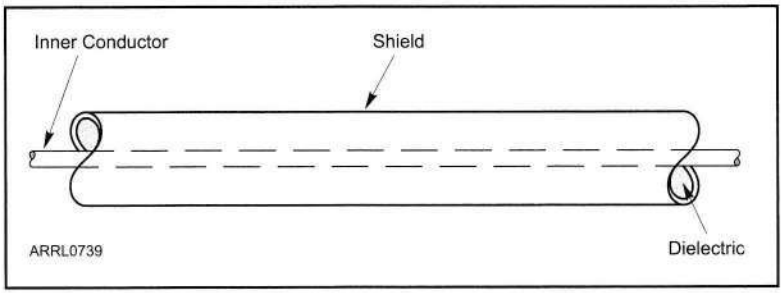

Figure 3.1 – Sketch of a typical coaxial transmission line.

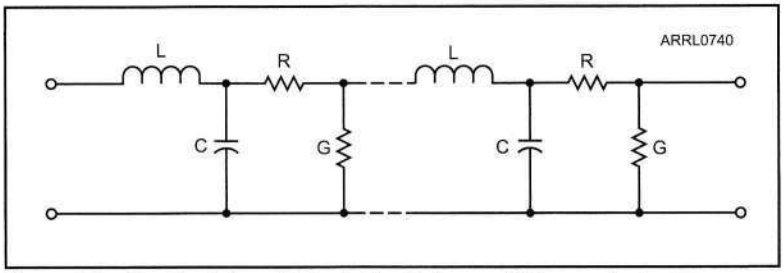

Figure 3.2 – Electrical dc equivalent circuit of a coaxial transmission line. At higher frequencies the series resistance increases because of skin effect. The length of each section can be changed by scaling the values. For many analysis applications, having 10 sections per wavelength will provide reasonable accuracy, thus the one-foot sections might be usable up to around 100 MHz, if the resistance were corrected for skin effect.

to air-insulated cable. The total area of each conductor is a function of the cable length, so the capacitance is usually specified in terms of capacitance per unit length, notated in this country in pF/ft. For example, the usual 50 Ω coax cable (which will be discussed shortly) might have a capacitance of 29 pF/ft.

Similarly, any piece of wire will have a certain inductance, and that includes the conductors making up a coaxial cable. Again, since the inductance is also a function of the cable length, it too is usually expressed in terms of inductance per unit length. For typical lines as above, it will be about 72.5 nH/ft.

The conductors will also have electrical resistance. Because of their relative sizes, this will predominantly be the resistance of the inner conductor. At very low frequencies, the resistance will be around the dc resistance of the inner conductor, perhaps 1.8 mΩ/ft depending on conductor size. There will also be some loss in the dielectric, increasing with frequency. This is represented as the conductance G. We thus could model a transmission line as an electrical circuit such as that shown in **Figure 3.2**.

CHARACTERISTIC IMPEDANCE

The characteristic impedance (Z_0) of a transmission line is one of its most significant parameters. If we consider the line model shown in Figure 3.2 and imagine a dc voltage connected to one end, a current will start to flow, regardless of what is happening at the other end. If the line were just capacitive, the initial current would be very high, as it tried to charge the capacitance. If it were entirely inductive, the initial current would be zero because of the back EMF. Because it is a combination, the initial current will be in between the two values, also limited by the resistance, and not usually a significant portion of the effect. That current will continue until the leading edge of the current pulse gets to the far end and returns with an indication of the effect of the load. The current pulse will travel at somewhat less than the speed of light in free space.

The amount of the current will be the same as if the source were connected to an impedance — generally close to being a resistor — during the initial period. The value of that resistor is called the *characteristic impedance* of the line, usually referred to as its Z_0. If the far end of the line were connected to an actual resistor equal to the Z_0, the same current would continue to flow until the source was disconnected, just as though it were an infinite length of line.

If we use the transmission line for the carrying of an RF signal rather than dc, the same kind of thing happens. For example, using Ohm's law, if we put a 1 V_{RMS} RF signal on one end of a line with a Z_0 of 50 Ω, the initial current would be 1/50 = 0.02 A or 20 mA. If the line were lossless (the R in the model = 0) and terminated at the far end with a 50 Ω resistor, the same 20 mA would flow into the resistor. This is known as a *matched* condition. If the termination were different than a 50 Ω resistor, we could no longer still have 1 V_{RMS} and 20 mA into the load, because it would violate Ohm's law for a different value resistor. Some fraction of the signal would be reflected from the end so that the combination of the forward and reflected signals would result in a voltage and current at the load that satisfies Ohm's law.

The sum of the forward and reflected wave is referred to as a *standing wave*, because the amplitude at any point along the line stays constant, just as it has to stay constant at the termination. This means that the voltage and current along the line will vary, repeating every half wavelength until it is back to the source (as shown in **Figure 3.3**). The impedance at the source will not be the value of the termination nor the line Z_0, but a function of the termination impedance and the distance from it (in wavelengths).

The ratio of maximum voltage (or current) to the minimum voltage (or current) on the line is called the standing wave ratio (SWR), a major consideration in most systems. By having a termination equal to the line

I Know What's Happening at the Shack — What's Happening at the Other End of my Feed Line?

If you want to find out — here's the easy way, using TLW.

Joel R. Hallas, W1ZR
Technical Editor, QST

I'm told that one of the more frequent questions received by *QST*'s "Doctor" has to do with folks wanting to determine the impact of transmission line losses on the effectiveness of their antenna system. These questions are often along the lines of, "I measure an SWR of 2.5:1 at the transmitter end of 135 feet of RG-8X coaxial cable. My transceiver's auto-tuner can tune it to 1.1, but how can I tell what my losses are?" or "How much difference will I have if I have a tuner at the antenna instead of using the built-in tuner?"

These are important questions that almost every amateur operator is faced with from time to time. An approximate answer can be obtained by using the graphs found in any recent edition of *The ARRL Antenna Book* showing the loss characteristics of many transmission line types, plus adding in the effect of an SWR greater than 1:1. The SWR at the antenna end can be determined from the bottom end SWR and the cable loss. Using these graphs requires a bit of interpolation or Kentucky windage, but can result in useful data.

But There's an Even Better Way!

Packaged with each of the last few editions of *The ARRL Antenna Book* is a CD containing the pages of the whole *Antenna Book* as well as some very useful software. The program that I use almost daily is one written by *Antenna Book* Editor R. Dean Straw, N6BV, called *TLW*, for *Transmission Line for Windows*.

TLW provides a very easy-to-operate mechanism to determine everything I usually need to know about what's happening on a transmission line. When you open the program, you are presented with a screen as shown in **Figure A**. This has the values plugged in from the last time you used it, often saving a step. Let's take a quick tour of the inputs:

Cable Type — This allows you to select the cable you would like to analyze. A drop-down box provides for the selection of one of 32 of the most common types of coax and balanced lines. An additional entry is provided for User Defined Transmission Lines that can be specified by propagation velocity and attenuation.

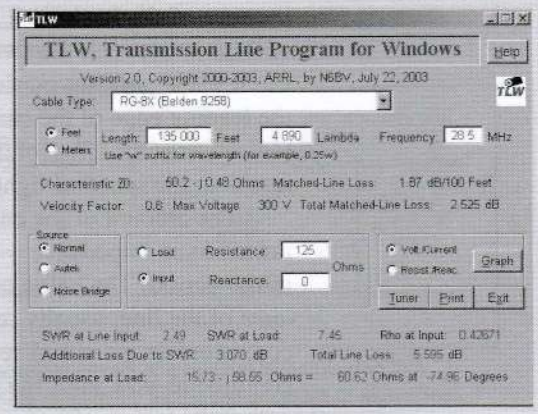

Figure A — The opening screen of *TLW*, illustrating the process described in the article.

Length — In feet or meters, your choice.

Frequency — This is an important parameter when dealing with transmission line effects.

Source — This defines the form of the input impedance data. Generally, you can use NORMAL.

Impedance — The impedance can be specified as what you measure, resistive (real) and reactive (imaginary, minus means capacitive). This could come from your antenna analyzer at either end of the transmission line. Note, if you only know the SWR, not the actual impedance, all is not lost — see below.

Now for the Outputs

SWR — The SWR is provided at each end of the cable. This is an important difference that many

people miss, important even with a moderate SWR at the transmitter end, as we'll see — the SWR at the antenna will be much higher due to the cable loss. With *TLW*, you instantly know the SWR at both ends, and the loss in the cable itself.

Rho at Load — This is the reflection coefficient, the fraction of the power reflected back from the load.

Additional Loss Due to SWR — This is one of the answers we were after.

Total Loss — And this is the other, the total loss in the line, including that caused by the mismatch.

But Doctor, What if I can Only Measure the SWR — Not the Actual Impedance?

Often the only measurement data available is the SWR at the transmitter end of the cable. Because the losses are a function of the SWR, not the particular impedance, you can just put in an arbitrary impedance with that same SWR and click the INPUT button. An easy arbitrary impedance to use is just the SWR times the Z0 of the cable, usually 50 Ω. For example, you could use a resistance of 125 Ω to represent an SWR of 2.5:1. This is what we've done in Figure A, using 135 feet of popular Belden RG-8X.

The results are interesting. Note that the 2.5:1 SWR as seen at the radio on 28.5 MHz results from a 7.45:1 SWR at the antenna — perhaps this is an eye-opener! Note that of the 5.6 dB loss, more than half, or 3.1 dB, is due to the mismatch. Note that if we used something other the actual measured impedance, we can't make use of the impedance data that *TLW* provides. We can use the SWR and loss data, however, but that's probably what we wanted to find out.

We can now do some "what ifs." We can see how much loss we have on other bands by just changing the frequency. For example, on 80 meters, with the same 2.5:1 at the transmitter end, the SWR at the antenna is about 3:1 and the loss is slightly more than 1 dB. We could also plug in an impedance calculated at the antenna end and see what difference other cable types would make. For example, with the same 28.5 MHz SWR of 7.45 at the antenna and 135 feet of ½ inch Andrew Heliax, we will have a total loss of 1.5 dB at 28.5 MHz. Note that the SWR seen at the bottom will now be 5.5:1 and our radio's auto-tuner might not be able to match the new load.

But Wait, There's More!

You can also click the GRAPH button and get a plot of either voltage and current or resistance and reactance along the cable. Note that these will only be useful if we have started with actual impedance, rather than SWR.

Pushing the TUNER button results in a page asking you to select some specifications for your tuner parts. *TLW* effectively designs a tuner of the type you asked for at the shack end of the cable. It also calculates the power lost in the tuner and gives a summary of the transmitted and lost power in watts, so you don't need to calculate it!

When you've finished, be sure to hit the EXIT button; don't just close the window. Otherwise *TLW* may not start properly the next time you want to use it.

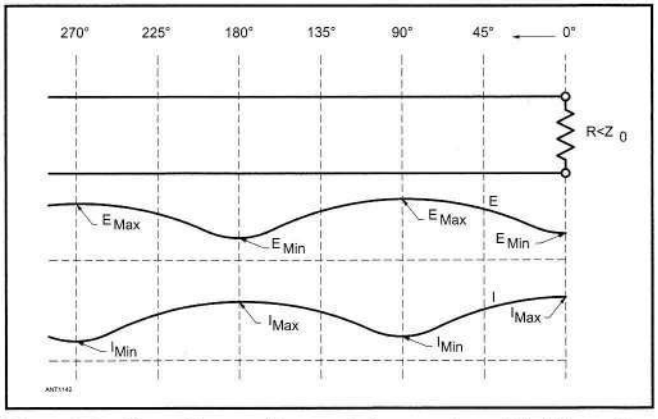

Figure 3.3 – The voltage and current along a mismatched line will vary, repeating every half wavelength.

Z_0, the standing wave doesn't exist and the SWR is 1:1. For a number of reasons, this is a desirable condition and cable with different values of Z_0 are available, including most commonly 35 Ω, 50 Ω, 75 Ω, and 93 Ω.

FIELDS WITHIN COAX

We need to briefly consider both the electric and magnetic fields in coax to understand how and why it works as it does. The electric field, just as with the plates of any capacitor with an applied voltage, exists between the outside of the center conductor and the inside of the outer conductor (see **Figure 3.4**). Because the outer conductor surrounds the inner conductor, all the electric field terminates on the inside of the shield and does not couple to, nor is it affected by, nearby conductors. Thus, the outside of the cable is effectively shielded from the effects of the electric field within the cable — one of the major benefits of coax.

As in any conductor, a magnetic field surrounds the two current-carrying conductors. For properly operating coaxial cable, the two currents will be equal and opposite; thus, the fields will cancel in the region outside the cable (see **Figure 3.5**), so the net magnetic field surrounding the cable will be zero. This, combined with the shielding of the electric field, results in a transmission line that is independent of the electrical conditions of its surroundings. This means it can be coiled, bundled with other cables, or run within metal conduit without any problems — as long as the currents are balanced and the shield is solid.

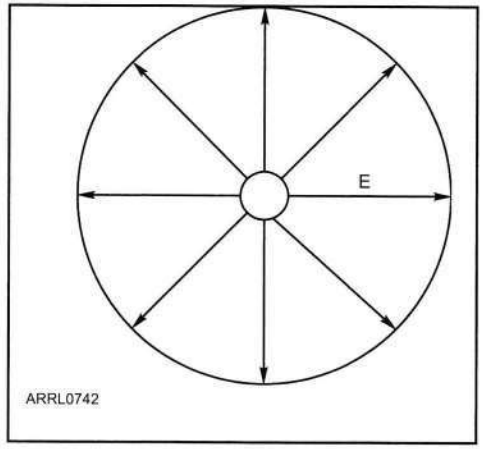

Figure 3.4 – The electric field within a coaxial transmission line. Note that if the shield is solid, it exists only within the cable, resulting in a part of the shielding effect.

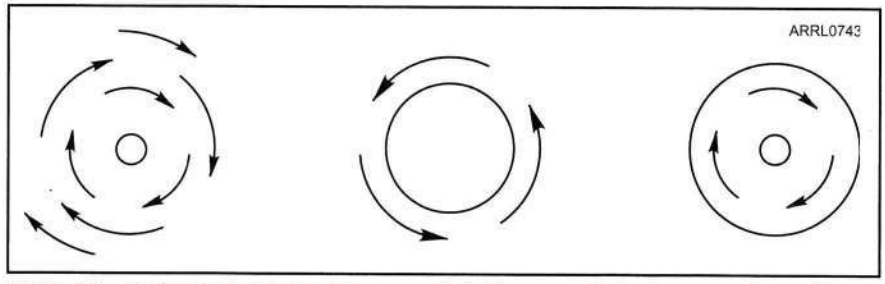

Figure 3.5 – As in any conductor, the magnetic field surrounds the two current-carrying conductors. On the left, the magnetic field surrounding a single isolated conductor is shown. The center image shows the magnetic field surrounding the outer conductor, and at right is shown the magnetic field surrounding the inner conductor. For properly operating coaxial cable, the two currents will be equal and opposite, as shown, and thus the fields will cancel outside the cable.

SHIELDING LIMITATIONS OF REAL COAX

Coax in the real world can be quite close to the ideal in most respects, but there are some limitations. The electric field shielding effectiveness is a function of the shield coverage. The best shielded cables are those with a solid tubular outer conductor. These can be considered a 100% shield, although loose or improperly installed connectors can be leakage points.

Unfortunately, solid tubular coax is not applicable to the many applications that require flexible cable. Probably the next best type, in terms of shielding effectiveness, is the type used by the cable television industry. It usually has multiple shields, generally one of wrapped aluminum foil and another of braided tinned copper. This is also quite effective — and has to be, otherwise cable signals, which occupy most of the radio spectrum,

would interfere with other users, including such critical systems as aircraft communications and navigation.

The rest of the coax world uses braided copper shielding. This can be adequate for most applications, although the quality varies considerably among brands and types. In many cases the manufacturer will specify the shielding coverage, usually in terms of a percentage, with 100% meaning fully covered. Some cable types have double shields — two independent braided shields, one around the other, in electrical contact over their length. These can be very close to 100% effective. Less expensive cables can have effectiveness as low as in the 80% range. The less completely shielded cables allow a partial leakage of the electric field, allowing some coupling to and from nearby circuits.

Another coupling mechanism occurs if the shield current is different from the current on the inner conductor. This can occur in a number of ways, typically due to a termination in which the outside of the shield acts like a separate conductor from the inside of the shield. Currents on the outside can also be induced by proximity to an antenna system.

TYPES OF COAXIAL CABLE

Coaxial cable came into common use during World War II, mainly in military radar and radio applications. A set of standards was developed during the period for radio guide (RG) cable, with that designation followed by a series number. The most common in radio use over the years have been 50 Ω characteristic Z_0 RG-8 and RG-58. Each has a copper center conductor, a polyethylene dielectric, a braided copper shield, and an outer jacket, originally made from black vinyl but more often of PVC or polyethylene today. The primary difference between the two is size, with the RG-8 having an outside diameter of 0.405 and RG-58 having one of 0.195 inches. The smaller cable has higher attenuation and lower voltage and power ratings, but offers lighter weight, additional flexibility, and handling convenience.

The next most frequently encountered early cables were those with 75 Ω characteristic impedance, most commonly RG-11 at 0.405 inches and RG-59 at 0.242 inches. A suffix "U" indicates cable that is universal (usable for multiple functions), while other suffixes indicate special characteristics or construction differences. Probably the most common coax in use today is RG-6 type (see below), an RG-59-size 75 Ω cable with a more effective foil shield, used for in-house connection of cable television equipment.

These characteristics were documented in a US military procurement manual that was cancelled in 2001, so the early numbers are no longer subject to official standardization. Thus cable that is called "RG-8U type"

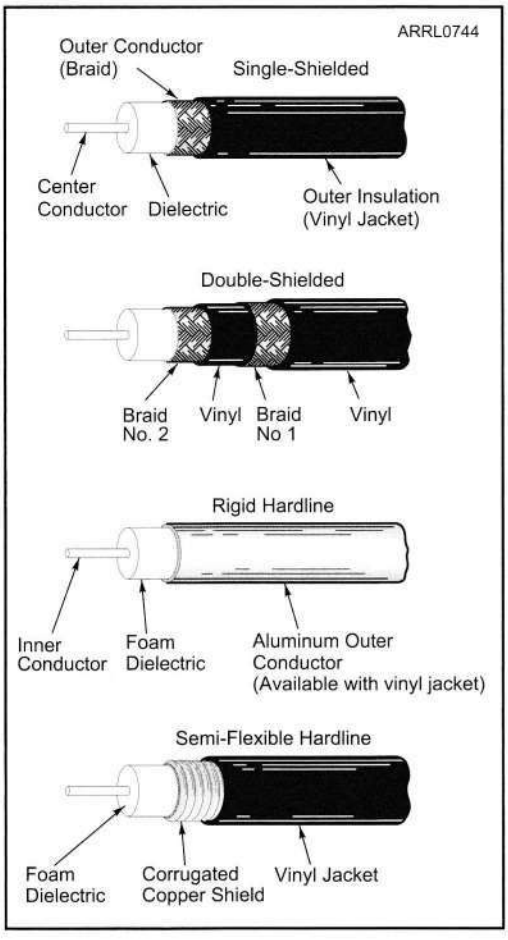

Figure 3.6 – Construction of a number of common types of coaxial cable.

is a manufacturer's designation that may mean the cable is somewhat like RG-8, but does not guarantee that it meets either early or current military standards. It may have a less dense shield or lower quality jacket, for example. Later standards include MIL-DTL-17H from August 19, 2005, which superseded MIL-C-17G of March 9, 1990. These standards refer to newer standard cable series that have replaced the earlier types. For example, today one would obtain RG-223 instead of RG-58, and RG-213 instead of RG-8. As in the earlier series, the word "type" is a manufacturer's escape clause that allows them to skirt military specifications.

Table 3.1 is a listing of many of the types of coaxial transmission line, as well as other types that we will discuss later. Note that within a type of cable, there are multiple cables from different manufacturers, with quite different characteristics. Some have a foamed polyethylene dielectric (FPE) instead of solid polyethylene. FPE is partly air and thus has a lower relative dielectric constant and less loss than standard cable. The foam also makes for a less sturdy cable that is more susceptible to water migration and cannot be flexed as tightly as the solid dielectric coax. The construction of a number of coaxial cable types is shown in **Figure 3.6**.

KEY CABLE PARAMETERS

The headings in Table 3.1 give insight into the differences between cable types. Each is described briefly below.

Nominal Z_0 (Ω) — As was discussed earlier, Z_0 is a primary transmission line parameter. Most systems specify the design impedance for various connections, and typically that will align with a standard cable Z_0. The usual practice is to use a cable with that Z_0 to connect to equipment to a load with the same impedance, although we will discuss exceptions. In most cases, particularly at lower frequencies, the difference between a Z_0 of 50, 51, 52, or 53 Ω, as shown in the RG-58 types, will not be significant. For coaxial cable, the Z_0 can be determined by the dimensions as follows:

Table 3.1

Nominal Characteristics of Commonly Used Transmission Lines

G or Type	Part Number	Nom. Z_0 Ω	VF %	Cap. pF/ft	Cent. Cond. AWG	Diel. Type	Shield Type	Jacket Material	OD inches	Max V (RMS)	Matched Loss (dB/100') 1 MHz	10	100	1000
RG-6	Belden 1694A	75	82	16.2	#18 Solid BC	FPE	FC	P1	0.275	600	0.2	0.7	1.8	5.9
RG-6	Belden 8215	75	66	20.5	#21 Solid CCS	PE	D	PE	0.332	2700	0.4	0.8	2.7	9.8
RG-8	Belden 7810A	50	86	23.0	#10 Solid BC	FPE	FC	PE	0.405	600	0.1	0.4	1.2	4.0
RG-8	TMS LMR400	50	85	23.9	#10 Solid CCA	FPE	FC	PE	0.405	600	0.1	0.4	1.3	4.1
RG-8	Belden 9913	50	84	24.6	#10 Solid BC	ASPE	FC	P1	0.405	600	0.1	0.4	1.3	4.5
RG-8	CXP1318FX	50	84	24.0	#10 Flex BC	FPE	FC	P2N	0.405	600	0.1	0.4	1.3	4.5
RG-8	Belden 9913F7	50	83	24.6	#11 Flex BC	FPE	FC	P1	0.405	600	0.2	0.6	1.5	4.8
RG-8	Belden 9914	50	82	24.8	#10 Solid BC	FPE	FC	P1	0.405	600	0.2	0.5	1.5	4.8
RG-8	TMS LMR400UF	50	85	23.9	#10 Flex BC	FPE	FC	PE	0.405	600	0.1	0.4	1.4	4.9
RG-8	DRF-BF	50	84	24.5	#9.5 Flex BC	FPE	FC	PE	0.405	600	0.1	0.5	1.6	5.2
RG-8	WM CQ106	50	84	24.5	#9.5 Flex BC	FPE	FC	P2N	0.405	600	0.2	0.6	1.8	5.3
RG-8	CXP008	50	78	26.0	#13 Flex BC	FPE	S	P1	0.405	600	0.1	0.5	1.8	7.1
RG-8	Belden 8237	52	66	29.5	#13 Flex BC	PE	S	P1	0.405	3700	0.2	0.6	1.9	7.4
RG-8X	Belden 7808A	50	86	23.5	#15 Solid BC	FPE	FC	PE	0.240	600	0.2	0.7	2.3	7.4
RG-8X	TMS LMR240	50	84	24.2	#15 Solid BC	FPE	FC	PE	0.242	300	0.2	0.8	2.5	8.0
RG-8X	WM CQ118	50	82	25.0	#16 Flex BC	FPE	FC	P2N	0.242	300	0.3	0.9	2.8	8.4
RG-8X	TMS LMR240UF	50	84	24.2	#15 Flex BC	FPE	FC	PE	0.242	300	0.2	0.8	2.8	9.6
RG-8X	Belden 9258	50	82	24.8	#16 Flex BC	FPE	S	P1	0.242	600	0.3	0.9	3.1	11.2
RG-8X	CXP08XB	50	80	25.3	#16 Flex BC	FPE	S	P1	0.242	300	0.3	0.9	3.1	14.0
RG-9	Belden 8242	51	66	30.0	#13 Flex SPC	PE	SCBC	P2N	0.420	5000	0.2	0.6	2.1	8.2
RG-11	Belden 8213	75	84	16.1	#14 Solid BC	FPE	S	PE	0.405	600	0.2	0.4	1.3	5.2
RG-11	Belden 8238	75	66	20.5	#18 Flex TC	PE	S	P1	0.405	600	0.2	0.7	2.0	7.1
RG-58	Belden 7807A	50	85	23.7	#18 Solid BC	FPE	FC	PE	0.195	300	0.3	1.0	3.0	9.7
RG-58	TMS LMR200	50	83	24.5	#17 Solid BC	FPE	FC	PE	0.195	300	0.3	1.0	3.2	10.5
RG-58	WM CQ124	52	66	28.5	#20 Solid BC	PE	S	PE	0.195	1400	0.4	1.3	4.3	14.3
RG-58	Belden 8240	52	66	28.5	#20 Solid BC	PE	S	P1	0.193	1900	0.3	1.1	3.8	14.5
RG-58A	Belden 8219	53	73	26.5	#20 Flex TC	FPE	S	P1	0.195	300	0.4	1.3	4.5	18.1
RG-58C	Belden 8262	50	66	30.8	#20 Flex TC	PE	S	P2N	0.195	1400	0.4	1.4	4.9	21.5
RG-58A	Belden 8259	50	66	30.8	#20 Flex TC	PE	S	P1	0.192	1900	0.4	1.5	5.4	22.8

G or Type	Part Number	Nom. Z_0 Ω	VF %	Cap. pF/ft	Cent. Cond. AWG	Diel. Type	Shield Type	Jacket Material	OD inches	Max V (RMS)	Matched Loss (dB/100') 1 MHz	10	100	1000
RG-59	Belden 1426A	75	83	16.3	#20 Solid BC	FPE	S	P1	0.242	300	0.3	0.9	2.6	8.5
RG-59	CXP 0815	75	82	16.2	#20 Solid BC	FPE	S	P1	0.232	300	0.5	0.9	2.2	9.1
RG-59	Belden 8212	75	78	17.3	#20 Solid CCS	FPE	S	P1	0.242	300	0.6	1.0	3.0	10.9
RG-59	Belden 8241	75	66	20.4	#23 Solid CCS	PE	S	P1	0.242	1700	0.6	1.1	3.4	12.0
RG-62A	Belden 9269	93	84	13.5	#22 Solid CCS	ASPE	S	P1	0.240	750	0.3	0.9	2.7	8.7
RG-62B	Belden 8255	93	84	13.5	#24 Flex CCS	ASPE	S	P2N	0.242	750	0.3	0.9	2.9	11.0
RG-63B	Belden 9857	125	84	9.7	#22 Solid CCS	ASPE	S	P2N	0.405	750	0.2	0.5	1.5	5.8
RG-142	CXP 183242	50	69.5	29.4	#19 Solid SCCS	TFE	D	FEP	0.195	1900	0.3	1.1	3.8	12.8
RG-142B	Belden 83242	50	69.5	29.0	#19 Solid SCCS	TFE	D	TFE	0.195	1400	0.3	1.1	3.9	13.5
RG-174	Belden 7805R	50	73.5	26.2	#25 Solid BC	FPE	FC	P1	0.110	300	0.6	2.0	6.5	21.3
RG-174	Belden 8216	50	66	30.8	#26 Flex CCS	PE	S	P1	0.110	1100	1.9	3.3	8.4	34.0
RG-213	Belden 8267	50	66	30.8	#13 Flex BC	PE	S	P2N	0.405	3700	0.2	0.6	1.9	8.0
RG-213	CXP213	50	66	30.8	#13 Flex BC	PE	S	P2N	0.405	600	0.2	0.6	2.0	8.2
RG-214	Belden 8268	50	66	30.8	#13 Flex SPC	PE	D	P2N	0.425	3700	0.2	0.6	1.9	8.0
RG-216	Belden 9850	75	66	20.5	#18 Flex TC	PE	D	P2N	0.425	3700	0.2	0.7	2.0	7.1
RG-217	WM CQ217F	50	66	30.8	#10 Flex BC	PE	D	PE	0.545	7000	0.1	0.4	1.4	5.2
RG-217	M17/78-RG217	50	66	30.8	#10 Solid BC	PE	D	P2N	0.545	7000	0.1	0.4	1.4	5.2
RG-218	M17/79-RG218	50	66	29.5	#4.5 Solid BC	PE	S	P2N	0.870	11000	0.1	0.2	0.8	3.4
RG-223	Belden 9273	50	66	30.8	#19 Solid SPC	PE	D	P2N	0.212	1400	0.4	1.2	4.1	14.5
RG-303	Belden 84303	50	69.5	29.0	#18 Solid SCCS	TFE	S	TFE	0.170	1400	0.3	1.1	3.9	13.5
RG-316	CXP TJ1316	50	69.5	29.4	#26 Flex BC	TFE	S	FEP	0.098	1200	1.2	2.7	8.0	26.1
RG-316	Belden 84316	50	69.5	29.0	#26 Flex SCCS	TFE	S	FEP	0.096	900	1.2	2.7	8.3	29.0
RG-393	M17/127-RG393	50	69.5	29.4	#12 Flex SPC	TFE	D	FEP	0.390	5000	0.2	0.5	1.7	6.1
RG-400	M17/128-RG400	50	69.5	29.4	#20 Flex SPC	TFE	D	FEP	0.195	1400	0.4	1.1	3.9	13.2
LMR500	TMS LMR500UF	50	85	23.9	#7 Flex BC	FPE	FC	PE	0.500	2500	0.1	0.4	1.2	4.0
LMR500	TMS LMR500	50	85	23.9	#7 Solid CCA	FPE	FC	PE	0.500	2500	0.1	0.3	0.9	3.3
LMR600	TMS LMR600	50	86	23.4	#5.5 Solid CCA	FPE	FC	PE	0.590	4000	0.1	0.2	0.8	2.7
LMR600	TMS LMR600UF	50	86	23.4	#5.5 Flex BC	FPE	FC	PE	0.590	4000	0.1	0.2	0.8	2.7
LMR1200	TMS LMR1200	50	88	23.1	#0 Copper Tube	FPE	FC	PE	1.200	4500	0.04	0.1	0.4	1.3

G or Type	Part Number	Nom. Z_0 Ω	VF %	Cap. pF/ft	Cent. Cond. AWG	Diel. Type	Shield Type	Jacket Material	OD inches	Max V (RMS)	Matched Loss (dB/100') 1 MHz	10	100	1000
Hardline														
½"	CATV Hardline	50	81	25.0	#5.5 BC	FPE	SM	none	0.500	2500	0.05	0.2	0.8	3.2
½"	CATV Hardline	75	81	16.7	#11.5 BC	FPE	SM	none	0.500	2500	0.1	0.2	0.8	3.2
⅞"	CATV Hardline	50	81	25.0	#1 BC	FPE	SM	none	0.875	4000	0.03	0.1	0.6	2.9
⅞"	CATV Hardline	75	81	16.7	#5.5 BC	FPE	SM	none	0.875	4000	0.03	0.1	0.6	2.9
LDF4-50A Heliax –½"		50	88	25.9	#5 Solid BC	FPE	CC	PE	0.630	1400	0.05	0.2	0.6	2.4
LDF5-50A Heliax –⅞"		50	88	25.9	0.355" BC	FPE	CC	PE	1.090	2100	0.03	0.10	0.4	1.3
LDF6-50A Heliax – ¼"		50	88	25.9	0.516" BC	FPE	CC	PE	1.550	3200	0.02	0.08	0.3	1.1
Parallel Lines														
TV Twinlead (Belden 9085)		300	80	4.5	#22 Flex CCS	PE	none	P1	0.400	**	0.1	0.3	1.4	5.9
Twinlead (Belden 8225)		300	80	4.4	#20 Flex BC	PE	none	P1	0.400	8000	0.1	0.2	1.1	4.8
Generic Window Line		405	91	2.5	#18 Solid CCS	PE	none	P1	1.000	10000	0.02	0.08	0.3	1.1
WM CQ 554		420	91	2.7	#14 Flex CCS	PE	none	P1	1.000	10000	0.02	0.08	0.3	1.1
WM CQ 552		440	91	2.5	#16 Flex CCS	PE	none	P1	1.000	10000	0.02	0.08	0.3	1.1
WM CQ 553		450	91	2.5	#18 Flex CCS	PE	none	P1	1.000	10000	0.02	0.08	0.3	1.1
WM CQ 551		450	91	2.5	#18 Solid CCS	PE	none	P1	1.000	10000	0.02	0.08	0.3	1.1
Open-Wire Line		600	92	1.1	#12 BC	none	none	none	**	12000	0.02	0.06	0.2	0.7

Approximate Power Handling Capability (1:1 SWR, 40°C Ambient):

	1.8 MHz	7	14	30	50	150	220	450	1 GHz
RG-58 Style	1350	700	500	350	250	150	120	100	50
RG-59 Style	2300	1100	800	550	400	250	200	130	90
RG-8X Style	1830	840	560	360	270	145	115	80	50

Legend:

**	Not Available or varies	FC	Foil + Tinned Copper Braid	S	Single Braided Shield
ASPE	Air Spaced Polyethylene	FEP	Teflon® Type IX	SC	Silver Coated Braid
BC	Bare Copper	Flex	Flexible Stranded Wire	SCCS	Silver Plated Copper Coated Steel
CC	Corrugated Copper	FPE	Foamed Polyethylene	SM	Smooth Aluminum
CCA	Copper Cover Aluminum		Heliax Andrew Corp Heliax	SPC	Silver Plated Copper
CCS	Copper Covered Steel	N	Non-Contaminating	TC	Tinned Copper
CXP	Cable X-Perts, Inc.	P1	PVC, Class 1	TFE	Teflon® Systems
D	Double Copper Braids	P2	PVC, Class 2	UF	Ultra Flex
DRF	Davis RF	PE	Polyethylene	WM	Wireman

$$Z_0 = \left(\frac{138}{\sqrt{\varepsilon_r}}\right) \times \log_{10}\left(\frac{D}{d}\right)$$

Where D and d are the diameters of the shield and center conductor respectively in the same units. ε_r is the relative dielectric constant of the dielectric (for air, $\varepsilon_r = 1$, for polyethylene $\varepsilon_r = 2.26$).

VF (%) — This is the velocity factor as a percentage of the speed of light in free space (300,000,000 m/s). This is largely a function of the relative dielectric constant of the insulation material. For polyethylene dielectric, the VF is usually 66%, in the 80th percentile for foamed poly, depending on density, and close to 100% for air-insulated lines. In many applications, the velocity is not particularly important, with two notable exceptions — it is critical if lines are used for delay or phasing lines, and it also directly affects the required length of lines used as impedance transformers (covered later). The velocity factor can be found as shown below.

$$VF = 100/\sqrt{\varepsilon_r}$$

Cap (pF/ft) — This is the capacitance between the inner and outer conductors of the cable. It is a function of the ratio of the diameters and the dielectric constant. Note that the ratio of diameters also determines the Z_0, so it's not surprising that cables of the same Z_0 with similar dielectrics have the same capacitance. Sometimes pieces of transmission line are used as capacitors in circuits; otherwise this is not often important.

Dimensions and Materials — These are often major considerations. It is critical to know the dimensions if determining connector or adapter types. The abbreviations are listed at the bottom of the table. Note that some center conductors are indicated as being flexible — a prime attribute in many applications.

Max V (RMS) — This is the maximum Root Mean Square, or effective voltage that can be safely applied to the cable. Note that this doesn't equate to power, which is listed separately at the bottom and applies for a matched (SWR = 1:1) condition. This voltage might occur briefly for any reason (the maximum peak voltage is 1.4 times the listed voltage), and above that, arcing is possible. The power is generally more of a thermal issue. For example, the listed voltage for RG-58, 300 V_{RMS}, would translate to a power of 1800 W in a 50 Ω system, while the maximum power (at 1.8 MHz) is listed as 1350 W.

Matched Loss (dB/100 feet) — This is the attenuation of 100 feet of the cable when matched to its Z_0. Note that the cable loss increases with frequency and is shown for four frequencies across the spectrum. The loss

is linearly related to length, so 200 feet has twice the loss, and 50 feet has half the loss. This is a key differentiator between cable types. Keep in mind that a 1 dB loss represents about a 20% reduction in power, a 3 dB loss is a 50% reduction in power, and 10 dB is a 90% reduction. All things being equal, larger cables have less loss (due to less conductor resistance) as do cables with higher velocity (less dielectric loss). The matched loss of major cable types is shown graphically in **Figure 3.7**.

ADDITIONAL LOSS DUE TO MISMATCH

You may have noticed that all the loss figures stated in Table 3.1 and shown in Figure 3.7 were for the case of a transmission line terminated in its Z_0. The additional loss due to mismatch is a function of both amount of the mismatch (SWR) and the loss if matched. **Figure 3.8** shows the additional loss in dB that occurs as a result of a line not being matched.

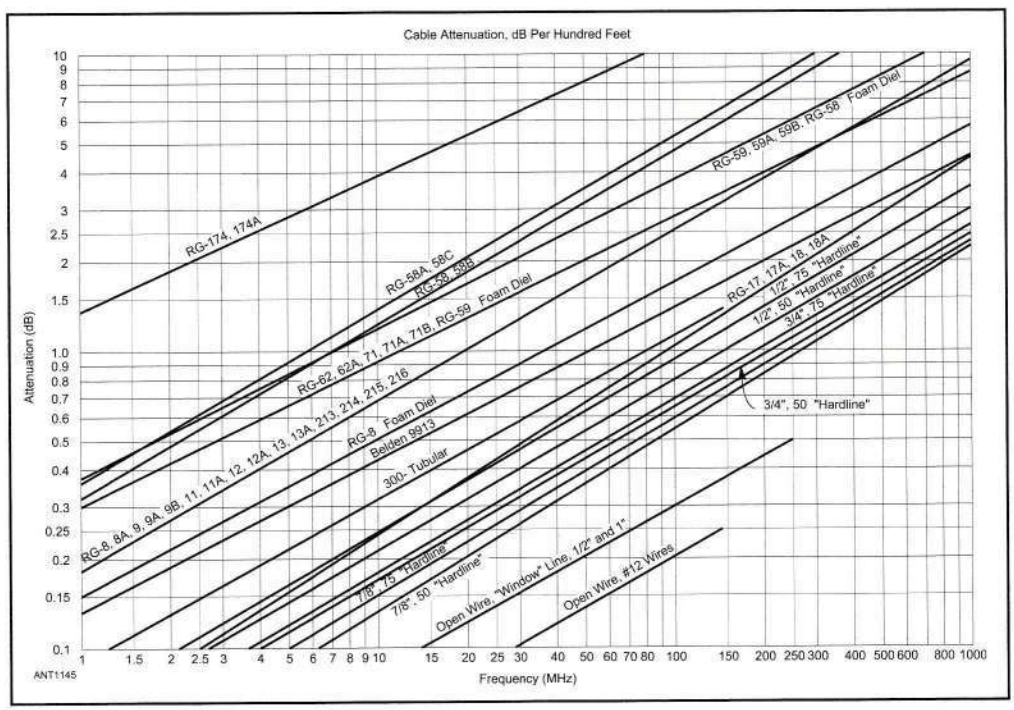

Figure 3.7 – Matched nominal loss of various transmission line types in dB/100 feet of representative transmission line types. As you choose transmission line, it is important to note that this data is representative — the variation between attenuation of different manufacturers and even different part numbers from the same manufacturer can be striking. Check the manufacturer's website for the data sheet of the transmission line you are considering to be sure you know what you are getting. For lengths other than 100 feet, the loss scales linearly. For example, if a line has a matched loss of 2 dB at 100 feet, the same line at the same frequency will have a loss of 1 dB if 50 feet long, and 5 dB if 250 feet long.

Note that the SWR shown is the SWR as measured or calculated at the load, and not the SWR measured at the transmitter end of the cable. This is particularly important in the case of a lossy line, since the loss will reduce both the power reaching the antenna and the power of the reflected wave that is used to determine the SWR. This can give very optimistic and erroneous results.

To give an example of this effect, consider a 100 W transmitter driving 100 feet of coax with a loss of 3 dB (50% loss). The antenna will see 50 W of power. Let's say 20% of the power is reflected due to the antenna mismatch. That will result in 10 W being reflected back toward the source. The 3 dB loss results in 5 W showing up as reflected power at the bottom of the cable. This is quite different than if the 100 W were applied to the antenna on lossless line — in

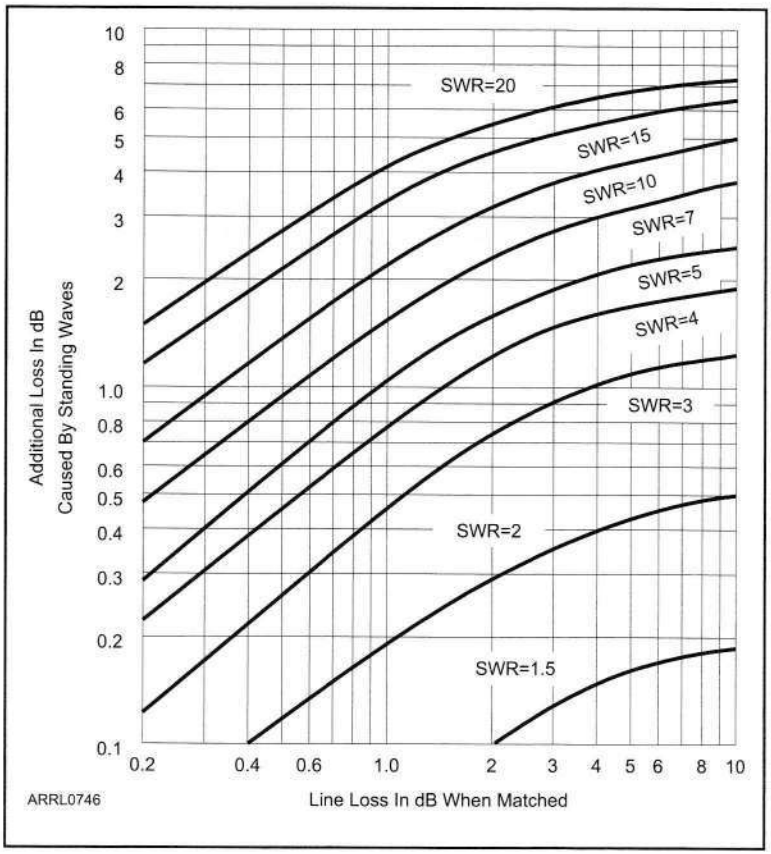

Figure 3.8 – Additional loss of a transmission line when mismatched. This loss needs to be added to the loss in Figure 3.7 for mismatched lines.

Table 3.2
Forward and Reflected Power and SWR as Seen at Each End of a Transmission Line With 3 dB Loss

Measurement	*Bottom of Cable*	*Top of Cable*
Forward Power (W)	100	50
Reflected Power (W)	5	10
Indicated Reflection Coefficient	0.224	0.447
Indicated SWR	1.6	4.0

that case, a reflected power of 20 W, not 5 W, would show up at the SWR measurement device.

Table 3.2 summarizes what we have at the two locations. Note the rather distressing result. A very acceptable measurement of an SWR of 1.6:1 at the bottom of the coax is the result of an unpleasant SWR of 4:1 at the antenna. In this example, our 100 W of power results in only 40 W radiated from the antenna — yet all of our measurements make us think we're doing well. Unfortunately, this example is not unusual, especially at the upper end of HF into the VHF range. If it happens at higher frequencies, it is usually more evident since nothing much ends up going in or out of the system! The sidebar discusses ways that this can be calculated, and perhaps avoided, through the use of software.[3]

Notes

[1]J. Hallas, W1ZR, *Basic Antennas*. Available from your ARRL dealer or the ARRL Bookstore, ARRL order no. 9994. Telephone 860-594-0355, or toll-free in the US 888-277-5289; **www.arrl.org/shop**; **pubsales@arrl.org**.
[2]B. Shackleford, W6YE, "Custom Open-wire Line — It's a Snap," *QST*, Jul 2011, pp 33-36.
[3]J. Hallas, W1ZR, "I Know What's Happening at the Shack — What's Happening at the Other End of My Feed Line?" *QST*, Feb 2007, p 63.

Chapter 4

Other Types of Unbalanced Transmission Line

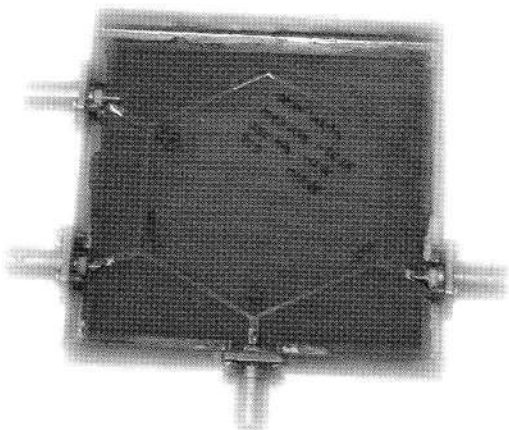

This microwave circulator is constructed of microstrip transmission line. Microstrip is easily implemented as part of PC board fabrication. The lines shown are single-sided stripline with the foil on the other side of the board serving as the "shield."

While coaxial cable is the most frequently encountered type of unbalanced transmission line, it is not the only type. This chapter will briefly introduce some other types of line in that category.

MICROSTRIP TRANSMISSION LINE

Microstrip is a form of transmission line that takes advantage of the properties of printed circuit (PC) boards. PC assemblies are a common and efficient method of circuit fabrication that has largely displaced the hand wiring of most electronic systems. The technique employs a thin piece of insulating material, the *substrate*, that serves as the mechanical strength member of the assembly and that supports all the components. Professional and military equipment generally makes use of a fiberglass-based material, while less critical consumer products are often made of phenolic resin.

A thin layer of copper that will eventually be transformed into component interconnections is bonded to the substrate. More common double-sided PC board has copper on both sides of the substrate. The PC designer (a person or software), working from the schematic of the circuit, lays out the board by specifying where each component will be placed and which pins need to be interconnected. The interconnections are made by removing

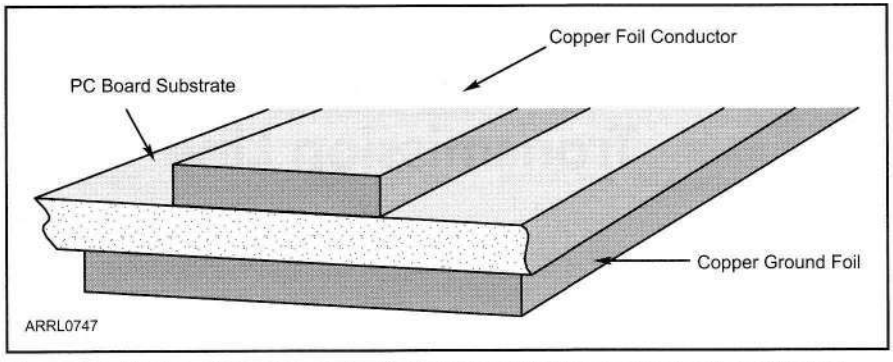

Figure 4.1 – Sketch of a typical microstrip transmission line as etched onto a PC board.

the copper that isn't needed. Often connections are established on both sides of double-sided board, but sometimes one side is used as a ground reference across the board. The unneeded copper is removed by using one of a number of methods of applying "resist" material to the areas that need to be kept. The board is then submerged in an acid bath to remove the excess copper. Following etching, the resist material is removed and the components are mounted to complete the circuit. While this sounds like an arduous process, compared to hand-wiring, it is easily automated and very efficient, especially if multiple boards are required for a production run.

RF circuits within a board, or leaving the board, can be interconnected using miniature coaxial cable with ends connected through holes in the board to the appropriate termination points just as other components with wire leads can be connected. Alternately, a microstrip transmission line can be formed on double-sided board during the printed circuit process. The line must be fabricated above a region that has a ground area on the bottom foil of the board, and merely consists of a conductor etched above the ground foil interconnecting to two end points. This is shown in **Figure 4.1**, along with the electric field between the conductors.

Note that unlike the case of the fields within a coax cable, the fields, while concentrated between the conductors, are not entirely contained there. This is a major limitation of microstrip line — it is not totally shielded. Therefore, care should be taken to make sure that coupling does not occur to sensitive circuits. This can usually be managed at the time of board layout.

In operation it is important that the connections of both input and output ends of the line include direct connections to the end of the "center conductor" and the ground plane directly beneath it.

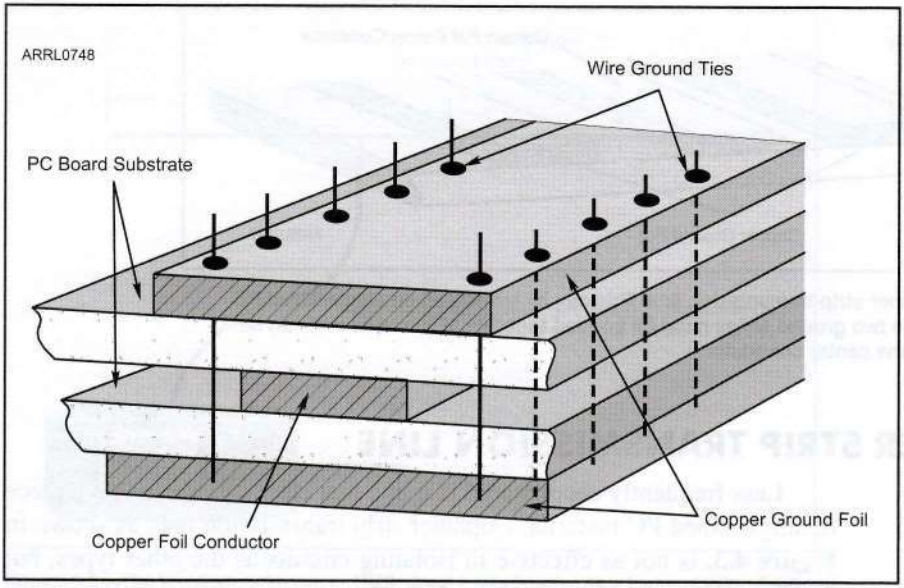

Figure 4.2 – Stripline transmission line, adding another ground layer to microstrip. Note the periodic connections between the two ground strips. These can improve the isolation to close to that of coax.

Characteristic Impedance

The characteristic impedance (Z_0) of microstrip line and the effective dielectric constant of the insulation are determined by the sizes of the conductors and the material used as the dielectric in a manner similar to coaxial cable.

STRIPLINE TRANSMISSION LINE

A variation of microstrip that actually was developed first is called stripline. It is just a microstrip "sandwich," formed by adding another piece of board with a ground foil above the single board in microstrip. Alternately, it can be formed as part of a multilayer board. It can have additional isolation from nearby conductors since the fields are more tightly constrained. It can approach coax in this regard if the two shield foils are tied together along the edge with frequent wires, as shown in **Figure 4.2**. In this case, the ground side of each end termination must connect directly to both ground foils in the area near the inner conductor.

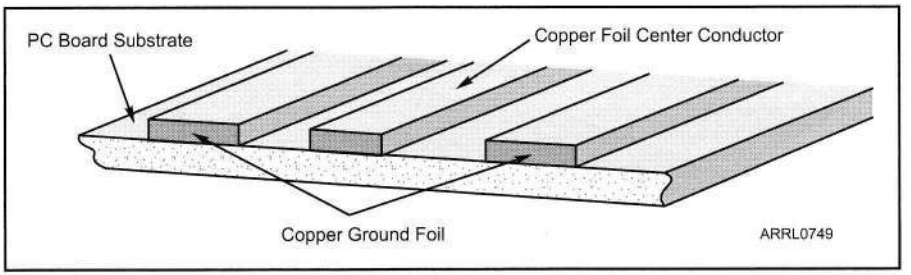

Figure 4.3 – Coplaner strip transmission line. This can be fabricated on single-sided PC board material. The two ground strips must be bonded together at the ends and can be much larger than the center conductor.

COPLANER STRIP TRANSMISSION LINE

Less frequently encountered is a line that can be deployed on a piece of single-sided PC material. Coplaner strip transmission line, as shown in **Figure 4.3**, is not as effective in isolating circuits as the other types, but may be usable in some situations. Note that in this case, the dielectric is a mix of the board substrate below and air above. Again, the ground side of the connection at each end must connect to both ground strips. This can be built into the PC board etching process.

SINGLE WIRE OVER A GROUND PLANE

An insulated wire located close to a metal chassis, or even a piece of PC material with a ground foil, can act like a microstrip line. (See **Figure 4.4**.) This is commonly employed in equipment that is hand-wired in the traditional manner between components on a metal chassis — in many cases without the builder thinking in terms of transmission lines. The effectiveness can be increased by locating the wire in a corner.

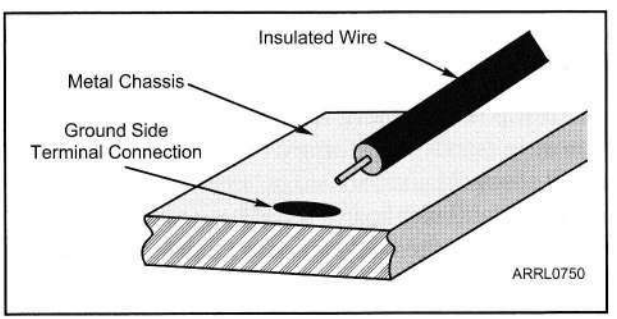

Figure 4.4 – An insulated wire positioned tightly against a chassis or other metal surface can serve as a transmission line similar to a microstrip line.

As with microstrip, while the end-to-end transmission is predictable and efficient, there can easily be unplanned and undesired coupling to other circuits within the chassis since the fields are not completely contained close to the wire. If there are other sensitive circuits close by, a piece of miniature coax can often fit in the same place and, if properly terminated, can reduce the coupling.

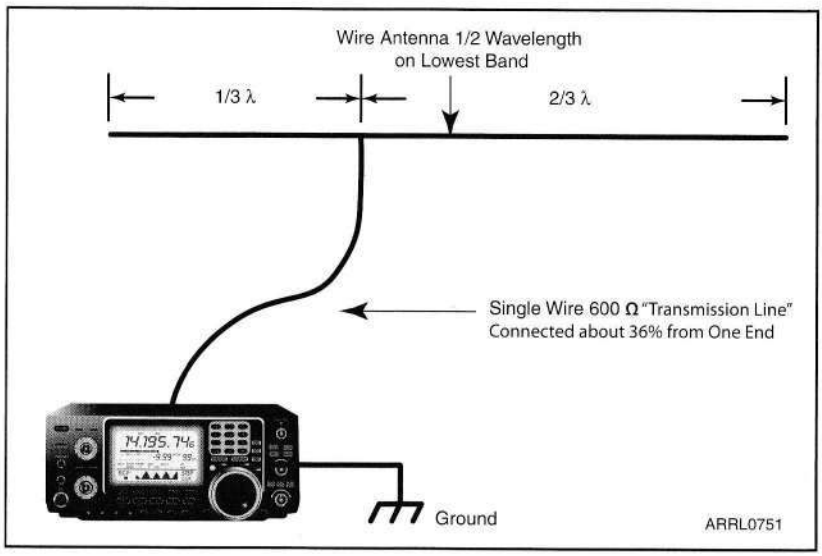

Figure 4.5 – The Windom antenna, c. 1929, used a single wire as a transmission line. There is controversy even today as to whether it really acts as a transmission line, or as a top-loaded vertical monopole.

SINGLE WIRE ISOLATED FROM GROUND

A popular multiband amateur antenna before World War II and continuing in popularity in different versions today is the Windom, as shown in **Figure 4.5**. It was described in detail in a 1929 *QST* article by L. G. Windom, based on work by others, and still carries his name.[1] The idea was that an antenna a half wavelength long on 80 meters could also be used on the other three HF bands of the time — 40, 20, and 10 meters.

However, there was a wide variation in the impedance at the center of such an antenna as the bands were changed. The solution was to feed it off center, at approximately one third of its length. The antenna would then provide a reasonable match to the line on all four bands.

The current in the "transmission line" has no direct return path to cancel its radiation, so it will radiate as well as (or perhaps better) than the antenna, depending on the band. In the typical configuration, this makes for a combination of vertically polarized radiation from the feed line and horizontally polarized radiation from the antenna. This may or may not be useful, depending on where the signal's desired destination is, but the RF at the bottom of the feed is almost never a good idea for the radio equipment or operators.

Recent Windom Implementations

More recently, Windom-type antennas have substituted high-impedance transmission lines for the single wire line. Some use a transformer at the antenna connection point to transform the impedance to 50 Ω for connection to coax. In both cases the lack of a balanced connection point at the antenna results in common mode current on the transmission line that will radiate. The coax-fed variety uses a choke at the bottom of the feed line to keep the current from the station. In both cases, the vertical section will radiate — commercial versions proclaim this as a selling point and have many happy users. One thing to keep in mind is that in Windom's day, we had four harmonically related bands. We still have those, but we've added five more, making an "all-band" antenna design even more of a challenge now than in 1929.

So while such a single wire may serve in some ways as a low-cost transmission line, and may have met the needs of early amateurs, it is not in the same category as lines in current use. It should thus be used with caution, if at all.

[1]L. Windom, W8GZ/W8ZG, "Notes on Ethereal Adornments — Practical Design Data for the Single-Wire-Fed Hertz Antenna," *QST*, Sep 1929, pp 19-23, 84.

Chapter 5

Let's Examine Balanced Transmission Line

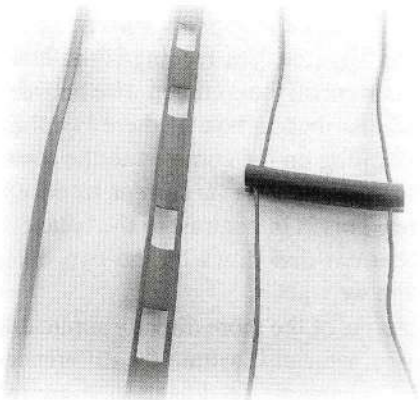

Three examples of balanced transmission line. From left, 300 Ω TV type twinlead, nominal 450 Ω "window" line and 600 Ω open-wire line.

In an unbalanced line of the type we have been discussing, the signal is applied between a conductor and a common conductor, often a shield or a ground plate. The voltage on the *hot* conductor is specified with respect to the common conductor. In a balanced line, there are two conductors, both at a potential with respect to ground. If properly balanced, both signals are of the same magnitude, but of opposite phase, so the total line voltage is twice the voltage of either with respect to ground.

This may be easier to grasp for those familiar with standard US household wiring. The transformer on the pole, which serves perhaps five houses, takes the multi kV distribution voltage and transforms it to 240 V ac. The secondary of the transformer has a center tap that is the *common* connection. The balanced pair and common are connected to the house, usually via a twisted wire cable. At the house end, the cable goes through a usage meter for billing purposes, then to the household distribution and circuit breaker or fuse box. The common connection is tied to the box frame, which is also tied to a ground connection at that point. Consider **Figure 5.1**, in which we portray the usual connectivity from the line to the primary ac distribution panel.

The two outer conductors are used to provide a balanced (with respect to common) 240 V feed for such heavy appliances as ovens, electric clothes dryers, or electric heating systems. Either outer conductor, fed with the common circuit, can be used to provide a 120 V unbalanced source for standard

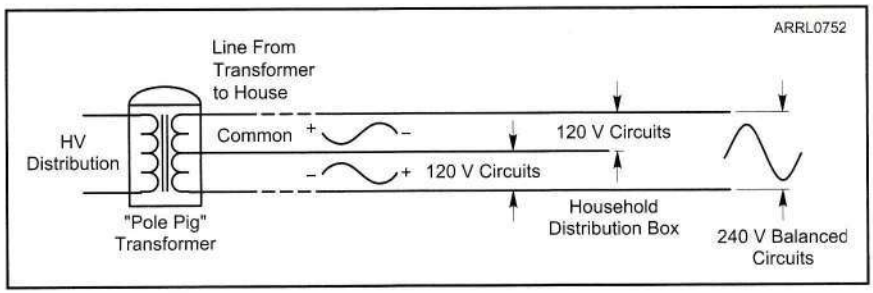

Figure 5.1 – Typical household ac power connectivity illustrates the concepts of balanced and unbalanced transmission lines. The 120 V circuits are unbalanced with a common return, while the 240 V circuits and their transmission system are balanced with respect to the common.

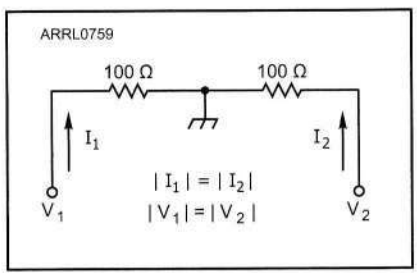

Figure 5.2 – Perfectly balanced load, where both the current and voltage on each side will be in balance.

wall outlets with the common serving as a return. This is exactly analogous to radio transmission lines. Note that while each 120 V circuit returns its current on the common wire, if the two sides are feeding equal loads there will be no net current on the common wire between the transformer and distribution box. If there is unbalance, the current returning on the common to the transformer is referred to as *common mode* current, a concept we will discuss later. This is in contrast to the balanced *differential mode* current that flows on the two outer wires — that's where we want it.

In terms of the more directly applicable radio uses, we can illustrate the differences as well. For example, feeding the non-ground end of two 100 Ω resistors (see **Figure 5.2**) that have the other end grounded will result in a balanced 200 Ω system. In such a case, the voltage on each side will be the same magnitude, but 180° out of phase. The magnitude of the currents on each side will also be the same, since the voltages and resistances are equal.

Note that the system would be balanced even without the ground connection. No current flows in the ground lead of the perfectly balanced system, so it could be removed without changing the operational properties. **Figure 5.3** shows two examples of inherently balanced antennas, one with a central ground

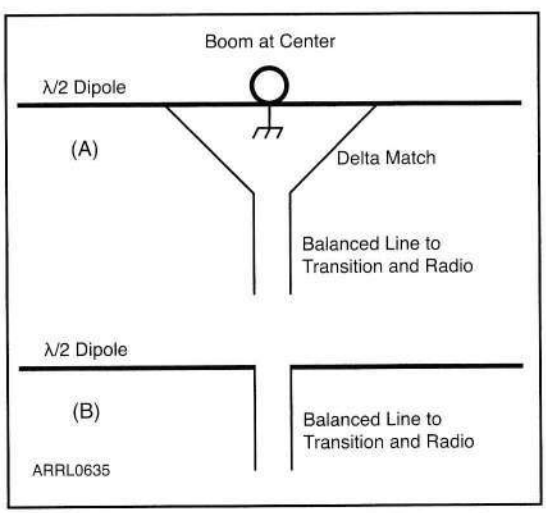

Figure 5.3 – Two examples of inherently balanced antennas, one (delta matched dipole) with a central ground (A) and one (split dipole) without (B).

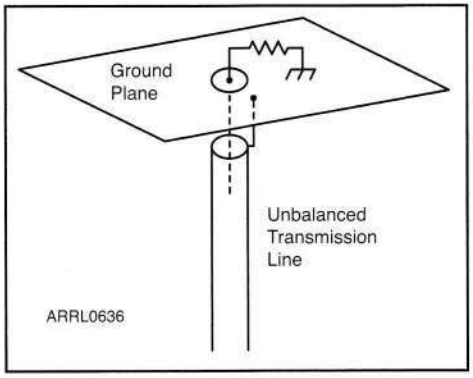

Figure 5.4 – Unbalanced resistive load. The signal is applied with reference to ground.

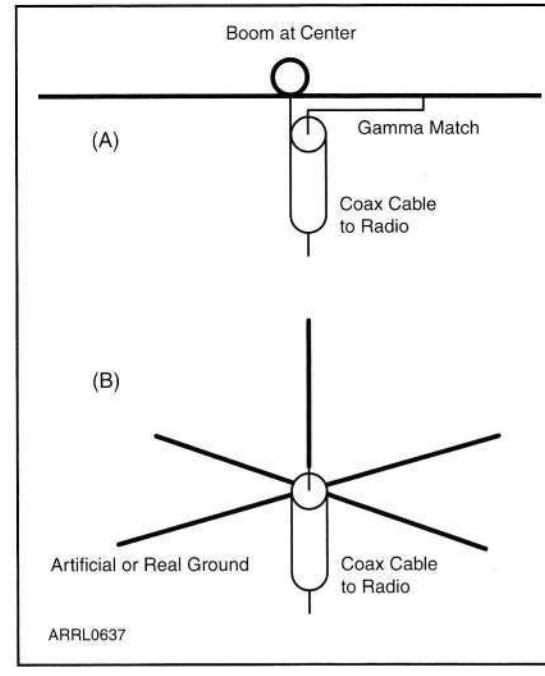

Figure 5.5 – Two examples of inherently unbalanced antennas, a gamma matched dipole at (A) and a vertical monopole at (B).

(A) and one without (B). The ground in the first is not actually necessary, but can be beneficial for lightning protection purposes. For both cases, some kind of transition is required to shift to an unbalanced system for connection to the radio. The types of transition will be the subject of a later chapter.

An unbalanced system, on the other hand, is fed with respect to ground. That is, one side of the load is at ground potential. **Figure 5.4** gives an example of an unbalanced resistive load, and **Figure 5.5** shows two antennas with inherently unbalanced feed points.

TYPES OF BALANCED LINE

Balanced transmission line is generally of relatively simple construction. Think two-wire lamp cord or speaker wire — both common examples of wire construction that could be used as balanced transmission line. Early receiving balanced line was typically a twisted pair of wires used to connect a dipole antenna to the commonly found balanced input of a receiving set of the time.

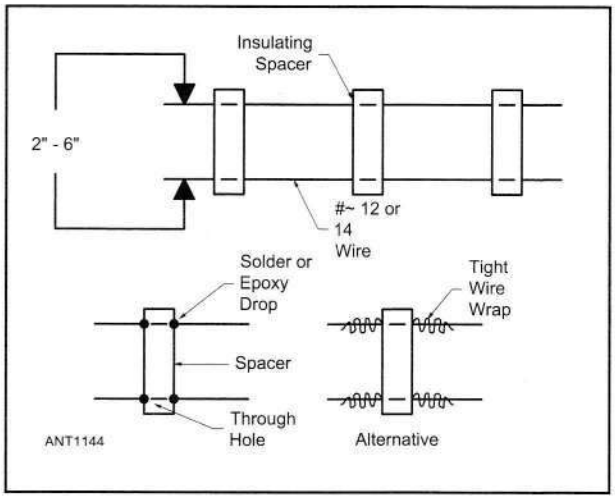

Figure 5.6 – Construction method of open-wire transmission line. Basically, just two parallel wires with a sufficient quantity of spacers to hold them apart.

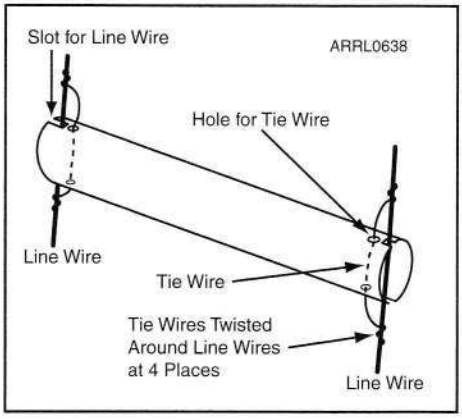

Figure 5.7 – Modern homemade open-wire line often uses PVC tubing as the insulating spacers. Easier fabrication is possible if the wires are in slots rather than being pulled through holes. The small tie wires run through holes to secure the line to the spacer.

For transmitting use, open-wire line was usually employed. It is still popular today for many applications and offers simplicity of construction, as shown in **Figures 5.6** and **5.7**. In the earliest days, the spacers were often made of wood that was boiled in paraffin to reduce the penetration of water. During World War II, and for some time after, porcelain spacers were made for the purpose. They are still ideal in many ways, but no longer in production.

Modern commercial balanced line is often made using a molded polyethylene web as both spacer and insulator. As shown in **Figure 5.8**, such line comes in several varieties. The twinlead types have continuous insulation, while the window line (also available in 300 Ω versions) has "windows" punched out periodically to make it almost equivalent to open-wire line. Twinlead at 300 Ω was originally developed as a transmission line for television reception, and was popular for connections to TV antennas until inexpensive low-loss coax overtook it in the marketplace

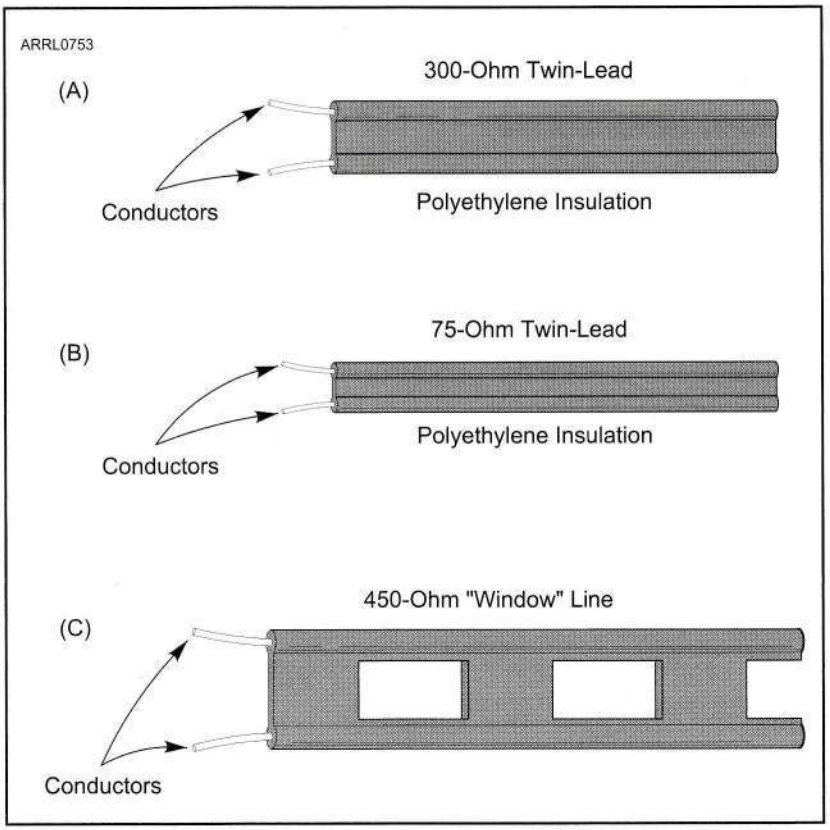

Figure 5.8 – Examples of balanced transmission line made with a molded polyethylene insulating webbing. Window line is made the same way, except that "windows" are punched out periodically to make the characteristics more similar to open-wire line.

in the 1970s. It is still available at electronic retailers, as are TV and FM antennas designed to use it. Open-wire line, constructed much like that shown in Figure 5.7, is available commercially as well.

There are a few varieties of shielded twinlead around as well. These have been in use for some time, first in military systems with various RG numbers, including RG-22 and RG-97 with a Z_0 of 95 Ω. Later, shielded 300 Ω twinlead was offered for TV antenna use in areas that would not be appropriate for usual balanced lines. Unfortunately, both have the advantages and disadvantages of unbalanced coax. They are easy to route through materials that would give problems to standard twinlead, but because of their construction, they also have loss characteristics similar to coax. If needed, a similar balanced transmission line can be fabricated from two coax cables,

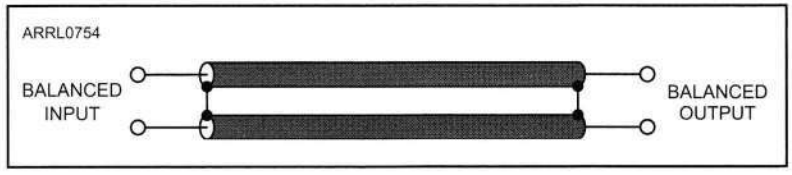

Figure 5.9 – Balanced transmission line made from two equal-length pieces of coax with shields tied together at each end. While it offers the installation flexibility of coax, it also has similar loss.

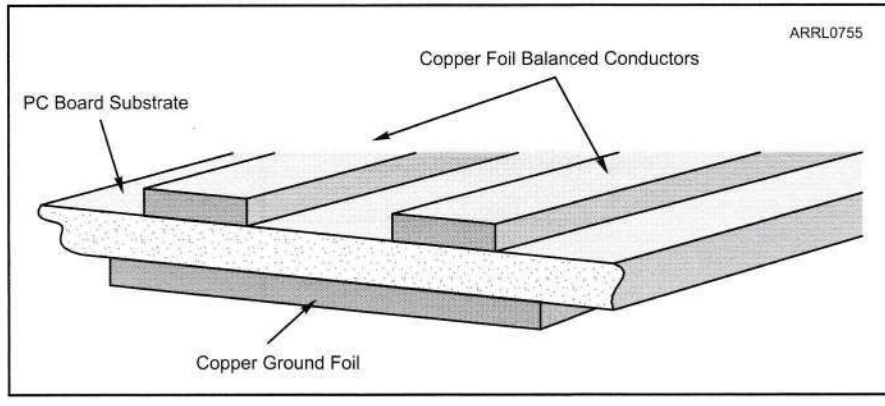

Figure 5.10 – Balanced microstrip line fabricated as part of a printed circuit.

as shown in **Figure 5.9**. The Z_0 is just twice the Z_0 of the individual cables. Note that if the shields are tied together at both ends, there will be no fields between the two cables, so they can even be run along different routes, as long as they are the same length. The loss will be the same as for coax.

Printed circuit board fabrication of stripline, or microstrip line, is also adaptable to balanced systems. The balanced microstrip line shown in **Figure 5.10** utilizes a balanced pair of conductors on the opposite side of the substrate from a ground foil to help contain the fields; however, a balanced pair on single-sided board is also possible.

THE BENEFITS OF BALANCED LINE

Balanced line has two primary benefits in comparison to coaxial cable. Most balanced lines, especially those with large portions of air dielectric, such as window line or ladder line, have a significantly lower loss than most coaxial cables.

Balanced line is often very conveniently connected to balanced antennas and is most often encountered in that application. It is also frequently found in very long runs from unbalanced antennas in which the losses (or

cost) of coax would be prohibitive. In that case, it may be worth the effort to transition from unbalanced to balanced near the antenna and then back to unbalanced at the radio end.

Most balanced line is relatively inexpensive when compared to coax — often an important consideration. Excellent homemade open-wire line can be fabricated at low cost from two rolls of wire (stranded works very well, particularly if subject to flexing) and insulators made from inexpensive household PVC tubing.

THE DOWNSIDES OF BALANCED LINE

As might be expected, there are downsides to balanced line. While coax cable, with its fields contained within the shield, can be rolled, buried (if it has a direct burial rating), or installed within or near pipes without impacting performance, this is not true of balanced line. With balanced line, the fields conveying the signal down the line exist in a region around the two lines several times the distance between them. This means that balanced line can't be placed on the ground, run in metal ducts, run through lossy material, or be rolled up without causing additional loss or change in characteristics.

FIELDS BETWEEN CONDUCTORS OF BALANCED LINE

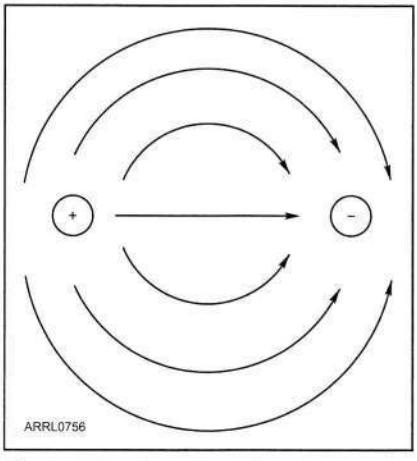

Figure 5.11 – Representation of the electric field between the conductors of balanced transmission line. The magnetic fields that surround each conductor are equal and of opposite sense if the currents are balanced.

The fields between the conductors of balanced lines are not constrained within a boundary, as is the case with coax. The strongest fields are in the space directly between the conductors, but the total fields between are similar to that shown in **Figure 5.11**. Outside the region between the conductors, the fields will tend to cancel in the plane at the center between and perpendicular to the wire axis. Coupling to other circuits will be strongest near either wire until the distance is large compared to the spacing. The coupling will be minimal for most purposes at a distance of two to three times the conductor spacing.

In the heyday of twinlead for TV use, tubular twinlead was popular for critical applications. This provided an elliptical cross-section of air space in the region between the conductors in an attempt to minimize losses in the region in which the fields are strongest.

While fields at a distance from balanced line are small, nearby fields can cause interference to other systems, particularly those interconnected by wiring.

In addition, balanced line run too close to computers and other potential RFI-generating systems can pick up interfering signals during reception.

ELECTRICAL CHARACTERISTICS OF BALANCED LINE

As with coax, a lumped circuit model of balanced transmission line can be generated based on the per unit electrical characteristics. A schematic diagram of the result is shown in **Figure 5.12**. According to Kraus, the per unit inductance of a balanced pair of similar wires removed from ground and with an air dielectric is:

$$L = 0.92 \times \log^{10} (D/r)\ \mu H/m, \text{ if } D>>r$$

Where D is the center-center spacing, and r is the radius of each conductor in the same units.[1]

The characteristic impedance, under the same conditions, is:

$$Z_0 = 276 \times \log^{10} (D/r)\ \Omega$$

Since Z_0 also equals $\sqrt{(L/C)}$, we can easily find the capacitance as $C = L/Z_0^2$.

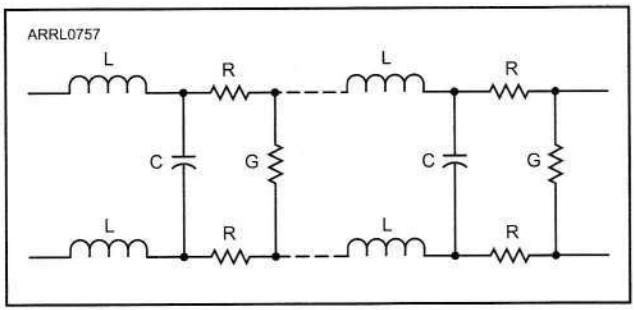

Figure 5.12 – Lumped element model of a balanced transmission line.

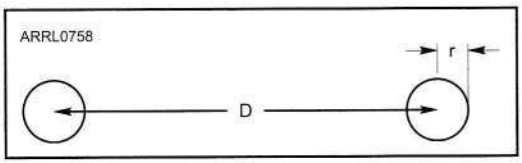

Figure 5.13 – Dimensions used to calculate transmission line parameters.

The series resistance is just the dc resistance of the wire at low frequencies, increasing at higher frequencies due to skin effect forcing current to the outer region of the conductors with corresponding reduction in effective surface area of the conductors.

The shunt conductance is the result of the losses in the dielectric. This is usually minimal in air dielectric line.

MATCHED LINE LOSS OF BALANCED LINES

The loss of matched balanced transmission line is provided in Table 3.1 in Chapter 3. It is worth making a note of the difference between the matched loss of coaxial cables shown in comparison to the losses of window line. Looking at the loss per 100 feet column of coax cable at 10 MHz, we note that most are in the range of 0.5 to 1.5 dB/100 feet. There are very large and very small cables outside this range, but typical matched loss

would be around 1 dB/100 feet. The balanced lines shown are in the range of 0.06 to 0.3 dB/100 feet, with window and open-wire line all in the 0.06 to 0.08 dB/100 foot range. At the 100 MHz point, the difference is perhaps even more striking. Flexible (non-hardline) coax, in the usual sizes, runs from around 1 dB to more than 5 dB/100 feet, while the window lines are all 0.3 dB/100 feet or less.

MISMATCHED LINE LOSS IN BALANCED LINES

The low matched loss results in dramatically lower total line loss for window line in comparison to the usual coax. Let's compare two lines with an SWR of 10:1. If we had 100 feet of coax with a 5 db loss (see Figure 3.8 in Chapter 3), we would add an additional 4 dB of loss due to the mismatch for a total of 9 dB. For window line with a matched loss of 0.3 dB, we would add only 0.95 dB, for a total of about 1.3 dB.

If we put 100 W of transmit power into the coax, at the far end we will have 12.6 W available to radiate from our antenna — a loss of 87.4 W in the transmission line as heat. With the window line, the antenna will get 74.1 W, a loss of 35.9 W in the transmission line. While 1 dB is usually just perceivable, 9 db can make a big difference.

This is the big strength of balanced line, particularly window and open-wire lines at HF where the matched loss is dramatically small. With window line, antenna systems can be designed to operate with high SWR, making it easy to cover multiple bands, for example. Coax, on the other hand, is generally limited to uses with an SWR of no more than 2 or 3:1 to avoid excessive loss. It is particularly noteworthy that the best window line generally costs less than even inexpensive coax.

POWER HANDLING CAPABILITY OF BALANCED LINE

Table 3.1 does not provide any information about the power rating of the various balanced lines. While the dielectric strength of polyethylene will be well into the megavolt per inch range, the line breakdown will likely be limited by the dielectric strength of air at most interfaces, about 76 kV/inch. The wire will also fuse at some current, around 82 A for #18 AWG copper wire.

Keep in mind that both the maximum voltage and current on the line will go up with the square root of the SWR, compared to what they would be for a matched line. As an example, consider a 450 Ω window line at 1500 W, the US amateur power limit. The voltage if matched would be:

$V = \sqrt{(Z_0 \times P)} = \sqrt{(450 \times 1500)} =$ 822 V, with a 100:1 SWR, a maximum

of 8222 V at some locations along the line.

The line current would be:

$I = \sqrt{(P / Z_0)} = \sqrt{(1500 / 450)} = 3.3$ A, with a 100:1 SWR, a maximum of 33 A at some locations along the line.

Neither of these quantities would be a problem for the physical characteristics of the line; however, the components to which they are connected in terminal equipment could be a very different story. Note that the maximum of one parameter in mismatched line will occur at the location along the line of the minimum of the other, with the maximums separated by ½ wavelength. Thus the maximums need not be encountered at all, and the line length can be designed to avoid maximums at sensitive locations, but only if the system will be used at a particular frequency. Multiband systems are likely to hit some maximum on some band.

[1]J. Kraus, W8JK (SK), *Electromagnetics*, McGraw-Hill Book Company, New York, 1953.

Chapter 6

Transmission Line Connectors

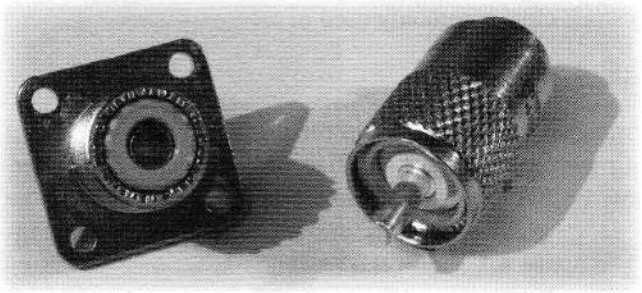

The popular "UHF" connector series is synonymous with "coax connector" for many, yet it is not always appropriate.

The most usual application of transmission lines is interconnecting different subsystems such as radios to antennas, interconnecting video systems or any functions that need to be interconnected in a well-defined way. A transmission line only becomes useful if the ends are properly prepared to interconnect with equipment at each end.

Generally, purchased equipment will include one side of the connector that the designer feels is appropriate for the application as part of the equipment. It is the responsibility of the systems integrator or installer to research the connector type and make sure the transmission line is terminated in a connector that will mate with the one on the equipment at each end to allow the connections to be made. Note that with different equipment types, the connector at each end of the cable may be different.

If you are designing the entire system, you have the flexibility to select the connector types as part of your design. It is important to select connectors that do not degrade system performance. This chapter will discuss the various connector types and their properties to help in that determination.

There are many types of connectors especially designed for termination of coaxial cables. These cables first came into widespread use in radio and video (radar screen data, for example) systems around the time of World War II due to the use of higher frequencies for communications and navigation systems for the military. In subsequent years there have been many new types developed for special purposes, some of which have come into general use.

"UHF" SERIES COAXIAL CONNECTORS

The UHF connector series was defined at a time when the "ultra high frequencies" meant anything above 30 MHz. Since we now consider VHF the range between 30 and 300 MHz and UHF from 300 to 3000 MHz, the designation is no longer appropriate, hence my use of quotation marks in the heading.

The first use of the UHF connector series was for broadband video systems such as radar signals. It allowed a termination of RG-8 sized coaxial cable into a continuously shielded interconnection across an interface. This was a significant improvement compared to the open screw terminals, binding posts, or Fahnestock clips commonly used in the prewar era.

The Basic UHF Connector Series

The connector consists of a center pin for the center conductor that plugs into a spring tensioned socket the size of a "banana" jack, surrounded by a screw-on backshell that provides the connection for the shield and holds the connection in place. **Figure 6.1** shows the basic elements of the system. The basic cable-terminating plug is still known by its World War II-era nomenclature, PL-259. The matching flange-type socket, nomenclature SO-239 (note difference in center digit), is normally used on the equipment side and mounts to a chassis or panel with four machine screws or other fasteners at the corners of the flange, which also serves as the shield termination.

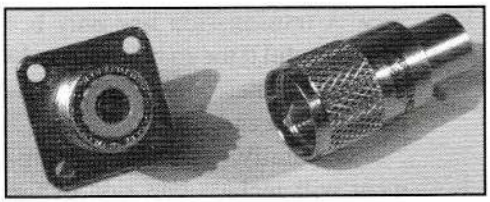

Figure 6.1 – The basic elements of the UHF coaxial connector series. A PL-259 UHF plug is on the right, with a mating SO-239 socket on the left.

The original PL-259 design called for the center conductor to be soldered to the inside of the hollow pin while the outer conductor or shield is soldered inside the outer shell through the holes provided. The inside of the outer shell of a PL-259 includes course threads that can help secure the cable jacket if tightly screwed in before soldering. **Figure 6.2** shows a typical application of a UHF connector pair.

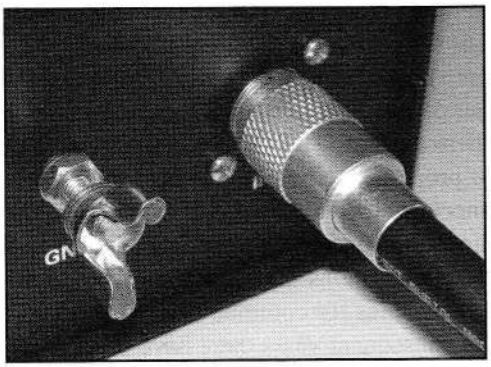

Figure 6.2 – A PL-259 plug attaches a cable to an SO-239 jack on a piece of equipment in the author's station.

Additional UHF Connector Types

Over the years there have been additional types of UHF connectors added to the series, some officially and some designed to meet particular needs.

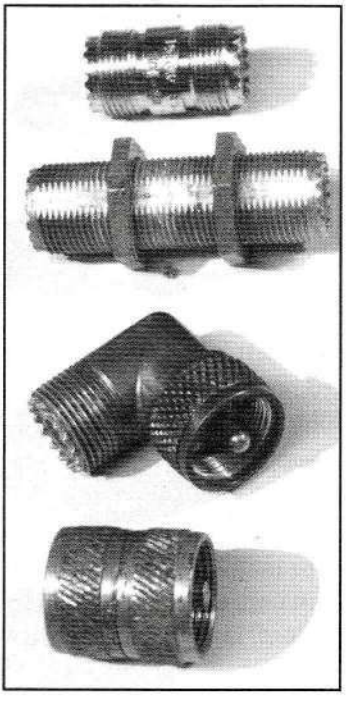

Figure 6.3 – Additional UHF series connector types. At the top is a PL-258 coax splice with an extended version below. Next is a UHF male-female elbow adapter that allows a change in cable direction — handy with heavy cables. At the bottom a double-male adapter.

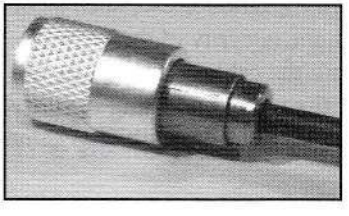

Figure 6.4 – A PL-259 with UG-175 reducer and an installed RG-58 cable.

Double Female Adapter: Probably the first was a double female adapter that allowed the interconnection of two male connectors, effectively splicing two cables together. This has a military designation of PL-258 and is shown at the top of **Figure 6.3**. Because of their shape, they are often referred to as *barrel* connectors. An unofficial expansion of the PL-258 concept is a somewhat similar double female connector that is made longer with a continuously threaded outer surface. These are usually provided with matching nuts (see one below the standard PL-258 in Figure 6.3) designed to secure them going through panels, partitions, or even walls. I have seen them up to 1 foot long.

Elbow Connectors: A male-female elbow connector (below the PL-258s in Figure 6.3) is often useful for changing a cable's angle of entry into equipment. This will allow a cable to hang straight down behind equipment without requiring a tight radius bend.

Double Male Adapter: Not surprisingly, double male adapters (shown at the bottom of Figure 6.3) are occasionally encountered as well, although the need to interconnect two pieces of equipment at close range is less common.

Reducing Adapters: The sizing of both the inside of the pin and the inside of the shell is just right for the 0.405 inch outside diameter of RG-8 or RG-11 and their inner conductors, or for their successor types of cables of similar size.

In many applications, it is desirable to use the smaller, more flexible RG-58 or RG-59 cables, especially for short patch cables. The shields of these cables are too small to be properly soldered to the inside of the PL-259 plug shell.

UHF connector adapters are available that screw into the back of the shell and provide a proper fit to the outer jacket of the smaller cable. The shield is then folded back over the adapter to appear at the plug solder holes. While the center conductor is also smaller, generally the pin can be filled with solder to complete the connection. The adapters, sometimes called reducers, are available in a number of sizes with the most common being the UG-175 for RG-58 size cables and UG-176 for RG-59 size cables including RG-8X. A UG-176 adapter with a PL-259 and an installed cable end are shown in **Figure 6.4**.

T Connectors: There are also triple-connector T connectors, sometimes with all three ports female, sometimes with the center port a male plug. These are useful for bridging cable

connections, but consider the implications of parallel impedances to the system SWR. Another variation that is frequently encountered is a jack with a threaded body that mounts through a panel hole much like half of the extended double female.

Jack Hood: In order to address the unshielded nature of the standard SO-239 panel jack, a special hood is also available that provides a solder connection to the shield and a shielded surrounding of the center conductor. While this can improve isolation, it exacerbates the Z_0 issue because of the changing outer conductor diameter of the hood's conical shape.

Jacks Without Flange: Jacks are available that mount into a single ⅝ inch diameter hole. The threads for the backshell are extended to the rear of the connector, and a shoulder is located on the panel side. It looks superficially like a PL-258, but has a center solder terminal.

Limitations of UHF Series Connectors

That the UHF connector is as popular as it is may be a testament to the power of being early on the scene. While it can be useful, it does have many limitations and weaknesses, none of which make it unsuitable, but all of them need to be taken into account. The major limitations, in my view, are listed below.

◆ The characteristic impedance of the connector itself is not the same as that of the usual coaxial cables with which it is used. The connector pair Z_0 is typically 30-40 Ω for perhaps an inch of length. While there actually are 36 Ω cables for which this would be a plus, they are rarely encountered. This results in an "impedance bump" that can cause a change in the impedance at the input to the system, depending on the electrical length.

The significance of this limitation will depend on how critical the cable impedance match, or SWR, is to the system operation. It is also true that it will be much more significant at frequencies with wavelengths above about 10 times that length or 10 inches. This corresponds to just above 1 GHz, within the UHF range. Many elect to use other connector series above 6 or 2 meters.

◆ UHF connectors are not waterproof. This is not usually a problem with their use indoors, but can be a serious problem for outdoor use, such as on antennas. Water not only causes problems with the integrity of the connector itself, but can also result in water migration into the cable. While water in a cable is never a good thing, it gets worse over time, often resulting in corrosion and contamination of the dielectric. This can result in additional cable loss over the years.

Fortunately, the connectors can be waterproofed using various tape-like products intended for the purpose. This is an extra step and one that impedes the connection and disconnection of outdoor equipment.

◆ The shield connection primarily occurs at the perpendicular surface between the two connectors, augmented by the backshell itself. The integrity of both aspects of this connection is dependent on the tightness of the backshell. In mobile systems, or others subject to vibration, this can result in loose, high resistance, or even disconnected shields over time. Such conditions result in excessive loss, noise, undesired coupling, and functionally the loss of all benefit of coax in the first place. Many recommend the use of pliers for an extra bit of torque, rather than just hand-tightening the backshells.

◆ Availability of low-quality products. While this is not a fault of the connector design, it is a fact that the UHF series is relatively easy to duplicate. It has also been around long enough so that there are many substandard UHF connectors in the marketplace, which may present the following issues:

- Inner conductor plug pins that are too narrow to accommodate RG-8 center conductors.
- Inner conductor plug pins or connector sockets that fall out of the body.
- Plug insulation that melts while soldering.
- Poor-quality metal parts, including insufficient or improper material plating.
- Jack spring fingers that lose tension after a few insertions.

The solution is simple — only buy products from manufacturers known to make high-quality products. The one that I know is always of high quality is Amphenol, although I'm sure there are others. All major Amateur Radio dealers offer Amphenol UHF connectors, and the prices are reasonable. I recommend avoiding electronic retail store house brands, as well as any connectors found at flea markets that don't show a known high-quality brand.

TYPE N COAXIAL CONNECTORS

The Type N connectors are of a similar size to their UHF counterpart, but these connectors are seriously designed for UHF operation. They were designed in the 1940s by Paul Neill of Bell Laboratories to overcome the limitations associated with the UHF type, particularly with respect to higher frequency operation. While originally specified to work well up to 1 GHz, they are routinely used at frequencies more than 10 times that high. The nomenclature is in appreciation of Neill's name.

The Basic Type N Connector Series

Only a very close look at a connected pair will indicate that it's not a UHF pair, however, once they are apart, the difference is clear. The biggest difference is that the shield interconnection is primarily made via a spring

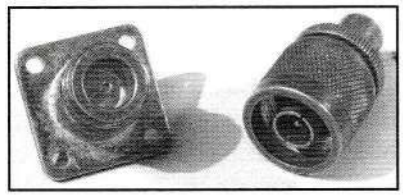

Figure 6.5 – A Type N connector pair — a good choice as an alternate in any application for which a UHF type would be used, but especially beneficial in the current UHF range or in wet conditions.

fingered sleeve surrounding the male pin that fits snugly into a matching cylinder in the female jack. This means the shield will be connected even if the backshell is loose.

A Type N connector pair is shown in **Figure 6.5**. The concentric shield connection on each side is evident in the photo. The size of the shield connection, the air space in between, and the mated pin/socket combination make for a constant-impedance, low-loss match.

There are two versions available; one with center pin and socket diameters that have a Z_0 of 50 Ω, generally used for RF work, and another at 75 Ω intended for video applications. The constant impedance avoids the impedance bump associated with the UHF series — the major frequency limiting factor of the UHF series. To put frosting on the cake, properly assembled Type N connectors are also waterproof.

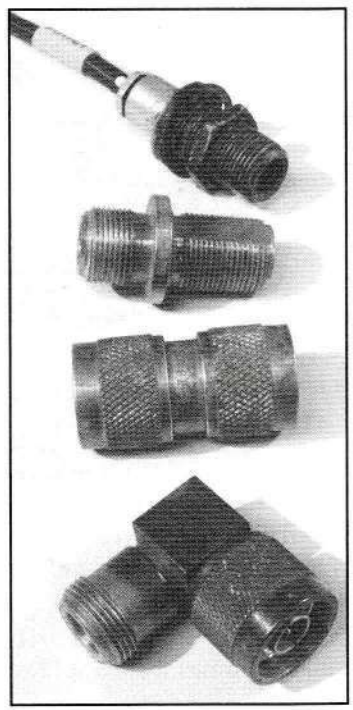

Figure 6.6 –Type N series connector variations. At the top, a Type N cable socket, below double female, double male and right angle adapters. Not shown — T adapters. All of the varieties of UHF connectors are also available in Type N.

As discussed detail in the *Coaxial Connector Assembly* chapter, the traditional Type N connector is assembled in a different manner than the soldered UHF type. A clamping arrangement is used to assemble the connector with the shield compressed between a washer and the shoulder of both sides of the connector. This avoids the melting cable dielectric insulation problem encountered with the soldering of shields to some kinds of connectors, but at a cost of requiring more careful measurement of trimming dimensions to make all the pieces come together in the right place. The only soldering required is of the low mass center conductor to its pin.

Other Varieties of Type N Connectors

Virtually all the different connector types described in the section under UHF connectors are also available for Type N connectors. A selection of Type N connectors is shown in **Figure 6.6**. In addition, the Type N series also offers a cable jack that looks like a cable plug, but is of opposite gender. This is significant because it allows the fabrication of extension cables that can be spliced together without the need for a barrel, or double female adapter. This is beneficial because each connector interface contributes to system loss and reduction of system reliability.

Limitations of Type N Connectors

Here we have a much shorter section than for UHF connectors. As with all connector types, there is a power limitation associated with the connectors, basically related to its physical dimensions.

Power Limits

The peak power is limited by the voltage breakdown across the air gap between the center pin and the shield connection, with a safe recommendation of at least 1000 V_{RMS} corresponding to a power level of 50 kW, while the average power is based on the heating of the conductors, limited by the current in the center pin. Skin effect concentrates the current in thinner and thinner outer regions of the pin as frequency increases, resulting in a typical average power rating around 5 kW at 20 MHz, decreasing with frequency to around 500 W at 2 GHz. Check the connector manufacturer's (as well as the cable manufacturer's) specifications if you expect to approach these limits.

Impedance Variation

This is a more insidious issue. The two different versions of the Type N connector have exactly the same size backshell and shield connection arrangement. The difference between them is strictly with the diameter of the center conductor, the 75 Ω version being thinner to result in a higher Z_0, as you would expect.

This means that a 75 Ω plug will mechanically fit into a 50 Ω Type N socket without difficulty. Unfortunately, it will not make a good contact. I am aware of one case in which the assembly alignment of the two was so perfect that it didn't make contact at all, leading to a lot of head-scratching.

The problem in the other direction is actually worse, in a way. Inserting a 50 Ω Type N plug into a 75 Ω socket will cause the center female socket to open further than it should. It will likely work in this situation, however, if a 75 Ω plug is ever inserted, it will no longer make good contact.

This problem is exacerbated by the fact that the connector types have no distinguishing marks to identify them. The only reason that this doesn't often come up is that the two varieties are generally used in different domains — 50 Ω in RF work — 75 Ω in video systems. Should you find yourself in a mixed environment — over-the-air television transmission comes to mind — I suggest adopting a color-coded or tagging standard for all Type N connectors so that this is less likely to happen. Better yet, select a different connector type for one or the other application.

Assembly Process

Some would consider it an advantage for UHF connectors that most experienced technicians can strip the outer and inner insulation and terminate a plug by eyeballing the dimensions, while the Type N requires careful measurement to assemble properly. Especially with full size cable, the Type N has an advantage in not needing soldering of the shield connection,

a time-consuming and failure-prone part of the operation. I would call it about even — but others will have their own opinion, especially if in the field without a rule or stripping guide.

BNC COAXIAL CONNECTORS

The BNC connector is perhaps the second most popular RF coaxial connector type in Amateur Radio circles. It was developed in 1951 and is related to the Type N, but has a smaller outer structure and a snap-on "bayonet" mount rather than the screw-on backshell of the Type N and UHF (see **Figure 6.7**). Its size is a perfect fit for the smaller (RG-58/59/8X) cables, although versions are available for smaller (e.g. RG-174) and larger (e.g. RG-8) sized cables.

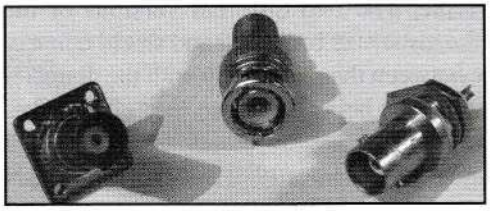

Figure 6.7 – The basic elements of the BNC coaxial connector series. On the left is a BNC flange mounting jack. On the right is a BNC through-hole mount jack and in the middle, a plug.

The connector was invented by Paul Neill of Bell Laboratories (of Type N fame) and Carl Concelman (inverter of the Type C connector, below) of Amphenol. BNC stands for Bayonet — Neill — Concelman. The flexibility of the small cables and the easy to attach mechanism of the bayonet backshell, make BNC cables ideal for patch panel use.

When originally designed, the connector was just made to match 50 Ω systems — in fact the inner pin and shield connecting portion is the same size as that of the Type N (in fact, a Type N plug can be inserted into a BNC socket). Later a 75 Ω version was added, although the 50 Ω is much more frequently encountered. So now there are both 50 and 75 Ω versions of the BNC connector. However, this time they were cleverly designed to be interchangeable without destruction or connectivity issues.

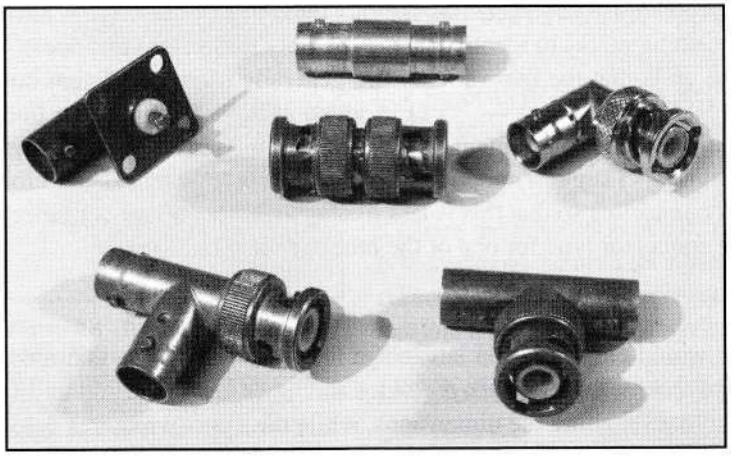

Figure 6.8 – Additional BNC series connector types. All the usual suspects are available.

The ratings of the BNC are quite similar to those of the Type N, since it has the same electrical dimensions, although its shielding is

somewhat less effective so its upper frequency limit is around 2 GHz. In fact, the voltage rating may be higher because an insulating sleeve surrounds the center pin, making for a longer air path between conductors. All of the usual variations and special fittings for other connector types are available for the BNC (see **Figure 6.8**)

RCA CONNECTORS

The RCA connector, sometimes called a *phono* (for phonograph, an early music playback system) connector is probably more frequently encountered than any other type in Amateur Radio equipment because it is used for many other purposes besides terminating coaxial cables.

This connector was initially developed as an audio connector by the Radio Corporation of America to connect phonographs to amplifiers. Its structure is inherently coaxial with some jack configurations designed to ground shield connections directly to panels, so it has appeared as an RF connector as well. It is most frequently encountered as a receive antenna connector, especially in lower-priced equipment. As a transmit RF connector, it generally is found at power levels of 100 W or less, also in lower-priced gear.

A notable exception is the series of high-end Collins Radio SSB transmitters, receivers, and transceivers introduced in the late 1950s. These used RCA connectors for audio and RF interconnections. This highlights one aspect of this connector series — they are made in many forms. The RCA jacks on the Collins gear were of very high quality, using ceramic dielectric insulators. Some have been described as "RF rated" — a noble thought, but by no means a standard designation. Most usually encountered RCA connectors are not as well fabricated, but they can do the job if carefully selected and properly installed. A selection of different types is shown in **Figure 6.9**.

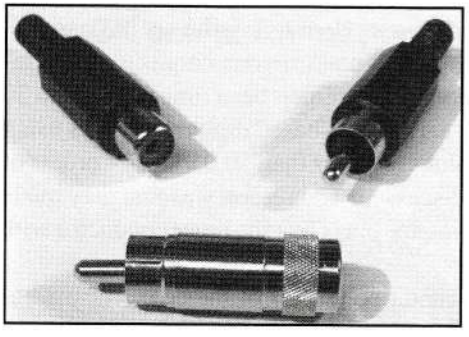

Figure 6.9 – Examples of RCA connectors. The plug at the bottom has a shielded backshell, more suited for RF use.

Unlike any of the previously described coaxial connectors, the RCA pair has no mechanical locking mechanism to retain the connections if subject to any pull on the cable. Since the BNC is similar in size, it may be a good alternative if that is likely to be an issue.

Since RCA connectors are so ubiquitous, it is worth mentioning that they are not, in my opinion, a very good choice for power interconnections. I have what is otherwise high-quality equipment that has RCA connectors as power accessory sockets and companion equipment with a panel jack designed to

accept 12 V dc from an RCA plug. Of course if the equipment is on while making this connection, as soon as the pin strays to the outer conductor on insertion, it blows a fuse deep in the source equipment.

OTHER COAXIAL CONNECTORS

While the connectors described in the earlier sections are those most frequently encountered as coaxial cable terminations, there are many other types that will be encountered from time to time. I think it's worth a bit of ink to let you know something about them.

SMA Coaxial Connectors

SMA connectors — short for *sub-miniature type A* — are found on a significant number of handheld transceivers as antenna connections (see **Figure 6.10**). These small threaded coax connectors are designed for operation well into the microwave region — typically to 13 GHz, but some varieties go much higher. Outside of amateur handheld antennas, they are mostly found used as interconnections between chassis of microwave equipment, often on the ends of miniature semi-rigid coax.

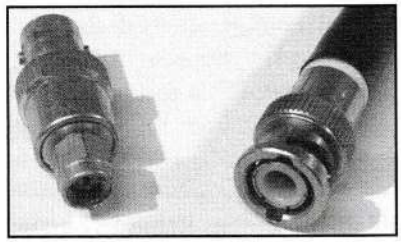

Figure 6.10 – A handheld transceiver BNC connected antenna compared to an SMA connector.

Their electrical properties are quite suitable for amateur handheld antennas, however, they are typically rated for 500 to 600 connect-disconnect cycles, so care should be taken with their mechanical properties. The alternate connector in this application is the BNC, which is my preference for a number of reasons, especially durability. An SMA handheld antenna is shown in Figure 6.10.

Type F Coaxial Connectors

Anyone who has ever hooked up a modern television set has encountered the Type F connector. This is a great mass-market connector — as inexpensive as possible for millions of users. I remember a time (more than 30 years ago when I was working on early cable-based digital networks using cable TV components) when the plugs cost less than $0.05/unit — orders of magnitude less than some we've discussed. The reason was that they made large quantities and the center conductor pin is just the inner conductor wire of the coax (see **Figure 6.11**).

With a center pin that is the center conductor of the coax, the assembly is trivial. The cable is stripped — fancy tools that do it in one step are available — the shield is crimped to the outer conductor shell of the connector (while soldering is possible with some varieties, anyone using these

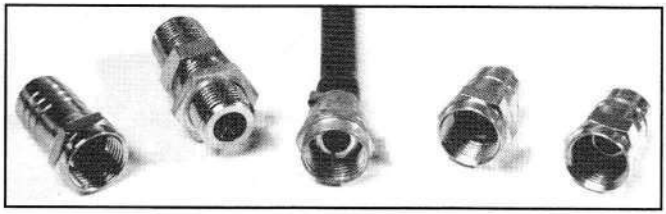

Figure 6.11 – Examples of Type F connectors as used in cable TV installations.

frequently uses a crimp tool), and you're done. The disadvantage is that the inner conductor must be solid wire and that it has no corrosion resistance. Special waterproof versions are available for outdoor use.

Type F connectors are not often encountered in Amateur Radio, with one notable and worthwhile exception. TV-type coax cable, often described as RG-6 type but made with aluminum foil shields, is actually pretty good coax. Modern cable TV systems operate well into the UHF range, so they are designed for low loss. They are often available at low cost, or even prewired within a house begging to be used for amateur antenna access. The problem is that most connectors of the type used in Amateur Radio can't deal with connections to the aluminum foil shield. Often the best approach is to either use the F connectors on the cable, or crimp some on and then use between series adapters (see below) to transition to the connector that will mate with your termination.

TNC Coaxial Connector

The TNC (Threaded — Neill — Concelman) is essentially a BNC with a threaded rather than a bayonet backshell. It thus is essentially a smaller Type N connector, but with the inner connecting surfaces the same size. It extends the 2 GHz frequency limit of the BNC up to 10 GHz or higher, and takes less panel space. It is a natural for heavy duty requirements with smaller cables.

Type C Coaxial Connector

This connector, honoring just Concelman, is essentially a TNC for larger cables. It is about the size of a Type N, but with a bayonet backshell and larger diameter inner components. It would seem to be a natural for patch panels for those running high power, but it has never caught on in the amateur community, that I'm aware of. In fact I hardly see them anywhere, which is too bad.

Motorola Connectors

These are the coaxial connectors designed and almost exclusively used to connect automotive antennas to automotive broadcast radios (see

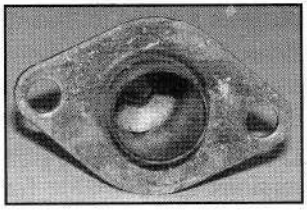

Figure 6.12 – A Motorola jack. These are commonly used in automotive broadcast receivers as antenna connectors.

Figure 6.12). They became popular for amateur use in the 1950s, at which time most HF voice used full carrier amplitude modulation. A number of companies offered tunable converters, designed for steering-column mounting, that translated amateur HF signals to the upper broadcast band.

The auto antenna, with its Motorola connector, plugged into the converter and a patch cable went from the converter to the antenna jack of broadcast radio. Usually, each had a Motorola connector. Apparently because of the converter connection, I have seen these connectors also used in home station VHF converters.

Type HN Coaxial Connector

The Type HN connector is similar in design and layout to the Type N, but is a bit larger. It has higher voltage breakdown and power ratings than the type N. It is a good match to the cables that are somewhat larger than RG-8 size and finds some amateur use in high power stations with long cable runs.

General Radio Connectors

The General Radio type 874 or GR connector is most frequently seen on test equipment made by that company, later GenRad through the 1970s. It is still popular in university physics and engineering laboratories because it is unique (to my knowledge) as a genderless coaxial connector. Both the inner and outer connection arrangements are made of four spring leaves in two pairs, with one pair of each separated further than the other (see **Figure 6.13**). In this way, by rotating 90 degrees, any two connectors can be mated resulting in a solid, matched connection without the need for gender converters (see **Figure 6.14**). The downside is that there is no locking arrangement, so it's not particularly suitable for long-term connections, but it's perfect for lab use.

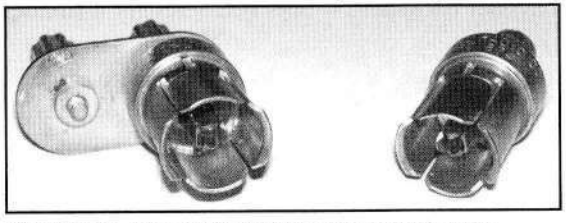

Figure 6.13 – The GR-874 genderless coaxial cable connector — popular for use with laboratory test equipment for many years.

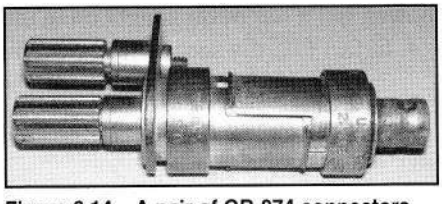

Figure 6.14 – A pair of GR-874 connectors mated.

Between Series Adapters

Virtually every coax connector type of either gender is available in a short adapter with a connector of every other type. These adapters allow equipment with one type of coax connector to be attached to cables

Figure 6.15 – Representative example of coaxial between series adapters.

terminated with another type. A collection of representative examples is shown in **Figure 6.15**.

These are best used for temporary test or measurement applications, although some find use in long-term applications. Every additional part, especially connectors, reduces the overall system reliability by adding another potential failure point.

There are a few exceptions, in my opinion, to this rule. One is that some equipment supplied with UHF jacks makes use of lower-cost parts in which the fingers give out quickly. While the best solution is to replace them with higher-quality units, sometimes that is not feasible and will likely void any equipment warranty. An adapter with a UHF plug and Type N socket is perfect for this situation, especially if the cable can be equipped with a Type N plug. This works best if done before the spring contacts get limp.

BALANCED LINE INTERCONNECTIONS

Considering how much longer balanced transmission line has been in use than coaxial cable, you might think there would be at least as many choices of connector. As it happens, that's not the case, but a few standards have evolved over the years.

Screw Terminals — Most Amateur Radio equipment designed for balanced transmission line offered screw terminals, as did most television receivers until the shift to coaxial cable interconnection made TV twinlead almost obsolete.

Screw terminals have the advantage of being nearly universal, in that virtually any reasonably sized wire size can fit under the screw head and may stay in place and not short during tightening. Still, the connection is not a terribly reliable one.

Most amateur receivers actually had three screw terminals. Two were for a balanced antenna, the third was a chassis ground (see **Figure 6.16**). The chassis ground should be connected to the power system safety ground, since many receivers had two-wire ac plugs. If an unbalanced antenna were

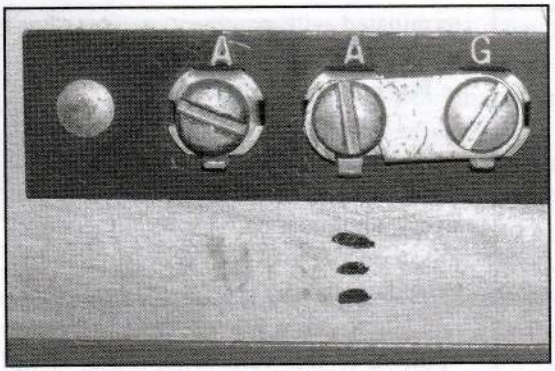

Figure 6.16 – Terminal strip on a 1950s communication receiver. There are two terminals for a balanced transmission line. If an unbalanced antenna is used, the ground terminal is jumpered to one of the antenna terminals as shown.

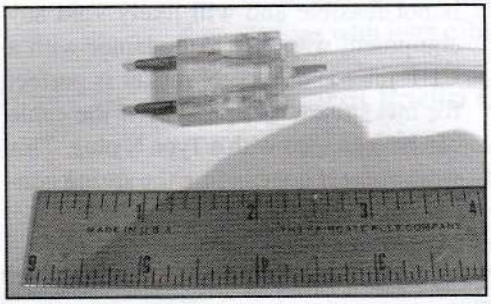

Figure 6.17 – A plug designed to terminate 300 Ω TV type twinlead.

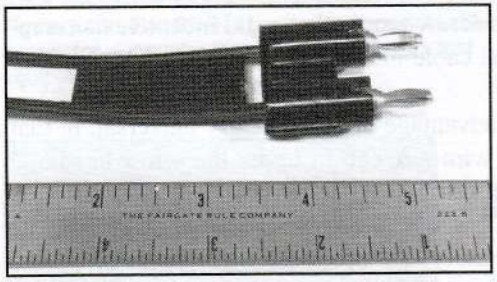

Figure 6.18 – The double banana plug, designed for low frequency balanced test equipment. It is a great fit with 450 Ω window line.

used, the ground should also be jumpered to one of the antenna connections, sometimes a link was provided for the purpose.

While wires under screw heads can be particularly unreliable, in my experience, a better solution is available in the use of crimped or soldered spade lugs under the screw terminals.

TV Twinlead Connectors

There actually was a type of connector especially designed for use with TV type 300 Ω twinlead (see **Figure 6.17**). For some reason, it never became popular for use with TV receivers, but was encountered in some peripheral equipment, such as UHF converters, before they were required to be included. The plug had two 0.093 inch soldered pins spaced at 0.486 inches. This is the same spacing as the pins of an FT-243 crystal holder, so would fit into a crystal socket, or two pins (with one in between) of an octal tube socket.

Double Banana Plug and Jack

A connector type that is not especially designed for the purpose is the double banana plug. A banana plug is a robust spring loaded plug of a size that happens to fit nicely into the center conductor of a UHF socket. A popular test equipment connectivity arrangement is two banana plugs within a common insulating housing spaced 0.75 inches (see **Figure 6.18**). This spacing is very convenient for use with most window-type transmission line.

Jacks are available in various forms, including panel mounting types and even combination plug and jack sets that also have screw terminals to clamp wire leads. Another handy arrangement is a kind of terminal that is sometimes called a "five-in-one." This mounts through a single hole into a panel and has a banana socket surrounded

Figure 6.19 – A five-in-one terminal accepts a banana plug, loose wire, or terminal lugs. If two are spaced at 0.75 inches, they will also accept the handy double banana plug.

by a nut arrangement that surrounds a threaded surface that includes a hole for wire or tip insertion. Thus it can accept a banana plug, a spade lug, a wire bent around the threads or a wire pushed through the perpendicular hole. If two are installed on ¾ inch centers, it will also accept the double banana plug, but can deal with loose wire ends, or lugs as well (see **Figure 6.19**).

Notes

[1]J. Kraus, W8JK (SK), *Electromagnetics*, McGraw-Hill Book Company, New York, 1953.

Chapter 7

Installing Coaxial Connectors on Cable

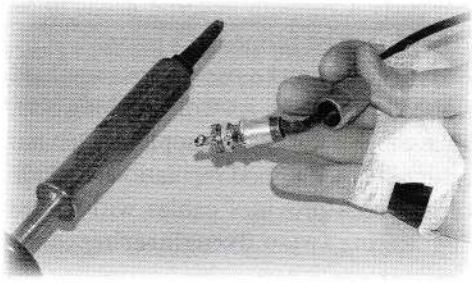

No coaxial cable run is any better than the installation of the connectors on its ends. Connector installation takes care and attention, but need not result in a trip to the emergency room.

The installation of transmission line connectors is looked on by some with dread, since it is both important and requires special care and moderate precision in order to do the job properly. Of course, any connector installation will be no better than the quality of the connector being used. Connector failures are surely the leading cause of problems with coax cables, although there are certainly other ways to ruin a coax run.

Standard or Crimp Connectors?

The "standard" coaxial cable designs are generally assembled by soldering. In the case of the PL-259 UHF plug, both the center conductor and shield are soldered, while standard Type N, BNC, and TNC connectors have a center pin that must be soldered and an integral tightened clamp for shield connection. TheType F television coax connector is a bit different. The center conductor of the coax is used directly as the center pin, while the shield is almost always crimped.

Alternative connector types are available in each series that use crimping for connection. In many cases, both the center conductor and shield are crimped, while some have a crimped shield and soldered inner conductor. I have seen no evidence that a crimped connector is inferior to a soldered one. With either type, poor assembly practices can yield poor results.

The issue with crimped connectors is that they require a crimping tool that is matched to the sizes of the crimped surfaces. Most quality crimping tools are relatively expensive and fit a limited series of cables and connectors. Some have dies that include multiple sizes of crimping holes, making

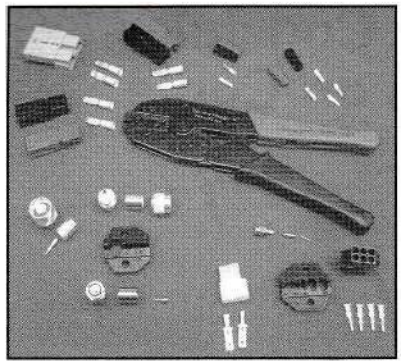

Figure 7.1 — The Andy-Crimp Pro™ tool, showing some of the available interchangeable dies along with a sampling of the different coax and power connectors that it can crimp with the right dies.

them more useful. The Andy-Crimp Pro™ tool — available from High Sierra Antennas (**www.hamcq.com**) or Quicksilver Radio (**www.qsradio.com**) — has available interchangeable dies that will also fit in other similar tools, such as the Powerpole crimper sold by West Mountain Radio (**www.westmountainradio.com**). In addition to the two die sets available for coax connections, there are sets available for the multiple sizes of popular Anderson Powerpole dc power connectors, and another set for Molex connectors and other crimp terminals (see **Figure 7.1**).

The crimping process is very effective if the proper tools and connectors that match the cable are all at hand. Some vendors have offered crimping arrangements for standard connectors, but these can result in fractures of the solid connector body. Crimping material needs to be pliable enough to be able to be formed in a press.

Another possibility is to make use of preassembled coaxial cables with the connectors already installed. As with anything else, the quality will vary depending on the capabilities of the supplier, often but not always indicated by the price. Suppliers with good reputations include ABR Industries (**www.abrind.com**), which provides cables with either UHF or N connectors, and DX Engineering (**www.dxengineering.com**), which provides cables with UHF connectors. These cable assemblies are available in different lengths and made from different types of cable, for a cost that is not much higher than the cost of the cable plus the connectors if you were to make them yourself. Both offer custom lengths and free shipping if a sufficient quantity is ordered.

The sections that follow will focus on installing standard coaxial connectors, with the exception of one representative sample of an Amphenol crimp-type UHF plug. If you decide to use crimp-type connectors and associated tools, the manufacturer should provide the cable and connector specific trimming dimensions. While the crimp diameters have moved toward industry standards, the details, especially of ferrule length, may result in different stripping lengths. Look at the website of LNL Distributors (**www.lnl.com/howto.htm**) to see some representative examples.

INSTALLING UHF SERIES COAXIAL CONNECTORS

UHF series connectors include cable-mounted plugs (the PL-259 type is the original pattern, although there have been others through the years) and chassis-mounted sockets (the SO-239 — note the difference in the center digit — being the standard type, although there are others here as well).

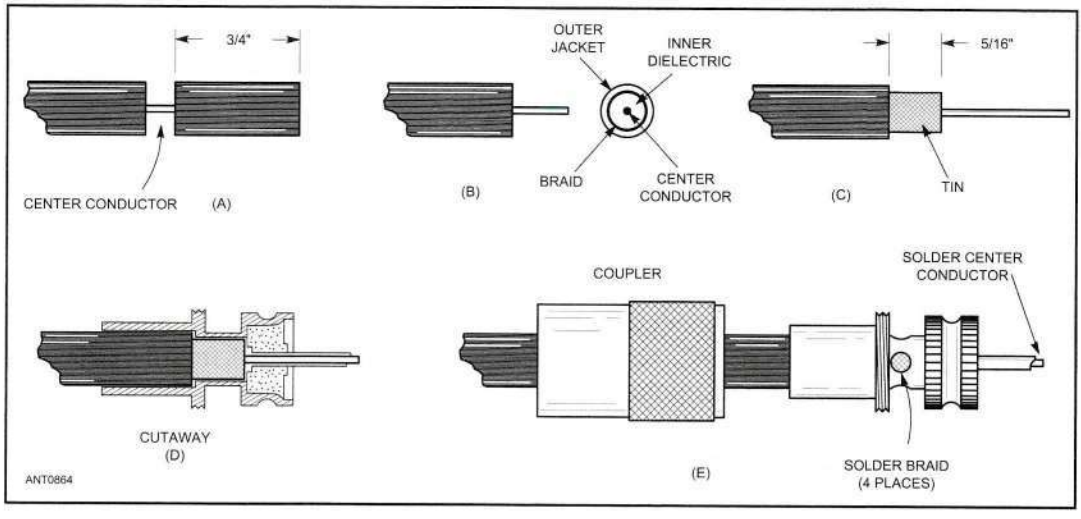

Figure 7.2 — The PL-259 or UHF plug is the most popular coax connector in Amateur Radio. Here the steps required for installation on RG-8/11/213 size (0.405-inch outer diameter) are shown. See the main text for a description of each step.

Most of the problems people have assembling these are with the plugs, so we'll start there.

UHF Plugs with Standard Cable

The standard PL-259 plug is designed to fit the common larger sizes of coax, such as RG-8, 11, 213 and RG-214, with an outer diameter of 0.405 inches. Note that this includes both 50 and 75 Ω types. Adapters are available for smaller cable types, discussed below. The installation of such coax into a PL-259 is illustrated in **Figure 7.2**.

In Step (A), the coax is stripped through the outer jacket, shield, and dielectric down to the center conductor starting ¾ of an inch back from the end, as shown. The hard part is cutting through all those layers and not also cutting some of the center conductor strands. This looks easier than it is with normal hand tools, but it is dramatically easier using a special tool. One by Ripley Brothers, the Cablematic UT-8000, works like a handheld pencil sharpener and makes a remarkably clean and straight cut.

By using a sharp knife, and going slow with a lot of patience, it is possible to work your way through the layers. Special tools are available that make this quite easy. It is also possible to use a tubing cutter with a sharp blade, at least to get through the outer jacket. Often, by the time you get all of that off, you will find that you have lost a strand or two of the center

conductor. The purist would start over; you may decide to define your own quality control standard and decide to allow the loss of a strand, as it will not make much difference in the scope of things. (The perfectionist will certainly start over; it's always a good idea — one of many reasons to start with a somewhat longer cable than you think you might need.)

As shown in (B), remove the cut pieces together, if possible. Sometimes a bit of a tug with electricians' pliers is helpful. Once all of the dielectric is removed, carefully check, with a magnifier if needed, to make sure that there are no strands of the shield hanging about and that the center conductor strands aren't nicked.

In step (C), score the outer jacket 5/16 of an inch back from the earlier cut without nicking the shield, and remove that section of the jacket. Sometimes a longitudinal cut from the score to the end makes it a bit easier to remove. Now *very lightly* tin the exposed shield. This is a very tricky step since:

- The shield has to be hot enough for the solder to flow into the wires without melting the dielectric. This is a particular challenge with foam dielectric type cables.
- The tinned shield needs to be almost the width of an untinned tightly woven shield in order to fit inside the barrel of the connector. This is a difficult step, since once the solder flows, it tends to wick into the shield. Recheck for any loose strands of shield that could short out the cable later. Some installers prefer to lightly tin the center conductor; this is not a bad idea, but also needs to be done sparingly to make sure the center conductor still fits within the pin. This can be checked from the pin side of the connector.

Now slide the coupling ring onto the cable, making sure that it is oriented in the proper direction. If doing both ends of the cable, this step can be delayed until the second end — just don't forget to do it. There is almost nothing less useful than a PL-259 without a coupling ring (or perhaps even worse, one remembered but installed backwards).

In step (D), the coax cable is inserted into the body of the connector. Again, check that the coupling ring hasn't fallen off. The connector should be installed with a clockwise turning motion in order that the threaded portion of the body screws onto the outer jacket. This can be a bit of an effort. Sometimes inserting the connector into the jack of a T connector will provide additional purchase, if the sharp points are engaged. Alternately, there are tools available, such as the DX Engineering UT-80P, that provide a good grip without chewing up the connector with pliers. The connector is on far enough if the center conductor is protruding from the pin and the shield is beyond the four solder holes. Recheck that the coupling ring is still there and oriented properly — this is your last chance for an easy correction.

Step (E) is the last part of the assembly process — soldering everything in place. First, support the cable and connector solidly, preferably in a way that doesn't draw off the heat from the connector body. Make sure that the cable weight is not pulling it downward, or else the heat from soldering will allow the dielectric to melt and the inner conductor to migrate through.

Use a heavy soldering iron of at least 150 W with a tip that will fit into the groove containing the solder holes. Since heat flows upward by convection, apply the iron to the bottom of the area and start flowing the solder into the top hole when the braid reaches melting temperature. Continue with the other holes, turning the cable carefully to reach the bottom hole. Let the cable and connector cool significantly before moving to the next step.

Check that the cable is not shorted by checking the resistance between the connector body and the inner conductor protruding from the pin. It should indicate infinite resistance, unless there is something providing connectivity at the far end. Now insert the connector in the vise with the open end of the pin pointing below the horizontal. Apply the soldering iron to the outside of the pin and gently apply solder to the junction of the center conductor and pin until it fills the void. When heated, the solder will flow between the inside of the pin and the center conductor by capillary action. If the pin were pointed the other way, it would flow down the outside of the pin and make it too thick it fit.

Let it cool and recheck the resistance. Trim the center conductor flush with the center pin and use a fine-tooth file to remove any solder from the outside of the pin. You're finally done — congratulations!

Another Opinion

Noted Amateur Radio contester Tim Duffy, K3LR, operator of one of the major multi-multi (multiple operator, multiple simultaneous transmitter) contest stations in the US, has another approach to assembling PL-259 plugs with the larger size cable, which he credits to William Maxson, N4AR. Tim has assembled an extreme antenna farm, visible from US Route 80 in Western Pennsylvania, and has terminated more coax cables than most people. Space considerations don't allow inclusion of all of his material, which can be seen on his website at **www.k3lr.com/engineering/pl259/**.

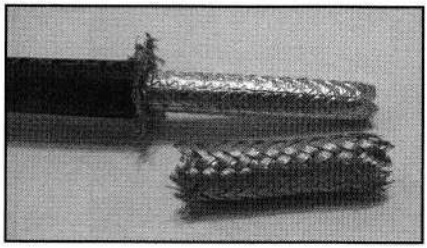

Figure 7.3 — After removing the outer jacket with a sharp knife, Tim carefully removes all but about ¼ inch of braid and fans out the remainder. [ROBERT BASTONE, WC3O]

Tim first measures a connector against the RG-8 or other 0.405-inch cable and removes just the outer jacket with a sharp knife. He then pulls the braid back all the way by fanning it out (as shown in **Figure 7.3**) and

wraps three to four turns of Scotch brand 88 black electrical tape around the dielectric up against the fanned-out braid (**Figure 7.4**). Using wire strippers, he removes the remaining dielectric from the center conductor (**Figure 7.5**). Then he installs the fully assembled PL-259 onto the center conductor and over the 88 tape. The back of the PL-259 body should rest on the fanned-out shield. He then solders the center conductor.

This done, he fans out the shield and cuts it to ¼-inch long and folds it over the back of the PL-259 (**Figure 7.6**). He solders the shield all the way around to the back of the PL-259 body. While the back is still hot, he wraps two turns of 88 electrical tape around the soldered shield to seal it all (**Figure 7.7**).

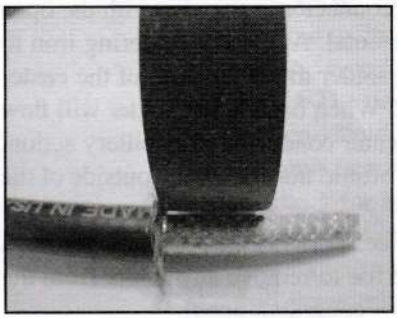

Figure 7.4 — Tim wraps three to four turns of electrical tape around the dielectric up against the fanned-out braid. [ROBERT BASTONE, WC3O]

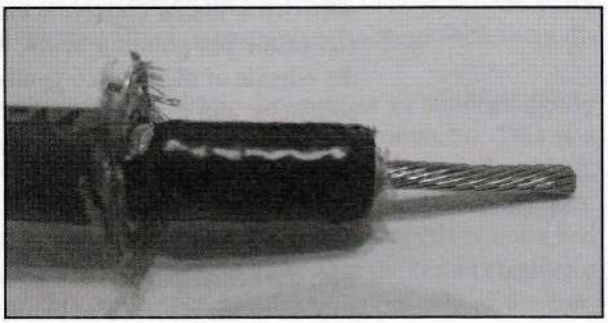

Figure 7.5 — The dielectric around the center conductor is removed from the area in front of the tape. [ROBERT BASTONE, WC3O]

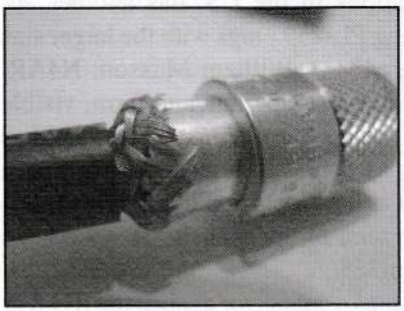

Figure 7.6 — Tim screws the connector onto the cable until it is fully seated, trims the shield, and solders the center conductor. [ROBERT BASTONE, WC3O]

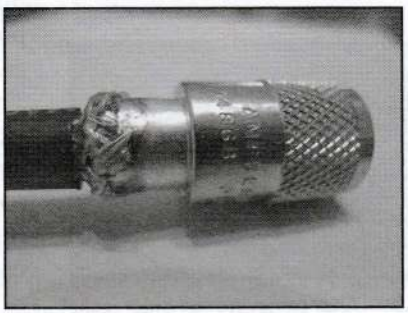

Figure 7.7 — The shield is soldered to the outside of the rear of the connector body and will be wrapped with tape while still warm to provide a seal. [ROBERT BASTONE, WC3O]

UHF Plugs with Smaller Cable

83-1SP (PL-259) Plug with Adapters (UG-176/U or UG-175/U)

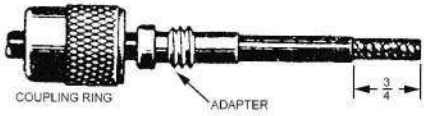

1. Cut end of cable even. Remove vinyl jacket 3/4" - don't nick braid. Slide coupling ring and adapter on cable.

2. Fan braid slightly and fold back over cable.

3. Position adapter to dimension shown. Press braid down over body of adapter and trim to 3/8". Bare 5/8" of conductor. Tin exposed center conductor.

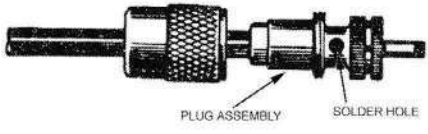

4. Screw the plug assembly on adapter. Solder braid to shell through solder holes. Solder conductor to contact sleeve.

5. Screw coupling ring on plug assembly.

ARRL0908

The PL-259 can easily be adaped to smaller cable types such as RG-58, 59 or RG-8X through the use of an adapter (some call it a reducer) that fits into the threaded portion of the plug. In many ways, this is easier to accomplish than the connection of the larger cables, even though the steps are similar. The cable is somewhat easier to handle and easier to strip since the dielectric is thinner and doesn't need to be cut through in one step. The shield also has less thermal mass to deal with while soldering. The process is illustrated in **Figure 7.8**.

Just as with the coupling ring and the larger cables, it is very important to slide both the coupling ring and the adapter onto the cable before progressing very far. It is also very important to support the connector and cable during soldering so it won't bend and allow the center conductor to migrate through the dielectric.

In Step 3 of Figure 7.8, it is important to trim the shield so that it doesn't extend over the threaded portion of the adapter; otherwise strands will jam the threads. Following Step 4, after the connector cools, make sure that the shield is soldered to both the adapter and the connector body. If it isn't properly soldered, you will be able to turn the adapter in the body. If that happens, just reheat the rear of the connector body and apply more solder into the holes when it's ready to flow. As with any connector installation, check for shorts with an ohmmeter.

Figure 7.8 — The procedure for assembly of UHF plugs with smaller coaxial cable. The UG-175/U adapter is for RG-58 size cable with 0.195-inch outer diameter. The UG-176/U adapter is for RG-59 size cable with 0.242-inch outer diameter, including RG-8X and RG-62. [AMPHENOL ELECTRONICS, RF DIVISION]

UHF Plugs with Crimped Connections

PL-259 compatible connectors are available with crimped rather than soldered connections for both large and small cable sizes. Each requires different size ferrules and different crimping tools. Some types have a center conductor that is soldered while the shield is crimped, while others have crimp arrangements for both conductors. If you use a type with a crimped center pin, make sure the center conductor extends all the way to the bottom of the pin, or the connection won't be solid. (See **Figure 7.9** for assembly details.)

UHF Sockets

The standard SO-239 panel socket mated with the PL-259 is a flange mount arrangement with a center pin and only four mounting holes for shield connection. The usual practice is to mount the connector using four machine screws, lock washers, and nuts. This provides a connection to a metal panel. If it is desired to continue with coax inside the panel, the usual practice is to connect the shield, via as short a connection as possible, to a solder lug under one (or more) of the mounting nuts.

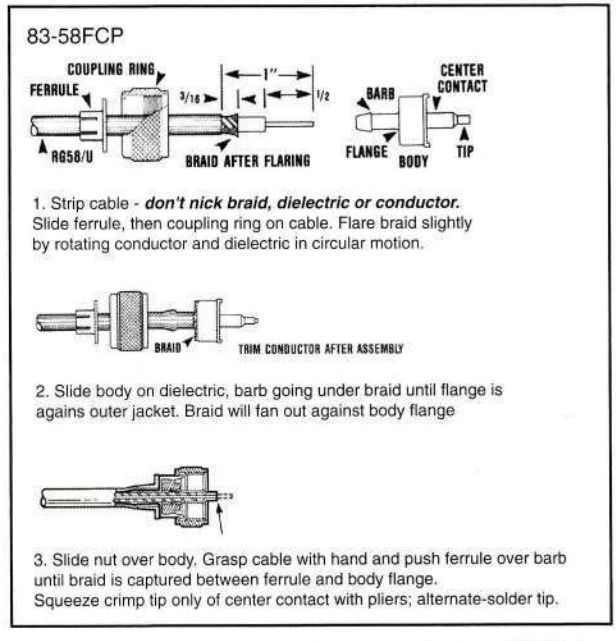

Figure 7.9 — The procedure for assembly of one type of crimped UHF plug with smaller coaxial cable. The 83-58 family of connectors are available in multiple versions for different cable types with different ferrule diameters requiring different crimp dies. Some have a soldered center conductor, some (as shown) have an inner conductor that can be crimped or soldered. [AMPHENOL ELECTRONICS, RF DIVISION]

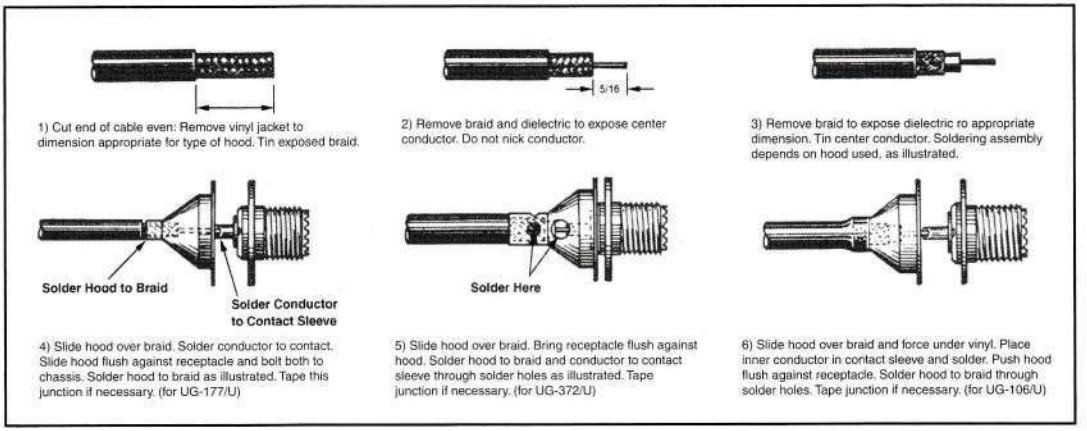

Figure 7.10 — The official procedure and dimensions for assembly of a shielding hood for SO-239 flange mount jacks. The different part numbers are for different cable types.

This arrangement is obviously not satisfactory if high frequency shielding is required. Using a shield hood can result in a properly shielded connection. (Details are shown in **Figure 7.10**.)

In addition to flange mounting, one-hole mount sockets are available. These are constructed much like the threaded PL-258 barrel connectors and are secured with nuts that fit the backshell threads. A center pin solder connection is provided inside the panel and if a shield connection is required, it is often made using a large solder lug that fits around the connector body. To extend a shielded connection with a one-hole mount, a PL-258 type double female connector with matching nuts can be used. The coax inside the panel is then terminated with a PL-259 plug.

INSTALLING TYPE N COAXIAL CONNECTORS

The Type N coaxial connector series is superficially similar in size and operation to the UHF series, but it corrects the major deficiencies of the earlier UHF type:

◆ Unlike the UHF, the Type N connectors maintain a constant characteristic impedance through the connector.

◆ The construction is such that the shield connection is not dependent on a tight backshell. Of course, if the backshell is removed far enough, the connectors can be pulled apart and break contact.

◆ The gaskets of the Type N prevent water penetration, a major factor in the deterioration of coax cables.

A Type N plug is actually easier to assemble than the UHF counterpart.

So why don't more amateurs switch over to Type N? Simple: They are more expensive (typically around $6, compared to $2 for a high-quality plug) and many installers don't know how to deal with them. The more expensive part is relative — what's it worth to save a trip up the tower in the winter?

Select the Correct Connector

Type N connectors come in 50 and 75 Ω versions. Be sure to select the right series, and get the right connector for your cable type if you are concerned about maintaining impedance. The insidious problem with having 50 and 75 Ω versions is that they look identical, and can be made to mate with each other, to a degree. As with the RG-8 (50 Ω) and RG-11 (75 Ω) type cables themselves, the connectors have the same outside and shield contact diameters. In order to maintain the constant impedance, the 75 Ω N connectors have a smaller diameter center conductor pin.

If a 50 Ω plug is inserted into a 75 Ω socket, the socket's inner conductor will be spread open too far, making it unreliable for use any later use with its proper 75 Ω a plug. While inserting a 75 Ω plug into a 50 Ω socket will not cause damage, it will result in an uncertain center conductor connection. If the pin is in perfect alignment, there will actually be no contact at all.

Installing a Type N Plug or Socket

Unlike the standard UHF connector arrangements that just have cable plugs and panel jacks, the Type N is available with similarly installed cable plugs and cable jacks. This makes coaxial "extension cords" feasible without the need for a double female adapter.

The installation instructions for a Type N plug or cable socket are shown in **Figure 7.11**. To add clarification here, we expand upon these steps using an Amphenol connector, part number 82-202-RFX, designed for a number of 0.405-inch diameter 50 Ω coax cables, including RG-8 and RG-213. Note that the suffix RFX indicates it is a commercial version rather the 82-202, which is the full military type at about three times the price. (Visit their website at **www.amphenolrf.com** to find the right kind for your cable.) A step-by-step installation process follows.

◆ *Lay it out* — Slide the nut, washer, and gasket over the cable jacket — in the correct order.

◆ *Remove the outer jacket* — Measure 9/16 inch of the outer jacket and carefully cut and remove it with a razor knife, without nicking the braid.

◆ *Comb out the braid* — Using an awl or a metal comb, straighten out the shield wires and slide on the clamp until it stops on the jacket, as shown in **Figure 7.12**.

◆ *Strip the dielectric* — Remove enough of the dielectric to leave

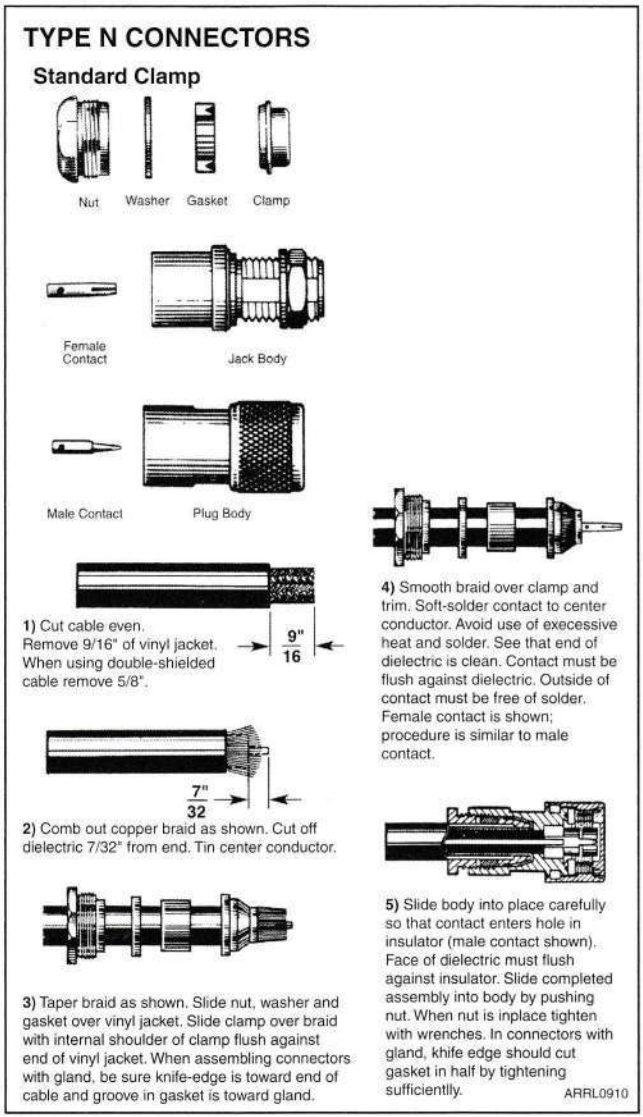

Figure 7.11 — The official procedure and dimensions for assembly of a standard Type N plug or cable jack.

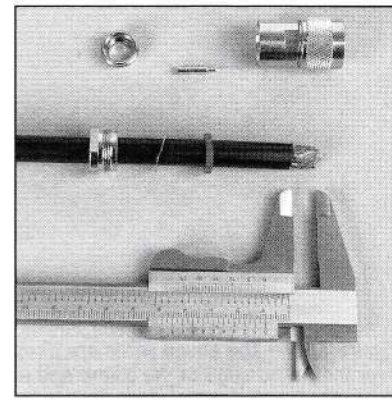

Figure 7.12 — The nut, washer, and gasket are in place on the cable jacket, in the correct order. The right amount of outer jacket is removed, and the shield wires are combed out straight.

7/32 of an inch between the end of the dielectric and the end of the inner conductor.

◆ *Trim the shield wires* — Use sharp diagonal cutters to trim the shield wires to make them just the right length to cover the round portion of the clamp (**Figure 7.13**).

◆ *Tin the center conductor and solder the pin* — Lightly tin the center conductor. Check to make sure it fits in the pin, and lightly dress it with a fine file, removing enough solder so that it fits fully into the pin. The bottom of the pin should rest against the dielectric and, with the pieces pushed together (as shown in **Figure 7.14**), the pin should be flush with the end of the housing. Now is the time to adjust as needed, then solder the pin and remove any solder on the outside of the pin with the file or emery cloth.

◆ *Final assembly* — Insert the pin into the connector body dielectric by pushing on the cable. Turn the nut until the threads start. Hold the connector

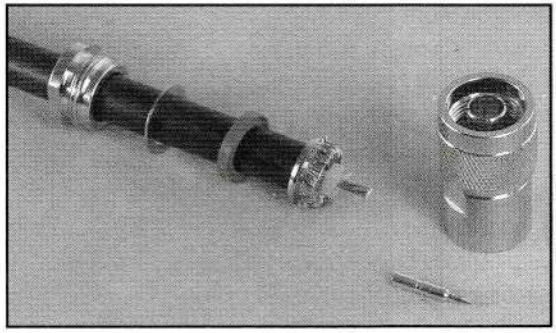

Figure 7.13 — The shield wires are trimmed to fit over the round edge of the clamp and enough of the dielectric is removed to allow the pin to fit flush.

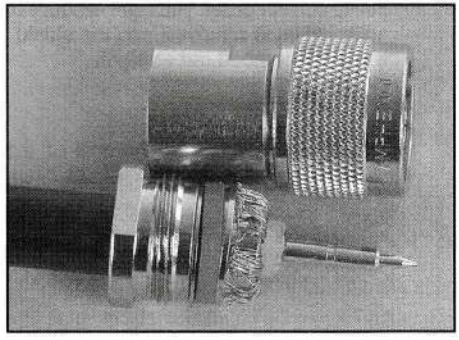

Figure 7.14 — Lightly tin the center conductor, make a final check of dimensions, and then solder on the pin.

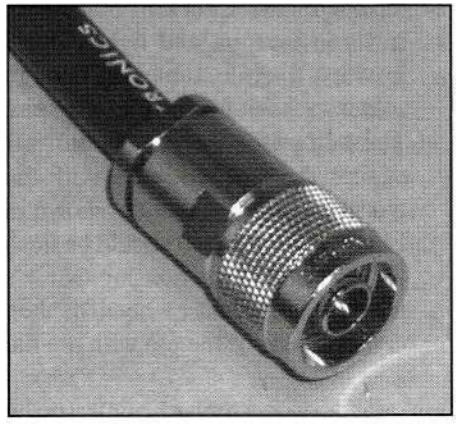

Figure 7.15 — The fully assembled connector.

body with a wrench and turn the nut with another wrench until tight. The pin should be about flush with the end of the coupling, the connector should not easily turn on the cable, and you should not be able to pull it off the cable (**Figure 7.15**).

Type N Jacks

As previously noted, the Type N offers cable jacks that assemble in the same manner as cable plugs. They also offer panel jacks in a few configurations. There are types that are similar to the open frame SO-239 panel jack, but there are also panel jacks that maintain the characteristic impedance and shielding integrity, more appropriate for critical RF applications. These assemble in the same manner as the other plugs and jacks, and are best installed in the panel after assembly.

Some Observations

Note that with the Type N, we have avoided the step of soldering to the connector body. This avoids the risk of melting the cable dielectric, a frequent problem with UHF connectors. Also, it is possible to modify the procedure slightly and solder on the pin, push the cable with pin attached through a small bulkhead hole, and then assemble the connector on the other side. With a UHF PL-259 connector, you need to do the soldering on the far side of the wall.

Unless there is a lot of working room, it is not recommended to replace UHF connectors on equipment with Type N. Adding a UHF to Type N adapter to a UHF connector, however, especially when the UHF is still new, can avoid some of the typical problems of loose coax connections later on.

For cables of the RG-58, 59, and 8X variety, the BNC connector is a good choice. It offers many of the benefits of the Type N in a smaller, bayonet-attached package. Type N connectors are also available for virtually all types of coax the amateur is likely to

encounter, although they will be harder to find and may not be available in the less-expensive commercial series. A BNC connector with a BNC to N between series adapter may be a good solution.

Type N Plugs for the Dedicated UHF Plug User

It is no wonder that hams are wedded to the ubiquitous PL-259 UHF series plug, since most HF and a large portion of VHF equipment provides matching UHF sockets for connection to antennas. However, there is a line of Type N plugs that assemble in almost the same way as a PL-259 plug. In fact, as seen in **Figure 7.16**, the shield is connected in exactly the same way, whether the cable is RG-8 or RG-8X. The same UG-176 adapter for RG-59 or similar sized coax that fits a PL-259 also fits in this Type N connector, as does the UG-175 for RG-58.

The same techniques that are used to prepare either size cable for a PL-259 are also used here. The same tools, such as the Ripley UT-8000 jacket and dielectric stripper, can be used to prepare the larger cables, or the traditional knife and pliers approach will work as well for this connector.

The connector comes in two pieces: an inner body where all the soldering takes place that includes a captive pin, and a housing that includes the backshell and the shield connection arrangement. As with a PL-259, this Type N can be disassembled, cleaned out, and reused. The usual Type N includes a gasket that is destroyed upon first assembly, and those can't be found either.

With the backshell removed, the soldered connector interior has a diameter of 0.6 inches, significantly less than assembled Type N at 0.83 inch,

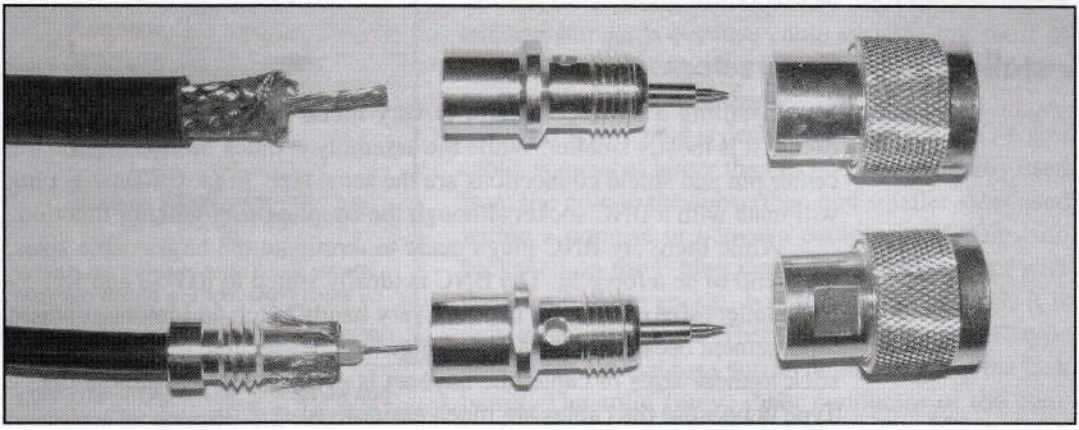

Figure 7.16 — RG-213 and RG-8X cable about to be assembled into UHF-like Type N plugs.

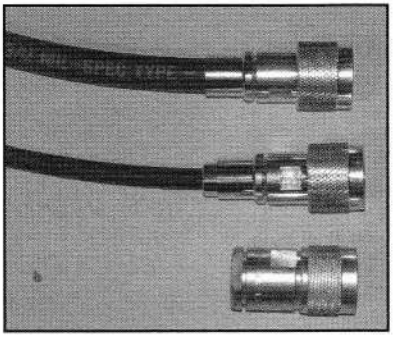

Figure 7.17 — Fully assembled Type N coax connectors on RG-213 and RG-8X cable. A standard clamp-type Type N plug is shown for comparison.

or even PL-259 at 0.74 inch. This can make it easier to route cables through smaller holes in partitions. The standard Type N can be soldered to its pin and routed through holes as small as the cable itself, but the final assembly has to be completed on the far side of the partition. Of course the current connector also needs final assembly, but it's just the threaded backshell piece. This can easily be tightened up using two 7/16-inch open-end wrenches, or one wrench and a vise.

The only difference between assembling this connector and a PL-259 is that the center conductor wire has a maximum length before it bottoms out inside the center pin. It must be trimmed until it can be screwed in far enough that the shield appears beyond the solder holes, as the connector is screwed onto the coax or the UG-175/6 adapter. **Figure 7.17** shows the assembled connectors in comparison to the size of a standard solder and clamp Type N plug.

These connectors cost between $5 and $7, about twice what a quality PL-259 costs, but about the same as the standard solder and clamp Type N plugs. They are somewhat longer than the usual Type N, which may be an issue in some installations. The standard N plug is about 1.5 inches long, while the item under discussion is 1.785 inches, 1.96 with a UG-176 adapter.

INSTALLING BNC AND OTHER COAXIAL CONNECTORS

Each coaxial connector type has its own installation requirements, although the BNC is quite similar to the Type N connector described in the last section.

Installing BNC Connectors

Installing a BNC connector is very much like installing a Type N, except it is mostly smaller. While the assembly is much more compact, the center pin and shield connections are the same size. In fact, a Type N plug will mate with a BNC socket although the coupling ring will not function.

While there are BNC plugs made to terminate the larger cable sizes, they tend to be a force fit. The BNC is ideally suited to RG-58 and RG-59 (or smaller) size cables and makes a very handy patch and interequipment arrangement because of its quick-change bayonet-secured backshell. If you stick to these sizes of cable, the bayonet is even easier to assemble than a Type N because the cables are much easier to work with.

As with others, the BNC is available in both crimp and clamp styles.

BNC CONNECTORS

Standard Clamp

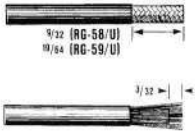

1. Cut cable even. Strip jacket. Fray braid and strip dielectric. ***Don't nick braid or center conductor.*** Tin center conductor.

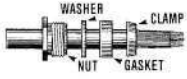

2. Taper braid. Slide nut, washer, gasket and clamp over braid. Clamp inner shoulder should fit squarely against end of jacket.

3. With clamp in place, comb out braid, fold back smooth as shown. Trim center conductor.

4. Solder contact on conductor through solder hole. Contact should butt against dielectric. Remove excess solder from outside of contact. Avoid excess heat to prevent swollen dielectric which would interfere with connector body.

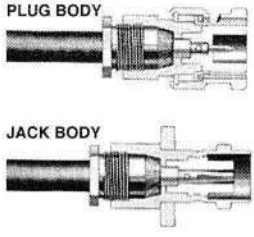

5. Push assembly into body. Screw nut into body with wrench until tight. ***Don't rotate body on cable to tighten.***

ARRL0911

Figure 7.18 — The official procedure and dimensions for assembly of a standard BNC plug or cable jack.

The solder (pin) and clamp (shield) are so easy to do with smaller cable, and are recommended if you can read a ruler and have power for a soldering iron. A notable exception would be cables with foil (or mostly foil) shields. The foil is somewhat less suitable for the shield clamp and a good match with a crimp arrangement.

Figure 7.18 provides the step-by-step instructions for BNC assembly. As with the Type N, both cable and panel jacks are available that assemble in the same way. There are open-frame jacks available in both flange type and one-hole mount styles.

Beware of electronic retailer "BNC" plugs that have a BNC-size backshell but use the center conductor of the cable as the pin. While they advertise them as "no solder" types, the wire is not the correct size to mate with a BNC jack.

Type F Connectors

Probably the most common coaxial connector ever made is the Type F, described in Chapter 6. While rarely encountered in Amateur Radio equipment, it appears in virtually all television and consumer video equipment made since the 1970s. It may be encountered in amateur video, or in making use of cables originally intended for other services. Because of its high volume, and the nature of the consumer marketplace, it was designed to be inexpensive and easy to install. In spite of this, cable systems using the connector must meet stringent leakage standards because cable systems use most of the spectrum allocated to over-the-air services and they must not interfere with them.

The Type F plug is designed for use with RG-6 size cable, somewhat larger than RG-59 and generally used from the pole to the subscriber, and smaller sizes used within a premise or between equipment. A screw-on backshell on the F plug maintains shield contact with the barrel of the socket, but as with the PL-259, it is only effective if tight. There is also a "push-on" type plug available that uses spring fingers to grasp the jack barrel. The solid (only) inner conductor of the coax pushes into a spring contact on the jack, generally with

significant through clearance so the length is not critical, unless it doesn't make the spring contact.

Cable TV-type flexible coax provides a large fractional shield coverage through the use of a wrapped aluminum foil shield, sometimes in combination with a loose wire shield. This arrangement pretty much rules out soldering of the shield connection and provides either a clamp or, more often, a crimp-on connection. Again, a number of different proprietary types of plugs with proprietary tools are available for such applications as waterproof outdoor use, although the very basic types are not very fussy about the crimp tool used. Still, a good fit makes for a better and neater connection.

RCA (Phono) Connectors

The RCA connector (see Chapter 6) was originally employed to connect a low-level phonograph cartridge signal, via a coax-like shielded wire, to an amplifier. As such, it has an inherently coaxial structure with the plug having a hollow pin and the shield connected via four springy petals, making a non-threaded almost, but just barely, backshell.

The connector type is most frequently encountered in Amateur Radio applications as a between-equipment connection arrangement for auxiliary functions, such as carrying reference and oscillator signals as well as switching, control and sometimes low voltage dc lines. In the 1950s and 1960s, it was sometimes also found used in place of a UHF connector as an antenna connection on receivers and transmitters at or below 100 W PEP.

While crimp-type connectors may be available, loose connectors tend to be the solder type. The basic connector consists of a center conductor soldered within the hollow center pin and the shield soldered over the outside of the shield fingers in K3LR fashion. Such connectors provided as part of preassembled audio cables with molded housings may be of a different arrangement.

In addition to the basic type, there are some with a metal screw-on back cover and interior terminal for the shield. These are neater and easier to grasp, but don't offer any electrical advantages over the basic configuration.

Chapter 8

Determining Which Line is Best Suited for a Particular Application

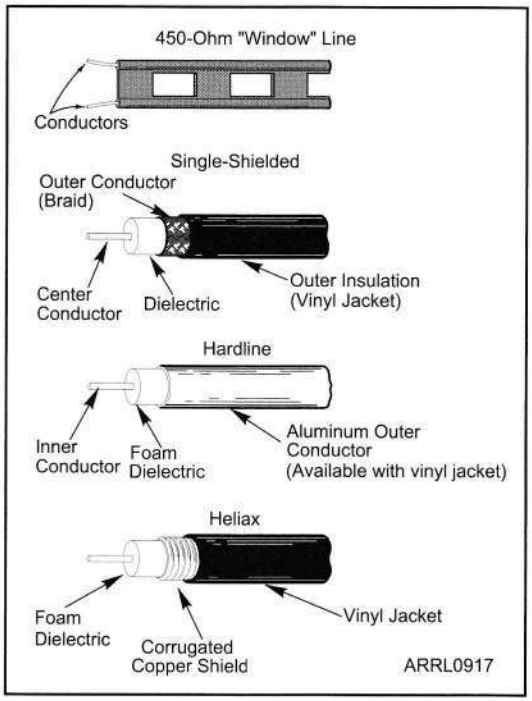

Not every line is right for every application — picking the right one may offer improved performance and longer cable life.

The choice of the best transmission line for an application may make a big difference in how well the system works. Some application problems appear immediately, sometimes with dramatic results, while other, more insidious ones manifest themselves gradually over time and can be easily overlooked.

GETTING THE SIGNAL TO THE FAR END OF THE LINE

What we usually want most from our transmission line is to get the signal to come out the far end looking as much as possible like the signal with which we started. In the realm of radio signals, this statement is mostly about transmission line loss. In other applications, such as pulsed data systems, we may have other concerns, including preserving pulse shape without distortion, but here we will focus on transmission of RF energy. As we have discussed, the selection of line type plays a crucial role in how successful we will be.

We spend a lot of money to have a transmitter to generate a radio signal, and we want that signal to arrive at our antenna and leave as radiated RF energy — not be radiated as heat from our transmission line. There are many factors that contribute to line loss, most of which we have already covered in detail. Here we will discuss which is most important for a particular application.

Characteristic Impedance

The characteristic impedance (Z_0) of a transmission line is one of the most fundamental attributes of a transmission line, and often considered first in selecting a line. While the Z_0 does relate directly to loss (higher Z_0 lines generally have somewhat less loss, all other things being equal), the matched loss due to the Z_0 is usually less important than the extent to which the Z_0 matches the load.

The Matched Case — In the most common configuration, the load is of approximately the same impedance that the equipment is designed to drive. That impedance is most often 50 Ω for radio equipment and 75 Ω for video equipment. Not coincidentally, the most common coaxial transmission lines are available with those Z_0 and the obvious choice for Z_0 is the one that matches the actual Z impedance of the equipment at both ends. Any other Z_0 will result in an SWR greater than 1:1, which will increase cable loss and not properly load the equipment.

Once we know the Z_0, we have a number of other considerations — how much loss will our system design tolerate, and what power rating does the cable need to meet. **Table 8.1** shows representative data on these parameters for some of the most popular 50 Ω cables. Note the dependence on operating frequency for both of these parameters.

If losses are of a particular concern, it is possible to change cable types to meet particular requirements. For example, if the load is a rotary antenna, it is usually necessary to feed it with a loop of flexible cable to avoid fatigue as the rotator turns back and forth. Since the lowest loss cable types do not tend to be very flexible, it is possible to change types (within the same Z_0) if the run is long enough to make a difference. At most frequencies, there is

Table 8.1
Attenuation and Power Handling Capability for Various 50 Ω Coax Cables vs Frequency

Cable	*Frequency (MHz)*	*Attenuation (dB/100')*	*Power Rating (W)*	*Minimum Bend Radius (")*
RG-58*	10	1.2	1937	2
	100	4.3	542	
LMR-195**	10	1.1	1430	
	100	3.6	450	
RG-8*	10	0.6		4.5
	100	1.9	800	
LMR-400**	10	0.39	5800	
	100	1.2	1810	

*Belden data from **www.belden.com**
Times Wire and Cable data from **www.timesmicrowave.com.

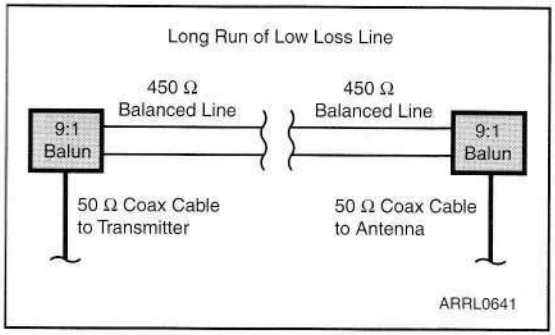

Figure 8.1 – The transition from coax to low loss, air dielectric, balanced transmission line can reduce loss if the loss reduction in the line is greater than the loss in the baluns. Here 9:1 (450: 50 Ω) baluns are used to transform the 50 Ω end impedances to the 450 Ω impedance of the window line.

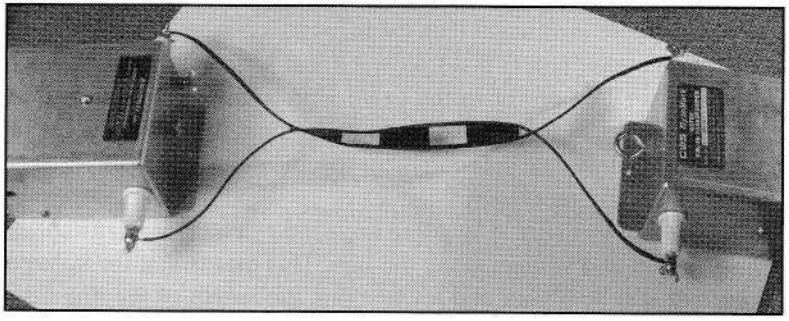

Figure 8.2 – Physical model of the 9:1 baluns from Figure 8.1 and a short window line section set up for laboratory loss testing.

negligible additional loss due to the connectors required; however, they do become additional points of potential failure as well as points of possible water ingress, if precautions aren't taken.

It is also possible to change to a very low loss medium if the length is sufficient. For example, the loss of 450 Ω window line, or 600 Ω open-wire line, is significantly less than that of coax, particularly as the frequency goes up. A balanced to unbalanced impedance transformer (balun) can be used to transform the impedance of the low loss medium to the desired 50 Ω at each end of the run as shown in **Figure 8.1** and **Figure 8.2**. The trade-off here is that the transformers will have some loss.

ARRL Lab measurements during the experiment pictured conclude that the pair of HF baluns had a total loss of less than 1.0 dB. Thus the run needs to be long enough so that the difference in loss between the cable types is greater than 1.0 dB in order for this to make sense. It is also necessary that the balanced line be installed so that it is away from the ground and not subject to other interfering objects.

Mismatched Case — If the transmission line isn't matched to the load or the equipment, a number of additional considerations need to be addressed. The three main areas are:

◆ *Additional Cable Loss.* As noted in Chapter 3, a mismatched transmission line will have more loss than a matched one. This is not generally a problem with a reasonable mismatch, perhaps 2:1 or 3:1, but it all depends on how high the matched loss would have been for the cable type, length and frequency.

◆ *Equipment Limitations.* Many radio transceivers will engage foldback circuitry if the load is different than that specified. This circuitry is designed to protect the output stages of a transmitter from the higher voltages or currents that could be present in a mismatched environment. While some radios are happy to drive loads with 2:1 or higher SWR, some start reducing power at 1.5:1. In terms of getting a signal to the end of the cable, this can be even more significant than cable loss.

Some types of equipment that follow a linear source impedance model will also deliver less power to the cable with a mismatch than if it is matched. The answer to these issues is to understand the requirements of your equipment and translate the equipment specifications into requirements for your transmission line system.

◆ *Stress on Components.* A standing wave ratio greater than 1:1 implies a changing current and voltage along the line. This means that the voltage and the current will be higher and lower along the length of the line than they would be if the line were matched. Fortunately, the locations of high current will be the locations of low voltage, and vice versa.

If the complex impedance of the load and the line propagation velocity and length are known, it is possible to determine the actual voltage and current at the end of the line. However, these values will hold for a single frequency, so in a multiband system, each may appear anywhere. The maximum voltage and current will each be equal to the values in a matched system times the square root of the SWR. If the termination equipment is specified to handle the resulting value, there should be no problem. As an example, with a matched 50 Ω, 1500 W system, the line voltage will be about 274 V, the current about 5.5 A. With a 4:1 SWR, the maximum voltage and maximum current will be twice those values at some points along the line.

OUTDOOR ISSUES

Generally, all modern transmission lines can be successfully operated indoors or outdoors. There have been types of TV twinlead, available years ago, specifically intended for indoor use because they were less visible. After a few seasons in sunlight, they would crack and eventually disintegrate. While modern cables last much longer outdoors, they do suffer degradation to different extents due to sunlight (primarily UV radiation) and moisture. The main degradation mechanism is the breakdown of the

outer jacket, the rate of breakdown being dependent on the characteristics of the jacket material.

Jacket Contamination

As part of the jacket manufacturing process, plasticizers and other compounds may be left within the jacket material. These materials can leach and migrate from and within the cable, changing the characteristics and causing degradation of both the shield and the inner dielectric. This process is accelerated by the temperature rise resulting from sunlight exposure. Cables identified as *non-contaminating*, such as those with non-contaminating vinyl (NCV) jackets, are resistant to these chemical effects. High-quality PVC and other materials can provide good protection to both UV and high temperature degradation mechanisms.

Polyethylene is another jacket choice that does not have plasticizers and is inherently resistant to UV, as well as offering additional abrasion resistance. Good-quality PVC jacketed cable can be expected to last 9 to 14 years before it suffers significant degradation, while polyethylene jacketed cable can last about twice as long. Low-quality cable can be expected to degrade significantly faster.

Water Penetration

Coaxial cable jackets are made of different materials suitable for different environments. A major problem with many types of coax, as well as some connectors on the ends, is water penetration. Water within the coax can cause the dielectric to become lossy and result in corrosion of the shield and even the inner conductor.

Water enters coaxial cable in at least two ways. Gaseous water vapor can migrate through the outer jacket. Liquid water can also enter through jacket pinholes left from the manufacturing process, or from abrasion resulting from rough handling.

In most cases, the entry of water into the cable from the connector ends is a more significant issue. While BNC and Type N connectors are designed to be waterproof, PL-259s are not. In order to avoid problems, a PL-259 must be sealed by means external to the connector. In addition, it is particularly critical that a drip loop be included at each end of every cable run that goes downward. A drip loop (see **Figure 8.3**) is any local low point before the connector so that water running down the outside of the cable can drip or run off before it gets to the connector. Without the loop, water will pour onto the connector, sometimes coming right into the equipment if connections aren't tight.

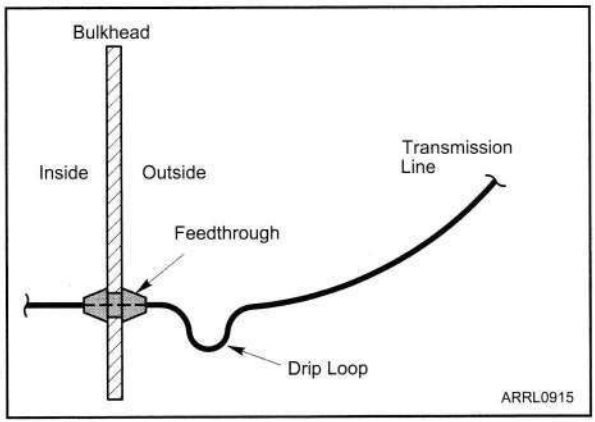

Figure 8.3 – A drip loop is an intended local low point in the cable before the connector so water running down the outside of the cable can run off before it gets to the connector.

There are a number of commercial products available for waterproofing connectors, although some make later connector removal very difficult, so make sure the connection is right before you seal it. High-quality cable will have fewer pinholes and be less subject to vapor migration, but improper connector installation can negate the benefits.

Direct Burial Coax

Most types of coax are designed for above-ground use, but some are rated for direct burial. This is mostly a statement about abrasion resistance. The usual ground near the surface moves with seasonal changes as well as with differences of surface load. Any shifting of the ground will tend to result in jacket abrasion from rocks or other debris in the soil.

Note that direct burial does not mean "submersible." Only special submarine cables, out of financial reach for most amateurs, are designed to spend time in the water. Direct burial cable doesn't promise lack of pinholes. This can result in problems for cables in any kind of ground without good drainage, such as clay. If the older houses in the area are made of brick, check your soil carefully before you bury any coax cable.

Some installers use conduit to avoid abrasion problems with below-ground cable. While this can reduce abrasion, it can result in other problems, such as water accumulation. Water can enter conduit through the ends or, more likely, through condensation. Without proper drainage, the coax ends up in the water. To avoid this problem, implement one of the following:

◆ Use conduit or drainage pipe with drainage holes on the bottom side. Prepare the trench with a layer of gravel above sand or earth with good drainage. Lay the conduit in the trench, hole-side down, and use elbows on the entrance and exit points to avoid direct water entry (see **Figure 8.4**).

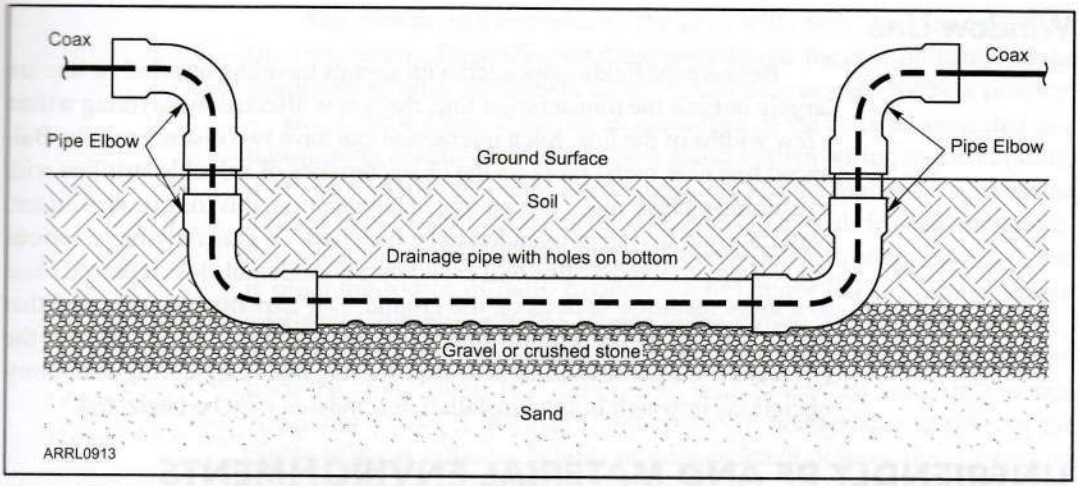

Figure 8.4 – A problem with burying coax in conduit is the accumulation of water in the conduit. By using drainage pipe with holes on the bottom side over good drainage material, such as the gravel and sand shown, any water can be moved away from the cable.

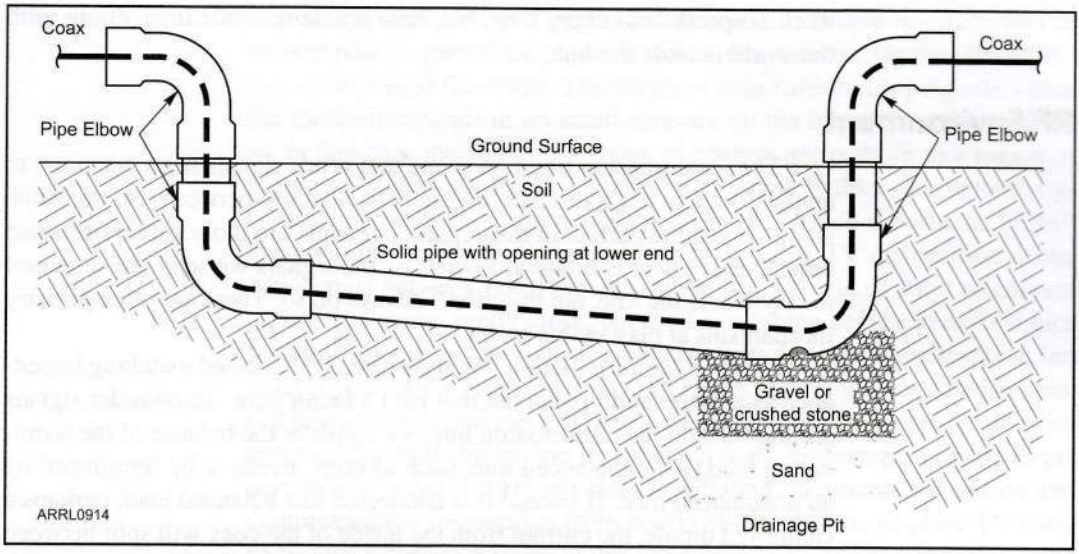

Figure 8.5 – Another solution to the problem of accumulation of water in the conduit is to use a pitched conduit with one or more low points able to drain into drainage pits.

◆ Lay the conduit with a pitch so that all water will run to one end, or to a midpoint. Have a drain at that point into a pit with gravel and sand in sufficient quantity to absorb the expected water. Follow up with a look at the drainage pit after some wet weather (see **Figure 8.5**).

Window Line

Because the fields associated with signals traveling on window line are largely outside the transmission line, the line is affected by anything within a few widths of the line. Such interaction can have two distinct results. Balanced line near metal takes on the characteristics of a double stripline with a resulting change in Z_0. Depending on application, this may be significant, particularly if a system intended to be matched. Of generally more serious consequences, window line will experience considerable loss if placed close to a lossy medium, such as on the ground. Our experiments indicated that the loss in 100 feet of window line on dry ground was 10 to 20 dB over the HF region. This is something to watch out for, especially during temporary operations in which normal installation standards may be neglected.[1]

UNFRIENDLY RF AND MATERIAL ENVIRONMENTS

To a greater or lesser extent, all transmission lines are subject to effects of their external environment. Some of these are obvious. For example, a transmission line that melts in a high-temperature environment will not work at specification very long, but there are more subtle interactions with the world outside the line.

RF Environment

The ideal transmission line is one that sends signals from one point to another without any interference from or to what's in between. No transmission line is quite perfect in this regard, but some are more susceptible than others. This effect is bilateral as well — the signals we send are supposed to stay inside the line, but they don't always do so. There are three primary mechanisms at play in this realm.

Proper Line Termination. We have already discussed matching impedance as a termination issue, but that isn't a factor here. To consider signals getting outside the transmission line, we consider the balance of the terminating load. An unbalanced line, such as coax, needs to be terminated by an unbalanced load. If instead it is connected to a balanced load, perhaps a center-fed dipole, the current from the inside of the coax will split between the half-antenna connected there and the outside of the coax, acting like another wire in parallel.

The amount of current going on the outside of the coax, which — because of skin effect — acts like a separate conductor from the inside surface of the shield, depends on the relative impedances of the two connection paths. This will depend on the frequency, the length of the coax, and the impedance of the ground termination of the shield at the far end.

Any current on the outside of the coax will result in radiation, just as from an antenna. Depending on the system design, the environment, and the sensitivity of other equipment close by, this may or may not be a problem — and in some cases, it can be an advantage. If the coax is connected to a transmitting antenna, and it runs past alarm system wiring in the building, it can be a serious problem. If you spent lots of time tuning a Yagi antenna for best front-to-back ratio and the coax picks up signals from all directions, you will also not find it a plus. This can be a problem in either direction, and is often the source of radio frequency interference (RFI) from household appliances as the coax works its way to the station.

Balanced transmission line, such as the popular window line, suffers from the same issues. It is designed to feed a balanced load, such as that center-fed dipole. If the load is not balanced, perhaps due to sides of the dipole being at different heights or near different objects, the currents on the two conductors will not be equal and opposite. Any resulting difference current due to imbalance will act like a separate antenna current on the line, and radiate just as will the coax described above, resulting in all the same issues. In addition, the unshielded balanced line, while its balanced currents cancel at distance, even if perfectly balanced can couple to conductors or objects near its path if the object is closer to one conductor than the other.

Coax Shield Coverage. The ability of coax cable to keep signals within the medium depends in no small measure on the integrity of the medium — in this case the shield. For coax to operate perfectly in this regard, it requires a perfect shield. This would be an infinitely thick, zero resistivity-conducting medium surrounding the dielectric, which unfortunately isn't available for purchase. Some coax, such as cable TV distribution cable, which runs between poles down a street, has a shield of solid aluminum tubing that comes pretty close, but it takes a tubing bender to make a nice corner — not what the typical amateur wants for many applications, but great if you want a long, low-loss, 75 Ω coax run out to your antenna field. Cable companies make use of, and must avoid interference to, frequencies assigned for over-the-air use by other services. Government agencies get particularly upset if there are signals radiating on aircraft navigation and communication frequencies from poorly shielded coax, so cable TV companies have been sensitized to this issue.

Most coax used by amateurs has a braided copper shield with an effectiveness related to the percentage of coverage — often a parameter listed by manufacturers. Note that even 100% coverage by braid will not quite equal the shielding effectiveness of tubing. Still, all things being equal, more coverage means more effective shielding. The 75 Ω RG-6 cable, often used as "drop cable" between the street and an end user, typically has a dual shield

— one layer aluminum foil, the other tinned copper braid. While the braid is usually quite sparse, the combination meets the strict cable TV emission requirements. Unfortunately, it doesn't work well with soldered connectors, but is appropriate for crimp-on types.

Connector Continuity. Particularly with UHF and F-type connectors, in which the connection of the shield is dependent on connector backshell tightness, improper tightening of connectors can nullify part of the effectiveness of shield coverage. Any resistance in the shield connection acts like a coupling mechanism between the inside and outside of the shield. This can get worse with time, due to vibration or oxidation of the surfaces.

Material Environment

Coax cable pretty much has the advantage here. The fields between the conductors of coax, except as noted above, stay largely within the cable itself. Thus coax is pretty impervious to normal outside influences — other than water or abrasion as outlined previously. Still, each cable has a temperature rating that should be observed, as well as some sensitivity to some types of chemical vapor environments that can attack the outer jacket or permeate and degrade the shield or inner materials.

Window line, with most of its fields outside the physical location of the wires, is very susceptible to signal degradation of various types due to proximity effects. This should be carefully considered in selecting appropriate line for a particular application. As noted previously, the attenuation of window line closer than a few inches from dry ground is very high — perhaps 10–20 dB in about 100 feet, based on our measurements.

If window line is routed close to metal surfaces, it will have a major change in characteristic impedance, as well as the possibility of coupling signals to undesired objects. Similarly, window line can be a problem in getting through walls or other partitions in which the lossiness of the materials in the partition may be unknown. One solution may be to use short sections of dual coax (see Figure 5.9 in Chapter 5); however, they should be quite short if the coax loss is to be negligible.

Notes

[1]B. Allison, WB1GCM, J. Hallas, W1ZR, "Getting on the Air — A Closer Look at Window Transmission Line," *QST*, Nov 2009, pp 66-68.

Chapter 9

Application and Installation Notes

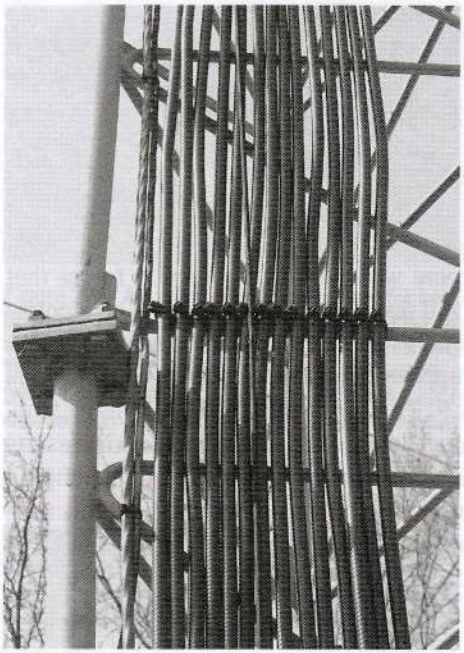

Coaxial cables going up a tower at W1AW, the ARRL Headquarters.

Once you have decided on a transmission line with the features you want, it is important to install it properly. Poor installation practices can result in more rapid degradation of transmission lines due to additional stress or inappropriate environmental factors. Implementing some of the following elements can help extend the life of your transmission line.

SUPPORTING LINE RUNS

Transmission lines are not generally intended to be structural members, yet they are often treated as such. A transmission line, particularly a coaxial cable, is not light and, in typical lengths, can be fairly heavy. **Table 9.1** provides some of the physical characteristics of typical coaxial cables. A quick glance indicates that each type should be able to withstand the tension of at least a 1000-foot vertical run; however, that's not quite the whole story.

Vertical Transmission Line Runs

While the cable itself may be able to withstand the tension of its own weight, whatever is used to secure the upper end will need to exert some kind of force on something to help it defy the forces of gravity. While a connector should also be able to support the weight, (assuming proper installation and no vibration that will cause it to break free in time), hanging a long line on a connector is not generally a great idea. The only thing worse is to have everything hanging directly on the soldered connections between the antenna and the cable.

Table 9.1
Physical Properties of Selected Transmission Line Types*

Cable Type (Belden PN)	*Weight/1000 feet (pounds)*	*Max Tension (pounds)*	*Minimum Bend Radius (inches)*
RG-213U (8267)	104	184	4.0
RG-8U (8237)	104	190	4.5
RG-8U Foam (9913)	97	300	6.0
RG-8U Foam (8214)	106	230	4.0
RG-8X Foam (9258)	35	75	2.4
RG-58 (7807)	22	25.4	1.9

*www.belden.com

The usual clamping arrangement will exert perpendicular forces that will distort the shape of the cable and result in a combination of concentration of tension forces and reduced ability to withstand the tension.

One good way to provide support to a coaxial transmission line is shown in **Figures 9.1 through 9.5**. This was described by Lyle Nelson, ABØDZ, in a *QST* "Hints and Kinks" column.[1] This method distributes the tension along a length of the cable and doesn't require any tight clamping to hold it securely in place. To further reduce tension on the line, this may be repeated as often as desired so each section of the cable is just holding up itself.

Horizontal Transmission Line Runs

A horizontal run adds the force required to avoid sag in the run. In fact, strictly speaking, it is only possible to have a horizontal run if there is infinite tension on each end to result in zero sag. All practical runs over horizontal spans are actually in the shape of a catenary, the shape that a cable takes on if its weight is supported at each end (see **Figure 9.6**).

To determine the amount of tension needed for a particular amount of sag, use the nomograph shown in **Figure 9.7**. The operation is performed in two steps:

Step 1. Lay a ruler between the two outside scales, with one end on the desired span length, and the other on the cable weight (in the same units as in Table 9.1). Make a dot on the "Work Axis."

Step 2. Rotate the ruler, keeping an edge on the dot from Step 1. At each position there will be a value for the tension and the corresponding half-span sag. Use a tension that is comfortably below the maximum tension shown in Table 9.1.

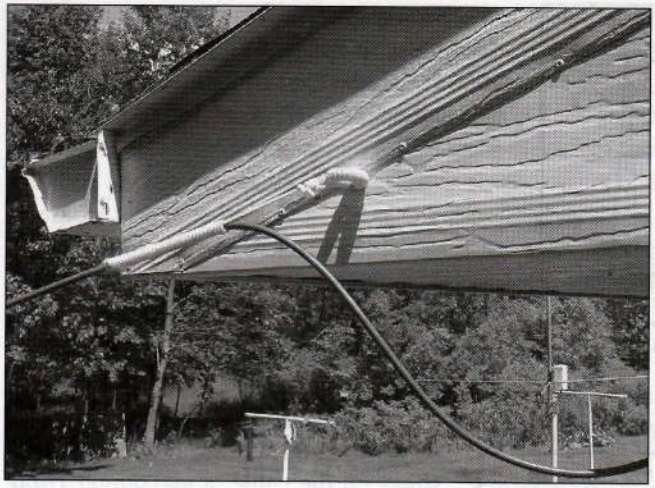

Figure 9.1 – An attachment mechanism for securing coaxial cable that distributes the tension of a length of the line to avoid excessive stretch. This can be used for either horizontal or vertical cable runs. The contributor recommends a 40-inch length of ⅛ -inch braided nylon rope for RG-8X size cable, 60 inches for RG-8 size, with an overhand knot at each end and the ends melted to avoid fraying. [LYLE NELSON, ABØDZ]

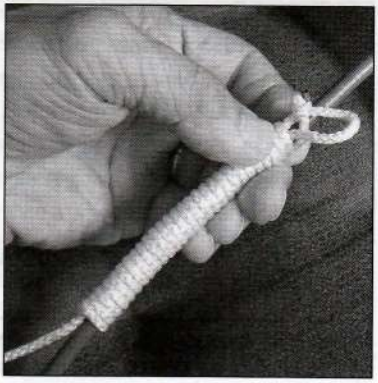

Figure 9.4 – Wind turns until you have about 3½ inches of the loop covered. [LYLE NELSON, ABØDZ]

Figure 9.2 – Start by making about a 5-inch loop along the cable. [LYLE NELSON, AB0DZ]

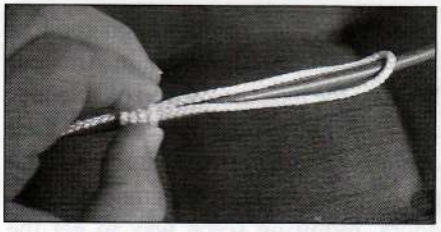

Figure 9.3 – Wind the cable in tight wraps starting at the open end of the loop. [LYLE NELSON, ABØDZ]

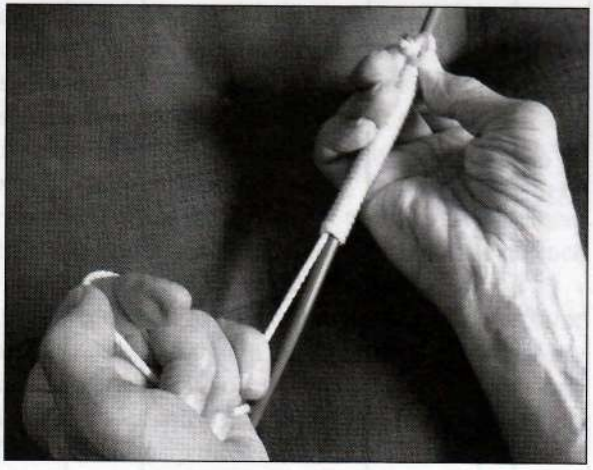

Figure 9.5 – Stick the end through the remaining loop and pull the rope from the other end until you have it tightly secured. The "tail" left out is then used to tie the cable to a screw eye or other support. [LYLE NELSON, ABØDZ]

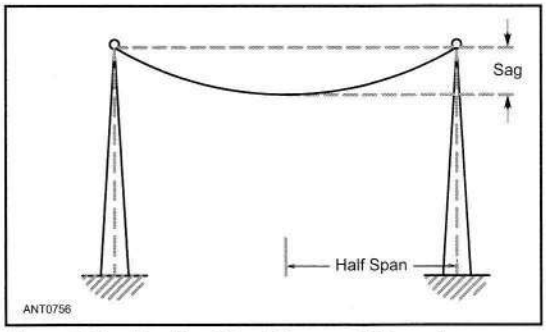

Figure 9.6 – A horizontal cable run with less than infinite tension on the ends will assume the shape of a catenary, as shown.

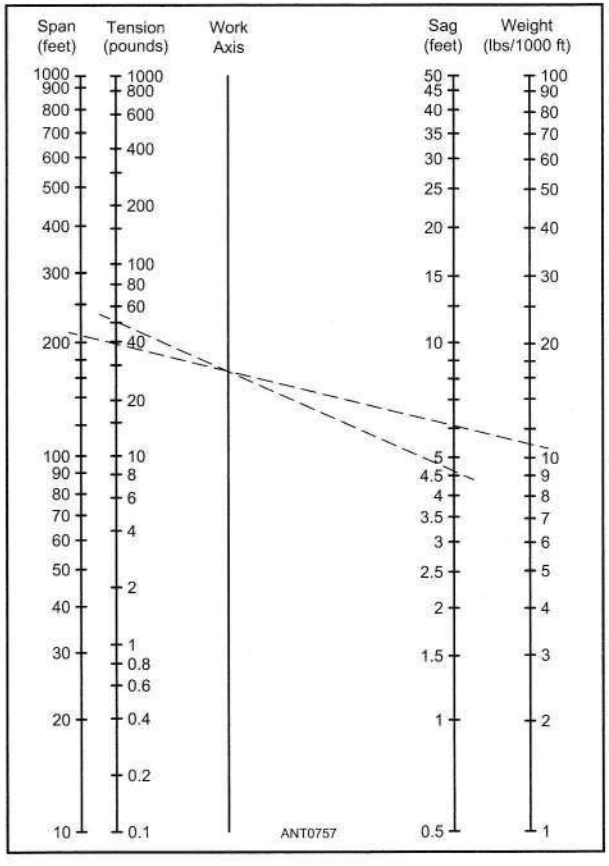

Figure 9.7 – Nomograph for determining sag in a cable run based on cable weight and span distance. [JOHN ELENGO, JR, K1AFR]

The dashed lines on Figure 9.7 are for an example with a cable weight of 11 pounds per 1000 feet and a span of 210 feet. The second line indicates that for a tension of 50 pounds, a sag of 4.7 feet will result.

Note that all of this assumes the end supports are fixed. If the end supports are trees, or other objects that will shift in the wind, the system needs to be laid out as if the trees were both at the position of furthest separation. The result will be additional sag in the rest position.

If the resulting sag is not satisfactory, or if you wish to reduce physical stress on the cable, a *messenger cable* can be used to support the cable run. This is just a kind of line with a high tension capability that is installed in the same path with correspondingly reduced sag. The transmission line(s) are then secured to the messenger cable every few feet so it assumes the shape of the messenger.

Keep in mind that the tension applied to the cable will also be applied to whatever anchor is supporting the end. This doesn't work if the tension pulls out the fasteners, or the wall they are attached to.

BUILDING ENTRANCE ARRANGEMENTS

One of the most common applications of transmission lines in Amateur Radio is the interconnection of antennas and radio equipment. By virtue of their operating characteristics, antennas tend to be outdoors and radio equipment indoors, requiring some way to get the line from one to the other. This can be

a bit tricky in the case of housing — it happens that most houses are especially designed to not have holes in their walls for running cables.

Of course, there are already such penetrations provided for utility power, telephone service drop lines and coaxial cable for CATV or satellite TV service, as well as non-electrical facilities such as water, gas, sewage and heating flues. If you are the owner of the property, you have the option of observing the techniques used by those services and doing something similar for radio antenna connecting transmission lines, although some techniques may be much easier to accomplish before the dwelling is completed.

Drilling Holes in Walls

As the owner, or with the permission of an owner, you can usually drill holes in walls. I have done this many times and have learned a few things in the process.

Be Sure You Know What's Between Outside and Inside

There are few things worse for the amateur constructor than drilling through a wall and running through a water supply or water heating pipe. Of course these can be repaired, but usually the damage extends far and wide before you can get the water turned off. If you will need professional help to recover, a good operating rule is to not attempt something like that on a Sunday!

The best way to avoid such problems, be they caused by pipes or wiring, is to make sure you know what's there before you drill. One way that works for me is to make all such penetrations into unfinished space, such as the wall above a basement foundation. Coming in near ground level also has potential benefit in terms of your lightning protection plan, which we will discuss in the next section. My station is usually in the basement, so this is a natural; however, if it's not, it may be easier to make the basement entrance and then go between floors, since most floors either have no such obstacles, or they can be easily seen (more on this later).

If you don't have a basement, or if basement entry won't work for some other reason, you will need to come through in higher ground. Here it is very important to know what you are doing. If you are not familiar with construction techniques, find a house under construction that has similar characteristics. Look it over before they close up the walls. You will see some places that make sense to drill through. Note that (in my experience) every window and door is surrounded by a pair of 2 × 4 or other framing lumber. This means that a hole drilled next to a door or window, or beneath a window will be wood the whole way through — generally no pipes or wiring. In addition, you can probably come through a piece of molding, which is a good idea.

I like to drill so that there is wood on both sides, so the inside hole comes out in a wooden molding. This way the hole is solid and pulling cable won't rip up plaster or sheetrock. It is also very easy to patch after you are done, especially for painted woodwork — a few applications of spackle will usually make even the biggest hole disappear. If you want to be even more solid, drive a dowel in to just below the surface, to be a base for the spackle. Adding a bit of trim paint is much easier than repainting or papering the whole room. If next to a window, you often have the added benefit of having the cable entrance hidden by draperies.

Note that your usual twist drill will not be long enough for the task. Invest in a couple of 12-inch or longer drill bits in sizes that slowly come up to the cable size. An exterior wall will be the thickness of the framing studs, plus the sheetrock or paneling on the inside, plus the inside molding. On the outside you may have underlayment or sheathing and then multiple layers of shingles, for example. Another advantage of drilling through solid wood is that you can then just push the cable through the hole. If you are drilling through a hollow wall, you will have to snake your way through the insulation and then pull the wire through — not the end of the world, but certainly an extra hassle. Make sure you drill the hole at a slight angle downward going outward, so no water will run into the house through the hole or follow the cable in.

If You're Doing More Than One, Combine Them

Somehow it seems that most amateurs eventually have a need for more than one such penetration. Even if you start out with one, your interests and capabilities will likely grow as you get further into Amateur Radio. While one can just keep punching holes in different places, at some point some kind of entrance facility may make more sense. We'll discuss some in the context of lightning protection, but even independent of that, a single entrance facility may be a better idea. For example, interior and exterior electrical boxes on each side of the exterior sheathing and attached on the inside to a stud may make a professional-looking arrangement that is easy to add to just by popping off the covers on both sides. If you're not up to the task, having an hour of discussion time with a contractor or electrician may pay for itself in the long run.

Making a Window Entrance

If walls won't work, another possibility is a window entrance. While I have seen descriptions of ways to drill holes in glass, I've never attempted it. Instead, I've unglazed and removed the pane of glass, and replaced it with a piece of ⅛-inch polycarbonate sheet. The light transmission is just a bit

less than through window glass, but not dramatically so. Still, I would avoid windows that highlight the appearance of a major room.

The polycarbonate is easy to work with using the usual tools, such as a reciprocating saw to cut it to size. Holes can be easily drilled, either for transmission line directly, or for PL-258 type or other feed-through connectors. If the holes are near the window edge, the cables may be able to be hidden by curtains or draperies as they go toward the floor. When it's time to move, recovery couldn't be simpler. Just remember where you stashed the pane of glass and swap it out with some glazing points and compound, and no one is the wiser.

Another possibility is to drill through the window sash itself. Carefully drill through a wooden sash in a spot that will be in the clear if the window is closed and that will not try to run through the glass. This can be accomplished with a short drill, is not likely to encounter plumbing or electrical runs and is easy to patch, if the surfaces are painted. While this is not quite in the same "no damage" category as the temporary board described below, it can be repaired to be almost invisible very quickly.

Temporary or "No Damage" Entrance Arrangements

If your circumstances are such that you can make no changes to the structure, or aren't even authorized to do any of this, there are still ways to bring antenna connections into the house. Some avoid the problem by using indoor or attic antennas. While that can keep you on the air, the chances are that you can have better results with an outdoor antenna. Here are a few possibilities.

Make the Connections Just When You Need Them

Most amateurs don't operate all the time, so they don't need an antenna connection all the time either. A transmission line connection can be just outside a window or door with its mate on the other side. When it's time to operate, just open the door, hook things up and leave the door open a crack while operating. Unless you are faced with heavy mosquito activity, this can work well. In fact some amateurs have the antenna, such as a short loaded vertical, just inside a patio door and move it all outside when it's time to operate — and when no one is looking.

Pinch Your Cable Under a Window Sash

Those using single-wire feed or window line can often put the line under a double-hung window and, if there's any gap or slop, just close the window on it, if it can still be latched. This is not ideal for a number of reasons, but is pretty easy to do. Perhaps a bit of "dressing" with a file can take the hard corner off the edge to make it less likely to damage the cable.

Add a Removable Panel Under a Window Sash

An improvement on the above that is almost as easy, is to get a small piece of trim board the width of your window sash and fit it under the lower sash, or above the upper sash so the window closes on it. Now you can notch (especially for cables with connectors) or drill as many holes as needed in your board for coax or other cables, or for feed-through connectors. If you don't want to build your own, MFJ offers a preassembled unit (see **Figure 9.8**) that can be cut to fit vertical or horizontal windows up to 48 inches wide and has feed-through arrangements for both coax and balanced lines. See **www.mfjenterprises.com**, and look for MFJ-4603.

There are two complications that need to be dealt with using this method. The first is that the security latch will no longer operate. This is pretty easy to fix. Either cut a piece of wood that can be jammed between the movable sash and frame, or install a small hardware store angle bracket so the window can't move. The screw hole can be easily spackled when it's time to move. The other problem is that there will be an open passage between panes of the two sashes that will allow insects to come through. Mosquitoes are particularly prone to do so, since they are attracted by the focused emission of CO_2 from people breathing inside the house. This is the same problem that occurs with window air conditioners and yields to the same solution — just a piece of foam strip pushed into the space (get one from an air conditioner dealer, or in a pinch, it's a great use for rolled-up surplus T-shirts).

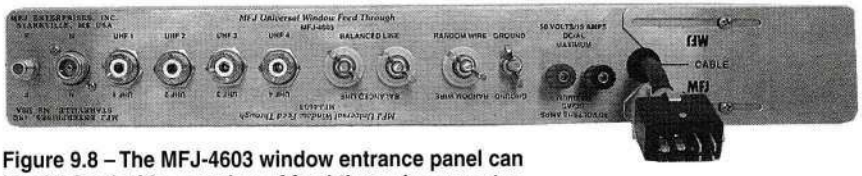

Figure 9.8 – The MFJ-4603 window entrance panel can be obtained with a number of feed-through connector configurations, or you can make your own from a piece of 1 x 2 lumber.

Drip Loops

With any cable entrance arrangement, it is critical that a drip loop be provided. This is easy to do; just make sure that the cable has a lower point before it enters the entrance arrangement. Otherwise, rainwater will follow the cable down and run into the wall or the feed-through mechanism. The drip loop allows a lower path from which the water will drip harmlessly onto the ground.

Extending the Route Between Floors or Rooms

If the entrance arrangement can't be on the same floor or in the same room as the station equipment, it is often fairly easy to continue on. If you

can't make permanent holes, look for existing ones that you can follow. A building with central heating usually has ducts or pipes that run from room to room, or between floors. In my experience, there is often space to follow, especially with the thinner varieties of coax. If you can't push it through without losing it in the space between wall surfaces, try pushing a straightened coat hanger through from the other side. Then tape the coax to the hanger with electrical tape, making a point of the tape — along with tapering the coax end in extreme cases — so the coax won't be pushed off, and then pull it back.

If you can drill a path, you may be able to find a good path — again, be alert for the possibility of wiring or plumbing. An unfinished basement ceiling is the easiest to get through since it is only one surface thick (usually subfloor plus finished flooring, perhaps 2 inches total). My favorite technique is to go through under an interior wall with a molding. First checking to make sure you won't end up in a floor joist, start the hole through the molding at an angle to enter the basement slightly offset. This way results in an easy-to-patch hole in the molding, rather than having to deal with patching a hole in a finished floor.

Going between upper floors is a bit trickier to do without making a mess. In many cases, following existing penetrations may be the best way. If not, my next choice is to find closets one above another. A discreet hole between floors in a corner adjacent to the door, or even next to the door molding, is usually not too obvious, especially if the cable is then painted the same color as the wall surface. If you're not comfortable with any of this, a competent residential electrician can likely do it all for you, once he understands exactly what you want. If possible, do it in such a way that you can pull the cables out and replace them or add to them. Ask the electrician to leave a loose piece of cord along the path so you can add additional cables as your needs expand — and they will.

Bringing Balanced Transmission Lines In from the Cold

All the techniques that we discussed for coax can also be applied to balanced lines, with just a few caveats. Balanced lines need to avoid a number of situations that wouldn't bother coax. Conditions to watch for are runs that are within a few inches of metal ducting, pipes, or wiring. Also, lossy material that will absorb energy from the fields around the line must be avoided. Perhaps most critical is inadvertent coupling to and from signal lines, including telephone, network, or alarm systems.

If it is not possible to avoid such environments, it is possible to employ a section of dual coax balanced line, as discussed in Chapter 5 and illustrated in Figure 5.9. While this will be an unmatched section resulting in an

impedance bump, that is not at all critical in the usual unmatched balanced line configuration, but should be considered if dealing with a matched condition, such as a 600 Ω feed to a rhombic antenna, or a 300 Ω feed to a folded dipole. The other consideration is that the loss will be that of unmatched coax, likely significant, so the length of this section should be as short as possible. For example, I used about 4 feet on one side of a rhombic feed as it went through a potentially lossy wall sill, just above the foundation line, without any problems.

GROUNDING AND LIGHTNING PROTECTION

While not a "transmission line" issue, per se, transmission lines that bring signals in from antennas can also bring in lightning energy if not properly protected. We will not go completely into lightning protection here, since that is arguably a subject for a book of its own; rather, we will briefly discuss ways to minimize what may be coming down the line as it comes inside.

A key to understanding lightning effects is to appreciate that with peak lightining strike current intensities from perhaps 20,000 A (50th percentile) to 200,000 A (90th percentile), it's not a question of where the current will go, but rather how much is left after you've gotten rid of as much as you can outside, before it heads toward the shack. This requires consideration of tower and antenna grounding with a low enough impedance to drain as much of the current as possible.

Still, it won't all go there — it will divide between paths to ground based inversely on impedance. Some will always go on the coax or other transmission line towards the station. It will show up in two forms; common mode current, essentially on the outside of the coax shield, and differential mode, between the inner conductor of the coax and the shield. In most environments, the common mode is a much larger fraction of the lightning current than the differential mode and can be reduced by low impedance grounding of the shields of coax as it comes into the building.

The Grounded Entrance Panel

The way to achieve this is to have the cable entrance at ground level and have as close to zero length conductivity as possible to a good ground structure at that point. This is not the usual solitary ground rod required by the National Electric Code (NEC), but a network of ground rods interconnected by buried, heavy, bare conductors that help distribute the current to the Earth's surface. The amount and extent needed for a desired grounding effectiveness will depend on the electrical characteristics of the soil at each location. The NEC, written into most local building codes, requires that all

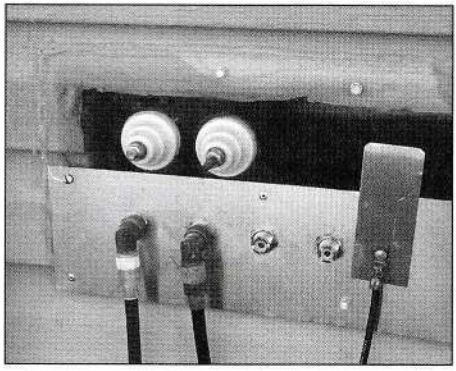

Figure 9.9 – The grounded entrance panel at amateur station K8CH.

grounds be bonded together. Thus your radio ground system should be bonded to the ground used at the electric utility panel — preferably connected via a short heavy conductor (sized per the local building code) running outside the building.

The best way to provide maximum protection, in my opinion, is to have all cables enter through a common ground level entrance panel, as shown in **Figure 9.9**. By having the panel at ground level, it is possible to have the lowest impedance ground connection arrangement by having the ground system start right at the panel. Instead of using feed-through connectors, my ground level entrance panel (shown in Figure 8.3) has commercial lightning arresters that serve double duty and are bonded to an aluminum plate that is grounded to an extensive ground system tied to a rod at the window and extending outward to multiple rods through buried bare ground wires.

The window line entrance (not shown in Figure 8.3, but similar to the two feed-through insulators visible in Figure 9.9) goes to a balanced feed arrestor just inside the panel. It is also possible to use two coaxial lightning arrestors to protect the equipment tied to the balanced feed line, with one conductor on each arrestor. Just make sure you calculate how high the operating voltage will be, and select appropriate arrestors so that they won't fire during normal transmission.

At my station, I have push-on type UHF coax connectors on my coax cables going to the inside connection of the arrestors (available from **www.americanradiosupply.com** and others) and double banana type going to the balanced arrestor. I routinely keep them disconnected when not actually on the air. In addition, I keep my ARRL All Risk equipment insurance policy up to date (see **arrlinsurance.com**).

Above-Ground Entrance Arrangements

A station located on an upper story without ground-level access has a different set of challenges. While it may be tempting to reduce transmission line length by making runs directly to the station, arguably it is the worst case from a lightning protection perspective, since all lightning currents on transmission lines are forced to go through the station. A better arrangement is to run the cables to ground level with an appropriate grounding and surge protection interface at that point, as shown in **Figure 9.10**. It's not bad to have additional arrestors at the station end, but the ground-level ones are the most important, in my view.

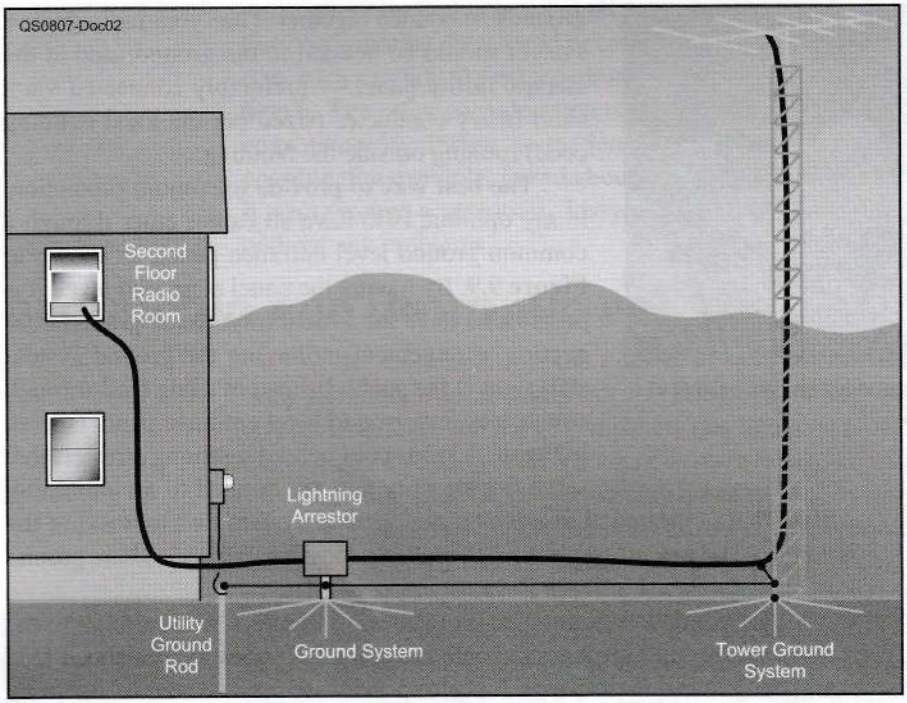

Figure 9.10 – Suggested arrangement for lightning protection grounding of an upper-story cable entrance. By running the cables first to grounding and lightning protection at ground level, the lowest impedance ground connection is provided.

TRANSMISSION LINE CARE AND MAINTENANCE

Fortunately, transmission lines tend to be rather low maintenance, however, that's not quite the same as "no maintenance." Transmission lines can last for many years, but none last forever, with typical expected useful lives of 10 to 20 years. That, of course, assumes proper installation and care.

Premature Line Degradation

Environmental factors are the major cause of early line degradation. Probably the most significant are the result of water penetration that occurs due to insufficient sealing of ends, or through jacket penetration resulting from abrasion. The insidious aspect of this is that such gradual degradation is not easily noticed through normal operation until it goes quite far. While we will pay lots of money for an additional 2 or 3 dB of antenna gain, we are not too likely to notice 2 or 3 dB of additional transmission line loss. In fact, the additional line loss results in lower SWR at the station end, along

with easier tune up and wider bandwidth — each of which could be, but probably aren't, noticed due to the gradual change.

Line Inspection

A regular program of physical inspection of transmission lines is most appropriate. Areas that are becoming abraded, show signs of insulation cracking, or from which waterproofing material is becoming unsealed can be readily addressed before they cause serious problems. A good application of electrical tape can provide additional coverage, as well as additional layers in areas subject to abrasion.

Be aware of areas that are bent more tightly than the allowed bending radius shown in Table 9.1. Foam dielectric cable, while lower in loss than cables with solid polyethylene dielectric, is subject to migration of the center conductor and possible shorting, if bent too much.

Another potential problem area is any solder connections that are exposed to the elements. Solder oxidizes in nature and can erode over time, eventually making for intermittent or failed connections.

Routine Measurement

It is a good idea to take and record a complete SWR run across frequencies of each antenna and transmission line system at installation. If nothing degrades, the values should stay unchanged over time. As a general rule, if the SWR goes up, look to the antenna for changes. If the SWR goes down, check for additional transmission line loss, since antennas rarely retune themselves, left to their own devices.

Checking Line Operation

Perhaps the best way to evaluate a line's operational characteristics is to measure the loss and SWR before installation, and then again during regular inspection periods. Just put a signal into a dummy load and wattmeter at the radio end, without the line and repeat the measurement at the far end. Any reduction in power delivered should be noted, and the loss calculated and recorded. Additional loss over time is an indication of degradation.

Checking Line Loss from One End

While measuring loss as described above is the most accurate method, sometimes it is not feasible to get equipment to the far end. In that case we can get a good measure of line loss from one end by measuring the SWR at the frequency of interest with the coax either open or shorted. If we had ideal lossless coax, our measured SWR would be infinite, since all the power would be reflected and would return to the source. With losses

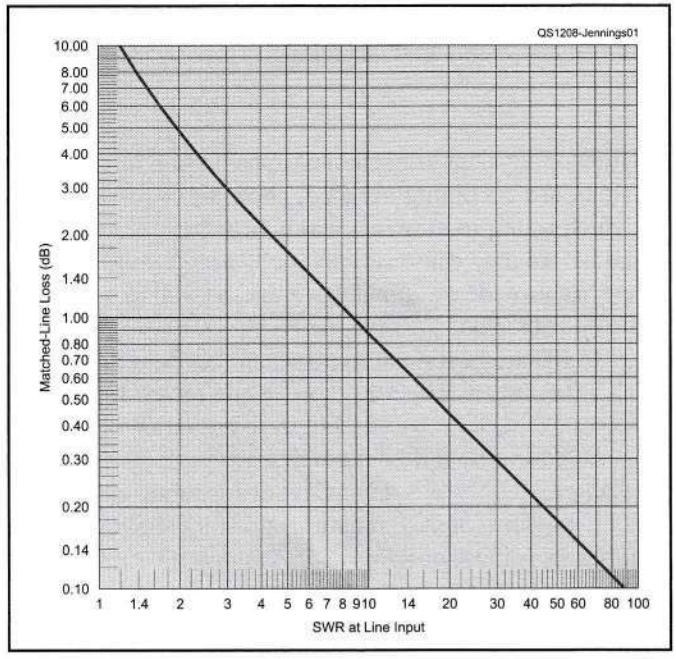

Figure 9.11 – Graph of the apparent SWR versus losses in a coax measured terminated in an open or short. Find the SWR value you measured on the horizontal axis. then go straight up and read the one way matched loss in dB on the vertical axis where the SWR reading crosses the diagonal line. Note that if the line is not matched, the loss can increase significantly.

in the coax, something else happens. Whatever signal power we put into one end will arrive at the other end with the same power, less the amount of line loss. Because the short or open at the far end of the coax provides a total reflection, the signal then reverses its direction and returns to the source end. On the return trip, the power level at the far end of the coax will be again reduced by the losses in the coax.

The reduced reflected power will show up in real coax as an SWR that is less than infinite. The higher the loss in the coax, the lower the measured SWR as read at the test end. Carried to extremes, a very high loss in a length of coax (such as the losses at UHF for a 500 foot long piece of RG-58) will result in an SWR of nearly 1:1 with the far end of the coax open or shorted.

Figure 9.11 shows a graph from the 16th edition of *The ARRL Antenna Book* of the SWR versus matched loss in a coax measured with a short or open at the far end. The section also provides an equation to determine the one-way matched loss from the measured SWR: L_M is the one-way matched line loss in decibels at the measurement frequency.

$$L_M = 10 \times \log_{10} \{(SWR + 1)/(SWR - 1)\}$$

In other words, if you measured an SWR of 3:1 with a length of open or shorted coax, either Figure 9.11 or the above equation indicates that the cable loss will be 3 dB at the frequency of interest.

To make the measurement, first make sure the antenna end of the coax is not connected to anything, and that any shorts you placed there during the ohmmeter tests have been removed. Follow the instructions in the manual for the antenna analyzer to make the SWR measurement.

As an example, let's say we measured the SWR of a 50 foot length of

RG-213 used at a dual-band VHF/UHF repeater site. At 147 MHz the open circuit SWR was 6.6:1. This indicates a loss of about 1.3 dB, compared to 1.4 dB predicted by *TLW* for 50 feet of RG-213 (Belden 8267).[2] At 445 MHz, the measured SWR was 1.4, indicating a loss of 7.78 dB, much worse than the 2.6 dB predicted by *TLW*. Thus this coax, while useful on 2 meters, will not be very good on 70 cm and is probably in the process of degrading.

What if the Antenna is Up in the Air?

The tests described previously are great if you have access to both ends of the coax, but sometimes you would like to find out about that coax without going up the tower. While you don't have control over the far end, you likely know what's there, if it's your antenna. For example, I have a 2 meter Yagi with a T matching section. While that provides a nice 50 Ω termination at 2 meters, it should look like a short at dc, and an ohmmeter continuity test should show a very low resistance, almost as low as if it were a short. A split feed Yagi or dipole should look like an open at dc.

The SWR at 2 meters won't tell us much about loss, in fact the lossier it is, the better the SWR will look. On the other hand, it will look a lot like a short at 1/10 the frequency or at 20 meters. A measurement there should give us a good, but not precise, idea of the 14 MHz loss. If the cable is good there, chances are it is also good at 2 meters. Other types of antenna connections may be trickier to make use of, but if you measure the SWR on other frequencies when the cable is new, and store the data in your archives, any change in later years may mean either the antenna or transmission line has undergone a change that merits investigation.

Another trick is to sweep your analyzer frequency looking for the worst SWR. That probably indicates either a very high or very low impedance termination and the loss at that frequency will be no better than that indicated by the SWR.

A Cautionary Note — Note that all of the loss results based on measured SWR are no better than the data provided by the SWR analyzer. *The ARRL Antenna Book* notes: "The instruments available to most amateurs lose accuracy at SWR values greater than about 5:1, so this method is useful principally as a go/no go check on lines that are fairly long." That really is the only question you need answer — do we want to keep this coax, or is it time for a replacement? These tests should give you enough information to make those decisions.

Notes

[1] L Nelson, AB0DZ, "Hints & Kinks — Anchoring Coaxial Feed Line," *QST*, Aug 2009, p 60.

[2] *The ARRL Antenna Book*, 16th Edition.

[3] *TLW, Transmission Line Program for Windows* software is provided on a CD with *The ARRL Antenna Book*.

Eliminate Line Loss!

Transmission lines are an integral part of the art of radio. Designed to carry RF power over short to medium distances with minimal loss, properly selected and installed transmission lines can be as important as radio equipment and antennas are for a station's success.

The Care and Feeding of Transmission Lines is a radio amateur's guide to understanding transmission lines. It includes an introduction to the various types of transmission lines, key parameters of coaxial cable and balanced line types, as well as the different types of connectors. With this book, you'll learn how to select the most appropriate transmission line for an application and how to install it, as well as maintenance techniques to help extend the useful life of the line.

Includes:

- **What is a Transmission Line and Why Do We Need One?**
- **Let's Examine Coaxial Transmission Line**
- **Other Types of Unbalanced Line**
- **Let's Examine Balanced Transmission Line**
- **Transmission Line Interconnections**
- **Determining Which Line is Best Suited for a Particular Application**
- **Application and Installation Notes**
- **Transmission Line Care and Maintenance**

About ARRL and the Amateur Radio Service

Amateur (Ham) Radio provides the broadest and most powerful wireless communications capability available to any private citizen anywhere in the world. The principles of this federally licensed radio service include public service, radio experimentation, and international goodwill. ARRL is the national membership association for Amateur Radio operators. ARRL has books, software, online courses and other resources for licensing, operating and training.

ISBN 978-0-87259-478-4
52795
9 780872 594784
USA $27.95 ARRL Order No. 4784

Published by:
ARRL The national association for AMATEUR RADIO®
225 Main Street, Newington, CT 06111-1494 USA
www.arrl.org

ELECTRONIC WARFARE FUNDAMENTALS

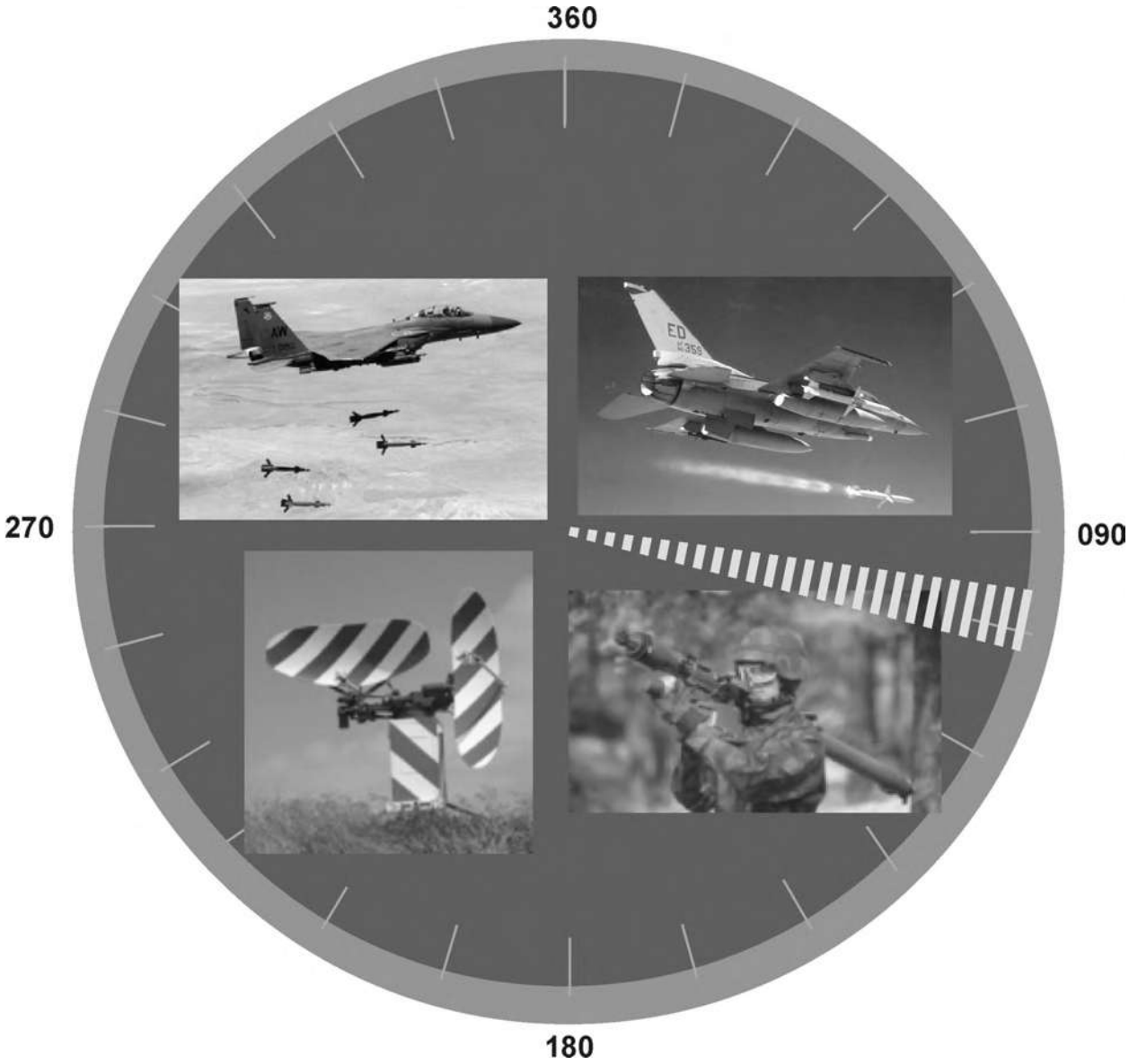

NOVEMBER 2000

PREFACE

Electronic Warfare Fundamentals **is a student supplementary text and reference book that provides the foundation for understanding the basic concepts underlying electronic warfare (EW). This text uses a practical building-block approach to facilitate student comprehension of the essential subject matter associated with the combat applications of EW.**

Since radar and infrared (IR) weapons systems present the greatest threat to air operations on today's battlefield, this text emphasizes radar and IR theory and countermeasures. Although command and control (C^2) systems play a vital role in modern warfare, these systems are not a direct threat to the aircrew and hence are not discussed in this book. This text does address the specific types of radar systems most likely to be associated with a modern integrated air defense system (IADS).

To introduce the reader to EW, ***Electronic Warfare Fundamentals*** **begins with a brief history of radar, an overview of radar capabilities, and a brief introduction to the threat systems associated with a typical IADS. The two subsequent chapters introduce the theory and characteristics of radio frequency (RF) energy as it relates to radar operations. These are followed by radar signal characteristics, radar system components, and radar target discrimination capabilities. The book continues with a discussion of antenna types and scans, target tracking, and missile guidance techniques.**

The next step in the building-block approach is a detailed description of countermeasures designed to defeat radar systems. The text presents the theory and employment considerations for both noise and deception jamming techniques and their impact on radar systems. This is followed by a chapter on decoys, both for defeating an IADS as well as for self-protection. Then, the next chapter discusses chaff characteristics, employment, and impact on specific radar systems.

The following two chapters are dedicated to the IR threat. The first covers IR theory, IR target detection and tracking, and advanced IR missile flare rejection techniques. The second chapter presents IR countermeasures to include flare employment, maneuvers, and missile warning equipment.

Electronic Warfare Fundamentals **then addresses an important aspect of EW, specifically electronic protection (EP). This section includes a description of the most common radar EP techniques designed to counter noise jamming, deception jamming, and chaff employment. The book concludes with an overview of the basic components and limitations of a typical radar warning receiver (RWR), current geolocation techniques, and it finally discusses the basic components of a self-protection jamming system.**

In addition to the textual material, the book also contains a detailed glossary of EW-related terms and acronyms for quick reference. A list of references is provided to acknowledge the source material used in the preparation of this text. These sources also provide the interested student with a supplementary reading list to learn more about a specific topic.

For information or comments on this document, please contact:

Det 8, ACC TRSS
4349 Duffer Drive, Ste 437
Nellis AFB NV 89191-7007

DSN: 682-4897
DSN FAX: 682-7391
Comm: (702) 652-4897
Comm FAX: (702) 652-7391

TABLE OF CONTENTS

CHAPTER 1. INTRODUCTION TO RADAR 1-1
1. INTRODUCTION 1-1
2. HISTORY 1-1
3. TARGET DISCRIMINANTS 1-2
4. INTRODUCTION TO INTEGRATED AIR DEFENSE SYSTEMS (IADS) 1-6
5. SUMMARY 1-10

CHAPTER 2. CHARACTERISTICS OF RF RADIATION 2-1
1. INTRODUCTION 2-1
2. FREQUENCY 2-1
3. WAVELENGTH 2-2
4. POLARIZATION 2-2
5. DOPPLER EFFECT 2-5
6. ELECTROMAGNETIC SPECTRUM 2-7
7. RF PROPAGATION 2-9
8. SUMMARY 2-14

CHAPTER 3. RADAR SIGNAL CHARACTERISTICS 3-1
1. INTRODUCTION 3-1
2. PULSE WIDTH (PW) 3-1
3. PULSE RECURRENCE TIME (PRT) 3-1
4. PULSE REPETITION FREQUENCY (PRF) 3-2
5. RADAR RECEIVER CHARACTERISTICS 3-3
6. DUTY CYCLE 3-4
7. PEAK POWER 3-4
8. AVERAGE POWER 3-5
9. MODULATION 3-6
10. SUMMARY 3-8

CHAPTER 4. RADAR SYSTEM COMPONENTS 4-1
1. INTRODUCTION 4-1
2. PULSE RADAR SYSTEM 4-1
3. CONTINUOUS WAVE (CW) RADAR 4-7
4. PULSE DOPPLER RADAR 4-9
5. MONOPULSE RADAR 4-10
6. SUMMARY 4-13

CHAPTER 5. RADAR PRINCIPLES 5-1
1. INTRODUCTION 5-1
2. RADAR RANGE 5-1
3. AZIMUTH DETERMINATION 5-7
4. ELEVATION DETERMINATION 5-11
5. RADAR RESOLUTION CELL 5-12
6. PULSE DOPPLER VELOCITY DETERMINATION 5-14
7. BASIC RADAR EQUATION 5-18
8. SUMMARY 5-21

CHAPTER 6. ANTENNA CHARACTERISTICS AND SCANS 6-1
1. INTRODUCTION 6-1
2. PARABOLIC ANTENNA 6-1
3. CASSEGRAIN ANTENNA 6-3
4. PHASED ARRAY ANTENNA 6-5
5. ANTENNA GAIN 6-9
6. POWER DENSITY 6-11
7. CIRCULAR SCAN 6-12
8. LINEAR SCAN 6-16
9. UNIDIRECTIONAL SCAN 6-16
10. BIDIRECTIONAL SCAN 6-17
11. CONICAL SCAN 6-18
12. TRACK-WHILE-SCAN 6-20
13. IMPACT OF TERRAIN ON RADAR SCANS 6-23
14. SUMMARY 6-26

CHAPTER 7. TARGET TRACKING 7-1
1. INTRODUCTION 7-1
2. RANGE TRACKING 7-2
3. CONICAL SCAN 7-4
4. TRACK-WHILE-SCAN (TWS) 7-6
5. LOBE-ON-RECEIVE-ONLY (LORO) 7-11
6. MONOPULSE RADAR 7-12
7. CONTINUOUS WAVE (CW) RADARS 7-16
8. PULSE DOPPLER RADAR 7-20
9. SUMMARY 7-24

CHAPTER 8. RADAR MISSILE GUIDANCE TECHNIQUES 8-1
1. INTRODUCTION 8-1
2. COMMAND GUIDANCE 8-3
3. SEMI-ACTIVE GUIDANCE 8-6
4. ACTIVE GUIDANCE 8-9
5. SEEKER-AIDED GROUND GUIDANCE/TRACK-VIA-MISSILE GUIDANCE ... 8-11

6. ANTIAIRCRAFT ARTILLERY (AAA) 8-12
7. SUMMARY 8-15

CHAPTER 9. INTRODUCTION TO RADAR JAMMING 9-1
1. INTRODUCTION 9-1
2. RADAR JAMMING TYPES 9-1
3. RADAR JAMMING EMPLOYMENT OPTIONS 9-3
4. FUNDAMENTALS OF RADAR JAMMING 9-7
5. SUMMARY 9-15

CHAPTER 10. RADAR NOISE JAMMING 10-1
1. INTRODUCTION 10-1
2. RADAR NOISE JAMMING EFFECTIVENESS 10-1
3. RADAR NOISE JAMMING GENERATION 10-4
4. BARRAGE JAMMING 10-5
5. SPOT JAMMING 10-6
6. SWEPT-SPOT JAMMING 10-7
7. COVER PULSE JAMMING 10-8
8. MODULATED NOISE JAMMING 10-10
9. SUMMARY 10-11

CHAPTER 11. DECEPTION JAMMING 11-1
1. INTRODUCTION 11-1
2. FALSE TARGET JAMMING 11-3
3. RANGE DECEPTION JAMMING 11-5
4. ANGLE DECEPTION JAMMING 11-8
5. VELOCITY DECEPTION JAMMING 11-11
6. MONOPULSE DECEPTION JAMMING 11-17
7. TERRAIN BOUNCE 11-23
8. SUMMARY 11-24

CHAPTER 12. DECOYS 12-1
1. INTRODUCTION 12-1
2. SATURATION DECOYS 12-1
3. TOWED DECOYS 12-3
4. EXPENDABLE ACTIVE DECOYS 12-6
5. SUMMARY 12-7

CHAPTER 13. CHAFF EMPLOYMENT 13-1
1. INTRODUCTION 13-1
2. CHAFF CHARACTERISTICS 13-2
3. CHAFF OPERATIONAL EMPLOYMENT 13-9
4. SUMMARY 13-16

CHAPTER 14. IR FUNDAMENTALS 14-1
1. INTRODUCTION 14-1
2. BASIC IR THEORY 14-1
3. IR SIGNATURE SOURCES 14-5
4. IR SEEKER CHARACTERISTICS 14-7
5. IR SEEKER TYPES 14-9
6. IR MISSILE FLARE REJECTION 14-12
7. SUMMARY 14-18

CHAPTER 15. IR COUNTERMEASURES 15-1
1. INTRODUCTION 15-1
2. FLARE CHARACTERISTICS 15-1
3. ADVANCED FLARES 15-3
4. FLARE EMPLOYMENT 15-4
5. IRCM TACTICS 15-5
6. MISSILE APPROACH WARNING SYSTEMS (MAWS) 15-6
7. SUMMARY 15-8

CHAPTER 16. RADAR ELECTRONIC PROTECTION (EP) TECHNIQUES 16-1
1. INTRODUCTION 16-1
2. RADAR RECEIVER PROTECTION 16-1
3. JAMMING SIGNAL AVOIDANCE 16-4
4. JAMMING SIGNAL EXPLOITATION 16-5
5. OVERPOWERING THE JAMMING SIGNAL 16-6
6. PULSE DURATION DISCRIMINATION 16-7
7. ANGLE DISCRIMINATION 16-7
8. BANDWIDTH DISCRIMINATION 16-8
9. DOPPLER DISCRIMINATION 16-9
10. TIME DISCRIMINATION 16-9
11. SUMMARY 16-10

CHAPTER 17. RADAR WARNING RECEIVER (RWR) BASIC OPERATIONS AND GEOLOCATION TECHNIQUES 17-1
1. INTRODUCTION 17-1
2. RWR ANTENNAS 17-1
3. RWR RECEIVER/AMPLIFIERS 17-3
4. SIGNAL PROCESSOR 17-6
5. EMITTER IDENTIFICATION (EID) TABLES 17-8
6. RWR SCOPE DISPLAY 17-8
7. RWR AUDIO 17-9
8. RWR INTERFACE CONTROL UNIT (ICU) 17-10
9. RWR LIMITATIONS 17-10
10. THREAT GEOLOCATION TECHNIQUES 17-15
11. SUMMARY 17-20

CHAPTER 18. SELF-PROTECTION JAMMING SYSTEM OPERATIONS 18-1
1. INTRODUCTION 18-1
2. RECEIVE ANTENNAS 18-2
3. RECEIVER SECTION 18-2
4. SYSTEM PROCESSOR 18-3
5. JAMMING TECHNIQUES GENERATOR 18-4
6. TRANSMIT ANTENNAS 18-4
7. C-9492 CONTROL INDICATOR UNIT 18-5
8. JAMMING POD CONSIDERATIONS 18-5
9. SUMMARY 18-7

ANNEX A. GLOSSARY A-1

ANNEX B. EC-RELATED ABBREVIATIONS AND ACRONYMS B-1

LIST OF REFERENCES

CHAPTER 1. INTRODUCTION TO RADAR

1. INTRODUCTION

The word "RADAR" is an acronym for RAdio Detection And Ranging. As it was originally conceived, radio waves were used to detect the presence of a target and to determine its distance or range (Figure 1-1).

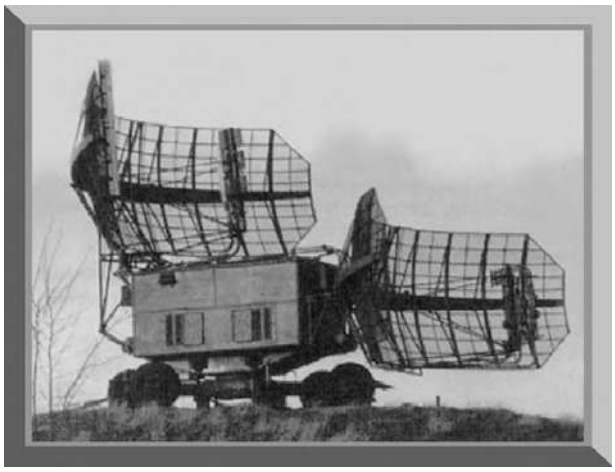

Figure 1-1. Radar System

2. HISTORY

The reflection of radio waves by objects was first noted more than a century ago. In 1903, the reflection of radio waves was employed in Germany to demonstrate detection of ships at sea (Figure 1-2). In 1922, Marconi presented the same idea in Britain but received little official interest. These early experiments used continuous wave, or CW, transmissions and relied on the reflection of a transmitted wave from a target to indicate the presence of a target. CW transmissions can detect the presence of an object and, if the radio wave is formed into a narrow beam, can also provide azimuth information. CW transmissions cannot provide range.

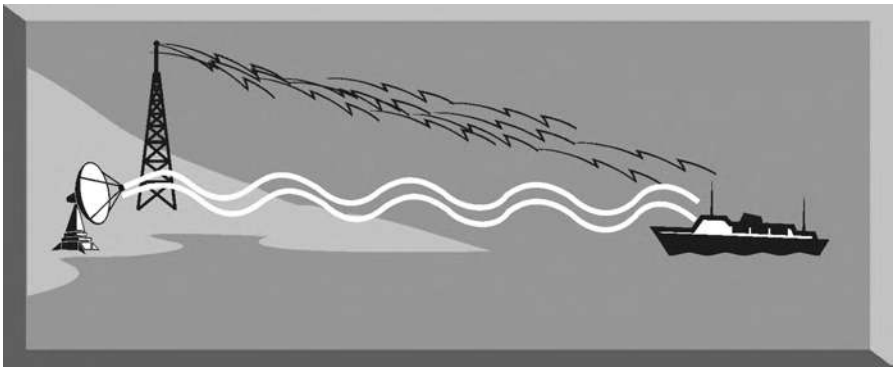

Figure 1-2. Early Continuous Wave Radar Experiments

a. The lack of range information was a serious limitation but was finally overcome by modulating the radio wave transmissions to send out a train of short pulses (Figure 1-3). The time between pulse transmission and an echo return to the receiver provides a direct measurement of range. Practical development of the pulse radar began in the 1930s, principally in the United States, Britain, and Germany. Due to deteriorating relations with Germany and the threat of invasion, the British intensified their efforts to develop a pulse radar in 1935. These efforts culminated in the development and deployment of multiple radar stations which formed the Chain Home System. These radar installations provided critical information to British pilots on the size and location of German bomber formations during the Battle of Britain.

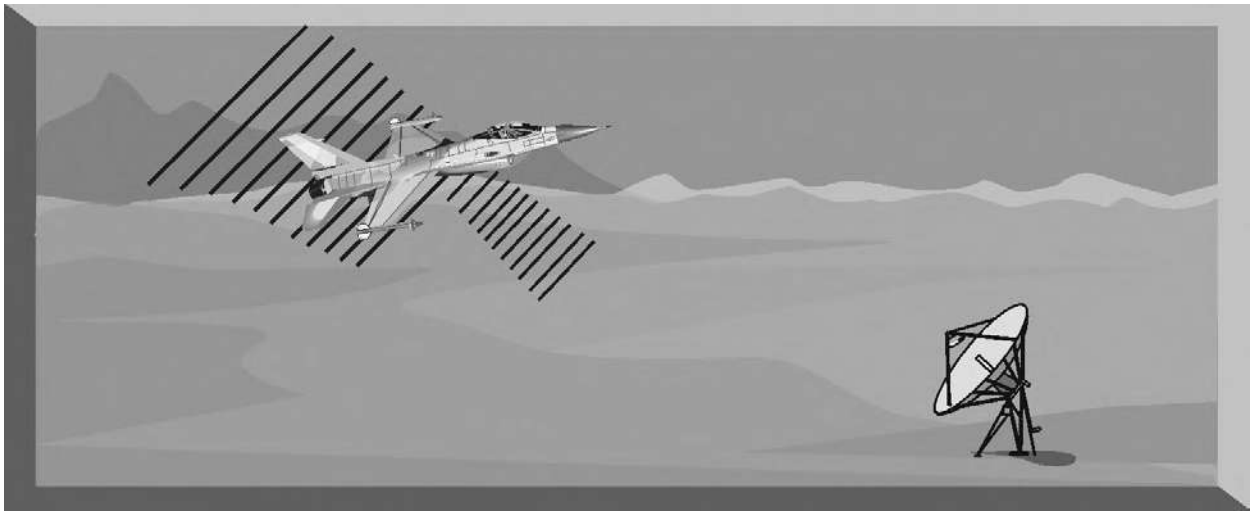

Figure 1-3. Pulse Radar Operation

b. The Chain Home System is considered the first integrated air defense system, or IADS. Radar development, with its obvious military and civilian applications, has continued unabated to the present day.

3. TARGET DISCRIMINANTS

The widespread military and civilian application of radar is based on its inherent advantages over the human eye (Figure 1-4). Radar can "see" farther than the human eye and more accurately assess the range or distance of an object. Radar works well in all-weather conditions and is relatively immune to smoke, haze, and clouds. What's more, radar works 24 hours a day because it can transmit its own energy and does not have to rely on sunshine or ambient radiation. There are some disadvantages of radar when compared to the human eye. First, radar does not have the resolution that the human eye has. While radar can detect the presence of an airplane, the human eye can discern, in great detail, the shape, size, color, and even markings. This can be a serious limitation if positive identification is required prior to engagement.

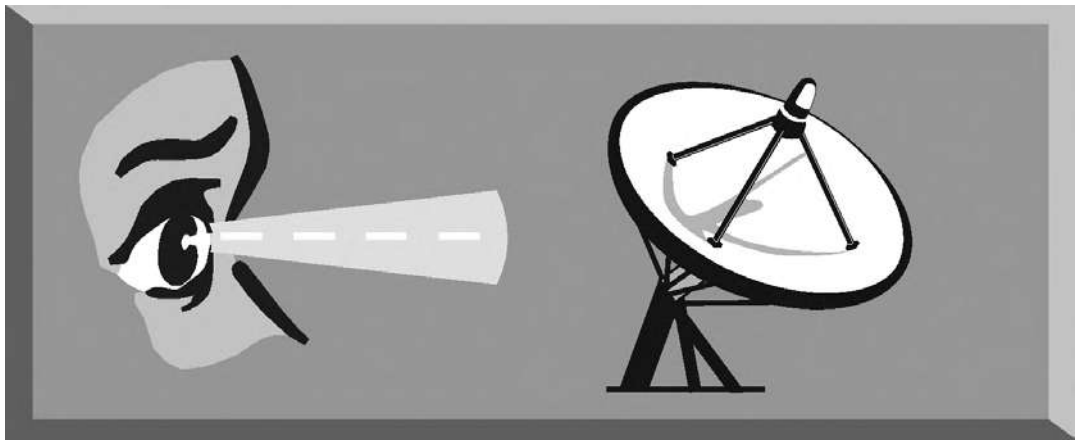

Figure 1-4. Radar Advantages and Disadvantages

Second, the human eye is not bothered by undesirable reflections, called clutter, the way radar sometimes is. Although metal is the best reflector of radio frequency (RF) energy, nearly any material will reflect some RF energy. Mountains, trees, buildings, rain, birds, and chaff all reflect RF energy. Radar systems must use target discriminants to isolate the desired target return from the clutter. These target discriminants include range, velocity, and angle (Figure 1-5).

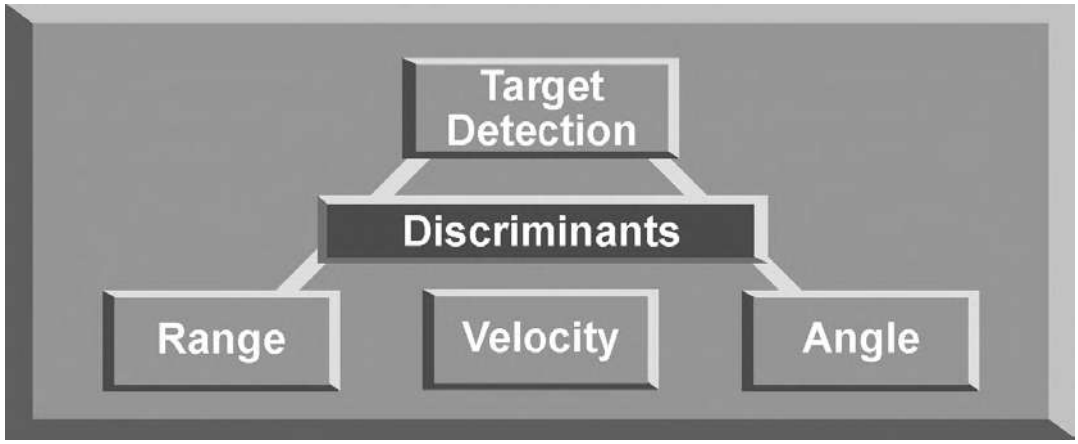

Figure 1-5. Radar Target Discriminants

a. The first target discriminant is range. The time an RF wave takes to go to, and return from, a target allows measurement of the range to that target. We know that RF energy travels at the speed of light, or "c" which is 3 x 10^8 meters per second. Target range can be determined by using the basic radar range equation (Equation 1-1), target range equals measured time, multiplied by the speed of light ("c"), divided by 2.

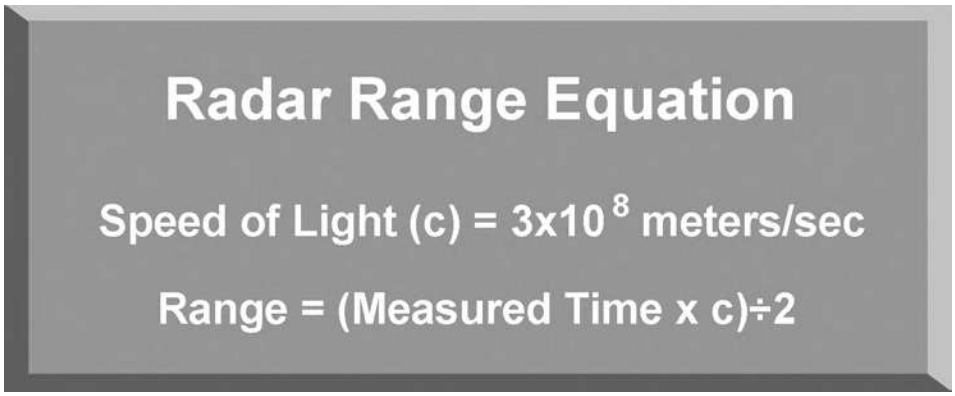

Equation 1-1. Basic Radar Range Equation

b. Target angle discrimination is another critical capability of radar systems. In order for a radar system to detect a target, the antenna must be pointed at the target during the transmission and reception of RF energy. The ability of a radar system to accurately determine angle is a function of the horizontal beamwidth of the antenna. If the radar sweep is referenced to true North, the angle of a radar return can be measured relative to true North (Figure 1-6).

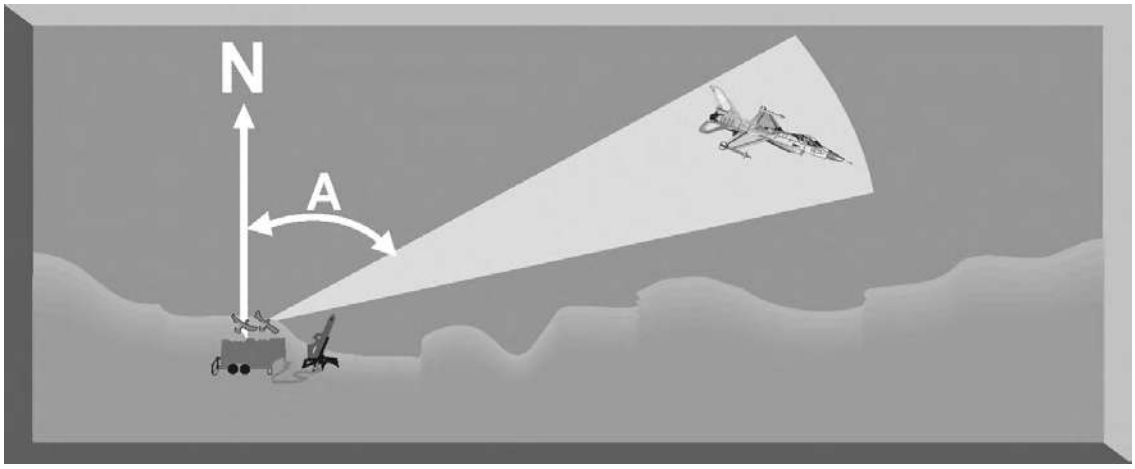

Figure 1-6. Angle Discrimination

c. Velocity discrimination is a specific capability of CW and pulse Doppler radar systems. The transmitters of CW radars send out continuous RF at a specific frequency (Figure 1-7). The reflected signal frequency is changed, or shifted, by a specific amount by a moving target. This frequency shift, called the Doppler effect, allows the measurement of the velocity of that target relative to the radar. The receiver measures this frequency difference which equates to a specific radial velocity. Pulse Doppler radars can measure the Doppler effect while still obtaining the range.

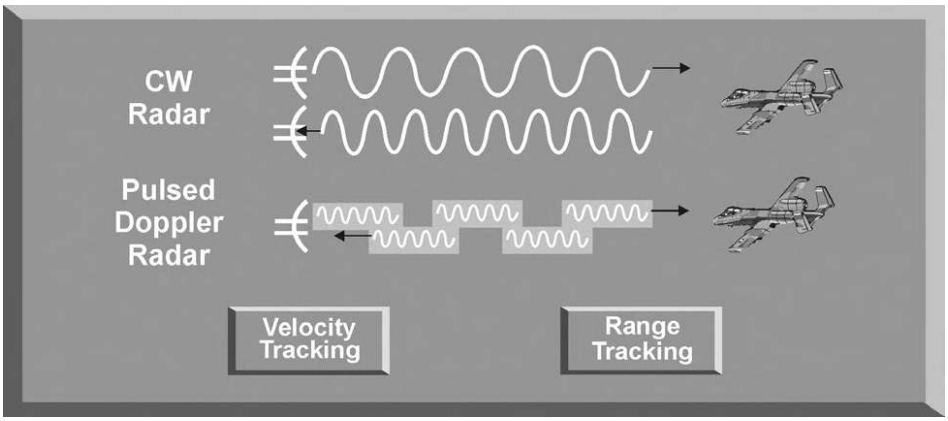

Figure 1-7. Velocity Discrimination

d. A basic pulse radar system consists of a transmitter, antenna, receiver, and a master timer (Figure 1-8). The transmitter sends electromagnetic energy (RF) to the antenna. This energy is radiated through the atmosphere. When this RF energy is interrupted by any object, such as a plane, ship, or the earth, a portion of the RF energy is reflected back to the antenna and processed by the receiver.

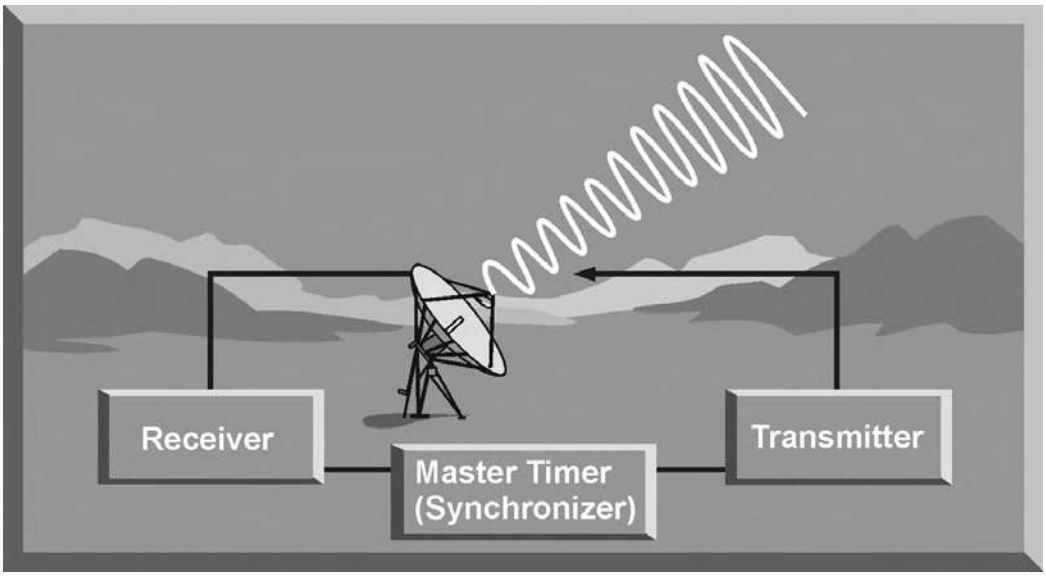

Figure 1-8. Basic Radar Operation

The reflection is called an echo, and the object interrupting the RF energy is called a target. The presence of an echo indicates target detection. If the target detected is the desired target, the echo is referred to as a target signal. If the echo is from undesired targets, such as the earth, the echo is referred to as clutter. This is especially true when the undesirable echoes make the detection of the desired target difficult. The capability of the antenna to focus the RF energy

affects the angular discrimination of the radar. The ability of the master timer to determine the time between RF transmission and target echo reception impacts the range determination capability of the radar. The ability of the receiver to analyze the Doppler frequency shift in the target echo determines the velocity discrimination capability of the radar and the ability of the radar to reject clutter.

4. INTRODUCTION TO INTEGRATED AIR DEFENSE SYSTEMS (IADS)

Radar systems have the inherent capability to determine accurate range, azimuth, and/or velocity information on airborne targets. Radar systems can provide this information in nearly all types of weather, day or night, and at distances that far exceed the capabilities of the human eye. Military commanders have taken advantage of these capabilities by employing radar systems to provide air defense for high-value targets. The primary missions of radar systems employed for air defense are attack warning and threat engagement.

a. Radar systems specifically designed to provide attack warning are called early warning (EW) radars (Figure 1-9). These radars are characterized by high power output, large antennas, and low frequencies. These same characteristics limit the accuracy of the target parameters available from early warning radars. The long-range detection of aircraft and the earliest possible attack warning capabilities of early warning radars provide the first line of defense for the air defense system.

Figure 1-9. Early Warning Radar System

b. Radar systems designed to provide target engagement information include ground control intercept (GCI) radars, acquisition radars, target tracking radars (TTRs), and airborne interceptor (AI) radars.

(1) GCI radars are designed to provide sufficiently accurate target aircraft range, azimuth, and altitude information to vector AI assets to intercept and destroy attacking aircraft (Figure 1-10). To provide this data, early warning radars can be deployed along with specialized height finder radars. This combination of radar systems is commonly referred to as a GCI site. Newer GCI radar systems, employing phased array antennas and Doppler processing, can provide the required 3-dimensional target information. Any radar system, or combination of radar systems, that can determine 3-dimensional target data, and is equipped with the communication equipment to pass this information to AI assets, can act as a GCI site. GCI radar systems can be used to supplement early warning radar systems to provide critical attack warning.

Figure 1-10. GCI Radar

(2) Acquisition radar systems are designed to act as GCI radars for ground based TTRs. Acquisition radar systems generally have shorter range capability than early warning radars and operate at higher frequencies. These radar systems provide accurate target range and azimuth data to TTRs to facilitate target engagement. Acquisition radars can be a distinct radar system (Figure 1-11) or be incorporated as part of the TTR (Figure 1-12).

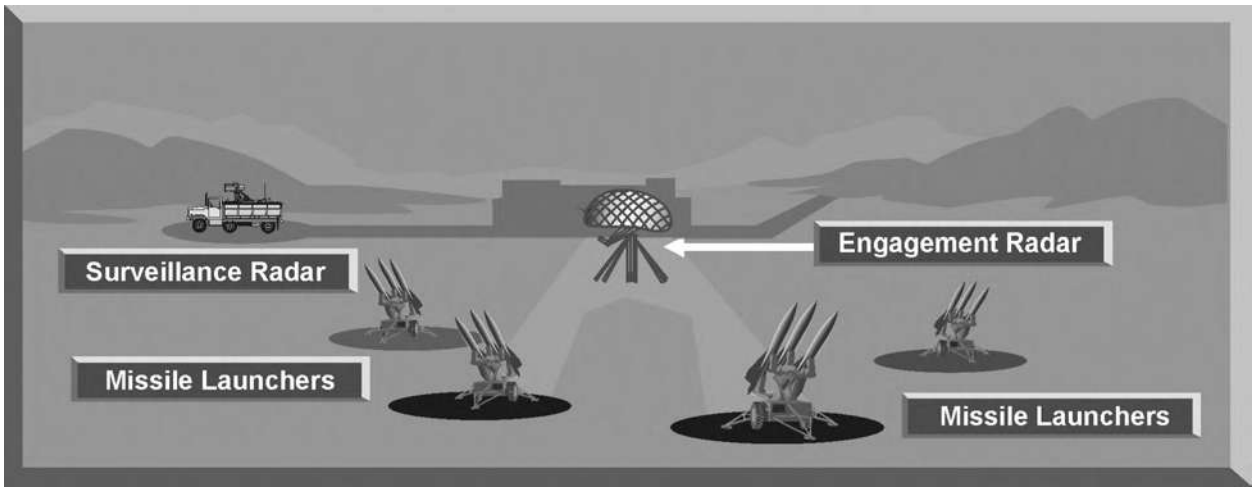

Figure 1-11. Acquisition Radar and TTR

Figure 1-12. TTR with Acquisition

(3) The primary role of TTRs, in support of an air defense system, is to provide continuous and accurate target parameters to a fire control computer. The fire control computer uses this data to guide missiles or aim antiaircraft artillery (AAA) to destroy attacking aircraft. TTRs employ various tracking techniques to continuously update target parameters. TTRs generally employ high frequencies, narrow beamwidths, and computer signal processing to enhance the accuracy of target parameters provided to the fire control computer.

(4) AI radar systems are TTRs employed by fighter aircraft to engage and destroy airborne targets (Figure 1-13). These radar systems are characterized by high frequency, sophisticated computer processing, and accurate target tracking capability. They are designed to allow the AI asset to employ air-to-air missiles and guns/cannons. TTRs and AI radars constitute the highest radar threat associated with an air defense system.

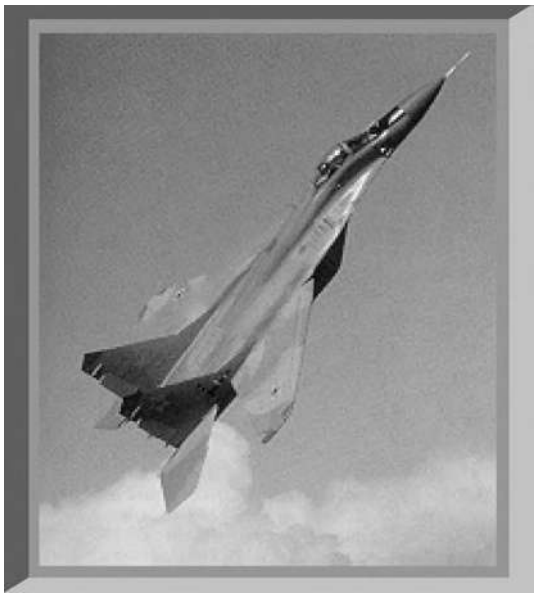

Figure 1-13. MiG-29

(5) Another growing lethal threat associated with an air defense system is infrared (IR) missiles. IR missile systems can be man-portable (Figure 1-14), mounted on vehicles, or employed by AI assets. These missile systems guide on the distinctive IR signature of aircraft. The recent proliferation and enhanced performance of IR systems has increased the contribution of these systems to air defense.

Figure 1-14. IR System

c. All these radar systems can be deployed to provide air defense for a particular country or geographical area. When the employment of these radar systems is integrated by a command and control (C^2) structure, this constitutes an IADS (Figure 1-15). The C^2 structure allows the military commander to take advantage of the threat warning provided by early warning radars. Based on this threat warning, the military commander can allocate specific assets (GCI and AI assets, or acquisition radars and TTRs) to engage airborne targets. This allocation decision is based on the capabilities of these systems and the tactical situation. This allocation process enables the military commander to maximize the capabilities of his forces to engage and destroy attacking aircraft.

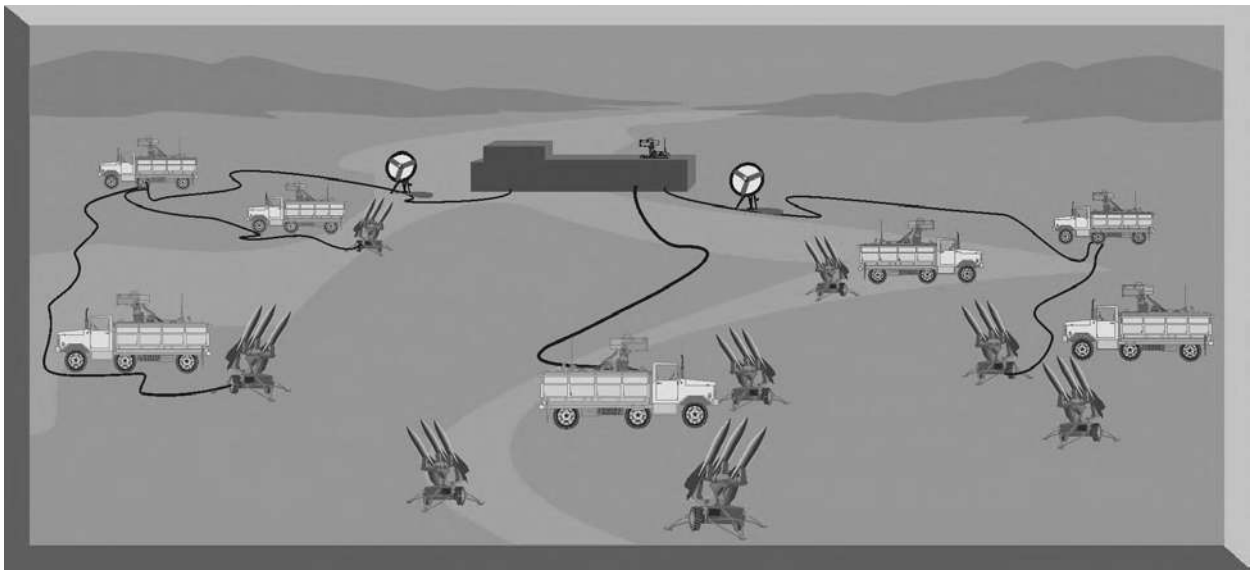

Figure 1-15. A Typical IADS

5. SUMMARY

Radar systems are the cornerstones of a modern IADS. Radar and IR threat systems operate at frequencies that span most of the electromagnetic spectrum. Each system has unique capabilities and operating characteristics that enable it to accomplish assigned tasks in support of the IADS. In order to effectively employ offensive air power on the modern battlefield, the systems that support the IADS must be negated. A basic knowledge of how radar and IR systems operate, their capabilities, limitations, and the available countermeasures is the key to defeating these systems. The purpose of this book is to provide this information.

CHAPTER 2. CHARACTERISTICS OF RF RADIATION

1. INTRODUCTION

In order for a radar system to determine range, azimuth, elevation, or velocity data, it must transmit and receive electromagnetic radiation. This electromagnetic radiation is referred to as radio frequency (RF) radiation. RF transmissions have specific characteristics that determine the capabilities and limitations of a radar system to provide these target discriminants, based on an analysis of the characteristics of the target return. The frequency of transmitted RF energy affects the ability of a radar system to analyze target return, based on time, to determine target range. RF frequency also affects the ability of the transmitting antenna to focus RF energy into a narrow beam to provide azimuth and elevation information. The wavelength and frequency of the transmitted RF energy impact the propagation of the radar signal through the atmosphere. The polarization of the RF signal affects the amount of clutter the radar must contend with. The ability of a radar system to use the Doppler effect in analyzing the radar return impacts the velocity discrimination capability of the radar. These characteristics of RF radiation will be discussed in this chapter.

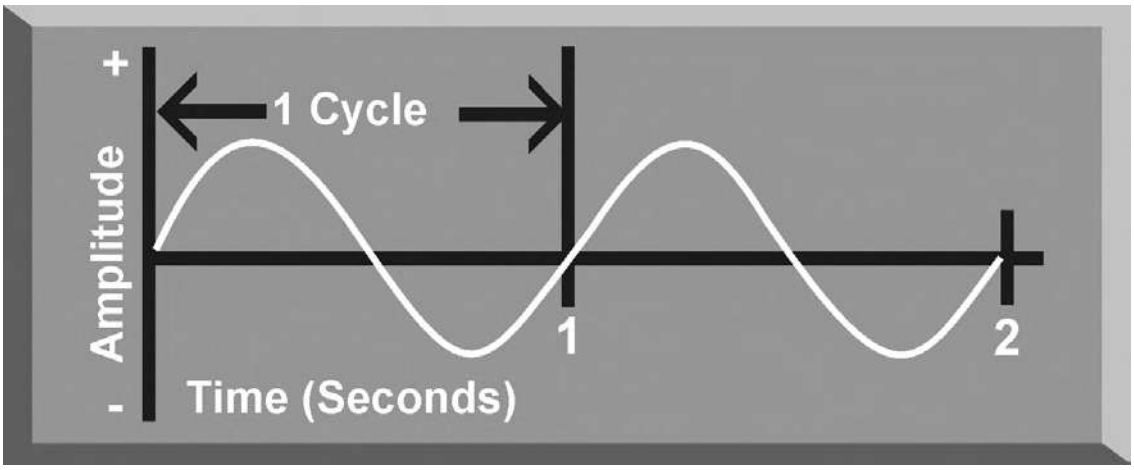

Figure 2-1. Radio Frequency

2. FREQUENCY

The output signal from a typical radio or radar system has several important characteristics that affect the capabilities and limitations of radio or radar systems. The first characteristic considered is usually RF. The frequency of the transmitted signal is the number of times per second the RF energy completes one cycle. The RF signal depicted in Figure 2-1 has a frequency of one cycle per second. The basic unit of measurement is the hertz (Hz). One hertz equals one cycle per second. Most radars have an RF in the millions of hertz, or megahertz (MHz).

3. WAVELENGTH

A characteristic of any RF signal is wavelength. Wavelength is a measure of the physical distance between peaks of a sine wave propagated in space (Figure 2-2).

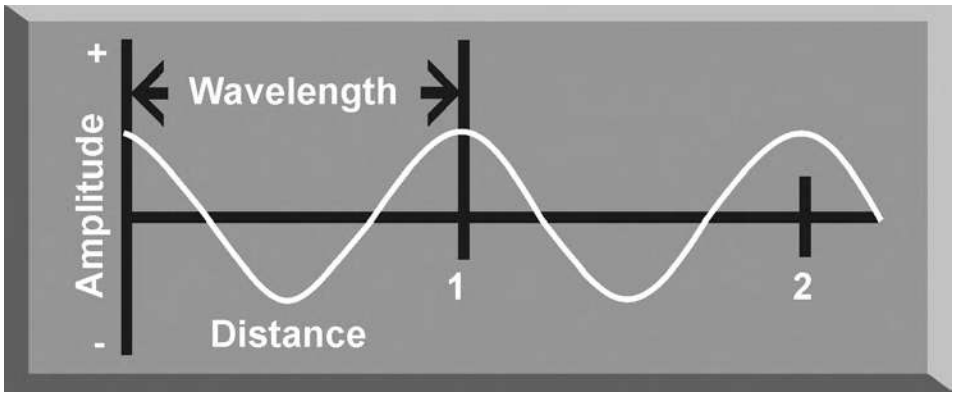

Figure 2-2. Radar Signal Wavelength

Though wavelength is measured in meters, most radar signals have wavelengths measured in centimeters or millimeters. The wavelength of a radar signal can be computed using the equation shown in Equation 2-1. The relationship between wavelength and frequency is inverse: the higher the frequency, the shorter the wavelength. In early radio and radar terminology, wavelength was used instead of frequency to describe operating characteristics of a system. Today, wavelength is used to describe systems operating at very high frequencies, such as millimeter wave, and for describing infrared (IR) systems.

$$\text{Wavelength } (\lambda) = \frac{c \text{ (Speed of Light)}}{f \text{ (Radar Frequency)}}$$

Equation 2-1. Basic Wavelength Equation

4. POLARIZATION

Another characteristic of a radio frequency wave is polarization. Polarization is determined by the radar antenna and refers to the orientation of the RF wave as it travels through space. There are two types of polarization: linear and circular.

a. Traveling electromagnetic energy has two components: an electrostatic field and a magnetic field. These two fields are always perpendicular to each other and perpendicular to the direction of travel. The polarization of the wave is defined in terms of the orientation to the electrostatic field. Many radar antennas are linearly polarized, either vertically or horizontally. The signal depicted in Figure 2-3 is vertically polarized.

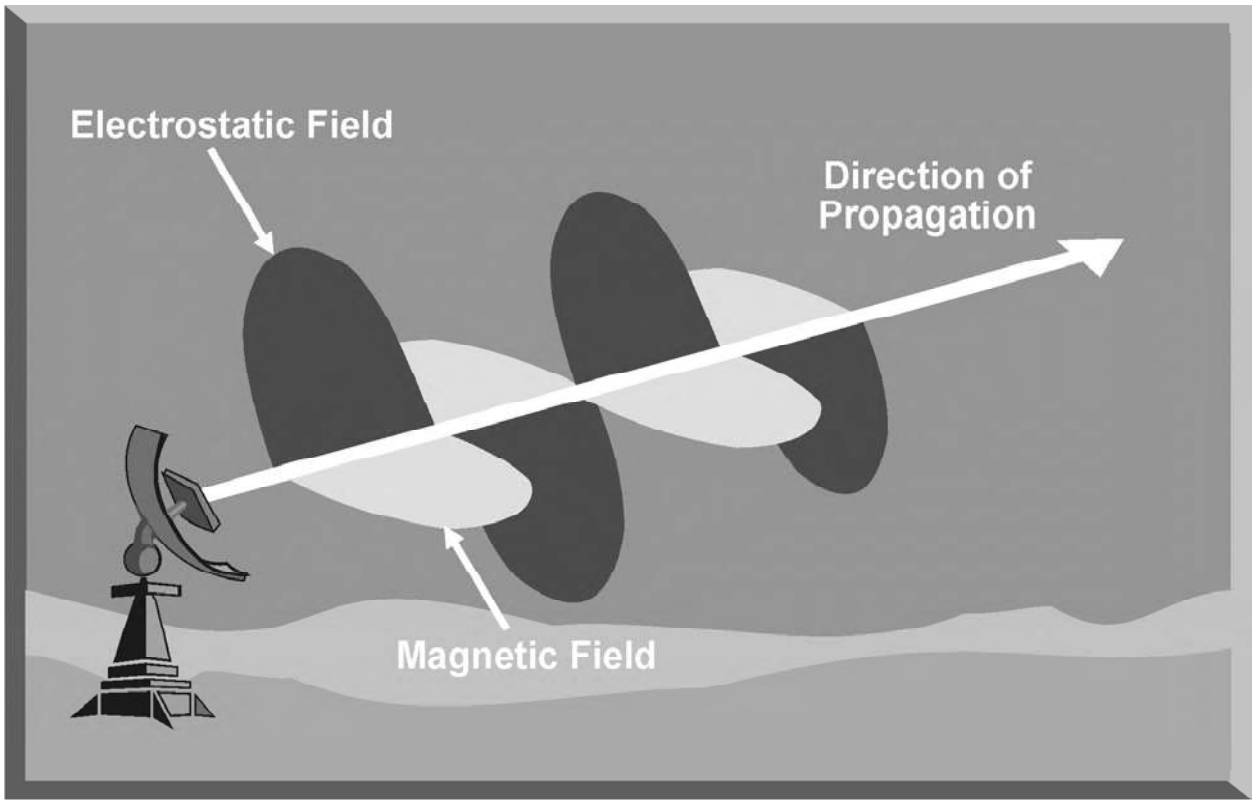

Figure 2-3. Radar Signal Vertical Polarization

b. Some radars use circular polarization to improve target detection in rain. Circular polarization can be right-hand, or left-hand orientation. For circular polarization, the direction of the electrostatic field varies with time and traces a circular locus about a fixed plane perpendicular to the direction of propagation. For a right-hand circular polarized signal, the electrostatic vector appears to rotate in a clockwise direction. For a left-hand circular polarized signal, the rotation is counterclockwise. Circular polarization can be visualized by pointing the thumb of either hand in the direction of propagation and curling the fingers in the direction of electrostatic field rotation (Figure 2-4).

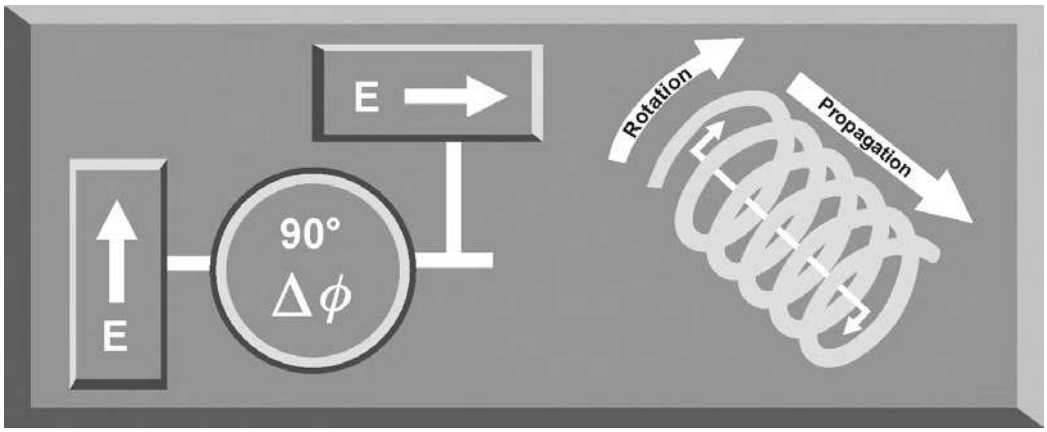

Figure 2-4. Circular Polarization

c. The impact of polarization on receivers and transmitters is fairly straightforward. If an antenna is designed to receive a particular polarization, it will have difficulty receiving a signal with an opposite polarization. This situation is defined as cross polarization (Figure 2-5).

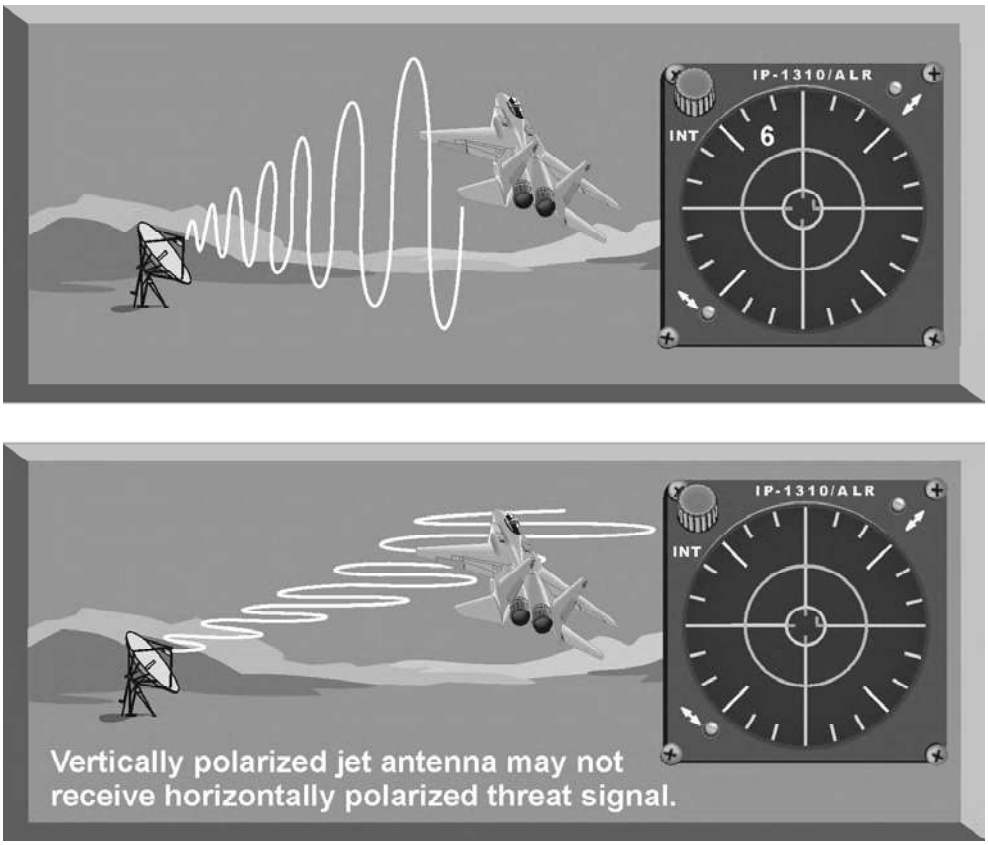

Figure 2-5. Impact of Polarization

The impact of cross polarization on electronic combat can be dramatic. If a radar warning receiver antenna is polarized to receive vertically polarized signals, a threat system employing a horizontally polarized radar signal may not be detected, or may be displayed on the scope well after the threat has acquired the aircraft. In addition, if the jamming antenna on an electronic attack (EA) system is also vertically polarized, it may not be able to jam this system. Fortunately, this potentially lethal situation rarely occurs, but future threat systems may take advantage of this situation. Table 2-1 details the impact of polarization on selected transmit and receive antenna combinations.

Table 2-1. Antenna Polarization Loss

Transmit Antenna Polarization	Receive Antenna Polarization	Percent Lost
Vertical	Vertical	0
Vertical	Slant (45° or 135°)	50
Vertical or Horizontal	Horizontal or Vertical	75
Vertical	Circular (right-hand or left-hand)	50
Horizontal	Horizontal	0
Horizontal	Slant (45° or 135°)	50
Horizontal	Circular (right-hand or left-hand)	50
Circular (right-hand)	Circular (right-hand)	0
Circular (right-hand)	Circular (left-hand)	94
Circular (right-hand or left-hand)	Slant (45° or 135°)	50

5. DOPPLER EFFECT

The "Doppler effect" takes advantage of the fact that the frequency of RF waves will be changed or shifted when reflected from a target moving relative to the radar. The shifted frequency of the returning RF wave depends on the movement of the aircraft in relation to the radar. In Figures 2-6, 2-7, and 2-8, f_o is the transmitted frequency of the radar, and f_t is the frequency of the reflected RF

wave from the target. For a stationary target, the frequency of the reflected signal will equal the frequency of the transmitted signal (Figure 2-6).

Figure 2-6. Zero Doppler Effect – Stationary Target

a. For a target moving toward the radar, the frequency of the reflected signal will be higher than the transmitted signal (Figure 2-7).

Figure 2-7. Doppler Effect – Closing Target

b. The reflected frequency for a target moving away from the radar will be lower than the transmitted frequency (Figure 2-8).

Figure 2-8. Doppler Effect – Opening Target

6. ELECTROMAGNETIC SPECTRUM

The portion of the electromagnetic spectrum (Figure 2-9) that today's electronic combat systems must deal with starts with radio waves and encompasses microwaves, infrared, and a small portion of the ultraviolet region. Communications systems generally operate in the HF, UHF, and VHF regions. Some satellite communications operate in the SHF region. Radars operate in the microwave region, normally from 0.2 – 200 gigahertz. Infrared systems operate in the region just below visible light.

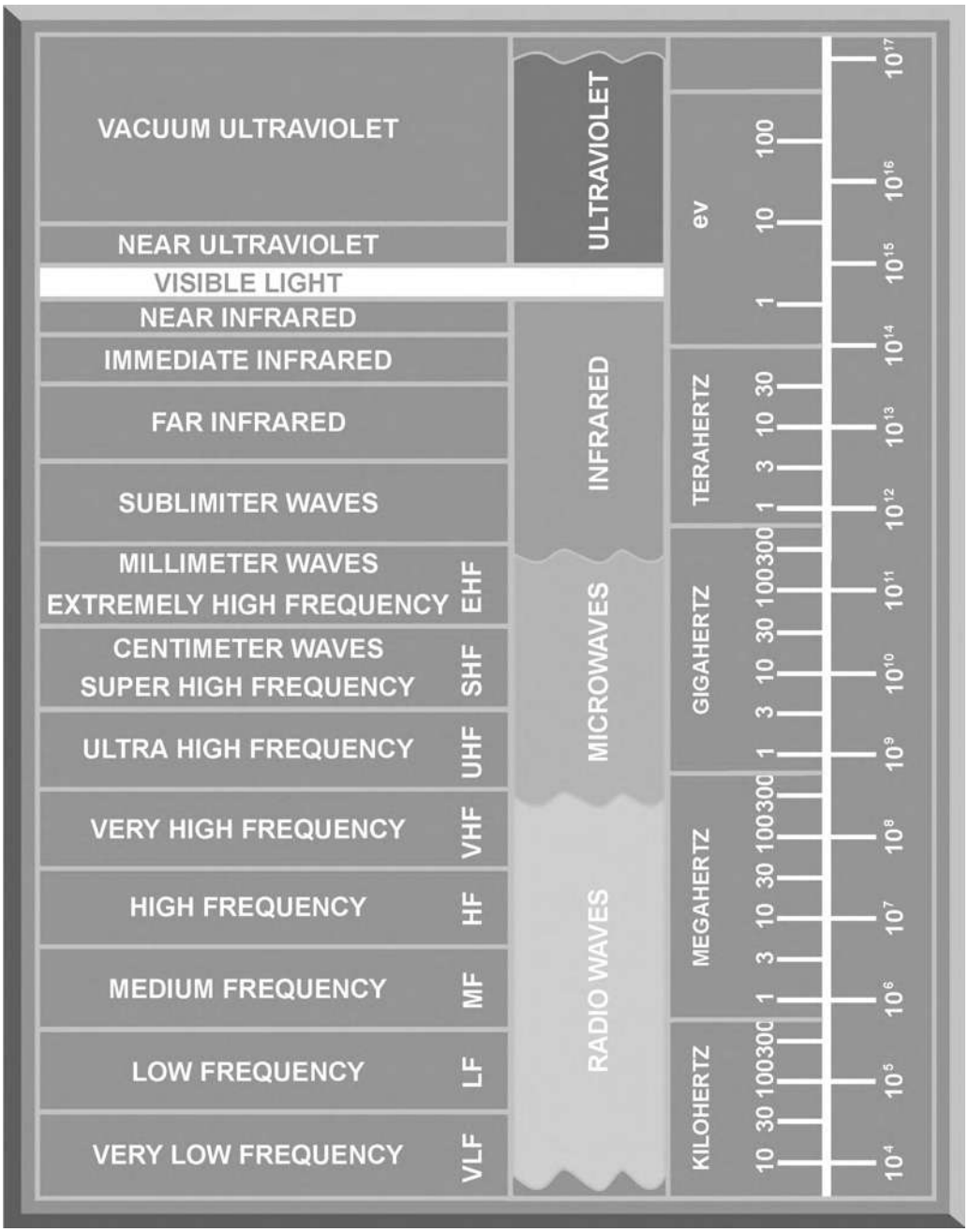

Figure 2-9. Electromagnetic Spectrum

a. Table 2-2 lists prefixes commonly used to indicate scientific notation and their abbreviations. These prefixes are often used when dealing with extremely high frequency radar signals or RF waves with extremely small wavelengths. For example, when dealing with extremely high frequency RF, it is simpler to use gigahertz, or GHz. One gigahertz is one thousand megahertz (MHz). For example, a radar operating at 3150 MHz is also operating at an RF of 3.150 GHz.

Table 2-2. Commonly Used Prefixes for Scientific Notation

Unit Designations			
Prefix	Symbol	Unit	Measure
Tetra	T	10^{12}	One Trillion
Giga	G	10^{9}	One Billion
Mega	M	10^{6}	One Million
Kilo	k	10^{3}	One Thousand
Cent	c	10^{-2}	One Hundred
Milli	m	10^{-3}	One Thousandth
Micro	u	10^{-6}	One Millionth

b. Frequency bands are often used when discussing radars and electronic combat systems. Radar designers use a frequency band designation system entirely different from the one used in electronic combat. Table 2-3 depicts both frequency band designation systems and the corresponding frequency ranges.

Table 2-3. Radar Frequency Band Designations

Frequency Range	EW Frequency Band	Radar Design Frequency Band
0-250 MHz	A	HF/VHF
250-500 MHz	B	UHF
500-1000 MHz	C	UHF
1-2 GHz	D	L
2-3 GHz	E	S
3-4 GHz	F	S
4-6 GHz	G	C
6-8 GHz	H	C
8-10 GHz	I	X (8-12.5 GHz)
10-20 GHz	J	Ku (12.5-18 GHz)
20-40 GHz	K	K (18-26.5 GHz)
40-60 GHz	L	Ka (26.5-40 GHz)
60-100 GHZ	M	40-100 Millimeter

7. RF PROPAGATION

Propagation characteristics of RF energy are profoundly affected by the earth's surface and atmospheric conditions. Any analysis of radar performance must take into account the propagation phenomena associated with RF radiation in a "real world" environment. The most important propagation phenomena include refraction, anomalous propagation (ducting), and attenuation.

a. In a vacuum, RF waves travel in a straight line. However, RF waves propagating within the earth's atmosphere do not travel in a straight line. The earth's atmosphere bends, or refracts, RF waves. One impact of the atmospheric refraction of RF waves is an increase in the line of sight (LOS) of the radar. This increase in radar LOS effectively extends the range of the radar system (Figure 2-10).

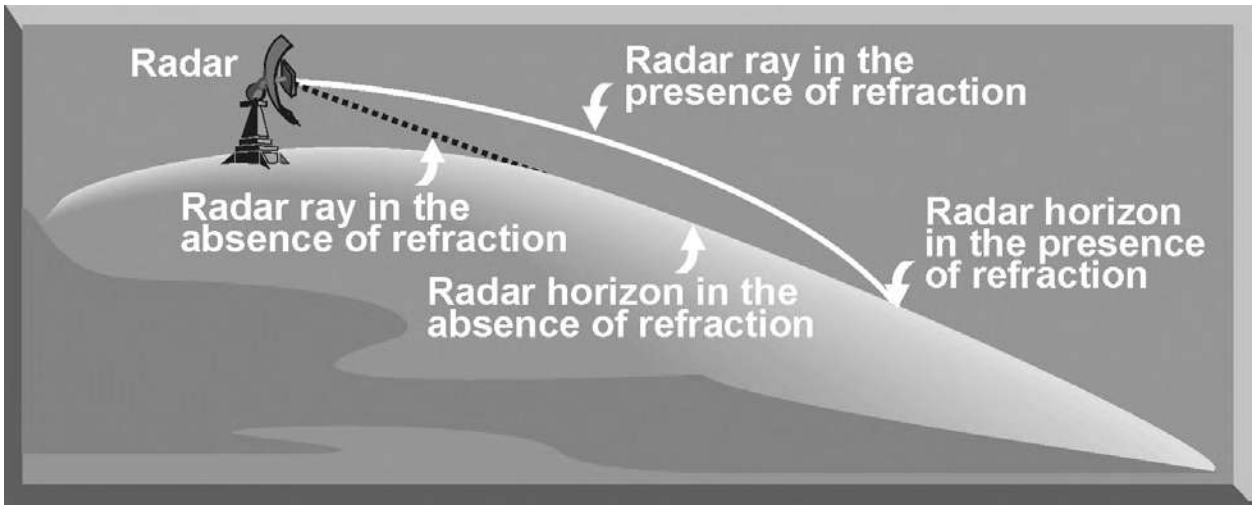

Figure 2-10. Impact of Refraction on RF Propagation

Atmospheric refraction of RF energy can also induce elevation measurement errors in radar systems (Figure 2-11).

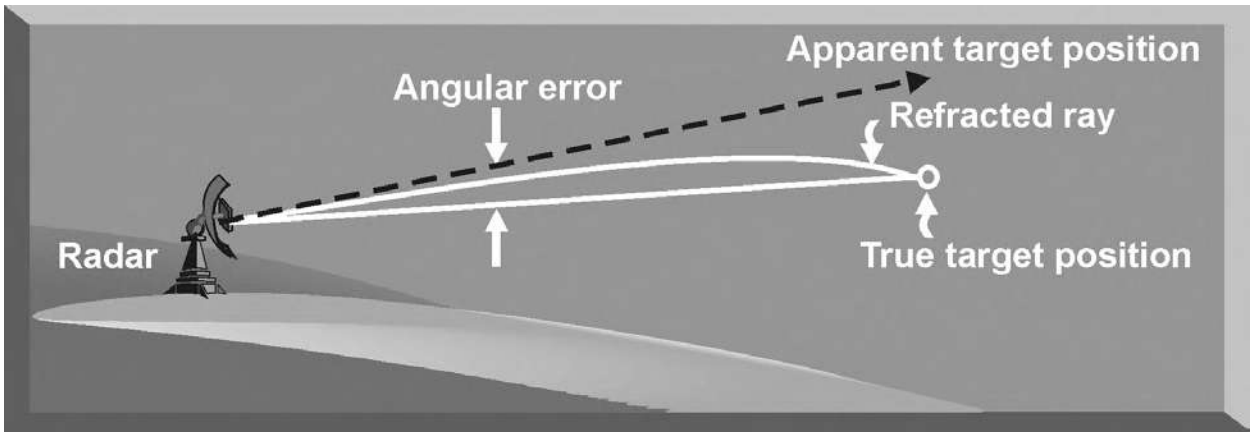

Figure 2-11. Impact of Refraction on Target Elevation Determination

(1) The refraction of RF waves in the atmosphere is caused by the variation in the velocity of propagation with altitude. The index of refraction (n) is used to describe this velocity variation and is defined by Equation 2-2.

$$\text{Index of Refraction (n)} = \frac{\text{Velocity of Propagation in a Vacuum}}{\text{Velocity of Propagation in the Atmosphere}}$$

Equation 2-2. Index of Refraction

(2) The term refractivity (N) is used for predicting the impact of refraction on RF wave propagation. Refractivity is a "scaled up" expression for the index of refraction and is used by radar designers to calculate the impact of refraction on actual radar systems. At normal radar operating frequencies, the refractivity for air containing water vapor can be computed using Equation 2-3.

$$\text{Refractivity (N)} = (n-1)\times 10^6 = \frac{77.6\,p}{T} + \frac{3.75\times 10^5 e}{T^2}$$

n = index of refraction
p = barometric pressure
e = partial pressure of water vapor
T = absolute temperature (degrees K)

Equation 2-3. Refractivity of RF Waves (Normal Radar Frequencies)

(3) As altitude increases, the barometric pressure and water vapor content decrease rapidly. At the same time, the absolute temperature decreases slowly based on the standard lapse rate. Using Equation 2-3, it can be seen that the refractivity of the atmosphere decreases with increasing altitude. This decrease in refractivity means that the velocity of RF waves increases with altitude. The result is a downward bending, or refraction, of RF waves as depicted in Figure 2-10. RF wave refraction primarily affects ground-based radar systems at low antenna elevation angles, especially at or near the horizon. For most radar applications, refraction is not a factor at elevation angles above 5 degrees.

b. The term anomalous, or nonstandard, propagation is used to describe atmospheric conditions that extend the propagation of RF waves and increase radar range. The most common anomalous propagation phenomena is called superrefraction, or ducting.

(1) A superrefracting duct is formed when the refractivity of the atmosphere (Equation 2-2) rapidly decreases with altitude. Based on Equation 2-2, this occurs when the temperature increases with altitude and/or the water vapor content decreases with altitude. An increase in temperature with altitude is called a temperature inversion. To produce a duct, the temperature inversion must be very pronounced.

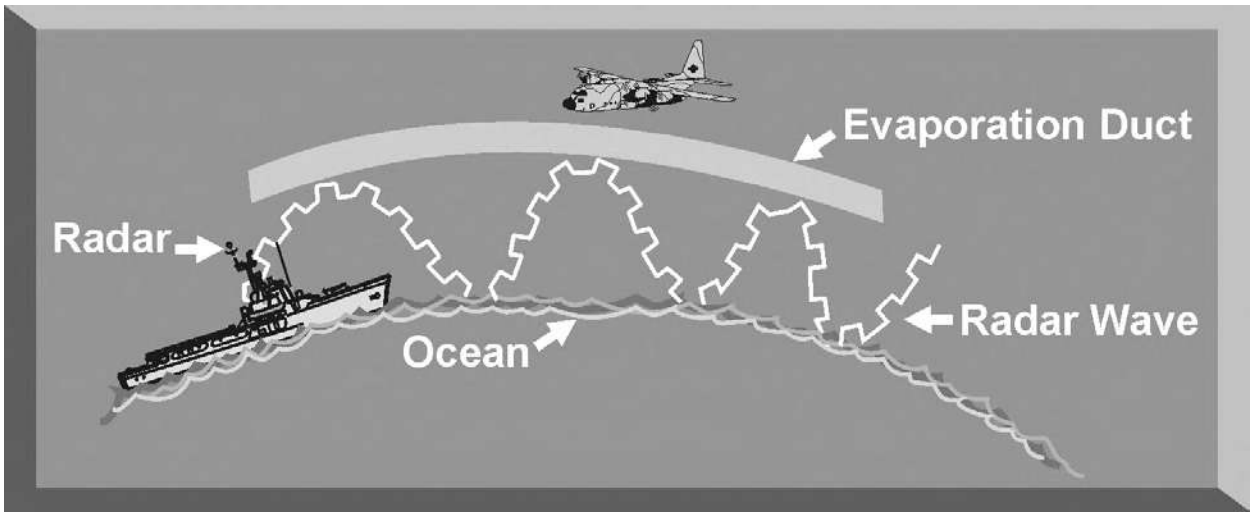

Figure 2-12. Superrefracting Surface Duct

(2) A superrefracting duct acts like a wave guide which traps the RF wave (Figure 2-12). This channels the radar signal and reduces attenuation. In order for an RF wave to propagate within a duct, the angle of the radar signal, in relation to the duct, should be less than one degree. The RF waves trapped by the duct take advantage of the decrease in refractivity and travel much further than normal. This can greatly extend the range of a radar system.

(3) The extension of radar range inside a duct can result in a reduction of radar coverage outside the duct. The area of reduced radar coverage because of ducting is called a radar hole. Due to radar holes, the extended radar range caused by ducting may result in a decrease in radar coverage along other paths of propagation. These holes can seriously degrade the effectiveness of early warning radar systems. For example, a radar system is taking advantage of a duct formed at the surface to extend low altitude radar range (Figure 2-12). Airborne targets flying just above the duct would normally be detected, but because of ducting, these targets may be missed.

(4) Water vapor content is a significant factor in producing ducts. Consequently, most ducts are formed over water and in warm climates. Any atmospheric phenomenon that results in a pronounced increase in temperature and/or a decrease in water vapor content as altitude increases can generate a superrefracting duct, of which there are three types. A superrefracting duct which is formed just above the surface of the earth is referred to as a surface duct. A surface duct formed just above the surface of the ocean is called an evaporation duct. A duct which is formed well above the surface of the earth is known as an elevated duct.

(a) Surface ducts formed over land are usually a result of the nighttime radiation of heat from the earth. Duct formation is especially prevalent during the

summer months when the ground is moist. As the earth loses heat, a temperature inversion is created at the surface coupled with a sharp decrease in the moisture content. These conditions are favorable to the formation of a surface duct. A superrefracting duct can also be produced by the diverging downdraft under a thunderstorm. The cool air that is dispersed creates a local temperature inversion while the water vapor content decreases due to rain. Surface ducts formed in conjunction with thunderstorms are difficult to predict and normally persist for a short period of time.

(b) A superrefracting surface duct that lies just above the surface of the ocean is a result of evaporated water, thus the term evaporation duct. The air in contact with the ocean is saturated with water vapor, while the air several feet above the ocean contains a much lower level. This rapid decrease in water vapor pressure with an increase in altitude creates an evaporation duct. An evaporation duct exists over the ocean almost all the time. The height of this duct varies from 20 to 100 feet based on the season, time of day, and wind speed. One positive aspect of an evaporation duct is the extended range available to a shipborne radar system with a properly aligned antenna. This extended range coverage against surface ships and low altitude aircraft is a definite advantage of ducted propagation.

(c) An elevated duct is generally formed by a temperature inversion in the upper atmosphere. To take maximum advantage of the increased radar range inside an elevated duct, both the radar and the target should be inside the elevated duct. In addition, radar systems operating below an elevated duct may also experience enhanced range performance.

(4) The presence of surface ducts and elevated ducts, especially over land, are extremely difficult to predict and may persist for very short periods of time. The atmospheric conditions favorable to duct formation are difficult to predict using conventional weather forecasting techniques.

c. The attenuation of RF energy in a clear atmosphere is due to the presence of oxygen and water vapor. Attenuation results when a portion of the RF energy strikes these molecules and is absorbed as heat. Figure 2-13 details the RF attenuation loss due to atmospheric gasses based on the frequency of the RF energy.

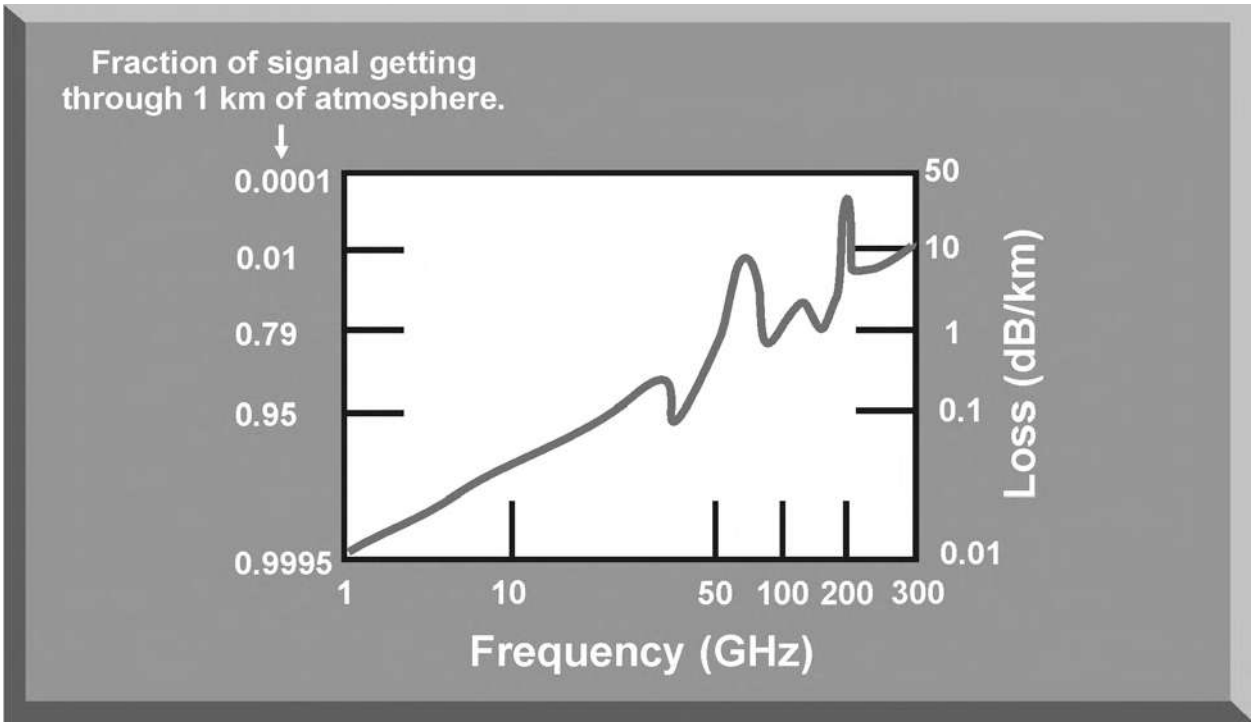

Figure 2-13. RF Atmospheric Attenuation

(1) At frequencies below 1 GHz, the effect of atmospheric attenuation is negligible. Above 10 GHz, atmospheric attenuation increases dramatically. This dramatic signal loss impacts the maximum detection range of radars operating in the millimeter wavelength band.

(2) RF energy attenuation decreases as altitude increases. The RF attenuation experienced by an air-to-air radar will depend on the altitude of the target as well as target range. For a ground-based radar, RF attenuation will decrease as antenna elevation increases.

8. SUMMARY

Since all radar operations depend on the transmission and reception of RF energy, a basic knowledge of RF frequency, wavelength, and polarization provides the basis for understanding the more complex radar characteristics. Since most modern radar systems employ some form of Doppler signal processing, the concept of the Doppler effect is fundamental to understanding modern radar operation. The concepts of refraction, anomalous propagation (ducting), and atmospheric attenuation are key to understanding how RF waves propagate in the atmosphere. The topics in this chapter provide a foundation for understanding radar and jamming system operation.

CHAPTER 3. RADAR SIGNAL CHARACTERISTICS

1. INTRODUCTION

Every radar produces a radio frequency (RF) signal with specific characteristics that differentiate it from all other signals and define its capabilities and limitations. Pulse width (pulse duration), pulse recurrence time (pulse repetition interval), pulse repetition frequency, and power are all radar signal characteristics determined by the radar transmitter. Listening time, rest time, and recovery time are radar receiver characteristics. An understanding of the terms used to describe these characteristics is critical to understanding radar operation.

2. PULSE WIDTH (PW)

Figure 3-1 depicts the output from a typical pulse radar. PW, sometimes called pulse duration (PD), is the time that the transmitter is sending out RF energy. PW is measured in microseconds. It has an impact on range resolution capability, that is, how accurately the radar can discriminate between two targets based on range.

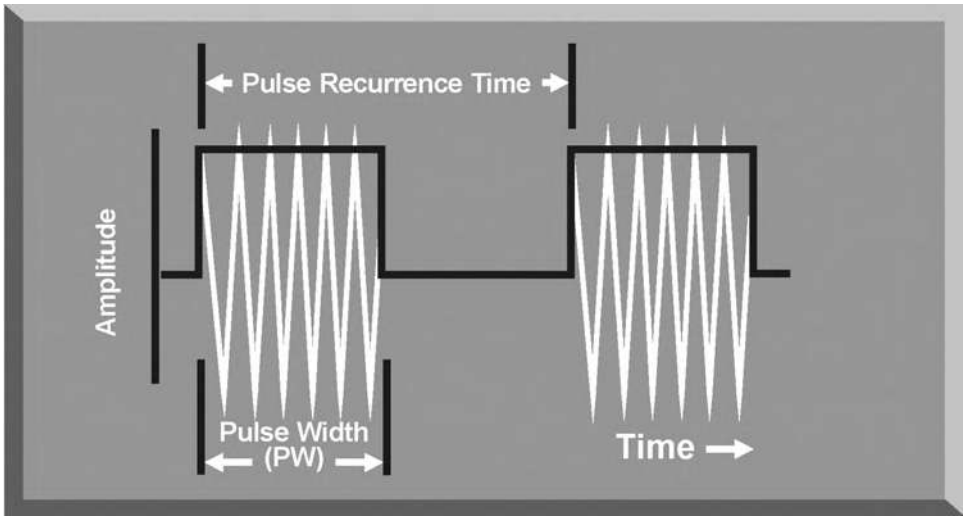

Figure 3-1. Typical Radar Pulse

3. PULSE RECURRENCE TIME (PRT)

Pulse recurrence time is also known as pulse repetition time. PRT is the time required for a complete transmission cycle. This is the time from the beginning of one pulse of RF energy to the beginning of the next. PRT is measured in microseconds. PRT is the same as pulse repetition interval (PRI), which is used in radar warning receivers and other electronic warfare support (ES) assets to discriminate between radar systems. It also affects maximum radar range.

4. PULSE REPETITION FREQUENCY (PRF)

One of the most important characteristics of a pulse radar signal is pulse repetition frequency. PRF is the rate at which pulses or pulse groups are transmitted. Generally, PRF is the number of pulses generated per second and is expressed in hertz (Hz). PRF and PRI are related in that PRI is the inverse of PRF. A word of caution—do not confuse the operating frequency of the radar, which is measured in Hz, with the pulse repetition frequency, which is also measured in Hz. They are entirely different characteristics of a pulsed radar signal.

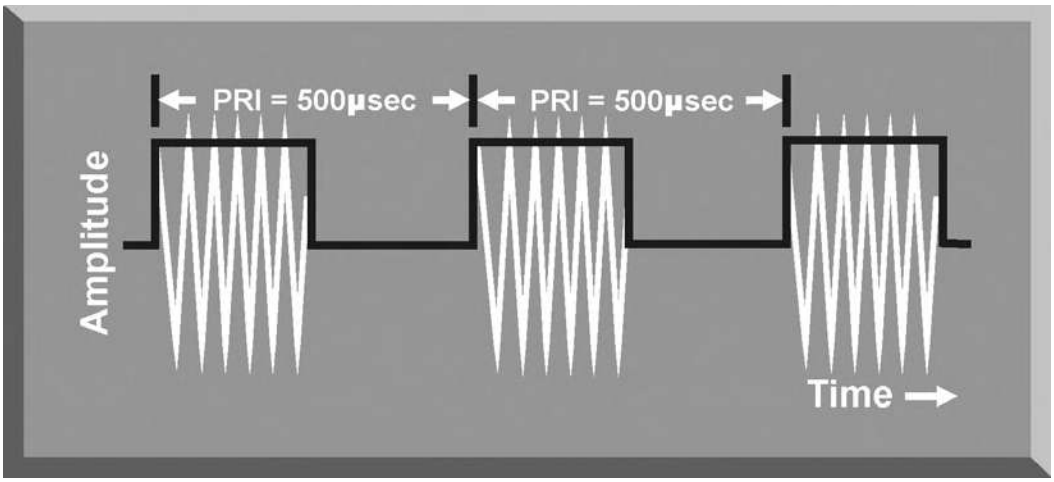

Figure 3-2. Constant PRF Radar Pulse

a. A pulse radar operating at an unvarying PRF is called a constant PRF radar (Figure 3-2). Pulse radar systems can employ PRF stagger or PRF jitter as an electronic protection (EP) technique against repeater or synchronous jammers. The time between each pulse is the PRI.

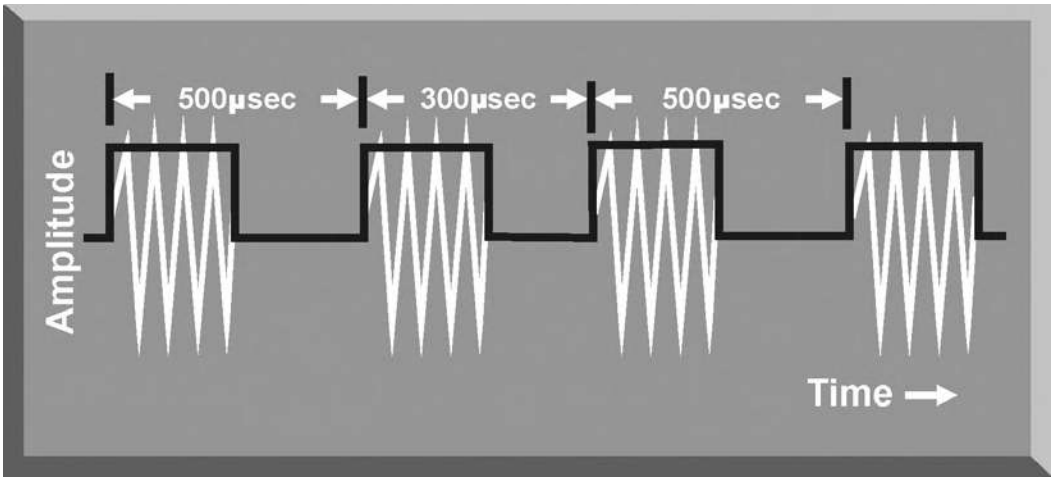

Figure 3-3. PRF Stagger

b. PRF stagger is accomplished by assuring that no adjacent PRIs are equal. The number of different PRIs generated is called the "position" of the stagger. Two-position stagger would have two PRI values, for example, 300 microseconds and 500 microseconds (Figure 3-3).

c. PRF jitter may be considered a random stagger. It is also an EP technique to counter synchronous jammers. PRF jitter has no repeating pattern of PRI values (Figure 3-4).

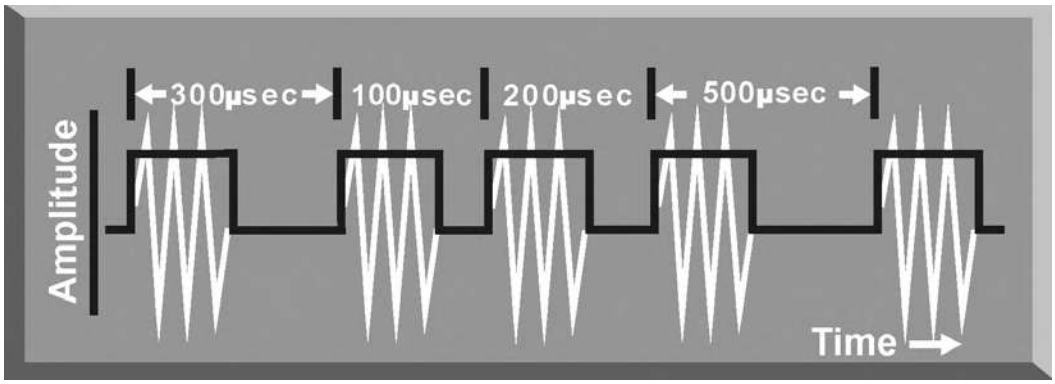

Figure 3-4. PRF Jitter

5. RADAR RECEIVER CHARACTERISTICS

Pulse repetition frequency, pulse recurrence time, and pulse width are determined by the transmitter. The pulse radar signal characteristics that relate to receiver operation are rest time, recovery time (RT), and listening time (LT) (Figure 3-5).

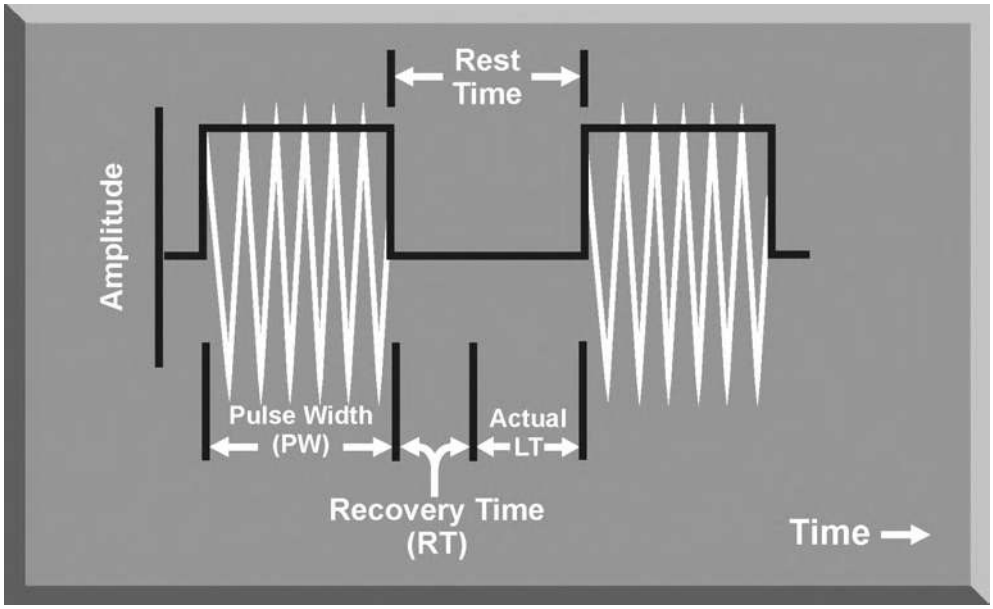

Figure 3-5. Basic Radar Pulse

a. Rest time is the time between the end of one transmitted pulse and the beginning of the next. It represents the total time that the radar is not transmitting. Rest time is measured in microseconds.

b. Recovery time (RT) is the time immediately following transmission time during which the receiver is unable to process returning radar energy. RT is determined by the amount of isolation between the transmitter and receiver and the efficiency of the duplexer. A part of the high power transmitter output spills over into the receiver and saturates this system. The time required for the receiver to recover from this condition is RT.

c. Listening time (LT) is the time the receiver can process target returns. Listening time is measured from the end of the recovery time to the beginning of the next pulse, or PRT minus (PW + RT). Listening time is measured in microseconds.

6. DUTY CYCLE

Duty cycle is the ratio of the time the transmitter operates to the time it could operate during a given transmission cycle. The duty cycle of a radar can be computed by dividing the PW by the PRT, or by multiplying the PW times the PRF. Duty cycle has no units (Equation 3-1). CW radars have a duty cycle of 100%, while early warning radars may have a duty cycle of around 1%.

$$\text{Duty Cycle} = \frac{PW}{PRT} \text{ or Duty Cycle} = PW \times PRF$$

Equation 3-1. Duty Cycle

7. PEAK POWER

The power output of a radar is normally expressed in terms of peak power or average power (Figure 3-6). Peak power is the amplitude, or power, of an individual radar pulse. It is simply the power, measured in watts or megawatts, that is radiated when the transmitter is on. The power a radar transmits is normally used to determine the maximum detection range of that radar. However, it is the energy in a radar pulse that determines maximum radar detection range. Since power is the rate of flow of energy, the energy in a radar pulse is equal to the peak power multiplied by the time the radar is transmitting, or pulse width (Equation 3-2).

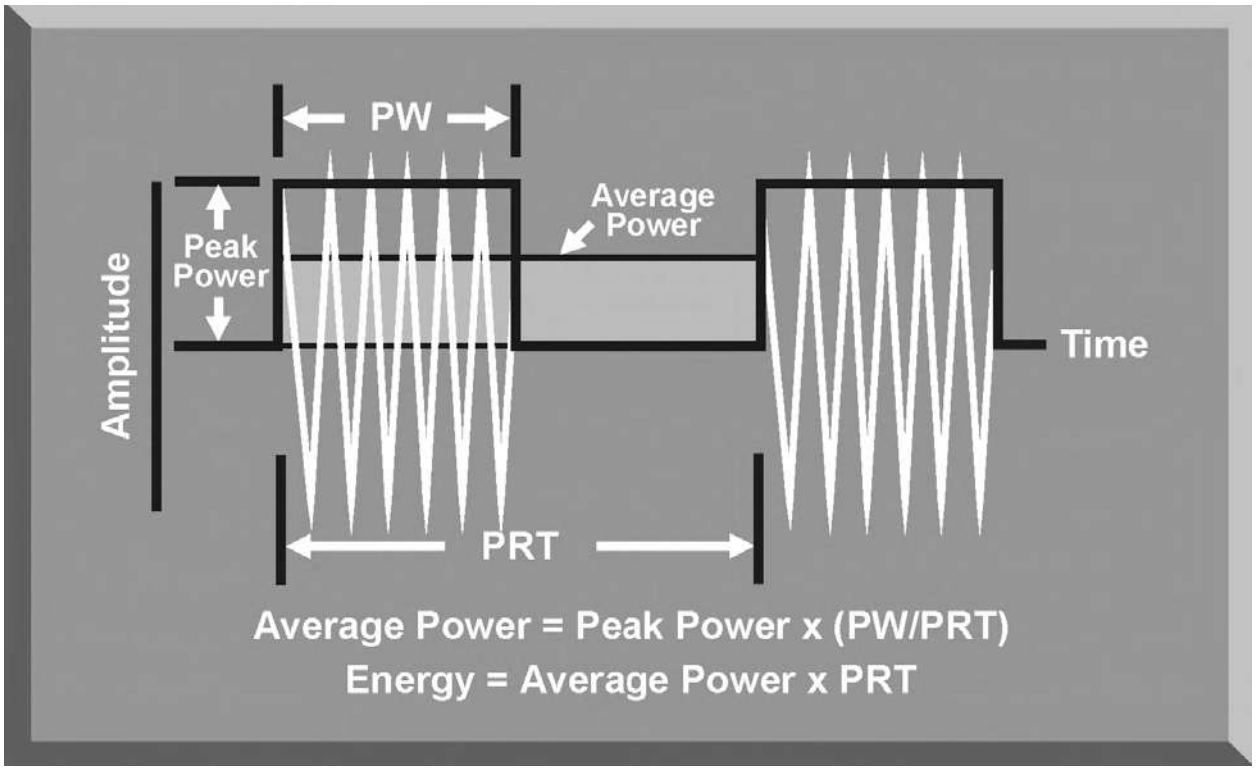

Figure 3-6. Peak Power and Average Power

Equation 3-2. Energy Per Pulse

8. AVERAGE POWER

Average power is the power distributed over the pulse recurrence time. It can be computed using the formula in Figure 3-6. The energy transmitted by average power can be computed by multiplying average power by PRT. Since the energy in a set of pulses determines detection range, average power or energy provides a better measure of the detection range of a radar than does peak power. Average power can be increased by increasing the PRF, by increasing the pulse width, or by increasing peak power (Figure 3-7).

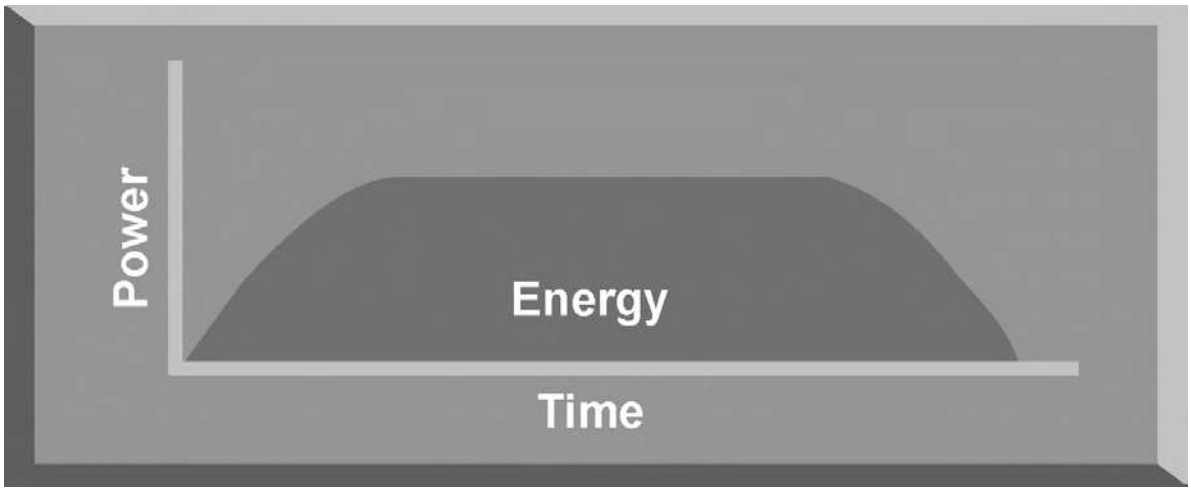

Figure 3-7. Radar Power and Energy

9. MODULATION

The characteristics of an RF signal must be changed in order to transmit information on the signal. This process is called modulation. Modulation is accomplished by combining a basic RF signal, called a carrier wave, with a modulating signal that contains the desired information. The resulting waveform is then used to transmit the desired information.

a. One basic modulation technique is amplitude modulation (AM). The carrier wave is combined with a modulating signal containing information of varying amplitude. Waveforms produced have the same frequency as the carrier wave but with a varying amplitude based on the information from the modulating signal. AM is used extensively in communications and broadcast radio transmissions (Figure 3-8).

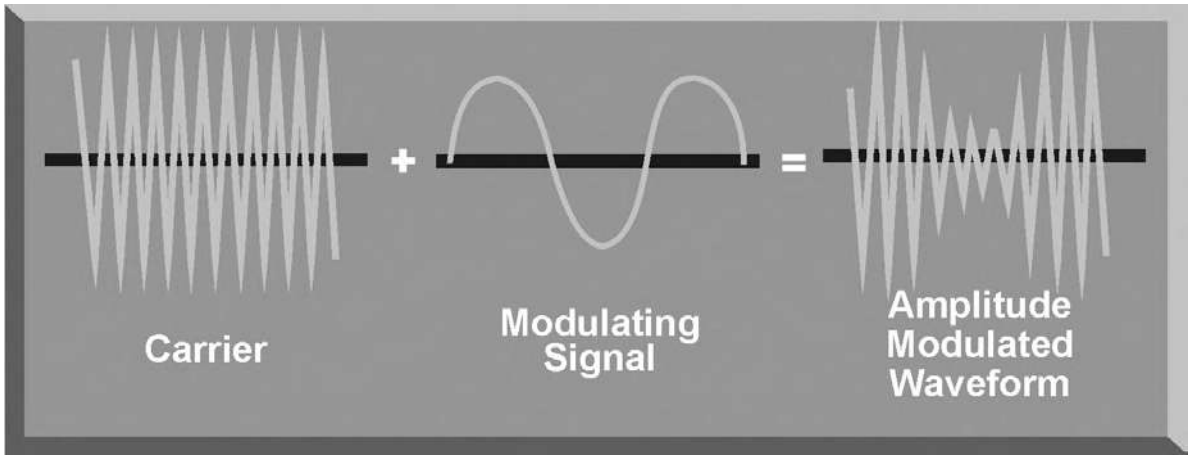

Figure 3-8. Amplitude Modulation

b. Frequency modulation (FM) is another means of impressing information on a carrier wave. Frequency modulation is accomplished by combining the carrier wave with a modulating signal containing information of varying frequency. The waveform produced has the same amplitude as the carrier wave, but the frequency varies based on the information from the modulating signal (Figure 3-9). FM is used extensively in communications and commercial radio. FM is also used with continuous wave (CW) radars to make them more resistant to jamming and to add range determination capability.

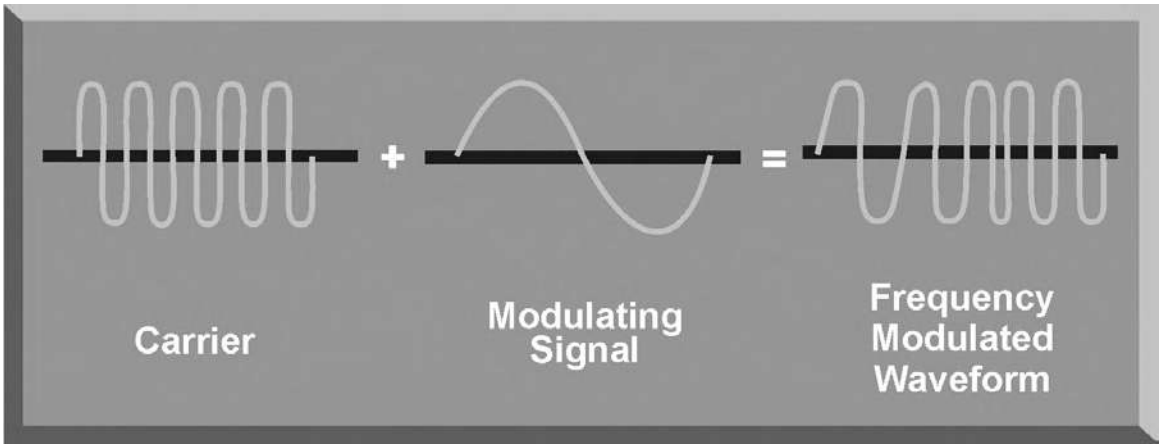

Figure 3-9. Frequency Modulation

c. A type of amplitude modulation known as pulse modulation (PM) is used in pulse radars to produce the short, powerful bursts of RF energy. PM combines the carrier wave with a rectangular pulse that acts like a switch. PM turns the transmitter on, leaves it on for a predetermined time, and then turns it off. The result is a waveform that produces radar pulses that can be used to measure range and angle to the target (Figure 3-10).

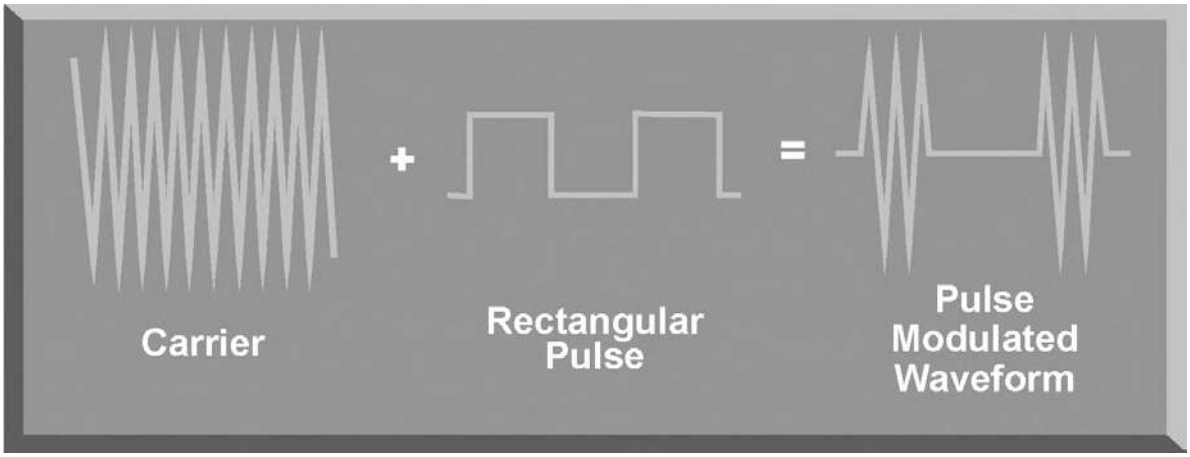

Figure 3-10. Pulse Modulation

10. SUMMARY

The radar signal characteristics of PW, PRI, PRF, and power determine the maximum range and the range resolution capability of a specific radar. When combined with the frequency of the carrier wave of the radar signal, these parameters provide a unique signature to identify a specific radar signal. Modulation is the method used to put information on an RF carrier wave. The primary modulation techniques used in radar signal generation include amplitude, frequency, and pulse modulation. The radar signal characteristics of PRF, PRI, power, and modulation are the keys to understanding radar operation and jamming techniques.

CHAPTER 4. RADAR SYSTEM COMPONENTS

1. INTRODUCTION

The individual components of a radar determine the capabilities and limitations of a particular radar system. The characteristics of these components also determine the countermeasures that will be effective against a specific radar system. This chapter will discuss the components of a basic pulse radar, a continuous wave (CW) radar, a pulse Doppler radar, and a monopulse radar.

2. PULSE RADAR SYSTEM

The most common type of radar design is the pulse radar system. The name describes a process of transmitting discrete bursts of RF energy at the frequency of the radar system. The time that pulses are transmitted determines the pulse repetition frequency (PRF) of the radar system. A pulse radar system can figure out range and azimuth. Range is determined by the time that it takes a pulse to go to a target and return. Target azimuth is determined by the relative position, or antenna orientation, when the pulse strikes the target. Figure 4-1 is a basic block diagram of a simple pulse radar system.

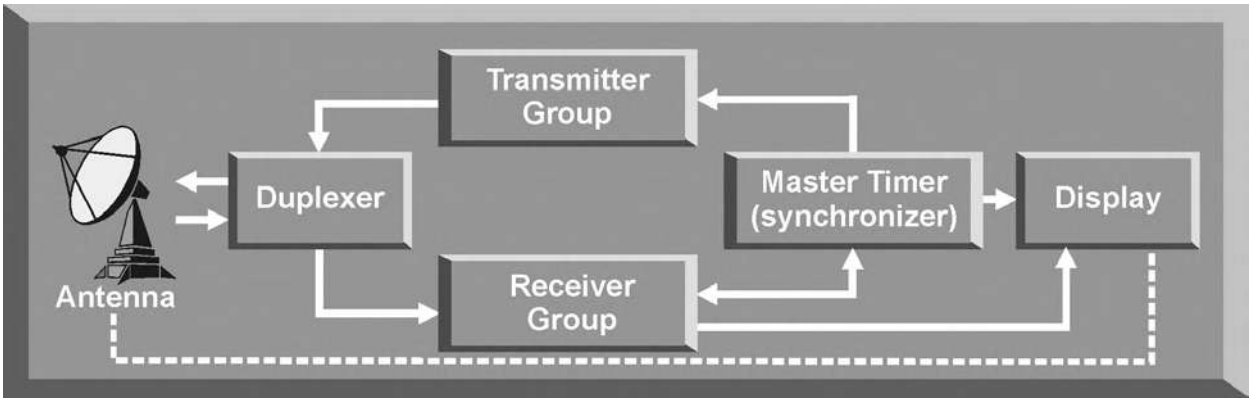

Figure 4-1. Pulse Radar Block Diagram

a. The purpose of the transmitter is to deliver a series of high-energy bursts of radio frequency (RF) energy to the antenna. The transmitter group of a modern pulse radar normally consists of a pulse generator or waveform generator, a modulator, and some kind of power amplifier (Figure 4-2).

(1) The purpose of the waveform generator is to generate the proper waveform or pulse, normally at a low power level, before delivery to the modulator. It is much easier to generate complex waveforms at a lower power level. These complex waveforms are required for coherent systems employing digital moving target indicator techniques and for pulse Doppler radar operations.

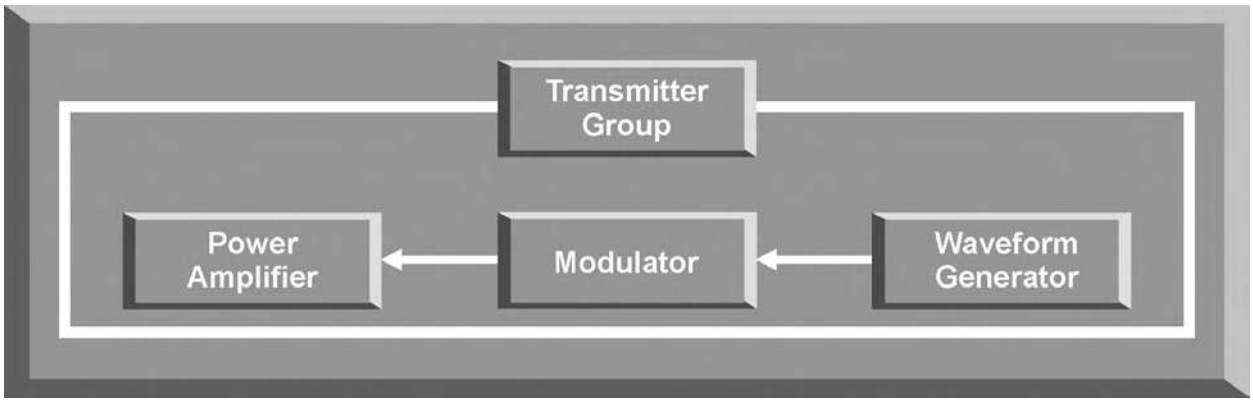

Figure 4-2. Transmitter Group

(2) The modulator is a major portion of the transmitter. The modulator provides an extremely powerful, very short pulse of direct current (DC) voltage to the power amplifier. This is similar to the ignition system of an automobile but with very stringent requirements. The modulator has an energy storage device and a switch. Between pulses, during the resting time of the transmitter, energy is accumulated and stored in the storage device. When keyed by the master timer, all this energy is switched to the power amplifier as a pulse. The waveform of this pulse is determined by the waveform generator.

(3) The power amplifier for a modern radar is normally a klystron, traveling wave tube, cross field amplifier, or solid state amplifier. Most common pulse radars use a klystron power amplifier. No matter what power amplifier is used, the purpose of the transmitter group is to produce a series of pulses at the correct amplitude, at the proper interval, with the exact waveform, and at the operating frequency of the radar.

b. A duplexer is required when both the transmitter and receiver use the same antenna. The duplexer acts as a rapid switch to protect the sensitive receiver from damage when the high-power transmitter is on. When the transmitter is off, the duplexer directs the weak target signals to the receiver. The duplexer's main purpose is to minimize power loss and maximize isolation. Power lost in the duplexer during transmission reduces the maximum detection range of the radar. Isolation refers to the amount of transmitter power that "bleeds through" the duplexer to the receiver during transmission. This "bleed through" must be extremely small to avoid receiver saturation or damage.

c. The capabilities of the receiver group are critical to radar performance (Figure 4-3). The ability of the radar receiver to detect the presence of the target return and extract the required information is limited primarily by noise. Noise can enter the receiver through the antenna along with the target return. This type of noise is called external noise. Noise generated within the receiver is called thermal noise. Radar noise can never be completely eliminated. Minimizing noise

is the most important consideration in the design of the sensitive receivers used with modern radars. In addition, relative immunity to noise makes a radar system more resistant to jamming.

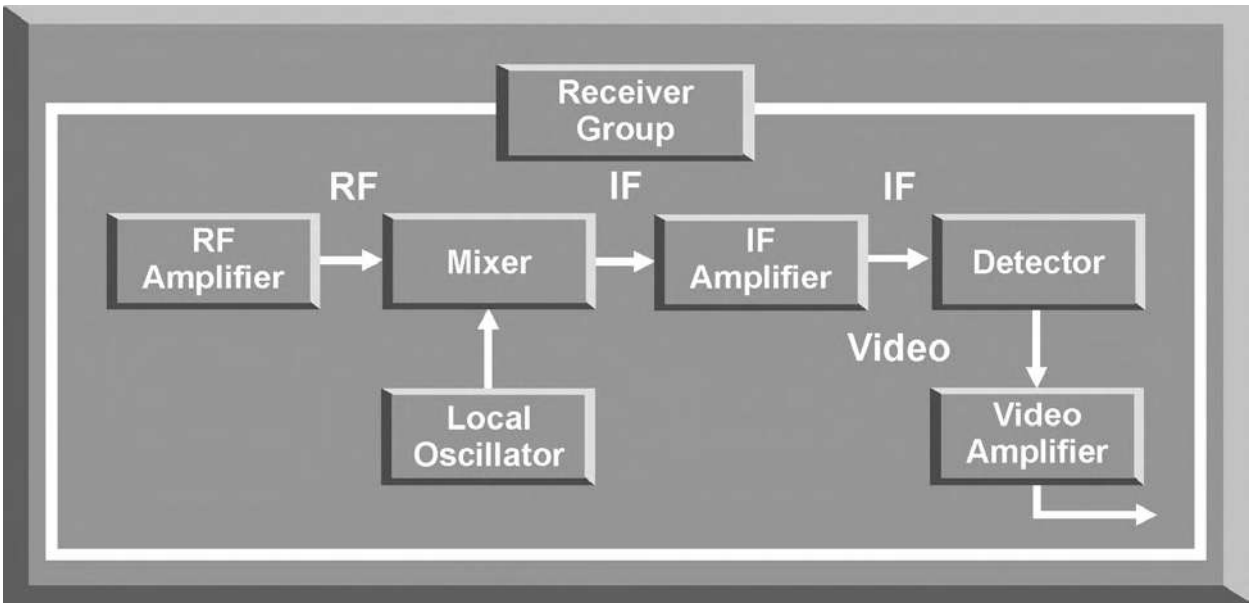

Figure 4-3. Receiver Group

(1) The most common pulse radar receiver is the superheterodyne receiver. A superheterodyne receiver consists of an RF amplifier, a mixer and local intermediate frequency (IF) amplifier, a detector, and a video amplifier.

(2) Radar target returns enter the receiver group via the antenna and duplexer. Since these signals are normally very low power, the RF amplifier boosts the signal gain and filters out as much external noise as possible. The capability of the RF amplifier to minimize noise determines the receiver sensitivity. The boosted RF signal is sent to the mixer where it is converted to a lower IF. This is accomplished by mixing the RF signal with the signal from the local oscillator to produce an IF that is easier to process. The IF amplifier increases the IF signal level and includes a matched filter. The matched filter maximizes the signal-to-noise ratio which enhances detection of the target return. The detector, which is usually a crystal diode, extracts the video modulation from the IF or converts the IF to a video signal.

d. The brain of a basic pulse radar is the master timer, or synchronizer, which coordinates the operation of the various parts of the radar (Figure 4-4). Exact timing within the radar is necessary to get accurate range. The master timer is an oscillator that triggers the transmitter to initiate transmission of a pulse. Simultaneously, the master timer sends a signal to initialize the display to ensure that range and azimuth information is accurately displayed.

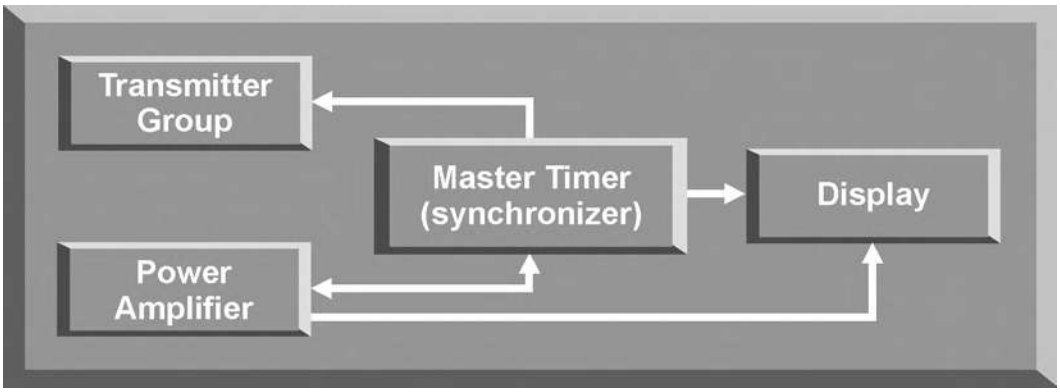

Figure 4-4. Master Timer/Synchronizer

e. The function of the antenna during transmission is to concentrate the radar energy from the transmitter into a shaped beam that points in the desired direction (Figure 4-5). During reception, or listening time, the function of the antenna is to collect the returning radar energy contained in the echo signals, and deliver these signals to the receiver. Radar antennas are characterized by directive beams that are usually scanned in a recognizable pattern.

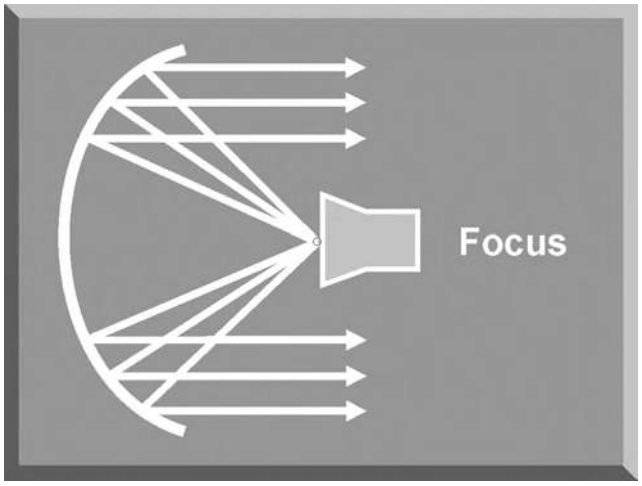

Figure 4-5. Parabolic Antenna

f. The purpose of the radar display is to take the information derived from a radar target in the receiver group and present it to the operator in a usable format. There are many different types of scope displays depending on the purpose of the radar and how the radar information is to be used. There are four basic types of radar displays: the A scope, B scope, range height indicator (RHI) scope, and plan position indicator (PPI) scope.

(1) The A scope is used to display target range or velocity (Figure 4-6). Threat systems using A scope displays include air interceptors (AIs) with range-only radar, surface-to-air missiles (SAMs), and radar-directed antiaircraft artillery (AAA) systems. SAM and AAA systems may use the A scope for range or velocity information, and other radar displays for azimuth and elevation data. The A scope displays range or velocity in relation to amplitude. The operator must distinguish the target return from other returns, including ground return and noise.

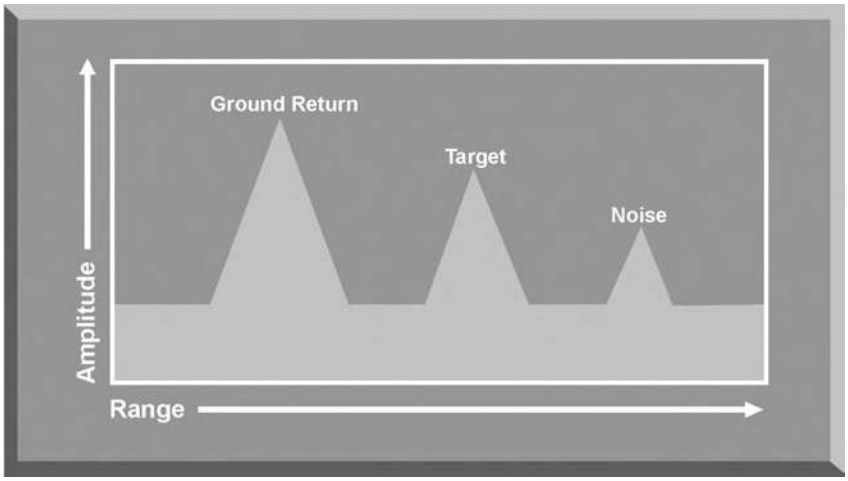

Figure 4-6. A Scope Display

(2) The B scope is used to display target range and azimuth (Figure 4-7). Threat systems using B scope displays include AI and SAM systems. The position of the target return to the right or left of the centerline of the screen shows the azimuth of the target. The position of the target return in relation to the bottom of the display, or zero range, shows target range.

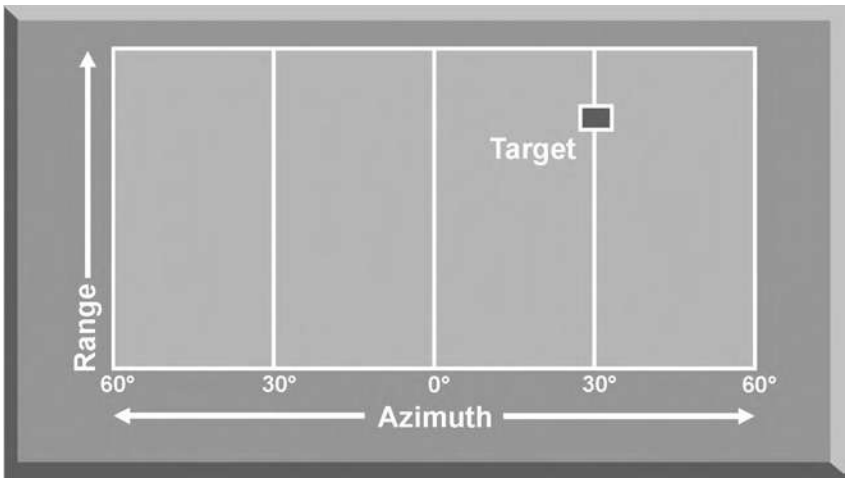

Figure 4-7. B Scope Display

(3) The RHI scope is used to display range and elevation (Figure 4-8). The RHI scope is used with height finder radars, and a modified RHI scope is used for ground-controlled approach (GCA) radars. The sweep trace of the display produces a fan-shaped display with the vertex at the lower left of the scope. The antenna sweeps up and down and is synchronized with the display.

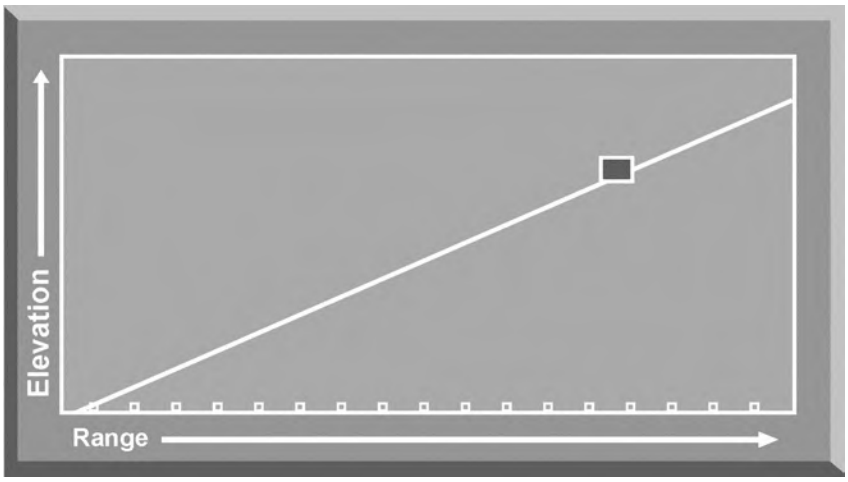

Figure 4-8. RHI Scope Display

(4) The PPI display is probably the best known radar display (Figure 4-9). The display represents a map picture of the area scanned by the radar beam, usually 360 degrees. The PPI display is used by early warning, acquisition, ground-controlled intercept (GCI), and SAM radar systems. The target return's angular position shows target azimuth, while distance from the center of the display shows range.

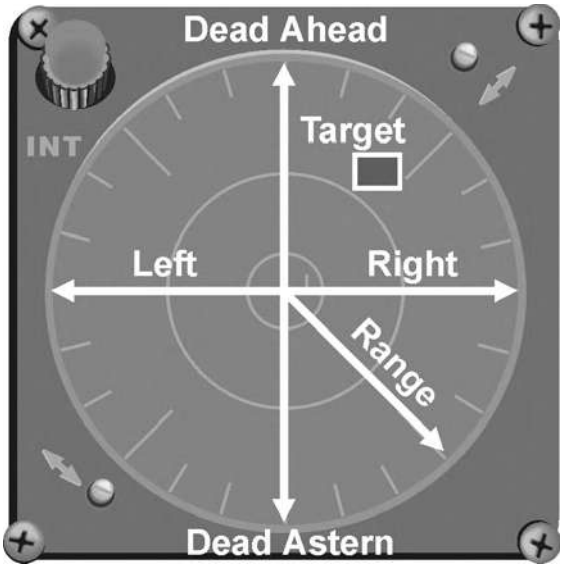

Figure 4-9. PPI Scope Display

3. CONTINUOUS WAVE (CW) RADAR

A continuous radar transmission from the antenna requires that classic CW radars have two antennas, one for transmission and one for reception (Figure 4-10). Since a continuous transmission results in a continuous echo signal, it is impossible to tell what part of the echo is associated with any particular part of the transmission. This makes conventional range determination (based on timing) impossible. However, the simple application of the Doppler principle provides a means for a CW radar to track a target. The Doppler principle deals with the fact that a radar return from a moving target will be shifted in frequency by an amount proportional to its radial velocity relative to the radar site. Using the difference in frequency from the transmitted signal to the received signal, a CW radar can separate the target return from clutter, based on a change in frequency. This type of radar is called a CW Doppler radar.

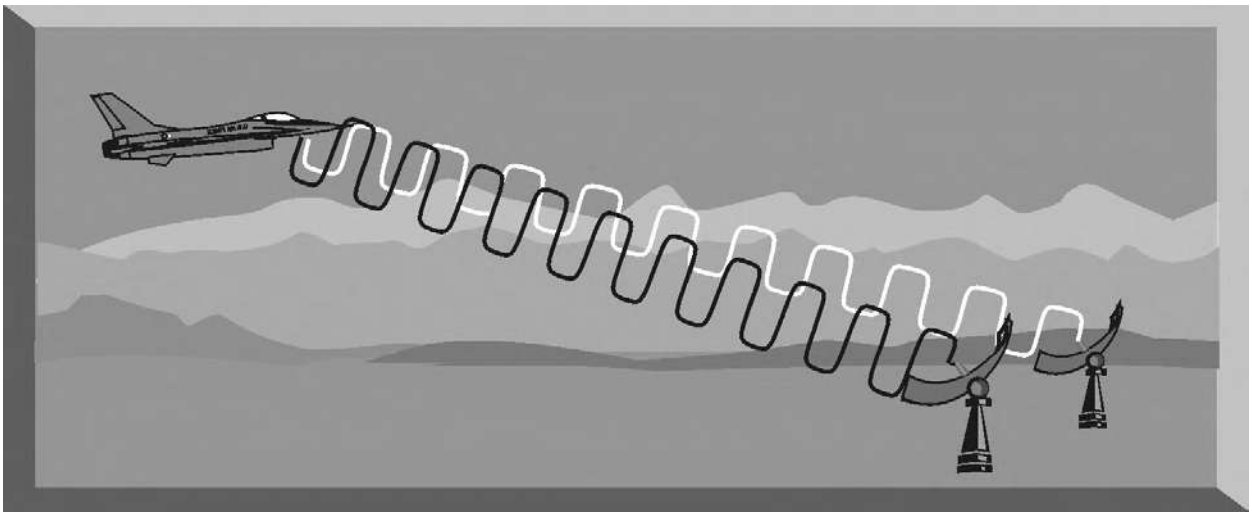

Figure 4-10. Continuous Wave Radar

a. Figure 4-11 depicts a basic CW Doppler radar. In a simple CW Doppler radar, the transmitter transmits a continuous signal at the radar's operating frequency. This signal is reflected by a moving target and travels back to the receiving antenna. The frequency of the reflected signal (f_d) is the frequency change due to the Doppler effect. This target frequency is passed to the detector. The transmitted frequency (f_o) is also fed to the detector as a reference. The detector notes the difference between the transmitted and received frequencies and passes this frequency to the Doppler filters. The Doppler filters only allow Doppler frequencies within a certain range to pass through. A filter is required for each Doppler frequency. The number of Doppler filters determines the number of targets that the radar can resolve in velocity.

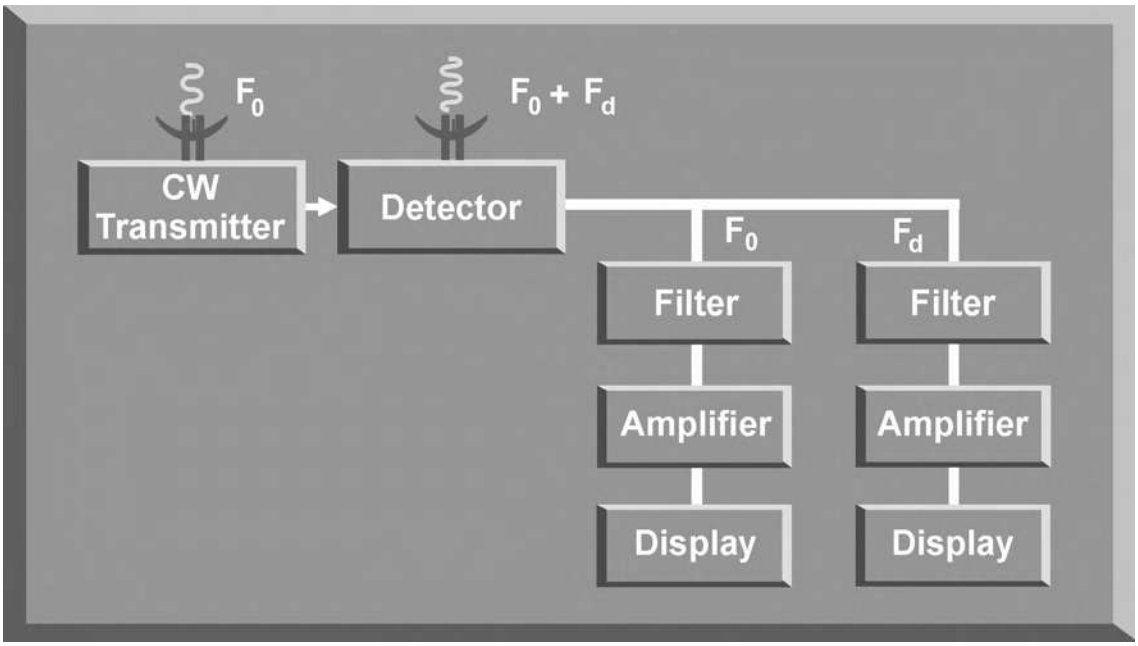

Figure 4-11. Basic CW Doppler Radar

b. The output of each Doppler filter is amplified and passed to its own display. The display is normally an A scope as shown in Figure 4-12.

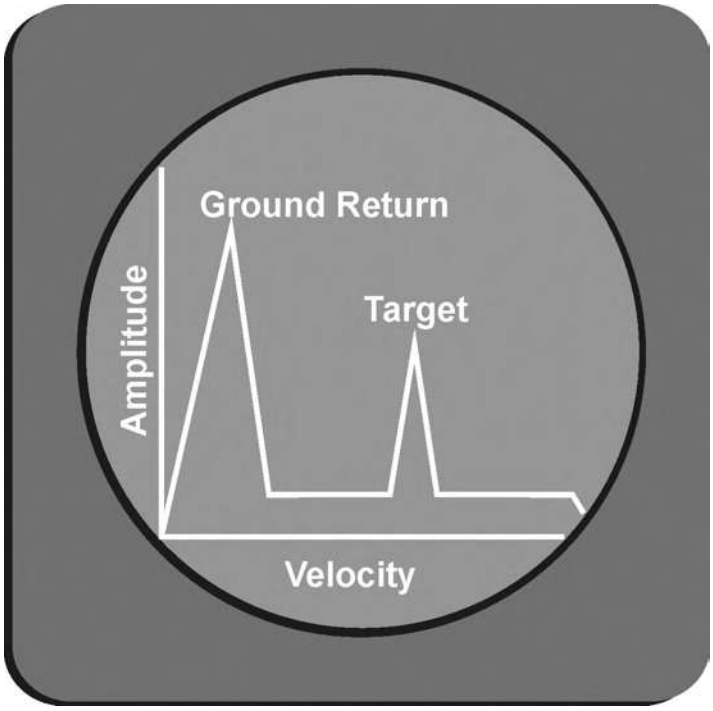

Figure 4-12. CW Doppler Radar Display

4. PULSE DOPPLER RADAR

Pulse Doppler radars combine the advantages of both pulse and Doppler radar systems (Figure 4-13). Because the signal is pulsed, the radar can determine range, azimuth, and elevation, similar to a conventional pulsed radar. A pulse Doppler radar can also compute overtake, or rate of closure, relative to the radar system on a pulse-to-pulse basis. Pulse Doppler radars also use multiple PRFs to eliminate target eclipsing and for range determination in medium PRF. The beauty of a pulse Doppler radar is that it eliminates ground clutter and provides range, azimuth, and velocity resolution.

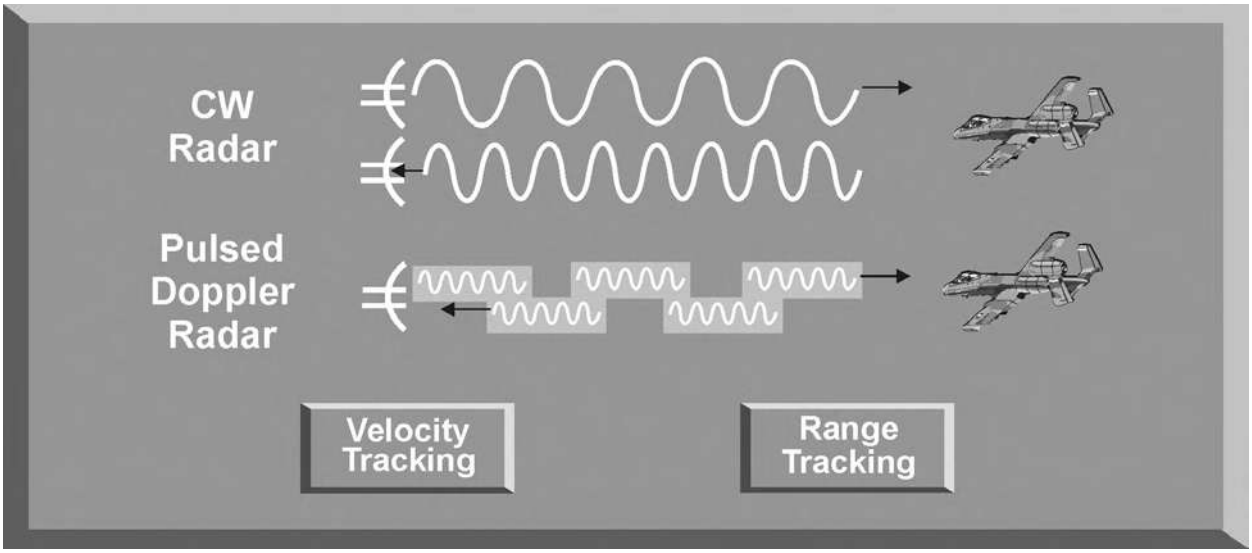

Figure 4-13. CW and Pulse Doppler Radar Comparison

a. A pulse Doppler radar transmits a box, or pulse, of coherent RF energy at the operating frequency of the radar. The frequency inside these boxes reacts the same way as the continuous waves of a CW radar. However, since the RF waves are pulsed, range determination can be accomplished by measuring the time it takes for the reflected pulse to return from the target. Velocity determination and tracking are accomplished by capturing and quantifying the Doppler shift of the frequencies in each box or pulse.

b. The basic block diagram of a coherent pulse Doppler radar (Figure 4-14) is similar to a pulse radar except for the addition of an exciter, a radar computer, and a digital signal processor. The exciter generates a continuous stable low power signal at the desired frequency and phase for the transmitter. It also sends this signal as a reference to the receiver. The digital signal processor performs the adding and subtracting functions required to find, track, and sort targets with respect to velocity and range. The radar computer performs all routine functions of the radar such as changing modes and accounting for aircraft flight parameters.

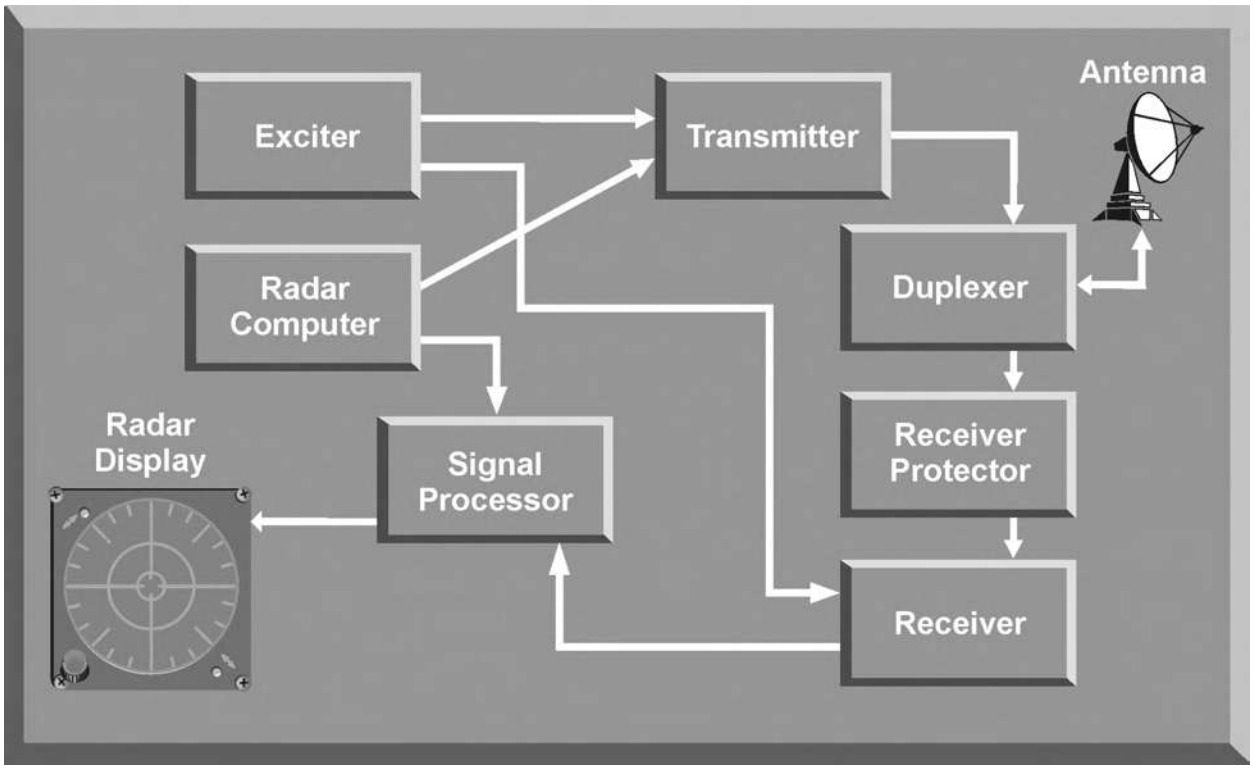

Figure 4-14. Basic Pulse Doppler Radar Diagram

5. MONOPULSE RADAR

The primary functions of monopulse radars include target tracking and weapon guidance. Monopulse radars were developed to overcome the limitations and jamming susceptibility of scanning radar systems. A monopulse radar typically receives returned radar energy in two, three, or four separate receivers, or channels, each looking at a different area. By comparing the returns from each receiver, track errors can be determined. For example, in Figure 4-15, this radar compares the amplitude, or signal strength, in each channel. Obviously, an aircraft in area "A" will produce a stronger return in receiver "A" since that receiver is focused in that direction. Since this type of system uses signal strength to determine position, typical noise jamming will only highlight an aircraft'' position. Other coherent radars can measure phase differences verses the amplitude differences used in the last example. If a signal is directly ahead of the antenna, each quadrant will receive the returned signal at exactly the same time and therefore the same exact phase. However, if a return is off-center, the returned signal will strike part of the antenna slightly ahead of the opposite side and each quadrant will measure a different phase. This phase difference is used to determine azimuth error.

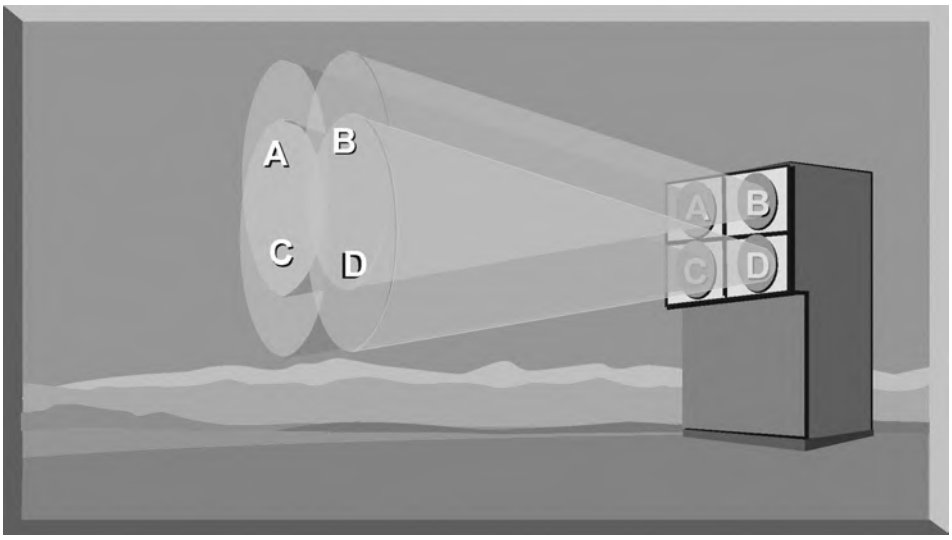

Figure 4-15. Monopulse Radar

a. Monopulse radars operate by comparing the amplitude or the phase of the received signal in each of the transmitted beams. A complex set of comparator circuits, called magic T's, do the addition and subtraction of the received signals based on the orientation of the magnetic field, or H-plane, and the electrostatic field, or E-plane (Figure 4-16). The received signal from antenna A enters the magic T in the H-plane arm while the signal from antenna B enters the magic T in the E-plane arm.

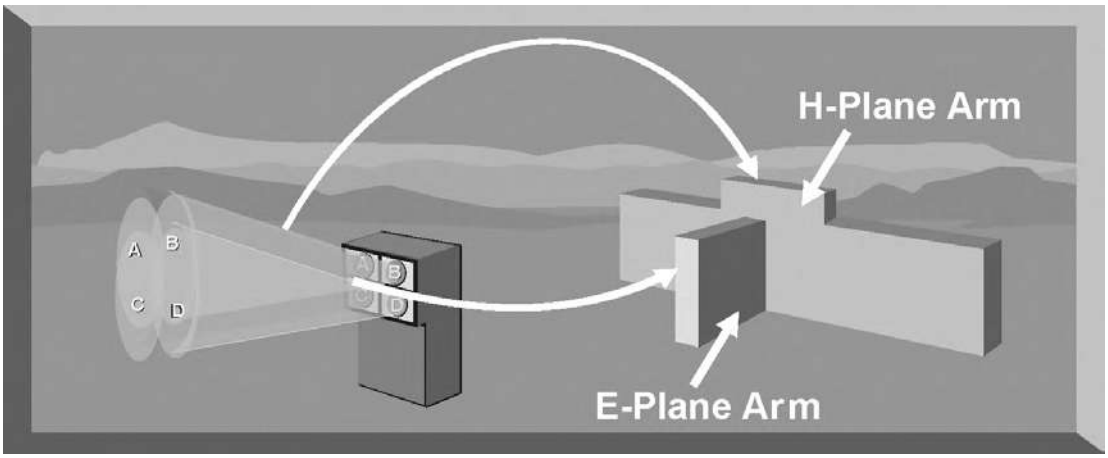

Figure 4-16. Monopulse Magic T's

b. Figure 4-17 depicts the output of a magic T. Output is the sum and difference of the two input signals. These sum and difference values, in amplitude or phase, are used to generate azimuth and elevation error signals and to compute range.

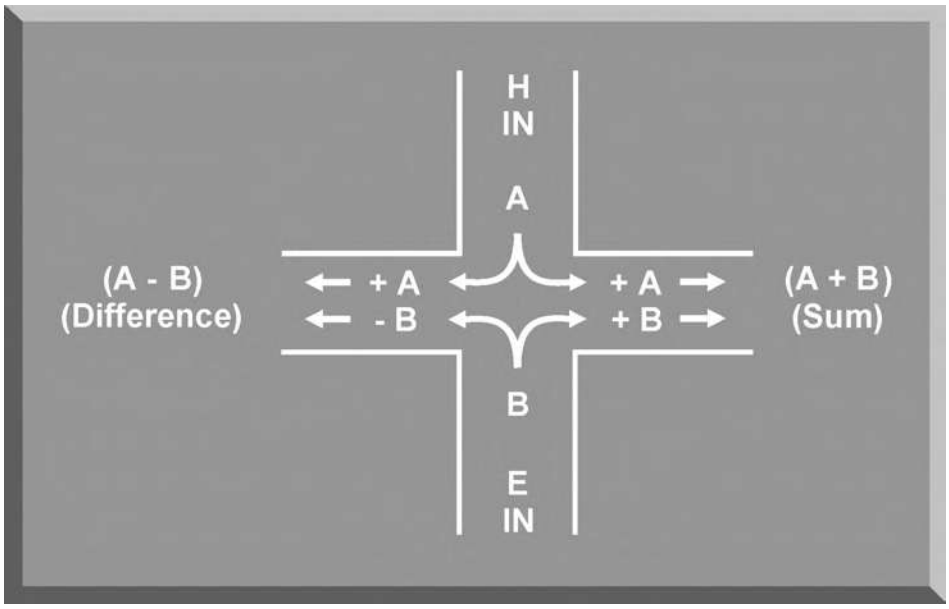

Figure 4-17. Magic T Output Signals

c. These sum and differences computed by the magic T's are sent as signals to the monopulse tracking servos to generate both azimuth and elevation corrections to keep the monopulse antenna centered on the target (Figure 4-18). Target range is computed by calculating the difference of signal transmission time with the reception time of the target echo. Range information is displayed to the operator for range tracking.

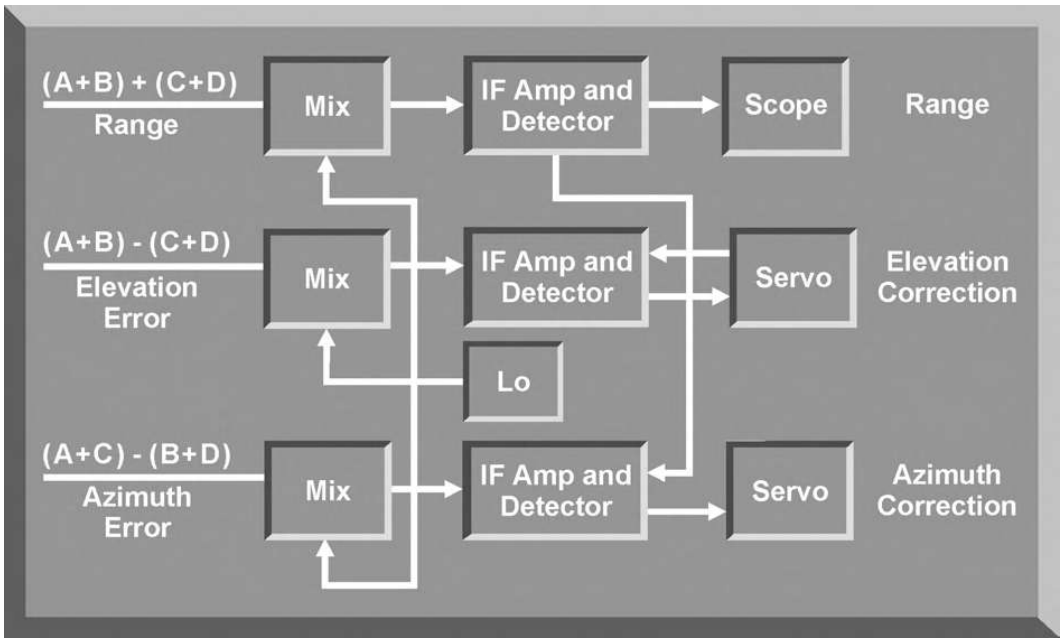

Figure 4-18. Monopulse Radar Track

d. If the signal in antenna A equals the signal in antenna B, equals the signal in antenna C, and equals the signal in antenna D, the target is in the center of the four radar beams (Figure 4-19). This is the condition the monopulse tracker attempts to maintain when tracking a target.

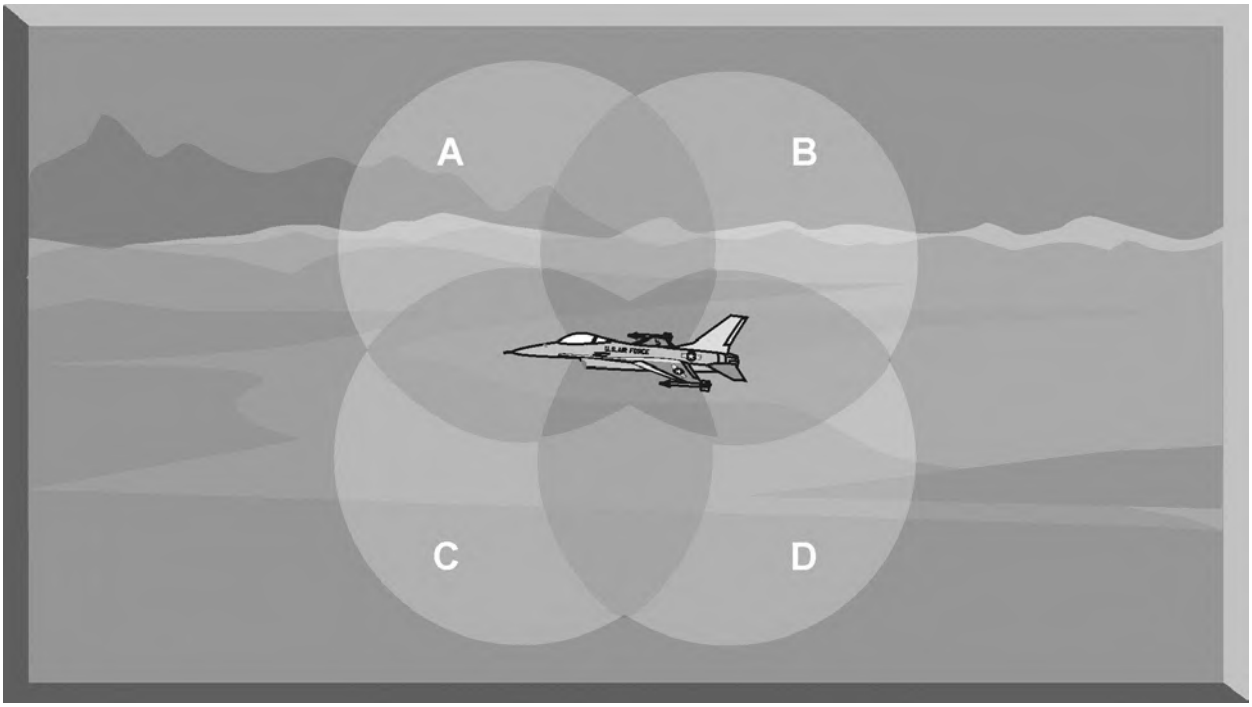

Figure 4-19. Monopulse Radar Track Logic

6. SUMMARY

This chapter has discussed the basic components of a simple pulse radar, a continuous wave radar, a pulse Doppler radar, and a monopulse radar. The characteristics of these components determine the capabilities and limitations of a particular radar system.

CHAPTER 5. RADAR PRINCIPLES

1. INTRODUCTION

The primary purpose of radar systems is to determine the range, azimuth, elevation, or velocity of a target. The ability of a radar system to determine and resolve these important target parameters depends on the characteristics of the transmitted radar signal. This chapter explains the relationship of radar frequency (RF), pulse repetition frequency (PRF), pulse width (PW), and beamwidth to target detection and resolution.

2. RADAR RANGE

A basic pulse radar system consists of four fundamental elements: the transmitter, the receiver, the antenna, and the synchronizer, or master timer.

a. The transmitter, through the antenna, sends out a pulse of RF energy at a designated frequency. The presence of a target is revealed when the RF energy bounces off the target, returns to the radar antenna, and goes into the receiver (Figure 5-1). The master timer measures the time between the transmission of a pulse and the arrival of a target echo.

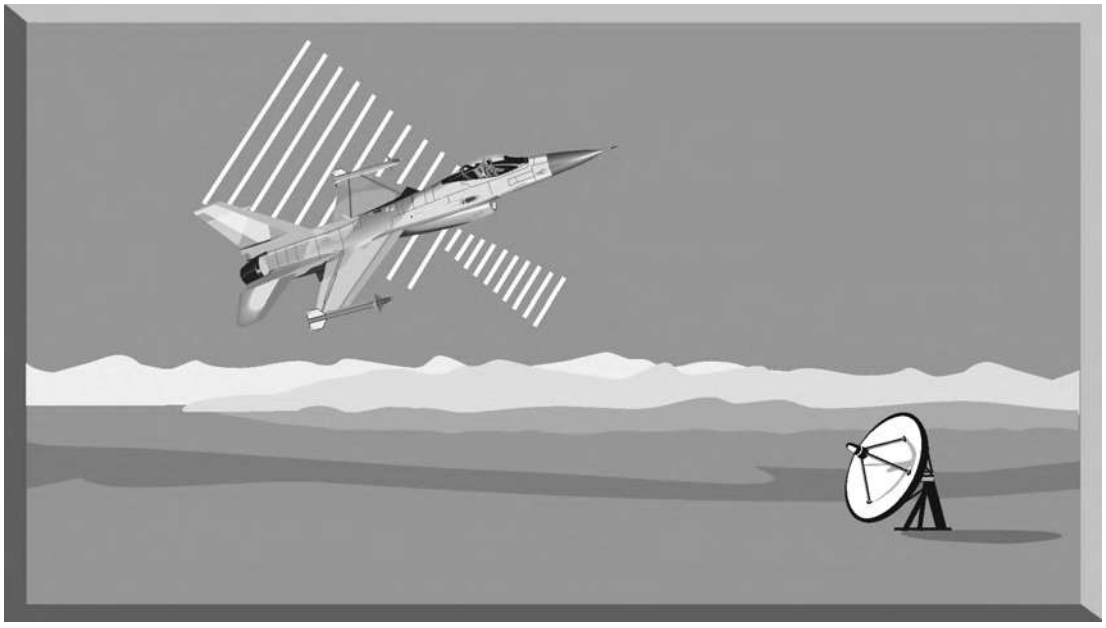

Figure 5-1. Basic Radar Pulse

(1) RF energy travels at the speed of light (c) which is 3 x 10^8 meters per second. Target range can be computed by using the basic radar range determination equation (Equation 5-1).

$$\text{Target Range} = \frac{\text{Measured Time x Speed of Light (c)}}{2}$$

Equation 5-1. Basic Radar Range Determination Equation

(2) Another useful measurement is the radar mile, which is the round trip time for an RF wave to travel to and from a target one nautical mile away (Figure 5-2). Solving the radar range equation for time results in Equation 5-2. Substituting the appropriate values into the equation and solving for time gives measured time of 12.4 microseconds for a one nautical mile (1853 meters) round trip.

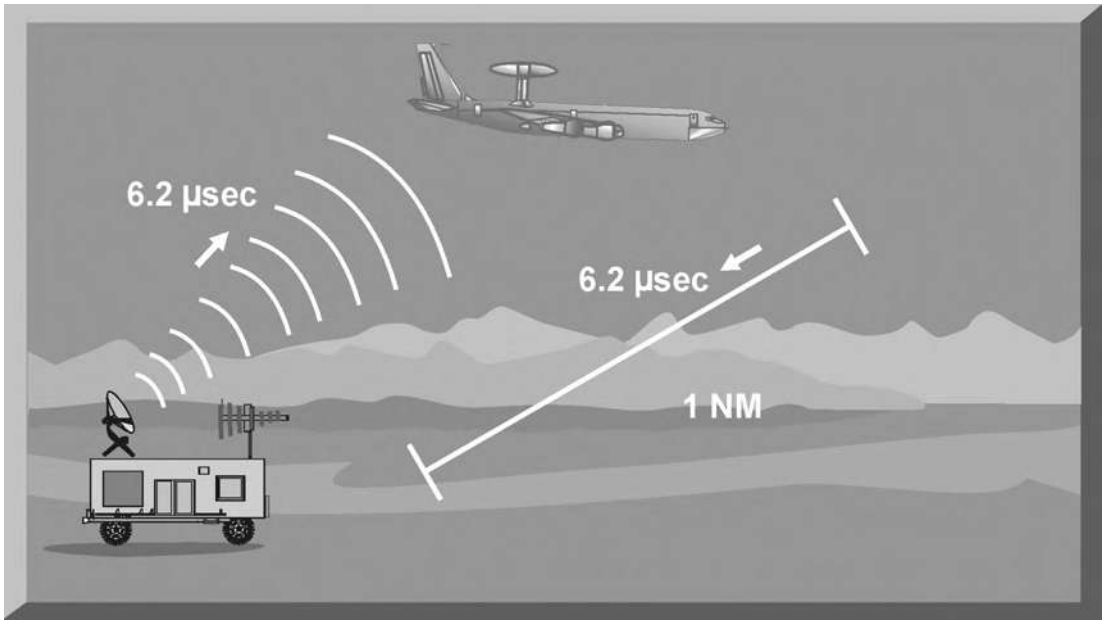

Figure 5-2. Radar Mile

$$\text{Measured Time} = \frac{\text{Target Range x 2}}{\text{Speed of Light (c)}} = \frac{\text{1853 meters x 2}}{3 \times 10^{8}\ \text{meters/second}} = 12.4\,\mu\text{sec}$$

Equation 5-2. Radar Mile

(3) A limitation on radar detection range is the concept of a second time around echo. A second time around echo occurs when a target echo associated with a particular radar pulse arrives at the antenna after another radar pulse has been transmitted. The radar master timer always assumes the target echo is associated with the last pulse transmitted. This makes the target echo ambiguous in range. Figure 5-3 depicts a radar signal with a pulse recurrence time (PRT) of 248 microseconds. Radar pulse A takes 372 microseconds to travel to the target and return. Using the range determination equation, actual target range is 30 nautical miles (nm). However, before the target echo returns to the antenna, radar pulse B is transmitted. The master timer associates the target echo of pulse A with radar pulse B, and calculates a target range of 10 nm. This ambiguous and false range is displayed to the operator.

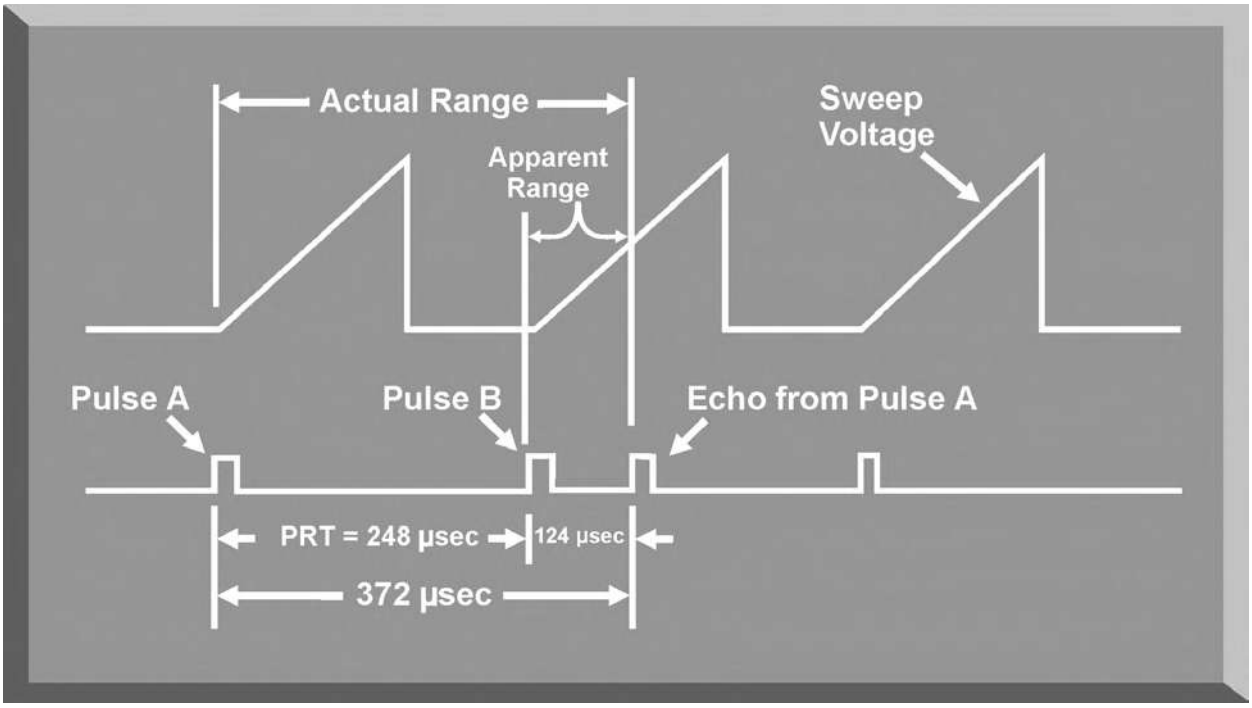

Figure 5-3. Second Time Around Echo

(4) Range ambiguities caused by second time around echoes limit the maximum unambiguous range of a radar system. This important capability can be calculated by using Equation 5-3. An analysis of this equation shows that a radar system designed for long-range detection should transmit a radar signal with a large PRT. In addition, as the PRF of a radar signal increases, the PRT decreases, and the maximum unambiguous range decreases.

$$\text{Maximum Unambiguous Range} = \frac{\text{PRT (µsecs)}}{\text{12.4 (µsecs/nm)}}$$

Equation 5-3. Maximum Unambiguous Range

b. A critical aspect of range determination is range resolution. Range resolution is the ability of a radar to separate two targets that are close together in range and are at approximately the same azimuth (Figure 5-4). The range resolution capability is determined by pulse width. Pulse width is the time that the radar is transmitting RF energy. Pulse width is measured in microseconds.

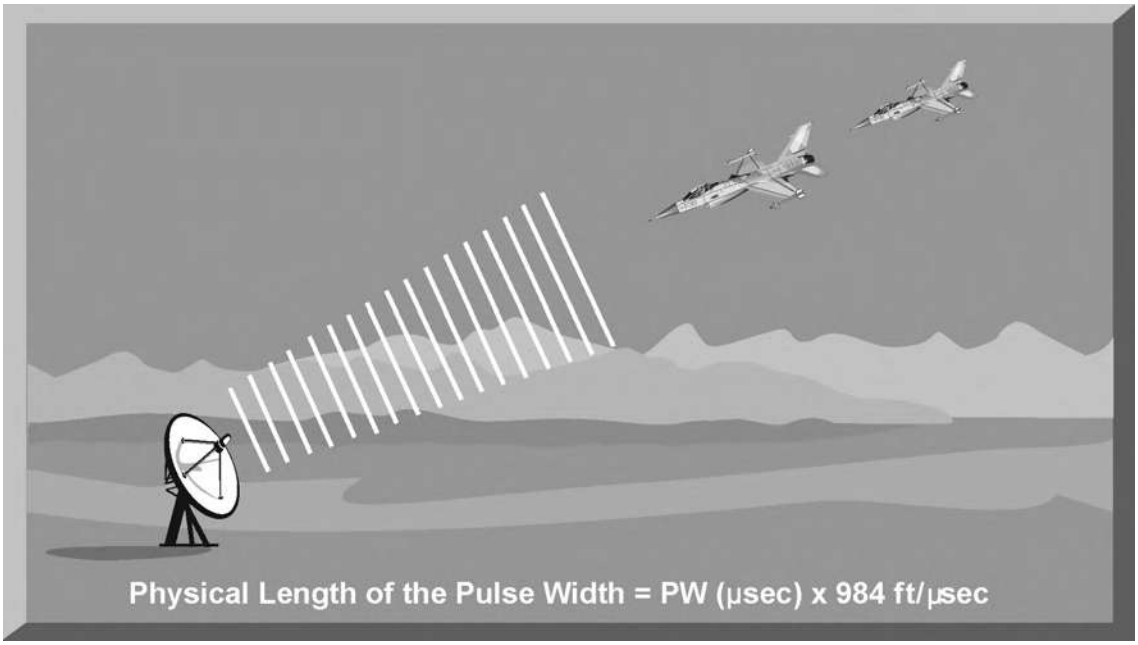

Figure 5-4. Radar Pulse

(1) A radar pulse in free space occupies a physical distance equal to the pulse width multiplied by the speed of light, which is about 984 feet per microsecond. If two targets are closer together than one-half of this physical distance, the radar cannot resolve the returns in range, and only one target will be displayed.

(2) To illustrate range resolution, consider Figure 5-5, in which two aircraft are separated by a distance of one-half the pulse width or less. At T1, the leading edge of the radar pulse hits the lead aircraft.

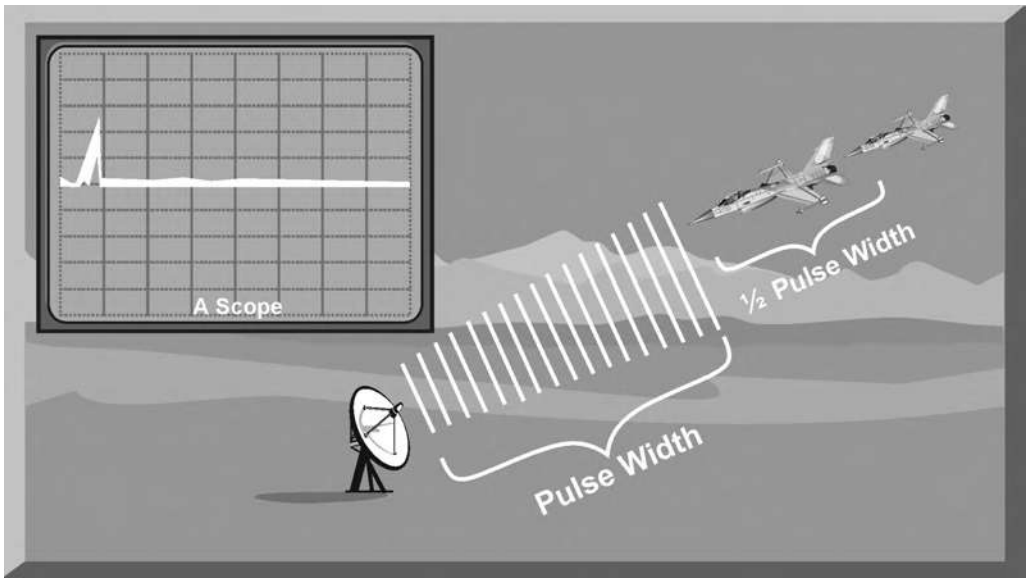

Figure 5-5. Radar Pulse at T1

(3) In Figure 5-6, at T2 the leading edge of this same pulse hits the trailing aircraft. Since the trailing aircraft is less than one-half the pulse width from the lead aircraft, the return echo from the lead aircraft is received by the antenna before the entire pulse has left the trailing aircraft.

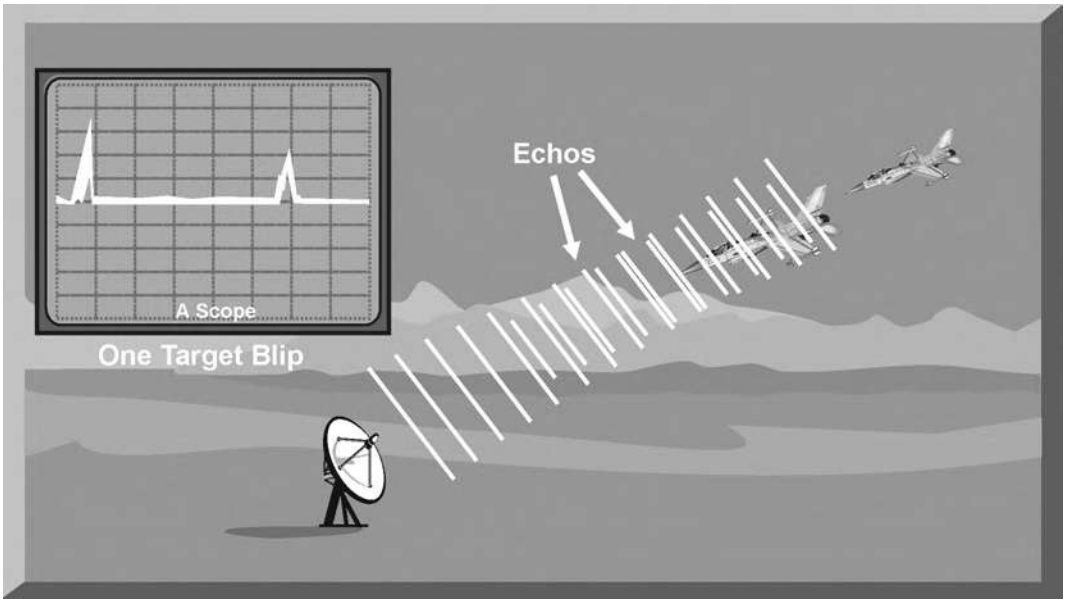

Figure 5-6. Radar Pulse at T2

(4) T3 depicts the merging target echoes at the radar (Figure 5-7). The radar would display only one target in this situation, such as the one shown on the radar scope in Figure 5-6.

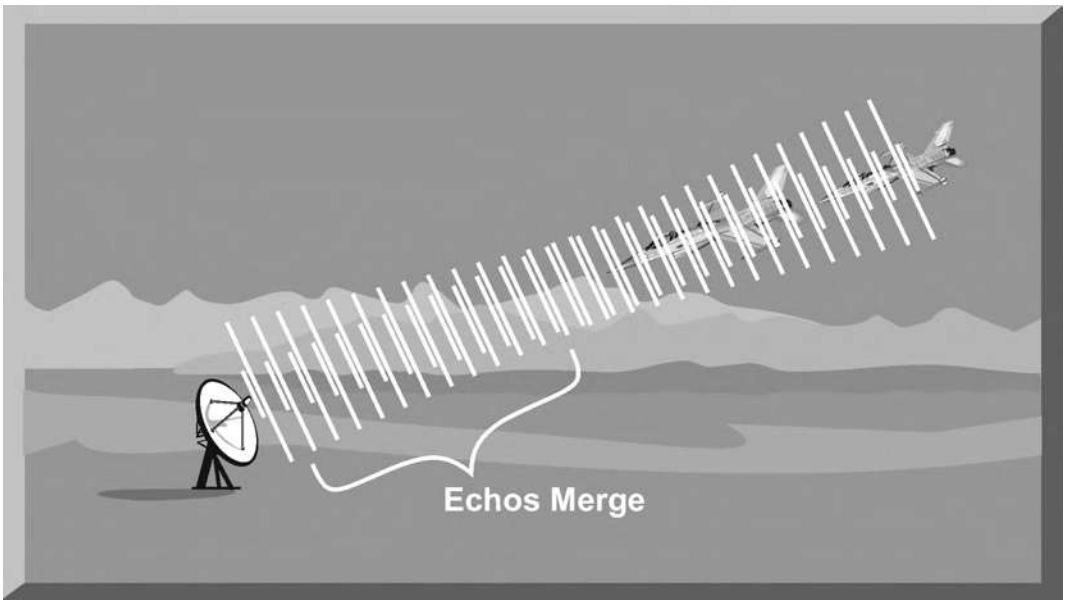

Figure 5-7. Radar Pulse at T3

(5) Two targets separated by more than one-half the pulse width, as in Figure 5-8, will be displayed as two targets. In this case, the transmitted pulse is completely past the lead aircraft before the return echo from the trailing aircraft reaches the antenna.

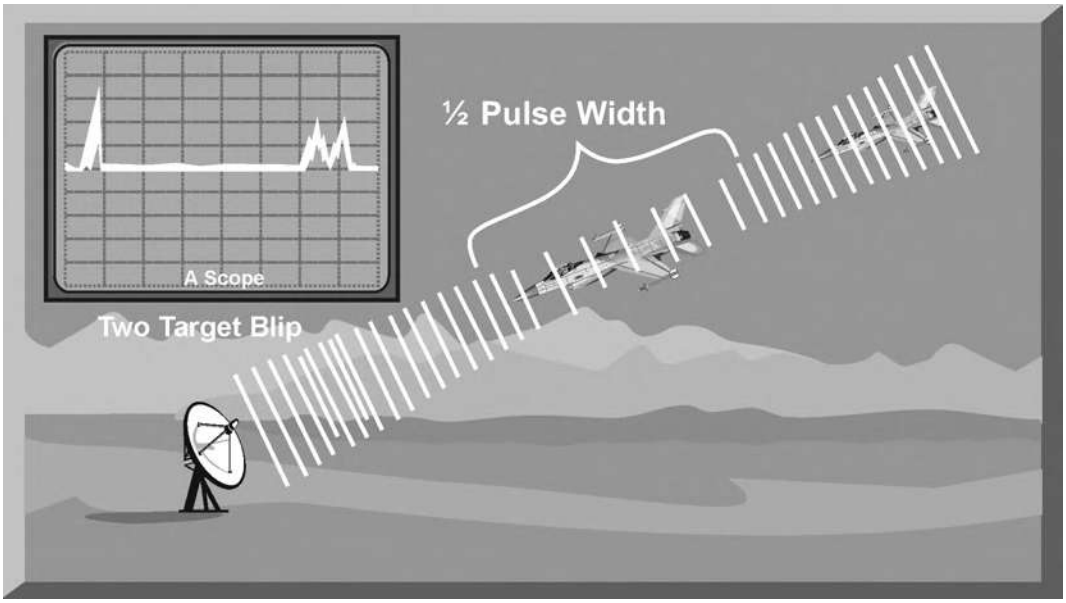

Figure 5-8. Radar Range Resolution

(6) The range resolution of the radar is usually expressed in feet and can be computed using Equation 5-4. It is the minimum separation required between two targets in order for the radar to display them separately on the radar scope.

$$\text{Range Resolution} = \frac{\text{Pulse Width} \times 984 \text{ feet}}{2}$$

Equation 5-4. Range Resolution

3. AZIMUTH DETERMINATION

The beamwidth of a radar system is the horizontal and vertical thickness of the radar beam (Figure 5-9). Beamwidth depends on antenna design and is normally measured in degrees from the center of the beam to the point at which the power drops off by half. This half-power point is -3 dB in power drop-off. Beamwidth governs the azimuth and elevation accuracy and resolution capability of a radar system in the same way that pulse width governs radar range accuracy and resolution.

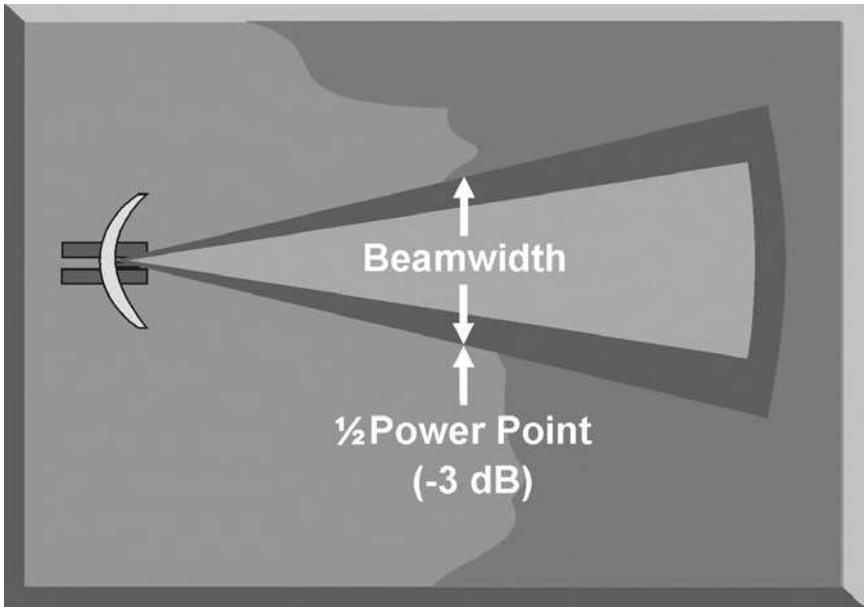

Figure 5-9. Radar Beamwidth

a. In order for a radar system to figure out target azimuth, the antenna must be aligned with a point of reference and pointed at the target during the transmission and reception of several pulses of radar energy. If the antenna is

referenced to true North, the azimuth of the target can be measured relative to true North (Figure 5-10). Azimuth determination is based on the position of the antenna when the target is being illuminated.

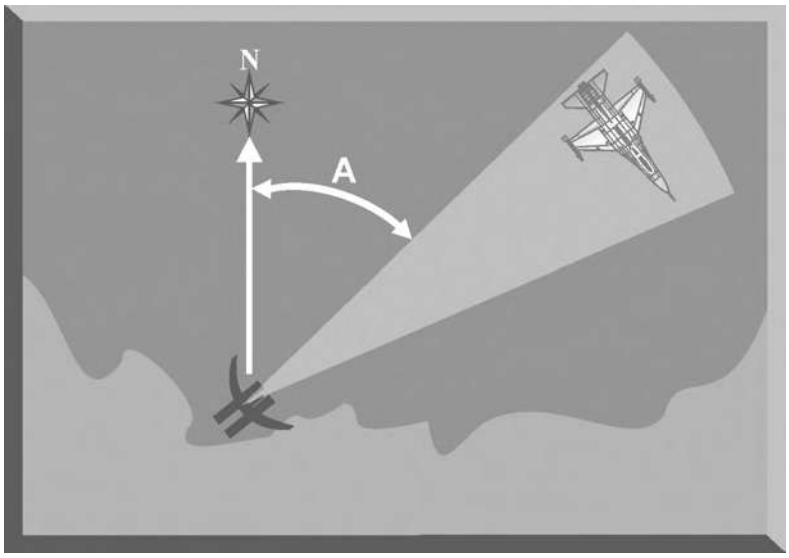

Figure 5-10. Azimuth Determination

(1) To provide accurate azimuth determination over a large area, many radars employ a narrow beam and scan the antenna in a predictable pattern. The most common scan pattern is a 360° circular scan at a constant rate (Figure 5-11). The plan position indicator (PPI) radar scope display is normally associated with this scan pattern. As the radar beam sweeps, a target is detected and displayed. The position of the antenna, when the target is displayed, shows the relative azimuth.

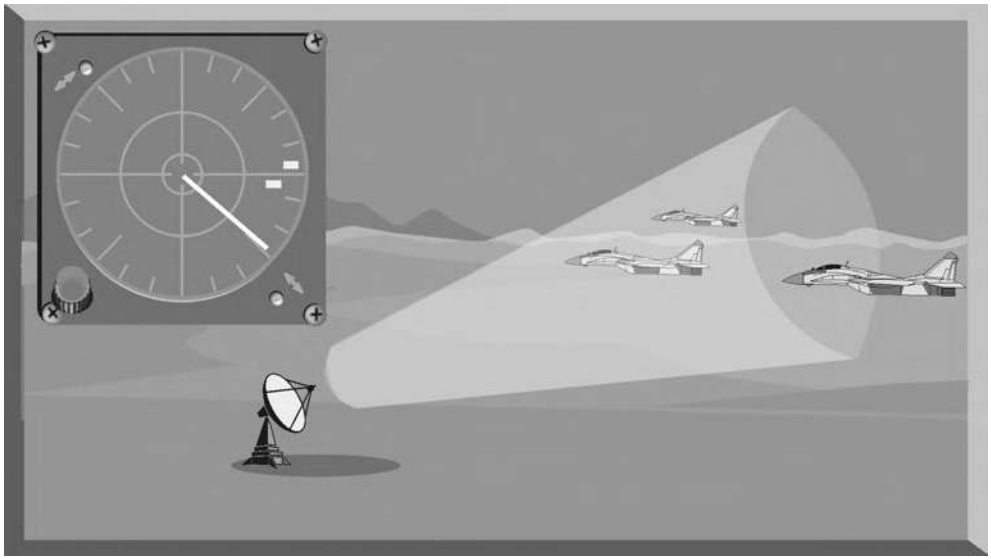

Figure 5-11. Antenna Scan

(2) The azimuth accuracy of a radar system is determined by the horizontal beamwidth (HBW). In Figure 5-12, radar system A has a horizontal beamwidth of 10°. As the beam sweeps, the target is illuminated for as long as it is in the beam. This means that the target covers 10° in azimuth on the PPI scope. Radar system B has a beamwidth of 1°. A target displayed on the PPI scope will cover 1° in azimuth. The narrower the horizontal beamwidth, the better the azimuth accuracy.

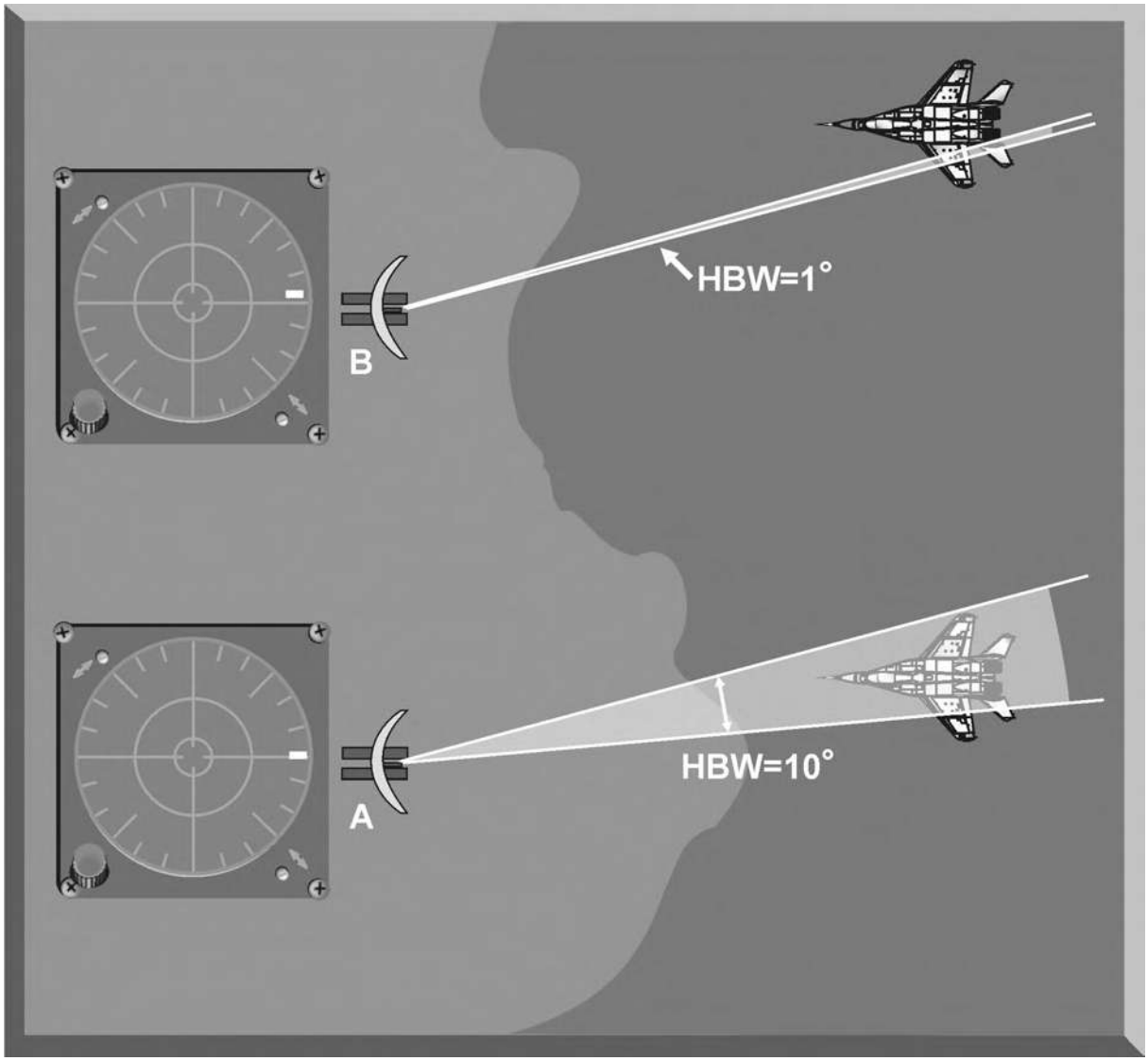

Figure 5-12. Horizontal Beamwidth Comparison

b. Azimuth resolution is the ability of a radar to display two targets flying at approximately the same range with little angular separation, such as two fighters flying line-abreast tactical formation. The azimuth resolution capability is usually expressed in nautical miles and corresponds to the minimum azimuth separation

required between two targets for separate display. Azimuth resolution depends on the horizontal beamwidth of the radar. The radar system in Figure 5-13 has a horizontal beamwidth of 10°. The two targets are so close in azimuth that the return echoes are blended into one return.

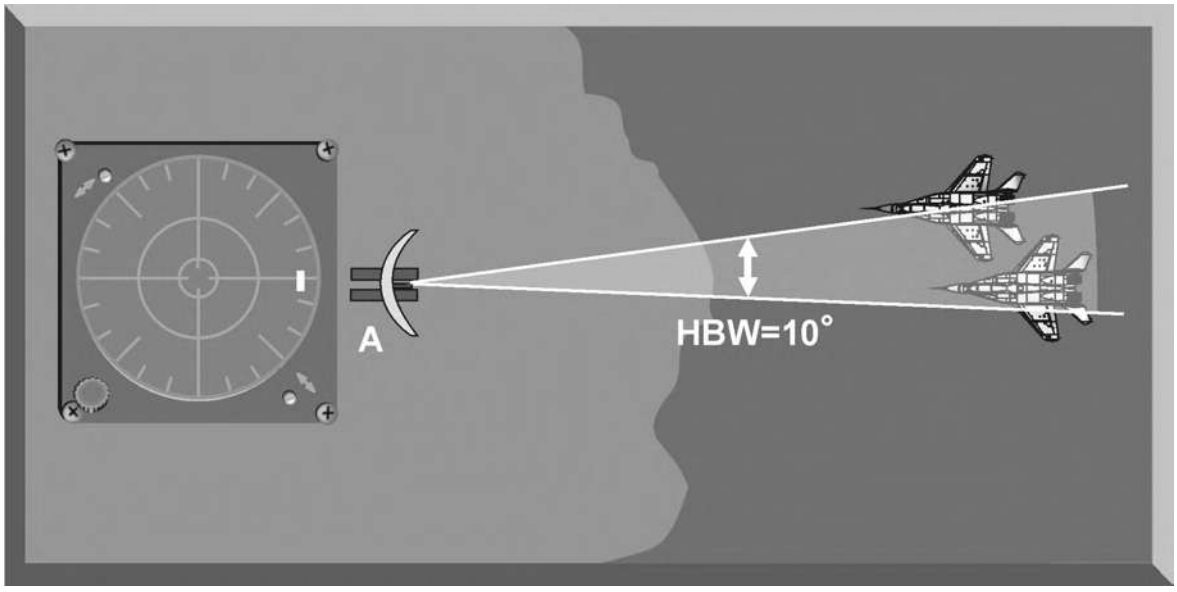

Figure 5-13. Horizontal Beamwidth and Azimuth Resolution

(1) The radar system in Figure 5-14 has a horizontal beamwidth of 1°. The radar beam not only hits the targets, but passes between them without causing a return. This allows the radars to display two distinct radar returns. A small horizontal beamwidth improves azimuth resolution.

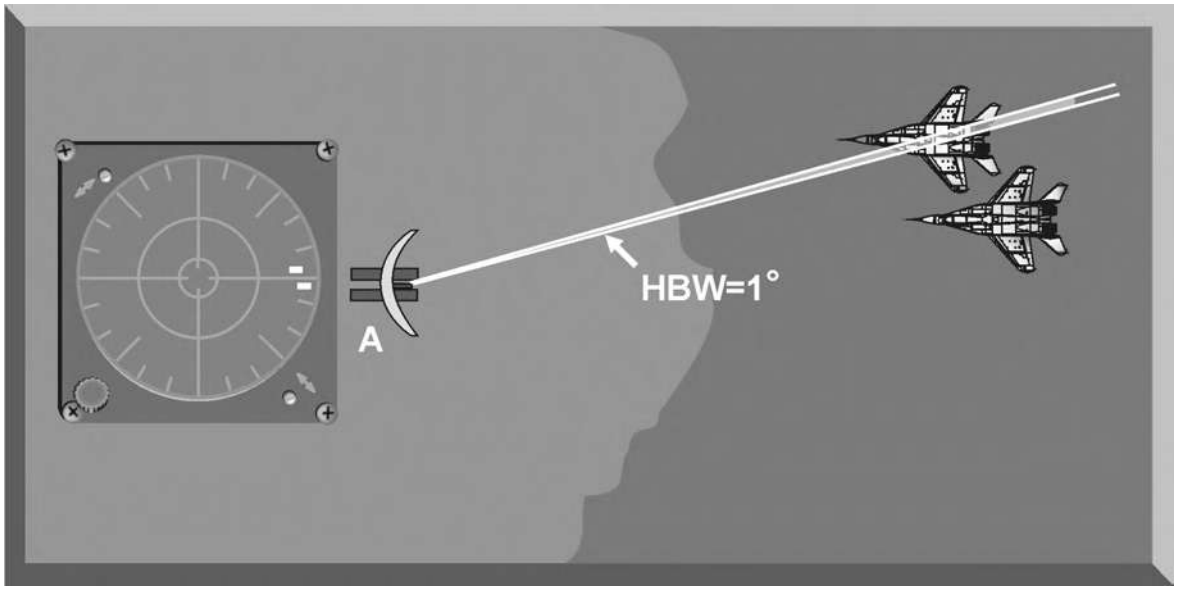

Figure 5-14. Azimuth Resolution

(2) Azimuth resolution, in nautical miles, can be computed using Equation 5-5. Notice that this equation is the "60 to 1 rule" used for navigation. A 1° beamwidth will yield a one-mile-wide cell at 60 nautical miles.

$$\text{Azimuth Resolution} = \frac{\text{Horizontal Beamwidth} \times \text{Range}}{60}$$

Equation 5-5. Azimuth Resolution

4. ELEVATION DETERMINATION

Since a radar beam is three-dimensional, the vertical beamwidth is the primary factor in determining altitude resolution capability. Altitude resolution is the ability of a radar to display two targets flying at approximately the same range and azimuth with little altitude separation, such as two fighters flying a vertical stack formation. The altitude resolution capability is usually expressed in feet and corresponds to the minimum altitude separation required between two targets for separate display. The radar system in Figure 5-15 has a vertical beamwidth of 10°. The two targets are so close in altitude that the return echoes depicted on the range height indicator (RHI) are blended into one.

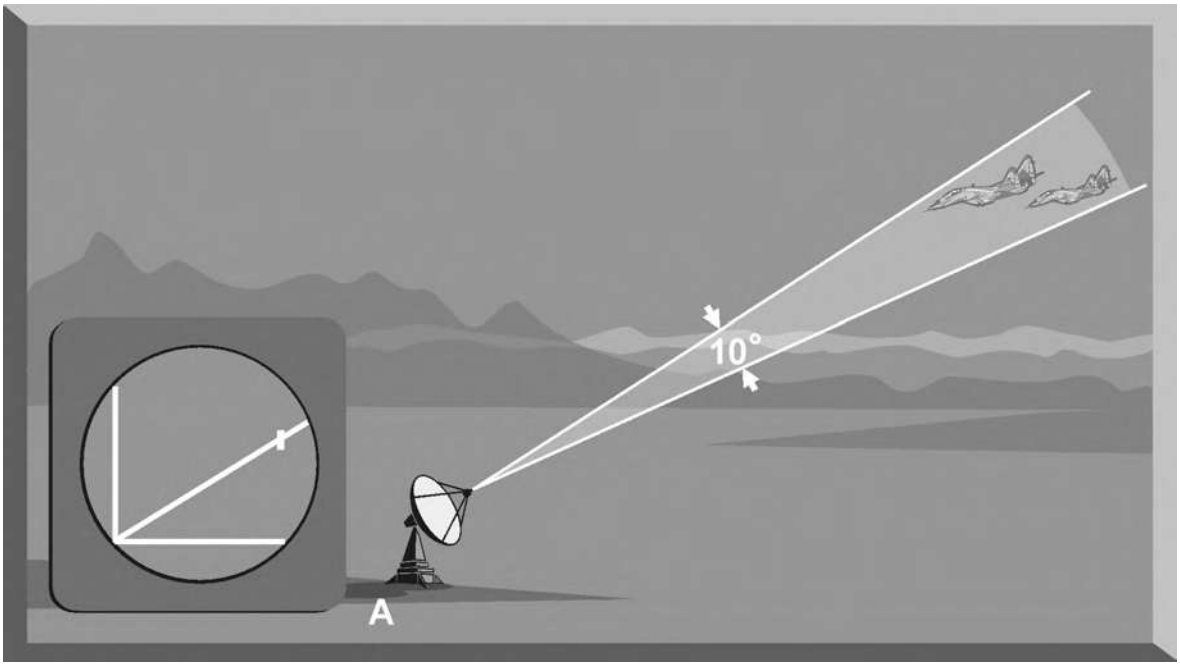

Figure 5-15. Vertical Beamwidth and Elevation Resolution

a. The radar system depicted in Figure 5-16 has a vertical beamwidth of 1°. This small beam not only hits the targets, but passes between them without causing a return. This allows the radar to display two distinct targets.

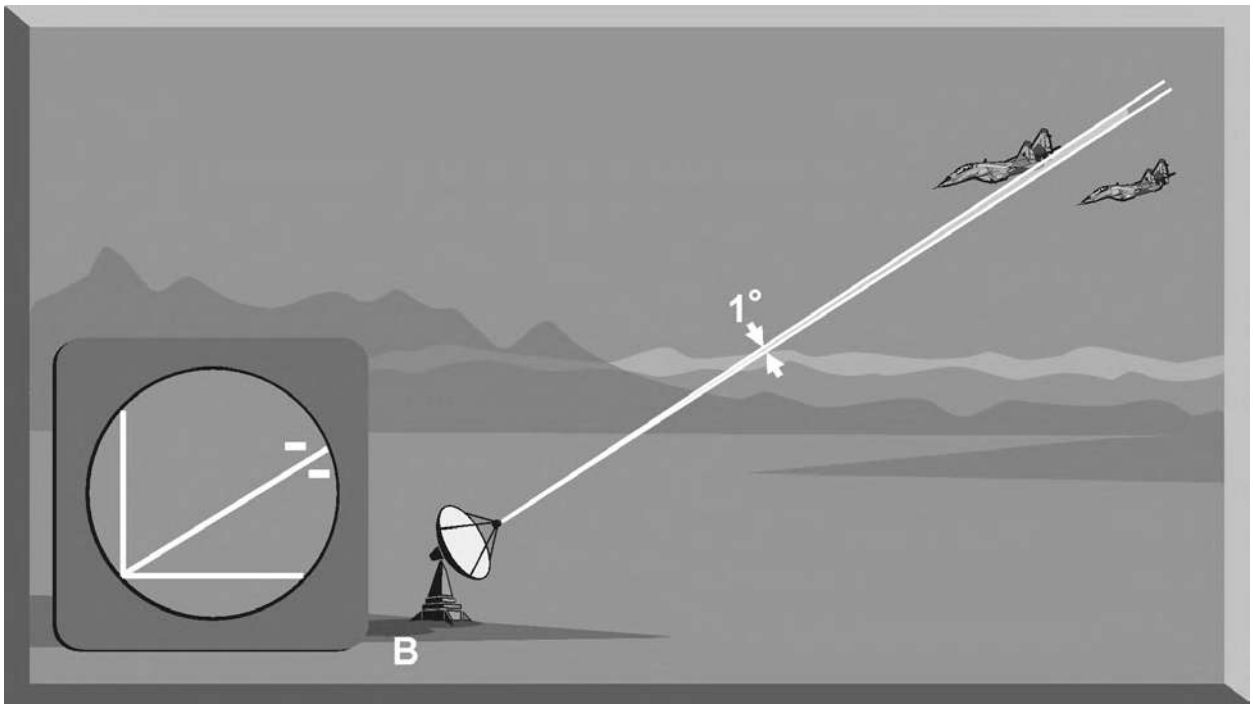

Figure 5-16. Elevation Resolution

b. Altitude/elevation resolution, in thousands of feet, can be computed using Equation 5-6.

$$\text{Altitude Resolution} = \frac{\text{Vertical Beamwidth} \times \text{Range}}{60}$$

Equation 5-6. Altitude Resolution

5. RADAR RESOLUTION CELL

A radar's pulse width, horizontal beamwidth, and vertical beamwidth form a three-dimensional resolution cell (RC) (Figure 5-17). A resolution cell is the smallest volume of airspace in which a radar cannot determine the presence of more than one target. The resolution cell of a radar is a measure of how well the radar can resolve targets in range, azimuth, and altitude. The horizontal and vertical

dimensions of a resolution cell vary with range. The closer to the radar, the smaller the resolution cell.

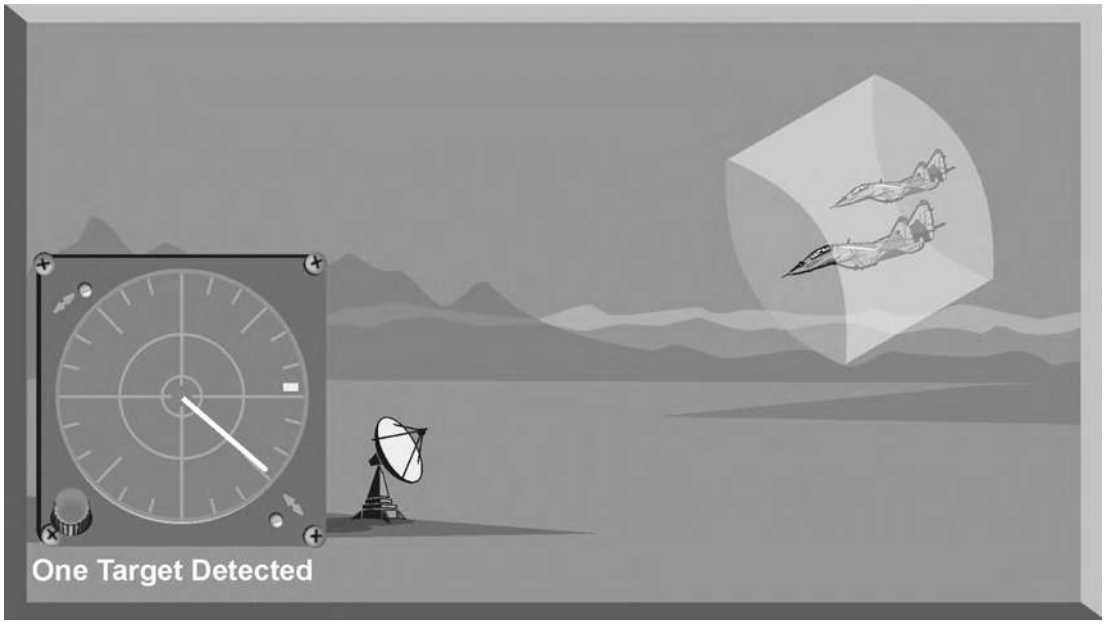

Figure 5-17. Radar Resolution Cell

a. The physical dimensions of a radar's resolution cell can be computed. For a radar with a pulse width of 1 microsecond, a horizontal beamwidth of 1°, and a vertical beamwidth of 10°, the formulas for range resolution, azimuth resolution, and altitude resolution can be used to compute the dimensions of the resolution cell. In the example in Figure 5-18, at a target range of 10 nm, the physical dimensions of the radar's resolution cell are 492 feet in range, by 1000 feet in azimuth, and 10,000 feet in altitude. These figures can be confirmed by using Equations 5-4, 5-5, and 5-6.

$$A = \text{Pulse Width} \times \frac{\text{Speed of Light}}{2}$$

$$A = 1 \text{ Microsecond} \times \frac{984 \text{ feet per microsecond}}{2}$$

$$A = 492 \text{ feet}$$

Figure 5-18. Radar Resolution Cell Dimensions

b. Based on these computations, two, or more, aircraft flying a trail formation closer than 492 feet would be displayed as a single target. Two, or more, aircraft flying line abreast closer than 1000 feet would be displayed as a single target. Two, or more, aircraft flying a vertical stack closer than 10,000 feet would be displayed as a single target. This also shows that the shorter the pulse width, the better the range resolution capability of a radar system. The narrower the horizontal beamwidth, the better the azimuth resolution capability. The narrower the vertical beamwidth, the better the altitude resolution capability.

c. Another type of resolution is velocity resolution. For a Doppler radar aircraft flying within the conventional resolution cell described above can be distinguished as separate targets if they have enough speed differential. Paragraph 6 below will describe how this is carried out.

6. PULSE DOPPLER VELOCITY DETERMINATION

To fully understand how a pulse Doppler radar determines target velocity, it is necessary to know more about the pulsed waveform. To generate a pulse modulated wave, a continuous carrier sine wave, like the output from a CW radar, is combined with a rectangular wave, like that of a pulse radar, to produce the pulse modulated waveform. Figure 5-19 depicts pulse modulation.

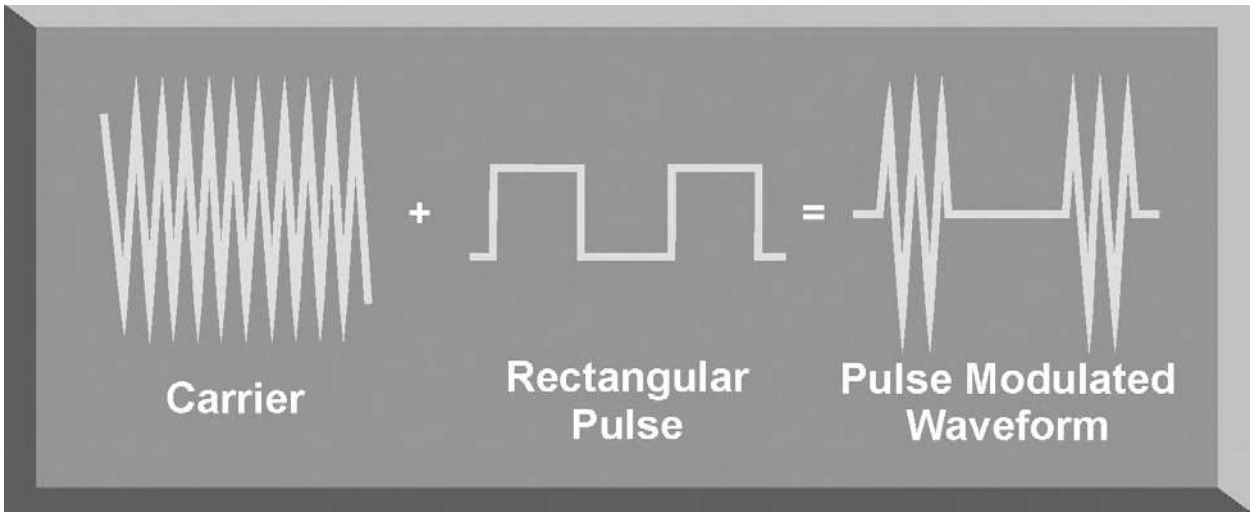

Figure 5-19. Pulse Modulation

a. Mathematically, any waveform other than a sine wave is composed of many different pure sine waves added in the proper amplitude and phase relationships (Figure 5-20). In a pulsed modulated waveform, the sine waves correspond to the fundamental frequency, which is the PRF, and the sum of all harmonics in the proper amplitude and phase. The frequency of the harmonic is the basic frequency plus or minus a multiple of the PRF.

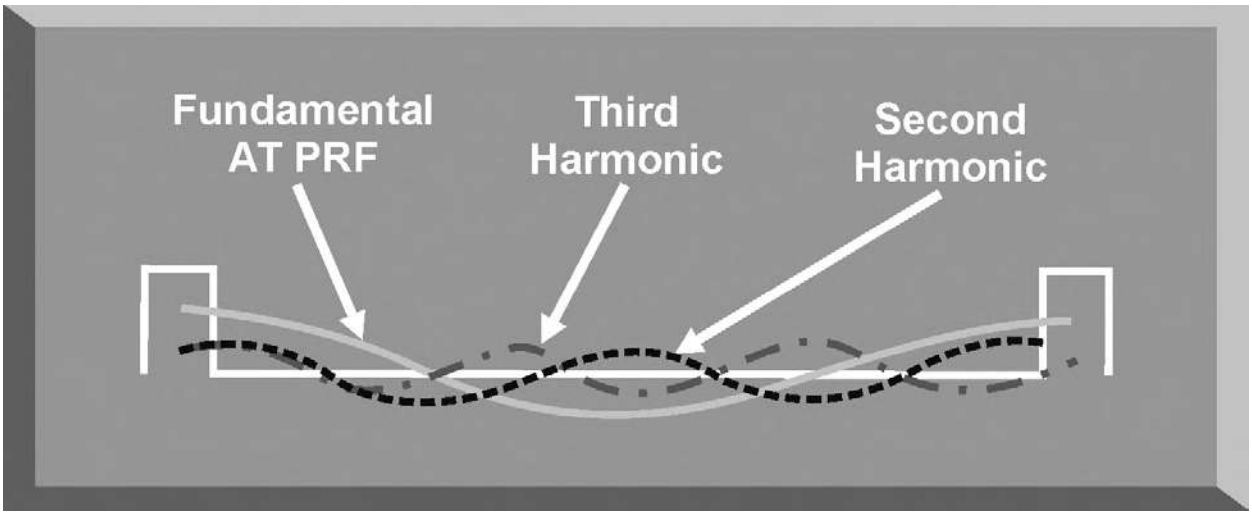

Figure 5-20. Harmonics of a Pulse Modulated Waveform

(1) Figure 5-21 is a plot of the harmonic content of a pulse modulated waveform operating at a carrier frequency of 2800 megahertz (MHz) with a PRF of 1 MHz. Note the loops of frequencies on either side of the carrier frequency. These are the additions and subtractions of all the frequencies in the rectangular pulse to the carrier frequency. The important thing to remember is that there are many frequencies present, and a pulse Doppler radar must deal with a crowded frequency spectrum. This becomes even more important when one considers the fact that every frequency present will experience a Doppler shift when it is reflected by a moving target. The individual frequencies shown are called spectral lines.

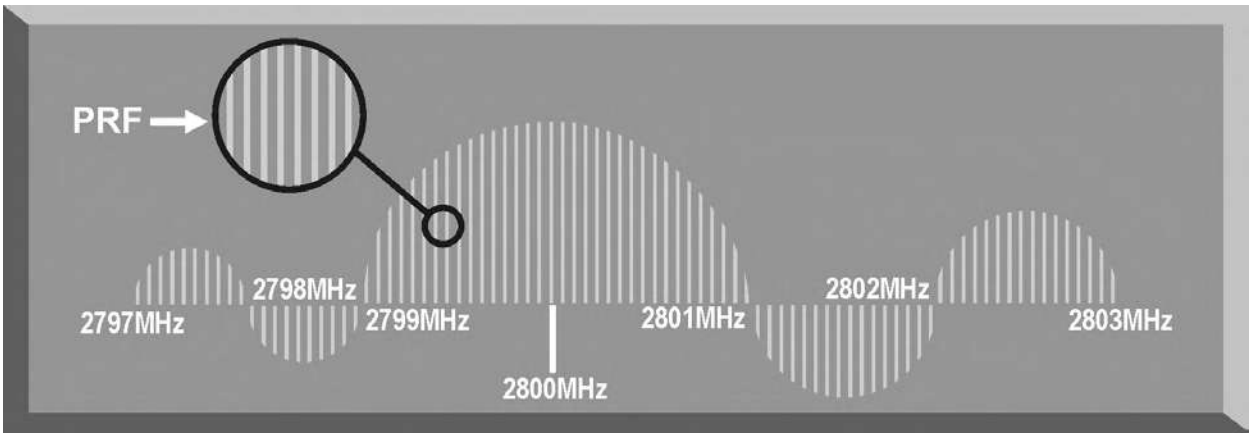

Figure 5-21. Harmonic Content

(2) For a pulse Doppler radar to accurately measure velocity, it must compare the frequency change, or Doppler shift, between the carrier frequency

and the frequency returning from the target. It is a difficult task for the radar to differentiate between the returning carrier and all the harmonic frequencies (Figure 5-22).

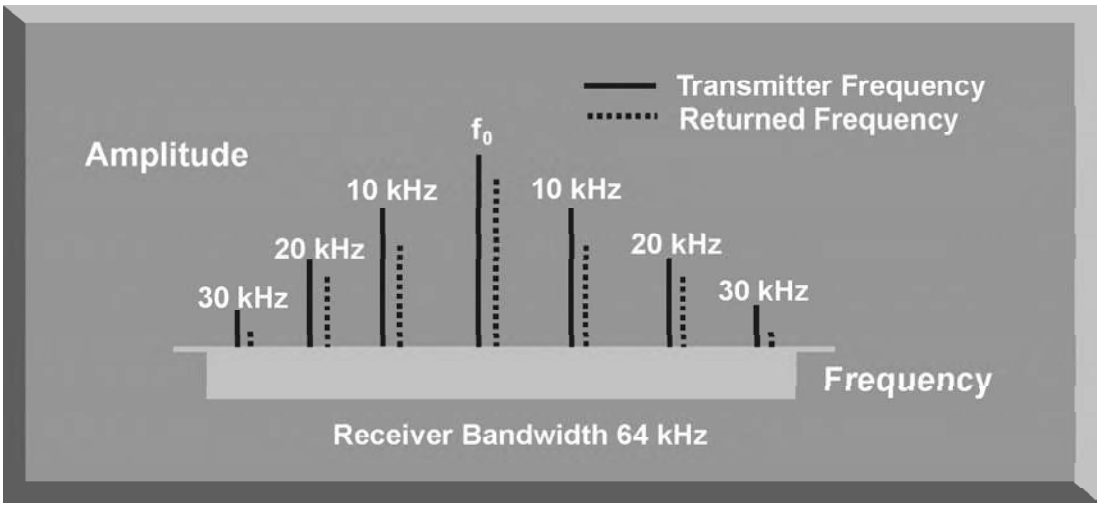

Figure 5-22. Spectral Line Frequencies

b. The radar differentiates between the returning carrier frequencies and all other harmonic frequencies by using clutter cancellers, or filters, at the known harmonic frequencies (Figure 5-23). The radar cannot process frequencies cancelled by these filters. The filters create "blind speeds" for the radar. The closer together the spectral lines, the more "blind speeds" the radar will have.

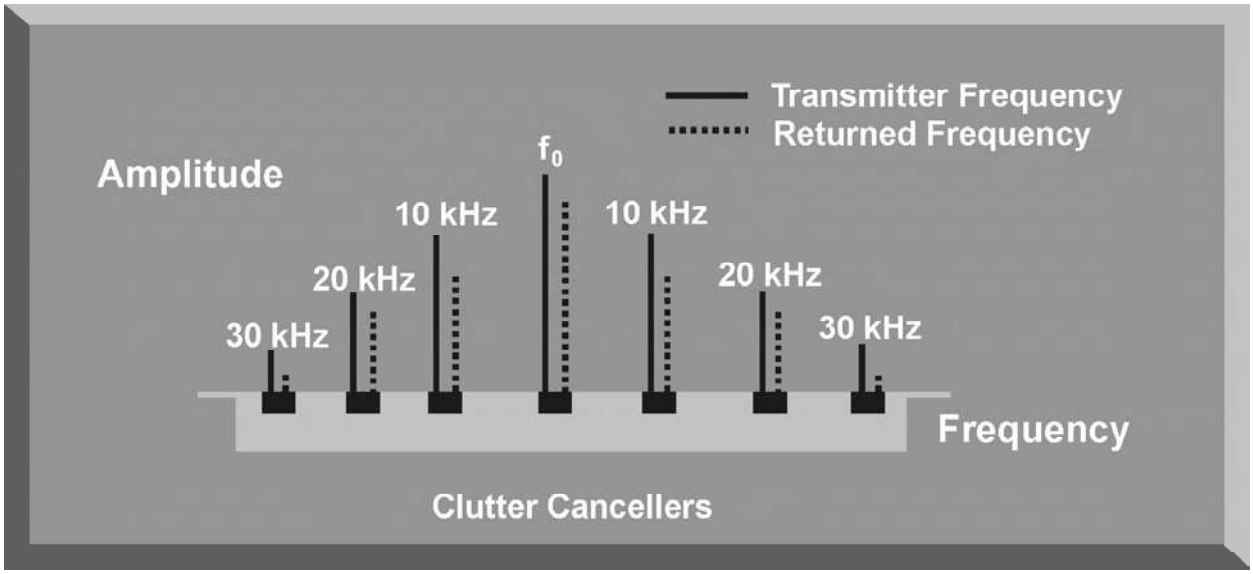

Figure 5-23. Selective Clutter Canceling

(1) Since the position of the harmonics in relation to the carrier frequency is based on PRF, the number of blind speeds can be reduced by changing the PRF of the radar. The higher the PRF, the wider the spacing of the spectral lines and the fewer blind speeds due to selective clutter canceling. However, a high PRF increases the problem of range ambiguities. Most modern pulse Doppler radars employ a medium and high PRF mode. Medium PRF equates to fewer range ambiguities but more blind speeds. High PRF has fewer blind speeds but more range ambiguities (Figure 5-24).

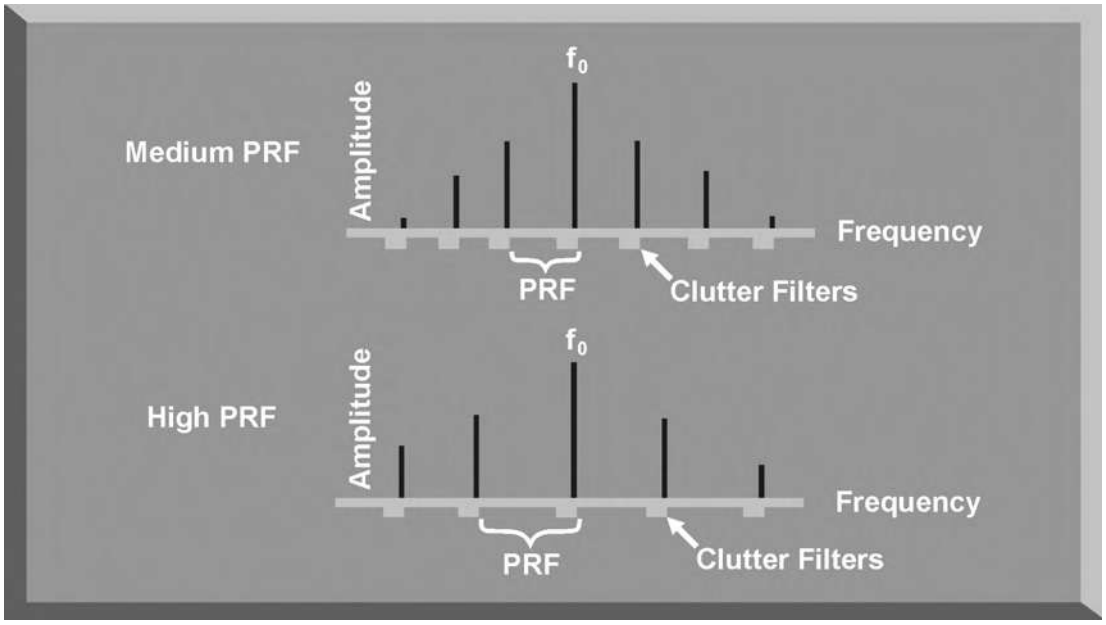

Figure 5-24. PRF and Spectral Lines

(2) To separate the returning target frequency shifts from all other frequencies in the returning waveform, the pulse Doppler radar employs filters to cancel the known harmonic frequency shifts. In addition, the radar cancels out all returns with no frequency shift, which equates to canceling all returns with no movement relative to the radar. However, if the radar has too many clutter filters, this creates multiple blind speeds, and targets will be missed. In Figure 5-25, the detection filters allow target frequencies to be processed, and clutter filters cancel unwanted frequency shifts. Target 1 will be detected, but Target 2 will be canceled.

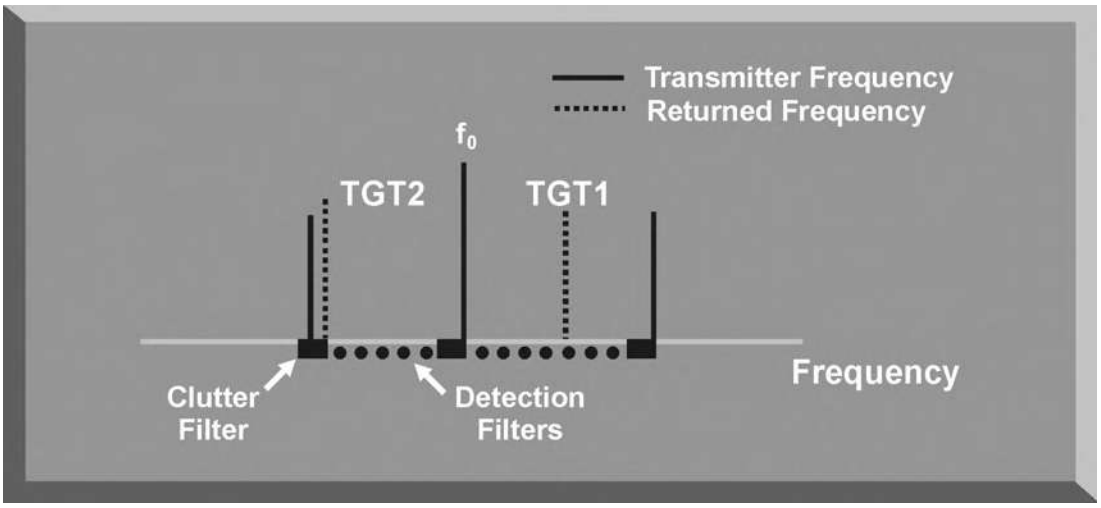

Figure 5-25. Pulse Doppler Filters

7. BASIC RADAR EQUATION

The basic radar equation relates the range of a radar system to the characteristics of the transmitter, receiver, antenna, and the target. The radar equation provides a means not only to figure out the maximum range of a particular radar system, but it can be used to understand the factors that affect radar operation. In this section, the simple forms of the radar equation are developed, starting with the power density of the transmitting antenna to the power received by the receiving antenna.

a. Power density is the power of a radio wave per unit of area normal to the direction of propagation. The power density generated by a practical antenna can be expressed in Equation 5-7.

$$\text{Power Density from Antenna} = \frac{P_T \times G}{4\pi r^2}$$

P_T = transmitted power
G = antenna gain
r = radius of the antenna

Equation 5-7. Power Density From an Antenna

b. As the radar beam propagates through space, it arrives at a target at some range (R) from the antenna. As the radar beam travels through space, the wavefront of the beam expands to a very large cross-sectional area, especially in relation to the target dimensions. The power density of the radar beam, across this wide area, at the target, is detailed in Equation 5-8.

$$\text{Power Density at Target} = \frac{P_T \times G}{4\pi R^2}$$

P_T = transmitted power
G = antenna gain
R = range to the target

Equation 5-8. Power Density at the Target

c. Since the cross-sectional area of the radar beam is so large, only a small portion of the total power in the beam can be reflected toward the antenna. The rest of the radar energy continues through space and is dissipated, absorbed, or reflected by other targets. The small portion of the radar beam that hits the target is reradiated in various directions. The measure of the amount of incident power intercepted by the target and reradiated back in the direction of the antenna depends on the radar cross section (RCS) of the target. Equation 5-9 details the power density of the target echo signal reflected back to the radar antenna.

$$\text{Power Density at Antenna} = \frac{P_T \times G}{4\pi R^2} \times \frac{\sigma}{4\pi R^2}$$

P_T = transmitted power
G = antenna gain
σ = RCS
R = range to the target

Equation 5-9. Power Density at the Antenna

d. As the target echo reaches the antenna, part of the echo is captured by the antenna based on the effective aperture (A_e). Equation 5-10 details the actual signal power received by the radar system. This is one form of the basic radar equation and is the signal strength of a radar return from a specific target at range (R) from the radar.

$$\text{Signal Power Density (S)} = \frac{P_T G \sigma A_e}{(4\pi)^2 R^4}$$

P_T = transmitted power
G = antenna gain
σ = RCS
R = range to the target
A_e = antenna aperture area

Equation 5-10. Signal Power Density

e. A detailed analysis of this equation is not required to draw some basic conclusions about the factors affecting the detection of an aircraft. If any factor in the numerator, such as transmitted power, is increased by a factor of three, the signal received by the radar will increase by only 30 percent. This clearly shows why radar system operation is characterized by the transmission of megawatts of power and the reception of microwatts of returning power. In addition, this equation shows that the most critical factor in determining radar detection is target range.

f. The maximum radar range (R_{MAX}) occurs when the signal power density received just equals the minimum detectable signal (S_{MIN}) for the receiver. Solving Equation 5-11 for range, and substituting S_{MIN}, yields the basic radar equation for R_{MAX} for a specific target. This is another form of the basic radar equation.

$$R_{MAX} = \frac{\left[P_T G \sigma A_e\right]^{1/4}}{\left[(4\pi)^2 S_{MIN}\right]}$$

P_T = transmitted power
G = antenna gain
σ = RCS
A_e = antenna aperture area
R = range to the target

Equation 5-11. Basic Radar Equation

g. It is important to note that the basic radar equations do not consider such factors as meteorological conditions, changes in aircraft RCS, the impact of clutter on gain, or operator abilities. The radar equation does explain why a radar system designed for long-range detection should transmit a very high power signal, concentrated into a narrow beam, collected by a large antenna, and processed by a very sensitive receiver.

8. SUMMARY

This chapter has discussed the methods employed by radar systems to determine target range, azimuth, elevation, and velocity. The relationship between pulse width and range resolution, beamwidth and azimuth/elevation resolution, and PRF and velocity resolution have been explained. In addition, an explanation of the complex radar equation has been presented. The capabilities and limitations of a specific radar system to determine these critical target parameters is the key to understanding the countermeasures designed to defeat this system.

CHAPTER 6. ANTENNA CHARACTERISTICS AND SCANS

1. INTRODUCTION

The function of the antenna during transmission is to concentrate the radar energy from the transmitter into a shaped beam that points in the desired direction. During reception, or listening time, the function of the antenna is to collect the returning radar energy, contained in the echo signals, and deliver these signals to the receiver. Radar antennas are characterized by directive beams that are usually scanned in a recognizable pattern. The primary antenna types in use today fall into three categories: parabolic, Cassegrain, or phased array antennas. Additionally, the method radar antennas employ to sample the environment is a critical design feature of the radar system. The scan type selected for a particular radar system often decides the employment of that radar in an integrated air defense system (IADS). The process the radar antenna uses to search airspace for targets is called scanning or sweeping. This chapter discusses circular, unidirectional, bidirectional, helical, raster, Palmer, and conical scans, and track-while-scan (TWS) radar systems.

2. PARABOLIC ANTENNA

One of the most widely used radar antennas is the parabolic reflector (Figure 6-1). The parabola-shaped antenna is illuminated by a source of radar energy, from the

Figure 6-1. Parabolic Antenna

transmitter, called the feed. The feed is placed at the focus of the parabola, and the radar energy is directed at the reflector surface. Because a point source of energy, located at the focus, is converted into a wavefront of uniform phase, the parabola is well suited for radar antenna applications. By changing the size and shape of the parabolic reflecting surface, a variety of radar beam shapes can be transmitted.

a. The antenna depicted in Figure 6-1 generates a nearly symmetrical pencil beam that can be used for target tracking.

b. Elongating the horizontal dimensions of the parabolic antenna creates a radar antenna called the parabolic cylinder antenna (Figure 6-2). The pattern of this antenna is a vertical fan-shaped beam. Combining this antenna pattern with a circular scan technique creates a radar system well suited for long-range search and target acquisition.

Figure 6-2. Parabolic Cylinder Antenna

c. Elongating the vertical dimensions of the parabola creates a radar antenna that generates a horizontal fan-shaped beam with a small vertical dimension (Figure 6-3). This type of antenna is generally used in height-finding radar systems.

Figure 6-3. Height-Finder Parabolic Antenna

d. Another variation of the basic parabolic antenna includes using an array of multiple feeds instead of a single feed (Figure 6-4). This type of parabolic antenna can produce multiple radar beams, either symmetrical or asymmetrical, depending on the angle and spacing of the individual feeds.

Figure 6-4. Multiple-Feed Parabolic Antenna

3. CASSEGRAIN ANTENNA

A Cassegrain antenna uses a two-reflector system to generate and focus a radar beam (Figure 6-5). The primary reflector uses a parabolic contour, and the secondary reflector, or subreflector, has a hyperbolic contour. The antenna feed

is located at one of the two foci of the hyperbola. Radar energy from the transmitter is reflected from the subreflector to the primary reflector to focus the radar beam. Radar energy returning from a target is collected by the primary reflector and reflected as a convergent beam to the subreflector. The radar energy is rereflected by the subreflector, converging at the position of the antenna feed. The larger the subreflector, the closer it can be to the primary reflector. This reduces the axial dimensions of the radar but increases aperture blockage due to the subreflector. A small subreflector reduces aperture blockage, but it must be positioned at a greater distance from the primary reflector.

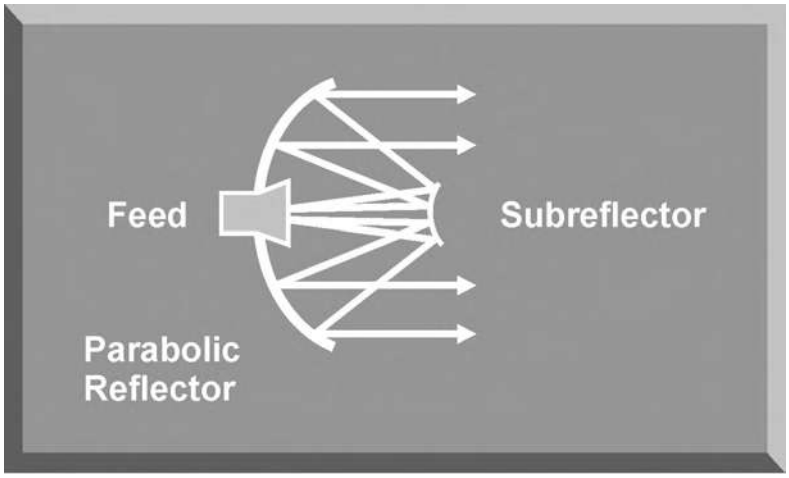

Figure 6-5. Cassegrain Antenna

a. To reduce the aperture blockage by the subreflector and to provide a method to rapidly scan the radar beam, the flat plate Cassegrain antenna was developed. This type of Cassegrain antenna is depicted in Figure 6-6.

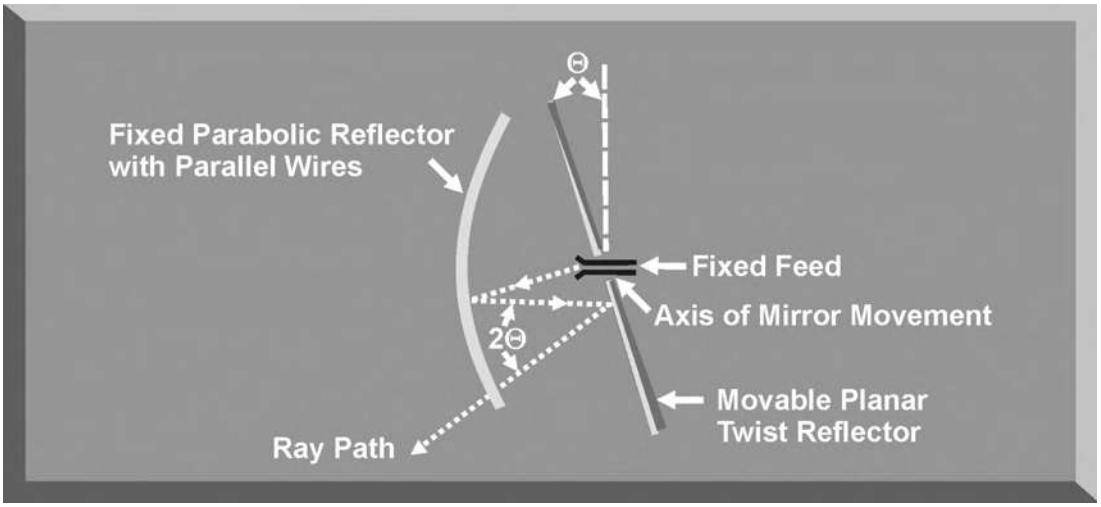

Figure 6-6. Flat Plate Cassegrain Antenna

The fixed parabolic reflector is made up of parallel wires spaced less than a half wavelength apart and supported by a low-loss dielectric material. This makes the fixed parabolic reflector polarization sensitive. It will completely reflect one type of linear polarization and be transparent to the orthogonal polarization. The fixed antenna feed, in the middle of the moveable mirror, transmits a radar signal polarized to be reflected by the parabolic reflector. The moveable mirror is constructed as a twist reflector that changes the polarization of the radar signal by 90°. The signal from the feed is reflected by the parabolic reflector to the mirror, which rotates the polarization 90°. This rotation makes the transmitted signal transparent to the parabolic reflector, and the signal passes through with minimal attenuation. The radar beam can be scanned over a wide area by rotating the moveable mirror. A deflection of the mirror by the angle θ results in the beam scanning through an angle of 2θ.

b. The geometry of the Cassegrain antenna is especially well suited for monopulse tracking radar applications. Unlike the parabolic antenna, the complex feed assembly required for a monopulse radar can be placed behind the reflector to avoid aperture blocking.

4. PHASED ARRAY ANTENNA

The phased array radar is a product of the application of computer and digital technologies to the field of radar design. A phased array antenna is a complex arrangement of many individual transmitting and receiving elements in a particular pattern. A phased array antenna can, in effect, radiate more than one beam from the antenna by using a computer to rapidly and independently control groups of these individual elements. Multiple beams and computer processing of radar returns give the phased array radar the ability to track-while-scanning and engage multiple targets simultaneously. Figure 6-7 is a view of the phased array radar antenna.

Figure 6-7. Phased Array Antenna

a. A phased array radar uses the principle of radar phase to control the individual transmitting and receiving elements. When two transmitted frequencies are in-phase, their amplitudes add together, and the radiated energy is doubled. When two transmitted frequencies are out-of-phase, they cancel each other. Phased array radars use this principle to control the shape of the transmitted radar beam (Figure 6-8).

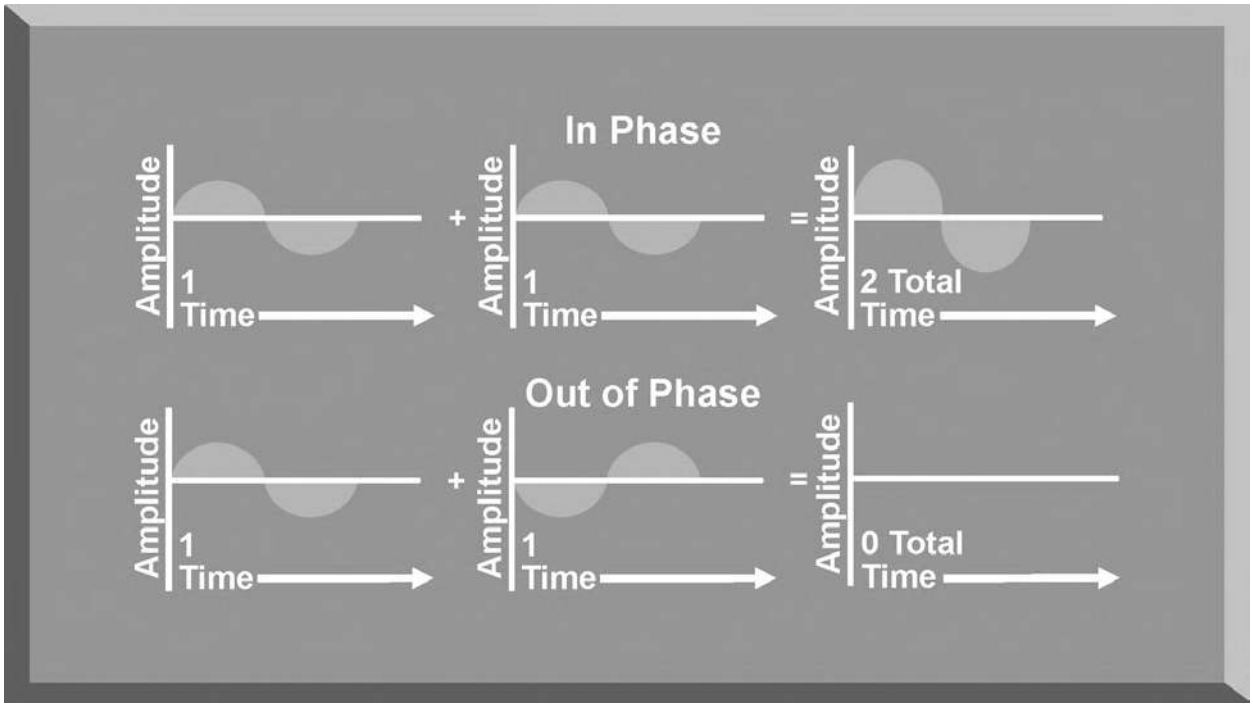

Figure 6-8. Phase Relationships

b. Phase relationships and antenna element spacing determine the orientation of the transmitted beam. In Figure 6-9, antenna elements A and B are separated by one-half wavelength and are radiating in-phase, that is, when one is at the positive peak, the other is also at a positive peak. Since the elements are one-half wavelength apart, when the positive peak radiated by A reaches B, B will be radiating a negative peak. As the peaks propagate along the X axis, they will cancel each other out. The total radiated power along that axis will be zero. Along the Y axis, however, the positive peaks from A will add to the positive peaks from B, causing the total radiation along this axis to be at its maximum value. This type of array is called a "broadside array" because most of the radiation is in the direction that is broadside to the line of the antenna array.

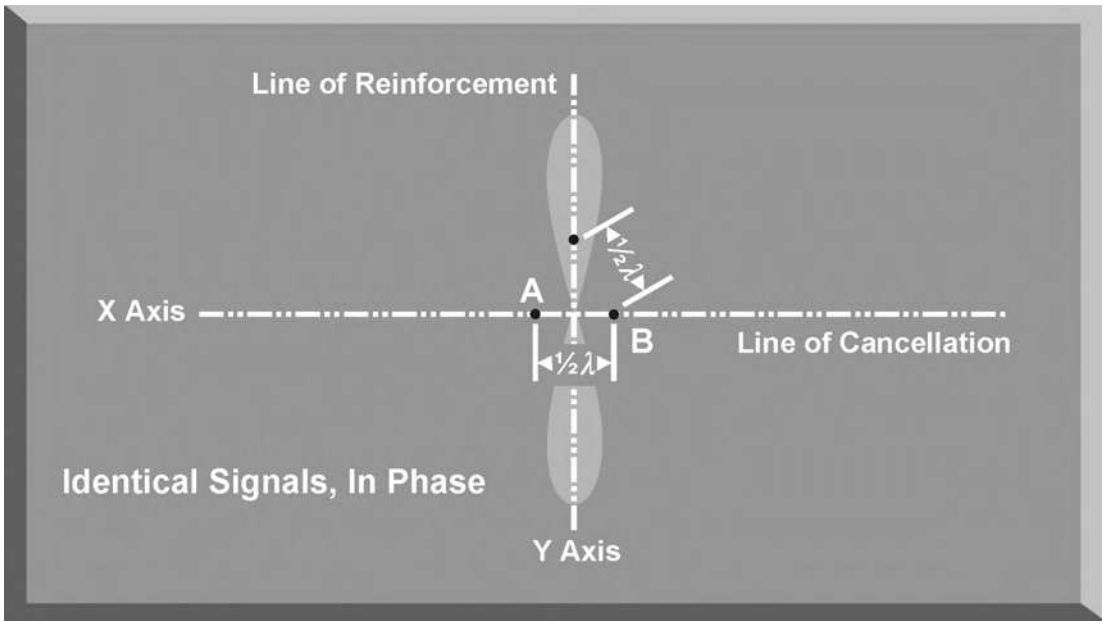

Figure 6-9. Broadside Array

c. If the same antenna elements are fed out-of-phase, the principal direction of radiation will be along the axis of the antenna elements. In Figure 6-10, when the positive peak from A arrives at B, B is now positive also. These energies interact to strengthen the energy being radiated from the ends of the array. Meanwhile, when the positive peak from A, radiating along the Y axis, meets the negative peak from B, they are canceled. This type of array is called an "end-fire array."

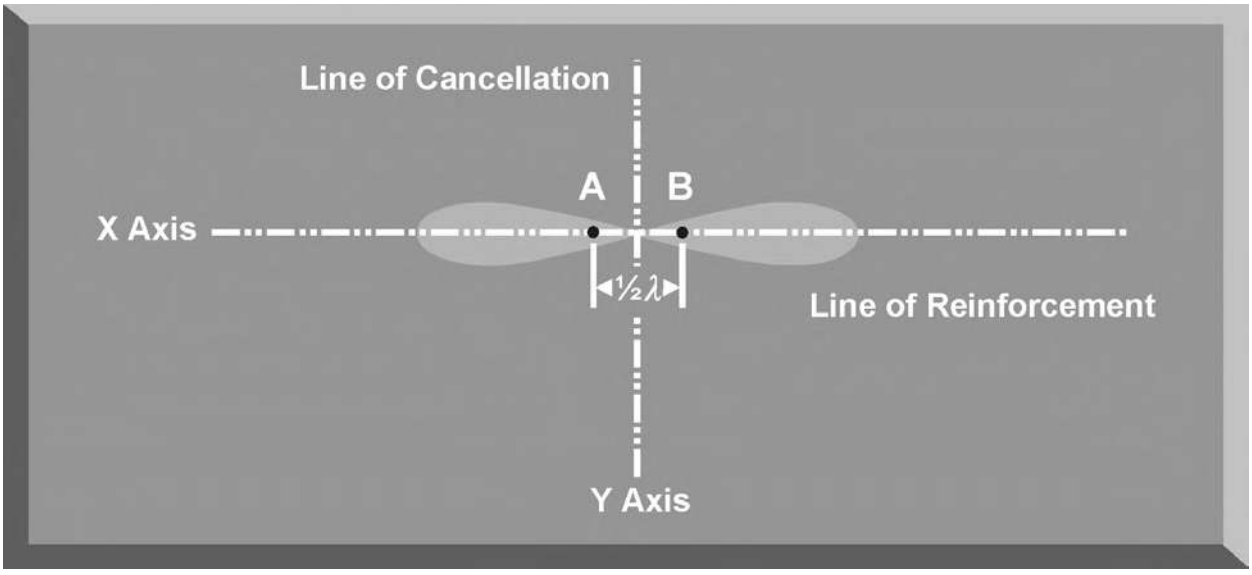

Figure 6-10. End-Fire Array

d. The computer controlling the phase of the signal delivered to each transmitting and receiving element of a phased array antenna controls the direction and shape of the radiated beam (Figure 6-11). By shifting the phase of the signals between 0° and 180°, the beam sweeps. This is the basic means of producing an antenna scan. In addition, the amplitude, or power, of the signal applied to each element can be varied to control the sidelobes. This alters the shape of the beam which affects the range capability and angular resolution of the radar.

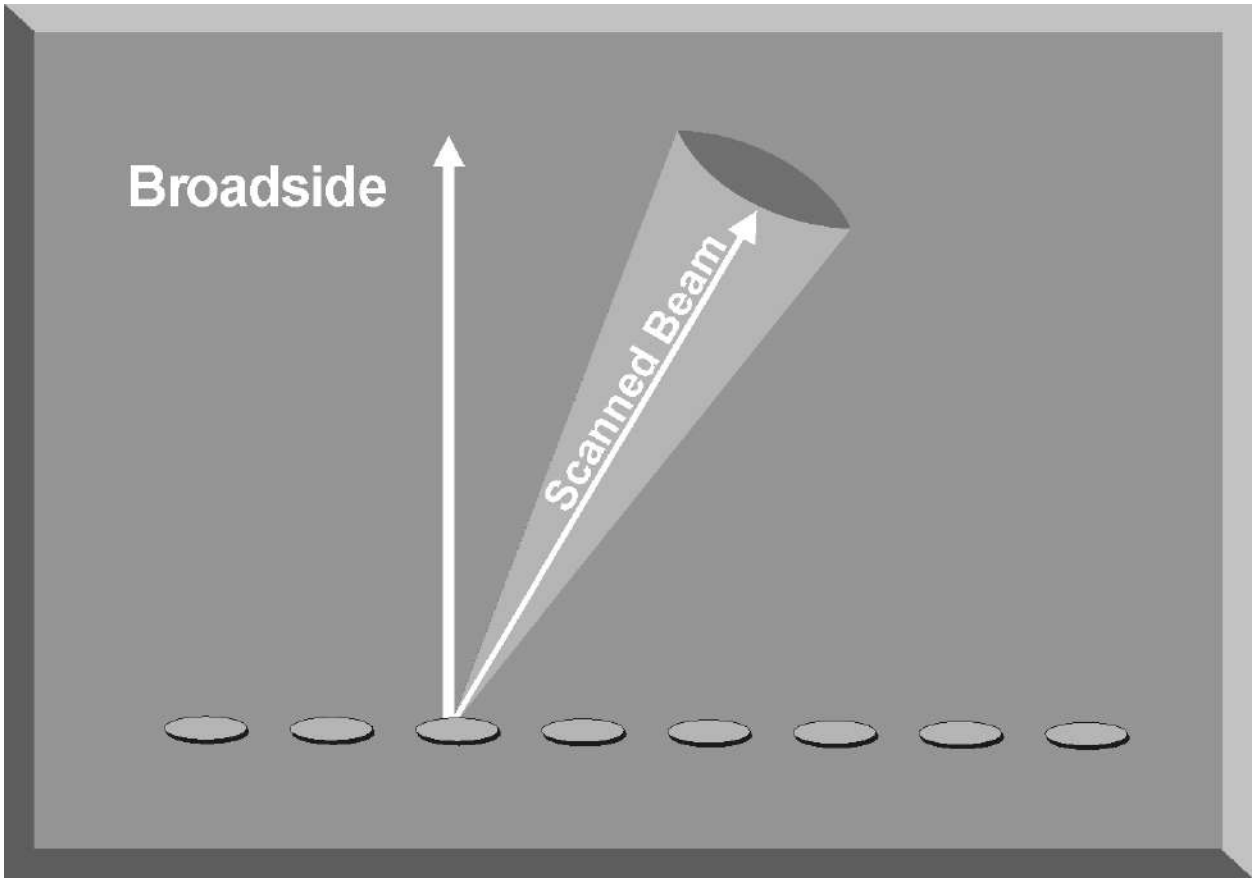

Figure 6-11. Phased Array Antenna Scan

e. Figure 6-12 depicts a variation of the phased array antenna, known as a planar array antenna. A planar array antenna uses transmit and receive elements in a linear array, but, unlike the phased array radar, the elements are smaller and are placed on a movable flat plate. The ability to simultaneously track several targets is one advantage of this type of radar.

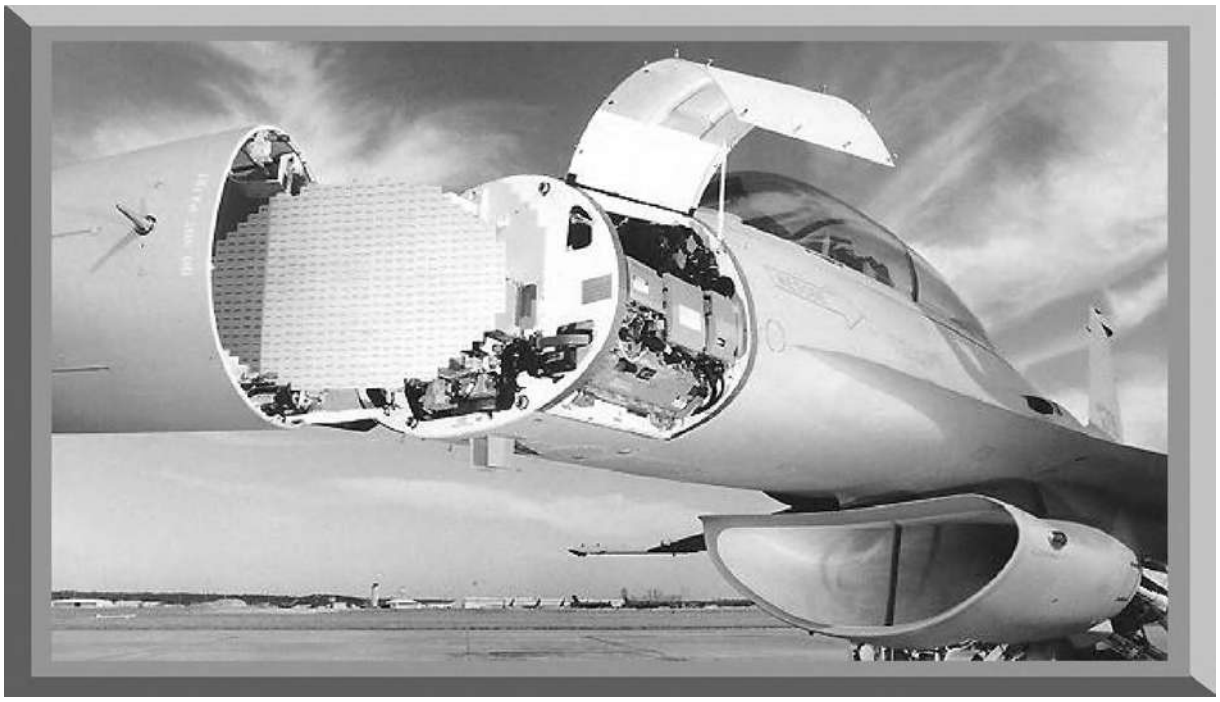

Figure 6-12. Planar Array Antenna

5. ANTENNA GAIN

The most important characteristic of any type of antenna is antenna gain. Antenna gain is a measure of the ability of an antenna to concentrate energy in the desired direction. Antenna gain should not be confused with receiver gain, which is designed to control the sensitivity of the receiver section of a radar system. There are two types of antenna gain: directive and power.

a. The directive gain of a transmitting antenna is the measure of signal intensity radiated in a particular direction. Directive gain is dependent on the shape of the radiation pattern of a specific radar antenna. The directive gain does not take into account the dissipative losses of the antenna. Directive gain is computed using Equation 6-1.

$$G_D \text{ (Directive Gain)} = \frac{\text{Maximum Radiation Intensity (Desired Direction)}}{\text{Average Radiation Intensity}}$$

Equation 6-1. Directive Gain

b. The power gain does include the antenna dissipative losses and is computed using Equation 6-2.

$$G\ (\text{Power Gain}) = \frac{\text{Maximum Radiation Intensity (Practical Antenna)}}{\text{Radiation Intensity of an Isotropic Antenna}}$$

Equation 6-2. Power Gain

c. The term isotropic antenna describes a theoretical spherical antenna that radiates with equal intensity in all directions. This results in a spherical radiation pattern. The power density for any point on an isotropic antenna is the radiation intensity and can be calculated by dividing the total power transmitted (P_T) by the total surface area of the sphere, as shown in Equation 6-3.

$$\text{Power Density (Isotropic Antenna)} = \frac{P_T\ (\text{Watts})}{4\pi r^2\ (\text{Centimeters}^2)}$$

Equation 6-3. Power Density for an Isotropic Antenna

d. The radiation pattern of an isotropic, or spherical, antenna would provide neither azimuth or elevation resolution and would be unusable for radar applications. To provide azimuth and elevation resolution, a practical antenna must focus the radar energy. The power density of a practical antenna differs from the isotropic antenna only in terms of antenna gain (G). Solving Equation 6-3 for the power density of a practical antenna yields Equation 6-4.

$$\text{Power Density (Practical Antenna)} = \frac{P_T\ G}{4\pi r^2}$$

Equation 6-4. Power Density for a Practical Antenna

e. The actual power gain (G) of a practical antenna can be calculated by using Equation 6-5.

$$G = \frac{4\pi A_e}{\lambda}$$

A_e = effective area of aperture

λ = wavelength of the radar

NOTE: The effective area of aperture (A_e) is the effective antenna area presented to the returning radar echo.

Equation 6-5. Power Gain of a Practical Antenna

6. POWER DENSITY

The power density and gain of an antenna are a function of the antenna pattern of a radar system. Figures 6-13 and 6-14 illustrate the antenna pattern of a typical parabolic antenna. Most of the power density of the radar is concentrated in the main beam. However, since the radar is not a perfect reflector, some radar energy is transmitted in the sidelobes. In addition, there is spillover radiation due to the energy radiated by the feed that is not intercepted by the reflector. Finally, the radar has a back lobe caused by diffraction effects of the reflector and direct signal leakage. Sidelobes and backlobes are all undesirable radiations that adversely affect the maximum radar range and increases the vulnerability of the radar to certain jamming techniques.

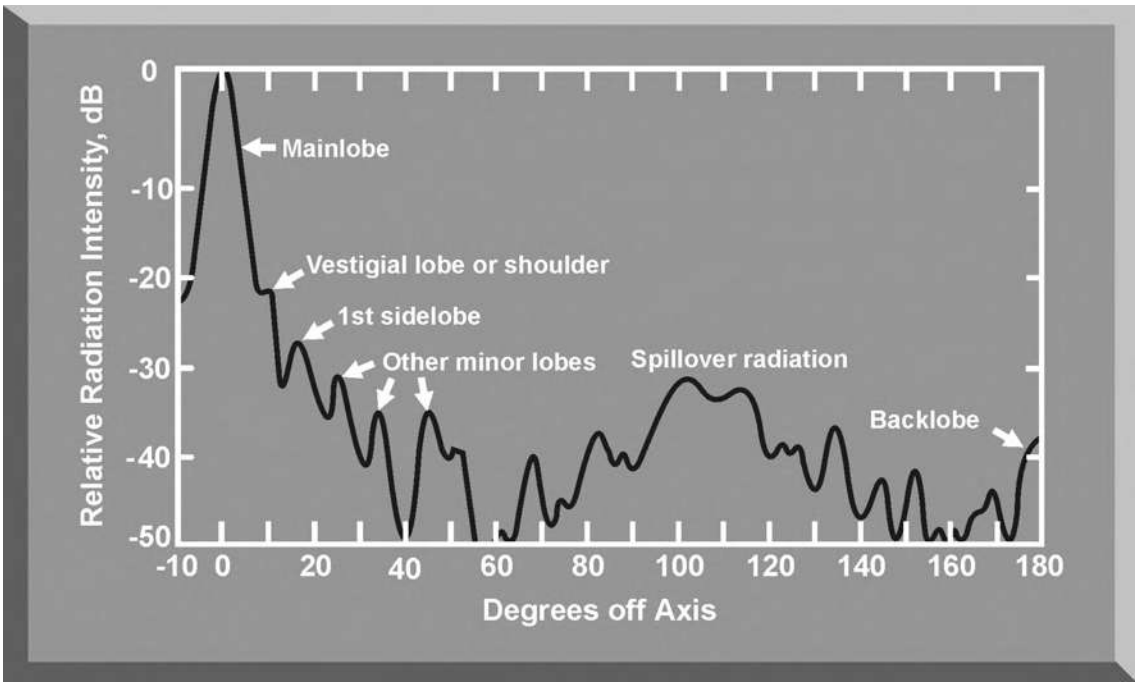

Figure 6-13. Radiation Pattern for a Parabolic Antenna

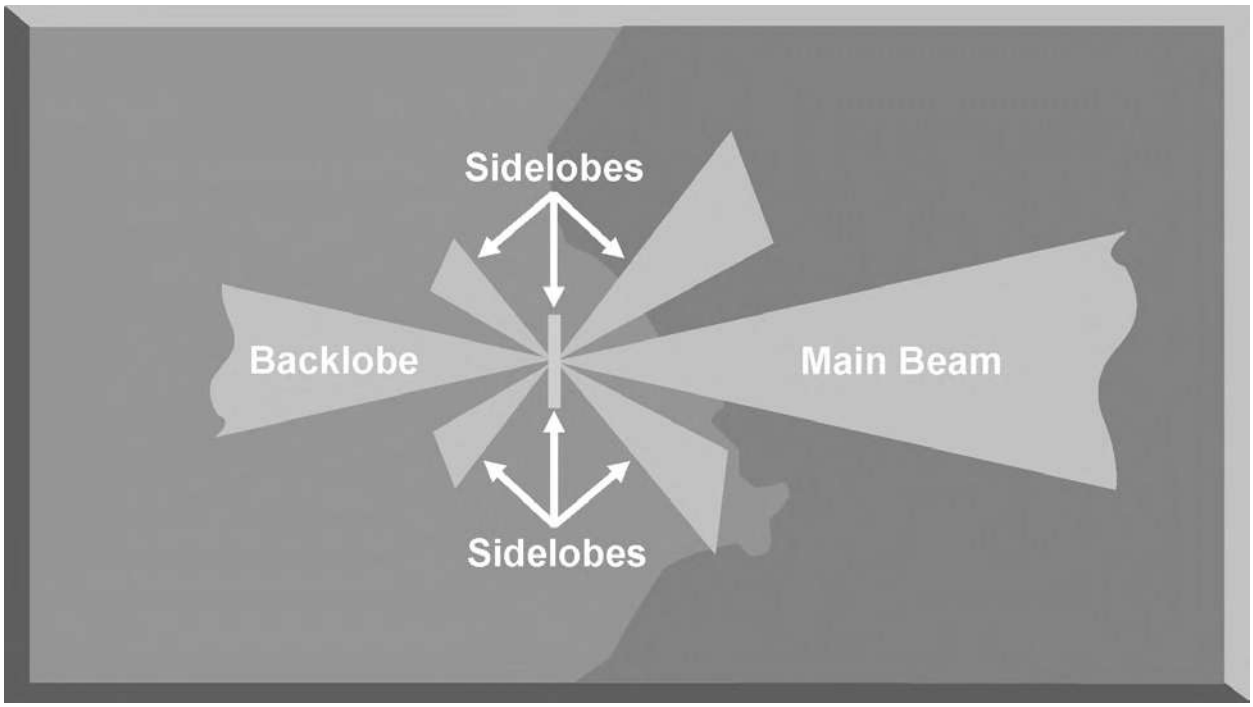

Figure 6-14. Radar Antenna Pattern

a. All radars have a primary main beam, which is where the radar has the most power and where target detection usually occurs. The dimensions of this main beam are highly dependent on the design of the antenna.

b. Besides the main beam, all radars have what is called a backlobe. This lobe is directly opposite to the location of the main beam. The sensitivity and signal strength associated with the backlobe is significantly less than that in the main beam.

c. Sidelobes add another dimension to the radar pattern. As with the backlobe, sidelobes do not have the signal strength or sensitivity associated with the main beam. Normally, the sensitivity associated with the sidelobes is 40-50 decibels (dBs) less than the main beam. The radar signal weakness in the backlobe and sidelobes of the main beam make these areas of the radar signal vulnerable to jamming. It is much easier to introduce jamming into these areas because of the reduced jamming-to-signal ratio needed to be effective. It is difficult for jamming to be effective in the main beam because the radar signal is very powerful in that region.

7. CIRCULAR SCAN

A circular scanning radar uses an antenna system that continuously scans 360° in azimuth (Figure 6-15). The time required for the antenna to sweep one complete 360° cycle is called the scan rate. Scan duration is the number of "hits per scan,"

or the number of pulses, reflected by a target as the radar beam crosses it during one full scan. Most pulse radars require 15 to 20 hits per scan to obtain sufficient information to display a target. The factors that determine the number of hits per scan the radar receives include pulse repetition frequency (PRF), antenna beamwidth, and scan duration.

Figure 6-15. Circular Scan Radar

a. Circular scan radars provide accurate target range and azimuth information. This makes these radars ideal for the roles of early warning and initial target acquisition. To accomplish these missions, the antenna generates a fan beam that has a large vertical beamwidth and a small horizontal beamwidth. Since elevation information will normally be provided by height finder radars, the size of the vertical beamwidth is not a limitation. This antenna scan allows the radar to scan large volumes of airspace for early target detection. Since early detection is the primary goal of early warning radars, accurate altitude and azimuth resolution are secondary considerations.

b. Circular scan radars designed for early warning transmit a radar signal with a low PRF. A low PRF allows sufficient time for the radar pulse to travel long distances, and return, before another pulse is transmitted. This gives the radar system a long, unambiguous range capability. Circular scan radars with low PRFs generally use long pulse widths in order to increase their average power and long-range detection capability. The scan durations of early warning radars are relatively long to provide the required "hits per scan" for long-range target

detection. The plan position indicator (PPI) scope display is normally used with a circular scan radar (Figure 6-16).

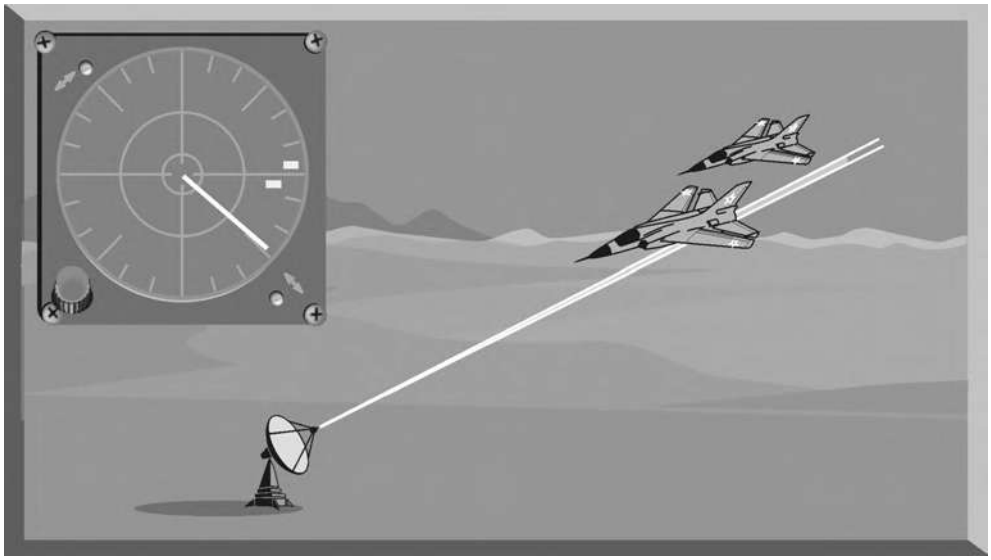

Figure 6-16. PPI Scope Display

c. In order to provide coverage for a large volume of airspace, the beamwidth associated with a circular scan radar is relatively wide. This wide beamwidth, coupled with the long pulse width and low PRF, gives the circular scan radar a large resolution cell, especially at long ranges (Figure 6-17). This limitation can be exploited to mask force size and composition. However, as range decreases, the dimensions of the resolution cell decrease, and a circular scan radar will begin to break out target formations.

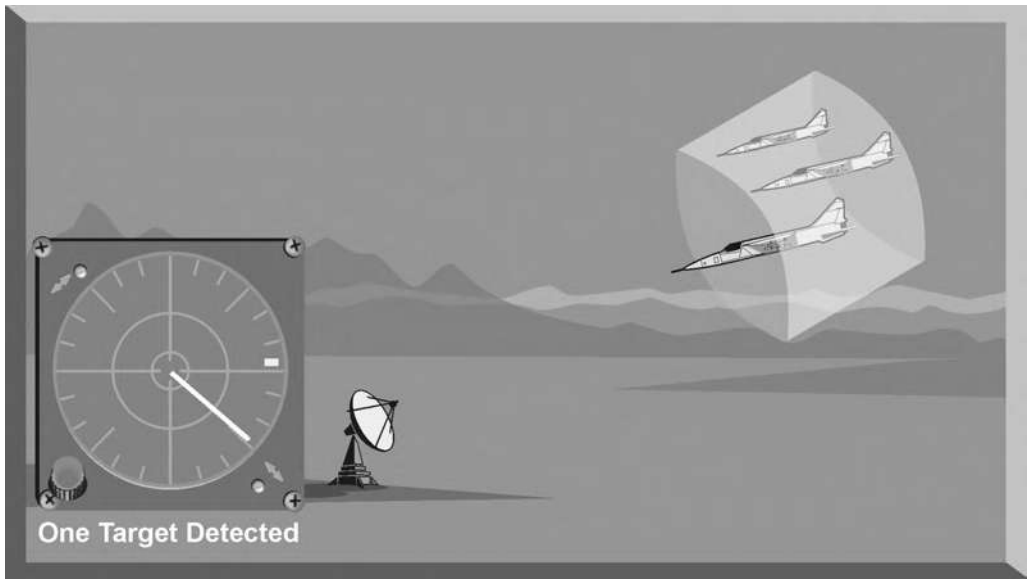

Figure 6-17. Resolution Cell

d. Circular scan radars provide range and azimuth information for both early warning and acquisition roles. Modified circular scan radars that can also provide elevation information may be used for ground control intercept (GCI) roles. Two modified circular scan radars that determine range, azimuth, and elevation are the V-beam and the stacked beam.

(1) The V-beam radar transmits two fan-shaped beams that are swept together (Figure 6-18). A vertical beam provides range and azimuth information. A second beam, rotated at some convenient angle, provides a measure of the altitude of the target.

Figure 6-18. V-Beam Radar

(2) A stacked beam radar (Figure 6-19) employs a vertical stack of fixed elevation "pencil" beams which rotate 360°. Elevation information is obtained by noting which beam contains the target return. Range and azimuth information is determined in the same manner as in an early warning radar.

Figure 6-19. Stacked Beam Radar

8. LINEAR SCAN

Linear scan is a method used by some radar systems to sweep a narrow radar beam in a set pattern to cover a large volume of airspace. Linear scans can be oriented in a vertical direction for height finder radars or in a horizontal direction, or raster, for acquisition and target tracking radars. A unidirectional linear radar scans in a single direction then begins its sweep all over again (Figure 6-20). Generally, linear scans offer excellent single-axis coverage, and the narrow beam offers enhanced azimuth and elevation resolution.

Figure 6-20. Unidirectional Linear Scan

9. UNIDIRECTIONAL SCAN

A helical scan is a unidirectional scan pattern that allows a "pencil" beam to search a 360° pattern. In Figure 6-21, the antenna sweeps a 360° sector in a clockwise direction. After each complete revolution, the antenna elevation is increased. This scan pattern is repeated for a specified number of revolutions, in this case, three, 360° sweeps. At the end of the scan pattern, the antenna elevation is reset to the initial elevation and the scan is repeated. A helical scan pattern is commonly used as a target acquisition mode for radar systems with narrow vertical and horizontal beamwidths.

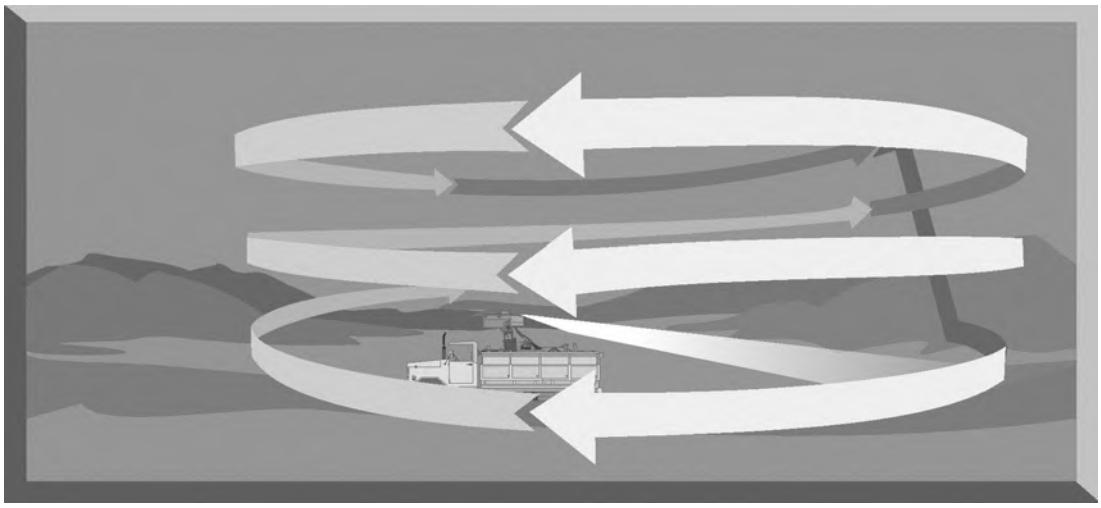

Figure 6-21. Helical Scan

10. BIDIRECTIONAL SCAN

A bidirectional linear scan, such as a raster scan, sweeps both horizontally and vertically (Figure 6-22). A raster scan uses a thin beam to cover a rectangular area by horizontally sweeping the area. The angle of elevation is incrementally stepped up or down with each horizontal sweep of the desired sector. After the sector has been covered, the angle of elevation is reset to the original value and the process is repeated. The number of raster bars is set by the number of horizontal sweeps in the basic raster pattern. Figure 6-22 shows a four-bar raster scan, which is normally associated with an airborne interceptor (AI) radar.

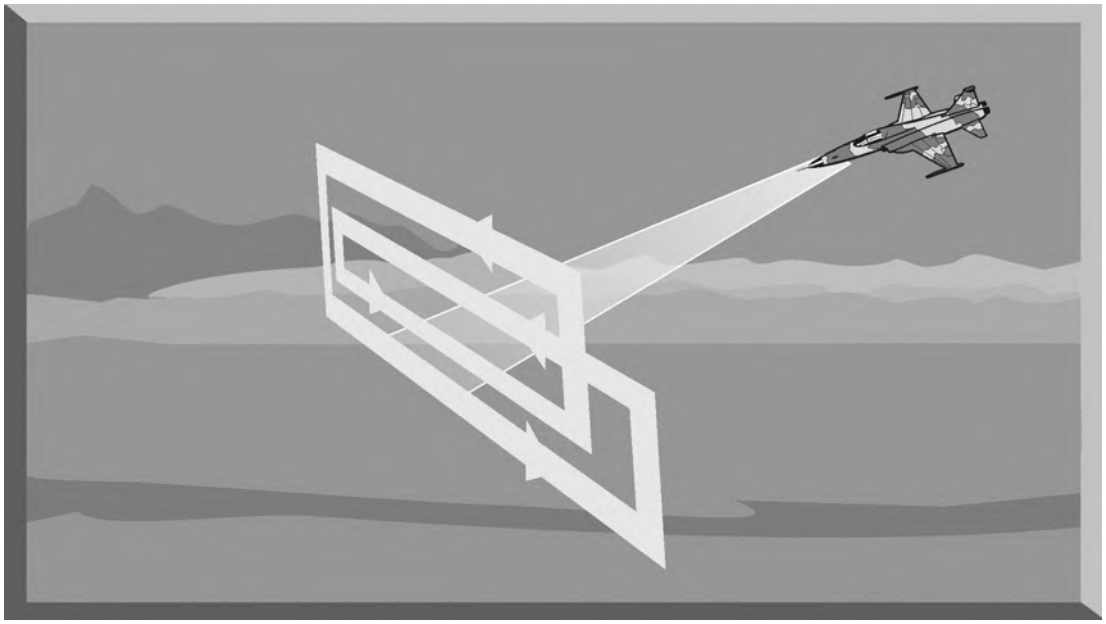

Figure 6-22. Raster Scan

11. CONICAL SCAN

A conical scan, or conscan, radar is generally used for precision target tracking. A conical scan radar (Figure 6-23) employs a pencil beam of radar energy that is continuously rotated around the target. This circular rotation of a pencil beam generates a cone-shaped scan pattern with the apex of the cone located at the antenna. Thus, the name conical scan.

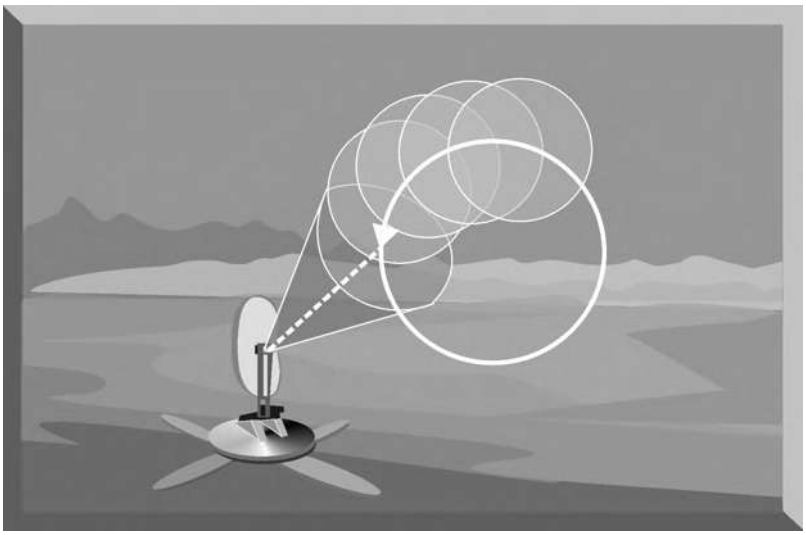

Figure 6-23. Conical Scan

a. As the pencil beam rotates, the circular scan patterns overlap in the center. This creates a central tracking area that has a much smaller effective beamwidth than the rotating pencil beam (Figure 6-24). This results in a very precise tracking solution.

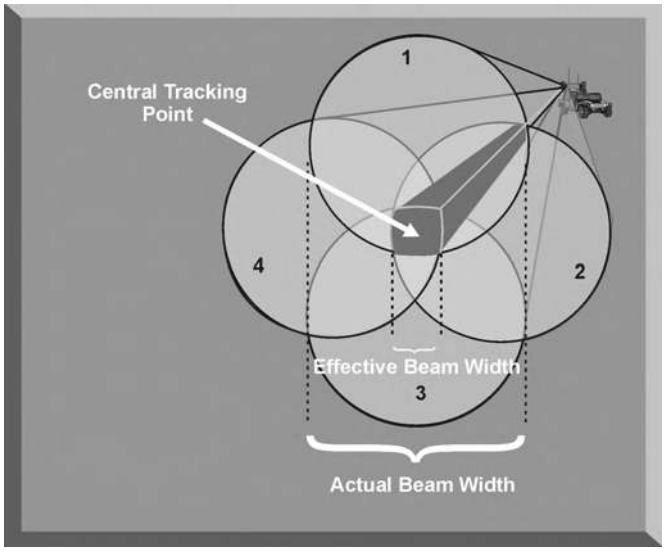

Figure 6-24. Conical Scan Tracking Area

b. Since conical scan radars are designed for precision target tracking, these radars normally operate at high frequencies, high PRF, narrow pulse widths, and narrow beamwidths. The rotation rate of the pencil beam can exceed 1,800 revolutions per minute. This means that both azimuth and elevation data can be updated about 30 times per second.

c. The combination of conical scan and raster scan is called a Palmer-raster scan (Figure 6-25). A Palmer-raster scan uses a thin beam, employing a conical scan searching pattern, for a specific sector of airspace. With each sweep of the sector, the angle of elevation is incrementally stepped up or down. After the vertical sector has been covered, the angle of elevation is set at the original elevation and the process is repeated. The number of bars is determined by the number of vertical search scans.

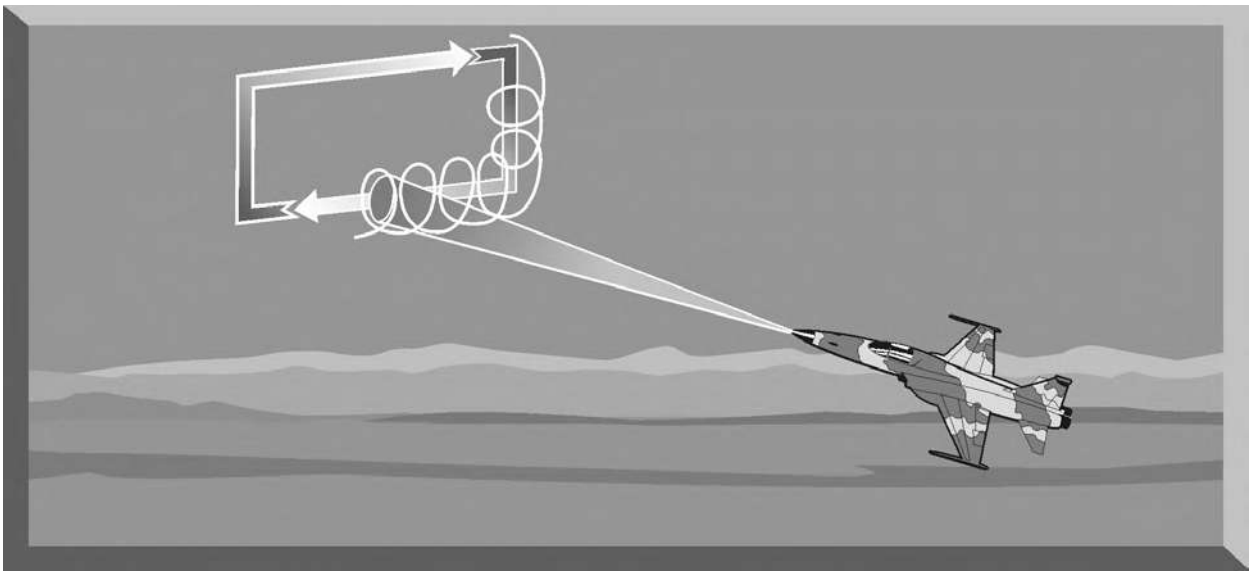

Figure 6-25. Palmer-Raster Scan

d. The combination of a conical scan and a circular scan is called a Palmer scan. Palmer scans incorporate a circular scanning antenna to search the entire horizon while simultaneously performing a conical scan. If the radar antenna is also performing a unidirectional altitude search in conjunction with this scan, it is employing a Palmer-helical scan (Figure 6-26).

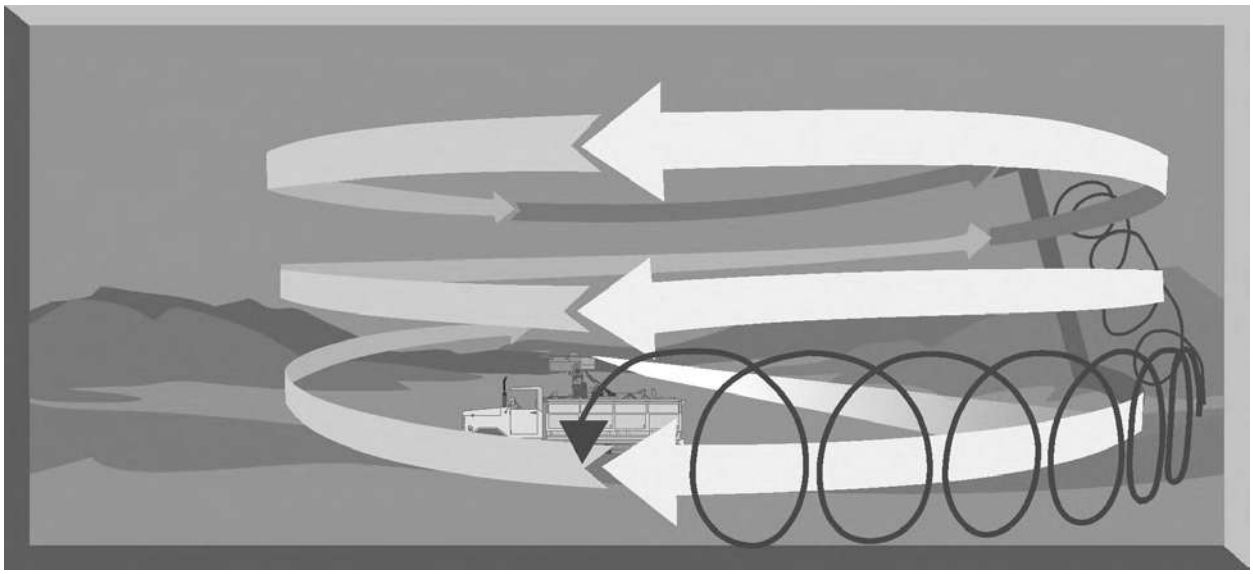

Figure 6-26. Palmer-Helical Scan

12. TRACK-WHILE-SCAN

A track-while-scan (TWS) system uses a technique that allows a radar to track one or more targets while scanning for others. Radar systems with a TWS capability must be able to generate two or more distinct radar beams.

a. A conventional TWS radar employs two antennas that work with each other to perform the scan function (Figure 6-27). Each antenna produces a separate unidirectional beam. Each beam is transmitted at a different frequency. The vertical antenna generates a beam employing a vertical sector scan similar to a height finder radar except the beamwidth is narrower and it scans at a higher rate. The horizontal antenna generates an identical beam employing a horizontal sector scan at a different frequency. The track function is accomplished in the area where the two beams pass through each other. A target that is within this center area is tracked, and positional information on range, elevation, and azimuth is updated each time the beams sweep through the area.

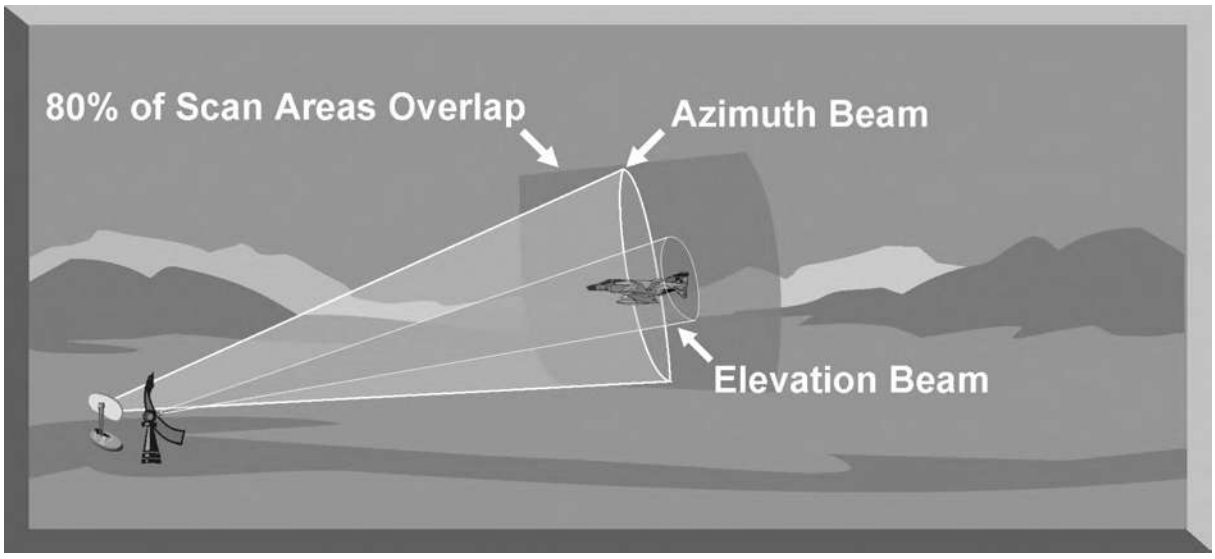

Figure 6-27. Conventional TWS Radar

b. The phased array radar is a product of the application of computer and digital technologies to the field of radar design. A phased array is a complex arrangement of many individual transmitting and receiving elements in a particular pattern (Figure 6-28). Common arrays include linear, planar, curved, and conformal, with linear being the most common. By using a computer to rapidly and independently control groups of these individual elements, a phased array antenna can, in effect, radiate more than one beam from the antenna. Multiple beams and computer processing of radar returns give the phased array radar the ability to perform the TWS function. The most common employment of the TWS capability of the phased array radar is in the air-to-air arena.

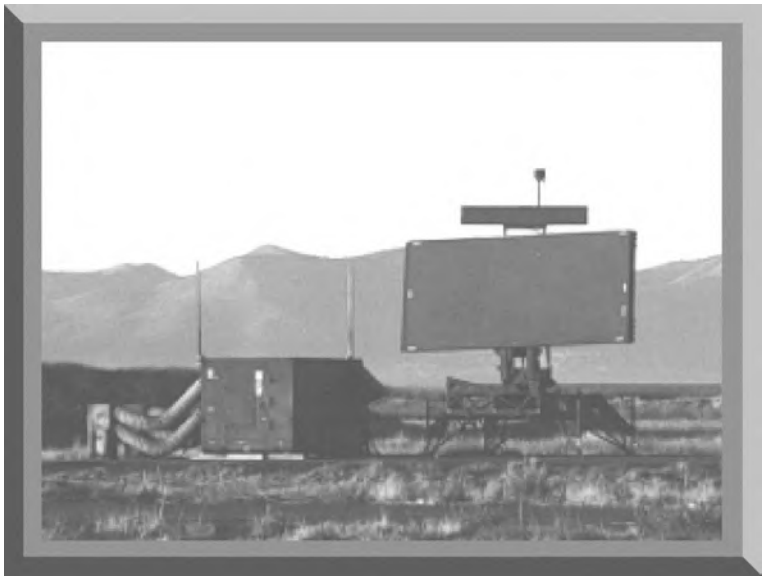

Figure 6-28. Phased Array Antenna

(1) The number of individual transmitting and receiving elements is limited by the size of the radar antenna. The number of targets a phased array radar can track is limited by the number of independent beams the antenna can generate. Many phased array radars, especially air-to-air radars, do not track and scan simultaneously, but rapidly switch between the two modes to overcome this limitation (Figure 6-29).

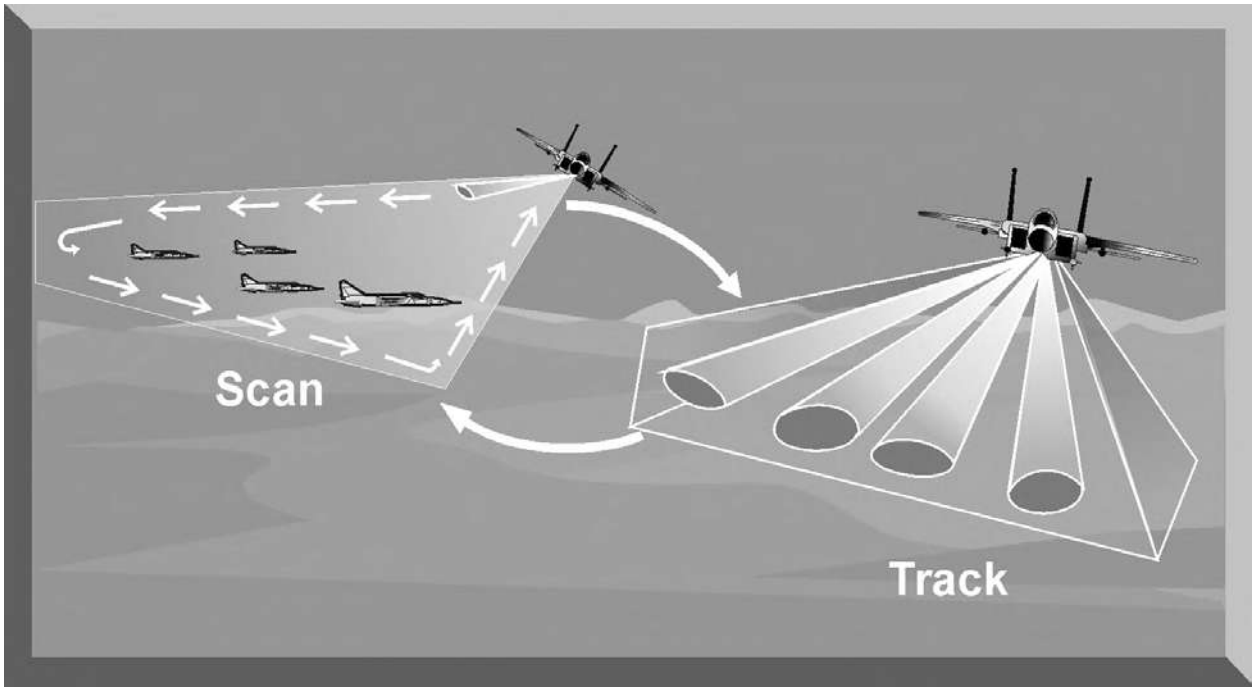

Figure 6-29. Phased Array TWS

(2) Modern TWS radars employ computer signal processing and complex computer algorithms to simplify the problem of target correlation (Figure 6-30). An air-to-air radar typically uses a raster scan to search a volume of airspace. In the search mode, the radar simply presents all targets detected in this airspace to the pilot on his radar display. In the TWS mode, the radar employs computer processing to figure out target correlation and update target information. This is done automatically, and the results are presented on the display.

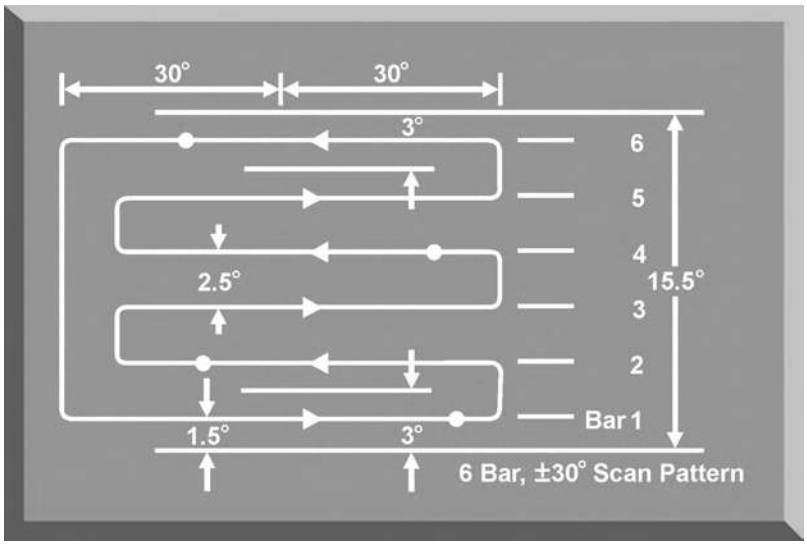

Figure 6-30. Phased Array TWS Radar Display

13. IMPACT OF TERRAIN ON RADAR SCANS

No matter what type of scan a radar system employs, terrain can limit radar line of sight (LOS) and target detection. The concepts of radar horizon, direct terrain masking, and indirect terrain masking are important factors in radar target detection and mission planning.

a. RF waves traveling in the atmosphere are bent, or refracted, and do not travel in a straight line. However, the degree of refraction depends on atmospheric conditions which vary significantly and are difficult to accurately quantify and predict. For these reasons, most radar computations are based on the assumption that RF waves travel in a straight line. The concept of the radar horizon is based on this assumption.

(1) The radar horizon shown in Figure 6-31 is the maximum range a radar system can detect a target due to the curvature of the earth. The distance (d) to the horizon for a radar antenna at a height (h) can be computed using Equation 6-6.

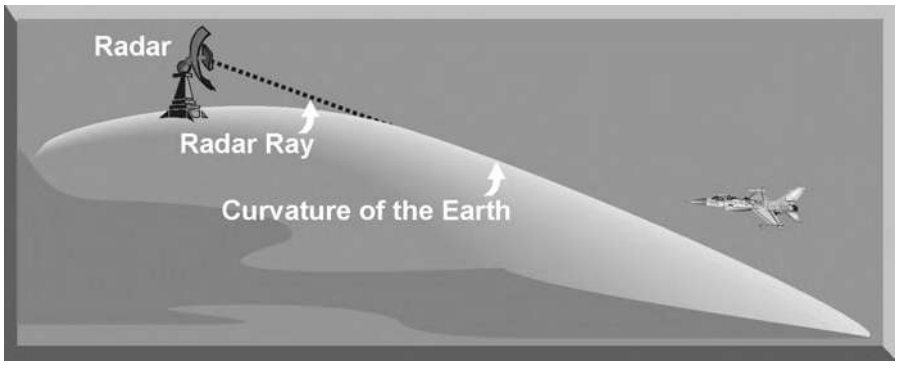

Figure 6-31. The Radar Horizon

$$\text{Distance to Horizon (d)} = \sqrt{2kah}$$

k = constant (4/3)
a = radius of earth
h = height of radar antenna

Equation 6-6. Basic Radar Horizon Equation

(2) In Equation 6-6, the constant, k, is commonly used to compensate for the assumption of straight line propagation of RF waves. Using the assumption that the height of the radar antenna is small compared to the radius of the earth, distance is measured in nautical miles (nm), and height is measured in feet, then Equation 6-6 reduces to Equation 6-7.

$$\text{Distance to Horizon (d)} = 1.06\sqrt{h}$$

Equation 6-7. Simplified Radar Horizon Equation

(3) Another application of Equation 6-7 is in calculating the range at which a radar antenna will achieve LOS with a low-altitude target. To compute this distance (D), Equation 6-8 can be used.

$$\text{Target Detection Distance (D)} = 1.06\,(\sqrt{h} + \sqrt{\text{target altitude}})$$

Equation 6-8. Target LOS Distance

(4) To illustrate the use of Equations 6-7 and 6-8, consider the example of a radar antenna located at a height of 25 feet and a target aircraft flying at an altitude of 100 feet. From Equation 6-7, the radar horizon for this system would be 5.3 nm. From Equation 6-8, the radar antenna will have LOS with the target aircraft at 16 nm.

b. The previous discussions of the radar horizon assumes the radar is operating over water or level terrain. Radar operations over rough terrain can present other radar LOS limitations. As illustrated in Figure 6-32, prominent terrain features can limit radar detection. In this illustration, a mountain acts as a radar horizon and limits target LOS in one sector of the radar scan. This situation is called direct terrain masking. Placing prominent terrain features between the aircraft and threat radar systems effectively negates these systems and is an integral part of threat avoidance during combat mission planning.

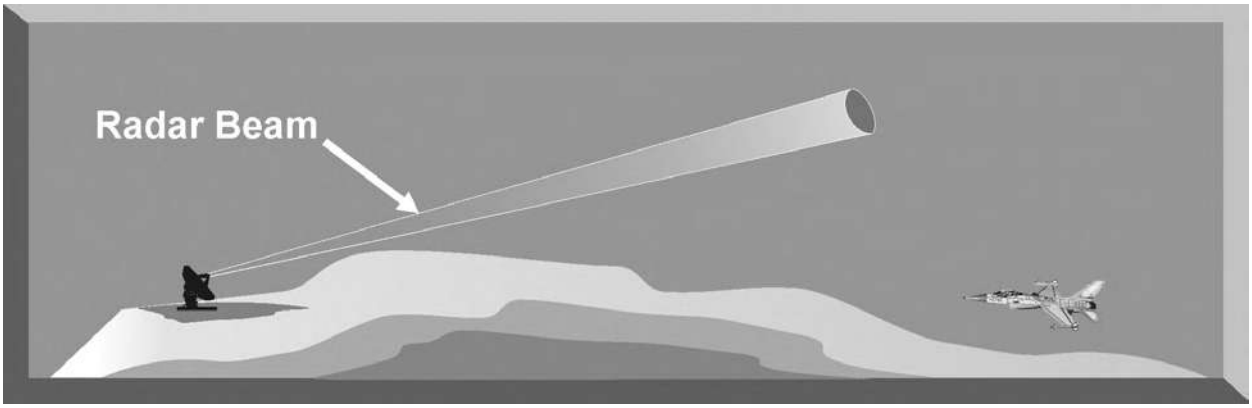

Figure 6-32. Direct Terrain Masking

c. Figure 6-33 depicts another impact of terrain on target detection/indirect terrain masking. When both the aircraft and a prominent terrain feature are illuminated by a radar beam, a pulse radar system may not be able to differentiate the target return from the return generated by the terrain. Indirect terrain masking is most effective when the aircraft is flying abeam the radar site. Pulse Doppler radars and radar systems employing moving target indicator (MTI) circuits may be able to negate the effectiveness of indirect terrain masking. However, indirect terrain masking is another important consideration for threat avoidance during combat mission planning.

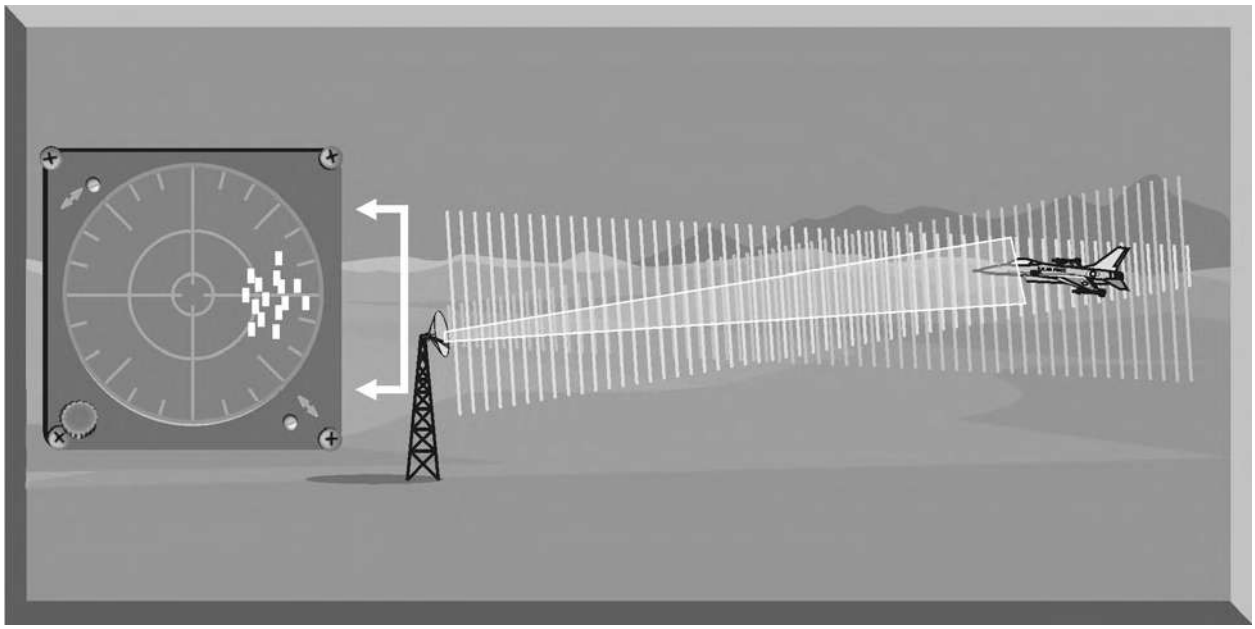

Figure 6-33. Indirect Terrain Masking

14. SUMMARY

This chapter has introduced basic antenna characteristics and how these characteristics influence their employment. The concepts of antenna gain and power density were also explained. The remainder of the chapter discussed the different types of radar scans. A radar's scan pattern is designed to enhance target detection and facilitate target tracking. The radar horizon, direct terrain masking, and indirect terrain masking are LOS limitations to all radar scans. The scan pattern chosen for a specific radar system determines the ability of that radar to provide accurate range, azimuth, elevation, or velocity of the detected target.

CHAPTER 7. TARGET TRACKING

1. INTRODUCTION

A target tracking radar (TTR) is designed to provide all the necessary information to guide a missile or aim a gun to destroy an aircraft. Once a target has been detected, either by a dedicated search radar or by using an acquisition mode, the TTR is designed to provide accurate target range, azimuth, elevation, or velocity information to a fire control computer.

a. A typical TTR has individual tracking loops to track a target in range, azimuth, elevation, or velocity. The antenna of the TTR is pointed at a single target, and the radar initiates acquisition and target track. TTRs normally employ automatic trackers to continuously measure target data. The range tracking loop employs an early gate/late gate range tracker to maintain automatic range tracking. The azimuth and elevation tracking loops generate error signals to position the antenna and maintain constant target illumination. The velocity tracking loop found on pulse Doppler and CW radars is used to reject clutter and generate accurate target radial velocity information. All this critical information is passed to a fire control computer for weapons employment.

b. The fire control computer is programmed with critical information on the capability of the weapon to be employed. For a missile, the fire control computer is programmed with the aerodynamic and range capabilities of the missile. For antiaircraft artillery (AAA), the fire control computer is programmed with the ballistics for the gun, rate of fire, and tracking rate. The fire control computer uses the precise target information from the TTR and the programmed weapon's parameters to compute a firing solution. Once a firing solution has been computed, the fire control computer either fires the weapon automatically or alerts the operator, who fires the weapon. For missile employment, the fire control computer may continue to provide missile guidance and fusing commands until missile impact or initiation of an active missile guidance mode. For AAA engagement, the fire control computer computes the required lead angle, aims the guns, and initiates firing.

c. To provide the required azimuth and elevation resolution, most TTRs use a high frequency to provide narrow antenna beamwidths for accurate target tracking. High frequency operation also allows the radar to transmit wide bandwidths. To provide the required range resolution, most TTRs employ narrow pulse widths and high pulse repetition frequencies (PRFs) to rapidly update target information. In this chapter, the target tracking techniques of conical scan, track-while-scan, lobe-on-receive-only, monopulse, Doppler radars, and pulse Doppler radars will be discussed.

2. RANGE TRACKING

In most TTR applications, the target is continuously tracked in range, azimuth, and elevation. Range tracking can be accomplished by an operator who watches an "A" scope presentation and manually positions a handwheel to maintain a marker over the desired target return. The setting of the handwheel is a measure of target range and is converted to a voltage used by the fire control computer. As target speeds and maneuvers increase, the operator may have extreme difficulty maintaining manual target range tracking. To avoid this situation, most TTRs employ an automatic range tracking loop. All pulse TTRs, which includes conical scan, track-while-scan, monopulse, and pulse Doppler radars, employ either a split gate or leading-edge automatic range tracking system. In a TTR, automatic range tracking serves two essential functions: (1) it provides the critical value of target range, and (2) it provides a target acceptance range gate that excludes clutter and interference from other returns. Since radar range is normally the first target discriminator used to initiate automatic target tracking, the second function is essential to the proper operation of the other tracking loops.

a. A range gate circuit is simply an electronic switch that is turned on for a period of time after a pulse has been transmitted. The time delay for switch activation corresponds to a specific range. Any target return that appears inside this range gate is automatically tracked. The most common type of automatic range tracking is accomplished by a split-gate tracker. Two range gates are generated as shown in Figure 7-1. The automatic range tracking loop attempts to keep the amount of energy from the target return in the early gate and late gate equal. The range tracking error is computed by subtracting the output of the late gate from the output of the early gate. The amount of the range tracking error signal is the difference between the center of the pulse and the center of the range gate. The sign of the error signal determines the direction in which the gates must be repositioned to continue to track the target.

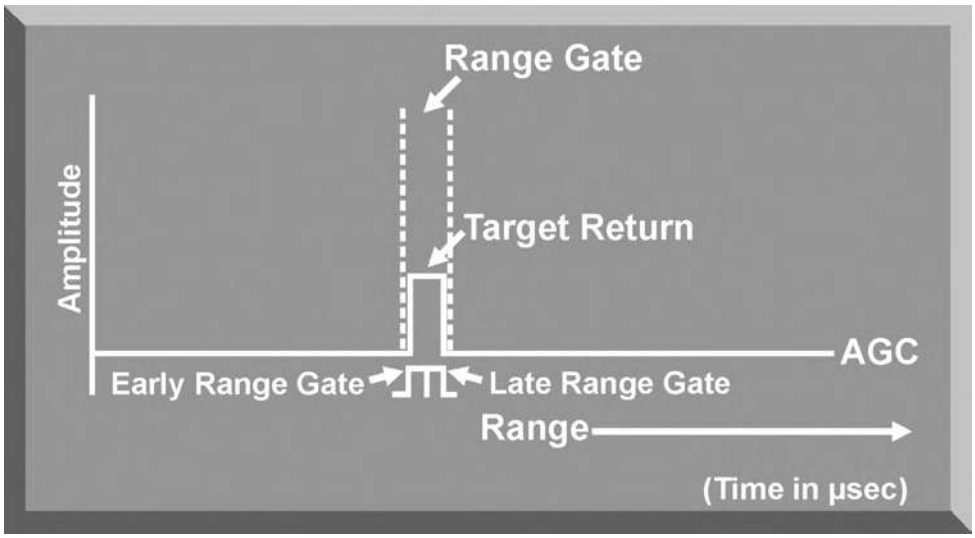

Figure 7-1. Split-Gate Range Tracker

b. Leading-edge range tracking is an electronic protection (EP) technique used to defeat range-gate-pull-off (RGPO) jamming. Figure 7-2 illustrates the application of leading-edge tracking. The leading-edge tracker obtains all range data from the leading edge of the target return. All RGPO cover pulse jamming tends to lag the target return by some increment of time (see (a) in Figure 7-2). By differentiating the entire return with respect to time, the target return can be separated from the jamming pulse (see (b) in Figure 7-2). Employing a split-gate tracker electronically positioned at the initial pan, or leading edge, of the returning pulse, the range tracking loop can track the target return and ignore any jamming signals. The range tracking loop then uses split-gate tracking logic to determine the magnitude and direction of range tracking errors and reposition the range gate.

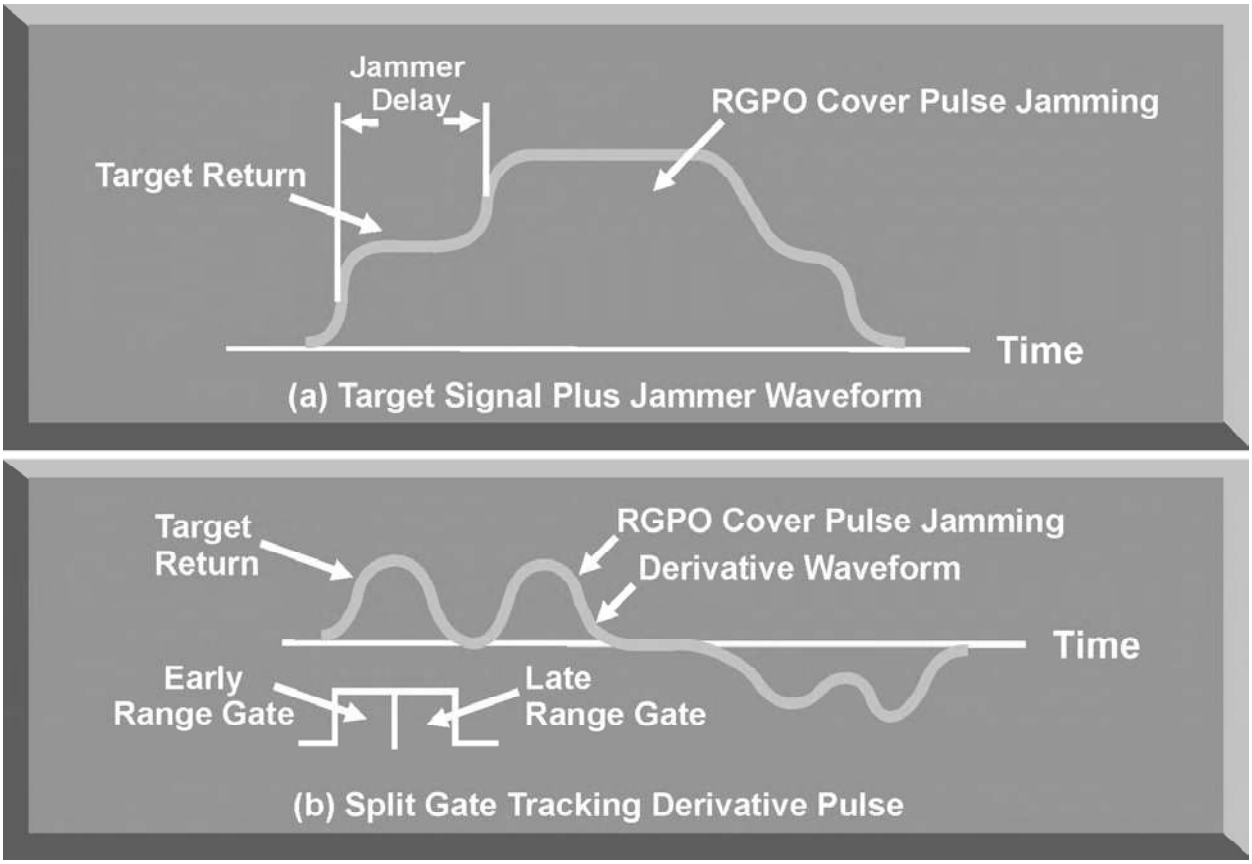

Figure 7-2. Leading-Edge Range Tracker

c. The width of the tracking gate is an important radar design consideration. The range gate should be sufficiently narrow to effectively isolate the target from other returns at different ranges. It should be wide enough to allow sufficient energy from the target echo to be displayed. The width of the range tracking gate is normally equal to the pulse width of the radar.

d. Nearly all range tracking gates employ some form of automatic gain control (AGC). AGC is designed to limit target clutter and glint. It is also designed to avoid excessive false alarms.

3. CONICAL SCAN

A conical scan tracking system is a special form of sequential lobing. Sequential lobing implies that the radar antenna beam is sequentially moved between beam positions around the target to develop angle-error data. For a conical scan radar to generate azimuth and elevation tracking data, the beam must be switched between at least four beam positions as shown in Figure 7-3.

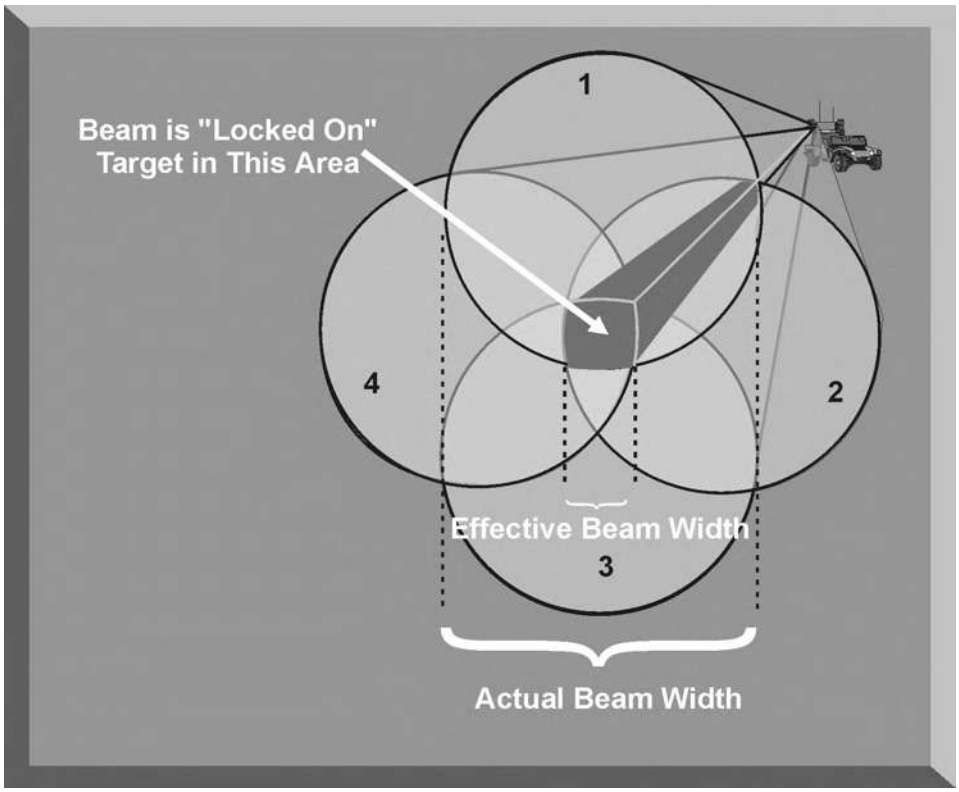

Figure 7-3. Conical Scan Positions

a. One of the simplest conical scan antennas is a parabola with an offset rear feed that rotates, or nutates, to maintain the plane of signal polarization. The radar beam is rotated at a fixed frequency around the target. The angle between the axis of rotation (normally the axis of the antenna) and the axis of the antenna beam is called the squint angle.

b. A conical scan radar first tracks the target aircraft in range. For azimuth and elevation tracking, the target return is modulated at a frequency equal to the rotation frequency of the radar beam. This results in a target signal output that resembles a sine wave (Figure 7-4). The azimuth and elevation tracking loops

drive servo motors to position the antenna to keep the energy level in each of the four positions equal. The amount of the modulated signal determines how far the target is off the antenna boresight while the phase of the modulation (positive or negative) determines the direction.

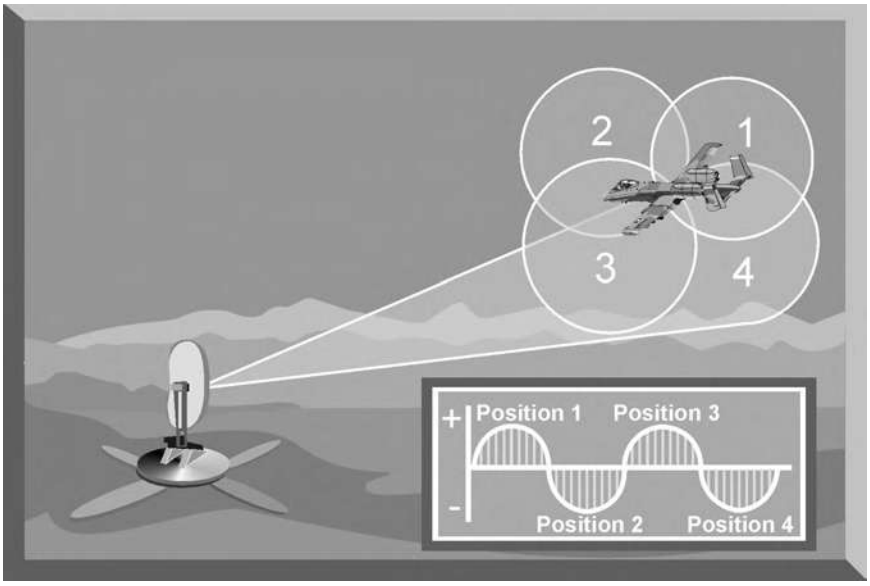

Figure 7-4. Conical Scan Modulation

c. In Figure 7-5, most of the target energy is in position 1, with a small amount of energy in position 4. The output from the elevation tracking loop is positive and drives the antenna servos upward. The output from the azimuth tracking loop moves the antenna to the right.

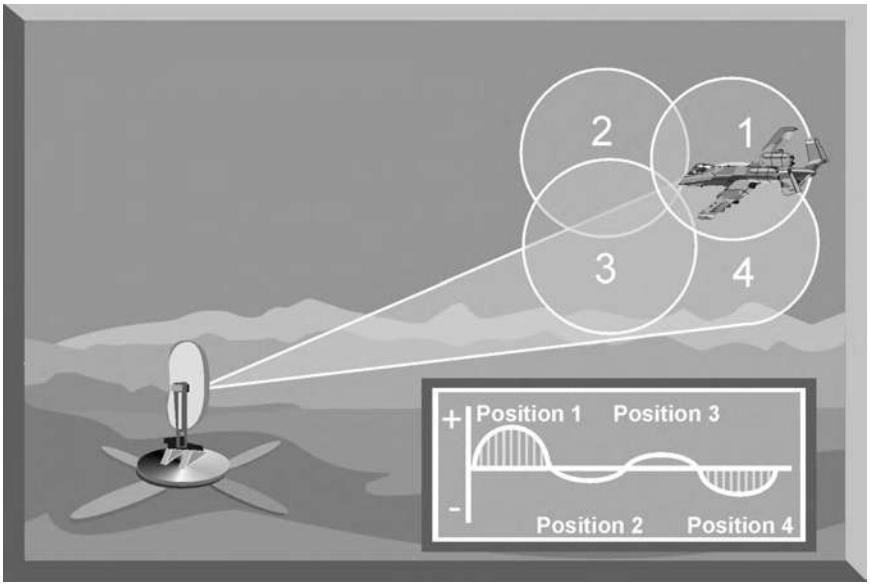

Figure 7-5. Conical Scan Tracking Errors

d. Once a balance of target energy in each scan position is achieved, the target is in the central tracking area (Figure 7-6). The azimuth and elevation tracking circuits continue to drive the antenna servos to maintain this energy balance which keeps the radar beam on the target.

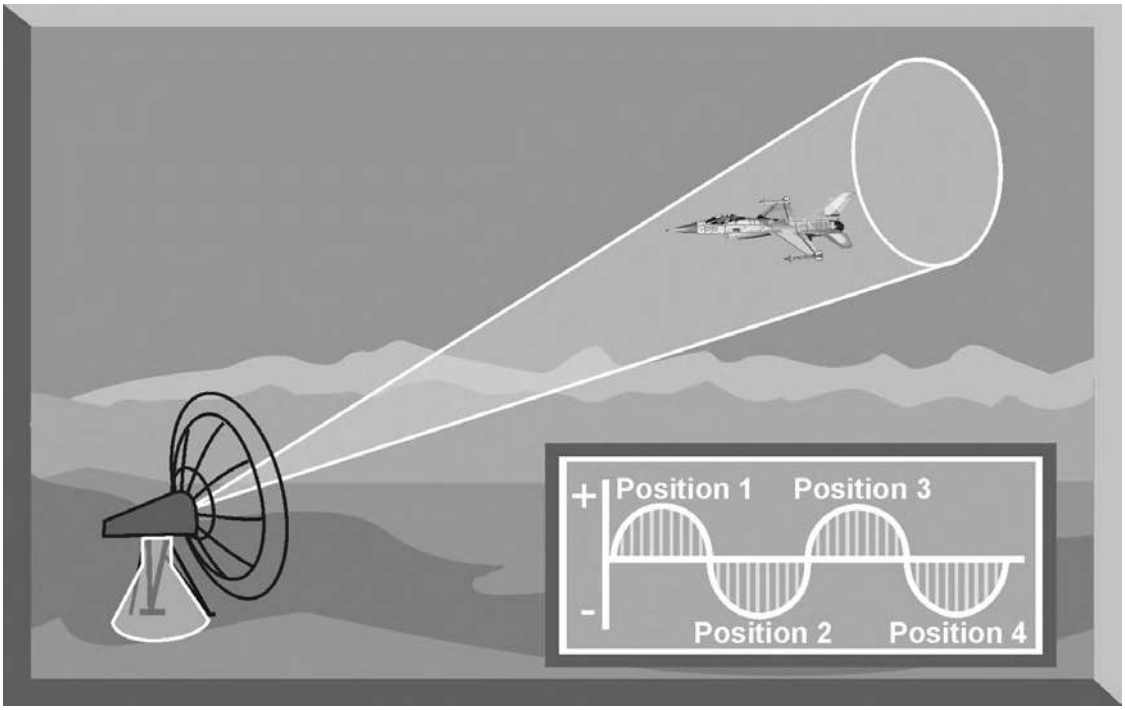

Figure 7-6. Conical Scan Tracking

e. The primary advantage of a conical scan radar is the small beamwidth which provides extremely accurate target tracking information. The primary disadvantages of conical scan include the following: (1) the narrow beamwidth makes target acquisition a problem. Even using a Palmer-helical scan, it may take considerable time to find and initiate track on a target; (2) conical scan radars are vulnerable to inverse gain modulation jamming based on the scanning frequency of the rotating beam; (3) a conical scan radar must analyze many radar return pulses to generate a tracking solution.

4. TRACK-WHILE-SCAN (TWS)

TWS is a combined search and tracking mode that sacrifices the continuous target observation capability of the dedicated tracker in return for the ability to monitor a finite sector of airspace. This is accomplished while maintaining tracks on multiple targets moving through the covered airspace. There are two types of radar systems capable of TWS operation: conventional and phased array.

a. Conventional track-while-scan threat radars use two separate antennas to generate two separate beams (Figure 7-7). These beams operate at two different

frequencies and are sectored so they overlap the same region of space. This overlap area provides a tracking area for a single target. One beam is sectored in the vertical plane to give range and elevation. The other beam is sectored in the horizontal plane to provide range and azimuth. Each beam scans its sector at a rate of 5 to 50 times per second. This provides a rapid update on target range, azimuth, and elevation.

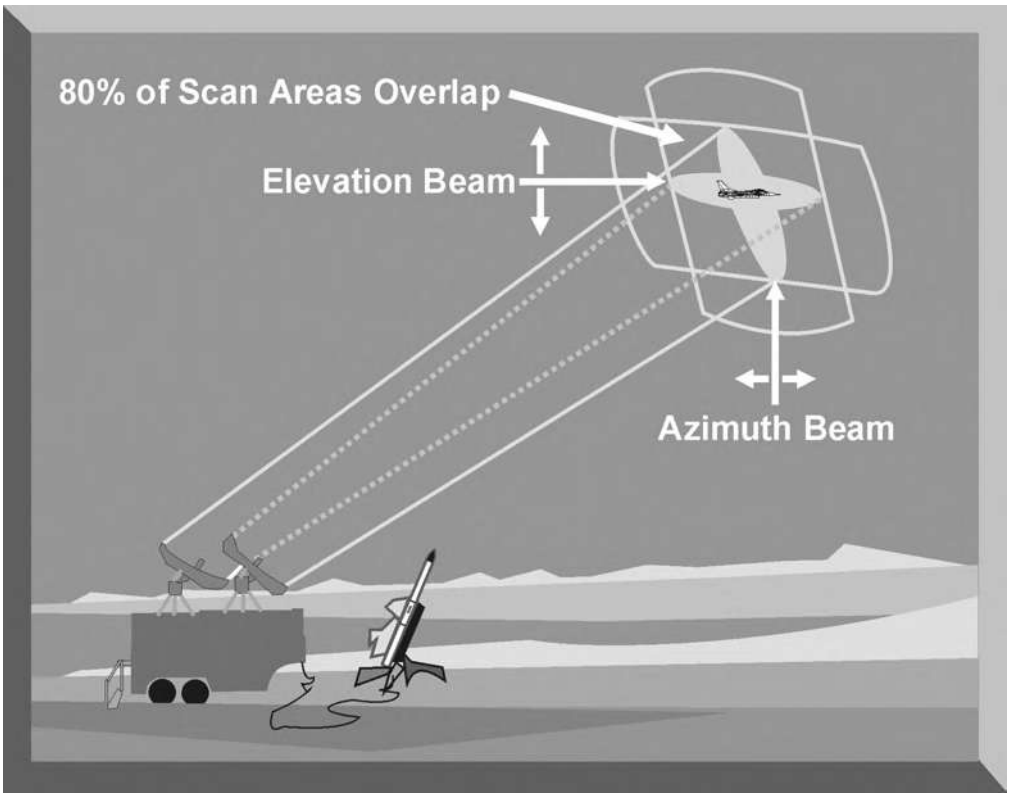

Figure 7-7. Conventional TWS Radar Beams

(1) The two TWS antennas generate their beams using an electro-mechanical principle. Each antenna provides inputs to its own display and provides angle and range information for all targets in the coverage of the radar. The display from the elevation beam is calibrated in range and elevation, while the display from the azimuth beam is calibrated in azimuth and range. Operators position a cursor over the returns on these displays using range as the primary parameter. Once a target has been designated for engagement, the radar automatically attempts to keep the tracking axis of the radar beams centered on the target.

(2) Once the target is designated by the operator, the range gate is enabled and tracks the target using a split-gate tracker. The azimuth and elevation tracking loops receive information only from targets inside the range gate. As the beams scan across the target, a burst of pulse returns is received that have an

amplitude envelope corresponding to the beam pattern. The azimuth beam pattern is shown in Figure 7-8.

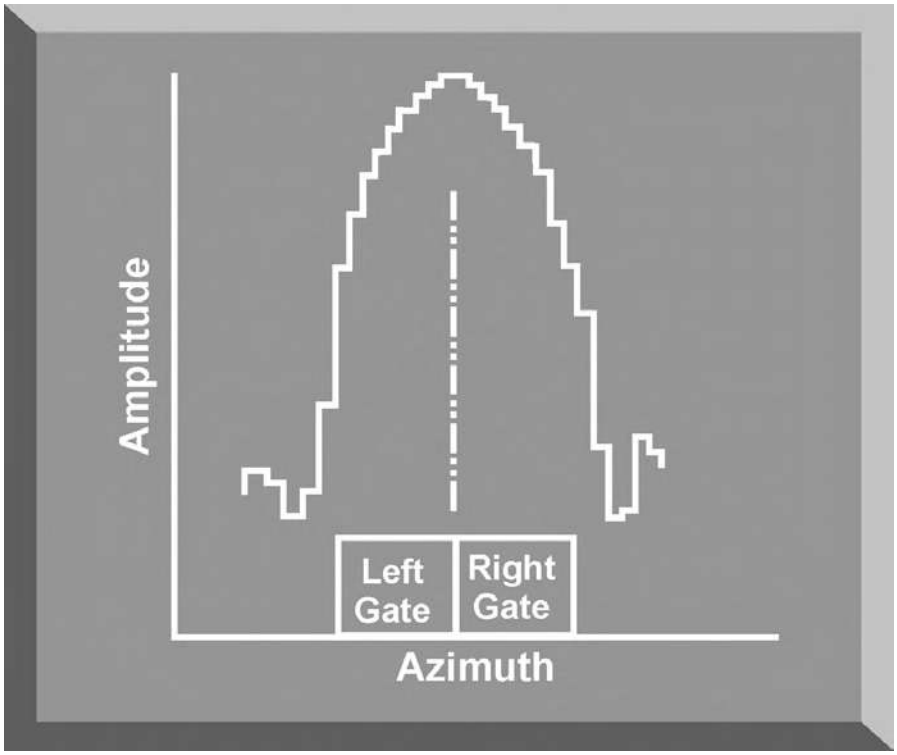

Figure 7-8. Conventional TWS Azimuth Tracking

(a) The azimuth tracker is typically a split-gate tracker, identical in concept to a split-gate range tracker. However, range delay time is replaced by azimuth scan time. The azimuth tracker uses a left gate and right gate. Each gate integrates its share of the target return to generate a voltage/time value. When the azimuth gate is centered on the target, the areas are equal and the error signal (right gate minus left gate) is zero. The azimuth tracking loop sends signals to the antenna servos to keep the target centered in the scan area.

(b) Elevation tracking is accomplished in the same manner by using an up gate and a down gate. The elevation tracking loop also sends signals to the antenna servos to keep the target centered in the scan area.

(3) Once the target is designated and the radar is automatically keeping the radar return centered in the tracking area, target range, azimuth, and elevation information is sent to a fire control computer. The radar continues to provide information on other targets in the scan area. The fire control computer indicates the firing solution has been achieved for the designated target, and a missile is launched. The radar tracks the target and the missile and provides in-flight corrections to the missile right up to the moment of missile impact. These corrections are based on both target and missile azimuth, range, and elevation

information. Information is passed to the missile from a dedicated antenna on the radar to special antennas on the missile. Commands from the radar to the missile are called uplink guidance commands. Information from the missile back to the radar and fire control computer is called downlink information.

(4) The advantages of a conventional TWS radar include the following: (1) TWS radars have the ability to maintain radar contact with all targets in the sector scan area while maintaining target track on a single target, and (2) the rapid sector scan rate provides a rapid update on target parameters. The primary disadvantages of a conventional TWS radar include: (1) a large resolution cell due to the wide azimuth and elevation beams, and (2) vulnerability to modulation jamming based on the scan rate of the independent beams.

b. Many modern radars employing a planar or phased array antenna system have a TWS mode. The radar does not really track and scan simultaneously, but rapidly switches between search and track (Figure 7-9).

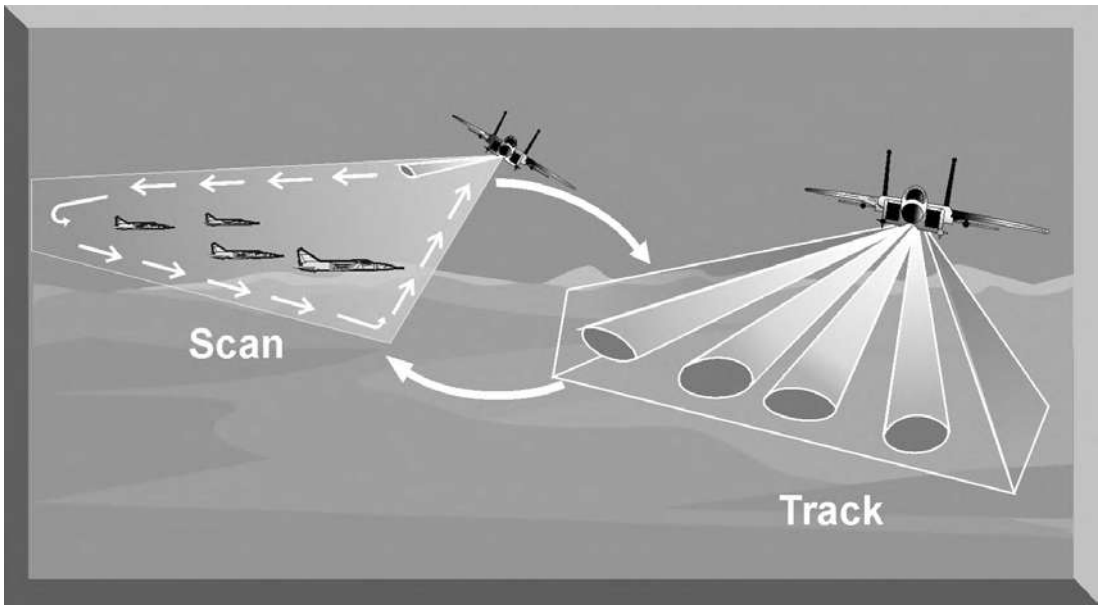

Figure 7-9. Phased Array TWS

(1) The most common air-to-air radar system uses a planar array antenna. In the scan mode, the radar antenna generates a pencil beam and uses a raster scan to detect targets in the search area. Targets detected are presented to the pilot on the aircraft's radar display (Figure 7-10).

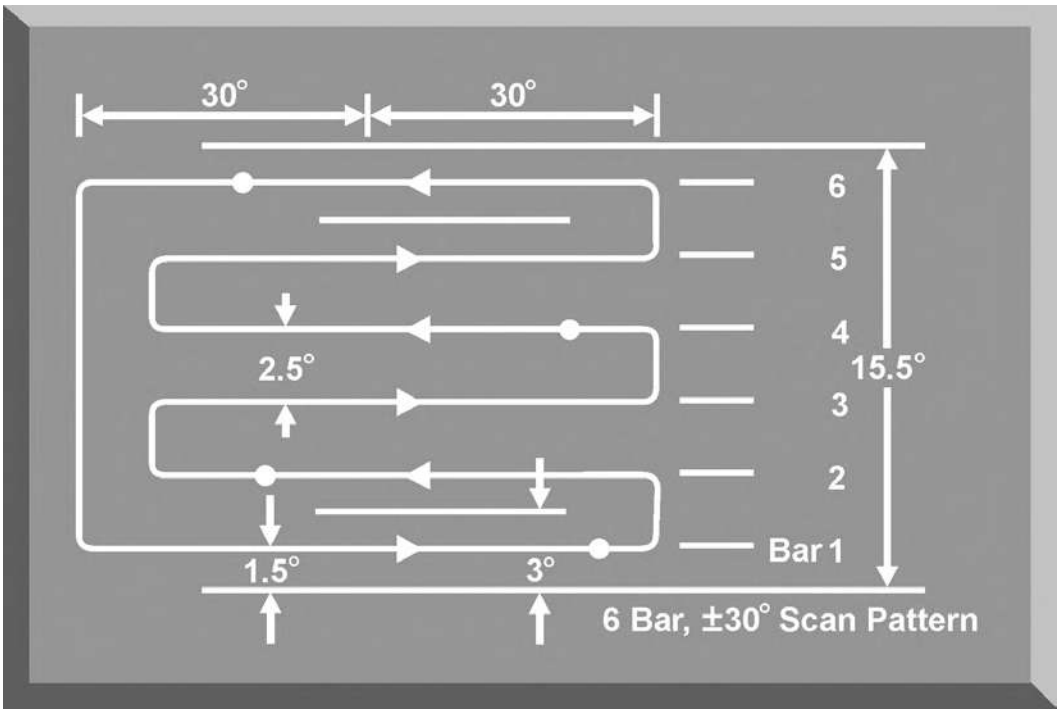

Figure 7-10. Air-to-Air TWS Display

(a) In the track mode, the antenna generates multiple beams to illuminate individual targets. The radar typically uses monopulse or pulse Doppler techniques to update target range, azimuth, elevation or velocity. These tracking techniques will be covered later in this chapter. The radar initiates a track file on each detected target that contains all current data on the target and an estimate of future target position.

(b) As the radar switches between track and scan modes, target parameters are updated in the tracking loop (Figure 7-11). The new target information is compared to the predicted information in the measurement data processing cell. If the two sets of data agree within certain limits, target position and information are updated. This process is called gating.

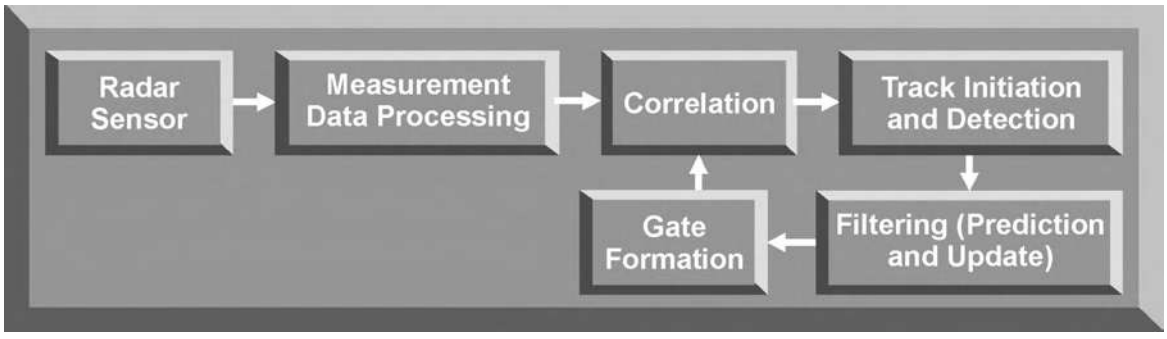

Figure 7-11. Planar/Phased Array TWS Tracking Loop

(c) If the updated target information does not correspond to the predicted values, the information is sent to the correlation processor. The correlation processor attempts to resolve the conflict based on further refinement of target data. If the correlation processor cannot assign the target parameters to an existing track file, a new track file is generated and displayed.

(2) The obvious advantage of a planar/phased array TWS radar is that it can search a large volume of airspace while tracking individual targets. The number of targets that can be tracked is limited by the number of beams the radar can generate. Planar/phased array radars have increased peak and average power when compared to pulse radar systems. Since the radar beam of a planar/phased array radar is electronically controlled and can rapidly change beams and scans, it is resistant to many jamming techniques. The primary disadvantages of a planar/phased array TWS radar include its complexity, cost, and reliance on computer processing.

5. LOBE-ON-RECEIVE-ONLY (LORO)

LORO is a mode of radar operation developed as an EP feature for a track-while-scan radar. LORO can be employed by any radar that has the capability to passively track a target. In a LORO mode, the radar transmits a continuous signal from a set of illuminating antennas. This continuous signal hits the target, and the return echo is received by a different set of receive antennas (Figure 7-12). The receive antennas are passive and generate azimuth and elevation tracking signals by electronically scanning the reflected signal. The tracking signals are sent to the antenna servos to keep the illuminating antennas pointed at the target and centered in the receive antenna tracking area. The range tracking circuit uses the time delay between the transmission and reception of the illuminating antenna signals. A split-gate tracker is used to provide range tracking.

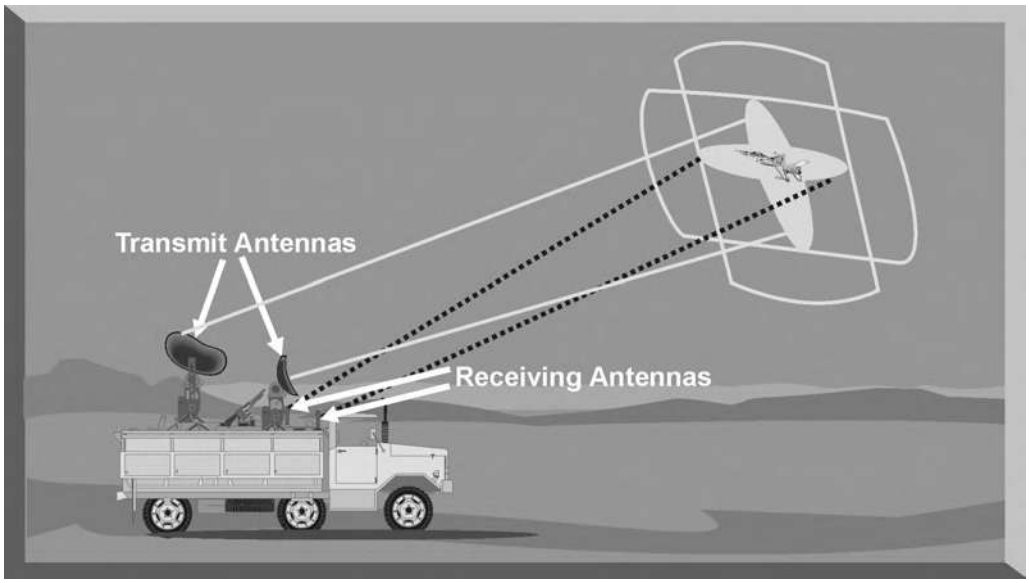

Figure 7-12. LORO Mode

a. The illuminating antennas used in the LORO mode have very narrow beamwidths and transmit at a high power level. This reduces the effectiveness of noise jamming techniques against a radar employing a LORO mode. In addition, the continuous signal from the illuminating antennas negate the effectiveness of most angle deception jamming techniques designed to defeat TWS radars. These specialized jamming techniques exploit the scan rate of TWS antennas. In the LORO mode, the illuminating antennas do not have a scan rate. The limited effectiveness of both noise and deception jamming techniques is the major advantage of the LORO mode.

b. The LORO mode also provides a track-on-jam (TOJ) capability to exploit noise jamming techniques. In a TOJ mode, the receive antennas passively track any detected noise jamming signals. The radar assumes that the most intense jamming signal is the target. The receive antennas process the strongest jamming signal as if it were a target echo from the transmit antenna signal. The receive antennas generate azimuth and elevation tracking signals to keep the jamming signal centered in the tracking area. The TOJ mode does not provide target range.

6. MONOPULSE RADAR

Monopulse radars are among the most complex radar systems. From a single pulse, a monopulse radar can derive all the data needed to update a target's position. It does this by comparing the relationship of two or more radar beams that are transmitted together from the same antenna but received separately. By comparing the phase or amplitude of the energy in these returned beams, target azimuth and elevation can be found. The speed that a monopulse radar updates the target's position, coupled with its azimuth/elevation accuracy and resistance to jamming, make this a popular choice amongst many newer TTRs.

a. The Magic T circuit allows monopulse radars to gather and process information from a single pulse that is transmitted and received using separate antennas. Figure 7-13 depicts a four-beam monopulse radar system. The Magic T is a sophisticated wave guide that can separate multiple signals by their phase relationships. This allows the radar tracking computer to compare the signal amplitude from the reflected pulses in several distinct ways. As the reflected energy enters the Magic T, it is separated by phase. The energy in the "H" arm will be in-phase and will exit from ports 1 and 2. The received energies entering the wave guide in the "E" arm exit at the number 1 port. This energy is exactly 180° out-of-phase with energy entering the H arm. This ensures there is no transfer of energy between the E and H plane arms. A typical monopulse radar would have eight Magic T's.

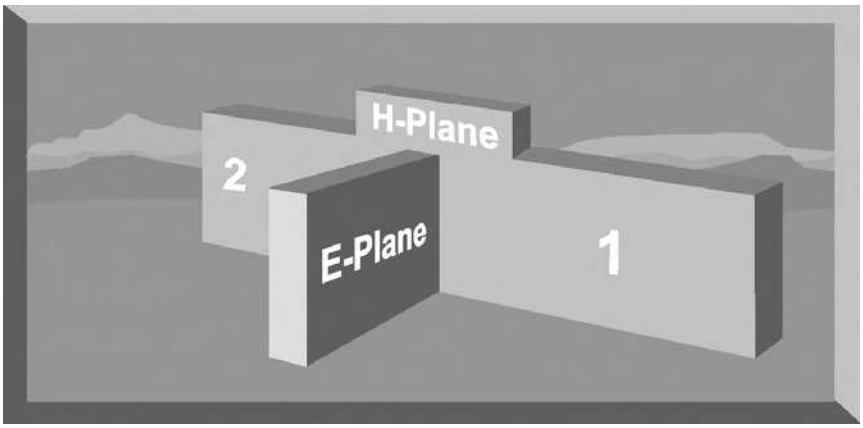

Figure 7-13. Monopulse Magic T

b. The output of a Magic T is the sum and difference of the two signals. These sum and difference values in amplitude or phase are used to generate azimuth and elevation error signals as well as to compute range. Monopulse radars may split the incoming signal as depicted in Figure 7-14. Upper antennas receive the A and B signals. Lower antennas receive the C and D signals. The various combinations of signals are processed and compared by simple addition and subtraction of the signal characteristics. From these steps, azimuth, range and elevation data are computed.

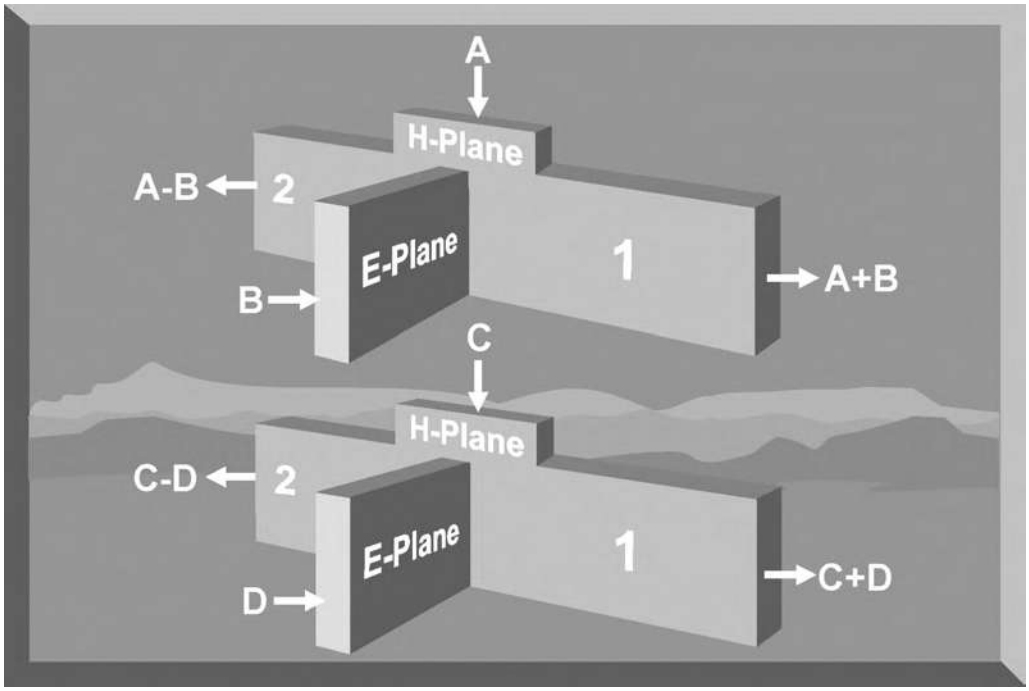

Figure 7-14. Magic T Output Signals

(1) The top equation in Figure 7-15 is used to compute target range. Target range is derived by adding the signal from the A scan to the signal from the B scan. This value is then added to the sum of the C and D scan signals. The output of these combinations is then passed to the range circuit which figures out the range of the target and displays it to the operator. Monopulse range tracking is accomplished by using either a leading-edge or split-gate tracking loop.

(2) Target elevation tracking error is derived using the middle equation from Figure 7-15. The signal from the A scan is added to the signal from the B scan. The signals from the C and D scans are also added. This time, however, the sum of A+B is subtracted from the sum of C+D. This value is then passed to the elevation circuit. Elevation signals are sent to the operator display and the servo mechanism, which corrects to the updated position of the target.

(3) The bottom equation from Figure 7-15 is used to compute the azimuth error. The signal from the A scan is added to the signal from the C scan. The B and D scans are also added together. The sums of these values are subtracted from each other. This difference equals the tracking error in azimuth. The radar system will then position the search beam to even the energy level between the two pairs of sums. When this occurs, the azimuth tracking error is zero.

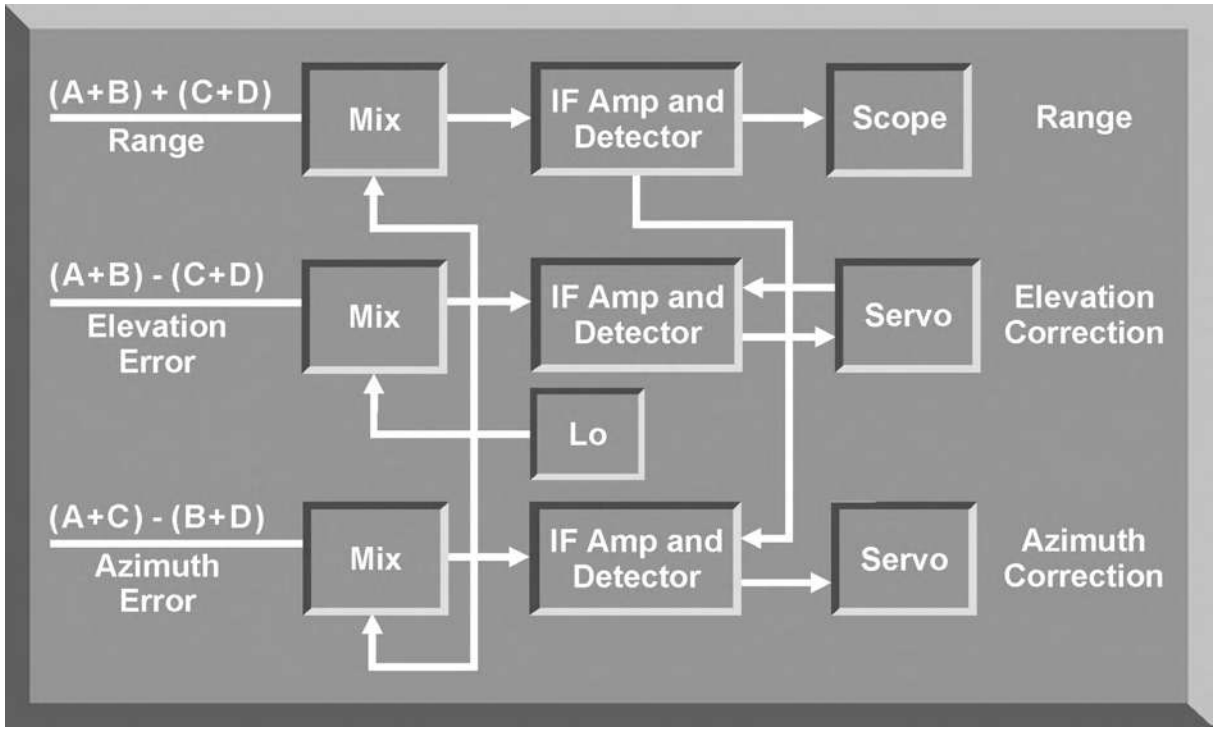

Figure 7-15. Monopulse Tracking Loops

c. A further illustration of the idea of signal combinations can be seen by referring to the F-16 in Figure 7-16. All the energy is received in the B scan area.

The A scan signal is added to the B scan signal. The signals from the C and D scans are also added. However, the sum of A+B is now subtracted from the sum of C+D. In this case, the values from the A scan and the C scan are zero. This total value of (A+B) - (C+D) is then passed to the elevation circuit.

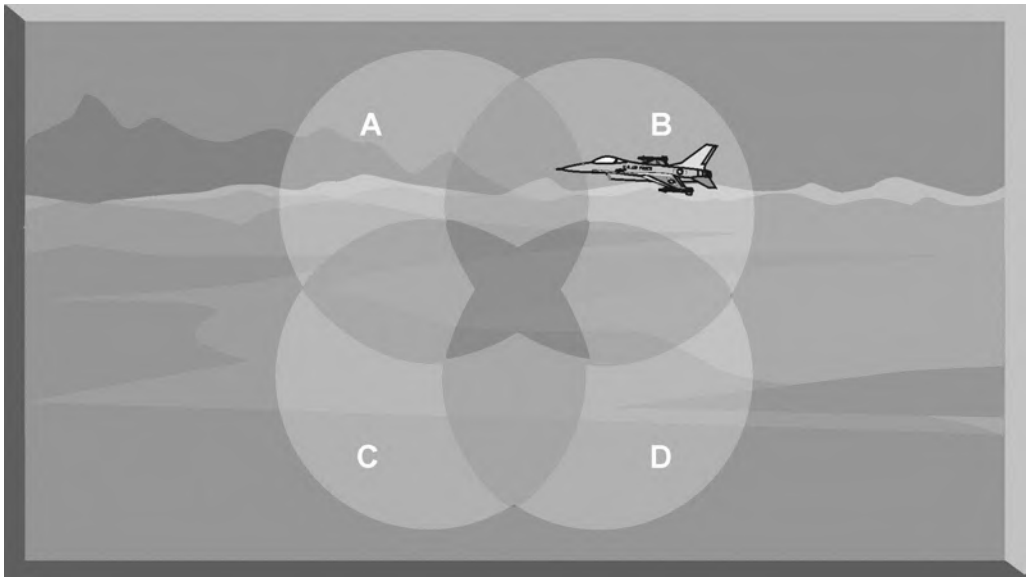

Figure 7-16. Monopulse Elevation Tracking Error

(1) The comparison in Figure 7-17 shows that all the energy is in the B scan. The radar will reposition the scan vertically to balance the energy between the B and D scans. When the energy level is balanced, the elevation error is zero.

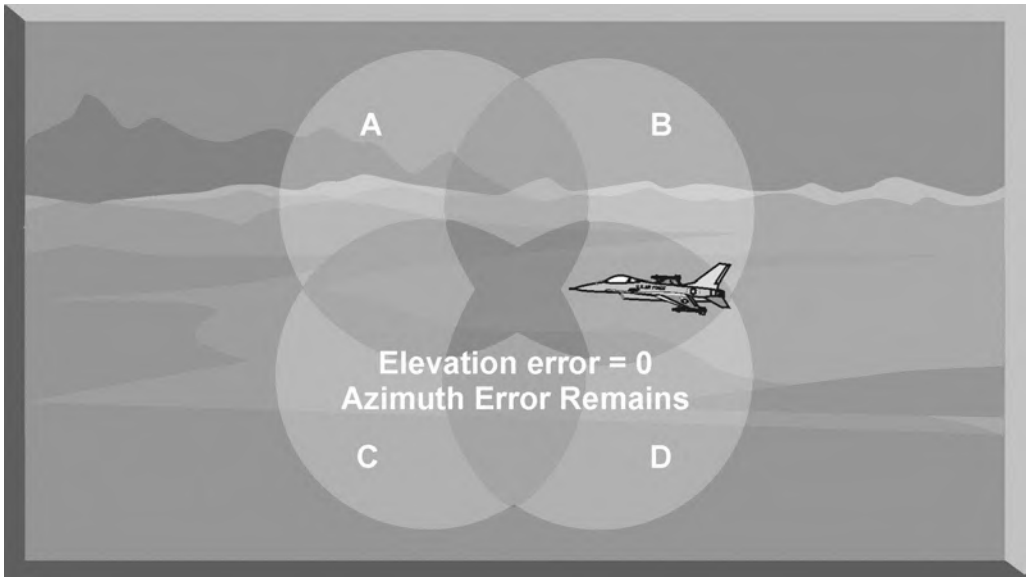

Figure 7-17. Monopulse Elevation Track

(2) Using the azimuth error equation from Figure 7-15, the azimuth tracking loop computes the azimuth error and repositions the antenna to equalize the received energy in all the beams. The monopulse radar has now established a tracking solution (Figure 7-18). All these computations are done instantaneously on a pulse-to-pulse basis.

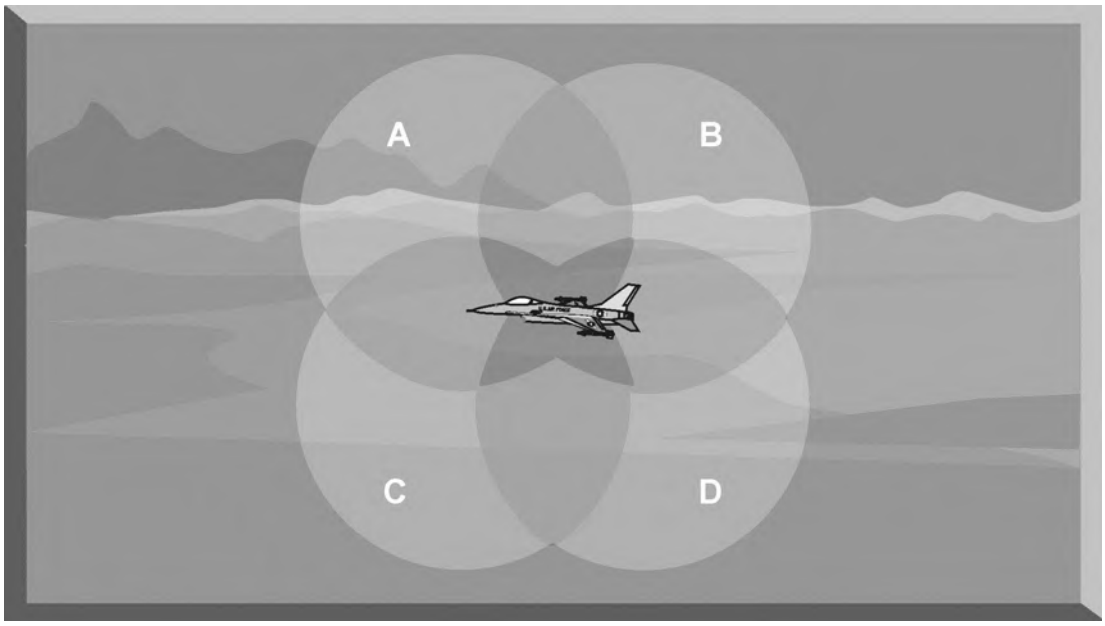

Figure 7-18. Monopulse Azimuth Track

7. CONTINUOUS WAVE (CW) RADARS

CW radar was one of the earliest forms of radar systems. Unlike pulse radar systems, CW radars emit a continuous beam of RF energy with no interruptions in the transmissions to detect returning echoes. A continuous radar transmission from the antenna requires that a classic CW radar have two antennas, one for transmission and one for reception (Figure 7-19).

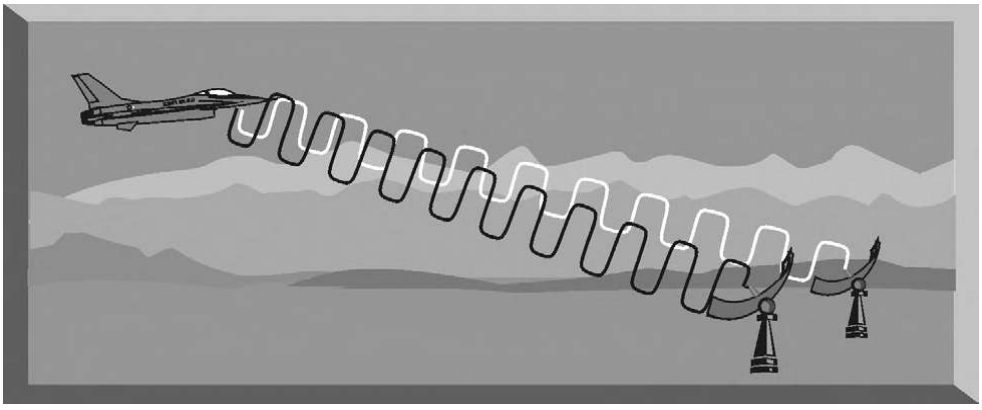

Figure 7-19. CW Radar

a. Since a continuous transmission results in a continuous echo signal, it is impossible to tell what part of the echo is associated with any particular part of the transmission. This makes range typical determination impossible. The azimuth and elevation tracking capability of a CW radar is based on the antenna position when the target is illuminated. The simple application of the Doppler principle provides a means for a CW radar to track a target in velocity and reject clutter. The Doppler principle deals with the fact that a radar return from a moving target will be shifted in frequency by an amount proportional to its radial velocity compared with the radar site. Using the difference in frequency from the transmitted signal to the received signal, a CW radar can separate the target return from clutter based on a change in frequency. This type of radar is called a CW Doppler radar.

b. The most serious disadvantage of a simple CW Doppler radar is that it does not provide any range information on the target. One method of obtaining range information from a CW radar uses frequency modulation (FM). The modulation can be sinusoidal, sawtooth, triangular, or any shape, as long as the rate of frequency change is known. The transmitter emits a continuous signal, but the frequency is changed in a known pattern. When the echo returns from the target, it is then compared to the frequency being transmitted. This frequency difference is directly proportional to the range of the target.

(1) Figure 7-20 shows how a FM CW radar measures range. Using a triangular wave for modulation, a plot of transmitted frequency over time would look like the solid line. It is important to note that this is not a depiction of the transmitted wave but a plot of how the frequency of the wave varies with time. For a target, without any relative motion, the frequency returning to the receiver is depicted by the dotted line. The target echo frequency lags the transmitted frequency by time (t). There is also a frequency difference between the transmitted and received signals. Range to the target may be computed by measuring this frequency difference and dividing by the rate of change of the transmitted frequency. The result is time. Dividing this time by 12.4 microseconds per radar mile yields range to the target. The frequency difference is constant for a target, without any relative motion, except for the brief intervals when the change in frequency goes from a positive to a negative slope. These "ditches" are negligible and can be disregarded when calculating range. The average amplitude is equal to target range.

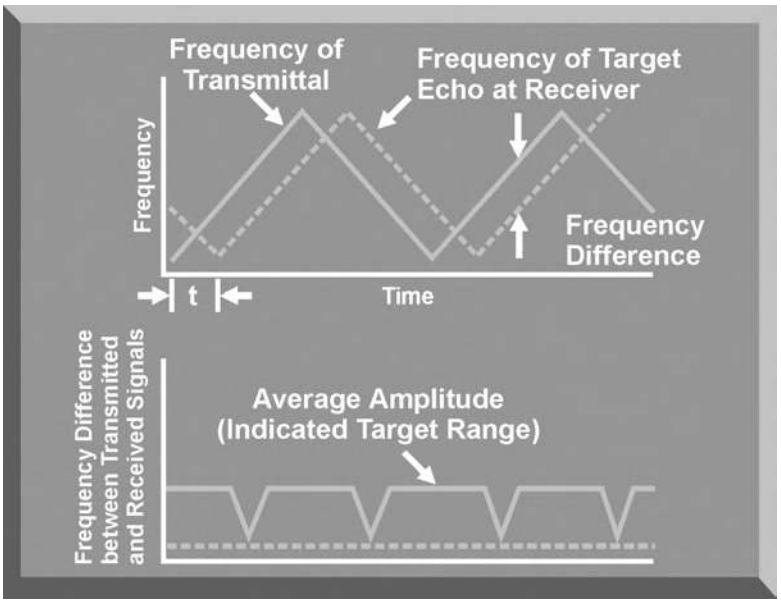

Figure 7-20. FM CW Radar Range Determination (No Relative Motion)

(2) For a target moving toward the radar, the FM CW radar measures both target range and velocity. In Figure 7-21, the frequency of the return signal will be increased as depicted by the dotted line. Remember, this is a graph of frequency versus time, not a depiction of the radar wave. For a moving target, this results in a varying frequency difference. A plot of the frequency difference over time provides target range by averaging the difference, while target velocity is found by comparing the two frequency differences.

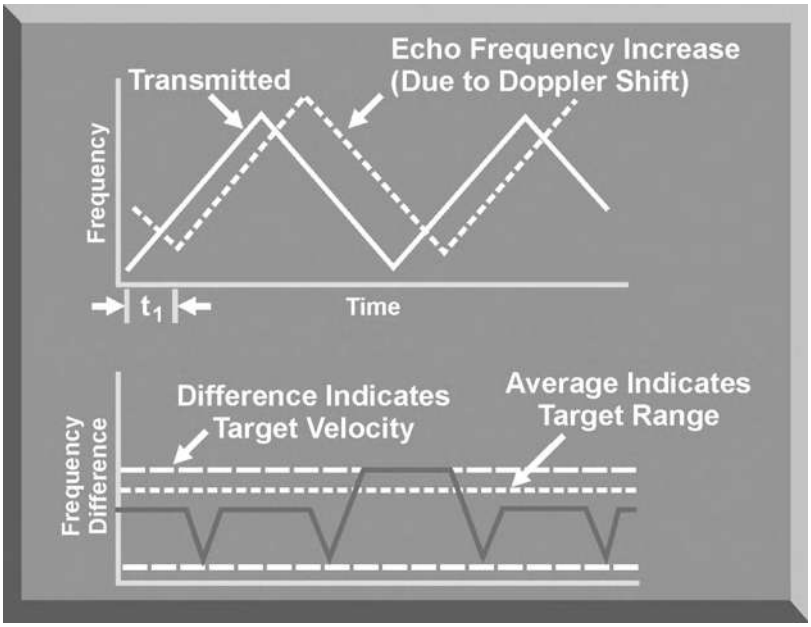

Figure 7-21. FM CW Radar Range Determination (Relative Motion)

c. The primary advantage of the FM CW Doppler radar is its ability to combine the clutter rejection features of a simple CW Doppler radar with the capability to detect range. The widest application of FM CW Doppler radars is in radar altimeters for aircraft. In addition, the HAWK missile system uses an FM CW Doppler acquisition radar and a CW target illuminator.

d. Another method used for clutter rejection in a pulse radar system is to employ special circuits, or Doppler processing, to identify and reject clutter. These special circuits are added to the receiver section of a pulse radar and are called moving target indicators (MTIs). There are two types of MTIs, non-coherent and coherent.

(1) The earliest form of MTI was called non-coherent MTI or "area" MTI. Non-coherent MTI radars do not process Doppler frequencies. The returns from one scan are subtracted from returns from the next scan. All targets that move at least one resolution cell in the time between scans are displayed. All stationary objects, including fixed clutter, are cancelled and not displayed. In this type of MTI, clutter cancellation is based on the size and movement of the return. Due to changes in the clutter cross section, instabilities in radar operations, variations such as rain or clouds, and noise from the transmitter, clutter cancellation is never complete. In another form of non-coherent MTI, the radar returns from moving targets are compared to the returns from fixed targets, and the fixed targets are cancelled. These non-coherent MTIs are simple, but they do not provide the clutter rejection available from coherent MTI radars.

(2) A coherent MTI uses the fact that Doppler shifts appear to a pulse radar as phase shifts on the received target pulse. Coherent MTI uses sophisticated circuitry, including stable local oscillators (STALOs) and coherent local oscillators (COHOs) to capture and process these phase shifts. Further processing of these phase shifts yields velocities for each return. Those velocities associated with stationary targets are rejected and only moving targets are displayed. Coherent MTIs have a major problem called "blind speeds." Blind speeds occur for all target Doppler frequencies that are the exact PRF, or any multiple of the PRF, of the radar signal. When a target is moving at a velocity that produces this Doppler frequency, its return is cancelled along with fixed returns.

(3) There are three techniques to limit "blind speeds." The first technique is to use a PRF stagger. By staggering the PRF, the blind speed associated with one PRF will be covered by the other PRF. The second method is called the delay line and canceler. This involves delaying each pulse so it can be compared to the next pulse before processing. This method enhances Doppler frequency comparison and rejects clutter more effectively. The third way is to use range gates and Doppler filters. A range gate is simply a switch that opens for a time corresponding to the time a radar return would arrive for a target at a specific range. For example, a range gate for all targets between 10 and 11 nautical miles would open 124 microseconds after the transmitted pulse (12.4 microseconds per mile) and close 12.4 microseconds later. A target return at this range would trip

this gate and be processed by Doppler filters to find velocity. Fixed targets would trip the range gate and be eliminated by the Doppler filters. This is a sophisticated technique that is also used by pulse Doppler radars.

8. PULSE DOPPLER RADAR

Pulse Doppler radars combine the advantages of both pulse and Doppler radar systems. Because the signal is pulsed, the radar can find range, azimuth, and elevation, similar to a conventional pulsed radar. A pulse Doppler radar can also compute overtake, or rate of closure, compared with the radar system on a pulse-to-pulse basis. A pulse Doppler radar operates much like an MTI, and the terms are sometimes used interchangeably. However, an MTI uses Doppler frequency shifts only to reject clutter while a pulse Doppler radar uses Doppler frequency shifts to reject clutter and to track targets in velocity. A pulse Doppler radar transmits a box or pulse of RF energy at the operating frequency of the radar (Figure 7-22). The frequency inside these boxes reacts the same way as the continuous waves of a CW radar, but since the RF waves are pulsed, range determination can be accomplished by measuring the time it takes for the reflected pulse to return from the target. Velocity determination and tracking are accomplished by capturing and quantifying the Doppler shift of the frequencies in each pulse.

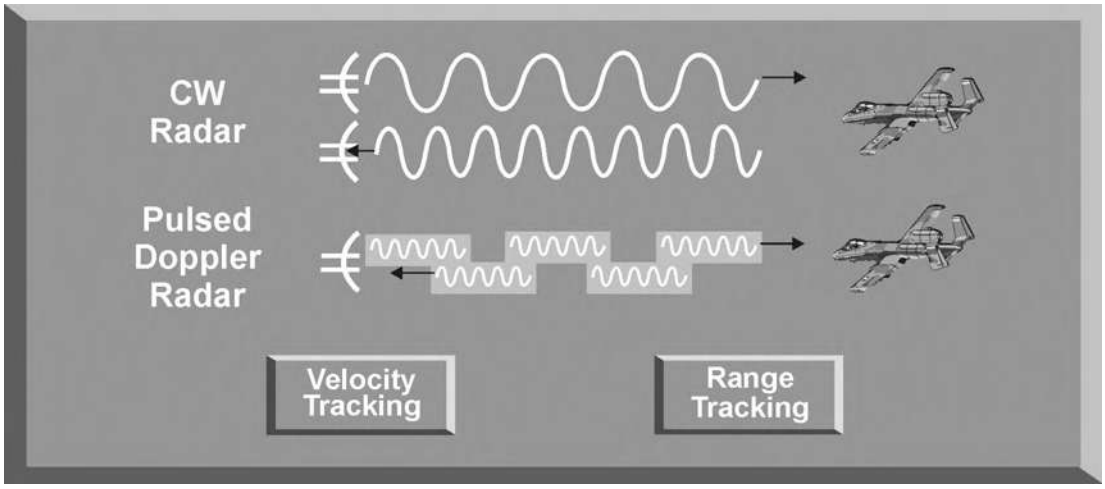

Figure 7-22. Comparison of CW Radar and Pulse Doppler Radar

a. A pulse Doppler radar tracks a single target in azimuth and elevation by employing either conical scan (sequential lobing) or monopulse tracking. Angle and elevation tracking employing these techniques is covered in Sections 3 and 6 of this chapter. The error signals generated by these techniques are sent to the antenna servos to keep the target return centered in the antenna beam.

b. Range tracking of a single target in a pulse Doppler radar is normally accomplished by a split-gate or leading-edge range tracking loop. Some pulse

Doppler radars employ an FM technique to provide range information during high PRF operations.

c. For velocity tracking, each range gate has a complete set of Doppler filter banks as depicted in Figure 7-23. Each pulse of RF energy is composed of many frequencies. To separate the returning target frequency from all other frequencies in the returning waveform, the pulse Doppler radar employs filters to cancel the unwanted frequencies. In addition, it cancels out all returns with no frequency shift, which equates to canceling all returns with no movement relative to the radar.

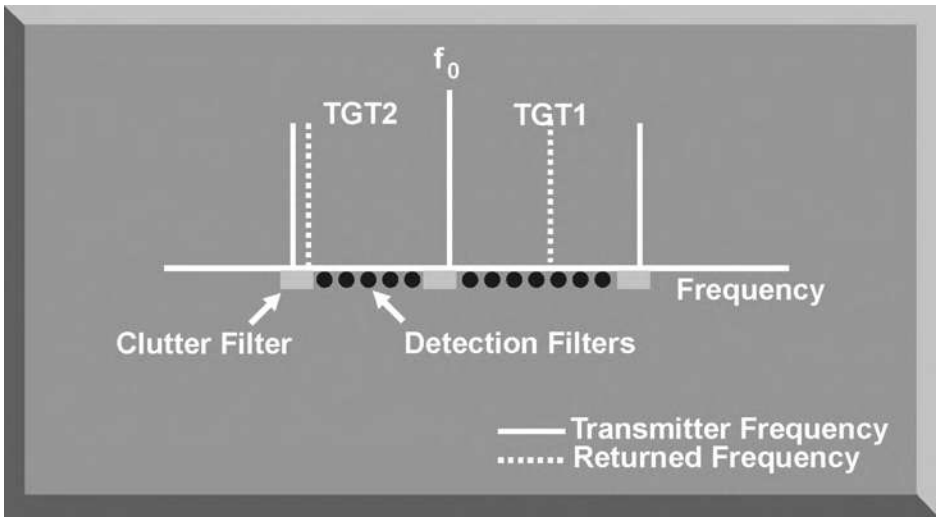

Figure 7-23. Range Ambiguity

d. The ability of a pulse Doppler radar to accomplish range, azimuth, and velocity tracking is dependent on the PRF of the radar. Table 7-1 summarizes these capabilities based on PRF. Low PRF tracking in velocity is extremely difficult due to the spacing of the spectral lines. Low PRF gives accurate range and azimuth as well as long, unambiguous range. Medium PRF tracking in range, azimuth, and velocity is easy for the radar to handle. High PRF provides excellent velocity resolution, but range ambiguities become a problem.

Table 7-1. Pulse Doppler Tracking Capabilities

Prefix	Velocity	Range	Azimuth
Low PRF	Poor	Good	Good
Med PRF	Good	Good	Good
High PRF	Excellent	Poor	Good

e. Weaknesses of pulse Doppler radars include velocity blind speeds, range ambiguity, and range eclipsing.

(1) The primary operator exploitable weakness of a pulse Doppler radar takes advantage of the pulse Doppler radar's biggest strength. The pulse Doppler is designed to eliminate ground returns so that the attacker is able to track an aircraft that used to be able to hide in ground clutter. To remove the ground clutter and avoid tracking unwanted targets like cars on a road, a filter is designed in the radar to eliminate all targets with a low velocity relative to the radar. The key to breaking track of a pulse Doppler radar is to place the aircraft in a speed less than the speed gate relative to the radar (Figure 7-24), commonly referred to as the Doppler notch.

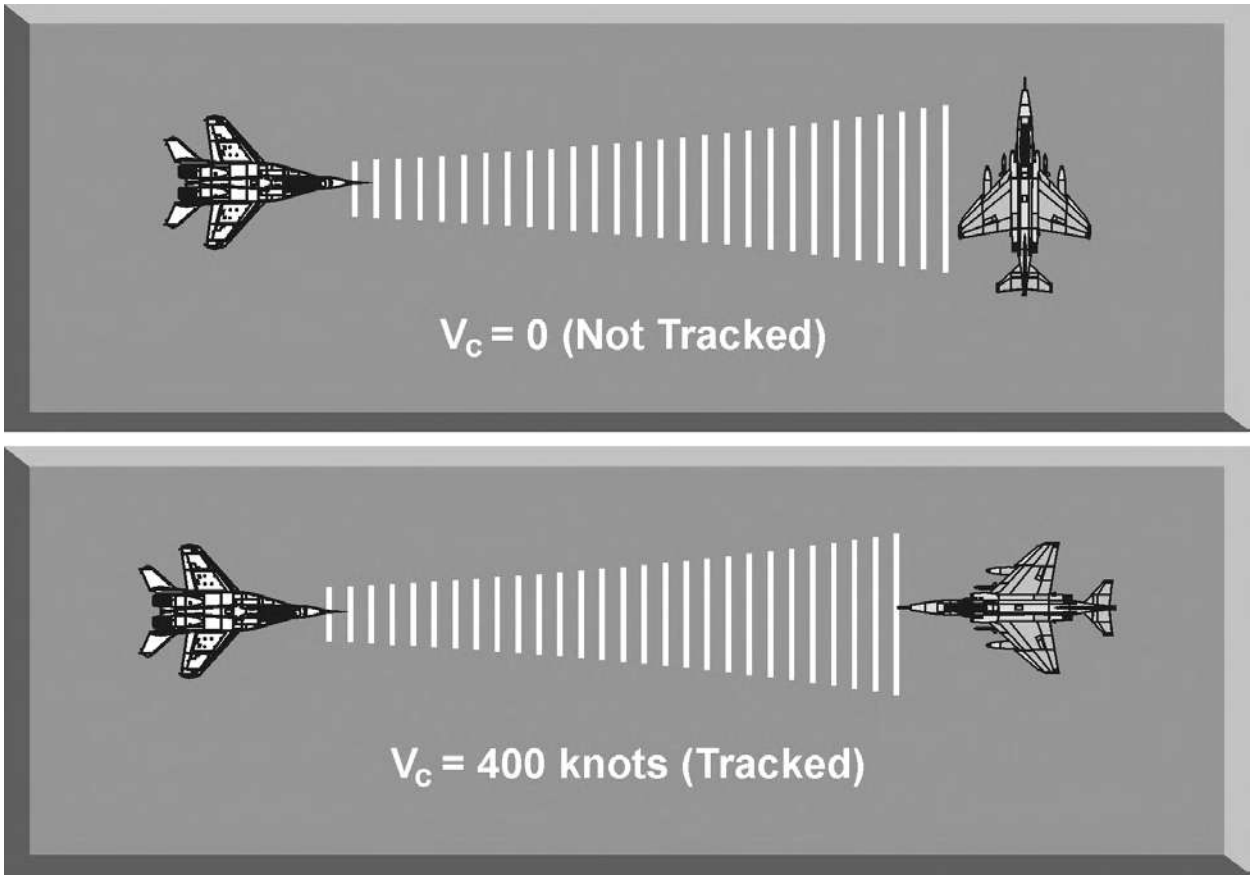

Figure 7-24. Pulse Doppler Speed Gate

(2) Range ambiguity occurs primarily with long-range targets when the return comes back to the radar after another pulse has already been transmitted (Figure 7-25). The radar will see this return and base its range calculations on the transmission time of the immediately preceding pulse, instead of the pulse that generated the return. The result will be an incorrect range calculation.

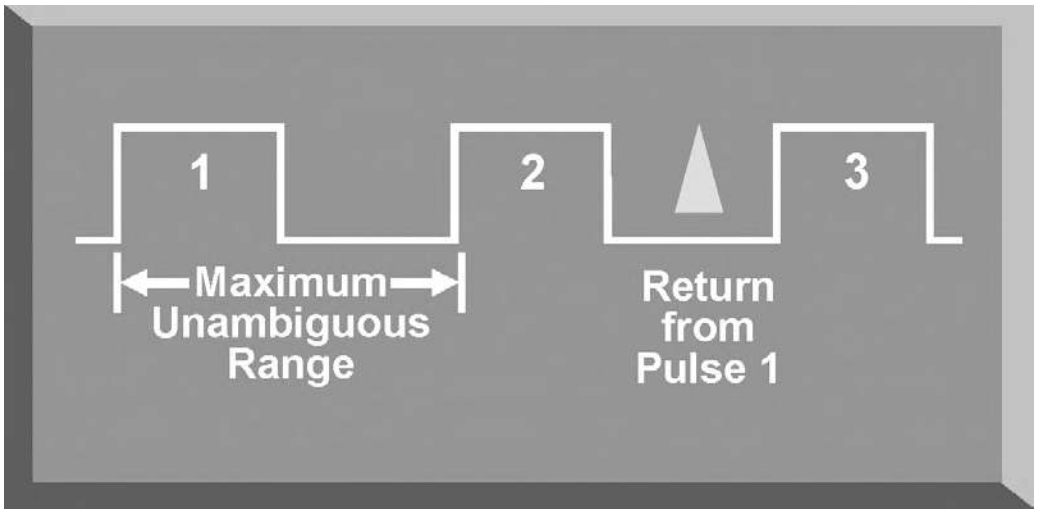

Figure 7-25. Range Ambiguity

(3) Range eclipsing occurs when a target return comes back to the radar antenna while a pulse is being transmitted (Figure 7-26). Since the radar cannot receive while transmitting, the return will not be displayed.

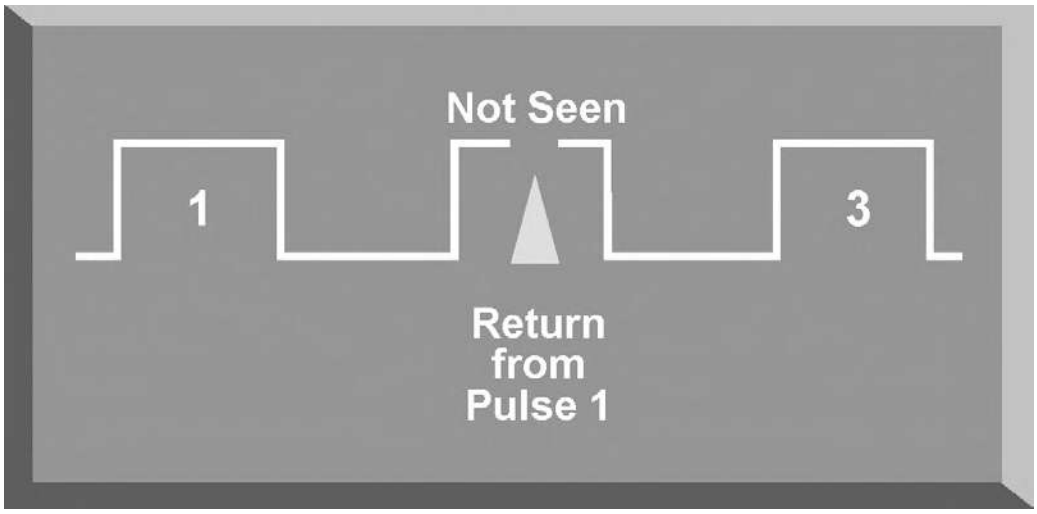

Figure 7-26. Range Eclipsing

(4) To solve the problems of range ambiguity and eclipsing, a pulse Doppler radar employs different PRFs and computer logic. In Figure 7-27, at PRF 1, the return from target 1 is eclipsed, and target 2 is ambiguous. By changing the PRF slightly, these range problems can be resolved. Notice that at PRF 2, neither target is eclipsed, and at PRF 3, target 2 is eclipsed. The computer logic needs to be extremely advanced to compensate for these problems. These simplistic examples show the complex problem of using multiple PRFs.

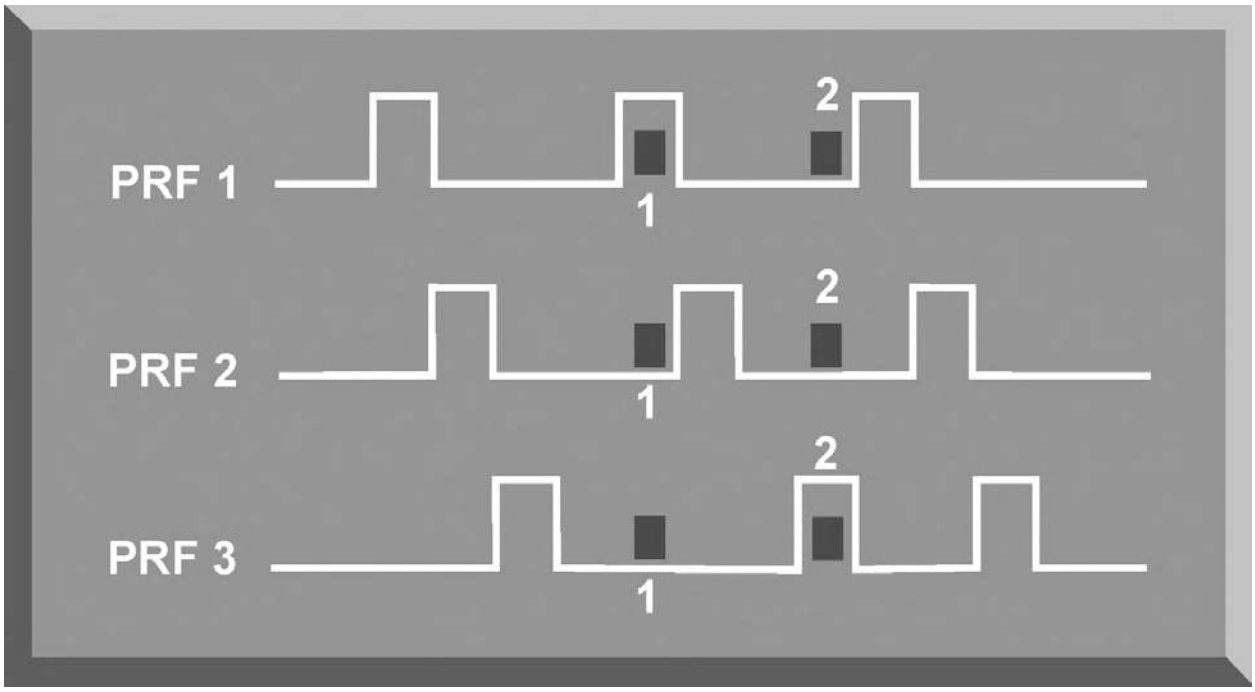

Figure 7-27. Resolving Range Ambiguity and Eclipsing

9. SUMMARY

This chapter has discussed the range, azimuth, elevation, and velocity tracking techniques employed by conical scan, TWS, LORO, monopulse, CW Doppler, and pulse Doppler radar systems. The method used by a specific radar system to track a target determines the type of jamming technique required to counter this system. A basic understanding of the target tracking techniques will enable you to understand the basic jamming techniques employed to defeat these threats.

CHAPTER 8. RADAR MISSILE GUIDANCE TECHNIQUES

1. INTRODUCTION

Once a target has been designated, acquired, and tracked by a radar system, the final stage in target engagement is to guide a missile or projectile to destroy the target. There are three basic requirements for successful missile guidance: (1) precise target tracking by a target tracking radar (TTR) to provide target parameters (range, azimuth, elevation, velocity, etc.), (2) a method to track the position of the missile compared with the target, and (3) a fire control computer to generate missile guidance commands based on target and missile position. The missile guidance techniques employed by modern air-to-air and surface-to-air missile (SAM) systems will be covered in this chapter. In addition, the target engagement techniques employed by antiaircraft artillery (AAA) systems will also be discussed. There are three distinct phases in any missile intercept: boost, mid-course, and terminal.

a. Nearly all missiles are unguided during the initial boost phase (Figure 8-1). During the boost phase, the missile electrical and hydraulic systems are activated and are coming up to operating parameters. The missile is gathering speed and normally will be in an unguided mode of flight.

Figure 8-1. Initial Boost Phase

b. During the mid-course phase, the missile is actively being guided to the target using some type of guidance signal (Figure 8-2). Guidance signals deflect

the control vanes of the missile to change its direction. These vanes change the roll, pitch, and yaw, in some combination, to control the missile flight path. Normally a gas grain generator powers a small hydraulic pump that deflects the control vanes in response to guidance signals. Each missile carries a limited supply of hydraulic fluid for maneuvering. The fluid is expended through vents with every control surface activation. The limited quantity of hydraulic fluid can be a significant factor during a long-range missile intercept.

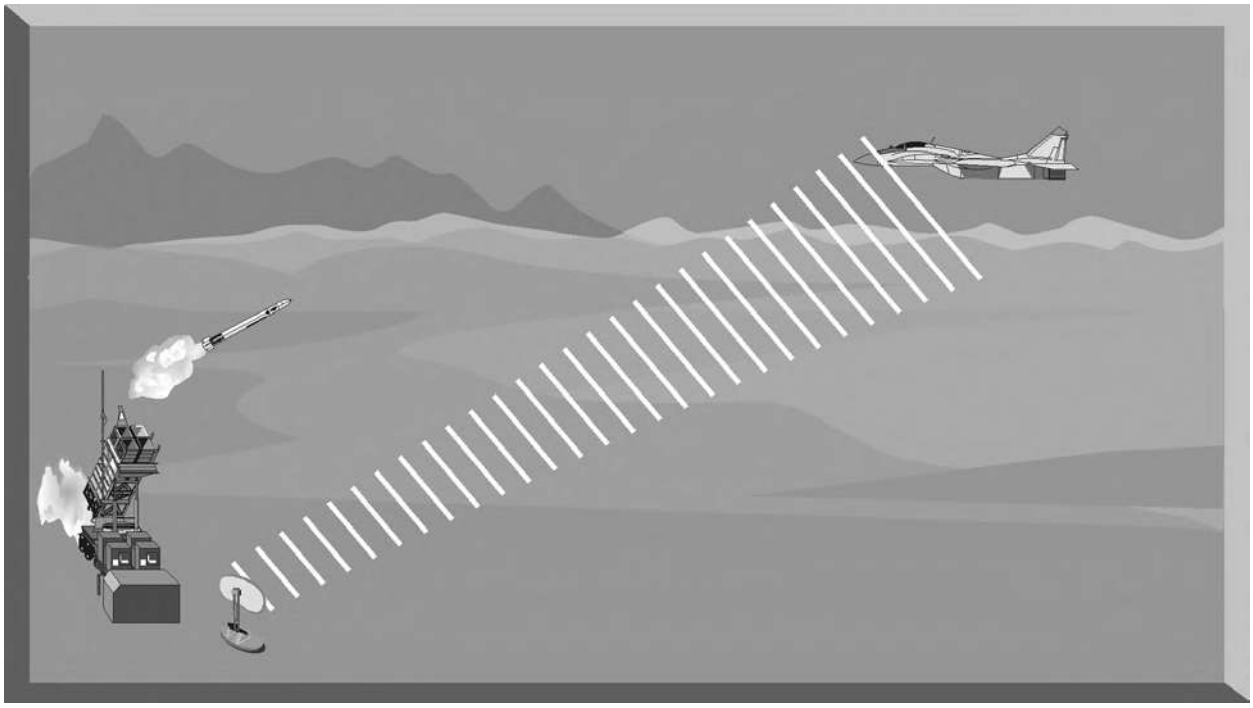

Figure 8-2. Mid-Course Guidance Phase

c. The final phase of an intercept is the terminal phase (Figure 8-3). During this phase, the missile attempts to pass close enough to the target to detonate the fuse while the target is within the lethal radius of the warhead. Modern missiles employ both a contact fuse and some type of proximity fuse. Proximity fuses range from command detonation for command-guided missiles, fractional Doppler gates for semi-active guided missiles, to active laser fuses for IR-guided missiles.

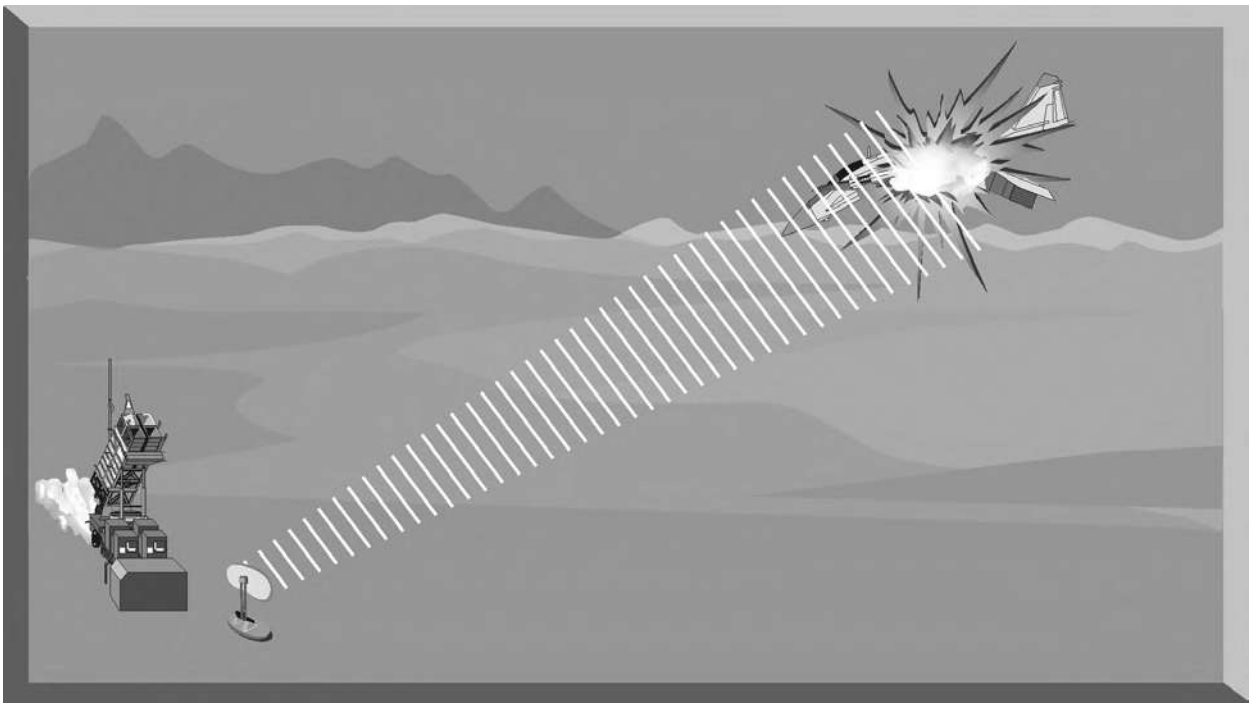

Figure 8-3. Terminal Guidance Phase

2. COMMAND GUIDANCE

Command guidance uses a fire control computer to constantly send course correction commands to the missile throughout its flight. These commands are a series of electrical missile guidance pulses called doublets or triplets. These pulses provide steering commands to the missile by varying the spacing between each guidance pulse. Each pulse, or pulse combination, relays some roll, pitch, and yaw command to the missile. These inputs are constantly corrected for the spatial relationship between the missile and the target's present position and rate of motion. Guidance commands are passed to the missile by specialized antennas on the TTR and an antenna installed on the missile, called a missile beacon. The beacon is a special radio receiver and transmitter that is attached to the rear of the missile. It acts like a transponder in that the TTR tracks and receives guidance commands. The guidance frequency may be widely separated from the target tracking radar frequency to minimize interference. This beacon is usually masked until missile booster separation. This results in the missile being launched unguided for the first 2-3 seconds. This type of delay is one of the reasons that all command-guided missile systems have a minimum launch range. Command guidance is used by the SA-2, SA-3, SA-4, and SA-8.

a. Command-guided missiles will generally fly a rectified (full or half) or three-point pursuit geometry during the mid-course portion of the intercept (Figure 8-4). However, a command-guided missile may transition to a pure pursuit geometry during the terminal phase of the intercept. Rectified geometry involves the prediction of where the target and the missile will be at some point in the future.

The target's direction and rate of movement is tracked and predicted. The missile is then launched, pulls lead on the target, and is guided to the point in the sky where the intercept is predicted to take place. This profile requires the constant update of both the target and missile positions.

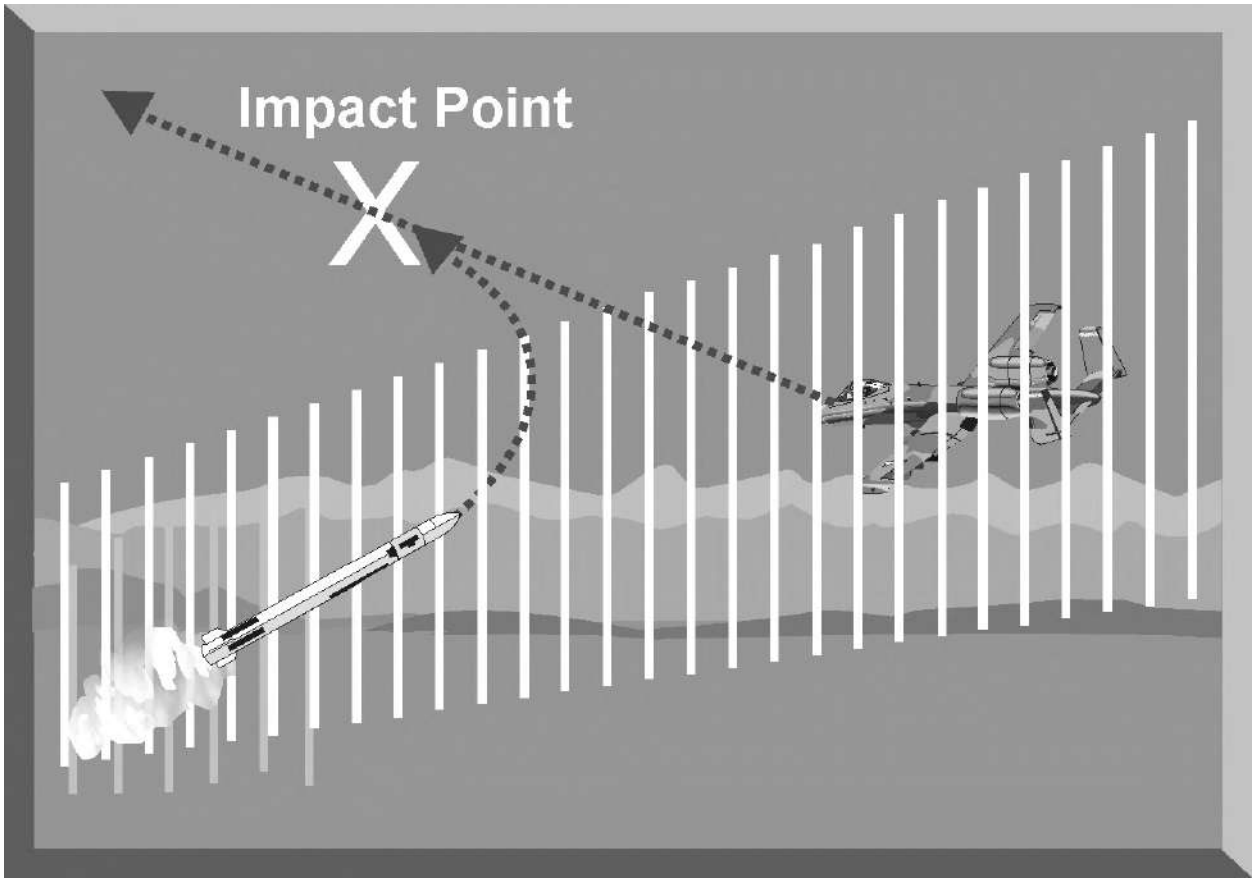

Figure 8-4. Rectified Flight Profile

b. Three-point pursuit geometry is often used when there is incomplete range tracking data on the target. In this case, it will be impossible to predict exactly where the target will be at some point in the future. In this profile, the target tracking radar constantly tracks the target. The missile location will be updated by the missile beacon. The fire control computer will direct the missile to fly directly down the tracking radar beam toward the target. In this geometry, the missile may start out on a direct intercept course and, depending on the target's direction and rate of movement, transition to a pure pursuit intercept. The three points in three-point missile geometry are depicted in Figure 8-5. Point one is the target tracking radar, point two is the missile itself, and point three is the target. By keeping all three points always in a line, the missile will intercept the target at some point, although the range of the target is unknown.

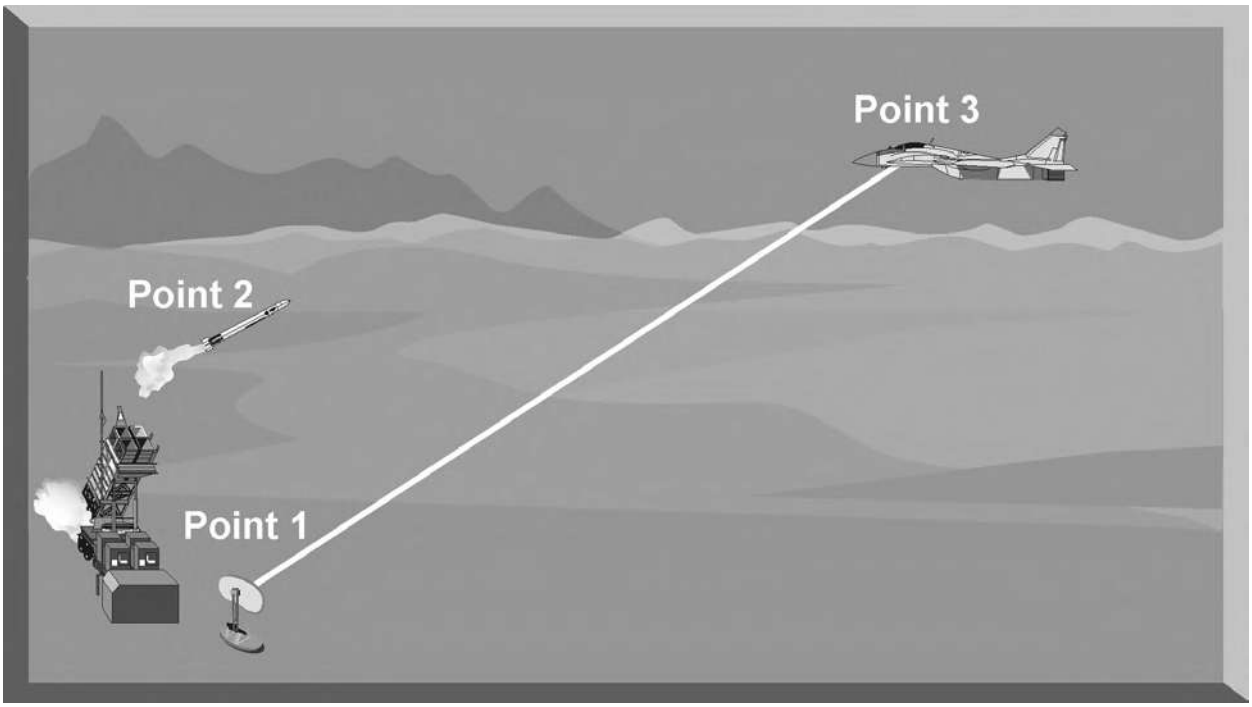

Figure 8-5. Command Guidance: Three-Point Pursuit

c. Command guidance techniques have many advantages. First, command-guided missiles can adjust their flight geometry throughout an intercept profile. Second, the missiles are uncomplicated since they do not carry onboard computers or target tracking equipment. The fire control computer associated with the TTR accomplishes all intercept calculations. Third, the primary intercept profile, a full- or half-rectified intercept, is the fastest and most fuel-efficient intercept. Fourth, command guidance is difficult to jam since the missile beacon antenna is at the rear of the missile and can be relatively high-powered. And finally, an intercept is possible even without accurate range information by using the three point intercept profile.

d. Command guidance has several disadvantages. First, the use of a missile beacon delays the capture of the missile by the tracking radar. This can cause a large dead zone which equates to a larger minimum engagement range. Second, the accuracy of the intercept geometry is only as good as the tracking information provided by the target tracking radar. Jamming, interference, or loss of signal will adversely affect the intercept accuracy. In addition, normal radar characteristics could produce sufficient errors to cause the missile to miss the target, especially at longer ranges. Third, with insufficient range information, the three-point intercept profile is very slow and could result in the missile running out of energy before it gets to the target. Fourth, command guidance is reactive. The fire control computer constantly updates the intercept geometry based on target maneuvering. This results in missile maneuvering lagging target maneuvers.

3. SEMI-ACTIVE GUIDANCE

Semi-active guidance is significantly different from command guidance, but only after launch. The first requirement is still for the target tracking radar to maintain a solid target track, with the tracking data being supplied to the fire control computer. The fire control computer then directs a target illumination antenna to point at the target and illuminates it with CW energy. The missile then passively homes on the reflected CW energy.

a. The missile used by a threat system that uses CW homing is vastly different from the missile being guided by a command guidance signal. The missile that homes on CW energy must be equipped with a seeker section composed of an antenna and an internal receiver. The seeker section processes and computes the necessary course corrections as it flies toward the target. It can do this by knowing the zero boresight line of the antenna within the missile (Figure 8-6). As the reflected CW energy is received by the seeker, there is normally some deviation from the zero reference position. The onboard computer then directs the control surfaces to change the flight path to reduce the reference errors in the antenna to zero, if possible. When the error between the antenna position and the boresight position is zero, the missile is pointed directly at the target.

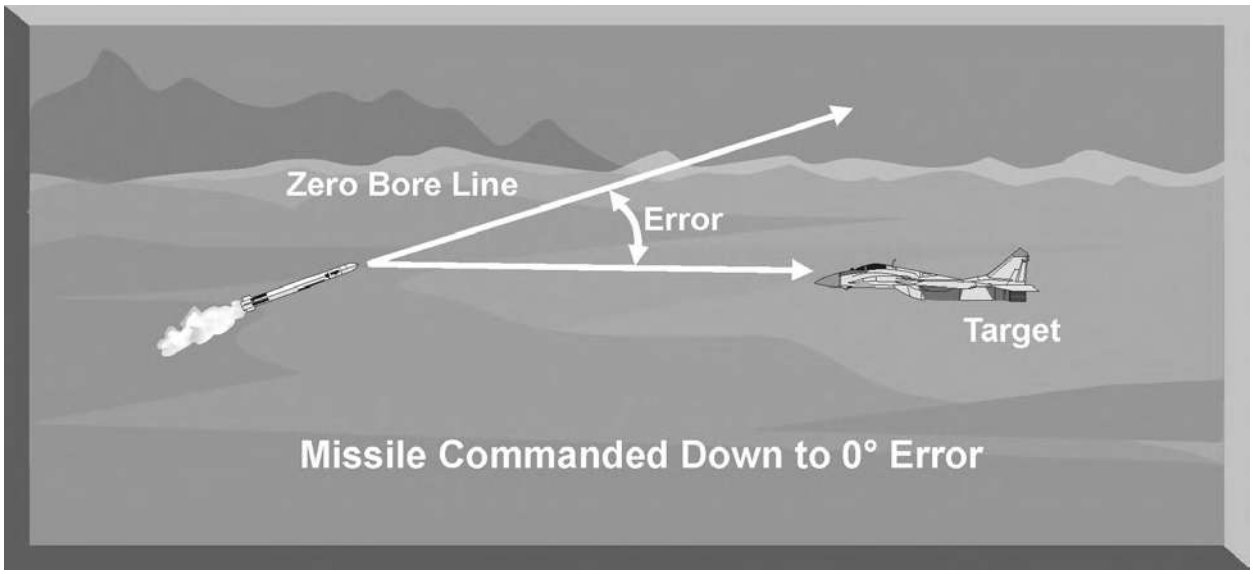

Figure 8-6. Semi-Active Guided Missile

b. Missile systems that use semi-active guidance normally use velocity as the primary target discriminator during the intercept. The missile seeker locks onto a reference Doppler signal provided by the fire control computer before launch. This Doppler signal establishes a tracking gate around the velocity of the target. After the missile is launched, it initially compares the reference Doppler to the target Doppler signal.

c. The mid-course phase for a semi-active missile is also different from that of a command-guided missile. A semi-active guided missile follows the reflected CW energy during the mid-course phase of the intercept and normally attempts to fly a lead pursuit profile to the target (Figure 8-7). If the target maneuvers, however, the missile may transition to a pure pursuit flight path. Unlike a command-guided missile, a semi-active guided missile does not use a missile beacon. The fire control computer does not need to know where the missile is to compute course corrections since all that is necessary is to illuminate the target with the CW illuminator. This also means that the missile can begin to track and guide when it is launched and locked on to the reference Doppler gate. Semi-active guidance is the primary mode of guidance for many surface-to-air missiles, and almost all radar-guided air-to-air missiles.

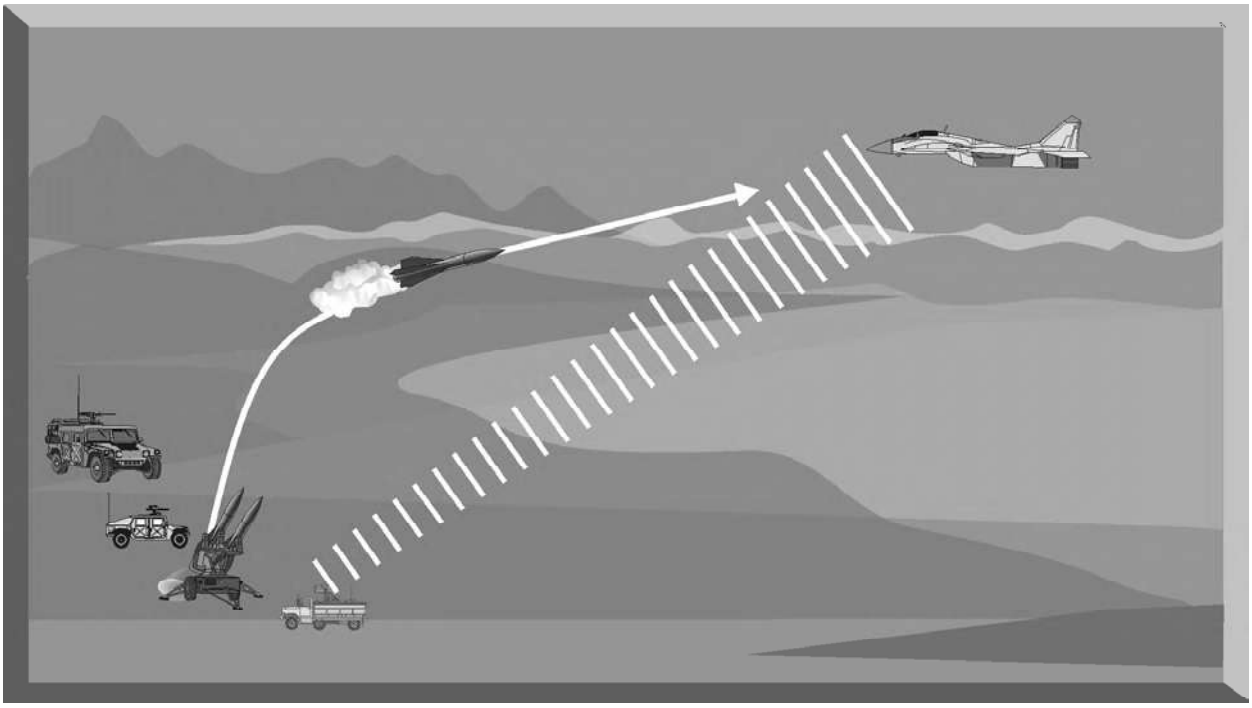

Figure 8-7. Semi-Active Guidance (Mid-Course)

d. As the missile enters the terminal phase of the intercept, there is no change in the guidance mode used by a CW homing missile. The missile may complete the terminal phase of the intercept geometry by going to a pure pursuit flight path, if necessary (Figure 8-8). The missile continues to home in on the reflected CW signal until it passes close enough for the fuse to function.

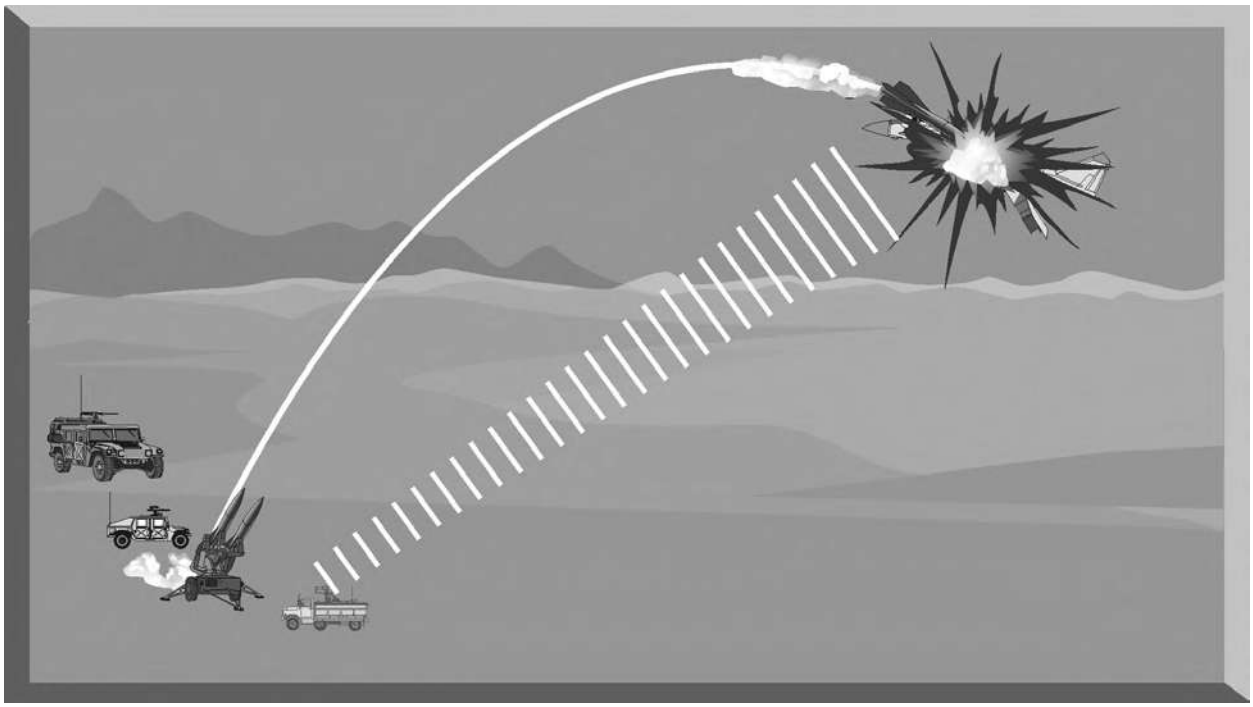

Figure 8-8. Semi-Active Guidance (Terminal Phase)

e. Semi-active missile guidance has many advantages. First, a semi-active guided missile is resistant to electronic jamming that may be used to deny range information. Second, a semi-active missile can be guided almost immediately after launch. This gives it a very small minimum range since it can maneuver almost as soon as it clears the launch rail. Third, it computes its own course corrections as necessary. This allows for a much quicker reaction to target maneuvers compared to a command-guided missile. Fourth, during a long-range intercept, a CW missile can be more accurate than a command-guided missile. This is accomplished by taking the inherent long-range radar tracking errors out of the equation. The target tracking radar only has to keep the target illuminated so that it can point the CW antenna at the target.

f. Although semi-active missile guidance is generally considered an excellent guidance technique, it does have some disadvantages. First, a semi-active guided missile normally requires reference Doppler values to be entered into the missile computer before launch. Without this reference, a semi-active missile cannot be launched (Figure 8-9). Second, a semi-active homing missile must maintain a lock onto the target Doppler. The use of chaff and beam maneuvers, which result in a near zero target Doppler, may cause a missile or radar to break lock. Third, if a break-lock occurs, a CW homing missile normally cannot regain target track and complete the intercept.

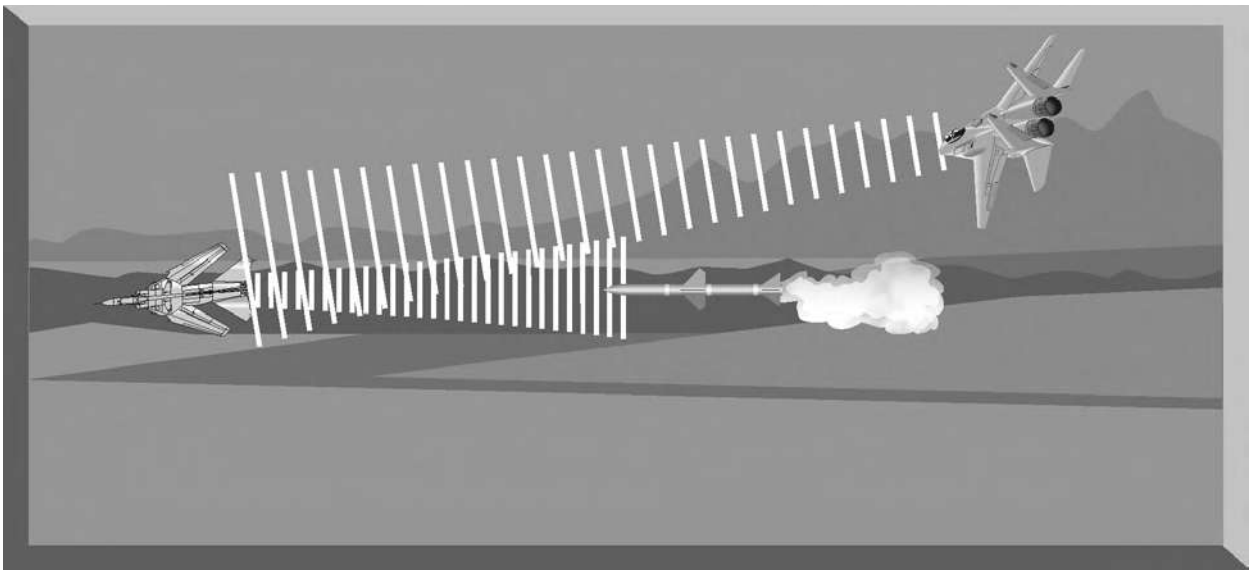

Figure 8-9. Semi-Active Guidance CW Reference Signal

4. ACTIVE GUIDANCE

Active guidance is an improvement that has been included in several new long-range missiles such as the AIM-54 Phoenix and the AIM-120 AMRAAM. This specialized guidance mode is only active during the terminal phase of flight. The mid-course phase usually employs semi-active or command guidance (Figure 8-10).

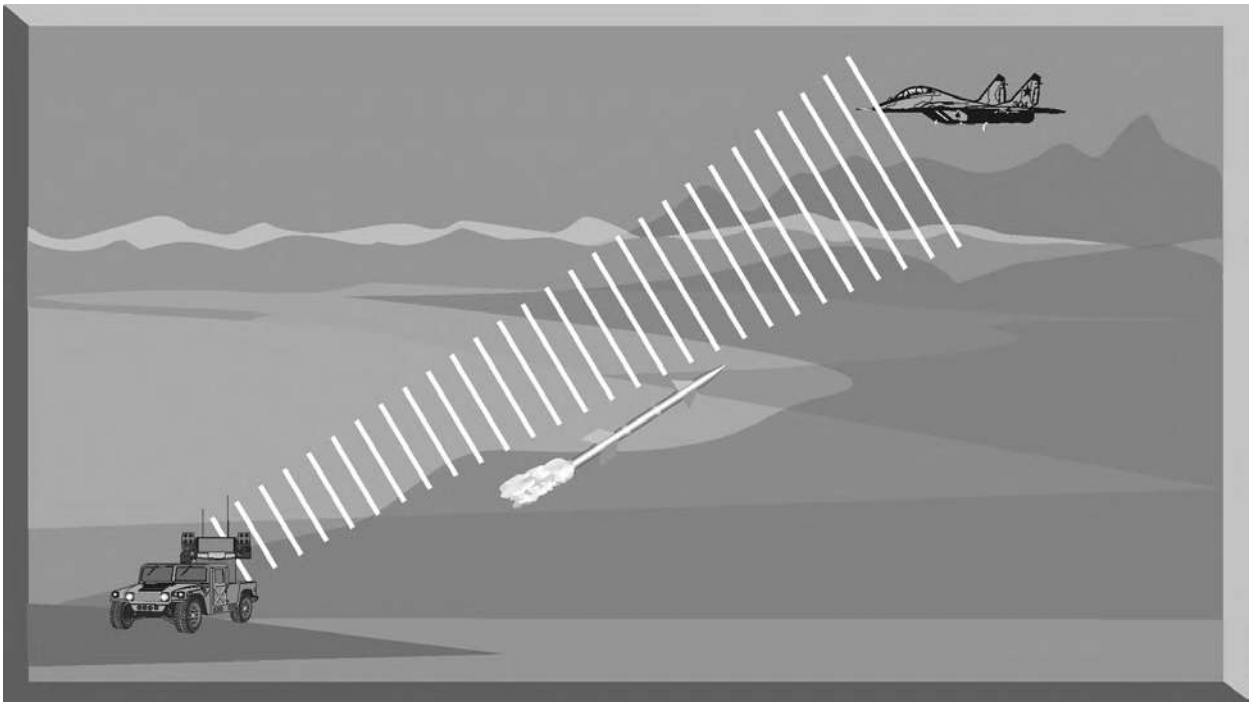

Figure 8-10. Active Guidance Mid-Course Intercept Phase

a. The range at which the missile goes "active" is dependent on the intercept geometry. High-aspect angle intercepts allow the activation of active guidance sooner than beam or tail-aspect intercepts. Missiles that employ active guidance carry a complete miniature radar system and fire control computer within the missile. As the missile nears the target, its internal radar system turns on and locks onto the target. The internal fire control computer directs control inputs to complete the intercept (Figure 8-11).

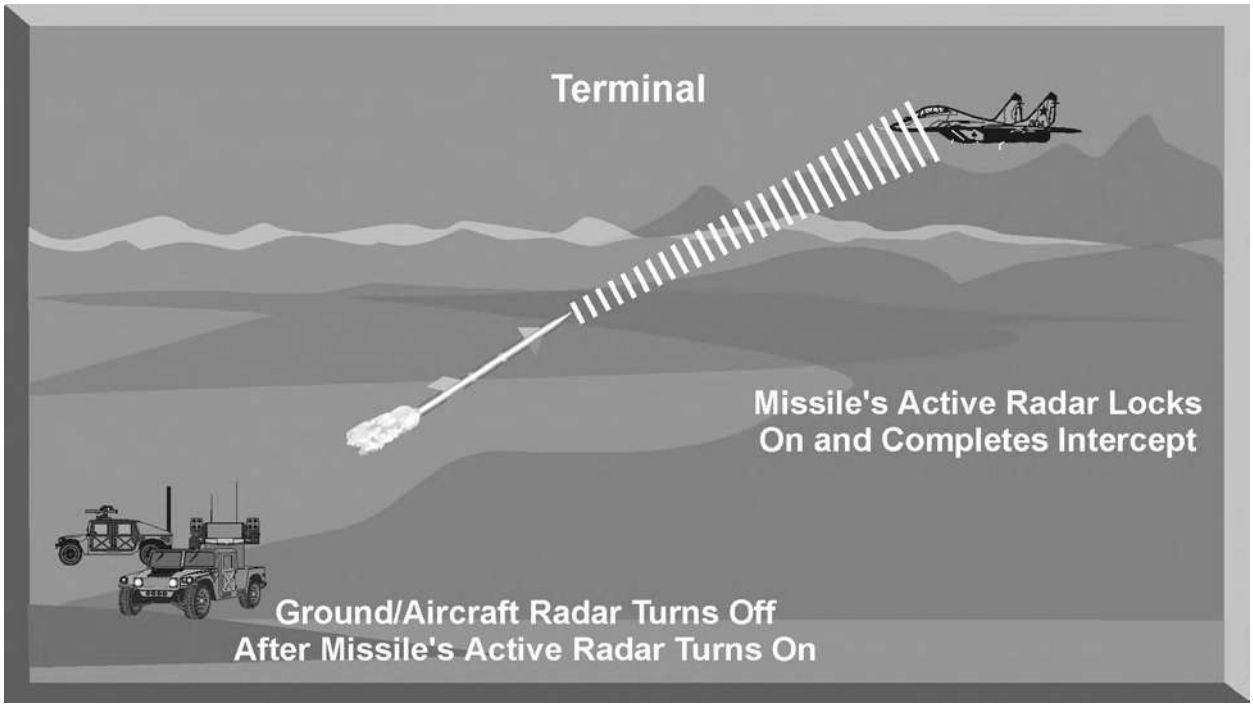

Figure 8-11. Active Guidance Phase

b. Active-guided missiles have many advantages. First, active-guided missiles are very accurate at long ranges. This is because they do not rely on the target tracking radar once their internal radar takes over the intercept. Second, an active missile is extremely difficult to jam. It uses a narrow beam and its relative power is constantly increasing as it nears the target. Third, an active-guided missile is a fire-and-forget weapon. Command or semi-active missile guidance requires the target tracking radar to maintain lock-on until the intercept is completed. In an air-to-air engagement, this means the interceptor is predictable until the missile hits the target, and vulnerable to an enemy missile attack. An interceptor with an active missile, however, may launch the missile and, once it goes "active," can then turn around or maneuver defensively.

c. Active-guided missiles have a few disadvantages as well. First, the active homing missile is a complex missile integrating both command and active guidance modes. Second, the missile may still be susceptible to electronic jamming during the mid-course phase of flight. Remember, during the mid-course

phase, the missile relies on command or semi-active guidance. Jamming the target tracking radar may affect the missile's ability to "see" the target near the terminal phase.

5. SEEKER-AIDED GROUND GUIDANCE/TRACK-VIA-MISSILE GUIDANCE

In seeker-aided ground guidance (SAGG) and track-via-missile (TVM) guidance, the target is illuminated by the ground-based radar and the missile receives reflected energy from the target. Unlike conventional semi-active homing, the missile does not generate its own guidance commands. Instead, the missile transmits raw engagement data to the ground-based fire control system (FCS) in order to generate uplink guidance commands. TVM is similar to SAGG; however, additional processing is done on-board the missile prior to transmitting the engagement data to the ground-based FCS.

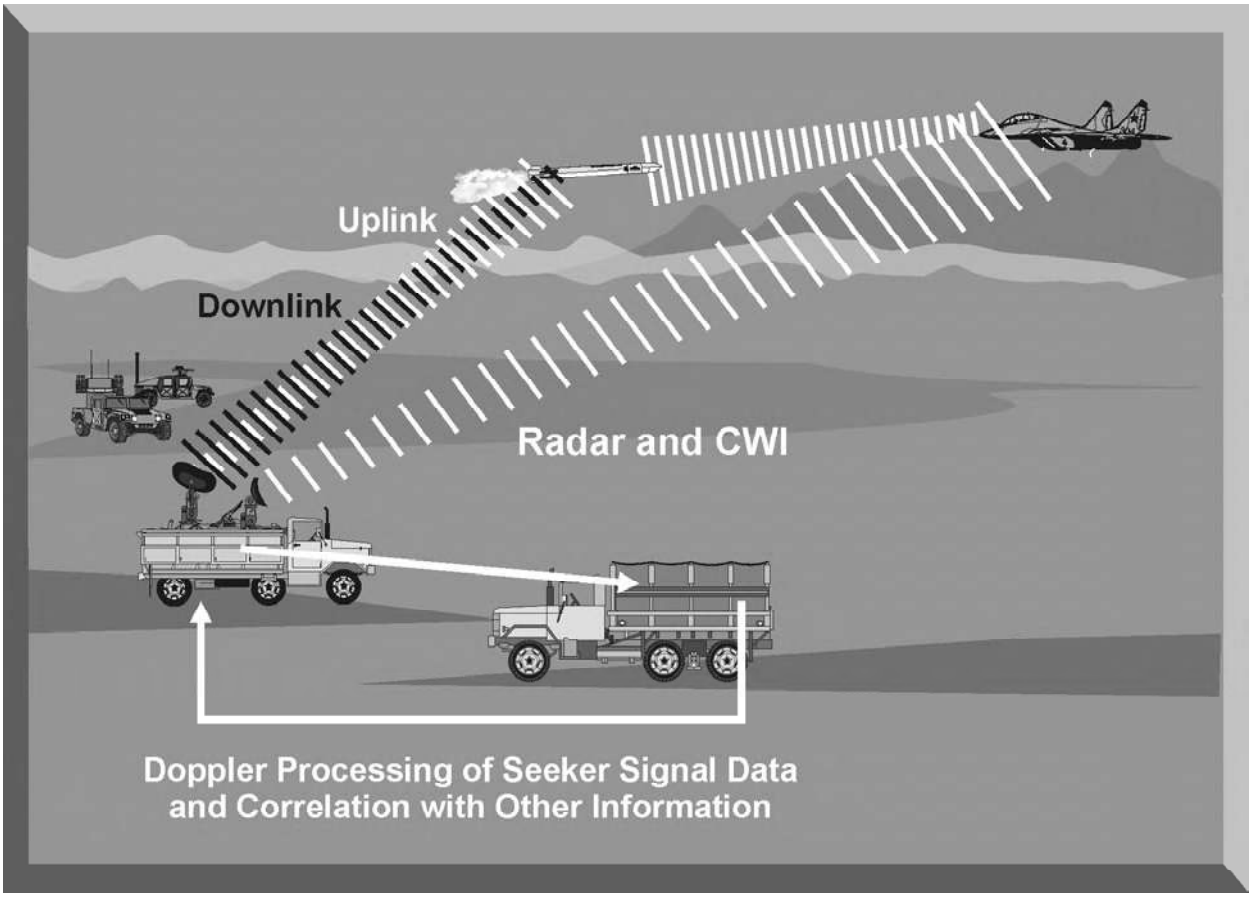

Figure 8-12. SAGG/Track-Via-Missile Guidance

a. Track-via-missile and seeker-aided ground guidance are two relatively new missile guidance techniques with similar advantages. First, they are extremely accurate at long ranges where the inherent radar tracking errors may be large

enough to cause a miss. Second, they can respond very quickly to any actions taken by the target since the missile seeker can track these changes and transmit the new position to the TTR fire control computer. Third, TVM and SAGG can be used with a large and capable fire control computer since most computations are accomplished by the TTR. Fourth, the integration of a phased array radar and the powerful TTR fire control computer allows the missile system to engage multiple targets. The Patriot missile battery, for example, can track and engage at least four targets simultaneously.

b. The major disadvantage of track-via-missile and seeker-aided ground guidance is that they are the most complex forms of missile guidance. They require the use of sophisticated computers to combine radar tracking data and data received from the missile. This required hardware is expensive and demands greater maintenance and logistical support. In addition, the missile itself needs to be large enough to store the appropriate hardware for computations and data transfer.

6. ANTIAIRCRAFT ARTILLERY (AAA)

The classic role of AAA is point defense. AAA systems provide close-in defense for high-value targets. AAA systems are deployed to defend cities, airfields, bridges, industrial centers, lines of communications, command and control centers, infantry/tank units, and SAM sites. There are two types of AAA systems: towed and mobile. Towed AAA is normally deployed in fixed sites around key targets. Mobile AAA systems are deployed to provide air defense for army units and to protect mobile SAM sites. The effectiveness of AAA systems, towed or mobile, depends on the ability of the system to predict an aircraft's future position to fire its unguided ballistic projectile to intercept the aircraft and destroy it. To accomplish this objective, AAA systems employ two primary tactics, aimed fire and sector/barrage fire.

a. Aimed AAA fire requires very accurate aircraft position information and an accurate prediction of future position. For aimed AAA fire, this information can be derived by using an optical sighting system on the gun or by employing a radar system coupled with a fire control computer. Smaller caliber AAA guns generally rely on optical target acquisition and firing (Figure 8-13). The high rate of fire, short range, and short projectile time of flight (TOF) simplifies the prediction and aiming problem for these systems. Smaller caliber AAA can also use tracer ammunition to help the gunner in correcting his optical firing solution. Larger caliber AAA systems, with slow rates of fire, long range, and long projectile TOF, generally use a TTR and a fire control computer to solve the problems associated with aimed fire (Figure 8-14).

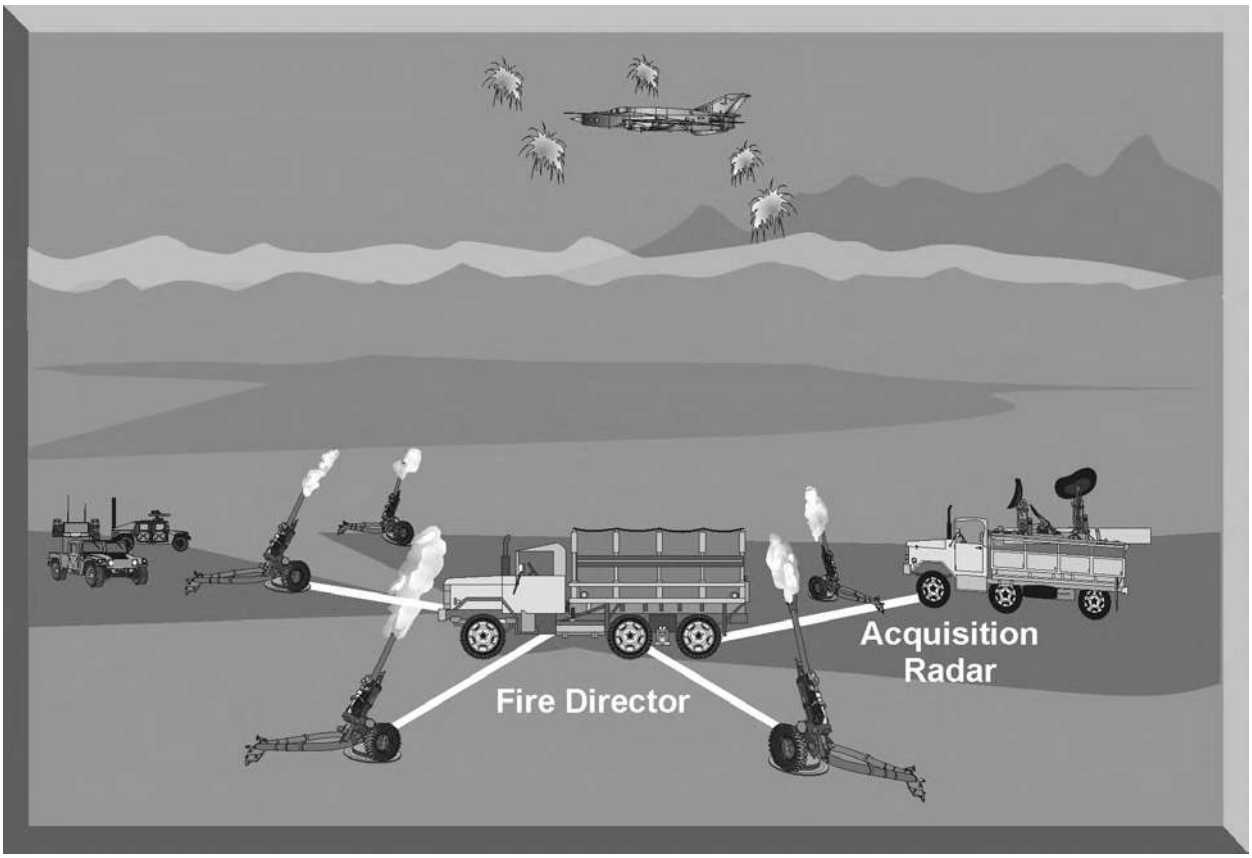

Figure 8-13. Optically Aimed AAA

(1) The typical engagement sequence for an aimed AAA engagement employing a TTR and fire control computer begins with initial target data from an acquisition radar. The guns and TTR are pointed toward the target. The TTR initiates search and lock-on to the target. The TTR associated with large caliber AAA is usually a conical scan radar to provide accurate target positioning information. Target information is fed into the fire control computer which calculates the aim point, points the guns, and initiates firing. The fire control computer uses the target kinematic data, gun ballistics, wind, air density, and projectile dispersion pattern to compute the required aim point. All these computations are based on the assumption that the target will continue on the same heading, at the same altitude, and at the same airspeed during the projectile TOF.

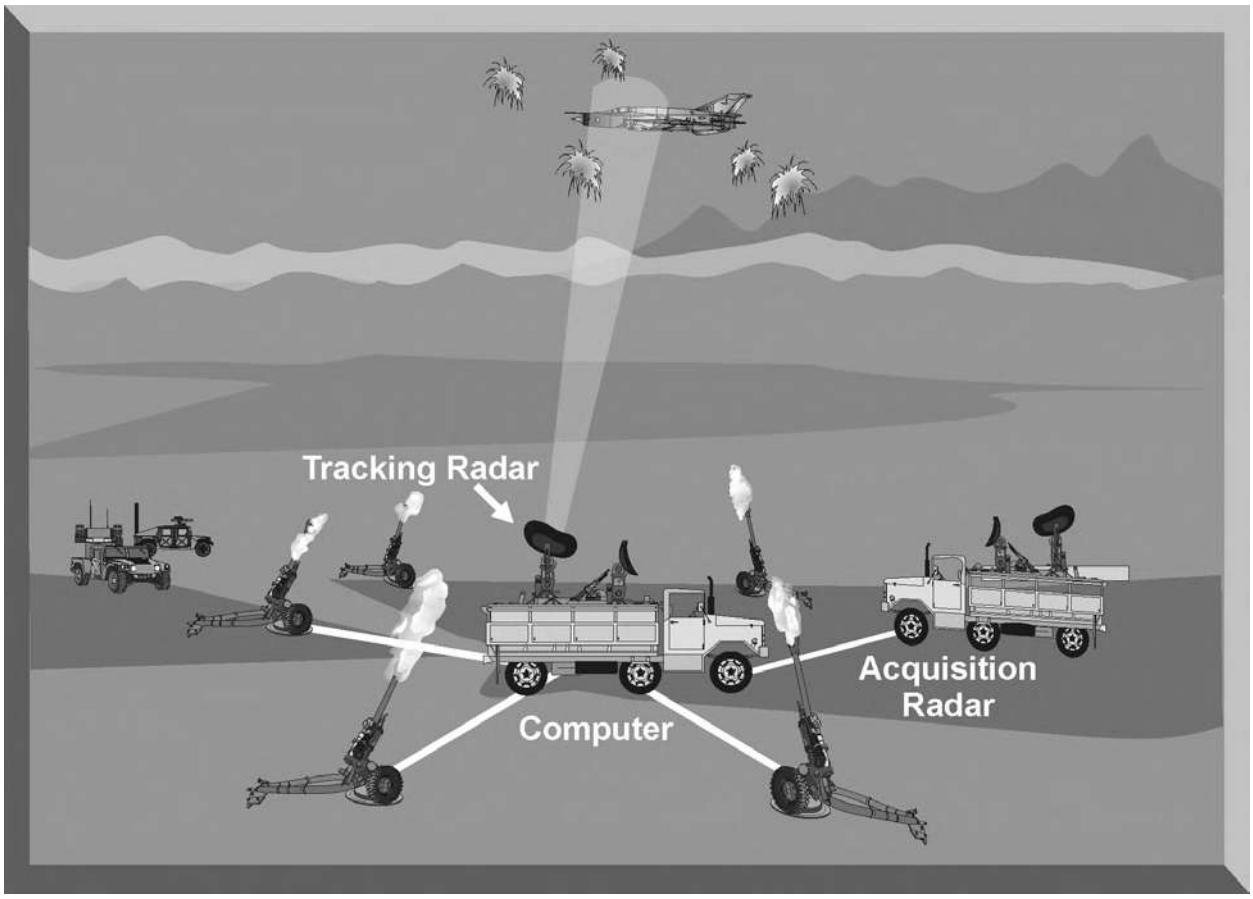

Figure 8-14. Radar-Directed AAA

(2) The typical engagement sequence for an aimed AAA engagement, employing optical target tracking begins with initial target information from an acquisition radar to the fire director. The fire director gives gross aiming commands to the individual guns. The gunners then visually search for the target and use the on-carriage gun sights to predict the required lead angle and initiate firing.

b. Sector or barrage fire tactics are employed when the aircraft cannot be accurately tracked (Figure 8-15). Acquisition information suggests an aircraft will traverse a volume of airspace or a specific sector. The fire director instructs the gunners to fire randomly into this sector in an effort to hit the aircraft with the barrage of AAA fire, or have the aircraft fly into a "curtain" of AAA fire. This tactic is especially effective for point defense for a fixed target. Attacking aircraft may have to fly a predictable flight path during weapons delivery. Sector/barrage fire can be directed to cover the expected attack directions and altitudes.

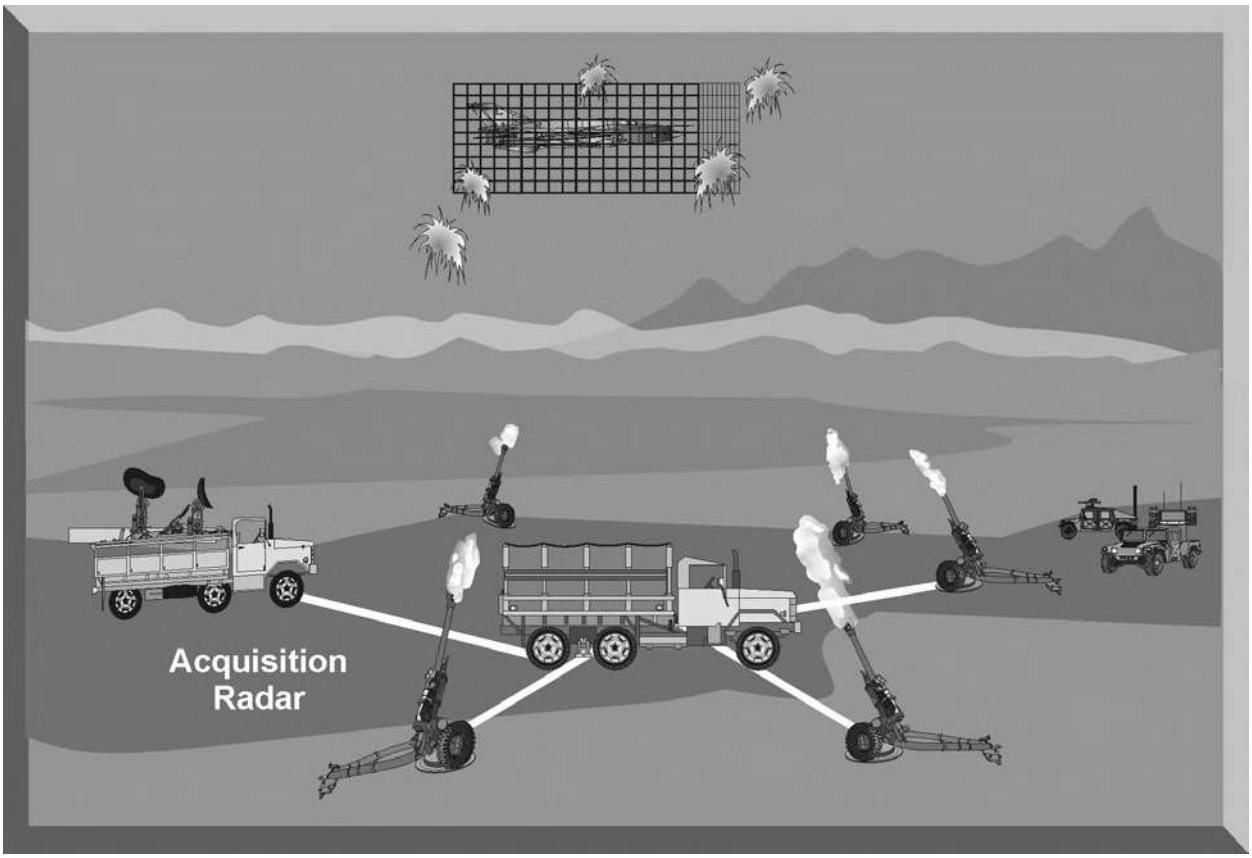

Figure 8-15. Sector/Barrage AAA

7. SUMMARY

This chapter has discussed the most common missile guidance techniques and AAA firing modes used by modern threat systems. A familiarity with the guidance technique employed by specific threat systems is the key to understanding the jamming techniques, chaff/flare employment settings, and tactical maneuvers designed to counter these systems.

CHAPTER 9. INTRODUCTION TO RADAR JAMMING

1. INTRODUCTION

Radar jamming is the intentional radiation or reradiation of radio frequency (RF) signals to interfere with the operation of a radar by saturating its receiver with false targets or false target information. Radar jamming is one principal component of electronic combat (EC). Specifically, it is the electronic attack (EA) component of electronic warfare (EW). Radar jamming is designed to counter the radar systems that play a vital role in support of an enemy integrated air defense system (IADS). The primary purpose of radar jamming is to create confusion and deny critical information to negate the effectiveness of enemy radar systems. This chapter will introduce the two types of radar jamming, the three radar jamming employment options, and discuss the fundamental principles that determine the effectiveness of radar jamming.

2. RADAR JAMMING TYPES

There are two types of radar jamming: noise and deception.

a. Noise jamming is produced by modulating a RF carrier wave with noise, or random amplitude changes, and transmitting that wave at the victim's radar frequency. It relies on high power levels to saturate the radar receiver and deny range and, occasionally, azimuth and elevation information to the victim radar (Figure 9-1). Noise jamming takes advantage of the extreme sensitivity of the radar receiver and the transmission pattern of the radar antenna to deny critical information to the victim radar.

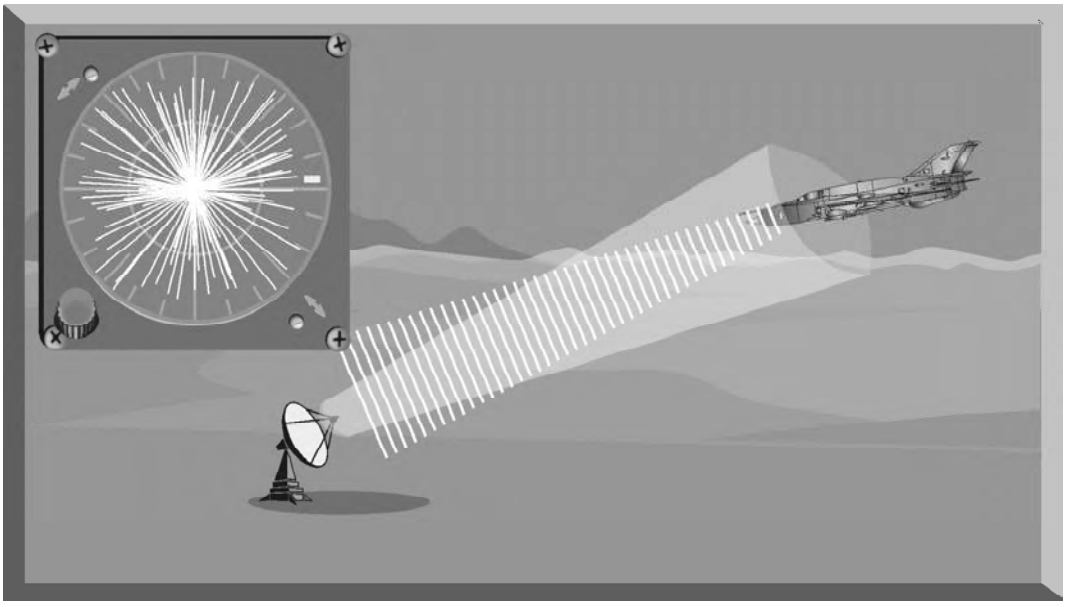

Figure 9-1. Noise Jamming

b. Deception jamming uses complex receiving and transmitting circuits to process and retransmit jamming pulses that appear as a real target to the victim radar. A deception jammer receives the signal from the victim radar and alters the signal to provide false range, azimuth, or velocity information. The altered signal is then retransmitted (Figure 9-2). The victim radar processes this signal, which disrupts the victim radar and confuses the radar operator. To be effective, deception jamming must match not only the victim radar's operating frequency, but all the other operating characteristics, including pulse repetition frequency (PRF), pulse repetition interval (PRI), pulse width, and scan rate.

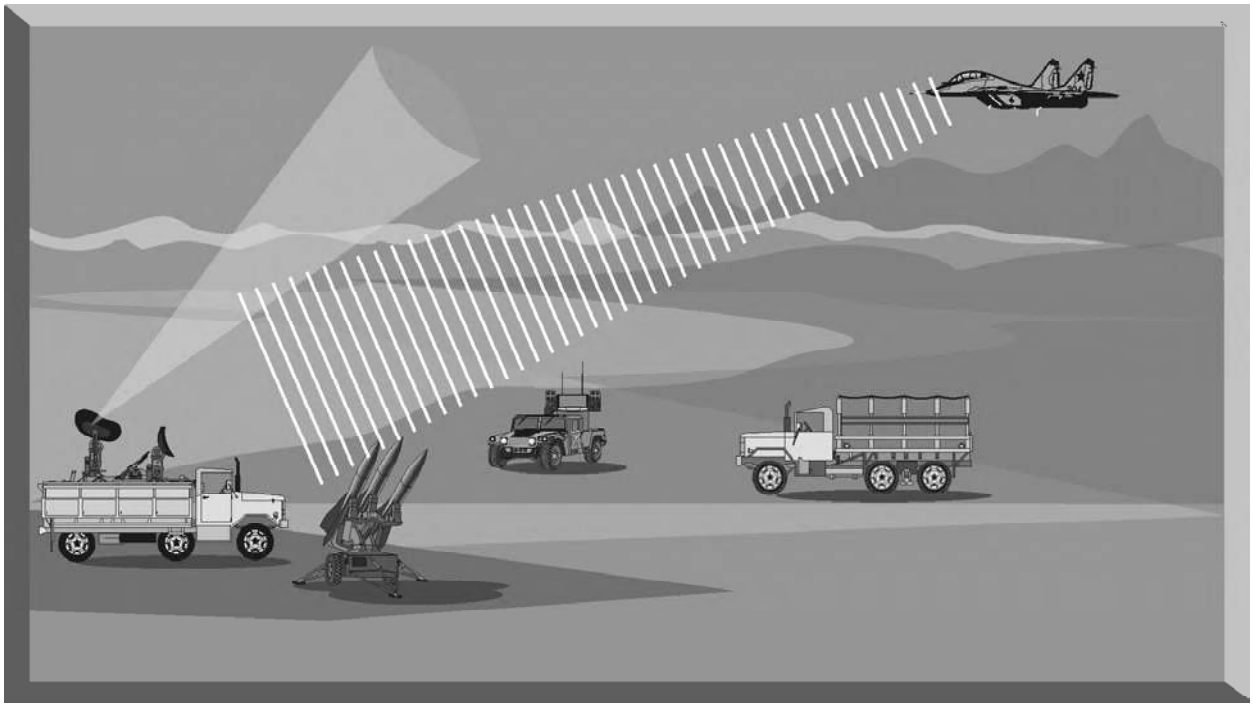

Figure 9-2. Deception Jamming

c. Both noise and deception jamming effectiveness are heavily dependent on another component of EW, specifically, electronic warfare support (ES). ES assets, either airborne or ground-based, provide the threat system specific radar parametric data and update this critical information based on observed threat system operations. This data provides the foundation for developing noise and deception jamming techniques. Intelligence and engineering assessment of this data are used to identify specific threat system weaknesses that can be exploited with the optimum noise, deception, or combination of jamming techniques. This information is then programmed into jamming systems to counter specific threats.

3. RADAR JAMMING EMPLOYMENT OPTIONS

There are currently two primary employment options for both noise and deception jamming techniques. These options are: (1) support jamming, and (2) self-protection jamming. Support jamming can be broken down further into stand-off jamming (SOJ), and escort jamming.

a. To counter early warning, ground control intercept (GCI), and acquisition radars associated with an enemy IADS, noise and deception jamming techniques are employed by specialized support jamming aircraft. The goal of support jamming is to create confusion and delays within the command and control structure of the IADS. Deny, delay or degrade the enemy's ability to engage friendly forces. Support jamming operations can be focused against a national level IADS through the use of a stand-off jamming (SOJ) profile (Figure 9-3) or against a target area threat array using an escort jamming profile.

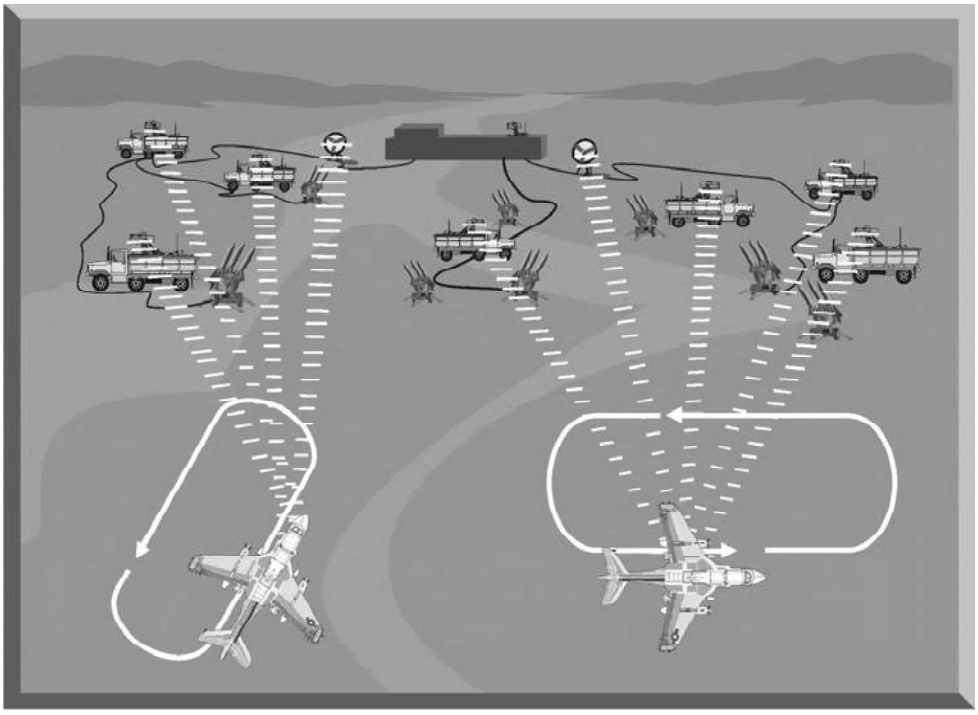

Figure 9-3. Stand-Off Jamming

(1) From an orbit area outside the surface-to-air missile (SAM) engagement zone, SOJ aircraft employ specialized jamming techniques to deny the enemy information about the attack package. SOJ aircraft employ specialized noise jamming techniques to generate jamming strobes on the victim radar display. This effectively denies range and azimuth information on aircraft ingressing and egressing the area covered by the noise jamming strobes. Intensity of the strobes is based on the power in the jamming. The area covered is based on the amount of jamming that can be injected into the main beam and sidelobes of the victim

radar. The effectiveness of SOJ noise jamming is determined by the power the jammer can generate relative to the power the victim radar can generate. This is called the jamming-to-signal (J/S) ratio.

(2) SOJ aircraft can also employ a deception technique to generate false targets to confuse the radar operator and mask the presence of real targets (Figure 9-4). In this specialized technique, the deception jammer must tune to the frequency, PRF, and scan rate of the victim radar. The jammer then transmits multiple jamming pulses that the victim radar receiver processes like real target returns. With enough power, the deception jammer can generate multiple false azimuth targets by injecting jamming pulses into the sidelobes of the victim radar. False moving targets and false range targets are generated by varying the time delay of the jamming pulses based on the PRF and scan rate of the victim radar.

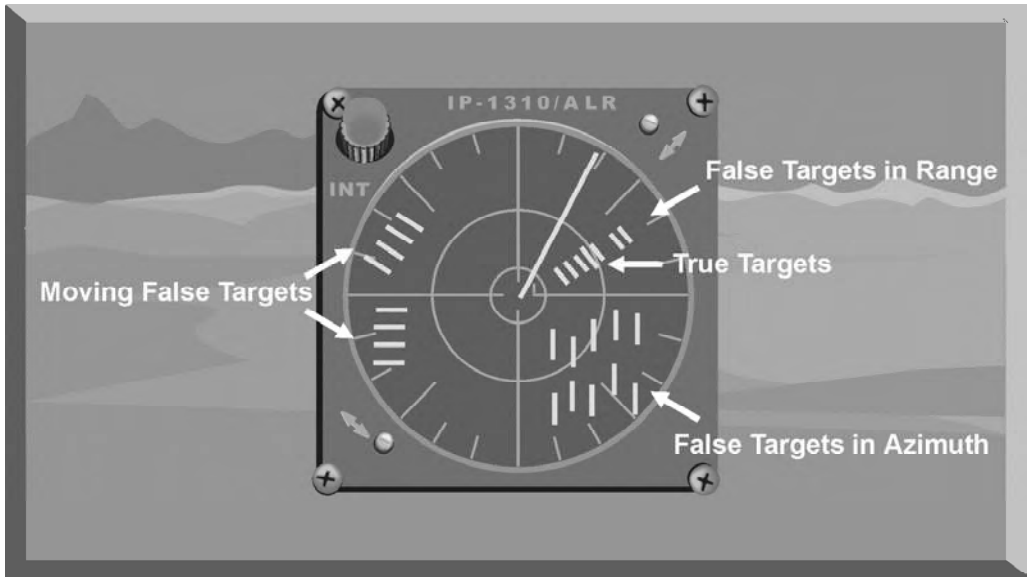

Figure 9-4. False Target Jamming

(3) Escort jamming is a specific tactic used by the EA-6B Prowler. The EA-6B is employed as an integral part of the attack package and is normally positioned behind and above the attack package (Figure 9-5).

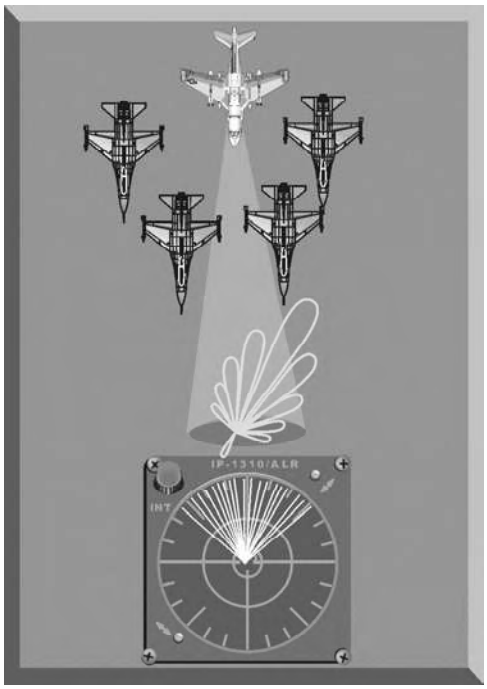

Figure 9-5. Escort Jamming

Using noise jamming, the EA-6B attempts to deny range and azimuth information to the victim radar by injecting high power signals into the main radar beam and sidelobes. To be effective, the EA-6B must be properly positioned in relation to the ingressing or egressing attack package (Figure 9-6).

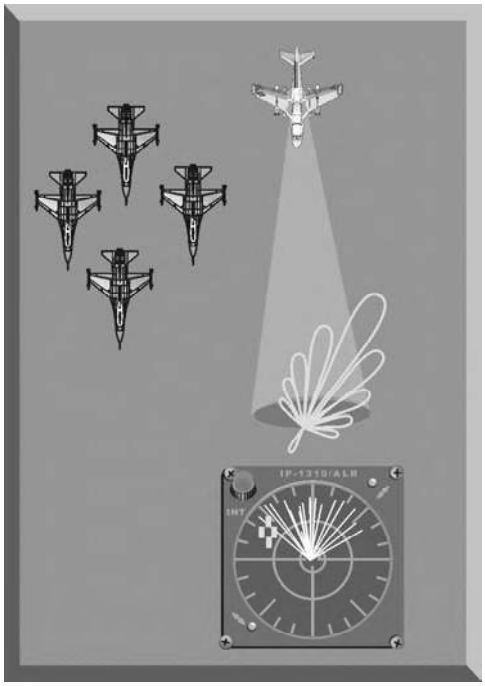

Figure 9-6. Escort Jamming Alignment

b. Self-protection radar jamming targets the radar systems that support jamming cannot negate. Self-protection jamming systems are part of a self-protection suite that includes a self-protection jamming pod, a chaff/flare dispenser, and on some aircraft, a towed decoy system. The overall purpose of these systems is individual aircraft survivability. These systems are designed to counter the individual SAM, AAA, and AI assets associated with the enemy IADS. They employ deception jamming techniques against the target tracking radars (TTRs) associated with these threats. They are designed to break the radar track or generate sufficient tracking errors to cause the missile or bullet to miss the aircraft.

(1) Self-protection radar jamming systems usually employ deception jamming techniques based on several factors. First, effective deception jamming techniques generally require less power than noise jamming techniques. Second, less power means less weight and space, which are very important considerations for modern tactical aircraft. Finally, deception jammers can be designed to jam multiple threats, which is a critical requirement for operations in a dense threat environment (Figure 9-7).

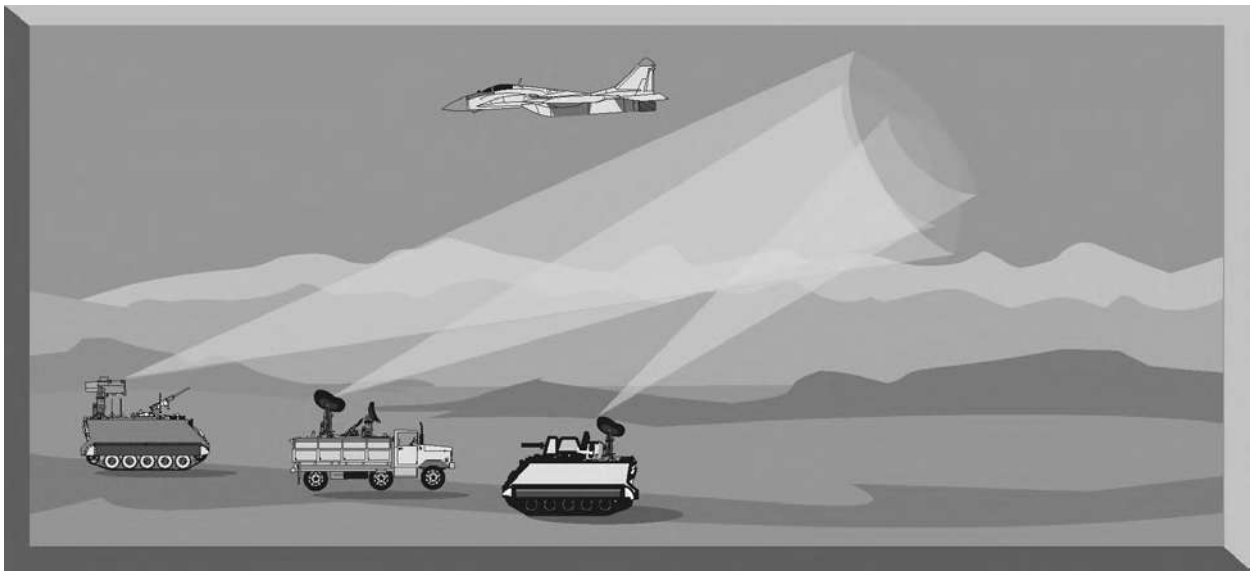

Figure 9-7. Self-Protection Jamming

(2) Despite the advantages of deception jamming techniques for self-protection jamming, there are some limitations that must be considered. First, deception jammers are complex electronic systems that must receive a victim radar's signal, memorize all its characteristics, modify the signal, and retransmit this modified signal at a high power level. Second, to be effective, deception jammers must be programmed with all the signal parameters (frequency, PRF, PRI, pulse width, scan rate, etc.) of the victim radar. Finally, because many deception techniques can be effective against specific threats, selecting optimum techniques to employ against these threats must be based on identified threat

system limitations. Identifying these specific threat systems limitations may be difficult.

4. FUNDAMENTALS OF RADAR JAMMING

There are some fundamental principles that apply to all types of jamming and to all jamming employment options. These principles are based on the characteristics of the jamming system and the characteristics of the victim radar. They include frequency matching, continuous interference, signal-to-noise ratio, jamming-to-signal ratio, and burnthrough range.

a. Based on the data provided by ES systems and intelligence evaluations, radar jamming systems must transmit signals at the frequency of the victim radar This applies to both noise and deception jamming. If a jamming signal does not match the transmitter frequency, the jamming signal is not received and displayed on the scope (Figure 9-8). When a jamming signal matches the transmitter frequency, the jamming signal is received and masks the target display (Figure 9-9).

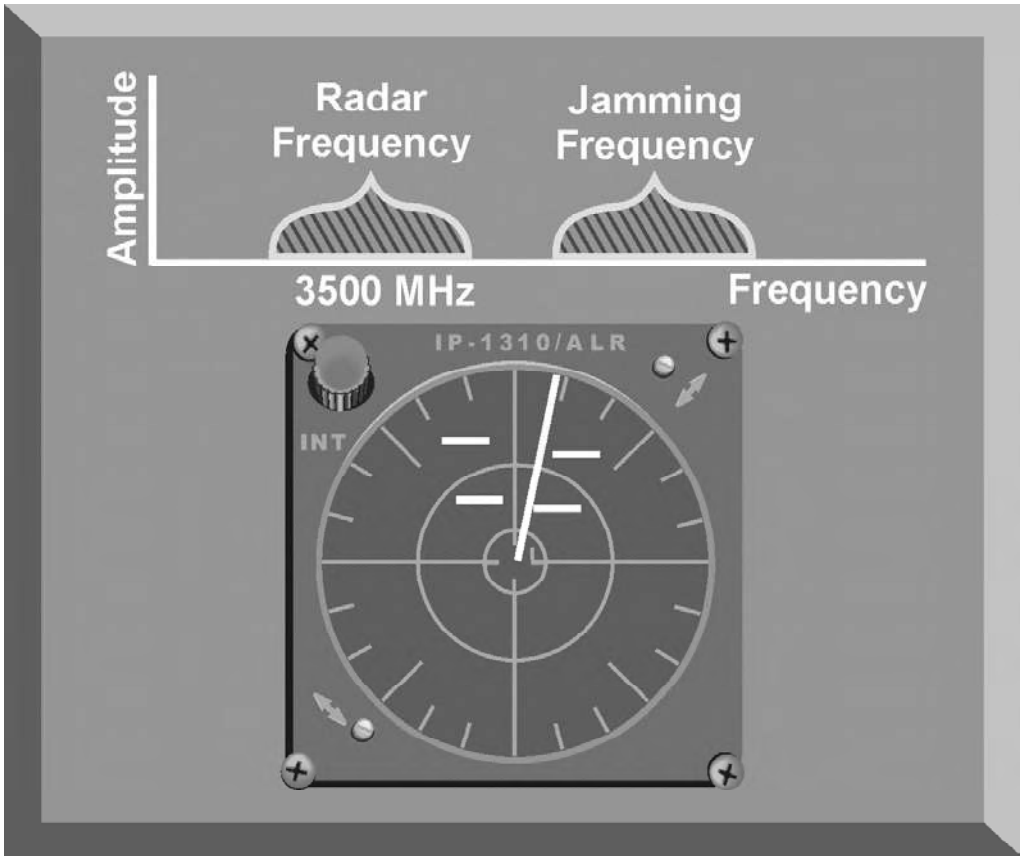

Figure 9-8. Jamming Frequency Error

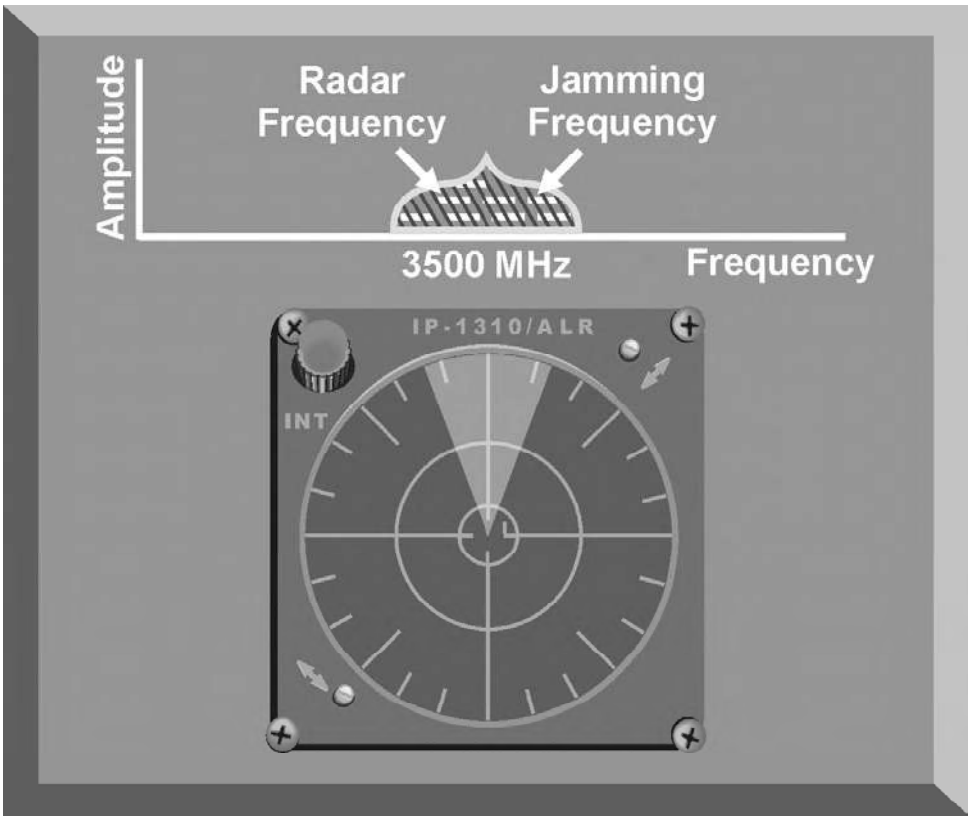

Figure 9-9. Correct Jamming Frequency Matching

b. For maximum effectiveness, a jamming transmitter should produce continuous interference. In much the same way intermittent static on a radio receiver does not completely block out a signal, intermittent jamming on a radar scope may not completely mask the target. An experienced radar operator or advanced automatic tracker can "read through" intermittent jamming and derive sufficient target information to negate jamming effectiveness. While true for noise jamming techniques, continuous interference also applies to deception techniques, especially when target reacquisition is considered.

c. The signal-to-noise (S/N) ratio is a measure of the ability of the victim radar to detect targets. It is also an indication of the vulnerability of the radar to certain jamming techniques, especially noise jamming.

(1) From the discussion of the basic radar equation in Chapter 5 (Equation 5-10), Equation 9-1 is the signal power density of a target return at the radar receiver. The signal power density of the target return is so weak that it requires very strong amplification before processing and display. Besides the signal power from the target, some level of thermal noise is also generated and amplified along with the target signal. For an "ideal" (no noise) amplifier, Equation 9-2 is used to compute the level of thermal noise generated by the amplifier.

$$\text{Signal Power Density} = \frac{P_T G \sigma A_e}{(4\pi)^2 R^4}$$

P_T = transmitted power
G = antenna gain
σ = target radar cross section (RCS)
A_e = antenna aperture area
R = range to the target

Equation 9-1. Signal Power Density

$$\text{Thermal Noise (N)} = KTBF$$

K = Boltzman's Constant
(1.38 x 10^{-23} watts/Hz degrees K)
T = standard temperature (290° K)
B = radar receiver equivalent bandwidth
F = radar receiver noise figure
(one for "ideal" receiver)

Equation 9-2. Thermal Noise

Note: The instantaneous bandwidth of a receiver is the frequency range over which the receiver can simultaneously amplify two or more signals to within a specified gain.

(2) The radar receiver amplifies both target signal and thermal noise. The output of the radar receiver will contain the target signal and the noise amplified across the bandwidth of the receiver. Separating the desired target signal from the undesired noise signal is one of the major problems confronting radar designers.

(3) Equation 9-3 is derived by dividing Equation 9-1 by Equation 9-2. Many factors in this equation fluctuate and must be estimated using statistical calculations. For example, target RCS fluctuates based on the changing angle of the antenna beam and corresponding changes in the reflected signal. Effective antenna aperture is also a statistical phenomenon based on the fluctuations in target RCS. The thermal noise generated by a receiver is also a fluctuating factor and must be treated statistically. This means that the S/N ratio is a statistical factor associated with a probability of target detection and a probability of a false alarm. A false alarm occurs when the radar operator or automatic tracking circuit designates a fluctuation in noise level as a target. The higher the S/N ratio, the

higher the probability of target detection with a corresponding reduction in the probability of a false alarm.

$$\text{Signal-to-Noise Ratio} = \frac{P_T G \sigma A_e \left(\frac{1}{(4\pi)^2 R^4} \right)}{KTBF}$$

P_T = transmitted power
G = antenna gain
σ = target radar cross section (RCS)
A_e = antenna aperture area
R = range to the target

K = Boltzman's Constant (1.38×10^{-23} watts/Hz degrees K)
T = standard temperature (290° K)
B = radar receiver equivalent bandwidth
F = radar receiver noise figure (one for "ideal" receiver)

Equation 9-3. Signal-to-Noise Ratio

(4) An analysis of Equation 9-3 suggests that any action that increases the power in the target signal (for example, increasing transmitted power, increasing antenna gain/aperture area, or decreasing target range) will improve the S/N ratio and improve the probability of target detection. It would also appear that decreasing the bandwidth of the radar receiver will increase the S/N ratio and enhance the probability of target detection. However, if the effective bandwidth of the receiver is reduced, this may eliminate a significant portion of the radar signal spectrum and decrease the probability of target detection.

(5) The S/N ratio is also an indication of the range at which a target will be detected. A plot of the receiver output of a typical radar is shown in Figure 9-10. The weak target signal at an extended range is just above the receiver noise level. The target at closer range is easily detected above the noise level. A radar operator or automatic target detector could mistake the very weak target return as a fluctuation in the receiver noise level. This could result in a missed detection. The lack of discrimination between noise and target returns because of a poor S/N ratio can also result in designating fluctuations in the noise level as actual target signals, known as false alarms.

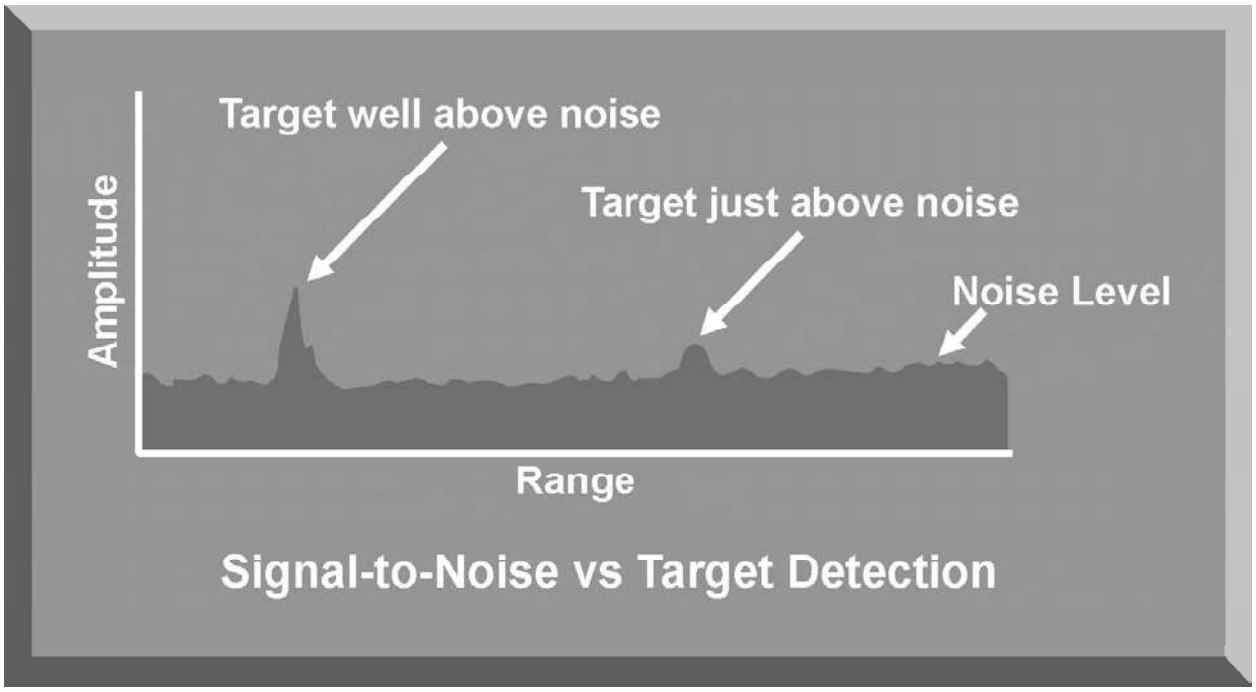

Figure 9-10. S/N Ratio and Target Detection

(6) To preclude, or minimize false alarms, the radar receiver may be equipped with electronic circuits to establish a false alarm threshold. If the signal strength of a radar return is below this threshold level, it will not be detected or displayed (Figure 9-11). This false alarm threshold also influences the probability of target detection. With the threshold set too high, many detected targets will not be displayed. Additionally, if the false alarm threshold is raised automatically in relation to the amplitude of the receiver noise, the radar receiver is more vulnerable to noise jamming.

Figure 9-11. Receiver False Alarm Threshold

(7) For any target return to be detected by the radar, the S/N ratio must be greater than one. If the S/N ratio is less than one, the target will not be detected above the receiver noise level. The purpose of noise jamming is to raise the level of noise in the radar receiver to reduce the S/N ratio to less than one. This masks the presence of the true target return. If a false alarm threshold is used, noise jamming raises this threshold to further complicate target detection. Figure 9-12 depicts a S/N ratio greater than one. Figure 9-13 depicts a S/N ratio of less than one due to noise jamming.

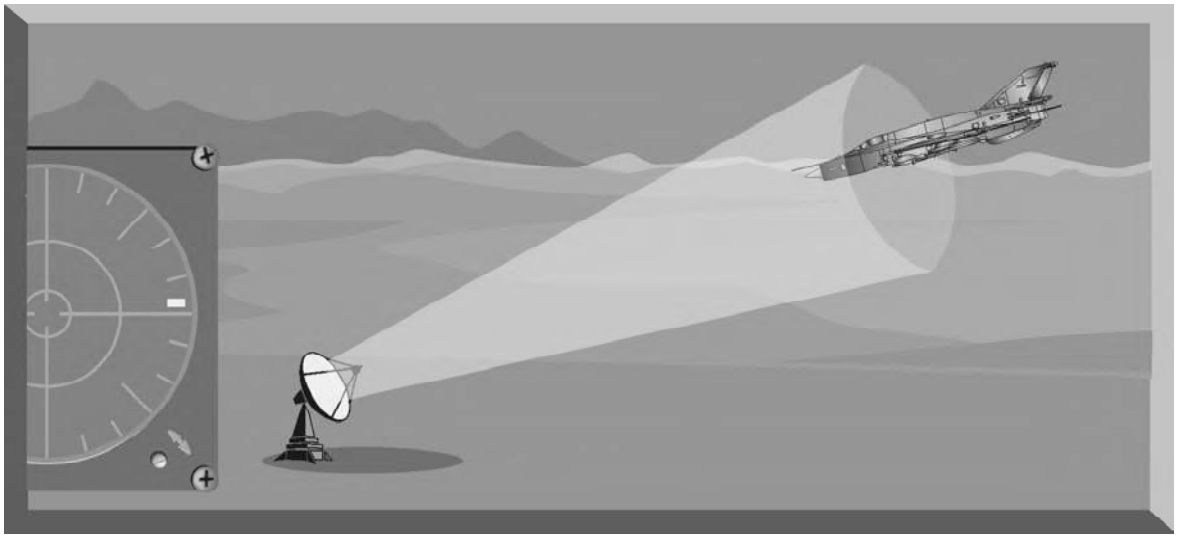

Figure 9-12. S/N Ratio Greater Than One

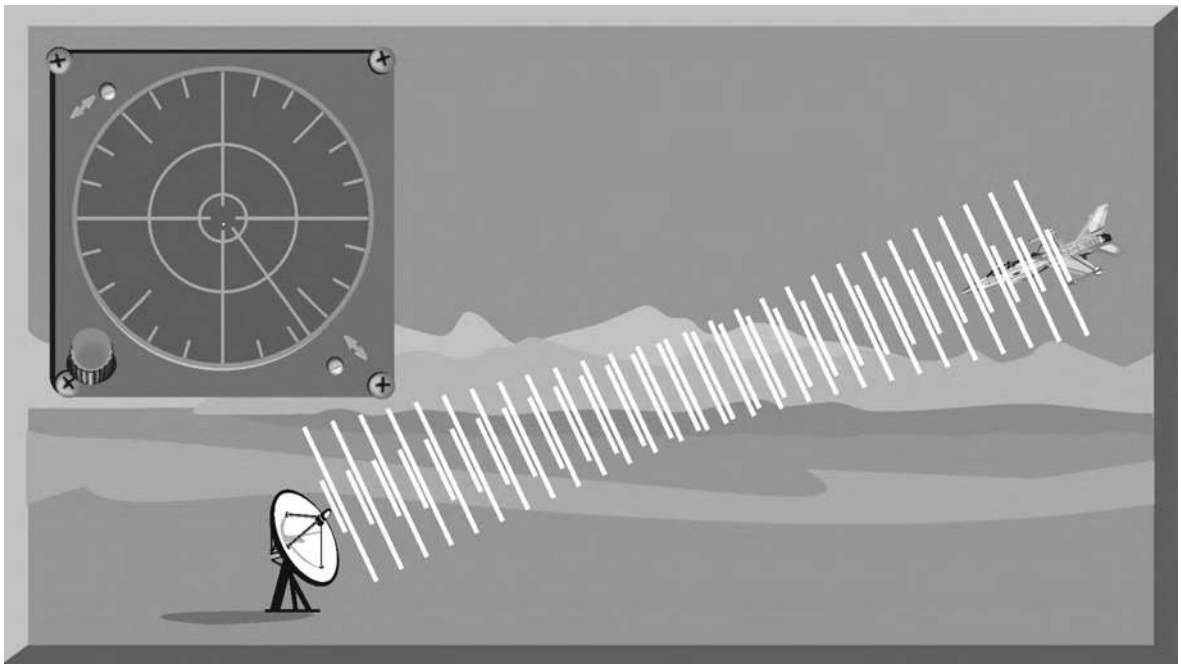

Figure 9-13. S/N Ratio Less Than One

d. The jamming-to-signal (J/S) ratio is a fundamental measure of jamming effectiveness. The J/S ratio compares the power in the jamming signal with the power in the radar return. Equation 9-4 is an expression of the J/S ratio. It is important to note that the J/S ratio should be measured at the output of the radar receiver. This will allow consideration of the receiver signal processing gain applied to the jamming signal.

$$\text{Jamming-to-Signal Ratio} = \frac{P_J G_J}{P_T G_T} \times \frac{4\pi R^2}{\sigma}$$

P_J = jamming power transmitted
G_J = jamming antenna gain
P_T = peak power transmitted by the radar
G_T = radar antenna gain
R = range from jammer to radar
σ = aircraft RCS

Equation 9-4. Jamming-to-Signal Ratio

(1) The most critical factor in both the S/N and the J/S ratios is range. The S/N ratio is calculated based on R to the fourth power. This equates to a signal traveling from the radar to the target, and back to the radar receiver. The J/S ratio is calculated using R to the second power. This factor reflects the "one way" transmission of the jamming pulse from the jammer to the victim radar's receiver.

(2) For a jamming signal to be effective, the J/S ratio must be greater than one. In general, threat radars, especially ground-based radars, transmit much more power than does an airborne jamming system. However, this power must travel twice as far as the airborne jamming signal. At long ranges, a low power jamming system can generate a J/S ratio much greater than one. In Figure 9-14, the jamming pulse completely masks the target return. As the jamming system approaches the target, the distance the radar pulse travels decreases with a corresponding increase of power in the radar return. This reduces the J/S ratio to a value less than one and the radar "sees" the target. This is called the burnthrough range (Figure 9-15).

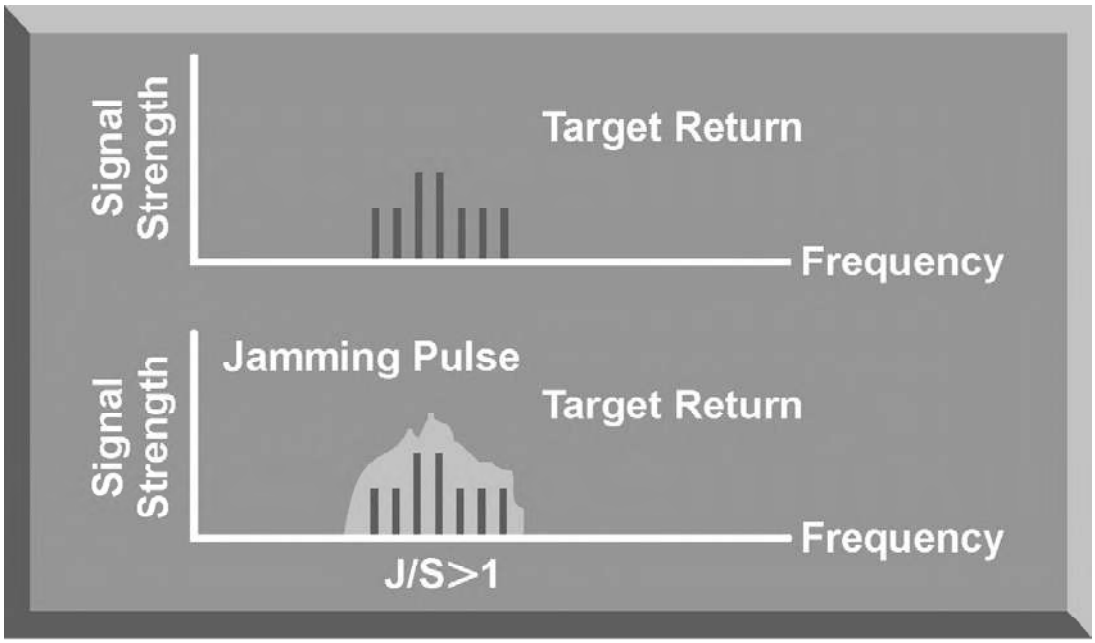

Figure 9-14. J/S Ratio Greater Than One

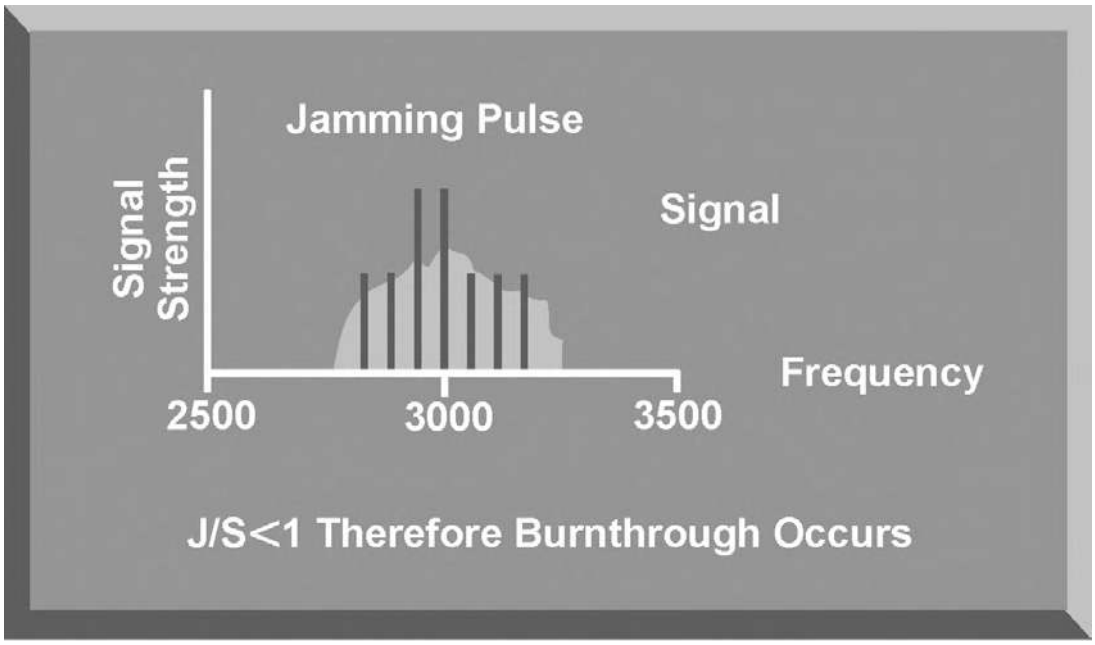

Figure 9-15. J/S Ratio Less Than One

e. Burnthrough occurs when the power in the reflected target signal exceeds the power in the jamming signal. Even when an optimum and continuous jamming technique is transmitting on the exact frequency of the victim radar, the jamming starts to lose effectiveness as it nears the radar. For a particular radar

jamming technique, burnthrough range depends on the detection capability of the victim radar, expressed as the S/N ratio, and the capability of the aircraft's jamming system, expressed as the J/S ratio. The idea of burnthrough range explains why a jamming technique, especially noise jamming, loses its effectiveness as the aircraft approaches the radar. When plotting the jamming and signal power versus range (Figure 9-16), these two values intersect at the point where the J/S ratio is one. At closer ranges, the jamming pulse is no longer masking the aircraft, and the aircraft can be detected. Burnthrough range is the point where the radar can see through the jamming.

Figure 9-16. Burnthrough Range

5. SUMMARY

The purpose of radar jamming is to confuse or deny critical data to the radar systems that play a vital role in supporting the mission of an integrated air defense system. Two types of radar jamming, noise and deception, can be employed in a support-jamming role, or in a self-protection role for individual aircraft. The effectiveness of a jamming technique depends on the ability of the jamming system to generate a jamming signal that replicates the parameters of the victim radar, especially its frequency. The signal-to-noise ratio of the victim radar determines the vulnerability of the radar receiver to jamming while the jamming-to-signal ratio is an indication of the ability of the jamming system to effectively jam the victim radar. These basic radar jamming concepts are fundamental to understanding the impact of specific jamming techniques on radar systems.

CHAPTER 10. RADAR NOISE JAMMING

1. INTRODUCTION

A radar noise jamming system is designed to generate a disturbance in a radar receiver to delay or deny target detection. Since thermal noise is always present in the radar receiver, noise jamming attempts to mask the presence of targets by substantially adding to this noise level. Radar noise jamming can be employed by support jamming assets or as a self-protection jamming technique. Radar noise jamming usually employs high-power jamming signals tuned to the frequency of the victim radar. This chapter will discuss the factors that determine the effectiveness of radar noise jamming, radar noise jamming generation, and the most common noise jamming techniques. These noise jamming techniques include barrage, spot, swept spot, cover pulse, and modulated noise jamming.

2. RADAR NOISE JAMMING EFFECTIVENESS

The effectiveness of radar noise jamming depends on numerous factors. These factors include the jamming-to-signal (J/S) ratio, power density, the quality of the noise signal, and the polarization of the transmitted jamming signal (Figure 10-1).

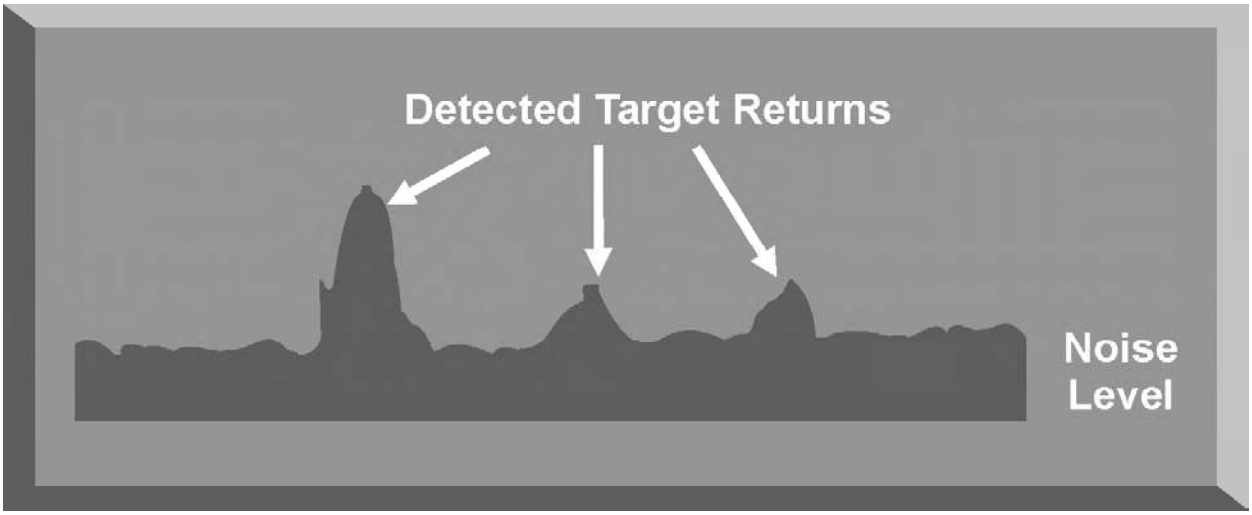

Figure 10-1. Noise Level in a Typical Radar Receiver Output

a. One of the most important factors that impacts the effectiveness of radar noise jamming is the J/S ratio (Figure 10-2). As discussed in Chapter 9, the power output of the noise jammer must be greater than the power in the target return, as measured at the output of the radar receiver. To achieve this level of jamming power, radar noise jammers usually generate high-power jamming signals. These high-power jamming signals can be introduced into the victim radar's main beam

to deny range information and into the victim radar's sidelobes to deny azimuth information.

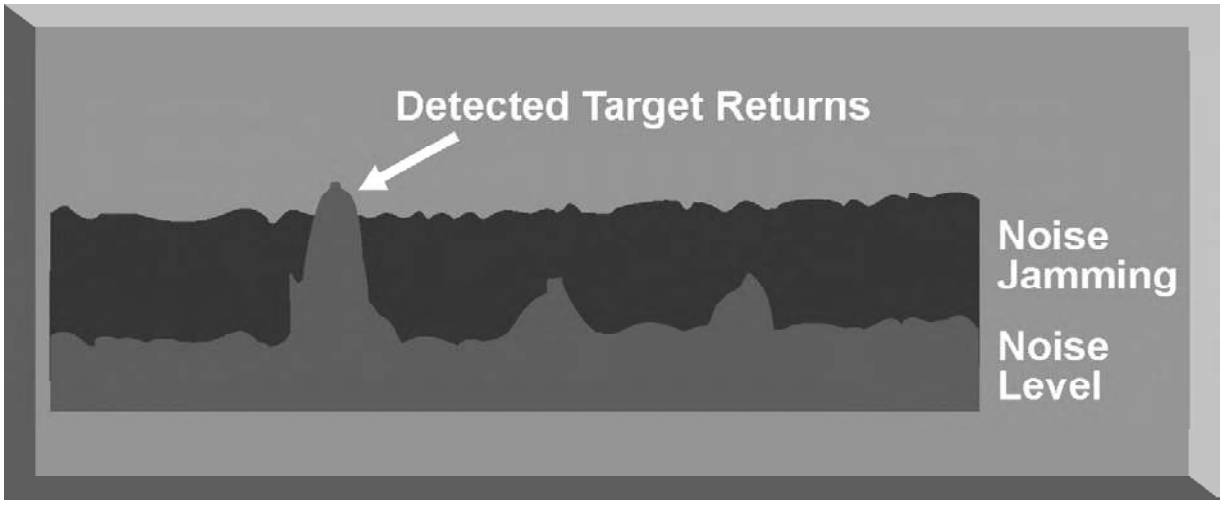

Figure 10-2. Impact of Noise Jamming

b. Another factor which impacts the effectiveness of radar noise jamming is the power density. The power density of the noise jamming signal has a direct relation to the J/S ratio.

(1) If the noise jamming signal is centered on the frequency and bandwidth of the victim radar, the jamming signal has a high power density. The ability of a noise jammer to concentrate the jamming signal depends on the ability of the jammer to identify the exact frequency and bandwidth of the victim radar (Figure 10-3).

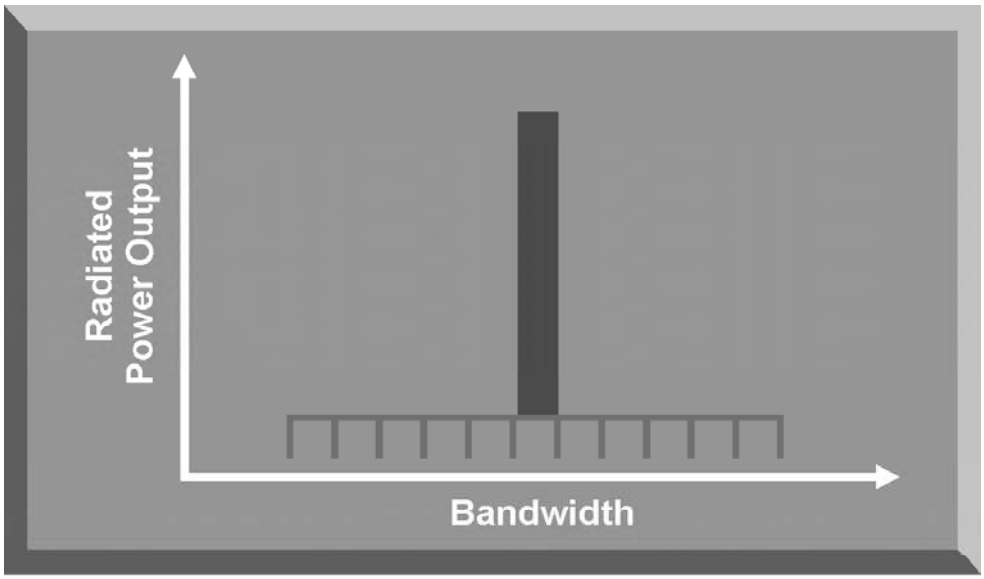

Figure 10-3. Power Density – Narrow Bandwidth

(2) If the generated noise jamming signal has to cover a wide bandwidth or frequency range, the power density at any one frequency is reduced (Figure 10-4). Radar systems that are frequency agile or that employ a wide bandwidth can reduce, or negate, the effectiveness of noise jamming by reducing the power density of the jamming signal.

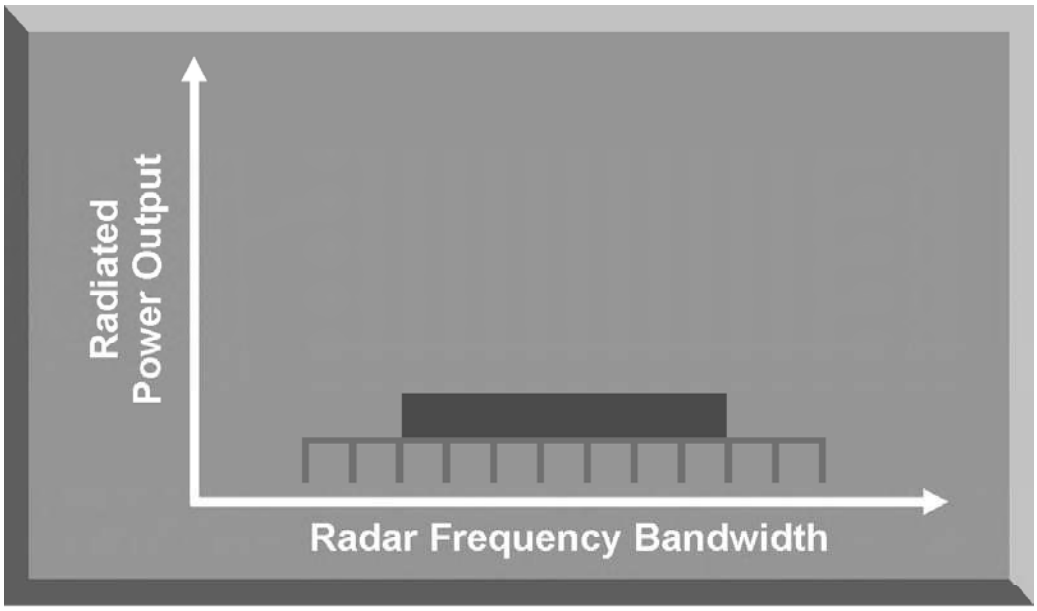

Figure 10-4. Power Density – Wide Bandwidth

c. The quality of the noise jamming also determines its effectiveness. To effectively jam a radar receiver with noise, the jamming signal must emulate the thermal noise generated by the receiver. This ensures that the radar operator or automatic detection circuit cannot distinguish between the noise jamming and normal thermal noise. Thermal noise is referred to as white noise and has a uniform spectrum. All of the frequencies in the bandwidth of the receiver have the same spectrum and an amplitude that varies based on Gaussian distribution. A Gaussian distribution is simply a bell-shaped distribution of amplitudes. In order to be effective, the jamming signal should exactly match the characteristics of the thermal noise signal of the victim radar receiver.

d. Polarization of the noise jamming signal is another significant factor that impacts its effectiveness. As discussed in Chapter 2, if the polarization of the jamming signal does not match the antenna polarization of the victim radar, there is a significant power loss in the jamming signal. Noise jamming systems designed to counter multiple threat radars, with various polarizations, generally use a transmitting antenna with a 45° slant or use circular polarization. Most threat systems are horizontally or vertically polarized. This results in a 50% reduction in effective radiated power (ERP) for most threat systems. A more serious power loss, nearly 100%, in ERP occurs when the jamming antenna is

orthogonally polarized with the victim antenna. The polarization of the noise jamming signal impacts the J/S ratio and the power density.

3. RADAR NOISE JAMMING GENERATION

Noise jamming is produced by modulating an RF carrier wave with random amplitude or frequency changes, called noise, and retransmitting that wave at the victim radar's frequency. Since noise from numerous sources is always present and displayed on a radar scope, noise jamming adds to the problem of target detection. Reflected radar pulses from target aircraft are extremely weak. To detect these pulses, a radar receiver must be very sensitive and be able to amplify the weak target returns. Noise jamming takes advantage of this radar characteristic to delay or deny target detection.

a. The simplest method of generating a high-power Gaussian noise jamming signal is to employ a highly amplified diode to generate a noise signal at the frequency of the victim radar. This signal is filtered and directly amplified to the maximum power that can be generated by the transmitter. This method is called direct noise amplification (DINA). The DINA method of noise generation has a serious limitation. The maximum power available from linear wideband power amplification is extremely limited. Employing any other form of power amplification would alter the Gaussian distribution of the jamming signal. This method of generating radar noise jamming was used extensively during WW II.

b. Modern noise jamming systems generate noise jamming signals by frequency modulating a carrier wave at the frequency of the victim radar. FM noise jammers employ a receiving antenna to intercept the victim's radar signal. The antenna passes the victim radar signal to the receiver for identification. The receiver also tunes the jamming signal generator to the correct frequency. The receiver uses an automatic frequency control (AFC) circuit to tune the voltage-controlled oscillator (VCO) to the frequency of the victim radar. A noise signal is generated by the jamming signal generator and added to the tuning voltage of the VCO to get an FM jamming signal. This signal is sent to a traveling wave tube (TWT) power transmitter. The TWT is normally operated in a saturated mode which produces a high-power jamming signal that covers a wider bandwidth than the victim radar. This reduces the power density of the signal, but the high power levels available from the TWT amplification of an FM signal compensate for this loss. The signal is sent to the transmitting antenna and directed toward the victim radar.

c. Figure 10-5 highlights an important feature of a modern radar noise jamming system: a look-through capability. A look-through mode allows the receiver to periodically sample the signal environment. The objective of the look-through mode is to allow the jammer to update victim radar parameters and change the jamming signal to respond to changes in the signal environment. This greatly enhances the effectiveness of noise jamming systems. One method used to provide a look-through capability is to isolate the transmit and receive

antennas to allow continuous operation of the receiver to update signal parameters. Another method is to switch off the jammer for a brief period to allow the receiver to sample the signal environment. Since this latter look-through method eliminates the jamming signal, the amount of time the jammer is switched off must be kept to a minimum.

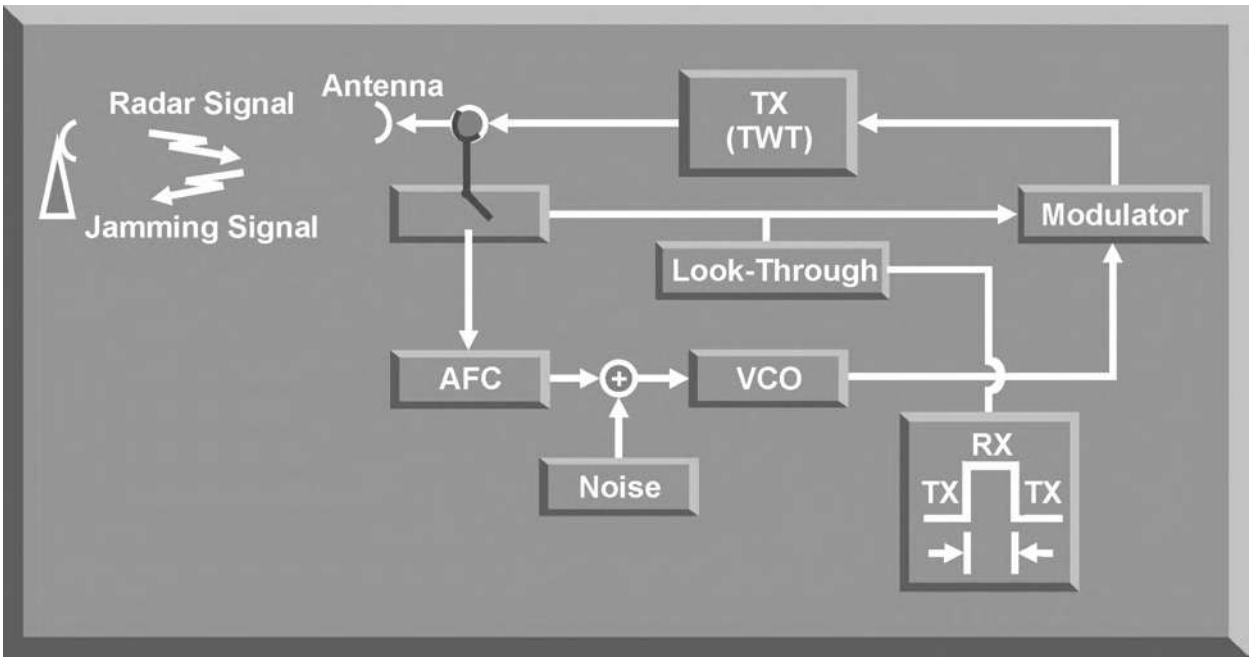

Figure 10-5. Frequency Modulated (FM) Noise Jamming System

4. BARRAGE JAMMING

An important aspect of jamming power is power density. Noise jamming depends on power density for its effectiveness. Power density is a function of the frequency range, or bandwidth, of the jamming signal. If a jammer covers a narrow frequency range, it can concentrate energy in a narrow band. If a jammer covers a wide frequency range, the energy is spread over that entire range. Since the jammer has fixed radiated power, this lowers the effective jamming power at a given frequency. Barrage jamming is a jamming technique where high power is sacrificed for the continuous coverage of several radar frequencies (Figure 10-6). The jamming signal is spread over a wide frequency range, which lowers the ERP at any one frequency. This type of jamming is useful against frequency-agile radars, against a radar system that uses multiple beams, or against multiple radar systems operating in a specific frequency range. By spreading the jamming over a wide frequency range, there is some level of jamming no matter what frequency the radar uses. Barrage jamming was used extensively during World War II. Advantages of barrage jamming are its simplicity and ability to cover a wide portion of the electromagnetic spectrum. The primary disadvantage is the low power density, especially when a high J/S ratio is needed against modern radars.

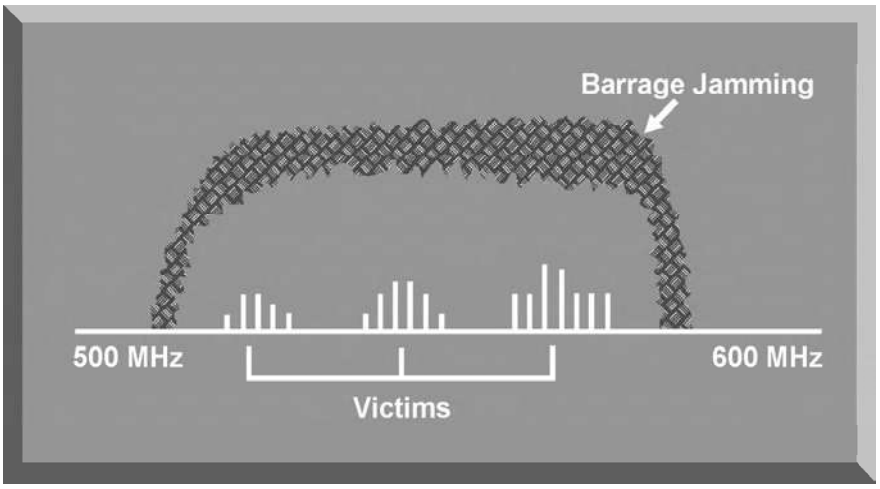

Figure 10-6. Barrage Jamming

5. SPOT JAMMING

One way to take advantage of the noise jammer's simplicity, but raise the jamming signal power, is to use a spot jammer. The earliest spot jammers were very narrow band jammers covering a bandwidth of 10 megahertz or less (Figure 10-7). This narrow band spot jammer was tuned to the anticipated frequency of the target radar. When it is necessary to jam a number of radars at different frequencies, more than one jammer is used. One problem that developed was of carrying the required number of spot jammers to counter a modern IADS. Also, radars that change their operating frequency, or are frequency-agile, defeat the spot jammer. Today, intercept panoramic receivers work with spot jammers to determine the frequency of the victim radar. A look-through capability is included in the system so that the target radar signal can be monitored to assess jamming effectiveness. The jamming signal can be adjusted for any changes in the operating frequency of the radar.

Figure 10-7. Spot Jamming

a. The primary advantage of spot jamming is its power density. Radar or communications receivers can be countered at longer ranges than when using a barrage jammer of equal output power (Figure 10-8).

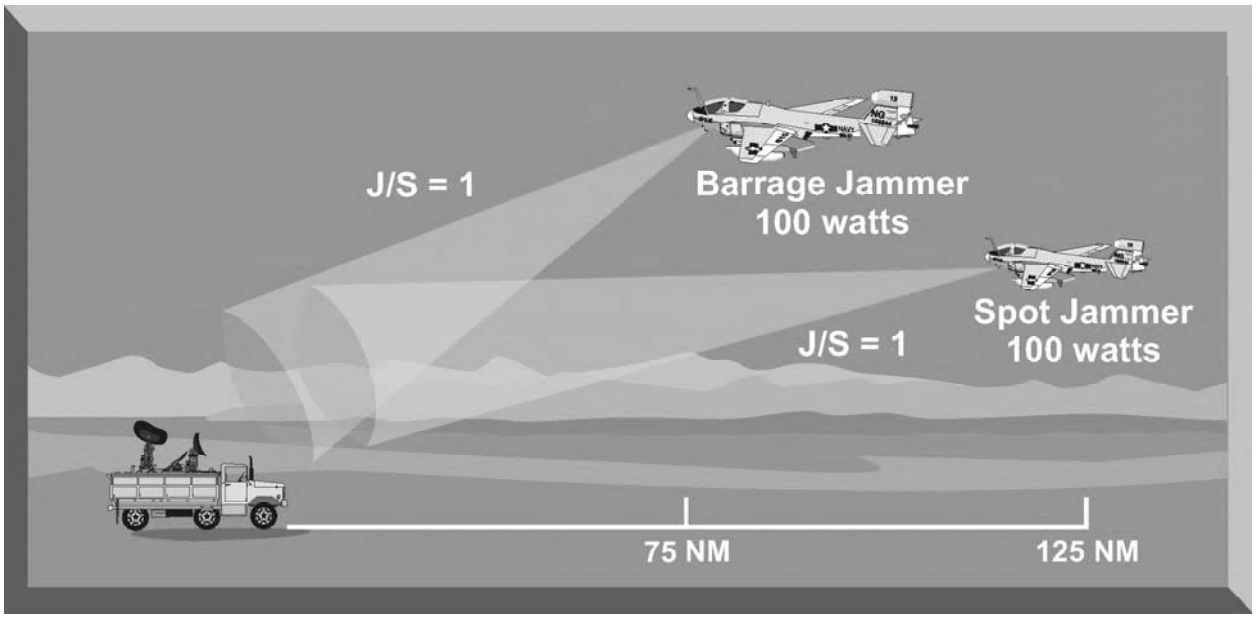

Figure 10-8. Spot Jamming Effectiveness

b. A disadvantage of the spot jammer is its coverage of a narrow band of the frequency spectrum. An operator or computer in the receiver must constantly monitor and tune the jamming signal to the target radar's frequency. The complexity of this process increases when jamming frequency-agile radars that can change frequencies with every pulse.

6. SWEPT-SPOT JAMMING

When high power density is required over a large bandwidth, one solution is to take spot jamming and sweep it across a wide frequency range (Figure 10-9). This preserves the high power density but allows the jamming to cover a large bandwidth. The jamming spot is swept across a broad frequency range at varying speeds. With this technique, a number of radar systems can be covered. Because of their high jamming power, swept-spot jammers are able to cover a number of radars operating in a broad frequency range. However, jamming is not continuous. Fast swept-spot jamming can approximate continuous jamming by causing a phenomenon known as "ringing." Fast sweeping spot noise is like a burst of energy which sets up vibrations within the receiver section. When these vibrations last until the next burst of energy is received, this is known as ringing. Three factors determine swept-spot jamming effectiveness. The first is the power in the spot. The next is the bandwidth, or frequency range, the spot covers. The last is the sweep rate.

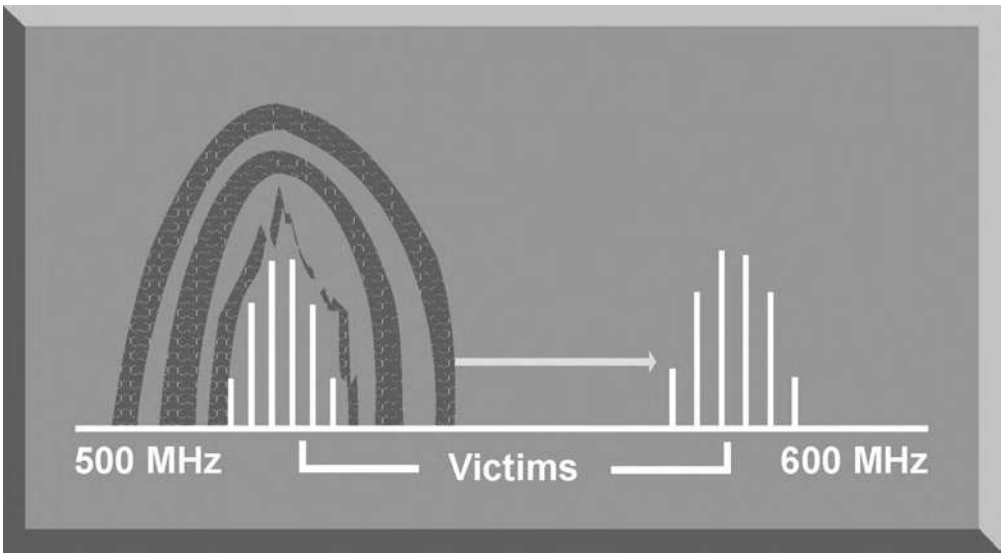

Figure 10-9. Swept-Spot Jamming

7. COVER PULSE JAMMING

Cover pulse jamming is a modification of swept-spot jamming. This is a "smart noise" technique that is responsive for a short period of time (Figure 10-10). A repeater jammer acts as a transponder. It receives several radar pulses and determines the PRF of the victim radar. It then uses this data to predict when the next radar pulse should arrive. Using an oscillator that is gated for a period of time based on predicted pulse arrival time, a noise-modulated signal is amplified and transmitted. This process works against a radar with a steady PRF, and allows a low-powered repeater to respond to a number of threats by time-sharing.

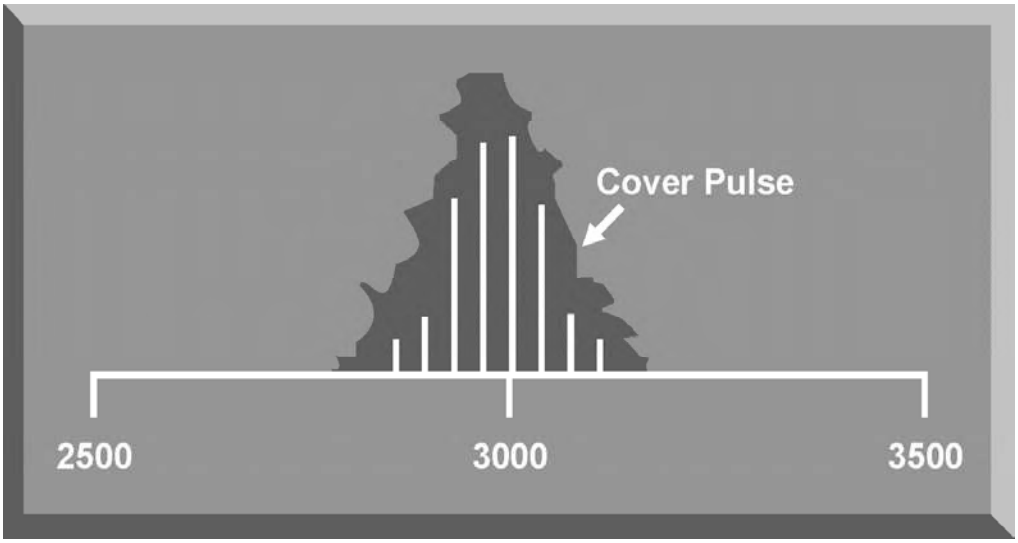

Figure 10-10. Cover Pulse Jamming

a. Cover pulse jamming is used to initiate a range gate pull-off (RGPO) deception jamming technique. The deception jammer transmits a noise jamming signal, or cover pulse, that is much stronger than the target return. The cover pulse raises the automatic gain inside the range gate, and the range tracking loop initiates tracking on the cover pulse. The deception jammer then increases the time delay in the jamming pulse and moves the range tracking gate away from the real target (Figure 10-11).

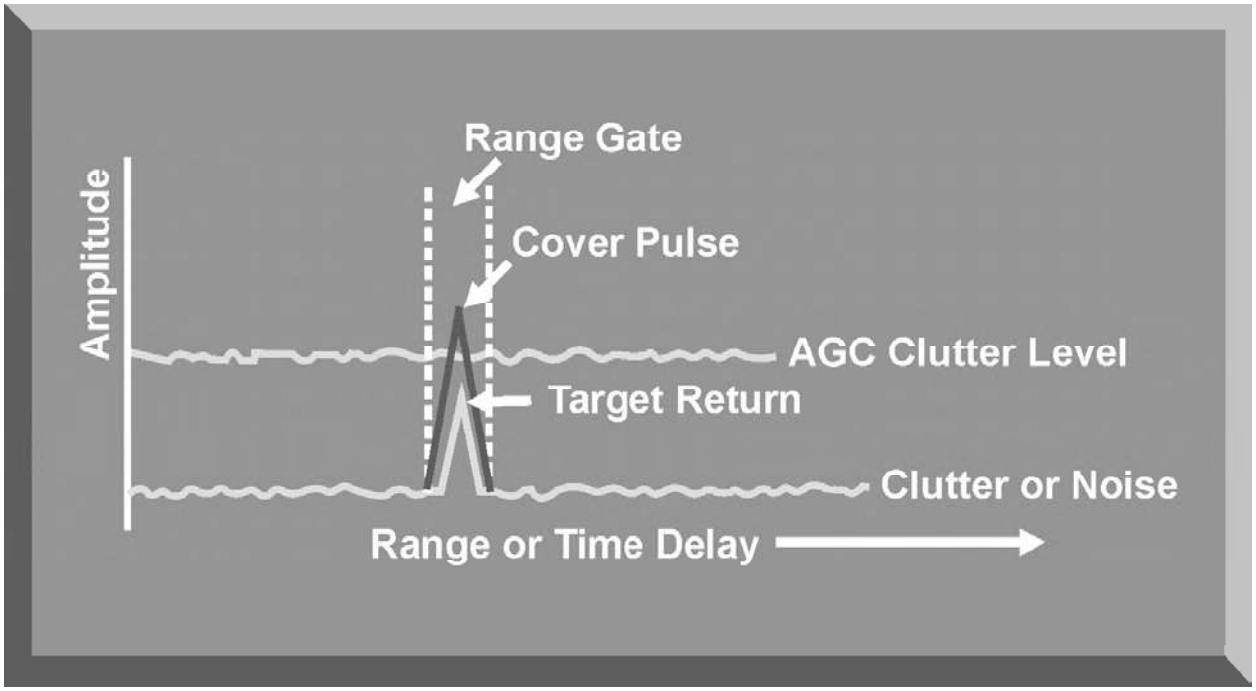

Figure 10-11. Range Gate Pull-Off Cover Pulse

b. A form of cover pulse jamming is also used to initiate a velocity gate pull-off (VGPO) technique against continuous wave and pulse Doppler radars. The cover pulse, in this case, is a strong jamming signal with the same frequency shift as the aircraft return. This cover pulse steals the velocity tracking gate and sets up the velocity tracking loop to steal the velocity tracking gate based on false target Doppler shifts (Figure 10-12).

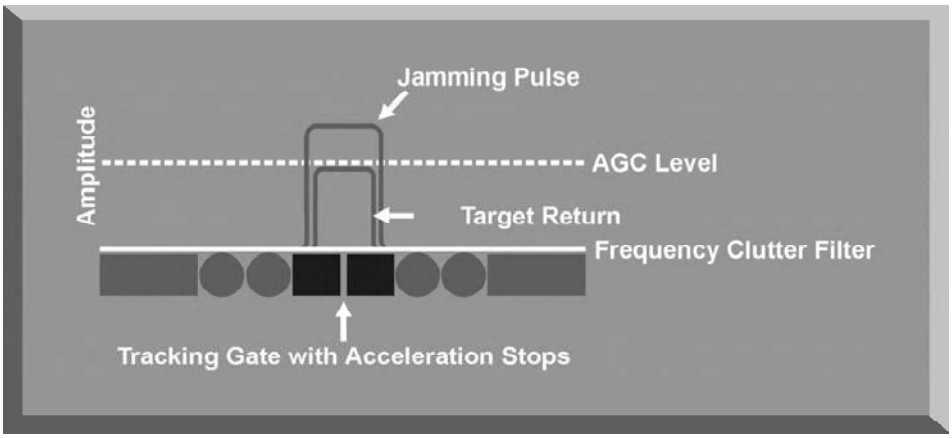

Figure 10-12. Velocity Gate Pull-Off Cover Pulse

8. MODULATED NOISE JAMMING

Modulated jammers are special hybrid jammers which employ noise jamming that is either amplitude or frequency modulated. The purpose of this modulated noise is to defeat target tracking radars (TTRs) rather than deny range information. Modulated noise jamming has proven effective against conical scan and track-while-scan (TWS) TTRs.

a. Modulated jamming alters the noise jamming signal at a frequency that is related to the scan rate of the target radar. If modulated jamming is used against a conical scan radar, a sine wave signal is used (Figure 10-13). The frequency of the sine wave is slightly higher than the scan rate of the victim radar. The amplitude difference results in a constantly varying phase between the radar and the jamming signal. This phase differential produces false targets with a strong signal amplitude everywhere the signals reinforce each other. This causes the conical scan radar to track the false returns and lose the real target return. For this technique to work, the scan rate of the intended victim radar must be known.

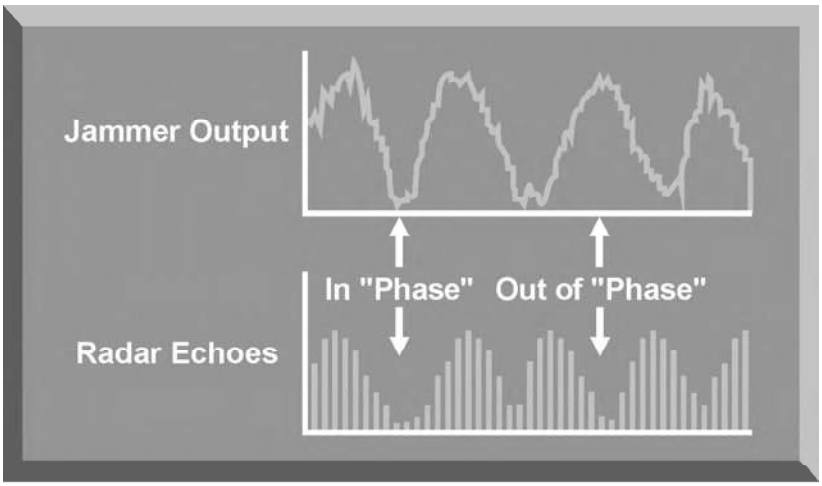

Figure 10-13. Conical Scan Modulated Jamming

b. Against a TWS radar, a rectangular waveform is used to modulate the noise signal. The PRF of the modulation is set at some harmonic of the TWS rate. This synchronization results in a number of jamming strobes on the radar scope. Each jamming strobe is at a different azimuth or elevation depending on which radar beam is being jammed. The number of jamming strobes depends directly on the harmonic used to modulate the signal. In Figure 10-14, a modulating signal frequency that is four times the scan rate of the radar will produce four jamming strobes on the scope. If the jamming is slightly out of tune with the scan rate, the jamming strobes will appear to roll across the radar scope.

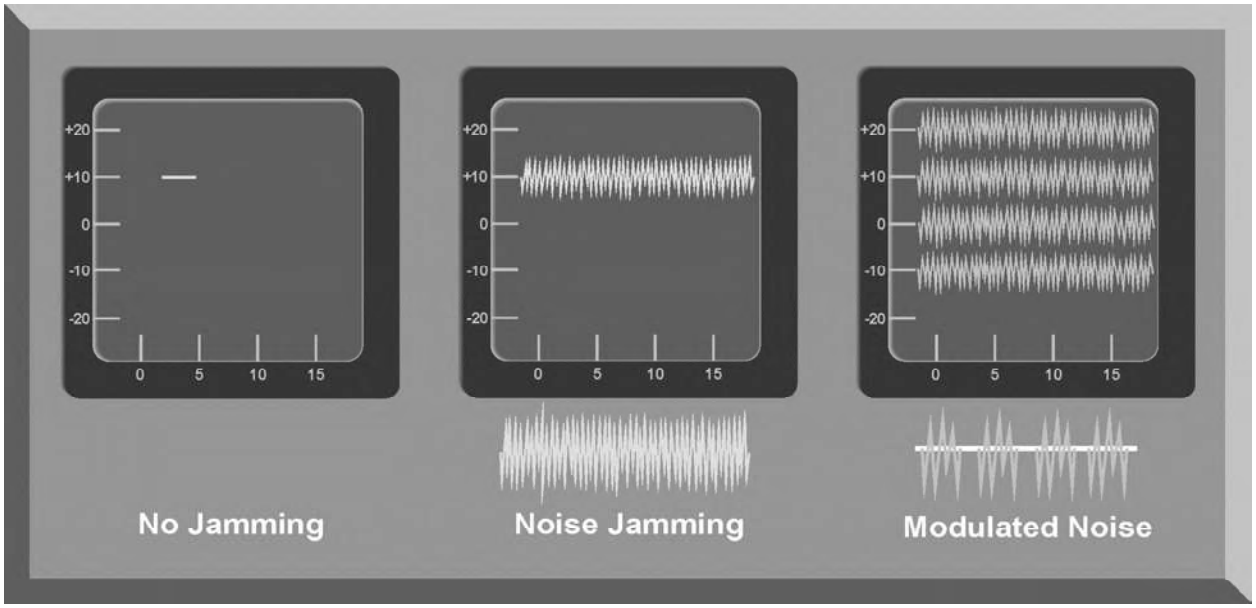

Figure 10-14. TWS Modulated Jamming

9. SUMMARY

Radar noise jamming is employed to deny target acquisition and target tracking data to a victim radar. This is accomplished by injecting amplitude or frequency modulated noise jamming signals into the victim radar's receiver. The radar noise jamming techniques discussed in this chapter included barrage, spot, swept-spot, cover pulse, and modulated jamming. The effectiveness of these noise jamming techniques depends on the power density of the jamming signal compared to the power in the radar return, or the J/S ratio. Radar noise jammers are generally simple, high-power systems which can be effectively employed in a support or self-protection role. Radar noise jamming can be employed in conjunction with deception jamming techniques to maximize the impact of jamming on victim radars.

CHAPTER 11. DECEPTION JAMMING

1. INTRODUCTION

Deception jamming systems are designed to inject false information into a victim radar to deny critical information on target azimuth, range, velocity, or a combination of these parameters. To be effective, a deception jammer receives the victim radar signal, modifies this signal, and retransmits this altered signal back to the victim radar. Because these systems retransmit, or repeat, a replica of the victim's radar signal, deception jammers are known as repeater jammers. The retransmitted signal must match all victim radar signal characteristics including frequency, pulse repetition frequency (PRF), pulse repetition interval (PRI), pulse width, and scan rate. However, the deception jammer does not have to replicate the power of the victim radar system.

a. A deception jammer requires significantly less power than a noise jamming system. The deception jammer gains this advantage by using a waveform that is identical to the waveform the radar's receiver is specifically designed to process. Therefore, the deception jammer can match its operating cycle to the operating cycle of the victim radar instead of using the 100% duty cycle required of a noise jammer. To be effective, a deception jammer's power requirements are dictated by the average power of a radar rather than the peak power required for a noise jammer. In addition, since the jammer waveform looks identical to the radar's waveform, it is processed like a real return. The jamming signal is amplified by the victim radar receiver, which increases its effectiveness. The reduced power required for effective deception jamming is particularly significant when designing and building self-protection jamming systems for tactical aircraft that penetrate a dense threat environment. Deception jamming systems can be smaller, lighter, and can jam more than one threat simultaneously. These characteristics give deception jammers a great advantage over noise jamming systems.

b. Although deception jammers require less power, they are much more complex than noise jammers (Figure 11-1). Memory is the most critical element of any deception jammer. The memory element must store the signal characteristics of the victim radar and pass these parameters to the control circuitry for processing. This must be done almost instantaneously for every signal that will be jammed. Any delay in the memory loop diminishes the effectiveness of the deception technique. Using digital RF memory (DRFM) reduces the time delay and enhances deception jammer effectiveness. Deception jamming employed in a self-protection role is designed to counter lethal radar systems. To be effective, deception jamming systems must be programmed with detailed and exact signal parameters for each lethal threat.

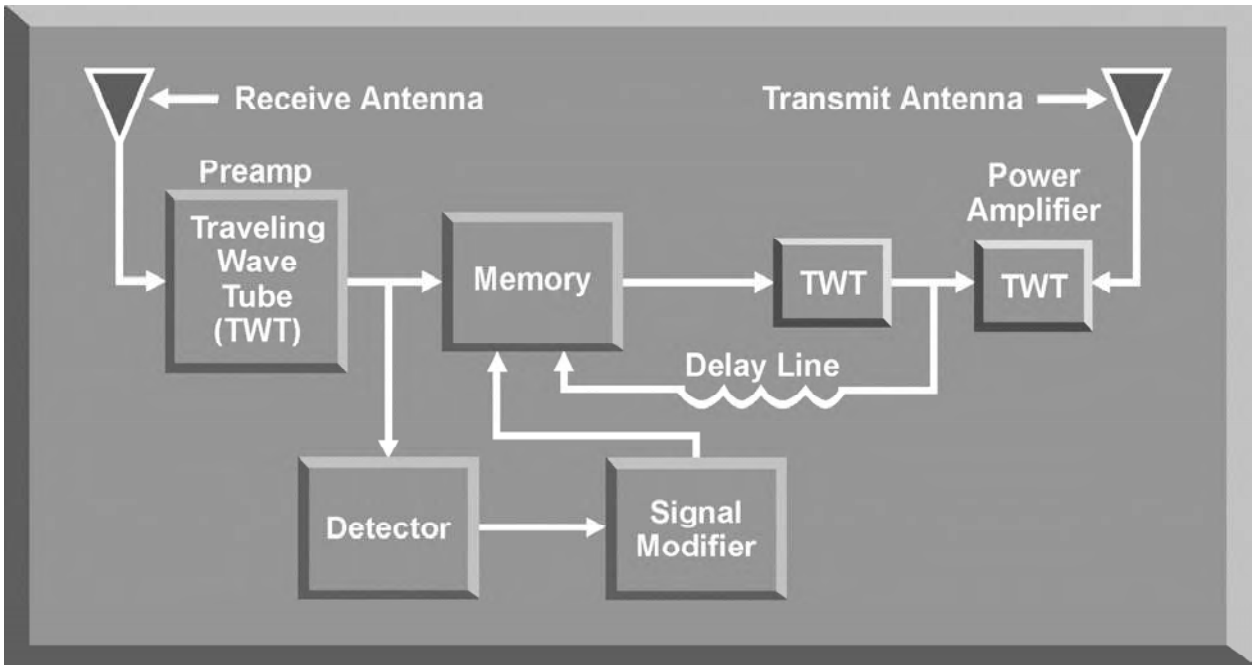

Figure 11-1. Deception Jamming System

c. The requirement for exact signal parameters increases the burden on electronic warfare support (ES) systems to provide and update threat information on operating frequency, PRF, PRI, power pulse width, scan rate, and other unique signal characteristics. An electronic intelligence (ELINT) architecture is required to collect, update, and provide changes to deception jamming systems. In addition, intelligence and engineering information on exactly how a specific threat system acquires, tracks and engages a target is essential in identifying system weaknesses. Once a weakness has been identified, an effective deception jamming technique can be developed and programmed into a deception jammer. For example, if a particular radar system relies primarily on Doppler tracking, a Doppler deception technique will greatly reduce its effectiveness. Threat system exploitation is the best source of detailed information on threat system capabilities and vulnerabilities. Effective deception jamming requires much more intelligence support than does noise jamming.

d. Most self-protection jamming techniques employ some form of deception against a target tracking radar (TTR). The purpose of a TTR is to continuously update target range, azimuth, and velocity. Target parameters are fed to a fire control computer that computes a future impact point for a weapon based on these parameters and the characteristics of the weapon being employed. The fire control computer is constantly updating this predicted impact point based on changes in target parameters. Deception jamming is designed to take advantage of any weaknesses in either target tracking or impact point calculation to maximize the miss distance of the weapon or to prevent automatic tracking. This chapter will discuss the most commonly employed deception jamming

techniques, including false target jamming, range deception jamming, angle deception jamming, velocity deception jamming, and monopulse jamming.

2. FALSE TARGET JAMMING

False target jamming is an effective jamming technique employed against acquisition, early warning, and ground control intercept (GCI) radars. The purpose of this type of jamming is to confuse the enemy radar operator by generating many false target returns on the victim radar scope. When false target deception jamming is successfully employed, the radar operator cannot distinguish between false targets and real targets (Figure 11-2).

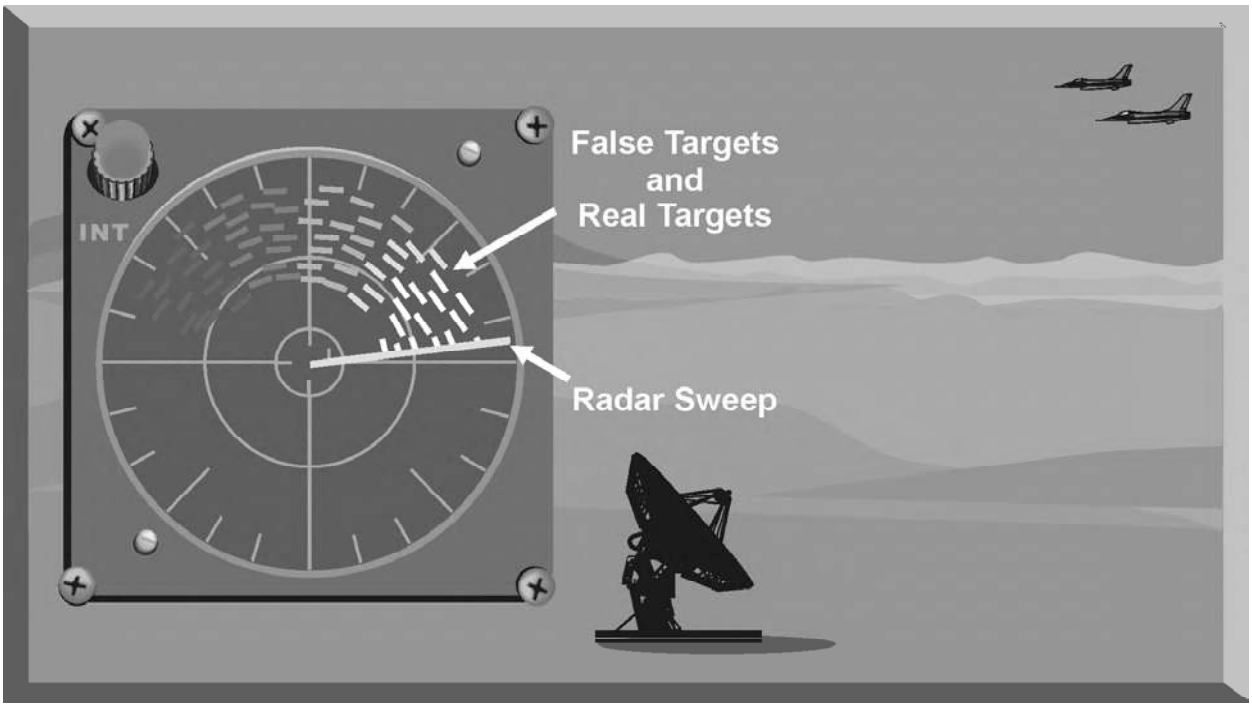

Figure 11-2. False Target Generation

a. To generate false targets, the deception jammer must tune to the frequency, PRF, and scan rate of the victim radar. The jamming pulse must appear on the radar scope exactly like a radar return from an aircraft. Multiple false targets greater in range than the jammer are generated by delaying the transmission of a jamming pulse until after the victim radar pulse has been received. False targets closer in range are generated by anticipating the arrival of a radar pulse and transmitting a jamming pulse before the victim radar pulse hits the aircraft. If the victim radar employs a jittered PRF, only targets greater in range can be generated.

b. To generate different azimuth false targets, the deception jammer synchronizes its transmitted pulse with the victim radar's sidelobes. Due to their

reduced power, when compared to the main beam, sidelobes are difficult to detect and analyze. The receiver in the deception jammer must be sensitive enough to detect these sidelobes and not be saturated by the power in the main radar beam. A false target deception jammer must inject a jamming pulse that looks like a target return into these sidelobes. To penetrate the radar sidelobes requires a lot of power. However, the power must be judiciously used. If a powerful jamming pulse is injected into the main beam, the false targets will be easy to detect. Most false target jammers vary the power in the jamming pulse inversely with the power in the received signal, on a pulse-by-pulse basis. This means the repeater jamming signal is at minimum power when the main beam of the victim radar is on the aircraft and at maximum power when the sidelobes are being jammed. To effectively generate false azimuth targets, the jammer must have a receiver with a wide dynamic range to detect both the main beam and the sidelobes. In addition, the jamming system must be able to generate high power that can be effectively controlled by the receiver.

c. To generate moving false targets, the deception jammer must synchronize with the main beam and the sidelobes in frequency, pulse width and PRF. Amplitude modulated jamming signals, with variable time delays, are transmitted into the sidelobes of the victim radar. The variable time delay provides a false target that changes range, either toward or away from the radar, depending on the time delay. The amplitude modulation provides false azimuth targets that appear to be moving.

d. The effectiveness of false target generation is based on the credibility of the generated false radar returns. If the victim radar can easily distinguish between false returns and target returns, the technique is a failure. The false returns must look identical to an aircraft return. The radar return on the victim radar scope should have the same intensity, depth, and width as a target return.

(1) Power determines the false target intensity when it is displayed on the victim radar scope. Varying jammer output power inversely with received power ensures that each false target has nearly the same intensity as a true target return. The depth, or thickness, of the false target depends on the pulse width of the victim radar. By matching the pulse width of the jamming pulse with the pulse width of the victim radar, the jammer can generate false targets with the same depth as a real target return.

(2) The width of the false target depends on the antenna pattern of the victim radar. This can pose a problem for false-target deception jammers. Because the jamming pulse is transmitted the entire time the radar beam is on the jammer, the width of a false target will tend to be greater than a real target return. Aircraft radar return varies with main beam cross-section. To correct this problem, most false target deception jammers use random modulation in the power of the transmitted pulses. This will vary the width of the false targets and make them look more like the variable returns of actual targets.

3. RANGE DECEPTION JAMMING

Although a specific TTR can track multiple targets and direct multiple weapons, the tracking circuit must select a single target return and track it while ignoring all other returns. Target selection is done by using gate bins. The range gate is used as the primary gate for target selection. A range gate is an electronic switch that is turned on for a period of microseconds based on a certain range or time delay after a pulse is transmitted (Figure 11-3).

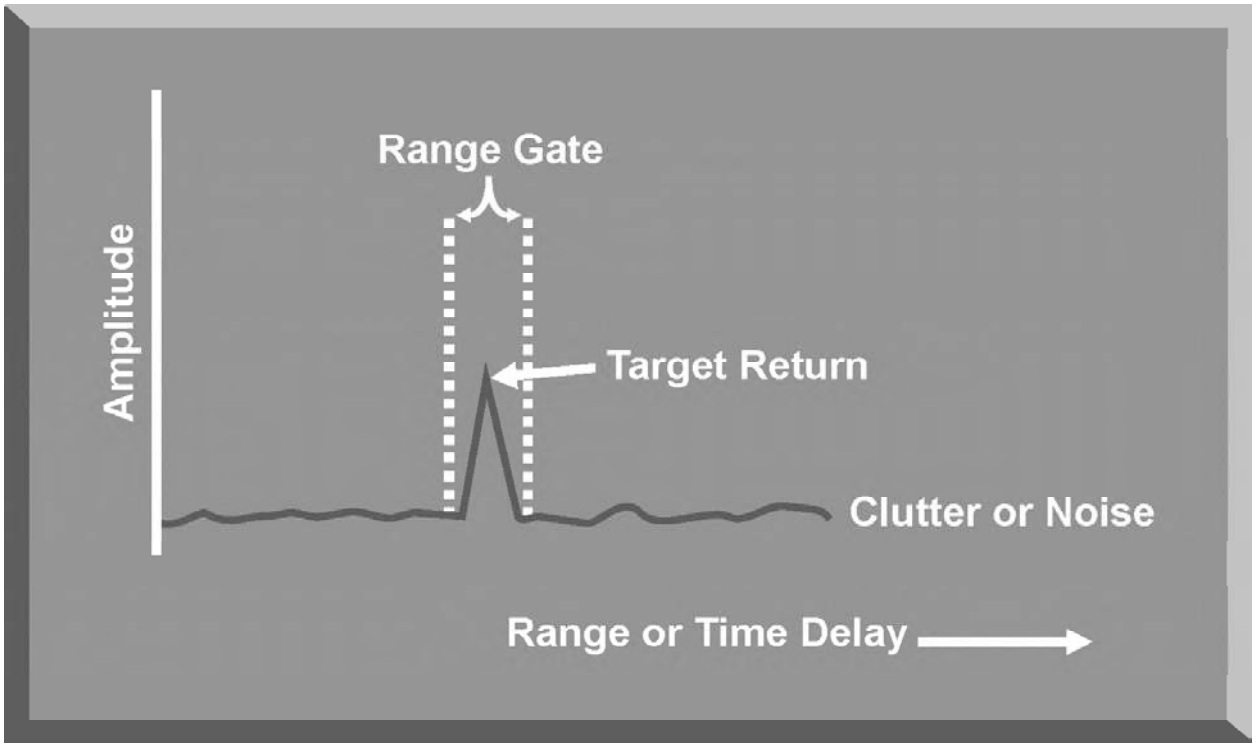

Figure 11-3. Range Gate Tracking

a. Range deception jamming exploits any inherent weakness in a TTR's automatic range gate tracking circuits. When a TTR's range gate locks on to an aircraft, the range deception jammer detects the radar signal. The range deception jammer then amplifies and retransmits a signal much stronger than the radar return. This retransmitted signal, called a cover pulse, is displayed in the range gate with the target signal (Figure 11-4).

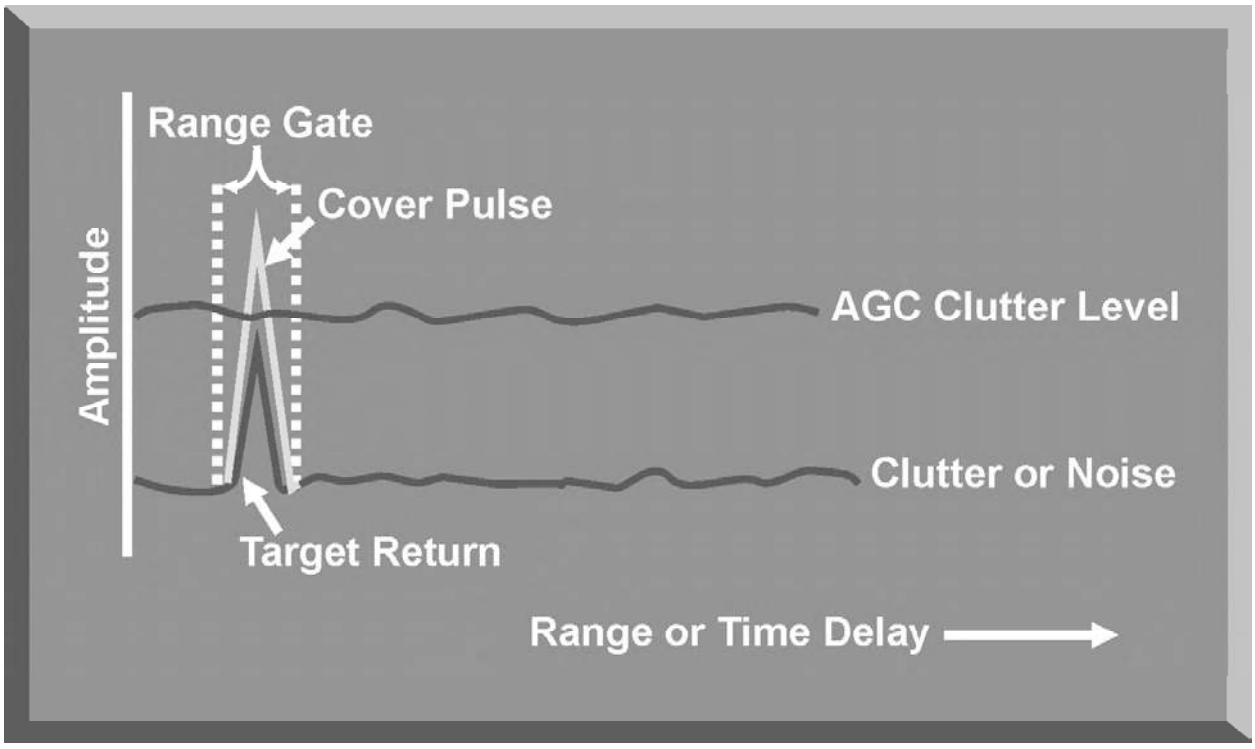

Figure 11-4. Range Gate Jamming Cover Pulse

b. The automatic gain control (AGC) circuit lowers the gain in the range tracking gate to control the amplitude of the cover pulse in the range gate. Reduced gain causes the real target return to be lost, and the range gate only tracks the jamming signal. This is known as range gate capture.

c. Once the range gate is captured by the cover pulse, a technique called range gate pull-off (RGPO) is employed (Figure 11-5). The deception jammer memorizes the radar signal and introduces a series of time delays before retransmitting. By increasing these time delays, the range gate will detect an increase in range and automatically move off to a false range. Once the range gate has moved well away from the real target, the range deception jammer shuts down, and the radar range gate is left with no target to track. The range gate breaks lock and the TTR must again go through the process of search, acquisition, and lock-on to re-engage the target.

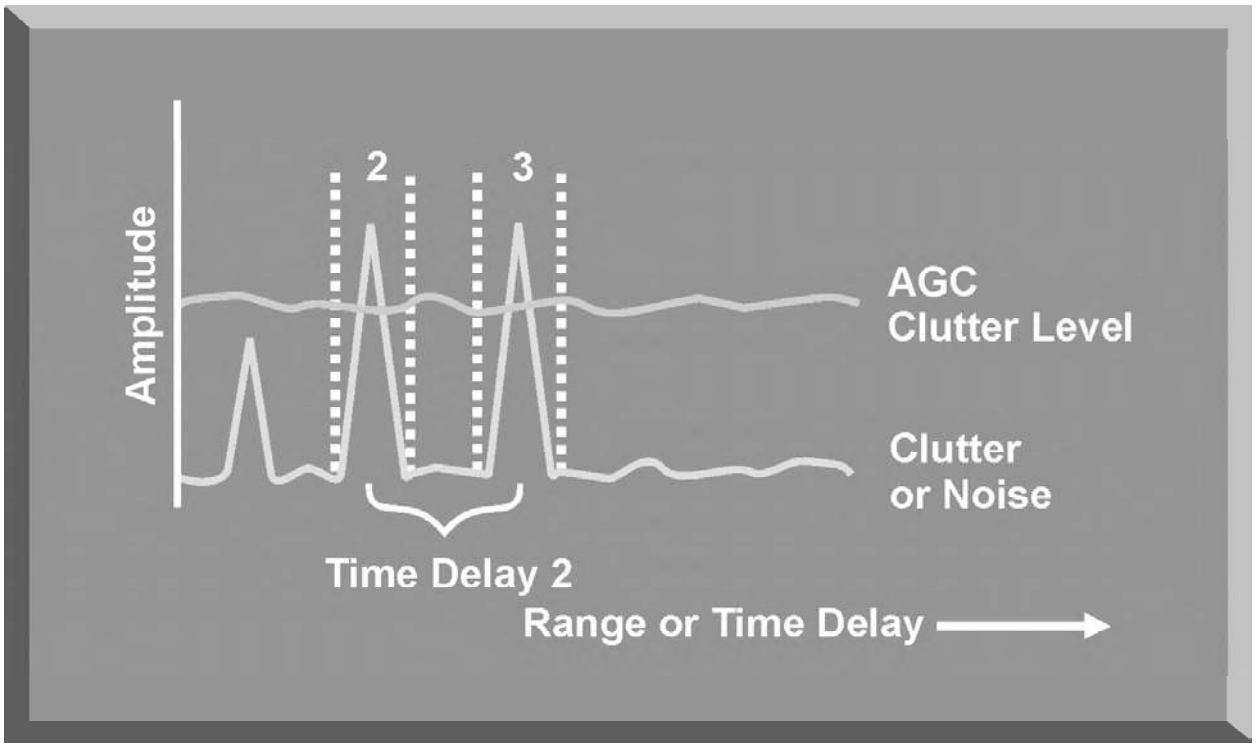

Figure 11-5. Range Gate Pull-Off

d. There are several advantages of range deception jamming, especially when used as a self-protection technique. It can generate sufficient errors to deny range information and is effective against most automatic range tracking systems. This technique does not require a large amount of power, just enough to cover the radar return of the aircraft. If the time delays are not exaggerated, an operator may not detect the loss of range lock-on until after a missile has been fired. The insidious nature of range deception jamming may generate enough miss distance to save the aircraft and pilot.

e. There are disadvantages to using range deception jamming. First, it can be defeated by a trained radar operator. If the operator detects a problem with the automatic range tracking circuit, the system can be switched to manual range tracking mode to defeat RGPO. Also, if the threat system is still able to track the aircraft's azimuth and elevation, range information may not be required to complete target engagement. To maximize range deception jamming effectiveness, it should be employed in conjunction with azimuth and elevation jamming. Finally, this type of range deception jamming is not effective against a leading-edge range tracking system. A leading-edge tracker will not see the delayed cover pulse. As the cover pulse moves off the target, AGC circuits reset the gain to continue tracking the real target. The only way to defeat a leading-edge range tracker is with a deceptive jammer that anticipates the next radar pulse and sends a jamming cover pulse before it reaches the aircraft. This jamming technique can also be defeated by randomly varying the radar PRF.

4. ANGLE DECEPTION JAMMING

Angle deception jamming is designed to exploit weaknesses in the angle tracking loop of the victim radar. The specific technique depends on the tracking method used to derive azimuth and elevation information. Inverse amplitude modulation jamming is the main angle deception technique used against TWS radars. For conical scan radars, scan rate modulation and inverse gain jamming are used. Swept square wave (SSW) jamming is used against LORO tracking radars. Monopulse angle deception jamming will be covered separately.

a. The azimuth and elevation tracking loop for a TWS radar is based on target signal amplitude modulation. The inverse amplitude modulation jammer generates a signal with modulation exactly opposite the expected return. To accomplish this, the angle deception jammer must receive the radar signals from the tracking beams. The jammer responds with a signal of the same frequency, PRF, and scan rate synchronized to the inverse of the radar antenna pattern (Figure 11-6). This induces an error in the angle tracking gate that, over a series of scans, causes the radar to lose target angle tracking.

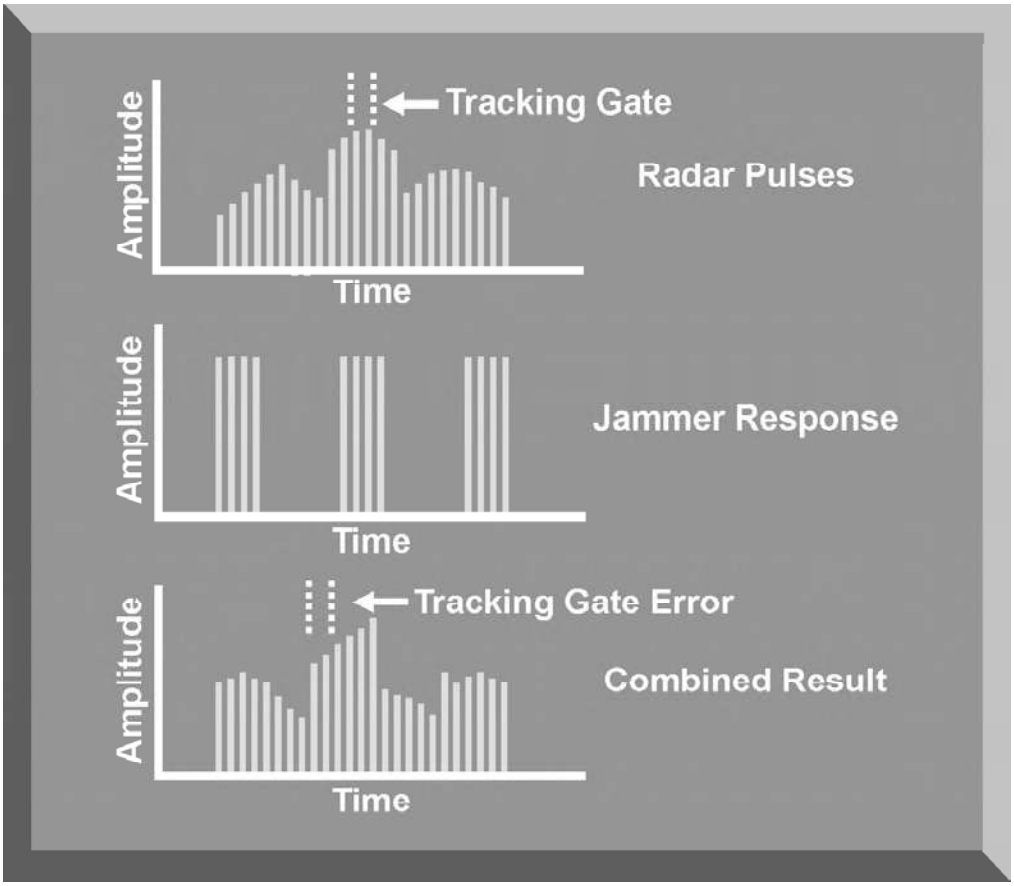

Figure 11-6. Inverse Amplitude Modulation Jamming

b. Inverse gain jamming is also effective against conical scan radars. Since conical scan radars use the phase of the target returns to generate error signals, an inverse gain deception jammer attempts to alter the phase by inducing fake signals into the antennas. In addition, by altering the amplitude of the signal, the jammer induces large errors into the tracking loop. To accomplish this, the jammer must determine the frequency, PRF, and scan rate of the victim radar. It then transmits signals that change the phase and amplitude of the target signal, resulting in a signal 180 degrees out of phase with the actual target (Figure 11-7). This 180-degree error rapidly drives the antenna off the target and causes break-lock.

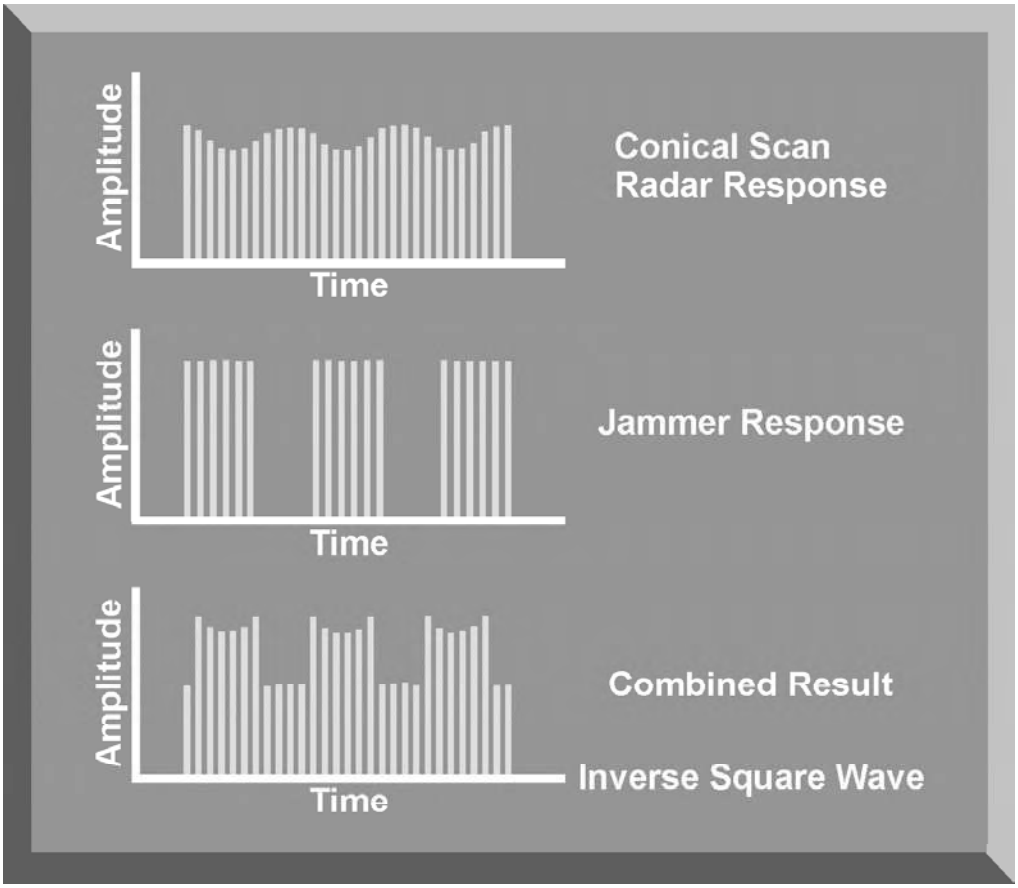

Figure 11-7. Inverse Gain Jamming

c. Scan rate modulation is also used against conical scan radars. This angle deception technique modulates the jamming pulse at or near the victim radar nutation frequency. As the modulation approaches the radar's nutation frequency, large error signals appear in the radar servo tracking loops, producing random gyrations in the antenna system, causing break-lock. This technique is most effective if the modulation jamming is slowly swept in frequency until it matches the nutation rate.

d. Both inverse scan and scan rate modulation jamming require very little power and have proven extremely effective against TWS and conical scan radars. To be effective, however, the angle deception jammer must find the precise scan rate of the victim radar. The jammer must concentrate on one signal at a time, limiting the number of threat systems that can be jammed simultaneously. In a dense threat environment, this can be a severe limitation.

e. The effectiveness of inverse gain and scan rate modulation jamming led radar designers to employ antennas that scan only during the receiving function of the radar system. Generally, this is accomplished by using two antennas. The transmitting antenna illuminates the target. Receiving antennas scan to produce the amplitude modulation of the reflected signal for effective angle tracking. This technique is called Lobe-On-Receive-Only (LORO). Since the transmitting antenna does not nutate, or scan, angle deception jammers cannot detect the modulation required to generate effective inverse gain modulation. Swept square wave (SSW) jamming is the angle deception technique developed to counter LORO angle tracking.

f. SSW jamming continuously varies the frequency of amplitude modulation on the jamming pulse over an expected range of nutation or scanning frequencies. This range is established by either electronic intelligence (ELINT) data on a particular system, or by exploitation. The dotted line in Figure 11-8 shows a threat's nutation or scan frequency. As the frequency of the modulated jamming pulse approaches the threat scan frequency, it induces errors in the angle tracking loop of the victim radar. The longer the SSW jamming stays near the scan frequency, the greater the induced errors. It is important that the sweep rate of the modulating jamming be slow enough to maximize its impact on the victim radar.

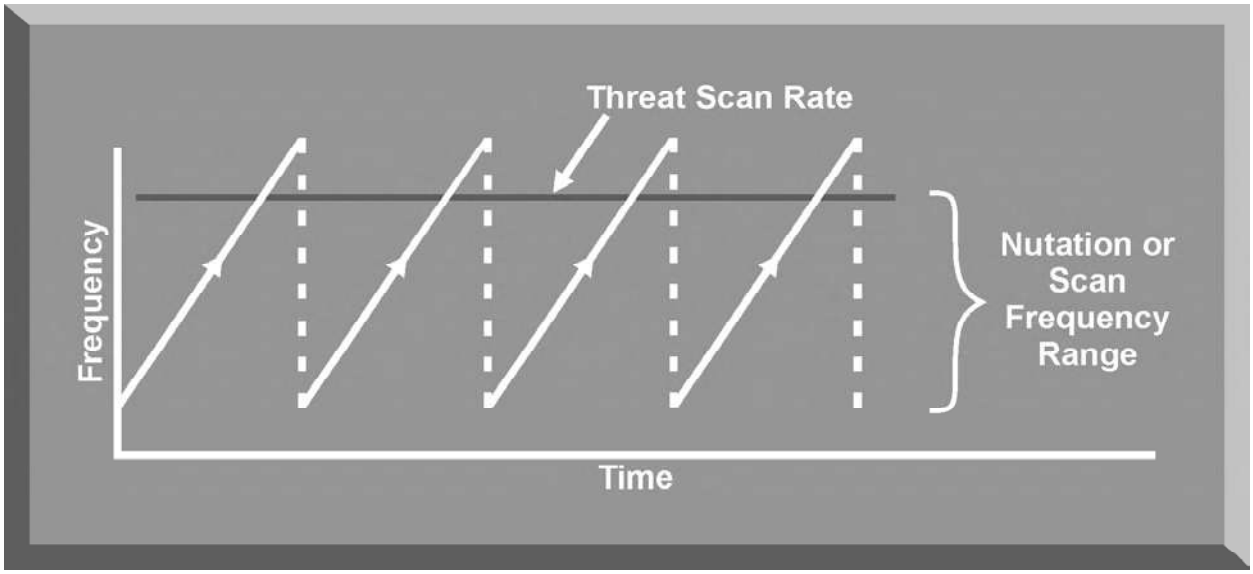

Figure 11-8. Swept Square Wave Jamming

5. VELOCITY DECEPTION JAMMING

Pulse Doppler and continuous wave (CW) radars track targets based on velocity or Doppler-shifted frequency (Figure 11-9). The objective of velocity deception jamming is to deny velocity tracking information and generate false velocity targets. The primary techniques include velocity gate pull-off (VGPO), Doppler noise, narrowband Doppler noise, and Doppler false targets.

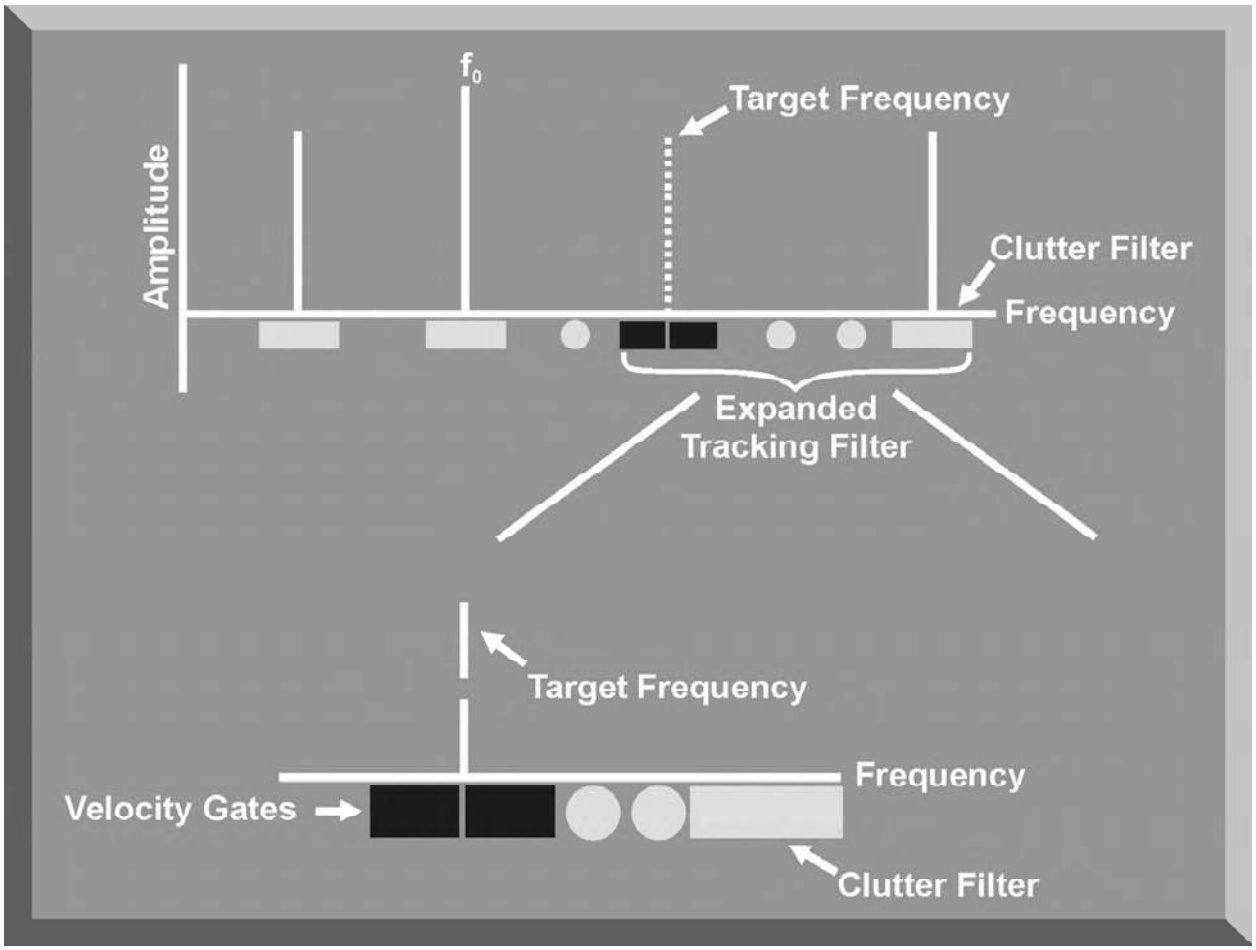

Figure 11-9. Velocity Tracking Gate

a. Velocity gate pull-off counters pulse Doppler or CW radars by stealing the velocity gate of their automatic tracking loop. The objective of VGPO is to capture the Doppler velocity tracking gate by transmitting an intense false Doppler signal. Then the frequency of the false signal is changed to move the tracking gate away from the true target Doppler. This is analogous to the RGPO technique used against the range gate tracking loop.

(1) To accomplish an effective VGPO technique, the jammer receives the CW or pulse Doppler signal. It then retransmits a CW or pulse Doppler signal that is higher in power than the return from the aircraft, but at approximately the same

Doppler frequency (Figure 11-10). It is important that the frequency of this initial jamming pulse appears within the same velocity tracking filters as the target return or the victim radar will disregard it. The frequency band of the Doppler tracking filters is an important piece of intelligence information. The velocity tracking gates are quite narrow, roughly 50 to 250 MHz. Once the jamming pulse appears in the tracking gate, the automatic gain control circuit gains out the target return, and the jamming pulse has captured the velocity gate.

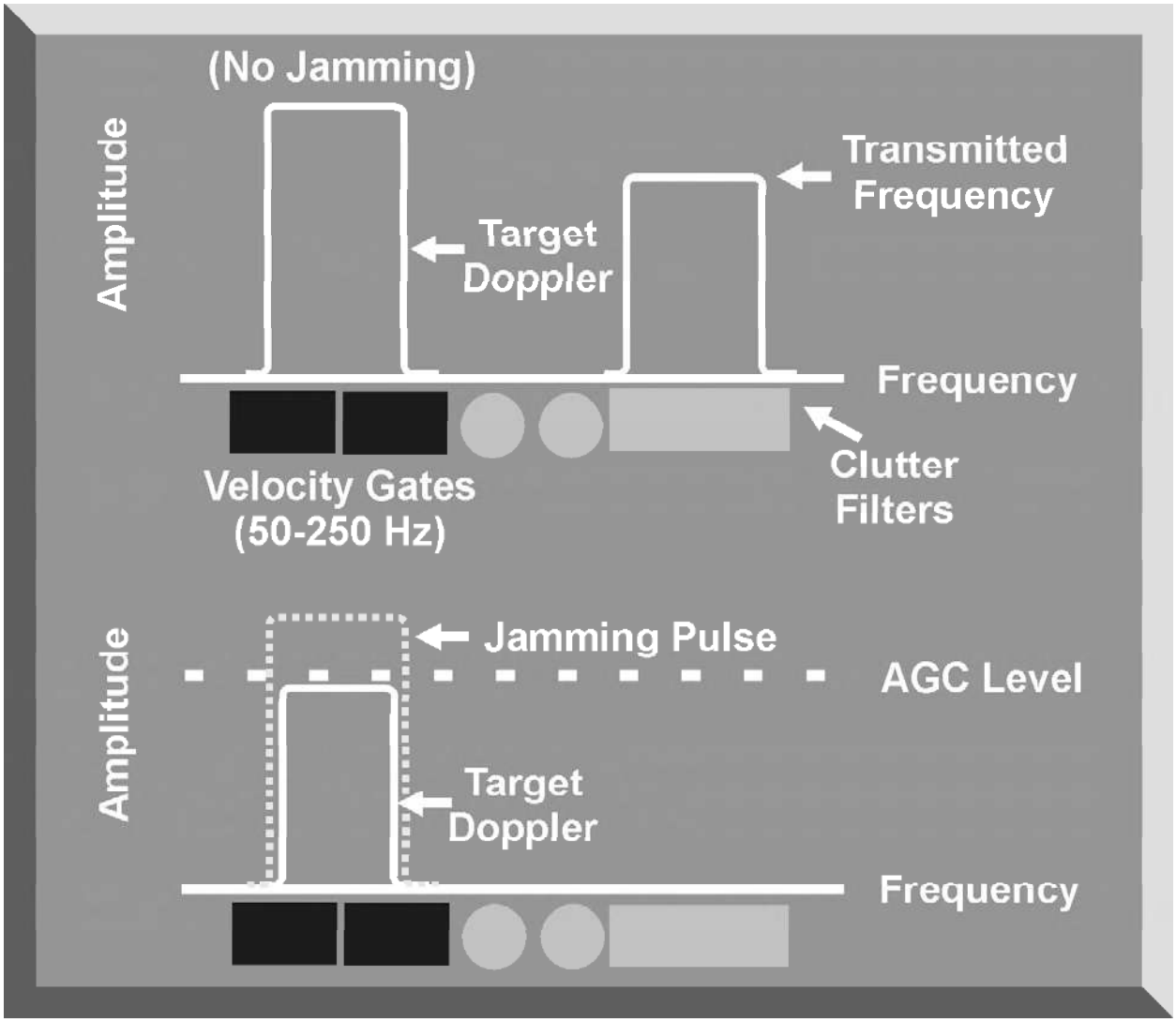

Figure 11-10. Velocity Gate Capture

(2) Once the jamming pulse has captured the tracking gate, the deception jammer slowly changes the Doppler frequency (Figure 11-11). This frequency shift is accomplished by several methods. The most common method uses frequency modulation (FM) within the jammer's traveling wave tube (TWT). By varying the TWT voltage, the Doppler frequency of the jamming pulse is changed

linearly, and the radar tracking gates follow the jamming pulse. By using FM, the jamming pulse can be moved in either a positive or negative direction, depending on the slope of the voltage. By slowly changing the frequency of the modulation, the jamming pulse pulls the tracking gates off the target. When the maximum offset has been achieved, nominally 5 to 50 kHz, the FM is "snapped back" to a minimum value, and the process is repeated to preclude target reacquisition.

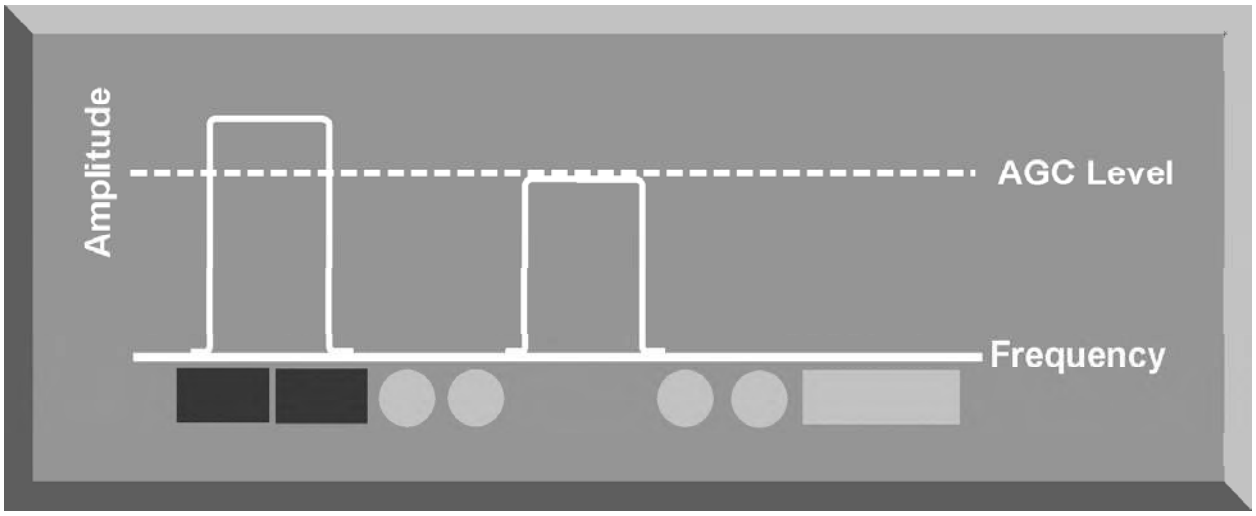

Figure 11-11. Velocity Gate Pull-Off

(3) The rate of change of frequency offset in a VGPO pulse is an extremely critical parameter. Many CW and pulse Doppler radars employ acceleration stops as part of the tracking gates. By differentiating the velocity outputs of the velocity tracking gates with respect to time, the velocity tracker computes target acceleration. Acceleration stops detect and reject unusually large changes in target acceleration. If the VGPO technique changes the frequency of the jamming pulse too rapidly, the tracking loop, with acceleration stops, will reject the jamming pulse and stay on the target. This means that an effective VGPO technique may take from one to ten seconds.

b. Doppler noise differs from most noise techniques in that it is a repeater technique. The jamming system must receive the pulse Doppler radar signal in order to generate an appropriate jamming pulse. Also, noise jamming output is done on a pulse-by-pulse basis and only lasts as long as the pulse duration, or pulse width, of the victim radar signal (Figure 11-12). The Doppler noise jammer receives each pulse and applies a random frequency shift, either positive or negative, to each pulse.

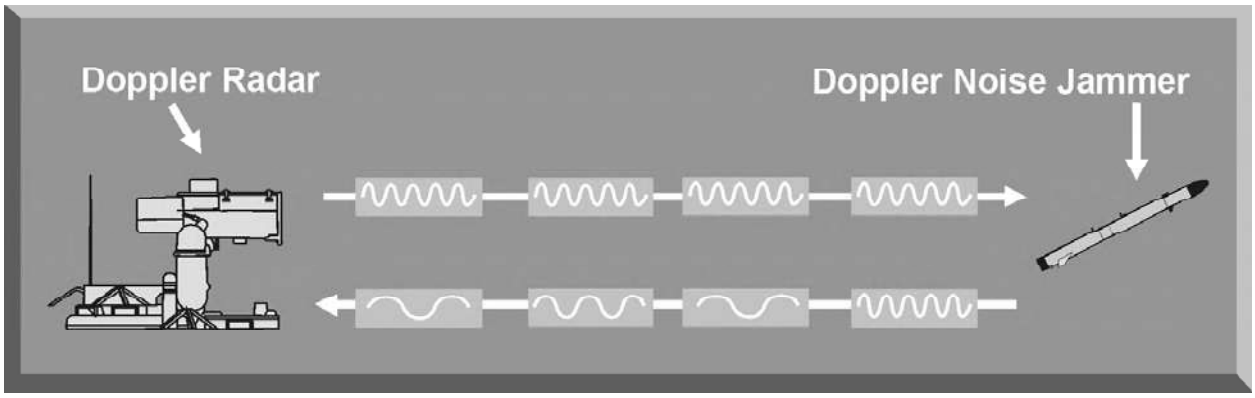

Figure 11-12. Doppler Noise Jamming

(1) When Doppler noise jamming pulses are processed by the signal processor, and the Doppler frequencies are sent to the velocity tracking gate, there are so many different velocities that the tracking gate cannot distinguish the target from the jamming. The random distribution of target velocities effectively masks the true target Doppler velocity. If the velocity tracking loop is not saturated, multiple false targets traveling at different speeds will be displayed.

(2) When a technique called Doppler noise blinking is employed, it interferes with the angle and velocity tracking within most semi-active radar missiles. Doppler noise blinking is accomplished by rapidly transmitting bursts of Doppler noise jamming (Figure 11-13).

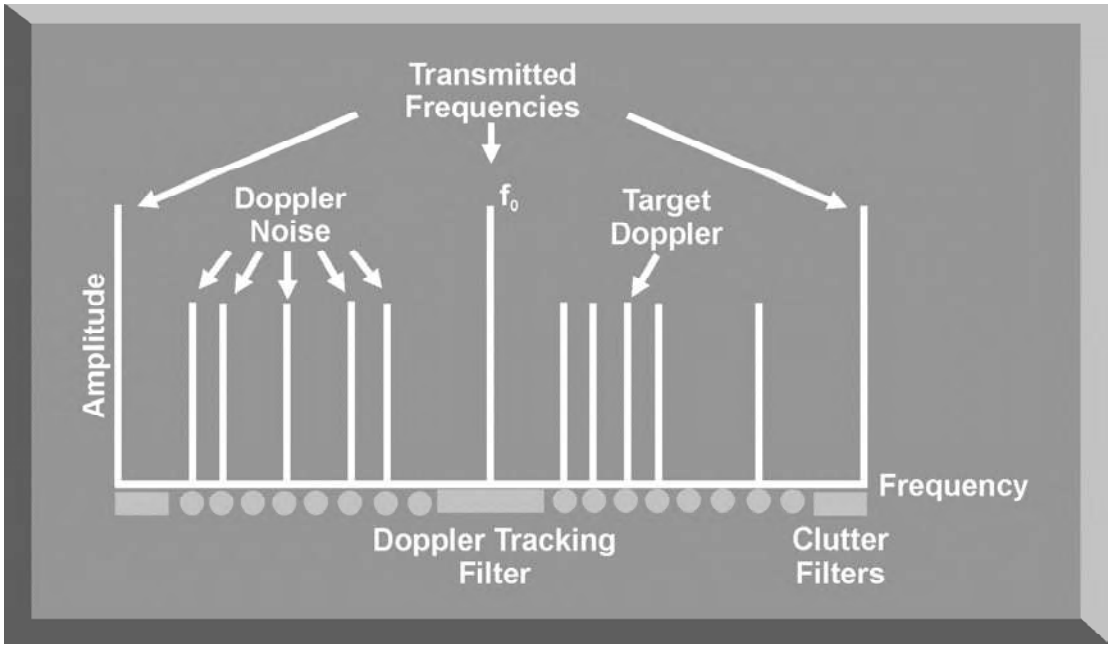

Figure 11-13. Impact of Doppler Noise Jamming

(3) Doppler noise jamming is effective against most pulse Doppler radars and the semi-active missiles employed with these radars. One disadvantage, however, is that it is only effective against the velocity tracking loop. If range tracking is still available to the radar, Doppler noise may highlight the jamming aircraft. Another disadvantage is that Doppler noise requires a sophisticated jammer able to receive the victim radar pulse, generate random positive and negative frequency modulations on this pulse, and retransmit the jamming pulses at the PRF and pulse width of the victim radar. This requires an extremely fast signal processing capability and detailed intelligence information on the victim radar.

c. Narrowband Doppler noise is also a repeater technique. The jamming system receives the pulse Doppler radar signal and generates a noise jamming signal on a pulse-by-pulse basis (Figure 11-14). Narrowband Doppler noise requires detailed information on the frequency coverage of an individual velocity tracking filter, or velocity bin, employed by the victim radar. Once this frequency range is known, the jammer receives each pulse from the victim radar and transmits jamming pulses with a higher and lower frequency shift based on the real target Doppler. These frequency shifts are always within the frequency range of the velocity bin.

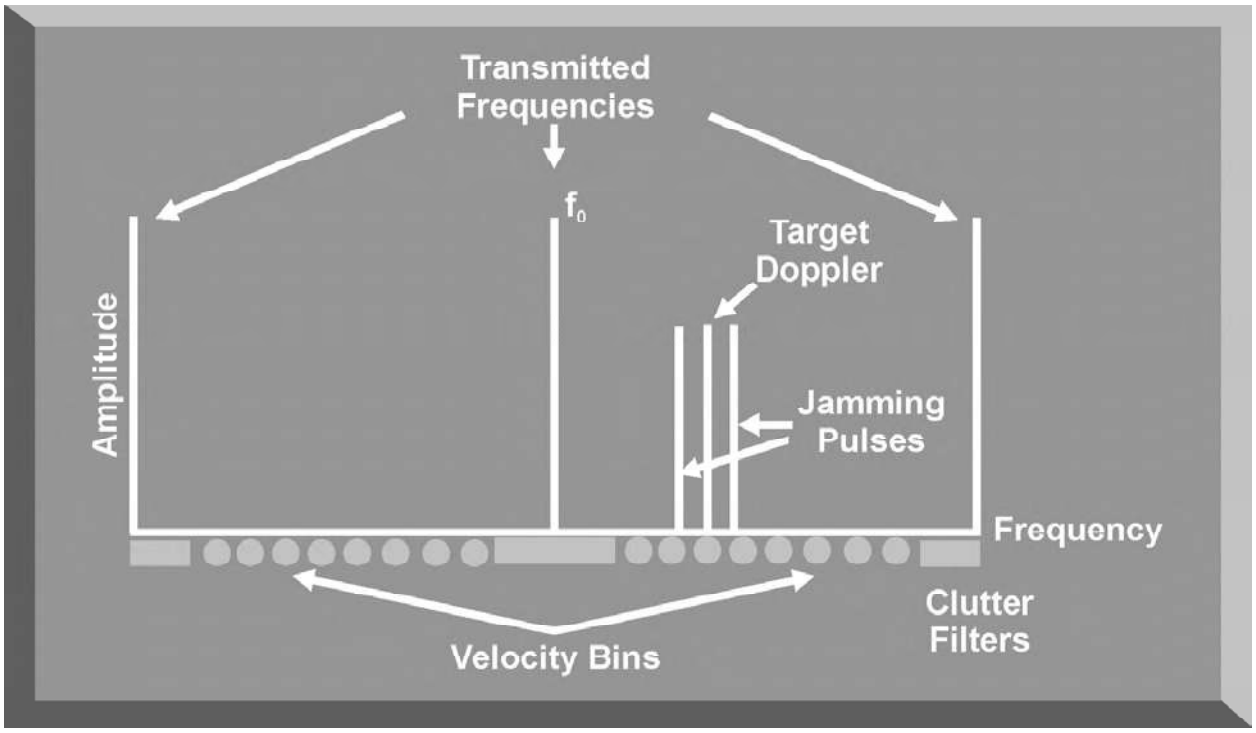

Figure 11-14. Narrowband Doppler Noise

(1) When these pulses are processed by the signal processor and the Doppler signals are sent to the velocity tracking gates, the particular bin that

contains the target Doppler also contains several other targets generated by the jammer. The victim radar signal processor attempts to distinguish the target Doppler from the jamming pulses. It raises the gain in the velocity tracking bins, thinking that the signal with the highest amplitude is the target. But, as the signal gain is increased, the target is "gained out" with the jamming signals and no target is displayed. This is called velocity bin masking and can completely deny target information to a pulse Doppler radar (Figure 11-15).

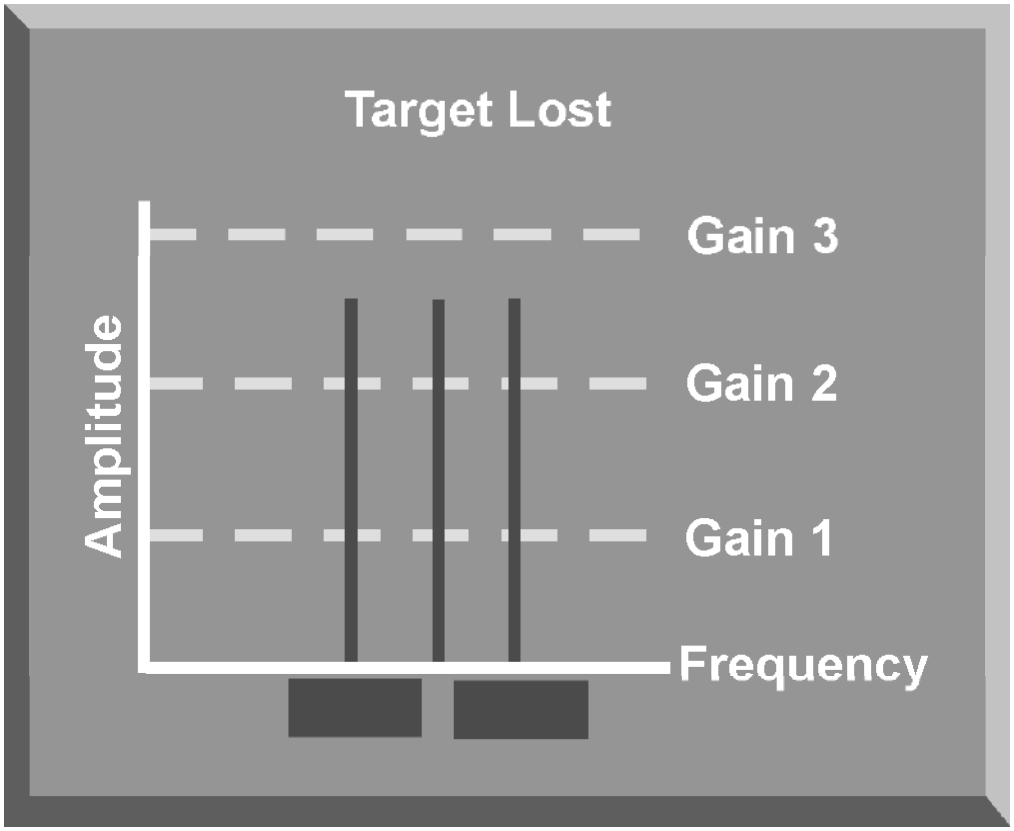

Figure 11-15. Velocity Bin Masking

(2) The advantage of narrowband Doppler noise is that it completely masks an aircraft's velocity from a pulse Doppler radar. The disadvantages include the following: When the victim radar can range-track an aircraft, narrowband Doppler noise highlights the aircraft's presence. To be effective, narrowband Doppler noise requires knowledge of the frequency range of the victim radar's velocity tracking bins, or filters. This detailed information may be available only through threat system exploitation. Finally, sophisticated signal processing and jamming systems are required to receive and transmit in the very narrow frequency band of the velocity bin.

d. Doppler false target jamming is normally used with narrowband Doppler noise or other deception techniques. Its purpose is to initially confuse the radar signal processor with multiple targets and then force the radar signal processor

to raise its gain levels in the velocity tracking loop. The Doppler false target jammer receives each pulse of the victim radar and applies a random frequency shift to a selected number of these pulses (Figure 11-16).

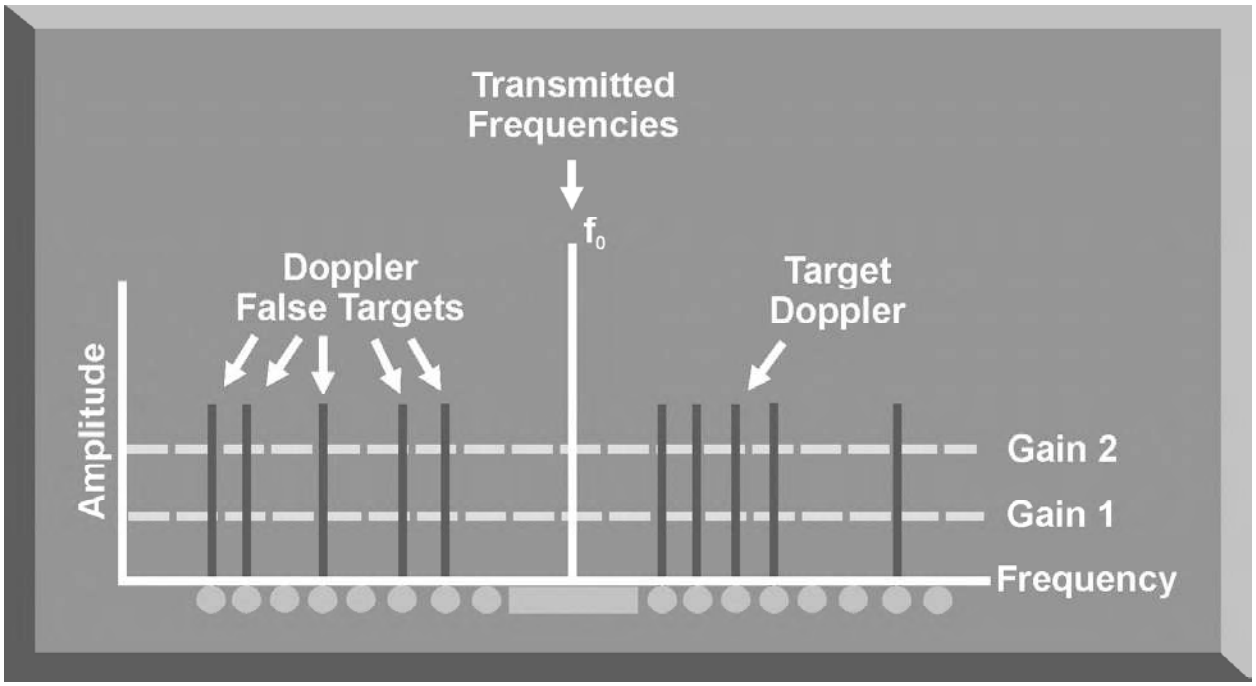

Figure 11-16. Impact of Doppler False Target Jamming

(1) The selected pulses are processed by the signal processor, and multiple Doppler frequencies are sent to the velocity tracking gate. In an attempt to distinguish the target from the jamming pulses, the signal processor increases the gain in each tracking filter, assuming the target Doppler has a higher amplitude than the jamming pulses. This increase in gain sets up the velocity tracking loop for a narrowband Doppler noise technique that will cause the real target to be lost among the generated false targets.

(2) The advantage of Doppler false target jamming is that it can initially confuse the radar signal processor and the radar operator as to the velocity of the real target. It also sets up the radar for narrowband Doppler noise technique and increases its effectiveness. The disadvantage is that the signal processor or the radar operator will eventually be able to distinguish the real target from the false targets based on its velocity. This jamming technique is much more effective when used in conjunction with other Doppler jamming techniques.

6. MONOPULSE DECEPTION JAMMING

The ability of monopulse tracking radars to obtain azimuth, range, and elevation information on a pulse-by-pulse basis make them extremely difficult to jam

(Figure 11-17). Amplitude modulation jamming used against conical scan or TWS radars, such as inverse scan and swept square wave, highlights a target, making monopulse tracking easier. Frequency modulation techniques, such as RGPO and VGPO, are equally ineffective. They serve as a beacon that aids the monopulse radar's target tracking ability. The monopulse radar may be able to track the jammer with more accuracy than tracking actual radar returns because target glint effects are absent from the jamming pulse. Monopulse angle jamming techniques can be divided into two main categories, system-specific and universal. Examples of system-specific jamming techniques include skirt frequency jamming, image jamming, and cross-polarization jamming. These techniques attempt to exploit weaknesses in the design and operation of specific monopulse radars. Cross-eye jamming, a universal technique, attempts to exploit all monopulse radar systems.

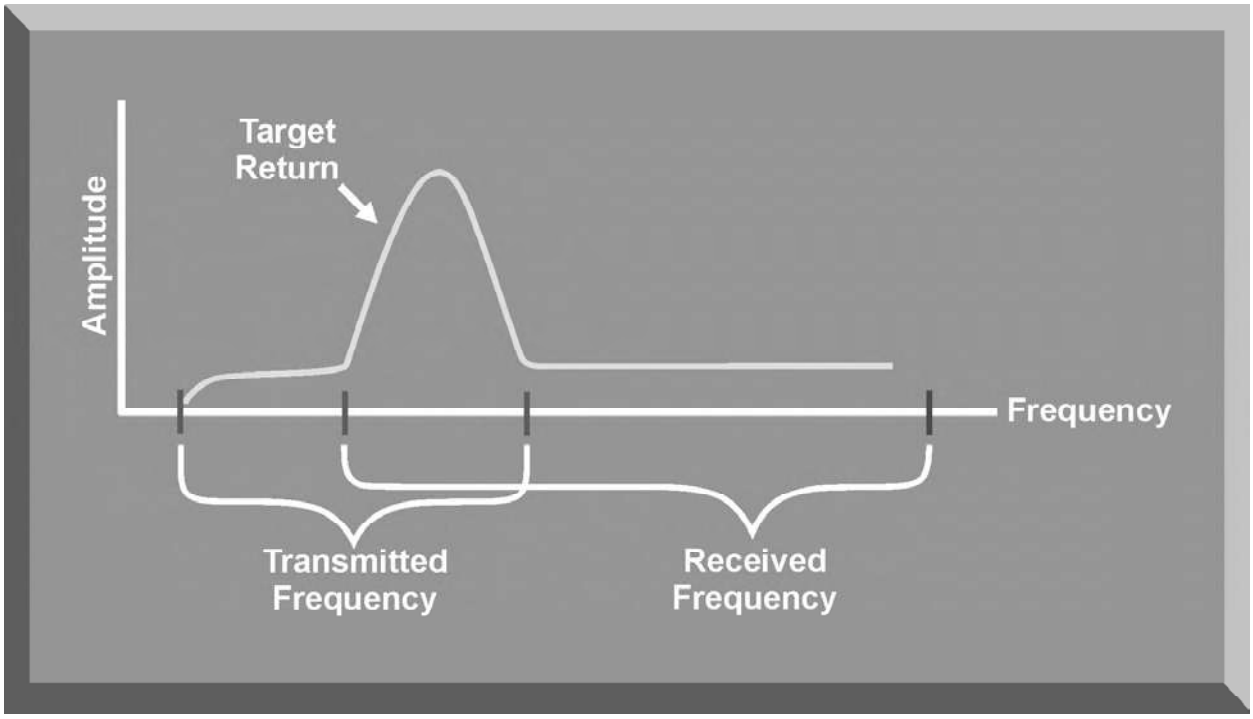

Figure 11-17. Monopulse Radar Receiver

a. Skirt frequency jamming, or filter skirt jamming, is designed to counter the monopulse receiver. Skirt frequency jamming is based on the fact that the intermediate frequency (IF) filter of the monopulse receiver must be correctly tuned to the transmitting frequency of the monopulse radar. It these two components are not exactly tuned, the target signal may be presented on the edge, or skirt, of the receiver IF filter. This offers an opportunity to inject a jamming signal into this skirt (Figure 11-18).

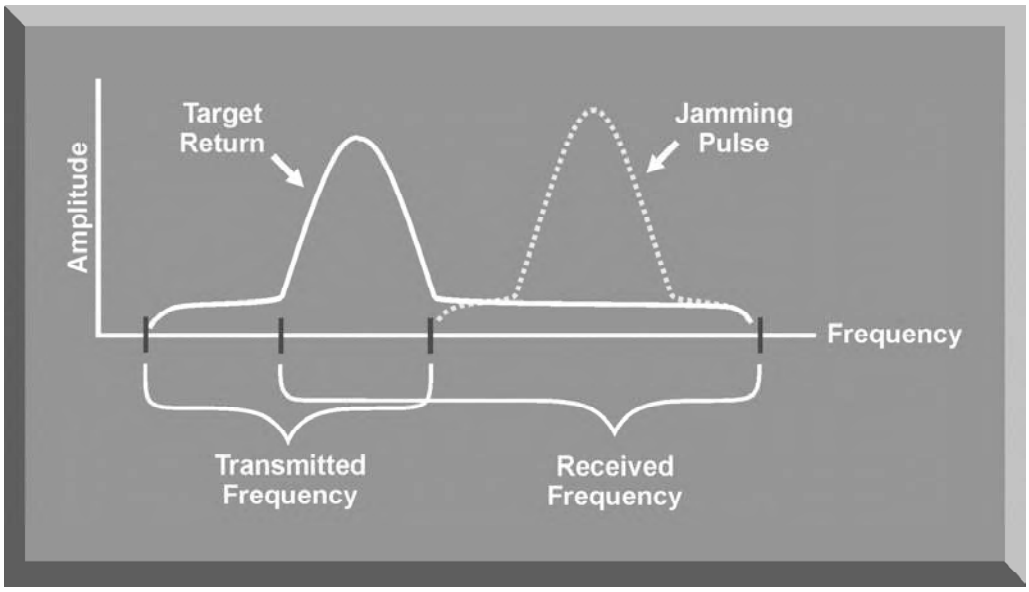

Figure 11-18. Filter Skirt Jamming Pulse

(1) Filter skirt jamming attempts to take advantage of this frequency imbalance by transmitting a jamming pulse tuned slightly off the radar transmitted frequency and in the middle of the receiver IF filter. This jamming pulse will generate a false error signal and drive the antenna away from the true target return.

(2) A well designed and maintained monopulse system does not have a frequency imbalance. The transmitter and IF filter frequencies will be identical. Jamming signals that are even slightly out of this narrow frequency range will not affect the monopulse tracking capability of the radar (Figure 11-19).

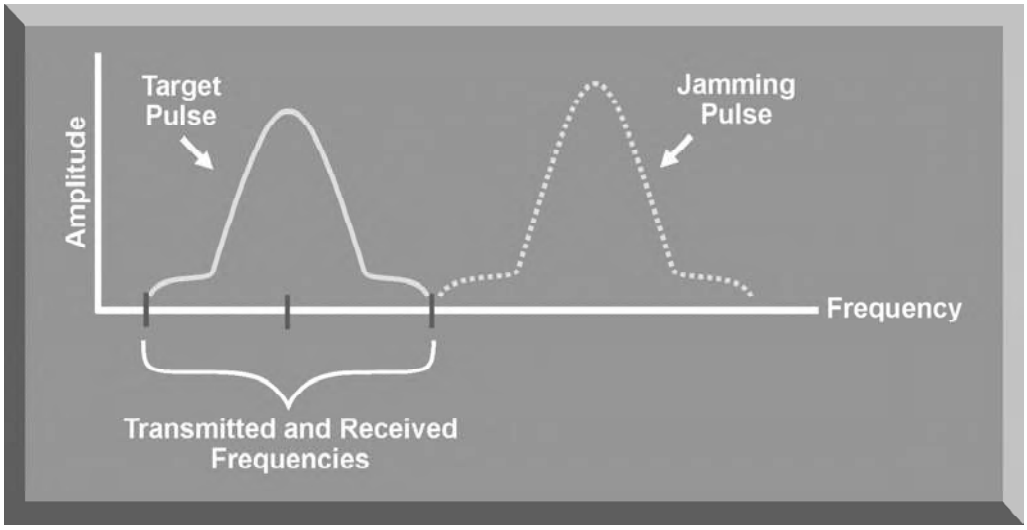

Figure 11-19. Ineffective Filter Skirt Jamming

(3) Effective filter skirt jamming requires extensive knowledge of the internal operation of the IF filter. This information can normally be obtained only by system exploitation. Variances from radar to radar and frequency imbalance exists from one radar IF filter to another. This creates a high degree of uncertainty in the effectiveness of this technique.

b. Image jamming exploits another potential weakness in the monopulse receiver (Figure 11-20). Some monopulse receivers have a wide-open front end with no preselection before the mixer. If the jammer transmits a pulse at the intermediate, or image, frequency, but out of phase with this frequency, the phase of the target tracking signal will be reversed and the antenna will be driven away from the target (Figure 11-21). Effective image jamming requires detailed information on the operation of the monopulse receiver. Of particular importance is the image, or intermediate, frequency and whether the local oscillation frequency is above or below the transmitted frequency. This may require exploitation of the monopulse threat system. In addition, a well-designed monopulse system has preselection in the front end and will reject signals that are out of phase with the transmitted frequencies. This capability renders image jamming ineffective.

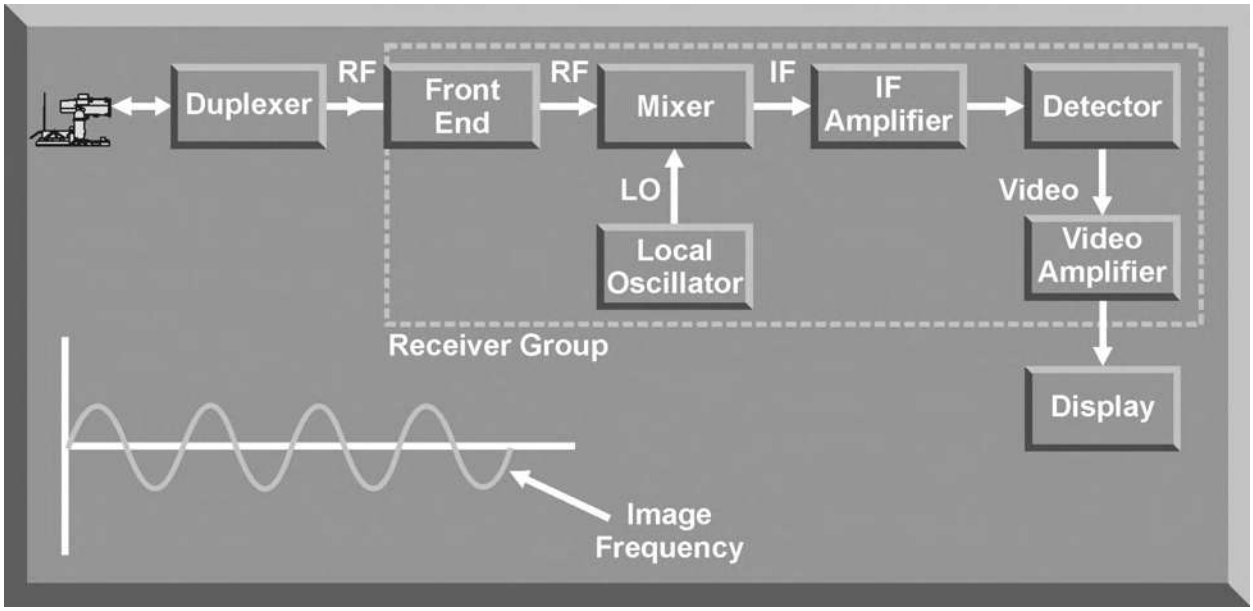

Figure 11-20. Monopulse Image Frequency

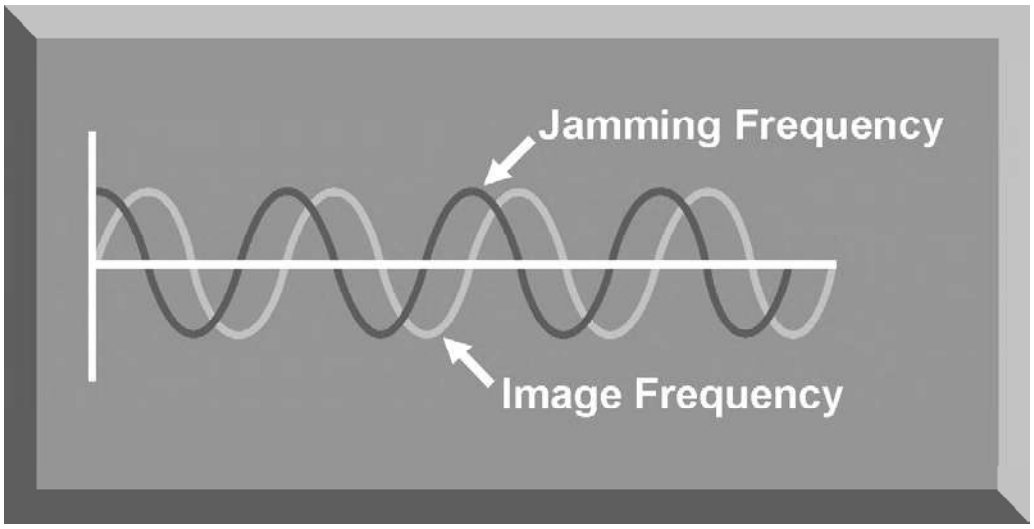

Figure 11-21. Monopulse Image Jamming

c. Cross-polarization jamming exploits the difference in the monopulse antenna pattern for a jamming pulse that is polarized orthogonal to the design polarization. The antenna pattern for a two-channel monopulse radar using sigma and delta beams shows the tracking point to be between the two beams (Figure 11-22). This is true if the radar is using its design polarization. However, the radar antenna also has a receiving pattern for a signal that is cross-polarized with the design frequency. For a cross-polarized signal, the tracking point is shifted one beamwidth to the right. This shift in the tracking point results in a target tracking signal that is 180° out of phase with the real signal. To be effective, a jamming signal polarized orthogonally to the design frequency of the radar would have to be 25 to 30 decibels, or about 1000 times, stronger than the radar signal.

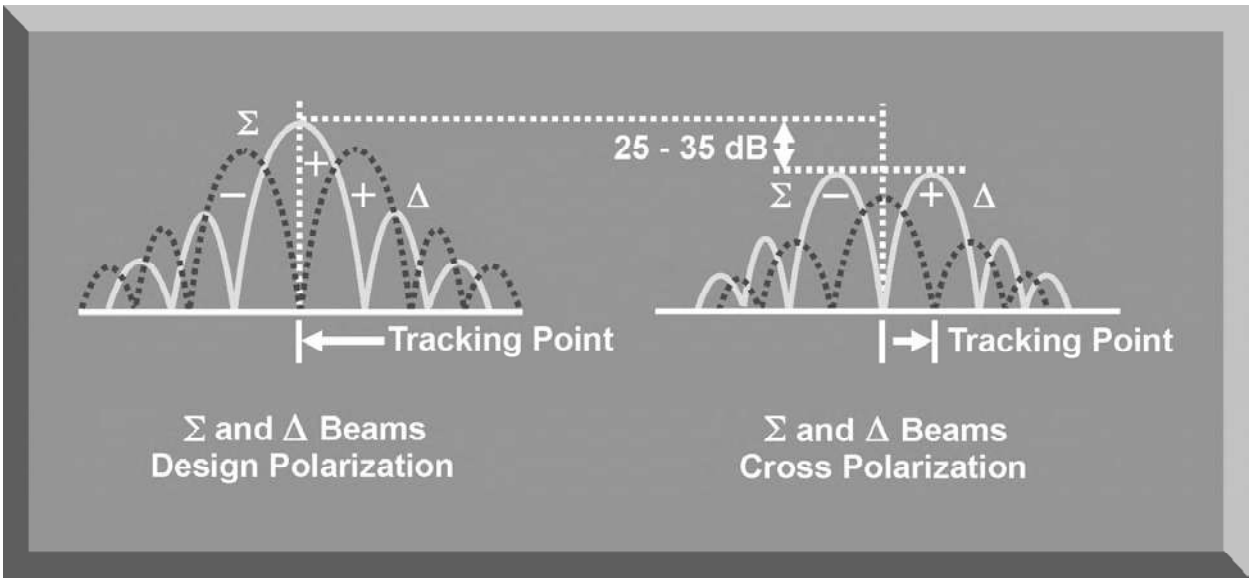

Figure 11-22. Cross-Polarization Antenna Pattern

(1) A cross-polarized jammer must receive and measure the polarization of the victim monopulse radar. The jammer then transmits a very high power jamming signal at the same frequency, but orthogonally polarized, to the victim radar. As a rule, the jamming signal must be 25 to 30 dBs stronger than the target return to exploit the tracking errors in the cross-polarized antenna pattern. Additionally, it must be as purely orthogonal to the design polarization as possible. Any jamming signal component that is not purely orthogonal will highlight the target and require more jamming power to cover the target return.

(2) A cross-polarized jammer must be able to generate a powerful jamming pulse that is polarized orthogonal to the victim radar. A cross-polarized jammer that generates the power and purity of polarization required to defeat monopulse angle tracking poses extreme technological challenges.

d. Cross-eye jamming is a complex technique that attempts to distort the wavefront of the beams in a monopulse radar and induce angle tracking errors. It exploits two basic assumptions of monopulse tracking logic in comparing target returns on a pulse-by-pulse basis. The first assumption is that a target return will always be a normal radar pulse echo. The second assumption is that any shift in amplitude or phase in a target return is due to the tracking antenna not pointing directly at a target. This condition generates an error signal and the antenna tries to null, but the amplitude or phase shifts.

(1) Cross-eye jamming attacks the two assumptions through a process of receiving and transmitting jamming pulses from different antennas separated as far apart as possible. In Figure 11-23, the phase front of a monopulse signal is received by the number 1 receive antenna, amplified by the repeater, and transmitted by the number 2 transmit antenna. The same phase front then hits receive antenna number 2, is shifted 180°, amplified by the repeater, and transmitted by the number 1 transmit antenna. These two out-of-phase signals must be matched in amplitude and must exceed the amplitude of the target return.

(2) When these jamming signals arrive at the victim radar, the tracking loop attempts to null out the amplitude and phase differences. With two widely spaced jamming sources at different phases, the antenna never achieves a null position or tracking solution. The distance between antenna pairs is an important parameter that determines the effectiveness of cross-eye jamming. The wider the spacing between antenna pairs, the more distortion in the victim's wave front near the true radar return. Most fighter aircraft do not provide sufficient spacing between the antennas to maximize effectiveness. Effectiveness is also lost when the aircraft is abeam or going away from the radar. To further complicate matters, when the radar is directly in front of the aircraft, the jamming pulses must have a power at least 20 dBs above the target return. Cross-eye jamming can also be defeated with a leading-edge tracker that rejects jamming signals arriving at the antenna behind the target return.

(3) Countering monopulse angle tracking is the greatest challenge for self-protection jamming systems. Skirt jamming and image jamming have had limited success. Cross-polarization and cross-eye jamming techniques require complex and sophisticated circuitry and much power.

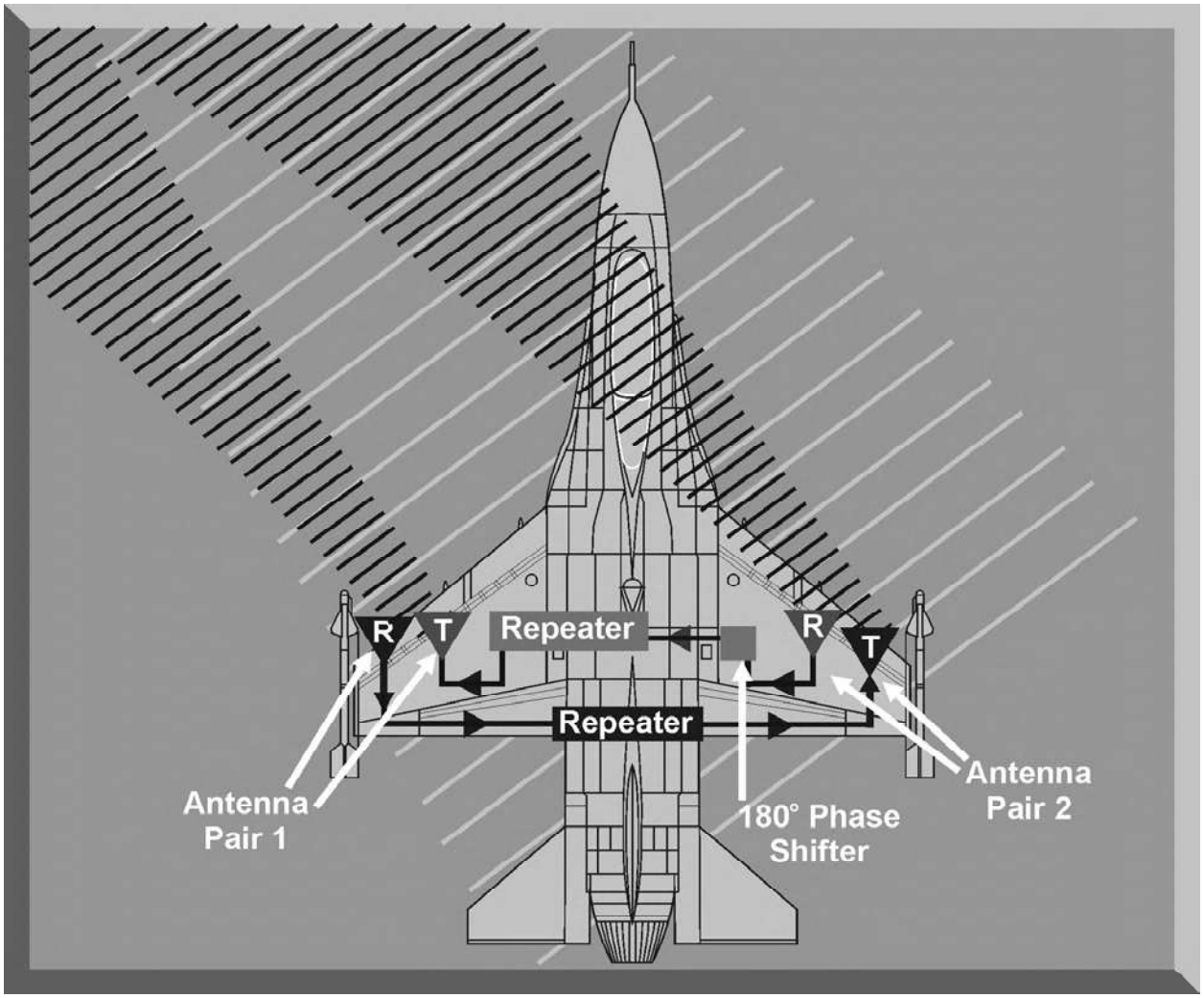

Figure 11-23. Cross-Eye Jamming

7. TERRAIN BOUNCE

Terrain bounce is a jamming technique used primarily at low altitude. It is used to counter semi-active, air-to-air missiles and monopulse tracking radars. The technique involves a repeater jammer that receives the radar or missile guidance signal. The jammer amplifies and directs this signal to illuminate the terrain directly in front of the aircraft. The missile or radar tracks the reflected energy from the spot on the ground instead of the aircraft (Figure 11-24).

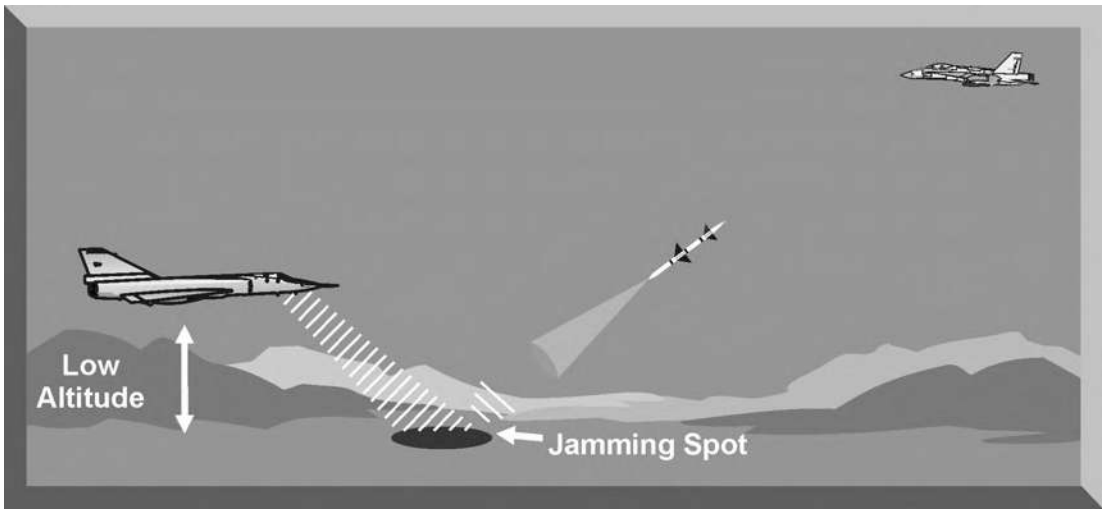

Figure 11-24. Terrain Bounce

a. To be effective, the terrain bounce jamming antennas should have a narrow elevation beamwidth and a broad azimuth beamwidth. This transmission pattern maximizes the energy directed toward the ground and minimizes the energy transmitted toward the missile or radar. To overcome signal losses associated with uncertain terrain propagation, the jamming system should also generate high jamming power. This ensures the energy reflected from the terrain is higher than the energy in the aircraft return. The terrain bounce jamming antennas should have very low sidelobes to preclude activation of any home-on-jam (HOJ) missile capability. For an air-to-air missile, the terrain bounce technique should be activated at long range. This will initially put the aircraft and the jamming spot in the same resolution cell. As the range decreases, the missile will be decoyed by the higher power in the jamming spot.

b. Some problems associated with terrain bounce jamming include the uncertainty of the signal scattering parameters of the various terrain features and the possible changes in signal polarization caused by terrain propagation. In addition, terrain bounce jamming can place maneuvering restrictions and maximum altitude limitations on the aircraft.

8. SUMMARY

There are several deception jamming techniques that can be employed to counter threat radar systems. The effectiveness of these techniques can be enhanced when they are employed in combination. For example, the effectiveness of an RGPO technique is enhanced when an angle deception technique is also employed. Determining the most effective deception technique, or combination of techniques, can present a challenge to intelligence and engineering analysts. However, when employed with maneuvers and chaff, deception techniques can mean the difference between success and failure on the modern battlefield.

CHAPTER 12. DECOYS

1. INTRODUCTION

A decoy is a device designed to look to an enemy radar more like an aircraft than the actual aircraft itself. Decoys do three primary missions: they saturate the enemy's integrated air defense system (IADS), coerce the enemy into exposing his forces prematurely, and defeat tracking by enemy radar. This chapter will discuss saturation decoys, towed decoys, and expendable active decoys. Chaff and flare systems will be discussed in separate chapters.

2. SATURATION DECOYS

A saturation decoy is usually an expendable vehicle designed to emulate a penetrating aircraft. Its mission is to deceive and saturate an enemy's IADS. Employing multiple saturation decoys can force an IADS to devote critical resources to engage these false targets. This depletes enemy assets available to engage penetrating aircraft. In addition, ground or air launched saturation decoys can be used to stimulate the IADS, to collect intelligence data, or to initiate attacks by suppression of enemy air defense (SEAD) assets. The three main characteristics of saturation decoys are their electronic signature, their flight program, and their mission type.

a. Saturation decoys must present an electronic signature, or radar return, that is indistinguishable from the aircraft they are protecting. Decoys can do this by either passive or active measures, or use a combination of both. A passive decoy is essentially a flying radar reflector. The size, shape, and materials used in the decoy are optimized to ensure that the proper amount of radar energy is returned to the enemy radars. Active decoys employ radar repeater systems to receive the enemy radar signal, amplify it and send back a radar return of the proper size to confuse the enemy. Reflecting or transmitting the proper size radar return is critical for both passive and active decoys. A return that is too large or too small will allow the enemy radar operator to differentiate between decoys and aircraft, causing the decoys to be ignored.

b. To continue deceiving an enemy IADS, a decoy must do more than provide the proper-sized radar return. Possessing flight characteristics similar to the aircraft it is protecting increases the probability that the decoy will effectively deceive an IADS for a sustained period of time. Modern decoys can either be powered with rockets, miniature engines, or simply glide for very long distances based upon the altitude and airspeed of the jet that releases them. Additionally, their flight paths can be pre-programmed into an onboard autopilot, allowing the decoy to fly an independent ground track, thus increasing their appearance as attack aircraft worth tracking.

c. Saturation decoys carry out two of the three decoy missions. Launched in significant numbers, they can saturate or overburden an IADS. Meanwhile, their realistic electronic image and preprogrammed flight paths entice the enemy to turn on radars and show his forces.

(1) Saturation decoys launched in coordination with an attacking strike package force the enemy to take time to process meaningless tracks and tie up critical assets. In this role, decoys primarily work against the early warning network of the enemy IADS by presenting the IADS with numerous targets to sort and track. Resources committed to tracking decoys may not be available to track actual aircraft. Additionally, if an enemy knows that decoys are present, he may not commit any resources against targets for fear they are just decoys.

(2) Time of radiation or "emission control" is a critical factor for acquisition and target tracking radars. To be effective and survive on the battlefield, ground threat radars radiate as little as possible; too much time radiating allows ELINT collectors to find their location and either direct aircraft to avoid them or call in an attack upon them. Therefore, when a decoy can get a radar to emit, the radar is now essentially compromised and can be avoided or attacked. Getting the enemy's radars to emit is called "stimulating the IADS," which is generally a precursor to any threat suppression mission.

(3) An extremely successful example of using decoys to stimulate the IADS was carried out in the Bekaa Valley in 1982. The Israelis opened the conflict by launching saturation decoys to successfully simulate an attack. While the Syrians reloaded, Israeli fighters attacked, destroying 17 of 19 Syrian SA-6s in the beginning of the battle. With the ground threat neutralized, the Israeli Air Force went on to destroy 85 Syrian fighters in the pure air-to-air conflict that resulted.

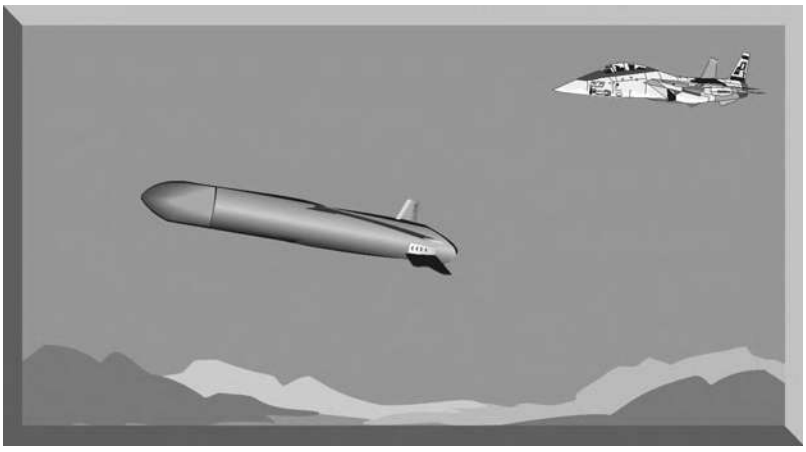

Figure 12-1. Tactical Air Launched Decoy

d. Two examples of saturation decoys are the Navy's Tactical Air Launched Decoy (TALD) in Figure 12-1 and the Air Force's proposed Miniature Air Launched

Decoy (MALD) in Figure 12-2. Both of these decoys can work actively or passively and both have pre-programmable flight paths. The TALD is an unpowered decoy normally launched from an F-14 Tomcat. The Air Force's MALD is a smaller jet-powered decoy also designed to be used by fighter aircraft. The MALD is 90 inches long, 6 inches in diameter, and has 25-inch wings that are foldable–essentially it is the size of an air-to-air missile. Because of its small size, the MALD can be carried into the target area before it is launched. Once launched it uses its speed, independent flight path, and electronically manipulated radar signature to make acquisition radars and target tracking radars mistake it for one of the attacking aircraft.

Figure 12-2. Miniature Air Launched Decoy (MALD)

3. TOWED DECOYS

A towed decoy is a small jammer that is physically attached to the aircraft (Figure 12-3). Unlike the saturation decoys that work against the IADS, the towed decoys are for individual aircraft survival. Towed decoys are designed to defeat enemy missiles in the final stages of an engagement; therefore, towed decoys, as well as other expendables, are known as endgame countermeasures. While towed decoys are primarily designed to provide sufficient miss distance between an attacking semi-active radar missile and the protected aircraft, they may also be effective against pulse Doppler radars and monopulse radars.

a. To be effective, the towed decoy must turn on within the threat radar's resolution cell after the radar is tracking the protected target. To successfully decoy the missile, the towed decoy must return radar signals with sufficient power to simulate a radar cross section (RCS) significantly larger than that of the

protected target. There are currently two generations of towed decoys on the market. Their primary difference lies in the connection each has with the aircraft towing it.

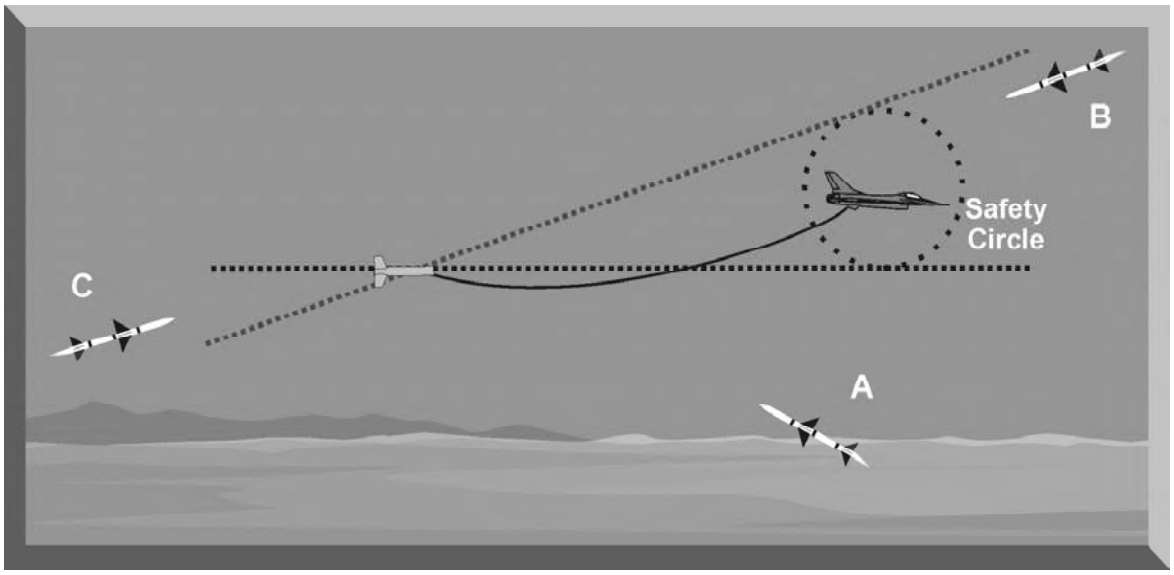

Figure 12-3. Towed Decoy

(1) The first generation of towed decoys contains a simple repeater jammer that enhances any signal it receives in the proper frequency range. The enhanced signal is stronger than the aircraft signal so the missile is lured towards the decoy. These decoys are stand-alone units that contain all the electronics, processors, receivers and transmitters within them. The only tie to the aircraft is for power and status. One of the big advantages of these simple repeater devices is that they do not require the exact frequency of the enemy radar systems to be effective, they will enhance any signal coming at them. An area of concern with the use of towed decoys is possible conflict between the onboard jamming system and the towed decoy. The onboard system could overpower the decoy, causing the attacking missile to ignore the decoy and track the aircraft.

(2) The second generation of decoys is tethered to the aircraft via fiber optic cable. Through this cable travels the different jamming modulations to be used by the decoy. These fiber optic towed decoys (FOTD) only contain the transmitters; the remaining items are in the jet or the pod. This system allows for more complex jamming through the decoy, including cooperative jamming between the aircraft and the decoy.

b. The separation required between the decoy and the aircraft is a primary consideration in developing a towed decoy system. The towed decoy should be positioned far enough behind the aircraft to preclude warhead fragments from missiles guiding on the decoy from also impacting the aircraft. Missile A in Figure

12-3 depicts a situation where the missile will detonate well outside of the aircraft's safety circle. From a pilot perspective, any restrictions on aircraft maneuvering imposed by a towed decoy are very important. The number of decoys that can be carried and the time required for decoy deployment are also important employment considerations.

c. Achieving 360° coverage is a primary limitation of a towed decoy system. When an aircraft equipped with a towed decoy is abeam a threat radar, the radar may be able to discriminate between the aircraft and the decoy. This is a function of the resolution cell of the radar. In addition, missiles approaching from a high-aspect angle, and above the aircraft (Figure 12-3 - Missile B), may fuse on the aircraft while guiding to the decoy. Missiles approaching from a low-aspect angle (Figure 12-3 - Missile C) may not fuse on the decoy and subsequently acquire and fuse on the aircraft. Finally, if the decoy is destroyed or lost, the time required to deploy a replacement decoy is critical, especially if the aircraft is engaged by multiple missiles.

d. An example of a fielded towed decoy system is the AN/ALE-50 (Figure 12-4). This first generation towed decoy system is found on Air Force F-16 and B-1 aircraft, and there is a version that is integrated into the ALQ-184 pod.

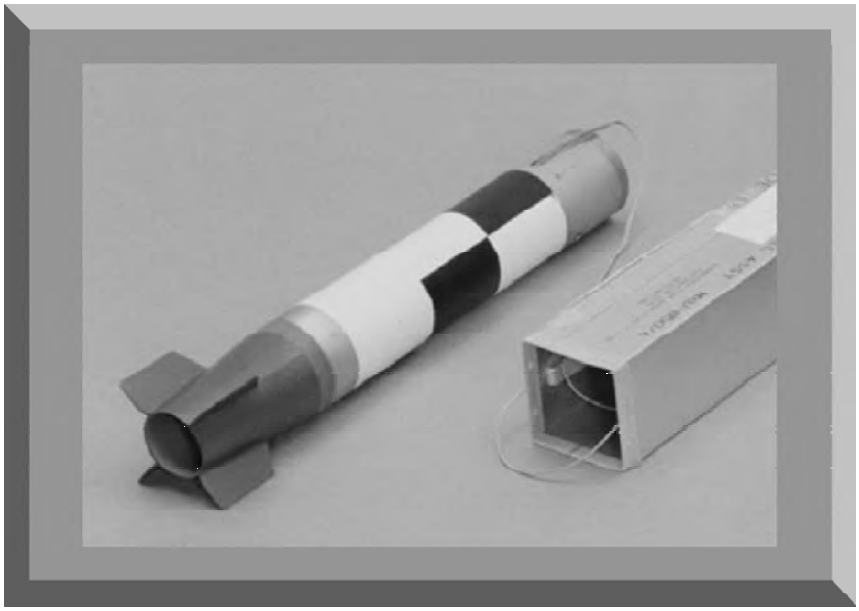

Figure 12-4. AN/ALE-50 System

(1) The system consists of a launch controller subsystem and towed decoys. The launch controller houses the decoy before it is launched, provides power to the decoy, and provides for the monitoring of the electronics. The decoy body is a factory sealed, self-contained unit with everything except for power. Power comes through the tether from the host aircraft; the decoy sends its operating status back through the tether to the aircraft.

(2) ALE-50 decoy use is cleared throughout the flight regime of the F-16 and B-1. Decoys can be deployed without being turned on, but once a decoy has been deployed, it cannot be reeled back in and must be severed before landing. Procedures are in place to reduce the chance that the onboard jamming system will negate the decoy.

(3) The ALE-50 towed decoy is a wideband RF repeater that provides self-protection EA by receiving, electronically amplifying, and retransmitting enemy radar RF signals. Upon receiving a threat radar signal, this simple repeater amplifies the signal and retransmits it. This provides the radar with two signals, one reflected from the aircraft and a stronger one from the decoy. With the signal from the decoy being the more attractive, the radar or missile guides towards the decoy. During combat operations over Kosovo, ALE-50 decoys were credited with saves for both F-16s and B-1s.

4. EXPENDABLE ACTIVE DECOYS

Expendable active decoys are designed to lure the tracking gates of an enemy's radar away from the aircraft. They are endgame countermeasures like towed decoys, but they differ in that expendable decoys free-fall or glide to the ground as opposed to being towed behind the aircraft.

a. Expendable decoys are small, active jamming systems designed to be expended by existing aircraft chaff and flare dispensers, such as the AN/ALE-40 or the AN/ALE-47. Expendable decoys can employ noise or deception jamming with noise jamming being the most common. Deception jamming techniques can be employed to enhance effectiveness against pulse Doppler radars. There are two challenges associated with expendable jammers: the amount of the time the jammer is effective and the packaging (Figure 12-5).

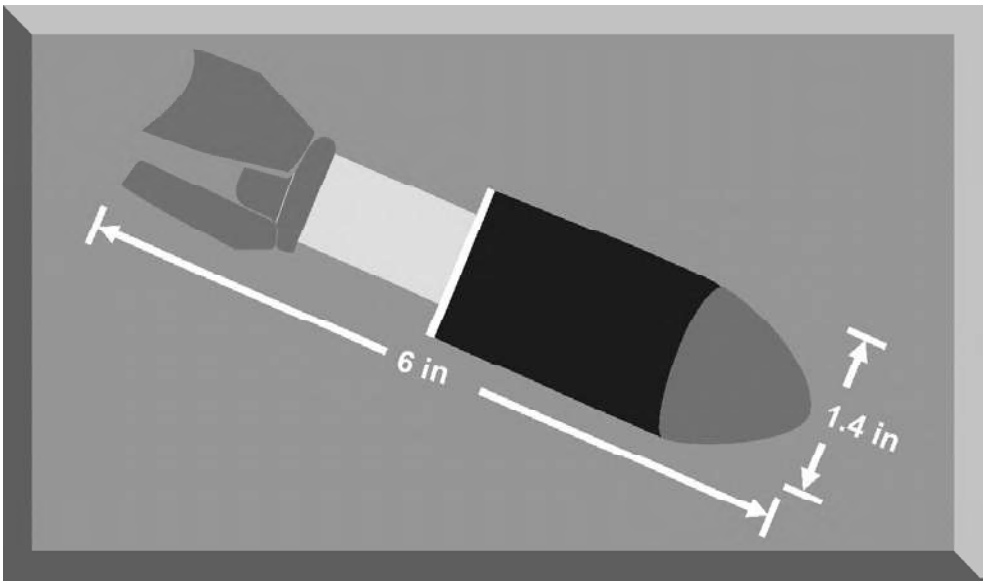

Figure 12-5. Generic Expendable

b. Expendable decoys are designed to provide protection for the dispensing aircraft for a specific period. The dispensing altitude and rate of fall determine this period of effective coverage. Expendable decoys can employ small parachutes of aerodynamic design to slow the rate of fall and increase the time of effective coverage. If the period of coverage is too short, multiple expendable decoys must be employed. This places a premium on timely employment and expendables management.

c. The primary components of an expendable decoy are the transmit and receive antennas, techniques generator, amplifier, and power supply. The transmit and receive antennas should be isolated and capable of high gain, wide bandwidth, and should use compatible polarization with the victim radar. The techniques generator must recognize the victim radar signal and generate the appropriate jamming response. The amplifier must be capable of generating a high power jamming signal over a wide frequency range. To meet these requirements, sophisticated computer and miniaturization techniques are used, and the components packaged to all fit in the aircraft dispenser. These factors impact the cost of expendable decoys and may limit the availability of these assets.

d. The Generic Expendable, RTE-1489, commonly called the GEN-X decoy is a fielded expendable active decoy. The decoy is sized to fit into a 1.4 x 1.4 x 5.8 inch cartridge and take advantage of new microwave/millimeter-wave integrated circuit (MMIC) technology. The GEN-X is programmable and features a broadband antenna and wide frequency coverage. After ejection, the decoy extends three small fins for stability. Its battery ignites to provide power, the receiver locks on to the threat radar signal, and a deception signal is generated and transmitted.

5. SUMMARY

Decoys simply provide the enemy with more targets to process. In the case of saturation decoys, this forces the enemy to commit resources against false targets, or show his defenses. For towed decoys and expendable active decoys, it makes the missile or tracking radar separate a real target from more electronically attractive decoys.

CHAPTER 13. CHAFF EMPLOYMENT

1. INTRODUCTION

Chaff was first used during World War II when the Royal Air Force, under the code name "WINDOW," dropped bales of metallic foil during a night bombing raid in July 1943 (Figure 13-1). The bales of foil were thrown from each bomber as it approached the target. The disruption of German AAA fire control and ground control intercept (GCI) radars rendered these systems almost totally ineffective. Based on this early success, chaff employment became a standard bomber tactic for the rest of the war.

Figure 13-1. "WINDOW" – The First Operational Employment of Chaff

a. Chaff is one of the most widely used and effective expendable electronic attack (EA) devices. It is a form of volumetric radar clutter consisting of multiple metalized radar reflectors designed to interfere with and confuse radar operation. It is dispensed into the atmosphere to deny radar acquisition, generate false targets, and to deny or disrupt radar tracking. Chaff is designed to be dispensed from an aircraft and function for a limited period.

b. Even with the development and deployment of advanced radar threat systems, chaff continues to be an extremely effective EA device. Experience gained during the Vietnam conflict, the 1973 Yom Kippur War, and DESERT STORM clearly shows that chaff effectiveness against radar threats is still a factor with which the enemy must contend. This is especially true when chaff is employed with self-protection jamming and aircraft maneuvers.

c. Chaff screening and self-protection are the two basic chaff employment tactics. Chaff screening tactics, including area saturation and chaff corridor employment, are designed to confuse and deny acquisition information to the early warning, GCI, and acquisition radars supporting surface-to-air missile (SAM) systems. Self-protection tactics are designed to counter acquisition and target tracking radars (TTRs). When used with jamming and maneuvers, chaff can cause TTRs to break lock or generate survivable miss distances if a SAM is fired at the aircraft.

2. CHAFF CHARACTERISTICS

To understand how chaff affects radar systems, it is important to understand its characteristics. The most important chaff characteristics are radar cross section (RCS), frequency coverage, bloom rate, Doppler content, polarization, and persistence.

a. RCS is a measure of the net reradiated energy from a target to the illuminating radar. The RCS of an aircraft varies based on the size, shape, type of skin surface, configuration, and aspect to the illuminating radar. Figure 13-2 shows the effect of aspect on aircraft RCS. The RCS is greatest when the aircraft aspect is 90°, or abeam the radar. The lowest RCS occurs near the 30-70° and 110-150° of aspect. Since the aircraft RCS also varies based on frequency, the victim radar's frequency is a key factor. To be effective, chaff must be dispensed in large enough quantities to create an RCS greater than the aircraft RCS.

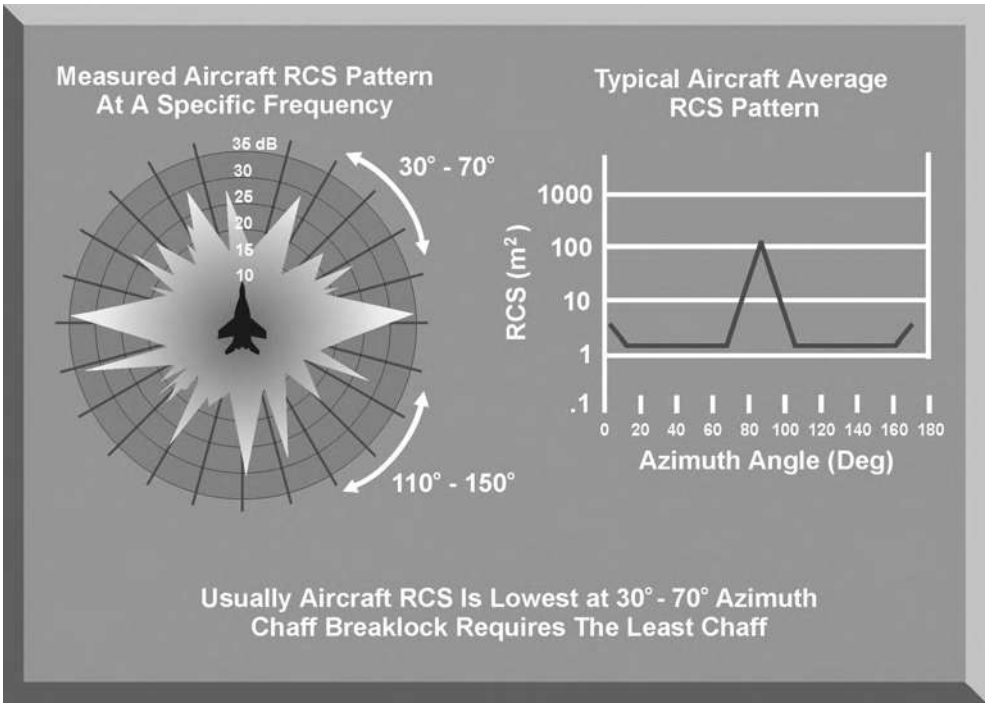

Figure 13-2. Aircraft Radar Cross Section (RCS)

(1) The RCS of a chaff bundle depends on the frequency of the victim radar and the dispensing aircraft's relative position, or aspect. Figure 13-3 shows the RCS of a single RR-170 chaff cartridge based on frequency. It shows that the largest RCS occurs at about 3 GHz. However, for the spectrum between 2-18 GHz, which includes most SAM TTRs, the RCS of the RR-170 cartridge is over 50 square meters. Since the typical fighter aircraft RCS varies between 1 and 10 square meters, depending upon frequency and aspect, the RR-170 chaff cartridge should provide a sufficient RCS to mask the aircraft RCS.

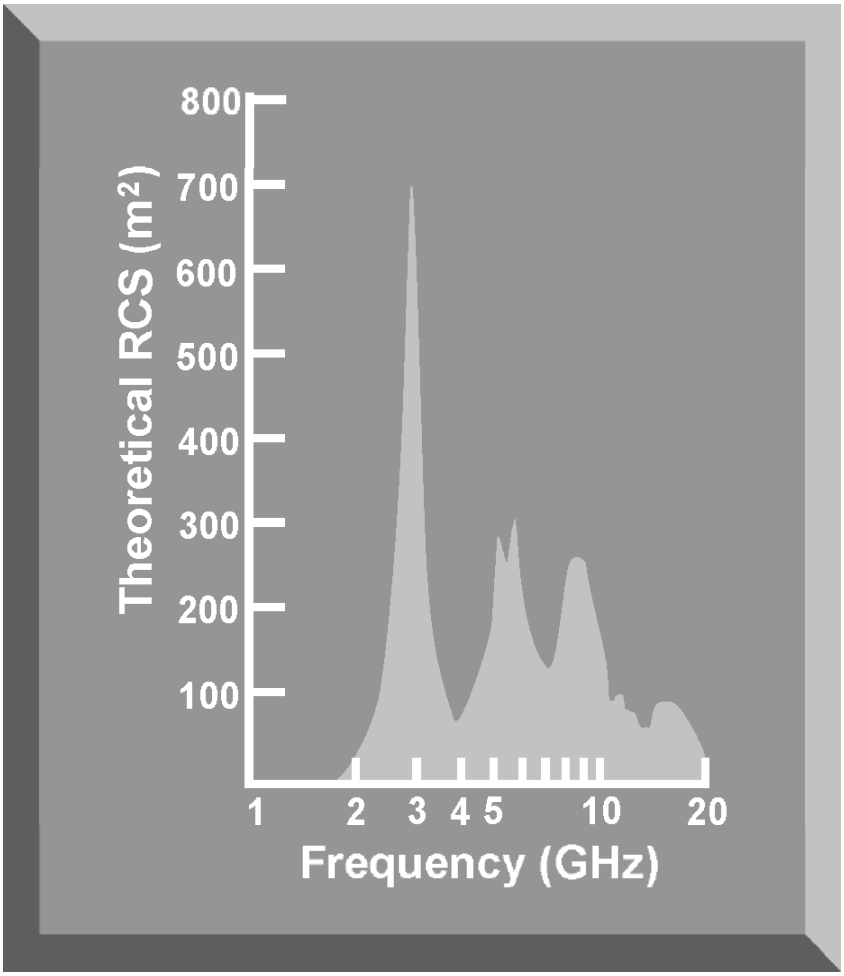

Figure 13-3. RR-170 Chaff Cartridge RCS

(2) The angular relationship, or aspect, between the aircraft and chaff bundle affects the chaff RCS presented to the victim radar. Chaff RCS is greatest when the chaff bundle and the aircraft are abeam the threat radar. It is smallest when the threat radar is off the nose or tail of the aircraft. Aspect is important when developing self-protection maneuvering and chaff dispensing tactics against threat radars (Figure 13-4).

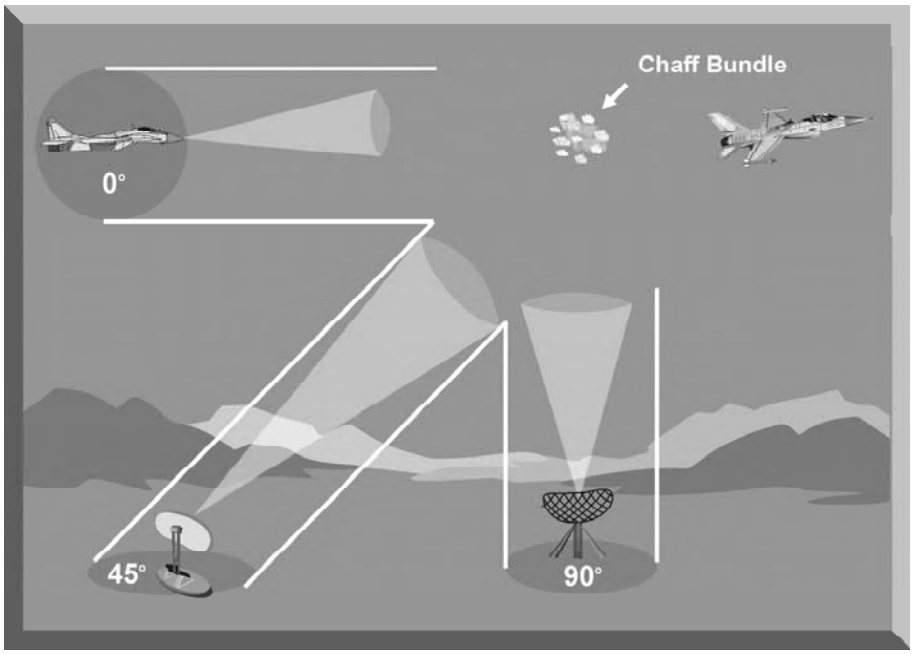

Figure 13-4. Threat Radar Aspect and Chaff RCS

(3) Dispensing multiple chaff bundles simultaneously does not necessarily increase chaff RCS. Multiple bundles increase the density of the chaff but do not directly enhance self-protection capabilities (Figure 13-5). This is an important consideration when developing chaff dispenser rates to counter threats.

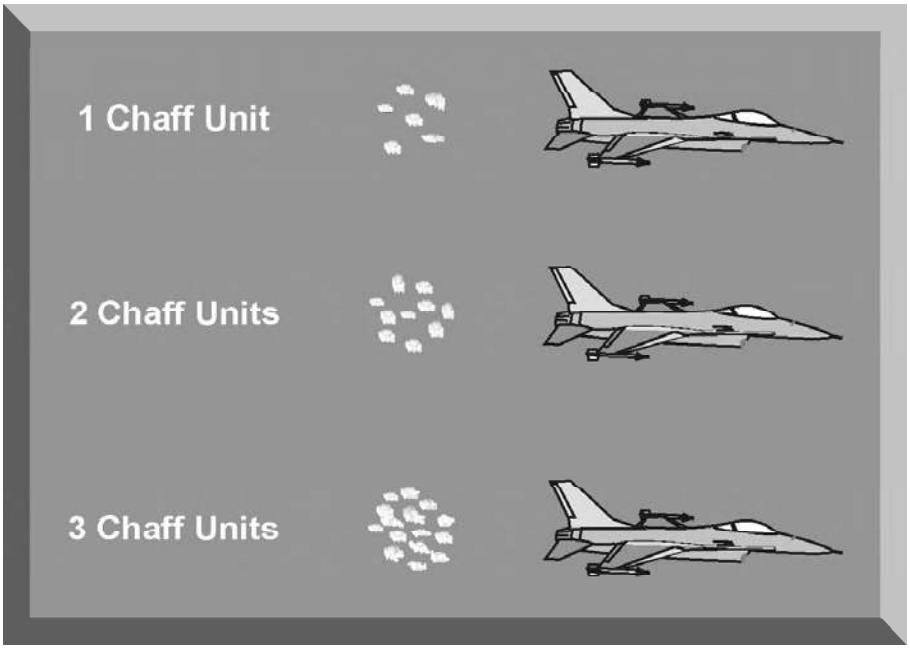

Figure 13-5. Impact of Multiple Chaff Cartridge Employment on Chaff RCS

b. Each strip of chaff is a dipole reflector that reradiates the electromagnetic energy received from an emitting radar and creates a radar echo. The optimum size is cut to about one-half the wavelength of the victim radar's RF. Since a single cut length is restricted in effectiveness to a narrow range of frequencies, different lengths are normally packaged together to provide coverage over a wide range of frequencies (Figure 13-6).

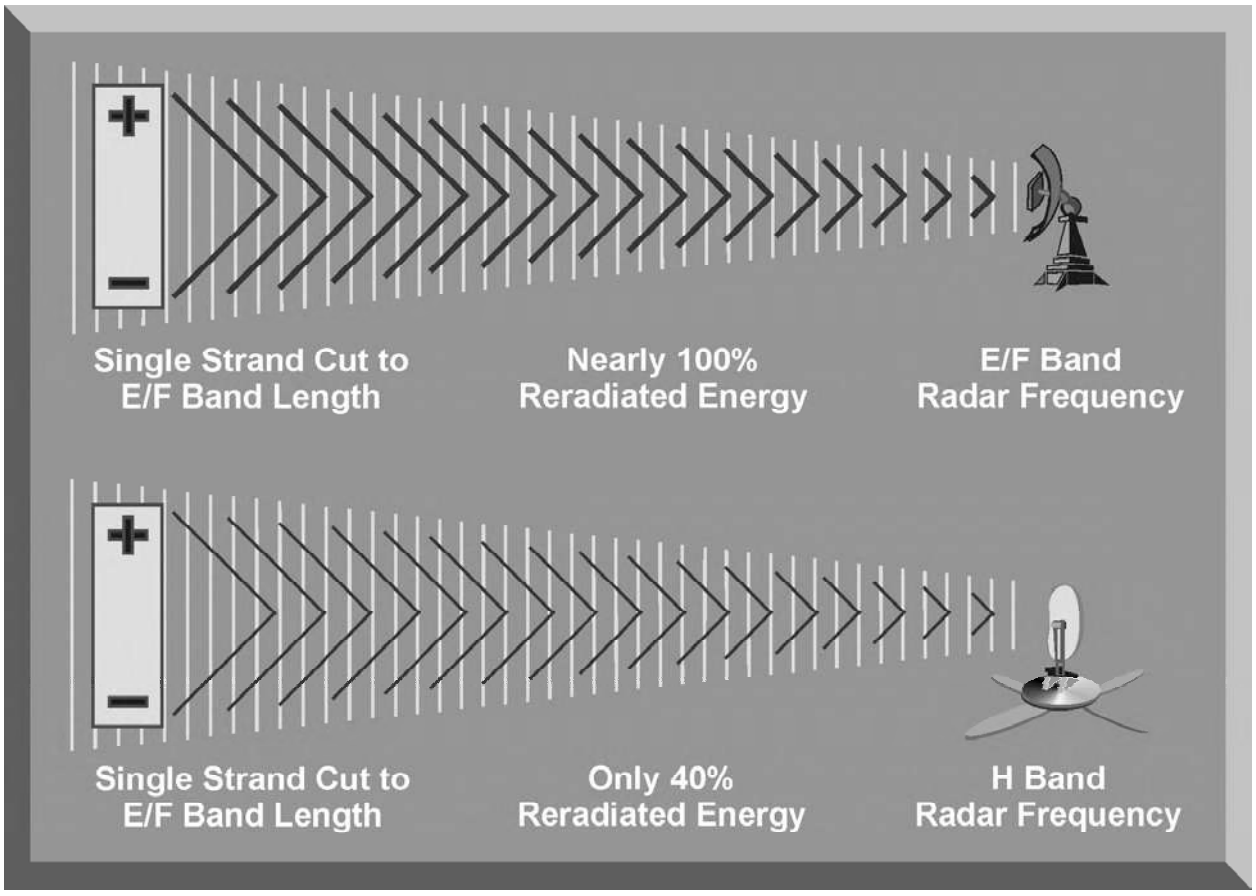

Figure 13-6. Chaff Length and Frequency Coverage

(1) Considerable research and development has reduced the size and increased the effectiveness of self-protection chaff. There are various chaff sizes, shapes, and materials. Most chaff carried on fighter aircraft are made of small aluminum strips, coated strips of nylon, or fiberglass. These strips are cut to various lengths and compressed into bundles that are small and light enough to allow the aircraft to carry and dispense multiple chaff bundles. These cuts of chaff are packaged into chaff cartridges and inserted into a dispenser on the aircraft. An explosive squib assembly ejects the cartridges from the dispenser and disperses the chaff (Figure 13-7).

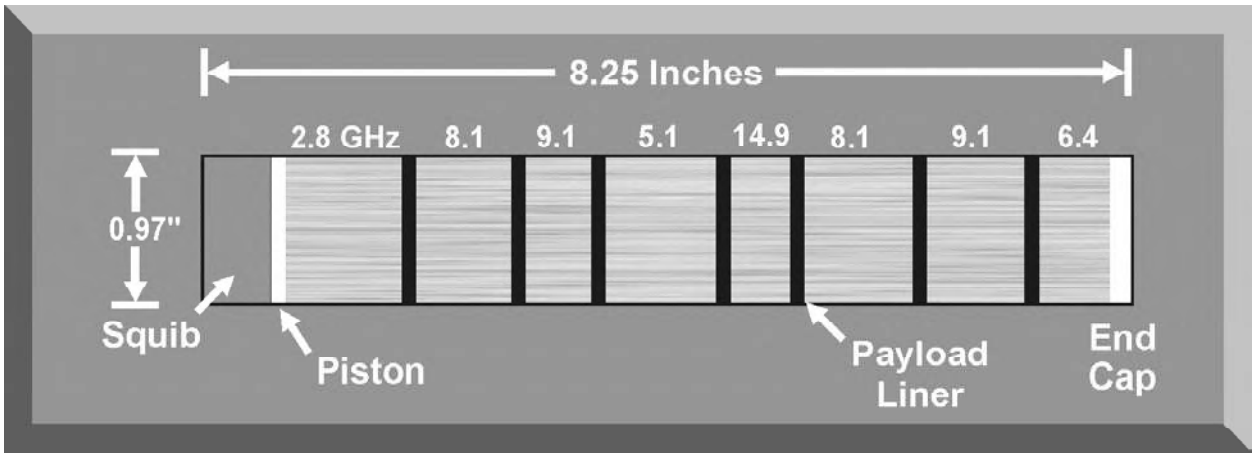

Figure 13-7. RR-170 Chaff Cartridge

(2) To provide as many dipoles as possible and present the maximum radar cross section, each chaff bundle has numerous chaff cuts to match a predetermined range of frequencies. Each chaff cartridge contains almost 3 million dipoles packaged in an eight inch by one-inch cartridge. The dipole frequencies cover the frequency range where most SAM TTRs and air-to-air radars operate (2 - 18 GHZ).

c. Bloom rate, the rate at which chaff will scatter, is also a very important characteristic of self-protection chaff. Self-protection chaff effectiveness is based on the relationship of bloom rate, chaff RCS, aircraft RCS, and the resolution cell of the threat radar system. The ability of chaff to effectively defeat a target tracking radar is directly related to the chaff dispense rate, which determines the chaff RCS, which should be larger than the aircraft's RCS. The chaff bundles must also bloom within the resolution cell of the radar.

(1) Chaff bloom rate is dependent on aerodynamic factors associated with the chaff type, the location of the dispenser on the aircraft, and the aircraft wake or turbulence. Heavy or dense chaff falls faster and blooms slower than lighter and less dense chaff. The location of the chaff dispenser on the aircraft affects the airflow in which the chaff will be dispensed. The ideal position for the dispenser is in the area where there is the most turbulence from the aircraft. Turbulence behind the aircraft is probably the most important factor affecting bloom rate. The more turbulent the airflow, the greater the bloom rate (Figure 13-8). Maneuvering the aircraft while dispensing chaff also enhances the chaff bloom rate.

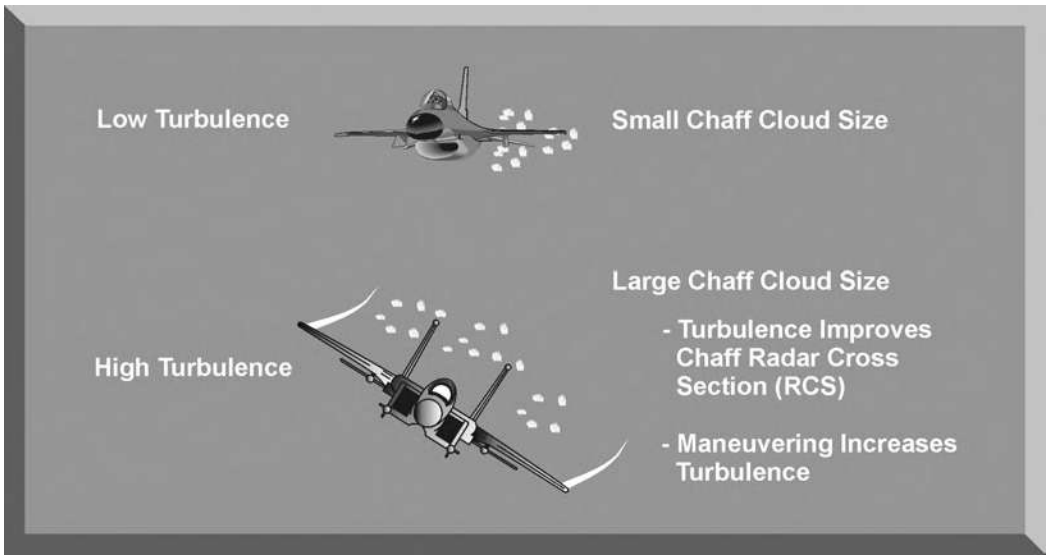

Figure 13-8. Impact of Turbulence and Chaff Bloom Rate

(2) To ensure that the victim radar is decoyed or that it transfers automatic tracking to the chaff, the chaff must bloom within the radar resolution cell. This resolution cell is a three-dimensional spheroid with dimensions based on the pulse width, horizontal beamwidth, vertical beamwidth, and the range of the aircraft (Figure 13-9). There are some rules of thumb that can be used when considering the bloom rate of chaff and the resolution cell of a particular radar. The shorter the pulse width of a radar, the faster the chaff has to bloom to be effective. The narrower the horizontal and vertical beamwidths, the faster the chaff has to bloom to be effective.

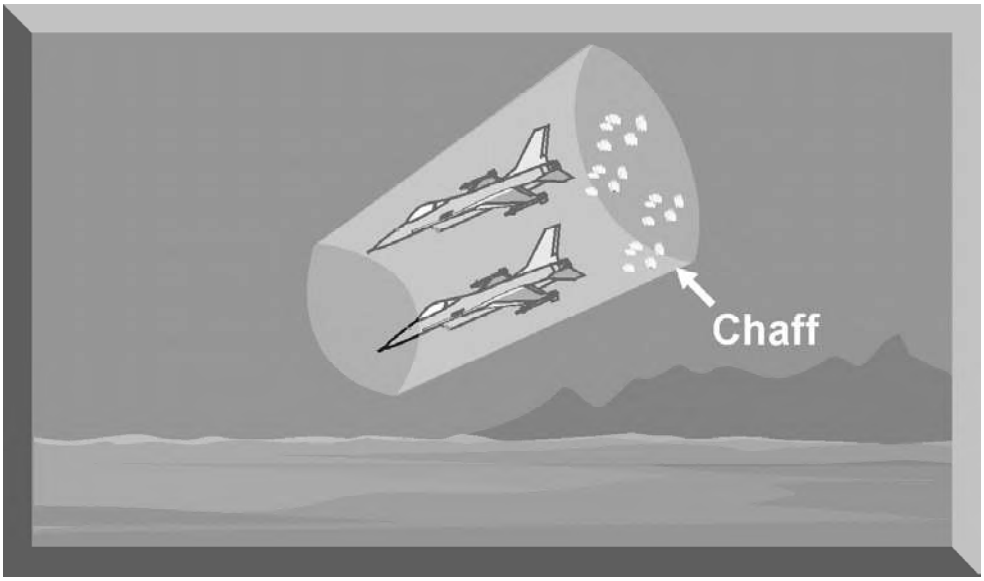

Figure 13-9. Chaff Bloom Rate and Radar Resolution Cell

d. Against Doppler radars, self-protection chaff is most effective when dispensed at or near the beam, relative to the threat radar. When chaff is dispensed in the airstream, the drag on an individual dipole is so great compared to its mass that it slows to the velocity of the surrounding air mass almost instantly. Since the relative velocity of the chaff, in relation to the radar, is zero, radar systems employing Doppler processing and tracking will not display the chaff. Doppler processing radars will continue to track the aircraft unless it also has a relative velocity of zero. This occurs when the aircraft is abeam the radar. Chaff corridor and area saturation tactics against Doppler tracking radars will have limited effectiveness.

e. Chaff persistence and polarization are two additional characteristics that are important employment considerations for area saturation or chaff corridor operations. These individual chaff element characteristics are directly related to the combined effects of aerodynamic, atmospheric, and gravitational influences.

(1) Chaff persistence is the length of time the chaff is at an effective altitude to screen ingressing aircraft during area saturation or chaff corridor operations. The time span depends on the fall rate of the chaff and varies according to the density of the dipoles. The prevailing atmospheric conditions, such as wind and temperature also affect chaff persistence. Generally, the longer cuts used for lower frequency radars fall faster than the shorter cuts used for higher frequency radars. Each type has its own rate of fall based on these conditions. The rate of fall is a critical mission planning consideration for determining the amount of time between chaff corridor or area saturation initiation and the arrival of the aircraft being screened. If the chaff is employed too early, it may not be at the correct altitude or may have dispersed to the point that it is not effective to screen ingressing aircraft.

(2) Each chaff strand is a polarized dipole with positive and negative ends. The orientation of these strands determine their polarity (Figure 13-10). Chaff cuts with the positive and negative ends oriented vertically are vertically polarized. Chaff cuts with the positive and negative ends oriented horizontally are horizontally polarized. Since chaff strands are initially buffeted by turbulence and airstream vortices, the dipole orientation and polarization, changes rapidly and randomly. Eventually, the strands separate into two groups; one descending horizontally, and one descending vertically. Since the vertically oriented strands tend to fall faster, the lower part of the chaff cloud tends to become more vertically polarized, while the upper portion is horizontally polarized. A threat radar that uses vertical polarization will receive minimal affects from the upper (horizontally polarized) portion of the chaff cloud. If the aircraft being screened are flying within this portion of the chaff cloud, they may be detected and engaged. This is another mission planning consideration for chaff area saturation or chaff corridor operations.

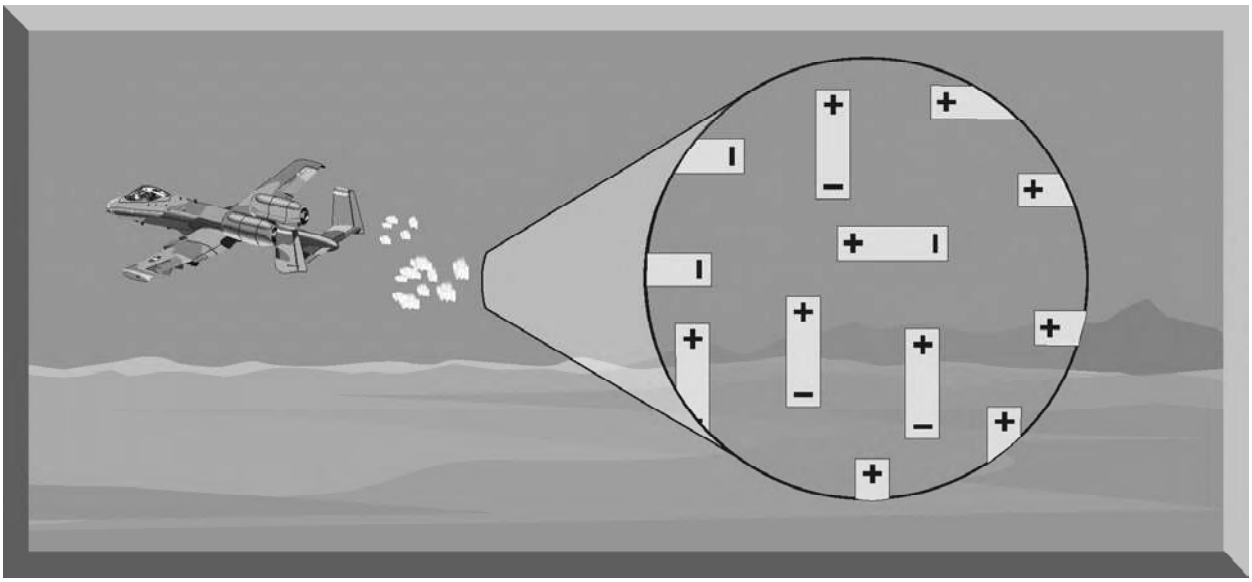

Figure 13-10. Impact of Chaff Polarization

3. CHAFF OPERATIONAL EMPLOYMENT

The two primary chaff employment tactics are force screening and self-protection. Force screening tactics include area saturation and corridor operations. Self-protection tactics include the reactive employment of chaff to negate a potentially lethal engagement. Different chaff dispensing techniques are used for each employment tactic and are important planning considerations for all chaff employment tactics. This section will discuss area saturation, corridor operations, and self-protection chaff employment.

a. The objective of area saturation operations is to present multiple false targets in a specific area in order to saturate radar systems and confuse the enemy integrated air defense system (IADS). Area saturation can be accomplished by fighter aircraft or drones equipped with chaff pods employing random chaff dispensing techniques. The chaff dispenser is set to release random bursts of chaff along the ingress and egress route of the attack package. Chaff pods may be supplemented with chaff bombs containing special fuses that provide false targets at varying altitudes. Attack aircraft can also contribute to area saturation by randomly dispensing self-protection chaff as they ingress and egress. However, this tactic can deplete the number of chaff bundles an attack aircraft may need to defeat a potentially lethal radar system encountered at a later time in the mission.

(1) The chaff cuts must provide frequency coverage for the threat radar systems. Also the RCS of each chaff burst should be large enough to present a realistic target to the victim radars. Multiple false targets created by chaff area saturation may confuse threat system operators and encourage them to expend missiles on false chaff targets.

(2) Saturation also masks the number of attacking aircraft (Figure 13-11). When used with false target deception jamming, area saturation can greatly enhance mission success. However, the technique is resource-intensive since aircraft employing chaff pods and chaff bombs cannot attack targets. These aircraft are vulnerable to attack and should be supported by standoff jamming. Area saturation tactics may have limited success against Doppler processing radars.

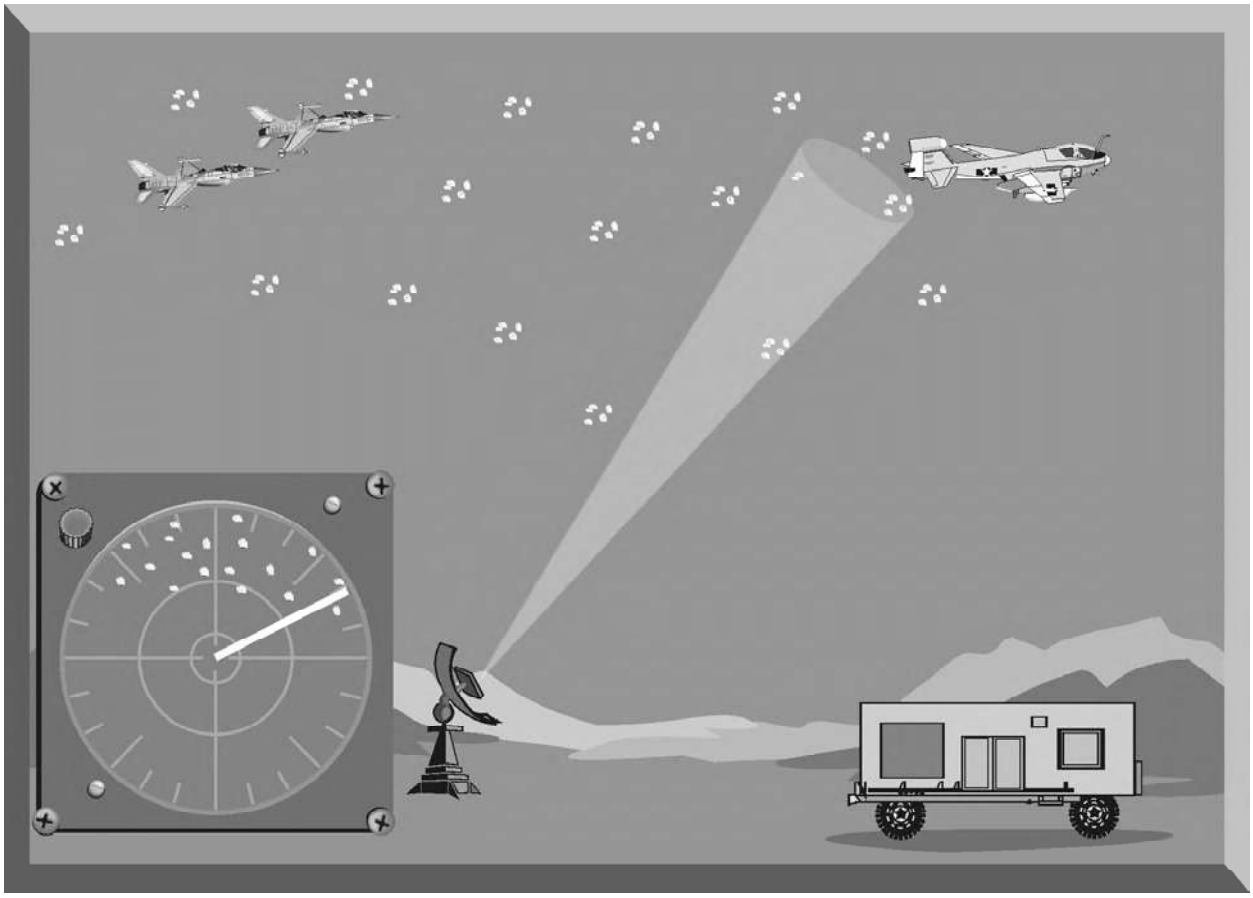

Figure 13-11. Area Saturation Tactics

b. The objective of chaff corridor operations is to screen the ingress and egress of an attack package by dispensing large quantities of chaff in a continuous "ribbon." Fighter aircraft, or drones equipped with chaff pods such as the ALE-38, employ a stream chaff dispensing technique to "lay" the chaff corridor. The pods are set to provide a continuous line of chaff dense enough to hide ingressing and egressing aircraft. The chaff cuts should provide frequency coverage for the radar systems that must be countered. Timing for the chaff aircraft in relation to the attack package must consider the fall rate and persistency of the chaff to ensure that the chaff corridor covers the required altitude for a time sufficient to allow the attack package to ingress and egress. An effective chaff corridor completely denies a radar's ability to distinguish between

the chaff and the attack aircraft. To do this, the radar cross section, or RCS, of the chaff within the resolution cell of the radar must exceed the RCS of the aircraft. This condition must be met throughout the length of the chaff corridor. When this condition is met, the chaff corridor will appear as a continuous return on the victim radar scope, and the attack package cannot be detected (Figure 13-12).

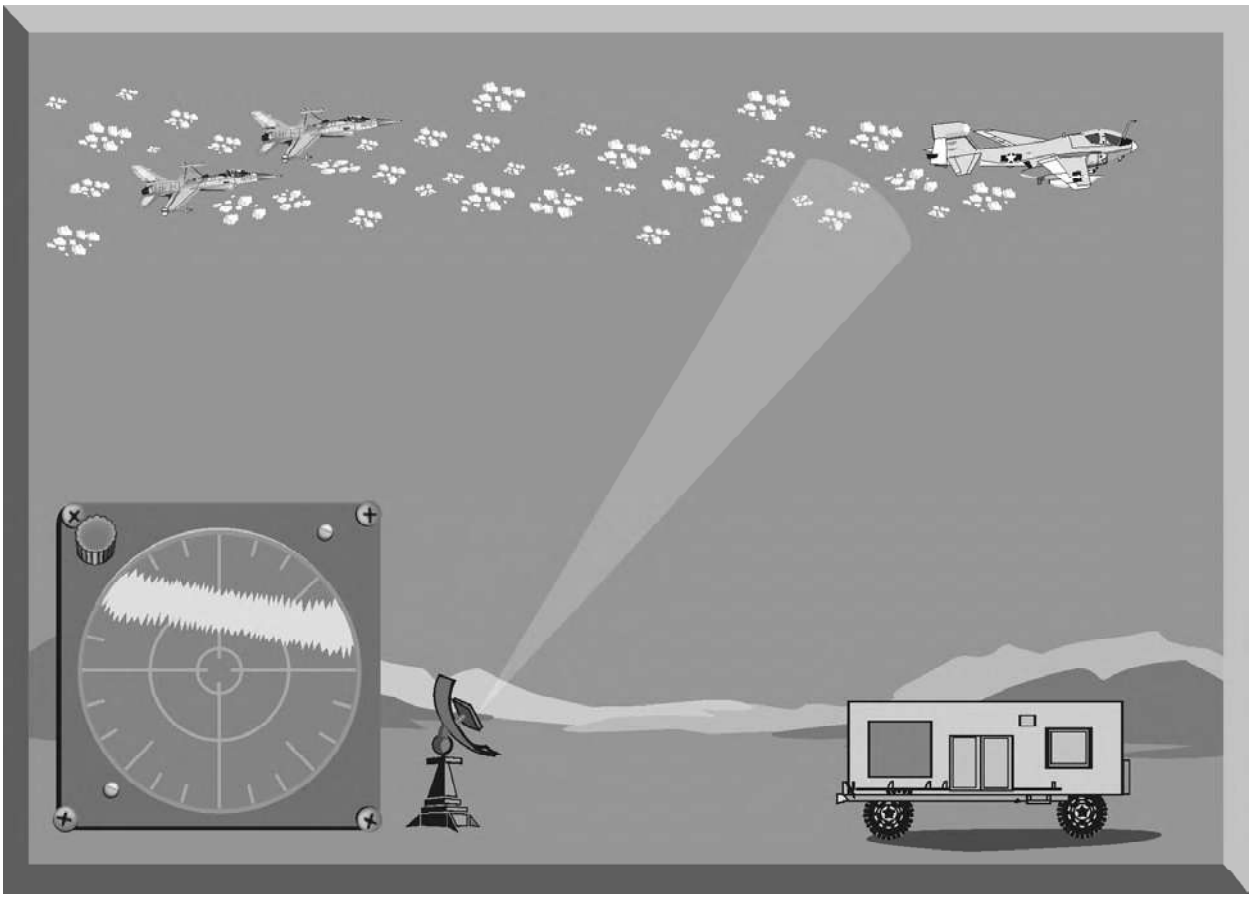

Figure 13-12. Chaff Corridor Tactics

(1) One advantage of a chaff corridor is that it can screen ingressing and egressing aircraft from pulse radar systems. However, chaff corridors are resource-intensive. Aircraft "laying" the corridor cannot strike critical targets. The chaff aircraft are also vulnerable to attack. Therefore, standoff jamming and self-protection jamming systems should be employed to provide some screening and protection for the chaff dispensing aircraft. Finally, chaff corridors may not be effective against radars with Doppler processing.

(2) To be effective, chaff corridor operations require detailed planning. Electronic combat (EC) planners must first determine that a chaff corridor is the most effective way to screen the attack force. This decision is based on the vulnerability of the attack aircraft to the anticipated threat radar systems and the availability of chaff assets. Once the decision is made to employ a chaff corridor,

planners must select the location, determine the length of the chaff corridor, select the ingress and egress altitudes, and establish the timing for the chaff aircraft and the attack package. Once the location of the chaff corridor is determined, planners must assess the threat radar systems that must be countered. The specific operating frequencies of the threat radars will determine the cuts of chaff that must be dispensed. The resolution cells of the threat radars will determine the density of chaff required. The length of the chaff corridor and the chaff density will determine the number of chaff aircraft required to seed the chaff corridor. The chaff fall rate and the atmospheric conditions impact the timing between the chaff aircraft and the attack package, and the altitude that the chaff dispensing aircraft must fly.

c. Self-protection chaff tactics are based on the use of chaff dispensers that use burst chaff dispensing techniques to defeat a TTR. Burst chaff dispensing, employed during the final phase of an engagement by air-to-air or surface-to-air weapons, can generate tracking errors or a radar break-lock. Burst chaff effectiveness is greatly enhanced when accompanied by jamming and evasive maneuvers (Figure 13-13).

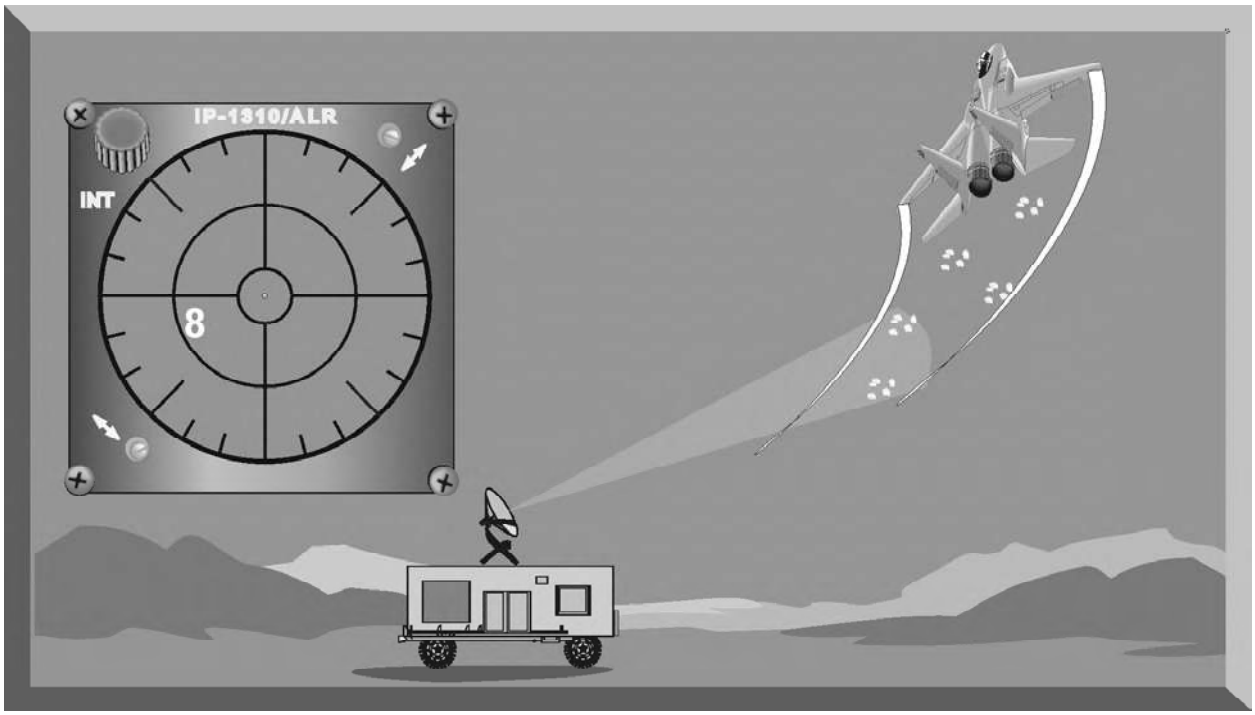

Figure 13-13. Self-Protection Chaff Tactics

(1) Self-protection chaff has proven effective against all pulse radar threat systems when employed with maneuvers and jamming. This is especially true for TTRs operating in an automatic tracking mode.

(a) Chaff employed against a track-while-scan (TWS) radar is designed to put multiple targets, with an RCS greater than the aircraft, in the resolution cell of the horizontal and vertical radar beams (Figure 13-14). Since the tracking loop tracks the largest return, the TWS radar will automatically switch to the chaff. After dispensing chaff, the pilot can maneuver vertically or horizontally to move the aircraft out of the resolution cell.

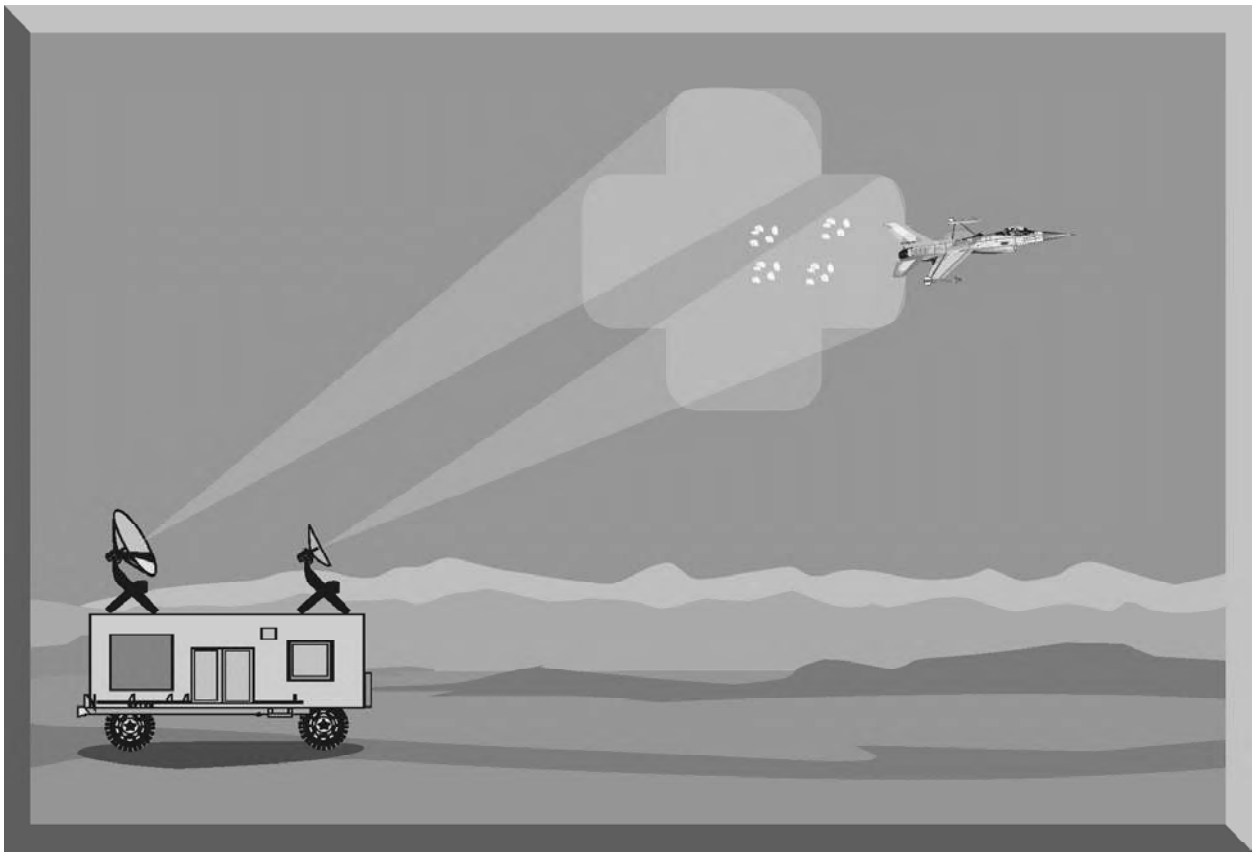

Figure 13-14. Self-Protection Chaff Effect on a TWS Radar

(b) Against a conical scan radar, chaff puts multiple, large RCS targets within the separate scans of the radar (Figure 13-15). These multiple targets generate error signals in the tracking loop and drive the separate scans off the aircraft return. As the conical scan radar tracking loop attempts to resolve these error signals, it will eventually lock on to the chaff. Maneuvering outside the overlapping scan area enhances chaff effectiveness and facilitates the transfer of radar lock-on to the chaff.

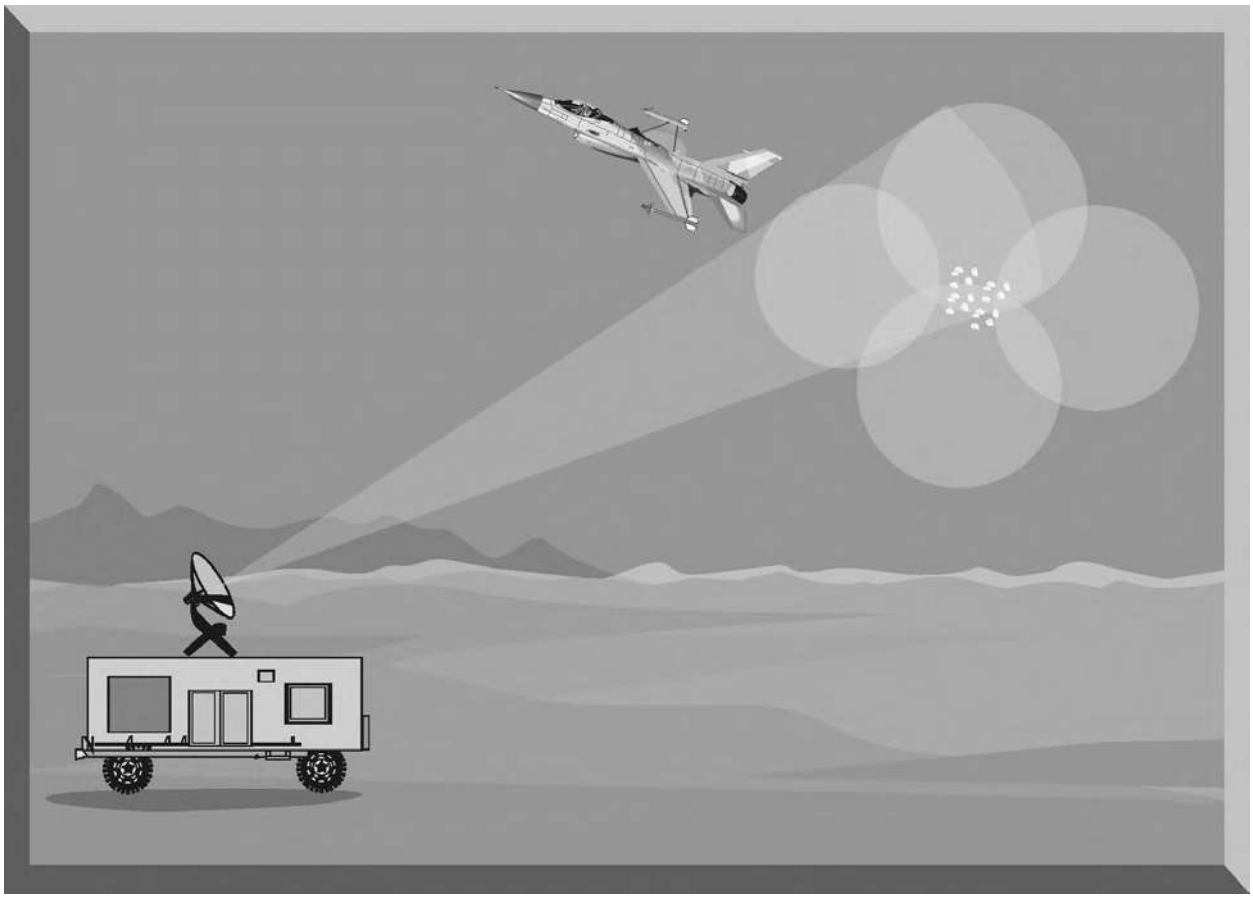

Figure 13-15. Self-Protection Chaff Impact on a Conical Scan Radar

(c) Chaff employed against a monopulse radar is designed to put multiple targets in at least two of the tracking beams (Figure 13-16). This generates errors in the azimuth, elevation, and range tracking circuits. Multiple chaff targets continue to generate azimuth and elevation errors that can eventually generate a break-lock condition, as the radar transfers lock-on to the chaff. Chaff is most effective against monopulse radars when employed on the beam in order to create the maximum angular tracking error.

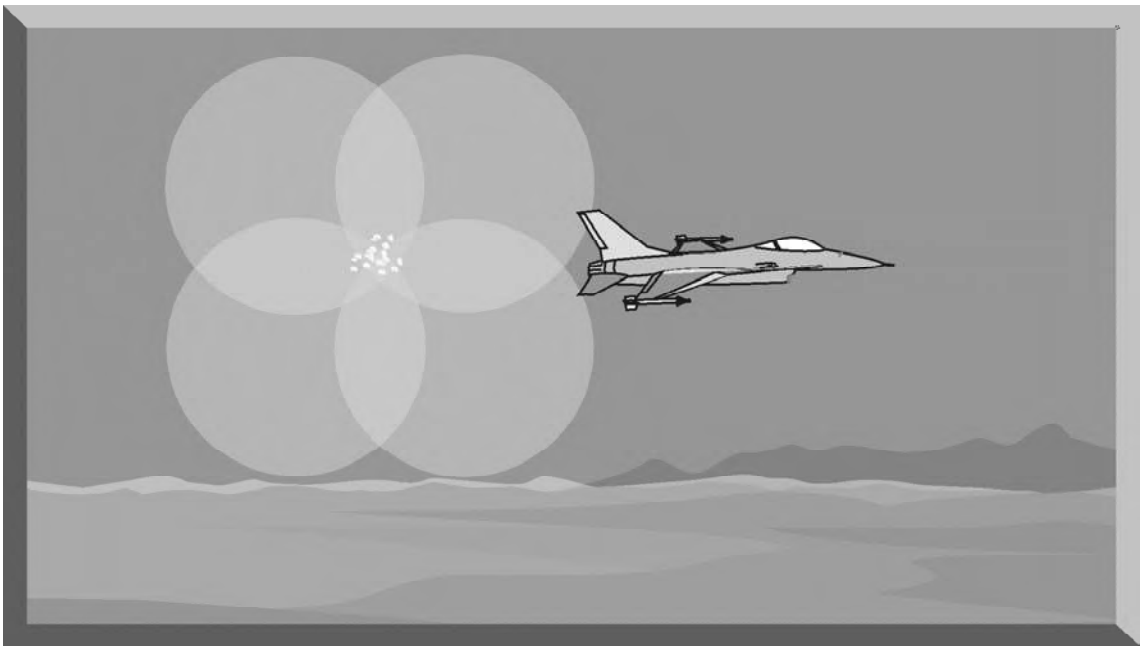

Figure 13-16. Self-Protection Chaff Impact on a Monopulse Radar

(d) Modern radars may employ some form of Doppler filtering to negate the effectiveness of chaff and other sources of clutter. Pulse Doppler and continuous wave radar systems track targets based on target velocity relative to the radar. Radars employing a moving target indicator (MTI) use relative target velocity to distinguish between targets and clutter. Chaff slows to near zero relative velocity almost immediately after dispensing. For self-protection chaff to be effective, the aircraft velocity relative to the radar site must also be near zero This occurs when the aircraft's aspect to the radar is 90°, or on the beam. By maneuvering to a beam aspect against a Doppler radar, the pilot is exploiting the "notch" where radar cannot discriminate targets based on Doppler frequency shift (Figure 13-17).

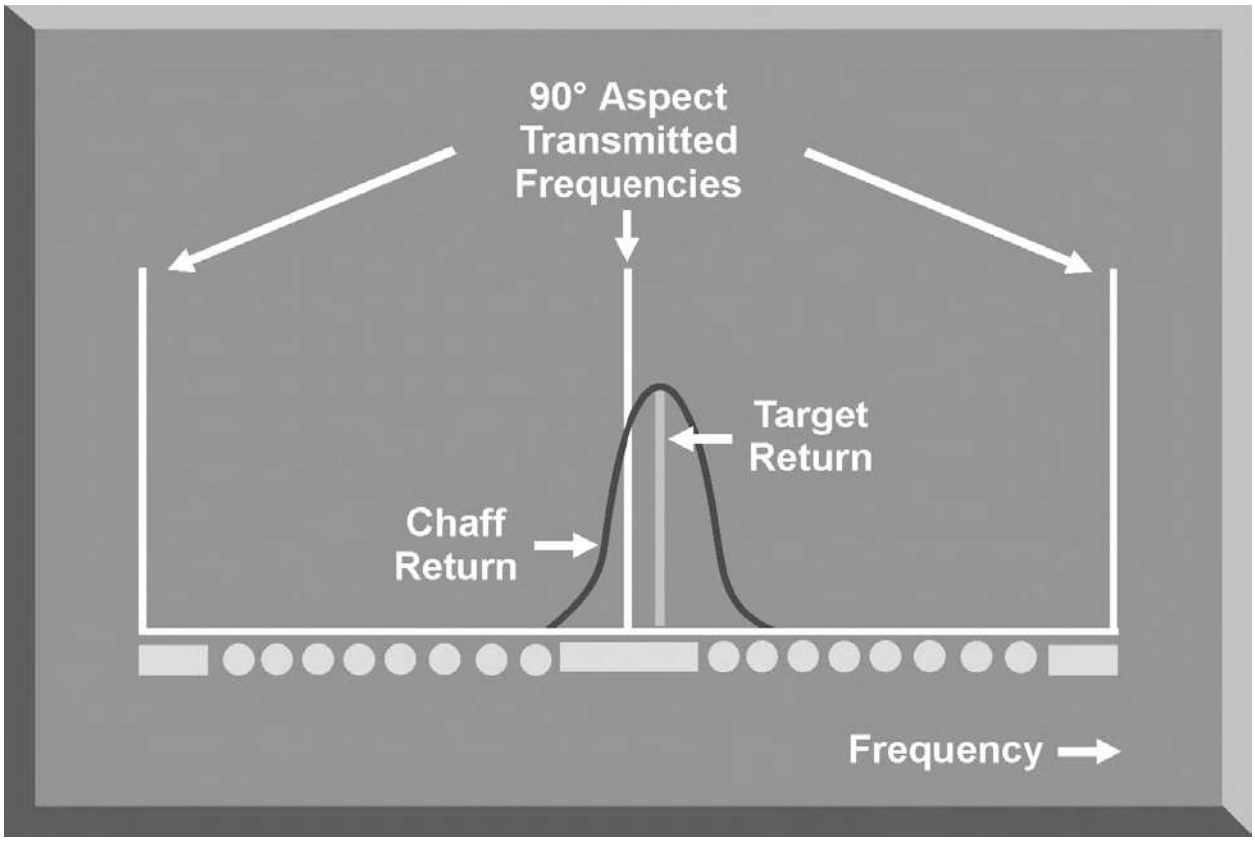

Figure 13-17. Self-Protection Chaff Impact on a Doppler Radar

4. SUMMARY

Chaff is one of the oldest and most effective pulse radar countermeasures. The fundamental characteristics of chaff (RCS, frequency coverage, bloom rate, Doppler content, polarization, and persistence) determine the effectiveness of chaff employment. The primary chaff employment tactics of force screening and self-protection are designed to maximize the impact of chaff on threat radar systems. Self-protection chaff, together with jamming and maneuvers, is often the "last line of defense" against lethal radar threat systems.

CHAPTER 14. IR FUNDAMENTALS

1. INTRODUCTION

Since their introduction in the 1950s, infrared (IR) missiles have been an increasing threat from both ground-based and airborne systems. The range, reliability, and effectiveness of IR missiles have been continuously improved by advanced detector materials and computer technology. Since IR missiles are passive, they are relatively simple and inexpensive to produce. These characteristics have contributed to the proliferation of IR missiles in the combat arena. Nearly every aircraft flying in either the air-to-air or air-to-surface role now carries an all-aspect IR missile. Additionally, every infantry unit down to the platoon level is equipped with shoulder-fired IR missiles (Figure 14-1). This chapter will cover basic IR theory, IR missile detection, IR seekers, and conclude with a section on IR flare rejection.

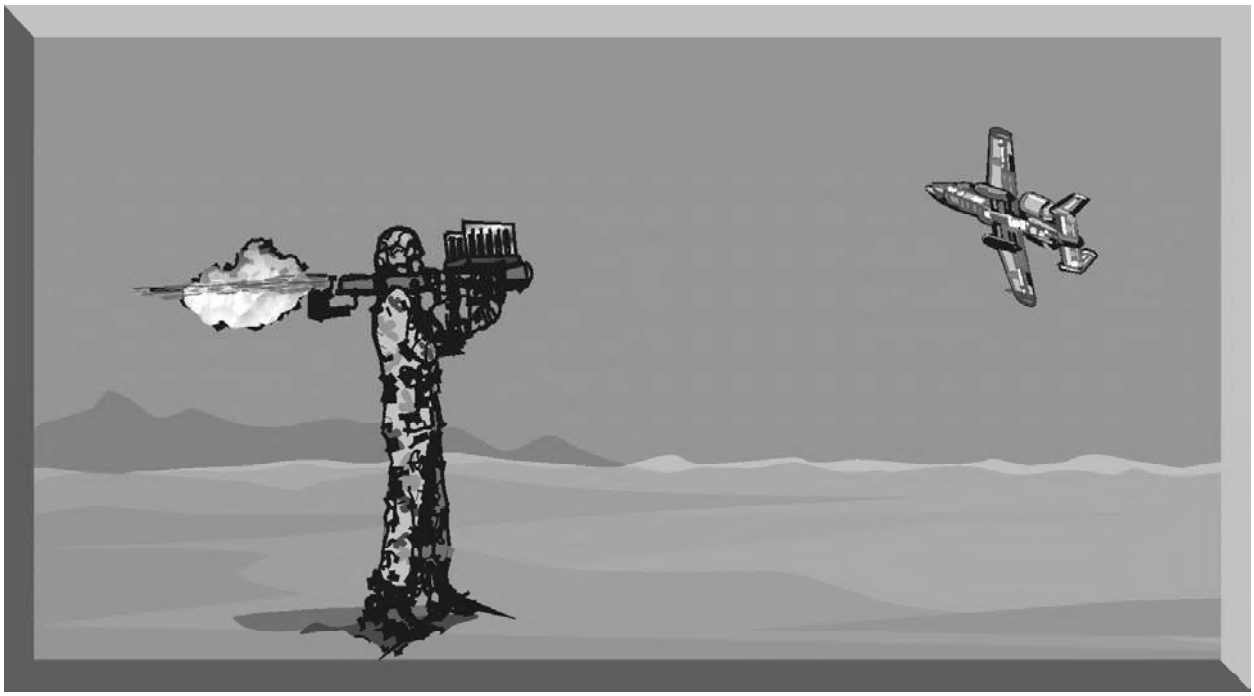

Figure 14-1. The IR Threat

2. BASIC IR THEORY

Because of its location in the frequency spectrum, IR radiation exhibits some of the characteristics and limitations of microwaves and visible light.

a. All warm objects emit IR energy. The object's temperature dictates the characteristics of this radiation. As the temperature of the material increases, the radiant intensity increases and shifts to shorter and shorter wavelengths or

higher and higher frequencies. The frequency band of IR radiation falls between the upper limit of microwaves and the lower limit of visible light. When discussing IR radiation, it is more convenient to refer to wavelength instead of frequency (Figure 14-2). The wavelength of the highest frequency IR is 0.72 x 10^{-6} meters. A unit of measure called the micron (μ), is one millionth, or 10^{-6}, of a meter and is used to designate IR wavelengths. IR energy falls in the electromagnetic spectrum between the wavelengths of 1000 and 0.72 microns, while visible light occupies the spectrum from 0.72 to 0.39 microns.

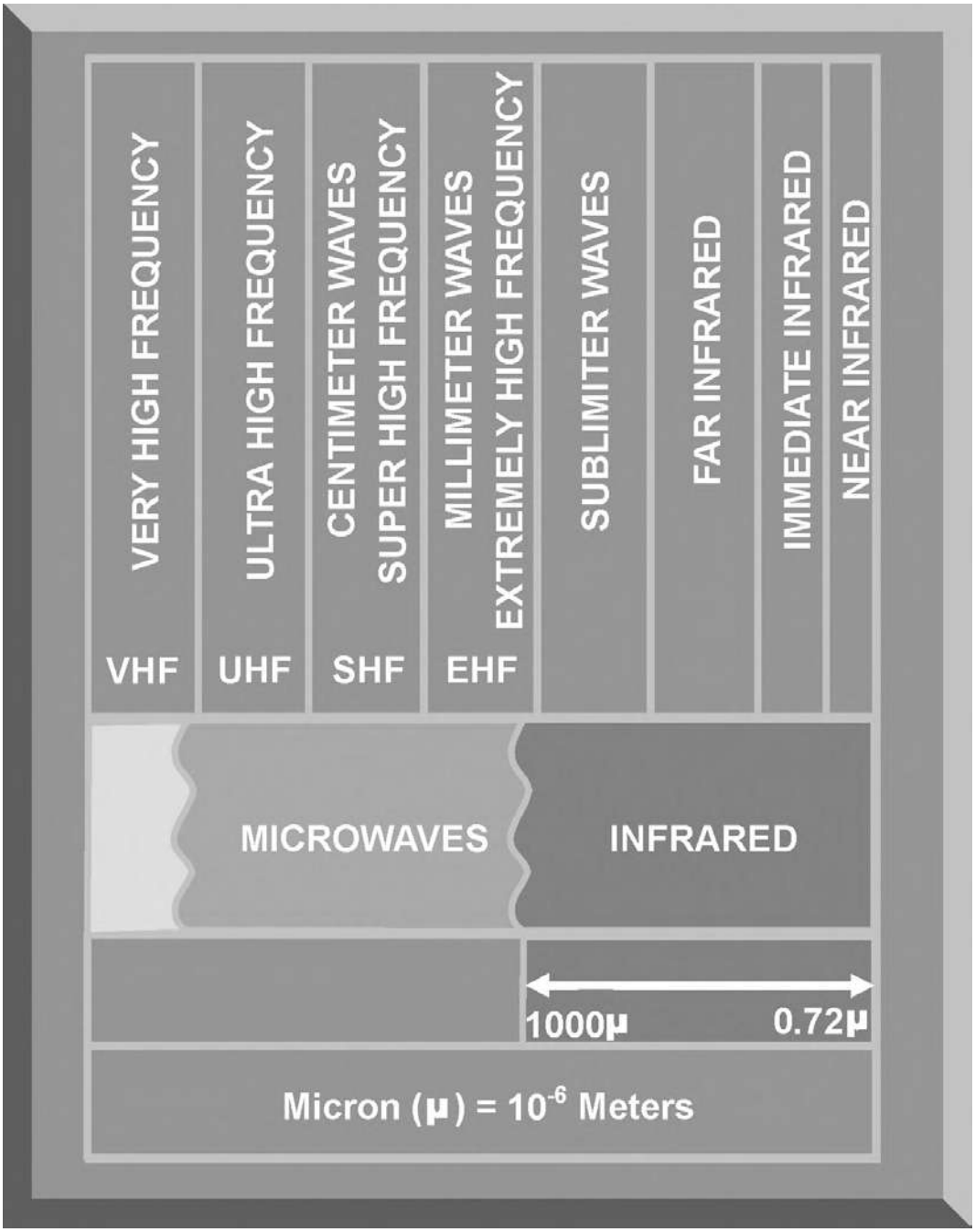

Figure 14-2. IR Frequency Band

b. As the IR energy travels through the atmosphere, certain wavelengths are absorbed or attenuated. The greatest IR attenuator is atmospheric water vapor, which varies as the weather conditions vary, with negligible absorption at altitudes above 30,000 feet. Another significant attenuator is carbon dioxide. The percentage of carbon dioxide in the atmosphere is practically constant up to a height of 30 miles. Carbon dioxide absorption is predictable and occurs only in the IR region. Scattering is another form of atmospheric attenuation and is caused by dust particles and water droplets. Scattering is also largely dependent on weather conditions and cannot be predicted. Most of the scattering occurs at lower altitudes and at the shorter wavelengths. Other atmospheric elements cause little or no attenuation of IR energy. Figure 14-3 shows atmospheric IR transmission at sea level. There is a relatively large window of IR transmission in the region from one to five microns. This is the region where the aircraft engine heat signature is at its maximum intensity and where most IR missiles are designed to operate.

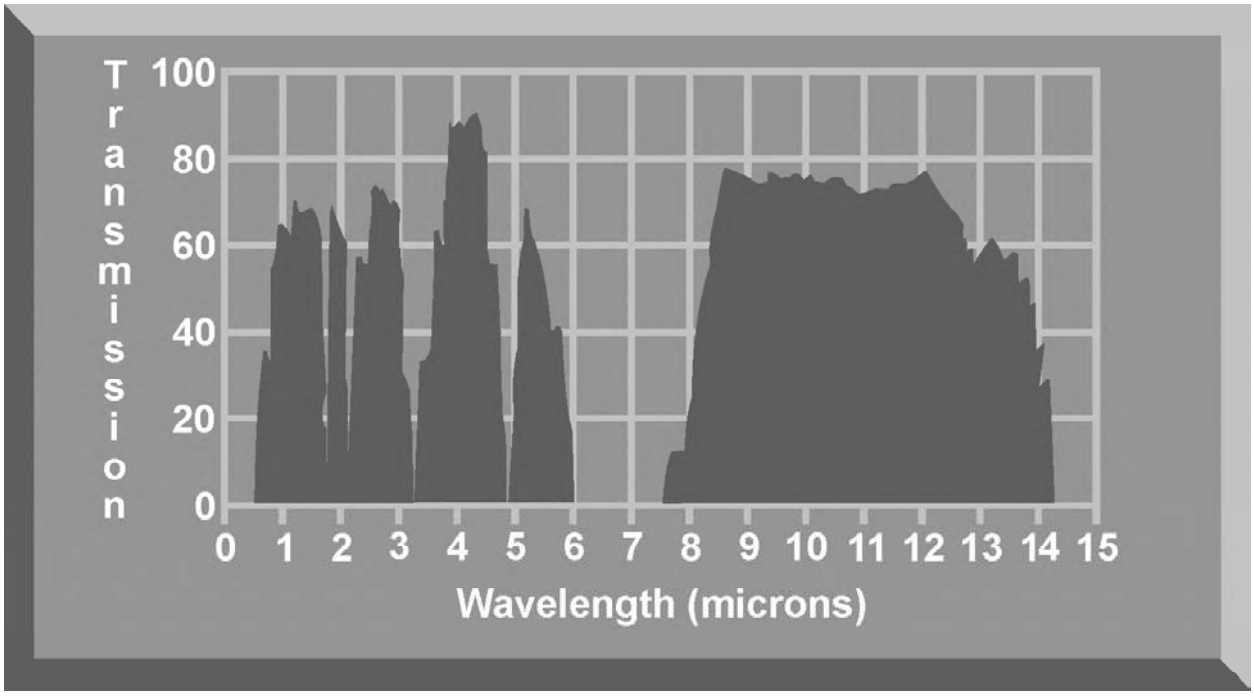

Figure 14-3. Atmospheric IR Transmission

c. IR energy exhibits some of the transmission characteristics of both RF energy and visible light. As with visible light, it can be optically focused by lenses and mirrors. This characteristic is used in the IR missile detector elements (Figure 14-4). As with RF energy, the intensity of IR radiation diminishes inversely with the square of the distance between the source and the receiver.

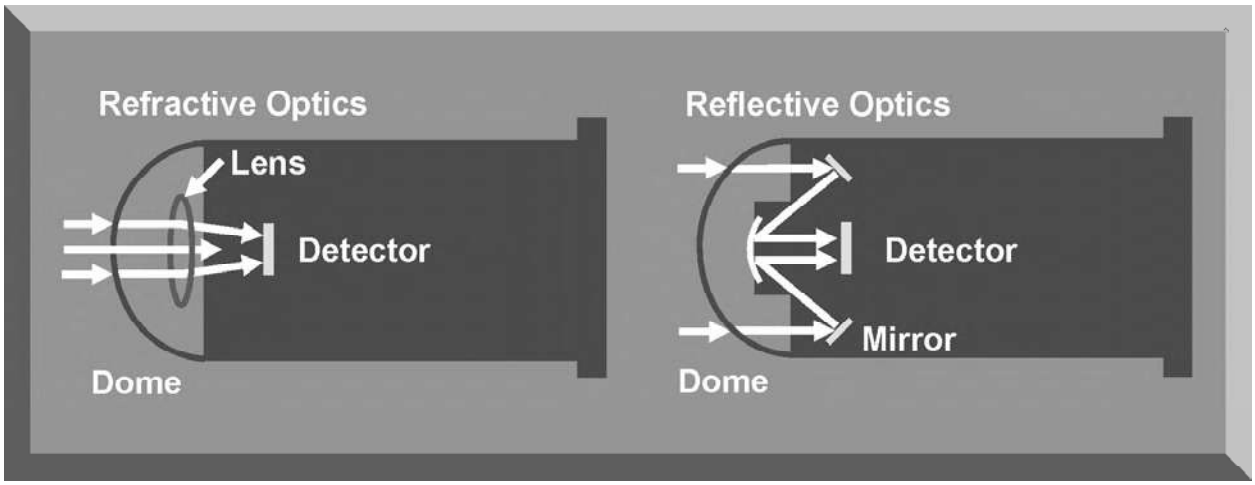

Figure 14-4. IR Missile Seeker

d. If the intensity of the aircraft's IR signature, while in the military power setting, is plotted in relation to wavelength, it reaches a peak at approximately 3 microns (Figure 14-5). In afterburner, the aircraft's IR intensity reaches a peak at approximately 1.5 microns. Since IR missiles are designed to detect and track the aircraft's IR signature, most IR missiles operate in the region of 1 to 5 microns. To be effective, the IR intensity of a flare must also fall within this micron region.

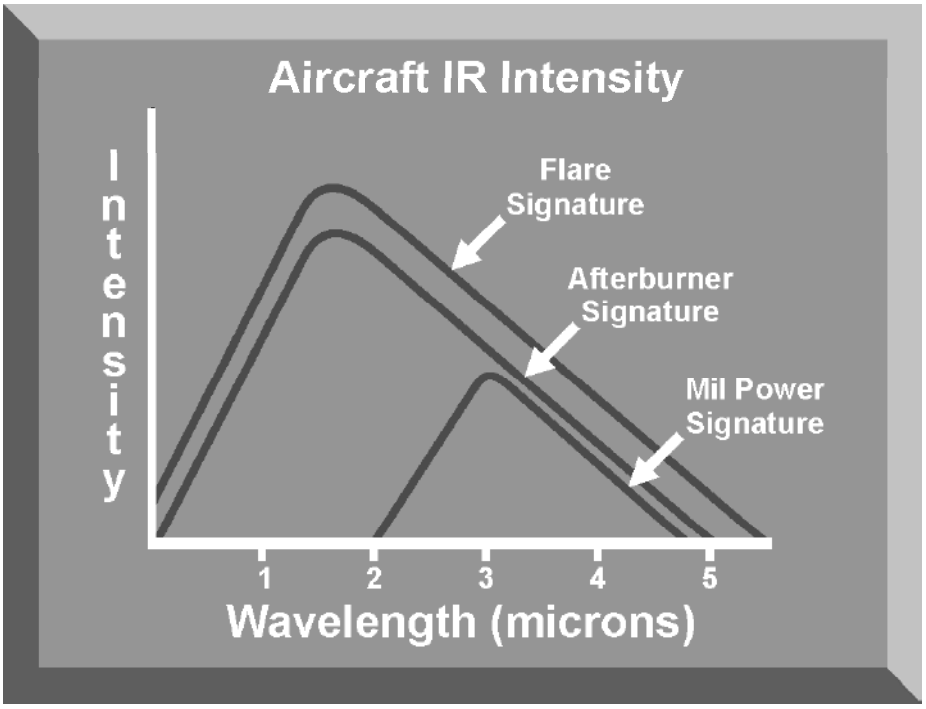

Figure 14-5. Aircraft IR Intensity

e. An aircraft's relative IR signature is based on aspect angle, airspeed, altitude, and afterburner status. The minimum relative IR intensity is at the nose and maximum at the tail. As airspeed increases, the relative IR intensity increases due to the heat generated by friction and increased engine temperatures. As altitude increases, the relative IR signature increases at all aspect angles, due to the reduction in atmospheric attenuation (Figure 14-6).

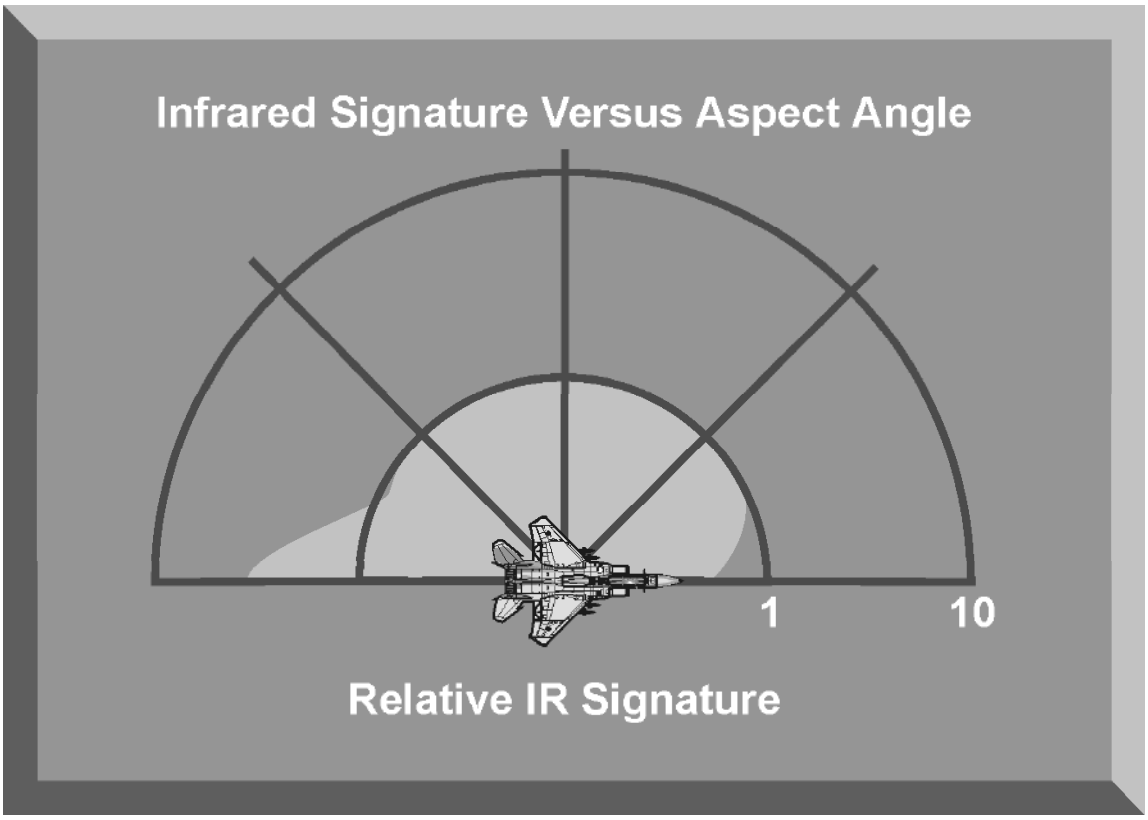

Figure 14-6. IR Signature Versus Aspect Angle

3. IR SIGNATURE SOURCES

IR guidance is based on the fact that every object with a temperature above zero degrees Kelvin emits IR radiation. The temperature of the object dictates the characteristics of this radiation. As the temperature of the object increases, the radiant intensity increases and shifts to higher and higher frequencies and correspondingly shorter and shorter wavelengths. The F-16 at Figure 14-7 demonstrates the different wavelengths found at different areas of the aircraft. Emissivity in Figure 14-7 is a relative measure of the IR energy emitted when a surface is directly viewed.

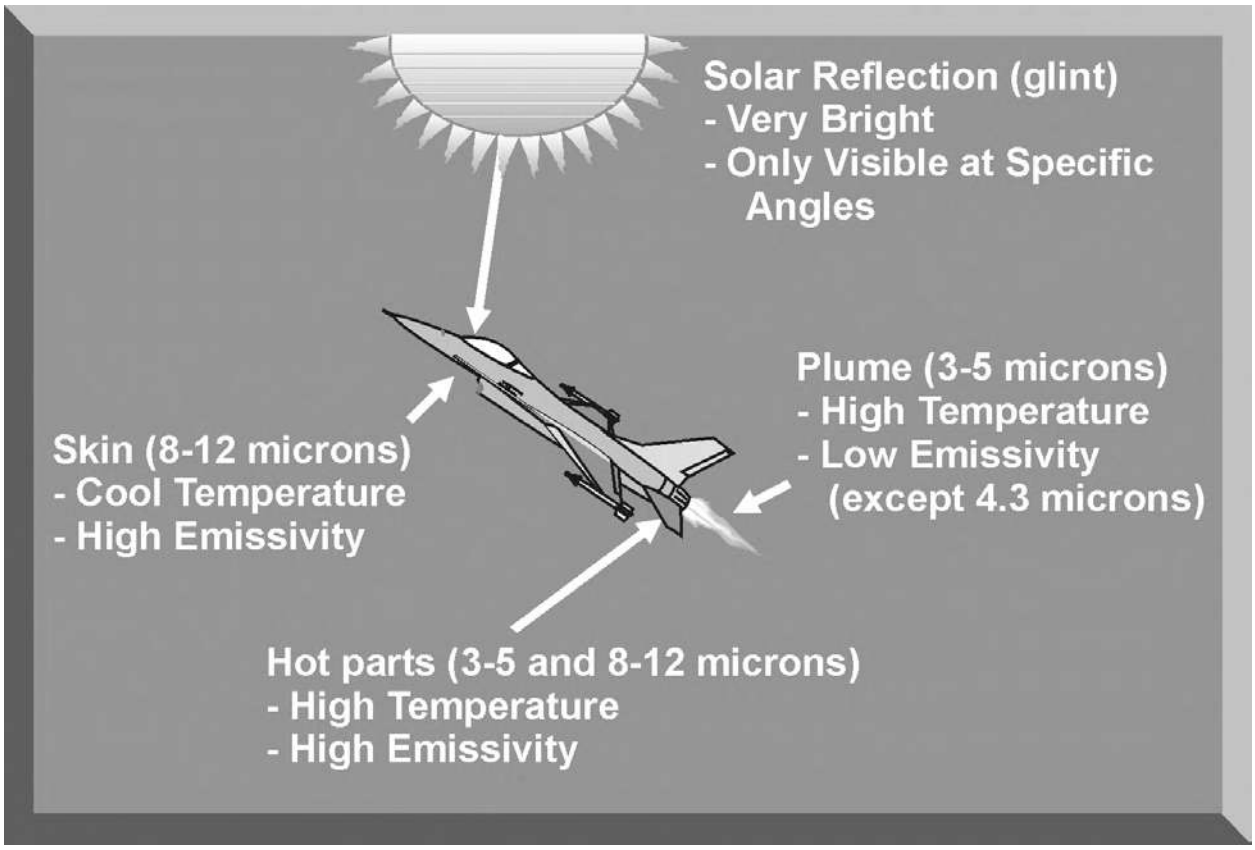

Figure 14-7. Target Signature Sources

a. The main aircraft signature sources are the plume, the engine hot parts, and the skin. The skin is large in area, but usually fairly cool. Thus the best detection of the aircraft skin is usually in the long wave IR band (8-12 microns).

b. The engine hot parts offer excellent detection when one is looking at the right angle. They have high temperatures and high emissivity. However, depending on the viewing angle, they may have a low perceived area.

c. The plume has high temperatures and a high perceived area. This large perceived area allows near all-aspect detection. Unfortunately, it has a relatively low emissivity except near 4.2 microns. It is the strategy of the new breed of all-aspect missiles to detect the plume in the mid-wave IR, around 4.2 microns.

d. Figure 14-8 shows some of the common IR detector materials. Note that the cooled detectors are sensitive to longer wavelength (lower energy) photons, as discussed earlier.

Material	Wave-Band
Lead Sulfide (PbS) - Uncooled	1.5 - 2.5 micrometers
Lead Sulfide (PbS) - Cooled	2.0 - 4.0 micrometers
Lead Selenide (PbSe) - Uncooled	2.0 - 4.2 micrometers
Lead Selenide (PbSe) - Cooled	3.0 - 5.0 micrometers
Indium Antimonide (InSb) - Cooled	2.0 - 5.0 micrometers
Mercury-Cadium-Telluride ($Hg_{(1-x)}Cd_{(x)}Te$) - Cooled	8.0 - 13.0 micrometers

Figure 14-8. IR Detection Materials

4. IR SEEKER CHARACTERISTICS

Guidance units are designed to detect and home in on the IR radiation of the aircraft. The job of the seeker is to view the scene and output the estimated target position. Figure 14-9 shows the hardware that makes up the seeker of a generic IR missile system.

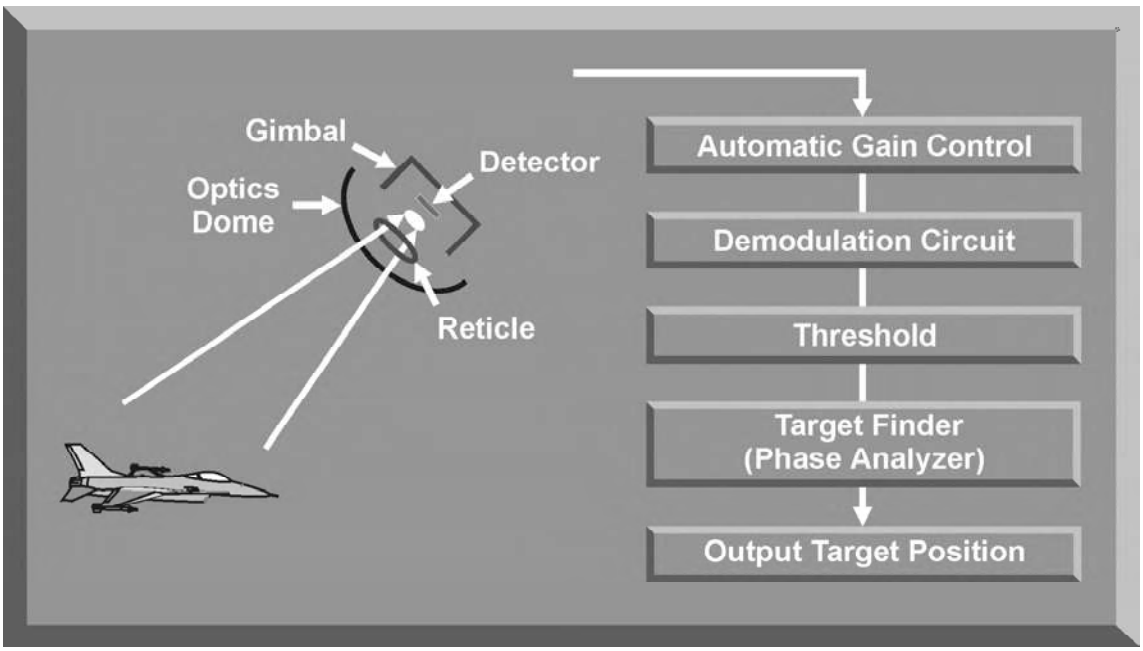

Figure 14-9. IR Missile Seeker

a. The dome acts as an IR transparent protective cover. Most IR missiles use the hemispherical dome because that shape does not alter the path of the incoming light rays. The optics focus the scene through the reticle onto the detector. The reticle pattern enables the detector output to "code" the position of the target.

b. The internal workings of the missile are similar to those found in a radar tracking system. There is an automatic gain control (AGC) to adjust the levels of the detector output so that it is not too large or too small. The demodulation circuit "decodes" the detector signal. The threshold circuit cancels signals that are below the specified threshold value, similar to the clutter rejection function found in radar systems. Finally, the phase analyzer reads the target position from the signal and sends the result to the autopilot. The autopilot then adjusts the missile's flight path to track the target.

c. IR systems employ filters and detectors to filter out unwanted IR radiation from the sun, sunlit clouds, smoke, the earth, and other background radiation sources (Figure 14-10). The detection unit is coupled with a guidance system to generate commands to the missile control vanes to keep the target centered in the field of view.

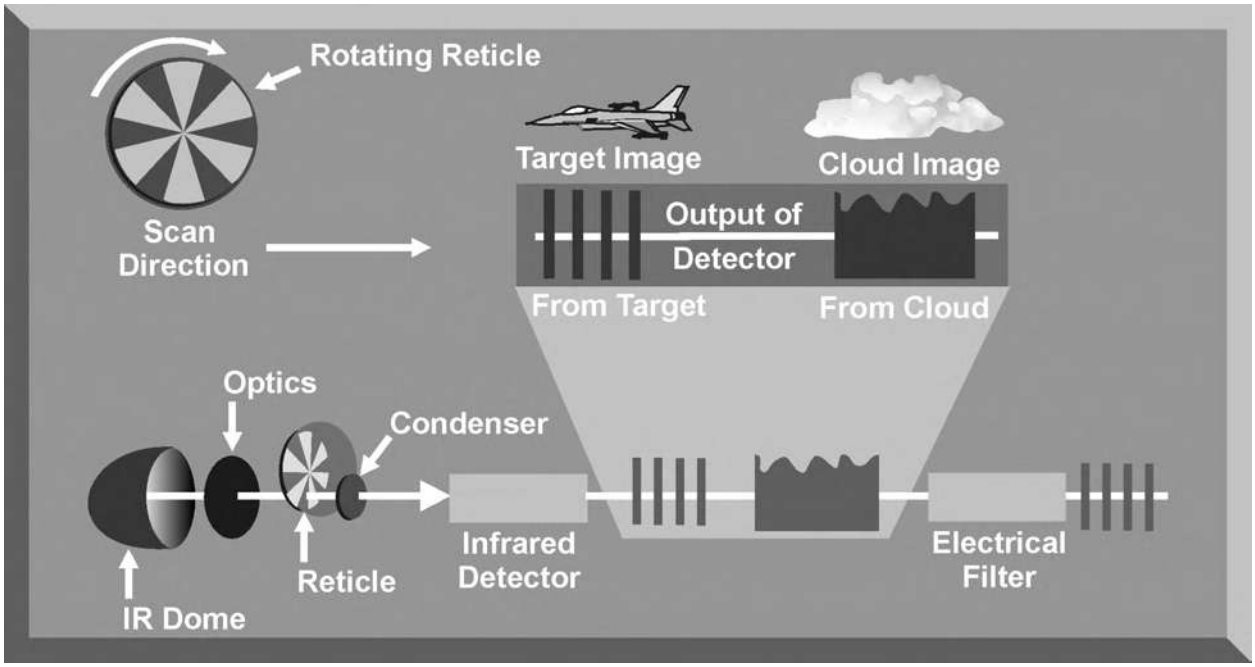

Figure 14-10. Spin Scan Reticle

d. A defining characteristic of an IR missile is its field of view (FOV) and field of regard (FOR) (Figure 14-11). The angular size of the image in degrees is called the field of view. To provide the greatest possibility of collecting IR radiation from the target, the receiver must have the greatest possible FOV. This in turn may

create problems. A large FOV increases the possibility that the receiver may not be able to distinguish the target from other sources of IR radiation. To avoid this problem, a relatively small FOV is scanned through a wider area. This wider area is referred to as the FOR. The gimbal enables the FOV to be scanned, so that an entire FOR can be searched.

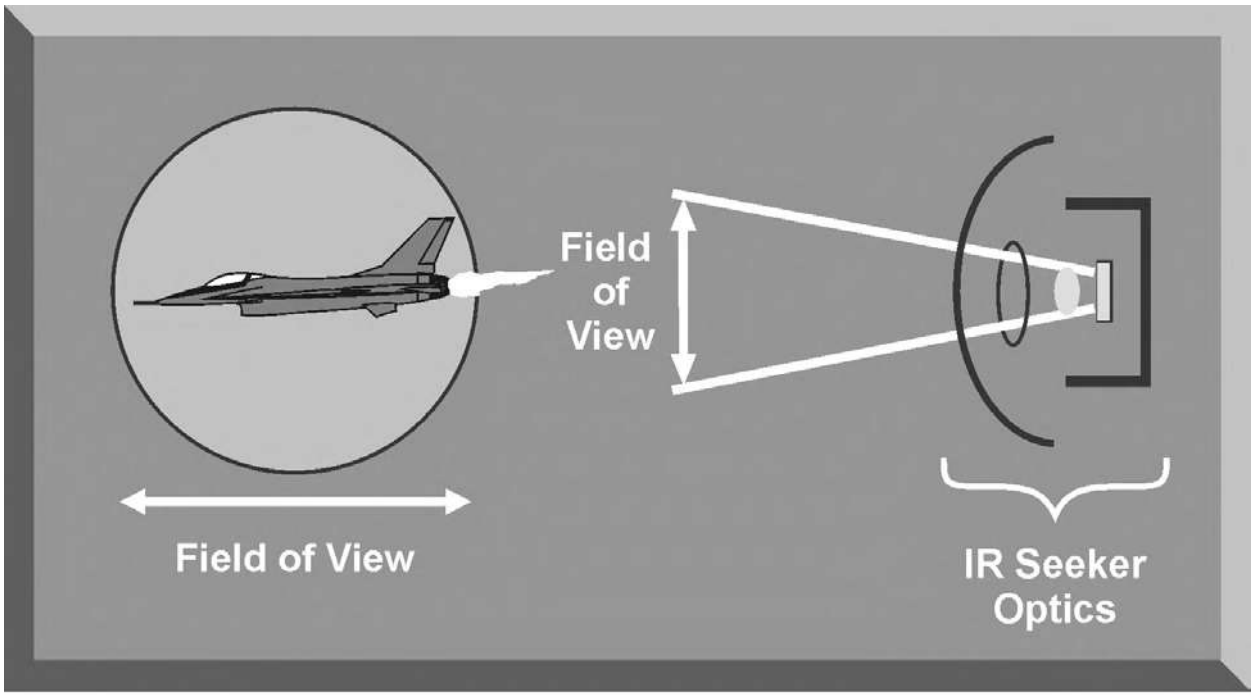

Figure 14-11. Missile Field of View

5. IR SEEKER TYPES

Through the years advances in seeker technology have resulted in significant changes to IR missile engagement tactics. This section will discuss spinning reticle, conical scan, cooled, and imaging IR seekers.

a. First generation IR missiles, like the SA-7, use a spinning reticle as the means to track the target. Due to their relatively low cost and ease of use, IR missiles of the first generation can still be encountered. The spinning reticle is inserted in the seeker just before the IR radiation reaches the detector. The reticle is a thin plate of optical material which has a transparent and opaque pattern on it. As the reticle is rotated, the IR energy is chopped at a rate determined by the reticle pattern. This system produces error signals when the target is not exactly centered in the field of view. Figure 14-12 is an example of a reticle pattern that can provide both azimuth and elevation information. If the target is located in the upper half of the pattern, the IR intensity on the detector is constant as the reticle rotates. As the pie-shaped half of the disc rotates over the target, the IR energy is pulsed and the amplitude of the pulses is an indication of relative elevation angle.

When the target moves to the right or left, the pulsing starts and stops at different times, indicating target azimuth. Center spun spin-scan seekers, also called center null reticles, are relatively insensitive when the target is in the center of the seeker scan where there is no tracking error. This is because the point target tends to bleed energy into all the spokes at once, eliminating the pulsed signal output of the detector. Once the target falls off the center of the reticle, the seeker generates an error signal that initiates guidance commands to recenter the target. This is the reason early IR missiles flew an undulating path toward the target.

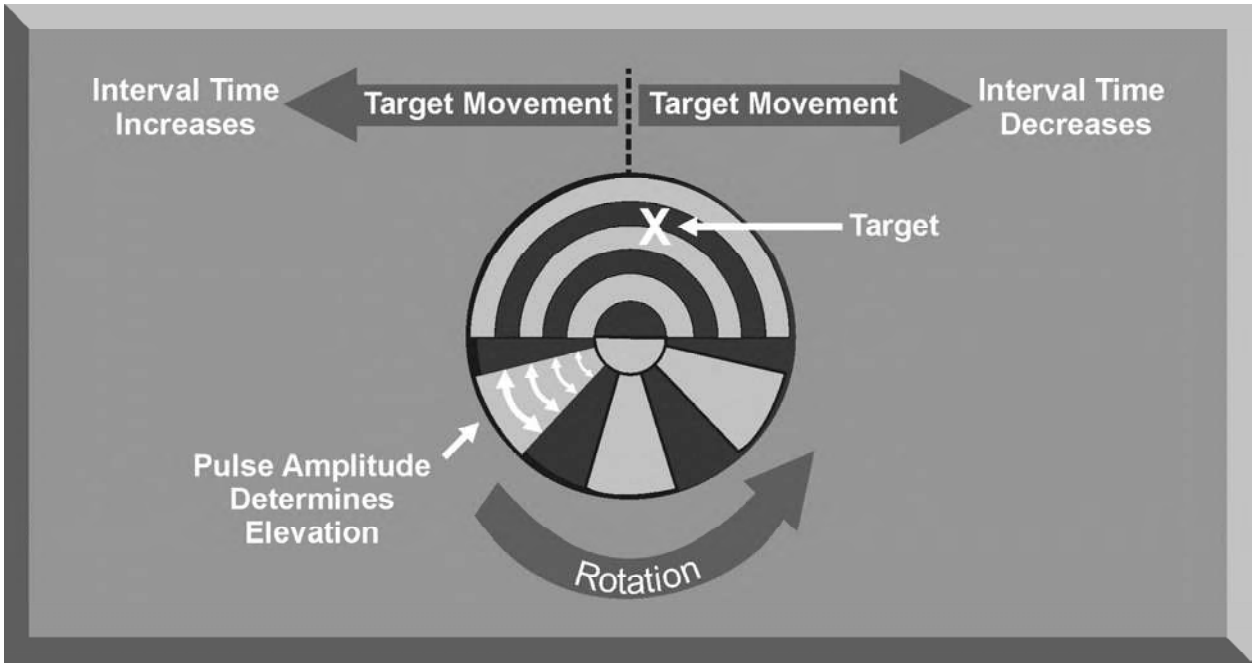

Figure 14-12. IR Missile Reticle

b. IR conical-scan (con-scan) seekers were developed to solve some of the problems with spin-scan seekers; notably the lack of error response when the target is near the center of the seeker field of view (FOV) (Figure 14-13). In a typical con-scan seeker, the reticle is fixed and does not spin. Instead, a secondary mirror is tilted and spun. This causes the target image to be scanned in a circular path around the outer edge of the reticle. When the target is centered in the seeker scan, the detector generates a pulsed output similar to that of the spin-scan seeker. However, as the target leaves the center, the output of the detector is a frequency modulated (FM) sine wave. The frequency of the modulation is directly proportional to the amount of target displacement from the center of the seeker scan. Con-scan optics are usually designed to spin the target very close to the edge of the reticle. This generates the greatest amount of FM modulation for a given target tracking error and gives the con-scan IR missile a more sensitive and tighter tracking loop. The center of the reticle is only used for acquisition.

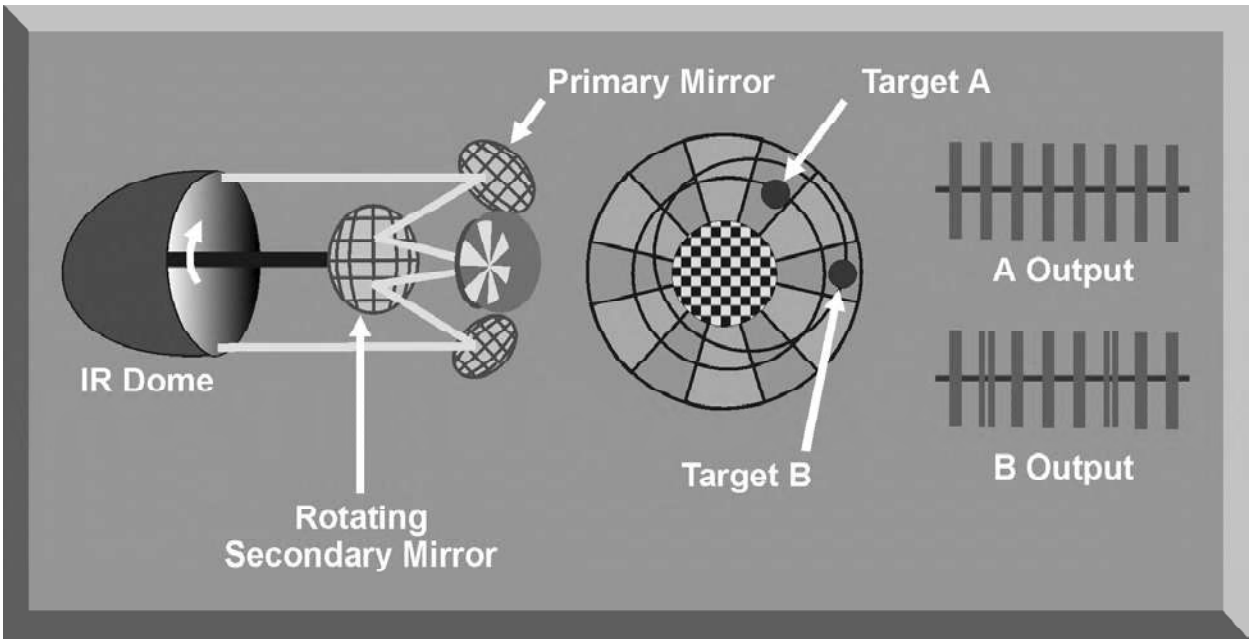

Figure 14-13. Conical Scan IR Seeker

c. A significant improvement to IR seekers resulted from the cooling of the detector with an inert gas such as argon. Older IR missiles, using uncooled lead-sulfide detectors, have a peak sensitivity in the 2 micron region. This limits these missiles, the SA-7 for example, to stern attacks because the missiles can only discriminate the IR signature of the engine turbine from background IR energy. By cooling the detector with an inert gas, like argon, the detectors of newer IR missiles can track longer wavelength IR radiation associated with airframe friction. Using newer detector materials like indium antimonide (InSb), require cooling to have increased target detection range and all-aspect tracking capability.

d. Imaging IR is the most recent advancement in IR seeker technology. The technology for these seekers is similar to that found in the AGM-65 Maverick missile. Imaging IR seekers are harder to decoy with flares than older seekers, and they are resistant to pulsed light jamming. Imaging detection involves creating an IR picture of the scene in one of two ways, scanning or staring. A scanning system uses one detector (or a mix of detectors and mirrors) which moves relative to the scene until the entire scene is scanned. This is an easy system to fabricate, but it can be noisy because the detector can't stay very long at each position, and it does not have a lot of time to measure the signal. A staring system uses many detectors, each of which detects a small portion of the scene. Each detector can "dwell" on its part of the scene for the entire frame time. However, such systems, also called focal plane arrays, are difficult to fabricate in a way such that each detector has the same sensitivity. One of the prime advantages with using imaging IR seekers is that they can be programmed

to track a particular IR shape or scene, significantly reducing the effectiveness of decoy flares.

6. IR MISSILE FLARE REJECTION

Flares are the primary countermeasure used to defeat the IR missile. Advanced IR missiles use different techniques to overcome the use of self-protection flares. There are two important characteristics of infrared (IR) missiles that influence the effectiveness of self-protection flares. The first is the ability of the IR missile seeker to discriminate between the IR signature of the aircraft and the IR signature of background interference, especially clouds. The second is the flare rejection capability built into the missile seeker and the missile guidance section.

a. The major source of IR background interference is sunlit clouds. Space filtering using a spinning reticle as described in the previous section is the method most widely used to suppress background interference and improve discrimination. IR energy from the target is gathered by the optical system and focused on the spinning reticle. The reticle chops the signal into a series of pulses that are focused onto the IR detector element. The signal output of a point source of IR energy, such as a target aircraft, will be a series of pulses. The signal output of a cloud, which covers several segments of the reticle, will be a single large pulse. An electrical filter eliminates the single large cloud pulse, and passes the multiple pulses generated by the target to the missile guidance section.

(1) IR missiles using spin-scan seekers have very little ability to reject flares. Flares provide the missile seeker with a hotter target than that of the aircraft, causing the spin-scan seeker to track the flare. The typical flare burns with a peak energy emission in the 2 micron range. Since the flare energy emission is greater than that of the target aircraft, the missile seeker transfers lock to the flare.

(2) Due to the scan pattern, con-scan seekers have some inherent resistance to flares. As described in the previous section, the reticle in a con-scan seeker is fixed and does not spin. Instead, a secondary mirror is tilted and spun. This causes the target image to be scanned in a circular path around the outer edge of the reticle. Because flares tend to drop away from the aircraft, they will drop off the con-scan reticle much faster than for a spin-scan reticle; therefore, flare resistance is built-in.

(3) Reducing the missile FOV is another method to help an IR missile discriminate the target IR signature from background IR (Figure 14-14). Limiting the FOV of the missile also makes the missile more resistant to flares. To decoy an IR missile seeker, the flare must create a heat source hotter than the aircraft and within the missile FOV. To decoy an IR missile with a narrow FOV, the flare must reach peak intensity almost immediately after ejection (Figure 14-15).

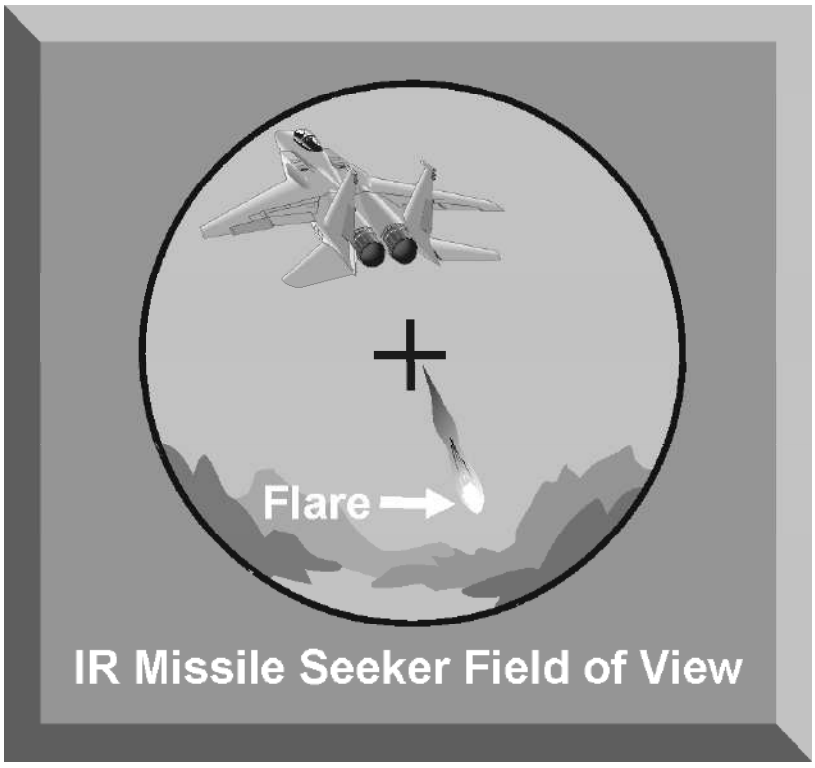

Figure 14-14. Impact of IR Missile Field of View

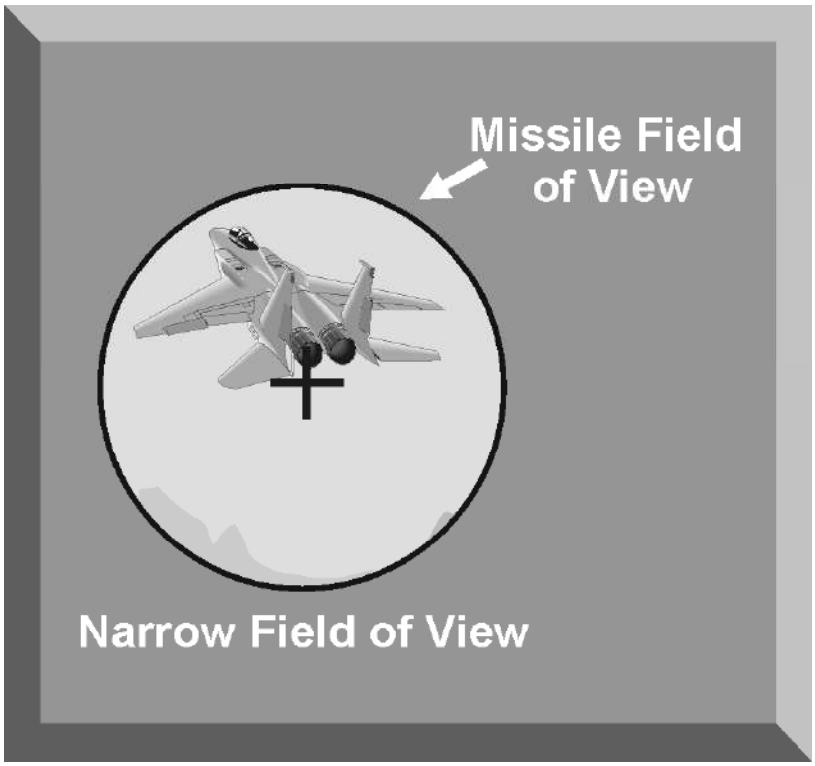

Figure 14-15. IR Missile – Narrow Field of View

(4) The detector also influences the ability of an IR missile to discriminate target IR from background IR. Newer IR seekers can track longer wavelength IR radiation. The seeker's ability to track through a wider frequency range forces flares to decoy that wider frequency range to be successful. Additionally, the cooled seeker's ability to track from all angles could cause geometry problems, the missile may never see a flare ejected from the bottom rear of an aircraft.

b. IR missile designers have combined computer signal processing and modern IR missile seekers to detect the presence of flares and reject them as targets. This flare rejection capability, or IR counter-countermeasure (IRCCM), allows newer IR missiles to track the aircraft IR signature while rejecting multiple flares. Flare rejection is based on two computer functions. The first is called the "trigger," which detects the flare in the seeker field of view. The "trigger" function activates the "response" computer processing, the action the seeker takes to reject the flare. Both the "trigger" and "response" must operate to successfully reject flares. Each advanced IR missile employs different computer techniques for both the "trigger" and "response." A flare technique developed to counter one IR missile may not work against another IR missile that uses different flare rejection computer techniques.

(1) There are several "trigger" techniques that can be used by IR missiles to detect flares. Advanced IR missiles may employ one or more of these techniques to detect the presence of a flare in the seeker FOV. These "trigger" techniques include rise time, two-color, kinematic, and spatial.

(a) An IR missile using a rise time "trigger" monitors the IR energy level of the target. A sharp rise in the received IR energy within a specified time limit indicates a flare in the IR seeker FOV. When the missile detects this rapid rise in IR energy, the rise-time "trigger" triggers a flare "response." The "response" is switched off when the received IR energy drops to its original level. The thresholds for the rise in IR energy and the response time are set to preclude activating the rise time "trigger" when the aircraft selects afterburner. An IR missile using the rise time "trigger" can be decoyed by multiple flares with slow rise times.

(b) IR missiles using a two-color "trigger" to detect flares sample the energy level in two different wavelength bands. In Figure 14-16, a non-afterburning target would have more IR intensity in band B than in band A. The typical flare produces more IR intensity in band A than band B. A sudden increase in band A intensity compared to band B intensity indicates a flare in the seeker FOV. The two-color "trigger" would then trigger a flare "response." Advanced IR missiles using a two-color "trigger" can employ different detectors composed of different materials to monitor the intensity in two bands. A lead sulfide detector could be used for band A and indium antimonide for band B. IR missiles using a single detector can employ a reticle with different bandpass filters to monitor IR intensity in both bands. To track the target, IR missiles employing a two-color "trigger" may use either band, or use data from both

bands of a dual-channel tracker. An IR missile using the two-color "trigger" can be decoyed by multiple flares that provide equal IR intensity in each band.

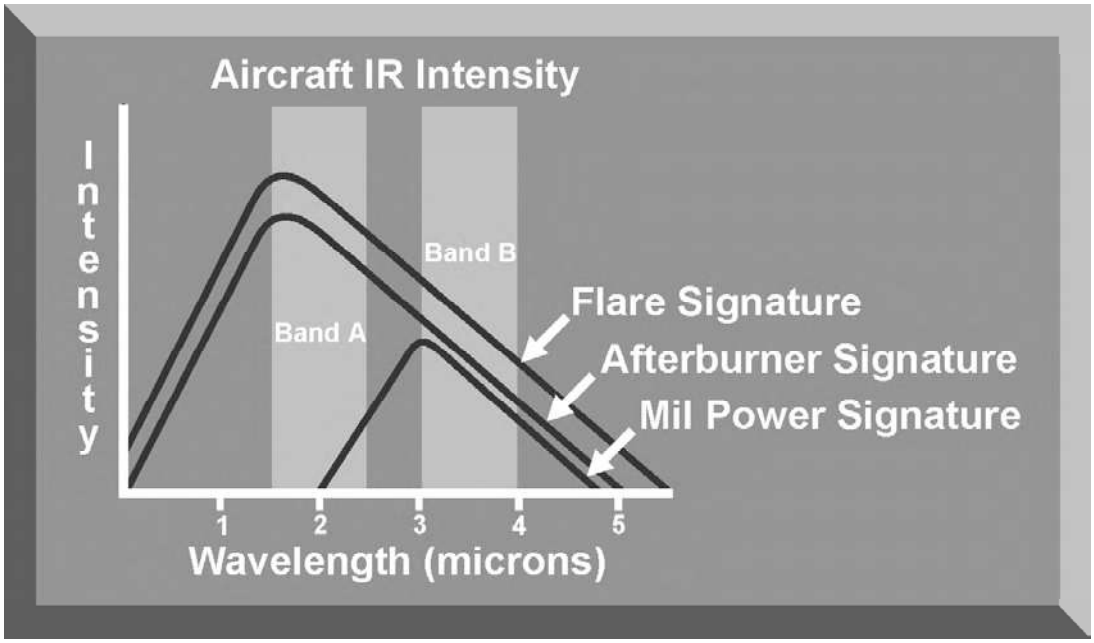

Figure 14-16. Two-Color IR "Trigger"

(c) A kinematic "trigger" takes advantage of the fact that flares separate very quickly from the dispensing aircraft due to aerodynamic drag. In a beam aspect engagement, an IR seeker that transfers track from the target to the flare will have a dramatic change in the line-of-sight rate due to the rapid separation of the flare from the aircraft. An IR missile employing a kinematic "trigger" detects this change and initiates the "response." IR missiles employing a kinematic "trigger" may have difficulty in flare detection in a head-on or stern engagement due to the small line-of-sight change between target and flare. Multiple flares dispensed at very short intervals will probably decoy an IR missile employing a kinematic "trigger".

(d) The spatial "trigger" operates like the kinematic "trigger" in that it uses the rapid separation of the flare from the aircraft to trigger the "response." An IR missile employing a spatial "trigger" uses the seeker to detect a flare. When the flare separates to the rear of the aircraft, the seeker will see the target on the edge of the FOV corresponding to the direction of target movement. The flare will be on the opposite side of the FOV. Once two hot objects on opposite sides of the FOV are distinguishable, the spatial "trigger" triggers the flare "response." IR missiles employing a spatial "trigger" can be decoyed by dispensing multiple flares at very short intervals.

(2) The seeker's "response" to the "trigger" is to reject the flare or limit its effect on target track. As long as the flare remains in the seeker FOV, the missile

is tracking the target in a degraded mode. Most IR seekers have a FOV of less than 2.5°. At long ranges, the flare will remain in the FOV for a relatively long period of time. At close range, the flare will be in the missile FOV for a relatively short period of time. Several different "response" techniques may be used, either alone or in combinations, to defeat a flare. These "response" techniques include simple memory, seeker push-ahead, seeker push-pull, and sector attenuation.

(a) When the simple memory "response" is initiated, the missile continues the maneuver it was performing just before the "trigger." This "response" assumes the flare will separate to the rear of the target. The missile rejects the seeker track data and maintains its motion relative to the target, waiting for the flare to leave the seeker FOV. The missile will continue to reject track data until the flare leaves the FOV or until the "trigger" times out. When the "trigger" times out, the "response" is discarded and the seeker operates in the normal track mode. If the "trigger" times out while a flare remains in the FOV, the seeker will usually transfer lock to the flare.

(b) The seeker push-ahead "response" causes the seeker gimbals to drive the seeker forward in the direction the target is moving (Figure 14-17). Pushing the seeker forward causes the flare to depart the FOV faster than with simple memory, minimizing the amount of time the missile is not tracking the target. The greater the amount of forward movement (called "bias"), the faster the flare will depart the FOV. If the amount of forward bias applied is too great, the seeker may be pushed forward of the target. This could cause both the target and the flare to depart the FOV and the missile would have to reacquire the target.

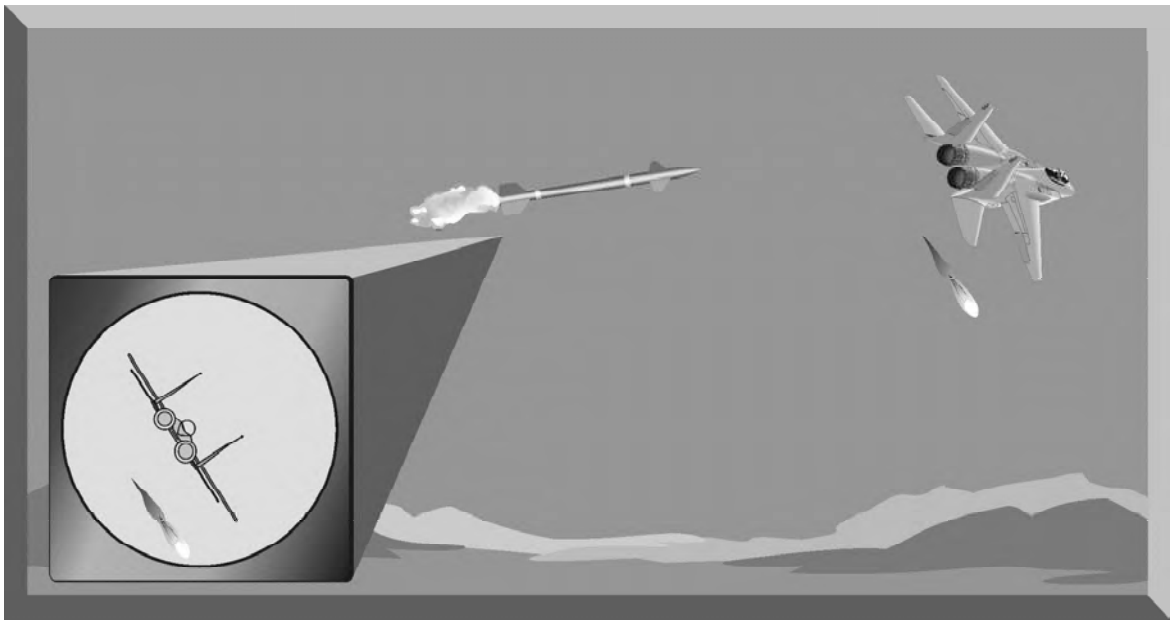

Figure 14-17. Seeker Push-Ahead "Response" Technique

(c) The seeker push-pull "response" assumes flares will have a higher intensity IR signature than the target. The "response" is initiated when the target and flare are on opposite sides of the seeker FOV (Figure 14-18). This corresponds to a spatial "trigger" condition. The received energy will rise and fall as the energy of the target and flare is scanned across the detector. When the flare energy is at a peak, the seeker gimbals drive the seeker away from the flare. When the lesser energy from the target is detected, the seeker's gimbals pull the seeker in the direction of the target. As a result, the seeker is moved away from the flare and toward the coolest IR source in the FOV, the target aircraft.

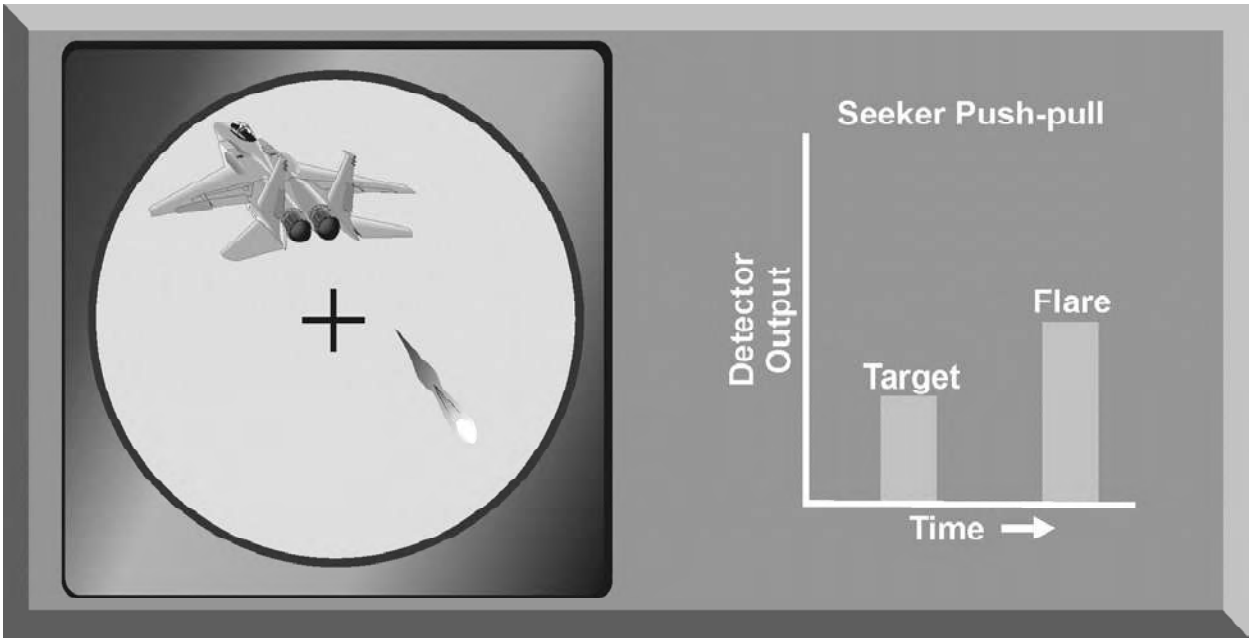

Figure 14-18. Seeker Push-Pull "Response" Technique

(d) The sector attenuation "response" is initiated by placing an attenuation filter across part of the seeker FOV (Figure 14-19). This filter reduces the seeker sensitivity in that part of the FOV. If the target being tracked is in the center of the FOV, then placing an attenuator in the quadrant below and to the rear of the target should reduce any energy received from a flare. If the attenuated flare energy is below that of the target energy, the seeker will continue to track the target.

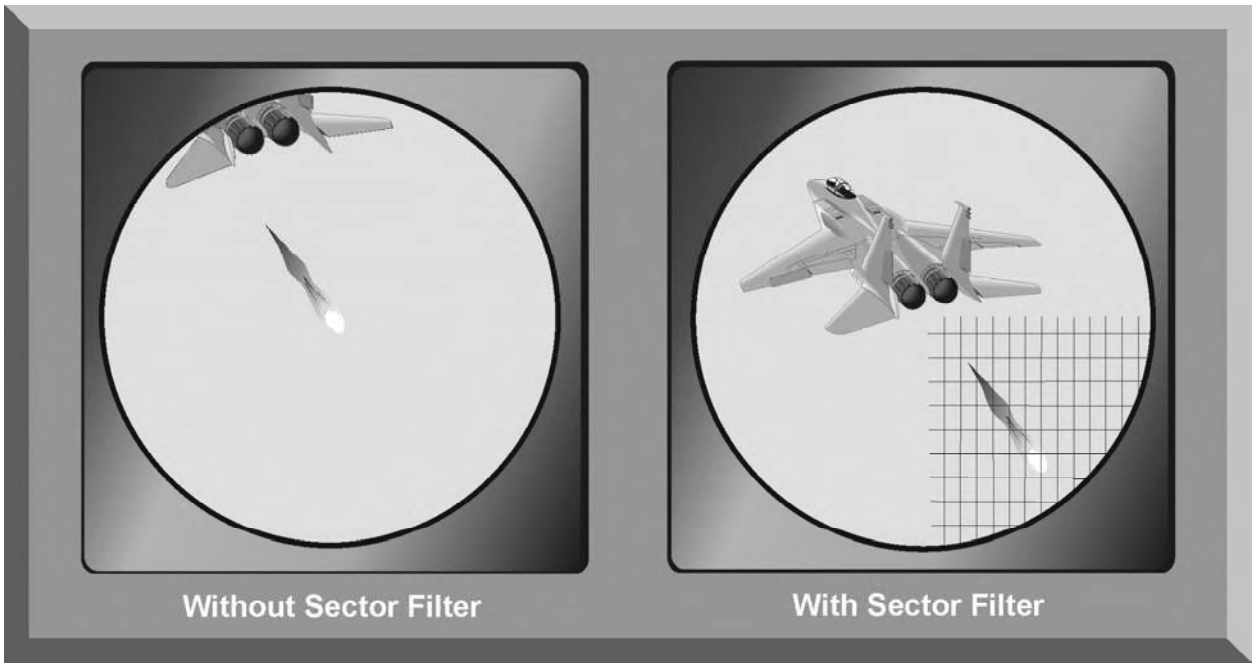

Figure 14-19. Sector Attenuation "Response" Technique

7. SUMMARY

This chapter provided some background on IR theory and IR detection, then went into some of the basics about the different types of IR missile seekers. Finally factors that impact the ability of an IR missile to reduce the effectiveness of self-protection flares were discussed. This ability depends on the discrimination capabilities of the missile seeker, the type of detector, the missile FOV, and the missile flare rejection capabilities. Modern IR missiles that employ sophisticated flare rejection techniques and advanced missile seeker technologies present a growing, and potentially lethal, threat.

CHAPTER 15. IR COUNTERMEASURES

1. INTRODUCTION

Defeating IR missiles used to be an afterthought placed well behind surviving the radar missile threat. Now with the proliferation of advanced IR missiles, defeating the IR threat is becoming more important and more difficult. The primary countermeasure used to defeat IR missiles is the self-protection flare. This chapter will discuss flare characteristics and employment considerations. One of the main difficulties in defeating an IR missile is knowing that one has been launched. This chapter will also discuss some of the methods currently available to detect an IR missile attack.

2. FLARE CHARACTERISTICS

Self-protection flares were developed to counter threat systems operating in the IR spectrum. Self-protection chaff and flare dispensers, such as the ALE-40, ALE-45, or the ALE-47, are designed to allow the pilot to dispense flare cartridges when engaged by an IR threat. These flare cartridges are pyrotechnic and pyrophoric devices designed to produce an IR source that is more attractive than the IR signature of the aircraft. To decoy an IR missile seeker, the flare must create a heat source more attractive than the aircraft, within the missile field of view. The most important flare characteristics that determine the ability of a flare to decoy an IR missile are IR wavelength matching, flare rise time, and flare burn time. The MJU-7 flare cartridge will be used as an example of a typical flare cartridge.

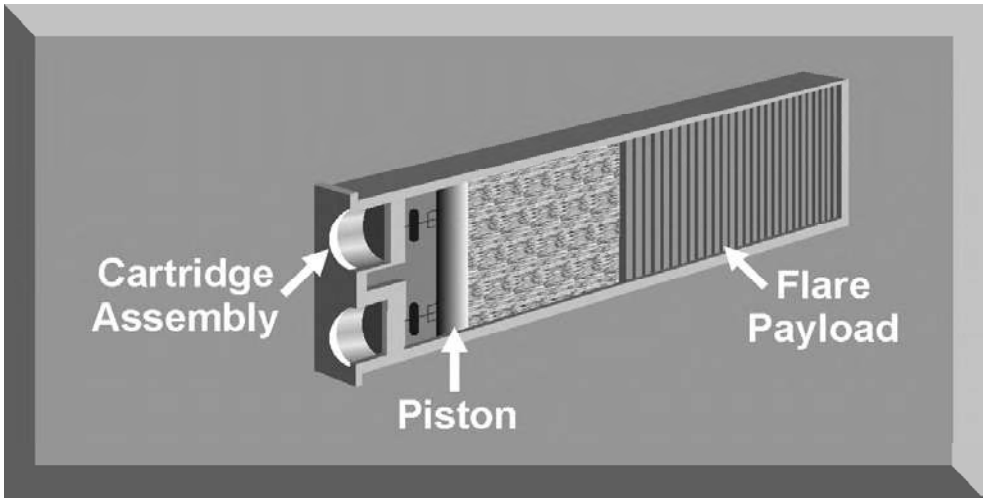

Figure 15-1. The MJU-7 Flare

a. The MJU-7 flare cartridge (Figure 15-1) is an example of a flare cartridge used in both the ALE-40 and the ALE-47 dispensers. The flare grain is composed of magnesium and tetraflouroethylene, or C_2F_4, which burns at 2000 to 2200°K. As the flare burns, it emits IR energy of different wavelengths from the luminous zone that emulates the aircraft IR signature. The burning flare also produces a large quantity of white smoke, which may highlight the position of the dispensing aircraft.

b. A flare must reach peak intensity shortly after ejection or it will not be effective in decoying the IR missile seeker. Flare rise time is the time required for the flare to reach peak intensity.

(1) To counter a short-range IR missile with a narrow field of view, a flare must reach peak intensity quickly. On the other hand, some advanced IR missiles now look for a rapid rise in IR energy as a trigger to know when a flare is trying to decoy it (Figure 15-2).

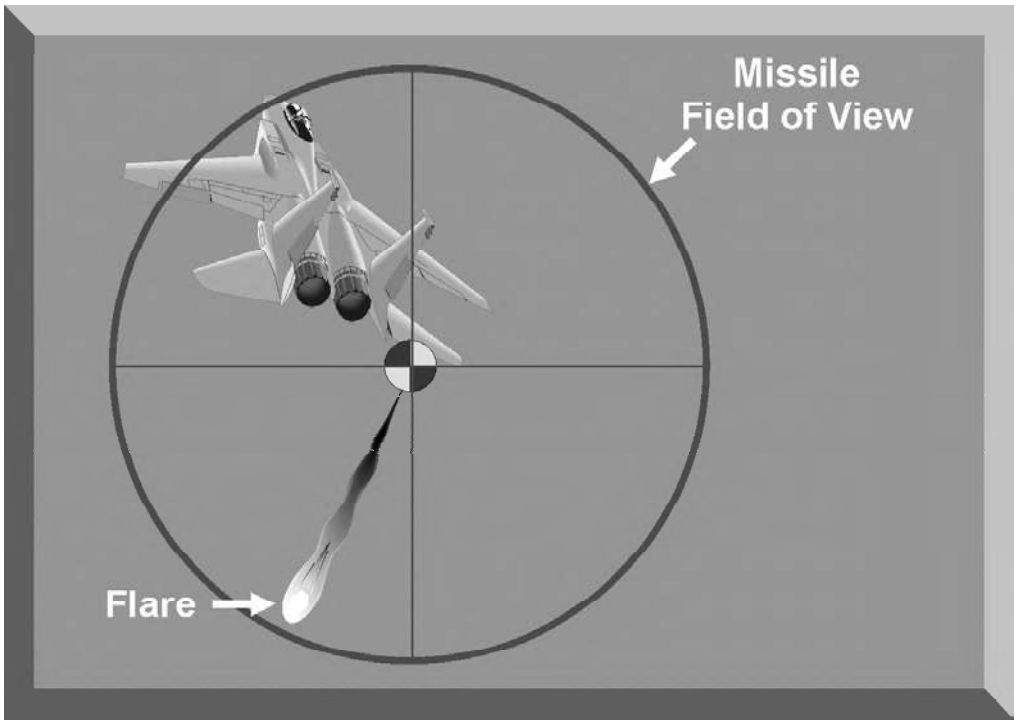

Figure 15-2. Impact of Flare Rise Time

(2) Flare rise time varies dramatically with altitude. The flare burns longer at high altitude, but it takes much longer to reach peak intensity. This increase in flare rise time at high altitude can impact the effectiveness of flares to decoy and defeat IR missiles particularly in the air-to-air combat environment.

c. Flare burn time is the time span that the flare burns and determines how far the IR seeker will be pulled off the target. The longer the burn time, the longer the

IR seeker is pulled off the target aircraft. The flare should burn long enough to ensure that the aircraft is no longer in the missile field of view. Flare burn time, like flare rise time, varies with altitude. A flare will burn longer, but at lower intensity, at higher altitudes. A longer flare burn time increases the probability the IR missile will be decoyed by a single flare.

3. ADVANCED FLARES

To counter the advances in IR missile seeker technology the Air Force and Navy formed the Advanced Strategic and Tactical Expendables program to develop and field advanced IR decoys. Two products to come out of this program are the kinematic flare, MJU-47, and the covert flare, MJU-50/51.

a. Kinematic Flares. A significant characteristic of conventional flares is that upon ejection they rapidly slow down and separate from the aircraft. As described in Chapter 14, modern IR missiles exploit this rapid separation between the aircraft and the flare. The rapid separation triggers a flare rejection response in the missile seeker causing it to ignore the flare and continue tracking the aircraft. The kinematic, or thrusted, flare delays the missile response by propelling itself in the direction of the aircraft and negating or delaying the missile's flare rejection trigger. The MJU-47 is the same size as the currently fielded MJU-10 flares. The flare's decoying pyrotechnics are vectored out the end of the flare to provide a means of propulsion (Figure 15-3).

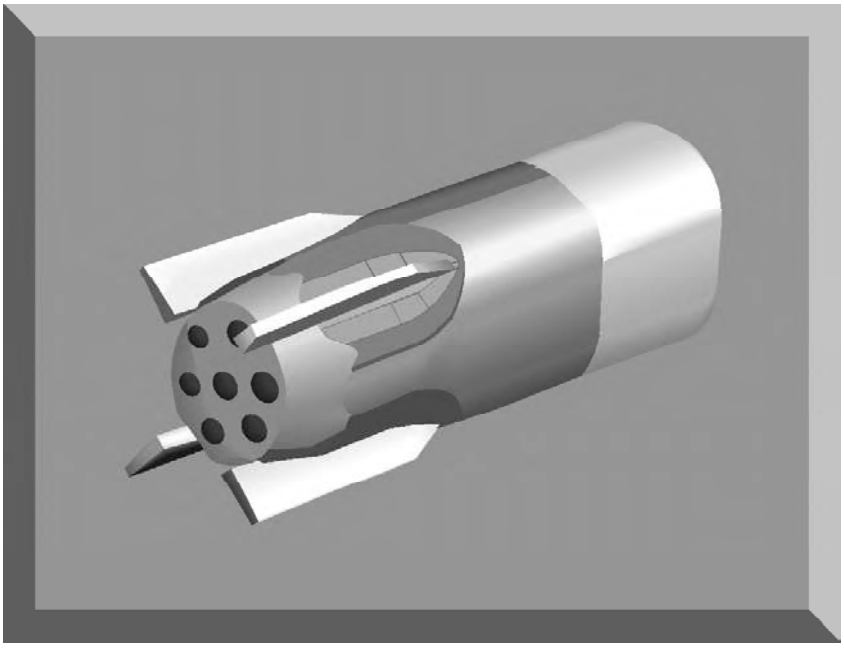

Figure 15-3. Kinematic Flare

b. Covert Flares. Though an effective tactic at defeating MANPADS, pre-emptively dropping flares in a target area carries a significant risk. The risk is that enemy air defense systems that may not have known the aircraft's location will surely see the flares, day or night, and any chance for surprise is lost. Figure 15-4 shows the visual signature of conventional flares. The danger of highlighting oneself becomes even more likely as aircraft become fitted with chaff and flare systems that automatically dispense expendables based upon inputs from the RWR or a missile attack warning system (MAWS). Automatic systems tend to error on the side of caution which means expendables will be dropped if there is any ambiguity. Visually covert flares, named the MJU-50 and MJU-51, remove this problem by not leaving a visual signature such as smoke or flame. These covert flares are made of material that oxidizes, pyrophoric instead of pyrotechnic, when released in the air. The MJU-50 is the size of the small M-206 flare while the MJU-51 is the size of the MJU-7 flare.

Figure 15-4. Flare Visual Signature

4. FLARE EMPLOYMENT

The purpose of employing a self-protection flare cartridge is to decoy the seeker head of an IR missile. This is accomplished by presenting the IR missile with a second heat source with an IR signature that exceeds the aircraft signature. The flare or IR source must appear in the field of view of the IR missile at the same time as the aircraft. As the flare separates from the aircraft, the IR missile seeker tracks the most intense IR signature, which ideally is the flare, and is decoyed away from the aircraft.

a. It is important to perform maneuvers along with flare employment to effectively defeat IR missiles. Maneuvers compound the IR missile's tracking problems and increase the distance between the aircraft and flare. Maneuvers that put the aircraft outside the IR missile field of view increase the ability of the flare to decoy the missile. When engaged by an IR threat, one tactic is to immediately dispense a flare and maneuver to put the missile on the beam. This increases the line-of-sight rate the missile guidance system must process and gives maximum separation between the aircraft and the flare (Figure 15-5).

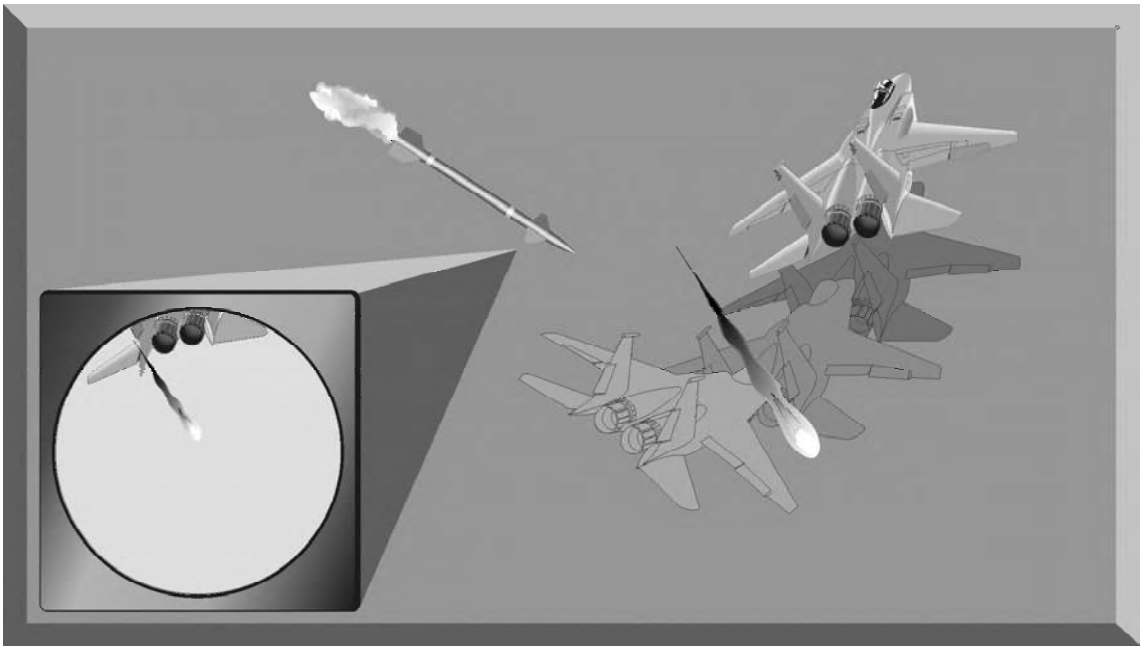

Figure 15-5. Initial Maneuver and Flare Employment

b. With the IR threat on the beam, the pilot has the best chance for achieving a "tally-ho" on the missile to determine range and keep the missile on the beam. Visually acquiring the missile increases the chances of surviving the encounter. Modern chaff and flare dispensers, such as the ALE-47 and ALQ-213, can be programmed to dispense flares in a sequence optimized to defeat specific IR missiles. Programs are selected by the pilot based upon the most likely threat. Classified tactics manuals provide aircraft specific maneuvers and flare dispensing programs to defeat the IR threat.

5. IRCM TACTICS

Besides maneuvers and flare employment, there are other IR countermeasures that can reduce the effectiveness of IR threat systems. The first is to reduce the intensity of the heat signature of the aircraft by reducing the power setting. The engines produce the largest IR signature and are the only source of IR radiation that the pilot can influence. By reducing the power setting, the IR signature is

reduced and the required flare intensity is thereby reduced. Use of afterburner should be minimized for exactly the same reason; the required flare intensity necessary to cover an aircraft in afterburner is difficult to obtain. The pilot should not reduce the power setting below the minimum required to maintain sufficient maneuvering airspeed.

a. Another effective IRCM is to use the sun. Maneuvering into the sun masks the aircraft's IR signature from most IR threat systems. When attacking a target defended by IR systems, an attack axis that places the sun behind the attacker may limit the effectiveness of these systems.

b. Clouds or smoke can also confuse IR threat systems (Figure 15-6). The water vapor making up clouds diffuses the IR energy making it difficult for an IR system to get a point to track, similar to how sun's light is diffused on a cloudy day. The particles found in smoke can have a similar effect on IR energy. The final IRCM is to reduce the IR signature of the aircraft by careful design of the engines and exhaust system. For example, the F-117 was specifically designed to provide the lowest possible IR signature.

Figure 15-6. IRCM

6. MISSILE APPROACH WARNING SYSTEMS (MAWS)

One of the most important factors in defeating an IR missile attack is knowing that an attack is in progress. Since IR threat systems are generally passive, the radar warning receiver (RWR) will provide no attack warning unless the threat uses some detectable radar energy for acquisition prior to launching an IR

missile. MAWS are designed to provide the crew some warning of an ongoing missile attack. These systems have been widely deployed on larger aircraft. Advances in technology allowing them to be smaller and promising lower false alarm rates have increased the possibility that fighter size aircraft may be outfitted with this equipment.

a. The two primary requirements for MAWS are timeliness and reliability. An IR missile engagement is an extremely short event providing very little time for the targeted aircraft to respond with maneuvers and flares. Secondly, there must be a very low false alarm rate. In earlier systems the sun, flares, or the wingman's aircraft have been known to cause false alarms. Aside from being annoying, a false alarm can become a tactical problem if the MAWS is tied directly into the countermeasures dispenser set allowing for automatic dispensing of chaff and flares when the MAWS senses an attack. False alarms in this type of scenario would only serve to highlight a previously untargeted aircraft.

b. MAWS detect incoming missiles either actively or passively. The active MAWS use a pulse Doppler radar to detect and track the in-flight approach of an attacking missile. Pulse Doppler radar is used for this purpose because of its ability to use relative velocity to pull targets out of clutter. An incoming missile will have a high velocity relative to the surrounding background. Range and time to impact are computed automatically, updated continuously, and provided to the crew to assist in defensive maneuvers (Figure 15-7). The down side to active MAWS is the requirement to continuously radiate for long periods of time to ensure protection. This contradicts the common tactic of keeping radar transmissions to a minimum to avoid being tracked via passive detection measures. This situation has led to the latest generation of MAWS being mostly of the passive type.

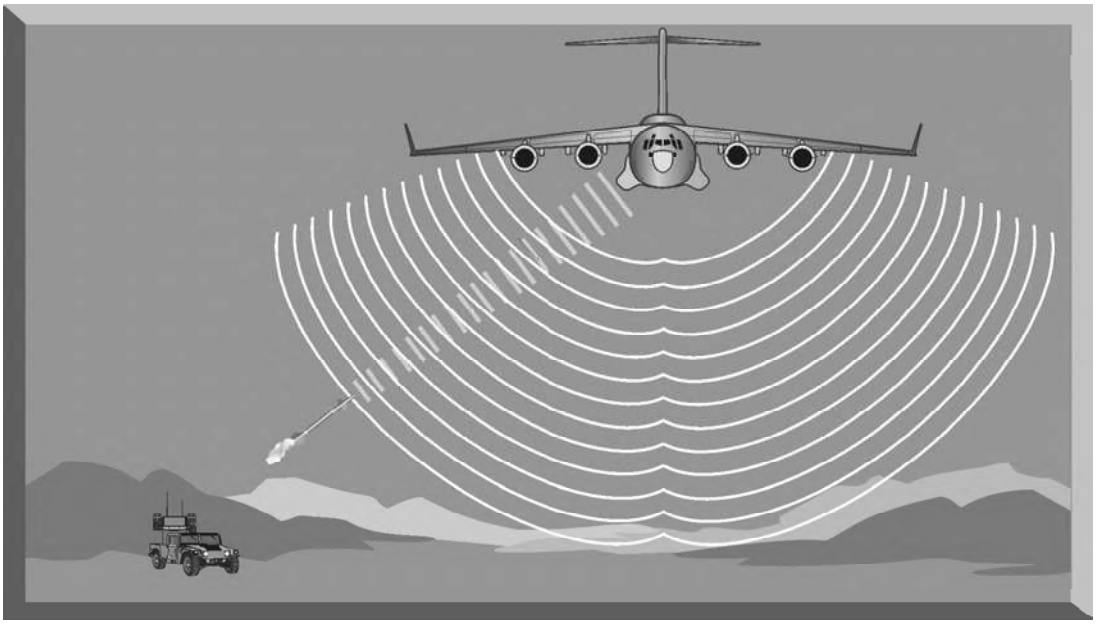

Figure 15-7. Missile Alert Warning System (MAWS)

c. The passive MAWS operate in either the ultraviolet, or the infrared frequency spectrum. These systems are tuned to look for the IR signature of a missile's rocket motor, then pass a warning and the position of the inbound threat to the pilot. To obtain all-aspect missile warning, multiple MAWS sensors must be positioned on the aircraft in a similar fashion to RWR antennas. All-aspect MAWS face the same challenges that RWR systems face: false multiple targets due to maneuvers and accurate threat position reporting, to name a few.

7. SUMMARY

The proliferation of IR threat systems has elevated the importance of IRCM to survival on the modern battlefield. The most effective IRCM is still the employment of flares in conjunction with maneuvers. The specific flare characteristics of IR spectrum coverage, rise time, and burn time are critical factors in determining flare effectiveness. Other IRCM tactics are designed to enhance the effectiveness of flares and take advantage of IR missile limitations. The effectiveness of all IRCM tactics depends on some type of attack warning. The new generation of MAWS should provide some measure of warning to the crews and in some cases automatically defeat the IR missile.

CHAPTER 16. RADAR ELECTRONIC PROTECTION (EP) TECHNIQUES

1. INTRODUCTION

Electronic warfare (EW) is defined as military action involving the use of electromagnetic and directed energy to control the electromagnetic spectrum or to attack the enemy. Nearly every military action, from command and control of an entire integrated air defense system (IADS) to precision guidance of an individual weapon, depends on effective use of the electromagnetic spectrum. Radar systems have become a vital element of nearly every military operation. Since these systems operate across the entire electromagnetic spectrum, much of the EW effort is concerned with countering radar systems. All of the jamming techniques discussed in Chapters 10 and 11 and the chaff employment options discussed in Chapter 13 are specifically designed to counter radar systems. These actions are classified as electronic attack (EA), which is a part of EW.

a. EW is somewhat like a chess game—a series of moves and countermoves within the electromagnetic spectrum. As we develop jamming techniques to counter radar systems, our adversaries develop counter-countermeasures to negate the effectiveness of these techniques. In response, we develop newer techniques and our adversaries respond with new modifications to their radar systems. This series of moves and countermoves can continue for decades. The development and application of radar counter-countermeasures are classified as electronic protection (EP), also a part of EW.

b. The continuing battle to control the electromagnetic spectrum for unrestricted radar employment has resulted in over 150 radar EP techniques. These techniques are designed to negate the effectiveness of electronic jamming and chaff on radar systems. These radar EP techniques can be incorporated into the design of a radar system or added to an existing radar system in response to a jamming technique. It is beyond the scope of this text to discuss all the radar EP techniques in use today. This chapter will discuss the most common EP techniques. They have been organized by function of the technique within the radar. These functions include radar receiver protection, jamming avoidance, jamming signal exploitation, overpowering the jamming signal, pulse duration discrimination, angle discrimination, bandwidth discrimination, Doppler discrimination, and time discrimination.

2. RADAR RECEIVER PROTECTION

The following are some of the most common radar counter-countermeasures designed to prevent receiver overload or saturation.

a. Sensitivity time control (STC) is used to counter close-in chaff or close-in clutter. Receiver gain is set at normal for long ranges and reduced for close-in ranges. One problem with using STC is that close-in targets may be missed if STC is improperly adjusted.

b. Automatic gain control (AGC) is used to counter chaff, clutter, and most types of transmitted jamming. AGC senses the signal level of a receiver's output and develops a back-bias, producing a constant output level. This technique has a slow response time compared to fast AGC and instantaneous AGC, both of which are employed instead of AGC. Also, it cannot maintain correct IF output levels for different intensity signals that are close in range because the bias voltage has a long buildup and decay time.

c. Fast automatic gain control (FAGC) is also employed against chaff, clutter, and most types of transmitted jamming. FAGC works by sensing the signal level of receiver output and develops a back-bias, tending to hold output constant. Response time is within milliseconds, permitting fast response and recovery as the antenna traverses the jammer's bearing. There are several precautions to note when using FAGC. First, targets may be suppressed and lost without the operator knowing that jamming is present. Second, a strong pulse or echo may cause ensuing weak targets to be lost. Lastly, FAGC has difficulty getting an accurate bearing on the jamming source.

d. Instantaneous automatic gain control (IAGC) is another technique to counter chaff, clutter, and most types of transmitted jamming. IAGC senses the signal level of each echo or jamming pulse and develops a back-bias that holds the stage output constant. Gain control response time is within milliseconds and extends the dynamic range of the receiver. There are several precautions to note when using IAGC. First, it is not effective against signals whose "in band" time is less than the IAGC response time. Also, with continuous duty cycle jammers, targets may be lost without the operator knowing that jamming is present. Finally, it is difficult to get an accurate bearing on the jamming source.

e. Automatic noise leveling (ANL) counters noise jamming and modulated or unmodulated constant wave jamming. ANL samples receiver noise content at the end of each PRF and sets the gain accordingly for the next pulse interval. Continuous jamming reduces gain to keep output the same as the original noise level. ANL also follows the scanning rate of the antenna so that receiver noise output is constant as the antenna rotates. When using ANL, targets may be suppressed and lost without the operator knowing that jamming is present. Also, receiver gain is unstable when pulses or swept jamming enter the sampling gate intermittently.

f. The logarithmic receiver (LOG) counters most types of transmitted jamming by amplifying and demodulating large dynamic-range signals in logarithmic amplifiers. This produces "amplitude compression" of the strong

signals. However, when using LOG, output is nearly constant so the operator cannot easily tell when jamming is present.

g. The logarithmic receiver with fast time constant (LOG-FTC) counters narrowband jamming, chaff, and clutter. This technique amplifies and demodulates large dynamic-range signals in logarithmic amplifiers, producing "amplitude compression" of the strong signals. Video is coupled through FTC circuits to eliminate rectified carrier and low frequency sideband products. There are problems with using LOG-FTC. First, the receiver output is nearly constant, so the operator cannot always tell when jamming is present. Second, LOG-FTC is not effective against wideband, or fast-swept, short pulse jamming. Lastly, LOG-FTC causes a broadening of displayed jam sector. as well as degrading bearing accuracy on the jam source.

h. Dicke-fix (DF) counters wideband and fast-swept jamming and is similar in employment to wideband limiting (WBL). DF amplifies without ringing, clips down all pulses to a common level, then amplifies the narrowband echo signal more than the wideband jamming. Noise level is held constant, independent of jamming intensity. There are precautions to note when using DF. Jamming that enters the wideband limiter can capture limiters, causing poor receiver sensitivity. Targets may be suppressed without the operator knowing that jamming is present. Also, resolution and target detection range are reduced, even in a non-jamming environment. Finally, DF is ineffective against extremely fast-swept spot jamming.

i. WBL is used to counter wideband jamming and fast-swept jamming. WBL amplifies without ringing, clips down all pulses to a common level, then amplifies the narrowband echo signal more than the wideband jamming. Noise level is held constant, independent of jamming intensity. However, jamming that enters the wideband limiter can capture limiters and cause poor receiver sensitivity. Resolution and target detection range is reduced, even in a clear environment. Targets may be suppressed without the operator knowing that jamming is present. Finally, WBL is ineffective against fast-swept spot jamming.

j. Adaptive video processing (AVP) counters chaff corridors, weather, sea clutter, and most types of transmitted jamming. AVP combines the adaptive threshold, beam-to-beam correlation, and wide-pulse blanking in frequency-scanning three-dimensional radars to avoid collapsing undesired returns on the PPI display. However, when using AVP, there is a decreased probability of detection in some multiple target situations. Also, targets may be suppressed without the operator knowing that jamming is present. Finally, AVP passes all point targets.

3. JAMMING SIGNAL AVOIDANCE

The following are some EP techniques used to avoid jamming signals.

a. Frequency agility (FA) counters narrowband jamming and some types of repeater and deception jamming. FA enables the radar to make rapid changes of transmitter and receiver operating frequency, sometimes on a pulse-to-pulse basis. Manual frequency changes may cause mutual interference with other radars and services.

b. Frequency diversity works against narrowband jamming and some types of repeaters and transponders. It is a multiple-radar coordination procedure in which radars are assigned operating frequencies that are separated to reduce mutual interference and their susceptibility to a single jammer. It is important to note that other radars may be operating at the same allocated operating frequency.

c. Polarization diversity is used to counter chaff, weather, and transmitted jamming. Polarization diversity attenuates jamming input to a radar receiver by using antenna polarization different from jammer polarization, and usually involves separate radars of different polarization. There are two precautions when using polarization diversity: (1) ground clutter worsens on vertical polarization, and (2) close coordination is necessary if separate radars are used; for example, one horizontally polarized search radar and one vertically polarized search radar.

d. Circular polarization (CP) works against chaff, weather, and transmitted jamming. CP attenuates jamming input to a radar receiver by using antenna polarization different from jammer polarization, and usually involves separate radars of different polarization. CP also improves target detection in rain clutter.

e. Conical-scan-on-receive-only (COSRO) is employed against inverse conical scan jamming to deny a jammer the ability to sense and upset scan angle tracking information. A constantly transmitted illumination beam is received and scanned to derive target angle information. However, the jammer can still degrade angle tracking if it can approximate the received signal scan rate.

f. Speedgate tracking is used against all types of transmitted jamming. The technique provides a very narrow bandpass having a center frequency related to Doppler shift. Only jamming within the restricted band is effective. It has the advantages of accurate target Doppler discrimination and good target tracking at low target levels. However, the speedgate can be stolen by gate stealers and some types of swept jamming.

g. Leading-edge track (LET) is used to counter an incoming target dropping chaff by allowing target tracking on the leading edge of the target. Trailing edge track (TET) is used to counter a receding target dropping chaff.

h. Track coast is used to counter chaff, clutter, multiple targets, range gate stealers, jam fades, and blinking jamming by placing tracking radar in a rate-aided coast condition. The system "estimates" target position to avoid interrupting the fire control solution. A lock-on or return to acquisition mode terminates the track coast condition. Track coast requires adequate storage of rate-aided information, and no true tracking information will be developed while track coast is operating.

i. Guard gates work against chaff, clutter, multiple targets, range gate stealers, jam fades, and blinking jamming. Guard gates provide automatic detection of a foreign signal and "estimates" target position to avoid interrupting fire control solutions. Like track coast, guard gates require an adequate store of rate-aided information with no true tracking information developed.

4. JAMMING SIGNAL EXPLOITATION

The following are some EP techniques that use the jamming signal for target acquisition and engagement.

a. Passive angle tracking (PAT) counters most types of transmitted jamming by allowing the radar to acquire and angle-track the source of jamming signals. There are some problems with this technique. Blinking jamming can cause severe instability, and the range of the jammer is unavailable until the target reaches burnthrough range.

b. Home-on-jamming (HOJ) counters most types of transmitted jamming by allowing the missile or radar to use the jamming signals, locate the source, and home on it. However, blinking jamming can cause severe instability, and the range of the jammer is unavailable until burnthrough.

c. Jamming signals produce recognizable sounds that help in their detection and identification. Aural recognition allows an operator to listen to the Doppler frequency associated with a moving target. It is used to counter most types of jamming.

d. The local oscillator off technique counters continuously transmitted jamming. No receiver output occurs unless a target echo signal and a jamming signal are present. Limitations of this technique include: targets only display in an area where jamming is present; and, if the antenna rotates away from the jammer, or if jamming is turned off, no targets are displayed on the radar scope.

e. The jamming strobe indicator counters any transmitted jamming with high-duty-cycle modulation. The indicator is a variable marker strobe on the radar display that moves in range proportional to jamming strength. The indicator traces an antenna lobe pattern on the display, showing the azimuth of the jamming source. There are some problems with the jamming strobe indicator. First, it interrupts normal video in some radars. Second, inverse or sidelobe

jamming can cause erroneous strobes. Finally, the jam strobe does not react to unmodulated CW or low-duty-cycle jamming for some radar systems.

f. The jamming indicator lamp, located on the operator console, is used on radars with automatic noise leveling (ANL) to counter continuous transmitted jamming. The lamp alerts the operator to the presence of jamming, and the ANL is manually shut off. This action allows the operator to determine jammer bearing.

g. Clean strobe generation (CSG) counters any transmitted jamming by using the sidelobe blanking circuits of a radar. An azimuth strobe appears when the jamming level in the main antenna exceeds the jamming level in the sidelobe auxiliary antennas. The operator is alerted to the presence and bearing of a jamming source, even with a constant false alarm radar (CFAR) receiver.

h. Jamming attenuation (JAM ATTEN) counters both clutter and any type of jamming. Receiver gain is reduced to avoid receiver saturation by inserting an attenuator pad that enables the operator to recognize presence, type, and bearing of a jamming source. When using JAM ATTEN, however, the reduced gain may cause loss of targets, even in non-jammed sectors. Also, any improvement in signal-to-jam ratio is not possible.

i. Receiver manual IF gain (MAN GAIN or IF GAIN) also counters clutter and jamming. Receiver gain is reduced to avoid jamming saturation by manually reducing stage gain, allowing the operator to identify jammer presence, type, and bearing. When using IF GAIN, the reduced gain may cause a loss of targets, even in non-jammed sectors. Also, any improvement in signal-to-jam ratio is not possible.

5. OVERPOWERING THE JAMMING SIGNAL

Following are some EP techniques a radar system can employ to overpower jamming and reduce the jamming-to-signal (J/S) ratio to less than one.

a. Burnthrough counters most types of transmitted jamming. Energy in the target pulse is raised by increasing the peak power, that is, the PRF or pulse width, or by increasing the time the radar illuminates the target by reducing the scan rate or scan angle. Some radars have modes in which the radar concentrates its power in narrow azimuth and elevation sectors about the suspected target position. However, burnthrough can degrade general radar performance by overloading the receiver if a large radar cross section target is detected. High power may impact radar operation in clutter or dense chaff environments.

b. Narrowband long pulse (NBLP or NLP) counters most types of transmitted jamming by using a high-energy long pulse. The signal uses a narrowband receiver for reception, and increases detection range for targets in jamming and

in the clear. Simultaneously, it reduces resolution, which causes poor radar performance in chaff and clutter.

6. PULSE DURATION DISCRIMINATION

The following are some radar counter-countermeasures that use pulse duration to discriminate between radar and jamming signals.

a. The fast time constant (FTC) is used to counter chaff, clutter, and narrowband jamming. A video circuit provides low frequency attenuation to reject carrier and low frequency modulation jamming. FTC passes normal radar pulse lengths with little attenuation, but causes some loss of receiver sensitivity.

b. Pulse width discrimination (PWD), clutter eliminate (CE), and wide pulse blanking (WPB) are designed to counter chaff, most types of jamming, EMI, and some types of deception jammers. A video coincidence gate, involving a delay line matched to the expected signal duration, senses if a return is the proper pulse width. PWD, CE, and WPB provide an enabling path for qualified signals. However, weak signals may be lost in the signal processing.

c. Pulse expansion-compression (PC) is used to counter most types of noise jamming and some types of deception jamming. An expanded pulse is coded for transmission. This expanded pulse is transmitted and decoded on return. Echo responses are then compressed in a decoding process. This expansion/compression is equivalent to NLP, which provides longer detection ranges, and wideband short pulse, which provides increased resolution. Using PC is not without problems. Unwanted residues may cause loss of weak targets. Additionally, range error proportional to the Doppler shift, or radial velocity, affects the accuracy of the PC.

7. ANGLE DISCRIMINATION

The following techniques use angle discrimination to distinguish between radar returns and jamming signals.

a. Sidelobe blanking (SLB) and sidelobe cancellation (SLC) are types of sidelobe suppression (SLS) used to counter sidelobe response to chaff, clutter, transmitted jamming, sidelobe jamming, and deception jamming. An auxiliary antenna approximates the pattern and gain of sidelobes of the main antenna and produces a signal for comparison with the signal received in the main antenna. If the signal in the auxiliary antenna is greater, the signal in the main antenna channel is blanked. This permits bearings to be obtained on a jamming source and rejects sidelobe jamming. SLB is useful only for determining the bearing to the jamming source.

b. Antenna manual positioning, antenna traverse and elevation angle offset, antenna jog, and antenna slow scan are EP techniques used to counter main

beam and sidelobe jamming and deception. These techniques are designed to increase the antenna scans across the jammed sector to increase the blip-scan ratio. These techniques increase the number of pulses integrated, as well as the operators' sorting capability.

8. BANDWIDTH DISCRIMINATION

The following are EP techniques that use bandwidth to distinguish between radar jamming and target returns.

a. Dicke-fix (DF) counters wideband and fast-swept jamming. A wideband limiter amplifies without ringing and clips all pulses down to a common level. Then an amplifier increases narrowband target echo signals more than the wideband jamming. There are some problems associated with DF. Any jamming entering the wideband limiter can "capture" the limiters and cause poor receiver sensitivity. Targets may be suppressed without the operator knowing that jamming is present. Resolution and target range is reduced, even in a clear environment. Finally, DF is ineffective, even harmful, when the jamming bandwidth is near the bandwidth of the desired echo signal.

b. Transmitter pulse lengthening (TPL) counters wideband and fast-swept jamming. TPL concentrates power into a narrow band about the carrier frequency by lengthening the transmitting pulse. While this allows use of a narrowband receiver, it impairs resolution, causing poor chaff and clutter performance.

c. Transmitter pulse shaping (TPS) counters wideband and fast-swept jamming. The sideband range is limited by shaping the transmitted pulse. This allows use of a narrowband receiver, but impairs resolution, causing poor performance in chaff and clutter.

d. Narrowband pulse limiting (NBLP or NLP) is a form of transmitter pulse lengthening that counters wideband jamming and fast-swept jamming. NBLP concentrates power into a narrow band in the carrier frequency by lengthening the transmitting pulse. This allows use of a narrowband receiver, but impairs resolution, causing poor chaff and clutter performance.

e. The fast time constant (FTC) is used to counter chaff, clutter, and narrowband jamming. A video circuit provides low frequency attenuation to reject carrier and low frequency modulation of jamming. FTC passes normal radar pulse lengths with little attenuation, but causes some loss of receiver sensitivity.

f. High video pass (HVP) is used to counter chaff, clutter, and narrowband jamming. It is similar to FTC. A video circuit provides low frequency attenuation to reject carrier and low frequency modulation jamming. HVP passes only the leading edge of the received pulses. HVP can cause some loss of receiver sensitivity.

g. The wideband short pulse (WSP) counters chaff, clutter, and narrowband jamming by transmitting a short pulse and using a wideband receiver for reception. Echo resolution and accuracy are improved, and performance against narrowband jamming is enhanced. However, the maximum detection range is decreased and system vulnerability to wideband jamming is increased.

h. Narrowband limiting (NBL) counters chaff, clutter and narrowband jamming. A narrowband filter positioned in the front of the amplifier section allows only the target signal bandwidth to enter the limiter, reducing wideband and off-frequency jamming. The limiter clips all signals and noise to a common level. This technique is useful only when followed by pulse compression or other "decode" techniques. NBL is not effective against wideband jammers capable of causing "ringing" of the NBL bandpass filters. Targets may be suppressed and lost without the operator knowing that jamming is present. Finally, target detection and resolution are poor.

9. DOPPLER DISCRIMINATION

EP techniques that use Doppler frequency discrimination between radar and jamming signals to negate jamming effectiveness include the following:

a. Moving target indication (MTI) is used to counter chaff and clutter. The phase of returned target echoes is compared on a pulse-to-pulse basis. Those with no phase change (no change in radial velocity) are cancelled using a delay-line canceler. Sensitivity using MTI is poor for weak targets, even in the clear. Also, it is blind to targets that have a Doppler frequency that is equal to a multiple of the radar PRF, unless PRF stagger is used. Finally, limited dynamic range does not allow full cancellation of strong clutter echoes.

b. Compensated coherent MTI, also known as compensated COHO MTI, counters chaff and clutter by comparing the phase of returned target echoes on a pulse-to-pulse basis. Those pulses with no phase change, that is, no change in radial velocity, are cancelled. Corrections to the coherent oscillator are applied to compensate for motion of the platform and radar antenna. Sensitivity is poor for weak targets, even in the clear, and it is blind to targets that have a Doppler frequency equal to, or a multiple of, the radar PRF, unless PRF stagger is used.

10. TIME DISCRIMINATION

The following EP techniques use time discrimination between radar and jamming signals to negate jamming effectiveness.

a. Video integration (VINT) and integrate-multiply (INT-MULT) counter any form of transmitted jamming not synchronous with radar PRF. The video continuously circulates through a delay line, delaying signals exactly one pulse recurrence time (PRT), then combines them with signals from the next PRT. Synchronous target signals add together to increase video output, but noise and

random pulses are suppressed. Unless MTI and FTC are employed, VINT and INT-MULT will enhance chaff, clutter, and jamming along with target returns. Also, feedback control, or loop gain, must be carefully adjusted for optimum results.

b. PRF stagger and jitter are EP techniques designed to counter quasi-synchronous jamming, EMI, MTI blind-speeds, "second trip" echoes, and repeater jammers simulating "closer-than-real" targets. The transmitter pulse interval is varied to break up synchronous patterns. Received signals must be "de-staggered" for use with MTI or integration. When using any of these techniques, video de-stagger balance must be accurate or "double video" occurs. These techniques are not effective against exact synchronous deception jamming.

c. Pulse-to-pulse correlation (PPC) is used to counter slow-swept blinking or pulsed jamming not synchronized with radar PRF, and some types of deception jammers. To be displayed, target video must exceed a threshold voltage for two successive pulses. The technique avoids displaying non-synchronous jamming and EMI, but is not effective against synchronous jamming, and may cause weak targets to be missed.

d. Beam-to-beam correlation (BBC) is used to counter slow-swept blinking or pulse jamming not synchronous with radar PRF and some types of repeaters and transponders. It is used in three-dimensional frequency scanning or frequency agile radars. To be displayed, the target return echo signal must exceed a threshold value in two adjacent antenna beams. BBC is not effective against synchronous jamming. It may also cause weak targets to be missed.

e. Single beam blanking (SBB) is used to counter slow-swept, blinking, pulsed jamming, and narrowband jamming. It is used in three-dimensional frequency scanning or frequency agile radars to avoid displaying vertical beams containing jamming. A blanking pulse is generated for vertical beams containing jamming so that they are not displayed. The technique is not used on RHI video. Also, it can cause a loss of targets at the jammed elevation angle on the PPI display.

11. SUMMARY

This chapter has discussed some of the most widely employed EP techniques designed to counter radar jamming. The capabilities of the individual radar operator were not discussed. However, the radar operator is as important as the EP techniques designed for the radar system. Many of the most effective EP techniques are designed to ease operator interpretation of the radar display. In the chess game of EW, the capabilities of individual radar operators can be as important as the sophisticated EP techniques in determining the final outcome.

CHAPTER 17. RADAR WARNING RECEIVER (RWR) BASIC OPERATIONS AND GEOLOCATION TECHNIQUES

1. INTRODUCTION

Radar surveillance and radar-directed weapons represent the biggest threat to aircraft survival on the modern battlefield. The first step in countering these threat systems is to provide the pilot or crew with timely information on the signal environment. The radar warning receiver (RWR) is designed to provide this vital information to the pilot. The RWR system is an example of an electronic warfare support (ES) system. The primary purpose of an RWR system is to provide a depiction of the electronic order of battle (EOB) that can have an immediate impact on aircraft survival. Though the RWR system is complex, the basic operations of the various components are straightforward. A step above RWR systems is threat geolocation. While an RWR provides the EOB for a single aircraft, threat geolocation systems can provide accurate threat location data for numerous aircraft over an entire region. Threat location data is used for aircraft threat avoidance and, more common today, the preemptive attacking of enemy radar sites. This chapter will discuss the functions of the various components of a RWR system including the antennas, receiver/amplifiers, signal processor, emitter identification (EID) tables, RWR scope, RWR audio, and limitations to RWR systems. This chapter will then go on to discuss three of the methods used to geolocate radar threat systems.

2. RWR ANTENNAS

Antennas are designed to receive radar pulses from threat radar systems. Factors that impact the operation of the RWR antennas include location, pattern, sensitivity, and polarization.

a. The physical location of the RWR antennas on the aircraft can affect its ability to detect a radar signal. Antennas are arranged to cover a predetermined area of horizontal and vertical space around the aircraft (Figure 17-1).

b. The antennas and their patterns play an essential part in displaying the spatial relationship of a threat radar to the aircraft. The antenna patterns are the areas, or "footprints," that the antennas are specifically designed to cover. These footprints are directly affected by the relative position of the antennas to the threat systems. This is because the signal processor measures and compares signal strength from all the aircraft antennas to compute threat signal location relative to the aircraft. This relative location is then presented on the RWR scope display. Aircraft movement and maneuvering shifts these relative positions during flight and can distort the true threat position on the RWR scope. Precise position determination is not possible with most RWRs.

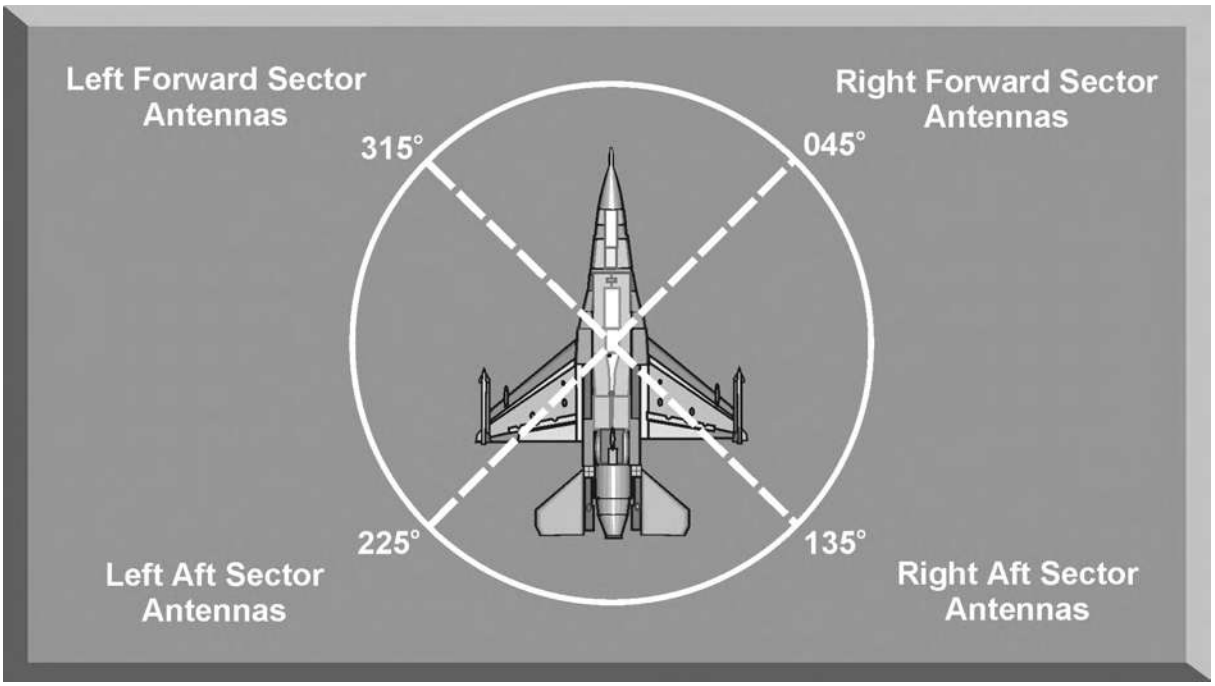

Figure 17-1. Radar Warning Receiver (RWR) Antennas

c. The sensitivity of an RWR antenna directly affects its ability to detect a radar signal. The more sensitive the antenna, the further it can detect a signal. The sensitivity of a system and its ability to intercept a radar signal is usually expressed in decibels relative to milliwatts or dBm units. A 10 dBm change in sensitivity can result in a 25 nm range difference in target detection. In general, sensitivity levels of -50 to -60 dBms are required to detect signals at long ranges (Figure 17-2).

Figure 17-2. RWR Antenna Sensitivity

d. Another factor affecting antenna detection range is the polarization of the antennas. If the polarization of the RWR antenna and the threat system antenna are mismatched, or cross-polarized, initial detection of a threat signal could be delayed until the aircraft is within the lethal range of a threat system. In this situation, the aircraft could be engaged with minimal warning (Figure 17-3).

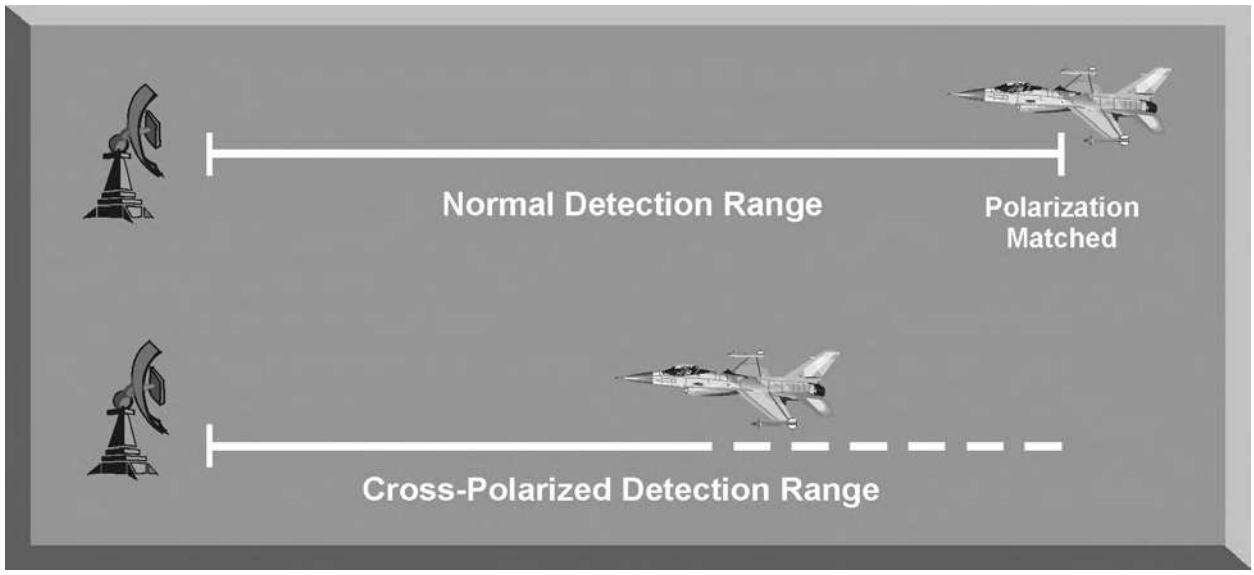

Figure 17-3. RWR Antenna Polarization

3. RWR RECEIVER/AMPLIFIERS

The RWR receiver/amplifier section processes the radar signals from the antennas. Most RWR systems use frequency bands to differentiate signals. Nominal band designations are summarized in Table 17-1. There are two types of receivers currently used in RWR systems: the crystal video receiver and the superheterodyne receiver.

Table 17-1. RWR Frequency Band Designators

RWR Frequency Band	EW Frequency Band
Band 0	Charlie-Delta Bands
Band 1	Echo-Foxtrot Bands
Band 2	Golf-Hotel Bands
Band 3	India-Juliet Bands

a. A crystal video receiver (CVR) is the simplest type of microwave receiver. It is used primarily for detection of pulse radar signals in the 2 to 18 GHz band. A CVR used in a radar warning receiver incorporates crystal detectors for each designated frequency band. A pulse radar signal is detected by the antenna and passed to the multiplexer. The multiplexer divides the received radar signals by frequency band and sends the signals to the appropriate band channel. The RF amplifier boosts the radar signal and passes it to the crystal detector (Figure 17-4).

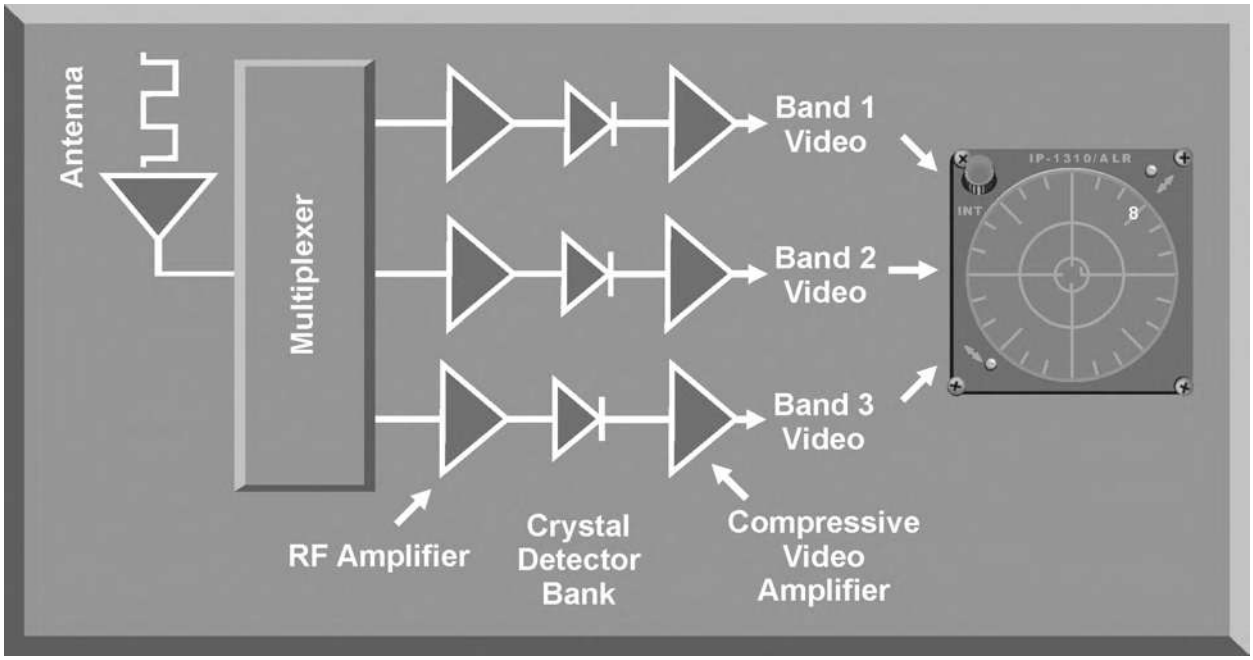

Figure 17-4. Crystal Video RWR Receiver

(1) The crystal detector is an RF diode, which converts the RF signal into a video signal. The voltage level of the output video signal is dependent only on the amplitude of the input signal and not on the frequency or phase. The sensitivity of a CVR is limited by the sensitivity of these crystal detectors. The sensitivity of crystal detectors currently available is generally adequate to detect main beam radiation from most threat radars. The video output of the crystal detectors is amplified by a high-grain compressive video amplifier and sent to the RWR scope for display.

(2) A CVR is extremely fast, sensitive, and covers a wide frequency range. These characteristics coupled with low cost and small size make CVRs ideal for use in radar warning receivers. The primary disadvantage of a CVR is that it is indiscriminate in reception and can be saturated in a dense signal environment. Multiple signals in the same band can cause amplitude distortion which can mask key threat signals.

b. A superheterodyne RWR receiver uses a pre-selector filter, mixer, and a local oscillator to translate the received signal to a lower intermediate frequency (IF). This lower IF allows the receiver to amplify and filter the received signal to provide greater sensitivity and frequency selectivity than a CVR (Figure 17-5).

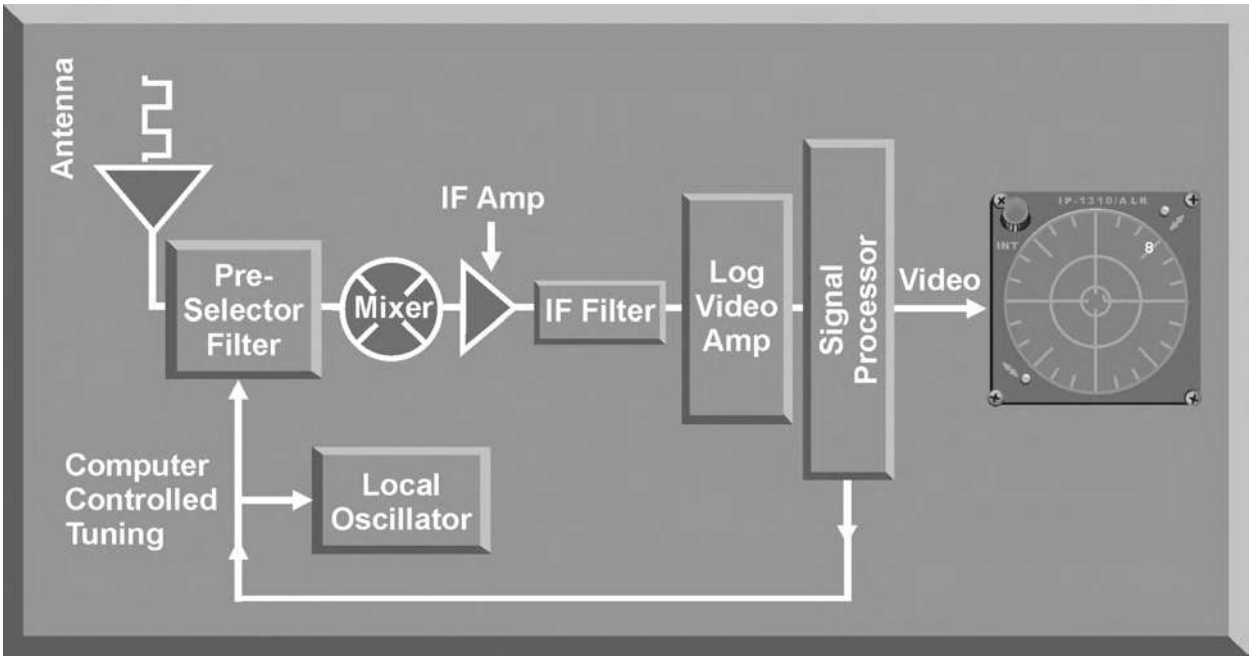

Figure 17-5. Superheterodyne RWR Receiver

(1) Superheterodyne RWR receivers use special scanning techniques controlled by the signal processor to tune the pre-selector filter and the local oscillator to rapidly scan selected threat system frequency bands. If the receiver detects activity in any of these bands, the scan stops to allow the processor to analyze the detected signals. The signal is combined with the local oscillator signal to lower the frequency to the IF. This signal is amplified, filtered, and amplified again before it reaches the signal processor. The signal processor classifies the threat and displays the proper threat symbol to the pilot. This entire process is accomplished in a matter of microseconds.

(2) The scanning superheterodyne receiver has important features that make it effective for RWR system application. It has excellent sensitivity and selectivity. It also has good frequency resolution. These features give the superheterodyne receiver a very low false alarm rate. The major disadvantage of the scanning superheterodyne receiver is its limited capability to receive signals from threat systems employing scanning antenna patterns. This limitation can be overcome with specific computer-controlled tuning to look for these threat signals.

4. SIGNAL PROCESSOR

The signal processor is the heart of the radar warning receiver. The signal processor is also known as the digital processor or analysis processor in different RWR systems. Its primary functions are to process numerous complex radar signals and identify, among the thousands of similar signals, those generated by lethal threat systems. The signal processor accomplishes this task continuously over the duration of the mission and displays the identified threat system to the aircrew almost instantly.

a. Signal processing begins when RF energy strikes the receive antennas on the aircraft. The received signals are then boosted in strength by intermediate amplifiers or antenna receivers. These amplified signals are then sent to the signal processor, or digital processor, where they are assigned a track file for reference to other signal characteristics. Data in these files is compared to those in the emitter identification (EID) table to process the signal for identification. Once identification is complete, a video and, if necessary, an audio signal, is sent to the cockpit display. The audio and video signals alert the aircrew to the electronic environment around the aircraft. This whole process takes less than a microsecond (Figure 17-6).

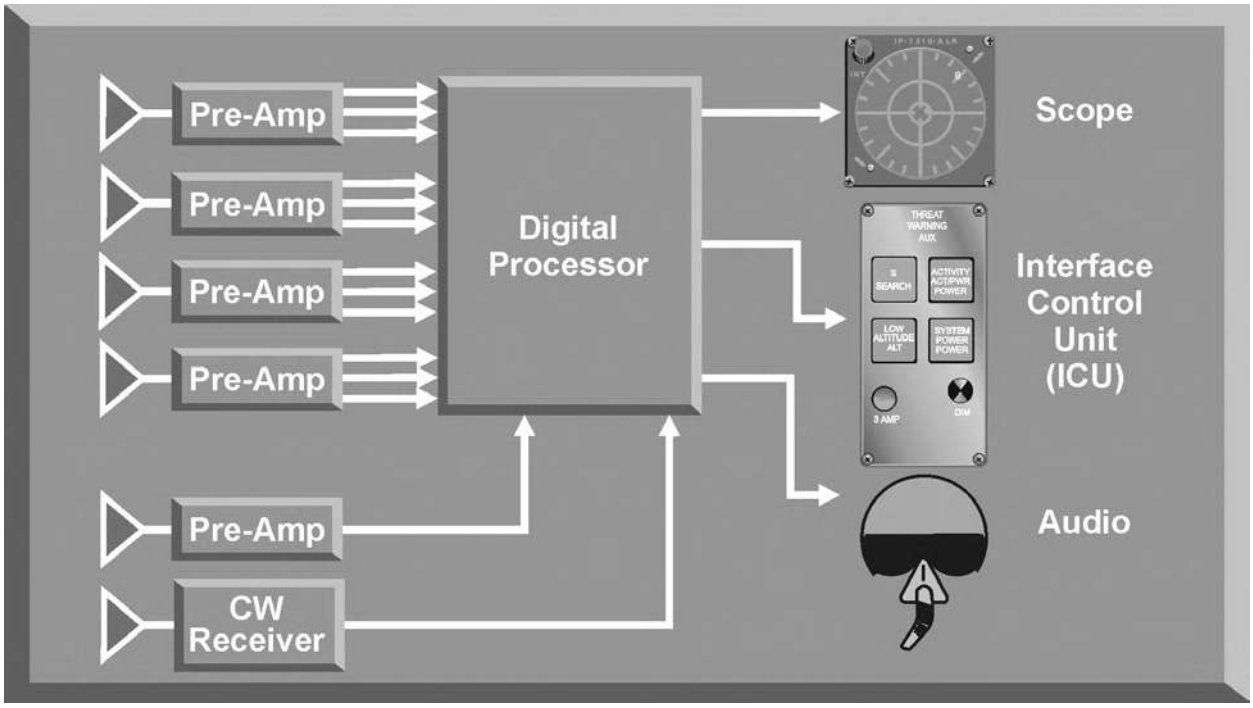

Figure 17-6. RWR System

b. Since many signals may be present, the amplifier detectors boost the signal strength, and also tag each signal by certain characteristics such as its time of arrival, direction of arrival, and/or frequency. These signals, along with their respective tags, are sent to the signal processor for further processing and

identification. The signal processor then makes a track file for each signal it receives from the amplifier detector.

c. The signal processor classifies each received signal and corresponding track file by its unique radar signal characteristics. Identifying characteristics used by a signal processor can include radio frequency, pulse width, pulse repetition frequency, EP techniques, and more. Characteristics of one signal may be identical to characteristics from different signals, while certain other characteristics can be as unique as a human fingerprint. The signal processor uses these primary characteristics to identify specific signals. When the primary characteristics of two or more signals are similar, the signal processor uses additional signal characteristics to resolve any confusion between two or more signals.

d. The signal processor ranks the track files based on priorities determined from tests it conducts on the signal characteristics and the threat priorities contained in the EID tables. It then quickly processes signals belonging to lethal threats before it processes signals belonging to non-lethal threats. For example, three signals enter the processor together and separate track files are established for each signal (Figure 17-7). A test on the first characteristic discriminant, frequency, will delay the further processing of Signal 3, since no lethal threat systems operate at a frequency less than 2000 megahertz. A further test on the remaining prioritized signals may eliminate Signal 2 as a threat system signal, leaving more processor time for the identification of the threat system which generated Signal 1. These tests do not stop the processor from attempting to identify all received signals. The signal processor merely delays the identifying sequence until all high priority signals have been processed.

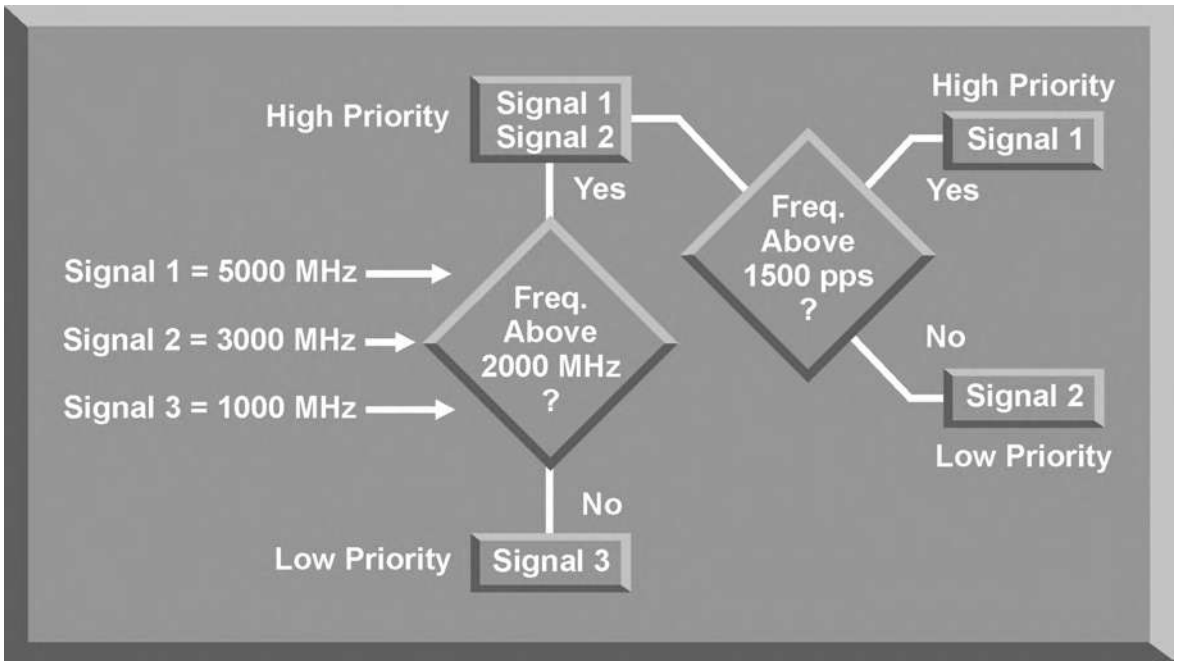

Figure 17-7. Signal Processor Signal Priority

5. EMITTER IDENTIFICATION (EID) TABLES

The signal characteristics in each track file are filled with processed data, and are constantly updated based on the time of arrival and location of the received signals. In addition, the track files are constantly compared to the EID table installed in the signal processor's computer memory. The EID table is a predefined table of radar characteristics associated with known radar systems (Figure 17-8). It is created from information gathered from electronic warfare support (ES) assets and intelligence sources. This table can be changed and updated as necessary to reflect the most current radar characteristics available for the anticipated threats in the planned theater of conflict. Each RWR system has unique procedures to reprogram the signal processor and update the EID tables. Emergency reprogramming actions, such as would be taken if a new threat appears that is not part of the current EID, are called a Pacer Ware.

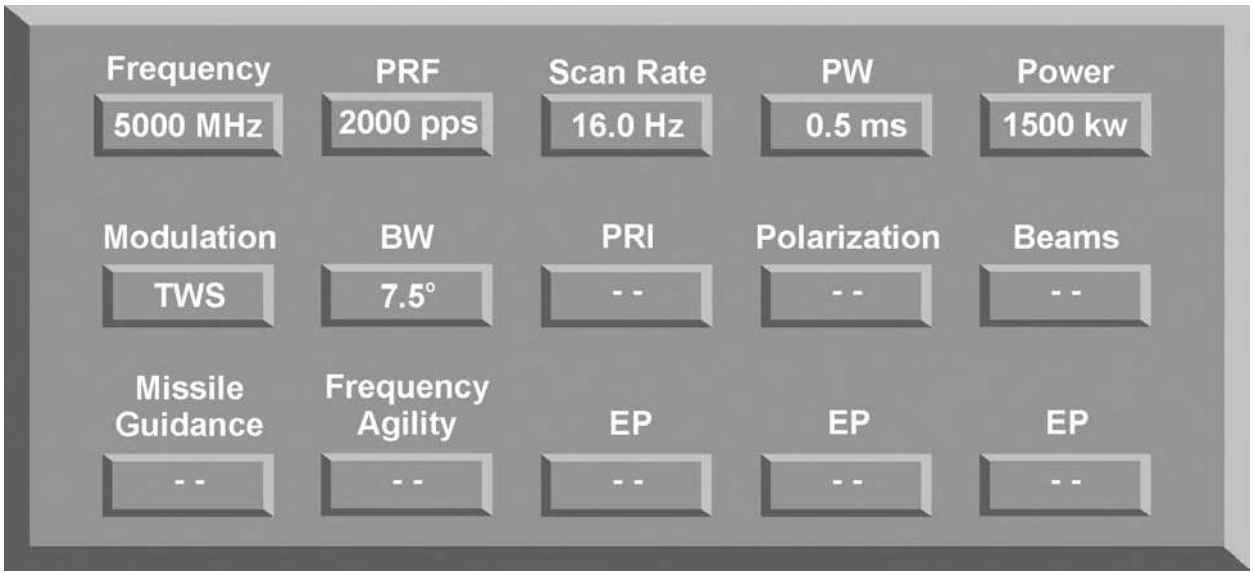

Figure 17-8. Sample EID Table

6. RWR SCOPE DISPLAY

The signal processor continually compares signal characteristics in the track files with the data in the EID tables. Once the signal processor has determined that enough of the signal characteristics match the information in the EID tables, it generates and positions a video symbol on the RWR scope. The video symbol represents a specific threat, and each threat system has its own unique symbol. In addition, an audio tone is generated to alert the pilot. The signal processor also generates symbols and audio associated with specific threat system actions, including search, track, and missile launch. The position of the threat symbol on the RWR scope always represents the relative position of the threat in relation to the aircraft which is the center of the RWR scope. The signal processor compares the received signal strength in the different antennas to determine the proper location of the threat symbol. Figure 17-9 depicts a situation where the two

forward antennas receive equal signal strength therefore the signal processor places the symbol at the 12 o'clock position.

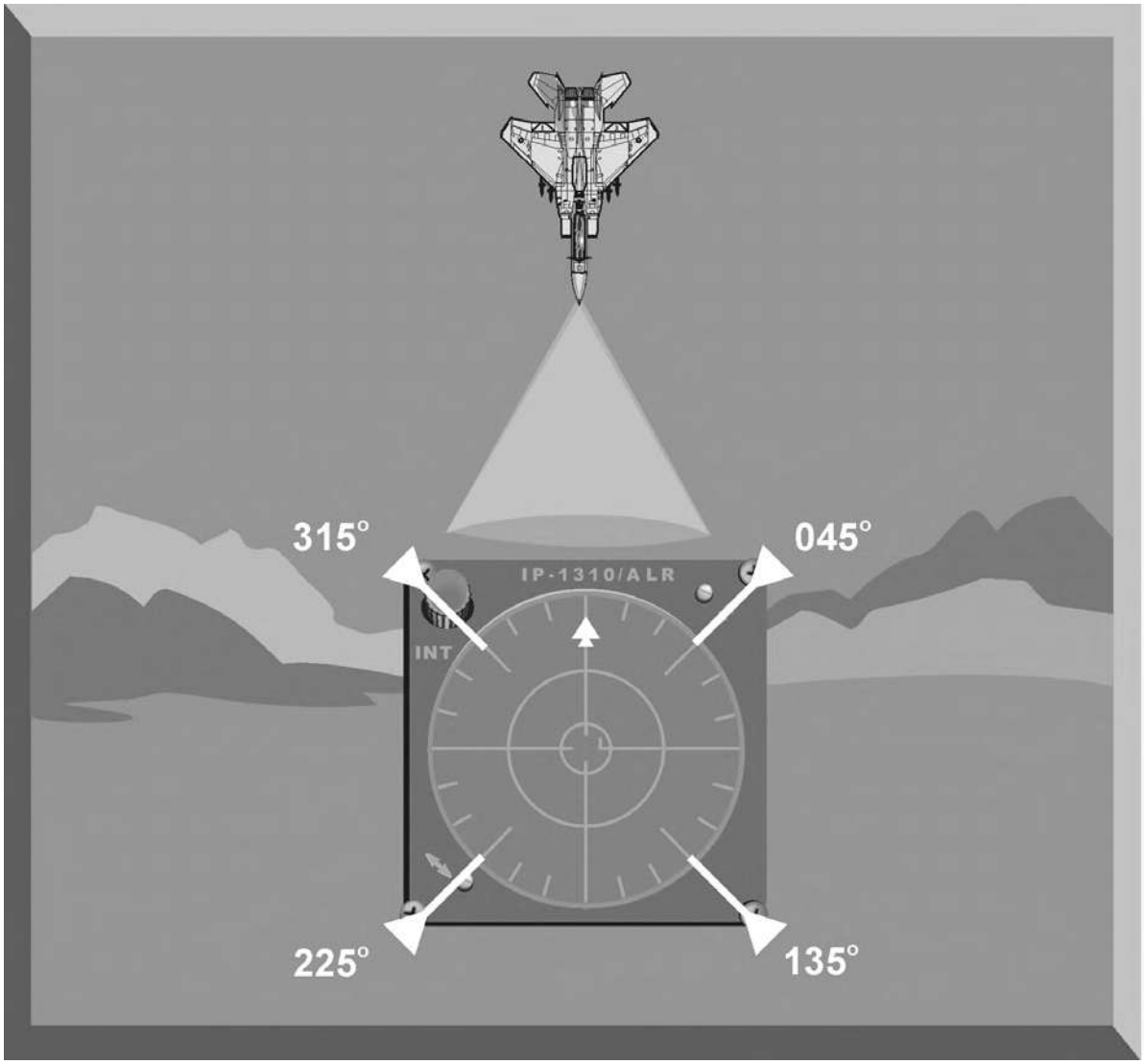

Figure 17-9. RWR Scope Azimuth Positioning

7. RWR AUDIO

In addition to generating threat symbols for each identified threat, the signal processor also generates threat audio. Threat audio first alerts the aircrew to the detection of a threat system. This RWR audio is generally referred to as "new guy" alert audio. The signal processor can also present constant audio from a selected threat. The aircrew controls this function through the interface control unit. The constant audio provided by an RWR system can be either "real" or synthetic. "Real" audio is normally based on the actual pulse repetition frequency (PRF) of the threat system radar whether the signal processor has identified it or not. Synthetic audio is based on the classification of the threat (SAM, AI, etc.) as

determined by the signal processor. The signal processor also generates a launch warning audio when the signal characteristics of the threat indicate a missile launch condition exists.

8. RWR INTERFACE CONTROL UNIT (ICU)

Every RWR system has some type of an ICU which provides the aircrew interface with the signal processor (Figure 17-10). The buttons on the ICU control specific functions of the signal processor. The ICU allows the aircrew to optimize the RWR system based on mission tactics. This optimization includes selecting appropriate priority lists based on ingress and egress tactics, controlling threat audio presentation, and determining the number and types of threats displayed. In addition, the ICU provides an additional visual indication of missile launch. All system test functions are controlled by the ICU to allow the aircrew to monitor the status of the RWR system.

Figure 17-10. RWR Interface Control Unit

9. RWR LIMITATIONS

There are several limitations associated with all RWR systems. The most important limitations include ambiguities, impact of maneuvering, and electromagnetic interference (EMI).

a. The sheer number and diversity of radar systems associated with an enemy IADS greatly compound the problem of threat identification and warning for RWRs. Adding to this problem is the fact that many different threat systems use operating modes that are parametrically similar. When an RWR processes a

radar signal that has the same characteristics of a signal from a different system, an ambiguity may occur. An RWR ambiguity is defined as the display of more than one symbol for a specific threat signal. RWR ambiguities may occur from both enemy and friendly radar systems.

(1) Figure 17-11 depicts a number of friendly and threat signals that operate between 8000 and 10,000 megahertz. On any given combat mission, it is quite possible that the RWR will receive signals from one or more of these threat systems at the same time. If frequency is the only signal characteristic available for processing, the RWR will not be able to determine which system the signal represents. Since threat systems operating in this frequency range are potentially lethal systems, the signal processor will attempt to match the frequency with a threat system from the EID table.

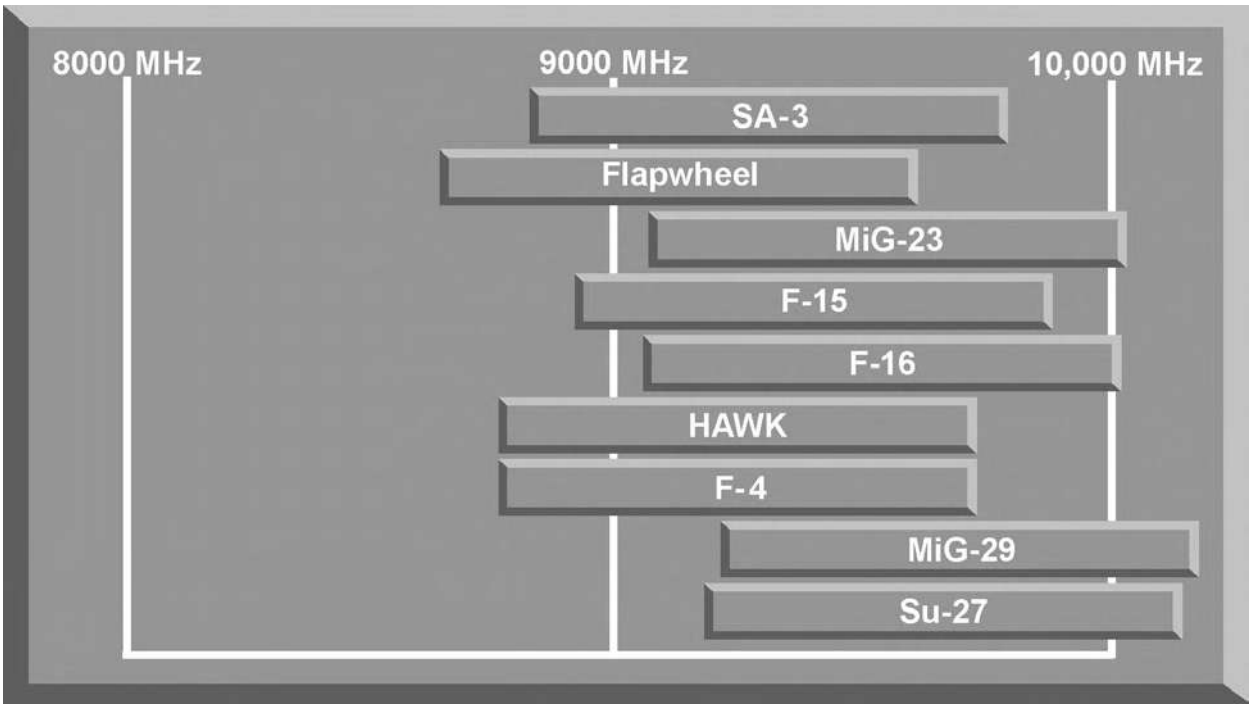

Figure 17-11. Signal Frequency Spectrum

(2) Matching partially processed signals to threat systems in the EID table may result in the wrong threat symbol being displayed, or numerous symbols being displayed on top of each other, making it difficult for the pilot to distinguish the exact threat. Incorrect threat symbology, or numerous combined symbols, are called RWR ambiguities.

b. RWRs are designed to provide accurate threat positioning information when the aircraft is flying straight and level. Most RWRs will also provide accurate threat positioning information when the aircraft is maneuvering up to certain limits of bank angle and turn rate. If aircraft maneuvering exceeds these

limits, RWR threat positioning data becomes unreliable. The two RWR limitations associated with aggressive maneuvering are inaccurate threat azimuth and multiple threat symbols.

(1) In Figure 17-12, the right forward and right aft RWR antennas detect a threat signal from a TTR. The left forward and left aft antennas are shielded by the aircraft and do not detect the signal. The signal processor determines the threat position, using the azimuth positioning algorithm, and displays the threat symbol at the 2 o'clock position.

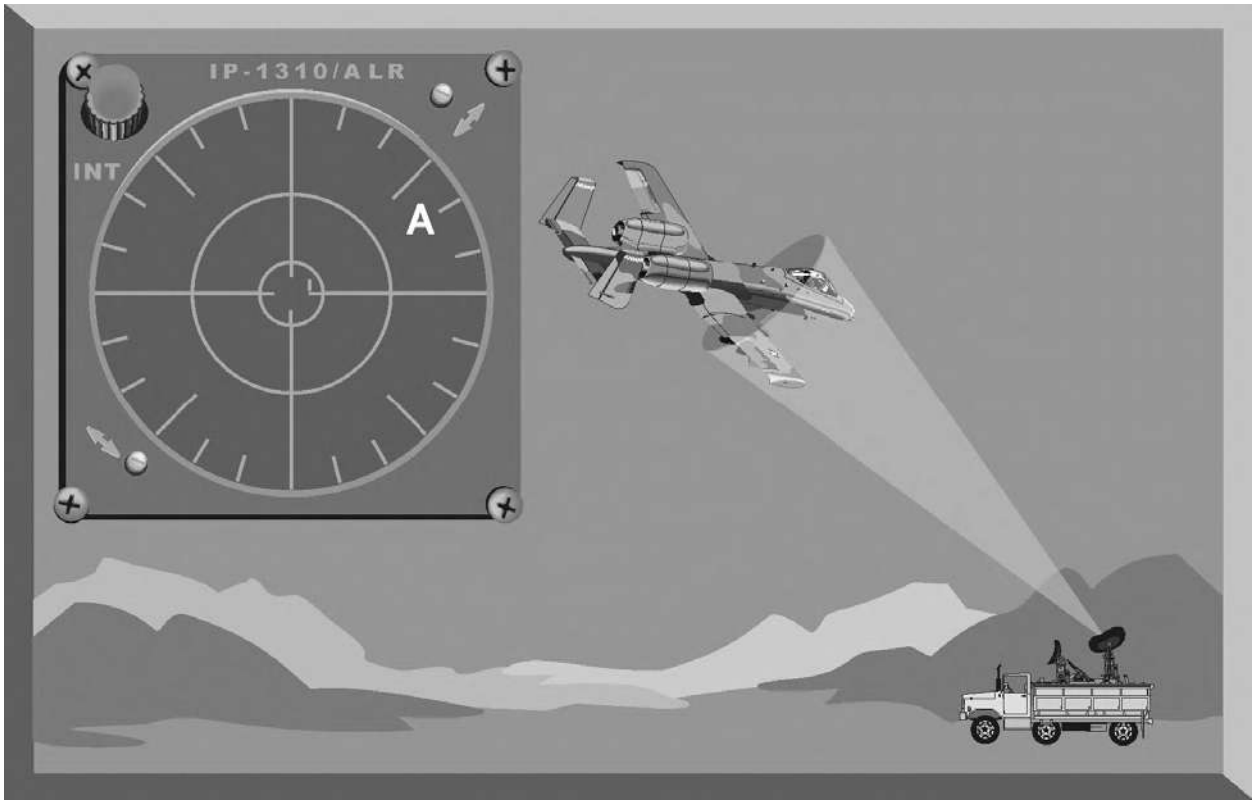

Figure 17-12. RWR Threat Azimuth Position Determination

(2) When the pilot maneuvers aggressively to put the threat symbol on the beam, he exceeds the RWR maneuvering limitations (Figure 17-13). Now all four RWR antennas detect the TTR signal. The signal strength in the right and left forward antennas is nearly equal. Based on this information, the signal processor displays the RWR symbol at the one o'clock position while the threat is actually at the three o'clock position.

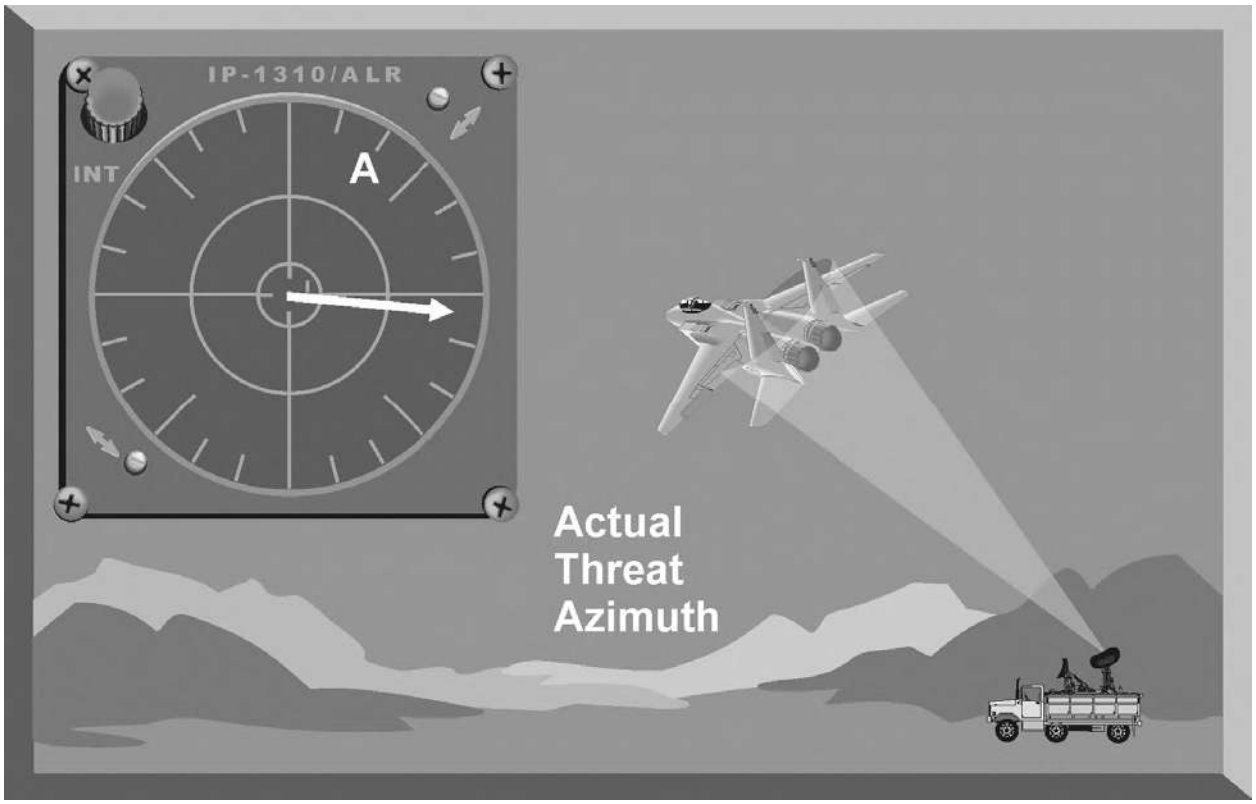

Figure 17-13. RWR Azimuth Error

(3) During aggressive maneuvering, the RWR signal processor may generate multiple symbols for a single threat emitter. In Figure 17-14, as the aircraft maneuvers, the relative azimuth of the threat position changes rapidly causing signal strength detected by each antenna to also change rapidly. The signal processor interprets these changing signals as new and different threat systems with the same signal characteristics. The number of "false" threat symbols displayed for a single threat is determined by the processing speed of the signal processor and a parameter called the symbol "age-out" time. Symbol age-out is the time, normally in seconds, that the RWR will continue to display a threat symbol after the signal processor has determined that the threat is no longer transmitting. The symbol age-out time is set for each threat in the EID tables.

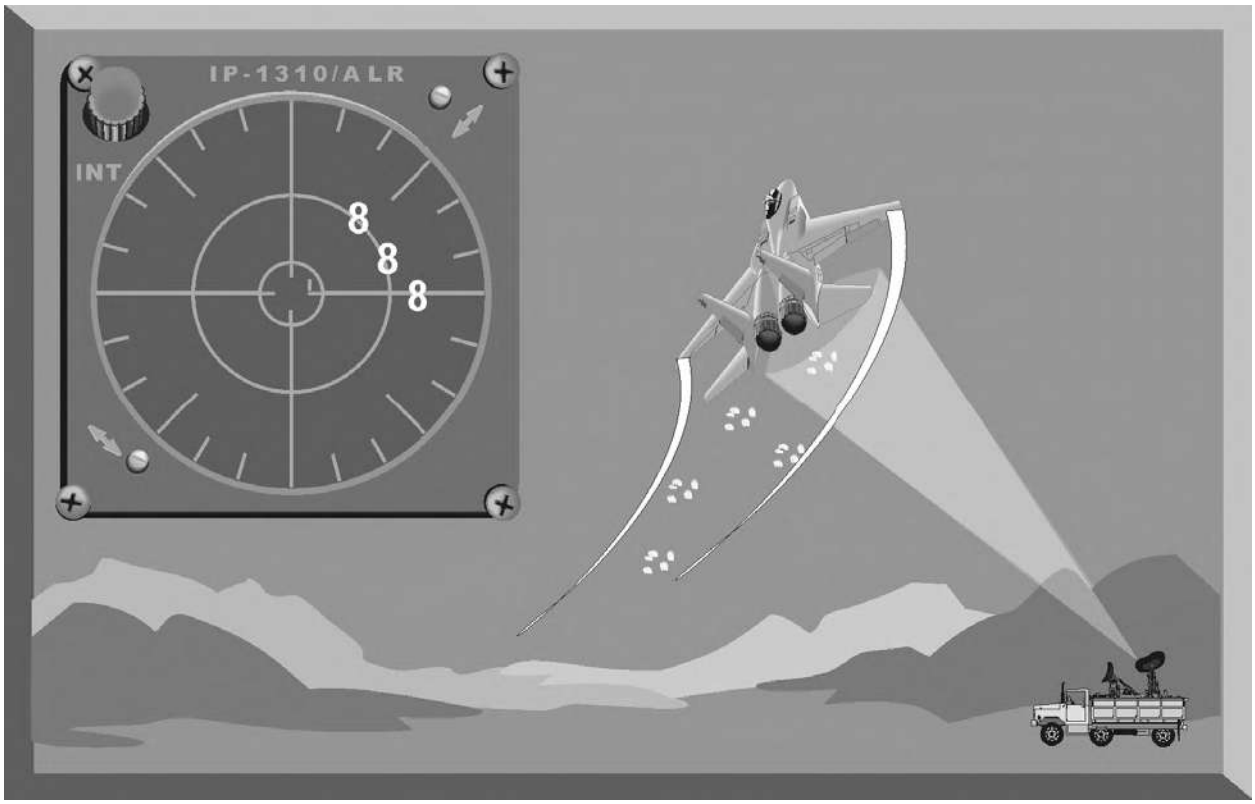

Figure 17-14. RWR Multiple Threat Symbols

c. Electromagnetic interference (EMI) is defined as any electromagnetic disturbance that interrupts, obstructs, or otherwise degrades or limits the effective performance of electronic systems. EMI can be induced intentionally, by way of jamming, or unintentionally as a result of spurious emissions and modulations. Certain RWR characteristics make them susceptible to EMI. Modern RWR systems are designed to receive and process signals in a wide frequency range, nominally 0.5 to 18 GHz, where most threats operate. This broad frequency coverage combined with the sensitive antennas make RWR systems susceptible to EMI. The primary source of EMI that impacts RWR operation is noise and deception jamming designed to counter enemy threat systems.

(1) High power noise jamming, such as that provided by a stand-off jamming aircraft, causes the RWR to raise the receiver threshold in the frequency band of the jamming. This effectively reduces the sensitivity of the RWR receiver and could delay the display of threat signals in that band. The reduction in sensitivity depends on the power that the jammer is transmitting, the beamwidth of the jamming beam, and the distance from the jammer to the aircraft. High power jamming may also generate multiple threat symbols on the RWR scope at the approximate azimuth to the jammer's position relative to the aircraft. Additionally, jamming from a wingman's self-protection system can generate multiple threat symbols and reduced sensitivity.

(2) A limitation of all RWR systems, related to EMI, is the problem of inaccurately identifying threat radar systems as friendly radar systems. This occurs when the parameters of a friendly radar are similar to the parameters of a threat radar system. The RWR will either display a threat radar symbol or an ambiguity associated with a threat radar. These RWR misidentifications are especially prevalent for AI radar systems.

(3) The impact of EMI on the operation of an RWR system depends on the signal environment. The pilot has little control over the number and diversity of friendly and enemy signals the RWR system must process. EMI is an unfortunate consequence of the reliance of modern military forces on operations in the electromagnetic spectrum. Aircrews should be keenly aware that EMI will impact RWR operation and be must be familiar with common RWR displays of EMI.

10. THREAT GEOLOCATION TECHNIQUES

The purpose of threat geolocation is to put a defined position, normally coordinates, on a threat radar. This information can be used to simply warn other aircraft about the threat or, if the coordinates are accurate enough, to allow for targeting and attack of the threat. Until recently, threat geolocation could only be performed by strategic assets and specialized tactical aircraft, specifically the F-4G Wild Weasel. Due to inherent time delays, data provided through strategic channels often did not apply to mobile threat systems. The mobile systems would relocate making the data obsolete. This section will discuss three techniques used to geolocate, also known as direction finding (DF), emitting radars that can be used by tactical assets to rapidly locate radar threat systems. The three are triangulation, interferometry, and time of arrival. All three techniques are heavily dependent upon the receiving aircraft's ability to accurately determine its present position, and the advent of GPS receivers has made this significantly easier.

a. Triangulation is the most basic form of DF available. It involves taking direction measurements from more than one source. The intersection of the azimuth measurements, called “lines of bearing”, is the likely location of the emitter (Figure 17-15). To be effective, the participating aircraft must have accurate data of their current positions when getting the lines of bearing.

(1) Triangulation can be carried out by multiple aircraft equipped with receiver equipment or by one aircraft over a period of time. The advantage of having multiple aircraft providing azimuth measurements is the increased angle-off and the speed of interception. In triangulation the best azimuth cuts are those that approach 90° angles. The speed of interception comes into play because threat emitters, knowing that DF operations are underway, attempt to transmit for as little time as possible. The disadvantage of multiple platforms is the communication required to ensure that all the platforms are measuring the same radar. In a dense radar environment this can be a difficult task.

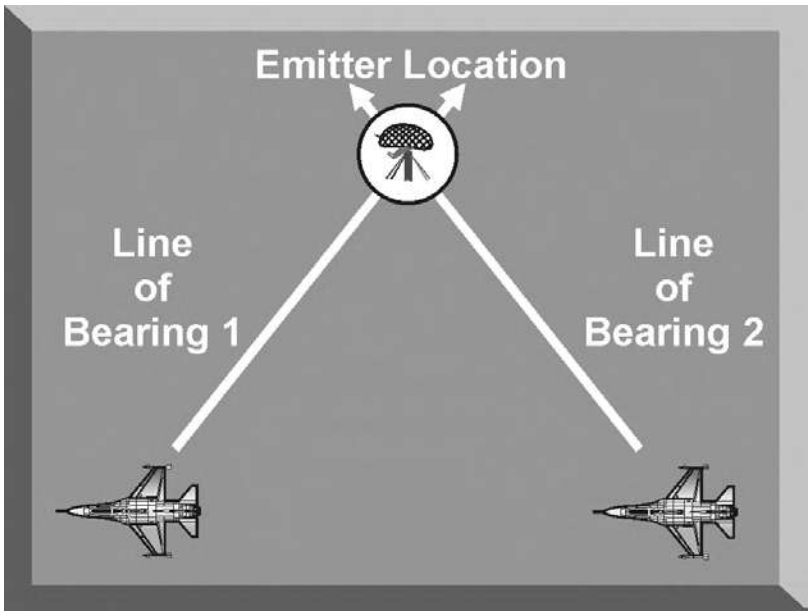

Figure 17-15. Triangulation

(2) Single aircraft triangulation eliminates the problem of signal coordination with other aircraft, but it also requires that the aircraft transit some distance to get multiple azimuth measurements. The accuracy of single ship DF operations is a function of the quality of the receiver equipment, distance away from the targeted radar, speed of the aircraft, and the amount of time that the targeted radar radiates.

b. The second technique is called interferometry. This technique is also known as phase interferometry, or phase difference of arrival. These systems operate by comparing the phase of a radar wave as it impacts two or more DF antennas; this phase difference is then used to compute an angle of arrival (AOA). For aircraft, the desire is to have these DF antennas on different parts of the same aircraft. Multiple AOA measurements are then used to provide the range and position of the threat.

(1) The key elements in an interferometer system are two antennas in fixed locations with matched receivers, a phase comparator, and a processor (Figure 17-16). An intermediate frequency output from each receiver is passed to a phase comparator, which measures the relative phase of the two signals. This relative phase position is passed to a processor, which calculates the AOA relative to the orientation of the two antennas (called the baseline). In most systems, the processor also accepts information about the orientation of the baseline (relative to true North or local horizontal) to determine the true azimuth or elevation angle to the emitter.

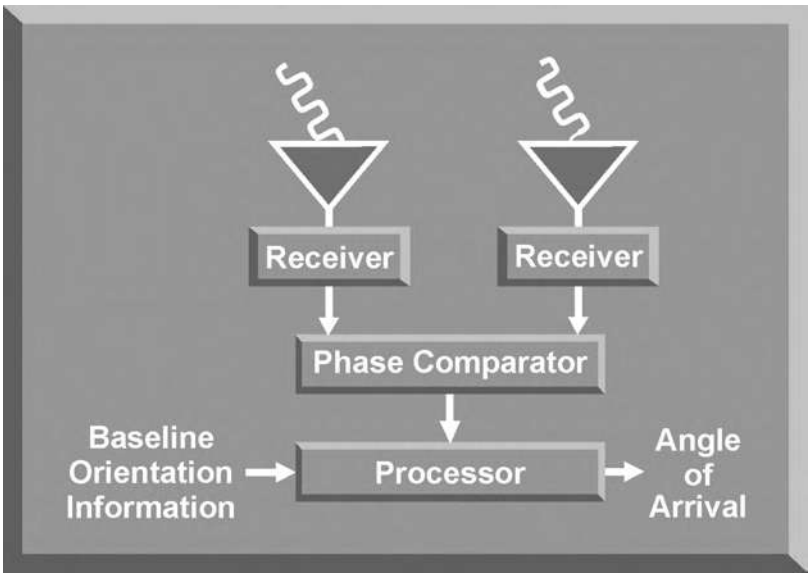

Figure 17-16. Interferometer Components

(2) To obtain rapid emitter locations some interferometer systems use multiple receive antennas in an array setup. This allows for simultaneous azimuth and elevation measurements to rapidly locate the emitter. An array allows for the mixing of long and short baselines in different patterns by selecting different pairs of antennas (Figure 17-17). The terms long baseline and short baseline are often used to designate the distance between the antenna elements in an interferometer system. Long baselines have the advantage of providing a quick and accurate location of the emitter, but they can suffer from ambiguities resulting from different wavefronts hitting the different antenna elements. In addition to the array depicted in Figure 17-17, a long baseline system could be created by using the existing RWR antennas on an aircraft, and supplementing these with a small short baseline system to compensate for the ambiguities.

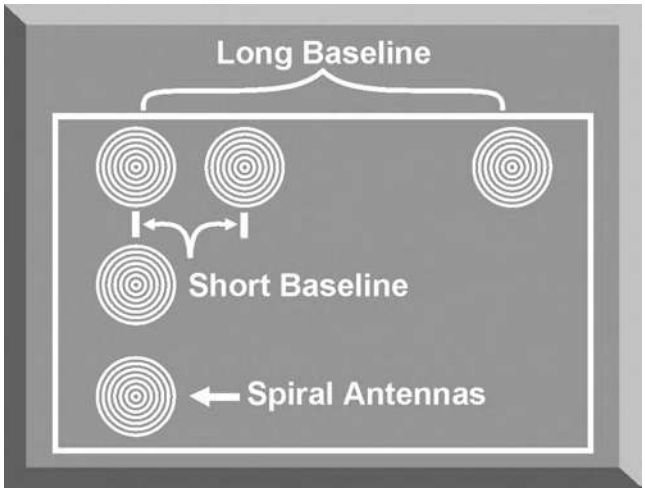

Figure 17-17. Interferometer Array

c. Time of arrival (TOA) and time difference of arrival (TDOA) techniques are the final type of location techniques to be covered in this section. Both techniques are based around the fact that radar signals travel at approximately the speed of light. Both techniques, using the speed of light as a constant, solve for the distance that the emitter is away from the receiver using the equation distance equals rate multiplied by time. Because there is not any directional information, the equation represents the radius of a circle around the receiving antenna; multiple distance measurements taken from multiple receivers are then overlayed. The intersection of the circles is the position of the emitter. If only two receivers are used, a simple DF technique can solve the ambiguity of which intersection represents the emitter (Figure 17-18).

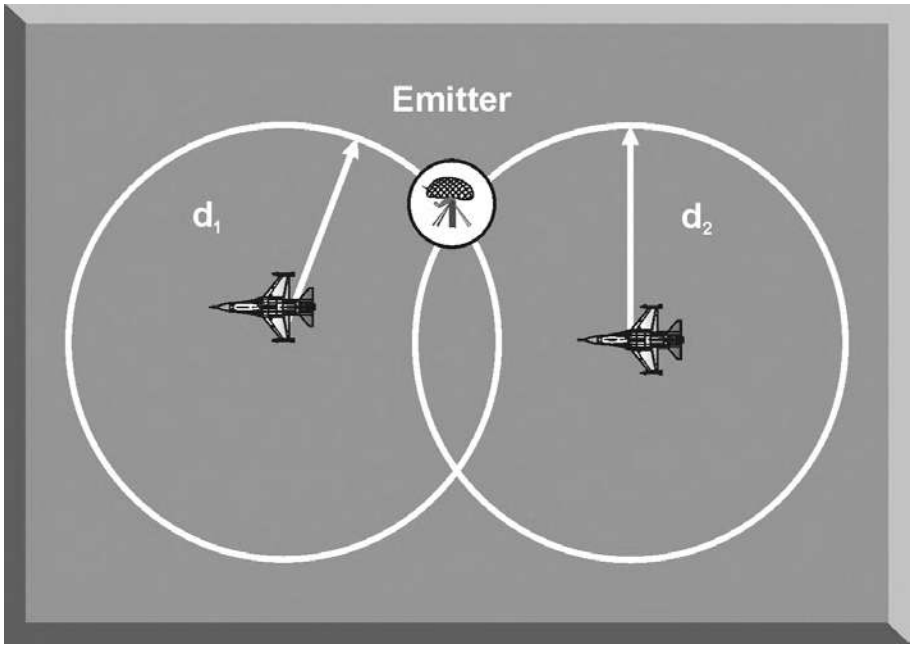

Figure 17-18. Time of Arrival Measurements

(1) TOA positioning is calculated by taking the time that a signal leaves a radar, measuring its arrival time at the receiver and mathematically solving for distance using the techniques described above. One of the primary challenges involved with TOA positioning is determining when the measured signal was transmitted, this requires either a very cooperative enemy or a radar signal with some type of exploitable time reference. Another challenge involves insuring that multiple receivers are timing the same signal. This is especially difficult in a threat intensive environment.

(2) TDOA is used when it is not possible to determine when a signal was transmitted. TDOA uses most of the same principles as TOA except that it must compensate for not knowing the time the signal was transmitted. It does this by using an extra receiver a known distance from the first receiver to generate a distance curve. The arrival of the signal is precisely measured at the two

receivers, the theory is that a signal that arrives at the two receivers at times t1 and t2 had to originate from a point on a curve defined by that difference in arrival time. For example, if the signal arrives at the two points at exactly the same time, then the transmitter must be equal distance from the two receivers. In this case the curve is actually a line of possible locations equal distance from the receivers and can easily be drawn. For situations where the signal arrives at different times at the receivers, a hyperbolic curve instead of a straight line denotes all the possible locations of the transmitter. Figure 17-19 shows an example of when the signal arrives at a different time, the constant value is the time difference multiplied by the speed of light yielding a distance. To solve for the emitter's location using TDOA another antenna receiver is required that is not in line with the first two receivers to generate an independent curve that will cross the first curve at the transmitter location.

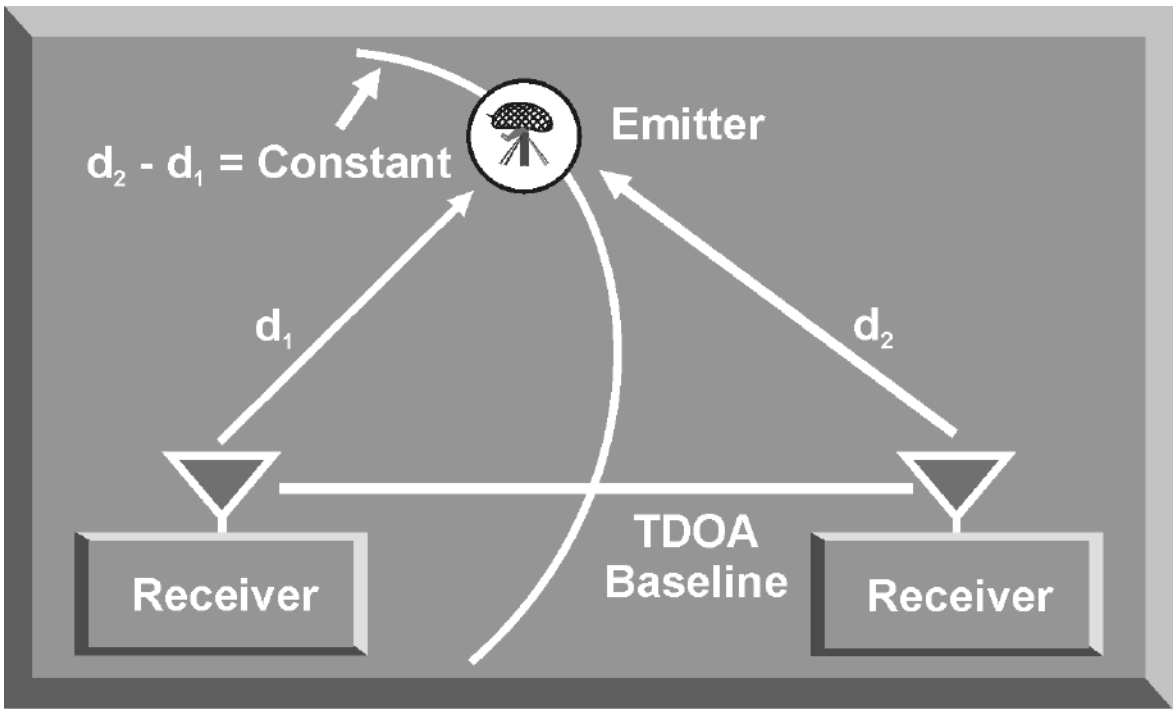

Figure 17-19. Time Difference of Arrival Measurements

(3) Timing techniques require very good timing accuracy in the receiving systems. If the receivers are far apart, such as different aircraft, then a separate time measurement is required at the source before sending to a processor. As with triangulation, one of the major challenges of multiple aircraft measurements is the coordination to ensure that the same signal is being looked at by all aircraft involved.

(4) Timing techniques are affected by the type of radar that they are trying to locate. Pure CW radars are not practical for a timing technique because there

is not a pulse to time. Pulsed signals, on the other hand, are much more susceptible to this type of location technique.

11. SUMMARY

An RWR system is designed to provide a picture of the electronic order of battle (EOB) operating in the vicinity of an aircraft. The signal processor is the heart of the RWR system and controls the function of all other system components. The signal processor, using inputs from the antennas and the receiver/amplifiers, compares the signal parameters with the parameters in the EID tables. The identified signals are displayed on the RWR scope with the appropriate audio. The ICU provides the aircrew interface with the signal processor to allow the aircrew to customize RWR operation for each combat mission. Modern RWR systems have some limitations that can effect aircrew survival. These limitations include ambiguous threat displays, maneuvering limitations, and EMI. Despite these limitations, an operational RWR system is one of the keys to survival on today's electronic battlefield. A product of advances on the electronic battlefield is rapid threat geolocation. New threat geolocation techniques are designed to provide advanced threat information to allow pilots to avoid, suppress, or destroy the mobile threat. The three most common techniques are basic triangulation using lines of bearing, interferometry using phase difference of arrival, and time difference of arrival using time differences to determine distance curves.

CHAPTER 18. SELF-PROTECTION JAMMING SYSTEM OPERATIONS

1. INTRODUCTION

Self-protection jamming systems are designed to counter surface-to-air missile (SAM), airborne interceptor (AI), and antiaircraft artillery (AAA) acquisition and target tracking radars. Self-protection jamming systems generate noise and deception jamming techniques to either deny threat system automatic tracking capability or generate sufficient tracking errors to prevent a successful engagement.

a. To counter the diverse array of threats and their associated frequencies in an integrated air defense system (IADS), a self-protection jamming system must be able to simultaneously jam multiple signals operating in a wide frequency range. The system must also be able to generate sufficient power to mask the radar return of the aircraft. Since many modern self-protection jamming systems are carried internally or externally on aircraft, their size, shape, and weight must be carefully controlled to minimize adverse effects on aircraft performance and handling. These design requirements may require a trade-off between additional power or capability and aircraft compatibility.

b. A self-protection jamming system must have receive antennas to receive radar signals, a system processor to identify received signals, a jamming techniques generator to produce an optimum jamming technique for the identified threat, and transmit antennas to transmit the required jamming techniques. These system components will be discussed in this chapter.

c. There are numerous internal and externally mounted self-protection jamming systems in use today. To simplify the discussion, the ALQ-184 pod will be used as an example of a modern, self-protection jamming system (Figure 18-1). The functions and operations of the ALQ-184 components are representative of currently deployed self-protection systems.

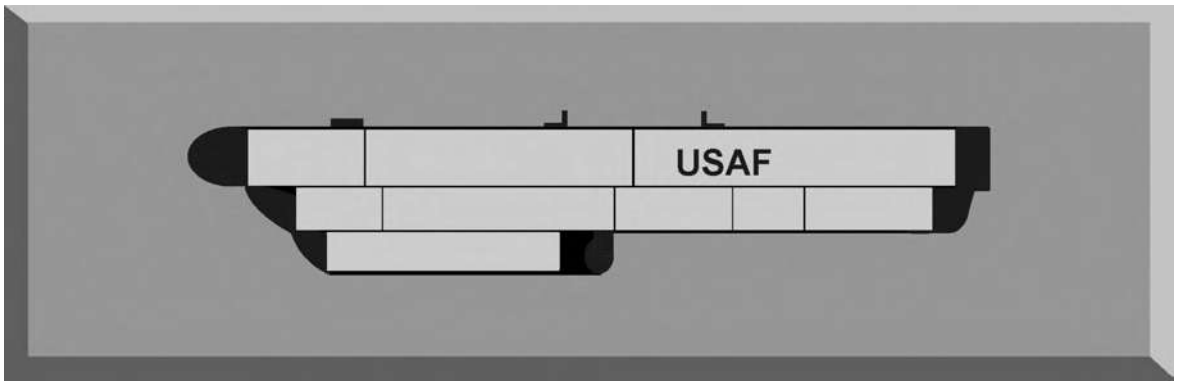

Figure 18-1. ALQ-184 Pod

2. RECEIVE ANTENNAS

The ALQ-184 pod has two sets of receive antenna assemblies located on the front and rear of the lower pod "gondola" (Figure 18-2). Each receive antenna assembly set consists of a low-band antenna and a mid/high-band antenna. The low-band antenna's signals are combined to form the input for the low-band receiver. The mid/high-band antennas provide signals to the separate mid/high-band portion of the pod.

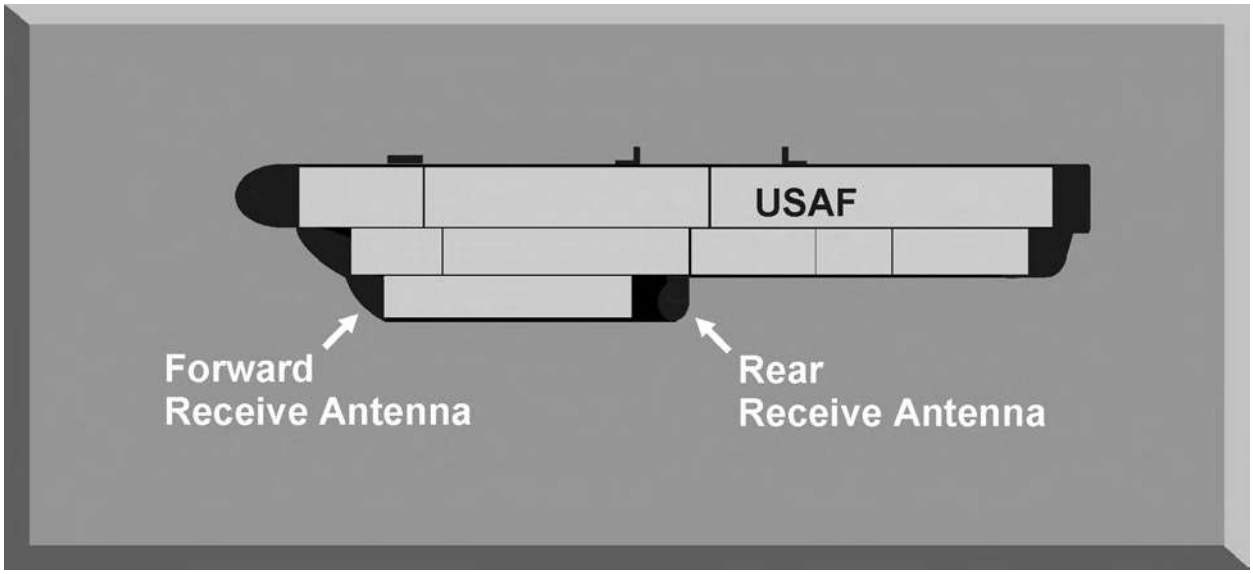

Figure 18-2. ALQ-184 Receive Antenna Location

a. The low-band receive antennas are circularly polarized spiral arrays. The mid/high-band receive antenna covers eight sub-bands via an eight element array that corresponds to the eight element transmit array. The mid/high-band antenna is also circularly polarized.

b. Each signal received via the receive antenna generates a corresponding transmit signal through a crystal video receiver. The angle of arrival (AOA) of each signal is determined by comparing the output of the crystal video receiver for each antenna.

3. RECEIVER SECTION

The forward and aft receive antennas detect radar signals and send them to the receiver section. The receiver section contains an AOA receiver and a multiplexer that separates frequencies. The AOA receiver determines the AOA of a signal based on the output signal level of each antenna element. The AOA data is passed to the system processor to control the angle of transmission of the jamming signal. The multiplexer separates all received threat signals into eight frequency sub-bands consisting of five mid-band and three high-band frequency

ranges. The multiplexer categorizes the received radar signals by sub-band and azimuth and then sends them to the system processor and the exciter.

4. SYSTEM PROCESSOR

The system processor is the "brain" of the ALQ-184 pod. It receives the threat signals from the receiver section that have already been categorized by sub-band and distinguished by AOA. Each received signal and its corresponding AOA is counted. When the signal count exceeds a pre-set threshold, the system processor validates the signal and identifies it using the emitter identification (EID) tables. Based on this threat identification, the system processor directs the techniques generator to initiate a jamming program through the exciter. At the same time, the system processor, through a signal switch control, directs the transmitter section to use either the forward or aft transmit antenna array, and specifies the transmit angle for the jamming program based on AOA.

a. The system processor also controls the low-band portion of the pod (Figure 18-3). The forward or aft low-band antenna receives and combines the threat signal and sends it to the multiplexer. The multiplexer channelizes this signal into one of two low sub-bands. The signal then passes to the modulator where the voltage controlled oscillators (VCOs) generate a jamming technique as directed by the system processor techniques generator. This ensures the jamming technique is at the proper frequency and modulation to provide maximum effect against the threat system. The generated jamming signal passes to a second multiplexer and then to a solid state amplifier for amplification. The amplified jamming signal is then sent to the two low-band traveling wave tubes (TWTs) and transmitted from the forward and aft low-band transmit antennas.

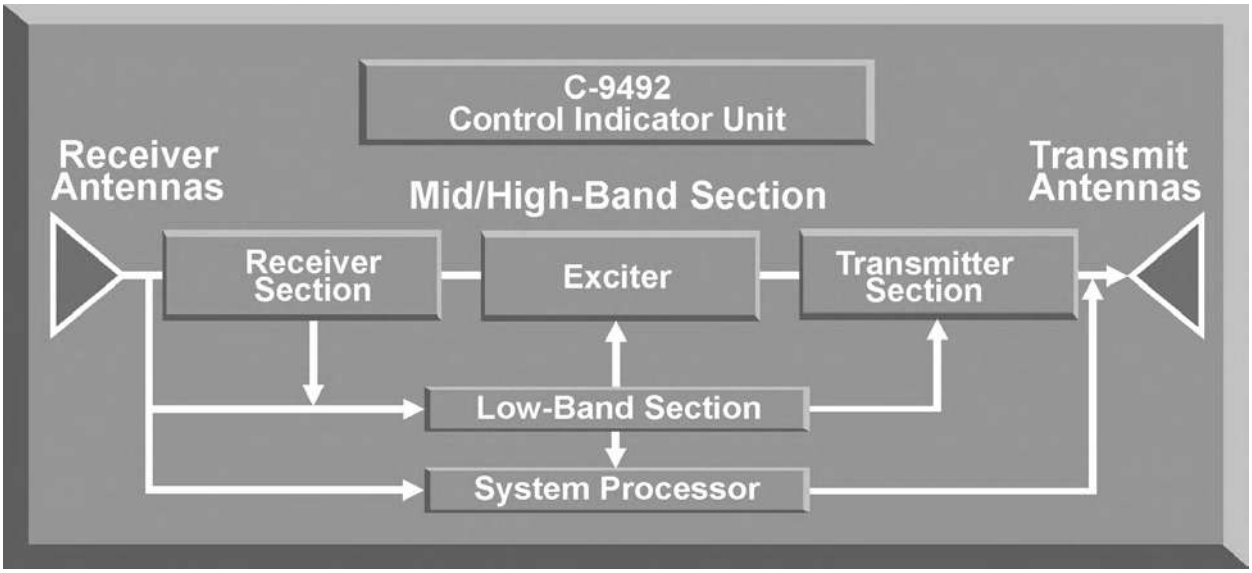

Figure 18-3. ALQ-184 Simplified Block Diagram

b. The system processor periodically performs a background built-in-test (B-BIT), to check the status and calibration of the ALQ-184. The system processor software is updated or reprogrammed as required from a memory loader verifier (MLV). The system processor uses two major software programs. The operational flight program (OFP) manages the receiver and transmitter functions, signal processing, and techniques generation. The mission data generator (MDG) contains the threat EID tables and the jamming techniques matrix for these threats.

5. JAMMING TECHNIQUES GENERATOR

The exciter section contains the VCOs and the keyed oscillators, which generate the jamming waveforms that are directed by the system processor. The exciter takes the threat signal from the receiver and modifies it with deception modulation or generates a noise program based on the techniques generator in the system processor. The selected jamming technique is then sent to the transmitter section.

6. TRANSMIT ANTENNAS

The transmitter section contains antenna switching circuits, a signal forming network, and TWTs. The antenna switching circuits are controlled by the system processor to ensure the transmitted jamming pulse is radiated at the proper azimuth. The signal-forming network controls the phase of each jamming signal. There are sixteen TWTs in the transmitter section, one for each front and aft antenna. The TWTs amplify the jamming signal for transmission from the appropriate transmit antenna.

a. The ALQ-184 has two sets of transmit antenna assemblies. One set is located on the front and one on the rear of the main pod assembly (Figure 18-4).

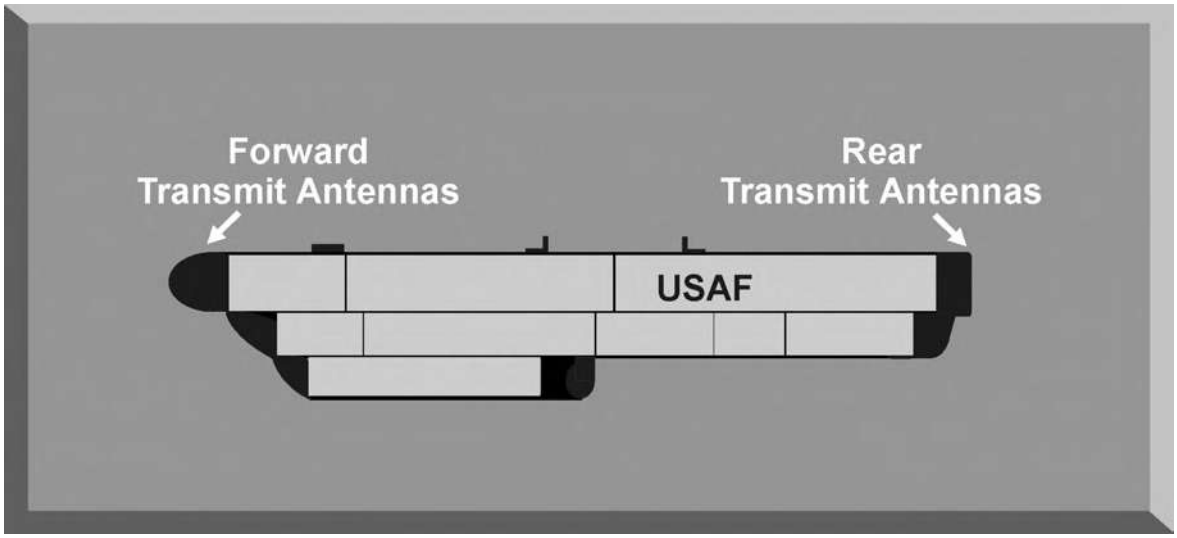

Figure 18-4. ALQ-184 Transmit Antenna Location

Each set has a low-band and mid/high-band antenna. The transmit antennas have opposite polarization from the receive antennas. This enables the pod to transmit and receive at the same time while preventing pod "ringing." Ringing occurs when the pod receives its own jamming signal and generates a jamming program to counter its own signal. This condition can highlight the aircraft to enemy radar and seriously degrade pod effectiveness.

b. The low-band transmit horn antennas are circularly polarized. The mid/high-band transmit antennas have the same eight-element array as the receive antennas. The transmit antennas generate a directional jamming signal for pulsed radar signals based on the AOA determined by the receive antennas. Detailed information on the antenna jamming pattern is contained in the ALQ-184 ECM Handbook.

7. C-9492 CONTROL INDICATOR UNIT

The C-9492 Control Indicator Unit (CIU) provides control of all functions of the ALQ-184. It allows the aircrew to control system power, select jamming techniques, and monitor system status (Figure 18-5).

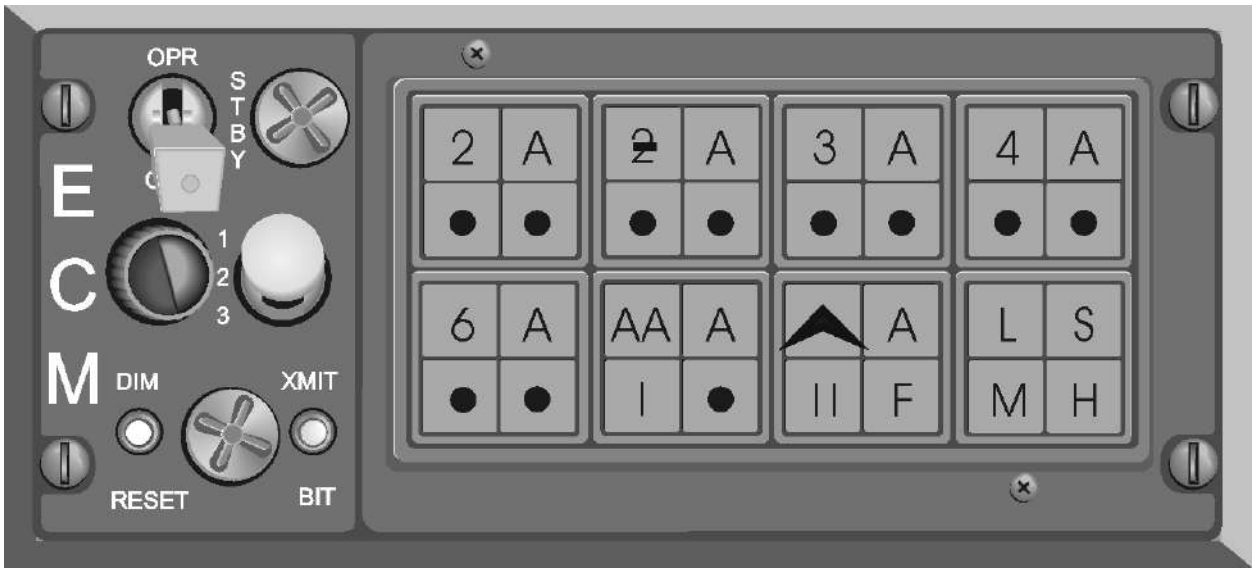

Figure 18-5. C-9492 Control Indicator Unit

8. JAMMING POD CONSIDERATIONS

Unfortunately, jamming pods do not make the aircraft completely invisible from enemy threat systems. When used in conjunction with the RWR, expendables, and threat countertactics they do drastically increase the probability of surviving a threat engagement. This section contains some items of consideration to ensure that your self-protection jamming is being properly utilized. These considerations include highlighting, burnthrough, and reprogramming.

a. If used improperly a self-protection pod can actually highlight the aircraft. This happens when a pod transmits a jamming program constantly or when another type of radar, not targeted for jamming but in the same frequency range, sees the jamming. Highlighting is normally associated with noise programs that transmit constantly. Most pods today avoid this by transmitting only when a threat requires it. Additionally, some aircraft have pod inhibit switches that allow the pod to remain in a standby condition until the pilot switches the pod to operate. What makes this system effective is that the switch is either on the stick or throttle allowing the pilot to rapidly go to operate without looking inside the cockpit (Figure 18-6).

Figure 18-6. F-16 ECM CMS

b. Burnthrough is described as the range that the aircraft's radar return is stronger than its jamming signal. Basically, the jet has gotten so close to the threat radar that the threat radar is overpowering the jamming pod. The range that this occurs varies for different radars, but it should be planned for particularly when there are threats in the target area. Burnthrough is also a consideration for support jamming systems; there is a range at which the support jammer's signal will be overpowered and the protected aircraft can be seen.

c. Many self-protection jamming systems are what is called software-reprogrammable. This means that jamming programs can be rapidly changed to adjust for changes in enemy radar systems. These updates can be made to

systems while they are still on the jet, and can take as little as 15 minutes using an MLV. The process of changing electronic warfare systems is known as a Pacer Ware change. An exercise to check the ability to make changes is known as a Serene Byte exercise. The pilot of the aircraft carrying the self-protection system has one responsibility in this process: to ensure that his jamming system is carrying the most current software program, usually referred to as a software version. While Pacer Ware changes are not common during peacetime operations, they do happen quickly during combat operations often to fine tune the jamming systems for the particular theater of combat.

9. SUMMARY

The effective employment of self-protection jamming is one of the factors that can mean the difference between success and failure on the modern battlefield. When employed in concert with chaff and maneuvers, self-protection jamming can be extremely effective in negating potentially lethal attacks. Despite their limitations, self-protection jamming systems are an important part of the "bag of tricks" aircrews can employ to put bombs on target.

ANNEX A
GLOSSARY

Absorption - Dissipation of energy of electromagnetic waves, sound, and light waves into other forms of energy because of interaction with matter. Absorption characteristics of specific materials are used as blankets, coatings, or structural and surface materials for aircraft to reduce effective radar cross-sections.

Acoustic jamming - The deliberate radiation of mechanical or electro-acoustic signals with the objectives of obliterating or obscuring signals which the enemy is attempting to receive, and of deterring enemy weapon systems.

Acquire –

1. When applied to acquisition radars: the process of detecting the presence and location of a target in sufficient detail to permit identification.

2. When applied to tracking radars: the process of positioning a radar beam so that a target is in that beam to permit the effective employment of weapons.

Acquisition radar - A radar set that detects an approaching target and feeds approximate position data to a fire control or missile guidance radar that then takes over the function of tracking the target.

Active array radar - A phased array radar in which each radiating element contains a transmitter and receiver front end, as opposed to a single transmitter/receiver serving all phased array elements. Advantages attributed to active array radars include efficient use of prime power, no waveguide losses, very wide bandwidth, and extreme reliability due to the lack of single point of failure.

Active homing guidance - A system of homing guidance in which both the source for illuminating the target, and the receiver for detecting the energy reflected from the target as the result of illumination, are carried within the missile.

Aerosols - Solid particles dispersed in the atmosphere that have resonant size particles with a high index of refraction. The particles both scatter and absorb visual and laser-directed energy so as to lessen the effect of weapon systems directed by these techniques.

Airborne early warning and control - Air surveillance and control provided by airborne early warning vehicles that are equipped with search and height finding radar and communications equipment for controlling weapons.

Airborne interceptor (AI) - A manned aircraft used for identification and/or engagement of airborne objects. (An AI may or may not be equipped with radar to assist in the interception.)

Airborne Warning and Control System (AWACS) - An aircraft suitably equipped to provide control, surveillance, and communications capability for strategic defense and/or tactical air operations.

Air defense - All defensive measures designed to destroy attacking enemy aircraft or missiles in the earth's envelope of atmosphere, or to nullify or reduce the effectiveness of such attack.

Air surveillance radar (ASR) - A radar displaying range and azimuth that is normally employed in a terminal area as an aid to approach and departure control.

Air-to-air missile (AAM) - A missile launched from an airborne carrier at a target above the surface.

Air-to-surface missile (ASM) - A missile launched from an airborne carrier to impact on a surface target.

Alternating current (AC) - An electric current that reverses its direction at regularly recurring intervals, the frequency being determined by the frequency of the alternator supplying the current.

AM-CW jamming - Jamming in which a carrier wave is modulated at a constant recurring rate. The recurrence rate of amplitude modulation is variable, and reflects a noticeable change in the radar scope. Because of the spiraling or chaining effect produced, AM-CW jamming is easily identified.

Amplifier - An electronic circuit usually used to obtain amplification of voltage, current, or power.

Amplitude shift keying - A method of impressing a digital signal upon a carrier signal by causing the carrier amplitude to take different values corresponding to the different values of the digital signal.

Amplitude modulation (AM) - **A method of impressing a message upon a carrier signal by causing the carrier amplitude to vary proportionally to the message waveform.**

Angle jamming - **A deception jamming technique used to deny azimuth and elevation information to a TTR by transmitting a jamming pulse similar to the radar pulse, but with modulation information out of phase with the returning target azimuth modulation information.**

Angle tracking - **Accomplished through the use of pulses to determine angular definition of a target.**

Antenna - **A device used for transmitting or receiving RF energy. The function of the antenna during transmission is to concentrate the radar energy from the transmitter into a shaped beam that points in the desired direction. During reception, or listening time, the function of the antenna is to collect the returning radar energy, contained in the echo signals, and deliver these signals to the receiver. Radar antennas are characterized by directive beams that are usually scanned in a recognizable pattern. The primary radar antenna types in use today fall into three categories: parabolic, Cassegrain, and phased array antennas.**

Antenna cross talk - **A measure of undesired power transfer through space from one antenna to another. Ratio of power received by one antenna to power transmitted by the other usually expressed in decibels.**

Antenna gain - **See Gain**

Antenna polarization - **See Polarization**

Antenna sidelobes - **See Sidelobes**

Antiaircraft artillery (AAA) - **Guns used to shoot unguided projectiles at airborne aircraft. Usually used in the air defense system.**

Anti-clutter circuits (in radar) - **Circuits that attenuate undesired reflections to permit detection of targets otherwise obscured by such reflections.**

Antiradiation missile (ARM) - **A missile that homes passively on a radiation source.**

Area defense - **The concept of locating defense units to intercept enemy attacks, remote from, and without reference to, individual vital installations, industrial complexes, or population centers.**

Asynchronous pulsed jamming - An effective form of pulsed jamming where the jammer nearly matches the PRF of the radar then transmits multiples of the PRF. It is more effective if the jammer pulse width is greater than that of the radar. Asynchronous pulsed jamming is similar to synchronous jamming except that the target lines tend to curve inward or outward and appear fuzzy in the jammed sector of the radar scope.

Attenuation - The decrease in amplitude of a signal during its transmission from one point to another. Attenuation increases as distance increases. The higher the frequency of the propagating signal, the higher the rate of attenuation.

Automatic frequency control (AFC) - Circuits in a receiver that automatically correct the local oscillator frequency to prevent receiver drift in tuned frequency.

Automatic gain control (AGC) –

1. A feature involving special circuitry designed to maintain the output of a radio, radar, or television receiver essentially constant, or to prevent its exceeding certain limits, despite variations in the strength of the incoming signal. In a radio receiver, in particular, though something of a misnomer, also known as automatic volume control.

2. A self-acting compensating device that maintains the output of a transmission system constant with narrow limits, even in the face of wide variations in the attenuation of the system.

3. A radar circuit that prevents saturation of the radar receiver by long blocks of receiver signals, or by a carrier modulated at low frequency.

Automatic search jamming - An intercept receiver and jamming transmitting system that automatically searches for and jams enemy signals of specific radiation characteristics.

Automatic tracking - Tracking in which a system employs some mechanism, e.g., servo or computer, to automatically follow some characteristics of the signal.

Azimuth resolution - The ability of a radar to distinguish two targets in close azimuth proximity and distance.

Backlobe - The portion of the radiation pattern of an antenna that is oriented 180° in relation to the main beam. The antenna backlobe is a result of diffraction effects of the reflector and direct leakage through the reflector surface.

Backward wave oscillator (BWO) - **A special traveling wave tube in which oscillatory currents are produced by using an oscillatory electromagnetic field to bunch the electrons as they flow from cathode to anode.**

Ballistic missile - **Any missile that does not rely upon aerodynamic surfaces to produce lift and consequently follows a ballistic trajectory when thrust is terminated.**

Bandpass filter - **A filter that allows a select range of frequencies to pass while attenuating all frequencies outside the range.**

Bandwidth - **The range of frequencies within which performance, with respect to some characteristics, falls with specific limits (i.e., the width of frequency of a barrage noise package).**

Barrage noise jamming - **Noise jamming spread in frequency to deny the use of multiple radar frequencies to effectively deny range information. Although this is attractive because it enables one jammer to simultaneously jam several radars of different frequencies, it does have the inherent problem that the wider the jamming spread, the less jamming power available per radar.**

Beam rider - **A missile guided by an electronic beam.**

Beam-to-beam correlation (BBC) - **Used by frequency scan radars to reject pulse jamming and jamming at swept frequencies. Correlation is made from two adjacent beams (pulses). The receiver rejects those targets (signals) that do not occur at the same place in two adjacent beams.**

Beamwidth - **The width of a radar beam measured between lines of half-power points on the polar pattern of the antenna. This width is measured at the 3 dB points.**

Beat frequency oscillator (BFO) - **Any oscillator whose output is intended to be mixed with another signal to produce a sum or difference beat frequency. Used particularly in reception of CW transmissions.**

Bistatic radar - **A radar where the transmitting and receiving antennas are separated by a considerable distance. Bistatic operation provides several advantages for its user. The covert positioning of the receivers poses problems for a potential attacking force since ELINT techniques locate the transmitter not the receiver. The proper placement of jamming assets is difficult, since the receiving sites are unknown. In addition, if a stand-off jammer is directed at the transmitter, its effectiveness in the direction of the covert receiver is diminished.**

Jammers not in the same beam as the wanted targets will be attenuated by the receiver's sidelobe protection and these targets will be more readily detected.

Blanking –

1. The cutting off of the electronic beam in a cathode-ray tube when the picture is not being formed. The beam is blanked while the spot is returning to the starting position (normally right to left).

2. Process of making a channel or device noneffective for a desired interval.

Blinking - A jamming technique employed by two aircraft separated by a short distance and within the same azimuth resolution to appear as one target to a tracking radar. The two aircraft alternately spot jam, causing the radar system to oscillate from one plane to another, making an accurate solution of fire control problem impossible. However, keep in mind that too high a blinking frequency can cause the tracker to average the data while too low a frequency will cause a missile to home-in on one of the jammers.

Broad pulse jamming - Transmission of broad pulses for control system jamming when little is known about the command pulse group. For example, a broad pulse might cover a whole group of command pulses, thus jamming that command.

Burnthrough range - The ability of a radar to see through jamming. Usually described as the point when the radar's target return is stronger than the jamming signal.

Burst chaff - The formation of a reflective volume of chaff from an individual bundle.

Buzzer - Code name for airborne jamming.

Capture - Where the jammer takes control over the guidance signal by active jamming.

Capture effect - The tendency of a receiver to suppress the weaker of two signals within its bandpass.

Capture of AGC - Domination of the radar's automatic gain control (AGC) level by a strong transmitted jamming signal.

Carrier frequency - Frequency of an unmodulated radio wave emanated from a radio, radar, or other type of transmitter.

Carrier wave - Electromagnetic radiation used to "carry" information from one point to another.

Centroid homing - When applied to antiradiation missiles, the effect on a missile that has two or more radiation sources in its field of view causing it to home on the centroid of the power from the radiating sources.

Chaff - Ribbon-like pieces of metallic materials or metalized plastic that are dispensed by aircraft to mask or screen other aircraft or to cause a tracking radar to break lock. The foil materials are generally cut into small pieces for which the size is dependent upon the radar interrogation frequency (approximately 1/2 wavelength of the victim radar frequency). Being 1/2 wavelength long, chaff acts as a resonant dipole and reflects much of the energy back to the radar.

Chaff corridor - Operational technique of dropping large quantities of chaff for a continuous period of time. This results in a "ribbon" or "stream" of returns many miles long on radar scopes. The penetrating strike force can then use the resulting chaff corridor to mask its penetration.

Chirp - A pulse compression technique characterized by linear frequency modulation on pulse (LFMOP).

Chirp radar - Radar in which a swept-frequency signal is transmitted, received from a target, and then compressed in time to give a final narrow pulse called the chirp signal. It has high immunity to jamming and an inherent rejection of random noise signals.

Circularly polarized jamming - The techniques of radiating jamming energy in both planes of polarization. With this method, there is a 3-dB loss of effective power in either plane, but the enemy cannot cross-polarize his antenna to escape jamming.

Circular scan - The pattern generated by an antenna that is continuously rotating in one direction.

Clipped noise modulation - A clipping action is performed to increase the. bandwidth of the jamming signal. Results in more energy in the sidebands, correspondingly less energy in the carrier, and an increase in the ratio of average power to peak power.

Clutter - Unwanted signals, echoes, or images on the face of a scope that interferes with the observation of desired signals. Also called noise. This tends to mask the true target from detection or cause a tracking radar to break lock.

Clutter elimination - The clutter eliminator circuit discriminates against any target echo that exceeds three times the transmitted pulse width, and will not display it on the indicator. It is normally employed on the lower beams of a high frequency radar. This will allow targets above a preset signal strength to be presented, while the clutter (land) will be eliminated.

Clutter gating - A technique that provides switching between MTI and normal videos. It results in the normal video being displayed in regions with no clutter and the MTI video being switched in only for the clutter areas. Clutter gating is achieved automatically by the PW discrimination or the use of storage tubes. It also can be achieved by a manually operated range azimuth gate. The clutter gate vastly increases the effectiveness of noncoherent MTI against chaff.

Coherent MTI (in radar MTI) - A system in which the target echo is selected based on its Doppler frequency when compared to a local reference frequency maintained by a coherent oscillator.

Coherent noise jamming - Noise-like jamming signal that is repetitive and in synch with the PRI of the radar.

Coherent repeater jammer - A jammer that uses the phase information of the receiver radar signal in creating false targets thus transmitting a signal that is acceptable to the receiver processor of a victim coherent radar.

Command and control warfare (C2W) - The integrated use of operations security (OPSEC), military deception, psychological operations (PSYOP), electronic warfare (EW), and physical destruction, mutually supported by intelligence to deny information, influence, degrade, or destroy adversary C^2 capabilities while protecting friendly C^2 capabilities.

Command, control, communications, and computer systems (C4) - The process of, and means for, the exercise of authority and direction by a properly designated commander over assigned forces in the accomplishment of the commander's mission.

Command guidance - A guidance system in which intelligence transmitted to the missile from an offboard source causes the missile to traverse a directed flight path.

Communications intelligence (COMINT) - Intelligence derived from the interception of enemy communications signals.

Communications security (COMSEC) - The protection resulting from all measures designed to deny unauthorized persons information of value that might be

derived from the possession and study of telecommunications, or to mislead unauthorized persons in their interpretation of the results of such possession and study. COMSEC includes: 1. Cryptosecurity; 2. transmission security; 3. emission security; and 4. physical security of communications security material and information.

1. Cryptosecurity - The component of communications security that results from the provision of technically sound cryptosystems and their proper use.

2. Transmission security - The component of communications security from which all measures designed to protect transmissions from interception and exploitation by means other than cryptoanalysis.

3. Emission security - The component of communications security that results from all measures taken to deny unauthorized persons information of value that might be derived from intercept and analysis of compromising emanations from crypto equipment and telecommunications systems.

4. Physical security - The component of communications security that results from all physical measures necessary to safeguard classified equipment, material, and documents from access thereto or observation thereof by being within a friendly power.

Complex pulse - A pulse train in which there is more than one pulse width and/or more than one pulse repetition interval.

Conformal antenna - An antenna which conforms to a surface whose shape is determined by considerations other than electromagnetic, for example, an antenna shaped to aerodynamically fit the side of an aircraft.

Conical scan (CONSCAN) - A type of scanning in which the axis of the RF beam is tilted away from the axis of the reflector and rotated about it, thus generating a cone.

Constant false alarm rate (CFAR) receiver - A radar receiver with automatic detection circuits designed to produce a constant number of erroneous target detections independent of noise level at the receiver input. CFAR techniques are intended to prevent receiver saturation and overload, to present clear video information to the display, and a constant noise level to an automatic detector. A device that accomplishes these objectives may respond to the signal-to-noise ratio, for example, rather than the absolute signal level above a fixed threshold. CFAR does not usually permit the detection of a target if the target is weaker than the jamming, but it does attempt to remove the confusing jamming effects.

Continuous wave (CW) - A constant, single-frequency, unmodulated carrier wave that is transmitted and then reflected. A good system for determining velocity.

Correlation detection (modulation systems) - Detection based on the averaged product of the received signal and locally generated function possessing some known characteristics of the transmitted wave. Note the following caveats:

1. The averaged product can be formed, for example, by multiplying and integrating, or by using a matched filter whose impulse response, when reversed in time, is the locally generated function.

2. Strictly, the above definition applies to detection based on cross-correlation. The term correlation detection may also apply to detection involving autocorrelation, in which case the locally generated function is merely a delayed form of the received signal.

Countdown - A technique for forcing the radar AGC to continuously change value and oscillate. The jammer rapidly changes the duty cycle of the deception pulses.

Countdown blink - Self-screening AGC deception using a gated repeater or noise source; the period of which is short compared to the victim's AGC time constant.

Cover pulse - A jammer covers the radar return with an AM pulse usually much wider than the radar pulse. Since tracking circuits are looking for largest return, they will transfer to the cover pulse, thereby denying range information.

Cross-eye - A jamming technique used to produce angular errors in monopulse and other passive lobing radars. Jammer is a two-source interferometer that causes the phase front of the signal reaching the radar to be highly distorted. With such a technique, it is difficult for the radar to determine the points from which the transmissions are originating. Requires a high jam-to-signal ratio or the skin echo will show up in the pattern nulls.

Cross-gated CFAR - A CFAR technique employed to achieve the fast switching required for an optimum combination of normal and MTI modes. Here, the MTI video signals are used to "gate" on the normal video when the MTI indicates a target in clutter. CFAR action is achieved by the wideband as in the zero-crossing and Dicke fix CFARs.

Cross polarization - or "Cross Pole," is a monopulse jamming technique where a cross-polarized signal is transmitted to give erroneous angle data to the radar. The component of the jamming signal with the same polarization as the radar must be very small.

Cross polarization jamming - A technique whereby the received signal is retransmitted cross-polarized and at a much higher power than the skin return- effective against some monopulse radars by generating erroneous angle information.

CW jamming - The transmission of constant-amplitude, constant-frequency, unmodulated jamming signals to change the signal-to-noise ratio of a radar receiver.

Data link - A communications link which permits automatic transmission of information in digital form.

Deception - Those measures designed to mislead the enemy by manipulation, distortion, or falsification of evidence to induce him to react in a manner prejudicial to his interests. (See Electronic Deception, or Manipulative Deception.)

Deception jamming - Any means of jamming consisting of false signals that have similar characteristics to the victim radar thereby deceiving the operator into erroneous conclusions.

Decibel (dB) - A dimensionless unit for expressing the ratio of two values, the number of decibels being 10 times the logarithm to the base 10 of a power ratio, or 20 times the logarithm to the base 10 of a voltage of current ratio. A power increase by 3 dB indicates a doubling of the original power.

(dBm) - Same as dBw except the reference level is one milliwatt instead of one watt.

(dBw) - Unit used to describe the ratio of the power at any point in a transmission system to a referenced level of one watt. The ratio expresses decibels above and below the reference level of one watt.

Defense suppression - A term applied to weapons systems that are intended to eliminate or degrade enemy detection, acquisition, or tracking equipment.

Delayed opening chaff - Chaff that blooms at a specific elapsed time after it is dispensed.

Detector balanced bias - Controlling circuit used in radar systems for anti-clutter purposes.

Dicke fix - A technique specifically designed to protect the receiver from ringing caused by noise, fast-sweep, or narrow-pulse jamming. The basic configuration

consists of a broadband limiting IF amplifier, followed by an IF amplifier of optimum bandwidth. The limit level is preset at approximately the peak amplitude of receiver noise. The bandwidth may vary from 10 to 20 MHz, depending on the jamming environment. The device provides excellent discrimination against fast-sweep jamming (10 - 500 MHz), usually something about 20 to 40 dB, without appreciable loss in sensitivity. However, strong CW jamming will seriously degrade the performance of the Dicke fix because the CW signal captures the radar signal in the limiter.

Dicke fix CFAR - Constant False Alarm Rate.

Dicke fix MT CFAR - An MTI CFAR technique similar to Dicke fix CFAR. Limiting and narrowbanding follow wideband amplification, phase detection, and cancellation so as not to impair the MTI performance.

Digital radio frequency memory (DRFM) - A computer-controlled digital device used in radar jamming systems. DRFM provides an extremely fast and accurate storage capability for victim radar signal parameters. Jamming systems employing DRFM can rapidly and accurately generate coherent jamming based on the memorized victim radar signal.

DINA - See Direct Amplified Noise.

Diode - An electron device having two electrodes, a cathode, and an anode.

Diplex - Two transmitters operating alternately on approximately the same RF and using a common antenna. The normal procedure is to pulse each transmitter at ½ the desired PRF, 180° out-of-phase. The advantage is that higher peak power per transmitter is possible because each transmitter is operating at ½ the normal duty cycle.

Dipole antenna - A straight, center-fed, ½ wavelength antenna. Horizontally polarized, it produces a figure-eight radiation pattern with maximum radiation at right angles to the plane of the antenna.

Direction finding (DF) - A procedure for obtaining bearings of radio frequency emitters with the use of a highly directional antenna and a display unit on an intercept receiver or ancillary equipment.

Direct amplified noise (DINA) - DINA without a carrier frequency is used for increasing (saturating) the radar receiver's noise level. This is called video stealing. The biggest danger from this type of jamming is that the radar operator may not realize he is being jammed when automatic gain control (AGC) or automatic noise leveling (ANL) are employed. This is a barrage type of jamming

with a bandwidth normally more than 50 MHz. DINA appears as a bright, high intensity wedge when the manual gain is employed. Thus, all useful radar scope information is lost.

Doppler (effect) - Continuous wave (CW) Doppler radar modules are sensors that measure the shift in frequency created when an object moves. A transmitter emits energy at a specific frequency which, when reflected, can indicate both speed and direction of the target. When objects move closer to the Doppler source, they increase in shift (positive value), and when they move further away, they decrease in shift (negative value).

Doppler radar - A radar system that measures the velocity of a moving object by the apparent shift in carrier frequency of the returned signal as it approaches or recedes.

Downlink - The signal from a transponder beacon located on a surface-to-air missile (SAM) used to provide a traceable radar return for missile guidance.

Downlink jamming (DLJ) - Some command guidance missiles carry a beacon (downlink) which is used by the parent radar to track the missile. If this beacon reply can be hidden from the parent tracking radar, the missile guidance solution can be defeated. Hence, downlink (beacon) jamming is intended to screen the missile beacon signal from the parent radar's view.

Ducting - The bending of radar rays due to atmospheric conditions. Ducting can either extend radar coverage beyond normal line of sight or it can deny the radar picture above a duct. Ducting is also called Anomalous Propagation.

Dummy antenna - A device that has the necessary impedance characteristics of an antenna and the necessary power-handling capabilities, but does not radiate or receive radio waves. Note: In receiver practice, that portion of the impedance not included in the signal generator is often called a dummy antenna.

Dummy load (radio transmission) - A dissipative but essentially nonradiating substitute device having impedance characteristics simulating those of the substituted device. This allows power to be applied to the radar unit without radiating into free space.

Duplex - In radar, a condition of operation when two identical and interchangeable equipments are provided—one in an active state, and the other immediately available for operation.

Duplexer - A switching device used in radar to permit alternate use of the same antenna for both transmitting and receiving.

Duty cycle - The ratio of the time the transmitter is actually on versus the time it could be on in a given transmission cycle. Mathematically, it can be expressed as:

$$\text{Duty Cycle} = \frac{PD}{PRT} \quad \text{or} \quad \text{Duty Cycle} = PD \times PRF$$

Dynamic range –

1. The difference, in decibels, between the overload level and the minimum acceptable signal level in a system or transducer. Note: The minimum acceptable signal level of a system or transducer is ordinarily fixed by one or more of the following: noise level, low-level distortion, interference, or resolution level.

2. Ratio of the specified maximum signal level capability of a system or component to its noise or resolution level, usually expressed in decibels.

Early warning radar - A radar set or system used near the periphery of a defended area to provide early notification of hostile aircraft approaching the area.

EA pod - A jamming system that is designed to be carried externally on an aircraft.

Effective radiated power (ERP) - Input power to antenna time multiplied by the gain of the antenna, expressed in watts.

Electromagnetic interference (EMI) - Any electromagnetic disturbance that interrupts, obstructs, or otherwise degrades or limits the effective performance of electronic systems. EMI can be induced intentionally, by way of jamming, or unintentionally because of spurious emissions and modulations.

Electromagnetic pulse (EMP) - The generation and radiation in a transmission medium of a very narrow and very high-amplitude pulse of electromagnetic noise. The term is associated with the high-level pulse because of a nuclear detonation and with an intentionally generated narrow, high-amplitude pulse for EA applications. In nuclear detonations, the EMP signal consists of a continuous spectrum with most of its energy distributed throughout the low frequency band of 3 to 30 kHz.

Electromagnetic radiation - Radiation made up of oscillating electric and magnetic fields and propagated with the speed of light. Includes gamma radiation, x-rays, ultraviolet, visible and infrared radiation, plus radar and radio waves.

Electromagnetic spectrum - The total range of frequencies (or wavelengths) over which any form of electromagnetic radiation occurs.

Electromagnetic test environment (EMTE) - A range complex of radars, such as those located at Eglin AFB, FL, operating in different frequency bands and modes to provide a very flexible test facility for evaluating aircraft antenna patterns, reflectivity measurements, infrared, reconnaissance, airborne interceptors, and electronic warfare devices and techniques.

Electronic attack (EA) - The use of electromagnetic energy, directed energy, or antiradiation weapons to attack personnel, facilities, or equipment with the intent of degrading, neutralizing, or destroying enemy combat capability. Action taken to reduce the enemy's effective use of the electromagnetic spectrum. EA is a division of electronic warfare (EW).

Electronic combat (EC) - Action taken in support of military operations against the enemy's electromagnetic capabilities. EC is task-oriented and includes electronic warfare (EW), command and control warfare (C2W), and suppression of enemy air defenses (SEAD).

Electronic protection (EP) - Active and passive means taken to protect personnel, facilities, and equipment from any effects of friendly or enemy employment of electronic warfare that degrade, neutralize or destroy friendly combat capability. EP is a division of electronic warfare (EW).

Electromagnetic deception - The deliberate radiation, reradiation, alteration, absorption, or reflection of electromagnetic radiations in a manner intended to mislead an enemy in the interpretation of, or use of, information received by his electronic systems. There are two categories of electronic deception:

1. Manipulative deception - The alteration or simulation of friendly electromagnetic radiation to accomplish deception.

2. Imitative deception - The introduction of radiations into enemy channels that imitate his own emissions.

Electronic intelligence (ELINT) - The intelligence information product of activities engaged in the collection and processing for subsequent intelligence purposes of foreign, noncommunications, electromagnetic radiations emanating from other than nuclear detonations or radioactive sources.

Electronic intelligence parameter limit list (EPL) - A compilation of identified signals with assigned ELINT notations.

Electronic jammers –

1. Expendable - A transmitter designed for special use such as being dropped behind enemy lines.

2. Repeater - A receiver-transmitter device that, when triggered by enemy radar impulses, returns synchronized false signals to the enemy equipment. The returned impulses are spaced and timed to produce false echoes or bearing errors in the enemy equipment. See Expendable and Repeater Jammers.

Electronic jamming - The deliberate radiation, reradiation, or reflection of electromagnetic energy with the object of impairing the use of electronic devices, equipment, or systems.

Electronic order of battle - A listing of all the electronic radiating equipment of a military force giving location, type function, and other pertinent data.

Electronic reconnaissance - Specific reconnaissance directed toward the collection of electromagnetic radiations. Examples:

COMINT	**Communications Intelligence**
ELINT	**Electronic Intelligence**
OPINT	**Optical Intelligence**
RINT	**Radiated Intelligence**
SIGINT	**Signal Intelligence**

Electronic warfare (EW) - Military action involving the use of electromagnetic energy and directed energy to control the electromagnetic spectrum. EW has three divisions: electronic attack (EA), electronic protection (EP), and electronic warfare support (ES).

Electronic warfare support (ES) - Actions taken to search for, intercept, identify, and locate sources of intentional radiated electromagnetic energy for the purpose of immediate threat recognition. Surveillance of the electromagnetic spectrum that directly supports an operational commander's electromagnetic information needs. ES is a division of EW.

Electro-optics (EO) - The interaction between optics and electronics leading to the transformation of electrical energy into light, or vice versa, with the use of an optical device.

Electro-optic counter-countermeasures (EOCCM) - Actions taken to ensure the effective friendly use of the electro-optic spectrum despite the enemy's use of countermeasures in that spectrum.

Emission control (EMCON) –

1. The management of electromagnetic radiations to counter an enemy's capability to detect, identify, or locate friendly emitters for exploitation by hostile action.

2. Controlling the radiation of an active system to minimize detection by enemy sensors.

Endgame - The period of military engagement 3-5 seconds before missile impact.

Endgame countermeasures (EGCM) - Actions taken to defeat a tracking missile. This includes expendables, decoys, and maneuvers.

Essential elements of information (EEI) - The critical items of information regarding the enemy and his environment needed by the commander by a particular time to relate with other available information and intelligence to be able to reach a logical decision.

Expendable jammer - A nonrecoverable jammer. Early expendables were limited to chaff and flare deployments; however, various radiating jamming systems exist that use noise or repeater techniques. These are dispensed by aircraft or other delivery systems and are designed to disrupt or deceive a victim radar for a short period of time.

Extremely high frequency (EHF) - Frequencies in the range of 30 to 300 GHz.

False target - Radiated bundle of electromagnetic energy that is displaced in time from the echo that creates a response in the receiver where no reflecting surface exists.

False target generator - Device for generating electromagnetic energy of the correct frequency of the receiver that is displaced in time from the reflected energy of the target.

Fast automatic gain control (FAGC) - An AGC scheme characterized by a response time that is long with respect to a PW and short with respect to the target. An ultra fast FAGC will reduce the CW capture effect on the Dicke fix.

Fast time constant circuit (in radar) –

1. A circuit with short time constant used to emphasize signals of short duration to produce discrimination against extended clutter, long-pulse jamming, or noise.

2. A resistance-capacitance differentiating network with a time constant about equal to the transmitted pulse width and employed in the video portion of the receiver to provide the discrimination against jamming with low modulating frequencies. FTC is effective against CW, long jamming pulses, swept jamming, and clutter. It is also fairly effective against chaff corridors. Based on time, the radar receiver will allow only pulses equal to its own pulse width to pass and be presented on the indicators as targets. Because of this, only the leading edges of long pulses will be displayed.

Fence –

1. Line or network of early warning radars.

2. Concentric steel fence erected around a ground radar transmitting antenna to serve as an artificial horizon and suppress ground clutter that would otherwise drown out weak signals returning at a low angle from the target.

Ferret - An aircraft, ship, or vehicle especially equipped for the detection, location, recording, and analyzing of electromagnetic radiations.

Field of view (FOV) - The maximum solid angle visible by an optical or electro-optic system.

Fire control radar - Specialized radar systems used to locate and track airborne and surface targets, compute an optimum weapons firing point, and control the firing and sometimes guidance of its weapons.

FM-by-noise modulation - A method of frequency modulating with effective jamming method against AM and fix-tuned FM receivers. Not very effective against continuously tunable PFM receivers; careful tuning can defeat a great portion of the jamming signal. For this reason, FM-by-noise is not considered optimum as a type of modulation for jamming FM receivers.

FM jamming - Technique consisting of a constant amplitude RF signal that is varied in frequency around a center frequency to produce a signal over a band of frequencies.

Forward edge of the battle area (FEBA) - The foremost limits of a series of areas in which ground combat units are deployed, excluding the areas in which the covering or screening forces are operating, designated to coordinate fire support, the positioning of forces, or the maneuver of units.

Frequency agility - A radar's ability to change frequency within its operating band, usually on a pulse-to-pulse basis. This is an EP technique employed to avoid spot jamming and to force the jammer to go into a less effective barrage mode.

Frequency band designations –

1. As decided upon by the Atlantic City Radio Convention of 1947, and later modified by Comite Consultatif International Radio (CCIR) Recommendation No. 142 in 1953:

Band	RF Range	Band	RF Range
VLF	0-30 kHz	VHF	30-300 MHz
LF	30-300 kHz	UHF	300-3000 MHz
MF	300-3000 kHz	SHF	3-30 GHz
HF	3-30 MHz	EHF	30-300 GHz

2. Electronic warfare uses the following designations:

A	0-250 MHz	H	6-8 GHz
B	250-500 MHz	I	8-10 GHz
C	500-1000 MHz	J	10-20 GHz
D	1000-2000 MHz	K	20-40 GHz
E	2-3 GHz	L	40-60 GHz
F	3-4 GHz	M	60-100 GHz
G	4-6 GHz		

Frequency bandpass - The number of hertz where maximum output is obtained between two limits usually defined and bounded by lower and upper half power (3 dB) points.

Frequency hopping - An anti-jamming technique used by a radar system. The carrier frequency of the pulsed transmissions are periodically or continuously shifted within limits on each successive pulse.

Frequency diversity - Method of transmission and/or reception using several frequencies simultaneously to minimize the effects of selective fading, deliberate jamming, or interference.

Frequency modulated CW (FM-CW) jamming - FM of a CW signal to produce a wide band of signals when the exact operating frequency of the victim is not known within the CW limits.

Frequency modulation (FM) - A method of impressing a message upon a carrier signal by causing the carrier frequency to vary proportionally to the message waveform.

Frequency shift keying (FSK) - A form of FM where the carrier is mined code. In multiple FSK, the carrier is shifted to more than two frequencies. FSK is used principally with teletype communications.

Frequency spectrum - The entire range of frequencies of electromagnetic radiation.

G - Acceleration due to gravity (32.2 ft/sec^2).

Gain (manual) - The receiver gain control allows the operator to vary the receiver sensitivity. It is not designed as an AJ feature; however, when properly employed it may greatly reduce the effects of jamming. The radar detection capability is also reduced by an equal amount.

Gain (transmission gain) - The increase in signal power in transmission from one point to another under static conditions. Note: Power gain is usually expressed in decibels.

Glint (in radar) –

1. The random component of target location error caused by variations in the phase front of the target signal (as contrasted with scintillation error). GLINT may affect angle, range of Doppler measurements, and may have peak values corresponding to locations beyond the true target extent in the measured coordinate.

2. Electronic countermeasures that use the scintillating, or flashing, effect of shuttered or rotating reflectors to degrade tracking or seeking functions of an enemy weapons system.

Ground controlled intercept (GCI) - Vectoring an interceptor aircraft to an airborne target by means of information relayed from a ground-based radar site that observes both the interceptor and target.

Guidance system (missile) - **A system that evaluates flight information, correlates it with target data, determines the desired flight path of the missile, and communicates the necessary commands to the missile flight control system.**

Guided missile - **An unmanned vehicle moving above the surface of the earth, whose trajectory of flight path is capable of being altered by an external or internal mechanism.**

Height finder - **A radar used to detect the angular elevation, slant range and height of objects in the vertical sight plane. An air defense ground radar used specifically to accurately determine aircraft altitude for tracking and ground controlled intercepts.**

Hertz (Hz) - **The unit of frequency, equal to one cycle of variation per second. It supersedes the unit cycle per second (cps).**

High frequency (HF) - **Frequencies from 3000 - 30,000 kHz.**

Home-on-jam (HOJ) - **A missile mode of operation in which a jamming signal is used to develop steering information for the missile to home in on the jamming source.**

Homing guidance - **A system by which a missile steers itself toward a target by means of a self-contained mechanism which is activated by some distinguishing characteristics of the target.**

Identification, friend or foe (IFF) - **A system using radar transmission to which equipment carried by friendly forces automatically responds, for example, by emitting pulses, thereby distinguishing themselves from enemy forces. It is the primary method or determining the friendly or unfriendly character of aircraft and ships by other aircraft and ships, and by ground forces employing radar detection equipment and associated identification, friend or foe units.**

Image frequency - **An undesired input frequency capable of producing the selected frequency by the same process. NOTE: An image frequency is a frequency which differs from, but has a certain symmetrical relationship to, that which a superheterodyne receiver is tuned. Consequently, the image frequency can be mistakenly accepted and processed as a true frequency by the receiver.**

Image jamming - **Jamming at the image frequency of the radar receiver. Barrage jamming is made most effective by generating energy at both the normal operating and imaging frequency of the radar. Image jamming inverts the phase of the response and is thereby useful as an eagle deception technique. Not effective if the radar uses image rejection.**

Imitative deception - The introduction of radiations into enemy channels which imitates their own emissions.

Imitative jamming - The jamming technique of transmitting a signal identical to the original guidance signal.

Infrared (IR) - That portion of the frequency spectrum lying between the upper end of the millimeter wave region and the lower (red) end of the visible spectrum. In wavelength, the IR lies between 0.78 and 300 microns; in frequency, it lies between one and 400 terahertz (THz).

Infrared counter-countermeasures (IRCCM) - Actions taken to effectively employ our own infrared radiation equipment and systems in spite of the enemy's actions to counter their use.

Infrared countermeasures (IRCM) –

1. Countermeasures used specifically against enemy threats operating in the infrared spectrum.

2. Actions taken to prevent or reduce the effectiveness of enemy equipment and tactics employing infrared radiation.

Instantaneous automatic gain control (IAGC) –

1. That portion of a system that automatically adjusts the gain of an amplifier with varying input pulse amplitudes. The adjustment is sufficiently fast to operate while a pulse is passing through the amplifier.

2. In radar, a quick-acting automatic gain control that responds to variations of mean clutter level, or jamming over different range or angular regions, avoiding receiver saturation (also known as back-bias). IAGC automatically adjusts the gain of the radar receiver so that strong signals do not block adjoining weak signals. IGAC is not quick enough to block short pulse jamming, extended clutter, or chaff.

Instantaneous frequency CFAR (IFCFAR) - A technique similar to the IF DICKE FIX CFAR, except for having a phase detector instead of a frequency discriminator. The primary use of this technique, combined with rapid random frequency changes, is to make chaff signals appear noise-like so they can be handled conventionally.

Instantaneous inverse gain - Pulse-by-pulse amplification, modulation, and reradiation of the victim's radar pulse to obscure angle data.

Intercept point - A computed point in space toward which an interceptor is vectored to complete an interception.

Interference (electronic) - An electrical or electromagnetic disturbance that causes undesirable responses on electronic equipment. Electrical interference refers specifically to interference caused by the operation of electrical apparatus that is not designed to radiate electromagnetic energy.

Interferometer - As pertains to radar, a receiving system which determines the angle of arrival of a wave by phase comparison of the signals received at separate antennas or separate points on the same antenna.

Interleaved jamming - Time sharing of a jammer's output around many threats usually to cover pulse jamming.

Intermediate frequency (IF) –

1. A fixed frequency to which all carrier waves are converted in a superheterodyne receiver.

2. A frequency to which a signaling wave is shifted locally as an intermediate step during transmission or reception.

3. A frequency resulting from the combination of the received signal and that of the local oscillator in a superheterodyne receiver.

Intermediate frequency jamming - Form of CW jamming that is accomplished by transmitting two CW signals separated by a frequency equal to the center frequency of the radar receiver IF amplifier.

Interrogator - A device used to transmit pulse-coded challenges to an IFF transponder and then evaluates the pulse-coded reply for identification purposes.

Intrapulse modulation repeater - A classified deception jamming technique.

Intrusion –

1. The entry of a nonfriendly aircraft or system into friendly air space.

2. The intentional interference in a communication system by which the intruder attempts to confuse, delay, or cause error by the selective introduction of additional data.

Inverse conscan - One method of confusing a radar operator or fire control radar system is to provide erroneous target bearings. This is accomplished by first sensing the radar antenna scan rate and then modulating repeater amplifier gain so that the weapons systems will fire at some bearing other than the true target bearing. The angle deception technique is used to break lock on CONSCAN radars.

Inverse gain - Amplification, inverse modulation, and reradiation of a radar's pulse train at the rotation rate of the radar scan. Deceives a conical scanning radar in angle.

Inverse-gain repeater jammer - A form of repeater in which the jammer creates false targets by varying the output power inverse with the strength of the received radar signal.

Jaff - Expression for the combination of electronic and chaff jamming. An ECM tactic involving the use of jammers to illuminate chaff corridors or chaff bursts to produce false targets.

Jam attenuator control - Used to prevent receiver saturation from any strong signals, including electronic jamming, chaff, or clutter. It also permits the determination of the bearing and elevation of jammers that would cause wide sectors of the scope to be obscured. The control reduces all signals equally, jamming as well as targets. This control should be used in the jammed sector only and not for an entire antenna revolution. Targets in the jammed sector would only be seen if they were stronger than the jamming. However, the jammed sector may be reduced enough in size to allow the operator to determine either bearing or elevation.

Jammer - A device used to deprive, limit, or degrade the use of communications or radar systems. Radio frequency jammers include noise, discrete frequency repeater, and deceptive equipment.

Jamming-to-signal (J/S) ratio - The relative power ratio of jamming to the radar return signal at the radar antenna. The inverse of the signal-to-jamming ratio.

Jam strobe - Also called JAVA (jamming amplitude versus azimuth). A circuit that generates a marker on the PPI to indicate signal strength as a function of bearing. It does this by sampling the jamming intensity once each repetition period. Besides showing the direction of the jammer, it also indicates the severity of main beam and sidelobe jamming.

Jet engine modulation (JEM) - Modulation present in the radar returns received from a jet aircraft, caused by the rotation of the fan or turbine blades of the aircraft's engines.

Jittered pulse repetition frequency (jittered PRF) - The PRF is rapidly varied at a random rate so that false targets appear to jitter or appear fuzzy on the scope. An alternative to jittered PRF is to change the PRF momentarily. This causes the false targets to change their position on the scope. It provides a discrimination against repeater-type jammers.

Klystron - A very stable microwave amplifier that provides high gain at good efficiency. This is accomplished by velocity modulating (accelerating a beam of electronics flowing from its cathode to its anode.

Laser target designation - The use of a laser to direct a light beam onto the target so that appropriate sensors can track or home on the reflected energy.

Leading-edge tracker - A tracking radar that obtains its data from the leading edge of the echo pulse from the target.

Light amplification by stimulated emission of radiation (LASER) - A process of generating coherent light. The process uses a natural molecular (and atomic) phenomenon whereby molecules absorb incident electromagnetic energy at specific frequencies. It then stores this energy for short but usable periods, then releases the stored energy as light at particular frequencies, and in an extremely narrow frequency band.

Lobe - One of the three-dimensional sections of the radiation pattern of a directional antenna bounded by 1-2 cones of nulls.

Lobe-on-receive-only (LORO) - Mode of operation consisting of transmitting on one antenna system and receiving the reflected energy on another system (TWS, conical, or monopulse).

Local oscillator off - A simple expedient of shutting off the local oscillator during barrage jamming. The barrage jammer will not be seen unless there is a beating signal such as a target; therefore, targets will appear. Since targets will not

appear in directions where no jamming arises, either an automatic azimuth switch or an additional receiver display is required.

Logarithmic fast time constant log (LOG-FTCL) - A device consisting of a logarithmic IF amplifier followed by an FTC circuit. The LOG-FTC combination is very effective in removing variations in the video output noise level caused by spot noise, wideband noise, and slow sweep noise modulated AM jamming.

Logarithmic receiver - A receiver whose response approximates the logarithm of the strength of the incoming signal. A special type of receiver having a large dynamic range of automatic gain control that gives considerable protection against receiver saturation by strong jamming on interference signals. Useful against weather, clutter, chaff, and spot jamming.

Look-down, shoot-down - Refers to an air interceptor (AI) equipped with a pulse Doppler radar, or a radar that has a moving target indicator (MTI) feature, that can detect and lock-on to a target within ground return clutter enabling the AI to track and shoot the target.

Look-through –

1. When jamming, a technique by which the jamming emission is interrupted irregularly for extremely short periods to allow monitoring of the victim signal during jamming operations.

2. When being jammed, the technique of observing or monitoring a desired signal during interruptions in the jamming signals.

Low frequency (LF) - Frequencies from 30 - 300 kHz.

Low power spread spectrum radar - A low power, high duty cycle radar whose spectrum is spread 100 MHz or more. Since this radar has a broad output spectrum and a high duty cycle, neither time nor frequency can be effectively used to resolve these signals. This leaves direction as the prime method of resolution. The spectrum of these radars is spread over the bandwidth by any of the pseudo random noise modulating techniques commonly used in communications. Techniques such as bi-phase modulation, quaternary phase modulation, chirp, random frequency jumping, etc., may be used to spread either a CW signal or a very high duty cycle signal. Such signals have a very good range resolution—approximately equal to the reciprocal of the bandwidth.

Magnetron - A radar microwave device whose operation is based on the motion of electrons (AC) under the influence of combined electric and magnetic fields.

Mainlobe - The lobe of a transmitting or receiving antenna centered on the directivity axis of the antenna.

Manipulative deception - The alteration or simulation of friendly electromagnetic radiations to accomplish the deception.

Meaconing, interference, jamming, and intrusion (MIJI) - An acronym of four component parts to determine the intent and technique of electromagnetic radiation.

Meaconing - a system of receiving radio beacon signals and rebroadcasting them on the same frequency to confuse navigation. Interference - unintentional electromagnetic radiation that may cause interference with electronic equipment.

Jamming - the deliberate radiation, reradiation, or reflection of electromagnetic energy with the intent of impairing the use of electronic devices, equipment, or systems being used by the enemy.

Intrusion - the intentional insertion of electromagnetic energy into transmission paths in any manner with the objective of deceiving operators or causing confusion.

Medium frequency (MF) - Frequencies from 300 to 3,000 kHz.

Micron - A unit of length equal to a micrometer (10^{-6} meters).

Microwave amplification by stimulated emission or radiation (MASER) - A low-noise, radio-frequency amplifier. The emission of energy stored in a molecular or atomic system by a microwave power supply is stimulated by the input signal.

Microwave communications - Line-of-sight communications, the frequency of which is higher than 300 MHz.

Millimeter waves - Frequencies (30 GHz to 300 GHz) in the millimeter portion of the electromagnetic spectrum.

Miss distance - The distance measured between the closest paths of a target and interceptor (i.e., aircraft and missile). One objective of self-protection jamming systems is to increase the miss distance to avoid destruction if missile launch cannot be prevented.

Missile approach warning system (MAWS) - A system used to detect and provide warning of approaching missiles. MAWS may be partitioned into active MAWS and passive MAWS.

1. Active missile approach warning system (AMAWS) - Generally employs pulse Doppler radar as its sensor. This radar is able to discern a moving target in stationary or slow-moving background clutter.

2. Passive missile approach warning system (PMAWS) - An ultraviolet (UV) or infrared-based detector system with the ability to detect and distinguish threat missiles from surrounding clutter and non-lethal missiles.

Modulated barrage jamming - A technique that varies the amplitude of the output power of a barrage jammer with sinusoidal or complex modulation.

Modulated CW jamming - A CW carrier waveform that has been modulated with another signal (such as noise, low, medium, or high frequencies), and is transmitted for the purpose of deception. May be AM, FM, pulse modulated (PM), etc.

Modulated PRF (MPRF) - The deliberate modulation of the interpulse spacing in a pulse train. See PRF Jitter and PRF Stagger.

Modulation - The variation of amplitude, frequency, or phase of an electromagnetic wave by impressing another wave on it.

Modulator - A device (such as an electron tube) for modulating a carrier wave or signal for the transmission of intelligence of some sort.

Monopinch - Anti-jam application of the monopulse technique where the error signal is used to provide discrimination against jamming signals.

Monopulse - A method of pulse generation that allows the simultaneous determining of azimuth, elevation and range, and/or speed from a single pulse.

Monopulse radar - A radar using a receiving antenna system having two or more partially overlapping lobes in the radiation patterns. Sum and difference channels in the receiver compare the amplitudes or the phases of the antenna outputs to determine the angle of arrival of the received signal relative to the antenna boresight. A well-designed monopulse tracking system will achieve a more accurate track under conventional jamming techniques than on the skin return. Certain monopulse trackers are susceptible to angular jamming techniques such as skirt and image jamming. Techniques such as "CROSS EYE" are designed to

attack all monopulse tracking systems. Monopulse deception is a major area of advanced R&D with no clear "best technique" yet in sight.

Moving target indicator (MTI) - A radar presentation that shows only targets that are in motion. Signals from stationary targets are subtracted out of the return signal by the output of a suitable memory circuit.

MTI CFAR - A technique that provides CFAR capability in an MTI receiver. The cancellation of ground clutter is not impaired during radar jamming.

Multiband radar - Radar that simultaneously operates on more than one frequency band through a common antenna. This technique allows for many sophisticated forms of video processing and requires that a jammer must jam all channels simultaneously.

Multiplex - Simultaneous transmission of two or more signals on a common carrier wave. The three types of multiplex are called time division, frequency division, and phase division.

Multitarget generator jamming - A technique where a generator takes the radar's PRF, scan rate, and antenna lobe pattern and computes when to transmit false targets at the radar's frequency. The targets appear as true targets, but normally only about 20 percent of the targets are programmed to give a logical course and speed. The many targets saturate the tracking operator's capability by the sudden appearance of multiple targets, and/or many targets either stationary or on illogical courses and speeds, or maneuvers such as 90 degree turns at high speeds but with no displacement. Also, targets may appear in back and sidelobe positions.

Music - In air intercept, a term meaning electronic jamming.

Narrowband (NB-1) - Narrows the receiver frequency making it more selective. It limits the target signals and the jamming signal to a set level of amplitude and reduces the level of a jamming signal if the jammer is not tuned to the radar's exact frequency.

Narrow pulse jamming - Jamming where the jammer pulse width is less than the radar's pulse width. Technique may be required by interleaved jamming.

Noise –

1. Any unwanted disturbance within a dynamic electrical or mechanical system, such as undesired electromagnetic radiation, and any transmission channel or device.

2. Uncontrolled random disturbances that arise in a guided missile system because of various physical phenomena.

Noise jamming - Direct (straight) AM or FM noise on a carrier frequency that has a highly variable bandwidth for the purpose of increasing (saturating) the radar receiver's noise level.

Nuclear effects - The electromagnetic phenomena resulting from a nuclear explosion. The phenomena are listed as follows:

1. Argus phenomena (trapped electrons). The trapping in the earth's magnetic field of electrons produced by a nuclear burst.

2. Blackout (radio frequency interference). An effect that is the result of ionization produced by a nuclear explosion in or above the atmosphere. This ionization can cause interference (blackout) by attenuating, reflecting, cluttering, and scattering radar electromagnetic pulses in a high-intensity burst of electromagnetic radiation, predominantly in the radio frequency range of the spectrum.

3. Optical phenomena. Intense radiations covering all parts of the optical spectrum are produced by the interactions between the atmosphere and the nuclear radiation and fission products resulting from a nuclear detonation. The resulting auroras and airglows are created as an optical background that can affect reconnaissance, tracking, warning and homing systems, and personnel.

4. Transient radiation effects on electronics. Nuclear radiation impinging on electronic systems or components can substantially alter the operation and output of these systems. The word transient refers to the type of environment and not to the duration of the effect since the effect may be either transient or permanent.

Nulls - Points of no radiation in an antenna radiation pattern.

Obscuration - Effects produced by masking-type jammers. Denial of either range or angle is achieved by submerging data interference caused by noise or noise-like signals.

Off-frequency spot jamming - A type of spot jamming in which the jammer frequency is off the radar operating frequency but still within the radar receiver bandpass.

Optical countermeasures - Applications of electronic countermeasures in the visible light portion of the electromagnetic spectrum. Actions taken to prevent or reduce an enemy's effective use of the visible spectrum.

Oscillator - Electronic circuit or device capable of converting direct current (DC) into alternating current (AC) at a frequency determined by the inductive and the capacitive constants of the oscillator.

Over-the-horizon radar - A radar system that makes use of the ionosphere to extend its range of detection beyond line-of-sight. Over-the-horizon radars may be either forward scatter or backscatter systems.

Palmer scan - Conical scan superimposed on another type of scan pattern-usually a spiral pattern.

Passive angle tracking (PAT) - A target may be tracked "passively" if that target emits electromagnetic radiation; i.e., jamming radio, radar signal of sufficient duration that a DF bearing may be obtained. The emission from the target is DF-ed in azimuth and/or elevation. No range information will be available unless cross DF techniques are used by two or more passively tracking sites.

Passive detection and tracking - By combining azimuth data on jamming strobes from several stations, intersections are obtained which indicate the position of the jammers. The number of ghosts can be reduced by increasing the number of friendly stations and obtaining elevation angles of strobes when available.

Passive electronic countermeasures - Electronic countermeasures based on the reflection, absorption or modification of the enemy's electromagnetic energy. This distinction between active and passive countermeasures is not currently used, but is based on the presence or absence of an electronic transmitter.

Passive homing guidance - A system of homing guidance in which the receiver in the missile uses radiations only from the target.

Peak power - Maximum power output during transmission time. Expressed in watts or megawatts.

Penetration aids - Techniques and/or devices employed by aerospace systems to increase the probability of weapon system penetration of any enemy defense.

Examples are: Low altitude profiles, trajectory adjustments, reduced radar cross-sections of attack vehicles, improved vehicle hardness to effects of defense engagements, terrain avoidance radar, bomber defense missiles, decoys, chaff, electronic countermeasures, etc. Penetration aids are used by an offensive system to penetrate enemy defenses more effectively. Also called PENAIDS.

Phase modulation - A method of impressing a message upon a carrier signal by causing the carrier phase to vary proportionally to the waveform.

Phase shift keying - A method of impressing a digital signal upon a carrier signal by causing the carrier phase to take different values corresponding to the different values of the digital signal.

Phased array radar - Radar using many antenna elements that are fed out-of-phase to each other. The direction of the beam can be changed as rapidly as the phase relationships (usually less than 20 μsec). Thus, the antenna remains stationary while the beam is moved electronically. The use of many antenna elements allows for very rapid and high directivity of the beam(s) with a large peak and/or average power.

Point defense - The defense of specified geographical areas, cities, and vital installations. One distinguishing feature of point defense missiles is that their guidance information is received from radars located near the launching sites.

Polarization - The direction of an electrical field is considered the direction of polarization. When a half-wave dipole antenna is horizontally oriented, the emitted wave is horizontally polarized. A vertical polarized wave is emitted when the antenna is erected vertically.

Polarization diversity - The variation of polarization (such as horizontal, vertical, circular, or elliptical for radar use) either simultaneously or singularly.

Power management - Generally classified methods to optimize all related EW activities and facilities-usually in reference to a coordinate, optimized EW suite.

PPI scope - A radar display yielding range and azimuth information via an intensity modulated display and a circular sweep of a radial line. The radar is located at the center of the display.

PRF jitter - PRF rapidly varied at a random rate so that false targets appear to jitter, or appear fuzzy, on the scope. An alternative to jittered PRF is to momentarily change the PRF. This causes the false targets to change their position on the scope.

PRF stagger - The technique of switching PRF or PRI to different values on a pulse-to-pulse basis such that the various intervals follow a regular pattern. This is useful in compensating for "blind speeds" in pulsed MTI radars. Interpulse intervals differ but follow a regular pattern.

Pseudo noise - A modulation technique resulting in low signal selectability and decreased vulnerability to jamming.

Pulse compression - A scheme whereby a specifically modulated, medium power long pulse is stretched and transmitted. The returned pulse is compressed in the receiver demodulation process to obtain the advantage of narrow pulse operation. Long pulses provide the advantage of long range detection and short (compressed) pulses provide the advantage of better resolution and accuracy. This technique uses matched filter techniques for discriminating against signals that do not correspond to the transmitted code. It permits an increase in average transmitted power (without an increase in peak power) with no loss in range resolution. Pulse compression is a special form of pulse coding and correlation.

Pulse deception jamming - Any of the many false target techniques used to deceive a pulse radar, as opposed to obscurative noise techniques.

Pulse discriminator - Device that responds only to a pulse that has a particular characteristic, such as duration or period.

Pulse Doppler radar - A highly complex radar system that employs a very high pulse repetition frequency (usually 10,000 PPS or higher) to reduce "blind speeds" and measure the Doppler frequency shift to resolve target velocity. Pulse Doppler is applied principally to radar systems requiring the detection of moving targets in a ground clutter environment. It uses pulse modulation to achieve higher peak power, greater range, less susceptibility to unfriendly detection, and enhanced range resolution.

Pulse duration - The time in microseconds that the radar set is transmitting RF energy. Generally, the greater the pulse duration, the higher the average power, but the poorer the range resolution. Also known as pulse width. More technically, it is the time interval, measured at the half-amplitude points, from the leading edge to the trailing edge of a pulse.

Pulse group - In complex pulse trains, two or more pulses that are recognizably distinct from the others.

Pulse interference suppression and blanking (PISAB) - An EP automatic interference blanking device that will blank all video signals not synchronous

with the radar PRF. PISAB does not require any trigger and operates on both normal and MTI modes. It is effective against random pulse signals.

Pulse jitter - Random variation of interpulse interval.

Pulse modulation (PM) - A special case of amplitude modulation in which the carrier wave is varied at a pulsed rate. This series of pulses is generally for transmitting data. The result is a short, powerful burst of electromagnetic radiation that can be used for measuring the distance from a radar set to a target.

Pulse modulated jamming - Use of jamming pulses of various widths and repetition rates.

Pulse position modulation - Modulation by variation of the interval that elapses between the pulse to be modulated in a group of pulses and a synchronizing pulse, usually the first pulse of the group.

Pulse repetition frequency (PRF) - The rate at which pulses or pulse groups are transmitted from a radar set. Generally, PRF is the number of pulses generated per second and is expressed in hertz (Hz).

Pulse repetition interval (PRI) - The interval of time between two transmitted radar pulses, usually expressed in microseconds. PRI is the inverse of PRF.

Pulse recurrence time (PRT) - Time elapsing between the start of one transmitted pulse and the start of the next. It is the reciprocal of PRF.

Pulse recurrence time (PRT) agility - Ability of the radar set to vary the number of pulses per set.

Pulse width (PW) - See Pulse Duration.

Pulse width discrimination (PWD) - An EP technique used to discriminate against received pulses that do not have the same duration as the radar transmitted pulse. PWD is used in eliminating the effects of pulse type interference when the interference pulses are not the same length as the real radar pulse. Since this circuit generates a blanking gate that shuts off the receiver whenever a pulse of improper length is sensed, loss of valid target data can result. PWD offers good discrimination against long-pulse jamming and jamming signals employing low frequency noise modulation. It affords little or no discrimination against short pulses and HF noise modulations.

Pulse width discriminator - A device that measures the pulse length of video signals and passes only those pulses whose time duration tails into some predetermined design tolerances. A pulse width discriminator will generally provide some gain against barrage jamming, similar to that of a matched filter in the video.

"Rabbits" - Interference from another radar on or near the frequency of the receiving radar. Shows on the indicators as interference at the rate of the relative PRF of the interfering radar.

Radar - From Radio Detection And Ranging. A device used to detect a distant target and determine and display its relative direction (azimuth) and its relative distance (range).

Radar absorbent material (RAM) - Material used as a radar camouflage device to reduce the echo area of an object.

Radar beacon - A receiver-transmitter combination that sends out a coded signal when triggered by the proper type of pulse enabling determination of range and bearing information by the interrogating station or aircraft.

Radar cross section - The equivalent area intercepted by a radiated signal and, if scattered uniformly in all directions, produces an echo at the radar receiver equal to that of the target. Typical radar cross sections of aircraft vary from one to over 1,000 square meters. The RCS of ships may exceed 10,000 square meters.

Radar definition - The accuracy with which a radar obtains target information such as range, azimuth, or elevation.

Radar homing - Homing on the source of a radar beam.

Radar homing and warning (RHAW) - Typically consists of an airborne, wideband video receiver designed to intercept, identify, and display the direction to pulse-type emitters.

Radar resolution - A measure of a radar's ability to separate targets that are close together in some aspect of range, azimuth, or elevation into individual returns.

Radar warning receiver (RWR) - A receiver onboard an aircraft that analyzes the hostile radar environment and determines radar threat by type, frequency, relative bearing, and relative distance. The threat is displayed to the aircrew by means of display lights, video symbols, and aural tones.

Radio frequency (RF) - Electromagnetic energy radiated at some frequency.

Radio frequency interference - An unintentional interfering signal capable of being propagated into electronic equipment, usually derived from sources outside the system.

Railing –

1. Pertains to radar pulse jamming at high recurrence rates (50 to 150 kHz). It results in an image on a radar indicator resembling fence railing.

2. The name given to that pattern produced on an "A" scope by CW modulated with a high frequency signal. Railings appear as a series of vertical lines resembling target echoes along the baseline.

Random modulation CW jamming - The use of a nonperiodic function to an AM, FM, or AM/FM CW carrier. The effects produced on a radar are similar to those produced by DINA.

Random noise - Electromagnetic energy having no particular modulation or pattern. May be generated by either natural atmospheric phenomena or by electromagnetic radiation devices.

Random pulse jamming - The technique by which a pulse transmission system is pulsed irregularly by random noise signals.

Range - The distance from one object to another.

Range gate - A gate voltage used to select radar echoes from a very short range interval.

Range gate capture - A jamming technique using a spoofer radar transmitter to produce a false target echo that can make a target tracking radar move off the real target and follow the false one.

Range gate pull-in (RGPI) - Same as range gate pull-off (see next text entry) except that the deceptive pulse is transmitted before the radar pulse is received. This is accomplished by digital storage of the pulse repetition period which must be extremely stable.

Range gate pull-off (RGPO) - A deception technique used against pulse tracking radars using range gates. The jammer initially repeats the skin echo with minimum time delay at a high power to capture the AGC circuitry. The delay is

progressively increased, forcing the tracking gates to be pulled away ("walked off") from the target echo. Frequency memory loops (FML) or transponders provide the variable delay.

Range gate tracker - A radar system that tracks targets in range by measuring the elapsed time from the transmitted pulse to the echo return.

Range tracking - Pulse radars measure the time difference between radar pulse transmission and echo reception. The range gate is positioned at a range where the target is expected. The receiver is blanked off except during the period where the range gate is positioned. Range tracking may occur at the leading edge of the return pulse or between ON and OFF gates.

Recovery time (RT) - The time that a radar requires to "get ready" to receive after a pulse is sent out. Time is required to get ready because the high-powered pulse tends to fill the sensitive radar receiver with RF energy, which prevents target returns from being seen. A short "damping out" period occurs after the pulse width during which time the RF energy dissipates, allowing weak target echoes to once again be detected.

Rectifier - A device (such as a vacuum tube) for converting alternating current (AC) into direct current (DC).

Repeater - A receiver-transmitter combination that amplifies the received signal and retransmits it.

Repeater jammer - Equipment used to confuse or deceive the enemy by causing his equipment to present false information. This is done by a system that intercepts and reradiates a signal on the frequency of the enemy equipment. The reradiated signal is modified to present erroneous data on azimuth, range, number of targets, etc.

Repeater jamming - Interception and reradiation of a signal with the reradiation of a signal being modified to give erroneous azimuth, range, velocity, acceleration, or number of targets.

Resolution - The ability of a system to distinguish between two adjacent objects and to display them separately.

Resolution cell - The minimum volume in space in which a radar can discriminate between targets. It is determined numerically-for a conventional radar-by the width of the beam in angle, the pulse width in range, and the velocity gate width in speed.

Response noise jammer - A repeater jammer that transmits spot noise over the received radar frequency even in the case of radar frequency agility.

Ringing - The undesired oscillation or triggering of an electrical device by its own transmitter.

Rope - An element of chaff consisting of a long roll of metallic foil or wire that is designed for broad low frequency response. (See Chaff.)

Rope chaff - Chaff that contains one or more rope elements. (See Chaff.)

Rotating polarization - The result of a rotating feed. This should not be confused with circular polarization where the electric field rotates about the axis of propagation at the radar frequency.

SAM - Surface-to-air missile.

Saturating signal - In radar, a signal of an amplitude greater than the dynamic range of the receiving system.

Sawtooth modulated jamming - Electronic countermeasure technique when a high-level jamming signal is transmitted, thus causing large AGC voltages to be developed at the radar receiver that, in turn, causes the target return and receiver noise to completely disappear.

Scan - The process of directing a beam of RF energy successively over a given region, or the corresponding process in reception.

Scan interval - The time interval from the peak of one mainlobe in a scan pattern to the peak of the next mainlobe.

Scan period - The time period of basic scan types (except conical and lobe switching) or the period of the lowest repetitive cycle of complex scan combinations. The basic unit of measurement is degrees/mils per second or seconds per cycle.

Scan rate modulation - Modulation of the deception jamming signal with one or more frequencies that are related to the scan rate of the radar.

Scan type - The path made in space by a point on the radar beam, for example, circular, helical, conical, spiral, or sector.

Search –

1. A term applied to that phase of radar operation when the lobe, or beam of radiated energy, is directed in such a way to search for targets in the area.

2. A systematic examination of space to locate and identify targets of interest.

Sector scan - A scan in which the antenna sweeps back and forth through a selected angle.

Selective identification feature (SIF) - A capability which, when added to the basic IFF system, provides the means to transmit, receive, and display selected coded replies.

Self-protection jamming - Jamming to protect the vehicle upon which the jammer is deployed.

Semiactive radar homing - Semiactive homing guidance combines principles from both the beam rider and the active radar homing missile. Track on the target is established by the AI's radar; the missile is launched when the target comes within its effective range. During missile flight, the AI maintains track on the target. Radar returns from the target are received by the missile. Guidance commands are generated within the missile from the radar returns.

Sensitivity time control (STC) - Programmed variation of the gain (sensitivity) of a radar receiver as a function of time within each pulse repetition interval or observation time. STC prevents overloading of the receiver by strong echoes from targets or clutter at close ranges. STC reduces the gain of the radar receiver for detection of close-in targets. It is particularly effective in removing close-in clutter and strong nearby signals. STC also refers to a circuit that reduces the gain of the radar receiver immediately following the transmission of the radar pulse so that the receiver is not saturated by strong radar returns from nearby objects.

Serrodyne - A method of "pulling off" the velocity gate of a Doppler radar by using a voltage-controlled phase shifter, usually a traveling wave tube (TWT). This introduces a frequency shift from zero to some maximum value, pulling the Doppler tracking gate away from the skin echo. The phase shift is usually accomplished by modulating the TWT's helix voltages.

Sidelobe - Part of the beam from an antenna, other than the mainlobe. Sidelobe gain is usually less than mainlobe gain. Given that the mainlobe radiates most of the power at zero degrees azimuth, sidelobes inherently radiate significant power in the direction of +20°, 90°, and 150° relative to the mainlobe.

Sidelobe blanking (SLB) - A device that employs an auxiliary wide angle antenna and receiver to sense whether a received pulse originates in the sidelobe region of the main antenna and to gate it from the output signal if it does. This technique uses an omnidirectional antenna and compares relative signal strength between the omni and the radar antenna. The omnichannel (plus receiver) has slightly more gain than the sidelobes of the normal channel, but less gain than the main beam. Any signal that is greater in the omnichannel must have been received from a sidelobe and is blanked. This technique is effective in removing spoofed signals with a duty cycle up to 50%.

Sidelobe canceller (SLC) - A device that employs one or more auxiliary antennas and receivers to allow linear subtraction of interfering signals from the desired output if they are sensed to originate in the sidelobe of the main antenna. This technique employs the same antenna and receiver configurations of the SLB, except that a gain matching and canceling process takes place. Extraneous signals entering the sidelobes of the main antenna are canceled while the targets remain. This type of system exhibits cancellation roughly 20 dB against a single noise jammer. With multiple jammers at various azimuths, the performance of this device rapidly deteriorates.

Sidelobe jamming - Jamming through a sidelobe of the receiving antenna in an attempt to obliterate the desired signal received through the mainlobe of the receiving antenna at fixed points.

Sidelobe suppression - The suppression of that portion of the beam from a radar antenna other than the mainlobe.

Sidewinder - A solid-propellant, air-to-air missile with nonnuclear warhead and an infrared guidance system. Designated as the AIM-9 missile.

Signal intelligence (SIGINT) - Intelligence derived from the interception of enemy communications and noncommunication signals. A generic term that includes both COMINT and ELINT.

Signal-to-jamming ratio (S/J) - The ratio of the signal power to the jamming power or intentional interference at some point in the system. This ratio is often expressed in decibels.

Signal-to-noise ratio (S/N) - Ratio of the power of the signal to the power of the noise.

Signature - The set of parameters that describes the characteristics of a radar target or an RF emitter and distinguishes one emitter from another. Signature

parameters include the RF of the carrier, the modulation characteristics (typically the pulse modulation code), and the scan pattern.

Sine-wave modulated jamming - Jamming signal produced by modulating a CW signal with one or more sine waves.

Single beam blanking (SBB) - Used by phased array radars as an alternative method of Beam to Beam Correlation (BBC). It is effective, to some degree, against many multiple target generators and swept frequency jammers. Because of overlapping beamwidths, a target signal will appear in more than one beam as the beams are scanned past a true target. When jamming signals are transmitted along one beam, that beam is blanked by the radar receiver.

Skirt jamming - Jamming that places the signal somewhat off the radar center frequency but within the IF skirts. The technique will degrade the tracking accuracy of some monopulse radars; however, good radar design makes the technique ineffective.

Smart jamming - Selective jamming of threat radars with an optimized modulation signal at a correct time. Power management techniques are used to control smart jamming systems.

Smith modulation - Deceptive technique that operates on the servo loop of the victim's radar. Two RF carriers are transmitted with a few cycles difference.

Spiral scan - A pencil beam scan which moves around a central axis describing the surface of a cone in an ever-increasing cone size.

Spot jamming - Narrow frequency band jamming concentrated against radar at a particular frequency. The jamming bandwidth is comparable to the radar bandpass. Used to deny range and sometimes angle information.

Spread spectrum - Use of broader frequency bandwidths than normally required to transmit information, in order to gain advantages in interference rejection (anti-jam), message privacy/security, low probability of intercept (LPI), deny frequency resolution, multiplexing of more than one message in the same bandwidth, or high resolution range measurement.

Spurious radiation - Emissions from a radio transmitter at frequencies outside its assigned or intended emission frequency. Spurious emission includes harmonic emission, parasitic emission, and intermodulation products, but excludes emissions in the immediate vicinity of the necessary band that are a result of the modulation process for the transmission of information.

Spurious response –

1. Any response, other than the desired response, of an electric transducer or device.

2. A term used in electronic warfare to describe the undesirable signal images in the intercept receiver resulting from the mixing of the intercepted signal with harmonics of the local oscillators in the receiver.

Staggered PRF - A technique of using more than one PRF to reduce the blind speeds associated with MTI radars. PRF switching occurs on a pulse-to-pulse basis.

Stand-off jammer (SOJ) - A powerful jammer that remains at a safe range while providing jamming coverage (masking) for the attacking elements. The Navy EA-6B is an example of a SOJ aircraft.

Stand-off jamming (SOJ) - A jamming aircraft that orbits outside the maximum range of the SAM threat. As the attack package penetrates, the jamming aircraft directs jamming against all significant radars in the area.

Stream - Dispensing of chaff (solid/random interval/bursts).

Stream chaff - Operational technique of dropping large quantities of chaff for a continuous period of time. This results in a "ribbon" or "stream" of returns many miles in length on victim radar scopes. The penetrating attack package can then use the resulting chaff corridor to mask their penetration.

Super high frequency (SHF) - Frequencies from 3 to 30 GHz.

Support jamming - A tactic by which aircraft carrying electronic jamming equipment orbit at a safe distance from the enemy threat defenses or fly escort with the strike force for the primary purpose of screening them from the threat radars.

Suppression of enemy air defenses (SEAD) - That activity which neutralizes, destroys, or temporarily degrades enemy air defense systems in a specific area by using physical attack, deception, and/or electronic warfare.

Surface-to-air missile (SAM) - A missile launched from a surface launcher at a target above the surface.

Sweep jammer - Electronic jammer that sweeps a narrow band of electronic energy over a broad bandwidth.

Sweep lock-on jammer - A transmitter in which a narrowband jamming signal can be tuned over a broad frequency band and the signal locked on a particular frequency.

Swept audio - Jamming technique usually employed against conical scan-on-receive-only (COSRO) radars. The received pulses are amplified and retransmitted by the target and amplitude modulated at a frequency close to the suspected receiver antenna scan frequency.

Swept jamming - An EA technique of barrage jamming in which a CW carrier or noise source is swept over a selected bandwidth.

Swept-spot jamming - A jamming technique in which an oscillator is swept over a specific range of frequencies in the band of interest in order to be assured of exciting a receiver tuned to any frequency in that band.

Synchronized-pulse jamming - The technique of attempting to insert jamming pulses into a receiver each time the receiver gate opens.

Synchronous-pulsed jamming - A jamming technique that matches exactly the PRF of the victim's radar; then transmits multiples of the PRF. It is most effective if the jammer also matches the PW of the radar. Synchronous-pulsed jamming is easily recognized since the spacing between successive target lines is equal and each target line is the same in depth from the center outward. The width of the jammed sector is dependent upon the range of the jammer from the radar.

Synthetic aperture radar (SAR) - A high-resolution ground mapping technique in which advantage is taken of the forward motion of a coherent pulsed radar to synthesize the equivalent of a very long sidelooking array antenna from the radar returns received over a period of up to several seconds or more.

Target acquisition - The detection, identification, and location of a target in sufficient detail to permit the effective employment of weapons.

Terminal guidance –

1. The guidance applied to a guided missile between mid-course and arrival in the vicinity of the target.

2. Electronic, mechanical, visual, or other assistance given to aircraft pilots to facilitate arrival at, operation within or over, landing upon or departure from an air landing or air drop facility.

Terminal threat - The weapon systems, generally near a target, used to directly engage an aircraft in order to destroy it.

Terrain-avoidance radar - An airborne radar that provides a display of terrain ahead of low-flying aircraft to permit horizontal avoidance of obstacles.

Terrain-following radar (TFR) - An airborne radar that provides a display of terrain ahead of low-flying aircraft to permit manual control, or signals for automatic control to maintain constant altitude above the ground.

Thermal crossover - The natural phenomenon which normally occurs twice daily when temperature conditions are such that there is a loss of contrast between two adjacent objects on infrared imagery.

Threshold - The minimum value of a signal that can be detected by a system or sensor under consideration.

Time-of-arrival (TOA) - A method of locating a distant pulse emitter by measuring the difference in the time-of-arrival of its pulses at three separate locations. This method is also called Inverse LORAN.

Track –

1. **A series of related contacts displayed on a plotting board.**

2. **To display or record the successive positions of a moving object.**

3. **To lock onto a point of radiation and obtain guidance from it.**

4. To keep a gun properly aimed, or to continuously point a target-locating instrument at a moving target.

5. The actual path of an aircraft above, or a ship on, the surface of the earth. The course is the path that is planned; the track is the path that is taken.

Tracking - The continuous monitoring of range, velocity, or position of a target in space from a reference position. This is accomplished via radar and/or optical means.

Tracking radar - A radar that measures the range, azimuth, elevation, and/or velocity of the target and provides data that may be used by the fire control computer to determine the target path and predict its future position.

Track-on-jam - A method of passive target tracking using the jamming signal emitted by the target.

Track-while-scan (TWS) radar - Although it is not really a tracking radar in the true sense of the word, it does provide complete and accurate position information for missile guidance by using two separate beams produced by two separate antennas on two different frequencies. The system uses electronic computer techniques whereby raw data are used to track an assigned target, compute target velocity, and predict its future position while maintaining normal sector scan.

Transceiver - A combined radio transmitter and receiver in which some circuits other than those of the power supply are common to both transmitter and receiver, and not providing for simultaneous transmission and reception.

Transponder - A transmitter-receiver capable of accepting the electronic challenge of an interrogator and automatically transmitting an appropriate reply.

Traveling wave tube (TWT) - An electron tube in which a beam of electrons interacts continuously with a guided electromagnetic wave to produce amplification at microwave frequencies. A TWT capable of providing high amplification (60 dB) in frequencies over several octaves without adjustment. TWTs are classified by:

1. Power Output:

Low (less than one watt)
High (more than 10 watts)
Intermediate (one to 10 watts)

2. **Noise Characteristics:**

   Low (less than 20 dB)

3. **Operating Mode:**

   Pulse
   CW
   Dual Mode (pulse or CW)

4. **Method of Focusing:**

   PPM (periodic permanent magnet)
   Solenoid (single electromagnet)
   Coupled Cavity

5. **Terms associated with TWT operation:**

   a. **Gain Compression: Change in amplification a device provides as it operates near saturation.**

   b. **Overdrive: TWT is operating beyond the point of saturation.**

   c. **Saturation Gain: Ratio of output power to input power when the device is being driven at maximum output.**

   d. **Serrodyne: Linear translation of the phase of a signal on the helix of a TWT by a linear sawtooth waveform that enables the TWT to operate as a single sideband frequency translator.**

   e. **Small Signal Gain: Ratio of output power to input power when the TWT is operating linearly.**

Two-signal jamming (also called straddle jamming) - Jamming whereby two signals are transmitted on two RF frequencies slightly separated. Effective against certain types of radar where receiver bandwidth is narrow enough to defeat noise jamming.

Ultra high frequency (UHF) - Frequencies from 300 to 3,000 MHz.

Unit prefixes - Prefixes used to indicate scientific units:

Multiple	Prefix	Symbol
10^{12}	tera	T
10^{9}	giga	G
10^{6}	mega	M
10^{3}	kilo	k
10^{2}	hecto	h
10^{1}	deka	da
10^{-1}	deci	d
10^{-2}	centi	c
10^{-3}	milli	m
10^{-6}	micro	μ
10^{-9}	nano	n
10^{-12}	pico	p
10^{-15}	femto	f
10^{-18}	atto	a

Unmodulated CW jamming - The transmission of a high power carrier frequency that causes an overload effect to occur in the radar receiver. Used against bandpass radars that have a limited tuning capability. Unmodulated CW jamming can be identified by a blackening of the scope background (no video present) in a wedge-shaped sector, or by a solid brightening of a wedge or sector, normally exceeding one bandwidth.

Uplink - The missile guidance signal that passes command guidance intelligence from the site to the missile.

Velocity gate pull-off (VGPO) - Method of capturing the velocity gate of a Doppler radar and moving it away from the skin echo. Similar to the RGPO, but used against Doppler radar systems. The target Doppler frequency, which is amplified and retransmitted, is shifted in frequency to provide an apparent rate change or Doppler shift.

Very high frequency (VHF) - Frequencies from 30 to 300 MHz.

Very low frequency (VLF) - Frequencies from 3 to 30 kHz.

Video frequency –

1. A band of frequencies extending from approximately 100 Hz to several MHz.

2. The frequency of the voltage resulting from television scanning. Range from zero to 4 MHz or more.

Warning receiver - A receiver with the primary function of warning the user that his unit is being illuminated by an electromagnetic signal of interest.

Wideband constant false alarm rate receiver (WB-1) - Used against individual or combinations of rapidly swept FM-CW, noise, or CW jamming. This mode has nonlinear limiting and gives poor resolution of overlapping targets.

Window –

1. Strips of frequency-cut metal foil, wire, or bars that may be dropped from aircraft or missiles, or expelled from shells or rockets as a radar countermeasure. A confusion reflector.

2. A passive radar deception or confusion device; usually consisting of some metallic structure, designed in size and shape to effectively reflect impinging signals, to simulate a true target.

3. British name for chaff.

Wobbulation - A periodic and usually slow variation of a parameter (such as frequency, amplitude, or period) about a central value. A low frequency modulation of a jamming carrier that appears on a radar display as a "wobbling" target. This effect is an undesired result of an angle deception or time-varying barrage technique.

Wooden round - An ordnance round (shell, missile, etc.) requiring no maintenance or preparation time prior to loading for firing.

Kenneth Vito Zichi

3018 Moyer Road
Williamston, MI 48895-9566

The ABC's of Propagation

As children, a lot of us thought of radio as a "magic" box. Just by turning a switch, voices and music from across the city, or state, would come drifting into our room. By the time most of us discover shortwave, we've outgrown the idea that supernatural forces were at work in our radios. Still, we remain awestruck at the idea that someone in Australia or South Africa could whisper into a microphone and we could hear it half a world away.

This decidedly non-supernatural method by which radio waves travel from point "A" to point "B" is called *propagation*. It is a concept basic to all radio communications. And despite popular myth, you do not need a Ph.D in physics to understand it.

Radio is a form of "electromagnetic radiation." That is a fancy way of saying that radio waves have both electrical and magnetic properties. If they are energetic enough, they can leave the confines of a conductor and travel freely through the air, a vacuum (like outer space), or other similar media. In this way, radio waves act much like light, which is another form of electromagnetic radiation, albeit higher in frequency than radio. In fact, light provides a very good analogy for explaining how radio waves propagate.

Types of Propagation

Like light, radio waves can propagate (travel) in several different ways. We've sketched out some of the most common types of propagation, how they work and on what band(s) you're likely to encounter them.

GROUND WAVE

The most common and reliable way for radio waves to travel is called "ground wave." This is a form of propagation that is common to *all* radio bands from VLF (Very Low Frequency) to radar. Simply put, when a radio wave travels directly from the transmitting antenna to the receiving antenna without bending, reflecting, or otherwise being diverted, it is traveling by ground wave.

Using the light analogy, imagine a lighthouse shining in the distance. So long as there is nothing between you and the light -- and you are not so far away that the curvature of the earth would place the lighthouse below the horizon -- you can see it. (See figure one, wave A).

You can increase the distance you can see the lighthouse by elevating either yourself (a receiver) or the light (a transmitter), but once these variables are fixed, there is a finite distance at which the light will be visible because of the earth's curvature.

Reception distance is therefore limited when using this form of propagation. However, this limitation is offset by the fact that groundwave reception is very reliable. Some examples of transmissions using ground wave reception are local AM and FM broadcasters, police communications and CB radio.

IONOSPHERIC ("Skip")

Another very common form of propagation is ionospheric propagation, which is also known as "skip" or "skywave." This common phenomenon of long distance communications on frequencies between .5 and 30 MHz is the result of the bending of radio waves in the earth's *ionosphere*.

The ionosphere is several regions of charged oxygen (and other gases) located some 60 and 200 miles above the ground. These layers have a number of unique properties, not the least is their ability to *refract* radio waves that enter it back toward the earth's surface.

To use the light analogy again, it is as if someone placed a huge mirror in the sky, and radio waves, which would ordinarily shoot off into space, are re-directed back to the earth's surface. (See figure one, wave B.)

Actually, this analogy is not quite correct since the ionosphere *refracts* radio waves and a mirror *reflects* light. At any rate, if a radio wave of the right frequency enters the ionosphere, it will be bent back to earth. The result is reception of the signal hundreds of miles away from the

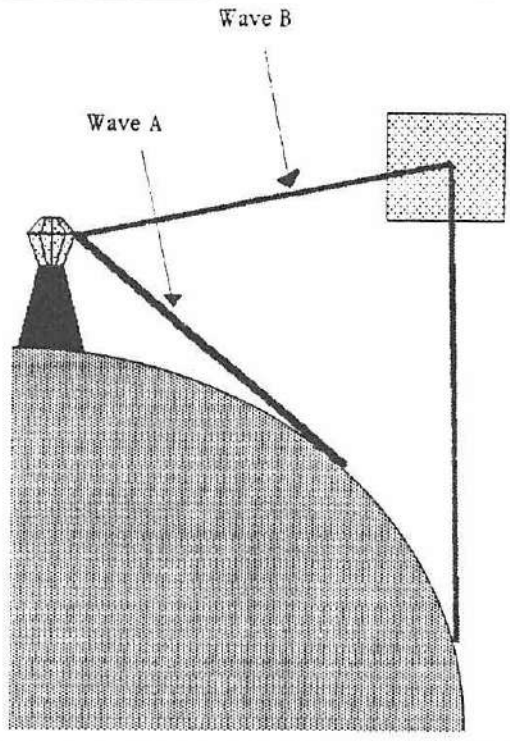

Figure One

Like the light from this lighthouse, radio waves travel only in straight lines. As a result of the curvature of the Earth, they can therefore only travel a finite distance (Wave "A").

Reception past the horizon can take place, but only if the radio waves are refracted or reflected off some surface, akin to someone in space holding amirror to allow you to see the lighthouse, as illustrated by wave "B."

Kenneth Vito Zichi

3018 Moyer Road
Williamston, MI 48895-9566

transmitter and well beyond the range possible by ground wave propagation.

Unfortunately, the ionosphere is also capable of absorbing or blocking reception of radio waves. Depending on the density of the ionosphere at a given time, the angle of the wave entering the ionosphere, and the frequency of the wave, long distance reception will be either enhanced or destroyed.

Too, the gap between where ground wave reception ends and the spot where the skywave signal hits the earth is also an area of non-reception. It is called the *skip zone* and the phenomenon is illustrated in figure two, with "S" denoting the skip zone.

Depending on the time of day and solar conditions (solar radiation is one of the major factors that cause gases in the upper atmosphere to ionize and form the ionosphere), different layers of ionized gas of varying intensity will be formed. Each layer affects radio waves slightly differently.

Lower frequency shortwave signals (eg. 2 through 9 MHz) will be absorbed if they pass through the ionosphere at low angles during the daylight hours. During this part of the day, there are more layers to the ionosphere and these layers are thicker. Thus, during the day, low frequencies do not propagate as well as higher frequencies (eg 11 through 25 MHz). Similarly, at night, the ionosphere is thinner and the low frequency waves are refracted without being absorbed. Then, the higher frequencies pass freely into space.

MULTI HOPS

Radio signals making the journey from transmitter to ionosphere to earth are said to have completed a "one hop" circuit. However, this is not necessarily the end of the trip. That same signal can be reflected from the earth, back up to the ionosphere once again, and down to earth, this time even further from the transmitter. If conditions are just right, a signal can go all the way around the world and double back on itself.

The "multi-hop" circuits do increase distances dramatically, but are less than single hops since they are subject to the uncertainties of the ionosphere more than once.

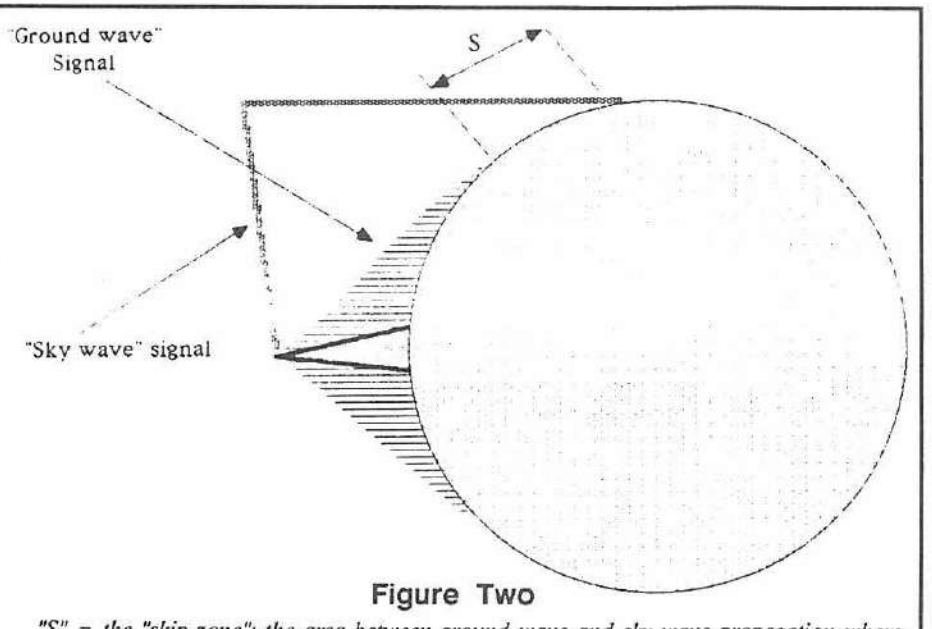

Figure Two

"S" = the "skip zone": the area between ground wave and sky wave propagation where reception of radio signals is difficult at best.

Drawing is not to scale! Actual distances for ground wave reception on the Earth would be about 300 km depending on effective height of transmitter and receiver antennae, not 1/4 of the planet's surface as indicated here!

EXOTIC STUFF

Lastly, there are numerous, less common ways that a radio wave can get from point A to point B.

One of these is called *sporadic E*. If it is sufficiently charged, the "E Layer" of the ionosphere is capable of refracting relatively high frequency radio waves. Occasionally, there will be "pockets" of highly charged particles within the E layer which allows for unusual reception.

This so called "sporadic E reception" is just that: sporadic. It is fairly common around local dusk and can boost reception of FM and TV signals well beyond their intended range. Sporadic E is also most common during the late spring and early summer in temperate latitudes but it is possible at any time of the year.

Moonbounce is a form of reception that's fascinating but rarely used now that man-made satellites populate the skies over planet earth. Pioneered by radio amateurs, it is a form of propagation in which signals are intentionally reflected off the moon's surface and back to earth.

Tropospheric Ducting is most common at relatively high frequencies and affects transmissions heard on FM, TV and scanners. It results when radio waves follow patterns of high and low pressure in the atmosphere (much the way weather patterns do). It allows for reception of signals slightly beyond the range you might otherwise expect.

Lastly, *Meteor Scatter* is probably one of the most unusual forms of propagation. Here, radio waves are bounced off the ionized trails of meteors. Like sporadic E reception, this results from a region of the atmosphere becomming supercharged, and thus refracting higher frequencies than normal back to earth. Reception of VHF signals using metero scatter can be very brief -- lasting in the order of seconds.

In short, there are a plethora of exotic reception techniques, but the ones outlined in the first part of this article are the ones you are most likely to run into, and should aid you in planning your listening to best enjoy the hobby.

■

2€

Wire Antennas that WORK!

A collection of details and descriptions of antennas
based on Spiderbeam fiberglass poles,
as described in greater detail on DJ0IP's Web Page:
WWW.DJ0IP.DE

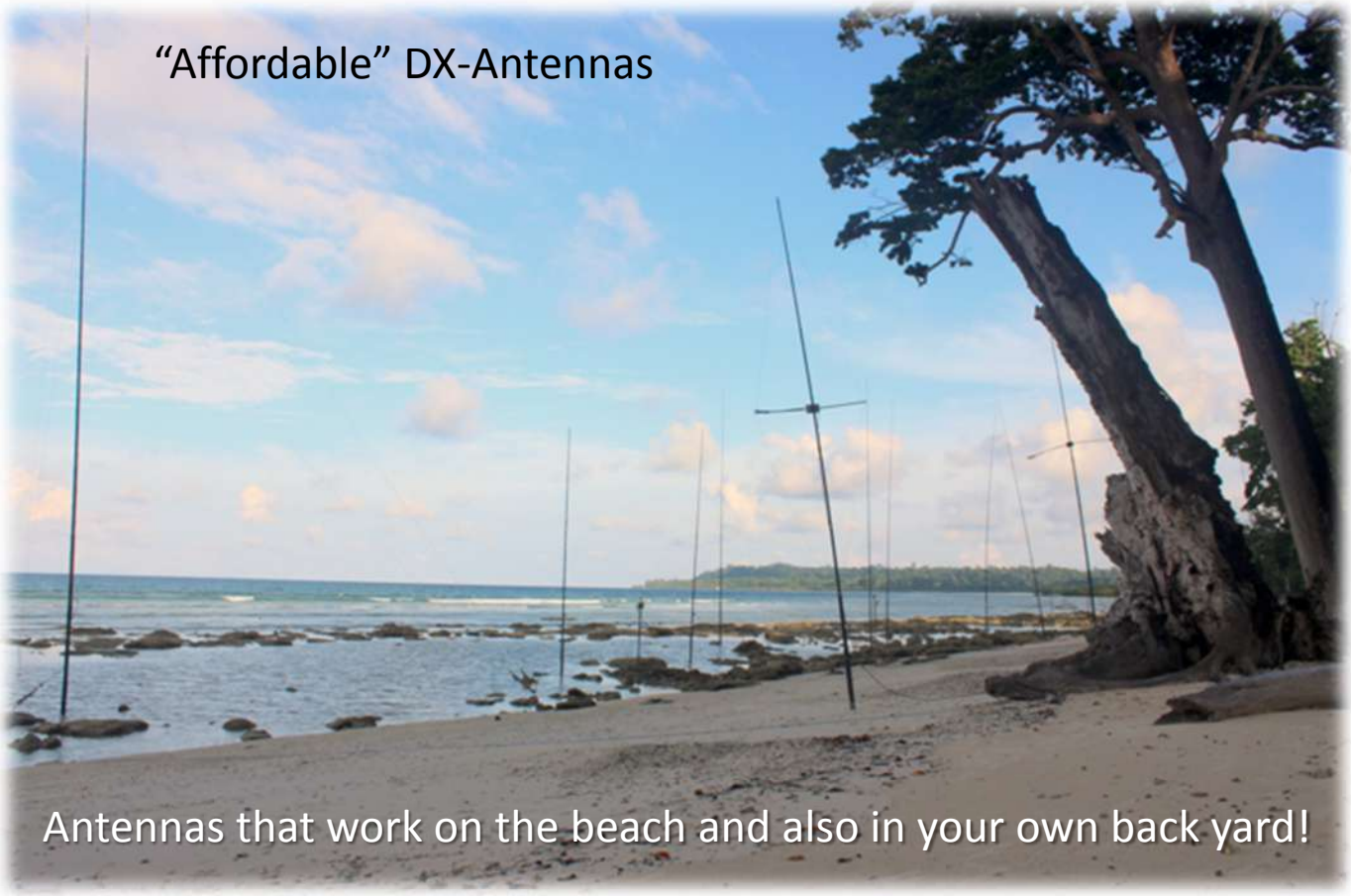

The antennas described in this booklet were designed to be efficient, yet simple enough for the average ham to build, using common hand tools. Several of these antennas are used regularly by DX-peditions to all corners of the world. All of these antennas have been built and tested by at least one of the Spiderbeam Team members: DF4SA / DF9GR / DJ0IP / DL9USA / DO5PNS / W4PA.

spiderbeam
high performance lightweight antennas

First Edition, June 2016 - © Spiderbeam GmbH

spiderbeam
high performance lightweight antennas

40m Vertical on 12m Pole
(Ground Radials)

Notes:

- Radials should be 6 to 10m long.
- It works great with just 8 radials.
- 16 or more radials is a little better.
- Space radials symmetrically around the pole.

Optional RF-Choke

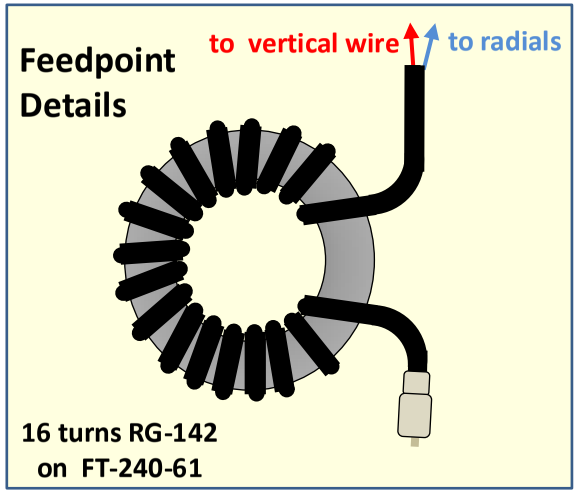

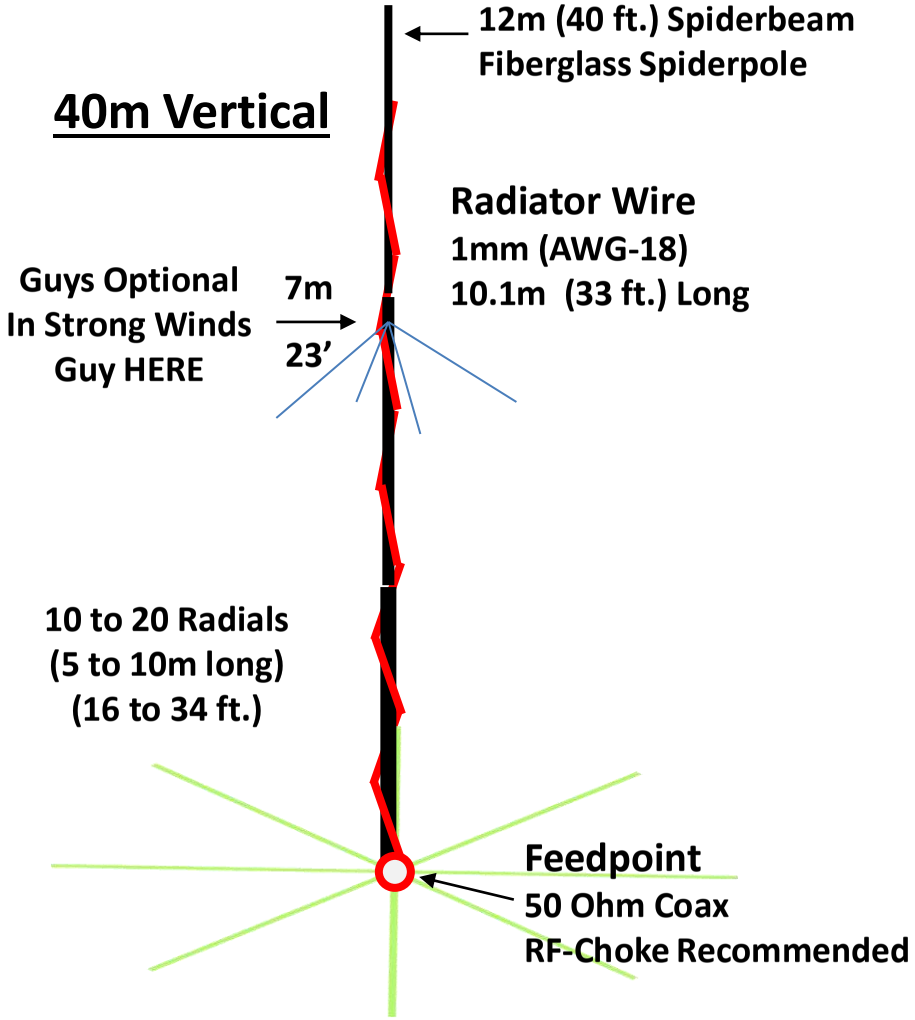

http://www.DJ0IP.de/vertical-antennas/

80m Vertical Antenna

On a Spiderbeam 12m HD Fiberglass Spiderpole

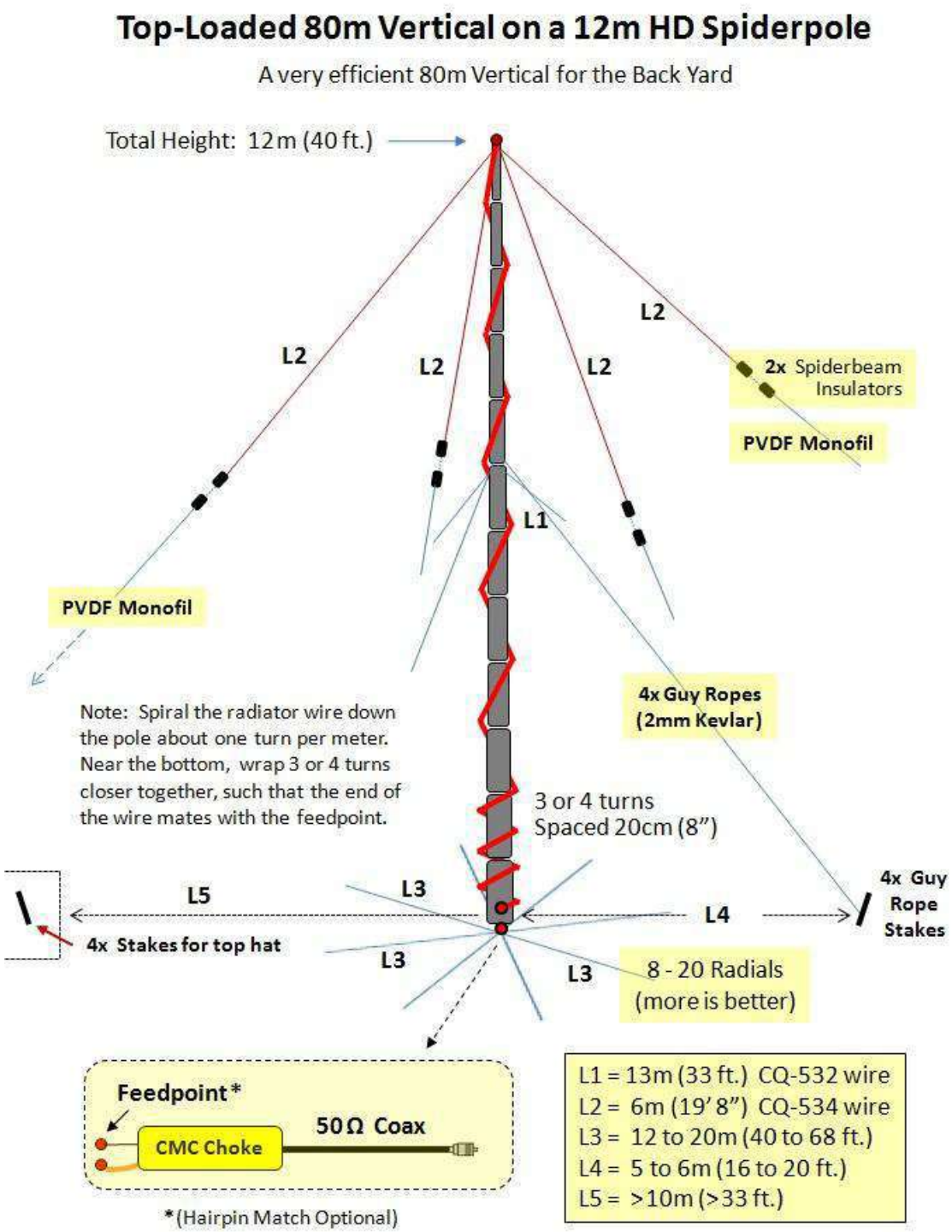

160m Inv-L on 12m Spiderpole

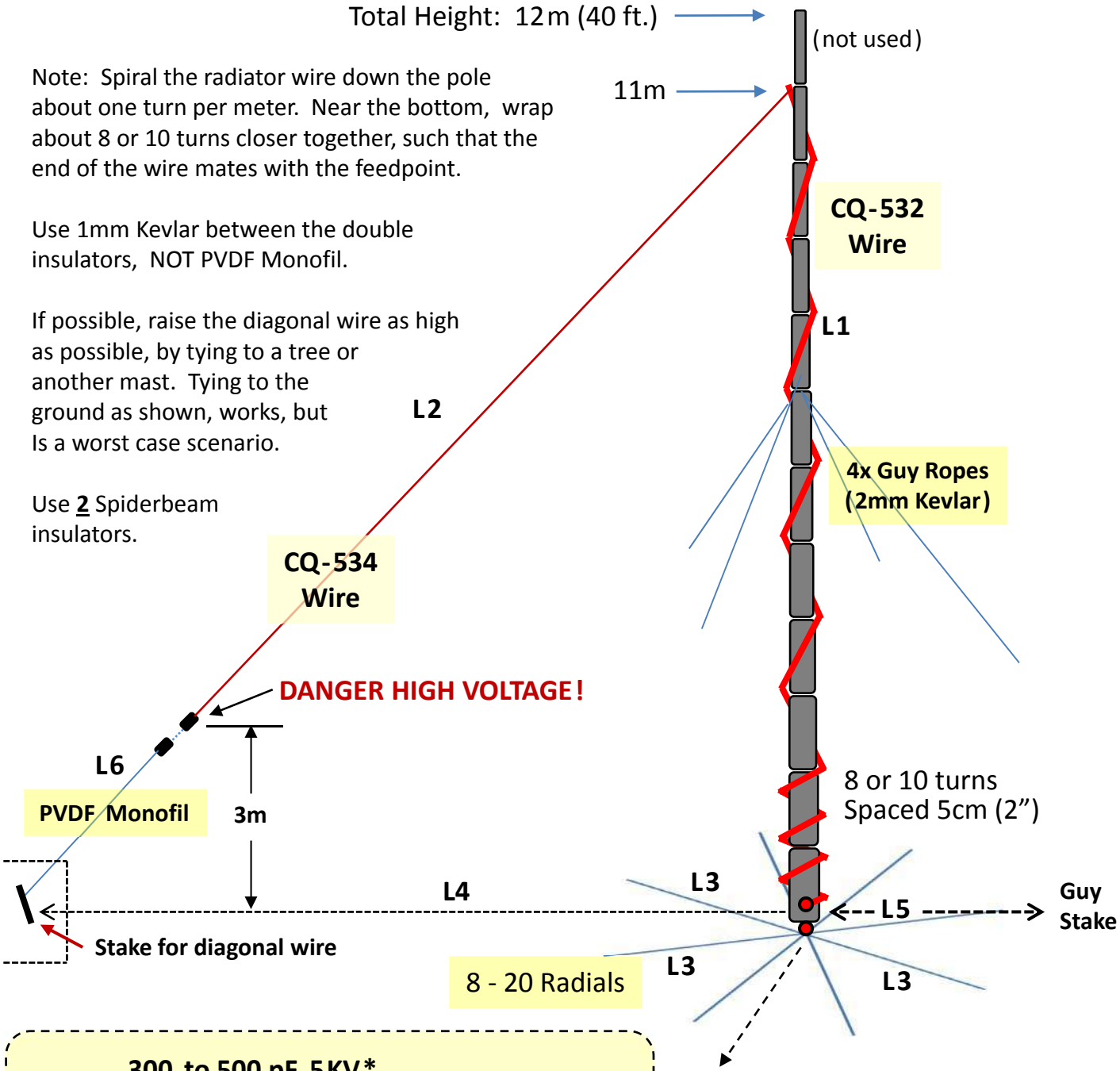

Note: Spiral the radiator wire down the pole about one turn per meter. Near the bottom, wrap about 8 or 10 turns closer together, such that the end of the wire mates with the feedpoint.

Use 1mm Kevlar between the double insulators, NOT PVDF Monofil.

If possible, raise the diagonal wire as high as possible, by tying to a tree or another mast. Tying to the ground as shown, works, but Is a worst case scenario.

Use **2** Spiderbeam insulators.

L1 = 13m (43 ft.) CQ-532 wire
L2 = 35m (115') CQ-534 wire[1]
L3 = 12 to 20m (40 to 66 ft.)
L4 = 35 to 50m (115 to 165 ft.)[2]
L5 = >10m (>33 ft.)
L6 = depends on stake[3]

*Not critical. Wire length will be adjusted for resonance.

[1] Adjust length for resonance.
[2] Adjust such that end of L2 is at least 3m high.
[3] Adjust as necessary.

DJ0IP

spiderbeam
high performance lightweight antennas

80m Vertical

using the **18m**
Fiberglass Pole

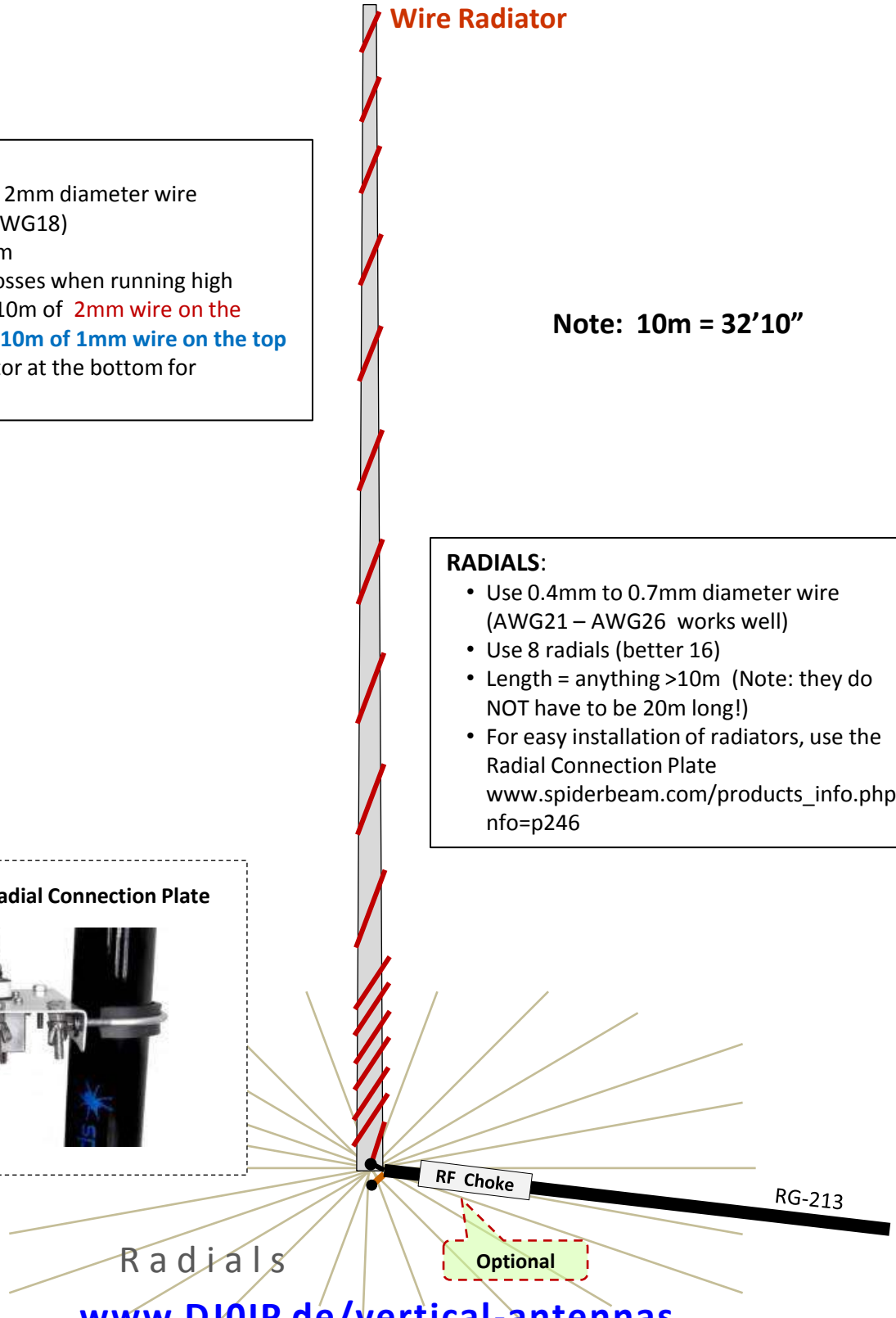

RADIATOR:

- Use 1mm to 2mm diameter wire (AWG12 – AWG18)
- Length = 20m
- For lowest losses when running high power, use 10m of 2mm wire on the bottom and **10m of 1mm wire on the top**
- Prune radiator at the bottom for resonance

Note: 10m = 32'10"

RADIALS:

- Use 0.4mm to 0.7mm diameter wire (AWG21 – AWG26 works well)
- Use 8 radials (better 16)
- Length = anything >10m (Note: they do NOT have to be 20m long!)
- For easy installation of radiators, use the Radial Connection Plate www.spiderbeam.com/products_info.php?info=p246

Optional Radial Connection Plate

www.DJ0IP.de/vertical-antennas

160 M Top-Loaded Spiderbeam Vertical on 18m Spiderbeam Pole

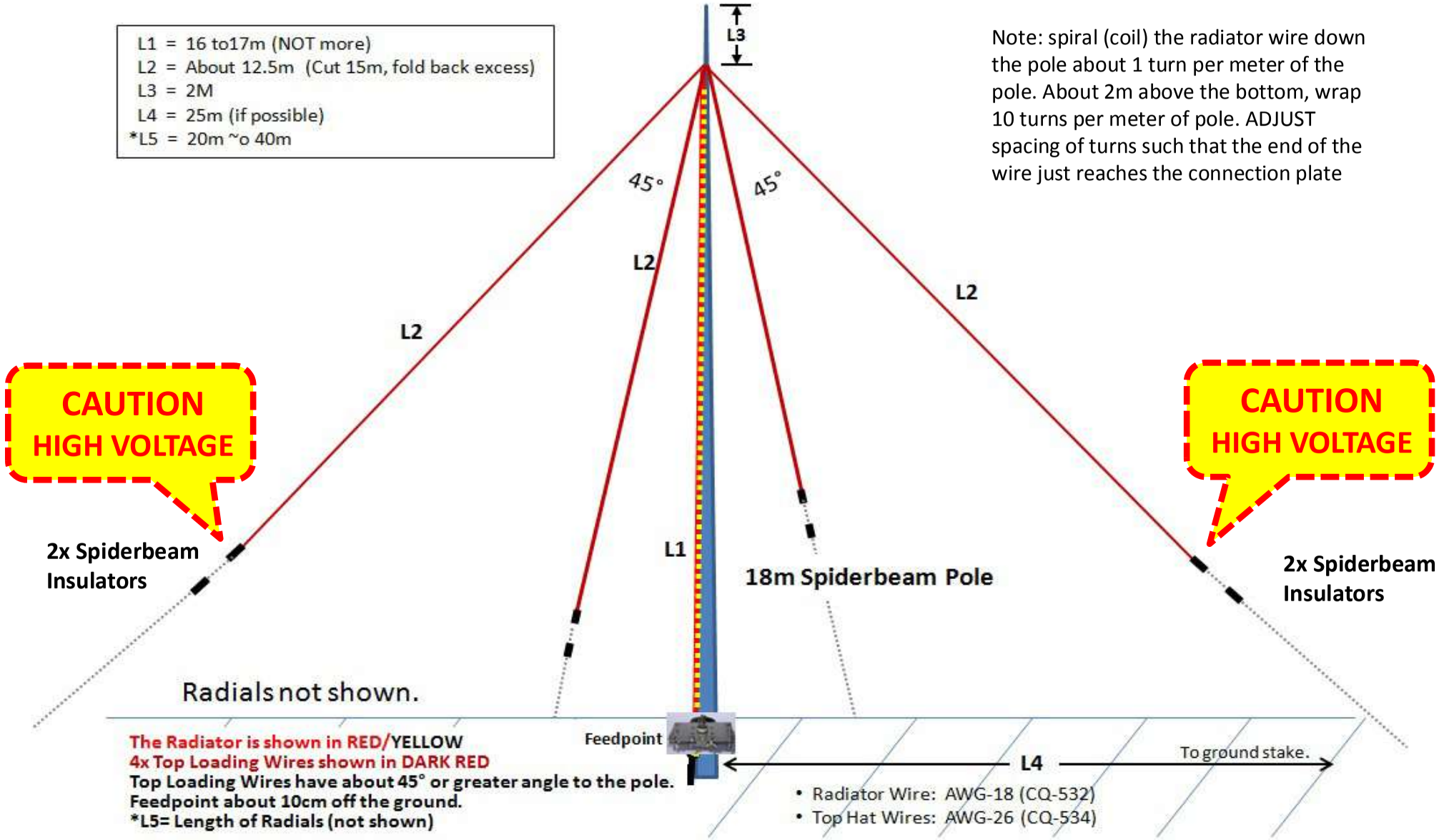

Note: spiral (coil) the radiator wire down the pole about 1 turn per meter of the pole. About 2m above the bottom, wrap 10 turns per meter of pole. ADJUST spacing of turns such that the end of the wire just reaches the connection plate

Start with L1 = 18m and trim to adjust frequency.

spiderbeam
high performance lightweight antennas

Simple 160m Inverted-L Antenna

on an 18m Spiderbeam Fiberglass Pole

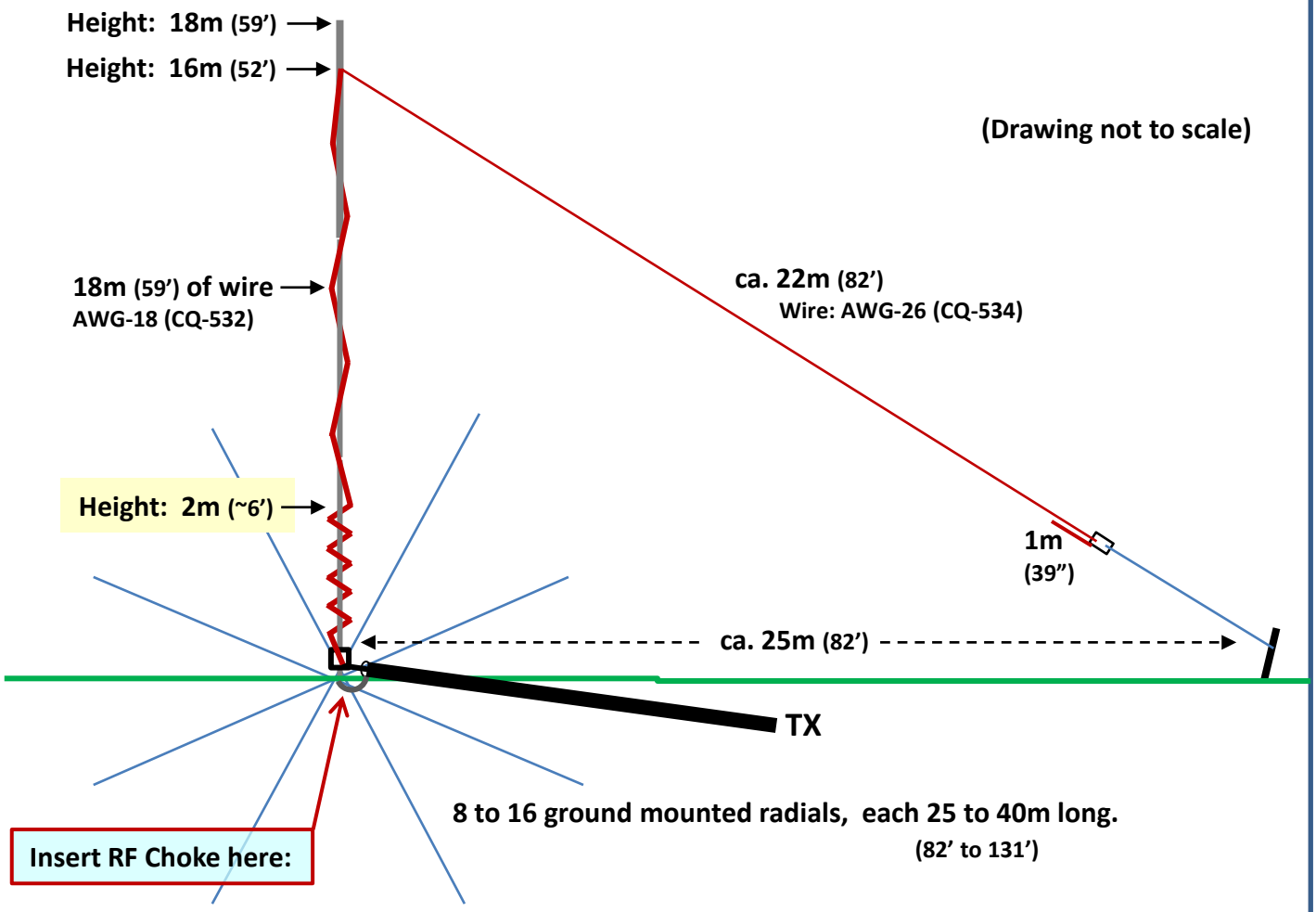

Antenna Details: http://www.dj0ip.de/vertical-antennas/

Choke Details: http://www.dj0ip.de/vertical-antennas/rf-cmc-choke/

Feedpoint Details

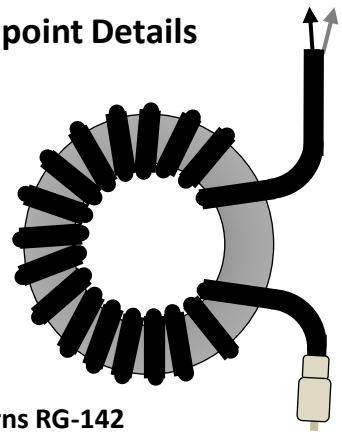

17 turns RG-142
on FT-240-43 (2x Cores for 1KW)

www.DJ0IP.de → and click on:

- Antennas
- Vertical-Antennas
  - "Inverted-L-Ant"
  (or)
  - "RF (CMC) Choke"

160m Vertical
on a Spiderbeam
26m Fiberglass Pole

Note: drawing not to scale !

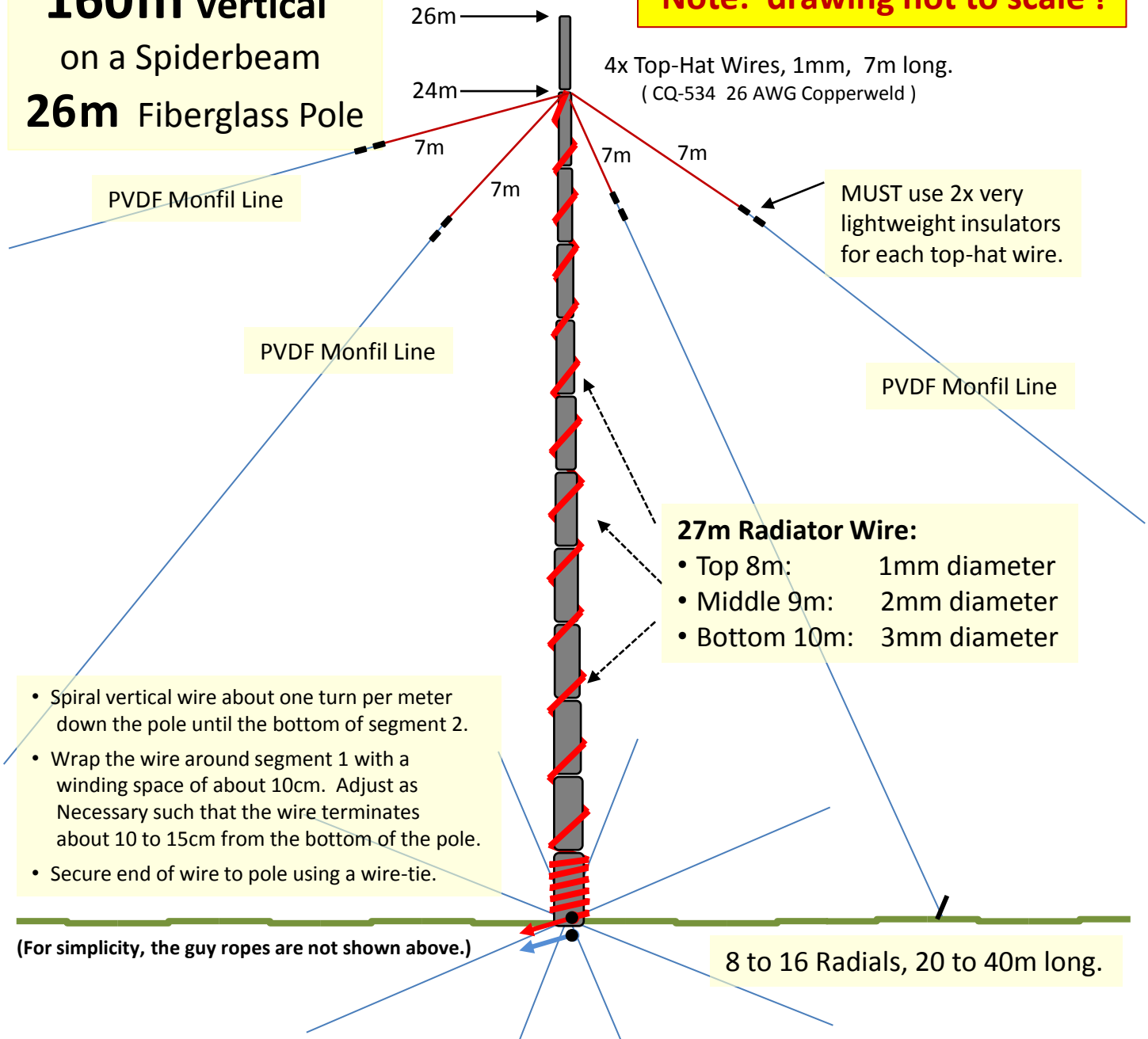

Feedpoint Details

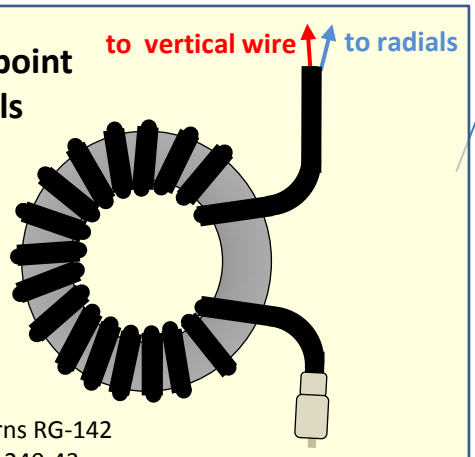

17 turns RG-142
on FT-240-43

Guying Info

- **4 levels**
- **4 directions**

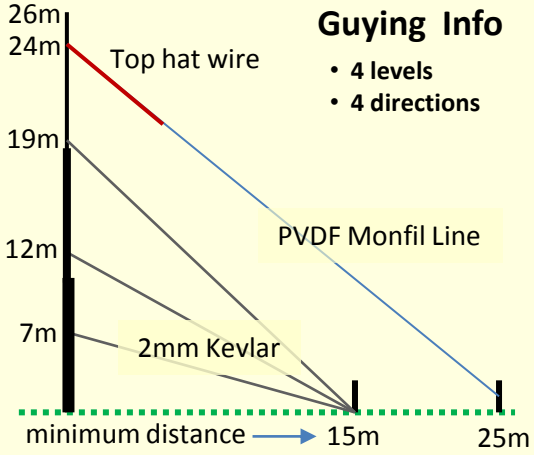

DUAL – BAND VERTICAL
80m / 40m

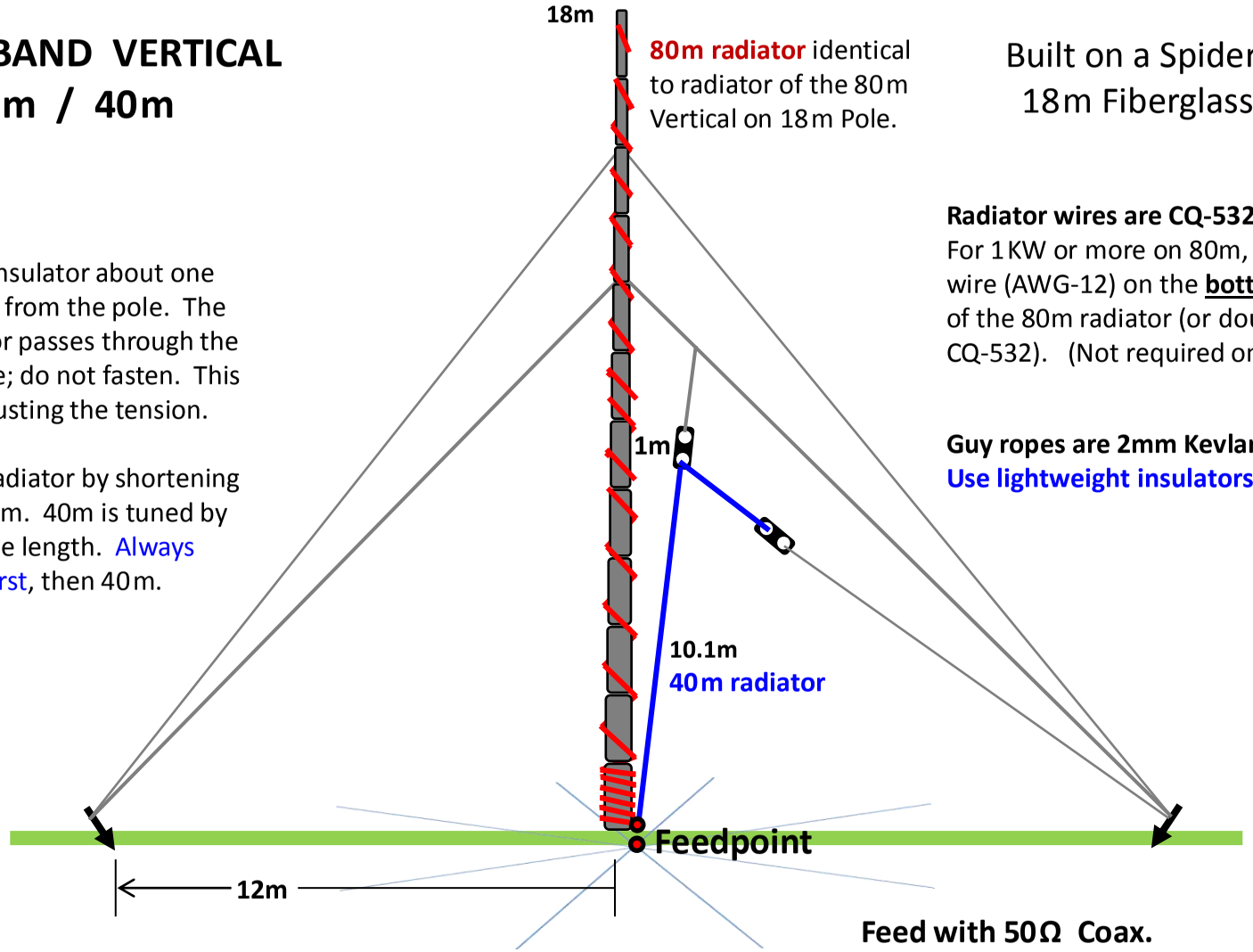

80m radiator identical to radiator of the 80m Vertical on 18m Pole.

Built on a Spiderbeam 18m Fiberglass Pole

Space first insulator about one meter away from the pole. The 40m radiator passes through the Bottom hole; do not fasten. This enables adjusting the tension.

Tune 80m radiator by shortening at the bottom. 40m is tuned by Adjusting the length. Always tune 80m first, then 40m.

Radiator wires are CQ-532 (AWG-18).
For 1KW or more on 80m, use 2mm wire (AWG-12) on the **bottom half** of the 80m radiator (or double the CQ-532). (Not required on 40m).

Guy ropes are 2mm Kevlar.
Use lightweight insulators!

Ground radials are required.

Use 8 to 16 ground radials (or more), 12 to 20m long. Space radials symmetrically around the pole.

Feed with 50Ω Coax.
Use optional CMC Choke (preferred).
Feedpoint ~5-10cm above ground.

info@spiderbeam.com

160m / 80m Dual-Band Vertical on Spiderbeam 18m Pole

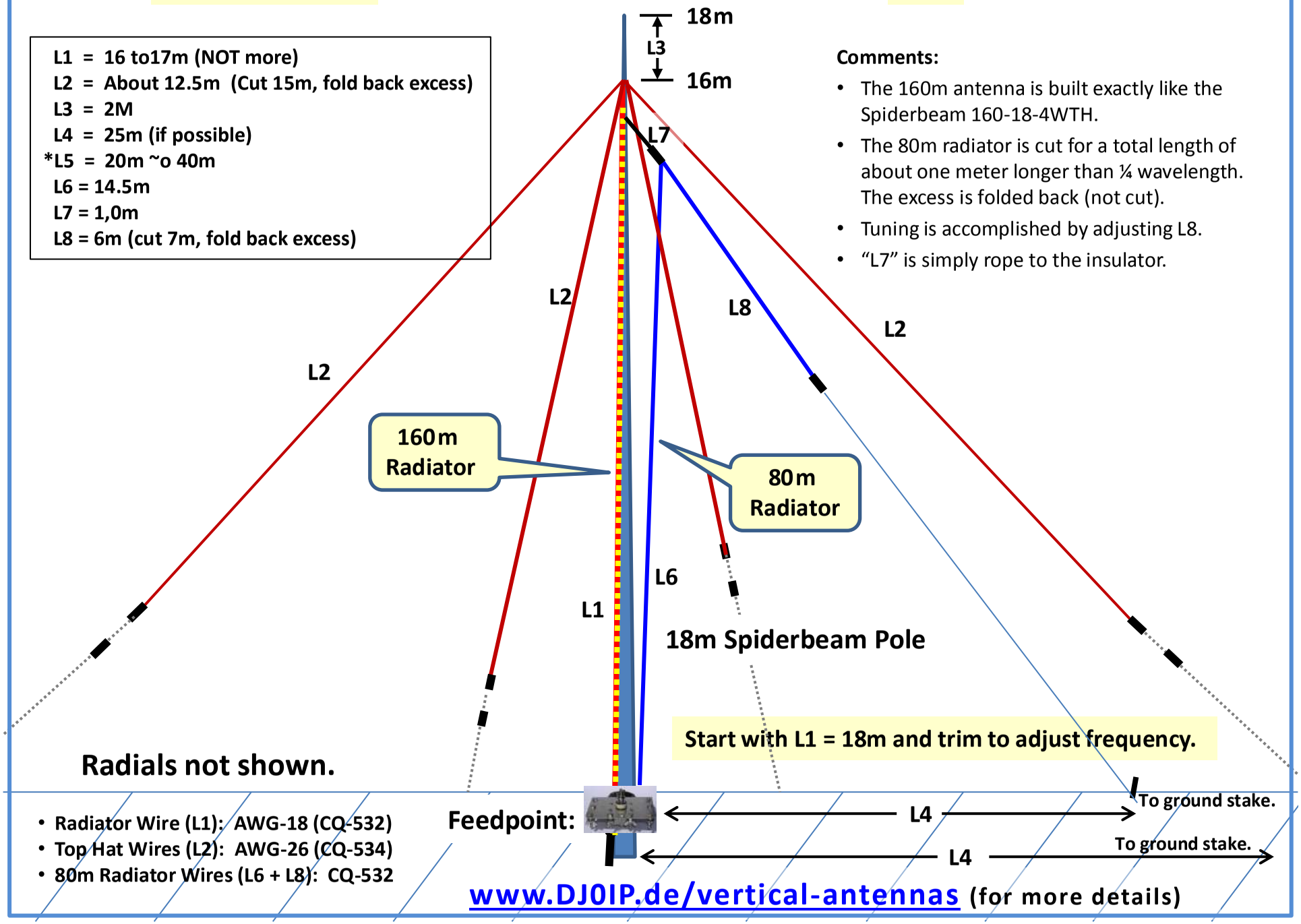

Comments:

- The 160m antenna is built exactly like the Spiderbeam 160-18-4WTH.
- The 80m radiator is cut for a total length of about one meter longer than ¼ wavelength. The excess is folded back (not cut).
- Tuning is accomplished by adjusting L8.
- "L7" is simply rope to the insulator.

- Radiator Wire (L1): AWG-18 (CQ-532)
- Top Hat Wires (L2): AWG-26 (CQ-534)
- 80m Radiator Wires (L6 + L8): CQ-532

www.DJ0IP.de/vertical-antennas (for more details)

Feeding Low Band Verticals

(Especially 160m)

Common Mode Current Choke

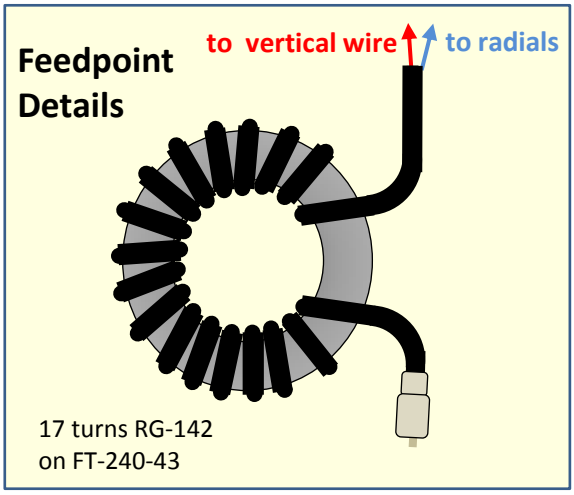

The choke is placed at the feedpoint of the Vertical. The drawing above shows how you can simply wrap coax on the toroid. Use RG-58 for a few hundred watts. For 1 KW use RG-142 (Teflon Coax). For 1.5 KW use 2x Toroids glued together. On the right you see a choke/balun usable for 40m and above. My choke looks similar to this, but has more windings in order to cover 160m. It is not necessary to cross-wind the coax, but sometimes it is more convenient.

A Hairpin Match (Shunt Match)

I've used the shunt match for nearly 50 years. It is a cheap and simple means of raising the feedpoint impedance from a low value (i.e. ~10Ω) to something closer to 50Ω. This is a great way to improve a low band vertical's match. Use thick soft-drawn copper wire or thin copper tubing. I wound about 10 turns onto a wine bottle. Tune by pushing the turns closer together or pulling them farther apart. My choke and Hairpin Match are shown on the right. (DJØIP)

spiderbeam
high performance lightweight antennas

HAIRPIN MATCH

(Shunt Match)

A quick and easy way to obtain a better SWR for short low-band Vertical Antennas.

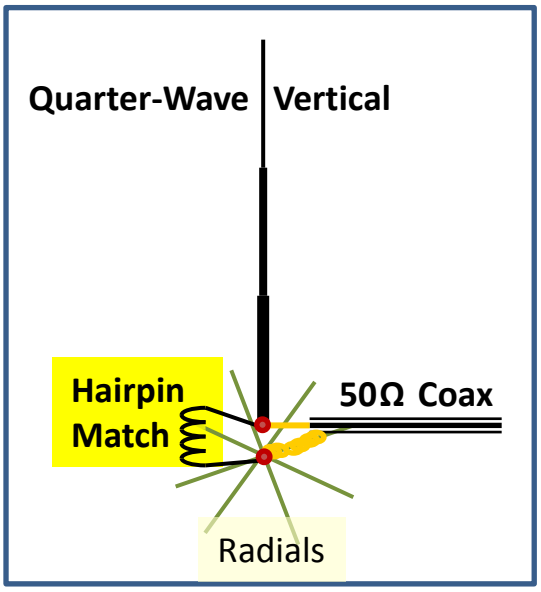

Wind thick wire or thin copper tubing
On a round object, such as a glass jar:

The Coil:

TUNING:

- Measure and record the SWR.
- Push the turns of the coil closer together and see if the SWR improves or gets worse.
- Pull the turns farther apart and check if the SWR gets worse or improves.
- Adjust for best SWR.
- Note: if spread too far apart and still not perfect, remove 1 or 2 windings from the coil.
- Note: if squeezed tightly together and still not perfect, add 1 or 2 windings to the coil.

http://www.DJ0IP.de/vertical-antennas/hairpin-match/

Multi-Band HF Vertical Dipole

On a Spiderbeam 12m HD Telescoping Fiberglass Pole

for: 80/40/30/20/17/15/12/10m

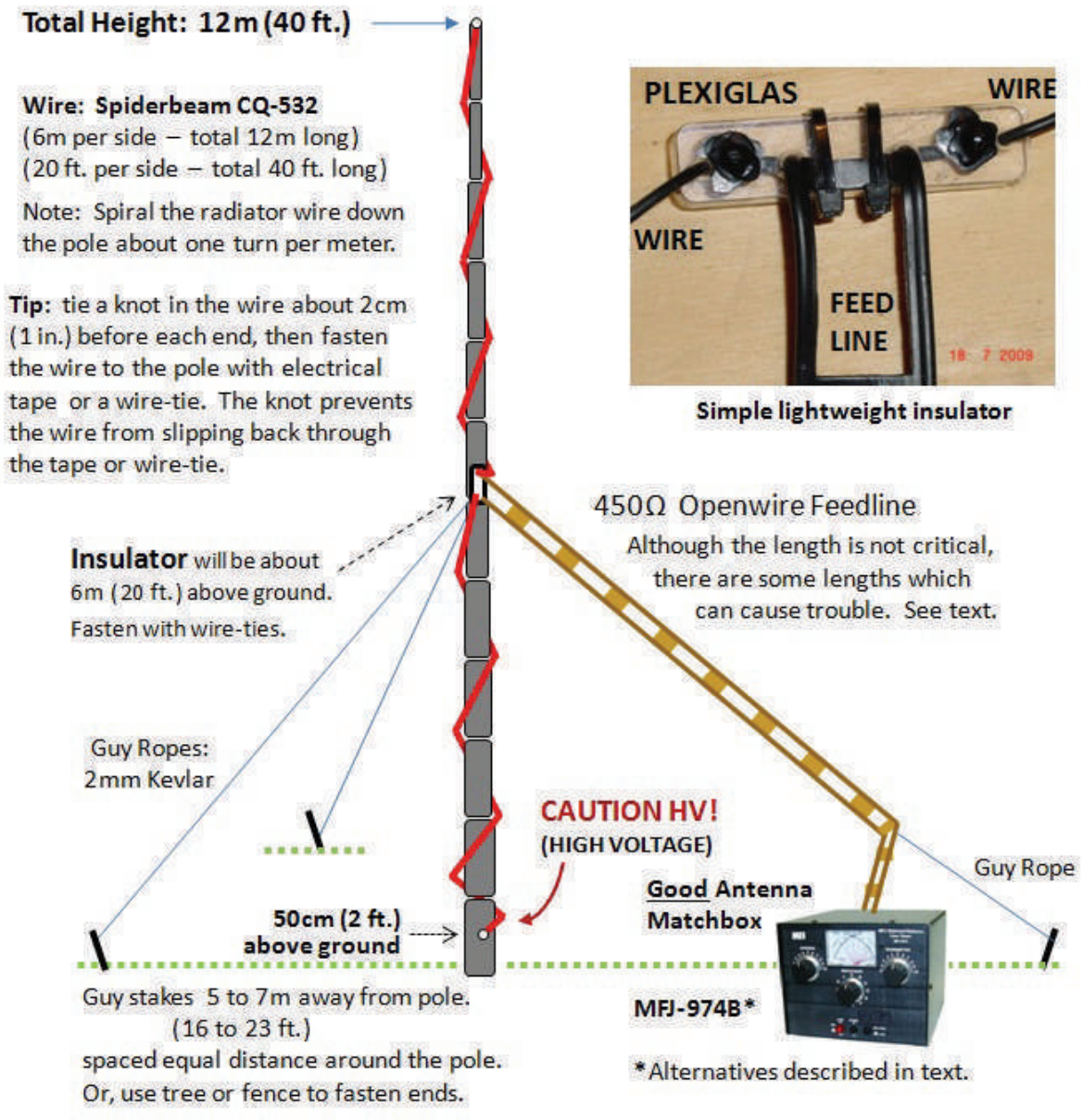

Spiraling the wire down the pole distributes its weight evenly around the pole and prevents it from flopping in the wind. Since the lower half of the pole is thicker (wider) than the upper half, the wire will end about 50cm above the ground.

IT IS IMPORTANT TO KEEP THE WIRE THIS DISTANCE FROM THE GROUND!

Spiderbeam 3 – Band Single-Loop Portable Quad

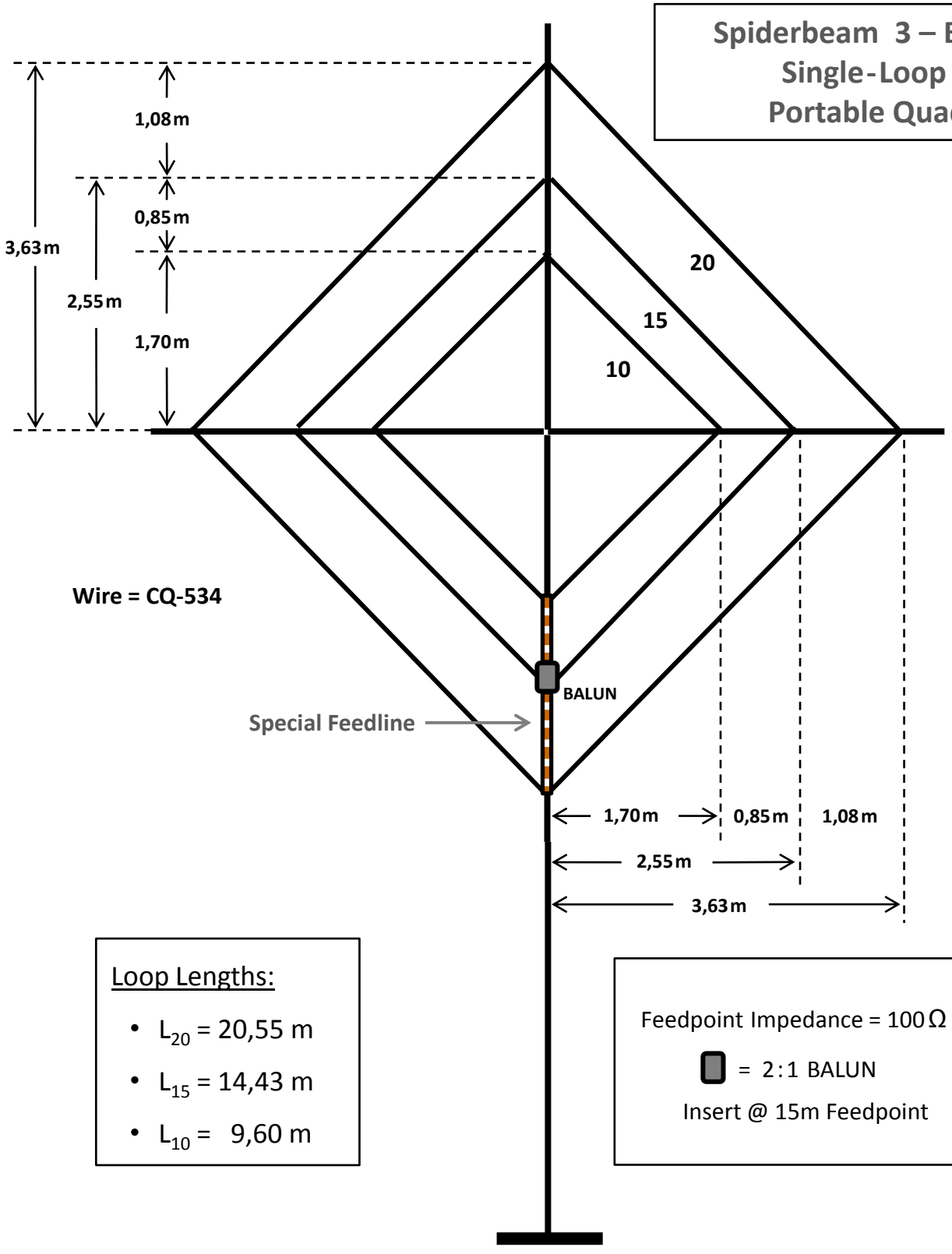

Loop Lengths:

- L_{20} = 20,55 m
- L_{15} = 14,43 m
- L_{10} = 9,60 m

Feedpoint Impedance = 100 Ω

= 2:1 BALUN

Insert @ 15m Feedpoint

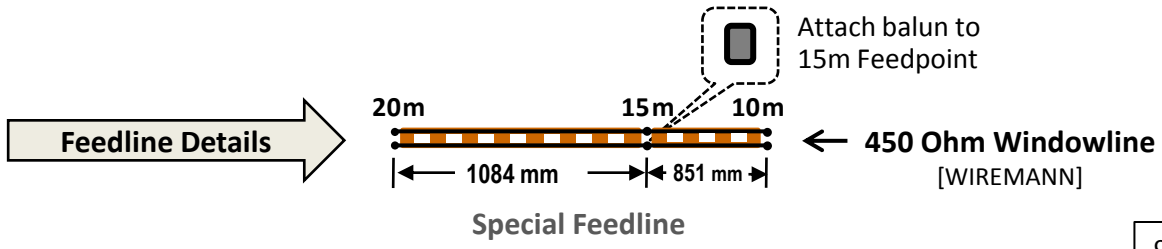

Special Feedline

9/07/2012

Mono – Loop Quad

A Vertically Oriented, Horizontally Polarized Loop

7 – Band Portable Antenna

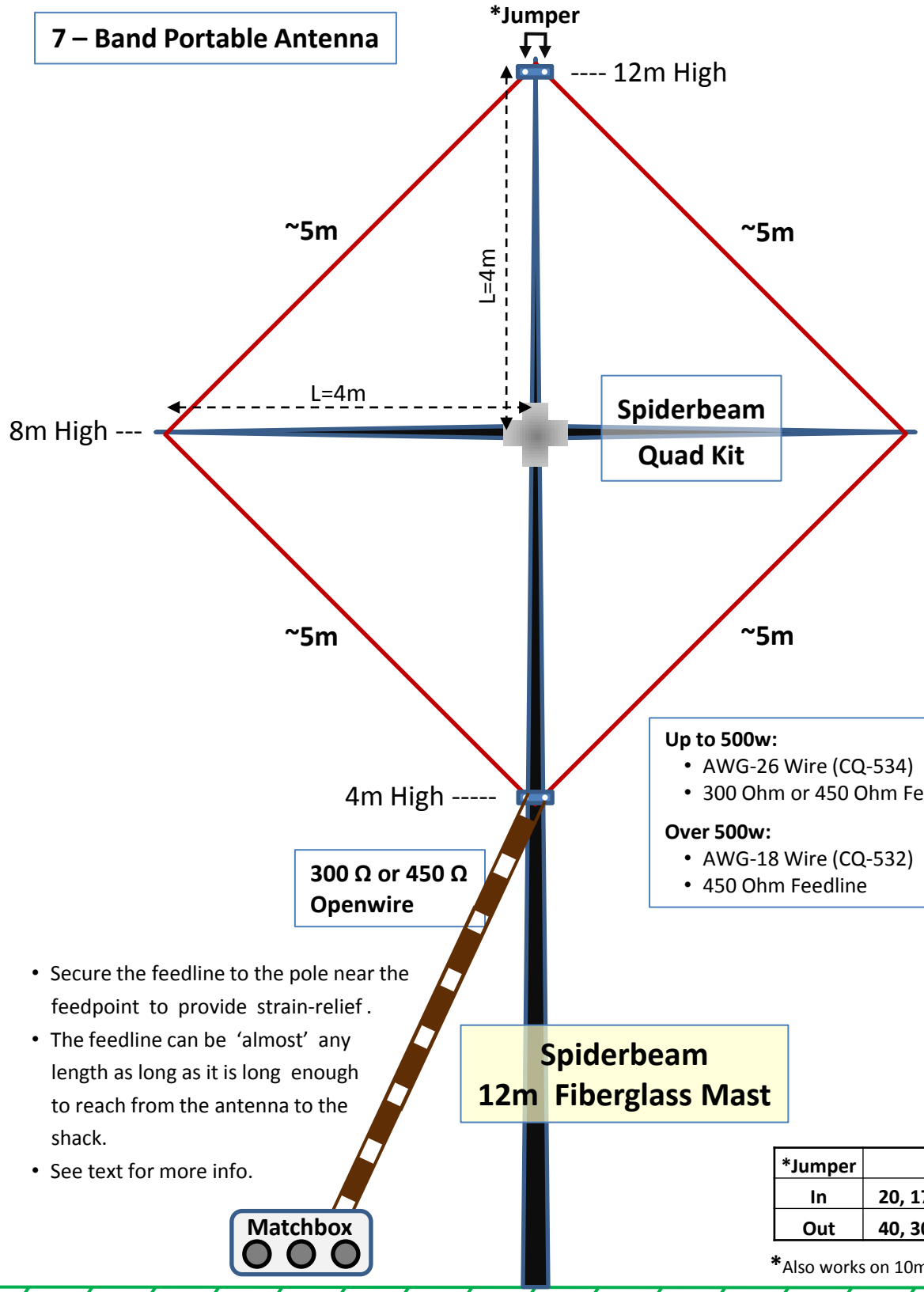

Up to 500w:

- AWG-26 Wire (CQ-534)
- 300 Ohm or 450 Ohm Feedline

Over 500w:

- AWG-18 Wire (CQ-532)
- 450 Ohm Feedline

- Secure the feedline to the pole near the feedpoint to provide strain-relief.
- The feedline can be 'almost' any length as long as it is long enough to reach from the antenna to the shack.
- See text for more info.

*Jumper	Band
In	20, 17, 15, 12m
Out	40, 30, 10*m

*Also works on 10m with jumper "in"

NOTE: Use Symmetrical Matchbox or Asymmetrical Matchbox with 1:1 or 4:1 Current Balun.

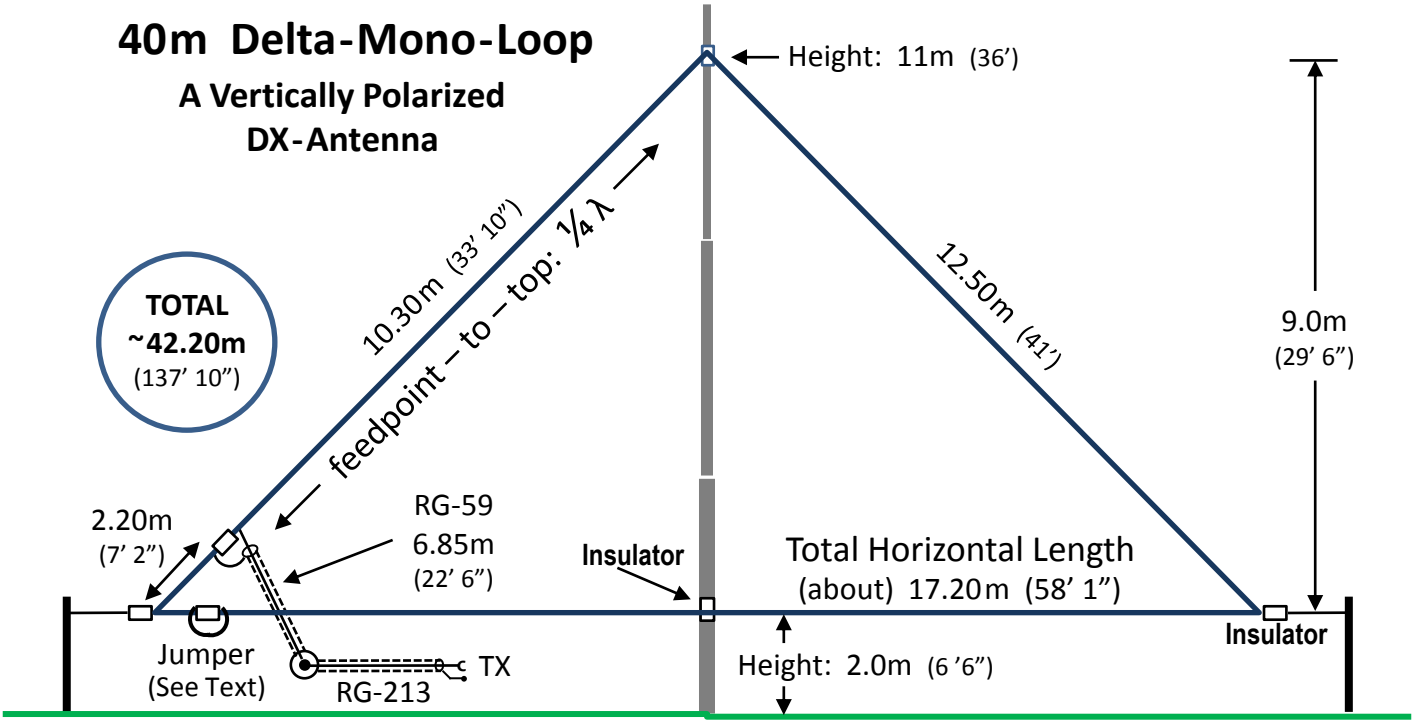

DESCRIPTION:

A **vertically polarized** full wavelength loop, with more or less **Omni-directional** radiation (due to the low height, requiring **NO RADIALS**. NOTE: though good for DX, stations within 500 miles may be stronger on a simple dipole.

CONSTRUCTION DETAILS:

- The pole should be about 12m high (minimum 11m). (39'4" to 36'). Higher is better, but then you will have to re-adjust the total length for resonance.
- The feedpoint is located in either diagonal side near one corner of the antenna, enabling vertical polarization. This makes the antenna an excellent DX antenna.
- The length of the diagonal is not very critical and may be adjusted to help find a better fit in the space available, but the distance from the feedpoint to the top should be **one quarter wavelength**.
- The exact total length will vary depending on ground conditions at your QTH. Begin with 42.7m (137' 10") and then shorten the horizontal leg to bring the resonance up to the desired frequency.
- Adjust total length by adjusting the length of the horizontal wire. (Easiest way).
- The horizontal leg of the antenna on the bottom should be 2 to 3m high (6'6" to 9'10") high enough for humans and animals to walk under. Changes to the height will require adjusting overall length.
- The insulator shown directly on the pole at the 2m level is for mechanical reasons. Secure the insulator to the pole, and then pass the horizontal leg through the insulator, reducing sag in the horizontal leg.
- The insulator in the horizontal leg near the left is an option for convenience. It enables easy adjustment for resonance by removing or adding wire. For disassembly, disconnect one side from the insulator and then roll the antenna as a single wire. Each time I changed my QTH, I had to re-adjust the length of the jumper. I just let the jumper wire hang down. For permanent use, you may leave this out.
- The antenna will have an impedance between 90Ω and 100Ω. A quarter wavelength matching stub of 75 Ohm coax will provide a good match to 50Ω. RG-59 is good enough for about 500w. If you want to run more power, use RG-11.

DJ0IP; Original source: CQDL article by DL1BU, April, 1979, page 154.

Donald Lee Smith

Don Smith is elderly and has suffered several serious strokes in the last few years. He is no longer able to respond to e-mails and his web site has been taken over by people who appear very keen to ensure that his work and information can no longer be accessed by members of the public.

At this point in time there is very little information available on Don's achievements. What I have been able to locate is four video recordings of lectures which he gave, plus a copy of his pdf document entitled "Resonance Energy Systems". There is also a web site with limited information. This site appears to have been set up by Don's son whom I suspect does not fully understand how his father's devices work. Don has produced at least forty eight different devices which draw energy from what Don prefers to call "the ambient background". His devices are capable of supplying kilowatts of excess energy and in most cases they do not require any input energy to be supplied by the user.

It is said that 40,000 copies of Don's pdf document have been sold worldwide, but it appears that it is no longer possible to buy a copy, and for that reason, a copy is contained within this document. Please be aware that Don states quite openly that he does not disclose all of the details on any of his devices in his public discussions. This is because the rights to each device have been assigned to a different company in which Don has a financial interest, and so it is not in his interests to disclose the full details. However, ha says that he discloses enough for somebody who is experienced in radio-frequency electronics to be able to deduce the things which he does not disclose and so build a device for his own use. If that is the case, then anybody who has succeeded in doing so has kept very quiet about it afterwards (which is understandable). Having said that, Tariel Kapanadze of Georgia appears to have replicated one of the designs although it is quite likely that Tariel deduced the operating principles for himself. These principles are clearly based on the work of Nikola Tesla.

In Don's work, he refers to the educational kit entitled "Resonant Circuits" No 10 - 416 from The Science Source at www.thesciencesiource.com. That kit now costs US$100 and they don't mention the fact that you need a signal generator capable of producing a 10 volt output at up to 1 MHz in order to be able to do resonance tests, and the kit now uses an LED rather than a neon bulb.

There is a "book" of Don's entitled "An Answer to America's Energy Deficit" but, being an earlier work than his pdf document, it does not appear to contain anything extra of any significance. Here is Don's pdf document, in it's original American-language wording with just minor clerical corrections:

RESONANCE ENERGY METHODS

Donald L. Smith
TransWorld Energy, CEO
September 23, 2002

Fax/Phone 281-370-4547 and e-mail donsm1@earthlink.net

DANGER
HIGH VOLTAGE

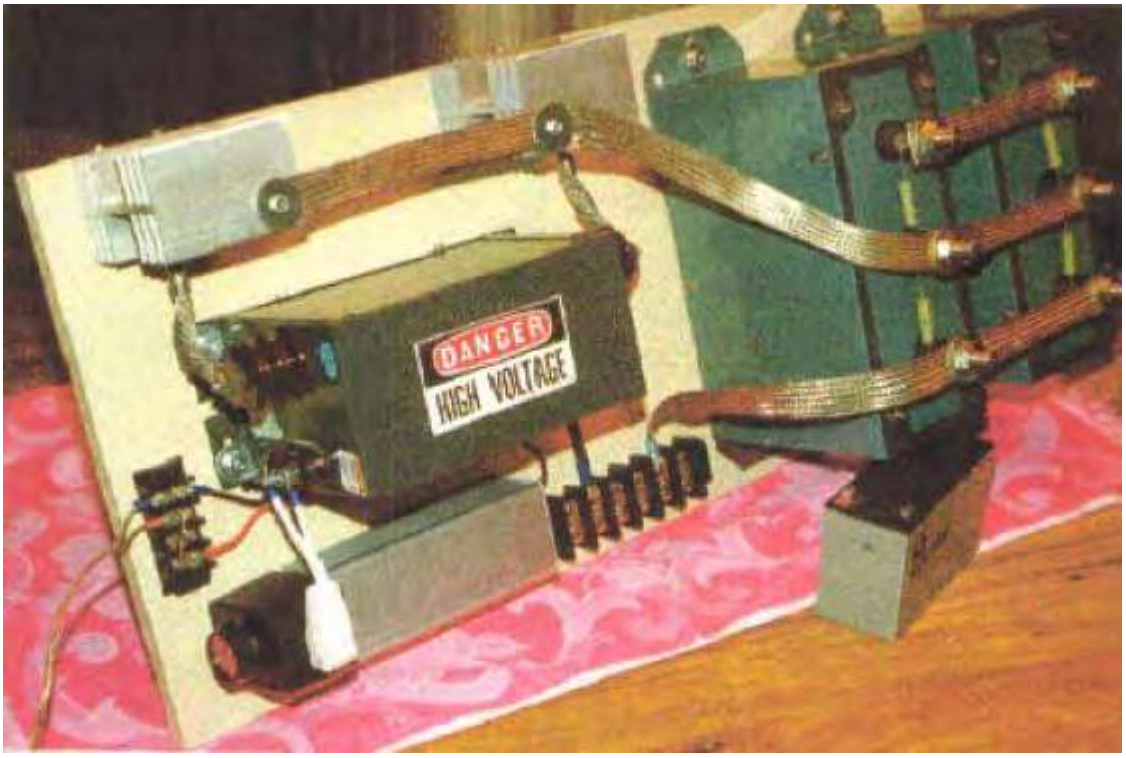
DANGER
HIGH VOLTAGE

DRI-VAR
LISTED
DRI-VAR
LISTED

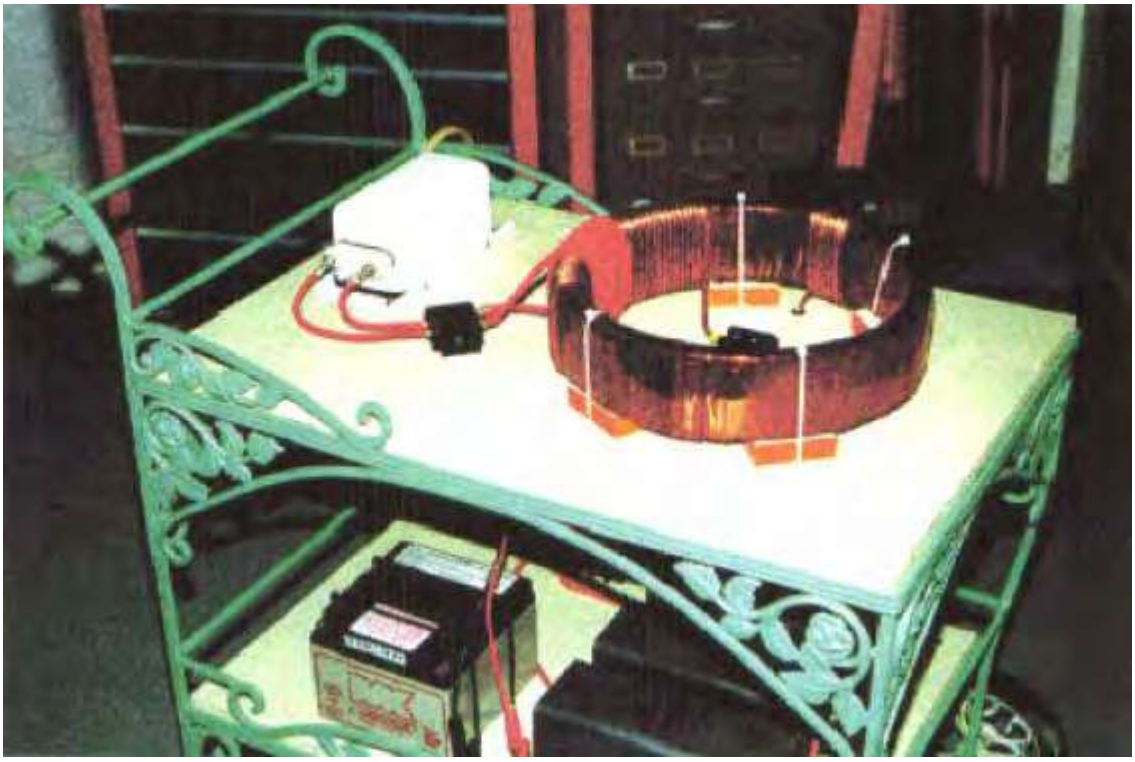

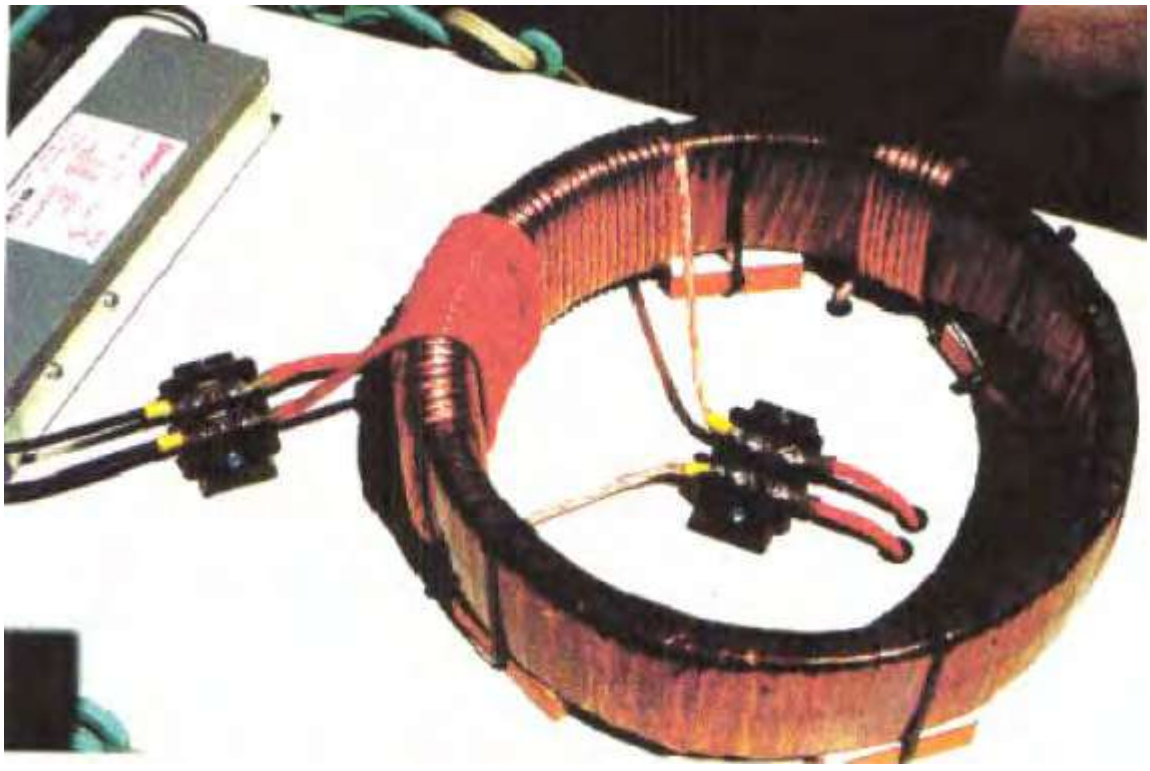

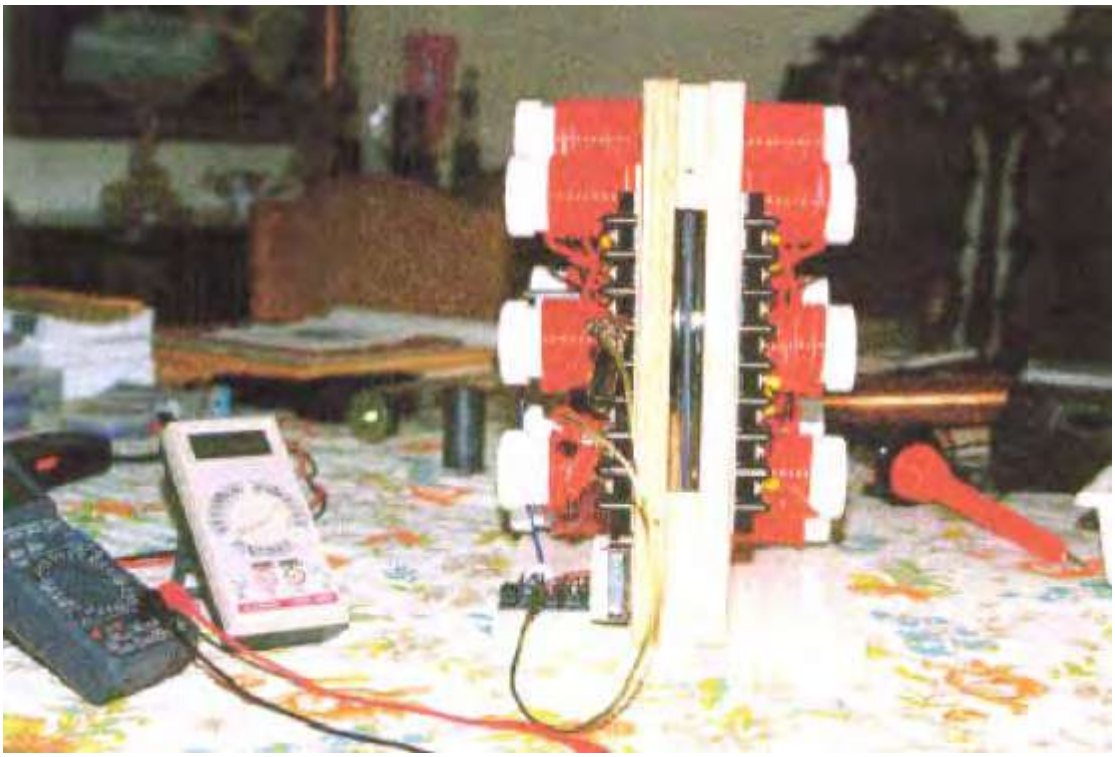

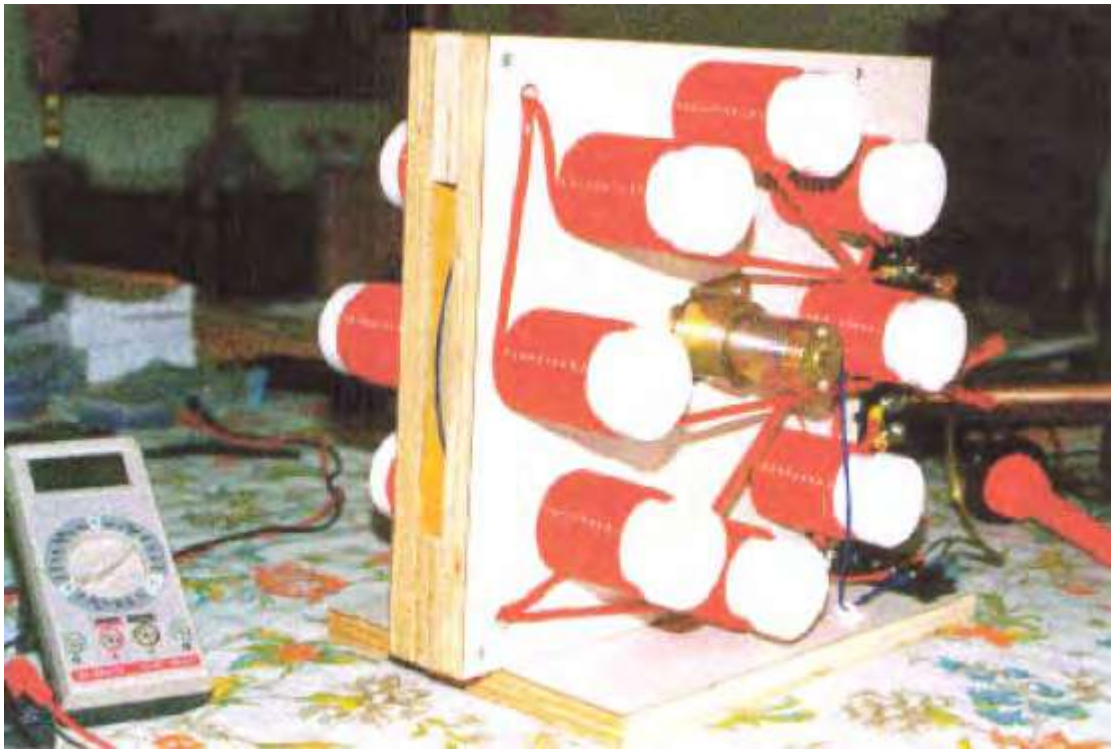

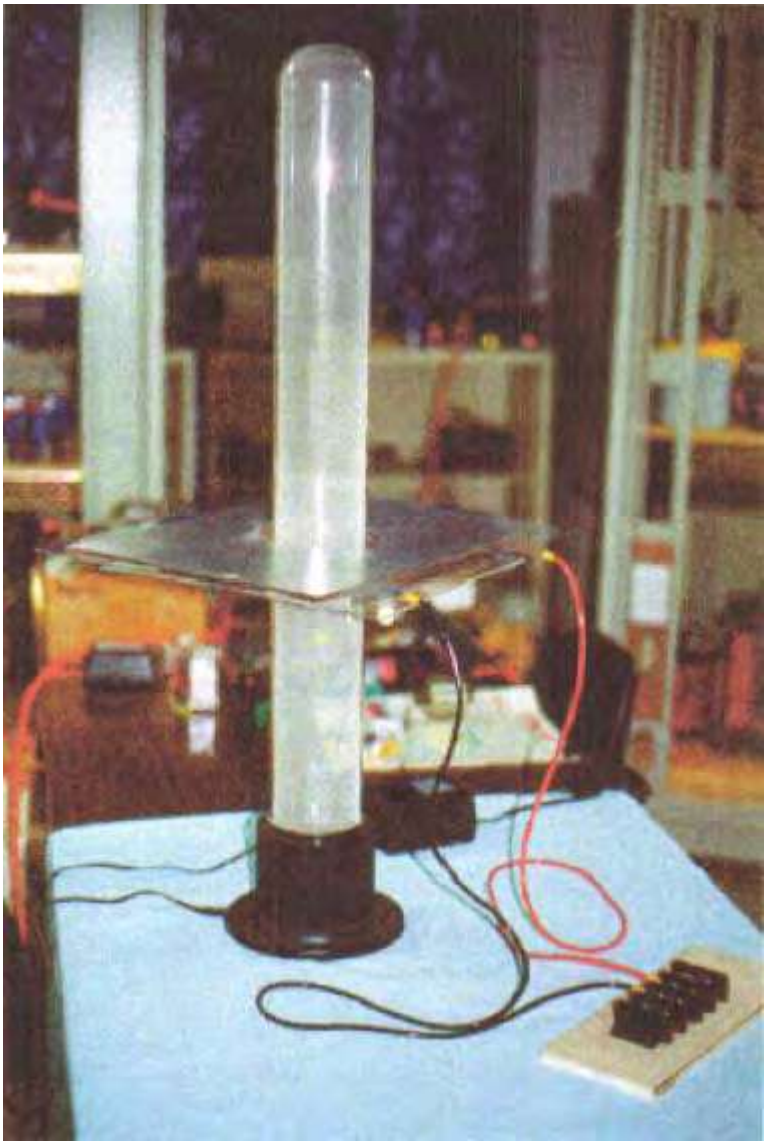

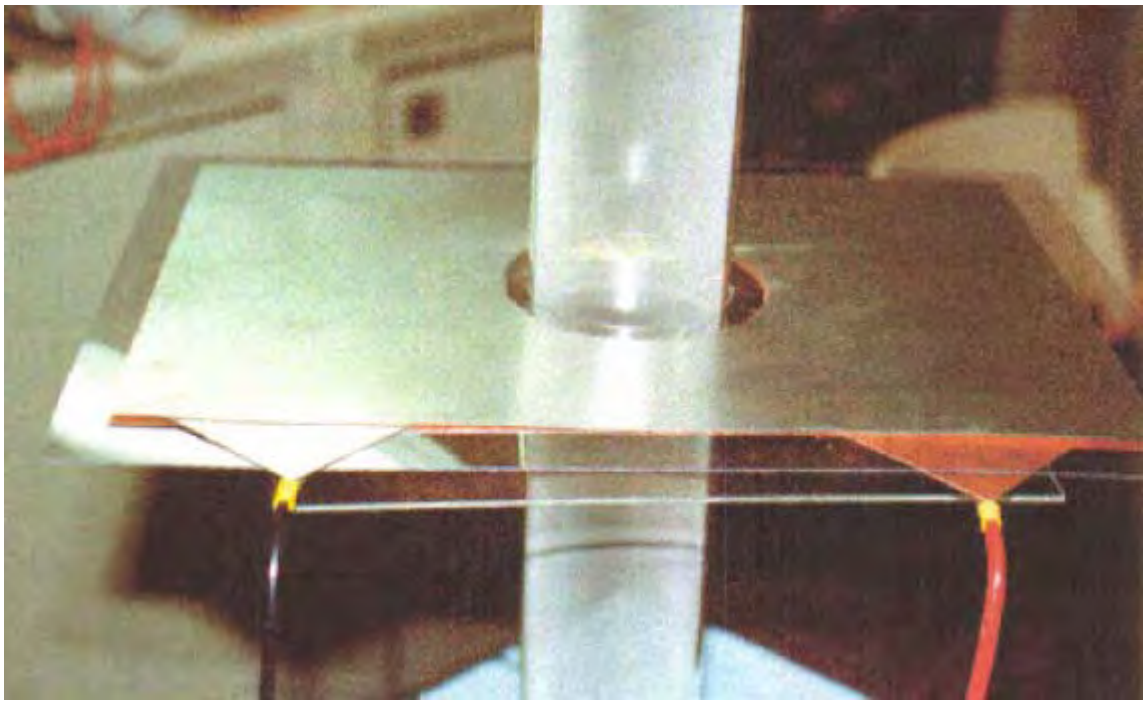

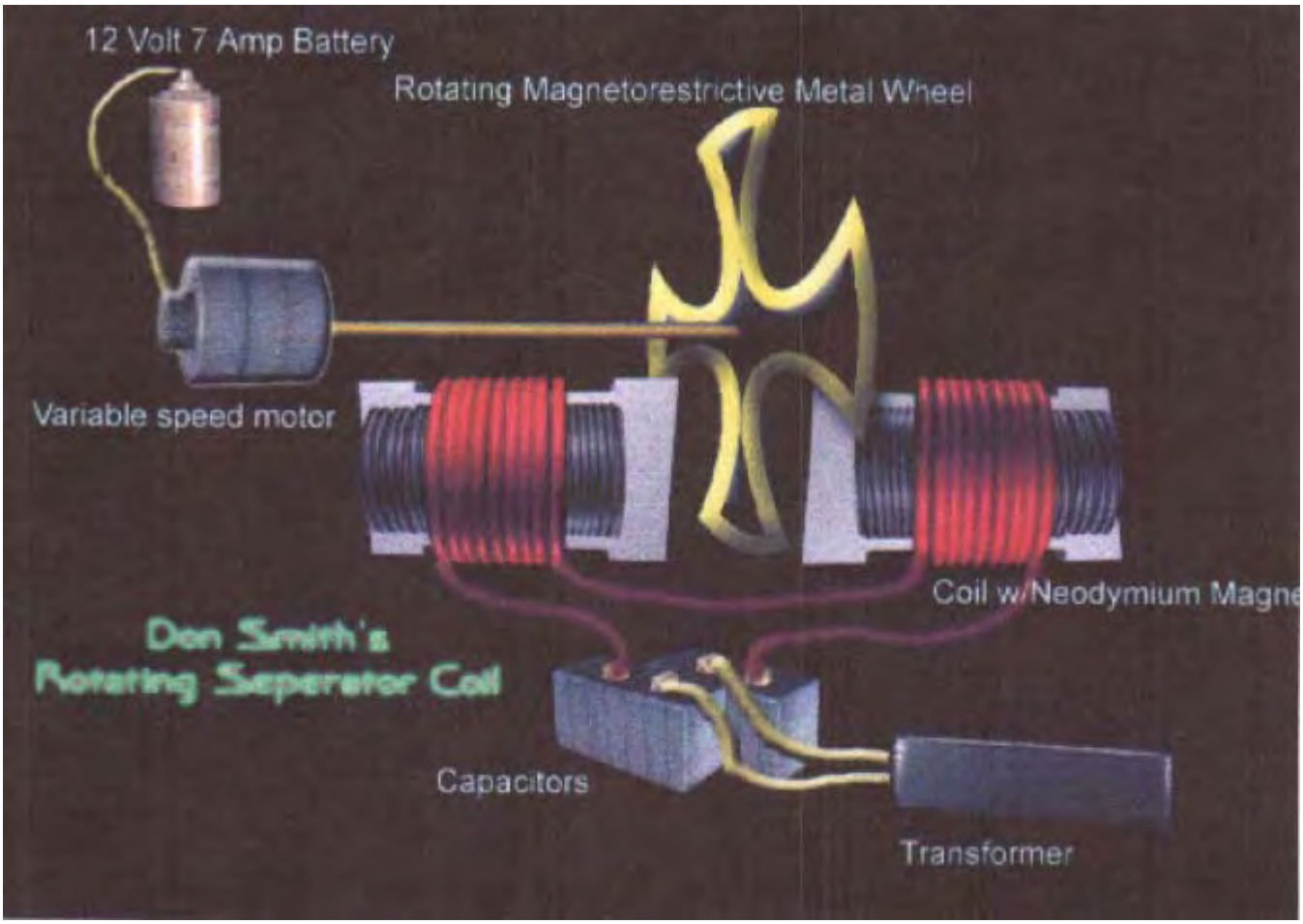
12 Volt 7 Amp Battery
Rotating Magnetorestrictive Metal Wheel
Variable speed motor
Coil w/Neodymium Magne
Don Smith's
Rotating Seperator Coil
Capacitors
Transformer

DIPOLE TRANSFORMER GENERATOR
DESCRIPTION

TECHNICAL FIELD:

The Invention relates to loaded Dipole Antenna Systems and their Electromagnetic radiation. When used as a transformer with an appropriate energy collector system it becomes a transformer generator. The invention collects and converts energy which, with conventional devices, is radiated and wasted.

BACKGROUND ART:

An International search of Patent Databases for closely related methods did not reveal any prior Art with an Interest in conserving radiated and wasted magnetic waves as useful energy.

DISCLOSURE OF INVENTION:

The Invention is a new and useful departure from transformer generator construction, such that radiated and wasted magnetic energy changes into useful electrical energy. Gauss Meters show that much energy from conventional electromagnetic devices is radiated back into the ambient background and wasted. In the case of conventional transformer generators, a radical change in the physical construction, allows better access to the energy available. It is found that creating a dipole and Inserting capacitor plates at right angle to the current flow, allows magnetic waves to change back to useful electrical (coulombs) energy. Magnetic waves passing through the capacitor plates do not degrade and the full impact of the available energy is accessed. One, or many sets of capacitor plates, may be used as desired. Each set of plates makes an exact copy of the full force and effect of the energy present in the magnetic waves. The originating source is not depleted or degraded as is common in conventional transformers.

BRIEF DESCRIPTION OF THE DRAWINGS:

The Dipole at right angle allows the magnetic flux surrounding it to intercept the capacitor plate, or plates, at right angles. The electrons present are spun in such a way that the electrical component of the electrons is collected by the capacitor plates. Essential parts are the South and North component of an active Dipole. Examples presented here, exist as fully functional prototypes, and were engineer constructed and fully tested for utility by the Inventor. Corresponding parts are utilized in each of the three examples as shown in the Drawings.

DRAWING 1 OF 4: VIEW OF THE METHOD

N = North and S = South of the Dipole

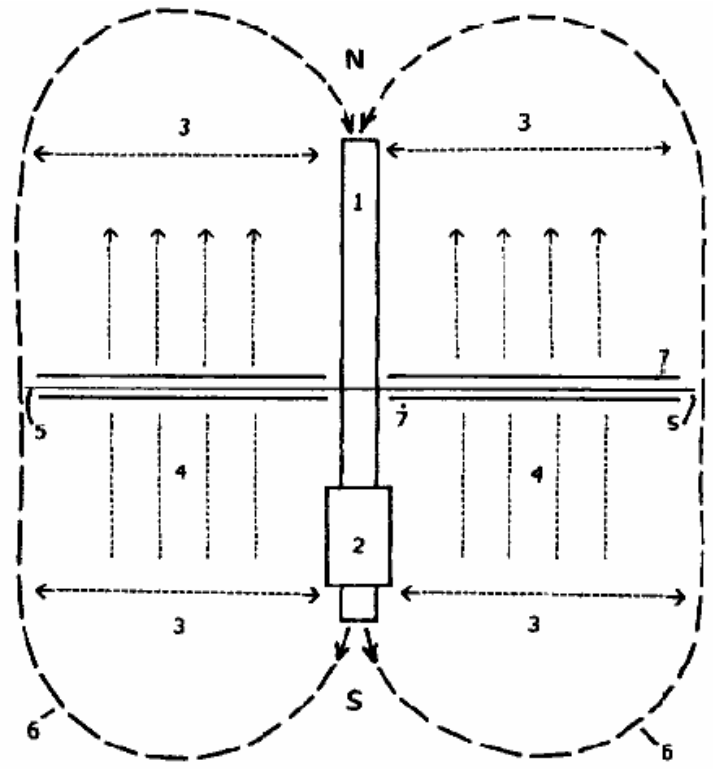

1. North and South component of the Dipole.
2. Resonate High Voltage induction coil.
3. Dipole's electromagnetic wave emission.
4. Heaviside current component.
5. Dielectric separator for the capacitor plates
6. For purposes of the drawing, a virtual limit of the electromagnetic wave energy.
7. Capacitor plates, with dielectric in between.

DRAWING 2 OF 4: COMPONENTS, 2A and 2B

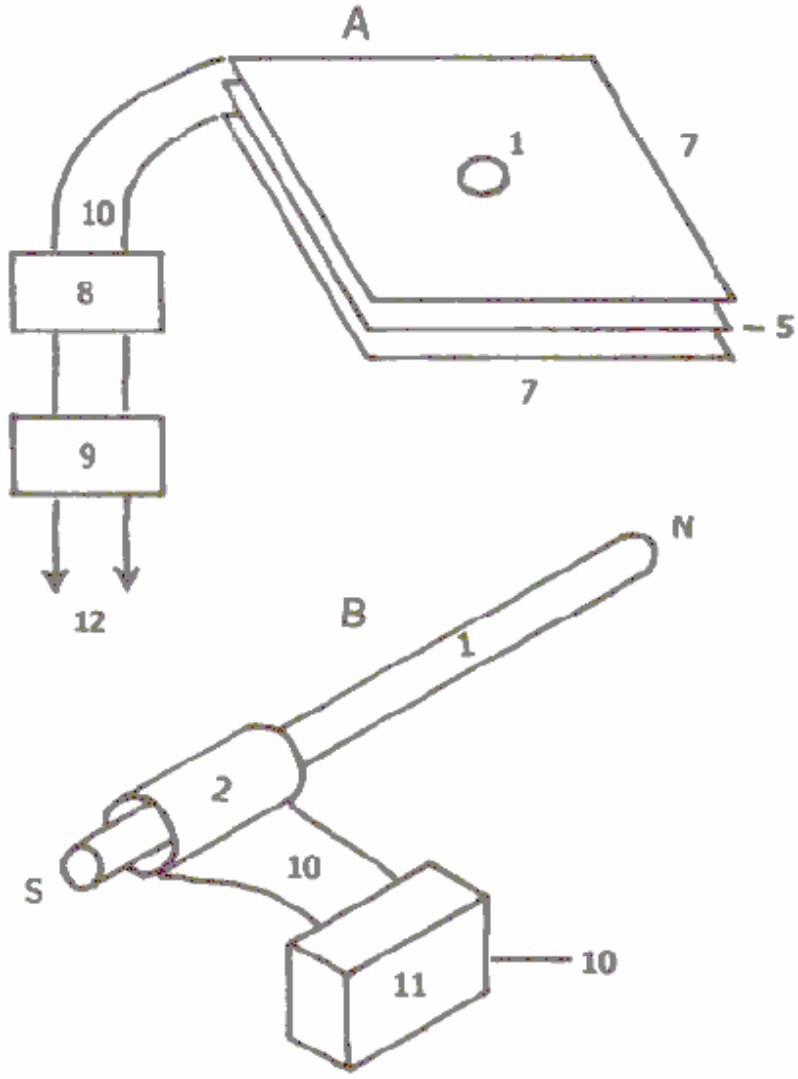

Fig.2-A:

1. Hole for mounting Dipole **B-1**.
2. Resonate high voltage induction coil.
5. Dielectric separator, a thin sheet of plastic separating the capacitor plates.
7. Capacitor plates, upper plate is aluminum and lower plate is copper.
8. Battery system, deep cycle.
9. Inverter. Input: Direct Current, output: 120 Volts at 60 cycles per second.
10. Connector wires.
12. Output to point of use being the load.

Fig.2-B N = North and S = South component of the Dipole

1. Metal rod, being soft magnetic metal such as iron.
2. Resonate high voltage induction coil.
10. Connector wires.
11. High Voltage input energy source such as a neon tube transformer.

DRAWING 3 OF 4 : Proof of Principle Device, using a Plasma Tube as an active Dipole.
N = North and S = South Components of the active Dipole.

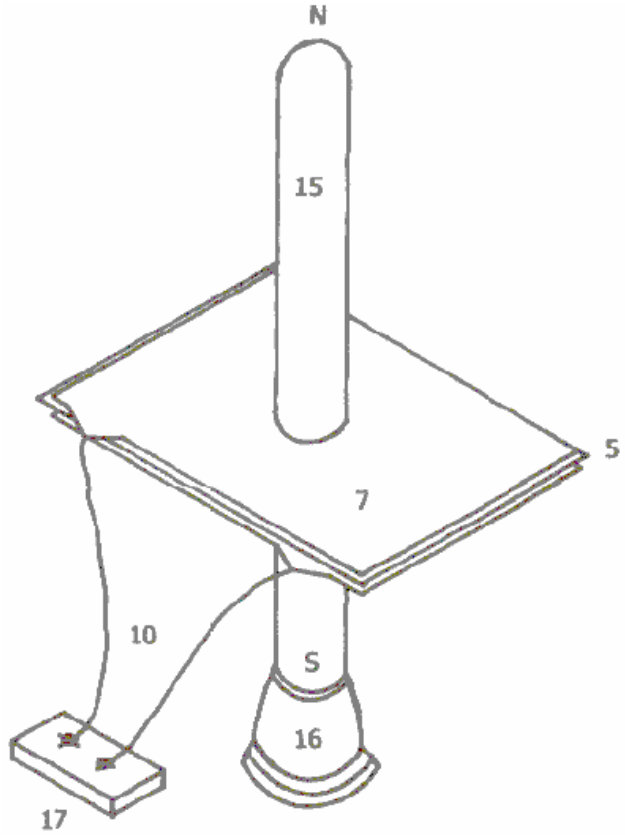

5. Dielectric separator of the capacitor plates.
7. Upper capacitor plate: upper plate is aluminum and lower plate is copper.
10. Connector wires.
15. Plasma Tube, 4 feet long and 6 inches in diameter.
16. High Voltage Energy source for the active Plasma Dipole.
17. Connector block: outlet for testing and use.

DRAWING 4 OF 4: Manufactures Prototype, Constructed and fully tested.

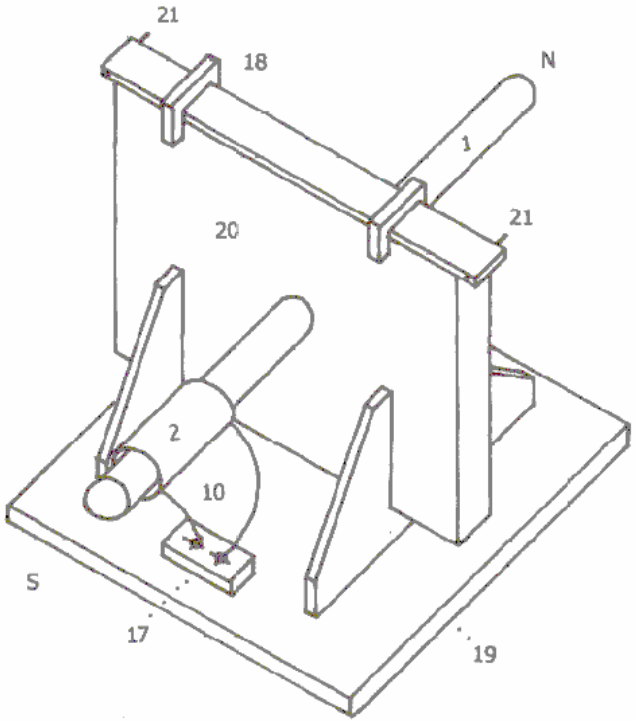

1. Metal Dipole rod.
2. Resonate High Voltage induction coil.
10. Connector wires.
17. Connector block for Input from high voltage energy source.
18. Clamps for upper edge of capacitor packet.
19. Support Device for The Dipole Transformer Generator.
20. Packet of Capacitor Plates.
21. Output connectors of the capacitor, producing energy into a deep cycle battery which then powers the inverter.

BEST METHOD OF CARRYING OUT THE INVENTION:

The Invention is applicable to any and all electrical energy requirements. The small size and high efficiency makes It an attractive option. It is particularly attractive for remote areas, homes, office buildings, factories, shopping centers, public places, transportation, water systems, electric trains, boats, ships and all things small or great Construction materials are readily available and the skill level required is moderate.

CLAIMS:

1. Radiated magnetic flux from the Dipole, when intercepted by capacitor plates at right angles, changes to useful electrical energy.
2. A Device and method for converting for use, normally wasted electromagnetic energy.
3. The Dipole of the Invention is any resonating substance such as Metal Rods, Coils and Plasma Tubes which have interacting Positive and Negative Components.
4. The Resulting Heaviside current component Is changed to useful electrical energy.

ABSTRACT

An Electromagnetic Dipole Device and Method, wherein, radiated and wasted energy is transformed into useful energy. A Dipole as seen in Antenna Systems is adapted for use with capacitor plates such that the Heaviside Current Component becomes a useful source of electrical energy.

TransWorld Energy
227 W. Airtex Blvd.
Houston, Tx. 77090

September 23.2002

Phone: (281)876-9200
Fax: (281)876-9216
Web-site: altenergy-pro.com
E-mail: donsm1@earthlink.net

Dear Reader:

TransWorld Energy is dedicated to improving the Human Condition in the Field of Energy which, at the same time, makes possible Healthy Water and increases the food Supply. A never-ending source of energy found throughout the universe is easily accessed with the minimum of effort and cost. The technology for doing this has been around since the 1820s. Selfish special interests have made sure that the technology remains discredited. People who control the Energy Sources control the World.

Extensive research and development by TransWorld and Associates has been progressing for more than 15 years. Numerous successful Energy Producing Devices have been produced and demonstrated throughout the World. Some of these can be viewed by the Web Site located using any major search engine (such as Lycos, Yahoo, Altavista, NorthenLight and more than 2,000 others throughout the World).

The Book which You are viewing has more than 40,000 copies in circulation. It has been translated and distributed in all major languages including Japanese, Arabic, Portuguese, French, Italian, Russian, Chinese, German, Spanish and many more. There are seven editions in circulation. An enormous interest is evident in the subject matter. An average of about fifty e-mails per day are received from the ends of the Earth (that is about 1,500 per month).

Once the Web Site and the book are viewed, it will become evident that abundant, self-sustainable energy is available everywhere for the taking. This is natural energy which does not harm the environment or those using it. The proper Device for Collecting is all that's required.

The Good News is that the problem is solved and with assistance, an ultimate source of energy which is environmentally benign, abundant throughout the universe and inexpensive to capture, is there for the taking.

Thank You for your consideration

_____

Donald L. Smith, CEO

Electrical Energy Generating System

Description and Function:
The Generation of Electrical Power requires the presence of electrons with various methods of stimulation, yielding magnetic and electrical impulses, collectively resulting in Electrical Energy (Power). In place of the mechanical - coils and magnet system, present in conventional electrical power generation, visible moving parts are replaced by resonate magnetic induction, using radio frequency. Transfer of energy by resonate induction is related to the ratio of the square of the cycles per second.

The Energy System, presented here, operates at millions of cycles per second verses the conventional 60 C.P.S. This tells us that it has a frequency advantage over conventional methods. This same advantage applies to the amount of electrical energy output. Therefore the Device is small in size and produces large amounts of Electrical Energy. The Electrons acquired, are from the surrounding Air and Earth Groundings, being the same source as in conventional methods. This is accomplished by magnetic resonate radio induction.

Applications:
This Electrical System adapts nicely to all Energy Requirements. It is a direct replacement for all existing Energy Systems. This includes such things as Manufacturing, Agricultural, Home Usage, Office Complexes, Shopping Centers, Rail Transportation, Automobiles, Electrical Power Grids, Municipalities, Subdivisions, and Remote Areas. Briefly, the only limiting factor is the imagination.

Economic Possibilities:
No Historical Reference Point exists for a comparison of the Possibilities of this System. One can see from the impacted applications listed above, that the magnitude exceeds any known invention, presently a part of the Human Experience.

Present and Future Plans:
The Energy System has been in the developmental stage during the past seven years. It is Patent Pending # 08/100,074 with the Patent Office. No prior art exists according to the Patent Office's response. The System is presently being introduced into the World Market.

Useful energy occurs as the result of imbalances in the ambient background energy, which is a transient phenomena. In the electrical field, it is a closed system subject to heat death, which severely limits it's utility. The flip side of the electron, produces magnetic waves which are an open system, not subject to heat death. These waves, being unrestricted, are the universal source of energy when unlimited resonate duplicates from this one source are available. Therefore, the key to unlimited energy, is Magnetic Resonance. In order to understand this, requires putting a stake through the Heart of Antique Physics. Non-linear and Open Systems are universally available in Magnetic Resonance Systems, Explosions of

any sort [including Atomic Explosions] and Combustibles of any type. Mechanical equivalents would be levers, pulleys and hydraulics. A highly obvious example is the Piano where the Key impacts the one note giving one sound level, which resonates with it's two side keys providing a much higher sound level. Magnetic Resonance Energy clearly amplifies itself, demonstrating more energy out, than in.

Ohmic resistance does not apply to Magnetic Resonance which travels unrestricted for great distances, therefore multitudes of electrons are disturbed, and their back-spin translates magnetic into usable electric energy. The right angle component which the magnetic flux provides, translates into useful electrical energy. Taken at right angles, the Magnetic Dipole provides an unlimited source of electrical energy. The writer is recognized world-wide for his knowledge and experience. See his Web Site at altenergy-pro.com .

Gravity is a function of spin phenomenon as observed in gravity separation of liquids. When spun, milk and cream separate. Therefore, relative specific gravity is function of mass versus spin. Magnetics and gravity are both spin related. In part, a top levitates when spun. Therefore, spinning magnetic fields are a functional motor source as in flying saucers.

ABSTRACT: Technology of New Energy:

Developments in the understanding of Electricity, along with Materials which were not previously available, allows the construction of Devices which collect energy in large quantities, from the Earth's Ambient Electrical Background. This Energy is naturally occurring, environmentally benign and is available everywhere. It is available wherever and whenever it is required. New Devices use Resonate Magnetic Waves which replicate upon spinning the locally present electrons, providing multiple duplicate copies of the Energy Present. Each electron when spun yields both magnetic and electric waves in equal proportion. The electrical component is a closed system limited by Ohms Law. The magnetic component is an open system not limited and it replicates multiple copies of the energy present.

Special materials and recent developments allow the magnetic energy to reproduce, through resonance, unlimited duplicate copies acquired from the ambient background. These Devices harvest the energy that has been, and is always present universally. Conventional methods consist of coils and magnets systems. Upon moving past each other, the magnetic flux field disturbs electrons which yield electricity, which is collected by the coils system. This is accomplished electronically with the new technology, without any moving parts and the energy is multiplied such that the Device becomes self-sustaining once it is started. This Technology, already presented Worldwide, will be shown at the Conference.

Dr. Smith
www.altenergy-pro.com
e-mail donsml@earthlink.net

"Putting a stake through the Heart" and thus removing the mental block created by antique physics is required. Conditions wherein this becomes necessary are non-linearity, resonance and explosions of any sort. Combustibles of any sort such gasoline and atomic explosions are good examples wherein more energy out than in, is obvious. You can add to that the non-linearity found in pulleys, hydraulics, steam power and suchlike. Magnetic resonance is a highly obvious source for multiplying energy output. The sound system present in the piano, demonstrates this very clearly. Energy amplification clearly present in the above, demonstrates the silliness attested to by many Physicists.

Ohmic resistance does not apply to magnetic resonance which travels unrestricted for great distances, therefore multitudes of electrons are disturbed, and their back-spin converts from magnetic energy to usable electric energy. These same electrons have been around from the beginning of time and they are undiminished and will remain so until the end of time.

ELECTRICAL ENERGY SYSTEMS PREFACE

Useful Electrical Energy is obtained directly from electron spin induced by incoming magnetic waves, or indirectly through mechanical exchange as in dynamo type devices. Simply put, electron spin converts from magnetic to electrical energy and vice versa. Nature provides grand scale magnetic wave induction throughout the universe, for free. In Electrical Systems, movement is at right angles to the direction of current movement. This explains the rotary movement of the Earth and other related Systems. The rate of Spin for the Earth is known as well as the mass (5.98×10^{24} Kg - "Physics for Scientist and Engineers", by Raymond A. Serway, Saunders College Publishing, 2nd Ed. page 288, Table 14.2), therefore the amount of incoming Electrical Energy which produces this action can be calculated.

It can be seen quite easily, that the incoming magnetic wave energy is Vast and Continuous. As an accretion mass, the Earth is an Energy Sink, getting it's energy from elsewhere, being Cosmic, Galactic and Solar. Conversion of incoming magnetic waves into electrical energy provides an unending, inexpensive and environmentally friendly source available to all. Cosmic and Galactic Energy is available twenty four hours per day. Large amounts of this Energy accumulates in the Earth's radiation belts. This Giant Energy Storage, when properly understood, provides a major source of free unending electrical energy. Each of My Inventions plugs into this vast energy source.

A perverse, Intentional Ignorance on the part of the Establishment, prevents recognition of the importance of the Energy Systems shown here. Any new system which is favorable towards the masses, is considered as disruptive, and therefore not allowed. Those who have the (Gold) Energy Rule (Golden rule) Mandated Destruction of all Humanity is not a consideration.

This Presenter will remove some of the Fog placed with the intention of preventing the recognition of this unending, environmentally clean, electrical energy Source, which is present everywhere throughout the Universe. The Cost of Harvesting and Using this Free Energy is a function of Human Stupidity.

RESONANCE CIRCUITS DEMO

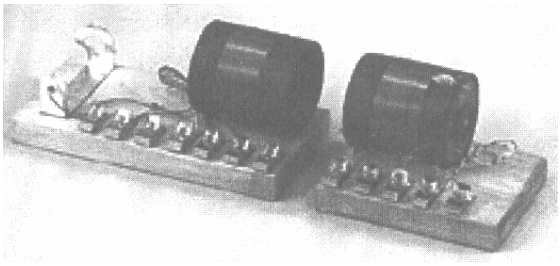

Used to demonstrate electromagnetic radiation between two UC circuits - one a transmitter and the other a receiver. When the 1.5 volt power transmitter is pulsed, the radiated signal is picked up by the remote receiver circuit which then lights up a 70 volt neon lamp.

With this apparatus, the student quickly understands some basic principles governing wireless communication, broadcasting, etc.

Kit: #10-416 $49.95

THE SCIENCE SOURCE
WALDOBORO, MAINE 04572
P.O. BOX 727

Tel. 1-800-299-5469
info@thesciencesource.com

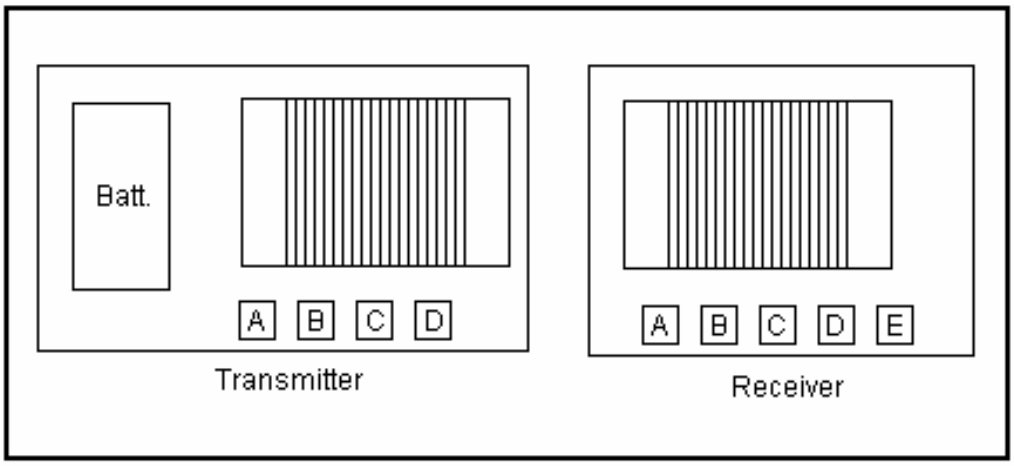

Diagram of transmitter and receiver coils

ULTIMATE ENERGY SOURCES

A human is a speck of dust on Earth, the Solar System is a speck of dust in the Galaxy and in turn, the Galaxy is a speck of dust in the Universe (Cosmos). All of these respectively represent vast ambient energy reservoirs. Awareness of the Sun, opens doors into other energy sources. Electromagnetic Energy which is present everywhere throughout the Universe, is accessed by catalytic activity, directly as in Solar Cells or indirectly as by mechanical means. Resonate, Magnetic Waves (Faraday's "Action at a Distance") allow Energy Activation Transfer to remote points of usage. The method of capture and use of this Energy is optional, and therefore it's cost is a function of Human Stupidity (Free-Energy).

Direct access is more desirable, and technology transfer from Solar Cell-type Devices provides the Catalyst. Enormously high Ambient Energy Levels are not detected by instruments that use the Ambient Background as a Reference Plane. A spoonful of water lifted from the Ocean does not define the Ocean. Incoming magnetic waves are reflected, Deflected or absorbed. Deflected Magnetic Waves spin electrons sideways producing useful Electrical Energy. Absorbed Wave Energy produces heat, therefore a hot interior for the Earth. In Electrical Systems physical movement is in the direction of current flow, frictional drag from inflow current defines gravity. Accretion masses resulting from Energy Sinks, provide all solid entities with their respective gravitational effect.

Increasing the tolerance level for Intellectual Awakening opens Doors of Reality. These doors blink into, and out of existence, and upon recognition, benefit Mankind. Opening some of these Doors, which at the present time are seen through a deep fog, is our purpose. Exploring Unrecognized Energy Sources, which are a Part of the Ambient Background, is another goal. Our Available Instruments do not use reference planes which allow recognition of this energy, as we shall see, vast Energy Sources that totally surround us are available through Technology Transfer. They are inexpensive (Free), fully self-renewable and environmentally benign.

Incoming Magnetic Wave Energy with Faraday's "action at a distance" will be looked at closely. Particle Physics will be left for the Astrophysics. Excited Electrons at point "A" the Sun (including the Galaxy and Cosmos) do not travel to point "B" the Earth, however a corresponding action occurs at point "B". The Electrons being disturbed at the Central Power Plant, in the same manner excite the Electrons at Your House, upon switching into an Earth grounding (known as "flipping the switch"). Correspondingly, there are Four Major Power Sources providing enormous amounts of Ambient Background Magnetic Wave Energy. They are The Cosmic, Galactic, Solar and Earth's Ambient Electromagnetic Backgrounds. The Earth's Electromagnetic Field comes from reflection, deflection and absorption as a result of action at a distance from the above.

Prescription Physics mandates that the Earth's background is of little interest. When we have Considered the evidence herein, it will become obvious that Special Interest's effort at keeping the People ignorant has, until now, largely succeeded.

Information for the entire World is available regarding the Magnetic Flux Background of the Earth's Surface (United State's Geological Survey, Colorado, USA, Office). When examined and properly understood, these Maps yield important information regarding reflection, deflection and absorption of incoming Magnetic Waves, plus action at a distance. When properly understood, these Maps reveal a very large Ambient Electromagnetic Energy Source. This is the Part of the Earth's Energy System that relates to the Bird on the High Voltage Line. When deflected, magnetic flux from electrons changes to electrical flux, providing the Motor System that spins or rotates the Earth. Physical movement by electrical systems is from inflow current movement. What level of current movement is required to spin the Earth? The Earth's Mass is 5.98×10^{24}. From this Information, the Watts of Electricity Required may be calculated! Absorbed microwave flux energy heats from the inside out, therefore a hot interior of the Earth results. Water is strongly diamagnetic, and on windless days, ocean waves provide visible Proof of the overhead incoming magnetic flux. From the information above, the Earth's weight and rate

of spin allows the calculation of the amount of incoming ambient background energy required. As You can see, it is not inconsequential as Prescription Physics mandates.

Astrophysicist are concerned with charged particles that whiz by, once every one hundred years, rather than Wave Phenomenon associated with action at a distance. This highly Active Wave Energy translates into Electrical Energy at point "B". The Galaxy is alive With Energy which is billions of times greater than that of the Sun. Visible Light is a very tiny part of the Electromagnetic Energy Spectrum. Frequencies present in the Galaxy and Cosmos allow Radio Telescope photographs of their existence and magnitude. One such 408 MHz photograph of the Electromagnetic Energy Spectrum shows that the Earth is a tiny speck of dust in this Enormous Ocean of Energy, and can be seen near the left end of the Central High Energy Area.

This Energy extends in all directions. Accretion and formation of Planets, Suns and Galaxies are results of energy sinks and variable sized black holes. Mass retains heat, and is cooked from the inside out by the microwave background energy provided by the Universe. Flux movement into energy sinks, provides the frictional force know as gravity. Spinning mass in the presence of incoming flux amplifies the gravitational effect.

At present, only Solar Energy is recognized. It is inconsistent, flaky and a very small Part of the Magnetic Wave Energy Present. Technology Transfer from Solar Power provides uncomplicated and inexpensive, direct access to the Other Greater Energy Sources. All Electromagnetic Energy harvesting methods include a Catalyst, a Collector and a Pump. Catalysts include sensitization through doping with certain elements, air and earth groundings. Collectors include temporary storage as in Capacitors, Coils and Transformers. The Pump System includes induced movement onward to the point of use. Conventional rotating coils and magnet systems activate electrons present, such that action at a distance can occur, therefore it is an energy activation pump. In Direct Access Systems such as Solar Cells, the same occurs without mechanical action. Direct access occurs when Magnetic Waves impact a catalyst, spinning the local electrons sideways, producing useful electrical energy.

Indirect acquisition of electrical energy by mechanical means is wasteful, troublesome, expensive and degrades the environment. The dynamo is a combination collector and pump of energy which is collected from the Earth's Ambient Energy Background. Generators do not. make electricity, they collect it from the Ambient Background and forward it, as in Faraday's "action at a distance". Energy Conservation Laws relating to these systems, relate to gray areas, and when understood, are excluded because of the existence of External forces, open and non-linear systems as per Einstein. The Knowledge Base just viewed, provides a Direct Understanding of the Requirements for Harvesting of unending, fully renewable, environmentally benign Sources of Electrical Energy.

Magnetic Resonance Power System
Suggestions for Construction

This is the Basic Sonar Power System which permits submarines to see approximately 50 miles distance. What is not commonly known is that it works better at higher frequencies in the Gigahertz range. Any Device that can radiate 50 miles plus, is producing an enormous electromagnetic disturbance from a small input into a rod of magnetostrictive material. Disturbing the Earth's Ambient Background plus the strong dipole being produced, turns the magnetostrictive rod into a combination of a receiving antenna and a vastly superior output transformer.

The Drawing is only the Key Unit. A power input module and an output inverter circuit (diode bridge plus output transformer) are also required. The metal core and the wire size of the output transformer, plus adjusting the Earth Grounding of the Load, will determine the Amperage.

The Ideal rod material is Terfenol-D (check the internet). However a 1.5" diameter 10" long rod, costs over $5,000 each. Less expensive alternatives are obvious. When constructing, use PVC tubing with removable caps. Wind the coils on it and insert the experimental rod. Use only magnetostrictive material. When you get it right, you will have exactly what the Doctor ordered:

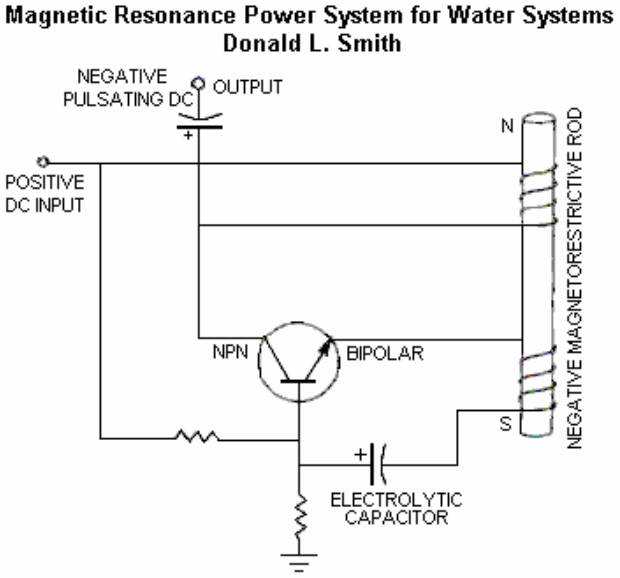

Magnetostriction oscillators work by magnetic resonance in a rod of magnetostriction material. This rod serves two purposes: It vibrates at the frequency of resonance oscillation, and it becomes the feedback transformer. Frequency is determined by items 4, 5, 6 and 8. The diameter, length and volume of the rod and output windings, determines the output. Item 2 provides feedback into the system. The negative magnetic character of item 8 plus the windings 2, in reaction to the magnetic flux field provided by 9, increases (amplifies or magnifies) the output. Magnetic permeability is the counterpart of negative resistance. Resonating with negative magnetic resistance, it pumps energy from the Earth's ambient background. Magnetic permeability is the ratio of flux density (Earth's B field) to the magnetizing force (H) in oersteds.

Magnetostrictive materials are piezoelectric in character, and have a very high resistance to electrical current flow. Examples are:

1. Permealloy Negative Magnetic Permeability	> 80,000
2. Sendust Negative Magnetic Permeability	30,000 -120,000
3. Metglas Negative Magnetic Permeability	> 200,000
4. Iron with (34%) Cobalt Magnetic Permeability	13,000
5. New Technology Magnetic Permeability	> 1,000,000

ELECTRICAL ENERGY SYSTEMS METHODS

1. DIRECT - Faraday's "Action at a Distance" incoming magnetic wave conversion to useful electrical energy. This includes Cosmic, Galactic, Solar and Magnets. Technology Transfer is from Solar Cell Technology.

2. INDIRECT - Electron Stimulation-Induced Electron Spin Systems, Electron Avalanche Pumping Systems

Primitive, Indirect Conversion from another form of energy. Coils and Magnet as in Dynamo Systems (Closed Systems). Chemical Systems, Atomic, Pons & Fleischman and etc.

Advanced, Direct Conversion, Magnetic Wave (Open Systems).

Ambient Sources
Air Core Coil Systems
Gaseous Tube Systems,
Solid State Marx Generator Avalanche Type Systems.
Leyden Bottle Capacitor Types inserted in Lakes and other.
Magnet Systems
Electron Beam Antenna Systems

3. TRANSFER MECHANISMS

Solids - as in metal conductors

Gaseous as in radio wave transmission, a form of ionization.

Sensitizing of Systems by use of Trace Doping with Radioactive elements, includes metal surfaces.

Open Systems, non-linear with external forces. Albert Einstein in a direct quote from his biography states that these are excluded from the conservation of energy laws.

Closed Systems Maxwellian Type Systems. Mathematics are predictable requiring deductive reasoning. Ohm's Law is King, and Establishment Intellectuals being comfortable with this, brand all else as a violation of the Laws of Nature by obtaining something for nothing. This is Dishonesty grand mal.

AMBIENT ENERGY SOURCES

Radiation System	*Diffusion Method*	*Magnetic Wave Energy*
1. Cosmic	**Reflection, Deflection and Absorption**	**Ultraviolet**
2. Galactic	**Reflection, Deflection and Absorption**	**Infrared**
3. Solar	**Reflection, Deflection and Absorption**	**Visible Light**
4. Earth	**Reflection, Deflection, Absorption, Faraday's "Action at a Distance" also, a Composite of all of the above**	**Earth's Electrical**

A deep fog pervades the entire Scientific Community with regards to the Significance of the Above Energy Sources. Magnetic Waves convert directly into Electrical Waves (useful electricity). Two sides of the electromagnetic system are always present and never separate. Local electron spin provides (action at a distance) the flip side of the incoming magnetic wave energy.

Enormous amounts of incoming magnetic wave energy becomes a part of the Ambient Background, and as such, cannot be measured directly. Reconstruction from indirect information, allows us to establish the actual energy levels which are present. Instruments provided by the Scientific Community measure only point "A" to "B", and when both are ambient, no potential energy is shown. This is the "bird sitting on the million volt power line and sensing nothing" approach. The Earth's actual ambient background has as it's Energy level multi-billions of Volts, which are conveniently and obliviously ignored by the scientific community. When properly understood, this enormous, never-ending source of environmentally-friendly energy becomes available.

ELECTRICAL ENERGY GENERATING SYSTEM

Patent Pending 08 / 100,074

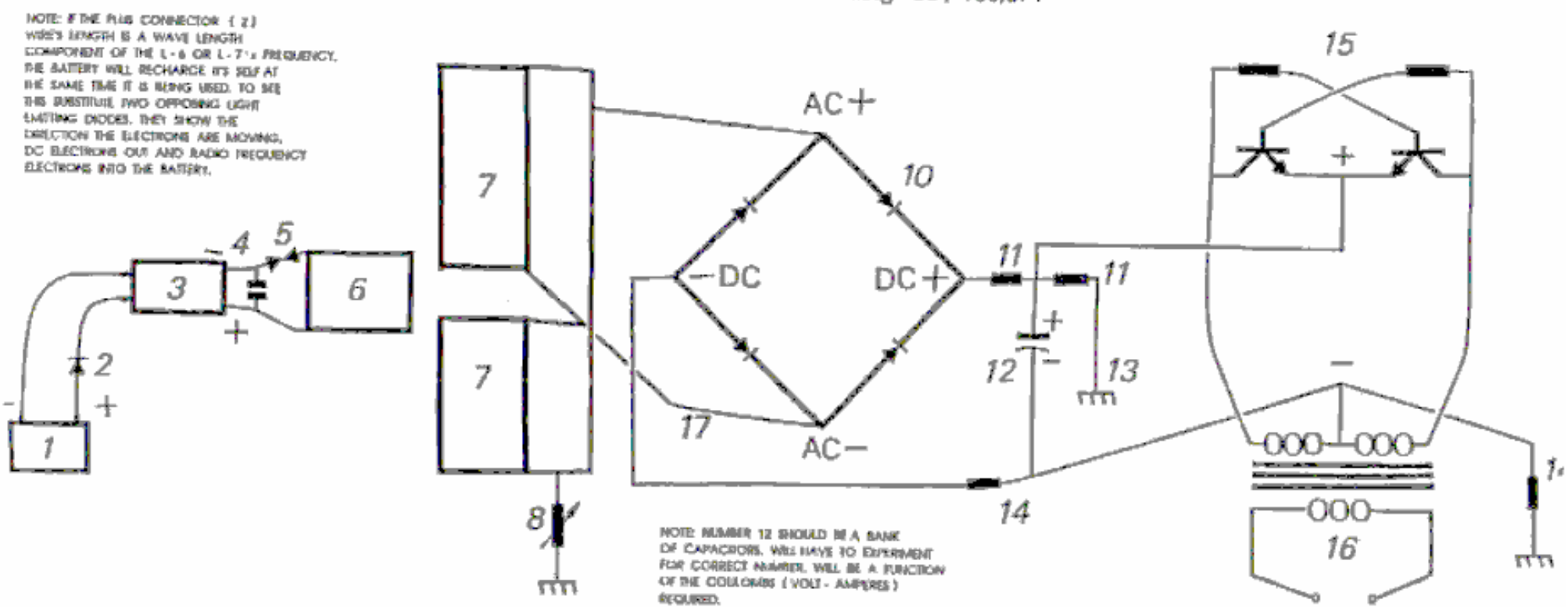

1. Geicel. 6 or 12 Volt,
2. Diode, Pass. use a Varactor.
3. High Voltage Module, Constituting the L-1 and L-2 Coils.
4. Capacitor, TDK 10.9 Pf., 30 KV,
5. Spark Gap, Small Engine Spark Plug, Gap = .0025 in.
6. Induction Transfer Coil L-3.
7. Induction Receiving Coil L-4.
8. Voltage Control Shunt.
9. Frequency Adjustor, prevents derating by Diode Bridge
10. Diode Bridge, 200 Nanosecond, R.F., > 100 KV .
11. Voltage Divider Circuit, corrects voltage for next stage.
12. Capacitor, electrolytic, smooths out DC + ripple effect.
13. Earth Ground.
14. Voltage Divider Curcit, corrects voltage for Transformer
15. Inverter Circuit, DC + in and 60 CPS to Transformer
16. Output from Transformer to Load (Work).
17. Center Tap

17 JANUARY, 1997

Electrical Energy System

Don L. Smith, Energy Consultant

At a meeting between J.P. Morgan, Edison and Tesla, Tesla proposed an Electrical Energy System which could he connected into directly, without using a meter. Tesla's Idea of "Free Energy" was not compatible with their thinking. Courtesy of Morgan and Edison, from that day foreword, a complete and total bastardization of the Idea has been in progress. Agents for Morgan and Friends include the U.S. Patent Office and Academia. Academia's bad habit of incestuous quoting of each other, eliminates them as a possibility in cleaning up the mess. This selective ignorance, permeates throughout the study of electricity.

Many people, otherwise known as "intellectuals", have a total blackout and become jabbering idiots when "free-energy" is mentioned. The term has been amended to say, "something which was never there is being harvested and that this violates the laws of physics". For the selectively ignorant, this seems the way to run. Those who choose Morgan's drum beat, have severely limited the possibilities built into electricity.

This paper will be an exercise in creative understanding, in placing updated knowledge at your disposal. Whether it becomes a useful tool or is selectively ignored is your choice.

Electrons are defined as being the practical source of electrical and magnetic energy. The electron as a particle, was postulated by professor J. Thompson in early 1900's. It is now universally accepted that the electron exists and that it is the source of electricity. When the electron is agitated it produces magnetic and negative electrical energy. Physics as it exists today, cannot explain why the electron remains intact and is not diminished by the energy it releases. This is a part of the built-in ignorance provided by the Morgan and Edison Camp.

One volts worth of electrons, when cycled, yields one volts worth of electricity. This can be repeated continuously forever and it never deplete or diminishes the electrons in question. They simply return to their air and/or earth source, waiting to do the whole thing again and again. Therefore, electrical energy is available, anywhere and everywhere humans go. People who intercede for profit, set the cost of electrical energy. Otherwise, all electrical energy is free, Morgan and Edison be damned.

Improving upon Professor Thompson's postulation, other obvious characteristics can be seen to further define the electron. It has both magnetic and electrical emanations resulting from a right-hand and left-hand spin. Since magnetism and amperage come as one package, this suggest, that electrons in their natural non-ionic state, exist as doublets. When pushed apart by agitation one spins and supplies electricity and the other spins and provides magnetic (amperage) energy. When they reunite, we have Volts x Amperage = Watts. This Idea, until now, has been totally absent from the knowledge base.

The number of times that an electron is cycled, sets the collective energy potential present. The electrical equivalent of $E = mC^2$ is $E = (\text{Volts} \times \text{Amperes}) \times (\text{Cycles Per Second})^2$. Those who choose, are now free to head for the bushes and make their usual contribution to humanity.

Prior to Tesla, there was a large group of people in Europe, who were building resonant coil systems for medical use. Amperage was dangerous in their coil systems. The Tesla Coil is only the Voltage half of their coil system, as will be demonstrated.

A short list of those (from 1860 onwards) active in resonate high frequency coil systems include; the Curies, Roentgen, Ruhmkoff, Oudin, Hertz, Levassor, Dumont, D'Arsonval and many others.

Peugeot, Panhard-Levassor, Bollee, Renault and others had successful electric automobiles in production using A C. motors. Various electrically-powered airships, including the Dirigible "France" were in service.

D'Arsonval, Professor of Experimental Medicine at the College of France, invented the electrocardiograph, oscilloscope, amp and volt meters, thermography and numerous other medical applications of high frequency electricity. As early as 1860, he was building high frequency coil systems, which he used in his experimental work. There is a strong connection between the work of Tesla and the people mentioned above.

Electric vehicles of all sorts, dominated until the 1920s, when the electric starter motor made the internal combustion engine practical. Prior to that, upon cranking, it frequently would break the owner's arm. At that point the use of batteries as a source of power was replaced by oil.

The establishment's carpet has some rather large lumps under it. Coulomb's and Newton's inverse square law is politely ignored and it's opposite is allowed to have only the most abstract status. Without opposites we have no definition.

The source value of a remote flux reading, requires the squaring of the distance, times the remote reading, to obtain the original value. The opposite of this, being the derivations relate to Energy equals Mass times the Velocity constant squared. The electrical equivalent, being Energy equal capacitance times voltage squared and Energy equals induction times amperes squared. Flux lines increase as the law of squares and then activate electron energy which was not previously a part of the sum. The cumulative capacitance and inductance increase as the outer ends of a Tesla coil are approached, and this results in output energy being greater than the input energy present. This Energy is real. It can be safely measured by magnetic flux methods and electrostatic voltmeters, based on the inverse square law

As seen above, flux lines result both from induction-henrys-amperage and capacitance-coulombs-volts, and define electrical energy. The non-linearity of this system does not obey Ohm's law, which is replaced with impedance and reactance for alternating current systems. Impedance is the sum of the system's resistance to AC current flow, and this becomes zero at resonance. In resonant induction systems, a cycles-per-second increase, invokes a second round for the law of squares.

The degree to which flux lines are present, disturbs an equal amount of electrons, upsetting the ambient background energy, resulting in useful electrical energy being obtained. The frequency at which the disturbance occurs, increases the useful energy available, and it obeys the law of squares. Two square-law components, *flux density* and *frequency* are involved. Enter resonance which cancels the resistive effect.

Only the electrical energy which is either above or below the ambient level is useful. For the Central U.S. going east to west, ambient as approximated by electro-static voltmeters and flux methods is 200,000 volts on a solar-quiet day. At night time, the ambient energy level drops to about one half of the daytime value. On a solar-active day, it may reach more than five times that of a solar-quiet day. Ambient background energy at the polar regions, is approximately 500,000 volts on a solar-quiet day. The background energy varies as it relates to the North-South component and the East-West continuum.

This leaves us with an interesting problem. Electrons, when disturbed, first produce magnetic flux and then produce electrical flux when they spin back to their normal position. Therefore any electron movement produces above ambient energy, being over unity.

ELECTRICAL ENERGY WITH ASSOCIATED PHENOMENA

1. Current-amperes results from the unequal distribution of negativity (electrons).

2. Electron spin causes electrical current and magnetic lines of force.

3. Magnetic imbalance causes the gravitational effect. This is evidenced in electric motors by magneto-gravitational displacement of mess, which causes the motor to rotate.

ENERGY LINES QF FLUX (FORCE) FIELDS & WAVES *

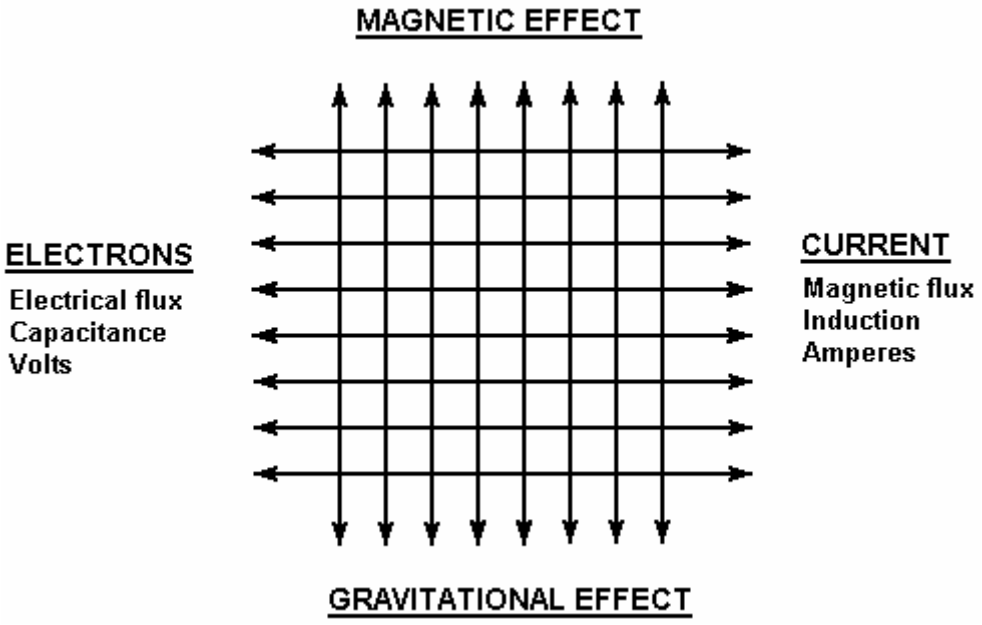

* Below 20,000 Cycles Per Second = **Fields**
Above 20,000 Cycles Per Second = **Waves** (Radio Frequency)

Derivation of Magnetic and Electrical Power

Analogous Relationships:

1. Potential Power is present in a bar magnet as shown:

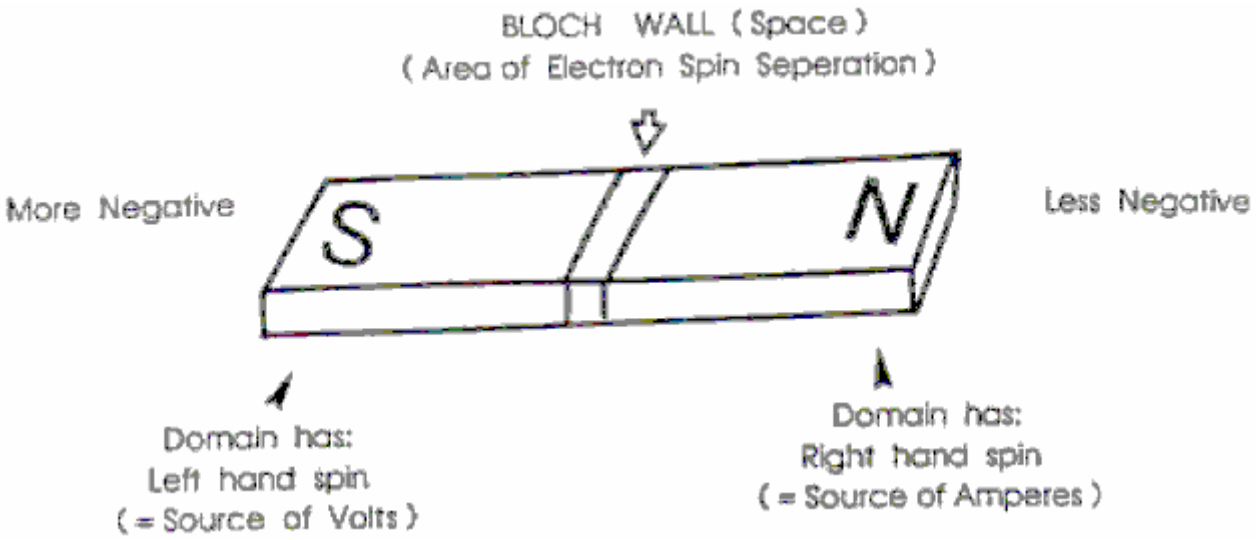

2. The Source of these Electrons being from the Solar Plasma, are non-ionic and occupy all Free Space. They are commonly obtained from Earth and Air Groundings. They exist in Doublet Pairs, one being more negative than the other. The more negative one has a Left Hand Spin. The less negative one has a Right Hand Spin.

3. Resonate Electrical Coil Systems (Tesla) are Analogous to the System observed in the Bar Magnet (above). The Bloch Wall Area is Located at the base of the L-2 Coil. The Left Spin portion of the coil (Voltage Only) Coil predominates. The Right hand Spin portion of the coil (Magnetic-Amperage) is mostly absent.

Tesla Coil Geometry *

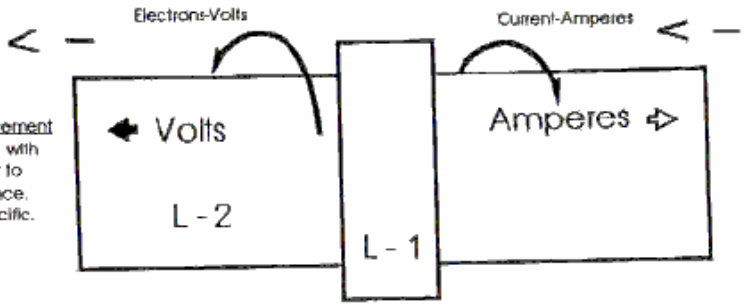

Correct Method of Measurement
Use the inverse square law with an Electrostatic Volt Meter to measure from a safe distance, they are frequency nonspecific.

Correct Method of Measurement
Use the inverse square law with Hall-Effect devices to measure from a safe distance, they are normally frequency nonspecific. The magnetic field they measure converts directly to Amperage

Volts dominate if the L-1 Coil is far right
Volts and Amperes about equal if L-1 Coil centered

This End Has Greater Voltage
Distributive Capacitance at Maximum
Capacitance-Coulombs-Voltage
Voltage has Electrons spinning to Left

This End Has Greater Amperage
Distributive Inductance at Maximum
Induction-Henrys-Amperage
Amperage has Electrons spinning to Right

Volts represent the more negative and Amperes the less negative. Therefore the electrical charge of more negative must seek the less negative to regain ambient.

* Contains proprietary information related to Patent Procedure
Geometry - properties of lines, surfaces and solids

Donald L. Smith
2 November, 1995

Induced Electrical Energy System

Collection and transfer of energy requires temporary storage, which occurs as capacitors and coils of a resonant circuit are cycled, on and off. The frequency at which the capacitors and coils are pumped, determines the amount of electrical energy that moves onward.

The amount of Energy transferred relates directly to the density of lines of flux present. The Kinetic Energy Formula is helpful in establishing the amount of energy present. This formula squares the velocity times mass. In the case of electrical energy, the intensity of voltage and amperes multiplied by the cycles per second, replace the velocity component.

Note that the "acceleration" of the Voltage "E" and Amperage "I", which increase as non-linear components, then obeys the Law of Squares.

Each unit of increase, causes a squaring of the flux lines present. The amount of energy transfer caused by this increase in flux lines is demonstrated below.

Increase in Flux Lines Present Symbolized

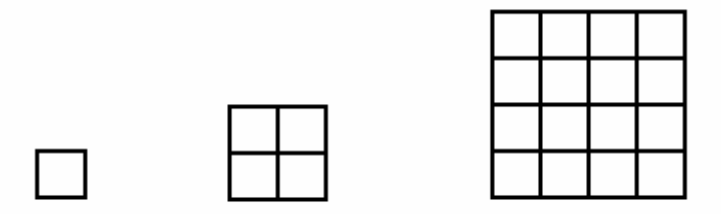

One Volt **Two Volts = Four** **Four Volts = Sixteen**

In resonant air-core coil energy transfer, the increase in flux lines present disturbs more electrons than previously, resulting in over-unity energy being present and available.

Energy stored, times the cycles per second, represents the energy being pumped by the system. Capacitors and inductors store electrons temporarily.

Capacitor formula: **W = 0.5 x C x E x Cycles per second** where:

W = energy in Joules (Watt Seconds)
C = capacitance in farads
E = applied potential in volts squared.

Inductor (Coil) formula: **W = 0.5 x L x I x Cycles per second** where:

W = energy in Joules (Watt Seconds)
L = inductance in henrys
I = current in amperes squared

Both one henry, and one farad, equal one volt. The higher the cycles per second, including the squaring of the flux lines, cause a large increase in the amount of energy being produced.

The above combined with a resonant energy induction system (where all electrons are moving in the same direction at the same time), make the next move into over-unity practical.

The dampening process of conventional electrical power generation, has all the available electrons bouncing randomly, mostly cancelling out each other. In that System, the useful energy available is a very small percentage of the energy which is present.

In the resonant induction system, a very high percentage of the energy present is useful. At resonance, (ohms-impedance-Z) becomes zero and all of the energy present is not degraded and becomes available to do useful work. "Ohms" is load or wasted energy, and "amperes" is the rate of that wasting of energy.

Using the previous information, if we now apply it to an air-core coil, resonant transformer energy system. L-1 and L-2 coils are now present. L-1 has a smaller number of turns and is several times the diameter of L-2. Input from a 12 volt high-voltage laser driver source, produces 8,000 volts with a low level of wasted energy, pushing amperage into, say, 4 turns of coil L-1. Each turn of the L-1 coil then acquires 2,000 volts of resonant potential. Consequently, each turn of L-2 is then exposed to the electric flux of 2,000 volts. Each turn at the bottom end of L-2 acquires 2,000 volts. The flux lines are squared and are additive as the voltage and amperage progresses towards the top end of L-2's large number of turns.

A huge number of additional flux lines which were not previously present become present at the top end of the L-2 coil. These flux lines excite the nearby electrons in it's earth and air and groundings. This high level of excitement above the ambient, causes a large number of electrons which were not previously a part of the energy present, to become available for use. At this point over-unity is present in large amounts.

The "bubble gum between the ears" response to this is: "this must be lots of volts but no amperes". Please recall that amperage is wasted energy, and that until that wasting occurs, there are no amperes. A good way to demonstrate this, would be to let the bubble gum crowd put their hands on the high-voltage end of the device while standing on wet ground (a people zapper). **Note: don't do this.**

This over-unity device produces energy at radio frequencies which range into the megahertz band. This allows the device to be small in size, and yet produce large amounts of energy. A megawatt-sized unit will sit comfortably on a breakfast table. This energy is changed to Direct Current and then switched to produce the desired working frequency AC.

Power Triangle

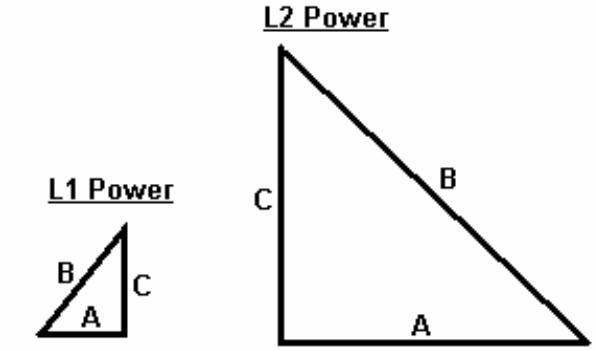

A: Volts x Amperes (the Available Power)

B: Volts x Ampres x Time (the Used Power)

C: Volts x Amperes x Recative (the Resinant Power)

1. Random movement of electrons in "A" and "B", mostly cancel each other out. This dampening, or wasteful concept of energy, is a source of much pleasure for the establishment.

2. "C" (Volt, Amperes, Reactive "V.A.R."), is the situation where all of the electrons move in the same direction at the same time. This results in near-unity energy output by resonant induction transfer.

3. Resonant induction transfer from one isolated power system, allows other resonant induction systems to duplicate the original source, which in no way diminishes the original source. Air-core coils (isolation-transformers) confirm this when they are a part of one of these functioning systems. A less perfect illustration would be the fact that the number of radio sets tuned to a particular radio transmission, does not alter the power required at the radio transmitter.

4. Resonant induction transfer, disturbs a large number of adjacent electrons which were not a part of the original input power source. The pulsating-pumping effect then draws in the newly available additional electrons into the on-going energy generation system. A near unity energy system of resonant air-core coils and the extra acquired electron-energy source constitute an over-unity system.

Electrical Power Generation / Points of Reference

Useful Electrical Power is Generated when Electrons from Earth and Air Groundings are disturbed by the movement of coils and magnets with reference to each other. The resulting electrical and magnetic energy is then changed to joules [watt-seconds: Volts x Amps x Seconds]. Each forward electron movement results in a magnetic impulse and each return movement causes an electrical impulse. The composite of the electrical energy impulses from these electrons yields useful energy [Power].

Let the above electron movement be represented by a room full of ping pong balls bouncing randomly. Most of the energy present cancels out by random impacts. This is the Classic Under-Unity approach to Electrical Power Generation, sanctioned by the Establishment.

In contrast to that, in the Electrical Energy Generation System presented here, the resonant Electrons are all moving in the same direction at the same time. This allows Near-Unity Electrical Power to Develop. This is the room-temperature equivalent of super conductivity.

The Energy System presented here, consists of a properly-adjusted and functional resonant air-core coil tank. The magnetic energy is stored in the coil system and the Electrical Energy is stored in capacitors. From Maxwell and others, we know that electrical-related energy has an equal amount of magnetic energy associated with it.

"The formula which establishes the Useful Energy of the System":

Joules = 0.5 x **C** x **V** squared x **C.P.S.** squared
units:
Joules (Volts x Amps x Seconds) Watt Seconds

C = Capacitance in microfarads
V = Potential in Volts
C.P.S. = Cycles per second

The transfer of Electrical Power by Resonant Induction is a direct function of the squaring of the cycles per second. For example, square 60 C.P.S. and then square the radio frequency C.P.S.s of the System here presented. Obviously, One Million Cycles per Second transfers more energy than Sixty Cycles per second. The Sanctioned Method of Electrical Power Generation uses the 60 C.P.S. Method. Using 60 C.P.S. and the random scattering of the Electrons System, assures the Establishment of it's desired Under-Unity Goal.

This random bouncing of the Electrons is the Ohms of Ohm's Law and is used to establish the rate of dissipation and/or Load [Work].

In the Resonant Tank Induction Energy Transfer System presented here, Impedance [system resistance] replaces the conventional ohm's usage. At Resonance, impedance becomes zero and the full force and effect of the Energy Transfer occurs. This is superconducting conditions at room temperature. At radio frequency the Electrons do not pass through the conductor as they do at lower frequencies. Instead, these Electrons encircle the conductor and are free of the conductor's resistance.

Let the Establishments Power Generation System be called 'A" and the System presented here be called "B".

With "A": Given 60 C.P.S. at 120 Volts using a 10 microfarad Capacitor:

Joules = [0.5 x 0.000010 x 120 squared] x C.P.S.s squared

(120 x 120 = 14,400)
[0.000010 x 14,400 = 0.144]
[0.144 x 0.5 = .072]
(0.072 x 3,600 = **259.2**]

Using the Inventor's Resonant Induction System, the Electrical Power available would then be 259.2 Joules [Watt-Seconds]. Using the Establishment's method only permits less than 10 Watt-Seconds of Useful Electrical Energy.

"B". Given One Million Cycles per second at 100,000 Volts, using a 10 microfarad Capacitor.

Joules = [0.5 x 0.000010 x 100,000 squared] x C.P.S.s squared

(100,000 x 100,000 = 10,000,000,000)
[0.000010 x 10,000,000,000 = 100,000]
(100,000 x 0.5 = 50,000]
(50,000 x One Million squared = **50,000,000,000,000,000**)

The useful Electrical Energy available is greater than 50 Mega Watts. Since the Resonant Electrons are non-impacting, all of the Energy is available for direct usage.

Benefits of the Inventor's System

1. Induction Energy transfer is enhanced by the squaring of the cycles per second produced by the System.

2. Induction Energy transfer is enhanced by the squaring the input voltage and amperage.

3. The increase of the flux lines occurring from the above, disturbing more electrons, causes more electrical energy to become available.

4. Resonant Induction has all of the Electrons moving unimpeded, resulting in superconductor conditions at room temperature.

5. A smaller amount of energy is used to disturb a larger number of Electrons. Electrons not originally a part of the System then contribute their energy, resulting in a net gain in available usable power.

6. The physical size of the System [Device] is small. The Device described in "B" sits comfortable on a breakfast table.

7. A small energy source is used to start the device and that source remains fully charged at all times by the System.

The Evidence Against Under Unity

1. Use of Logarithmic Scales on electrical measurement instruments. Linear measurement works fine where Ohm's Law applies (direct current). In alternating current, ohms are replaced by impedance and the measurements become non-linear.

2. Infinite "Q" at resonance confirms that voltage and amperage is squared, as in the kinetic energy formula. See the formulas of this report.

3. Square waves are clipped infinite "Q"s.

4. Maxwell and others show that magnetic-inductance-amperage and electrical-capacitance-voltage are two sides of the same coin. Magnetic-inductance is directly equal to amperage. Both obey the Law of Squares, which has over-unity built in.

5. Magnetic and electrical flux are present in enormous amounts at the outer ends of an operating Tesla Coil.

6. Ignorance of how to measure and relate magnetic and electrical flux, is the chief weapon of the under-unity gaggle.

7. The Cumulative inductance and capacitance of the Tesla Coil grounds itself out, if not properly utilized. See this report for the temporary energy storage accessible, when properly managed.

8. The Patent Office refers devices related to over-unity to their metering group, which is a sure indication that they are aware and accept the logarithmic measuring devices. This is direct and absolute evidence that they accept the square law as it relates to kinetic energy. This also indicates they are aware that over-unity exists. Since their bureaucratic brain is improperly motivated they continue to badger inventors who are working in the over-unity arena. Their level of intellectual dishonesty is sanctioned by, and is a real part of doing business with, a government which prides itself in being a hooliganistic bureaucracy.

Reading List

1. Alston, L.L. (Ed.), 1968, High-Voltage Technology, Oxford Univ. Press, London
2. Beck, E. 1954, Lightning Protection for Electric Systems, McGraw-Hill, N Y.
3. Bowdler, GAV. 1973, Measurements in High-voltage Test Circuits Pergamom, Oxford. L C. 72-86488
4. Brewley, L.V., 1951, Traveling Waves in Transmission Lines Pub: John Wiley. N.Y.
5. Chapman, S. and Barteis, J . 1940, Geomagnetism, two volumes, 1,000 plus pages, Oxford at the Clarendon press, England
6. Craggs. J.D. and Meek, J.M. 1954, High-Voltage laboratory Technique., Butterworth, London
7. EHV Transmission Line Reference Book, 1968 Edison Elcctric Institute, N.Y.
8. Farno, R.M., Chu. L.J., and Adler, R.B., 1968, Electromagnetic Fields, Energy and Forces, Pub: M.I.T Press, Cambridge, Mass.
9. Feinberg, R. (Ed.) 1979, Modern Power Transformer Practice, McMillan. London
10. Frungel, F., High Speed Pulse Technology, Vols 1 and 2, Pub: Academic Press. 1965, N.Y., and London
11. Gallagher, T.J. and Pearmain, AJ. 1983, ISBN 0-471-90096-6 High Voltage Measurement and Design, John Wiley, N.Y.
12. Hague, B., Alternating-Current Bridge Methods, 5 th. ed. Pub: Sir lsaac Pitman and Sons, 1959, London.
13. Hawley, W.G. 1959, Impulse-voltage Testing, Chapman and Hill, London.
14. Hayashi, Ch., Non-linear Oscillations in Physical Systems, Pub: McGraw-Hill, 1964. N.Y.
15. Henny, K. 1933-1959, Editor-in-Chief, Radio Engineering Handbook, five different copyrights, L.C. 58-11174, McGraw-Hill. N.Y.
16. Hudlestone, R.H. and Leonard, S.L., Plasma Diagnostics Techniques, Pub: Academic Press. N.Y.
17. Jacobs, J A., Editor, Geomagnetism, (a massive work) 3 large volumes, Pub: Academic Press, London.
18. Jeans, J.H. 1925, The Mathematics of Electricity and Magnetism, 5 th. Ed., Cambridge University Press,
19. Jones, B. 1972, New Approaches to the Design and Economics of EHV Transmission Plant, Pergamom, London.
20. Kind, D. 1978, An Introduction to High-voltage Experimental Technique, Viewieg, Braunschweig ISBN 3-528-08383-2
21. Knoepfel. H. 1970. Pulsed High Magnetic Fields, North-Holland, Amsterdam.
22. Kreuger, F H. 1964, Discharge Detection in High-Voltage Equipment, Temple Press, Heywood, London.
23. Kuffel, E. and Zacngl. W S. 1984, High-Voltage Engineering, Pergamom, ;London. ISBN 0-08-024213-8
24. Kupfmuller, K. 1957, Introduction to the Scientific Basis of Electrical Engineering, Pub Spinger. Berlin.
25. Lemon. H.B. and Ference, M. Jr., Analytical Experimental Physics " a major work" from The Ryerson Physical Laboratory at the University of Chicago, numerous copyrights 1933-1944. Printed as a text book by the University of Chicago Press
26. Lewis, I.A.D., and Well, F.H., Milli-microsecond Pulse Techniques Pub: Pergamom Press, N.Y. and London.
27. Malan, D.J. 1963, Physics of Lightning, English University Press, London.
28. Martin, T.L Jr., Physical Basis for Electrical Engineering, Prentice-Hall, N.J.
29. Matsusta, S. and Campbell, W.H . 1967 Physics of Geomagnetic Phenomena, Massive work in two volumes of 700 pages each. Academic Press, London.
30. National Physical laboratory, 1956, Notes on Applied Science ii 17, High Voltage Impulse Testing. HMSO.
31. Rather, H.. 1961, The Electron Avalanche and it's Generation, Pub: Vo. 33, Springer, Berlin.
32. Rokityansky, I.I., 1982. Geo-electromagnetic Investigation of the Earth's Crust and Mantle, Pub: Springer-Verlag, Berlin.
33. Salge, J., Pcier, D , Brilka, R., Schneider, D„ 1970, Applications of Inductive Energy Storage for the Production of Intense Magnetic Fields, Pub: Procedure of 6 th. Symp. on Fusion Technology, Aachen
34. Schulz, E.H., Anderson, L.T., and Leger, R.M., Experiments in Electronics and Communication Engineering, Copyrights, various, from 1943 thru 1954 LC 55-5033 Harper and Brothers, N.Y.
35. Schwab, AJ 1972, High-Voltage Measurement Techniques, The M I T. Press, Cambridge. Mass., ISBN 0262-19096-6
36. Sevin, L., 1965, Field Effect Transistors, McGraw-Hill, London.
37. Silsbee, F.B., 1942, Static Electricity, U.S. Department of Commerce, Washington. D C , U.S. Government Printing Office, (N.B.S. Circular C 438)
38. Smith, A. A., 1977, Coupling of External Electromagnetic Fields to Transmission Lines, ISBN 0-471-01995-X
39. Terman. F.E., Electronics and Radio Engineering, 4 th. ed., Copyrights 1932, 1937, 1947 and 1955 LC 55-6174 McGraw-Hill Book Co., N.Y
40. Thomas, R.T.,1970 High-Impulse Current and Voltage Measurement, Trans. I.E.E.E. EV1-19, pages 102-107
41. Thompson, Professor W, (titled Lord Kelvin) Reprint of Papers or. Electrostatics and Magnetism (original 1872) London.
42. Traister, R., 1983, The Experimenter's Guide to Solid State Diodes, Prentice-Hall, Inc. ISBN 0-13-295444
43. Valley, G.E, and Wallman. II . 1948, Vacuum Tube Amplifiers, McGraw-Hill, N.Y.
44. Weedy, B.M. 1980, Underground Transmission of Electrical Power, Wiley, London,
45. Weeks, W L. 1981, Transmission and Distribution of Electrical Energy, Harper and Row, N.Y.
46. Winch, R_P. Electricity and Magnetism (several printings) Composed in Copenhagen, Denmark, Prentice-Hall Physics Series
47. Zijlstra, H., 1957, Experimental Methods in Magnetism, two volumes, the North-Holland Publishing Co.. Amsterdam.

An Answer to America's Energy Deficit

Donald L. Smith

Energy Consultant

Energy, energy everywhere and not a Joule to Jounce. Conventional wisdom, when properly tuned will appreciate the nature of energy, as here presented. The basic unit of electricity (the electron) upon encountering a moving magnetic field (or wave) spins, giving off an electric impulse. When this impulse collapses, it spins back to it's natural position, giving off a magnetic impulse. Therefore, magnetic and electric are two sides of the same coin. When the magnetic side is pulsed, it yields electricity and conversely, pulsing of the electrical side yields a magnetic field. Moving one in relation to the other produces useful energy. When done consecutively, each cycle pushes (current) forward, while pulling electrons into the system... in much the same way as a water pump moves water. These electrons are obtained from Earth and air grounding.

The word "electric" comes from the Latin word electron "amber". When rubbed, amber develops an electrical charge, which can be transferred to a dissimilar substance. During the seventeenth and eighteenth centuries, a great deal of attention was centered on this attribute of amber. Amber was used to differentiate the non-metals. Carbon-related substances and other non-metals, when subjected to friction, give up negative electrical charges. On the other hand, metals when subjected to friction, simply conduct the charge. It is important to note that approximately 70% of the Earth's exposed crustal portions (surface) consist of silicone-related non-metals (electron donors) and become a direct source of electrical energy when properly agitated.

Useful electrical energy can be obtained by grounding into the Earth's non-metal crust and into it's atmosphere as a natural source of electrons. These electrons have accumulated from the solar plasma during the aging of the Earth for more than 4.5 billion years, at a rate exceeding 3.9 exajoules per year This indicates that the Earth's electrical field contains in excess of 17.6×10^{18} of cumulative exajoules of energy. One exajoule is the approximate energy equivalent of 125 million barrels of oil. The electrical energy in one display of lightning is approximately ten trillion joules. During each 24 hour period, the land portions of Earth's surface yields in excess of 200,000 emissions, which involves more than 2,000 quadrillion watts.

C.F. Gauss (1777-1855) and H.C. Oersted (1777-1851) were each separately trying to define the Earth's electrical field with all external influences removed. These external influences being solar-quiet periods and being remote from the land's surface. The air electricity background which they measured varies with latitude. Their European measurements correspond to approximately the latitude of Washington. D C. They were measuring magnetic field flux as an indicator of negative electron energy active and present. A related family of measurement are now presented. Units of measurement used to define flux fields include Gauss (one unit = 100,000 volts), Oersted (one unit = 50,000 volts), Tesla (one unit = 10,000 Gauss) and Gamma (one unit = 1/10,000 of a Gauss). Much confusion exists in electrical related publications about these units. As presented here they are correct with values taken from their original definitions.

The entire surface of the Earth has been surveyed by aerial magnetometer, in most cases using gamma or nano teslas. One gamma is the magnetic flux equivalent of 10 active volts of electricity. When the data is corrected for flight height it becomes obvious that there are numerous areas where the gamma readings exceed one trillion gammas. Lightning strikes from the ground up are in that energy range. With knowledge of these electron enriched areas, the quality of Earth grounding, becomes enhanced. The correction necessary for land surface data when acquired from aerial magnetometer maps (using Coulomb's law) requires that the remote distance be squared and then multiplied by the remote reading. As an example, if the remote reading is 1,600 gammas and the flight height being 1,000 feet. Take 1,000 x 1,000 = 1,000,000 x 1,600 gammas = 1.6 trillion gammas x 10 volts = 16 trillion volts equivalent for land surface data. Present day methodology requires mechanical energy in exchange for electrical energy. Once obtained, this energy is subject to Ohm's Law. Present Methodology obtains it's electrical energy from it's non-metal and air groundings.

This same energy can be obtained without the wasteful mechanical approach and at a much, much lower cost. Any required amount of electricity is available by resonant induction transfer from the

Earth's magnetic and electrical fields. The major difference is in the functioning of Ohm's Law in relation to resonant circuits. In the resonant induction system suggested here, system resistance (Z) becomes zero at resonance.

Therefore, Volts and Amperes are equal (V.A.R.) until work (load) is introduced.

Each cycling of this resonant induction system pulls in additional electrons from the Earth's electrical field, generating electrical energy in any required amount. In this system, a small amount of electrical energy is used to activate and pull a much larger amount of energy into the system.

This electrical advantage corresponds to the pulley and lever of the mechanical world. The electrical system presented here is extremely efficient. Using present methodology as a basis for comparison, with it's 60 cycles per second system. The resonant induction system, cycling at 60 million times per second produces one million times the energy which is produced by the present energy systems. A single small size unit of the resonant induction system has more usable electrical output than a major conventional unit. The radio frequency energy produced is easily changed to Direct Current, and then to the present 60 cycles per second system in preparation for commercial usage.

The Patent Pending on this system is #08/100,074, "Electrical Energy Generating System", dated 4 February, 1992.

Definitions: One **Joule** is one watt for one second
One **Watt** is one volt ampere
V.A.R. is Volt Amperes Reactive

Additional Reading:

Electricity and Magnetism by B.I. Bleany and B. Bleany Oxford University Press 1991 ISBN. 0-19-851172-8

Engineering Electromagnetics by W. H. Hayt. Jr. McGraw-Hill 1989 ISBN. 0-07-027406-1

Energy Methods in Electromagnetism by P. Hammond Oxford University Press 1986 ISBN. 0-19-859368-6

Energy in Electromagnetism by H. G. Booker Institution of Electrical Engineers by Peter Peregrinus Ltd. 1982 ISBN 0-900040-59-1

The American Radio Relay League Handbook for 1992 and 1993. 69th and 70th editions. Published by The American Radio Relay League. (For V.A.R. information) ISBN. 0-87259-169-7

Electron Paramagnetic Resonance, Techniques & Applications by R. S. Alger, U. S. Naval Radiological Defence Laboratory, San Francisco, California. Pub. Interscience Lib. Congress #67-20255

Geomagnetic Diagnosis of the Magnetosphere by A. Nishida, University of Tokyo 1978 Pub: Springer-Verlag ISBN. 0-387-08297-2

Energy and The Missing Resource by I. Dostrovsky. Pub: Cambridge University Press 1988 ISBN. 0-521-26592-4

High Voltage Measurement Techniques By A. Schwab, M.I.T.. 1971 I S.B.N. 0-262-19096

Environmental Magnetism by R. Thompson & F. Oldfield Pub: Allen & Unwin, London 1986 ISBN. 0-04-538003-1

Geo-electromagnetic Investigation of the Earth's Crust and Mantle. Translated from Russian, By I. I. Rokityansky. Institute of Geophysics, Kiev, U.S.S R. Pub: Springer-Verlag 1082. ISBN. 3-540-10630-8

Electron Paramagnetic Resonance of Transition Ions by A. Abragam and B. Bleaney Dover Publications, New York, N.Y. 1986

The Electromagnetic Field by A. Shadowitz, Dover Publications, New York, N.Y.

Geomagnetism, Several Volumes, Pub. Periodically by J.A. Jacobs, Institute of Earth Studies, Dyfed, U.K. Pub: Academic Press 1989-1990's.

Geomagnetism by S. Chapman and J. Bartels, 3 Volumes Oxford University Press, 1940

Physics of Geomagnetic Phenomena, Several Volumes by S. Matsushita and W. H. Campbell National Center for Atmospheric Research, Boulder, Colorado Library of Congress #67-23168 Pub: Academic Press, 1967

Physics Problems and How to Solve Them by C. E. Bennett, Professor Emeritus of Physics. University of Main (Particularly the sections on Electricity and Magnetism, and Units of Measure). Pub: Harper & Row ISBN. 0-06-460203-6

Units and Standards for Electromagnetics By P. Vigoureux, National Physical Laboratory Pub: Springer-Verlag 1071 ISBN. 0-387-91077-8

Surveyor's Guide to Electromagnetic Distance Measurement. Edited by J. J. Saastamoinen, Canada Pub: University of Toronto Press

Electromagnetic Distance Measurement by C. D. Burnside Pub: Granada, London 1971
ISBN. 0-258-96793-5

Der Magnetische Kreis "The Magnetic Circuit" By Von Heinz Rieger of Siemens AG. 1970 Berlin and Munchen, Germany I.S.B.N. 3-8009-4719 6

Electronic Modelling of Power Electronic Converters by J. A Ferreira Pub: Kluwer Academic 1989 33 AH Dordrecht, The Netherlands I.S.B.N. 0-7923-9034-2

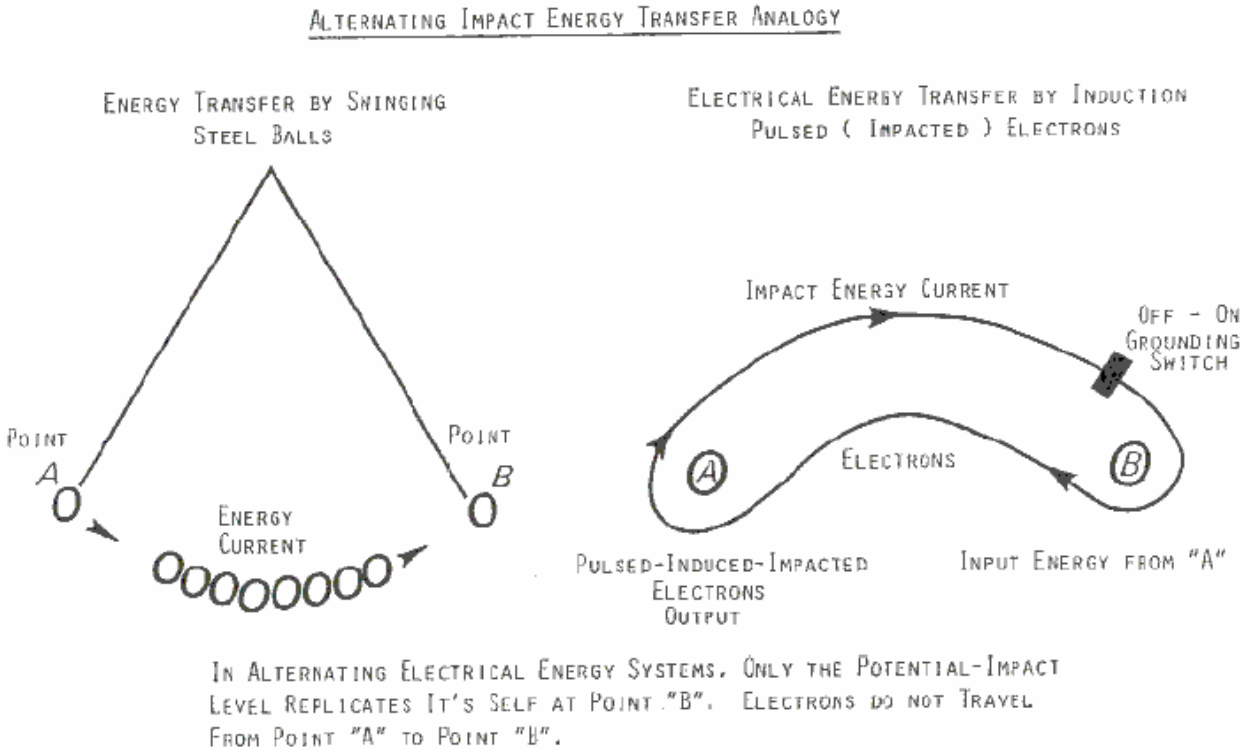

E.E.S. II, BACKGROUND INFORMATION & CONCEPT

With alternating electrical current, electrons do not move from point "A" to point "B" as commonly envisioned! Electrical potential (oscillating electrons) at point "A", results in harmonic electron activity at point "B", when the grounding switch (circuit) is closed. That is to say, point "B" supplies it's own electrons and mirrors the activity of point "A". Impulsing (turbulence) by magnetic induction causes electrons to be pulled into the system, which then oscillates. When the magnetic field collapses (becomes absent) the electrical potential returns to it's natural background level.

Several major flaws are present in the conventional 60 cycles per second method of electrical power generation and it's iron core transformer system. ***This system is handcuffed by the inverse relationship of volts to amperes.*** This represents a stodgy, inflexible inheritance, courtesy of Mr. T.A. Edison and his concept of electrical power generation.

Nikola Tesla stood, almost alone, against Edison and managed to prevail with his Alternating Current system. Without the alternating current system, electronic things in the modern sense would not exist.

This report will be concerned with some of the extensions and benefits of the alternating current electrical system. ***This study will limit it's scope to air core coil transformers at radio frequency and upwards. The electrical power produced by this method is inverted to Direct Current and then to Alternating Current as required for popular usage.*** There are several important advantages of this system over conventional power generation.

Start with two coils (separate-apart), one being a reactor coil (L-1) and a second coil (L-2), being the reactant coil. Magnetic field fluxing (off-on of the electrical source) causes inductive reactance of L-1 which replicates by induction in L-2. Pulsing of the magnetic field (from L-1) in the presence of L-2, generates electrical potential. For example, should the L-1 coil have ten turns, with an imposed AC. potential of 1,200 volts. This results in each turn of L-1 acquiring 120 volts of potential. This induced magnetic field, then replicates itself in each turn of the L-2 coil. The L-2 coil may have one or many hundreds of turns. Modern encapsulation techniques makes high frequency and high energy controllable.

Let's take another important step in this air-core transformer process. For purpose of discussion, let the value of inductive reactance at 60 cycles per second, equal one. Each time the frequency is doubled, the effectiveness of induction is squared. At about 20,000 Hz, ***when radio frequency is achieved, the electrons begin spinning free, outside of the inductor and they become increasingly free of the inverse relationship of volt-amperes.*** From this point on, they replicate by the inductive process as V.A.R.. *That is to say,* ***volts and amperes are equal, until resistance (work) is introduced. Therefore, additional, not previously available electrons become incorporated for a very large net gain in potential. This gain is real !***

The quality of the grounding system determines the effectiveness of this method of producing electricity. A handy reference to locate the negative grounding areas for power generation can be found in the Aeromagnetic Map Studies of the US Geological Survey. They provide an excellent method for locating the best sites for optimum negative grounding areas.

When this method is combined with the induction coil system, already described, it provides an electrical power generating system millions of times more efficient than any known conventional method.

This new system ("E.E.S. II") is uncomplicated, physically small and it is inexpensive to build. The technology required for it's construction already exists. Maintenance is near zero, as there are no moving parts. Once operating, this system could last forever.

Small mobile E.E.S. II units are already available as replacements for the batteries used in electric automobiles. Larger E.E.S. II units can be provided as a replacement source of power for hotels, office buildings, subdivisions, electric trains, manufacturing, heavy equipment, ships, and generally speaking, any present day application of electrical power.

Earth Electrical System II, Modular Units

The system consists of three separate modules. Reverse engineering is used in matching the modules to the desired usage.

HIGH VOLTAGE INDUCTION TRANSFORMER MODULE:

1. Preferably an off-the-shelf-unit similar to a TV flyback and/or automobile ignition type related coil (transformer).

2. Ratio of input to output may be from less than 1:100 to greater than 1:1,000 A voltage tripler may then be used.

3. A connection allowing the high voltage output to pass onward through the induction coil L-1 and then to it's grounding.

AN AIR CORE INDUCTION COIL TRANSFORMER MODULE:

1. There are two coils: the reactor coil L-1 and the reactant coil L-2. L-1 has a high voltage radio frequency capacitor between it and it's grounding.

2. Input into the L-1 inductor is divided by the number of turns in it. The magnetic flux field provided from each turn of L-1 replicates itself as an electrical potential in each turn of L-2.

3. L-2 may have one turn or many hundreds of turns. The net gain depends upon the number of turns in L-2. Output from L-2 is in V.A.R. ***With this type of output, volts and amperes are the same until work(resistivity) is introduced.***

THE INVERTER MODULE:

1. Inverts to direct current (D C.)

2. Inverts to alternating current (A C), as desired.

3. Provides customized output of electrical power ready for designated usage

EARTH ELECTRICAL SYSTEM II, DOMESTIC USE RANGE MODULE
UP TO TWO MILLION VOLT-AMPERES-REACTIVE OUTPUT *
PLAN "A", WITH VARIABLE CONTROLS
NOT TO SCALE

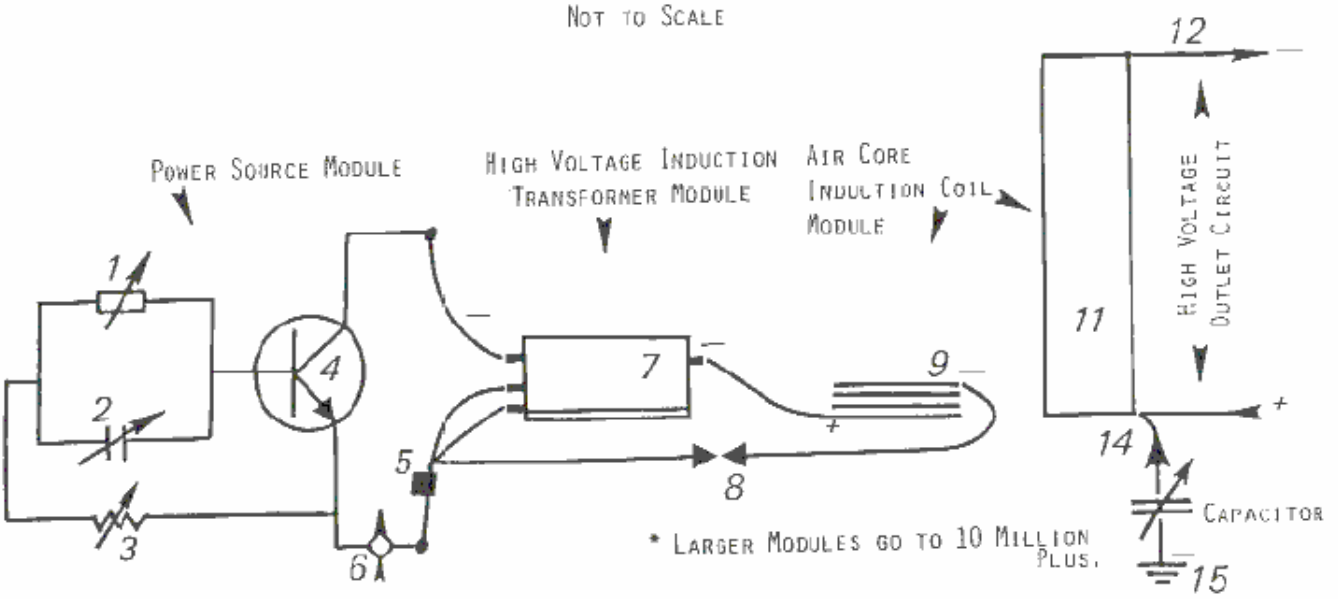

PARTS: 1. COIL, VARIABLE. 2. CAPACITOR, VARIABLE. 3. RESISTOR, VARIABLE. 4. TRANSISTOR, R.F., 5. BATTERY, RECHARGEABLE. 6. OFF-ON SWITCH, VARIABLE. 7. HIGH VOLTAGE TRANSFORMER, 8. FEED BACK WITH SPARK GAP. 9. REACTOR, INDUCTION COIL. 10. FEED BACK WITH SPARK GAP, 11. REACTANT COIL. 12. OUTPUT FOR # 11. 13. INPUT FOR ELEVEN. 14. GROUNDING FOR ELEVEN.

EARTH ELECTRICAL SYSTEM II, DOMESTIC USE RANGE MODULE
UP TO TWO MILLION VOLT-AMPERES-REACTIVE OUTPUT *
PLAN "B", ELECTRICAL AUTOMOBILE ENERGY SOURCE

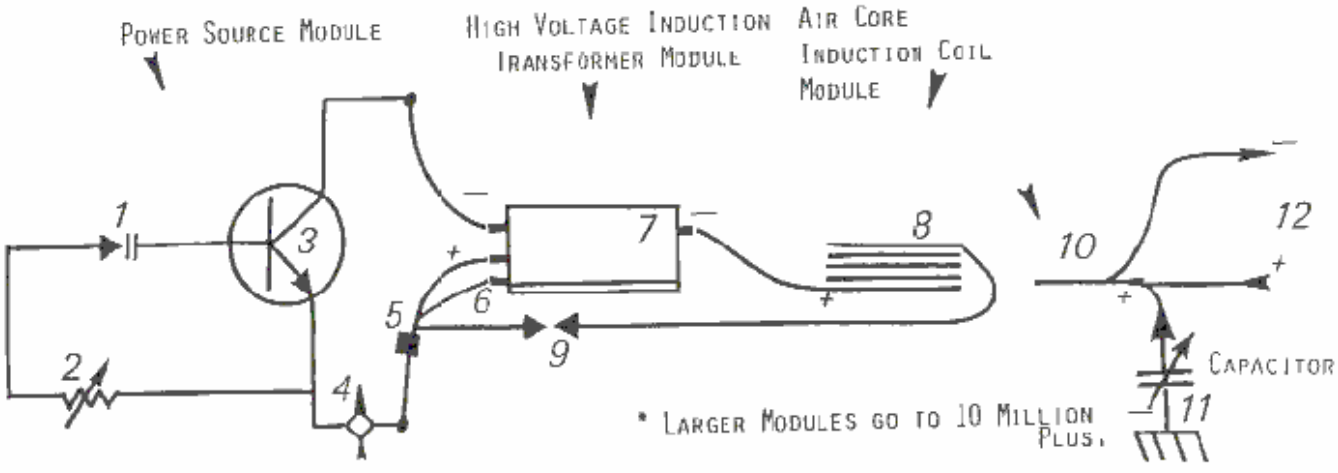

PARTS: 1. VARACTOR, RADIO FREQUENCY. 2. RESISTOR. 3. TRANSISTOR, RADIO FREQUENCY. 4. OFF-ON SWITCH, MULTI-POSITION. 5. BATTERY, RECHARGEABLE. 6. TRANSFORMER GROUNDING. 7. HIGH VOLTAGE INDUCTION TRANSFORMER. 8. REACTOR, INDUCTION COIL. 9. FEED BACK WITH SPARK GAP. 10. REACTANT, INDUCTION COIL. 11. GROUNDING FOR # 10. OUT-PUT CIRCUIT. IN VOLT-AMPERES-REACTIVE.

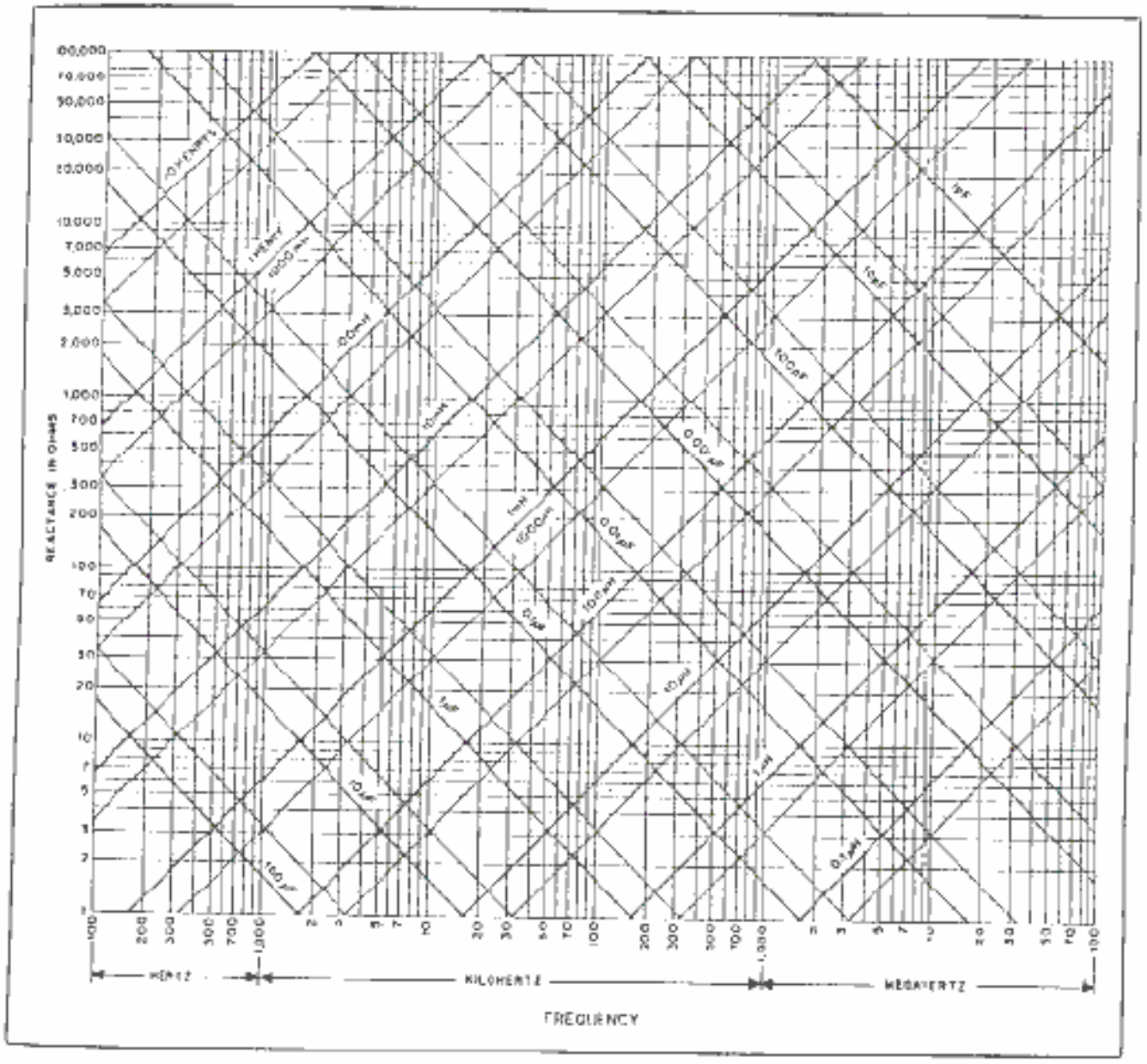

Fig. 44 — Inductive and capacitive reactance vs. frequency. Heavy lines represent multiples of 10, intermediate light lines multiples of five. For example, the light line between 10 μH and 100 μH represents 50 μH; the light line between 0.1 μF and 1 μF represents 0.5 μF, and so on. Intermediate values can be values within the chart range. For example, the reactance of 10 henrys at 60 Hz can be found by taking the reactance of 10 henrys at 600 Hz and dividing by 10 for the 10 × times decrease in frequency.

CHART, COURTESY OF A.R.R.L., 1992 ED.

Speech presented the evening of 23 July. 1994 at the
International Tesla Society Convention at Colorado Springs. Colorado.

DONALD L. SMITH
ENERGY CONSULTANT
8110 BENT OAK LANE
SPRING. TEXAS 77379

ELECTRICAL ENERGY REFERENCE POINTS

Electrical Energy Generating System
Patent Pending # 08/100.074. 2/4/92

The word "electric" comes from the Latin word electron "amber". When rubbed, amber develops an electrical charge, which can be transferred to a dissimilar substance. During the seventeenth and eighteenth centuries, a great deal of attention was centered on this attribute of amber. Amber was used

to differentiate the non-metals. Carbon-related substances and other non-metals, when subjected to friction, give up negative electrical charges. On the other hand, metals when subjected to friction, simply conduct the charge. It is important to note that approximately 70% of the Earth's exposed crustal portions (surface) consist of silicone related non-metals (electron donors) and therefore becomes a direct source of electrical energy when properly agitated.

Useful electrical energy is obtained by grounding into the Earth's non-metal crust and into it's atmosphere as a natural source of electrons. These electrons have accumulated from the solar plasma during the aging of the Earth for more than 4.5 billion years, at a rate exceeding 3.9 exajoules per year. This indicates that the Earth's electrical field contains in excess of 17.6×10^{18} power of cumulative exajoules of energy. One exajoule is the approximate energy equivalent of 125 million barrels of oil. The electrical energy in one display of lightning is approximately ten trillion joules. During each 24 hour period, the land portions of the Earth's surface yields in excess of 200,000 emissions, which involves more than 2,000 quadrillion watt-seconds of active energy on display.

This physical phenomenon indicates that the Earth's crust is an unending source of electrical energy. The surface area involved is a very small portion of the Earth's crust.

J.C. Maxwell (1891) suggested that an active electron field gives rise to an associated magnetic field. Therefore, both are present with pulsating current. Early studies, involving observation of compass needles by microscopy, revealed that the needle vibrates as with alternating current. More recent studies by A. Nishida and others, confirm that alternating current is common in the Earth's crust.

C.F. Gauss (1777-1855) and H.C. Oersted (1777-1851), both were separately trying to define the Earth's electrical field with all external influences removed. These external influences being solar-quiet periods and being remote from the land's surface. The air electricity background which they measured varies with latitude. Their European measurements correspond to approximately the latitude of Washington, D.C. They were measuring magnetic field flux as an indicator of negative electron energy active and present.

A related family of measurement is now presented. Units of measurement used to define flux fields include Gauss (one unit = 100,000 volts), Oersted (one unit - 50,000 volts), Tesla (one unit = 10,000 Gauss) and Gamma (one unit = 1/10,000 th of a Gauss). Much confusion exists in electrical related publications about these units. As presented here, they are correct with values taken from their original definitions.

The entire surface of the Earth has been surveyed by aerial magnetometer, in most cases using gamma or nano teslas. One gamma is the magnetic flux equivalent of 10 active volts of electricity. When this data is corrected for flight height, it becomes obvious that there are numerous areas where the gamma readings exceed one trillion gammas. Lightning strikes from the ground up are in that energy range. With knowledge of these electron enriched areas, the quality of Earth grounding, becomes enhanced.

The correction necessary for land surface data when acquired from aerial magnetometer maps (using the inverse square law) requires that the remote distance be squared and then multiplied by the remote reading. For example, if the reading is 1,600 gammas and the flight height is 1,000 feet. Take 1,000 x 1,000 = 1,000,000 x 1,600 gammas = 1.6 trillion gammas x 10 volts = 16 trillion volts equivalent for land surface data.

Present day methodology requires mechanical energy to be expended in exchange for electrical energy. Any required amount of electricity is available by resonant induction transfer from the Earth's magnetic and electrical fields. Each cycling of this resonant induction system pulls in additional electrons, generating energy in any required amount. A small amount of electrical energy is used to activate and pull into the system a much larger amount of energy.

ENERGY VERSUS MASS

Steady State	Unsteady State
Static "Pre-Energy "	Kinetic "Energy"
Mass attracts Mass, Gravity Dominates	Expanding, Magnetic Energy Dominates
	Electrons moving apart
	Pressure decreasing
	Cooling effect dominates
	Less scattering of Energy
	Negative resistance
	Contraction, Electrical Energy Dominates
	Electrons moving together
	Pressure increasing
	Heating effect dominates
	Scattering of Energy
	Positive resistance

Functions of active Electrons

Electrons become active when placed inside the critical distance allowed by their negativity.

Active Electrons provide:

1. Electricity
2. Magnetics
3. Gravitational thrust as in Electric Motors
4. The source of Visible Light
5. It's charge is Negative

They move in a closed loop as seen in the Icon for infinity, not in a circle as shown in many books. One half of the loop consist of a magnetic impulse and the return half consist of the electrical impulse. This is seen as the classic sine wave of alternating electrical energy.

A flash of light occurs when two electrons suddenly find they are too close together. Daylight results from the impingement of Electrons in the Earth's atmosphere with the Electrons of the Solar Plasma.

My Concept of the Forces of Nature differs from the conventional. It consist of a weak and a strong force, each being additionally composed of electrical, magnetic and gravitational (fields and waves). Any two of the three constitute the third member; Gravity "B" of the weak force competes with humans on a daily basis. Gravity "A" of the strong force is the force that holds the Solar System and the Universe in place. Energy from the Electrons represent the weak force. Energy inside the Atom represents the strong force "A". Controlled resonant induction of any two of the three, changes into the third and is the motor that runs the Universe. We see this in the electrically-induced magnetic thrust against gravity in electric motors.

Weak force is required to dislodge electrons and strong force (atomic) to dislodge protons. Unless dislodged, these particles are of little value in producing Conventional Electrical Energy.

Therefore, in conventional electrical energy production, the particle of importance is the negative electron. Electrons have a "grudging" relationship with other electrons. They like each other, especially at arms length. Like potentials repel each other, and unlike potentials attract. To demonstrate this, take two batteries of the same type, but of a different charge level (unequal potentials). Put the plus and

minus ends facing the same direction. Then with a volt meter, measure the electrical potential between the two negative ends and then the two positive ends. It is obvious that the "more negative" moves to the "less negative" is the correct concept for electrical energy generation. Electrical Energy flow consist of a higher concentration of electrons moving to an area of lesser concentration.

OHM'S LAW WITH CORRECTIONS:

A major obstruction in reference to the correct function of electrical energy is the establishment's incorrect interpretation of Ohm's Law. The corrected version is:

Volts = Energy Available (Potential)

Ohm = Scattering, dissipation of Energy (Load)

Ampere = the rate of, dissipation / scattering of energy

It is important to note that Ohm and Ampere are after the fact, and are not decisive except for the dissipation factor. High Voltage at low amperage simply means that the High Voltage is still intact for future usage. In no way is the potential diminished by low amperage.

EXAMPLES OF OVERUNITY

Dominos did not exist in England when the Laws of Conservation were originally put in place. Otherwise they might have been very different. For example, let us take a long row of upright dominos, (many thousands) and flip number one. The Energy required to flip the first domino must now be added with that of thousands more in order to have a correct assessment.

The Electron itself is an excellent example of over-unity. The electron provides various forms of energy continuously throughout eternity and is in no way diminished. It simply cycles through the system and is available thereafter.

In Electrical Systems, Electrons active at point "A" are not the same Electrons active at point "B". That is to say, the Electrons activated at the Central Electrical Energy Station are not the ones used at your house. When you ground your system by flipping the wall switch, you use your own electrons. In closed energy systems, electrons communicate with and replicate the activity of the overbalanced potential, when provided with Earth and or Air Groundings.

The number of Radio sets and Television sets running at any one time do not diminish, in any way the electrical output of the source station.

For example, let now use an Air Coil Resonant Induction System for the purpose of flipping some electrons. The flipping device (reactor coil L-1) is pulsed, which then provides a resonant induction pulse. In turn, this flips the electrons present at the (reactant L-2) Coil. The energy input in L-1 is divided by the number of turns present. The induced magnetic pulsing in turn flips the electrons in each turn of L-2. If more turns are present in L-2 than L-1, there is a net gain in the Energy present, as demonstrated by the dominos above. The farads and henrys of the resonant system provide the resonant frequency when pulsed by an external energy system. A system shunt in the resonant circuit sets the containment level for energy potential.

The Induction Process itself provides an excellent example of over-unity. When comparing rate of induction, the cycles per second must be squared and then compared to the square of the second System. Let us then compare the 60 c.p.s. System with my 220 MHz Device. Energy produced at radio frequency has several major advantages over the conventional system. Ohm's Law does not apply to a resonant air-core radio frequency system.

For example: When the system is resonant, the following is true:

EXPECTED RESULTS

$$\frac{\text{Energy Potential as Volts}}{\text{Dissipation}} = \text{Rate of Dissipation}$$

ACTUAL RESULTS

Superconductor Conditions take over

$$\frac{\text{Energy Potential as Volts}}{(\text{Dissipation})^*} = (\text{Rate of Dissipation})^*$$

*** OHMS / DISSIPATION IN AIR-COIL RESONANT INDUCTION SYSTEMS: RESISTIVITY BECOMES ZERO AT RESONANCE**

This is named the V.A.R. (Volt Amperes Reactive) System.

When compared to the Conventional Under-Unity iron-core transformer system, the results are over-unity. It is strange that mechanical advantage as in pulleys, gears, levers and others which correspond to the electrical advantage above mentioned, are not considered over-unity devices.

Let us take a closer look at resonant induction. As an example, let a room full of ping pong balls randomly bouncing at a high speed represent the Conventional method of under-unity energy generation. Suppose that by resonant induction the balls all move in the same direction at the same time. When this occurs a huge amount of energy not previously available is present. The resonant air-core coil system lines up the electrons in such a manner that the energy factor is nearly 100 % , and not the 2% or 3% of Conventional under-unity devices sanction by the establishment.

Some other devices where overunity is common would be resonant induction circuits present in conventional radio tubes (high plate voltage), negative-feedback systems found in Op-Amps and possibly others.

SUMMARY

Useful electrical energy is achieved when the electron density at point "A" becomes greater than at point "B", (being the more-negative moving to the less-negative concept). Coils moving through a magnetic field or vice versa causes this imbalance.

The mindset of the professional Electrical Engineer is restricted to non-resonant and iron-core coil resonant systems. Ohm's Law, when applied to resonant air-core induction systems, becomes, system resistivity (impedance, Z). "Z" becomes zero at resonance. Therefore, in this system, volts and amperes are equal until load (resistivity) is introduced. This is called the Volt Ampere Reactive (V.A.R.) System. With impedance being zero, the System grounding is coupled directly into the Earth's immense electrical potential. Efficiency of induction relates to the square of the cycles per second. Compare the ratio of the conventional 60 c.p.s. System and the 220 million plus cycles of my Earth Electrical System II.

Electrons which cycle through this system, after being used, are returned intact to their former state for future usage.

Electron spin causes electrical current and magnetic lines of force

The effect of current, results from the unequal distribution of negativity (electrons).

Magnetic imbalance causes the gravitational effect. This is evidenced in electric motors by magnet-gravitational displacement of mass which causes the motor to rotate.

The System is an extension of present technology.

The System and it's source utilizes magnetometer studies.

This System (Earth Electrical System II. "E E S . II") utilizes a fully renewable energy source.

This System utilizes a non-polluting energy source.

This System utilizes an universally available energy source.

Endorsement and Certification of The System can be anticipated by States with pollution problems.

AIR CORE INDUCTION COIL BUILDERS GUIDE

DONALD L. SMITH

Energy Consultant

1. Decide frequency. Considerations are: (economy of size)

a. Use radio frequency upward (above 20,000 Hz).

b. Use natural frequency (coils have both capacitance and inductance), that is match the wire length of the wire in the coil to the desired frequency.

c. Wire length is either one quarter, one half or full wave length.

d. To obtain the wire length (in feet) use the following: If using one quarter wave length divide 247 by the desired frequency (megahertz range is desirable). If using one half wave length divide 494 by the desired frequency. If using full wave length divide 998 by the desired frequency.

2. Decide number of turns, ratio of increase in number of turns sets the function. In the case of the L-1 coil, each turn divides the input voltage by the number of turns. In the case of L-2 coil, the resulting voltage in each turn of L-1 is induced into each turn of L-2, adding up with each turn. For example if the input into L-1 from a high voltage, low amperage module is 2,400 volts, and L-1, for example, has 10 turns, then each turn of L-1 will have 240 volts of magnetic induction which transfers 240 volts of electricity to each turn of L-2. L-2 may be one turn or many turns, such as 100 to 500 or more turns. At 100 turns, 24,000 volts would be produced. At 500 turns, 120,000 volts would be produced.

3. Decide the height and diameter of the coil system. The larger the diameter of the coil, the fewer turns are required, and the coil has a lesser height. In the case of L-2 this results in lowering the amplification of the induced voltage from L-1.

4. For example, if 24.7 MHz is the desired frequency output from L-2. One quarter wave length would be 247 divided by 24.7 which equals 10 feet of wire. The number of turns will be the amplification factor. The coil may be wound on standard size P.V.C. or purchased from a supplier. The supplier is normally a ham radio supply source. Once the length is determined and the number of turns decided, move to the next step. For example, let each turn of L-1 have 24 volts and desired output of L-2 be 640 volts. Therefore L-2 needs 26.67 turns. It has been determined that the wire length for one quarter wave length is 10 feet. The number of inches in 10 feet is 120. Using Chart "A" supplied look for next higher number of turns showing (being between 20 and 30 turns with a 2" diameter coil). This tells us to use a 2" coil. If ready-made as in the case of Barker and Williamson, 10 Canal Street, Bristol, Penna., 215-788-5581, the coils come in standard sizes of 4, 6 and 10 turns per inch. For higher "Q" use wider spacing of the turns. These coils come in a ready-made length of 10 inches. Select from the coil 30 turns and put input clamps on the base of the coil and at 30 turns. For exact determination of the correct position of the output clamp, use an externally grounded voltage probe. The node of maximum intensity, being the natural resonant point. Off the shelf multimeters are not radio frequency responsive. The easiest way to accomplish the above is to get from the hardware store or Radio Shack a voltage detector having a neon bulb system (Radio Shack Cat. No. 272-1100b, NE2-Neon Lamps) will work. With your hand as a ground, move the wire extension of the neon lamp along the coil surface until the neon is brightest. This is the desired point of resonance and it is the optimum connection point.

5. The input power now needs consideration. A 2,400 High Voltage module has been previously selected. This module can be made from a diode bridge or any combination of voltage amplifiers. The one used here is an off-the-shelf type, similar to those used for laser technology.

6. Construction of the input L-1 coil. It has already been decided that there will be 10 turns. The length of the wire here is not critical. Since the L-2 coil is 2-inches in diameter, the next off-the-shelf larger size may be used for L-1. Use a 3" diameter off-the-shelf coil which has 10 turns to the inch. Remove (cut) a 10 turn portion from the larger coil. Use an L.C.R. meter and measure the natural farads (capacitance) and henrys (inductance) values of the L-2 coil. Now do the same for the L-1 coil. It will be necessary to put a capacitor across the voltage input of L-1 in order to match the L-1 coil to the L-2 coil. A spark gap across L1 is also required to deal with the return voltage from L-1. A tuneable capacitor of the pad ("trimmer") type for L-1 is desirable.

7. The performance of the L-2 coil can be further enhanced by having an Earth grounding from the base of the coil. The maximum voltage output will be between the base and the top of the L-2 coil. Lesser voltages can be obtained at intermediate points along the length of the L-2 coil.

SUPPLY SOURCES

1. HAM RADIO SUPPLY STORES

2. COILS, AIR INDUCTOR IN HOUSTON

3. BAKER AND WILLIAMSON (READY MADE), BRISTOL. PENNA.
ALSO R.F. DUMMY LOADS AND WATTMETERS.

N O T E S

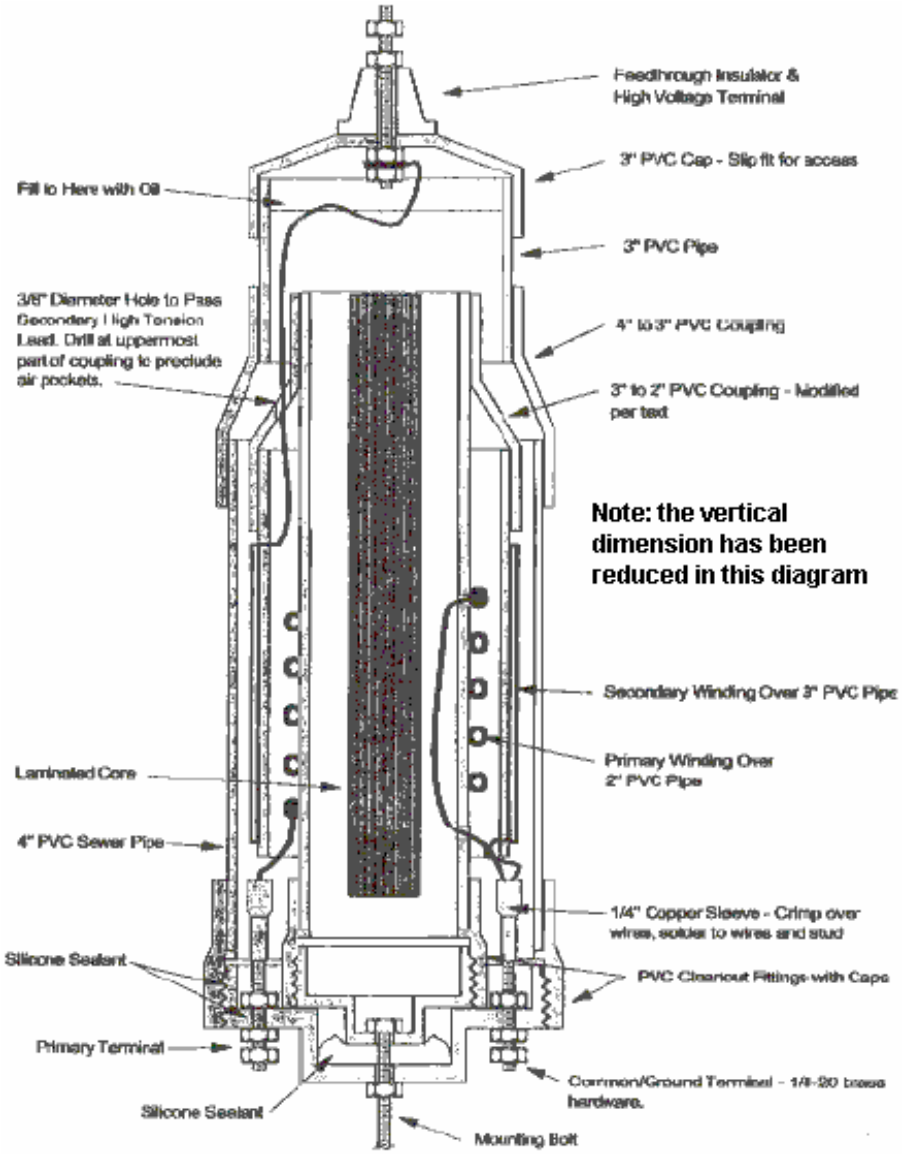

Impulse Transformer Assembly

ELECTRICAL PRINCIPLES: TERMINOLOGY & SAFETY

The use of electricity is so commonplace that most people assume that it will always be available on demand. To fully realize our dependence upon electricity, consider the ways in which electricity is being used each day in the home, on the farm and the ranch. Electricity is doing more to increase work efficiency and promote enjoyable living than any other single factor. The use of electricity has grown to the extent that an increasing portion of the home or business budget, is used in paying for this source of energy.

1. Definition of Electricity

Electricity can be defined in several ways. The layman defines electricity as a source of energy that can be converted to light, heat, or power. Electrical Engineers define electricity as a movement of electrons caused by electrical pressure or voltage. The amount of energy produced depends on the number of electrons in motion.

2. The Manufacture and Distribution of Electricity

Electricity is produced from generators that are run by water, steam, or internal combustion engines. If water is used as a source of power to turn generators, it is referred to as hydroelectric generation. There are a number of this type located in areas where huge dams have been built across large streams.

Steam is used as a source of power for generating much of today's electricity. Water is heated to a high temperature, and the steam pressure is used to turn turbines which generate electricity. These are referred to as thermal-powered generators. Fuels used to heat the water are coal, natural gas, and/or fuel oil.

Generators at the power plant generate from 13,800 to 22,000 volts of electricity. From the power plant, electricity is carried to a step-up sub-station which, through the use of transformers, increases the voltage from 69,000 to 750,000 volts. This increase in voltage is necessary for the efficient transmission of electricity over long distances. From the step-up sub-station, the electricity is carried on transmission lines to a step-down sub-station which reduces the voltage to 7,200 to 14,000 volts for distribution to rural and city areas.

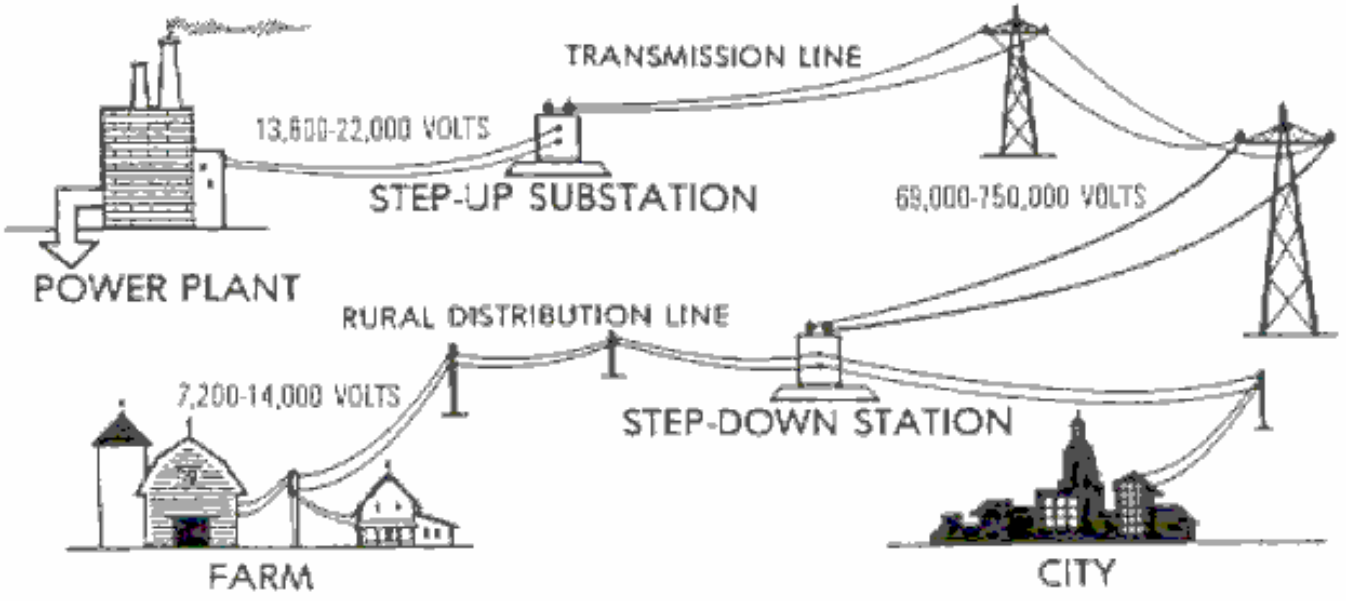

Transformers at the business or residence reduce the voltage to 120 or 240 volts to supply the meter of the customer:

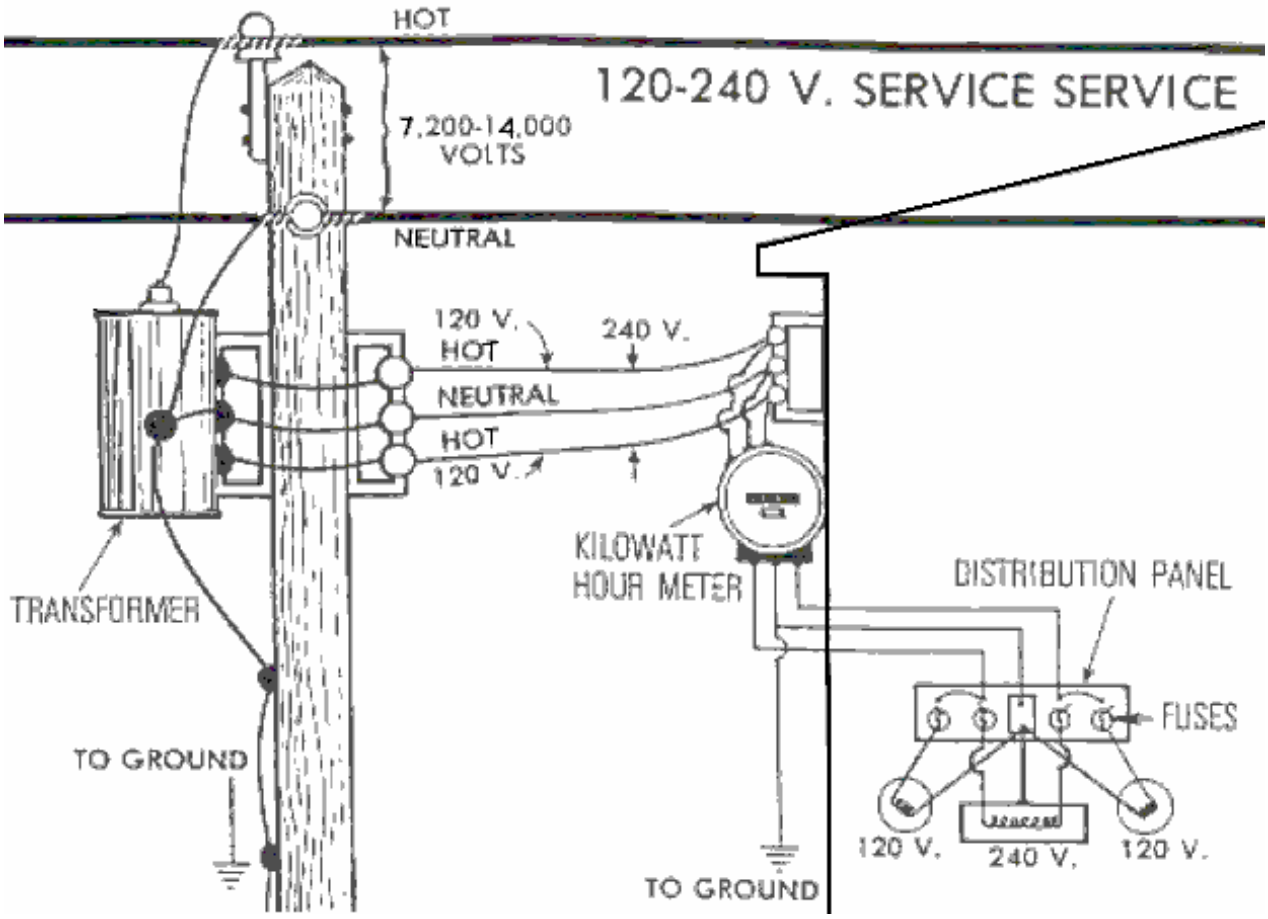

3. Common Electrical Terms

In order to work safely and efficiently with electricity and have the ability to converse on the subject, the following terms should be understood:

Ampere (Amp) - A measurement in units of the rate of flow of electrical current. This may be compared with the rate of flow of water in gallons per minute.

Example: A 60-watt incandescent lamp on a 120V circuit would pull 1/2 ampere of electricity (60 divided by 120 = 0.5 or 1/2, Formula: Amperes = Watts / Volts

Volt (V) - A unit of measure of electrical pressure. A given electrical pressure (V) causes a given amount of electrical current (Amps) to flow through a load of given resistance. Voltage may be compared to water pressure in pounds per square inch in a water system. Common service voltages are 120 volts for lighting and small appliance circuits and 240 volts for heating, air conditioning, and large equipment circuits.

Watt (W) - A unit of measure of electrical power. When applied to electrical equipment, it is the rate that electrical energy is transformed into some other form of energy such as light. Watts may be compared to the work done by water in washing a car. (Formula: Volts x Amps = Watts)

Kilowatt (KW) - A unit of measurement used in computing the amount of electrical energy used. Kilowatts are determined by dividing the number of watts by 1000 as 1 kilowatt = 1,000 watts.

Kilowatt-Hour (KWH) - A measure of electricity in terms of power in kilowatts and time in hours. One KWH is 1000 watts used for one hour.

Alternating Current (A.C.) - Electrical current that alternates or changes direction several times per second. The direction current moves depends on the direction in which the voltage forces it.

Cycle - The flow of electricity in one direction, the reverse flow of electricity in the other direction, and the start of the flow back in the other direction. The cycles per second are regulated by the power supplier and are usually 60 in America. Most electric clocks are built to operate on the mains frequency. More or fewer cycles per second would cause mains-operated clocks to gain or lose time. The present practice is to use the term Hertz (Hz) rather than "cycles per second".

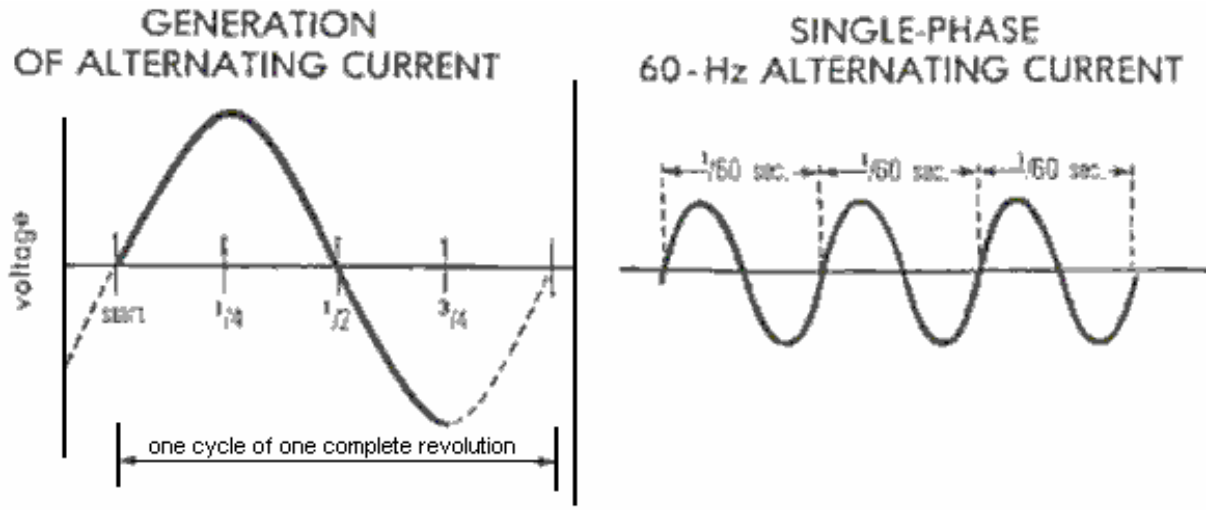

Direct Current (D.C.) - Electrical current flowing in one direction. Example: electrical circuits in automobiles and tractors.

Transformer - A device used to increase or decrease voltage.

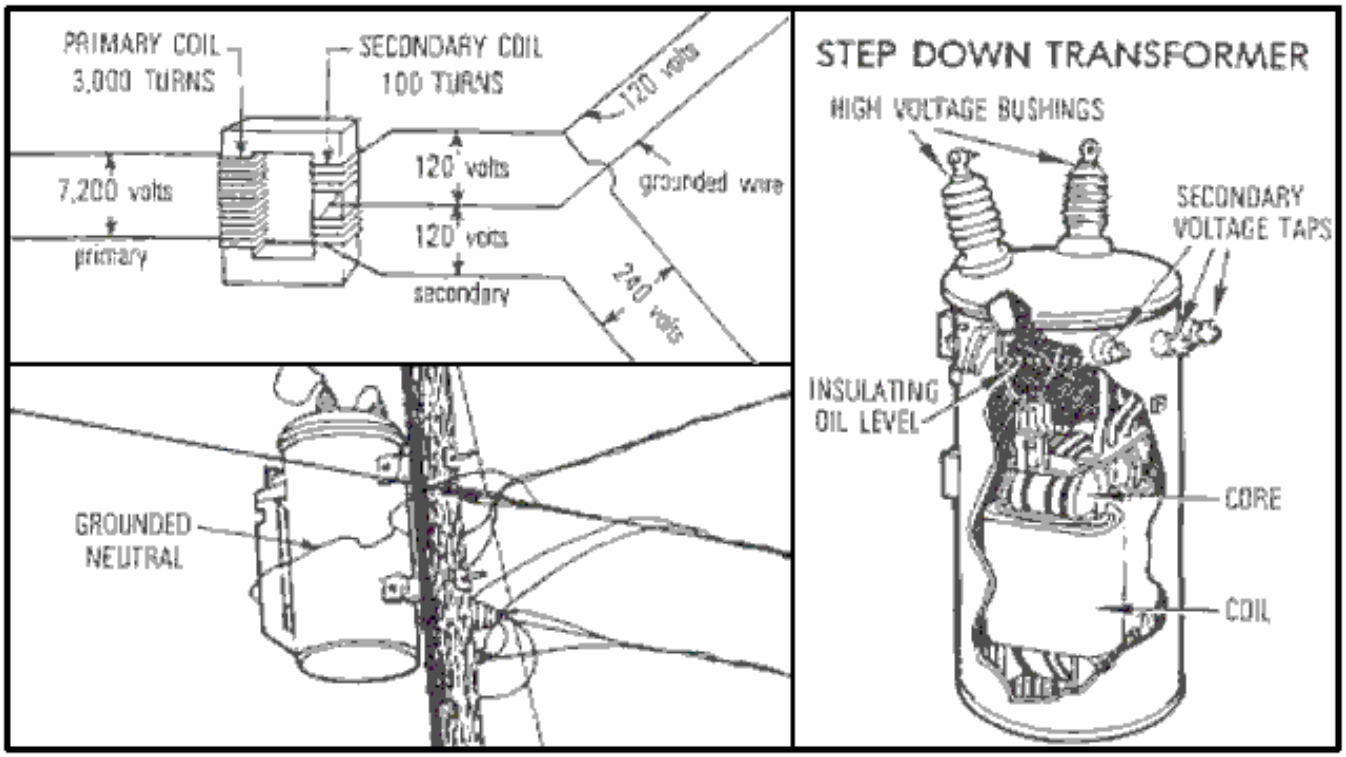

Single Phase - The most common type of electrical service or power available to consumers. One transformer is used between the distribution line and the meter. Usually

three wires, two "hot" and one neutral, are installed to provide 120V and 240V single-phase service. Single-phase service may also be supplied with a three-phase service.

Three-Phase - This type of service is designed especially for large electrical loads. It is a more expensive installation due to three wires and three transformers being required. The important advantage of three-phase power is that the total electrical load is divided among the three phases, consequently, the wire and transformers can be smaller. Other advantages exist in the design of three-phase motors.

Short Circuit - A direct connection (before current flows through an appliance) between two "hot" wires, between a "hot" and neutral wire, or between a "hot" wire and ground.

Voltage Drop - A reduction of current between the power supply and the load. Due to resistance, there will be a loss of voltage any time electricity flows through a conductor (wire). Factors that influence voltage drop are size of wire, length of wire, and the number of amps flowing. A drop in voltage may cause a loss of heat, light, or the full power output of a motor. It could cause motor burn-out unless the motor is properly protected (time-delay fuse).

Fuse - A device used to protect circuits from an overload of current.

Circuit Breaker - A device used to protect circuits from an overload of current. May be manually reset.

Time-Delay Fuse - A fuse with the ability to carry an overload of current for a short duration without disengaging the contacts or melting the fuse link.

Horsepower (hp) - A unit of mechanical power equal to 746 watts of electrical power (assuming 74.6% electric motor efficiency). Motors of one horsepower and above are rated at 1000 watts per hp while motors below one horsepower are rated at 1,200 watts per hp.

Conductor - The wire used to carry electricity (typically, copper or aluminum). Copper and aluminum should not be spliced together due to their incompatibility resulting in deterioration and oxidation.

Insulator - A material which will not conduct electricity and is usually made of glass, Bakelite, porcelain, rubber, or thermo-plastic.

"Hot" Wire - A current-carrying conductor under electrical pressure and connected to a fuse or circuit breaker at the distribution panel. (Color Code: usually black or red)

Neutral Wire - A current-carrying conductor not under electrical pressure and connected to the neutral bar at the distribution panel. (Color Code: usually white)

Grounding - The connection of the neutral part of the electrical system to the earth to reduce the possibility of damage from lightning and the connection of electrical equipment housings to the earth to minimize the danger from electrical shock. (Color Code: Can be green or bare wire).

Underwriters' Laboratory (U.L.) - An American national organization which tests all types of wiring materials and electrical devices to insure that they meet minimum standards for safety and quality.

National Electric Code (N.E.C.) - Regulations approved by the National Board of Fire Underwriters primarily for safety in electrical wiring installations. All wiring should meet the requirements of the national as well as the local code.

4. Computing Electrical Energy Use and Cost

If an estimate of cost for electricity used is desired, the name plate data on appliances and equipment and an estimate of operating time may be used. The following formulas should be used for determining watts, amps, volts, watt-hours, kilowatt-hours, and cost.

Watts = Volts x Amperes

Amperes = Watts / Volts

Volts = Watts / Amperes

Watt-Hours = Watts x Hours of operation

Kilowatt-Hours = Watt-Hours / 1000

Cost = Kilowatt-Hours x Local Rate per Kilowatt-Hour (or per "Unit")

Example:

Local electricity rate per Kilowatt-Hour: 8 cents
Equipment plate data: 120 Volts 5 Amps
Monthly hours of operation: 10

1. Watts = Volts x Amperes, so Watts = 120 x 5 = 600 watts
2. Watt-Hours = 600 x 10 = 6,000 watt-hours
3. Kilowatt-Hours = 5,000 / 1,000 = 6 kilowatt-hours (or 6 Units)
4. Cost = 6 x 8 = 48 cents

5. Electrical Circuits

An Electrical Circuit is a completed path through which electricity flows. Insulated conductors (wires) provide the path for the flow of electricity. A water system and an electrical circuit are similar in many respects. Water flows through pipes and is measured in gallons per minute, and electricity flows through conductors and is measured in amperes. A simple circuit is shown here:

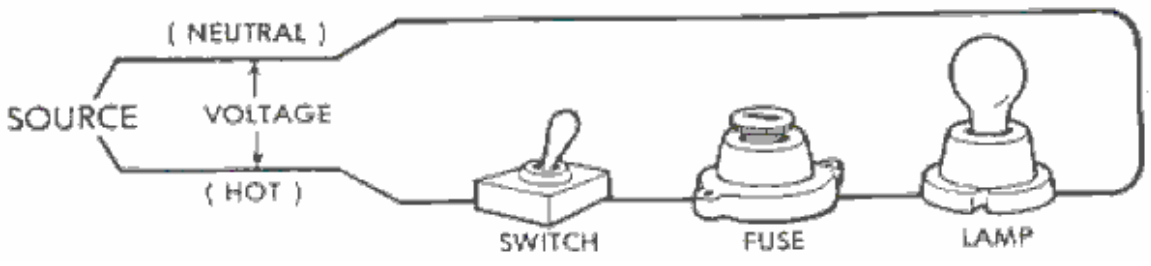

A circuit includes a "hot" wire (red or black) carrying current from the source through a switch, circuit protector (fuse or circuit-breaker), and an appliance. The neutral wire (white) conducts the current from the appliance to the source (ground).

There arc two methods for connecting devices in a circuit - "in series" or "in parallel". In a series circuit, all of the current must flow through each device in the circuit. Removing any one of the devices in a series circuit will stop the flow of current. In parallel circuits, the load (lights or appliances) are connected between the two wires of the circuit providing an independent path for the flow of current, and removing a lamp has no effect on the other lamps in the circuit.

Switches, fuses, and circuit breakers are always connected in series. In most cases, except for some Christmas tree lights, appliances and lights are connected in parallel.

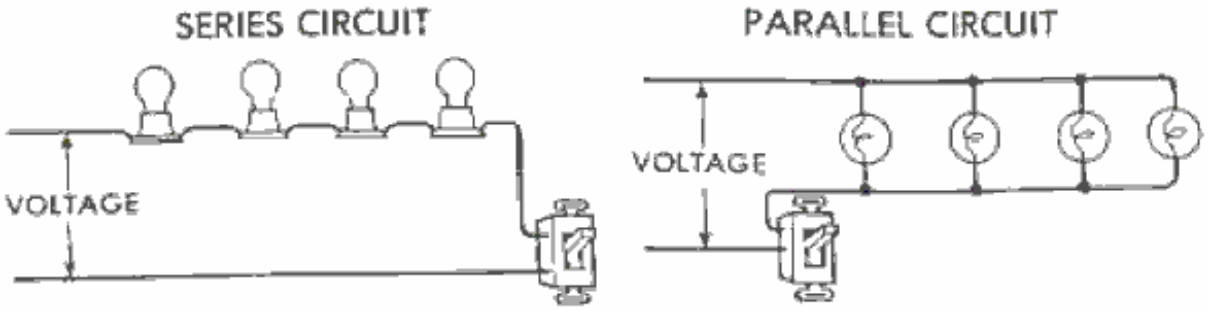

6. 120 Volt and 240 Volt Circuits

The 120V circuit has one "hot" and one neutral wire, with the switch and circuit protector in the hot line. The neutral wire from the appliance is connected to the neutral bar in the fuse or breaker box. For safety, the neutral wire should never be broken or interrupted with a switch or fuse.

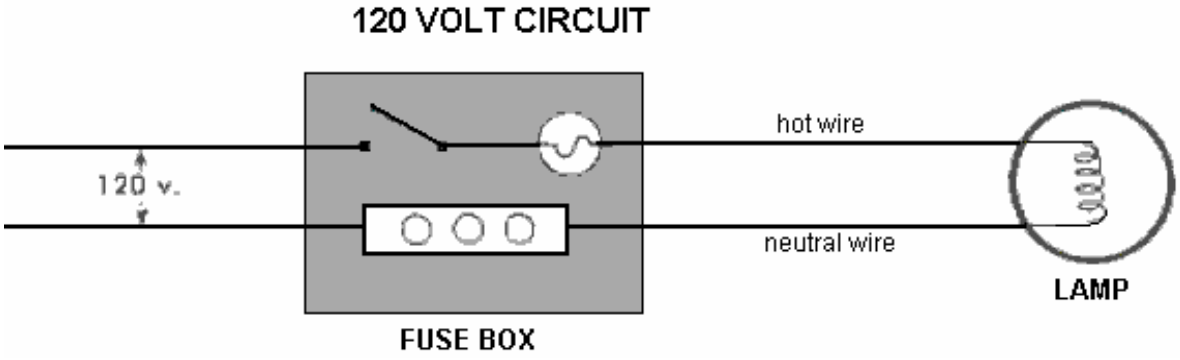

The voltage in a 120V circuit is measured with a voltmeter with one lead on the hot terminal and the other lead on the neutral bar. The number of amperes flowing may be measured with a clamp-on ammeter by encircling the hot or neutral wire with the jaws of the ammeter.

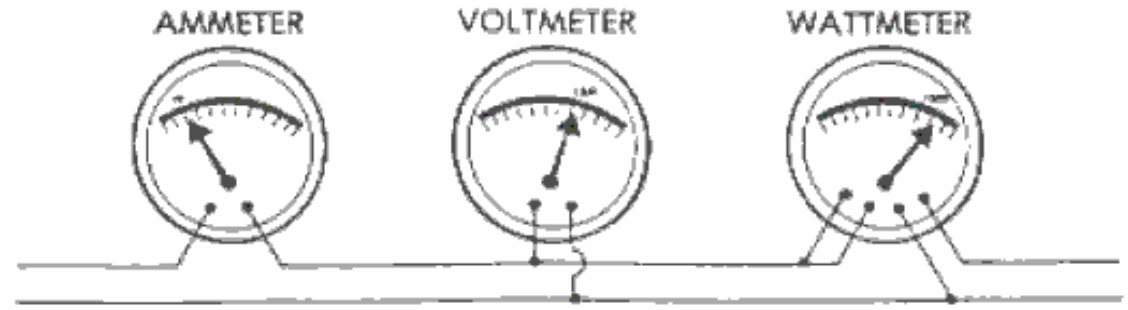

The 240V circuit has two hot wires and one safety-ground wire. Switches and fuses are installed in the hot lines. The two hot wires arc necessary for the operation of 240V welders and motors. The safety-ground wire, connected to the metal frame of the equipment or motor and to the neutral bar, does not carry current unless a "short" develops in the motor or welder. If a short should occur, one of the circuit protectors will burn-out or open, thus opening the circuit.

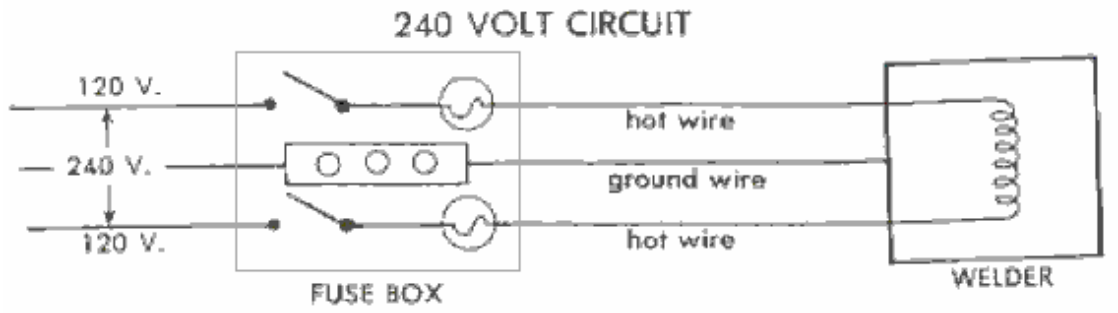

The voltage on a 240V circuit is measured by fastening a lead on the voltmeter to each of the hot wires. Voltage between either hot terminal and the neutral bar will be one-half of the voltage between the two hot wires. The number of amperes flowing can be measured by clamping an ammeter around either of the hot wires.

7. Safety Grounding of Electrical Equipment

Refer back, to the 240V circuit and note the ground wire from the metal frame to the neutral bar. The following illustration shows proper safety grounding when operating a drill in a 120V circuit. The safety-ground wire may be bare, but a three-wire cable is recommended. Safety-ground wire in three-wire cable is usually green in color. A current-carrying neutral wire should never be used for a safety-ground. Likewise, a safety-ground wire should never be used as a current-carrying hot or neutral wire.

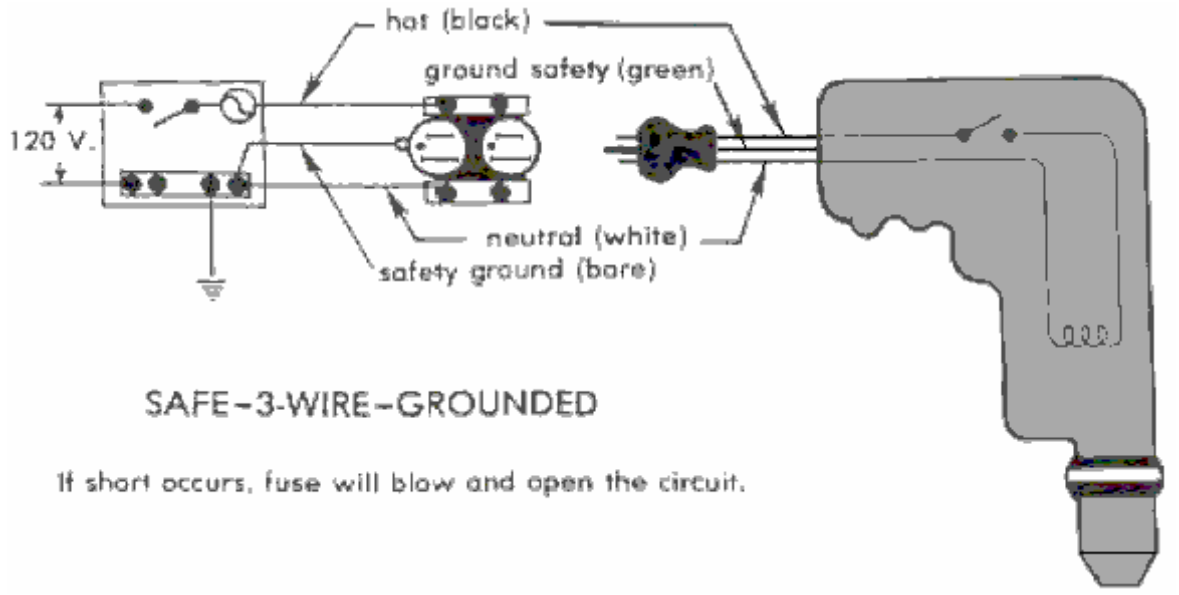

Using grounded receptacles and a safety-ground on all circuits will allow the safety-grounding of appliances when they are plugged into the outlet. An adapter must be used to properly ground appliances connected to receptacles which are not safety-grounded. If an adapter is used, the green pigtail wire must be connected to a known ground to give protection from electrical shock should a short-circuit occur.

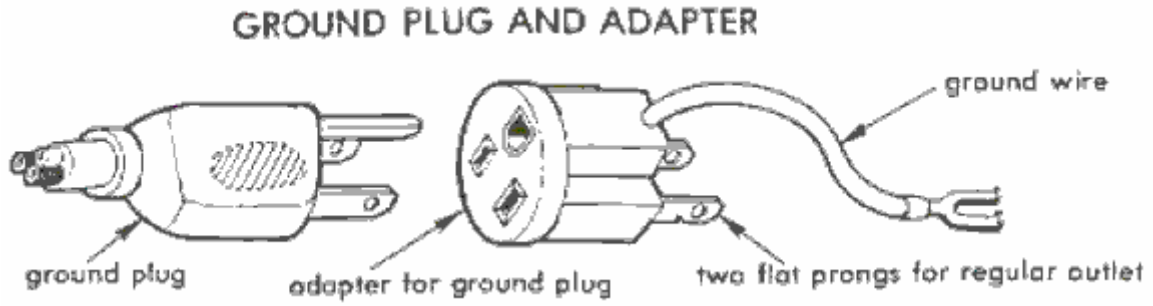

A test lamp can be used to check a circuit completed between a "hot" wire and a neutral wire. Use the test lamp to check appliances for shorts. With the appliance plugged into an outlet, touch the appliance frame with one lead of the test lamp while the other lead of the test lamp is grounded to a water or gas pipe. If the test light does not burn, reverse the appliance plug and check with the test lamp again. If the light burns, a short exists (the hot wire is touching the frame of the appliance). Unplug the appliance and repair or discard it.

8. Electrical Circuit Protection

Electrical circuits should be protected from an overload of amperes. Too many amperes flowing through an unprotected circuit will generate heat, which will deteriorate or melt the insulation and possibly cause a fire. The number of amperes that a given conductor can safely carry, depends upon the kind and size of wire, type of insulation, length of run in feet, and the type of installation. Charts are available in reference texts giving allowable current-carrying capabilities of various conductors.

The four types of circuit protection are: common fuses, fusetrons (time-delay), fustats (two-part time-delay), and circuit-breakers. Fuses are of two basic types: plug, and cartridge.

Common fuses contain a link made from a low-temperature melting alloy which is designed to carry current up to the rating of the fuse. Current higher than the amperage rating causes the link to heat above it's melting point. When the fuse "blows", the link melts and opens the circuit.

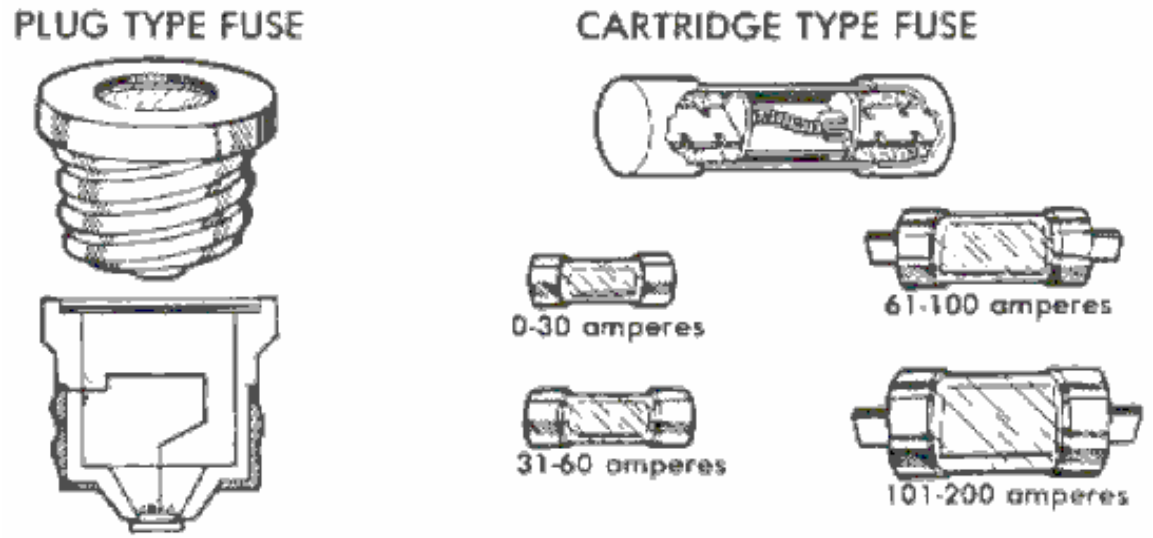

Fusetrons (time-delay fuses) are made to carry a temporary overload, such as the overload caused by the starting of an electric motor. The fuse, however, still provides protection for the circuit, and a short-circuit will melt the fuse link. If a common fuse is used, the fuse link will melt every time an electric motor starts. The use of a larger ampere common fuse will prevent the "blow" resulting from the temporary overload, but will not provide protection for the motor or the circuit.

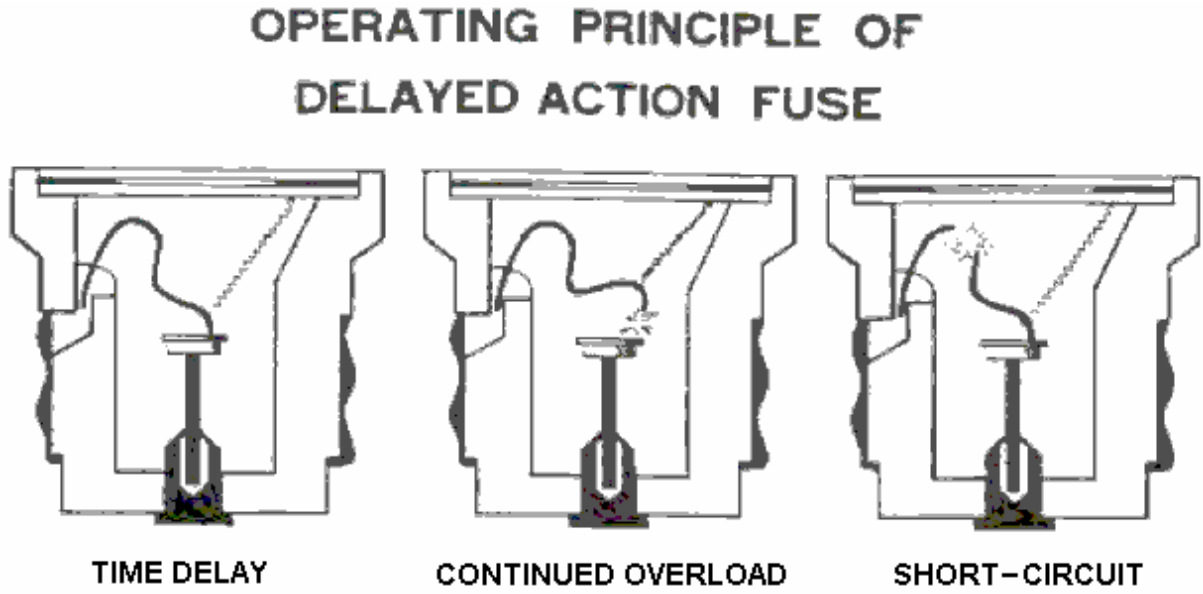

Fustats, non-tamperable fuses of the time-delay type, have a different size base and require a special adapter which is screwed into the standard fuse socket. After the adapter is installed, it cannot be removed. For example, the installation of a 15-ampere adapter allows only the use of 15-ampere or smaller fuse.

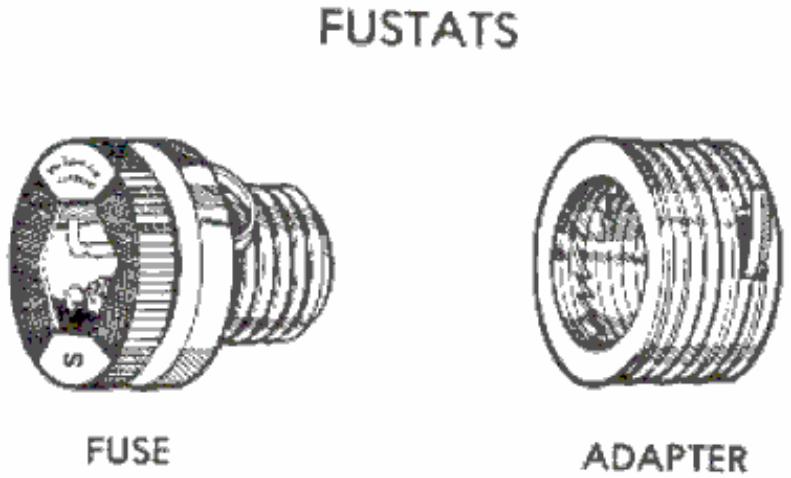

Circuit breakers eliminate the replacement of fuses and are commonly used even though a circuit breaker box costs more than a fuse box. Circuit breakers are of two types, thermal and magnetic. The thermal breaker has two contacts held together by a bi-metal latch. A current overload causes the bi-metallic strip to become heated, the latch releases, and the points spring open. After the bi-metallic strip cools, the switch is reset and service is restored.

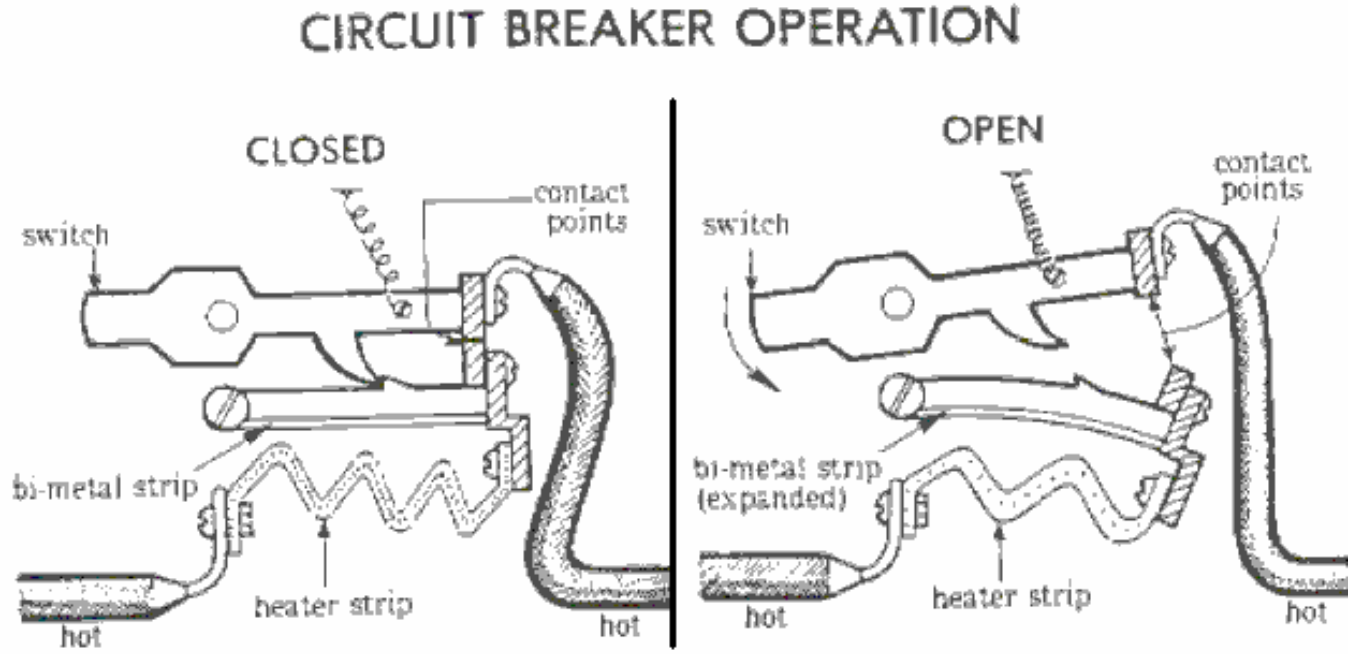

The magnetic breaker has contacts that are held together by a latch which is released by the action of an electromagnet. The amount of current flowing through the circuit will determine the size of the electromagnet. This type of circuit-breaker is reset by moving the toggle switch to the "on" position.

The following diagram shows the parts of a circuit breaker.

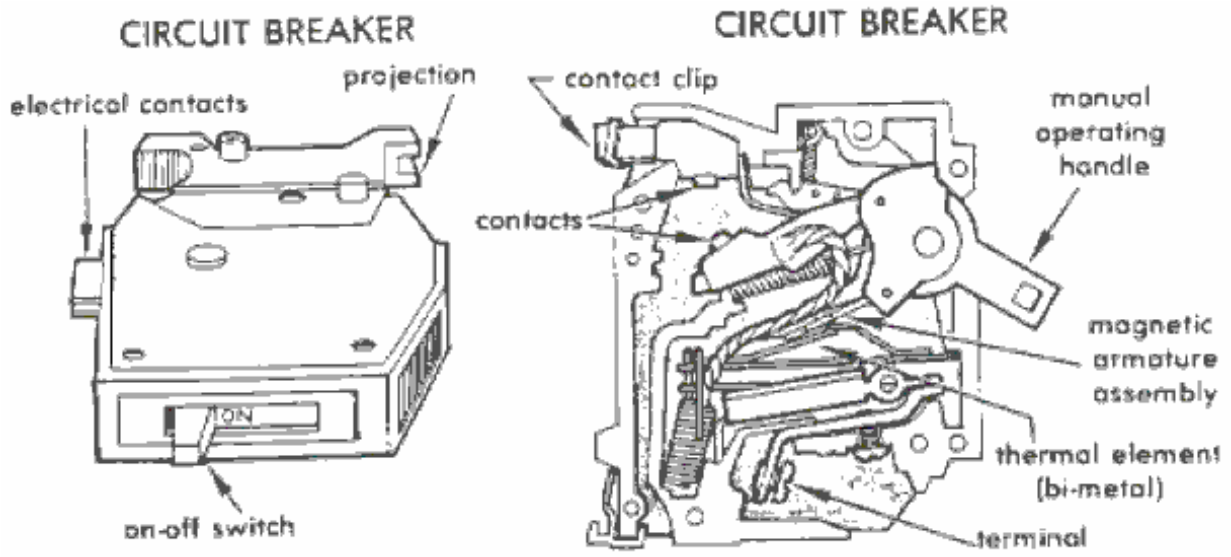

9. No Fault Grounding

Fuses and circuit-breakers are safety devices which limit current (amperage) in a circuit. Their main function is to protect equipment and wiring from overload. Ground fault circuit interrupters (GFI) are designed to protect humans, equipment, and/or electrical systems from injury or damage if electricity flows in an unintended path (a short-circuit).

A GFI is a very sensitive device that functions by comparing the current moving in the "hot" wire with that in the neutral wire. If these two currents are not equal, a fault exists, and current is "leaking" out of the circuit. If the difference in current between the two wires is 5/1000 of an ampere or greater,

the GFI will open the circuit, shutting off the power and eliminating any shock hazard.

The National Electrical Code requires GFI's for all 120V, single phase, 15 and 20 amp receptacles installed outdoors, in bathrooms, and in garages for residential buildings. A GFI is required at construction sites and some other applications. After correcting a circuit fault, the GFI may be reset for further use.

A variety of GFI equipment is made for 120 and 240 volt circuits:

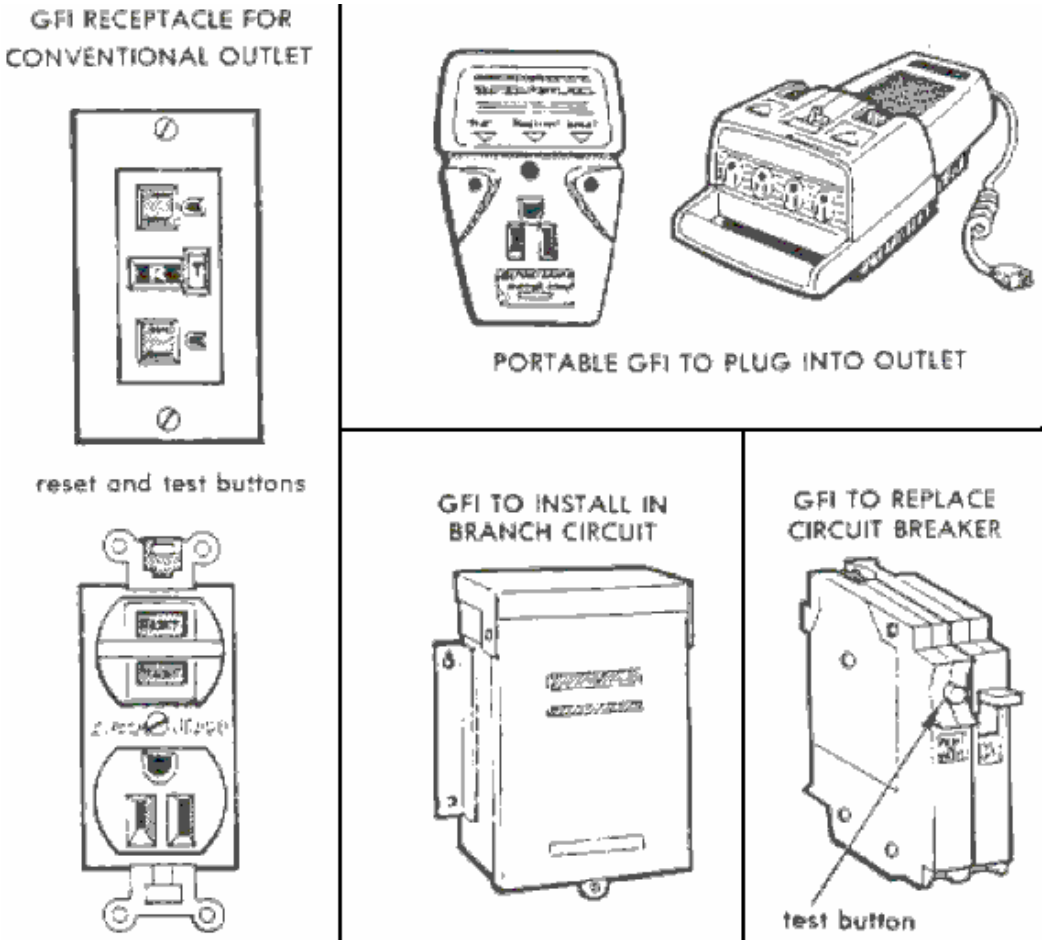

REFERENCES:

COOPER, ELMER L., *AGRICULTURAL MECHANICS: FUNDAMENTALS AND APPLICATIONS*. DELMAR PUBLISHERS INC., ALBANY, NEW YORK

ELECTRICAL WIRING - RESIDENTIAL, UTILITY BUILDINGS, SERVICE AREAS, AAVIM, ATHENS, GEORGIA.

Note: This electrical information does not apply directly to areas outside America and local regulations for electrical supply should be checked.

The following material is the section originally in Chapter 3 of "The Practical Guide to Free-Energy Devices" which deals with Don Smith's technology:

Don Smith. One of most impressive developers of free-energy devices is Don Smith who has produced many spectacular devices, generally with major power output. These are a result of his in-depth knowledge and understanding of the way that the environment works. Don says that his understanding comes from the work of Nikola Tesla as recorded in Thomas C. Martin's book "The Inventions, Researches, and Writings of Nikola Tesla" ISBN 0-7873-0582-0 available from http://www.healthresearchbooks.com and various other book companies. This book can be downloaded from http://www.free-energy-info.com as a pdf file, but a paper copy is much better quality and easier to work from.

Don states that he repeated each of the experiments found in the book and that gave him his understanding of what he prefers to describe as the 'ambient background energy' which is called the 'zero-point energy field' elsewhere in this eBook. Don remarks that he has now advanced further than Tesla in this field, partly because of the devices now available to him and which were not available when Tesla was alive.

Don stresses two key points. Firstly, a dipole can cause a disturbance in the magnetic component of the 'ambient background' and that imbalance allows you to collect large amounts of electrical power, using capacitors and inductors (coils). Secondly, you can pick up as many powerful electrical outputs as you want from that one magnetic disturbance, without depleting the magnetic disturbance in any way. This allows massively more power output than the small power needed to create the magnetic disturbance in the first place. This is what produces a COP>1 device and Don has created nearly fifty different devices based on that understanding.

Although they get removed quite frequently, there is one video which is definitely worth watching if it is still there. It is located at http://www.metacafe.com/watch/2820531/don_smith_free_energy/ and was recorded in 2006. It covers a good deal of what Don has done. In the video, reference is made to Don's website but you will find that it has been taken over by Big Oil who have filled it with innocuous similar-sounding things of no consequence, apparently intended to confuse newcomers. A website which I understand is run by Don's son is http://www.28an.com/altenergypro/index.htm and it has brief details of his prototypes and theory. You will find the only document of his which I could locate, here http://www.free-energy-info.com/Smith.pdf in pdf form and it contains the following patent on a most interesting device which appears to have no particular limit on the output power. This is a slightly re-worded copy of that patent as patents are generally worded in such a way as to make them difficult to understand.

Patent NL 02000035 A **20th May 2004** **Inventor: Donald Lee Smith**

TRANSFORMER GENERATOR MAGNETIC RESONANCE INTO ELECTRIC ENERGY

ABSTRACT

The present invention refers to an Electromagnetic Dipole Device and Method, where wasted radiated energy is transformed into useful energy. A Dipole as seen in Antenna Systems is adapted for use with capacitor plates in such a way that the Heaviside Current Component becomes a useful source of electrical energy.

DESCRIPTION

Technical Field:

This invention relates to loaded Dipole Antenna Systems and their Electromagnetic radiation. When used as a transformer with an appropriate energy collector system, it becomes a transformer/generator. The invention collects and converts energy which is radiated and wasted by conventional devices.

Background Art:

A search of the International Patent Database for closely related methods did not reveal any prior art with an interest in conserving radiated and wasted magnetic waves as useful energy.

DISCLOSURE OF THE INVENTION

The invention is a new and useful departure from transformer generator construction, such that radiated and wasted magnetic energy changes into useful electrical energy. Gauss meters show that much energy from conventional electromagnetic devices is radiated into the ambient background and wasted. In the case of conventional transformer generators, a radical change in the physical construction allows better access to the energy available. It is found that creating a dipole and inserting capacitor plates at right angles to the current flow, allows magnetic waves to change back into useful electrical (coulombs) energy. Magnetic waves passing through the capacitor plates do not degrade and the full impact of the available energy is accessed. One, or as many sets of capacitor plates as is desired, may be used. Each set makes an exact copy of the full force and effect of the energy present in the magnetic waves. The originating source is not depleted of degraded as is common in conventional transformers.

BRIEF DESCRIPTION OF THE DRAWINGS

The Dipole at right angles, allows the magnetic flux surrounding it to intercept the capacitor plate, or plates, at right angles. The electrons present are spun such that the electrical component of each electron is collected by the capacitor plates. Essential parts are the South and North component of an active Dipole. Examples presented here exist as fully functional prototypes and were engineer constructed and fully tested in use by the Inventor. In each of the three examples shown in the drawings, corresponding parts are used.

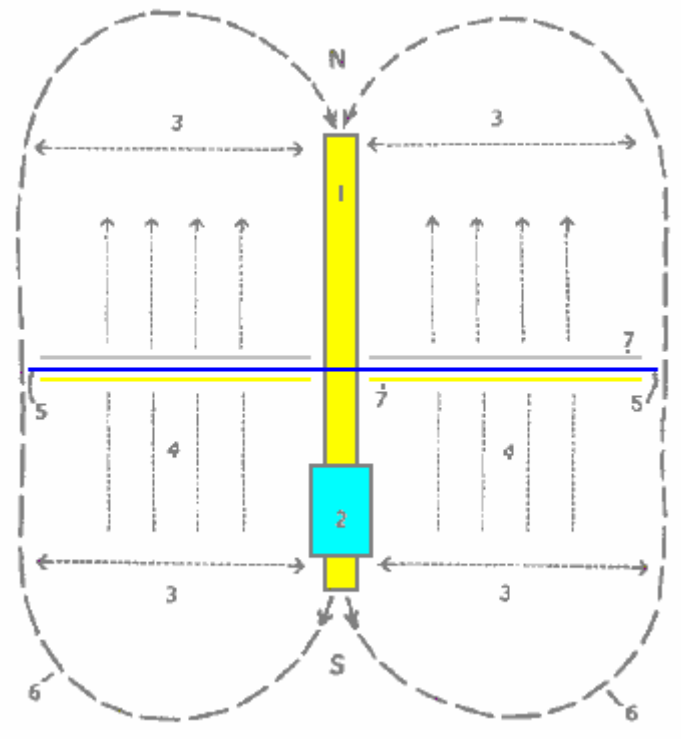

Fig.1 is a View of the Method, where **N** is the North and **S** is the South component of the Dipole.

Here, **1** marks the Dipole with its North and South components. **2** is a resonant high-voltage induction coil. **3** indicates the position of the electromagnetic wave emission from the Dipole. **4** indicates the position and flow direction of the corresponding Heaviside current component of the energy flow caused by the induction coil **2**. **5** is the dielectric separator for the capacitor plates **7**. **6** for the purposes of this drawing, indicates a virtual limit for the scope of the electromagnetic wave energy.

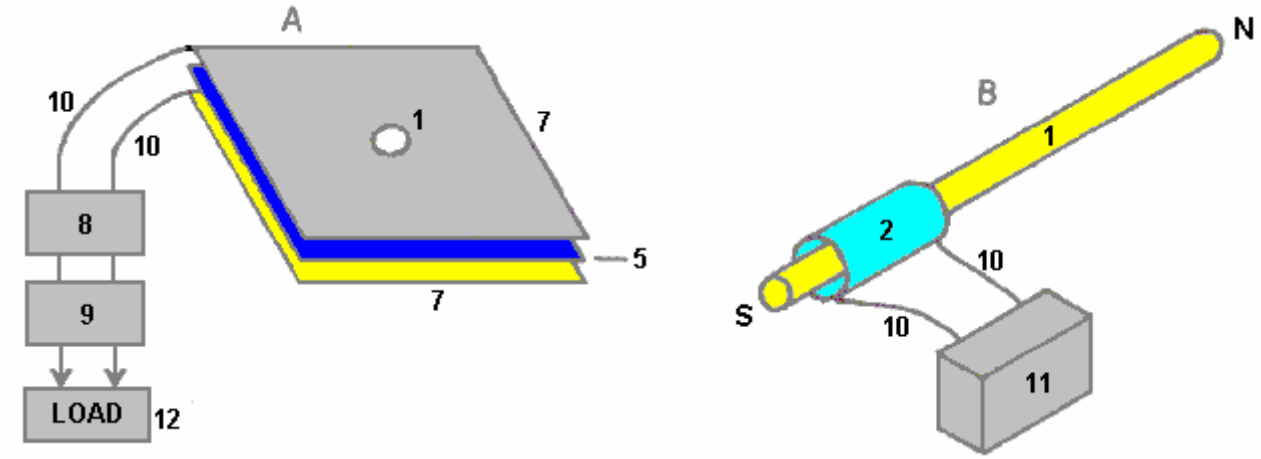

Fig.2 has two parts **A** and **B**.

In **Fig.2A 1** is the hole in the capacitor plates through which the Dipole is inserted and in **Fig.2B** it is the Dipole with its North and South poles shown. **2** is the resonant high-voltage induction coil surrounding part of the Dipole **1**. The dielectric separator **5**, is a thin sheet of plastic placed between the two capacitor plates **7**, the upper plate being made of aluminium and the lower plate made of copper. Unit **8** is a deep-cycle battery system powering a DC inverter **9** which produces 120 volts at 60 Hz (the US mains supply voltage and frequency, obviously, a 240 volt 50 Hz inverter could be used here just as easily) which is used to power whatever equipment is to be driven by the device. The reference number **10** just indicates connecting wires. Unit **11** is a high-voltage generating device such as a neon transformer with its oscillating power supply.

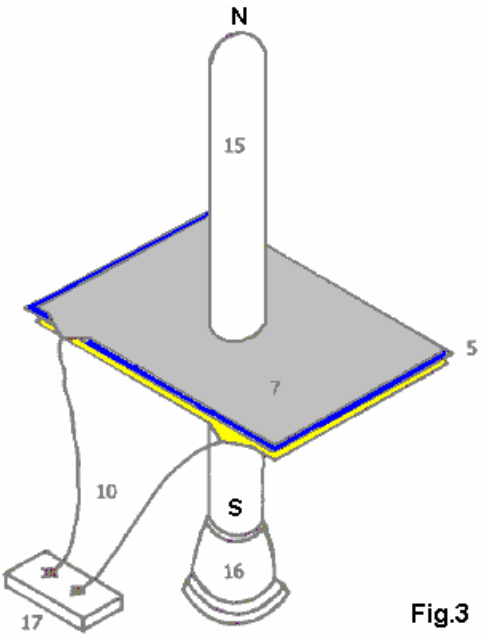

Fig.3

Fig.3 is a Proof Of Principal Device using a Plasma Tube as an active Dipole. In this drawing, **5** is the plastic sheet dielectric separator of the two plates **7** of the capacitor, the upper plate being aluminium and the lower plate copper. The connecting wires are marked **10** and the plasma tube is designated **15**. The plasma tube is four feet long (1.22 m) and six inches (100 mm) in diameter. The high-voltage energy source for the active plasma dipole is marked **16** and there is a connector box **17** shown as that is a convenient method of connecting to the capacitor plates when running tests on the device.

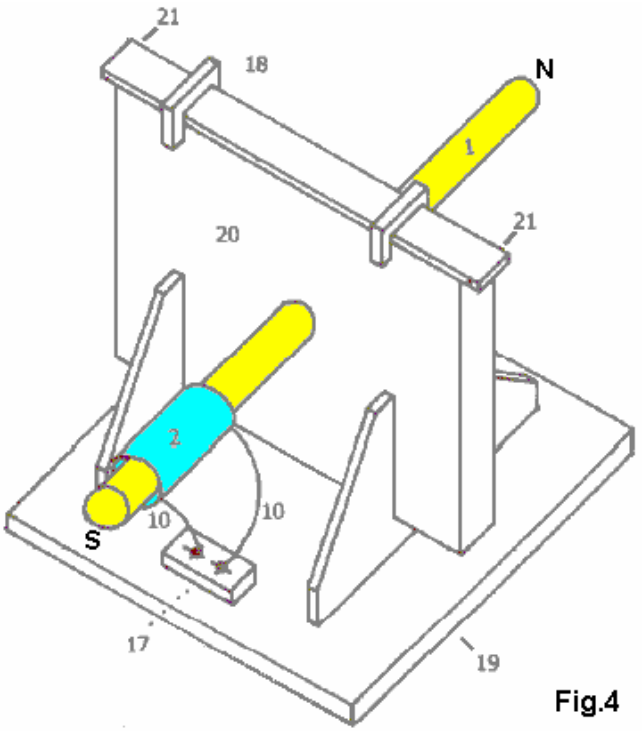

Fig.4

Fig.4 shows a Manufacturer's Prototype, constructed and fully tested. **1** is a metal Dipole rod and **2** the resonant high-voltage induction coil, connected through wires **10** to connector block **17** which facilitates the connection of it's high-voltage power supply. Clamps **18** hold the upper edge of the capacitor packet in place and **19** is the base plate with it's supporting brackets which hold the whole device in place. **20** is a housing which contains the capacitor plates and **21** is the point at which the power output from the capacitor plates is drawn off and fed to the DC inverter.

BEST METHOD OF CARRYING OUT THE INVENTION

The invention is applicable to any and all electrical energy requirements. The small size and it's high efficiency make it an attractive option, especially for remote areas, homes, office buildings, factories, shopping centres, public places, transportation, water systems, electric trains, boats, ships and 'all things great and small'. The construction materials are commonly available and only moderate skill levels are needed to make the device.

CLAIMS

1. Radiated magnetic flux from the Dipole, when intercepted by capacitor plates at right angles, changes into useful electrical energy.

2. A Device and Method for converting for use, normally wasted electromagnetic energy.

3. The Dipole of the Invention is any resonating substance such as Metal Rods, Coils and Plasma Tubes which have interacting Positive and Negative components.

4. The resulting Heaviside current component is changed to useful electrical energy.

****

This patent does not make it clear that the device needs to be tuned and that the tuning is related to its physical location. The tuning will be accomplished by applying a variable-frequency input signal to the neon transformer and adjusting that input frequency to give the maximum output.

Don Smith has produced some forty eight different devices, and because he understands that the real power in the universe is magnetic and not electric, these devices have performances which appear staggering to people trained to think that electrical power is the only source of power. One device which I understand is commercially produced in Russia, is shown here:

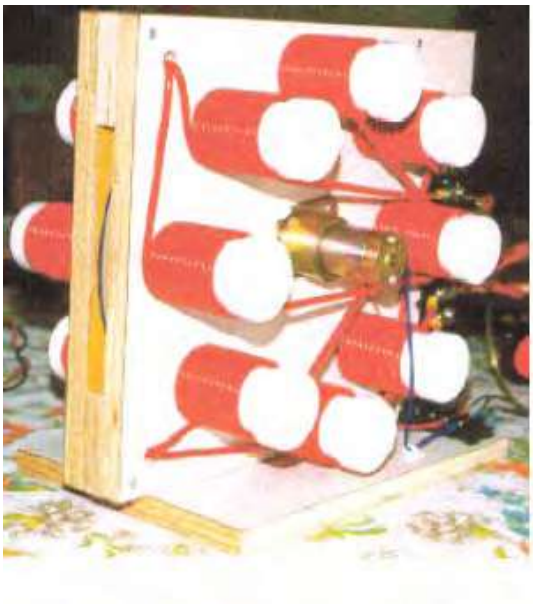

This is a small table-top device which looks like it is an experiment by a beginner, and something which would be wholly ineffective. Nothing could be further from the truth. Each of the eight coils pairs (one each side of the rotating disc) produces 1,000 volts at 50 amps (fifty kilowatts) of output power, giving a total power output of 400 kilowatts. It's overall size is 16" x 14.5" x 10" (400 x 370 x 255 mm). In spite of the extremely high power output, the general construction is very simple:

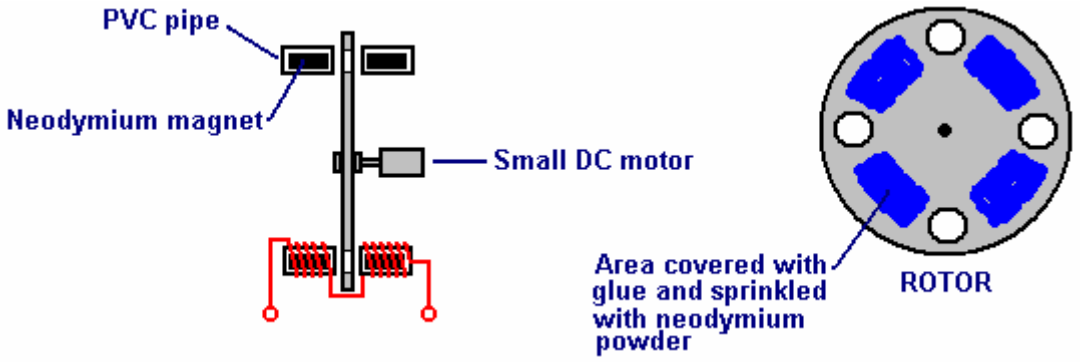

The device operates on a fluctuating magnetic field which is produced by a small low-power DC motor spinning a plastic disc. In the prototype shown above, the disc is an old vinyl record which has had holes cut in it. Between the holes is an area which was covered with glue and then sprinkled with powdered neodymium magnet material. It takes very little power to spin the disc, but it acts in a way which is very much like the Ecklin-Brown generator, repeatedly disrupting the magnetic field. The magnetic field is created by a neodymium magnet in each of the sixteen plastic pipes. It is important that the change in the magnetic flux between the matching magnets on each side of the disc is as large as possible. The ideal rotor material for this is "Terfenol-D" (tungsten zirconate) with slots cut in it but it is so expensive that materials like stainless steel are likely to be used instead. Please understand that all of Don's designs rely on resonant operation and so the coil impedance has to be matched to the pulse frequency used to drive the coil.

For Don Smith, this is not an exceptional device. The one shown below is also physically quite small and yet it has an output of 160 kilowatts (8000 volts at 20 amps) from an input of 12 volts 1 amp (COP = 13,333):

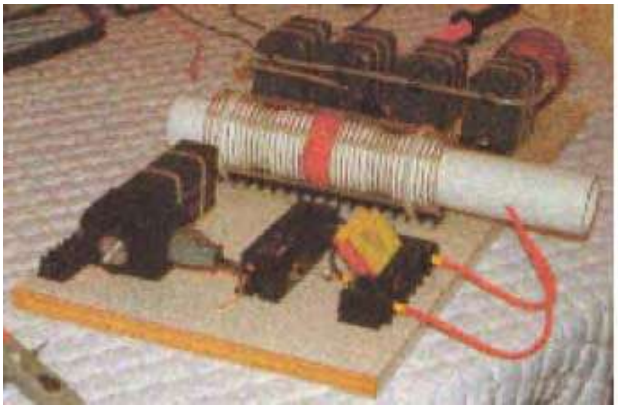

Again, this is a device which can be placed on top of a table and is not a complicated form of construction, having a very open and simplistic layout. However, some components are not mounted on this board. The twelve volt battery and connecting leads are not shown, nor is the ground connection, the step-down isolation transformer and the varistor used to protect the load from over-voltage by absorbing any random voltage spikes which might occur, but more of these things later on when a much more detailed description of this device is given. Again, please understand that Don does not reveal all of the details of any of his designs, and he deliberately omits to mention various important details, leaving us to deduce what is missing from our own understanding of how these devices work.

The device shown above is a typical example of this with various subtle points glossed over in spite of this being one device which Don says that we should be able to reproduce ourselves. Let me state here that reproducing this seemingly simple design of Don's is not an easy thing to do and it is not something which can be thrown together by a beginner using whatever components happen to be at hand at the time. Having said that, with careful study and commonsense application of some obvious facts, it should be possible to make one of these devices.

Another of Don's devices is shown here:

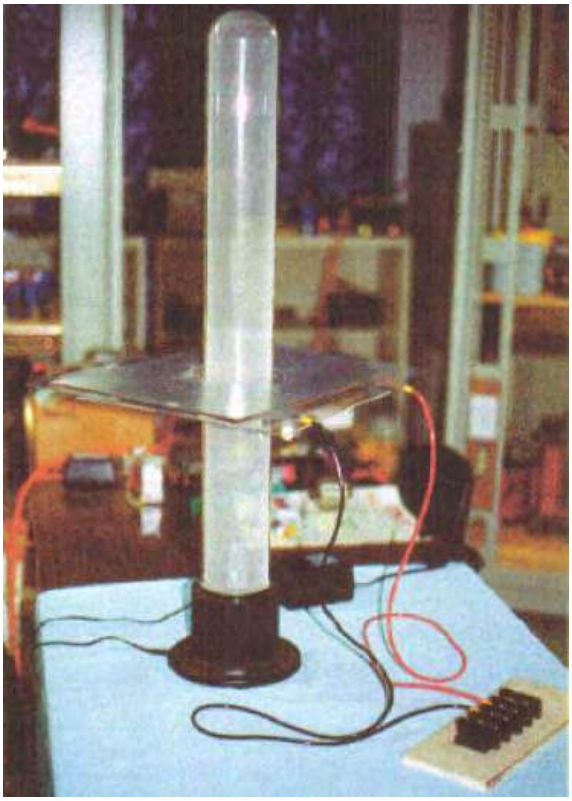

This is a larger device which uses a plasma tube four feet (1.22 m) long and 6 inches (100 mm) in diameter. The output is a massive 100 kilowatts. This is the design shown as one of the options in Don's patent. Being an Electrical Engineer, none of Don's prototypes are in the "toy" category. If nothing else is taken from Don's work, we should realise that high power outputs can be had from very simple devices.

There is one other brief document "Resonate Electrical Power System" from Don Smith which says:

Potential Energy is everywhere at all times, becoming useful when converted into a more practical form. There is no energy shortage, only grey matter. This energy potential is observed indirectly through the manifestation of electromagnetic phenomenon, when intercepted and converted, becomes useful. In nonlinear systems, interaction of magnetic waves amplify (conjugate) energy, providing greater output than input. In simple form, in the piano where three strings are struck by the hammer, the centre one is impacted and resonance activates the side strings. Resonance between the three strings provides a sound level greater than the input energy. Sound is part of the electromagnetic spectrum and is subject to all that is applicable to it.

"Useful Energy" is defined as "that which is other than Ambient". "Electric Potential" relates to mass and it's acceleration. Therefore, the Earth's Mass and Speed through space, gives it an enormous electrical potential. Humans are like the bird sitting unaware on a high voltage line. in nature, turbulence upsets ambient and we see electrical displays. Tampering with ambient, allows humans to convert magnetic waves into useful electricity.

Putting this in focus, requires a look at the Earth in general. During each of the 1,440 minutes of each day, more than 4,000 displays of lightning occur. Each display yields more than 10,000,000 volts at more than 200,000 amperes in equivalent electromagnetic flux. This is more than 57,600,000,000,000 volts and 1,152,000,000,000 amperes of electromagnetic flux during each 24 hour period. This has been going on for more than 4 billion years. The USPTO insist that the Earth's electrical field is insignificant and useless, and that converting this energy violates the laws of nature. At the same time, they issue patents in which, electromagnetic flux coming in from the Sun is converted by solar cells into DC energy. Aeromagnetic flux (in gammas) Maps World-Wide, includes those provided by the US Department of Interior-Geological Survey, and these show clearly that there is present, a spread of 1,900 gamma above Ambient, from reading instruments flown 1,000 feet above the (surface) source. Coulomb's Law requires the squaring of the distance of the remote reading, multiplied by the recorded reading. Therefore, that reading of 1,900 gamma has a corrected value of 1,900 x 1,000 x 1,000 = 1,900,000,000 gamma.

There is a tendency to confuse "gamma ray" with "gamma". "Gamma" is ordinary, everyday magnetic flux, while "gamma ray" is high-impact energy and not flux. One gamma of magnetic flux is equal to that of 100 volts RMS. To see this, take a Plasma Globe emitting 40,000 volts. When properly used, a gamma meter placed nearby, will read 400 gammas. The 1,900,000,000 gamma just mentioned, is the magnetic ambient equivalent of

190,000,000 volts of electricity. This is on a "Solar Quiet" day. On "Solar Active" days it may exceed five times that amount. The Establishment's idea that the Earth's electrical field is insignificant, goes the way of their other great ideas.

There are two kinds of electricity: "potential" and "useful". All electricity is "potential" until it is converted. The resonant-fluxing of electrons, activates the electrical potential which is present everywhere. The Intensity/CPS of the resonant-frequency-flux rate, sets the available energy. This must then be converted into the required physical dimensions of the equipment being used. For example, energy arriving from the Sun is magnetic flux, which solar cells convert to DC electricity, which is then converted further to suit the equipment being powered by it. Only the magnetic flux moves from point "A" (the Sun) to point "B" (the Earth). All electrical power systems work in exactly the same way. Movement of Coils and Magnets at point "A" (the generator) fluxes electrons, which in turn, excite electrons at point "B" (your house). **None of the electrons at point "A" are ever transmitted to point "B"**. In both cases, the electrons remain forever intact and available for further fluxing. This is not allowed by Newtonian Physics (electrodynamics and the laws of conservation). Clearly, these laws are all screwed up and inadequate.

In modern physics, USPTO style, all of the above cannot exist because it opens a door to overunity. The good news is that the PTO has already issued hundreds of Patents related to Light Amplification, all of which are overunity. The Dynode used to adjust the self-powered shutter in your camera, receives magnetic flux from light which dislodges electrons from the cathode, reflecting electrons through the dynode bridge to the anode, resulting in billions of more electrons out than in. There are currently, 297 direct patents issued for this system, and thousands of peripheral patents, all of which support overunity. More than a thousand other Patents which have been issued, can be seen by the discerning eye to be overunity devices. What does this indicate about Intellectual Honesty?

Any coil system, when fluxed, causes electrons to spin and produce useful energy, once it is converted to the style required by its use. Now that we have described the method which is required, let us now see how this concerns us.

The entire System already exists and all that we need to do is to hook it up in a way which is useful to our required manner of use. Let us examine this backwards and start with a conventional output transformer. Consider one which has the required voltage and current handling characteristics and which acts as an isolation transformer. Only the magnetic flux passes from the input winding to the output winding. No electrons pass through from the input side to the output side. Therefore, we only need to flux the output side of the transformer to have an electrical output. Bad design by the establishment, allowing hysteresis of the metal plates, limits the load which can be driven. Up to this point, only potential is a consideration. Heat (which is energy loss) limits the output amperage. Correctly designed composite cores run cool, not hot.

A power correction factor system, being a capacitor bank, maintains an even flow of flux. These same capacitors, when used with a coil system (a transformer) become a frequency-timing system. Therefore, the inductance of the input side of the transformer, when combined with the capacitor bank, provides the required fluxing to produce the required electrical energy (cycles per second).

With the downstream system in place, all that is needed now is a potential system. Any flux system will be suitable. Any amplification over-unity output type is desirable. The input system is point "A" and the output system is point "B". Any input system where a lesser amount of electrons disturbs a greater amount of electrons - producing an output which is greater than the input - is desirable.

At this point, it is necessary to present updated information about electrons and the laws of physics. A large part of this, originates from me (Don Smith) and so is likely to upset people who are rigidly set in the thought patterns of conventional science.

Non - Ionic Electrons

As a source of electrical energy, non-ionic electrons doublets exist in immense quantities throughout the universe. Their origin is from the emanation of Solar Plasma. When ambient electrons are disturbed by being spun or pushed apart, they yield both magnetic and electrical energy. The rate of disturbance (cycling) determines the energy level achieved. Practical methods of disturbing them include, moving coils past magnets or vice versa. A better way is the pulsing (resonant induction) with magnetic fields and waves near coils.

In coil systems, magnetic and amperage are one package. This suggests that electrons in their natural non-ionic state, exist as doublets. When pushed apart by agitation, one spins right (yielding Volts-potential electricity) and the other spins left (yielding Amperage-magnetic energy), one being more negative than the other. This further suggests that when they reunite, we have (Volts x Amps = Watts) useful electrical energy. Until now, this idea has been totally absent from the knowledge base. The previous definition of Amperage is therefore flawed.

Electron Related Energy

	Energy Available	Method of Storage	Common Unit	Units of Measure
Electrons	Electrical	Capacitor/Coulombs	Volts	Flux Units
	Spin / Gravity	Momentum	Torque	Ergs
	Magnetic	Coils/Amp. turns	Amperes	Flux Units
				Teslas, Gauss,
				Gammas, Oesteds
	Light	Laser	Lux ,	Photons/Gamma Rays
	Impact / resistance			
	Heat	Various	Fahrenheit/Celsius	Temp

Left hand spin of electrons results in Electrical Energy and right hand spin results in Magnetic Energy. Impacted electrons emit visible Light and heat.

Useful Circuits, Suggestions for Building an Operational Unit

1. Substitute a Plasma Globe such as Radio Shack's "Illumna-Storm" for the source-resonant induction system. It will have about 400 milligauss of magnetic induction. One milligauss is equal to 100 volts worth of magnetic induction.

2. Construct a coil using a 5-inch to 7-inch (125 to 180 mm) diameter piece of PVC for the coil former.

3. Get about 30 feet (10 m) of Jumbo-Speaker Cable and separate the two strands. This can be done by sticking a carpet knife into a piece of cardboard or wood, and then pulling the cable carefully past the blade to separate the two insulated cores from each other. (PJK Note: "Jumbo-Speaker Cable" is a vague term as that cable comes in many varieties, with anything from a few, to over 500 strands in each core. As Don points out that the output power increases with each turn of wire, it is distinctly possible that each of these strands acts the same as individual insulated turns which have been connected in parallel, so a 500-strand cable may well be far more effective than a cable with just a few strands).

4. Wind the coil with 10 to 15 turns of wire and leave about 3 feet (1 m) of cable spare at each end of the coil. Use a glue gun to hold the start and finish of the coil.

5. This will become the "L - 2" coil shown in the Circuits page.

6. When sitting on top of the Plasma Globe (like a crown) you have a first-class resonant air-core coil system.

7. Now, substitute two or more capacitors (rated at 5,000 volts or more) for the capacitor bank shown on the Circuits page. I use more than two 34 microfarad capacitors.

8. Finish out the circuit as shown. You are now in business !

9. Voltage - Amperage limiting resistors are required across the output side of the Load transformer. These are used to adjust the output level and the desired cycles per second.

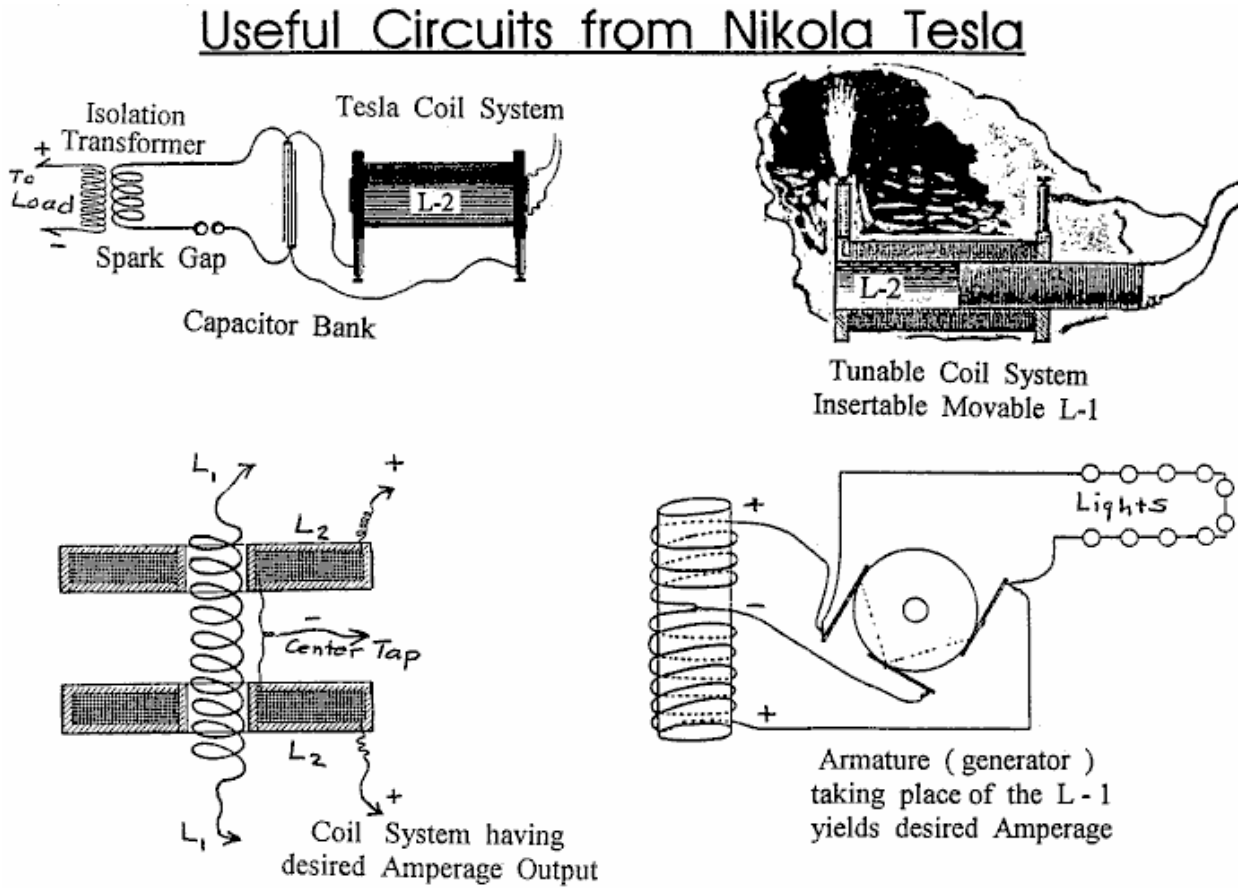

Don Smith's Suggestions: Get a copy of the "Handbook of Electronic Tables and Formulas", published by Sams, ISBN 0-672-22469-0, also an Inductance/Capacitance/Resistance meter is required. Chapter 1 of Don's pdf document has important time-constant (frequency) information and a set of reactance charts in nomograph style (*"nomograph": a graph, usually containing three parallel scales graduated for different variables so that when a straight line connects values of any two, the related value may be read directly from the third at the point intersected by the line*) which makes working, and approximating of the three variables (capacitance, inductance and resistance) much easier. If two of the variables are known, then the third one can be read from the nomograph.

For example, if the input side of the isolation transformer needs to operate at 60 Hz, that is 60 positive cycles and 60 negative cycles, being a total of 120 cycles. Read off the inductance in Henries by using the Inductance meter attached to the input side of the isolation transformer. Plot this value on the (nomographic) reactance chart. Plot the needed 120 Hz on the chart and connect these two points with a straight line. Where this line crosses the Farads line and the Ohms line, gives us two values. Choose one (resistor) and insert it between the two leads of the transformer input winding.

The Power Correction Factor Capacitor (or bank of more than one capacitor) now needs adjusting. The following formula is helpful in finding this missing information. The capacitance is known, as is the desired potential to pulse the output transformer. One Farad of capacitance is one volt for one second (one Coulomb). Therefore, if we want to keep the bucket full with a certain amount, how many dippers full are needed? If the bucket needs 120 volts, then how many coulombs are required?

$$\frac{\text{Desired Voltage}}{\text{Capacitance in Microfarads}} = \text{Required frequency in Hz}$$

Now, go to the nomograph mentioned above, and find the required resistor jumper to place between the poles of the Correction Factor Capacitor.

An earth grounding is desirable, acting as both a voltage-limiter and a transient spike control. Two separate earths are necessary, one at the Power Factor Capacitor and one at the input side of the isolation transformer. Off-the-shelf surge arrestors / spark gaps and varistors having the desired voltage/potential and amperage control are commonly available. Siemens, Citel America and others, make a full range of surge arrestors, etc. Varistors look like coin-sized flat capacitors. Any of these voltage limiters are marked as "V - 1" in the following text.

It should be obvious that several separate closed circuits are present in the suggested configuration: The power input source, the high-voltage module, a power factor capacitor bank combined with the input side of the isolation transformer. Lastly, the output side of the isolation transformer and its load. None of the electrons active at the power source (battery) are passed through the system for use downstream. At any point, if the magnetic flux rate should happen to vary, then the number of active electrons also varies. Therefore, controlling the flux rate controls the electron (potential) activity. Electrons active at point "A" are not the same electrons which are active at point "B", or those at point "C", and so on. If the magnetic flux rate (frequency Hz) varies, then a different number of electrons will be disturbed. This does not violate any Natural Law and it does produce more output energy than the input energy, should that be desirable.

A convenient high-voltage module is a 12 volt DC neon tube transformer. The Power Factor Correction Capacitors should be as many microfarads as possible as this allows a lower operating frequency. The 12-volt neon tube transformer oscillates at about 30,000 Hz. At the Power Correction Factor Capacitor bank we lower the frequency to match the input side of the isolation transformer.

Other convenient high-voltage sources are car ignition coils, television flyback transformers, laser printer modules, and various other devices. Always lower the frequency at the Power Factor Correction Capacitor and correct, if needed, at the input side of the isolation transformer. The isolation transformer comes alive when pulsed. Amperage becomes a part of the consideration only at the isolation transformer. Faulty design, resulting in hysteresis, creates heat which self-destructs the transformer if it is overloaded. Transformers which have a composite core instead of the more common cores made from many layers of thin sheets of soft iron, run cool and can tolerate much higher amperage.

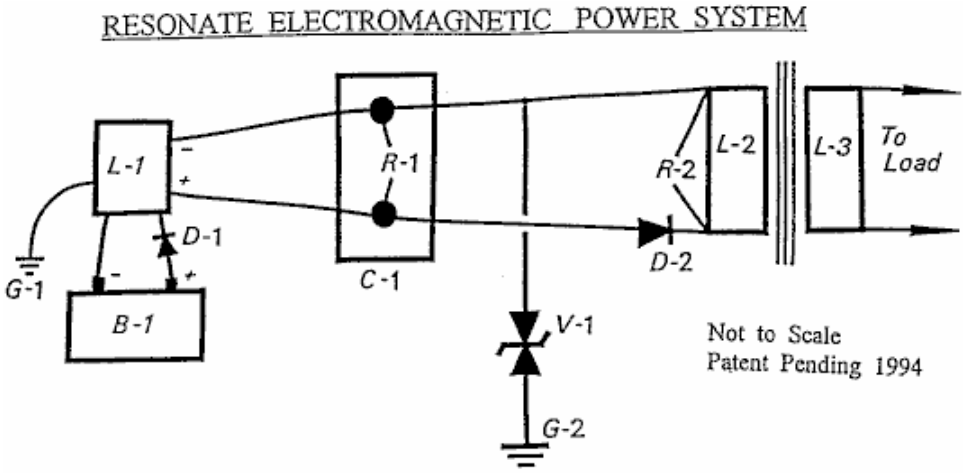

Power Source: B - 1 Gelcell, 12 Volt, 7 Amp Hour
D - 1 Kick back protection for L - 1
L - 1 Bertonee, NPS - 12D8, constant burn Neon Tube transformer, Bertonee, Boston, MS

Power Conditioner: C - 1, Capacitor or Capacitor Bank, 8,000 microfarads for 480 volts DC. R - 1, Resister used to set electron pump rate, frequency of the capacitor. Maintains the desired voltage level required to operate the system.

Voltage Control: V-1, Varistor, limits the voltage as required for the Output Transformer L -2. (480 V @ 60 Amps)

Output Transformer: Isolation Type, (L - 2 / L-3) with R - 2 (resistor) correcting the output frequency to 60 CPS, being 60 UP and 60 DN (120 total). (28.8 KVA)

Useful Timing Formulas:

T = frequency in cycles per second
C = capacitance in microfarads
L = Inductance in milliheneries
R = resistance in ohms

Therefore: $T = RC$ and $T = \frac{L}{R}$

The information shown above, relates to the small Suitcase Model demonstrated at the 1996 Tesla Convention, presented as Don Smiths' Workshop. This unit was a very primitive version and newer versions have atomic batteries and power output ranges of Gigawatts. The battery requirement is low level and is no more harmful than the radium on the dial of a clock. Commercial units of Boulder Dam size are currently being installed at several major locations throughout the world. For reasons of Don's personal security and contract obligations, the information which he has shared here, is incomplete.

Booker, H.G., " Energy in Electromagnetism ", Institute of Electrical Engineers, Peter Peregrinus, Ltd., 1982, I.S.B.N. 0-906048-59-1

Bleany and Bleany, " Electricity and Magnetism ", Oxford University Press, 1991, I.S.B.N. 0-19-851172-8

Chapman and Bartels, " Geomagnetism ", 3 vol., Oxford University Press, 1940

Hammond, P., " Energy Methods in Electromagnetism ", Oxford University Press, 1986, I.S.B.N. 0-19-859368-6

Matsushita and Campbell, " Physics of Geomagneic Phenomena ", several vols., National Center for Atmospheric Research, Boulder, Colorado, Academic press, 1967

Nashida, A., " Geomagnetic Diagnosis of the Magnetosphere ", University of Tokyo, Springer-Verlag, 1978, I.S.B.N. 0-387-08297-2

Rieger, Von Heinz., " Der Magnetisch Kreis ", Siemens A.G., Berlin and Munchen, Germany, I.S.B.N. 3-8009-4719-6

Rokityansky, I.I., " Geoelectrical investigation of the Earth's Crust and Mantel ", Institute of Geophysics, Kiev, U.S.S.R., Springer-Verlag, 1982, I.S.B.N. 3-540-10630-8

Vigoureux, P., " Units and Standards for Electromagnetics ", National Physical Laboratory, 1971, Springer-Verlag, I.S.B.N. 0-387-91077-8

Finnell, Woosley, " Solar Power Satellite Microwave Transmission and Receiver System. Energy Conversion Conference, Sept. 1981 pp 266-271

Glaser, " Satellite Solar Power Station " The Journal of Solar Energy and Technology, Vol. 12, No. 3., p. 353 .

Denmum et al, "A Microwave Power Transmission System for Space Satellite Power", Energy Conversion Conference Conference, Sept. 1977, pp 162-168

Nalos et al, "Microwave Power Beaming for long range energy transfer" "Proceedings of the 8 th European Microwave Conference" pp 573-578, 4 through 8 th. Sept., 1978

Angrist, S.W., " Direct Energy Conversion ", forth edition, Carnegie-Mellon University, Pub. Allyn and Bacon, Boston, London, Sidney and Toronto, ISBN 0-205-07758-7

Smith, D.L., " An Answer to Americas Energy Defict " , fifth edition, Pub. International Tesla Society, Colorado Springs, Co., 1996

Aspden, H. " The Law of Electrodynamics ", J. Franklin Inst., 287:179, 1969.

Sethian, J.D., " Anomalous Electron-Ion Energy Transfer ", Phys. Rev. Letters, vol. 40, No. 7, pp. 451-454 , 1978.

Westinghouse R. & D., "Electromagnetic Spectrum Chart"., Pub. The Exploratorium, San Francisco, CA 94123, Distributed by Edmond Scientific, Barrington, N.J. 06007 Order # 609-573-6250

I am most definitely not an expert in this area. However, it is probably worth mentioning some of the main points which Don Smith appears to be making. There are some very important points being made here, and grasping these may make a considerable difference to our ability to tap into the excess energy available in our local environment. There are four points worth mentioning:

1. Voltage
2. Frequency
3. Magnetic / Electric relationship
4. Resonance

1. Voltage. We tend to view things with an 'intuitive' view, generally based on fairly simple concepts. For example, we automatically think that it is more difficult to pick up a heavy object than to pick up a light one. How much more difficult? Well, if it is twice as heavy, it would probably be about twice as much effort to pick it up. This view has developed from our experience of things which we have done in the past, rather than on any mathematical calculation or formula.

Well, how about pulsing an electronic system with a voltage? How would the output power of a system be affected by increasing the voltage? Our initial 'off-the cuff' reaction might be that the power output might be increased a bit, but then hold on… we've just remembered that Watts = Volts x Amps, so if you double the voltage, then you would double the power in watts. So we might settle for the notion that if we doubled the voltage then we could double the output power. If we thought that, then we would be wrong.

Don Smith points out that as capacitors and coils store energy, if they are involved in the circuit, then the output power is proportional to the **square** of the voltage used. Double the voltage, and the output power is four times greater. Use three times the voltage and the output power is nine times greater. Use ten times the voltage and the output power is one hundred times greater !

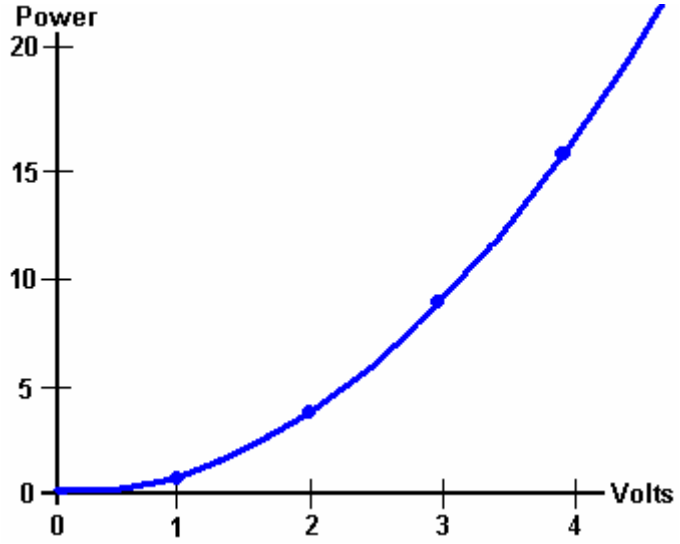

Don says that the energy stored, multiplied by the cycles per second, is the energy being pumped by the system. Capacitors and inductors (coils) temporarily store electrons, and their performance is given by:

Capacitor formula: **$W = 0.5 \times C \times V^2 \times Hz$** where:

W is the energy in Joules (Joules = Volts x Amps x seconds)
C is the capacitance in Farads
V is the voltage
Hz is the cycles per second

Inductor formula: **$W = 0.5 \times L \times A^2 \times Hz$** where:

W is the energy in Joules
L is the inductance in henrys
A is the current in amps
Hz is the frequency in cycles per second

You will notice that where inductors (coils) are involved, then the output power goes up with the square of the current. Double the voltage **and** double the current gives four times the power output due to the increased voltage and that increased output is increased by a further four times due to the increased current, giving sixteen times the output power.

2. Frequency. You will notice from the formulas above, that the output power is directly proportional to the frequency "Hz". The frequency is the number of cycles per second (or pulses per second) applied to the circuit. This is something which is not intuitive for most people. If you double the rate of pulsing, then you double the power output. When this sinks in, you suddenly see why Nikola Tesla tended to use millions of volts and millions of pulses per second.

However, Don Smith states that when a circuit is at it's point of resonance, resistance in the circuit drops to zero and the circuit becomes effectively, a superconductor. The energy for such a system which is in resonance is:

Resonant circuit: **$W = 0.5 \times C \times V^2 \times (Hz)^2$** where:

W is the energy in Joules
C is the capacitance in Farads
V is the voltage
Hz is the cycles per second

If this is correct, then raising the frequency in a resonating circuit has a massive effect on the power output of the device. The question then arises: why is the mains power in Europe just fifty cycles per second and in America just sixty cycles per second? If power goes up with frequency, then why not feed households at a million cycles per second? One major reason is that it is not easy to make electric motors which can be driven with power delivered at that frequency, so a more suitable frequency is chosen in order to suit the motors in vacuum cleaners, washing machines and other household equipment.

However, if we want to extract energy from the environment, then we should go for high voltage and high frequency. Then, when high power has been extracted, if we want a low frequency suited to electric motors, we can pulse the already captured power at that low frequency.

It might be speculated that if a device is being driven with sharp pulses which have a very sharply rising leading edge, that the effective frequency of the pulsing is actually determined by the speed of that rising edge, rather than the rate at which the pulses are actually generated. For example, if pulses are being generated at, say, 50 kHz but the pulses have a leading edge which would be suited to a 200 kHz pulse train, then the device might well see the signal as a 200 kHz signal with a 25% Mark/Space ratio, the very suddenness of the applied voltage having a magnetic shocking effect equivalent to a 200 kHz pulse train.

3. Magnetic / Electric relationship. Don states that the reason why our present power systems are so inefficient is because we concentrate on the electric component of electromagnetism. These systems are always COP<1 as electricity is the 'losses' of electromagnetic power. Instead, if you concentrate on the magnetic component, then there is no limit on the electric power which can be extracted from that magnetic component. Contrary to what you might expect, if you install a pick-up system which extracts electrical energy from the magnetic component, you can install any number of other identical pick-ups, each of which extract the same amount of electrical energy from the magnetic input, **without** loading the magnetic wave in any way. Unlimited electrical output for the 'cost' of creating a single magnetic effect.

The magnetic effect which we want to create is a ripple in the zero-point energy field, and ideally, we want to create that effect while using very little power. Creating a dipole with a battery which has a Plus and a Minus terminal or a magnet which has North and South poles, is an easy way to do create an electromagnetic imbalance in the local environment. Pulsing a coil is probably an even better way as the magnetic field reverses rapidly if it is an air-core coil, such as a Tesla Coil. Using a ferromagnetic core to the coil can create a problem as iron can't reverse it's magnetic alignment very rapidly, and ideally, you want pulsing which is at least a thousand times faster than iron can handle.

Don draws attention to the "Transmitter / Receiver" educational kit "Resonant Circuits #10-416" supplied by The Science Source, Maine. This kit demonstrates the generation of resonant energy and it's collection with a receiver circuit. However, if several receiver circuits are used, then the energy collected is increased several times without any increase in the transmitted energy. This is similar to a radio transmitter where hundreds of thousands of radio receivers can receive the transmitted signal without loading the transmitter in any way.

This immediately makes the Hubbard device spring to mind. Hubbard has a central "electromagnetic transmitter" surrounded by a ring of "receivers" closely coupled magnetically to the transmitter, each of which will receive a copy of the energy sent by the transmitter:

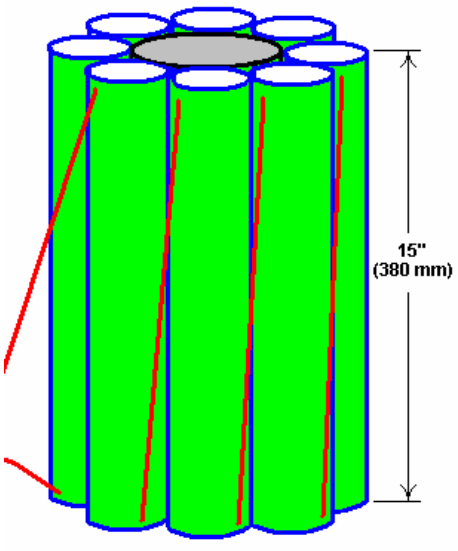

Don points to an even more clearly demonstrated occurrence of this effect in the Tesla Coil. In a typical Tesla Coil, the primary coil is much larger diameter than the inner secondary coil:

If, for example, 8,000 volts is applied to the primary coil which has four turns, then each turn would have 2,000 volts of potential. Each turn of the primary coil transfers electromagnetic flux to every single turn of the secondary winding, and the secondary coil has a very large number of turns. Massively more power is produced in the secondary coil than was used to energise the primary coil. A common mistake is to believe that a Tesla Coil can't produce serious amperage. If the primary coil is positioned in the middle of the secondary coil as shown, then the amperage generated will be as large as the voltage generated. A low power input to the primary coil can produce kilowatts of usable electrical power as described in chapter 5.

4. Resonance. An important factor in circuits aimed at tapping external energy is resonance. It can be hard to see where this comes in when it is an electronic circuit which is being considered. However, everything has it's own resonant frequency, whether it is a coil or any other electronic component. When components are connected together to form a circuit, the circuit has an overall resonant frequency. As a simple example, consider a swing:

If the swing is pushed before it reaches the highest point on the mother's side, then the push actually detracts from the swinging action. The time of one full swing is the resonant frequency of the swing, and that is determined by the length of the supporting ropes holding the seat and not the weight of the child nor the power with which the child is pushed. Provided that the timing is exactly right, a very small push can get a swing moving in a substantial arc. The key factor is, matching the pulses applied to the swing, to the resonant frequency of the swing. Get it right and a large movement is produced. Get it wrong, and the swing doesn't get going at all (at which point, critics would say "see, see …swings just don't work - this proves it !!").

Establishing the exact pulsing rate needed for a resonant circuit is not particularly easy, because the circuit contains coils (which have inductance, capacitance and resistance), capacitors (which have capacitance and a small amount of resistance) and resistors and wires, both of which have resistance and some capacitance. These kinds of circuit are called "LRC" circuits because "L" is the symbol used for inductance, "R" is the symbol used for resistance and "C" is the symbol used for capacitance.

Don Smith provides instructions for winding and using the type of air-core coils needed for a Tesla Coil. He says:

1. Decide a frequency and bear in mind, the economy of the size of construction selected. The factors are:

(a) Use radio frequency (above 20 kHz).
(b) Use natural frequency, i.e. match the coil wire length to the frequency - coils have both capacitance and inductance.
(c) Make the wire length either one quarter, one half of the full wavelength.
(d) Calculate the wire length in feet as follows:
If using one quarter wavelength, then divide 247 by the frequency in MHz.
If using one half wavelength, then divide 494 by the frequency in MHz.
If using the full wavelength, then divide 998 by the frequency in MHz.
For wire lengths in metres:
If using one quarter wavelength, then divide 75.29 by the frequency in MHz.
If using one half wavelength, then divide 150.57 by the frequency in MHz.
If using the full wavelength, then divide 304.19 by the frequency in MHz.

2. Choose the number of turns to be used in the coil when winding it using the wire length just calculated. The number of turns will be governed by the diameter of the tube on which the coil is to be wound. Remember that the ratio of the number of turns in the "L - 1" and "L - 2" coils, controls the overall output voltage. For example, if the voltage applied the large outer coil "L - 1" is 2,400 volts and L - 1 has ten turns, then each turn of L - 1 will have 240 volts dropped across it. This 240 volts of magnetic induction transfers 240 volts of electricity to every turn of wire in the inner "L - 2" coil. If the diameter of L - 2 is small enough to have 100 turns, then the voltage produced will be 24,000 volts. If the diameter of the L - 2 former allows 500 turns, then the output voltage will be 120,000 volts.

3. Choose the length and diameter of the coils. The larger the diameter of the coil, the fewer turns can be made with the wire length and so the coil length will be less, and the output voltage will be lower.

4. For example, if 24.7 MHz is the desired output frequency, then the length of wire, in feet, would be 247 divided by 24.7 which is 10 feet of wire (3,048 mm). The coil may be wound on a standard size of PVC pipe or alternatively, it can be purchased from a supplier - typically, an amateur radio supply store.

If the voltage on each turn of L - 1 is arranged to be 24 volts and the desired output voltage 640 volts, then there needs to be 640 / 24 = 26.66 turns on L - 2, wound with the 10 feet of wire already calculated.

Note: At this point, Don's calculations go adrift and he suggests winding 30 turns on a 2-inch former. If you do that, then it will take about 16 feet of wire and the resonant point at 10-feet will be at about 19 turns, giving an output voltage of 458 volts instead of the required 640 volts, unless the number of turns on L - 1 is reduced to give more than 24 volts per turn. However, the actual required diameter of the coil former (plus one diameter of the wire) is 10 x 12 / (26.67 x 3.14159) = 1.43 inches. You can make this size of former up quite easily if you want to stay with ten turns on the L - 1 coil.

5. Connect to the start of the coil. To determine the exact resonant point on the coil, a measurement is made. Off-the-shelf multimeters are not responsive to high-frequency signals so a cheap neon is used instead. Holding one wire of the neon in one hand and running the other neon wire along the outside of the L - 2 winding, the point of brightest light is located. Then the neon is moved along that turn to find the brightest point along that turn, and when it is located, a connection is made to the winding at that exact point. L - 2 is now a resonant winding. It is possible to increase the ("Q") effectiveness of the coil by spreading the turns out a bit instead of positioning them so that each turn touches both of the adjacent turns.

6. The input power has been suggested as 2,400 volts. This can be constructed from a Jacob's ladder arrangement or any step-up voltage system. An off-the-shelf module as used with lasers is another option.

7. Construction of the L - 1 input coil has been suggested as having 10 turns. The length of the wire in this coil is not critical. If a 2-inch diameter PVC pipe was used for the L - 2 coil, then the next larger size of PVC pipe can be used for the L - 1 coil former. Cut a 10-turn length of the pipe (probably a 3-inch diameter pipe). The pipe length will depend on the diameter of the insulated wire used to make the winding. Use a good quality multimeter or a specialised LCR meter to measure the capacitance (in Farads) and the inductance (in henrys) of the L - 2 coil. Now, put a capacitor for matching L - 1 to L - 2 across the voltage input of L - 1, and a spark gap connected **in parallel** is required for the return voltage from L - 1. A trimmer capacitor for L - 1 is desirable.

8. The performance of L - 2 can be further enhanced by attaching an earth connection to the base of the coil. The maximum output voltage will be between the ends of coil L - 2 and lesser voltages can be taken off intermediate points along the coil if that is desirable.

Don provides quite an amount of information on one of his devices shown here:

Without his description of the device, it would be difficult to understand it's construction and method of operation. As I understand it, the circuit of what is mounted on this board is as shown here:

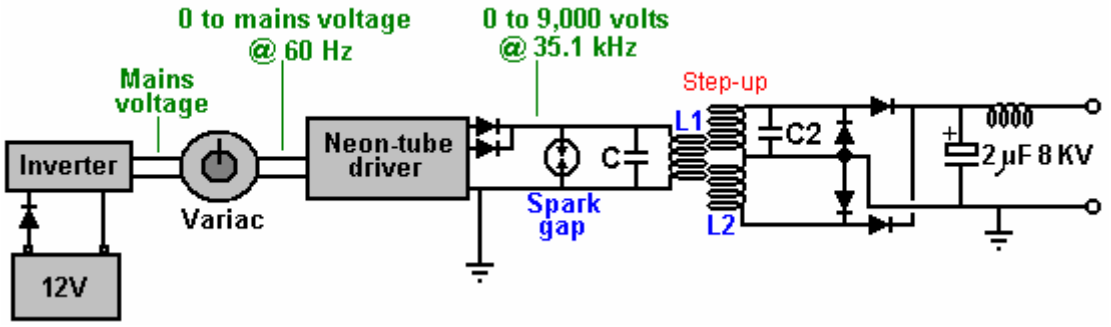

This arrangement has bothered some readers recently as they feel that the spark gap should be in series with the L1 coil, like this:

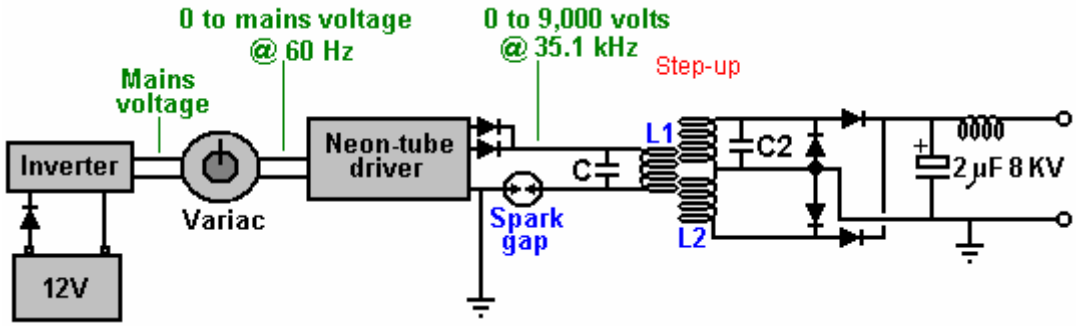

This is understandable, as there is always a tendency to think of the spark gap as being a device which is there to protect against excessive voltages rather than seeing it as an active component of the circuit, a component which is in continuous use. In 1925, Hermann Plauston was granted a patent for a whole series of methods for converting the high voltage produced by a tall aerial system into useable, standard electricity. Hermann starts off by explaining how high voltage can be converted into a convenient form and he uses a Wimshurst static electricity generator as an example of a constant source of high voltage. The output from a rectified Tesla Coil, a Wimshurst machine and a tall aerial are very much alike, and so Hermann's comments are very relevant here. He shows it like this:

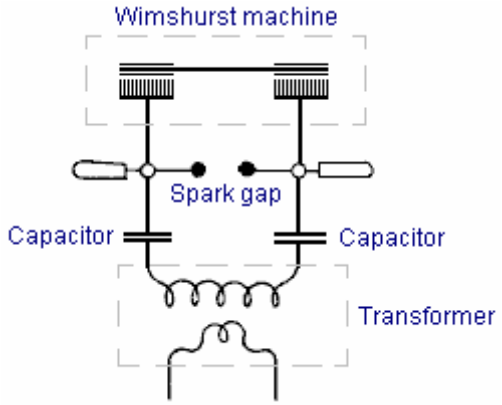

Here, the output of the Wimshurst machine is stored in two high-voltage capacitors (Leyden jars) causing a very high voltage to be created across those capacitors. When the voltage is high enough, a spark jumps across the spark gap, causing a massive surge of current through the primary winding of the transformer, which in his case is a step-down transformer as he is aimed at getting a lower output voltage. Don's circuit is almost identical:

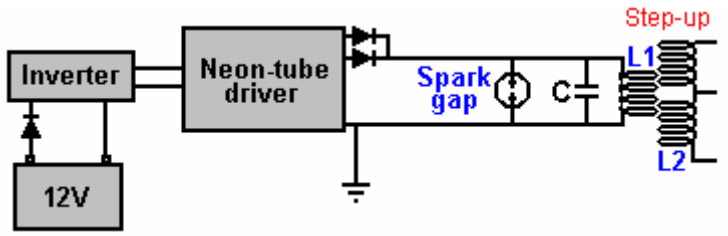

Here the high voltage comes from the battery/inverter/neon-tube driver/rectifiers, rather than from a mechanically driven Wimshurst machine. He has the same build up of voltage in a capacitor with a spark gap across the capacitor. The spark gap will fire when the capacitor voltage reaches its designed level. The only difference is in the positioning of the capacitor, which if it matched Hermann's arrangement exactly, would be like this:

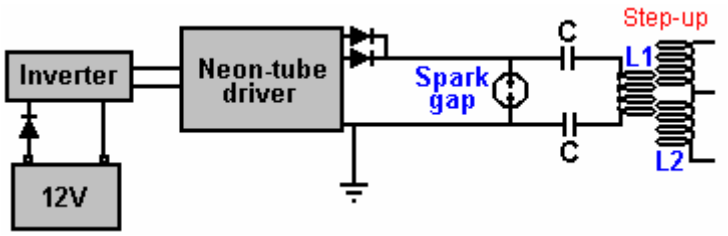

which would be a perfectly viable arrangement as far as I can see. You will remember that Tesla, who always speaks very highly of the energy released by the very sharp discharge produced by a spark, shows a high-voltage source feeding a capacitor with the energy passing through a spark gap to the primary winding of a transformer:

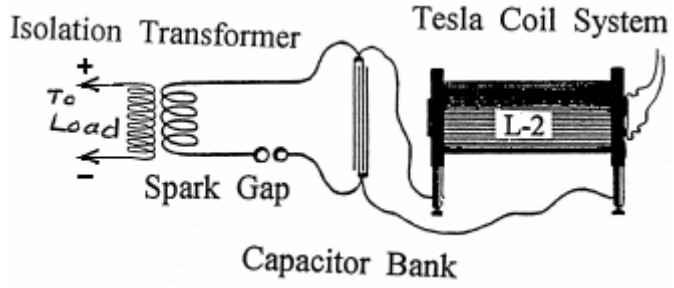

However, with Don's arrangement, it can be a little difficult to see why the capacitor is not short-circuited by the very low resistance of the few turns of thick wire forming the L1 coil. Well, it would do that if we were operating with DC, but we are most definitely not doing that as the output from the neon-tube driver circuit is pulsing 35,000 times per second. This causes the DC resistance of the L1 coil to be of almost no consequence and instead, the coil's "impedance" or "reactance" (effectively, it's AC resistance) is what counts. Actually, the capacitor and the L1 coil being connected across each other have a combined "reactance" or resistance to pulsing current at this frequency. This is where the nomograph diagram comes into play, and there is a much easier to understand version of it a few pages later on in this document. So, because of the high pulsing frequency, the L1 coil does not short-circuit the capacitor and if the pulsing frequency matches the resonant frequency of the L1 coil (or a harmonic of that frequency), then the L1 coil will actually have a very high resistance to current flow through it. This is how a crystal set radio receiver tunes in a particular radio station, broadcasting on it's own frequency.

Anyway, coming back to Don's device shown in the photograph above, the electrical drive is from a 12-volt battery which is not seen in the photograph. Interestingly, Don remarks that if the length of the wires connecting the battery to the inverter are exactly one quarter of the wave length of the frequency of the oscillating magnetic field generated by the circuit, then the current induced in the battery wires will recharge the battery continuously, even if the battery is supplying power to the circuit at the same time.

The battery supplies a small current through a protecting diode, to a standard off-the-shelf "true sine-wave" inverter. An inverter is a device which produces mains-voltage Alternating Current from a DC battery. As Don wants adjustable voltage, he feeds the output from the inverter into a variable transformer called a "Variac" although this is often made as part of the neon-driver circuit to allow the brightness of the neon tube to be adjusted by the user. This arrangement produces an AC output voltage which is adjustable from zero volts up to the full mains voltage (or a little higher, though Don does not want to use a higher voltage). The use of this kind of adjustment usually makes it essential for the inverter to be a true sine-wave type. As the power requirement of the neon-tube driver circuit is so low, the inverter should not cost very much.

The neon-tube (or "gas-discharge" tube) driver circuit is a standard off-the-shelf device used to drive neon tube displays for commercial establishments. The one used by Don contains an oscillator and a step-up transformer, which together produce an Alternating Current of 9,000 volts at a frequency of 35,100 Hz (sometimes written as 35.1 kHz). The term "Hz" stands for "cycles per second". Don lowers the 9,000 volts as he gets great power output at lower input voltages and the cost of the output capacitors is a significant factor. The particular neon-tube driver circuit which Don is using here, has two separate outputs, so Don connects them together and uses a blocking diode in each line to prevent either of them affecting the other one. Not easily seen in the photograph, the high-voltage output line has a very small, encapsulated, spark gap in it and the line is also earthed. This

device is commonly used as a lightning strike protection component and in Don's circuit it lights continuously when the device is running. It looks like this:

The output of the neon-tube driver circuit is used to drive the primary "L1" winding of a Tesla Coil style transformer. This looks ever so simple and straightforward, but there are some subtle details which need to have attention paid to them.

The operating frequency of 35.1 kHz is set and maintained by the neon-tube driver circuitry, and so, in theory, we do not have to do any direct tuning ourselves. However, we want the resonant frequency of the L1 coil and the capacitor across it to match the neon-driver circuit frequency. The frequency of the "L1" coil winding will induce exactly the same frequency in the "L2" secondary winding. However, we need to pay special attention to the ratio of the wire lengths of the two coil windings as we want these two windings to resonate together. A rule of thumb followed by most Tesla Coil builders is to have the same weight of copper in the L1 and L2 coils, which means that the wire of the L1 coil is usually much thicker than the wire of the L2 coil. If the L1 coil is to be one quarter of the length of the L2 coil, then we would expect the cross-sectional area of the L1 coil to be four times that of the wire of the L2 coil (as the area is proportional to the square of the radius, and the square of two is four)

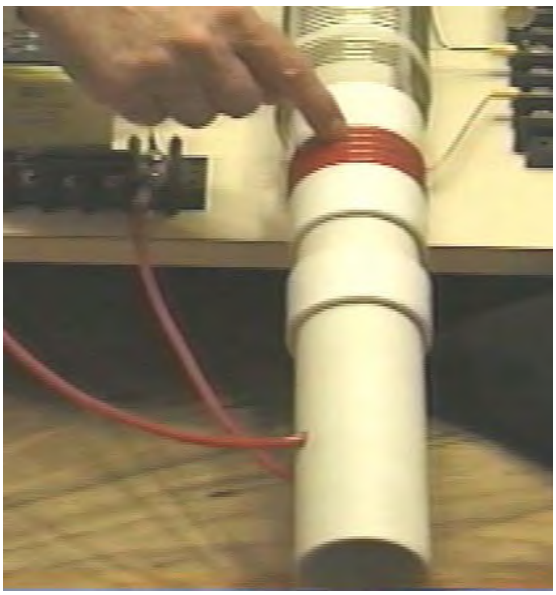

Don uses a plastic tube as the former for his "L1" primary coil winding. As you can see here, the wire is fed into the former, leaving sufficient clearance to allow the former to slide all the way into the outer coil. The wire is fed up inside the pipe and out through another hole to allow the coil turns to be made on the outside of the pipe. There appear to be five turns, but Don does not always go for a complete number of turns, so it might be 4.3 turns or some other value. The key point here is that the length of wire in the "L1" coil turns should be exactly one quarter of the length of wire in the "L2" coil turns.

The "L2" coil used here is a commercial 3-inch diameter unit from Barker & Williamson, constructed from uninsulated, solid, single-strand "tinned" copper wire. Don has taken this coil and unwound four turns at the centre of the coil in order to make a centre-tap. He then measured the exact length of wire in the remaining section and made the length of the "L1" coil turns to be exactly one quarter of that length. The wire used for the "L1" coil looks like Don's favourite "Jumbo Speaker Wire" which is a very flexible wire with a very large number of extremely fine uninsulated copper wires inside it.

You will notice that Don has placed a plastic collar on each side of the winding, matching the thickness of the wire, in order to create a secure sliding operation inside the outer "L2" coil, and the additional plastic collars positioned further along the pipe provide further support for the inner coil. This sliding action allows the primary coil "L1" to be positioned at any point along the length of the "L2" secondary coil, and that has a marked tuning effect on the operation of the system. The outer "L2" coil does not have any kind of tube support but instead, the coil shape is maintained by the stiffness of the solid wire plus four slotted strips. This style of construction produces the highest possible coil performance at radio frequencies. With a Tesla Coil, it is most unusual to have the L1 coil of smaller diameter than the L2 coil.

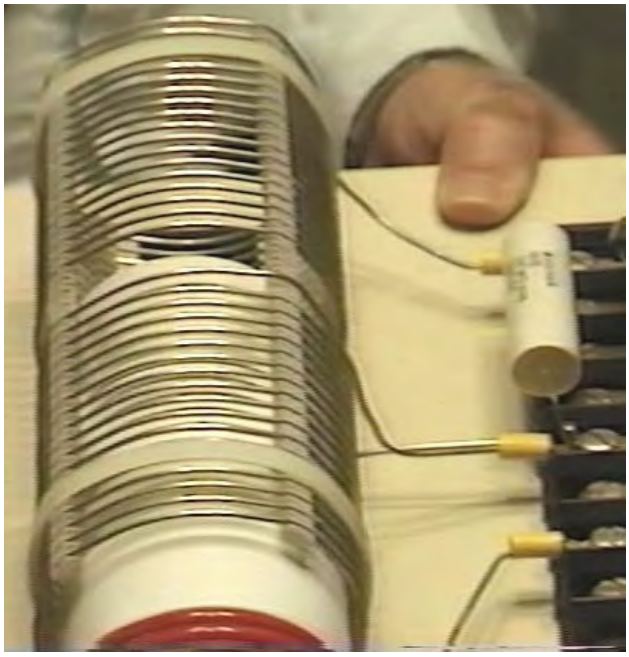

The "L2" coil has two separate sections, each of seventeen turns. One point to note is the turns are spaced apart using slotted strips to support the wires and maintain an accurate spacing between adjacent turns. It must be remembered that spacing coil turns apart like this alters the characteristics of the coil, increasing it's "capacitance" factor substantially. Every coil has resistance, inductance and capacitance, but the form of the coil construction has a major effect on the ratio of these three characteristics. The coil assembly is held in position on the base board by two off-white plastic cable ties. The nearer half of the coil is effectively connected across the further half as shown in the circuit diagram above.

One point which Don stresses, is that the length of the wire in the "L1" coil and the length of wire in the "L2" coil, must be an exact even division or multiple of each other (in this case, the "L2" wire length in each half of the "L2" coil is exactly four times as long as the "L1" coil wire length). This is likely to cause the "L1" coil to have part of a turn, due to the different coil diameters. For example, if the length of the "L2" coil wire is 160 inches and "L1" is to be one quarter of that length, namely, 40 inches. Then, if the "L1" coil has an effective diameter of 2.25 inches, (allowing for the thickness of the wire when wound on a 2-inch diameter former), then the "L1" coil would have 5.65 (or 5 and 2/3) turns which causes the finishing turn of "L2" to be 240 degrees further around the coil former than the start of the first turn - that is, five full turns plus two thirds of the sixth turn.

The L1 / L2 coil arrangement is a Tesla Coil. The positioning of the "L1" coil along the length of the "L2" coil, adjusts the voltage to current ratio produced by the coil. When the "L1" coil is near the middle of the "L2" coil, then the amplified voltage and amplified current are roughly the same. However, Don stresses that the "height" length of the coil (when standing vertically) controls the voltage produced while the coil "width" (the diameter of the turns) controls the current produced.

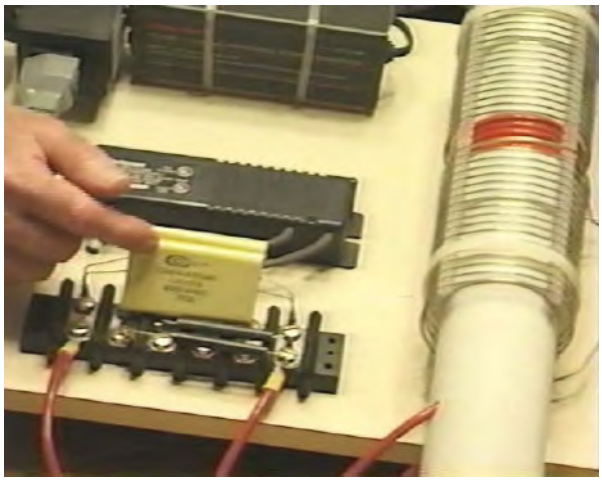

The exact wire length ratio of the turns in the "L1" and "L2" coils gives them an almost automatic synchronous tuning with each other, and the exact resonance between them can be achieved by the positioning of the "L1" coil along the length of the "L2" coil. While this is a perfectly good way of adjusting the circuit, in the 1994 build shown in the photograph, Don has opted to get the exact tuning by connecting a capacitor across "L1" as marked as "**C**" in the circuit diagram. Don found that the appropriate capacitor value for his particular coil build, was about 0.1 microfarad (100 nF) and so he connected two 47 nF high-voltage capacitors in parallel to get the value which he wanted. It must be remembered that the voltage across "L1" is very high, so a capacitor used in that position needs a voltage rating of at least 9,000 volts. Don remarks that the actual capacitors seen in the photograph of this prototype are rated at fifteen thousand volts, and were custom made for him using a "self-healing" style of construction.

Don has also connected a small capacitor across the "L2" coil, and that optional component is marked as "C2" in the circuit diagram and the value used by Don happened to be a single 47nF, high-voltage capacitor. As the two halves of the "L2" coil are effectively connected across each other, it is only necessary to have one capacitor for "L2":

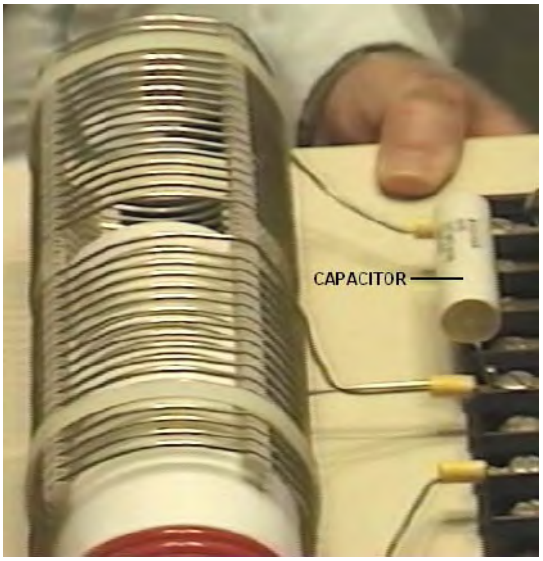

There are various ways of dealing with the output from the "L2" coil in order to get large amounts of conventional electrical power out of the device. The method shown here uses the four very large capacitors seen in the photograph. Each of these four capacitors are said to be 8 microfarad capacity with a 2,000 volt rating. In spite of the fact that they appear to be wired in parallel, Don states that they are in fact, wired in series to make a single capacitor of 2 microfarad capacity with an 8,000 volt rating. Don remarks that he has to be very careful to keep the voltage to the neon-tube driver circuit turned down in order to avoid getting more than 8,000 volts on these output storage capacitors.

This capacitor bank is fed through a diode which is rated for both high voltage and high current, as Don states that the device produces 8,000 volts at 20 amps, in which case, this rectifying diode has to be able to handle that level of power, both at start-up when the capacitor bank is fully discharged and "L2" is producing 8,000 volts, and when the full load of 20 amps is being drawn. The actual diodes used by Don happen to be rated at 25 KV but that is a far greater rating than is actually needed.

In passing, it might be remarked that the average home user will not have an electrical requirement of anything remotely like as large as this, seeing that 10 kW is more than most people use on a continuous basis, while 8 KV at 20 A is a power of 160 kilowatts. As the neon-tube driver circuit can put out 9,000 volts and since the L1 / L2 coil system is a step-up transformer, if the voltage fed to the capacitor bank is to be kept down to 8,000 volts, then the Variac adjustment must be used to reduce the voltage fed to the neon-tube driver circuit, in order to lower the voltage fed to the L1 / L2 coil pair, typically, to 3,000 volts.

A very astute and knowledgeable member of the EVGRAY Yahoo EVGRAY forum whose ID is "silverhealtheu" has recently pointed out that Don Smith says quite freely that he does not disclose all of the details of his designs, and it is his opinion that a major item which has not been disclosed is that the diodes in the circuit diagrams shown here are the wrong way round and that Don operates his voltages in reverse to the conventional way. In fact, the circuit diagram should be:

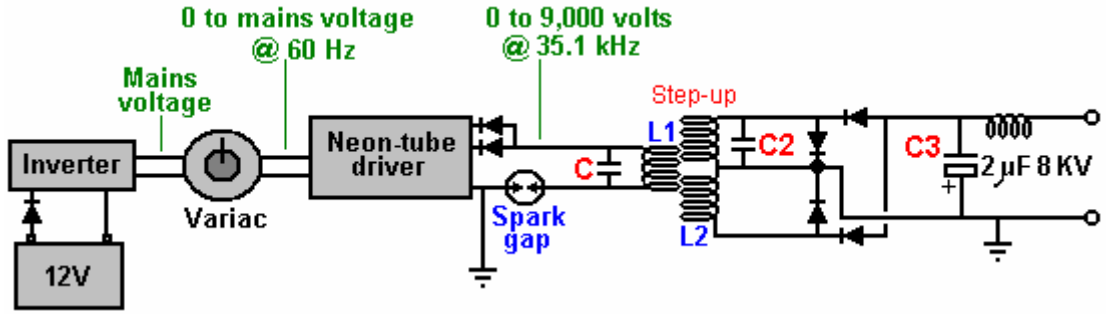

He comments: "the diodes leaving the Neon-tube Driver may need to be reversed as we want to collect the negative polarity. The spark gap will then operate on ambient inversion and the spark will look and sound totally different with a much faster crack and producing very little heat and even becoming covered in frost is possible.

The Variac should be raised up just enough to get a spark going then backed off slightly. Any higher voltage is liable to make the Neon-tube Driver think that it has a short-circuit condition, and the new electronic designs will then shut down automatically and fail to operate at all if this method is not followed.

When running, C, L1 and L2 operate somewhere up in the Radio Frequency band because the Neon-tube Driver only acts as a tank-circuit exciter. The large collection capacitor C3, should fill inverted to earth polarity as shown above. The load will then be pulling electrons from the earth as the cap is REFILLED back to ZERO rather than the joules in the capacitor being depleted.

Also remember that the Back-EMF systems of John Bedini and others, create a small positive pulse but they collect a super large NEGATIVE polarity spike which shoots off the bottom of an oscilloscope display. This is what we want, plenty of this stored in capacitors, and then let the ambient background energy supply the current when it makes the correction."

This is **a very important point** and it may well make a really major difference to the performance of a device of this nature.

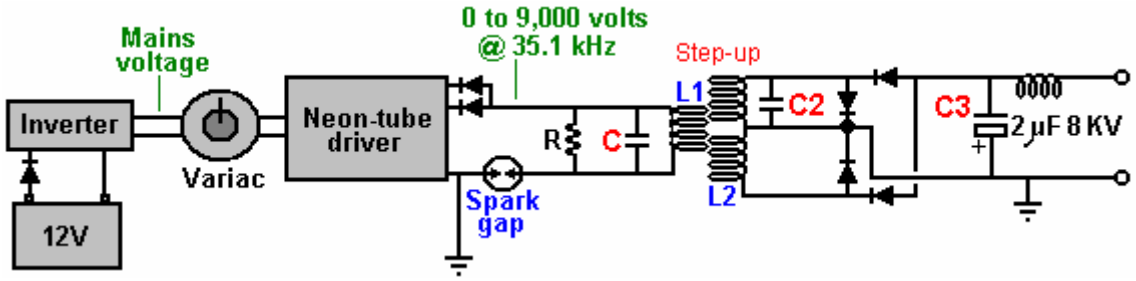

One reader has drawn attention to the fact that Don's main document indicates that there should be a resistor "R" across the L1 coil as well as the capacitor "C" and he suggests that the circuit should actually be as shown above, considering what Don said earlier about his "suitcase" design. Another reader points out that the wire in the output choke shown in the photograph below appears to be wound with wire that is far too small diameter to carry the currents mentioned by Don. I seems likely that a choke is not needed in that position, but a more powerful choke can easily be wound using larger diameter wire.

When the circuit is running, the storage capacitor bank behaves like an 8,000 volt battery which never runs down and which can supply 20 amps of current for as long as you want. The circuitry for producing a 220 volt 50 Hz AC output or a 110 volt 60 Hz AC output from the storage capacitors is just standard electronics. In passing, one option for charging the battery is to use the magnetic field caused by drawing mains-frequency current pulses through the output "choke" coil, shown here:

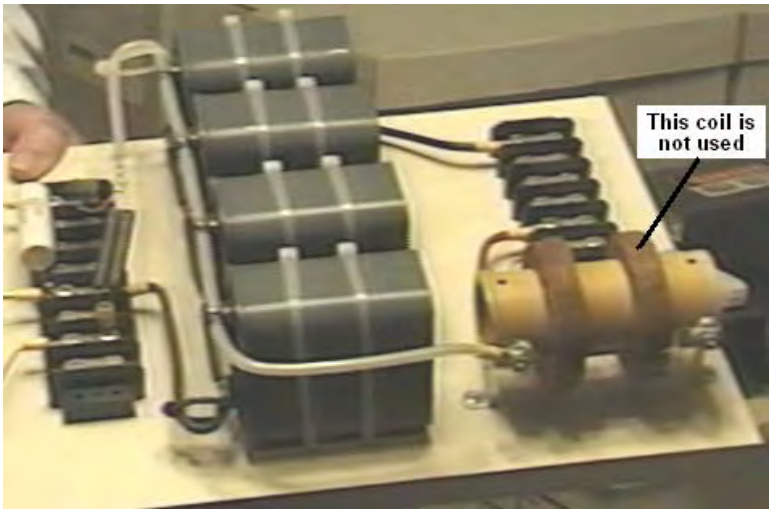

The output current flows through the left hand winding on the brown cylindrical former, and when the photograph was taken, the right-hand winding was no longer in use. Previously, it had been used to provide charging power to the battery by rectifying the electrical power in the coil, caused by the fluctuating magnetic field caused by the pulsing current flowing through the left hand winding, as shown here:

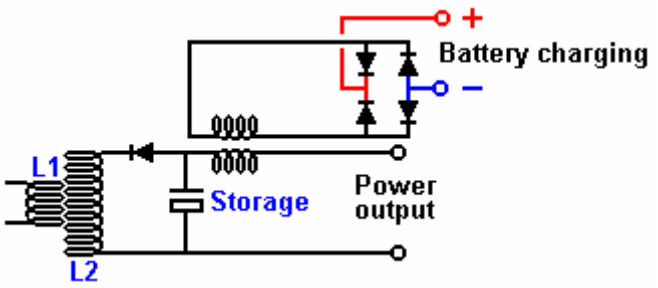

The DC output produced by the four diodes was then used to charge the driving battery, and the power level produced is substantially greater than the minor current drain from the battery. Consequently, it is a sensible precaution to pass this current to the battery via a circuit which prevents the battery voltage rising higher than it should. A simple voltage level sensor can be used to switch off the charging when the battery has reached its optimum level. Other batteries can also be charged if that is wanted. Simple circuitry of the type shown in chapter 12 can be used for controlling and limiting the charging process. The components on Don's board are laid out like this:

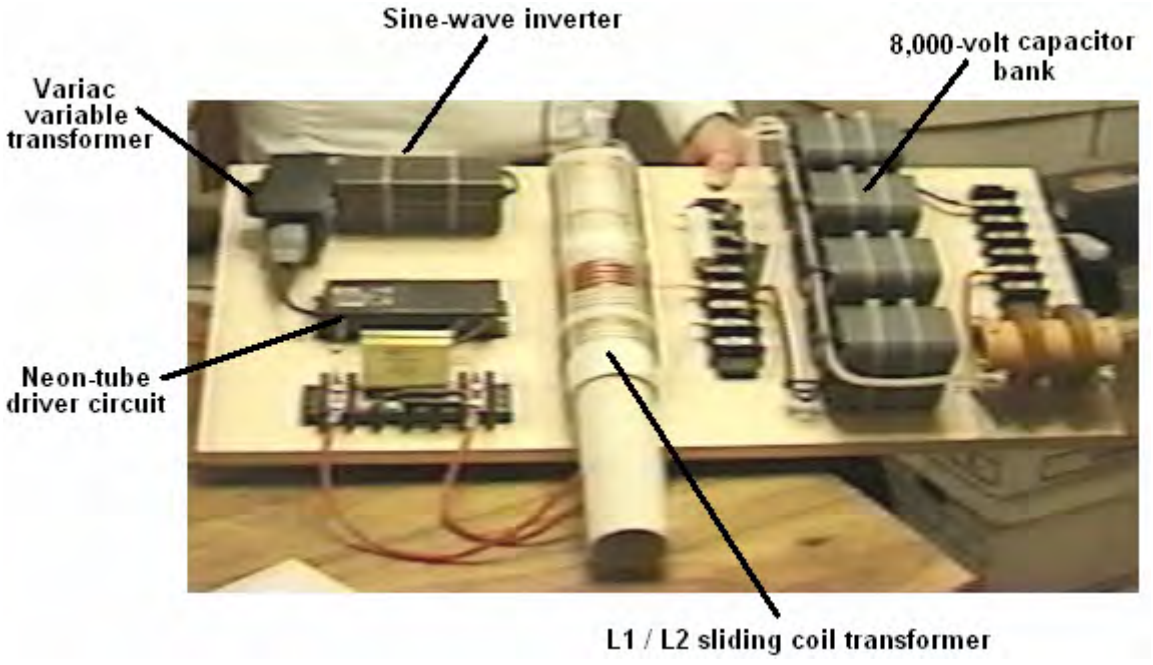

Don draws attention to the fact that the cables used to connect the output of "L2" to the output of the board, connecting the storage capacitors on the way, are very high-voltage rated cables with special multiple coverings to ensure that the cables will remain sound over an indefinite period. It should be remarked at this point, that the outer 3" diameter coil used by Don, is not wound on a former, but in order to get higher performance at high frequencies, the turns are supported with four separate strips physically attached to the turns - the technique described later in this document as being an excellent way for home construction of such coils.

Please bear in mind that the voltages here and their associated power levels are literally lethal and perfectly capable of killing anyone who handles the device carelessly when it is powered up. When a replication of this device is ready for routine use, it must be encased so that none of the high-voltage connections can be touched by anyone. This is not a suggestion, but it is a mandatory requirement, despite the fact that the components shown in the photographs are laid out in what would be a most dangerous fashion were the circuit to be powered up as it stands. Under no circumstances, construct and test this circuit unless you are already experienced in the use of high-voltage circuits or can be supervised by somebody who is experienced in this field. This is a "one hand in the pocket at all times" type of circuit and it needs to be treated with great care and respect at all times, so be sensible.

The remainder of the circuit is not mounted on the board, possibly because there are various ways in which the required end result can be achieved. The one suggested here is perhaps the most simple solution:

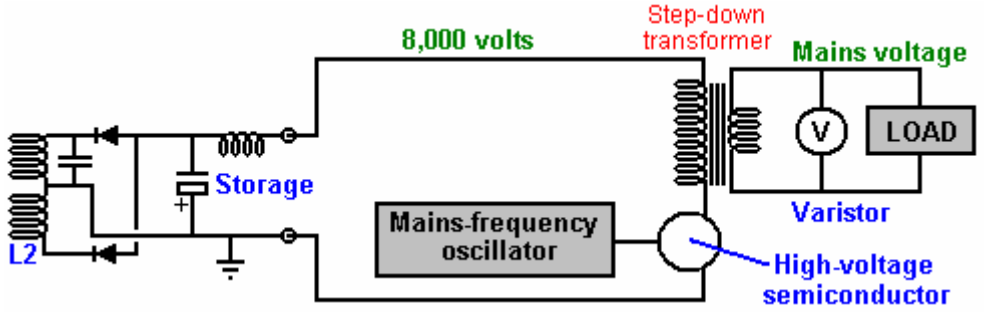

The voltage has to be dropped, so an iron-cored mains-frequency step-down transformer is used to do this. To get the frequency to the standard mains frequency for the country in which the device is to be used, an oscillator is used to generate that particular mains frequency. The oscillator output is used to drive a suitable high-voltage semiconductor device, be it an FET transistor, an IGBT device, or whatever. This device has to switch the working current at 8,000 volts, though admittedly, that will be a current which will be at least thirty six times lower than the final output current, due to the higher voltage on the primary winding of the transformer. The available power will be limited by the current handling capabilities of this output transformer.

As the circuit is capable of picking up additional magnetic pulses, such as those generated by other equipment, nearby lightning strikes, etc. an electronic component called a "varistor" marked "V" in the diagram, is connected across the load. This device acts as a voltage spike suppressor as it short circuits any voltage above its design voltage, protecting the load from power surges.

Don also explains an even more simple version of the circuit as shown here:

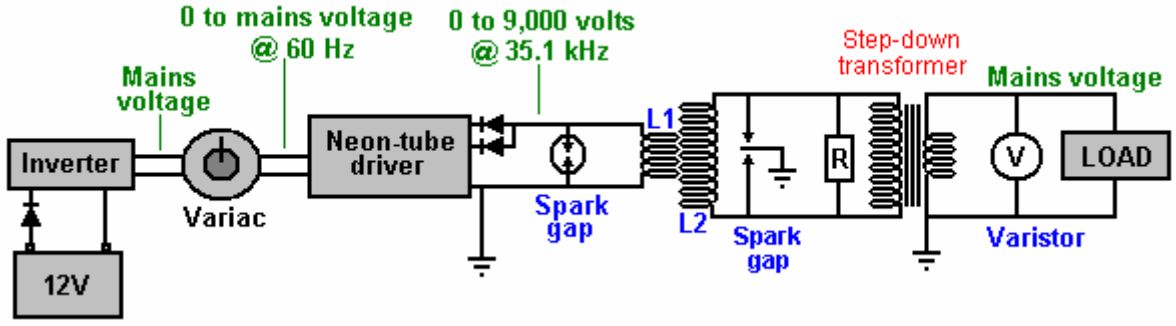

This simplified circuit avoids the need for expensive capacitors and the constraints of their voltage ratings, and the need for electronic control of the output frequency. The wire length in the turns of coil "L2" still needs to be exactly four times the wire length of the turns in coil "L1", but there is only one component which needs to be introduced, and that is the resistor "**R**" placed across the primary winding of the step-down isolation transformer. This transformer is a laminated iron-core type, suitable for the low mains frequency, but the output from "L2" is at much higher frequency. It is possible to pull the frequency down to suit the step-down transformer by connecting the correct value of resistor "R" across the output transformer (or a coil and resistor, or a coil and a capacitor). The

value of resistor needed can be predicted from the American Radio Relay League graph (shown as Fig.44 in Don's .pdf document which can be downloaded from the www.free-energy-info.com website). The sixth edition of the Howard Sams book "Handbook of Electronics Tables and Formulas" (ISBN-10: 0672224690 or ISBN-13**:** 978-0672224690) has a table which goes down to 1 kHz and so does not need to be extended to reach the frequencies used here. The correct resistor value could also be found by experimentation. You will notice that an earthed dual spark gap has been placed across "L2" in order to make sure that the voltage levels always stay within the design range. Don remarks that he intends this particular device to be built by anyone who wants to, providing power for that person's needs and he states that some two hundred replications have already been built.

Don also explains an even more simple version which does not need a Variac, high voltage capacitors or high voltage diodes. Here, a DC output is accepted which means that high-frequency step-down transformer operation can be used. This calls for an air-core transformer which you would wind yourself from heavy duty wire. Mains loads would then be powered by using a standard off-the-shelf inverter. In this version, it is of course, necessary to make the "L1" turns wire length exactly one quarter of the "L2" turns wire length in order to make the two coils resonate together. The operating frequency of each of these coils is imposed on them by the output frequency of the neon-tube driver circuit. That frequency is maintained throughout the entire circuit until it is rectified by the four diodes feeding the low-voltage storage capacitor. The target output voltage will be either just over 12 volts or just over 24 volts, depending on the voltage rating of the inverter which is to be driven by the system. The circuit diagram is:

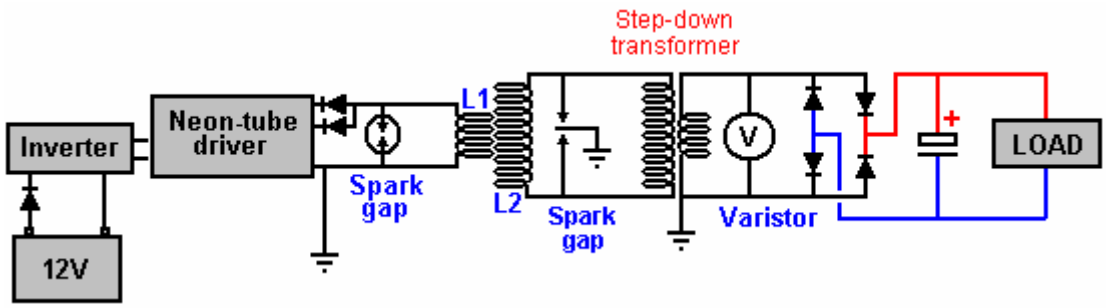

As many people will find the nomograph chart in Don's pdf document very difficult to understand and use, here is an easier version:

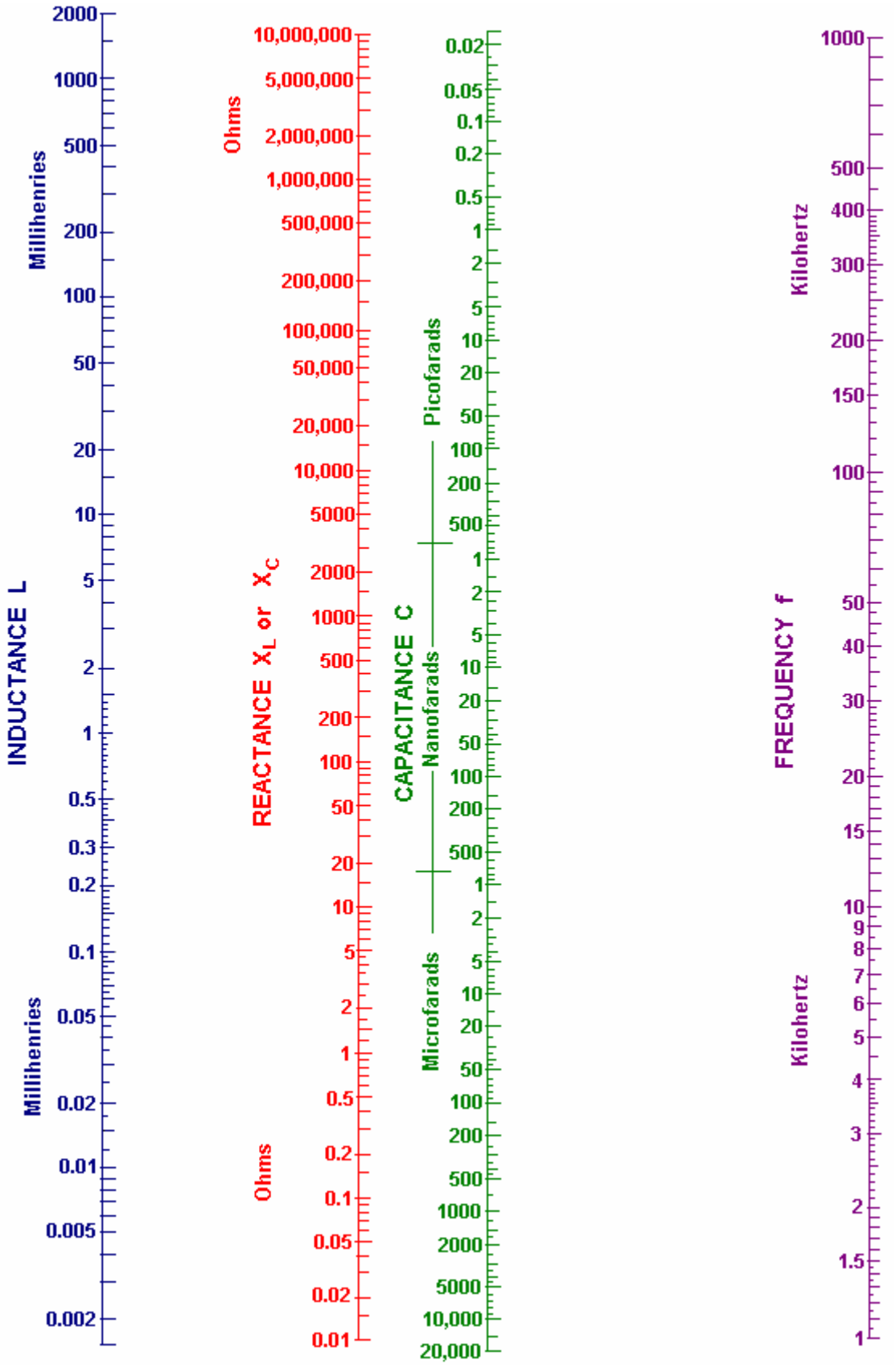

The objective here is to determine the "reactance" or 'AC resistance' in ohms and the way to do that is as follows:

Suppose that your neon-tube driver is running at 30 kHz and you are using a capacitor of 100 nF (which is the same as 0.1 microfarad) and you want to know what is the AC resistance of your capacitor is at that frequency. Also, what coil inductance would have that same AC resistance. Then the procedure for finding that out is as follows:

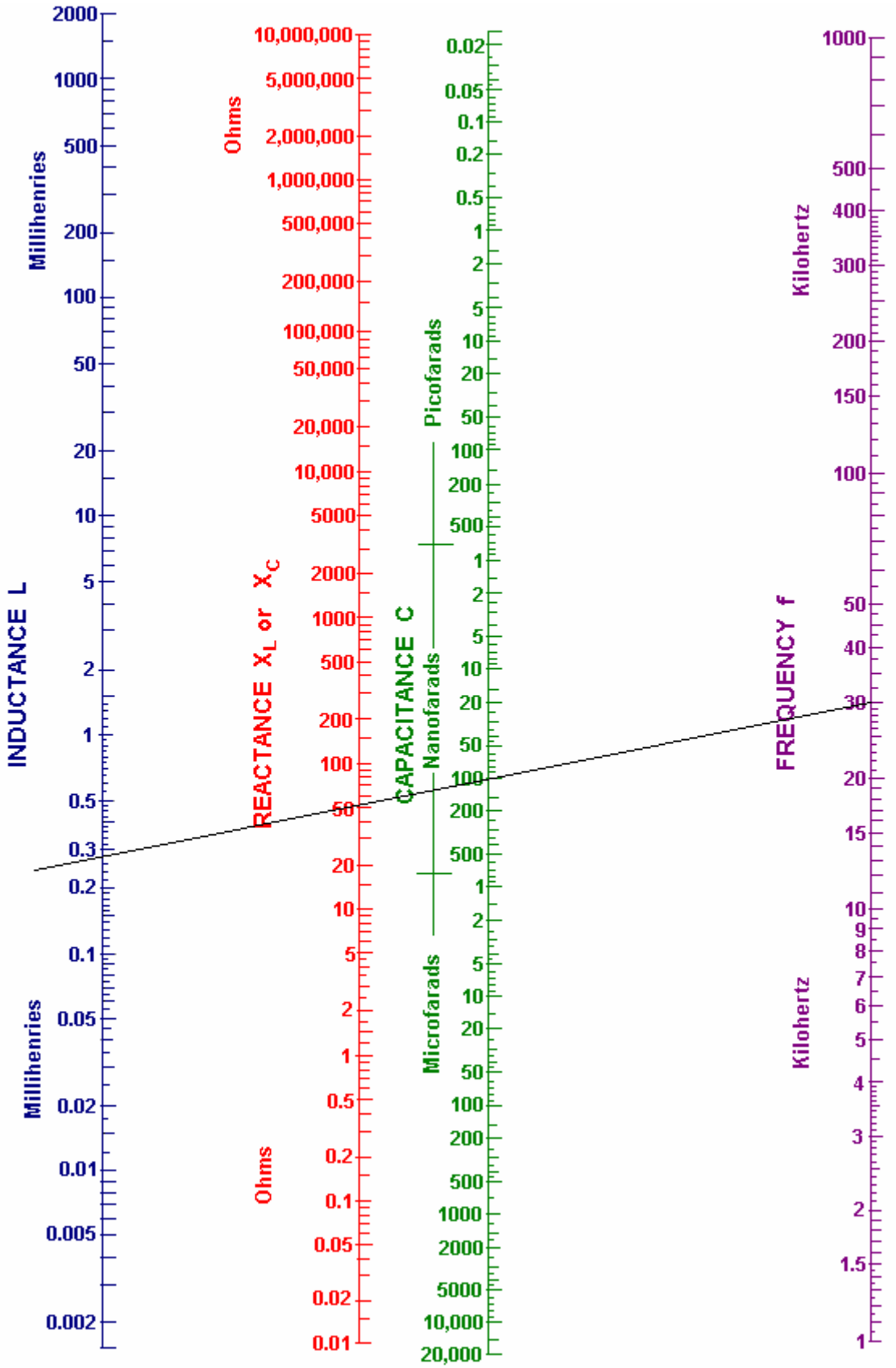

Draw a straight line from your 30 kHz frequency (purple line) through your 100 nanofarad capacitor value and carry the line on as far as the (blue) inductance line as shown above.

You can now read the reactance ("AC resistance") off the red line, which looks like 51 ohms to me. This means that when the circuit is running at a frequency of 30 kHz, then the current flow through your 100 nF capacitor will be the same as through a 51 ohm resistor. Reading off the blue "Inductance" line that same current flow at that frequency would occur with a coil which has an inductance of 0.28 millihenries.

I have been passed a copy of Don's circuit diagram for this device, and it is shown here:

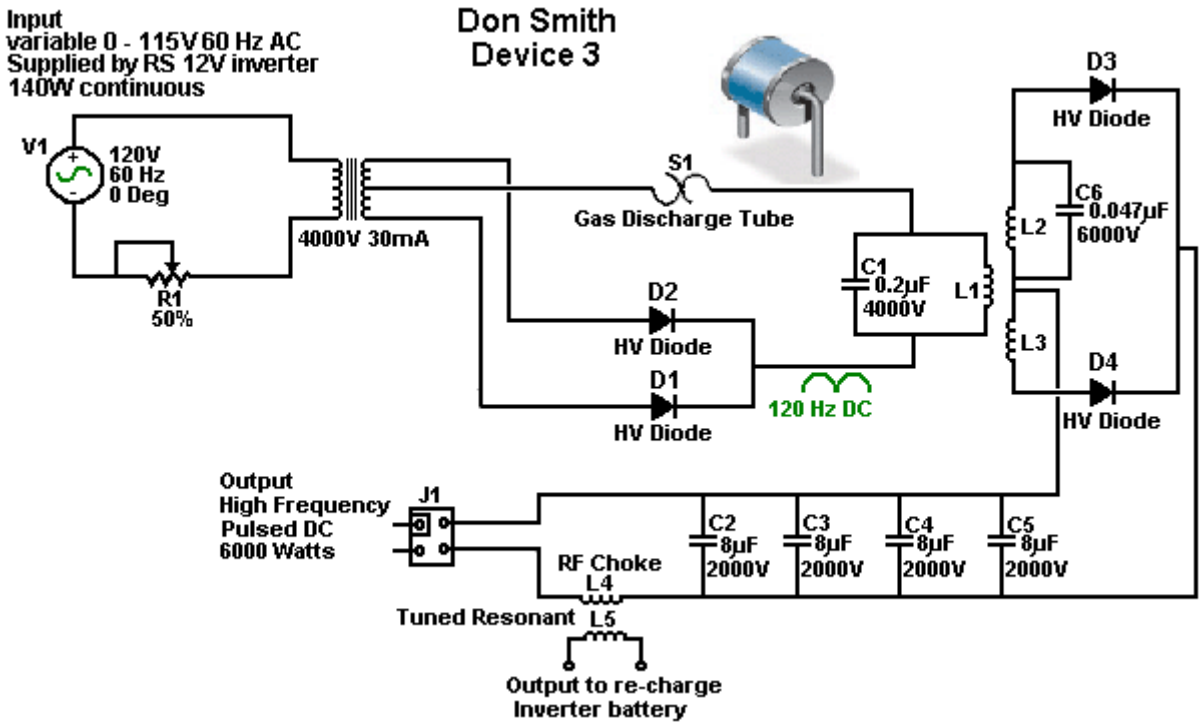

The 4000V 30mA transformer shown in this circuit diagram, may use a ferrite-cored transformer from a neon-tube driver module which steps up the voltage but it does not raise the frequency as that is clearly marked at 120 Hz pulsed DC. You will notice that this circuit diagram is drawn with Plus shown below Minus (which is most unusual).

Please note that when an earth connection is mentioned in connection with Don Smith's devices, we are talking about an actual wire connection to a metal object physically buried in the ground, whether it is a long copper rod driven into the ground, or an old car radiator buried in a hole like Tariel Kapanadze used, or a buried metal plate. When Thomas Henry Moray performed his requested demonstration deep in the countryside at a location chosen by the sceptics, the light bulbs which formed his demonstration electrical load, glowed more brightly with each hammer stroke as a length of gas pipe was hammered into the ground to form his earth connection.

Don also explains an even more simple version of his main device. This version does not need a Variac (variable voltage transformer) or high voltage capacitors. Here, a DC output is accepted which means that high-frequency step-down transformer operation can be used. This calls on the output side, for an air-core (or ferrite rod core) transformer which you would wind yourself from heavy duty wire. Mains loads would then be powered by using a standard off-the-shelf inverter. In this version, it is of course, very helpful to make the "L1" turns wire length exactly one quarter of the "L2" turns wire length in order to make the two coils automatically resonate together. The operating frequency of each of these coils is imposed on them by the output frequency of the neon-tube driver circuit. That frequency is maintained throughout the entire circuit until it is rectified by the four diodes feeding the low-voltage storage capacitor. The target output voltage will be either just over 12 volts or just over 24 volts, depending on the voltage rating of the inverter which is to be driven by the system.

As the circuit is capable of picking up additional magnetic pulses, such as those generated by other equipment, nearby lightning strikes, etc. an electronic component called a "varistor" marked "V" in the diagram, is connected across the load. This device acts as a voltage spike suppressor as it short-circuits any voltage above its design voltage, protecting the load from power surges. A Gas-Discharge Tube is an effective alternative to a varistor.

This circuit is effectively two Tesla Coils back-to-back and the circuit diagram might be:

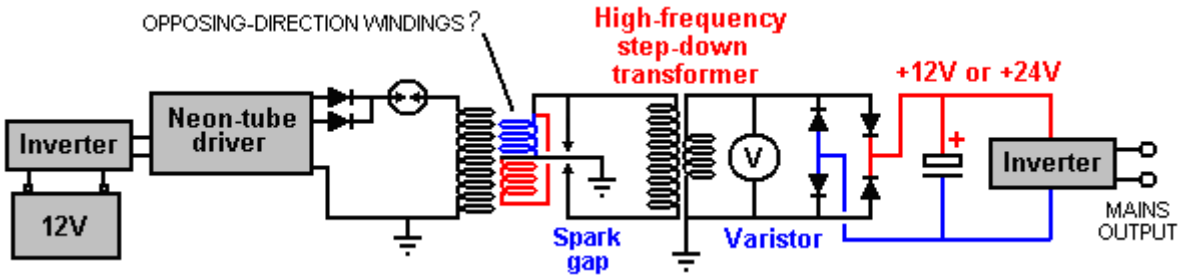

It is by no means certain that in this circuit, the red and blue windings are wound in opposing directions. The spark gap (or gas-discharge tube) in series with the primary of the first transformer alters the operation in a somewhat unpredictable way as it causes the primary to oscillate at a frequency determined by it's inductance and it's self-capacitance, and that may result in megahertz frequencies. The secondary winding(s) of that transformer **must** resonate with the primary and in this circuit which has no frequency-compensating capacitors, that resonance is being produced by the exact wire length in the turns of the secondary. This looks like a simple circuit, but it is anything but that. The excess energy is produced by the raised frequency, the raised voltage, and the very sharp pulsing produced by the spark. That part is straightforward. The remainder of the circuit is likely to be very difficult to get resonating as it needs to be in order to deliver that excess energy to the output inverter.

When considering the "length" of wire in a resonant coil, it is necessary to pay attention to the standing wave created under those conditions. The wave is caused by reflection of the signal when it reaches the end of the wire OR when there is a sudden change in the diameter of the wire as that changes the signal reflection ability at that point in the connection. You should pay attention to Richard Quick's very clear description of this in the section of his patent which is included later on in this chapter. Also, remember what Don Smith said about locating the peaks of the standing wave by using a hand-held neon lamp.

One very significant thing which Don pointed out is that the mains electricity available through the wall socket in my home, does **not** come along the wires from the generating station. Instead, the power station influences a local 'sub-station' and the electrons which flow through my equipment actually come from my local environment because of the influence of my local sub-station. Therefore, if I can create a similar influence in my home, then I no longer need that sub-station and can have as much electrical energy as I want, without having to pay somebody else to provide that influence for me.

A Practical Implementation of one of Don Smith's Designs

The objective here, is to determine how to construct a self-powered, free-energy electrical generator which has no moving parts, is not too expensive to build, uses readily available parts and which has an output of some kilowatts. However, under no circumstances should this document be considered to be an encouragement for you, or anyone else to actually build one of these devices. This document is presented solely for information and educational purposes, and as high voltages are involved, it should be considered to be a dangerous device unsuited to being built by inexperienced amateurs. The following section is just my opinions and so should not be taken as tried and tested, working technology, but instead, just the opinion of an inexperienced writer.

However, questions from several different readers indicate that a short, reasonably specific description of the steps needed to attempt a replication of a Don Smith device would be helpful. Again, this document must not be considered to be a recommendation that you actually build one of these high-voltage, potentially dangerous devices. This is just information intended to help you understand what I believe is involved in this process.

In broad outline, the following steps are used in the most simple version of the arrangement:

1. The very low frequency and voltage of the local mains supply is discarded in favour of an electrical supply which operates at more than 20,000 Hz (cycles per second) and has a voltage of anything from 350 volts to 10,000 volts. The higher voltages can give greater overall output power, but they involve greater effort in getting the voltage back down again to the level of the local mains voltage in order for standard mains equipment to be used.

2. This high-frequency high voltage is used to create a series of very rapid sparks using a spark gap which is connected to a ground connection. Properly done, the spark frequency is so high that there is no audible sound caused by the sparks. Each spark causes a flow of energy from the local environment into the circuit. This energy is not standard electricity which makes things hot when current flows through them, but instead this energy flow causes things to become cold when the power flows through them, and so it is often called "cold" electricity. It is tricky to use this energy unless all you want to do is light up a series of light bulbs (which

incidentally, give out a different quality of light when powered with this energy). Surprisingly, the circuit now contains substantially more power than the amount of power needed to produce the sparks. This is because additional energy flows in from the ground as well as from the local environment. If you have conventional training and have been fed the myth of "closed systems", then this will seem impossible to you. So, let me ask you the question: if, as can be shown, all of the electricity flowing into the primary winding of a transformer, flows back out of that winding, then where does the massive, continuous flow of electricity coming from the secondary winding come from? None of it comes from the primary circuit and yet millions of electrons flow out of the secondary in a continuous stream which can be supplied indefinitely. So, where do these electrons come from? The answer is 'from the surrounding local environment which is seething with excess energy' but your textbooks won't like that fact as they believe that the transformer circuit is a 'closed system' – something which probably can't be found anywhere in this universe.

3. This high-voltage, high-frequency, high-power energy needs to be converted to the same sort of hot electricity which comes out of a mains wall socket at the local voltage and frequency. This is where skill and understanding come into play. The first step is to lower the voltage and increase the available current with a step-down resonant transformer. This sounds highly technical and complicated, and looking at Don Smith's expensive Barker & Williamson coil, makes the whole operation appear to be one for rich experimenters only. This is not the case and a working solution can be cheap and easy. It is generally not convenient to get the very high voltage all the way down to convenient levels in a single step, and so, one or more of those resonant transformers can be used to reach the target voltage level. Each step down transformer boosts the available current higher and higher.

4. When a satisfactory voltage has been reached, we need to deal with the very high frequency. The easiest way to deal with it is to use high-speed diodes to convert it to pulsing DC and feed that into a capacitor to create what is essentially, an everlasting battery. Feeding this energy into a capacitor converts it into conventional "hot" electricity and a standard off-the-shelf inverter can be used to give the exact voltage and frequency of the local mains supply. In most of the world, that is 220 volts at 50 cycles per second. In America it is 110 volts at 60 cycles per second. Low-cost inverters generally run on either 12 volts or 24 volts with the more common 12 volt units being cheaper.

So, let's take a look at each of these step in more detail and see if we can understand what is involved and what our options are:

1. We want to produce a high-voltage, high-frequency, low-current power source. Don Smith shows a Neon-Sign Transformer module. His module produced a voltage which was higher than was convenient and so he used a variable AC transformer or "Variac" as it is commonly known, to lower the input voltage and so, lower the output voltage. There is actually no need for a Variac as we can handle the higher voltage or alternatively, use a more suitable Neon-Sign Transformer module.

   However, we have a problem with using that technique. In the years since Don bought his module, they have been redesigned to include circuitry which disables the module if any current flows out of it directly to earth, and as that is exactly what we would want to use it for, so most, if not all of the currently available neon-sign transformer modules are not suitable for our needs. However, I'm told that if the module has an earth wire and that earth wire is left unconnected, that it disables the earth-leakage circuitry, allowing the unit to be used in a Don Smith circuit. Personally, I would not recommend that if the module is enclosed in a metal housing.

   A much cheaper alternative is shown here: http://www.youtube.com/watch?v=RDDRe_4D93Q where a small plasma globe circuit is used to generate a high-frequency spark. It seems highly likely that one of those modules would suit our needs:

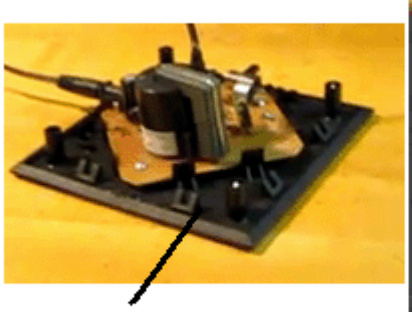

MODULE WITHOUT
THE PLASMA GLOBE

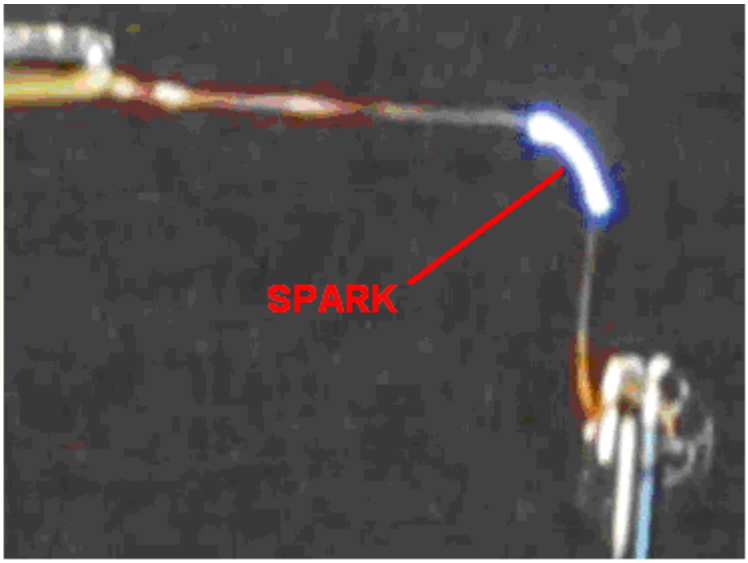

An alternative method is to build your own power supply from scratch. Doing that is not particularly difficult and if you do not understand any electronics, then perhaps, reading the beginner's electronics tutorial in chapter 12 (http://www.free-energy-info.com/Chapter12.pdf) will fill you in on all of the basics needed for understanding (and probably designing your own) circuits of this type. Here is a variable frequency design for home-construction:

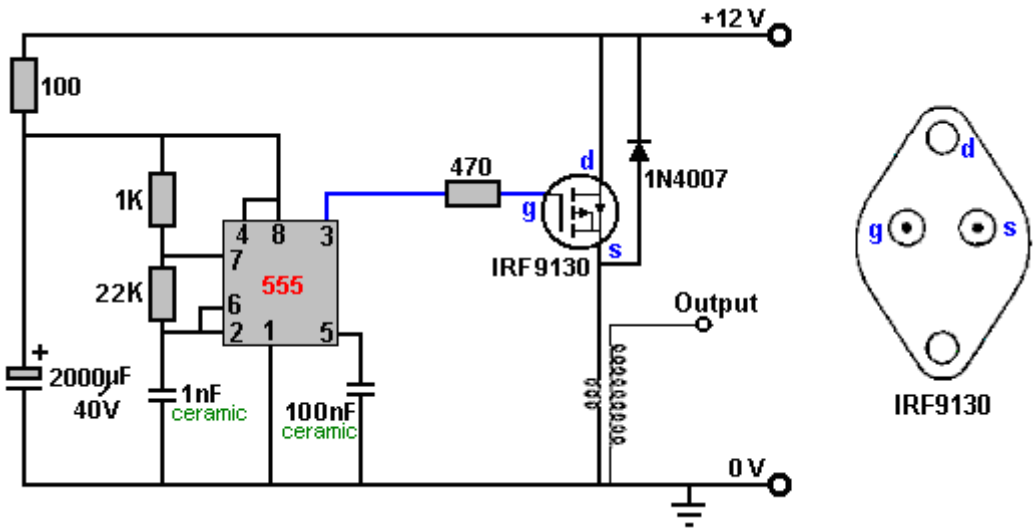

One advantage of this circuit is that the output transformer is driven at the frequency set by the 555 timer and that frequency is not affected by the number of turns in the primary winding, nor it's inductance, wire diameter, or anything else to do with the coil. While this circuit shows the rather expensive IRF9130 transistor, I expect that other P-channel FETs would work satisfactorily in this circuit. The IRF9130 transistor looks like this:

The circuit has a power supply diode and capacitor, ready to receive energy from the output at some later date if that is possible and desired. The 555 circuit is standard, giving a 50% Mark/Space ratio. The 10 nF capacitor is there to maintain the stability of the 555 and the timing section consists of two variable resistors, one fixed resistor and the 1 nF capacitor. This resistor arrangement gives a variable resistance of anything from 100 ohms to 51.8K and that allows a substantial frequency range. The 47K (Linear) variable resistor controls the main tuning and the 4.7K (Linear) variable resistor gives a more easily adjustable frequency for exact tuning. The 100 ohm resistor is there in case both of the variable resistors are set to zero resistance. The output is fed

through a 470 ohm resistor to the gate of a very powerful P-channel FET transistor which drives the primary winding of the output transformer.

The output transformer can be wound on an insulating spool covering a ferrite rod, giving both good coupling between the windings, and high-frequency operation as well. The turns ratio is set to just 30:1 due to the high number of primary winding turns. With a 12-volt supply, this will give a 360-volt output waveform, and by reducing the primary turns progressively, allows the output voltage to be increased in controlled steps. With 10 turns in the primary, the output voltage should be 3,600 volts and with just 5 turns 7,200 volts. The higher the voltage used, the greater the amount of work needed later on to get the voltage back down to the output level which we want.

Looking at the wire specification table, indicates that quite a small wire diameter could be used for the oscillator output transformer's secondary winding. While this is perfectly true, it is not the whole story. Neon Tube Drivers are very small and the wire in their output windings is very small diameter indeed. Those driver modules are very prone to failure. If the insulation on any one turn of the winding fails and one turn becomes a short-circuit, then that stops the winding from oscillating, and a replacement is needed. As there are no particular size constraints for this project, it might be a good idea to use enamelled copper wire of 0.45 mm or larger in an attempt to avoid this insulation failure hazard. No part of the transformer coil spool should be metal and it would not be any harm to cover each layer of secondary winding with a layer of electrical tape to provide additional insulation between the coil turns in one layer and the turns in the layer on top of it.

A plug-in board layout might be:

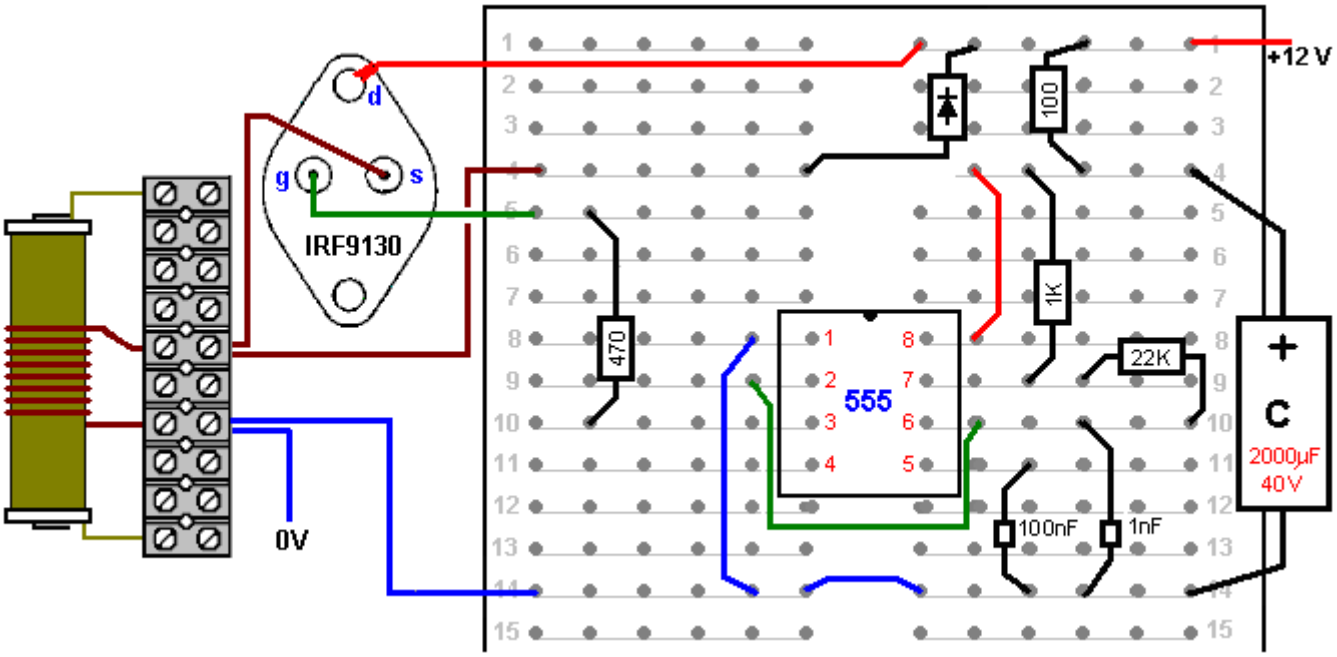

Please remember that you can't just stick your average voltmeter across a 4 kV capacitor (unless you really do want to buy another meter) as they only measure up to about a thousand volts DC. So, if you are using high voltage, then you need to use a resistor-divider pair and measure the voltage on the lower resistor. But what resistor values should you use? If you put a 10 Megohm resistor across your 4 kV charged capacitor, the current flowing through the resistor would be 0.4 milliamps. Sounds tiny, doesn't it? But that 0.4 mA is 1.6 watts which is a good deal more than the wattage which your resistor can handle. Even using this arrangement:

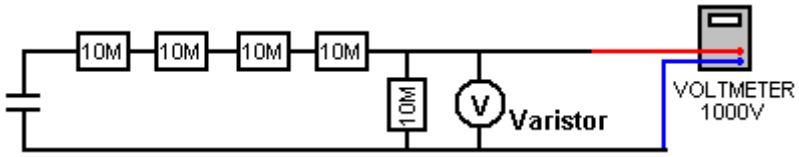

the current will be 0.08 mA and the wattage per resistor will be 64 mW. The meter reading will be about 20% of the capacitor voltage which will give a voltmeter reading of 800 volts. The input resistance of the meter needs to be checked and possibly, allowed for as the resistance in this circuit is so high (see chapter 12). When making a measurement of this type, the capacitor is discharged, the resistor chain and meter attached, and

then, and only then, is the circuit powered up, the reading taken, the input power disconnected, the capacitor discharged, and the resistors disconnected. High-voltage circuits are highly dangerous, especially so, where a capacitor is involved. The recommendation to wear thick rubber gloves for this kind of work, is not intended to be humorous. Circuits of this type are liable to generate unexpected high-voltage spikes, and so, it might be a good idea to connect a varistor across the meter to protect it from those spikes. The varistor need to be set to the voltage which you intend to measure and as varistors may not be available above a 300V threshold, two or more may need to be connected in series where just one is shown in the diagram above. The varistor should not have a higher voltage rating than your meter.

2. We now need to use this high voltage to create a strategically positioned spark to a ground connection. When making an earth connection, it is sometimes suggested that connecting to water pipes or radiators is a good idea as they have long lengths of metal piping running under the ground and making excellent contact with it. However, it has become very common for metal piping to be replaced with cheaper plastic piping and so any proposed pipe connection needs a check to ensure that that there is metal piping which runs all the way into the ground.

Neon

Gas-Discharge Tube

The spark gaps shown can be commercial high-voltage gas discharge tubes, adjustable home-made spark gaps with stainless steel tips about 1 mm apart, car spark plugs, or standard neon bulbs, although these run rather hot in this application. A 15 mm x 6 mm size neon bulb operates with only 90 or 100 volts across it, it would take a considerable number of them connected in series to create a high voltage spark gap, but it is probably a misconception that the spark gap itself needs a high voltage. Later on in this chapter, there is an example of a very successful system where just one neon bulb is used for the spark gap and an oscillating magnetic field more than a meter wide is created when driven by just an old 2,500 volt neon-sign transformer module. If using a neon bulb for the spark gap, then an experienced developer recommends that a 22K resistor is used in series with the neon in order to extend it's working life very considerably.

This circuit is one way to connect the spark gap and ground connection:

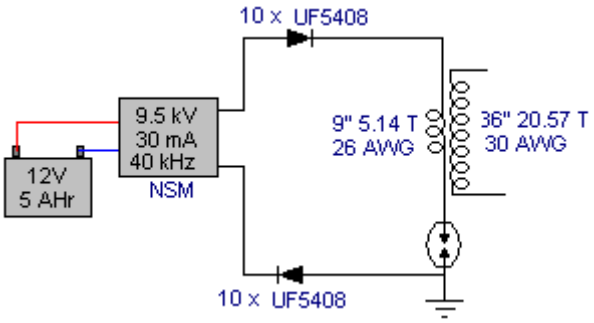

This is an adaption of a circuit arrangement used by the forum member "SLOW-'N-EASY" on the Don Smith topic in the energeticforum. Here, he is using a 'LowGlow' neon transformer intended for use on a bicycle. The diodes are there to protect the high-voltage power supply from any unexpected voltage spikes created later on in the circuit. The spark gap is connected between the primary winding of a step-up transformer and the earth connection. No capacitor is used. Seeing this circuit, we immediately think of Don Smith's large and expensive coils, but this experimenter does not use anything like that. Instead, he winds his transformer on a simple plastic former like this:

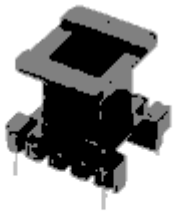

Ho Sung International. EI-2820 nylon bobbin. Core is 10 mm x 13 mm x 10 mm high. Top is 18.5 mm x 21.5 mm. Base is 22 mm x 26 mm. Four leads, 15 mm and 20 mm spacing

And to make matters 'worse' the primary winding wire is just 9 inches (228.6 mm) long and the secondary just 36 inches (914.4 mm) long, the primary being wound directly on top of the secondary. Not exactly a large or expensive construction and yet one which appears to perform adequately in actual tests.

This is a very compact form of construction, but there is no necessity to use exactly the same former for coils, nor is there anything magic about the nine-inch length of the L1 coil, as it could easily be any convenient length, say two feet or 0.5 metres, or whatever. The important thing is to make the L2 wire length exactly four times that length, cutting the lengths accurately. It is common practice to match the weight of copper in each coil and so the shorter wire is usually twice the diameter of the longer wire.

The circuit above, produces a cold electricity output of high voltage and high frequency. The voltage will not be the same as the neon transformer voltage, nor is the frequency the same either. The two coils resonate at their own natural frequency, unaltered by any capacitors.

3. The next step is to get the high voltage down to a more convenient level, perhaps, like this:

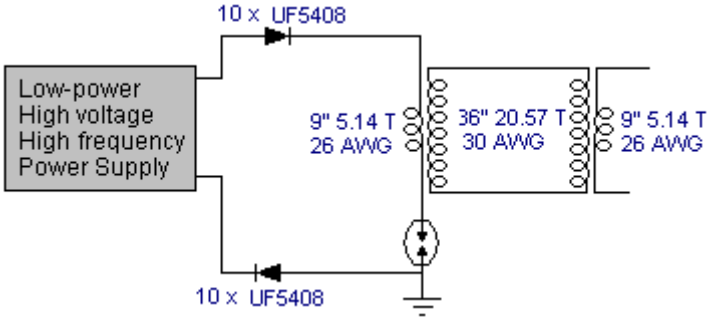

Here, an identical transformer, wound in exactly the same way, is used in reverse, to start the voltage lowering sequence. The wire length ratio is maintained to keep the transformer windings resonant with each other.

Supposing we were to wind the L2 coil of this second transformer in a single straight winding and instead of winding just one L1 winding on top of it, two or more L1 identical windings were placed on top of it – what would happen?:

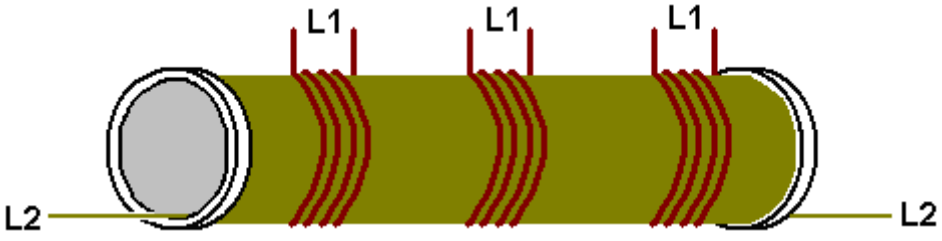

Now for a comment which will seem heretical to people steeped in the present day (inadequate) level of technology. The power flowing in these transformers is cold electricity which operates in an entirely different way to hot electricity. The coupling between these coils would be inductive if they were carrying hot electricity and in that case, any additional power take-off from additional L1 coils would have to be 'paid' for by additional current draw through the L2 coil. However, with the cold electricity which these coils are actually carrying, the coupling between the coils is magnetic and not inductive and that results in no increase in L2 current, no matter how many L1 coil take-offs there are. Any additional L1 coils will be powered for free. However, the position of the coils relative to each other has an effect on the tuning, so the L1 coil should be in the middle of the L2 coil, which means that any additional L1 coils are going to be slightly off the optimum tuning point.

4. Anyway, following through on just one L1 coil, there is likely to be at least one further step-down transformer needed and eventually, we need conversion to hot electricity:

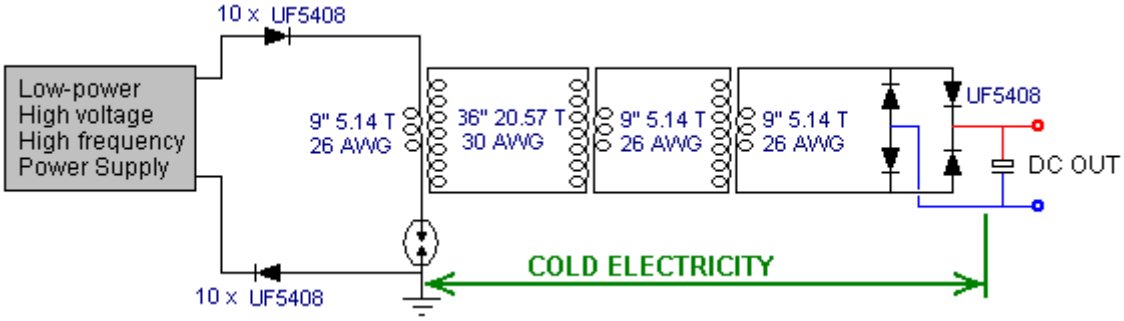

Probably the easiest conversion is by feeding the energy into a capacitor and making it standard DC. The frequency is still very high, so high-speed diodes (such as the 75-nanosecond UF54008) are needed here although the voltage level is now low enough to be no problem. The DC output can be used to power an inverter so that standard mains equipment can be used. It is not necessary to use just one (expensive) large-capacity inverter to power all possible loads as it is cheaper to have several smaller inverters, each powering it's own set of equipment. Most equipment will run satisfactorily on square-wave inverters and that includes a mains unit for powering the input oscillator circuit.

PVC pipe is not a great material when using high-frequency high-voltage signals, and grey PVC pipe is a particularly poor coil former material. The much more expensive acrylic pipe is excellent, but if using PVC, then performance will be better if the PVC pipe is coated with an insulating lacquer (or table tennis balls dissolved in acetone as show on YouTube).

However, there are some other factors which have not been mentioned. For example, if the L1 coil is wound directly on top of the L2 coil, it will have roughly the same diameter and so, the wire being four times longer, will have roughly four times as many turns, giving a step-up or step-down ratio of around 4:1. If, on the other hand, the coil diameters were different, the ratio would be different as the wire lengths are fixed relative to each other. If the L2 coil were half the diameter of the L1 coil, then the turns ratio would be about 8:1 and at one third diameter, 12:1 and at a quarter diameter 16:1 which means that a much greater effect could be had from the same wire length by reducing the L2 coil diameter. However, the magnetic effect produced by a coil is linked to the cross-sectional area of the coil and so a small diameter is not necessarily at great advantage. Also, the length of the L1 coil wire and number of turns in it, affect the DC resistance, and more importantly, the AC impedance which affects the amount of power needed to pulse the coil.

It is also thought that having the same weight of copper in each winding gives an improved performance, but what is not often mentioned is the opinion that the greater the weight of copper, the greater the effect. You will recall that Joseph Newman (chapter 11) uses large amounts of copper wire to produce remarkable effects. So, while 9 inches and 36 inches of wire will work for L1 and L2, there may well be improved performance from longer lengths of wire and/or thicker wires.

We should also not forget that Don Smith pointed out that voltage and current act (out of phase and) in opposite directions along the L2 coil, moving away from the L1 coil:

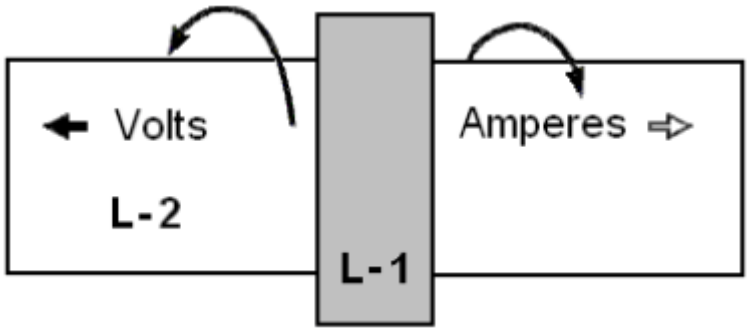

It has been suggested that a greater and more effective power output can be obtained by splitting the L2 coil underneath the L1 coil position, winding the second part of L2 in the opposite direction and grounding the junction of the two L2 windings. Don doesn't consider it necessary to reverse the direction of winding. The result is an L2 winding which is twice as long as before and arranged like this:

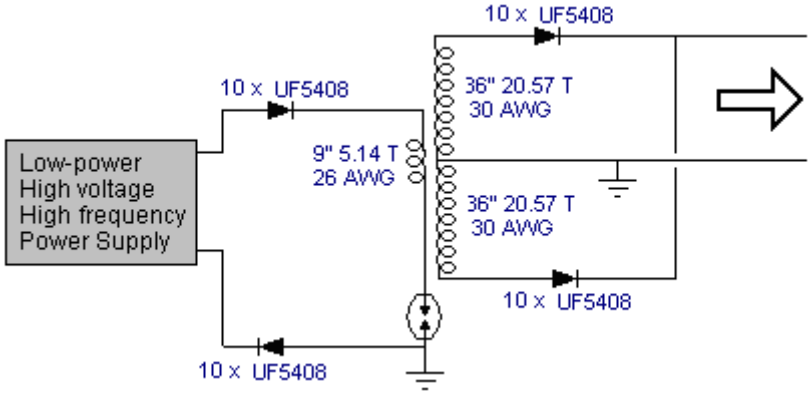

Here, the additional high-voltage diodes allow the two out of phase windings to be connected across each other. You will notice that this arrangement calls for two separate earth connections, both of which need to be high-quality connections, something like a pipe or rod driven deeply into moist soil or alternatively, a metal plate or similar metal object of substantial surface area, buried deep in moist earth, and a thick copper wire or copper braid used to make the connection. These earthing points need to be fairly far apart, say, ten metres. A single earth connection can't be used as that would effectively short-circuit across the L1/L2 transformer which you really do not want to do.

With this arrangement, the outline circuit becomes:

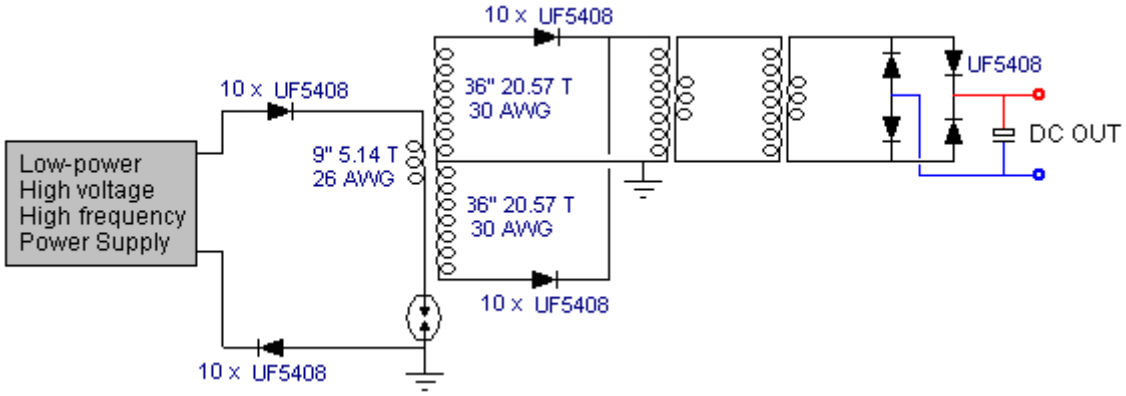

The thick earth wiring is helpful because in order to avoid the earth wire being included in the resonant wire length, you need a sudden change in wire cross-section:

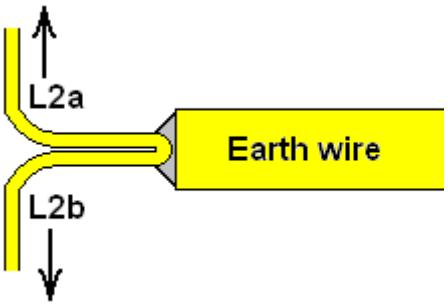

These are just some ideas which might be considered by some experienced developer who may be thinking of investigating Don Smith style circuitry.

To give you some idea of the capacity of some commercially available wires when carrying hot electricity, this table may help:

AWG	SWG	Diameter	Maximum Amps	220V kW	110V kW
1	2	7.01 mm	119	26.18	13.09
3	4	5.89 mm	75	16.50	8.25
4	6	4.88 mm	60	13.20	6.60
6	8	4.06 mm	37	8.14	4.07
8	10	3.25 mm	24	5.28	2.64
10	12	2.64 mm	15	3.30	1.65
12	14	2.03 mm	9.3	2.05	1.02
13	15	1.83 mm	7.4	1.63	801 watts
14	16	1.63 mm	5.9	1.30	650 watts
15	17	1.42 mm	4.7	1.03	515 watts
16	18	1.22 mm	3.7	814 watts	407 watts

It is recommended that the wire have a current carrying capacity of 20% more than the expected actual load, so that it does not get very hot when in use. The wire diameters do not include the insulation, although for solid enamelled copper wire, that can be ignored.

There is a most impressive video and circuit shown at http://youtu.be/Q3vr6qmOwLw where a very simple arrangement produces an immediately successful performance for the front end of Don's circuitry. The circuit appears to be:

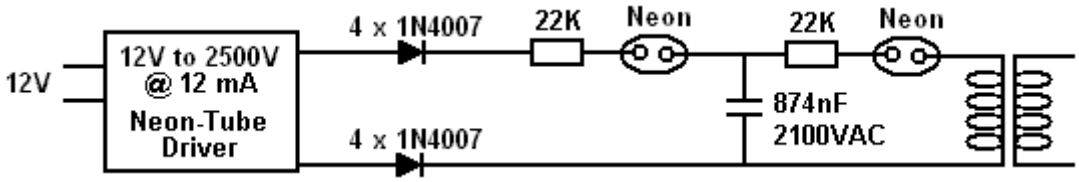

Here, a simple Neon Sign Transformer module which has no earth connection, is used to produce a 2.5 kV voltage with a frequency of 25 kHz and a maximum output current capacity of 12 mA. There is no difficulty in constructing the equivalent to that power supply unit. The two outputs from the module are converted to DC by a chain of four 1N4007 diodes in series in each of the two outputs (each chain being inside a plastic tube for insulation).

This output is fed through an optional 22K resistor via a neon lamp to a microwave oven capacitor which happens to be 874 nF with a voltage rating of 2,100 volts. You might feel that the voltage rating of the capacitor is too low for the output voltage of the neon sign module, but the neon has a striking voltage of just 90 volts and so the capacitor is not going to reach the output voltage of the power supply. The resistors are solely to extend the life of the neons as the gas inside the tube gets a considerable jolt in the first nanosecond after switch-on. It is unlikely that omitting those resistors would have any significant effect, but then, including them is a trivial matter. The second neon feeds the primary of the resonant transformer which is only shown in notional outline in the diagram above as the developer suggests that the primary acts as a transmitter and that any number of receiving coils can be used as individual secondaries by being tuned to the exact frequency of that resonating primary.

In the video showing this arrangement, the developer demonstrates the fluctuating, high-frequency field which extends for some four feet (1.2 m) around the coil. He also remarks that the single neons in his arrangement could each be replaced with two neons in series. In test which I ran, I found that I needed two neons in series ahead of the capacitor in order to get continuous lighting of the output neon. Also, one of the diodes needed to be reversed so that one faced towards the input and one away from it. It did not matter which diode was reversed as both configurations worked. Again, please note that this presentation is for information purposes only and it is **NOT** a recommendation that you should actually build one of these devices. Let me stress again that this is a high-voltage device made even more dangerous by the inclusion of a capacitor, and it is quite capable of killing

you, so, don't build one. The developer suggests that it is an implementation of the "transmitter" section of Don's Transmitter/multiple-receivers design shown below. However, before looking at that design, there is one question which causes a good deal of discussion on the forums, namely, if the centre-tap of the L2 secondary coil is connected to ground, then should that earth-connection wire length be considered to be part of the quarter length of the L1 coil? To examine this possibility in depth, the following quote from Richard Quick's very clear explanation of resonance in his US patent 7,973,296 of 5th July 2011 is very helpful.

However, the simple answer is that for there to be exact resonance between two lengths of wire (whether or not part, or all of those lengths of wire happen to be wound into a coil), then one length needs to be **exactly** four times as long as the other, and ideally, half the diameter as well. At both ends of both lengths of wire, there needs to be a sudden change in wire diameter and Richard explains why this is. But, leaving that detailed explanation for now, we can use that knowledge to explain the above simplified system in more detail. Here is the circuit again:

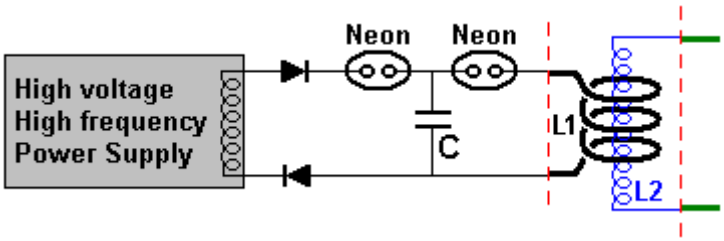

One very important point to note is that no earth connection is required and in spite of that, the performance shown on video is very impressive. While an earth connection can feed substantial power into the circuit, not needing one for the front end is an enormous advantage and potentially, opens the way for a truly portable device. Another very important point is the utter simplicity of the arrangement where only cheap, readily available components are used (and not many of those are needed). The resistors for extending the life of the neon bulbs are not shown, but they can be included if desired and the circuit operation is not altered significantly by having them there. If a higher spark voltage is wanted, then two or more neon bulbs can be used in series where these circuit diagrams show just one.

A point to note is that the lower diode is shown reversed when compared to the previous diagram. This is because the power supply shown is any generic power supply which drives a simple output coil which does not have a centre tap. The neon supply of the earlier diagram appears to have two separate outputs which will, presumably, be out of phase with each other as that is common practice for neon-sign driver modules. If you wish, the two diodes shown here could be replaced by a diode bridge of four high-voltage, high-speed diodes.

The wire lengths of L1 and L2 are measured very accurately from where the wire diameter changes suddenly, as indicated by the red dashed lines. The L2 wire length is exactly four times as long as the L1 wire length and the L2 wire diameter is half of the L1 wire diameter.

How long is the L1 wire? Well, how long would you like it to be? It can be whatever length you want and the radius of the L1 coil can be whatever you want it to be. The theory experts will say that the L1 coil should resonate at the frequency of the power feeding it. Well, good for them, I say, so please tell me what frequency that is. It is not going to be the frequency of the power supply as that will be changed by at least one of the neon bulbs. So, what frequency will the neon bulb produce? Not even the manufacturer could tell you that as there is quite a variation between individual bulbs which are supposedly identical.

Actually, it doesn't matter at all, because the L1 coil (and the L2 coil if you measure them accurately) has a resonant frequency all of its own and it will vibrate at that frequency no matter what the frequency feeding it happens to be. A coil resonates in very much the same way that a bell rings when it is struck. It doesn't matter how hard you strike the bell or how rapidly you strike it – the bell will ring at it's own natural frequency. So the L1 coil will resonate at it's own natural frequency no matter what rate the voltage spikes striking it arrive, and as the L2 coil has been carefully constructed to have exactly that same frequency, it will resonate in synchronisation with the L1 coil.

This means that the length of the wire for the L1 coil is the choice of the builder, but once that length is chosen it determines the length of the wire for the L2 coil as that is exactly four times as long, unless the builder decides to use an arrangement which has L2 wound in both the Clockwise and counter-clockwise directions, in which case, each half of the L2 coil will be four times the length of the wire in the L1 coil, like this:

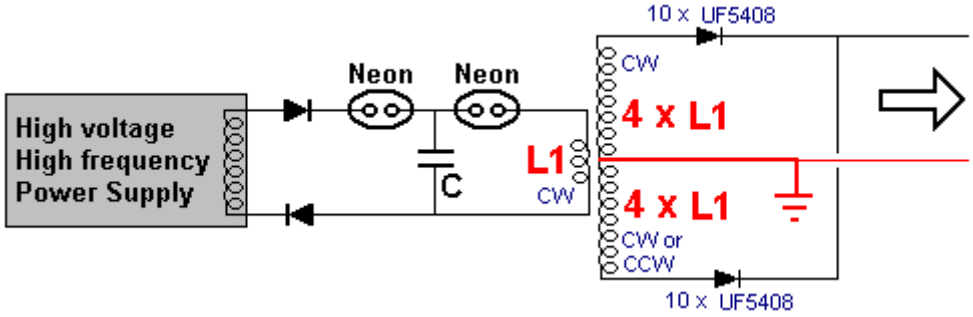

Mind you, there is one other factor to be considered when deciding what the most convenient wire length for L1 might be, and that is the number of turns in the L1 coil. The larger the ratio between the turns in L1 and the turns in L2, the higher the voltage boost produced by the L1/L2 transformer, and remember that the length of L2 is fixed relative to the length of L1.

So, a possible circuit style might be:

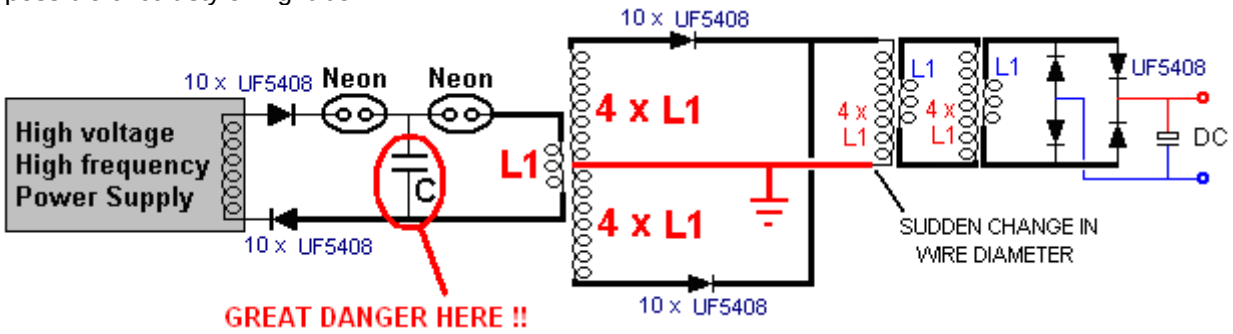

There are some important points to remember. One is that there must be a sudden change of wire diameter at both ends of each L1 coil and at the ends of each L2 coil. If there isn't, then the connecting wire length will form part of the coil and if there is some change in diameter but not very much, then it is anybody's guess what the resonant wire length for that coil will be. There can be as many step-down isolation air-core L1/L2 transformers as desired and these do not need to be particularly large or expensive.

The builder of this circuit put it together in just a few minutes, using components which were to hand, including the microwave oven capacitor marked "C" in the diagrams above. That capacitor is isolated on both sides by the neon bulb spark gaps and so it will have no modifying effect on the resonant frequency of any of the coils in this circuit. But it is vital to understand that the energy stored in that capacitor can, and will, kill you instantly if you were to touch it, so let me stress once again that this information is **NOT** a recommendation that you actually build this circuit. The DC output from the circuit is intended to power a standard inverter, which in turn, would be perfectly capable of powering the high voltage, high frequency input oscillator.

One final point is that as demonstrated in the video, the oscillating magnetic field produced by the L1 coil can power several identical L2 coils, giving several additional power outputs for no increase in input power, because the coupling is magnetic and not inductive as mentioned earlier in this chapter. Please notice that neither the L1 coil nor the L2 coil has a capacitor connected across it, so resonance is due solely to wire length and no expensive high-voltage capacitors are needed to get every L1/L2 coil pair resonating together. One possible arrangement might be like this:

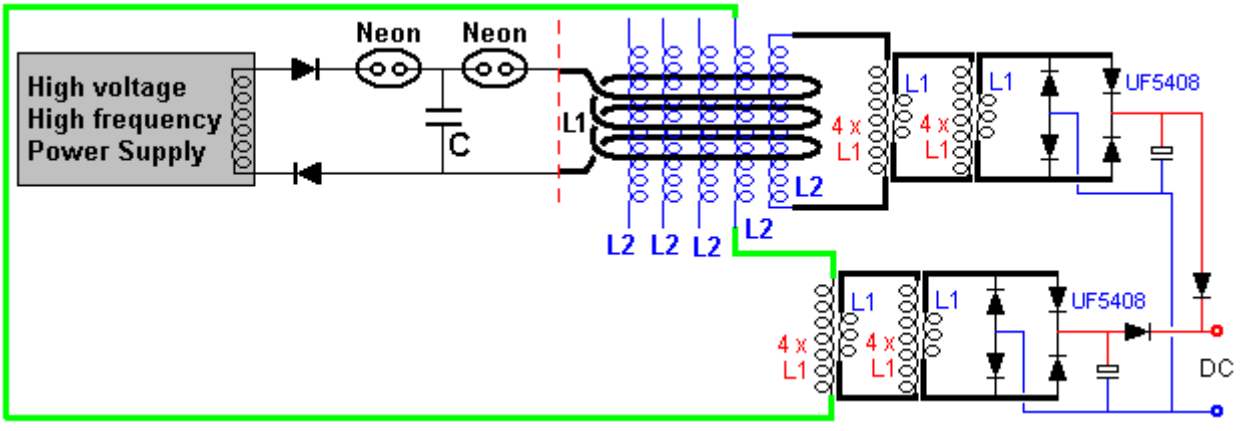

Where two of the L2 coils are shown connected together to give increased output power. This arrangement uses low-voltage inexpensive components for the output stages and there is no obvious limit to the amount of output power which could be provided. As the circuit operates at high frequency throughout, there is no particular need for additional L2 coils to be placed physically inside the L1 coil:

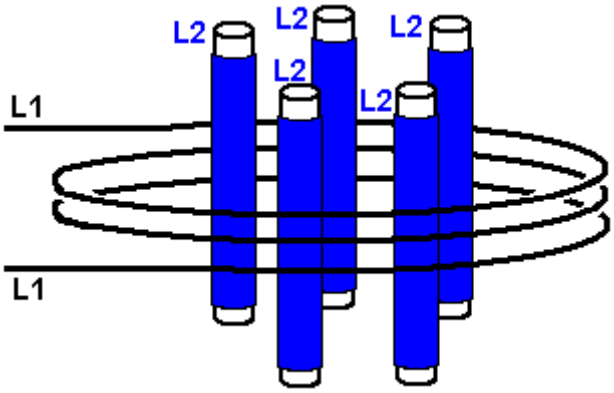

However, there can be an advantage to this arrangement in that the wire length of the L1 coil is greater, which in turn makes the wire length of each L2 coil greater (being four times longer). This gives greater flexibility when planning the turns ratio of the L1/L2 transformer. The voltage step-up or step-down of that transformer happens to be in the ratio of the turns, in spite of the fact that this is not inductive coupling and so standard transformer technology does not apply.

When you choose the number of turns and coil diameter for L1, that also gives the length of the L2 wire. In order to get the desired output voltage, if perhaps, the step-down ratio is needed to be an amount of 46:1, then you need 46 times the number of L1 turns on the L2 coil. That means that you know both the wire length and number of turns wanted in the L2 coil. But, as each turn will have a length of 3.14159 times the diameter, it follows then that the wanted diameter is the wire length per turn, divided by 3.14159. The wire sits on top of the tube on which it is wound and so has a greater diameter by one wire thickness, so the calculated tube diameter needs to be reduced by one wire diameter. For example, if the length per turn is 162 mm and the wire diameter 0.8 mm, then the tube diameter would be 162 / 3.14159 – 0.8 which is 50.766 mm (just over two inches).

Now for Richard's explanation of the resonant frequency of any length of wire:

"Quarter-Wave" Resonance; Standing Electromagnetic Waves"

One of the two main types is electrical resonance is referred to here as quarter-wave resonance. This type of resonance depends almost entirely on the length of a wire element For reasons described below, if a segment or length of wire is one quarter as long as the "voltage waves" which are travelling through the wire, then a set of "reflected" waves will be added to the emitted waves, in a synchronised alignment which creates stronger "superimposed waves".

Accordingly, an understanding of the "quarter-wave" phenomenon will help a reader understand how a straightforward and easily-controlled factor (i.e., the length of a wire ribbon which will be used to form a spiral coil) can help create a "quarter-wave" resonant response, which will create the types of electromagnetic pulses and fields referred to as "standing waves".

The speed at which a voltage impulse is transmitted through a metal wire is extremely fast. It is essentially the same as the speed of light, which travels 300 million meters (186,000 miles) in a single second (that distance would circle the earth more than 7 times).

If wavelength (in meters) is multiplied by frequency (cycles per second), the result will be the speed of light, 300 million meters/second. Therefore, the wavelength of an "alternating current" (AC) voltage, at some particular frequency, will be the speed of light, divided by which frequency.

Therefore, using simple division, if an alternating voltage operates at a frequency of 1 megahertz (MHz), which is a million cycles per second, then the "wavelength" at that frequency will be 300 meters. If the frequency halves become 500 kilohertz, the wavelength becomes twice as long (600 meters); and, if the frequency were to increase to 2 megahertz, the wavelength drops to 150 meters.

It should be noted which the term "cycles" is what scientists call "a dimensionless unit", which drops out and becomes silent when other physical terms are multiplied or divided.

At AC frequencies of 10 kilohertz or greater, the common references to "alternating current" (AC) voltage begin using a different term, which is "radio-frequency" (RF) voltage. Accordingly, RF voltage is a form (or subset) of AC voltage, which operates at frequencies higher than 10 kilohertz. RF power generators are readily available, and

are sold by numerous companies which can be easily located by an Internet search, using the term “RF power generator”. For example, Hotek Technologies Inc. (hotektech.com) sells two RF power generators, called the AG 1024 and AG 1012 models, which can provide output power at frequencies ranging from 20 kHz to 1 MHz; the 1012 model has a power output of 1000 watts, while the 1024 model has a power output of 2000 watts. The output frequency of any such RF power supply can be adjusted and “tuned” across the entire range of operating frequencies, merely by turning knobs or manipulating other controls in a power supply of this type.

In a wire having a fixed and unchanging length, the easiest way to create a “standing wave” is to adjust the RF frequency emitted by a power supply with an adjustable frequency, until the “tuned” frequency creates a wavelength which is 4 times as long as the wire. This principle is well-known to physicists, and it is commonly referred to as “quarter-wave” behaviour, since the length of the wire segment must be one quarter as long as the wavelength. Since it is important to this invention, the principles behind it are illustrated in a series of drawings provided in **Fig.1** to **Fig.4**, all of which are well-known prior art.

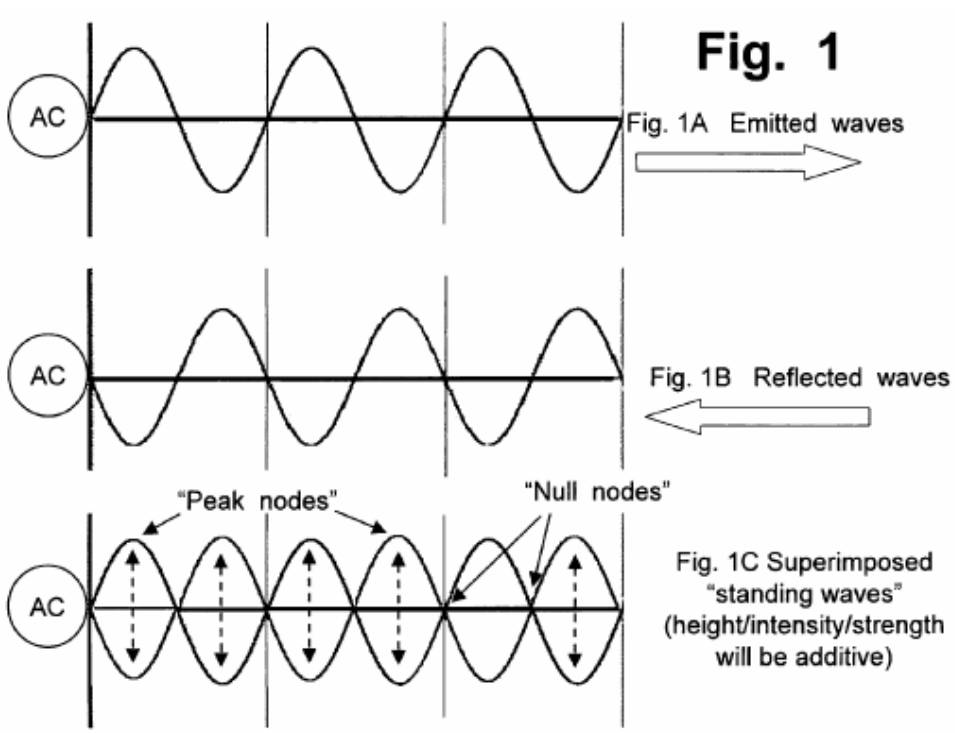

Fig.1A indicates an idealized wavelength of an alternating voltage, depicted by a sine wave which is being sent from an AC power supply (shown by a circle at the left end of a horizontal straight wire) into the “input” end of the wire. The voltage waves travel through the wire towards the right, as indicated by the block arrow in **Fig.1A**. When the waves reach the end of the wire, they cannot leave the wire (at least, not in a simplified and “ideal” system, which is being assumed and used here to explain the principle of how a simple straight wire can create a standing wave). Therefore, the voltage wave will effectively “bounce” or “reflect” back from the tip of the wire, and the “reflected wave” will begin travelling back through the wire, going in the opposite direction, as indicated by the left-pointing block arrow in **Fig.1B**.

Because of the laws of conservation of energy, the reflection and “return travel” of these types of waves, when they bounce off the tip of a wire, is actually quite good, and rather efficient, as discussed below, provided which the wire tip does not emit sparks, arc discharges, or other forms of “escaping” electrical energy.

Accordingly, **Fig.1A** depicts a set of “emitted waves” travelling towards the right, while **Fig.1B** depicts an idealised set of “reflected waves” travelling toward the left along the same wire.

Fig.1C illustrates what happens when both sets of waves (emitted and reflected) are superimposed on each other. Since the two sets of waves are travelling at exactly the same speed, and since they have exactly the same wavelength, they will create a “standing wave” pattern when they are added together. As can be visualised from **Fig.1C**, there will be a set of locations, along the length of the wire, which can be referred to as “peak nodes”, where the AC voltage reaches it’s maximum.

At a location halfway between a pair of adjacent “peak nodes”, there will be a spot which can be called a “null node”, a “zero node”, a trough or valley node, or similar terms. At each “null node” location, the AC voltage will appear to be not fluctuating at all. Those are the sites, along the length of the wire, where each “positive” hump (created by a sine wave travelling toward the right) will be counter-balanced and offset by a “negative hump” with exactly the same height, travelling at an identical speed toward the left.

As a result, this type of response within a wire creates a “standing wave”. If the instantaneous voltage is measured at a “null node”, it would appear that nothing is happening, in terms of fluctuating voltage. Furthermore, the “null node” will not be moving, along the length of the wire; instead, it will appear to be standing still.

This can be demonstrated, in a coil, by using a “grounded lead” to test for voltages along the length of a coil. If a “grounded lead” coupled to a volt meter is used to touch the surfaces of a series of strands in a non-insulated coil (such as a coil made of thin copper tubing, wrapped around a plastic cylindrical shape, as used in the types of large transformers used by hobbyists to create “Tesla coils” which will emit large and visually impressive electrical arcs), the “test lead” will detect no apparent voltage at a null node, which will occur at some particular strand in the coil. At a different strand of the coil, the “test lead” will detect an alternating voltage which has twice the strength and intensity of the voltage being emitted by the power supply.

If voltage is measured at a “peak node”, the voltage will be doing something which can be called, using vernacular or laymen's terms, “the full-tilt boogie”. The AC voltage levels will be moving back and forth, between: (i) a very high and intense positive voltage, to (ii) an equally intense negative voltage. This is indicated by the “bubble” shapes shown along the wire in **Fig.1C**.

The “bubbles” which are shown in **Fig.1C** can help someone understand how standing waves are created, and how they act in a synchronised manner. However, which drawing fails to show another result which is very important in what actually happens in a standing wave. For purposes of description and analysis at this introductory level, the system can be assumed to be “ideal”, which implies a perfect “mirror-image” reflection of each wave from the right end of the wire. An “ideal” system also implies that no reflections occur at the left hand end of the wire where the power supply is located, and all “reflected” wave activity simply ceases. In real circuits and wires of this type, second and third order reflections do in fact occur, and they are used to further increase the strength and power output of these types of systems; however, those additional factors and “harmonics” should be ignored until after the basic principles of this type of system have been grasped and understood.

In an ideal system, when the reflected waves (which are travelling toward the left, in the wire segments illustrated in **Fig.1**) are “superimposed” on the emitted waves (travelling toward the right), the “peak” positive voltage which will be instantaneously reached, at the highest point of each “bubble” shown in **Fig.1C**, will occur when the positive peak of an emitted wave crosses a mirror-image positive peak of a reflected wave, travelling in the opposite direction. Accordingly, when those two “positive peak” values are added to each other, the instantaneous positive peak voltage which will occur, in the wire, will actually be twice as intense as the “positive peak” voltage being emitted by the AC power supply.

An instant later, at that exact point on that segment of wire, a negative peak voltage will be created, which will be the sum of (i) the negative peak voltage emitted by the power supply, and (ii) the negative peak voltage of a reflected wave also will pass through, travelling toward the left. At which instant, when those two negative peak voltages are added to each other, the instantaneous negative voltage which will occur, in the wire, will be twice as intense as the “negative peak” voltage being generated by the AC power supply.

A more accurate and representative visual depiction of a “standing wave” in a wire would actually show the heights of the peaks as being twice as tall as the peaks of the emitted voltage waves, and the reflected voltage waves. However, which depiction might confuse people, so it usually is not shown in drawings of “standing waves”.

Accordingly, the instantaneous response in the wire, at a location halfway between two “null nodes”, is doing something which can fairly and properly be called “the full-tilt double double boogie”. The “double double” phrase (note which it contains not just one but two “doubles”) was added to that phrase, for two reasons:

(i) To emphasise the fact that each and every voltage peak (maximum positive, and maximum negative) will be twice as strong, and twice as intense, as the maximum positive and negative peak voltages emitted by the power supply; and,

(ii) to point out that the frequency of the superimposed “bubbles”, shown in **Fig.1C**, is actually twice as fast as the frequency of the AC cycle which is emitted by the power supply, as discussed below.

The “twice the intensity” result is directly comparable to what an observer will see, if a large mirror is placed behind a light bulb in an otherwise dark room. The mirror effectively keeps the room dark, everywhere behind the mirror, so there is no “magical doubling” of the light in the room; which would violate the basic law of conservation of energy. Instead, what the mirror does is to shift light away from the backside of the mirror, and keep that light energy on the reflective side of the mirror. Anyone standing in front of the mirror will see two apparent light bulbs. Both of those light bulbs (the original bulb, and the reflected image) will have the same brightness (if the mirror is perfect). Therefore, the mirror will double the intensity of the light energy reaching the observer.

That same effect, in a circuit, will happen if the end of a wire acts like a mirror. If a wire does not have any components which will cause it to become an active “emission source” (which is the behaviour of transmission antennas and certain other components), in a way which efficiently releases voltage-created energy into the atmosphere, then the basic rules which require conservation of energy will prevent that energy from simply disappearing and ceasing to exist. As a result, even if the end of a wire is not designed to be a perfect reflector, a

large portion of the voltage wave will indeed reflect off the wire tip, and travel back through the same wire, in a "second pass".

To understand adequately, the type and amount of "wave reflection" which occurs at a wire tip, consider what happens if a light bulb is shining in a room which has shiny, glossy white paint on all the walls and ceilings; then, consider how it would look if the same light bulb were located in a room with all of the walls and ceilings painted "matt black". The total amount of light which would be available, to carry out a task such as reading a newspaper, clearly would be much greater in the white room, because light reflects off white paint, even though white paint does not even begin to approach the type of "reflection quality or clarity" which a mirror creates. The difference in what happens, when light intensity in a room painted matt black is compared to a room painted a glossy white, does not arise from the presence or absence of "reflection quality or clarity"; instead, it is governed by the laws of conservation of energy. When light shines on to a surface which is painted matt black, the light energy is absorbed by the paint, and it literally warms the paint up. In contrast to that, glossy white paint will not absorb light energy, so it reflects the light back out, for a "second pass" through the air which fills a room.

Because of the laws of conservation of energy, and without depending on any "quality of reflectance" characteristic of wire tips, electrical energy cannot simply disappear, when it reaches the end of a wire. Instead, there are only two things which can happen to that energy:

(i) the electrical energy can be emitted into the surroundings, such as by emitting sparks, arcs, or radio-frequency signals which will carry energy; or

(ii) if the energy is not emitted by the tip of the wire, then, by simple necessity and because of the basic law of conservation of energy, it must be reflected back into the wire, and it will be forced to travel back through the wire again.

If a wire has a long and tapered tip, then the reflected wave might become somewhat diffused, and it might lose some portion of the "clarity" of the wave. However, since wavelengths in the frequencies of interest here are hundreds of meters long, the type of tip created by a conventional wire cutter will not create any significant diffusion, in a reflected wave. And, unlike the white-painted walls of a room, there is not a large area which is available, at the tip of a wire, which can create scatter, spread, or diffusion. As a result, the tip of a wire will be a relatively efficient mirror-type reflector, when an AC voltage is "pumped" into one end of the wire.

The second factor mentioned above, when the "double-double" boogie phrase was mentioned, relates to a doubling of the frequency of a standing wave. When a standing wave is created in a wire by reflection of an emitted AC voltage wave, the frequency of the standing wave is, quite literally, double the frequency of the emitted wave.

This can be seen, visually, by noting that in the emitted AC voltage, shown in **Fig.1A**, a single complete wavelength contains both a "positive hump" and a "negative hump". Accordingly, three complete sine waves, divided into three segments by the imaginary vertical lines, are shown in **Fig.1A**.

By contrast, each and every "bubble" shown in **Fig.1C** depicts a complete and total "wavelength", in a standing wave. Six of those standing wave "bubbles" fit into exactly the same length of wire which holds only 3 emitted wavelengths from the power supply.

The "frequency doubling" effect of standing waves is important, because AC systems can convey and release energy in a manner which increases, as the frequency of the AC voltage supply increases. To some extent, this is analogous to saying that, if a motor can be run at twice the speed (while still generating the same torque), then the work output of that motor can be twice as great, at the higher speed. That analogy is not entirely accurate, since work output from an electric device which uses AC power depends on "area of the curve" functions which occur when sine waves are involved. Nevertheless, as a general principle, if the frequency of the voltage peaks increases, then power output will also increase, in many types of electric circuit components.

In the three panels of **Fig.1**, the wire length is three times as long as the wavelength of the voltage from the power supply. However, to create standing waves, a wire length does not need to be any particular multiple of the wavelength of an AC voltage. As can be seen by considering **Fig.1C**, the same types of "bubbles" would be created: (i) if the wire length were exactly twice as long as the wavelength; or, (ii) if the wire length were the same length as the wavelength.

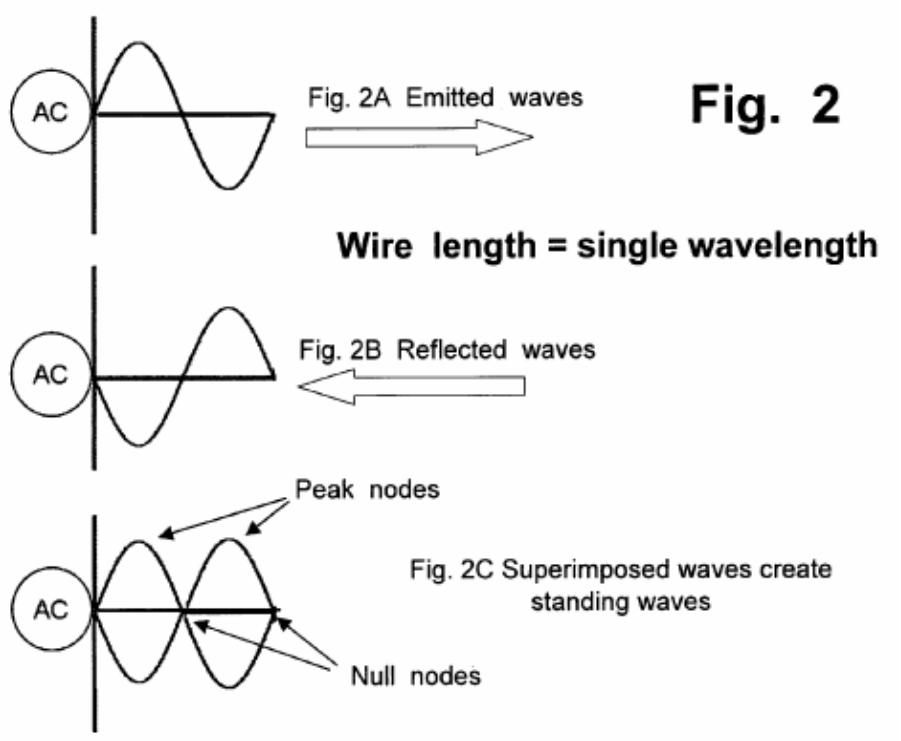

Accordingly, **Fig.2** (which includes **Fig.2A** showing an emitted wave, **Fig.2B** showing a reflected wave, and **Fig.2C** showing the superimposed "bubbles") shows what happens in a wire segment which has a length which is equal to a single wavelength from an AC voltage at a fixed frequency. A resonant standing wave will be formed, with a frequency which is double the frequency of the input AC voltage. which same result will apply, in a wire having any length which is an exact (integer) multiple (such as 1x, 2x, 3x, etc.) of the wavelength of the AC voltage being pushed (or forced, driven, pumped, etc.) into the wire segment.

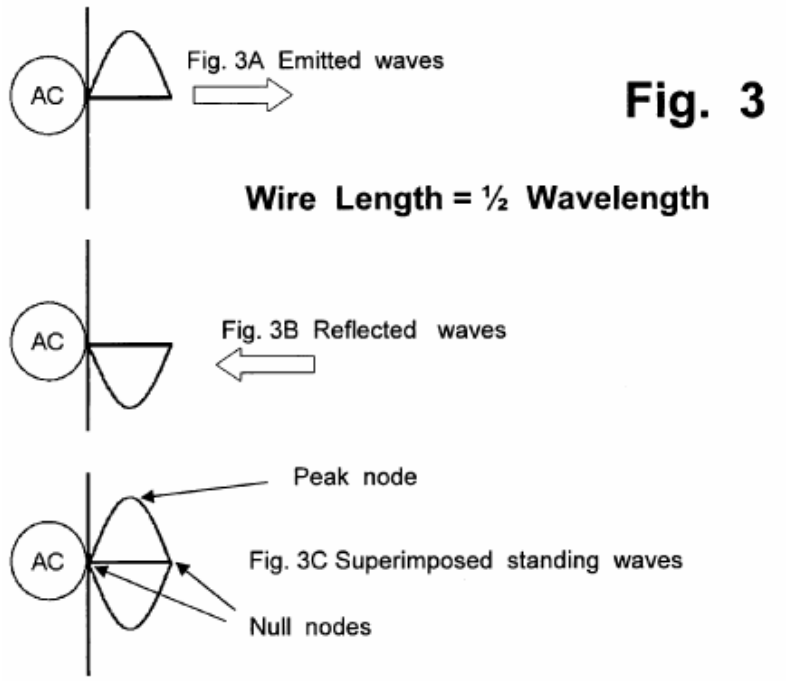

Moving to still shorter wires, the same principle also applies to any wire with a length equal to one half of an AC voltage wavelength. As shown in **Fig.3** (which includes **Fig. 3A** showing an emitted wave, **Fig. 3B** showing a reflected wave, and **Fig. 3C** showing the superimposed "bubbles"), if the wire length is one half of the wavelength, a natural and resonant standing wave will still form, with a frequency which is double the frequency of the input AC voltage.

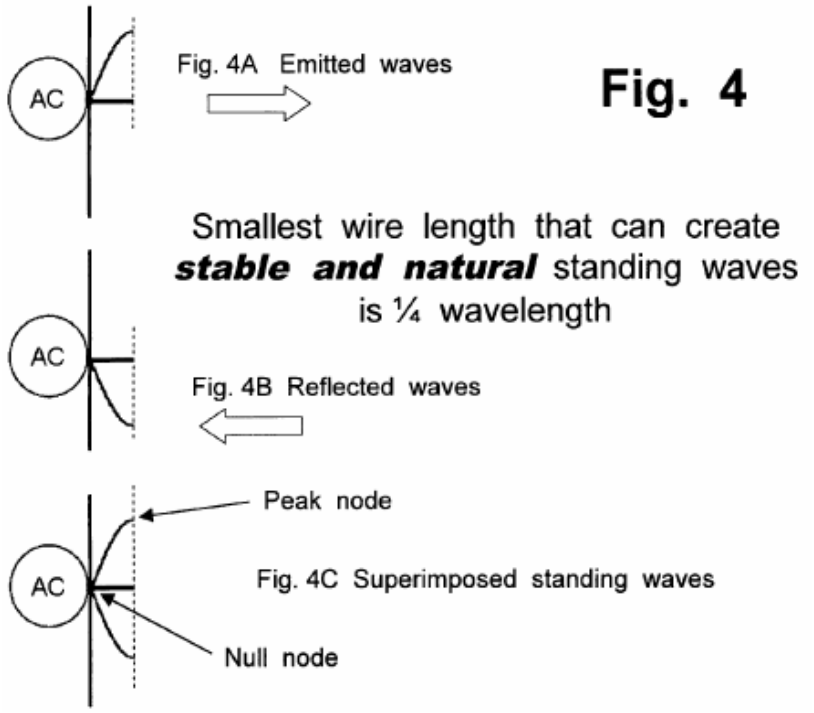

Finally, moving to a still shorter wire, the same principle also applies to any wire which has a length equal to one quarter of an AC voltage wavelength, as shown in **Fig.4A**, **Fig.4B**, and **Fig.4C** Even though it does not stretch across or cover a complete "bubble", the standing wave shown in **Fig.4C** is nevertheless a stable, natural, and resonant "standing wave", with a frequency which is exactly twice the frequency of the input AC voltage.

It is possible to create partially stable and semi-resonant responses, using one eighth, one sixteenth, or shorter lengths of wire, by using additional devices which can remove electrical power from the system, or which can generate effects which are usually called "harmonics". However, those are not the types of natural and stable responses which can be created by a simple, basic system consisting of nothing more than: (i) a wire having a fixed length and a "reflective" tip; and (ii) an AC power source with a frequency which can be "tuned" until it creates a resonant response in any wire segment having a suitable length.

Therefore, since quarter-wave wire lengths are the shortest lengths which can create natural and stable standing waves, the conventional term which is commonly used, to describe what happens when a wire creates a resonant standing-wave response, is a "quarter-wave" response.

In some devices, telescoping components (or other elements which can alter the effective length of a wire-type element) can be used to alter the ability of the element to respond to a fixed wavelength. Many types of antennas use this approach, if they need to process signals which are being transmitted on fixed and known frequencies. However, those examples are not relevant to spiral coil reactors, which will use an approach which involves tuning and adjusting the frequency of the voltage which is being supplied to a reactor, until a resonant response is observed in coils with fixed and unchanging lengths.

It should also be noted that certain types of "tuning" elements (such as capacitors, which can have either fixed or adjustable capacitance levels) can also be coupled electrically to a wire, in a manner which "emulates" adding more length to that wire. This approach can be used to alter (or increase the range of) the frequencies to which a wire circuit will respond resonantly.

So, if we have resonant standing-wave voltages in our L2 coil and some of that signal passes through the wire connecting one end of the coil to the earth, then what will happen? The best way to check it is to test the way which a prototype behaves, however, if I may express an opinion, I would suggest that the signal passing down the earth wire will be absorbed when it reaches the earth and that will prevent the signal being reflected back to the L2 coil to upset it's operation.

Another device of Don's is particularly attractive because almost no home-construction is needed, all of the components being available commercially, and the output power being adaptable to any level which you want. Don particularly likes this circuit because it demonstrates COP>1 so neatly and he remarks that the central transmitter Tesla Coil on its own is sufficient to power a household.

Another device of Don's is particularly attractive in that almost no home-construction is needed, all of the components being available commercially, and the output power being adaptable to any level which you want. Don particularly likes this circuit because it demonstrates COP>1 so neatly and he remarks that the central transmitter Tesla Coil on its own is sufficient to power a household.

The coil in the centre of the board is a power transmitter made from a Tesla Coil constructed from two Barker & Williamson ready-made coils. Three more of the inner coil are also used as power receivers. The outer, larger diameter coil is a few turns taken from one of their standard coils and organised so that the coil wire length is one quarter of the coil wire length of the inner coil ("L2").

As before, a commercial neon-tube driver module is used to power the "L1" outer coil with high voltage and high frequency. It should be understood that as power is drawn from the local environment each time the power driving the transmitter coil "L1" cycles, that the power available is very much higher at higher frequencies. The power at mains frequency of less than 100 Hz is far, far less than the power available at 35,000 Hz, so if faced with the choice of buying a 25 kHz neon-tube driver module or a 35 kHz module, then the 35 kHz module is likely to give a much better output power at every voltage level.

The "L1" short outer coil is held in a raised position by the section of white plastic pipe in order to position it correctly relative to the smaller diameter "L2" secondary coil. Again, it appears to have five turns:

The secondary coils are constructed using Barker & Williamson's normal method of using slotted strips to hold the tinned, solid copper wire turns in place.

As there are very slight differences in the manufactured coils, each one is tuned to the exact transmitter frequency and a miniature neon is used to show when the tuning has been set correctly.

The key feature of this device is the fact that any number of receiver coils can be placed near the transmitter and each will receive a full electrical pick up from the local environment, without altering the power needed to drive the Tesla Coil transmitter - more and more output without increasing the input power - unlimited COP values, all of which are over 1. The extra power is flowing in from the local environment where there is almost unlimited amounts of excess energy and that inflow is caused by the rapidly vibrating magnetic field generated by the

central Tesla Coil. While the additional coils appear to just be scattered around the base board, this is not the case. The YouTube video http://www.youtube.com/watch?v=TiNEHZRm4z4&feature=related demonstrates that the pick-up of these coils is affected to a major degree by the distance from the radiating magnetic field. This is to do with the wavelength of the signal driving the Tesla Coil, so the coils shown above are all positioned at exactly the same distance from the Tesla Coil. You still can have as many pick-up coils as you want, but they will be mounted in rings around the Tesla Coil and the coils in each ring will be at the same distance from the Tesla Coil in the centre.

Each of the pick up coils act exactly the same as the "L2" secondary coil of the Tesla Coil transmitter, each picking up the same level of power. Just as with the actual "L2" coil, each will need an output circuit arrangement as described for the previous device. Presumably, the coil outputs could be connected in parallel to increase the output amperage, as they are all resonating at the same frequency and in phase with each other. Each will have its own separate output circuit with a step-down isolation transformer and frequency adjustment as before. If any output is to be a rectified DC output, then no frequency adjustment is needed, just rectifier diodes and a smoothing capacitor following the step-down transformer which will need to be an air core or ferrite core type due to the high frequency. High voltage capacitors are very expensive. The http://www.richieburnett.co.uk/parts.html web site shows various ways of making your own high-voltage capacitors and the advantages and disadvantages of each type.

There are two practical points which need to be mentioned. Firstly, as the Don Smith devices shown above feed radio frequency waveforms to coils which transmit those signals, it may be necessary to enclose the device in an earthed metal container in order not to transmit illegal radio signals. Secondly, as it can be difficult to obtain high-voltage high-current diodes, they can be constructed from several lower power diodes. To increase the voltage rating, diodes can be wired in a chain. Suitable diodes are available as repair items for microwave ovens. These typically have about 4,000 volt ratings and can carry a good level of current. As there will be minor manufacturing differences in the diodes, it is good practice to connect a high value resistor (in the 1 to 10 megohm range) across each diode as that ensures that there is a roughly equal voltage drop across each of the diodes:

If the diode rating of these diodes were 4 amps at 4,000 volts, then the chain of five could handle 4 amps at 20,000 volts. The current capacity can be increased by connecting two or more chains in parallel.

Two DVDs containing video recordings of Don Smith's lectures are available for purchase via the website link: https://secure.netsolhost.com/nuenergy.org/product_catalog.htm

Various questions from readers indicate that the operation of AC circuits is not really understood, so electronics experts can skip this next section.

AC Circuits. This is a lightweight introduction to Alternating Current circuits and pulsed DC circuits for people who have not read Chapter 12 which is an electronics tutorial. Let me say again, that I am mainly self-taught, and so this is just a general introduction based on my present understanding.

Alternating Current, generally called “AC” is called that because the voltage of this type of power supply is not a constant value. A car battery, for instance, is DC and has a fairly constant voltage usually about 12.8 volts when in it’s fully charged state. If you connect a voltmeter across a car battery and watch it, the voltage reading will not change. Minute after minute it says exactly the same because it is a DC source.

If you connect an AC voltmeter across an AC power supply, it too will give a steady reading, but it is telling a lie. The voltage is changing all the time in spite of that steady meter reading. What the meter is doing is **assuming** that the AC waveform is a sine wave like this:

and based on that assumption, it displays a voltage reading which is called the “Root Mean Square” or “RMS” value. The main difficulty with a sine wave is that the voltage is below zero volts for exactly the same length of

time as it is above zero volts, so if you average it, the result is zero volts, which is not a satisfactory result because you can get a shock from it and so it can't be zero volts, no matter what the arithmetical average is.

To get over this problem, the voltage is measured thousands of times per second and the results squared (that is, the value is multiplied by itself) and then those values are averaged. This has the advantage that when the voltage is say, minus 10 volts and you square it, the answer is plus 100 volts. In fact, all of the answers will be positive, which means that you can add them together, average them and get a sensible result. However, you end up with a value which is far too high because you squared every measurement, and so you need to take the square root of that average (or "mean") value, and that is where the fancy sounding "Root Mean Square" name comes from – you are taking the (square) root of the (average or) mean value of the squared measurements.

With a sine wave like this, the voltage peaks are 41.4% higher than the RMS value which everyone talks about. This means that if you feed 100 volts AC through a rectifier bridge of four diodes and feed it into a capacitor the capacitor voltage will **not** be 100 volts DC but instead it will be 141.4 volts DC and you need to remember that when choosing the voltage rating of the capacitor. In that instance I would suggest a capacitor which is made to operate with voltages up to 200 volts.

You probably already knew all of that, but it may not have occurred to you that if you use a standard AC voltmeter on a waveform which is **not** a sine wave, that the reading on the meter is most unlikely to be correct or anywhere near correct. So, please don't merrily connect an AC voltmeter across a circuit which is producing sharp voltage spikes like, for instance, one of John Bedini's battery pulsing circuits, and think that the meter reading means anything (other than meaning that you don't understand what you are doing).

You will, hopefully, have learned that power in watts is determined by multiplying the current in amps by the voltage in volts. For example, 10 amps of current flowing out of a 12 volt power supply, represents 120 watts of power. Unfortunately, that only holds true for circuits which are operating on DC, or AC circuits which have only resistors in them. The situation changes for AC circuits which have non-resistive components in them.

The circuits of this type which you are likely to come across are circuits which have coils in them, and you need to think about what you are doing when you deal with these types of circuit. For example, consider this circuit:

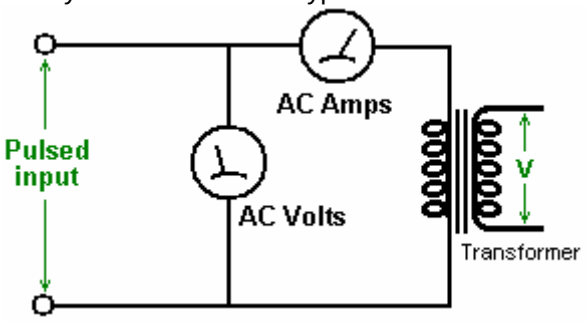

This is the output section of a prototype which you have just built. The input to the prototype is DC and measures at 12 volts, 2 amps (which is 24 watts). Your AC voltmeter on the output reads 15 volts and your AC ammeter reads 2.5 amps and you are delighted because 15 x 2.5 = 37.5 which looks much bigger than the 24 watts of input power. **But**, just before you go rushing off to announce on YouTube that you have made a prototype with COP = 1.56 or 156% efficient, you need to consider the real facts.

This is an AC circuit and unless your prototype is producing a perfect sine wave, then the AC voltmeter reading will be meaningless. It is just possible that your AC ammeter is one of the few types that can accurately measure the current no matter what sort of waveform is fed to it, but it is distinctly possible that it will be a digital meter which assesses current by measuring the AC voltage across a resistor in series with the output, and if that is the case, it will probably be assuming a sine wave. The odds are that both readings are wrong, but let's take the case where we have great meters which are reading the values perfectly correctly. Then the output will be 37.5 watts, won't it? Well, actually, no it won't. The reason for this is that the circuit is feeding the transformer winding which is a coil and coils don't work like that.

The problem is that, unlike a resistor, when you apply a voltage across a coil the coil starts absorbing energy and feeding it into the magnetic field around the coil, so there is a delay before the current reaches it's maximum value. With DC, this generally doesn't matter very much, but with AC where the voltage is changing continuously, it matters a great deal. The situation can be as shown in this graph of both voltage and current:

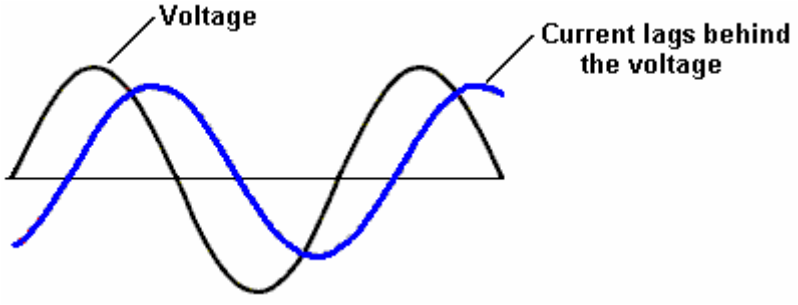

At first, this does not look like any great problem, but it has a very significant effect on the actual power in watts. To get the 37.5 watts output which we were talking about earlier, we multiplied the average voltage level by the average current level. But these two values do not occur at the same time and that has a major effect.

As this can be a little difficult to see, let's take the peak values rather than the averages as they are easier to see. Let's say that in our example graph that the voltage peak is 10 volts and the current peak is 3 amps. If this were DC we would multiply them together and say that the power was 30 watts. But with AC, this does not work due to the timing difference:

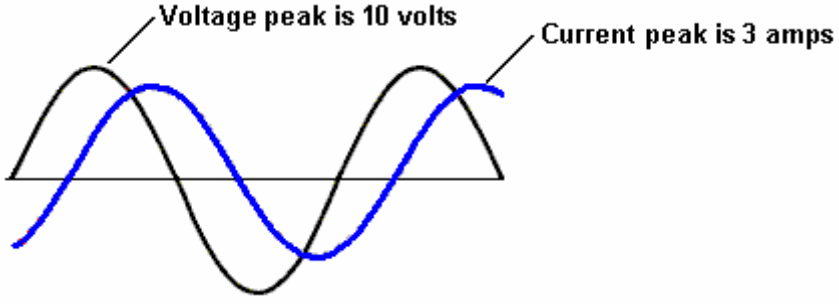

When the voltage is peaking, the current is nowhere near it's peak value of 3 amps:

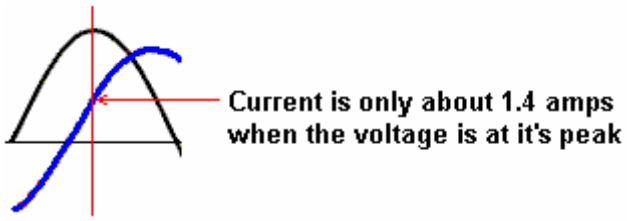

As a result of this, instead of getting our expected peak power at the top of the voltage peak, the actual power in watts is very much lower – less than half of what we were expecting. Not so good, but it gets worse when you look at the situation more closely. Take a look at what the voltage is when the current crosses the zero line, that is, when the current is zero. The output power is zero when the current is zero but this occurs when the voltage is at a very high value:

The same goes for when the voltage is zero. When the voltage is zero, then the power is also zero, and you will notice that this occurs when the current is at a high value:

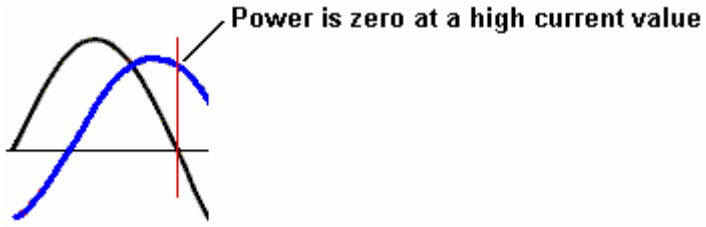

The power is **not** the average current multiplied by the average voltage if there is a coil involved in the circuit – it will be less than that by an amount known as the "power factor" and I'll leave you to work out why it is called that.

So, how do you determine what the power is? It is done by sampling the voltage and current many times per second and averaging those combined results:

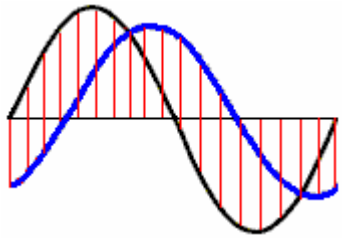

Both the voltage and the current are sampled at the times indicated by the vertical red lines and those figures are used to calculate the actual power level. In this example, only a few samplings are shown, but in practice, a very large number of samples will be taken. The piece of equipment which does this is known as a wattmeter as it measures watts of power. The sampling can be done by windings inside the instrument, resulting in an instrument which can be damaged by overloading without the needle being anywhere near full deflection, or it can be done by digital sampling and mathematical integration. Most digital sampling versions of these meters only operate at high frequencies, typically over 400,000 cycles per second. Both varieties of wattmeter can handle any waveform and not just sine waves.

The power company supplying your home, measures the current and assumes that the full voltage is present during all of the time that the current is being drawn. If you are powering a powerful electric motor from the mains, then this current lag will cost you money as the power company does not take it into account. It is possible to correct the situation by connecting one or more suitable capacitors across the motor to minimise the power loss.

With a coil (fancy name "inductor" symbol "L"), AC operation is very different to DC operation. The coil has a DC resistance which can be measured with the ohms range of a multimeter, but that resistance does not apply when AC is being used as the AC current flow is **not** determined by the DC resistance of the coil. Because of this, a second term has to be used for the current-controlling factor of the coil, and the term chosen is "impedance" or for people who like to make everything sound unduly complicated "reactance". I will stick with the term "impedance" as it is clear that it is the feature of the coil which "impedes" AC current flow through the coil.

The impedance of a coil depends on it's size, shape, method of winding, number of turns and core material. It also depends on the frequency of the AC voltage being applied to it. If the core is made up of iron or steel, usually thin layers of iron which are insulated from each other, then it can only handle low frequencies. You can forget about trying to pass 10,000 cycles per second ("Hz") through the coil as the core just can't change it's magnetic poles fast enough to cope with that frequency. A core of that type is ok for the very low 50 Hz or 60 Hz frequencies used for mains power, which are kept that low so that electric motors can use it.

For higher frequencies, ferrite can be used for a core and that is why some portable radios use ferrite-rod aerials, which are a bar of ferrite with a coil wound on it. For higher frequencies (or higher efficiencies) iron dust encapsulated in epoxy resin is used. An alternative is to not use any core material and that is usually referred to as an "air-core" coil. These are not limited in frequency by the core but they have a very much lower inductance for any given number of turns. The efficiency of the coil is called it's "Q" (for "Quality") and the higher the Q factor, the better. The resistance of the wire lowers the Q factor.

A coil has inductance, and resistance caused by the wire, and capacitance caused by the turns being near each other. However, having said that, the inductance is normally so much bigger than the other two components that we tend to ignore the other two. Something which may not be immediately obvious is that the impedance to AC current flow through the coil depends on how fast the voltage is changing. If the AC voltage applied to a coil completes one cycle every ten seconds, then the impedance will be much lower than if the voltage cycles a million times per second.

If you had to guess, you would think that the impedance would increase steadily as the AC frequency increased. In other words, a straight-line graph type of change. That is not the case. Due to a feature called resonance, there is one particular frequency at which the impedance of the coil increases massively. This is used in the tuning method for AM radio receivers. In the very early days when electronic components were hard to come by, variable coils were sometimes used for tuning. We still have variable coils today, generally for handling large currents rather than radio signals, and we call them “rheostats” and some look like this:

These have a coil of wire wound around a hollow former and a slider can be pushed along a bar, connecting the slider to different winds in the coil depending on it’s position along the supporting bar. The terminal connections are then made to the slider and to one end of the coil. The position of the slider effectively changes the number of turns of wire in the part of the coil which is being used in the circuit. Changing the number of turns in the coil, changes the resonant frequency of that coil. AC current finds it very, very hard to get through a coil which has the same resonant frequency as the AC current frequency. Because of this, it can be used as a radio signal tuner:

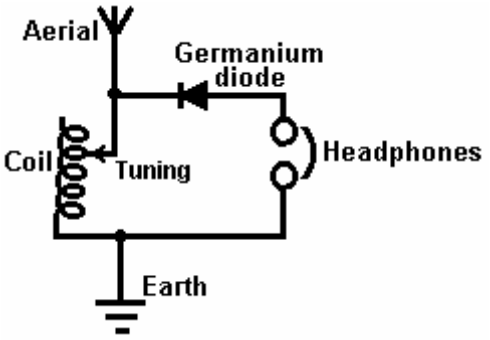

If the coil’s resonant frequency is changed to match that of a local radio station by sliding the contact along the coil, then that particular AC signal frequency from the radio transmitter finds it almost impossible to get through the coil and so it (and only it) diverts through the diode and headphones as it flows from the aerial wire to the earth wire and the radio station is heard in the headphones. If there are other radio signals coming down the aerial wire, then, because they are not at the resonant frequency of the coil, they flow freely through the coil and don’t go through the headphones.

This system was soon changed when variable capacitors became available as they are cheaper to make and they are more compact. So, instead of using a variable coil for tuning the radio signal, a variable capacitor connected across the tuning coil did the same job:

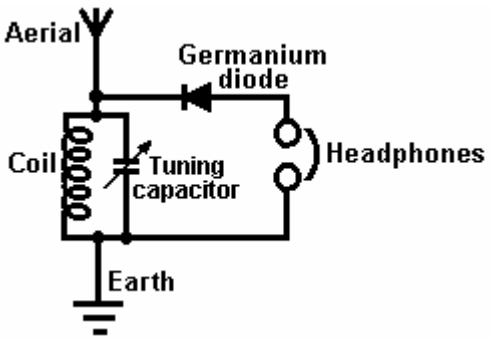

While the circuit diagram above is marked “Tuning capacitor” that is actually quite misleading. Yes, you tune the radio receiver by adjusting the setting of the variable capacitor, **but**, what the capacitor is doing is altering the

resonant frequency of the coil/capacitor combination and it is the resonant frequency of that combination which is doing exactly the same job as the variable coil did on it's own.

This draws attention to two very important facts concerning coil/capacitor combinations. When a capacitor is placed across a coil "in parallel" as shown in this radio receiver circuit, then the combination has a very high impedance (resistance to AC current flow) at the resonant frequency. But if the capacitor is placed "in series" with the coil, then there is nearly zero impedance at the resonant frequency of the combination:

This may seem like something which practical people would not bother with, after all, who really cares? However, it is a very practical point indeed. Remember that Don Smith often uses an early version, off-the-shelf neon-tube driver module as an easy way to provide a high-voltage, high-frequency AC current source, typically, 6,000 volts at 30,000 Hz. He then feeds that power into a Tesla Coil which is itself, a power amplifier. The arrangement is like this:

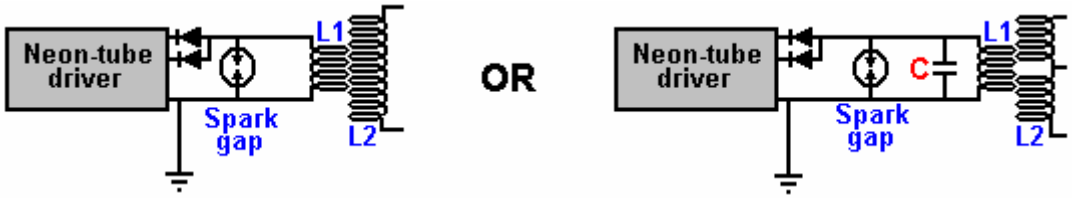

People who try to replicate Don's designs tend to say "I get great sparks at the spark gap until I connect the **L1** coil and then the sparks stop. This circuit can never work because the resistance of the coil is too low".

If the resonant frequency of the **L1** coil does not match the frequency being produced by the neon-tube driver circuit, then the low impedance of the **L1** coil at that frequency, will definitely pull the voltage of the neon-tube driver down to a very low value. But if the **L1** coil has the same resonant frequency as the driver circuit, then the **L1** coil (or the **L1** coil/capacitor combination shown on the right, will have a very high resistance to current flow through it and it will work well with the driver circuit. So, no sparks, means that the coil tuning is off. It is the same as tuning a radio receiver, get the tuning wrong and you don't hear the radio station.

This is very nicely demonstrated using simple torch bulbs and two coils in the YouTube video showing good output for almost no input power: http://www.youtube.com/watch?v=kQdcwDCBoNY and while only one resonant pick-up coil is shown, there is the possibility of using many resonant pick-up coils with just the one transmitter.

As it would not be unusual for many readers to feel that there is some "black magic" about the neon-driver circuit used by Don to drive the Tesla Coil section of his circuitry and that if a suitable unit could not be purchased then the circuit could not be reproduced or tested, it seems reasonable to show how it operates and how it can be constructed from scratch:

The circuit itself is made up of an oscillator to convert the 12-volt DC supply into a pulsating current which is then stepped up to a high voltage by a transformer. Here is a circuit which has been used for this:

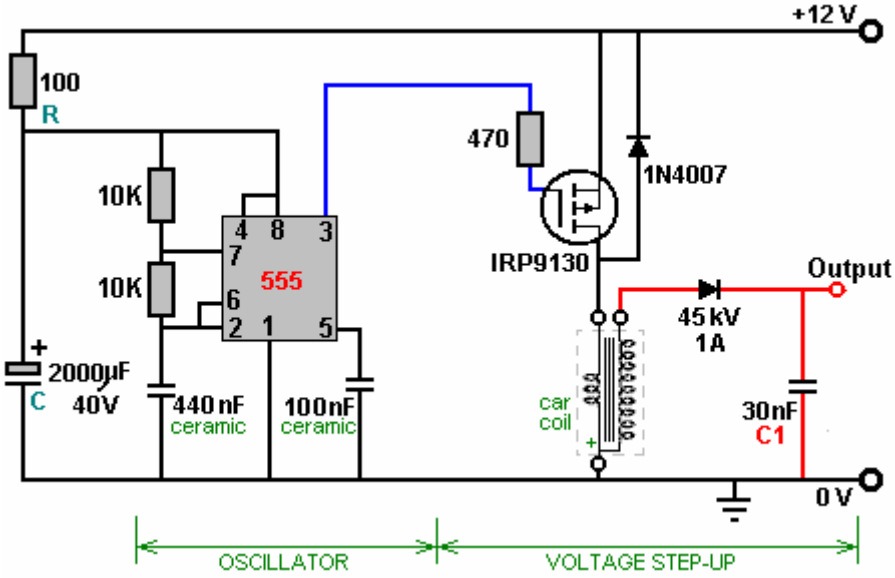

The supply for the 555 timer chip is protected against spikes and dips by the resistor "R" and the capacitor "C". The 555 timer chip acts as an oscillator or "clock" whose speed is governed by the two 10K resistors feeding the 440 nF capacitor. The step-up transformer is an ordinary car coil and the drive power to it is boosted by the IRP9130 FET transistor which is driven by the 555 chip output coming from it's pin 3.

The output from the (Ford Model T) car coil is rectified by the diode, which needs to have a very high voltage rating as the voltage at this point is now very high. The rectified voltage pulses are stored in a very high-voltage capacitor before being used to drive a Tesla Coil. As a powerful output is wanted, two car coils are used and their outputs combined as shown here:

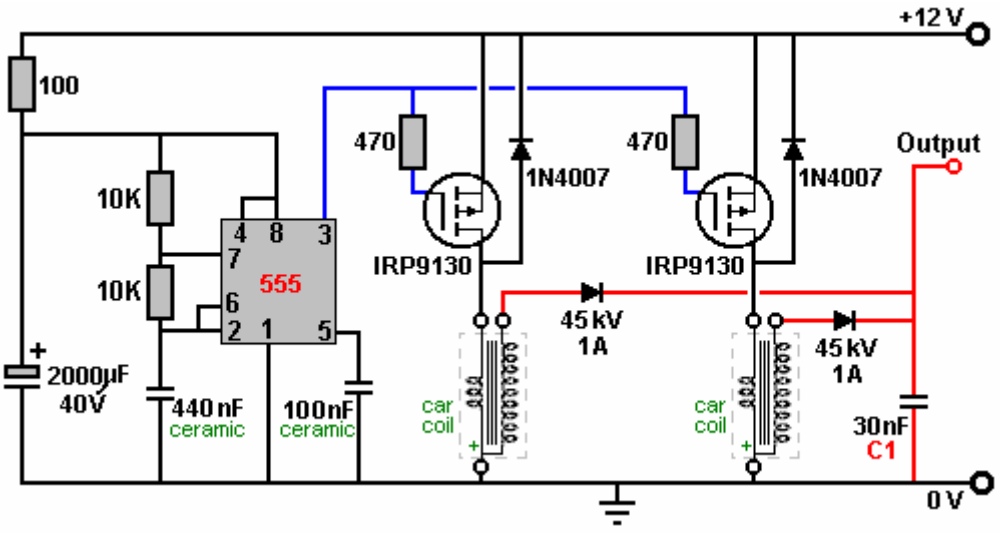

You will notice that the car coil has only three terminals and the terminal marked "+" is the one with the connection common to both of the coils inside the housing. The coil may look like this:

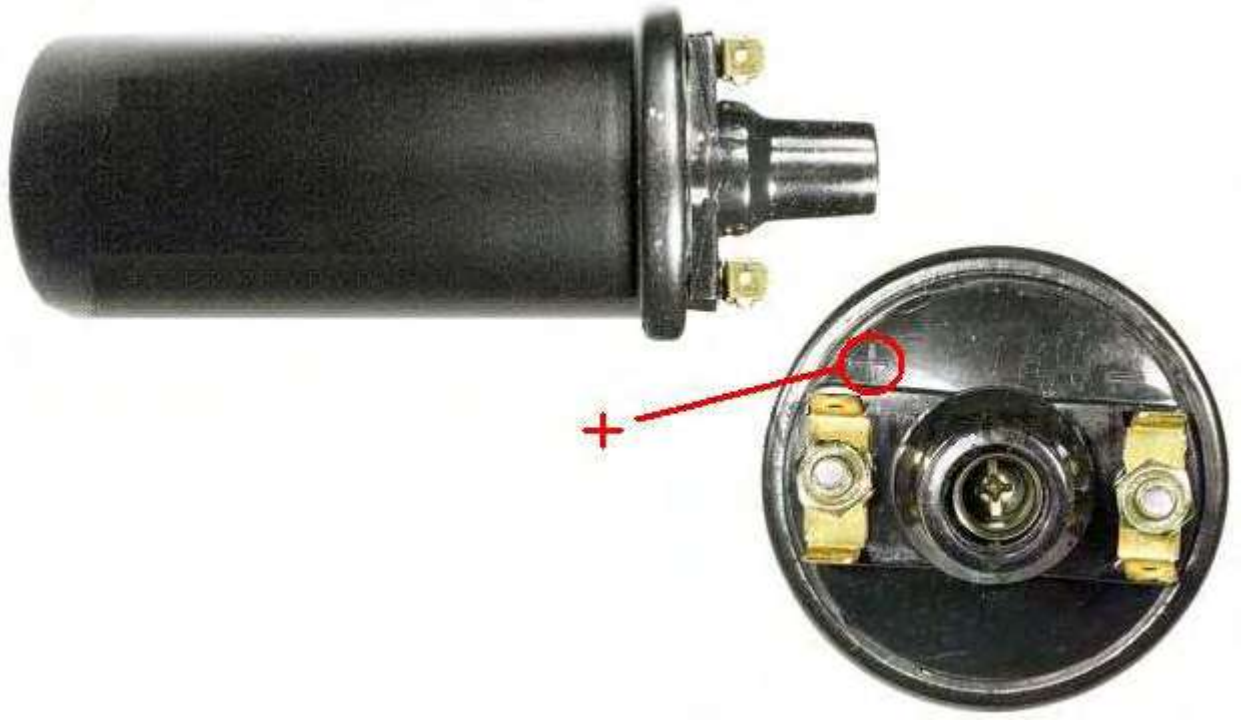

and the "+" is generally marked on the top beside the terminal with the two internal connections running to it. The circuit described so far is very close to that provided by a neon-tube driver circuit and it is certainly capable of driving a Tesla Coil.

There are several different way of constructing a Tesla Coil. It is not unusual to have several spark gaps connected in a chain. This arrangement is called a "series spark gap" because the spark gaps are connected "in series" which is just a technical way of saying "connected in a row". In the chapter on aerial systems, you will see that Hermann Plauston uses that style of spark gap with the very high voltages which he gets from his powerful aerial systems. These multiple spark gaps are much quieter in operation than a single spark gap would be. One of the possible Tesla Coil designs uses a pancake coil as the "L1" coil as that gives even higher gain. The circuit is as shown here:

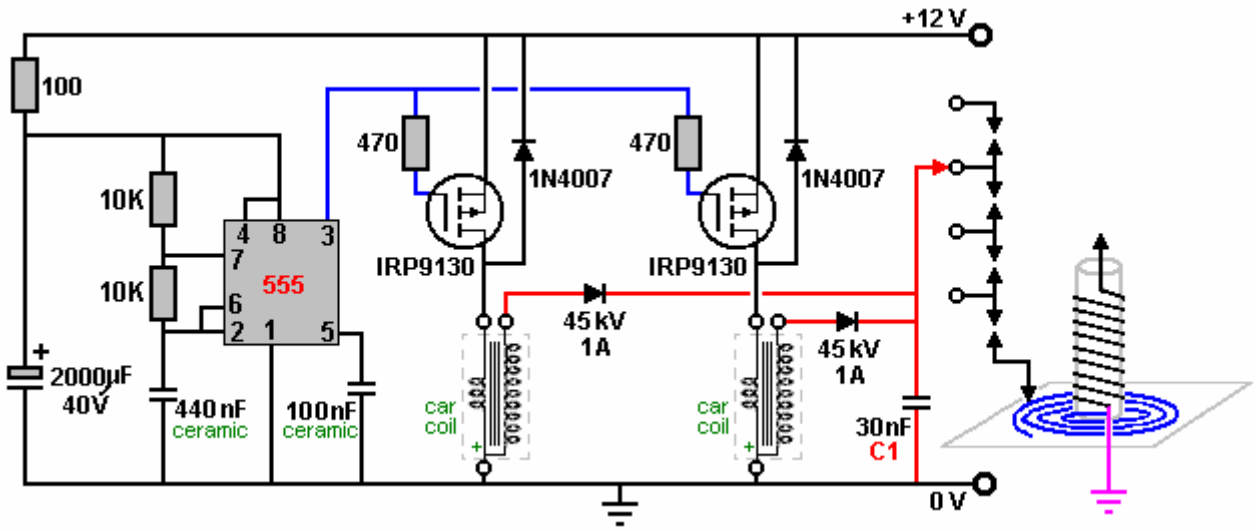

The connection to the pancake coil is by a moveable clamp and the two coils are tuned to resonance by careful and gradual adjustment of that connection. The series spark gap can be constructed in various ways, including using car spark plugs. The one shown here uses nuts and bolts projecting through two strips of a stiff, non-conducting material, as that is much easier to adjust than the gaps of several spark plugs:

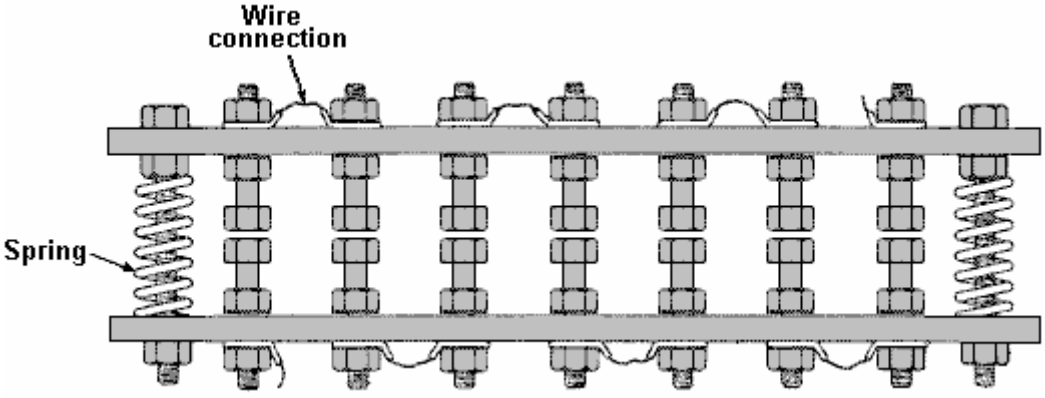

Tightening the bolts which compress the springs moves the bolt heads closer together and reduces all of the spark gaps. The electrical connections can be made to the end tags or to any of the intermediate wire connection straps if fewer spark gaps are required in the chain.

Let me remind you again that this is not a toy and very high voltages will be produced. Also, let me stress again that if you decide to construct anything, then you do so entire on your own responsibility. This document is only provided for information purposes and must not be seen as an encouragement to build any such device nor is any guarantee given that any of the devices described in this eBook will work as described should you decide to attempt to construct a replication prototype of your own. Generally, it takes skill and patience to achieve success with any free-energy device and Don Smith's devices are some of the most difficult, especially since he admits quite freely that he does not disclose all of the details.

The output capacitor marked "C1" in the circuit diagram above has to be able to handle very high voltages. There are various ways of dealing with this. Don dealt with it by getting very expensive capacitors manufactured by a specialist company. Some home-based constructors have had success using glass beer bottles filled with a salt solution. The outside of the bottles are wrapped in aluminium foil to form one of the contacts of the capacitor and bare wires are looped from deep inside each bottle on to the next one, looping from the inside of one bottle to the inside of the next one, and eventually forming the other contact of the capacitor. While that appears to work well, it is not a very convenient thing to carry around. An alternative is just to stand the bare bottles in a container which is lined with foil which forms the second contact of the capacitor.

One method which has been popular in the past is to use two complete rolls of aluminium foil, sometimes called "baking foil", laying them one flat, covering it with one or more layers of plastic cling film and laying the second roll of foil on top of the plastic. The three layers are then rolled up to form the capacitor. Obviously, several of these can be connected together in parallel in order to increase the capacitance of the set. The thicker the plastic, the lower the capacitance but the higher the voltage which can be handled.

The November 1999 issue of Popular Electronics suggests using 33 sheets of the thin aluminium used as a flashing material by house builders. At that time it was supplied in rolls which were ten inches (250 mm) wide, so their design uses 14" (355 mm) lengths of the aluminium. The plastic chosen to separate the plates was polythene sheet 0.062 inch (1.6 mm) thick which is also available from a builders merchants outlet. The plastic is cut to 11 inch (280 mm) by 13 inch (330 mm) and assembly is as follows:

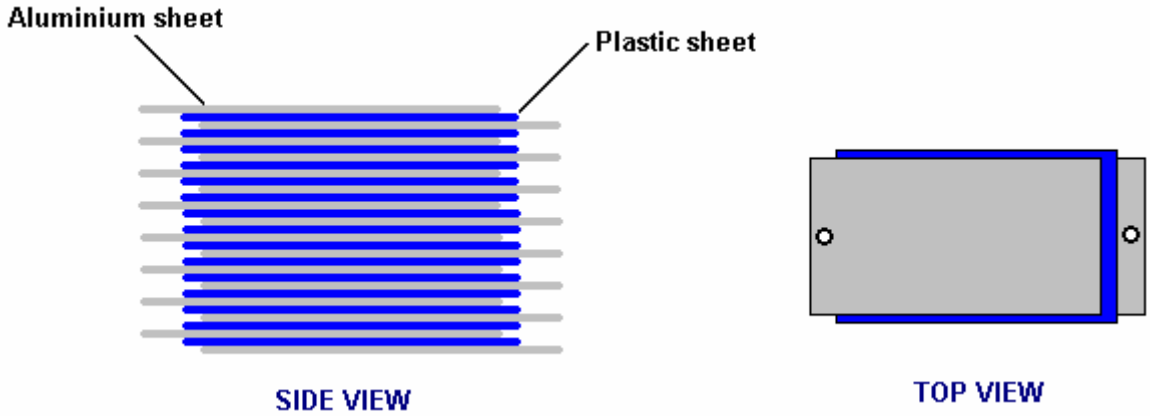

The sandwich stack of sheets is then clamped together between two rigid timber sheets. The tighter that they are clamped, the closer the plates are to each other and the higher the capacitance. The electrical connections are made by running a bolt through the projecting ends of the plates. With two thicknesses of plastic sheet and one of aluminium, there should be room for a washer between each pair of plates at each end and that would improve the clamping and the electrical connection. An alternative is to cut a corner off each plate and position them alternatively so that almost no plate area is ineffective.

As Don Smith has demonstrated in one of his video presentations, Nikola Tesla was perfectly correct when he stated that directing the discharge from a Tesla Coil on to a metal plate (or in Don's case, one of the two metal plates of a two-plate capacitor where a plastic sheet separates the plates just as shown above), produces a very powerful current flow onwards through a good earth connection. Obviously, if an electrical load is positioned between the plates and the earth connection, then the load can be powered to a high level of current, giving a very considerable power gain.

Coil Construction: The Barker & Williamson coils used by Don in his constructions are expensive to purchase. Some years ago, in an article in a 1997 issue of the "QST" amateur radio publication, Robert H. Johns shows how similar coils can be constructed without any great difficulty. The Electrodyne Corporation research staff have stated that off-the-shelf solid tinned copper wire produces three times the magnetic field that un-tinned copper does, so perhaps that should be borne in mind when choosing the wire for constructing these coils.

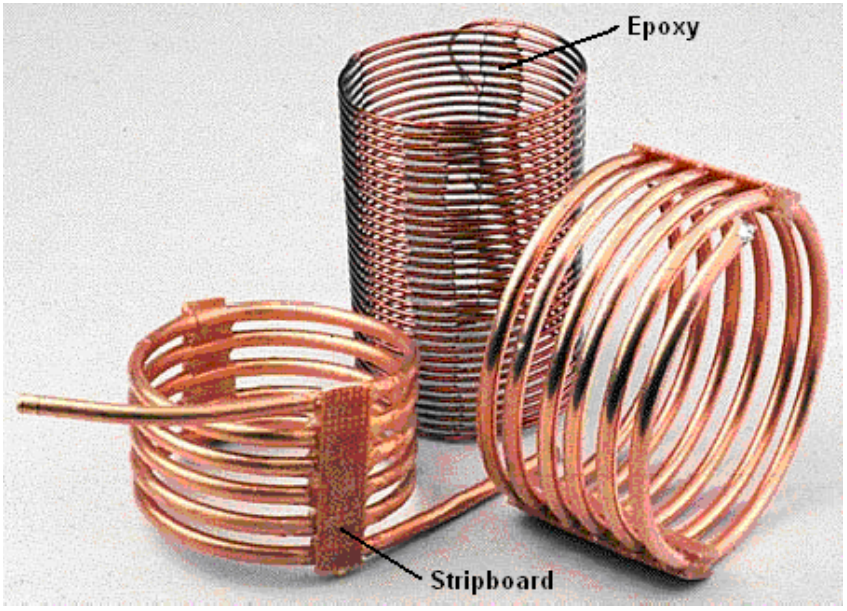

These home-made coils have excellent "Q" Quality factors, some even better than the tinned copper wire coils of Barker & Williamson because the majority of electrical flow is at the surface of the wire and copper is a better conductor of electricity than the silver tinning material.

The inductance of a coil increases if the turns are close together. The capacitance of a coil decreases if the turns are spread out. A good compromise is to space the turns so that there is a gap between the turns of one wire thickness. A common construction method with Tesla Coil builders is to use nylon fishing line or plastic strimmer cord between the turns to create the gap. The method used by Mr Johns allows for even spacing without using any additional material. The key feature is to use a collapsible former and wind the coil on the former, space the turns out evenly and then clamp them in position with strips of epoxy resin, removing the former when the resin has set and cured.

Mr Johns has difficulty with his epoxy being difficult to keep in place, but when mixed with the West System micro fibres, epoxy can be made any consistency and it can be applied as a stiff paste without any loss of it's properties. The epoxy is kept from sticking to the former by placing a strip of electrical tape on each side of the former.

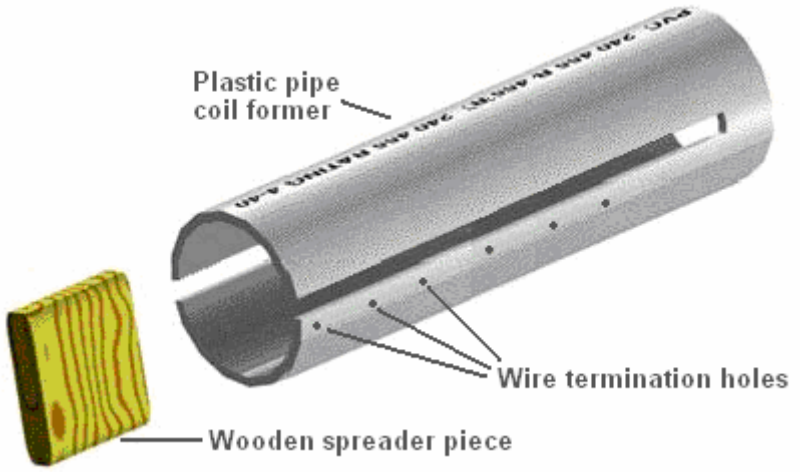

I suggest that the plastic pipe used as the coil former is twice the length of the coil to be wound as that allows a good degree of flexing in the former when the coil is being removed. Before the two slots are cut in the plastic pipe, a wooden spreader piece is cut and it's ends rounded so that it is a push-fit in the pipe. This spreader piece is used to hold the sides of the cut end exactly in position when the wire is being wrapped tightly around the pipe.

Two or more small holes are drilled in the pipe beside where the slots are to be cut. These holes are used to anchor the ends of the wire by passing them through the hole and bending them. Those ends have to be cut off before the finished coil is slid off the former, but they are very useful while the epoxy is being applied and hardening. The pipe slots are cut to a generous width, typically 10 mm or more.

The technique is then to wedge the wooden spreader piece in the slotted end of the pipe. Then anchor the end of the solid copper wire using the first of the drilled holes. The wire, which can be bare or insulated, is then wrapped tightly around the former for the required number of turns, and the other end of the wire secured in one of the other drilled holes. It is common practice to make the turns by rotating the former. When the winding is completed, the turns can be spaced out more evenly if necessary, and then a strip of epoxy paste applied all along one side of the coil. When that has hardened, (or immediately if the epoxy paste is stiff enough), the pipe is turned over and a second epoxy strip applied to the opposite side of the coil. A strip of paxolin board or strip-board can be made part of the epoxy strip. Alternatively, an L-shaped plastic mounting bracket or a plastic mounting bolt can be embedded in the epoxy ready for the coil installation later on.

When the epoxy has hardened, typically 24 hours later, the coil ends are snipped off, the spreader piece is tapped out with a dowel and the sides of the pipe pressed inwards to make it easy to slide the finished coil off the former. Larger diameter coils can be wound with small-diameter copper pipe.

The coil inductance can be calculated from:

Inductance in microhenrys $L = d^2n^2 / (18d + 40l)$

Where:
d is the coil diameter in inches measured from wire centre to wire centre
n is the number of turns in the coil
l is coil length in inches (1 inch = 25.4 mm)

Using this equation for working out the number of turns for a given inductance in microhenrys:

$$n = \frac{\sqrt{L(18d + 40l)}}{d}$$

Patrick Kelly
engpjk@gmail.com
http://www.free-energy-info.co.uk
http://www.free-energy-devices.com

03W-8605-5.qxd 12/10/09 10:23 AM Page 1

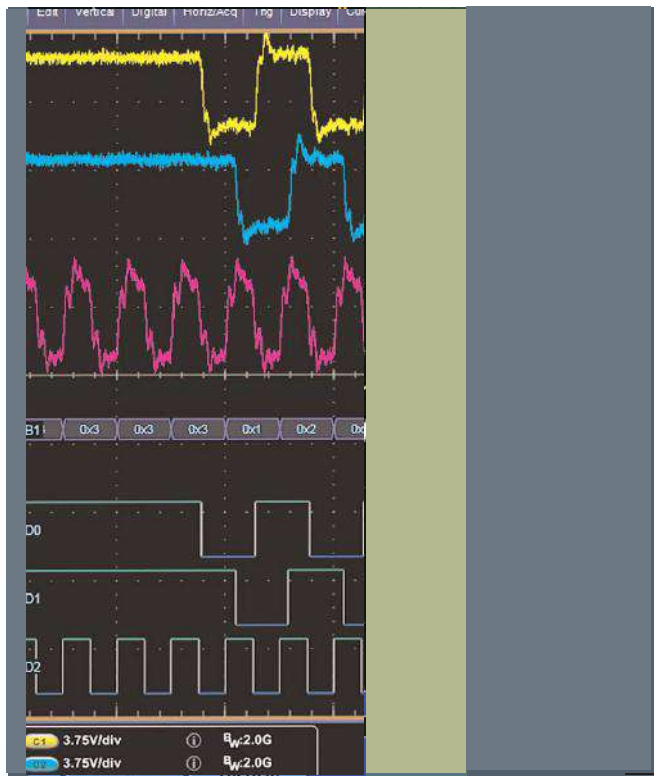

XYZs of Oscilloscopes

Primer

Tektronix®

03W-8605-5.qxd 12/10/09 10:23 AM Page 2

Table of Contents

Introduction 4

Signal Integrity . . . . . 5 - 6

The Significance of Signal Integrity 5
Why is Signal Integrity a Problem? 5
Viewing the Analog Origins of Digital Signals 6

The Oscilloscope . . . . . 7 - 12

Understanding Waveforms & Waveform Measurements . .7
Types of Waves 8
Sine Waves 9
Square and Rectangular Waves 9
Sawtooth and Triangle Waves 9
Step and Pulse Shapes 9
Periodic and Non-periodic Signals 9
Synchronous and Asynchronous Signals 9
Complex Waves 10
Waveform Measurements 11
Frequency and Period 11
Voltage 11
Amplitude 11
Phase 11
Waveform Measurements with Digital Oscilloscopes 12

Types of Oscilloscopes . . . . . .13 - 17

Digital Storage Oscilloscopes 13
Digital Phosphor Oscilloscopes 15
Mixed Signal Oscilloscopes 16
Digital Sampling Oscilloscopes 17

The Systems and Controls of an Oscilloscope .18 - 31

Vertical System and Controls 19
Position and Volts per Division 19
Input Coupling 19
Bandwidth Limit 19
Bandwidth Enhancement 20
Horizontal System and Controls 20
Acquisition Controls 20
Acquisition Modes 20
Types of Acquisition Modes 21
Starting and Stopping the Acquisition System 21
Sampling 22
Sampling Controls 22
Real-time Sampling Method 22
Equivalent-time Sampling Method 24
Position and Seconds per Division 26
Time Base Selections 26
Zoom/Pan 26
Search 26
XY Mode 26
Z Axis 26
XYZ Mode 26
Trigger System and Controls 27
Trigger Position 29
Trigger Level and Slope 29
Trigger Sources 29
Trigger Modes 30
Trigger Coupling 30
Trigger Holdoff 30
Display System and Controls 31
Other Oscilloscope Controls 31
Math and Measurement Operations 31
Digital Timing and State Acquisitions 31

03W-8605-5.qxd 12/10/09 10:23 AM Page 3

The Complete Measurement System . . . . . 32 - 34

Probes 32
Passive Probes 33
Active and Differential Probes 34
Logicl Probes 34
Specialty Probes 35
Probe Accessories 35

Performance Terms and Considerations . . . . . 35 - 42

Bandwidth 35
Rise Time 36
Sample Rate 37
Waveform Capture Rate 38
Record Length 38
Triggering Capabilities 39
Effective Bits 39
Frequency Response 39
Vertical Sensitivity 39
Sweep Speed 39
Gain Accuracy 39
Horizontal Accuracy (Time Base) 39
Vertical Resolution (Analog-to-Digital Converter) 39
Timing Resolution (MSO) 40
Connectivity 40
Expandability 40
Ease-of-use 42

Operating the Oscilloscope . . . . . 43 - 45

Proper Grounding 43
Setting the Controls 43
Calibrating the Instrument 44
Connecting the Probes 44
Compensating the Probes 44

Oscilloscope Measurement Techniques . . . . . 46 - 48

Voltage Measurements 46
Time and Frequency Measurements 47
Pulse Width and Rise Time Measurements 47
Phase Shift Measurements 48
Other Measurement Techniques 48

Written Exercises . . . . . 49 - 54

Part I
A. Vocabulary Exercises 49
B. Application Exercises 50

Part II
A. Vocabulary Exercises 51
B. Application Exercises 52

Answer Key 54

Glossary . . . . . 55 - 58

03W-8605-5.qxd 12/10/09 10:23 AM Page 4

Introduction

Nature moves in the form of a sine wave, be it an ocean wave, earthquake, sonic boom, explosion, sound through air, or the natural frequency of a body in motion. Energy, vibrating particles and other invisible forces pervade our physical universe. Even light – part particle, part wave – has a fundamental frequency, which can be observed as color.

Sensors can convert these forces into electrical signals that you can observe and study with an oscilloscope. Oscilloscopes enable scientists, engineers, technicians, educators and others to "see" events that change over time.

Oscilloscopes are indispensable tools for anyone designing, manufacturing or repairing electronic equipment. In today's fast-paced world, engineers need the best tools available to solve their measurement challenges quickly and accurately. As the eyes of the engineer, oscilloscopes are the key to meeting today's demanding measurement challenges.

The usefulness of an oscilloscope is not limited to the world of electronics. With the proper sensor, an oscilloscope can measure all kinds of phenomena. A sensor is a device that creates an electrical signal in response to physical stimuli, such as sound, mechanical stress, pressure, light, or heat. A microphone is a sensor that converts sound into an electrical signal. Figure 1 shows an example of scientific data that can be gathered by an oscilloscope.

Oscilloscopes are used by everyone from physicists to repair technicians. An automotive engineer uses an oscilloscope to correlate analog data from sensors with serial data from the engine control unit. A medical researcher uses an oscillscope to measure brain waves. The possibilities are endless.

The concepts presented in this primer will provide you with a good starting point in understanding oscilloscope basics and operation.

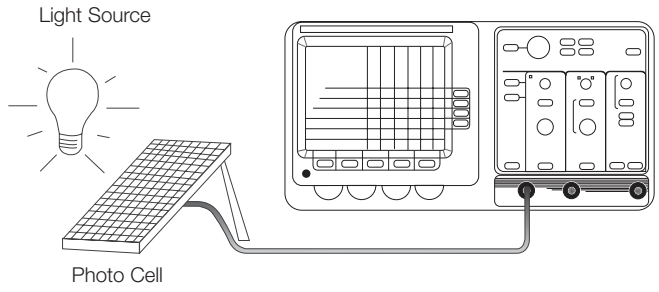

Figure 1. An example of scientific data gathered by an oscilloscope.

The glossary in the back of this primer will give you definitions of unfamiliar terms. The vocabulary and multiple-choice written exercises on oscilloscope theory and controls make this primer a useful classroom aid. No mathematical or electronics knowledge is necessary.

After reading this primer, you will be able to:

- Describe how oscilloscopes work
- Describe the differences between various oscilloscopes
- Describe electrical waveform types
- Understand basic oscilloscope controls
- Take simple measurements

The manual provided with your oscilloscope will give you more specific information about how to use the oscilloscope in your work. Some oscilloscope manufacturers also provide a multitude of application notes to help you optimize the oscilloscope for your application-specific measurements.

Should you need additional assistance, or have any comments or questions about the material in this primer, simply contact your Tektronix representative, or visit **www.tektronix.com**.

03W-8605-5.qxd 12/10/09 10:23 AM Page 5

Signal Integrity

The Significance of Signal Integrity

The key to any good oscilloscope system is its ability to accurately reconstruct a waveform – referred to as signal integrity. An oscilloscope is analogous to a camera that captures signal images that we can then observe and interpret. Two key issues lie at the heart of signal integrity.

- When you take a picture, is it an accurate picture of what actually happened?
- Is the picture clear or fuzzy?
- How many of those accurate pictures can you take per second?

Taken together, the different systems and performance capabilities of an oscilloscope contribute to its ability to deliver the highest signal integrity possible. Probes also affect the signal integrity of a measurement system.

Signal integrity impacts many electronic design disciplines. But until a few years ago, it wasn't much of a problem for digital designers. They could rely on their logic designs to act like the Boolean circuits they were. Noisy, indeterminate signals were something that occurred in high-speed designs – something for RF designers to worry about. Digital systems switched slowly and signals stabilized predictably.

Processor clock rates have since multiplied by orders of magnitude. Computer applications such as 3D graphics, video and server I/O demand vast bandwidth. Much of today's telecommunications equipment is digitally based, and similarly requires massive bandwidth. So too does digital high-definition TV. The current crop of microprocessor devices handles data at rates up to 2, 3 and even 5 GS/s (gigasamples per second), while some DDR3 memory devices use clocks in excess of 2 GHz as well as data signals with 35 ps rise times.

Importantly, speed increases have trickled down to the common IC devices used in automobiles, consumer electronics, and machine controllers, to name just a few applications.

A processor running at a 20 MHz clock rate may well have signals with rise times similar to those of an 800 MHz processor. Designers have crossed a performance threshold that means, in effect, almost every design is a high-speed design.

Without some precautionary measures, high-speed problems can creep into otherwise conventional digital designs. If a circuit is experiencing intermittent failures, or if it encounters errors at voltage and temperature extremes, chances are there are some hidden signal integrity problems. These can affect time-to-market, product reliability, EMI compliance, and more. These high-speed problems can also impact the integrity of a serial data stream in a system, requiring some method of correlating specific patterns in the data with the observed characteristics of high-speed waveforms.

Why is Signal Integrity a Problem?

Let's look at some of the specific causes of signal degradation in today's digital designs. Why are these problems so much more prevalent today than in years past?

The answer is speed. In the "slow old days," maintaining acceptable digital signal integrity meant paying attention to details like clock distribution, signal path design, noise margins, loading effects, transmission line effects, bus termination, decoupling and power distribution. All of these rules still apply, but…

Bus cycle times are up to a thousand times faster than they were 20 years ago! Transactions that once took microseconds are now measured in nanoseconds. To achieve this improvement, edge speeds too have accelerated: they are up to 100 times faster than those of two decades ago.

This is all well and good; however, certain physical realities have kept circuit board technology from keeping up the pace. The propagation time of inter-chip buses has remained almost unchanged over the decades. Geometries have shrunk, certainly, but there is still a need to provide circuit board real estate for IC devices, connectors, passive components, and of course, the bus traces themselves. This real estate adds up to distance, and distance means time – the enemy of speed.

03W-8605-5.qxd 12/10/09 10:23 AM Page 6

It's important to remember that the edge speed – rise time – of a digital signal can carry much higher frequency components than its repetition rate might imply. For this reason, some designers deliberately seek IC devices with relatively "slow" rise times.

The lumped circuit model has always been the basis of most calculations used to predict signal behavior in a circuit. But when edge speeds are more than four to six times faster than the signal path delay, the simple lumped model no longer applies.

Circuit board traces just six inches long become transmission lines when driven with signals exhibiting edge rates below four to six nanoseconds, irrespective of the cycle rate. In effect, new signal paths are created. These intangible connections aren't on the schematics, but nevertheless provide a means for signals to influence one another in unpredictable ways.

Sometimes even the errors introduced by the probe/instrument combination can provide a significant contribution to the signal being measured. However, by applying the "square root of the sum of the squares" formula to the measured value, it is possible to determine whether the device under test is approaching a rise/fall time failure. In addition, recent oscilloscope tools use special filtering techniques to de-embed the measurement system's effects on the signal, displaying edge times and other signal characteristics.

At the same time, the intended signal paths don't work the way they are supposed to. Ground planes and power planes, like the signal traces described above, become inductive and act like transmission lines; power supply decoupling is far less effective. EMI goes up as faster edge speeds produce shorter wavelengths relative to the bus length. Crosstalk increases.

In addition, fast edge speeds require generally higher currents to produce them. Higher currents tend to cause ground bounce, especially on wide buses in which many signals switch at once. Moreover, higher current increases the amount of radiated magnetic energy and with it, crosstalk.

Viewing the Analog Origins of Digital Signals

What do all these characteristics have in common? They are classic analog phenomena. To solve signal integrity problems, digital designers need to step into the analog domain. And to take that step, they need tools that can show them how digital and analog signals interact.

Digital errors often have their roots in analog signal integrity problems. To track down the cause of the digital fault, it's often necessary to turn to an oscilloscope, which can display waveform details, edges and noise; can detect and display transients; and can help you precisely measure timing relationships such as setup and hold times. Modern oscilloscopes can help to simplify the troubleshooting process by triggering on specific patterns in parallel or serial data streams and displaying the analog signal that corresponds in time with a specified event.

Understanding each of the systems within your oscilloscope and how to apply them will contribute to the effective application of the oscilloscope to tackle your specific measurement challenge.

03W-8605-5.qxd 12/10/09 10:23 AM Page 7

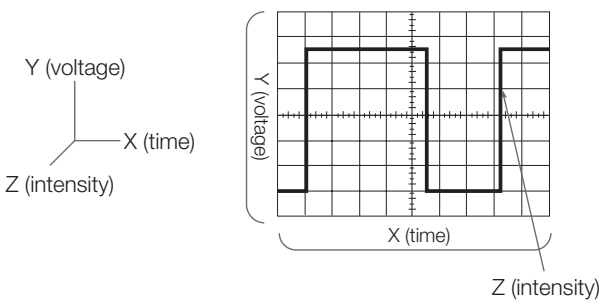

Figure 2. X, Y, and Z components of a displayed waveform.

The Oscilloscope

What is an oscilloscope and how does it work? This section answers these fundamental questions.

The oscilloscope is basically a graph-displaying device – it draws a graph of an electrical signal. In most applications, the graph shows how signals change over time: the vertical (Y) axis represents voltage and the horizontal (X) axis represents time. The intensity or brightness of the display is sometimes called the Z axis, as shown in Figure 2. In DPO oscilloscopes, the Z axis can be represented by color grading of the display, as seen in Figure 3.

This simple graph can tell you many things about a signal, such as:

- The time and voltage values of a signal
- The frequency of an oscillating signal
- The "moving parts" of a circuit represented by the signal
- The frequency with which a particular portion of the signal is occurring relative to other portions
- Whether or not a malfunctioning component is distorting the signal
- How much of a signal is direct current (DC) or alternating current (AC)
- How much of the signal is noise and whether the noise is changing with time

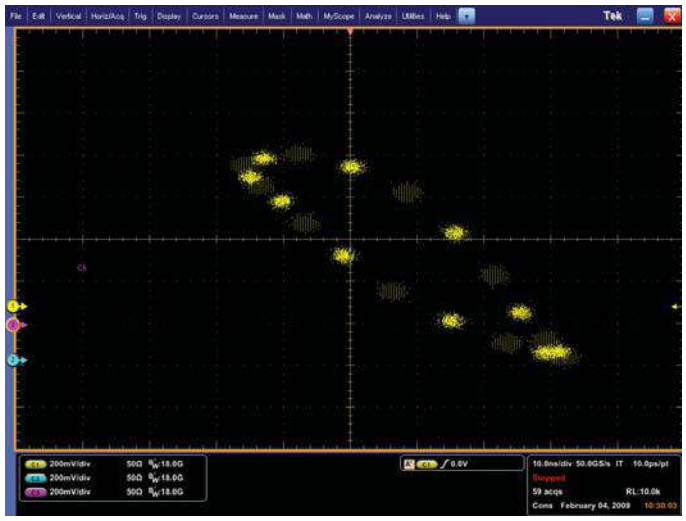

Figure 3. Two offset clock patterns with Z axis intensity grading.

Understanding Waveforms and Waveform Measurements

The generic term for a pattern that repeats over time is a wave – sound waves, brain waves, ocean waves, and voltage waves are all repetitive patterns. An oscilloscope measures voltage waves. Remember as mentioned earlier, that physical phenomena such as vibrations or temperature or electrical phenomena such as current or power can be converted to a voltage by a sensor. One cycle of a wave is the portion of the wave that repeats. A waveform is a graphic representation of a wave. A voltage waveform shows time on the horizontal axis and voltage on the vertical axis.

03W-8605-5.qxd 12/10/09 10:23 AM Page 8

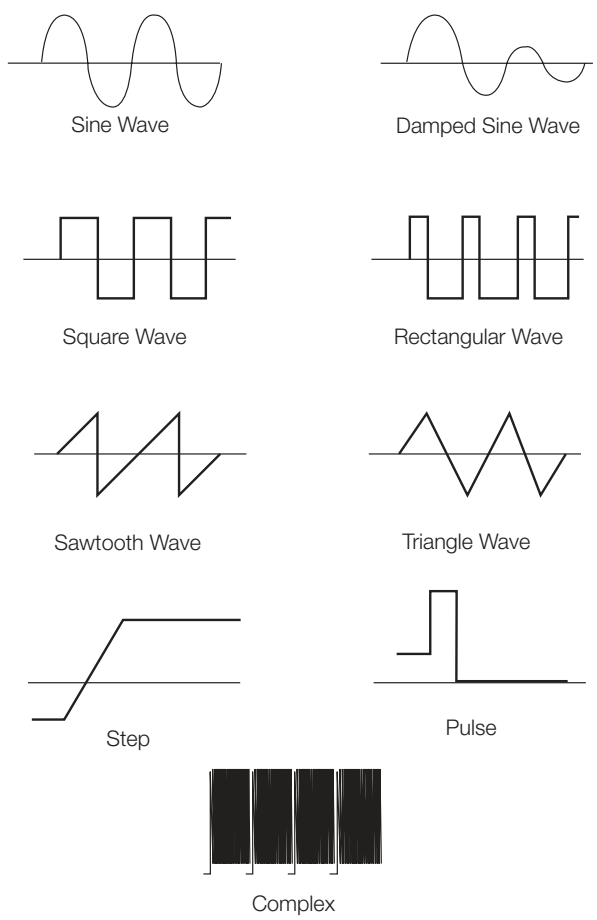

Figure 4. Common waveforms.

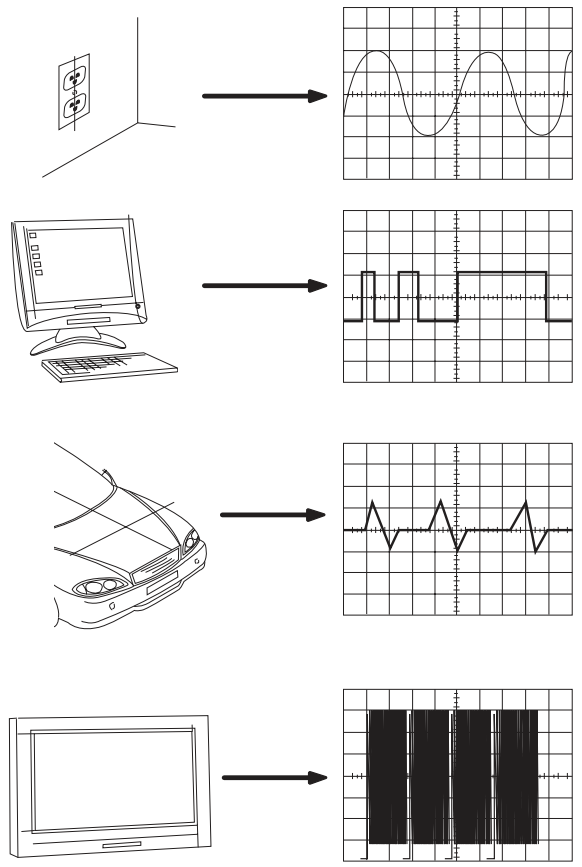

Figure 5. Sources of common waveforms.

Waveform shapes reveal a great deal about a signal. Any time you see a change in the height of the waveform, you know the voltage has changed. Any time there is a flat horizontal line, you know that there is no change for that length of time. Straight, diagonal lines mean a linear change – rise or fall of voltage at a steady rate. Sharp angles on a waveform indicate sudden change. Figure 4 shows common waveforms and Figure 5 displays sources of common waveforms.

Types of Waves

You can classify most waves into these types:

- Sine waves
- Square and rectangular waves
- Sawtooth and triangle waves
- Step and pulse shapes
- Periodic and non-periodic signals
- Synchronous and asynchronous signals
- Complex waves

03W-8605-5.qxd 12/10/09 10:23 AM Page 9

Sine Waves

The sine wave is the fundamental wave shape for several reasons. It has harmonious mathematical properties – it is the same sine shape you may have studied in trigonometry class. The voltage in your wall outlet varies as a sine wave. Test signals produced by the oscillator circuit of a signal generator are often sine waves. Most AC power sources produce sine waves. (AC signifies alternating current, although the voltage alternates too. DC stands for direct current, which means a steady current and voltage, such as a battery produces.)

The damped sine wave is a special case you may see in a circuit that oscillates, but winds down over time.

Square and Rectangular Waves

The square wave is another common wave shape. Basically, a square wave is a voltage that turns on and off (or goes high and low) at regular intervals. It is a standard wave for testing amplifiers – good amplifiers increase the amplitude of a square wave with minimum distortion. Television, radio and computer circuitry often use square waves for timing signals.

The rectangular wave is like the square wave except that the high and low time intervals are not of equal length. It is particularly important when analyzing digital circuitry.

Sawtooth and Triangle Waves

Sawtooth and triangle waves result from circuits designed to control voltages linearly, such as the horizontal sweep of an analog oscilloscope or the raster scan of a television. The transitions between voltage levels of these waves change at a constant rate. These transitions are called ramps.

Step and Pulse Shapes

Signals such as steps and pulses that occur rarely, or non-periodically, are called single-shot or transient signals. A step indicates a sudden change in voltage, similar to the voltage change you would see if you turned on a power switch.

A pulse indicates sudden changes in voltage, similar to the voltage changes you would see if you turned a power switch on and then off again. A pulse might represent one bit of information traveling through a computer circuit or it might be a glitch, or defect, in a circuit. A collection of pulses traveling together creates a pulse train. Digital components in a computer communicate with each other using pulses. These pulses may be in the form of serial data stream or multiple signal lines may be used to represent a value in a parallel data bus. Pulses are also common in x-ray, radar, and communications equipment.

Periodic and Non-periodic Signals

Repetitive signals are referred to as periodic signals, while signals that constantly change are known as non-periodic signals. A still picture is analogous to a periodic signal, while a moving picture can be equated to a non-periodic signal.

Synchronous and Asynchronous Signals

When a timing relationship exists between two signals, those signals are referred to as synchronous. Clock, data and address signals inside a computer are an example of synchronous signals.

Asynchronous is a term used to describe those signals between which no timing relationship exists. Because no time correlation exists between the act of touching a key on a computer keyboard and the clock inside the computer, these are considered asynchronous.

03W-8605-5.qxd 12/10/09 10:24 AM Page 10

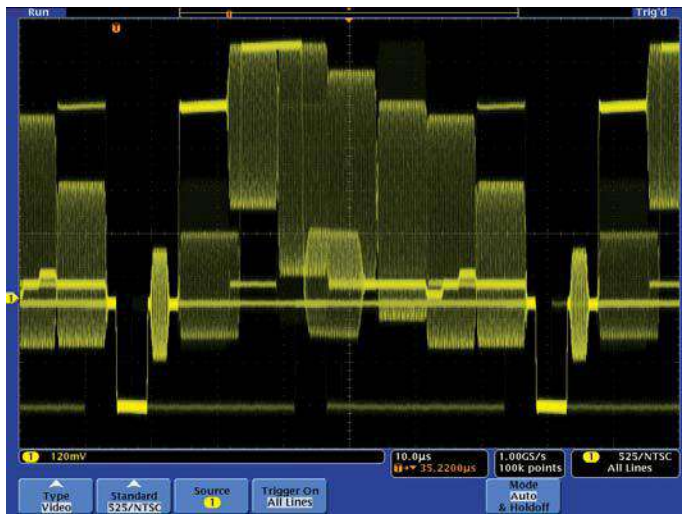

Figure 6. An NTSC composite video signal is an example of a complex wave.

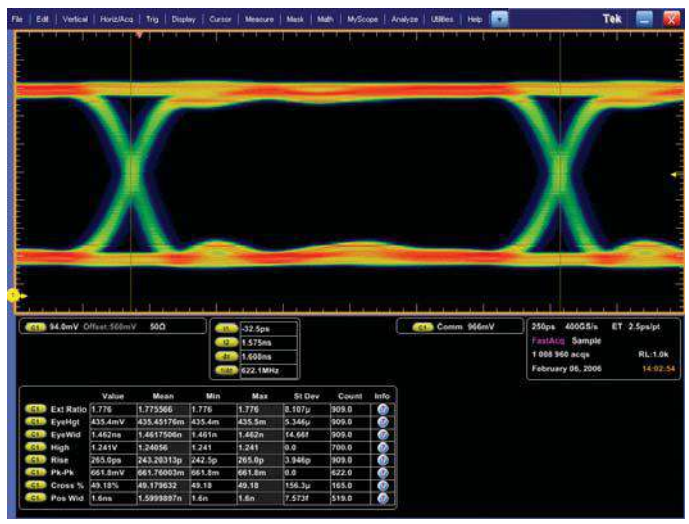

Figure 7. 622 Mb/s serial data eye pattern.

Complex Waves

Some waveforms combine the characteristics of sines, squares, steps, and pulses to produce complex waveshapes. The signal information may be embedded in the form of amplitude, phase, and/or frequency variations. For example, although the signal in Figure 6 is an ordinary composite video signal, it is composed of many cycles of higher-frequency waveforms embedded in a lower-frequency envelope.

In this example, it is usually most important to understand the relative levels and timing relationships of the steps. To view this signal, you need an oscilloscope that captures the low-frequency envelope and blends in the higher-frequency waves in an intensity-graded fashion so that you can see their overall combination as an image that can be visually interpreted. Digital phosphor oscilloscopes are most suited to viewing complex waves, such as video signals, illustrated in Figure 6. Their displays provide the necessary frequency-of-occurrence information, or intensity grading, that is essential to understanding what the waveform is really doing.

Some oscilloscopes allow for displaying certain types of complex waveforms in special ways. For example, telecommunications data may be displayed as an eye pattern or a constellation diagram.

Telecommunications digital data signals can be displayed on an oscilloscope as a special type of waveform referred to as an eye pattern. The name comes from the similarity of the waveform to a series of eyes, as seen in Figure 7. Eye patterns are produced when digital data from a receiver is sampled and applied to the vertical input, while the data rate is used to trigger the horizontal sweep. The eye pattern displays one bit or unit interval of data with all possible edge transitions and states superimposed in one comprehensive view.

A constellation diagram is a representation of a signal modulated by a digital modulation scheme such as quadrature amplitude modulation or phase-shift keying.

03W-8605-5.qxd 12/10/09 10:24 AM Page 11

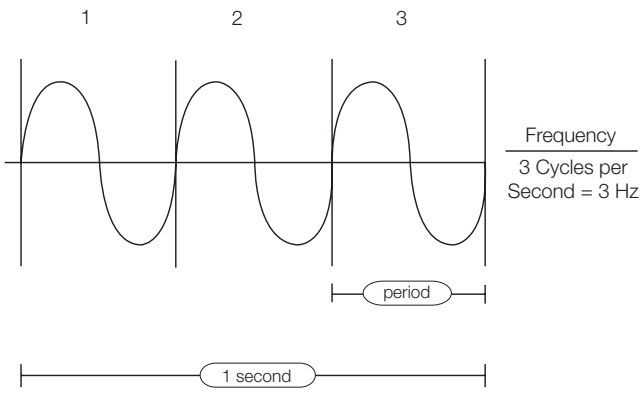

Figure 8. Frequency and period of a sine wave.

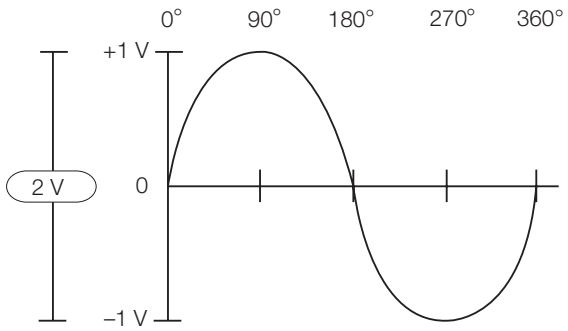

Figure 9. Amplitude and degrees of a sine wave.

Waveform Measurements

Many terms are used to describe the types of measurements that you make with your oscilloscope. This section describes some of the most common measurements and terms.

Frequency and Period

If a signal repeats, it has a frequency. The frequency is measured in Hertz (Hz) and equals the number of times the signal repeats itself in one second, referred to as cycles per second. A repetitive signal also has a period, which is the amount of time it takes the signal to complete one cycle. Period and frequency are reciprocals of each other, so that 1/period equals the frequency and 1/frequency equals the period. For example, the sine wave in Figure 8 has a frequency of 3 Hz and a period of 1/3 second.

Voltage

Voltage is the amount of electric potential, or signal strength, between two points in a circuit. Usually, one of these points is ground, or zero volts, but not always. You may want to measure the voltage from the maximum peak to the minimum peak of a waveform, referred to as the peak-to-peak voltage.

Amplitude

Amplitude refers to the amount of voltage between two points in a circuit. Amplitude commonly refers to the maximum voltage of a signal measured from ground, or zero volts. The waveform shown in Figure 9 has an amplitude of 1 V and a peak-to-peak voltage of 2 V.

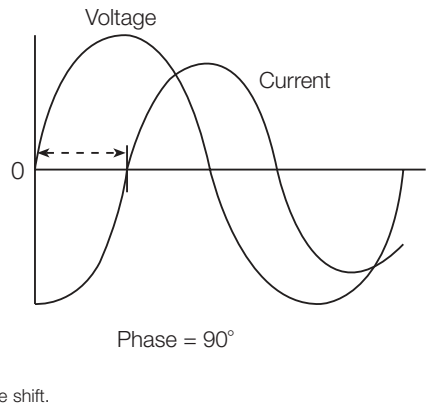

Figure 10. Phase shift.

Phase

Phase is best explained by looking at a sine wave. The voltage level of sine waves is based on circular motion. Given that a circle has 360°, one cycle of a sine wave has 360°, as shown in Figure 9. Using degrees, you can refer to the phase angle of a sine wave when you want to describe how much of the period has elapsed.

Phase shift describes the difference in timing between two otherwise similar signals. The waveform in Figure 10 labeled “current” is said to be 90° out of phase with the waveform labeled “voltage,” since the waves reach similar points in their cycles exactly 1/4 of a cycle apart (360°/4 = 90°). Phase shifts are common in electronics.

03W-8605-5.qxd 12/10/09 10:24 AM Page 12

Waveform Measurements with Digital Oscilloscopes

Modern digital oscilloscopes have functions that make waveform measurements easier. They have front-panel buttons and/or screen-based menus from which you can select fully automated measurements. These include amplitude, period, rise/fall time, and many more. Many digital instruments also provide mean and RMS calculations, duty cycle, and other math operations. Automated measurements appear as on-screen alphanumeric readouts. Typically these readings are more accurate than is possible to obtain with direct graticule interpretation.

Examples of fully automated waveform measurements:

- Period
- Frequency
- Width +
- Width -
- Rise time
- Fall time
- Amplitude
- Extinction ratio
- Mean optical power
- Duty Cycle +
- Duty Cycle -
- Delay
- Phase
- Burst width
- Peak-to-peak
- Mean
- Cycle mean
- Cycle area
- High
- Low
- Minimum
- Maximum
- Overshoot +
- Overshoot -
- RMS
- Cycle RMS
- Jitter

03W-8605-5.qxd 12/10/09 10:24 AM Page 13

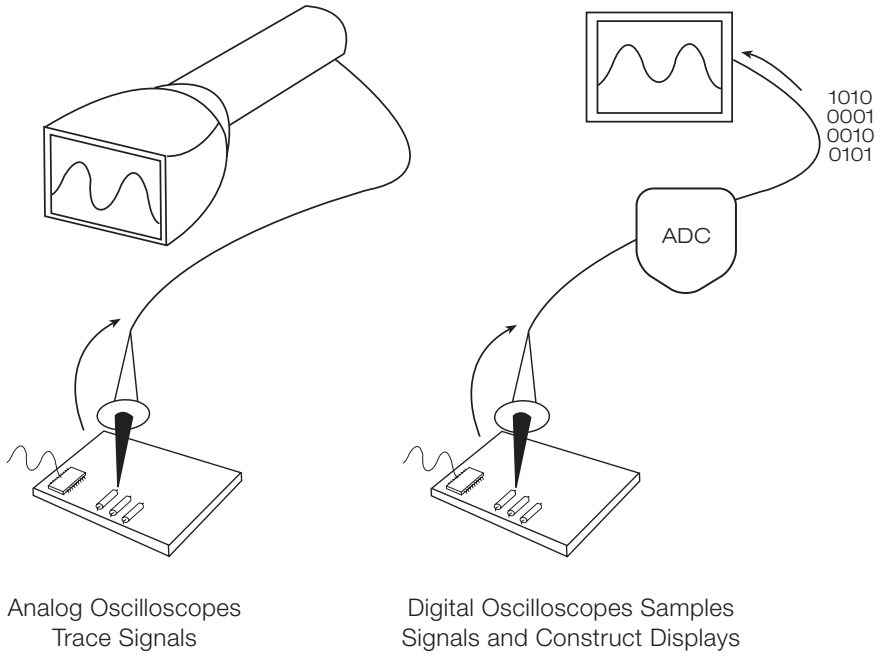

Figure 11. Analog oscilloscopes trace signals, while digital oscilloscopes sample signals and construct displays.

The Types of Oscilloscopes

Electronic equipment can be classified into two categories: analog and digital. Analog equipment works with continuously variable voltages, while digital equipment works with discrete binary numbers that represent voltage samples. A conventional phonograph is an analog device, while a compact disc player is a digital device.

Oscilloscopes can be classified similarly – as analog and digital types. In contrast to an analog oscilloscope, a digital oscilloscope uses an analog-to-digital converter (ADC) to convert the measured voltage into digital information. It acquires the waveform as a series of samples, and stores these samples until it accumulates enough samples to describe a waveform. The digital oscilloscope then re-assembles the waveform for display on the screen, as seen in Figure 11.

Digital oscilloscopes can be classified into digital storage oscilloscopes (DSOs), digital phosphor oscilloscopes (DPOs), mixed signal oscilloscopes (MSOs), and digital sampling oscilloscopes.

The digital approach means that the oscilloscope can display any frequency within its range with stability, brightness, and clarity. For repetitive signals, the bandwidth of the digital oscilloscope is a function of the analog bandwidth of the front-end components of the oscilloscope, commonly referred to as the –3 dB point. For single-shot and transient events, such as pulses and steps, the bandwidth can be limited by the oscilloscope's sample rate. Please refer to the Sample Rate section under Performance Terms and Considerations for a more detailed discussion.

Digital Storage Oscilloscopes

A conventional digital oscilloscope is known as a digital storage oscilloscope (DSO). Its display typically relies on a raster-type screen rather than the luminous phosphor found in an older analog oscilloscope.

Digital storage oscilloscopes (DSOs) allow you to capture and view events that may happen only once – known as transients. Because the waveform information exists in digital form as a series of stored binary values, it can be analyzed, archived, printed, and otherwise processed, within the oscilloscope itself or by an external computer. The waveform need not be continuous; it can be displayed even when the signal disappears. Unlike analog oscilloscopes, digital storage oscilloscopes provide permanent signal storage and extensive waveform processing. However, DSOs typically have no real-time intensity grading; therefore, they cannot express varying levels of intensity in the live signal.

03W-8605-5.qxd 12/10/09 10:24 AM Page 14

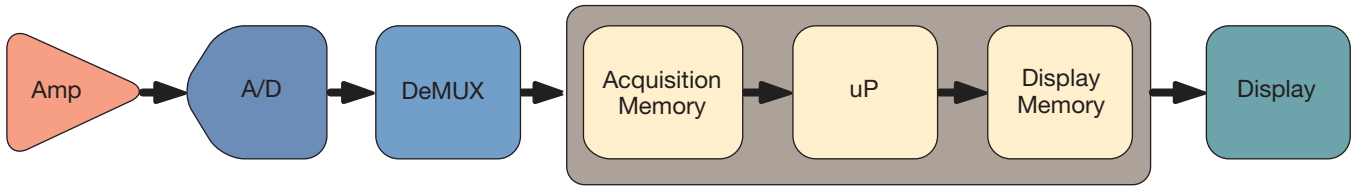

Figure 12. The serial-processing architecture of a digital storage oscilloscope (DSO).

Some of the subsystems that comprise DSOs are similar to those in analog oscilloscopes. However, DSOs contain additional data-processing subsystems that are used to collect and display data for the entire waveform. A DSO employs a serial-processing architecture to capture and display a signal on its screen, as shown in Figure 12. A description of this serial-processing architecture follows.

Serial-processing Architecture

Like an analog oscilloscope, a DSO's first (input) stage is a vertical amplifier. Vertical controls allow you to adjust the amplitude and position range at this stage. Next, the analog-to-digital converter (ADC) in the horizontal system samples the signal at discrete points in time and converts the signal's voltage at these points into digital values called sample points. This process is referred to as digitizing a signal.

The horizontal system's sample clock determines how often the ADC takes a sample. This rate is referred to as the sample rate and is expressed in samples per second (S/s).

The sample points from the ADC are stored in acquisition memory as waveform points. Several sample points may comprise one waveform point. Together, the waveform points comprise one waveform record. The number of waveform points used to create a waveform record is called the record length. The trigger system determines the start and stop points of the record.

The DSO's signal path includes a microprocessor through which the measured signal passes on its way to the display. This microprocessor processes the signal, coordinates display activities, manages the front panel controls, and more. The signal then passes through the display memory and is displayed on the oscilloscope screen.

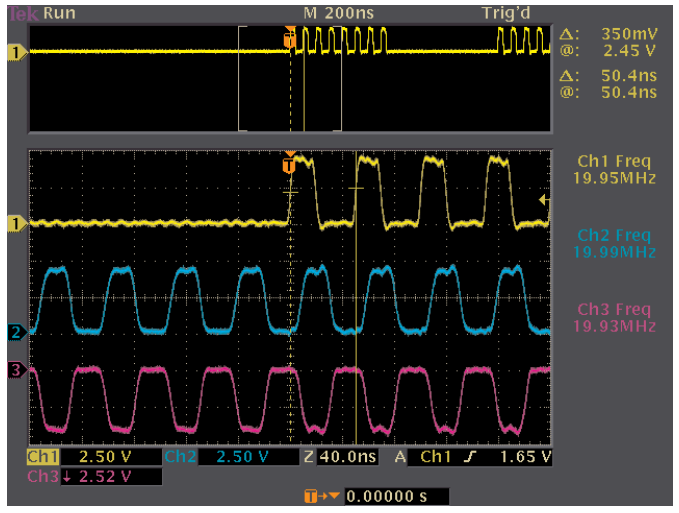

Figure 13. The digital storage oscilloscope delivers high-speed, single-shot acquisition across multiple channels, increasing the likelihood of capturing elusive glitches and transient events.

Depending on the capabilities of your oscilloscope, additional processing of the sample points may take place, which enhances the display. Pre-trigger may also be available, enabling you to see events before the trigger point. Most of today's digital oscilloscopes also provide a selection of automatic parametric measurements, simplifying the measurement process.

As shown in Figure 13, a DSO provides high performance in a single-shot, multi-channel instrument. DSOs are ideal for low-repetition-rate or single-shot, high-speed, multi-channel design applications. In the real world of digital design, an engineer usually examines four or more signals simultaneously, making the DSO a critical companion.

03W-8605-5.qxd 12/10/09 10:24 AM Page 15

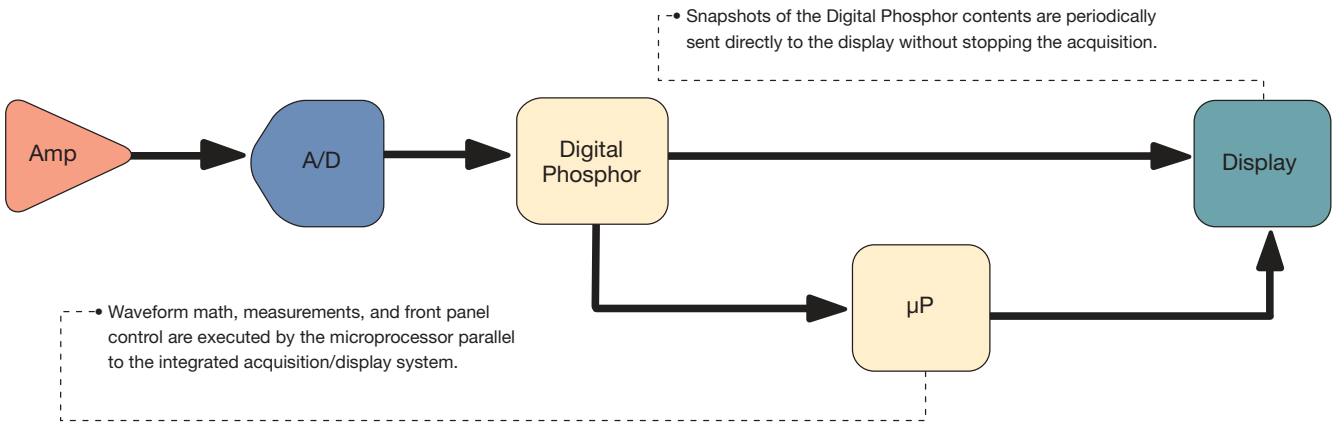

Figure 14. The parallel-processing architecture of a digital phosphor oscilloscope (DPO).

Digital Phosphor Oscilloscopes

The digital phosphor oscilloscope (DPO) offers a new approach to oscilloscope architecture. This architecture enables a DPO to deliver unique acquisition and display capabilities to accurately reconstruct a signal.

While a DSO uses a serial-processing architecture to capture, display and analyze signals, a DPO employs a parallel-processing architecture to perform these functions, as shown in Figure 14. The DPO architecture dedicates unique ASIC hardware to acquire waveform images, delivering high waveform capture rates that result in a higher level of signal visualization. This performance increases the probability of witnessing transient events that occur in digital systems, such as runt pulses, glitches and transition errors, and enables additional analysis capability. A description of this parallel-processing architecture follows.

Parallel-processing Architecture

A DPO's first (input) stage is similar to that of an analog oscilloscope – a vertical amplifier – and its second stage is similar to that of a DSO – an ADC. But, the DPO differs significantly from its predecessors following the analog-to-digital conversion.

For any oscilloscope – analog, DSO or DPO – there is always a holdoff time during which the instrument processes the most recently acquired data, resets the system, and waits for the next trigger event. During this time, the oscilloscope is blind to all signal activity. The probability of seeing an infrequent or low-repetition event decreases as the holdoff time increases.

It should be noted that it is impossible to determine the probability of capture by simply looking at the display update rate. If you rely solely on the update rate, it is easy to make the mistake of believing that the oscilloscope is capturing all pertinent information about the waveform when, in fact, it is not.

The digital storage oscilloscope processes captured waveforms serially. The speed of its microprocessor is a bottleneck in this process because it limits the waveform capture rate.

The DPO rasterizes the digitized waveform data into a digital phosphor database. Every 1/30th of a second – about as fast as the human eye can perceive it – a snapshot of the signal image that is stored in the database is pipelined directly to the display system. This direct rasterization of waveform data, and direct copy to display memory from the database, removes the data-processing bottleneck inherent in other architectures. The result is an enhanced "real-time" and lively display update. Signal details, intermittent events, and dynamic characteristics of the signal are captured in real-time. The DPO's microprocessor works in parallel with this integrated acquisition system for display management, measurement automation and instrument control, so that it does not affect the oscilloscope's acquisition speed.

A DPO faithfully emulates the best display attributes of an analog oscilloscope, displaying the signal in three dimensions: time, amplitude and the distribution of amplitude over time, all in real-time.

03W-8605-5.qxd 12/10/09 10:24 AM Page 16

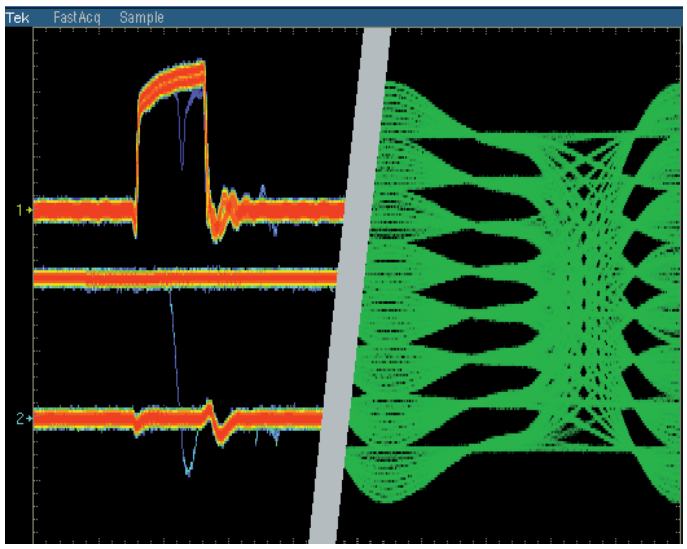

Figure 15. Some DPOs can acquire millions of waveform in just seconds, significantly increasing the probability of capturing intermittent and elusive events and revealing dynamic signal behavior.

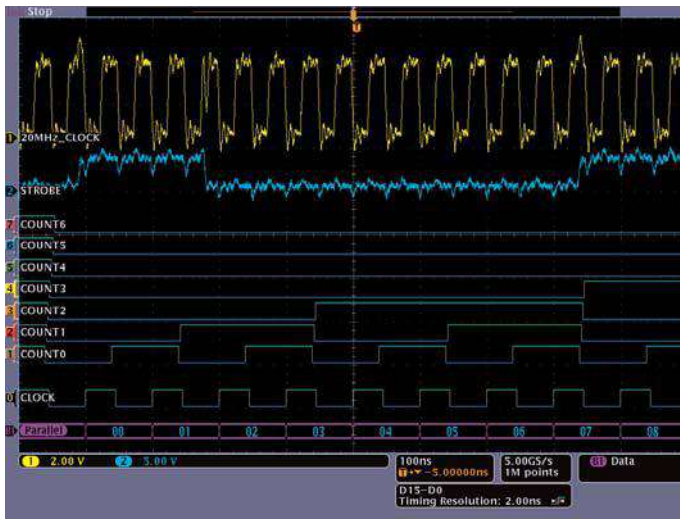

Figure 16. The MSO provides 16 integrated digital channels, enabling the ability to view and analyze time-correlated analog and digital signals.

Unlike an analog oscilloscope's reliance on chemical phosphor, a DPO uses a purely electronic digital phosphor that's actually a continuously updated database. This database has a separate "cell" of information for every single pixel in the oscilloscope's display. Each time a waveform is captured – in other words, every time the oscilloscope triggers – it is mapped into the digital phosphor database's cells. Each cell that represents a screen location and is touched by the waveform is reinforced with intensity information, while other cells are not. Thus, intensity information builds up in cells where the waveform passes most often.

When the digital phosphor database is fed to the oscilloscope's display, the display reveals intensified waveform areas, in proportion to the signal's frequency of occurrence at each point – much like the intensity grading characteristics of an analog oscilloscope. The DPO also allows the display of the varying frequency-of-occurrence information on the display as contrasting colors, unlike an analog oscilloscope. With a DPO, it is easy to see the difference between a waveform that occurs on almost every trigger and one that occurs, say, every 100th trigger.

Digital phosphor oscilloscopes (DPOs) break down the barrier between analog and digital oscilloscope technologies. They are equally suitable for viewing high and low frequencies, repetitive waveforms, transients, and signal variations in real-time. Only a DPO provides the Z (intensity) axis in real-time that is missing from conventional DSOs.

A DPO is ideal for those who need the best general-purpose design and troubleshooting tool for a wide range of applications, as seen in Figure 15. A DPO is exemplary for advanced analysis, communication mask testing, digital debug of intermittent signals, repetitive digital design and timing applications.

Mixed Signal Oscilloscopes

The mixed signal oscilloscope (MSO) combines the performance of a DPO with the basic functionality of a 16-channel logic analyzer, including parallel/serial bus protocol decoding and triggering. The MSO's digital channels view a digital signal as either a logic high or logic low, just like a digital circuit views the signal. This means as long as ringing, overshoot and ground bounce do not cause logic transitions, these analog characteristics are not of concern to the MSO. Just like a logic analyzer, a MSO uses a threshold voltage to determine if the signal is logic high or logic low.

The MSO is the tool of choice for quickly debugging digital circuits using its powerful digital triggering, high resolution acquisition capability, and analysis tools. The root cause of many digital problems is quicker to pinpoint by analyzing both the analog and digital representations of the signal, as shown in Figure 16, making a MSO ideal for verifying and debugging digital circuits.

03W-8605-5.qxd 12/10/09 10:24 AM Page 17

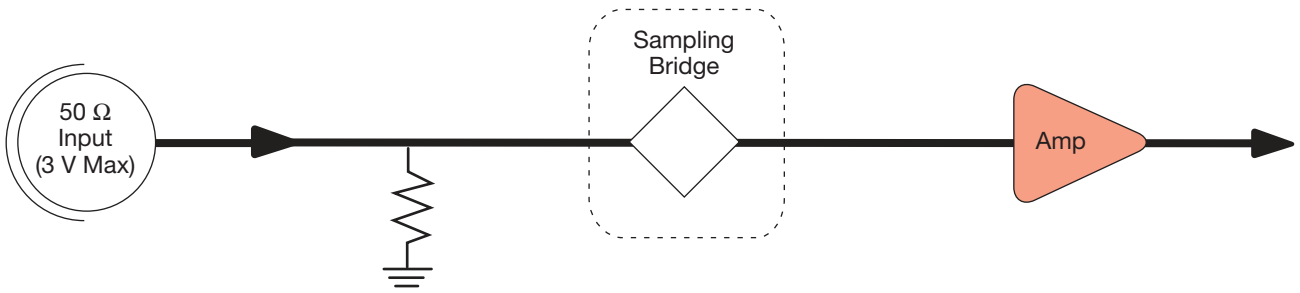

Figure 17. The architecture of a digital sampling oscilloscope.

Digital Sampling Oscilloscopes

In contrast to the digital storage and digital phosphor oscilloscope architectures, the architecture of the digital sampling oscilloscope reverses the position of the attenuator/amplifier and the sampling bridge, as shown in Figure 17. The input signal is sampled before any attenuation or amplification is performed. A low bandwidth amplifier can then be utilized after the sampling bridge because the signal has already been converted to a lower frequency by the sampling gate, resulting in a much higher bandwidth instrument.

The tradeoff for this high bandwidth, however, is that the sampling oscilloscope's dynamic range is limited. Since there is no attenuator/amplifier in front of the sampling gate, there is no facility to scale the input. The sampling bridge must be able to handle the full dynamic range of the input at all times. Therefore, the dynamic range of most sampling oscilloscopes is limited to about 1 V peak-to-peak. Digital storage and digital phosphor oscilloscopes, on the other hand, can handle 50 to 100 volts.

In addition, protection diodes cannot be placed in front of the sampling bridge as this would limit the bandwidth. This reduces the safe input voltage for a sampling oscilloscope to about 3 V, as compared to 500 V available on other oscilloscopes.

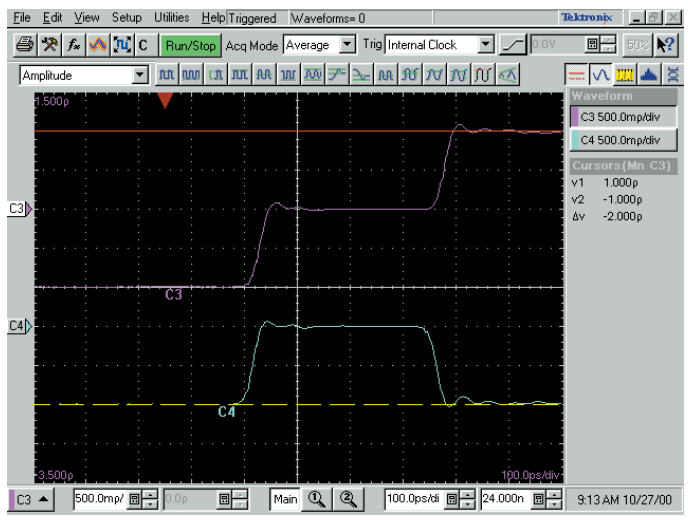

Figure 18. Time domain reflectometry (TDR) display from a digital sampling oscilloscope.

When measuring high-frequency signals, the DSO or DPO may not be able to collect enough samples in one sweep. A digital sampling oscilloscope is an ideal tool for accurately capturing signals whose frequency components are much higher than the oscilloscope's sample rate, as seen in Figure 18. This oscilloscope is capable of measuring signals of up to an order of magnitude faster than any other oscilloscope. It can achieve bandwidth and high-speed timing ten times higher than other oscilloscopes for repetitive signals. Sequential equivalent-time sampling oscilloscopes are available with bandwidths to 80 GHz.

03W-8605-5.qxd 12/10/09 10:24 AM Page 18

The Systems and Controls of an Oscilloscope

This section briefly describes the basic systems and controls found on analog and digital oscilloscopes. Some controls differ between analog and digital oscilloscopes; your oscilloscope probably has additional controls not discussed here.

A basic oscilloscope consists of four different systems – the vertical system, horizontal system, trigger system, and display system. Understanding each of these systems will enable you to effectively apply the oscilloscope to tackle your specific measurement challenges. Recall that each system contributes to the oscilloscope's ability to accurately reconstruct a signal.

The front panel of an oscilloscope is divided into three main sections labeled vertical, horizontal, and trigger. Your oscilloscope may have other sections, depending on the model and type. See if you can locate these front-panel sections in Figure 19, and on your oscilloscope, as you read through this section.

When using an oscilloscope, you need to adjust three basic settings to accommodate an incoming signal:

- Vertical: The attenuation or amplification of the signal. Use the volts/div control to adjust the amplitude of the signal to the desired measurement range.
- Horizontal: The time base. Use the sec/div control to set the amount of time per division represented horizontally across the screen.
- Trigger: The triggering of the oscilloscope. Use the trigger level to stabilize a repeating signal, or to trigger on a single event.

Figure 19. Front-panel control section of an oscilloscope.

Common vertical controls include:

- Termination
  - 1M ohm
  - 50 ohm
- Coupling
  - DC
  - AC
  - GND
- Bandwidth
  - Limit
  - Enhancement
- Position
- Offset
- Invert – On/Off
- Scale
  - Fixed steps
  - Variable

03W-8605-5.qxd 12/10/09 10:24 AM Page 19

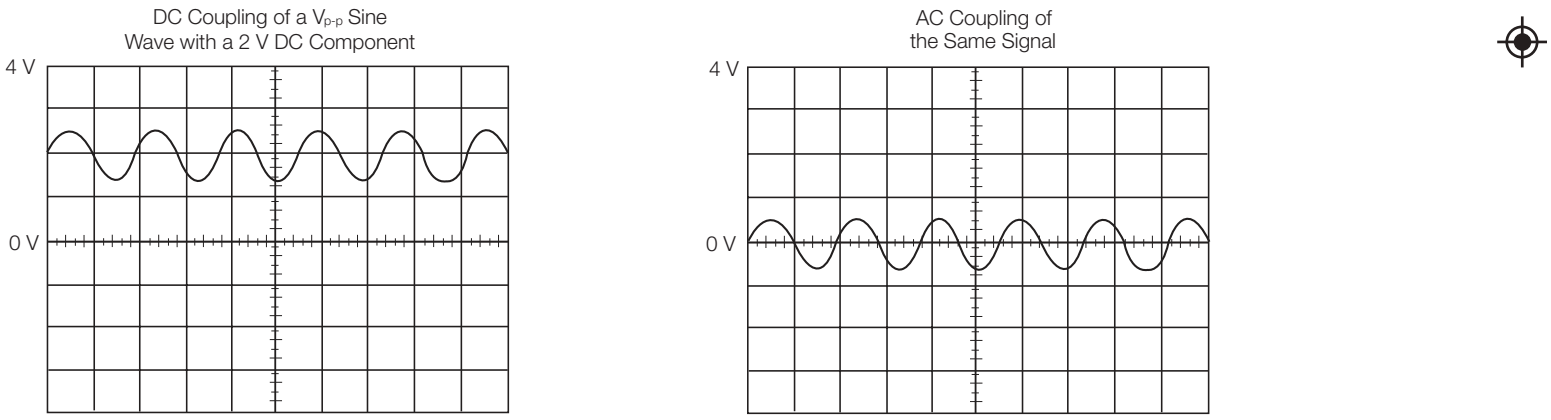

Figure 20. AC and DC input coupling.

Vertical System and Controls

Vertical controls can be used to position and scale the waveform vertically, set the input coupling, and adjust other signal conditioning.

Position and Volts per Division

The vertical position control allows you to move the waveform up and down exactly where you want it on the screen.

The volts-per-division setting (usually written as volts/div) is a scaling factor that varies the size of the waveform on the screen. If the volts/div setting is 5 volts, then each of the eight vertical divisions represents 5 volts and the entire screen can display 40 volts from bottom to top, assuming a graticule with eight major divisions. If the setting is 0.5 volts/div, the screen can display 4 volts from bottom to top, and so on. The maximum voltage you can display on the screen is the volts/div setting multiplied by the number of vertical divisions. Note that the probe you use, 1X or 10X, also influences the scale factor. You must divide the volts/div scale by the attenuation factor of the probe if the oscilloscope does not do it for you.

Often the volts/div scale has either a variable gain or a fine gain control for scaling a displayed signal to a certain number of divisions. Use this control to assist in taking rise time measurements.

Input Coupling

Coupling refers to the method used to connect an electrical signal from one circuit to another. In this case, the input coupling is the connection from your test circuit to the oscilloscope. The coupling can be set to DC, AC, or ground. DC coupling shows all of an input signal. AC coupling blocks the DC component of a signal so that you see the waveform centered around zero volts. Figure 20 illustrates this difference. The AC coupling setting is useful when the entire signal (alternating current + direct current) is too large for the volts/div setting.

The ground setting disconnects the input signal from the vertical system, which lets you see where zero volts is located on the screen. With grounded input coupling and auto trigger mode, you see a horizontal line on the screen that represents zero volts. Switching from DC to ground and back again is a handy way of measuring signal voltage levels with respect to ground.

Bandwidth Limit

Most oscilloscopes have a circuit that limits the bandwidth of the oscilloscope. By limiting the bandwidth, you reduce the noise that sometimes appears on the displayed waveform, resulting in a cleaner signal display. Note that, while eliminating noise, the bandwidth limit can also reduce or eliminate high-frequency signal content.

03W-8605-5.qxd 12/10/09 10:24 AM Page 20

Bandwidth Enhancement

Some oscilloscopes may provide a DSP arbitrary equalization filter which can be used to improve the oscilloscope channel response. This filter extends the bandwidth, flattens the oscilloscope channel frequency response, improves phase linearity, and provides a better match between channels. It also decreases rise time and improves the time domain step response.

Horizontal System and Controls

An oscilloscope's horizontal system is most closely associated with its acquisition of an input signal – sample rate and record length are among the considerations here. Horizontal controls are used to position and scale the waveform horizontally.

Acquisition Controls

Digital oscilloscopes have settings that let you control how the acquisition system processes a signal. Look over the acquisition options on your digital oscilloscope while you read this description. Figure 21 shows you an example of an acquisition menu.

Acquisition Modes

Acquisition modes control how waveform points are produced from sample points. Sample points are the digital values derived directly from the analog-to-digital converter (ADC). The sample interval refers to the time between these sample points. Waveform points are the digital values that are stored in memory and displayed to construct the waveform. The time value difference between waveform points is referred to as the waveform interval.

Common horizontal controls include:

- Time Base
- XY
- Scale
- Trace Separation
- Record Length
- Resolution
- Sample Rate
- Trigger Position
- Zoom/Pan
- Search

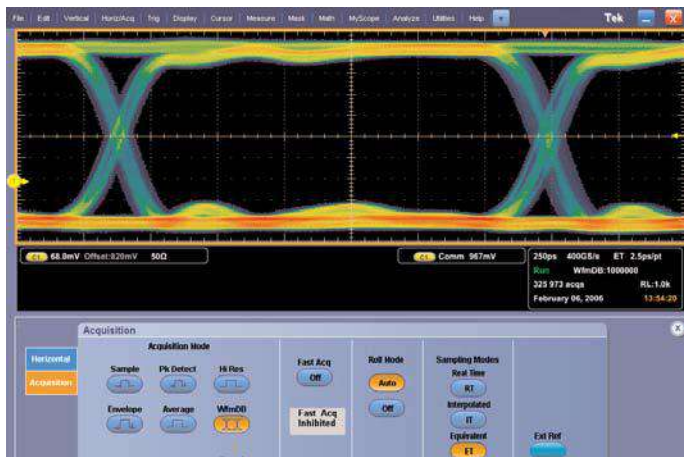

Figure 21. Example of an acquisition menu.

The sample interval and the waveform interval may, or may not, be the same. This fact leads to the existence of several different acquisition modes in which one waveform point is comprised of several sequentially acquired sample points.

Additionally, waveform points can be created from a composite of sample points taken from multiple acquisitions, which provides another set of acquisition modes. A description of the most commonly used acquisition modes follows.

03W-8605-5.qxd 12/10/09 10:24 AM Page 21

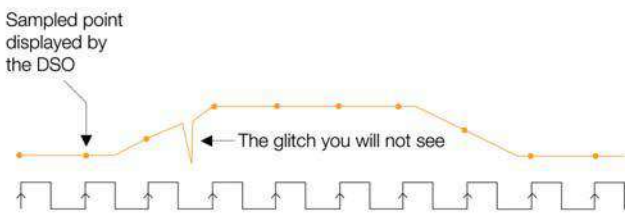

Figure 22. Sample rate varies with time base settings - the slower the time based setting, the slower the sample rate. Some digital oscilloscopes provide peak detect mode to capture fast transients at slow sweep speeds.

Types of Acquisition Modes

- Sample Mode: This is the simplest acquisition mode. The oscilloscope creates a waveform point by saving one sample point during each waveform interval.
- Peak Detect Mode: The oscilloscope saves the minimum and maximum value sample points taken during two waveform intervals and uses these samples as the two corresponding waveform points. Digital oscilloscopes with peak detect mode run the ADC at a fast sample rate, even at very slow time base settings (slow time base settings translate into long waveform intervals) and are able to capture fast signal changes that would occur between the waveform points if in sample mode, as shown in Figure 22. Peak detect mode is particularly useful for seeing narrow pulses spaced far apart in time, as demonstrated in Figure 23.
- Hi-Res Mode: Like peak detect, hi res mode is a way of getting more information in cases when the ADC can sample faster than the time base setting requires. In this case, multiple samples taken within one waveform interval are averaged together to produce one waveform point. The result is a decrease in noise and an improvement in resolution for low-speed signals. The advantage of Hi Res Mode over Average is that Hi-Res Mode can be used even on a single shot event.
- Envelope Mode: Envelope mode is similar to peak detect mode. However, in envelope mode, the minimum and maximum waveform points from multiple acquisitions are combined to form a waveform that shows min/max accumulation over time. Peak detect mode is usually used to acquire the records that are combined to form the envelope waveform.

Figure 23. Peak detect mode enables the oscilloscope to capture extremely brief transient anomalies.

- Average Mode: In average mode, the oscilloscope saves one sample point during each waveform interval as in sample mode. However, waveform points from consecutive acquisitions are then averaged together to produce the final displayed waveform. Average mode reduces noise without loss of bandwidth, but requires a repeating signal.
- Waveform Database Mode: In waveform database mode, the oscillocope accumulates a waveform database that provides a three-dimensional array of amplitude, time, and counts.

Starting and Stopping the Acquisition System

One of the greatest advantages of digital oscilloscopes is their ability to store waveforms for later viewing. To this end, there are usually one or more buttons on the front panel that allow you to start and stop the acquisition system so you can analyze waveforms at your leisure. Additionally, you may want the oscilloscope to automatically stop acquiring after one acquisition is complete or after one set of records has been turned into an envelope or average waveform. This feature is commonly called single sweep or single sequence and its controls are usually found either with the other acquisition controls or with the trigger controls.

03W-8605-5.qxd 12/10/09 10:24 AM Page 22

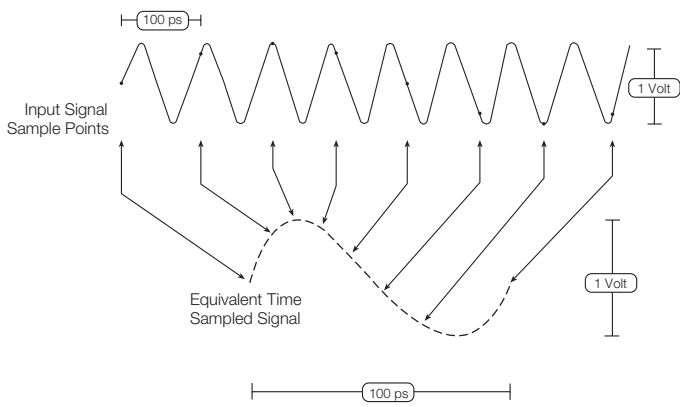

Figure 24. Basic sampling, showing sample points are connected by interpolation to produce a continuous waveform.

Sampling

Sampling is the process of converting a portion of an input signal into a number of discrete electrical values for the purpose of storage, processing and/or display. The magnitude of each sampled point is equal to the amplitude of the input signal at the instant in time in which the signal is sampled.

Sampling is like taking snapshots. Each snapshot corresponds to a specific point in time on the waveform. These snapshots can then be arranged in the appropriate order in time so as to reconstruct the input signal.

In a digital oscilloscope, an array of sampled points is reconstructed on a display with the measured amplitude on the vertical axis and time on the horizontal axis, as illustrated in Figure 24.

The input waveform in Figure 24 appears as a series of dots on the screen. If the dots are widely spaced and difficult to interpret as a waveform, the dots can be connected using a process called interpolation. Interpolation connects the dots with lines, or vectors. A number of interpolation methods are available that can be used to produce an accurate representation of a continuous input signal.

Sampling Controls

Some digital oscilloscopes provide you with a choice in sampling method – either real-time sampling or equivalent-time sampling. The acquisition controls available with these oscilloscopes will allow you to select a sample method to acquire signals. Note that this choice makes no difference for slow time base settings and only has an effect when the ADC cannot sample fast enough to fill the record with waveform points in one pass. Each sampling method has distinct advantages, depending on the kind of measurements being made.

Controls are typically available on modern oscilloscopes to give you the choice of three horizontal time base modes of operations. If you are simply doing signal exploration and want to interact with a lively signal, you will use the Automatic or interactive default mode that provides you with the liveliest display update rate. If you want a precise measurement and the highest real-time sample rate that will give you the most measurement accuracy, then the Constant Sample Rate mode is for you. It will maintain the highest sample rate and provide the best real-time resolution. The last mode is called the Manual mode because it ensures direct and independent control of the sample rate and record length.

Real-time Sampling Method

Real-time sampling is ideal for signals whose frequency range is less than half the oscilloscope's maximum sample rate. Here, the oscilloscope can acquire more than enough points in one "sweep" of the waveform to construct an accurate picture, as shown in Figure 25. Real-time sampling is the only way to capture fast, single-shot, transient signals with a digital oscilloscope.

03W-8605-5.qxd 12/10/09 10:24 AM Page 23

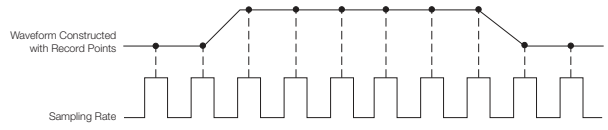

Figure 25. Real-time sampling method.

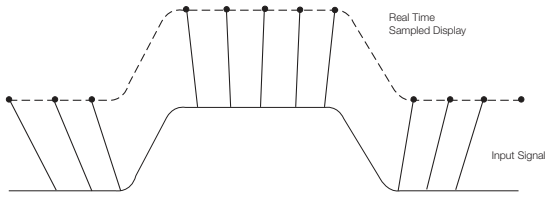

Figure 26. In order to capture this 10 ns pulse in real-time, the sample rate must be high enough to accurately define the edges.

Real-time sampling presents the greatest challenge for digital oscilloscopes because of the sample rate needed to accurately digitize high-frequency transient events, as shown in Figure 26. These events occur only once, and must be sampled in the same time frame that they occur.

If the sample rate isn't fast enough, high-frequency components can "fold down" into a lower frequency, causing aliasing in the display, as demonstrated in Figure 27. In addition, real-time sampling is further complicated by the high-speed memory required to store the waveform once it is digitized. Please refer to the Sample Rate and Record Length sections under Performance Terms and Considerations for additional detail regarding the sample rate and record length needed to accurately characterize high-frequency components.

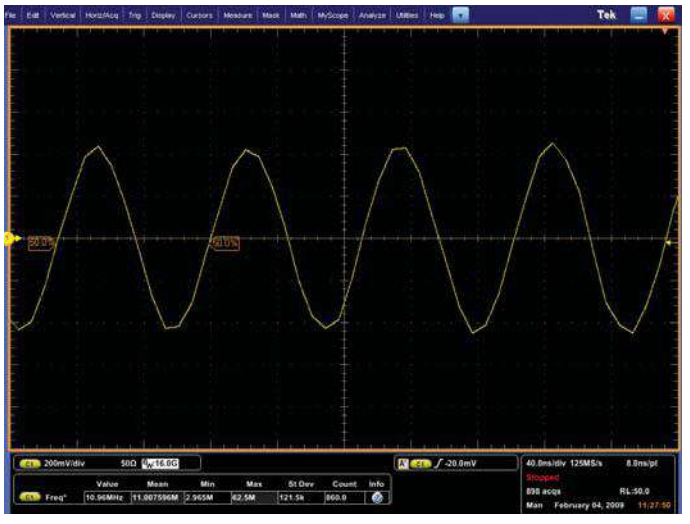

Figure 27. Undersampling of a 100 MHz sine wave introduces aliasing effects.

Real-time sampling with interpolation, dgital oscilloscopes take discrete samples of the signal that can be displayed. However, it can be difficult to visualize the signal represented as dots, especially because there can be only a few dots representing high-frequency portions of the signal. To aid in the visualization of signals, digital oscilloscopes typically have interpolation display modes.

In simple terms, interpolation "connects the dots" so that a signal that is sampled only a few times in each cycle can be accurately displayed. Using real-time sampling with interpolation, the oscilloscope collects a few sample points of the signal in a single pass in real-time mode and uses interpolation to fill in the gaps. Interpolation is a processing technique used to estimate what the waveform looks like based on a few points.

03W-8605-5.qxd 12/10/09 10:24 AM Page 24

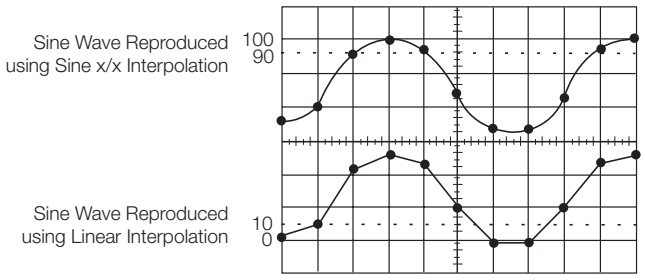

Figure 28. Linear and sin x/x interpolation.

Linear interpolation connects sample points with straight lines. This approach is limited to reconstructing straight-edged signals, as illustrated in Figure 28, which better lends itself to square waves.

The more versatile sin x/x interpolation connects sample points with curves, as shown in Figure 28. Sin x/x interpolation is a mathematical process in which points are calculated to fill in the time between the real samples. This form of interpolation lends itself to curved and irregular signal shapes, which are far more common in the real world than pure square waves and pulses. Consequently, sin x/x interpolation is the preferred method for applications where the sample rate is 3 to 5 times the system bandwidth.

Equivalent-time Sampling Method

When measuring high-frequency signals, the oscilloscope may not be able to collect enough samples in one sweep. Equivalent-time sampling can be used to accurately acquire signals whose frequency exceeds half the oscilloscope's sample rate, as illustrated in Figure 29. Equivalent-time

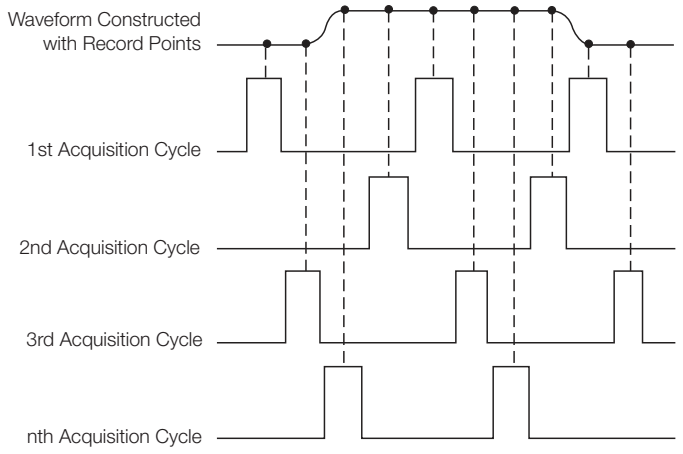

Figure 29. Some oscilloscopes use equivalent-time sampling to capture and display very fast, repetitive signals.

digitizers (samplers) take advantage of the fact that most naturally occurring and man-made events are repetitive. Equivalent-time sampling constructs a picture of a repetitive signal by capturing a little bit of information from each repetition. The waveform slowly builds up like a string of lights, illuminating one-by-one. This allows the oscilloscope to accurately capture signals whose frequency components are much higher than the oscilloscope's sample rate.

There are two types of equivalent-time sampling methods: random and sequential. Each has its advantages. Random equivalent-time sampling allows display of the input signal prior to the trigger point, without the use of a delay line. Sequential equivalent-time sampling provides much greater time resolution and accuracy. Both require that the input signal be repetitive.

03W-8605-5.qxd 12/10/09 10:24 AM Page 25

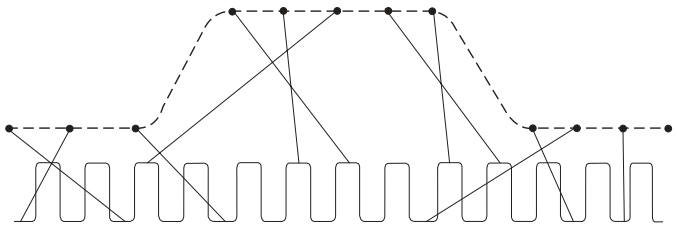

Figure 30. In random equivalent-time sampling, the sampling clock runs asynchronously with the input signal and the trigger.

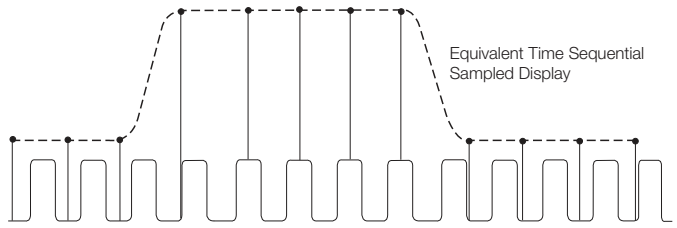

Figure 31. In sequential equivalent-time sampling, the single sample is taken for each recognized trigger after a time delay which is incremented after each cycle.

Random Equivalent-time Sampling

Random equivalent-time digitizers (samplers) utilize an internal clock that runs asynchronously with respect to the input signal and the signal trigger, as illustrated in Figure 30. Samples are taken continuously, independent of the trigger position, and are displayed based on the time difference between the sample and the trigger. Although samples are taken sequentially in time, they are random with respect to the trigger – hence the name “random” equivalent-time sampling. Sample points appear randomly along the waveform when displayed on the oscilloscope screen.

The ability to acquire and display samples prior to the trigger point is the key advantage of this sampling technique, eliminating the need for external pretrigger signals or delay lines. Depending on the sample rate and the time window of the display, random sampling may also allow more than one sample to be acquired per triggered event. However, at faster sweep speeds, the acquisition window narrows until the digitizer cannot sample on every trigger. It is at these faster sweep speeds that very precise timing measurements are often made, and where the extraordinary time resolution of the sequential equivalent-time sampler is most beneficial. The bandwidth limit for random equivalent-time sampling is less than for sequential-time sampling.

Sequential Equivalent-time Sampling

The sequential equivalent-time sampler acquires one sample per trigger, independent of the time/div setting, or sweep speed, as illustrated in Figure 31. When a trigger is detected, a sample is taken after a very short, but well-defined, delay. When the next trigger occurs, a small time increment – delta t – is added to this delay and the digitizer takes another sample. This process is repeated many times, with “delta t” added to each previous acquisition, until the time window is filled. Sample points appear from left to right in sequence along the waveform when displayed on the oscilloscope screen.

Technologically speaking, it is easier to generate a very short, very precise “delta t” than it is to accurately measure the vertical and horizontal positions of a sample relative to the trigger point, as required by random samplers. This precisely measured delay is what gives sequential samplers their unmatched time resolution. Since, with sequential sampling, the sample is taken after the trigger level is detected, the trigger point cannot be displayed without an analog delay line, which may, in turn, reduce the bandwidth of the instrument. If an external pretrigger can be supplied, bandwidth will not be affected.

03W-8605-5.qxd 12/10/09 10:24 AM Page 26

Position and Seconds per Division

The horizontal position control moves the waveform left and right to exactly where you want it on the screen.

The seconds-per-division setting (usually written as sec/div) lets you select the rate at which the waveform is drawn across the screen (also known as the time base setting or sweep speed). This setting is a scale factor. If the setting is 1 ms, each horizontal division represents 1 ms and the total screen width represents 10 ms, or ten divisions. Changing the sec/div setting enables you to look at longer and shorter time intervals of the input signal.

As with the vertical volts/div scale, the horizontal sec/div scale may have variable timing, allowing you to set the horizontal time scale between the discrete settings.

Time Base Selections

Your oscilloscope has a time base, which is usually referred to as the main time base. Many oscilloscopes also have what is called a delayed time base – a time base with a sweep that can start (or be triggered to start) relative to a pre-determined time on the main time base sweep. Using a delayed time base sweep allows you to see events more clearly and to see events that are not visible solely with the main time base sweep.

The delayed time base requires the setting of a time delay and the possible use of delayed trigger modes and other settings not described in this primer. Refer to the manual supplied with your oscilloscope for information on how to use these features.

Zoom/Pan

Your oscilloscope may have special horizontal magnification settings that let you display a magnified section of the waveform on-screen. Some oscilloscopes add pan functions to the zoom capability. Knobs are used to adjust zoom factor or scale and the pan of the zoom box across the waveform.

Search

Some oscilloscopes offer search and mark capabilities, enabling you to quickly navigate through long acquisitions looking for user-defined events.

XY Mode

Most oscilloscopes have an XY mode that lets you display an input signal, rather than the time base, on the horizontal axis. This mode of operation opens up a whole new area of phase shift measurement techniques, explained in the Measurement Techniques section of this primer.

Z Axis

A digital phosphor oscilloscope (DPO) has a high display sample density and an innate ability to capture intensity information. With its intensity axis (Z axis), the DPO is able to provide a three-dimensional, real-time display similar to that of an analog oscilloscope. As you look at the waveform trace on a DPO, you can see brightened areas – the areas where a signal occurs most often. This display makes it easy to distinguish the basic signal shape from a transient that occurs only once in a while – the basic signal would appear much brighter. One application of the Z axis is to feed special timed signals into the separate Z input to create highlighted “marker” dots at known intervals in the waveform.

XYZ Mode with DPO and XYZ Record Display

Some DPOs can use the Z input to create an XY display with intensity grading. In this case, the DPO samples the instantaneous data value at the Z input and uses that value to qualify a specific part of the waveform. Once you have qualified samples, these samples can accumulate, resulting in an intensity-graded XYZ display. XYZ mode is especially useful for displaying the polar patterns commonly used in testing wireless communication devices – a constellation diagram, for example. Another method of displaying XYZ data is XYZ record display. In this mode the data from the acquisition memory is used rather than the DPO database.

03W-8605-5.qxd 12/10/09 10:24 AM Page 27

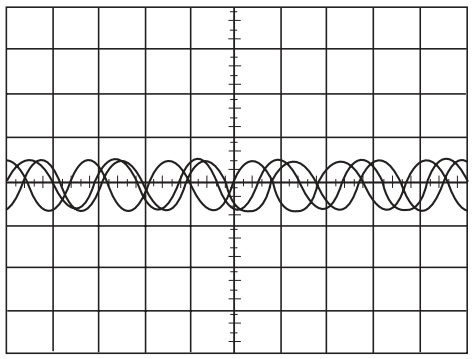

Figure 32. Untriggered display.

Trigger System and Controls

An oscilloscope's trigger function synchronizes the horizontal sweep at the correct point of the signal, essential for clear signal characterization. Trigger controls allow you to stabilize repetitive waveforms and capture single-shot waveforms.

The trigger makes repetitive waveforms appear static on the oscilloscope display by repeatedly displaying the same portion of the input signal. Imagine the jumble on the screen that would result if each sweep started at a different place on the signal, as illustrated in Figure 32.

Edge triggering, available in analog and digital oscilloscopes, is the basic and most common type. In addition to threshold triggering offered by both analog and digital oscilloscopes, many digital oscilloscopes offer numerous specialized trigger settings not offered by analog instruments. These triggers respond to specific conditions in the incoming signal, making it easy to detect, for example, a pulse that is narrower than it should be. Such a condition would be impossible to detect with a voltage threshold trigger alone.

Advanced trigger controls enable you to isolate specific events of interest to optimize the oscilloscope's sample rate and record length. Advanced triggering capabilities in some oscilloscopes give you highly selective control. You can trigger on pulses defined by amplitude (such as runt pulses), qualified by time (pulse width, glitch, slew rate, setup-and-hold, and time-out), and delineated by logic state or pattern (logic triggering).

Other advanced trigger functions include:

- **Pattern Lock Triggering:** Pattern lock triggering adds a new dimension to NRZ serial pattern triggering by enabling the oscilloscope to take synchronized acquisitions of a long serial test pattern with outstanding time base accuracy. Pattern lock triggering can be used to remove random jitter from long serial data patterns. Effects of specific bit transitions can be investigated, and averaging can be used with mask testing.
- **Serial Pattern Triggering:** Serial pattern triggering can be used to debug serial architectures. It provides a trigger on the serial pattern of an NRZ serial data stream with built-in clock recovery and correlates events across the physical and link layer. The instrument can recover the clock signal, identify transitions, and allow you to set the desired encoded words for the serial pattern trigger to capture.
- **A & B Triggering:** Some trigger systems offer multiple trigger types only on a single event (A event), with delayed trigger (B event) selection limited to edge type triggering and often do not provide a way to reset the trigger sequence if the B event doesn't occur. Modern oscilloscopes can provide the full suite of advanced trigger types on both A and B triggers, logic qualification to control when to look for these events, and reset triggering to begin the trigger sequence again after a specified time, state, or transition so that even events in the most complex signals can be captured.
- **Search & Mark Triggering:** Hardware triggers watch for one event type at a time, but Search can scan for multiple event types simultaneously. For example, scan for setup or hold time violations on multiple channels. Individual marks can be placed by Search indicating events that meet search criteria.
- **Trigger Correction:** Since the trigger and data acquisition systems share different paths there is some inherent time delay between the trigger position and the data acquired. This results in skew and trigger jitter. With a trigger correction system the instrument adjusts the trigger position and compensates for the difference of delay there is between the trigger path and the data acquisition path. This will eliminate virtually any trigger jitter at the trigger point. In this mode, the trigger point can be used as a measurement reference.

03W-8605-5.qxd 12/10/09 10:24 AM Page 28

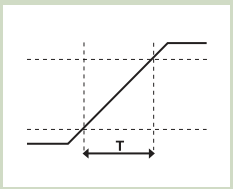

Slew Rate Triggering. High frequency signals with slew rates faster than expected or needed can radiate troublesome energy. Slew rate triggering surpasses conventional edge triggering by adding the element of time and allowing you to selectively trigger on fast or slow edges.

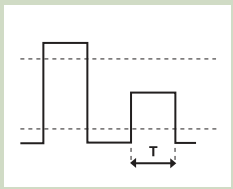

Runt Pulse Triggering. Runt triggering allows you to capture and examine pulses that cross one logic threshold, but not both.

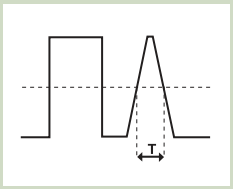

Glitch Triggering. Glitch triggering allows you to trigger on digital pulses when they are shorter or longer than a user-defined time limit. This trigger control enables you to examine the causes of even rare glitches and their effects on other signals

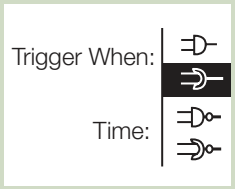

Logic Triggering. Logic triggering allows you to trigger on any logical combination of available input channels – especially useful in verifying the operation of digital logic.

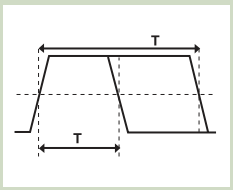

Pulse Width Triggering. Using pulse width triggering, you can monitor a signal indefinitely and trigger on the first occurrence of a pulse whose duration (pulse width) is outside the allowable limits.

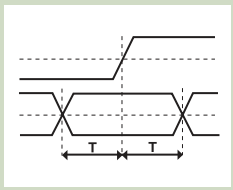

Setup-and-Hold Triggering. Only setup-and-hold triggering lets you deterministically trap a single violation of setup-and-hold time that would almost certainly be missed by using other trigger modes. This trigger mode makes it easy to capture specific signal quality and timing details when a synchronous data signal fails to meet setup-and-hold specifications.

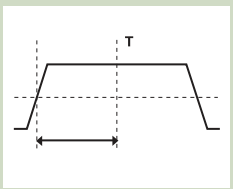

Time-out Triggering. Time-out triggering lets you trigger on an event without waiting for the trigger pulse to end, by triggering based on a specified time lapse.

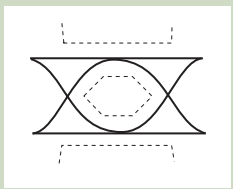

Communication Triggering. Optionally available on certain oscilloscope models, these trigger modes address the need to acquire a wide variety of Alternate-Mark Inversion (AMI), Code-Mark Inversion (CMI), and Non-Return to Zero (NRZ) communication signals.

Figure 33. Common trigger types.

- **Serial Triggering on Specific Standard Signals I²C, CAN, LIN, etc.)** - Some oscilloscopes provide the ability to trigger on specific signal types for standard serial data signals such as CAN, LIN, I²C, SPI, and others. The decode of these signal types is also available on many oscilloscopes today.
- **Parallel Bus Triggering** - Multiple parallel buses can be defined and displayed at one time to easily view decoded parallel bus data over time. By specifying which channels are the clock and data lines, you can create a parallel bus display on some oscilloscopes that automatically decodes bus content. Countless hours can be saved by using parallel bus triggers to simplify capture and analysis.

Optional trigger controls in some oscilloscopes are designed specifically to examine communications signals as well. Figure 33 highlights a few of these common trigger types in more detail. The intuitive user interface available in some oscilloscopes also allows rapid setup of trigger parameters with wide flexibility in the test setup to maximize your productivity.

03W-8605-5.qxd 12/10/09 10:24 AM Page 29

Trigger Position

Horizontal trigger position control is only available on digital oscilloscopes. The trigger position control may be located in the horizontal control section of your oscilloscope. It actually represents the horizontal position of the trigger in the waveform record.

Varying the horizontal trigger position allows you to capture what a signal did before a trigger event, known as pre-trigger viewing. Thus, it determines the length of viewable signal both preceding and following a trigger point.

Digital oscilloscopes can provide pre-trigger viewing because they constantly process the input signal, whether or not a trigger has been received. A steady stream of data flows through the oscilloscope; the trigger merely tells the oscilloscope to save the present data in memory.
In contrast, analog oscilloscopes only display the signal – that is, write it on the CRT – after receiving the trigger. Thus, pre-trigger viewing is not available in analog oscilloscopes, with the exception of a small amount of pre-trigger provided by a delay line in the vertical system.

Pre-trigger viewing is a valuable troubleshooting aid. If a problem occurs intermittently, you can trigger on the problem, record the events that led up to it and, possibly, find the cause.

Trigger Level and Slope

The trigger level and slope controls provide the basic trigger point definition and determine how a waveform is displayed, as illustrated in Figure 34.

The trigger circuit acts as a comparator. You select the slope and voltage level on one input of the comparator. When the trigger signal on the other comparator input matches your settings, the oscilloscope generates a trigger.

The slope control determines whether the trigger point is on the rising or the falling edge of a signal. A rising edge is a positive slope and a falling edge is a negative slope. The level control determines where on the edge the trigger point occurs.

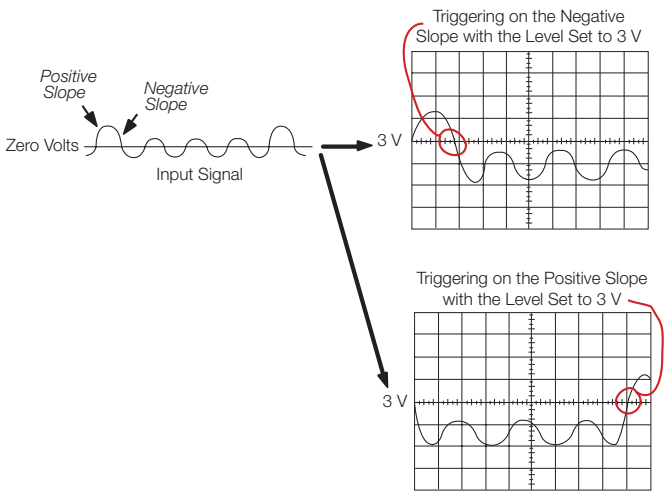

Figure 34. Positive and negative slope triggering.

Trigger Sources

The oscilloscope does not necessarily need to trigger on the signal being displayed. Several sources can trigger the sweep:

- Any input channel
- An external source other than the signal applied to an input channel
- The power source signal
- A signal internally defined by the oscilloscope, from one or more input channels

Most of the time, you can leave the oscilloscope set to trigger on the channel displayed. Some oscilloscopes provide a trigger output that delivers the trigger signal to another instrument.

The oscilloscope can use an alternate trigger source, whether or not it is displayed, so you should be careful not to unwittingly trigger on channel 1 while displaying channel 2, for example.

03W-8605-5.qxd 12/10/09 10:24 AM Page 30

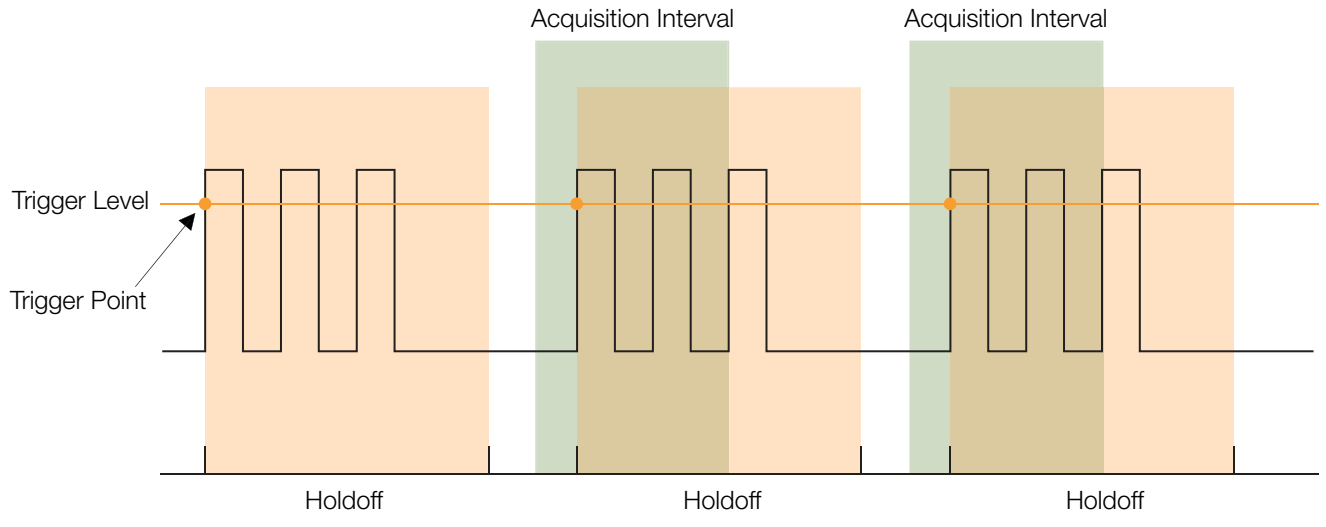

Figure 35. Trigger holdoff.

Trigger Modes

The trigger mode determines whether or not the oscilloscope draws a waveform based on a signal condition. Common trigger modes include normal and auto.

In normal mode the oscilloscope only sweeps if the input signal reaches the set trigger point; otherwise (on an analog oscilloscope) the screen is blank or (on a digital oscilloscope) frozen on the last acquired waveform. Normal mode can be disorienting since you may not see the signal at first if the level control is not adjusted correctly.

Auto mode causes the oscilloscope to sweep, even without a trigger. If no signal is present, a timer in the oscilloscope triggers the sweep. This ensures that the display will not disappear if the signal does not cause a trigger.

In practice, you will probably use both modes: normal mode because it lets you see just the signal of interest, even when triggers occur at a slow rate, and auto mode because it requires less adjustment.

Many oscilloscopes also include special modes for single sweeps, triggering on video signals, or automatically setting the trigger level.

Trigger Coupling

Just as you can select either AC or DC coupling for the vertical system, you can choose the kind of coupling for the trigger signal.

Besides AC and DC coupling, your oscilloscope may also have high frequency rejection, low frequency rejection, and noise rejection trigger coupling. These special settings are useful for eliminating noise from the trigger signal to prevent false triggering.

Trigger Holdoff

Sometimes getting an oscilloscope to trigger on the correct part of a signal requires great skill. Many oscilloscopes have special features to make this task easier.

Trigger holdoff is an adjustable period of time after a valid trigger during which the oscilloscope cannot trigger. This feature is useful when you are triggering on complex waveform shapes, so that the oscilloscope only triggers on an eligible trigger point. Figure 35 shows how using trigger holdoff helps create a usable display.

03W-8605-5.qxd 12/10/09 10:24 AM Page 31

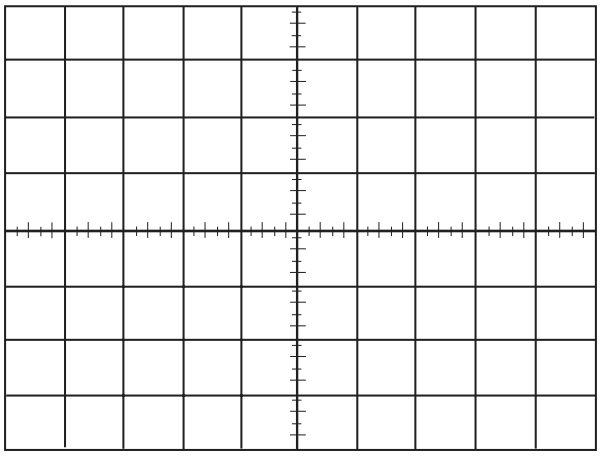

Figure 36. An oscilloscope graticule.

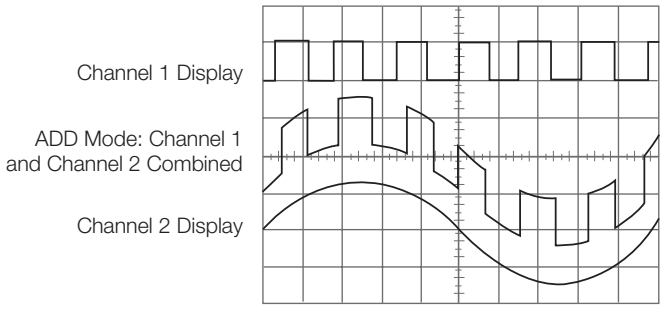

Figure 37. Adding channels.

Display System and Controls

An oscilloscope's front panel includes a display screen and the knobs, buttons, switches, and indicators used to control signal acquisition and display. As mentioned at the front of this section, front-panel controls are usually divided into vertical, horizontal and trigger sections. The front panel also includes input connectors.

Take a look at the oscilloscope display. Notice the grid markings on the screen – these markings create the graticule. Each vertical and horizontal line constitutes a major division. The graticule is usually laid out in an 8-by-10 or 10-by-10 division pattern. Labeling on the oscilloscope controls (such as volts/div and sec/div) always refers to major divisions. The tick marks on the center horizontal and vertical graticule lines, as shown in Figure 36, are called minor divisions. Many oscilloscopes display on the screen how many volts each vertical division represents and how many seconds each horizontal division represents.

Other Oscilloscope Controls

Math and Measurement Operations

Your oscilloscope may also have operations that allow you to add waveforms together, creating a new waveform display. Analog oscilloscopes combine the signals while digital oscilloscopes create new waveforms mathematically. Subtracting waveforms is another math operation. Subtraction with analog oscilloscopes is possible by using the channel invert function on one signal and then using the add operation. Digital oscilloscopes typically have a subtraction operation available. Figure 37 illustrates a third waveform created by combining two different signals.

Using the power of their internal processors, digital oscilloscopes offer many advanced math operations: multiplication, division, integration, Fast Fourier Transform, and more. This advanced signal processing capability can also perform functions such as the insertion of a filter block which can be used de-embed the characteristics of the fixture on the device under test or implement a filter block with desired frequency response such as a low pass filter. The processing block is flexible – not dedicated; it can perform as an arbitrary filter instead, for example for simulation of pre-emphasis/de-emphasis schemes.

Digital Timing and State Acquisitions

Digital channels provided by a mixed signal oscilloscope enable acquisition capabilities similar to those found on logic analyzers. There are two major digital acquisition techniques. The first technique is timing acquisition in which the MSO samples the digital signal at uniformly spaced times determined by the MSO's sample rate. At each sample point, the MSO stores the signal's logic state and creates a timing diagram of the signal. The second digital acquisition technique is state acquisition. State acquisition defines special times that the digital signal's logic state is valid and stable. This is common in synchronous and clocked digital circuits. A clock signal defines the time when the signal state is valid. For example, the input signal stable time is around

03W-8605-5.qxd 12/10/09 10:24 AM Page 32

the rising clock edge for a D-Flip-Flop with rising edge clocking. The output signal stable time is around the falling clock edge for a D-Flip-Flop with rising edge clocking. Since the clock period of a synchronous circuit may not be fixed, the time between state acquisitions may not be uniform as it is in a timing acquisition.

A mixed signal oscilloscope's digital channels acquire signals similar to how a logic analyzer acquires signals in timing acquisition mode. The MSO then decodes the timing acquisition into a clocked bus display, and event table which is similar to the logic analyzer's state acquisition display, providing you with important information during debug.

We have described the basic oscilloscope controls that a beginner needs to know about. Your oscilloscope may have other controls for various functions. Some of these may include:

- Automatic parametric measurements
- Measurement cursors
- Keypads for mathematical operations or data entry
- Printing capabilities
- Interfaces for connecting your oscilloscope to a computer or directly to the Internet

Look over the other options available to you and read your oscilloscope's manual to find out more about these other controls.

The Complete Measurement System

Probes

Even the most advanced instrument can only be as precise as the data that goes into it. A probe functions in conjunction with an oscilloscope as part of the measurement system. Precision measurements start at the probe tip. The right probes matched to the oscilloscope and the device-under-test (DUT) not only allow the signal to be brought to the oscilloscope cleanly, they also amplify and preserve the signal for the greatest signal integrity and measurement accuracy.

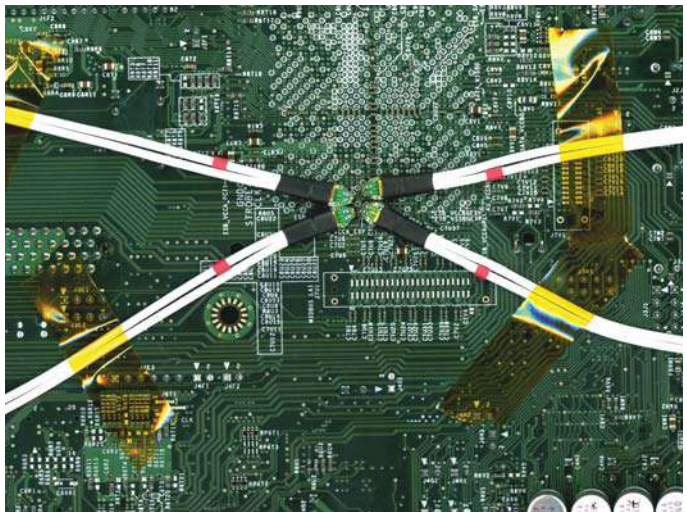

Figure 38. Dense devices and systems require small form factor probes.

To ensure accurate reconstruction of your signal, try to choose a probe that, when paired with your oscilloscope, exceeds the signal bandwidth by 5 times.

Probes actually become part of the circuit, introducing resistive, capacitive and inductive loading that inevitably alters the measurement. For the most accurate results, the goal is to select a probe with minimal loading. An ideal pairing of the probe with the oscilloscope will minimize this loading, and enable you to access all of the power, features and capabilities of your oscilloscope.

Another connectivity consideration is the probe's form factor. Small form factor probes provide easier access to today's densely packed circuitry, as shown in Figure 38.

A brief description of the types of probes follows. Please refer to the Tektronix ABCs of Probes primer for more information about this essential component of the overall measurement system.

03W-8605-5.qxd 12/10/09 10:24 AM Page 33

Figure 39. A typical passive probe with accessories.

Passive Probes

For measuring typical signal and voltage levels, passive probes provide ease-of-use and a wide range of measurement capabilities at an affordable price. The pairing of a passive voltage probe with a current probe will provide you with an ideal solution for measuring power.

Most passive probes have some attenuation factor, such as 10X, 100X, and so on. By convention, attenuation factors, such as for the 10X attenuator probe, have the X after the factor. In contrast, magnification factors like X10 have the X first.

The 10X (read as “ten times”) attenuator probe reduces circuit loading in comparison to a 1X probe and is an excellent general-purpose passive probe. Circuit loading becomes more pronounced for higher frequency and/or higher impedance signal sources, so be sure to analyze these signal/probe loading interactions before selecting a probe. The 10X attenuator probe improves the accuracy of your measurements, but also reduces the signal’s amplitude at the oscilloscope input by a factor of 10.

Because it attenuates the signal, the 10X attenuator probe makes it difficult to look at signals less than 10 millivolts peak-to-peak. The 1X probe is similar to the 10X attenuator probe but lacks the attenuation circuitry. Without this circuitry, more interference is introduced to the circuit being tested.

Use the 10X attenuator probe as your general-purpose probe, but keep the 1X probe accessible to measure slow-speed, low-amplitude signals. Some probes have a convenient feature for switching between 1X and 10X attenuation at the probe tip. If your probe has this feature, make sure you are using the correct setting before taking measurements.

Many oscilloscopes can automatically detect whether you are using a 1X or 10X probe and adjust their screen readouts accordingly. However with some oscilloscopes, you must set the type of probe you are using or read from the proper 1X or 10X marking on the volts/div control.

The 10X attenuator probe works by balancing the probe’s electrical properties against the oscilloscope’s electrical properties. Before using a 10X attenuator probe you need to adjust this balance for your particular oscilloscope. This adjustment is known as compensating the probe and is described in more detail in the Operating the Oscilloscope section of this primer.

Passive probes, such as the one shown in Figure 39, provide excellent general-purpose probing solutions. However, general-purpose passive probes cannot accurately measure signals with extremely fast rise times, and may excessively load sensitive circuits. The steady increase in signal clock rates and edge speeds demands higher speed probes with less loading effects. High-speed active and differential probes provide ideal solutions when measuring high-speed and/or differential signals.

03W-8605-5.qxd 12/10/09 10:24 AM Page 34

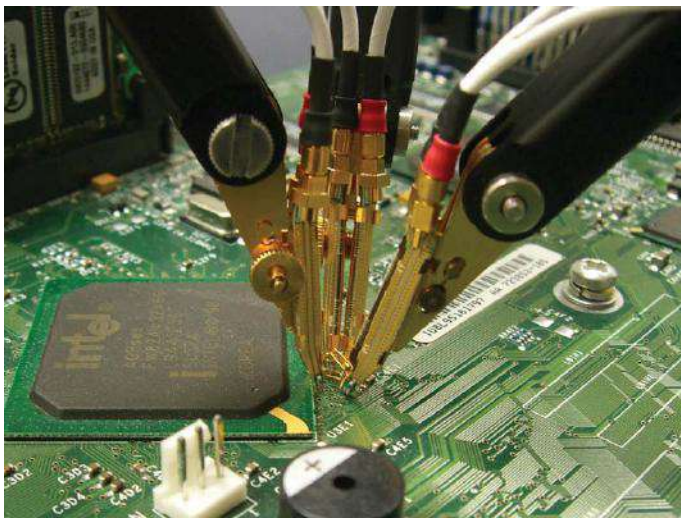

Figure 40. High-performance probes are critical when measuring the fast clocks and edges found in today's computer buses and data transmission lines.

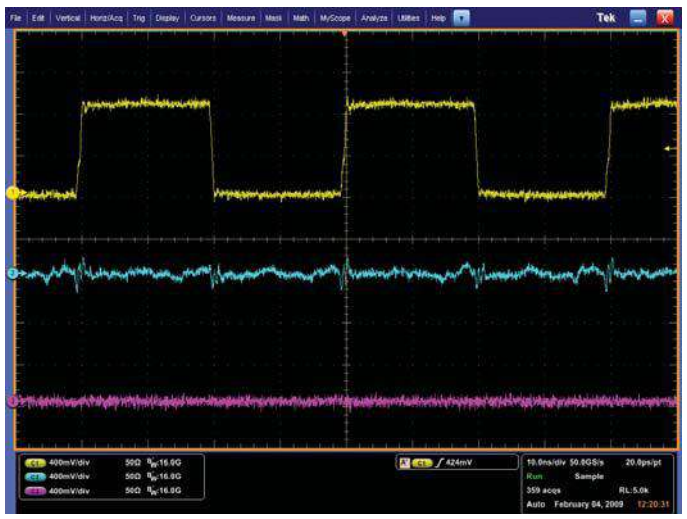

Figure 41 Differential probes can separate common-mode noise from the signal content of interest in today's fast, low-voltage applications - especially important as digital signals continue to fall below typical noise thresholds found in integrated circuits.

Active and Differential Probes

Increasing signal speeds and lower-voltage logic families make accurate measurement results difficult to achieve. Signal fidelity and device loading are critical issues. A complete measurement solution at these high speeds includes high-speed, high-fidelity probing solutions to match the performance of the oscilloscope, as shown in Figure 40.

Active and differential probes use specially developed integrated circuits to preserve the signal during access and transmission to the oscilloscope, ensuring signal integrity. For measuring signals with fast rise times, a high-speed active or differential probe will provide more accurate results, as highlighted in Figure 41.

Newer probe types provide the advantage of being able to use one setup, and get three types of measurements without adjusting probe tip connections. These probes can make differential, single-ended and common mode measurements from the same probe setup.

Logic Probes

The logic probe shown in Figure 42 offers two eight-channel pods. Each channel ends with a probe tip featuring a recessed ground for simplified connection to the device-under-test. The coax on the first channel of each pod is colored blue making it easy to identify. The common ground uses an automotive style connector making it easy to create custom grounds for connecting to the device-under-test. When connecting to square pins, you can use an adapter that attaches to the probe head extending the probe ground flush with the probe tip so you can attach to a header. These probes offer outstanding electrical characteristics with minimal capacitive loading.

Figure 42. Logic probes for a mixed signal oscilloscope (MSO) simplify digital connectivity to your device.

03W-8605-5.qxd 12/10/09 10:24 AM Page 35

Specialty Probes

In addition to the previously mentioned probe types, there are also a variety of other specialty probes and probing systems. These include current, high-voltage, and optical probes, just to name a few.

Probe Accessories

Many modern oscilloscopes provide special automated features built into the input and mating probe connectors. In the case of intelligent probe interfaces, the act of connecting the probe to the instrument notifies the oscilloscope about the probe's attenuation factor, which in turn scales the display so that the probe's attenuation is figured into the readout on the screen. Some probe interfaces also recognize the type of probe – that is, passive, active or current. The interface may act as a DC power source for probes. Active probes have their own amplifier and buffer circuitry that requires DC power.

Ground lead and probe tip accessories are also available to improve signal integrity when measuring high-speed signals. Ground lead adapters provide spacing flexibility between probe tip and ground lead connections to the DUT, while maintaining very short lead lengths from probe tip to DUT.

Please refer to the Tektronix ABCs of Probes primer for more information about probes and probe accessories.

Performance Terms and Considerations

As previously mentioned, an oscilloscope is analogous to a camera that captures signal images that we can observe and interpret. Shutter speed, lighting conditions, aperture and the ASA rating of the film all affect the camera's ability to capture an image clearly and accurately.

Like the basic systems of an oscilloscope, the performance considerations of an oscilloscope significantly affect its ability to achieve the required signal integrity.

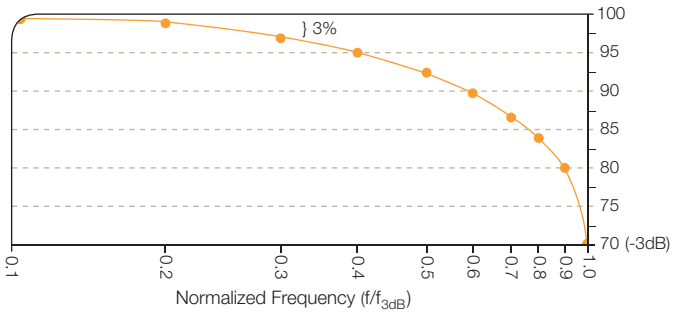

Figure 43. Oscilloscope bandwidth is the frequency at which a sinusoidal input signal is attenuated to 70.7% of the signal's true amplitude, known as the -3 dB point.

Learning a new skill often involves learning a new vocabulary. This idea holds true for learning how to use an oscilloscope. This section describes some useful measurement and oscilloscope performance terms. These terms are used to describe the criteria essential to choosing the right oscilloscope for your application. Understanding these terms will help you to evaluate and compare your oscilloscope with other models.

Bandwidth

Bandwidth determines an oscilloscope's fundamental ability to measure a signal. As signal frequency increases, the capability of the oscilloscope to accurately display the signal decreases. This specification indicates the frequency range that the oscilloscope can accurately measure.

Oscilloscope bandwidth is specified as the frequency at which a sinusoidal input signal is attenuated to 70.7% of the signal's true amplitude, known as the –3 dB point, a term based on a logarithmic scale, as seen in Figure 43.

Without adequate bandwidth, your oscilloscope will not be able to resolve high-frequency changes. Amplitude will be distorted. Edges will vanish. Details will be lost. Without adequate bandwidth, all the features, bells and whistles in your oscilloscope will mean nothing.

To determine the oscilloscope bandwidth needed to accurately characterize signal amplitude in your specific application, apply the "5 Times Rule."

$$\text{Oscilloscope Bandwidth} \geq \begin{matrix}\text{Highest Frequency} \\ \text{Component of Signal}\end{matrix} \; x \; 5$$

03W-8605-5.qxd 12/10/09 10:24 AM Page 36

Figure 44. The higher the bandwidth, the more accurate the reproduction of your signal, as illustrated with a signal captured at 250 MHz, 1 GHz and 4 GHz bandwidth levels.

An oscilloscope selected using the 5 Times Rule will give you less than ±2% error in your measurements – typically sufficient for today's applications. However, as signal speeds increase, it may not be possible to achieve this rule of thumb. Always keep in mind that higher bandwidth will likely provide more accurate reproduction of your signal, as demonstrated in Figure 44.

Some oscilloscopes provide a method of enhancing the bandwidth through digital signal processing. A DSP arbitrary equalization filter can be used to improve the oscilloscope channel response. This filter extends the bandwidth, flattens the oscilloscope's channel frequency response, improves phase linearity, and provides a better match between channels. It also decreases rise time and improves the time-domain step response.

Rise Time

In the digital world, rise time measurements are critical. Rise time may be a more appropriate performance consideration when you expect to measure digital signals, such as pulses and steps. As shown in Figure 45, your oscilloscope must have sufficient rise time to accurately capture the details of rapid transitions.

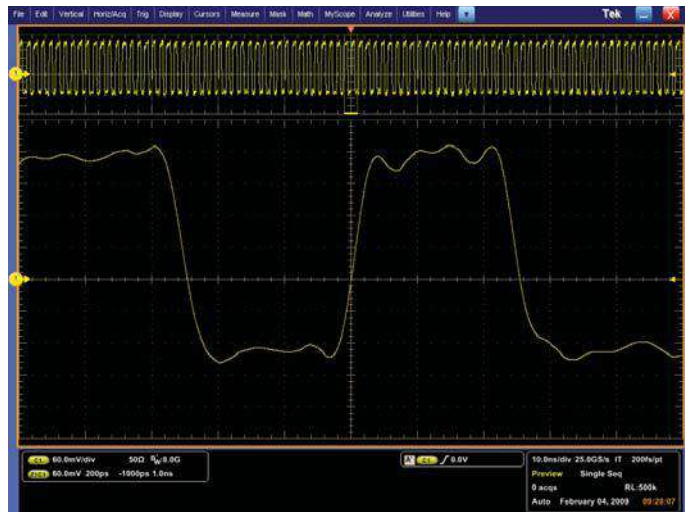

Figure 45. Rise time characterization of a high-speed digital signal.

Rise time describes the useful frequency range of an oscilloscope. To calculate the oscilloscope rise time required for your signal type, use the following equation:

$$\text{Oscilloscope Rise Time} \leq \text{Fastest Rise Time of Signal} \times \frac{1}{5}$$

Note that this basis for oscilloscope rise time selection is similar to that for bandwidth. As in the case of bandwidth, achieving this rule of thumb may not always be possible given the extreme speeds of today's signals. Always remember that an oscilloscope with faster rise time will more accurately capture the critical details of fast transitions.

In some applications, you may know only the rise time of a signal. A constant allows you to relate the bandwidth and rise time of the oscilloscope, using the equation:

$$\text{Bandwidth} = \frac{k}{\text{Rise Time}}$$

where k is a value between 0.35 and 0.45, depending on the shape of the oscilloscope's frequency response curve and pulse rise time response. Oscilloscopes with a bandwidth of <1 GHz typically have a 0.35 value, while oscilloscopes with a bandwidth of > 1 GHz usually have a value between 0.40 and 0.45.

03W-8605-5.qxd 12/10/09 10:24 AM Page 37

Logic Family	Typical Signal Rise Time	Calculated Signal Bandwidth
TTL	2 ns	175 MHz
CMOS	1.5 ns	230 MHz
GTL	1 ns	350 MHz
LVDS	400 ps	875 MHz
ECL	100 ps	3.5 GHz
GaAs	40 ps	8.75 GHz

Figure 46. Some logic families produce inherently faster rise times than others.

Some logic families produce inherently faster rise times than others, as illustrated in Figure 46.

Sample Rate

Sample rate – specified in samples per second (S/s) – refers to how frequently a digital oscilloscope takes a snapshot or sample of the signal, analogous to the frames on a movie camera. The faster an oscilloscope samples (i.e., the higher the sample rate), the greater the resolution and detail of the displayed waveform and the less likely that critical information or events will be lost, as shown in Figure 47. The minimum sample rate may also be important if you need to look at slowly changing signals over longer periods of time. Typically, the displayed sample rate changes with changes made to the horizontal scale control to maintain a constant number of waveform points in the displayed waveform record.

How do you calculate your sample rate requirements? The method differs based on the type of waveform you are measuring, and the method of signal reconstruction used by the oscilloscope.

In order to accurately reconstruct a signal and avoid aliasing, the Nyquist theorem states that the signal must be sampled at least twice as fast as its highest frequency component. This theorem, however, assumes an infinite record length and a continuous signal. Since no oscilloscope offers infinite record length and, by definition, glitches are not continuous,

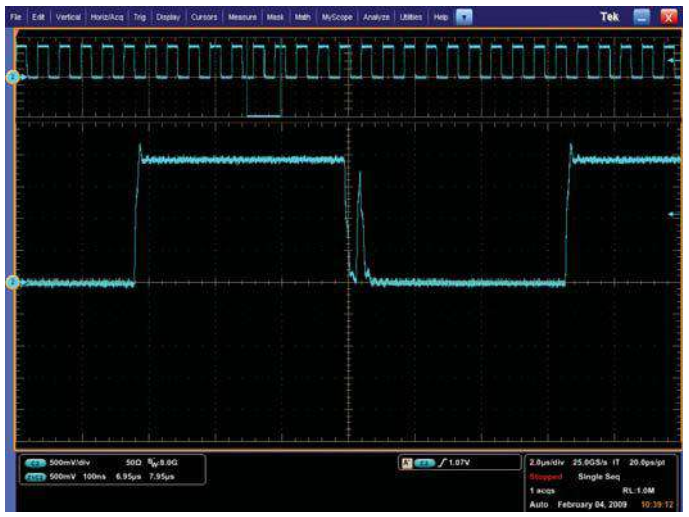

Figure 47. A higher sample rate provides greater signal resolution, ensuring that you'll see intermittent events.

sampling at only twice the rate of highest frequency component is usually insufficient.

In reality, accurate reconstruction of a signal depends on both the sample rate and the interpolation method used to fill in the spaces between the samples. Some oscilloscopes let you select either sin (x)/x interpolation for measuring sinusoidal signals, or linear interpolation for square waves, pulses and other signal types.

For accurate reconstruction using sin(x)/x interpolation, your oscilloscope should have a sample rate at least 2.5 times the highest frequency component of your signal. Using linear interpolation, the sample rate should be at least 10 times the highest frequency signal component.

Some measurement systems with sample rates to 50 GS/s and bandwidths to 20 GHz have been optimized for capturing very fast, single-shot and transient events by oversampling up to 5 times the bandwidth.

03W-8605-5.qxd 12/10/09 10:24 AM Page 38

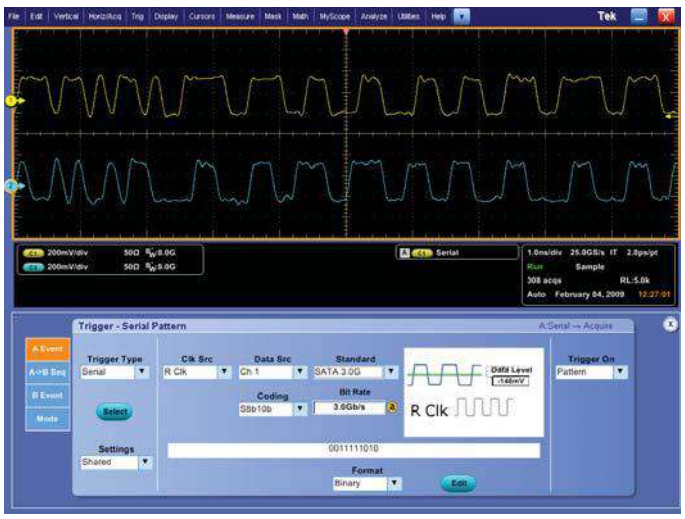

Figure 48. A DPO provides an ideal solution for non-repetitive, high-speed, multi-channel digital design applications.

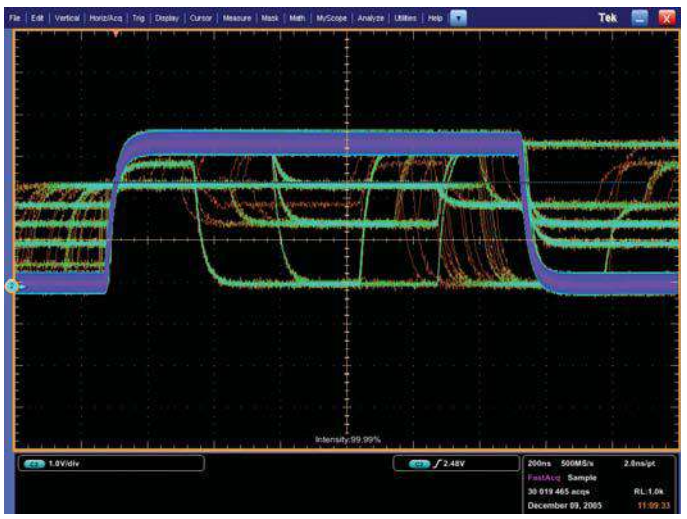

Figure 49. A DPO enables a superior level of insight into signal behavior by delivering vastly greater waveform capture rates and three-dimensional display, making it the best general-purpose design and troubleshooting tool for a wide range of applications.

Waveform Capture Rate

All oscilloscopes blink. That is, they open their eyes a given number of times per second to capture the signal, and close their eyes in between. This is the waveform capture rate, expressed as waveforms per second (wfms/s). While the sample rate indicates how frequently the oscilloscope samples the input signal within one waveform, or cycle, the waveform capture rate refers to how quickly an oscilloscope acquires waveforms.

Waveform capture rates vary greatly, depending on the type and performance level of the oscilloscope. Oscilloscopes with high waveform capture rates provide significantly more visual insight into signal behavior, and dramatically increase the probability that the oscilloscope will quickly capture transient anomalies such as jitter, runt pulses, glitches and transition errors.

Digital storage oscilloscopes (DSOs) employ a serial-processing architecture to capture from 10 to 5,000 wfms/s. Some DSOs provide a special mode that bursts multiple captures into long memory, temporarily delivering higher waveform capture rates followed by long processing dead times that reduce the probability of capturing rare, intermittent events.

Most digital phosphor oscilloscopes (DPOs) employ a parallel-processing architecture to deliver vastly greater waveform capture rates. As seen in Figure 48, some DPOs can acquire millions of waveforms in just seconds, significantly increasing the probability of capturing intermittent and elusive events and allowing you to see the problems in your signal more quickly. Moreover, the DPO's ability to acquire and display three dimensions of signal behavior in real time – amplitude, time and distribution of amplitude over time – results in a superior level of insight into signal behavior, as shown in Figure 49.

Record Length

Record length, expressed as the number of points that comprise a complete waveform record, determines the amount of data that can be captured with each channel. Since an oscilloscope can store only a limited number of samples, the waveform duration (time) will be inversely proportional to the oscilloscope's sample rate.

$$\text{Time Interval} = \frac{\text{Record Length}}{\text{Sample Rate}}$$

03W-8605-5.qxd 12/10/09 10:24 AM Page 39

Modern oscilloscopes allow you to select record length to optimize the level of detail needed for your application. If you are analyzing an extremely stable sinusoidal signal, you may need only a 500 point record length, but if you are isolating the causes of timing anomalies in a complex digital data stream, you may need a million points or more for a given record length, as demonstrated in Figure 50.

Triggering Capabilities

An oscilloscope's trigger function synchronizes the horizontal sweep at the correct point of the signal, essential for clear signal characterization. Trigger controls allow you to stabilize repetitive waveforms and capture single-shot waveforms.

Please refer to the Trigger section under Performance Terms and Considerations for more information regarding triggering capabilities.

Effective Bits

Effective bits represent a measure of a digital oscilloscope's ability to accurately reconstruct a sinewave signal's shape. This measurement compares the oscilloscope's actual error to that of a theoretical "ideal" digitizer. Because the actual errors include noise and distortion, the frequency and amplitude of the signal must be specified.

Frequency Response

Bandwidth alone is not enough to ensure that an oscilloscope can accurately capture a high frequency signal. The goal of oscilloscope design is a specific type of frequency response: Maximally Flat Envelope Delay (MFED). A frequency response of this type delivers excellent pulse fidelity with minimum overshoot and ringing. Since a digital oscilloscope is composed of real amplifiers, attenuators, ADCs, interconnects, and relays, MFED response is a goal that can only be approached. Pulse fidelity varies considerably with model and manufacturer.

Vertical Sensitivity

Vertical sensitivity indicates how much the vertical amplifier can amplify a weak signal – usually measured in millivolts (mV) per division. The smallest voltage detected by a general-purpose oscilloscope is typically about 1 mV per vertical screen division.

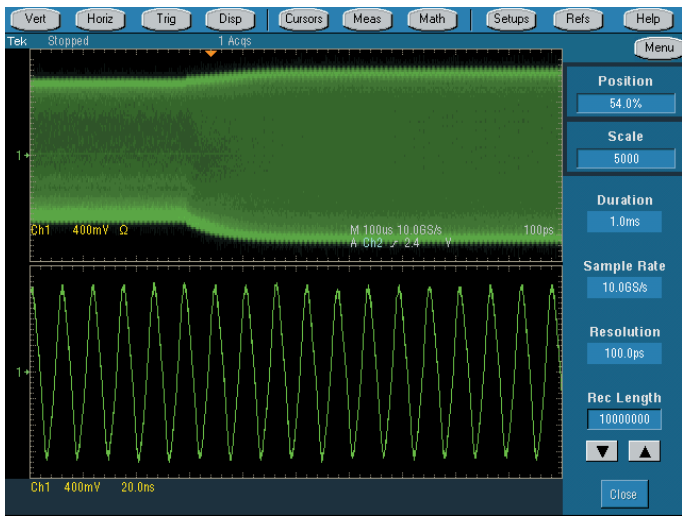

Figure 50. Capturing the high frequency detail of this modulated 85 MHz carrier requires high resolution sampling (100 ps). Seeing the signal's complete modulation envelope requires a long time duration (1 ms). Using long record length (10 MB), the oscilloscope can display both.

Sweep Speed

Sweep speed indicates how fast the trace can sweep across the oscilloscope screen, enabling you to see fine details. The sweep speed of an oscilloscope is represented by time (seconds) per division.

Gain Accuracy

Gain accuracy indicates how accurately the vertical system attenuates or amplifies a signal, usually represented as a percentage error.

Horizontal Accuracy (Time Base)

Horizontal, or time base, accuracy indicates how accurately the horizontal system displays the timing of a signal, usually represented as a percentage error.

Vertical Resolution (Analog-to-Digital Converter)

Vertical resolution of the ADC, and therefore, the digital oscilloscope, indicates how precisely it can convert input voltages into digital values. Vertical resolution is measured in bits. Calculation techniques can improve the effective resolution, as exemplified with hi-res acquisition mode.

03W-8605-5.qxd 12/10/09 10:24 AM Page 40

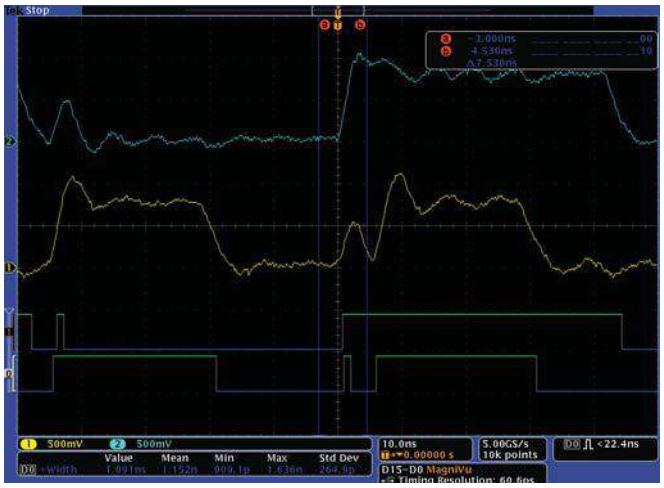

Figure 51. The MSO provides 16 integrated digital channels, enabling the ability to view and analyze time-correlated analog and digital signals. A high speed timing acquisition provides more resolution to reveal narrow events such as glitches.

Timing Resolution (MSO)

An important MSO acquisition specification is the timing resolution used for capturing digital signals. Acquiring a signal with better timing resolution provides a more accurate timing measurement of when the signal changes. For example, a 500 MS/s acquisition rate has 2 ns timing resolution and the acquired signal edge uncertainty is 2 ns. A smaller timing resolution of 60.6 ps (16.5 GS/s) decreases the signal edge uncertainty to 60.6 ps and captures faster changing signals.

Some MSOs internally acquire digital signals with two types of acquisitions at the same time. The first acquisition is with standard timing resolution, and the second acquisition uses a high speed resolution. The standard resolution is used over a longer record length while the high speed timing acquisition offers more resolution around a narrow point of interest, as shown in Figure 51.

Connectivity

The need to analyze measurement results remains of utmost importance. The need to document and share information and measurement results easily and frequently has also grown in importance. The connectivity of an oscilloscope delivers advanced analysis capabilities and simplifies the documentation and sharing of results. As shown in Figure 52, standard interfaces (GPIB, RS-232, USB, Ethernet) and network communication modules enable some oscilloscopes to deliver a vast array of functionality and control.

Figure 52. Today's oscilloscopes provide a wide array of communications interfaces, such as a standard Centronics port and optional Ethernet/RS-232, GPIB/RS-232, and VGA/RS-232 modules. There is even a USB port (not shown) on the front panel.

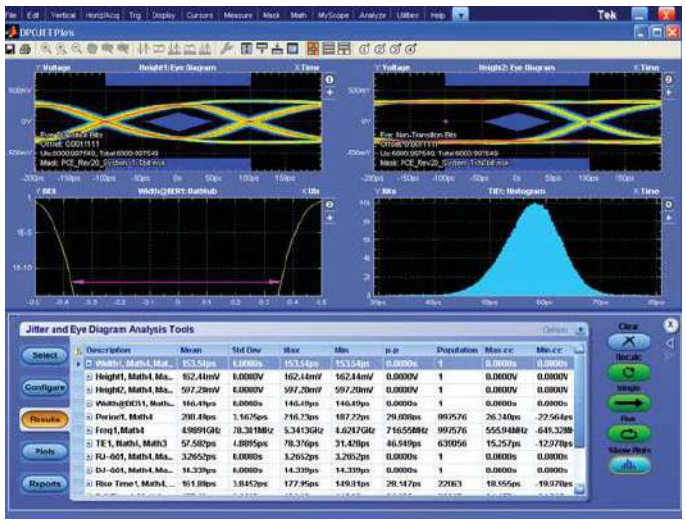

Figure 53. Analysis software packages are specifically designed to meet jitter and eye measurement needs of today's high-speed digital designers.

Some advanced oscilloscopes also let you:

- Create, edit and share documents on the oscilloscope – all while working with the instrument in your particular environment
- Access network printing and file sharing resources
- Access the Windows® desktop
- Run third-party analysis and documentation software
- Link to networks
- Access the Internet
- Send and receive e-mail

Expandability

An oscilloscope should be able to accommodate your needs as they change. Some oscilloscopes allow you to:

03W-8605-5.qxd 12/10/09 10:24 AM Page 41

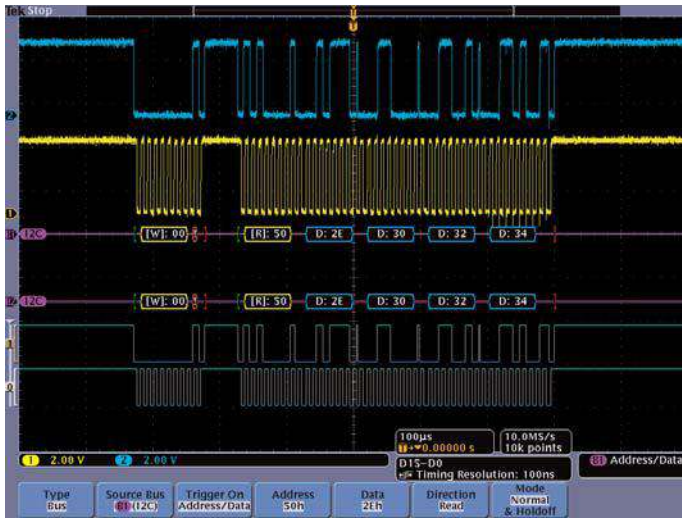

Figure 54. Serial bus analysis is accelerated with automated trigger, decode, and search on serial packet context.

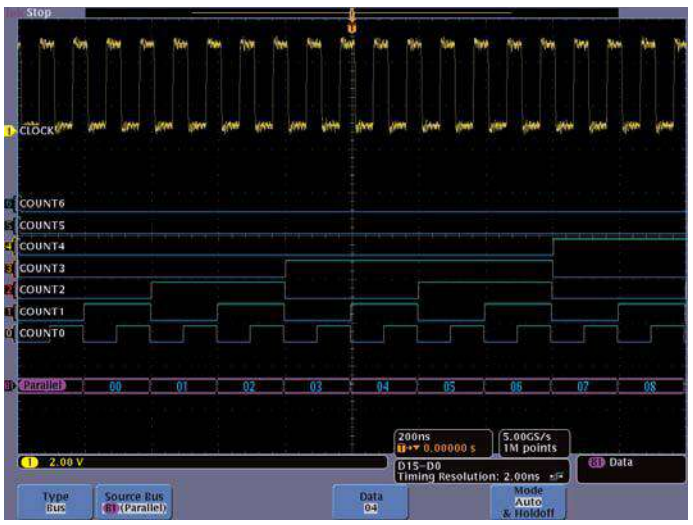

Figure 55. Automatically trigger, decode, and search on clocked or unclocked parallel bus data.

- Add memory to channels to analyze longer record lengths
- Add application-specific measurement capabilities
- Complement the power of the oscilloscope with a full range of probes and modules
- Work with popular third-party analysis and productivity Windows-compatible software
- Add accessories, such as battery packs and rackmounts

Application modules and software may enable you to transform your oscilloscope into a highly specialized analysis tool capable of performing functions such as jitter and timing analysis, microprocessor memory system verification, communications standards testing, disk drive measurements, video measurements, power measurements and much more. Figures 53 - 58 highlight a few of these examples.

Figure 56. Advanced DDR analysis tools automate complex memory tasks like separating read/write bursts and performing JEDEC measurements.

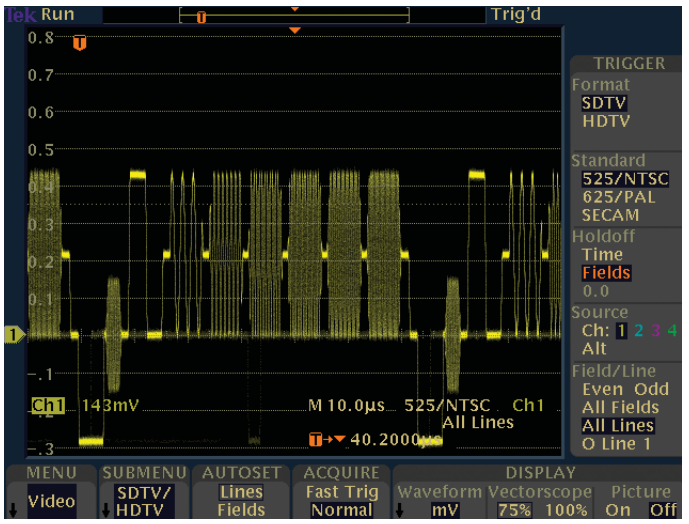

Figure 57. Video application modules make the oscilloscope a fast, tell-all tool for video troubleshooting.

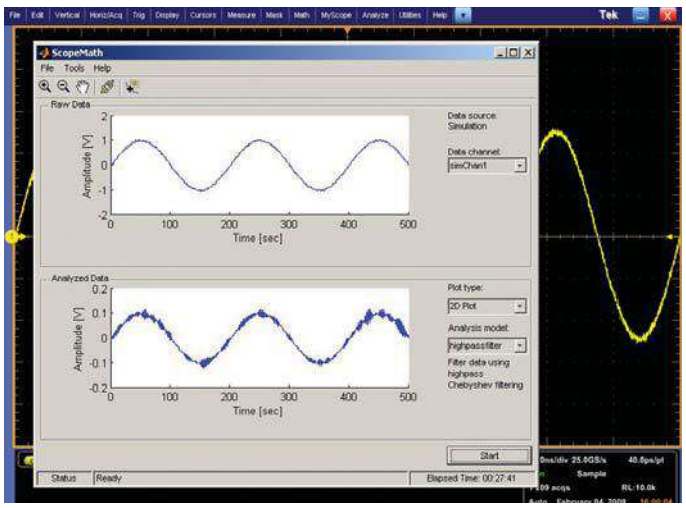

Figure 58. Advanced analysis and productivity software, such as MATLAB®, can be installed in Windows-based oscilloscopes to accomplish local signal analysis.

03W-8605-5.qxd 12/10/09 10:24 AM Page 42

Figure 59. Traditional, analog-style knobs control position, scale, intensity, etc. – precisely as you would expect.

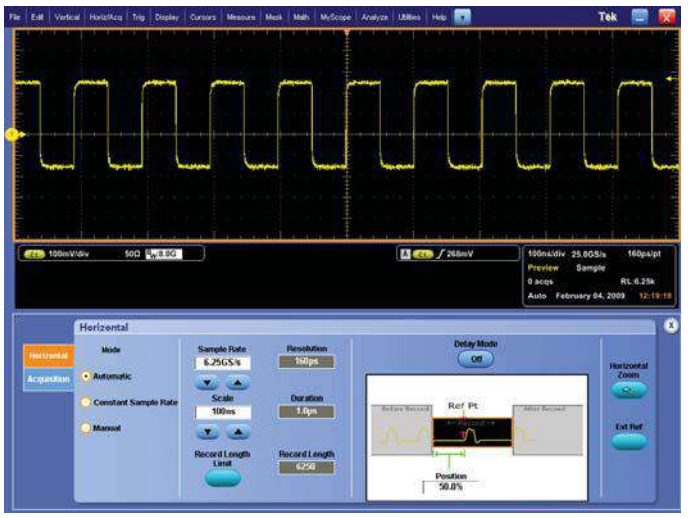

Figure 60. Use graphical control windows to access even the most sophisiticated functions with confidence and ease.

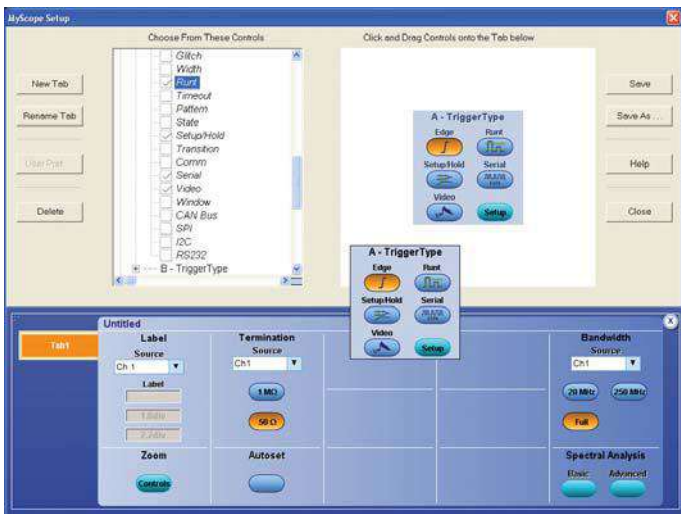

Figure 61. Touch-sensitive display naturally solves issues with cluttered benches and carts, while providing access to clear, on-screen buttons.

Ease-of-Use

Oscilloscopes should be easy to learn and easy to use, helping you work at peak efficiency and productivity. Allowing you to focus on your design, rather than the measurement tools. Just as there is no one typical car driver, there is no one typical oscilloscope user. Regardless of whether you prefer a traditional instrument interface, or that of a Windows® interface, it is important to have flexibility in your oscilloscope's operation.

Many oscilloscopes offer a balance between performance and simplicity by providing the user with many ways to operate the instrument. A front-panel layout, in Figure 59, provides dedicated vertical, horizontal and trigger controls. An icon-rich graphical user interface, as shown in Figure 60, helps you understand and intuitively use advanced capabilities. Touch-sensitive displays solve issues with cluttered benches and carts, while providing access to clear, on-screen buttons, as seen in Figure 61. Online help provides a convenient, built-in reference manual. Intuitive controls allow even occasional oscilloscope users to feel as comfortable driving the oscilloscope as they do driving a car, while giving full-time users easy access to the oscilloscope's most advanced features. In addition, many oscilloscopes are portable, such as the one shown in Figure 62, making the oscilloscope efficient in many different operating environments – in the lab or in the field.

03W-8605-5.qxd 12/10/09 10:24 AM Page 43

Figure 62. The portability of many oscilloscopes makes the instrument efficient in many operating environments.

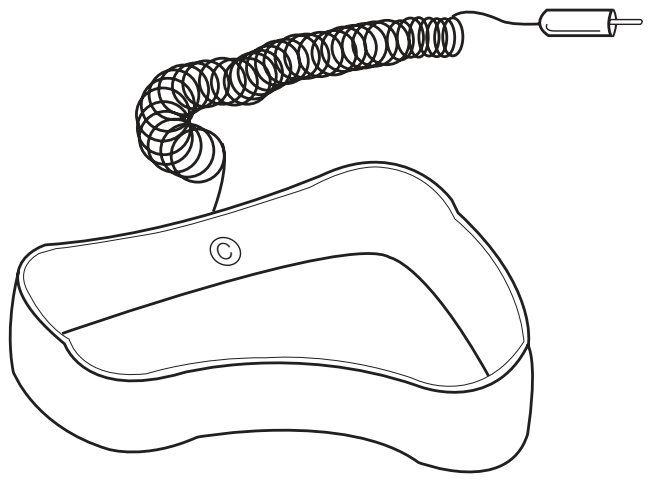

Figure 63. Typical wrist-type grounding strap.

Operating the Oscilloscope

This section briefly describes how to set up and start using an oscilloscope – specifically, how to properly ground the oscilloscope and yourself, set the oscilloscope controls, calibrate the oscilloscope, connect the probes, and compensate the probes.

Proper grounding is an important step when setting up to take measurements or work on a circuit. Proper grounding of the oscilloscope protects you from a hazardous shock and grounding yourself protects your circuits from damage.

Proper Grounding

To ground the oscilloscope means to connect it to an electrically neutral reference point, such as earth ground. Ground your oscilloscope by plugging its three-pronged power cord into an outlet grounded to earth ground.

Grounding the oscilloscope is necessary for safety. If a high voltage contacts the case of an ungrounded oscilloscope – any part of the case, including knobs that appear insulated – it can give you a shock. However, with a properly grounded oscilloscope, the current travels through the grounding path to earth ground rather than through you to earth ground.

Grounding is also necessary for taking accurate measurements with your oscilloscope. The oscilloscope needs to share the same ground as any circuits you are testing.

Some oscilloscopes do not require separate connection to earth ground. These oscilloscopes have insulated cases and controls, which keeps any possible shock hazard away from the user.

If you are working with integrated circuits (ICs), you also need to ground yourself. Integrated circuits have tiny conduction paths that can be damaged by static electricity that builds up on your body. You can ruin an expensive IC simply by walking across a carpet or taking off a sweater and then touching the leads of the IC. To solve this problem, wear a grounding strap, as shows in Figure 63. This strap safely sends static charges on your body to earth ground.

Setting the Controls

After plugging in the oscilloscope, take a look at the front panel. As described previously, the front panel is typically divided into three main sections labeled vertical, horizontal, and trigger. Your oscilloscope may have other sections, depending on the model and type.

Notice the input connectors on your oscilloscope – this is where you attach the probes. Most oscilloscopes have at least two input channels and each channel can display a

03W-8605-5.qxd 12/10/09 10:24 AM Page 44

waveform on the screen. Multiple channels are useful for comparing waveforms. As mentioned earlier, MSOs also have digital inputs as well.

Some oscilloscopes have AUTOSET and/or DEFAULT buttons that can set up the controls in one step to accommodate a signal. If your oscilloscope does not have this capability, it is helpful to set the controls to standard positions before taking measurements.

General instructions to manually set up the oscilloscope in standard positions are as follows:

- Set the oscilloscope to display channel 1
- Set the vertical volts/division scale and position controls to mid–range positions
- Turn off the variable volts/division
- Turn off all magnification settings
- Set the channel 1 input coupling to DC
- Set the trigger mode to auto
- Set the trigger source to channel 1
- Turn trigger holdoff to minimum or off
- Set the horizontal time/division and position controls to mid-range positions
- Adjust channel 1 volts/division such that the signal occupies as much of the 10 vertical divisions as possible without clipping or signal distortion

Calibrating the Instrument

In addition to proper oscilloscope setup, periodic instrument self-calibration is recommended for accurate measurements. Calibration is needed if the ambient temperature has changed more than 5° C (9° F) since the last self-calibration or once a week. In the oscilloscope menu this can sometimes be initiated as “Signal Path Compensation”. Refer to the manual that accompanied your oscilloscope for more detailed instructions.

Connecting the Probes

Now you are ready to connect a probe to your oscilloscope. A probe, if well-matched to the oscilloscope, will enable you to access all of the power and performance in the oscilloscope and will ensure the integrity of the signal you are measuring.

Measuring a signal requires two connections: the probe tip connection and the ground connection. Probes often come with a clip attachment for grounding the probe to the circuit under test. In practice, you attach the grounding clip to a known ground in the circuit, such as the metal chassis of a product you are repairing, and touch the probe tip to a test point in the circuit

Compensating the Probes

Passive attenuation voltage probes must be compensated to the oscilloscope. Before using a passive probe, you need to compensate it – to balance its electrical properties to a particular oscilloscope.

You should get into the habit of compensating the probe every time you set up your oscilloscope. A poorly adjusted probe can make your measurements less accurate. Figure 64 illustrates the effects on a 1 MHz test signal when using a probe that is not properly compensated.

Most oscilloscopes have a square wave reference signal available at a terminal on the front panel used to compensate the probe. General instructions to compensate the probe are as follows:

- Attach the probe to a vertical channel
- Connect the probe tip to the probe compensation, i.e. square wave reference signal
- Attach the ground clip of the probe to ground
- View the square wave reference signal
- Make the proper adjustments on the probe so that the corners of the square wave are square

03W-8605-5.qxd 12/10/09 10:24 AM Page 45

Probe Undercompensated.

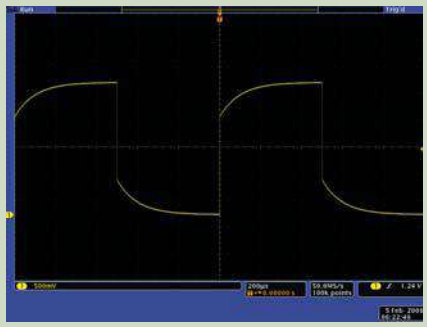

Probe Adjustment Signal

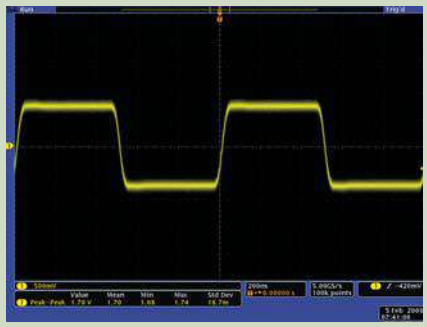

Note Reduced Amplitude

Probe Compensated Correctly.

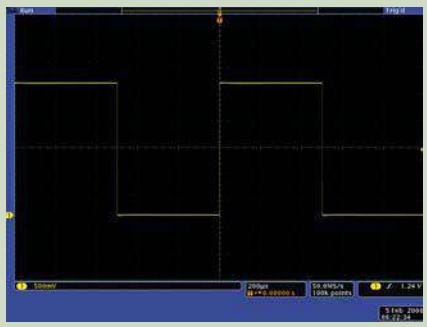

Probe Adjustment Signal

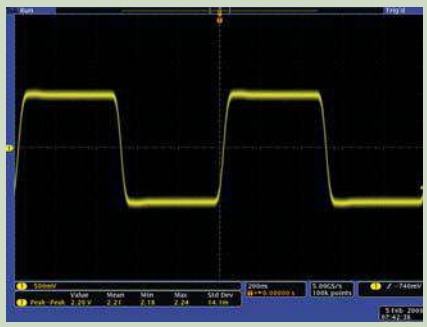

Note Proper Amplitude

Probe Overcompensated.

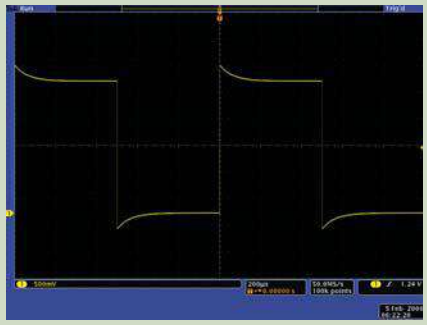

Probe Adjustment Signal

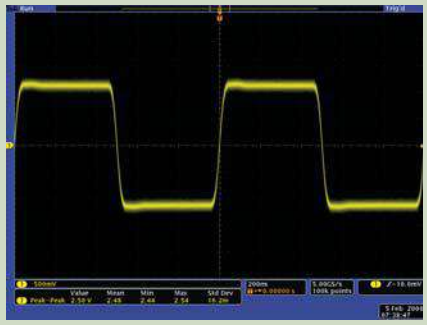

Note Increased Amplitude

Figure 64. The effects of improper probe compensation.

When you compensate the probe, always attach any accessory tips you will use and connect the probe to the vertical channel you plan to use. This will ensure that the oscilloscope has the same electrical properties as it does when you take measurements.

03W-8605-5.qxd 12/10/09 10:24 AM Page 46

Oscilloscope Measurement Techniques

This section reviews basic measurement techniques. The two most basic measurements you can make are voltage and time measurements. Just about every other measurement is based on one of these two fundamental techniques.

This section discusses methods for taking measurements visually with the oscilloscope screen. This is a common technique with analog instruments, and also may be useful for “at-a-glance” interpretation of digital oscilloscope displays.

Note that most digital oscilloscopes include automated measurement tools that simplify and accelerate common analysis tasks, thus improving the reliability and confidence of your measurements. However, knowing how to make measurements manually as described here will help you understand and check the automatic measurements.

Voltage Measurements

Voltage is the amount of electric potential, expressed in volts, between two points in a circuit. Usually one of these points is ground (zero volts), but not always. Voltages can also be measured from peak-to-peak – from the maximum point of a signal to its minimum point. You must be careful to specify which voltage you mean.

The oscilloscope is primarily a voltage-measuring device. Once you have measured the voltage, other quantities are just a calculation away. For example, Ohm’s law states that voltage between two points in a circuit equals the current times the resistance. From any two of these quantities you can calculate the third using the following formula:

$$\text{Voltage} = \text{Current} \times \text{Resistance}$$

$$\text{Current} = \frac{\text{Voltage}}{\text{Resistance}}$$

$$\text{Resistance} = \frac{\text{Voltage}}{\text{Current}}$$

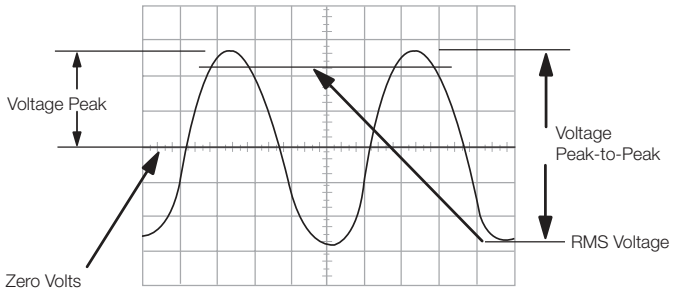

Figure 65. Voltage peak (V_p) and peak-to-peak voltage (V_{p-p})

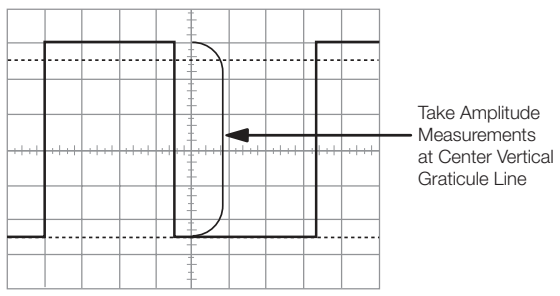

Figure 66. Measure voltage on the center vertical graticule line.

Another handy formula is the power law, which states that the power of a DC signal equals the voltage times the current. Calculations are more complicated for AC signals, but the point here is that measuring the voltage is the first step toward calculating other quantities. Figure 65 shows the voltage of one peak (V_p) and the peak-to-peak voltage (V_{p-p}).

The most basic method of taking voltage measurements is to count the number of divisions a waveform spans on the oscilloscope’s vertical scale. Adjusting the signal to cover most of the display vertically makes for the best voltage measurements, as shown in Figure 66. The more display area you use, the more accurately you can read the measurement.

Many oscilloscopes have cursors that let you make waveform measurements automatically, without having to count graticule marks. A cursor is simply a line that you can move across the display. Two horizontal cursor lines can be moved up and down to bracket a waveform’s amplitude for voltage measurements, and two vertical lines move right and left for time measurements. A readout shows the voltage or time at their positions.

03W-8605-5.qxd 12/10/09 10:24 AM Page 47

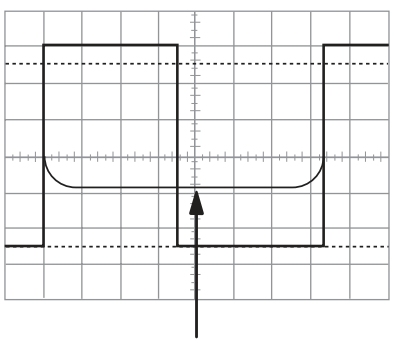

Figure 67. Measure time on the center horizontal graticule line.

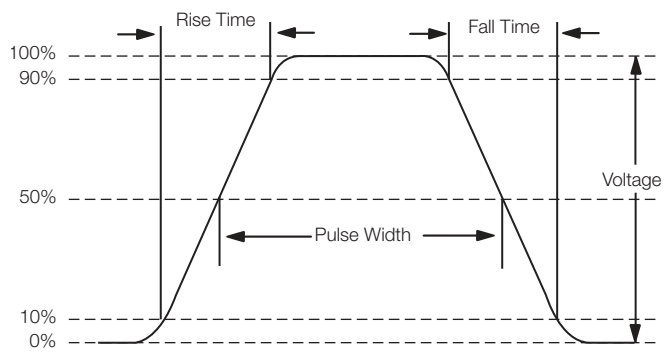

Figure 68. Rise time and pulse width measurement points.

Time and Frequency Measurements

You can make time measurements using the horizontal scale of the oscilloscope. Time measurements include measuring the period and pulse width of pulses. Frequency is the reciprocal of the period, so once you know the period, the frequency is one divided by the period. Like voltage measurements, time measurements are more accurate when you adjust the portion of the signal to be measured to cover a large area of the display, as illustrated in Figure 67.

Pulse Width and Rise Time Measurements

In many applications, the details of a pulse's shape are important. Pulses can become distorted and cause a digital circuit to malfunction, and the timing of pulses in a pulse train is often significant.

Standard pulse measurements are pulse rise time and pulse width. Rise time is the amount of time a pulse takes to go from a low to high voltage. By convention, the rise time is measured from 10% to 90% of the full voltage of the pulse. This eliminates any irregularities at the pulse's transition corners. Pulse width is the amount of time the pulse takes to go from low to high and back to low again. By convention, the pulse width is measured at 50% of full voltage. Figure 68 illustrates these measurement points.

Pulse measurements often require fine-tuning the triggering. To become an expert at capturing pulses, you should learn how to use trigger holdoff and how to set the digital oscilloscope to capture pretrigger data, as described in the Systems and Controls of an Oscilloscope section. Horizontal magnification is another useful feature for measuring pulses, since it allows you to see fine details of a fast pulse.

03W-8605-5.qxd 12/10/09 10:24 AM Page 48

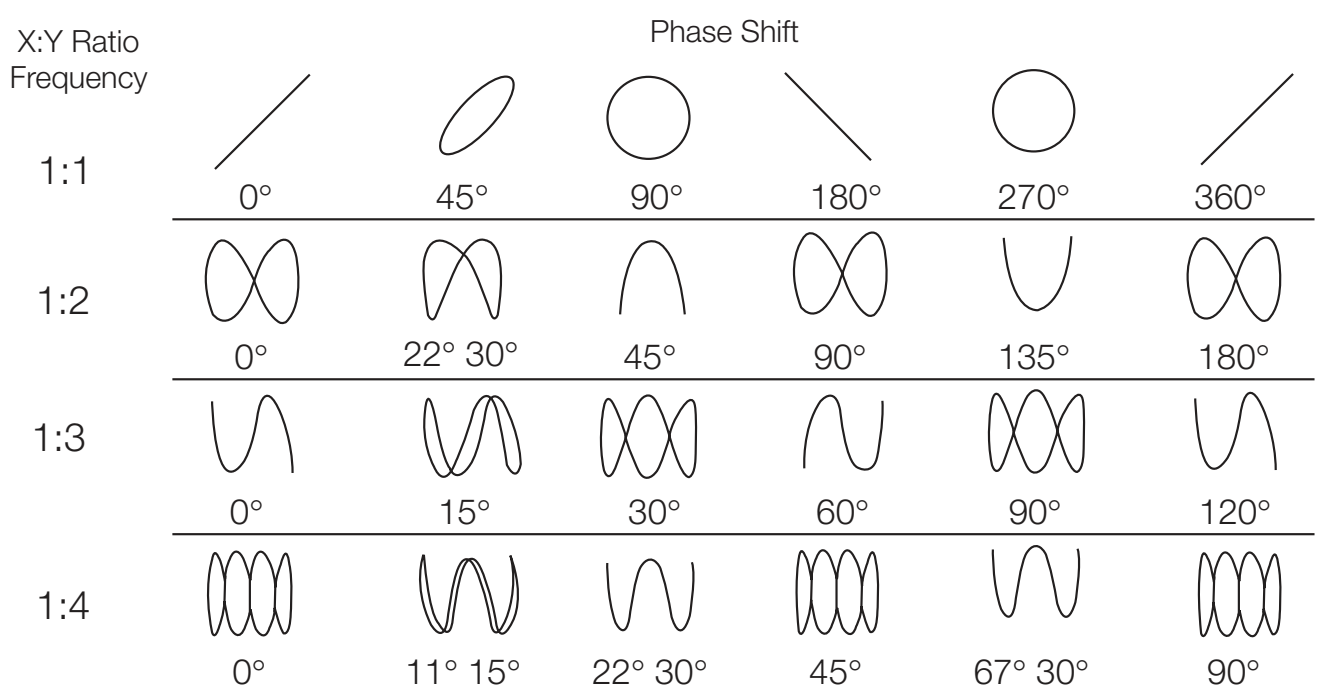

Figure 69. Lissajous patterns.

Phase Shift Measurements

One method for measuring phase shift – the difference in timing between two otherwise identical periodic signals – is to use XY mode. This measurement technique involves inputting one signal into the vertical system as usual and then another signal into the horizontal system – called an XY measurement because both the X and Y axis are tracing voltages. The waveform that results from this arrangement is called a Lissajous pattern (named for French physicist Jules Antoine Lissajous and pronounced LEE–sa–zhoo). From the shape of the Lissajous pattern, you can tell the phase difference between the two signals. You can also tell their frequency ratio. Figure 69 shows Lissajous patterns for various frequency ratios and phase shifts.

The XY measurement technique originated with analog oscilloscopes. DSOs may have difficulty creating real-time XY displays. Some DSOs create an XY image by accumulating triggered data points over time, then displaying two channels as an XY display.

DPOs, on the other hand, are able to acquire and display a genuine XY mode image in real-time, using a continuous stream of digitized data. DPOs can also display an XYZ image with intensified areas. Unlike XY displays on DSOs and DPOs, these displays on analog oscilloscopes are typically limited to a few megahertz of bandwidth.

Other Measurement Techniques

This section has covered basic measurement techniques. Other measurement techniques involve setting up the oscilloscope to test electrical components on an assembly line, capturing elusive transient signals, and many others. The measurement techniques you will use will depend on your application, but you have learned enough to get started. Practice using your oscilloscope and read more about it. Soon its operation will be second nature to you.

03W-8605-5.qxd 12/10/09 10:24 AM Page 49

Written Exercises

This section contains written exercises that cover information in this primer. These are divided into two parts, Part I and Part II, with vocabulary and application exercises for each.

Check how well you have absorbed the information in these sections by verifying your responses against the answer key at the end of this section on page 54.

Part I covers information presented in these sections:

- The Oscilloscope
- Performance Terms and Considerations

Part II covers information presented in sections:

- The Systems and Controls of an Oscilloscope
- Operating the Oscilloscope
- Measurement Techniques

Part I A: Vocabulary Exercise

Write the letter of the definitions in the right column next to the correct words in the left column.

	Term		Definition
1.	___ Acquisition	**A**	The unit of electric potential difference.
2.	___ Analog	**B**	A performance measurement indicating the precision of an ADC, measured in bits.
3.	___ Bandwidth	**C**	Term used when referring to degree points of a signal's period.
4.	___ Digital Phosphor	**D**	The number of times a signal repeats in one second.
5.	___ Frequency	**E**	The amount of time it takes a wave to complete one cycle.
6.	___ Glitch	**F**	A stored digital value that represents the voltage of a signal at a specific point in time on the display.
7.	___ Period	**G**	A common waveform shape that has a rising edge, a width, and a falling edge.
8.	___ Phase	**H**	A performance measurement indicating the rising edge speed of a pulse.
9.	___ Pulse	**I**	Oscilloscope circuitry that controls the timing of the sweep.
10.	___ Waveform Point	**J**	An intermittent spike in a circuit.
11.	___ Rise Time	**K**	A signal measured by an oscilloscope that only occurs once.
12.	___ Sample Point	**L**	The oscilloscope's process of collecting sample points from the ADC, processing them, and storing them in memory.
13.	___ Digital Storage	**M**	Something that operates with continuously changing values.
14.	___ Time Base	**N**	Digital oscilloscope that captures 3 dimensions of signal information in real-time.
15.	___ Transient	**O**	Digital oscilloscope with serial processing.
16.	___ ADC Resolution	**P**	A sine wave frequency range, defined by the – 3 dB point.
17.	___ Volt	**Q**	The raw data from an ADC used to calculate and display waveform points.

03W-8605-5.qxd 12/10/09 10:24 AM Page 50

Part I B: Application Exercise

Circle the best answers for each statement. Some statements have more than one right answer.

1. With an oscilloscope you can:

a. Calculate the frequency of a signal.

b. Find malfunctioning electrical components.

c. Analyze signal details.

d. All the above.

2. The difference between analog and digitizing oscilloscopes is:

a. Analog oscilloscopes do not have on-screen menus.

b. Analog oscilloscopes apply a measurement voltage directly to the display system, while digital oscilloscopes first convert the voltage into digital values.

c. Analog oscilloscopes measure analogs, whereas digitizing oscilloscopes measure digits.

d. Analog oscilloscopes do not have an acquisition system.

3. An oscilloscope's vertical section does the following:

a. Acquires sample points with an ADC.

b. Starts a horizontal sweep.

c. Lets you adjust the brightness of the display.

d. Attenuates or amplifies the input signal.

4. The time base control of the oscilloscope does the following:

a. Adjusts the vertical scale.

b. Shows you the current time of day.

c. Sets the amount of time represented by the horizontal width of the screen.

d. Sends a clock pulse to the probe.

5. On an oscilloscope display:

a. Voltage is on the vertical axis and time is on the horizontal axis.

b. A straight diagonal trace means voltage is changing at a steady rate.

c. A flat horizontal trace means voltage is constant.

d. All the above.

6. All repeating waves have the following properties:

a. A frequency measured in Hertz.

b. A period measured in seconds.

c. A bandwidth measured in Hertz.

d. All the above.

7. If you probe inside a computer with an oscilloscope, you are likely to find the following types of signals:

a. Pulse trains.

b. Ramp waves.

c. Sine waves.

d. All the above.

8. When evaluating the performance of an analog oscilloscope, some things you might consider are:

a. The bandwidth.

b. The vertical sensitivity.

c. The ADC resolution.

d. The sweep speed.

9. The difference between digital storage oscilloscopes (DSO) and digital phosphor oscilloscopes (DPO) is:

a. The DSO has a higher bandwidth.

b. The DPO captures three dimensions of waveform information in real-time.

c. The DSO has a color display.

d. The DSO captures more signal details.

03W-8605-5.qxd 12/10/09 10:24 AM Page 51

Part II A: Vocabulary Exercise

Write the letter of the definitions in the right column next to the correct words in the left column.

	Term		Definition
1. ___	Averaging Mode	**A**	The unintentional interaction of the probe and oscilloscope with the circuit being tested which distorts a signal.
2. ___	Circuit Loading	**B**	A conductor that connects electrical currents to the Earth.
3. ___	Compensation	**C**	A sampling mode in which the digital oscilloscope collects as many samples as it can as the signal occurs, then constructs a display, using interpolation if necessary.
4. ___	Coupling	**D**	A sampling mode in which the digital oscilloscope constructs a picture of a repetitive signal by capturing a little bit of information from each repetition.
5. ___	Earth Ground	**E**	A device that converts a specific physical quantity such as sound, pressure, strain, or light intensity into an electrical signal.
6. ___	Equivalent-Time	**F**	A test device for injecting a signal into a circuit input.
7. ___	Graticule	**G**	A processing technique used by digital oscilloscopes to eliminate noise in a displayed signal.
8. ___	Interpolation	**H**	The method of connecting two circuits together.
9. ___	Real Time	**I**	A “connect-the-dots” processing technique to estimate what a fast waveform looks like based on only a few sampled points.
10. ___	Signal Generator	**J**	The grid lines on a screen for measuring oscilloscope traces.
11. ___	Single Sweep	**K**	A trigger mode that triggers the sweep once, must be reset to accept another trigger event.
12. ___	Sensor	**L**	A probe adjustment for 10X attenuator probes that balances the electrical properties of the probe with the electrical properties of the oscilloscope.

03W-8605-5.qxd 12/10/09 10:24 AM Page 52

Part II B: Application Exercise

Circle the best answers for each statement. Some statements have more than one right answer.

1. To operate an oscilloscope safely, you should:

a. Ground the oscilloscope with the proper three-pronged power cord.

b. Learn to recognize potentially dangerous electrical components.

c. Avoid touching exposed connections in a circuit being tested even if the power is off.

d. All the above.

2. Grounding an oscilloscope is necessary:

a. For safety reasons.

b. To provide a reference point for making measurements.

c. To align the trace with the screen's horizontal axis.

d. All the above.

3. Circuit loading is caused by:

a. An input signal having too large a voltage.

b. The probe and oscilloscope interacting with the circuit being tested.

c. A 10X attenuator probe being uncompensated.

d. Putting too much weight on a circuit.

4. Compensating a probe is necessary to:

a. Balance the electrical properties of the 10X attenuator probe with the oscilloscope.

b. Prevent damaging the circuit being tested.

c. Improve the accuracy of your measurements.

d. All the above.

5. The trace rotation control is useful for:

a. Scaling waveforms on the screen.

b. Detecting sine wave signals.

c. Aligning the waveform trace with the screen's horizontal axis on an analog oscilloscope.

d. Measuring pulse width.

6. The volts per division control is used to:

a. Scale a waveform vertically.

b. Position a waveform vertically.

c. Attenuate or amplify an input signal.

d. Set the numbers of volts each division represents.

7. Setting the vertical input coupling to ground does the following:

a. Disconnects the input signal from the oscilloscope.

b. Causes a horizontal line to appear with auto trigger.

c. Lets you see where zero volts is on the screen.

d. All the above.

8. The trigger is necessary to:

a. Stabilize repeating waveforms on the screen.

b. Capture single-shot waveforms.

c. Mark a particular point of an acquisition.

d. All the above.

9. The difference between auto and normal trigger mode is:

a. In normal mode the oscilloscope only sweeps once and then stops.

b. In normal mode the oscilloscope only sweeps if the input signal reaches the trigger point; otherwise the screen is blank.

c. Auto mode makes the oscilloscope sweep continuously even without being triggered.

d. All the above.

10. The acquisition mode that best reduces noise in a repeating signal is:

a. Sample mode.

b. Peak detect mode.

c. Envelope mode.

d. Averaging mode.

03W-8605-5.qxd 12/10/09 10:24 AM Page 53

11. The two most basic measurements you can make with an oscilloscope are:

a. Time and frequency measurements.

b. Time and voltage measurements.

c. Voltage and pulse width measurements.

d. Pulse width and phase shift measurements.

12. If the volts/division is set at 0.5, the largest signal that can fit on the screen (assuming an 8 x 10 division screen) is:

a. 62.5 millivolts peak-to-peak.

b. 8 volts peak-to-peak.

c. 4 volts peak-to-peak.

d. 0.5 volts peak-to-peak.

13. If the seconds/division is set at 0.1 ms, the amount of time represented by the width of the screen is:

a. 0.1 ms.

b. 1 ms.

c. 1 second.

d. 0.1 kHz.

14. By convention, pulse width is measured:

a. At 10% of the pulse's peak-to-peak (pk-pk) voltage.

b. At 50% of the pulse's peak-to-peak (pk-pk) voltage.

c. At 90% of the pulse's peak-to-peak (pk-pk) voltage.

d. At 10% and 90% of the pulse's peak-to-peak (pk-pk) voltage.

15. You attach a probe to your test circuit but the screen is blank. You should:

a. Check that the screen intensity is turned up.

b. Check that the oscilloscope is set to display the channel that the probe is connected to.

c. Set the trigger mode to auto since norm mode blanks the screen.

d. Set the vertical input coupling to AC and set the volts/division to its largest value since a large DC signal may go off the top or bottom of the screen.

e. Check that the probe isn't shorted and make sure it is properly grounded.

f. Check that the oscilloscope is set to trigger on the input channel you are using.

g. All of the above.

03W-8605-5.qxd 12/10/09 10:24 AM Page 54

Answer Key

This section provides the answers to all written exercises in the previous section.

Part IA: Vocabulary Exercise Answers

1. L	5. D	9. G	13. O
2. M	6. J	10. F	14. I
3. P	7. E	11. H	15. K
4. N	8. C	12. Q	16. B
			17. A

Part IB: Application Exercise Answers

1. D	3. D	5. D	7. A
2. B,D	4. C	6. A,B	8. A,B,D
			9. B

Part IIA: Vocabulary Exercise Answers

1. G	4. H	7. J	10. F
2. A	5. B	8. I	11. K
3. L	6. D	9. C	12. E

Part IIB: Application Exercise Answers

1. D	5. C	9. B,C	13. B
2. A,B	6. A,C,D	10. D	14. B
3. B	7. D	11. B	15. G
4. A,C	8. D	12. C	

03W-8605-5.qxd 12/10/09 10:24 AM Page 55

Glossary

A

Acquisition Mode – Modes that control how waveform points are produced from sample points. Some types include sample, peak detect, hi res, envelope, average, and waveform data base.

Alternating Current (AC) – A signal in which the current and voltage vary in a repeating pattern over time. Also used to indicate signal coupling type.

Amplification – An increase in signal amplitude during its transmission from one point to another.

Amplitude – The magnitude of a quantity or strength of a signal. In electronics, amplitude usually refers to either voltage or power.

Analog-to-Digital Converter (ADC) – A digital electronic component that converts an electrical signal into discrete binary values.

Analog Oscilloscope – An instrument that creates a waveform display by applying the input signal (conditioned and amplified) to the vertical axis of an electron beam moving across a cathode-ray tube (CRT) screen horizontally from left to right. A chemical phosphor coated on the CRT creates a glowing trace wherever the beam hits.

Analog Signal – A signal with continuously variable voltages.

Attenuation – A decrease in signal amplitude during its transmission from one point to another.

Averaging – A processing technique used by digital oscilloscopes to reduce noise in a displayed signal.

B

Bandwidth – A frequency range, usually limited by –3 dB.

C

Circuit Loading – The unintentional interaction of the probe and oscilloscope with the circuit being tested, distorting the signal.

Compensation – A probe adjustment for passive attenuation probes that balances the capacitance of the probe with the capacitance of the oscilloscope.

Coupling – The method of connecting two circuits together. Circuits connected with a wire are directly coupled (DC); circuits connected through a capacitor or transformer are indirectly (AC) coupled.

Cursor – An on–screen marker that you can align with a waveform to make more accurate measurements.

D

Delayed Time Base – A time base with a sweep that can start (or be triggered to start) relative to a pre-determined time on the main time base sweep. Allows you to see events more clearly and to see events that are not visible solely with the main time base sweep.

Digital Signal – A signal whose voltage samples are represented by discrete binary numbers.

Digital Oscilloscope – A type of oscilloscope that uses an analog-to-digital converter (ADC) to convert the measured voltage into digital information. Types include: digital storage, digital phosphor, mixed signal, and digital sampling oscilloscopes.

Digital Phosphor Oscilloscope (DPO) – A type of digital oscilloscope that closely models the display characteristics of an analog oscilloscope while providing traditional digital oscilloscope benefits (waveform storage, automated measurements, etc.) The DPO uses a parallel-processing architecture to pass the signal to the raster-type display, which provides intensity-graded viewing of signal characteristics in real time. The DPO displays signals in three dimensions: amplitude, time and the distribution of amplitude over time.

Digital Sampling Oscilloscope – A type of digital oscilloscope that employs equivalent-time sampling method to capture and display samples of a signal, ideal for accurately capturing signals whose frequency components are much higher than the oscilloscope's sample rate.

Digital Signal Processing – The application of algorithms to improve the accuracy of measured signals.

Digital Storage Oscilloscope (DSO) – A digital oscilloscope that acquires signals via digital sampling (using an analog-to-digital converter). It uses a serial-processing architecture to control acquisition, user interface, and the raster display.

Digitize – The process by which an analog-to-digital converter (ADC) in the horizontal system samples a signal at discrete points in time and converts the signal's voltage at these points into digital values called sample points.

Direct Current (DC) – A signal with a constant voltage and/or current. Also used to indicate signal coupling type.

Division – Measurement markings on the oscilloscope graticule indicating major and minor marks.

03W-8605-5.qxd 12/10/09 10:24 AM Page 56

E

Earth Ground – A conductor that will connect electrical currents to the Earth.

Effective Bits – A measure of a digital oscilloscope's ability to accurately reconstruct a sine wave signal's shape. This measurement compares the oscilloscope's actual error to that of a theoretical "ideal" digitizer.

Envelope – The outline of a signal's highest and lowest points acquired over many displayed waveform repetitions.

Equivalent-time Sampling – A sampling mode in which the oscilloscope constructs a picture of a repetitive signal by capturing a little bit of information from each repetition. Two types of equivalent-time sampling: random and sequential.

F

Focus – The analog oscilloscope control that adjusts the cathode-ray tube (CRT) electron beam to control the sharpness of the display.

Frequency – The number of times a signal repeats in one second, measured in Hertz (cycles per second). The frequency equals 1/period.

Frequency Response – Frequency response curves of an oscilloscope define the accuracy in amplitude representation of the input signal in function of the signals frequency. In order to obtain maximum signal fidelity, it is important that the oscilloscope has a flat (stable) frequency response across the entire specified oscilloscopes bandwidth.

G

Gain Accuracy – An indication of how accurately the vertical system attenuates or amplifies a signal, usually represented as a percentage error.

Gigahertz (GHz) – 1,000,000,000 Hertz; a unit of frequency.

Glitch – An intermittent, high-speed error in a circuit.

Graticule – The grid lines on a display for measuring oscilloscope traces.

Ground –

1. A conducting connection by which an electric circuit or equipment is connected to the earth to establish and maintain a reference voltage level.
2. The voltage reference point in a circuit.

H

Hertz (Hz) – One cycle per second; the unit of frequency.

Horizontal Accuracy (Time Base) – An indication of how accurately the horizontal system displays the timing of a signal, usually represented as a percentage error.

Horizontal Sweep – The action of the horizontal system that causes a waveform to be drawn.

I

Intensity Grading – Frequency-of-occurrence information that is essential to understanding what the waveform is really doing.

Interpolation – A "connect-the-dots" processing technique to estimate what a fast waveform looks like based on only a few sampled points. Two types: linear and sin x/x.

K

Kilohertz (kHz) – 1,000 Hertz; a unit of frequency.

L

Loading – The unintentional interaction of the probe and oscilloscope with the circuit being tested which distorts a signal.

Logic Analyzer – An instrument used to make the logic states of many digital signals visible over time. It analyzes the digital data and can represent the data as real-time software execution, data flow values, state sequences, etc.

M

Megahertz (MHz) – 1,000,000 Hertz; a unit of frequency.

Megasamples per second (MS/s) – A sample rate unit equal to one million samples per second.

Microsecond (µs) – A unit of time equivalent to 0.000001 seconds.

Millisecond (ms) – A unit of time equivalent to 0.001 seconds.

Mixed Signal Oscilloscope (MSO) – A type of digital oscilloscope that combines the basic functionality of a 16-channel logic analyzer with the trusted performance of a 4-channel digital phosphor oscilloscope.

03W-8605-5.qxd 12/10/09 10:24 AM Page 57

N

Nanosecond (ns) – A unit of time equivalent to 0.000000001 seconds.

Noise – An unwanted voltage or current in an electrical circuit.

O

Oscilloscope – An instrument used to make voltage changes visible over time. The word oscilloscope comes from "oscillate," since oscilloscopes are often used to measure oscillating voltages.

P

Peak (V_p) – The maximum voltage level measured from a zero reference point.

Peak Detection – An acquisition mode available with digital oscilloscopes that enables you to observe signal details that may otherwise be missed, particularly useful for seeing narrow pulses spaced far apart in time.

Peak-to-peak (V_{p-p}) – The voltage measured from the maximum point of a signal to its minimum point.

Period – The amount of time it takes a wave to complete one cycle. The period equals 1/frequency.

Phase – The amount of time that passes from the beginning of a cycle to the beginning of the next cycle, measured in degrees.

Phase Shift – The difference in timing between two otherwise similar signals.

Pre-trigger Viewing – The ability of a digital oscilloscope to capture what a signal did before a trigger event. Determines the length of viewable signal both preceding and following a trigger point.

Probe – An oscilloscope input device, usually having a pointed metal tip for making electrical contact with a circuit element, a lead to connect to the circuit's ground reference, and a flexible cable for transmitting the signal and ground to the oscilloscope.

Pulse – A common waveform shape that has a fast rising edge, a width, and a fast falling edge.

Pulse Train – A collection of pulses traveling together.

Pulse Width – The amount of time the pulse takes to go from low to high and back to low again, conventionally measured at 50% of full voltage.

R

Ramps – Transitions between voltage levels of sine waves that change at a constant rate.

Raster – A type of display.

Real-time Sampling – A sampling mode in which the oscilloscope collects as many samples as possible from one triggered acquisition. Ideal for signals whose frequency range is less than half the oscilloscope's maximum sample rate.

Record Length – The number of waveform points used to create a record of a signal.

Rise Time – The time taken for the leading edge of a pulse to rise from its low to its high values, typically measured from 10% to 90%.

S

Sampling – The conversion of a portion of an input signal into a number of discrete electrical values for the purpose of storage, processing and/or display by an oscilloscope. Two types: real-time sampling and equivalent-time sampling.

Sample Point – The raw data from an ADC used to calculate waveform points.

Sample Rate – Refers to how frequently a digital oscilloscope takes a sample of the signal, specified in samples per second (S/s).

Sensor – A device that converts a specific physical quantity such as sound, pressure, strain, or light intensity into an electrical signal.

Signal Integrity – The accurate reconstruction of a signal, determined by the systems and performance considerations of an oscilloscope, in addition to the probe used to acquire the signal.

Signal Source – A test device used to inject a signal into a circuit input; the circuit's output is then read by an oscilloscope. Also known as a signal generator.

03W-8605-5.qxd 12/10/09 10:24 AM Page 58

Sine Wave – A common curved wave shape that is mathematically defined.

Single Shot – A signal measured by an oscilloscope that only occurs once (also called a transient event).

Single Sweep – A trigger mode to display one triggered screen of a signal and then stop.

Slope – On a graph or an oscilloscope display, the ratio of a vertical distance to a horizontal distance. A positive slope increases from left to right, while a negative slope decreases from left to right.

Square Wave – A common wave shape consisting of repeating square pulses.

Sweep – One horizontal pass of an anlog oscilloscope's electron beam from left to right across the CRT screen.

Sweep Speed – Same as the time base.

T

Time Base – Oscilloscope circuitry that controls the timing of the sweep. The time base is set by the seconds/division control.

Trace – The visible shapes drawn on a CRT by the movement of the electron beam.

Transient – A signal measured by an oscilloscope that only occurs once (also called a single–shot event).

Trigger – The circuit that references a horizontal sweep on an oscilloscope.

Trigger Holdoff – A control that allows you to adjust the period of time after a valid trigger during which the oscilloscope cannot trigger.

Trigger Level – The voltage level that a trigger source signal must reach before the trigger circuit initiates a sweep.

Trigger Mode – A mode that determines whether or not the oscilloscope draws a waveform if it does not detect a trigger. Common trigger modes include normal and auto.

Trigger Slope – The slope that a trigger source signal must reach before the trigger circuit initiates a sweep.

V

Vertical Resolution (Analog-to-Digital Converter) – An indication of how precisely an analog-to-digital converter (ADC) in a digital oscilloscope can convert input voltages into digital values, measured in bits. Calculation techniques, such as hi res acquisition mode, can improve the effective resolution.

Vertical Sensitivity – An indication of how much the vertical amplifier can amplify a weak signal – usually measured in millivolts (mV) per division.

Volt – The unit of electric potential difference.

Voltage – The difference in electric potential, expressed in volts, between two points.

W

Wave – The generic term for a pattern that repeats over time. Common types include: sine, square, rectangular, sawtooth, triangle, step, pulse, periodic, non-periodic, synchronous, asynchronous.

Waveform – A graphic representation of a voltage varying over time.

Waveform Capture Rate – Refers to how quickly an oscilloscope acquires waveforms, expressed as waveforms per second (wfms/s).

Waveform Point – A digital value that represents the voltage of a signal at a specific point in time. Waveform points are calculated from sample points and stored in memory.

Writing Speed – The ability of an analog oscilloscope to provide a visible trace of the movement of a signal from one point to another. This ability is restrictive for low-repetition signals that have fast-moving details, such as digital logic signals.

XY Mode – A measuremenbt technique that involves inputting one signal into the vertical system, as usual, and one into the horizontal system to trace voltages on both the X and Y axis.

Z

Z Axis – The display attribute on an oscilloscope that shows brightness variations as the trace is formed.

03W-8605-5.qxd 12/10/09 10:24 AM Page 59

03W-8605-5.qxd 12/10/09 10:24 AM Page 60

Contact Tektronix:

ASEAN / Australasia (65) 6356 3900
Austria 00800 2255 4835*
Balkans, Israel, South Africa and other ISE Countries +41 52 675 3777
Belgium 00800 2255 4835*
Brazil +55 (11) 3759 7600
Canada 1 (800) 833-9200
Central East Europe, Ukraine and the Baltics +41 52 675 3777
Central Europe & Greece +41 52 675 3777
Denmark +45 80 88 1401
Finland +41 52 675 3777
France 00800 2255 4835*
Germany 00800 2255 4835*
Hong Kong 400-820-5835
India (91) 80-42922600
Italy 00800 2255 4835*
Japan 81 (3) 6714-3010
Luxembourg +41 52 675 3777
Mexico, Central/South America & Caribbean 52 (55) 53 35 10 85
Middle East, Asia and North Africa +41 52 675 3777
The Netherlands 00800 2255 4835*
Norway 800 16098
People's Republic of China 400-820-5835
Poland +41 52 675 3777
Portugal 80 08 12370
Republic of Korea 82 (2) 6917-5000
Russia & CIS +7 (495) 7484900
South Africa +27 11 206 8360
Spain 00800 2255 4835*
Sweden 00800 2255 4835*
Switzerland 00800 2255 4835*
Taiwan 886 (2) 2722-9622
United Kingdom & Ireland 00800 2255 4835*
USA 1 (800) 833-9200
* European toll-free number. If not accessible, call: +41 52 675 3777

Contact List Updated 09 December 2009

For Further Information
Tektronix maintains a comprehensive, constantly expanding collection of application notes, technical briefs and other resources to help engineers working on the cutting edge of technology. Please visit **www.tektronix.com**

Copyright © 2009, Tektronix. All rights reserved. Tektronix products are covered by U.S. and foreign patents, issued and pending. Information in this publication supersedes that in all previously published material. Specification and price change privileges reserved. TEKTRONIX and TEK are registered trademarks of Tektronix, Inc. All other trade names referenced are the service marks, trademarks or registered trademarks of their respective companies.
12/09 JS 03W-8605-5
TEK1511

Tektronix®

MORE ELECTRONIC GADGETS FOR THE EVIL GENIUS

40 NEW BUILD-IT-YOURSELF PROJECTS

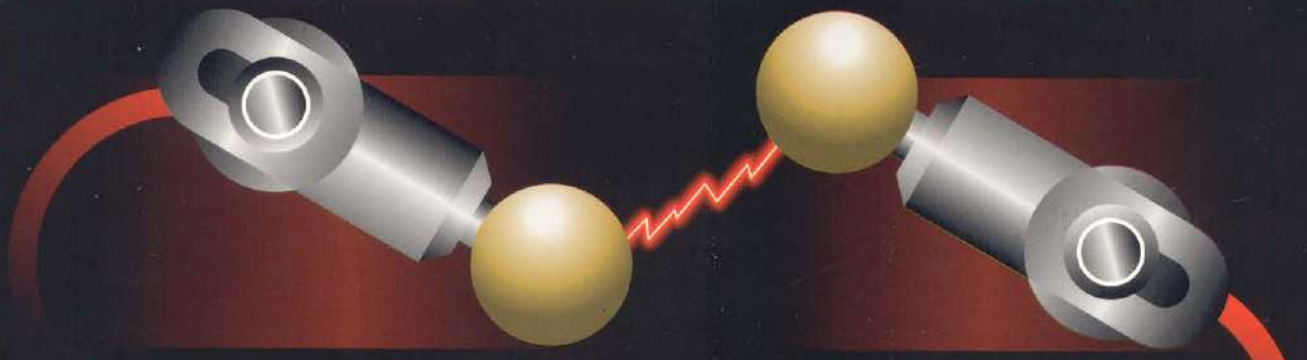

- Every project includes a list of materials, sources for obtaining parts, schematics, documentation, and clear instructions
- Projects are fun and inexpensive, but challenging enough for an electronics wiz
- Build your own lasers, surveillance devices, ultrasonic generators, display and detection devices

TAB ELECTRONICS

BOB IANNINI

Contents

Chapter One Battery-Powered Infrared Pulsed Laser 1
Theory of Operation 2
Circuit Theory of Operation 2
Current Monitor 5
Charging Circuits 5
Chassis Assembly 5
Assembly Testing 7
Final Assembly 8
Special Note 8

Chapter Two High-Speed Laser Pulse Detector 11
Circuit Description 12
System Assembly 13
Assembly Testing 15
Final Assembly 16
Special Note 17
Special Note on Photo Detectors 17

Chapter Three Ultra-Bright Green Laser Project 19
Assembly Steps 20

Chapter Four 115 VAC, 5- to 50-Watt Pulsed Infrared Laser 25
Theory of Operation 25
Circuit Theory of Operation 26
Notes on SCR 28
Notes on the Storage Capacitor 28
Notes on Layout Wiring 28
Notes on Circuit Monitoring 30
Assembly Steps 30
Assembly Testing 33
Final Assembly Steps 35

Chapter Five Laser Property Guard 37
System Installation Suggestions 39

Chapter Six 30-Milliwatt, 980-Nanometer Infrared Laser 43
Assembly 44
Collimator and Final Assembly 47

Chapter Seven High-Voltage, High-Frequency Driver Module 51
Electrical and Mechanical Specifications 51
Circuit Description 52
Construction 52
Board Assembly Steps 52
Testing Steps 56

Chapter Eight Negative Ion Machine with Reaction-Emitting Rotor 59
Benefits of Negative Ions 59
Circuit Description 60
Assembly Steps 61
Notes 62

Chapter Nine Kirlian Imaging Project 65
Assembly Steps 66
Testing Steps for the Circuit 66
Notes 67

Chapter Ten Plasma Etching and Burning Pen 69
Driver Circuit Description 69
Drive Circuit Assembly 70
Driver Board Testing 71
Mechanical Assembly 72
Sample Demonstration 72

Chapter Eleven How to Electrify Objects and Vehicles 75
Supplementary Electrification Data and Information 76
Assembly of Suggested Power Sources 81
Circuit Description of Pulsed Shocker 81
Construction Steps for Pulsed Shocker 81
Notes Pulsed Shocker 85
Construction of Continuous Shocker 85

Chapter Twelve Electromagnetic Pulse (EMP) Gun 87
Basic Theory Simplified 87
Circuit Description 89
Circuit Assembly 89
Notes 89

Chapter Thirteen Microwave Cannon 93

Chapter Fourteen Induction Heater 103
Circuit Operation 103
Project Assembly 104
Project Testing 108
Using the Heater Project 108

Chapter Fifteen 50-Kilovolt Laboratory DC Supply 113
Basic Description 113
Circuit Operation 114
Assembly of the Driver Section 114
Pretesting the Driver Section 116
Assembly of the Multiplier Section 121
Final Testing 125
Applications 129

Chapter Sixteen Magnetic High-Impact Cannon 133
Theory of Operation 133
Circuit Theory 134
Assembly Steps 136
Circuit Testing 136
Assembly of the Completed System 137
Testing and Operation of the Cannon 143

Chapter Seventeen Vacuum Tube Tesla Coil Project 151
Basic Description 153
Assembly Steps 154
Testing and Operating 167
Notes 167

Chapter Eighteen Universal Capacitance Discharge Ignition (CDI) Driver 169
Circuit Description 169
Assembly Steps 170
Test Steps 175
Notes on Operation 175

Chapter Nineteen Long-range Telephone Conversation Transmitter 177
Circuit Description 177
Assembly of the Circuit Board 179
Notes 180

Chapter Twenty Line-Powered Telephone Conversation Transmitter 183
Circuit Description 183
Assembly of the Circuit Board 185
Notes 186

Chapter Twenty-One Remote Wireless FM Repeater 187
Circuit Description 187
Assembly 188
Notes 189

Chapter Twenty-Two Tracking and Homing Transmitter 191
Circuit Description 191
Assembly of the Circuit Board 192
Notes 194

Chapter Twenty-Three Snooper Phone Room-Listening Device 195
Circuit Operation 195

Construction Steps 196
Final Assembly 197
Testing Steps 198
Notes 199

Chapter Twenty-Four Long-Range FM Voice Transmitter 201
Circuit Description 201
Assembly Steps 202
Notes 204

Chapter Twenty-Five FM Pocket Radio and TV Disrupter 205
Circuit Theory 206
Assembly Steps 206

Chapter Twenty-Six Ozone Generator for Water Treatment 209
Introduction to the Benefits of Ozone 209
Ozone for Water Applications 210
Ways to Generate Ozone 210

Chapter Twenty-Seven Therapeutic Magnetic Pulser 213
Circuit Description 214
Assembly 215

Chapter Twenty-Eight Noise Curtain Generator 219
Circuit Description 220
Assembly Steps 220
Testing Steps 221

Chapter Twenty-Nine Mind-Synchronizing Generator 223
Information on Mind Control 223
Operating a Mind Machine 225
Circuit Theory 226
Assemble the Board 227

Chapter Thirty Alternative Health Multiwave Machine 231
Theory of Operation 231
Construction of the Multiwave Coil and Antenna 233
Operation 234

Chapter Thirty-One Mind Mangler 237
Circuit Operation 237
Construction Steps 238
Testing 239

Chapter Thirty-Two 500-Milligram Ozone Air Purification System 241
The Story of Ozone 241
Ozone for Treating Air 242
Construction Steps 242
Special Notes 244

Chapter Thirty-Three Invisible Pain-field Generator 249
Circuit Description 250
Construction 251

Chapter Thirty-Four Canine Controller 257
Device Description 257
Circuit Description 258
Circuit Assembly 260
Testing the Circuit 263

Chapter Thirty-Five Ultrasonic Phaser Pain-Field Generator 265
Basic Device Description 265
Circuit Theory 266
Construction Steps 267
Testing the Assembly 268
Basic Operating Instructions 269
Information on the System 272
A Word of Caution 272
General Information on Ultrasonics 272
Application Supplement 272

Chapter Thirty-Six Magnetic Distortion Detector 275
Circuit Description 276
Assembly Steps 277
Pretesting the Sense Head 278

Construction of the Control Box 279
Control Box Protesting 279
Applications 281
Optional Ultra-Sensitive Vibration and Tremor Detector 283

Chapter Thirty-Seven Body Heat Detector 285
Description 285
Body Heat Detector Modes 286
Circuit Description 286
Assembly Instructions 288
Operating Instructions 290
Final Notes 291

Chapter Thirty-Eight Ion and Field Detector 293
Circuit Description 293
Construction Steps 294
Applications 298

Chapter Thirty-Nine Light Saber Recycling Stand 301
Circuit Description 301
Assembly 302
Parts Fabrication 302
Operation 303

Chapter Forty Andromeda Plasma Lamp 309
Circuit Description 309
Assembly Board Wiring 310

Index 317

Chapter One

Battery-Powered Infrared Pulsed Laser

This project shows how to construct a low-powered, portable, solid-state, pulsed infrared laser. The system uses a gallium arsenide laser diode and provides pulse powers from 10 to 100 watts, depending on the diode used. The device operates from batteries and is completely self-contained. It may be built in a pistol, rifle, or a simple tubular configuration. The device is intended as a source of adjustable-frequency pulses from 10 to 1,000 repetitions per second of infrared energy at 900 nanometers

The system is shown in Figure 1-1 as being built on a perforated board assembly and combination copper ground plane that all fits into a tubular enclosure with a lens and holder for a collimator. The housing serves as the enclosure for the batteries and contains the control panel at its rear. It may be fitted with a handle that can hold an optional trigger switch when the device is designed in a gun configuration. A conventional sighting system is also easily adapted to the device.

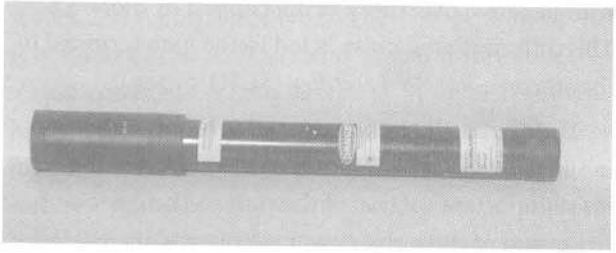

Figure 1-1 *Photograph of laser*

The laser is intended as a rifle-type simulated weapon, whose range can be several miles or as a long-range, laser-beam protection fence with a similar range of several miles. It is intended to be used with our high-speed laser pulse detector described in Chapter 2.

The laser, when assembled as shown, is a class 3B FDA certified device and requires the appropriate labeling and several included safety functions, as described in the assembly instructions. At no time should it be pointed at anyone without protective eyewear or at anything that could reflect the pulses. Never look into the unit when the power is on. The device is intended to be used for ranging, simulated weapons practice, intrusion detection, communications and signaling, and a variety of related scientific, optical experiments and uses.

This is an intermediate- to advanced-level project requiring electronic skills and basic electronic shop equipment. Expect to spend $100 to $150. All parts are readily available, with specialized parts obtainable through Information Unlimited (www.amazing1.com), and they are listed in Table 1-1.

Theory of Operation

A laser diode is nothing more than a three-layer device consisting of a *pn* junction of *n*-type silicon, a *p* type of gallium arsenide, and a third *p* layer of doped gallium arsenide with aluminum. The *n*-type material contains electrons that readily migrate across the *pn* junction and fill the holes of the *p*-type material. Conversely, holes in the *p* type migrate to the *n* type and join with electrons. This migration causes a potential hill or barrier consisting of negative charges in the *p*-type material and positive charges in the *n*-type material that eventually ceases growing when a charge equilibrium exists. In order for current to flow in this device, it must be supplied at a voltage to overcome this potential barrier. This is the forward voltage drop across a common diode. If this voltage polarity is reversed, the potential barrier is simply increased, assuring no current flow. This is the reversed bias condition of a common diode.

A diode without an external voltage applied to it contains electrons that move and wander through the lattice structure at a low, lazy average velocity as a function of temperature. When an external current at a voltage exceeding the barrier potential is applied, these lazy electrons increase their velocity so that some of them, by colliding, acquire a discrete amount of energy and become unstable. They eventually emit the acquired energy in the form of a photon after returning to a lower-energy state. These photons of energy are random both in time and direction; hence, any radiation produced is incoherent, such as that of an LED.

The requirement for coherent radiation is that the discrete packets of radiation must be in the form of a lockstep phase and in a definite direction. This demands two essential requirements: first, sufficient electrons at the necessary excited energy levels, and second, an optical resonant cavity capable of trapping these energized electrons to stimulate more electrons and give them direction. The amount of energized electrons is determined by the forward diode current. A definite threshold condition exists where the device emits laser light rather than incoherent light, such as in an LED. This is why the device must be pulsed with high current. The radiation from these energized electrons is reflected back and forth between the square-cut edges of the crystal that form the reflecting surfaces due to the index of refraction of the material and air.

The electrons are initially energized in the region of the *pn* junction. When these energized electrons drift into the *p*-type transparent region, they spontaneously liberate other photons that travel back and forth in the optical cavity interacting with other electrons, commencing laser action. A portion of the radiation traveling back and forth between the reflecting surfaces of these mirrors escapes and constitutes the output of the device.

Circuit Theory of Operation

Figure 1-2 shows the inverter section increasing the 12 volts of the portable battery pack to 200 to 300 volts performed by the circuit, which consists of a switching transistor (Q1) and step-up transformer (T1). Q1 conducts until saturated for a time until the base reverse biases and can no longer sustain it at an on state and Q1 turns off. This causes the magnetic field in its collector winding (COL) to collapse, thus producing a stepped-up voltage in the secondary (SEC) of proper phase. The variable resistor (R3) controls the charging current to the capacitor (C2), the transistor turnoff time, and consequently system power.

The stepped-up square wave voltage on the secondary of T1 is rectified by diode (D1) and integrated onto the storage capacitor (C3). The trigger circuit determines the pulse rep rate of the laser and uses a timer (I1) whose pulse rate is determined by the timing resistor and capacitor (R9 and C6). R9 is adjustable for changing the laser pulse rate. The output trigger pulse is differentiated by capacitor (C4) with negative overshoot being clipped by diode D2. This differentiated pulse is fed to the gate terminal of the *silicon controlled rectifier* (SCR) switch.

The discharge circuit generates the current pulse in the laser diode (LD1) and consequently is the most important section of the pulser. The basic configuration of the pulse power supply is shown in the system schematic. The current pulse is generated by the charging storage capacitor C3 being switched through the SCR and laser diode LD1. The rise time

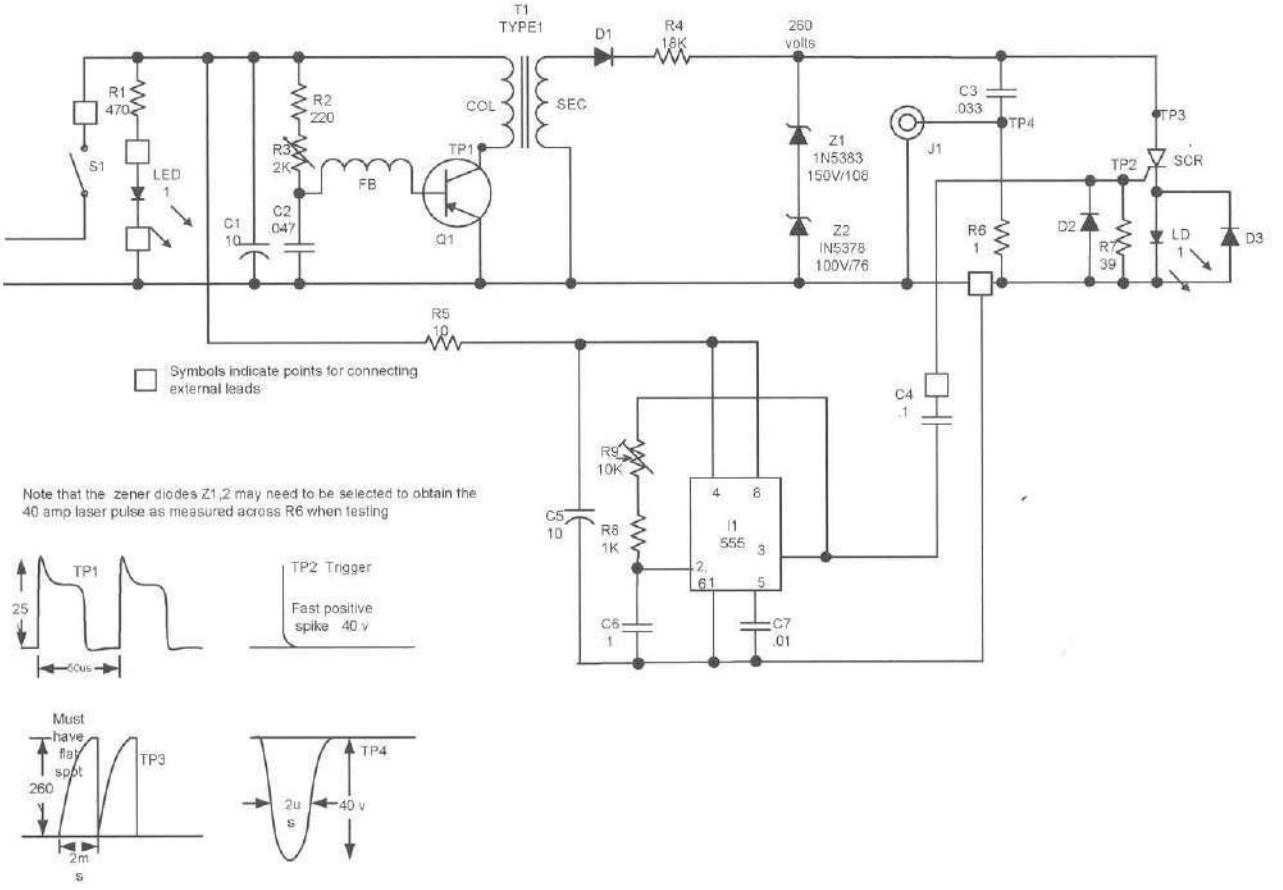

Figure 1-2 *Circuit schematic*

of the current pulse is usually determined by the SCR, while the fall time is determined by the capacitor value and the total resistance in the discharge circuit.

Figure 1-3 shows the typical anode voltage and current waveforms of the SCR during the current pulse through the diode laser. The peak current, pulse width, and voltage of the capacitor discharge circuit are related for various load and capacitance values. The peak laser current and charged capacitor voltage relationships are given for several different capacitor values and typical laser types. The voltage and current limits of the SCR are also shown. Short pulse widths provide less time for the SCR to turn on than longer pulse widths; therefore, the SCR impedance is higher and more voltage is required to generate the same current. Also shown are the current pulse waveforms for the three different values of the capacitance. The capacitor is charged to the same voltage in all three cases, that is, 400 volts.

In conventional SCR operation, the anode current, initiated by a gate pulse, rises to its maximum value in about 1 microsecond. During this time, the anode-to-cathode impedance drops from an open circuit to a fraction of an ohm. In injection laser pulsers, however, the duration of the anode-cathode pulse is much less than the time required for the SCR to turn on completely. Therefore, the anode-to-cathode impedance is at the level of 1 to 10 ohms throughout most of the conduction period.

The major disadvantage of the high SCR impedance is that it causes low circuit efficiency. For example, at a current of 40 amps, the maximum voltage would be across the SCR, while only 9 volts would be across the laser diode. These values represent very low circuit efficiency.

The efficiency of a laser array is greater due to its circuit impedance being more significant. Because the SCR is used unconventionally, many of the standard specifications such as peak current reverse

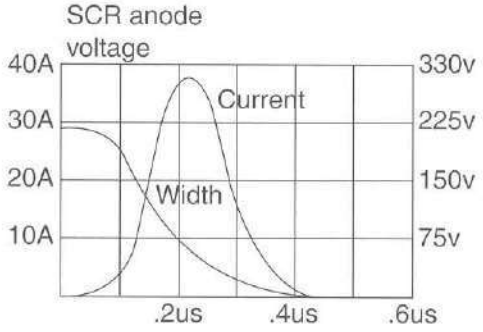

SCR operating curves

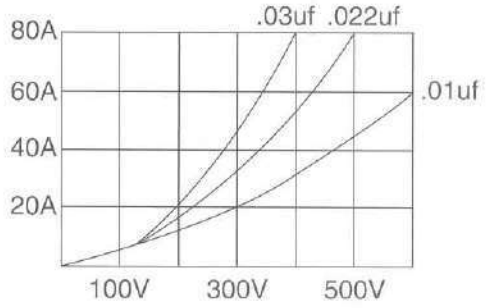

Capacitor voltage versus current peak

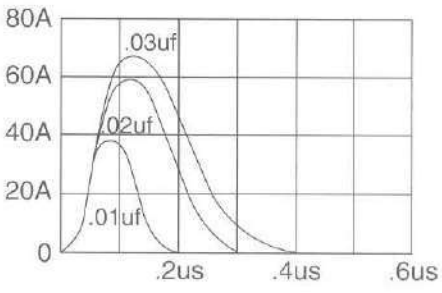

Capacitor value versus current peak

Typical curves and parameters for laser pulses using SCR silicon controlled rectifier and capacitor discharges

Figure 1-3 *SCR operating curves*

voltage, on-state forward voltage, and turn-off time are not applicable. In fact, it is difficult to select an SCR for a pulsing circuit on the basis of normally specified characteristics. The specifications important to laser pulser applications are the forward-blocking voltage and current rise time. A *use test* is the best and often the only practical method of determining the suitability of a particular SCR.

The voltage rating of the storage capacitor must be at least as high as the supply voltage. With the exception of ceramic types, most capacitors (metallized paper, mica, etc.) will perform well in this circuit. Ceramic capacitors have noticeably greater series resistance but are usable in slower speed pulsing circuits.

Lead lengths and circuit layout are very important to the performance of the discharge circuit. Lead inductance affects the rise time and peak value of the current, and it can also produce ringing and undershoot in the current waveform that can destroy the laser. A well-built discharge circuit might have a total lead length of only 1 inch and therefore an inductance of approximately 20 nanohenries. If the current rises to 75 amperes in 100 nanoseconds, the inductive voltage drop across this lead can be 15 volts. It is now obvious that if proper care is not taken in wiring the discharge circuits, high-inductive voltage drops will result.

A 1-ohm resistor in the discharge circuit will greatly reduce the current undershoot in single-diode lasers. Laser arrays usually have sufficient resistance to eliminate undershoot. The small resistance in the discharge circuit is also useful in monitoring the laser current, as described in the following section.

A clamping diode (D3) is added in parallel with the laser to reduce the current undershoot. Its polarity should be opposite that of the laser. Although the clamping diode is operated above its usual maximum current rating, the current undershoot caused by ringing is very short and the operating life of the diode is satisfactory.

Current Monitor

The current monitor in the discharge circuit provides a means of observing the laser current's waveform with an oscilloscope. A resistive-type monitor (R6) reduces circuit ringing and current undershoot, but the lead inductance of the resistor may cause a current reading that is higher than it actually is. A current transformer such as the Tektronix CT-2 can also be used to monitor the current and is not affected by lead inductance. Because the transformer does not respond to low-frequency signals, it should be used with fast waveforms that have a short pulse width and a fast fall time.

Charging Circuits

The second major section of the pulser is the charging circuit. This circuit charges the capacitor to the supply voltage during the time interval between the laser current pulses. It also isolates the supply voltage from the discharge circuit during the laser current pulse, thereby allowing the SCR to recover to the blocking state. Because the response times of the charging circuit are relatively long, lead lengths are not important and the circuit can be remotely located from the discharge circuit.

The simplest charging circuit is a resistor-cap combination. The resistor must limit the current to a value less than the SCR holding current, but it should be as low as practical, because this resistance also determines the charging time of the capacitor, C3.

Chassis Assembly

The following is a list of steps to construct the laser project.

1. Fabricate the copper chassis, as shown in Figure 1-4. This part is shown in Table 1-1 as being available.

2. Assemble the board as shown in Figure 1-5. Lay out and identify all the parts and pieces. Separate the components that go to the assembly board and fabricate the (PB1) perfboard from a 1.4 × 5-inch piece of .1 × .1 grid. Note the two holes for attachment to the copper chassis section from Figure 1-6.

3. Assemble the components as shown and observe the polarity of the capacitors and semiconductors.

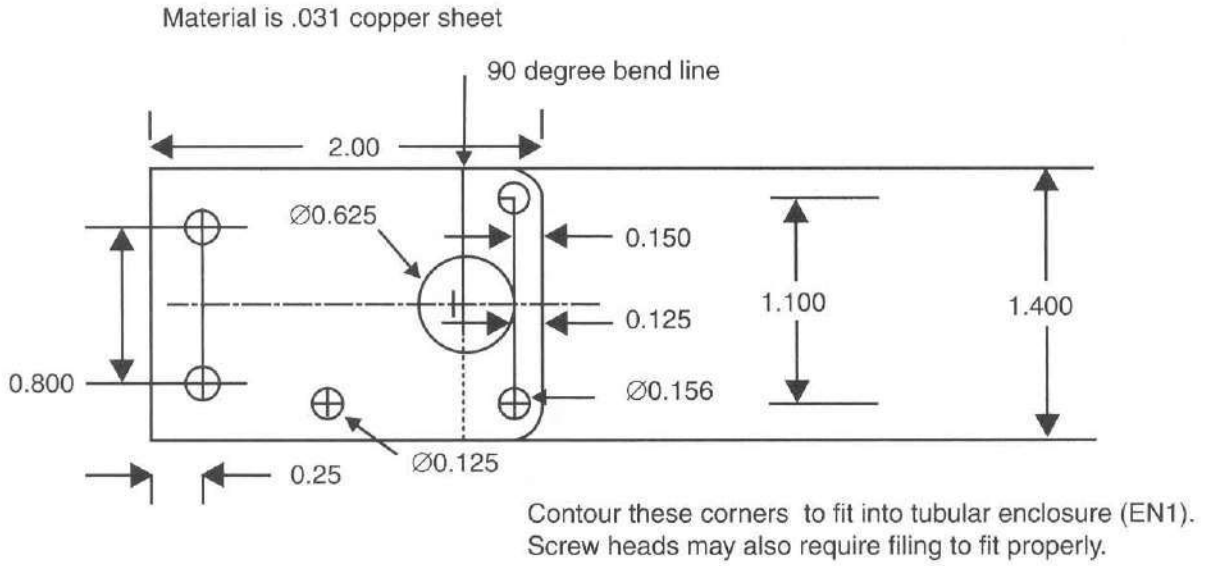

Figure 1-4 *Fabrication of laser chassis*

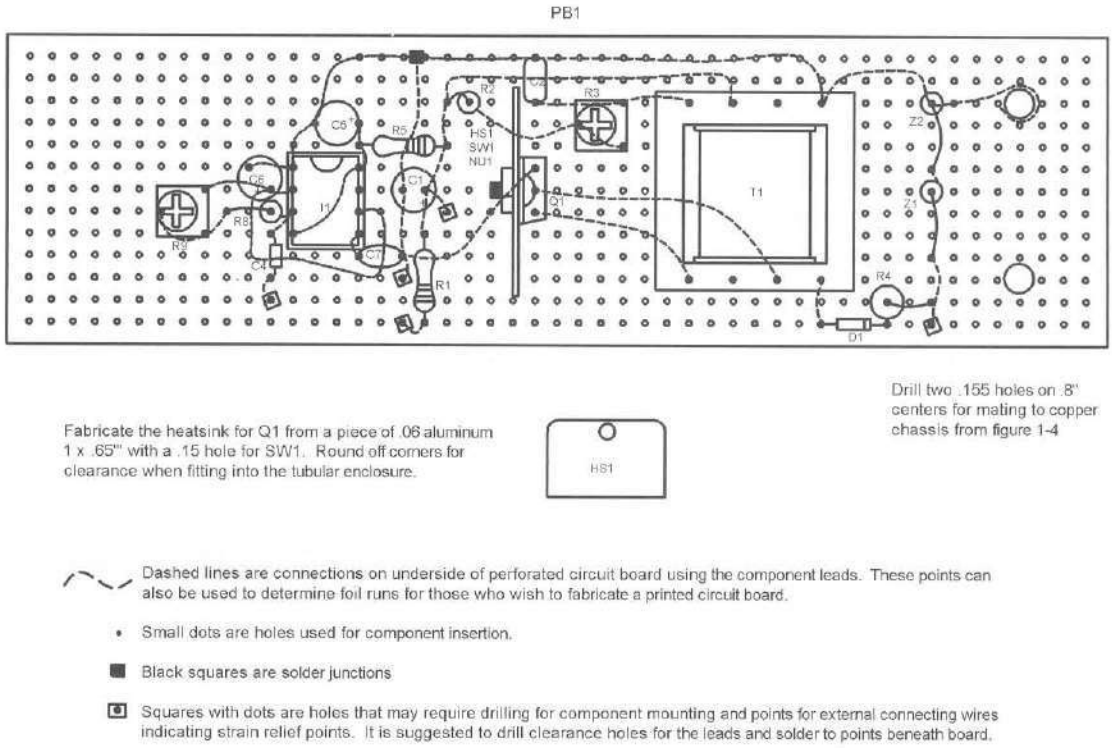

Figure 1-5 *Assembly board parts identification*

4. Connect the components using their actual leads wherever possible. Follow the layout and avoid bare-wire bridges.

5. Figure 1-6 shows the wiring of the copper chassis (COPCHA1). This type of wiring is preferred for high-frequency, sensitive, low-noise circuitry. It is used in this circuit due to the high-current pulses with fast rise times.

   Start by forming the leads and soldering to the copper plate. You will need a good hot soldering iron to do this correctly. The components themselves serve as anchor points and will be self-supporting when soldered to one another.

6. Figure 1-7 shows the interconnection of the copper chassis and the perforated assembly board via the two screws and nuts. Attach and connect the external leads and components as shown.

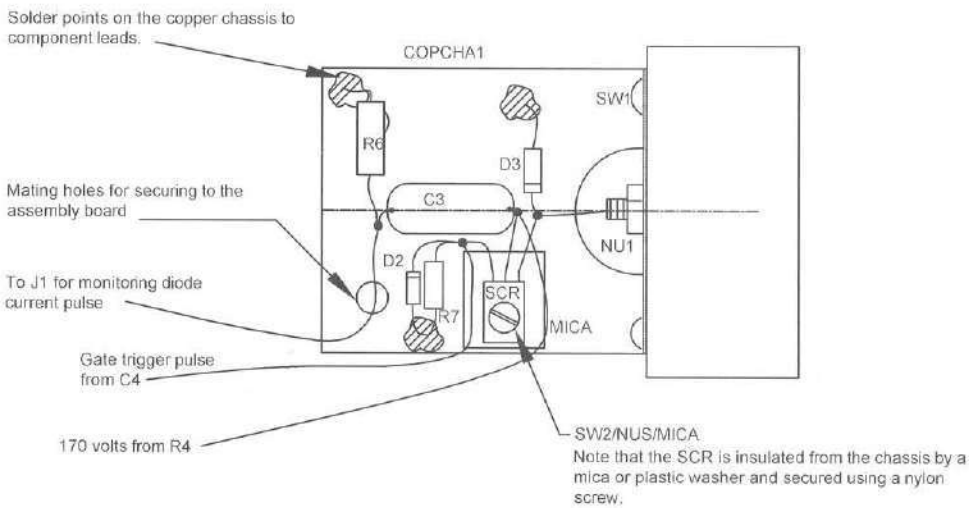

Figure 1-6 *Assembly of laser chassis*

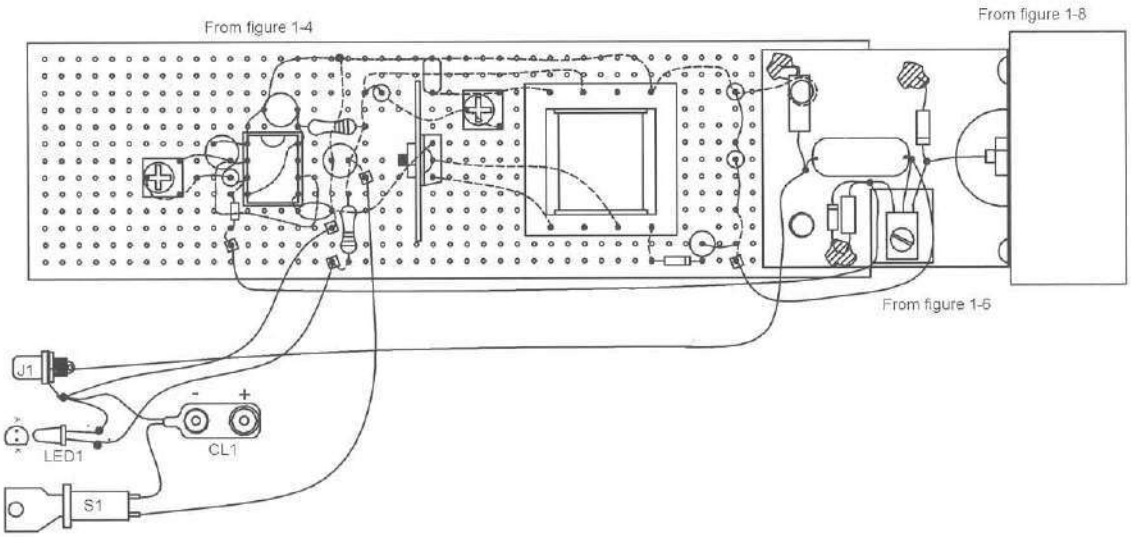

Figure 1-7 *Interconnecting the assembly board to the laser chassis*

7. Fabricate the LAHOLD1, as shown in Figure 1-8. Mount laser diode LD1 into the center hole and secure via a nut (NU1). Secure this assembly to the bent-down flange of the copper chassis. Use two 1/4-inch screws as shown.
8. A collimator adapter is shown and is optional.

Assembly Testing

The following steps will require basic testing equipment.

1. It is assumed at this point that the assembly is complete, as shown in Figure 1-7. Verify the circuit and preset the two trimpots R3 and R9 to midrange.
2. Obtain a 12-volt bench power supply and connect the 12 volts to the battery clip CL1. Turn on the key switch and note the LED coming on. A current meter on the bench supply should read approximately 300 milliamps.
3. Connect a scope to TP1, as shown in Figure 1-2, and adjust R3 for the waveshape as shown.
4. Connect the scope to TP2 and note a spiky waveform that verifies the trigger pulse to the SCR.
5. Connect the scope to TP3 and note the waveform, which is the voltage across the SCR. Note the flat spot indicating that capacitor C3 has reached full charge before the SCR is triggered. The top of this waveshape is affected by the pulse repetition rate and should support 500 repetitions per second when set by R9.
6. Connect the scope to TP4 and set it for a negative-going fast pulse, indicating the current waveform through the LD1 laser diode. If you have followed the instructions and your assembly of the copper chassis is secure with short leads, you should see a picture-perfect waveform as shown.

   Note that the current pulse is 40 amps and corresponds to 1 amp for every volt read at TP4. If you find the pulse is less, you can increase the voltage ratings on one of the zener diodes. The laser diode specified requires 40 amps for full output. Any value over 40 amps will greatly shorten the useful life of this part.
7. Verify the laser output by using a night vision scope or a video camera. You should see an indication of the output. Screw in LEN1 so it is flush with the holder and adjust for the smallest footprint at over 50 feet. Our lab model adjusted to about two turns below being flush with the holder for the best results. The output should be a sharp, narrow bar shape with the diode specified.

Material can be preferably aluminum or fabricated from a PVC rod.

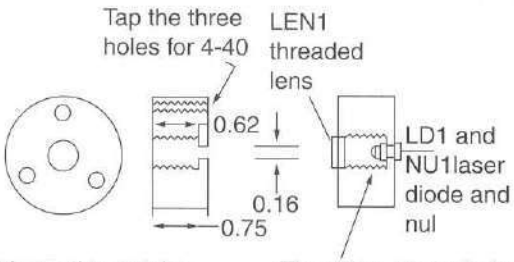

This section can be mated to section B when using a collimator with a C mount fitting.

Thread to .5" depth to mate with lens as supplied.

Optonal "C" mount collimator adapter fabricated from aluminum

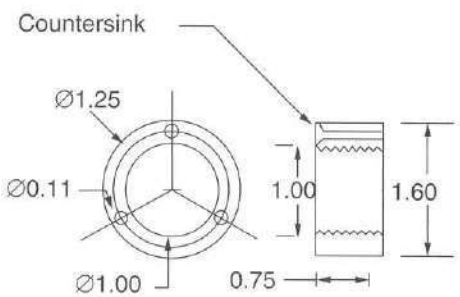

Section B adapter for fitting to the lens holder when using the optional collimator

Three mounting holes of .11 on a 1.25" diameter reference 120 degrees are mated to those in above

Thread for C lens at 1" diameter 32 tpi to a minimum of .375"

Figure 1-8 *Laser diode and lens holder*

Final Assembly

Create the EN1 enclosure from a 12 × 1.5-inch inner diameter plastic or aluminum tube (see Figure 1-9). Enclose the assembly and label it as shown in Figure 1-10. You may want to construct a mounting block or another assembly to mechanically connect the laser to a good, sturdy video tripod for future use.

Special Note

This laser is rated at 10 to 20 watts and is not to be confused with a continuous-output device rated at this power level. The advantage of this system is that the pulses are optically equivalent to 10 to 20 watts, and a suitable detection system will see them at this power level.

The equivalent energy output is related to the repetition rate times the peak power times the pulse duration and is approximately equal to joules. A joule is a watt second and is energy. If that energy is released in 1 microsecond as a pulse, the power of that pulse is now 1 megawatt.

A very suitable detector for this pulsed laser is our laser light detector described in Chapter 2, and a useful application for it as a laser property security fence is described in Chapter 5. Note that a laser pointer is 5 milliwatts, meaning the pulsed laser is 5,000 times more detectable.

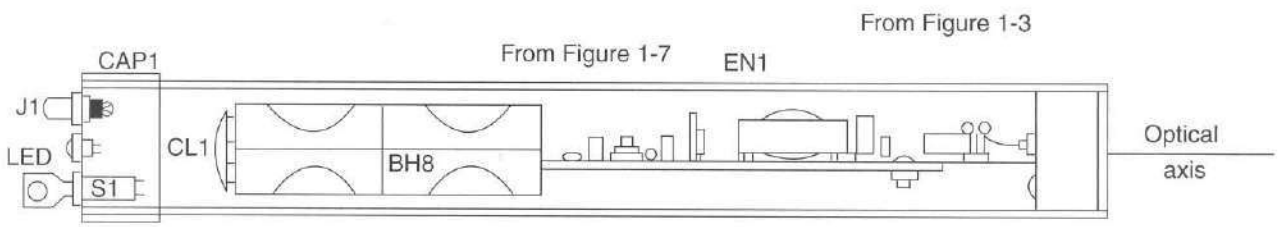

Figure 1-9 *X-ray view of enclosure*

CAUTION: Viewing of laser beam of direct reflections require the use of protective eye wear available through Information Unlimited at www.amazing1.com

Instruction

1. Turn key switch counterclockwise to verify unit is off. Note key is easily removed in the "off" position
2. Remove CAP1 and insert 8 AA batteries into holder.
3. Turn key clockwise and note LED lighting. If not, check the battery holder. Note key cannot be removed in the on position. Laser energy is infrared and can not be seen with the eye. You must use infrared detection devices such as our laser pulse detector or suitable night vision devices. Video cameras will often detect the laser.
4. Adjust collimator for desired effect if you are using.

Note that collimator will expand beam at near field but greatly reduce it at far field.

Compliance tests
1. Verify correct labels as shown
2. Key switch — nonremoval in off position
3. Beam indicator LED indicates beam emission

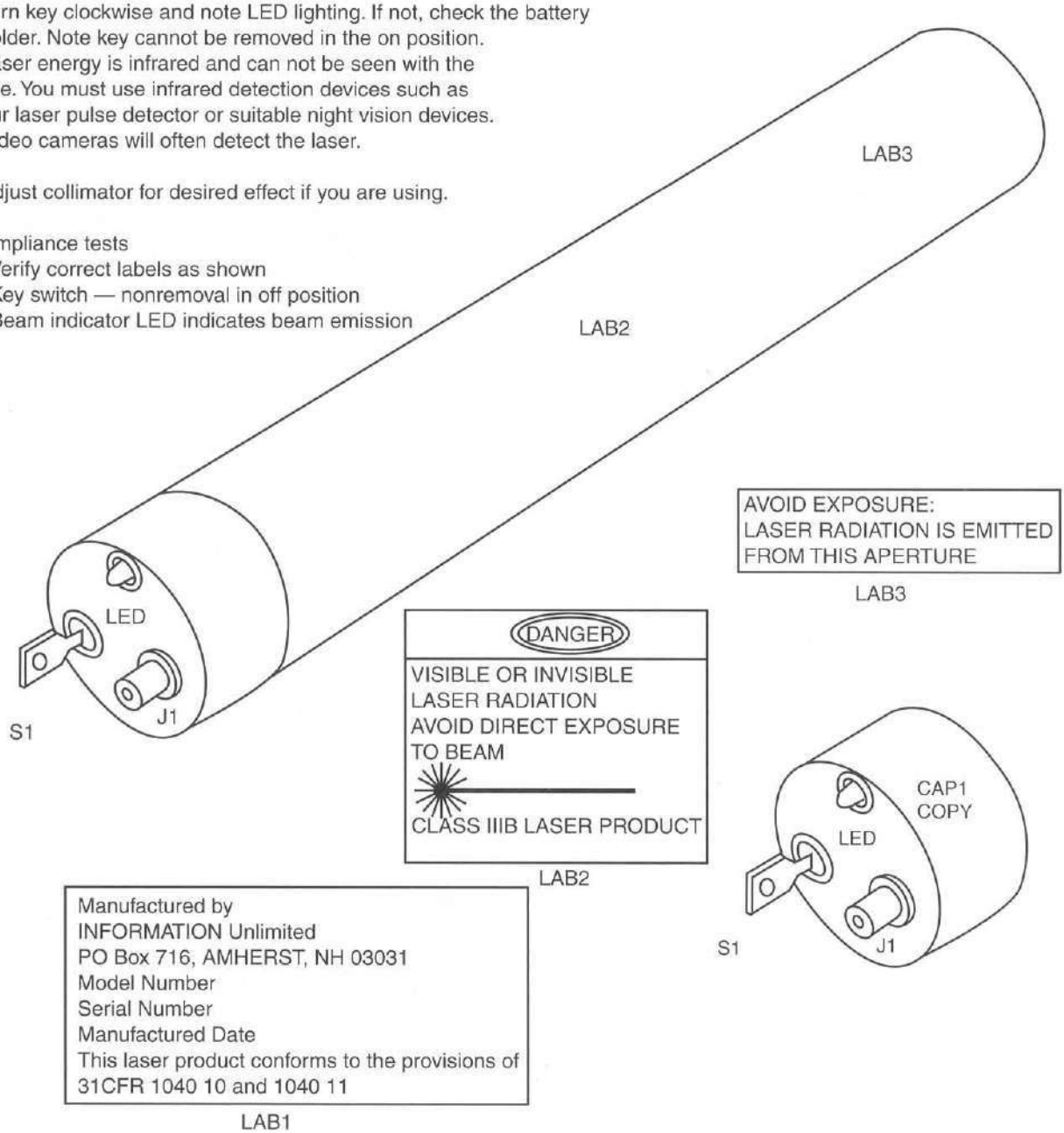

Figure 1-10 *Final assembly view and labels*

Table 1-1 Battery-Operated Infrared Laser Parts List

Ref. #	Description	DB Part #
R1	470 1/4-watt resistor (yel-pur-br)	
R2	220 1/4-watt resistor (red-red-br)	
R3	2K horizontal trimmer resistor	
R4	18K, 3-watt metal oxide resistor	
R5	10-ohm, 3/4-watt resistor (br-blk-blk)	
R6	1-ohm, 1/2-watt carbon resistor (br-blk-gold)	
R7	39 1/4-watt resistors (or-wh-blk)	
R8	1K 1/4-watt resistor (br-blk-red)	
R9	10K horizontal trimmer resistor	
C1,5	Two 10-microfarad, 50-volt vertical electrolytic capacitors	
C2	.047-microfarad, 50-volt plastic capacitor 473	
C3	.033-microfarad, 250-volt polypropylene capacitor	
C4	.1-microfarad, 50-volt plastic capacitor	
C6	1-microfarad, 50-volt vertical electrolytic capacitor	
C7	.01-microfarad/50-volt plastic capacitor (103)	
D1,3	Two 1N4937 1-kilovolt, 1-amp diode	
D2	IN914 silicon diode	
LED1	Bright green *light-emitting diode* (LED)	
LD1	40-amp, 10- to 20-watt, 904-nanometer TO18 pack laser diode	DB# LD650
SCR1	C106M 600-volt, 4-amp *silicon-controlled rectifier* (SCR)	DB# C106M
Z1	100/76-volt, 5-watt zener diode 1N5378	
Z2	150/108-volt, 5-watt zener diode 1N5383	
Q1	MJE3055T NPN power transistor in TO220 case	
I1	555 *dual inline package* (DIP) timer	
T1	400-volt square-wave-switching transformer	DB# TYPE1PC
PB1	1.4 × 5-inch, .1 × .1 grid perforated board	
S1	Key switch with non-removable key in on position	DB# KEYSWSM
J1	RCA phono jack	
COPCHAS1	Copper chassis, created in Figure 1-4	DB# COPCHAS1
LAHOLD	Laser and lens holder, created in Figure 1-8	DB# LAHOLD1
LENS13	Threaded lens	DB# LENS13
EN1	1 1/2-inch inner diameter × 1/32-inch wall × 12-inch plastic or aluminum housing tube	
CAP1,2	1 5/8-inch plastic caps, reworked as shown in Figure 1-9	
BH8	Eight AA cell holder	
SW1	Five 6-32 × 1/4-inch screws	
NU1	Four 6-32 hex nuts	
SW2	4-40 × 3/8-inch nylon screw	
MICA	Mica insulating washer	
NU2	4-40 hex nut	
HSINK	Heatsink tab for Q1	

Chapter Two

High-Speed Laser Pulse Detector

This project shows how to build a specialized device capable of detecting fast, high-speed optical pulses. A suitable laser generating these pulses is described in Chapters 1 and 4 and can have a range, limited only by the curvature of the earth. Its uniqueness is its ability to resolve these pulses with rise times in the nanosecond range. This capability makes it possible to transmit large amounts of information within a small period of time.

The heart of this device is the actual front-end detector, in this case a PIN diode device. PIN comes from *positive negative* (PN) junction with intrinsic layer (I). The characteristics of this detector are low capacitance, high resistance, and low leakage when operating in the reverse bias mode. It may also be used as a photo cell when operated in the forward mode.

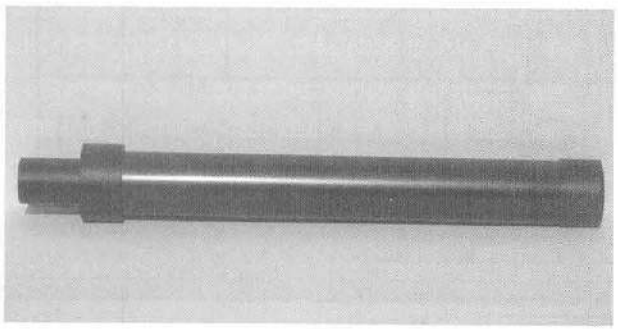

Figure 2-1 *The high-speed laser pulse detector*

The first part of the circuit is built on a piece of thin copper and uses discrete components. The builder may choose to build on a fully copper-clad circuit board if available, and a facsimile output can be set up via a phono jack or a BNC connector. A signal-conditioning circuit is shown built on a normal perforated circuit board and is designed to actuate a relay in the absence of the laser pulses. This mode of operation allows its use as a long-range laser perimeter or invisible fence intrusion detector, as described in Chapter 5.

Optics are shown for those wanting to operate at long ranges. Machined fittings are shown to mate with the 1.5-inch inner-diameter plastic enclosure used for the housing.

This is an intermediate- to advanced-level project requiring certain electronic skills, and one should expect to spend $35 to $70. All parts are readily available, with specialized parts obtainable through Information Unlimited (www.amazing1.com), and they are listed in Table 2-1.

Circuit Description

The circuit in Figure 2-2 utilizes a pin photodiode (LPIN) reverse biased by resistor R3. The reverse-biased photodiode produces a voltage across bias resistor R2. The response of the PIN photo detector is determined by the resistance of R2 and is relatively low due to the nanosecond rise time of the laser pulses detected. Capacitor C3 couples the positive-going detected laser pulses to the gate of a preamplifying *field effect transistor* (FET) Q1 where the negative-going pulse is amplified and fed into a second FET (Q2) for further amplification. NPN transistor Q3 again amplifies the positive-going pulse for Q2 to a negative pulse. This amplified signal is a reasonably good facsimile of the actual laser pulse and can be monitored or further processed via phono jack J1.

The negative-going pulses are also fed to a Schmidt discriminator that is in an untriggered state, providing that transistor Q4 continues to see these pulses. When the pulses are interrupted by an object in the laser path, Q4 turns on due to a positive bias set by trimpot resistor R15 and turns transistor Q5 off, regenerating the trigger state of the Schmidt discriminator. R15 allows the adjustment of a trigger threshold if required. The triggering time of the circuit also helps prevent false triggering such as flying birds, windblown debris, and insects.

The output of the Schmidt is DC coupled into the base of the emitter-follower transistor Q6 where the signal is inverted by transistor Q7. The negative-going level at the collector of Q7 now triggers timer I1 on for a preset time that controls an alarm or another function resulting from a qualified laser beam interruption. A relay (RE1) is shown in the circuit and can be used as normal open or normal closed contacts for control of external circuit functions. This is shown in the phasor pain field generator in Chapter 35.

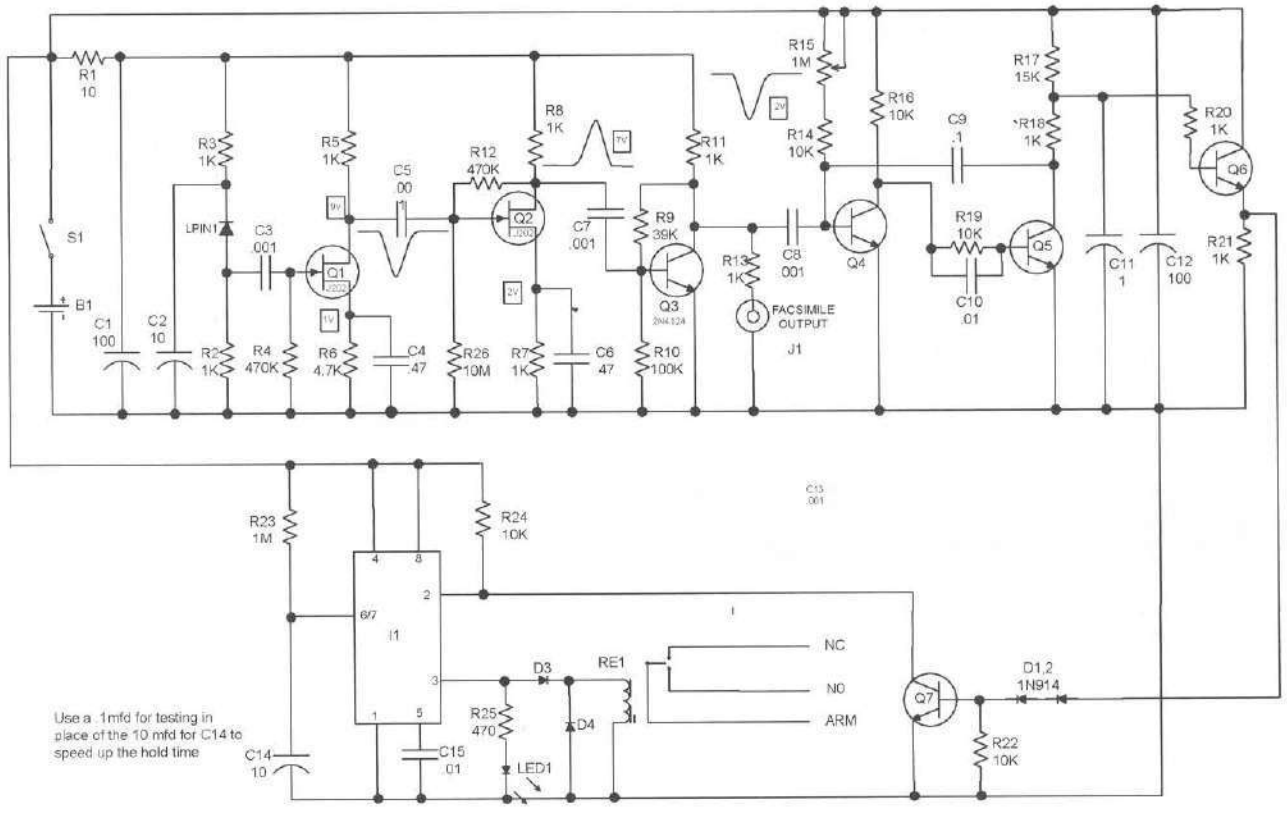

Figure 2-2 *Circuit schematic*

System Assembly

1. Assemble the board, as shown in Figure 2-3. Lay out and identify all the parts and pieces. Separate the components that go to the assembly board and create the PB1 perfboard from a 1½ × 5½-inch piece of .1 × .1 grid. Note the two holes for attachment to the copper chassis section.
2. Assemble the components as shown and observe polarity of the capacitors and semiconductors.
3. Connect the components using their actual leads wherever possible. Follow the layout and avoid bare-wire bridges. Note that Figure 2-3 shows pieces of #20 bus lead used as VC+ and COMMON rails. This approach is easier for wiring as it gives a direct route for the component leads.
4. Create the copper chassis as shown in Figure 2-4. This part is listed as a fabricated piece in Table 2-1.
5. Figure 2-5 shows the wiring of the COPCHA1 copper chassis. This type of wiring is preferred for high-frequency and sensitive, low-noise circuitry. It is used in this circuit due to the fast-rise-time, low-level-voltage pulses.

   Start by forming the leads and soldering to the copper plate. You will need a good, hot soldering iron to do this correctly. The components themselves serve as anchor points and will be self-supporting when soldered to one another.
6. Figure 2-6 shows the connection of the copper chassis and the perforated assembly board via the two screws and nuts. Attach and connect the external leads and components as shown.

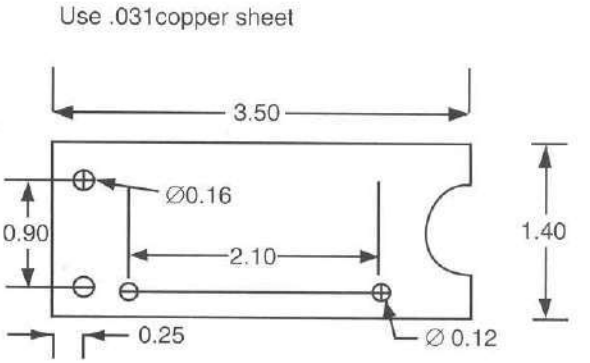

Figure 2-4 *Fabrication of the laser chassis*

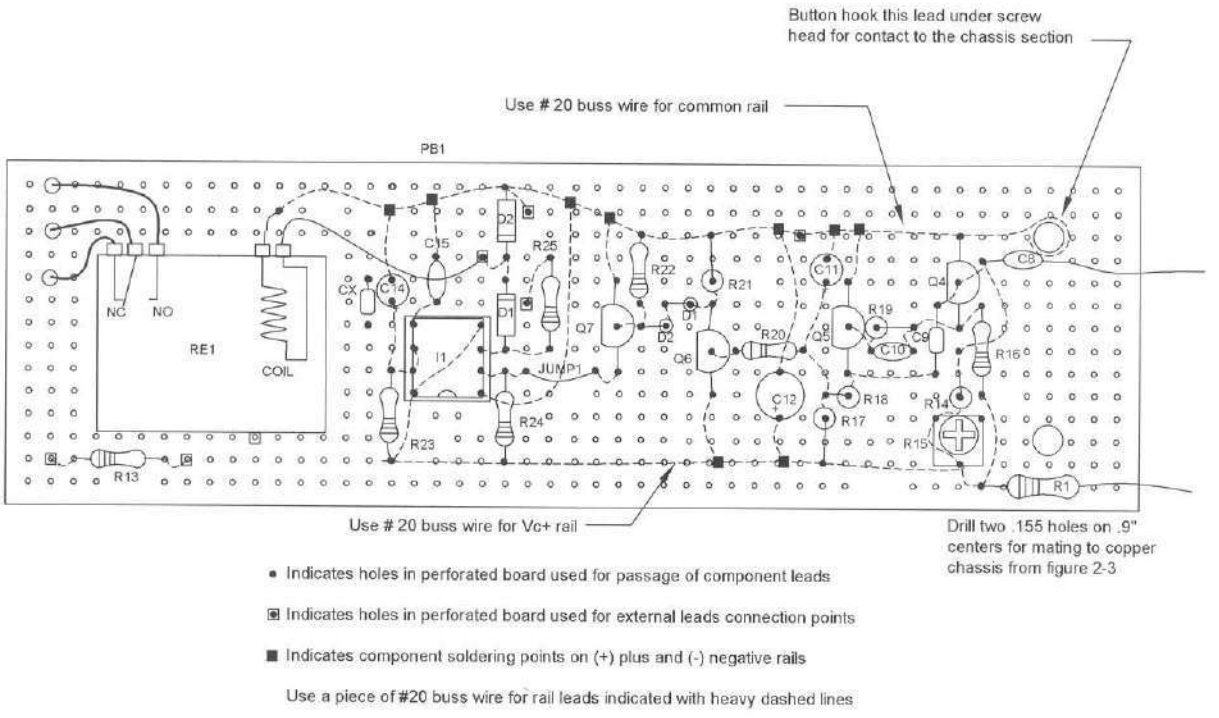

Figure 2-3 *Assembly board parts identification*

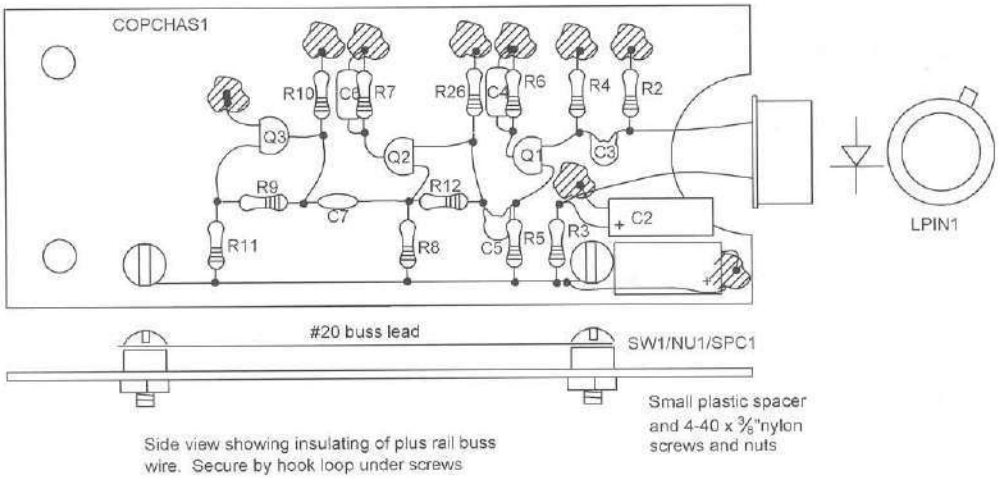

Figure 2-5 *Assembly of the laser chassis*

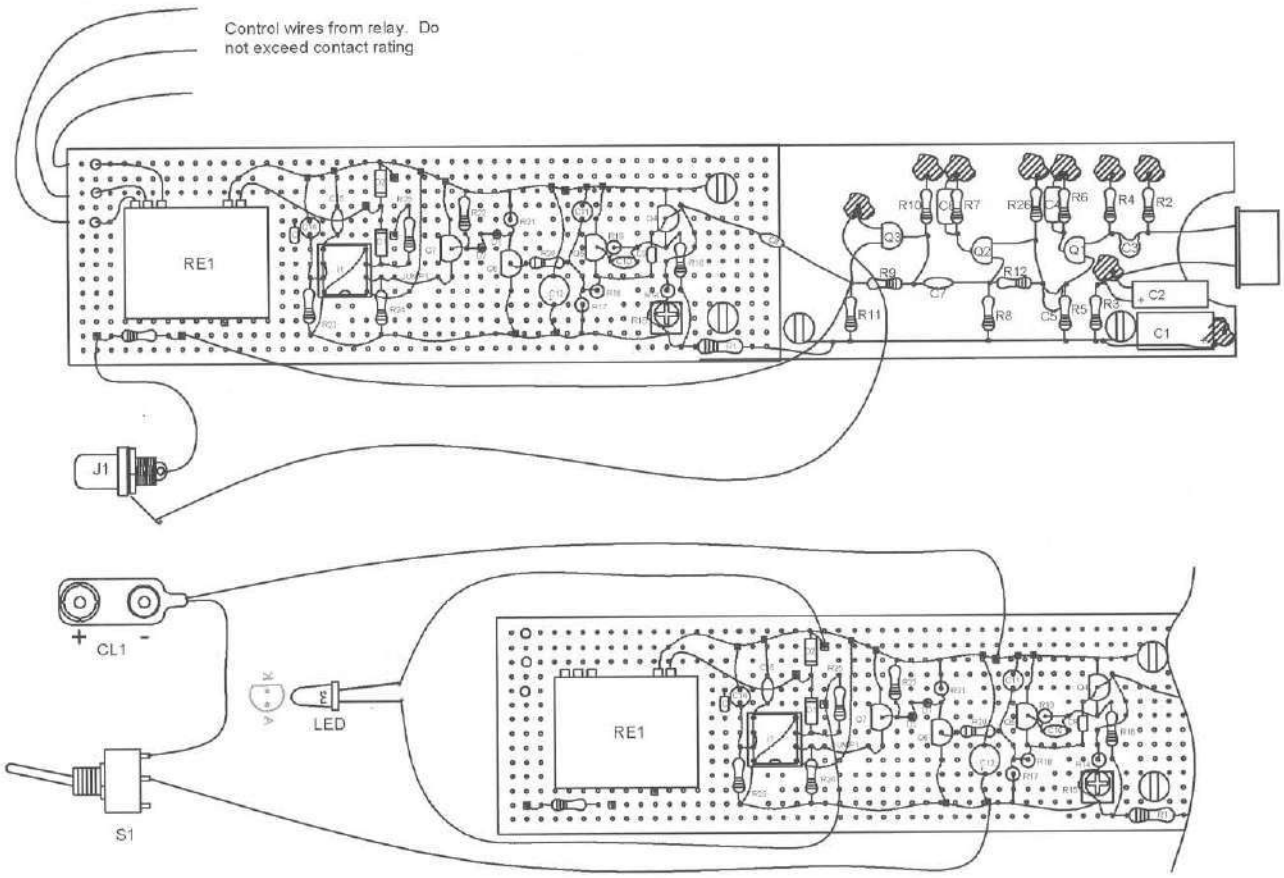

Figure 2-6 *Connection of board to chassis*

Assembly Testing

Testing of the laser receiver involves the use of a compatible laser transmitter to provide the necessary high-speed pulses. The laser described in Chapter 1 is recommended.

1. It is assumed at this point that the assembly is complete, as shown in Figure 2-6. Verify the circuit and preset the R15 trimpot to midrange. This test is performed *without* the circuitry installed and without a lens. You should temporarily replace C14 with a .1-microfarad value.
2. Obtain a 12-volt bench power supply and connect the 12 volts to the battery clip CL1. Turn on the S1 switch and note the LED coming on and flashing erratically. A current meter on the bench supply should read approximately 10 milliamps.
3. Measure the DC voltage levels, as indicated in Figure 2-2, noted in the squares. These values should be within 10 to 15 percent of those indicated.

At this point, you will need an optical laser pulse transmitter, such as that described in Chapter 1. Any suitable laser or optical transmitter will work with a fast pulse rise of 1 usec or so. The detector, as shown, uses a silicon PIN diode with a spectral sensitivity peak at 960 nanometers. This is very close to the spectral output of the lasers described in Chapters 1 and 4.

4. Position the laser pulse generator source so that it is pointing in the direction of the laser receiver being tested. You will need to connect a scope at the drain of Q1 and then attempt to position the receiver so it is receiving the pulses and is secure in this position. This may be tricky and require patience. When the laser is perfectly aligned with the receiver, the signal will block the Q1 and produce an overloaded waveshape. Carefully adjust the receiver off axis until the scope indicates the negative-going facsimile pulse as shown. Continue through the circuit and observe the waveshapes as shown, again adjusting the receiver off axis to obtain the required waveshape.

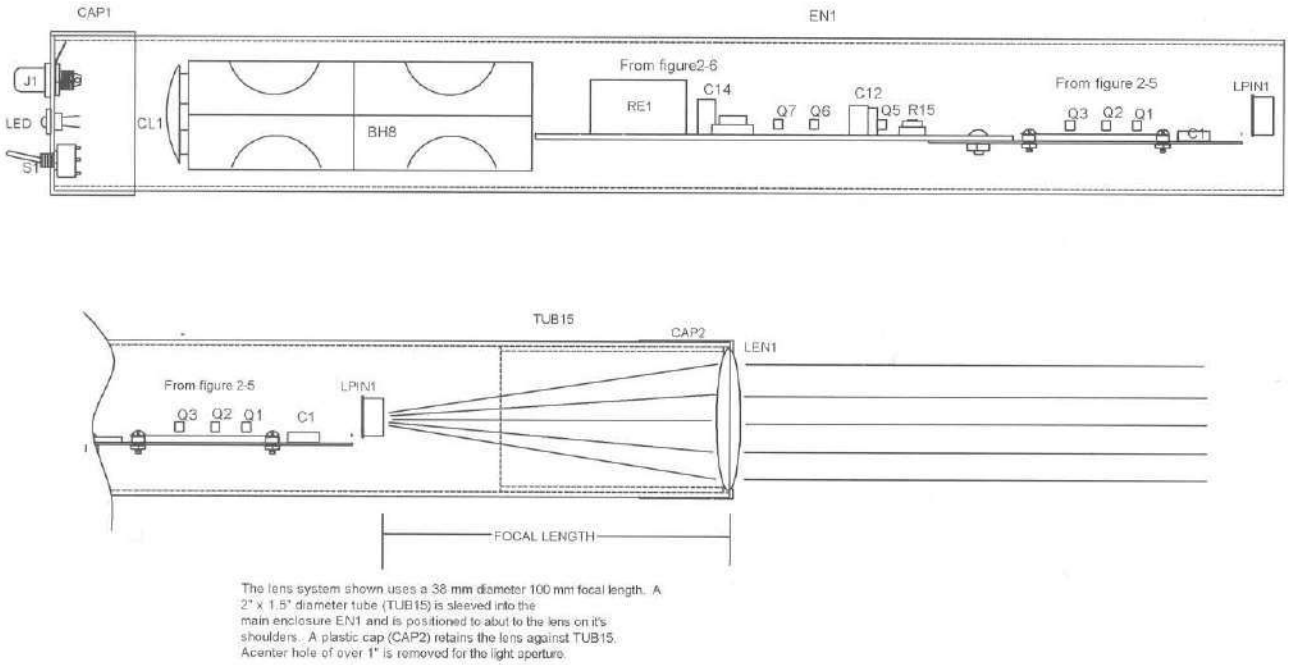

Figure 2-7 *X-ray view of enclosure*

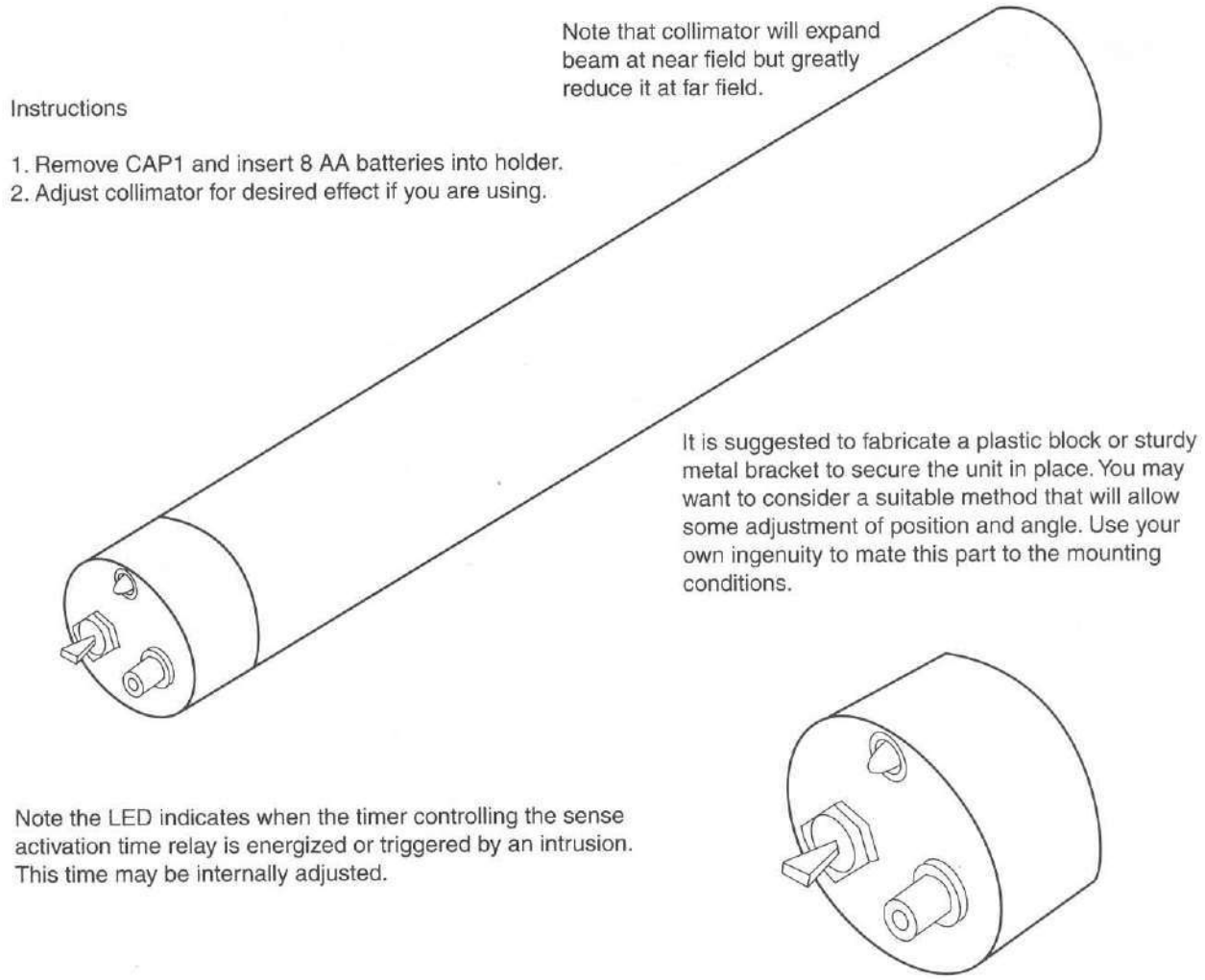

Figure 2-8 *Final assembly view*

Note that the LED will be off if the circuit is working and will come on if you block the light with a solid object.

5. Verify that the discriminator works and you can set the sensitivity trip level via R15. Verify the timer trips when the light beam is broken, activating the relay for a preset time as determined by the value of C14. This feature now allows external circuitry to be activated when the laser beam is broken, powering alarms or deterrents. The relay as shown provides a normally closed and open circuit that can be selected by the user. Do not switch loads that exceed the relay contact rating.

Final Assembly

Fabricate the EN1 enclosure from a 15 × 1.5-inch ID plastic or aluminum tube. Enclose the assembly as shown in Figure 2-7. You may want to create a mounting block or another assembly to mechanically connect the laser to a good, sturdy video tripod for future use

The system as shown is enclosed in a long tube that includes the batteries. You may separate the batteries and relay control circuits from the actual detection section consisting of the copper chassis and optics. This approach will be a two-part system that is connected via a cable or cord.

Special Note

This laser pulse detector receiver, when used with a pulsed laser like that described in Chapter 1, can have a control range exceeding that allowed by the curvature of the earth when used with suitable optics. Alignment is about as critical as sighting a high-powered rifle and requires extreme mechanical stability once set. The alignment of a long-range system requires patience, perseverance, and a little black magic.

Chapter 5 describes how to use both the laser pulser from Chapter 1 and the above assembly in a multiple-reflection property protection device with an ultrasonic shock deterrent.

Special Note on Photo Detectors

Two photo detectors are referenced in Table 2-1. LPIN is the low-cost piece that will usually provide the necessary operating parameters for most hobbyist laser projects. LPINX is more expensive and has a much lower dark current rating. It is used for lower noise and more sensitive circuitry.

Table 2-1 Laser Pulse Detector Parts List

Ref. #	*Description*	*DB Part #*
R1	10 ohms, 1/4 watt (br-blk-blk)	
R2, 3, 5, 7, 8, 11, 13, 18, 20, 21	Ten 1K, 1/4-watt resistors (br-blk-red)	
R4, 12	Two 470K, 1/4-watt resistors (yel-pur-yel)	
R6	4.7K, 1/4-watt resistor (yel-blk-red)	
R9	39K, 1/4-watt resistor (or-wh-or)	
R10	100K, 1/4-watt resistor (br-blk-yel)	
R14, 16, 19, 22, 24	Five 10K, 1/4-watt resistors (br-blk-or)	
R15	1M horizontal trimmer resistor	
R17	15K, 1/4-watt resistor (br-blk-or)	
R23	1M, 1/4-watt resistor (br-blk-grn)	
R25	470-ohm, 1/4-watt resistor (yel-pur-br)	
R25	10M, 1/4-watt resistor (br-blk-blue)	
C1, 12	Two 100-microfarad, 50-volt vertical electrolytic capacitors	
C2, 14	Two 10-microfarad, 50-volt vertical electrolytic capacitors	
C3, 5, 7, 8	Four .001-microfarad, 100-volt disc capacitors	
C4, 6	Two .47-microfarad, 50-volt plastic capacitors	
C9, 13	Two .1-microfarad, 50-volt plastic capacitors	
C10, 15	Two .01-microfarad, 50-volt plastic capacitors (103)	
C11	1-microfarad, 50-volt vertical electrolytic capacitor	
Q1, 2	Two J202 N-channel FET transistors	
Q3	2N4124 *negative positive negative* (NPN) high-frequency transistor	
Q4,5,6,7	Four PN2222 NPN general-purpose transistors	
D1,2	Two IN914 silicon diodes	
D3,4	Two IN4007 1-kilovolt, 1-amp diodes	
I1	555 *dual inline package* (DIP) timer integrated circuit	
LED1	High-brightness *light-emitting diode* (LED)	
*LPIN1	Silicon PIN photodiode dark current less than .10 nano-amp (see text)	DB# PIN
*LPIN1X	Silicon photo diode dark current less than .02 nano-amp (see text)	DB# PINX
RE1	12-volt coil, 400-ohms, 120 VAC 15-amp contacts	DB# RE12115
COPCHAS1	1.4 × 3.5-inch .031 copper plate (see Figure 2-4)	
SW1/NU1	Four 4-40 × 3/8 nylon screws and metal hex nuts	
SPC1	Two 1/4-inch plastic spacers	
PB1	5½" × 1½" .1 × .1 grid perforated circuit board	
J1	Chassis mount RCA phono jack	
S1	Small *single pole, single throw* (SPST) toggle switch	
CL1	Battery clip	
BH8	Holder for 8 AA cell battery	
EN1	1 1/2-inch inner diameter × 1/32-inch wall plastic or aluminum tube	
CAP1, 2	Two 1 5/8" plastic caps reworked as shown in Figure 2-8	
LEN1	38 mm × 100 mm focal length DCX glass lens	DB# 38100
RET1	Reworked 1 1/2-inch plastic cap for retaining lens	
TUB15	2-inch length of 1.5-inch outer diameter plastic or aluminum tube	

Chapter Three

Ultra-Bright Green Laser Project

This ultra-bright green laser project, as shown in Figure 3-1, is intended for the laser experimenter who desires to add a simple optical system that provides far-field focusing, beam collimation, or beam expanding.

Construction parts such as tubing, handles, brackets, and hardware are all readily available from most local hardware stores (see Table 3-1). Our suggested lab approach is to locate some telescopic tubing of metal or plastic, or a combination of both, and fabricate the laser and lens holders from a suitable sized plastic rod or equivalent. The center holes of the holders must be as true as possible or the optical system's integrity will be greatly degraded.

Figure 3-1 *Photo of green laser project*

The grip or handle is created from a 1-inch-thick piece of finished pine that has a section carefully removed for the battery holder and push-button switch. Passage holes for the power leads are drilled as shown. You may also use a suitable sized plastic box. A clear piece of Lexan (polycarbonate) sheet is formed with a flange at a 90-degree bend and is the surface for mounting the switch. This cover is screwed to the wooden handle and makes an attractive design if done with care and precision. The handle can be constructed with a contoured shape to match the curvature of the tube, and you may also add rings, fins, and other décor to make a space-age optical ray gun.

The operation of the laser allows usage without any optics, providing similar performance to a high-quality laser pointer. The addition of the lens system allows far-field focusing, close range expansion, and far-field collimation where the beam spot impact will be reduced by the collimating power of the system. As an example, the bare foot beam diameter (or operation without external optics) at 300 meters will be approximately a 50-centimeter diameter spot. With an ×10 collimator, the diameter can be reduced to 5 centimeters.

This is a class iiia beginner's laser project that uses a working laser module. Class iiia is a classification for lasers under 5 milliwatts of output power

Never point it at vehicles, aircraft, or directly at people. Expect to spend $40 to $50 for this very rewarding laser project.

Assembly Steps

1. Rework the laser module (LM1) as shown in Figure 3-2.
2. Wire the laser module with pushbutton switch (SW1) and battery clip (CL1) as shown in Figure 3-3.
3. Make final assembly as shown in Figure 3-4.
4. Connect batteries and activate SW1. Note a green impact point. Adjust lenses as shown for desired beam profile.

The green laser module has a built in push button switch that may be bypassed by adding a connection lead as shown. This added lead is the negative input. The spring connection is also the negative input but now requires activation of the built in switch. The positive input can be a mechanical connection to the brass housing by wrapping a bare lead around the slot. You may also carefully solder a lead as shown for this positive input point.

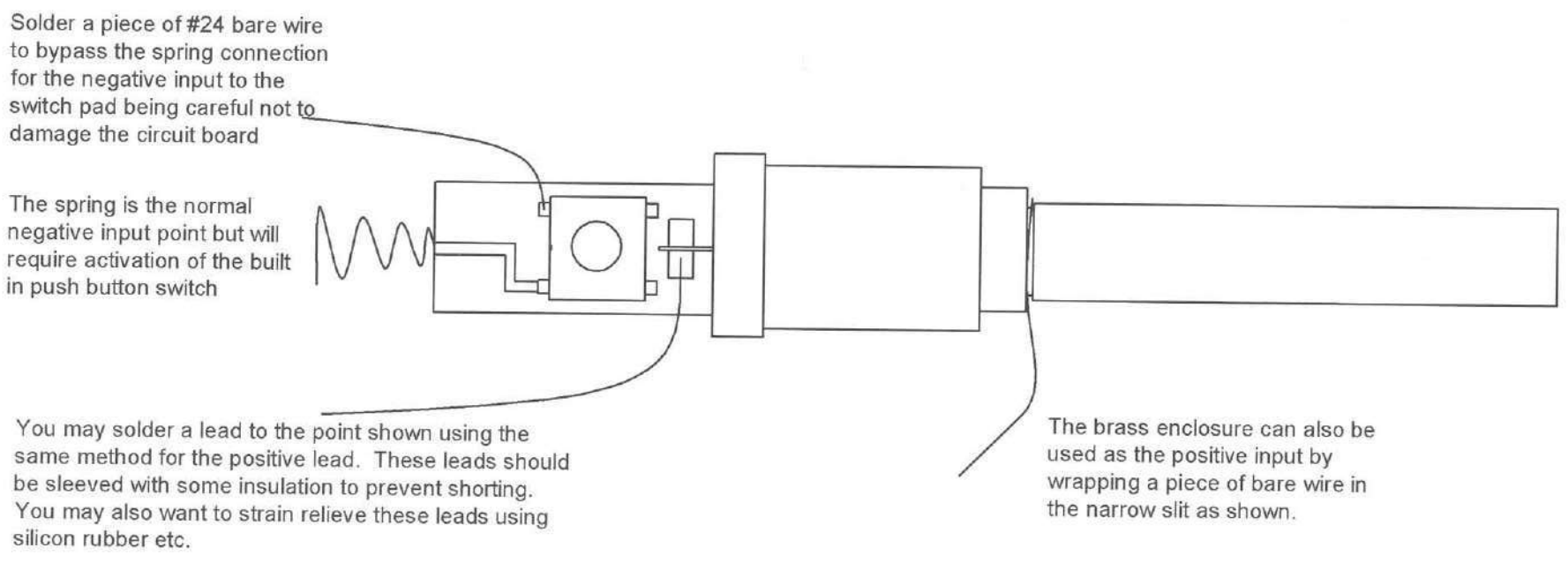

Figure 3-2 *Laser module rework*

LEN2 position will depend on focal lengths and focus distance of target. LEN1 lens distance from module is not critical, but attempt to get close to module as this will limit overall length of system. Lenses are mounted inside of fabricated bushings/holders and secured in place by small trace amounts of glue. Lenses must be perfectly centered for proper operation. The magnification value of the system is determined by the focal length of the convex lens divided by that of the concave lens. This value expands the beam width but decreases the beam divergence by the same factor greatly increasing the range capability producing a much smaller spot size at far field.
Approximate position shown for lenses supplied with kit. Adjustment is by varying the seperation distance between LEN1 and LEN2. Start at a distance (fx) of approx 6.25mm (2.5")

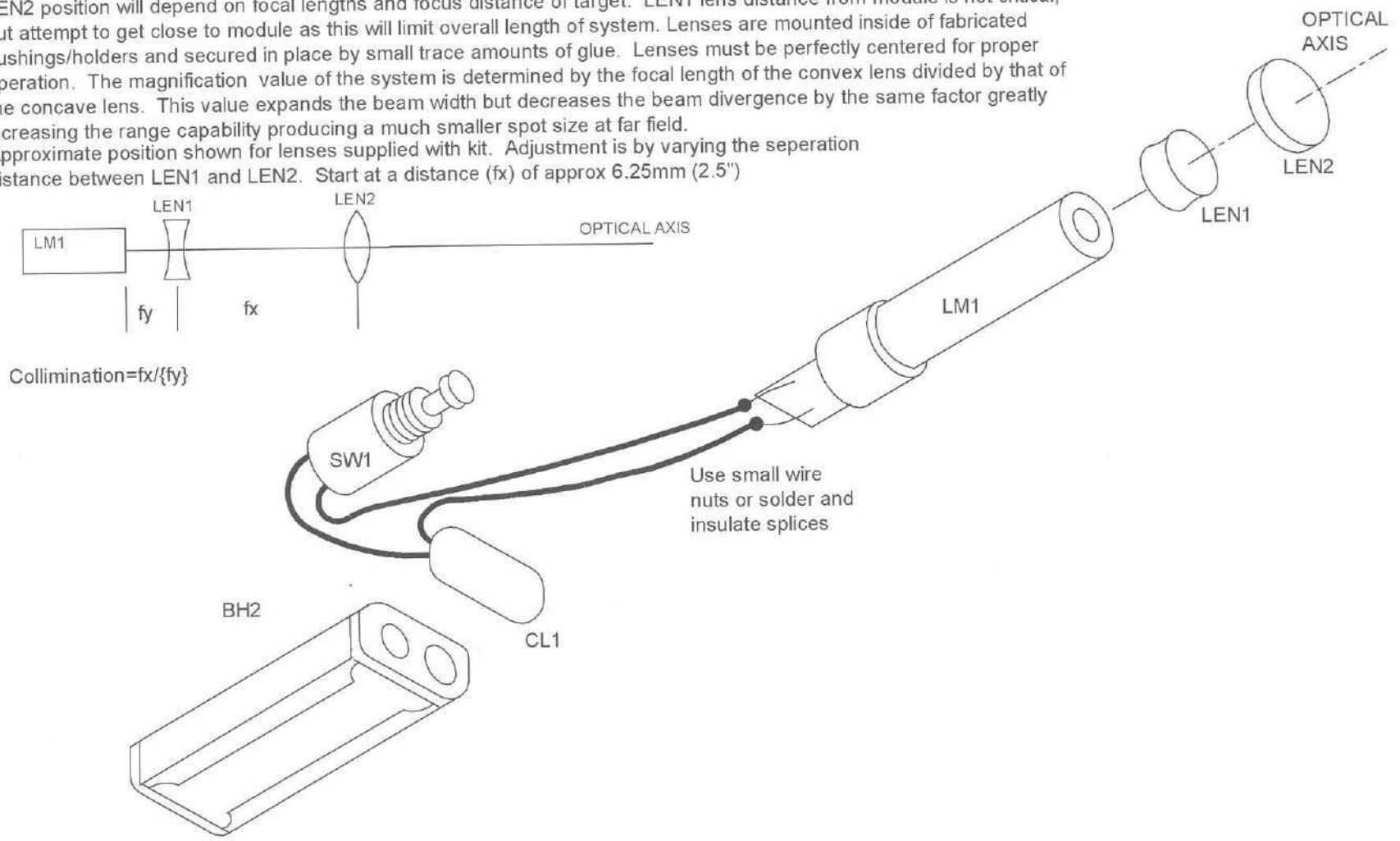

The green laser module has a built in push button switch that may be bypassed by adding a connection lead as shown. This added lead is the negative input. The spring connection is also the negative input but now requires activation of the built in switch. The positive input can be a mechanical connection to the brass housing by wrapping a bare lead around the slot. You may also carefully solder a lead as shown for this positive input point.

Figure 3-3 *Ultra bright green isometric assembly*

Holders for laser module and lenses may be made from fabricating wooden or plastic dowels to the required dimensions.

Fabricate OD to a snug sliding fit to ID of housing tube

Fabricate ID to snug fit to OD of lens or laser module

The BRK1 is formed over TUB1 and secures this assembly to the wooden handle via four small #6 screws

Tubing pieces should telescopically fit for easy adjustment of collimator. Start with around a 1" diameter section for TUBE1 and obtain a suitable size for TUBE2. You may ream out the larger tube or turn down the smaller for a suitable sliding fit. Note that clear plastic tube provides a good transparent housing that may enhance your science project.
Note the dimensions may be varied to fit available sizes of lenses etc.

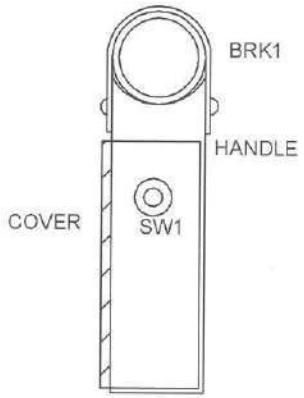

Front view looking into laser.

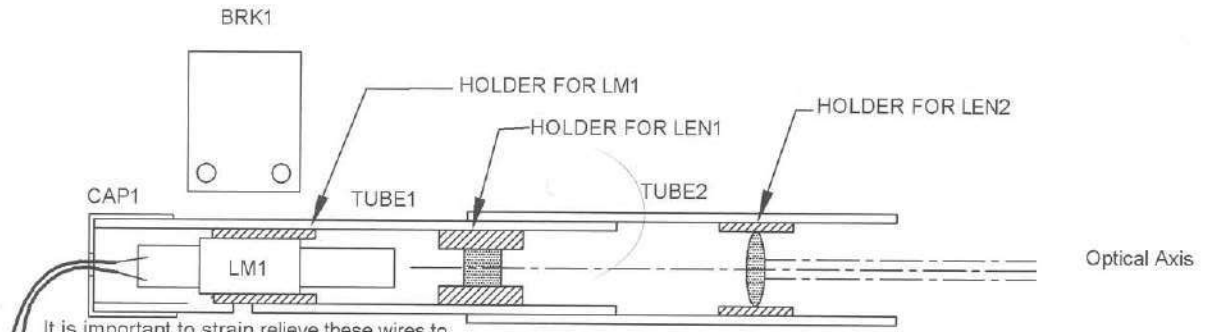

It is important to strain relieve these wires to the module as connections to the board are very fragile

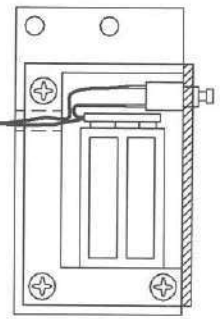

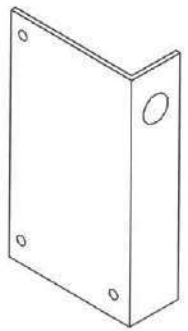

The handle can be fabricated from a piece of 1" pine removing a section with a chisel or jig saw to form out a compartment for the battery holder and switch. A plastic cover fits over the cut out section and is fabricated as shown. This forms a neat appearing and transparent assembly. File to fit contour of tubing.

Clear piece of formable plastic such as lexan or equivalent. Fab as shown

Figure 3-4 *Ultra bright green optical laser gun suggested final design*

Table 3-1 Ultra-Bright Green Laser Parts List

Ref. #	*Description*	*DB Part #*
SW1	Pushbutton NO switch	
BH2AA	Two-cell AA battery holder	
CL1	Battery snap clip	
LM1	5-milliwatt green laser module	DB# LM-532-P5
LEN1	Concave lens .6 × -.75-inch focal length	DB# LE15
LENS	Convex lens .9 × 3.5-inch focal length	DB# LE2475
LAB1	Class 3a danger laser label	
LAB2	Certification label	
LAB3	Aperture label	
The mechanical parts you get yourself; they are not critical and those shown represent our finalized lab approach.		
TUBE1	1-inch OD thin-walled plastic tubing	
TUBE2	Tube for telescope over TUBE1	
HANDLE	2 × 4 × 1-inch piece of soft pine	
COVER	Piece of 1/16-inch clear plastic sheet	
BRK1	1/32 × 1/2-inch aluminum bracket	
LENS HOLDERS	Wood or plastic dowels	
SCREWS	Small wood	

Chapter Four

115 VAC, 5- to 50-Watt Pulsed Infrared Laser

This project shows how to construct a laboratory-use, solid-state, pulsed infrared laser (see Figure 4-1). The system utilizes a gallium arsenide laser diode providing pulse powers of 10 to 100 watts depending on the diode used. The device operates from the 115 VAC line via an isolation transformer and is constructed in two parts. The laser is an excellent source of variable-frequency pulses adjustable from 10 to 2,500 repetitions per second of infrared energy.

The laser, when assembled as shown, is a class iiib device and requires the appropriate labeling and several included safety functions, as described in the assembly instructions. At no time should it be pointed at anyone without protective eyewear or at anything that could reflect these pulses. Also, never look into the unit when the power is on. It is intended to be used for ranging, simulated weapons practice, intrusion detection, communications and signaling, and a variety of related scientific, optical experiments and uses.

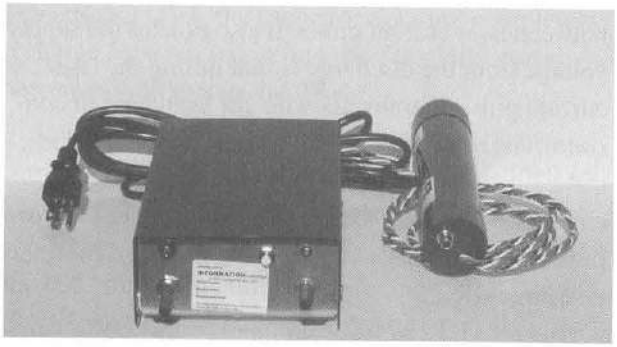

Figure 4-1 *IR laser*

This is an intermediate- to advanced-level project requiring electronic skills and basic electronic shop equipment. Expect to spend $100 to $150. All parts are readily available, with specialized parts obtainable through Information Unlimited (www.amazing1.com), and they are listed in Table 4-1.

Theory of Operation

A laser diode is nothing more than a three-layer device consisting of a *pn* junction of *n*-type silicon, a *p*-type of gallium arsenide, and a third *p* layer of doped gallium arsenide with aluminum. The *n*-type material contains electrons that readily migrate across the *pn* junction and fill the holes of the *p*-type material. Conversely, holes in the *p*-type migrate to the *n*-type and join with electrons. This migration causes a potential hill or barrier consisting of negative charges in the *p*-type material and positive charges in the *n*-type material that eventually cease growing when a charge equilibrium exists. In order for current to flow in this device, it must be supplied at a voltage to overcome this potential barrier. This is the forward voltage

Table 4-1

INFO #	*Pulse width*	*Package*	*Diodes*	*Peak current*	*Emitting area*	*Peak power*	*Duty factor*	*Beam symmetry*	*Spectral width*
LD660	200 ns	TO18	1	40 amps	9 × 1	12 watts	.1%	15 × 20	3.5 nm
LD780	200 ns	TO5	2	40 amps	21 × 1	20 watts	.1%	15 × 20	3.5 nm
LD1630	200 ns	TO5	2	40 amps	21 × 1	30 watts	.1%	15 × 20	3.5 nm

drop across a common diode. If this voltage polarity is reversed, the potential barrier is simply increased, assuring no current flow. This is the reversed bias condition of a common diode.

A diode without an external voltage applied to it contains electrons that move and wander through the lattice structure at a low, lazy average velocity as a function of temperature. When an external current at a voltage exceeding the barrier potential is applied, these lazy electrons now increase their velocity to where some, by colliding, acquire a discrete amount of energy and become unstable, eventually emitting this acquired energy in the form of a photon after returning to a lower energy state. These photons of energy are random both in time and direction; hence, any radiation produced is incoherent, such as that of a *light-emitting diode* (LED).

The requirements for coherent radiation are that the discrete packets of radiation must be in the form of a lockstep phase and in a definite direction. This demands two essential requirements; first, sufficient electrons at the necessary excited energy levels and, second, an optical resonant cavity capable of trapping these energized electrons for stimulating more and giving them direction. The amount of energized electrons is determined by the forward diode current. A definite threshold condition exists where the device emits laser light rather than incoherent light, such as in an LED. This is why the device must be pulsed with a high current. The radiation from these energized electrons is reflected back and forth between the square-cut edges of the crystal that form the reflecting surfaces due to the index of refraction of the material and air.

The electrons are initially energized in the region of the *pn* junction. When these energized electrons drift into the *p*-type transparent region, they spontaneously liberate other photons that travel back and forth in the optical cavity interacting with other electrons commencing laser action. A portion of the radiation traveling back and forth between the reflecting surfaces of these mirrors escapes and constitutes the output of the device.

Circuit Theory of Operation

AC power, as shown in Figure 4-2, is obtained via polarized plug CO1 through fuse FH1. Proper grounding of the green cord lead is a necessity to prevent an unnecessary shock hazard along with usage of grounded test and measuring equipment. S1 is a key switch type where the key can be removed only in the off position. Transformer T1 provides a one-to-one ratio and isolation from the power line, while step-down transformer T2 provides the low voltages necessary for the control circuits. The power indicator lamp consists of neon lamp NE1 and associated current-limiting resistor R1.

Diodes D1 and D2, along with capacitors C1 and C2, comprise a voltage doubler. The voltage across C1 and C2 is 1.4 × 230 or approximately 340 volts.

A major section of this laser pulser is the charging circuit. This circuit charges the pulse discharge capacitor (C10) to the supply voltage during the time interval between laser current pulses. It also isolates the supply voltage from the discharge circuit during the laser current pulse, thereby allowing the switching *silicon-controlled rectifier* (SCR) to recover to the blocking state. Because the response times of the charging circuit are relatively long, lead lengths are not important, and the circuit can be remotely located from the discharge circuit.

The simplest charging circuit is a resistor-capacitor combination. In this simple case, the resistor must limit the current to a value less than the SCR holding

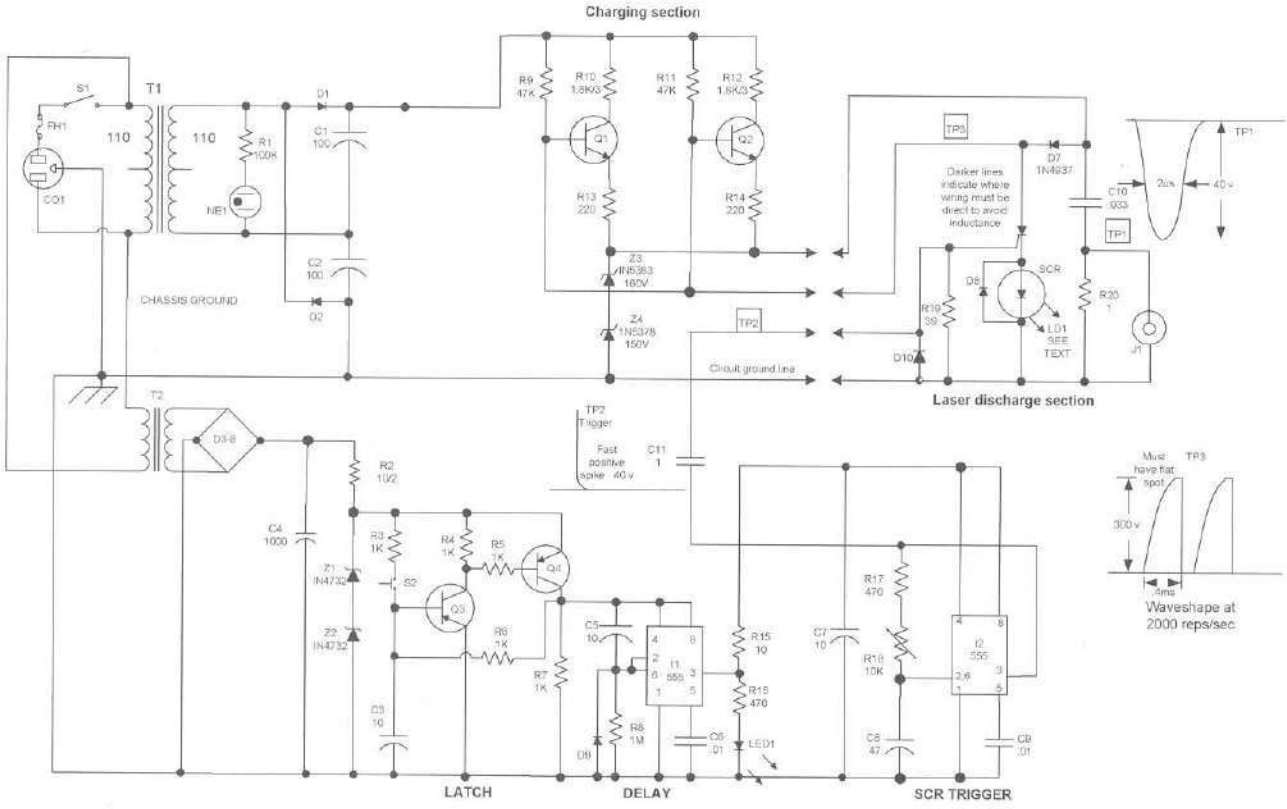

Figure 4-2 *Circuit schematic*

current but should be as low as practical because this resistance also determines the charging time of the capacitor C10, thus determining the available laser pulse repetition rate at full energy. For example, a resistance of 40 kilo-ohms limits the current to 10 milliamps from a 400-volt supply. This current value is just at the holding level of an average SCR. A time of almost 4 milliseconds is required to charge C10, a 0.033-microfarad capacitor, to the supply voltage in three time constants through a 40-kilo-ohm resistor. Therefore, the *pulse repetition rate* (PRR) of the pulsing circuit is limited to less than 250 Hz. If the PRR exceeds this value, the capacitor does not completely recharge between pulses and the peak laser current decreases with increasing PRR.

Varying the supply voltage may control the peak current in the discharge circuit, provided the PRR is low enough to allow the capacitor to fully recharge between current pulses. Both the supply voltage and the PRR determine the peak laser current. A considerable risk exists in increasing the supply voltage to compensate for an insufficient recharge time. If the PRR is decreased while the supply voltage is high, the capacitor again recharges completely, and the laser pulse current increases to a value that may damage or destroy the laser diode.

The needs for a variable voltage supply and the low PRR limit are the major disadvantages of the resistive-type charging network. Therefore, the limitations of the simple resistor drivers are that a resistor large enough to keep the current below the holding current of the SCR also limits the pulse repetition rate.

The frequency capability of the pulse power supply can be greatly improved with the charging circuits, as described. Capacitor C10 is charged to the supply voltage when the SCR is not conducting. Diode D7 is in the off state, because no current flows through it during this period. At the onset of a pulse trigger at the gate, the impedance of the SCR drops rapidly and capacitor C10 discharges toward ground potential. During this period, current is surging through diode D7, causing zero biasing of the current-control transistors (Q1, Q2) by shorting the bias resistors (R9, R11). The SCR now turns off when the current drops below its holding current. The voltage across capacitor

C10 then charges back to the supply voltage. During the capacitor charge cycle, diode D7 passes no current, and Q1 and Q2 are forward biased into the saturation region. Obviously, the charging time of C10 is now shorter due to being charged through the smaller-value resistors (R10, R12). The emitter resistors R13 and R14 balance the current through Q1 and Q2.

Zener diodes (Z3, Z4) are selected to regulate and provide the proper required current pulse for the laser diode in operation. The zener diodes provide a maximum charge voltage of 310 volts that produces 40 amps through laser diode LD1 for up to 2,500 laser pulses per second.

Other laser diodes may require a selection of other voltage-rated zener diodes. The builder may wish to provide a multiposition switch to select these various combinations of zener diodes externally via a front panel control.

The trigger circuit consists of an astable timer (I2) that derives its power through the output of timer I1, which provides a delay time required for FDA laser compliance. The trigger and delay circuitry, as well as the timers, are powered by 12 VDC from transformer T2 and rectifier diodes D3 through D6. Capacitor C4 filters the rectified wave and steps up the voltage to 15 VDC. Resistor R2 drops the 15 volts to the zener voltage of zener diodes Z1 and Z2 of regulated 12 VDC.

Operation of the laser requires activating pushbutton switch S2, which latches transistor Q4 upon supplying power to timer I1. The timer must time out to 10 seconds, as determined by resistor R8 and capacitor C5. The emission indicator LED1 comes on simultaneously with power to the trigger timer I2, which pulses the laser diode LD1. The laser pulse rate is determined by external pot R18.

Notes on SCR

In the conventional operation of an SCR, the anode current, initiated by a gate pulse, rises to its maximum value in about 1 microsecond. During this time, the anode-to-cathode impedance drops from open circuit to a fraction of an ohm. In injection laser pulsers, however, the duration of the anode-cathode pulse is much less than the time required for the SCR to turn on completely. Therefore, the anode-to-cathode impedance is at the level of 1 to 10 ohms throughout most of the conduction period. The major disadvantage of the high SCR impedance is that it causes low circuit efficiency. For example, at a current of 40 amps, the maximum voltage would be across the SCR, while only 9 volts would be across the laser diode, which represents very low circuit efficiency. The efficiency of a laser array is greater due to its circuit impedance being more significant.

Because the SCR is used unconventionally, many of the standard specifications such as peak current reverse voltage, on-state forward voltage, and turn-off time are not applicable. In fact, it is difficult to select an SCR for a pulsing circuit on the basis of normally specified characteristics. The specifications important to laser pulser applications are forward-blocking voltage and current rise time. A usage test is the best and many times the only practical method of determining the suitability of a particular SCR.

Notes on the Storage Capacitor

The voltage rating of the storage capacitor must be at least as high as the supply voltage. A high-quality metallized capacitor must be used for this part as peak currents are in the tens of amps.

Notes on Layout Wiring

Lead lengths and circuit layout are very important to the performance of the discharge circuit. Lead inductance affects the rise time and peak value of the current and can also produce ringing and undershoots in the current waveform that can destroy the laser. A well-built discharge circuit might have a total lead length of only 1 inch and therefore an inductance of approximately 20 nanohenries. If the current rises to 75 amperes in 100 nanoseconds, the inductive voltage drop will be $e = L\, di/dt$. If proper care is not taken in wiring the discharge circuits, high-inductance voltage drops will result.

A 1-ohm resistor (R20) in the discharge circuit will greatly reduce the current undershoot in single-diode lasers. Laser arrays usually have sufficient resistance

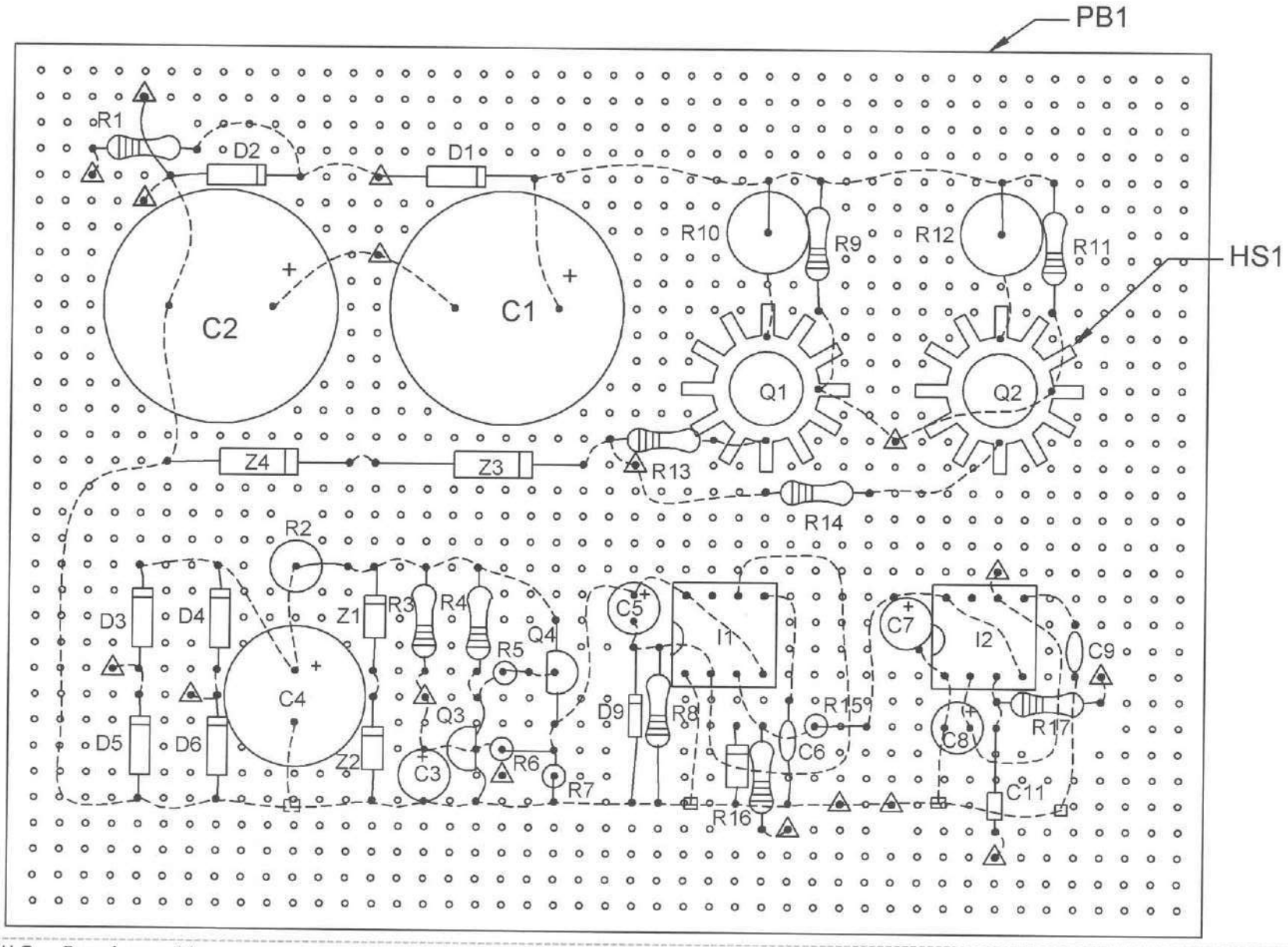

Figure 4-3 *Board assembly*

115 VAC, 5- to 50-Watt Pulsed Infrared Laser

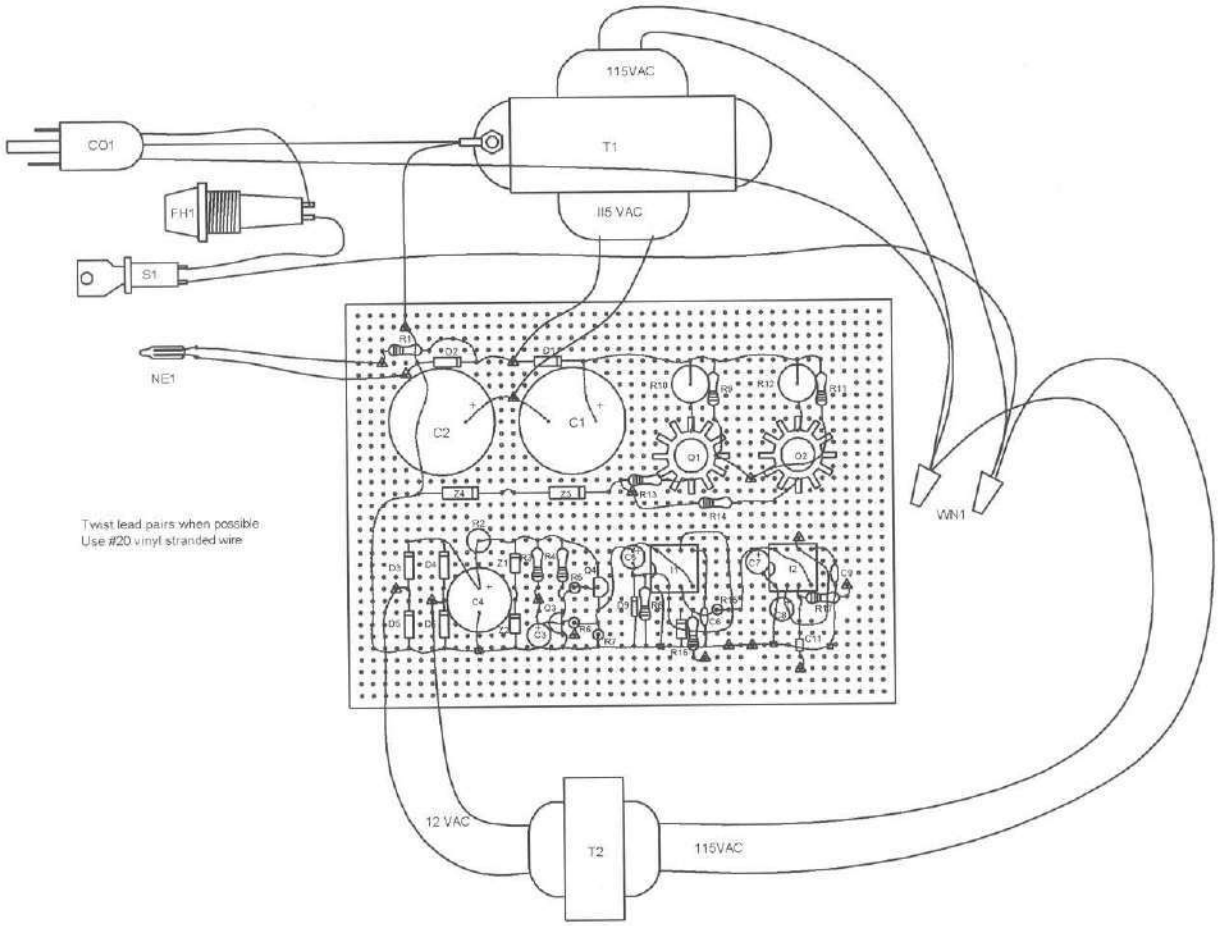

Figure 4-4 *Board input power wiring.*

to eliminate an undershoot. The small resistance in the discharge circuit is also useful in monitoring the laser current, as described in the following section.

A clamping diode (D8) is added in parallel with the laser to reduce the current undershoot. Its polarity should be opposite that of the laser. Although the clamping diode is operated above its usual maximum current rating, the current undershoot caused by ringing is very short and the operating life of the diode is satisfactory.

Notes on Current Monitoring

The current monitor in the discharge circuit provides a means of observing the laser current waveform with an oscilloscope. A resistive-type monitor (R20) reduces circuit ringing and current undershoot, but the lead inductance of the resistor may cause a higher than actual current reading. A current transformer such as the Tektronix CT-2 can also be used to monitor the current and is not affected by lead inductance. Because the transformer does not respond to low-frequency signals, it should be used with fast, short-pulse-width, fast fall-time waveforms.

Assembly Steps

Assembly of the laser system is straight forward and will require basic tools and test equipment.

1. Lay out and identify all parts and pieces. Verify them with the parts list, and separate the resistors as they have a color code to determine their value. Colors are noted on the parts list.
2. Cut a piece of .1-inch grid perforated board to a size of 5.8 × 3.5 inches, as shown in Figure 4-3.

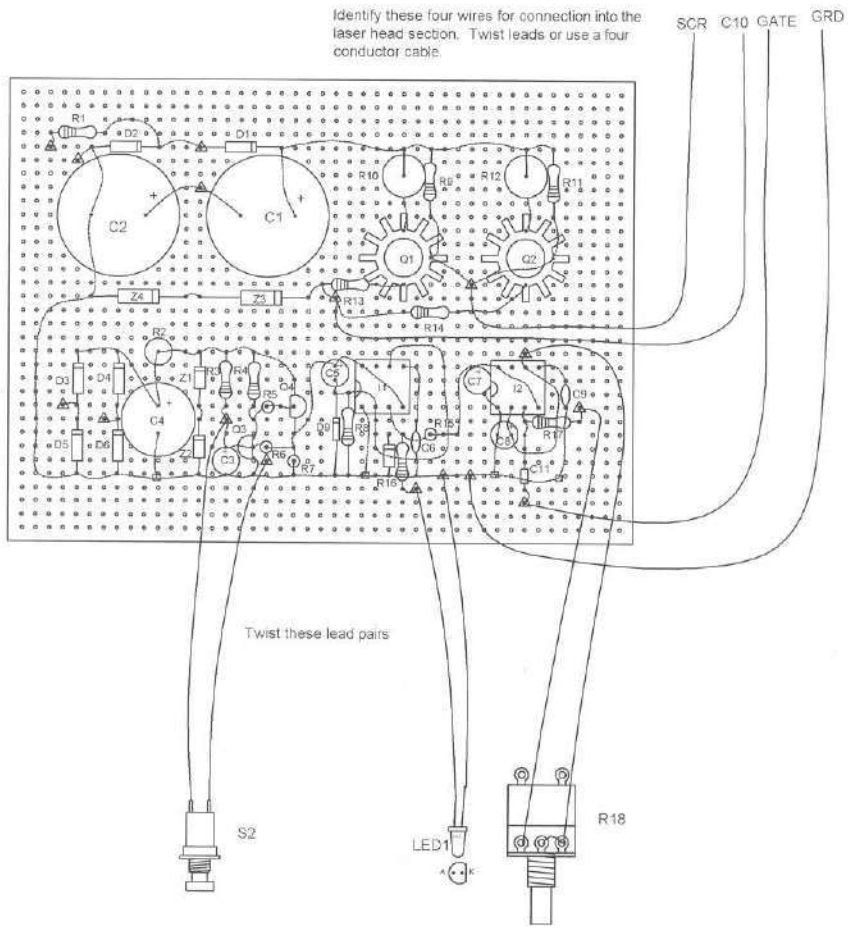

Figure 4-5 *Board output and control wiring*

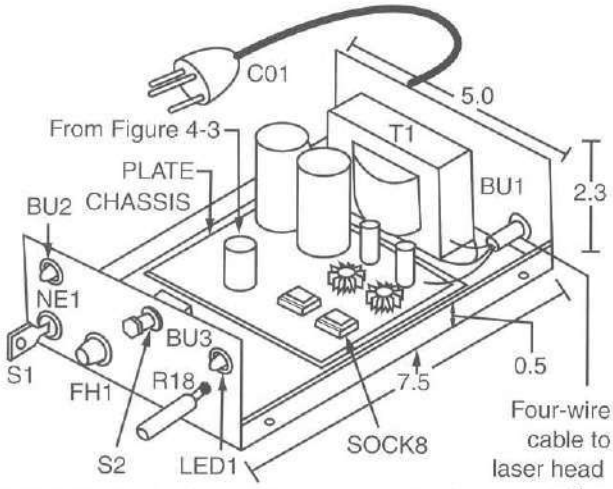

Figure 4-6 *Fabrication and chassis assembly*

3. If you are building from a perforated board, insert the components, starting in the lower left-hand corner as shown. Pay attention to the polarity of the capacitors that have polarity signs and all semiconductors. Use eight-pin sockets for I1 and I2.

   Route the leads of the components as shown and solder as you go, cutting away unused wires. Attempt to use certain leads as the wire runs or use pieces of the #24 bus wire. Follow the dashed lines on the assembly drawing as these indicate the connection runs on the underside of the assembly board. The heavy dashed lines indicate the use of thicker #20 bus wire, as this is a high-current discharge path.

4. Attach the external leads as shown in Figure 4-4 to the external components. Note the chassis grounding to the green lead of the power cord (CO1) and the use of wire nuts (WN1) for the junction of the transformer's primary inputs.

5. Attach the external leads as shown in Figure 4-5 to the external components. Note the four leads that go to the laser head assembly. These

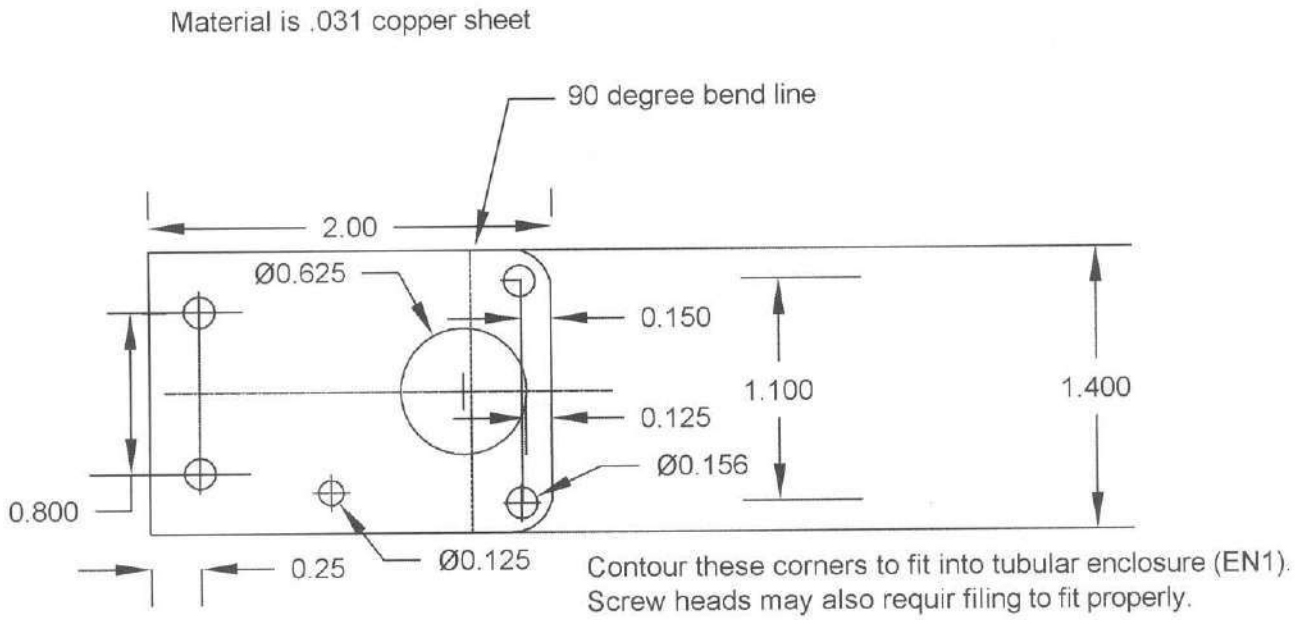

Figure 4-7 *Assembly of laser chassis*

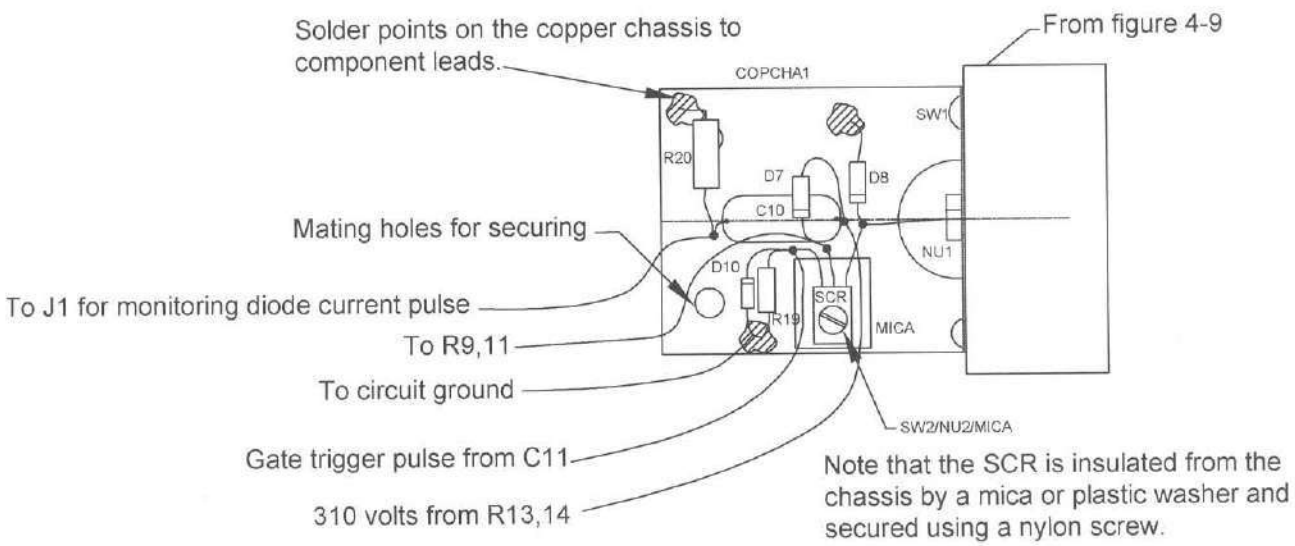

Figure 4-8 *Fabricate the laser holder*

are suggested to be 24 to 36 inches in length as well as twisted and identified. You may use a four-conductor cable.

6. Double-check the accuracy of the wiring and the quality of the solder joints. Avoid wire bridges, shorts, and close proximity to other circuit components. If a wire bridge is necessary, sleeve some insulation onto the lead to avoid any potential shorts.

7. Fabricate the chassis, as shown in Figure 4-6. Then position and drill the front and rear panel holes to fit the necessary external components. Use appropriate bushings for the power cord and wires to the laser head. Also, place an insulating piece (PLATE) under the assembly board to prevent contact with the metal chassis.

8. Fabricate the laser chassis, as shown in Figure 4-7, from a .031 piece of copper sheet metal.

9. Assemble the laser chassis, as shown in Figure 4-8. This section takes advantage of the ground plane effect of using the copper for

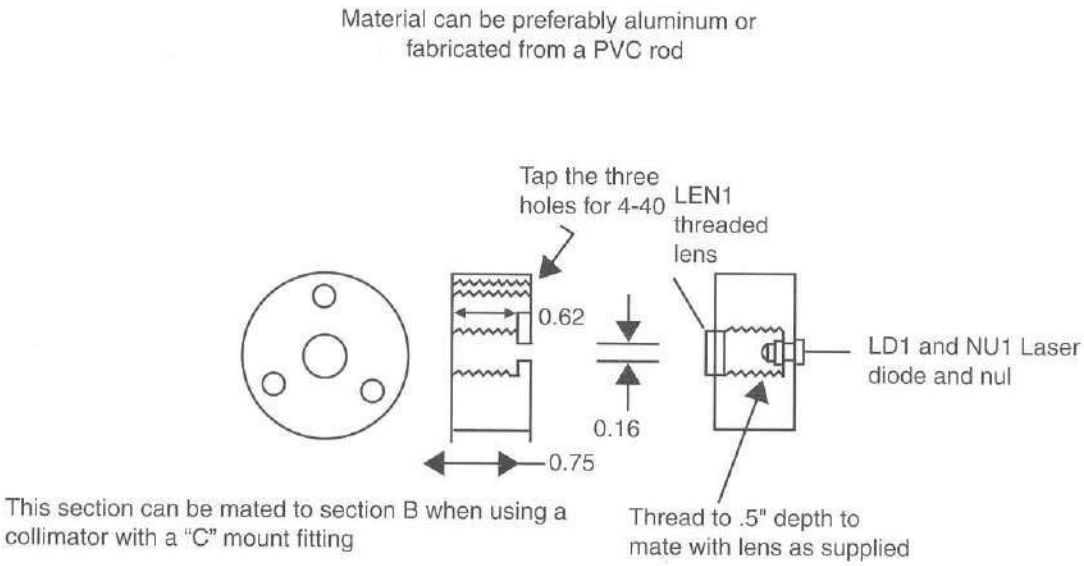

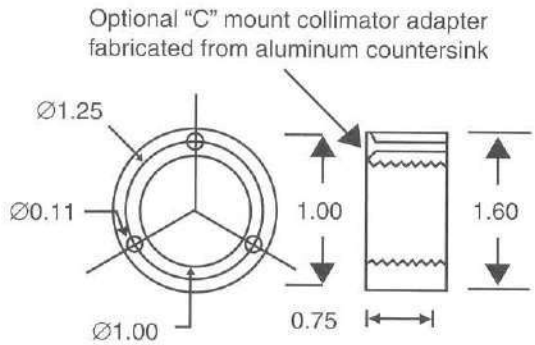

Section B adapter for fitting to the lens holder when using the optional collimator.

Three mounting holes of .11 on a 1.25" diameter 120 degres are mated to those in above.

Thread for "C" lens at 1" diameter 32 tpi to a minimum of .375".

Figure 4-9 *Laser diode and lens holder*

direct solder points. It is important to maintain a good waveshape because the switching currents are 40 amps and any undershoot is undesirable across the laser diode. Do not install the laser diode at this point.

10. Create the laser holder (LAHOLD), as shown in Figure 4-9. This assembly is attached to the bent-up lip of the chassis section by two small screws.

Assembly Testing

Testing will involve the use of an oscilloscope with a 100 MHz bandwidth and infrared detection equipment such as a night vision scope or camera.

1. It is assumed at this point that the electronic assembly is complete. Verify the circuit and preset the two trimpots, R3 and R9, to midrange.

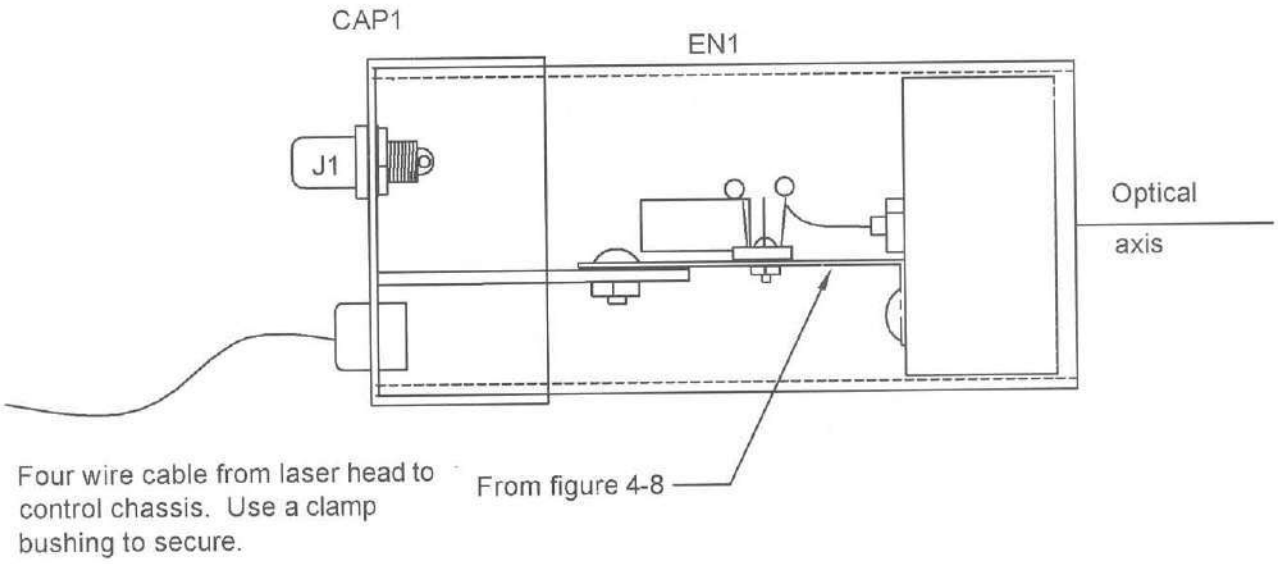

Figure 4-10 *Final head assembly*

2. Insert a .5-amp fuse into the fuse holder. Verify that the key switch is off and R18 is fully counterclockwise. Plug in a ballasted, 25-watt, 115-volt, 60 Hz power source. This is nothing more than the cord with a 25-watt lamp in series with the black lead. It protects the circuitry from the catastrophic currents of the power line should a major fault occur. Obtain a 1N4007 power diode and temporarily wire it in place of the laser diode LA1. The diode simulates the actual laser diodes and avoids costly replacement should a gross error exist. The actual laser diode is not to be wired in at this point. Turn on the key switch and note the NE1 coming on. The ballast lamp should not be lit.

13. Connect the scope to TP2 and note a spiky waveform that verifies the trigger pulse to the SCR, as shown in Figure 4-2.

14. Connect the scope to TP3 and note the waveform, which is the voltage across the SCR. Notice the flat spot indicating that capacitor C10 has reached a full charge before the SCR is triggered. The top of this waveshape is affected by the pulse repetition rate and should support 2,500 repetitions per second when set by R18 (see Figure 4-2).

15. Connect the scope to TP1 and set it up for a negative-going fast pulse, indicating the current waveform through the LD1 laser diode. If you have followed the instructions and your assembly of the copper chassis is secure with short leads, you should see a picture-perfect waveform, as shown.

    Note that the current pulse is 40 amps and corresponds to 1 amp for every volt read at TP1. If you find the pulse is less, you can increase the voltage ratings on one of the zener diodes, Z3 or Z4. The laser diode specified requires 40 amps for full output. Any value over 40 amps will greatly shorten the useful life of this part. The range of the pulse rep rate should be 200 to 2,500 pulses per second. The pulse amplitude should only vary several percent throughout this range. You will note that the amplitude will slightly decrease as the rep rate is increased.

16. At this point, you should be wearing your safety glasses. Remove the test diode D5 and connect the laser diode. Place an infrared indicator several inches from the diode and note an orange glow when the unit is turned on. Then recheck the pulse shape and amplitude.

17. Verify the laser output by using a night vision scope or a video camera. Screw in LENS13, so it is flush with the holder. Adjust it to find the smallest footprint at over 50 feet. Our lab model adjusted to about two turns below being flush with the holder for the best results. The output should be a sharp, narrow bar shape with this diode specified.

Please note that laser diodes are very easily destroyed by current pulses that are too large and overshoot. Pay attention to the correct current pulse shown in Figure 4-2.

The recommended laser diodes are available from Information Unlimited and are shown in Table 4-1.

Final Assembly Steps

Final assembly of head section as shown in Figure 4-10. For final assembly place the label as shown and verifying the compliance tests in Figure 4-11

Compliance Tests

1. Verify correct labels as shown.
2. Key switch — nonremoval in off position.
3. Beam indicator LED indicates beam emission.

Instruction

1. Turn key switch counterclockwise to verify unit is off. Note key is easily removed in the off position.
2. Plug unit into 115 vac.
3. Turn key clockwise and note NE1 lighting. Note key cannot be removed in the on position Laser energy is infrared and cannot be seen with the eye. You must use infrared detection devices such as our laser pulse detector or suitable night-vision devices. Video cameras will often detect the laser.
4. Adjust collimator for desired effect if you are using.

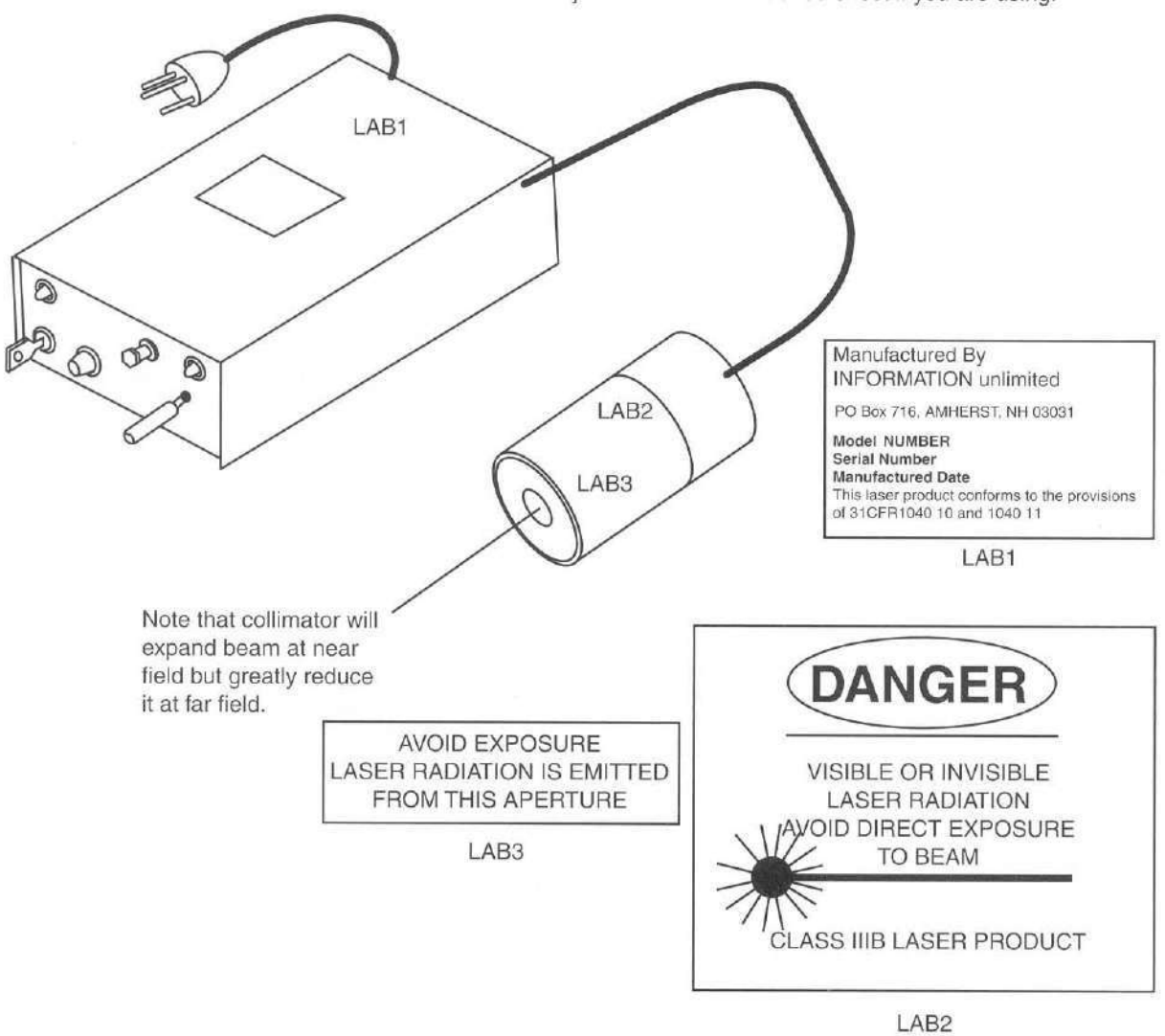

Figure 4-11 *Isometric of final view*

Table 4-2 Parts List for Pulsed Laser

Ref #	Description	DB Part #
R1	100K, ¼ –watt resistor (br-blk-yel)	
R2	10-ohm, 1-watt resistor (br-blk-blk)	
R3, 4, 5, 6, 7	Two 1K ¼-watt resistors (br-blk-red)	
R8	1M, ¼-watt resistor (br-blk-gr)	
R9, 11	47K, ¼-watt resistor (yel-pur-or)	
R10, 12	1.8K, 3-watt mox resistor	
R13, 14	220, 1/2-watt resistor (red-red-br)	
R15	10-ohm, ¼-watt resistor (br-blk-blk)	
R16, 17	470-ohm, ¼-watt resistor (yel-pur-br)	
R18	10K, 10 mm potentiometer	
R19	39-ohm, ¼-watt resistor (or-wh-blk)	
R20	1-ohm, ½-watt carbon resistor (br-blk-gold)	
C1, 2	Two 330 mfd, 16-volt vertical electrolytic capacitor	
C4	1,000 mfd, 25-volt vertical electrolytic capacitor	
C3, 5, 7	10 mfd, 25-volt vertical electrolytic capacitor	
C6, 9	.01 mfd, 50-volt disc capacitor	
C10	.033 mfd, 400-volt polypropylene capacitor	
C11	.1 mfd 50-volt plastic capacitor	
D1, 2	1N4007 1KV, 1-amp rectifier diodes	
D3–6	Four 1N4001 50-volt 1-amp rectifier	
D7, 8	1N4937 fast recovery 1KV, 1-amp diode	
D9, 10	Two 1N914 signal diodes	
Z1, 2	1N4735 6.2-volt zener diode	
Z3	1N5383 150-volt, 5-watt zener diode	
Z4	1N5384 160-volt, 5-watt zener diode	
Q1, 2	Two 2N3439 NPN high-voltage transistors	
Q3	PN2907 PNP general-purpose transistor	
Q4	PN2222 NPN general-purpose transistor	
I1, 2	Two timer dip integrated circuits LM555	
LED1	Green LED	
NE1	Neon indicator lamp	
SCR1	12-amp, 800-volt SCR S8012R	DB# S8012R
LD1	Laser diode 40-amp, 10–20-watt, 904 nm TO18 package	DB# LD650
LAHOLD	Laser and lens holder fabricated as shown in Figure 4-9	
LENS13	Threaded lens	
T1	115/115 volt, 15-volt-amp isolation transformer	DB# TR115/115
T2	115/12 volt, 1-amp transformer	DB# 12DC/.1
J1	RCA phono jack	
CO1	Three-wire #18 power cord	
S1	Compliant key switch	DB# KEYSWSM
S2	Pushbutton no switch	
FH1	Panel-mount fuse holder	
FS1	1-amp fuse	
WN1	Two small Hi3 wire nuts	
PB1	4.8 × 3.5-inch .1 × .1 perforated circuit vector board	
SOCK8	Two 8-pin integrated circuit sockets	

Chapter Five

Laser Property Guard

This project, as shown in Figure 5-1, allows the user to protect a perimeter of over 1,000 meters. The system utilizes a laser transmitter, as described in Chapter 1, and a laser receiver, described in Chapter 2. The system can easily control any deterrent to an invader, such as flood lighting, alarms, man-trap systems, or our phaser pain field generator, as described in Chapter 35.

The operation of the laser property guard is simple. The laser beam is directed through the area to be protected, using front-surface mirrors located on sturdy and secure mounts and at the points necessary to obtain the required coverage (see Figure 5-2). The receiver is normally quiescent when receiving this beam. Once the beam is broken by an intrusion, the receiver now processes the interruption as a fault and powers the desired deterrent or alarm.

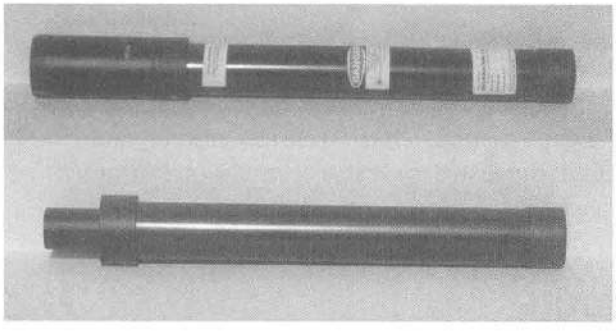

Figure 5-1 *Laser property guard protector components*

This project requires assembly of the laser devices, as described in Chapters 1 and 2. The setup requires basic mechanical skills and installation of the optical reflecting mirrors, and the hookup requires basic electrical skills. Expect to spend $25 to $50 after the assembly of the necessary components. All parts are readily available, with specialized parts obtainable through Information Unlimited (www.amazing1.com) and listed in Table 5-1.

The laser property guard system, as shown in Figure 5-3, utilizes a pulsed infrared laser to provide a perimeter path of programmed light pulses that, when interrupted, will sound an alarm, create an alert, or trigger a deterrent. The trigger fault signal actually triggers a timer or a latching circuit, which drives a switch for the external control of other functions. The timer mode allows the adjustment of the alarm period and automatically resets. The latch mode requires a manual reset.

Even though the laser pulses are rated in tens of watts, the overall energy over a period of 1 second is in the milliwatts. Installing the system at short ranges of only one to two reflection points is reasonably simple. Longer ranges requiring multiple reflections can be challenging.

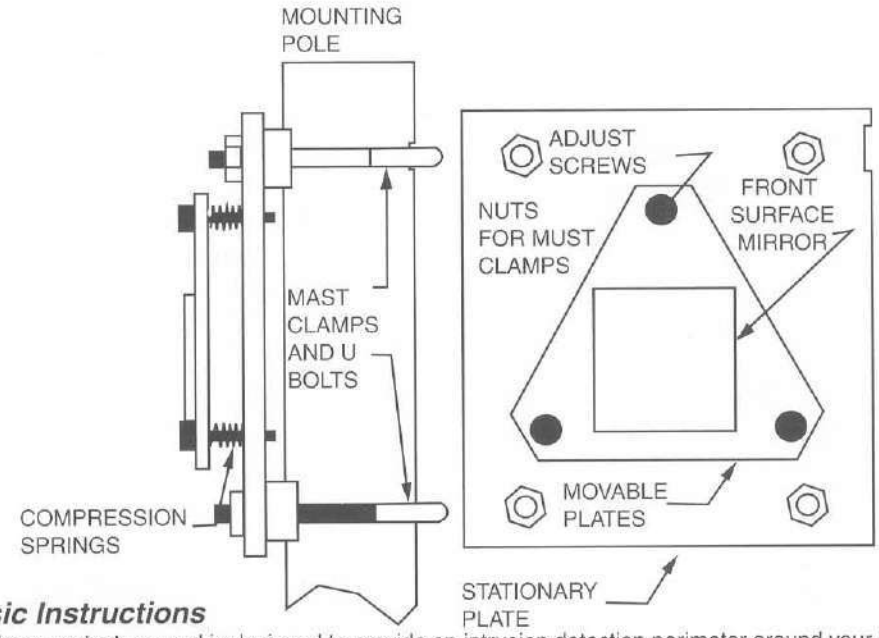

Basic Instructions

Your laser protector guard is designed to provide an intrusion detection perimeter around your home or target area. It uses a Class iiia pulsed diode laser to minimize but not eliminate any optical hazard. A low-liability sonic shock field generator such as that described in Chapter 35 is suggested as a deterrent. Caution: Check local laws for proper posting of this equipment on your property. Remember if you injure a criminal, even if he is robbing you, it can result in a stiff penalty in certain states for violating his rights.

System Setup

1. Obtain the following equipment listed in the latest Information Unlimited catalog.
   - ❑ Class iiia pulsed diode laser as described in Chapter 1.
   - ❑ Optical light detector and controller with built-in alarm as described in Chapter 2.
   - ❑ Low-liability sonic shock pain field generator as described in Chapter 35.

2. Examine the area you want to protect. Attempt to position beam travel over level terrain to eliminate possible easy-to-sneak-under points.

3. Establish corner points of property where mirrors are to be positioned. Note that a clear view of adjacent mirrors, laser and receiver must be maintained in all weather conditions for reliable operation.

4. Determine the corner where you want to position the actual laser and laser detector at. Note: There should be access to these devices for powering and control.

5. Construct mirror mounts using your own ingenuity. Allow for adjustment and stability. Rough align mirror to approximate position.

6. Turn on laser and position to hit center of first mirror. Secure laser in place.

Adjust first mirror to hit center of second and repeat for remaining mirrors all the way back to the optical receiver. Secure in place as you go.

Special note: Large areas may require an optical collimator at the laser output to reduce beam width at longer ranges. The collimator can be a rifle scope, telescope, binocular, etc., positioned in axial alignment with the laser. Beam divergence will be reduced by the magnification factor of the system used, however the actual beam will be expanded by same factor. The net result is a smaller cross-section at longer ranges.

Figure 5-2 *Low-cost, adjustable mirror mount*

System Installation Suggestions

There are many ways to align an optical system of this type. The use of a visible laser module as listed in Table 5-1 can simplify the initial setup and positioning of the mirrors. Those fortunate to have night vision equipment will find this a considerable advantage.

- Determine the area you want to protect. Flat land is the most desirable, as gullies and hills are difficult to cover without using more mirrors.
- You must also consider the position of the laser transmitter and receiver, noting the power and connection into the alarm or the deterrent section. Weather exposure and convenience must also be taken into consideration, and mounting must be stable and somewhat adjustable.
- Determine the path that the light must travel to provide acceptable coverage. Always attempt to use as few mirrors as possible and consider the laser transmitter's and receiver's positions. If you are lucky, you may have some objects to mount the mirrors to. They must be stable and allow placement at the required height for your application.

  The mirrors used for this project must be the front-surface-coated type if multiple reflections are required. Regular household mirrors can be used up to two reflection points, but they will cause multiple reflections. A low, adjustable-cost mirror mount is shown in Figure 5-2. You may in certain cases use a good-quality automotive mirror, as they are easily adjustable.
- Evaluate the wildlife in your area and determine the best laser height that will provide minimal false alarms from the animal population. Obviously, deer will always be a problem, as their height may be close to that of the target intruder.
- Determine the deterrent you wish to use against the intruder. You can activate bright lights, sonic pain generators (described in Chapter 35), alarms, or just alerts so you can take further action. For more serious applications, you can activate shocking devices, such as those described in Chapter 11, nonlethal kinetic devices, or explosive charges for shock and surprise. Very serious deterrents can consist of deadly force, such as high-powered kinetic devices, shotgun traps, high-powered shocking devices, and buried explosives for lethality.

Caution: As man trapping is illegal in the United States, it may also be so in your country. Always check your laws before ever implementing a deterrent that can cause injury.

- The quality of the mirrors and their mounts cannot be overstressed when designing a high-integrity system. Here we discuss a low-cost system that may suffice in smaller installations but may be limited for use in larger, more reliable systems.

The initial alignment requires a visible, low-power laser to align the mirrors. The laser may have to be collimated for larger multiple reflection systems.

Optics on the laser light transmitter and receiver, as shown, may be sufficient for small systems. They do not have to be high-cost precision devices, as the only objective is to establish a properly aligned, position-stable beam spot.

Once the preliminary alignment is accomplished, you can put the laser transmitter in place and, with a night vision scope, recheck the alignment. The laser receiver, as constructed here, has an indicating *light-emitting diode* (LED). This function can be eliminated if required. The actual control of external functions is via a set of normally open or closed relay contacts that can handle 115 VAC at 10 amps AC.

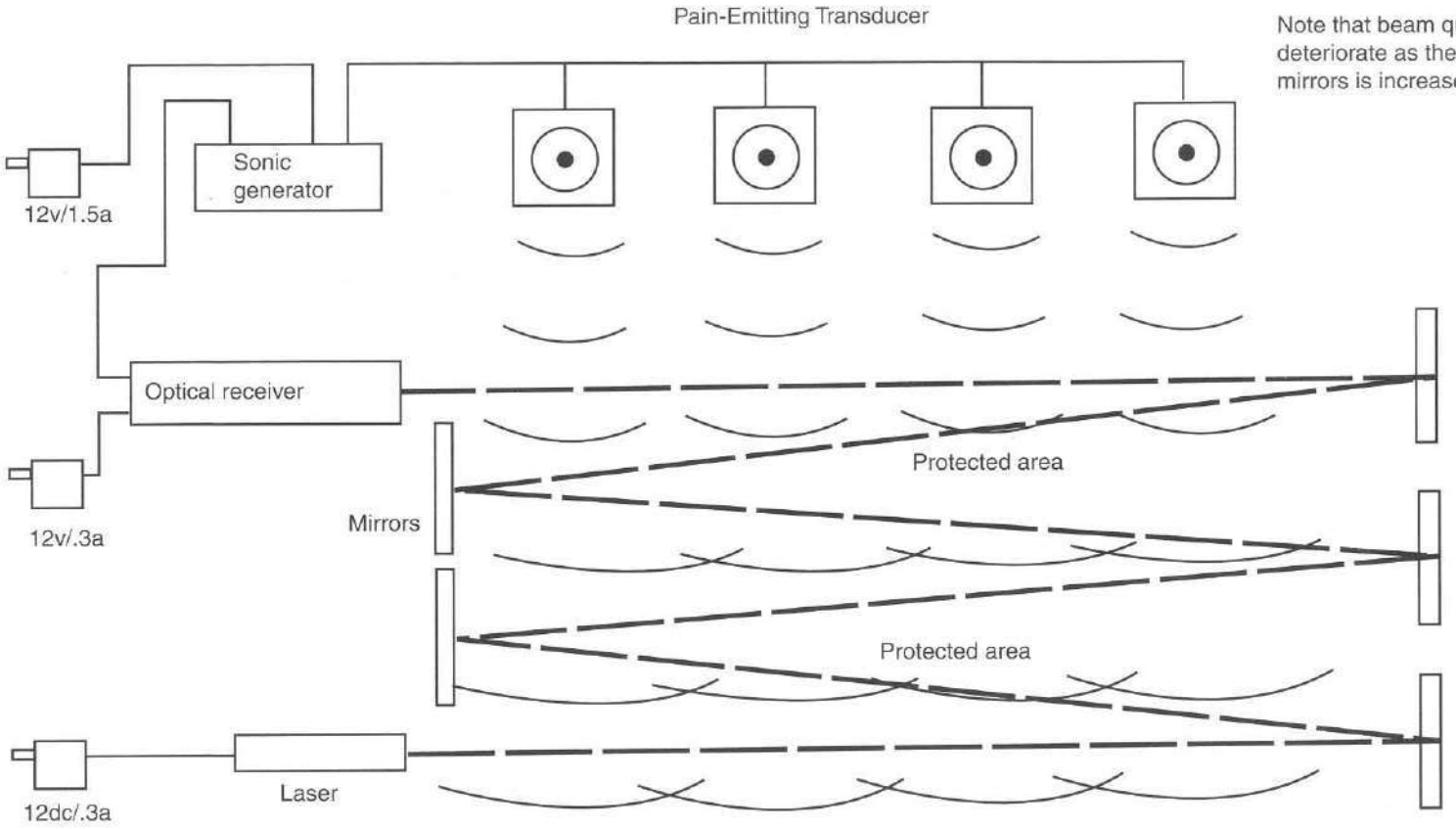

Laser beam is reflected back and forth in the protected area via strategically placed mirrors. Once the beam is broken by an intruder the optical receiver detects and sends a level to the sonic generator where the transducers are activated producing an intolerable sonic pain field discouraging the intrusion.

Even though there is no lasting effect from exposure to the transducers, it is always best to check with local laws before implementing this system.

Figure 5-3 *Example of system layout*

Table 5-1 Laser Property Guard Parts List

Ref. #	*Description*	*DB Part #*
MIRROR	3 × 4-inch front surface mirrors	DB# MIR FRSUR
LRG4K	Pulsed infrared laser kit, as in Chapter 1	DB# LRG4K
LRG40	Assembled pulsed infrared laser, as in Chapter 1	DB# LRG40
LSD4K	Laser detector kit, as in Chapter 2	DB# LSD4K
LSD40	Assembled laser detector, as in Chapter 2	DB# LSD40
PPF4K	Pain field generator kit, as in Chapter 35	DB# PPF4K
PPF40	Assembled pain field generator, as in Chapter 35	DB# PPF40
SHOCK1K	Kit of shockers, as in Chapter 11	DB# PFSHK1K
SHOCK10	Assembled shockers, as in Chapter 11	DB# PFSHK10
LM650-3	Visible red laser module for alignment aid	DB# LM650-Description P3System

Chapter Six

30-Milliwatt, 980-Nanometer Infrared Laser

The laser project shown in Figure 6-1 is a continuous infrared device providing a continuous 30-milliwatt output at 980 nanometers. The laser, when built as shown, should comply with a class 3 laser-compliant system. The completed laser can be very optically dangerous, and eye protection must be worn to prevent direct or scattered reflections to the eyes.

The project can be used for many optical applications, including illuminating a surface, such as a window, for laser listening. Laser listening is were a laser beam illuminates a window and a sensitive receiver picks up the light reflections and processes them into audio signals similar to the picked-up voices that vibrate the illuminated window glass. A system such as this is described on www.amazing1.com. It should be noted that using a class 3b laser for this application can be an optical hazard to anyone in the target area.

Converting illumination using night vision cameras and spectrally compatible viewers is another potential application, again being fully aware of a possible optical hazard. Other applications are invisible target identification, voice and data communication, and optical signaling and experimenting.

Figure 6-1 *The infrared laser module*

This is an intermediate-level project requiring basic electronic skills. Safety glasses are strongly advised, as the laser can cause eye damage if viewed directly or via direct reflections. Expect to spend $75 to $150. All parts are readily available, with specialized parts obtainable through Information Unlimited (www.amazing1.com), and they are listed in Table 6-1.

For those wanting to use this project as an illuminating laser for window bounce listeners, it is suggested that you refer to Chapter 13 in *Electronic Gadgets for the Evil Genius*, published by McGraw-Hill, ISBN 0-07-142609-4.

Circuit Description

Figure 6-2 shows the laser module LM1 and associated support circuitry. The system is powered by batteries B1 and B2 and is controlled by an internal key switch (S1) or external enabling control leads. A light-emitting diode (LED1) and a current-limiting resistor (R1) indicate the presence of laser emission.

The system will require S1 to be a key switch with a nonremovable key in the activated position if the assembly is integrated as a fully functional laser system. The power line or bench operation will require a

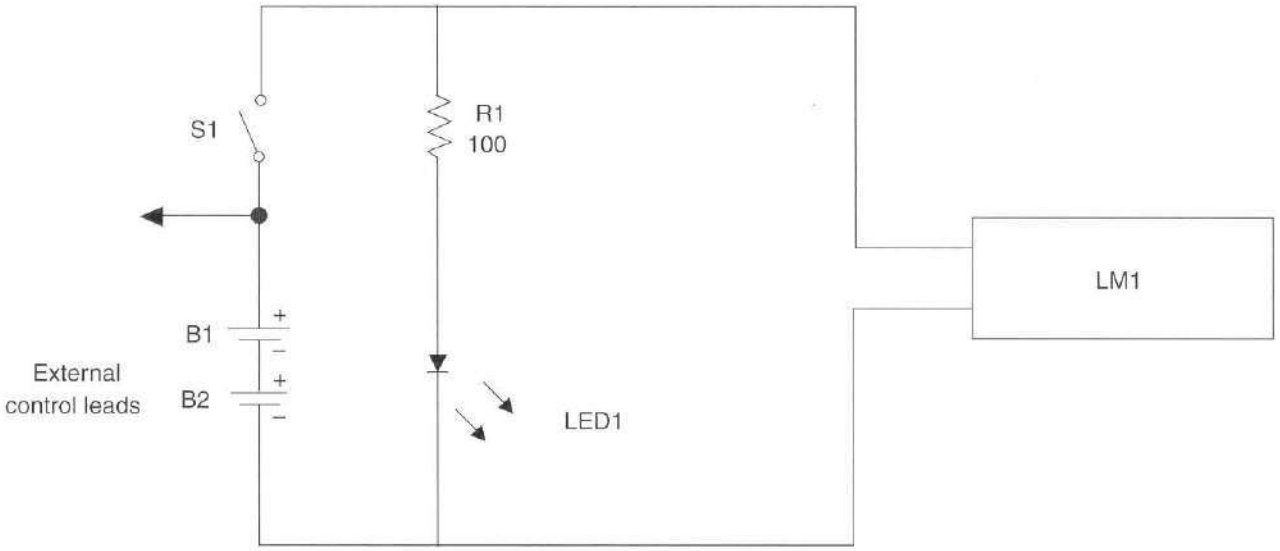

Laser current should be 50 to 60 milliamps at 3 volts input.

Warning: If you overvolt or reverse polarity on your laser module, you will ruin it!!

Assembly shows a battery-operated compliant laser system. You may wire direct to a 3-volt source that now contains the key switch and a built-in time delay necessary for compliance and safety.

Figure 6-2 *Circuit schematic*

key switch for external enabling and associated control circuitry that may require an emission delay and automatic resetting should a loss of power occur.

Assembly

1. Rework the laser module, as shown in Figure 6-3. This step requires care as it is easy to damage the module if one is not very careful.
2. Connect the soldered leads to a source of 3 volts, paying attention to the correct polarity. If you have a current meter, you can measure 40 milliamps.

   Output can be detected using infrared photosensitive paper or a night vision scope. Certain video cameras may also detect the laser output.

   Danger! Do not view directly or indirectly without safety glasses.
3. Fabricate the laser holder (HOLD1), as shown in Figure 6-4.
4. Fabricate the laser module tube (TUB1) from a piece of 3-inch × 1-inch OD × 1/16-inch wall plastic tubing, as shown in Figure 6-5.

   Fabricate the two spacing washers (WASH1, 2) from 1/16-inch plastic. Note the inner hole is 1 inch to allow for the sleeving onto TUB1 as shown. The outer diameter fits into the inner diameter of the main enclosure (EN1). It is these two spacer washers that position and secure TUB1 into the center of EN1. Space the two washers as shown.
5. Insert the laser module LM1 as shown and wire it up to the circuitry as shown. It is a good idea to leave enough lead length to allow one to pull out the battery holder for battery replacement by removing the rear cap (CAP1). Use a piece of foam to secure the battery holder in place.
6. Verify the proper circuit operation so that when the key switch is activated, the LED emits, indicating laser emission.

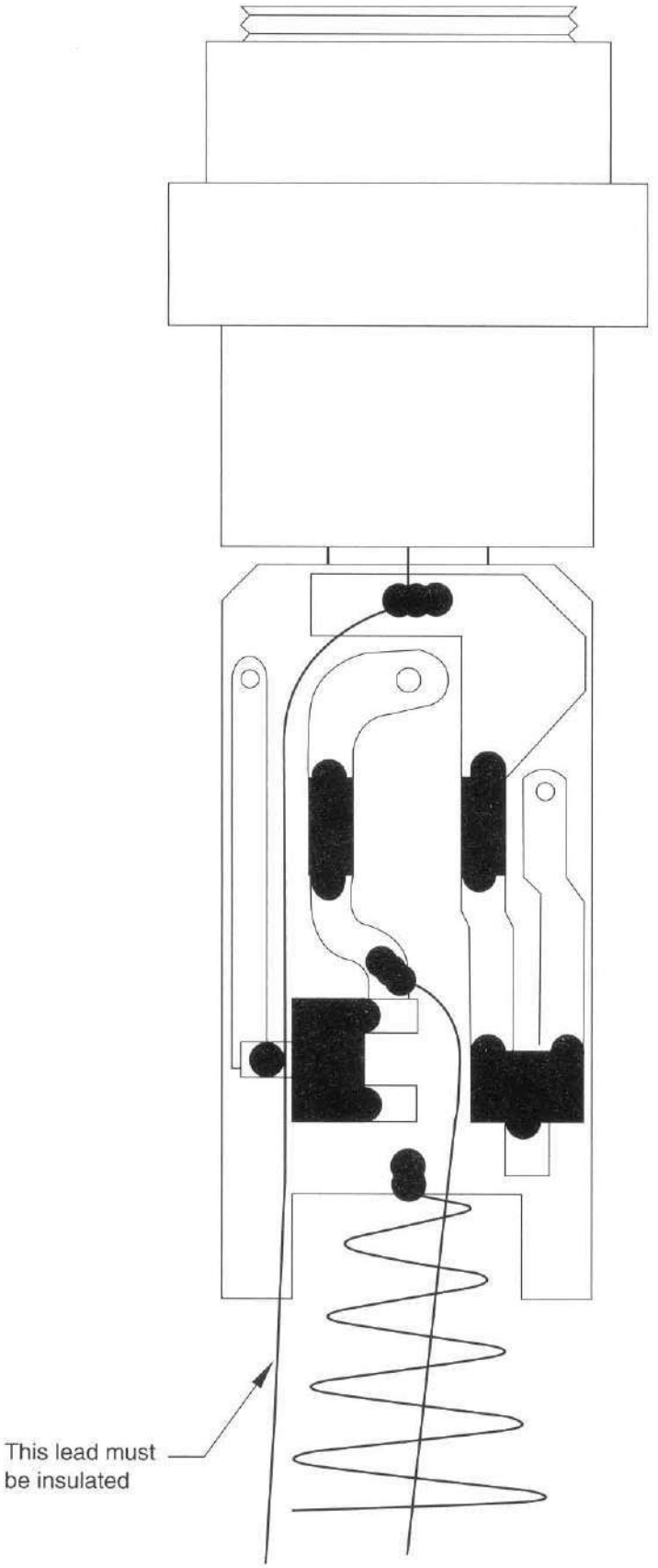

Very carefully attach #24 bare bus leads to the solder pads as shown. It is necessary to insulate the positive lead using a piece of insulation stripped from a piece of wire or insulated tubing.

Note that the brasshead of the laser is the positive connection and the spring the negative. Activation will require now depressing the on-board pushbutton switch. You may connect to these points if unsure of soldering to the small foils on the printed circuit board.

Warning: If you overvolt or reverse polarity on you laser module, you will ruin it!!

Figure 6-3 *Laser module rework*

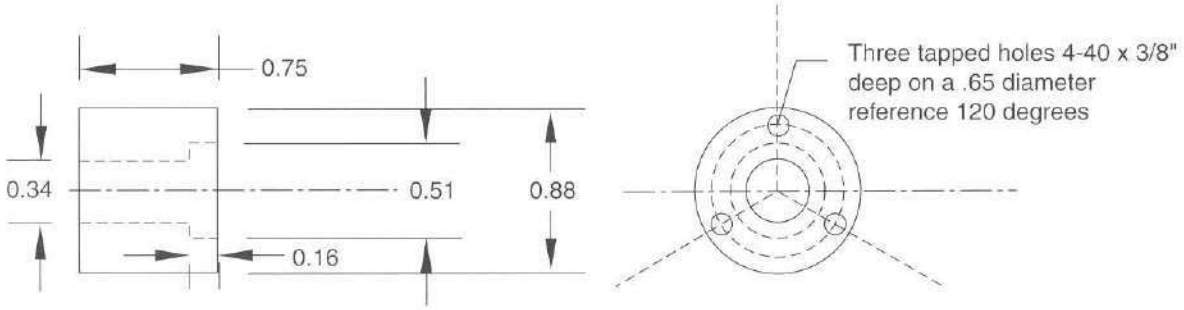

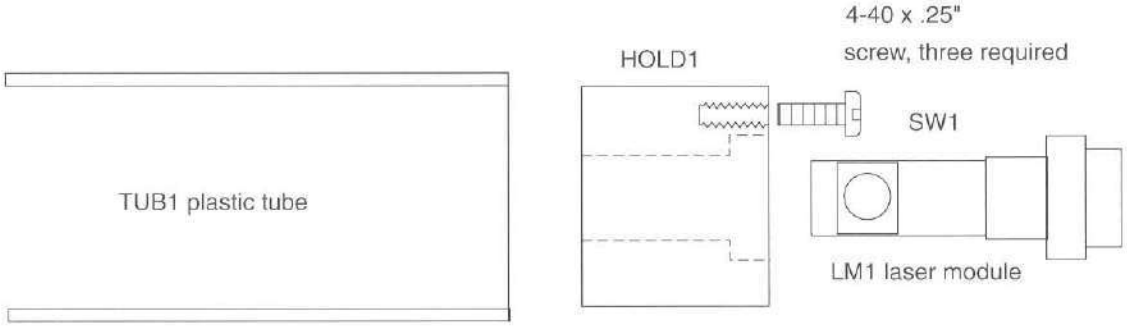

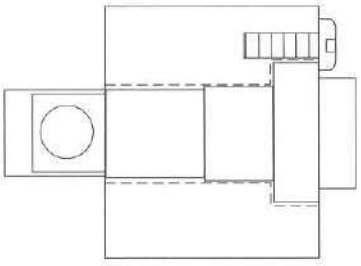
X-ray view showing assembled LM1 laser module inserted into HOLD1 holder with three retaining screws SW1

Figure 6-4 *Creation of laser module holder and retaining washer*

This is our approach to assembling this laser project with external optics. The builder may use his own ingenuity noting that the objective is optical stability and safety.

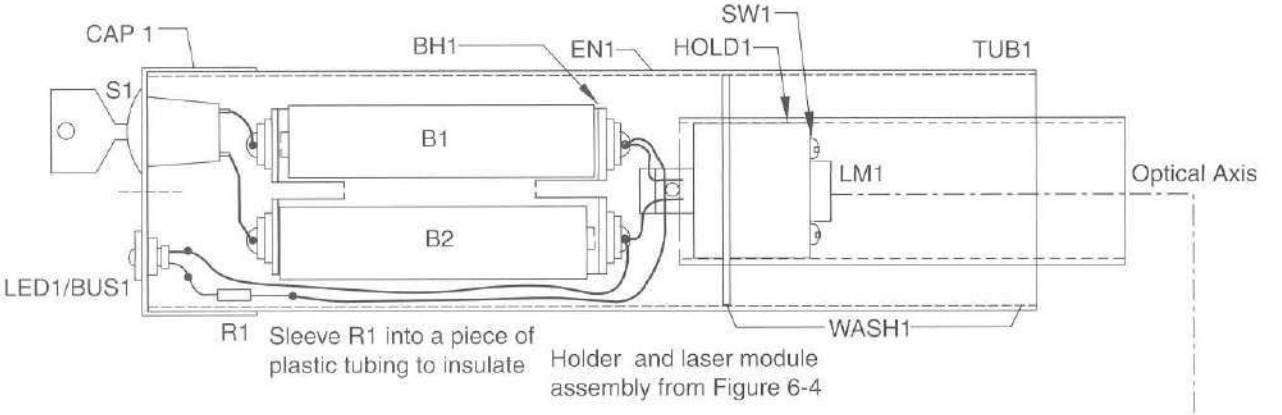

Note if the system is to be completely integrated, that the key switch will be necessary for FDA compliance in requiring this part with nonremovable key in the on position.

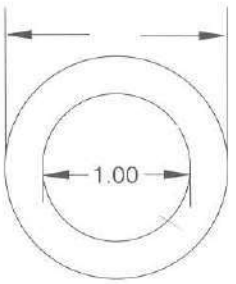

Fabrication of the two WASH1 spacing washers. Use 1/16" Lexan.

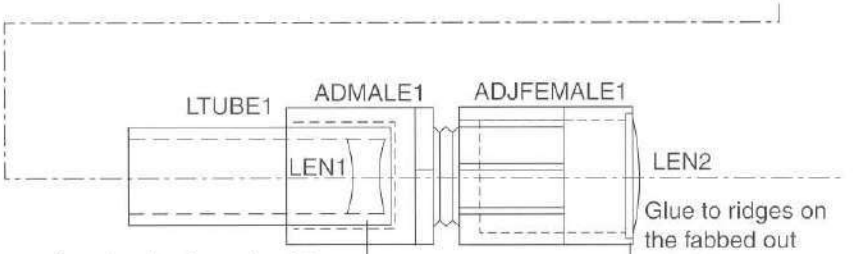

X-ray view showing innards of the optional low-cost X7 collimator

Glue to ridges on the fabbed out shoulder recess. ***Caution!!*** Lenses must be clean and free of finger prints!!

The objective is to get the proper seperation distance between the two lenses to allow proper adjustment within the range of the threaded sections of the male and female pieces.

Figure 6-5 *X-ray of complete assembly*

Collimator and Final Assembly

1. Glue the larger lens LEN2 into ADFE-MALE1 as shown, using silicon rubber glue or an equivalent. Clean the lens before gluing.
2. Insert LEN1 into the laser output end of the LTUB1 assembly as shown. Do not glue at this time.
3. Fully insert the LTUB1 into the 1-inch tube TUB1. Shim it with tape for a secure but removable fit.
4. Finish the assembling and label it as shown in Figure 6-6.
5. Point the laser at a target around 100 meters away and adjust the collimator to the smallest spot. This should be done in low light, preferably at night, using a night vision device and only looking at the beam impact point. Note

Instructions

1. Turn key switch full ccw. Note switch has several positions–only two are used in this version.
2. Remove CAP1 and insert 2 AA batteries into holder.
3. Turn on key two positions cw and note LED lighting. If not check the battery holder.
4. Adjust coliminator for desired effect.

Note that coliminator will expand the beam at near field but greatly reduce it at far field. Laser module may require beam adjustment over time using the special tool.

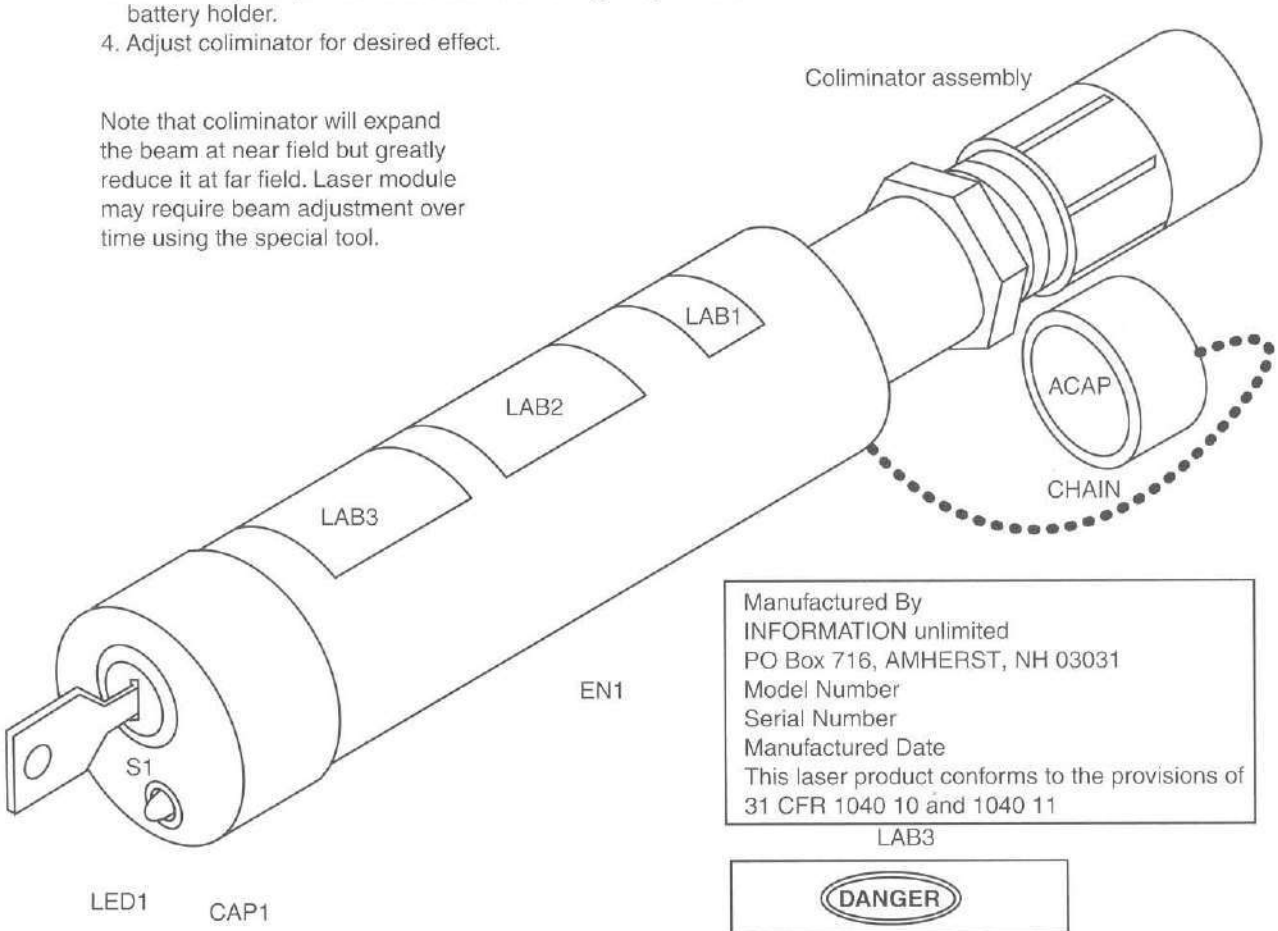

Compliance test

1. Verify correct labels as shown
2. Key switch–nonremoval in off position
3. Beam indicator LED indicates after delay
4. Aperture cap included

WARNING: Do not under any circumstances point this device at people, vehicles, or especially aircraft. YOU WILL BE PROSECUTED IF CAUGHT!!!

Figure 6-6 *Final assembly view*

that the adjustment should be about 1/2 to 3/4 turns from being fully tight for a mechanically stable operation. If it is too far out, the assembly will be loose. You may have to use a wire brush on the threads and lube with dry teflon for smooth action. You may compensate the distance between lenses by changing the length of TUBE1. You may now glue LEN1 in place as noted.

The collimator will expand the beam width but decrease the divergence by the same ratio. This greatly reduces the far-field beam diameter.

Note that the laser module is at a wavelength of 980 nanometers and is invisible to the eye. Also, note that most of the mechanical parts used in this project can be obtained through most hardware stores.

Table 6-1 Infrared Laser Parts List

Ref. #	*Description*	*DB Part #*
R1	220-ohms, 1/4-watt resistor (red-red-br)	
LED1	High-brightness green LED	
LM1	30-milliwatt, 980-nanometer infrared laser module	DB# LM980-25
S1	Key switch with nonremovable key in "on" position	
BH1	Dual, side-by-side two-AA battery holder	
WR24	12-inch #24 bus wire	
WR22	24-inch #22 vinyl hookup wire	
HOLD1	Fabricated holder with washer for laser module	DB# HOLD1
SWI/NU1	Two 4-40, 1.25-inch machine screws and nuts	
TUB1	3 × 1-inch OD × .875-inch plastic or metal tube	
WASH1	Two fabricated plastic spacing washers, 1.5 OD with 1-inch center hole	
EN1	6-inch × 1.625 OD × 1.5-inch ID plastic or metal tube	
CAP1	1 5/8-inch plastic slip on cap	

Parts for low-cost collimator

LEN1	6 mm × (-1) double-concave negative glass lens	DB# LENS13
LEN2	24 mm × 75 mm plano/convex glass lens	DB# LE2475
*LTUB1	625-inch ID × 2-inch schedule 40 PVC tube	
*ADMALE1	1/2-inch PVC schedule 40 slip fit to male thread, GENOVA 30405	
*ADFEMALE1	1/2-inch PVC schedule 40 slip fit to female threads, GENOVA 30305	
*ACAP1	Plastic cap and chain for aperture cap	
LAB1	Aperture label	
LAB2	Classification label	
LAB3	Certification label	

*Available in most hardware stores

Chapter Seven

High-Voltage, High-Frequency Driver Module

Figure 7-1 shows that a universal, high-voltage, modular power supply project will provide you with many options. This "sweetheart" of a circuit has features that make it a priceless tool for the high-voltage researcher and experimenter.

The circuit operates on 11 to 15 volts DC, drawing 3 amps under a full load, allowing a portable battery or 115 volts AC via a converter. The output voltage is a 60 KHz, high-frequency current that is fully short-circuit protected. The high-frequency output also makes it possible to use low-energy voltage multiplier stacks for high-voltage DC sources, and it can also serve as an excellent plasma driver when used directly. The output current is fully adjustable via a control pot.

The unit is excellent for powering neon and all types of gas-filled vessels using one or two electrodes, or it can power objects simply by proximity. It easily retrofits to our voltage multipliers' modules that provide DC voltages up to 100 kilovolts and currents of up to .3 milliamperes. The current-limiting and control features make this combination an excellent choice for charging capacitors for low loss charging, utilizing 12-volt portable or 115 vac line operation. Also, the device is an excellent choice for powering large and small antigravity craft, ozone air purification, and other applications requiring a high-voltage current-controlled source. The module is shown built on both a rugged *printed circuit board* (PCB) and a vector perforated box. It is mounted in a plastic channel.

Figure 7-1 *Completed assembly module*

The module is used for several projects in this book. In order not to waste a lot of space, we show it as a common subassembly for the following chapters:

- Chapter 12, "Electro-magnetic (EMP) Gun"
- Chapter 32, "100-Milligram Ozone Machine"

Electrical and Mechanical Specifications

- Open-circuit voltage, 7,500 peak at 60 KHz
- Short-circuit current, 10 milliamperes short-circuit protected
- Input 11 to 15 volts DC at 3 amps fully loaded

- Adjustable current by duty-cycle-controlled pulse
- Compact size, 7 × 2⅛ × 1⅛ inches, weighing less than 5 ounces
- Easily retrofits to our voltage multipliers

This is an intermediate-level project requiring basic electronic skills and should cost between $25 and $50. All parts are readily available, with specialized parts obtainable through Information Unlimited (www.amazing1.com), and they are listed in Table 7-1.

High-voltage DC output is obtained from this module using a Cockcroft-Walton voltage multiplier with multiple stages of multiplication as required. Note that this method of obtaining high voltages was used in the first atom smasher that ushered in the nuclear age.

The multiplier section requires a high-voltage AC source for input supplied by the circuit transformer (T1) producing 6 to 8 kilovolts at approximately 60 KHz. You will note that this transformer is of a unique design, being owned by our company Information Unlimited. The part is very small, versatile, and lightweight for the power produced.

Circuit Description

The primary of T1 is current driven through inductor L1 and switched at the desired frequency by FET switch Q1. Capacitor C6 is resonated with the primary of T1 and zero voltage switches when the frequency is properly adjusted. (This mode of operation is very similar to class E operation.) The timing of the drive pulses to Q1 is therefore critical to obtain optimum operation (see Figure 7-2).

The drive pulses are generated by a 555 timer circuit (I1) connected as an astable multivibrator with a rep rate determined by the setting of trimpot R1 and the fixed-value timing capacitor C2.

The timer circuit is now turned on and off by a second timer, I2. This timer operates at a fixed frequency of 100 Hz but has an adjustable duty cycle (a ratio of on to off time) determined by the setting of control pot R10. I1 is now gated on and off with this controlled pulse now providing an adjustment of output power.

When the unit is interfaced with a DC voltage multiplier, an over-voltage protection spark gap is placed across the output and is easily set to break down at a preset voltage level for circuit protection. Even though the output is short-circuit protected against continuous overload, constant hard discharging of the output can cause damage and must be limited. A pulse-current-limiting resistor (R17) helps to protect the unit from these catastrophic current spikes.

Power input is controlled by switch S1, which is part of control pot R10. Actual power can be a small battery- capable of supplying up to 2 amps or a 12-volt, 2 to 3-amp converter for 115-volt operation.

Construction

The circuit is shown using the more challenging *perforated circuit board* often required for a science fair project. A *printed circuit board* is also individually available, requiring that you identify only the particular part and insert it into the respective holes as noted. The PCB is plainly marked with the part identification, and soldering is now very simple as you solder the component leads to the conductive metal traces on the underside of the board.

The perforated board approach is more challenging, as now the component leads must be routed and used as the conductive metal traces. We suggest that the builder closely follow the figures in this section and mark the actual holes with a pen before inserting the parts. Start from a corner, using it as a reference, and proceed from left to right. Note that the perforated board is the preferred approach for science projects, as the system looks more homemade.

Board Assembly Steps

If you are a beginner it is suggested to obtain our *GCATI General Construction Practices and Techniques*. This informative literature explains basic practices that are necessary in proper construction of electromechanical kits and is listed in Table 7-1.

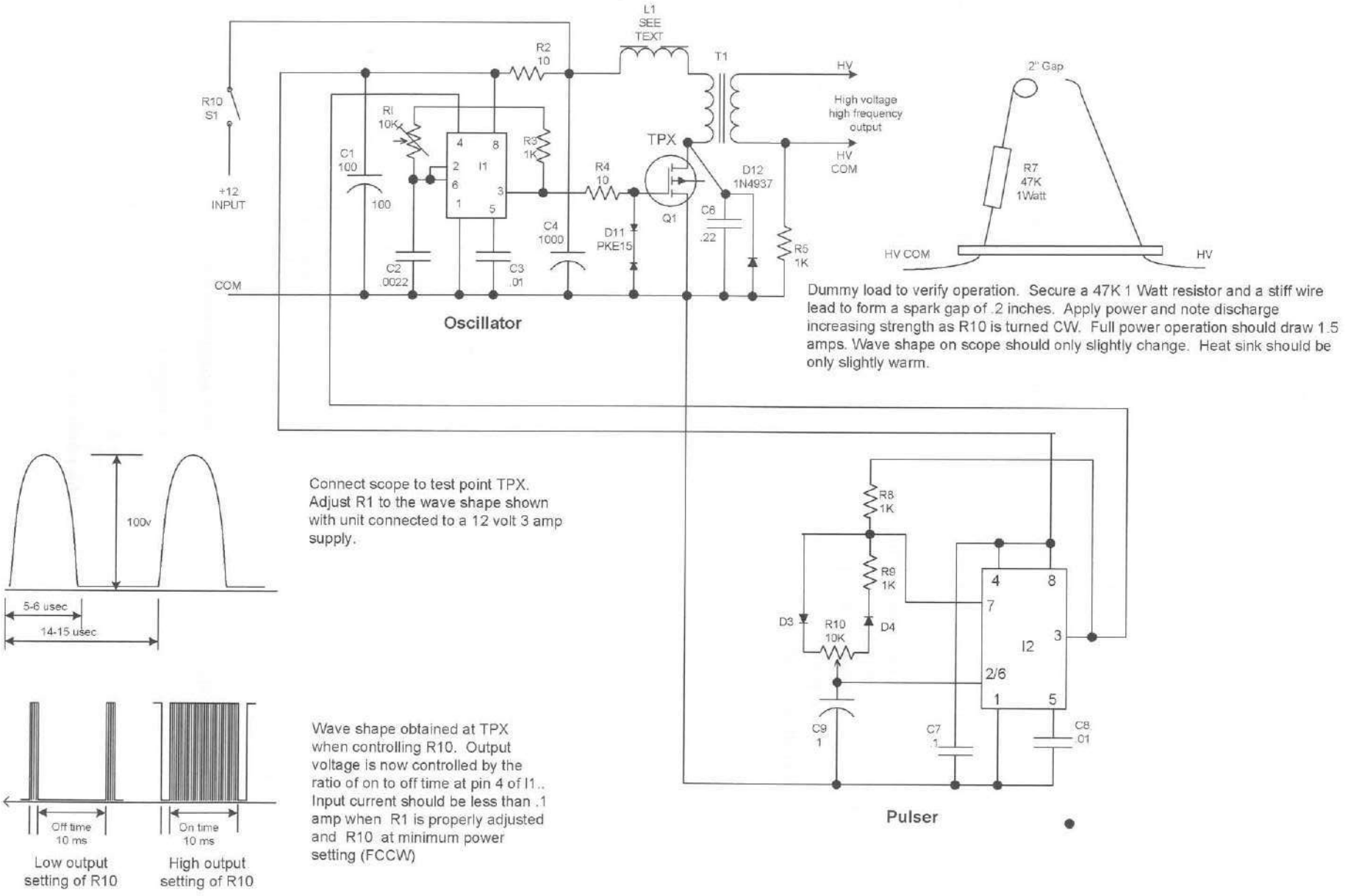

Figure 7-2 *Circuit schematic*

1. Lay out and identify all the parts and pieces. Verify them with the parts list, and separate the resistors, as they have a color code to determine their value. Colors are noted on the parts list.
2. Cut a piece of .1-inch grid perforated board to a size of 5 × 3 inches. Locate and drill the holes, as shown in Figure 7-3. An optional PCB is individually available (refer to Table 7-1).
3. Fabricate a metal heatsink for Q1 from a piece of .063 aluminum, at 1.5 × .75 inches, as shown in the inset of Figure 7-4.
4. Assemble L1 as shown in the Figure 7-4 inset. This part is individually available and listed in Table 7-1
5. If you are building from a perforated board, it is suggested that you insert components starting at the lower left-hand corner, as in Figure 7-5. Pay attention to the polarity of the capacitors with polarity signs and all semiconductors. Route the leads of the components as shown and solder as you go, cutting away unused wires. Attempt to use certain leads as the wire runs or use pieces of the #24 bus wire. Follow the dashed lines on the assembly drawing, as these indicate connection runs on the underside of the assembly board. The heavy dashed lines indicate the use of thicker #20 bus wire, as this is a high-current discharge path.

   Figures 7-6 and 7-7 show the available PCB, which is also listed as an available part in Table 7-1.
6. Attach external leads as shown in Figure 7-5.
7. Double-check the accuracy of the wiring and the quality of the solder joints. Avoid wire bridges, shorts, and close proximity to other circuit components. If a wire bridge is necessary, sleeve some insulation onto the lead to avoid any potential shorts.

These three holes for attaching optional multiplier board

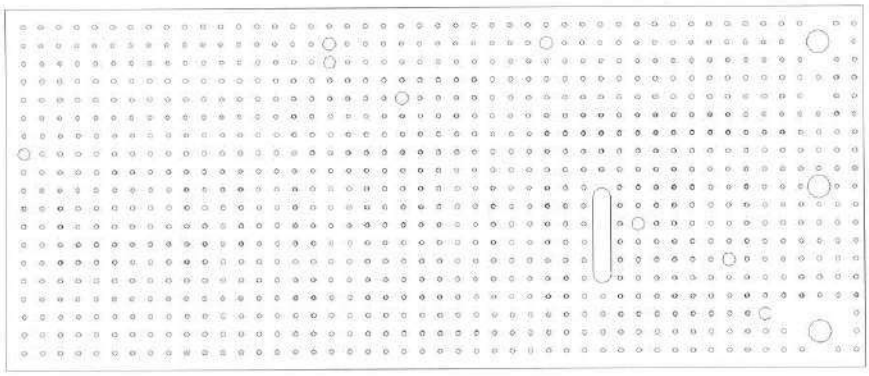

The circuit section is 4.8" x 2.9" .1 x .1 perforated board. Drill eight .063" holes in this perforated section and eleven in the

Drill the three .125" holes for attaching to the optional multiplier board used for high voltage dc applications.

Drill and drag the .125" slot as shown. This cutout and the enlarged holes are for mounting transformer T1.

Hole diameters are not critical.

Always use the lower left hand corner of perf board for position reference.

Figure 7-3 *Perforated board*

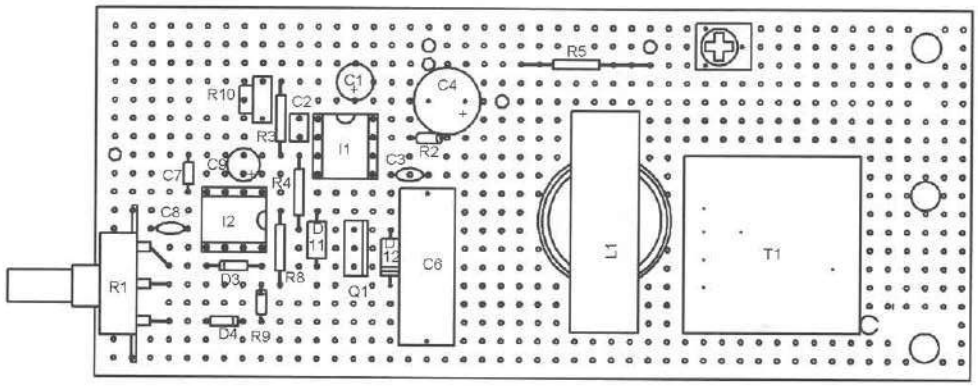

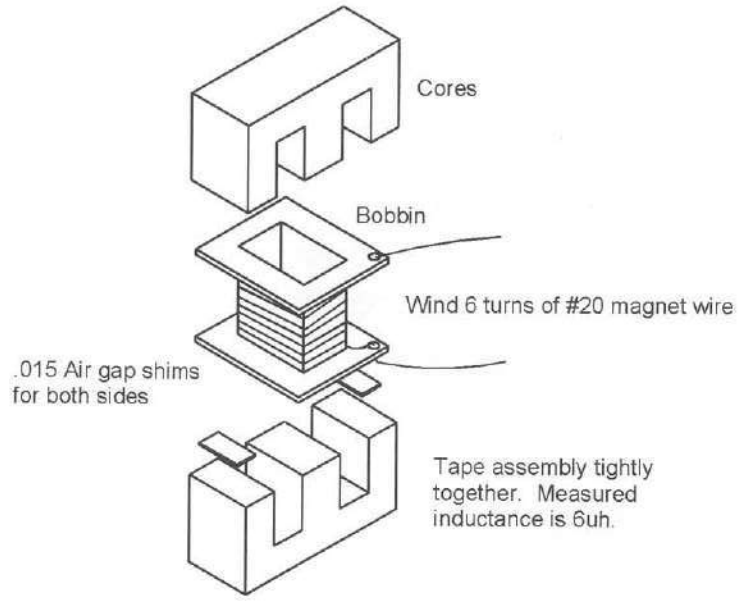

Note polarity of C1,C4,C9,D3,D4, D12 and D20A-D20J

Note position of I1,I2,Q1

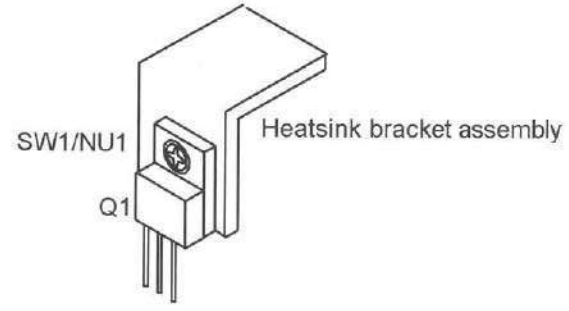

HSINK Bracket fabricated as per
step 3 from 1/16" aluminium piece.
Note hole for attaching tab of Q1

Figure 7-4 *Parts assembly and fabrication*

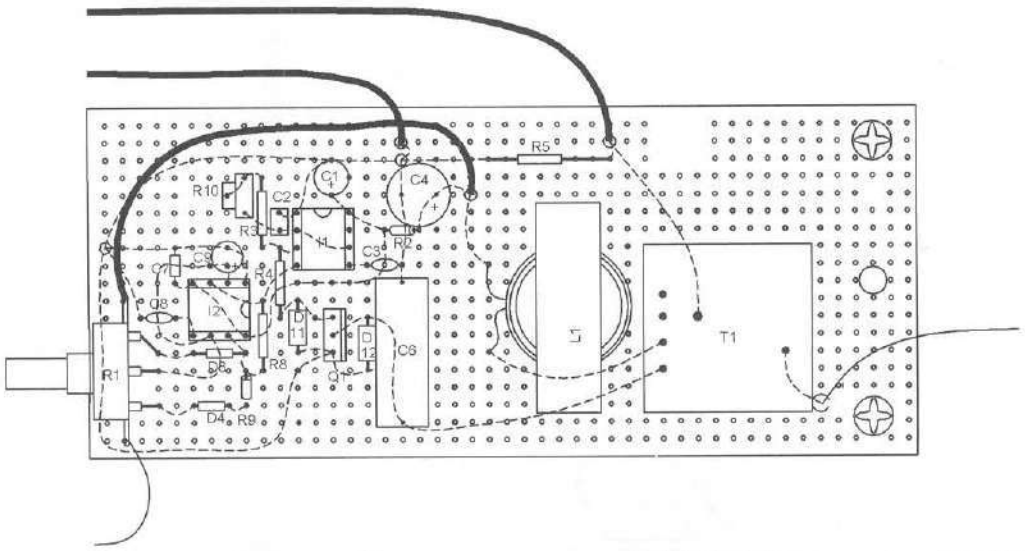

Thick dashed lines are direct connection runs beneath board of #20 buss wire (WR20BUSS) and are extended for the spark switch electrodes.

Thinner dashed lines are #24 buss wire (WR24BUSS) and component leads wherever possible.

Triangles are direct connection point junctions.

Solid black lines are external leads for input and output lines. Use red (WR20R) for +12 input. Use green (WR20G) for lifter - connection. Use black (WR20B) for com -12 input

Use 1/8-3/16 wide smooth globular solder joints for connections to C20A-J and D20A-J, R7 and HV output points. Thisis contrary to normal soldering but is necessary to prevent corona leakage.

Figure 7-5 *Wiring connections and external leads*

8. Fabricate a channel from a piece of 1/16-inch plastic material. Place it in the assembly and secure it at the corners using silicon rubber adhesive. You may also enclose it in a suitable plastic box.

   This step may not be required when used for another project referenced in this book.

Testing Steps

This step will require basic electronic laboratory equipment including a 60 MHz oscilloscope.

1. Preset the trimpot R1 to midrange and R10 to full counterclockwise. Short out the output leads using a short clip lead.
2. Obtain a 47K, 1-watt resistor and construct the spark gap "dummy load," as shown in Figure 7-2.
3. Obtain a 12-volt DC, 3-amp power converter* or a 12-volt, 4-amp rechargeable battery.*

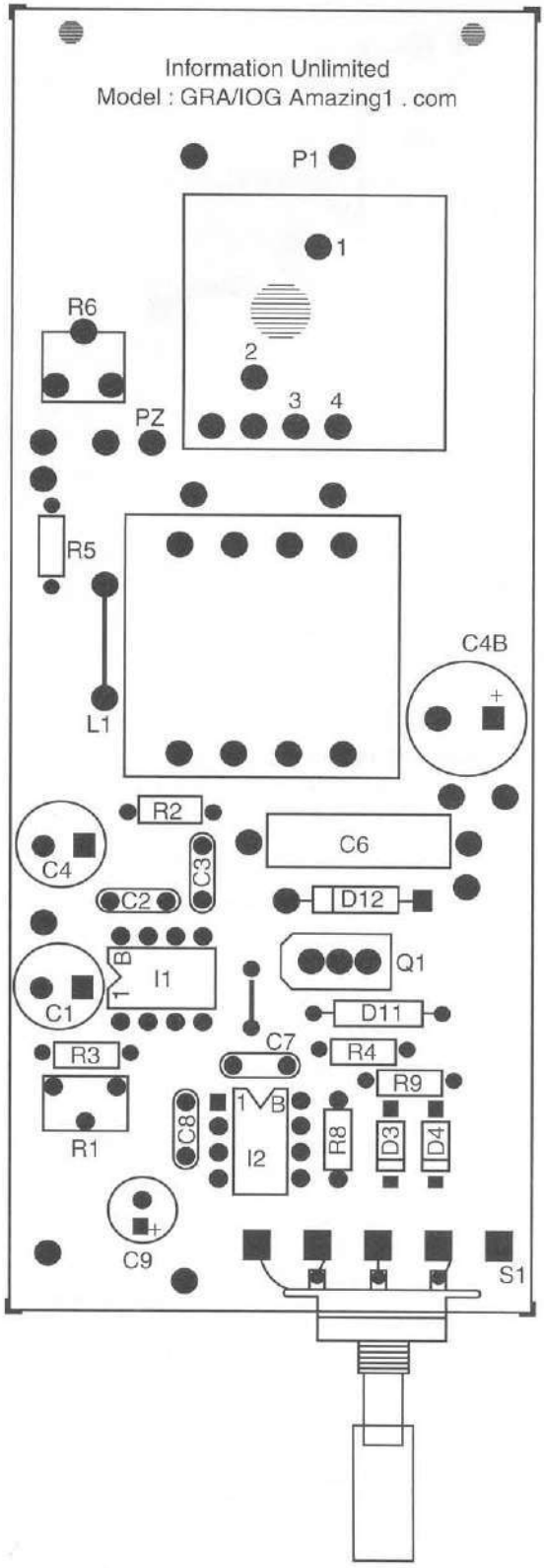

Figure 7-6 *PCB part identification*

4. Connect the input to the power converter and connect the scope, set to read 100 volts and with a sweep time of 5 usecs, to the drain of Q1.

5. Apply power and quickly adjust R1 to the waveshape shown in the inset of Figure 7-2. Note an input current dip of 100 milliamps or less. Check the heatsink of Q1, noting only warm to touch or slightly above 110 degree F.

   Note our laboratory-built units usually tune in with the pot set to 11 o'clock.

6. Remove the clip lead short in step 9 and connect the dummy load. Apply power and rotate R10 clockwise, noting the input current smoothly increasing to 1.5 amps and the spark increasing in energy. This control varies the ratio of off to on time and nicely controls the system current. Note that this system can easily provide 30 watts of usable power.

Table 7-1 High-Voltage, High-Frequency Driver Module Parts List

Ref. #	*Description*	*DB Part #*
R1	10K vertical trimpot	
R2, R4	Two 10-ohm, 1/4-watt resistor (br-blk-blk)	
R3, 5, 8, 9	Four 1K, 1/4-watt resistor (br-blk-red)	
R7	47K, 1-watt resistor (yel-pur-or)	
R10/S1	10K, 17 millimeter pot and switch	
C1	100-microfarad, 25-volt vertical electroradial leads	
C2	.0022-microfarad, 50-volt green plastic cap (222)	
C3,8	Two .01-microfarad, 50-volt disks (103)	
C4	1,000-microfarad, 25-volt vertical electrolytic capacitor	
C6	.22-microfarad, 250-volt metallized polypropylene	
C9	1-microfarad, 25-volt vertical electro cap	
C7	.1-microfarad, 50-volt cap, INFO#VG22	
D3, 4	Two IN914 silicon diodes	
D11	One PKE15, 15-volt transient suppressor	

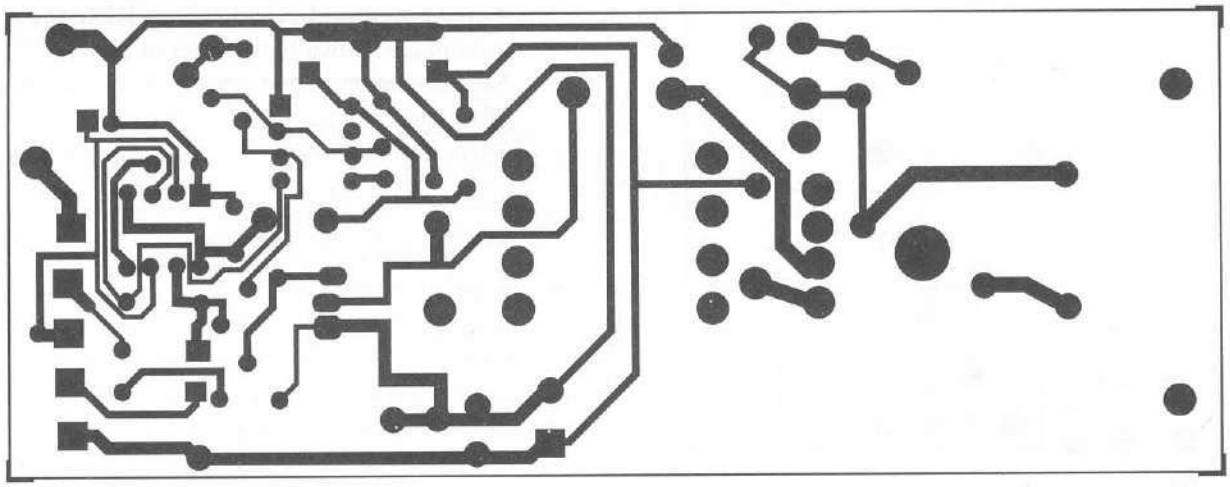

Figure 7-7 *PCB foil traces*

D12	1N4937 fast-switching 1-kilovolt diode	
Q1	IRF540 *metal-oxide-semiconductor field effect transistor* (MOSFET) transistor TO220	
I1, 2	Two 555 DIP timers	
T1	7-kilovolt, 10-milliamp mini-switching transformer	DB# IU28K089
L1	6 uH inductors (see text on assembly)	DB# IU6UH
PBOARD	5 × 2.8 × .1-inch grid perforated board; build to size per Figure 7-2	
PCGRA	Optional PCB	DB# PCGRA
WR20R	12-inch #20 vinyl red wire for positive input	
WR20B	12-inch #20 vinyl black wire for negative input	
WR20G	12-inch #20 vinyl green wire for output ground to craft return	
WR20KV	Four 20 kilovolt silicon high-voltage wires for output	
WR20BUSS	18 inches of #20 bus wire for spark gap and heavy leads (see Figure 7-5)	
WR24BUSS	12 inches of #24 bus wire for light leads (see Figure 1-5)	
HSINK	1.5 × 1-inch .063 AL plate created as per Figure 7-4	
SW1	One 6-32½ Philips screw	
NUT	Four 6-32 keep nuts	
12DC/7	115 VAC to 12 VDC, 3-amp converter	DB# 12DC/7
BAT12	12-volt, 4-amp, hour rechargeable battery	DB# BAT12
BC12K	Battery charger kit for above BAT12	DB# BC12K
GCAT1	*GENERAL CONSTRUCTION PRACTICES*	DB# GCAT1

Chapter Eight

Negative Ion Machine with Reaction-Emitting Rotor

Figure 8-1 shows a new concept in negative ion generation. A spinning rotor powered by the emitted ions themselves generates copious amounts of beneficial ions. Large volumes of ions can now be produced, as the area circumscribed by the rotor greatly reduces the local charge flux. This feature allows many times more ions without ozone-producing voltages.

Negative ions are highly beneficial and cause a sense of well-being, as well as rid the air of pollen and other breathable irritants. This is an excellent device for people suffering from asthma and other bronchial problems. It is also a nice conversation piece with a desktop unit's spinning rotor silently reaching a relatively high rotational velocity. The device operates from 115 VAC/12 VDC or a battery. The project utilizes a 25-kilovolts negative output power module requiring 12 volts DC at 500 milliamps along with our proprietary rotating emitter.

This is a beginner- to intermediate-level project requiring basic electronic skills, and one should expect to spend $25 to $50. All the parts are readily available, with specialized parts obtainable from Information Unlimited (www.amazing1.com), and they are listed in Table 8-1.

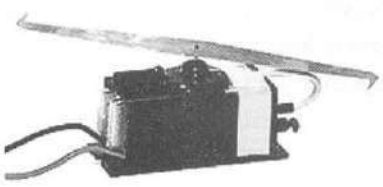

Figure 8-1 *The ion machine*

Precautions: Do not use this device in explosive or flammable atmospheres, as spark discharges may cause dangerous ignitions.

Benefits of Negative Ions

In the last several decades, a medical controversy has evolved pertaining to the beneficial effects of these minute electrical particles. As with any device that appears to affect people in a beneficial sense, there are those who sensationalize and exaggerate these claims as a cure for all aliments and ills. Such people manufacture and market these devices under these false pretenses and consequently give the products an adverse name. The Food and Drug Administration now steps in on these claims, and the product, along with its beneficial facets, goes down the tubes.

People are affected by the property of these particles, which increase the activity rate of cilia, whose function is to keep the trachea clean from foreign objects, thus enhancing oxygen intake and increasing the flow of mucus. This property neutralizes the

effects of cigarette smoking, which slows down this activity of the cilia. Hay fever and bronchial asthma victims are greatly relieved by these particles, and burn and surgery patients are relieved of pain and heal faster.

Tiredness, lethargy, and general worn-out feelings are replaced by a sense of well-being and renewed energy. Negative ions destroy bacteria and purify the air with a country-air freshness. They also cheer people up by decreasing the serotonin content of the blood. As can be seen in countless articles and technical writings, negative ions are a benefit to humans and their environment.

Negative ions occur naturally from static electricity, the wind, waterfalls, crashing surf, cosmic radiation, radioactivity, and ultraviolet radiation. Positive ions are also produced from some of these phenomenon and both of them usually cancel each other out as a natural statistical occurrence. However, many manmade objects and devices have a tendency to neutralize the negative ions, thus leaving an abundance of positive ions, which create sluggishness and most of the opposite physiological effects of its negative counterpart.

One method for producing negative ions is by obtaining a radioactive source rich in beta radiation (negative electrons). Alpha and gamma emissions from this source produce positive ions that are neutralized electrically. The resulting negative ions are directed by electrostatic forces to the output exit of the device and are further dispersed by the action of a fan (this method has recently come under attack by the Bureau of Radiological Health and Welfare for the use of tritium or other radioactive salts). This approach appears to be the more hazardous of the two according to the Consumer Product Safety people. The second method is to produce a potential level of negative high-voltage electricity without ozone and allow the creation of negatively charged particles by the high voltage.

Your negative ion generator produces ions via a high-potential, low-current source of DC power. The high potential causes negative charges to be produced at the sharp emission points of the rotor blade. The reactionary force of the emitted particles now causes the rotor to spin, allowing these negative ions to escape into the air stream due to the high-charge density at the sharp, pointed rotor tips. (The point of a pin will have a much higher charge density than a larger diameter spheroid for the same potential.) Ozone is kept at a minimum by keeping the voltage relatively low while allowing a sufficient charge density lets the negative particles escape into the air.

Circuit Description

The circuit (MOD25KV) consists of a high-frequency, high-voltage oscillator being fed into a multistage Cockcroft-Walton multiplier. This energy is converted into a potential of up to a negative 25,000 volts. The high-frequency stage consists of a transistor connected as a simple oscillator where its collector drives the primary winding of the resonant transformer (T1).

The high-frequency output of T1 is fed into a voltage multiplier stage consisting of a diode string (D1 to D5) and a capacitor string (C1 to C5). A 12-volt DC wall adapter (T2) powers the unit. A separate ground is required for optimum performance and involves connecting the negative 12 volts to earth ground. This is done by connection to the AC receptacle plate or ground pin. This ground provides a virtual ground for the ions.

A charge concentration occurring at the ends of the rotor blade's points now produces ions, and reactionary forces move the rotor at a high speed. Ions are produced at a high rate as the effective emitter area is equal to that of the rotating rotor. Also, charge neutralization is minimal using this method and a high ion current is generated.

The output of the unit can be approximated by the fact that a Coulomb charge equals the current multiplied by the seconds. There are also 6.25 × E18 negative chargers per Coulomb and the maximum current to the emitters is 400 microamps. Therefore, the unit can produce 6.25 × E18 × 200 × E-6 = 2.5 × 10E15

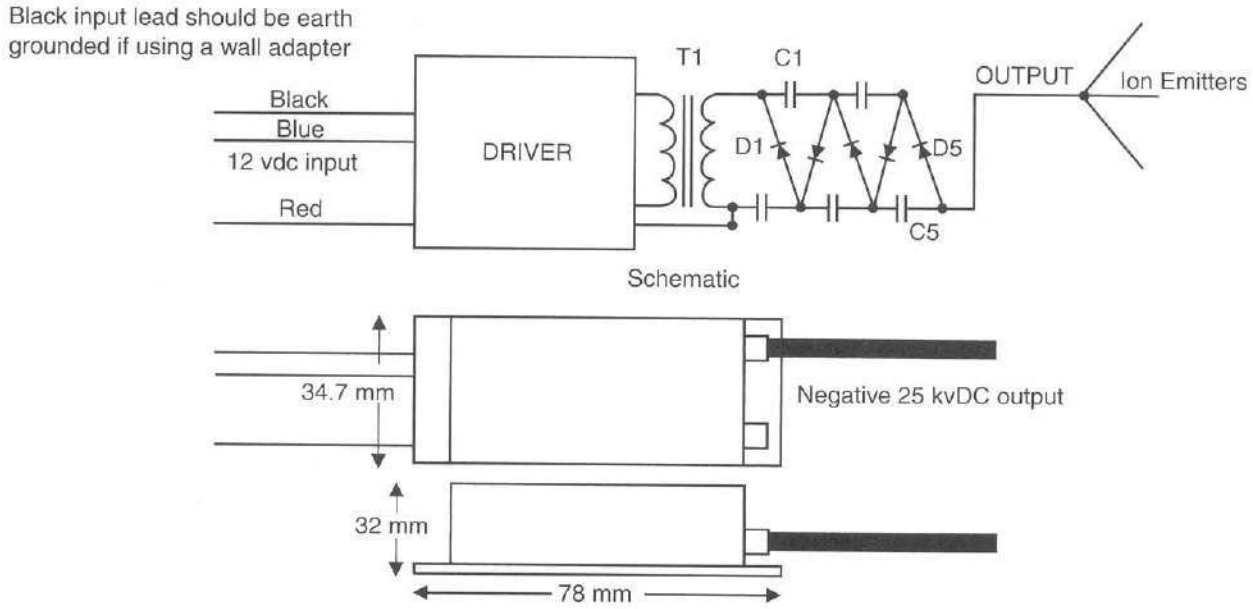

Function	Value	Notes	Other
Input Voltage	12 vdc		
Input Current (No load)			
Input Current (load)	400 ma		
Input Watt (No load)			
Input Watt (load)			
Output Volts	–20 kvDC		
Output Configuration	Single Output		
Internal Operating Frequency	35 KHz		

Use a 12 vdc/.5 amp DC wall adapter or other suitable power supply.
Always check entire system for any excessive heating.

Figure 8-2 *Circuit schematic*

negative charges per second. This is usually sufficient for a large room.

Assembly Steps

1. Lay out and identify all parts and pieces. Verify them with the parts list.
2. Carefully fabricate the rotor blade as shown in Figure 8-3 and note that it must be balanced for optimum rotational velocity and ion emission.
3. Position a common plastic pushpin (PIN1) and hot glue or epoxy to the module as shown. Glue is more forgiving if should you ever wish to replace the pin.
4. Carefully strip about 3/4 of an inch of insulation from the output lead. Tin and solder it to the bottom of the actual pin. This connection point must allow complete clearance of the entire bearing section of the rotor assembly when in place.
5. Wire up the wall adapter (T2) and ground the lead using (WN1) wire nuts, as shown in Figure 8-4.

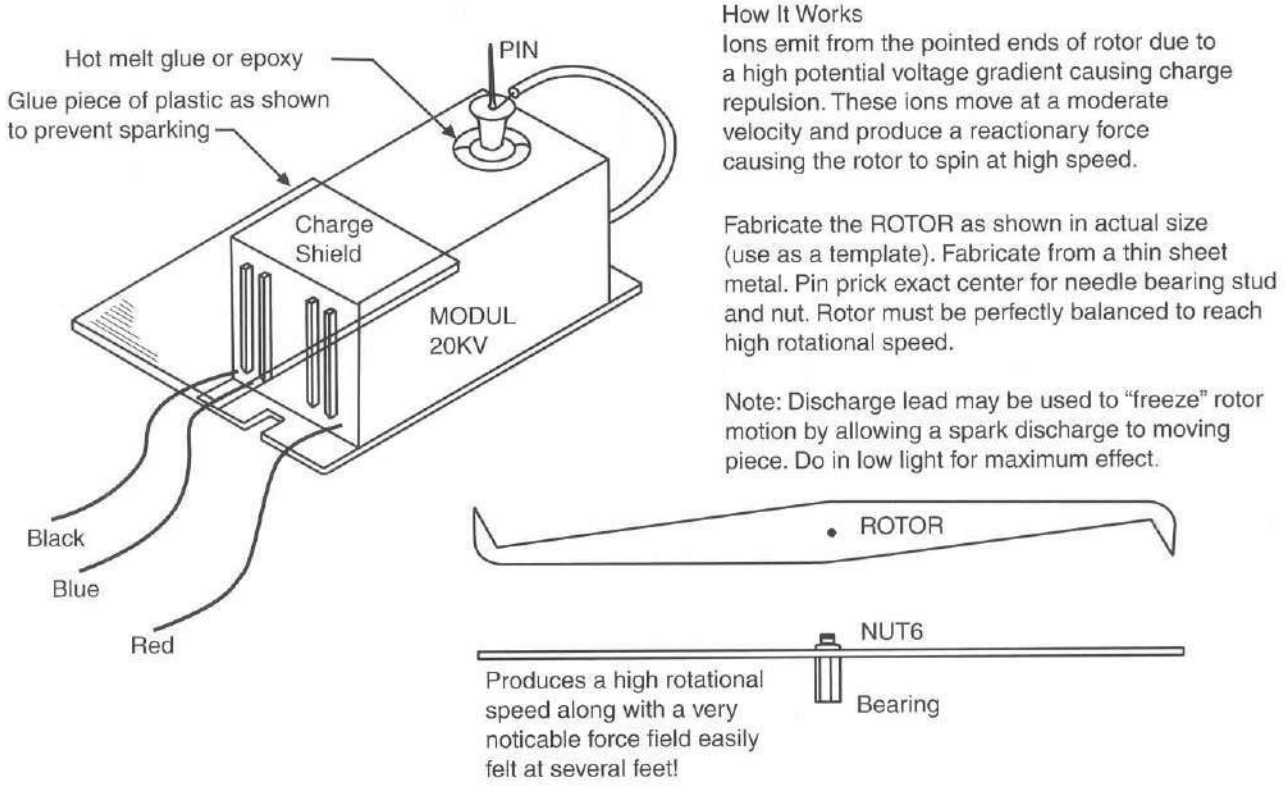

Figure 8-3 *Isometric view of the overall unit*

6. Glue on the CS1 charge shield plate to prevent premature sparking to the metal heatsink of the module. Also, stick on the rubber feet.
7. The unit is perfectly usable. However, you may want to enclose it in some sort of plastic box. Always use good ventilation and make sure the box is large enough or about 1½ times the diameter of the rotor.
8. Find a suitable location, such as a nonmetallic table, to place the unit on. Place the rotor blade on the pin and verify it is unobstructed. Then connect the grounding lead to the receptacle mounting screw and plug in the T2 adapter. The rotor should begin rotating and quickly reach a high speed.

Notes

Ions are now being emitted into the air and can easily be detected by holding a fluorescent tube or a small neon indicating lamp (LA1) near the unit, noting a flashing. This must be done in the dark. You can also place a piece of paper near the base of the unit and note the force field generated that tries to pull the paper.

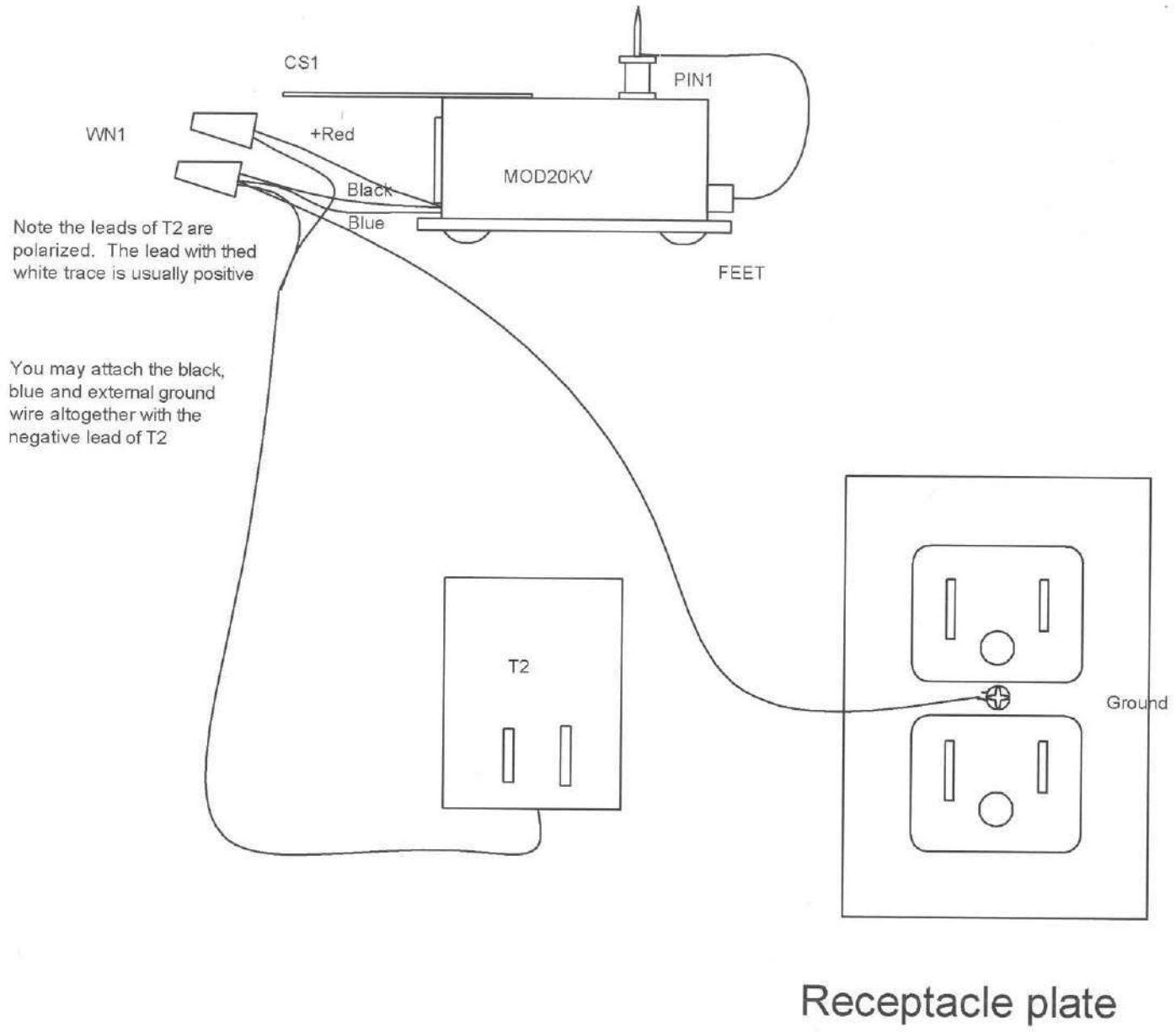

Figure 8-4 *Side view showing power connections*

Table 8-1 Negative Ion Machine Parts List

Ref. #	*Description*	*DB Part #*
MODULE	Negative 20-kilovolt module reworked	DB# MOD20KV
T2	12-volt DC, 500-milliamp wall adapter	DB# 12DC/.5
ROTOR	Metal fabricated rotor	DB# ROTOR
PIN	Common plastic pushpin	
BEARING	#6-32 threaded standoff	
NUT6	6-32 hex nut	
CS1	2¼ × 1½-inch-thin, 1/16 to ⅛-inch-thick plastic	
WN1	Small wire nuts	
FEET	Four stick-on rubber feet	

Chapter Nine

Kirlian Imaging Project

Kirlian photography uses *cold electron emission* to expose a photographic film. Cold electron emission is the result of electrons accelerating in an electric field. These accelerated electrons ionize the air and recombine producing ultraviolet light that is mostly invisible to the naked eye. This phenomenon is commonly known as *corona*. Many living objects are claimed to emit this radiation that will vary according to the health and condition of the object being exposed. This in itself is now subject to scientific research in material analysis. A more "psychic application" can be seen in the practice of radiation being referred to as an aura and being dependent on other more metaphysical functions. This project describes a simple method of producing Kirlian images of small objects and is an introduction to those who want to explore this interesting field. Kirlian imaging ranges from the psychic to materials analysis. Often it is used for experiments in which it is claimed that objects all possess a unique aura signature. This depends on the subject's mental makeup and condition at the time. Basically, it is a form of corona discharge that occurs as a precursor to a dielectric breakdown by most conductive objects when placed in a high-frequency, high-voltage field. Corona is a form of electrical leakage occurring without actual air breakdown such as a spark discharge. A corona discharge possesses ultraviolet emissions that easily develop film and thermographic paper, producing an image print.

This is an intermediate-level project requiring basic electronic skills and one can expect to spend $25 to $50. All parts are readily available, with specialized parts obtainable through Information Unlimited (www.amazing1.com). The parts are listed in Table 9-1.

The system is simple and built from readily available parts (see Figure 9-1). The builder may deviate from what is shown as long as the basics are adhered to. The system requires a high-voltage, high-frequency module, as shown in Chapter 10 where it will be used to supply the burning plasma for the plasma pen project.

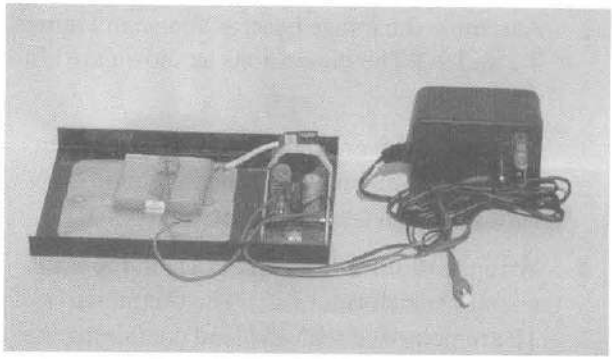

Figure 9-1 *A complete unit*

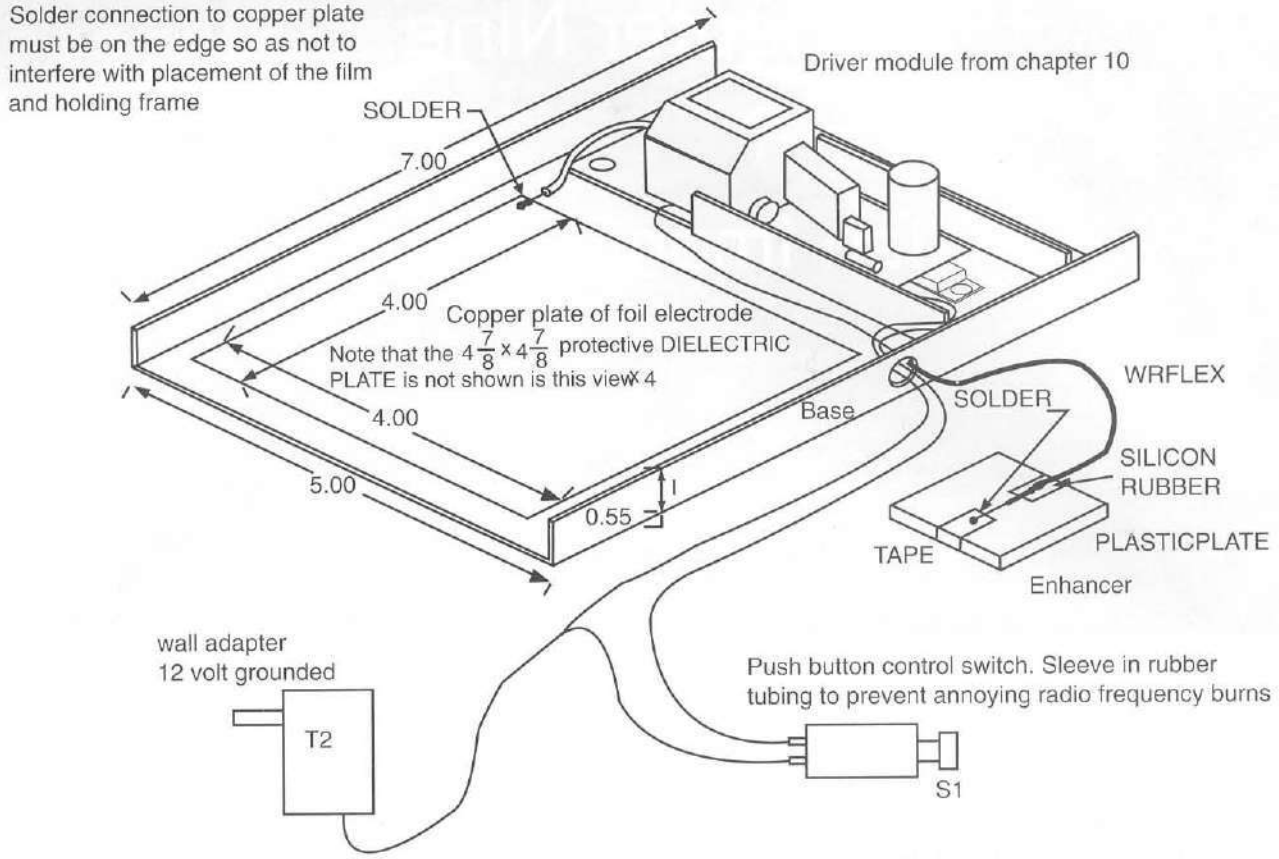

Figure 9-2 *Isometric of the image base and charge plate*

Assembly Steps

If you are a beginner, it is suggested to obtain our *GCAT1 General Construction Practices and Techniques*. This informative literature explains basic practices that are necessary in proper construction of electromechanical kits and is listed in Table 9-1.

1. Assemble the driver module, as shown in Figures 10-2 and 10-3 in Chapter 10. Verify proper operation before using.
2. Assemble the image base, as shown in Figures 9-2 and 9-3. The dimensions as shown are not critical.
3. Mount the driver module and solder the output lead as shown. Route the input and high-voltage return lead to the ENHANCER.
4. Wire the pushbutton switch (S1) to the wall adapter transformer (T2). The output wires of T2 are polarized with the lead containing the white trace, usually the positive. It is a good idea to cover the entire body of S1 except the plastic actuator; any contact to metal will result in small, very annoying burns. The wall adapter recommended has a third pin being an isolated ground for the high-frequency return.

Testing Steps for the Circuit

These steps usually will not require any special testing equipment.

1. Power up the unit and activate S1. Place your finger on the insulated plate and note a bluish corona discharge occurring under your finger. You may feel some heat or a tingling sensation. Try this for only up to 20 seconds.
2. Obtain some thermographic fax paper and place it on the dielectric plate. Place your finger on the paper and energize the circuit for 10 to 20 seconds. You will note an image on the paper.

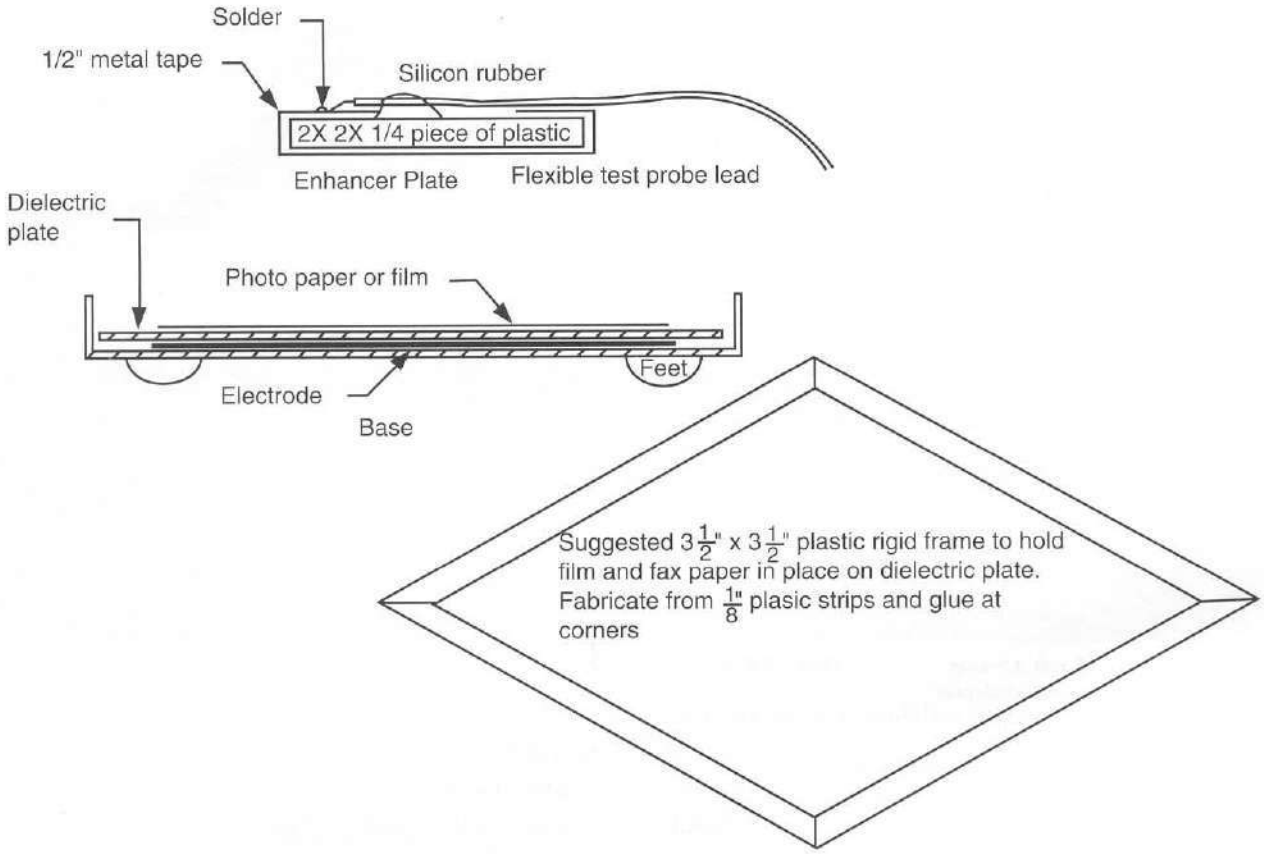

Figure 9-3 *Image base and charge plate*

Try it again with a metal object such as a coin on the dielectric plate and place the enhancer on the object. Push the button for 5 to 10 seconds and note an image forming.

3. You can upgrade your image to an actual photograph by using actual camera film. The old Polaroid 600 or other similar instant film will work. You must work entirely in the dark to avoid film exposure to any ambient light. The objective is to place the film on the dielectric plate along with the object to be photographed and the enhancer placed on top.

Notes

You will note that a few variables here can affect performance: the output voltage of the driver module and the dielectric plate's thickness and dielectric properties. The dielectric plate is important because it must form a high enough capacity between the object and the contacts to allow an adequate corona current to flow to create an image. The thinner the plastic dielectric plate, the more corona current. However, you must not allow a breakdown to occur by using material that is too thin, as this can produce a painful burn.

Many different sources of information, including some excellent books, are available on the applications, methods, and uses of Kirlian photography. You are encouraged to continue to investigate this unusual electronic phenomenon.

Table 9-1 Kirlian Imaging Parts List

Ref. #	*Description*	*DB Part #*
DRIVER	Driver module from Chapter 10	DB# MINIMAX7
BASE	6 × 7-inch plastic piece, formed as shown in Figure 9-2	
COPPER ELECTRODE	4 × 4-inch, thin piece of copper	
DIELECTRIC PLATE	5 × 5 × .02-inch piece of polypropylene sheet	DB# POLYP20
PLASTIC PLATE	2 × 2 × 1/4-inch plastic plate	
TAPE	Four inches of 1/2-inch solderable metal sticky tape	
FEET	Four sticky rubber feet	
T2	12-volt, 1.5-amp groundedadapter with third pin	DB# 12DC/1.5G
FRAME PIECES	Four strips of 1/8-inch plastic to fabricate the frame as shown in Figure 9-3	
WRFLEX	12 inches of flexible test lead wire	
S1	Push-button switch reworked as shown to prevent burns	
GCAT1	General construction practices	DB# GCAT1

Chapter Ten

Plasma Etching and Burning Pen

A plasma pen uses high frequency, high voltage to burn or etch permanent markings into many different materials (see Figure 10-1). With a little practice, the user can create many intriguing designs of fine, lace-like etches. Names and other text can easily be etched into almost any organic material. Wood, paper, plastics, pumpkins, gourds, eggs, and leaves can all be marked with fine and fancy designs or inscriptions. The pen's other applications include Kirlian photography, aura enhancing, and magically lighting household fluorescent and neon tubes, all without any connecting wires, providing a great magic act. You can also use this for plasma experimentation or even removing warts.

This is an intermediate-level project requiring basic electronic skills. Expect to spend $25 to $35. All parts are readily available, with specialized parts obtainable through Information Unlimited (www.amazing1.com), and all of them are listed in Table 10-1.

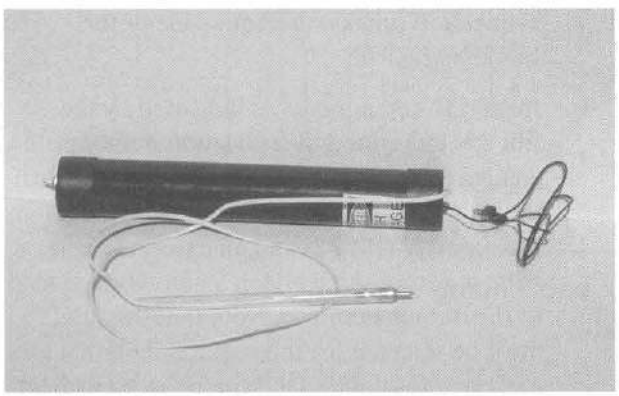

Figure 10-1 *Photo of assembly*

The system is shown in two parts: the power driver and the pen or etching section. These are connected together via a suitable, flexible, high-voltage wire. The power driver consists of the electronics module and the internal batteries for portable use. A jack is provided for external use from a 12 VDC wall adapter or another suitable source. This section is housed in a tubular enclosure with plastic end caps as shown.

Driver Circuit Description

The circuit is a frequency, high-voltage oscillator that consists of transistor Q1 connected as a simple oscillator where its collector drives the primary winding PR1 of the resonant transformer T1. Feedback is obtained via a second winding (FB) and fed to the base of Q1 through a current-limiting resistor (R1). Resistor R2 biases Q1 into conduction and initiates the oscillation (see Figure 10-2).

Capacitor C3 speeds up the turn-off time of Q1, while resistor R3 and capacitor C5 provide a filter to prevent oscillation at the self-resonant frequency of T1. Resonating capacitor C4 resonates the transformer

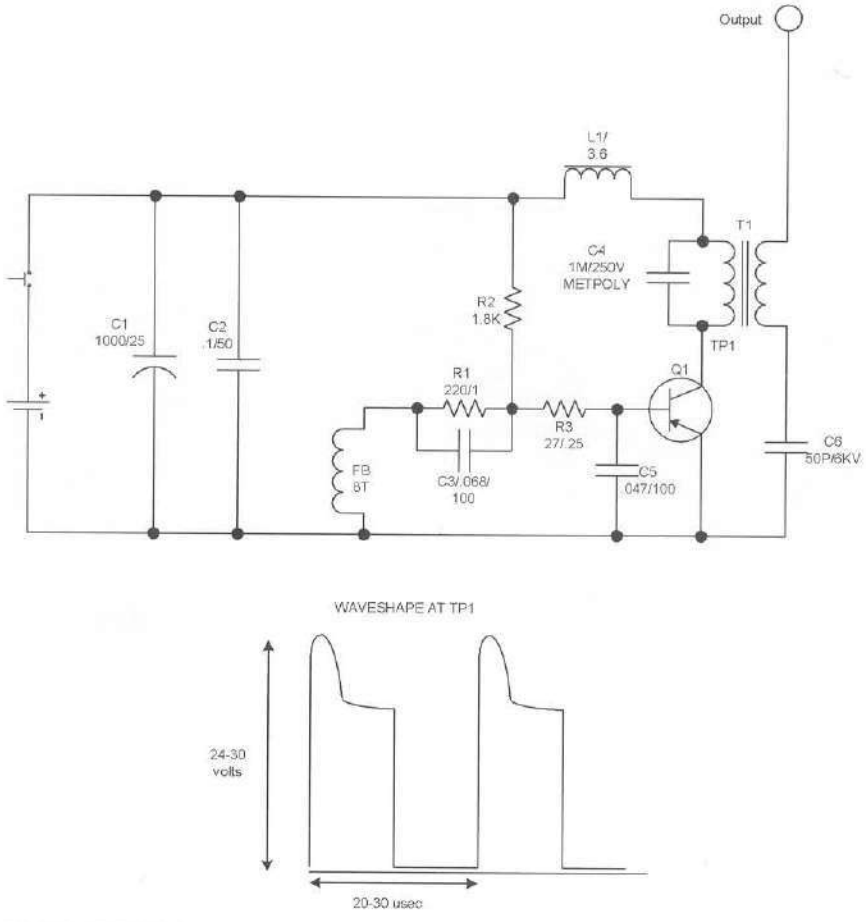

Figure 10-2 *Circuit schematic*

to around 35 KHz. The current-limiting inductor L1 limits the short-circuit current to a noncatastrophic value, and capacitors C1 and C2 bypass any signal to ground.

Driver Circuit Assembly

1. Lay out and identify all the parts and pieces. Verify them with the parts list, and separate the resistors as they have a color code to determine their value. Colors are noted on the parts list.
2. Obtain the available *printed circuit board* (PCB), as shown in Figure 10-3, or fabricate a piece of perforated circuit board to the PC as laid out on the PCB. Note the size of the PCB is $3\frac{1}{2} \times 1\frac{3}{8}$ inches and contains the silk screening that shows the positioning of the mounted parts.
3. If you are building from a perforated circuit board, it is suggested that you insert the components starting in the lower left-hand corner. Pay attention to the polarity of the capacitors that have polarity signs and all semiconductors. Route the leads of the components as shown and solder as you go, cutting away unused wires. Attempt to use certain leads as the wire runs and follow the foil traces on the drawing as these indicate the connection runs on the underside of the assembly board.
4. Insert the components as indicated by the silk-screen printed identification numbers and compare this with the bill of materials. Attach three 6-inch, #22-20 leads as shown for the input power (P1, P2) and an external high-voltage return. Also attach a high-voltage lead to the output as shown. Note that this lead must be selected for the required length. Use a silicon, 20-kilovolt DC wire or an equivalent.

Note the ground lead that connects to the metal frame under the screw head as shown.

5. Double-check the accuracy of the wiring and the quality of the solder joints. Avoid wire bridges, shorts, and close proximity to other circuit components. If a wire bridge is necessary, sleeve some insulation onto the lead to avoid any potential shorts.
6. Cut the metal bracket (BRK1) from a piece of .062 sheet aluminum and make the final assembly, as shown in Figure 10-4. Note that the metal tab of Q1 must be insulated from the bracket as shown on the mounting scheme. This piece is also the heatsink for Q1.

Driver Board Testing

This step will require basic electronic laboratory equipment. A 60 MHz oscilloscope is suggested.

1. Obtain a 12-volt DC source, preferably with a volt and ammeter. Leave the output leads as open circuit and apply power. Note a current draw of less than 250 milliamps. If you have a scope, observe the waveshape at the collector of Q1, as shown in Figure 10-2.
2. Contact the high-voltage output lead to the bracket and note that you can draw a ½-inch arc with the input current going to 1 amp. This completes this module.

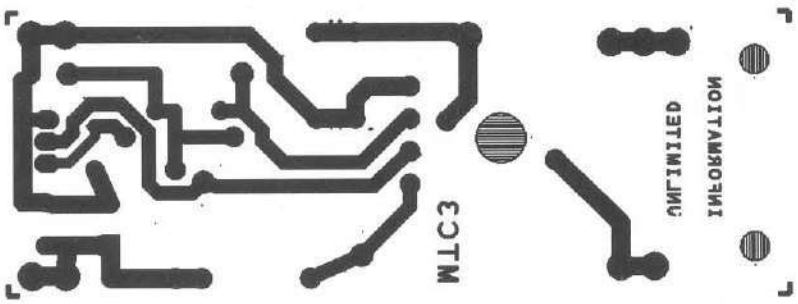

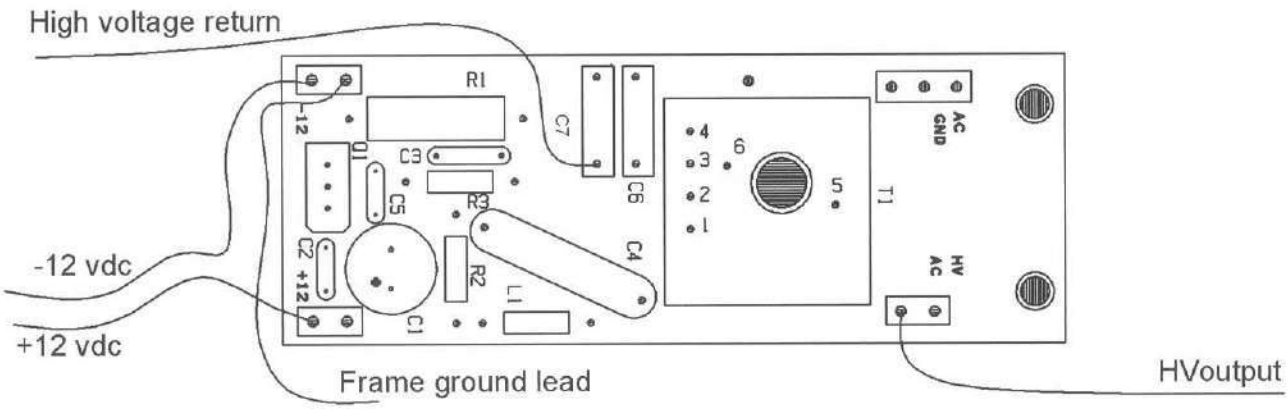

Figure 10-3 *Assembly board*

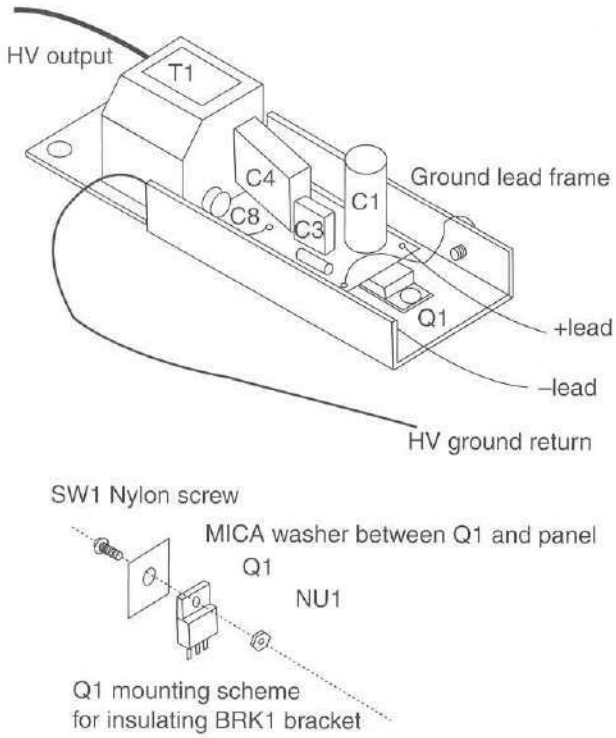

Figure 10-4 *Isometric of assembly*

Mechanical Assembly

You will need some basic cutting tools for the following steps.

1. Fabricate TUB2, as shown in Figure 10-5, and then make the caps CA1 and CA2 for passage of the output leads and for switch S1, jack J1, and indicator lamp LA1.
2. Insert the components and wire them up as shown. Note the current-limiting resistor R10. The exiting leads should be tied in a knot to relieve any strain.
3. Assemble the pen section as shown and solder the lead to the brass POINT. Shim the lead and POINT, and mechanically secure them in place.

Sample Demonstration

1. Obtain a 4 × 6-inch square piece of ¼-inch masonite plywood, as shown in Figure 10-6. Moisten it with a sponge and place it on top of an approximately equal-size metal plate attached to the ground lead.
2. Contact the surface with the plasma pen and note the burning action. Experiment for the best results with other materials.

Note that your pen will light fluorescent lamps in your house just from its proximity to them, and it can also be used for Kirlian photography.

Switch S1 selects either internal batteries or external 12 volts, jack J1 is for the external 12 volts. LED indicates when the system is powered up. Resistor R1 limits the LED current. These components are mounted on the rear cap CAP2.

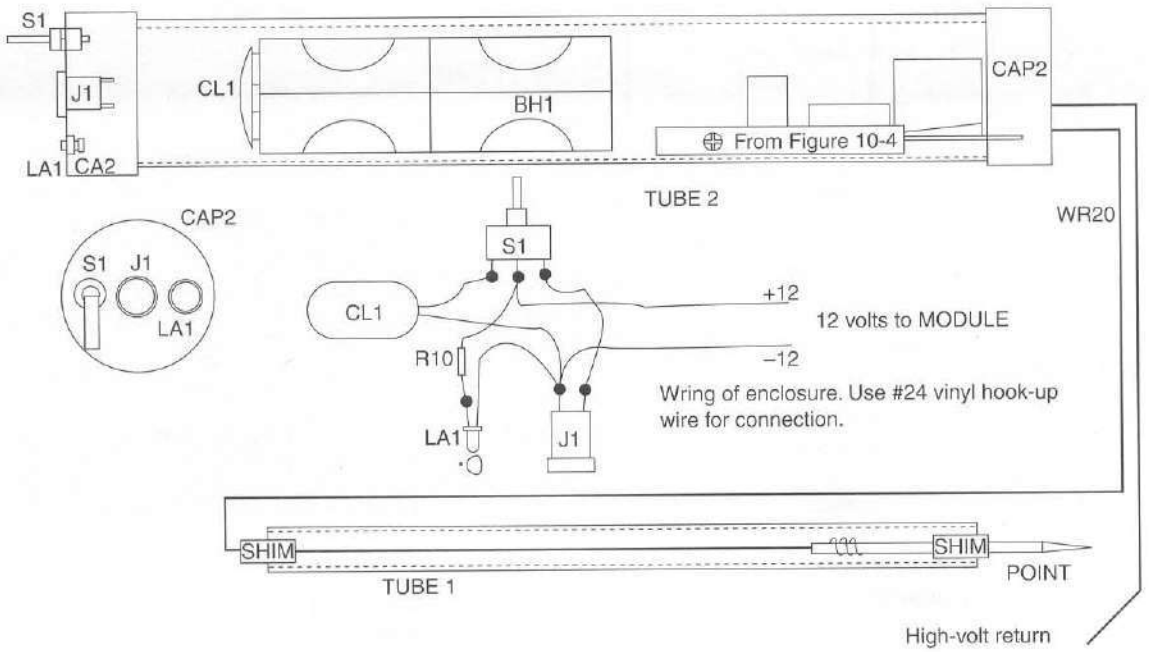

The POINT can be a 1/5 to 1/4 brass rod that can be soldered to. The SHIMS can be rubber tubing that strain relieve and position the feed lead and burning point. TUBE1 can be a 3/8" diameter plastic tube.

Figure 10-5 *Final enclosure and wiring*

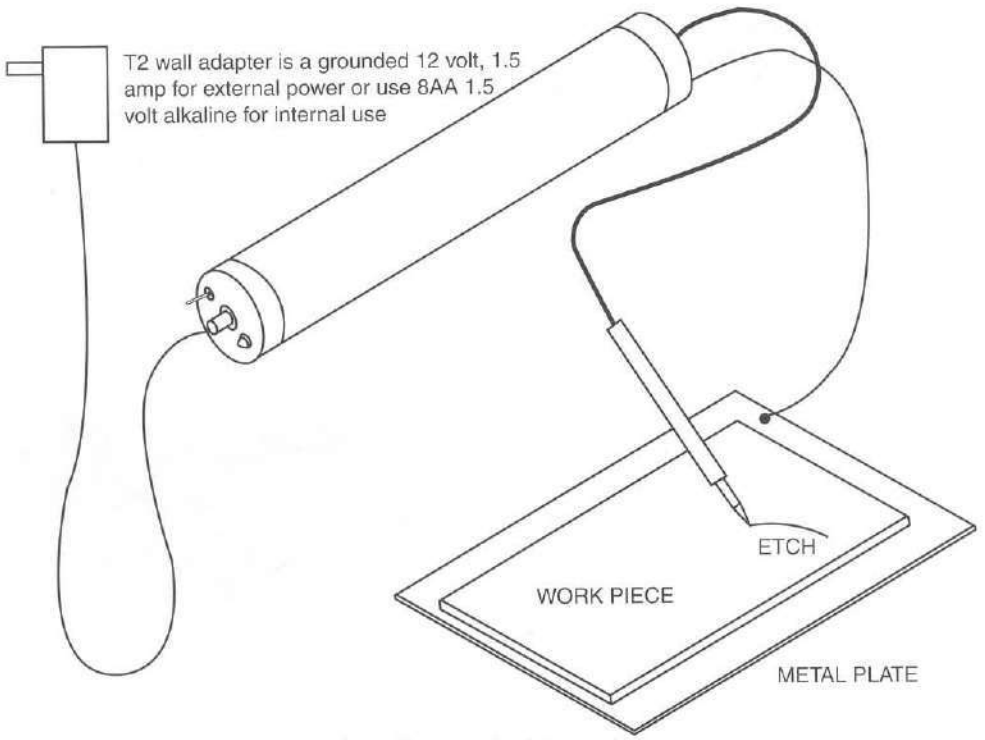

For optimum performance, use a piece of marisonite, thin wood, etc.
Place on top of metal plate connected to the high-voltage ground lead.
You may moisten the beginning area to start the etch.

Figure 10-6 *Sample demonstration*

Table 10-1 Plasma Etching and Burning Pen Parts List

Ref. #	*Description*	*DB Part #*
R1	220 ohms, 1 watt (red-red-br)	
R2	1.8K, 1/4-watt (br-gray-red)	
R3	27 ohms, 1/4-watt (red-pur-blk)	
C1	1,000-microfarad, 25-volt vertical electrolytic capacitor	
C2	.1-microfarad/50-volt small, plastic, capacitor	
C3	.068-microfarad, 50-volt plastic capacitor (683)	
C4	1-microfarad, 250-volt metallized foil large, blue, plastic capacitor	
C5	.047-microfarad, 100-volt plastic capacitor (473)	
C6, 7	Two 25-picofarad, 6-kilovolt ceramic capacitors or a single 50-picofarad, 6-kilovolt unit	
Q1	MJE3055T TO220 power tab NPN transistor	
T1	Special high-frequency transformer	DB# 28K089
WR20	24-inch #22-20 vinyl stranded hookup wire	
PCMTC	MTC3 printed circuit board or use a 3 1/2 × 1 1/2 × .1-inch grid perf board	DB# PCMTC
BRKT1	Create as shown in Figure 10-4	
TUBE2	12 × 2-inch ID schedule, 40 PVC tubing	
TUBE1	3/8 × 1/4-inch ID length of plastic tubing	
CA1, 2	Two mating flat-end caps for TUBE1	
POINT	1/8 × 3-inch brass rod filed to shape	
LA1	*Light-emitting diode* (LED), any color	
R10	220 1/4-watt resistor (red-red-br)	
CL1	Battery snap clip	
BH8	Eight-AA-cell battery holder	
S1	*Single pole, double throw* (SPDT) small toggle switch	
J1	Chassis-mounting DC power jack	
WR24	48-inch, #24 vinyl hookup wire	
WR20	24-inch, 20-kilovolt, silicon, high-voltage wire	
NEONX21	Assembled high-voltage module (see Figure 10-3)	DB# NEON21

Chapter Eleven

How to Electrify Objects and Vehicles

Figure 11-1 shows two board-level devices capable of producing electrical shocks. The larger circuit generates low-energy, 20,000-volt pulses similar to an automotive ignition system. Although these pulses are nonlethal, they can still be very painful when contacted. The smaller circuit generates a steady 5-milliamp, low current at 2,000 volts. By itself, it is not lethal but again can produce a painful shock. If the output is allowed to charge a capacitor to a sufficient energy level, then the rules change and a potentially lethal situation exists. This level usually is any value over 25 joules as computed from W (joules) = half of C (capacitance in farads) $\times$ V^2 (in volts) that the capacitor is allowed to charge too.

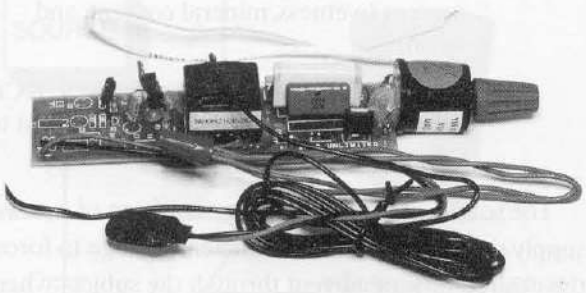

Figure 11-1 *Photograph of devices*

Caution: The use of electrification to prevent human intrusion is illegal. This application is legally referred to as "man trapping." Consult legal advice before using this if human contact is intended!

Warning: Never expose any person wearing a pacemaker or having a known physical condition to any form of electrical shock.

Data shows how to use several shocking systems with different types of outputs and applications. Even though the energy levels may be well below dangerous levels, secondary reactions can cause severe injury. Use caution if intended for human contact, and never connect the DC output version to a capacitor as a lethal charge may exist.

The following information is intended to serve as a guide to those contemplating using our equipment or other devices capable of producing a mild, severe, or possibly lethal electric shock. Any device of this nature, if used against people, may be considered a potential weapon. Remember that what may be a mild shock to one person could be harmful to another. Secondary effects, resulting from involuntary action, must also be considered.

The devices sold are intended for laboratory experiments or for use against animals. They should only be used for intimidation purposes to prevent an encounter. Human contact must be totally justified,

as serious consequences can result from the illegality of their use.

Even though our electronic devices provide an average current below what is considered lethal to the average person, circumstances such as a person's heart condition or other physical parameters can influence both the immediate effect and after contact reaction.

Table 11-1 shows certain effects from various electrical currents. Remember that the indicated current must have an appropriate voltage behind it to flow through a given resistance, such as the human body. When working with sources that have storage capacitors (especially dangerous sources), one must take into account the high peak current that can result for a period of time and result in possible electrocution if this duration of time is sufficient.

Table 11-1 Electrical current scale

Voltage	*Degree of pain*	*Examples*
.01 to 1 ma	Tingling to annoying	Static electric shocks
1 to 5 ma	Annoying to painful	Spark plugs, TV picture tubes, trip current of GFI
5 to 20 ma	Painful to very painful	Oil burner ignition, bug killers, stun guns
20 to 50 ma	Very painful to possibly lethal	Neon sign transformer, old tube radios
50 to 100 ma	Possibly lethal to lethal	Low-powered transmitters, capacitor charges for lasers
100 to 500 ma	Lethal to deadly	Medium-powered transmitters, laboratory power supplies
500 ma to 1amp (+)	Deadly, with usually no second chance	Electric chair, 220-volt house current under certain circumstances

Supplementary Electrification Data and Information

The following information explains how to place an electrical charge on an object to protect against animal damage, intrusion, or theft, and the construction of several energy sources is referenced. These must be treated with caution and never be used on human beings without proper discretion due to potential injury or electrocution. Accidental contact must also be avoided. Many laws unfortunately are made to protect the criminal, and therefore any attempt made to protect oneself or property using these devices could result in a suit by the criminal if he or she can prove injury.

The methods for electrifying objects and areas will be shown as several examples that the user may adapt to his or her own needs. To successfully electrify, an object requires the following conditions to exist. Note that the following pertains to flowing electric current and not to static or super-high voltages. Figure 11-2 provides the basic explanation.

- The object of contact must be of a conductive nature such as metal, conductive paint, or wet ground.
- The subject (the intruder or animal) must supply the link to complete the circuit; that is, his or her physical extremities must come in contact with the object, along with a second common surface such as the ground, water, or another object anticipating simultaneous contact. No current flows unless contact is made to complete the circuit by the subject physically touching the object.
- The electric current flows from the +lead of SOURCE to the −lead. In doing so, it flows from the object to the point of contact by the subject to the ground and back to SOURCE via the −lead. This produces a current flow through the subject, developing an electrical shock. The severity of this shock is dependent on:
  - How well the ground will conduct this current (wetness, mineral content, and so on)
  - The electrical parameters of the SOURCE, that is, the voltage and available current to support this voltage

The source of electrical energy is a form of a power supply made to generate a sufficient voltage to force the desired flow of current through the subject when contact is made. This can take on many different forms depending on the applications and the desired results. If a system was built to kill a human being, a power supply with a current supply capability of ½ to 20 amps would be necessary to support a voltage high

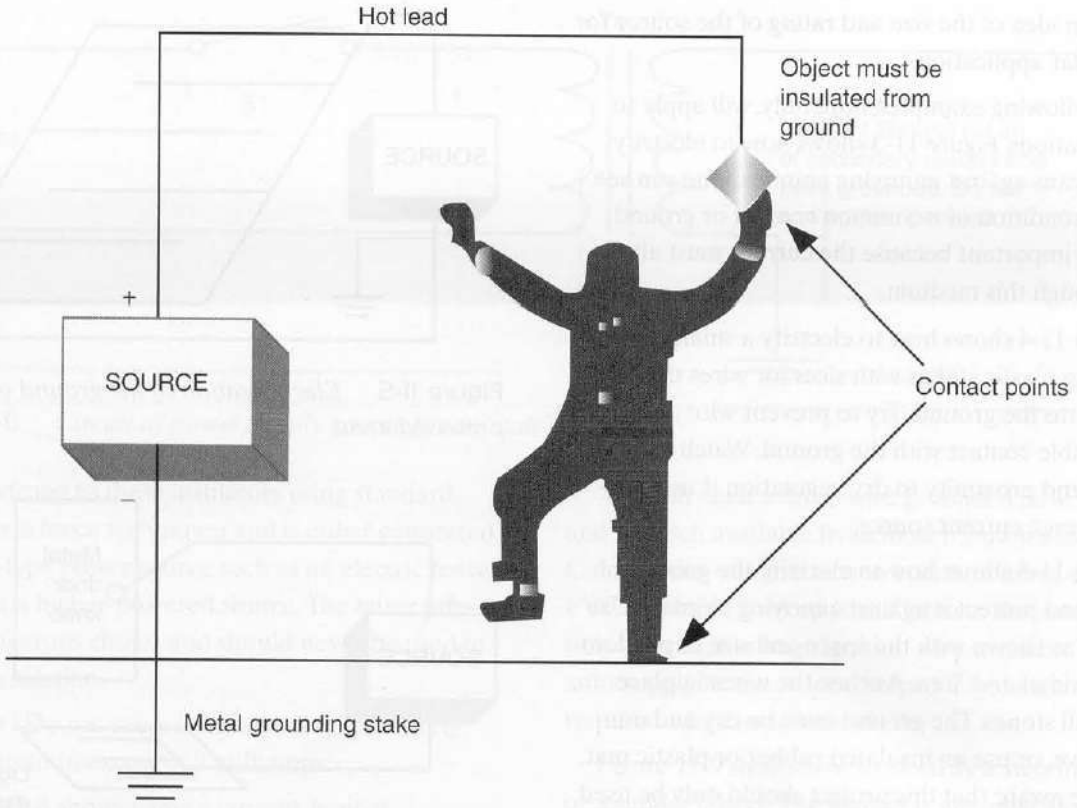

Figure 11-2 *Electrification principle*

enough to cause this current to flow, usually several thousand volts. (These parameters are similar to those used in electric chairs.) Currents of more than 1/10 of an amp are considered lethal to the average human under certain circumstances, 1/100 of an amp produces intense pain, and 1/1,000 of an amp is felt with no difficulty and is very annoying.

Special pulse-type energy sources, similar to capacitor discharge ignitions, can be used relatively safely as peak currents are high, yet the average is low. A source of this type is the pulsed model described in this project. This source is capable of generating the high-peak current pulses and maintaining a substantial voltage on the body of a vehicle in spite of leakages due to steel-belted tires and so on. The source is also relatively safe to exposure but will produce moderate shocks. With these parameters, one

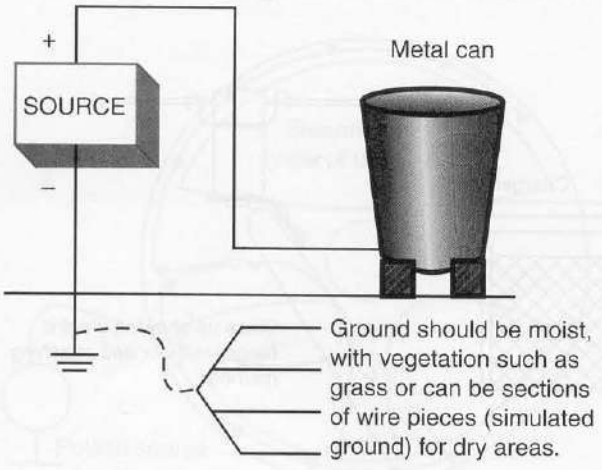

Figure 11-3 *Electrification of a garbage can or similar object*

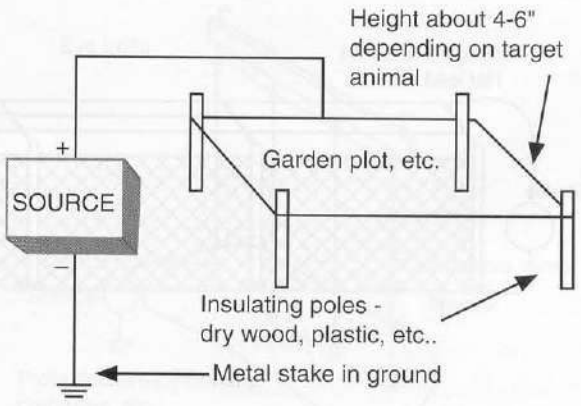

Figure 11-4 *Electrification of a small area*

can get an idea of the size and rating of the source for a particular application.

The following examples, hopefully, will apply to most situations. Figure 11-3 shows how to electrify garbage cans against annoying animals. One can see that the condition of a common contact or ground system is important because the current must also flow through this medium.

Figure 11-4 shows how to electrify a small garden area using plastic stakes with slots for wires that are pushed into the ground. Try to prevent wire droop and possible contact with the ground. Watch for fire hazards and proximity to dry vegetation if using a high, average current source.

Figure 11-5 shows how to electrify the ground of an area and protect it against annoying animals. Use #20 wire as shown with the space and size dependent on the animal and area. Anchor the wires in place with small stones. The ground must be dry and non-conductive, or use an insulated rubber or plastic mat. Please be aware that this project should only be used with a low-energy pulsed system or a hand-cranked magneto. Do not create this system if you have a heart condition.

Figure 11-6 shows a prank, but this is only to be done using a low-energy pulsed system or a hand-cranked magneto. The victim stands on a rug to open a door and zap! You turn the power on.

Figure 11-7 shows the electrification of a fence. This method is for educational use only, as serious injury can result either from the electric shock or the physical reaction. The intended use would be for military or other high-security situations.

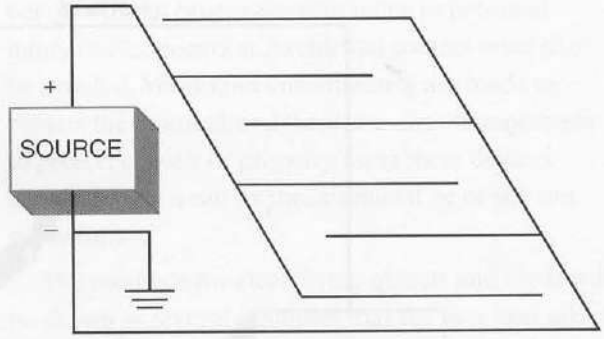

Figure 11-5 *Electrification of the ground or protected areas*

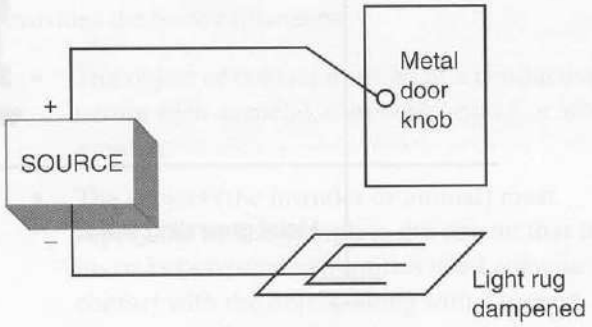

Figure 11-6 *Door knob prank*

The object here is to electrify the top-most wire of a chain-link fence, as anyone attempting to crawl over will no doubt come in contact with the top wire. This is a very effective method and can cause severe injury and even death from electrocution or physical injury from falling. The best method is to simply replace the original top-most wire with a standard, electrical farm fence insulator, as shown in Figure 11-7. The wire is

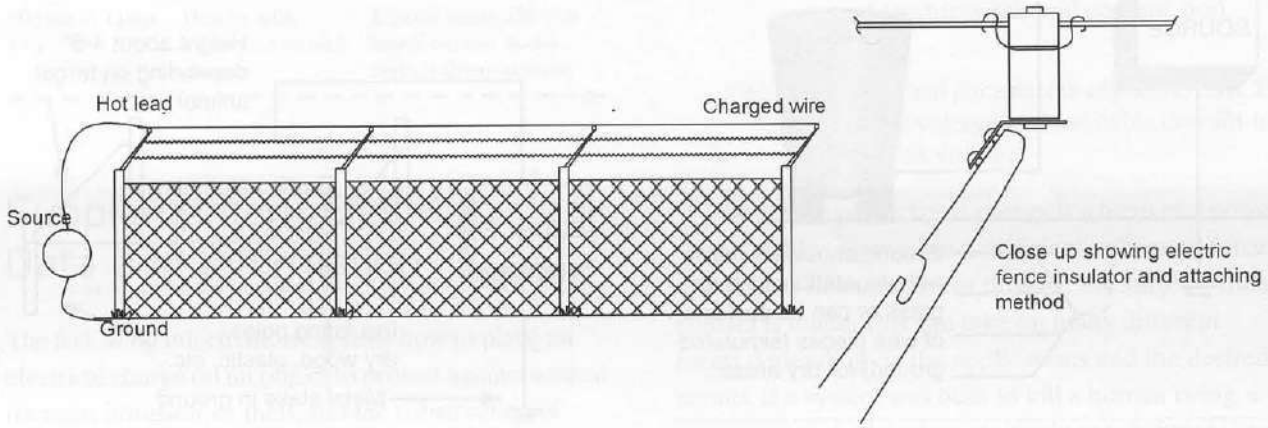

Figure 11-7 *Electrification of a chain-link or similar fence*

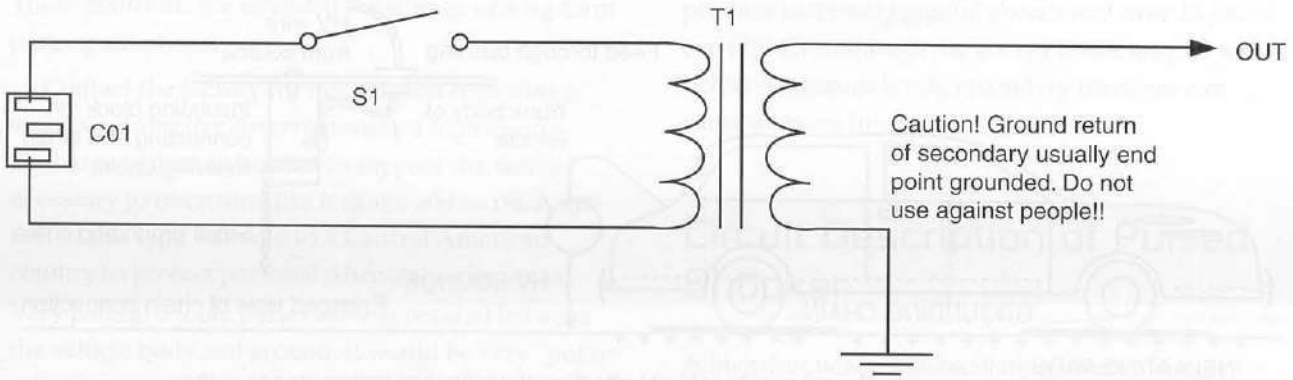

Figure 11-8 *Circuit of power supply source for animals only*

then just strung to these insulators using standard, electric farm fence techniques and is either connected to a farm-type power source such as an electric fence charger or a higher-powered source. The latter presents a dangerous choice and should never be used in a normal situation.

Danger! Do not use a transformer with a short-circuit current in excess of 9 milliamps.

Figure 11-8 shows using a current-limited transformer powered by 115 VAC. The following are suggested power sources for the circuit shown in Figure 11-8.

4KV/009: T1 −4 KV, 9 ma, 115 VAC, current-limited floating secondary Database #4 KV/.03 A

6KV/02: T1 6.5 KV, 20 ma, 115 VAC, current-limited floating secondary Database #6 KV/.02 A

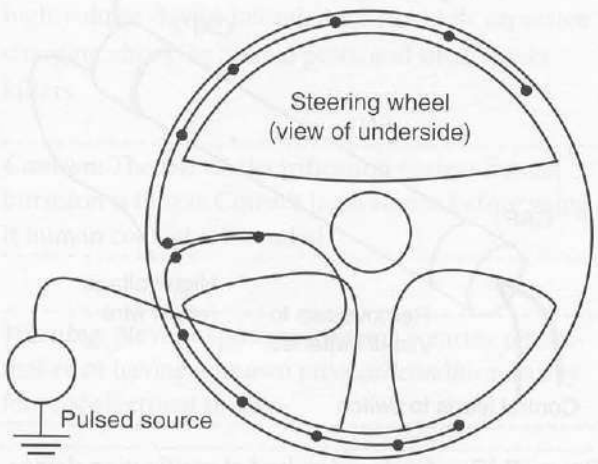

Figure 11-9 *Electrification of a steering wheel or similar object*

You will need a three-wire grounded power cord and a switch available from most hardware stores. Connect the −connection to common using standard PVC or plastic hookup wire. Connect the +connection via a high-voltage ignition wire available from an auto supply house. A weatherproof system is required when installed outside.

Figure 11-9 shows how to electrify a steering wheel or a similar object. The project is intended as a theft or unauthorized use deterrent. Use a low-energy, pulsed, high-voltage source.

The subject sits in the seat and activates the pressure switch to the source. When he grabs the steering wheel, he experiences a mild pulse-type shock between his hand and rear end. The voltage return is via metal springs in the seat. To create this project, please follow these steps:

1. Tape some thin, bare wire on the underside of the steering wheel. Secure it with small pieces of tape, wax, or silicon rubber.

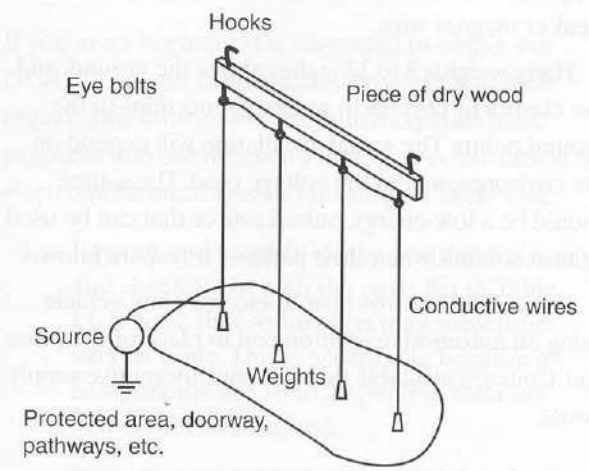

Figure 11-10 *Space or field electrification*

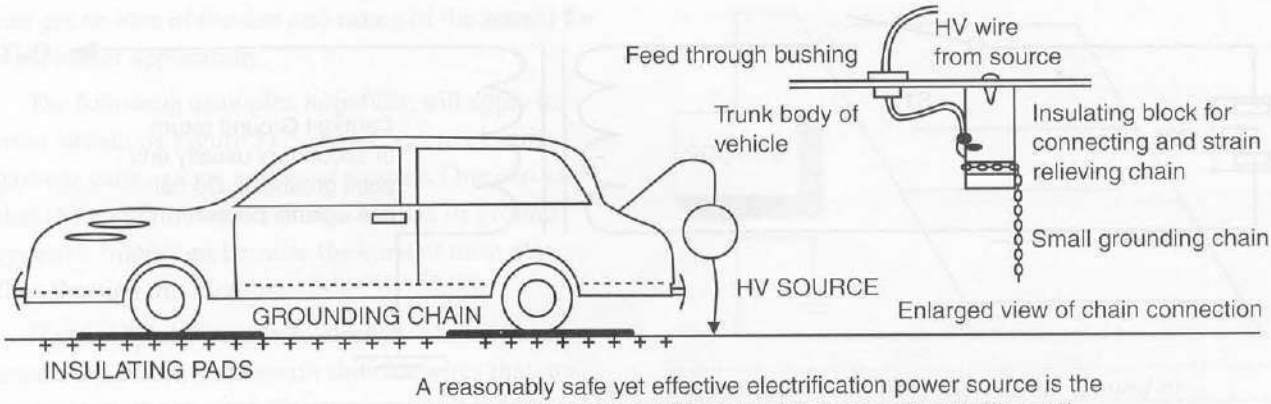

A reasonably safe yet effective electrification power source is the pulsed version shown, with a standard automotive ignition coil replacing the small trigger coil. This approach lengthens the pulse to overcome the electrical capacity of the vehicle body and provides a better overall effect.

Figure 11-11 *Electrification of a vehicle or similar object*

2. Run a concealed connecting wire up the steering column to the bare wire. This wire should be insulated and connect to the output of the source.
3. Conceal an activation switch as desired and don't forget to de-energize it before entering the car. You may want to rig up a pressure-sensitive switch on the seat so when the thief gets in the unit it activates before he starts the car. Important caution: The unit must be activated without the car being in motion or serious accidents may result.
4. The use of our pulsed low-power source is suggested.

Figure 11-10 shows how to protect an area, doorway, or paths using space or field electrification. Hanging supports use ultra-thin steel wire for strength or weaker magnet wire.

Hang weights 8 to 12 inches above the ground, and use elastics or O-rings to secure connections to the ground points. The actual installation will depend on the environment and the voltage used. The source should be a low-energy, pulsed source that can be used against animals when their paths of travel are known.

Figure 11-11 shows how to electrify any vehicle using an automotive ignition coil in place of the pulse coil. Coils are available through any automotive supply house.

A remote switch must be mounted so that it is accessible from the outside of the vehicle. This may be actuated via an insulating object such as a plastic comb or something similar. An override switch may be installed to actuate this system while one is inside the vehicle in order to discourage certain encounters involving contact while driving or stopped at a light.

The suitable method for connecting to earth ground as the common terminal is accomplished via a grounding chain. This is shown strain relieved via a plastic insulating block. The user is asked to use his or her own ingenuity to create other methods of implementation.

Insulated platforms for wheels should be used if the tires have steel-belted radials or if roads are salty.

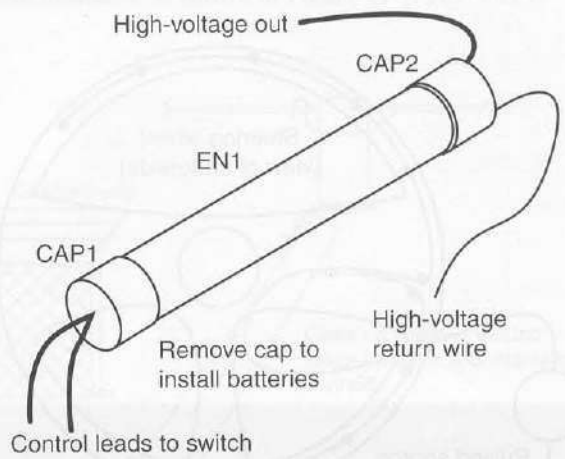

Figure 11-12 *Enclosed pulsed electrification device*

These platforms are intended for storage or long-term parking situations.

Contact the factory for information regarding a serious automotive deterrent using a high-energy discharge system to be able to support the voltage necessary to overcome tire leakage and so on. A system of this type was sold to a Central American country to protect personal when in hostile areas. Very painful 5 joule pulses were generated between the vehicle body and ground. It would be very "politically incorrect" if it were used in this country. This system produces high-current pulses of several tens of amperes for short durations. This is necessary as most tires offer considerable leakage at these high voltages, and a steady-state supply would no doubt burn off the tires and be very lethal to the perpetrator.

Assembly of Suggested Power Sources

The *pulsed version* shown in Figure 11-12 can also be used as a high-voltage trigger for triggering spark gaps, flash tubes, chemical igniters, Kirklian photography, and for electrification in animal control. The unit is housed in a tubular enclosure and powered by built-in batteries or by an external 12 VDC wall adapter. The device produces 20,000-volt pulses for electrifying objects, fences, and so on. Dual-mode operation produces low-energy pulses of .02 joules at a repetition rate of 30 per second or medium-energy pulses of .2 joules at a repetition rate of 4 per second.

The *continuous version* generates a steady, high-voltage device intended for research, capacitor charging, shocking animal pests, and small insect killers.

Caution: The use of electrification against human intrusion is illegal. Consult legal advice before using if human contact is intended.

Warning: Never expose any person wearing a pacemaker or having a known physical condition to any form of electrical shock.

Danger! Never charge a capacitor and use it for shocking humans. Energy storage over 5 joules can produce extremely painful shocks and over 25 joules can kill! Even though the energy levels may be well below dangerous levels, secondary reactions can cause a severe injury.

Circuit Description of Pulsed Shocker

A high-frequency, self-oscillating inverter circuit comprised of switching transistor Q1 and stepup transformer T1 produces a high-voltage high frequency at the secondary winding. This high-voltage AC is rectified by diode D1 and charges up storage capacitor C3 or C4 through isolation resistor R3. When this voltage charges up to the breakdown potential of SIDAC (SID1), the energy stored in the capacitors is "dumped" into the primary of the high-voltage pulse transformer T2, producing a high-voltage pulse at the output terminals (see Figure 11-13).

The oscillator circuit utilizes a winding on T1 to produce the necessary positive feedback to the base of Q1 to sustain oscillation. Resistor R1 initiates Q1 to turn on while resistor R2 and C2 control the base current and operating point.

A charging circuit consisting of the current-limiting resistor R4 and rectifier diode D2 allows external charging of battery B1 when *nickle cadmium* (NiCad) or other rechargeable batteries are used.

Construction Steps for Pulsed Shocker

If you are a beginner it is suggested to obtain our *GCATI General Construction Practices and Techniques*. This informative literature explains basic practices that are necessary in proper construction of electromechanical kits and is listed on Table 11-2.

1. Lay out and identify all the parts and pieces, and check them with the parts list in Table 11-2. Note that some parts may sometimes vary in value. This is acceptable because all components are 10 to 20 percent tolerant unless otherwise noted.

   Some kits contain a length of insulated wire.

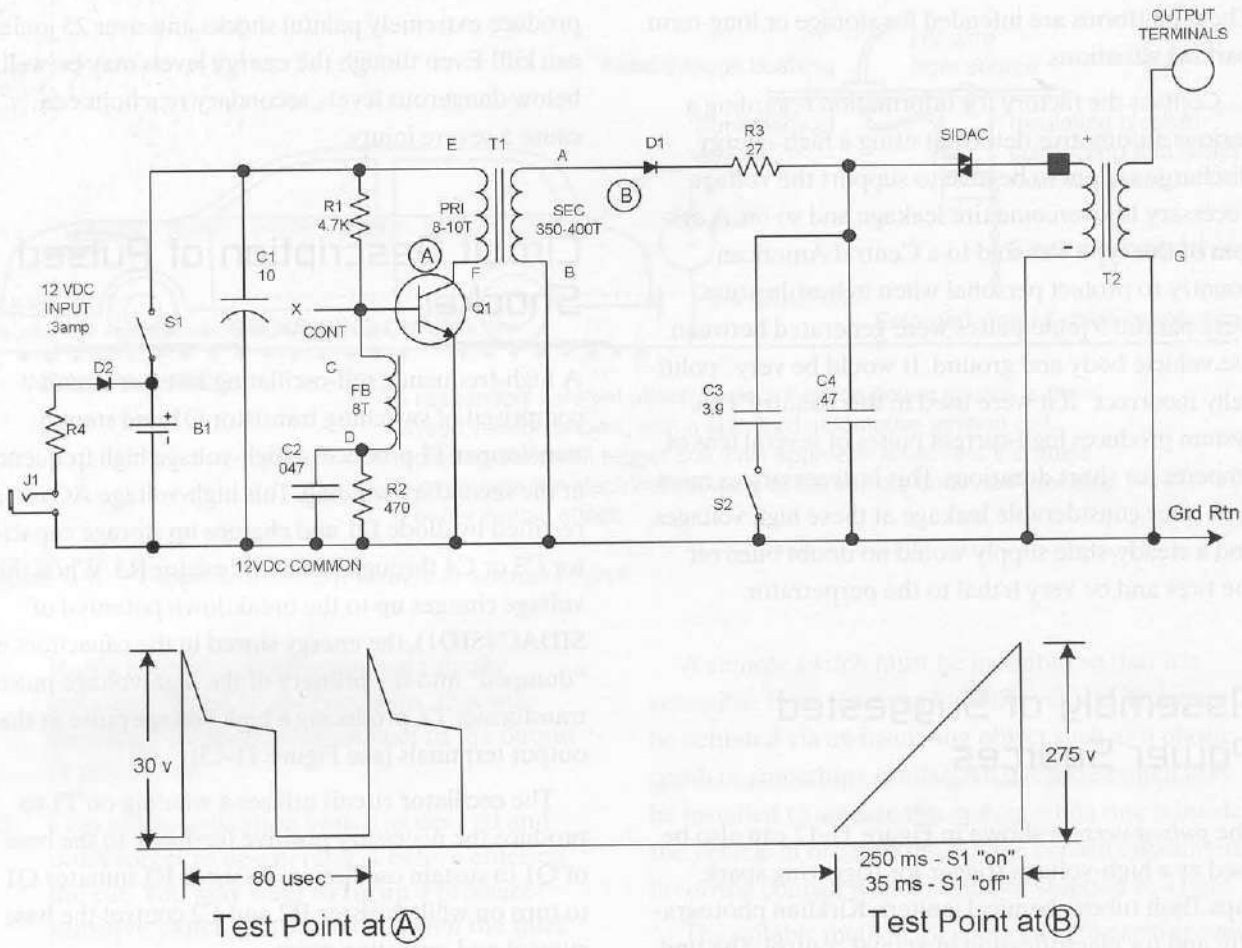

Figure 11-13 *Circuit schematic*

This must be cut, stripped, and tinned according to where it is used.

2. Assemble the board as shown in Figure 11-14. Insert the components into the board holes as shown, proceeding from left to right. Note the polarity of the components.

Note: Certain leads of the actual components will be used for connecting points and circuit runs. Do not cut or trim them at this time. It is best to temporarily fold the leads over to secure the individual parts from falling out of the board holes for now.

3. Verify the wiring, proper components, and polarity to the schematics. Check for cold solder, excess solder, and bare-wire bridge shorts. Now the unit is ready to test.

4. Test the unit as per the following:

A. Position the bare end of the ground return lead (GRD RTN) to allow a 1/2- to 3/4-inch air gap between the output pins of T2.

B. Connect 12 volts from a bench power supply or use eight AA NiCads at 1.25 volts each or eight AA alkalines at 1.5 volts for 12 volts.

C. Note with S2 open a fast pulsing action will produce a thin, bluish discharge. This can cause a very mild electrical shock and could be safely used within reason as a prank.

D. Note a thick, slow pulsing discharge when S2 is closed. This can produce a painful shock and is intended for use against animals.

E. The current draw with the unit properly operating should be approximately 250 milliamps.

F. Check the power tabs of both Q1 and SIDAC. These should be cool to warm to the touch.

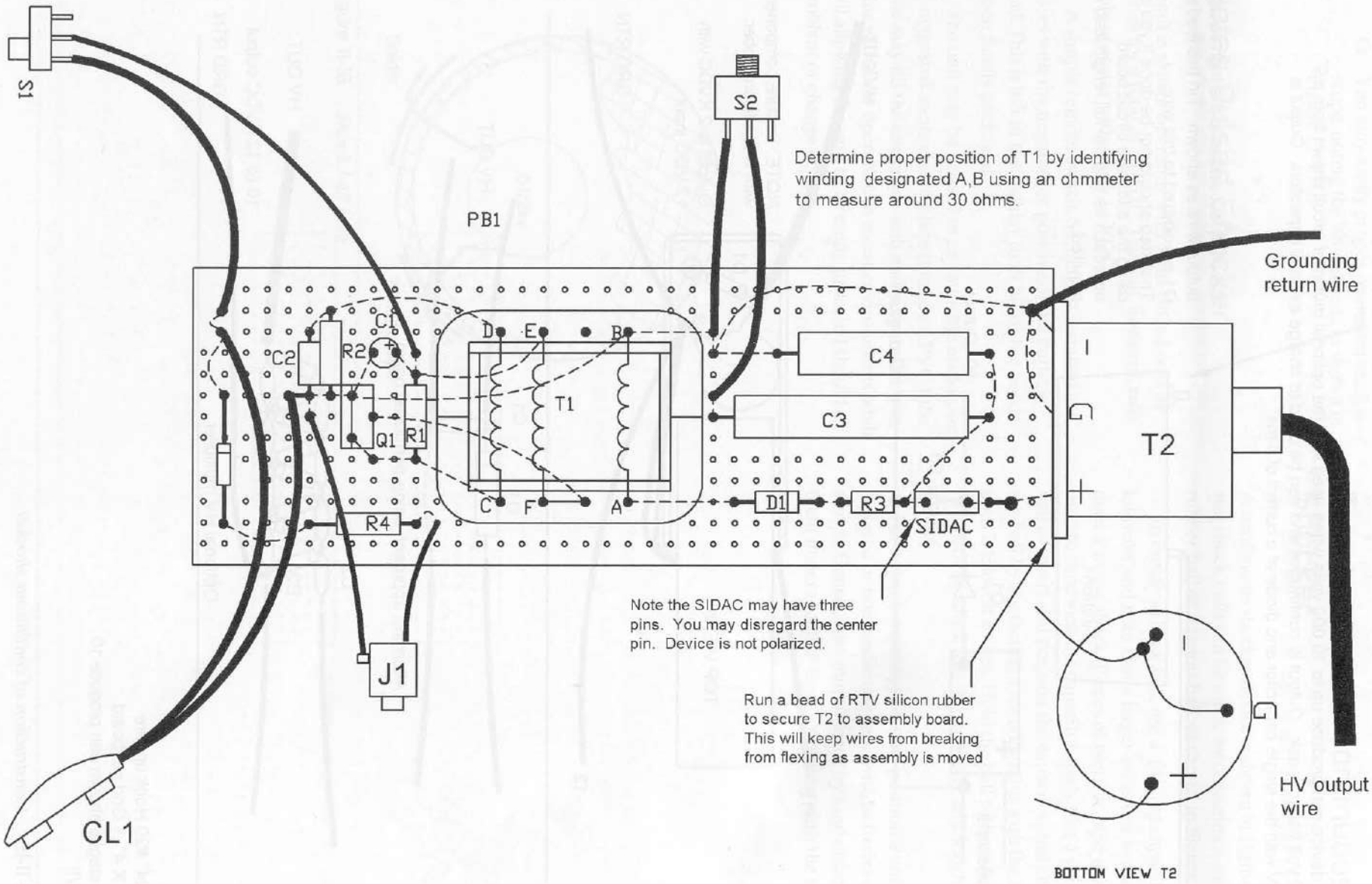

Figure 11-14 *Assembly board*

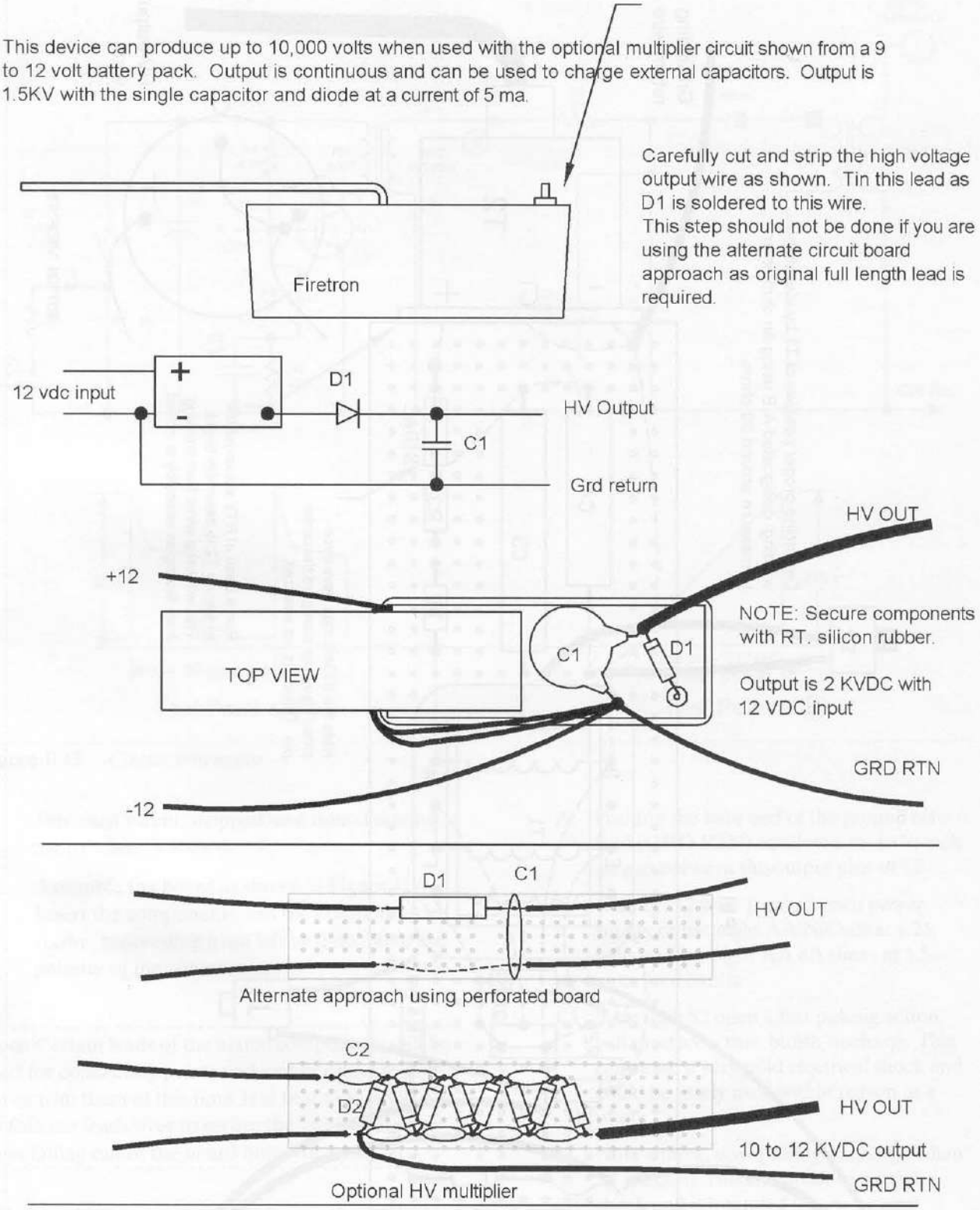

WR1 24" #20 Hook up wire
PB1 1 X 4" .1 Grid perfboard
Note 4 stages shown can produce 10 to12 KV!!

Figure 11-15 *Construction of continuous shocker*

G. You may verify proper operation using a scope, noting the waveshapes as shown in Figure 11-13.

Notes Pulsed Shocker

Input is shown operating with eight NiCad cells in series for a total of 10 VDC. The unit, however, reliably operates within 8 to 14 VDC.

A simple remote switch, S1, may be installed in series with the negative or positive of the battery lead. This is left to the builder to fit his or her needs when finally packaged.

The unit may be housed in any suitable enclosure. A suggested method is to place it inside a PVC tube You may fill the enclosure with melted paraffin wax. This will allow operation in moist environments while still allowing the unit to be easily unsealed should a problem or change occur

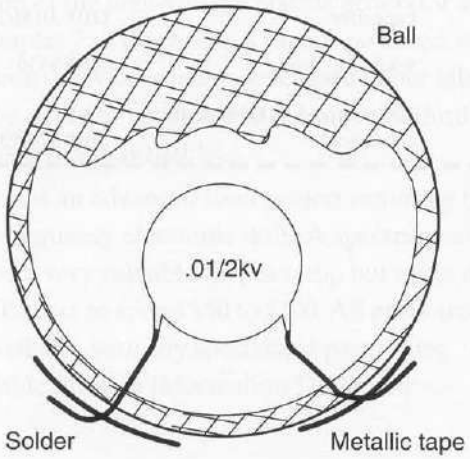

Figure 11-16 *Shock ball joke*

Construction of Continuous Shocker

A continuous shocker device is shown in Figure 11-15, and shock balls can be made by obtaining a small rubber ball or a tennis ball, as shown in Figure 11-16.

To create a shock ball, use a .01-amp capacitor at 2 kilovolts and note that a larger capacitor would produce a worse shock. Pieces of metallic tape must be used to sandwich the capacitor leads. Cut a slit in the ball to insert and position the capacitor, and charge the ball by contacting a metallic strip with the continuous 2-kilovolt source. Hold the ball without touching the metallic strips, toss it to a buddy, and watch the results.

For a shock wand application, position a unit inside a plastic or nonconductive tube with batteries and a switch. Connect the output leads by sandwiching them under metallic tape for contact with the target subject.

Table 11-2 Parts List for Shockers

Ref. #	Description	DB Part #
R1	4.7K, 1/4-watt carbon film resistor (yel, pur, red)	
R2	470 ohm, 1/4-watt carbon film resistor (yel, pur, br)	
R3	27-ohm, 1/4-watt carbon film resistor (red, pur, blk)	
R4	100-ohm, 1/4-watt carbon film resistor (br, blk, br)	
C1	10-microfarad, 25-volt electrolytic capacitor vertical mount	
C2	.047-microfarad, 50-volt polyester capacitor	
C3	3.9 to 4-microfarad, 350-volt polyester capacitor	
C4	.47-microfarad, 250-volt polyester capacitor	
Q1	MJE3055 NPN transistor TO220	
D1, 2	Two IN4007 1-kilovolt rectifier diode	
SIDAC	300-volt Sidactor switch	SIDAC
T1	400-volt switching square-wave transformer	DB# TYPE1PC
T2	25-kilovolt pulse transformer	DB# CD25B
S1, 2,	Two *single pole, single throw* (SPST) 3-amp toggle switch or equivalent	
PB1	5 × 1.5 × .1-inch grid perforated circuit board	
PCLITE	Optional *printed circuit board* (PCB)	DB# PCLITE
WR20B	36-inch #20 vinyl stranded hookup wire, black	
WR20R	36-inch #20 vinyl stranded hookup wire, red	
WRHV20	12-inch 20-kilovolt wire	
CL1	Battery clip	
CAP1, 2	Two 1⅝-inch plastic caps	
EN1	12 inches of 1⅝ × 1½ × 12 plastic tube	
BH1	Eight-AA-cell battery holder	
J1	3.5-millimeter mono jack	
12DC/.3	Optional 12 VDC, .3-amp wall adapter	DB# 12DC/.3

Parts for the continuous version

FIRETRON	Firetron 2,000-volt module	DB# FIRETRON
C1	.01-microfarad, 2,000-volt disc capacitor	DB# .01M/2KV
D1	6-kilovolt diode	DB# VG6
C2	270-picofard, 3,000-volt disc capacitor	DB# 270P/3KV

Chapter Twelve

Electromagnetic Pulse (EMP) Gun

Figure 12-1 shows the construction of a low-power pulse gun that will provide kilowatts of peak power at frequencies up to 100 MHz with harmonics. The unit shown is battery powered and uses a modified version of the high-voltage plasma generator shown in Chapter 7 of this book. A higher powered, more functional device is being developed in our labs and will be ready to be copied at the time the third book of this series is available.

This is an advanced level project requiring basic high-frequency electronic skills. A spectrum analyzer can be a very valuable tool in setup but is not necessary. Expect to spend $50 to $100. All parts are readily available, with any specialized parts being available through Information Unlimited (www.amazing1.com) as listed in the parts list at the end of this chapter.

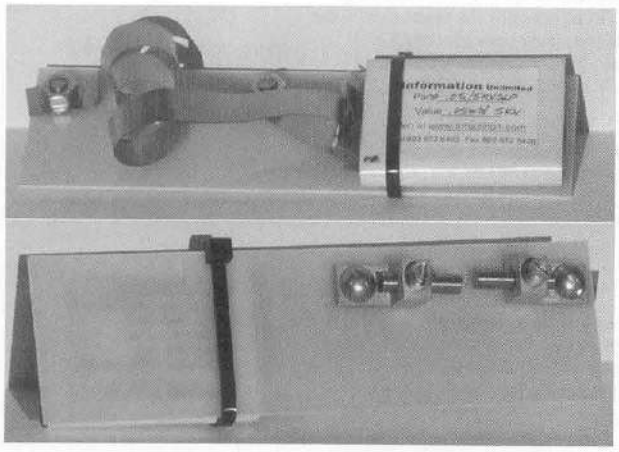

Figure 12-1 *Electromagnetic pulse gun*

Basic Theory Simplified

The ability of a signal to disrupt sensitive circuitry requires several properties. Most microprocessors consist of *field effect transistors* (FET) operating at very low voltages. Once these voltages are exceeded, catastrophic failure becomes imminent. Forgiveness to an overvoltage fault is practically nonexistent due to a microthin metal oxide between controlling elements. Any overvoltage generated across these elements consequently produces permanent damage or, in some less severe cases, causes deprogramming. To generate these damaging voltages from an external source requires a wave that can produce a standing wave of energy across circuit board traces, components, and other key points. The external signal energy therefore must be high enough for the circuitry geometry to be a significant part of energy at the wavelength. Therefore microwaves having fast rise times (high Fourier equivalents) and burst duration help to maximize the effect. The energy required is great, as it must be sufficient to enhance damage. A good measure would be the quotient of energy/wavelength. A high-power pulse of microwaves can be generated in several ways.

Explosive flux compression-driven virtual cathode oscillators and their generic relatives can produce gigawatts of peak power from only hundreds of kilojoules. This is where a seed current is pulsed into an inductor and at its peak is compressed by a shaped explosive charge thereby trapping the flux and creating a source of high energy. The coil must be compressed both along its axis and along its radius using a high-detonation velocity explosive such as the cyclotrimethyltrinitramine, its derivatives PETN, or some other equivalent energetic explosive. This trapped flux now produces an energy gain that is conditioned into the final peak-powered pulse of microwave power (HEPM). Flux compression like that of a nuclear initiation requires precise timing of the explosive chargers. For flux compression, Krytron switches or similar can be used instead of the more radiation-hardened Sprytrons that are used in nuclear initiations where ionizing radiation is produced from the inherent fissionable materials.

A virtual cathode oscillator can also easily be energized from a small Marx impulse generating 200 to 400 kilovolts. The fast current rise and high peak power can produce a powerful burst of microwaves.

Other methods include exploding wires where energy is allowed to flow into a LCR circuit and then is rapidly disrupted by the explosion of the feed wire as it vaporizes at near the peak injection current. A very fast and energetic pulse is produced, which is capable of generating an *electromagnetic pulse* (EMP).

Microwave pulses are excellent candidates for damaging sensitive electronic circuitry. But much lower frequencies are better for disrupting power grids and other similarly sized systems, as now the lengths of the conductive elements are more conducive to generating the high standing voltage waves. Obviously more energy is now required, as breakers, switches, and transformers require more energetic pulses

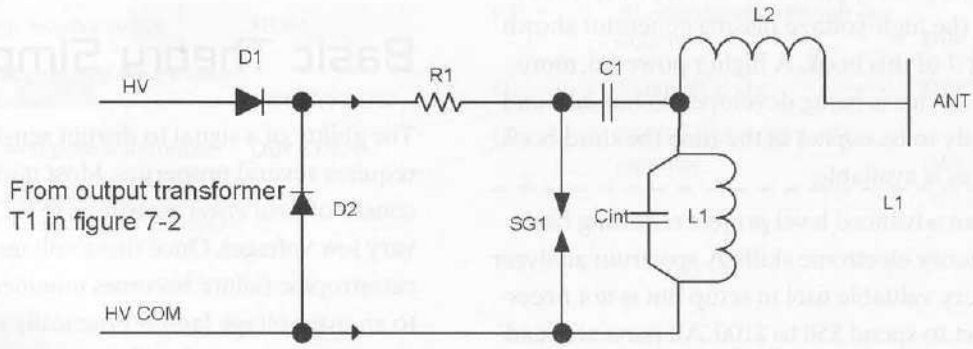

The ideal peak power of this circuit can be approximated by evaluating the product of the charge voltage across C1 x the peak current as determined by Ipk = Epk x the square root of the capacitance of C1/the total inductance of the discharge circuit. This expression implies no resistance (R) in the discharge circuit that now is only in an ideal situation. In all actuality the resistance in the real world will now be a factor in where e to the -(pi/square root of L/C) / R must be a factor in the above ideal condition. This now implies a damped waveform.

Diodes D1,2 are 10 kv 10 ma fast recovery
Resistor R1 is three 47k 1 watt resistors in series and isolate the diodes from the dv/dt of the discharge.
L2 inductor tunes out the capacitive reactance of the antenna at the desired resonant frequency

Capacitor C1 is a "slapper" capacitor. These are used to produce a very fast rise time necessary to detonate initiators necessary for initiating high explosive. Its claim to fame is the high peak current discharge current. The capacitor is constructed as strip lines with the connection leads exiting a common end.

Figure 12-2 *Circuit schematic*

Circuit Description

The circuit shown in Figure 12-2 shows a simple method of obtaining a high-power pulse with Fourier equivalents above 100 MHz. Even though the power and frequency are relatively low, close range effects are possible on many target circuits.

The project uses a high-frequency plasma source, which is converted to a direct current charging source and is short circuited functionally by the use of lossless reactive ballasting. This means that the capacitor can be charged without the use of an energy-robbing resistor, as only the real part of the complex current is seen by the battery supply.

The modified source now supplies a current charge to the reservoir capacitor (C1) to a value where the spark discharges across SG1. Current through L1 rapidly rises and rings along with the circuit and lumped capacitance (Cint). Spark gap SG1 must turn off and allow the energy to circulate in the discharge in order to generate a resonant peak of power that is now coupled into the system emitter. Experimentation of the gap settings is necessary to obtain an optimum effect.

Circuit Assembly

1. Fabricate a piece of Lexan plastic or G10 circuit board, as shown in Figure 12-3, to a 7 × 2 inch plate for PL1. Locate the two 1/4-inch spark-gap-holder (SGH1, 2) screws holes as shown. The holes are spaced 2 3/4 inches from one another.

2. Form a three-turn 1-inch diameter coil (L1) from 1/2-inch sheet copper or #14 solid copper wire, as shown in Figure 12-4. Note the leads as attached to the capacitor (C1) and the end gap holder.

3. Connect an output port at the junction of C1 and L1 as shown. This point is now considered the output and can be connected to the radiating emitter.

4. Connect it to the converted plasma driver in the manner shown in Chapter 7 to the generator (see the schematic Figure 12-2). Note the added diodes D1 and D2 for converting the output to direct current

5. You will note a coil (L2) connected in series with the output lead. This inductor tunes out the capacitive reactance of the lead and the end capacitance. Experiment using a radio wave or absorption wave meter to determine the resonant frequency of L1/C1. Select a value for L2 to provide maximum radiation from a distance.

6. Experiment on various electronic devices and observe the effects at various distances.

Notes

A low-cost spectrum analyzer would be a great aid in setting up this system. Please note this is a low-power device intended as an introductory project for those desiring to experiment with shock pulse and EMP research. Several more functional and sophisticated devices will be featured in the next book in this series.

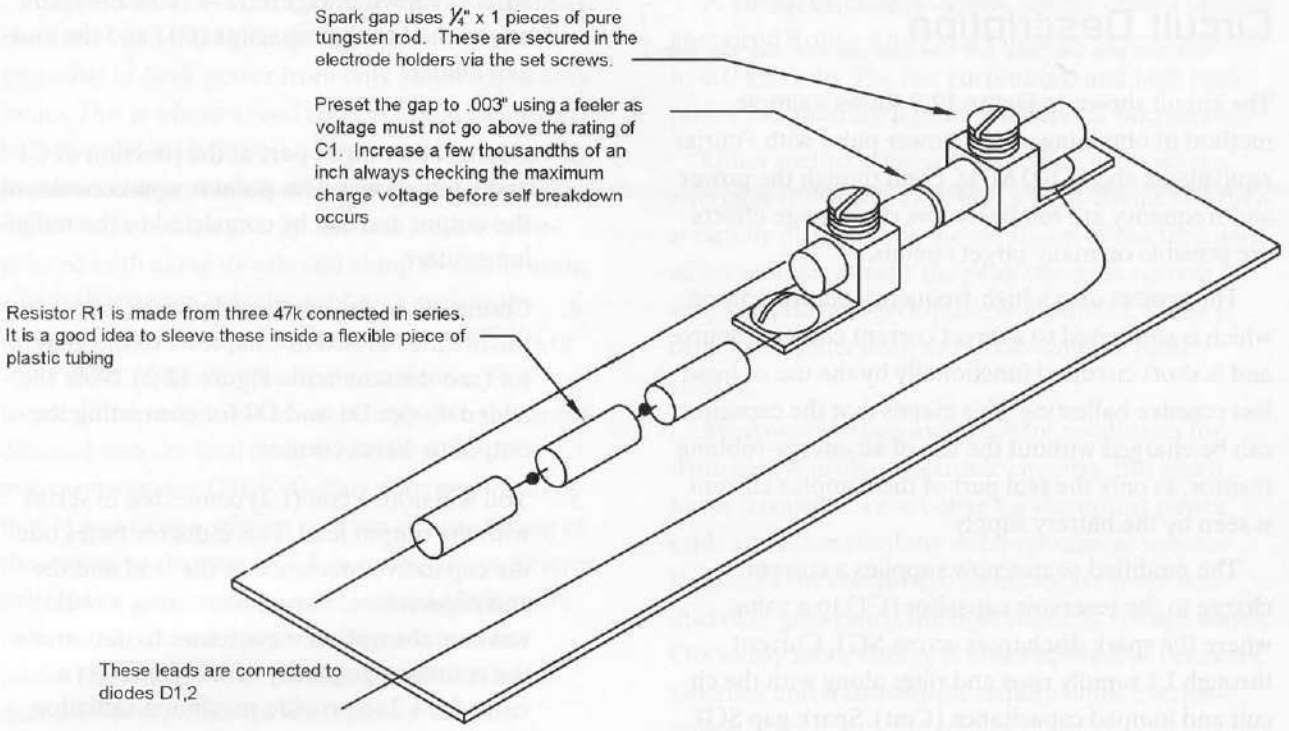

Figure 12-3 *Generator board bottom view*

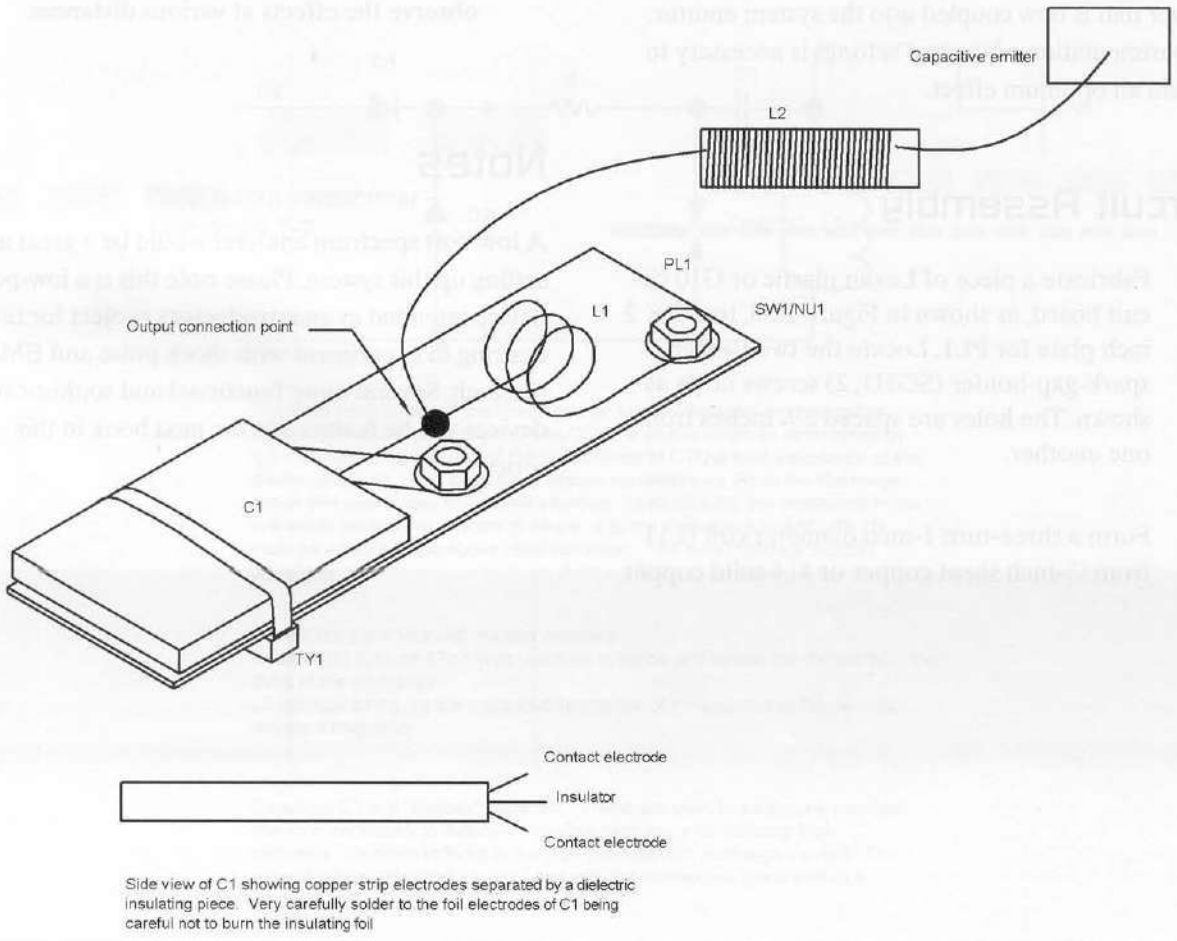

Figure 12-4 *Generator board bottom view*

Table 12-1 EMP Gun Parts List

Ref. #	Description	DB part #
R1	Three 47K, 1-watt resistors (yel-pur-or) connected in series	
D1, D2	Two 16 KV, 10 ma fast-recovery high-voltage rectifiers	DB# VG16
C1	.05 mfd, 5 KV stripline capacitor	DB#.05M/5KV
L1	Inductor 3-turn, 1-inch diameter use #12 copper wire	
L2	Inductor wind, as directed in text	
ELECTRODES	Two ½ × 1 inch pure tungsten electrodes	DB# TUNG141B
PL1	7 × 2 inch × .063 Lexan or G10 plastic	
TYE1	10-inch nylon tie wraps	
SW1/NU1	Two ¼ × 1 inch brass screw and nuts	
GRAVDRIV1K	Plasma driver kit	DB# GRAVDRIV1K
GRAVDRIV10	Plasma driver assembly	DB# GRAVDRIV10

Chapter Thirteen

Microwave Cannon

This project shows how to build a powerful microwave transmitter intended to be a useful laboratory resource or as a device for disrupting bothersome stereos, boom boxes, and other annoyances perpetrated by inconsiderate hip-hop miscreants. This chapter was prepared by Dr. Barney Vincellete, who holds several doctorate degrees in the electrical sciences. It is a very useful tutorial involving the design of a microwave system, going into basic mathematical details for those who are interested. The system can be built from the parts of a microwave oven.

Warning: The project uses dangerously high voltages and can be a radiation hazard at close range if not used with protective shielding. This is an advanced project intended for experienced builders and must not be attempted by anyone unfamiliar with high voltages or high-power radio frequency circuitry.

Figure 13-1 *Microwave cannon*

The microwave cannon consists of three parts: the parabolic reflector horn, the electric field focusing lens, and the magnetron. The horn focuses the magnetic oscillations that circumscribe the magnetron antenna into a narrow beam in order to concentrate the radiation into a two-dimensional space. It also prepares the electric field oscillations for the lens to concentrate the radiation in the third dimension. Because the electric field and magnetic field are orthogonal, calculations upon them and the modifications that we will perform upon them can be done on one without altering the other.

In designing the horn, we will assign the Cartesian coordinate system with the z axis along the longitudinal axis of the horn; that is, the z axis will occupy the center of the shaft of radiation that will be fired into your cultural tyrants' stereos. The Poynting vector will be on the z axis, and the x axis will be directed horizontally to the left and right of the z axis. The x axis will, during the calculations for the shape of the horn, be given an absolute value; that is, it will be endowed with a positive value whether it increases to the left or right of the z axis. This is because its values will be the square root of x squared, and it will be symmetrical to the left and right of the z axis. The origin will be located at the vertex of the parabola that will define the sides of the horn.

The y axis will be in the vertical direction to complete the basic vectors in our discourse and

calculations. It will pass through the z axis at the mouth of the horn, rather than through the vertex, as the x axis does. It too will have only positive values because, due to its symmetry about the z axis, there is no need to consider negative values of y (see Figure 13-2).

The dimensions of the sides of the horn will be performed first. In building the wooden mold upon which the sheet copper will be formed, an adjustment will be made to correct for the flare that can be seen in Figure 13-3.

The horn will be made of 20-inch-wide sheet copper that can be purchased from a roofing supply house. Because the dimensions of the parabolic sides shown in Figure 13-2 are fixed by the top and bottom pieces of copper that will be soldered to the copper side pieces, the top and bottom pieces will be cut to a parabolic shape with an extra ¼-inch margin on the sides that will be bent into a ridge that will be soldered to the side piece. The actual parabola will have a maximum width of 19.5 inches, or the maximum value of x will be 9.75 inches. Also, for structural rigidity, a half-inch lip will be bent along the front edge of the top and bottom pieces.

The parabola will contain the magnetron antenna aligned parallel to the y axis and positioned at the focal point of the parabola. The focal point will be one-eighth of the wavelength of the magnetron frequency, which, when the wavelength is computed by dividing the speed of light by the frequency or 2.45 GHz, gives us a wavelength of 2.45 inches and a focal length of 0.6 inches. The parabola is described by the equation x squared = 4 pz, where *p* equals the focal length. When *p* equals .6 inches, *r* equals 2.4 z. From this, we construct Table 13-1.

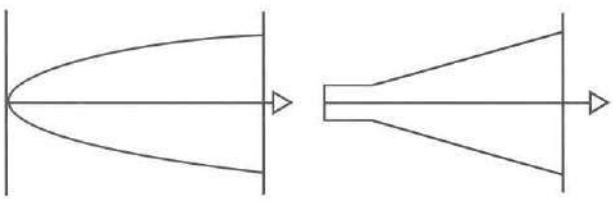

Figure 13-2 *Top and side horn templates*

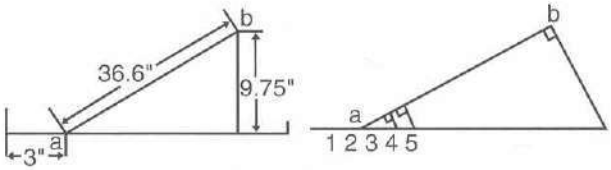

Figure 13-3 *Flair angle template*

Table 13-1 Parabolic Dimensions (measurements in inches)

z	x	z	x	z	x	z	x	z	x
.125	.55	3	2.68	8	4.38	16	6.2	29	8.34
.25	.77	4	3.1	9	4.65	18	6.57	32	8.76
.5	1.1	5	3.46	10	4.9	20	6.93	35	9.17
1	1.55	6	3.79	12	5.37	23	7.43	38	9.55
2	2.19	7	4.1	14	5.8	26	7.9	39.6	9.75

When regarding the side view of the horn (Figure 13-2), it can be seen that plotting the parabola, which is done by cutting the wooden sheets used for making a mold of the horn, will require an adjustment so that the sides of the parabola are not distorted where z is greater than 3 inches. The dimensions of z, if projected from the z axis to the top and bottom of the horn where z is greater than 3 inches, will have to be enlarged by dividing each inch by the direction cosine of the angle between the z axis and the top (also the bottom) of the horn. This can be done by drawing upon a sheet of 2 by 4 foot particle board, as shown in Figures 13-3.

After you have marked the board, as shown in Figure 13-3, you will begin plotting dots measured above and below the z axis at distances of x from Table 13-1 measured with a carpenter's square. You will connect these dots with a ruler, and when you cut out the parabola, the saber saw that you use will make a curved path that will very closely approximate the parabolic shape needed. After you cut out the parabola, you will make another cut along the locus of points where z equals 3 inches.

You will trace these pieces and cut duplicates from another piece of particle board, as shown in Figure 13-4. With nails, screws, glue, and two trapezoidal-shaped pieces of particle board, you will put together

the form that you will use to build the copper horn (see Figure 13-5).

Stand the wooden form on its end, where z is 39.6 inches against the floor, and make a template from poster paper that has been taped together to form large enough pieces. Make a template that will wrap about the sides, and trim it to fit so that it matches the sides. Make another template for the top (also the bottom) piece the same way, as shown in Figure 13-6.

You will need 15 feet of copper roofing sheet metal to cut the pieces that you will solder together. Trace and cut the long piece from the template you made from the sides and rear of the wooden form. Add a half-inch to the length of each side so that you can bend a lip that will make the front of the sides rigid. This lip will also provide a place where you can attach the sides of a wooden frame that will make the horn more stable. Then trace the top and bottom pieces against the copper and draw a 1/4-inch additional margin surrounding the parabola you just traced. Also add a half-inch to the front that you can bend into a lip to make the top and bottom more rigid. Cut out two of these pieces, one for the top and one for the bottom.

With a pair of pliers, bend a 90-degree lip from the 1/4-inch margin you traced. You can cut notches in this lip to make this bending easier. This lip will be soldered to the piece that will form the sides of the horn. Bend the half-inch lip at the front edges of the pieces that you will solder together, and clean the insides of the lip that you will be soldering to the sides of the horn using steel wool or sand paper. Clean the exterior 1/4-inch sides of the horn to which you will be soldering the top piece. Apply a thin coat of soldering paste and clamp the sides and top securely into place on the wooden form you built. Hammer the side lip against the sides of the horn for a tight fit. You do not need a sharp crease where the horn begins to flare out where *z* is 3 inches; a modest bend will do. You are now ready to begin soldering the seam, as shown in Figure 13-7.

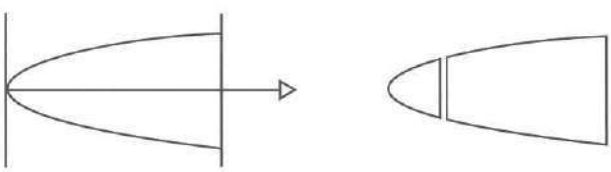

Figure 13-4 *Templates for forming the horn pieces*

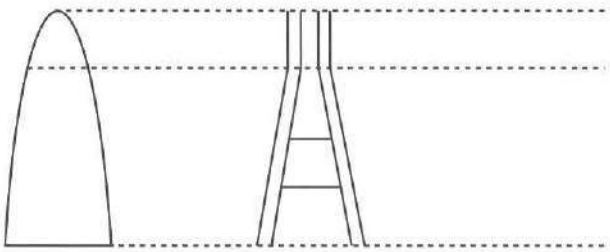

Figure 13-5 *Poster paper template*

Begin with a propane torch and plumber's solder. Apply the flame to a spot and, as soon as it is hot enough to draw in some solder, let just enough solder draw into the seam to fill the gap. Use more hammer taps to close any open spots where the lip is not tightly against the side piece. As soon as you have an inch or two soldered, remove the flame and solder another place a few inches away. Do not use enough solder to cause it to form drips or beads on the inside of the horn. Continue until the entire seam is soldered. After this is done, remove the clamps and sheet copper structure you soldered together. If you see any lumps of solder on the interior seam, you can melt it away by applying a flame.

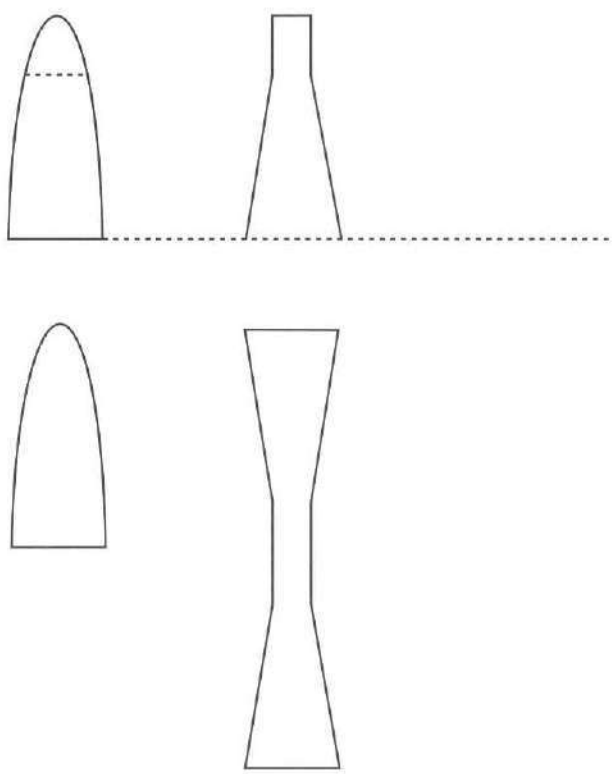

Figure 13-6 *Top template*

Now you must locate the point on the center axis at the top of the horn. This can be done by measuring the center of the front of the top section of the horn, measuring 2 feet along each side of the horn's interior, drafting a line between these points that are 2 feet back from the front, and bisecting it. You bisect the width of the front to find one point. You then measure 2 feet back on each side and draw a line between the ends. You bisect the line for the second point. This will provide two points to extend back to the vertex of the parabola's interior.

Now measure, as punctiliously as you can, 0.6 inches from the vertex. Drill a pilot hole and cut a circle that is $1^3/_{16}$ inches in diameter. With a hammer and a piece of pipe, tap on the interior of this hole so that its edges flare outward to make a good seal with the brass wool gasket on the magnetron you will be using (see Figure 13-8).

At this point, solder the bottom piece into place and complete the construction of the copper horn. A wooden frame must be built to make the front edges of the horn more rigid, to provide a structure for mounting the lens, and to provide a place for the front of an aluminum rail where a telescopic rifle sight will be mounted.

Here you have great artistic liberty in how you will build this cabinetry. Half-inch plywood is the most practical material to use, and cedar has the most pulchritudinous finish to stain, varnish, and paint. You can paint or carve artwork upon this frame, and you can also upholster the rear or sides with velvet and sunken buttons. In the most unlikely event the cannon becomes an exhibit in court, these characteristics will humor the jury, many of whom will be as hostile as you against the music the neighbors were forcing into your home. If it becomes newsworthy enough to attract a television crew, it will be a splendid show for the millions of people whom you will inspire to follow your example and join the revolution against cultural tyranny.

The rear of the frame will protect the operator from the deadly 4,500-volt wires between the power supply and the magnetron. It will also provide a place to mount the rear of the aluminum rail for the telescopic rifle sight.

Let us digress to a disquisition on the flair angle formed by the sides of the cannon. In order to form the best possible cancellation of standing waves, due to the impedance vicissitudes where the horn begins to flair at the mouth of the horn, the following equation must be emulated within approximately 10 percent. The dimensions of the horn must match this within a percent.

$$0.25 = [a/(2\lambda)]\tan(\theta/2)$$

where a is the dimension of the mouth in the horn in the y direction: 20 inches. λ is the wavelength in

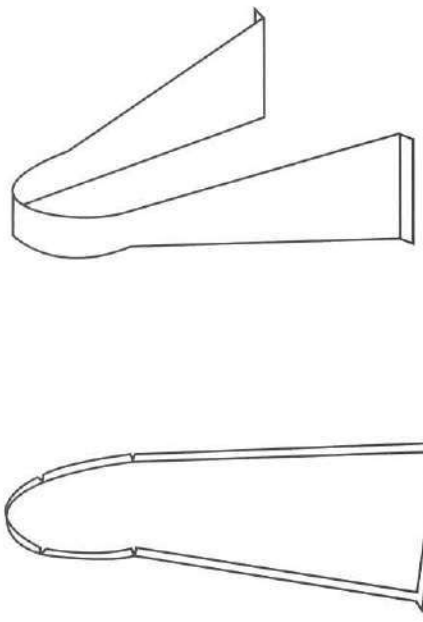

Figure 13-7 *Copper side with top and bottom pieces*

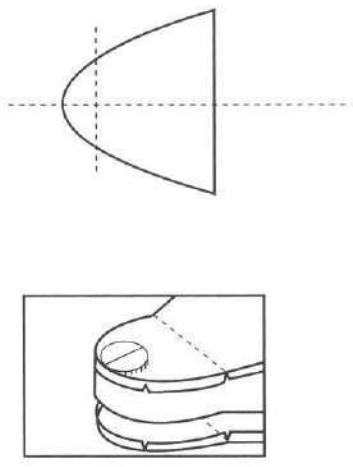

Figure 13-8 *Position of aperture hole for magnetron probe*

inches. θ is the angle between the z axis and the top (or bottom) side of the horn.

Let us now examine the efficiency of the parabolic sides of the horn for their focus of the magnetic field. The antenna is circumscribed by a magnetic field that propagates from a line source at the center of the antenna. The radiation either reflects off the sides of the parabola formed by the horn or it radiates directly from the antenna out the mouth of the horn. The latter is not useful because it dissipates rapidly with distance from the cannon. The former, the reflected radiation, is projected parallel to the zy plane, and because it originates from a line source parallel to the y axis, no diffraction occurs off the sides of the horn's mouth. The fraction of the radiation that is reflected is 92.2 percent of the total from the antenna. This is far superior to the typical 40 percent efficiency given by radar dishes that use large sizes to achieve gain.

The focusing of the electric field can now be performed by placing a lens in front of the cannon's mouth, and a description of the electric field must be provided. On the surface of a conductor there can be no voltage parallel to the surface of that conductor, because any voltage would be short-circuited out. This makes the components of the gradient of any voltage parallel to that surface zero. Since the electric field is the negative gradient of the voltage, the electric field near a conducting surface must perforce be perpendicular to that surface. As the electric field propagates forward, it forms a cylindrical-shaped wavefront in the flared part of the horn. At the mouth of the horn, this cylinder has a radius of 41 inches. A lens will convert this cylindrical wavefront to a flat wavefront, and that will complete the focusing of the radiation.

The lens will be constructed of metal plates that will be aligned parallel to the y and z axis 4 inches apart. Between these plates, any wave vector, $k = 2n/\pi$, can be the vector sum of two components, kx and kz. In the x direction, the sine wave of the wave vector will be zero every 4 inches, because at the plates the electric field in the y direction must be zero. Taking recourse to the Pythagorean theorem, the wavelength in the z direction is dilated by the inverse of the refraction index, that is, the refraction index, $n =$ [1−(λ/8 inches)E2]E−.5 = 0.8 (λ = 4.8 inches). See Figure 13-9.

The cylinder formed by the cylindrical-shaped wavefront plus the refraction index times the distance parallel to the z axis between the lens elements to a flat plane in front of the lens is to be constant so that the electric field will be in phase on the flat front of the lens. The y axis is shifted to the most concave depth of the lens elements, and the z axis is directed rearward. The algebra for calculating the concave curve to cut into the rear of the lens plates is rudimentary. From the following equation, the dimensions of the lens are shown in Figure 13-10.

[(47" - z)E2 + y]E.5 + 0.8 z = 47" from which z = {18.8 - [(18.8)E2 - (1.44y)E2] E.5} {1/.72}

The lens plates mounted against the far right and far left sides of the lens frames should be cut from leftover sheet copper and glued to wooden sides, also cut to the shape of the lens element. The other lens elements should be made from 0.025-inch sheet aluminum. They should be 21 inches long in order to mount them to the wood lens frame you will build. Small wooden blocks can hold the ends of lens plates in place. Pieces of wood with grooves cut into them will also work.

The efficiency of the lens can also be calculated. This efficiency is due to the reflection of radiation that takes place when radiation passes from a medium of one refraction index into a medium of a different refraction index where the space impedance is changed. Two reflections occur, one when the radiation enters the rear of the lens and a second reflection when the radiation exits the front of the lens. The second reflection is in opposite phase with the first reflection, so it is 2π radians out of phase with the first reflection. The appropriate Fresnel equation for calculating the power reflected when the electric field

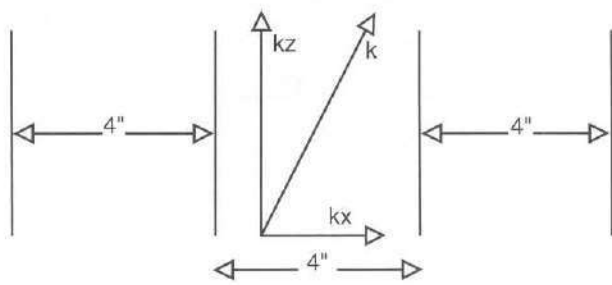

Figure 13-9 *Focus plate geometry*

is parallel to the plane containing the angle of incidence, θi, and the angle of transmission, θt, is as follows:

$$R = \{[-\cos\theta i + (n1/n2)\cos\theta t] \div [\cos\theta i + (n1/n2)\cos\theta t]\}E2$$

θt is arctan dz/dy, as can be seen in Figure 13-11. θi is θt − arctan $[y/(47 - z)]$.

In the second reflection, θi and θt are both zero. n1 is 1 and nt is 0.8. The second reflection that must be subtracted from the first one is cos [2π radians $2(z + .25'')\lambda z]T$, where T is the fraction of the power transmitted into the lens and λz is 4.8 inches/0.8. Since the total reflected power is almost everywhere less than a percent, we can make the approximation that T equals 1. If the reflected power is calculated every inch for y, the average power reflected is approximately half a percent. Thus, the gain of the horn is

$$4\pi A/\Lambda E2 = 218 \text{ or } 23.4 \text{ db}$$

With the ideal horn and lens system having been designed so that the common man can build it without having to know all the electromagnetic laws of physics that make it work, we direct our attention to the choice of a microwave source. The cardinal rule of electronic warfare is that the radiation must convey noise in order to disrupt the signals in the circuits you will be attacking. This requires modulation that will drown out enough of the unwanted music and interfere with the digital signals in disc players to make them useless. Half-wave rectification of the current through the radiation generator is subjectively the most disrupting. The lower frequencies promoted by stereo manufacturers and music producers seem to be designed to most effectively penetrate the walls of apartments and homes for the purpose of destroying the privacy and cultural autonomy of all but the wealthiest who can afford the enormous cost of solitude.

The 60-cycle voltage from a household wall socket offers a nearly ideal source of modulation to create this disruption, because in a microwave oven it is half-wave rectified by a voltage-doubling circuit. This provides a splendid spectrum of Fourier frequencies that concentrate upon the lower frequencies but distribute themselves upward through the audio range, and it gives the utmost modulation of amplitude. It also reduces the duty cycle of the magnetron while preserving the maximum power in each pulse it shoots into the neighbor's stereo for the best range.

The first inclination is to choose a magnetron that will have the highest output power. The best choice would be a radar magnetron, which might offer 30 to 100 kilowatts in pulses that are only a microsecond or two in duration. However, tests using radar against a compact disc player yield disappointing results. The Fourier series expansion on a series of microsecond-long pulses modulates less than 1 percent in the audio band. The series of ticking sounds that it introduces into a stereo amplifier is scarcely noticeable, and not enough pulses occur to put sufficient errors in the digital circuits of the compact disc player to do any good. Also, audio circuits are not as sensitive to the

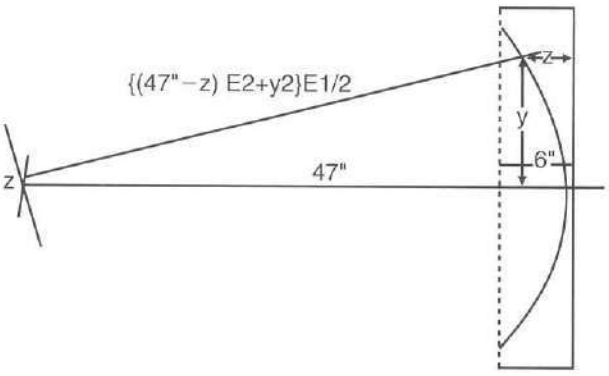

Figure 13-10 *Wavefront and electric lens geometry*

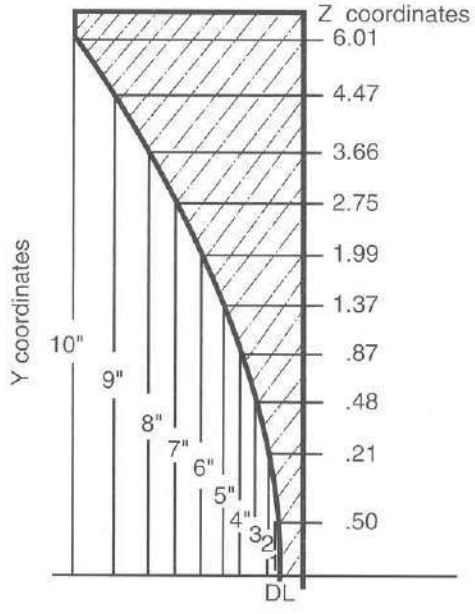

Figure 13-11 *Calculated lens dimension*

higher frequencies of radar as they are to microwave oven frequencies.

We might also be inclined to consider the higher-powered magnetrons used in industrial heaters and plasma generators, but this can be problematic. First, higher power is achieved more by increasing the duty cycle than by increasing the peak output power we desire. The 3,000-watt Panasonic 2M265 magnetron has a 7-kilowatt peak output power, but it runs on pulse-modulated direct current for a longer duty cycle than the half-wave voltage doubler of a microwave oven. Its operation is more critical; the cathode heater must have its voltage adjusted to the power output, and the cathode is more brittle in these more powerful magnetrons. It also costs as much as $1,000 and the power supply is even more expensive. The 6,000-watt Toshiba E3328 magnetron runs on filtered direct current and it has even more expensive computer controls that adjust an electromagnet to control the current. The peak output power is less than that of the 3,000-watt magnetron.

Another problem occurs with these magnetrons as well. They are so unforgiving of such things as a large metal object near the cannon in which they might be installed that reflections could mismatch the impedance enough to shorten the service life. The manufacturers recommend that they have a branch off of a waveguide to a dummy load that will absorb any energy due to such an impedance mismatch in order to protect the magnetron. This makes the parabolic horn impossible to use because it is not practical to feed with a waveguide. A pyramidal horn would be needed and it only has two-thirds of the gain of the parabolic horn. Thus, the 6,000-watt magnetron would be as good as a 4,000-watt one in a parabolic horn, and the 3,000-watt magnetron would be as good as two-thirds of 7,000 watts in a parabolic horn. Several vastly cheaper household oven magnetrons can easily outclass the more expensive and difficult-to-operate choices that appear more attractive until they are examined with greater perspicacity.

Another difficulty with purchasing industrial magnetrons also exists. Companies will not sell them to private individuals out of fear that they might be used for negative or hateful enterprises, such as in machines designed to sabotage overly loud stereos. Although almost any magnetron and power supply from any microwave oven will work, the best oven magnetron for our purposes is the 2M121A, which has its number conflated with the number 53 or 57. These last two numbers make no difference in the choice of editions of the 2M121A you procure. They are used in the following ovens: the Panasonic 1030, the Brother MF5000 and MF7000, and the Merrichef models 136M, 165M, and 206M. It has a peak output power of 5,800 watts, better than the 2,000-watt magnetrons that cost more than twice as much. It can be ordered from the Expert Appliance site (www.expertappliance.com) under the part number Z9-Panasonic NEI 030-412 if you type in Panasonic NEI 030 for the type of oven for which you are purchasing parts. The transformer number is 210 Panasonic NEI 030-5414. Global Microwave Parts has voltage-doubling capacitors that are 0.85 microfarads rated at 2,500 volts AC and diodes. You should use one rated at half an ampere. Magnetrons and parts are available and listed in Table 13-2. You will need copper and aluminum sheeting, along with mat-erials available from hardware or building suppliers.

The magnetron is attached to the antenna, as shown in Figure 13-12. Follow the instructions closely and observe that the brass washer is flush with the copper conductive surface.

The power supply is a simple voltage-doubler circuit, shown in Figure 13-13. It must be understood that the voltages in the wires will be in the thousands and can produce a spark that can jump through the air and through an insulator, conveying enough current that it would probably cause electrocution. Accordingly, the wires should be positioned where they will not be approached or touched. The magnetron and horn must be securely grounded or it will be 4,500 volts above ground potential. The frame that you must build around it will keep people's hands away from these wires. Also, after the cannon is shut off, four of the capacitors can hold a charge that would inflict a shock unless it is discharged, either through a bleeder resistor that may be built into the capacitor or it can be discharged with a safety discharge probe.

The magnetron must also have a fan to cool it during operation. The 2M121A requires at least 85 cubic feet per minute of air directed through its fins for best operation.

When your microwave cannon is completed, testing it is little more than a matter of switching on the power and aiming it at a fluorescent tube or a

small 120-volt lightbulb. The lightbulb should be no more than 25 watts and should glow slightly when it is within a few feet of the mouth of the cannon. Fluorescent lamp tubes should light up as far as 10 feet away.

You should not put any body parts directly in front of the cannon at close range because, after a few seconds to a few minutes, you could burn yourself, but a distance of over 50 feet away would provide safety. However, prolonged overheating of internal organ tissue is remotely possible and the cornea of the eye can be damaged by overheating. Also, testicles can overheat, and at close enough range for the *root mean square* (RMS) microwave field to exceed 4,000 watts per square meter, a 5-minute uninterrupted exposure is supposed to build up enough internal steam pressure to cause the testicles to explode. However, the possibility of having a hot spot this intense a few inches in front of the cannon is marginal.

When testing or using your microwave cannon, you can do so with utmost safety to yourself by constructing a gown out of metal screen from a hardware store. The gown should include a hood that completely covers the head and should extend over the torso down to just below the vaudevillian parts of the body. The sex organs should be stuffed into a tin can, the mouth of which can be lined with fake fur to make it more comfortable. (Obviously, the ladies need not take recourse to this expedient.) This is more than enough to prevent any harm when performing experiments that last half an hour or more and is probably hundreds of times the protection you will need.

It can be advantageous to test the cannon in your backyard. Sooner or later the neighbors will see it, and if they see a mysterious-looking machine that lights up fluorescent tubes 10 or more feet away and they see you dressed in a wire screen gown complete with a tin can, it will frighten the emunctory indiscretions out of them. Further, when they complain to the authorities they will sound much the same way mental patients sound as they describe exotic macrunes, stereos malfunctioning, strange costumes complete with tin cans, and the like. It is even slightly possible

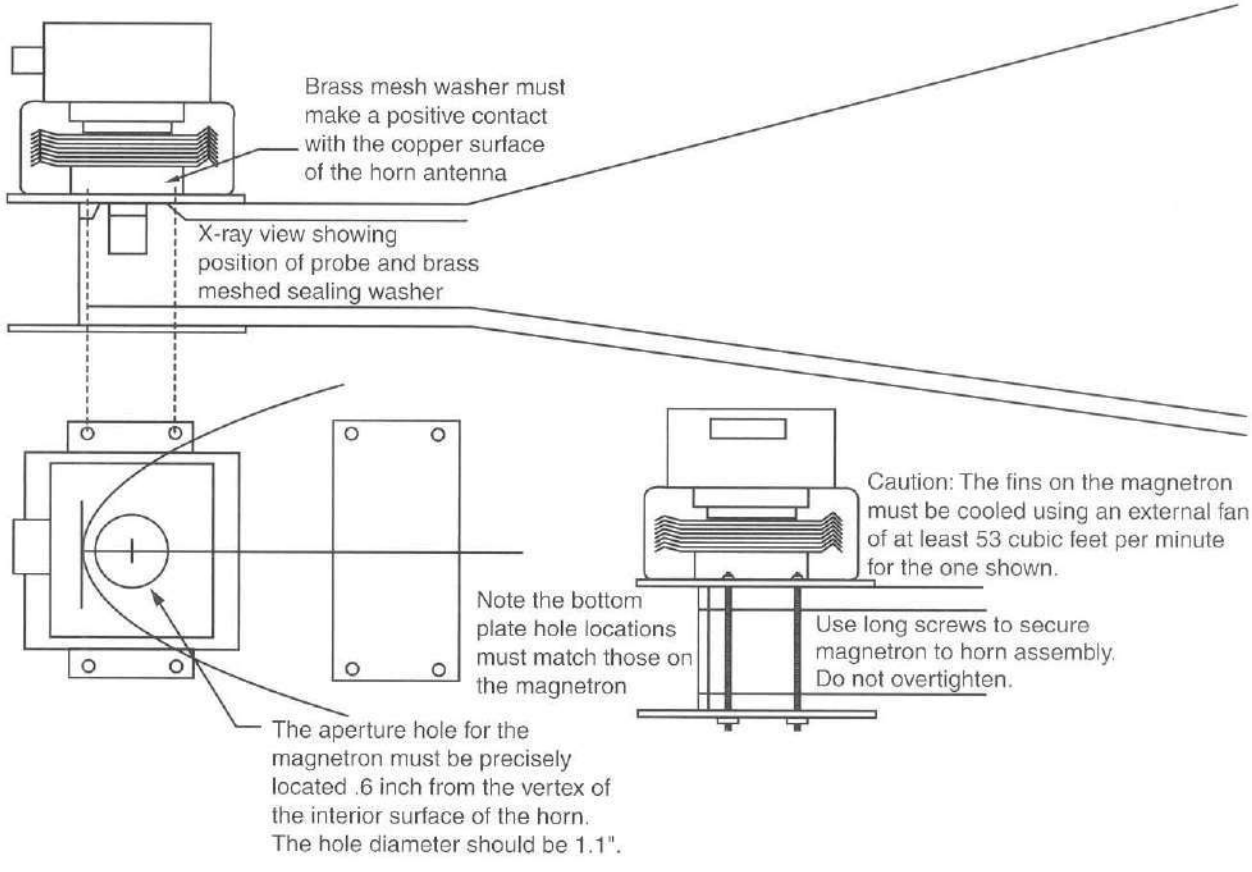

Figure 13-12 *Attaching the magnetron*

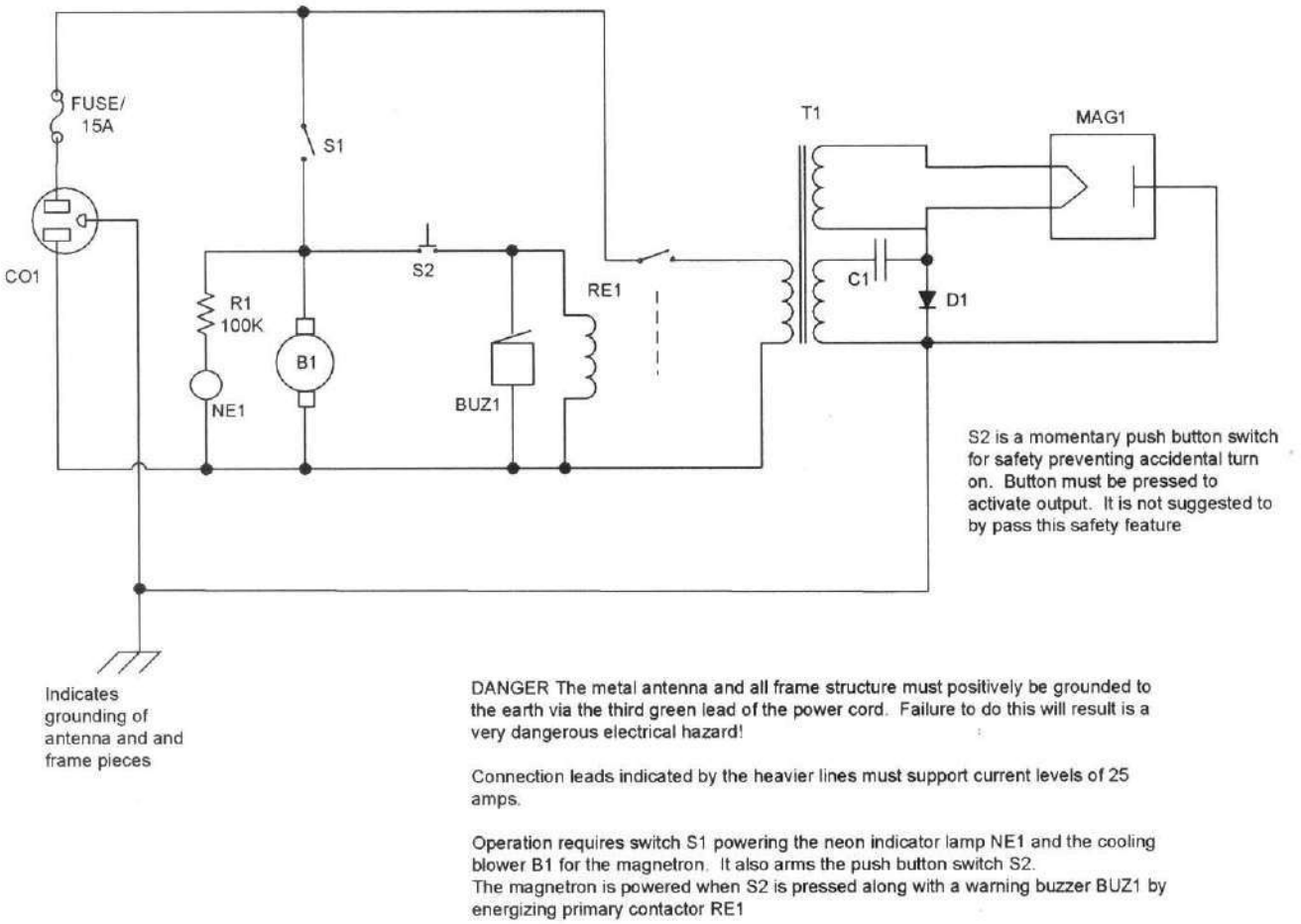

Figure 13-13 *Microwave cannon schematic*

that they might be invited to undergo observation at the local state psychiatric hospital, where, if you are really ambitious, you could locate their room, aim your microwave cannon, and make their stereo buzz whenever the psychiatrist's back is turned and cause a diagnosis that will keep them out of the neighborhood for a longer time. But in the remote case you get caught doing this, it will be almost impossible to prosecute you because no state legislature has the time to write and process special laws against shooting microwaves into peoples' stereos. The television publicity possible if the state attempts to prosecute you will be a disaster for the system that supports cultural tyranny because it will inspire countless television viewers to join in the revolution to make the world a better place by building more microwave cannons and shooting down more obnoxious stereos. And even if they can win a battle in court, they will ultimately lose the war that they started against human dignity.

Table 13-2 Microwave Cannon Parts List

Ref. #	*Description*	*DB Part #*
R1	100K ¼-watt resistor (br-blk-yel)	
CO1	Heavy-duty, 15-amp, three-wire power cord	
FUSE/15	15-amp fuse and holder	
B1	85 cubic feet/minute or better cooling fan for magnetron fins	
S1	*Single pole, single throw* (SPST), 5-amp, 115 VAC toggle switch	
S2	Momentary push-button switch (see note on Figure 13-13)	
NE1	Neon indicator lamp with leads or equivalent	
BUZ1	120 VAC high output safety buzzer	
RE1	10- to 20-amp contacter or relay	
T1	Magnetron power transformer NEI030-5414	DB# MAGTRAN
C1	.85-microfarad, 2500 VAC voltage-doubler capacitor	DB# MAGCAP
D1	5 kilovolt, ½-amp diode	DB# MAGDIODE
MAG1	2M121A magnetron	DB# MAGNETRON

Chapter Fourteen

Induction Heater

This device shown in Figure 14-1 shows an induction heater capable of heating metals to over 1,500 degrees Fahrenheit. It can be used in the processing of gas discharge tubes often used for plasma, neon displays, laser discharge tubes, and spectrum tubes. These tubes usually require electrodes that must be heated to drive out the impurities that are now sucked out by a vacuum system. The induction heater heats these electrodes directly through the glass.

The completed system consists of a donut-shaped heating coil head connected via an umbilical cord, which is in turn connected to the power-conditioning and control box. The system is powered directly from 115 VAC and requires caution when building and using. The head is a coil of wire that surrounds the target area to be heated. As shown, it is an air-cooled system that requires a waiting time for processing between operations because the coil will get hot. The common circuit ground is above ground and requires an isolation transformer or an ungrounded scope to view the waveforms from a grounded scope.

This is an advanced-level project requiring electronic skills and the use of an oscilloscope. Expect to spend $35 to $75. All the parts are readily available, with specialized parts obtainable through Information Unlimited (www.amazing1.com), and they are listed in Table 14-1.

Figure 14-1 *Induction heater*

Circuit Operation

The power cord CO1 supplies 115/220 VAC from a wall receptacle where the third, green wire, grounding lead must be securely attached to the metal chassis (CHASSIS) for safety (see Figure 14-2).

Switch SW1 energizes the primary circuits, and fuse FUS1 protects the main circuit from any catastrophic faults. Indicator lamp NEON1 requires the current-limiting resistor R12 and lights up when SW1 is turned on. The peak charging current to capacitors C10 and C11 is limited by in-rush resistor Rx. The rectifiers D1, D2, D3, and D4 are shown in a

full-bridge configuration when used for 220 VAC input. For 115 VAC operation, only D1 and D3 are used along with the JUMP jumper in a voltage-doubler configuration. The output voltage across C10 and C11 is 300 volts DC and is referred to as the positive and negative rails.

Dropping resistors R2 and R3 provide voltage to the oscillator driver IC1 with zener diode Z1 regulating the voltage at 15 volts. Switch SW2 is normally closed, shorting out this voltage across Z1. Capacitor C2 provides the high instant of current for the output pulses and must be physically close to IC1. Operation requires SW2 being pressed, allowing 15 volts to be applied to the oscillator driver generating the drive pulses.

These drive pulses turn the main MOSFET switches, Q1 and Q2, off and on. The switching frequency is determined by the time constant of power control pot R10 and timing capacitor C3. A limit resistor, R11, prevents driving the circuit beyond the intended limits.

The switching circuit is in a half-bridge configuration where the MOSFET connected to the positive end (+ rail) must be driven with its source pin referenced at 150 volts above the common end (− rail). This is accomplished by biasing a bootstrap capacitor (C4) through an ultrafast diode (D5), providing the correct DC level to fully control Q1. Resistors R6 and R7 eliminate the high-frequency parasitic oscillation that occurs as a result of rapidly switching the capacitive load of the MOSFET gates. Capacitor C40 limits the current flow to a second neon indicator light, NEON2, which is connected in series and is energized by the output frequency when the heating cycle is activated by SW2.

A network consisting of capacitor C7 and resistor R8 slows down the transition time of the switched pulses across Q1 and Q2. The resultant time constant limits the rate of voltage rise, dv/dt, that could cause a premature turn-on at the wrong switch, creating a catastrophic fault mode.

Capacitors C5 and C6 provide a voltage midpoint and produce the necessary storage energy to maintain the voltage level of the individual pulses. The output is taken at the junction of Q1/Q2 and C5/C6 and is a square wave fed to the induction heating coil L1. A current rise through L1 now commences as a function of Et/L where E is the voltage of the drive pulse, t is the applied time, and L is the inductance of L1. This changing current now induces eddy currents in the target piece to be heated as a function of $E = L\ di/dt$. These circulating currents quickly heat up the target piece.

Project Assembly

1. Assemble the heating head coil, as shown in Figure 14-3. This coil must be tightly and evenly wound for optimal performance. It may be difficult for the beginner and is available in three sizes, as indicated in Table 14-1.
2. Assemble the circuit board, as shown in Figure 14-4. Note that you should allow a half-inch for the Q1 and Q2 pins. This is necessary to allow these parts to be placed flat against the chassis when mounting as they exit at the midsection of the part.

   It is also strongly suggested that you use an eight-pin IC socket (SO8) because IC1 is very sensitive to static electricity and possible errors during the assembly.

   Note that if you are building from a perforated or vector circuit board, it is suggested that you use the indicated traces for the wire runs and insert components starting in the lower left-hand corner. Pay attention to the polarity of capacitors with polarity signs and all semiconductors.

   Route the leads of the components as shown and solder as you go, cutting away the unused wires. Attempt to use certain leads as the wire runs or use pieces of the #24 bus wire. The heavy foil runs should use the thicker #20 bus wire because these are the high-current discharge paths.
3. Double-check the accuracy of the wiring and the quality of the solder joints. Avoid wire bridges, shorts, and close proximity to other circuit components. If a wire bridge is necessary, sleeve some insulation onto the lead to avoid any potential shorts.

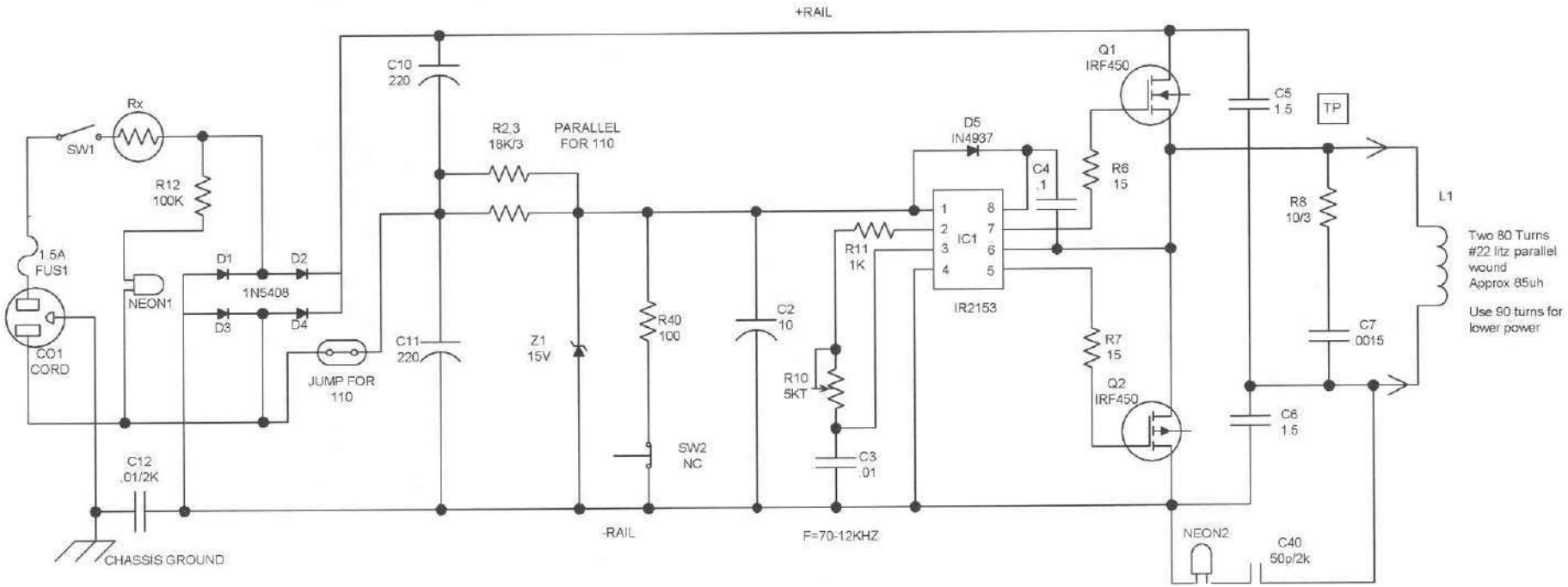

Figure 14-2 *Induction heater schematic*

4. Connect the external components as shown in Figure 14-5. Use 6-inch lengths of the wire size as noted.

5. Create the chassis, as shown in Figure 14-6, from a piece of .065-inch 5052 bendable aluminum. Note to trial-fit and measure the diameters of the components before drilling the holes. Pay attention to the holes for mounting Q1 and Q2 because these must be reasonably accurate to align with the layout of the PCB. Also, there must be at least 1/8 inch of clearance between the board and the chassis for sandwiching in the PLASTPL plastic plate. This prevents grounding out of the board wiring traces to the metal chassis.

6. The final assembly is shown in Figure 14-7. Note the mounting scheme for Q1 and Q2, as they must be insulated from the chassis using the thermo pads, THERM1. These pads allow heat transfers and provide electrical insulation from the metal chassis.

   Drill the hole for grounding lug LUG1 and solder the green grounding lead from the power cord and circuit board's earth ground.

The heating head coil assembly can be built to accommodate a diameter from a 1/2" to a 1" object. The assembly with the material shown is intended for using enclosed electrodes in glass tubes such as those used in neon tubes, laser tubes, and spectrum tubes. High-temperature materials may be used if you are anticipating using for other applictions.

The coil should be wound with high-frequency wire to limit heating losses. Use #22 litz wire consisting of multiple strands of #36 magnet wire.

1. Fabricate the winding bobbin from 1.25" lengths of 1/16" wall GT fiber glass tubing of your diameter choice of 1/2, 5/8, 3/4, 7/8 or 1".
2. Wind an even 1" layer of the #22 litz wire. Glue the start wire with a fast-curing glue. Tape the finished winding using a single layer of high-temperature glass tape.
3. Continue winding layers and repeat step 2 until there are 80 turns. You may truncate the successive layers by several turns at each end to keep from slipping off or use a quick-curing glue.
4. Attach the input leads and attach by gluing and taping into place.

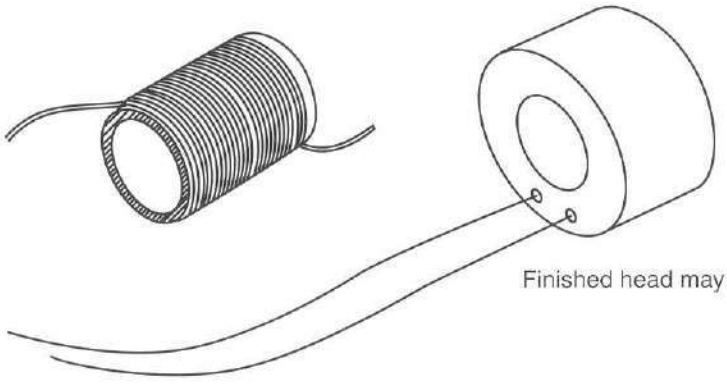

Finished head may be potted in epoxy or sealed in plastic caps

The inductances of the various heads will vary as a function of the diameter. Ideal current through the head is 20 amps peak. You should therefore adjust the frequency of R10 to maintain this value when changing the head sizes as the following:

1/2" head	50 uh	75 KHz
5/8" head	75 uh	50 KHz
3/4" head	100 uh	40 KHz
7/8" head	125 uh	35 KHz
1" head	150 uh	30 KHz

These heads are available assembled for those not wanting to attempt winding their own. They are listed in Table 14-1.

Figure 14-3 *Heater head coil assembly*

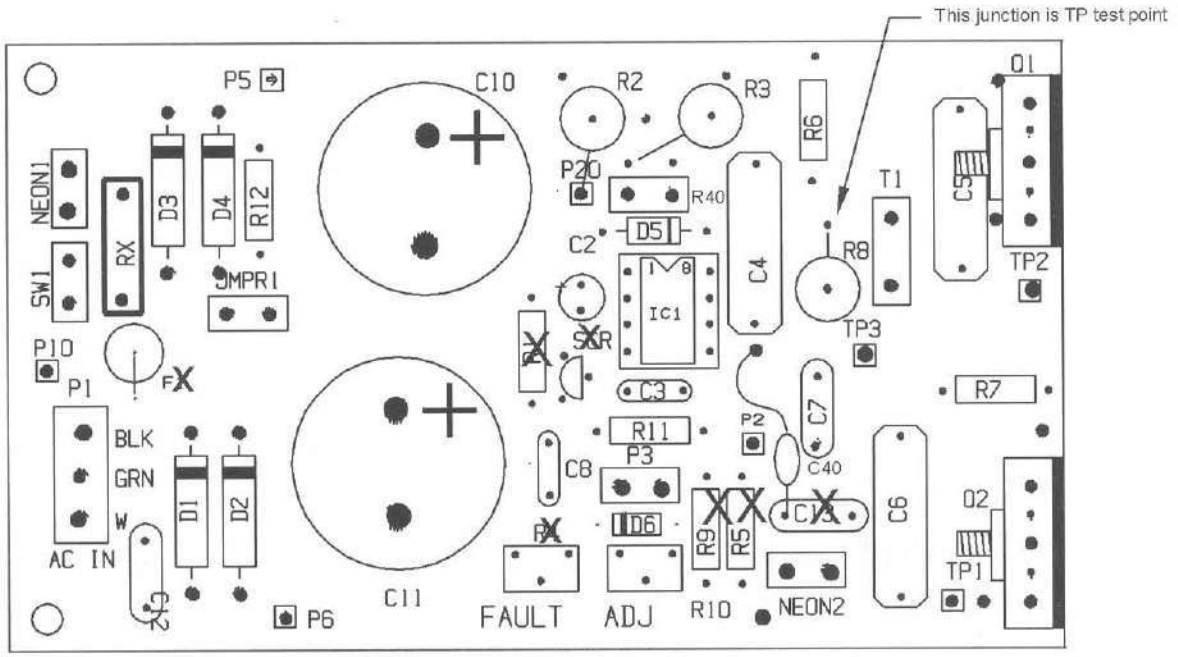

1. Black dots are connections points to external leads as shown figure 14-5

2. The PC board as shown is used in several projects and does not use all the components as indicated. Those indicated by an X are omitted for this project. R40 and C40 are added to the pads as shown and are not identified on the PC board printing

3. This circuit uses a 8 pin socket for IC1 as it is prone to failing if there are circuit faults

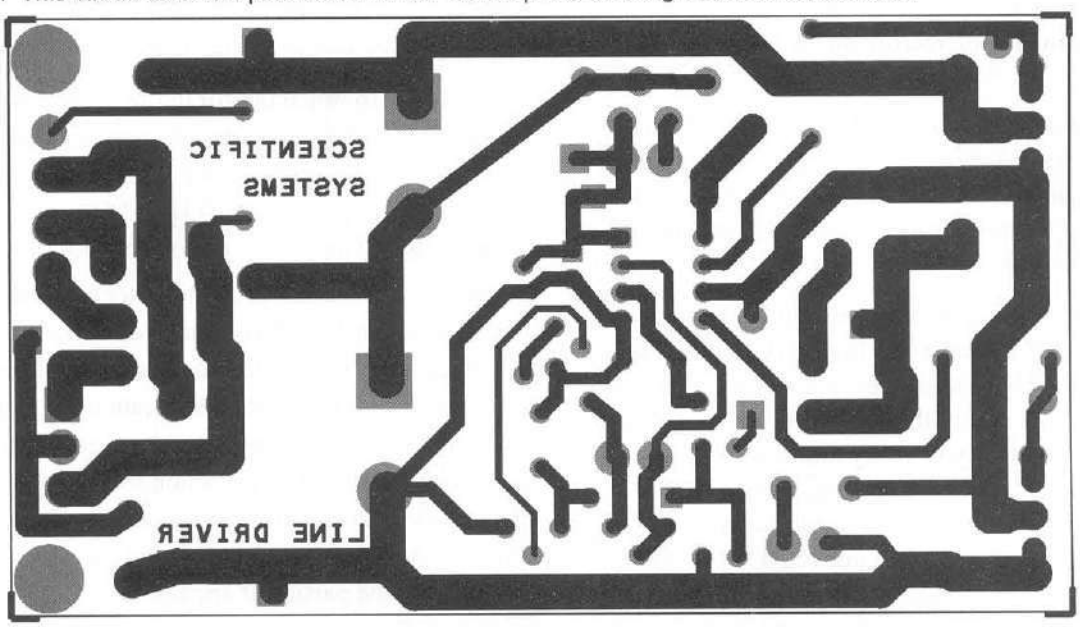

Assembly of the board assembly is shown using a printed circuit board available through www.amazing1.com Builders may use a vector board and use the component leads to duplicate the foil traces as shown.

On all IND40 assembly boards this jump lead is to be the first part on the board. Once the unit is final assembled with the heating head connected in place the jump now can now be disconnected. This step prevents static electric damage to the semiconductors.

Figure 14-4 *Assembly of the circuit board*

Note that we have shown the use of plastic bushings (BU38) for the neon indicator lamps and output leads, and also BU58CL clamp bushing for the line cord.

7. Assemble the test jig as shown in Figure 14-8. This is a very useful fixture for any 115 VAC project up to 300 watts.
8. Now fabricate the cover to fit the chassis section. Use bendable plastic or a thin, perforated aluminum sheet. Secure it to the chassis via four screws (SW1) on the folded-up lip in this section.

Project Testing

Caution: The circuit commonly noted as −RAIL is electrically above earthground by over 150 volts. It is strongly recommended that you obtain a 200-watt isolation transformer before proceeding and testing this or other similar direct line powered circuits. Experienced experimenters working on dry, wooden floors may choose to unground their test equipment. This can be a dangerous shock hazard!

1. Connect the ungrounded scope to the TP test point, as noted in the Figure 14-2 schematic or in Figure 14-4. The lead of R8 is shown connected to the junction of the drain and the source of Q1 and Q2 respectively.
2. Verify that the main power switch S1 is off and insert a 2-amp fuse into FH1. Then adjust trimpot R10 to midrange and connect CO1 to the female end of the cord on the test jig. It is important that you verify that the test jig is not shorting the ballast lamp. Plug the jig into the output of the isolation transformer. Quickly turn on S1 and notice NEON1 lighting up and the ballast lamp not lighting. If it lights, you must troubleshoot and find your error before proceeding.

Press and hold PB1, noting a picture-perfect square wave on the scope with the lamp only dimly lighting. Quickly adjust R10 for a 20-usec pulse period. This corresponds to 50 kHz. NEON2 will indicate when PB1 is activated. Experienced builders may wish to monitor the current to the head using a current probe attachment to the scope. This wave shape should be another picture-perfect sawtooth of 20 amps maximum.

Using the Heater Project

Obtain a gas discharge tube with an electrode to fit into the head size you chose in assembly.

At this point, it is a good idea to have a meter capable of measuring the AC line current, as this value is very dependent on the object that you place into the head and should not exceed 2 amps. You can drop this value by increasing the frequency, which is done by adjusting R10. When heating electrodes, you will note the ampmeter dropping in level when the electrode is red hot. This is due to the change in the magnetic characteristics of the heated material.

Something to watch out for in this project is overheating the head coil. You may implement a cooling fan stand when using the device for multiple tasks. Also, the chassis panel where Q1 and Q2 are mounted should not be uncomfortably hot to touch.

Those experienced can create other heads for different heating tasks and you can even make a "quick" heat solder pot. Just make sure you keep the switching current below the maximum of 20 amps. The inductance of the head should not go below 80 uh. Alternate head construction must always take into consideration heating fatigue and the eventual failure of the head wires, bobbin, and construction materials for the particular application.

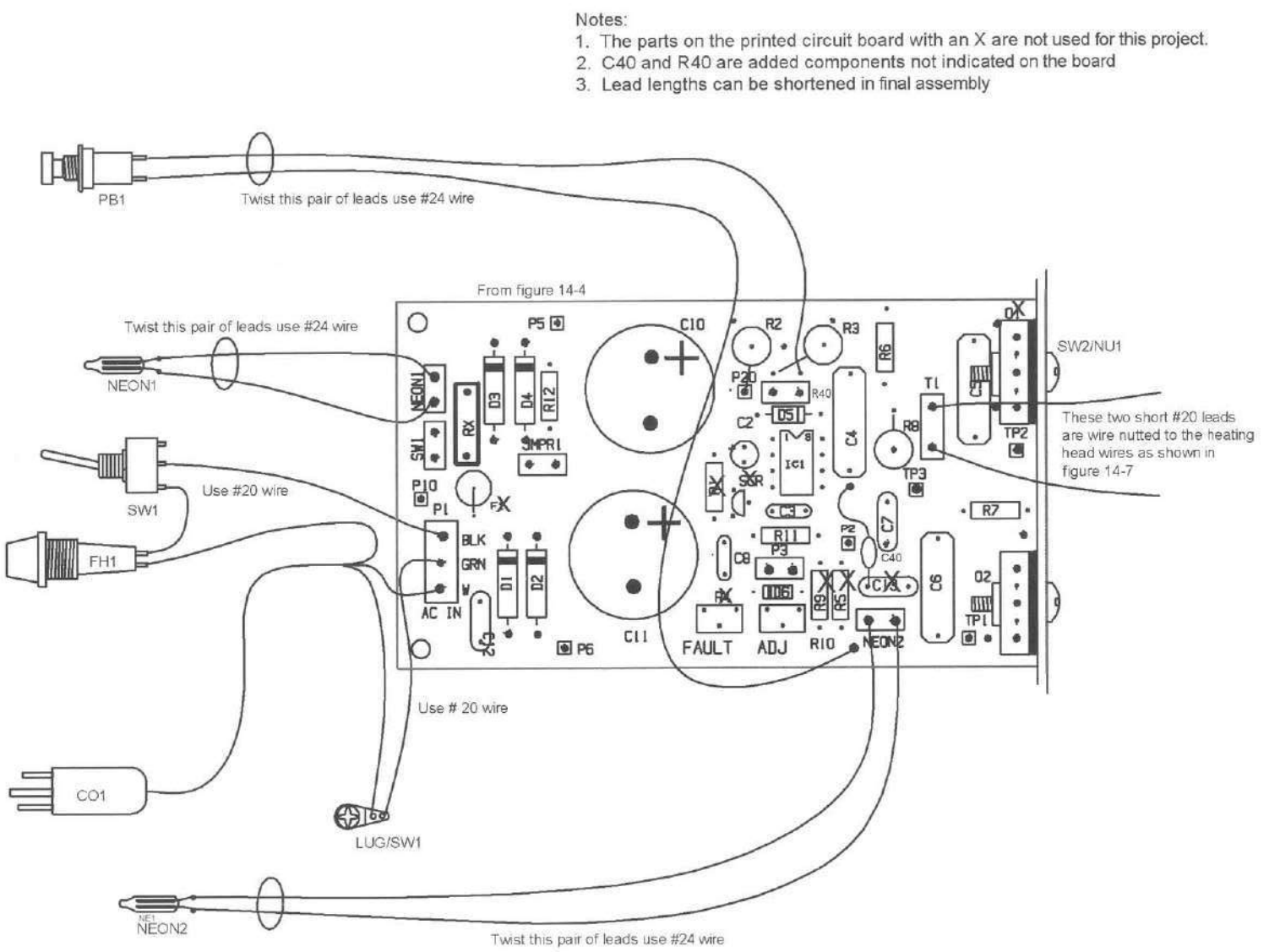

Figure 14-5 *External wiring*

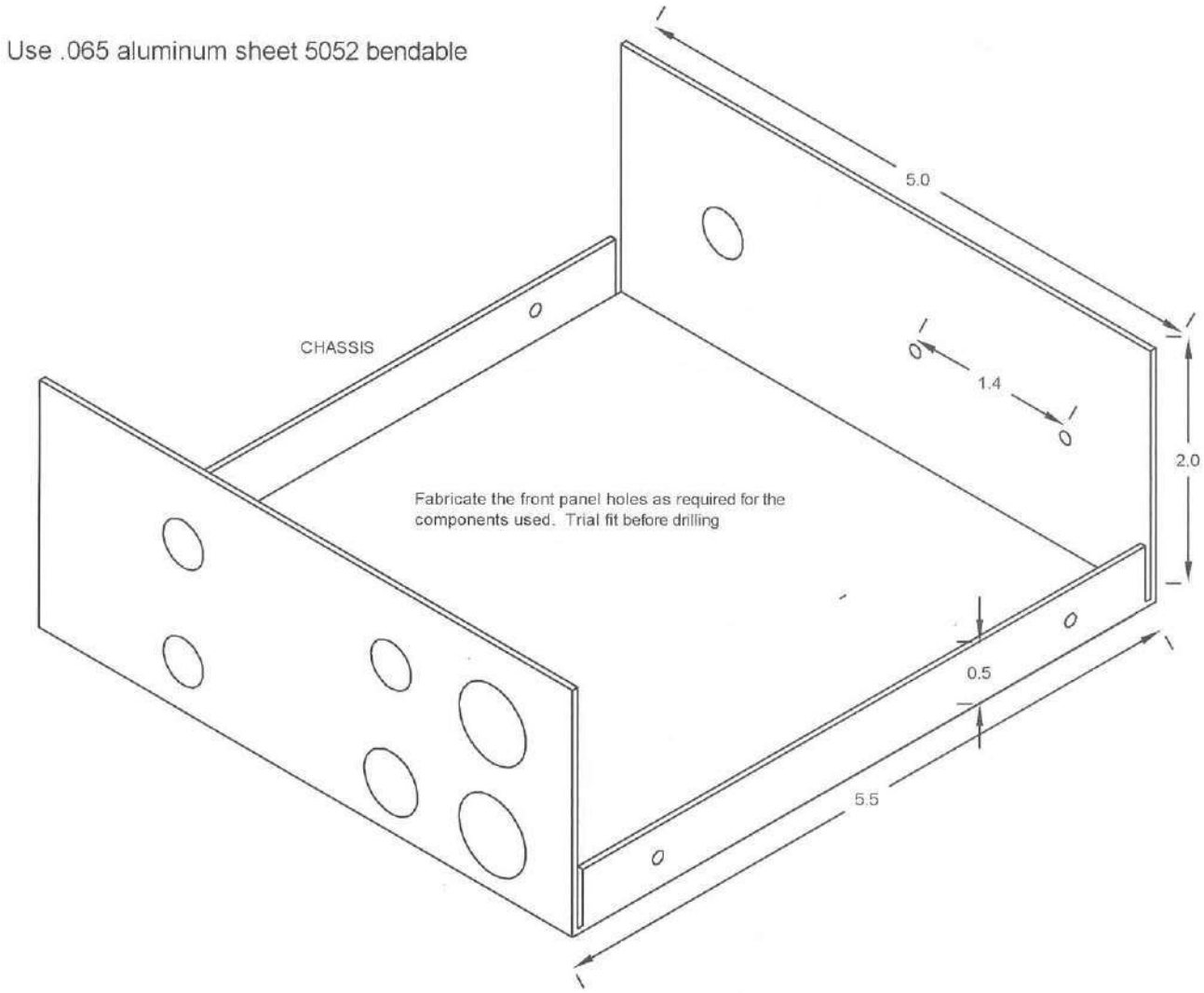

Figure 14-6 *Chassis fabrication*

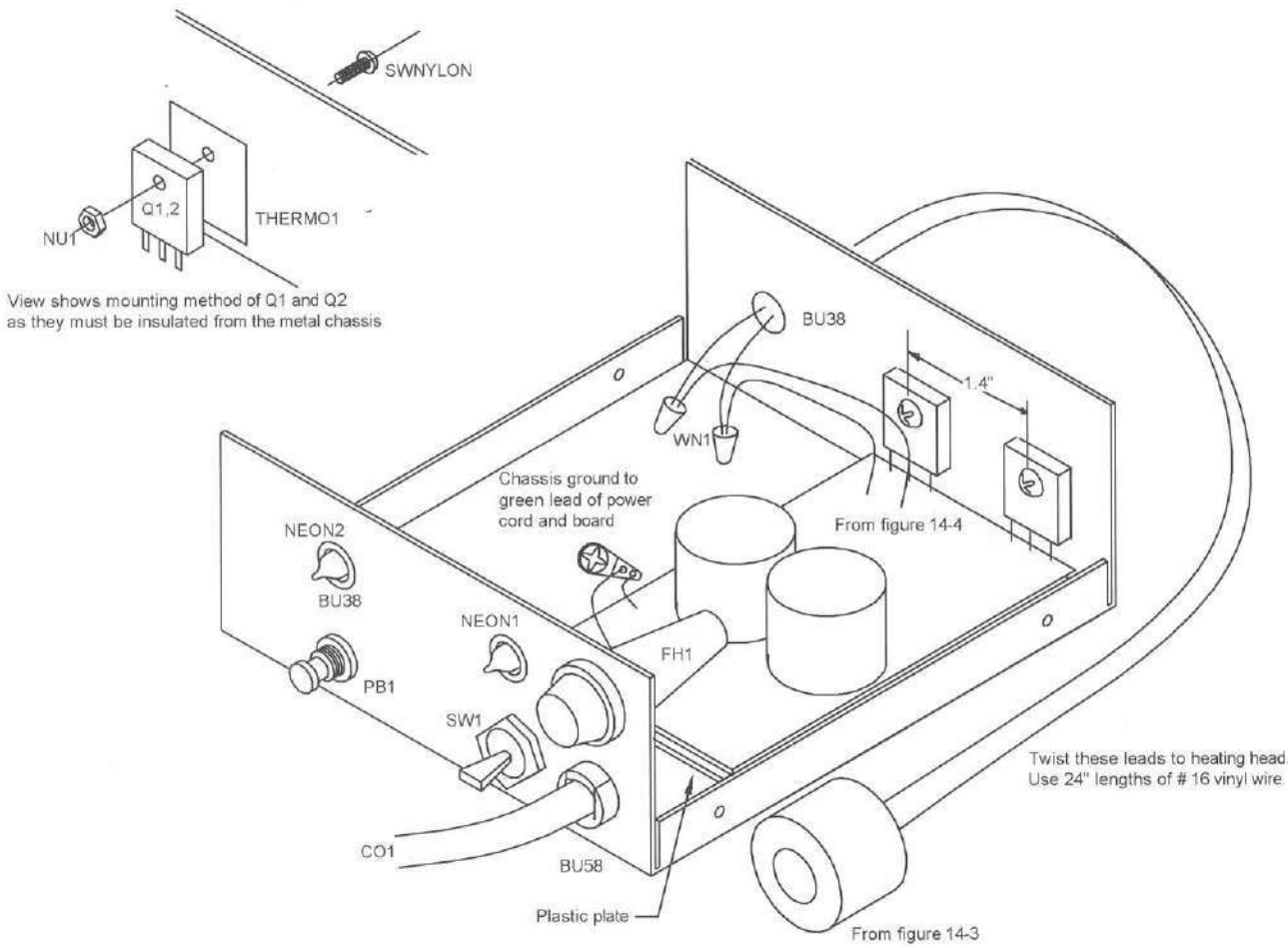

Figure 14-7 *Isometric of final assembly*

This test jig as shown prevents catastrophic damage to AC powered circuitry in the event of a fault when first assembled. Basically it uses a 60-watt lamp as a ballast, connected in series with the hot wire of the AC line. The lamp will usually allow ample current to flow for operational circuit verification yet limit short circuit current to that of the lamp should the circuit have a catastrophic fault. It is suggested that the serious experimenter construct this test jig and enclose it in a suitable container with receptacle for plugging in any AC circuit under test.

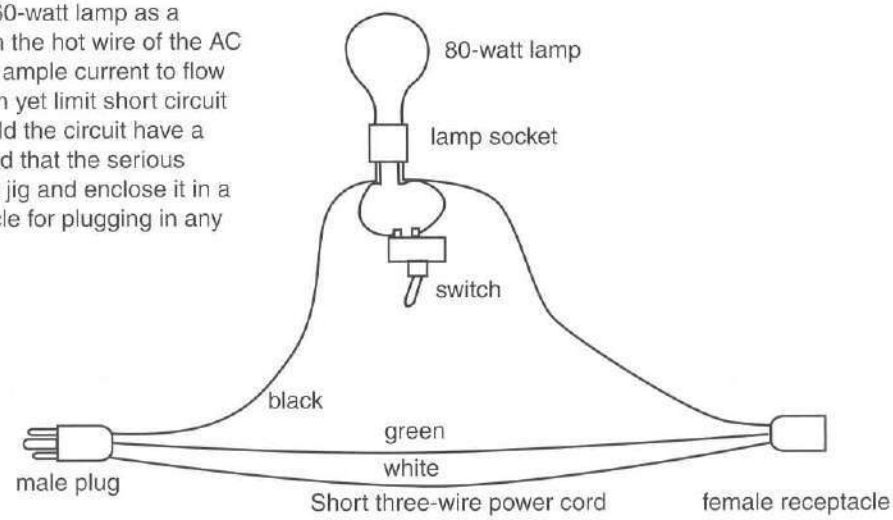

Figure 14-8 *Useful test jig for line-drive circuits*

Table 14-1 Induction Heater Parts List

Ref. #	Description	DB Part #
R2, 3	Two 18K 3-watt resistor	
R4	100-ohm, 1/4-watt resistor (br-blk-br)	
R6, 7	Two 15 1/4-watt resistor (br-grn-blk)	
R8	10-ohm, 3-watts metal oxide resistor	
R10	5K vertical trimmer	
R11	1 K 1/4-watt resistor (br-blk-red)	
R12	100 K 1/4-watt resistor (br-blk-yel) or 10-ohm 3-watt metal oxide resistor	
Rx	5-amp in-rush limiter (KC006L-ND)	
C2	10-microfarad, 50-volt vertical electrolytic capacitor	
C3	.01- microfarad, 50-volts plastic capacitor (103)	
C4	.1-microfarad, 600-volt plastic capacitor	
C5, 6	Two 1.5-microfarad, 400-volt metal polyester capacitors	
C7	.0015-microfarad, 600-volt polypropylene capacitor	
C10, 11	Two 200- to 800-microfarad, 200-volt vertical electrolytic capacitors	
C12	.01-microfarad, 2-kilovolt disc capacitor	
C40	50-picofarad, 6-kilovolt ceramic capacitor	
D1, 2, 3, 4	Four 1,000-volt, 3-amp rectifiers (1N5408)	
D5	1-kilovolt, 1-amp fast diode (1N4937)	
Z1	15-volt, .5-watt zener diode (1N5245)	
Q1, 2	IRFP450/460 *metal-oxide-semiconductor field effect transistors* (MOSFET)	
IC1	IR2153 half-bridge driver	
NEON1, 2	Two neon indicator bulbs with leads	
FH1	Fuse holder panel mount	
FUS1	2-amp slow blow 3AG fuse	
PB1	Normally closed push-button switch	
SW1	*Single pole, single throw* (SPST) toggle switch	
CO1	Three-wire line cord	
LUG1	#6 solder lug	
SO8	Eight-pin *integrated circuit* (IC) socket	
THERM1	Two thermo mounting pads for Q1 and Q2	
PCLINE	*Printed circuit board* (PCB)	DB# PCLINE
WN1	Two small wire nuts	
CHASSIS	Chassis fabricated from .065-inch aluminum sheet per Figure 14-6	
COVER	Cover fabricated from plastic sheet to fit chassis (see Figure 14-6)	
BU38	Three 3/8-inch plastic bushings	
BU58CL	5/8-inch clamp bushing for cord CO1	
SW1	Five #6 × 3/8-inch sheet metal screws for cover and LUG1	
SW2/NU1	Two 6-32 × 1/2-inch nylon screws and nuts	
WR24	24 inches of #24 vinyl stranded hookup wire	
WR20	24 inches of #20 vinyl stranded hookup wire	
WR16	48 inches of #16 vinyl stranded hookup wire	
PLASTIC	2 × 4-inch plastic insulating plate for under PC board	
HEAD12	Head with 1/2-inch clearance hole	DB# HEAD12
HEAD58	Head with 5/8-inch clearance hole	DB# HEAD58
HEAD34	Head with 3/4-inch clearance hole	DB# HEAD34
HEAD78	Head with 7/8-inch clearance hole	DB# HEAD78
HEAD10	Head with 1-inch clearance hole and head parts for those wanting to attempt assembly	DB# HEAD10
WR22LITZ	#22 LITZ of multiple strands of #36 enamel wire	
BOBBIN	1.25 inches of 5/8-inch GT tubing	

Chapter Fifteen

50-Kilovolt Laboratory DC Supply

This project, as shown in Figure 15-1, provides the high-voltage experimenter or researcher a DC source of 5 to 60 kilovolts at 5 milliamps. The system is short-circuit protected and current limited by inductive ballasting. This circuitry is excellent for high-energy capacitor charging intended for high-power applications. The charging current is fully adjustable and easily converts to a voltage source by the addition of load resistors. It is an excellent device for large gravity and lifter research, as well as normal, high-voltage laboratory functions.

This is an advanced-level project requiring electronic skills and high-voltage experience. Expect to spend $100 to $250. All parts are readily available, with specialized parts obtainable through Information Unlimited (www.amazing1.com), and they are listed in Table 15-1.

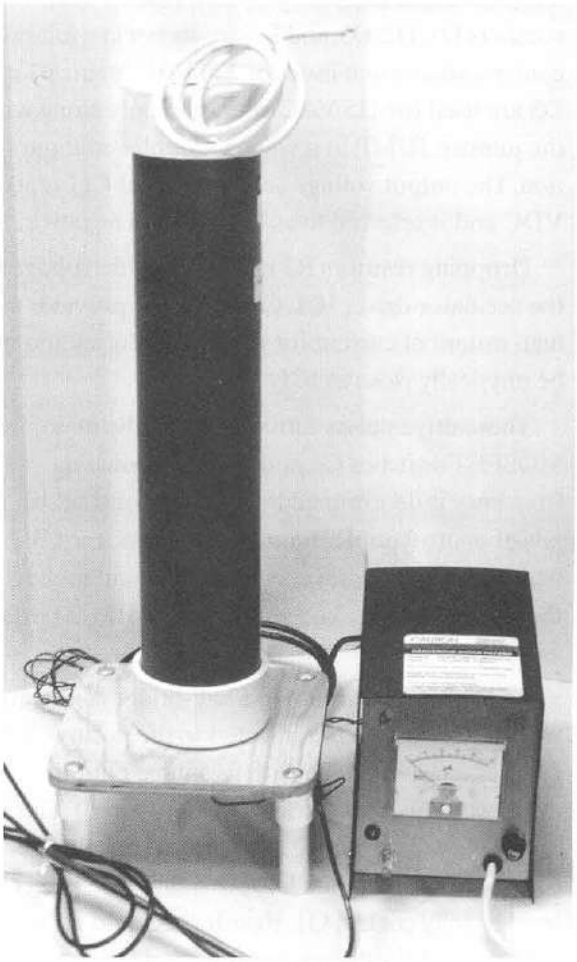

Figure 15-1 *50-Kilovolt power supply*

Basic Description

This project is shown constructed in two sections. The first section is the power conditioning and control circuitry. This is where the 115 VAC level is converted to a variable-frequency, high-voltage current source between 15 and 30 kHz. The second section is the high-voltage multiplier circuitry interconnected via a short umbilical cable from the power control section.

The multiplier section is a Cockcroft-Walton half-wave circuit consisting of 10 capacitors and diodes connected in the ladder configuration, along with a peak-current, high-voltage-limiting resistor.

Circuit Operation

The power cord (CO1) supplies 115/220 VAC from a wall receptacle where the third, green, grounding lead wire must be securely attached to the metal chassis (CHASSIS) for safety (see Figure 15-2).

Switch S1 energizes the primary circuits and fuse FUS1 protects the main circuit from any catastrophic faults. The indicator lamp NEON1 requires current-limiting resistor R12 and lights up when SW1 is turned on. The peak charging current to capacitors C10 and C11 is limited by in-rush resistor Rth. The rectifiers D1, D2, D3, and D4 are shown in a full-bridge configuration when used for 220 VAC input. D1 and D3 are used for 115 VAC operation only along with the jumper, JUMP, in a voltage-doubler configuration. The output voltage across C10 and C11 is 300 VDC and is referred to as the plus and negative rails.

Dropping resistors R2 and R3 provide voltage to the oscillator driver IC1. Capacitor C2 provides the high instant of current for the output pulses and must be physically close to IC1.

These drive pulses turn off and on the main MOSFET switches Q1 and Q2. The switching frequency is determined by the time constant of power control pot R21 and timing capacitor C3. A limit resistor R11 prevents driving the circuit beyond the intended limits. You will note that R21 is part of switch S1.

The switching circuit is in a half-bridge configuration where the MOSFET connected to the positive end (+ rail) must be driven with its source pin referenced at 150 volts above the common end (− rail). This is accomplished by biasing a bootstrap capacitor C4 through ultrafast diode D5, providing the correct DC level to fully control Q1. Resistors R6 and R7 eliminate the high-frequency parasitic oscillation that occurs as a result of rapidly switching the capacitive load of the MOSFET gates. The transition time of the switched pulses across Q1 and Q2 is slowed down by a network consisting of capacitor C7 and resistor R8. The resultant time constant limits the rate of voltage rise dv/dt rate, which could cause premature turn-on at the wrong switch, creating a catastrophic fault mode.

Capacitors C5 and C6 provide a voltage midpoint and produce the necessary storage energy to maintain the voltage level of the individual pulses. The output is taken at the junction of Q1/Q2 and C5/C6 and is a square wave fed to the primary of transformer T1, inducing the high-voltage output in the secondary winding.

A safety shutdown circuit, consisting of a spark breakover switch, fires when the voltage exceeds a certain level and is fed to isolation transformer T2. The output is now rectified by diode D6 and integrated onto capacitor C8. When this voltage exceeds a preset level controlled by trimpot R4, a trigger level now turns on the silicon switch, SCR, and crowbars the voltage to the drive chip IC1, shutting it down and disabling the high voltage until reset by power removal.

The 15,000-volt, high-frequency output is fed to the voltage multiplier stack, consisting of capacitors C14 through C21 and diodes D7 through D14. The resultant 50,000-volt DC output is in series with peak-current-limiting resistors (R17 through R20).

Assembly of the Driver Section

1. Assemble the circuit board as shown in Figure 15-3. Note to allow a length of a half-inch for the pins of Q1 and Q2. This is necessary to allow these parts to be placed flat against the chassis when mounting.

   It is also strongly suggested that you use an eight-pin integrated circuit socket (SO8) because IC1 is very sensitive to static electricity and possible errors during assembly.

   Note that if you are building from a perforated or vector circuit board, it is suggested that you use the indicated traces for the wire runs and insert components starting in the lower left-hand corner. Pay attention to the polarity of the capacitors with polarity signs and all the semiconductors.

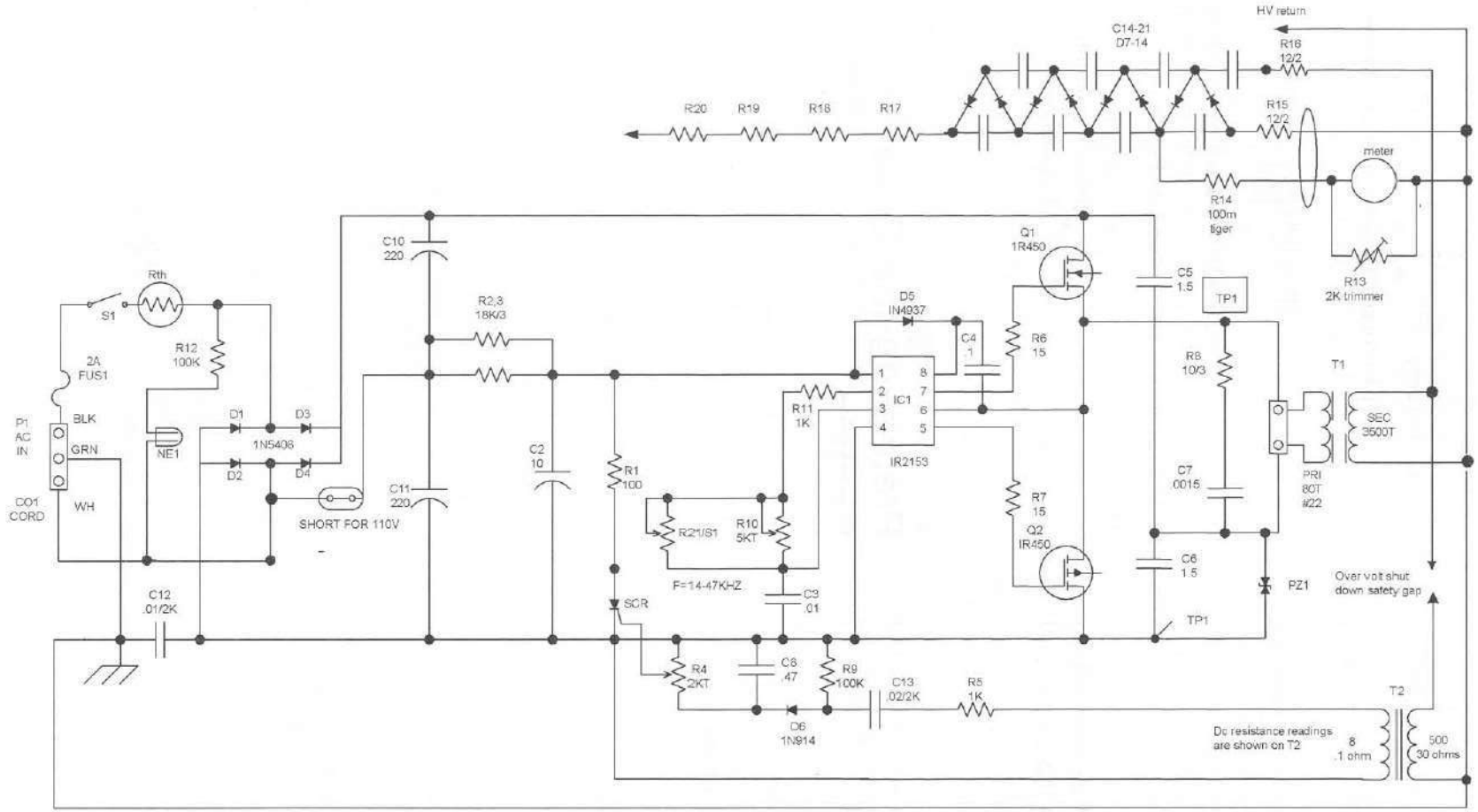

TRANSFORMER				
PRIMARY	80	#22 LITZ	9MH	4.75MH
XFMR	TURNS	WIRE	Lsc	Lcc
SECONDARY	3500	#39 MAG	3HY	9H
AIR GAPS	2 MILS/SIDE			

Figure 15-2 *Circuit schematic*

Route the leads of the components as shown and solder as you go, cutting away unused wires. Attempt to use certain leads as the wire runs or use pieces of the #24 bus wire. The heavy foil runs should use the thicker
#20 bus wire as these are the high-current discharge paths.

2. Double-check the accuracy of the wiring and the quality of the solder joints. Avoid wire bridges, shorts, and close proximity to other circuit components. If a wire bridge is necessary, sleeve some insulation onto the lead to avoid any potential shorts.
3. Assemble the transformer as shown in Figure 15-4, or you may purchase this part as noted on the parts list.
4. Connect the external components as shown in Figure 15-5.
5. Fabricate the chassis as shown in Figure 15-6 from a piece of .035-inch 5052 bendable aluminum. Note to trial-fit and measure the diameters of the components before drilling the holes. Pay attention to the holes for mounting Q1 and Q2, as these must be reasonably accurate to align with the layout of the PCB. Also, there must be at least 1/8 inch of clearance between the board and chassis for sandwiching in the PLASTPL plastic plate. This prevents grounding out of the board's wiring traces.
6. Fabricate the plastic base from a 9 × 6-inch piece of 1/16-inch Lexan sheet, as shown in Figure 15-7.
7. Fabricate the parts as shown in Figure 15-8 for the over-voltage shutdown switch.
8. Attach the metal chassis to the plastic base via four screws and nuts, SW12/NU1 (see Figure 15-9).
9. Attach the shutdown switch assembly from Figure 15-8 using sheet metal screws SW1.
10. Mount the assembled PCB, as in Figure 15-3. Note that Q1 and Q2 are mounted using the insulating THERMO1 pads with the nylon screws. Mount the prewired front panel components, as in Figure 15-5.
11. Mount transformer T1 via an 8-inch tie wrap. Note the cores of T1 are wrapped with a single turn of #18 bus wire and this is connected to the ground lug electrically grounding the core.
12. Mount transformer T2 using a piece of double-sided foam tape or glue it in place.
13. Mount the remaining hardware, wiring lugs, and so on.
14. Proceed to wire everything as shown in Figure 15-10. Use twist pairs where noted or tie-wrap to neaten its appearance (see Figure 15-11).
15. Double-check the wiring for any obvious errors. You should have a finished assembly resembling Figure 15-12. The unit is now ready for the basic pretest.

Pretesting the Driver Section

This step will require basic electronic laboratory equipment including a 60 MHz oscilloscope

1. Assembly the test jig as shown in Chapter 14 Figure 14-8. This fixture is a very useful for any 115 VAC project up to 300 watts.

Caution: The circuit commonly noted as −RAIL is electrically above ground by over 150 volts. It is strongly recommended that you obtain a 200-watt isolation transformer before proceeding and that you test this or similar direct-line-powered AC circuits. Experienced people working on dry, wooden floors may choose to unground their test equipment. This still can be a dangerous shock hazard!

---

2. Connect the scope to the test points as noted in the Figure 15-2 schematic or as shown in Figure 15-4. The lead of R8 is shown connected to the junction of the drain and the source of Q1 and Q2 respectively.
3. Short out the output leads.

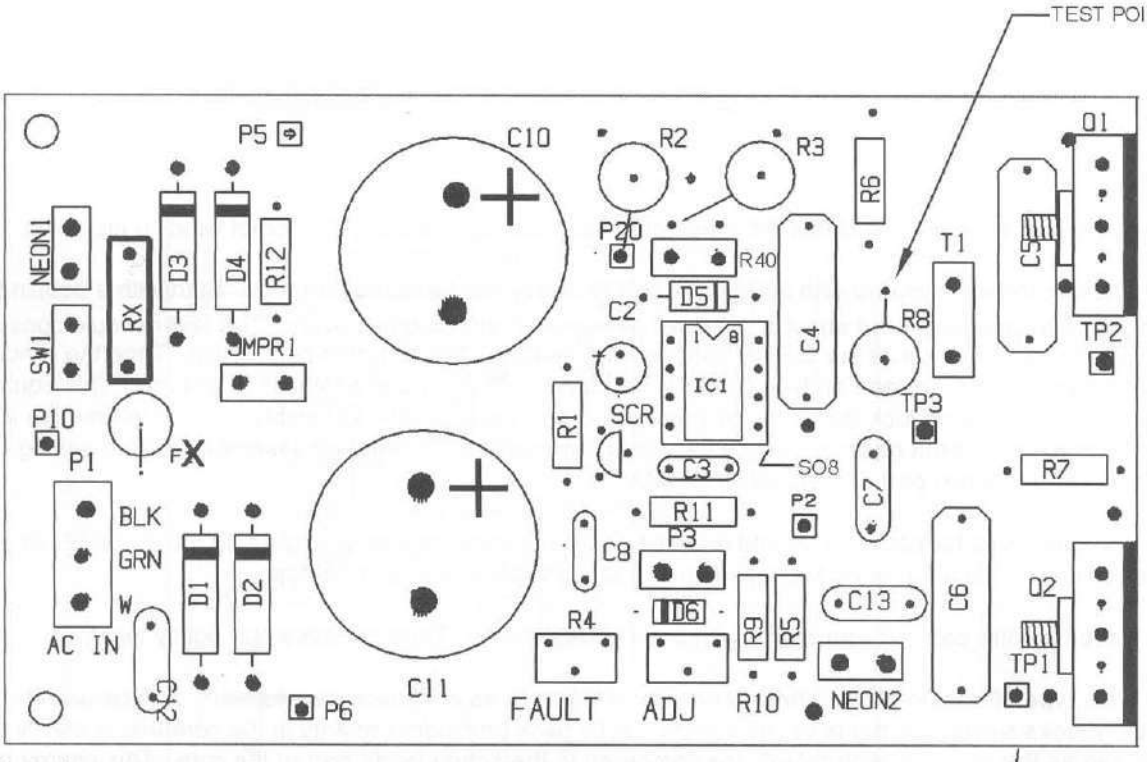

1. Black dots are connections points to external leads as shown figure 15-5

2. The PC board as shown is used in several projects and may not use all the components as indicated.

3. This circuit uses a 8 pin socket for IC1 as it is prone to failing if there are circuit faults

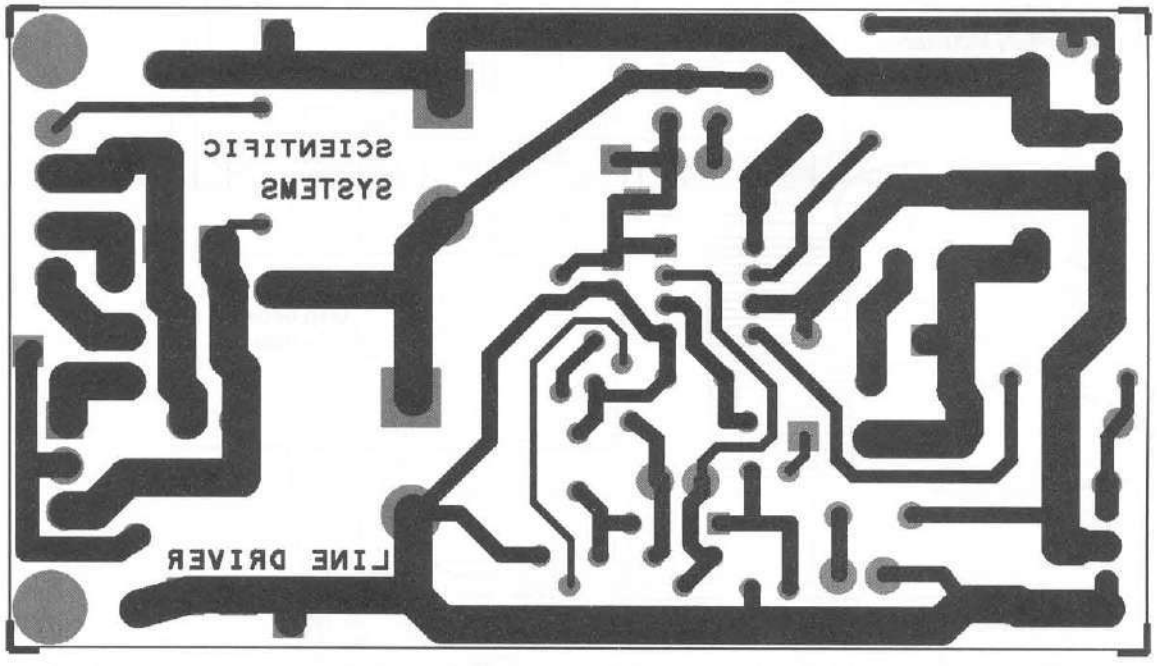

Assembly of the board is shown using a printed circuit board available through www.amazing1.com Builders may use a vector board and use the component leads to duplicate the foil traces as shown.

Figure 15-3 *Assembly of the circuit board*

The special ferrite transformer used in this project is available ready to use and is listed on table 15-1. The transformer is designed with a certain amount of leakage reactance between the primary and secondary winding to allow limited short circuit current. This approach allows charging capacitors without the use of lossy resistors. While this is an advantage in circuit protection is has the disadvantage of requiring transistor switches (FETS) that now must switch the reactive leakage current in addition to the real load current. We show our circuit using high current switches that alleviate this problem.

The design specifications are shown for those advanced builders desiring to attempt winding their own.

1. The secondary is wound with 3500 turns of #39 heavy insulated magnet wire. Start with a bobbin that will fit over the cores and wind about a ¾" layer evenly and without cross overs. The layer should consist of about 200 turns. Note to exit the start of your winding as this is the common connection. Tape the winding using 2 mil polypropylene tape and wind the second layer until you have a total of 3500 turns. This equates out to 18 layers!! (good luck doing this by hand) You now must pot the assembly and this will require a cup to hold the windings and out gassing using a vacuum pump on both the winding assembly and the potting material. We use a two part silicon rubber GE#627.

2. The primary is far easier to do and requires another bobbin now only winding 80 turns of #22 Litz high frequency wire. This will require two layers and is taped together using mylar tape.

3. Assemble the core set and space with 5 mil (.005)" shims. Tape the assembly tightly together.

Note: This type of transformer is often incorrectly referred to as a "flyback transformer". A flyback unit physically looks similar but this is where it ends. A fly back unit stores energy in the core that is mainly across the air gap as this is a very high reluctance compared to the actual ferrite part of the core. This energy builds up as long as the transistor is on and then "flies back" when the transistor switches off.

Measured parameters:

Open circuit primary inductance.....5.5 mH
short circuit primary inductance..... 1 mH
Open circuit secondary inductance.....10 H
Short circuit secondary inductance..... 2 H

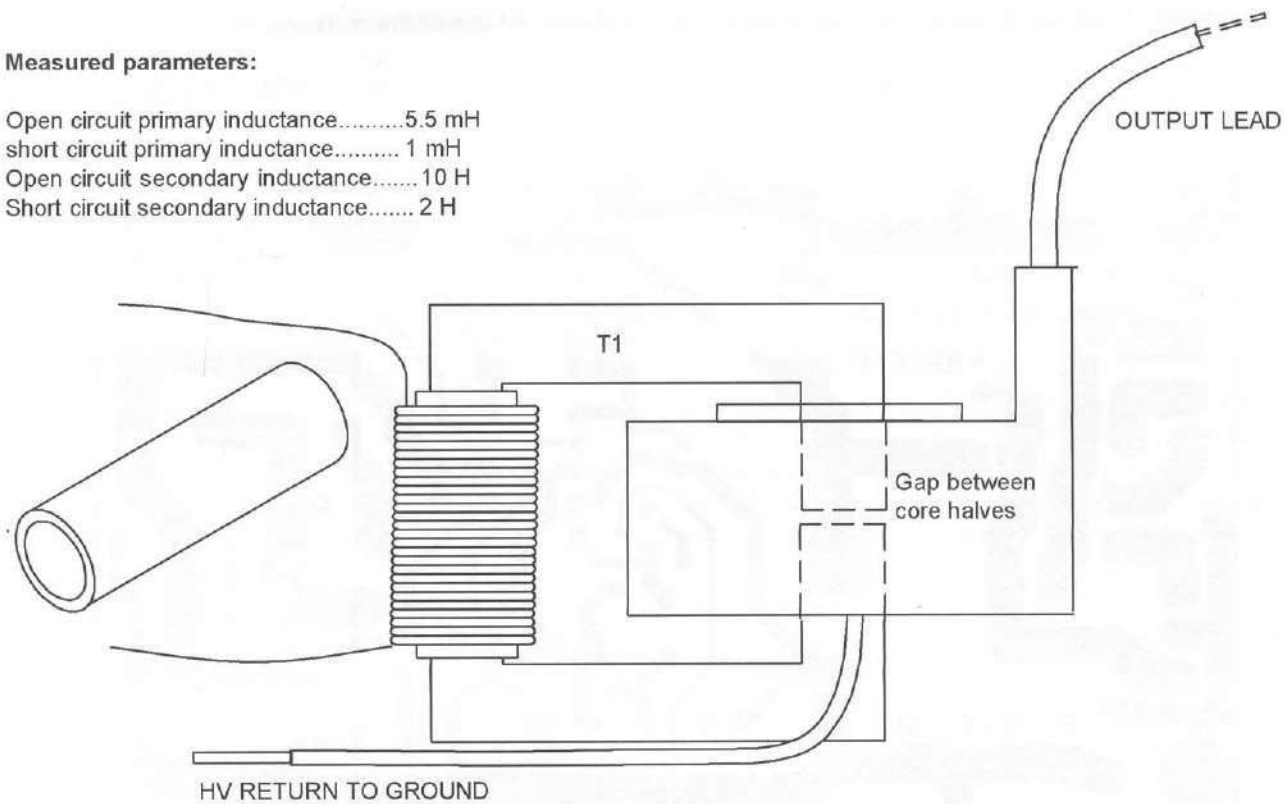

*#18 solid magnet wire can be used however high frequency LITZ wire will give a slight improvement. You can make this wire by obtaining 6 pieces of #26 magnet wire and twist together as a single wire.

Figure 15-4 *Assembly of transformer*

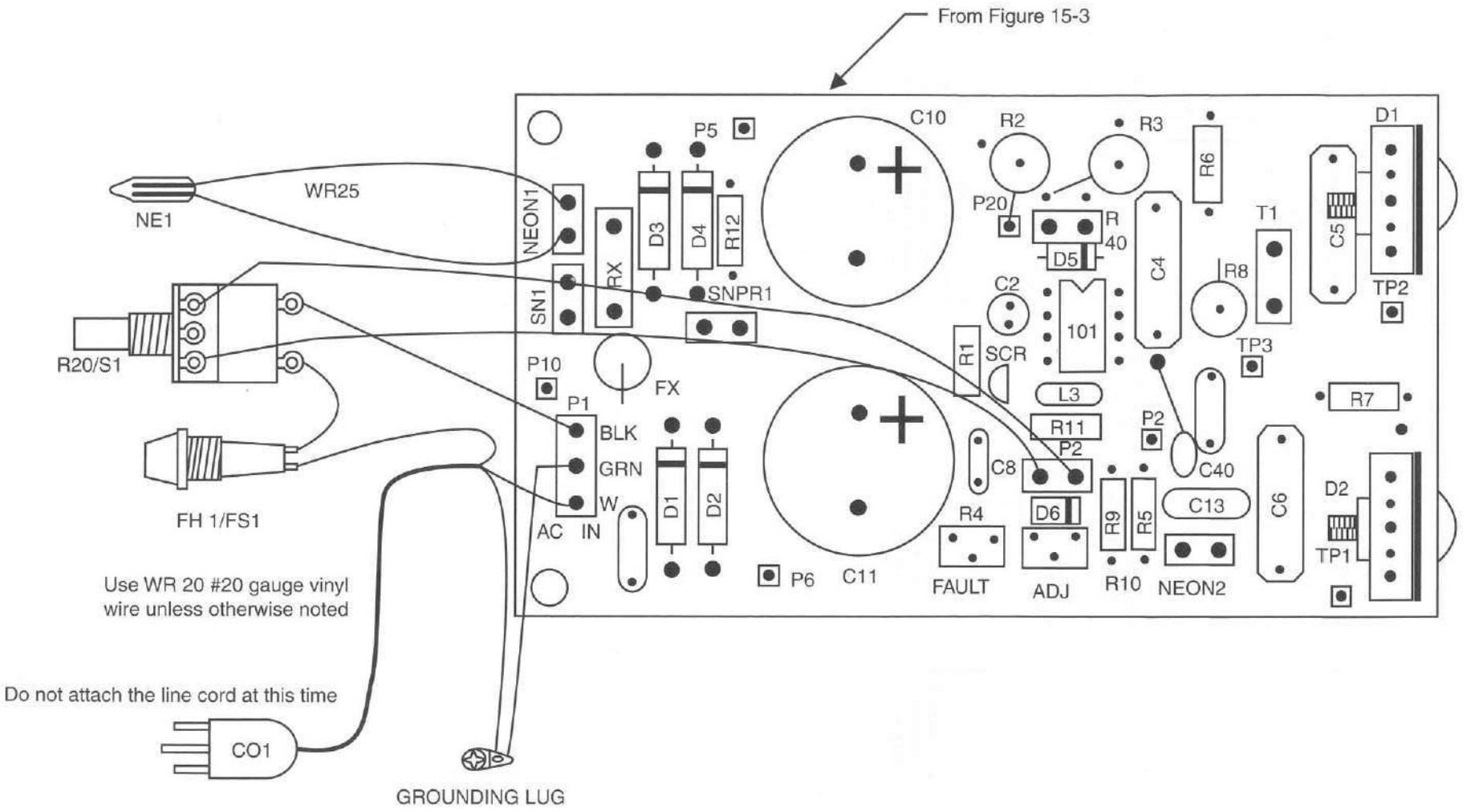

Figure 15-5 *External wiring*

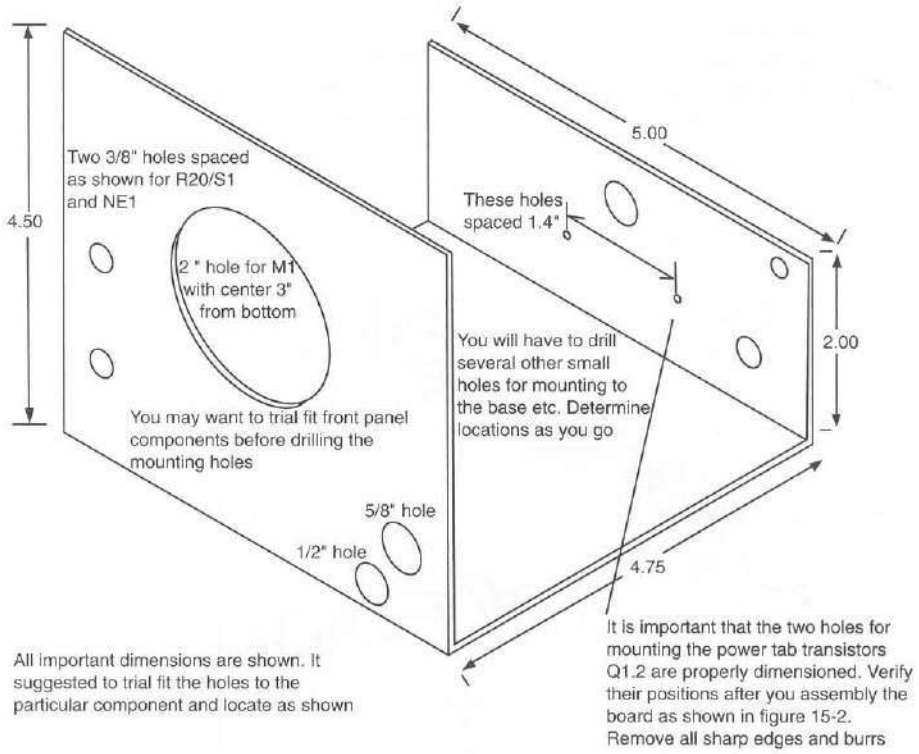

Figure 15-6 *Chassis fabrication*

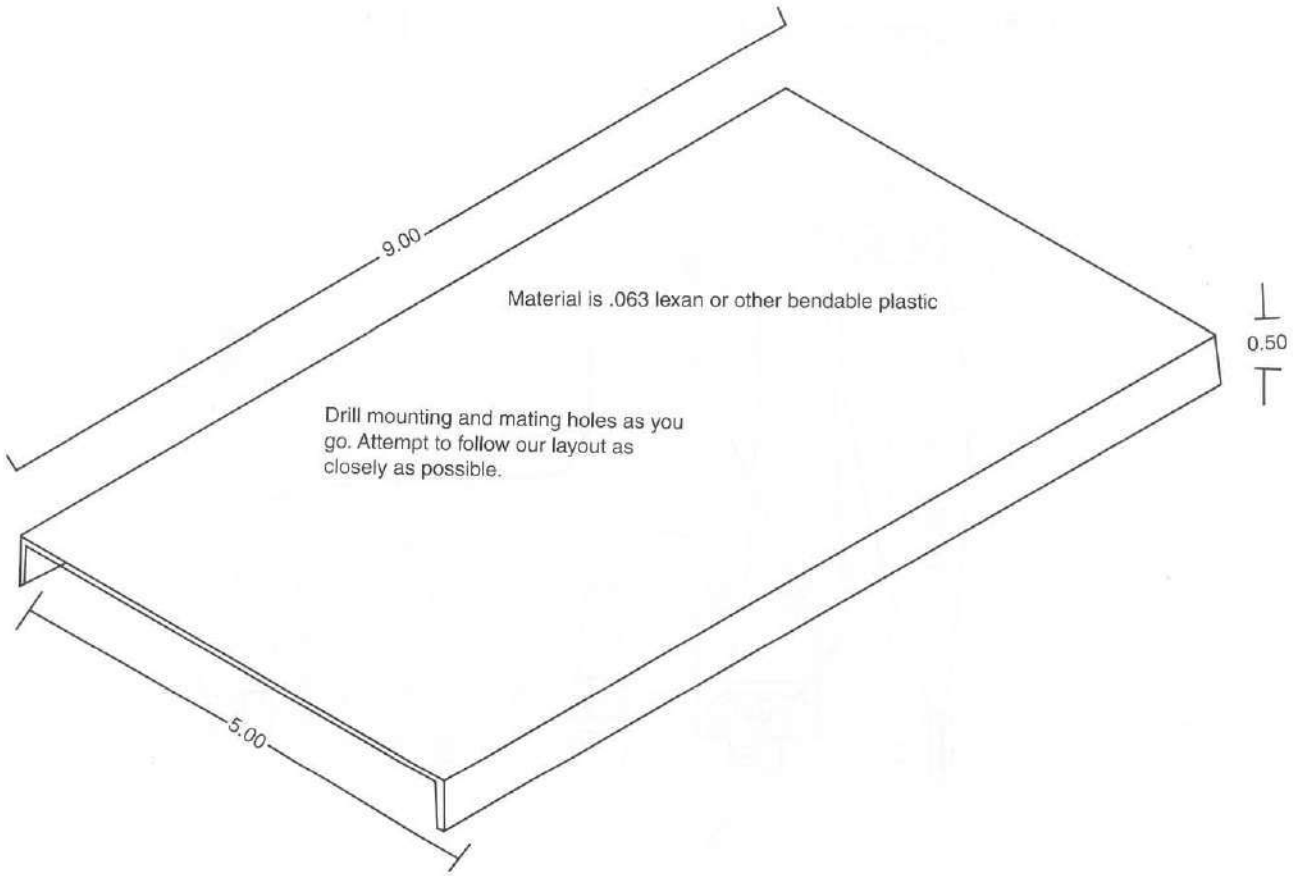

Figure 15-7 *Plastic base fabrication*

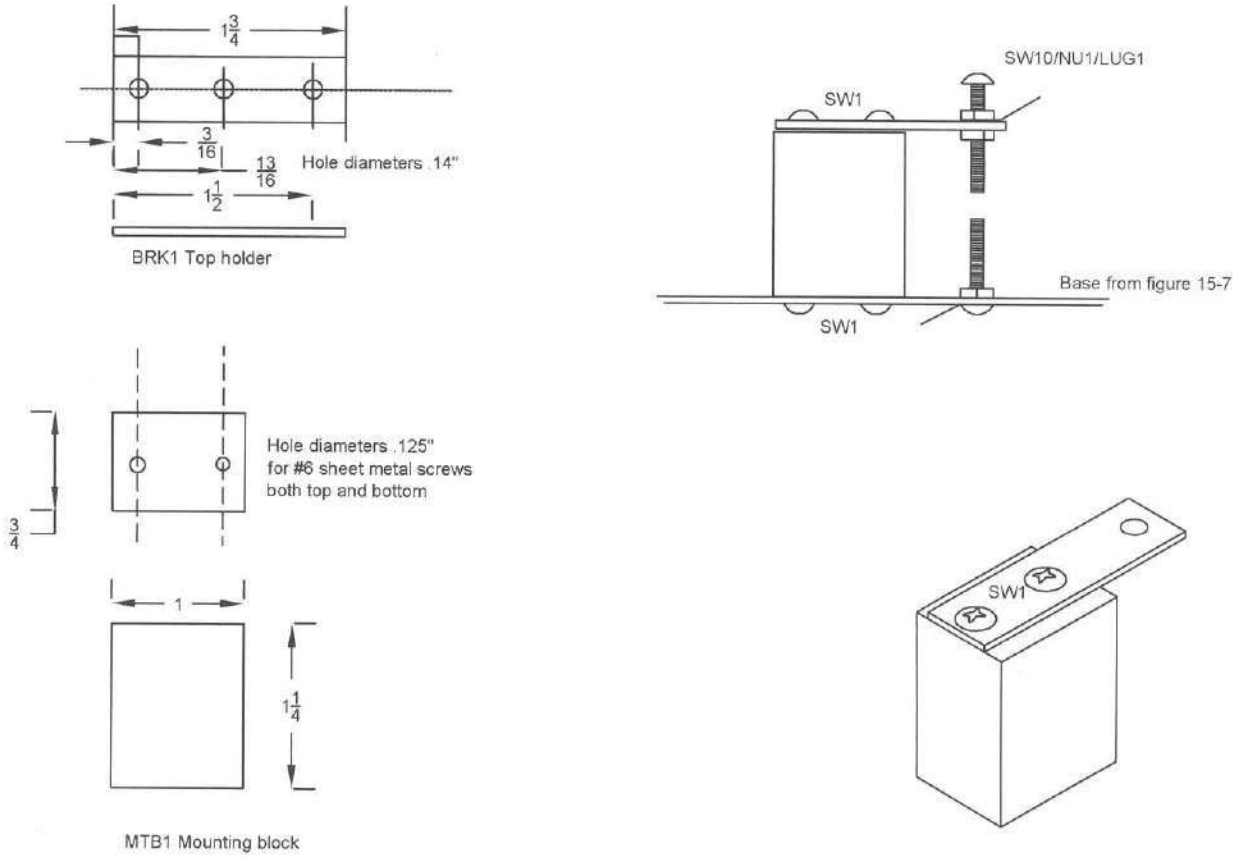

Figure 15-8 *Creating the shutdown switch*

4. Verify the main power switch S1 is off and insert a 2-amp fuse into FH1. Connect CO1 to the female end of the cord on the test jig and adjust both trimpots to midrange. Verify the test jig is not shorting the ballast lamp and plug the jig into the output of the isolation transformer. Quickly turn on S1 and note NEON1 lighting and the ballast lamp not lighting. If it brightly lights up, you must troubleshoot and find your error before proceeding. Otherwise, note a picture-perfect square wave on the scope with the lamp only dimly lighting. Adjust R21 full clockwise and adjust trimpot R10 for an 80-usec pulse period. This corresponds to 12.5 kHz. Experienced builders may wish to monitor the current to T1 using a current probe attachment to the scope. This waveshape should be another picture-perfect saw tooth of 8 amps maximum. This is a reactive current and is not reflected as an input current due to the phase angle.
5. Turn the unit off and unshort the output leads. Adjust the spark switch screws 1/8 of an inch.
6. Turn on R21/S1 and very quickly rotate clockwise, noting the unit shutting down as apparent by the absence of the waveshape at the test point. If this does not occur instantly, you will need to readjust the switch gap or trimpot R4 clockwise until the shutdown activates. If it does not, you must troubleshoot the circuit. This completes the driver section of this system.

Assembly of the Multiplier Section

Assembly of this section requires solder joints to be large, smooth, and globular. This is contrary to normal soldering practices but is necessary to reduce hv leakage.

1. Fabricate the MULTIBOARD board and two BRK2 brackets, as shown in Figure 15-13.
2. Assemble the diodes and components as shown in Figure 15-14, but do not solder at

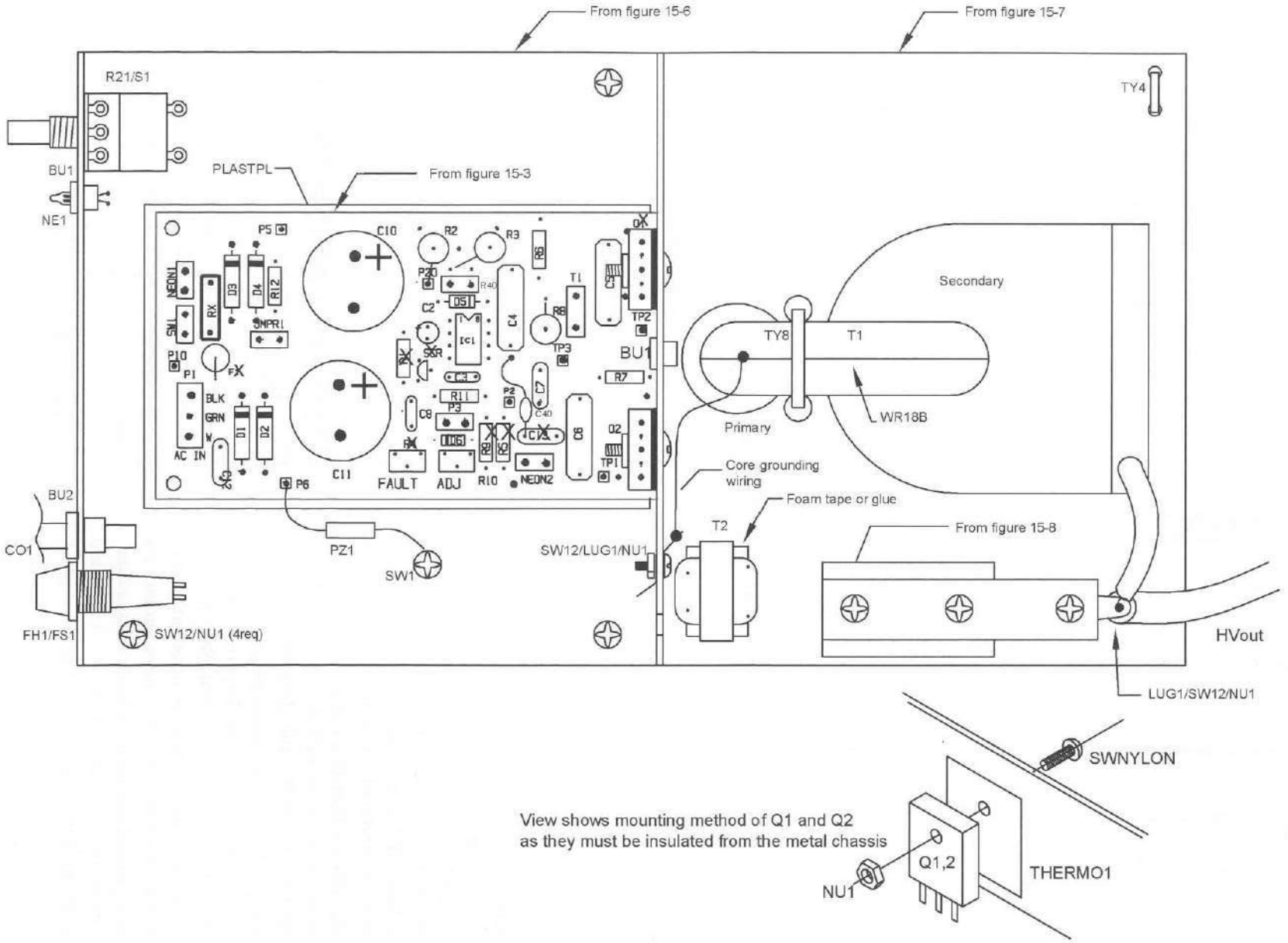

Figure 15-9 *Parts layout to driver*

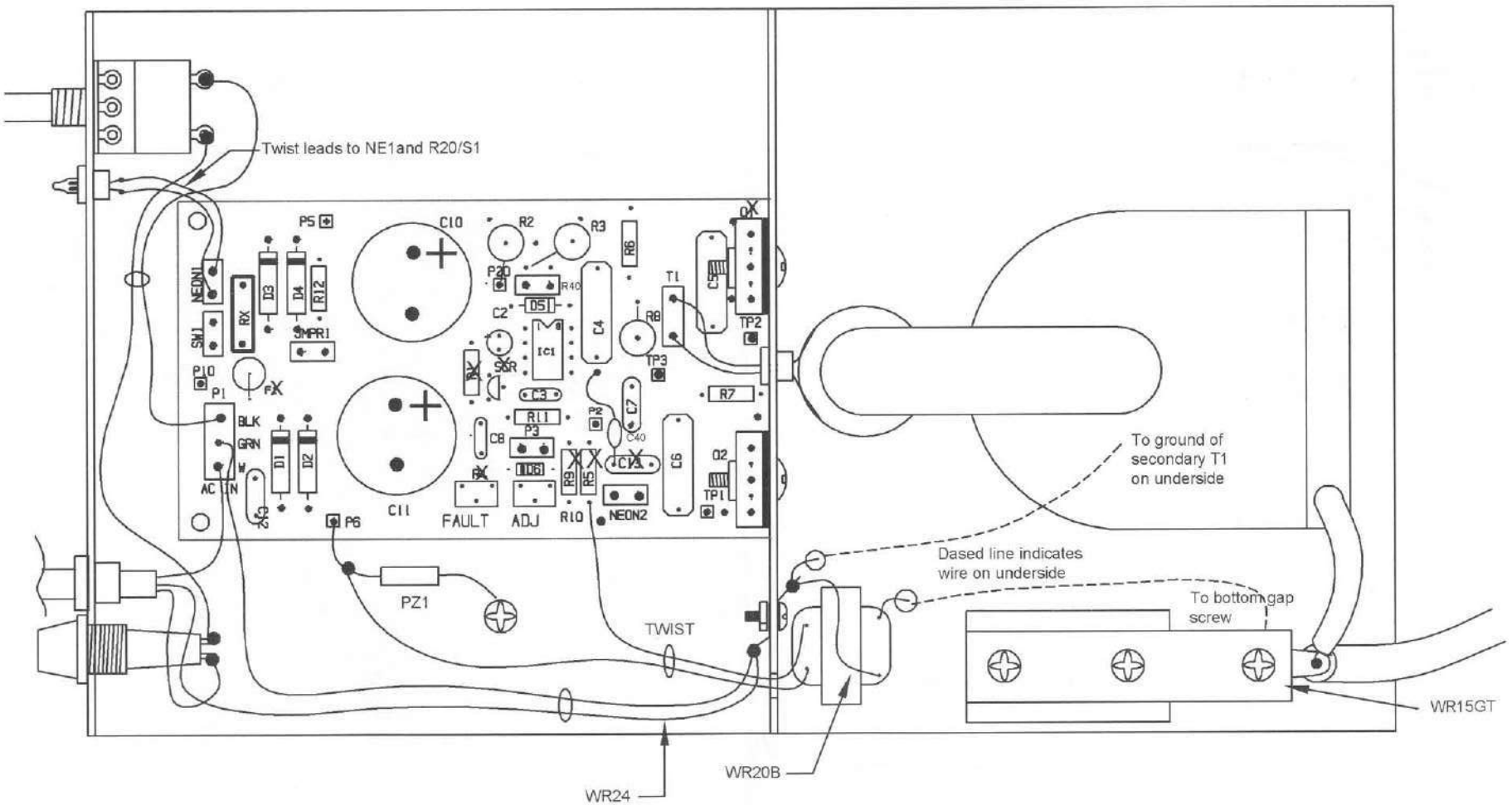

Figure 15-10 *Primary wiring aid*

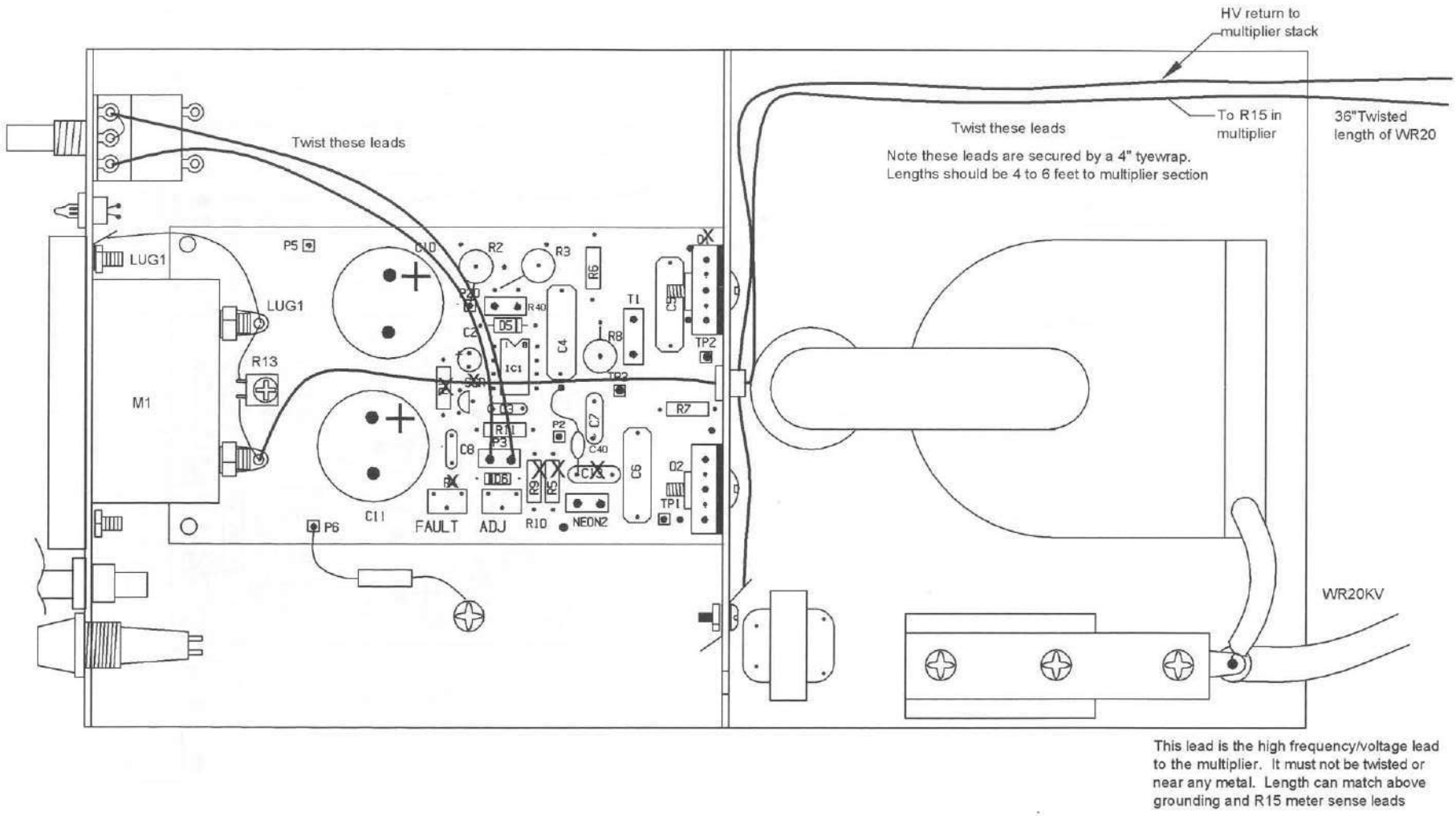

Figure 15-11 *Secondary wiring aid*

this time. Assemble the resistor tube for R17-20 as shown.

3. Mount the capacitors C14 through C21 and the remaining components as shown in Figure 15-15. Insert the BAF1 baffle plate to insulate and separate the left and right rows.

   Proceed to solder all the joints, noting that the capacitor and diode connections should be smooth, round balls of solder 1/8 to 3/16 of an inch wide. This may be tricky with all the leads but should be done to avoid leakage, especially the last four capacitors.

4. Sleeve resistor R14 into a plastic sleeve, as shown in Figure 15-16.

5. The final assembly is shown in Figure 15-17. Note you have a choice of an output lead or a spherical terminal.

Final Testing

This step requires basic electronic laboratory equipment including a 60 MHz oscilloscope along with a high-voltage meter with a 40 kilovolt dc rating. You will need a high-voltage load resistor to verify output power capabilities.

1. Connect the driver and multiplier sections together and separate them by at least 3 feet. Keep the high-voltage wire from the driver away from other conductive objects. Follow Figure 15-11 for the driver and Figure 15-17 for the multiplier interconnecting wiring.

2. Obtain a load resistor of around 10 megohms of at least 100 watts. This resistor must be able to support at least 50,000 volts. Our laboratory load resistor consists of 180 47k, 1-watt resistors connected in series and then inserted into

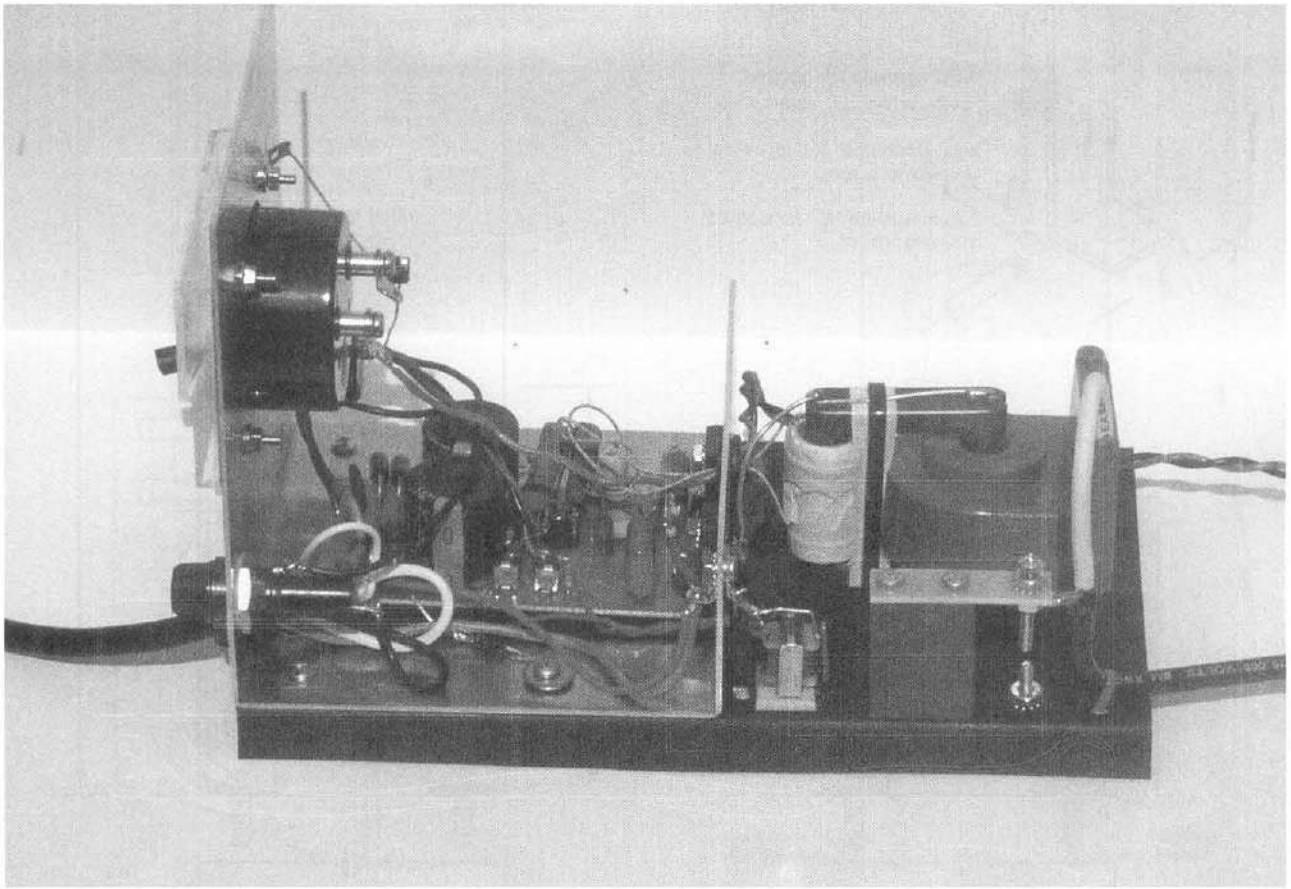

Figure 15-12 *Driver section*

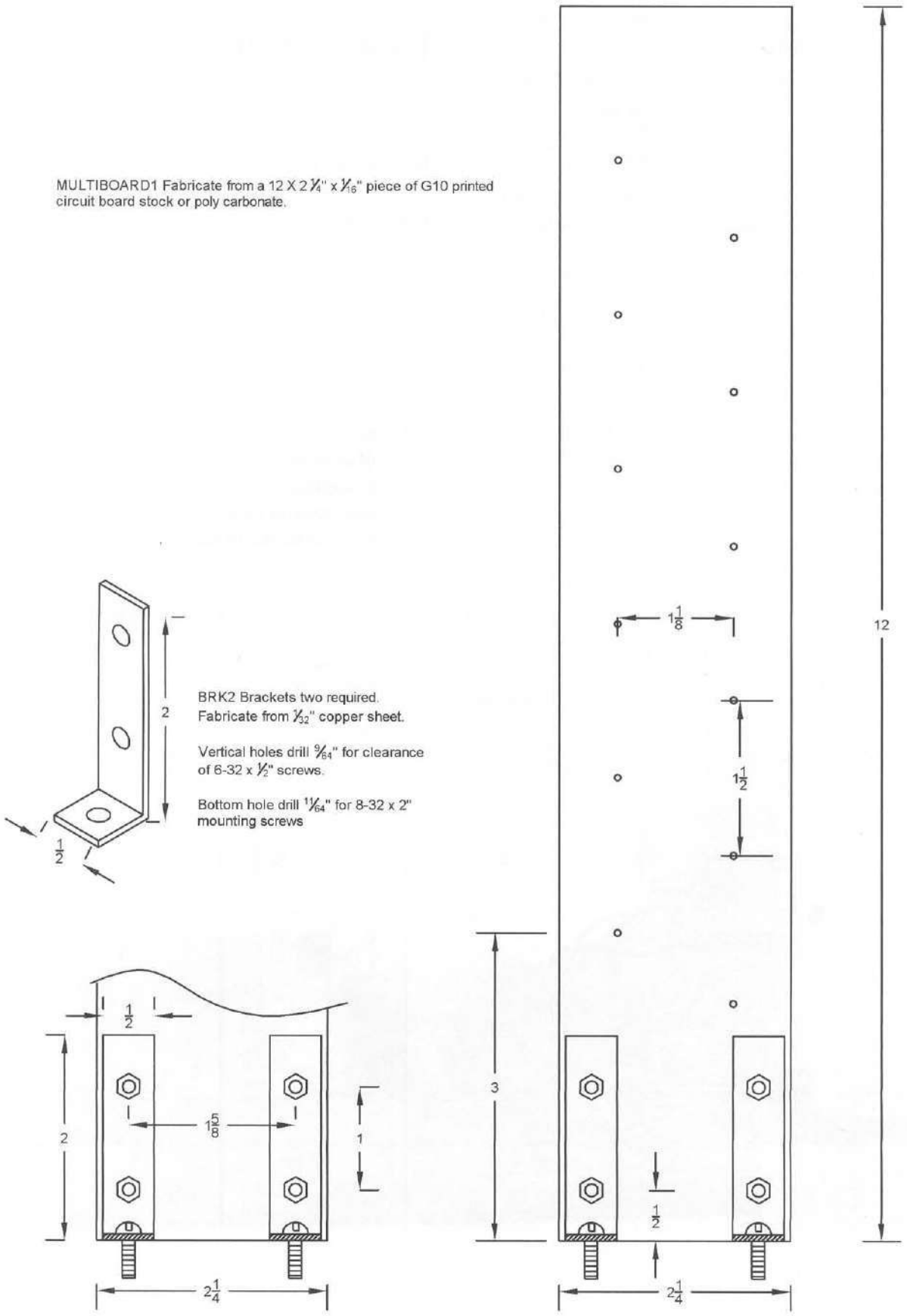

Figure 15-13 *Creating the multiplier board*

some polyethylene tubing, along with the terminating high-voltage leads. The tubing is then coiled, maintaining adequate clearance of the terminating leads. This is a very tedious assembly but works well for powers up to 300 watts at 100 kilovolts. Connect the load to the output and common leads.

3. Assuming that the driver is properly functioning, proceed to apply power and slowly turn the power control pot R21 to full clockwise, noting a line current draw of about 2 amps. Very carefully measure around 35 kilovolts at the output using a 40-kilovolt probe such as an HV44 or similar. The load resistors should start to get warm.

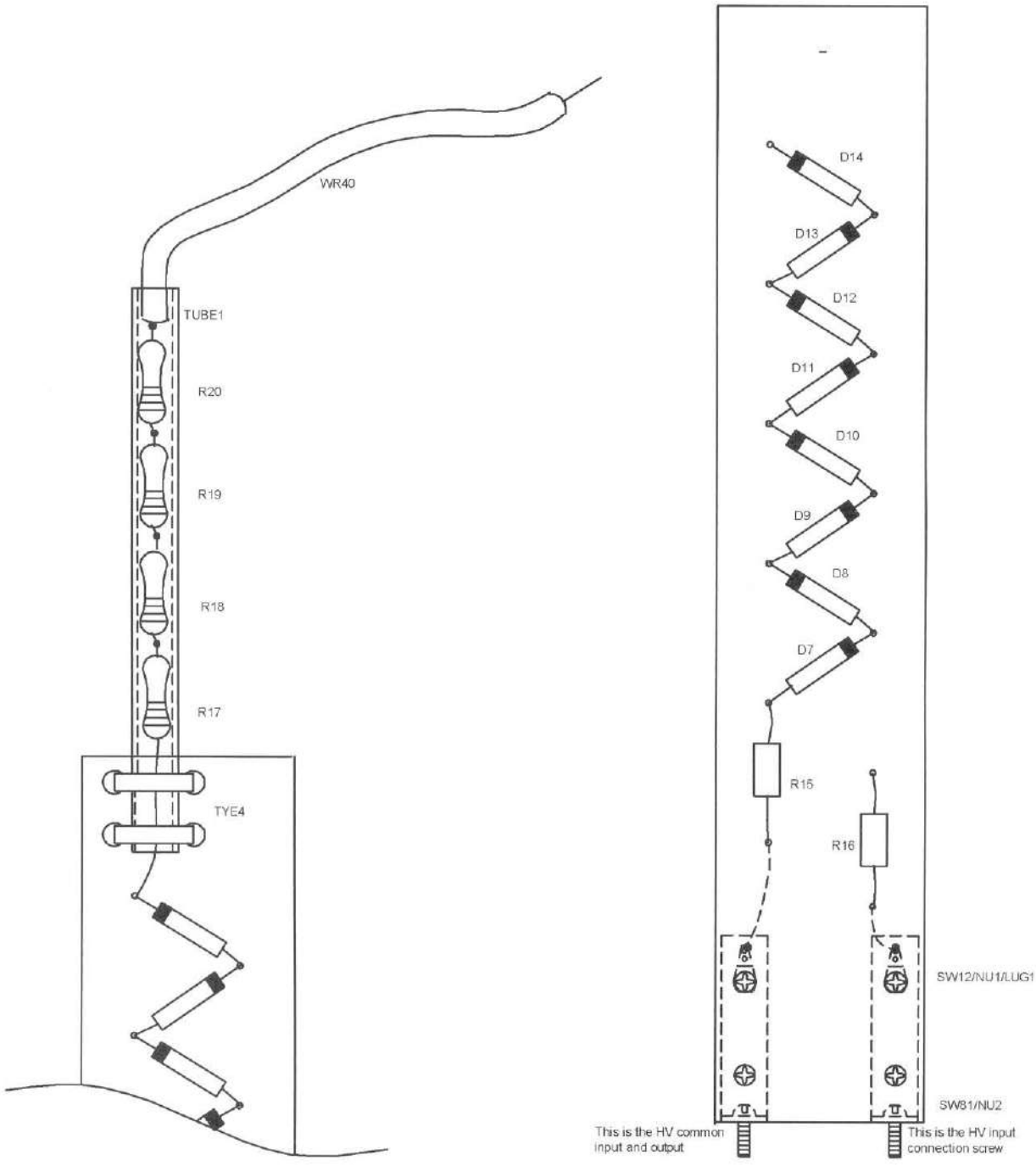

Figure 15-14 *Diode layout and wiring*

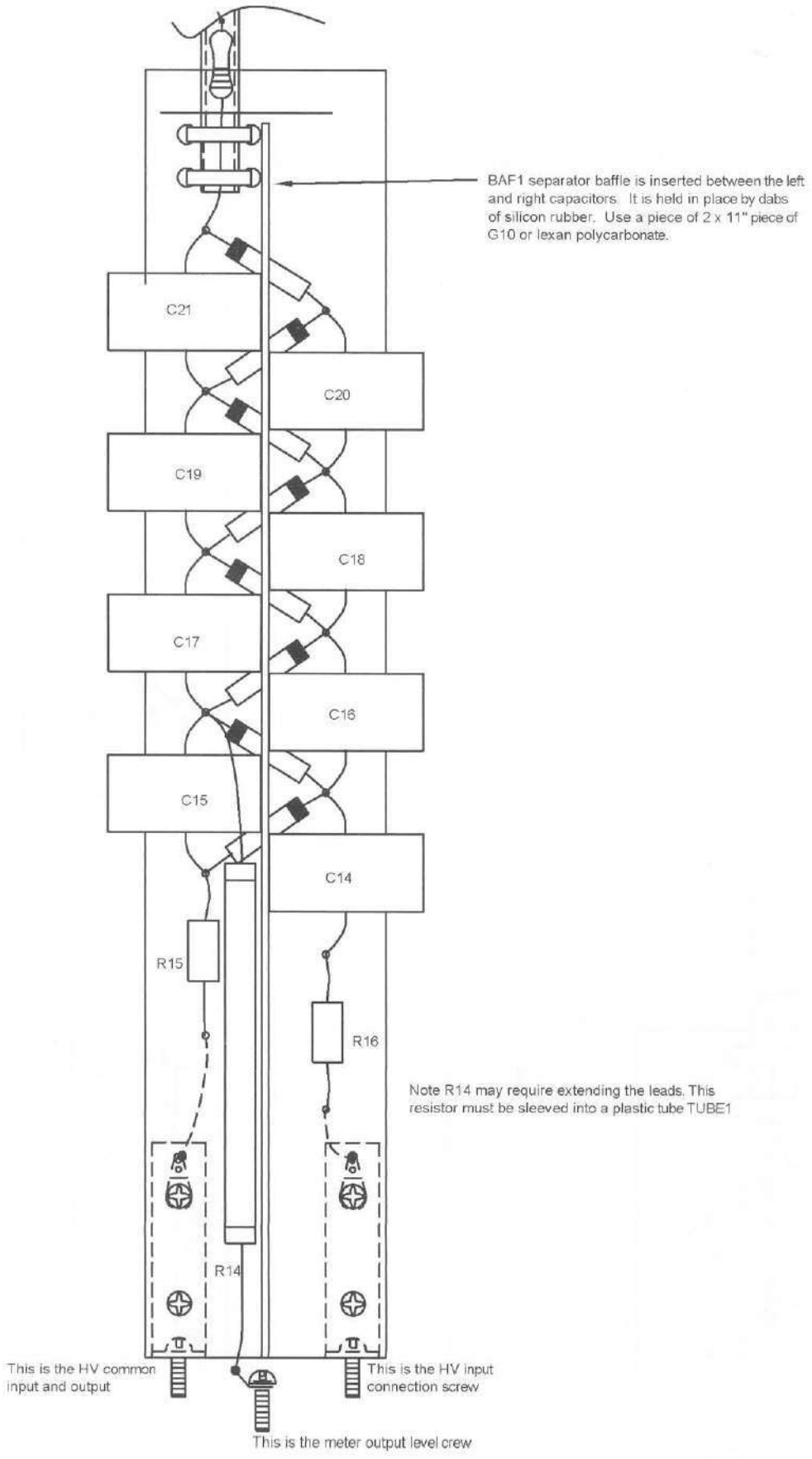

Figure 15-15 *Mount capacitors and remaining components as shown here.*

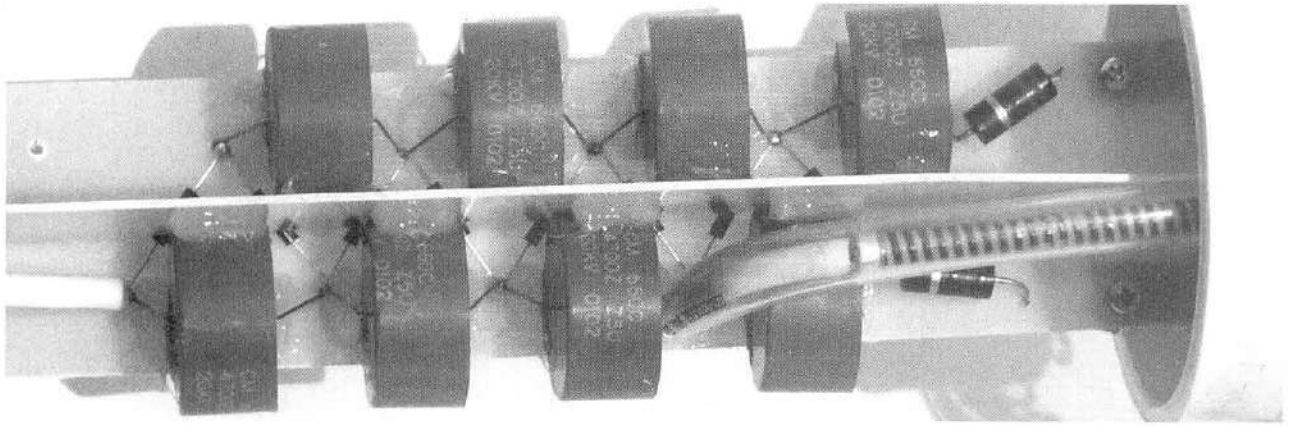

Figure 15-16 *Multiplier internal photo*

4. Allow to it run for several minutes and note that Q1 and Q2 are only slightly warm to the touch.
5. Reverify the operation of the shutdown circuit to prevent damage to the circuit components in the event of over-volting.

Applications

This unit is excellent to use for powering large anti-gravity lifters because it is not damaged by short-circuiting the output. It can also be used for charging capacitors up to 50,000 volts or as a voltage source with a load resistor of 20 megohms. The charging current is 4 to 5 milliamps and charges as a current source.

DANGER! Improper contact or use of high-energy capacitors can result in death by electrocution or injury due to explosive discharges.

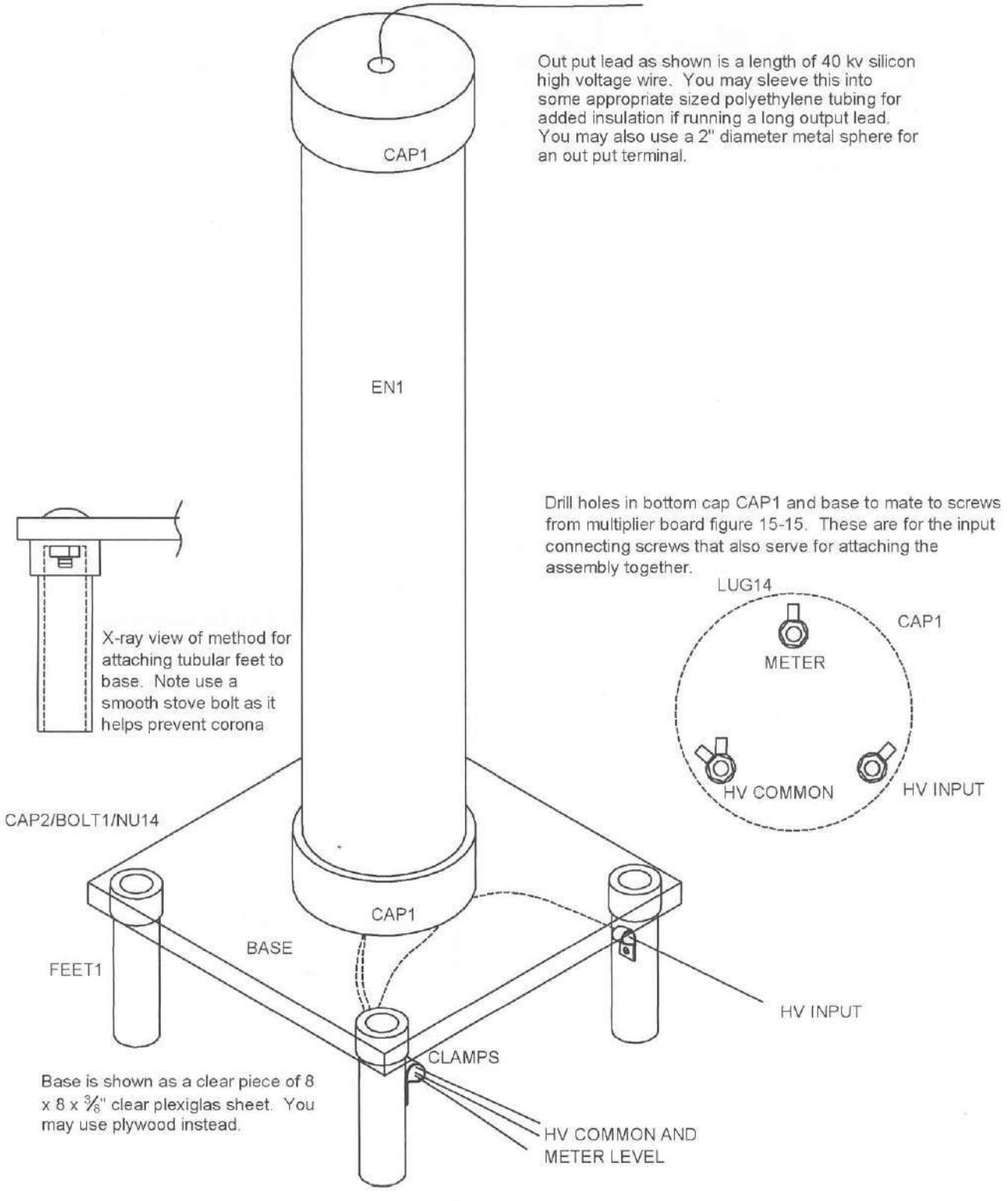

Figure 15-17 *Final assembly*

Table 15-1 50-Kilovolt Power Supply

Ref. #	Description	DB Part #
R1	100-ohm, 1/4-watt resistor (br-blk-br)	
R2, 3	Two 18K, 3-watt resistors	
R4, 13	Two 2K vertical trimmers	
R6, 7	Two 15 1/4-watt resistors (br-grn-blk)	
R8	10-ohm, 3-watt metal oxide resistor	
R10	5K vertical trimmer	
R5, 11	Two 1K 1/4-watt resistors (br-blk-red)	
R9, 12	Two 100K 1/4-watt resistors (br-blk-yel)	(KC006-LND)
Rth	limiter 5-amp in-rush	
R15, 16	Two 12-ohm, 2-watt carbon resistors (br-red-blk)	
R14	100 meg, 20-kilovolt tiger resistor	
R17–20	4 100K, 2-watt ceramic resistor	DB# 100KCER
R21/S1	10K pot and 115 VAC switch	
C2	10-microfarad, 50-volt vertical electrolytic capacitor	
C3	.01-microfarad, 50-volt plastic capacitor (103)	
C4	.1-microfarad, 600-volt plastic capacitor	
C5, 6	Two 1.5-microfarad, 400-volt metal polyester capacitors	
C7	.0015-microfarad, 600-volt polypropylene capacitor	
C8	.47-microfarad, 50-volt plastic capacitor	
C10, 11	Two 200- to 800-microfarad, 200-volt vertical electrolytic capacitors	
C12, 13	Two .01-microfarad, 2-kilovolt disc capacitor	
C14–21	Eight .0047-microfarad, 20-kilovolt ceramic capacitors	DB#.0047/20 KV
PZ1	420-volt suppressor	
D1, D2, D3, D4	Four 1,000-volt, 3-amp rectifier (1N5408)	
D5	1-kilovolt, 1-amp fast diode (1N4937)	
D6	1N914 small-signal diode	
D7–14	Eight 30-kilovolt, 5-milliamp fast-recovery diodes	DB# 3VG30
SCR	EC103 A, 12 uamp sensitive gate *silicon-controlled rectifier* (SCR)	
Q1, 2	IRFP450/460 *metal-oxide-semiconductor field effect transistor* (MOSFET)	
IC1	IR2153 half-bridge driver	
T1	High-volt transformer assembled as shown in Figure 15-4	DB# FLYPVM
T2	8/500-ohm audio transformer	
SO8	Eight-pin DIP socket	
NE1	Neon indicator bulb with leads	
FH1	Fuse holder panel mount	
FUS1	3-amp slow blow 3AG fuse	
METER	50 uamp, 3-panel meter	DB# METER50L
CO1	Three-wire line cord	
LUG1	Eight #6 solder lugs	
LUG14	Three 1/4-20 lugs	
THERM1	Two thermo mounting pads for Q1 and Q2	
PCLINE	*Printed circuit board* (PCB)	DB# PCLINE
BU38	Three 3/8-inch plastic bushings	
BU58CL	5/8-inch clamp bushing for cord CO1	
WR15GTO	4 feet of 15-kilovolt GTO flexible wire	
WR40KV	12 inches of 40-kilovolt high-voltage silicon wire	DB# WR40KV
WR20	10 feet of #20 vinyl hookup wire	
WR24	12 inches of # 24 vinyl hookup wire	
WR20B	12 inches of # 20 bus wire	
WR18B	24 inches of #18 bus wire	

Table 15-1 *continued*

Fabrication

Ref. #	*Description*	*DB Part #*
CHASSIS	Chassis created from .065-inch aluminum as per Figure 15-6	
COVER	Cover created from plastic sheet to fit chassis	
BASEPLATE	Base plate created from .065-inch Lexan per Figure 15-7	
BRK1	Bracket created from .035-inch copper per Figure 15-8	
BRK2	Two brackets created from .035-inch copper per Figure 15-13	
MTB1	Mounting block created from .75-inch PVC plastic	
PLASTPL	4.5 × 2.5 piece of insulating plastic, shown in Figure 15-9	
MULTIBOARD1	Multiplier board created from .065-inch Lexan per Figure 15-13	
BASE	Base created from 8 × 8 × 3/8-inch Plexiglas per Figure 15-17	
BAF1	Baffle separator created from .065-inch Lexan per Figure 15-15, available from a hardware store	
SW1	Five #6 1/4-inch sheet metal screws for cover and MTB1	
SWNYLON	Two 6-32 1/2-inch nylon screws	
SW12	Ten 6-32 1/2-inch screws	
SW10	Two 6-32 × 1-inch screws	
SW81	Three 8-32 × 2-inch screws	
BOLT1	Four 1/4-20 × 1 1/2-inch stove bolts	
NU1	Sixteen 6-32 keep nuts	
NU2	Six 8-32 keep nuts	
NU14	Four 14-20 hex nuts	
CAP1	Two 3-inch PVC flat caps (GENOVA# 70153)	
CAP2	Four 1/2-inch PVC flat caps (GENOVA# 30155)	
FEET1	Four pieces of 1/2 × 3-inch PVC tubing	
EN1	3 × 15-inch PVC tubing	
TUBE1	10 inches of 3/8 ID × 1/2 OD flexible plastic tubing	

Chapter Sixteen

Magnetic High-Impact Cannon

This very advanced project (shown in Figure 16-1) is intended for the experienced experimenter and researcher in the field of high-voltage and high-energy circuitry. The magnetic cannon accelerates a projectile at high velocities with considerable kinetic energy; this is accomplished strictly from a magnetic pulse. Not only is this project a dangerous electrical device, it is also kinetically hazardous, as the accelerated projectile can cause serious injury and even death. The same consideration and respect given to a firearm must be given to this project. A video demonstration of this device blasting large holes through a wall can be seen at www.amazing1.com.

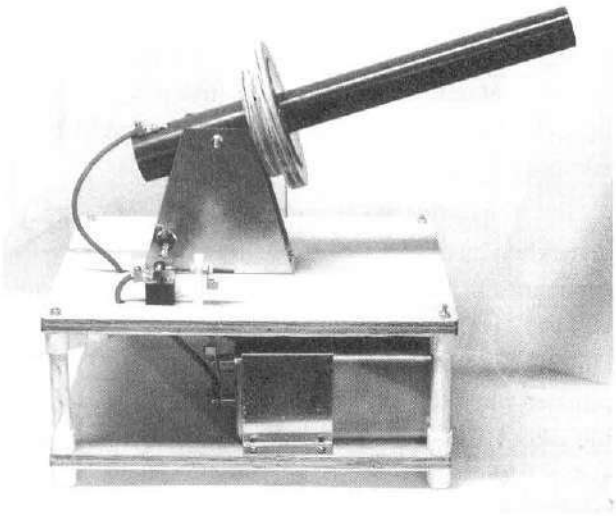

Figure 16-1 *The magnetic cannon*

Under the correct supervision, the magnetic cannon can provide a high-action science project demonstrating several important electrical laws that involve electromagnetic reactions. Lenz's law and the Lorentz JXB forces are clearly utilized in this device. The system as shown can provide the experienced hobbyist hours of fun and entertainment by experimenting with its effect (its impact) on various objects.

This is an advanced level project requiring electronic skills and high-voltage experience. Expect to spend $300 to $500 unless you have access to the surplus market. All parts are readily available and any specialized parts are available through Information Unlimited (www.amazing1.com) and are listed in the parts list at the end of the chapter.

Theory of Operation

A nonmagnetic conductor such as aluminum is placed in a time-variant magnetic field. Induced currents in the aluminum produce currents that, in turn, produce opposing magnetic fields thereby causing a moment of acceleration of the aluminum piece. In this project the aluminum piece is in the form of a large flat washer that is the projectile. The aluminum projectile has a hole in its center with a mandrel guide to keep it traveling in a straight line.

The heart of this project is the accelerating coil. It is what couples the energy (the electrical current) to the aluminum ring (the projectile). Optimum efficiency is dependent on the coupling to achieve maximum projectile kinetic energy. This requires a minimal proximity of the projectile to the coil along with minimal air gaps (such as the spacing between the wires of the coil and the geometry of the coil as related to the dimensional format of the projectile). Also the inductive value of the coil is related to the storage capacity to provide the current rise over a time period that is dependent on the physical parameters of the projectile. The associated second-order differential equations that mathematically determine these parameters are beyond the scope of this material. Although the mathematical purist will find a deviation from maximum efficiency by using different materials, practically speaking, there are materials of different sizes and materials that offer a cost-effective compromise. An example is the use of square magnetic wire in place of conventional round stock wire. Using square magnetic wire for the coil, when properly wound, will provide more kinetic energy to the projectile due to reduced air space (reluctance); however it is quite difficult to wind and usually requires purchasing a significant amount at a healthy price.

The shape and timing parameters of the coil-magnetizing pulse must be related to the projectile to achieve optimum efficiency. A current rise that is too fast will cause slippage (magnetic cavitation). Note that one definite disadvantage of this method of acceleration is that the projectile is influenced over a very short distance. Velocity, now being the square root of the acceleration times the distance, is limited. To achieve high resultant velocities requires a very high moment of acceleration. Projectiles using conventional explosives current detonators and boosters could be prone to sympathetic initiation by these high g accelerating forces at the time of launching.

Circuit Theory

This project as shown in Figure 16-2 is constructed operating from 115 vac household current. It also can be built to operate from 12 volts or built-in batteries.

A high-voltage current-limited 60 Hz transformer (T30) steps up the 115 vac to 6,500 vac and is rectified by high-voltage diodes (D31 through D34). DC current now charges the energy storage capacitors (C30) through the isolation resistor (R30) to a programmable value, as selected by the operator. It is this stored energy that is discharged into the accelerator coil (L1) as it is switched by the spark gap (GAP1). Once switched into the coil, the now rapidly rising current wave induces a current into the aluminum ring projectile (PROJ1). It is this induced current that now generates a very high magnetic moment and repels the initial field in the accelerator coil, causing a moment of intense accelerative forces. Those not familiar with this concept often ask why an aluminum ring? The answer is that a magnetic material would now be attracted and thus would neutralize the repulsion.

The initializing of the circuit commences by turning on the key switch (S2). This switch is intended to keep unauthorized personnel from powering up the system. The key switch controls 12 volts of DC power necessary to energize the relay (RE1), with normally open contacts controlling power to the high-voltage transformer (T30).

The controlling system, as shown, consists of momentary pushbutton switches that start the charging action (S4) and can stop this action via switch (S5). Triggering the momentary pushbutton switch (S3) supplies power to the trigger module (TRIG10) and firing trigger gap (GAP2), thereby initiating the main gap GAP2 and switching the energy from the storage capacitors C30 into the accelerator coil L1. Charging voltage to C30 is controlled by the potentiometer R14. Once set, the voltage will maintain its preset level until triggered or readjusted. Meter M1 indicates the charge voltage and is calibrated by the trimpot (R16).

The transformer (T1) supplies 12 volts of AC that is rectified by diodes (D1 through D4), filtered by capacitor C4, and regulated by zener diodes (Z1 and Z2) to 12 volts dc in order to power the control circuits. The indicator *light-emitting diode* (LED1) illuminates when the key switch is energized. The second indicator LED (LED2) illuminates when charging of C30 is taking place. A buzzer (BUZ1) sounds whenever there is a charge voltage on C30. This is a safety

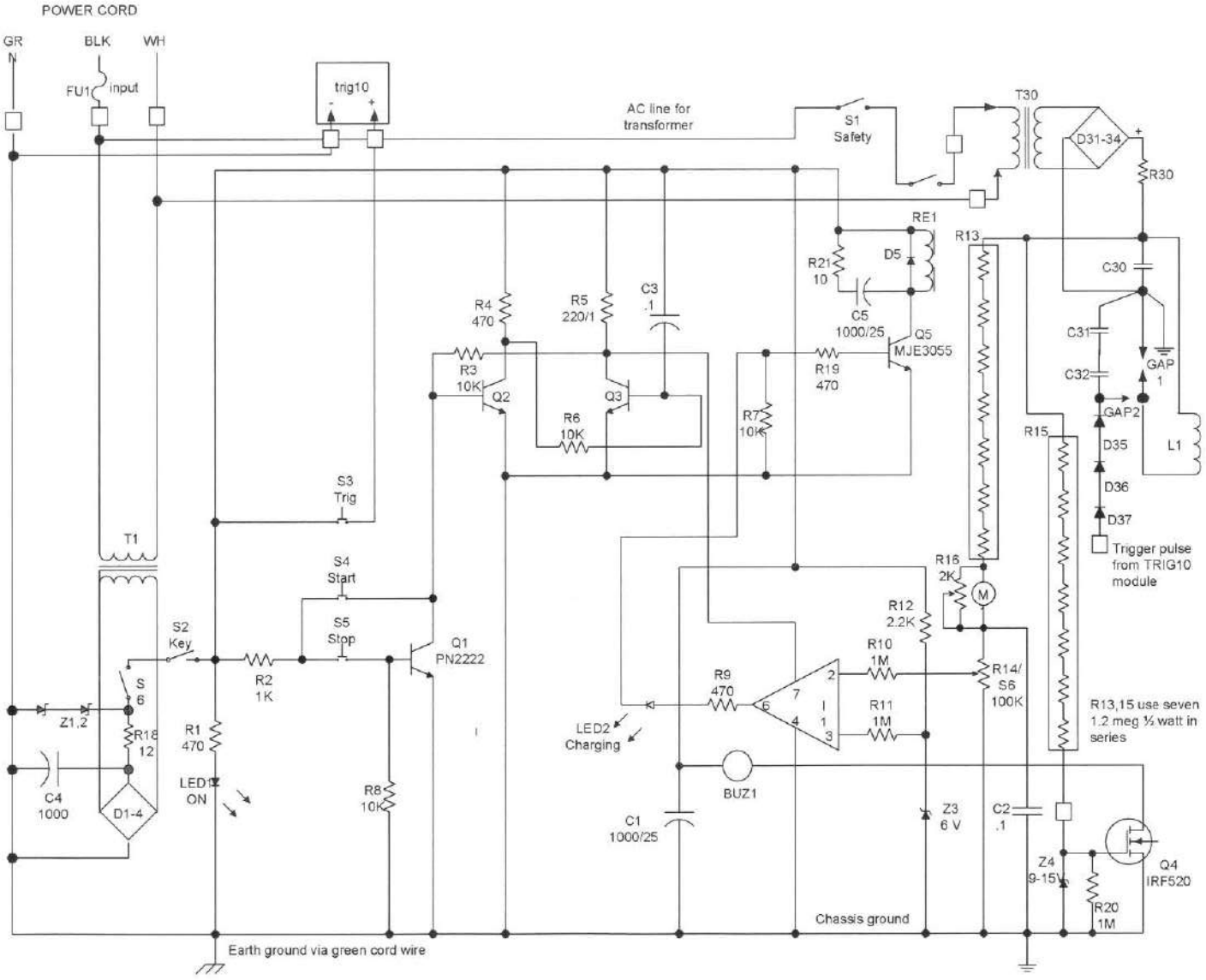

Figure 16-2 *Schematic*

device to warn the operator that a voltage exists on the storage capacitors. Sense voltage is obtained for the meter and charge voltage control circuit via string resistor R13. The safety level voltage is obtained through the resistor string (R15).

Assembly Steps

1. Cut a piece of .1 × .1 grid perforated circuit board (PB1) 6 × 4½ inch. You will have to drill holes for transformer T1 and relay RE1.
2. Insert the components as shown in Figure 16-3, starting from the lower left-hand corner. Count the perforated holes as a guide. Note the polarity marks on capacitors and diodes. It is suggested that you use a socket (SO8) for the LM741 integrated circuit (I1).
3. Wire the components as shown in Figure 16-3 using the leads of the actual components as the connection runs. These are indicated by the dashed lines. Always avoid bare-wire bridges and globby solder joints. Check for cold or loose solder joints. Note the symbols indicating wires to external components and to solder junctions beneath board.
4. Assemble the resistor dividers (R13 and R15) as shown in Figure 16-4 from seven 1.2 meg, ½-watt resistors that are all connected in series and sleeved into a ¼-inch ID flexible plastic tubing. Place these along with the connecting leads. The leads connected to R30 must be rated for 10 kilovolts. Connect the external components using #20 vinyl-jacketed, stranded wire. Attach and solder shunt resistor R16 across meter M1. Sleeve in the connection.
5. Connect the three high-voltage diodes (D35, D36, and D37) in series as shown in Figure 16-5. Make sure there are no sharp edges on solder joints and then sleeve into a plastic tube with a short piece of high-voltage wire lead.

   Connect the remaining components, noting that some may have to be unsoldered when routing through the panel, as shown. Verify proper lengths of connecting leads with other figures in the project.
6. Fabricate the chassis from a sheet of .063 aluminum as shown in Figure 16-6. The front panel holes are shown to approximate layout and size. These should be verified with all parts for hole size and location.
7. Fabricate a 6 × 7½ inch sheet of plastic (PLATE1) to insulate the assembly board connections as shown in Figure 16-7. Assemble T30 to the chassis using screws and nuts. Include solder lugs for grounding the power cord and assembly board.
8. Fabricate a 2¼ × 7 inch piece of plastic (PLATE2) for mounting the four rectifiers (D31 through D34) and resistor R30. Use two-sided sticky tape or silicon rubber to secure. Use a long screw or piece of threaded rod with an insulating washer on top side of resistor.
9. Assemble components to the front panel, as shown in Figure 16-8, and then finalize the wiring to complete assembly. Use pieces of 10 kilovolt-rated wire for those that are shown as heavy traces. Other leads are made from #20 vinyl-jacketed, stranded wire. The grounding leads shown are from the power cord, assembly board, and D33/D34 to the lug on T30. Output leads are shown as the TRIGGER, COMMON GROUND, and HV OUTPUT. Observe all notes on this figure.

Circuit Testing

10. Obtain a ballasted 115 vac power source. You can make this simply by placing a 60-watt lightbulb in series with the hot side of the power line, which is usually designated by the black lead. Do not eliminate the green earth ground connection.
11. Verify all switches are off and then insert a 3-amp fuse into FU1. Temporarily connect the high-voltage output to the chassis ground. Output is current limited by the leakage inductance of T30.

12. Plug into the ballasted 115 vac source. Turn on S6 and the key switch. Note LED1 lighting. Check control of both these switches as they are connected in series.
13. Push S3 and note a high-voltage spark at the trigger output lead.
14. Push S4 and note the relay latching and 60-watt lamp starting to light. The unit may chatter in this mode. LED2 should light in coincidence with the relay.

This concludes the basic test of this circuit but does not verify the programming voltage function, meter reading and calibration, or the safety buzzer.

Assembly of the Completed System

15. Fabricate the upper and lower deck pieces, as shown in Figure 16-9. Fabricate four pieces of 5½-inch PVC tubing for the pillar spacers located at each corner.

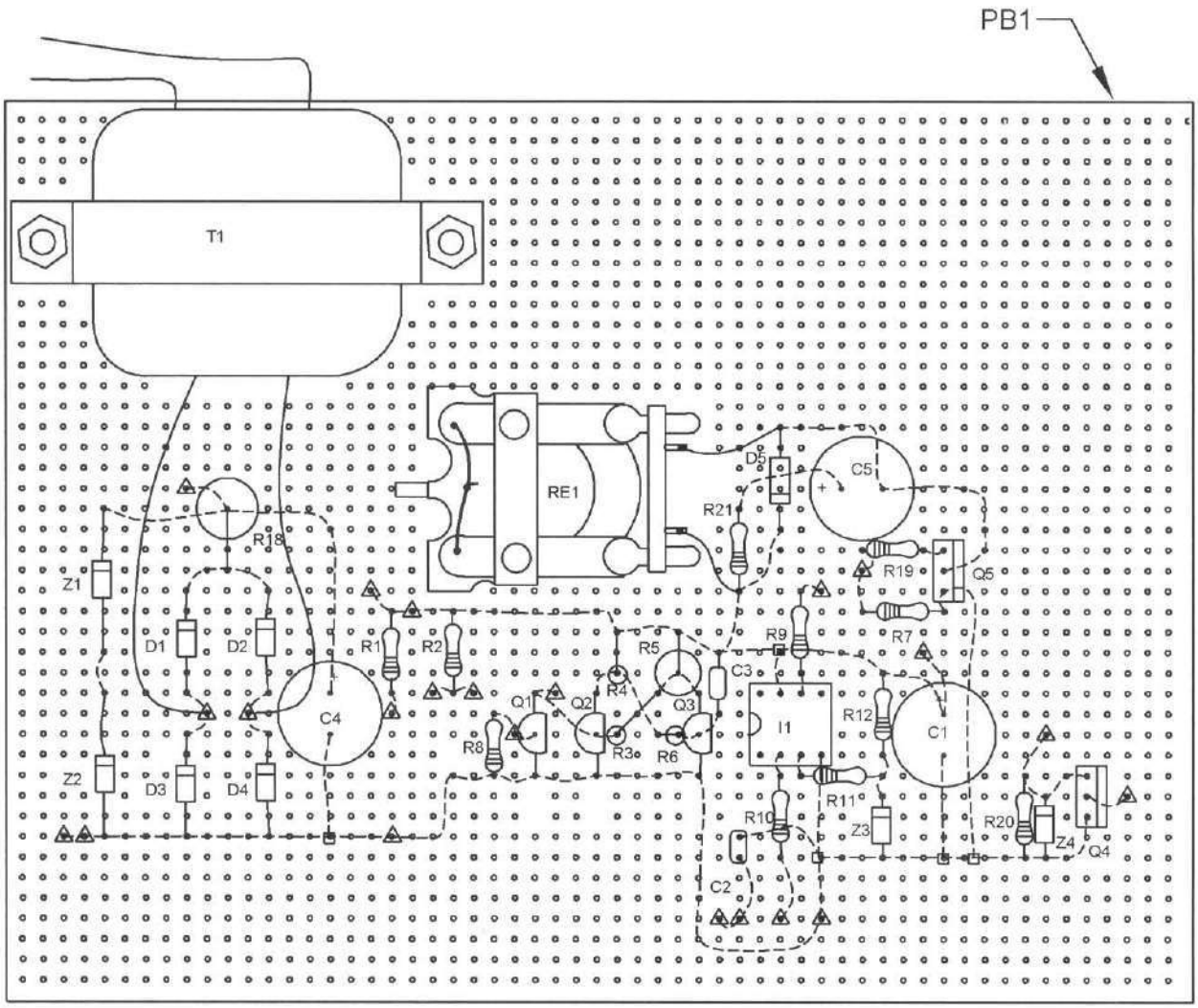

Figure 16-3 *Assembly board parts layout*

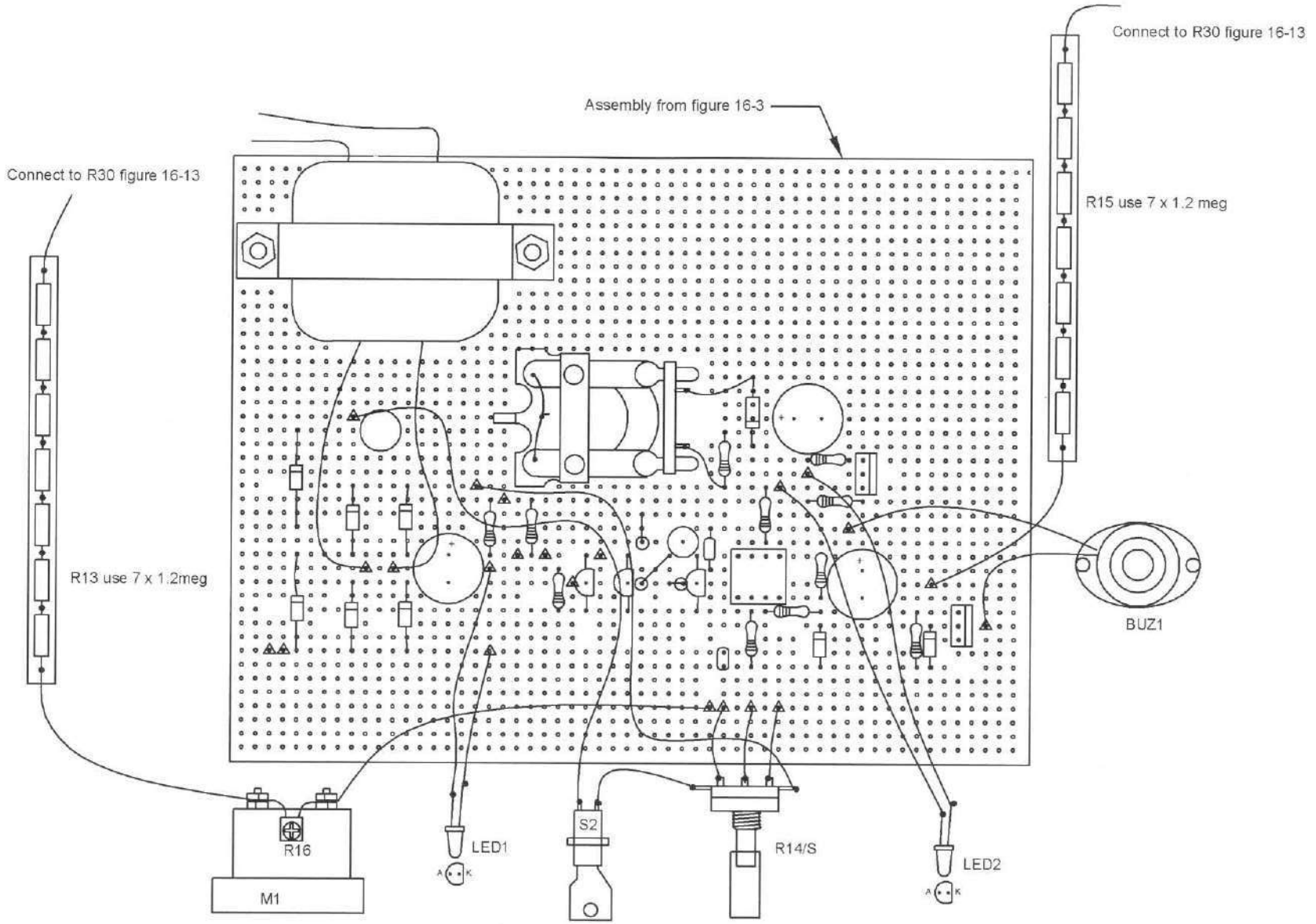

Figure 16-4 *Assembly board external wiring first level*

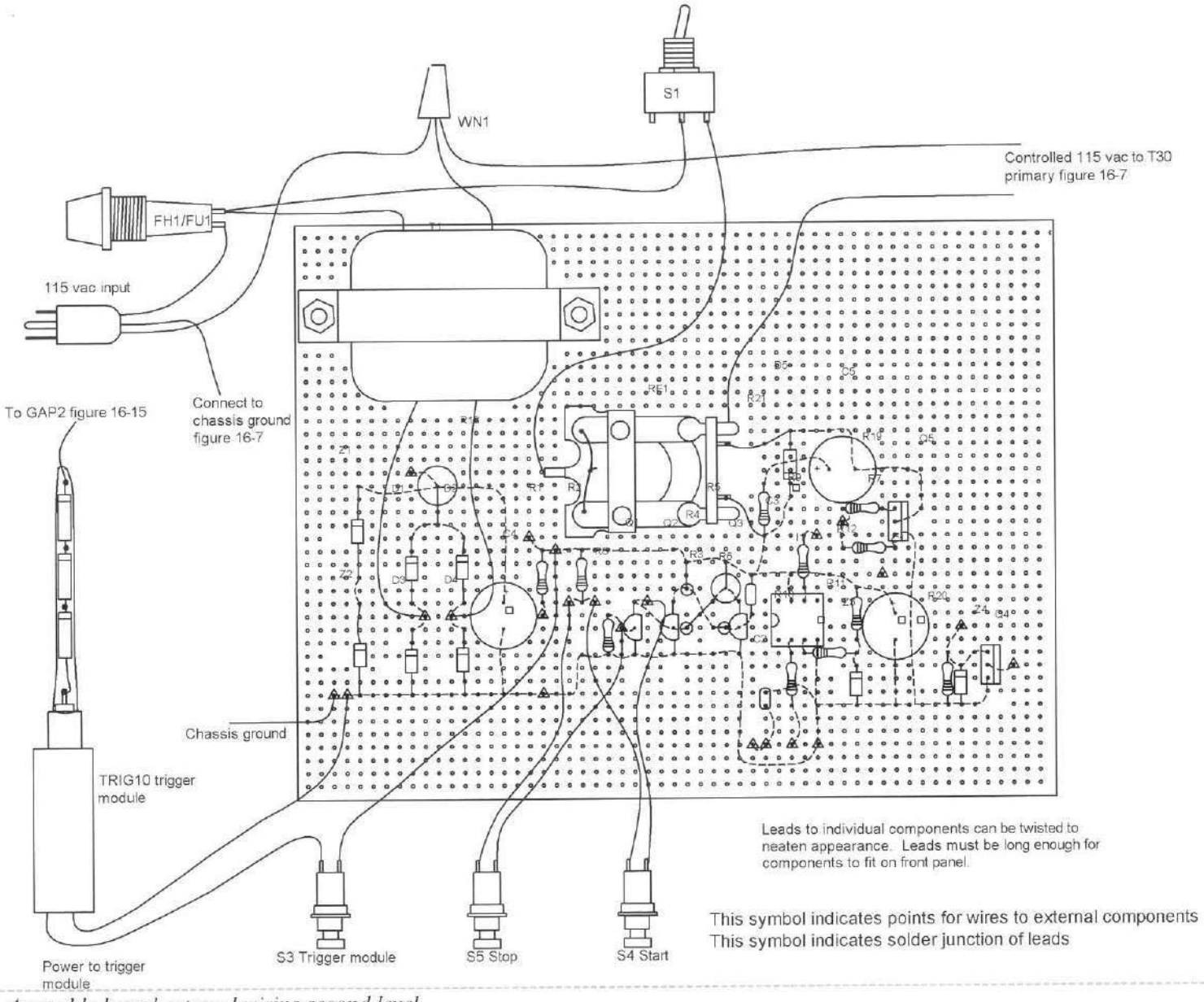

Figure 16-5 *Assembly board external wiring second level*

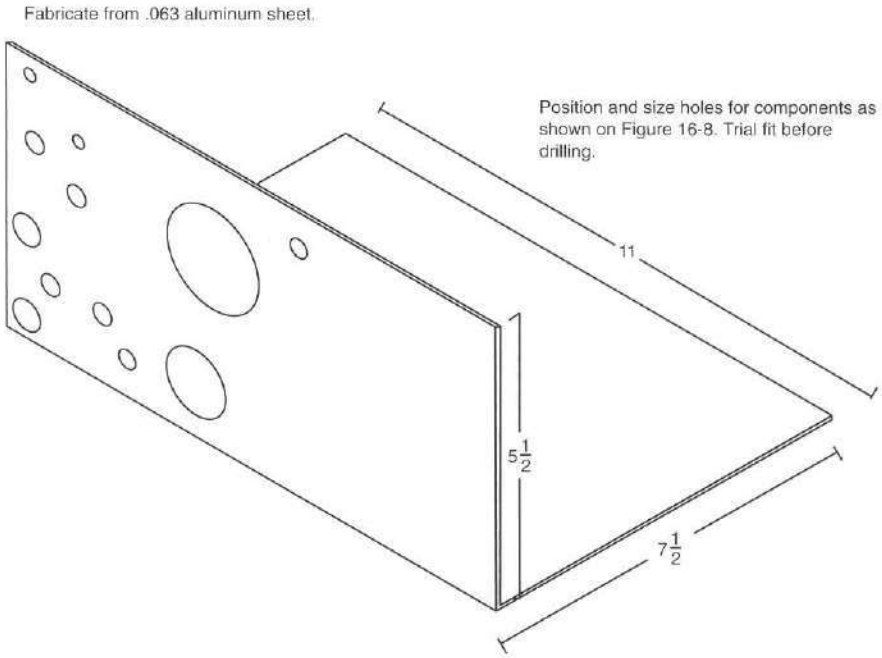

Figure 16-6 *Fabrication of chassis*

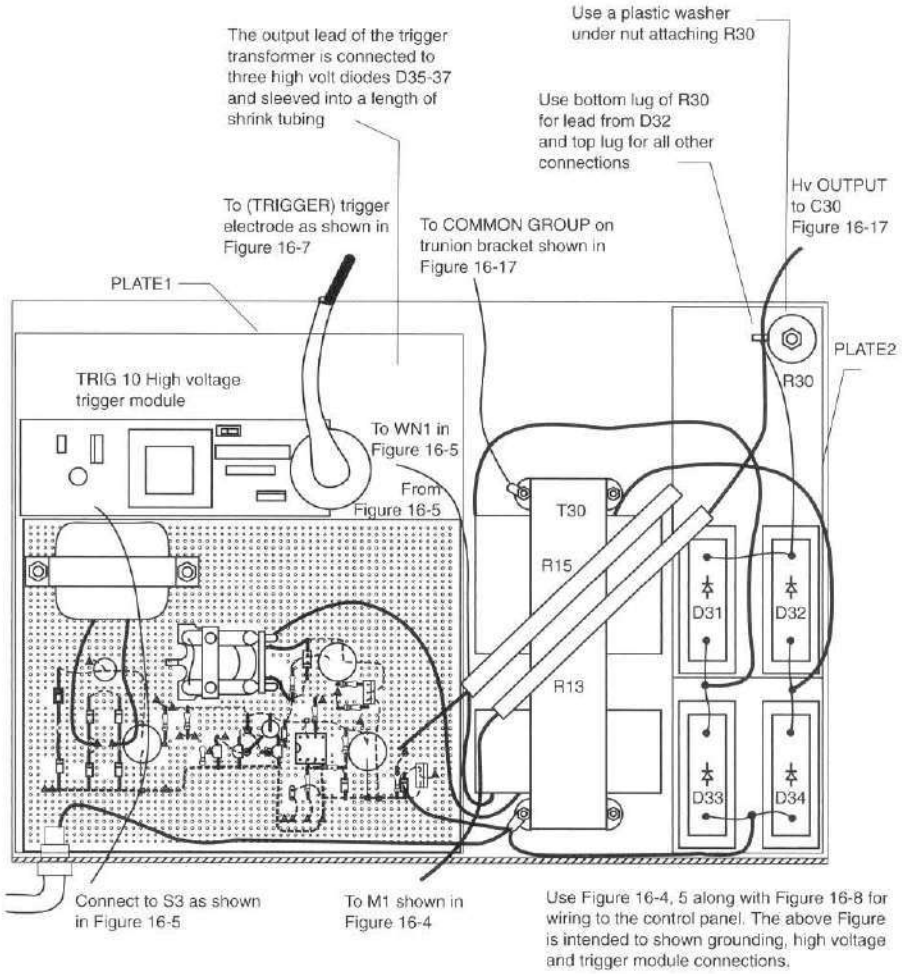

Figure 16-7 *Assembly and wiring of chassis*

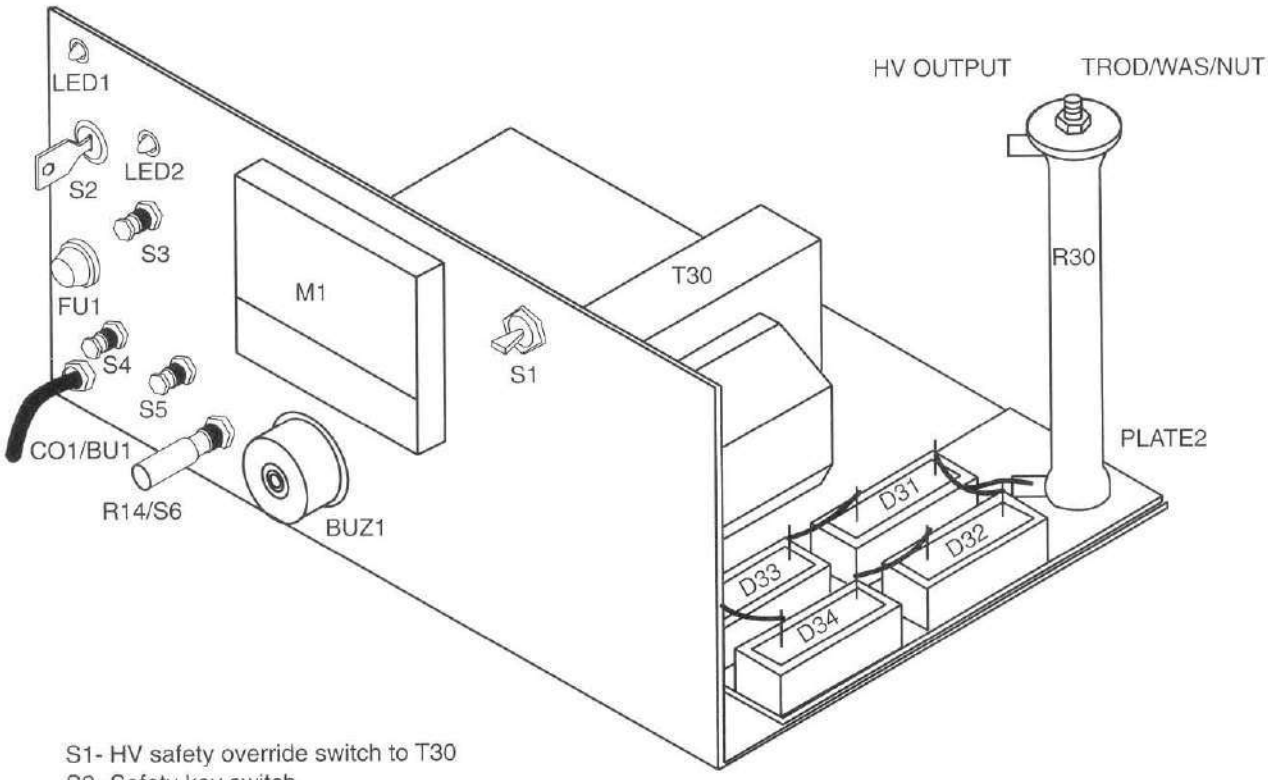

S1- HV safety override switch to T30
S2- Safety key switch
S3- Trigger "fire" switch
S4- Charge start switch
S5- Charge abort switch
S6- Low control voltage switch
LED1- Power "on" indicator
LED2- Charging cycle "on" indicator
R14- Programmed charge voltage level control
FU1- 3 amp fuse holder
BUZ1- High voltage presence audible warning
M1- Charge voltage meter.. 5 kilovolt full scale
CO1/BU1- Clamp bushing for power cord CO1

Note that it is a good idea to label the controls

Figure 16-8 *Front-panel controls and wiring*

16. Fabricate the capacitor bracket, as shown in Figure 16-10. This piece secures the three energy storage capacitors C10A, C10B, and C10C on the bottom deck.

17. Fabricate the trunion bracket, as shown in Figure 16-11. This piece secures the actual flyway and accelerating coil and therefore must be able to withstand the kinetic recoil from the accelerating reaction of the projectile. This bracket is the central electrical grounding point of the discharge circuit and must also be actively grounded to earth ground via the power cord green wire. There is also a 3/8-inch hole for the electrode holding collar (COLLAR1) for the ground electrode (TUNG38) of the main spark switch (GAP1). This part must be centered and carefully soldered in place using a propane torch.

18. Fabricate the front and rear disk section, as shown in Figure 16-12. You may also fabricate the projectile (PROJ1) from a piece of aluminum, as shown.

19. Wind the coils, as shown in Figure 16-13. It is a good idea to study Figures 16-12, 16-13, and 16-14 before attempting this step. Make sure to leave connection leads that are a minimum of 10 inches long.

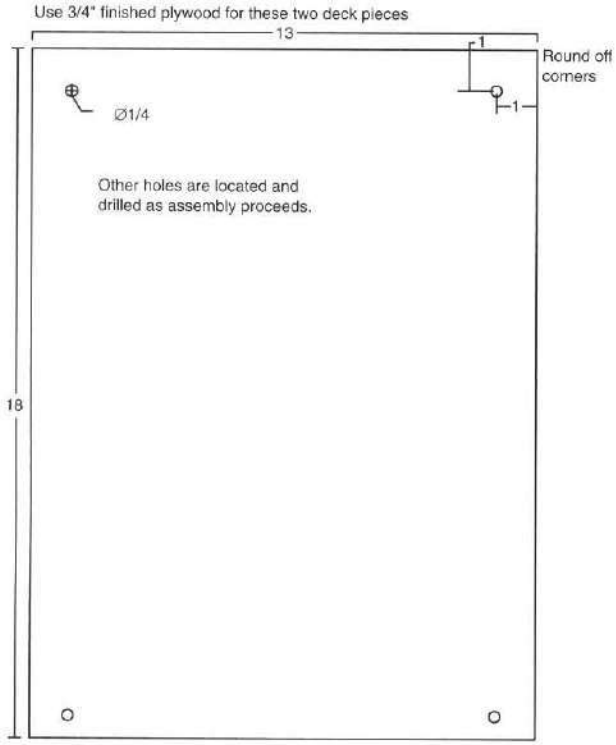

Figure 16-9 *Fabrication of deck sections*

20. Assemble the flyway and breech, as shown in Figure 16-14. Study the notes on this figure.

21. Fabricate the two plastic blocks (PVCBLK and TFBLK), as shown in Figure 16-15, to the suggested dimensions. Note that the heights of these pieces must allow close alignment of the electrodes as dictated by the position of the soldered collar on the trunion bracket. C31 and C32 are wired in place and must be spread apart to prevent sparking. The blocks are secured to the top deck using sheet metal screws. Use two screws for the PVC block. Do not allow these screws to penetrate more than 1/2 inch into the plastic material. Note the clearance hole in the deck for the high-voltage lead from the trigger module, shown in Figure 16-7.

22. Assemble the three energy-discharge capacitors (shown in Figure 16-16) along with the charger and control module.

23. Make the final assembly steps and wire, as shown in Figure 16-17. Note the direct and

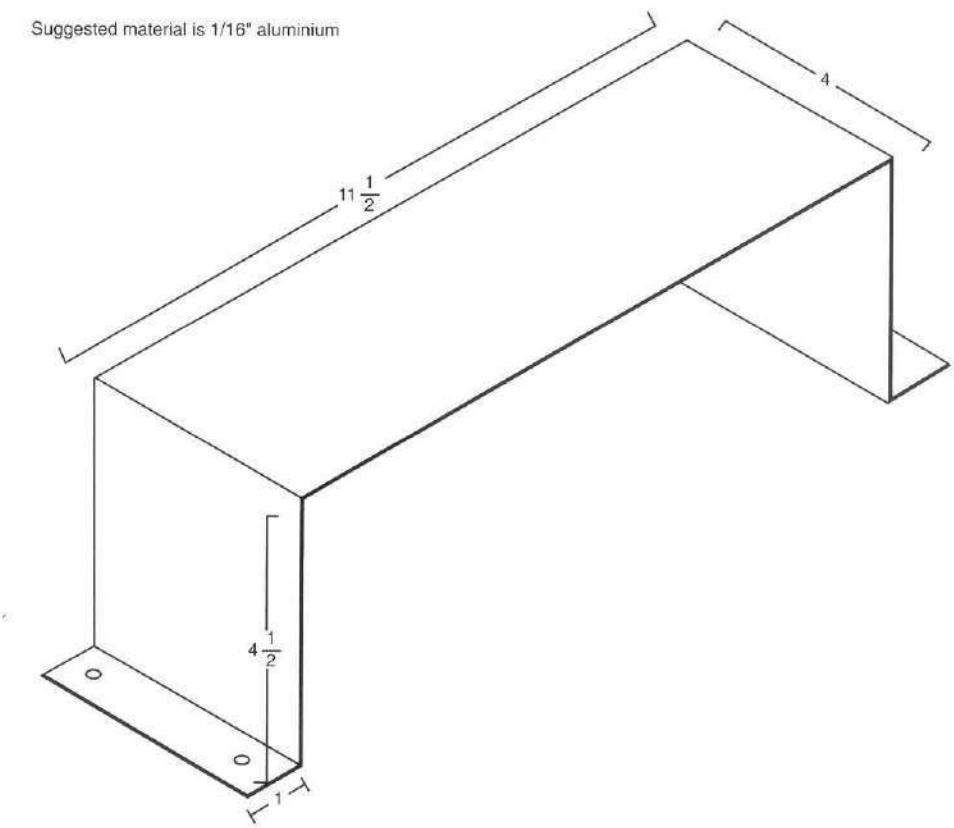

Figure 16-10 *Fabrication of the capacitor bracket*

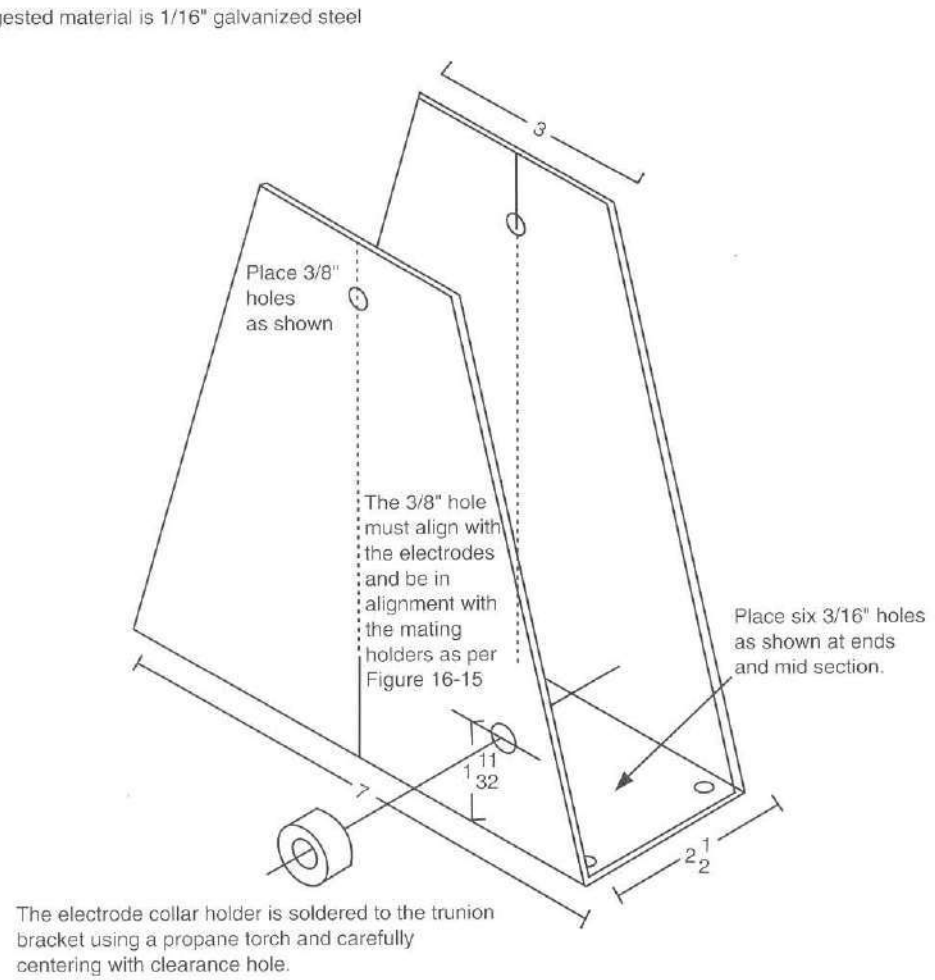

Figure 16-11 *Fabrication of the trunion bracket*

heavy leads for the discharge path. You may want to sleeve some plastic tubing over these leads, as they are rated only for 600 volts.

Note: The trunion bracket is the common grounding point for the system. It is very important that the earth ground green lead of the power cord be firmly attached at this point to ensure system operating safety.

24. Verify and use the diagram shown in Figure 16-18 as a wiring aid and reconfirm grounding and general circuitry and integrity.

Testing and Operation of the Cannon

25. Locate a test site with a backstop capable of stopping the projectile. Obtain a 5,000 volt DC reading meter to set M1. It is assumed that the circuitry is correctly assembled and the basic electrical pretest as described in steps 10 through 14 was successively performed. Preset the main gap to 1/16 inch and the trigger gap to 1/8 inch.

26. Preset all switches shown back in Figure 16-8 to the off position. Familiarize yourself with these controls

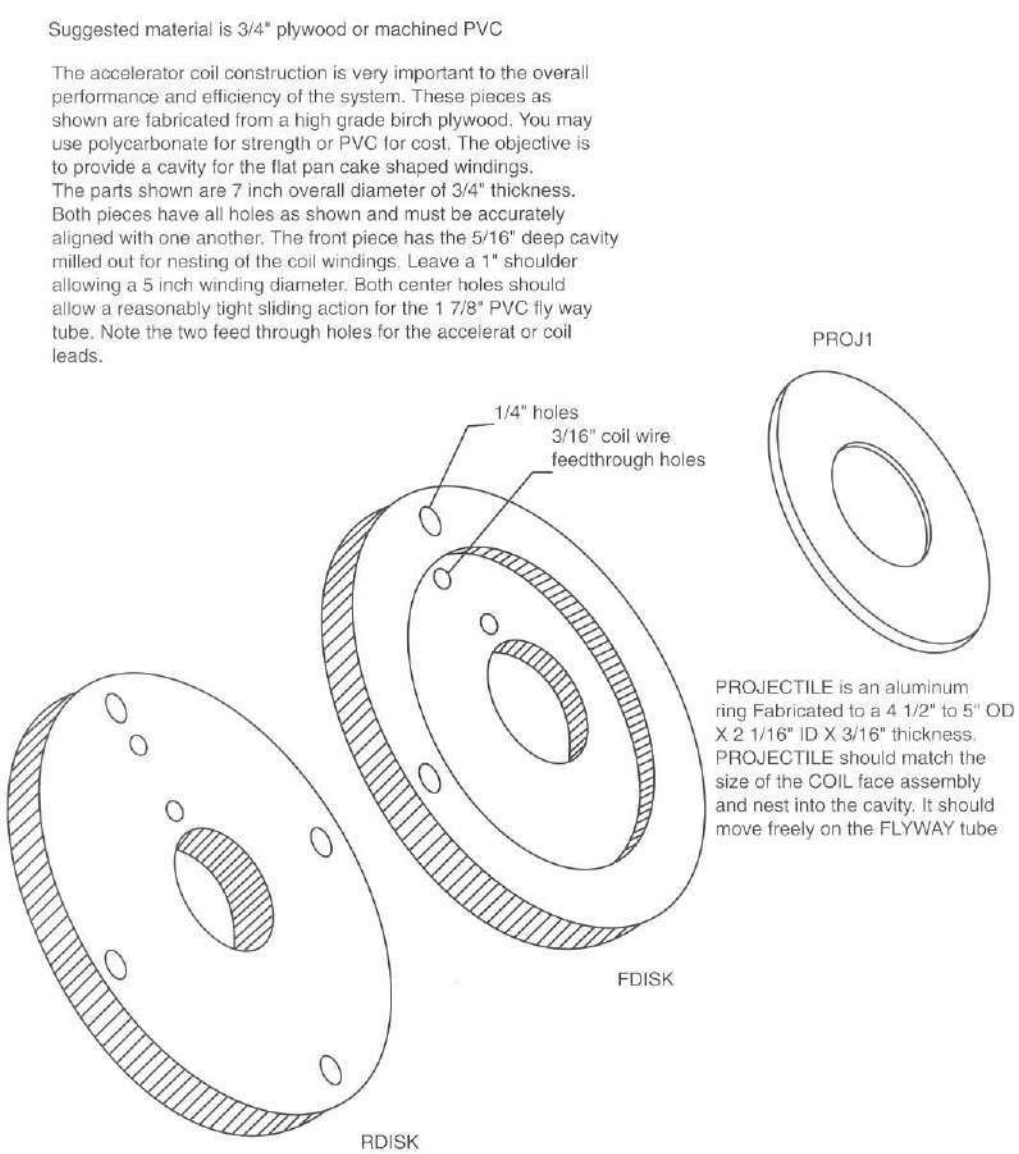

Figure 16-12 *Fabrication of the accelerator coil holder*

Danger: The next steps involve exposure to dangerous high voltages. Failure to take any of the following described steps will require a complete shutdown and power removal, along with a shorting of C30 before performing any trouble shooting.

27. Connect the test meter from chassis ground to the output end of resistor R30. Plug the unit into 115 vac and turn on S6. Turn on the key switch S2 and note LED1 lighting. Place the projectile over the accelerator coil.

28. Depress pushbutton switch S3 and note a spark occurring in both gaps.

29. Verify S1 safety switch is off. Depress pushbutton switch S4 and note the relay RE1 energizing and LED2 lighting. Depress pushbutton switch S5 and note RE1 de-energizing and LED2 turning off. Verify these on and off functions of S4 and S5 several times before the next steps.

    S5 is important as it must stop the charging action in the event that you choose to quickly abort the cycle.

30. Turn on toggle switch S1. Restart the system by again depressing R4, noting a voltage reading on both the panel meter M1 and the external test meter. This voltage will build up to a level as set by the charge-voltage level control R14 and then shut down, only to restart the charge cycle when the voltage charge level

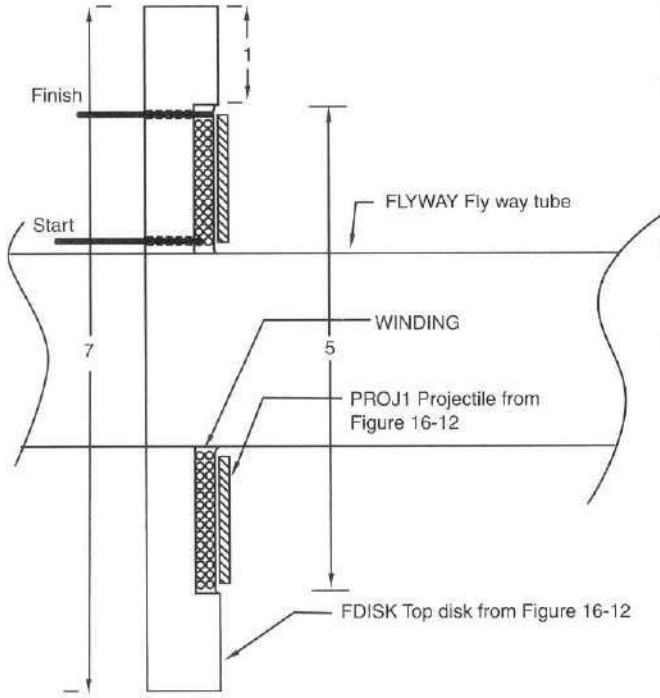

1. Fabricate the FLYWAY from a 18" piece of 2" PVC tubing
2. Wind a coil of 30 turns of #12 in fifteen layers of 2 turns each. Finished coil must be in a tight pancake configuration and have 10 inch connection leads. *You may have to make up a temporary bobbin jig for this step.* Hold together with tape etc.
3. Place COIL section into cavity routing the leads as shown. COIL section should nest into cavity and be positioned flat.
4. Seal all points that can leak as epoxy must be carefully poured over the COIL forming a 1/16" layer on top.

Figure 16-13 *Side view showing winding*

Suggested material is ¾" plywood or machined PVC

You will note that the front disk housing the accelerator coil is allowed to move over the flyway tube and against the springs to absorb some of the recoil. The rear disk abuts to the shoulder of the breech tube that is non movable along with the flyway tube.

This feature in important if you are intending to repetitively fire high energy shots..

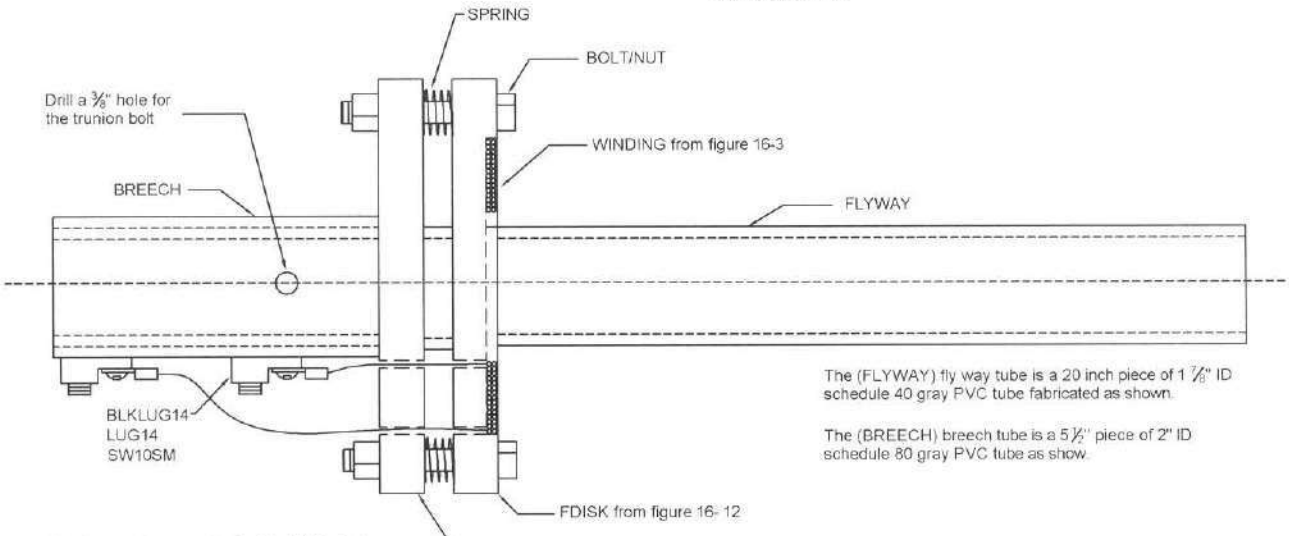

The (FLYWAY) fly way tube is a 20 inch piece of 1 ⅞" ID schedule 40 gray PVC tube fabricated as shown.

The (BREECH) breech tube is a 5½" piece of 2" ID schedule 80 gray PVC tube as show.

Discharge wires are attached to ¼" block lugs (BLKLUG) via the set screw. The coil wires are soldered to ¼" spade lugs that are secured to the block lugs via #10 x ⅜" sheet metal screws, screwed into both the FLYWAY and BREECH tube.

The bare leads from the coil should be individually sleeved into plastic tubing to prevent catastrophic contact

Figure 16-14 *Assembly of the breech and flyway*

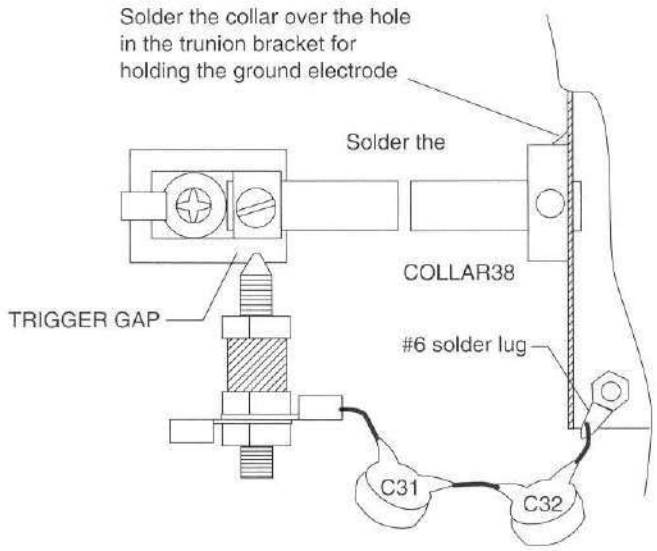

Solder gap switch assembly top view

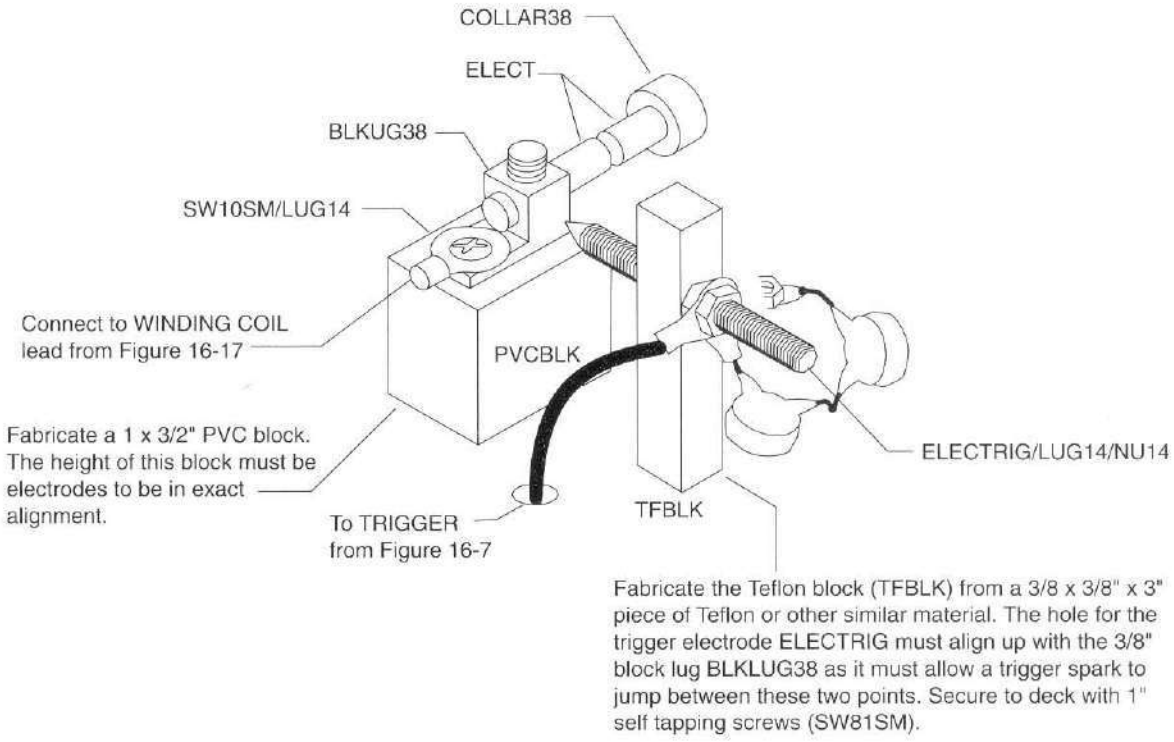

Spark gap switch is o view

Figure 16-15 *Details of the spark and trigger switches*

falls below the set level. Obviously there is an amount of hysteresis that prevents off-and-on chatter. With R14 set to full counterclockwise (CCW), this voltage should reset at less than 1,000 volts. The buzzer BUZ1 should be producing an annoying sound, thus alerting you to a charge presence on the capacitors.

31. Slightly turn R14 clockwise and allow it to cycle, repeating up to 1,500 volts as read on the external test meter. Depress the trigger

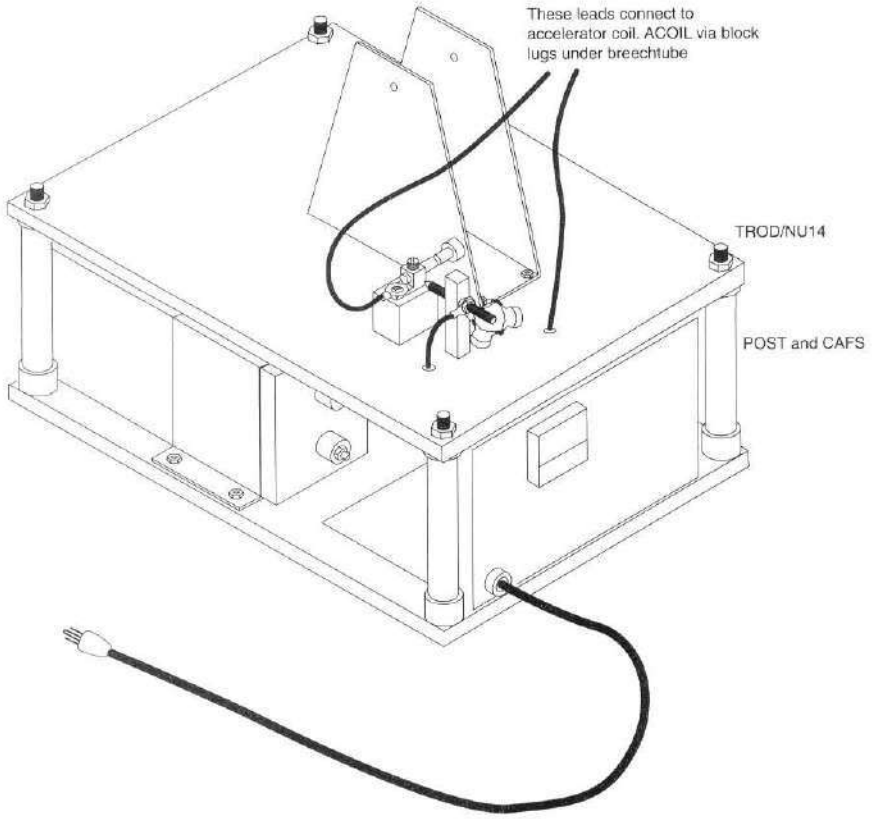

Figure 16-16 *Final assembly isometric view*

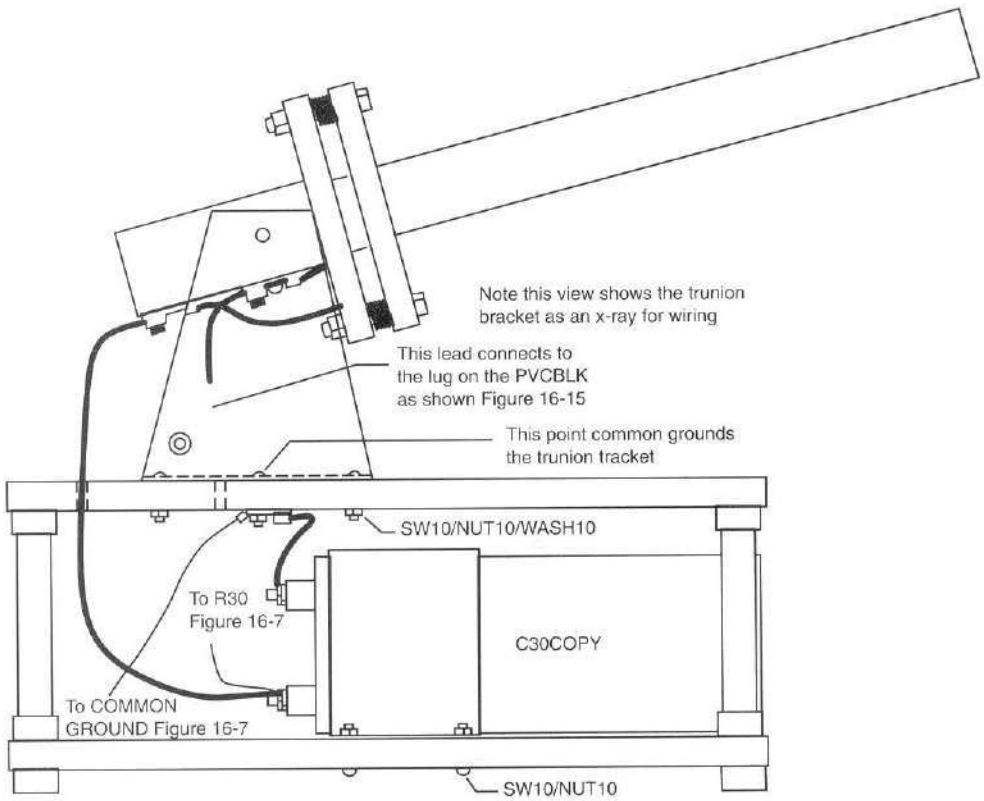

Figure 16-17 *Final assembly side view*

fire pushbutton S3 and note the projectile shooting into the backstop. Immediately press the stop switch S5 unless you want it to charge up for the next shot.

Note: The system will automatically recharge to the 1,500-volt present level unless the stop switch is activated.

---

32. Repeat the cycle, increasing the charge voltage up to 2,500 volts, and then adjust the trimpot R16 on the meter M1 to agree with the test meter.

33. Repeat this step allowing the charge voltage to go up to 5,000 volts, noting the impact of the projectile.

34. Verify the unit is not breaking apart as a result of recoil. Rethink the recoil springs if a problem exists.

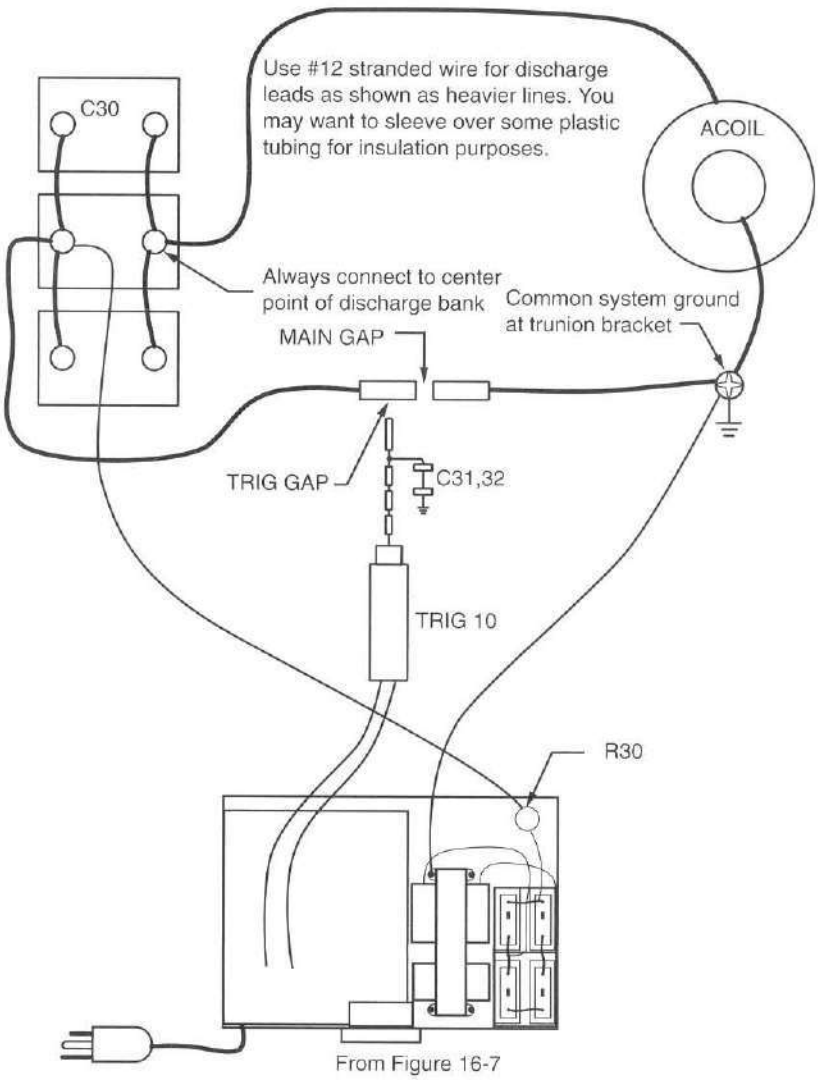

Figure 16-18 *Overall system wiring diagram*

Table 16.1 Magnetic Cannon Part List

Ref. #	Description	DB Part #
R1, 4, 9, 19	Four 470, 1/4-watt resistors (yel-pur-br)	
R2	1K, 1/4-watt resistor (br-blk-red)	
R3, 6, 7, 8	Four 10 kilohm, 1/4-watt resistors (br-blk-or)	
R5	220, 1/4-watt resistor (red-red-br)	
R10, 11	Two 10M, 1/4-watt resistors (br-blk-bl)	
R12	2.2K, 1/4-watt resistor (red-red-red)	
R13, 15	Fourteen 1.2M, 1/4-watt resistors (br-red-gr) (see schematic in Figure 16-2)	
R14/S6	100K potentiometer, 17 mm with low-volt switch	
R16	2K trimpot	
R20	1M, 1/4-watt resistor (br-blk-gr)	
R21	10-ohm, 1/4-watt resistors (br-blk-blk)	
R18	12-ohm, 3-watt resistor	
R30	16K, 50-watt power resistor	DB# 16K50W
C1, 4, 5	Three 1,000 mfd, 25-volt vertical electrolytic capacitors	
C2, 3	Two .1 mfd, 50-volt plastic capacitors	
*C30A	Three 32 mfd, 4,500-volt oil-filled cans in parallel for 96 mfd/4.5 kv	DB# 32m/4500
*C30B	Four 24 mfd, 5,200-volt oil-filled cans in parallel for 96 mfd/5 kv	DB# 24m/5200
I1	741 op-amp DIP IC	
Q1, 2, 3	Three PN2222 GP NPN transistors	
Q4	IRF520 Mosfet	
Q5	MJE3055 NPN power transistor	
D1-4	Four 1N4001 50-volt 1-amp diodes	
D5	1N4007 1,000-volt, 1-amp diode	
D31-34	Four 8-kilovolt, 100 ma standard recovery diodes	DB# H407
D35-37	Three 30 kilovolt, 10 ma diodes	DB# VG30
Z1, 2, 3	Three 1N4733 6-volt zener diodes	
Z4	1N4745 15-volt zener diode	
LED1	Red LED indicator	
LED2	Green LED indicator	
S1	SPST toggle switch	
S2	Key switch	
S3, 4, 5	Three pushbutton NO switches	
RE1	12-volt, 5-amp relay	
BUZ1	12-volt buzzer	DB# BUZROUND
Q1	100-volt IRF540 MOSFET	
T1	12-volt, 100 ma transformer	DB# 12/.1
T2	6,500-volt, 20 ma current-limited transformer	DB# 6kv/20
*L10	Accelerator coil assembly, as shown in Figures 16-12 and 16-13	DB# ACCOIL
*GAP1	Main gap assembly, as shown in Figure 16-15	DB# GAPMAIN
*GAP2	Trigger gap assembly, as shown in Figure 16-15	DB# GAPTRIG
CHASSIS1	Metal chassis fabricated as shown in Figure 16-6	
PLATE1	6 × 7 1/2 × 1/16 inch plastic insulating plate	
PLATE2	2 1/4 × 7 1/2 × 1/16 inch plastic insulating plate	
TAPE1	12 inches of 1-inch wide, thin sticky tape	
PLTUBE	18 inches of 1/4-inch ID vinyl flexible tubing for R13, R15, and trigger diodes	
CO1	6 feet of 3-wire #18 power cord	
HVWIRE	12 inches 20 kv silicon high-voltage wire	DB# WIRE20KV
BUSSWIRE	24 inches #20 bare busswire	

WR20	10 feet #20 vinyl stranded hook-up wire	
WN1	Medium wire nut	
BU2, 3	Two bushings for LEDS	
BU1	Power cord clamp bushing	
SW6	Six 6-32 × 3/4-inch screws	
SW1	6-32 × 1/4-inch screw for mounting relay	
NU6	Six #6 hex nuts	
LUG6	#6 solder lug	
TROD	5-inch length of 1/4-20 threaded rod, 2 nuts, and plastic washers	
TRIG10	Assembled trigger pulse module	DB# TRIG10
TRIG1K	Kit of trigger pulse module	DB# TRIG1K

Parts List to Final System

DECKS	Two fabricated pieces of 7/8-inch birch plywood 13 × 17 inches
POSTS	Four fabricated pieces of 5 3/4 × 7/8 inch PVC tubing
PLATE1	Fabricate a piece of 1/16-inch plastic sheet 6 × 7 inches
PLATE2	Fabricate a piece of 1/16-inch plastic sheet 2 1/4 × 7 inches
BRKCAP1	Fabricate the capacitor bracket seen in Figure 16-10
BRKTRUN1	Fabricate the trunion bracket seen in Figure 16-11
RDISK	Fabricate the rear disk seen in Figure 16-12
FDISK	Fabricate the front disk seen in Figure 16-12
PROJ1	Fabricate the projectile seen in Figure 16-12
BLKELECT	Fabricate the electrode holding block seen in Figure 16-15
BLKTRIG	Fabricate the trigger electrode holding block seen in Figure 16-15
FLYWAY	Fabricate the flyway tube seen in Figure 16-14
BREECH	Fabricate the breech tube seen in Figure 16-14
CAPS	Twelve 7/8-inch PVC caps for posts and feet seen in Figure 16-1
SPRINGS	Four 1/2-inch diameter × 3/4-inch stiff compression springs
COLLAR	3/8-inch shaft collar
BLKLUG25	Three 1/4-inch block lugs for breech connections
BLKLUG38	3/8-inch block lug for electrode
LUG14	Five 1/4-inch wide solder lugs
ELECTRGAP	Two 3/8 × 2-inch tungsten or tool steel electrodes
ELECTRTRIG	1/4-20 × 3-inch threaded rod with point
TROD	Four 1/4-20 × 8-inch threaded rod
BOLT/NUT	Five 3 1/2 × 3/8-inch bolt and nut
NUT14	Eleven 1/4 × 20 nuts for trigger gap and posts
SW10M	Five #10 × 1/2-inch sheet metal screws
SW10	Ten #10-32 × 1.5-inch machine screw
NU10	Ten #10-32 nuts
WASH10	Twenty #10 wide shoulder washers
WIRE12	4 feet #12 stranded, vinyl-covered wire
WIRE12	30 feet #12 heavy-coated, magnetic wire for winding ACOIL

Chapter Seventeen

Vacuum Tube Tesla Coil Project

This advanced project, as shown in Figure 17-1, is similar to a coil made by John Weisner some years ago. The geometry of the secondary not being the most efficient is a good compromise for wireless energy transmission and also provides a reasonable output display. The project is intended for the experienced experimenter and researcher in the field of high-voltage and high-frequency circuitry. Not only is this project a dangerous electrical device, but it can also be a bothersome source of radio interference, especially in the standard AM broadcast band and should be used in a shielded enclosure or a Faraday cage if operated on a continuous basis. A gas discharge lamp such as a standard household fluorescent lamp will glow up to 10 feet away when this device is used. Annoying burns are experienced when contact is made with conductive objects up to similar distances.

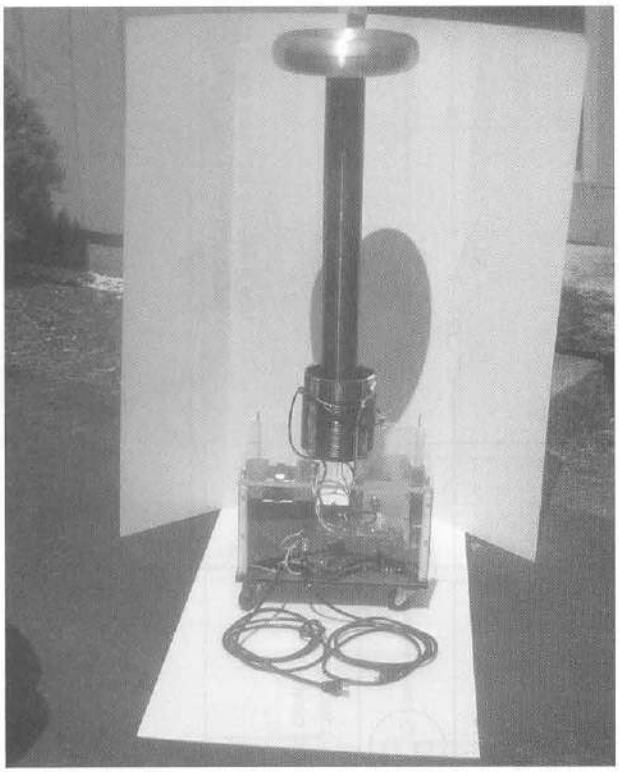

Figure 17-1 *The vacuum tube Tesla coil*

We also have built coils using 304TH, 450TH, and parallel 2500THs with a full 5,000 watts of plate dissipation. This coil produced spectacular flaming arcs up to 8 feet long with 8 kilowatts of input. A video showing the operation is on our web site. The coil shown here will easily produce 1 to 2 feet of flaming arcs.

This system can provide the experienced hobbyist with hours of fun and entertainment experimenting with terminals and settings to generate wireless energy as well as output arcs and sparks. This is an advanced-level and potentially expensive project requiring electronic skills and high-voltage experience. Expect to spend $300 to $750. All the parts are readily available, with specialized parts obtainable through Information Unlimited (www.amazing1.com), and they are listed in Table 17-1.

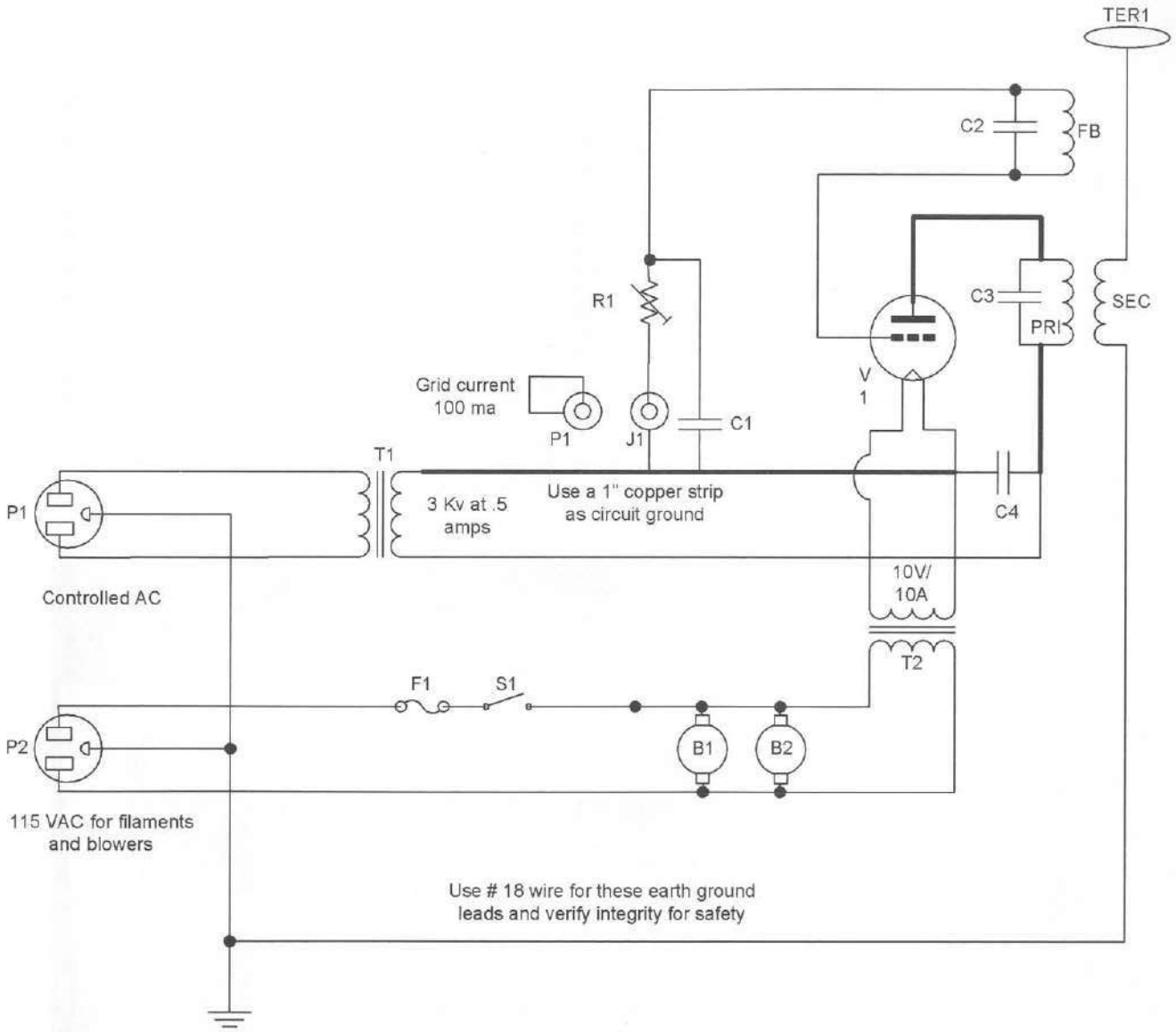

Figure 17-2 *Circuit schematic*

Feed back winding is 10 to 20 turns of #18 stranded vinyl wire. Open circuit inductance is approximately 75 micro-henries

Primary windings are 20 to 22 turns of #8 insulated wire. Open circuit inductance 55 micro-henries

Secondary winding is a 33" length of tightly wound #28 magnet wire for about 2000 turns. Free standing resonant frequency is approximately 200 kHz.

Resistor R1 is 5000 ohms at 100 watts

Basic Description

These spectacular display devices produce arcs and sparks quite unlike the undamped spark gap-driven Tesla coils. Operation does not require a noisy spark gap that produces copious amounts of *radio frequency interference* (RFI) but operates efficiently at the quarter-wave frequency of the secondary coil. Vacuum tubes, while large and requiring filament power, do offer robust and forgiving operation and are intended as a good starter approach to solid-state Tesla coils.

This approach is far less temperamental than the solid-state *metal-oxide-semiconductor field effect transistors* (MOSFET) or *insulated gate bipolar transistor* (IGBT) drivers. However, once these FET devices are debugged and tweaked, one can obtain some excellent results. Our lab FET coil generates over 4-foot sparks using only 3 kilowatts. The output frequency tracks within 5 percent of the resonant point using one of our proprietary circuits that will be on our site in the late spring of 2006 with the complete system scheduled for publishing in the third edition of this book series.

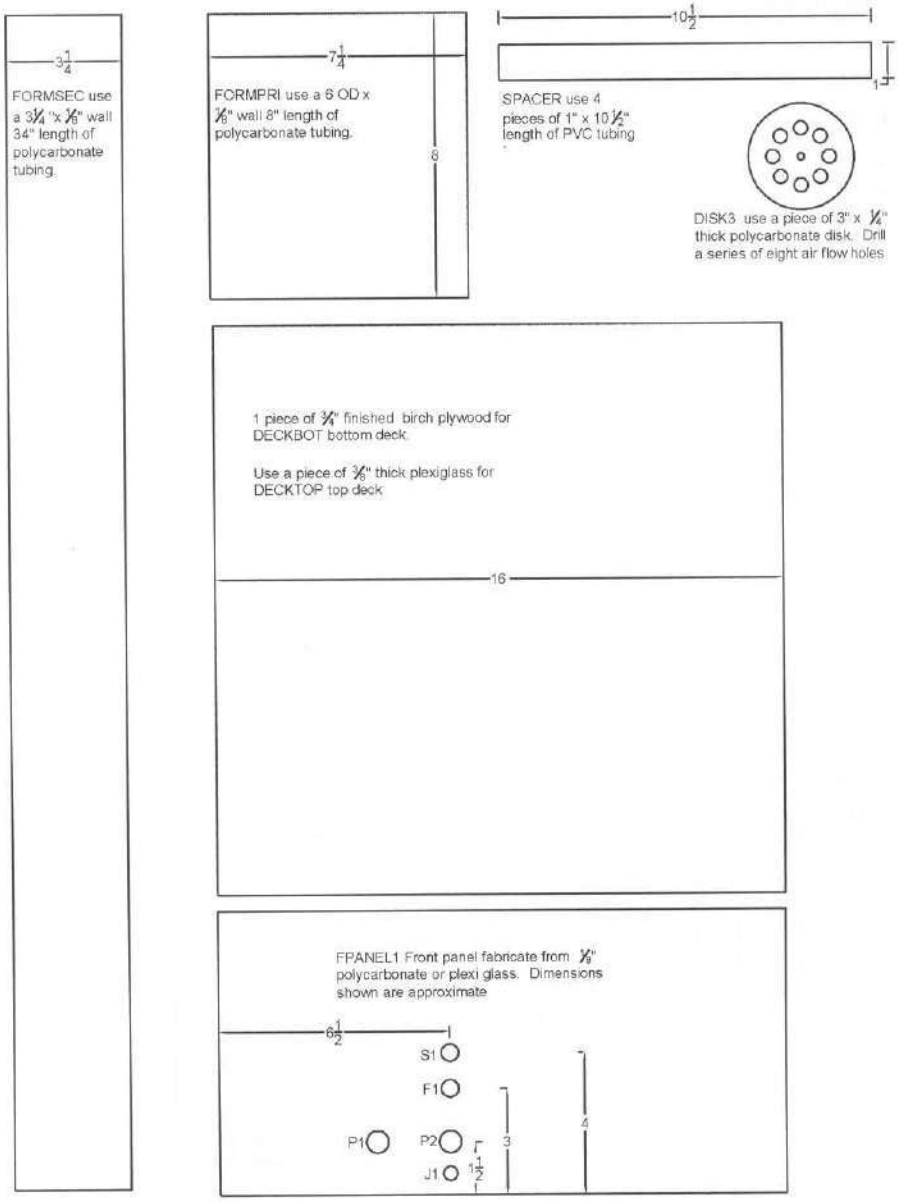

Figure 17-3 *Creating the major parts*

The circuit as shown on the schematic in Figure 17-2 of the vacuum tube device is nothing more than a medium-powered Hartley radio frequency oscillator tuned to the resonant frequency of the secondary coil. The circuit uses a medium-powered, readily available 833A triode transmitting tube that inherently has a high grid to plate capacitance necessary for self-oscillation. The plate load is a resonant transformer with both the primary and secondary tuned to the approximate identical frequencies. The output potential is now a function of the secondary-to-primary coil inductances times the peak primary plate voltage. This system generates voltages at frequencies sufficient to cause air breakdown, thus producing the sparks and arc jumping into open air.

The output of the oscillator is relatively closely coupled to the secondary coil designed for high Q performance and self-resonant to the quarter-wave of the oscillator frequency. The voltage distribution is now that of a quarter section with a current node at the base and voltage node at the top. The input power to the coil is raw, unrectified AC at 3,000 volts *root mean square* (rms) with a current of .5 amps. The peak voltage is over 4,000 volts and is supplied by a conventional plate transformer being fed by a voltage-adjustable variac, which allows you to adjust the output voltage of the system. A pulse signal is also shown that controls the grid of the tube, allowing a wide range of spark texture variation by changing the duty cycle and frequency.

Assembly Steps

1. Fabricate the secondary coil form (FORMSEC) from a 3 1/4 × 1/8-inch wall polycarbonate tubing, as shown in Figure 17-3. It is not suggested that you use PVC tubing due to moisture retention and breakdown.

   Fabricate the primary coil form (FORMPR1)as shown in Figure 17-3 from a length of 7 1/2 × 1/4-inch wall plastic tubing. Polycarbonate tubing is preferred.

   Fabricate two 3-inch diameter discs (DISK3) as shown in Figure 17-3 from 1/4-inch polycarbonate. These pieces are for the ends of the secondary coil and are secured via three #6 × 3/8-inch brass wood screws. Drill air passage holes as shown for the blower (B2).

   Fabricate four 10.5-inch spacers (SPACER) as shown in Figure 17-3 from lengths of 1-inch OD PVC tubing.

   Fabricate the 16 × 16-inch square bottom deck (DECKBOT) as shown in Figure 17-3 from a piece of 3/4-inch finished plywood and paint it black.

   Fabricate the 16 × 16-inch deck top (DECKTOP) as shown in Figure 17-3 from a 3/8-inch-thick Plexiglas or you may use plywood.

2. Fabricate the parts as shown in Figure 17-4. Note to use 1/16-inch G10 or another high-temperature plastic for the actual tube

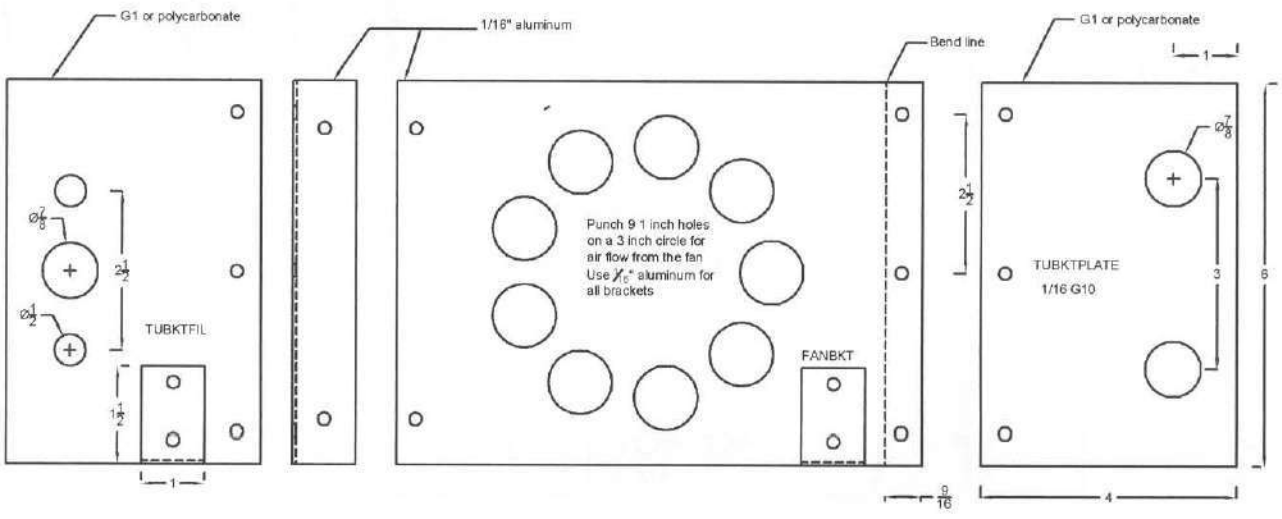

Figure 17-4 *Assembly of the tube and mounting bracket*

holders (TUBKTFIL and TUBKTPLATE). Use 1/16-inch aluminum for the other parts. Note the mating holes for assembling them together, as shown in Figure 17-4.

3. Assemble the fan and tube-mounting bracket from the parts in Figure 17-5. Use thirteen 6-32 × 1/2-inch screws and nuts. Foot brackets secure the assembly to the wooden deck via four #8 × 1/2-inch wood screws. TUBKTPLATE must be disassembled to insert the tube V1 in place. The blower fan B1 is centered to maximize air flow across the plate section of V1. It is mounted using four 8-32 × 1/2-inch screws and nuts. The entire assembly

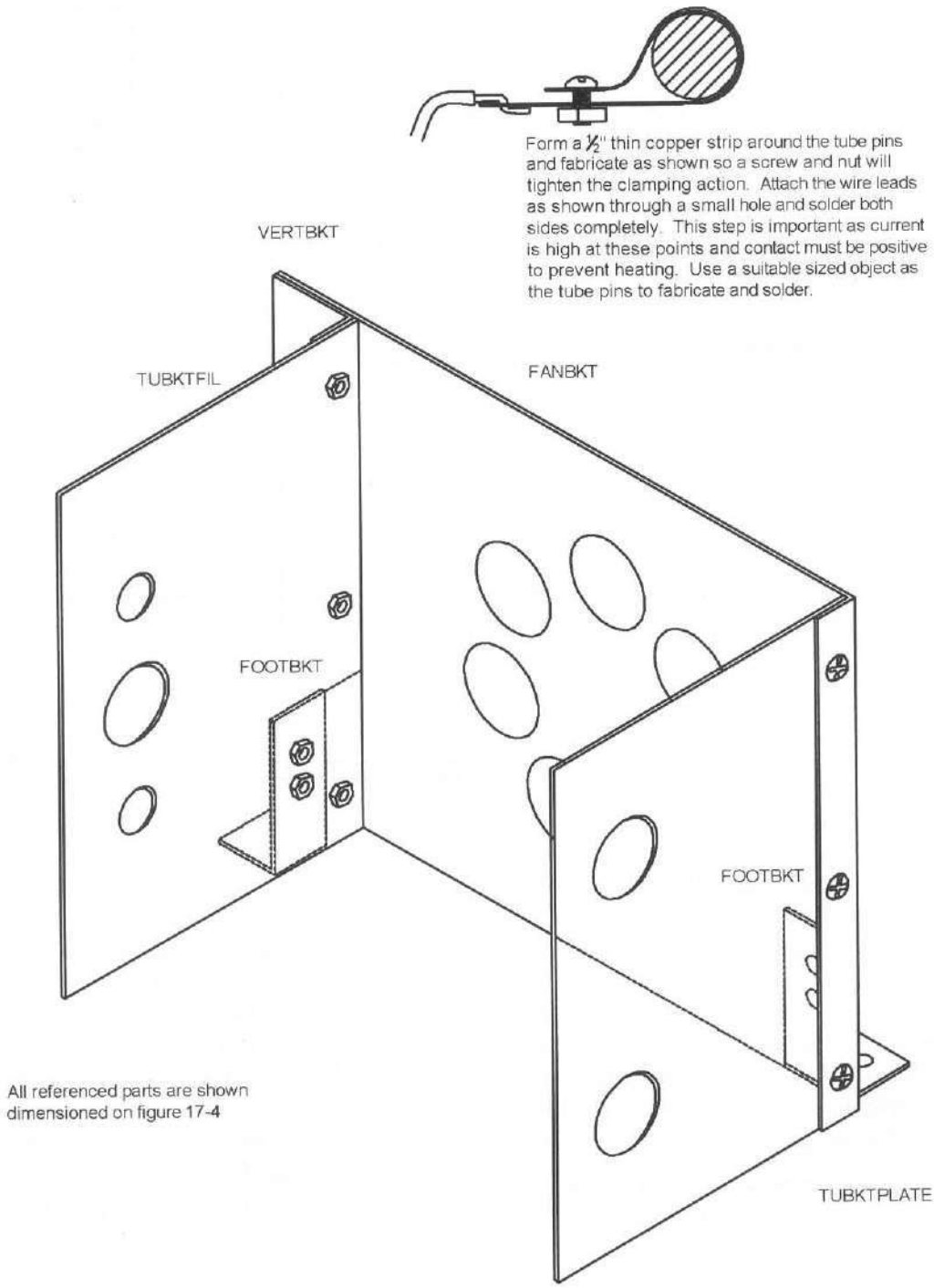

Figure 17-5 *Assembly of the tube-holding bracket*

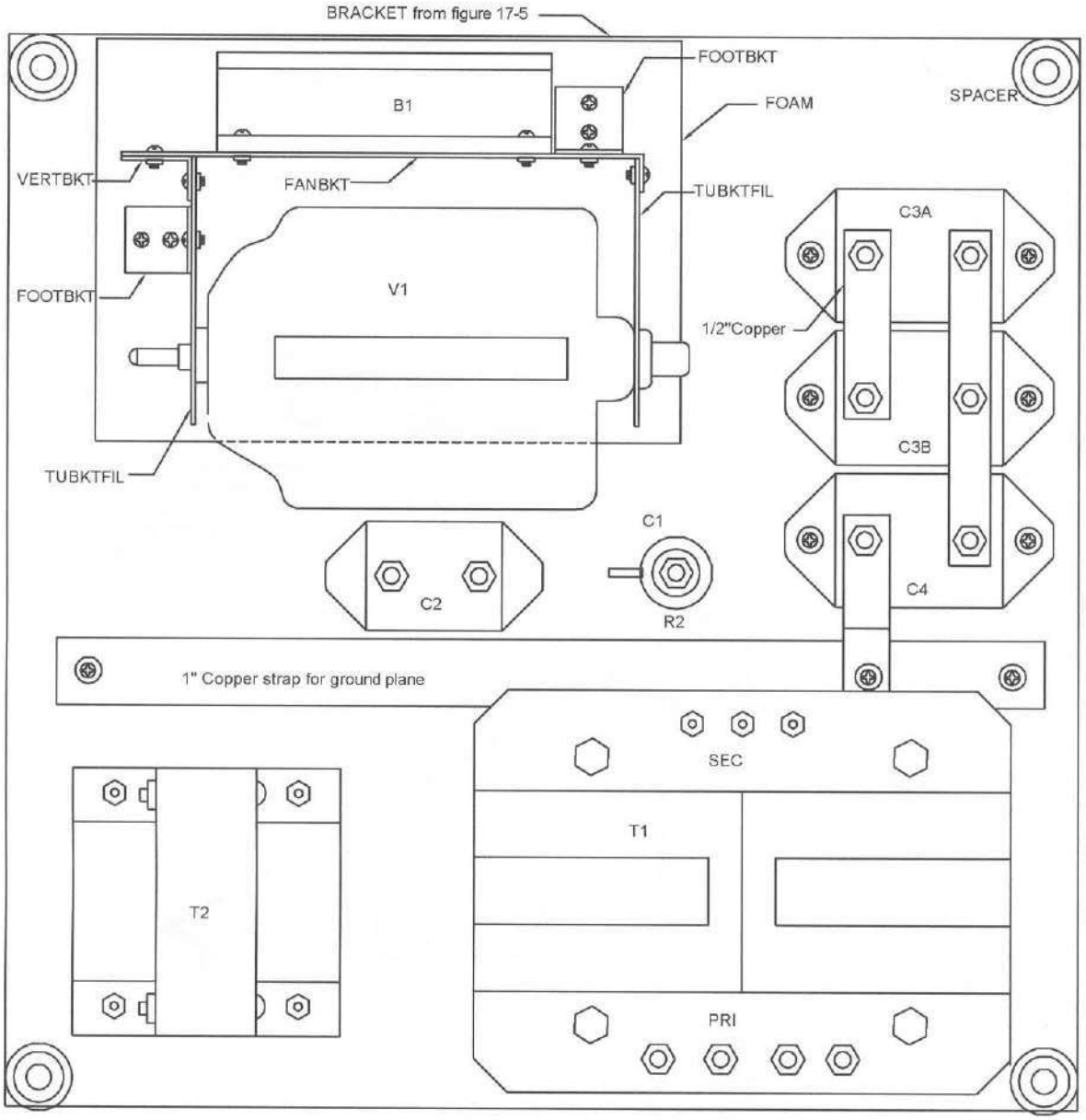

Figure 17-6 *Bottom deck assembly*

must set on a 1/4-inch foam rubber pad to avoid any vibration. Fabricate the tube pin connections from 1/2-inch strips of thin copper in the form of clamping connectors. Use screws to tighten the clamps securely around the tube pins. Crimp the connecting wires in place and carefully solder the connecting leads completely. This is important as the tube pins must pass a high current.

4. Lay out the bottom deck DECKBOT and trial-fit the components, as shown in Figure 17-6. (You may want to consider castors at the corners for system mobility.) Cut a 14-inch length of a 1-inch-wide copper strip for the main ground plane. Secure it via two wood screws at the end points. Secure the plate transformer (T1) using four 1/4-20 × 1 1/2-inch bolts with flat washers on the bottom side of the wooden deck. Mount the three mica capacitors (C3A, C3B, and C4) using 6-32 × 1 1/2-inch screws, nuts, and washers. Cut 1/2-inch lengths of copper straps and attach them as shown. Note the grounding piece on C4 must be shaped and formed to have a flat surface abutting the ground plane strap and fitting as shown.

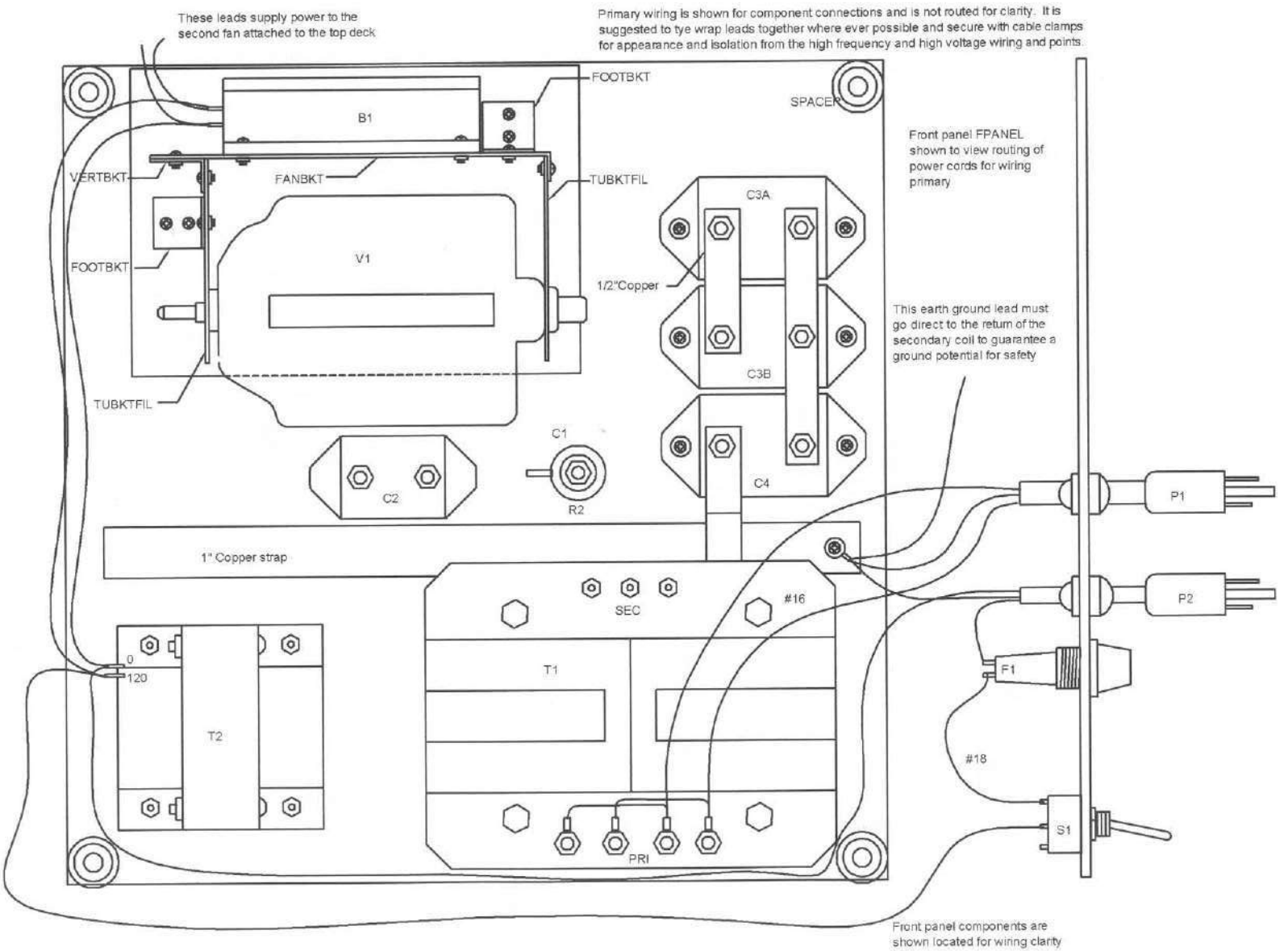

Figure 17-7 *Bottom deck primary wiring*

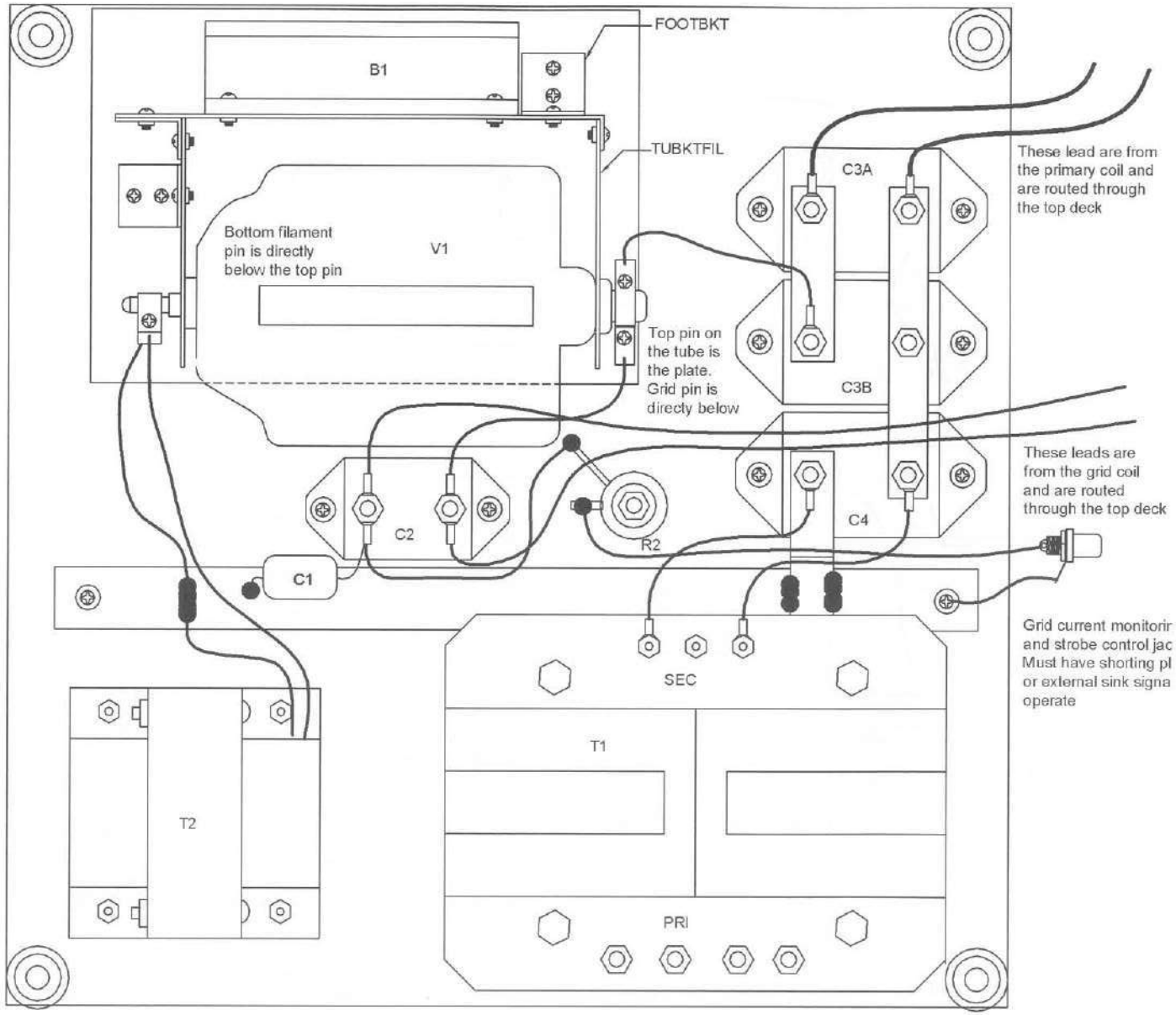

Figure 17-8 *Bottom deck high-voltage wiring*

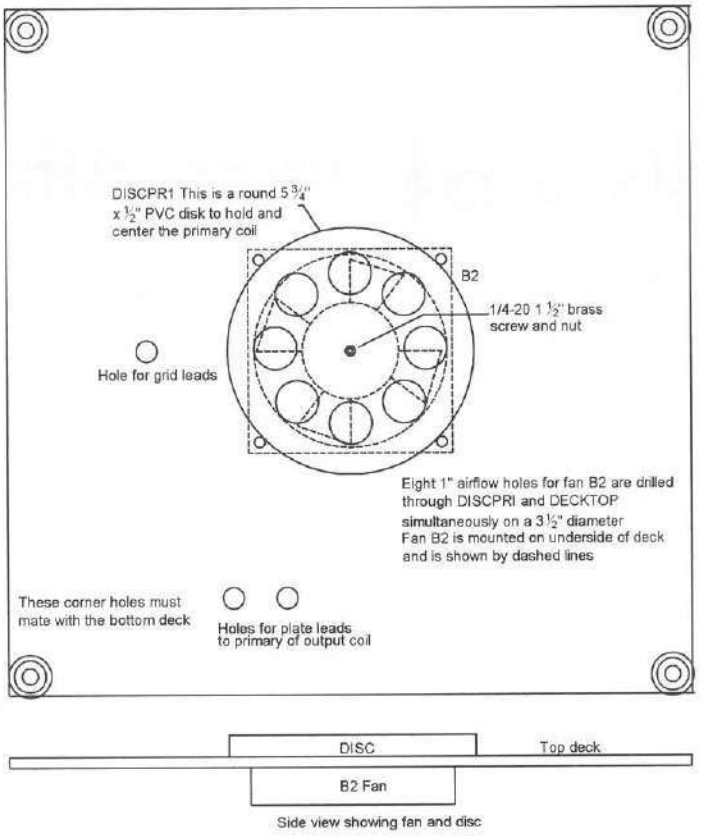

Figure 17-9 *Top deck fabrication and assembly*

Do not tighten the nuts at this time. Mount mica capacitor C2 using similar hardware and grid resistor R2 vertically using a long 1/4-inch bolt or a threaded rod. Do not overtighten. Secure the filament transformer T2 using four 8-32 × 1 1/2-inch screws and nuts. Secure the tube and fan bracket via four #8 × 1/2-inch wood screws through the two foot brackets FOOBKT. Also note the foam rubber mount FOAM. Drill holes for the 1/4-inch −20 threaded rods for the deck spacer.

5. Thread the power cords (P1, P2) through the clamp bushings (BU1, BU2) as shown in Figure 17-7 on the front-panel section (FPANEL). The actual location on the panel section is shown in Figure 17-3. Figure 17-7 is shown to clarify the wiring. Power cord P1 must be a heavy-duty, #16, three-wire cord, with P2 being a #18, three-wire cord. Connect the two green ground leads to a crimp lug along with a 24-inch piece of #18 stranded wire that eventually connects to the center ground lug of the secondary coil. Solder this lug and verify the integrity as this is mandatory for electrical safety. Proceed to wire as shown using #18 stranded wires. Note that the two leads eventually connect to the second blower (B2) mounted on the top deck. Use crimp lugs and solder wherever shown. Route the wires, tie wrap, and clamp into place for appearance and isolation from other components.

6. Wire the filament clips to the 10-volt output leads of T2 as shown in Figure 17-8. These clips are shown in Figure 17-5. You will note that insulation is removed from one of these leads, and the uncovered section is soldered to the 1-inch copper strip. Solder in the bypass resistor (C1) to the copper strip and to a lug with the other leads to R2. High-voltage wire should be used from transformer T2 to capacitor C4. Proceed to complete the wiring using crimp lugs and soldering. Two pairs of wires are shown from the primary and grid coil. These are not actually connected at this time as they are part of the top deck assembly (DECKTOP). Jack (J1) is attached to the front panel shown located in Figure 17-3.

7. Fabricate the DECKTOP, as shown in Figure 17-9. This piece was originally shown as being

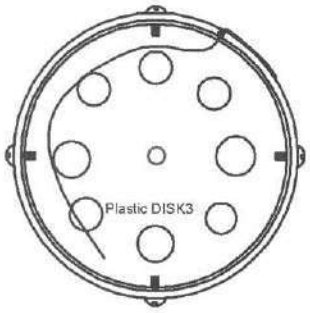

The secondary is wound on the form as shown for FORMSEC in figure 17-3.
Special note: The coil form must be totally clean both inside and out. Use isopropyl alcohol and allow the form to completely dry. Coat with a layer of orange shellac should do this on a dry day or in a dehumidified area.

Start by inserting the polycarbonate disk DISK3 into the output end of the coil form flush with the end. Secure using 3 or 4 small plastic screws. Do not use metal on the coil output end as arcing will occur.

Insert a 1" width aluminum bracket into the base end with a 1/4-20 tapped hole for screwing on to the brass screw from figure 17-9. Bend down ½" 90 degree ends to attach to inner diameter of coil via brass screws and nuts.

Position roll of #28 heavy magnet wire and thread into holes on base end of form. Attach free end to bracket via one of the screws. Drill small holes at each end of the coil form ½" from ends for threading the "start" and "finish" leads of the windings.

Start to wind the turns and continue for 33" in length being careful to keep the wire tight, free of kinks and avoiding any overlaps. Do approximately several inches at a time and shellac in place using orange shellac. Always secure lead with a piece of good adhesive sticky tape as an "unwind" will be disastrous. Winding this coil with two people is much easier.

Completed coil should contain approximately 2400 turns and tune to around 200 khz when free standing. Note winding should be in the same direction as primary coil LP1

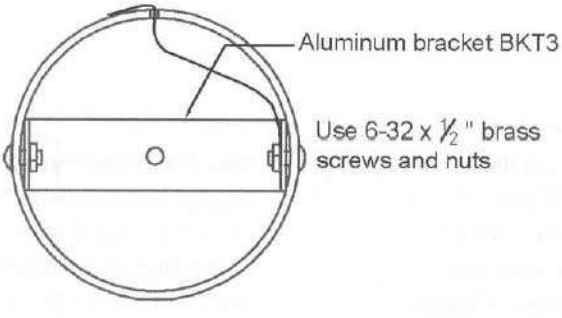

Figure 17-10 *Assembly of the secondary coil*

a 3/8-inch Plexiglas square from Figure 17-3. Fabricate a 5¾-inch PVC disc (DISCPRI) from ½-inch-thick sheet. This piece is for securing and centering the primary coil assembly, shown later in the plans. Secure it in place on the deck via a ¼-20 × 1-inch brass screw and nut. This will be the grounding point for the bottom of the secondary coil and

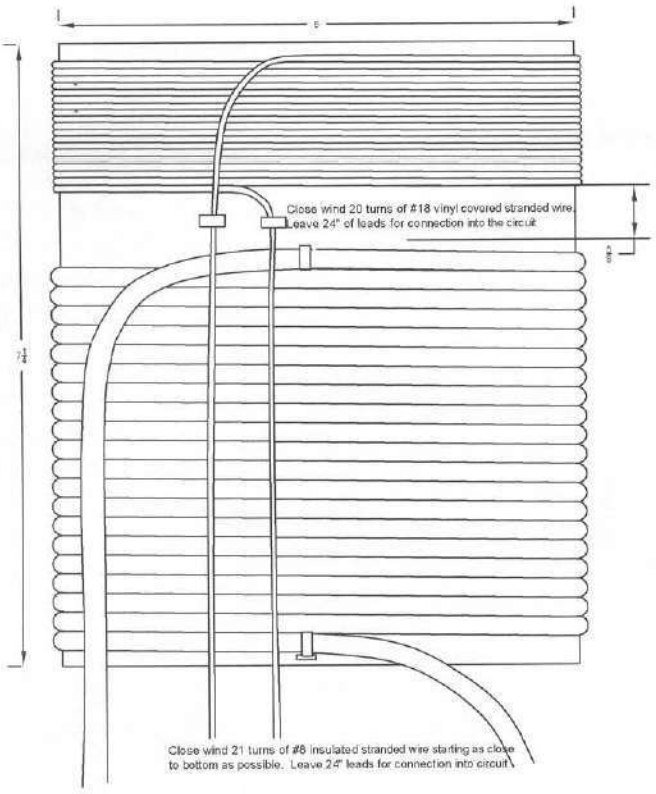

Figure 17-11 *Assembly of the primary coil*

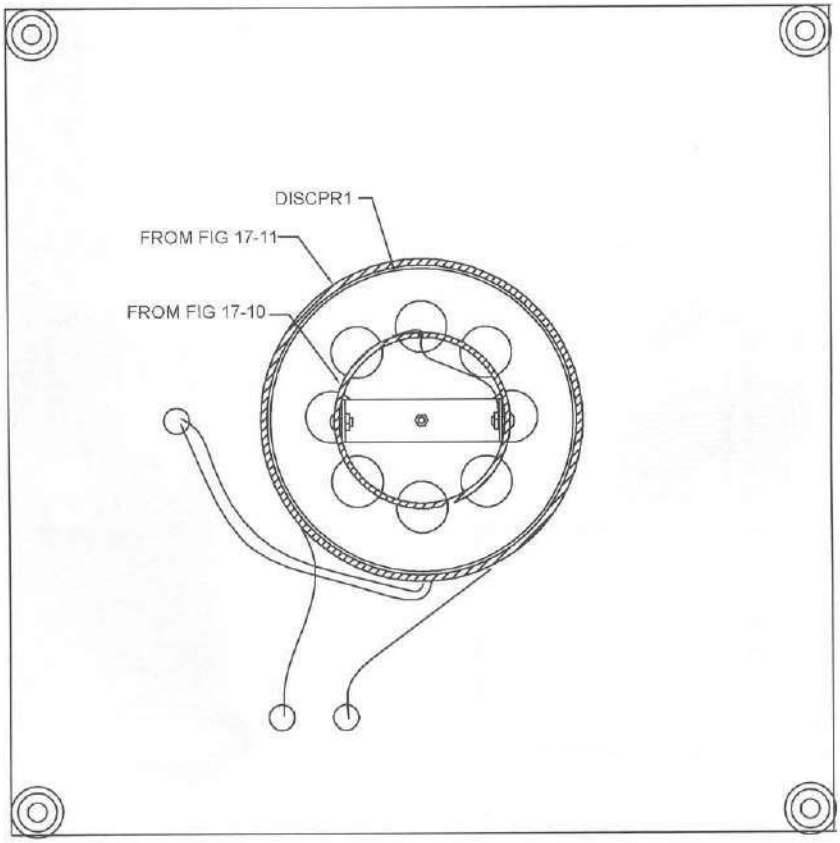

Figure 17-12 *Final assembly of top deck*

goes to earth ground, as shown in Figure 17-7. Proceed to drill the eight 1-inch air flow holes.

At this time, the builder should be aware that if his or her coil is to be used on a continuous basis, the second blower mounted on the underside of the top deck is necessary to keep the bottom of the coils cool. They will heat up over time due to the resonant rise of current associated with the base of a quarter-wave resonator. If your coil is to be used for a short-time operation of several minutes, the part involving the drilling of the air flow holes and the second fan may be omitted.

8. Assemble and wind the secondary coil as shown in Figure 17-10. Proper winding of the coil is mandatory for achieving optimal operation. Kinks and overlaps will seriously affect output.

9. Assemble the primary coil assembly, as shown in Figure 17-11. Start at the bottom and tightly wind the turns. Use tie wraps to secure the start and finish of this heavier 21 turns of the #8 stranded wire. You may want to place dabs of silicon rubber to secure them in place. Start

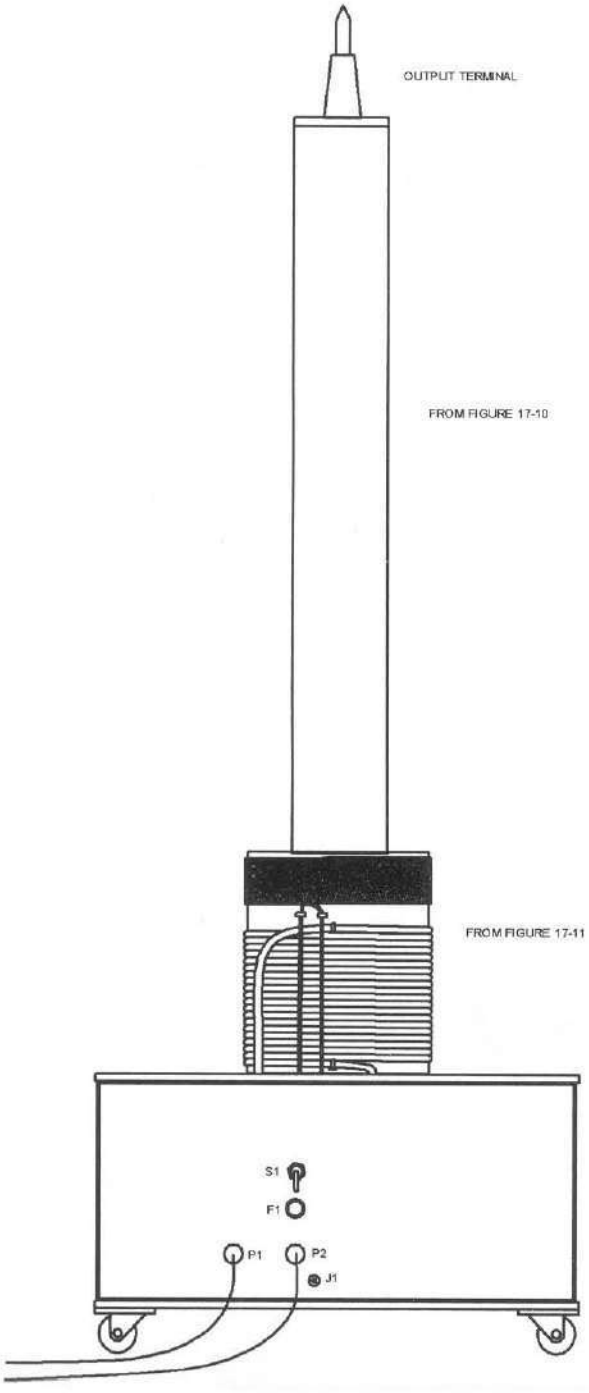

Figure 17-13 *Side view of final assembly*

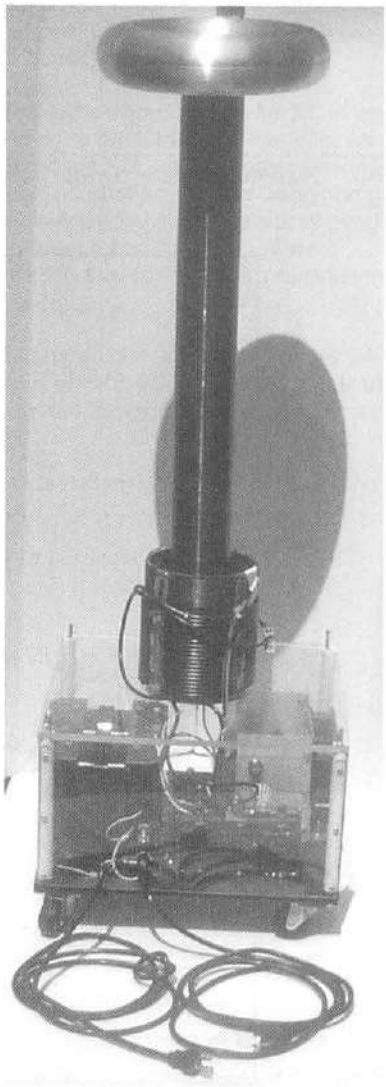

Figure 17-14 *The final assembly*

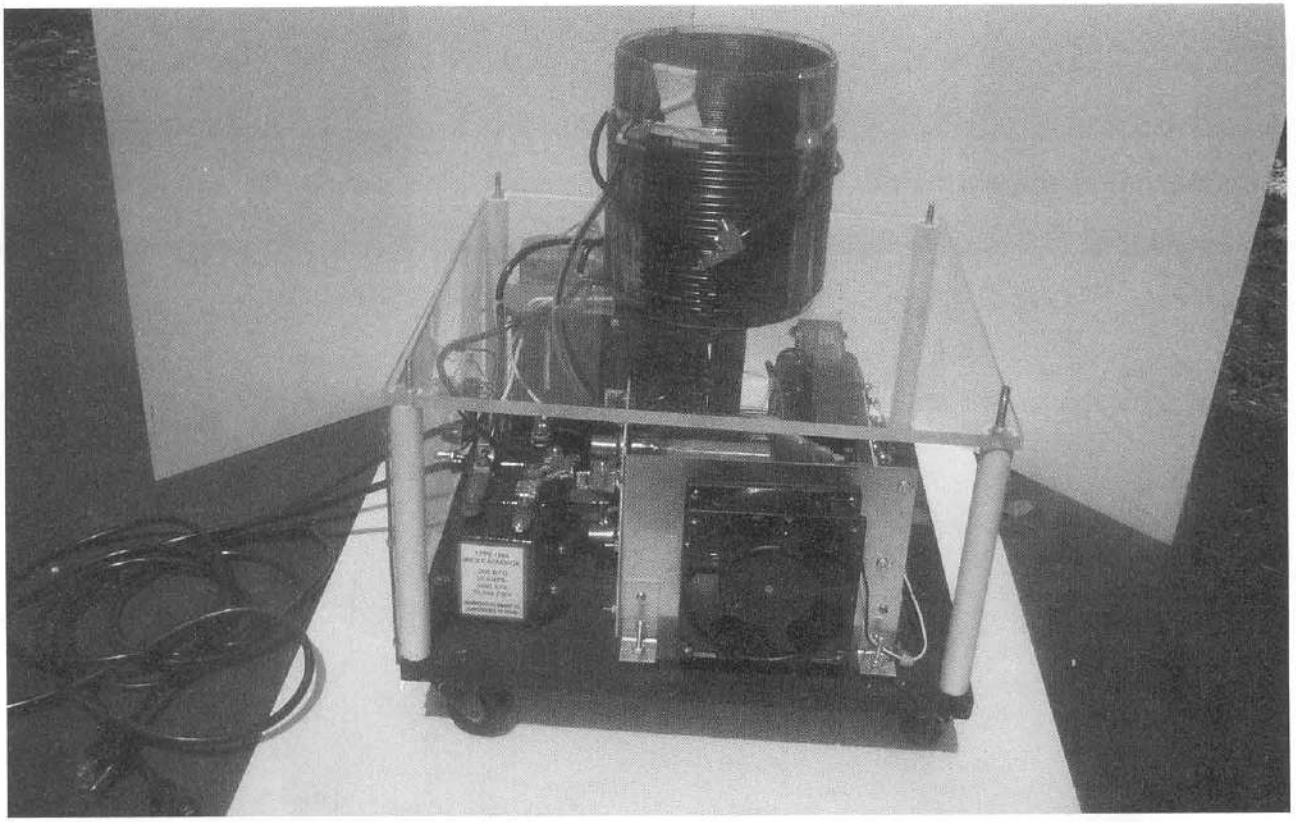

Figure 17-15 *The right-side view*

from the top and wind 20 turns of #18 vinyl-covered stranded wire and tie wrap it in place. Note that there must be at least ½-inch between the closest proximities of these two coils as a flashover (or spark break) could damage the vacuum tube. Leave at least 2 feet of extra leads for connections, as shown in Figure 17-8.

10. Finally, assemble the top deck, as shown in Figure 17-12. The primary coil section slips over the disc DISCPRI, as shown in Figure 17-8. The tapped hole in the bracket of the secondary coil screws onto the center brass screw shown in Figure 17-8. It is this screw that grounds and secures the secondary coil.

    Route the leads from the coils through their respective holes for connection into the circuit. You will note back in Figure 17-8 that the heavy plate leads are shown connected to C3A via heavy crimp lugs and are also soldered. The same applies for the smaller grid leads that connect across C2. These leads may require switching during the test steps. Both sets of these leads carry high-frequency energy with the heavier leads carrying high-radio-frequency voltages and currents. These heavier leads must be as short and direct as possible and not be in close proximity to other objects.

    Figure 17-13 shows the completed graphic of the coil assembly with an insulator and a pointed discharge pin. Any suitable feed through the insulator around 2 to 3 inches in height can be used. You may also use a piece of polycarbonate or Teflon rod for this part. Other plastics may carbonize and burn.

    The following figures are actual photos showing different views of the assembly apart and intact. They are intended as assembly aids.

Figure 17-14 shows a 12 × 3-inch toroid as the output terminal. You will note the two power cords exiting through the front panel.

Figure 17-15 shows the right side with a view of the blower B1 and tube-mounting bracket.

Figure 17-16 shows the left side with a view of the filament and plate transformers.

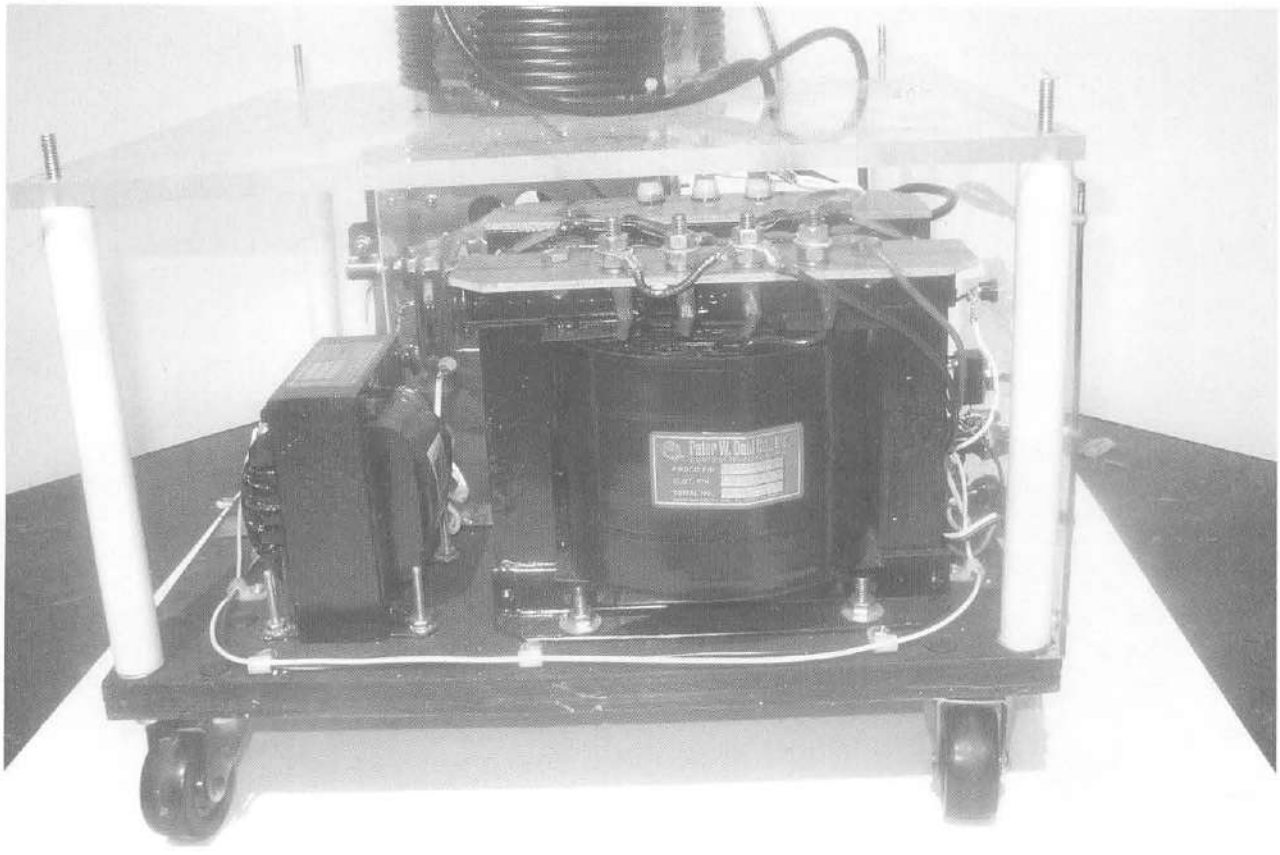

Figure 17-16 *The left-side view*

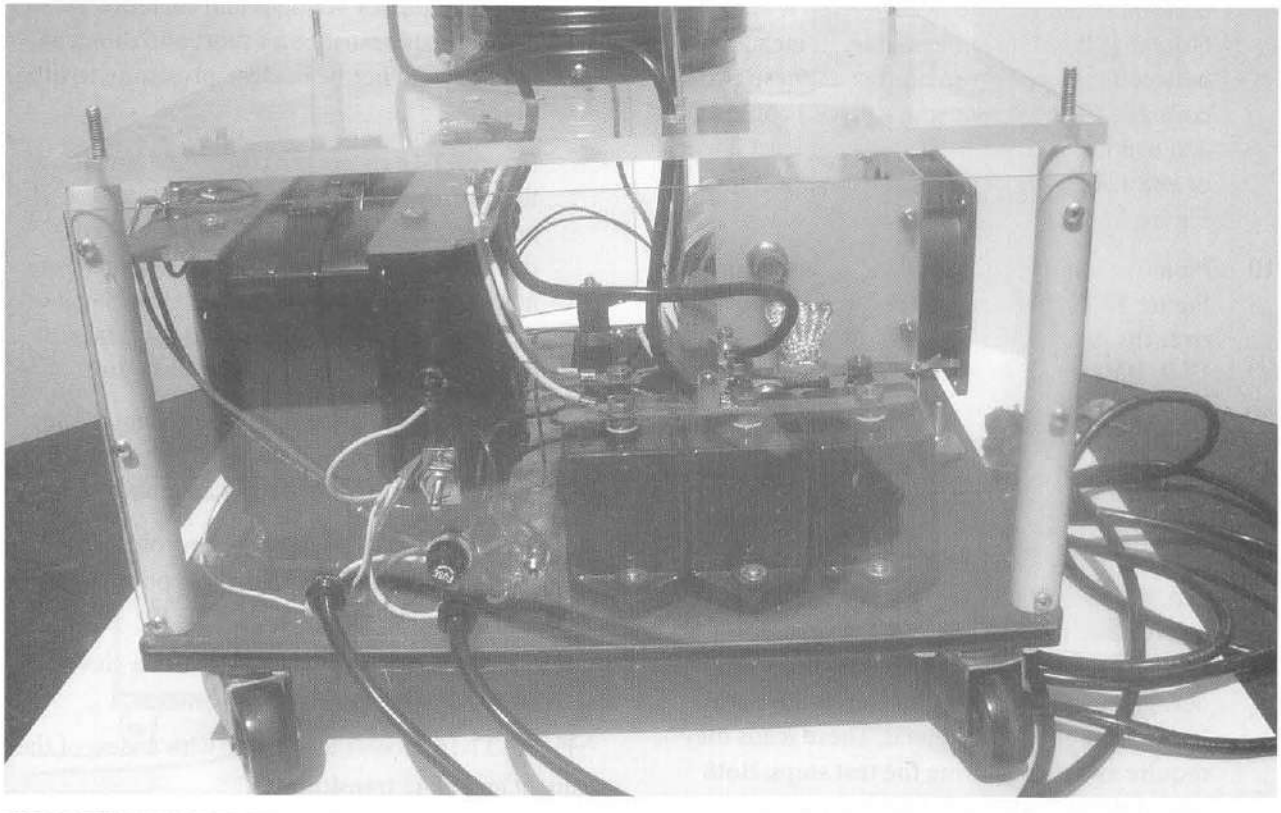

Figure 17-17 *The front view*

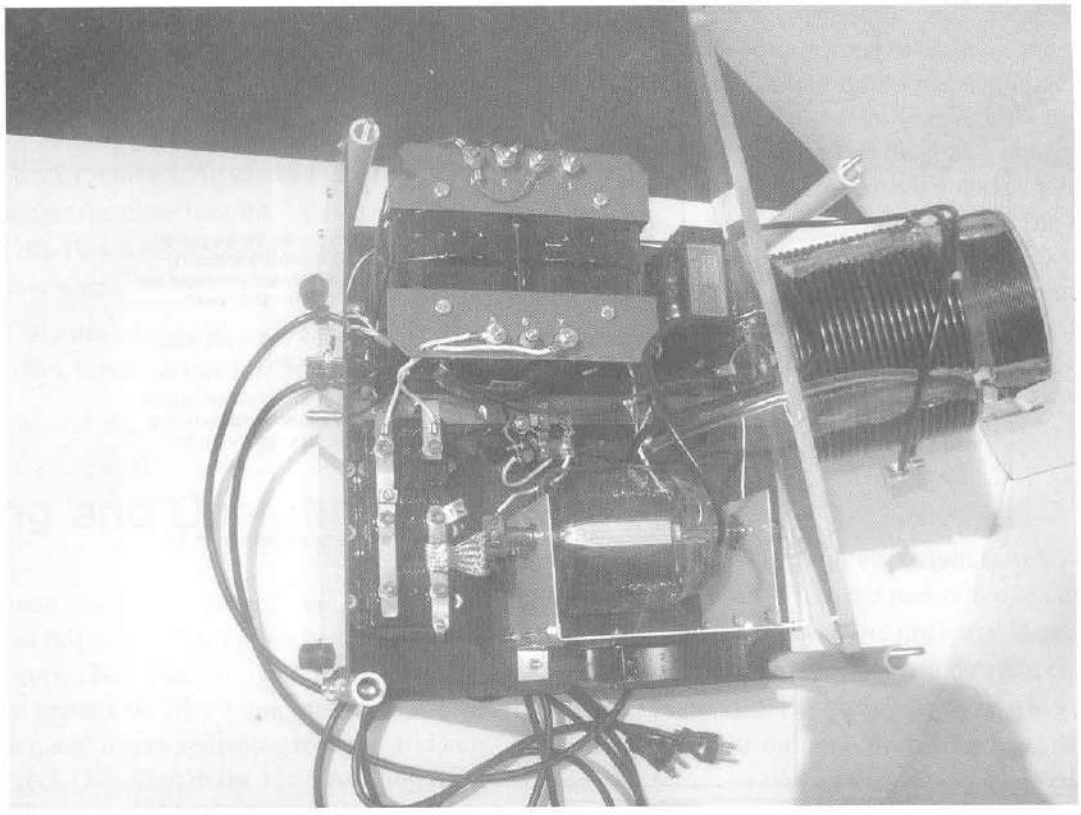

Figure 17-18 *The top view*

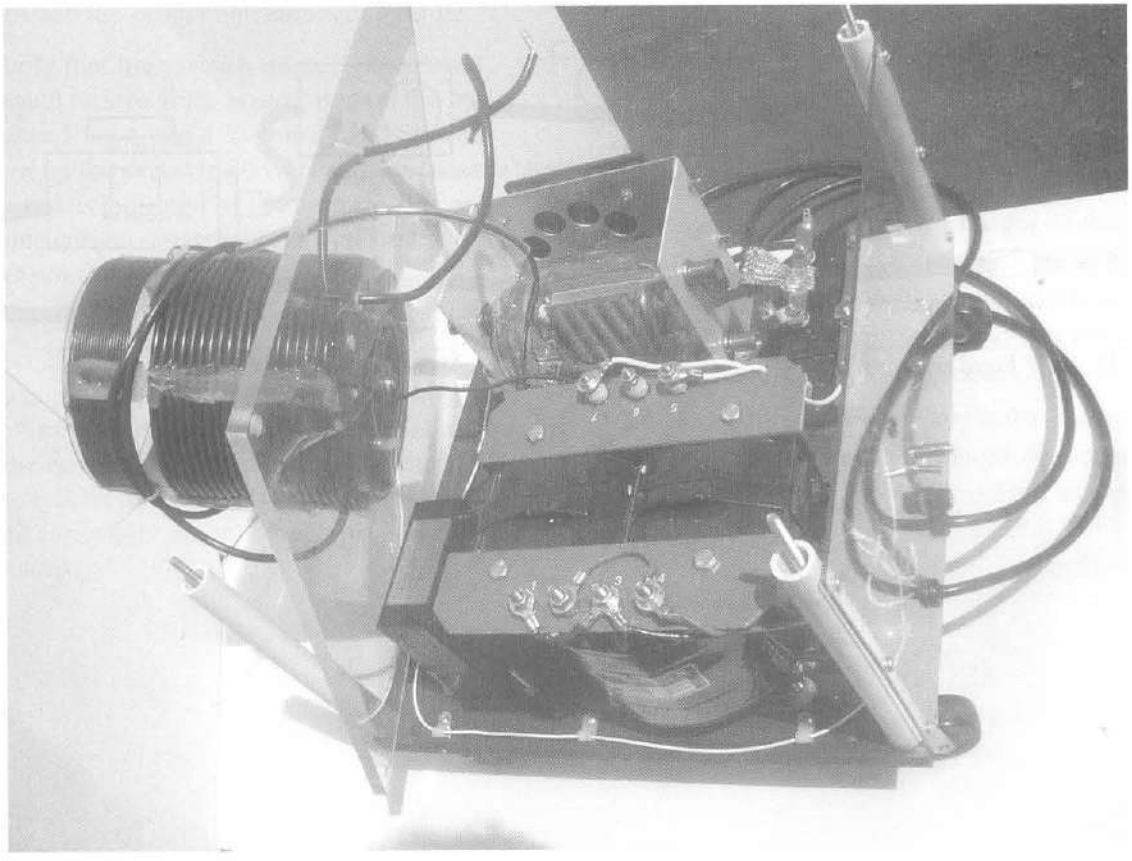

Figure 17-19 *Another top view*

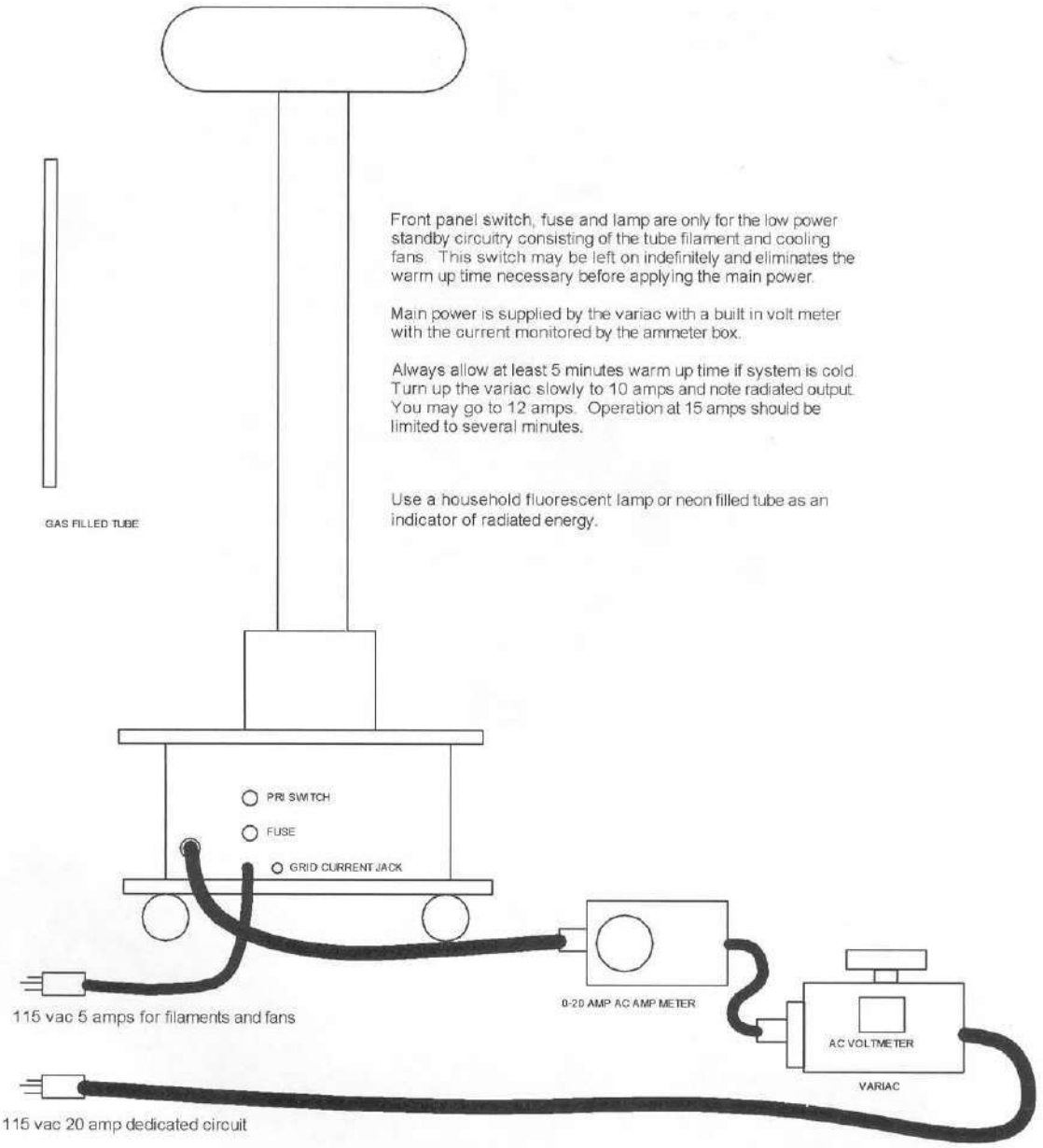

Figure 17-20 *Final system setup*

Figure 17-17 shows the front view through the clear plastic panel. Note the three mica capacitors C3A, C3B, and C4.

Figure 17-18 shows the top view with the clear plastic top deck removed. We used a piece of shielded strap to connect the plate terminal of the tube to C3A and C3B. This is not necessary and may be heavy flexible wire.

Figure 17-19 also shows the top view with the clear plastic top deck removed but at a different angle.

Testing and Operating

1. You will need a dedicated 20-amp line to obtain full output. Set up the system as shown in Figure 17-20. Place the unit away from metal objects, insert a 7-amp fuse in the holder, and insert a shorting into the grid current jack (J1). Plug in the 115 VAC plug for the filament and blower fans, and wait for the tube to glow and the fans to blow. Always allow at least 3 minutes for the tube filament to reach the proper emission temperature.
2. Verify that the variac is properly wired and turned to zero volts, as indicated on the voltmeter. Plug it into a 20-amp circuit. Slowly turn up the variac to 30 volts and verify some output as indicated by the bulb glowing or some corona discharge occurring on the output pin.

   If you do not observe some output, it will be necessary to completely shut the system down by unplugging both plugs, reversing the grid coil wires that attach to C2, and repeating the previous step. This is referred to as phasing the system. You should get substantial output and easily light the tube when properly phased.
3. Once you verify that the coil is properly phased, you may start to increase the voltage, noting the output discharge, the input current, and the applied AC voltage as indicated on the variac meter. You must also observe that the plate of the tube does not start to glow, as this is an indication of mistuning. The tube may have a very soft glow at full 120 VAC where the output should be 15 inches or more. The input current will approach 20 amps.

Notes

Tuning the coil for maximum output is tricky and may take some effort on the part of the builder. The tuning values will vary as the discharge increases due to the virtual capacitance of the ionization cloud at the top of the coil. The output terminal will also greatly effect the output tuning. Try adding or subtracting a turn or two on the primary plate coil, as this will change the resonant drive signal. You will need more inductance as the output increases, and the trick is to select the optimum value at the desired input power.

A 12-inch toroid or another large capacitive terminal will cause larger circulating currents within the coil and greatly enhance the wireless transmission of energy, as can be demonstrated by observing the distance that is possible for lighting the gas discharge tube without a wire. This will eliminate the air breakdown discharge when operating in this mode as the terminal voltage drops unless you increase the input power to overcome this loading effect.

The geometry of the secondary coil as shown is not the optimum for maximum length discharges. A squatter size would be more efficient but would radiate less.

Table 17-1 Vacuum Tube Tesla Coil Parts List

Ref. #	*Description*	*DB Part #*
R2	5K, 100-watt wire-wound resistor	
C1	.004-microfarad, 1,000-volt polypropylene capacitor	DB# .0039/400
C2	.003-microfarad, 3-kilovolt mica capacitor	DB# .003/3 KVM
C3A, B, C4	Three .01-microfarad, 10-kilovolt mica capacitors	DB# .01/10 KVM
V1	833A Triode vacuum tube	DB# 833A
T1	3,000-volt, .5-amp plate transformer	DB# 3KV/.5A
T2	10-volt, 10-amp filament transformer	DB# 10V/10A
B1, 2	5 × 5-inch muffin fan and 5 × 5-inch high-output muffin fan	DB # FAN1
S1	*Single pole, single throw* (SPST) 5-amp toggle switch	
F1/FS1	Panel-mount fuse holder and 5-amp fuse	
P1	8-foot #16 three-wire power cord	
P2	8-foot #18 three-wire power cord	
AMPMETER	20-amp AC panel mount ammeter	
VARIAC	18-amp variac with built-in meter	DB# VARIAC18A
TUBE	15-inch neon tube	DB# NE15
TER1	12 × 3-inch toroidal terminal	DB# TO12

Chapter Eighteen

Universal Capacitance Discharge Ignition (CDI) Driver

Figure 18-1 shows how to construct a very useful driver circuit that can be used to pulse most induction and ignition coils in the forward direction. High-quality automotive ignition coils can produce 50- to 75,000-volt pulses capable of jumping several inches. The system allows control of the pulse repetition rate up to 100 reps/second and individual pulse energy up to .3 joules. A maximum power output of over 30 watts is possible. Our laboratory model has generated discharges of up to 10 inches from some high-performance ignition coils.

The advantage of a *capacitance discharge ignition* (CD) system is its ability to produce high peak currents and voltages simultaneously. This property is well understood and appreciated in the automotive industry where fouled spark plugs are prevented by the brisance of the discharge. Electric fences burn away vegetation growth from contacting the wire by using high current pulses. Stun guns use these high peak current pulses to thwart the neuromuscular system. All this peak power with very low resultant energy allows many useful applications where battery-operated systems can be efficiently utilized.

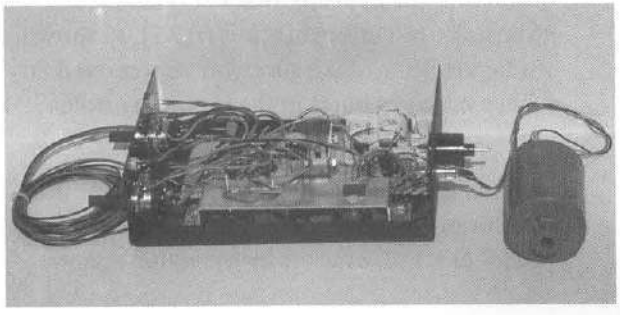

Figure 18-1 *The capacitor discharge driver*

This is an intermediate-level project requiring basic electronic skills and one should expect to spend $25 to $50. All the parts are readily available, with specialized parts obtainable through Information Unlimited (www.amazing1.com), and they are listed in Table 18-1.

Circuit Description

Figure 18-2 shows the complete circuit schematic of the adjustable energy and repetition rate capacitor discharge driver. The adjustable voltage regulator I2 controls the operating voltage to the system via control pot R9/S1 from 6 to 12 volts. Input to I2 is a 12-volt DC wall adapter transformer with a current rating of 1 to 2 amps being controlled by switch S1. This adjustable voltage is fed to the switching transistors Q1 and Q2 via the center tap of stepup transformer T1. The switching action of these transistors is controlled by a complementary pulse driver circuit I1 with its frequency controlled by trimpot R3. This circuit generates a high-frequency signal that alternates between the two primary windings, in turn inducing a higher voltage in the secondary winding.

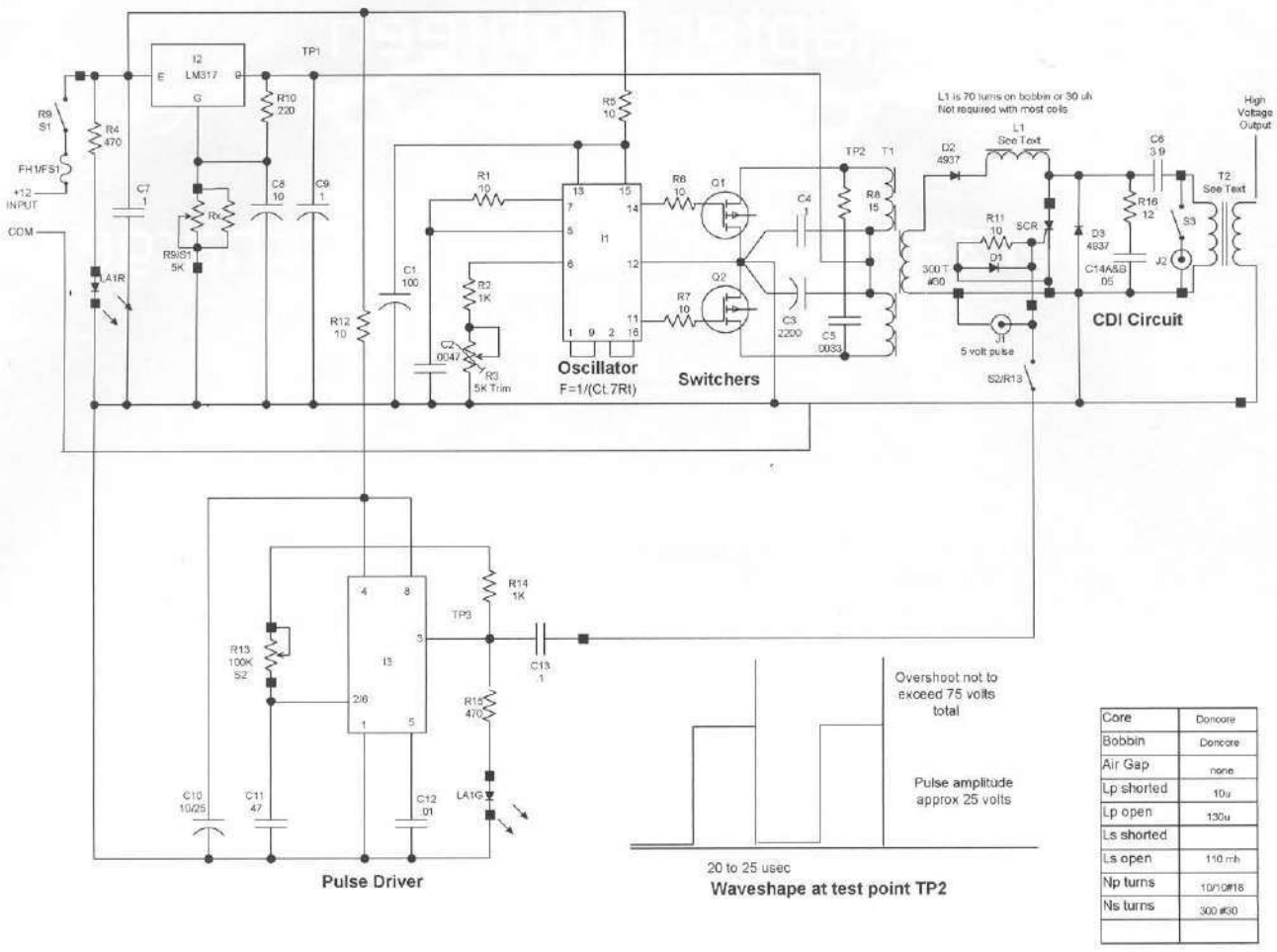

Figure 18-2 *Circuit schematic*

T1 is a transformer with a preset, built-in leakage reactance that controls the short-circuit-charging current to discharge capacitor C6 through rectifying diode D2. Once C6 is charged, it can be discharged by the silicon controlled rectifier switch (SCR) through the primary high-voltage pulse transformer T2. The SCR is controlled by timer chip I3, connected as a variable pulse generator via pulse rate adjust pot R13/S2. It is these pulses that trigger the SCR to switch energy from C6 into T2, generating the high-voltage output pulses. You may also externally switch the SCR via a pulse signal at input jack J1. R13/S2 must be off for this external function. The pulse transformer is shown as a low-power unit in the parts list.

The real intention of the circuit is the ability to pulse-drive many different ignition coils at different energy levels as selected by R9 and pulse repetition rates as selected by R13. We have obtained sparks up to 4 inches with conventional automotive coils.

Assembly Steps

1. Assemble the switching transformer as shown in Figure 18-3.
2. Fabricate the heatsink bracket (HS1) and transistor-mounting bracket (BR1), as shown in Figure 18-4. Make sure you've removed any sharp edges or burrs in the mounting holes that could break through the insulating pads.
3. Attach Q1 and Q2 as shown, noting that the mounting tabs are insulated from the actual metal heatsink bracket by the nylon screws.

1. Bifilar (parallel) wind two different color #18 magnet wire for 10 turns on the primary bobbin. Tape in place leaving 8" leads. Note that different colors will help identifying the lead ends.
   #18 solid magnet wire can be used however high frequency LITZ wire will give a slight improvement. You can make this wire by obtaining 6 pieces of #26 magnet wire and twist together as a single wire.

2. Wind 300 turns of #30 magnet wire in the 10 segments of the secondary bobbin. Wind 30 turns per segment and attach the start and finish leads to the connection lugs

3. Place the wound coils onto the cores as shown and tape tightly into place.

4. You may verify the inductance as follows secondary open:
   A to B&C are around 130 micro henries.
   D to B&C are around 130 micro henries
   Secondary winding 110 millihenrys

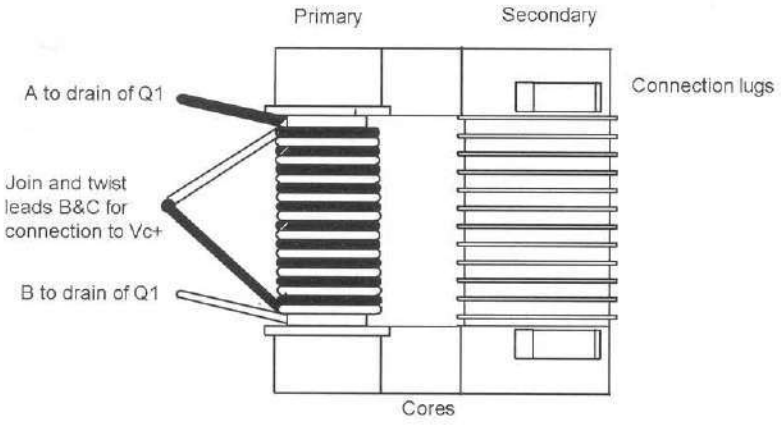

#18 solid magnet wire can be used however high frequency LITZ wire will give a slight improvement. You can make this wire by obtaining 6 pieces of #26 magnet wire and twist together as a single wire.

Figure 18-3 *T1 Transformer construction*

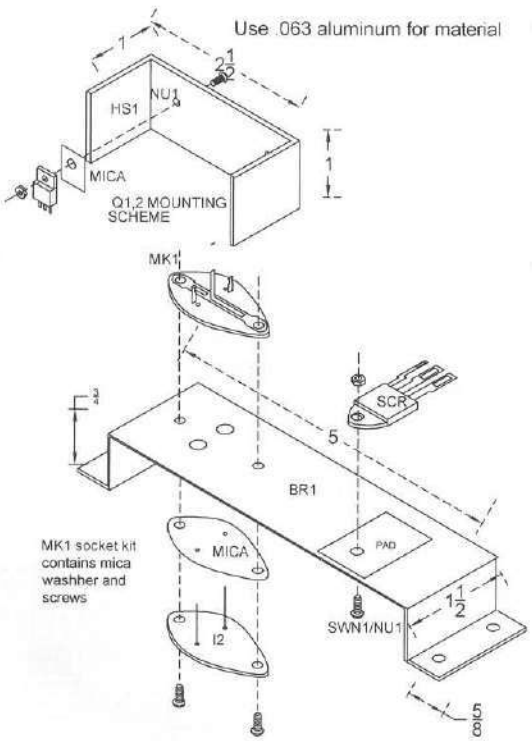

Figure 18-4 *Assembly of brackets*

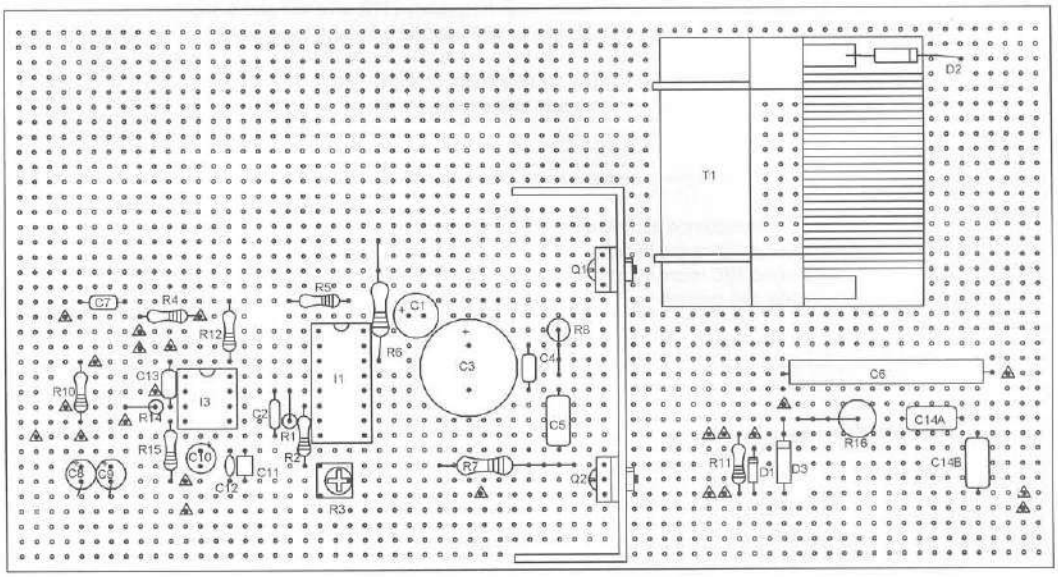

Figure 18-5 *Assembly board and parts location*

Attach I2 using the socket assembly kit (MK1) and attach the SCR using a nylon screw and an insulating pad (PAD).

4. Cut a piece of .1 × .1 grid perforated circuit board (PB1) at 7 × 3.8 inches.

5. Insert the components as shown in Figure 18-5, starting from the lower left-hand corner. Count the perforated holes for a guide. Note the polarity marks on C1, C3, C8, C9, and C10 and diodes D1, D2, and D3. It is suggested that you use sockets SO16 for I1 and SO8 for I3.

6. Wire the components as shown in Figure 18-6 using the leads of the actual components as the connection runs, which are indicated by the dashed lines. Always avoid bare-wire bridges and messy solder joints. Check for cold or loose solder joints and secure T1 using double-sided sticky tape or plastic tie wraps.

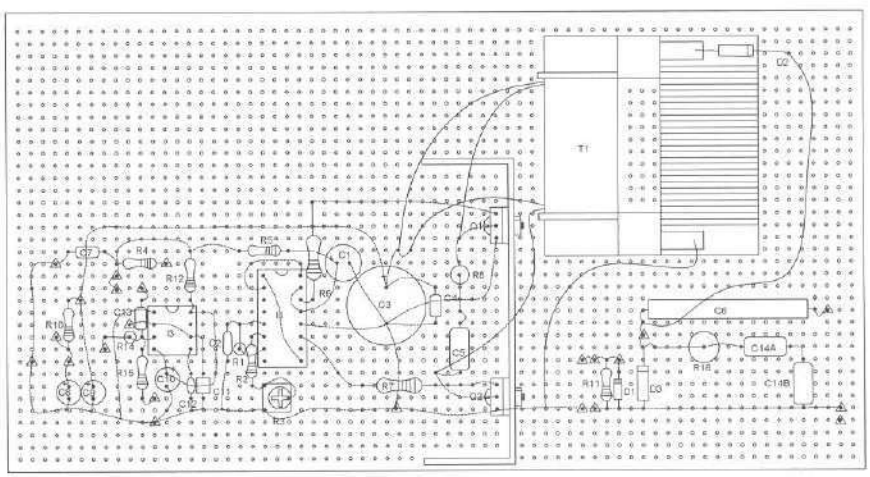

Figure 18-6 *Internal onboard wiring*

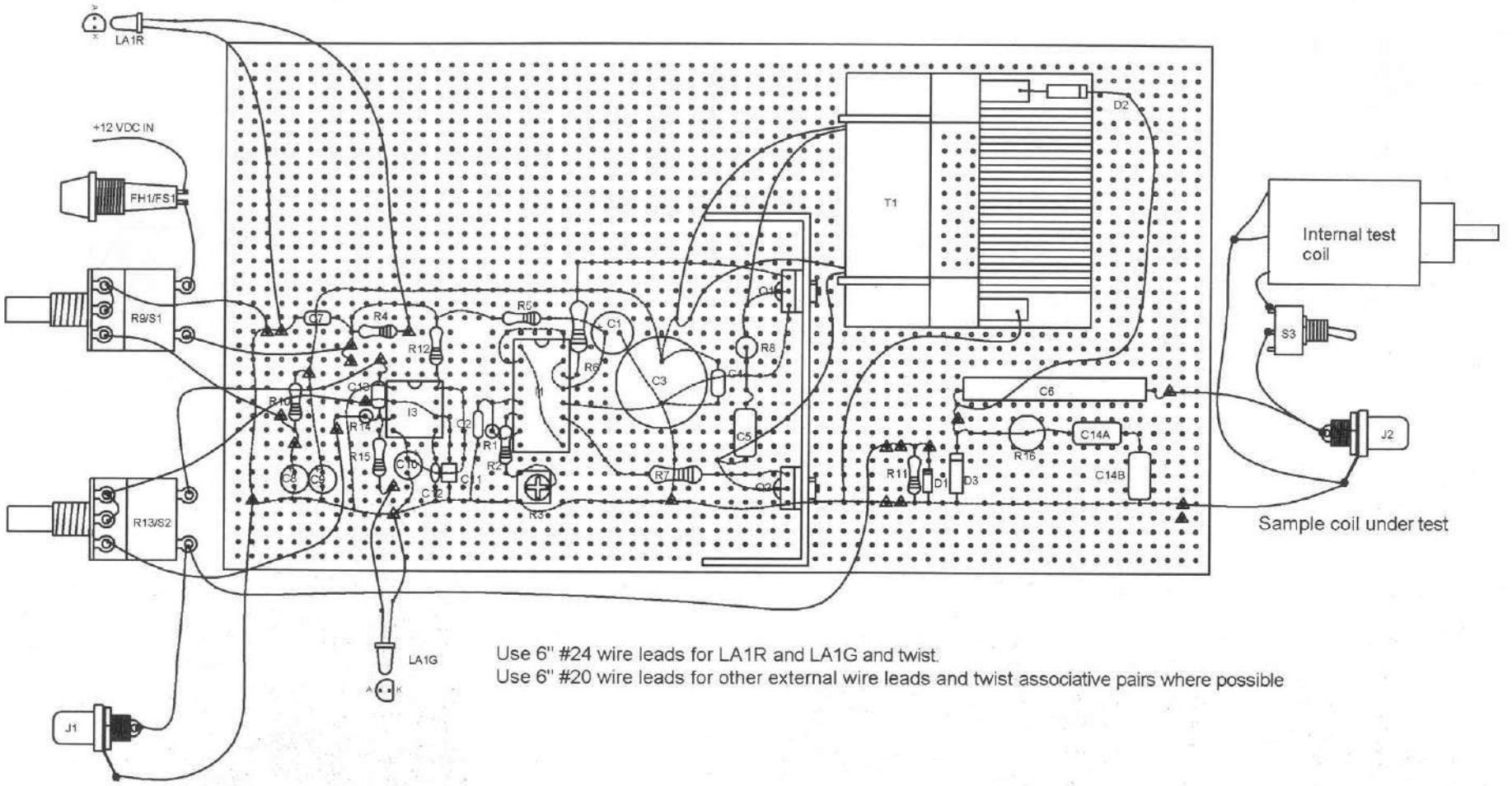

Figure 18-7 *External wiring to controls and input*

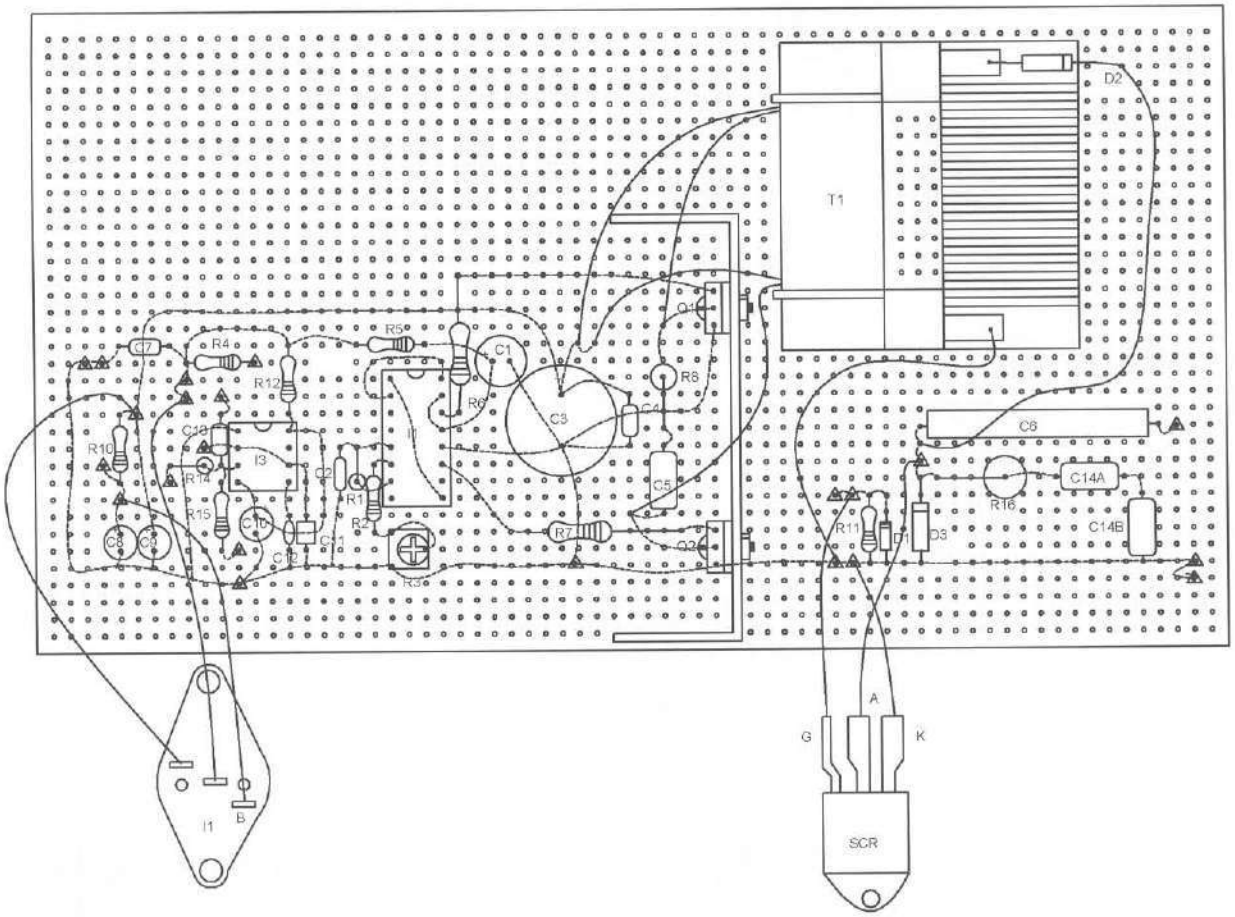

Figure 18-8 *External wiring to transistor modules*

The external coil of choice is connected to J3 using short lengths of #18 wire. It is a good idea to rig a ground return for the output spark to jump to. Always use one of the primary leads of the external coil as the ground return point. Other points used for ground may cause voltage loops that can damage the unit. We use a dedicated gap with connection leads containing clips. The gap is adjustable from ½ to 3".

S3 disables the internal test coil.

J1 is intended for input from an external trigger and requires R13 to be fully off.

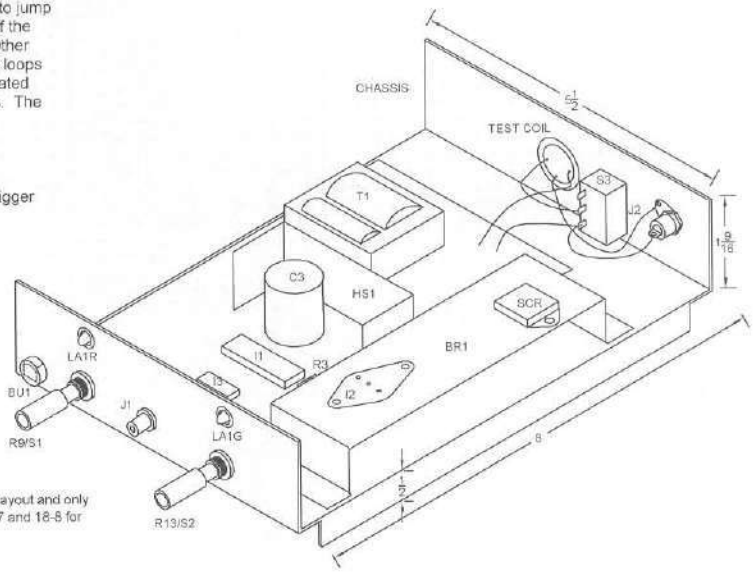

Note this view is intended to show the general layout and only indicates certain components. Use figures 18-7 and 18-8 for wiring of the specific parts as shown

Figure 18-9 *Final assembly*

7. Wire the external components as shown in Figure 18-7.
8. Wire the transistors from the assembled bracket, as shown in Figure 18-8 and detailed in Figure 18-4.

Fabricate the mounting chassis at the overall dimensions shown in Figure 18-9. Trial-fit the remaining components, proceeding to drill and locate with the proper sized holes. Attempt to follow the figure and note the position of the BR1 bracket assembly and front panel controls. Route and twist all lead pair to neaten appearance. You may want to splice in some output leads to replace the connections to the test pulse transformer T2. These should be #18 wire and as short as physically possible to the external ignition coil. Also create a suitable cover if required and ventilate it with holes for air cooling.

Test Steps

This step will require basic electronic laboratory equipment, including a 60 MHz oscilloscope.

1. Turn off both controls R9 and R13. Set the R3 trimpot at midrange.
2. Connect a scope to TP2 and a voltmeter to TP1.
3. Apply 12 VDC to the input leads and turn on R9/S1. Adjust the meter for 5 volts and adjust the period of the waveshape at TP2 to a 25 us period. The input current should be less than .2 amps on a 12-volt power supply.
4. Note that the LED indicators are on with LA1G flashing at the pulse repetition rate determined by the R13 setting. This occurs even with R13/S2 fully off.
5. Turn on R13 and adjust it for 10 volts. Note the test coil sparking over its outer surface. Rotate R13 and notice the pulse rate increasing. Only operate the test coil to test circuit performance.

Notes on Operation

The unit is intended to drive larger ignition and induction coils. Jack J2 is intended as the output to the external coil under operation.

Note that the test coil must be disabled for external operation and may be disconnected by unsoldering or using a suitable high-current switch that may be mounted on the rear panel adjacent to J2.

When using unknown coils, it is advised that you monitor the DC voltage across the SCR. It should never exceed 400 volts, as the storage capacitor will be overrated. The SCR can handle up to 800 volts.

A change occurs in the charging voltage as the pulse repetition rate is changed. It decreases as the repetition rate increases. You can compensate for this by adjusting R9, but you must be careful to turn it down before lowering the repetition rate. Always start with the voltage control R9 at the lowest setting and increase as necessary. Additionally, jack J1 is intended for external triggering and must be used with R13/S2 in the off position.

Table 18-1 Parts List for CDI Driver

Ref. #	Description	DB Part #
R1, 5, 6, 7, 11, 12	Six 10-ohm 1/4-watt resistors (br-blk-blk)	
R2, 14	Two 1K, 1/4-watt resistors (br-blk-red)	
R3	5K horizontal trimmer	
R4, 15	Two 470 ohm, 1/4-watt resistors (yel-pur- br)	
R8	15-ohm, 3-watt metal oxide resistor	
R9/S1, R13/S2	Two 10K pots and switches	
R10	220-ohm 1/2-watt resistor (red-red-br)	
R16	12-ohm, 2-watt metal oxide resistor	
Rx	Select a 1/4-watt resistor to shunt R9 to improve range	
C1	100-microfarad, 25-volt vertical electrolytic capacitor	
C2	4,700-picofarad, 50-volt polyester capacitor	
C3	2,200-microfarad, 25-volt vertical electrolytic capacitor	
C4, 7, 13	Three .1-microfarad, 50-volt polyester capacitors	
C5	.0033-microfarad, 250-volt polypropylene capacitor	
C6	3- to 5-microfarad, 350-volt polyester capacitor	DB# 3.9M/350
C9	1-microfarad, 25-volt vertical electrolytic capacitor	
C8, 10	Two 10-microfarad, 25-volt vertical electrolytic capacitors	
C11	.47-microfarad, 50-volt polyester capacitor	
C12	.01-microfarad, 50-volt disc capacitor	
C14	.05-microfarad, 400-volt metalized polypropylene	
I1	*Integrated circuit* (IC) driver and pulse-width modulator (LM3525)	
I2	1.5-amp adjustable voltage regulator (LM317)	
I3	Timer *dual inline package* (DIP) IC (LM555)	
Q1, 2	Two 100-volt *metal-oxide-semiconductor field effect transistors* (MOSFETS) (IRF540)	
SCR1	70-amp, 700-volt *silicon-controlled rectifier* (SCR)	DB# S8070W
D1	IN914 small-signal diode	
D2, 3	Two IN4937 fast-recovery, 1,000-volt, 1-amp diodes	
LA1R	Red *light-emitting diode* (LED)	
LA1G	Green LED	
T1	Inverter high-voltage transformer, as shown in Figure 18-3	DB# TRANCDI
T2	20-kilovolt pulse transformer (see text)	DB# CD25B
FH1	Panel-mount fuse holder	
FS1	3-amp fuse	
J1, 2	RCA phono jack	
S3	*Single pole, single throw* (SPST) 5-amp or more toggle switch	
PB1	7 × 3.8 × .1-inch perforated circuit vector board	
SOCK8	Eight-pin IC socket	
SOCK16	16-pin IC socket	
MK1	TO3 transistor mounting kit	
PAD	Thermo pad insulator	
CHASSIS	#20-gauge aluminum chassis, as shown in Figure 18-9	
HS1	Heatsink, as shown in Figure 18-4	
BR1	Transistor-mounting bracket, as shown in Figure 18-4	
MICA	Two Mica insulating pads for Q1 and Q2	
SWN1	Two 6-32 × 1/2-inch nylon screws	
SW1	6-32 × 1/2-inch screws	
NU1	Seven 6-32 nuts	
WIRE20B	12 inches of #20 bus wire	
WR20	Six feet of #20 vinyl hookup wire	
BU1	Small clamp bushing	
BU2, 3	Two 3/8-inch plastic bushings for LED	

Chapter Nineteen

Long-range Telephone Conversation Transmitter

Figure 19-1 shows a device that allows the user to monitor a phone's incoming and outgoing calls without any connecting wires. The system is intended to transmit both sides of a telephone conversation to any FM radio or headset-type receiver, such as a Walkman radio. It allows the user to perform outside activities such as mowing the lawn or working outside the house while completely monitoring the telephone over the radio.

The unique feature of this device is that activation occurs only when the phone is off the hook. This eliminates transmitting a continuous signal, thus preventing potential interference and unnecessarily wearing down the batteries. It also eliminates dead-tape listening time, as now the tape only records voices when the telephone is used. You may also listen to a radio station while monitoring the telephone. When the phone is used, the radio station is replaced by the transmission of the unit.

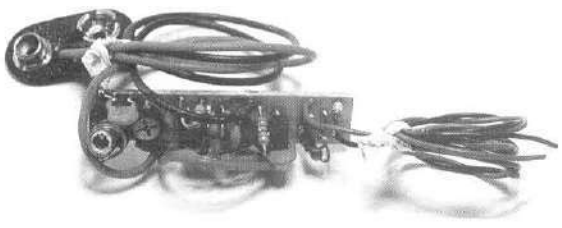

Figure 19-1 *Wireless circuit*

The device is shown assembled on a perforated circuit board and may be housed in a small plastic enclosure. Potting (or encapsulating with epoxy) and sealing is at the discretion of the builder.

Circuit Description

This chapter shows how to build a mini-powered FM transmitter that transmits both sides of a telephone conversation to a nearby FM radio. The circuit consists of a *radio-frequency* (RF) oscillator section combined with a telephone-activated switch section that controls the oscillator power (see Table 19-1). Transistor Q1 forms a relatively stable RF oscillator whose frequency is determined by the values of coil L1 and tuning capacitor C4. The C4 setting determines the desired operating frequency and is in the standard FM broadcast band with tuned circuit design, favoring the high end up to 110 MHz. Capacitor C2 supplies the necessary feedback voltage developed across resistor R3 in the emitter circuit of Q1, sustaining an oscillating condition. Resistors R1 and R2 provide the necessary bias of the base emitter junction for proper operation, while capacitor C1 bypasses any RF to ground fed to the base circuit. Capacitor C3 provides an RF return path for the tank circuit of L1 and C4 while blocking the DC supply voltage fed to the collector of Q1 (see Figure 19-2).

You will note that the junction of the base bias resistors R1 and R2 is a feed point consisting of capacitor C5 and resistor R4. This point is where the speech voltage from the telephone is applied. Because of the nature of the oscillator frequency being subject to change by varying the base bias condition, a varying AC voltage superimposed at this point causes a corresponding frequency shift (FM) along with an amplitude-modulated (AM) condition. It is this property that allows the circuit to be FM modulated by the speech occurring on the telephone lines. The signal is clearly detected by any FM receiver when properly tuned.

Be aware that before the phone receiver is lifted off the hook, a DC voltage of approximately 50 volts along with some AC hum is measured across the green and red wires of the phone line. This 50 volts is used to keep transistors Q2 and Q3 "off" by preventing forward biasing of the Q2 junction. The zener diode Z1 reverse voltage is exceeded as long as the voltage on the telephone lines remains above the zener voltage. When the phone is off the hook, the voltage is now below the zener voltage, and resistor R5 now biases Q2 "on," which turns Q3 on and clamps the common return of the oscillator to the negative of the battery, commencing operation by turning on.

Note that Q2 and Q3 make a simple DC switch that produces a minimal battery current during the on-hook conditions. When the receiver is lifted, commencing normal conversation, this DC voltage drops to less than 10 volts, and an existing AC voltage corresponding to the speech conversation now modulates the oscillator as described. You will also note Q2 and Q3 being a simple DC switch that only allows a minimal battery current during the on-hook condition.

Capacitor C5 is necessary to block the DC component of the phone line when an on-hook condition exists and allows little attenuation of the varying AC speech voltage. Resistor R4 is necessary for attenuation of this speech voltage that could cause overmodulation and unnecessary serious sidebands if not properly selected.

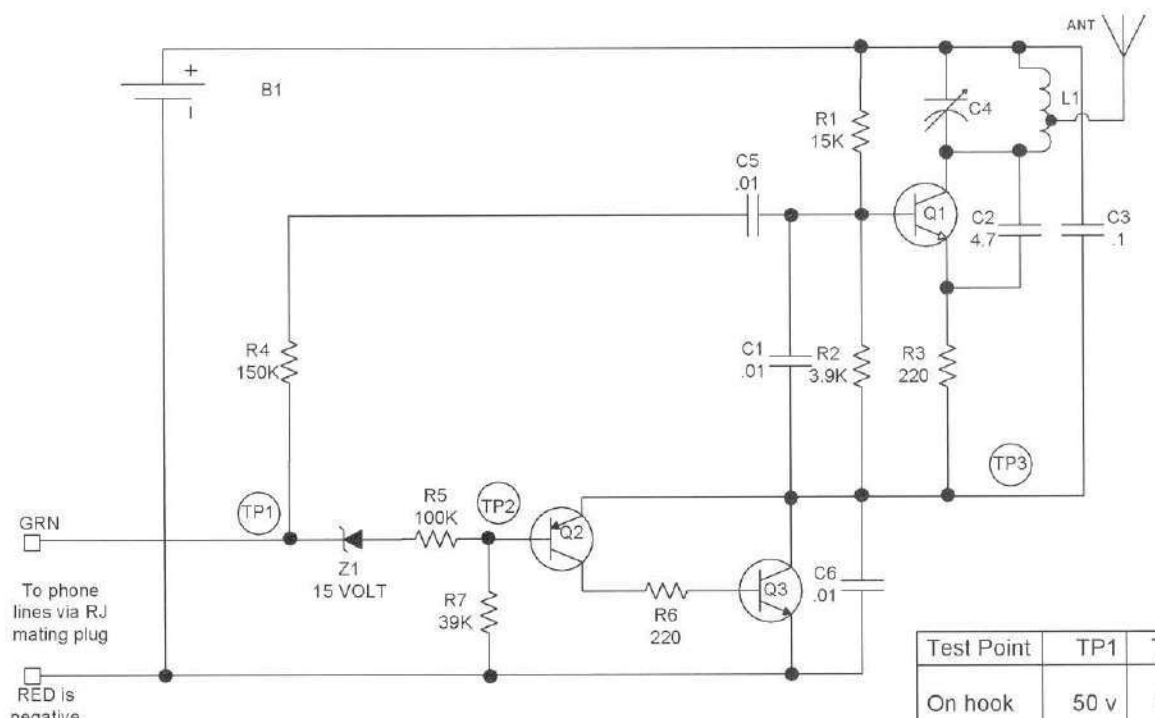

Test Point	TP1	TP2	TP3
On hook	50 v	10 v	9 v
Off hook	8 v	.7 v	.1 v

Measured from negative battery lead

Figure 19-2 *Circuit schematic*

Assembly of the Circuit Board

Assemble the circuit as shown in Figure 19-3.

1. Fabricate a piece of .1-inch grid perforated board to a size of 2 × 1 inches.
2. Form L1 by tightly wrapping eight turns of #16 bus wire on a #8 wood screw. This produces an eight-turn coil with an inner diameter of approximately .135 inches and is about .625 inches in length. Insert it in the proper hole and solder as shown.
3. Insert trimmer capacitor C4 into the holes as shown. You may put this component on either side of the PC board. This choice is up to you and should be determined by the final packaging scheme you require. Three holes are available for the part, with two of them electrically the same point. This is necessary as some trimmers may have three pins. Make sure that the common pins are connected to the same electrical points with the odd pin to the other point.
4. If you are building from a perforated board, it is suggested that you insert components starting in the lower left-hand corner. Pay attention to the polarity of the capacitors with polarity signs and all the semiconductors. Route the leads of the components as shown and solder as you go, cutting away unused wires. Attempt to use certain leads as the wire runs or use pieces of the #24 bus wire. Follow the dashed lines on the assembly drawing as these indicate connection runs on the underside of the assembly board.
5. Attach the external leads of battery clip CL1 and the RJ cable and plug them into the phone connection jack.
6. Double-check the accuracy of the wiring and the quality of the solder joints. Avoid wire bridges, shorts, and close proximity to other circuit components. If a wire bridge is necessary, sleeve some insulation onto the lead to avoid any potential shorts.
7. Tune an FM receiver to a fairly strong station at the high end of the band (108 MHz or higher). Turn up the volume and position it at a distance of 25 to 50 feet.
8. If a multimeter or 50-milliamp meter is available, connect it in series with the battery lead.

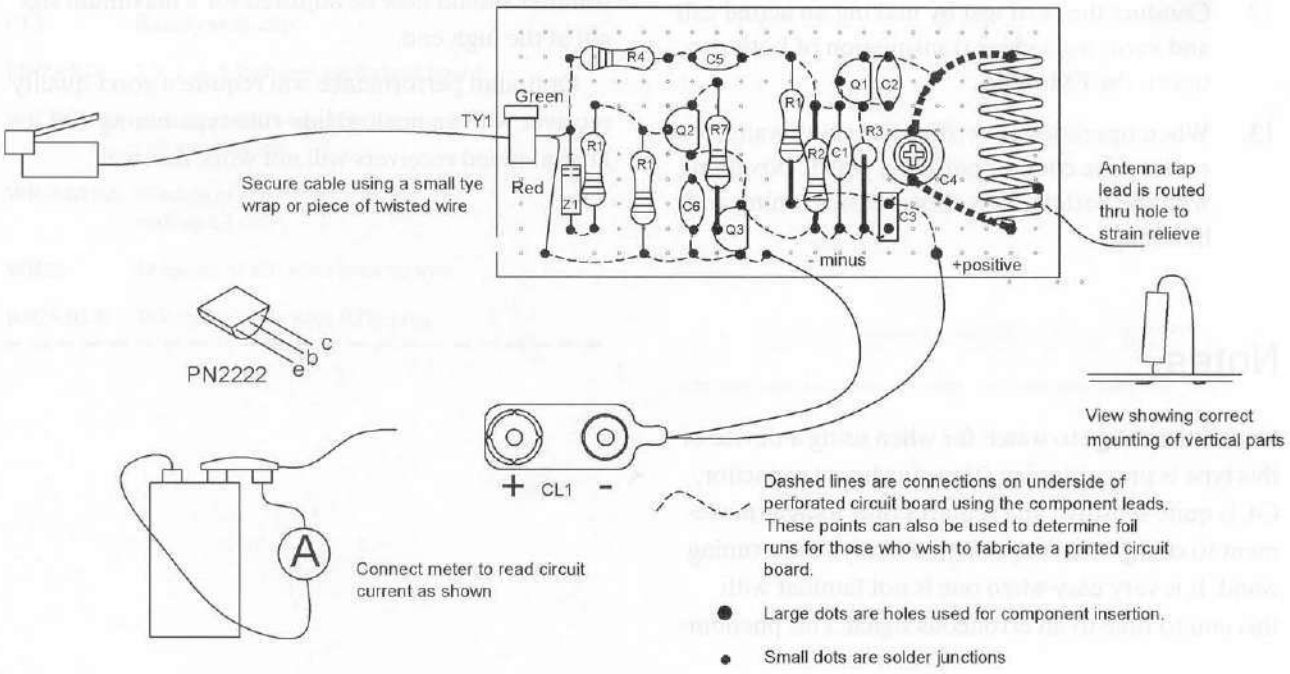

Figure 19-3 *Assembly of circuit board*

This can be done by removing one of the clip fasteners and connecting the meter to the free contacts, as shown in Figure 19-3. The meter should read 5 to 7 milliamps. Use a short piece of bare wire to touch the coil L1 a turn at a time, starting from the C3 end. Note that as you progress turn by turn away from C3 that the indicated meter current will drop or change.

9. Connect the operating unit to the phone line with the phone on hook and notice the meter reading dropping to almost nothing. You may have to reverse the connections to the phone lines. Check the following voltage points indicated on the schematic to verify proper circuit operation, as shown in Figure 19-2.
10. Take the phone off the hook and tune C4 with a tuning wand until you hear the telephone tone. It may be difficult at first to spot the signal as this adjustment is very touchy. It is important to know that several spots in the adjustment may be erroneous and will be weak and unstable. The correct signal will be strong, stable, and clear, and it can be verified by distance-of-transmission testing.
11. Once the desired setting of C4 is found, the position should be marked on the adjustment capacitor with the frequency noted.
12. Conduct the final test by making an actual call and verifying a clear transmission of both parties to the FM radio.
13. When operation is verified, you may want to enclose the circuit board in a plastic box along with the battery. This allows easier tuning and handling.

Notes

One of the things to watch for when using a device of this type is proper tuning. The adjustment capacitor, C4, is quite sensitive and requires only a slight movement to change the frequency, so always use a tuning wand. It is very easy when one is not familiar with this unit to tune to an erroneous signal. This phenomenon is likely to occur when the unit is close to the monitoring receiver. As stated previously, an erroneous signal will be weak, distorted, and unstable (often it is mistaken for the main signal and the unit is blamed for poor performance), and the main signal will be strong, stable, and undistorted, if modulated.

Several experiments in tuning the unit should be done before attempting to use it for the desired application. Also, whenever possible, the unit should be used around 108 to 109 MHz, which is at the boundary of the aircraft band and upper FM broadcast band. When the approximate desired spot is found, final touchup tuning should be done at the receiver end for clarity. In most areas, these upper frequencies are clear and allow uninterrupted use in contrast to the lower ones in the FM band where a slight change in frequency from a clear spot results in the unit being drowned out by a strong broadcast station. Do not go above 108 MHz if near an airport or air traffic lane.

Most available FM radios can easily be detuned slightly to shift the dial readings down to where the dial reading of 108 MHz is actually 109 MHz. This is accomplished by carefully adjusting the "oscillator," the padding trimmer located on the main tuning capacitor, and "walking" a known station down the necessary megahertz or two. An antenna-peaking trimmer should now be adjusted for a maximum signal at the high end.

Optimum performance will require a good-quality receiver with an analog slide-rule-type tuning dial. Digital tuned receivers will not work that well.

Table 19-1 Long-Range Phone Conversation Transmitter Parts List

Ref. #	Description	DB Part #
R1	15K, 1/4-watt resistor (br-gr-or)	
R2	3.9K, 1/4-watt resistor (or-wh-red)	
R3, 6	Two 220 ohm, 1/4-watt resistor (red-red-br)	
R4	150K, 1/4-watt resistor (br-gr-yel)	
R5	100K, 1/4-watt resistor (br-blk-yel)	
R7	39K, 1/4-watt resistor (or-wh-or)	
C1, 5, 6	Three .01-microfarad, 50-volt disc capacitors	
C2	4- to 6-picofarad small silver mica disk (4.7)	DB# 4.7P
C3	.1-microfarad, 50-volt disc capacitor	
C4	6- to 35-picofarad trimmer capacitor	DB# 635P
Z1	15-volt zener diode (1N5245)	
Q1, 3	Two PN2222 NPN general-purpose transistors	
Q2	PN2907 PNP general-purpose transistor	
L1	Coil wound as described in assembly steps	DB# COIL8T
CL1	Battery snap clip	
PBOARD	2 × 1 × .1-inch grid perforated board	
WR24BUSS	12 inches of #24 bus wire for wiring and antenna tap	
WR16BUSS	6 inches of #16 bus wire for making L1 coil	
WR20	24 inches of #20 vinyl hookup wire	
RJCABLE	Telephone cable with RJ11 plug	

Chapter Twenty

Line-Powered Telephone Conversation Transmitter

This project shown in Figure 20-1 is similar to that described in Chapter 19, but this one can be permanently implanted in a telephone and can operate indefinitely, as it does not require batteries. The circuit as shown derives its power from the phone lines once the receiver is lifted off of the hook. Operating range is limited to several hundred feet, far less than the battery-powered version.

The unique features of this device is that it does not require a battery, and activation occurs only when the phone is off the hook. This eliminates transmitting a continuous signal, thus preventing potential interference and eliminates dead-tape listening time. You may also listen to a radio station while monitoring the telephone. When the phone is used, the radio station is replaced by the transmission of the unit. The device is shown assembled on a perforated circuit board and may be housed in a small plastic enclosure. Potting and sealing is at the discretion of the builder.

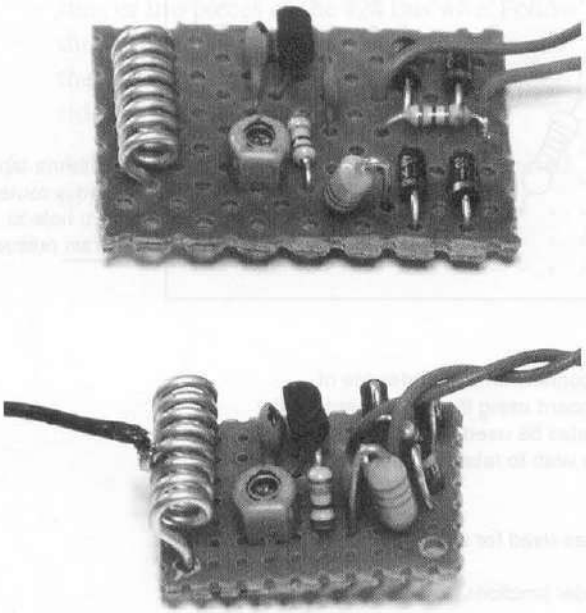

Figure 20-1 *Photograph of circuit*

Circuit Description

This chapter shows how to build a mini-powered FM transmitter that transmits both sides of a telephone conversation to a nearby FM radio. The circuit consists of a *radio-frequency* (RF) oscillator section combined with a telephone power conditioner that powers the oscillator (see Table 20-1). Transistor Q1 forms a relatively stable RF oscillator whose frequency is determined by the value of coil LI and tuning capacitor C3. The setting of C3 determines the desired operating frequency and is in the standard FM broadcast band with tuned circuit design favoring the high end up to 110 MHz. Capacitor C2 supplies the necessary feedback voltage necessary to sustain oscillation. Resistor R2 provides the necessary bias of the base emitter junction for proper operation, while

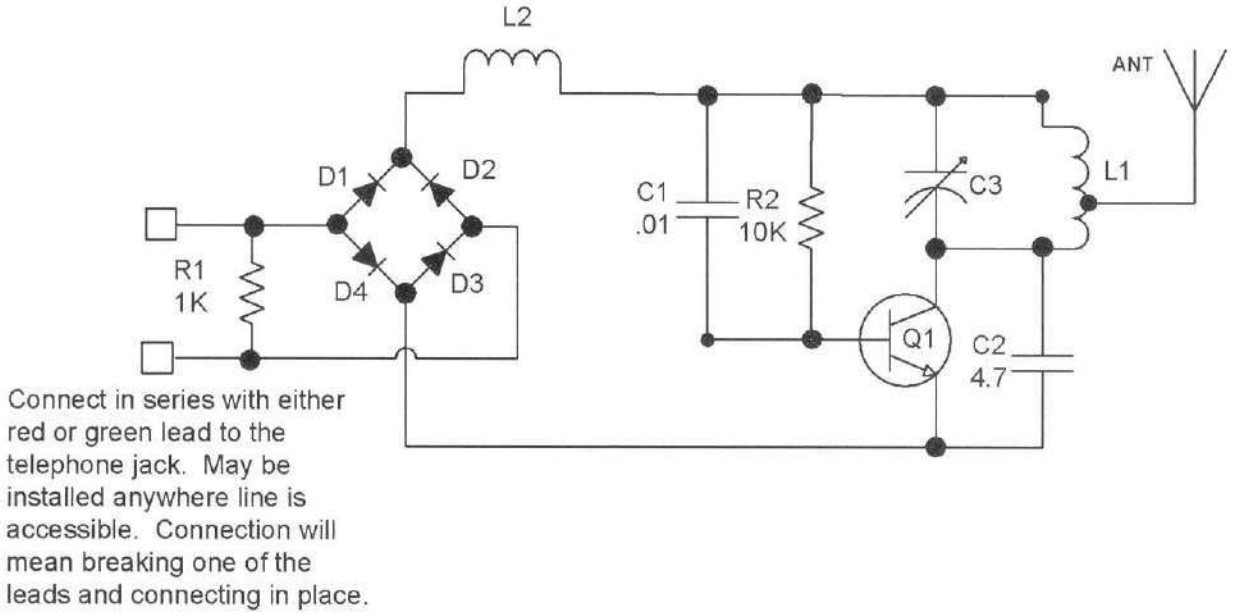

Figure 20-2 *Circuit schematic*

capacitor C1 bypasses any RF to ground. Choke L2 blocks the signal energy from going back to the phone lines yet allows DC power to Q1 (see Figure 20-2).

Connecting the circuit requires breaking one of the lines and connecting the input leads in series with the telephone. It is this method that leaches voltage from the series load resistor R1 when the telephone is in use, as current now flows across R1. The bridge diodes consisting of D1 through D4 polarize the audio voltages necessary to modulate the oscillator.

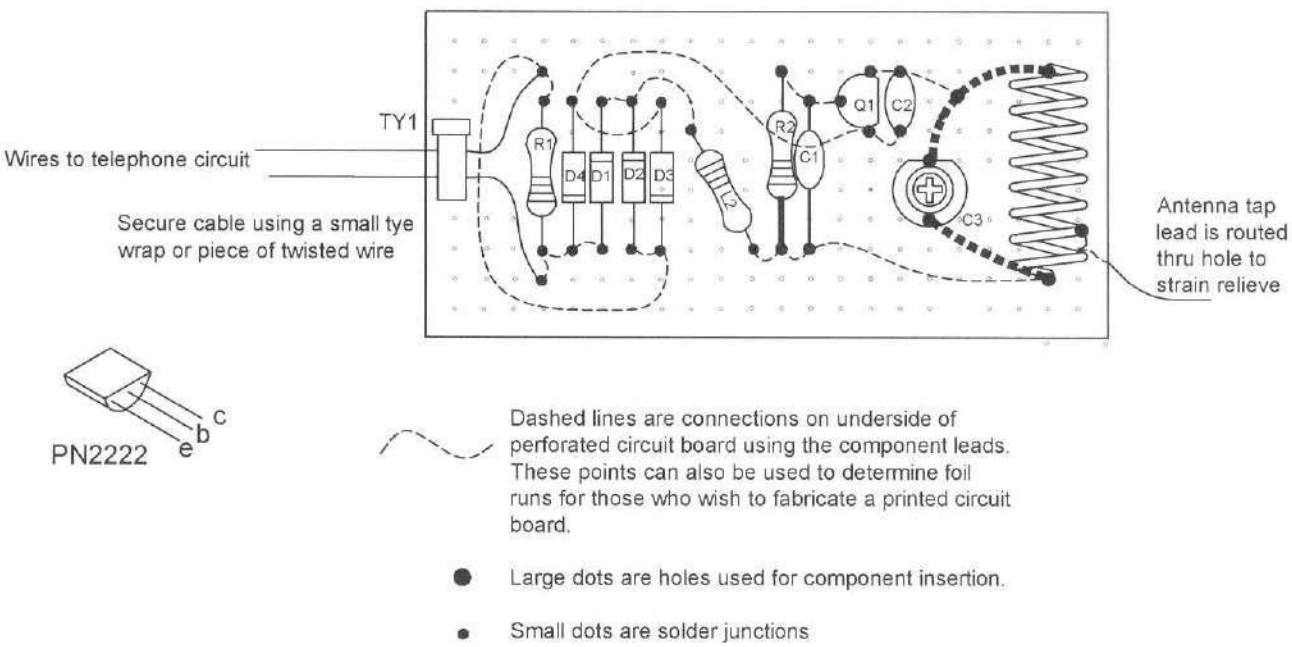

Figure 20-3 *Assembly of circuit board*

Assembly of the Circuit Board

Assemble the circuit as shown in Figure 20-3:

1. Cut a piece of .1-inch grid perforated board to 2 × 1 inches.
2. Form L1 by tightly wrapping eight turns of #16 bus wire on a #8 wood screw. This produces an eight-turn coil with an inner diameter of approximately .135 inches and is about .625 inches in length. Insert it in the proper hole and solder as shown.
3. Insert trimmer capacitor C4 into the holes as shown. You may put this component on either side of the PC board. The choice is up to you and should be determined by the final packaging scheme you require. Three holes are available for the part, with two of them electrically the same point. This is necessary, as some trimmers may have three pins. Make sure that the common pins are connected to the same electrical points, with the odd pin to the other point.
4. If you are building from a perforated board, it is suggested that you insert the components starting in the lower left-hand corner. Pay attention to the polarity of the capacitors that have polarity signs and all the semiconductors. Route the leads of the components as shown and solder as you go, cutting away unused wires. Attempt to use certain leads as the wire runs or use pieces of the #24 bus wire. Follow the dashed lines on the assembly drawing as these indicate connection runs on the underside of the assembly board.
5. Attach the external leads that are connected to the telephone lines.
6. Double-check the accuracy of the wiring and the quality of the solder joints. Avoid wire bridges, shorts, and close proximity to other circuit components. If a wire bridge is necessary, sleeve some insulation onto the lead to avoid any potential shorts.
7. Tune an FM receiver to a fairly strong station at the high end of the band (108 MHz or higher). Turn up the volume and position it 25 to 50 feet away from the transmitter.
8. Connect the operating unit to the phone line with the phone on the hook. Remove the phone and adjust C3 until you hear the dial tone. Tuning the trimmer must be done with an insulating tuning wand. It is best to tune the unit by placing it on a nonconductive surface and securing it with a sponge or a piece of rubber.

   It may be difficult at first to spot the signal as this adjustment is very touchy. Also note that several spots in the adjustment may be erroneous and will be weak and unstable. The correct signal will be strong, stable, and clear and can be verified through distance-of-transmission testing.
9. Once the desired setting of C4 is found, it should be marked, with the frequency noted.
10. Conduct a final test by making an actual call and verifying the clear transmission of the FM radio to both parties.
11. When operation is verified, it may be a good idea to enclose the circuit board in a plastic box. This allows easier tuning and handling.

Notes

Please see notes in Chapter 19.

Table 20-1 Line-Powered Telephone Conversation Transmitter Parts List

Ref. #	*Description*	*DB Part #*
R1	1K 1/4-watt resistor (br-blk-red)	
R2	10K 1/4-watt resistor (br-blk-or)	
C1	.01-microfarad, 50-volt disc capacitor	
C2	4- to 6-picofarad small silver mica disk (4.7)	DB# 4.7P
C3	6- to 35-picofarad trimmer capacitor	DB# 635P
D1–4	100-volt diodes IN4002	
Q1	PN2222 NPN general-purpose transistor	
L1	Coil wound as described in assembly steps	DB# COIL8T
L2	3.6 microhenry inductor	DB# 3.6U
PBOARD	2 × 1 × .1-inch grid perforated board	
WR24BUSS	12 inches of #24 bus wire for wiring and antenna tap	
WR16BUSS	6 inches of #16 bus wire for making L1 coil	
WR20	24 inches of #20 vinyl hookup wire	

Chapter Twenty-One

Remote Wireless FM Repeater

Figure 21-1 shows a wireless FM transmitter designed to transmit the output of a tape recorder, VCR, DVD, or any device having composite audio and video outputs to a nearby radio or TV tuned to the unit's frequency. Assembly is built on a piece of circuit board and may be placed in any suitable plastic container along with a 9-volt battery.

Figure 21-1 *The completed device*

Circuit Description

The parts for this project are listed in Table 21-1. Transistor Q1 forms a relatively stable *radio-frequency* (RF) oscillator whose frequency is determined by the value of coil L1 and tuning capacitor C4. The C4 setting determines the desired operating frequency and is in the standard FM broadcast band with tuned circuit design favoring the high end up to 110 MHz. Capacitor C2 supplies the necessary feedback voltage developed across emitter resistor R3 in the emitter circuit of Q1, sustaining an oscillating condition. Resistor R1 and R2 provide the necessary bias of the base emitter junction for proper operation, while capacitor C1 bypasses any RF to ground fed to the base circuit. Capacitor C9 provides an RF return path for the tank circuit of L1 and C4 while blocking the DC supply voltage fed to the collector of Q1 (see Figure 21-2). R4 is connected in series with DC-blocking capacitor C5 to the input cable and plug.

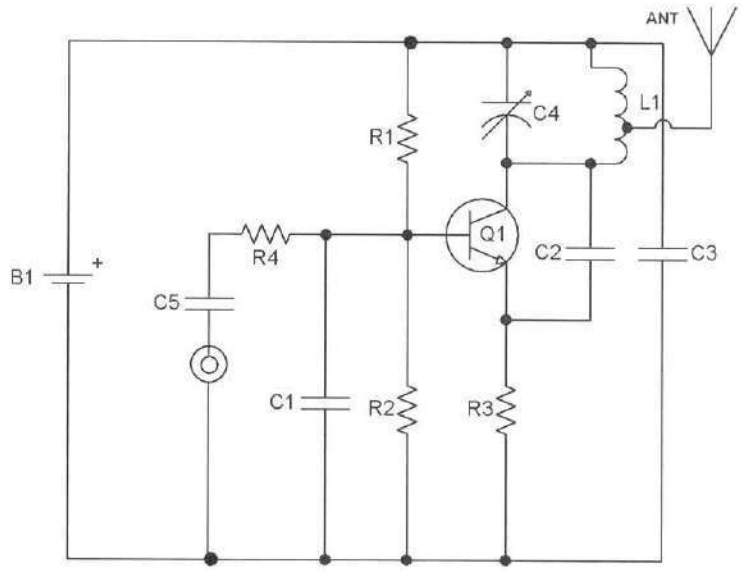

Figure 21-2 *Circuit schematic*

Assembly

Assemble the circuit as shown Figure 21-3.

1. Cut a piece of .1-inch grid perforated board to a size of 2 × 1 inches.
2. Form L1 by tightly wrapping eight turns of #16 bus wire on a #8 wood screw. This produces an eight-turn coil with an inner diameter of approximately .135 inches and a length of .625 inches. Insert it in the proper hole and solder as shown.
3. Insert trimmer capacitor C4 into the holes as shown. You may put this component on either side of the PC board. This choice is up to you and should be determined by the final packaging scheme you require. Three holes are available for the part with two of them electrically the same point. This is necessary, as some trimmers may have three pins. Make sure that the common pins are connected to the same electrical points with the odd pin to the other point.
4. If you are building from a perforated board, it is suggested that you insert components starting in the lower left-hand corner. Pay attention to the polarity of the capacitors that have polarity signs and all the semiconductors. Route the leads of the components as shown and solder as you go, cutting away unused wires. Attempt to use certain leads as the wire runs or use pieces of the #24 bus wire. Follow the dashed lines on the assembly drawing as these indicate the connection runs on the underside of the assembly board.
5. Attach the external leads of the battery clip (CL1) and shielded cable (WR10).
6. Double-check the accuracy of the wiring and the quality of the solder joints. Avoid wire bridges, shorts, and close proximity to other circuit components. If a wire bridge is necessary, sleeve some insulation onto the lead to avoid any potential shorts.
7. Tune an FM receiver to a fairly strong station at the high end of the band (108 MHz or higher). Turn up the volume and position the receiver about 25 to 50 feet from the transmitter circuit.
8. If a multimeter or 50-milliamp meter is available, connect it in series with a battery lead. This can be done by removing one of the clip fasteners and connecting the meter to one of the free contacts, as shown in Figure 21-2. The meter should read 5 to 7 milliamps. Pick up a short piece of bare wire and touch coil L1. Touch it a turn at a time, starting from the C3

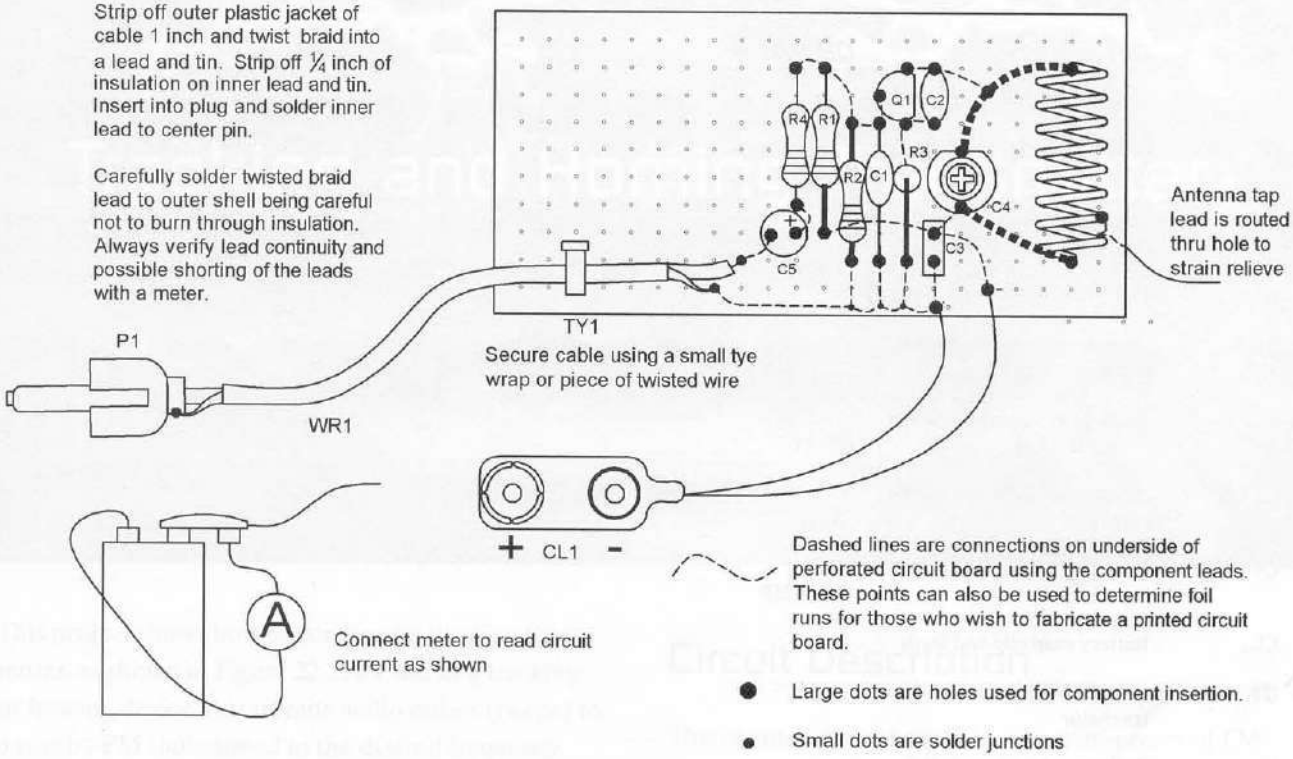

Figure 21-3 *Assembly of board*

end. Note that as you progress turn by turn away from C3 that the indicated meter current will drop or change.

9. Connect the cable into an audio source such as a recorder or another radio. Slowly rotate C4 with an insulated tuning wand until the station being received by the radio is at approximately 108 MHz. It may be difficult at first to spot the signal, as this adjustment is very touchy. Also note that several spots in the adjustment may be erroneous and will be weak and unstable. The correct signal will be strong, stable, and clear and can be verified by distance-of-transmission testing.
10. Once the desired setting of C4 *is* found, it should be marked with the frequency noted.
11. When the operation is verified, it may be desired to pot the assembly as shown. This allows easier tuning and handling.

Notes

Please refer to the notes in Chapter 19 on operation of wireless circuits.

Table 21-1 Remote Wireless FM Repeater Parts List

Ref. #	*Description*	*DB Part #*
R1	15K, 1/4-watt resistor (br-gr-or)	
R2	3.9K, 1/4-watt resistor (or-wh-red)	
R3	220-ohm, 1/4-watt resistor (red-red-br)	
R4	1K, 1/4-watt resistor (br-blk-red)	
C1, 5	Two .01-microfarad, 50-volt disc capacitors	
C2	Small 4- to 6-picofarad silver mica disk (4.7)	DB #4.7P
C3	.1-microfarad, 50-volt plastic capacitor	
C4	6- to 35-picofarad trimmer capacitor	DB #635P
CL1	Battery snap clip and leads	
Q1	PN2222 NPN general-purpose transistor	
L1	Coil wound as described in assembly steps	DB #Coil8T
PBOARD	2 × 1 × .1-inch grid perforated board	
WR24BUSS	12 inches of #24 bus wire for wiring and antenna tap	
WR16BUSS	6 inches of #16 bus wire for making L1 coil	
WR1	12 inches of shielded cable	
P1	RCA phono plug	

Chapter Twenty-Two

Tracking and Homing Transmitter

This project shows how to construct a beeping transmitter, as shown in Figure 22-1, for use as a tracking or homing device. It transmits audio pulses (beeps) to a nearby FM radio tuned to the desired frequency. The unit is intended to be used in transmitter hunt games or as a homing beacon for hunters or hikers. It is suggested that you mark a bearing heading on a small but good-quality FM radio and use it as a low-cost receiver for determining the direction of the signal pickup. The range of the device, when used as a homing device with a quarter-wave vertical placed on top of a metal roof, such as a vehicle, can be in excess of 3 miles when using a quality analog FM receiver.

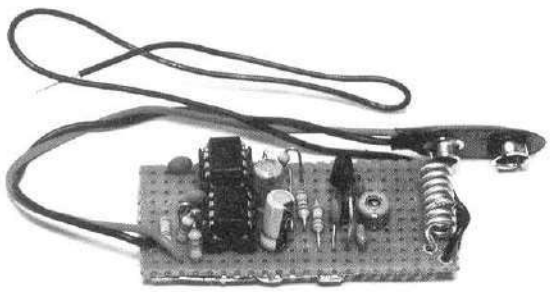

Figure 22-1 *Transmitter circuit*

Circuit Description

This chapter shows how to build a mini-powered FM transmitter that transmits audio pulses for tracking and homing applications (see Figure 22-2). The circuit consists of a *radio-frequency* (RF) oscillator section interfaced with a tone modulator and a pulse-switching section that controls the oscillator power. Transistor Q1 forms a relatively stable RF oscillator whose frequency is determined by the value of coil LI and tuning capacitor C4. The C4 setting determines the desired operating frequency and is in the standard FM broadcast band with the tuned circuit design favoring the high end up to 110 MHz. Capacitor C2 supplies the necessary feedback voltage developed across resistor R3 in the emitter circuit of Q1, sustaining an oscillating condition. Resistors R1 and R2 provide the necessary bias of the base emitter junction for proper operation, while capacitor C1 bypasses any RF to ground fed to the base circuit. Capacitor C3 provides an RF return path for the tank circuit of LI and C4 while blocking the DC supply.

You will note that the junction of the base bias resistors R1 and R2 is a feed point consisting of resistor R4. This point is where the beeping tone from the tone generator chip I2 is applied. Because of the

nature of the oscillator frequency being subject to change by varying the base bias condition, a pulsed voltage superimposed at this point causes a corresponding frequency shift (FM) along with an amplitude modulated shift (AM) condition. It is this property that allows the circuit to be FM modulated, producing the tone frequency. The signal is clearly detected on any FM receiver when the receiver is properly tuned. The tone frequency is the pulse repetition rate of I1 wired as an astable pulse generator. This repetition rate is determined by timing resistor R5 and capacitor C6.

The ratio of beeping on to off time is controlled by chip I1, wired as a free-running astable device with duty cycle control. This function is determined by the ratio of resistors R7 and R8 and timing capacitor C8. The output of I1 controls the bias voltage of oscillator Q1 through resistor R1, turning the oscillator on and off (see Figure 22-2).

Assembly of the Circuit Board

Assemble the circuit as shown in Figure 22-3.

1. Cut a piece of .1-inch grid perforated board to a size of 2 × 1 inches.
2. Form L1 by tightly wrapping eight turns of #16 bus wire on a #8 wood screw. This produces an eight-turn coil with an inner diameter of .135 inches and a length of .625 inches. Insert it in the proper hole and solder as shown.
3. Insert trimmer capacitor C4 into the holes as shown. You may put this component on either side of the PC board. The choice is up to you and should be determined by the final packaging scheme you require. Three holes are available for the part, with two of them electrically the same point. This is necessary, as some trimmers may have three pins. Make sure that the common pins are connected to the same electrical points with the odd pin to the other point.
4. If you are building from a perforated board, it is suggested that you insert components, starting in the lower left-hand corner. Pay atten-

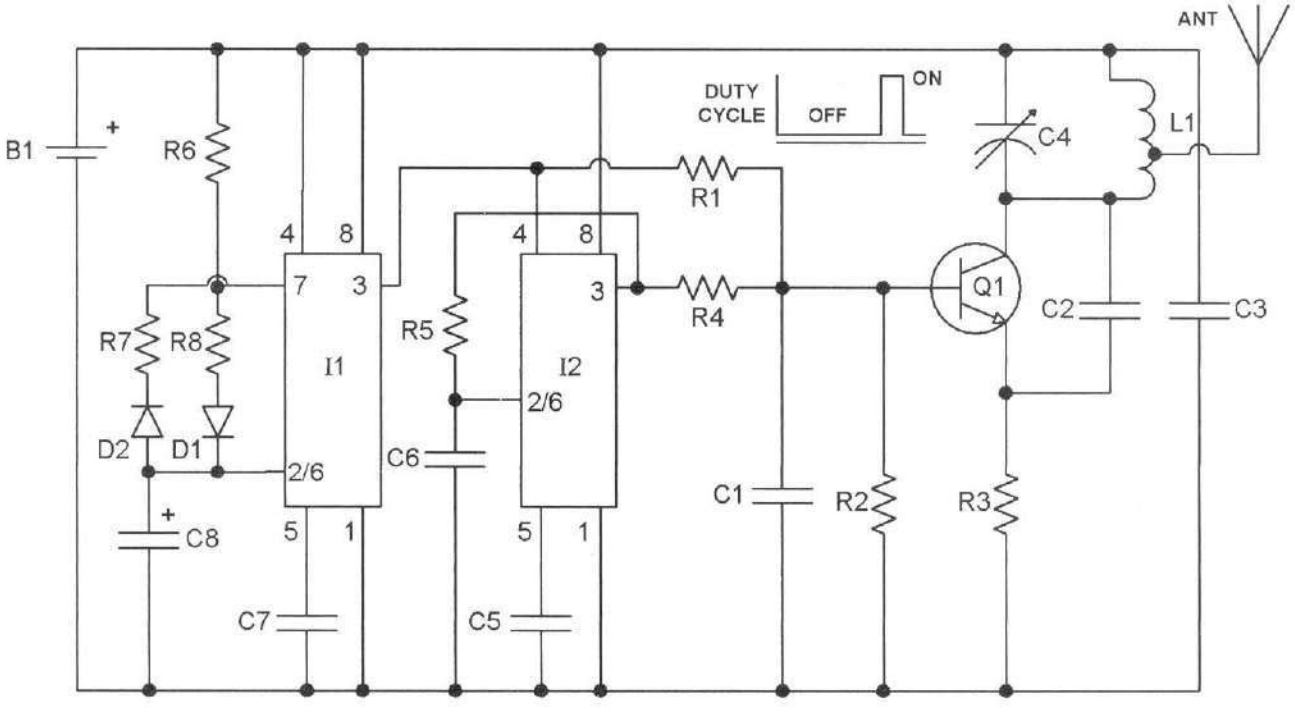

Figure 22-2 *Circuit schematic*

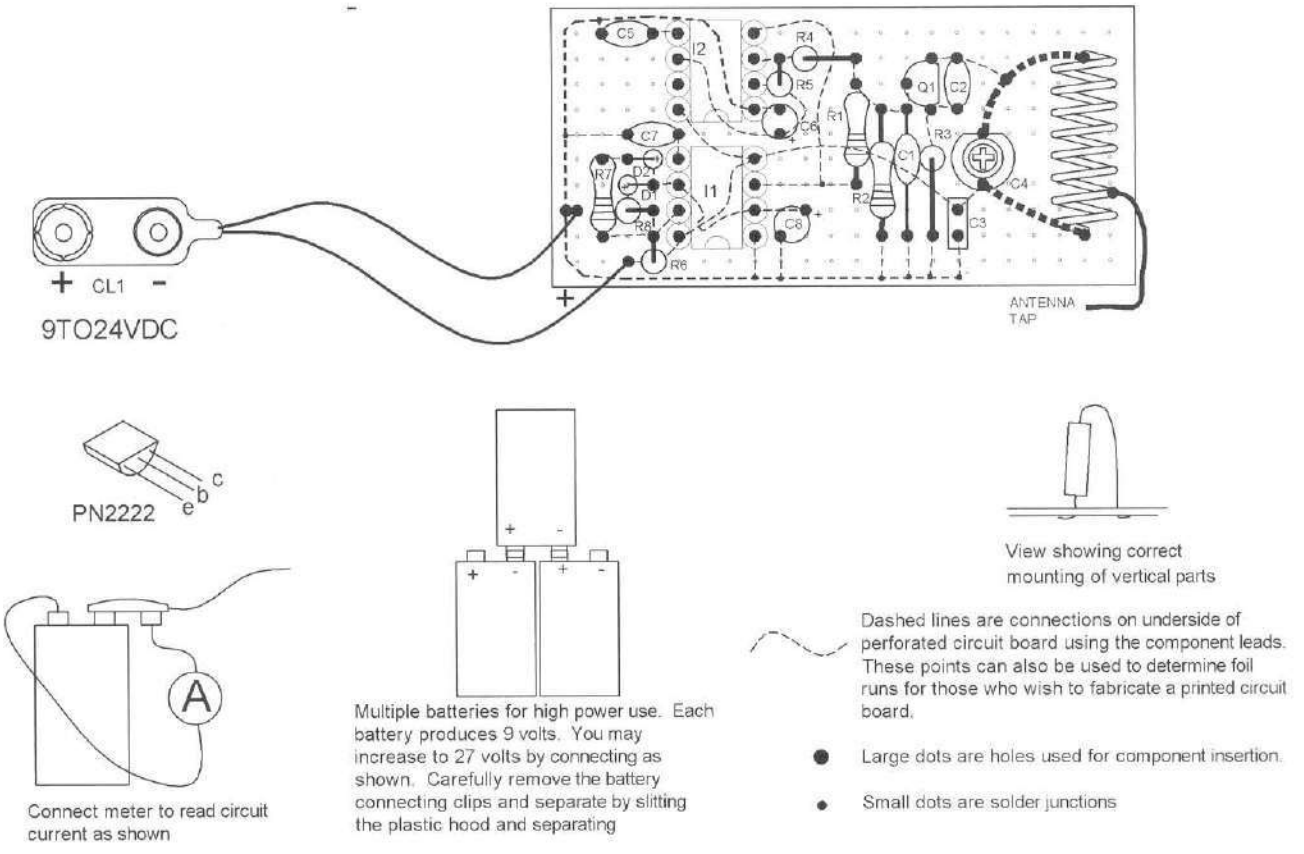

Figure 22-3 *Assembly of the circuit board*

tion to the polarity of the capacitors with polarity signs and all the semiconductors. Route the leads of the components as shown and solder as you go, cutting away the unused wires. Attempt to use certain leads as the wire runs or use pieces of the #24 bus wire. Follow the dashed lines on the assembly drawing as these indicate the connection runs on the underside of the assembly board.

5. Attach the external leads of battery clip CL1.
6. Double-check the accuracy of the wiring and the quality of the solder joints. Avoid wire bridges, shorts, and close proximity to other circuit components. If a wire bridge is necessary, sleeve some insulation onto the lead to avoid any potential shorts.
7. Tune an FM receiver to a fairly strong station at the high end of the band (108 MHz or higher). Turn up the volume and position the receiver 25 to 50 feet from the transmitter circuit.
8. If a multimeter or 50-milliamp meter is available, connect it in a series with a battery lead. This can be done by removing one of the clip fasteners and connect the meter to the free contacts, as shown in Figure 22-2. The meter should read a pulsing of 5 to 7 milliamps. Use a short piece of bare wire to touch the coil L1 a turn at a time, starting from the C3 end. Note that as you progress turn by turn away from C3 that the indicated meter current will drop or change.
9. Tune C4 with an insulated tuning tool until you hear the beeping tone. It may be difficult at first to spot the signal, as this adjustment is very touchy. Also note that several spots in the adjustment may be erroneous and will be weak and unstable. The correct signal will be strong, stable, and clear and can be verified by distance-of-transmission testing.

10. Once the desired setting of C4 is found, it should be marked with alignment marks, with the frequency noted.
11. Finally, test the unit using a good-quality FM analog receiver. Note to place an arrow on the radio once you determine the proper positioning to obtain the maximum signal strength. Do this step from a distance of at least several hundred feet.
12. When operation is verified, it may be desired to enclose the circuit board into a plastic box along with the battery. This allows easier tuning and handling.

Notes

Please see the notes in Chapter 19 on operating.

Table 22-1 Tracking and Homing Transmitter Parts List

Ref. #	*Description*	*DB Part #*
R1	Two 10K, 1/4-watt resistor (br-gr-or)	
R2	3.9K, 1/4-watt resistor (or-wh-red)	
R3	220-ohm, 1/4-watt resistor (red-red-br)	
R5	1K, 1/4-watt resistor (br-blk-red)	
R6	39K, 1/4-watt resistor (or-wh-or)	
R7	100K, 1/4-watt resistor (br-blk-yel)	
R8	22K, 1/4-watt resistor (red-red-or)	
C1, 5, 7	Three .01-microfarad, 50-volt disc capacitors	
C2	Small, 4- to 6-picofarad, silver mica disk (4.7)	DB# 4.7P
C3	.1-microfarad, 50-volt plastic capacitor	
C4	6- to 35-picofarad trimmer capacitor	DB# 635P
C6	.47-microfarad, 25-volt vertical electrolytic capacitor	
C8	4.7-microfarad, 25-volt vertical electrolytic capacitor	
D1, 2	Two 1N914 small-signal diodes	
I1, 2	Two 555 timers in a *dual inline package* (DIP)	
CL1	Battery snap clip and leads	
Q1	PN2222 NPN general-purpose transistor	
L1	Coil wound as described in assembly steps	DB# COIL8T
PBOARD	2 × 1 × .1-inch grid perforated board	
WR24BUSS	12 inches of #24 bus wire for wiring and antenna tap	
WR16BUSS	6 inches of #16 bus wire for making L1 coil	

Chapter Twenty-Three

Snooper Phone Room-Listening Device

Figure 23-1 shows a simple electronic device intended to be an intrusion detector and listening device for checking a home or office while away or on vacation. It may also be used to trigger other electrical devices. The circuitry does not require a tone encoder, so it does not provide selected activation by a particular caller. Thus, it limits the device from being used for illegal purposes and allows the sale of the kit or fully assembled unit without the requirement of special authorization.

This is an intermediate-level project requiring basic electronic skills. Expect to spend $25 to $40. All parts are readily available, with specialized parts obtainable through Information Unlimited (www.amazing1.com), and they are listed in Table 23-1.

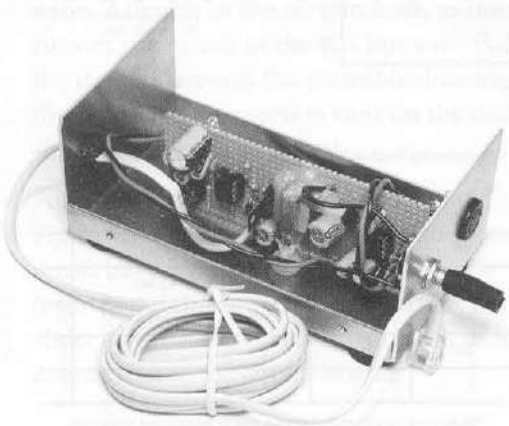

Figure 23-1 *The snooper phone*

Unlike the controversial Infinity transmitter, our system does not utilize decoder and encoder circuitry. Once connected to the phone lines, it will open a microphone to anyone who happens to dial the number. This feature obviously reduces the potential use of the device for illegal interception of oral communication. Even though the phone does not ring, it would not be long before the potential victim of an illegal surveillance would be aware of the setup. It is therefore quite obvious that the applications are strictly limited to use as a security device that checks for unauthorized intrusion or checks household appliances by placing a pickup device in certain favorable locations to overhear these desired sounds and noises. I am sure that anyone with this capability would breathe a sigh of relief to be able to dial his or her home or office phone while being away and hear the familiar sounds of appliances and other systems properly performing their duties and functions.

Circuit Operation

Your circuit consists of a high-gain amplifier (I1) fed into the telephone lines via transformer T1. The circuit is initiated by the action of a voltage transient pulse occurring across the phone line at the instant of

a telephone circuit connection being made. This transient is a voltage change of about 48 to 5 VDC and usually occurs before the ring signal. It is this change that immediately forward-biases diode D1 and triggers pin 2 of timer I2, whose output pin 3 goes positive, turning on transistors Q1 and Q2. Timer I2 now remains in this state for a period depending on the values of timing resistor R12 and the selected value of the capacity determined by the activated time of switch S2. This four-position switch allows time selections of 10, 30, 100, and 1,000 seconds by the selection of the respective capacitors C12 through C15 (see Figure 23-2).

You will note that when Q2 is turned on by timer I2 that a simulated off-hook condition exists by the switching action connecting the 500-ohm winding of the transformer directly across the phone lines. Simultaneously, Q1 clamps the ground of the I1 amplifier to the negative return of battery B1, enabling this amplifier section. System power is controlled by switch S1 being part of the pickup sensitivity control R1.

Electret microphone M1 picks up the sounds fed to operational amplifier I1 with the output coupled by capacitor C6 to the 1,500-ohm winding of T1, and R1 controls the pickup sensitivity of the system. The system described will operate when any incoming call is received without the phone ever ringing.

Construction Steps

If you are a beginner, it is suggested to obtain our *GCAT1 General Construction Practices and Techniques*. This informative literature explains basic practices that are necessary in proper construction of electromechanical kits and is listed in Table 23-1.

1. Lay out and identify all the parts and pieces. Verify them with the parts list, and separate the resistors as they have a color code to determine their value. Colors are noted on the parts list.
2. Cut a piece of .1-inch grid perforated board to a size of 4.2 × 1.5. Locate and drill the holes as shown in Figure 23-3.

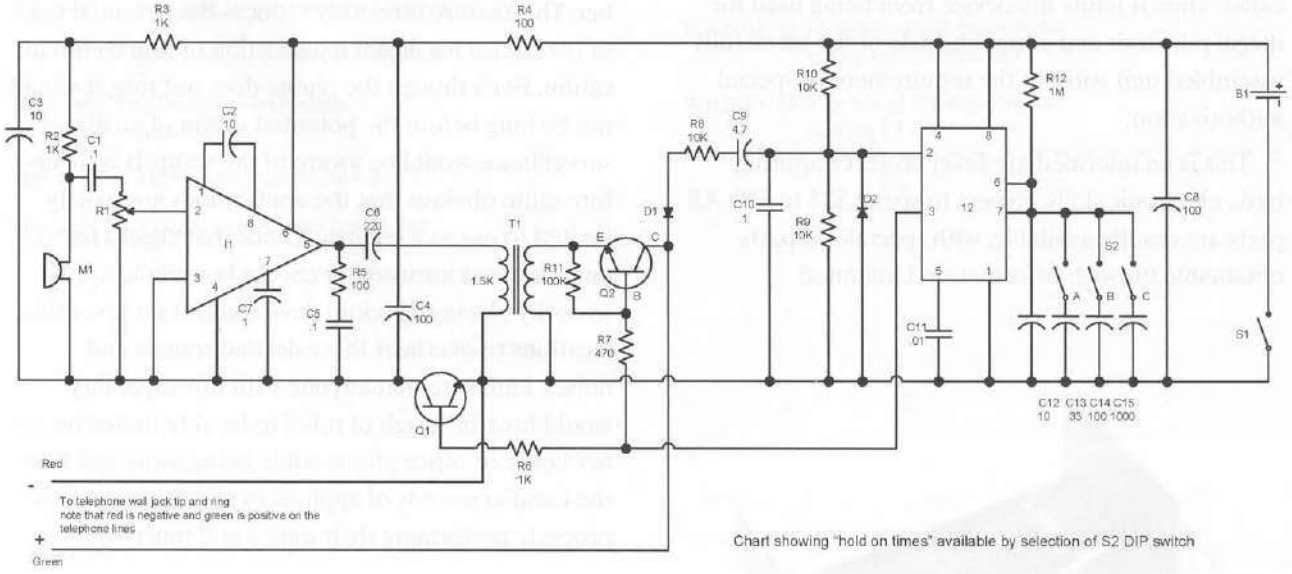

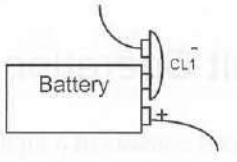

Measure circuit current by connecting a milliamp meter to the unconnected battery and battery clip contact

Chart showing "hold on times" available by selection of S2 DIP switch

S2A	S2B	S2C	*TIME
off	off	off	10 sec
on	off	off	43 sec
on	on	off	145 sec
on	on	on	1145 sec

*times may vary from that shown due to component variances

Figure 23-2 *Circuit schematic*

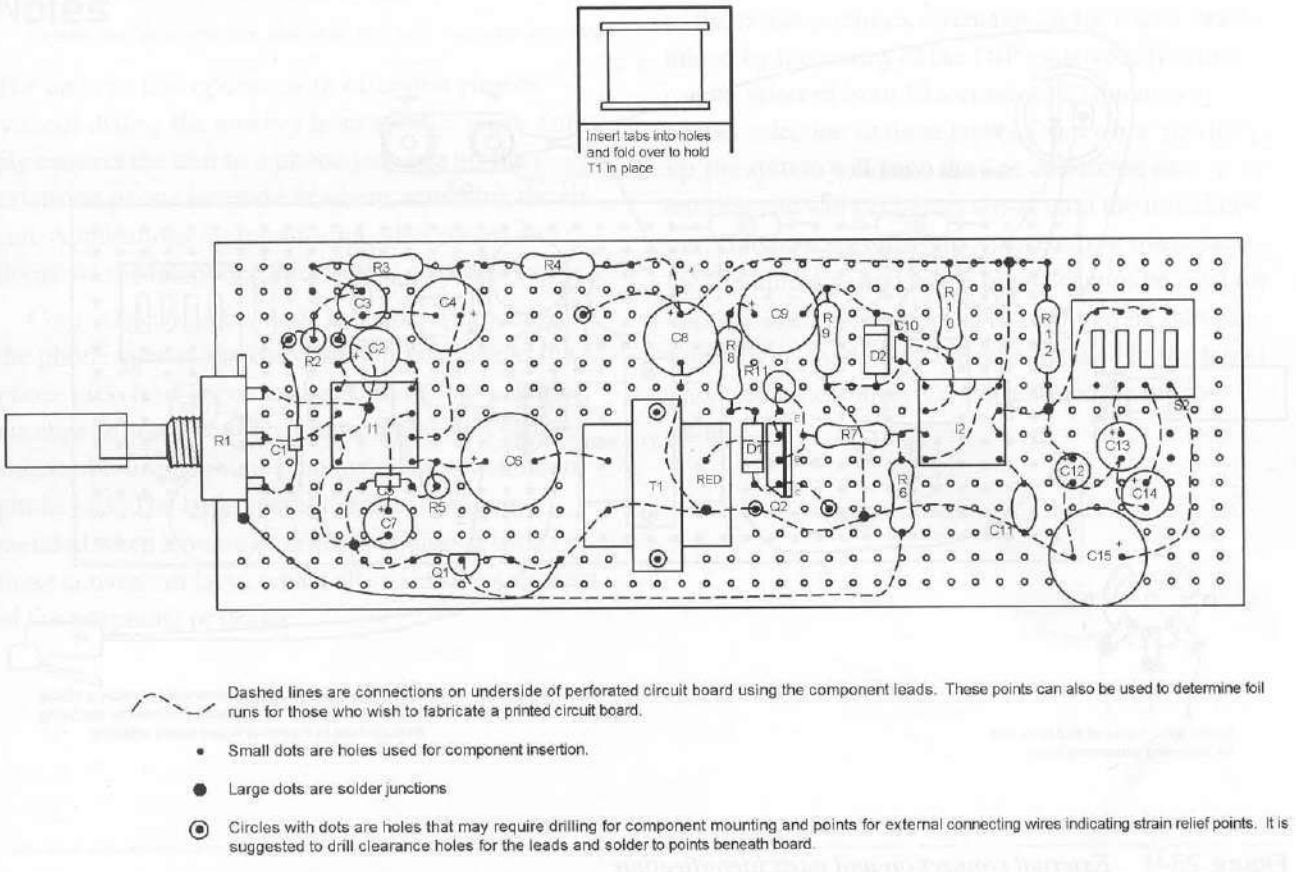

Figure 23-3 *Assembly board layout*

3. If you are building from a perforated board, it is suggested that you insert the components starting in the lower left-hand corner (see Figure 23-3). Pay attention to the polarity of the capacitors with polarity signs and all the semiconductors.

   Route the leads of the components as shown and solder as you go, cutting away unused wires. Attempt to use certain leads as the wire runs or use pieces of the #24 bus wire. Follow the dashed lines on the assembly drawing as these indicate connection runs on the underside of the assembly board.

4. Attach the external leads as shown in Figure 23-4. You may relieve any strain they might have by drilling holes to allow the insertion of the entire wire. Note that the short pieces of bus wire are soldered to R1 for connection to the circuit board.

5. Double-check the accuracy of the wiring and the quality of the solder joints. Avoid wire bridges, shorts, and close proximity to other circuit components. If a wire bridge is necessary, sleeve some insulation onto the lead to avoid any potential shorts.

Final Assembly

Create a suitable housing from a piece of aluminum or purchase a ready-made aluminum box approximately 5 × 3 × 2 inches. Drill the holes as required for the microphone grommet GR1, gain control R1, and strain relief bushing for the phone line cable assembly RJ11. The metal box should be grounded to the circuit common line to reduce hum pickup. Note that a piece of Velcro sticky tape can be used to secure the battery or use your own ingenuity.

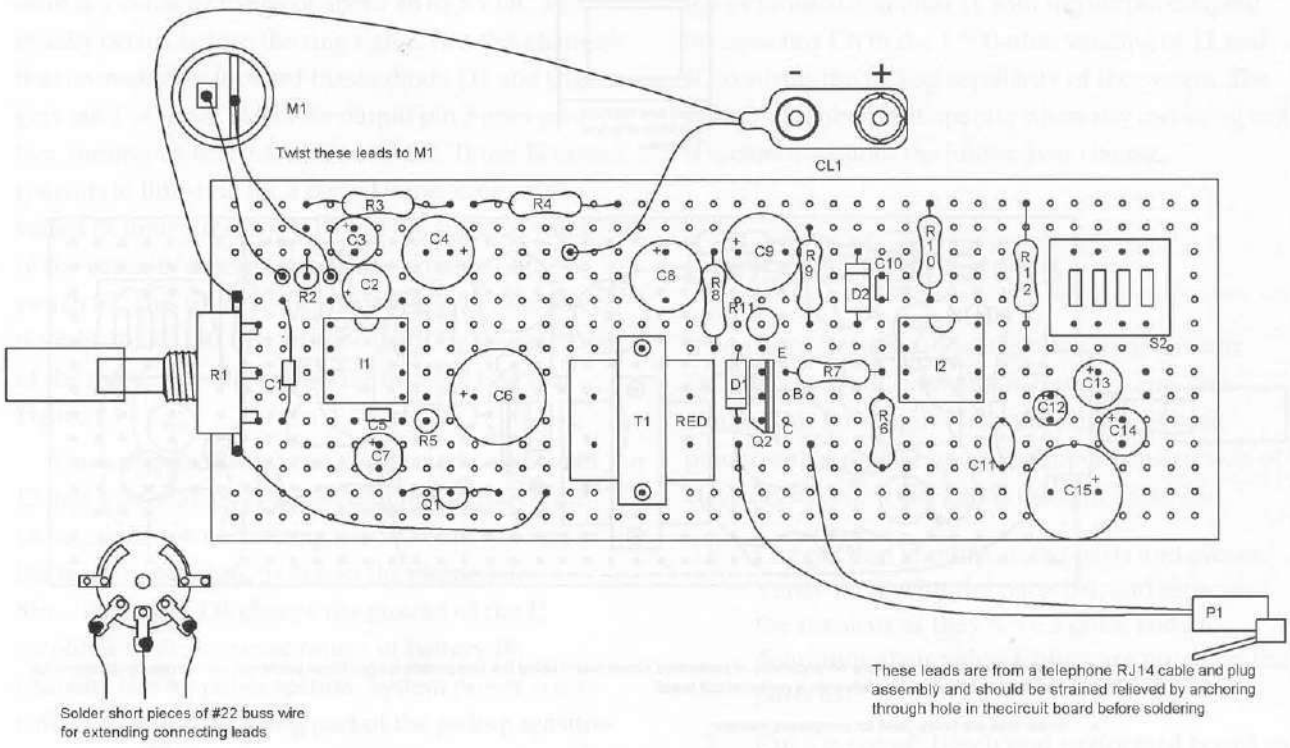

Figure 23-4 *External connection and parts identification*

Testing Steps

This step will require basic electronic laboratory equipment including a 60 MHz oscilloscope if trouble shooting the circuit is necessary.

1. Turn the unit off by rotating R1 full counter-clockwise, noting the click of the switch. Verify that all the DIP switch levers of S2 are down (off). Connect the battery as shown in series with a current meter and note zero current flow. Turn the unit on and note a current of 5 milliamps, which may momentarily jump to 30 milliamps as the unit times out.
2. Locate a phone jack so that you can monitor the DC voltage. Connect a meter across the tip and ring leads (green and red), and note the 40 to 50 volts with the phone on the hook. Also note the green lead is positive and the red is negative. This is the opposite of conventional wiring. Lift the phone and notice the 40 to 50 volts dropping down to 8 to 12 volts. This step verifies a properly working phone line.
3. Turn the unit off and connect it to the phone line. Rotate the R1 so that it just clicks on, and note the voltage remaining as or timing out to read the on-hook 40 to 50 volts. Preset R2 to midway.
4. Call the target phone using a cell or another telephone. The unit should connect at the beginning of the ring signal before the phone has a chance to ring. You should clearly hear sounds until the unit times out, at which time the device disconnects and restores the phone to normal operation. Adjust R1 for desired pickup sensitivity. The timeout time should be only about 10 seconds for the presetting of S2, as instructed in step 1. You may lengthen these times as shown in Figure 23-2.

Notes

The unit can also operate with extension phones without dialing the number from another place. Simply connect the unit to a phone jack and lift the extension phone located elsewhere, activating the circuit. Applications for monitoring other rooms and floors via the telephone lines now is possible.

Connections can be made in simple ways across the phone lines at any convenient point, such as the phone jack, lead-in box, or inside the telephone itself via clips or lugs. They can also be made via a simple, standard four-pin phone plug mated to any standard phone jack. The latter method is usually recommended when a home or office is equipped with these convenient jacks, which allow simple placement of the telephone or device.

When the phone activates, allowing you to listen to the target premises, it remains on for a time determined by the setting of the DIP switch S2. This time can be selected from 10 seconds to 20 minutes by proper selection of these levers. Even when you hang up, the system will keep the line connected so another call will get a busy signal until the unit times out. One now sees the importance of not overselecting the timing period as the phone cannot be used for either incoming or outgoing calls. Outgoing calls can normally be made with the unit installed to the target phone, but incoming calls will activate the microphone.

Table 23-1 Snooper Phone Room-Listening Device Parts List

Ref. #	*Description*	*DB Part #*
R1/S1	10K, 17-millimeter pot and switch	
R2, 3, 6	Four 1K, 1/4-watt resistors (br-blk-red)	
R4, 5	One 100-ohm, 1/4-watt resistor (br-blk-br)	
R7	470 1/4-watt resistor (yel-pur-br)	
R8, 9, 10	Three 10K, 1/4-watt resistors (br-blk-or)	
R11	100K, 1/4-watt resistor (br-blk-yel)	
R12	1M 1/4-watt resistor (br-blk-gr)	
C1, 5, 10	Three .1-microfarad, 50-volt caps	
C2, 3, 12	Three 10-microfarad, 25-volt vertical electro radial leads	
C4,8,14	Three 100-microfarad, 25-volt vertical electro radial leads	
C6	.22-microfarad, 250-volt metalized polypropylene	
C7	.1-microfarad, 50-volt cap	
C9	1-microfarad, 25-volt vertical electro cap	
C13	33-microfarad, 25-volt vertical electro radial leads	
C11	.01-microfarad, 50-volt disk (103)	
C15	1,000-microfarad, 25-volt vertical electrolytic capacitor	
C6	.22-microfarad, 250-volt metallized polypropylene	
C9	1-microfarad, 25-volt vertical electro cap	
C7	.1-microfarad, 50-volt cap (INFO#VG22)	
D1, 2	Two 1N4007 1-kilovolt diodes	
I1	LM386 operational amplifier *dual inline package* (DIP) *integrated circuit* (IC)	
I2	555 timer DIP IC	
Q1	PN2222 NPN small-signal transistor	
Q2	D40D5 high-voltage transistor	
T1	1.5K, 500-ohm audio interstage transformer	
M1	Electret microphone	
S2	4PST DIP switch	
PBOARD	4.2 × 1.5 × .1-inch grid perforated board, sized per chapter	
GR1	1/2-inch rubber grommet	
BUSCLP	1/4-inch Heyco clamp bushing	
CL1	9-volt battery clip with leads	
RJ11	RJ11 telephone plug and cable assembly	
WR20R	12 inches of #20 vinyl red wire for positive input	
WR20B	12 inches of #20 vinyl black wire for negative input	
ENC1	5 × 3 × 2-inch aluminum box and cover	

Chapter Twenty-Four

Long-Range FM Voice Transmitter

This project shows how to construct an electronic device that can transmit low-level sounds over a considerable distance (see Figure 24-1). It is intended for use as a security system when entry sounds are broadcasted over a standard FM radio, providing an early warning of an intrusion. It may be used to monitor children, swimming pools, sick and invalid people, and animals. The device can also be used for nature listening, which is made possible by the wide frequency response of the audio section, allowing good-quality reproducibility of rare bird calls, for example. An excellent application, when one is living in hostile areas, is to install the unit in one's home. This allows monitoring of the premises before possibly being surprised by a burglar.

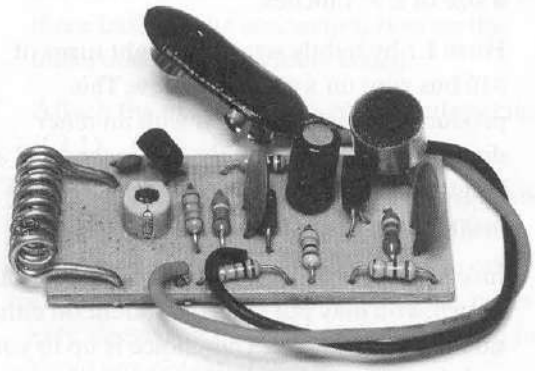

Figure 24-1 *Long-range FM voice transmitter*

The assembled transmitter is small enough to be placed at the foci of a sonic reflector, creating a highly directional wireless mike for targeting particular areas of interest. (The Audubon Society purchased 25 of these systems for monitoring bird and animal calls in mosquito-infested swamp areas.)

Circuit Description

This circuit shows how to build a super-sensitive, mini-powered FM transmitter consisting of a *radio frequency* (RF) oscillator section interfaced with a high-sensitivity, wide pass-band audio amplifier and capacitance mike with a built-in *field effect transistor* (FET) that modulates the base of the RF oscillator transistor (see Figure 24-2). Transistor Q1 forms a relatively stable RF oscillator whose frequency is determined by the value of coil L1 and tuning capacitor C4. The setting of C4 determines the desired operating frequency and is in the standard FM broadcast band with the tuned circuit design favoring the high end up to 110 MHz. Capacitor C2 supplies the necessary feedback voltage developed across resistor R3 in the emitter circuit of Q1, sustaining an oscillating condition. Resistors R1 and R2 provide the necessary bias of the base emitter junction for proper operation, while capacitor C1 bypasses any RF to ground fed to the base circuit. Capacitor C3 provides an RF return path for the tank circuit of L1 and C4 while

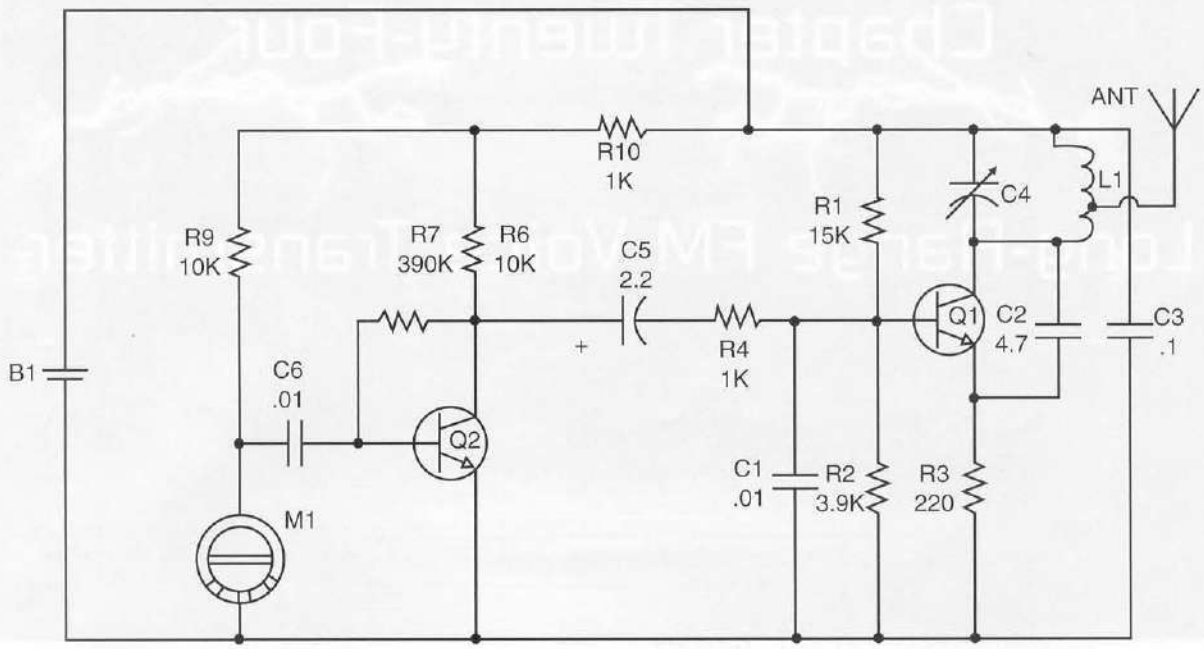

Note that the microphone M1 has polarity. You can identify the ground pad by the connection tabs to the outer shell.

Figure 24-2 *Circuit schematic*

blocking the DC supply voltage fed to the collector of Q1.

The audio section utilizes a high-sensitivity capacitance mike (M1) and built-in FET transistor (field effect) and will clearly pick up all low-level sounds in the speech audio spectrum. The speech voltage developed across resistor R9 by M1 is capacitively coupled by C6 to the base of audio amplifier transistor Q2. You will note the base of oscillator transistor Q1 is biased by resistors R1 and R2. A signal voltage now developed across resistor R6 is capacity coupled through nonpolarized capacitor C5 to the base of Q1 through resistor R4. The gain of Q2 is controlled by the ratio of R7 and R6. The operating point is set to allow full excursion of the collector to the amplified signal. The amplified speech signal now causes FM and AM modulation of the oscillator circuit by slight shifting of the operating point of the base section. Resistor R10 decouples the oscillator and audio circuits and is necessary to prevent feedback and other undesirable effects.

When properly assembled, the circuit should produce crystal-clear quality when the receiver is properly tuned to the unit. Note that a shunt capacitor may be connected across the base lead of Q1 to reduce sensitivity. The circuit with the components listed operates best in the upper FM band. This is a clear spot without interference from FM radio stations. However, satisfactory performance is obtained above 110 MHz for limited range use. Use caution as this is the aircraft band and should not be used if near an airport (see Table 24-1).

Assembly Steps

Assemble the circuit as shown in Figure 24-3.

1. Cut a piece of .1-inch grid perforated board to a size of 2 × 1 inches.
2. Form L1 by tightly wrapping eight turns of #16 bus wire on a #8 wood screw. This produces an eight-turn coil with an inner diameter of approximately .135 inches and a length of about .625 inches. Insert it in the proper hole and solder as shown.
3. Insert trimmer capacitor C4 into the holes as shown. You may put this component on either side of the PC board. This choice is up to you and should be determined by the final packaging scheme you require. Three holes are available for the part with two of them electrically the same point. This is necessary as some

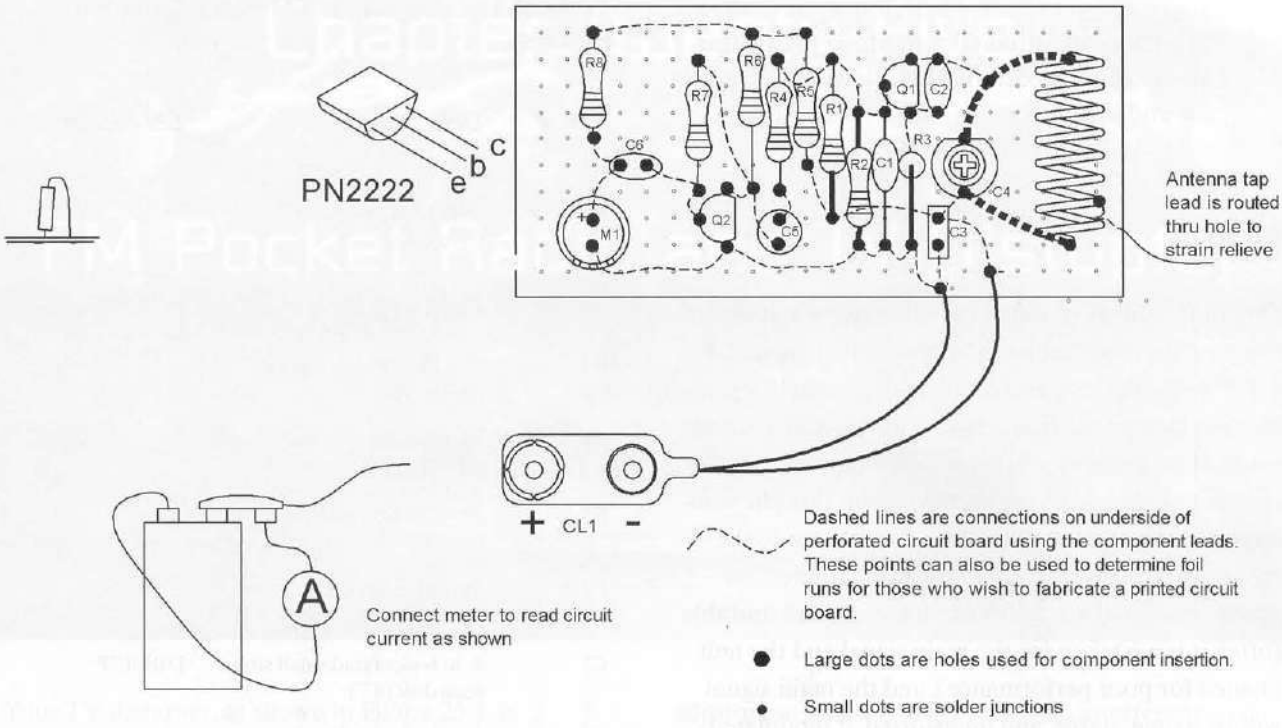

Figure 24-3 *Assembly board*

trimmers may have three pins. Make sure that the common pins are connected to the same electrical points with the odd pin to the other point.

4. If you are building from a perforated board, it is suggested that you insert components starting in the lower left-hand corner. Pay attention to the polarity of the capacitors with polarity signs and all the semiconductors. Route the leads of the components as shown and solder as you go, cutting away unused wires. Attempt to use certain leads as the wire runs or use pieces of the #24 bus wire. Follow the dashed lines on the assembly drawing as these indicate the connection runs on the underside of the assembly board.
5. Attach the external leads of the battery clip (CL1).
6. Double-check the accuracy of the wiring and the quality of the solder joints. Avoid wire bridges, shorts, and close proximity to other circuit components. If a wire bridge is necessary, sleeve some insulation onto the lead to avoid any potential shorts.
7. Tune an FM receiver to a fairly strong station at the high end of the band (108 MHz or higher). Turn up the volume and position the receiver 25 to 50 feet from the circuit.
8. If a multimeter or 50-milliamp meter is available, connect it in series with a battery lead. This can be done by removing one of the fasteners of the clip and connecting the meter to the free contacts, as shown in Figure 24-3. The meter should read 5 to 7 milliamps. Use a short piece of bare wire to touch the coil L1 a turn at a time, starting from the C3 end. Note that as you progress turn by turn away from C3 that the indicated meter current will drop or change.
9. If the device performs as follows with the battery connected, slowly rotate C4 with an insulated tuning wand until the station being received by the radio at approximately 108 MHz breaks out in audio feedback or is blocked out. It may be difficult at first to spot the signal as this adjustment is very touchy. Also note that several spots in the adjustment may be erroneous and will be weak and unstable. The correct signal will be strong, stable, and clear and can be verified by distance-of-transmission testing.
10. Once the desired setting of C4 is found, it should be marked with the frequency noted.

11. When operation is verified, it may be desired to enclose the circuit board into a plastic box along with the battery. This allows easier tuning and handling.

Notes

One of the things to watch for when using a device of this type is proper tuning. The adjustment capacitor, C4, is quite sensitive and requires only a slight movement to change the frequency, so always use a tuning wand. It is very easy when one is not familiar with this unit to tune to an erroneous signal. This phenomenon is likely to occur when the unit is close to the monitoring receiver. As previously mentioned, an erroneous signal will be weak, distorted, and unstable (often it is mistaken for the main signal and the unit blamed for poor performance), and the main signal will be strong, stable, and undistorted, if modulated. Several experiments in tuning the unit should be done before attempting to use it for the desired application.

Also, whenever possible, the unit should be used around 108 to 109 MHz, which is at the boundary of the aircraft band and upper FM broadcast band. When the approximate desired spot is found, final touchup tuning should be done at the receiver end for clarity. In most areas, these "upper" frequencies are clear and allow uninterrupted use in contrast to the lower ones in the FM band where a slight change in frequency from a clear spot results in the unit being drowned out by a strong broadcast station. Do not go above 108 MHz if near an airport or air traffic lane.

Most available FM radios can easily be detuned slightly to shift the dial readings down where 108 is 109. This is accomplished by carefully adjusting the "oscillator," the padding trimmer located on the main tuning capacitor, and "walking" a known station down the necessary megahertz or two. An antenna-peaking trimmer should now be adjusted for maximum signal at the high end.

Optimum performance will require a good-quality receiver with an analog slide-rule-type tuning dial. Digital tuned receivers will not work that well.

Table 24-1 Long-Range FM Voice Transmitter Part List

Ref. #	*Description*	*DB Part #*
R1	15K, 1/4-watt resistor (br-gr-or)	
R2	3.9K, 1/4-watt resistor (or-wh-red)	
R3	220-ohm, 1/4-watt resistor (red-red-br)	
R4, 5	Two 1K, 1/4-watt resistors (br-blk-red)	
R6, 9	Two 10K, 1/4-watt resistors (br-blk-or)	
R7	390K, 1/4-watt resistor (or-wh-yel)	
C1, 6	Two .01-microfarad, 50-volt disc capacitors	
C2	4- to 6-picofarad small silver mica disk (4.7)	DB# 4.7P
C3	.1-microfarad, 50-volt plastic capacitor	
C4	6- to 35-picofarad trimmer capacitor	DB# 635P
C5	2.2-microfarad, 25-volt vertical nonpolarized electrolytic capacitor	
CL1	Battery snap clip and leads	
Q1, 2	Two PN2222 NPN general-purpose transistors	
L1	Coil wound as described in assembly steps	DB# COIL8T
PBOARD	2 × 1 × .1-inch grid perforated board	
WR24BUSS	12 inches of #24 bus wire for wiring and antenna tap	
WR16BUSS	6 inches of #16 bus wire for making L1 coil	
M1	Special FET-bypassed microphone	DB# FETMIKE
PCXFM1		DB# PCXFM

Chapter Twenty-Five

FM Pocket Radio and TV Disrupter

Your TV disrupter, as shown in Figure 25-1, is designed and built on a piece of perforated circuit board that can fit inside a small plastic case. It operates using two standard, 9-volt transistor batteries in series. A unique pulsing circuit causes carrier deviation at 1,000 Hz, which creates a highly effective interfering device. The unit is tuned to a certain channel or frequency via a miniature tuning capacitor and then is controlled by a slight action of hand movement for further control.

This device is intended as a barroom joke and must not be abused. No attempts should be made to add an antenna because the range can be excessive and become a highly illegal device. When used as a harmless gag, such as in a bar, you can drive the bartender crazy because just as he is about to make an adjustment to a TV to get rid of the interference, you simply detune the device to make an adjustment to get rid of the interference and take the disrupter off the channel. When he thinks the problem is solved and continues his other duties, you hit it again. You can only begin to imagine the enjoyment (as a gag) of creating such havoc and being completely unnoticed.

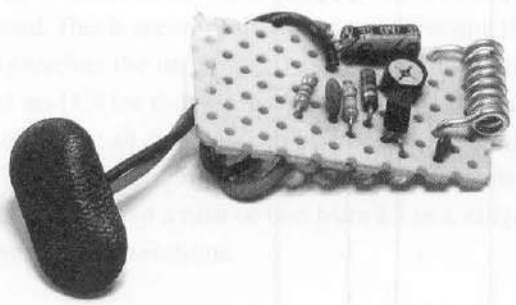

Figure 25-1 *Assembly board*

Also, any FM radio station can be interrupted with a 1,000 Hz tone that is many times louder than the normal received station. Obviously, a fun-loving person can use his or her imagination and come up with many harmless uses for the device.

It must be stated that using a device of this nature could be considered illegal, and discretion should be used at all times because a good gag can become a hateful nuisance. Also note that when cable TV is used, it may be necessary to get as close to the set as possible for maximum effect.

The following plans show how a miniature, simple, inexpensive electronic circuit can disrupt TV and radio communications in a very limited area. The unit can also be used to blank out those tiresome commercials.

Circuit Theory

The I1 timer generates positive pulses that occur across R4. The frequency of those pulses is a function of R1 and C1 and consequently establishes the pulse repetition rate of the device. This frequency modulates the base of Q1, which is a variable oscillator whose frequency is determined by C6 (see Figure 25-2). See Table 25-1 for the parts list.

Assembly Steps

Lay out and identify the parts with the bill of materials. Insert the components as shown in Figure 25-3, starting from one end of the perforated circuit board, and follow the locations using the holes as guides. Use the leads of the actual components as the connection runs, which are indicated by the dashed lines. It is a good idea to trial-fit the parts before actual soldering. Always avoid bare wire bridges and globby solder joints, and check for cold or loose solder joints. Always pay attention to the capacitors with polarity signs and all the semiconductors.

To adjust for frequency, set the TV to channel 2 and turn C6 for maximum capacitance (for a preliminary frequency, when adjusting, it is advisable to use a lower voltage due to the possibility of interfering with other than TV or radio stations such as police or aircraft bands). Adjust L1 by compressing turns until the interference is noted on channel 2. Turn to other channels, turn on C4, and note the complete coverage. Channels above 6 are covered by the harmonic output of the device.

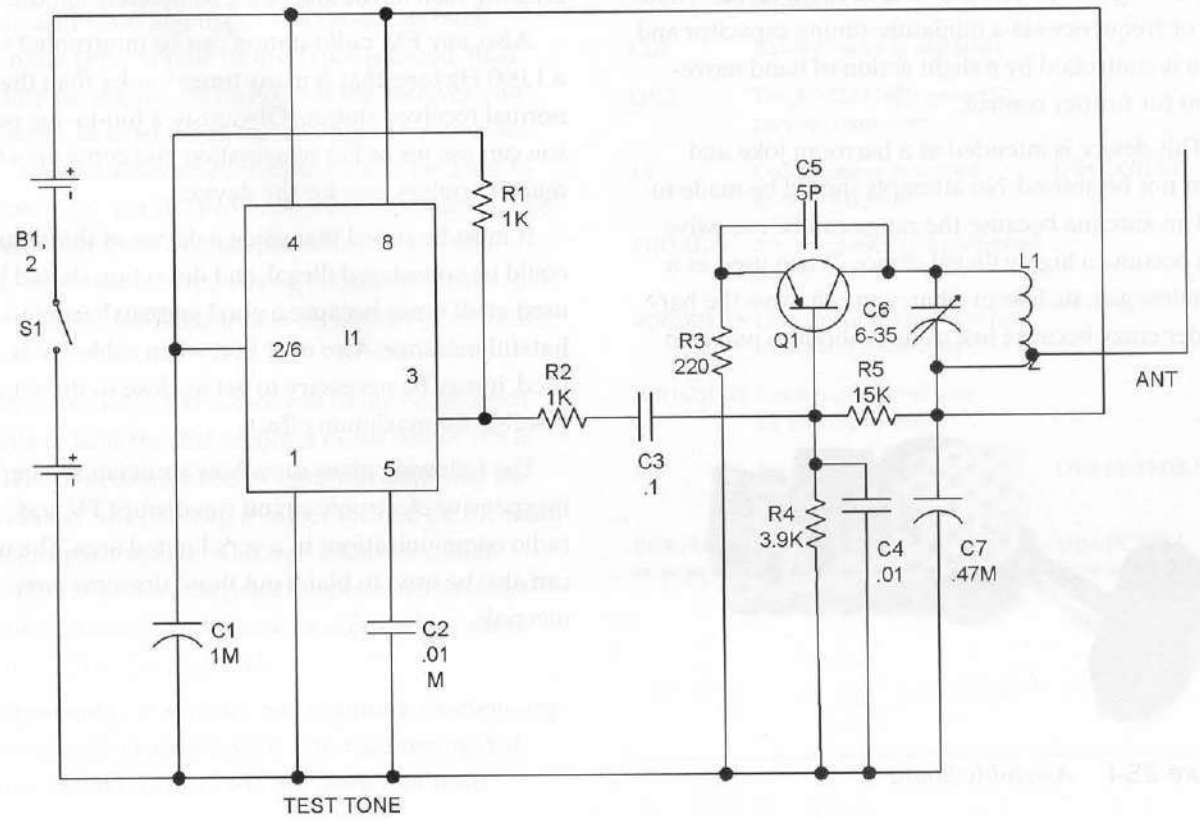

Figure 25-2 *Circuit schematic*

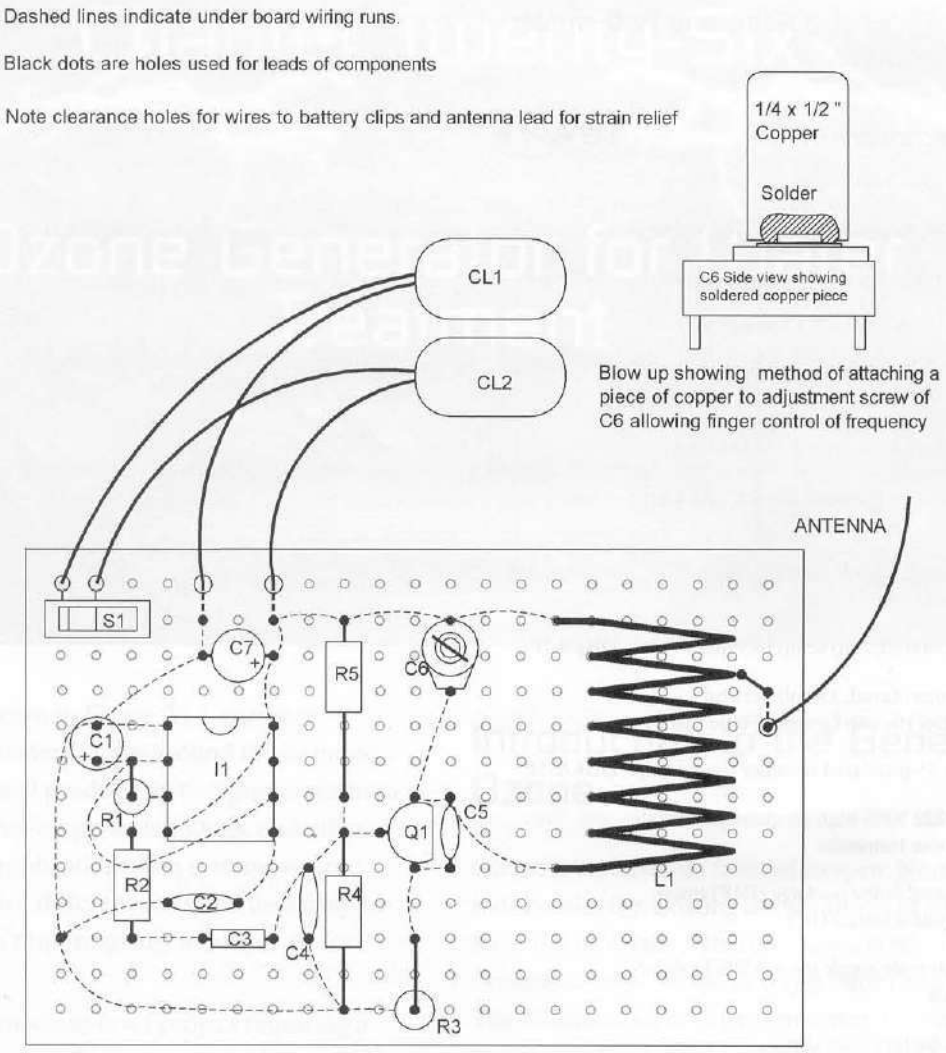

Figure 25-3 *Assembly board*

Several points of interest should be mentioned here, one being the ability to tune the unit on or off of a particular channel with just hand capacity (slight movement near L1); that is, the ability to detune the circuit with your hand creates a virtual capacitance. The other is the ability to also cover the FM radio band. This is accomplished by decompressing the coil (spreading the turns apart) and eventually adjusting L1 and C4 for the necessary coverage. It should be noted that all channels can be covered along with the FM band when properly adjusted. It may be necessary to remove a turn or two from L1 to a range on the FM radio stations.

Cable and satellite TV will often require the unit to be very close to cause an effect. There is no control over this, as the unit is designed to interfere with the actual frequency of the station being received, as was the case before cable and satellite services.

Table 25-1 FM Pocket Radio and TV Disrupter Parts List

Ref. #	Description	DB Part #
R1, 2	Two 1K, 1/4-watt resistors (br-blk-red)	
R3	220-ohm, 1/4-watt resistor (red-red-br)	
R3	100-ohm, 1/4-watt resistor (br-blk-br)	
R4	3.9K, 1/4-watt resistor (or-wh-red)	
R5	15K, 1/4-watt resistor (br-gr-or)	
C1	1-microfarad, 35-volt vertical electrolytic cap (green or blue can)	
C2, 4	Two .01-microfarad, 25-volt disk caps (103)	
C3	.1-meter, 50-volt ceramic cap (blue tablet .1)	
C5	6-picofarad, zero temp (4.7 disk)	DB# 4.7P
C7	.47-microfarad, 35-volt vertical electrolytic cap (green or blue can)	
C6	6- to 35-picofarad trimmer tuning Cap	DB# 635P
Q1	PN2222 NPN high-frequency, general-purpose transistor	
I1	555 *dual inline package* (DIP) timer *integrated circuit* (IC)	
S2	*Single pole, single throw* (SPST) slider switch	
CL1	Two-battery snap clip	
WR1	9 inches of #16 buss wire; wind seven turns on a pencil-sized object	
WR2	12 inches of #24 vinyl hookup wire	
PB1	2.5 × 1.5 × .1-inch grid perforated circuit board	
L1	Coil as shown	DB# COIL8T

Chapter Twenty-Six

Ozone Generator for Water Treatment

This project, as shown in Figure 26-1, can very effectively purify water for use around the home or farm. The system will produce up to 5 grams per hour sufficient for swimming pools, laundries, and other medium-volume applications. The system covered here is shown in five different sizes and uses easy-to-construct modules requiring only a flow of air for operation.

This is an intermediate-level project requiring a basic electrical hookup. Expect to spend $50 to $250 depending on the size of the system chosen and the availability of the required air source. All parts are readily available, with specialized parts obtainable through Information Unlimited at www.amazing1.com, and they are listed in the parts list at the end of the chapter.

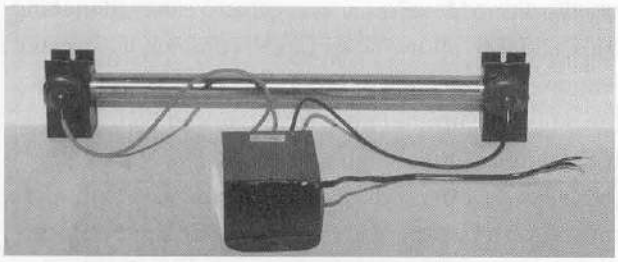

Figure 26-1 *The water treatment system*

Introduction to the Benefits of Ozone

Ozone is an unstable form of oxygen. Normal oxygen is diatomic (0_2), existing as two atoms of oxygen that form the molecule. Whereas ozone is tri-atomic (0_3), existing as three atoms of oxygen for the molecule. The tri-atomic form of oxygen is very unstable, wanting to lose the third oxygen atom and combine with whatever atom it can (oxidization). This property makes it the most active oxidizer known, with the exception of the very hazardous fluorine gas.

Ozone at normal pressures is colorless and produces a pleasing, fresh-air odor often like that after an old-fashioned thunderstorm. Under pressure, it becomes a bluish gas.

Ozone is also a very powerful bactericide. It is not affected by pH, as is chlorine, thus making it an excellent candidate for pools, spas, laundries, and general water treatment applications. It is many times more soluble in water, further enhancing its purifying effect. Ozone will combine with diatomic nitrogen N^2, forming nitrous oxide, 2NO. This oxide quickly combines with water, forming nitric acid, HNO_3. This is often a very undesirable effect when used with straight air. Pure oxygen greatly minimizes this effect and is often required in many applications. However, those requiring a supply of concentrated nitric acid

for nitration may wish to consider ozone and air with a condensing apparatus to obtain this useful acid. A condensing apparatus takes vapor from the ozone gas along with water and nitrogen to form a liquid by contacting them with cooler surfaces. The liquid (now nitric acid) flows down into a collection container by gravity. In the same way the old timers made moonshine, this uses a simple and basic chemical reaction where $2O^3 + 2N^2 + 2H_2O$ yields $2H(NO^3) + H_2O + 2NO$.

Ozone for Water Applications

It is estimated that 20 percent of all ground water is contaminated by pesticides, benzene, and phenol derivatives along with other undesirable organic substances. Ozone can oxidize many of these compounds, along with deactivating many viruses and harmful bacteria. Ozone will also oxidize certain inorganic compounds, such as iron and manganese, making them more easily removable by filtration.

Chlorine and bromine are often the choice of disinfectant for swimming pools and spas. The effect of these halogens is often dictated by pH, temperature, and agitation. Extreme heat and agitation can produce chloroform, a very toxic carcinogenic. The *Environmental Protection Agency* (EPA) is already taking a look at these chemicals for this use.

Ozone-treated water will destroy fungus, mold, and many pathogens found in water when used for washing fruits and vegetables in packing lines. When discharged, ozone causes little change to the beneficial bacteria in sewage treatment facilities.

Additionally, freshly caught fish will last longer when washed with ozone-treated water, and ozone's oxidizing action can eliminate odors from stored cheese. Egg storage time is increased, and wine can be aged faster. The removal of odors produced by the bleaching of beeswax, starch, flour, straw, bones, and feathers are all aided by ozone treatment. Also, the grease and wax on cotton and wool fibers can be decomposed by ozone, and gray mold on the surface of fruits and vegetables can be controlled by ozone.

Ways to Generate Ozone

Ozone can be produced by an electrical discharge or by a high-frequency electromagnetic wave. A high frequency requires the wave to be in the ultraviolet spectrum where Planck's energy formula, $W = hc/v$, starts to become effective. This is where energy in a wave packet in ergs is equal to Planck's constant times the speed of light in centimeters divided by the wavelength in centimeters. It is this energy that causes the stable O_2 to break up and recombine with other O_2 to form unstable O_3. Germicidal lamps operating at 253.7 nanometers can produce ozone.

The method presented here utilizes the ozone-producing properties of an electrical discharge. We have all, at one time, smelled the by-products of ozone. After a thunderstorm, it can be detected, as well as on certain days where electrical activity is spawning a storm. A sparking electric discharge such as brushes on a motor will create ozone also.

Our method uses a metal tube with a conductor running down the center. The conductor and the tube are insulated by one another and must support the high frequency and high voltage necessary to create a corona without breaking down into an arc. The ozone produced in the tubular cavity must be made to flow using moving air for cooling and replenishing air to be converted.

This method, while producing usable ozone, has several disadvantages. First, normal air contains nitrogen that likes to combine with the ozone to produce nitrous oxides. Second, air contains water in the form of moisture. Without getting into basic chemistry, we know that water plus nitrous oxide forms nitric acid, which is corrosive and undesirable for air purification applications. However, a very effective way of making this acid is to allow the oxides to combine with water vapor or steam and condense in a cooling tube, producing concentrated nitric acid that can be used in the manufacture of high explosives. The 5 gram per hour system can produce enough nitric acid that, when mixed with battery acid (sulfuric acid), can produce usable amounts of high explosives by the simple nitration of many organic compounds.

Select the system you require from Figure 26-2. Note that each is complete with the mating power supply.

Wire up the system as directed in Figure 26-3. Obtain a suitable air supply and connect up the hoses as shown. Use ozone-resistant material for connections to the cell.

Turn on the air supply and note a bubbling from the output hose immersed under the water. Apply power to the high voltage and note a distinct smell coming from the hose when pulled out of the water. Reinsert and rig the hose end to stay under the water. The unit is now ozonating the water.

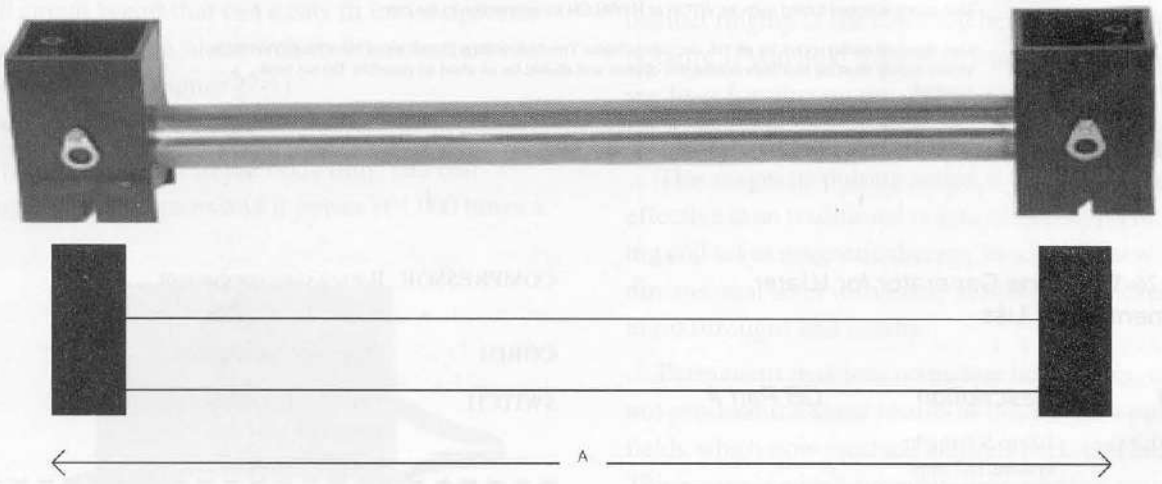

DATA BASE#	LENGTH A	OZONE OUTPUT/HR	AIR/O3 FLOW/MIN	INPUT V	INPUT I
OZONE300	182mm	100-500 mg/hr	.25-.55 CFM*	115 Vac	.2 Amps
OZONE800	282mm	500-1000 mg/hr	.35-.7 CFM*	115 Vac	.6 Amps
OZONE2000	382mm	1000-2500 mg/hr	1-1.5 CFM*	115 Vac	.9 Amps
OZONE5000	482mm	2500-5000 mg/hr	1.5-3 CFM*	115 Vac	I.2 Amps

* Multiply CFM by 28.3 to get Liters per minute

Each DATA BASE# system is complete with a matching power supply and ready to connect up as shown on figure 26-3

Figure 26-2 *System selection specifications*

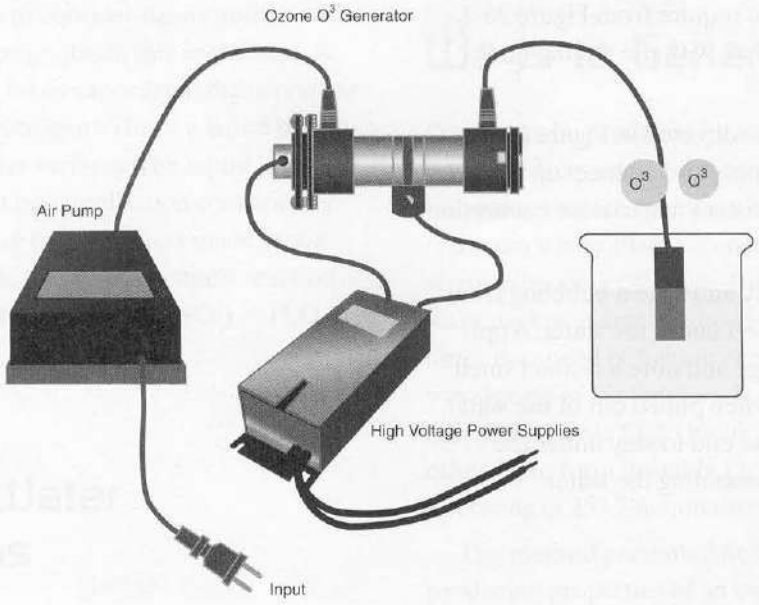

The high voltage power supplies used in these systems operate from normal 115 Vac 60 Hz. They are listed with the appropriate ozone cell on figure 26-2

The air pumps used can be that appropriate for the volume of the particular syste. A flow meter should be used when first setting up the system to verify proper air flow. Pure oxygen works the best and is available in cylinders with regulator valves and optional flow meters. Large aquarium air pumps may be used with the smaller systems while rotary vane air compressors are suggested for the larger systems. Note to multiply cubic feet per minute (CFM) by the factor 28.3 when converting to liters per minute.

Use ozone resistant tubing such as VITOR or HYPALON for connection to the cell

Use standard wiring codes for all 115 vac connections. The high voltage output wires from the high voltage power supply must be free from conductive objects and should be as short as possible. Do not twist together.

Figure 26-3 *Ozone system diagram*

Table 26-1 Ozone Generator for Water Treatment Parts List

Ref. #	*Description*	*DB Part #*
OZONE300	100 to 500 mg/hr system/182 mm/ 115 VAC @ .2 amps	DB# OZONE500
OZONE800	500 to 1,000 mg/hr system/282 mm/ 115 VAC @ .6 amps	DB# OZONE800
OZONE2000	1,000 to 2,000 mg/hr system/382 mm/ 115 VAC @ .9 amps	DB# OZONE2000
OZONE5000	2,500 to 5,000 mg/ hr system/482 mm/ 115 VAC @ .2 amps	DB# OZONE5000
HOSE	Connecting hoses, use ozone-resistant VITOR or HYPALON	
COMPRESSOR	Rotary vane compressor at required airflow	
CORD1	Three-wire power cord	
SWITCH	Two switches to control air compressor and high-voltage supply	

Chapter Twenty-Seven

Therapeutic Magnetic Pulser

This project shows how to build a battery-powered magnetic pulser that can provide relief from aches and pains, as well as improve upon many different health concerns and conditions. The unit is built on a small circuit board that can easily fit into a cigarette pack-size enclosure, along with its 9-volt battery or wall adapter (see Figure 27-1).

This magnetic pulser is designed so the magnetic north pole is applied to the body only. The coil strength is 10,000 gauss and it pulses at 1,000 times a second. A small switch can be used to turn the device off or you may simply unsnap the battery clip.

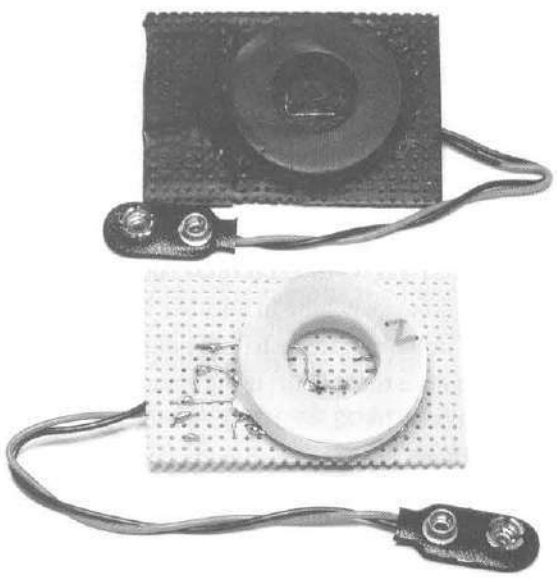

Figure 27-1 *The thermomagnetic pulser*

When an aluminum beer or pop can is held between your ear and this pulser, you hear a strong, distinct ringing as the can itself becomes the opposing polarity. If you hold the coil in front of a TV, you can see lines forming on the screen. On some TVs, the lines are visible when it's held as far away as 3 inches.

This magnetic pulsing action is more powerful and effective than traditional magnetic therapy. The pulsing coil takes magnetic therapy to a whole new dimensional level with many yet-to-explore exciting breakthroughs and results.

Permanent magnets, no matter how strong, will not produce the same results as this device's pulsed fields, which now produce induced back-emf currents. This requires a high-intensity, time-varying, magnetic impulse, not just a steady-state magnetic field.

Permanent magnets have their uses, but they work in different ways with different results. Equally important is the fact that we have "electric-powered" brains: All our thoughts and perceptions consist of complex networks of electrical signals and electromagnetic fields that pulse and sweep throughout the brain. So it then makes sense that harmonic electrical revitalization of the brain can harmonically influence your mental state and positively alter mental effectiveness.

Externally applied magnetic pulses to the lymphatic system, spleen, kidney, and liver help neutralize germinating, latent, and incubating parasites of all types, helping to block reinfection. This speeds up the elimination of disease, restores the immune system, and supports detoxification. The movement of the lymphatic system is essential in purifying, detoxifying, and regenerating the body, supporting the immune system, and maintaining health. Normally, the lymph is pumped by the movement of our body's electromagnetic field with vigorous exercise and physical activity. However, a clogged, sluggish, or weak lymphatic system prevents the body from circulating vital fluids and eliminating toxic wastes, thus weakening the immune system. It makes us vulnerable to infections and diseases. In order to be healthy, it is essential to keep the energy balanced and fluids moving so that the body's natural intelligence may operate at its full healing capacity. In addition, each cell must be enlivened with its own unique energetic frequencies and harmonic energy state and be harmonically connected to the life-force energy throughout the rest of the body.

Pulsed electromagnetic fields influence cell behavior by inducing electrical changes around and within the cell. Improved blood supply increases the oxygen pressure, activating and regenerating cells. Improved calcium transport increases the absorption of calcium in bones and improves the quality of cartilage in joints, decreasing pain dramatically. Acute and even chronic pain may disappear completely.

This device uses complex energy pulses of magnetic waves to stimulate certain body functions. It accelerates the production of vitally important hormones often providing miraculous effects. Magnetic pulsing aids in human growth hormone production and neotransmitter production. The results are remarkable, increasing vitality, sexuality, and accelerated healing. It also helps learning and the reduction of memory loss with reports of increased psychic ability for some people. The magnetic pulser also revitalizes and rejuvenates. As we get older, hormone production drops off considerably and is a reason why we age.

Users are experiencing faster healing of injuries, including bone fractures, carpal tunnel, and arthritis. The pulsed magnetic field stimulates blood flow and cellular respiration in the area applied. Reports have also documented that people's migraine headaches have ceased after magnetic therapy has been applied.

This pulser can be worn, held, or wrapped to any part of the body or held in place with a tension bandage. You can use your pulser while driving and on the go, rather than having to stop and apply it when sitting or lying down, as is necessary when using a 110-volt, standard magnetic pulser. The product is currently being sold only for experimental research and testing.

This is a simple, basic-level project requiring minimal electronic skills. Expect to spend $15 to $20. All parts are readily available, with specialized parts obtainable through Information Unlimited (www.amazing1.com), and they are listed in the parts list at the end of the chapter.

Circuit Description

Figure 27-2 shows a 555 timer (I1) connected as a free-running, astable pulse generator. The output pulses are nonsymmetrical with a ratio of low to high time of 10 to 1. Discharge resistor R3 and forward-conducting diode D2 control the low time, whereas charge resistor R2 and forward-conducting diode D1 control the high time. Timing capacitor C2 is common to both states of the pulse being alternately charged and discharged.

Magnetic energy is produced when the timer I1 turns on transistor Q1. The current now has the "on" time of the pulse to build up and then collapse in the flux coil L1 when Q1 is turned off. The stored energy is returned to the circuit by diode D3. The result is a steady train of magnetic pulses at 1,000 pulses per second.

The switch S1 allows the unit to be turned on and off and also allows switching in another range, dropping the pulse repetition to 100 per second. It is interesting to note that claims using specific pulse repetition rates of 20, 72, 95, 100, 125, 146, 440, 600, 660, and 727 have proven very beneficial. Do not attempt to extend the frequency without first determining the current rise in the coil. Current may be excessive and will require more turns as the frequency is lowered.

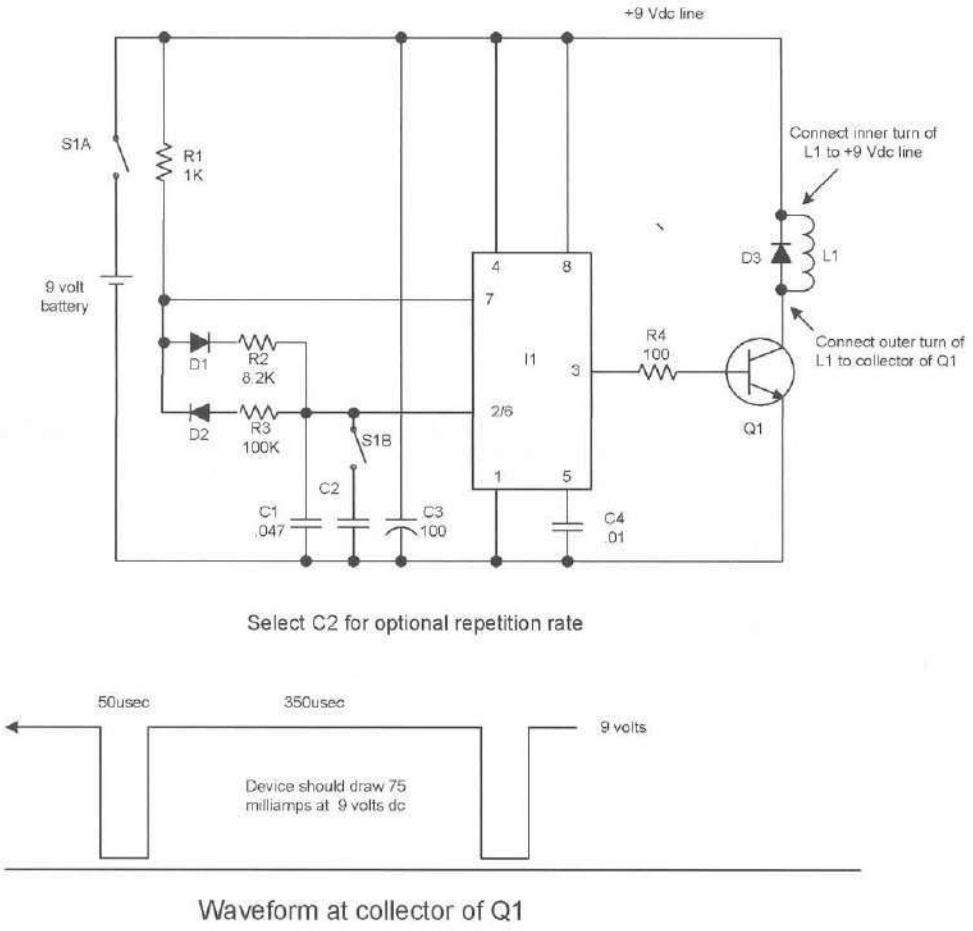

Figure 27-2 *Circuit schematic*

Assembly

1. Assemble the flux coil as shown in Figure 27-3 by first drilling a small hole adjacent to the inner diameter so that the "start" lead can exit the winding. Carefully wind 100 turns of #24 magnet wire in even windings. This is not necessary but makes for a neat-looking construction. Note to wind the wire so that its direction is the same as the figure with the leads routed as directed. This will guarantee the correct polarity as shown.
2. Cut a piece of .1-inch grid perforated board to a size of 2.6 × 1.8 inches, as shown in Figure 27-4. Locate and drill the holes as shown for the leads of battery clip CL1.
3. When building from a perforated board, it is suggested that you insert the components starting in the lower left-hand corner as shown. Pay attention to the polarity of the capacitors with polarity signs and all the semiconductors.

   Route the leads of the components as shown and solder as you go, cutting away unused wires. Attempt to use certain leads as the wire runs or use pieces of the #24 bus wire. Follow the dashed lines on the assembly drawing as these indicate the connection runs on the underside of the assembly board.
4. Attach the external leads from the battery clip and flux coil. Note the polarity of the leads on this part as indicated in Figures 27-2 and 27-4.
5. Double-check the accuracy of the wiring and the quality of the solder joints. Avoid wire bridges, shorts, and close proximity to other circuit components. If a wire bridge is necessary, sleeve some insulation onto the lead to avoid any potential shorts.
6. You are now ready to test the unit. Connect it to a 9-volt battery and note a current draw of 60 to 80 milliamps. Place the coil of the unit

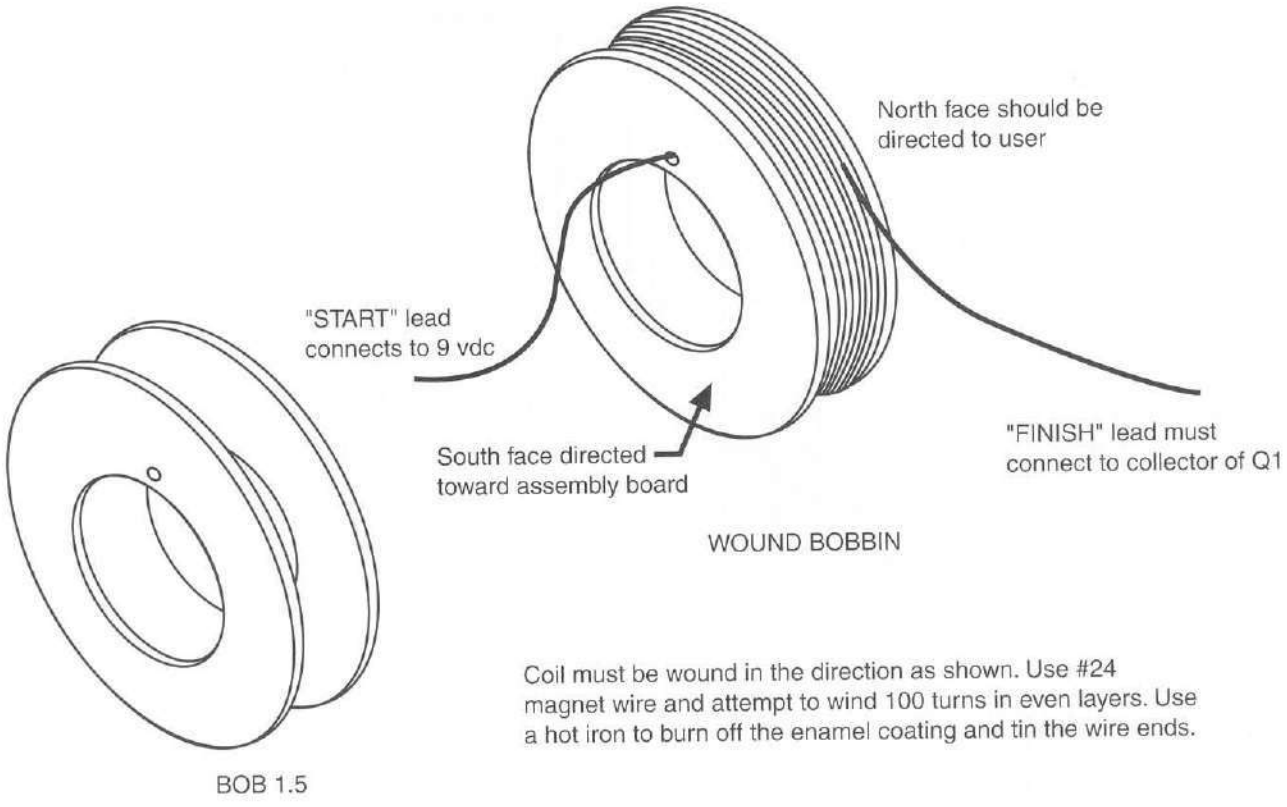

Figure 27-3 *Flux coil assembly*

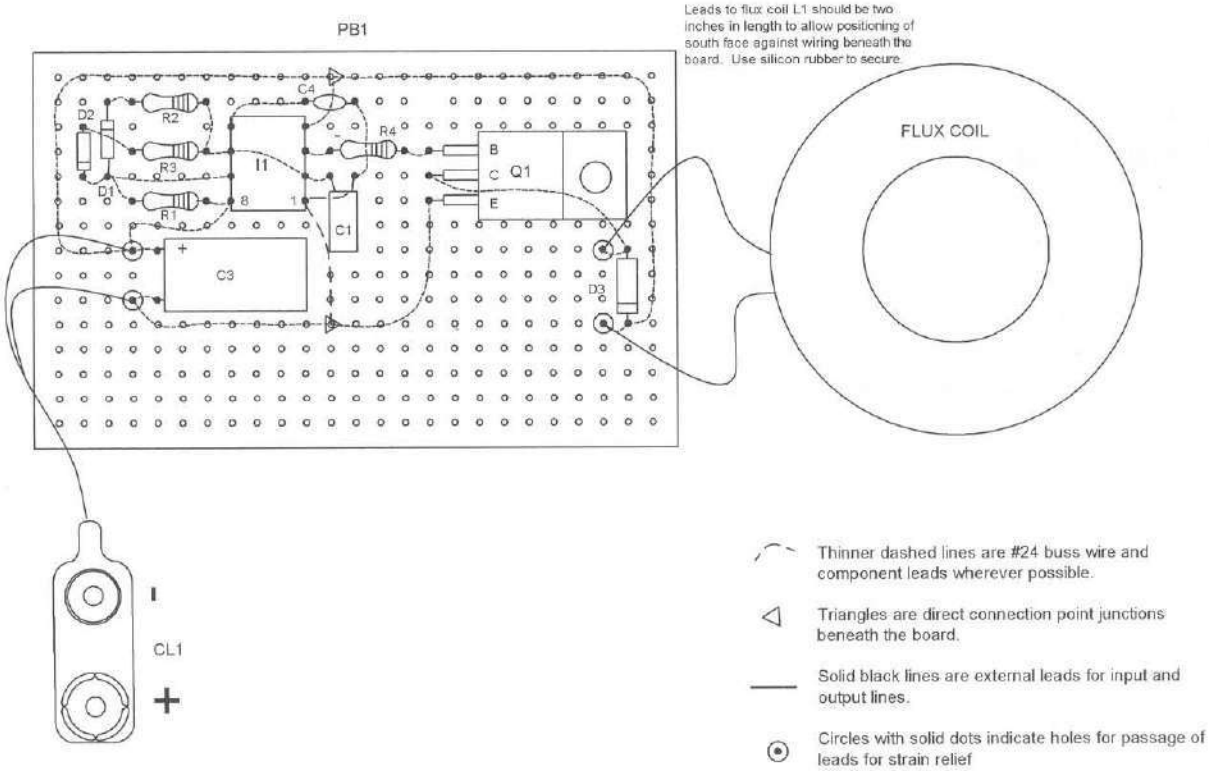

Figure 27-4 *Board assembly*

near a television screen and note the lines appearing. You may also put a metal can onto the coil head and place your ear to the can, noting a 1 to 2 KHz tone. If you have a scope, note the waveshape shown in Figure 27-2.

7. To use the unit, simply place the north face of the coil to the target area and allow exposure for several hours.

Table 27-1 Therapeutic Magnetic Pulser Parts List

Ref. #	*Description*	*DB Part #*
R1	1K, ¼-watt resistor (br-blk-red)	
R2	8.2K, ¼-watt resistor (gray-red-red)	
R3	100K, ¼-watt resistor (br-blk-yel)	
R4	100-ohm, ¼-watt resistor (br-blk-br)	
C1	.047-microfarad, 50-volt plastic capacitor	
C2	1-microfarad, 25-volt vertical electrolytic capacitor	
C3	100-microfarad, 25-volt vertical electrolytic capacitor	
C4	.01-microfarad, 50-volt disk capacitor (103)	
D1, 2	Two IN914 silicon diodes	
D3	1-kilovolt, 1-amp diode 1N4007	
Q1	TIP31 NPN TO-220 power transistor	
I1	555 dual inline package (DIP) timer	
BOB1.5	1.5 × .3 × .75-inch ID nylon bobbin (see Figure 27-3)	DB# BOB1.5
L1	Flux coil (see Figure 27-3)	DB# FLUXCOIL
PBOARD	2.6 × 1.8 × .1-inch grid perforated board as shown in Figure 27-4	
CL1	9-volt battery snap clip	

Chapter Twenty-Eight

Noise Curtain Generator

This unique circuit shown in Figure 28-1 is designed to produce a relaxing sound like that of a breaking surf. It is technically known as pink noise, being defined as a random distributor of equal sounds in the audible spectrum, favoring the higher-frequency end.

Pink noise has a spectral intensity that is inversely proportional to frequency for a given range. Therefore equal power is dissipated into a fixed resistance in any octave bandwidth in that range. White noise is random noise, which is typically thermal and shot noise, has a constant energy per unit bandwidth, and is independent of the central frequency at the band.

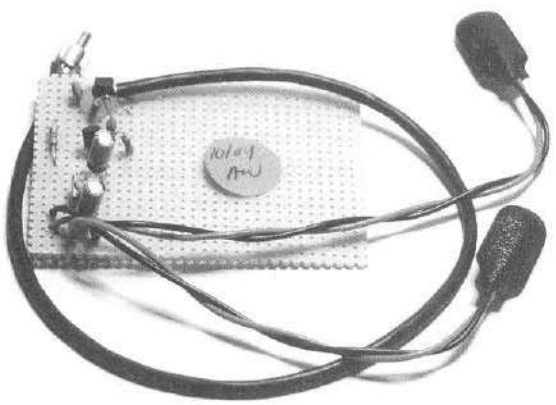

Figure 28-1 *The board-level generator*

This device is intended for use as a relaxing source of sound and also as a mask for certain types of surveillance equipment. Crashing surf is an excellent example of naturally produced pink noise that has a great relaxing effect. Due to the nearly equal amplitude of all the frequencies generated, the electronic equipment of an acoustical nature becomes easily overloaded and saturated, whereby normal voice sounds of varying amplitude and of limited bandwidth are much more finite and are unable to be processed by the equipment. In other words, the noise jams the microphone and audio preamplifier circuitry, thus rendering it unable to detect normal voices. (It should be noted that in certain instances a running shower will sometimes help simulate pink noise.)

The signal from the device is intended to be fed into the input of any amplifier, radio, or tape deck. It is easily connected to the center arm of the volume control if an input jack is not provided in a regular radio. (You will note the phono plug attached.) Also, the two batteries used are left on permanently, due to the fact that so little power is used.

The optional "speaker amplifier" reference schematic in Figure 28-2 is built on a piece of perfboard using standard audio-frequency wiring techniques. When used as a totally self-contained system, the electronics may be housed along with all batteries into a case or enclosure determined by the builder. This approach provides a convenient portable unit.

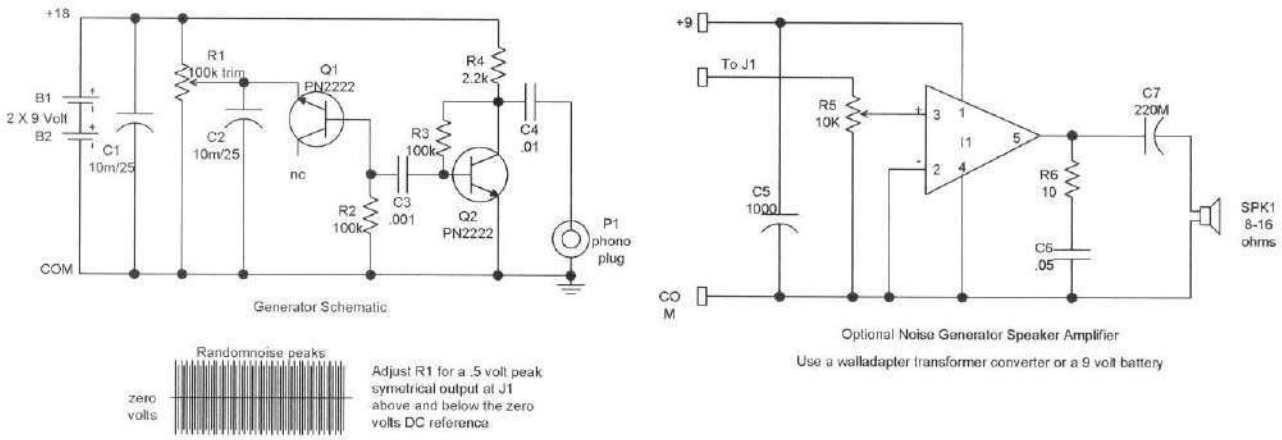

Figure 28-2 *Circuit schematic*

Circuit Description

Pink noise is a form of white noise that is the Gaussian distribution of all possible frequencies, the difference being that pink noise is more weighted to the audio spectrum. This form of noise has some very interesting properties, one being the ability to cause relaxation and a sense of well-being. Another property is that it provides a background that will completely mask an annoying device, rendering it unable to affect normal conversation. The device described is designed to work with any sound system with an audio input or is easily adapted to drive a loudspeaker by connecting it to a normal radio or building an optional speaker amp, as shown in the accompanying plans, making a complete system (see the parts list at the end of the chapter).

The circuit works in the following manner: A base emitter junction of transistor Q1 is reversed biased through a current-limiting resistor into breakdown (avalanche) condition. The random shot noise created is fed to the common emitter amplifier transistor, Q2, and to a filter, which in turn provides a low-level signal output. The unit module board and the batteries are placed in a plastic case with pieces of foam rubber or plastic. The outlet leads are fed out per the builder's requirements. The batteries are permanently installed and left on because the operating current is so low that there is no reason for a switch. Note that Jl is *not* required if using the optional speaker and amplifier circuit.

Assembly Steps

If you are a beginner it is suggested you obtain our *GCAT1 General Construction Practices and Techniques*. This informative manual explains basic practices that are necessary in the proper construction of electromechanical kits and is listed in Table 28-1.

1. Lay out and identify all the parts and pieces. Verify them with the parts list, and separate the resistors as they have a color code to determine their value. Colors are noted on the parts list.
2. Cut a piece of .1-inch grid perforated board to a size of 3 × 2.4 inches. Locate and drill the holes as shown in Figure 28-3 for the leads of the battery clips.
3. If you are building from a perforated board, it is suggested that you insert the components starting in the lower left-hand corner as shown in Figure 28-3. Pay attention to the polarity of the capacitors with polarity signs and all the semiconductors. Route the leads of the components as shown and solder as you go, cutting away unused wires. Attempt to use certain leads as the wire runs or use pieces of the #24 bus wire. Follow the dashed lines on the assembly drawing as these indicate connection runs on the underside of the assembly board.

4. Attach the external leads as shown in Figure 28-4. Notice the special note on the shielded cable.
5. Double-check the accuracy of the wiring and the quality of the solder joints. Avoid wire bridges, shorts, and close proximity to other circuit components. If a wire bridge is necessary, sleeve some insulation onto the lead to avoid any potential shorts.

Testing Steps

Insert the two battery clips and plug the output cable into the microphone or auxiliary jack of the existing system. Note the rushing sound and adjust the trimpot R1 to the desired effect. If you have a scope, make the adjustment as shown in Figure 28-2. If you build the speaker amplifier section, simply connect it as shown for a self-contained system suitable for nightstand use.

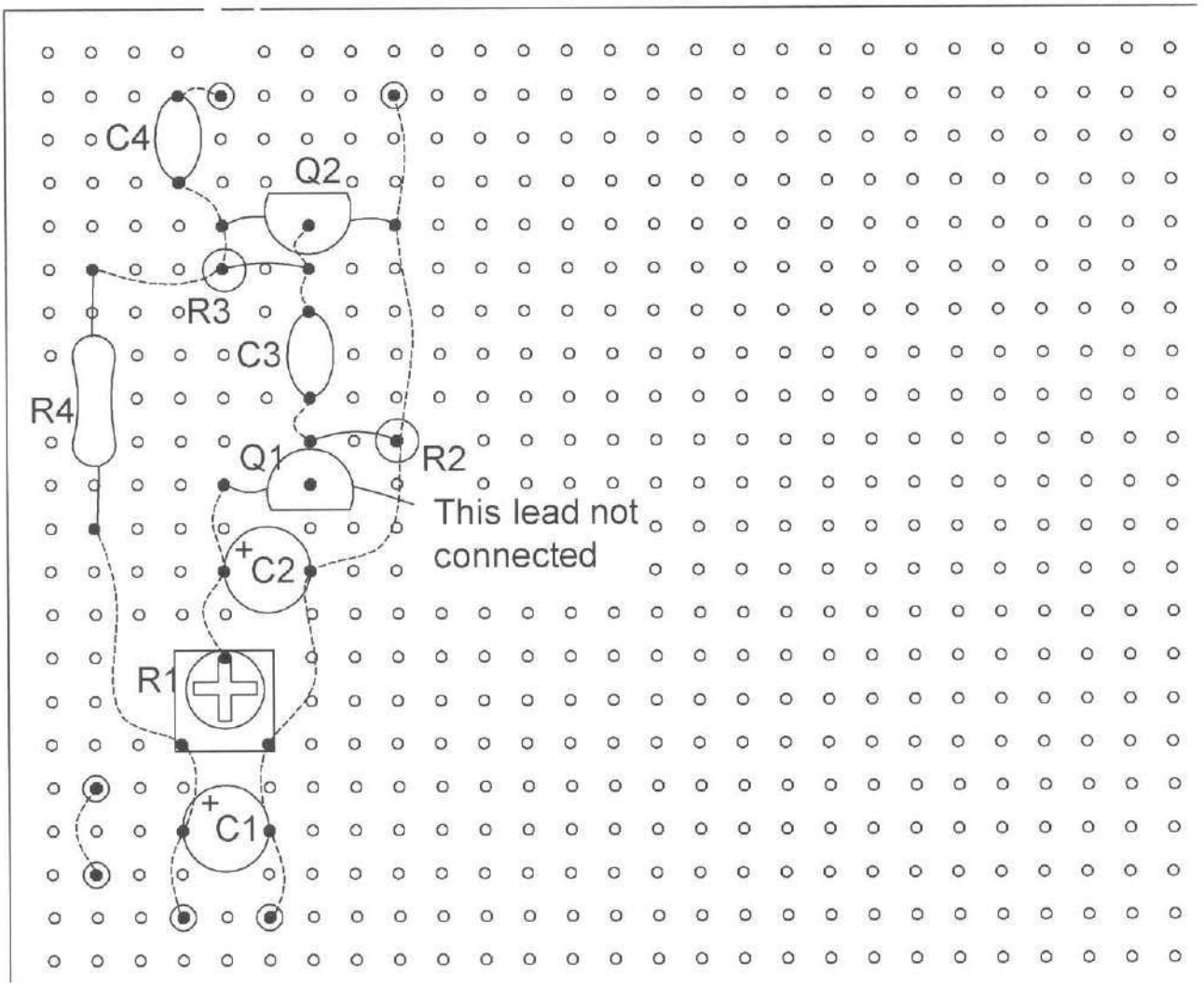

Figure 28-3 *Assembly board layout*

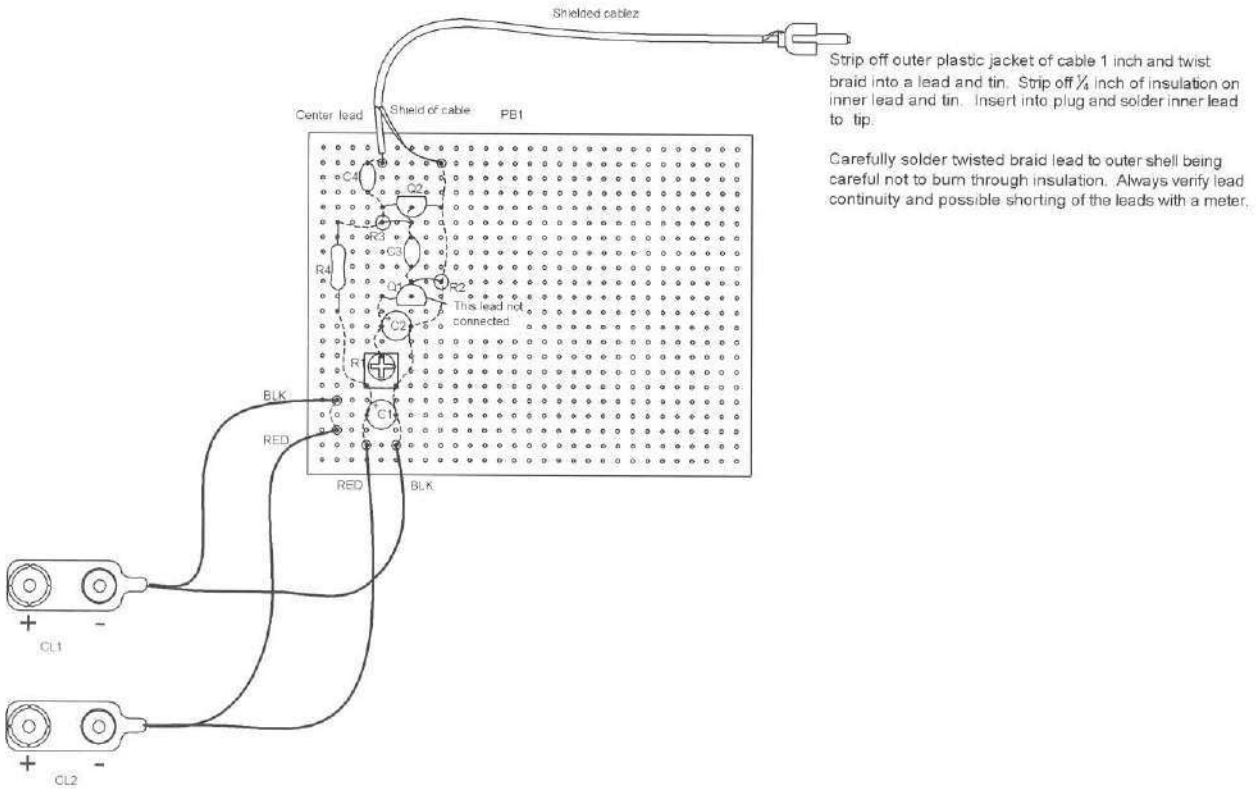

Figure 28-4 *Assembly showing external leads*

Table 28-1 Noise Curtain Generator Parts List

Ref. #	*Description*	*DB Part #*
R1	100K trimpot vertical mount	
R2, 3	Two 100K, ¼-watt resistors (br-blk-yel)	
R4	2.2K, ¼-watt resistor (red-red-red)	
R5	10K trimpot vertical mount	
R6	10-ohm, ¼-watt resistor (br-blk-blk)	
C1, 2	10-microfarad, 50-volt vertical electrolytic capacitor	
C3	.001-microfarad, 50-volt disc capacitor	
C4	.01-microfarad, 50-volt disk capacitor	
C5	1,000-microfarad, 25-volt vertical electrolytic capacitor	
C6	.047-microfarad, 50-volt plastic capacitor	
C7	220-microfarad, 25-volt vertical electrolytic capacitor	
Q1, 2	Two PN2222 NPN general-purpose transistors	
I1	LM386 dual inline package (DIP) operational amplifier	
PB1	2.25 × 3 × .1 × .1-inch grid perforated circuit board	
SPK1	Small 8- to 16-ohm speaker	
CL1, 2	Two 9-volt battery clips and leads	
P1	RCA phono plug	
SHC1	12-inch shielded microphone cable	

Chapter Twenty-Nine

Mind-Synchronizing Generator

Caution: This machine can trigger epileptic seizures and should be avoided at all costs by anyone who suspects even slightly that they are epileptic.

Your mind synchronizer is designed to be a completely self-contained unit with built-in batteries (see Figure 29-1). The system produces a variable-rate, flashing, monochromatic, directional, "shaped" light source (a light source with a variable ratio of off to on times), and a complementary synchronized audio pulser with tone-shaping control. The unit may be used so that a group can be exposed to light and sound pulses. For individual use, headphones can be used, along with special assembled light glasses. These are shown made from an existing pair of sunglasses. Optimum performance requires a quiet and reasonably low light condition, and distractions must be at a minimal. The mind-synchronizer can produce strange and bizarre hallucinations, as well as provide a sense of relaxation and well-being.

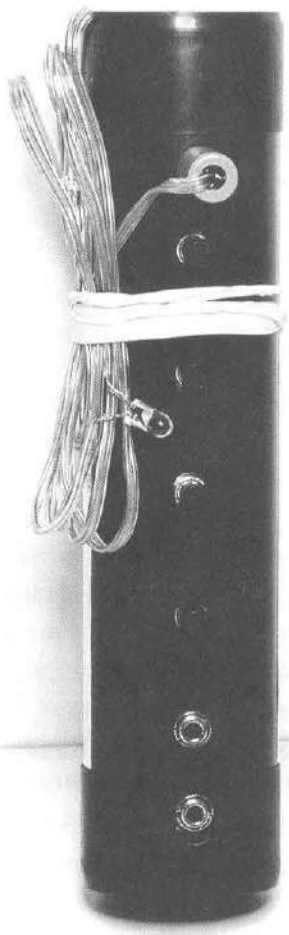

Figure 29-1 *Photograph of unit*

Information on Mind Control

Today's work environment demands that we have the ability to excel, to compete, and to resolve problems. Hence, the most important tool we possess is our mind. To optimize our potential, we now offer our low-cost mind-synchronizing unit.

After 25 years of research, Dr. Axel Bruck of Berlin, Germany, created a machine that can enhance, develop, and perfect the qualities within you in order to attain the goal of mental fitness. It has been found that external stimulation evokes a mental reaction in people that is either active or passive. The mind synchronizer can determine automatically the kind of person you are. An evaluation is performed via the means of a hand sensor using a technique called biofeedback, which is sensitive to the flow of blood. This knowledge is very important for providing optimal stimulation to the users.

Having determined the kind of person you are, the mind synchronizer now uses "programmed" light pulses and "shaped" sound to help you reach a required mental condition, be it relaxation or efficiency. It has been known for hundreds of years that an external rhythm of light and sound has an effect on your mental condition. The mind synchronizer is a modern version of a drum and a flickering fireplace.

Through extensive scientific measurements, experiments, and results, the mind synchronizer can improve your performance level by using the right stimuli:

- Deep relaxation to the point of sleeping
- Relaxation
- Equilibrium
- Activation of muscles doing physical movements
- Efficiency

Whether in sports, professions, or personal lives, the development of personality and identity is vital to personal success and satisfaction. The mind synchronizer trains and perfects your mental and psychic abilities so that you have a stable way of thinking with a healthy outlook. The mind synchronizer teaches you the technique of concentration, stress handling, focusing, visualization, relaxation, and self-awareness

When using the mind synchronizer, you learn to set a goal and concentrate on this goal completely. You eliminate all distractions and thereby maintain your concentration over a long period of time. By doing so, you improve your power of concentration. In the long run, you will think clearly, make better decisions, and deal more effectively with life itself.

The program of relaxation combats stress, tension, and direct pressure. Almost everything we do causes stress. Stress means that the body is in a chaotic condition. The opposite of stress is relaxation. The right kind of relaxation is an optimization of mind, concentration, learning ability, performance, and health.

In reality, a relaxed person saves more than half a billion heartbeats over a nervous or hectic person, according to Professor Prinzinger's theory of the Quiet Pulse. Professor Prinzinger performed much research into the various relaxed states of the body and the relationship of relaxation to heart rate and blood pressure. The body consumes less energy, organs are burdened less, and life expectancy increases.

The program of efficiency is a newly developed psycho-active technique: the indication of unconscious eye movement and the employment of rhythm displacement. Certain stimulating rhythms such as that of a strobing light can produce nausea when strobing at 20 repetitions per minute. Other stimulating rhythms of lower repetitions per minute can produce relaxation and the feeling of well being. In such a case, eye movement usually follows at the lower repetition rates. The combination of visual effects (flashing *light-emitting diodes* [LEDs]) with audio input (via a headset) produces high-efficiency performance. The mind synchronizer establishes physical and mental readiness to attain this goal of high performance.

The program of activation involves more optic, visual patterns than acoustic ones to provide "imagination journeys." To experience associations with your own history and your own personality, you will be able to discover your emotional condition and personality.

The program of equilibrium allows for meditation with your eyes open. You would observe attentively, simply, and exactly each individual light source and its changes. The mind synchronizer will bring you the healthy balance you desire through light and sound.

Mind machines are available from a wide variety of sources today. Often referred to as hemispheric synchronizers or cortical-frequency entertainment devices, they all basically perform one basic function: They lead the brain to synchronize both hemispheres and then lead those synchronized hemispheric frequencies to a specific target frequency. In order to

understand why anyone would want to do such a thing, let's examine what frequencies the brain produces and what people experience when the brain is at these frequencies.

Generally, brain waves are broken down into four different levels. They are referred to as beta, alpha, theta, and delta. With respect to frequency, they are as follows:

Beta: 13 cycles per second or more

Alpha: 8 to 12 cycles per second

Theta: 5 to 7 cycles per second

Delta: 1 to 4 cycles per second

Profound changes take place in a person's conscious experience at each of these levels. The beta frequency is the "normal" waking frequency, the drive-in-the-city, go-to-work, drink-coffee frequency, and it can range as high as 40 cycles per second. It is *not* a relaxing frequency.

The alpha frequency is a realm of relaxed awareness. It has been shown in a concrete fashion that this frequency is associated with an increased capacity for learning, comprehension, and retention. It is in the alpha state that the best learning occurs.

Theta is a hypnotic state often associated with meditation, a zen-like state of waking dreaminess. It can be a profoundly relaxed state where internal associations and thoughts can form ideas with clarity that could never have emerged in the normal, high-noise environment of the beta state. This is also the range that many native shamans have been found to enter when engaging in healing trance work. It is a state of profound tranquility.

The delta state is much simpler to define; you're asleep. When your brain waves are in the delta range, you're in a sound and restful sleep.

A number of studies have been done that indicate that a flashing light has a profound impact on the entire brain, more so than a pulsing sound or feeling. When the brain is exposed for a time (as short as 2 to 5 minutes) to a flashing light at a speed close to the brain's existing operating frequency, the brain will begin to synchronize with the stimulation. Moreover, both hemispheres, which are often operating at different frequencies, will harmonize. This has also been shown clinically and statistically to be an aid to mental functioning. Many books are available on the market on this subject for anyone who would like more detailed information on these studies.

Operating a Mind Machine

Now with the previous information in mind, the operation of the mind machine in all of its forms is basically the same. Start the machine off at a frequency that is roughly equivalent to the operating frequency of your brain at the time. (Use your own feelings as a gauge. If you're frazzled, start at maximum frequency; if you're pretty mellow, start at about half-frequency.) Allow yourself about 3 to 4 minutes at this frequency, and then slowly begin bringing the frequency down, very slowly. You should take about 7 to 10 minutes to bring the control all the way down. When you reach a minimum, leave it there for about 5 to 7 minutes.

After you've gotten to the bottom range, you can either lead yourself back to normal, in which case you will feel what you may consider a "good normal." If you so choose, you can exit directly from the lowest setting. If you do, have taken your time getting to it, and stayed there for several minutes, you will notice that it may be very hard to begin to move. Your limbs may feel very heavy, as if your body were asleep. If you manage to get to your feet, you may notice that things won't feel as solid; they'll seem to have a rubbery quality to them. These sensations can be quite pleasant as long as you're prepared and expect them (and don't have to drive or operate heavy machinery afterward!).

The visual effects are the most stunning and can only be likened to the experience of ingesting certain mind-altering substances. As the frequencies change, you will notice colors. Yes, two little flashing red lights in front of your closed eyes will create the illusion of fantastic, swirling colors and geometric designs ranging from ultimate simplicity to incredible complexity. One effect will be observed as myriads of little shapes that form and begin to slowly spiral around your field of vision, first clockwise, then counterclockwise, then back again. You will see dreamy, smooth, cloudlike fields of frosty blue-white, deep blues, deep reds, electric greens, yellows, whites, and purples, all in balls,

stripes, stars, and triangles, dancing and moving like the most intense kaleidoscope you can imagine. The imagery is absolutely fascinating and can transfix you with the dazzling display. You will be absolutely amazed and impressed with the fact that it is your brain that produces this light show.

This unit is designed to take you from a medium-level beta down to a low theta. You can use these states as you desire. You may wish to stop the frequency decrease early and remain in the alpha state before an exam, prior to entering a class, or when trying to learn something important. You can continue on down and enter the theta level and create healing imagery in your mind to assist your body's own natural healing processes.

Most of all, play with your unit and enjoy the show. Built right, it will provide many years' worth of reliable service. Through usage, you can become familiar with the settings and be able to use the machine in a way that's exactly right for you. Always leave yourself plenty of time to use the machine and at least a half-hour after to "normalize." Use the unit to help you drift off to sleep; you can actually lead your brain down into relaxation and turn the unit off after you've gone into a deep theta, and if you're ready to sleep away, it's only a short slide from theta into the peaceful slumber of delta.

Circuit Theory

Integrated circuit I1 is an astable oscillator with a pulse rate being controlled from approximately 3 to 40 reps per second by external pot R2. The output of Ul now triggers integrated circuit I2 being connected as a monostable circuit that controls these pulses' ratios of on to off time. This duty cycle control is via external pot R5. Light-emitting diodes (LEDl and LED2) are connected to the output pin 3 of I2 through brightness control pot R7. These are the diodes you install in the sunglasses or they can be a single ultrabright LED for group use. The result is a variable flash rate from 3 to 40 pulses per second with a variable duty cycle rate (ratio of on to off time).

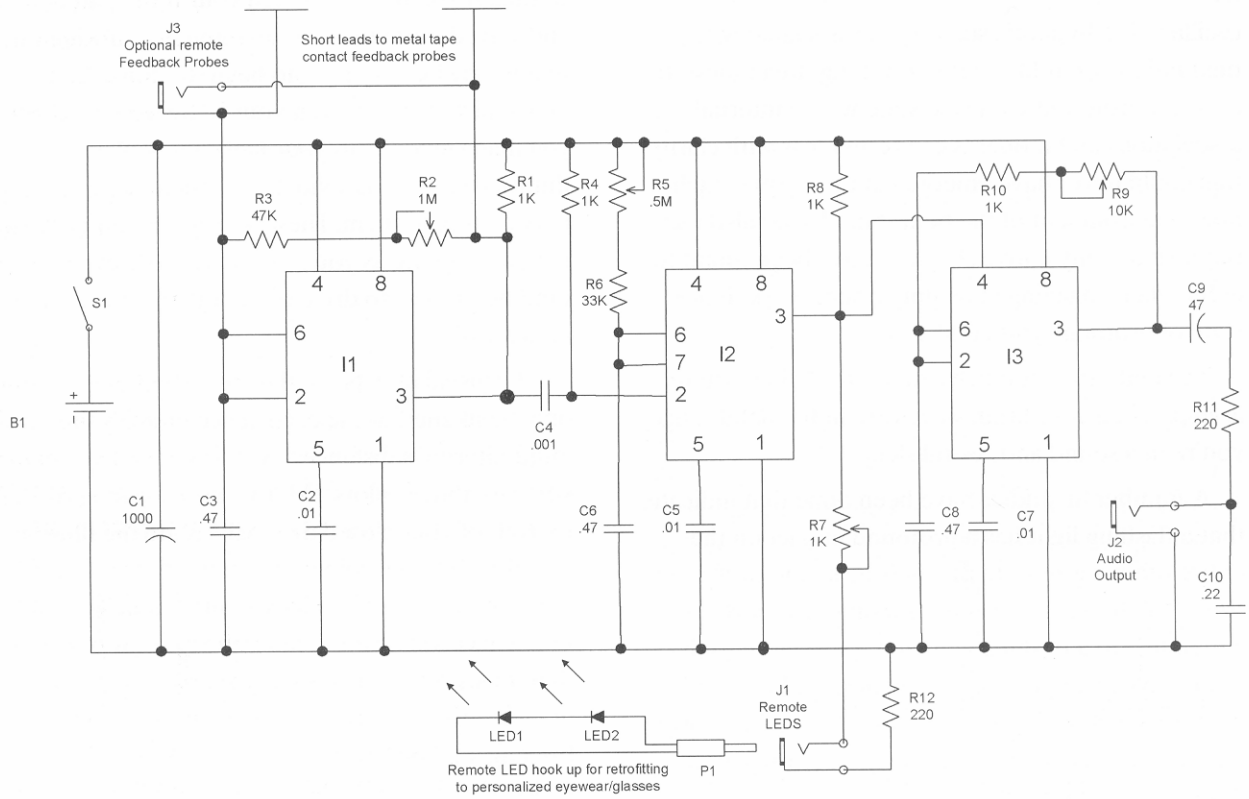

Figure 29-2 *Circuit schematic*

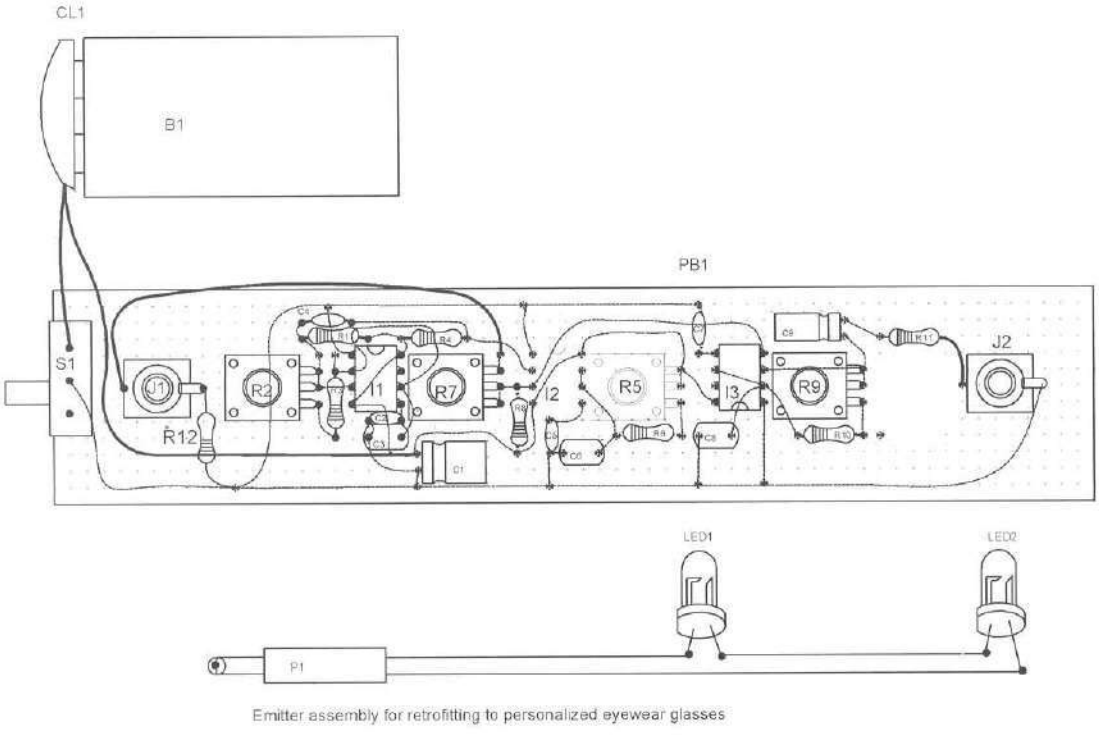

Figure 29-3 *Assembly board*

Note it is best to experiment with and record the duty cycle settings and their effects (see Figure 29-2).

The circuit also includes integrated circuit I3 connected as a variable-rate, sonically "shaped" audio oscillator. The output is via jack J2 driving a set of 32-ohm headphones.

The feedback circuit consists of two external pieces of metallic tape providing points of contact for the user's hand. Body resistance now partially controls the pulse rate of I1. An uptight situation provides lower contact resistance and consequently raises the pulse rate. As one relaxes, this resistance becomes higher and lowers the pulse rate. An external jack (J3) provides a connection for other bodily contact probes to the feedback system. These contact probes are left to the discretion of the user. This jack is omitted when using the external tape probes. Switch S1 controls power to the circuit and should be off when not in use to conserve the internal batteries.

Assemble the Board

If you are a beginner, it is suggested to obtain our *GCAT1 General Construction Practices and Techniques*. This informative manual explains basic practices that are necessary in proper construction of electromechanical kits and is listed in Table 29-1.

1. Lay out and identify all the parts and pieces. Verify them with the parts list, and separate the resistors as they have a color code to determine their value. Colors are noted on the parts list at the end of the chapter.

2. Cut a piece of .1-inch grid perforated board to a size of $6\frac{1}{4} \times 1\frac{1}{4}$ inches, as shown in Figure 29-3. An optional PCB is individually available.

   The circuit is shown with the more challenging perforated circuit board often required for a science fair project. A PCB is also available and requires that you only identify the particular part and insert it into the respective holes as noted. The PCB is plainly marked with the part identification. Soldering is very simple as you solder the component leads to the conductive metal traces on the underside of the board.

   The perforated board approach is more challenging as now the component leads must be routed and used as the conductive metal traces. We suggest that the builder closely follow the drawings on this section and mark the actual holes with a pen before inserting the

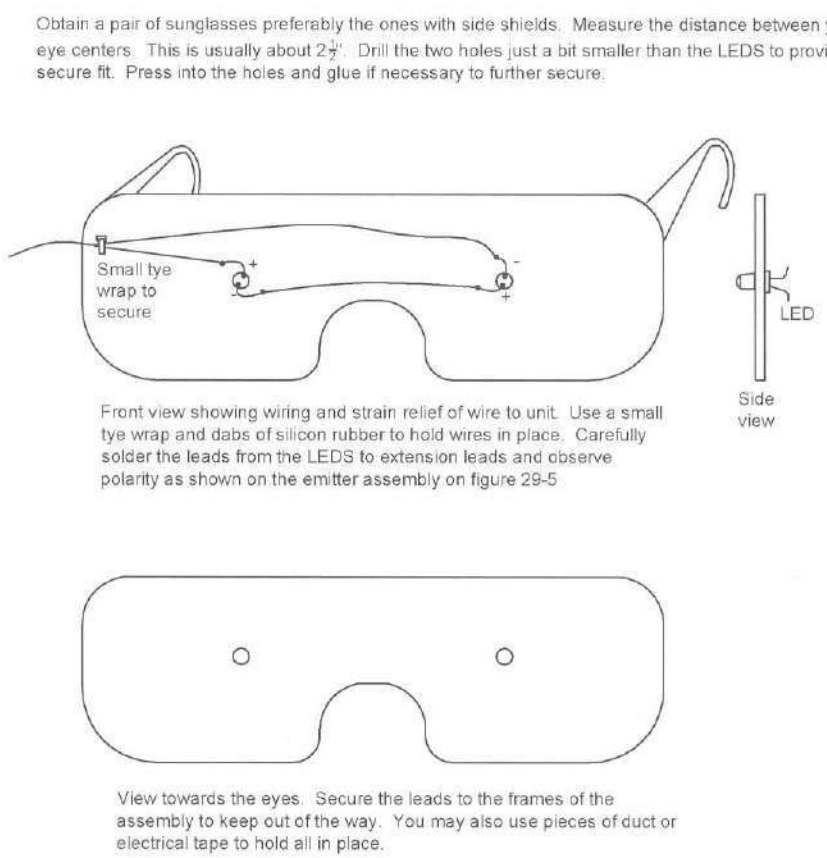

Figure 29-4 *Assembly of glasses*

parts. Start from a corner, using it as a reference, and proceed from left to right. Note that the perforated board is the preferred approach for science projects as the system looks more homemade.

3. If you are building from a perforated board, it is suggested that you insert the components, starting in the lower left-hand corner, as shown in Figure 29-3. Pay attention to the polarity of the capacitors with polarity signs and all the semiconductors. Resistor RI2 is connected from the pin of 11 to the PC board. Note the control pots R2, R5, R7, and R9 and jacks J1, J2, and J3 should be positioned to closely match the holes, as shown in Figure 29-5. Route the leads of the components as shown and solder as you go, cutting away unused wires. Attempt to use certain leads as the wire runs or use pieces of the #24 bus wire. Follow the dashed lines on the assembly drawing as these indicate the connection runs on the underside of assembly board.
4. Attach the external leads to the battery holder as shown.
5. Double-check the accuracy of the wiring and the quality of the solder joints. Avoid wire bridges, shorts, and close proximity to other circuit components. If a wire bridge is necessary, sleeve some insulation onto the lead to avoid any potential shorts.
6. Assemble an LED to cable P1 as shown. Also, retrofit to the eyewear as per Figure 29-4.
7. Fabricate the enclosure tube (TUB1) as shown in Figure 29-5 and insert the assembly board and battery. Verify that the controls mounted on the assembly board will match the drilled holes with the dimensions as shown. Note the dimensions are shown for use with the optional PCB and may be changed. The unit is secured attaching the adjustment pots via nuts.
8. The final assembly is shown in Figure 29-6 and should be operated as instructed.

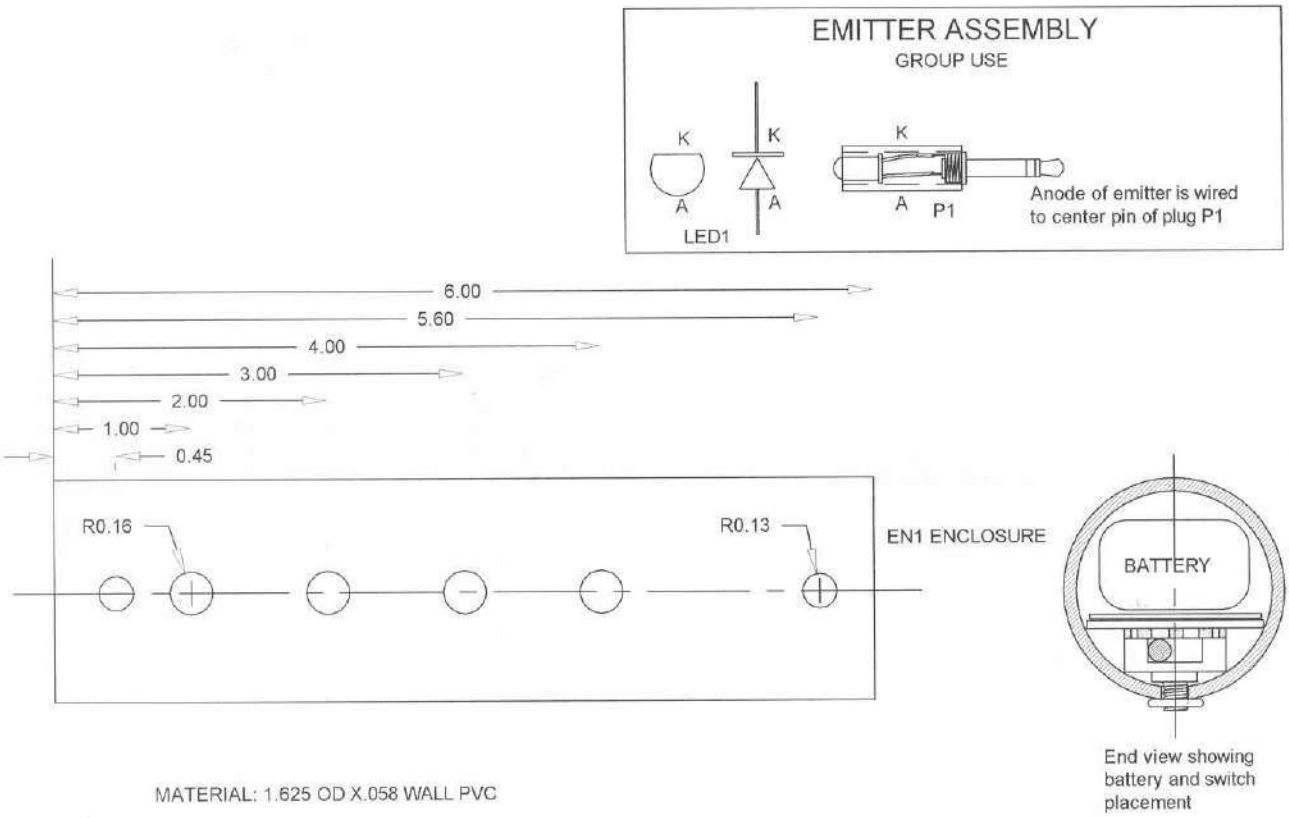

Figure 29-5 *Fabrication of enclosure*

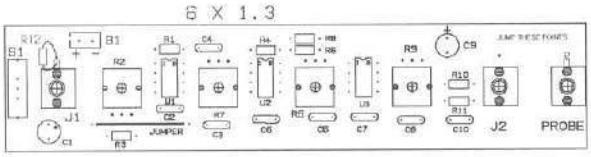

Figure 29-6 *Final assembly on PC Board*

Table 29-1 Mind-Synchronizing Generator Parts List

Ref. #	*Description*	*DB Part #*
R1, 4, 8, 10	Four 1K, ¼-watt resistors (br-blk-red)	
R2, 5	.5-1 meg potentiometer resistor	
R3	47K, ¼-watt resistors (yel-pur-or)	
R6	33K resistor (or-w-or)	
R7	1K pot resistor	
R9	10K pot resistor	
RI1, 12	Two ¼-watt 220- to 330-ohm, resistors (red-red-br)	
CI	1,000-microfarad, 25-volt vertical electrolytic capacitor	
C2, 5, 7	Four .01-microfarad, 50-volt disc capacitors	
C4	.001 mfd, 50-volt disk capacitor	
C3, 6, 8	Three .47-microfarad, 50-volt mylar capacitors	
C9	47-microfarad, vertical electrolytic capacitor	
C10	.22-microfarad, 50-volt mylar capacitor	
Il, 2, 3	Three 555 dual inline package (DIP) timers	
*LED1, 2	Two bright-red LEDs or use single, optional 15,000 mcd assembled as shown	
S1	Single pole, single throw (SPST) PC switch	
CLI	9-volt battery snap	
11, 3	Two 3.5 mm mono jacks	

Operation and explanation of controls

1. Slide of bottom cap and insert a 9 volt battery

2. Plug in 30 ohm headsets into J2

3. Plug in cable to LEDS in glasses

4. Identify and study the functions of the four controls

   R2-Frequency control allows setting from 1-24 reps

   R7-Allows setting of LED brightness

   R5-Sets the ratio of "off to on" time. Will interact with R2 if set to long "on" time. Suggest to preset full CW and then set for desired effect

   R9- Allows tone adjustment or sound shaping.

5. Adjust the unit to produce a test tone of about 3 pulses per second. Grab feed back probes being the metal strips along the side of the unit and note pulse rate increasing. It is suggested to become familiar with the operation and resulting effects before attempting to use the feedback functions.

6. Unit is easily hand held with all controls accessible

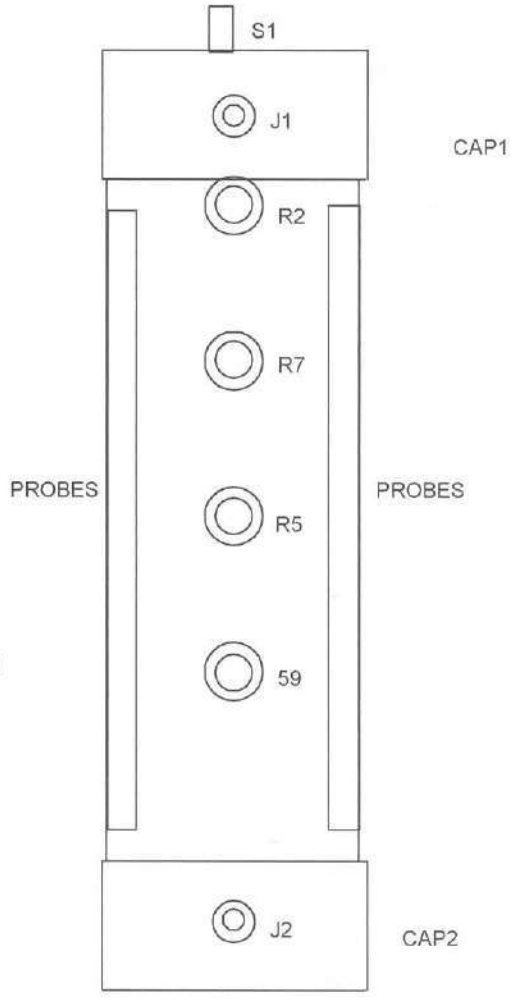

Figure 29-7 *Operation and Explanation of Controls*

J2	3.5 mm stereo jack
WR1	12 inches of #24 hookup wire
WR2	24 inches of #24 bus wire
WR3	48 inches of two-cord speaker wire
PB1	.1 × 6¼ × 1¼-inch grid perforated board
PCBOARD	Optional printed circuit board (PCB) with printing DB# PBMIND
EN1	Enclosure, sized at 1⅞ OD × 1⅞ ID × 7 inches
CA1, 2	Two 1⅞ inch plastic caps #A 1⅞
P1	3.5 mm plug for LED cable to eyewear
HEADSETS	Stereo or mono, 32-ohm, cushioned headphones
TAPE	4 × ½-inch metallic silicon tape229

Chapter Thirty

Alternative Health Multiwave Machine

Figure 30-1 shows how to construct a Lakhovsky multiwave alternative health system. Dr. Lakhovsky was a Russian researcher who experimented with the effects of high-frequency electromagnetic radiation on various parts of the living organism. This controversial system is claimed to cure many health ills, including cancer. Its claim to fame is that all cells in a living body possess an intrinsic, vibrating resonant frequency that can be energized by an external means. Diseased cells appear to have a weaker and different frequency that can be brought back into step with the adjacent nondiseased cells. Antiaging appears to occur when cells are exposed to this full-spectrum electromagnetic vibratory energy. It is of special interest that this method of cellular regeneration has generated considerable interest in several research fields as a possible cure for cancer.

This project shows how to construct the multiwave radiating coil and antenna from readily available parts and pieces. System operation will require a working BTC30 12-inch-spark Tesla coil, as described in Chapter 14 of *Electronic Gadgets for the Evil Genius*. This Tesla coil is also available through plans, a kit, or as a complete and ready-to-use coil on the Information Unlimited Web site at amazing1.com.

It is suggested that the builder obtain the Lakhovsky handbook as listed in the parts list at the end of this chapter and study the methods of application and testimonials on the use of this controversial health machine before using it on one's self or others.

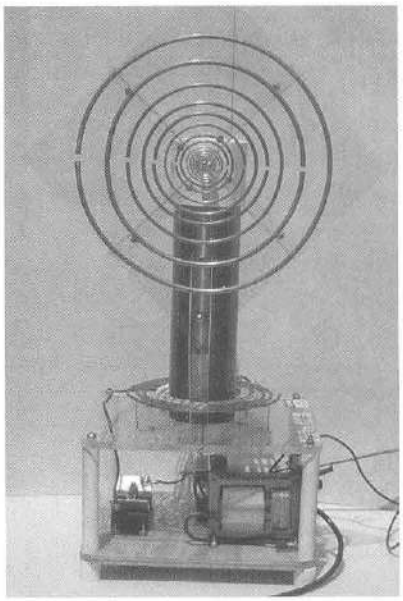

Figure 30-1 *The multiwave antenna*

Theory of Operation

Figure 30-2 shows a block diagram of the radiating coil and Tesla driver. The antenna coil contains a series of concentrically wound coil rings mounted in a flat plane. These coils all possess an inherent resonant

L1 to Ln represents the inductance of all of the coils.
C1 to Cn reprasents the capacity of all of the coils.
R1 to Rn is the radiation resistance of each section.
Frequency are the sum of the resonant sections ranging up to the gigahertz.

L is the sum of L1 to Ln
C is the sum of C1 to Cn
R is the sum of R1 to Rn and is mainly the radiation resistance.

The undamaged current wave from the output of the Tesla driver induces voltages at many frequencies into the multicoils of the antenna.

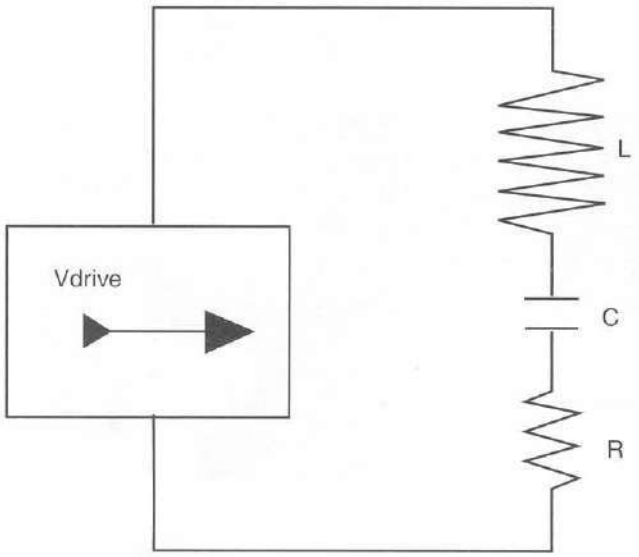

Figure 30-2 *Diagram of system*

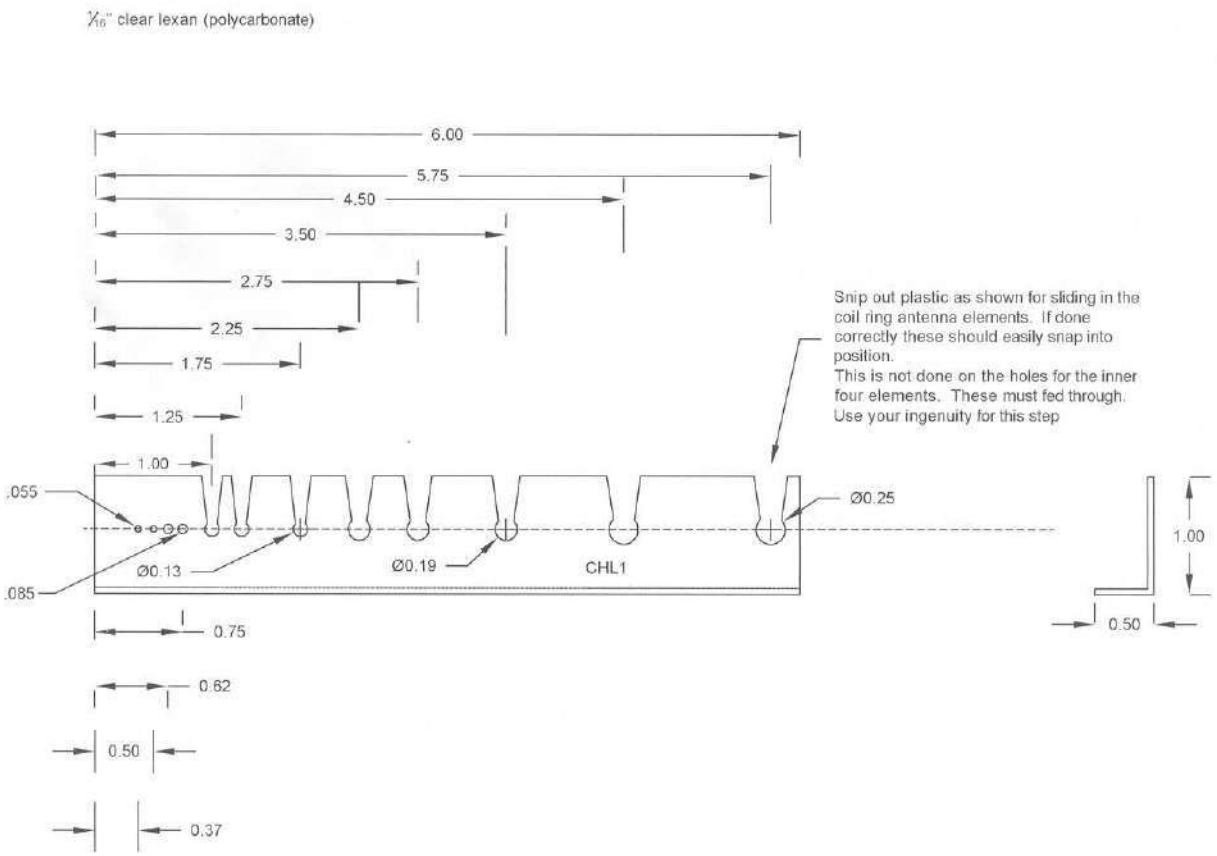

Figure 30-3 *Fabricating the four coil holders*

frequency as a function of their physical parameters. Harmonics are also produced and with all the coils oscillating they create a near-continuous spectrum of radio-frequency energy. A spark-driven Tesla coil is required for optimum results, as it generates many fast steps of current rich in harmonic content that drives the antenna coil.

Construction of the Multiwave Coil and Antenna

1. Create the four coil holders (CHOLD1) as shown in Figure 30-3. Use 1/16-inch Lexan polycarbonate.
2. Create the 12 × 12-inch main plate (MP1) from a piece of 1/16-inch Lexan sheet, as shown in Figure 30-4.
3. Mount the coil holders as shown and carefully drill the mounting holes. Use nylon or brass screws and nuts for mounting the holders to the plate. It is very important to have these holders as exact as possible or the wound coils will not fit properly in their predrilled slots.
4. Form the circular coil rings from the appropriate diameter copper tube and snap the tubing into place. Again attempt to form circles as perfect as possible for proper operation and esthetics. The inner coil rings are formed pieces of bus wire and are threaded through their respective holes. Note a 1/8-inch gap at the coil ends.
5. Attach a PVC cap (CAP1) using a small metal screw, solder lug, and nut. This screw is the high-voltage feed point to the antenna and is connected to a piece of wire soldered to the innermost coil ring (see Figure 30-5).
6. The antenna may be used with any suitable high-voltage, high-frequency generator. It is shown in Figure 30-6 with our BTC30 250-kilovolt Tesla coil, as described in Chapter 14 of *Electronic Gadgets*. It is available as a kit or completed system as noted in Table 30-1.

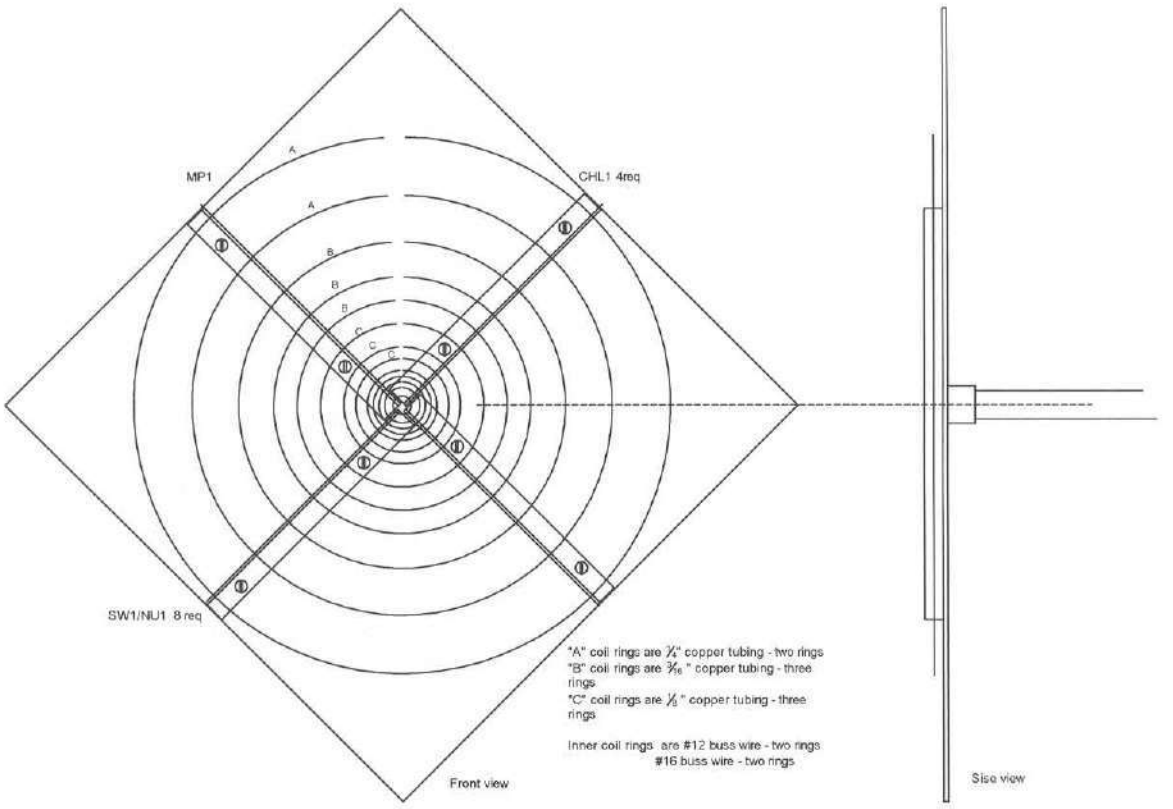

Figure 30-4 *Creating the base*

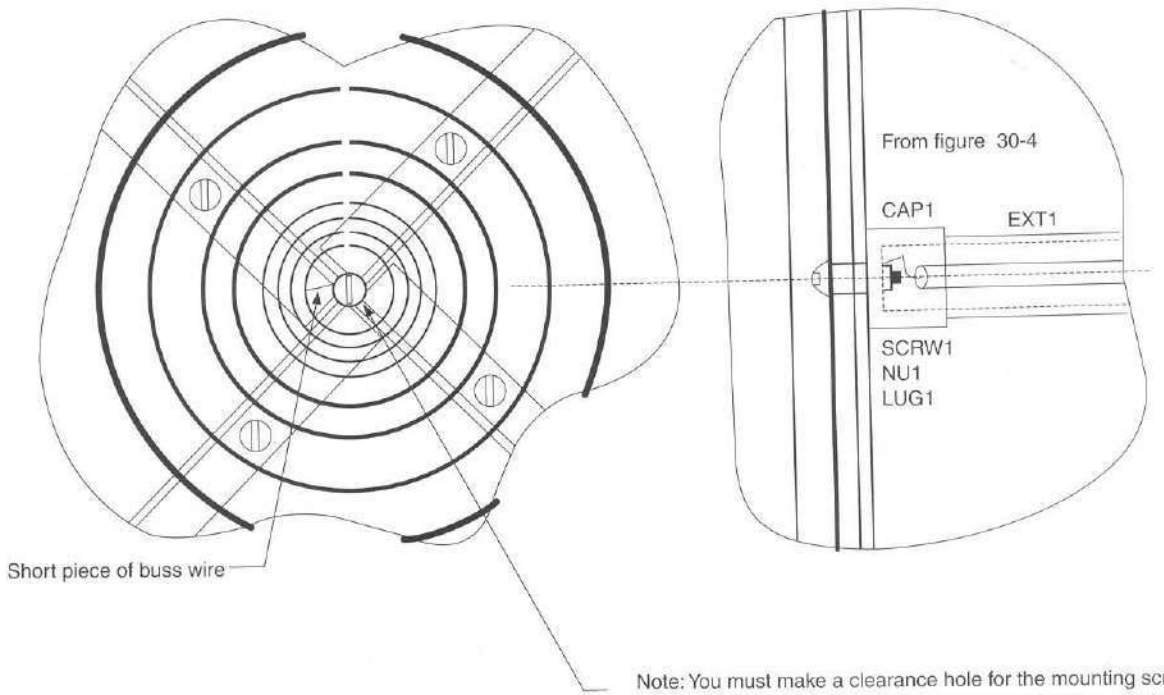

Figure 30-5 *Mounting and feeding details*

7. If you intend to use our coil, you will need to obtain a 3-inch slip cap (SLP1) and drill a hole for the extension arm tube (EXT1). You will also need the plastic stabilizing bracket (BRK1) required to keep the coil assembly upright.
8. The connection between the output of the Tesla coil and the antenna is made via the wire sleeved through the extension tube that connects to the mounting screw and exits through the rear to make contact with the Tesla coil output lead.

Operation

The following instructions reference the use of our 250-kilovolt Tesla coil as listed in Table 30-1 or as described in Chapter 14 of *Electronic Gadgets*.

1. Preset the spark gap on the Tesla coil to no more than 1/16 of an inch. Connect the tap lead for maximum inductance.
2. Turn on the switch on the Tesla coil and note all the antenna coil rings adjacently sparking and arcing between one another. Note that the outer ring may be grounded to the chassis to increase output activity.

At this point, it is recommended that you obtain the referenced book (LSK1), the *Lakhovsky Multiple Wave Oscillator Handbook*, as referenced in the parts list and familiarize yourself with the potentials, treatments, and experiments possible with this system.

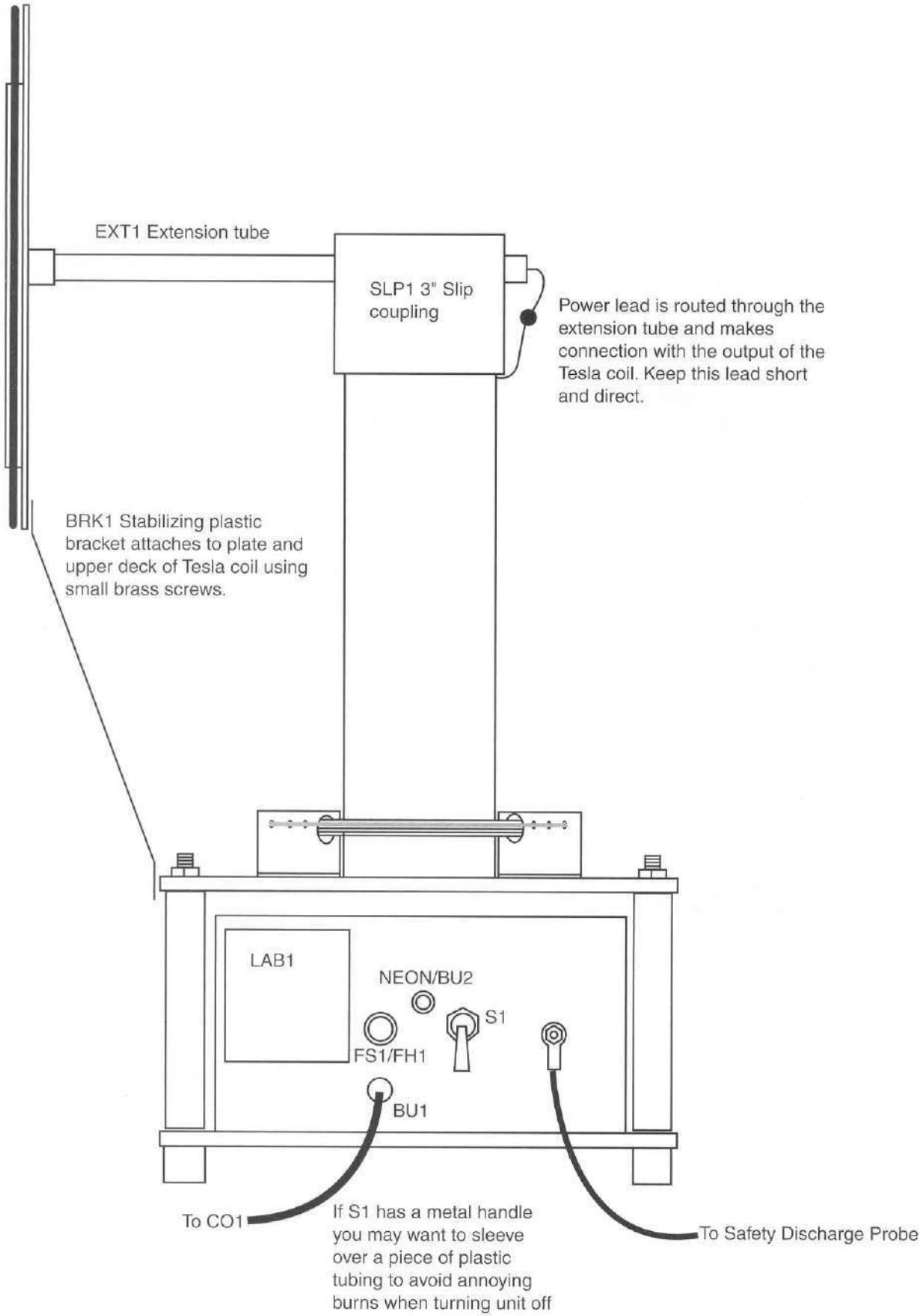

Figure 30-6 *Completed system*

Table 30-1 Multiwave Machine Parts List

Ref. #	*Description*	*DB Part #*
CHL1	Four coil-ring holders shown in Figure 30-3	DB# CHL1LAK
MP1	Mounting plate shown in Figure 30-4	
ARING	Two ¼-inch copper, soft drawn tubings	
BRING	Three 3/16-inch copper, soft drawn tubings	
CRING	Three ⅛-inch copper, soft drawn tubings	
INNERRING	Two #12 bus wire circular rings	
INNERRING SMALL	Two #16 bus wire circular rings	
SW1/NU1	106-32 × ½-inch brass or nylon screws and nuts	
SCRW1/NU1	6-32 × ¾-inch brass screw and nut	
LUG1	#6 solder lug	
WR20	24 inches of #20 bus wire	
BRK1	Stabilizing bracket shown in Figure 30-6	
CAP1	½-inch PVC slip cap	
SLP1	3 inches of PVC slip coupling	
EXT1	18 inches of ½-inch PVC tubing	
BTC3K	250-kilovolt Tesla coil generator kit and plans	DB# BTC3K
BTC30	250-kilovolt Tesla coil generator ready to use	DB# BTC30
LSK1	Book on Lakhovsky, 144 pages	DB# LSK1

Chapter Thirty-One

Mind Mangler

This board-level device, as shown in Figure 31-1, when properly assembled, can be a great prank. When placed in one's bedroom under normal light condition, it does nothing. As soon as the lights are turned off, it comes to life, producing pulses of high-frequency sound much like an insect. These control pulses can be timed to occur about every minute. When the unsuspecting victim attempts to locate it by turning on the lights, it ceases operation. Even using a flashlight will disable it. The long time between pulses also makes it very difficult to detect. Properly hidden, it can take a long time to locate and may turn a prank into a nasty situation.

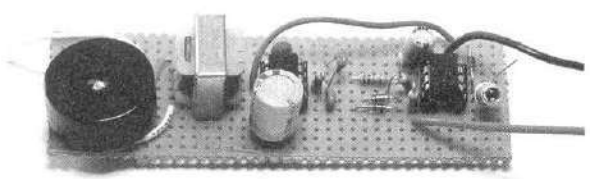

Figure 31-1 *Board-level view of the mind mangler*

Circuit Operation

Figure 31-2 shows a timer, I1, as a free-running, astable pulse generator producing a symmetrical 10-second, off and on pulse controlling the second timer, I2. Timer I1 has a phototransistor Q1 connected in series with the reservoir capacitor C1. As long as there is light on Q1, C1 can never discharge due to the conductance of Q1. Therefore, pin 3 is at a low and I2 is disabled. When the lights go out, C1 now is allowed to discharge and pin 3 goes high, turning on I2 and producing the high-frequency sound to the output transducer TD1. The high-audio frequency is determined by resistor R3 and C3, and can be changed by altering these values. The output signal from I2 is stepped up by transformer T1 (see the parts list at the end of the chapter).

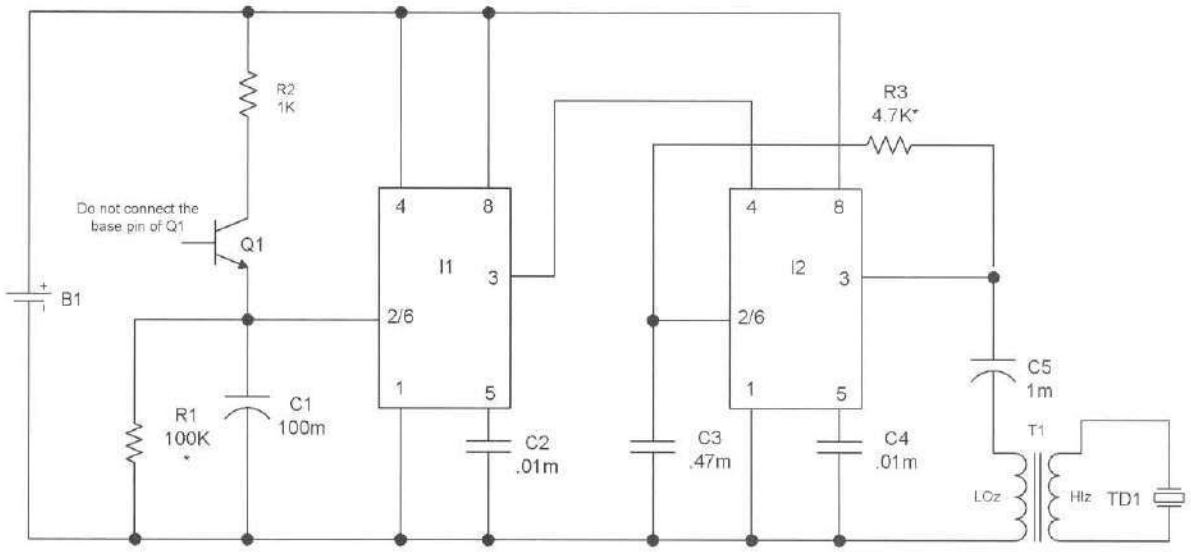

*The value of R1 May be changed to adjust for dark and light conditions. You may want to replace with a 500 K trimpot

Figure 31-2 *Circuit schematic*

Construction Steps

1. Identify all the parts and pieces and verify them with the bill of materials.
2. Insert the components starting from one end of the perforated circuit board and follow the locations shown in Figure 31-3 using the individual holes as guides. Use the leads of the actual components as the connection runs, which are indicated by the dashed lines. It is a good idea to trial-fit the larger parts before actually starting to solder. Always avoid bare wire bridges, globby solder joints, and potential solder shorts. Also check for cold or loose solder joints.

Additionally, pay attention to the polarity of the capacitors with polarity signs and all the semiconductors. The transformer position is determined using an ohmmeter.

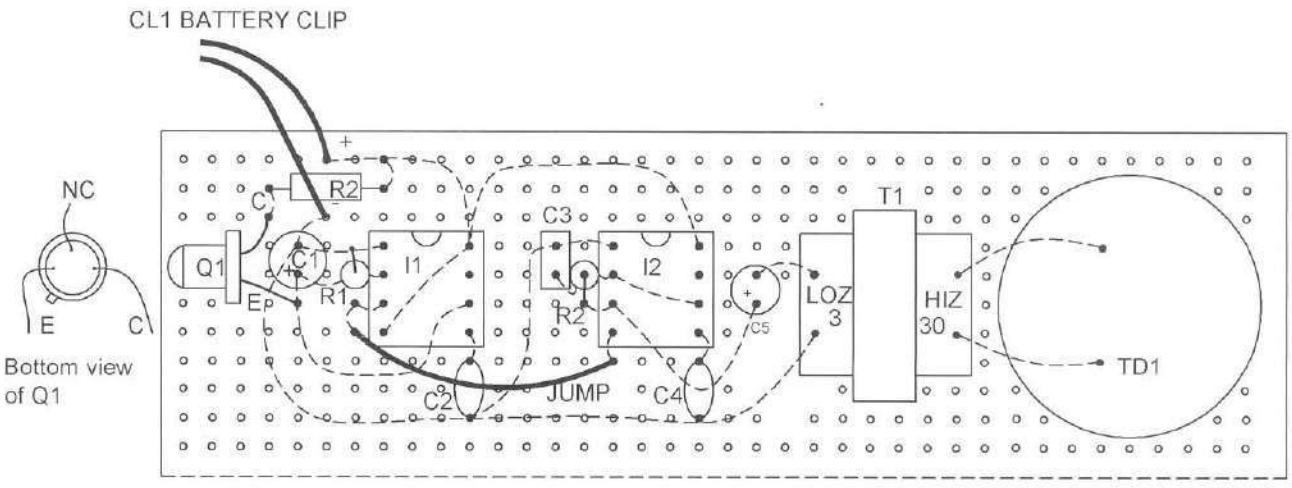

You can determine the low impedance side of T1 with an ohmeter. It will always read as the lower of the two

Figure 31-3 *Assembly board*

Testing

Verify the wiring accuracy and connection. Insert a 9-volt battery into the clip, cover the lens of Q1 or turn off the lights, and note the unit emitting a low-level, raspy, clicking tone like a sick cricket. Uncover the lens of Q1 and note the circuit shutting down. There will be a delay that is dependent on the level of light and dark. You may vary the response by changing the value of R1. Decreasing its value will require more light to shut down and vice versa.

Table 31-1 Mind Mangler Part List

Ref. #	*Description*	*DB Part #*
R1	100K, ¼-watt resistor (br-blk-yel)	
R2	1K, ¼-watt resistor (br-blk-yel)	
R3	4.7K, ¼-watt resistor (yel-pur-red)	
C1	100-microfarad, 25-volt vertical electrolytic capacitor	
C2, 4	Two .01-microfarad, 50-volt plastic capacitors (103)	
C3	.47-microfarad, 50-volt vertical electrolytic capacitor	
C5	1-microfarad, 50-volt vertical electrolytic capacitor	
I1, 2	Two 555 timer dual inline packages (DIP)	
Q1	L14P phototransistor	
CL1	9-volt battery clip	
TD1	Small piezo transducer	
T1	Small audio transformer, 8 to 1K	
PB1	4 × 1.5 × .1-inch grid perforated circuit board	

Chapter Thirty-Two

500-Milligram Ozone Air Purification System

Figure 32-1 shows a useful home device that generates ozone for eliminating odors, killing bacteria and mold, and disinfecting unsanitary areas such as pet boxes and bathrooms.

This project shows how you can build a system that could cost over $300 for less than $50. Its simple and basic design uses two 12-volt fans to blow air over a unique ozone-producing cell that is powered by a variable-output, high-voltage, high-frequency power supply. The power supply is featured in Chapter 7 of this book and is used in several other projects.

This is a beginner- to intermediate-level project requiring minimal basic electronic skills. Expect to spend $40 to $60. All the parts are readily available, with specialized parts obtainable through Information Unlimited (www.amazing1.com), and they are listed in Tables 32-1 and 7-1 at the end of this chapter and Chapter 7.

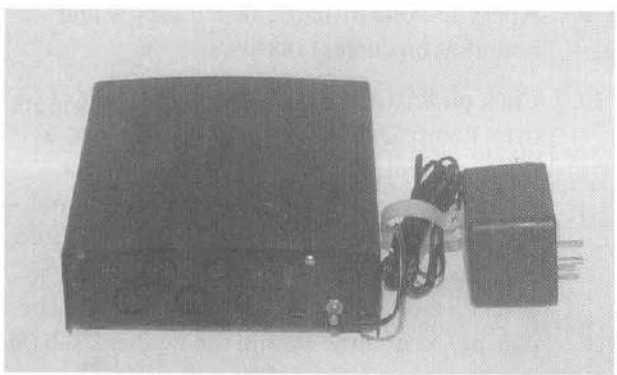

Figure 32-1 *Ozone purification system*

The Story of Ozone

Ozone is an unstable form of oxygen. Normal oxygen is diatomic (0_2), existing as two atoms of oxygen making up the molecule. Ozone is triatomic (0_3), existing as three atoms of oxygen for the molecule. The triatomic form of oxygen is very unstable, wanting to lose the third oxygen atom and combine with whatever atom it can (oxidization). This property makes it the most active oxidizer known, with the exception of the very hazardous fluorine gas. Ozone at normal pressures is colorless and odorless, yet it produces a pleasing, fresh-air odor as a result of the nitrous oxides it produces. The odor is usually noticeable after an old-fashioned thunderstorm. Under pressure, it becomes a bluish gas.

Ozone is also a very powerful bactericide. It is not affected by pH, as is chlorine, thus making it an excellent candidate for pools, spas, laundries, and general water treatment applications. It is many times more soluble in water, further enhancing its purifying effect. Ozone will combine with diatomic nitrogen, N_2, forming nitrous oxide, 2NO. This oxide quickly combines with water, forming nitric acid, HNO_3. This is often a very undesirable effect when used with

straight air. Pure oxygen greatly minimizes this effect and is often required in many applications.

However, those requiring a supply of concentrated nitric acid for the nitration of many carbohydrates, such as cellulose, glycerine, hexamine, phenol, and toluene, may wish to consider combining ozone and air with a condensing apparatus to obtain this useful acid.

Ozone for Treating Air

Air pollution is one of the most serious environmental issues that we face. Visible and detectable smoke, dust, mildew, mold, and toxic odors, bacteria, pollen, and static electricity, along with the more elusive and invisible chemicals, have become a serious health threat. As buildings and homes are constructed with tighter air sealants for energy conservation, the problem will become even more severe. Often the effects from these problems include burning eyes, headaches, dizziness, depression, allergies, and general lethargy, all of which are usually attributed to colds and viruses. Air filters, such as the overpriced Sharper Image unit currently being advertised, are only partially effective, with some producing undesirable positive ions.

Ozone purifies the air from these undesirable pollutants by oxidization, as most pollutants readily combine with this highly reactive tri-atomic form of oxygen and break down into water and other nontoxic compounds. Ozone is produced artificially by electricity and is many times more antiseptically effective than oxygen.

Construction Steps

1. The system is shown using the high-voltage, high-frequency driver shown in Chapter 7. It is built on a printed circuit board or a more difficult perforated board. The PCB version is the easiest, as construction involves placing the correct components into the correct holes and soldering. The more difficult approach is also shown and uses a perforated circuit board. This is far more challenging and is intended for the experienced assembler. Figure 32-2 shows the board with the necessary changes for use with this circuit.
2. Create the base section, as shown in Figure 32-3. You can use sheet aluminum or bendable plastic sheets. Design a mating cover with a slight overhang over the front and rear panels. Use similar material and mount using #6 sheet metal screws along the lip of the base.
3. Fabricate the fan and cell mounting bracket as shown in Figure 32-4. Use clear 1/16-inch polycarbonate plastic and initially layout the piece, marking off the bend and cutting lines. You may fabricate separate pieces for the cell brackets and fans if you do not have access to the necessary equipment. Note dimensions and cuts must result in a single piece, as shown.
4. Cut out a piece of window screen large enough to cover the input air holes and secure it from the inside of the base enclosure using screws and silicon rubber cement.
5. Mechanically assemble the components, as shown in Figure 32-5. Verify all proper fittings and the clearance of components, especially the high-voltage points on the cell. Finally, wire everything as shown and verify the accuracy and any potential errors. Note: Figure 32-6 shows the wiring using the perforated board approach. Do not connect the 12 DC/1.5 adapter wall transformer at this time.
6. Obtain a 12-volt, 3-amp bench power supply with a voltage and current meter. Connect it to where the adapter's plus and minus wires go.
7. Connect a scope to the test points, as shown in Figure 32-5.
8. Preset the trimpot R1 to midrange and control pot R10 to full counterclockwise and click off.
9. Apply 12 volts from the bench supply and note that no current occurs.
10. Click on R10 and note a pulsing current of over 1 amp. Quickly adjust the trimpot to a dip in current, as noted on the meter. Our model was tuned correctly when the trimpot was set to one to two o'clock. The fans should both be in full operation and you should detect a faint, bluish glow coinciding with the pulsing. At no time should the heatsink tab on the power transistor Q1 be hot.

It will be necessary to construct the printed circuit assembly board as shown in chapter 7 with the following below list of revisions.

Wind L1 using 10 turns of #22 magnet wire. Air gap core with .007 (7mils) shims. Measured inductance should be between 15 -16 micro-henries.

Trimpot R6 is not used

Replace R5 with a wire jump

Replace C2 from a .0022 to a .0047 microfarad capacitor

Replace C6 from a .22 to a .47 microfarad 250 volt capacitor

Capacitor C4 is not used. insert a short piece of buss wire for a test point ground

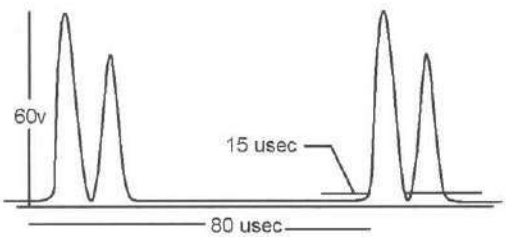

Correct wave shape measured at the drain of Q1 and test ground point

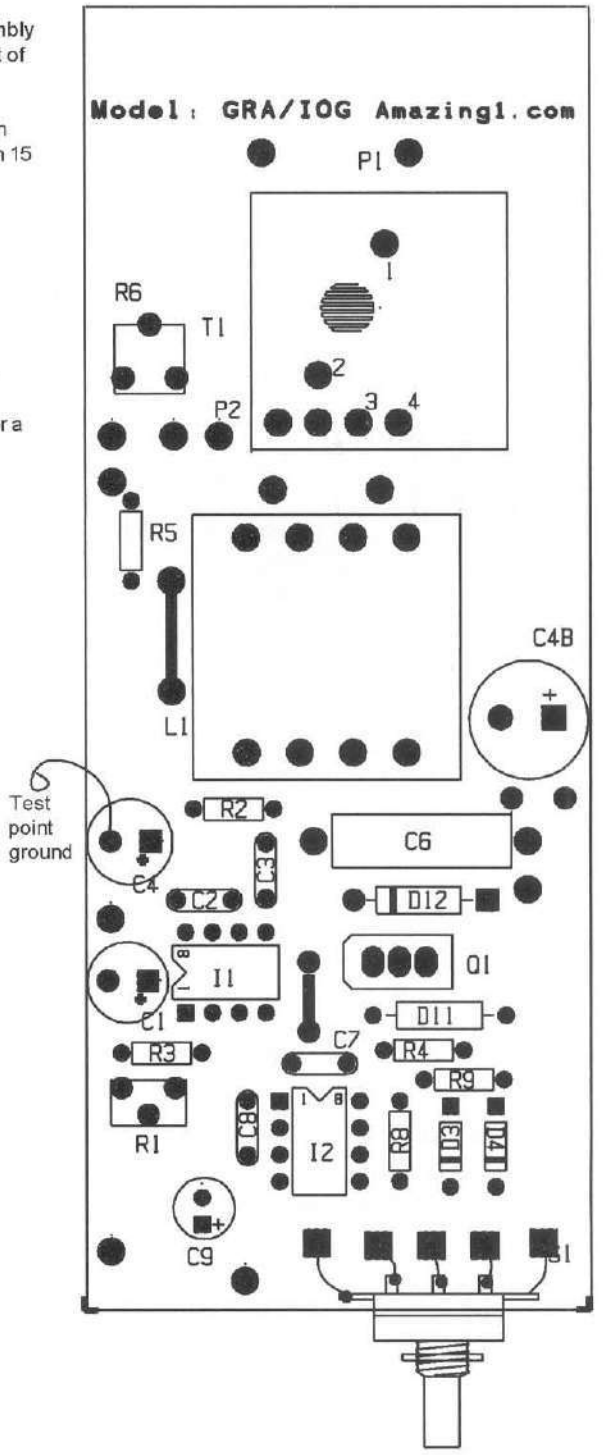

Figure 32-2 *PCB rework*

11. Turn R10 full clockwise and note the on time of the pulse increasing with the current but not exceeding 1.5 amps at these pulse peaks. Allow it to operate for 30 minutes and note ozone being produced, a soft, bluish, even glow on the cell, and the heatsink not getting too hot to touch.
12. Once this is verified, you can hook in the 12 VDC/1.5-amp adapter transformer. Allow it to operate and verify that the adapter does not get hot.
13. Attach the cover and place the unit in the target area.

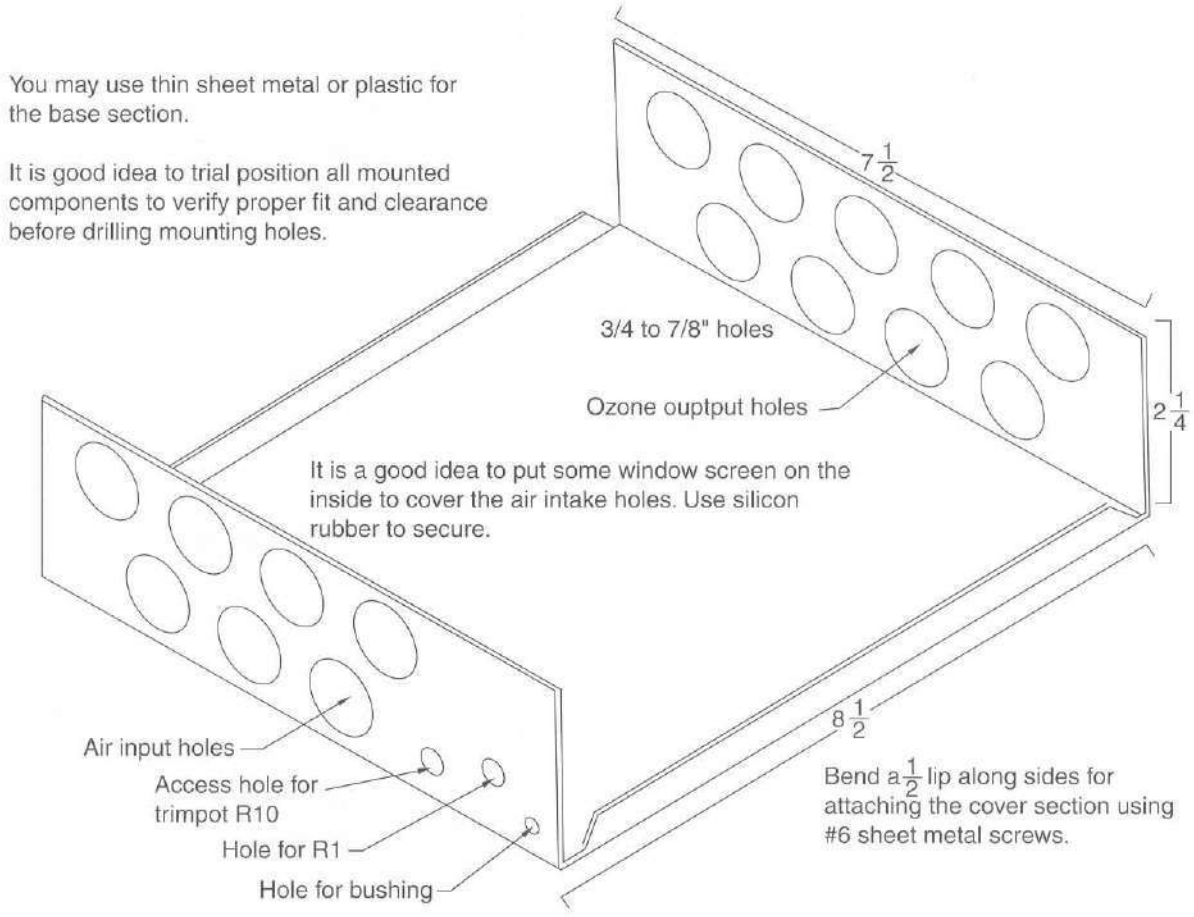

Figure 32-3 *Base section creation*

14. Place the unit with the output directed toward the center of the area.
15. Plug in the wall adapter and rotate the control switch to on. Note the fan rotating and freely turning without obstructions. It should produce a good air flow.
16. Adjust the control a full clockwise turn and note a smell of fresh air emitting from output ports. You will observe a purplish glow around the cell when viewed in darkness.
17. Allow it to run for several hours and adjust the control to where the fresh air smell is just detectable.
18. Check both the unit and the wall adapter for excessive heating. They should only be warm to the touch.
19. This unit may need cleaning from dust. Use compressed dry air or a soft cleaning brush.

Special Notes

You should never operate the unit when the odor becomes pungent or domineering. Ozone is a colorless, odorless gas composed of unstable diatomic oxygen. The smell of fresh air is not the ozone, but the result of secondary reactions with other chemicals.

The unit can be adapted to 12 VDC operation for vehicle or battery use. Simply remove the adapter and splice in some 12-volt connections. Use caution when observing the polarity. You may request a factory modification for this step.

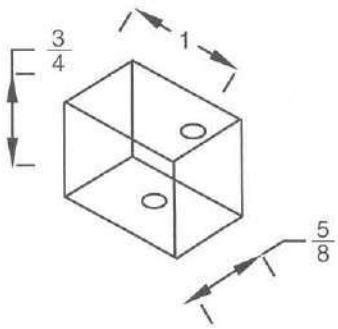

Ozone cell-mounting blocks (2) use PVC or another suitable insulting plastic. You will note the position of the bottom hole mounting the blocks of the base is at their geometrical center. The top hole is offset to this location so as not to be adjacent to one another avoiding possible voltage breakdown.

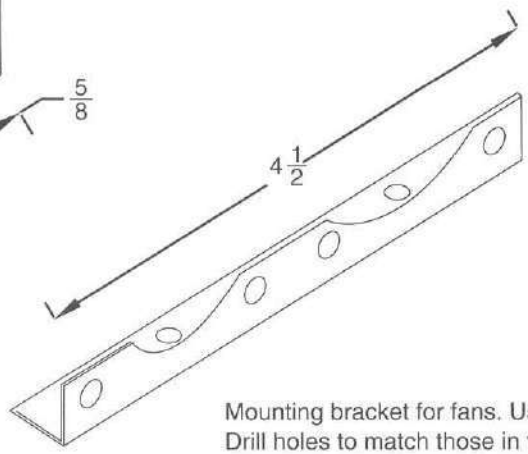

Mounting bracket for fans. Use $\frac{1}{32}$ aluminum or plastic. Drill holes to match those in the fan assemblies.

Figure 32-4 *Fabricated parts*

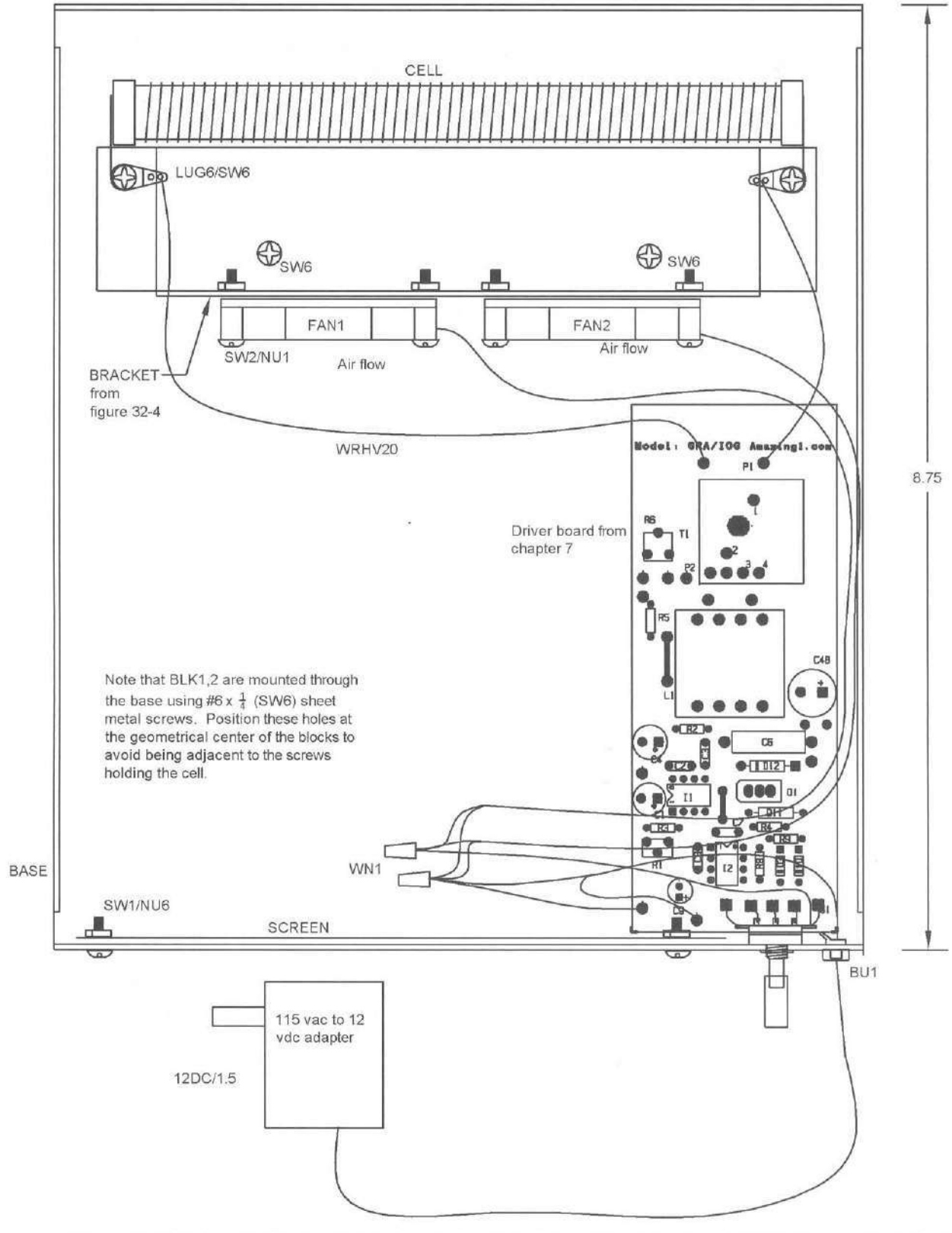

Figure 32-5 *Mechanical layout showing wiring when using the PCB*

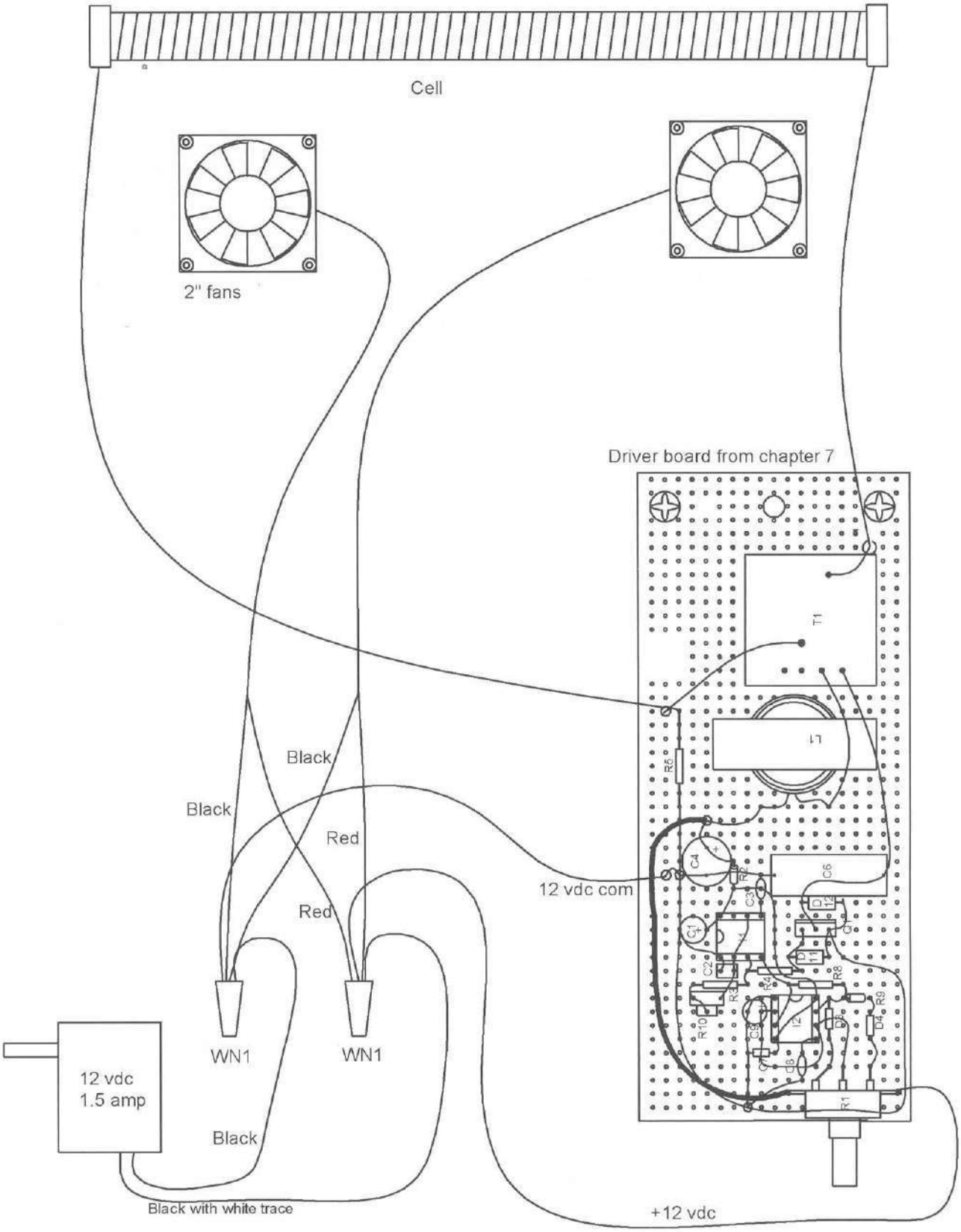

Figure 32-6 *Final wiring using a perforated board*

Table 32-1 500-Milligram Ozone Machine Parts List

Ref. #	*Description*	*DB Part #*
DRIVER	Modified high-voltage assembly from Chapter 7	DB# GRADRIV10
BASE	Base section fabricated per Figure 32-3	
COVER	Fabricated to fit BASE section	
BLOCKS	Two blocks fabricated per Figure 32-4	
BRACKET	Bracket fabricated per Figure 32-4	
FAN1, 2	Two small, 2 × 2-inch, 12-volt fans	DB# FAN2
CELL500	500-milligram ozone corona cell	DB# CELL500
SCREEN	2 × 5-inch piece of window screen	
12DC/1.5	12-volt, 1.5-amp wall adapter transformer	DB# 12 DC/1.5
WRHV20	6-inch, 20-kilovolt, high-voltage wire	
WN1,2	Two small wire nuts	
BU1	Small Heyco bushing #2P-4	
SW6	10 #6 × ¼-inch sheet metal screws for cover and blocks	
SW2/NU2	Four #4-40 × ¾-inch machine screws and nuts for fans	
SW1/NU1	Two #6-32 × ½-inch machine screws	
LUG6	Two #6 solder lugs	
WR22	12 inches of #22 vinyl hookup wire	
FEET	Four stick-on rubber feet for base section	

Chapter Thirty-Three

Invisible Pain-Field Generator

The invisible pain-field generator device shown Figure 33-1 is a handheld, battery-operated sonic, shock-wave generator that produces a *sound pressure level* (SPL) of up to 125 decibels (db) at 30 centimeters. The shock wave frequencies are user presettable at 25, 16, and 12 KHz. A sweep function is included in the circuitry where the selected center frequency varies between two set limits at an adjustable rate, providing a complex sonic signal that further enhances the effect.

Applications of the device can range from the routing out of agricultural pests in silage bins, chicken houses, grain bins, or wherever rats are a problem. The optimum frequency for this particular application is 16 KHz or just above that of human hearing. Many farmers use these devices for determining the effectiveness of pesticides, noting the reduction in infestation levels. Other applications include spooking birds and animals from unwanted areas and discouraging dogs and deer from decimating shrubs and ornamentals.

Figure 33-1 *Pain-field generator*

Adjustment of the frequency down to 12 KHz (within the range of human hearing) will produce extremely painful and annoying affects. The unit is excellent for disbursing crowds of potentially unruly people. A simple test is to point the device at an unsuspecting subject and momentarily push the button. You will notice a very positive response. Unfortunately maximum affect seems to favor younger women; older men seem to be less sensitive.

The unit is very directional when used outside, but it looses this property when used inside due to reflections from walls, ceilings, and furniture.

The unit is shown assembled into a small plastic enclosure that includes the electronics emitter transducer and the 9-volt battery. A removable plastic cover allows access in order to change the battery. Controls include a pushbutton emission control and sweep-activation pushbutton switches located on the top of the enclosure. The size of the main enclosure is $4 \times 2 \times 1$ inches. The weight is only about 6 ounces with batteries installed

The unit can be used as a research tool for producing an effect on certain animals for their control and experimentation. The device has been successfully used for controlling certain dogs or other vicious animals by joggers or other outdoors enthusiasts. The unit has also been used in flushing out rats.

Caution: Caution must be used, as the effect on most people causes pain, headache, nausea, and extreme irritability. (Younger women are especially affected.) Do not, under any circumstances, point the unit at a person's ears or head at close range, as severe discomfort and possible ear damage may result. This also applies to dogs and other animals.

Include a caution label on the device to avoid exposure over 105 db for any continuous period of time. When using the device around people, you must be careful, as unjustified harassment is illegal and can result in prosecution.

This is an intermediate-level project requiring basic electronic skills. Expect to spend $25 to $50. All parts are readily available, and any specialized parts are available through Information Unlimited (www.amazing1.com) and are listed in Table 33-1 at the end of the chapter.

Circuit Description

A timer (IC2) is connected as an astable free-running multivibrator whose frequency is internally controlled by trimpot (R9). Resistor R8 selects the range limit of R9. The square-wave output of IC2 is via pin 3 and is directly coupled to power amplifier Q2. The drain of Q2 is DC biased through audio-frequency blocking chokes (L1A and L1B), providing a high impedance to the AC component of the signal.

DIP switches (S1,2,3) preselect the internal frequency for the required application and are shown in Figure 33-2. These switches select resonating inductors L2 and L3 connected in series with the output transducer TD1. The resonant action between the inherent capacity of TD1 and these selected inductances now produces a sinusoidal-shaped wave

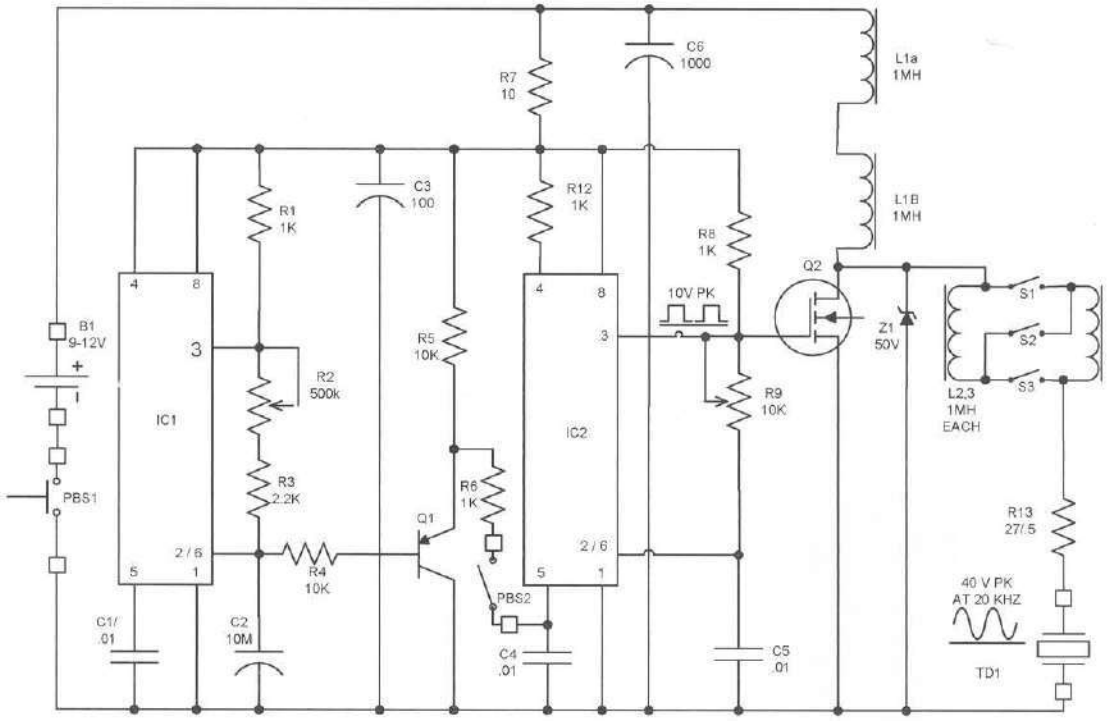

ma	freq	1	2	3	usec
225	25khz	on	off	on	tune max 40-50 u
175	16khz	on	off	off	tune max 60-70 u
150	12khz	off	on	off	tune max 80-90u

Figure 33-2 *Pain-field generator circuit schematic*

peaking around the upper limit of the tuning range. This *signal* waveform now has a peak-to-peak voltage several times that of the *original* square wave. Transducer TD1 now can take advantage of these peak voltages to produce the high sound-pressure levels necessary without exceeding the high RMS ratings of an equivalent voltage-level square wave. Zener diode Z1 clips any excessive overshoots across Q2.

Timer IC1 is similarly connected as an astable running multivibrator and is used to produce the sweeping voltage necessary for modulating the frequency of IC2. This sweep repetition rate is controlled by trimpot R2. Resistor R3 limits the range of this repetition time. C2 sets the sweep time range. Output for IC1 is via pins 6 and 2, where the signal ramp function voltage is resistively coupled to inverter transistor Q1 via resistor R6. The output of Q1 is fed to pin 5 of IC2 and provides the output modulation voltage necessary to vary the frequency as required. Note that the modulation signal is enabled by pushbutton PBS2.

Power to the system is via battery B1 and pushbutton PBSl. Capacitor C6 guarantees an AC return path for the output signal. Power to the driver circuits IC1 and IC2 is thru a decoupling network consisting of resistor R7 and capacitor C3.

Construction

1. Layout and identify all parts and pieces. Verify with parts list. Separate resistors, as they have a color code to determine their value. Colors are noted on the parts list.
2. If you are building from a perforated board, use Figure 33-3 as a parts placement guide and insert components starting in the lower left-hand corner as shown. Pay attention to polarity of capacitors and all semiconductors. It is suggested you use sockets for integrated circuits IC1 and IC2.

   Route leads of components, as shown, and solder as you go, cutting away unused wires. Attempt to use certain leads as the wire runs or use pieces of the #24 buss wire. Follow dashed lines on assembly drawing, as these indicate connection runs on underside of assembly board. The heavy dashed lines indicate use of thicker #20 buss wire, as this is a high-current discharge path.

   Please note that this circuit is very cramped, and it is suggested you obtain the optional printed circuit board shown in the parts list.
3. Attach external leads to components as shown in Figure 33-4, noting the individual lengths and twisted pairs.
4. Double-check accuracy of wiring and quality of solder joints. Avoid wire bridges, shorts, and close proximity to other circuit components. If a wire bridge is necessary, sleeve some insulation onto the lead to avoid any potential shorts.
5. Connect an ohm meter between CLI contacts and pushbutton PBSl. Note a reading of several thousand ohms. This may vary but should not indicate a short circuit. Preset trimpots R2 and R7 to midrange.
6. Connect a 9-volt battery and note a current of 200 to 250 milliamps when R9 is set to midrange. The meter can be connected across PBSl for this step.
7. Simultaneously press both PBS2 and PBSI and note a piercing sweeping tone coming from the transducer TD1. Turn R9 fully ccw and note the decrease in signal tone.
8. Frequency range should be approximately 10 to 25 KHz, with a sweep of approximately 1 to 20 times per second selectable by trimpot R2.
9. Check the waveshapes as shown at pin 3 of the output timer IC2. This is determined by the following formula: $F = 1/(1.57 \times R9 \times C5)$.
10. Check the waveshapes as shown across transducer TD1. This waveshape is approximately 40 to 50 volts, peak to peak, and approaches a sine wave. This is the approximate resonant frequency point of the selected values of series inductances within the inherent capacitance of the transducer. A voltage-peaking effect will be noted, as the frequency is varied by trimpot R9. As the frequency is varied off of resonance, this wave will severely distort but will not damage the circuitry. Note the chart in Figure 33-2 showing the selection

It may be a good idea to use SOCK 1, 2 sockets for IC1, 2 to avoid unsoldering if you make an error.

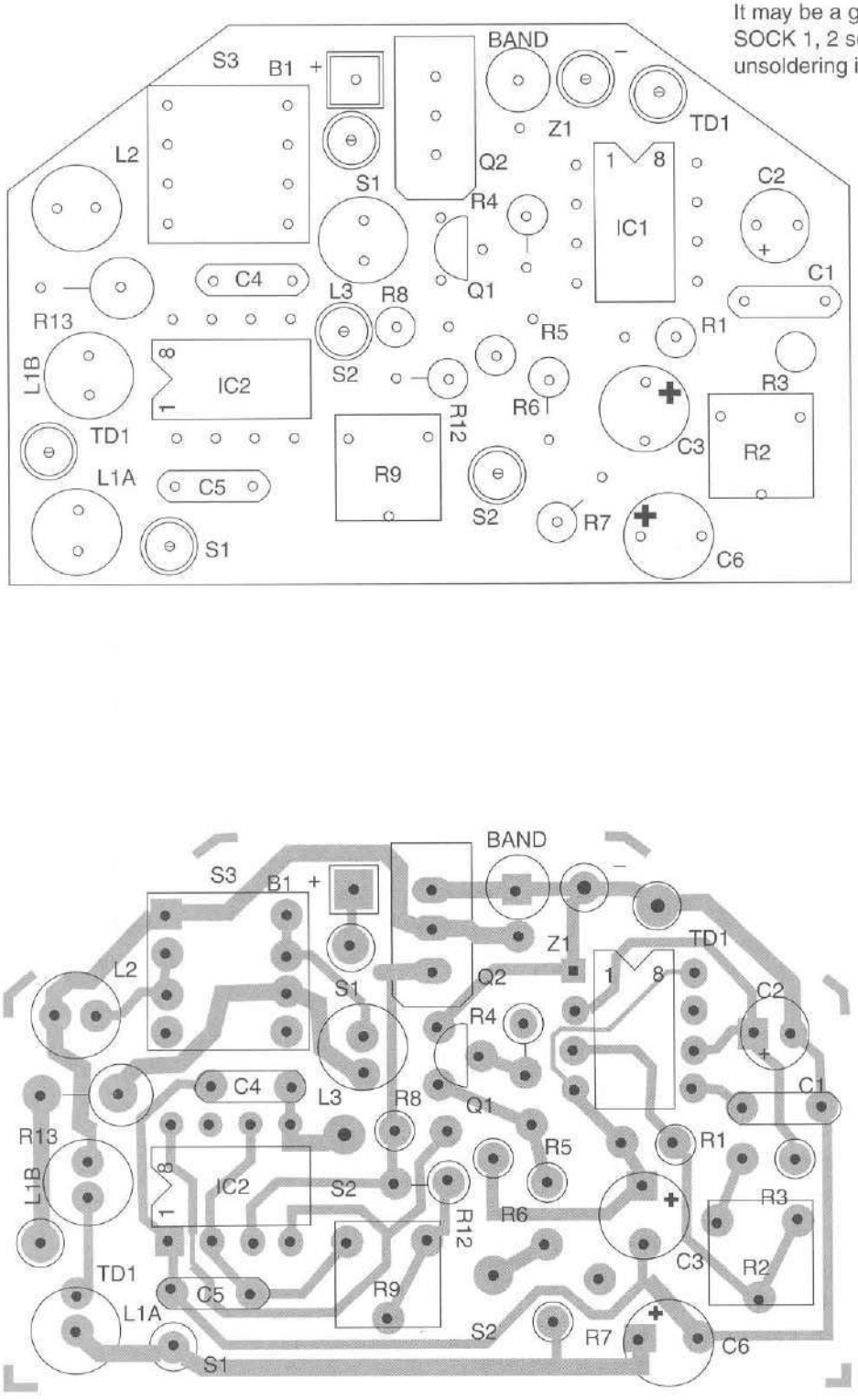

BAND
S3
B1
+
−
Z1
TD1
L2
Q2
S1
1
8
C2
R4
C4
L3
R8
Q1
C1
R13
R5
R1
L1B
8
IC2
1
S2
R3
R6
R12
C3
R2
TD1
C5
R9
L1A
S2
R7
C6
S1

Figure 33-3 *Printed circuit board parts and wiring*

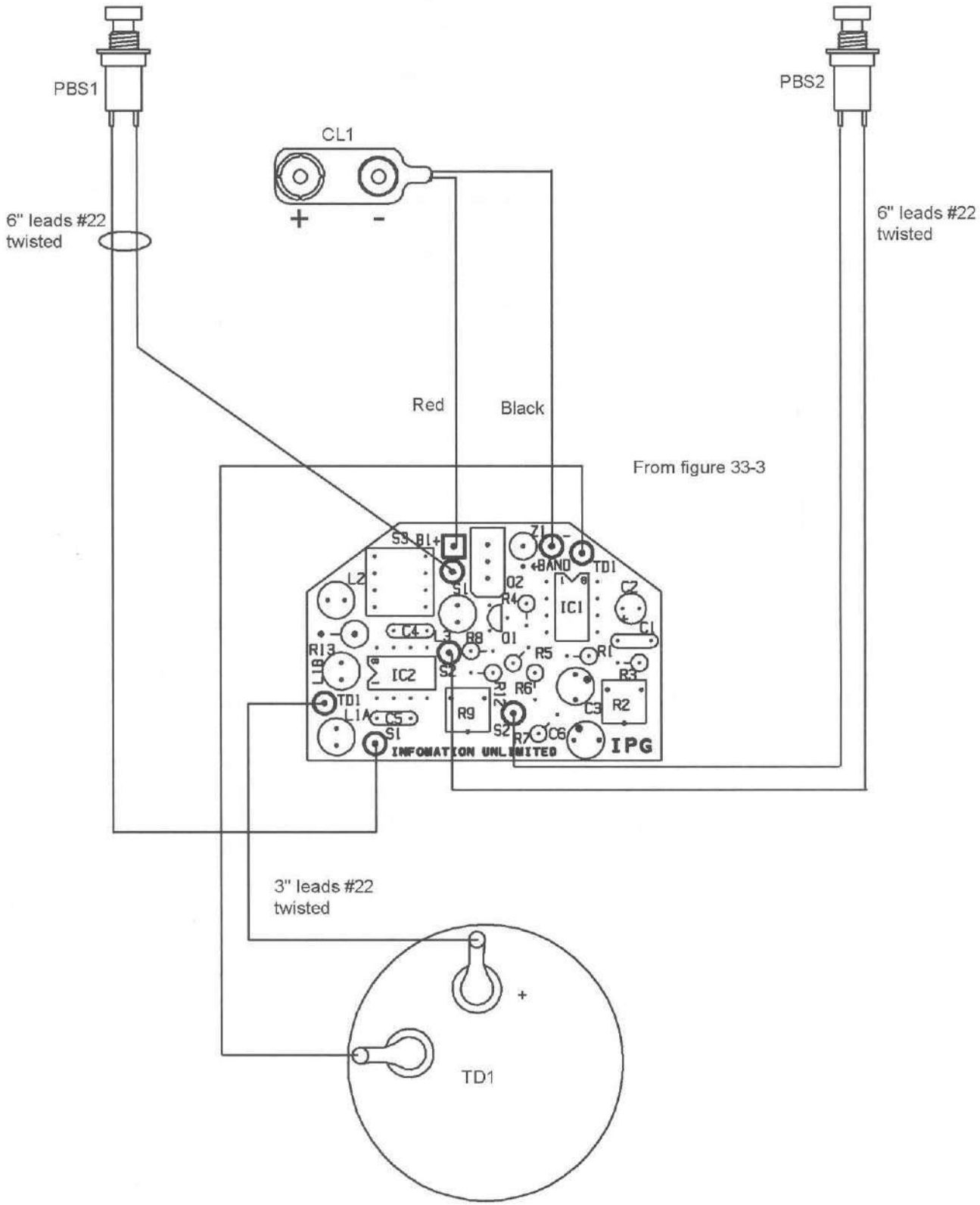

Figure 33-4 *External wiring*

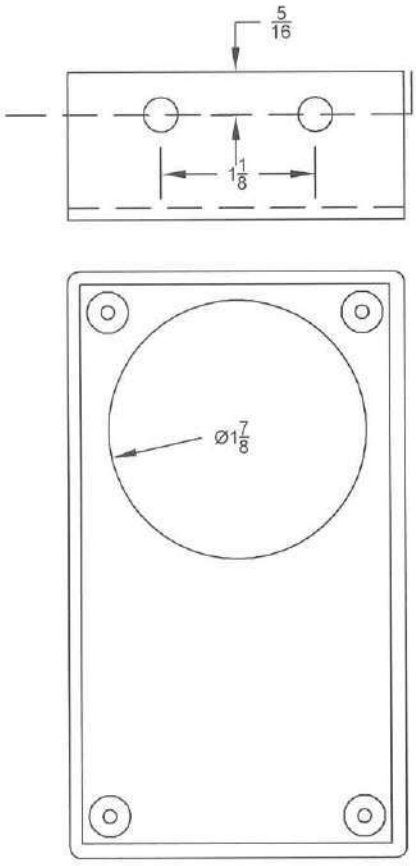

Operating instructions:

Remove rear cover and insert a 9 volt alkaline battery. Note that proper positioning is required for cover to properly fit without bowing.

Default settings of the two trimpots is midrange. To change for obtaining the maximum effect on the target you may adjust trimpots using a small plastic tuning tool or screw driver.

Simply direct unit transducer opening towards the target and push the control button. You should notice an immediate effect. The range will depend on the acoustical sensitivity of the target subject.

Use the sweep button to possible enhance the effect on the target.

This unit is designed for generating intermittent bursts of ultrasonic and high frequency acoustical energy.
Do not direct at people.
Use out side as walls and ceilings will cause the signal to loose directional characteristics and effect the user.
Use in 2 to 5 second bursts.

Figure 33-5 *Fabrication of plastic case*

of the inductances for the choice of operating frequencies that provide the maximum output.

Use a scope for these measurements. These steps are not necessary if the unit appears to function as described.

11. A sound pressure measurement of approximately 125 db was measured at 10 KHz at a distance of 16 inches on our model. Voltage across TD1 was measured at 40 volts peak.

This completes the electronic testing of the unit.

12. Fabricate the EN1 enclosure, as shown in Figure 33-5. Note 1⅞-inch hole for the aperture of TDI. This hole should be made with a large punch or hole saw using a drill press. The hole may also be cut out with a sharp knife. Drill ¼-inch holes for PBSl and PBS2, as shown.

13. Cut a piece of 2⅛ × 2⅛-inch window screen and secure it along with transducer TDI. Use RTV or suitable adhesive.

14. Make final assembly, as shown Figure 33-6, and secure assembly board with two-sided foam tape.

15. Attach the battery and position as shown. Note: The battery must be up against the enclosure with all leads properly routed or the rear cover will not fit properly.

16. See Figure 33-5 for operating instructions.

Figure 33-6 *Final assembly into EN1 enclosure*

Table 33-1 Invisible Pain-Field Generator Parts List

Ref#	*Description*	*DB Part #*
R1,6,8,12	Four 1 K, ¼-watt resistors (br-blk-red)	
R2	500 K vertical trimpot	
R3	2.2 K, ¼-watt resistor (red-red-red)	
R4,5	Two 10 K, ¼-watt resistors (br-blk-or)	
R7	10-ohm, ¼-watt (br-blk-blk)	
R9	10 K vertical trimpot	
R13	27-ohm, ½-watt resistor (red-pur-blk)	
C1,4	Two .01 mfd, 50-volt disc capacitors	
C2	10 mfd, 50-volt vertical electrolytic capacitor	
C5	.01 mfd, 50-volt plastic capacitor	
C3	100 mfd, 50-volt vertical electrolytic capacitor	
C6	1,000 mfd, 25-volt vertical electrolytic capacitor	
IC1,2	Two 555 timer DIP integrated circuits	
Q1	PN2907 PNP TO92 transistor	
SOCK1,2	Two 8-pin DIP sockets for above IC1,2 (Not shown)	
Q2	IRF540 Mosfet TO220	
L1AB,2,3	Four 1-millihenry inductors	DB# 1MH
Z1	50-volt, 1-watt Zener diode	
PBS1,2	Two pushbutton switches	
S1,2,3	3 or 4 section DIP switch	
CL1	Battery snap clip	
TD1	Special polarized transducer	DB# 1020A
PCB1	Printed circuit board	DB# PCIPG9
CASE	4 × 2 ⅜ × 1⅛-inch plastic enclosure	
SCREEN	2.5 × 2.5 inch piece of window screen	

Chapter Thirty-Four

Canine Controller

This very useful device, as shown in Figure 34-1, is intended for those who are bothered by nearby barking dogs. The control section is a modification of a circuit made by Bob Gaffigan in 1993. The project is intended to detect the dog's bark, which triggers a high-output, pain-field sonic generator, as described in Chapter 35, producing very uncomfortable sounds to the animal's sensitive hearing.

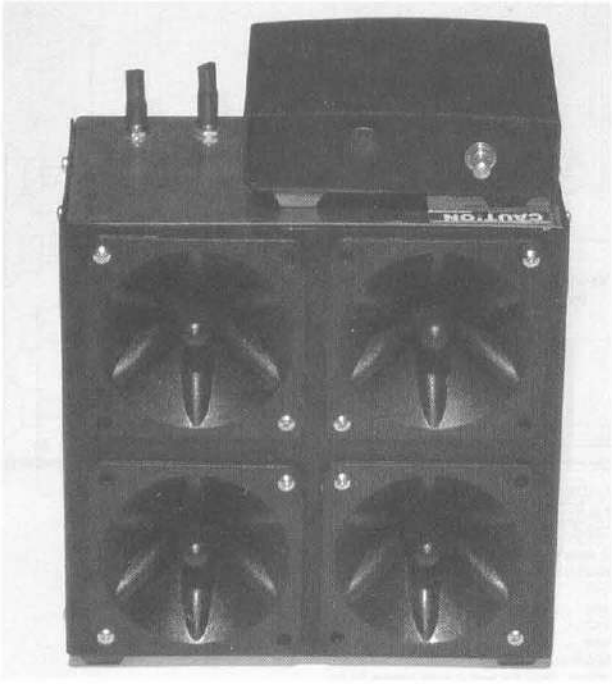

Figure 34-1 *The canine controller system with our sonic blaster*

The system may be covertly used without the dog owners knowing or it can even be tuned to bother the owners every time their mutt goes into a barking frenzy. The user can implement many options to discourage these constant barkers or give some of these inconsiderate owners a taste of their own medicine.

This is an intermediate-level project requiring basic electronic skills. Expect to spend $25 to $50. All the parts are readily available, with the specialized parts obtainable through Information Unlimited (www.amazing1.com), and they are listed in the parts list in Table 34-1 at the end of the chapter.

Device Description

A directional device picks up the dog's bark and processes it so that it turns on the sonic burst pain-field generator pointed in the offending animal's direction. The animal now experiences a very uncomfortable sound, much like a person would find the scratching of chalk on a blackboard. Eventually, the animal associates this sound with his barking, thus conditioning him to stop. The device contains adjustments that actually count the number of yelps so that it can be set not to trigger, thereby discouraging the animal from a normal barking trend that may be the warning of an intrusion or other important event.

The unit is easily mounted in any convenient location and operates from internal batteries, an external 12 volts, or 115 VAC via a wall adapter converter. The detection system contains adjustments for bark-level sensitivity, the number of barks detected before triggering, and the length of the triggered on time of the sonic burst. The pain-field generation section, as described in Chapter 35, has controls for the frequencies of the burst, sweep rate, sweep on/off, and main power control. The canine controller section is designed to easily connect to the existing jacks on the sonic generator section via a three-conductor cable. It may be mechanically attached as a single unit for a compact integrated system. The pickup microphone may even be placed at the focal point of a parabolic dish, providing very discrete selection of the target. As in any device such as this, many variables will enter into the equation that defines the overall performance. The suggested effective range will vary but can be up to 100 feet.

Special Note: In some circumstances, the owner is more to blame than the actual animal. As previously stated, the unit may be tuned to a frequency that the owner him- or herself finds very uncomfortable.

Circuit Description

Figure 34-2 shows the block diagram where the mic picks up the bark and amplifies it. A filter favors the assumed frequencies of the bark and feeds them to a bark counter. This circuit contains a selector switch to preset the necessary number of barks to trigger the bark period timer. The time of the bark period is also selectable by a switch. The bark period timer gates on the MOSFET switch transistor turns on the sonic generator, which drives the four transducers that now produce the directional, uncomfortable sound pain-field shockwaves.

Figure 34-3 shows the complete schematic of the controller section circuit, and the sonic pain-field generator section schematic is shown in Chapter 35. The bark is detected by microphone M1 and amplified by operational amplifier IC2A. The DC follower IC2D sets the midpoint bias, and resistor R2 sets the gain of this stage. The output level at this stage is controlled by potentiometer R5 and fed to amplifier/filter IC2C with a passband set by resistors R8 and R9 and capacitors C8 and C9. Schmidt discriminators

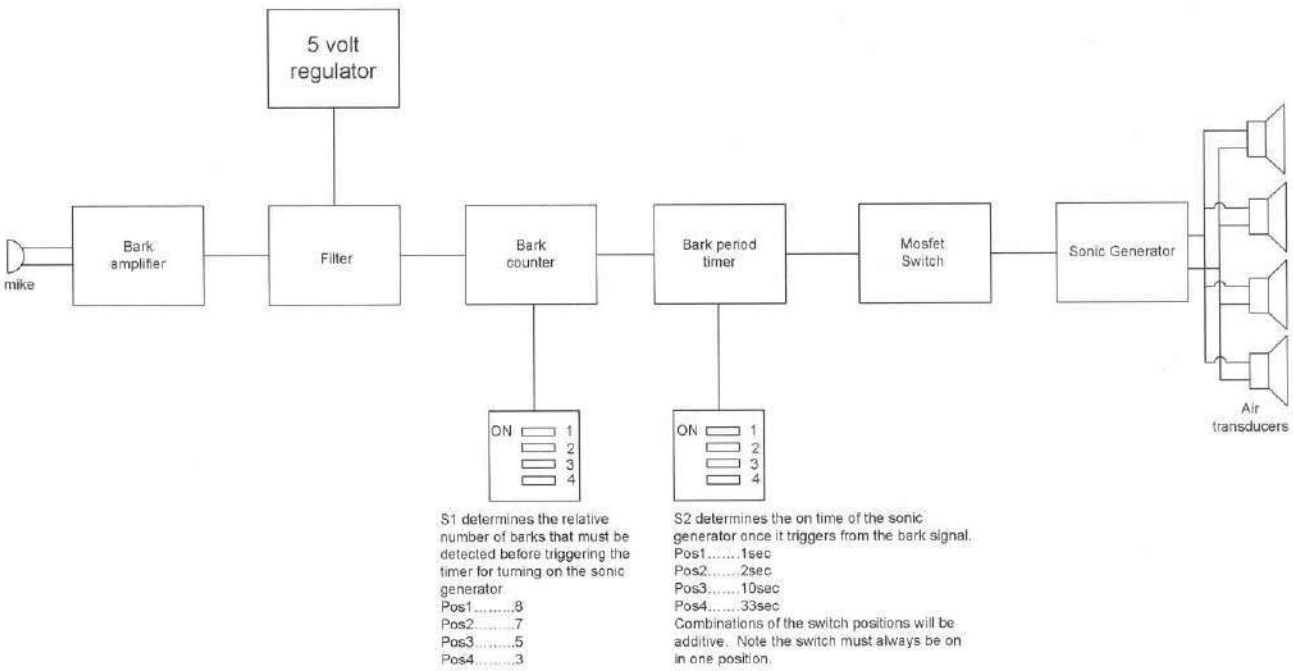

Figure 34-2 *Circuit block diagram*

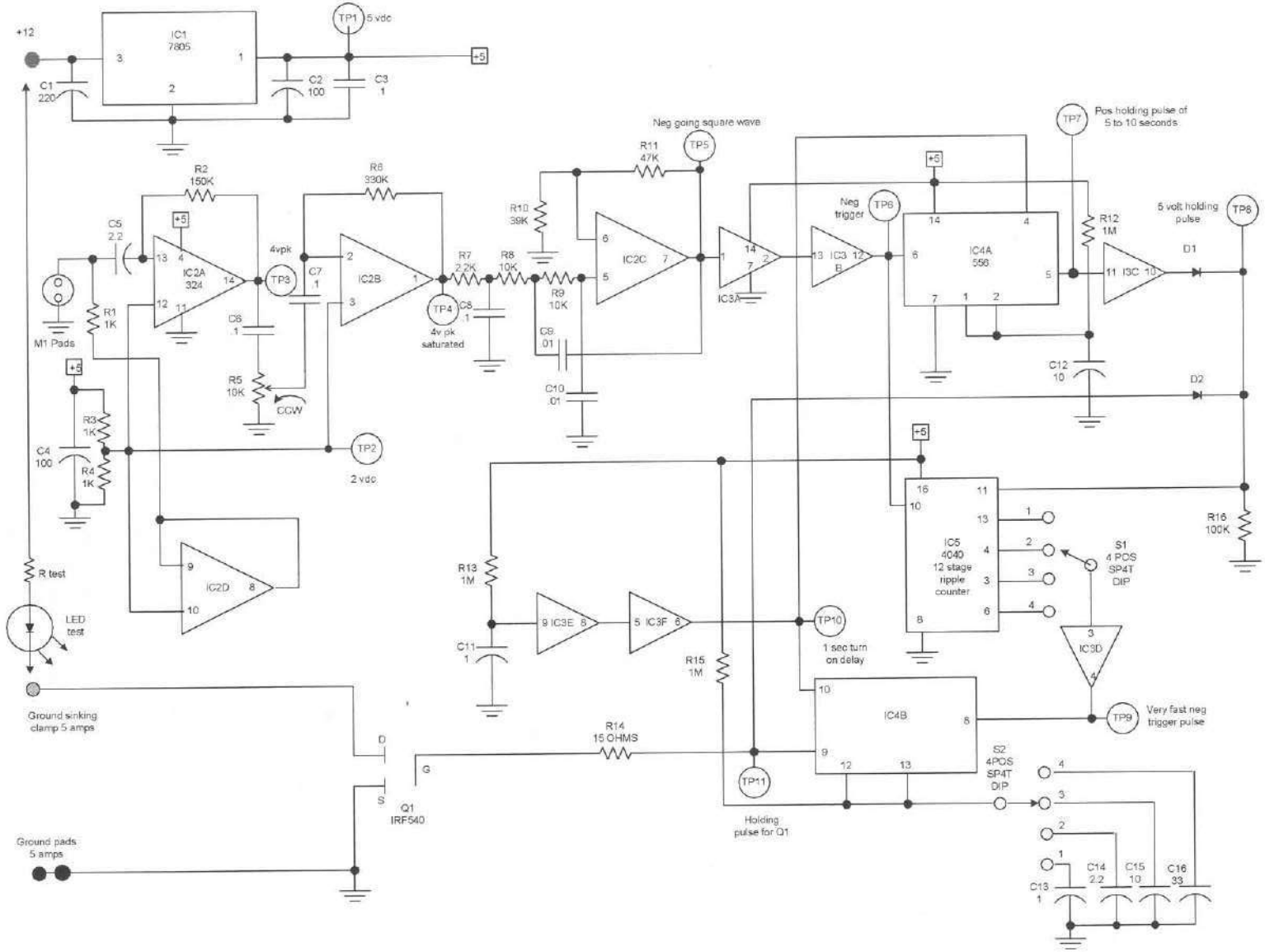

Figure 34-3 *Circuit schematic*

IC3A and IC3B trigger the signal, provide a defined level of the correct polarity to initiate timer IC4A, and enable ripple counter IC5 to count the barks within a time period determined by IC4A. If the number of barks exceeds a limit set by bark count switch S1, timer IC4B is initiated, turning on MOSFET switch Q1 for a predetermined amount of time selected by switch S2, enabling the sonic pain-field deterrent signal to be sent toward the target and then resetting. You will note that control of the sonic pain-field generator is made by sinking the negative return lead into the ground.

Circuit Assembly

1. Assemble the circuit board as shown in Figure 34-4. Note that Figure 34-5 shows the foil traces of the printed circuit. It is not recommended that you assemble this circuit on a perforated vector board unless you are an advanced assembler.

   Note that if you are building from a perforated or vector circuit board, it is suggested that you use the indicated traces for the wire runs and insert components starting at the lower left-hand corner. Pay attention to the polarity of the capacitors with polarity signs and all the semiconductors. It is a good idea to use sockets for all the integrated circuits.

   Route the leads of the components as shown and solder as you go, cutting away unused wires. Attempt to use certain leads as the wire runs or use pieces of the #26 bus wire. The heavy foil runs should use the thicker #24 bus wire, as these are the high-current discharge paths.

2. Double-check the accuracy of the wiring and the quality of the solder joints. Avoid wire

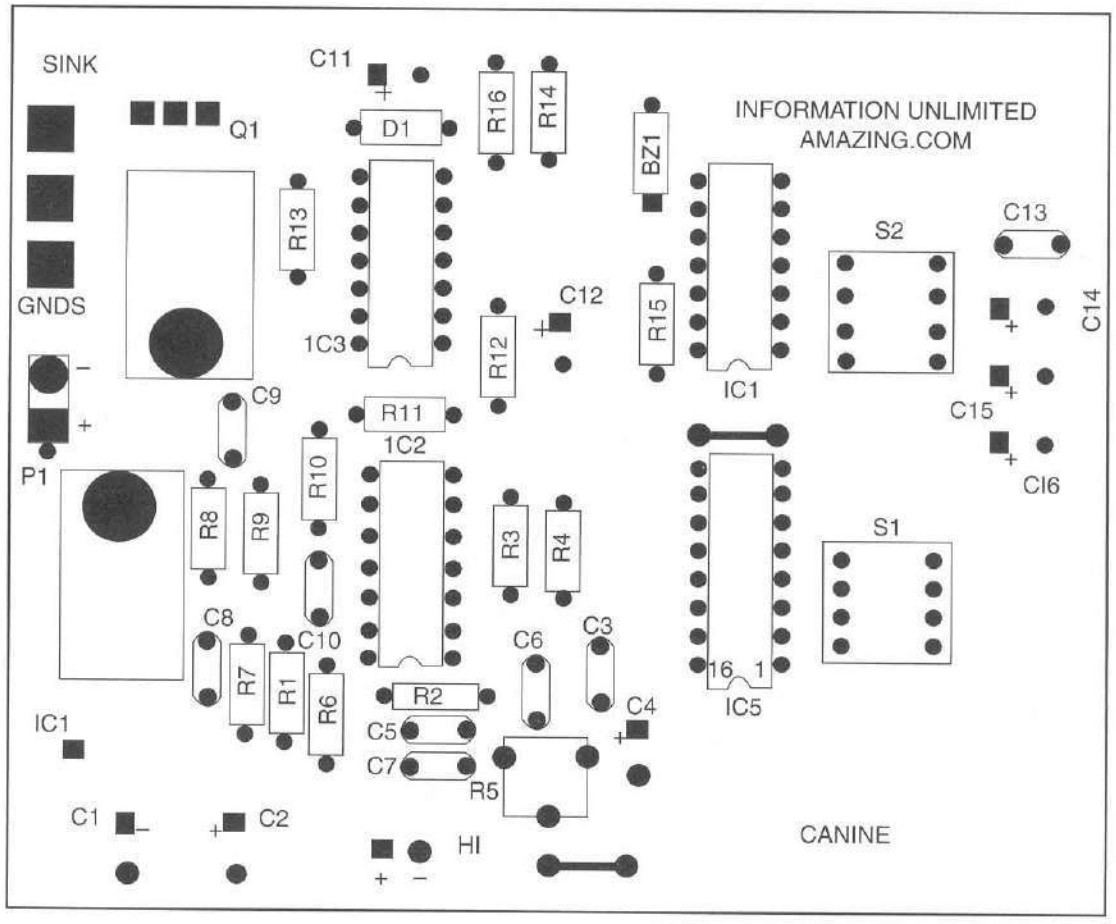

Figure 34-4 *Assembly of the circuit board*

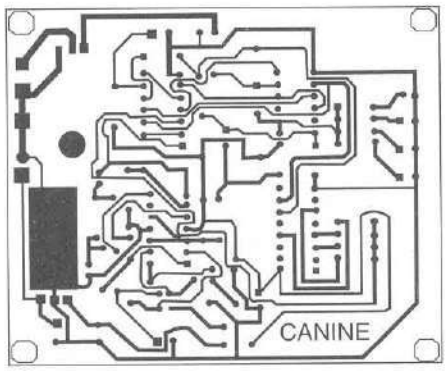

Figure 34-5 *Assembly circuit board traces*

bridges, shorts, and close proximity to other circuit components. If a wire bridge is necessary, sleeve some insulation onto the lead to avoid any potential shorts.

3. Connect the external components as shown in Figure 34-6. Use shielded microphone cable if you are not installing it on the actual board.
4. Fabricate the chassis as shown in Figure 34-7 from a piece of .035-inch 5052 bendable aluminum or plastic. If you use metal, you will need a piece of plastic material under the assembly board to prevent shorting the foil traces.
5. Create a mating cover and finally assemble everything as shown in Figure 34-8. Note the hole for the microphone with a screen. Wire the P1 plug and cable for interconnecting the controller and the sonic blaster using desired lengths per your requirements. Leave the other end with leads that will eventually connect to the sonic blaster.

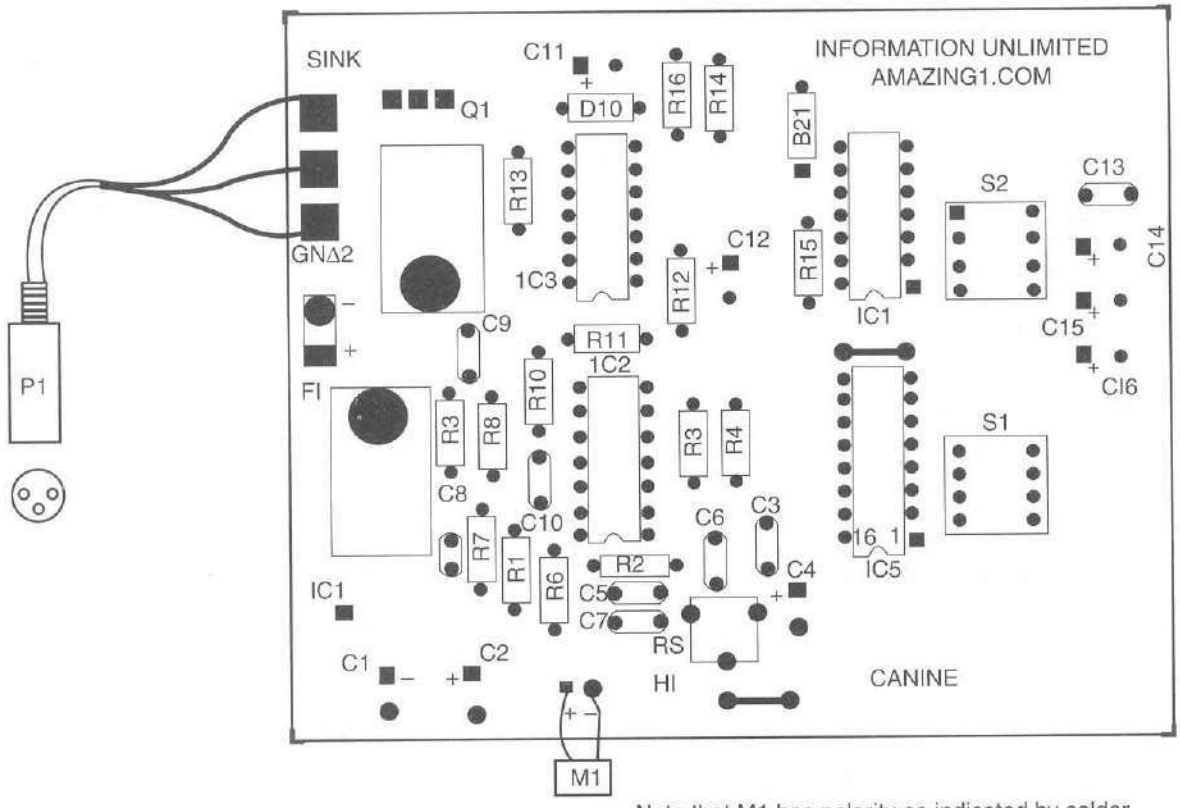

Bottom view showing pads

Note that M1 has polarity as indicated by solder pad connected to the main enclosure. This contact is ground indicated by the – sign. Be very careful when soldering o these pads. Use #22 wire or smaller. If leads are longer than one several inches it is suggested to use shielded microphone cable.

Figure 34-6 *External wiring*

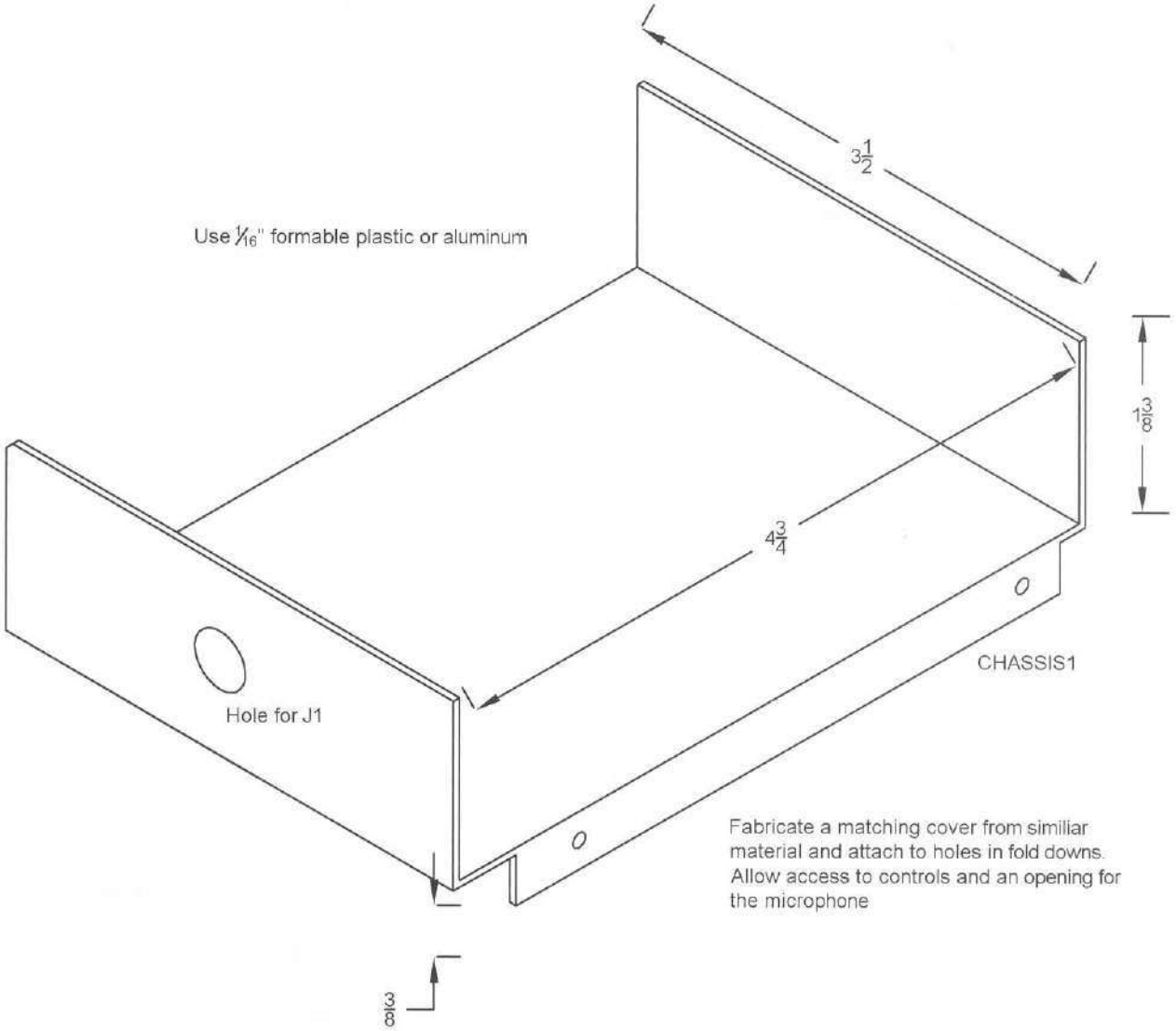

Figure 34-7 *Chassis fabrication*

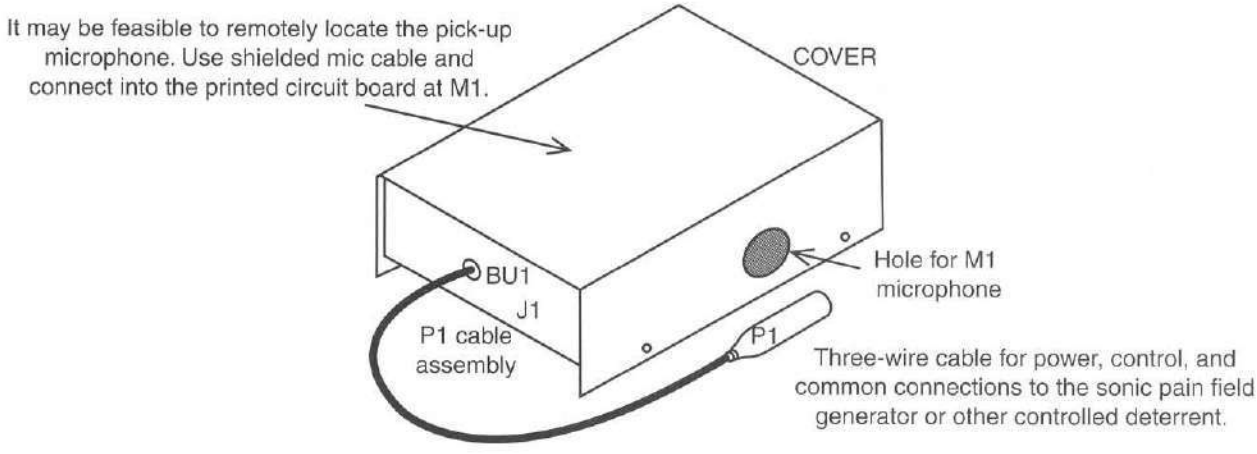

Figure 34-8 *Isometric of final assembly*

Testing the Circuit

1. Assemble the test jig, referring back to Figure 34-3. If the circuit is correct, you may go right to the connection of the test jig as shown and perform the following steps:

   a. Preset S1 to position 4 (the lowest number of barks for activation).

   b. Preset S2 to position 1 (the shortest time for the sonic generator).

   c. Preset R5 to midrange.

2. Apply a 12 VDC input and note a low-current draw of less than 10 milliamps, which is the same value as the quiescent operating current. C cell batteries will work approximately 30 days before requiring replacement.

3. Simulate a bark and note the test LED momentarily coming on. If this occurs, you may want to test the various positions of S1 and S2. Also verify the sensitivity control, R5.

4. If the circuit does not work, you may need a scope to test the various test points as shown in Figure 34-3. They should have the following values:

   TP1: +5 volts DC

   TP2: 2 to 3 volts DC

   TP3: 4-peak-volt audio level

   TP4: Saturated audio signal

   TP5: Negative-going pulse

   TP6: Negative-going square wave

   TP7: Positive 10-second holding pulse

   TP8: Positive holding pulse

   TP9: Very fast negative trigger pulse

   TP10: 1-second turn-on delay

   TP11: Holding pulse for Q1

10. Once the controller operation is verified, you may connect the system as shown in Figure 34-9. You will need a properly working sonic pain-field generator, as described in Chapter 35.

    It is suggested that you experiment with the system before actually installing it. Once familiar with it, you may position the system for the best effect. You also have the option of adjusting the sonic generator when the dog starts barking so that it can also be very annoying to the animal owners when their mutt goes into an uncontrolled barking rage. Use your own judgment as you can get tagged for harassment!

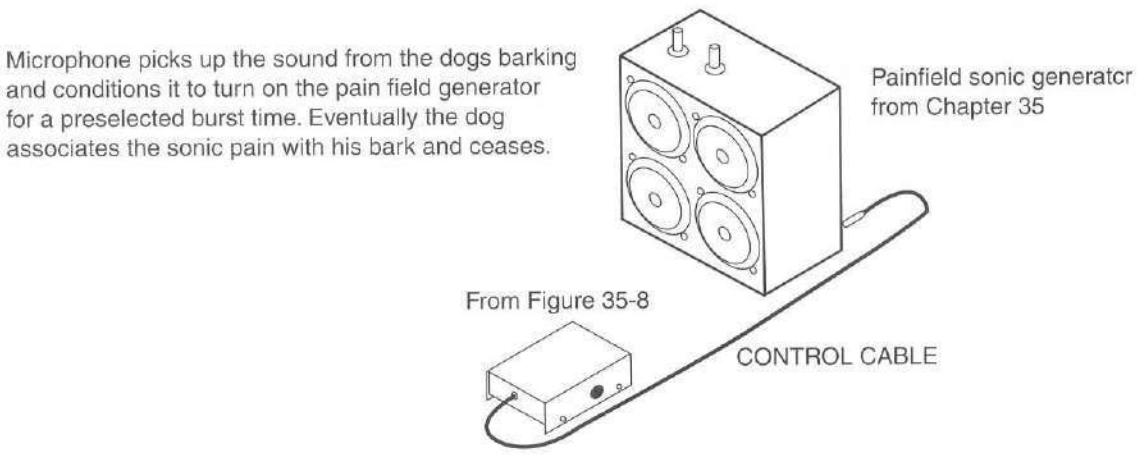

Figure 34-9 *Systems view*

Table 34-1 Canine Controller Parts List

Ref. #	Description	DB Part #
R1, 3, 4	Three 1K, ¼-watt resistors (br-blk-red)	
R2	150K, ¼-watt resistor (br-gr-yel)	
R5	10K pot and 12-volt switch, 17 mm	
R6	330K, ¼-watt resistor (or-or-yel)	
R7	2.2K, ¼-watt resistor (red-red-red)	
R8, 9, 10	Three 10 kilo-ohm, ¼-watt resistors (br-blk-or)	
R11	47 kilo-ohm, ¼-watt resistor (yel-pur-or)	
R12, 13, 15	Three 1M, ¼-watt resistors (br-blk-gr)	
R14	15-ohm, ¼-watt resistor (br-gr-blk)	
R16	100K, ¼-watt resistor (br-blk-yel)	
C1	220-microfarad, 25-volt vertical electrolytic capacitor	
C2, 4	Two 100-microfarad, 25-volt vertical electrolytic capacitors	
C3, 6, 7, 8	Four .1-microfarad, 50-volt plastic capacitors	
C5, 14	Two 2.2-microfarad, 50-volt vertical electrolytic capacitors	
C9, 10	Two .01-microfarad, 50-volt plastic capacitors	
C11, 13	Two 1-microfarad, 50-volt vertical electrolytic capacitors	
C12, 15	Two 10-microfarad, 50-volt vertical electrolytic capacitors	
C16	33-microfarad, 50-volt vertical electrolytic capacitor	
D1, 2	Two IN914 silicon diodes	
IC1	7805 5-volt regulator TO220	
IC2A, B, C, D	LM324 quad amp in dual inline package (DIP)	
IC3A, B, C, D, E, F	40106 hex Schmidt in DIP	
IC4	556 dual timer in DIP	
IC5	4040 complementary metal oxide semiconductor (CMOS) PLL phase lock loop in DIP	
Q1	100-volt IRF540 metal-oxide-semiconductor field effect transistor	MOSFET
M1	FET mic element	DB# FETMIK
S1, 2	Two four-position single-throw DIP switches	
PCCANINE	Printed circuit board (PCB)	DB# PCCANINE
CHASSIS1	Metal or plastic chassis as shown in Figure 34-7	
COV1	Cover fabricated as shown in Figure 34-8	
J1/P1	Three-pin chassis mount jack and mating plug	
WR3C	3-inch three-conductor cable for interconnecting	
PPF4K	Pain-field generator kit as described in Chapter 35	DB# PPF4K
PPF40	Pain-field generator assembled as described in Chapter 35	DB# PPF40

Chapter Thirty-Five

Ultrasonic Phaser Pain-Field Generator

This project, as shown in Figure 35-1, shows how to construct a moderately high powered sonic generator that can be used for tasks that range from animal control to discouraging personal encounters. It can be used as part of our laser property protection guard described in Chapter 5 or as the deterrent for use with the canine controller, as described in Chapter 34. The unit can generate a variable rate of complex waves from 5 to 25 kHz well into the ultrasonic range. These waves can be very painful or disorientating to animals and people, depending on where the controls of the unit are set.

This is an excellent device for use in animal control as well as a low-liability deterrent in anti-intrusion alarms and detection systems. This is an intermediate-level project requiring basic electronic skills. Expect to spend $50 to $75. All parts are readily available, with specialized parts obtainable through Information Unlimited at www.amazing1.com, and they are listed in the parts list at the end of the chapter.

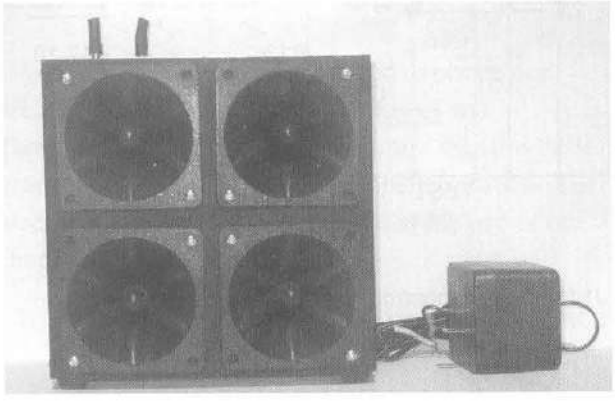

Figure 35-1 *The phaser pain-field generator*

Basic Device Description

This chapter demonstrates how to create a variable-sweep-frequency, ultrasonic, pain-field generator capable of producing the equivalent of 400 watts of resultant power such as that obtainable from a conventional dynamic transducer system. This is possible due to recently developed piezoelectric ceramic devices. The high efficiency requires very little driving power, consequently resulting in a lightweight, portable, handheld device that is battery driven and capable of producing high sound pressure. It is a directional device and can be set up in a target area such as a field or garden to discourage any sound-sensitive animals. It is also capable of being powered by a car's 12-volt system and can be mounted on the hood or roof of the vehicle. Transducers are mounted in an array for a concentration of energy in one direction.

It should be understood that certain people subjected to different degrees of exposure are affected more than others, some to a point where they may vomit or experience severe headaches and cranial

pains. Some people will experience severe pain in the ear, teeth, or lower head. Statistically, women and younger children are many times more sensitive to this device than the average male adult. With this in mind, the user must exercise consideration when testing and using the device for animal control, as many people will not be aware of the source of this pain and attribute it to a headache or other physical ailment. Also, certain people are affected mentally to a point of actually losing their tempers completely or becoming extremely quick-tempered. Some will experience a state of extreme anxiety when overly exposed. Therefore, consideration must be used at all times when testing or using this or similar devices.

It should also be noted that using the transducers in an array configuration may be damaging to hearing at close range. The array approach produces high sound-pressure density occurring on or near the output axis.

Circuit Theory

Figure 35-2 shows a timer, IC2, connected as an astable free-running multivibrator whose frequency is externally controlled by pot R9. Resistor R10 selects the range limit of R9, and capacitor C5 determines the frequency range of the device along with the previous resistors.

The square wave output of IC2 is via pin 3 and is directly coupled to power amplifier Q2. The drain of Q2 is DC biased through choke L1.

The square wave output signal is then fed into transducer TD1 in series with parallel combination of resonating coils L2 and L3. The resonant action between the inherent capacity of TD1, the C7 tuning capacitor, and the inductance now produces a sinusoidal-shaped wave peaking around 25 kHz or the

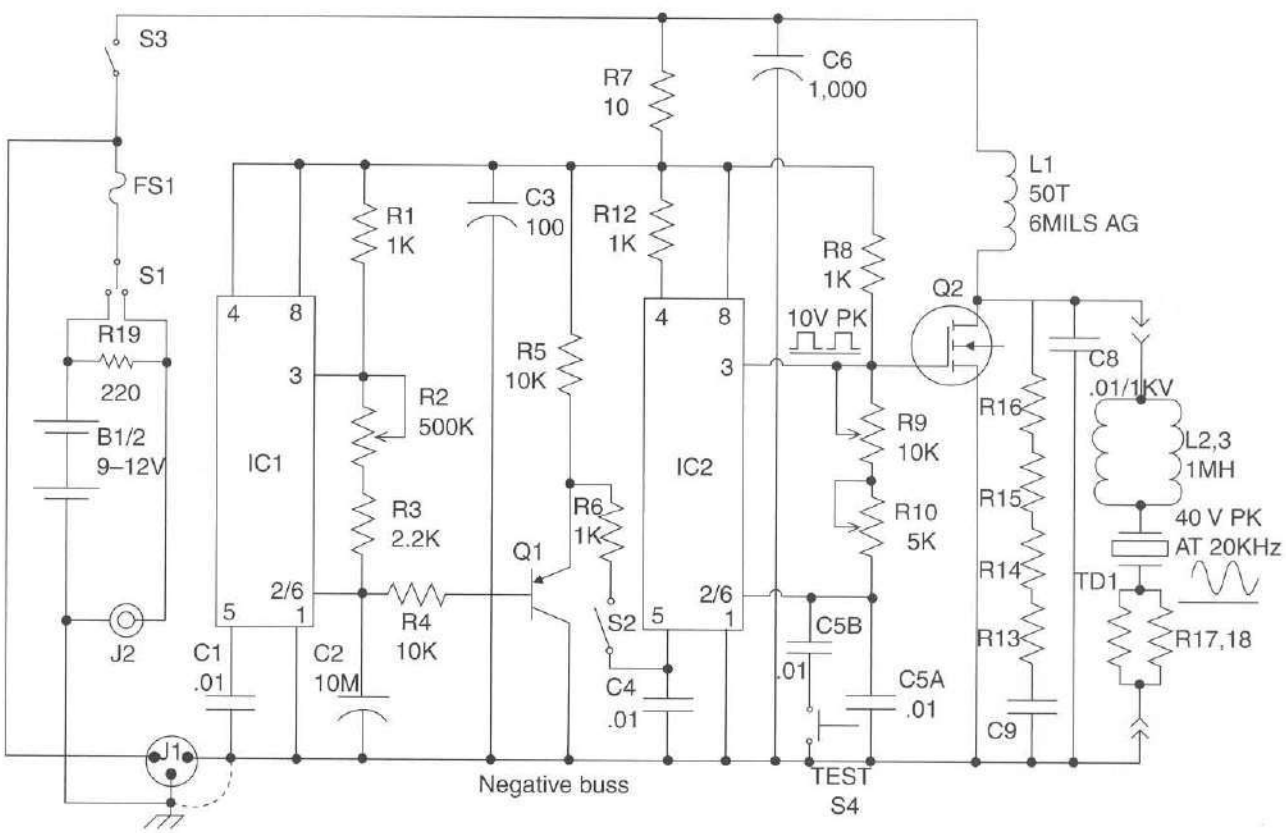

Dashed line indicates bypass connection when not using J1 for external control. You may also short these pins using a mating plug with pins connected together.

Note four transducers and associated networks.

Figure 35-2 *Schematic of the phaser pain-field generator*

upper limit of the tuning range. This signal waveform now has a peak-to-peak voltage several times that of the original square wave. Transducer TD1 now can take advantage of these peak voltages to produce the high sound-pressure levels necessary without exceeding the high *root means square* (rms) ratings of an equivalent voltage-level square wave.

Timer IC1 is similarly connected as an astable, running multivibrator and is used to produce the sweeping voltage necessary for modulating the frequency of IC2. This sweep repetition rate controlled by pot R2 and resistor R3 limits the range of this repetition time. Resistor R1 selects the duty cycle of the pulse, while capacitor C2 sets the sweep time range. The output for IC1 is via pins 6 and 2 where the signal ramp function voltage is resistively coupled to inverter transistor Q1 via resistor R4. The output of Q1 is fed to pin 5 of IC2 and provides the output modulation voltage necessary to vary the frequency as required. Note that the modulation signal is easily disabled via R2/S2.

Capacitor C6 guarantees an AC return path for the output signal. Power to driver circuits IC1 and IC2 is through a decoupling network consisting of resistor R7 and capacitor C3.

Power to the system is via internal battery B1 or an external 12 VDC such as from a vehicle. Three-way switch S1 selects between these two power sources or shuts the unit off in the center position. Resistor R19 provides a trickle charge to the internal battery when using an external source. Jack J1 allows a connection that is similar to our canine controller, turning on the unit when it detects a barking dog.

Construction Steps

If you are a beginner it is suggested to obtain our *GCAT1 General Construction Practices and Techniques*. This informative literature explains basic practices that are necessary in proper construction of electromechanical kits and is listed at the end of the chapter.

1. Lay out and identify all the parts and pieces, and check them with the parts list. Note that certain parts may sometimes vary in value. This is acceptable as all components are 10 to 20 percent tolerant unless otherwise noted.
2. Fabricate the heatsink bracket (HS1) as shown in Figure 35-3 from a .75 × 2 × .065-inch aluminum piece. Bend it 90 degrees at its midsection and drill a hole for the SW1/NU1 screw and nut. Attach it to Q2 as shown.
3. Assemble the L1 choke coil as shown in Figure 35-4 by wrapping 50 turns of #24 magnet wire on the nylon bobbin as evenly as possible. Leave 2 inches of leads for a connection to the circuitry. Assemble the E core as shown and shim each side with pieces of yellow cardboard strips of 3 mils each for a total of 6 mils. If you have an LCR bridge, measure 1 millihenry.
4. Assemble the PCB as shown in Figure 35-5. Note the two wire jumps and component polarity. Wire in inductor L1 and secure it to the board with *room temperature vulcanizing* (RTV) silicon rubber or another suitable adhesive.

   If you are building from a perforated or vector circuit board, it is suggested that you use the indicated traces for the wire runs and insert the components starting in the lower left-hand corner. Pay attention to the polarity of the capacitors with polarity signs and all the semiconductors.

   Route the leads of the components as shown and solder as you go, cutting away unused wires. Attempt to use certain leads as the wire

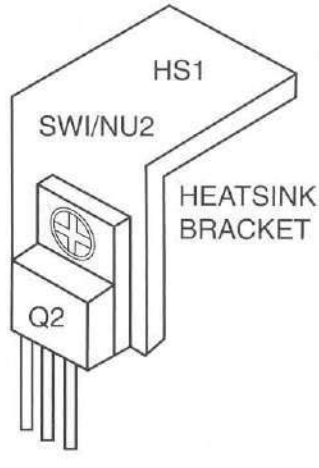

Figure 35-3 *Fabrication of heatsink*

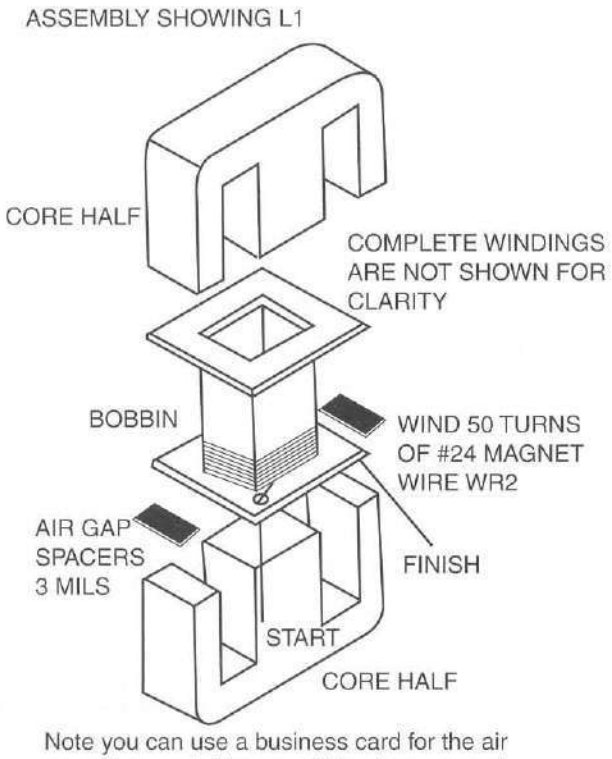

Figure 35-4 *Assembly of L1 inductor*

runs or use pieces of the #24 bus wire. The heavy foil runs should use the thicker #20 bus wire as these are the high-current discharge paths.

It is suggested that you use an 8-pin integrated circuit socket (SO8) for IC1 and IC2.

5. Double-check the accuracy of the wiring and the quality of the solder joints. Avoid wire bridges, shorts, and close proximity to other circuit components. If a wire bridge is necessary, sleeve some insulation onto the lead to avoid any potential shorts.

6. Fabricate the chassis and cover, as shown in Figure 35-6 from 1/16-inch Lexan plastic or aluminum. Use a large punch or circle saw to cut out the four holes for the transducers. Drill the remaining holes as you assemble it, verifying the proper clearances and sizes with components.

7. Complete the final assembly shown in Figure 35-7 and mount the assembly board, battery holders, switch S1, jacks J1 and J2, and fuse holder FS1. It is a good idea to trial-fit all the parts in this section before actually drilling or making any mounting holes. Note a piece of plastic (SPACER) that insulates the bottom solder connections of the PCB from shorting out to the metal chassis base. Also note resistor R19 across S1. Secure the battery holders using pieces of two-sided foam sticky tape (TAPE). Wire using #20 vinyl wire as shown.

8. Mount the transducers as shown in Figure 35-8 using SW2/NU2 6-32 × 1/2-inch screws and nuts.

   Twist the leads of the two inductors L2 and L3 together, effectively paralleling these components. Repeat this for resistors R17 and R18. You should end up with four sets of these parallel components. These components should be self-supporting by being connected to stiff pieces of bus wire. Take caution to observe any potential shorts. Solder the two 18-inch connecting leads and connect them to point P6 on the assembly board.

9. The final assembly is shown in Figure 35-9. Do not attach the cover until you have tested the unit.

Testing the Assembly

10. Turn the pots counterclockwise, set the switch to mid position (off), and install eight fresh batteries into the battery holders. If you have access to a bench supply of 12 VDC at 2 amps, it may be connected to J2 via a mating plug, eliminating the need for the batteries in the preliminary test. Short out the chassis ground and negative bus pins of J1. This jack is for connection to the canine controller module or other remote control devices.

Note: A variable bench supply capable of 12 VDC at 2 amps with a voltmeter and current meter can be a great convenience for the remaining steps and the testing of other similar circuits.

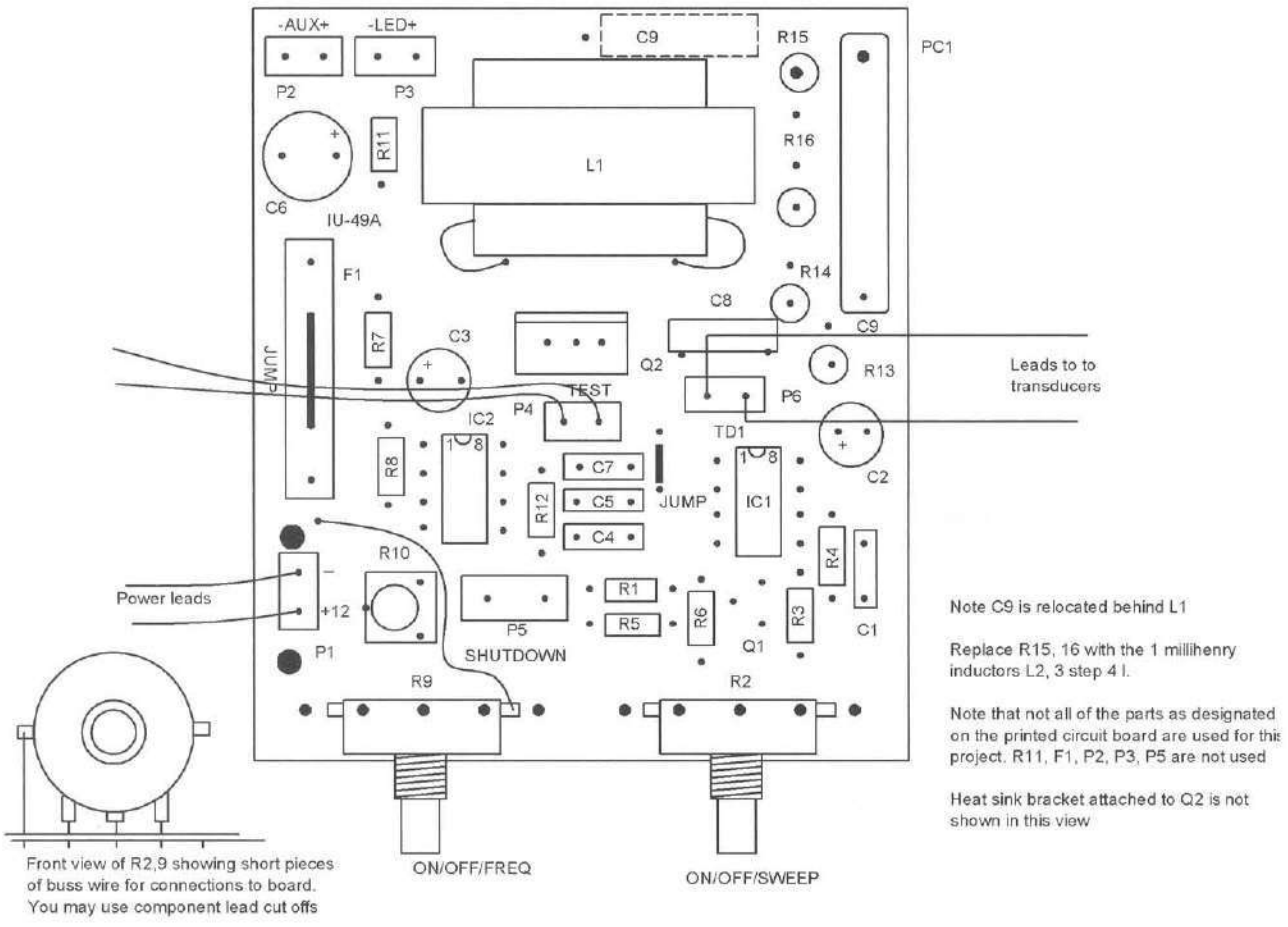

Figure 35-5 *Assembly of PCB*

11. Press push button S1 and note a loud, piercing wave coming from TD1. Measure a current of 500 to 600 milliamps in series with a battery or bench supply. Note that the switch position when up should be power supplied by internal batteries, and the down position being supplied by the external 12 VDC supply. This function may be reversed but should be noted, as the external position will automatically trickle charge the internal batteries.

12. Rotate R9 and note the frequency increasing to above the audible range; measure a current of 400 to 800 milliamps. You may preset the limit of the high range by the R9 setting. The normal factory setting is 25 kHz maximum with R10 full clockwise. Note the wave shapes shown in Figure 35-2 for those who have a scope.

13. Turn on sweep control R2/S2 and note the frequency being modulated by a changing rate as this control is adjusted. Use caution as certain sweep rates may cause epileptic seizures and other undesirable effects. Sweep rates between 7 to 20 per sec should be used with caution.

Basic Operating Instructions

14. Connect a 12-volt source capable of supplying 2 amps of current to designated leads or use internal *nickel cadmium* (NiCad) batteries that are type C cells. These will provide approximately 3½ hours continuous operation at slightly reduced output.

15. The battery-charging function occurs when the system is connected to an external power source and will charge the NiCad batteries at a 100-milliamp rate, taking about 14 hours to fully charge.

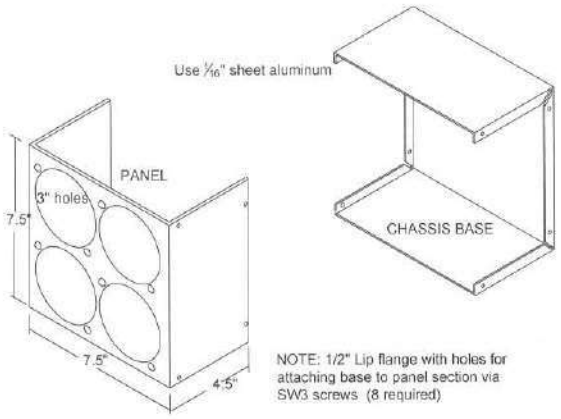

Figure 35-6 *Chassis fabrication*

16. If continued use is anticipated via the external 12 volts, it is a good idea to remove the internal batteries' connections as overcharge may occur that will ruin the batteries or actually cause them to explode. The recommended method of setting the controls is the following:

    a. Determine the frequency limits per the application. These types of devices have two basic applications. When used as an anti-intrusion device to discourage unauthorized entrance, adjustments are made for maximum human annoyance, usually with frequencies from 10 to 15 kHz.

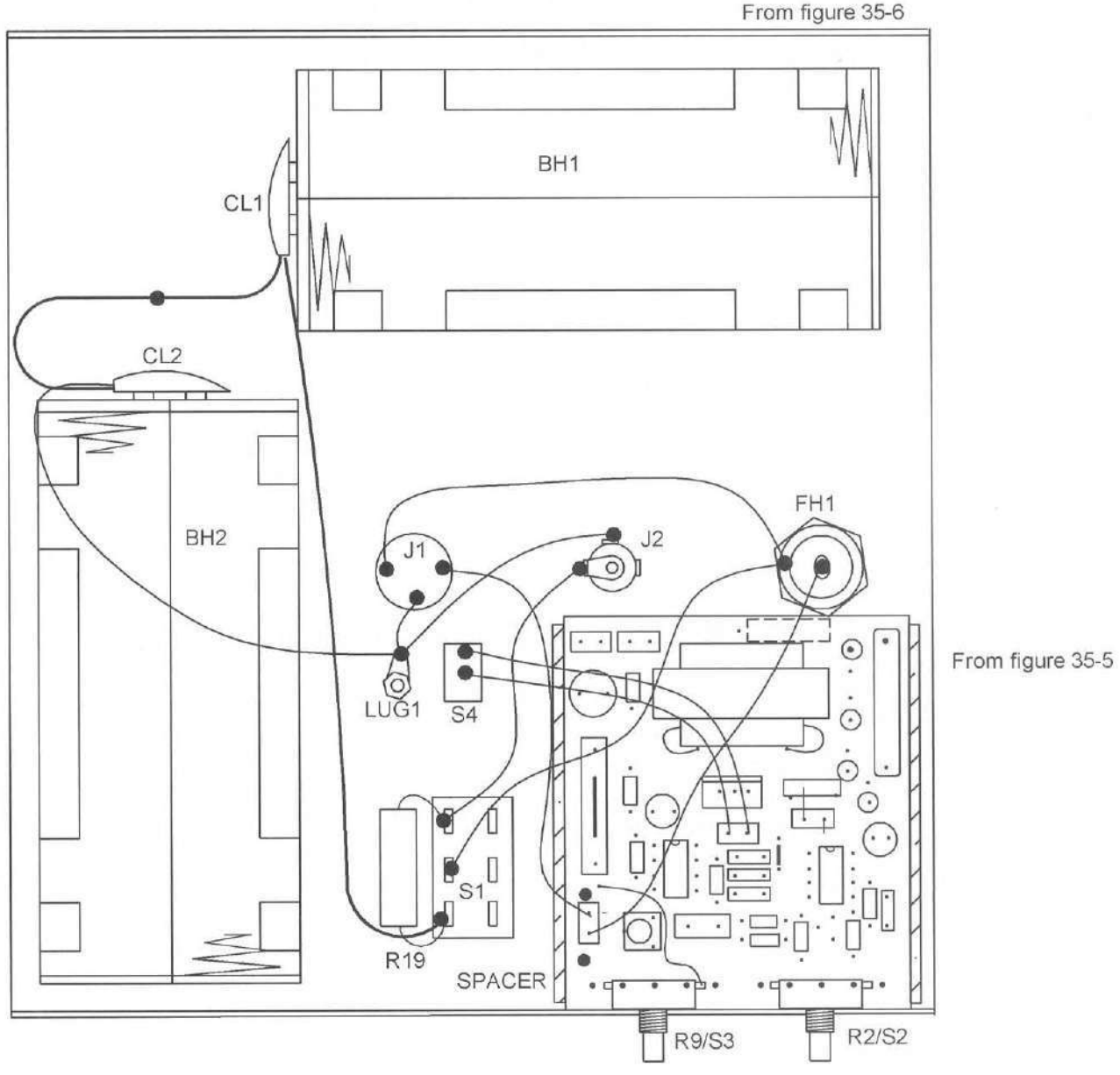

Figure 35-7 *Chassis wiring*

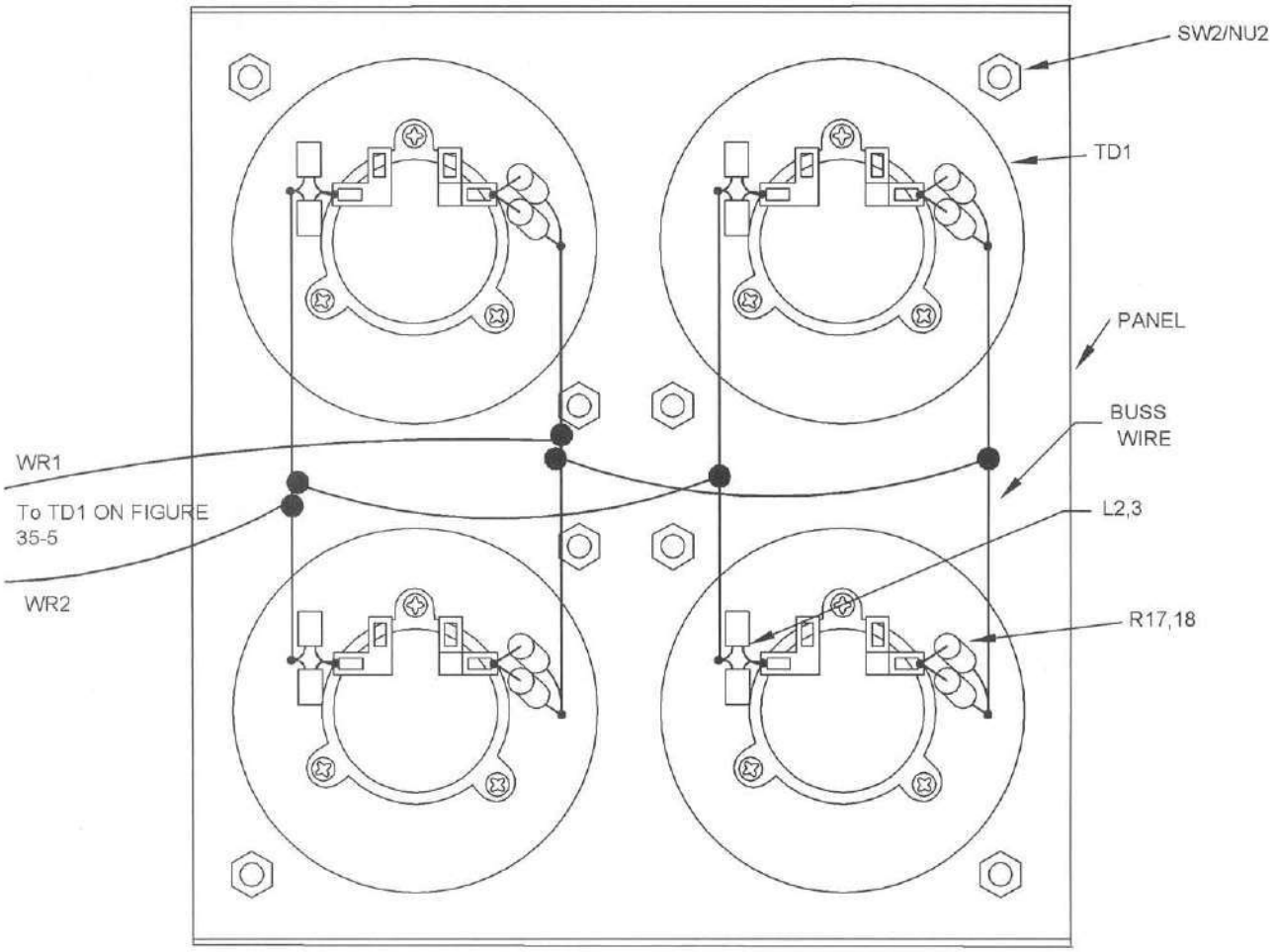

Figure 35-8 *Transducer panel wiring*

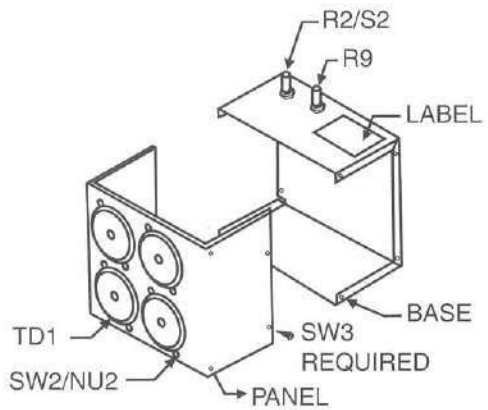

NOTE: 1/2" Lip flange with holes for attaching base to panel section via SW3 screws (8 required)

Figure 35-9 *Final assembly*

When used as a rodent device, we have found that the lowest tolerable frequency to humans usually has the greatest effect on the common species of rats. This is not always true but serves as a starting point in initially setting the adjustments. A frequency setting of 15 to 20 kHz for nonhuman living areas and 20 to 25 kHz for areas where people are present usually suffices for good rat control. Note that at no time should the unit be set higher than 25 kHz.

Dog control is usually around 18 kHz, but experimenting with the target animal may be necessary for optimum effect. Stubborn dog owners fall into the category of anti-intrusion if they will not cooperate.

b. Turn the SWP control off. Adjust the TONE control so that the output is detectable by the human ear or just above the point of annoyance.

c. Set the TEST switch to an audible verification. Note that experimentation is required for optimizing any effect on a given set of target applications.

Information on the System

Your phaser system is capable of operating in two modes. Mode one is at a frequency that is known to produce paranoia, nausea, disorientation, and many other physiological effects. Mode two allows using the system as an audible alarm to frighten off intruders or warn the user of an intrusion. Both modes may be used in combination and are easily rear-panel-controlled by the user.

A Word of Caution

Ultrasonics is a grey area in many respects when an application involves the control of animals or even a deterrent to unauthorized intrusion. It is always best to consult with local municipal and state laws before using this device to protect home or property. Remember many state laws lean more towards the right of the criminal rather than the victim.

General Information on Ultrasonics

Numerous requests have been made for information on the effect of these devices on people. First, let us make it clear that no device such as this should purposely be used on humans, and we discourage this use due to the possibility of acoustically sensitive people being highly irritated.

None of these devices has the ability to stop a person with the same effect as a gun, club, or more conventional weapon. They will, however, produce an extremely uncomfortable, irritating, sometimes painful effect in most people. Everyone will experience this effect to some degree. Unfortunately, younger women are much more affected than older men due to being more acoustically sensitive. The range of the device depends on many variables and is normally somewhere between 10 and 100 feet depending on the acoustical sensitivity of the target.

One possible use of the device (which deserves careful consideration) is the installation of all transducers in an area to protect against unauthorized intrusion. This would produce an irritating and painful feeling for the intruder, along with a condition of paranoia of not knowing what to expect next.

Application Supplement

The following describes an acoustical, ultrasonic device for dispersing potentially unruly crowds or gatherings. The reason for using the higher-frequency energy is that it is easily directed without being diffracted in all directions. Therefore, the use of directional-type transducers producing a front-to-back relative signal ratio of 20 to 30 dbs is easily achieved. The higher-frequency sound can produce nausea, headaches, and depression without the subject necessarily being able to determine the source. This effect no doubt presents an advantage to law enforcement when using these devices.

It is a known fact that the development of any type of demonstration in "psychological crowd control" follows the natural laws of growth and decay, in that a positive influx of people encourages a crowd growth, whereas a negative outflux creates a diminishing situation. One must realize that differences exist among most people regarding sound level and frequency sensitivity. When sampling a group or crowd as to the overall sensitivity of these devices, it is usually found that certain ones may not be affected to the same degree as others. However, taking into consideration that those who find the effect intolerable does generate the negative outflux that usually terminates the gathering.

This method, to this date, produces no permanent, lasting effects or symptoms and therefore becomes a more humane means of dispersing potentially unruly crowds. It should also be mentioned that younger people appear to be many times more sensitive to this effect. This usually goes hand in hand in most

demonstrations, since younger people are more apt to become unruly.

This section encompasses many of the methods for applying this device via a permanent installation where transducers can be placed and adjusted to produce the necessary sound-pressure levels at distances to achieve the desired effects. This method could prove effective as an intrusion deterrent for a certain protected area.

Another method could be a handheld directional device similar to a megaphone where the amount of transducers used would be determined by the affects desired. This device would take into consideration the highly directional characteristics of this energy, being able to be directed at problem areas as a handheld portable system.

Another method for effective control would be clusters or arrays of transducers with these systems being mounted to vehicles via conventional roof mounts or on the hoods of these vehicles. Operation could take further advantage of the fair to good soundproofing found in most automobiles and vehicles could approach problem areas, taking advantage of close-proximity situations.

It has been found that certain frequencies also can be made to produce intense irritability in certain types of people. This method could justify the eventual use of more severe methods of restraint, assuming that the target subjects would eventually become more aggressive or violent, thus warranting this action. This is only to be considered as a potential extreme use of the device.

The objective here is to describe a similar method whereby the sound-pressure levels and frequencies can be obtained economically and efficiently, using state of the art methods and easily available parts, yet they can still be portable and easily handled for complete operational flexibility. Construction is based around the use of the piezoelectric tweeter transducers. These lightweight devices are easily driven and produce a conversion efficiency of over six times their electromagnetic counterpart. Being lightweight, economical, and easy to use when driving, they are an excellent candidate for this type of system. Higher driving impedance versus frequency is the inverse of the electromagnetic type.

The system, as described, contains several modes of operation. The first mode is a steady state of a certain frequency determined by the operator. This mode is termed *manual frequency control* and is adjusted by its appropriate control. The next mode is *low speed sweep*, which consists of the unit starting at a low frequency and automatically increasing to its higher limit where it again repeats itself. The remaining modes are controlled rates of this sweep, determined by the appropriate control referred to as *sweep rate control*. It is these controls that can be remotely operated from the inside of a vehicle when high-powered, outside arrays in clusters are used. As was mentioned before, certain frequencies combined with certain sweep rates can cause different degrees of effectiveness. It is not the objective of this information to analyze the potential types of effect and behavior versus control setting, but to describe the working system as a generator of these controlled sounds.

Table 35-1 Pain-Field Generator Parts List

Ref. #	Description	DB Part #
R1, 6, 8, 12	Four 1K, ¼-watt resistors (br-blk-red)	
R2/S2	500K, 1 meg pot/switch, 17 mm	
R3	2.2K, ¼-watt resistor (red-red-red)	
R4, 5	Two 10K, ¼-watt resistors (br-blk or)	
R7	10-ohm, ¼-watt resistor (br-blk-blk)	
R9/S3	10K pot/switch, 17 mm	
R10	5K horizontal trimpot	
R13–16	Four 4.7-ohm, 3-watt resistors (yel-pur-sil-gold)	
R17, 18, 19	Nine 120-ohm, 5-watt resistors (br-red-br); use two per transducer and one across S1	
C1, 4	Two .01-microfarad, 50-volt disk capacitors (103)	
C3	100-microfarad, 25-volt vertical electrolytic capacitor	
C2	10-microfarad, 25-volt vertical electrolytic capacitor	
C5A, B	Two .01-microfarad, 50-volt polyester capacitor	
C6	1,000-microfarad, 25-volt vertical electrolytic capacitor	
C8	.01-microfarad, 2-kilovolt disk capacitor	
C9	.22-microfarad, 250-volt polypropylene capacitor	
L2, 3	Eight 1 mh inductors (6080), 2 used per transducer, in place of R15 and R16 as marked on PC board	DB# 1MH
L1	Inductor: two Hitachi 30.48 E cores and mating bobbin assembled and wound L1 inductor	DB# PPPL1L1
Q1	PN2907 PNP GP transistor	
Q2	IRF530 or 540 N-channel metal-oxide-semiconductor field effect transistor (MOSFET)	
IC1, 2	Two 555 dual inline package (DIP) timers	
HS1	Heatsink bracket, created as shown	
SW1	6-32 × ¼-inch screw	
SW2	Eight 6-32 × ½-inch screw	
SW3	Eight #8 × ¼-inch sheet metal screw	
NU2	Nine 6-32 hex nuts	
FH1/FS1	Fuse holder and 2-amp fuse	
J1	Three-pin din chassis mount jack	
J2	DC 2.5 mm jack panel mounting	
CL1, 2	Two battery 9-volt clips	
BH1, 2	Two four-C-Cell holders	
S1	Single pole, single throw (SPDT) power switch	
S4	Small SPST toggle switch	
PC1	Printed circuit board (PCB) or use perforated vector board	DB# PCSONIC
TD1	Four polarized 130 db piezo transducer	DB# MOTRAN
WR1/2	36 inches of #20 vinyl hookup wire, red and black	
CHASSISBASE	Create as shown in Figure 35-6	
PANEL	Create as shown in Figure 35-6	
TAPE	8 inches of two-sided 1-inch foam tape for securing battery holders to base	
SPACER	3 × 3-inch piece of plastic sheet to insulate assembly board from metal BASE	
LABULTRA	Label, ultrasonic warning	

Chapter Thirty-Six

Magnetic Distortion Detector

The following project, as shown in Figure 36-1, describes an excellent, low-cost device that has amazing sensitivity in its ability to detect magnetic disturbances down into the microgauss. A microgauss is one millionth of a gauss. The earth's magnetic field is 500 milligauss where a milligauss is one thousandth of a gauss. The unit easily detects sunspot activity and auroras, and it can even be used as a vibration sensor that can detect a person's finger tapping on a rock. It can also detect moving aircraft and vehicles, as well as other changing electric and magnetic phenomena.

Actual detection is accomplished via an analog meter that responds to the relative strength of the changing magnetic fields. An audible alarm also allows the presetting of an activation level where it will alert the user of certain activity. An output port is included for connecting to a chart recorder.

The magnetic fields produced by many devices, both manmade and natural, are detectable by this system. Interesting results are produced when this unit is placed near anything electrical or magnetic such as a car, motor, or TV. The sensitivity is impressive when one sees the results of a 1-amp pulse of electrical current through a wire located a meter away from the unit. (This corresponds to a milligauss. Earth's magnetic field is .5 gauss). When the system is properly installed, it will detect passing automobiles, aircraft, or any moving, ferrous source that will cause the terrestrial magnetic field to distort. The unit is an excellent science fair project and can supply the amateur scientist with hours of knowledgeable entertainment in listening and detecting magnetic fields and their abnormalities.

Figure 36-1 *The magnetic distortion detector*

Construction is shown to be as flexible as possible. It is built in two sections: the sensing head and the control box, which are interconnected via a length of shielded cable. The maximum usable sensitivity requires the sensing head to be placed away from power lines and other potential disturbances. The sensing head, which must be securely mounted to prevent interference from mechanical movement due to wind and vibration, can cause erroneous signals as it shifts position through the earth's magnetic field. The unit can also be made as a sensitive magnetic probe by installing the sensing head and the control box together, bearing in mind that the usable sensitivity will be decreased due to erroneous movement near magnetic materials when moving its position. The detection of field changes produces a moderately loud alarm along with a relative indication from an analog meter located on the panel. An optional jack

is used for an X/Y chart recorder, and the system is fully battery powered.

This is an intermediate to advanced-level project requiring basic electronic skills. Expect to spend $45 to $65. All parts are readily available, with specialized parts obtainable through Information Unlimited at www.amazing1.com, and they are listed in the parts list at the end of the chapter.

Circuit Description

Figure 36-2 shows a coil (L1) consisting of many thousands of turns is wound on a 2-inch bobbin and placed over a soft iron core of about 1 to 2 feet in length. Any magnetic changes induce small voltages to occur at the output of this coil. This output signal is fed into a nano-amp, sensitive DC amplifier (I1), providing a current gain of 500 times the original. The iron core of L1 serves to concentrate the magnetic flux lines by offering a lower reluctance path than that of air. The input of I1 is protected by overvoltage and transients via clipping diodes Dl and D2. The output of I1 is forced to near zero via a multiturn trimpot (R4) for balancing and compensating any offset.

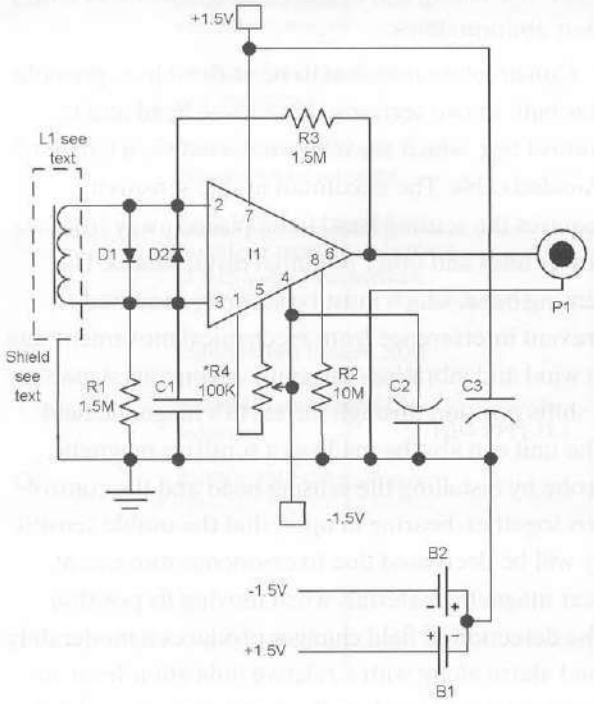

Figure 36-2 *Sense head schematic*

Power for I1 consists of batteries Bl and B2, which are left in the circuit permanently as current drain is very low and replacement can be on a yearly basis. It should be noted that if the sensing head is to be located in a hard-to-get area the builder might use D-size cells, as these will last that much longer.

The sense head output is fed to the control box via any reasonable length of shielded cable, WR10. As mentioned before, the sensing head should be located away from any potential magnetic interfering devices, such as anything electrical and large, ferrous objects.

Aluminum foil can be wrapped around the sense coil and is connected to the circuit common line. This reduces the capacitive pickup of unwanted signals.

Again, the sensing head and control box may be assembled together and used as a probe. This configuration may reduce the system's sensitivity due to erroneous movements and interaction of the circuits such as magnetic speakers and meters. This method is not encouraged due to these erroneous readings.

Figure 36-3 shows the control box providing another amplifier, I2, with a gain of 200 times the original amount, which gives the system an overall gain of 100,000. Full-scale meter deflection of the 50 ua meter (M1) occurs when a current of .5 nano-amp is obtained from L1. It is obvious that with the many thousands of turns on L1 that a detectable signal can occur with very minute flux changes, such as the result of changes in the microgausses. It should be noted that the earth's magnetic field is only .5 gauss.

I1 is connected as a conventional DC operational amplifier with its output DC coupled to I2 via a shielded cable. This cable is necessary to separate the sense head and the control box by at least 6 feet. This is necessary to prevent magnetic coupling from the speaker SPK1. Sensitivity control pot R5 controls the system gain and is usually set at maximum.

You will note that meter deflection pot R11 also is ganged with switch S1, which controls the +6-volt power to the control box section. R11 controls the deflection of meter M1 with diode D3 and capacitor C6, serving to smooth out and average the signal. The voltage level at jack J2 is also controlled by R11 and is an auxiliary jack intended for a chart or other recorder. The audible alarm activation point is controlled by pot R12 that is ganged with switch S2.

Switch S2 controls the −6 volt power to the control box.

The alarm is nothing more than a reflex-type oscillator consisting of transistors Q2 and Q3 with its feedback paths consisting of resistor R15 and capacitor C8. Trimpot resistor R16 is set for a reliable, clean-sounding signal.

Assembly Steps

1. Figure 36-4 shows coil L1 wound with thousands of turns of fine magnet wire. This may be difficult to do and it is suggested that the builder locate a high-voltage oil burner ignition, neon sign, bug killer, or other similar transformer and carefully remove the high-voltage secondary winding. The parameters of these transformers are usually around 5,000 volts at 10 to 20 milliamps. These are available from junkyards and other places. Many are rejected due to radio and TV interference and yet have intact secondary winding suitable for this project.

   The objective is to obtain one with as many turns as possible; however, most will work quite well. A quick test is to measure the DC resistance of between 5 and 20K across the coil. A relay coil of high impedance such as 5 to 10K may also work. The coil must have connecting leads and these should be secured with *room temperature vulcanizing* (RTV) adhesive, wax, or something similar to prevent breaking that may render the coil useless. A soft iron core of 1 to 2 feet is inserted through the coil and serves to offer a lower reluctance to the magnetic flux lines. It is these lines that, as they change in the core, induce a voltage due to magnetic induction. Note to shield the coil from electrical and capacitive pickup by wrapping it in aluminum foil and connecting the foil to the circuit ground. A special custom-made coil is available from Information Unlimited and is noted in the parts list.

2. Lay out and identify all the parts and pieces, and check them with the parts list. Note that some parts may sometimes vary in value. This is acceptable as all components are 10 to 20 percent tolerant unless otherwise noted.

3. Assemble the board by inserting components into the board holes as shown in Figure 36-5.

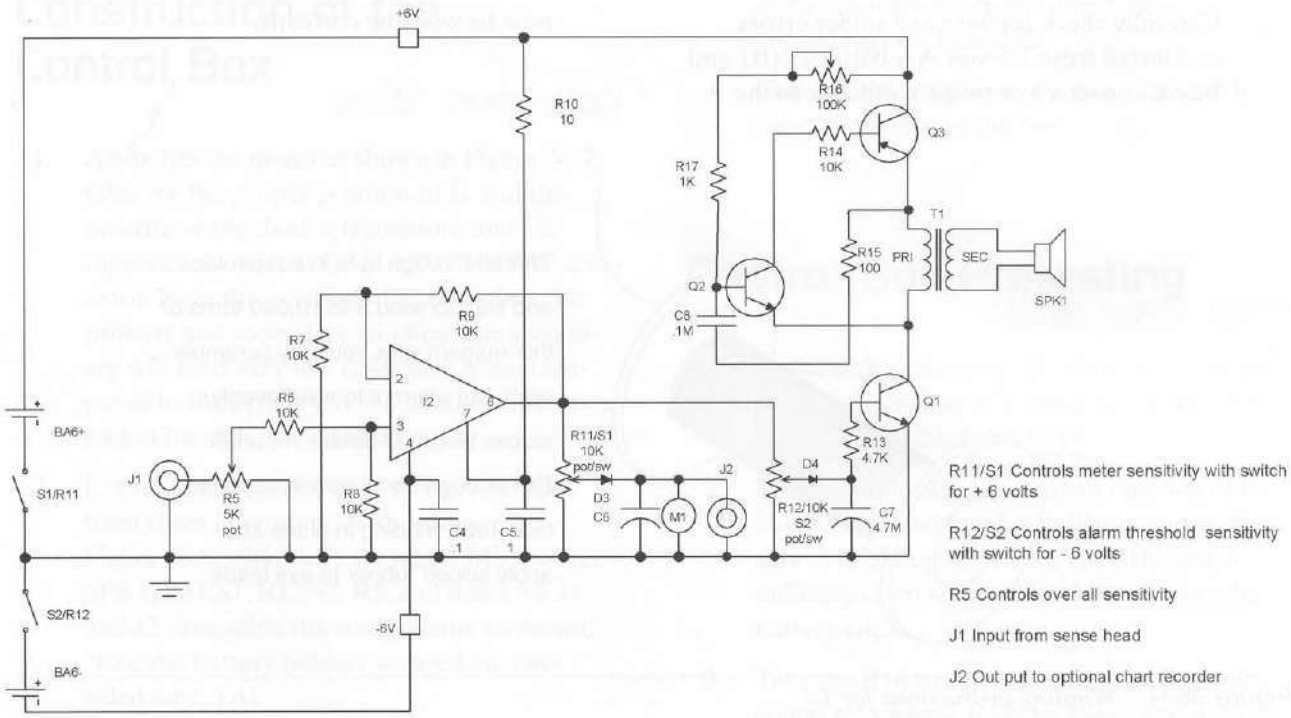

Figure 36-3 *Control box schematic*

Proceed from left to right, attempting to obtain the layout. Note the polarity of the components as indicated. Certain leads of the actual components are to be used for connecting points and circuit runs. Do not cut or trim them at this time. It is best to temporarily fold the leads over to secure the individual parts from falling out of the board holes for now. Solder as required and clip off excess leads. Some kits contain a length of insulated wire. This must be cut, stripped, and tinned according to where it is used.

4. Wire in the 6-foot length of shielded cable, being careful not to burn through the insulation and short out the cable.
5. Attach the battery clip HOLD1 using silicon rubber.
6. Attach the L1 coil to the PB1 perforated board as shown in Figure 36-5 and secure it with RTV adhesive. You will have to drill a hole for the iron core. The core should fit snuggly and can be glued in place in the final assembly.

Pretesting the Sense Head

1. Carefully check for wire and solder errors, and install fresh 1.5-volt AA batteries (B1 and B2). Connect a low-range voltmeter to the leads of the output cable and adjust the 25-turn pot (R4) for as close to a near-zero reading as possible. Finally, adjust the lowest range of the meter, preferably the 50 microamp range. This should be done outside away from power lines.
2. With the meter still connected, observe a reading when a piece of iron is moved near sensing coil L1 and moved about. If the piece of iron contains any magnetism, the effect will be enhanced.
3. Wrap the sense coil with several layers of aluminum foil and ground the foil to the negative circuit. Diodes D1 and D2 will require shading against light sources as the junction behaves like photodiodes at these low signal levels.
4. Create enclosure EN1, as shown in Figure 36-6, from an 8 × 3½-inch outer-diameter piece of plastic tubing.

   Note the small, ⅜-inch access holes for adjusting R4 are drilled when all is in place. Create the brackets as required for mounting the sense head.
5. Install the assembly into EN1 with caps CP1 and CP2 as shown. Recheck it by connecting the meter across P1. Readjust R4 through the access hole if needed. The sense head should now be working correctly.

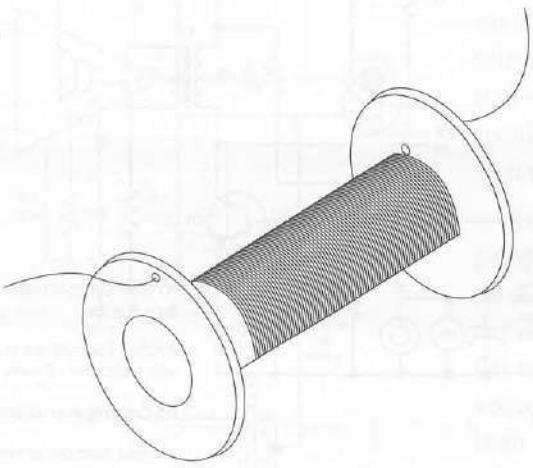

Figure 36-4 *Winding instructions for L1*

Strip off outer plastic jacket of cable 1 inch and twist braid into a lead and tin. Strip off 1/4 inch of insulation on inner lead and tin. Insert into plug and solder inner lead to lin tip.

Carefully solder twisted braid lead to outer shell being careful not to burn through insulation. Always verify lead continuity and possible shorting of the leads with a meter.

Dashed lines are connections on underside of perforated circuit board using the component leads. These points can also be used to determine foil runs for those who wish to fabricate a printed circuit board.

• Small dots are holes used for component insertion.

◉ Circles with dots are holes that may require drilling for component mounting and points for external connecting wires, indicating strain relief points. It is suggested to drill clearance holes for the leads and solder to points beneath board.

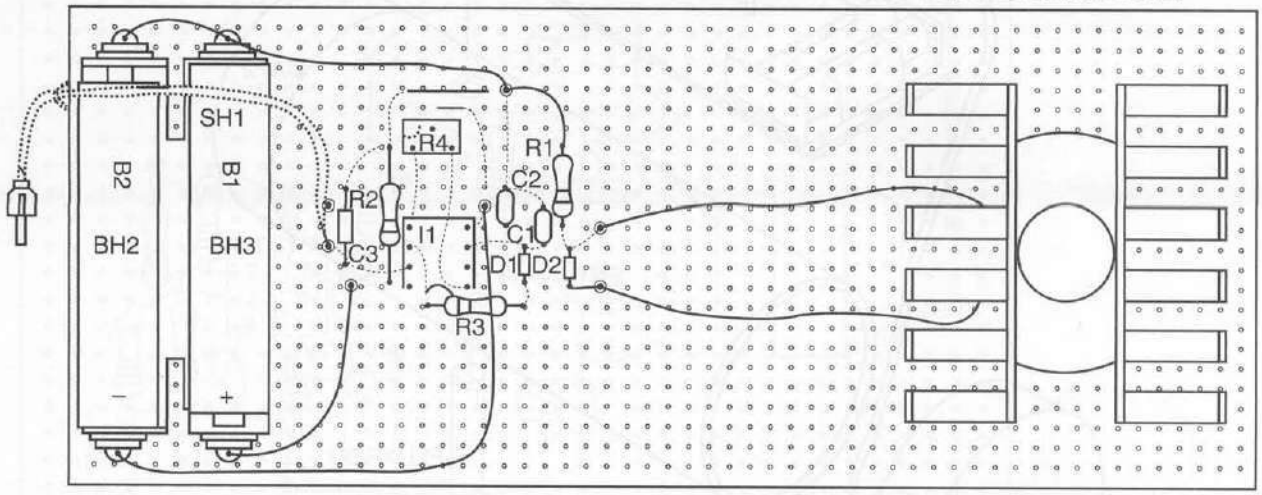

Note: The sense head as shown in this sketch is wound from a transformer bobbin. Any plastic bobbin 2"x1" will usually suffice. See Figure 36-4.

Figure 36-5 *Assembly of the sense board section*

Construction of the Control Box

1. Assemble the board as shown in Figure 36-7. Observe the proper position of I1 and the polarity of the diodes, transistors, and C6 capacitor. Note that Q3 is a PNP PN2907 transistor. Note the position of T1 regarding the primary and secondary winding. The secondary will read very low resistance when compared to the primary. It is a good idea to use a socket for the integrated circuit.
2. Create the enclosure base section (BASE) from sheet aluminum, as shown in Figure 36-8, with holes for meter M1, speaker SPK1, R11/S1, R12/S2, R5, and holes for J1 and J2. Assemble the components as shown. Note the battery holders secured via two-sided tape, TA1.
3. Attach the interconnecting leads, as shown in Figure 36-9. Twist the leads whenever possible and keep them short and direct. Note the ground lugs on J1 and J2.
4. Connect the leads from the board assembly to the components in the box.

Control Box Pretesting

1. Position the board, but do not secure it at this point. Turn S1 and S2 off and insert four AA batteries into BH2 and BH3.
2. Turn on both switches, unsnap one side of the battery clip, and insert a milliamp meter. Measure .5 milliamps (−6 volts) at BH2 and .8 milliamps (+6 volts) at BH3. Reconnect the battery clips.
3. Turn the R16 trimpot to midrange, R11 full counterclockwise, R12 clockwise, and note the meter remaining at zero and the alarm

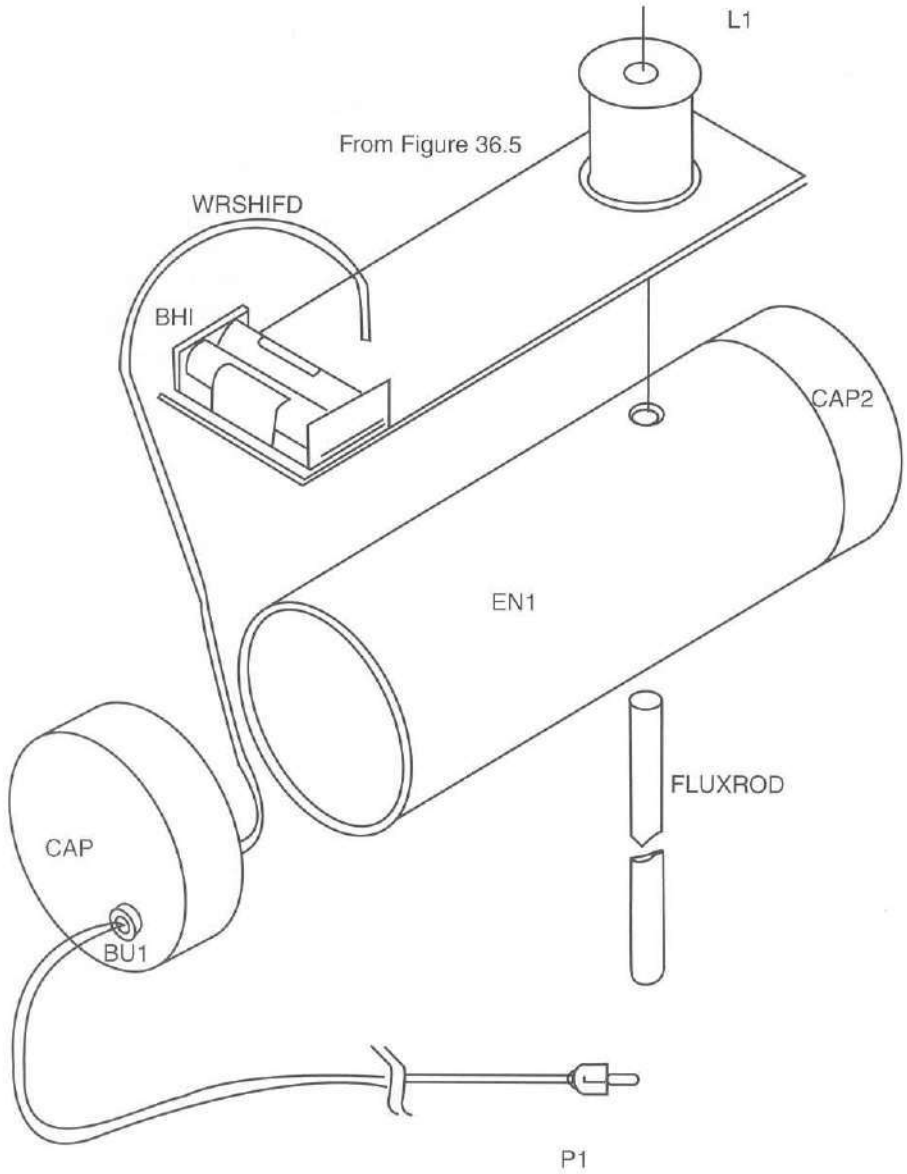

Figure 36-6 *Sense head enclosure assembly*

remaining silent. Now turn R11 clockwise and note the meter deflecting to full scale.

The following steps will require the sense head located away from electrical wiring and other potential sources of magnetic interference. The distance should be at least 5 feet from the control box to avoid feedback from the meter and speaker magnets.

4. Turn both R11 and R12 full clockwise. Plug in P1 from the sense head J2. Note the meter may pin, or jump off scale, and the alarm may sound. Have a friend slowly rotate R4 on the sense head to attempt to bring the meter into range. You may have to desensitize the circuit by turning R11 counterclockwise until the meter reads midrange and turn R12 to deactivate the alarm as it can be annoying during testing. Note that R5 is an overall sensitivity control and should be turned fully on in most applications for maximum sensitivity. The meter and alarm can be ranged by their respective controls, R11 and R12.

When properly set, the reading will constantly fluctuate and is the result of sunspots or other phenomena distorting the earth's magnetic field.

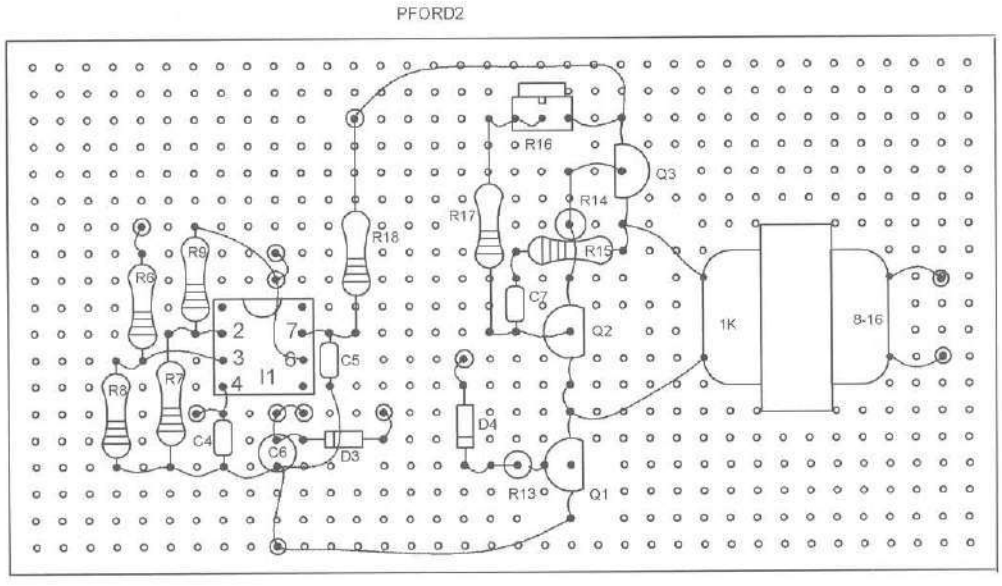

Figure 36-7 *Assembly control board*

If you choose a magnetically noisy location, you will have an added signal as the result of power lines, motors, and other magnetic disturbance. Note that if R11 cannot bring the meter into range without overly desensitizing it, it may be necessary to internally readjust R4 for proper ranging.

5. Preset R14 at midrange and adjust R12 until the alarm sounds. Readjust R16 for a clean, desirable-sounding tone if necessary.

Appreciating the sensitivity of this unit requires operation in a magnetically quiet location where all the controls can be advanced fully. Under the conditions of a low magnetic background, the unit can detect automobiles, manmade devices, and natural magnetic disturbances. Also, simply moving a piece of iron near the sensing head should produce an indication. (Note low-level-detection sensitivity may be difficult during the peak of the sunspot cycle due to the high background signal fluctuations.)

Jack J2 may be used to drive an XY recorder when observing sunspots or other time-related disturbances.

Note: No steps were taken to filter out 60 HZ disturbances, as it appears that many uses of this device involve the detection of power lines and other related equipment.

Applications

The uses of this device are obviously only appreciated by those who can understand its sensitivity to a minute change in magnetic flux. The unit can be made to detect the motion of large steel bodies as they distort the existing earth's magnetic field. Many applications and experiments are therefore possible with the device. Any high-impedance headphones

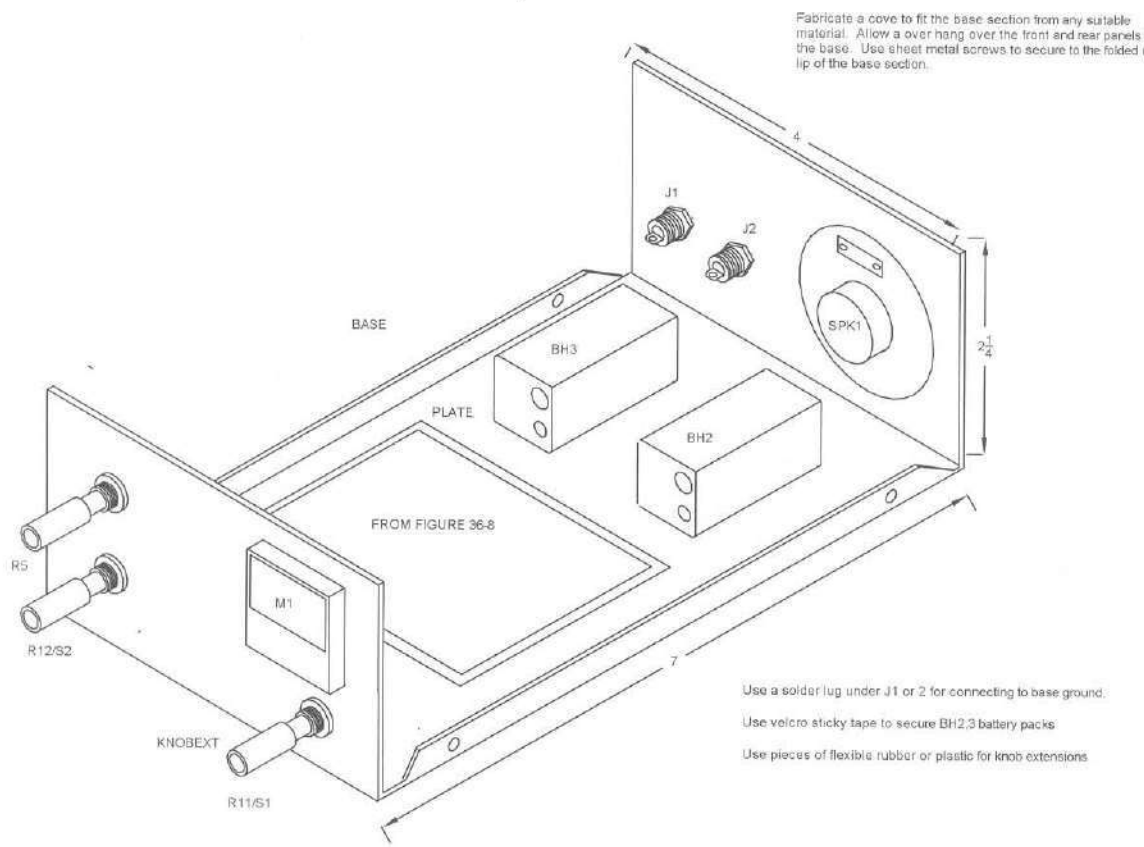

Figure 36-8 *Control box base section fabrication and layout*

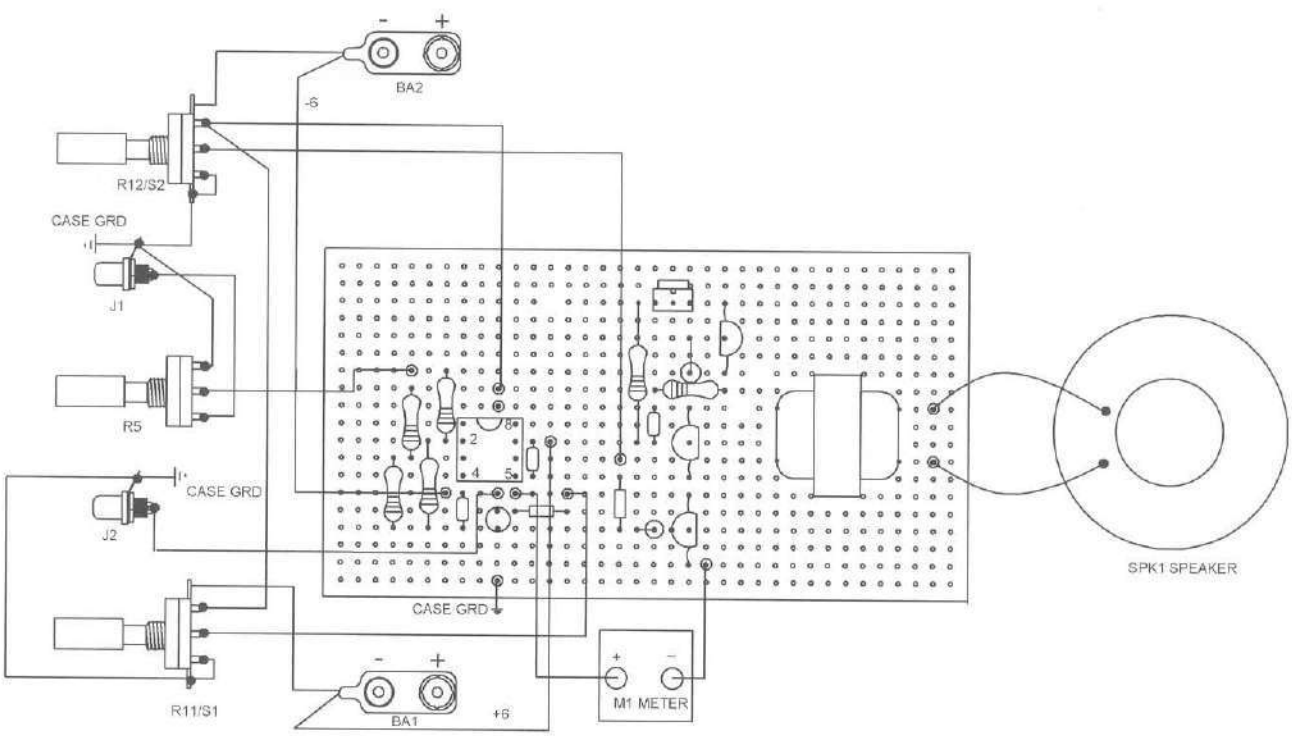

Figure 36-9 *Final assembly control box*

can be plugged into J2 where the experimenter can actually "listen in" and hear the field changing.

One verifying test that is easily done to determine the system's ability to detect the earth's magnetic field is the following. Rotate the sensing head with short, quick jerks in a clockwise direction. Note the meter pinning, and as rotation is continued a point will be found where the meter will respond less. This nulling point should occur with the fluxrod pointed in a north/south direction. If rotation is continued, it will be found that the short, quick jerks must occur in a counterclockwise direction to obtain a positive meter movement. This is similar to an electrical generator using the earth as its field magnet and the sensing head core as the moving armature.

Optional Ultra-Sensitive Vibration and Tremor Detector

You may easily convert this device to a vibration detector by simply modifying the sense head so it can be mounted to a rigid object such as a rock. The trick now is to place a magnet adjacent to the end of the sense coil, L1. The magnet should be held in place by elastic or other means whereby it is mechanically isolated relative to the sense coil. It should be very close to the sense coil for optimum sensitivity.

The theory is simple. Positioning a powerful magnet near a coil with many turns produces a signal. It is now the relative motion between this magnet and the coil that produces a voltage by the familiar equation $E = Nd0/dt$, where E is volts, N is the coil turns, 0 theta is the flux of the magnet, and t is the rate of relative motion in seconds. The combination of the high-resultant signal volts and the amplification sensitivity of the circuit provides amazing results.

Many variations are possible with the common objective being to obtain the highest reading for a given tremor. This unit will easily detect earthquakes occurring anywhere on the planet; however, the builder must experiment with motion dampening and other schemes to differentiate between manmade vibrations in order to isolate these signals. This is an excellent, low-cost project for any interested individual to learn by experimentation.

Table 36-1 Magnetic Distortion Detector Parts List

Ref. #	Description	DB Part #
R1, 3	Two 1.5M, ¼-watt resistors (br-gr-gr)	
R2	Two 10M, ¼-watt resistors (br-blk-bl)	
R4	100-kilo-ohm, 10-turn vertical trimmer	
R5	5K linear pot	
R6, 7, 8, 9, 14	Five 10K, ¼-watt resistor (br-blk-or)	
R10	10-ohm, ¼-watt resistor (br-blk-blk)	
R11/S1, 12/S2	Two 10K linear pots and switches	
R13	4.7K, ¼-watt resistor (yel-pur-red)	
R15	100-ohm ¼-watt resistor (br-blk-br)	
R16	100-kilo-ohm vertical trimmer	
R17	1-kilo-ohm, ¼-watt resistor (br-blk-red)	
C1, 2, 3, 4, 5, 8	Six .1-microfarad, 50-volt plastic capacitors	
C6	1-microfarad, 50-volt vertical electrolytic capacitor	
C7	4.7-microfarad, 50-volt vertical electrolytic capacitor	
I1	LM4250 nano-amp operational amplifier in a dual inline package (DIP)	
I2	LM741 operational differential amplifier in DIP	
D1, 2, 3, 4	Four IN914 small-signal diodes	
Q1, 2	Two PN2222 NPN GP silicon transistors	
Q3	PN2907 PNP GP silicon transistor	
T1	1K to 8-ohm, small audio transformer	
M1	50 uamp panel meter	DB# METER50S
SPK1	2-inch, 8- to 16-ohm speaker	
J1, 2	Two RCA panel-mount phono jacks	
P1, 2	Two RCA mating phono plugs	
CL1, 2	Two 9-volt battery clips	
SH1	3 feet of single-conductor, shielded mike cable	
WIRE24	4 feet of #24 vinyl stranded hookup wire	
BH1	Two-AA-battery holder	
BH2, 3	Two 4-AA-battery holders	
BU1	Small, plastic feed-through bushing	
L1SENSE	Sense coil per Figure 36-4	DB# SENSE
PBORD1	6¼ × 2½-inch, .1 × .1-inch grid perforated vector board	
PBORD2	4½ × 2-inch, .1 × .1-inch grid perforated vector board	
EN1	7½ × 3-inch schedule 40 PVC tubing	
CAP1	Two 3½-inch black plastic caps	
TAP1	4 inches of 4 × 1-inch strips of Velcro sticky tape	
KNOBEXT	4 inches of 3/16-inch inner-diameter plastic or rubber tubing for shafts	
FLUXROD	6 inches of ¼ × 20-inch steel-threaded rod and two mating nuts	
BASE	Created as shown in Figure 36-8 from .063 aluminum	
COVER	Cut to fit BASE section	
PLATE	5 × 2½-inch piece of insulating plastic to mount under board	

Chapter Thirty-Seven

Body Heat Detector

This project, as shown in Figure 37-1, shows how to construct a useful device that can detect human or animal motion up to several hundred meters. It provides a narrow field of view and can be used for paths and walkways. Farmers use these devices to detect when a predator comes into range, taking the necessary action when the alarm sounds. It may also be used as a medium-sensitive thermal detector for lab and research use. The device is an excellent science project demonstrating medium-sensitivity detection of relatively low temperatures.

This is an intermediate-level project requiring basic electronic skills. Expect to spend $30 to $45. All the parts are readily available, with specialized parts obtainable through Information Unlimited at www.amazing1.com. These are listed in the parts list at the end of the chapter.

Figure 37-1 *Body heat detector*

Description

Your body heat detector is a device capable of sensing an object at a temperature increase slightly over ambient. It is this property that allows it to detect a living body at a considerable distance. The sensitivity of the device corresponds to a black body wavelength of 10 microns, corresponding to a temperature of 100° Fahrenheit. Black-body radiation defines color temperature in wavelengths below what is visible to the naked eye. All objects above absolute zero radiate energy as a function of their temperature to the fourth power. This radiation decreases in wavelength as the radiating body becomes hotter. This radiation will consist of the visible color spectrum for a given range of temperatures. Hotter bodies will show visible color such as blue being on the hotter side of red. A body hot enough to glow red is around 900 degrees F. Black bodies radiate in the infrared (invisible) and lower as the generating temperatures are near ambient being above 70 degrees F. All objects above absolute zero radiate energy as a function of the fourth power of temperature, and body heat energy is in the infrared region at around 100° degrees F.

The applications for this device are numerous and as an example you could a create motion detection system for home security. These are normally short-range, wide-angle detection systems and are limited in performance. Our system would be mounted similar to an optical scope on a rifle or a tripod. A living target now can easily be ferreted out in darkness or under moderate cover due to heat reflections. A predator, as it approaches its target victim, is easily detected, alerting the farmer or rancher to take the next step of action. Garden pests, as they emerge from their burrow, and downed game can easily be detected by the device.

The ability to detect hot spots is an extremely useful function. An example of sensitivity can easily be demonstrated by the following. Obtain a piece of cardboard or plastic approximately 6 × 12 inches. Place your hand on one end of this piece for several seconds to produce a hot spot of your hand print. Then place the piece in front of the unit, noting a detected signal increase on the surface previously touched by your hand due to the heat stored. (Don't touch the other end of the piece). Note that as time continues, the hot spot dissipates into the object thereby reducing the temperature differential and the signal pickup on the cardboard piece becomes evenly distributed. The differences in temperature detection capability is in the millidegrees. You can now realize the many useful applications of this unit.

Body Heat Detector Modes

Your body heat detector operates in two modes:

- **MODE A:** This mode is used to detect moving bodies such as animals, people, and so on. It is intended for sensing intrusions along pathways and into areas where a narrow field of view is necessary at long ranges (100 meters or so). This mode is the most stable of the two and rejects steady background sources of thermal energy. Detected bodies, however, must be moving.
- **MODE B:** Operation in this mode allows the detection of stationary hot spots and is most useful with a "cold background" such as at night. It is useful for ferreting out thermal sources such as hidden persons and animals. Hot object spots and areas are easily detected, but unfortunately this mode is so sensitive that often signals appear to be erroneous and mask the target object.

Both modes of operation require a camera tripod for reliable and simple operation. Very often a panning action can be used to reject or detect the desired targets.

Circuit Description

The heart of the detector is a pyroelectric detector (PYR1) capable of detecting very minute temperature changes. This device is responsive to temperatures of 100° Fahrenheit equivalent to approximately 10 microns. Unfortunately, its response speed is relatively slow, peaking at about .1 Hz. This is shown in Figure 37-2.

The pyroelectronic effect utilizes dual crystals of lithium tantalum oxide (LiTa 02). These crystals are polarized in an electric field below the Curie point. Electrodes attached to the crystal become electrically charged and eventually neutralize due to the surroundings. When the neutralized crystal is exposed to an infrared signal, its temperature changes, producing a charge on the electrodes and hence a detected signal. This signal is amplified by a built-in, low-noise *field effect transistor* (FET) and becomes the output. It is important to note that only a changing infrared signal can produce output; therefore, a chopper must be used for stationary sources. A chopper is nothing more than a mechanical wheel that has vanes to periodically interrupt the heat radiation signal to the pyrodetector, simulating a moving object. A moving source obviously produces a changing signal. The dual crystals will also cancel out signals produced from sunlight as they are oppositely polarized in the detector.

The output of the detector is connected to the input of a low-frequency, dual-stage amplifier and filter (U1) with a gain of approximately 2,500. This amplifier is designed to respond to a frequency of .1 to 10 Hz, peaking at about 1 Hz. This matches the response of the pyrodetector and the signal commonly generated by a living, moving body in the field of detection.

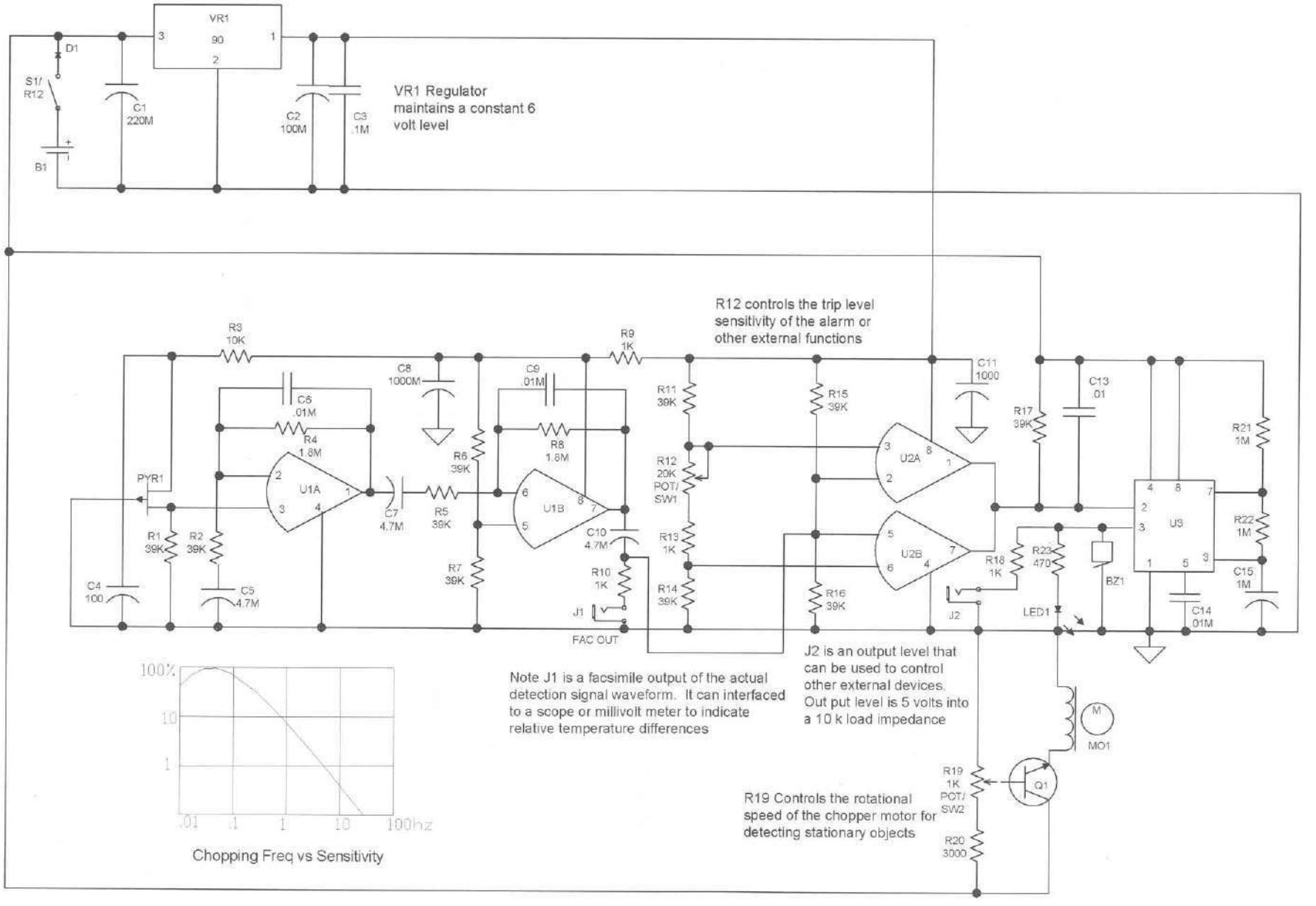

Figure 37-2 *Circuit schematic*

The changing AC output of the dual-signal amplifier (U1A and U1B) is capacitive coupled to output jack J1. It is this signal that is measured by an external AC millivolt meter and provides an analog indication of signal strength. This signal may be further processed for ultra-low-sensitive detection or maybe demodulated where the resulting DC level can control a VCO for audible detection via a changing tone. This AC signal is also fed to the dual plus and minus ("window") comparator (U2A and U2B). A threshold control (R12) presets the trip voltage or sensitivity of activation. The output of these two comparators is "anded" together and fed to the trigger input of the timer (U3). The output of U3 now activates audible buzzer BZ1 and visual indicator LED1. The buzzer on time is controlled by timing resistors R21 and R22 and capacitor C15.

An optional motor speed control for the chopper consists of Q1 and speed control pot R19. Jack J2 provides a 5-volt level through 1K resistor R18 and is used to trigger other systems.

Assembly Instructions

1. Lay out and identify all the parts and pieces, and verify them within the parts list at the end of the chapter.
2. Examine the PC board, as shown in Figure 37-3 and 37-4.
3. Proceed to assemble the device by inserting and soldering all the fixed resistors.
4. Insert and solder the capacitors, carefully noting the polarity on all the electrolytics: C1, C2, C4, C5, C7, C8, C10, C11, and C15. The other capacitors are not polarized.
5. Insert and solder in the semiconductors (D1 and VR1) and Q1. Note the polarity.
6. Identify and note the position marks on the integrated circuits U1, U2, and U3. Insert and carefully solder them, avoiding solder shorts between the pins. It is suggested to always use sockets for these components.
7. Identify the pots R12 and R9 and solder them in place. Note the switch section, S1, of R12. These connections are made using short pieces of cut leads to the pads directly beneath. Note these pots must be properly installed to allow final alignment with the PANEL plate.
8. Insert the wire jumps using short pieces of the cut leads of components that were used priorly.

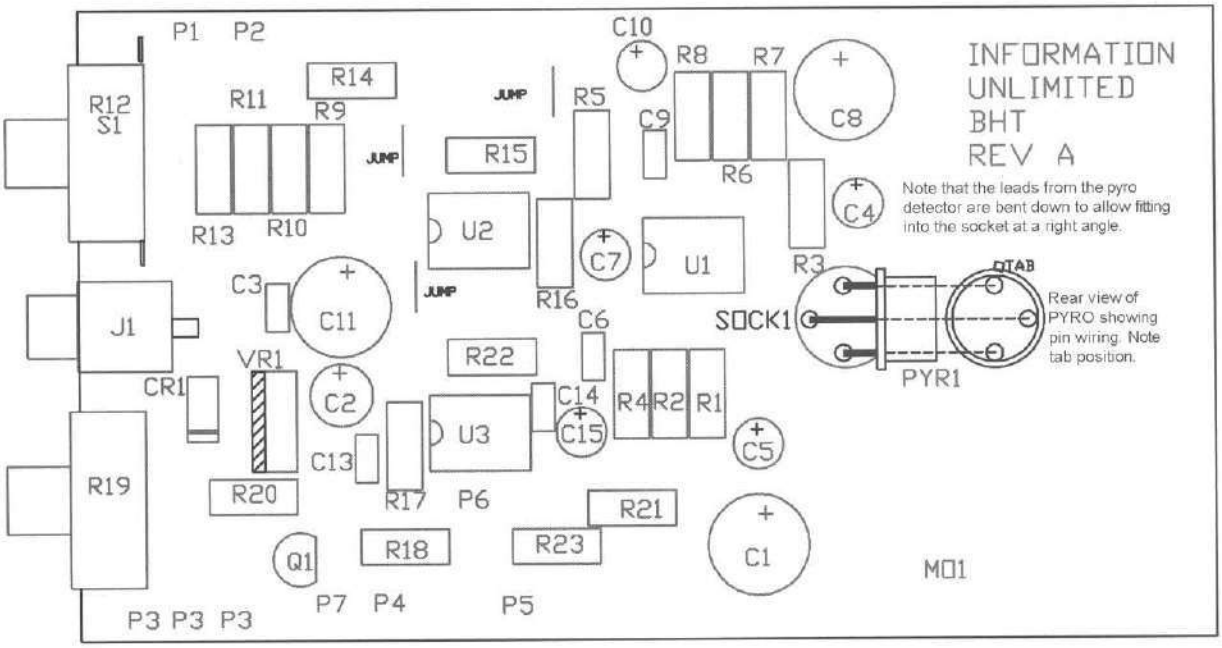

Figure 37-3 *PCB wiring and assembly*

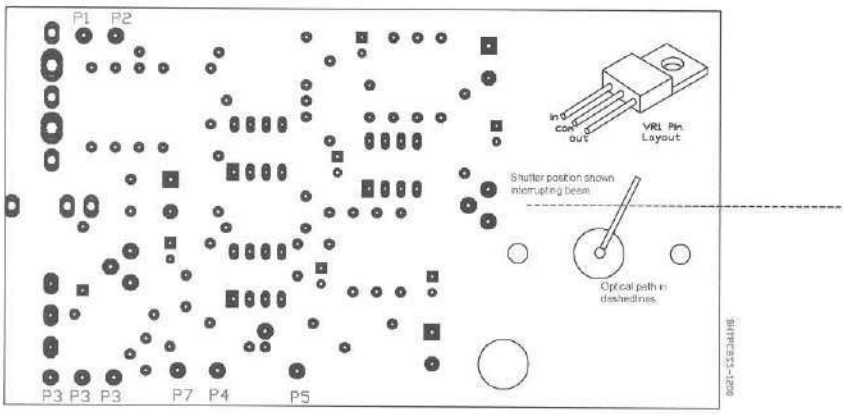

Figure 37-4 *Pad and connections*

9. Insert J1 and note the rear connection lead requiring a short piece of bare wire to connect to the board pad directly beneath.

10. Insert the SOCK1 pyrodetector socket as shown. Carefully form the three leads of the pyrodetector at 90°. Do not sharply bend it. Note the proper leads, and position the tab as shown. This part must be at the optical center of the system for proper operation.

11. Connect the BZ1 buzzer using its leads, as shown in Figure 37-5.

12. Connect output control jack J2 and indicator light-emitting diode (LED1) using a 3-inch length of #22 vinyl wire. Note the cathode lead of LED1 directly connecting to the ground lug of J2. Note these parts eventually will be mounted to the panel.

13. Connect the leads from the chopper motor MO1 and battery clip CL1 as shown.

14. Create the panel, as shown in Figure 37-6. Attach it to the PC board via the two pots and the jack. The panel and PC board should be flush to one another. Attach the remaining J2 and LED1 to the panel. Note to use a bushing for the LED.

15. Create the shutter flap (FLAP), as directed in Figure 37-6.

16. Recheck all wiring for shorts, accuracy, and correctness of parts. Also check for solder joints. You are now ready to bench test the assembly.

17. Connect a 9-volt supply to the battery clip.

18. Rotate R12 to on, and note the shutter flap rotating with R19 full counterclockwise. It should slow down as R12 is turned in a clockwise direction. This rotation should be variable in the range of 10 *revolutions per second* (rps), down to stalling at less than 1 rps. The motor will stall if there is any obstruction.

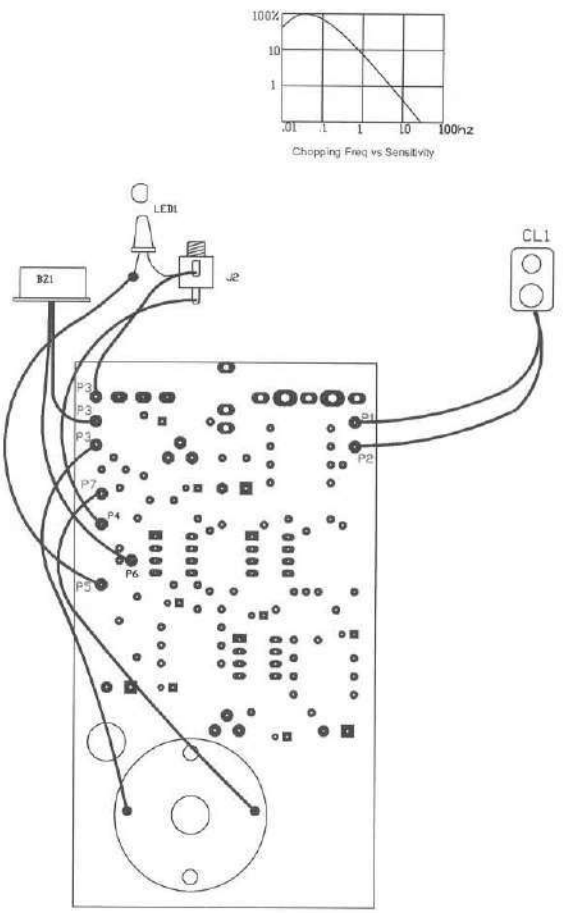

Figure 37-5 *Final wiring to external components*

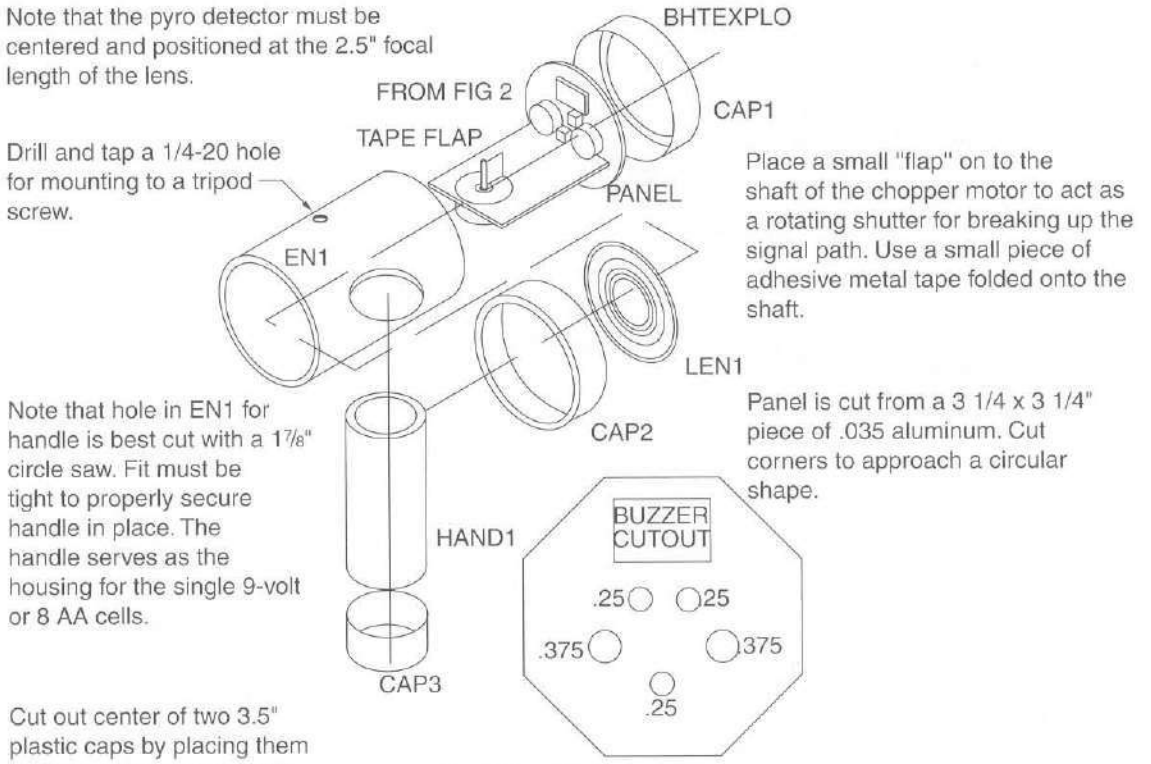

Figure 37-6 *Final housing setup*

Make sure the flap is clear and not touching the bearing bottom.

19. Connect a scope to J1 and note a changing level as your hand or another warm object is waved in view of the detector. Note the signal responding to a stationary source with the shutter flap or to some form of motion with the shutter flap stopped. Check the sensitivity control pot R12 and then verify a DC output level at J2, occurring when a body is detected. This function is for control of external alarms and alerts.

20. Check that the buzzer and light emitter activate when detecting a thermal source. Use your solder iron as a heat source and experiment with different sources.

21. Finally, assemble the device as shown in Figure 37-7 and proceed to use it as outlined in the instruction section.

Operating Instructions

1. Turn all controls fully counterclockwise to off.

2. Remove the battery compartment cover and slide out the eight-cell holder. Insert fresh batteries and reinstall.

3. Rotate the chopper control fully clockwise. View the shutter through the access hole and note how it is positioned in the figure.

4. Slowly turn the sensitivity control clockwise until the alarm sounds. If the unit does not respond, try moving your hand in front of it, noting its response. Turn the control back, just to the point where the unit does not respond.

5. Turn the chopper control until the unit starts to respond. You are now measuring the thermal background as indicated by the periodic sounding of the alarm as the shutter interrupts the heat path.

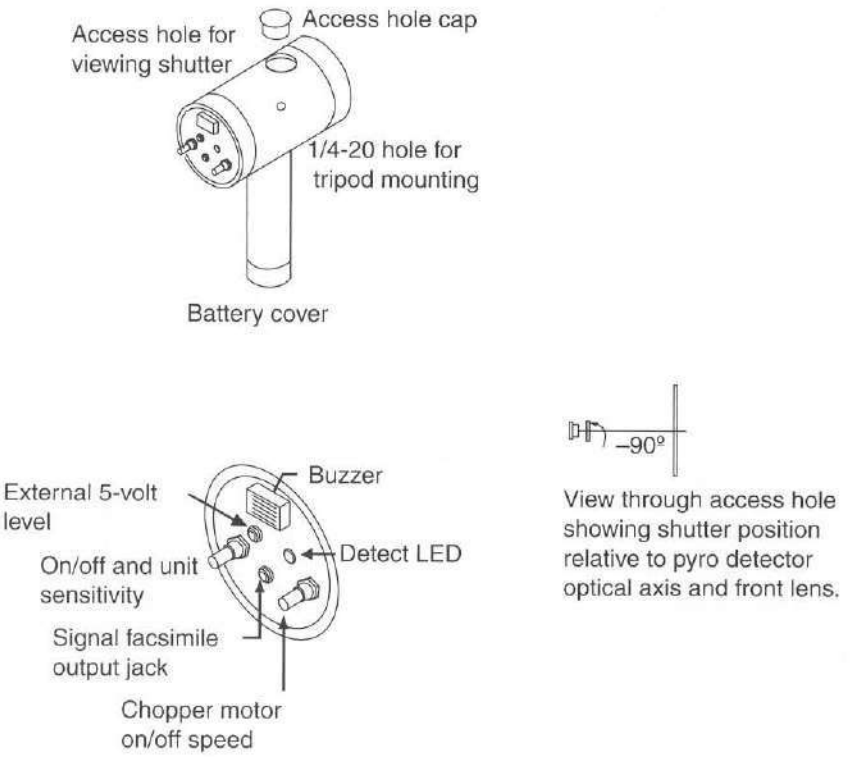

Figure 37-7 *Final assembly view*

6. Connect a standard 3.5-millimeter plug into the 5-volt level jack and measure a positive 5-volt level every time the alarm responds. This output is through a 1K resistor and is intended for triggering other alarms or external functions.

7. Connect a standard 3.5-millimeter plug into the signal facsimile jack and connect it to a scope input set on the AC millivolt scale. Note the changing voltage level indicating the slightest amount of differential thermal energy. Check this level with and without the chopper and try it with various thermal sources, noting the voltage levels. This output port is intended for the lab technician desiring to explore low-level thermal sources. It requires a scope or a sensitive AC millivolt meter capable of measuring 10 to 100 millivolts.

The previous steps are performed without considering the thermal stabilizing of the unit or its immediate surroundings. Maximum sensitivity will not be obtainable under these conditions.

8. Select a target area and mount the unit on a tripod, using the 1/4-20 mounting hole located on the side of the unit. This scheme will place the handle in the horizontal plane (off to the side) but should not pose a problem. The access hole will be opposite the handle.

9. Point the unit at the target area and allow it several hours to thermally stabilize. Do not touch the enclosure and try not to get too close to the front of the system, as this can destabilize the system for low-level detection.

10. Point and pan the unit at some known source to verify the anticipated range of operation. Experiment with the chopper speed or no shutter to obtain the optimum results for your application.

11. Handheld operation will vary considerably due to the many variables in the thermal background. We can only suggest that you get accustomed by trial and error to determine your application.

Final Notes

The access hole for the chopper shutter is necessary in order to prevent the blockage of the thermal path when the chopper motor is off. There is no guarantee

that the shutter will not randomly stop at the wrong place, blocking the detector and preventing normal operation. In such cases, the shutter must be manually moved with a pencil or some object.

The unit must be temperature stable to optimize maximum sensitivity. This usually takes about an hour if the unit has been recently handled or placed near radiant sources.

For actual body detection, the best performance will occur on a cold night. This does not mean that the unit will not work on a warm night, but that it might be less sensitive.

The detection of stationary objects may vary with chopper motor speed and background temperature. The maximum response of the pyrodetector is around .1 chops per second. This is very slow for many applications and we suggest increasing it to 1 to 3 per second.

The field of view may be narrow due to the Fresnel lens used, but you may change to other suitable lenses of polyethylene. Also, a panning action allows zeroing in on certain target subjects.

Table 37-1 Body Heat Detector Parts List

Ref.#	Description	DB Part #
R1, 2, 5, 6, 7, 11, 14, 16, 17	Ten 39K, ¼-watt resistors (or-wh-or)	
R3	10K, ¼-watt resistor (br-blk-or)	
R4, 8	Two 1.8-megohm ¼-watt resistors (br-gray-gr)	
R9, 10, 13, 18	Four 1K, ¼-watt resistors (br-blk-red)	
R20	4.7K, ¼-watt resistor (yel-pur-red)	
R21, 22	Two 1-megohm, ¼-watt resistor (br-blk-gr)	
R12/S1	20K pot and 12 VDC switch	
R19	500 to 1-kilohm pot	
R23	470-ohm, ¼-watt resistor (yel-pur-br)	
C1	220-microfarad, 25-volt vertical electrolytic capacitor	
C2, 4	Two 100-microfarad, 25-volt vertical electrolytic capacitors	
C3	.1-microfarad, 50-volt plastic capacitor	
C5, 7, 10	Three 4.7-microfarad, 25-volt vertical electrolytic capacitors	
C6, 9, 13, 14	Four .01-microfarad, 50-volt plastic capacitors (103)	
C8, 11	Two 1,000-microfarad, 25-volt vertical electrolytic capacitors	
C15	1-microfarad, 25-volt vertical electrolytic capacitor	
PC1	Printed circuit board (PCB)	DB# PCBHT
SOCK1	Three-pin TO5 socket	
Q1	PN2222 NPN transistor	
U1	LM358 dual-operational-amplifier integrated circuit	
U2	LM393 dual-comparator integrated circuit	
U3	LM555 timer integrated circuit	
VR1	7805 5-volt regulator TO220 package	
MO1	Low-voltage chopper motor	DB# CHOPMOT
PYR1	Pyroelectric detector	DB# PYR1
BZ1	Piezoelectric buzzer	
LED1	High-brightness light emitter	
J1, 2	Two 3.5-millimeter panel-mount jacks	
CL1	Battery clip and 9-inch leads	
PANEL	3.25 × 3.25-inch aluminum as shown	
EN1	6 × 3.5-inch OD schedule 40 PVC tubing as shown	
HANDLE	6 × 1.875-inch schedule 40 PVC tubing as shown	
CAP1, 2	Two 3 ½-inch plastic caps, as shown in Figure 37-6	
CAP3	2-inch plastic cap for retaining batteries in handle section	
LEN1	3-inch Fresnel polyethylene lens	DB# FRELEN3
BU1	Lens holder for LED1 or use a ⅜-inch bushing	
BHOLD1	8-AA-cell, 4 × 2 battery holder with snaps	
WR20B	24 inches #22 black vinyl hookup wire	

Chapter Thirty-Eight

Ion and Field Detector

This chapter focuses on a device capable of detecting and indicating the relative amount of free ions in the air (see Figure 38-1). It can determine the output of ion generators, high-voltage leakage points, static electrical conditions electric field gradients, and any other application where the presence of ions or a measurement of their relative flux density is required. It can also be used as a very sensitive lightning indicator, showing dangerous electric field levels.

Figure 38-1 *Ion and field detector*

The unit is handheld and enclosed in a plastic enclosure about the size of a king-size pack of cigarettes. A sensitivity control with an on/off switch, a high flux indicator lamp, and a meter are located on the front panel. A telescoping antenna exits a hole in the top of the unit and is used as a moving probe or a stationary pickup point for these charge fields. Grounding the unit is a strip of metallic foil on the outside of the enclosure that contacts the user's hand or may be directly connected to earth ground via a wire. Please note that the performance of this unit can be seriously affected by high humidity conditions.

Circuit Description

As shown in Figure 38-2, ions are accumulated on the collector probe ANT1 and cause a minute, negative base current to flow in transistor Q1 connected as a PNP Darlington pair with transistor Q2. Capacitor C1 and resistor R1 form a time constant to eliminate any rapid fluctuations. The response of the time constant can be changed for various applications and is discussed in Figure 38-2. Diodes D1 and D2 prevent excessive voltage from destroying Q1 by clamping any transients to ground. The collector of Q2 is DC

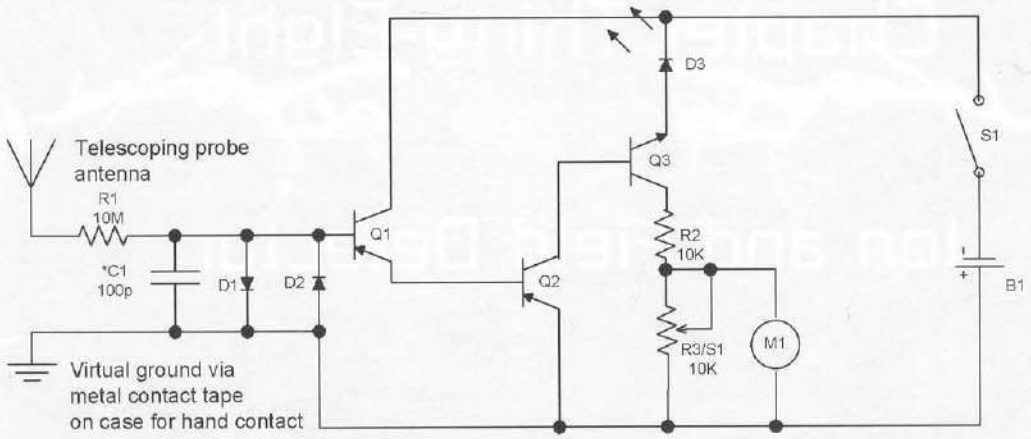

C1 is used to slow down the response and can be eliminated when detecting fast discharge fields such as lightning etc

Unit is shown wired for positive ion detection. You may change to negative by replacing the PN2222 transistors with PN2907 and the opposite. For a quick indication you may grab the antenna and use the body of the unit to detect the negative ions

Please note that the antenna probe on you unit is a telescoping antenna properly secured and electrically isolated. It is important to remember that any type of leakage around the input of QI can reduce the sensitivity. You may wish to coat the circuitry with a good quality varnish etc. Make sure unit is dry and clean before sealing.

Figure 38-2 *Circuit schematic*

coupled to the base of NPN transistor Q3 in series with current-limiting resistor R2 and meter sensitivity pot R3. Current flowing through Q3 now causes a voltage to develop across R3, driving the indicator meter M1. *Light-emitting diode* (LED) D3 is connected in series with the emitter of Q3 and serves as a visual indicator of strong charge fields. It should be noted that the meter serves only as a relative indicator of ion flux and is not totally that linear.

A threshold voltage, as a result of the base emitter, drops off Q1 and Q2 is only noticeable at almost non-detectable levels. It should be noted that in order for the unit to operate properly, some sort of ground is usually required. Metallic tape is used as shown and provides contact to the operator's hand, providing a partial ground. If the unit is placed remotely, it should be earth grounded to a water pipe, for example.

Measuring positive ions simply involves holding the antenna, using the body of the unit as the probe, or reversing the polarity of the transistors. A *double pole, double throw* (DPDT) switch may be optionally installed for polarity reversal, allowing reversal at the flick of a switch. Be aware that a ceramic or quality switch must be used to avoid leakage in high humidity conditions.

Construction Steps

1. Lay out and identify all the parts and pieces. Verify them with the parts list, and separate the resistors as they have a color code to determine their value. Colors are noted in the parts list at the end of the chapter.
2. Cut a piece of .1-inch grid perforated board to 2 × 1 inches. Locate and drill the holes as shown in Figure 38-3. If you are building from a perforated board, it is suggested that you insert the components starting in the lower left-hand corner as shown. Pay attention to the polarity of all the semiconductors. Route

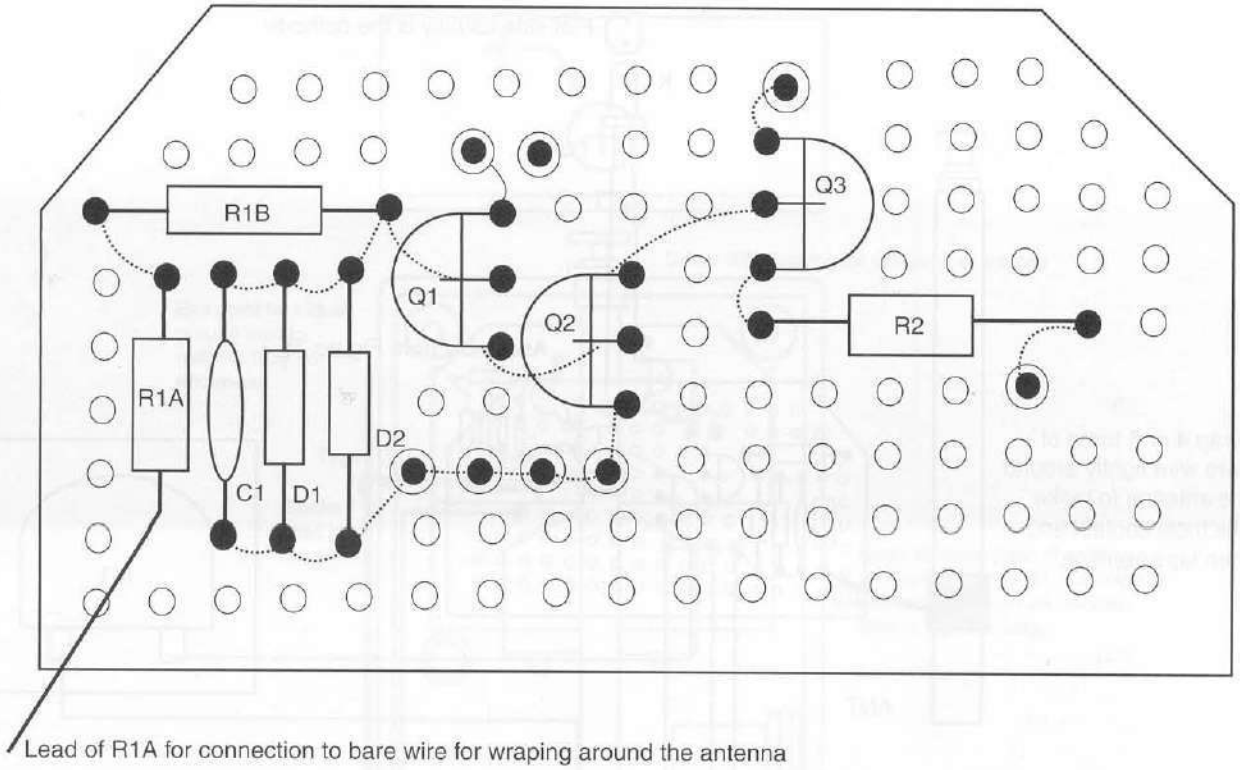

Figure 38-3 *Assembly board wiring*

the leads of the components as shown and solder as you go, cutting away unused wires. Attempt to use certain leads as the wire runs or use pieces of the #24 bus wire. Follow the dashed lines on the assembly drawing as these indicate the connection runs on the underside of the assembly board.

3. Attach the external leads and components as shown in Figure 38-4.

4. Double-check the accuracy of the wiring and the quality of the solder joints. Avoid wire bridges, shorts, and close proximity to other circuit components. If a wire bridge is necessary, sleeve some insulation onto the lead to avoid any potential shorts.

5. Create the plastic case, as shown in Figure 38-5. Note the 1-inch meter hole centered and located approximately 1½ inch from the top as shown. Holes for the switches are centered and located 1 inch below the meter line. Location is not critical, but make sure everything is clear and fits together.

6. Place a strip of foil tape as shown, noting a hole for the connection to the common circuit

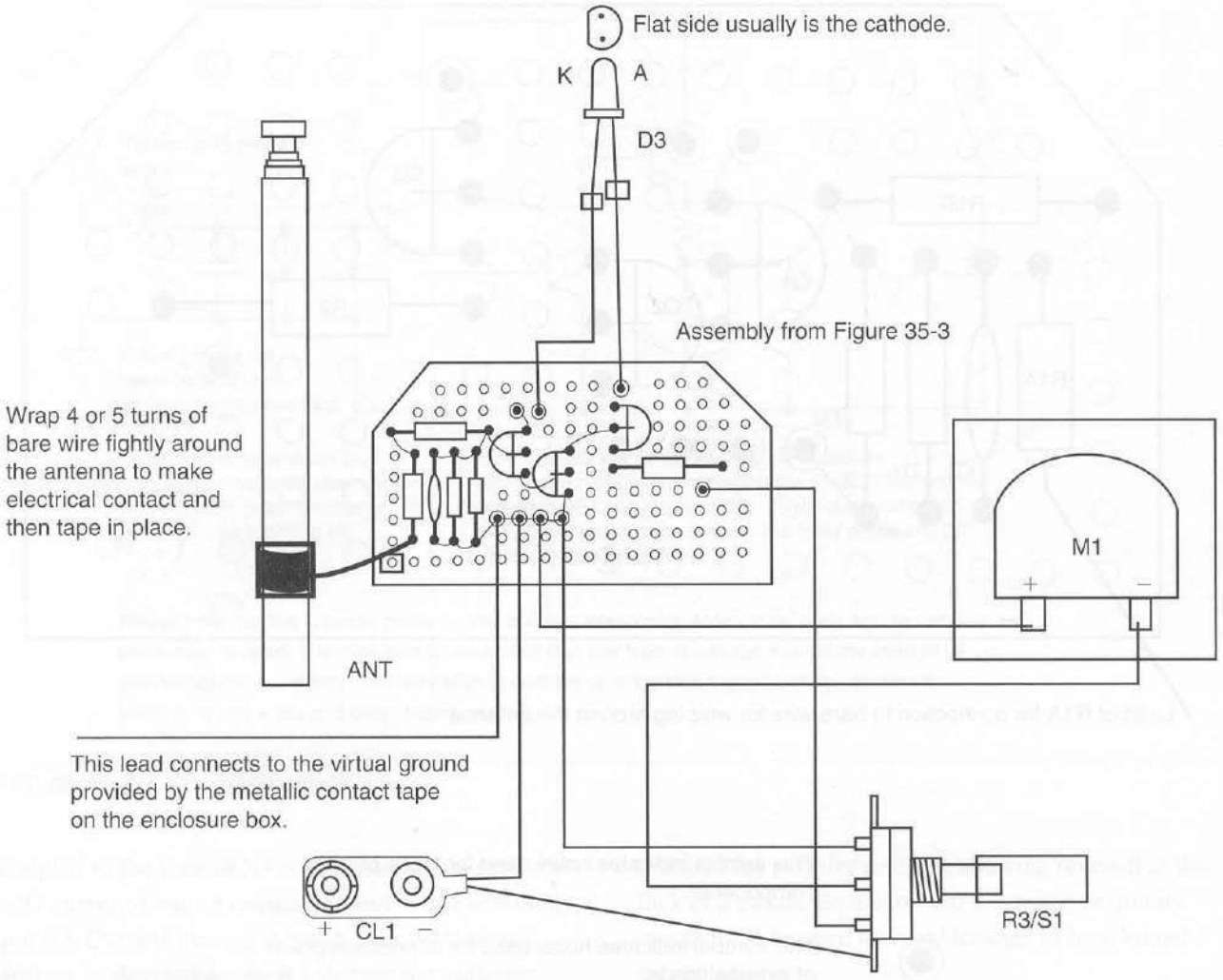

Figure 38-4 *Final wiring and assembly*

point. Secure the assembly board with double-sided tape after circuit operation has been verified.

7. Install battery B1 as shown and turn on the control. Rotate R3 fully clockwise and note the meter showing a slight indication. This is due to transistor and circuit leakage and should not be considered an indication of the ions. If meter sensitivity responds in the opposite way, you may have to reverse the wires across the outer terminals of R3 or the meter leads.
8. Extend the antenna about 6 inches and adjust R3 fully clockwise. Obtain a plastic comb and run it through your hair or rub a plastic object with a dry cloth. Place it near the probe and note the meter indicating a strong charge and the diode lighting. This effect may be reduced if the air is damp or moist.
9. Make the final assembly, as shown in Figure 38-6.

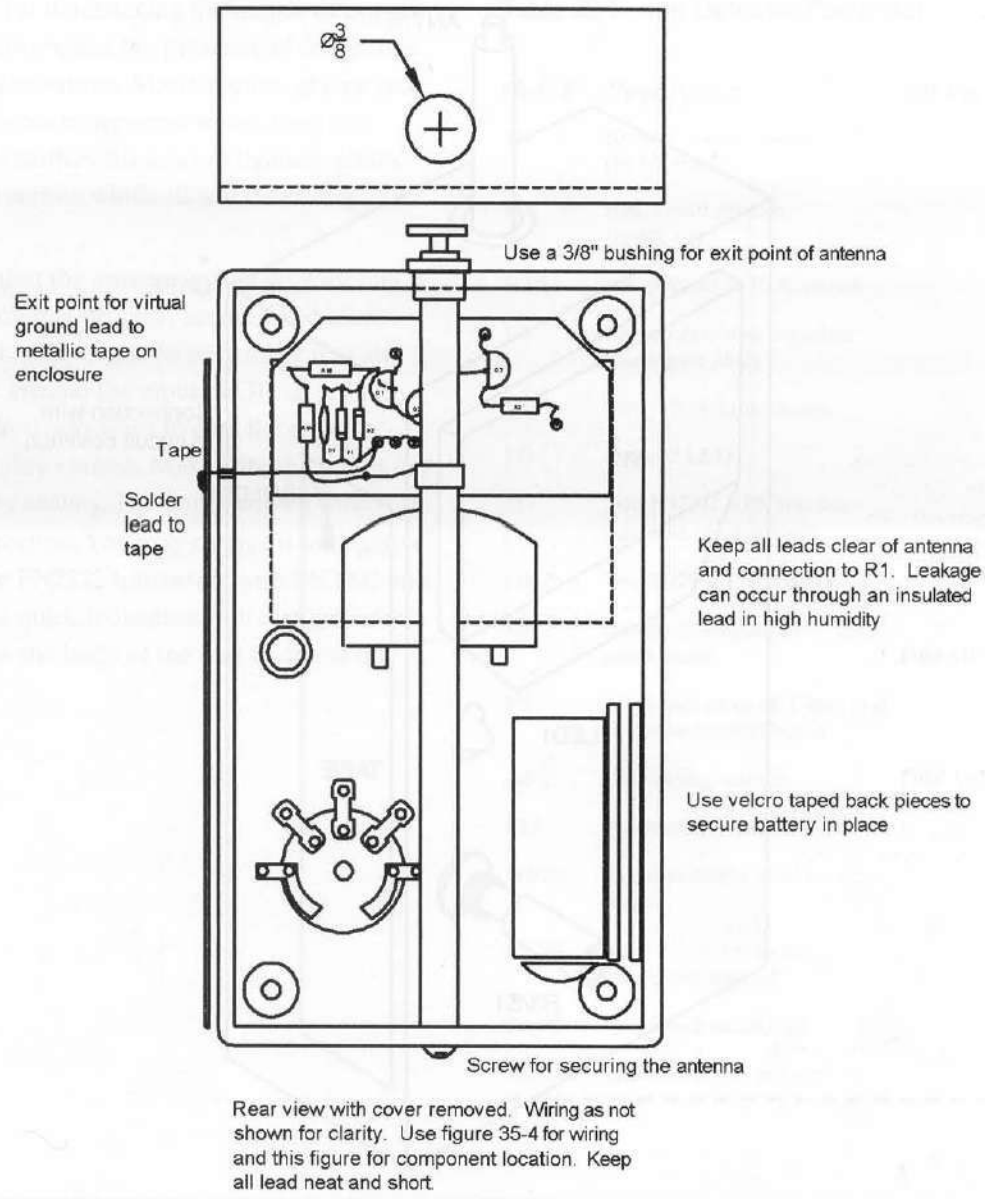

Figure 38-5 *Final assembly*

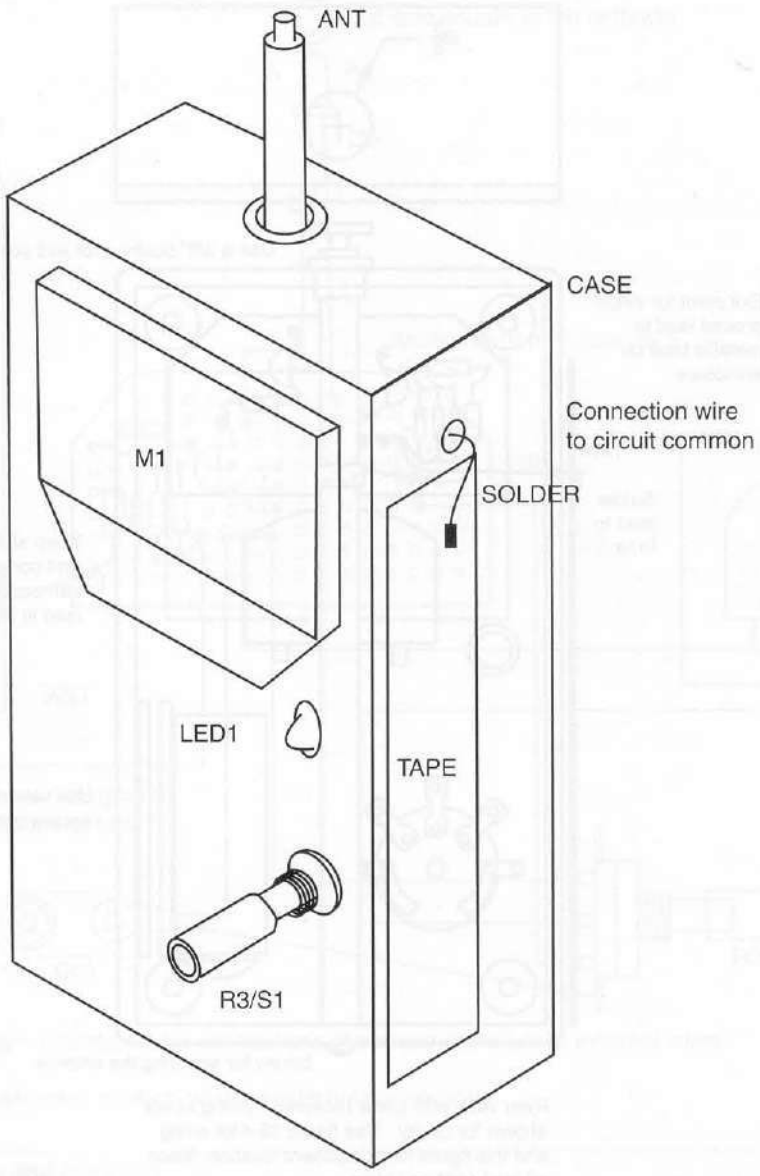

Figure 38-6 *Completed unit*

Applications

Your ion detector is a very, very sensitive ion-measuring device. It can be used for relative measurement but is not designed for absolute measurement.

For quick indications of the presence of a negative ion field, the unit may be handheld and actually used to determine where the source is. The sensitivity of this device can be realized by the simple experiment of running a plastic comb through one's hair and laying it near the probe, as described above.

Those who are familiar with the metallic leaf electroscope will soon realize the advantage of portability and sensitivity. When used for indicating or testing the relative strength of ion sources, the unit should be hard wire grounded for the best results. Adjustments to an ion source to determine the ion output may be made, noting the meter reading and then readjusting R3 to bring the meter reading to scale.

A very interesting phenomenon will be noted when using this device for detecting residual ion fields, the shielding of ions, field direction, static charges, resultant polarity, and the intensity of static charges, as well as a host of others. The unit is an

invaluable tool for determining the output of ion generators, any purifiers, and the presence of dangerous static electricity situations. Many sources of charged particles soon become apparent when using the device. People's clothes, fluorescent lighting, plastic containers, and certain winds all will indicate a charge.

Please note that the antenna probe on your unit is a telescoping antenna properly secured and electrically isolated. It is important to remember that any type of leakage around the input of Ql can reduce the sensitivity. You may want to coat the circuitry with a good-quality varnish. Make sure the unit is dry and clean before sealing. The unit is shown wired for positive ion detection. You may change it to negative by replacing the PN2222 transistors with PN2907 and vice versa. For a quick indication, you may grab the antenna and use the body of the unit to detect the negative ions.

Table 38-1 Ion Detector Parts List

Ref. #	*Description*	*DB Part #*
R1	10 meg, ¼-watt resistor (br-blk-blue)	
R2	10K, 1-watt resistor (br-blk-or)	
R3/S1	10K pot and 12 VDC switch	
C1	100-picofard disk capacitor (see Figure 38-2)	
D1, 2	Two 1N914 signal diodes	
D3	Colored LED	
Q3	Two PN2222 NPN transistor (see note on reversing)	
Q1, 2	Two PN2907 PNP transistors	
M1	100-micro-amp, small panel meter	DB# METER50S
PB1	1 × 2-inch piece of .1-inch grid perforated circuit board	
ANT	Telescoping antenna	DB# ANT1
CL1	9-volt battery clip	
WR24	24 inches of #24 vinyl hookup wire	
CASE	4⅜ × 2⅞ × 1¼-inch plastic box with lid	
TAPE	4 × ½-inch metal tape	
WR24B	12 inches of #24 bus wire	

Chapter Thirty-Nine

Light Saber Recycling Stand

This project is intended for those who have built or purchased a light saber from Information Unlimited or who have built one from our first book as directed in Chapter 21 in this series of three.

The saber stand recycles your saber where the plasma display travels up the tube, appearing to evaporate into open space (see Figure 39-1). It then retracts into the hilt and continues repeating until power is removed. The effect is very relaxing and provides an excellent display piece or prop for a bar, a point-of-purchase display, an attention getter, a conversation piece, or just a nightlight for a bedroom.

Operation is powered from a 12-volt wall adapter and is completely safe for children. This is an intermediate-level project requiring basic electronic skills. Expect to spend $20 to $30. All the parts are readily available, with specialized parts obtainable through Information Unlimited (www.amazing1.com), and are listed in the parts list at the end of the chapter.

Circuit Description

Figure 39-2 shows a 12-volt wall adapter (T1) being fed into a voltage regulator chip (I2) where a regulated 9 volts is applied to the remaining circuitry. Capacitors C1 and C2 smooth out the voltage waveform. An astable pulse generator using a timer (I1) provides an uneven "on to off" time determined by the ratio of resistors R2 and R3. The output pulse repetition rate is a function of timing capacitor C3 with

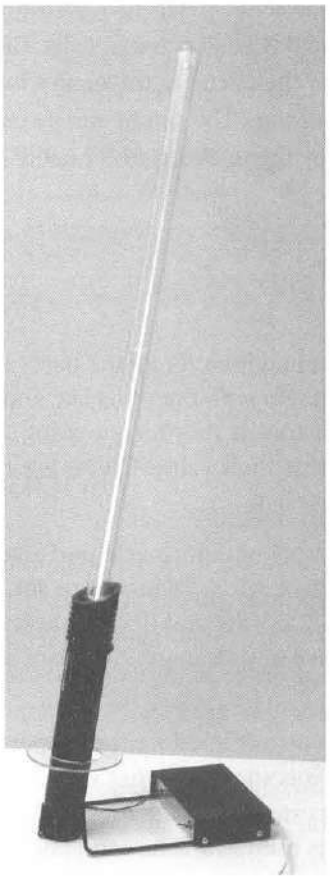

Figure 39-1 *The saber recycling stand*

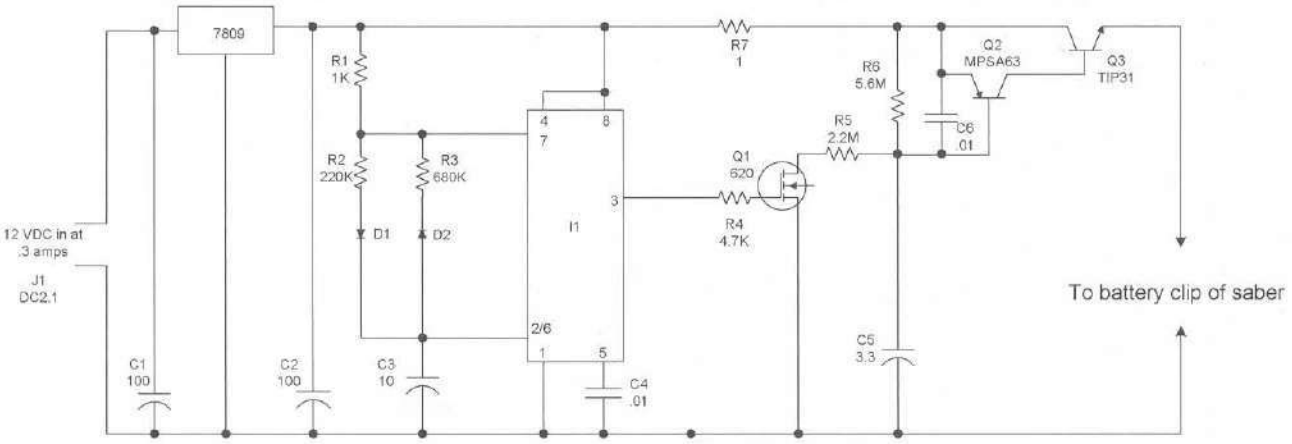

Figure 39-2 *Circuit schematic*

output at pin 3 of I1. The pulse output serves as a gate for MOSFET switch Q1, creating a charging and discharging of low-leakage capacitor C5. A quasi-linear voltage ramp now appears across C5, controlling the current through a high beta Darlington transistor (Q2) in turn controlling the main-current pass transistor Q3. It is this ramping up and down of current that now powers the saber electronics, allowing the plasma to flow up and down, all automatically. The cycling action is set by the circuit to travel up a half-second and down 3 seconds. This timing can be changed to some extent by the selection of R2 and R3.

Assembly

1. Lay out and identify all the parts and pieces. Verify them with the parts list, and separate the resistors as they have a color code to determine their value. Colors are noted on the parts list.
2. Cut a piece of .1-inch grid perforated board to a size of 3.1 × 1.8 inches, as shown in Figure 39-3. Locate and drill the holes as shown to relieve any strain on the input and output leads.
3. When you are building from a perforated board, it is suggested that you insert the components starting in the lower left-hand corner, which is used as a reference, and proceed to the opposite corner.

   Pay attention to the polarity of the capacitors with polarity signs and all the semiconductors.

   Route the leads of the components as shown and solder as you go, cutting away unused wires. Attempt to use certain leads as the wire runs or use pieces of the #24 bus wire. Follow the dashed lines on the assembly drawing as these indicate the connection runs on the underside of the assembly board.
4. Attach the external leads for battery clip CL1 and the leads to input power jack J1. *Important!* The battery clip CL1 must be wired in reverse by connecting the red lead to the circuit ground and the black lead to the emitter of Q3.
5. Double-check the accuracy of the wiring and the quality of the solder joints. Avoid wire bridges, shorts, and close proximity to other circuit components. If a wire bridge is necessary, sleeve some insulation onto the lead to avoid any potential shorts.

Parts Fabrication

1. Create the chassis shown in Figure 39-4. This is attached to the BASE section using four #6 sheet metal screws.
2. Create the base section from a piece of plastic or aluminum, as shown in Figure 39-5. Note

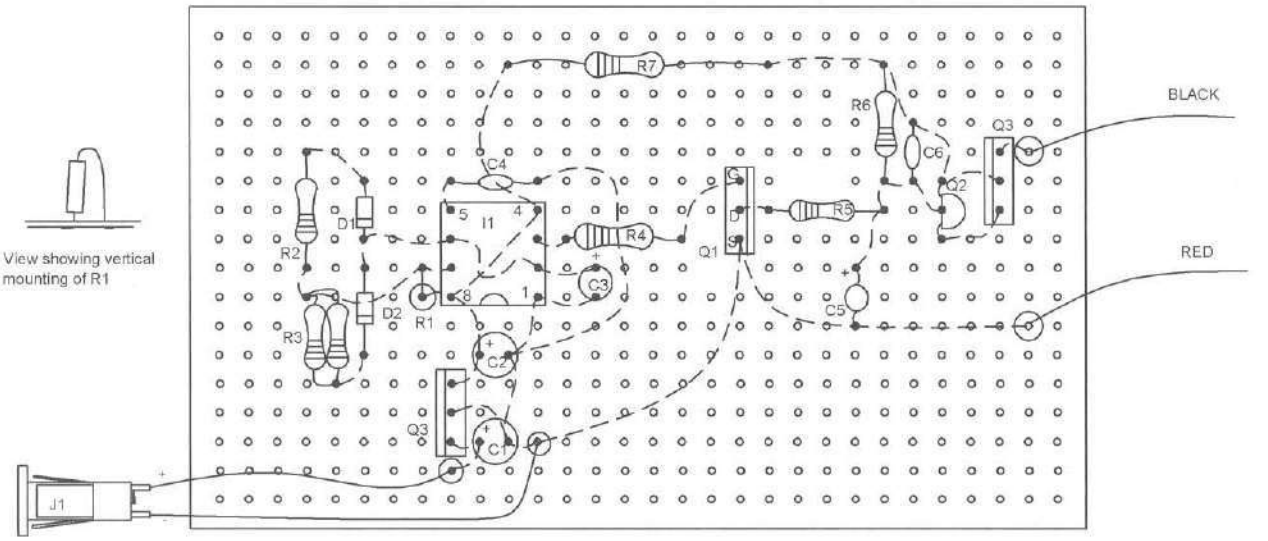

Notes

The looped dashed lind connecting pins 2 and 6 of I1 must have a sleeve of insulated tubing to prevent shorting the lead between pins 4 and 8.

Dashed lines are connections on underside of perforated circuit board using the component leads. These points can also be used to determine foil runs for those who wish to fabricate a printed circuit board.

Small dots are holes used for component insertion.

Large dots are solder junctions

Circles with dots are holes that may require drilling for component mounting and points for external connecting wires indicating strain relief points. It is suggested to drill clearance holes for the leads and solder to points beneath board.

Figure 39-3 *Board assembly*

the four holes for mounting the chassis section, two holes for the holder section, and two holes for the tie wraps.

3. Create the holder from a piece of 2⅜-inch, schedule 40 gray PVC tubing. Note the slight angle cut for aesthetics being congruent with the light saber when in the stand. This piece is mounted to the base using two #6 × ⅜-inch sheet metal screws.

4. Form the frame as shown in Figure 39-6 from 3/16-inch cold roll steel rod or an equivalent. The frame must be formed to provide a stable assembly with the saber in place in the stand. The longer 36-inch blade unit is the most critical, requiring the most attention. Attempt to follow the dimensions as shown and determine the base angle as a final adjustment with the saber in place.

   The frame is secured in place by inserting the horizontal members through the corner holes in the chassis section. The front section of the frame is secured in place by two small tie wraps, as shown in Figure 39-5.

10. Finish the assembly, as shown in Figures 39-7 and 39-8.

Operation

Remove the cap at the rear of the saber hilt and remove both batteries. Take out one of the battery clips and snap it into the mating clip of the saber stand. Position the saber in the stand and verify its mechanical stability. Plug in the wall adapter and turn on the switch. The plasma should immediately go to the end and then drop down into the hilt. Recycling should commence and continue until power is removed.

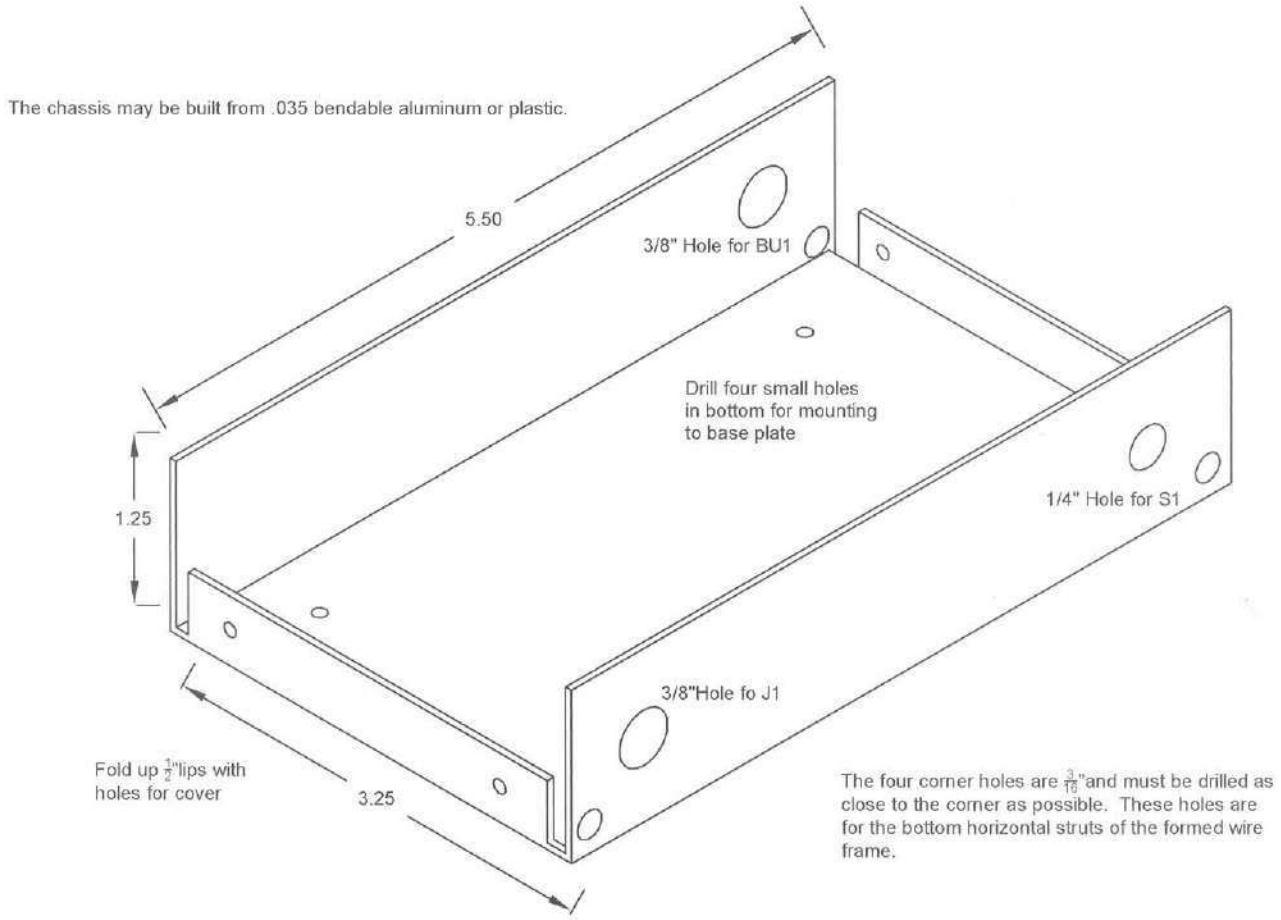

Figure 39-4 *Chassis fabrication*

Light sabers are available from Information Unlimited at www.amazing1.com in 24- or 36-inch lengths in colors of phasor green, photon blue, starfire purple, neon red, or solar yellow.

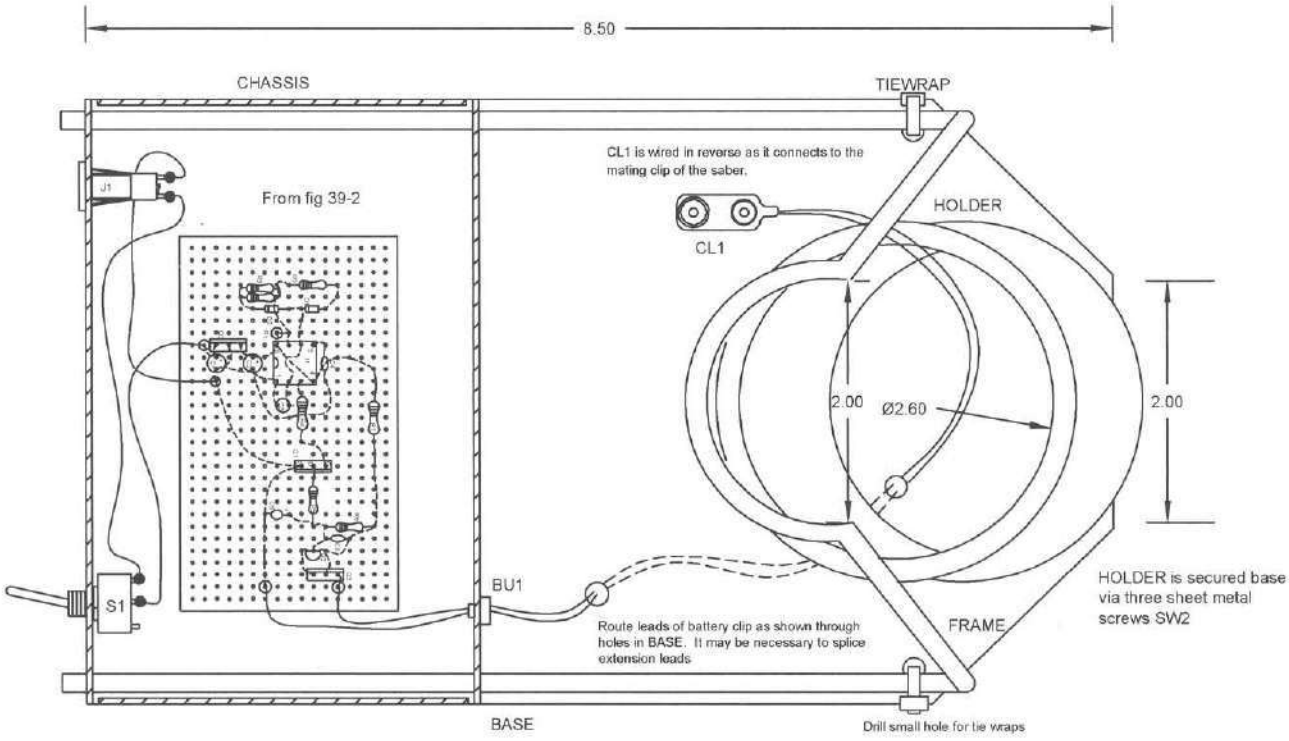

Figure 39-5 *Base fabrication*

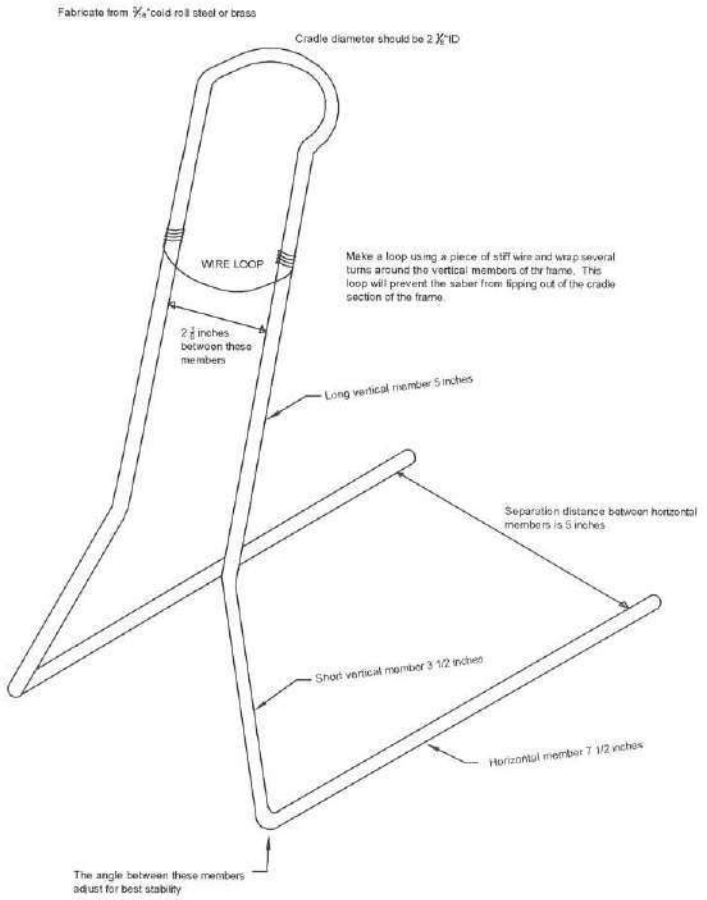

Figure 39-6 *Frame section*

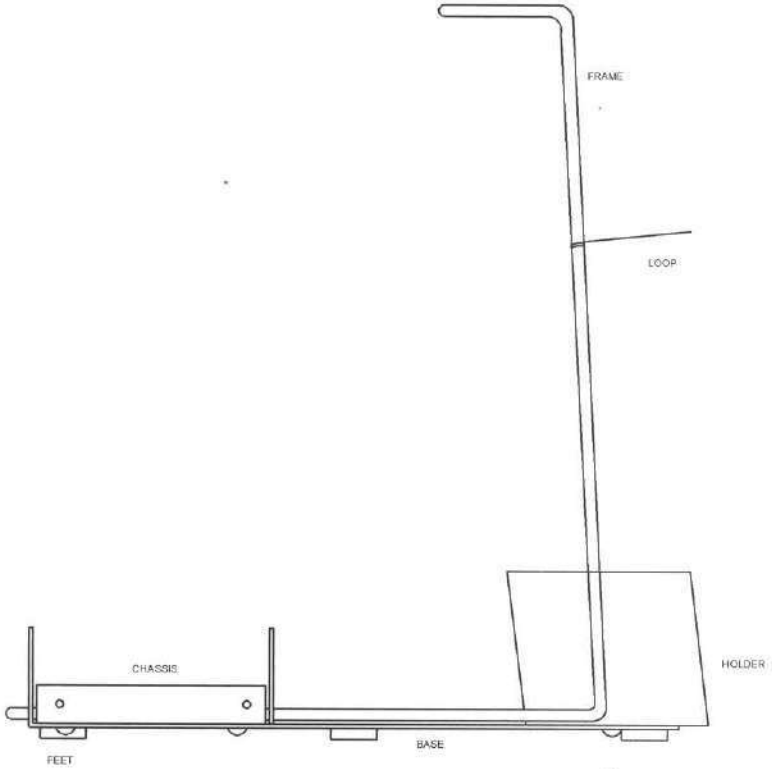

Figure 39-7 *Side view of assembly*

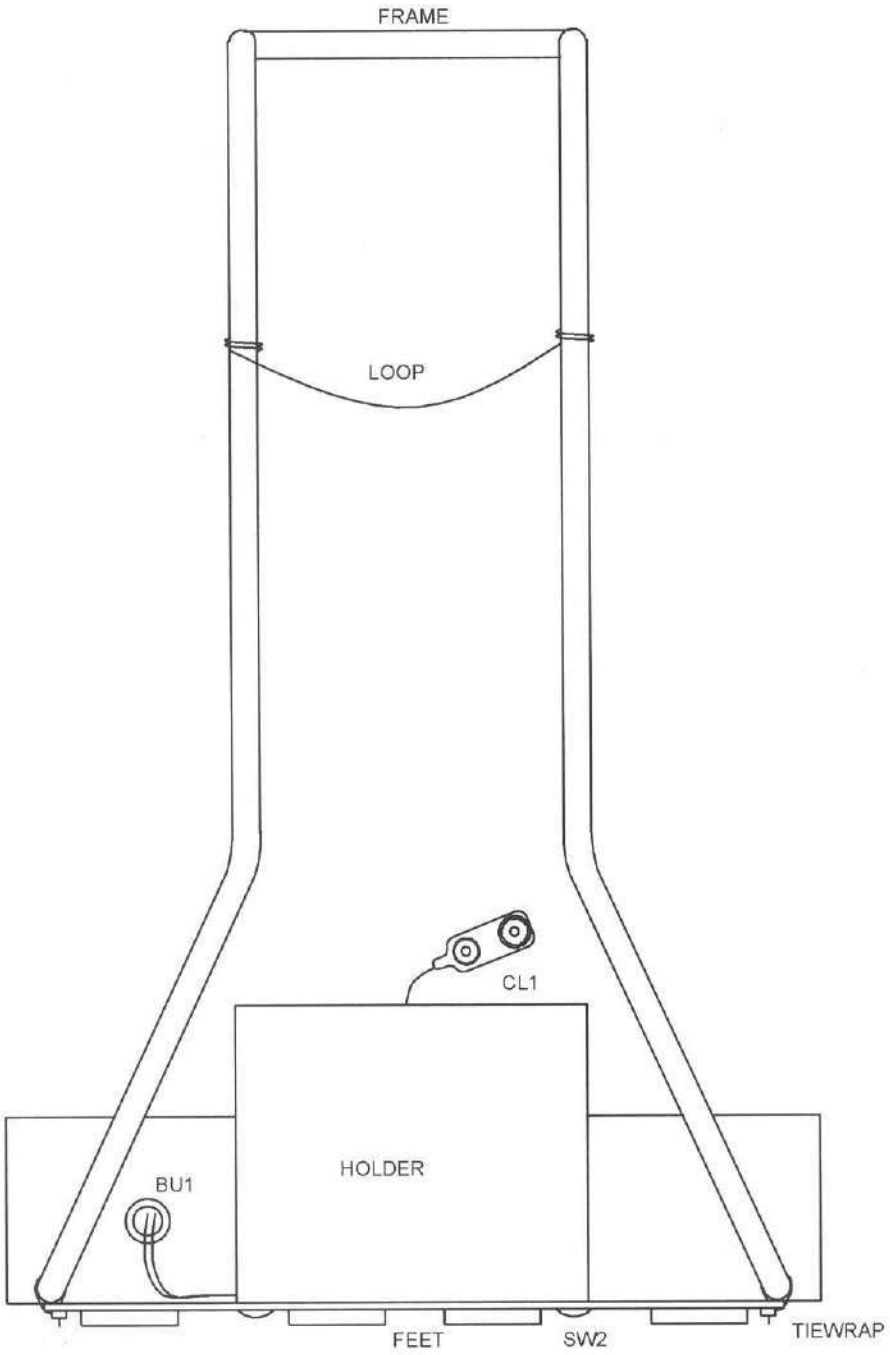

Figure 39-8 *Front view of assembly*

Table 39-1 Light Saber Stand Parts List

Ref. #	Description	DB Part #
R1	1K, ¼-watt resistor (br-blk-red)	
R2	220K, ¼-watt resistor (red-red-yel)	
R3	680K, ¼-watt resistor (blue-gray-yel)	
R4	4.7K, ¼-watt resistor (yel-pur-red)	
R5	2.2 m, ¼-watt resistor (red-red-gr)	
R6	5.6 m, ¼-watt resistor (gr-blue-gr)	
R7	1-ohm, ¼-watt resistor (br-blk-gold)	
C1, 2	Two 100-microfarad, 25-volt vertical electrolytic capacitors	
C3	10-microfarad, 25-volt vertical electrolytic capacitor	
C4, 6	Two .01-microfarad, 50-volt disc capacitors	
C5	3.3-microfarad, 35-volt tantalum capacitor	
D1, 2	Two IN914 silicon diodes	
I1	555 dual inline package (DIP) timer integrated circuit	
I2	7809 T0220 9-volt regulator	
Q1	IRF620 metal-oxide-semi-conductor field effect transistor (MOSFET)	
Q2	MPSA63 PNP Darlington transistor	
Q3	TIP31 T0220 NPN transistor	
J1	Snap-in DC panel, 2.5 mm jack	
S1	Single pole, single throw (SPST) small toggle switch	
PB1	3.5 × 2 .1 × .1-inch grid perforated board; trim to size	
CL1	Battery clip with 12-inch leads or extend shorter leads	
TIEWRAP	Two small tie wraps	
CHASSIS	Create as shown in Figure 39-4 from .035-inch aluminum	
BASE	Create as shown in Figure 39-5 from .035-inch plastic	
HOLDER	Create from a length of 2⅜-inch schedule 40 gray PVC	
FRAME	Create as shown in Figure 39-6	
FEET	Six large, rubber stick-on feet	
SW2	Six #6 × ⅜-inch sheet metal screws	
BU1	Two ⅜-inch plastic bushings	
LIGHT SABER	36- or 24-inch saber in blue, green, red, or purple	

Chapter Forty

Andromeda Plasma Lamp

This project shows how to build a unique type of outside lamp suitable for illuminating driveways, pools, gardens, walkways, docks, or any place where colorful or functioning illumination is desired. The lamps are patented by the author and are currently in preproduction.

The lamp's features are high efficiency as five individual lamps can be powered by a single, conventional, 12-volt wall adapter as the lamps require only 3 watts each. The lamps provide a high amount of useful illumination and must not be compared to the low-light, solar-powered accent lamps.

Another feature of the lamp is that it never needs replacing and should last a lifetime. Other lamps such as incandescent ones are always burning out filaments, whereas conventional fluorescents darken and fail to start due to metallic sputtering.

The third feature is that the lamps are available in pure spectral colors of green, blue, purple, yellow, red, and cool and warm white. These are vivid colors and not the result of filters or paint. Their color is the result of the true spectral emission.

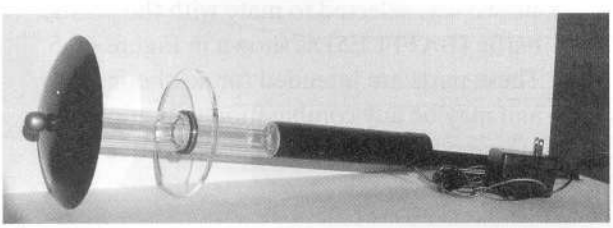

Figure 40-1 *The Andromeda plasma lamp*

This is an intermediate-level project requiring basic electronic skills. Expect to spend $25 to $35. All the parts are readily available, with specialized parts obtainable through Information Unlimited at www.amazing1.com, which are listed in the parts list at the end of the chapter.

Circuit Description

Transistor Q1 forms a self-oscillating circuit where current rises in the collector, COL, winding transformer T1 and inducing a voltage in the feedback (FB). This also causes a winding that keeps Q1 on until T1 saturates and the feedback voltage can no longer be induced. The collector current rapidly falls and forces the base to go negative further, turning Q1 off. When the collector current falls to zero, Q1 is turned on by bias-set resistors R1 and R2, which must charge up timing capacitor C2. The setting of trimpot R1 determines the power output by controlling the number of cycles per second, and capacitor C1 bypasses any residual signal voltage to ground (see Figure 40-2).

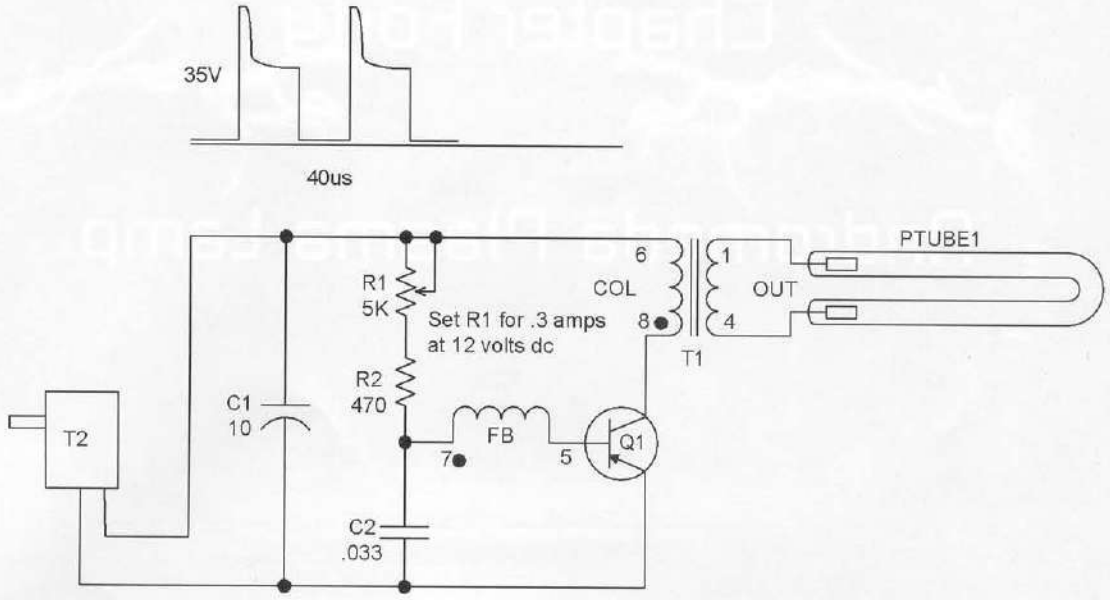

Figure 40-2 *Circuit schematic*

Assembly Board Wiring

1. Cut a piece of .1 × .1 grid vector circuit board to 1 × 4.5 inches, as shown in Figure 40-3.
2. Whenever you are using a perforated board, it is suggested that you insert components starting in the lower left-hand corner. Pay attention to the polarity of the capacitors with polarity signs and all the semiconductors. Route the leads of the components as shown and solder as you go, cutting away unused wires. Attempt to use certain leads as the wire runs or use pieces of the #24 bus wire. Follow the dashed lines on the assembly drawing as these indicate the connection runs on the underside of the assembly board.
3. Double-check the accuracy of the wiring and the quality of the solder joints. Avoid wire bridges, shorts, and close proximity to other circuit components. If a wire bridge is necessary, sleeve some insulation onto the lead to avoid any potential shorts.
4. Attach leads from the plasma tube PT1, being careful not to stress the glass enclosure. Note the small tie wraps (TY1) securing the tube to the perforated board. Again, do not cause any stress to the glass. Make sure that when tightening the wraps they do not stress the tube. When soldering, you must not allow the glass or metal seal to get too hot. Leave at least a half-inch lead between the tube and the connection. Use flux and make the solder joints quickly.
5. Connect the input power leads to a 12-volt DC source and note the lamp lighting. Quickly adjust trim pot R1 to 300 milliamps of current. The lamp should be very bright and the heatsink tab on Q1 should only be warm. Allow it to run for several hours and check adapter transformer T2 for excessive heating.
6. Create the EN1 enclosure tube and the STK1 mounting stake, as shown in Figure 40-4. Note the two mating holes for attaching the stake and the $^{5}/_{16}$-inch hole for the rubber tubular bushing for routing the input power leads.
7. Obtain a top canopy (CANOPY7). The one shown was selected to mate with the plastic baffle (BAFFLE5) as shown in Figure 40-5. These parts are intended for aesthetics only and may be any combination that appears pleasing to the builder. A good source is a

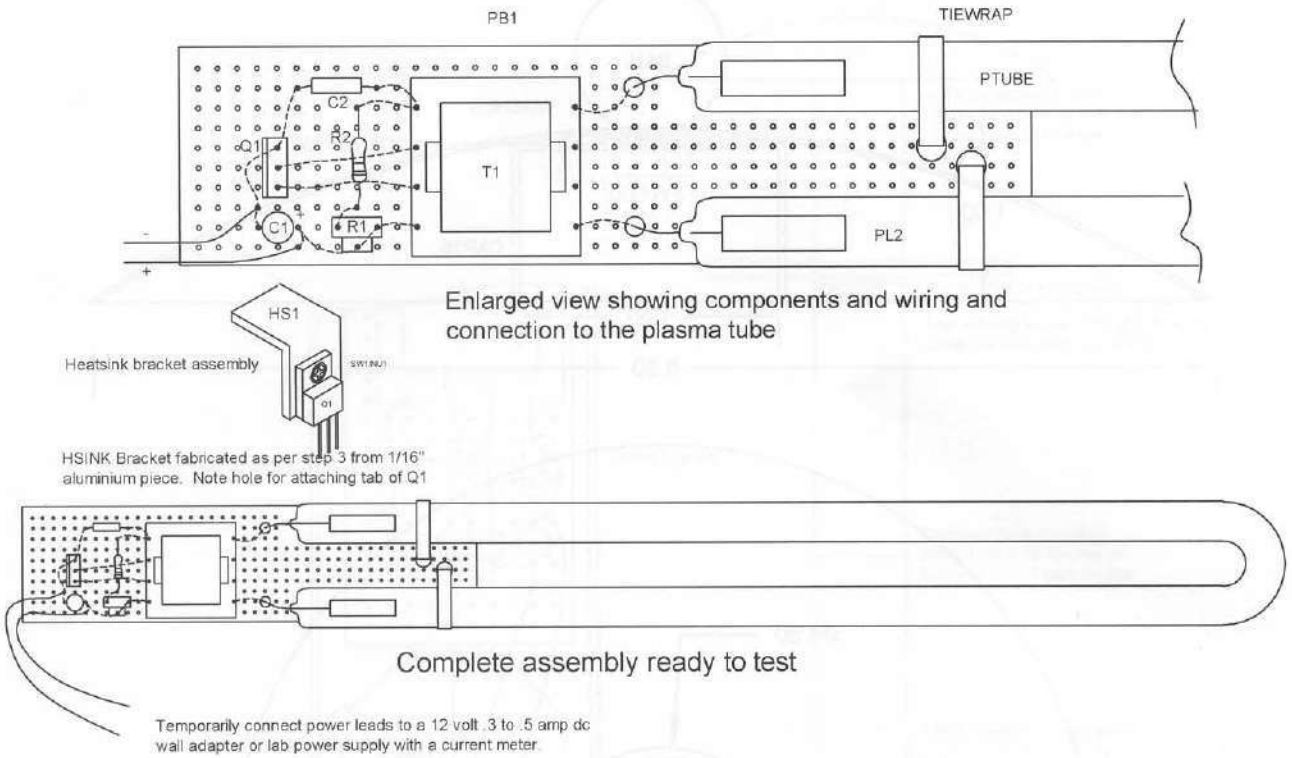

Figure 40-3 *Assembly board*

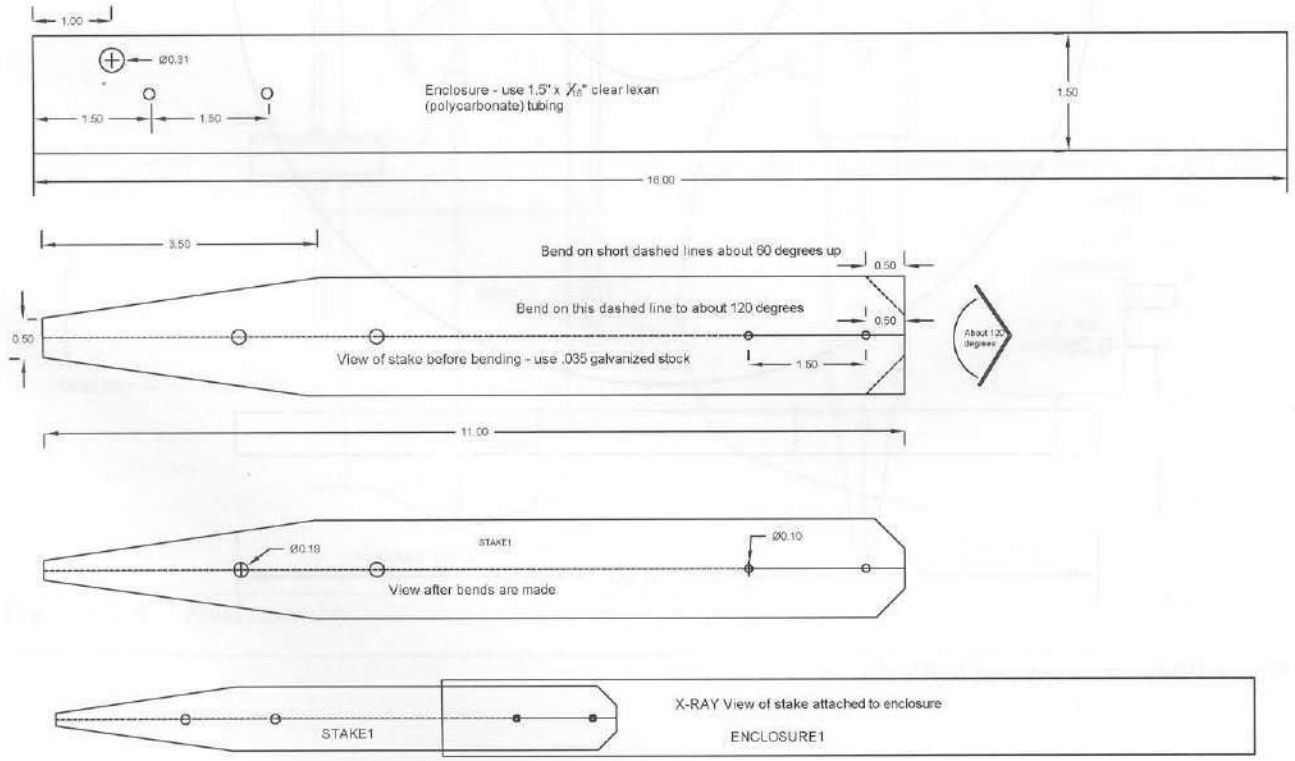

Figure 40-4 *Creating the mounting stake and enclosure*

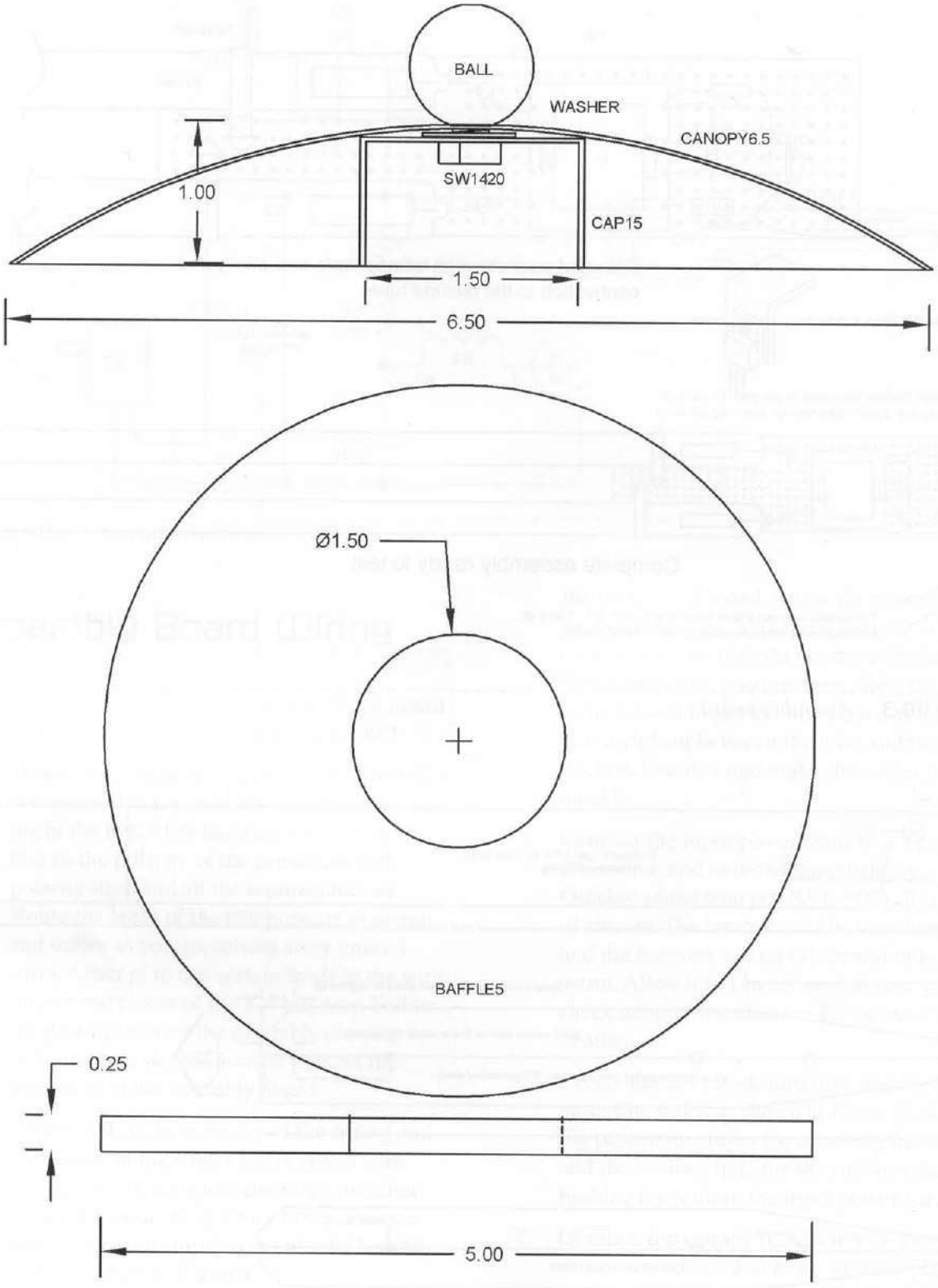

Figure 40-5 *Canopy and baffle design*

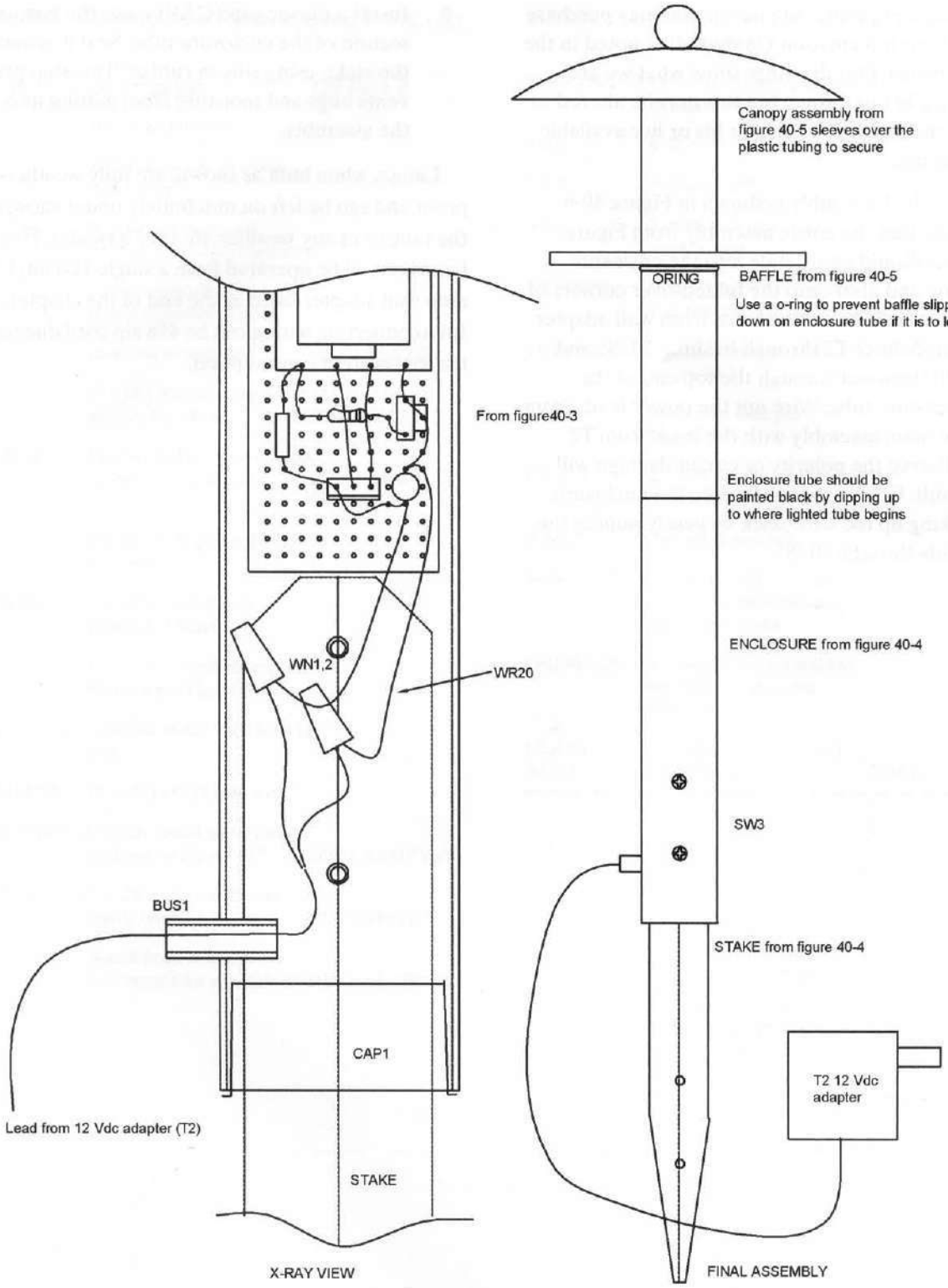

Figure 40-6 *Final assembly*

lamp or lighting supplier or you may purchase it from Information Unlimited, as noted in the parts list. Our drawings show what we are using in our design, but this may be altered to fit the builder's choice or his or her available sources.

8. The final assembly is shown in Figure 40-6. Note that the entire assembly from Figure 40-3 should easily slide into the enclosure tube and abut onto the folded-over corners of the stake. Thread the leads from wall adapter transformer T2 through bushing BUS1 and pull them out through the top end of the enclosure tube. Wire nut the power leads from the main assembly with the leads from T2. Observe the polarity or circuit damage will result. Gently slide them into the enclosure, taking up the wire slack by gently pulling the leads through BUS1.
9. Insert a plastic cap (CAP1) into the bottom section of the enclosure tube. Seal it around the stake using silicon rubber. This step prevents bugs and moisture from getting into the assembly.

Lamps, when built as shown, are fully weatherproof and can be left on indefinitely under snow, in the rain, or in any weather, short of a twister. Five lamps can all be operated from a single 12-volt, 1.5-amp wall adapter listed at the end of the chapter. Interconnecting wiring can be #18 zip cord due to the low-current consumption.

Table 40-1 Andromeda Plasma Lamp Parts List

Ref. #	Description	DB Part #
R1	5K vertical trimmer	
R2	470-ohm, ¼-watt resistor (yel-pur-br)	
C1	10-microfarad, 50-volt vertical electrolytic capacitor	
C2	.033-microfarad, 50-volt plastic capacitor (332)	
T1	Inverting transformer	DB# ANQP2824
T2	12 VDC, 300-milliamp wall adapter transformer	DB# 12 DC/.3
PTUBE-C	Cool white/blue/green/purple/red/yellow plasma tube	DB# PTUBE-COLOR
Q1	PN3055 NPN power T0-220 transistor	
PBOARD	1 × 4.5 × .1-inch grid perforated board	
HS1	1.5 × 1 × 1/16-inch aluminum heatsink per Figure 40-3	
WR20	12 inches of #20 vinyl hookup wire	
WR24BUSS	12 inches of #24 buss wire	
CANOPY6.5	6.5-inch, round metal canopy, as shown in Figure 40-5	DB# CANOPY65
BAFFLE	5 × .25-inch, round, clear plastic baffle	DB# BAFFLE5
BALL	⅞-inch brass ball with a hole tapped for a ¼-20 bolt	DB# BALL78
STAKE1	Metal stake created as shown in Figure 40-4	
ENCLOSURE	Plastic tube created as shown in Figure 40-4	
SW1	6-32 ¼ Phillips screw	
NUT	6-32 keep nut	
SW3	Two #6 × ¼-inch sheet metal screws	
SW1420X1	¼-20 × 1-inch hex bolt for attaching the ball (see Figure 40-5)	
TIEWRAP	Two tie wraps used per Figure 40-3	
CAP1	Plastic cap used per Figure 40-6	
CAP1.5	1.5-inch plastic cap shown in Figure 40-6	
WN1, 2	Two small wire nuts	
BUS1	5/16 OD × 3/16 ID × 1-inch length of rubber tubing (see Figure 40-6)	
ORING1.25	1¼-inch O-ring for holding the baffle in place per Figure 40-6	
5 LAMP ADAPTER	12 VDC, 1.5-amp adapter for five lamps	DB# 12/1 .5

Burn things out, mess things up—that's how you learn.

Learn by Discovery

Make: Electronics

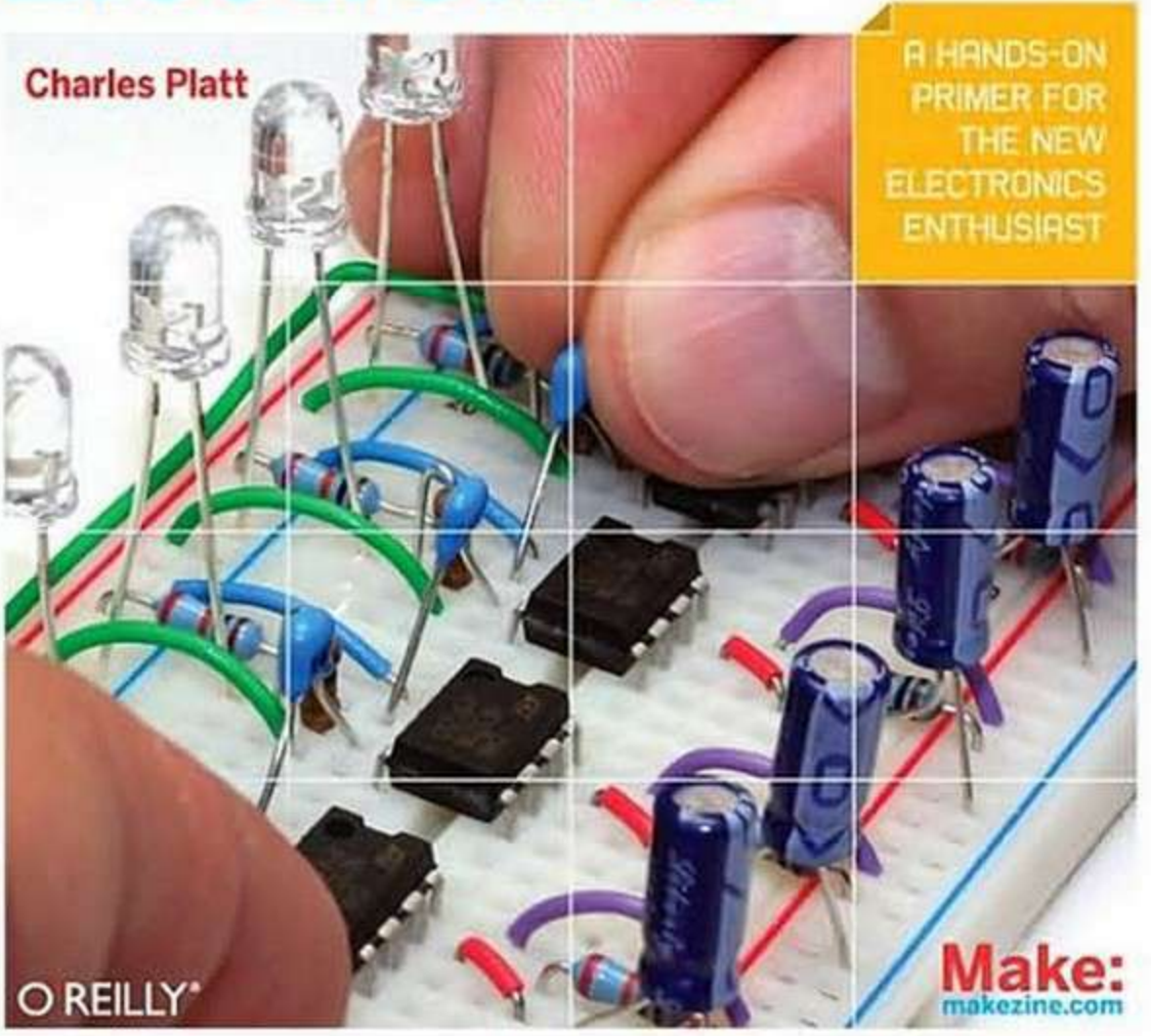

Contents

Preface ix

1. Experiencing Electricity 1
Shopping List: Experiments 1 Through 5 1
Experiment 1: Taste the Power! 5
Experiment 2: Let's Abuse a Battery! 9
Experiment 3: Your First Circuit 13
Experiment 4: Varying the Voltage 18
Experiment 5: Let's Make a Battery 32

2. Switching Basics and More 39
Shopping List: Experiments 6 Through 11 39
Experiment 6: Very Simple Switching 43
Experiment 7: Relay-Driven LEDs 55
Experiment 8: A Relay Oscillator 60
Experiment 9: Time and Capacitors 68
Experiment 10: Transistor Switching 73
Experiment 11: A Modular Project 82

3. Getting Somewhat More Serious 95
Shopping List: Experiments 12 Through 15 95
Experiment 12: Joining Two Wires Together 104
Experiment 13: Broil an LED 114
Experiment 14: A Pulsing Glow 117
Experiment 15: Intrusion Alarm Revisited 127

4. Chips, Ahoy! 147
Shopping List: Experiments 16 Through 24 147
Experiment 16: Emitting a Pulse 153
Experiment 17: Set Your Tone 162
Experiment 18: Reaction Timer 170
Experiment 19: Learning Logic 181
Experiment 20: A Powerful Combination 197
Experiment 21: Race to Place 205
Experiment 22: Flipping and Bouncing 211
Experiment 23: Nice Dice 214
Experiment 24: Intrusion Alarm Completed 223

5. What Next? 227
Shopping List: Experiments 25 Through 36 228
Customizing Your Work Area 228
Reference Sources 233
Experiment 25: Magnetism 236
Experiment 26: Tabletop Power Generation 239
Experiment 27: Loudspeaker Destruction 242
Experiment 28: Making a Coil React 246
Experiment 29: Filtering Frequencies 249
Experiment 30: Fuzz 257
Experiment 31: One Radio, No Solder, No Power 262
Experiment 32: A Little Robot Cart 268
Experiment 33: Moving in Steps 284
Experiment 34: Hardware Meets Software 293
Experiment 35: Checking the Real World 306
Experiment 36: The Lock, Revisited 311
In Closing 317

Appendix. Online Retail Sources and Manufacturers 319

Index 325

Preface

How to Have Fun with This Book

Everyone uses electronic devices, but most of us don't really know what goes on inside them.

Of course, you may feel that you don't need to know. If you can drive a car without understanding the workings of an internal combustion engine, presumably you can use an iPod without knowing anything about integrated circuits. However, understanding some basics about electricity and electronics can be worthwhile for three reasons:

- By learning how technology works, you become better able to control your world instead of being controlled by it. When you run into problems, you can solve them instead of feeling frustrated by them.
- Learning about electronics can be fun—so long as you approach the process in the right way. The tools are relatively cheap, you can do all the work on a tabletop, and it doesn't consume a lot of time (unless you want it to).
- Knowledge of electronics can enhance your value as an employee or perhaps even lead to a whole new career.

Learning by Discovery

Most introductory guides begin with definitions and facts, and gradually get to the point where you can follow instructions to build a simple circuit.

This book works the other way around. I want you to start putting components together right away. After you see what happens, you'll figure out what's going on. I believe this process of *learning by discovery* creates a more powerful and lasting experience.

Stay Within the Limits!

Although I believe that everything suggested in this book is safe, I'm assuming that you will stay within the limits that I suggest. Please always follow the instructions and pay attention to the warnings, denoted by the icon you see here. If you go beyond the limits, you will expose yourself to unnecessary risks.

Learning by discovery occurs in serious research, when scientists notice an unusual phenomenon that cannot be explained by current theory, and they start to investigate it in an effort to explain it. This may ultimately lead to a better understanding of the world.

We're going to be doing the same thing, although obviously on a much less ambitious level.

Along the way, you will make some mistakes. This is good. Mistakes are the best of all learning processes. I want you to burn things out and mess things up, because this is how you learn the limits of components and materials. Since we'll be using low voltages, there'll be no chance of electrocution, and so long as you limit the flow of current in the ways I'll describe, there will be no risk of burning your fingers or starting fires.

Figure P-1. *Learning by discovery allows you to start building simple circuits right away, using a handful of cheap components, a few batteries, and some alligator clips.*

How Hard Will It Be?

I assume that you're beginning with no prior knowledge of electronics. So, the first few experiments will be ultra-simple, and you won't even use solder or prototyping boards to build a circuit. You'll be holding wires together with alligator clips.

Very quickly, though, you'll be experimenting with transistors, and by the end of Chapter 2, you will have a working circuit that has useful applications.

I don't believe that hobby electronics has to be difficult to understand. Of course, if you want to study electronics more formally and do your own circuit design, this can be challenging. But in this book, the tools and supplies will be inexpensive, the objectives will be clearly defined, and the only math you'll need will be addition, subtraction, multiplication, division, and the ability to move decimal points from one position to another.

Moving Through This Book

Basically there are two ways to present information in a book of this kind: in tutorials and in reference sections. I'm going to use both of these methods. You'll find the tutorials in sections headed as follows:

- Shopping Lists
- Using Tools
- Experiments

You'll find reference sections under the following headings:

- Fundamentals
- Theory
- Background

How you use the sections is up to you. You can skip many of the reference sections and come back to them later. But if you skip many of the tutorials, this book won't be of much use to you. Learning by discovery means that you absolutely, positively have to do some hands-on work, and this in turn means that you have to buy some basic components and play with them. You will gain very little by merely imagining that you are doing this.

It's easy and inexpensive to buy what you need. In almost any urban or suburban area in the United States, chances are you live near a store that sells electronic components and some basic tools to work with them. I am referring, of course, to RadioShack franchises. Some Shacks have more components than others, but almost all of them have the basics that you'll need.

You can also visit auto supply stores such as AutoZone and Pep Boys for basics such as hookup wire, fuses, and switches, while stores such as Ace Hardware, Home Depot, and Lowe's will sell you tools.

If you prefer to buy via mail order, you can easily find everything you need by searching online. In each section of the book, I'll include the URLs of the most popular supply sources, and you'll find a complete list of URLs in the appendix.

Fundamentals

Mail-ordering components and tools

Here are the primary mail-order sources that I use myself online:

http://www.radioshack.com
: RadioShack, a.k.a. The Shack. For tools and components. Not always the cheapest, but the site is easy and convenient, and some of the tools are exactly what you need.

http://www.mouser.com
: Mouser Electronics.

http://www.digikey.com
: Digi-Key Corporation.

http://www.newark.com
: Newark.

Mouser, Digi-Key, and Newark are all good sources for components, usually requiring no minimum quantities.

http://www.allelectronics.com
: All Electronics Corporation. A narrower range of components, but specifically aimed at the hobbyist, with kits available.

http://www.ebay.com
: You can find surplus parts and bargains here, but you may have to try several eBay Stores to get what you want. Those based in Hong Kong are often very cheap, and I've found that they are reliable.

http://www.mcmaster.com
: McMaster-Carr. Especially useful for high-quality tools.

Lowe's and Home Depot also allow you to shop online.

Figure P-2. *You'll find no shortage of parts, tools, kits, and gadgets online.*

Companion Kits

Maker Shed (*www.makershed.com*) offers a number of *Make: Electronics* companion kits, both toolkits and bundles of the various components used in the book's experiments. This is a simple, convenient, and cost-effective way of getting all the tools and materials you need to do the projects in this book.

Comments and Questions

Please address comments and questions concerning this book to the publisher:

O'Reilly Media, Inc.
1005 Gravenstein Highway North
Sebastopol, CA 95472
800-998-9938 (in the United States or Canada)
707-829-0515 (international or local)
707-829-0104 (fax)

We have a web page for this book, where we list errata, examples, larger versions of the book's figures, and any additional information. You can access this page at:

http://oreilly.com/catalog/9780596153748

To comment or ask technical questions about this book, send email to:

bookquestions@oreilly.com

For more information about our books, conferences, Resource Centers, and the O'Reilly Network, see our website at:

http://oreilly.com

Safari® Books Online

Safari Books Online is an on-demand digital library that lets you easily search over 7,500 technology and creative reference books and videos to find the answers you need quickly.

With a subscription, you can read any page and watch any video from our library online. Read books on your cell phone and mobile devices. Access new titles before they are available for print, and get exclusive access to manuscripts in development and post feedback for the authors. Copy and paste code samples, organize your favorites, download chapters, bookmark key sections, create notes, print out pages, and benefit from tons of other time-saving features.

O'Reilly Media has uploaded this book to the Safari Books Online service. To have full digital access to this book and others on similar topics from O'Reilly and other publishers, sign up for free at *http://my.safaribooksonline.com*.

1 Experiencing Electricity

I want you to get a taste for electricity—literally!—in the first experiment. This first chapter of the book will show you:

- How to understand and measure electricity and resistance
- How to handle and connect components without overloading, damaging, or destroying them

Even if you have some prior knowledge of electronics, you should try these experiments before you venture on to the rest of the book.

IN THIS CHAPTER

Shopping List: Experiments 1 Through 5
Experiment 1: Taste the Power!
Experiment 2: Let's Abuse a Battery!
Experiment 3: Your First Circuit
Experiment 4: Varying the Voltage
Experiment 5: Let's Make a Battery

Shopping List: Experiments 1 Through 5

If you want to limit your number of shopping trips or online purchases, look ahead in the book for additional shopping lists, and combine them to make one bulk purchase.

In this first chapter, I will give you part numbers and sources for every tool and component that we'll be using. Subsequently, I won't expect you to need such specific information, because you will have gained experience searching for items on your own.

Maker Shed (www.makershed.com) *has put together a series of* Make: Electronics *companion kits. These include all of the tools and components used in book's experiments. This is a quick, simple, and cost-effective way of getting everything you need to complete the projects in this book.*

Tools

Small pliers

RadioShack Kronus 4.5-inch, part number 64-2953 or Xcelite 4-inch mini long-nose pliers, model L4G.

Or similar. See Figures 1-1 through 1-3. Look for these tools in hardware stores and the sources listed in the preface. The brand is unimportant. After you use them for a while, you'll develop your own preferences. In particular, you have to decide whether you like spring-loaded handles. If you decide you don't, you'll need a second pair of pliers to pull the springs out of the first.

Wire cutters

RadioShack Kronus 4.5-inch, part number 64-2951, or Stanley 7-inch model 84-108.

Or similar. Use them for cutting copper wire, not harder metals (Figure 1-4).

Figure 1-1. *Generic long-nosed pliers are your most fundamental tool for gripping, bending, and picking things up after you drop them.*

Figure 1-2. *Longer-nosed pliers: these are useful for reaching into tiny spaces.*

Figure 1-3. *Sharp-pointed pliers are designed for making jewelry, but are also useful for grabbing tiny components.*

Figure 1-4. *Wire cutters, sometimes known as side cutters, are essential.*

Multimeter

Extech model EX410 or BK Precision model 2704-B or Amprobe model 5XP-A.

Or similar. Because electricity is invisible, we need a tool to visualize the pressure and flow, and a meter is the only way. A cheap meter will be sufficient for your initial experiments. If you buy online, try to check customer reviews, because reliability may be a problem for cheap meters. You can shop around for retailers offering the best price. Don't forget to search on eBay.

The meter must be digital—don't get the old-fashioned analog kind with a needle that moves across a set of printed scales. This book assumes that you are looking at a digital display.

I suggest that you do not buy an autoranging meter. "Autoranging" sounds useful—for example, when you want to check a 9-volt battery, the meter figures out for itself that you are not trying to measure hundreds of volts, nor fractions of a volt. The trouble is that this can trick you into making errors. What if the battery is almost dead? Then you may be measuring a fraction of a volt without realizing it. The only indication will be an easily overlooked "m" for "millivolts" beside the large numerals of the meter display.

On a manual-ranging meter, you select the range, and if the source that you are measuring is outside of that range, the meter tells you that you made an error. I prefer this. I also get impatient with the time it takes for the autoranging feature to figure out the appropriate range each time I make a measurement. But it's a matter of personal preference. See Figures 1-5 through 1-7 for some examples of multimeters.

Figure 1-5. *You can see by the wear and tear that this is my own favorite meter. It has all the necessary basic features and can also measure capacitance (the F section, for Farads). It can also check transistors. You have to choose the ranges manually.*

Figure 1-6. *Mid-priced RadioShack meter, which has the basic features; however, the dual purpose for each dial position, selected with the SELECT button, may be confusing. This is an autoranging meter.*

Figure 1-7. *An autoranging meter from Extech offers basic functions, plus a temperature probe, which may be useful to check whether components such as power supplies are running unduly hot.*

Supplies

Batteries

9-volt battery. Quantity: 1.

AA batteries, 1.5 volts each. Quantity: 6.

The batteries should be disposable alkaline, the cheapest available, because we may destroy some of them. You should *absolutely not* use rechargeable batteries in Experiments 1 and 2.

Battery holders and connectors

Snap connector for 9-volt battery, with wires attached (Figure 1-8). Quantity: 1. RadioShack part number 270-325 or similar. Any snap connector that has wires attached will do.

Battery holder for single AA cell, with wires attached (Figure 1-9). Quantity: 1. RadioShack part number 270-401 or Mouser.com catalog number 12BH410-GR, or similar; any single-battery holder that has thin wires attached will do.

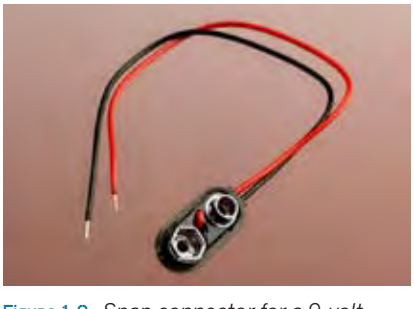

Figure 1-8. *Snap connector for a 9-volt battery.*

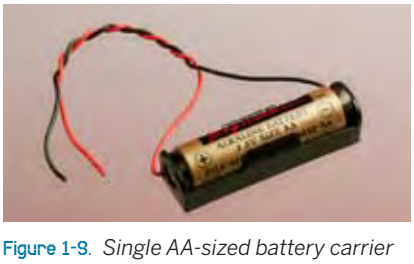

Figure 1-9. *Single AA-sized battery carrier with wires.*

Figure 1-10. *Battery carrier for four AA cells, to be installed in series, delivering 6 volts.*

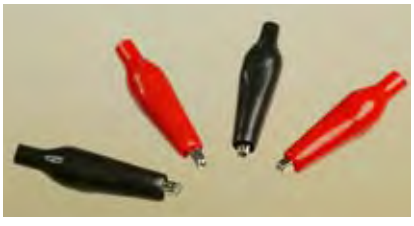

Figure 1-11. *Alligator clips inside vinyl sheaths, which reduce the chance of accidental short circuits.*

Figure 1-12. *A 3-amp fuse intended primarily for automotive use, shown here larger than actual size.*

Figure 1-13. *Potentiometers come in many shapes and sizes, with different lengths of shafts intended for different types of knobs. For our purposes, any style will do, but the larger-sized ones are easier to play with.*

Battery holder for four AA cells, with wires attached (Figure 1-10). Quantity: 1. All Electronics catalog number BH-342 or RadioShack part 270-391 or similar.

Alligator clips

Vinyl-insulated. Quantity: at least 6. All Electronics catalog number ALG-28 or RadioShack part number 270-1545 or similar (Figure 1-11).

Components

You may not know what some of these items are, or what they do. Just look for the part numbers and descriptions, and match them with the photographs shown here. Very quickly, in the learning by discovery process, all will be revealed.

Fuses

Automotive-style, mini-blade type, 3 amps. Quantity: 3. RadioShack part number 270-1089, or Bussmann part ATM-3, available from automotive parts suppliers such as AutoZone (Figure 1-12).

Or similar. A blade-type fuse is easier to grip with alligator clips than a round cartridge fuse.

Potentiometers

Panel-mount, single-turn, 2K linear, 0.1 watt minimum. Quantity: 2. Alpha part RV170F-10-15R1-B23 or BI Technologies part P160KNPD-2QC25B2K, from Mouser.com or other component suppliers (Figure 1-13).

Or similar. The "watt" rating tells you how much power this component can handle. You don't need more than 0.5 watts.

Resistors

Assortment 1/4-watt minimum, various values but must include 470 ohms, 1K, and 2K or 2.2K. Quantity: at least 100. RadioShack part number 271-312.

Or search eBay for "resistor assorted."

Light-emitting diodes (LEDs)

Any size or color (Figures 1-14 and 1-15). Quantity: 10. RadioShack part number 276-1622 or All Spectrum Electronics part K/LED1 from Mouser.com.

Or similar. Just about any LEDs will do for these first experiments.

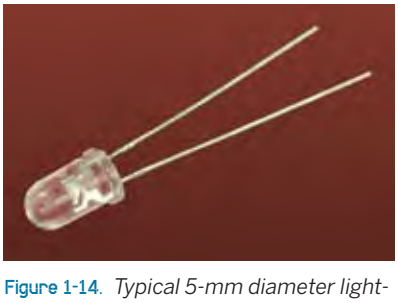

Figure 1-14. *Typical 5-mm diameter light-emitting diode (LED).*

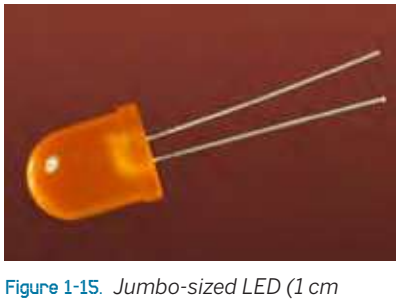

Figure 1-15. *Jumbo-sized LED (1 cm diameter) is not necessarily brighter or more expensive. For most of the experiments in this book, buy whatever LEDs you like the look of.*

Experiment 1: Taste the Power!

Can you taste electricity? Maybe not, but it feels as if you can.

You will need:

- 9-volt battery
- Snap connector for battery terminals
- Multimeter

No More Than 9 Volts

A 9-volt battery won't hurt you. But do not try this experiment with a higher-voltage battery or a larger battery that can deliver more current. Also, if you have metal braces on your teeth, be very careful not to touch them with the battery.

Procedure

Moisten your tongue and touch the tip of it to the metal terminals of a 9-volt battery. The sudden sharp tingle that you feel is caused by electricity flowing from one terminal of the battery (Figure 1-16), through the moisture on and in your tongue, to the other terminal. Because the skin of your tongue is very thin (it's actually a mucus membrane) and the nerves are close to the surface, you can feel the electricity very easily.

Now stick out your tongue, dry the tip of it very thoroughly with a tissue, and repeat the experiment without allowing your tongue to become moist again. You should feel less of a tingle.

What's happening here? We're going to need a meter to find out.

Figure 1-16. *Step 1 in the process of learning by discovery: the 9-volt tongue test.*

Tools

Setting up your meter

Check the instructions that came with the meter to find out whether you have to install a battery in it, or whether a battery is preinstalled.

Most meters have removable wires, known as *leads* (pronounced "leeds"). Most meters also have three sockets on the front, the leftmost one usually being reserved to measure high electrical currents (flows of electricity). We can ignore that one for now.

The leads will probably be black and red. The black wire plugs into a socket labeled "COM" or "Common." Plug the red one into the socket labeled "V" or "volts." See Figures 1-17 through 1-20.

The other ends of the leads terminate in metal spikes known as *probes*, which you will be touching to components when you want to make electrical measurements. The probes detect electricity; they don't emit it in significant quantities. Therefore, they cannot hurt you unless you poke yourself with their sharp ends.

If your meter doesn't do autoranging, each position on the dial will have a number beside it. This number means "no higher than." For instance if you want to check a 6-volt battery, and one position on the voltage section of the dial is numbered 2 and the next position is numbered 20, position 2 means "no higher than 2 volts." You have to go to the next position, which means "no higher than 20 volts."

Figure 1-17. *The black lead plugs into the Common (COM) socket, and the red lead plugs into the red socket that's almost always on the righthand side of a multimeter.*

If you make a mistake and try to measure something inappropriate, the meter will show you an error message such as "E" or "L." Turn the dial and try again.

Figure 1-18

Figure 1-19

Figure 1-20. *To measure resistance and voltage, plug the black lead into the Common socket and the red lead into the Volts socket. Almost all meters have a separate socket where you must plug the red lead when you measure large currents in amps, but we'll be dealing with this later.*

FUNDAMENTALS

Ohms

We measure distance in miles or kilometers, weight in pounds or kilograms, temperature in Fahrenheit or Centigrade—and electrical resistance in ohms. The ohm is an international unit.

The Greek omega symbol (Ω) is used to indicate ohms, as shown in Figures 1-21 and 1-22. Letter K (or alternatively, KΩ) means a kilohm, which is 1,000 ohms. Letter M (or MΩ) means a megohm, which is 1,000,000 ohms.

Number of ohms	Usually expressed as	Abbreviated as
1,000 ohms	1 kilohm	1KΩ or 1K
10,000 ohms	10 kilohms	10KΩ or 10K
100,000 ohms	100 kilohms	100KΩ or 100K
1,000,000 ohms	1 megohm	1MΩ or 1M
10,000,000 ohms	10 megohms	10MΩ or 10M

A material that has very high resistance to electricity is known as an *insulator*. Most plastics, including the colored sheaths around wires, are insulators.

A material with very low resistance is a *conductor*. Metals such as copper, aluminum, silver, and gold are excellent conductors.

Figure 1-21. *The omega symbol is used internationally to indicate resistance on ohms.*

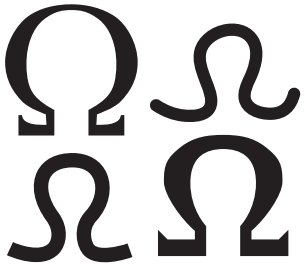

Figure 1-22. *You'll find it printed or written in a wide variety of styles.*

Procedure

We're going to use the meter to discover the electrical resistance of your tongue. First, set your meter to measure resistance. If it has autoranging, look to see whether it is displaying a K, meaning kilohms, or M, meaning megohms. If you have to set the range manually, begin with no less than 100,000 ohms (100K). See Figures 1-23 through 1-25.

Touch the probes to your tongue, about an inch apart. Note the reading, which should be around 50K. Now put aside the probes, stick out your tongue, and use a tissue to dry it very carefully and thoroughly. Without allowing your tongue to become moist again, repeat the test, and the reading should be higher. Finally, press the probes against the skin of your hand or arm: you may get no reading at all, until you moisten your skin.

When your skin is moist (for instance, if you perspire), its electrical resistance decreases. This principle is used in lie detectors, because someone who knowingly tells a lie, under conditions of stress, tends to perspire.

A 9-volt battery contains chemicals that liberate electrons (particles of electricity), which want to flow from one terminal to the other as a result of a chemical reaction inside it. Think of the cells inside a battery as being like two water tanks—one of them full, the other empty. If they are connected with a pipe, water flows between them until their levels are equal. Figure 1-26 may help you visualize this. Similarly, when you open up an electrical pathway between the two sides of a battery, electrons flow between them, even if the pathway consists only of the moisture on your tongue.

Electrons flow more easily through some substances (such as a moist tongue) than others (such as a dry tongue).

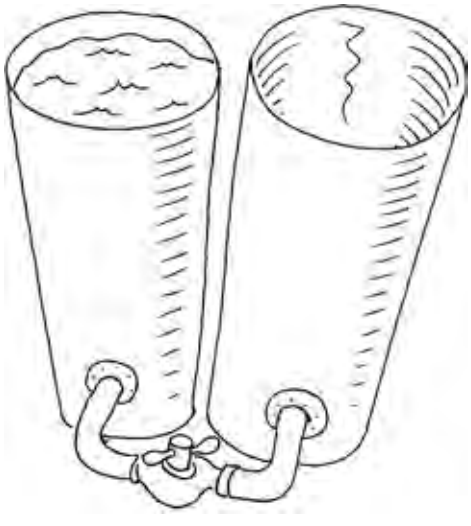

Figure 1-26. *Think of the cells in a battery as being like two cylinders: one full of water, the other empty. Open a connection between the cylinders, and the water will flow until the levels are equal on both sides. The less resistance in the connection, the faster the flow will be.*

Figure 1-23

Figure 1-24

Figure 1-25. *To measure ohms, turn the dial to the ohm (omega) symbol. On an autoranging meter, you can then press the Range button repeatedly to display different ranges of resistance, or simply touch the probes to a resistance and wait for the meter to choose a range automatically. A manual meter requires you to select the range with the dial (you should set it to 100K or higher, to measure skin resistance). If you don't get a meaningful reading, try a different range.*

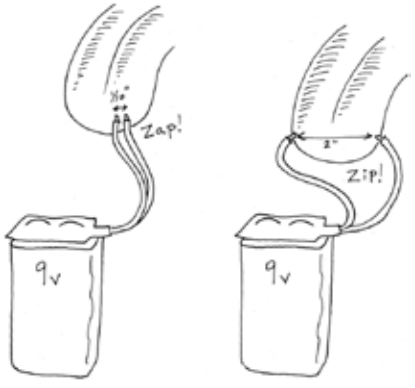

Figure 1-28. *Modifying the tongue test to show that a shorter distance, with lower resistance, allows greater flow of electricity, and a bigger zap.*

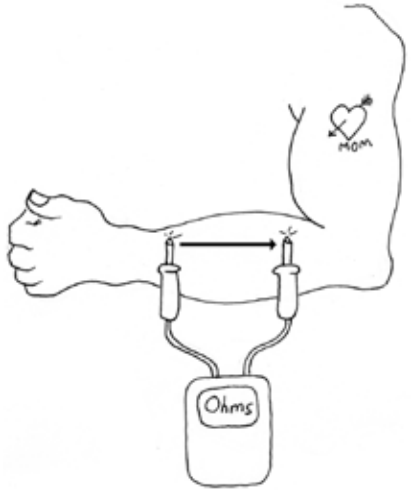

Figure 1-29. *Moisten your skin before trying to measure its resistance. You should find that the resistance goes up as you move the meter probes farther apart. The resistance is proportional to the distance.*

BACKGROUND

The man who discovered resistance

Georg Simon Ohm, pictured in Figure 1-27, was born in Bavaria in 1787 and worked in obscurity for much of his life, studying the nature of electricity using metal wire that he had to make for himself (you couldn't truck on down to Home Depot for a spool of hookup wire back in the early 1800s).

Despite his limited resources and inadequate mathematical abilities, Ohm was able to demonstrate in 1827 that the electrical resistance of a conductor such as copper varied in proportion with its area of cross-section, and the current flowing through it is proportional to the voltage applied to it, as long as temperature is held constant. Fourteen years later, the Royal Society in London finally recognized the significance of his contribution and awarded him the Copley Medal. Today, his discovery is known as Ohm's Law.

Figure 1-27. *Georg Simon Ohm, after being honored for his pioneering work, most of which he pursued in relative obscurity.*

Further Investigation

Attach the snap-on terminal cap (shown earlier in Figure 1-8) to the 9-volt battery. Take the two wires that are attached to the cap and hold them so that the bare ends are just a few millimeters apart. Touch them to your tongue. Now separate the ends of the wires by a couple of inches, and touch them to your tongue again. (See Figure 1-28.) Notice any difference?

Use your meter to measure the electrical resistance of your tongue, this time varying the distance between the two probes. When electricity travels through a shorter distance, it encounters less total resistance. As a result, the current (the flow of electricity per second) increases. You can try a similar experiment on your arm, as shown in Figure 1-29.

Use your meter to test the electrical resistance of water. Dissolve some salt in the water, and test it again. Now try measuring the resistance of distilled water (in a clean glass).

The world around you is full of materials that conduct electricity with varying amounts of resistance.

Cleanup and Recycling

Your battery should not have been damaged or significantly discharged by this experiment. You'll be able to use it again.

Remember to switch off your meter before putting it away.

Experiment 2: Let's Abuse a Battery!

To get a better feeling for electrical power, you're going to do what most books tell you not to do. You're going to short out a battery. A short circuit is a direct connection between the two sides of a power source.

Short Circuits

Short circuits can be dangerous. Do not short out a power outlet in your home: there'll be a loud bang, a bright flash, and the wire or tool that you use will be partially melted, while flying particles of melted metal can burn you or blind you.

If you short out a car battery, the flow of current is so huge that the battery might even explode, drenching you in acid (Figure 1-30).

Lithium batteries are also dangerous. Never short-circuit a lithium battery: it can catch fire and burn you (Figure 1-31).

Use only an alkaline battery in this experiment, and only a single AA cell (Figure 1-32). You should also wear safety glasses in case you happen to have a defective battery.

You will need:

- 1.5-volt AA battery
- Single-battery carrier
- 3-amp fuse
- Safety glasses (regular eyeglasses or sunglasses will do)

Procedure

Use an alkaline battery. Do not use any kind of rechargeable battery.

Put the battery into a battery holder that's designed for a single battery and has two thin insulated wires emerging from it, as shown in Figure 1-32. Do not use any other kind of battery holder.

Use an alligator clip to connect the bare ends of the wires, as shown in Figure 1-32. There will be no spark, because you are using only 1.5 volts. Wait one minute, and you'll find that the wires are getting hot. Wait another minute, and the battery, too, will be hot.

Figure 1-30. *Anyone who has dropped an adjustable wrench across the bare terminals of a car battery will tell you that short circuits can be dramatic at a "mere" 12 volts, if the battery is big enough.*

Figure 1-31. *The low internal resistance of lithium batteries (which are often used in laptop computers) allows high currents to flow, with unexpected results. Never fool around with lithium batteries!*

Figure 1-32. *Shorting out an alkaline battery can be safe if you follow the directions precisely. Even so, the battery is liable to become too hot to touch comfortably. Don't try this with any type of rechargeable battery.*

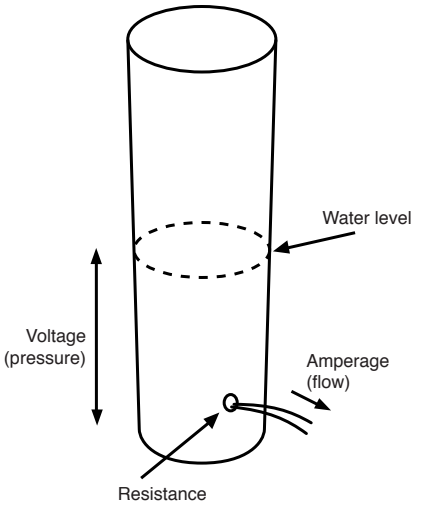

Figure 1-33. *Think of voltage as pressure, and amperes as flow.*

The heat is caused by electricity flowing through the wires and through the electrolyte (the conductive fluid) inside the battery. If you've ever used a hand pump to force air into a bicycle tire, you know that the pump gets warm. Electricity behaves in much the same way. You can imagine the electricity being composed of particles (electrons) that make the wire hot as they push through it. This isn't a perfect analogy, but it's close enough for our purposes.

Chemical reactions inside the battery create electrical pressure. The correct name for this pressure is *voltage*, which is measured in volts and is named after Alessandro Volta, an electrical pioneer.

Going back to the water analogy: the height of the water in a tank is proportionate to the pressure of the water, and comparable to voltage. Figure 1-33 may help you to visualize this.

But volts are only half of the story. When electrons flow through a wire, the flow is known as *amperage*, named after yet another electrical pioneer, André-Marie Ampère. The flow is also generally known as current. It's the current—the amperage—that generates the heat.

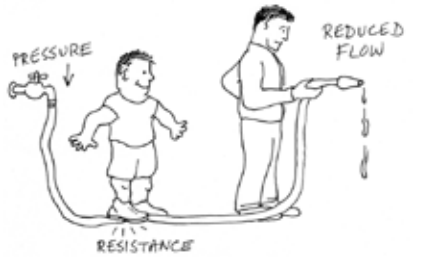

Figure 1-34. *Larger resistance results in smaller flow—but if you increase the pressure, it may overcome the resistance and increase the flow.*

BACKGROUND

Why didn't your tongue get hot?

When you touched the 9-volt battery to your tongue, you felt a tingle, but no perceptible heat. When you shorted out a battery, you generated a noticeable amount of heat, even though you used a lower voltage. How can we explain this?

The electrical resistance of your tongue is very high, which reduces the flow of electrons. The resistance of a wire is very low, so if there's only a wire connecting the two terminals of the battery, more current will pass through it, creating more heat. If all other factors remain constant:

- Lower resistance allows more current to flow (Figure 1-34).
- The heat generated by electricity is proportional to the amount of electricity (the current) that flows.

Here are some other basic concepts:

- The flow of electricity per second is measured in amperes, or amps.
- The pressure of electricity causes the flow, measured in volts.
- The resistance to the flow is measured in ohms.
- A higher resistance restricts the current.
- A higher voltage overcomes resistance and increases the current.

If you're wondering exactly how much current flows between the terminals of a battery when you short it out, that's a difficult question to answer. If you try to use your multimeter to measure it, you're liable to blow the fuse inside the meter. Still, you can use your very own 3-amp fuse, which we can sacrifice because it didn't cost very much.

First inspect the fuse very carefully, using a magnifying glass if you have one. You should see a tiny S-shape in the transparent window at the center of the fuse. That S is a thin section of metal that melts easily.

Remove the battery that you short-circuited. It is no longer useful for anything, and should be recycled if possible. Put a fresh battery into the battery carrier, connect the fuse as shown in Figure 1-35, and take another look. You should see a break in the center of the S shape, where the metal melted almost instantly. Figure 1-36 shows the fuse before you connected it, and Figure 1-37 depicts a blown fuse. This is how a fuse works: it melts to protect the rest of the circuit. That tiny break inside the fuse stops any more current from flowing.

Figure 1-35. *When you attach both wires to the fuse, the little S-shaped element inside will melt almost instantly.*

Figure 1-36. *A 3-amp fuse, before its element was melted by a single 1.5-volt battery.*

Figure 1-37. *The same fuse after being melted by electric current.*

FUNDAMENTALS

Volt basics

Electrical pressure is measured in volts. The volt is an international unit. A millivolt is 1/1,000 of a volt.

Number of volts	Usually expressed as	Abbreviated as
0.001 volts	1 millivolt	1 mV
0.01 volts	10 millivolts	10 mV
0.1 volts	100 millivolts	100 mV
1 volt	1,000 millivolts	1V

Ampere basics

We measure electrical flow in amperes, or amps. The ampere is an international unit, often referred to as an "amp." A milliamp is 1/1,000 of an ampere.

Number of amperes	Usually expressed as	Abbreviated as
0.001 amps	1 milliamp	1 mA
0.01 amps	10 milliamps	10 mA
0.1 amps	100 milliamps	100 mA
1 amp	1,000 milliamps	1A

BACKGROUND

Inventor of the battery

Alessandro Volta (Figure 1-38) was born in Italy in 1745, long before science was broken up into specialties. After studying chemistry (he discovered methane in 1776), he became a professor of physics and became interested in the so-called galvanic response, whereby a frog's leg will twitch in response to a jolt of static electricity.

Using a wine glass full of salt water, Volta demonstrated that the chemical reaction between two electrodes, one made of copper, the other of zinc, will generate a steady electric current. In 1800, he refined his apparatus by stacking plates of copper and zinc, separated by cardboard soaked in salt and water. This "voltaic pile" was the first electric battery.

Figure 1-38. *Alessandro Volta discovered that chemical reactions can create electricity.*

FUNDAMENTALS

Direct and alternating current

The flow of current that you get from a battery is known as *direct current*, or DC. Like the flow of water from a faucet, it is a steady stream, in one direction.

The flow of current that you get from the "hot" wire in a power outlet in your home is very different. It changes from positive to negative 50 times each second (in Great Britain and some other nations, 60 times per second). This is known as *alternating current*, or AC, which is more like the pulsatile flow you get from a power washer.

Alternating current is essential for some purposes, such as cranking up voltage so that electricity can be distributed over long distances. AC is also useful in motors and domestic appliances. The parts of an American power outlet are shown in Figure 1-39. A few other nations, such as Japan, also use American-style outlets.

For most of this book I'm going to be talking about DC, for two reasons: first, most simple electronic circuits are powered with DC, and second, the way it behaves is much easier to understand.

I won't bother to mention repeatedly that I'm dealing with DC. Just assume that everything is DC unless otherwise noted.

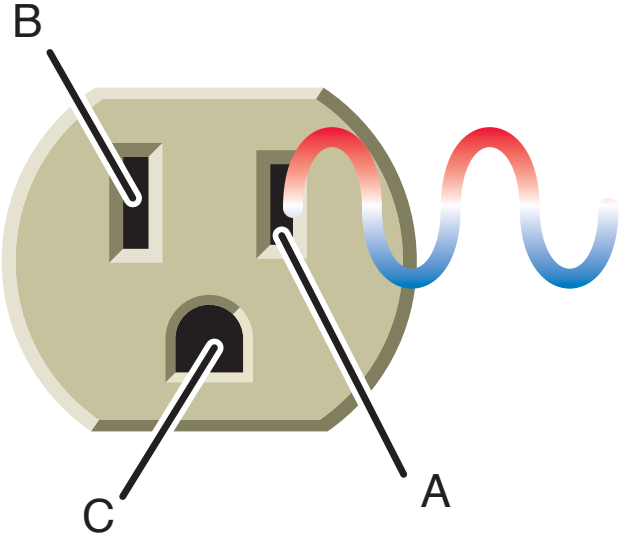

Figure 1-39. *This style of power outlet is found in North America, South America, Japan, and some other nations. European outlets look different, but the principle remains the same. Socket A is the "live" side of the outlet, supplying voltage that alternates between positive and negative, relative to socket B, which is called the "neutral" side. If an appliance develops a fault such as an internal loose wire, it should protect you by sinking the voltage through socket C, the ground.*

Cleanup and Recycling

The first AA battery that you shorted out is probably damaged beyond repair. You should dispose of it. Putting batteries in the trash is not a great idea, because they contain heavy metals that should be kept out of the ecosystem. Your state or town may include batteries in a local recycling scheme. (California requires that almost all batteries be recycled.) You'll have to check your local regulations for details.

The blown fuse is of no further use, and can be thrown away.

The second battery, which was protected by the fuse, should still be OK. The battery holder also can be reused later.

Experiment 3: Your First Circuit

Now it's time to make electricity do something that's at least slightly useful. For this purpose, you'll use components known as resistors, and a light-emitting diode, or LED.

You will need:

- 1.5-volt AA batteries. Quantity: 4.
- Four-battery holder. Quantity: 1.
- Resistors: 470Ω, 1K, and either 2K or 2.2K (the 2.2K value happens to be more common than 2K, but either will do in this experiment). Quantity: 1 of each resistor.
- An LED, any type. Quantity: 1.
- Alligator clips. Quantity: 3.

Setup

It's time to get acquainted with the most fundamental component we'll be using in electronic circuits: the humble resistor. As its name implies, it resists the flow of electricity. As you might expect, the value is measured in ohms.

If you bought a bargain-basement assortment package of resistors, you may find nothing that tells you their values. That's OK; we can find out easily enough. In fact, even if they are clearly labeled, I want you to check their values yourself. You can do it in two ways:

- Use your multimeter. This is excellent practice in learning to interpret the numbers that it displays.
- Learn the color codes that are printed on most resistors. See the following section, "Fundamentals: Decoding resistors," for instructions.

After you check them, it's a good idea to sort them into labeled compartments in a little plastic parts box. Personally, I like the boxes sold at the Michaels chain of crafts stores, but you can find them from many sources.

BACKGROUND

Father of electromagnetism

Born in 1775 in France, André-Marie Ampère (Figure 1-40) was a mathematical prodigy who became a science teacher, despite being largely self-educated in his father's library. His best-known work was to derive a theory of electromagnetism in 1820, describing the way that an electric current generates a magnetic field. He also built the first instrument to measure the flow of electricity (now known as a *galvanometer*), and discovered the element fluorine.

Figure 1-40. *Andre-Marie Ampere found that an electric current running through a wire creates a magnetic field around it. He used this principle to make the first reliable measurements of what came to be known as amperage.*

FUNDAMENTALS

Decoding resistors

Some resistors have their value clearly stated on them in microscopic print that you can read with a magnifying glass. Most, however, are color-coded with stripes. The code works like this: first, ignore the color of the body of the resistor. Second, look for a silver or gold stripe. If you find it, turn the resistor so that the stripe is on the righthand side. Silver means that the value of the resistor is accurate within 10%, while gold means that the value is accurate within 5%. If you don't find a silver or gold stripe, turn the resistor so that the stripes are clustered at the left end. You should now find yourself looking at three colored stripes on the left. Some resistors have more stripes, but we'll deal with those in a moment. See Figures 1-41 and 1-42.

Figure 1-41. *Some modern resistors have their values printed on them, although you may need a magnifier to read them. This 15K resistor is less than half an inch long.*

Figure 1-42. *From top to bottom, these resistor values are 56,000 ohms (56K), 5,600 ohms (5.6K), and 560 ohms. The size tells you how much power the resistor can handle; it has nothing to do with the resistance. The smaller components are rated at 1/4 watt; the larger one in the center can handle 1 watt of power.*

Starting from the left, the first and second stripes are coded according to this table:

Black	0
Brown	1
Red	2
Orange	3
Yellow	4
Green	5
Blue	6
Violet	7
Gray	8
White	9

The third stripe has a different meaning: It tells you how many zeros to add, like this:

Black	-	No zeros
Brown	0	1 zero
Red	00	2 zeros
Orange	000	3 zeros
Yellow	0000	4 zeros
Green	00000	5 zeros
Blue	000000	6 zeros
Violet	0000000	7 zeros
Gray	00000000	8 zeros
White	000000000	9 zeros

FUNDAMENTALS

Decoding resistors (continued)

Note that the color-coding is consistent, so that green, for instance, means either a value of 5 (for the first two stripes) or 5 zeros (for the third stripe). Also, the sequence of colors is the same as their sequence in a rainbow.

So, a resistor colored brown-red-green would have a value of 1-2 and five zeros, making 1,200,000 ohms, or 1.2MΩ. A resistor colored orange-orange-orange would have a value of 3-3 and three zeros, making 33,000 ohms, or 33KΩ. A resistor colored brown-black-red would have a value of 1-0 and two additional zeros, or 1KΩ. Figure 1-43 shows some other examples.

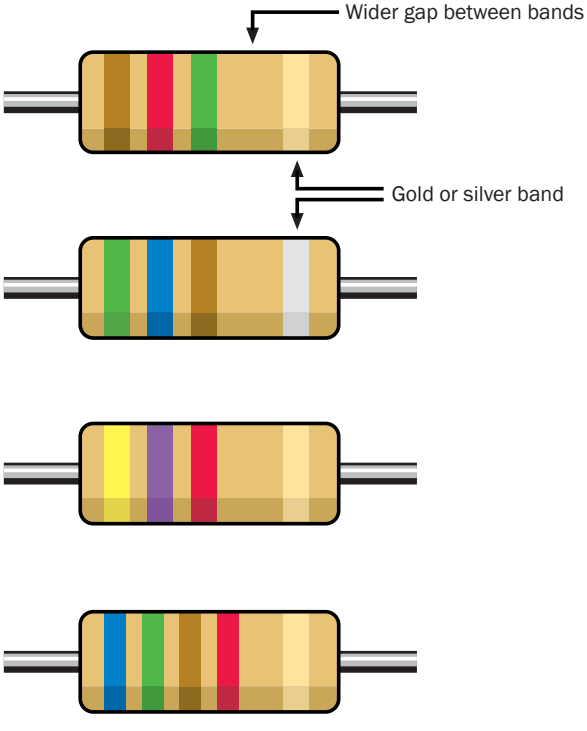

Figure 1-43. *To read the value of a resistor, first turn it so that the silver or gold stripe is on the right, or the other stripes are clustered on the left. From top to bottom: The first resistor has a value of 1-2 and five zeros, or 1,200,000, which is 1.2MΩ. The second is 5-6 and one zero, or 560Ω. The third is 4-7 and two zeros, or 4,700, which is 4.7KΩ. The last is 6-5-1 and two zeros, or 65,100Ω, which is 65.1KΩ.*

If you run across a resistor with four stripes instead of three, the first *three* stripes are digits and the *fourth* stripe is the number of zeros. The third numeric stripe allows the resistor to be calibrated to a finer tolerance.

Confusing? Absolutely. That's why it's easier to use your meter to check the values. Just be aware that the meter reading may be slightly different from the claimed value of the resistor. This can happen because your meter isn't absolutely accurate, or because the resistor is not absolutely accurate, or both. As long as you're within 5% of the claimed value, it doesn't matter for our purposes.

Lighting an LED

Now take a look at one of your LEDs. An old-fashioned lightbulb wastes a lot of power by converting it into heat. LEDs are much smarter: they convert almost all their power into light, and they last almost indefinitely—as long as you treat them right!

An LED is quite fussy about the amount of power it gets, and the way it gets it. Always follow these rules:

- The *longer* wire protruding from the LED must receive a *more positive* voltage than the shorter wire.
- The voltage difference between the long wire and the short wire must not exceed the limit stated by the manufacturer.
- The current passing through the LED must not exceed the limit stated by the manufacturer.

What happens if you break these rules? Well, we're going to find out!

Make sure you are using fresh batteries. You can check by setting your multimeter to measure volts DC, and touching the probes to the terminals of each battery. You should find that each of them generates a pressure of at least 1.5 volts. If they read slightly higher than this, it's normal. A battery starts out above its rated voltage, and delivers progressively less as you use it. Batteries also lose some voltage while they are sitting on the shelf doing nothing.

Load your battery holder (taking care that the batteries are the right way around, with the negative ends pressing against the springs in the carrier). Use your meter to check the voltage on the wires coming out of the battery carrier. You should have at least 6 volts.

Now select a 2KΩ resistor. Remember, "2KΩ" means "2,000 ohms." If it has colored stripes, they should be red-black-red, meaning 2-0 and two more zeros. Because 2.2K resistors are more common than 2K resistors, you can substitute one of them if necessary. It will be colored red-red-red.

Wire it into the circuit as shown in Figures 1-44 and 1-45, making the connections with alligator clips. You should see the LED glow very dimly.

Now swap out your 2K resistor and substitute a 1K resistor, which will have brown-black-red stripes, meaning 1-0 and two more zeros. The LED should glow more brightly.

Swap out the 1K resistor and substitute a 470Ω resistor, which will have yellow-violet-brown stripes, meaning 4-7 and one more zero. The LED should be brighter still.

This may seem very elementary, but it makes an important point. The resistor blocks a percentage of the voltage in the circuit. Think of it as being like a kink or constriction in a flexible hose. A higher-value resistor blocks more voltage, leaving less for the LED.

Figure 1-44. *The setup for Experiment 3, showing resistors of 470Ω, 1KΩ, and 2KΩ. Apply alligator clips where shown, to make a secure contact, and try each of the resistors one at a time at the same point in the circuit, while watching the LED.*

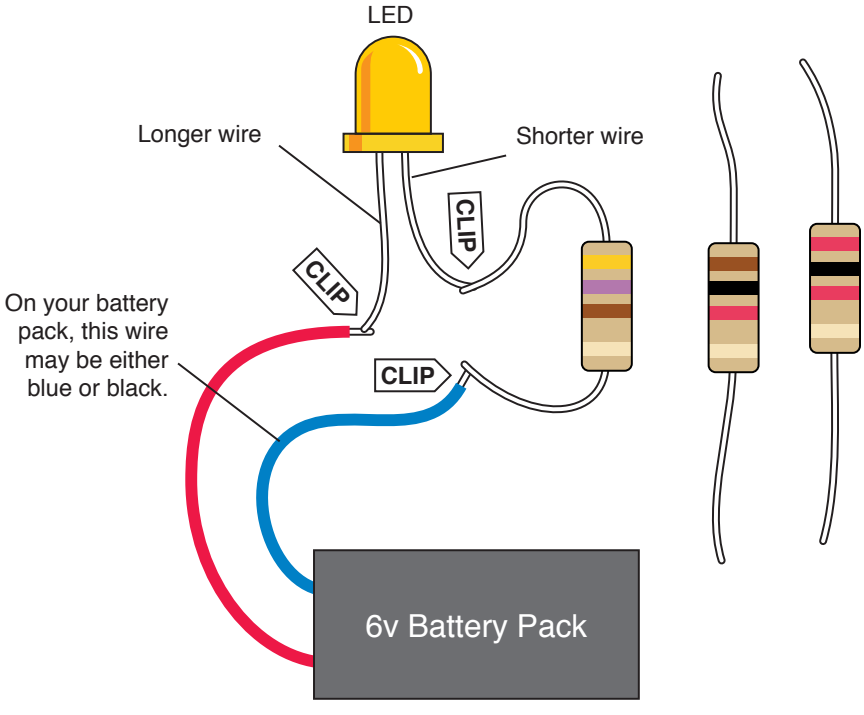

Figure 1-45. *Here's how it actually looks, using a large LED. If you start with the highest value resistor, the LED will glow very dimly as you complete the circuit. The resistor drops most of the voltage, leaving the LED with insufficient current to make it shine brightly.*

Cleanup and Recycling

We'll use the batteries and the LED in the next experiment. The resistors can be reused in the future.

Experiment 4: Varying the Voltage

Potentiometers come in various shapes and sizes, but they all do the same thing: they allow you to vary voltage and current by varying resistance. This experiment will enable you to learn more about voltage, amperage, and the relationship between them. You'll also learn how to read a manufacturer's data sheet.

You will need the same batteries, battery carrier, alligator clips, and LED from the last experiment, plus:

- Potentiometer, 2KΩ linear. Quantity: 2. (See Figure 1-46.) Full-sized potentiometers that look like this are becoming less common, as miniature versions are taking their place. I'd like you to use a large one, though, because it's so much easier to work with.
- One extra LED.
- Multimeter.

Look Inside Your Potentiometer

The first thing I want you to do is find out how a potentiometer works. This means you'll have to open it, which is why your shopping list required you to buy two of them, in case you can't put the first one back together again.

Most potentiometers are held together with little metal tabs. You should be able to grab hold of the tabs with your wire cutters or pliers, and bend them up and outward. If you do this, the potentiometer should open up as shown in Figures 1-47 and 1-48.

Figure 1-46

Figure 1-47

Figure 1-48. *To open the potentiometer, first pry up the four little metal tabs around the edge (you can see one sticking out at the left and another one sticking out at the right in Figure 1-47). Inside is a coil of wire around a flat plastic band, and a pair of springy contacts (the wiper), which conduct electricity to or from any point in the coil when you turn the shaft.*

Depending whether you have a really cheap potentiometer or a slightly more high-class version, you may find a circular track of conductive plastic or a loop of coiled wire. Either way, the principle is the same. The wire or the plastic

possesses some resistance (a total of 2K in this instance), and as you turn the shaft of the potentiometer, a wiper rubs against the resistance, giving you a shortcut to any point from the center terminal.

You can try to put it back together, but if it doesn't work, use your backup potentiometer instead.

To test your potentiometer, set your meter to measure resistance (ohms) and touch the probes while turning the potentiometer shaft to and fro, as shown in Figure 1-49.

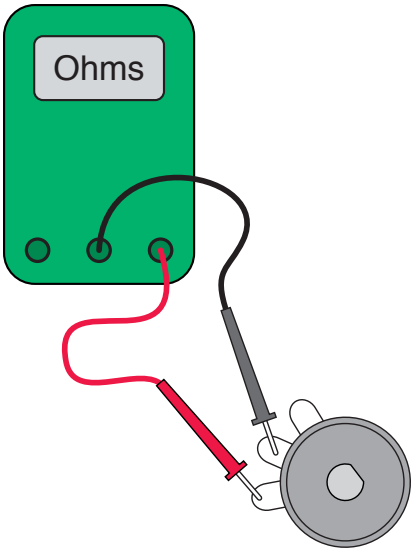

Figure 1-49. *Measure the resistance between these two terminals of the potentiometer while you turn its shaft to and fro.*

Dimming Your LED

Begin with the potentiometer turned all the way counterclockwise, otherwise you'll burn out the LED before we even get started. (A very, very small number of potentiometers increase and decrease resistance in the opposite way to which I'm describing here, but as long as your potentiometer looks like the one in Figure 1-48 after you open it up, my description should be accurate.)

Now connect everything as shown in Figures 1-50 and 1-51, taking care that you don't allow the metal parts of any of the alligator clips to touch each other. Now turn up the potentiometer *very* slowly. You'll notice the LED glowing brighter, and brighter, and brighter—until, oops, it goes dark. You see how easy it is to destroy modern electronics? Throw away that LED. It will never glow again. Substitute a new LED, and we'll be more careful this time.

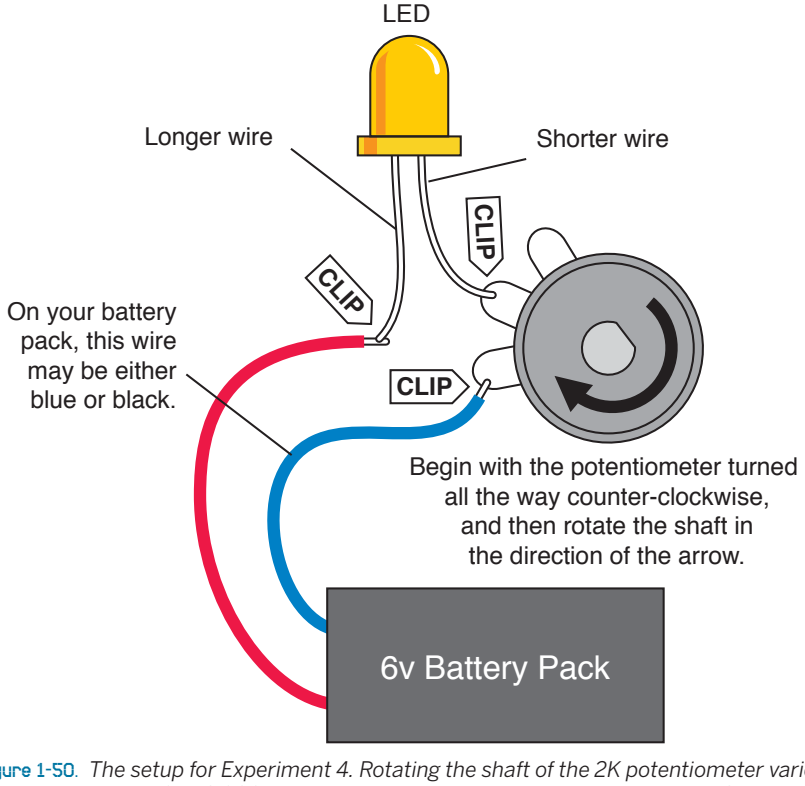

Figure 1-50. *The setup for Experiment 4. Rotating the shaft of the 2K potentiometer varies its resistance from 0 to 2,000Ω. This resistance protects the LED from the full 6 volts of the battery.*

Figure 1-51. *The LED in this photo is dark because I turned the potentiometer up just a little bit too far.*

Figure 1-52

Figure 1-53

Figure 1-54. *Each meter has a different way to measure volts DC. The manually adjusted meter (top) requires you to move a slider switch to "DC" and then choose the highest voltage you want to measure: In this case, the selected voltage is 20 (because 2 would be too low). Using the autoranging RadioShack meter, you set it to "V" and the meter will figure out which range to use.*

While the batteries are connected to the circuit, set your meter to measure *volts DC* as shown in Figures 1-52 through 1-54. Now touch the probes either side of the LED. Try to hold the probes in place while you turn the potentiometer up a little, and down a little. You should see the voltage pressure around the LED changing accordingly. We call this the *potential difference* between the two wires of the LED.

If you were using a miniature old-fashioned lightbulb instead of an LED, you'd see the potential difference varying much more, because a lightbulb behaves like a "pure" resistor, whereas an LED self-adjusts to some extent, modifying its resistance as the voltage pressure changes.

Now touch the probes to the two terminals of the potentiometer that we're using, so that you can measure the potential difference between them. The potentiometer and the LED share the total available voltage, so when the potential difference (the voltage drop) around the potentiometer goes up, the potential difference around the LED goes down, and vice versa. See Figures 1-55 through 1-57. A few things to keep in mind:

- If you add the voltage drops across the devices in the circuit, the total is the same as the voltage supplied by the batteries.
- You measure voltage relatively, between two points in a circuit.
- Apply your meter like a stethoscope, without disturbing or breaking the connections in the circuit.

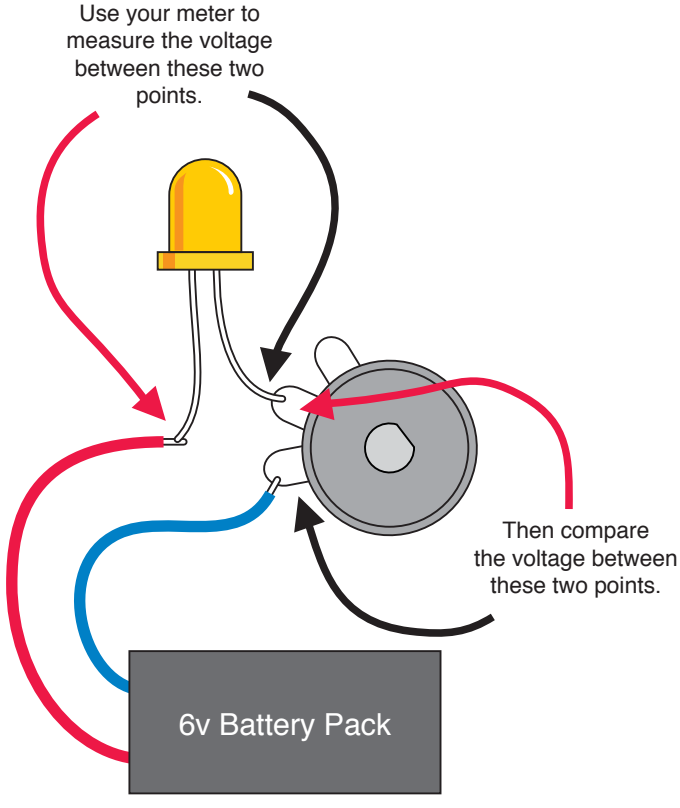

Figure 1-55. *How to measure voltage in a simple circuit.*

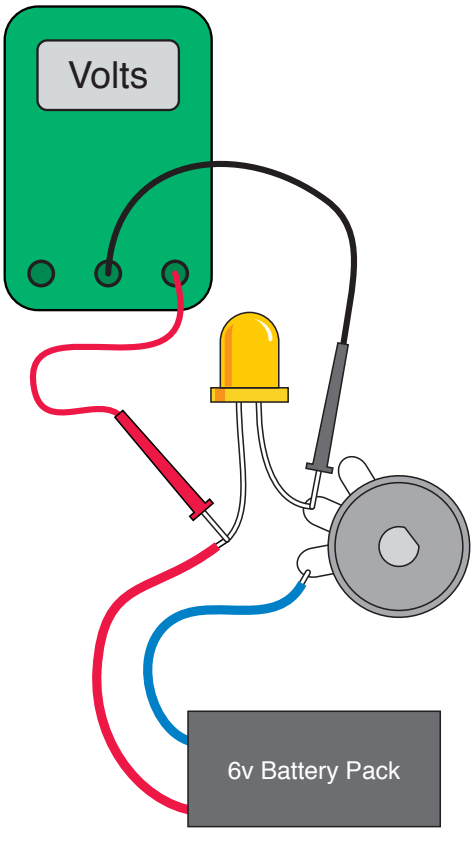

Figure 1-56. *The meter shows how much voltage the LED takes.*

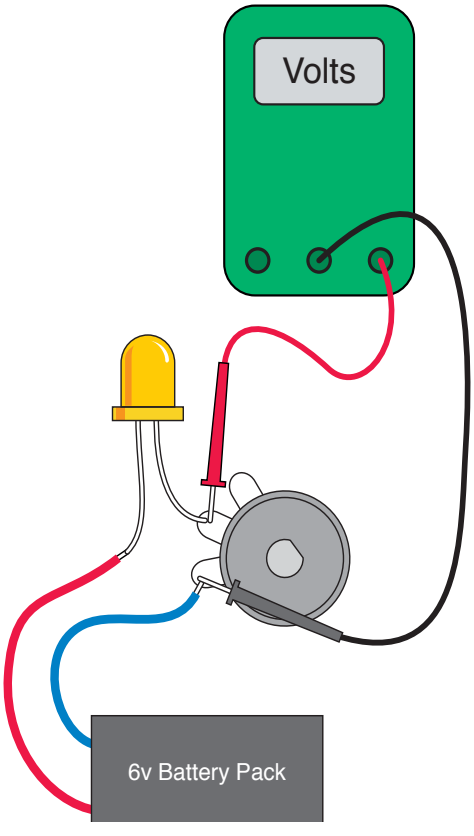

Figure 1-57. *The meter shows how much voltage the potentiometer takes.*

Checking the Flow

Now I want you to make a different measurement. I want you to measure the flow, or current, in the circuit, using your meter set to mA (milliamps). Remember, to measure current:

- You can only measure current when it passes *through* the meter.
- You have to insert your meter into the circuit.
- Too much current will blow the fuse inside your meter.

Make sure you set your meter to measure mA, not volts, before you try this. Some meters require you to move one of your leads to a different socket on the meter, to measure mA. See Figures 1-58 through 1-61.

Figure 1-58. *Any meter will blow its internal fuse if you try to make it measure too high an amperage. In our circuit, this is not a risk as long as you keep the potentiometer in the middle of its range. Choose "mA" for milliamps and remember that the meter displays numbers that mean thousandths of an amp.*

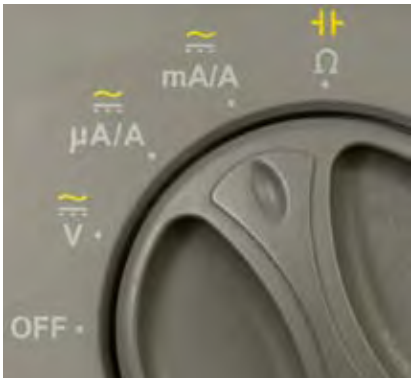

Figure 1-59

Figure 1-60

Figure 1-61. *A manual meter such as the one here may require you to shift the red lead to a different socket, to measure milliamps. Most modern meters don't require this until you are measuring higher currents.*

Insert your meter into the circuit, as shown in Figure 1-62. Don't turn the potentiometer more than halfway up. The resistance in the potentiometer will protect your meter, as well as the LED. If the meter gets too much current, you'll find yourself replacing its internal fuse.

As you adjust the potentiometer up and down a little, you should find that the varying resistance in the circuit changes the flow of current—the amperage. This is why the LED burned out in the previous experiment: too much current made it hot, and the heat melts it inside, just like the fuse in the previous experiment. *A higher resistance limits the flow of current, or amperage*.

Now insert the meter in another part of the circuit, as shown in Figure 1-63. As you turn the potentiometer up and down, you should get exactly the same results as with the configuration in Figure 1-64. This is because the current is the same at all points in a similar circuit. *It has to be, because the flow of electrons has no place else to go*.

It's time now to nail this down with some numbers. Here's one last thing to try. Set aside the LED and substitute a 1KΩ resistor, as shown in Figure 1-64. The total resistance in the circuit is now 1KΩ plus whatever the resistance the potentiometer provides, depending how you set it. (The meter also has some resistance, but it's so low, we can ignore it.)

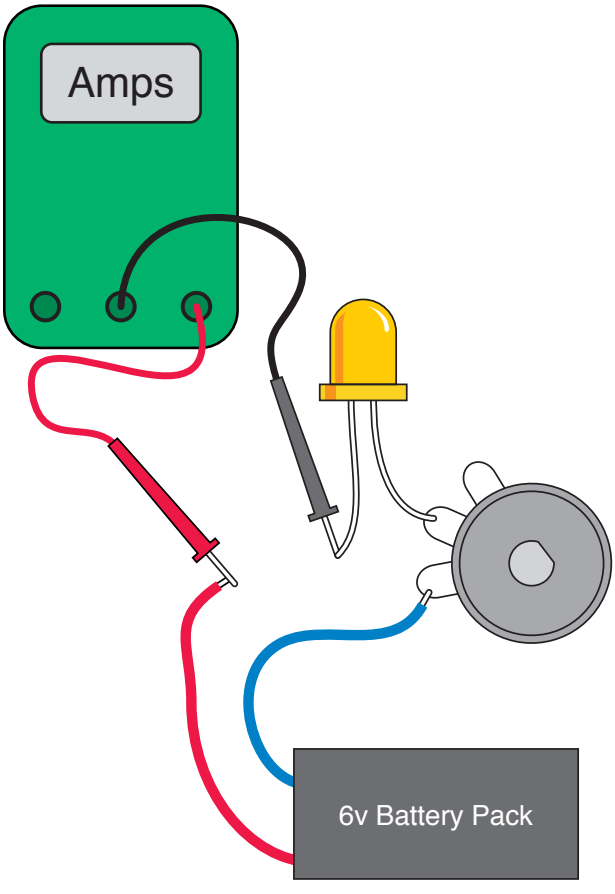

Figure 1-62. *To measure amps, as illustrated here and in Figure 1-63, the current has to pass through the meter. When you increase the resistance, you restrict the current flow, and the lower flow makes the LED glow less brightly.*

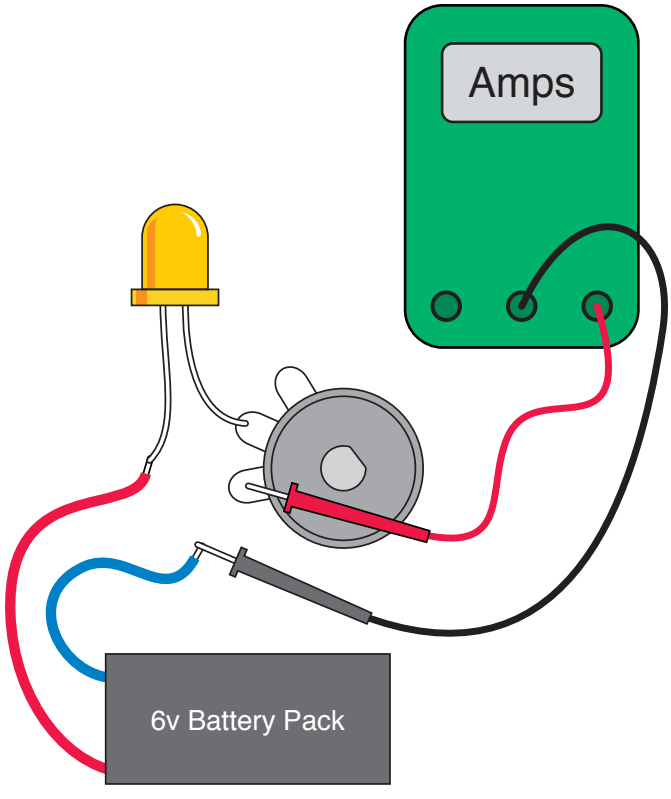

Figure 1-63

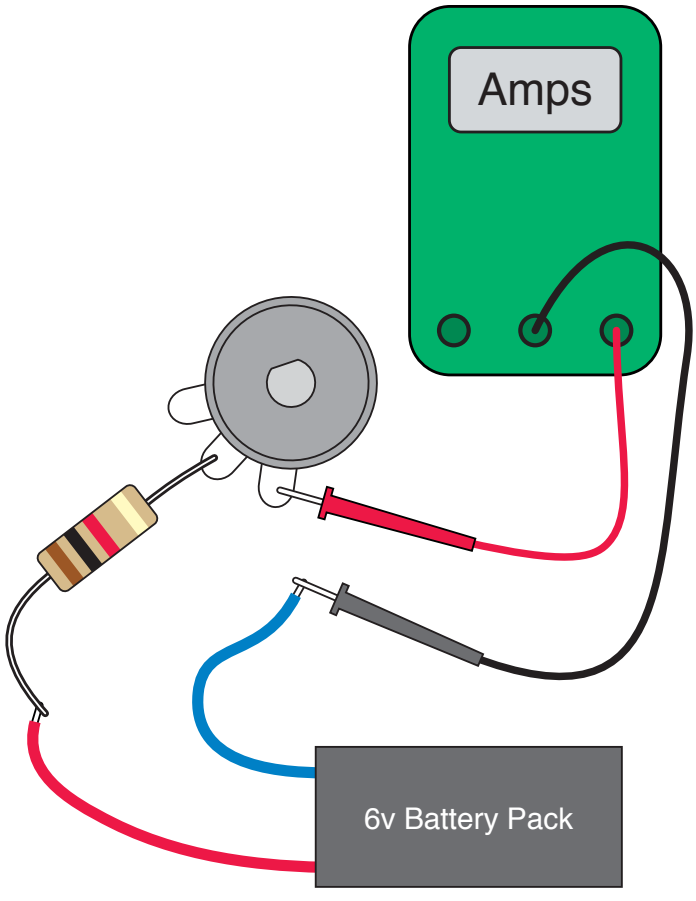

Figure 1-64. *If you substitute a resistor instead of the LED, you can confirm that the current flowing through the circuit varies with the total resistance in the circuit, if the voltage stays the same.*

Turn the potentiometer all the way counterclockwise, and you have a total of 3K resistance in the circuit. Your meter should show about 2 mA flowing. Now turn the potentiometer halfway, and you have about 2K total resistance. You should see about 3 mA flowing. Turn the potentiometer all the way clockwise, so there's a total of 1K, and you should see 6 mA flowing. You may notice that if we multiply the resistance by the amperage, we get 6 each time—which just happens to be the voltage being applied to the circuit. See the following table.

Total resistance	Current	Voltage
(KΩ)	(mA)	(Volts)
3	2	6
2	3	6
1	6	6

In fact, we could say:

voltage = kilohms × milliamps

But wait a minute: 1K is 1,000 ohms, and 1mA is 1/1,000 of an amp. Therefore, our formula should really look like this:

voltage = (ohms × 1,000) × (amps/1,000)

The two factors of 1,000 cancel out, so we get this:

volts = ohms × amps

This is known as Ohm's Law. See the section, "Fundamentals: Ohm's Law," on the following page.

FUNDAMENTALS

Series and parallel

Before we go any further, you should know how resistance in a circuit increases when you put resistors in series or in parallel. Figures 1-65 through 1-67 illustrate this. Remember:

- Resistors in series are oriented so that one follows the other.
- Resistors in parallel are oriented side by side.

When you put two equal-valued resistors in series, you double the total resistance, because electricity has to pass through two barriers in succession.

When you put two equal-valued resistors in parallel, you divide the total resistance by two, because you're giving the electricity two paths which it can take, instead of one.

In reality we don't normally need to put resistors in parallel, but we often put other types of components in parallel. Lightbulbs in your house, for instance, are all wired that way. So, it's useful to understand that resistance in a circuit goes down if you keep adding components in parallel.

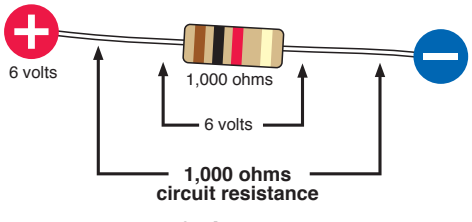

Figure 1-65. *One resistor takes the entire voltage, and according to Ohm's Law, it draws v/R = 6/1,000 = 0.006 amps = 6mA of current.*

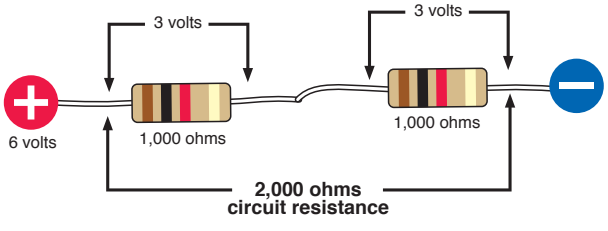

Figure 1-66. *When two resistors are in series, the electricity has to pass through one to reach the other, and therefore each of them takes half the voltage. Total resistance is now 2,000 ohms, and according to Ohm's Law, the circuit draws v/R = 6/2,000 = 0.003 amps = 3mA of current.*

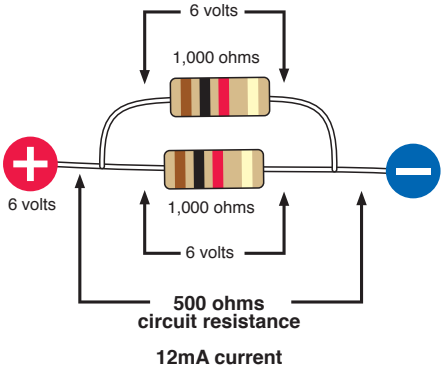

Figure 1-67. *When two resistors are in parallel, each is exposed to the full voltage, so each of them takes 6 volts. The electricity can now flow through both at once, so the total resistance of the circuit is half as much as before. According to Ohm's Law, the circuit draws v/R = 6/500 = 0.012 amps = 12mA of current.*

FUNDAMENTALS

Ohm's Law

For reasons I'll explain in a moment, amps are normally abbreviated with the letter I. V stands for volts and R stands for resistance in ohms (because the omega symbol, Ω, is not easily generated from most keyboards). Using these symbols, you can write Ohm's Law in three different ways:

$V = I \times R$

$I = V/R$

$R = V/I$

Remember, V is a *difference* in voltage between two points in a simple circuit, R is the resistance in ohms *between* the same two points, and I is the current in amps flowing *through* the circuit between the two points.

Letter I is used because originally current was measured by its *inductance*, meaning the ability to induce magnetic effects. It would be much less confusing to use A for amps, but unfortunately it's too late for that to happen.

Using Ohm's Law

Ohm's Law is extremely useful. For example, it helps us to figure out whether a component can be used safely in a circuit. Instead of stressing the component until we burn it out, we can predict whether it will work.

For instance, the first time you turned the potentiometer, you didn't really know how far you could go until the LED burned out. Wouldn't it be useful to know precisely what resistance to put in series with an LED, to protect it adequately while providing as much light as possible?

How to Read a Data Sheet

Like most information, the answer to this question is available online.

Here's how you find a manufacturer's data sheet (Figure 1-68). First, find the component that you're interested in from a mail-order source. Next, Google the part number and manufacturer's name. Usually the data sheet will pop up as the first hit. A source such as *Mouser.com* makes it even easier by giving you a direct link to manufacturers' data sheets for many products.

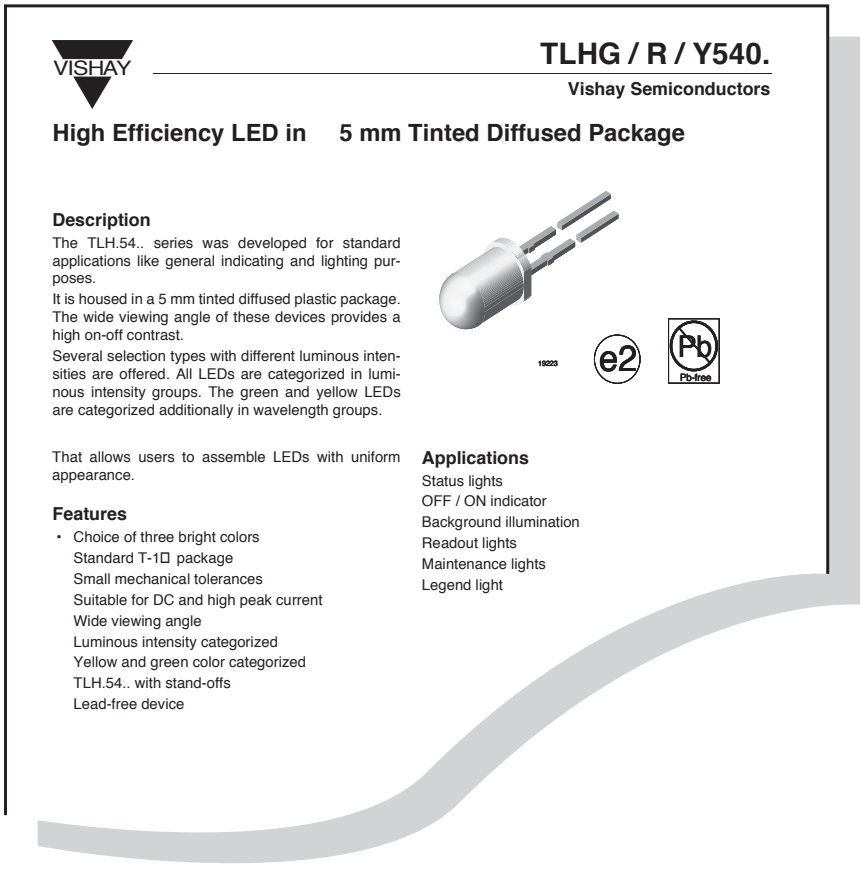

VISHAY

TLHG / R / Y540.

Vishay Semiconductors

High Efficiency LED in 5 mm Tinted Diffused Package

Description

The TLH.54.. series was developed for standard applications like general indicating and lighting purposes.

It is housed in a 5 mm tinted diffused plastic package. The wide viewing angle of these devices provides a high on-off contrast.

Several selection types with different luminous intensities are offered. All LEDs are categorized in luminous intensity groups. The green and yellow LEDs are categorized additionally in wavelength groups.

That allows users to assemble LEDs with uniform appearance.

Features

- Choice of three bright colors
  Standard T-1□ package
  Small mechanical tolerances
  Suitable for DC and high peak current
  Wide viewing angle
  Luminous intensity categorized
  Yellow and green color categorized
  TLH.54.. with stand-offs
  Lead-free device

Applications

Status lights
OFF / ON indicator
Background illumination
Readout lights
Maintenance lights
Legend light

Figure 1-68. *The beginning of a typical data sheet, which includes all relevant specifications for the product, freely available online.*

BACKGROUND

How much voltage does a wire consume?

Normally, we can ignore the resistance in electric wires, such as the little leads of wire that stick out of resistors, because it's trivial. However, if you try to force large amounts of current through long lengths of thin wire, the resistance of the wire can become important.

How important? Once again, we can use Ohm's Law to find out.

Suppose that a very long piece of wire has a resistance of 0.2Ω. And we want to run 15 amps through it. How much voltage will the wire steal from the circuit, because of its resistance?

Once again, you begin by writing down what you know:

$R = 0.2$

$I = 15$

We want to know V, the potential difference, for the wire, so we use the version of Ohm's Law that places V on the left side:

$V = I \times R$

Now plug in the values:

$V = 15 \times 0.2 = 3$ volts

Three volts is not a big deal if you have a high-voltage power supply, but if you are using a 12-volt car battery, this length of wire will take one-quarter of the available voltage.

Now you know why the wiring in automobiles is relatively thick—to reduce its resistance well below 0.2Ω. See Figure 1-69.

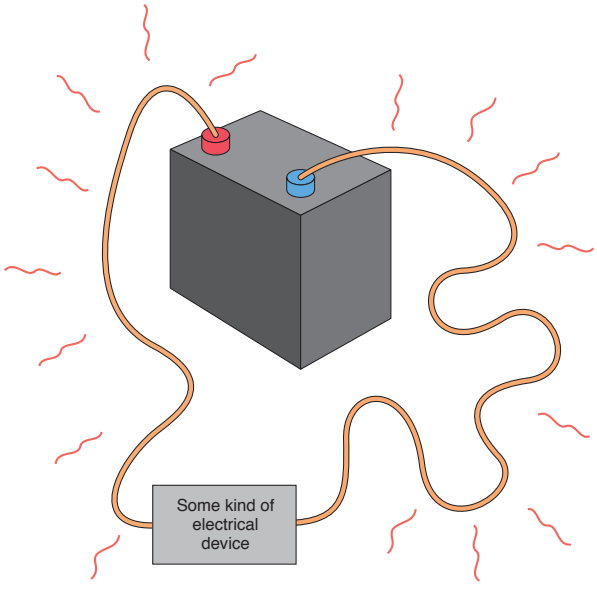

Figure 1-69. *When a 12-volt car battery runs some kind of electrical device through a long piece of thin wire, the resistance of the wire steals some of the voltage and dissipates it as heat.*

BACKGROUND

The origins of wattage

James Watt (Figure 1-70) is known as the inventor of the steam engine. Born in 1736 in Scotland, he set up a small workshop in the University of Glasgow, where he struggled to perfect an efficient design for using steam to move a piston in a cylinder. Financial problems and the primitive state of the art of metal working delayed practical applications until 1776.

Despite difficulties in obtaining patents (which could only be granted by an act of parliament in those times), Watt and his business partner eventually made a lot of money from his innovations. Although he predated the pioneers in electricity, in 1889 (70 years after his death), his name was assigned to the basic unit of electric power that can be defined by multiplying amperes by volts. See the Fundamentals section, "Watt Basics," on page 31.

Figure 1-70. *James Watt's development of steam power enabled the industrial revolution. After his death, he was honored by having his name applied to the basic unit of power in electricity.*

Here's an example. Suppose I want a red LED, such as the Vishay part TLHR5400, which has become such a common item that I can buy them individually for 9 cents apiece. I click the link to the data sheet maintained by the manufacturer, Vishay Semiconductor. Almost immediately I have a PDF page on my screen. This data sheet is for TLHR, TLHG, and TLHY types of LED, which are red, green, and yellow respectively, as suggested by the R, G, and Y in the product codes. I scroll down and look at the "Optical and Electrical Characteristics" section. It tells me that under conditions of drawing a current of 20 mA, the LED will enjoy a "Typ," meaning, typical, "forward voltage" of 2 volts. The "Max," meaning maximum, is 3 volts.

Let's look at one other data sheet, as not all of them are written the same way. I'll choose a different LED, the Kingbright part WP7113SGC. Click on the link to the manufacturer's site, and I find on the second page of the data sheet a typical forward voltage of 2.2, maximum 2.5, and a maximum forward current of 25 mA. I also find some additional information: a maximum reverse voltage of 5 and maximum reverse current of 10 uA (that's microamps, which are 1,000 times smaller than milliamps). This tells us that you should avoid applying excessive voltage to the LED the wrong way around. If you exceed the reverse voltage, you risk burning out the LED. Always observe polarity!

Kingbright also warns us how much heat the LED can stand: 260° C (500° F) for a few seconds. This is useful information, as we'll be putting aside our alligator clips and using hot molten solder to connect electrical parts in the near future. Because we have already destroyed a battery, a fuse, and an LED in just four experiments, maybe you won't be surprised when I tell you that we will destroy at least a couple more components as we test their limits with a soldering iron.

Anyway, now we know what an LED wants, we can figure out how to supply it. If you have any difficulties dealing with decimals, check the Fundamentals section "Decimals," on the next page, before continuing.

How Big a Resistor Does an LED Need?

Suppose that we're use the Vishay LED. Remember its requirements from the data sheet? Maximum of 3 volts, and a safe current of 20mA.

I'm going to limit it to 2.5 volts, to be on the safe side. We have 6 volts of battery power. Subtract 2.5 from 6 and we get 3.5. So we need a resistor that will take 3.5 volts from the circuit, leaving 2.5 for the LED.

The current flow is the same at all places in a simple circuit. If we want a maximum of 20mA to flow through the LED, the same amount of current will be flowing through the resistor.

Now we can write down what we know about the resistor in the circuit. Note that we have to convert all units to volts, amps, and ohms, so that 20mA should be written as 0.02 amps:

V = 3.5 (the potential drop across the resistor)
I = 0.02 (the current flowing through the resistor)

We want to know R, the resistance. So, we use the version of Ohm's Law that puts R on the left side:

$$R = V/I$$

Now plug in the values:

$$R = 3.5/0.02$$

Run this through your pocket calculator if you find decimals confusing. The answer is:

$$R = 175\Omega$$

It so happens that 175Ω isn't a standard value. You may have to settle for 180 or 220Ω, but that's close enough.

Evidently the 470Ω resistor that you used in Experiment 3 was a very conservative choice. I suggested it because I said originally that you could use any LED at all. I figured that no matter which one you picked, it should be safe with 470Ω to protect it.

Cleanup and Recycling

The dead LED can be thrown away. Everything else is reusable.

FUNDAMENTALS

Decimals

Legendary British politician Sir Winston Churchill is famous for complaining about "those damned dots." He was referring to decimal points. Because Churchill was Chancellor of the Exchequer at the time, and thus in charge of all government expenditures, his difficulty with decimals was a bit of a problem. Still, he muddled through in time-honored British fashion, and so can you.

You can also use a pocket calculator—or follow two basic rules.

Doing multiplication: combine the zeros

Suppose you need to multiply 0.04 by 0.005:

1. Count the total number of zeros following both of the decimal points. In this case, three zeros.
2. Multiply the numbers which follow the zeros. In this case, $4 \times 5 = 20$.
3. Write down the result as 0 followed by a decimal point, followed by the number of zeros, followed by the multiplication result. Like this: 0.00020, which is the same as 0.0002.

Doing division: cancel the zeros

Suppose you need to divide 0.006 by 0.0002:

1. Shift the decimal points to the right, in both the numbers, by the same number of steps, until both the numbers are greater than 1. In this case, shift the point four steps in each number, so you get 60 divided by 2.
2. Do the division. The result in this case is 30.

THEORY

Doing the math on your tongue

I'm going to go back to the question I asked in the previous experiment: why didn't your tongue get hot?

Now that you know Ohm's Law, you can figure out the answer in numbers. Let's suppose the battery delivered its rated 9 volts, and your tongue had a resistance of 50K, which is 50,000 ohms. Write down what you know:

V = 9

R = 50,000

We want to know the current, I, so we use the version of Ohm's Law that puts this on the left:

I = V/R

Plug in the numbers:

I = 9/50,000 = 0.00018 amps

Move the decimal point three places to convert to milliamps:

I = 0.18 mA

That's a tiny current that will not produce much heat at 9 volts.

What about when you shorted out the battery? How much current made the wires get hot? Well, suppose the wires had a resistance of 0.1 ohms (probably it's less, but I'll start with 0.1 as a guess). Write down what we know:

V = 1.5

R = 0.1

Once again we're trying to find I, the current, so we use:

I = V/R

Plug in the numbers:

I = 1.5/0.1 = 15 amps

That's 100,000 times the current that may have passed through your tongue, which would have generated much more heat, even though the voltage was lower.

Could that tiny little battery really pump out 15 amps? Remember that the battery got hot, as well as the wire. This tells us that the electrons may have met some resistance inside the battery, as well as in the wire. (Otherwise, where else did the heat come from?) Normally we can forget about the internal resistance of a battery, because it's so low. But at high currents, it becomes a factor.

I was reluctant to short-circuit the battery through a meter, to try to measure the current. My meter will fry if the current is greater than 10A. However I did try putting other fuses into the circuit, to see whether they would blow. When I tried a 10A fuse, it did not melt. Therefore, for the brand of battery I used, I'm fairly sure that the current in the short circuit was under 10A, but I know it was over 3A, because the 3A fuse blew right away.

The internal resistance of the 1.5-volt battery prevented the current in the short circuit from getting too high. This is why I cautioned against using a larger battery (especially a car battery). Larger batteries have a much lower internal resistance, allowing dangerously high currents which generate explosive amounts of heat. A car battery is designed to deliver literally hundreds of amps when it turns a starter motor. That's quite enough current to melt wires and cause nasty burns. In fact, you can weld metal using a car battery.

Lithium batteries also have low internal resistance, making them very dangerous when they're shorted out. High current can be just as dangerous as high voltage.

FUNDAMENTALS

Watt basics

So far I haven't mentioned a unit that everyone is familiar with: watts.

A watt is a unit of work. Engineers have their own definition of work—they say that work is done when a person, an animal, or a machine pushes something to overcome mechanical resistance. Examples would be a steam engine pulling a train on a level track (overcoming friction and air resistance) or a person walking upstairs (overcoming the force of gravity).

When electrons push their way through a circuit, they are overcoming a kind of resistance, and so they are doing work, which can be measured in watts. The definition is easy:

watts = volts × amps

Or, using the symbols customarily assigned, these three formulas all mean the same thing:

$W = V \times I$

$V = W/I$

$I = W/V$

Watts can be preceded with an "m," for "milli," just like volts:

Number of watts	Usually expressed as	Abbreviated as
0.001 watts	1 milliwatt	1mW
0.01 watts	10 milliwatts	10 mW
0.1 watts	100 milliwatts	100 mW
1 watt	1,000 milliwatts	1W

Because power stations, solar installations, and wind farms deal with much larger numbers, you may also see references to kilowatts (using letter K) and megawatts (with a capital M, not to be confused with the lowercase m used to define milliwatts):

Number of watts	Usually expressed as	Abbreviated as
1,000 watts	1 kilowatt	1 KW
1,000,000 watts	1 megawatt	1 MW

Lightbulbs are calibrated in watts. So are stereo systems. The watt is named after James Watt, inventor of the steam engine. Incidentally, watts can be converted to horsepower, and vice versa.

THEORY

Power assessments

I mentioned earlier than resistors are commonly rated as being capable of dealing with 1/4 watt, 1/2 watt, 1 watt, and so on. I suggested that you should buy resistors of 1/4 watt or higher. How did I know this?

Go back to the LED circuit. Remember we wanted the resistor to drop the voltage by 3.5 volts, at a current of 20 mA. How many watts of power would this impose on the resistor?

Write down what you know:

V = 3.5 (the voltage drop imposed by the resistor)

I = 20mA = 0.02 amps (the current flowing through the resistor)

We want to know W, so we use this version of the formula:

$W = V \times I$

Plug in the values:

$W = 3.5 \times 0.02 = 0.07$ watts (the power being dissipated by the resistor)

Because 1/4 watt is 0.25 watts, obviously a 1/4 watt resistor will have about four times the necessary capacity. In fact you could have used a 1/8 watt resistor, but in future experiments we may need resistors that can handle 1/4 watt, and there's no penalty for using a resistor that is rated for more watts than will actually pass through it.

Experiment 5: Let's Make a Battery

Long ago, before web surfing, file sharing, or cell phones, kids were so horribly deprived that they tried to amuse themselves with kitchen-table experiments such as making a primitive battery by pushing a nail and a penny into a lemon. Hard to believe, perhaps, but true!

This is seriously old-school—but I want you to try it anyway, because anyone who wants to get a feel for electricity should see how easy it is to extract it from everyday objects around us. Plus, if you use enough lemons, you just *might* generate enough voltage to power an LED.

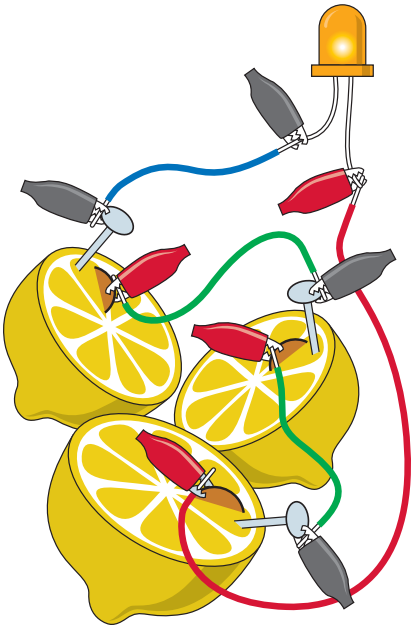

Figure 1-71. *A three-lemon battery. Don't be too disappointed if the LED fails to light up. The lemons have a high electrical resistance, so they can't deliver much current, especially through the relatively small surface area of the nails and the pennies. However, the lemon battery does generate voltage that you can measure with your meter.*

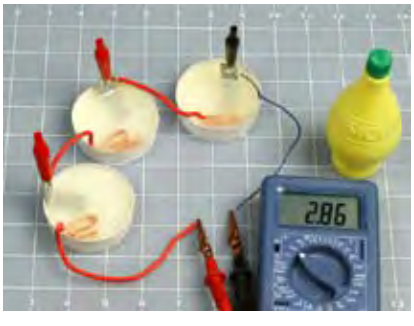

Figure 1-72. *Bottled lemon juice seems to work just as well as fresh lemon juice. I cut the bottoms off three paper cups, inserted a galvanized bracket into each, and used heavyweight stranded copper wire to make the positive electrodes*

The basic components of a battery are two metal electrodes immersed in an electrolyte. I won't define these terms here (they're explained in the following section "Theory: The nature of electricity"). Right now all you need to know is that lemon juice will be your electrolyte, and copper and zinc will be your electrodes. A penny provides the necessary copper, as long as it is fairly new and shiny. Pennies aren't solid copper anymore, but they are still copper-plated, which is good enough.

To find some metallic zinc, you will have to make a trip to a hardware store, where you should ask for roofing nails. The nails are zinc-plated to prevent them from rusting. Small metal brackets or mending plates also are usually zinc-plated. They should have a slightly dull, silvery look. If they have a mirror-bright finish, they're more likely to be nickel-plated.

Cut a lemon in half, set your multimeter so that it can measure up to 2 volts DC, and hold one probe against a penny while you hold the other probe against a roofing nail (or other zinc-plated object). Now force the penny and the nail into the exposed juicy interior of the lemon, as close to each other as possible, but not actually touching. You should find that your meter detects between 0.8 volts and 1 volt.

You can experiment with different items and liquids to see which works best. Immersing your nail and penny in lemon juice that you have squeezed into a shot glass or egg cup may enhance the efficiency of your battery, although you'll have a harder time holding everything in place. Grapefruit juice and vinegar will work as substitutes for lemon juice.

To drive a typical LED, you need more than 1 volt. How to generate the extra electrical pressure? By putting batteries in series, of course. In other words, more lemons! (Or more shot glasses or egg cups.) You'll also need lengths of wire to connect multiple electrodes, and this may entail skipping ahead to Chapter 2, where I describe how to strip insulation from hookup wire. Figures 1-71 and 1-72 show the configuration.

If you set things up carefully, making sure than none of the electrodes are touching, you may be able to illuminate your LED with two or three lemon-juice batteries in series. (Some LEDs are more sensitive to very low currents than others. Later in the book I'll be talking about very-low-current LEDs. If you want your lemon-juice battery to have the best chance of working, you can search online for low-current LEDs and buy a couple.)

THEORY

The nature of electricity

To understand electricity, you have to start with some basic information about atoms. Each atom consists of a nucleus at the center, containing protons, which have a positive charge. The nucleus is surrounded by electrons, which carry a negative charge.

Breaking up the nucleus of an atom requires a lot of energy, and can also liberate a lot of energy—as happens in a nuclear explosion. But persuading a couple of electrons to leave an atom (or join an atom) takes very little energy. For instance, when zinc reacts chemically with an acid, it can liberate electrons. This is what happens at the zinc electrode of the chemical battery in Experiment 5.

The reaction soon stops, as electrons accumulate on the zinc electrode. They feel a mutual force of repulsion, yet they have nowhere to go. You can imagine them like a crowd of hostile people, each one wanting the others to leave, and refusing to allow new ones to join them, as shown in Figure 1-73.

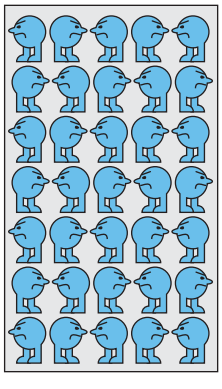

Figure 1-73. *Electrons on an electrode have a bad attitude known as mutual repulsion.*

Now consider what happens when a wire connects the zinc electrode, which has a surplus of electronics, to another electrode, made from a different material, that has a shortage of electrons. The electrons can pass through the wire very easily by jumping from one atom to the next, so they escape from the zinc electrode and run through the wire, propelled by their great desire to get away from each other. See Figure 1-74. This mutual force of propulsion is what creates an electrical current.

Now that the population of electrons on the zinc electrode has been reduced, the zinc-acid reaction can continue, replacing the missing electrodes with new ones—which promptly imitate their predecessors and try to get away from each other by running away down the wire. The process continues until the zinc-acid reaction grinds to a halt, usually because it creates a layer of a compound such as zinc oxide, which won't react with acid and prevents the acid from reacting with the zinc underneath. (This is why your zinc electrode may have looked sooty when you pulled it out of the acidic electrolyte.)

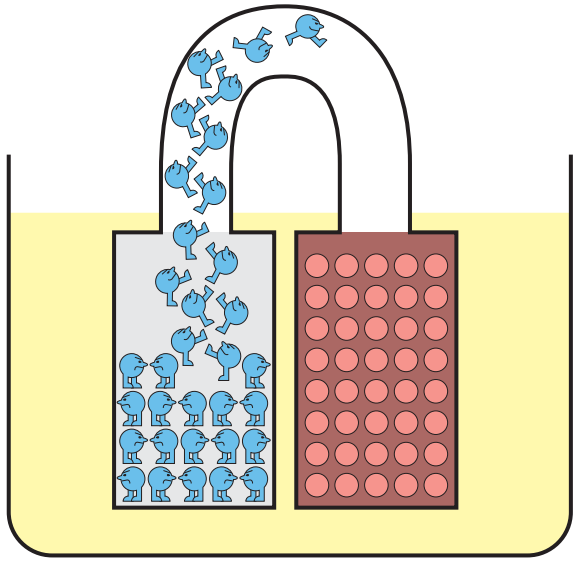

Figure 1-74. *As soon as we open up a pathway from a zinc electrode crowded with electrons to a copper electrode, which contains "holes" for the electrons, their mutual repulsion makes them try to escape from each other to their new home as quickly as possible.*

This description applies to a "primary battery," meaning one that is ready to generate electricity as soon as a connection between its terminals allows electrons to transfer from one electrode to the other. The amount of current that a primary battery can generate is determined by the speed at which chemical reactions inside the battery can liberate electrons. When the raw metal in the electrodes has all been used up in chemical reactions, the battery can't generate any more electricity and is dead. It cannot easily be recharged, because the chemical reactions are not easily reversible, and the electrodes may have oxidized.

In a rechargeable battery, also known as a secondary battery, a smarter choice of electrodes and electrolyte does allow the chemical reactions to be reversed.

How much current is being generated in your lemon battery? Set your meter to measure milliamps, and connect it between the nail and the penny. I measured about 2mA, but got 10mA when I used some #10 stranded copper wire instead of a penny and a large mending plate instead of a roofing nail, immersed in a cup of grapefruit juice. When a larger surface area of metal makes better contact with the electrolyte, you get a greater flow of current. (Don't ever connect your meter to measure amps directly between the terminals of a real battery. The current will be too high, and can blow the fuse inside your meter.)

What's the internal resistance of your lemon? Put aside the copper and zinc electrodes and insert your nickel-plated meter probes into the juice. I got a reading of around 30K when both probes were in the same segment of the lemon, but 40K or higher if the probes were in different segments. Is the resistance lower when you test liquid in a cup?

Here are a couple more questions that you may wish to investigate. For how long will your lemon battery generate electricity? And why do you think your zinc-plated electrode becomes discolored after it has been used for a while?

Electricity is generated in a battery by an exchange of ions, or free electrons, between metals. If you want to know more about this, check the section "Theory: The nature of electricity" on the previous page.

Cleanup and Recycling

The hardware that you immersed in lemons or lemon juice may be discolored, but it is reusable. Whether you eat the lemons is up to you.

BACKGROUND

Positive and negative

If electricity is a flow of electrons, which have a negative charge, why do people talk as if electricity flows from the positive terminal to the negative terminal of a battery?

The answer lies in a fundamental embarrassment in the history of research into electricity. For various reasons, when Benjamin Franklin was trying to understand the nature of electric current by studying phenomena such as lightning during thunderstorms, he believed he observed a flow of "electrical fluid" from positive to negative. He proposed this concept in 1747.

In fact, Franklin had made an unfortunate error that remained uncorrected until after physicist J. J. Thomson announced his discovery of the electron in 1897, 150 years later. Electricity actually flows from an area of greater negative charge, to some other location that is "less negative"—that is, "more positive." In other words, electricity is a flow of negatively charged particles. In a battery, they originate from the negative terminal and flow to the positive terminal.

You might think that when this fact was established, everyone should have discarded Franklin's idea of a flow from positive to negative. But when an electron moves through a wire, you can still think of an equal positive charge flowing in the opposite direction. When the electron leaves home, it takes a small negative charge with it; therefore, its home becomes a bit more positive. When the electron arrives at its destination, its negative charge makes the destination a bit less positive. This is pretty much what would happen if an imaginary positive particle traveled in the opposite direction. Moreover, all of the mathematics describing electrical behavior are still valid if you apply them to the imaginary flow of positive charges.

As a matter of tradition and convenience we still retain Ben Franklin's erroneous concept of flow from positive to negative, because it really makes no difference. In the symbols that represent components such as diodes and transistors, you will actually find arrows reminding you which way these components should be placed—and the arrows all point from positive to negative, even though that's not the way things really work at all! Ben Franklin would have been surprised to learn that although most lightning strikes occur when a negative charge in clouds discharges to neutralize a positive charge on the ground, some forms of lightning are actually a flow of electrons from the negatively charged surface of the earth, up to a positive charge in the clouds. That's right: someone who is "struck by lightning" may be hurt by *emitting* electrons rather than by receiving them, as shown in Figure 1-75.

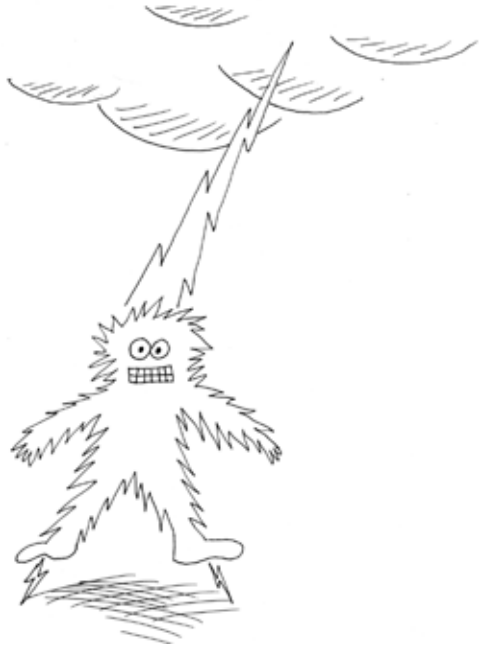

Figure 1-75. *In some weather conditions, the flow of electrons during a lightning strike can be from the ground, through your feet, out of the top of your head, and up to the clouds. Benjamin Franklin would have been surprised.*

THEORY

Basic measurements

Electrical potential is measured by adding up the charges on individual electrons. The basic unit is the *coulomb*, equal to the total charge on about 6,250,000,000,000,000,000 electrons.

If you know how many electrons pass through a piece of wire each second, this establishes the flow of electricity, which can be expressed in amperes. In fact 1 ampere can be defined as 1 coulomb per second. Thus:

1 ampere = 1 coulomb/second

= about 6.25 quintillion electrons/second

There's no way to "see" the number of electrons running through a conductor (Figure 1-76), but there are indirect ways of getting at this information. For instance, when an electron goes running through a wire, it creates a wave of electromagnetic force around it. This force can be measured, and we can calculate the amperage from that. The electric meter installed at your home by the utility company functions on this principle.

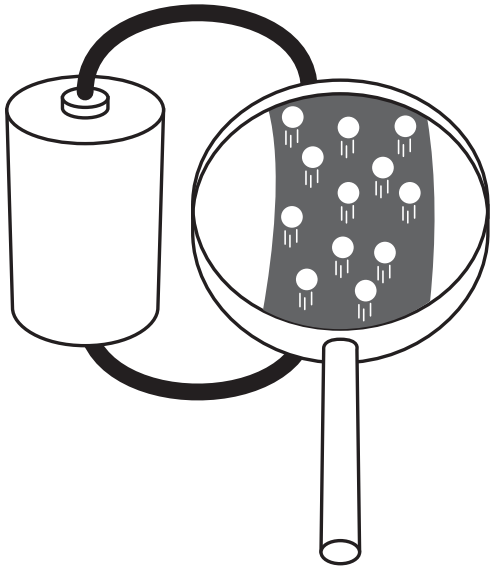

Figure 1-76. *If you could look inside an electric wire with a sufficiently powerful magnifying device, and the wire happened to be carrying 1 ampere of electron flow at the time, you might hope to see about 6.25 quintillion electrons speeding past each second.*

If electrons are just moving freely, they aren't doing any work. If you had a loop of wire of zero resistance, and you kick-started a flow of electrons somehow, they could just go buzzing around forever. (This is what happens inside a superconductor—almost.)

Under everyday conditions, even a copper wire has some resistance. The force that we need to push electrons through it is known as "voltage," and creates a flow that can create heat, as you saw when you shorted out a battery. (If the wire that you used had zero resistance, the electricity running through it would not have created any heat.) We can use the heat directly, as in an electric stove, or we can use the electrical energy in other ways—to run a motor, for instance. Either way, we are taking energy out of the electrons, to do some work.

One volt can be defined as the amount of pressure that you need to create a flow of 1 ampere, which does 1 watt of work. As previously defined, 1 watt = 1 volt × 1 ampere, but the definition actually originated the other way around:

1 volt = 1 watt/1 ampere

It's more meaningful this way, because a watt can be defined in nonelectrical terms. Just in case you're interested, we can work backward through the units of the metric system like this:

1 watt = 1 joule/second

1 joule = a force of 1 newton acting through 1 meter

1 newton = the force required to accelerate 1 kilogram by 1 meter per second, each second

On this basis, the electrical units can all be anchored with observations of mass, time, and the charge on electrons.

Practically Speaking

For practical purposes, an intuitive understanding of electricity can be more useful than the theory. Personally I like the water analogies that have been used for decades in guides to electricity. Figure 1-77 shows a tall tank half full of water, with a hole punched in it near the bottom. Think of the tank as being like a battery. The height of the water is comparable to voltage. The volume of flow through the hole, per second, is comparable to amperage. The smallness of the hole is comparable to resistance. See Figure 1-79 on the next page.

Where's the wattage in this picture? Suppose we place a little water wheel where it is hit by the flow from the hole. We can attach some machinery to the water wheel. Now the flow is doing some work. (Remember, wattage is a measurement of work.)

Maybe this looks as if we're getting something for nothing, extracting work from the water wheel without putting any energy back into the system. But remember, the water level in the tank is falling. As soon as I include some helpers hauling the waste water back up to the top of the tank (in Figure 1-78), you see that we have to put work in to get work out.

Similarly, a battery may seem to be giving power out without taking anything in, but the chemical reactions inside it are changing pure metals into metallic compounds, and the power we get out of a battery is enabled by this change of state. If it's a rechargeable battery, we have to push power back into it to reverse the chemical reactions.

Going back to the tank of water, suppose we can't get enough power out of it to turn the wheel. One answer could be to add more water. The height of the water will create more force. This would be the same as putting two batteries end to end, positive to negative, in series, to double the voltage. See Figure 1-80. As long as the resistance in the circuit remains the same, greater voltage will create more amperage, because amperage = voltage/resistance.

What if we want to run two wheels instead of one? We can punch a second hole in the tank, and the force (voltage) will be the same at each of them. However, the water level in the tank will drop twice as fast. Really, we'd do better to build a second tank, and here again the analogy with a battery is good. If you wire two batteries side by side, in parallel, you get the same voltage, but for twice as long. The two batteries may also be able to deliver more current than if you just used one. See Figure 1-81.

Summing up:

- Two batteries in series deliver twice the voltage.
- Two batteries in parallel can deliver twice the current.

All right, that's more than enough theory for now. In the next chapter, we'll continue with some experiments that will build on the foundations of knowledge about electricity, to take us gradually toward gadgets that can be fun and useful.

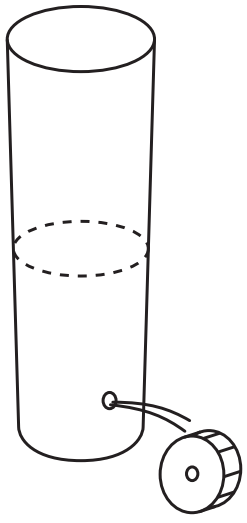

Figure 1-77. *If you want to get work out of a system...*

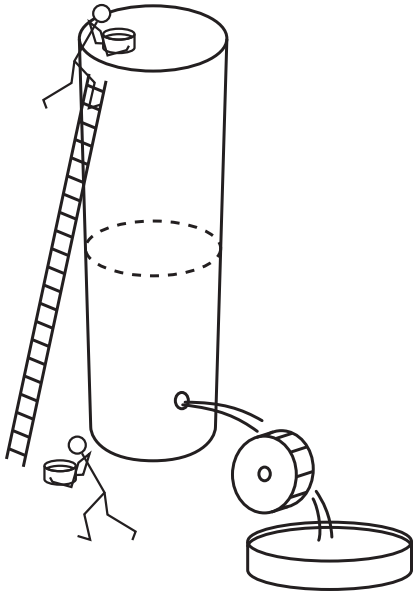

Figure 1-78. *. . . somehow or other you have to put work back into it.*

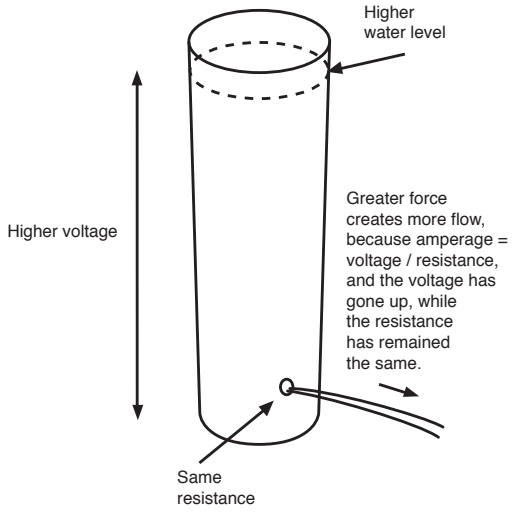

Figure 1-79. *Greater force generates more flow, as long as the resistance remains the same.*

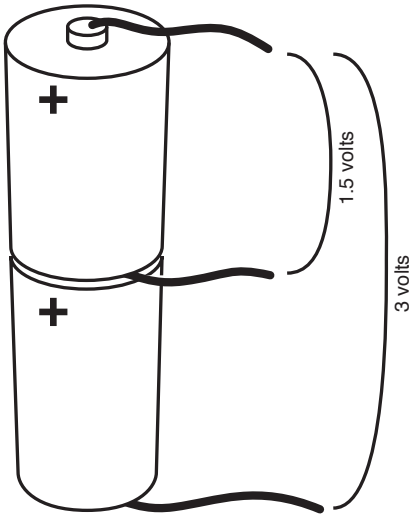

Figure 1-80. *When you place two equal batteries in series, you double the voltage.*

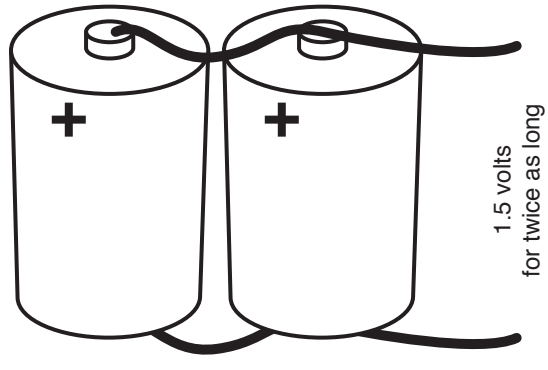

Figure 1-81. *Two equal batteries that are wired in parallel will deliver the same voltage for twice as long as one.*

2

Switching Basics and More

The concept of switching is fundamental in electronics, and I'm not just talking about power switches. By "switching," I mean using one flow of electricity to switch, or control, another. This is such an important principle that no digital device can exist without it.

Today, switching is mostly done with semiconductors. Before I deal with them, I'll back up and illustrate the concept by introducing you to relays, which are easier to understand, because you can see what's going on inside them. And before I get to relays, I'll deal with everyday on/off switches, which may seem very simple—but we have to nail down the basics.

Also in this chapter, I'll deal with capacitance, because capacitance and resistance are fundamental to electronic circuits. By the end of the chapter, you should have a basic grounding in electronics and be able to build the noise-making section of a simple intrusion alarm. This will be your first circuit that does something genuinely useful!

IN THIS CHAPTER

Shopping List: Experiments 6 Through 11
Experiment 6: Very Simple Switching
Experiment 7: Relay-Driven LEDs
Experiment 8: A Relay Oscillator
Experiment 9: Time and Capacitors
Experiment 10: Transistor Switching
Experiment 11: A Modular Project

Shopping List: Experiments 6 Through 11

As in the previous shopping list, you should visit the various online suppliers for availability and pricing of components and devices. Manufacturers seldom sell small numbers of parts directly. Check the appendix for a complete list of URLs for all the companies mentioned here.

Devices

- Power supply/universal AC adapter, 3 to 12 volts at 1A (1,000 mA). See Figure 2-1. Part number 273-029 from RadioShack, part PH-62092 by Philips, or similar.
- Breadboard suitable for integrated circuits. Quantity: 1. See Figures 2-2 and 2-3. Part 276-002 from RadioShack, model 383-X1000 made by PSP, part 923252-I by 3M, or similar. A breadboard that has screw terminals mounted beside it will be a little easier to use but more expensive than one that does not have terminals.

Figure 2-1. *This AC adapter delivers DC from 3 to 12 volts, and is ideal for electronics projects.*

Figure 2-2. *This "breadboard" for quickly constructing electronic circuits has a metal base, and screw terminals for attaching wires from a power supply.*

Figure 2-3. *A breadboard without screw terminals is almost as convenient, and is cheaper.*

Tools

Wire strippers

Ideal model 45-121 wire strippers for 16- to 26-gauge wire, or similar. See Figure 2-4. (The "gauge" of the wire tells you how thick it is. A higher gauge means a thinner wire. In this book, we will mainly be using thin wire of 20- to 24-gauge.)

You may also consider the Kronus Automatic Wire Strippers, part 64-2981 from RadioShack, or GB Automatic Wire Strippers, part SE-92 from Amazon.com. See Figure 2-5.

The Kronus and GB wire strippers are functionally identical. The advantage of their design is that it enables you to strip insulation from a wire with one hand. But they do not work well on really thin wire.

Figure 2-4. *To use these wire strippers, insert a piece of insulated wire in the appropriate-sized hole between the jaws, grip the handles, and pull a section of insulation away. See page 45.*

Figure 2-5. *These automatic wire strippers enable one-handed operation, but are not suitable for very small wire diameters. See page 44.*

Supplies

Hookup wire

Solid-conductor, 22-gauge, minimum 25 feet of each color. See Figure 2-6. Part 278-1222 from RadioShack, catalog item 9948T17 from McMaster-Carr, or check eBay for deals.

It's easy to buy the wrong kind of wire. You need solid-core wire, which has a single conductor inside the plastic insulation, not stranded, which has multiple, thinner conductors. See Figures 2-7 and 2-8. You're going to be pushing wires into little holes in a "breadboard," and stranded wire won't let you do this. You will also have problems if you buy wire thicker than 22-gauge. Remember: the lower the gauge number, the thicker the wire.

For a little extra money, you can buy an assortment of precut sections of wire, with ends stripped and ready for use. Try catalog item JW-140 (jumper wire assortment) from All Electronics or search eBay for "breadboard wire." See Figure 2-9.

Patch cords

Patch cords are not strictly necessary but very convenient. You don't want audio or video patch cords, which have a plug on each end; you want wires with alligator clips on each end, also sometimes referred to as "test leads." Try catalog item 461-1176-ND from Digi-Key or catalog item MTL-10 from All Electronics. See Figure 2-10.

Figure 2-6. *Using hookup wire with different colors of plastic insulation will help you to distinguish one wire from another in your circuits.*

Figure 2-7. *Solid-conductor wire of 22 or 24 gauge is suitable for most of the experiments in this chapter.*

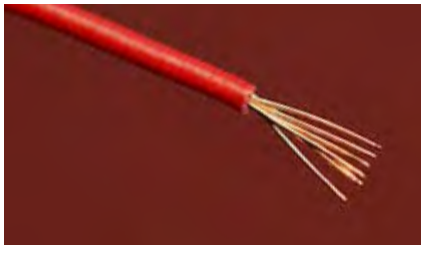

Figure 2-8. *Stranded is more flexible, but cannot be used easily with breadboards.*

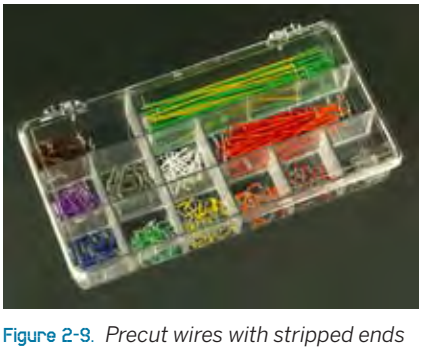

Figure 2-9. *Precut wires with stripped ends can save a lot of time and trouble—if you don't mind paying a little extra.*

Figure 2-10. *Patch cords, sometimes known as test leads, consist of wires preattached to alligator clips. This is another of those little luxuries that reduces the hassle factor in hobby electronics.*

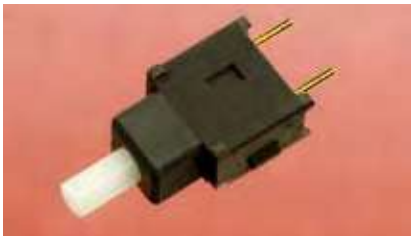

Figure 2-11. *The terminals protruding from this tiny pushbutton are spaced 0.2 inches apart, making it ideal for the "breadboard" that you'll be using.*

Figure 2-12. *This relatively large toggle switch made by NKK has screw terminals, which will reduce the inconvenience of attaching it to hookup wire.*

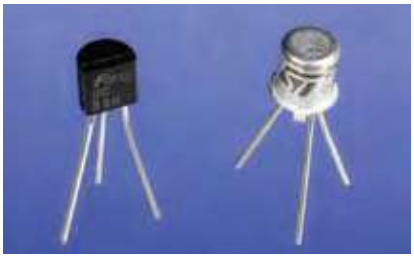

Figure 2-13. *Transistors are commonly sold either in little metal cans or sealed into little lumps of plastic. For our purposes, the packaging makes no difference.*

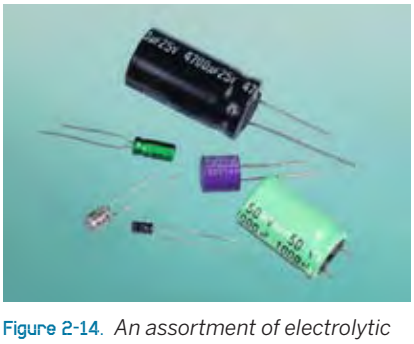

Figure 2-14. *An assortment of electrolytic capacitors.*

Components

Pushbutton

Momentary-on, SPST, sometimes referred to as OFF-(ON) or (ON)-OFF type. Must be PCB- or PC-mount, meaning is extremely small with thin spiky contacts on the bottom. Quantity: 1. See Figure 2-11.

Examples are part number AB11AP by NKK, part MPA103B04 by Alco-switch, or part EP11SD1CBE by C&K. If you have a choice, buy the cheapest, as we're going to switch very low current.

Switches

Toggle switch, single-pole, double-throw (SPDT), sometimes referred to as ON-ON type. Quantity: 2. See Figure 2-12.

Model S302T-RO by NKK is ideal; it has screw terminals that will eliminate the need for alligator clips. Other options are catalog item MTS-4PC from All Electronics or part 275-603 from RadioShack.

We won't be switching large currents or high voltages, so the exact type of switch is unimportant. However, the terminals on larger-size switches are spaced wider apart, which makes them easier to deal with.

Relays

DPDT, nonlatching, 12v DC. Quantity: 2.

It's important to get the right kind of relay—one whose configuration matches the pictures I'll be using. Look for parts FTR-F1CA012V or FTR-F1CD012V by Fujitsu, G2RL-24-DC12 by Omron, or OMI-SH-212D by Tyco. Avoid substitutions.

Potentiometer

1 megohm linear potentiometer, Part number 271-211 from RadioShack, part number 24N-1M-15R-R from Jameco, or similar.

Transistors

NPN transistor, general-purpose, such as 2N2222 by STMicroelectronics, part PN2222 by Fairchild, or part 2N2222 from RadioShack. Quantity: 4. See Figure 2-13.

2N6027 programmable unijunction transistor manufactured by On Semiconductor or Motorola. Quantity: 4.

Capacitors

Electrolytic capacitors, assorted. Must be rated for a minimum of 25 volts and include at least one capacitor of 1,000 µF (microfarads). If you search on eBay, make sure you find *electrolytic* capacitors. If they're rated for higher voltages, that's OK, although they will be physically larger than you need. See Figure 2-14.

Ceramic capacitors, assorted. Make sure you get at least one rated at 0.0047 µF (which can also be written as 47 nF). See Figure 2-15.

Resistors

If you bought only a minimal selection for experiments 1 through 5, now's the time to buy a larger assortment, so that you won't be stuck needing the one value that you don't have. 1/4-watt minimum.

Loudspeaker

Any 8Ω, 1-inch miniature loudspeaker such as part 273-092 from RadioShack. See Figure 2-16.

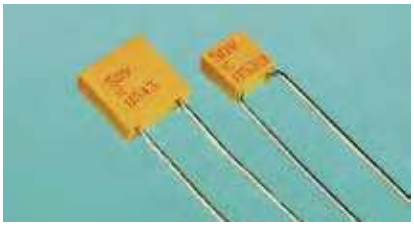

Figure 2-15. *Ceramic capacitors mostly look like this, although many of them are round or bead-shaped instead of square. The packaging shape is unimportant to us.*

Figure 2-16. *This miniature loudspeaker, just over 1 inch in diameter, is useful for verifying audio output direct from transistor circuits.*

Experiment 6: Very Simple Switching

You will need:

- AA batteries. Quantity: 4.
- Battery carrier for 4 AA batteries. Quantity: 1.
- LED. Quantity: 1.
- Toggle switches, SPDT. Quantity: 2. See Figure 2-12.
- 220Ω or similar value resistor, 1/4-watt minimum. Quantity: 1.
- Alligator clips. Quantity: 8.
- Wire or patch cords. See Figure 2-10, shown previously.
- Wire cutters and wire strippers if you don't use patch cords. See Figure 2-4, shown previously.

In Experiment 3, you illuminated an LED by attaching a battery, and switched it off by removing the battery. For greater convenience our circuits should have proper switches to control power, and while I'm dealing with the general topic of switches, I'm going to explore all the varieties, using a circuit to suggest some possibilities.

Assemble the parts as shown in Figures 2-17 and 2-18. The long lead on the LED must connect with the resistor, because that is the more positive side of the circuit.

You'll notice that you have to include a couple lengths of wire. I suggest green wire to remind you that these sections are not connected directly to positive or to negative power. But you can use any color you like. You can also substitute patch cords, if you have them. However, learning to strip insulation from pieces of wire is a necessary skill, so let's deal with that now.

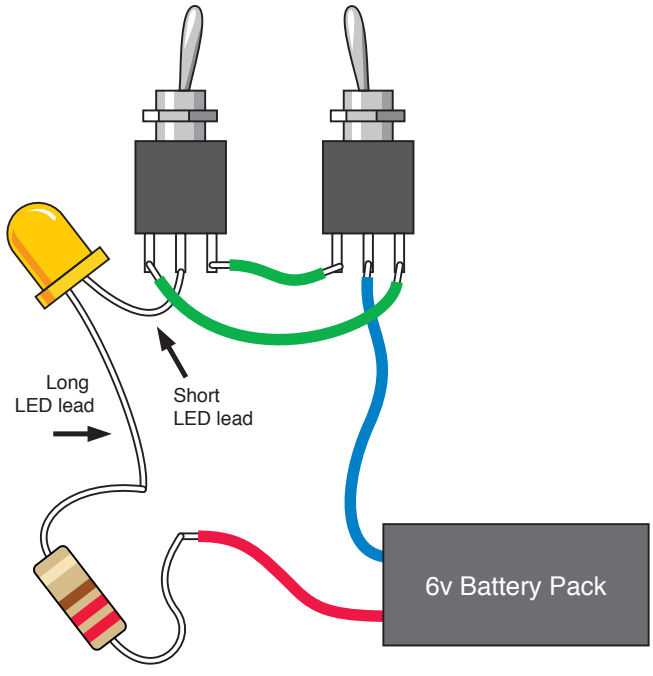

Figure 2-17. *If the LED is on, flipping either of the switches will turn it off. If the LED is off, either of the switches will turn it on. Use alligator clips to attach the wires to each other, and to the switches if your switches don't have screw terminals. Be careful that the clips don't touch each other.*

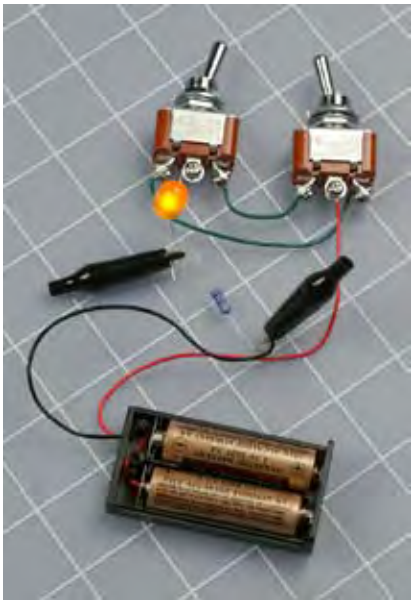

Figure 2-18. *Full-size toggle switches with screw terminals make it easy to hook up this simple circuit.*

Figure 2-19. *Using automatic wire strippers, when you squeeze the handles the jaw on the left clamps the wire, the sharp grooves on the right bite into the insulation. Squeeze harder and the jaws pull away from each other, stripping the insulation from the wire.*

Tools

If automatic wire strippers (Figure 2-19) don't grip skinny 22-gauge wire very effectively, try the Ideal brand of wire strippers shown back in Figure 2-4, or use plain and simple wire cutters as shown in Figure 2-20. When using wire cutters, you hold the wire in one hand and apply the tool in your other hand, squeezing the handles with moderate pressure—just enough to bite into the insulation, but not so much that you chop the wire. Pull the wire down while you pull the cutters up, and with a little practice you can rip the insulation off to expose the end of the wire.

Macho hardware nerds may use their teeth to strip insulation from wires. When I was younger, I used to do this. I have two slightly chipped teeth to prove it. Really, it's better to use the right tool for the job.

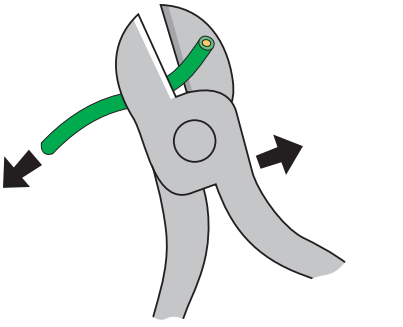

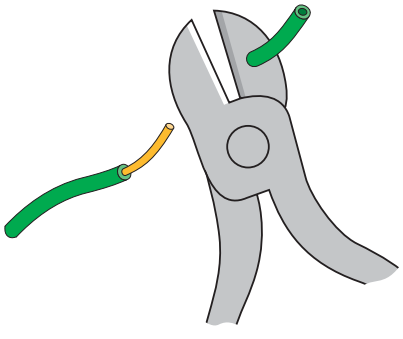

Figure 2-20. *To remove insulation from the end of a thin piece of wire, you can also use wire cutters. This takes a little practice.*

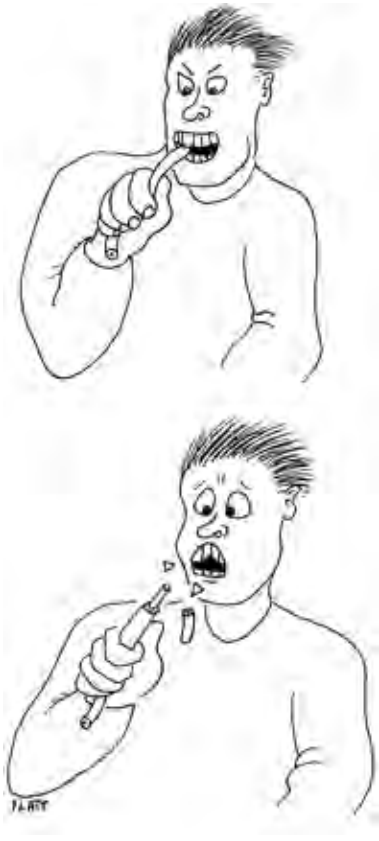

Figure 2-21. *Those who tend to misplace tools, and feel too impatient to search for them, may feel tempted to use their teeth to strip insulation from wire. This may not be such a good idea.*

Connection Problems

Depending on the size of toggle switches that you are using, you may have trouble fitting in all the alligator clips to hold the wires together. Miniature toggle switches, which are more common than the full-sized ones these days, can be especially troublesome (see Figure 2-22). Be patient: fairly soon we'll be using a breadboard, which will eliminate alligator clips almost completely.

Testing

Make sure that you connect the LED with its long wire toward the positive source of power (the resistor, in this case). Now flip either of the toggle switches. If the LED was on, it will go off, and if it was off, it will go on. Flip the other toggle switch, and it will have the same effect. If the LED does not go on at all, you've probably connected it the wrong way around. Another possibility is that two of your alligator clips may have shorted out the battery.

Assuming your two switches do work as I described them, what's going on here? It's time to nail down some basic facts.

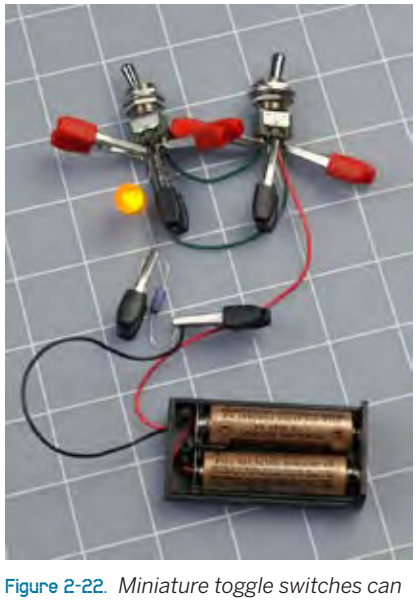

Figure 2-22. *Miniature toggle switches can be used—ideally, with miniature alligator clips—but watch out for short circuits.*

FUNDAMENTALS

All about switches

When you flip the type of toggle switch that you used in Experiment 6, it connects the center terminal with one of the outer terminals. Flip the switch back, and it connects the center terminal with the other outer terminal, as shown in Figure 2-23.

The center terminal is called the pole of the switch. Because you can flip, or throw, this switch to make two possible connections, it is called a *double-throw switch*. As mentioned earlier, a single-pole, double-throw switch is abbreviated *SPDT*.

Some switches are on/off, meaning that if you throw them in one direction they make a contact, but in the other direction, they make no contact at all. Most of the light switches in your house are like this. They are known as *single-throw switches*. A single-pole, single-throw switch is abbreviated *SPST*.

Some switches have two entirely separate poles, so you can make two separate connections simultaneously when you flip the switch. These are called *double-pole switches*. Check the photographs in Figures 2-24 through 2-26 of old-fashioned "knife" switches (which are still used to teach electronics to kids in school) and you'll see the simplest representation of single and double poles, and single and double throws. Various toggle switches that have contacts sealed inside them are shown in Figure 2-27.

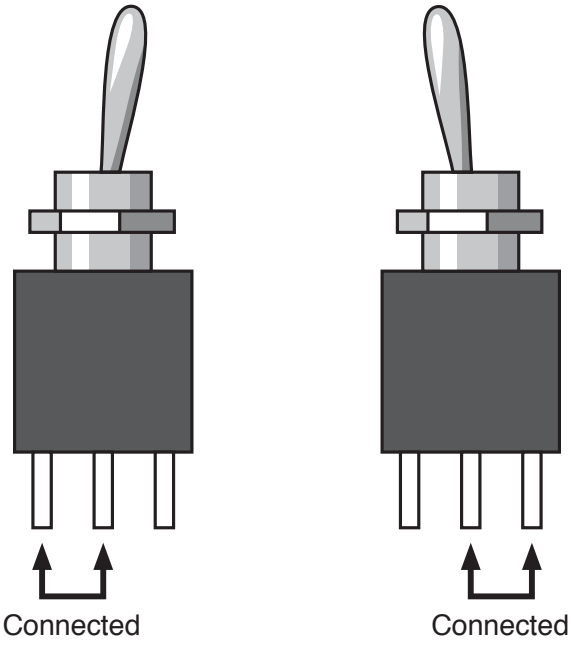

Figure 2-23. *The center terminal is the pole of the switch. When you flip the toggle, the pole changes its connection.*

Figure 2-24. *This primitive-looking single-pole, double-throw switch does exactly the same thing as the toggle switches in Figures 2-23 and 2-27.*

Figure 2-25. *A single-pole, single-throw switch makes only one connection with one pole. Its two states are simply open and closed, on and off.*

Figure 2-26. *A double-pole, single-throw switch makes two separate on/off connections.*

FUNDAMENTALS

All about switches (continued)

Figure 2-27. *These are all toggle switches. Generally, the larger the switch, the more current it can handle.*

To make things more interesting, you can also buy switches that have three or four poles. (Some rotary switches have even more, but we won't be using them.) Also, some double-throw switches have an additional "center off" position.

Putting all this together, I made a table of possible types of switches (Figure 2-28). When you're reading a parts catalog, you can check this table to remind yourself what the abbreviations mean.

	Single Pole	Double Pole	3-Pole	4-Pole
Single Throw	SPST ON-OFF	DPST ON-OFF	3PST ON-OFF	4PST ON-OFF
Double Throw	SPDT ON-ON	DPDT ON-ON	3PDT ON-ON	4PDT ON-ON
Double Throw with Center Off	SPDT ON-OFF-ON	DPDT ON-OFF-ON	3PDT ON-OFF-ON	4PDT ON-OFF-ON

Figure 2-28. *This table summarizes all the various options for toggle switches and pushbuttons.*

Now, what about pushbuttons? When you press a door bell, you're making an electrical contact, so this is a type of switch—and indeed the correct term for it is a momentary switch, because it makes only a momentary contact. Any spring-loaded switch or button that wants to jump back to its original position is known as a momentary switch. We indicate this by putting its momentary state in parentheses. Here are some examples:

- OFF-(ON): Because the ON state is in parentheses, it's the momentary state. Therefore, this is a single-pole switch that makes contact only when you push it, and flips back to make no contact when you let it go. It is also known as a "normally open" momentary switch, abbreviated "NO."
- ON-(OFF): The opposite kind of momentary single-pole switch. It's normally ON, but when you push it, you break the connection. So, the OFF state is momentary. It is known as a "normally closed" momentary switch, abbreviated "NC."
- (ON)-OFF-(ON): This switch has a center-off position. When you push it either way, it makes a momentary contact, and returns to the center when you let it go.

Other variations are possible, such as ON-OFF-(ON) or ON-(ON). As long as you remember that parentheses indicate the momentary state, you should be able to figure out what these switches are.

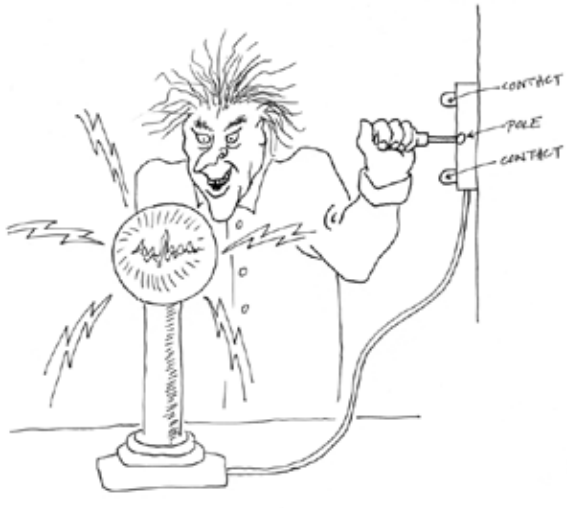

Figure 2-29. *This evil mad scientist is ready to apply power to his experiment. For this purpose, he is using a single-pole, double-throw knife switch, conveniently mounted on the wall of his basement laboratory.*

FUNDAMENTALS

All about switches (continued)

Sparking

When you make and break an electrical connection, it tends to create a spark. Sparking is bad for switch contacts. It eats them until the switch doesn't make a reliable connection anymore. For this reason, you must use a switch that is appropriate for the voltage and amperage that you are dealing with. Electronic circuits generally are low-current, and low-voltage, so you can use almost any switch, but if you are switching a motor, it will tend to suck an initial surge of current that is at least double the rating of the motor when it is running constantly. You should probably use a 4-amp switch to turn a 2-amp motor on and off.

Checking a switch

You can use your meter to check a switch. Doing this helps you find out which contacts are connected when you turn a switch one way or the other. It's also useful if you have a pushbutton and you can't remember whether it's the type that is normally open (you press it to make a connection) or normally closed (you press it to break the connection). Set your meter to measure ohms, and touch the probes to the switch terminals while you work the switch.

This is a hassle, though, because you have to wait while the meter makes an accurate measurement. When you just want to know whether there is a connection, your meter has a "continuity tester" setting. It beeps if it finds a connection, and stays silent if it doesn't. See Figures 2-30 through 2-32 for examples of meters set to test continuity. Figure 2-33 offers an example of a toggle switch being tested for continuity.

> *Use the continuity-testing feature on your meter only on circuits or components that have no power in them at the time.*

Figure 2-30

Figure 2-31

Figure 2-32. *To check a circuit for continuity, turn the dial of your meter to the symbol shown. Only use this feature when there is no power in the component or the circuit that you are testing.*

Figure 2-33. *When the switch connects two of its terminals, the meter shows zero resistance between them and will beep if you have set it to verify continuity.*

BACKGROUND

Early switching systems

Switches seem to be such a fundamental feature of our world, and their concept is so simple that it's easy to forget that they went through a gradual process of development and refinement. Primitive knife switches were quite adequate for pioneers of electricity who simply wanted to connect and disconnect electricity to some apparatus in a laboratory, but a more sophisticated approach was needed when telephone systems began to proliferate. Typically, an operator at a "switchboard" needed a way to connect any pair of 10,000 lines on the board. How could it be done?

In 1878, Charles E. Scribner (Figure 2-34) developed the "jack-knife switch," so called because the part of it that the operator held looked like the handle of a jackknife. Protruding from it was a plug, and when the plug was pushed into a socket, it made contact inside the socket. The socket, in fact, was the switch.

Figure 2-34. *Charles E. Scribner invented the "jack-knife switch" to satisfy the switching needs of telephone systems in the late 1800s. Today's audio jacks still work on the same basis.*[*]

Audio connectors on guitars and amplifiers still work on the same principle, and when we speak of them as being "jacks," the term dates back to Scribner's invention. Switch contacts still exist inside a jack socket.

Today, of course, telephone switchboards have become as rare as telephone operators. First they were replaced with relays—electrically operated switches, which I'll talk about later in this chapter. And then the relays were superceded by transistors, which made everything happen without any moving parts. Before the end of this chapter, you'll be switching current using transistors.

* The photo on which this drawing is based first appeared in *The History of the Telephone* by Herbert Newton Casson in 1910 (Chicago: A. C. McClurg & Co.).

Introducing Schematics

In Figure 2-35, I've redrawn the circuit from Experiment 6 in a simplified style known as a "schematic." From this point onward, I will be illustrating circuits with schematics, because they make circuits easier to understand. You just need to know a few symbols to interpret them.

Larger versions of all schematics and breadboard photos are available online at this book's website: http://oreilly.com/catalog/9780596153748.

Compare the schematic here with the drawing of the circuit in Figure 2-17. They both show exactly the same thing: Components, and connections between them. The gray rectangles are the switches, the zigzag thing is the resistor, and the symbol with two diagonal arrows is the LED.

The schematic LED symbol includes two arrows indicating that it emits light, because there are some kinds of diodes, which we'll get to later, that don't. The triangle inside the diode symbol always points from positive to negative.

Trace the path that electricity can take through the circuit and imagine the switches turning one way or the other. You should see clearly now why either switch will reverse the state of the LED from on to off or off to on.

This same circuit is used in houses where you have a switch at the bottom of a flight of stairs, and another one at the top, both controlling the same lightbulb. The wires in a house are much longer, and they snake around behind the walls, but because their connections are still the same, they could be represented with the same basic schematic. See Figure 2-36.

A schematic doesn't tell you exactly where to put the components. It just tells you how to join them together. One problem: Different people use slightly different schematic symbols to mean the same thing. Check the upcoming section, "Fundamentals: Basic schematic symbols," for the details.

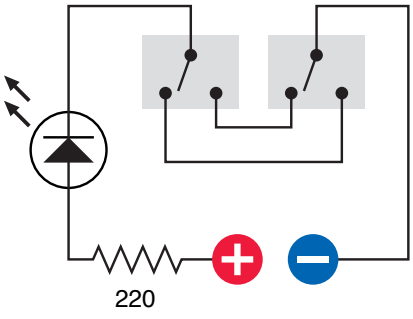

Figure 2-35. *This schematic shows the same circuit as in Figure 2-17 and makes it easier to see how the switches function.*

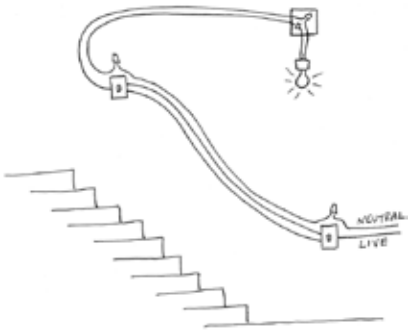

Figure 2-36. *The two-switch circuit shown in Figures 2-17 and 2-35 is often found in house wiring, especially where switches are located at the top and bottom of a flight of stairs. This sketch shows what you might find inside the walls. Wires are joined with "wire nuts" inside boxes that are hidden from everyday view.*

FUNDAMENTALS

Basic schematic symbols

Schematic symbols are like words in a language: they have mutated over the years into a confusing range of variations. A simple on/off (single-pole, single-throw, or SPST) switch, for instance, can be represented by any of the symbols shown in Figure 2-37. They all mean exactly the same thing.

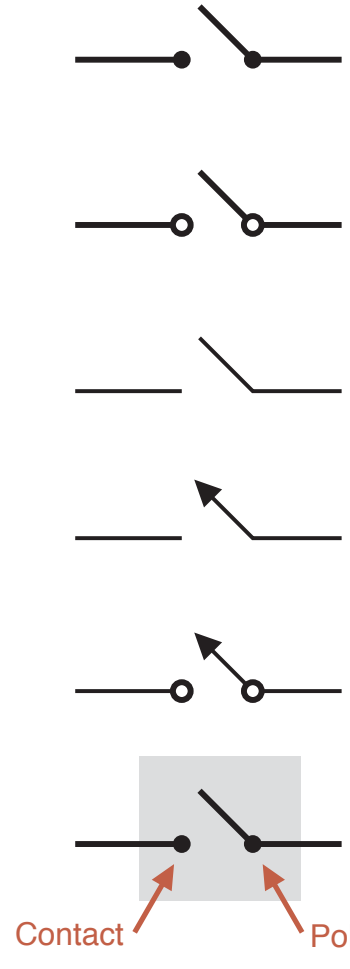

Figure 2-37. *Variations on a theme: Just some of the different styles used to depict a single-pole, single-throw switch in schematic diagrams. The bottom version is the style used in this book.*

Figure 2-38 shows double-pole, double-throw switches. A dotted line indicates a mechanical connection inside the switch, so that when you flip it, you affect both the poles simultaneously. Remember, the poles are electrically isolated from each other.

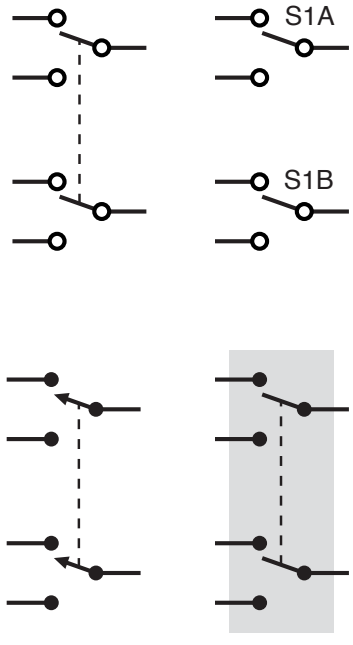

Figure 2-38. *More variations: some different styles for depicting a double-pole, double-throw switch. The style at bottom-right is used in this book.*

Once in a while, you may find a schematic in which switches seem to be scattered around, but the way they are identified (such as S1A, S1B, S1C, and so on) tells you that this is really all one switch with multiple poles.

In the schematics in this book, I'll place a gray rectangle behind each switch. This gray rectangle is not a standard symbol; you won't find it in other books. I'm just including it to remind you that the parts inside are all contained in one package.

A very important stylistic variation in schematics is the way they show whether wires make a connection with each other. Old schematics used to show a little semicircular bump in a wire if it crossed another wire without making a connection. Because modern circuit-drawing software doesn't create this style of schematic, it is no longer often used. The modern style, which you are likely to find if you browse through schematics online, can be summarized like this:

- A dot joining two wires indicates an electrical connection.
- No dot indicates no connection.

FUNDAMENTALS

Basic schematic symbols (continued)

The problem is that this is not very intuitive, especially when you're just beginning to use schematics. When you see two wires crossing, you can easily imagine that they are making a connection, even though there's no dot at the intersection. Therefore, in the interests of clarity, I've chosen to use the old "semicircular bump" style of schematic in this book (see Figure 2-39). It can be summarized like this:

- A dot joining two wires indicates an electrical connection.
- A bump in a wire that crosses another wire indicates no connection.

In this book, you won't find wires crossing each other without either a dot or a bump.

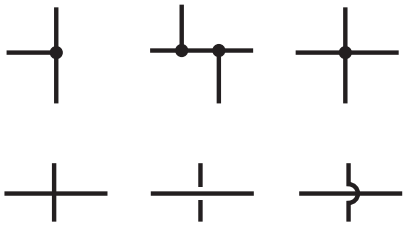

Figure 2-39. *In wiring schematics, a dot always indicates an electrical connection. However, the cross-shaped intersection of wires at top-right is considered bad style because if the dot is accidentally omitted or poorly printed, the intersection can be mistaken for the type shown at bottom left, in which the wires do not make a connection. All three of the configurations in the bottom row indicate no connection, the first example being the most common style, the center example being least common, and the third being the most old-fashioned—although for reasons of clarity, it is used in this book.*

In a battery-powered circuit, you may find a battery symbol, but more often you will find a little note indicating where positive voltage enters the system, while negative is indicated by a "ground" symbol. In fact there may be ground symbols all over the place. You have to remember that when you build a circuit, all the wires leading to grounds must actually be connected together, to the negative side of the voltage supply.

The idea of the ground symbol dates back to the time when electronic gadgets were mounted on a metal chassis, which was connected to the negative side of the power supply. The ground symbol really meant "connect to the chassis." Some variants in the ground symbol are shown in Figure 2-40.

Figure 2-40. *All of these symbols are used to mean the same thing: connect the wire to "ground" or "chassis" or the negative side of the power source. The far-right symbol is used in this book.*

In this book, we have color throughout, so I'll show a red positive and blue negative to clarify where the power is connected, and I won't use ground symbols. Once again, my purpose is to minimize the risk of misunderstandings, because I know how frustrating it is to build a circuit that doesn't work.

A big inconsistency in schematics is the way in which they show resistors. The traditional zigzag symbol has been abandoned in Europe. Instead they use a rectangle with a number inside indicating the number of ohms. See Figure 2-41. The Europeans also changed the way in which decimal points are represented: they omit them as much as possible, because in badly printed schematics, the little dots tend to get lost (or can be confused with dust and dirt). So, a 4.7KΩ resistor will be listed as 4K7, and a 1.2MΩ resistor will be 1M2. I like this notation, so I'm going to be using it myself, but I'll be keeping the zigzag resistor symbol, which remains widely used in the United States.

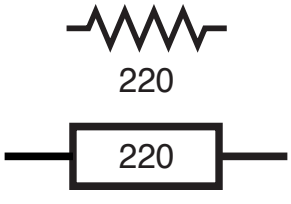

Figure 2-41. *Two styles for depicting a 220Ω resistor. The upper version is traditional, and still used in the United States. The lower version is European.*

FUNDAMENTALS

Basic schematic symbols (continued)

Potentiometers suffer from the same inconsistent style between the United States and Europe, but either way, you'll find an arrow showing where the wiper (usually, the center terminal) touches the resistance. See Figure 2-42. And sometimes LEDs are shown inside circles, and sometimes not. I prefer circles, myself. See Figure 2-46.

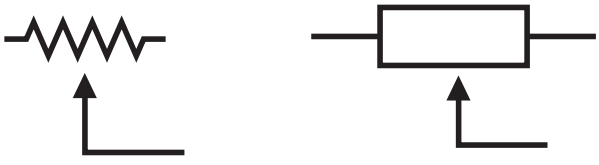

Figure 2-42. *Potentiometer symbols: the left is traditional and used in the United States, the right is European. In both cases the arrow indicates the wiper (usually the center terminal).*

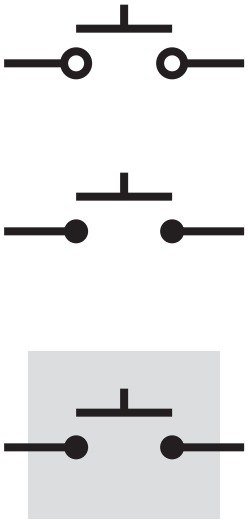

Figure 2-43. *Three ways of indicating a pushbutton switch.*

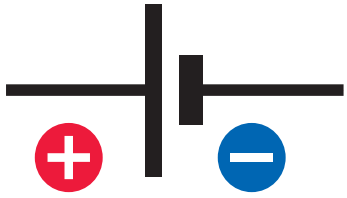

Figure 2-44. *The battery symbol is usually shown without + and – symbols. I've added them for clarity.*

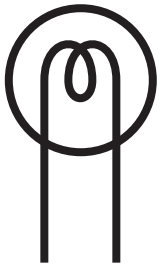

Figure 2-45. *Symbol for an incandescent lightbulb.*

I'll explore other symbol variants later in the book. Meanwhile, the most important things to remember are:

- The positions of components in a schematic are not important.
- The styles of symbols used in a schematic are not important.
- The connections between the components are extremely important.

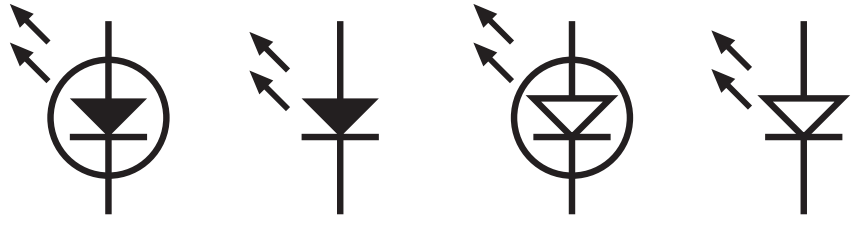

Figure 2-46. *Sometimes an LED is shown with a circle around it; sometimes not. In this book, I will include the circle. The arrows indicate emitted light.*

FUNDAMENTALS

Basic schematic symbols (continued)

For example, the three LED circuits that I have included in Figure 2-47 show components in different positions, using different symbols, but all three circuits function exactly the same way, because their connections are the same. In fact, they all depict the circuit that you built in Experiment 4, shown in Figure 1-50.

Often the symbols in a schematic are placed so that the circuit is most intuitively easy to understand, regardless of how you may build it with actual components. Compare the example in Figure 2-48, showing the two DPDT switches, with the version shown back in Figure 2-35. The previous one looked more like your bench-top version of it, but Figure 2-48 shows the flow of electricity more clearly.

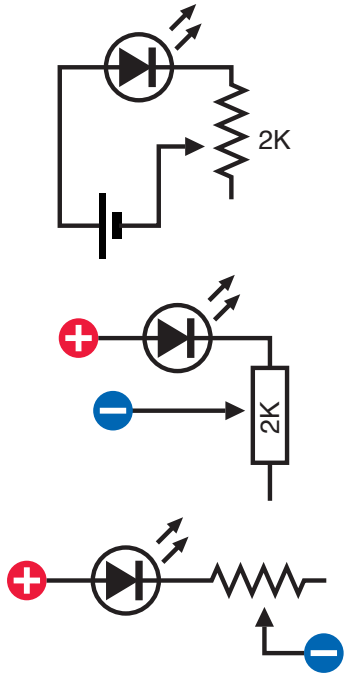

Figure 2-47. *These three schematics all depict the same basic circuit. It's the circuit that you built with the potentiometer in Experiment 4.*

In many schematics, the positive side of the power supply is shown at the top of the diagram, and negative or ground at the bottom. Many people also tend to draw a schematic with an input (such as an audio input, in an amplifier circuit) at the left side, and the output at the right. So, "positive voltage" flows from top to bottom while a signal tends to pass from left to right.

When I was planning this book, initially I drew the schematics to conform with this top-to-bottom, left-to-right convention, but as I started building and testing the circuits, I changed my mind. We use a device known as a "breadboard" to create circuits, and its internal connections require us to lay out components very differently from a typical schematic. When you're starting to learn electronics, it's very confusing to try to rearrange components from a schematic in the configuration that you need for a breadboard.

Therefore, throughout this book, you'll find that I have drawn the schematics to imitate the way you'll wire them on a breadboard. I believe the advantages of doing things this way outweigh the disadvantages of being a little different from the schematic styles that are used elsewhere.

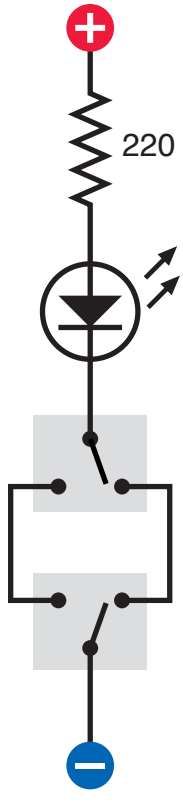

Figure 2-48. *This schematic is just another, clearer, simpler way of showing the circuit that appeared in Figure 2-35.*

Experiment 7: Relay-Driven LEDs

You will need:

- AC adapter, wire cutters and strippers.
- DPDT relay. Quantity: 2.
- LEDs. Quantity: 2.
- Resistor, 680Ω approx. Quantity: 1.
- Pushbutton, SPST. Quantity: 1.
- Hookup wire, 22 gauge, or patch cords.
- Alligator clips. Quantity: 8.
- Utility knife.

The next step in our exploration of switching is to use a remote-controlled switch. By "remote-controlled," I mean one to which you can send a signal to turn it on or off. This kind of switch is known as a *relay*, because it relays an instruction from one part of a circuit to another. Often a relay is controlled by a low voltage or small current, and switches a larger voltage or higher current.

This setup can be cost-effective. When you start your car, for instance, a relatively small, cheap switch sends a small signal down a relatively long, thin, inexpensive piece of wire, to a relay that is near the starter motor. The relay activates the motor through a shorter, thicker, more expensive piece of wire, capable of carrying as much as 100 amps.

Similarly, when you raise the lid on an a top-loading washing machine during its spin cycle, you close a lightweight switch that sends a small signal down a thin wire to a relay. The relay handles the bigger task of switching off the large motor spinning the drum full of wet clothes.

Before you begin this experiment, you need to upgrade your power supply. We're not going to use batteries anymore, because most relays require more than 6 volts, and in any case you should have a power supply that can give you a variety of voltages on demand. The simplest way to achieve this is by using an AC adapter.

First you'll set up the AC adapter. After you have it running, you'll use it to power the relay. Initially the relay will just switch between two LEDs, but then you'll modify the circuit to make the LEDs flash automatically. Finally you'll rebuild the circuit on a breadboard, and say goodbye to alligator clips, for most of the time at least.

Preparing Your AC Adapter

An AC adapter plugs into the wall and converts the high-voltage AC supply in your home into a safe, low DC voltage for electronic devices. Any charger that you use with your cell phone, or iPod, or laptop computer is a special-purpose AC adapter that delivers only one voltage via a specific type of plug. I've asked you to buy a general-purpose adapter that delivers many different voltages, and we're going to begin by getting rid of its plug.

Figure 2-49. *Preparing an AC adapter. First, cut off the little low-voltage plug and throw it away.*

Figure 2-50. *Second, strip the wires, making one shorter than the other to reduce the risk of them touching. Color one of the adapter wires red with a marker, to identify it as the positive one.*

1. It's important to make sure that your AC adapter is not plugged into the wall!
2. Chop off the little plug at the end of its wire. See Figure 2-49.
3. Use a box cutter or utility knife or scissors to make a half-inch cut between the two conductors, and then pull the conductors apart a couple of inches.
4. Use wire cutters to trim one of the conductors shorter than the other, so that after you strip away a little of the insulation, the exposed copper wires cannot easily touch each other. This is a precaution against short-circuiting your AC adapter and burning it out.
5. Strip the two conductors using your wire strippers. Twist the copper strands between finger and thumb so that there are no loose strands sticking out. See Figure 2-50.
6. Make sure that the two wires are not touching each other, and plug your AC adapter into a wall outlet. Set your meter to DC volts and apply the meter probes to the wires from the adapter. If the voltage is preceded with a minus sign, you have the probes the wrong way around. Reverse them and the minus sign should go away. This tells you which wire is positive.
7. Mark the positive wire from the adapter. If the wire has white insulation, you can mark it with a red marker. If it has black insulation, you can tag it with a label. The positive wire will remain positive regardless of which way up you plug the AC adapter into a wall outlet.

The Relay

The type of relay that I want you to use has little spiky legs on the bottom, in a standardized layout. If you buy some other kind of relay, you will have to figure out for yourself which pins are connected to the coil inside, which pins go to the poles of the switch inside it, and which go to the normally closed and normally open contacts. You can check the manufacturer's data sheet for this purpose, but I strongly suggest you use one of the relays mentioned in the shopping list, so that you can follow the instructions here more easily.

I asked you to buy two relays so that you can use one for investigational purposes—meaning that you can break it open and take a look inside. If you do this very, very carefully, the relay should still be usable afterward. If not, well, you still have a spare.

The easiest way to open the relay is with a box cutter or utility knife. Figures 2-52, 2-53, and 2-54 show the technique. Shave the edges of the plastic shell containing the relay, beveling them until you see just a hair-thin opening. Don't go any farther; the parts inside are very, very close to its housing. Now pop the top off. You can use needle-nosed pliers to nibble the rest of the shell away. Read the following section, "Fundamentals: Inside a relay," and then apply power to the relay to see how it works.

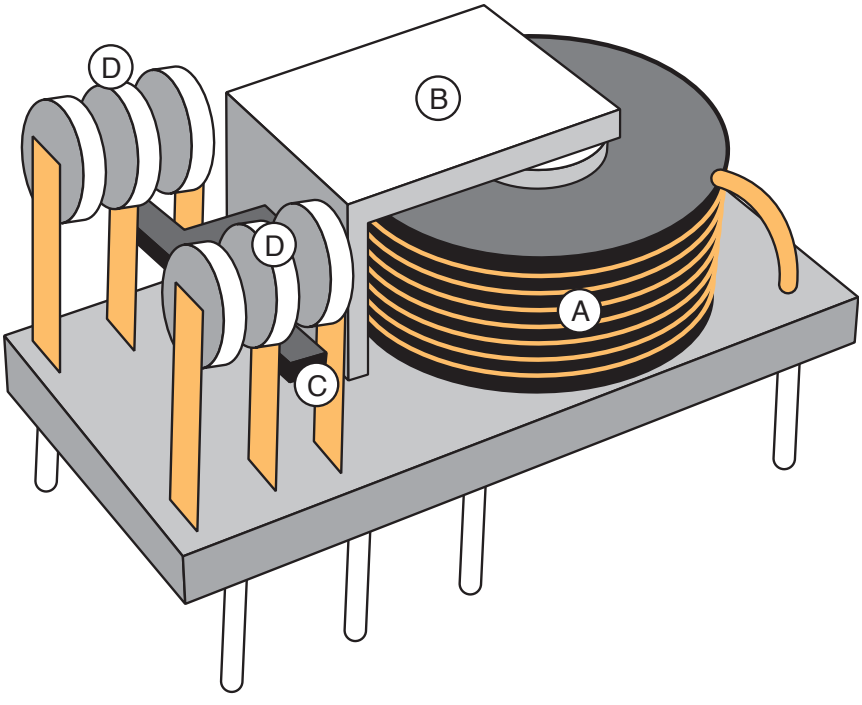

Figure 2-51. *This is one way that the parts inside a relay can be arranged. The coil, A, generates a magnetic attraction pulling lever B downward. A plastic extension, C, pushes outward against flexible metal strips and moves the poles of the relay, D, between the contacts.*

Figure 2-52. *To look inside a sealed relay, shave the top edges of the plastic package with a utility knife til you open a thin crack.*

Figure 2-53. *Insert the blade of your knife to pry open the top, then repeat the procedure for the sides.*

Figure 2-54. *If you are really, really careful, the relay should still work after you open it.*

Figure 2-55

Figure 2-56. *Patience is essential when carving the edges of a relay package in order to open it. Faster methods such as a tomahawk or a flamethrower will satisfy the emotional needs of those with a short attention span, but results may be unpredictable.*

Figure 2-57. *Four assorted 12-volt relays, shown with and without their packages. The automotive relay (far left) is the simplest and easiest to understand, because it is designed without much concern for the size of the package. Smaller relays are more ingeniously designed, more complex, and more difficult to figure out. Usually, but not always, a smaller relay is designed to switch less current than a larger one.*

FUNDAMENTALS

Inside a relay

A relay contains a coil of wire wrapped around an iron core. When electricity runs through the coil, the iron core exerts a magnetic force, which pulls a lever, which pushes or pulls a springy strip of metal, closing two contacts. So as long as electricity runs through the coil, the relay is "energized" and its contacts remain closed.

When the power stops passing through the coil, the relay lets go and the springy strip of metal snaps back into its original position, opening the contacts. (The exception to this rule is a latching relay, which requires a second pulse through a separate coil to flip it back to its original position; but we won't be using latching relays until later in the book.)

Relays are categorized like switches. Thus, you have SPST relays, DPST, SPDT, and so on.

Compare the schematics in Figure 2-58 with the schematics of switches in Figure 2-38. The main difference is that the relay has a coil that activates the switch. The switch is shown in its "relaxed" mode, when no power flows through the coil.

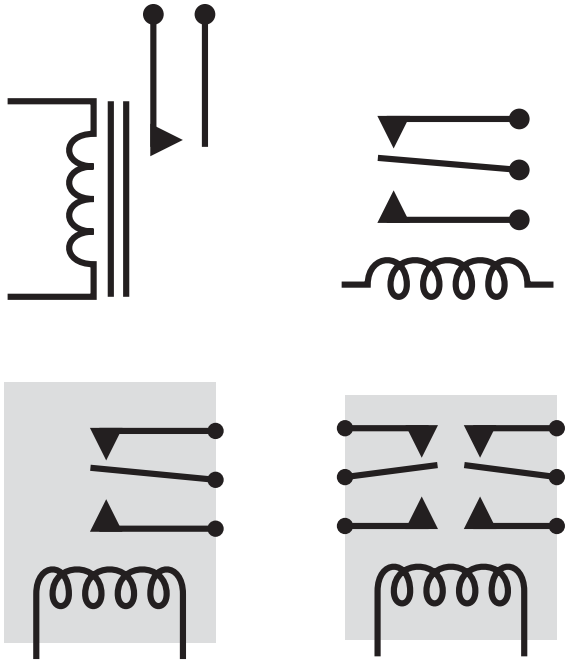

Figure 2-58. *Various ways to show a relay in a schematic. Top left: SPST. Top right and bottom left: SPDT. Bottom right: DPDT. The styles at bottom-left and bottom-right will be used in this book.*

The contacts are shown as little triangles. When there are two poles instead of one, the coil activates both switches simultaneously.

Most relays are nonpolarized, meaning that you can run electricity through the coil in either direction, and the relay doesn't care. You should check the data sheet to make sure, though. Some relay coils work on AC voltage, but almost all low-voltage relays use direct current—a steady flow of electricity, such as you would get from a battery. We'll be using DC relays in this book.

Relays suffer from the same limitations as switches: their contacts will be eroded by sparking if you try to switch too much voltage. It's not worth saving a few dollars by using a relay that is rated for less current or voltage than your application requires. The relay will fail you when you need it most, and may be inconvenient to replace.

Because there are so many different types of relays, read the specifications carefully before you buy one. Look for these basics:

Coil voltage
: The voltage that the relay is supposed to receive when you energize it.

Set voltage
: The minimum voltage that the relay needs to close its switch. This will be a bit less than the ideal coil voltage.

Operating current
: The power consumption of the coil, usually in milliamps, when the relay is energized. Sometimes the power is expressed in milliwatts.

Switching capacity
: The maximum amount of current that you can switch with contacts inside the relay. Usually this is for a "resistive load," meaning a passive device such as light bulb. When you use a relay to switch on a motor, the motor takes a big initial surge of current before it gets up to speed. In this case, you should choose a relay rated for double the current that the motor draws when it is running.

Procedure

Turn the relay with its legs in the air and attach wires and LEDs as shown in Figure 2-59, with a 680Ω resistor (a 1K resistor will be OK if you don't have the correct value). Also attach a pushbutton switch. (Your pushbutton switch may look different from the one shown, but as long as it is a SPST pushbutton with two contacts at the bottom, it will work the same way.) When you press the pushbutton, the relay will make the first LED go out and the second LED light up. When you release the pushbutton, the first LED lights up and the second one goes out.

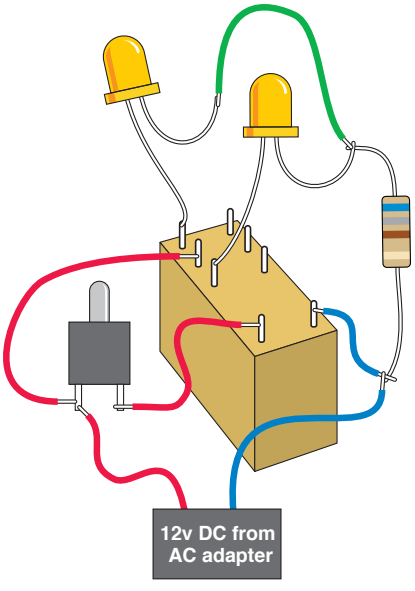

Figure 2-59. *As before, you can use patch cords, if you have them, instead of some of the wired connections shown here.*

How It Works

Check the schematic in Figure 2-60 and compare it with Figure 2-59. Also see Figure 2-62, which shows how the pins outside the relay make connections inside the relay when its coil is energized, and when it is not energized.

This is a DPDT relay, but we are only using one pole and ignoring the other. Why not buy a SPDT relay? Because I want the pins to be spaced the way they are when you will upgrade this circuit by transferring it onto a breadboard, which will happen very shortly.

On the schematic, I have shown the switch inside the relay in its relaxed state. When the coil is energized, the switch flips upward, which seems counterintuitive, but just happens to be the way that this particular relay is made.

When you're sure you understand how the circuit works, it's time to move on to the next step: making a small modification to get the relay to switch itself on and off, as we'll do in Experiment 8.

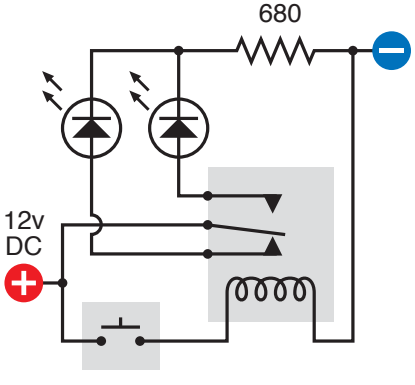

Figure 2-60. *Same circuit, shown in schematic form.*

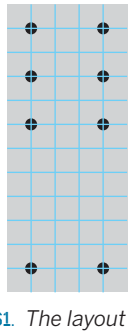

Figure 2-61. *The layout of the pins of the relay, superimposed on a grid of 1/10-inch squares. This is the type of relay that you will need in Experiment 8.*

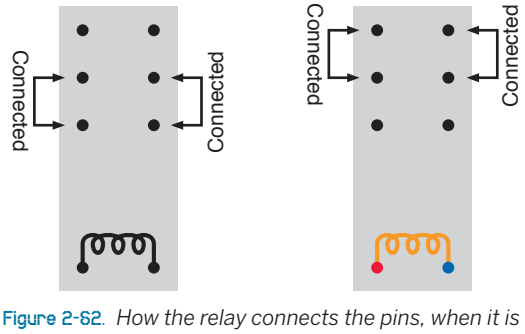

Figure 2-62. *How the relay connects the pins, when it is not energized (left) and when it is energized (right).*

Larger versions of all schematics and breadboard photos are available online at this book's website: http://oreilly.com/catalog/9780596153748.

Experiment 8: A Relay Oscillator

You will need:

- AC adapter, breadboard, wire, wire cutters and strippers.
- DPDT relay. Quantity: 1.
- LEDs. Quantity: 2.
- Pushbutton, SPST. Quantity: 1.
- Alligator clips. Quantity: 8.
- Resistor, approximately 680Ω. Quantity: 1.
- Capacitor, electrolytic, 1,000 µF. Quantity: 1.

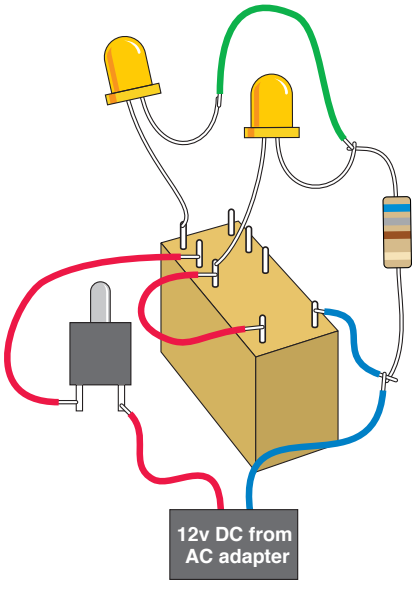

Figure 2-63. *A small revision to the previous circuit causes the relay to start oscillating when power is applied.*

Look at the revised drawing in Figure 2-63 and the revised schematic in Figure 2-64 and compare them with the previous ones. Originally, there was a direct connection from the pushbutton to the coil. In the new version, the power gets to the coil by going, first, through the contacts of the relay.

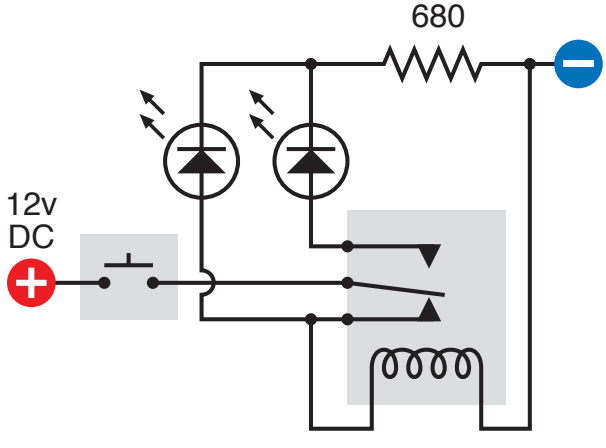

Figure 2-64. *The oscillator circuit shown in schematic form.*

Now, when you press the button, the contacts in their relaxed state feed power to the coil as well as to the lefthand LED. But as soon as the coil is energized, it opens the contacts. This interrupts the power to the coil—so the relay relaxes, and the contacts close again. They feed another pulse of power to the coil, which opens the contacts again, and the cycle repeats endlessly.

Because we're using a very small relay, it switches on and off extremely fast. In fact, it oscillates perhaps 50 times per second (too fast for the LEDs to show what's really happening). Make sure your circuit looks like the one in the diagram, and then press the pushbutton very briefly. You should hear the relay make a buzzing sound. If you have impaired hearing, touch the relay lightly with your finger, and you should feel the relay vibrating.

When you force a relay to oscillate like this, it's liable to burn itself out or destroy its contacts. That's why I asked you to press the pushbutton briefly. To make the circuit more practical, we need something to slow the relay down and prevent it from self-destructing. That necessary item is a capacitor.

Adding Capacitance

Add a 1,000 µF electrolytic capacitor in parallel with the coil of the relay as shown in the diagram in Figure 2-65 and the schematic in Figure 2-66. Check Figure 2-14 if you're not sure what a capacitor looks like. The 1,000 µF value will be printed on the side of it, and I'll explain what this means a little later.

Make sure the capacitor's *short* wire is connected to the *negative* side of the circuit; otherwise, it won't work. In addition to the short wire, you should find a minus sign on the body of the capacitor, which is there to remind you which side is negative. Electrolytic capacitors are fussy about this.

When you press the button now, the relay should click slowly instead of buzzing. What's happening here?

A capacitor is like a tiny rechargeable battery. It's so small that it charges in a fraction of a second, before the relay has time to open its lower pair of contacts. Then, when the contacts are open, the capacitor acts like a battery, providing power to the relay. It keeps the coil of the relay energized for about one second. After the capacitor exhausts its power reserve, the relay relaxes and the process repeats.

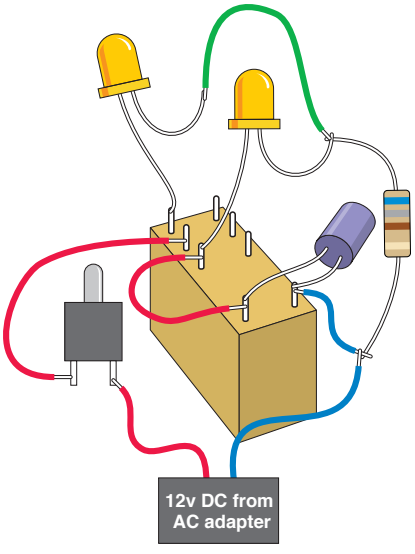

Figure 2-65. *Adding a capacitor makes the relay oscillate more slowly.*

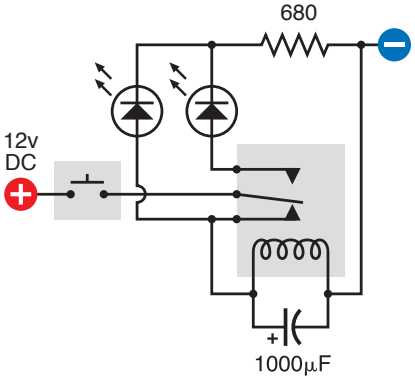

Figure 2-66. *The capacitor appears at the bottom of this schematic diagram.*

FUNDAMENTALS

Farad basics

The Farad is an international unit to measure capacitance. Modern circuits usually require small capacitors. Consequently it is common to find capacitors measured in microfarads (one-millionth of a farad) and even picofarads (one-trillionth of a farad). Nanofarads are also used, more often in Europe than in the United States. See the following conversion table.

0.001 nanofarad	1 picofarad	1 pF
0.01 nanofarad	10 picofarads	10 pF
0.1 nanofarad	100 picofarads	100 pF
1 nanofarad	1,000 picofarads	1,000 pF
0.001 microfarad	1 nanofarad	1 nF
0.01 microfarad	10 nanofarads	10 nF
0.1 microfarad	100 nanofarads	100 nF
1 microfarad	1,000 nanofarads	1,000 nF
0.000001 Farad	1 microfarad	1 µF
0.00001 Farad	10 microfarads	10 µF
0.0001 Farad	100 microfarads	100 µF
0.001 Farad	1,000 microfarads	1,000 µF

(You may encounter capacitances greater than 1,000 microfarads, but they are uncommon.)

FUNDAMENTALS

Capacitor basics

DC current does not flow through a capacitor, but voltage can accumulate very quickly inside it, and remains after the power supply is disconnected. Figures 2-67 and 2-68 may help to give you an idea of what happens inside a capacitor when it is fully charged.

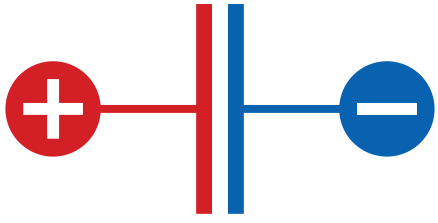

Figure 2-67. *When DC voltage reaches a capacitor, no current flows, but the capacitor charges itself like a little battery. The positive and negative charges are equal and opposite.*

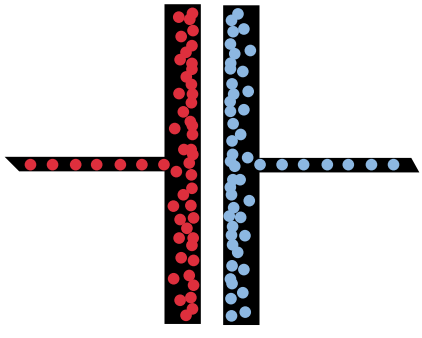

Figure 2-68. *You can imagine positive "charge particles" accumulating on one side of the capacitor and attracting negative "charge particles" to the opposite side.*

In most modern electrolytic capacitors, the plates have been reduced to two strips of very thin, flexible, metallic film, often wrapped around each other, separated by an equally thin insulator. Disc ceramic capacitors typically consist of just a single disc of nonconductive material with metal painted on both sides and leads soldered on.

The two most common varieties of capacitors are ceramic (capable of storing a relatively small charge) and electrolytic (which can be much larger). Ceramics are often disc-shaped and yellow in color; electrolytics are often shaped like miniature tin cans and may be just about any color. Refer back to Figures 2-13 and 2-14 for some examples.

Getting Zapped by Capacitors

If a large capacitor is charged with a high voltage, it can retain that voltage for a long time. Because the circuits in this book use low voltages, you don't have to be concerned about that danger here, but if you are reckless enough to open an old TV set and start digging around inside (which I do not recommend), you may have a nasty surprise. An undischarged capacitor can kill you as easily as if you stick your finger into an electrical outlet. Never touch a large capacitor unless you really know what you're doing.

FUNDAMENTALS

Capacitor basics (continued)

Ceramic capacitors have no polarity, meaning that you can apply negative voltage to either side of them. Electrolytics do have polarity, and won't work unless you connect them the right way around.

The schematic symbol for a capacitor has two significant variants: with two straight lines (symbolizing the plates inside a capacitor), or with one straight line and one curved line, as shown in Figure 2-69. When you see a curved line, that side of the capacitor should be more negative than the other. The schematic symbol may also include a + sign. Unfortunately, some people don't bother to draw a curved plate on a polarized capacitor, yet others draw a curved plate even on a nonpolarized capacitor.

Figure 2-69. *The generic schematic for a capacitor is on the left. The version on the right indicates a polarized capacitor which requires its left plate to be "more positive" than its right plate. The plus sign is often omitted.*

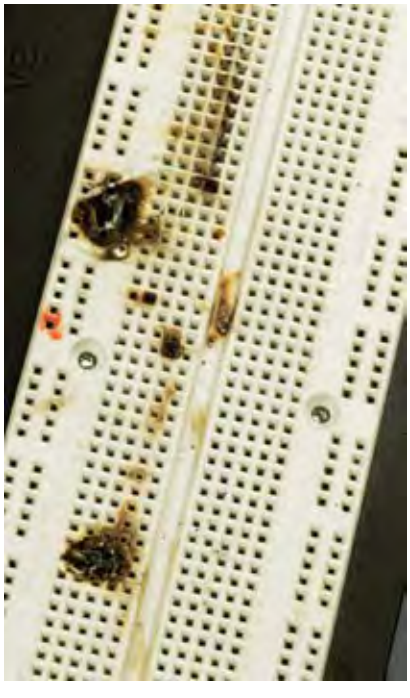

Figure 2-70. *A tantalum capacitor was plugged into this breadboard, accidentally connected the wrong way around to a power source capable of delivering a lot of current. After a minute or so of this abuse, the capacitor rebelled by popping open and scattering small flaming pieces, which burned their way into the plastic of the breadboard. Lesson learned: observe polarity!*

Capacitor Polarity

You must connect an electrolytic capacitor so that its longer wire is more positive than its shorter wire. The shell of the capacitor is usually marked with a negative sign near the shorter wire.

Some capacitors may behave badly if you don't observe their polarity. One time I connected a tantalum capacitor to a circuit, using a power supply able to deliver a lot of current, and was staring at the circuit and wondering why it wasn't working when the capacitor burst open and scattered little flaming fragments of itself in a 3-inch radius. I had forgotten that tantalum capacitors can be fussy about positive and negative connections. Figure 2-70 shows the aftermath.

BACKGROUND

Michael Faraday and capacitors

The earliest capacitors consisted of two metal plates with a very small gap between them. The principle of the thing was simple:

- If one plate was connected to a positive source, the positive charges attracted negative charges onto the other plate.
- If one plate was connected to a negative source, the negative charges attracted positive charges onto the other plate.

Figures 2-67 and 2-68, shown previously, convey the basic idea.

The electrical storage capacity of a capacitor is known as its *capacitance*, and is measured in farads, named after Michael Faraday (Figure 2-71), another of the pantheon of electrical pioneers. He was an English chemist and physicist who lived from 1791 to 1867.

Although Faraday was relatively uneducated and had little knowledge of mathematics, he had an opportunity to read a wide variety of books while working for seven years as a bookbinder's apprentice, and thus was able to educate himself. Also, he lived at a time when relatively simple experiments could reveal fundamental properties of electricity. Thus he made major discoveries including electromagnetic induction, which led to the development of electric motors. He also discovered that magnetism could affect rays of light.

His work earned him numerous honors, and his picture was printed on English 20-pound bank notes from 1991 through 2001.

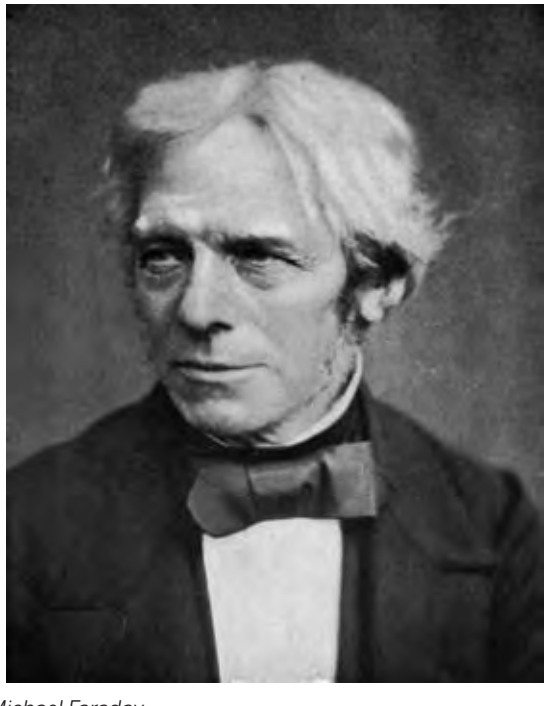

Figure 2-71. *Michael Faraday*

Breadboarding the Circuit

I promised to free you in time from the frustrations of alligator clips, and that time has come. Please turn your attention to the block of plastic with lots of little holes in it that I asked you to buy. For reasons that I do not know, this is called a *breadboard*. When you plug components into the holes, hidden metal strips inside the breadboard connect the components for you, allowing you to set up a circuit, test it, and modify it very easily. Afterward you can pull the components off the breadboard and put them away for future experiments.

Without a doubt, breadboarding is the most convenient way to test something before you decide whether you want to keep it.

Almost all breadboards are designed to be compatible with integrated circuit chips (which we will be using in Chapter 4 of this book). The chip straddles an empty channel in the center of the breadboard with rows of little holes either side—usually five holes per row. You insert other components into these holes.

In addition, the breadboard should have columns of holes running down each side. These are used to distribute positive and negative power.

Take a look at Figures 2-72 and 2-73, which show the upper part of a typical breadboard seen from above, and the same breadboard seen as if with X-ray vision, showing the metal strips that are embedded behind the holes.

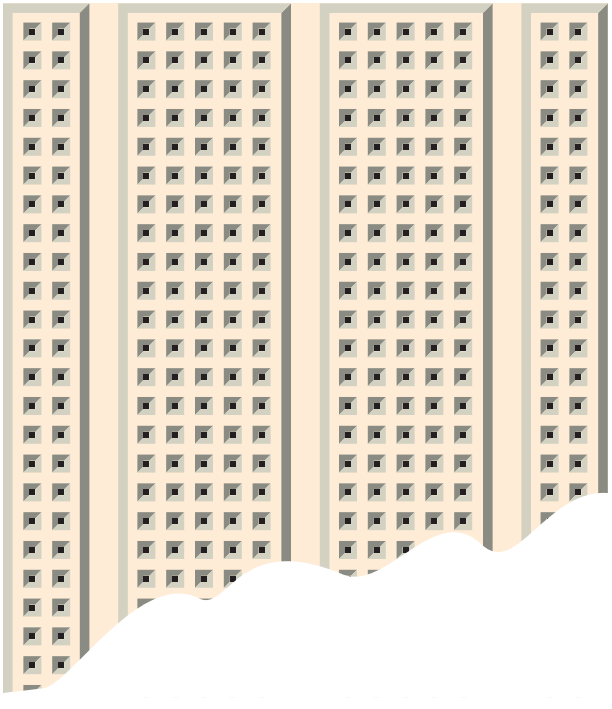

Figure 2-72. *A typical breadboard. You can plug components into the holes to test a circuit very quickly.*

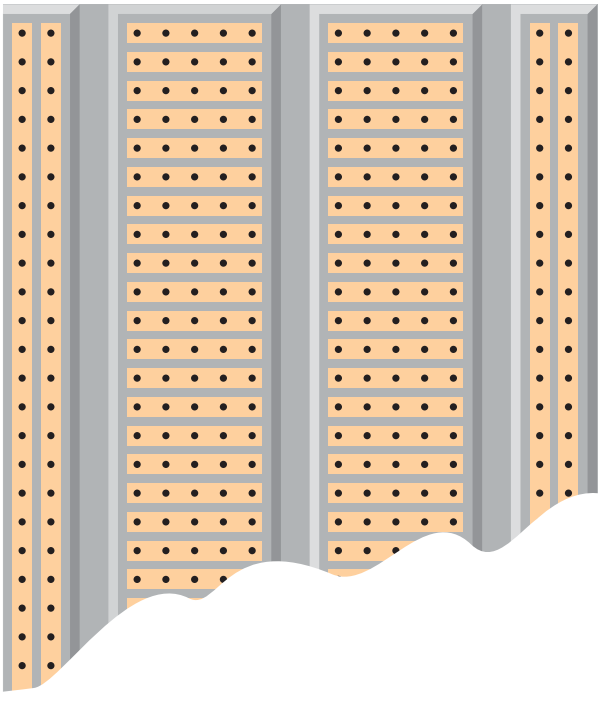

Figure 2-73. *This X-ray-vision view of the breadboard reveals the copper strips that are embedded in it. The strips conduct electricity from one component to another.*

Important note: some breadboards divide each vertical column of holes, on the left and the right, into two separate upper and lower sections. Use your meter's continuity testing feature to find out if your breadboard conducts power along its full length, and add jumper wires to link the upper and lower half of the breadboard if necessary.

Figure 2-74 shows how you can use the breadboard to replicate your oscillating relay circuit. To make this work, you need to apply the positive and negative power from your AC adapter. Because the wire from your AC adapter is almost certainly stranded, you'll have difficulty pushing it into the little holes. A way around this is to set up a couple of pieces of bare 22-gauge wire, and use them as terminals to which you clip the wire from the adapter, as in Figure 2-75. (Yes, you still need just a couple of alligator clips for this purpose.) Alternatively, you can use a breadboard with power terminals built into it, which is more convenient.

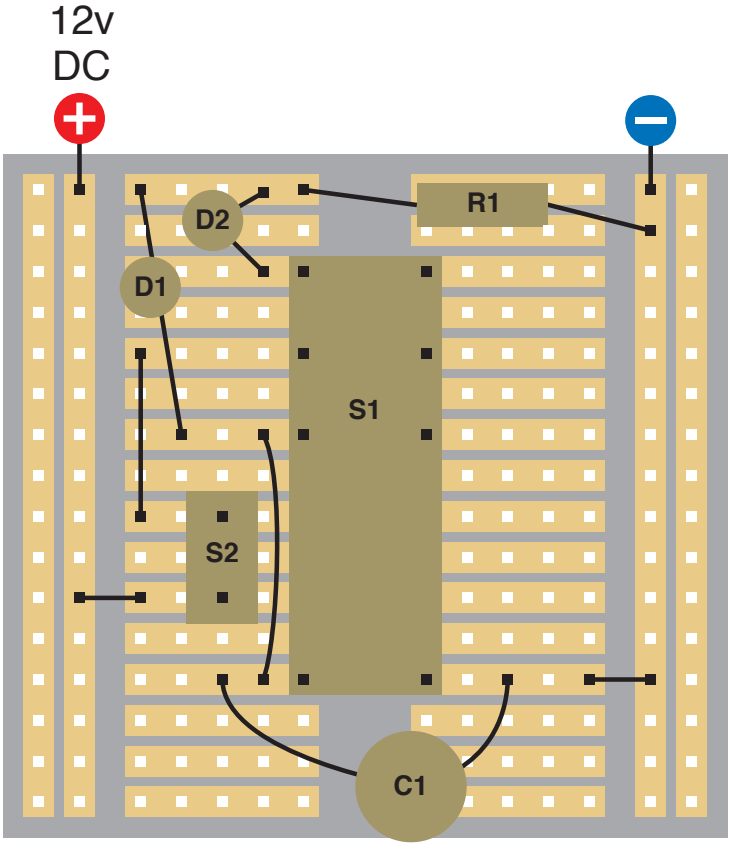

Figure 2-74. *If you place the components on your breadboard in the positions shown, they will create the same circuit that you built from wire and alligator clips in Experiment 8. Component values:*

D1, D2: Light-emitting diodes
S1: DPDT relay
S2: SPST momentary switch
C1: Electrolytic capacitor, 1,000 µF
R1: Resistor, 680Ω minimum

Figure 2-75. *If your breadboard doesn't have screw terminals, insert two short pieces of solid-core wire with stripped ends and then attach the stranded wires from the adapter using alligator clips.*

You'll need some more 22-gauge wire, or some precut hookup wire, to supply the power to your components, which are plugged into the breadboard as shown in Figures 2-76 and 2-77. If you get all the connections right, the circuit should function the same way as before.

The geometry of the metal connecting strips in the breadboard often forces you to connect components in a roundabout way. The pushbutton, for instance, supplies power to the pole of the relay but cannot be connected directly opposite, because there isn't room for it.

Remember that the strips inside the breadboard that don't have any wires or components plugged into them are irrelevant; they don't do anything.

I'll include some suggested breadboard layouts for circuits as you continue through this book, but eventually you'll have to start figuring out breadboard layouts for yourself, as this is an essential part of hobby electronics.

Larger versions of all schematics and breadboard photos are available online at this book's website: http://oreilly.com/catalog/9780596153748.

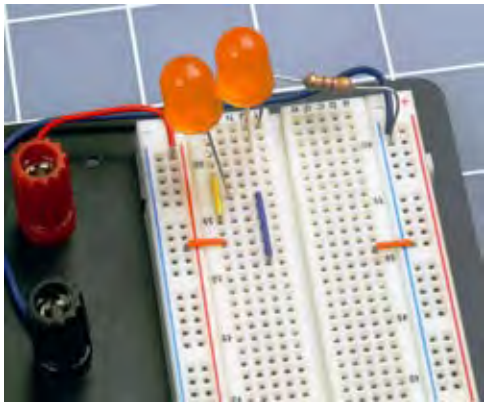

Figure 2-76. *Two oversized LEDs, one resistor, and the necessary jumper wires have been added to the breadboard.*

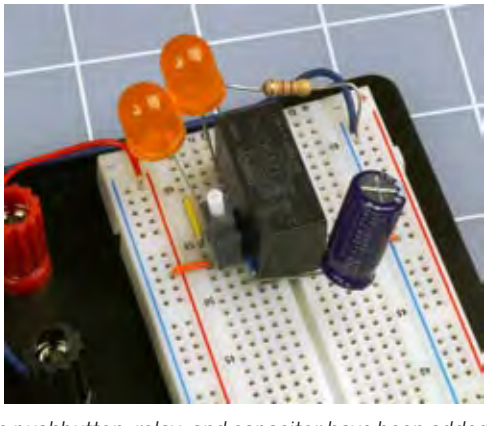

Figure 2-77. *Now the pushbutton, relay, and capacitor have been added to complete the circuit shown in the diagram and the schematic. When the pushbutton is pressed, the relay oscillates and the LEDs flash.*

Experiment 9: Time and Capacitors

You will need:

- AC adapter, breadboard, wire, wire cutters, and strippers.
- Multimeter.
- Pushbutton, SPST. Quantity: 1.
- Resistors and electrolytic capacitors, assorted.

In Experiment 8, when you put a capacitor in parallel with the coil of the relay, the capacitor charged almost instantly before discharging itself through the relay coil. If you add a resistor in series with a capacitor, the capacitor will take longer to charge. By making a capacitor take longer to charge, you can measure time, which is a very important concept.

Clean the components off your breadboard and use it to set up the very simple circuit shown in Figure 2-78, where C1 is a 1,000 µF capacitor, R1 is a 100K resistor, R2 is a 100Ω resistor, and S1 is the pushbutton that you used previously. Set your meter to measure volts DC, place the probes around the capacitor, and hold down the pushbutton. You should see the meter counting upward as the voltage accumulates on the capacitor. (This is easier with a meter that doesn't have autoranging, because you won't have to wait while the meter figures out which range to apply.) Resistor R1 slows the charging time for the capacitor.

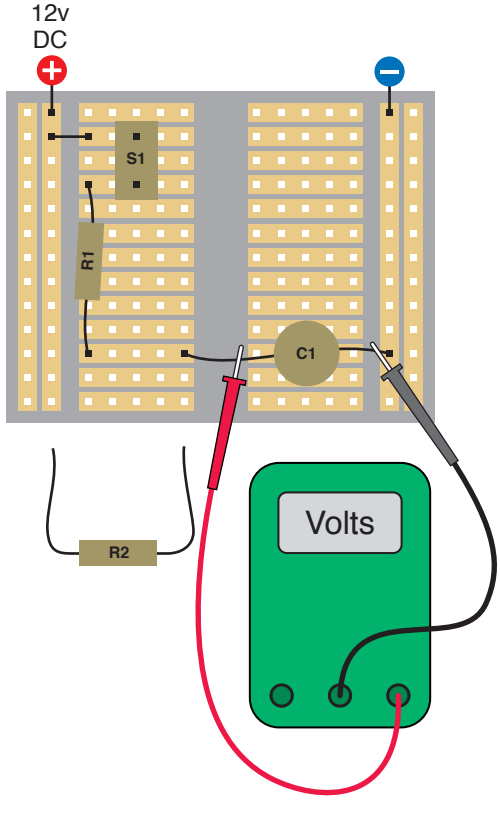

Figure 2-78. *Watch the voltage building up on the capacitor while you hold down the pushbutton. Substitute other values for R1, discharge the capacitor by touching R2 across it, and then repeat your measurement process.*

S1: Momentary pushbutton, OFF (ON)
R1: 100K initially
R2: 100Ω
C1: 1,000 µF

Release the pushbutton, set aside your meter, and discharge the capacitor by touching R2 across it for a second or two. Now substitute a 50K resistor for R1, and repeat the measurement. The meter should count upward almost twice as fast as before.

Voltage, Resistance, and Capacitance

Think of the resistor as a faucet, and the capacitor as a balloon that you are trying to fill with water. When you screw down the faucet until only a trickle comes through, the balloon will take longer to fill. But a slow flow of water will still fill the balloon completely if you wait long enough, and (assuming the balloon doesn't burst) the process ends when the pressure inside the balloon is equal to the water pressure in the pipe supplying the faucet. See Figure 2-79.

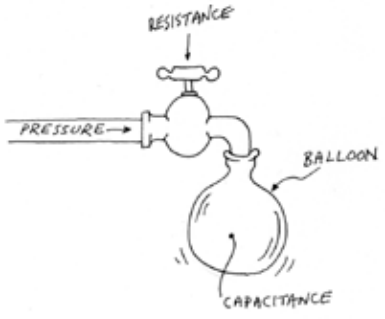

Figure 2-79. *When the faucet is closed half-way, the balloon will take longer to fill, but will still contain as much water and as much pressure in the end.*

Similarly, in your circuit, if you wait long enough, eventually the voltage across the capacitor should reach the same value as the voltage of the power supply. In a 12-volt circuit, the capacitor should eventually acquire 12 volts (although "eventually" may take longer than you think).

This may seem confusing, because earlier you learned that when you apply voltage at one end of a resistor, you get less voltage coming out than you have going in. Why should a resistor deliver the full voltage when it is paired with a capacitor?

Forget the capacitor for a moment, and remember how you tested just two 1K resistors. In that situation, each resistor contained half the total resistance of the circuit, so each resistor dropped half the voltage. If you held the negative probe of your meter against the negative side of your power supply and touched the positive probe to the center point between the two resistors, you would measure 6 volts. Figure 2-80 illustrates this.

Now, suppose you remove one of the 1K resistors and substitute a 9K resistor. The total resistance in the circuit is now 10K, and therefore the 9K resistor drops 90% of the 12 volts. That's 10.8 volts. You should try this and check it with your meter. (You are unlikely to find a 9K resistor, because this is not a standard value. Substitute the nearest value you can find.)

Now suppose you remove the 9K resistor and substitute a 99K resistor. Its voltage drop will be 99% of the available voltage, or 11.88 volts. You can see where this is heading: the larger the resistor, the larger its contribution to voltage drop.

However, I noted previously that a capacitor blocks DC voltage completely. It can accumulate an electrical charge, but no current passes through it. Therefore, a capacitor behaves like a resistor that has infinite resistance to DC current.

(Actually the insulation inside the capacitor allows a little bit of "leakage," but a perfect capacitor would have infinite resistance.)

The value of any resistor that you put in series with the capacitor is trivial by comparison. No matter how high the value of the resistor is, the capacitor still provides much more resistance in the circuit. This means that the capacitor steals almost the complete voltage drop in the circuit, and the voltage

difference between one end of the resistor and the other will be zero (assuming that we ignore little imperfections in the components). Figure 2-80 may help to clarify this concept.

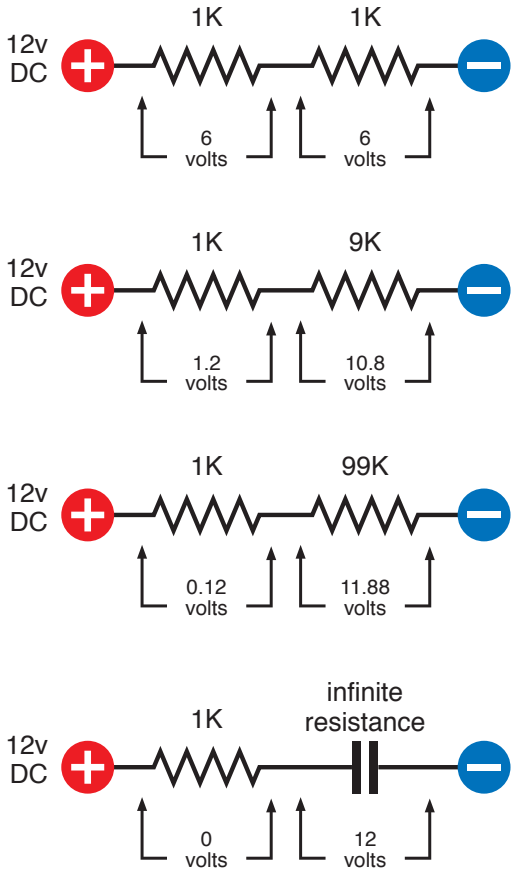

Figure 2-80. *When two resistances are in series, the larger one drops the voltage more than the smaller one. If the larger resistance becomes infinite (as in the case of a capacitor), the smaller one no longer has any measurable contribution to the voltage drop, and the voltage is almost exactly the same at both ends.*

You should try this using real resistors and capacitors—although if you do, you will run into a little problem. When you use your meter in its "DC volts" mode, it diverts a little of the current in the circuit—just a tiny taste—in the process of measuring it. The meter steals such a small amount, it doesn't affect the reading significantly when you are checking voltage across a resistor. The internal resistance of the meter is higher than the values of most resistors. However, remember that the internal resistance of a capacitor is almost infinite. Now the internal resistance of the meter becomes significant. Because you can never have an ideal meter, any more than you can have an ideal capacitor or resistor, your meter will always interfere with the circuit slightly, and you will get only an approximate indication.

If you try to measure the voltage on a capacitor that has been charged but is now not connected to anything else, you'll see the number slowly falling, as the capacitor discharges itself through the meter.

THEORY

The time constant

You may be wondering if there's a way to predict exactly how much time it takes for various capacitors to charge, when they are paired with various resistors. Is there a formula to calculate this?

Of course, the answer is yes, but the way we measure it is a bit tricky, because a capacitor doesn't charge at a constant rate. It accumulates the first volt very quickly, the second volt not quite as quickly, the third volt even less quickly—and so on. You can imagine the electrons accumulating on the plate of a capacitor like people walking into an auditorium and looking for a place to sit. The fewer seats that are left, the longer people take to find them.

The way we describe this is with something called a "time constant." The definition is very simple:

$$TC = R \times C$$

where TC is the time constant, and a capacitor of C farads is being charged through a resistor of R ohms.

Going back to the circuit you just tested, try using it again, this time with a 1K resistor and the 1,000 µF capacitor. We have to change those numbers to farads and ohms before we can put them in the formula. Well, 1,000 µF is 0.001 farads, and 1K is 1,000 ohms, so the formula looks like this:

$$TC = 1{,}000 \times 0.001$$

In other words, TC = 1—a lesson that could not be much easier to remember:

> ***A 1K resistor in series with a 1,000 µF capacitor has a time constant of 1.***

Does this mean that the capacitor will be fully charged in 1 second? No, it's not that simple. TC, the time constant, is the time it takes for a capacitor to acquire *63%* of the voltage being supplied to it, if it starts with zero volts.

(Why 63%? The answer to that question is too complicated for this book, and you'll have to read about time constants elsewhere if you want to know more. Be prepared for differential equations.) Here's a formal definition for future reference:

> TC, the time constant, is the time it takes for a capacitor to acquire 63% of the difference between its current charge and the voltage being applied to it. When TC=1, the capacitor acquires 63% of its full charge in 1 second. When TC=2, the capacitor acquires 63% of its full charge in 2 seconds. And so on.

What happens if you continue to apply the voltage? History repeats itself. The capacitor accumulates *another* 63% of the *remaining* difference between its current charge, and the voltage being applied to it.

Imagine someone eating a cake. In his first bite he's ravenously hungry, and eats 63% of the cake in one second. In his second bite, not wanting to seem too greedy, he takes just another 63% of the cake that is left—and because he's not feeling so hungry anymore, he requires the same time to eat it as he took to eat the first bite. In his third bite, he takes 63% of what still remains, and still takes the same amount of time. And so on. He is behaving like a capacitor eating electricity (Figure 2-81).

Figure 2-81. *If our gourmet always eats just 63% of the cake still on the plate, he "charges up" his stomach in the same way that a capacitor charges itself. No matter how long he keeps at it, his stomach is never completely filled.*

THEORY

The time constant (continued)

The cake eater will always have a few crumbs to eat, because he never takes 100% of the remainder. Likewise, the capacitor will never acquire a full charge. In a perfect world of perfect components, this process would continue for an infinite time.

In the real world, we say rather arbitrarily:

> After 5 × TC the capacitor will be so nearly fully charged, we won't care about the difference.

In the table is a calculation (rounded to two decimal places) showing the charge accumulating on a capacitor in a 12-volt circuit where the time constant is 1 second.

Here's how to understand the table. V1 is the current charge on the capacitor. Subtract this from the supply voltage (12 volts) to find the difference. Call the result V2. Now take 63% of V2, and add this to the current charge (V1) and call the result V4. This is the new charge that the capacitor will have after 1 second, so we copy it down to the next line in the table, and it becomes the new value for V1.

Now we repeat the same process all over again. Figure 2-82 shows this in graphical form. Note that after 5 seconds, the capacitor has acquired 11.92 volts, which is 99% of the power supply voltage. This should be close enough to satisfy anyone's real-world requirements.

If you try to verify these numbers by measuring the voltage across the capacitor as it charges, remember that because your meter steals a little current, there will be a small discrepancy that will increase as time passes. For practical purposes, the system works well enough.

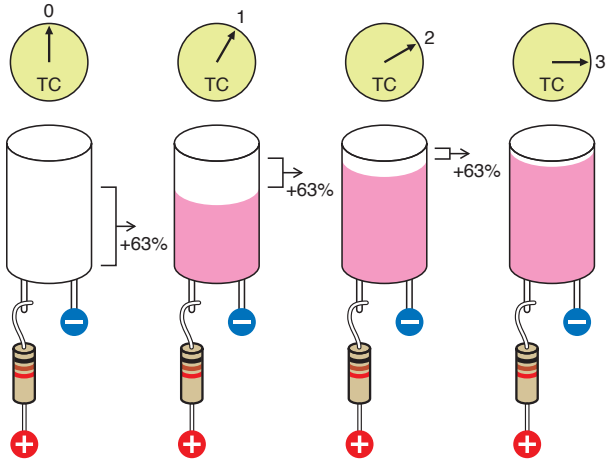

Figure 2-82. *A capacitor starts with 0 volts. After 1 time constant it adds 63% of the available voltage. After another time constant, it adds another 63% of the remaining voltage difference, and so on.*

Time in secs	V1: Charge on capacitor	V2: 12 – V1	V3: 63% of V2	V4: V1 + V3
0	0.00	12.00	7.56	7.56
1	7.56	4.44	2.80	10.36
2	10.36	1.64	1.03	11.39
3	11.39	0.61	0.38	11.77
4	11.77	0.23	0.15	11.92
5	11.92			

Experiment 10: Transistor Switching

You will need:

- AC adapter, breadboard, wire, and meter.
- LED. Quantity: 1.
- Resistors, various.
- Pushbutton, SPST. Quantity: 1.
- Transistor, 2N2222 or similar. Quantity: 1.

A transistor can switch a flow of electricity, just like a relay. But it's much more sensitive and versatile, as this first ultra-simple experiment will show.

We'll start with the 2N2222 transistor, which is the most widely used semiconductor of all time (it was introduced by Motorola in 1962 and has been in production ever since).

First, you should get acquainted with the transistor. Because Motorola's patents on the 2N2222 ran out long ago, any company can manufacture their own version of it. Some versions are packaged in a little piece of black plastic; others are enclosed in a little metal "can." (See Figure 2-83.) Either way, it contains a piece of silicon divided into three sections known as the collector, the base, and the emitter. I'll describe their function in more detail in a moment, but initially you just need to know that in this type of transistor, the collector receives current, the base controls it, and the emitter sends it out.

Use your breadboard to set up the circuit shown in Figure 2-85. Be careful to get the transistor the right way around! (See Figure 2-84.) For the three brands I have mentioned in the shopping list, the flat side should face right, if the transistor is packaged in black plastic, or the little tab should face toward the lower left, if the transistor is packaged in metal.

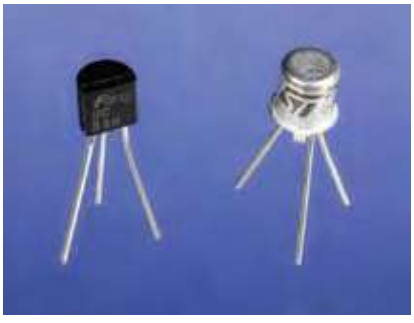

Figure 2-83. *A typical transistor is packaged either in a little metal can or a molded piece of black plastic. The manufacturer's data sheet tells you the identities of the three wire leads, relative to the flat side of a black plastic transistor or the tab that sticks out of a metal-can transistor.*

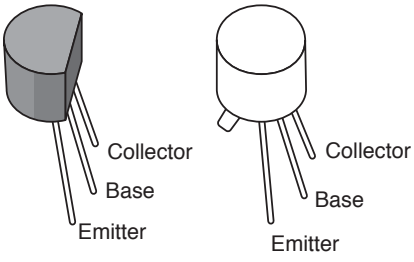

Figure 2-84. *The 2N2222 transistor may be packaged in either of these formats. Left: RadioShack or Fairchild. Right: STMicroelectronics (note the little tab sticking out at the lower-left side). If you use a different brand, you'll have to check the manufacturer's data sheet. Insert the transistor in your breadboard with the flat side facing right, as seen from above, or the tab pointing down and to the left, seen from above.*

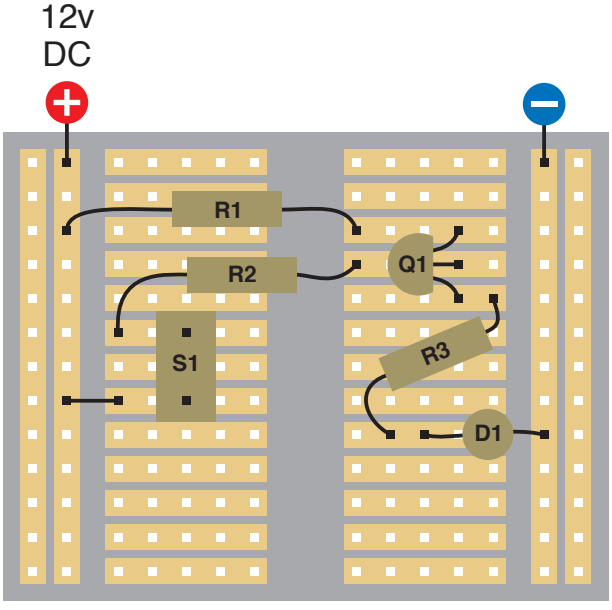

Figure 2-85. *The transistor blocks voltage that reaches it through R1. But when pushbutton S1 is pressed, this tells the transistor to allow current to pass through it. Note that transistors are always identified with letter Q in wiring diagrams and schematics.*

S1: Pushbutton, momentary, OFF (ON)
R1: 180Ω
R2: 10K
R3: 680Ω
Q1: 2N2222 or similar
D1: LED

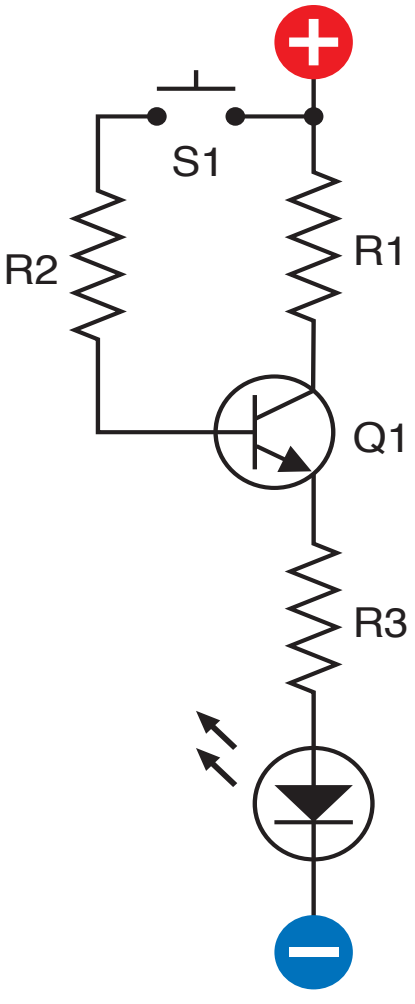

Figure 2-86. *This shows the same circuit as the breadboard diagram in Figure 2-85.*

Initially, the LED should be dark. Now press the pushbutton and the LED should glow brightly. Electricity is following two paths here. Look at the schematic in Figure 2-86, which shows the same circuit more clearly. I've shown positive at the top and negative at the bottom (the way most schematics do it) because it helps to clarify the function of this particular circuit. If you view the schematic from the side, the similarity with the breadboard layout is easier to see.

Through R1, voltage reaches the top pin (the collector) of the transistor. The transistor only lets a tiny trickle of it pass through, so the LED stays dark. When you press the button, voltage is also applied along a separate path, through R2 to the middle pin (the base) of the transistor. This tells the transistor to open its solid-state switch and allow current to flow out through its third pin (the emitter), and through R3, to the LED.

You can use your meter in volts DC mode to check the voltage at points in the circuit. Keep the negative probe from the meter touching the negative voltage source while you touch the positive probe to the top pin of the transistor, the middle pin, and the bottom pin. When you press the button, you should see the voltage change.

Fingertip Switching

Now here's something more remarkable. Remove R2 and the pushbutton, and insert two short pieces of of wire as shown in Figure 2-87. The upper piece of wire connects with the positive voltage supply; the lower piece connects with the middle pin of the transistor (its base). Now touch the tip of your finger to the two wires. Once again, the LED should glow, although not as brightly as before. Lick the tip of your finger, try again, and the LED should glow more brightly.

Never Use Two Hands

The fingertip switching demo is safe if the electricity passes just through your finger. You won't even feel it, because it's 12 volts DC from a power supply of 1 amp or less. But it's not a good idea to put the finger of one hand on one wire, and the finger of your other hand on the other wire. This would allow the electricity to pass through your body. Although the chance of hurting yourself this way is extremely small, you should never allow electricity to run through you from one hand to the other. Also, when touching the wires, don't allow them to penetrate your skin.

Your finger is conducting positive voltage to the base of the transistor. Even though your skin has a high resistance, the transistor still responds. It isn't just switching the LED on and off; it is *amplifying the current* applied to its base. This is an essential concept: *a transistor amplifies any changes in current that you apply to its base*.

Check Figure 2-88 to see more clearly what's happening.

If you studied the section "Background: Positive and negative" in Chapter 1, you learned that there is really no such thing as positive voltage. All we really have is negative voltage (created by the pressure of free electrons) and an absence of negative voltage (where there are fewer free electrons). But because the idea of a flow of electricity from positive to negative was so widely believed before the electron was discovered, and because the inner workings of a transistor involve "holes" which are an absence of electrons and can be thought of as positive, we can still pretend that electricity flows from positive to negative. See the following section, "Essentials: All about NPN and PNP transistors," for more details.

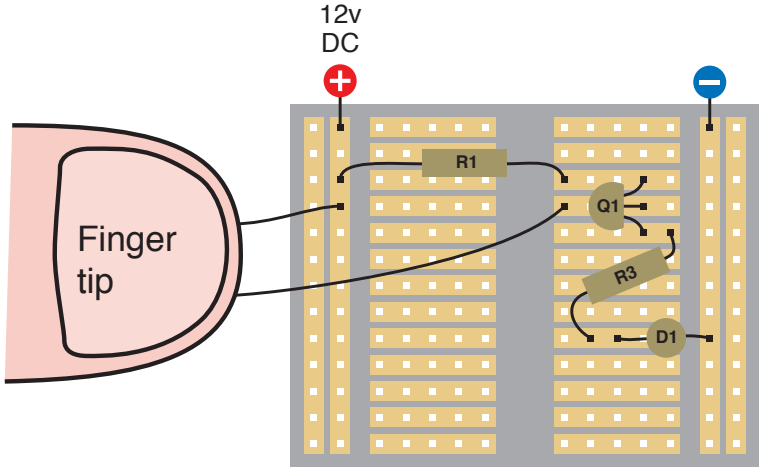

Figure 2-87

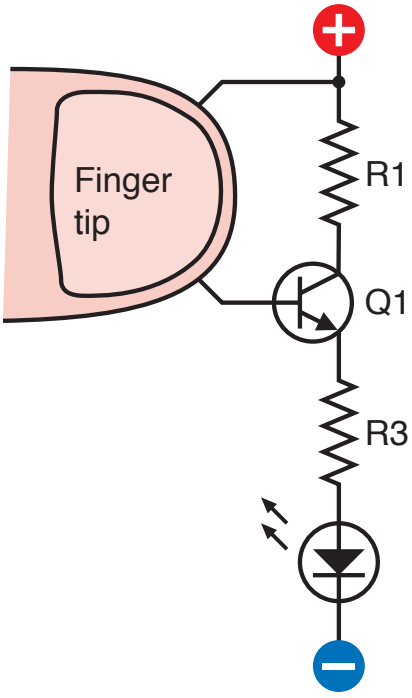

Figure 2-88. *These two diagrams show the same components as before, with a fingertip substituted for R2. Although only a trickle of voltage now reaches the base of the transistor, it's enough to make the transistor respond.*

ESSENTIALS

All about NPN and PNP transistors

A transistor is a semiconductor, meaning that sometimes it conducts electricity, and sometimes it doesn't. Its internal resistance varies, depending on the power that you apply to its base.

NPN and PNP transistors are bipolar semiconductors. They contain two slightly different variants of silicon, and conduct using both polarities of carriers—holes and electrons.

The NPN type is a sandwich with P-type silicon in the middle, and the PNP type is a sandwich with N-type silicon in the middle. If you want to know more about this terminology, and the behavior of electrons when they try to cross an NP junction or a PN junction, you'll have to read a separate source on this subject. It's too technical for this book. All you need to remember is:

- All bipolar transistors have three connections: Collector, Base, and Emitter, abbreviated as C, B, and E on the manufacturer's data sheet, which will identify the pins for you.
- NPN transistors are activated by *positive* voltage on the base relative to the emitter.
- PNP transistors are activated by *negative* voltage on the base relative to the emitter.

In their passive state, both types block the flow of electricity between the collector and emitter, just like an SPST relay in which the contacts are normally open. (Actually a transistor allows a tiny bit of current known as "leakage.")

You can think of a bipolar transistor as if it contains a little button inside, as shown in Figures 2-89 and 2-90. When the button is pressed, it allows a large current to flow. To press the button, you inject a much smaller current into the base by applying a small voltage to the base. In an NPN transistor, the control voltage is positive. In a PNP transistor, the control voltage is negative.

NPN transistor basics

- To start the flow of current from collector to emitter, apply a relatively positive voltage to the base.
- In the schematic symbol, the arrow points from base to emitter and shows the direction of positive current.
- The base must be at least 0.6 volts "more positive" than the emitter, to start the flow.
- The collector must be "more positive" than the emitter.

PNP transistor basics

- To start the flow of current from emitter to collector, apply a relatively negative voltage to the base.
- In the schematic symbol, the arrow points from emitter to base and shows the direction of positive current.
- The base must be at least 0.6 volts "more negative" than the emitter, to start the flow.
- The emitter must be "more positive" than the collector.

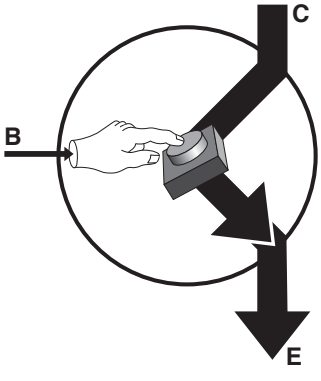

Figure 2-89. *You can think of a bipolar transistor as if it contains a button that can connect the collector and the emitter. In an NPN transistor, a small positive potential presses the button.*

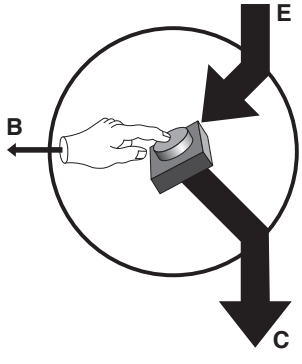

Figure 2-90. *In a PNP transistor, a small negative potential has the same effect. The arrows point in the direction of "positive current flow."*

ESSENTIALS

All about NPN and PNP transistors (continued)

All-transistor basics

- Never apply a power supply directly across a transistor. You can burn it out with too much current.
- Protect a transistor with a resistor, in the same way you would protect an LED.
- Avoid reversing the connection of a transistor between positive and negative voltages.
- Sometimes an NPN transistor is more convenient in a circuit; sometimes a PNP happens to fit more easily. They both function as switches and amplifiers, the only difference being that you apply a relatively positive voltage to the base of an NPN transistor, and a relatively negative voltage to the base of a PNP transistor.
- PNP transistors are used relatively seldom, mainly because they were more difficult to manufacture in the early days of semiconductors. People got into the habit of designing circuits around NPN transistors.
- Remember that bipolar transistors amplify current, not voltage. A small fluctuation of current through the base enables a large change in current between emitter and collector.
- Schematics sometimes show transistors with circles around them, and sometimes don't. In this book, I'll use circles to draw attention to them. See Figures 2-91 and 2-92.
- Schematics may show the emitter at the top and the collector at the bottom, or vice versa. The base may be on the left, or on the right, depending on what was most convenient for the person drawing the schematic. Be careful to look carefully at the arrow in the transistor to see which way up it is, and whether it is NPN or PNP. You can damage a transistor by connecting it incorrectly.
- Transistors come in various different sizes and configurations. In many of them, there is no way to tell which wires connect to the emitter, the collector, or the base, and some transistors have no part numbers on them. Before you throw away the packaging that came with a transistor, check to see whether it identifies the terminals.
- If you forget which wire is which, some multimeters have a function that will identify emitter, collector, and base for you. Check your multimeter instruction booklet for more details.

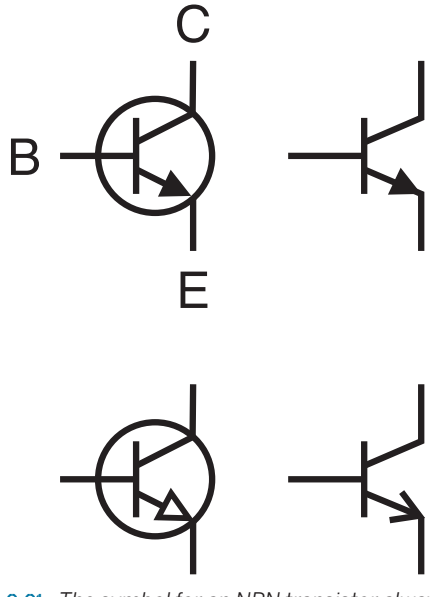

Figure 2-91. *The symbol for an NPN transistor always has an arrow pointing from its base to its emitter. Some people include a circle around the transistor; others don't bother. The style of the arrow may vary. But the meaning is always the same. The top-left version is the one I use in this book.*

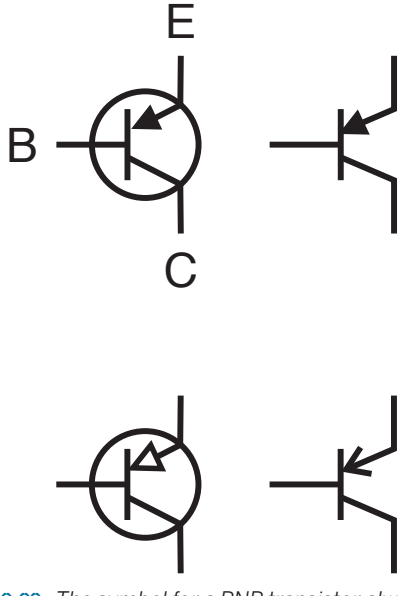

Figure 2-92. *The symbol for a PNP transistor always has an arrow pointing from its emitter to its base. Some people include a circle around the transistor; others don't bother. The style of the arrow may vary. But the meaning is always the same. The top-left version is the one I use in this book.*

BACKGROUND

Transistor origins

Though some historians trace the origins of the transistor back to the invention of diodes (which allow electricity to flow in one direction while preventing reversal of the flow), there's no dispute that the first working transistor was developed at Bell Laboratories in 1948 by John Bardeen, William Shockley, and Walter Brattain (Figure 2-93).

Shockley was the leader of the team, who had the foresight to see how potentially important a solid-state switch could be. Bardeen was the theorist, and Brattain actually made it work. This was a hugely productive collaboration—until it succeeded. At that point, Shockley started maneuvering to have the transistor patented exclusively under his own name. When he notified his collaborators, they were—naturally—unhappy about this idea.

A widely circulated publicity photograph didn't help, in that it showed Shockley sitting at the center in front of a microscope, as if he had done the hands-on work, while the other two stood behind him, implying that they had played a lesser role. In fact Shockley, as the supervisor, was seldom present in the laboratory where the real work was done.

The productive collaboration quickly disintegrated. Brattain asked to be transferred to a different lab at AT&T. Bardeen moved to the University of Illinois to pursue theoretical physics. Shockley eventually left Bell Labs and founded Shockley Semiconductor in what was later to become Silicon Valley, but his ambitions outstripped the capabilities of the technology of his time. His company never manufactured a profitable product.

Eight of Shockley's coworkers in his company eventually betrayed him by quitting and establishing their own business, Fairchild Semiconductor, which became hugely successful as a manufacturer of transistors and, later, integrated circuit chips.

Figure 2-93. *Photographs provided by the Nobel Foundation show, left to right, John Bardeen, William Shockley, and Walter Brattain. For their collaboration in development of the world's first working transistor in 1948, they shared a Nobel prize in 1956.*

ESSENTIALS

Transistors and relays

One limitation of NPN and PNP transistors is that they are naturally "off" until you turn them "on." They behave like a normally open pushbutton, which conducts electricity only for as long as you hold it down. They don't normally behave like a normal on switch, which stays on until you apply a signal to turn it off.

A relay offers more switching options. It can be normally open, normally closed, or it can contain a double-throw switch, which gives you a choice of two "on" positions. It can also contain a double-pole switch, which makes (or breaks) two entirely separate connections when you energize it. Single-transistor devices cannot provide the double-throw or double-pole features, although you can design more complex circuits that emulate this behavior.

Here's a list of transistor and relay characteristics.

	Transistor	Relay
Long-term reliability	Excellent	Limited
Configurable for DP and DT switching	No	Yes
Ability to switch large currents	Limited	Good
Able to switch alternating current (AC)	Usually not	Yes
Can be triggered by alternating current (AC)	Usually not	Optional
Suitability for miniaturization	Excellent	Very limited
Sensitive to heat	High	Moderate
Ability to switch at high speed	Excellent	Limited
Price advantage for low-voltage low-current	Yes	No
Price advantage for high-voltage high-current	No	Yes
Current leakage when "off"	Yes	No

The choice between relays or transistors will depend on each particular application.

THEORY

See the current

If you want to get a more precise understanding of how a transistor works, you should try this little test. It shows the precise behavior and limits of the 2N2222 transistor that you used in the previous experiment.

I've said that in an NPN transistor, the collector should always be more positive than the emitter and that the base should have a potential somewhere between those two voltages. Figure 2-94 shows this rather vague relationship. Now I want to substitute some numbers for these general statements.

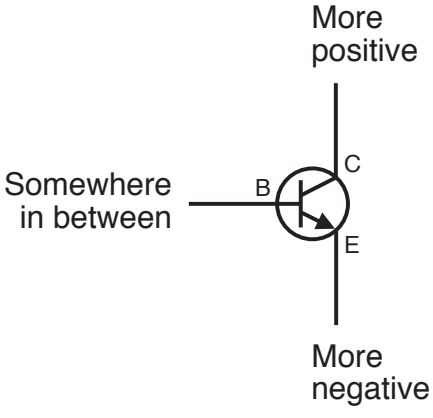

Figure 2-94. *The proper functioning of an NPN transistor requires you to maintain these voltage relationships.*

Take a look at the schematic in Figure 2-95, and check the component values. Notice that the total resistance above the transistor, from R1 + R2, is the same as the total resistance below it, from R3 + R4. Therefore the potential on the base of the transistor should be halfway between the two extremes—until you use potentiometer P1 to adjust the voltage of the base of the transistor up and down.

The two 180Ω resistors, R1 and R3, protect the transistor from passing excessive current. The two 10K resistors, R2 and R4, protect the base when the potentiometer is turned all the way up or all the way down.

I would like you to see what the transistor is doing by measuring the amperage flowing into the base at the position marked A1, and the total amperage flowing out through the emitter at the position marked A2. To do this, it would be really helpful if you had two meters. As that may be impractical, the breadboard diagrams in Figures 2-96 and 2-97 show how you can swap one meter between the two locations.

Remember that to measure milliamps, you have to pass electricity through the meter. This means that the meter must be inserted into the circuit, and whenever you remove the meter, you have to remake the connection where the meter was. The breadboard diagram shows how you can do this. Fortunately, it's very easy to remove and replace wires in a breadboard. Where wires are connected to the potentiometer, you may need to revert to using alligator clips.

Begin with the potentiometer turned about halfway through its range. Measure at A1 and A2. Turn the potentiometer up a bit, and measure current at the two locations again. Following is a table showing some actual readings I obtained at those two locations, using two digital meters simultaneously.

Milliamps passing through location A1	Milliamps passing through location A2
0.01	1.9
0.02	4.9
0.03	7.1
0.04	9.9
0.05	12.9
0.06	15.5
0.07	17.9
0.08	19.8
0.09	22.1
0.10	24.9
0.11	26.0
0.12	28.3

There's a very obvious relationship. The current emerging from the emitter of the transistor, through location A2, is about 24 times the current passing through location A1, into the base. The ratio of current coming out from the emitter of an NPN transistor to current going into the base is known as the *beta value* for a transistor. The beta value expresses the transistor's amplifying power.

It's a very constant ratio, until you push it a little too far. Above 0.12 mA, this particular transistor becomes "saturated," meaning that its internal resistance cannot go any lower.

THEORY

See the current (continued)

In my little experiment, I found that the maximum current at A2 was 33mA. A simple calculation using Ohm's Law showed me that this meant the transistor's internal resistance was near zero. This is why you should protect a transistor with some additional resistance in the circuit. If you don't, its low internal resistance would allow a huge current flow that would immediately burn it out.

What about the other end of its range? When it passes only 1.9 mA, the transistor has an internal resistance of around 6,000Ω. The conclusion is that depending how much current you apply to this transistor, its internal resistance varies between zero and 6,000Ω, approximately.

So much for the theory. Now what can we do with a transistor that's fun, or useful, or both? We can do Experiment 11!

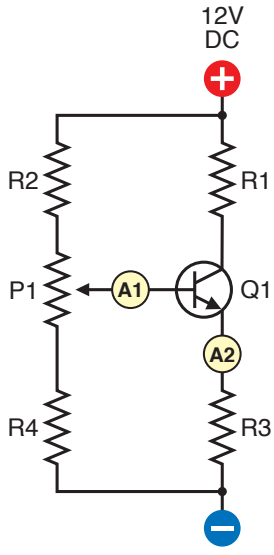

Figure 2-95. *This is basically the same as the previous circuit, with a potentiometer added and the LED removed. Component values:*

R1: 180Ω
R2: 10K
R3: 180Ω
R4: 10K
P1: 1M linear potentiometer
Q1: 2N2222 transistor

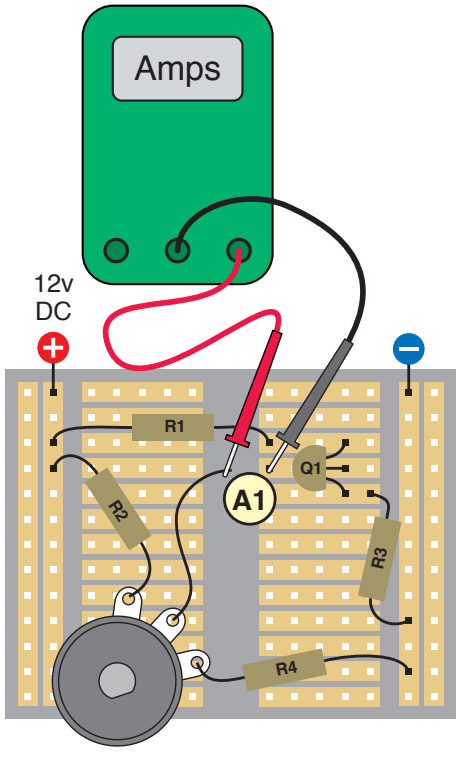

Figure 2-96. *The meter is measuring current flowing from the potentiometer into the base of the transistor at position A1 (see Figure 2-95).*

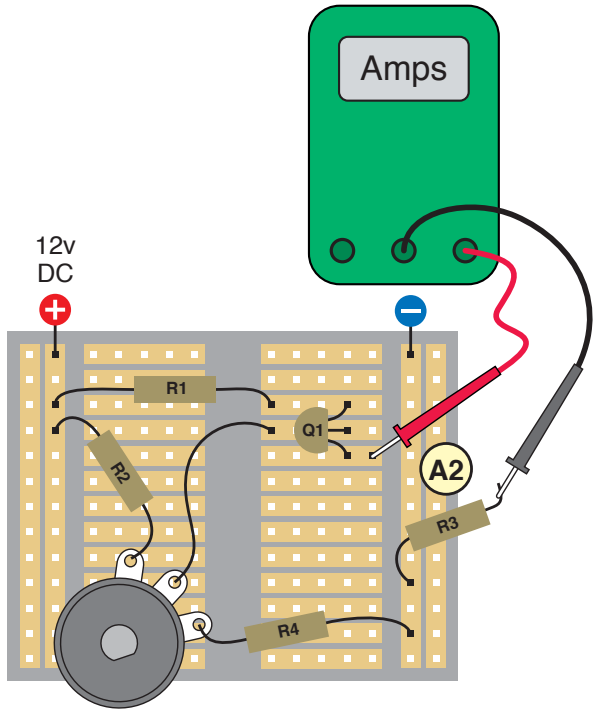

Figure 2-97. *One end of resistor R3 has been unplugged from the breadboard so that the meter now measures current flowing out through the emitter of the transistor, into R3, at position A2.*

Experiment 11: A Modular Project

You will need:

- AC adapter, breadboard, wire, and meter.
- LED. Quantity: 1.
- Resistors, various.
- Capacitors, various.
- Transistor, 2N2222 or similar. Quantity: 2.
- 2N6027 programmable unijunction transistor (PUT). Quantity: 2.
- Miniature 8Ω loudspeaker. Quantity: 1.

So far, I've described small circuits that perform very simple functions. Now it's time to show how modules can be combined to create a device that does a bit more.

The end product of this experiment will be a circuit that makes a noise like a small siren, which could be used in an intrusion alarm. You may or may not be interested in owning an alarm, but the four-step process of developing it is important, because it shows how individual clusters of components can be persuaded to communicate with each other.

I'll begin by showing how to use a transistor to make a solid-state version of the oscillating circuit that you built with a relay in Experiment 8. The relay, you may remember, was wired in such a way that the coil received power through the contacts of the relay. As soon as the coil was energized, it opened the contacts, thus cutting off its own power. As soon as the contacts relaxed they restored the power, and the process repeated itself.

There's no way to do this with a single bipolar transistor. You actually need two of them, switching each other on and off, and the way that this works is quite hard to understand. An easier option is to use a different thing known as a programmable unijunction transistor, or PUT.

Unijunction transistors were developed during the 1950s, but fell into disuse when simple silicon chips acquired the ability to perform the same kinds of functions, more accurately and more cheaply. However, the so-called programmable unijunction transistor is still widely available, often used in applications such as lamp dimmers and motor controllers. Because its primary use is in generating a stream of pulses, it's ideal for our purposes.

If you put together the components shown in Figure 2-98, the LED should start flashing as soon as you apply power.

Note that this circuit will work on 6 volts. You won't damage anything if you run it with 12 volts, but as we continue adding pieces to it, you'll find that it actually performs better at 6 volts than at 12. If you read the next section, "Essentials: All about programmable unijunction transistors," you'll find out how the circuit works.

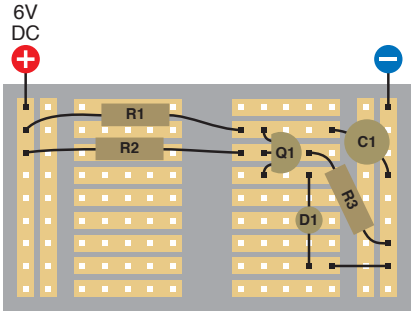

Figure 2-98. *Assemble these components, apply power, and the LED should start flashing.*

R1: 470K
R2: 15K
R3: 27K
C1: 2.2 µF electrolytic capacitor
D1: LED
Q1: 2N6027 programmable unijunction transistor

ESSENTIALS

All about programmable unijunction transistors

The schematic symbol for a programmable unijunction transistor, or PUT, looks very different from the symbol for a bipolar transistor, and its parts are named differently, too. Nevertheless, it does have a similar function as a solid-state switch. The symbol and the names of the three connections are shown in Figure 2-99.

Note that this is a rare case (maybe the only one in the whole of electronics!) in which you won't run into confusing variations of the basic schematic symbol. A PUT always seems to look the way I've drawn it here. Personally I think it would be clearer if we added a circle around it, but no one seems to do that, so I won't, either.

The 2N6027 is probably the most common PUT, and seems to be standardized in its packaging and pin-outs. I've only seen it in a plastic module rather than a little tin can. Figure 2-100 shows the functions of the leads if your 2N6027 is manufactured by Motorola or On Semiconductor. If you have one from another source, you should check the data sheet.

Note that the flat side of the plastic module faces the opposite way around compared with the 2N2222 bipolar transistor, when the two devices are functioning similarly.

The PUT blocks current until its internal resistance drops to allow flow from the "anode" to the "cathode." In this way, it seems very similar to an NPN transistor, but there's a big difference in the circumstances that cause the PUT to lower its resistance. The voltage at the anode determines when the PUT allows current to flow.

Suppose you start with, say, 1 volt at the anode. Slowly, you increase this voltage. The transistor blocks it until the anode gets close to 6 volts. Suddenly this pressure breaks down the resistance and current surges from the anode to the cathode. If the voltage goes back down again, the transistor reverts to its original state and blocks the flow.

I've included another version of the "finger on the button" drawing to convey this concept. The voltage on the anode is itself responsible for pushing the button that opens the pathway to the cathode. See Figure 2-101.

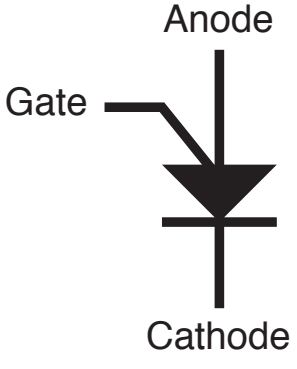

Figure 2-99. *The schematic symbol for a PUT.*

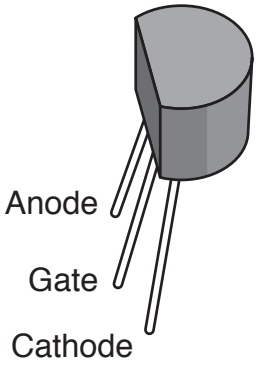

Figure 2-100. *In PUTs manufactured by On Semiconductor and Motorola, the leads have these functions.*

ESSENTIALS

All about programmable unijunction transistors (continued)

This may cause you to wonder what the function of the gate is. You can think of it as "assisting" the finger on the button. In fact, the gate is the "programmable" part of a PUT. By choosing a voltage for the gate, you establish the threshold point when current starts to flow.

Here's a simple take-home summary:

- The anode has to be more positive than the cathode, and the gate should be between those two extremes.
- If anode voltage increases above a threshold point, current bursts through and flows from the anode to the cathode.
- If anode voltage drops back down below the threshold, the transistor stops the flow.
- The voltage you apply to the gate determines how high the threshold is.
- The gate voltage is adjusted with two resistors, shown as R1 and R2 in the simple schematic in Figure 2-102. Typically, each resistor is around 20K. The PUT is protected from full positive voltage by R3, which can have a high value, 100K or greater, because very little current is needed to bias the transistor.
- You add your input signal in the form of positive voltage at the anode. When it exceeds the threshold, it flows out of the cathode and can work some kind of output device.

The only remaining question is how we make a PUT oscillate, to create a stream of on/off pulses. The answer is the capacitor that you included in the circuit that you breadboarded at the beginning of Experiment 11.

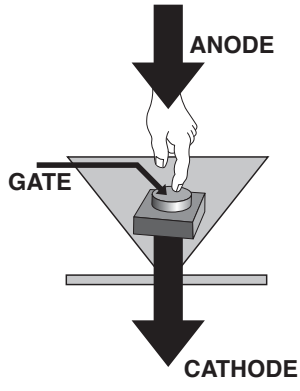

Figure 2-101. *When voltage at the anode of a PUT crosses a threshold (determined by a preset voltage at the gate), current breaks through and surges from the anode to the cathode. In this sense, the anode voltage acts as if it presses a button itself to open a connection inside the PUT, with some assistance from control voltage at the gate.*

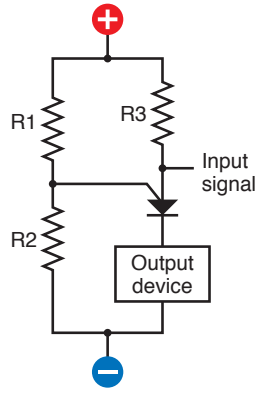

Figure 2-102. *This simple schematic shows how a PUT is used. R1 and R2 determine the voltage at the gate, which sets the threshold point for the input at the anode. Above the threshold, current flows from anode to cathode.*

Step 1: Slow-Speed Oscillation

Figure 2-103 is a schematic version of the previous PUT breadboard circuit shown in Figure 2-98, drawn so that the layout looks as much like the breadboard as possible.

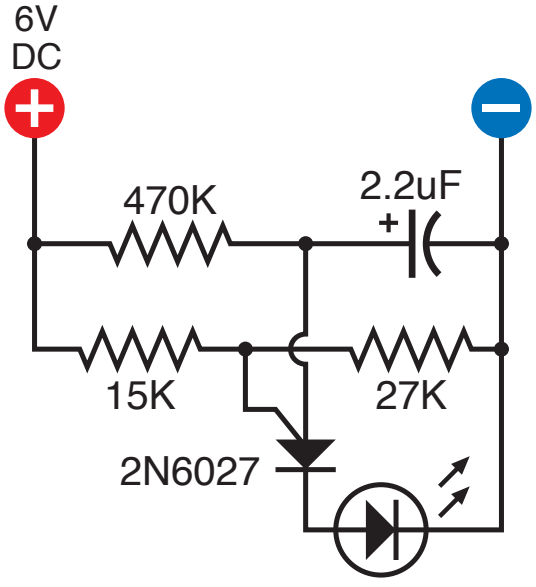

Figure 2-103. *This makes it easier to see what's happening in the breadboard version.*

The 15K resistor and 27K resistor establish the voltage at the gate. The 470K resistor supplies the anode of the PUT, but the PUT begins in its "off" condition, blocking the voltage. So the voltage starts to charge the 2.2 µF capacitor.

You may remember that a resistor slows the rate at which a capacitor accumulates voltage. The bigger the resistor and/or the larger the capacitor, the longer the capacitor takes to reach a full charge. In this circuit, the capacitor takes about half a second to get close to 6 volts.

But notice that the PUT is connected directly with the capacitor. Therefore, whatever voltage accumulates on the capacitor is also experienced by the PUT. As the voltage gradually increases, finally it reaches the threshold, which flips the PUT into its "on" state. The capacitor immediately discharges itself through the PUT, through the LED (which flashes), and from there to the negative side of the power supply.

The surge depletes the capacitor. The voltage drops back down, and the PUT returns to its original state. Now the capacitor has to recharge itself all over again, until the whole process repeats itself.

If you substitute a 22 µF capacitor, the charge/discharge cycle should take about 10 times as long, which will give you time to measure it. Set your meter to measure volts DC and place its probes on either side of the capacitor. You can actually watch the charge increasing until it reaches the threshold, at which point the capacitor discharges and the voltage drops back down again.

So now we have an oscillator. What's next?

Step 2: Beyond the Persistence of Vision

If you substitute a much smaller capacitor, it will charge much more quickly, and the LED will flash faster. Suppose you use a capacitor of 0.0047 µF (which can also be expressed as 47 nanofarads, or 47 nF). This seems like an odd number, but it's a standard value for a capacitor. This will reduce the capacitance by a factor of more than 500, and therefore the LED should flash about 500 times as fast, which should be about 1,000 times per second. The human eye cannot detect such rapid pulses. The human ear, however, can hear frequencies up to 10,000 per second and beyond. If we substitute a miniature loudspeaker for the LED, we should be able to hear the oscillations.

Figure 2-104 shows how I'd like you to make this happen. Please leave your original, slow-flashing circuit untouched, and make a duplicate of it farther down the breadboard, changing a couple of component values as indicated. In the schematic in Figure 2-105, the new part of the circuit is in solid black, while the previous section is in gray.

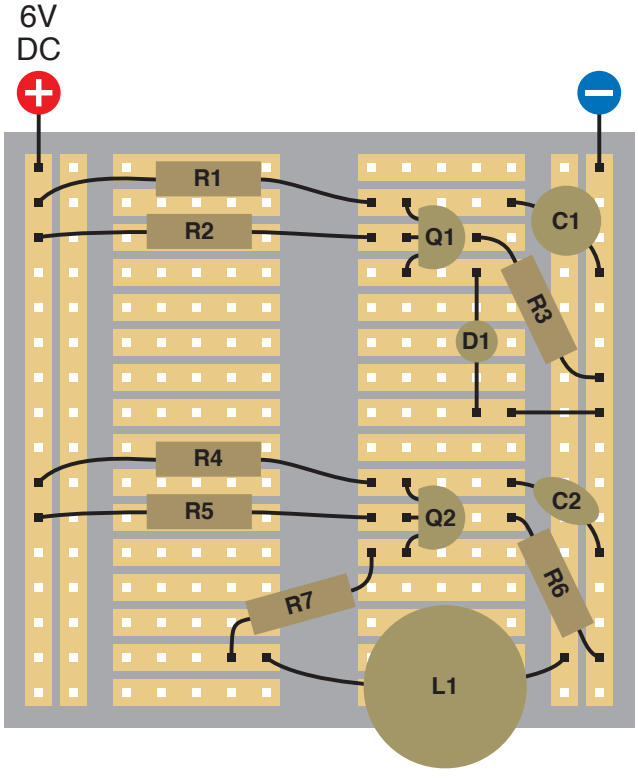

Figure 2-104. *The extra components which have been added at the lower half of the breadboard have the same functions as the components at the top, but some values are slightly different:*

R4: 470K
R5: 33K
R6: 27K
R7: 100Ω
C2: 0.0047 µF
Q2: 2N6027
L1: 8Ω 1-inch loudspeaker

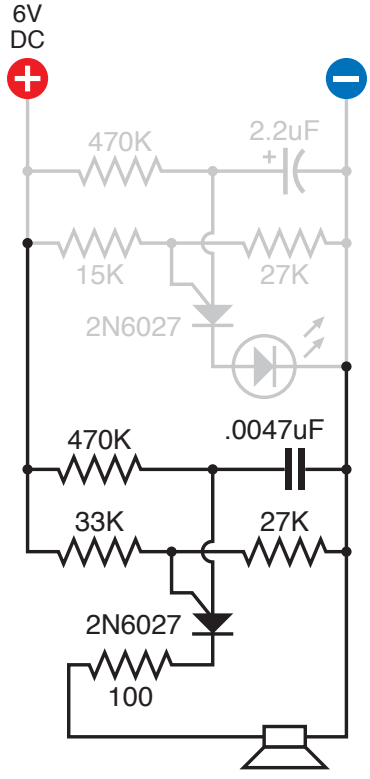

Figure 2-105. *The previous section that you built is shown in gray. Just add the new section in black.*

I want you to keep the slow-flashing circuit separately, untouched, because I have an idea to make use of it a little later. You can leave the LED blinking.

The loudspeaker should be wired in series with a 100Ω resistor to limit the current that flows out of the PUT. The loudspeaker doesn't have any polarity, even though it is fitted with a red wire and a black wire. You can connect it either way around.

Initially, you may be disappointed, because the circuit will not seem to be doing anything. However, if you place your ear very, very close to the loudspeaker, and if you wired the circuit correctly, you should hear a faint buzz, like a mosquito. Obviously, this isn't loud enough to serve any practical purpose. We need to make it louder. In other words, we need to amplify it.

Maybe you remember that the 2N2222, which you played with previously, can function as an amplifier. So let's try using that.

Step 3: Amplification

Disconnect the loudspeaker and its 100Ω series resistor. Then add the 2N2222, which is linked with the output from the PUT via a 1K resistor to protect it from excessive current. See Figure 2-107.

The emitter of the 2N2222 is connected to ground, and the collector is supplied through the loudspeaker and its 100Ω series resistor. This way, small fluctuations in the output from the PUT are sensed by the base of the 2N2222 which converts them into bigger fluctuations between the collector and the emitter, which draw current through the loudspeaker. Check the schematic in Figure 2-108.

Now the sound should be louder than an insect buzz, but still not really loud enough to be useful. What to do?

Well—how about if we add another 2N2222? Bipolar transistors can be placed in series, so that the output from the first one goes to the base of the second one. The 24:1 amplification of the first one is multiplied by another 24:1, giving a total amplification of more than 500:1.

There are limits to this technique. The 2N2222 can only conduct so much current before getting overloaded, and excess amplification can cause distortion. But when I built this circuit, I used a meter to verify that we're still within the design limits of a 2N2222, and for this project, I don't care whether the sound is slightly distorted.

BACKGROUND

Mounting a loudspeaker

The diaphragm or cone of a loudspeaker is designed to radiate sound, but as it oscillates to and fro, it emits sound from its back side as well as its front side. Because the sounds are opposite in phase, they tend to cancel each other out.

The perceived output from a loudspeaker can increase dramatically if you add a horn around it in the form of a tube to separate the output from the front and back of the speaker. For a miniature 1-inch loudspeaker, you can bend and tape a file card around it. See Figure 2-106.

Better still, mount it in a box so that the box absorbs the sound from the rear of the loudspeaker. For purposes of these simple experiments, I won't bother to go into the details of vented enclosures and bass-reflex designs.

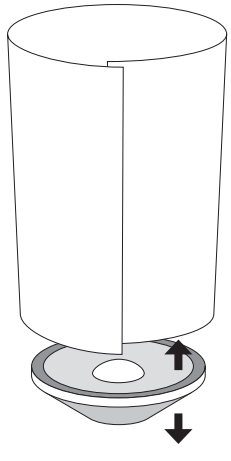

Figure 2-106. *A loudspeaker emits sound from its bottom surface as well as its top surface. To increase the perceived audio volume, use a cardboard tube to separate the two sound sources, or mount the speaker in a small box.*

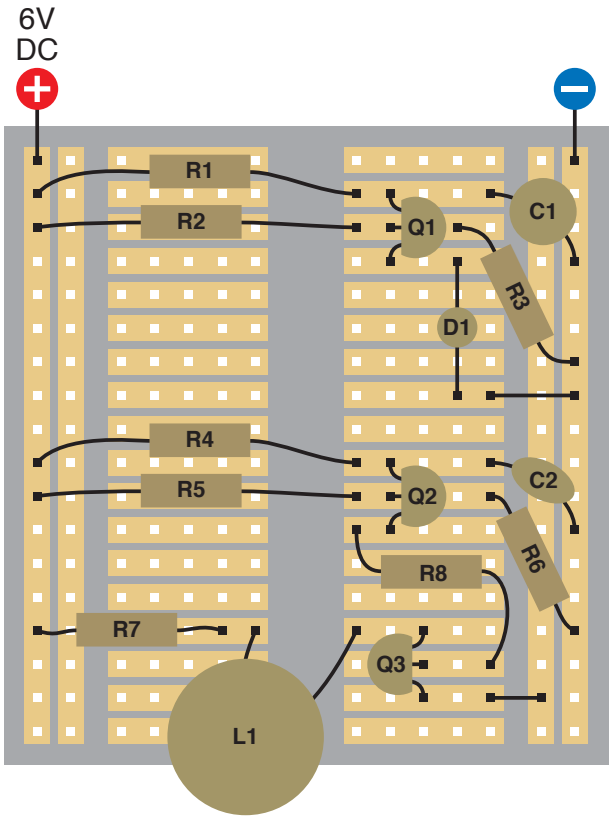

Figure 2-107. *By adding a 2N2222 general-purpose transistor, we amplify the signal from Q2:*

R8: 1K
Q3: 2N2222

Other components are the same as in the previous step in constructing this circuit.

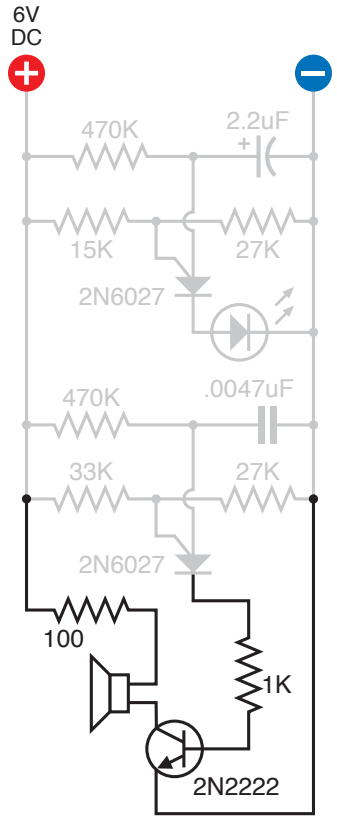

Figure 2-108

Add the second 2N2222 as shown in Figure 2-109. In Figure 2-110, once again the previously wired section is in gray.

If the accumulation of electrical components is beginning to seem confusing, remember that each cluster of parts has a separate defined function. We can draw a block diagram to illustrate this, as in Figure 2-112.

Using the second 2N2222, you should find that the output is more clearly audible, at least within the limits of your tiny 1-inch loudspeaker. Cup your hands around it to direct the sound, and you'll find that the volume seems to increase. You can also try using a 3-inch loudspeaker, which will create a generally better audio output while still remaining within the limits of the little 2N2222 transistor. See Figure 2-106, shown previously, and Figure 2-111.

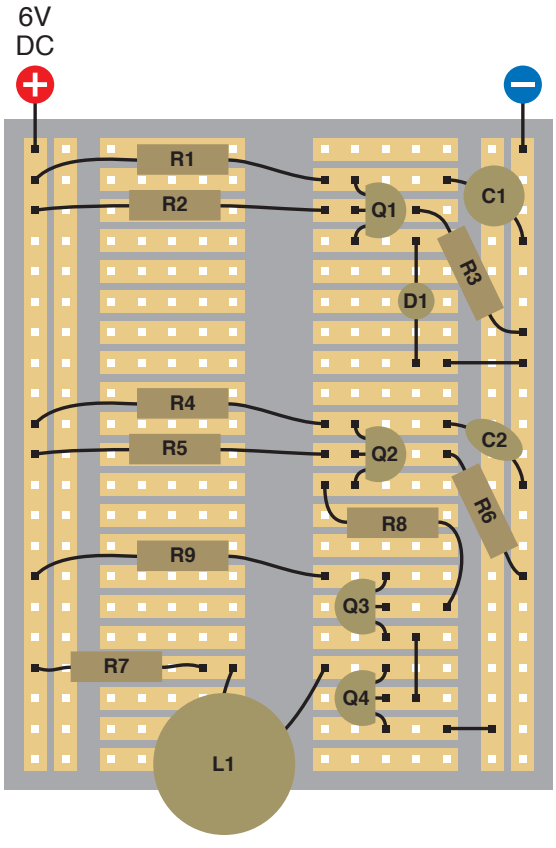

Figure 2-109. *Q4 is another 2N2222 transistor that further amplifies the signal. It receives power through R9: 2.2K.*

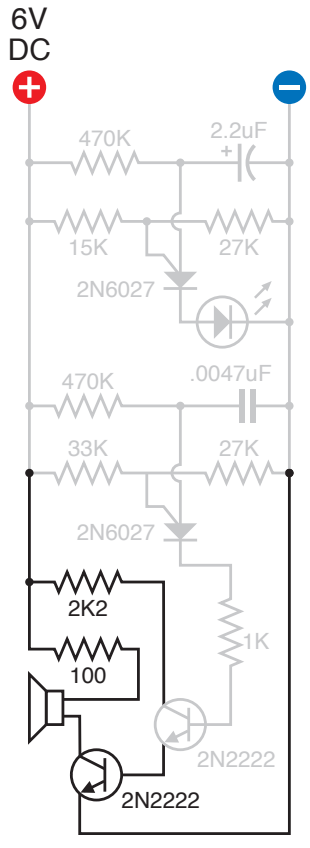

Figure 2-110. *This schematic is comparable with the component layout in Figure 2-109.*

Figure 2-111. *The 2N2222 transistor is quite capable of driving a 3-inch loudspeaker, which will create much better sound than a 1-inch speaker.*

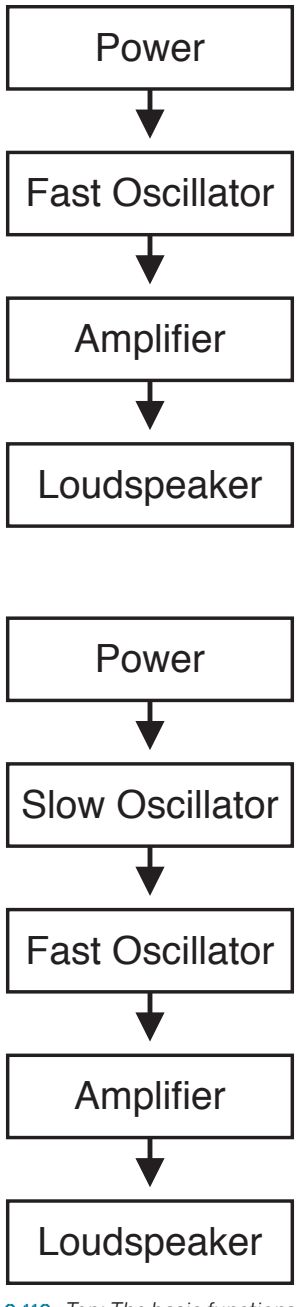

Figure 2-112. *Top: The basic functions of the noisemaking oscillator circuit shown as a block diagram. Bottom: The same functions with a slow oscillator added to control the fast oscillator.*

Step 4: Pulsed Output

If you wanted to use this audio signal as some kind of an alarm, a steady droning noise is not very satisfactory. A pulsing output would be a much better attention-getter.

Well, the first section of the circuit that you assembled created a pulsing signal about twice per second. You used it to flash an LED. Maybe we can get rid of the LED and feed the output from the first section to the second section. The lower block diagram in Figure 2-112 explains this concept.

Can it really be that simple? Well, yes and no. The trick is to make the output from the first section compatible with the input to the second section. If you simply connect a wire from the cathode of the first PUT to the anode of the second PUT, that's not going to work, because the second PUT is already oscillating nicely between low and high voltage, about 1,000 times each second. Add more voltage, and you will disrupt the balance that enables oscillation.

However, remember that the voltage on the gate of a PUT affects its threshold for conducting electricity. Maybe if we connect the output from Q1 to the gate of Q2, we'll be able to adjust that threshold automatically. The voltage still has to be in a range that the PUT finds acceptable, though. We can try various resistors to see which one works well.

This sounds like trial and error—and that's exactly what it is. Doing the math to predict the behavior of a circuit like this is far too complicated—for me, anyway. I just looked at the manufacturer's data sheet, saw the range of resistor values that the PUT would tolerate, and chose one that seemed as if it should work.

If you remove the LED and substitute R10 as shown in the breadboard diagram in Figure 2-113, you'll find that the fluctuating output from Q1 makes Q2 emit a two-tone signal. This is more interesting, but still not what I want. I'm thinking that if I make the pulses out of Q1 less abrupt, the result could be better, and the way to smooth a pulsing output is to hook up another capacitor that will charge at the beginning of each pulse and then release its charge at the end of each pulse. This is the function of C3 in Figure 2-114, and it completes the circuit so that it makes a whooping sound almost like a "real" alarm.

If you don't get any audio output, check your wiring very carefully. It's easy to make a wrong connection on the breadboard, especially between the three legs of each transistor. Use your meter, set to DC volts, to check that each section of the circuit has a positive voltage relative to the negative side of the power supply.

Figure 2-115 shows how your circuit should actually look on the breadboard.

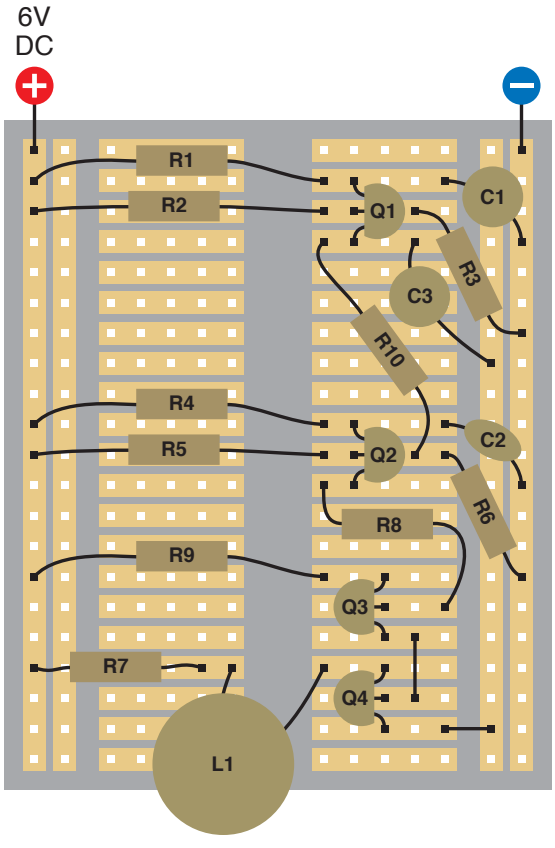

Figure 2-113. *R10 connects the slow-running oscillator at the top of the breadboard to the gate of Q2, the PUT in the middle of the breadboard. This modulates the audio oscillator, with addition of a smoothing capacitor.*

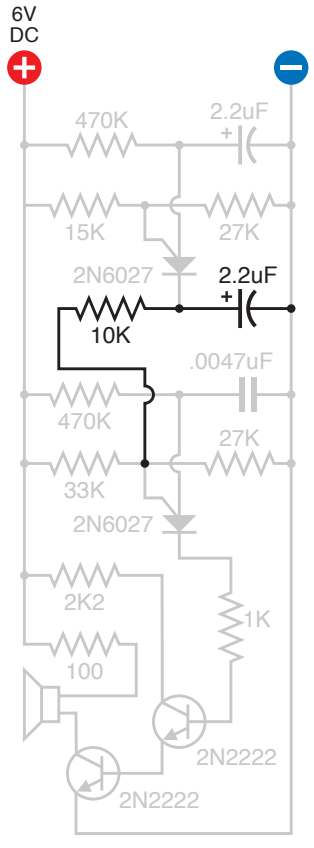

Figure 2-114. *This schematic shows the same circuit as in Figure 2-113:*

R10: 10K
C3: 2.2 µF

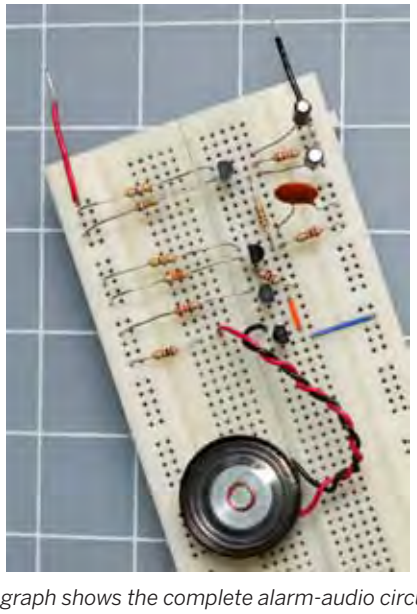

Figure 2-115. *This photograph shows the complete alarm-audio circuit on a breadboard.*

Tweaking it

There's still a lot of room for creativity here:

- Adjust the frequency of the sound: Use a smaller or larger capacitor instead of C2 (half or twice the current value). Use a smaller or larger value for R5.
- Adjust the pulsing feature: Use a smaller or larger capacitor instead of C1 (half or twice the current value). Use a smaller or larger value for R2.
- General performance adjustments: try a larger value for R1. Try smaller or larger values for C3.
- Try running the circuit at 7.5 volts, 10 volts, and 12 volts.

The circuits in this book are suggested as only a starting point. You should always try to tweak them to make them your own. As long as you follow the general rule of protecting transistors and LEDs with resistors, and respecting their requirements for positive and negative voltage, you're unlikely to burn them out. Of course, accidents will happen—I myself tend to be careless, and fried a couple of LEDs while working on this circuit, just because I connected them the wrong way around.

Step 5: Enhancements

A noisemaking circuit is just the output of an alarm. You would need several enhancements to make it useful:

1. Some kind of an intrusion sensor. Maybe magnetic switches for windows and doors?
2. A way to start the sound if any one of the sensors is triggered. The way this is usually done is to run a very small but constant current through all of the switches in series. If any one switch opens, or if the wire itself is broken, this interrupts the current, which starts the alarm. You could make this happen with a double-throw relay, keeping the relay energized all the time until the circuit is broken, at which point, the relay relaxes, opening one pair of contacts and closing the other pair, which can send power to the noisemaker.

   The trouble is that a relay draws significant power while it's energized, and it also tends to get hot. I want my alarm system to draw very little current while it's in "ready" mode, so that it can be powered by a battery. Alarm systems should never depend entirely on AC house current.

   If we don't use a relay, can we use a transistor to switch on the rest of the circuit when the power is interrupted? Absolutely; in fact, one transistor will do it.
3. But how do we arm the alarm in the first place? Really, we need a three-step procedure. First, check a little light that comes on when all the doors and windows are closed. Second, press a button that starts a 30-second countdown, giving you time to leave, if that's what you want to do. And third, after 30 seconds, the alarm arms itself.

4. If the alarm is triggered, what then? If someone forces open a window, should the alarm stop sounding as soon as the window is closed again? No, the alarm should lock itself on, until you turn it off.
5. How do you turn it off? Some kind of secret-code keypad would be good.
6. But to avoid driving everyone crazy if the alarm is triggered when you're not there, it should eventually stop itself, perhaps after about 10 minutes. At that point it should remain quiet but should light an LED to tell you what happened. You can then press a reset button to switch off the LED.

Implementing the Wish List

I've compiled a wish list that seems likely to make the project at least five times as complicated as it is already. Well, that's what tends to happen when you go beyond little demo circuits and try to design something that will be useful in everyday life. Suddenly you find yourself having to accommodate all kinds of circumstances and situations.

Actually, I can and will show you how to take care of all the enhancements on the wish list, but I'm thinking that they will require us to get a little more serious about electronics projects in general first. If you're going to build something ambitious, you'll want to make it more permanent, and probably more compact, than a breadboard with components pushed into it.

You will need to know how to connect everything permanently with solder, on a piece of perforated board that you can install in a neat little project box with switches and lights on the outside.

I'm going to deal with soldering and packaging in the next chapter. After that, we'll get back to the alarm project.

Getting Somewhat More Serious

3

I don't know how far you'll want to delve into electronics, but I do know that I've shown you about as much as I can with just a handful of components, some wires, a breadboard, and a few tools. To continue, you'll need:

- Some more tools and supplies
- Basic soldering skills
- Additional knowledge about:
  - Integrated circuits
  - Digital electronics
  - Microcontrollers
  - Motors

The tools are not particularly exotic or expensive, and the soldering skills are easily acquired. Learning to join wires with solder is far easier than mastering high-level crafts such as jewelry making or welding.

As for additional areas of knowledge about electronics, they are no more challenging than those that I have covered already.

By the end of this section, you should be able to transplant components from a breadboard onto perforated board, where you will solder everything together, and then mount the board in a little box with switches and warning lights on the front, for everyday use.

IN THIS CHAPTER

Shopping List: Experiments 12 Through 15
Experiment 12: Joining Two Wires Together
Experiment 13: Broil an LED
Experiment 14: A Pulsing Glow
Experiment 15: Intrusion Alarm Revisited

Shopping List: Experiments 12 Through 15

Tools

Each of the following tools is rated Essential, Recommended, or Optional. The Essential tools will take you through this chapter of the book. If you supplement them with the Recommended tools, they should be sufficient to get you to the end of the book. The Optional tools will make your work easier, but whether they're worth the money is for you to decide. Remember that URLs for manufacturers and sources of supply are all listed in the appendix.

Figure 3-1. *The low wattage of this pencil-style soldering iron enables you to use it safely on sensitive components, and the sharp tip helps to apply heat selectively.*

Figure 3-2. *This higher-wattage soldering iron delivers the additional heat necessary for thicker wire or larger components. The discoloration quickly occurs as a result of everyday use and has no effect on the capability of the iron, as long as the tip of it is clean.*

Figure 3-3. *The helping hand is fitted with two alligator clips to hold your work. The metal spiral is a safe place to holster a hot soldering iron, and you use the sponge to wipe its tip.*

I am assuming that you already have some commonly used workshop basics, such as an electric drill.

Essential: Pencil-type 15-watt soldering iron

Examples are RadioShack part 64-2051, McMaster-Carr catalog item 7016A34, or Xytronic model 252. See Figure 3-1. Soldering irons rated at 15 watts are less common than those that deliver 25 watts or more. Still, the 15-watt size is desirable for the small-scale work you'll be doing, and greatly reduces the risk of damaging components by inflicting excess heat.

When comparing prices, remember that a plated tip, which costs a little more, will last longer, will be easier to keep clean, and will conduct heat more reliably than a plain copper tip. If the manufacturer's specification doesn't mention a plated tip, the soldering iron probably doesn't have one.

Essential: General-duty soldering iron, 30 to 40 watts

Although most of the projects in this book entail small, heat-sensitive components and thin wire, at some point you're likely to want to make a solder joint with larger components and/or thicker wire. A 15-watt soldering iron will be unable to deliver enough heat. You should consider having a larger soldering iron in reserve, especially because they are relatively inexpensive.

Personally, I like the Weller Therma-Boost, shown in Figure 3-2, because it has an extra button that delivers more heat on demand. This is useful when you want the iron to get hot quickly, or if you are trying to solder very thick wire, which absorbs a lot of heat.

If you can't find or don't like the Weller, almost any 30-watt or 40-watt soldering iron will do. Check eBay or your local hardware store.

Essential: Helping hand

The so-called "helping hand" (or "third hand") has two alligator clips that hold components or pieces of wire precisely in position while you join them with solder. Some versions of the "helping hand" also feature a magnifying lens, a wire spiral in which you can rest your soldering iron, and a little sponge that you use to clean the tip of your iron when it becomes dirty. These additional features are desirable. Helping hands are available from all electronics hobby sources. Examples are the catalog item HH55 from Elenco or model 64-2991 from RadioShack. See Figure 3-3.

Essential: Magnifying lens

No matter how good your eyes are, a small, handheld, powerful magnifying lens is essential when you are checking solder joints on perforated board. The three-lens set in Figure 3-4 is designed to be held close to your eye, and is more powerful than the large lens on a "helping hand." The folding lens in Figure 3-5 stands on your workbench for hands-free operation. Both are available from RadioShack and similar items are stocked by art supply stores and hobby shops. Plastic lenses are quite acceptable if you treat them carefully.

Figure 3-4. *As long as you treat it carefully, a cheap set of plastic magnifying lenses is perfectly acceptable. Handheld magnification is essential for inspecting the solder joints that you make on perforated board.*

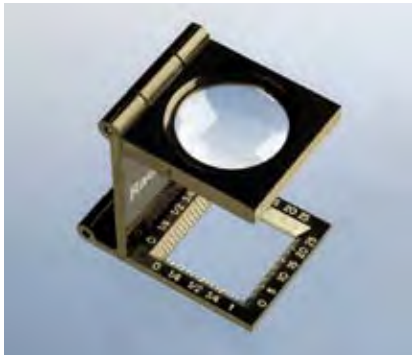

Figure 3-5. *This kind of folding magnifier can stand on your desktop and is useful for checking part numbers on tiny components.*

Essential: Clip-on meter test leads

The probes that came with your multimeter require you to hold them in contact while you make a reading. This requires both hands, preventing you from doing anything else at the same time.

When you use a pair of "minigrabber" probes with little spring-loaded clips at the end, you can attach the Common (negative) lead from your meter to the negative side of your circuit and leave it there, while you touch or attach the positive probe elsewhere.

The Pomona model 6244-48-0 (shown in Figure 3-6) from Meter Superstore and some other suppliers is what you need. If you have trouble finding it or you object to the cost, you may consider making your own by buying a couple of "banana plugs" (such as RadioShack part 274-721) that will fit the sockets on your meter, and then use 16-gauge or thicker stranded wire to connect the plugs with IC test clips, such as Kobiconn 13IC331 or RadioShack "mini hook clips," part number 270-372C. See Figures 3-7 and 3-8.

Figure 3-6. *These "minigrabber" add-ons for meter leads make it much easier to measure voltage or current. Push the spring-loaded button, and a little copper hook slides out. Attach it to a wire, release the button, and you have your hands free for other tasks. It's a mystery that meters are not supplied with these grabbers as standard equipment.*

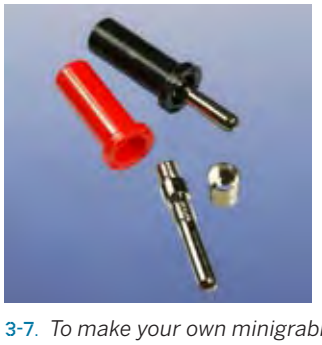

Figure 3-7. *To make your own minigrabber meter leads, first attach a banana plug to a wire by sliding the wire through the cap, into the plug, and out through a hole in the side.*

Figure 3-8. *Then screw a collar over the protruding piece of wire, and screw on the cap. The other end of the wire is soldered to a probe.*

Figure 3-9. *Like an overpowered hair dryer, the heat gun is used with heat-shrink tubing to create a snug, insulated sheath around bare wire.*

Essential: Heat gun

After you join two wires with solder, you often need to insulate them. Electrical tape, sometimes called insulating tape, is messy and tends to come unstuck. You'll be using heat-shrink tube, which forms a safe, permanent sheath around a bare-metal joint. To make the tube shrink, use a heat gun, which is like a very powerful hair dryer. They're available from any hardware supply source, and I suggest you buy the cheapest one you can find. See Figure 3-9.

Essential: Solder pump

This little gadget sucks up hot, melted solder when you are trying to remove a solder joint that you made in the wrong place. Available from All Electronics (catalog item SSR-1) or RadioShack 64-2086. See Figure 3-10.

Essential: Desoldering wick

Also known as desoldering braid. See Figure 3-11. You use this to soak up solder, in conjunction with the Solder Pump. Available from All Electronics (catalog item SWK) or RadioShack (part 64-2090).

Essential: Miniature screwdriver set

Dinky little electronic parts often have dinky little screws in them, and if you try to use the wrong size of screwdriver, you'll tend to mash the heads of the screws. I like the Stanley precision set, part number 66-052, shown in Figure 3-12. But any set will do as long as it has both small Phillips and straight-blade screwdrivers.

Recommended: Soldering stand

Like a holster for a gun, you rest your soldering iron in this stand when the iron is hot but not on use. Examples are catalog item 50B-205 from All Electronics, RadioShack model 64-2078, or check eBay. See Figure 3-13. This item may be built into the helping hand, but you need an extra one for your second soldering iron.

Figure 3-10. *To remove a solder joint, you can heat the solder until it's liquid, then suck it up into this squeezable rubber bulb.*

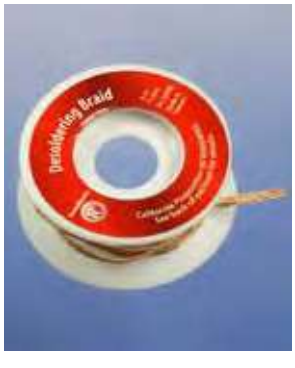

Figure 3-11. *An additional option for removing liquid solder is to soak it up in this copper braid.*

Figure 3-12. *A set of small screwdrivers is essential.*

Figure 3-13. *A safe and simple additional stand for a hot soldering iron.*

Recommended: Miniature hand saw

I assume that you will want to mount a finished electronics project in a decent-looking enclosure. Consequently, you are likely to need tools to cut, shape, and trim thin plastic. For example, you may want to cut a square hole so that you can mount a square power switch in it.

Power tools are not suitable for this kind of delicate work. A miniature handsaw (a.k.a. a "hobby saw") is ideal for trimming things to fit. X-Acto makes a range of tiny saw blades. I suggest the #15 blade, plus the handle that it fits in, shown in Figure 3-14. Available online from Tower Hobbies, Hobbylinc, ArtCity, and many other arts/crafts sources. Also look for the larger X-Acto saw blade, #234 or #239, which you can use for cutting perforated board.

Figure 3-14. *X-Acto makes a range of small saw blades that are ideal for cutting square holes to mount components in plastic panels.*

Recommended: Miniature vise

A miniature vise can do things that the helping hand cannot. I use mine when I'm sawing small pieces of plastic and as a dead weight to anchor a piece of perforated board while I'm working on it. See Figure 3-15.

Look for a cast-iron vise that is listed as being 1 inch or slightly larger, available from Megahobby, eBay, and other arts/crafts sources. Also consider the PanaVise, which has a tilting head to allow you to turn your work to any angle.

Figure 3-15. *This one-inch vise is available from the McMaster-Carr catalog.*

Recommended: Deburring tool

A deburring tool instantly smoothes and bevels any rough edge (when you have sawn or drilled a piece of plastic, for instance) and also can enlarge holes slightly. This may be necessary because some components are manufactured to metric sizes, which don't fit in the holes that you drill with American bits. Your small local hardware store may not stock deburring tools, but they are very inexpensively available from Sears, McMaster-Carr, KVM Tools, or Amazon. See Figure 3-16.

Optional: Hand-cranked countersink

You need a countersink to bevel the edges of screw holes to accept flat-headed screws. If you use a countersink bit in an electric drill, it won't give you precise control when you're working with thin, soft plastic.

Handheld countersinks that you grasp and turn like a screwdriver are easy to find, but McMaster-Carr (catalog item 28775A61) is the only source I've found for a hand-cranked tool that is much quicker to use. It comes with a set of bits, as shown in Figure 3-17.

Figure 3-16. *This cunning little blade, safety-tipped with a round bump on the end, removes rough edges from saw cuts with a single stroke, and can enlarge holes that are almost big enough—but not quite.*

Optional: Pick and hook set

Made by Stanley, part number 82-115, available from Amazon and hardware stores. You can find imported imitations for a few dollars less. See Figure 3-18.

Optional: Calipers

These may seem like a luxury, but are useful for measuring the external diameter of a round object (such as the screw thread on a switch or a potentiometer) or the internal diameter of a hole (into which you may want a switch or potentiometer to fit).

I like Mitutoyo calipers, and the low-end model 505-611 (shown in Figure 3-19) does everything I need. You can find cheaper brands, but economizing on precision measuring tools may not be a wise policy in the long term. The manufacturer's site will show you all their available models, after which you can Google "Mitutoyo" to find retail sources.

Figure 3-17. *You spin this countersink tool like a hand crank to add just the right amount of bevel to a hole, so that it will accommodate a flat-head screw.*

Figure 3-18. *This pick-and-hook set is useful in many unexpected ways.*

Figure 3-19. *Calipers can be digital (which automatically convert from millimeters to 1/64 inch to 1/1,000 inch), or analog like these (so you never need to worry about a dead battery).*

Supplies

Figure 3-20. *Spools of solder in various thicknesses.*

Solder

This is the stuff that you will melt to join components together on a permanent (we hope) basis. You need some very thin solder, size 0.022 inches, for very small components, and thicker solder, 0.05 inches, for heavier items. Avoid buying solder that is intended for plumbers, or for craft purposes such as creating jewelry. A range of solder thicknesses is shown in Figure 3-20. You want to make sure to get lead-free solder.

Electronics solder has a nonacidic rosin core that is appropriate for electronic components. Rolls of solder are available from all hobby-electronics sources including All Electronics, RadioShack, and Jameco, or search for "electronic solder" on Amazon.

Wire

You'll need some stranded wire to make flexible external connections with the circuit that you'll be building. Look for 22-gauge stranded hookup wire, in red, black, and green, 10 feet (minimum) of each.

If you want to install the intrusion alarm after completing that project in Experiment 15, you'll need white-insulated two-conductor wire of the type sold for doorbells or furnace controls. This is available by the foot

from Lowe's, Home Depot, Ace Hardware, and similar stores. You'll decide how much to buy after you measure the distances between the magnetic sensor switches that you decide to install.

Heat-shrink tube

For use in conjunction with your heat gun, described previously. You'll need a range of sizes in any colors of your choice. See Figure 3-21. Check RadioShack part 278-1627, other electronics suppliers, or your local hardware store. Prices will vary widely. You can buy the cheapest.

Copper alligator clips

These absorb heat when you are soldering delicate components. The Mueller BU-30C is a full-size solid copper alligator clip for maximum heat absorption. RadioShack sells smaller clips (part number 270-373, shown in Figure 3-22) that are suitable for tiny components.

Figure 3-21. *Slide heat-shrink tubing over a bare joint and apply heat from a heat gun to make a tight insulating seal around the joint.*

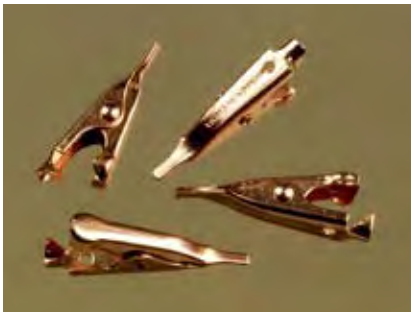

Figure 3-22. *These small clips absorb heat to protect components when you're soldering them.*

Perforated board

When you're ready to move your circuit from a breadboard to a more permanent location, you'll want to solder it to a piece of perforated board, often known as "prototyping board" but also called "perfboard."

You need the type that has copper strips etched onto the back, in exactly the same "breadboard layout" as the conductors hidden inside a breadboard, so that you can retain the same layout of your components when you solder them into place. Examples are RadioShack part 276-150 (shown in Figure 3-23) for small projects and part 276-170 (in Figure 3-24) for larger projects, such as Experiment 15.

For very small projects in which you will connect components using their wires alone, you need perfboard that isn't etched with copper strips connecting the holes. I like the Twin Industries 7100 range (available from Mouser.com) or Vectorboard from Newark Electronics, shown in Figure 3-25. You use a saw to cut out as small a piece as you need. Cheaper options are RadioShack part 276-147 (shown in Figure 3-26), or PC-1 from All Electronics. These have little copper circles around each hole that are not necessary for our purposes, but not a problem, either.

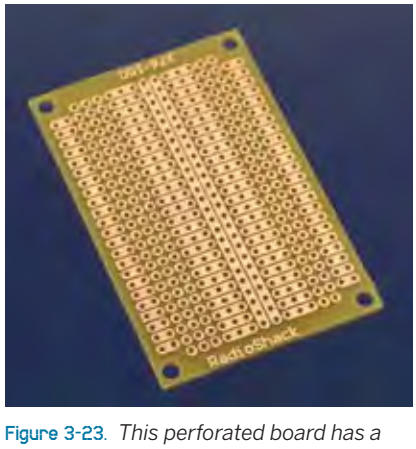

Figure 3-23. *This perforated board has a pattern of copper traces similar to the pattern inside a breadboard, so that you can lay out the components with minimal risk of wiring errors, when you're ready to create a permanently soldered version of your project.*

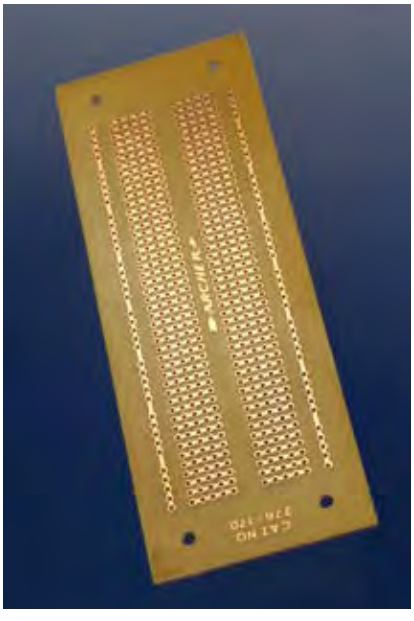

Figure 3-24. *A larger example of perforated board with breadboard geometry.*

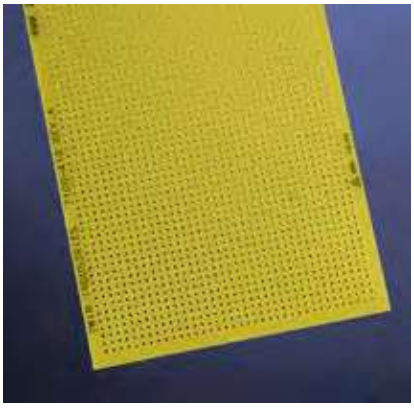

Figure 3-25. *Plain perforated board (with no copper traces) can be used for mounting components when you want to do point-to-point wiring.*

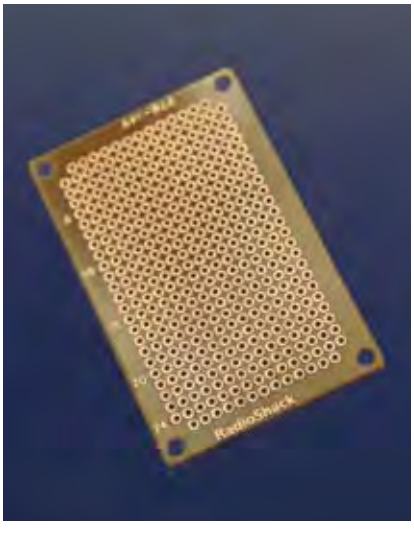

Figure 3-26. *A small piece of perforated board with individual copper solder pads to assist you in mounting components.*

Plywood

When you use a soldering iron, hot drops of solder tend to fall onto your table or workbench. The solder solidifies almost instantly, can be difficult to remove, and will leave a scar. Consider using a 2-foot square of half-inch plywood to provide disposable protection. You can buy it precut at Home Depot or Lowe's.

Machine screws

To mount components behind a panel, you need small machine screws (or "bolts"). They look nice if they have flat heads that fit flush against the panel. I suggest stainless-steel machine screws, #4 size, in 1/2-, 5/8-, 3/4-, and 1-inch lengths, 100 of each, plus 400 washers and 400 #4 locknuts of the type that have nylon inserts, so that they won't work loose. Check McMaster-Carr for a large and reasonably priced selection.

Project boxes

A project box is just a small box (usually plastic) with a removable lid. You mount your switches, potentiometers, and LEDs in holes that you drill through the box, and you attach your circuit on a perforated board that goes inside the box. Search All Electronics for "project box" or RadioShack for "project enclosure."

You need a box measuring approximately 6 inches long, 3 inches wide, and 2 inches high, such as RadioShack part 270-1805. Anything similar will do. I suggest you buy a couple other sizes as well, as they will be useful in the future.

Components

Power plugs, sockets, and binding posts

After you finish a project and put it in a box, you'll need a convenient way to supply it with power. Buy yourself a pair of insulated binding posts, such as RadioShack part 274-661, shown in Figure 3-27. Also obtain a panel-mounted power jack, size N, such as RadioShack part 274-1583, and DC power plug, size N, such as RadioShack 274-1573. The plug-and-socket pair is pictured in Figure 3-28.

Finally, you will need interconnects that are sized to fit a perforated board that is drilled at intervals of 1/10 inch. Sometimes known as "single inline sockets and headers," but also known as "boardmount sockets and pin-strip headers," they come in strips of 36 or more, and you can snip off as many as you need. Examples are Mill-Max part numbers 800-10-064-10-001000 and 801-93-050-10-001000, or 3M part numbers 929974-01-36-RK and 929834-01-36-RK. You can buy them from the usual electronics suppliers. Figure 3-29 shows headers before and after being snapped into small sections. Make sure that the interconnects have a terminal spacing of 0.1 inch.

Figure 3-27. *These terminals, also known as binding posts, enable a solderless connection with wires that have stripped ends. Also available in black.*

Figure 3-28. *The socket on the right can be mounted in a project box to receive power from the plug on the left.*

Battery

After you complete Experiment 15 at the end of this section of the book, if you want to use the project on a practical basis, you'll need a 12-volt battery. Search online for "12v battery" and you'll find many sealed, rechargeable lead-acid batteries that are designed for alarm systems, some measuring as small as 1×2×3-inch and costing under $10. You need a charger with it, which will probably cost you about $10.

Switches and relays

You will need the same DPDT relay and the same SPDT toggle switch that were mentioned in Chapter 2 shopping list.

For Experiment 15, you'll need magnetic switches that you can apply to doors or windows, such as the Directed model 8601, available from dozens of sources online.

Also you will need a DPDT pushbutton switch, ON-(ON) type, with solder terminals. Examples are model MPG206R04 by Tyco or model MB2061SS1W01-RO by NKK (with optional cap). Or search eBay for "DPDT pushbutton."

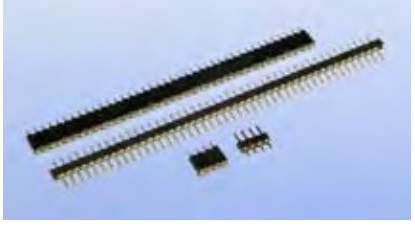

Figure 3-29. *Single inline sockets (top) and headers (middle) allow you to make very compact plug-and-socket connections to a PC board. They can be sawn, cut, or snapped into smaller sections (bottom). The terminals are 0.1 inch apart.*

Diodes

Buy at least half-a-dozen red 5 mm LEDs rated for approximately 2 volts, such as the Optek part number OVLFR3C7, Lumex part number SSL-LX-5093IT, or Avago part HLMP-D155. Buy half-a-dozen similar green LEDs at the same time.

In addition, you'll need a signal diode, type 1N4001 (any brand will do). Figure 3-30 shows an example, highly magnified. They're cheap, and likely to be useful in the future, so buy 10 of them.

Figure 3-30. *This 1N4001 diode is about 1/4 inch long and can handle up to 50 volts.*

Soldering Irons Get Hot!

Please take these basic precautions:

Use a proper stand (such as the one incorporated in your helping hands) to hold your soldering iron. Don't leave it lying on a workbench.

If you have infants or pets, remember that they may play with, grab, or snag the wire to your soldering iron. They could injure themselves (or you).

Be careful never to rest the hot tip of the iron on the power cord that supplies electricity to the iron. It can melt the plastic in seconds and cause a dramatic short circuit.

If you drop a soldering iron, don't be a hero and try to catch it. Most likely you will grab the hot part, which hurts. (I speak from experience.) When you burn your hand, you will instinctively let go of the iron, so you may as well let it drop freely without the intermediate step of burning yourself while it's on its way to the floor. Naturally, you should pick it up quickly after it does hit the floor, but by then you will have gained the necessary time in which to make a sensible decision to grab it by the cool end.

Always bear in mind that others in your home are more at risk of hurting themselves on a soldering iron than you are, because they won't know that it's hot. Most soldering irons have no warning lights to tell you that they're plugged in. As a general rule, always assume that a soldering iron is hot, even if it's unplugged. It may retain sufficient heat to burn you for longer than you expect.

Loudspeaker

To complete the project in Experiment 15, you'll need a loudspeaker small enough to fit inside your project box but louder than the 1-inch speaker that you used previously. It should be 2 inches or 2.5 inches (50 to 60 mm) in diameter. If you can find a 100Ω speaker, it will give you more output, but an 8Ω speaker will be acceptable.

Experiment 12: Joining Two Wires Together

Your adventure into soldering begins with the prosaic task of joining one wire to another, but will lead quickly to creating a full electronic circuit on perforated board. So let's get started!

You will need:

- 30-watt or 40-watt soldering iron
- 15-watt pencil-type soldering iron
- Thin solder (0.022 inches or similar)
- Medium solder (0.05 inches or similar)
- Wire strippers and cutters
- "Helping hand" gadget to hold your work
- Shrink-wrap tubing, assorted
- Heat gun
- Something to protect your work area from drops of solder

Your First Solder Joint

We'll start with your general-duty soldering iron—the one rated for 30 or 40 watts. Plug it in, leave it safely in its holder, and find something else to do for five minutes. If you try to use a soldering iron without giving it time to get fully hot, you will *not* make good joints.

Strip the insulation from the ends of two pieces of 22-gauge solid wire and clamp them in your helping hand so that they cross each other and touch each other, as shown in Figure 3-31.

To make sure that the iron is ready, try to melt the end of a thin piece of solder on the tip of the iron. The solder should melt instantly. If it melts slowly, the iron isn't hot enough yet.

Now follow these steps (shown in Figures 3-32 through 3-36):

1. Make sure the tip of the soldering iron is clean (wipe it on the moistened sponge in the base of your helping hand if necessary), then touch it against the intersection of the wires steadily for three seconds to heat them. If you have hard tap water, use distilled water to wet the sponge to avoid a buildup of mineral deposits on the tip of your soldering iron.
2. While maintaining the iron in this position, feed a little solder onto the intersection of the wires, also touching the tip of the soldering iron. Thus, the two wires, the solder, and the tip of the iron should all come together at one point. The solder should spread over the wires within another two seconds.
3. Remove the iron and the solder. Blow on the joint to cool it. Within 10 seconds, it should be cool enough to touch.
4. Unclamp the wires and try to tug them apart. Tug hard! If they defeat your best attempts to separate them, the wires are electrically joined and should stay joined. If you didn't make a good joint, you will be able to separate the wires relatively easily, probably because you didn't apply enough heat or enough solder to connect them.

The reason I asked you to begin by using the higher-powered soldering iron is that it delivers more heat, which makes it easier to use.

Figure 3-31. *A helping hand work aid is shown here holding two wires with their stripped ends touching. The magnifying glass has been hinged out of the way.*

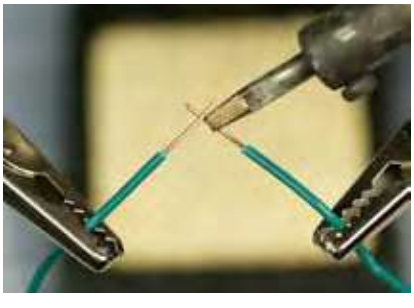

Figure 3-32

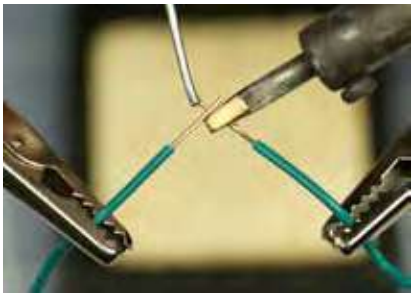

Figure 3-33

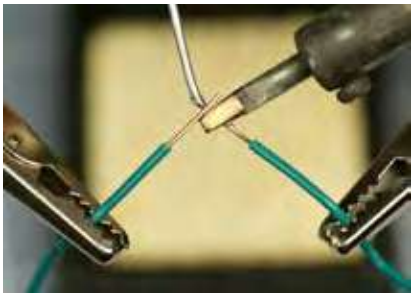

Figure 3-34

Figure 3-35. *This and the preceding three figures illustrate four steps to making a solder joint: apply heat to the wires, bring in the solder while maintaining the heat, wait for the solder to start to melt, and wait a moment longer for it to form a completely molten bead. The whole process should take between 4 and 6 seconds.*

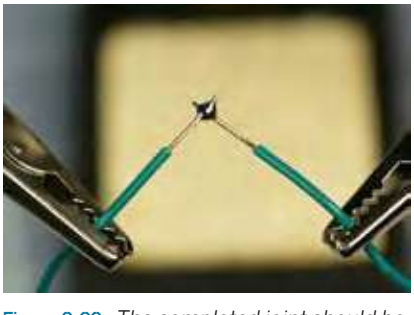

Figure 3-36. *The completed joint should be shiny, uniform, and rounded in shape.*

BACKGROUND

Soldering myths

Myth #1: Soldering is very difficult.

Millions of people have learned how to do it, and statistically, you are unlikely to be less coordinated than all of them. I have a lifelong problem with a tremor in my hands that makes it difficult for me to hold small things steadily. I also get impatient with repetitive detail work. If I can solder components, almost anyone should be able to.

Myth #2: Soldering involves poisonous chemicals.

Modern solder contains no lead. You should avoid inhaling the fumes for prolonged periods, but that also applies to everyday products such as bleach and paint. If soldering was a significant health hazard, we should have seen a high death rate among electronics hobbyists decades ago.

Myth #3: Soldering is hazardous.

A soldering iron is less hazardous than the kind of iron that you might use to iron a shirt, because it delivers less heat. In fact, in my experience, soldering is safer than most activities in a typical home or basement workshop. That doesn't mean you can be careless!

Soldering alternatives

As recently as the 1950s, connections inside electronic appliances such as radio sets were still being hand-soldered by workers on production lines. But the growth of telephone exchanges created a need for a faster way to make large numbers of rapid, reliable point-to-point wiring connections, and "wire wrap" became a viable alternative.

In a wire-wrapped electronics project, components are mounted on a circuit board that has long, gold-plated, sharp-cornered square pins sticking out of the rear. Special silver-plated wire is used, with an inch of insulation stripped from its ends. A manual or power-driven wire-wrap tool twirls the end of a wire around one of the pins, applying sufficient tension to "cold-weld" the soft silver plating of the wire to the pin. The wrapping process exerts sufficient pressure to make a very reliable joint, especially as 7 to 9 turns of wire are applied, each turn touching all four corners of the pin.

During the 1970s and 1980s, this system was adopted by hobbyists who built their own home computers. A wire-wrapped circuit board from a hand-built computer is shown in Figure 3-37. The technique was used by NASA to wire the computer in the Apollo spacecraft that went to the moon, but today, wire-wrapping has few commercial applications.

The widespread industrial use of "through-hole" components, such as the chips on early desktop computers, encouraged development of wave soldering, in which a wave or waterfall of molten solder is applied to the underside of a preheated circuit board where chips have been inserted. A masking technique prevents the solder from sticking where it isn't wanted.

Today, surface-mount components (which are significantly smaller than their through-hole counterparts) are glued to a circuit board with a solder paste, and the entire assembly is then heated, melting the paste to create a permanent connection.

Figure 3-37. *This picture shows some of the wire-wrapping in Steve Chamberlin's custom-built, retro 8-bit CPU and computer. "Back in the day," connecting such a network of wires with solder joints would have been unduly time-consuming and prone to faults. Photo credit: Steve Chamberlin.*

TOOLS

Eight most common soldering errors

1. Not enough heat.

   The joint looks OK, but because you didn't apply quite enough heat, the solder didn't melt sufficiently to realign its internal molecular structure. It remained granular instead of becoming a solid, uniform blob, and you end up with a "dry joint," also known as a "cold joint," which will come apart when you pull the wires away from each other. Reheat the joint thoroughly and apply new solder.

   A leading cause of underheated solder is the temptation to use the soldering iron to carry solder to the joint. This results in the cold wires reducing the temperature of the solder. What you should do is touch the soldering iron to heat the wires first, and then apply the solder. This way, the wires are hot and help to melt the solder, which wants to stick to them.

   Because this is such a universal problem, I'll repeat myself: *Never melt solder on the tip of the iron and then use it to carry the solder to the joint.*

   You don't want to put hot solder on cold wires. You want to put cold solder on hot wires.

2. Too much heat.

   This may not hurt the joint, but can damage everything around it. Vinyl insulation will melt, exposing the wire and raising the risk of short circuits. You can easily damage semiconductors, and may even melt the internal plastic components of switches and connectors.

   Damaged components must be desoldered and replaced, which will take time and tends to be a big hassle (see "Tools: Desoldering" on page 109 for advice).

3. Not enough solder.

   A thin connection between two conductors may not be strong enough. When joining two wires, always check the underside of the joint to see whether the solder penetrated completely.

4. Moving the joint before the solder solidifies.

   You may create a fracture that you won't necessarily see. It may not stop your circuit from working, but at some point in the future, as a result of vibration or thermal stresses, the fracture can separate just enough to break electrical contact. Tracking it down will then be a chore. If you clamp components before you join them, or use perforated board to hold the components steady, you can avoid this problem.

5. Dirt or grease.

   Electrical solder contains rosin that cleans the metal that you're working with, but contaminants can still prevent solder from sticking. If any component looks dirty, clean it with fine sandpaper before joining it.

6. Carbon on the tip of your soldering iron.

   The iron gradually accumulates flecks of black carbon during use, and they can act as a barrier to heat transfer. Wipe the tip of the iron on the little sponge mounted in the base of your soldering iron stand or your helping hand.

7. Inappropriate materials.

   Electronic solder is designed for electronic components. It will not work with aluminum, stainless steel, or various other metals. You may be able to make it stick to chrome-plated items, but only with difficulty.

8. Failure to test the joint.

   Don't just assume that it's OK. Always test it, by applying manual force if you can (see Figures 3-38 and 3-39 for the ideal protocol) or, if you can't get a grip on the joint, slip a screwdriver blade under it and flex it just a little, or use small pliers to try to pull it apart. Don't be concerned about ruining your work. If your joint doesn't survive rough treatment, it wasn't a good joint.

Of the eight errors, dry/cold joints are by far the worst, because they are easy to make and can look OK.

Figure 3-38. *Test result of a bad solder joint.*

Figure 3-39. *Test result of a good solder joint.*

Your Second Solder Joint

Time now to try your pencil-style soldering iron. Once again, you must leave it plugged in for a good five minutes to make sure it's hot enough. In the meantime, don't forget to unplug your other soldering iron, and put it somewhere safe while it cools.

This time I'd like you to align the wires parallel with each other. Joining them this way is a little more difficult than joining them when they cross each other, but it's a necessary skill. Otherwise, you won't be able to slide heat-shrink tubing over the finished joint to insulate it.

Figures 3-40 through 3-44 show a successful joint of this type. The two wires do not have to make perfect contact with each other; the solder will fill any small gaps. But the wires must be hot enough for the solder to flow, and this can take an extra few seconds when you use the low-wattage pencil-style iron.

Be sure to feed the solder in as shown in the pictures. Remember: don't try to carry the solder to the joint on the tip of the iron. Heat the wires first, and then touch the solder to the wires and the tip of the iron, while keeping it in contact with the wires. Wait until the solder liquifies, and you will see it running eagerly into the joint. If this doesn't happen, be more patient and apply the heat for a little longer.

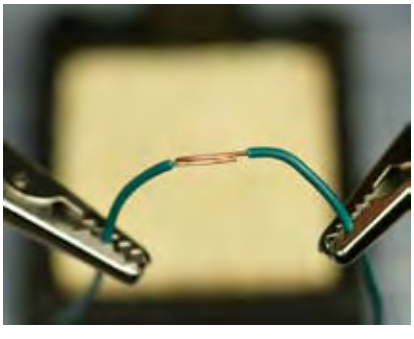

Figure 3-40

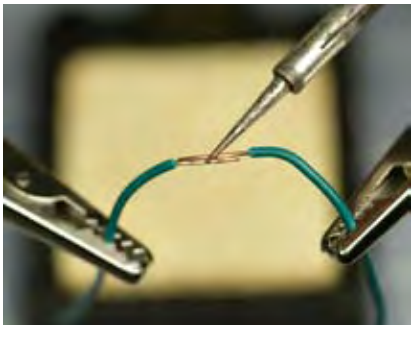

Figure 3-41

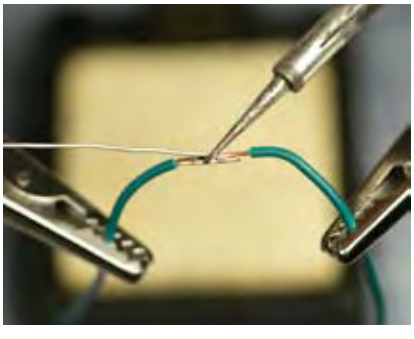

Figure 3-42

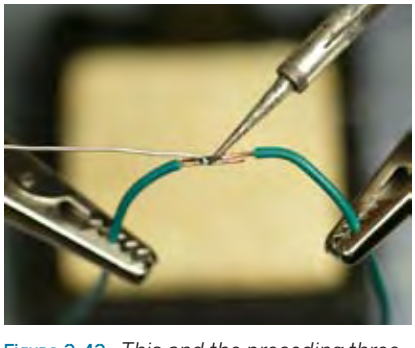

Figure 3-43. *This and the preceding three figures show how joining two wires that are parallel is more difficult, and the low-wattage, pencil-type soldering iron will require longer to heat them sufficiently for a good joint. Thinner solder can be used.*

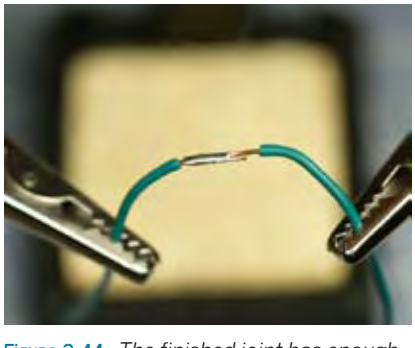

Figure 3-44. *The finished joint has enough solder for strength, but not so much solder that it will prevent heat-shrink tubing from sliding over it.*

THEORY

Soldering theory

The better you understand the process of soldering, the easier it should be for you to make good solder joints.

The tip of the soldering iron is hot, and you want to transfer that heat into the joint that you are trying to make. In this situation, you can think of the heat as being like a fluid. The larger the connection is between the soldering iron and the joint, the greater the quantity of heat, per second, that can flow through it.

For this reason, you should adjust the angle of the soldering iron so that it makes the widest possible contact. If it touches the wires only at a tiny point, you'll limit the amount of heat flow. Figures 3-45 and 3-46 illustrate this concept. Once the solder starts to melt, it broadens the area of contact, which helps to transfer more heat, so the process accelerates naturally. Initiating it is the tricky part.

The other aspect of heat flow that you should consider is that it can suck heat away from the places where you want it, and deliver it to places where you don't want it. If you're trying to solder a very heavy piece of copper wire, the joint may never get hot enough to melt the solder, because the heavy wire conducts heat away from the joint. You may find that even a 40-watt iron isn't powerful enough to overcome this problem, and if you are doing heavy work, you may need a more powerful iron.

As a general rule, if you can't complete a solder joint in 10 seconds, you aren't applying enough heat.

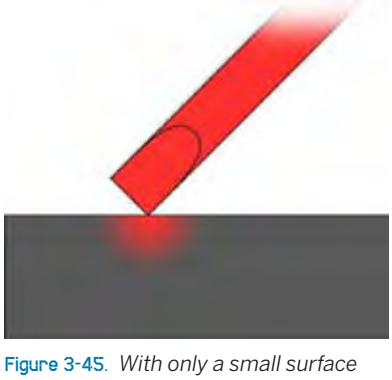

Figure 3-45. *With only a small surface area of contact between the iron and the working surface, an insufficient amount of heat is transferred.*

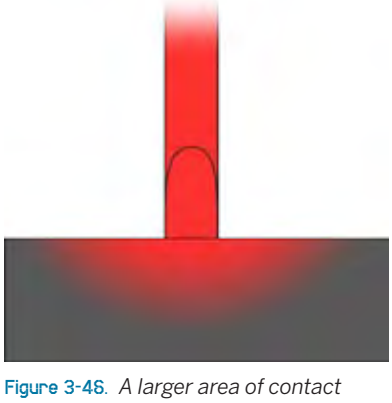

Figure 3-46. *A larger area of contact between the soldering iron and its target will greatly increase the heat transfer.*

TOOLS

Desoldering

Desoldering is much, much harder than soldering. Two simple tools are available:

- *Suction pump*. First, you apply the soldering iron to make the solder liquid. Then you use this simple gadget to try to suck up as much of the liquid as possible. Usually it won't remove enough metal to allow you to pull the joint apart, and you will have to try the next tool. Refer back to Figure 3-10.
- *Desoldering wick or braid*. Desoldering wick, also known as braid, is designed to soak up the solder from a joint, but again, it won't clean the joint entirely, and you will be in the awkward position of trying to use both hands to pull components apart while simultaneously applying heat to stop the solder from solidifying. Refer back to Figure 3-11.

I don't have much advice about desoldering. It's a frustrating experience (at least, I think so) and can damage components irrevocably.

Heat Guns Get Hot, Too!

Notice the chromed steel tube at the business end of your heat gun. Steel costs more than plastic, so the manufacturer must have put it there for a good reason—and the reason is that the air flowing through it becomes so hot that it would melt a plastic tube.

The metal tube stays hot enough to burn you for several minutes after you've used it. And, as in the case of soldering irons, other people (and pets) are vulnerable, because they won't necessarily know that the heat gun is hot. Most of all, make sure that no one in your home ever makes the mistake of using a heat gun as a hair dryer (Figure 3-47).

This tool is just a little more hazardous than it appears.

Adding Insulation

After you've succeeded in making a good inline solder connection between two wires, it's time for the easy part. Choose some heat-shrink tubing that is just big enough to slide over the joint with a little bit of room to spare.

Figure 3-47. *Other members of your family should understand that although a heat gun looks like a hair dryer, appearances may be deceptive.*

Slide the tubing along until the joint is centered under it, hold it in front of your heat gun, and switch on the gun (keeping your fingers away from the blast of superheated air). Turn the wire so that you heat both sides. The tubing should shrink tight around the joint within half a minute. If you overheat the tubing, it may shrink so much that it splits, at which point you must remove it and start over. As soon as the tubing is tight around the wire, your job is done, and there's no point in making it any hotter. Figures 3-48 through 3-50 show the desired result. I used white tubing because it shows up well in photographs. Different colors of heat-shrink tubing all perform the same way.

Figure 3-48. *Slip the tubing over your wire joint.*

Figure 3-49. *Apply heat to the tubing.*

Figure 3-50. *Leave the heat on the tubing until it shrinks to firmly cover the joint.*

I suggest you next practice your soldering skills on a couple of practical projects. In the first one, you can add color-coded, solid-core wires to your AC adapter, and in the second one, you can shorten the power cord for a laptop power supply. You can use your larger soldering iron for both of these tasks, because neither of them involves any heat-sensitive components.

Modifying an AC Adapter

In the previous chapter, I mentioned the irritation of being unable to push the wires from your AC adapter into the holes of your breadboard. So, let's fix this right now:

1. Cut two pieces of solid-conductor 22-gauge wire—one of them red, the other black or blue. Each should be about 2 inches long. Strip a quarter-inch of insulation from both ends of each piece of wire.
2. Trim the wire from your AC adapter. You need to expose some fresh, clean copper to maximize your chance of getting the solder to stick.

   I suggest that you make one conductor longer than the other to minimize the chance of the bare ends touching and creating a short circuit. Use your meter, set to DC volts, if you have any doubt about which conductor is positive.

Solder the wires and add heat-shrink tubing as you did in the practice session. The result should look like Figure 3-51.

Figure 3-51. *Solid-core color-coded wires, soldered onto the wires from an AC adapter, provide a convenient way to feed power to a breadboard. Note that the wires are of differing lengths to reduce the risk of them touching each other.*

Choose the Right Tubing

If you use heat-shrink tubing on 110v AC cord, as is being done in this experiment, make sure you use tubing that's been rated for 110v use.

Shortening a Power Cord

When I travel, I like to minimize everything. It always annoys me that the power cord for the power supply of my laptop is 4 feet long. The thinner wire that connects the power supply to the computer is also 4 feet long, and I just don't need that much wire.

After searching exhaustively I couldn't find any laptop power cables shorter than 3 feet, so I decided to shorten one myself. If you feel no need to do this, you should try the following procedure on an old extension cord, just as an exercise. You do need to go through these steps to acquire some practice in soldering heavier, stranded wire and using heat-shrink tubing:

1. Use your wire cutters to chop the wire, and then a utility knife to split the two conductors, with one shorter than the other. When splicing a power cord or similar cable containing two or more conductors, it's good to avoid having the joints opposite each other. They fit more snugly if they are offset, and there's less risk of a short circuit if a joint fails.

Figure 3-52

Figure 3-53

Figure 3-54

Figure 3-55

Figure 3-56

Figure 3-57

Figure 3-58. *Figures 3-52 through 3-58 illustrate the sequence of steps to prepare for making a shortened power cord for a laptop computer power supply.*

2. Strip off a minimal amount of insulation. One-eighth of an inch (3 mm) is sufficient. The automatic wire strippers that I mentioned in the shopping list in Chapter 1 are especially convenient, but regular wire strippers will do the job.
3. Cut two pieces of heat-shrink tubing, each 1 inch long, big enough to slide over the separate conductors in your cable. Cut a separate 2-inch piece of larger tubing that will slide over the entire joint when it's done. The steps described so far are illustrated in Figures 3-52 through 3-58.
4. Now for the most difficult part: activating your human memory. You have to remember to slide the tubing onto the wire *before* you make your solder joint, because the plugs on the ends of the wires will prevent you from adding any heat-shrink tubing later. If you're as impatient as I am, it's very difficult to remember to do this every time.

5. Use your helping hand to align the first joint. Push the two pieces of wire together so that the strands intermingle, and then squeeze them tight between finger and thumb, so that there are no little bits sticking out. A stray strand of wire can puncture heat-shrink tubing when the tubing is hot and soft and is shrinking around the joint.
6. The wire that you're joining is much heavier than the 22-gauge wire that you worked with previously, so it will suck up more heat, and you must touch the soldering iron to it for a longer time. Make sure that the solder flows all the way into the joint, and check the underside after the joint is cool. Most likely you'll find some bare copper strands there. The joint should become a nice solid, rounded, shiny blob. Keep the heat-shrink tubing as far away from the joint as possible while you're using the soldering iron, so that heat from the iron doesn't shrink the tubing prematurely, preventing you from sliding it over the joint later.

Figure 3-59

Figure 3-60

Figure 3-61

Figure 3-62

Figure 3-63

Figure 3-64

7. When the joint has cooled, slide the heat-shrink tubing over it, and apply the heat gun. Now repeat the process with the other conductor. Finally, slide the larger piece of tubing over the joint. You did remember to put the large tubing onto the wire at the beginning, didn't you?

Figures 3-59 through 3-65 show the steps all the way through to the end.

If you have completed the soldering exercises so far, you now have sufficient basic skills to solder your first electronic circuit. But first, I want you to verify the vulnerability of components to heat.

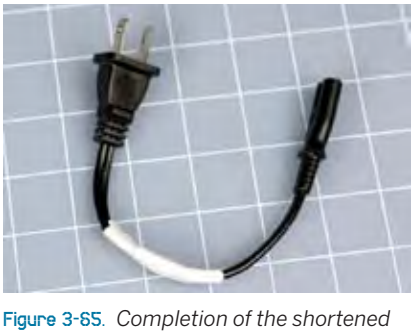

Figure 3-65. *Completion of the shortened power cord for a laptop power supply.*

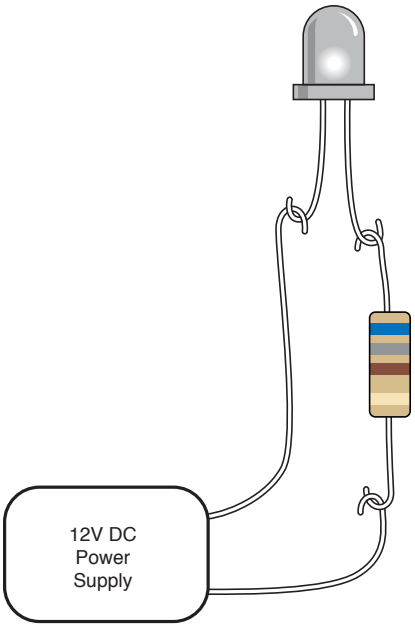

Figure 3-66. *By literally hooking together the leads from a resistor and a white-light LED, we minimize pathways for heat to escape during the subsequent test.*

Figure 3-67. *Applying heat with a 15-watt soldering iron. A typical LED should withstand this treatment for two or three minutes, but if you substitute a 30-watt soldering iron, the LED is likely to burn out in under 15 seconds.*

Experiment 13: Broil an LED

In Chapter 1, you saw how an LED can be damaged if too much current flows through it. The electricity caused heat, which melted the LED. Unsurprisingly, you can just as easily melt it by applying too much heat to one of its leads with a soldering iron. The question is: how much heat is too much? Let's find out.

You will need:

- 30-watt or 40-watt soldering iron
- 15-watt pencil-type soldering iron
- A couple of LEDs (that are expendable)
- 680Ω resistor
- Wire cutters and sharp-nosed pliers
- "Helping hand" gadget to hold your work

I don't want you to use alligator clips to join the LED to a power supply, because the alligator clip will divert and absorb some of the heat from your soldering iron. Instead, please use some sharp-nosed pliers to bend each of the leads from an LED into little hooks, and do the same thing with the wires on a 680Ω load resistor. Finally bend the new wires on your AC adapter so that they, too, are tiny hooks. Now you can put the hooks together like links in a chain, as shown in Figure 3-66.

Grip the plastic body of the LED in your helping hand. Plastic is not a good thermal conductor, so the helping hand shouldn't siphon too much heat away from our target. The resistor can dangle from one of the leads on the LED, and the wire from the AC adapter can hang from that, a little farther down. Gravity should be sufficient to make this work. Set your AC adapter to deliver 12 volts as before, plug it in, and your LED should be shining brightly. I used a white LED in this experiment, because it's easier to photograph.

Make sure your two soldering irons are really hot. They should have been plugged in for at least five minutes. Now take the pencil-style iron and hold its tip firmly against one of the leads on your glowing LED, while you check the time with a watch. Figure 3-67 shows the setup.

I'm betting that you can sustain this contact for a full three minutes without burning out the LED. This is why you use a 15-watt soldering iron for delicate electronics work—it doesn't endanger the components.

Allow your LED wire to cool, and then apply your more powerful soldering iron to the same piece of wire as before. Again, make sure it is completely hot, and I think you'll find that the LED will go dark after as little as 10 seconds (note, some LEDs can survive higher temperatures than others). This is why you *don't* use a 30-watt soldering iron for delicate electronics work.

The large iron doesn't necessarily reach a higher temperature than the small one. It just has a larger heat capacity. In other words, a greater quantity of heat can flow out of it, at a faster rate.

Throw away your burned-out LED. Substitute a new one, connected as before, but add a full-size copper alligator clip to one of the leads up near the body of the LED, as shown in Figure 3-68. Press the tip of your 30-watt or 40-watt soldering iron against the lead just *below* the alligator clip. This time, you should be able to hold the powerful soldering iron in place for a full two minutes without burning out the LED.

Imagine the heat flowing out through the tip of your soldering iron, into the wire that leads to the LED—except that the heat meets the alligator clip along the way, as shown in Figure 3-69. The clip is like an empty vessel waiting to be filled. It offers much less resistance to heat than the remainder of the wire leading to the LED, so the heat prefers to flow into the copper clip, leaving the LED unharmed. At the end of your experiment, if you touch the clip, you'll find that it's hot, while the LED remains relatively cooler.

The alligator clip is known as a heat sink, and it should be made of copper, because copper is one of the best conductors of heat.

Because the 15-watt soldering iron failed to harm the LED, you may conclude that the 15-watt iron is completely safe, eliminating all need for a heat sink. Well, this may be true. The problem is, you don't really know whether some semiconductors may be more heat-sensitive than LEDs. Because the consequences of burning out a component are so exasperating, I suggest you should play it safe and use a heat sink in these circumstances:

- If you apply 15-watt iron extremely close to a semiconductor for 20 seconds or more.
- If you apply a 30-watt iron near resistors or capacitors for 10 seconds or more. (Never use it near semiconductors.)
- If you apply a 30-watt iron near anything meltable for 20 seconds or more. Meltable items include insulation on wires, plastic connectors, and plastic components inside switches.

Rules for Heat Sinking

1. Full-size copper alligator clips do work better.
2. Clamp the alligator clip as close as possible to the component and as far as possible from the joint. (You don't want to suck too much heat away from the joint.)
3. Make sure there is a metal-to-metal connection between the alligator clip and the wire to promote good heat transfer.

Figure 3-68. *When a copper alligator clip is used as a heat sink, you should be able to apply a 30-watt soldering iron (below the clip) without damaging the LED.*

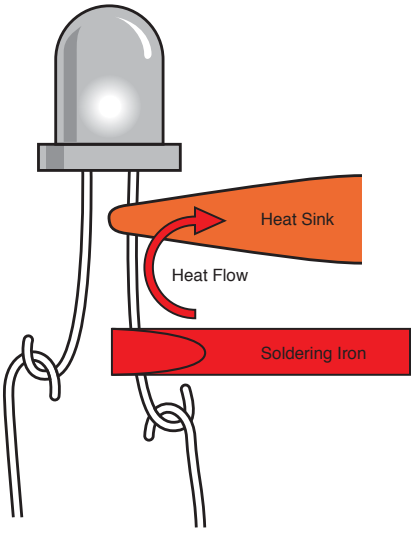

Figure 3-69. *The heat sink intercepts the heat, sucks it up, and protects the LED from damage.*

FUNDAMENTALS

All about perforated board

For the remainder of this book, you'll be using perforated board whenever you want to create permanent, soldered circuits. There are three ways to do this:

1. Point-to-point wiring. You use perforated board that has no connections behind the holes. Either the board has no copper traces on it at all, as in Figure 3-70, or you will find a little circular copper circle around each hole, as in Figure 3-71. These circles are not connected with each other and are used only to stabilize the components that you assemble.

   Point-to-point wiring allows you to place the components in a convenient, compact layout that can be very similar to a schematic. Under the board you bend the wires to link the components, and solder them together, adding extra lengths of wire if necessary. The advantage of this system is that it can be extremely compact. The disadvantage is that the layout can be confusing, leading to errors.

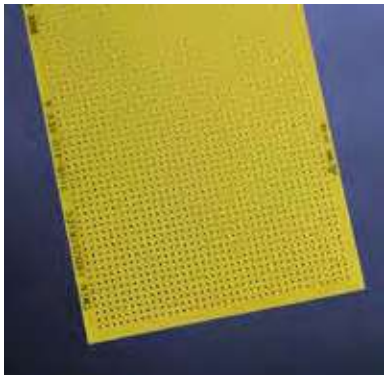

Figure 3-70

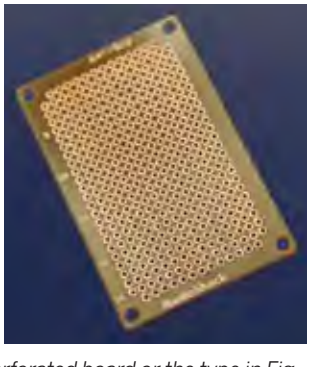

Figure 3-71. *Either this type of perforated board or the type in Figure 3-70 can be used for point-to-point wiring in Experiment 14.*

2. Breadboard-style wiring. Use perforated board that is printed with copper traces in exactly the same pattern as the conductors inside a breadboard. Once your circuit works on the breadboard, you move the components over to the perfboard one by one, maintaining their exact same positions relative to each other. You solder the "legs" of the components to the copper traces, which complete the circuit. Then you trim off the surplus wire. The advantage of this procedure is that it's quick, requires very little planning, and minimizes the possibility for errors. The disadvantage is that it tends to waste space. A cheap example is shown in Figure 3-72.
3. You can etch your own circuit board with customized copper traces that link your components in a point-to-point layout. This is the most professional way to complete a project, but it requires more time, trouble, and equipment than is practical in this book.

   Point-to-point wiring is like working with alligator clips, on a much smaller scale. The first soldered project will use this procedure.

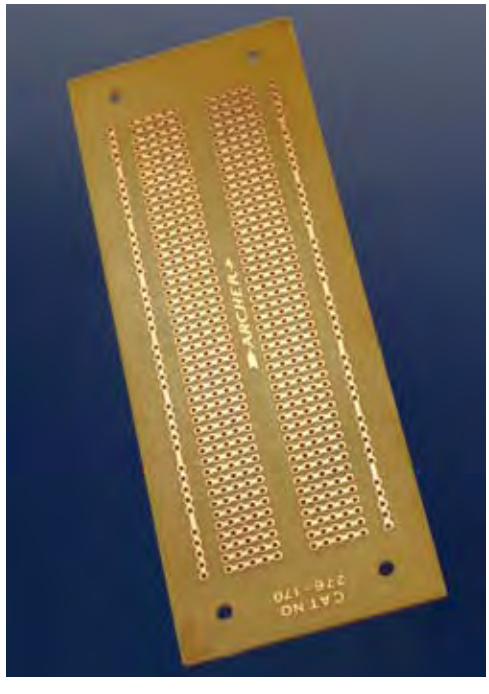

Figure 3-72. *Perforated board etched with copper in variants of a breadboard layout. This example is appropriate for Experiment 15.*

Experiment 14: A Pulsing Glow

You will need:

- Breadboard
- 15-watt pencil-type soldering iron
- Thin solder (0.022 inches or similar)
- Wire strippers and cutters
- Plain perforated board (no copper etching necessary)
- Small vise or clamp to hold your perforated board
- Resistors, various
- Capacitors, electrolytic, 100 µF and 220 µF, one of each
- Red LED, 5 mm, rated for 2 volts approximately
- 2N6027 programmable unijunction transistor

Your first circuit using a PUT was a slow-speed oscillator that made an LED flash about twice each second. The flashes looked very "electronic," by which I mean that the LED blinked on and off without a gradual transition between each state. I'm wondering if we can modify this circuit to make the LED pulse in a more gentle, interesting way, like the warning light on an Apple MacBook when it's in "sleep" mode. I'm thinking that something of this sort might be wearable as an ornament, if it's small enough and elegant enough.

I'm also thinking that this first soldering project will serve three purposes. It will test and refine your skill at joining wires together, will teach you point-to-point wiring with perfboard, and will give you some additional insight into the way that capacitors can be used to adjust timing.

Look back at the original schematic in Experiment 11, on page 82. Refresh your memory about the way it worked. The capacitor charges through a resistor until it has enough voltage to overcome the internal resistance in the PUT. Then the capacitor discharges through the PUT and flashes the LED.

If you drew a graph of the light coming out of the LED, it would be a thin, square-shaped pulse, as shown in Figure 3-73. How can we fill it out to make it more like the curve in Figure 3-74, so that the LED fades gently on and off, like a heartbeat?

One thing is obvious: the LED is going to be emitting a greater total amount of light in each cycle. Therefore, it's going to need more power. This means that C1, in Figure 3-75, must be a larger capacitor.

When we have a larger capacitor, it takes longer to charge. To keep the flashes reasonably frequent, we'll need a lower-value resistor for R1 to charge the capacitor quickly enough. In addition, reducing the values of R2 and R3 will program the PUT to allow a longer pulse.

Most important, I want to discharge the capacitor through a resistor to make the onset of the pulse gradual instead of sudden. Remember, when you have a resistor in series with a capacitor, the capacitor not only charges more slowly, but discharges more slowly.

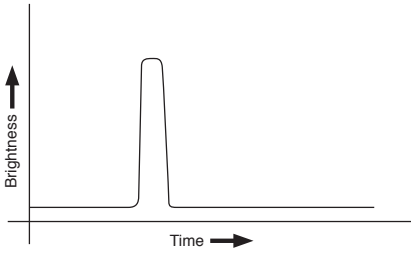

Figure 3-73

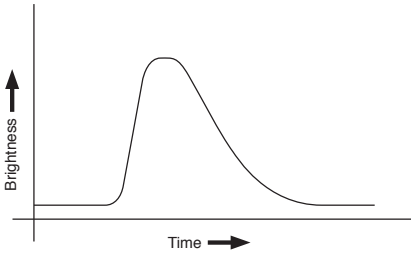

Figure 3-74. *The original PUT oscillator circuit in Experiment 11 made the LED emit sharp, short flashes. The upper graph shows what we might find if we measured light output over time. The second graph shows a gentler onset to each flash, followed by a slow fade-out. Capacitors can be used to create this effect.*

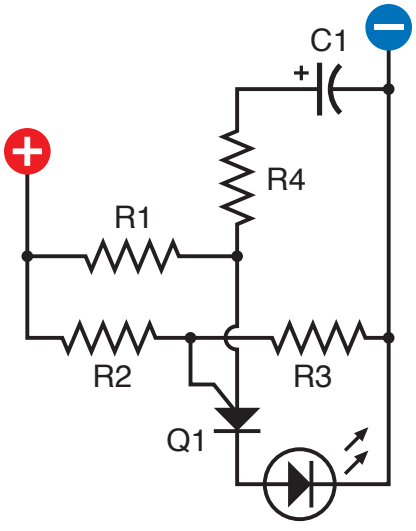

Figure 3-75. *The first step toward creating a gentler flashing effect is to use a larger capacitor for C1 and discharge it through a resistor, R4. Lower-value resistors are necessary to charge the capacitor rapidly enough.*

R1: 33K
R2: 1K
R3: 1K
R4: 1K
C1: 100 µF electrolytic
Q1: 2N6027

Figure 3-75 shows these features. Compare it with Figure 2-103 on page 85. R1 is now 33K instead of 470K. R2 and R3 are reduced to 1K. R4 also is 1K, to so that the capacitor takes longer to discharge through it. And C1 is now 100 µF instead of 2.2 µF.

Assemble this circuit on a breadboard, and compare the results when you include R4 or bypass it with a plain piece of jumper wire. It softens the pulse a bit, but we can work on it some more. On the output side of the PUT, we can add another capacitor. This will charge itself when the pulse comes out of the PUT, and then discharge itself gradually through another resistor, so that the light from the LED dies away more slowly.

Figure 3-76 shows the setup. C2 is large—220 µF—so it sucks up the pulse that comes out of the PUT, and then gradually releases it through 330Ω resistor R5 and the LED. You'll see that the LED behaves differently now, fading out inside of blinking off. But the resistances that I've added have dimmed the LED, and to brighten it, you should increase the power supply from 6 volts to 9 volts.

Remember that a capacitor imposes a smoothing effect only if one side of it is grounded to the negative side of the power supply. The presence of the negative charge on that side of the capacitor attracts the positive pulse to the other side.

I like the look of this heartbeat effect. I can imagine a piece of wearable electronic jewelry that pulses in this sensual way, very different from the hard-edged, sharp-on-and-off of a simple oscillator circuit. The only question is whether we can squeeze the components into a package that is small enough to wear.

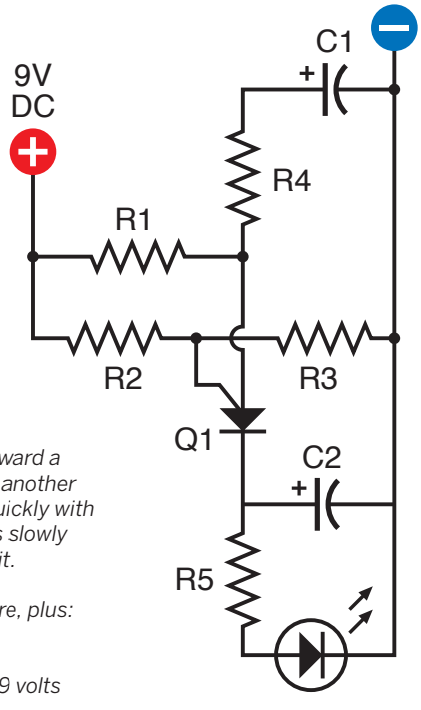

Figure 3-76. *The second step toward a gentler flashing effect is to add another capacitor, C2, which charges quickly with each pulse and then discharges slowly through R5 and the LED below it.*

Same components as before, plus:
R5: 330Ω
C2: 220 µF electrolytic
Power supply increased to 9 volts

Figure 3-77. *On a dark night in a rural area, the heartbeat flasher may be attractive in unexpected ways.*

Resizing the Circuit

The first step is to look at the physical components and imagine how to fit them into a small space. Figure 3-78 shows a 3D view of a compact arrangement. Check this carefully, tracing all the paths through the circuit, and you'll see that it's the same as the schematic. The trouble is that if we solder the components together like this, they won't have much strength. All the little wires can bend easily, and there's no easy way to mount the circuit in something or on something.

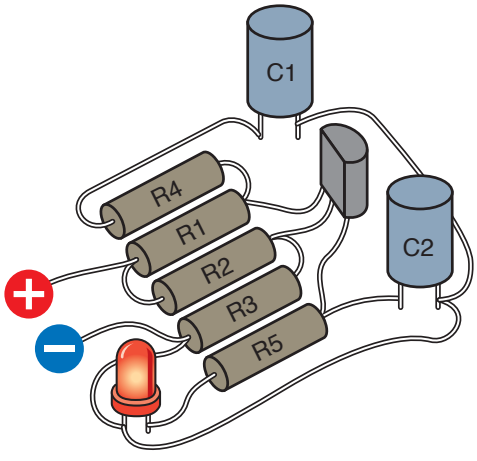

Figure 3-78. *This layout of components replicates their connections in the schematic diagram while squeezing them into a minimal amount of space.*

The answer is to put it on a substrate, which is one of those terms that people in the electronics field like to use, perhaps because it sounds more technical than "perfboard." But perforated board is what we need, and Figure 3-79 shows the components transferred onto a piece of board measuring just 1 inch by 0.8 inch.

The center version of this diagram uses dotted lines to show how the components will be connected with each other underneath the board. Mostly the leads that stick out from underneath the components will be long enough to make these connections.

Finally, the bottom version of the perfboard diagram shows the perfboard flipped left-to-right (notice the L and the R have been transposed to remind you, and I've used a darker color to indicate the underside of the board). Orange circles indicate where solder joints will be needed.

The LED should be unpluggable, because we may want to run it at some distance from the circuit. Likewise the power source should be unpluggable. Fortunately we can buy miniature connectors that fit right into the perforated board. You may have to go to large online retail suppliers such as Mouser.com for these. Some manufacturers call them "single inline sockets and headers," while others call them "boardmount sockets and pinstrip headers." Refer back to Figure 3-29 and check the shopping list for more details.

This is a very compact design that will require careful work with your pencil-style soldering iron. Because a piece of perforated board as small as this will tend to skitter around, I suggest that you apply your miniature vise to one end to anchor it with some weight while still allowing you to turn it easily.

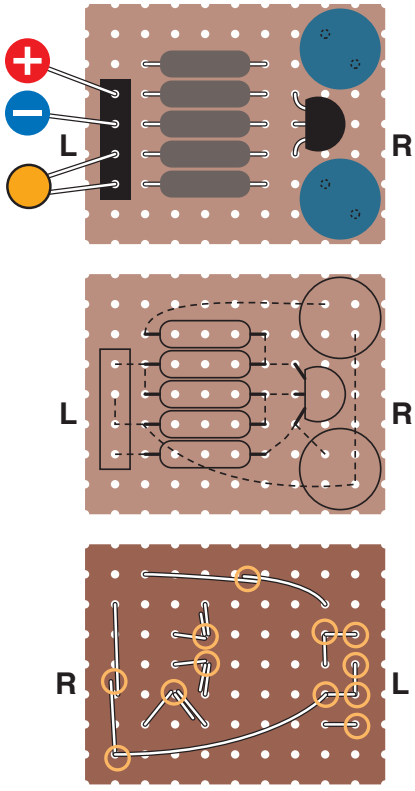

Figure 3-79. *Perforated board can be used to support the layout of components. Their leads are soldered together under the board to create the circuit. The middle diagram shows the wires under the board as dashed lines. The bottom diagram shows the board from underneath, flipped left to right. Orange circles indicate where solder joints will be necessary.*

When I'm working on this kind of project, I like to place it (with the vise attached) on a soft piece of polyurethane foam—the kind of slab that is normally used to make a chair cushion. The foam protects the components from damage when the board is upside-down, and again helps to prevent the work from sliding around unpredictably.

Step by Step

Here's the specific procedure for building this circuit:

1. Cut the small piece of perfboard out of a sheet that has no copper traces on it. You can cut the section using your miniature hobby saw, or you may be able to snap the board along its lines of holes, if you're careful. Alternatively, use a small ready-cut piece of perfboard with copper circles on it that are not connected to one another. You'll ignore the copper circles in this project. (In the next experiment, you'll deal with the additional challenge of making connections between components and copper traces on perforated board.)
2. Gather all the components and carefully insert them through holes in the board, counting the holes to make sure everything is in the right place. Flip the board over and bend the wires from the components to anchor them to the board and create connections as shown. If any of the wires isn't long enough, you'll have to supplement it with an extra piece of 22-gauge wire from your supply. You can remove all the insulation, as we'll be mounting the perfboard on a piece of insulating plastic.
3. Trim the wires approximately with your wire cutters.
4. Make the joints with your pencil soldering iron. Note that in this circuit, you are just joining wires to each other. The components are so close together that they'll prevent each other from wiggling around too much. If you are using board with copper pads (as I did), and some solder connects with them, that's OK—as long as it doesn't creep across to the neighboring component and create a short circuit.
5. Check each joint using a close-up magnifying glass, and wiggle it with pointed-nosed pliers. If there isn't enough solder for a really secure joint, reheat it and add more. If solder has created a connection that shouldn't be there, use a utility knife to make two parallel cuts in the solder, and scrape away the little section between them.

Generally, I insert three or four components, trim the wires approximately, solder them, trim their wires finally, then pause to check the joints and the placement. If I solder too many components in succession, there's a greater risk of missing a bad joint, and if I make an error in placing a component, undoing it will be much more problematic if I have already added a whole lot more components around it.

Figures 3-80 and 3-81 show the version of this project that I constructed, before I trimmed the board to the minimum size.

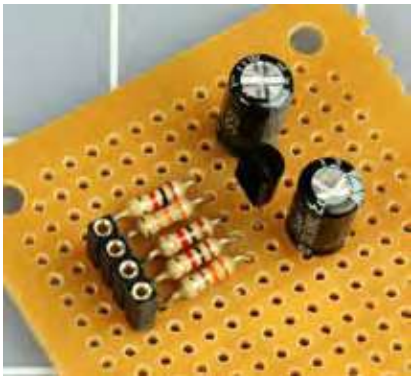

Figure 3-80. *Components mounted on a piece of perforated board.*

Figure 3-81. *The assembly seen from below. The copper circles around the holes are not necessary for this project. Some of them have picked up some solder, but this is irrelevant as long as no unintentional short circuits are created.*

Flying Wire Segments

The jaws of your wire cutters exert a powerful force that peaks and then is suddenly released when they cut through wire. This force can be translated into sudden motion of the snipped wire segment. Some wires are relatively soft, and don't pose a risk, but harder wires can fly in unpredictable directions at high speed, and may hit you in the eye. The leads of transistors are especially hazardous in this respect.

I think it's a good idea to wear safety glasses when trimming wires.

Finishing the Job

I always use bright illumination. This is not a luxury; it is a necessity. Buy a cheap desk lamp if you don't already have one. I use a daylight-spectrum fluorescent desk lamp, because it helps me identify the colored bands on resistors more reliably. Note that this type of fluorescent lamp emits quite a lot of ultraviolet light, which is not good for the lens in your eye. Avoid looking closely and directly at the tube in the lamp, and if you wear glasses, they will provide additional protection.

No matter how good your close-up vision is, you need to examine each joint with that close-up magnifier. You'll be surprised how imperfect some of them are. Hold the magnifier as close as possible to your eye, then pick up the thing that you want to examine and bring it closer until it comes into focus.

Finally, you should end up with a working circuit. You can insert the wires from your power supply into two of the tiny power sockets, and plug a red LED into the remaining two sockets. Remember that the two center sockets are negative, and the two outer sockets are positive, because it was easier to wire the circuit this way. You should color-code them to avoid mistakes.

So now you have a tiny circuit that pulses like a heartbeat. Or does it? If you have difficulty making it work, retrace every connection and compare it with the schematic. If you don't find an error, apply power to the circuit, attach the black lead from your meter to the negative side, and then go around the circuit with the red lead, checking the presence of voltage. Every part of this circuit should show at least some voltage while it's working. If you find a dead connection, you may have made a bad solder joint, or missed one entirely.

When you're done, now what? Well, now you can stop being an electronics hobbyist and become a crafts hobbyist. You can try to figure out a way to make this thing wearable.

First you have to consider the power supply. Because of the components that I used, we really need 9 volts to make this work well. How are you going to make this 9-volt circuit wearable, with a bulky 9-volt battery?

I can think of three answers:

1. You can put the battery in a pocket, and mount the flasher on the outside of the pocket, with a thin wire penetrating the fabric. Note that the tiny power connector on the perforated board will accept two 22-gauge wires if they are solid core, or if they are stranded (like the wires from a 9-volt battery connector) but have been thinly coated with solder.
2. You could mount the battery inside the crown of a baseball cap, with the flasher on the front.
3. You can put together three 3-volt button batteries in a stack, held in some kind of plastic clip. If you try this option, it may not be a good idea to try to solder wire to a battery. You will heat the liquid stuff inside the battery, which may not be good for it, and may not be good for you if the liquid starts boiling and the battery bursts open. Also, solder doesn't stick easily to the metallic finish on most battery terminals.

Most LEDs create a sharply defined beam of light, which you may want to diffuse to make it look nicer. One way to do this is to use a piece of transparent acrylic plastic, at least 1/4 inch thick, as shown in Figure 3-82. Sandpaper the front of the acrylic, ideally using an orbital sander that won't make an obvious pattern. Sanding will make the acrylic translucent rather than transparent.

Drill a hole slightly larger than the LED in the back of the acrylic. Don't drill all the way through the plastic. Remove all fragments and dust from the hole by blasting some compressed air into it, or by washing it if you don't have an air compressor. After the cavity is completely dry, get some transparent silicone caulking or mix some clear five-minute epoxy and put a drop in the bottom of the hole. Then insert the LED, pushing it in so that it forces the epoxy to ooze around it, making a tight seal. See Figure 3-82.

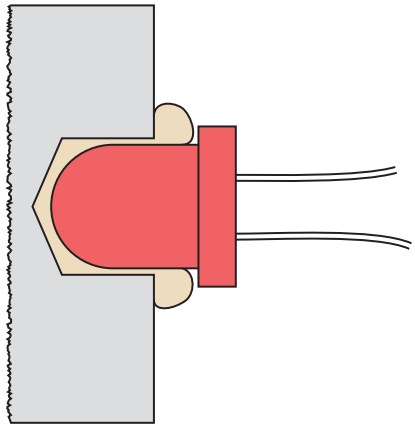

Figure 3-82. *This cross-sectional view shows a sheet of transparent acrylic in which a hole has been drilled part of the way from the back toward the front. Because a drill bit creates a hole with a conical shape at the bottom, and because the LED has rounded contours, transparent epoxy or silicone caulking can be injected into the hole before mounting the LED.*

Try illuminating the LED, and sand the acrylic some more if necessary. Finally, you can decide whether to mount the circuit on the back of the acrylic, or whether you want to run a wire to it elsewhere.

Because the LED will flash at about the speed of a human heart while the person is resting, it may look as if it's measuring your pulse, especially if you mount it on the center of your chest or in a strap around your wrist. If you enjoy hoaxing people, you can suggest that you're in such amazingly good shape, your pulse rate remains constant even when you're taking strenuous exercises.

To make a good-looking enclosure for the circuit, I can think of options ranging from embedding the whole thing in clear epoxy to finding a Victorian-style locket. I'll leave you to consider alternatives, because this is a book about electronics rather than handicrafts.

However, I will address one final issue: how long will this gadget continue flashing?

If you check the following section "Essentials: Battery life," you'll find that a regular alkaline 9-volt battery should keep the LED flashing for about 50 hours.

ESSENTIALS

Battery life

Any time you finish a circuit that you intend to run from a battery, you'll want to calculate the likely battery life. This is easily done, because manufacturers rate their batteries according to the "ampere hours" they can deliver. Keep the following in mind:

- The abbreviation for amp-hours is Ah, sometimes printed as AH. Milliampere-hours are abbreviated mAh.
- The rating of a battery in amp-hours is equal to the current, in amps, multiplied by the number of hours that the battery can deliver it.

Thus, in theory 1 amp-hour can mean 1 amp for 1 hour, or 0.1 amp for 10 hours, or 0.01 amp for 100 hours—and so on. In reality, it's not as simple as this, because the chemicals inside a battery become depleted more quickly when you draw a heavy current, especially if the battery gets hot. You have to stay within limits that are appropriate to the size of the battery.

For instance, if a small battery is rated for 0.5 amp-hours, you can't expect to draw 30 amperes from it for 1 minute. But you should be able to get 0.005 amps (i.e., 5 milliamps) for 100 hours without any trouble. Remember, though, that the voltage delivered by a battery will be greater than its rated voltage when the battery is fresh, and will diminish below its rated voltage while the battery is delivering power.

According to some test data that I trust (I think they are a little more realistic than the estimates supplied by battery manufacturers), here are some numbers for typical batteries:

- Typical 9 volt alkaline battery: 0.3 amp-hours, while delivering 100 mA.
- Typical AA size, 1.5-volt alkaline battery: 2.2 amp-hours, while delivering 100 mA.
- Rechargeable nickel-metal hydride battery: about twice the endurance of a comparably sized alkaline battery.
- Lithium battery: maybe three times the endurance of an alkaline battery.

BACKGROUND

Maddened by measurement

Throughout most of this book, I've mostly used measurements in inches, although sometimes I've digressed into the metric system, as when referring to "5-mm LEDs." This isn't inconsistency on my part; it reflects the conflicted state of the electronics industry, where you'll find inches and millimeters both in daily use, often in the very same data sheet.

The United States is the only major nation still using the old system of units that originated in England. (The other two holdouts are Liberia and Myanmar, according to the CIA's *World Factbook*.) Still, the United States has led many advances in electronics, especially the development of silicon chips, which have contacts spaced 1/10 inch apart. These standards became firmly established, and show no sign of disappearing.

To complicate matters further, even in the United States, you can encounter two incompatible systems for expressing fractions of an inch. Drill bits, for instance, are measured in multiples of 1/64 inch, while metal thicknesses may be measured in decimals such as 0.06 inch (which is approximately 1/16 inch).

The metric system is not necessarily more rational than the U.S. system. Originally, when the metric system was formally introduced in 1875, the meter was defined as being 1/10,000,000 of the distance between the North Pole and the equator, along a line passing through Paris—a quixotic, Francocentric conceit. Since then, the meter has been redefined three times, in a series of efforts to achieve greater accuracy in scientific applications.

As for the usefulness of a 10-based system, moving a decimal point is certainly simpler than doing calculations in 64ths of an inch, but the only reason we count in tens is because we happen to have evolved with that number of digits on our hands. A 12-based system would really be more convenient, as numbers would be evenly divisible by 2 and 3.

As we're stuck with the whimsical aspects of length measurement, I've created the charts in Figures 3-83 and 3-84 to assist you in going from one system to another. From these you will see that when you need to drill a hole for a 5 mm LED, a 3/16-inch drill bit is about right. (In fact, it results in a better, tighter fit than if you drill an actual 5 mm hole.)

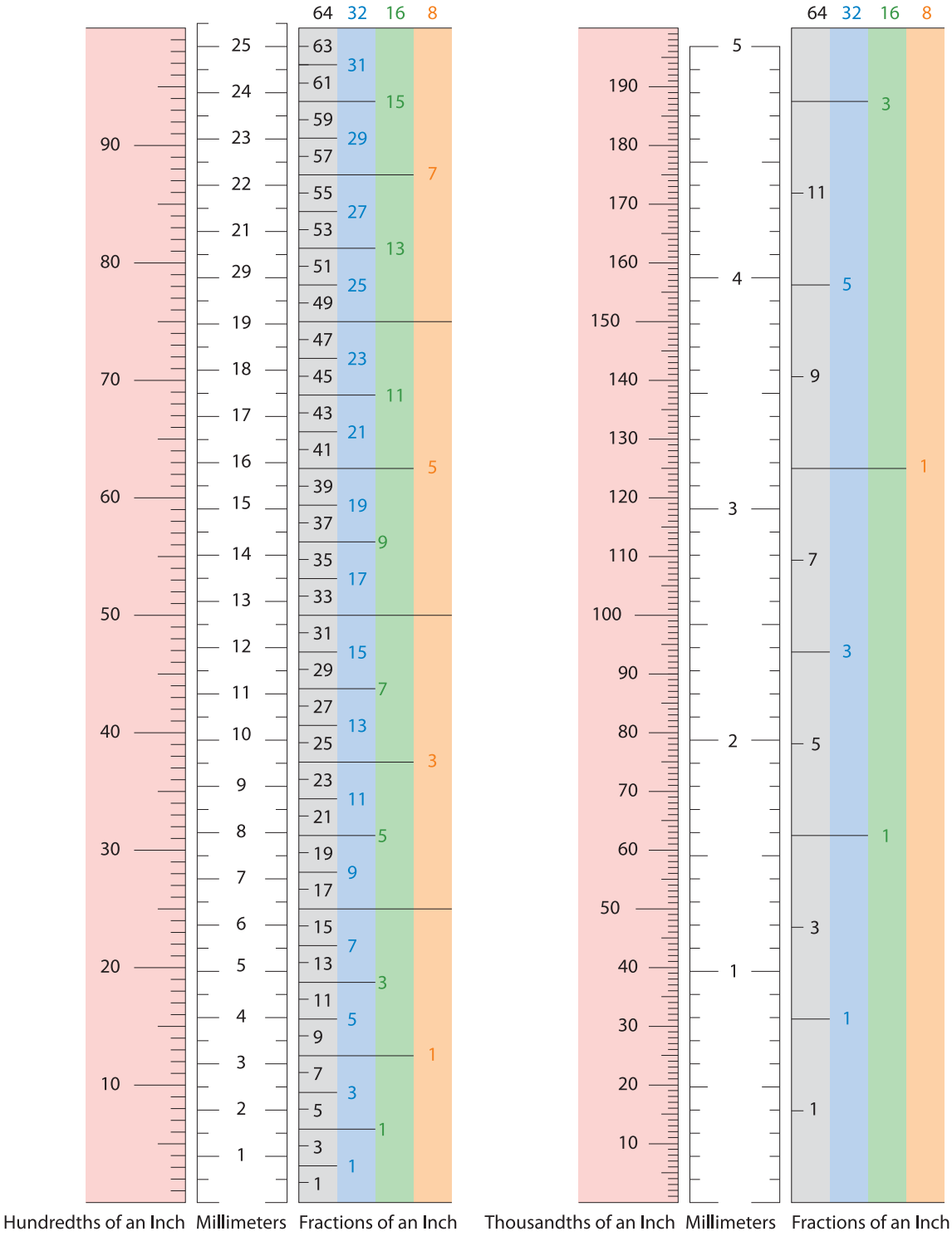

Figure 3-83. *Because units of measurement are not standardized in electronics, conversion is often necessary. The chart on the right is a 5x magnification of the bottom section of the chart on the left.*

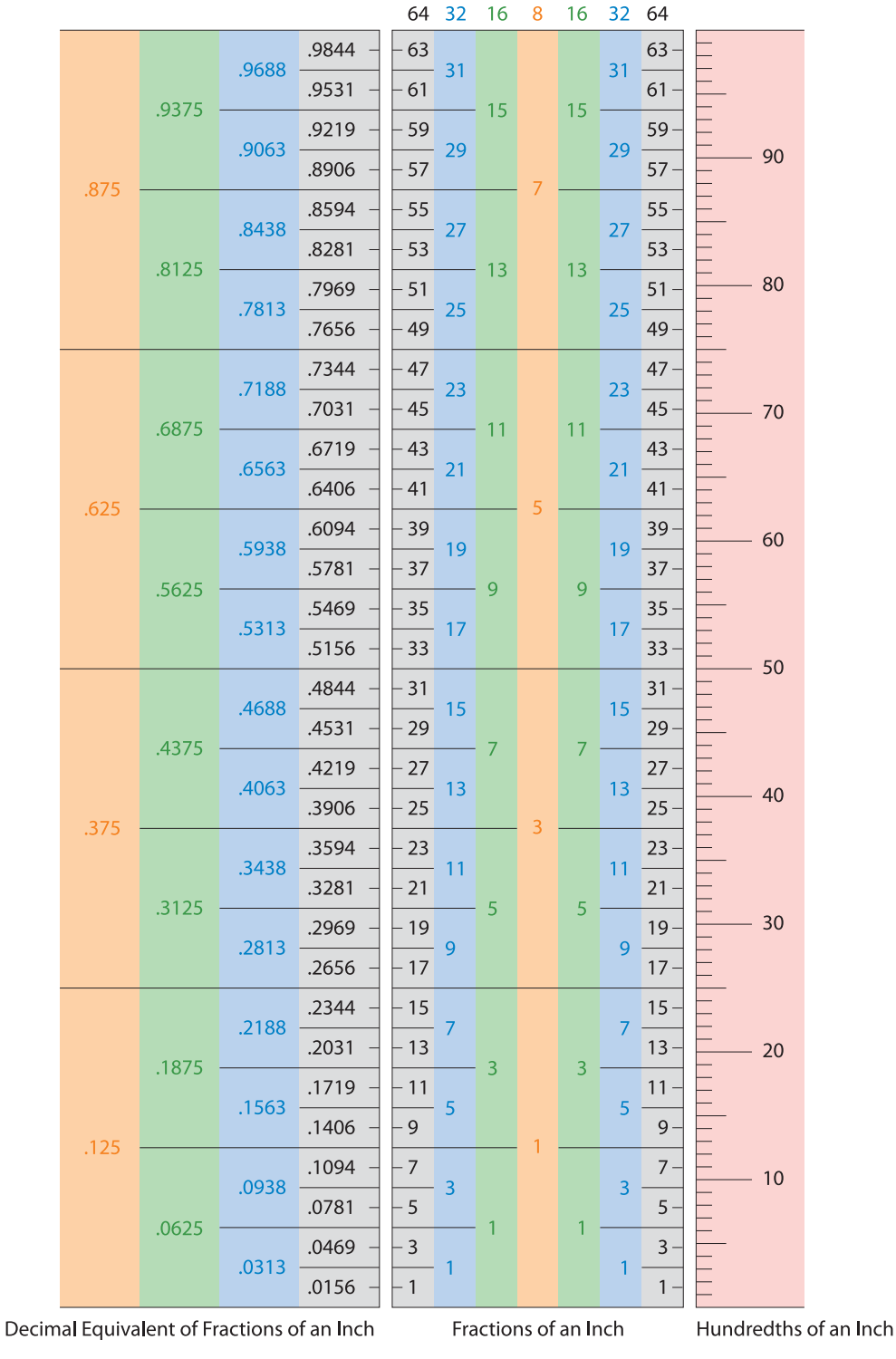

Figure 3-84. *This chart allows conversion between hundredths of an inch, conventional U. S. fractions of an inch, and fractions expressed in thousandths of an inch.*

Experiment 15: Intrusion Alarm Revisited

Time now to add some of the enhancements to the intrusion alarm that I discussed at the end of Experiment 11. I'm going to show you how the alarm can be triggered if you install various detectors on windows and doors in your home. I'll also show how the alarm can be wired so that it locks itself on and continues to make noise even after a door or window is reclosed.

This experiment will demonstrate the procedure for transferring a project from a breadboard to a piece of perforated board that has copper connections laid out identically to the ones inside the breadboard, as shown earlier in Figure 3-72. And you'll mount the finished circuit in a project box with switches and connectors on the front.

When all is said and done, you'll be ready for wholesale circuit building. The explanations in the rest of this book will get gradually briefer, and the pace will increase.

You will need:

- 15-watt pencil-type soldering iron
- Thin solder (0.022 inches or similar)
- Wire strippers and cutters
- Perforated board etched with copper in a breadboard layout
- Small vise or clamp to hold your perforated board
- The same components that you used in Experiment 11, plus:
  - 2N2222 NPN transistor. Quantity: 1.
  - DPDT relay. Quantity: 1.
  - SPDT toggle switch. Quantity: 1.
  - 1N4001 diode. Quantity: 1.
  - Red and green 5mm LEDs. Quantity: 1 each.
  - Project box, 6 × 3 × 2 inches.
  - Power jack, type N, and matching power socket, type N.
  - Binding posts.
  - Stranded 22-gauge wire, three different colors.
  - Magnetic sensor switches, sufficient for your home.
  - Alarm network wiring, sufficient for your home.

Magnetic Sensor Switches

Figure 3-85. *In this simple alarm sensor switch, the lower module contains a magnet, which opens and closes a reed switch sealed into the upper module.*

A typical alarm sensor switch consists of two modules: the magnetic module and the switch module, as shown in Figures 3-85 and 3-86. The magnetic module contains a permanent magnet, and nothing else. The switch module contains a "reed switch," which makes or breaks a connection (like a contact inside a relay) under the influence of the magnet. When you bring the magnetic module close to the switch module, you may faintly hear the reed switch click as it flips from one state to the other.

Like all switches, reed switches can be normally open or normally closed. For this project, you want the kind of switch that is normally open, and closes when the magnetic module is close to it.

Attach the magnetic module to the moving part of a door or window, and attach the switch module to the window frame or door frame. When the window or door is closed, the magnetic module is almost touching the switch module. The magnet keeps the switch closed until the door or window is opened, at which point the switch opens.

The only question is: how do we use this component to trigger our alarm? As long as a small current flows through all our magnetic sensor switches, the alarm should be off, but if the flow of current stops, the alarm should switch on.

We could use a relay that is "always on" while the alarm is armed. When the circuit is interrupted, the relay relaxes and its other pair of contacts closes, which could power up the alarm noisemaker.

But I don't like this idea. Relays take significant power, and they can get hot. Most of them are not designed to be kept "always-on." I'd prefer to handle the task using a transistor.

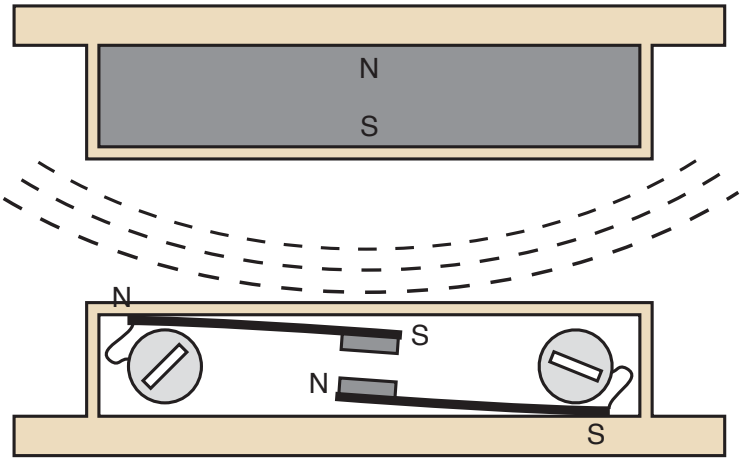

Figure 3-86. *This cutaway diagram shows a reed switch (bottom) and the magnet that activates it (top), inside an alarm sensor. The switch contains two flexible magnetized strips, the upper one with its south pole adjacent to an electrical contact, the lower one with its north pole adjacent to an electrical contact. When the south pole of the magnet approaches the switch, the magnetic force (shown as dashed lines) repels the south contact and attracts the north contact, causing them to snap together. Two screws on the outside of the casing are connected with the strips inside.*

A Break-to-Make Transistor Circuit

First, recall how an NPN transistor works. When the base is not sufficiently positive, the transistor blocks current between its collector and emitter, but when the base is relatively positive, the transistor passes current.

Take a look at the schematic in Figure 3-87, which is built around our old friend the 2N2222 NPN transistor. When the switch is closed, it connects the base of the transistor to the negative side of the power supply through a 1K resistor. At the same time, the base is connected with the positive side of the power supply through a 10K resistor. Because of the difference in resistances and the relatively high turn-on voltage for the LED, the base is forced below its turn-on threshold, and as a result, the transistor will not pass much current. The LED will glow dimly at best.

Now what happens when the switch is opened? The base of the transistor loses its negative power supply and has only its positive power supply. It becomes much more positive, above the turn-on threshold for the transistor, which tells the transistor to lower its resistance and pass more current. The LED now glows brightly. Thus, when the switch is turned off and breaks the connection, the LED is turned on.

This seems to be what we want. Imagine a whole series of switches instead of just one switch, as shown in Figure 3-88. The circuit will still work the same way, even if the switches are scattered all over your home, because the resistance in the wires connecting the switches will be trivial compared with the resistance of the 1K resistor.

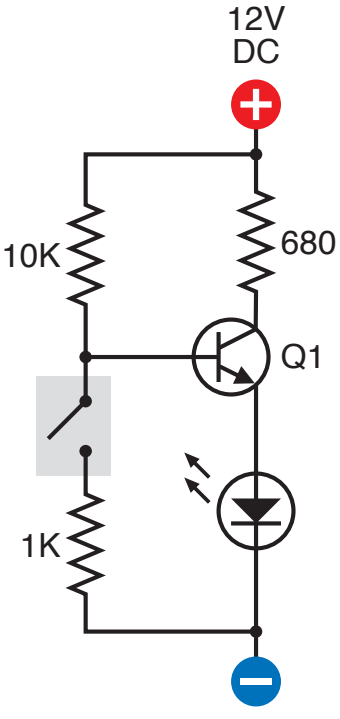

Figure 3-87. *In this demonstration circuit, when the switch is opened, it interrupts negative voltage to the base of the transistor, causing the transistor to lower its resistance, allowing current to reach the LED. Thus, when the switch is turned off, it turns on the LED.*

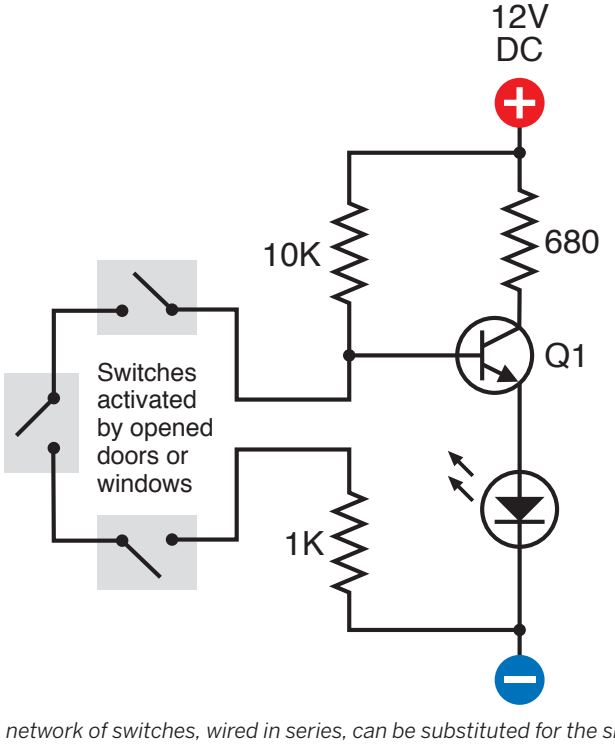

Figure 3-88. *A network of switches, wired in series, can be substituted for the single switch in Figure 3-87. Now any one switch will break continuity and trigger the transistor.*

I have shown the switches open, because that's the way the schematic for a switch is drawn, but imagine them all closed. The base of the transistor will now be supplied through the long piece of wire connecting all the closed switches, and the LED will stay dark. Now if just one switch is opened, or if anyone tampers with the wire linking them, the base of the transistor loses its connection to negative power, at which point the transistor conducts power and the LED lights up.

While all the switches remain closed, the circuit is drawing very little current—probably about 1.1 mA. So you could run it from a typical 12-volt alarm battery.

Now suppose we swap out the LED and put a relay in there instead, as shown in Figure 3-89. I don't mind using a relay in this location, because the relay will not be "always on." It will normally be off, and will draw power only when the alarm is triggered.

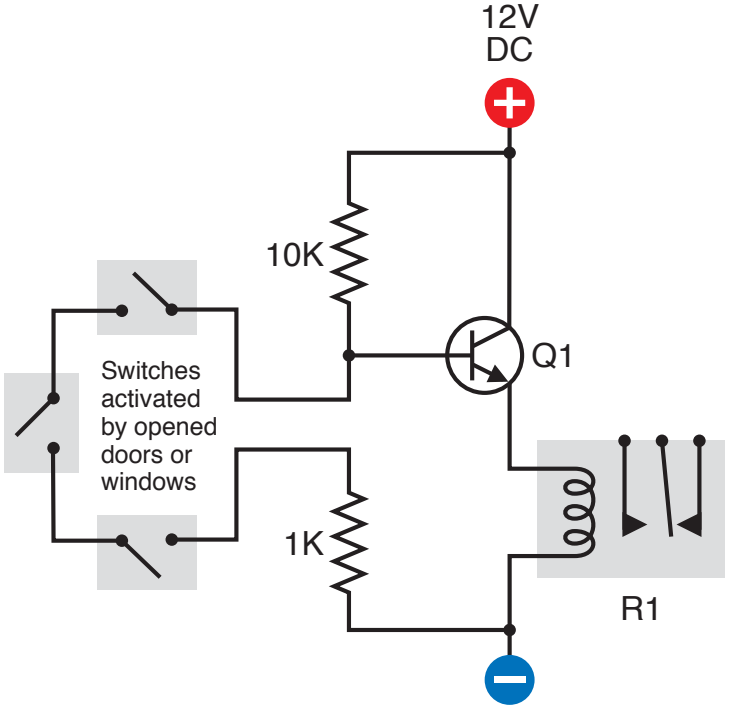

Figure 3-89. *If the LED and 680Ω resistor shown in are removed, and a relay takes their place, the relay will be activated when any switch in the sensor network is opened.*

Try one of the 12-volt relays that you used previously. You should find that when you open the switch, the relay is energized. When you close the switch, the relay goes back to sleep. Note that I eliminated the 680Ω resistor from the circuit, because the relay doesn't need any protection from the 12-volt power supply.

Self-Locking Relay

There's only one remaining problem: we want the alarm to continue making noise even after someone who has opened a door or window closes it again quickly. In other words, when the relay is activated, it must lock itself on.

One way to do this would be by using a latching relay. The only problem is that we would then need another piece of circuitry to unlatch it. I prefer to show you how you can make any relay keep itself switched on after it has received just one jolt of power. This idea will be useful to you later in the book as well.

The secret is to supply power to the relay coil through the two contacts inside the relay that are normally open. (Note that this is exactly opposite to the relay oscillator, which supplied power to its coil through the contacts that were normally closed. That setup caused the relay to switch itself off almost as soon as it switched itself on. This setup causes the relay to keep itself switched on, as soon as it has been activated.)

In Figure 3-90, the four schematics illustrate this. You can imagine them as being like frames in a movie, photographed microseconds apart. In the first picture, the switch is open, the relay is not energized, and nothing is happening. In the second, the switch has been closed to energize the coil. In the third, the coil has pulled the contact inside the relay, so that power now reaches the coil via two paths. In the fourth, the switch has been opened, but the relay is still powering its own coil through its contacts. It will remain locked in this state until the power is disconnected.

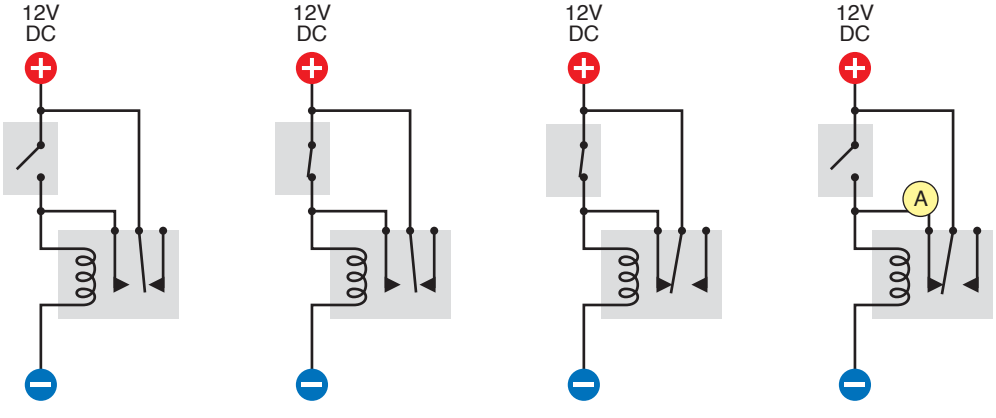

Figure 3-90. *This sequence of schematics shows the events that occur when a relay is energized. Initially, the switch is open. Then the switch is closed, activating the relay. The relay then powers itself through its own internal contacts. The relay remains energized even after the switch is opened again. Power switched by the relay can be taken from the circuit at point A.*

All we need to do, to make use of this idea, is to substitute the transistor for the on/off switch, and tap into the circuit at point A, running a wire from there to the noisemaking module.

Figure 3-91 shows how that would work. When the transistor is activated by any of the network of sensor switches, as previously explained, the transistor conducts power to the relay. The relay locks itself on, and the transistor becomes irrelevant.

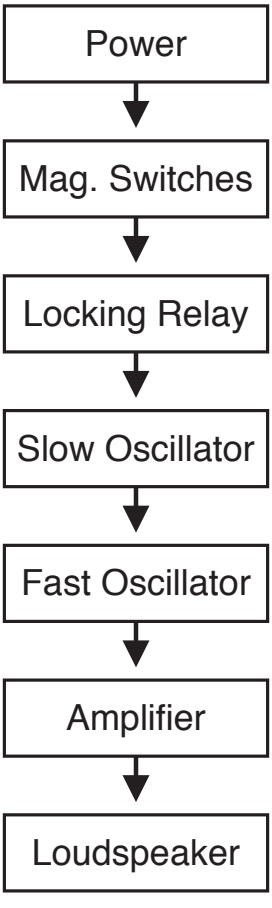

Figure 3-92. *This block diagram previously shown in Figure 2-112 on page 90 has been updated to include the magnetic-switch network and locking-relay control system.*

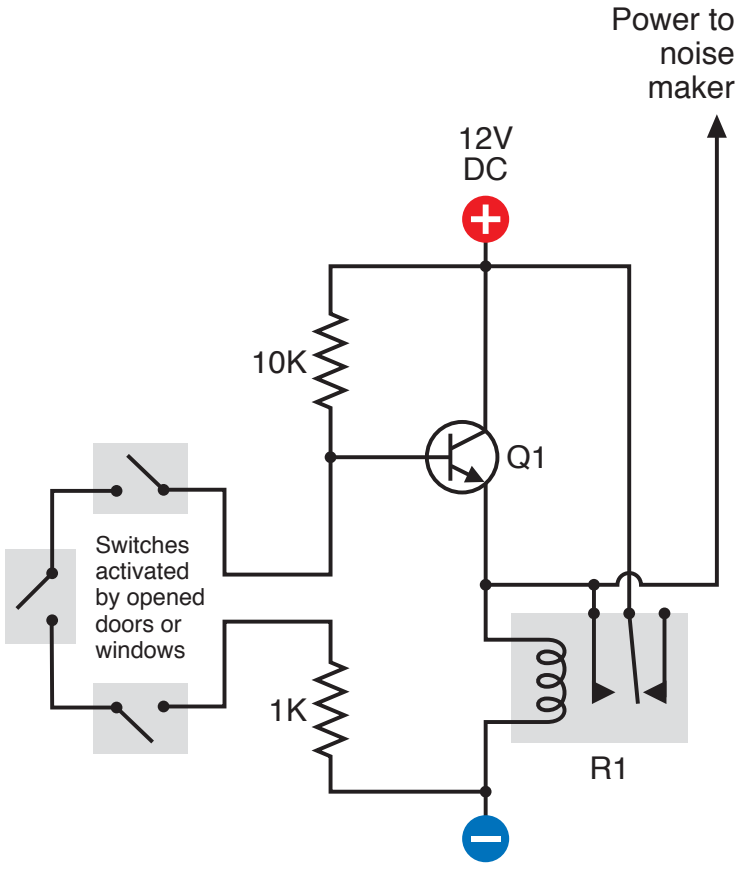

Figure 3-91. *The self-locking relay depicted in has been incorporated in the alarm circuit, so that if any switch in the network is opened, the relay will continue to power the noise maker even if the switch is closed again.*

Because I've been adding pieces to the original alarm noisemaker circuit, I've updated the block diagram from Figure 2-112 to show that we can still break this down into modules with simple functions. The revised diagram is shown in Figure 3-92.

Blocking Bad Voltage

One little problem remains: in the new version of the circuit, if the transistor goes off while the relay is still on, current from the relay can flow back up the wire to the emitter of the transistor, where it will try to flow backward through the transistor to the base, which is "more negative," as it is linked through all the magnetic switches and the 1K resistor to the negative side of the power supply.

Applying power backward through a transistor is not a nice thing to do. Therefore the final schematic in this series shows one more component, which you have not seen before: a diode, labeled D1. See Figure 3-93. The diode looks like the heart of an LED, and indeed, that's pretty much what it is, although some diodes are much more robust. It allows electricity to flow in only one direction,

from positive to negative, as shown by its arrow symbol. If current tries to flow in the opposite direction, the diode blocks it. The only price you pay for this service is that the diode imposes a small voltage drop on electricity flowing in the "OK" direction.

So now, positive flow can pass from the transistor, through the diode, to the relay coil, to get things started. The relay then supplies itself with power, but the diode prevents the positive voltage from getting back into the transistor the wrong way.

Perhaps a more elegant solution to the problem is to connect the NO leg of the relay via a 10k resistor to the base connection. When the relay is not energized, the NO leg is inert and simply behaves as a parasitic capacitance on the node. When the relay becomes energized, the NO leg shunts +12V through the common terminal via a 10k resistor into the base of the transistor. In this circuit configuration, the transistor is never exposed to a potentially harmful voltage and you are not depending on leakage currents of non-ideal elements to protect devices.

However, I needed an opportunity to introduce you to the concept of diodes. You can check the following section "Essentials: All about diodes" to learn more.

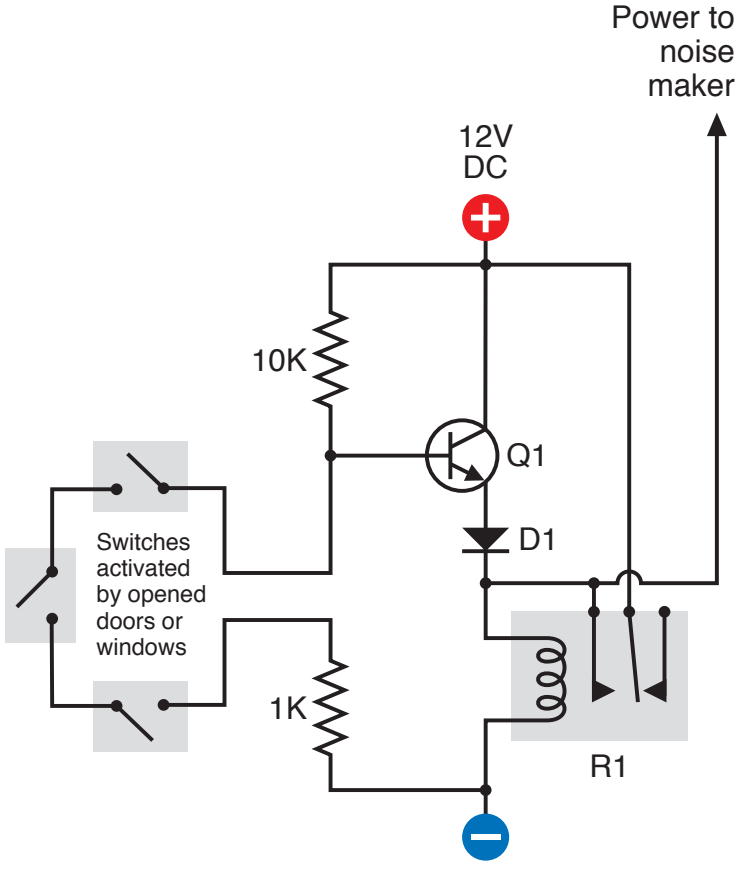

Figure 3-93. *Diode D1 has been added to protect the emitter of Q1 from positive voltage when the relay is energized.*

ESSENTIALS

All about diodes

A diode is a very early type of semiconductor. It allows electricity to flow in one direction, but blocks it in the opposite direction. (A light-emitting diode is a much more recent invention.) Like an LED, a diode can be damaged by reversing the voltage and applying excessive power, but most diodes generally have a much greater tolerance for this than LEDs. The end of the diode that blocks positive voltage is always marked, usually with a circular band, while the other end remains unmarked. Diodes are especially useful in logic circuits, and can also convert alternating current (AC) into direct current (DC).

A Zener diode is a special type that we won't be using in this book. It blocks current completely in one direction, and also blocks it in the other direction until a threshold voltage is reached—much like a PUT.

Signal diodes are available for various different voltages and wattages. The 1N4001 diode that I recommend for the alarm activation circuit is capable of handling a much greater load at a much higher voltage, but I used it because it has a low internal resistance. I wanted the diode to impose a minimal voltage drop, so that the relay would receive as much voltage as possible.

It's good practice to use diodes at less than their rated capacity. Like any semiconductor, they can overheat and burn out if they are subjected to mistreatment.

The schematic symbol for a diode has only one significant variant: sometimes the triangle is outlined instead of filled solid black (see Figure 3-94).

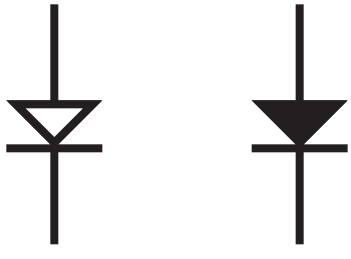

Figure 3-94. *Either of these schematic symbols may be used to represent a diode, but the one on the right is more common than the one on the left.*

Completing the Breadboard Alarm Circuit

It's time now to breadboard the control circuit for your alarm noisemaker. Figure 3-95 shows how this can be done. I am assuming that you still have the noisemaker, which functions as before. I'm assuming that you still have its relevant components mounted on the top half of the breadboard. To save space, I'm just going to show the additional components mounted on the bottom half of the same breadboard.

It's important to remember that you are not supplying power directly to the left and right "rails" on the breadboard anymore; you are supplying power to the relay-transistor section, and when the relay closes its contacts, the *relay* supplies power to the rails. These then feed the power up to the top half of the breadboard. So disconnect your power supply from the breadboard rails and reconnect it as shown in Figure 3-95.

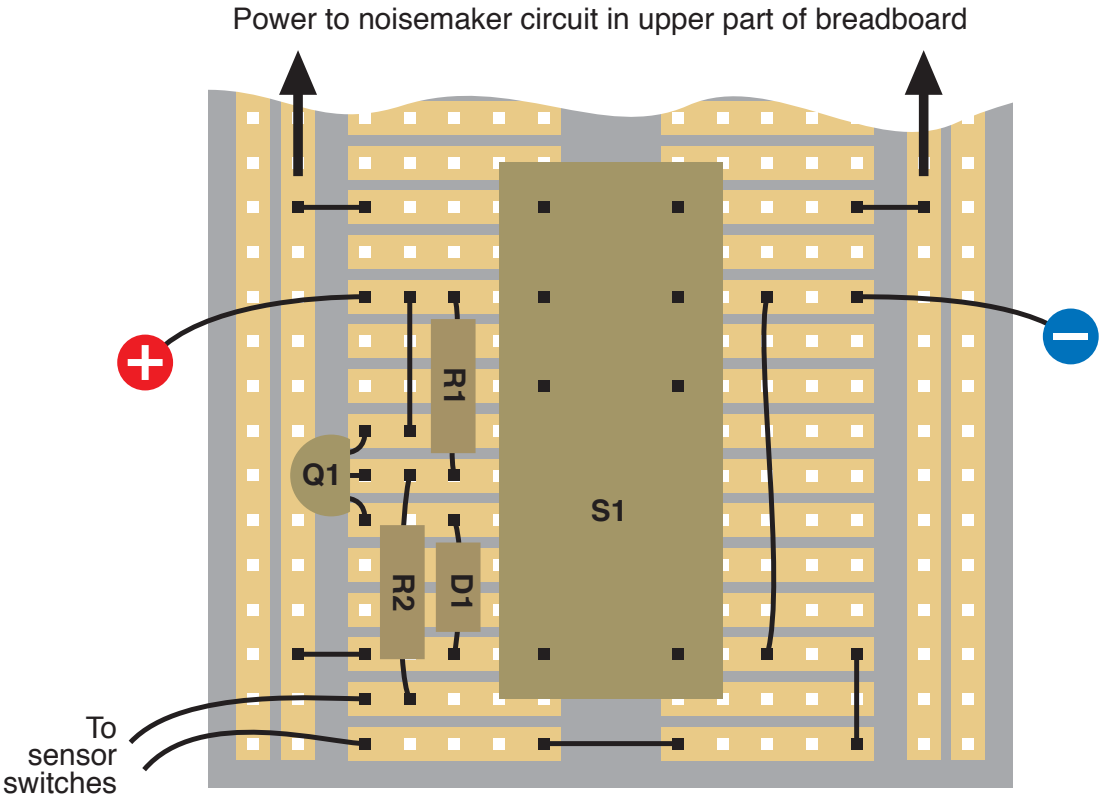

Figure 3-95. *The schematic that was developed in the previous pages can be emulated with components on a breadboard, as shown here. S1 is a DPDT relay. Wires to the sensor switch network and to the power supply must be added where shown.*

Because it's a double-pole relay, I am using it to switch negative as well as positive. This means that when the relay contacts are open, the noisemaking section of the circuit is completely isolated from the rest of the world.

The breadboarded relay circuit is exactly the same as the schematic in Figure 3-93. The components have just been rearranged and squeezed together so that they will fit alongside the relay. Two wires at the lower-left corner go to the network of magnetic sensor switches that will trip the alarm; for testing purposes, you can just hold the stripped ends of these two wires together to simulate all the switches being closed, and separate the wires to simulate a switch opening.

Two more wires bring power to the breadboard on either side of the relay. This is where you should connect your power supply during testing. The output from the relay, through its top pair of contacts, is connected with the rails of the breadboard by a little jumper wire at top left, and another at top right. Don't forget to include them! One more little wire at the lower-left corner (easily overlooked) connects the lefthand side rail to the lefthand coil terminal of the relay, so that when the relay is powering the noisemaker circuit, it powers itself as well.

When you mount the diode, remember that the end of it that is marked with a band around it is the end that blocks positive current. In this circuit, that's the lower end of the diode.

Try it to make sure that it works. Short the sensor wires together and then apply power. The alarm should remain silent. You can use your meter to check that no voltage exists between the side rails. Now separate the sensor wires, and the relay should click, supplying power to the side rails, which activates the noisemaker. Even if you bring the sensor wires back together, the relay should remain locked on. The only way to unlock it is to disconnect the power supply.

When the circuit is active, the transistor followed by the diode drops the voltage slightly, but the 12-volt relay should still work.

In my test circuit, trying three different relays, they drew between 27 and 40 milliamps at 9.6 volts. Some current still leaked through the transistor when it was in its "off" mode, but only a couple of milliamps at 0.5 volts. This low voltage was far below the threshold required to trip the relay.

Ready for Perfboarding

If the circuit works, the next step is to immortalize it on perforated board. Use the type of board that has a breadboard contact pattern etched on it in copper, as shown in Figure 3-72 on page 116. Check the following section, "Essentials: Perfboard procedure," for guidance on the best way to make this particular kind of solder joint—and the subsequent section for the most common problems.

ESSENTIALS

Perfboard soldering procedure

Carefully note the position of a component on your breadboard, and then move it to the same relative position on the perfboard, poking its wires through the little holes.

Turn the perfboard upside down, make sure that it's stable, and examine the hole where the wire is poking through, as shown in Figure 3-96. A copper trace surrounds this hole and links it with others. Your task is to melt solder so that it sticks to the copper and also to the wire, forming a solid, reliable connection between the two of them.

Take your pencil-style soldering iron in one hand and some solder in your other hand. Hold the tip of the iron against the wire and the copper, and feed some thin solder to their intersection. After two to four seconds, the solder should start flowing.

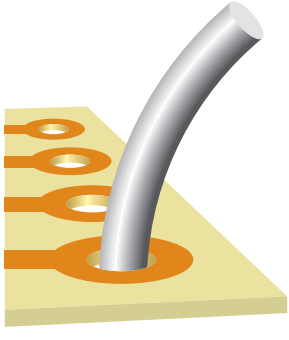

Figure 3-96

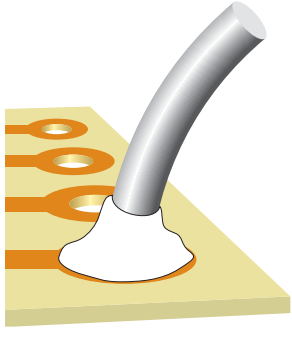

Figure 3-97

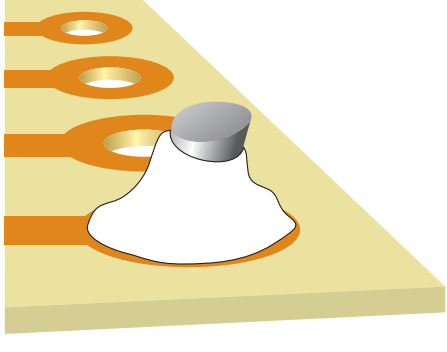

Figure 3-98. *To establish a connection between a section of wire and a copper trace on perforated board, the wire is pushed through the hole, and solder (shown in pure white for illustrative purposes) completes the connection. The wire can then be snipped short.*

Allow enough solder to form a rounded bump sealing the wire and the copper, as shown in Figure 3-97. Wait for the solder to harden thoroughly, and then grab the wire with pointed-nosed pliers and wiggle it to make sure you have a strong connection. If all is well, snip the protruding wire with your cutters. See Figure 3-98.

Because solder joints are difficult to photograph, I'm using drawings to show the wire before and after making a reasonably good joint, which is shown in pure white, outlined with a black line.

Actual soldered perfboard is shown in the photographs in Figures 3-99 and 3-100.

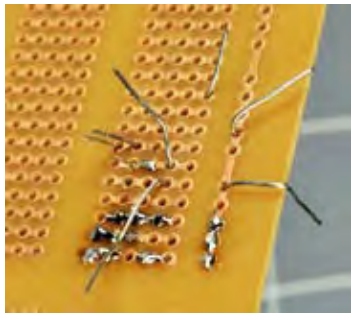

Figure 3-99. *This photograph was taken during the process of transferring components from breadboard to perforated board. Two or three components at a time are inserted from the other side of the board, and their leads are bent over to prevent them from falling out.*

Figure 3-100. *After soldering, the leads are snipped short and the joints are inspected under a magnifying glass. Another two or three components can now be inserted, and the process can be repeated.*

TOOLS

Four most common perfboarding errors

1. Too much solder

Before you know it, solder creeps across the board, touches the next copper trace, and sticks to it, as depicted in Figure 3-101. When this happens, you have to wait for it to cool, and then cut it with a utility knife. You can also try to remove it with a rubber bulb and solder wick, but some of it will tend to remain.

Even a microscopic trace of solder is enough to create a short circuit. Check the wiring under a magnifying glass while turning the perfboard so that the light strikes it from different angles (or use your solder wick to suck it away).

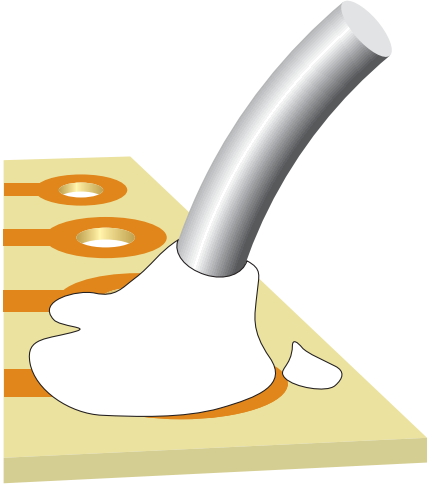

Figure 3-101. *If too much solder is used, it makes a mess and can create an unwanted connection with another conductor.*

2. Not enough solder

If the joint is thin, the wire can break free from the solder as it cools. Even a microscopic crack is sufficient to stop the circuit from working. In extreme cases, the solder sticks to the wire, and sticks to the copper trace around the wire, yet doesn't make a solid bridge connecting the two, leaving the wire encircled by solder yet untouched by it, as shown in Figure 3-102. You may find this undetectable unless you observe it with magnification.

You can add more solder to any joint that may have insufficient solder, but be sure to reheat the joint thoroughly.

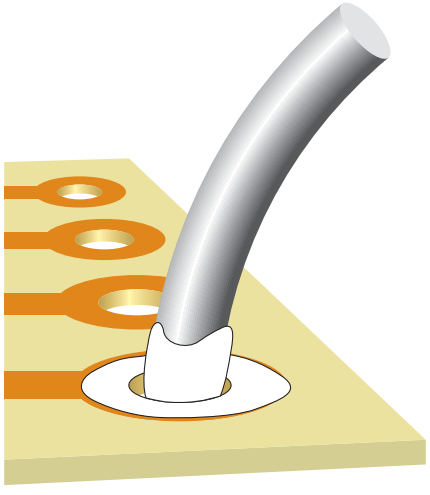

Figure 3-102. *Too little solder (or insufficient heat) can allow a soldered wire to remain separate from the soldered copper on the perforated board. Even a hair-thin gap is sufficient to prevent an electrical connection.*

3. Components incorrectly placed

It's very easy to put a component one hole away from the position where it should be. It's also easy to forget to make a connection.

I suggest that you print a copy of the schematic, and each time you make a connection on the perforated board, you eliminate that wire on your hardcopy, using a highlighter.

4. Debris

When you're trimming wires, the little fragments that you cut don't disappear. They start to clutter your work area, and one of them can easily get trapped under your perforated board, creating an electrical connection where you don't want it.

This is another reason for working with something soft, such as polyurethane foam, under your project. It tends to absorb or hold little pieces of debris, reducing the risk of you picking them up in your wiring.

Clean the underside of your board with an old (dry) toothbrush before you apply power to it, and keep your work area as neat as possible. The more meticulous you are, the fewer problems you'll have later.

Once again, be sure to check every joint with a magnifying glass.

Transferring components from the breadboard to the perforated board should be fairly simple, as long as you don't try to move too many at once. Follow the suggestions described in previous section "Essentials: Perfboard procedure," and pause frequently to check your connections. Impatience is almost always the cause of errors in this kind of work.

Figure 3-103 shows the noisemaker section of the circuit on perfboard, with the components positioned to minimize wasted space. Figure 3-104 shows the perfboard with the relay and its associated components added. The two black wires will go to the loudspeaker, the black-and-red pair of wires will bring power to the board, and the green wires will go to the magnetic sensor switches. Each wire penetrates the board, and its stripped end is soldered to the copper beneath.

Test it now, in the same way that you tested the same circuit on the breadboard. If it doesn't work, check the following section, "Essentials: Real-world fault tracing." If it does work, you're ready to trim the board and mount it in a project box.

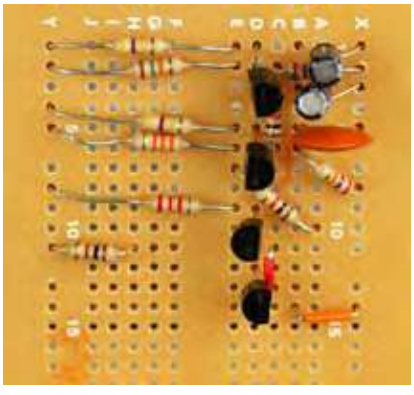

Figure 3-103. *The noisemaker circuit has been transplanted from breadboard to perforated board, with no additions or changes.*

Figure 3-104. *The relay-transistor control circuit has been added. Wires to external devices have been stripped and poked into the perforated board, where they are soldered in place. The green wires connect with the sensor network, the black wires go to the loudspeaker, and the red-and-black wires supply power.*

ESSENTIALS

Real-world fault tracing

Here's a real-life description of the procedure for tracing a fault.

After I assembled the perfboard version of the combined noisemaker and relay circuit, I checked my work, applied power—and although the relay clicked, no sound came out of the loudspeaker. Of course, everything had worked fine on the breadboard.

First I looked at component placement, because this is the easiest thing to verify. I found no errors. Then I flexed the board gently while applying power—and the loudspeaker made a brief "beep." Any time this happens, you can be virtually certain that a solder joint has a tiny crack in it.

The next step was to anchor the black lead of my meter to the negative side of the power supply, and then switch on the power and go through the circuit point by point, from top to bottom, checking the voltage at each point with the red lead of the meter. In a simple circuit like this, every part should show at least some voltage.

But when I got to the second 2N2222 transistor, which powers the loudspeaker, its output was completely dead. Either I had melted the transistor while soldering it (unlikely), or there was a bad joint. I checked the perfboard beneath the transistor with the magnifying glass, and found that solder had flowed around one of the leads of the transistor without actually sticking to it. The gap must have been less than one-thousandth of an inch, but still, that was enough. Probably, the problem had been caused by dirt or grease.

This is the kind of patient inquiry you need to follow when a circuit doesn't work. Check whether your components are placed correctly, check your power supply, check the power on the board, check the voltage at each stage, and if you are persistent, you'll find the fault.

Switches and Inputs for the Alarm

Now you need to make the system easy to use. The block diagram in Figure 3-105 shows one additional box near the top of the sequence: User Controls. These will consist of switches, LEDs, and connections to the outside world. To plan this part of the job, first I have to summarize the way in which our alarm system works at this point in its evolution.

A full-featured home alarm system normally has two modes: in-home and away-from-home:

- Using the in-home mode, you switch on the alarm while you are at home so that it will alert you if an intruder opens a door or window.
- Using the away-from-home mode, typically you enter a code number, after which you have 30 seconds to leave and close the door behind you. When you return, you trigger the alarm by opening the door, but now you have 30 seconds to go to the control panel and enter your code number again to stop the alarm from sounding.

So far, the alarm system that you've been building has only an in-home mode. Still, many people find this function useful and reassuring. Later in the book I'll suggest a way in which you can modify it to incorporate an away-from-home mode, but for now, making it practical for in-home use is enough of a challenge.

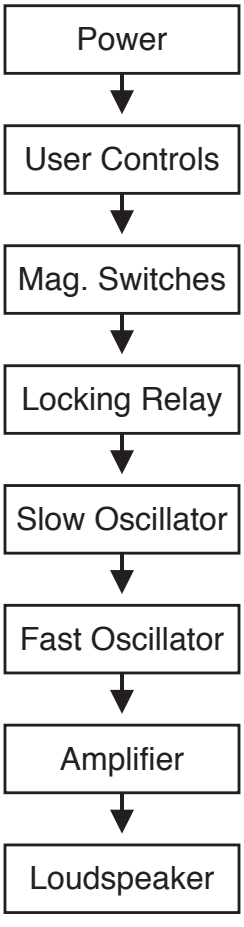

Figure 3-105. *The final block diagram for this phase of the project shows where user controls fit in the series of functions.*

Consider how it should be used on an everyday basis. It should have an on/off switch, naturally. When it's on, any of the magnetic sensor switches should trigger the alarm. But what if you switch it on without realizing that you've left a window open? At that time it won't be appropriate for the alarm to sound. What you really need is a circuit-test feature, to tell you if all the doors and windows are closed. Then you can switch on the alarm.

I think a pushbutton would be useful to test the alarm circuit. When you press it, a green LED should light up to indicate that the circuit is good. After you see the green light, you let go of the pushbutton and turn on the power switch, which illuminates a red LED, to remind you that the alarm is now armed and ready.

One additional feature would be useful: an alarm noisemaker test feature, so that you can be sure that the system is capable of sounding its alert when required to do so.

The circuit shown in Figure 3-106 incorporates all of these features. S1 is a SPDT switch; S2 is a DPDT momentary pushbutton of ON-(ON) type. The schematic shows it in its "relaxed" mode, when the button is not being pressed.

D1 is a red LED, D2 is a green LED, J1 is a power input jack (to be connected with an external 12-volt supply), and R1 is a 680Ω resistor to protect the LEDs. Note that J1 follows the usual practice of supplying positive voltage in its center contact, and negative in the circular shell around the center.

When S1 is in its Off position, it still supplies positive power through its upper contact to S2, the pushbutton. When the pushbutton is pressed, so that it goes into its "Test" position, the pole of S2 connects with the power and sends it out through the sensor switches on doors and windows. The wires to these switches will be attached via a couple of binding posts, shown here as two circles. If the sensor switches are all closed, power returns through the second binding post, passes through the lower set of contacts in S2, and lights D2, the green LED. Because S1 is not supplying power to the alarm circuit board, the alarm does not sound at this time.

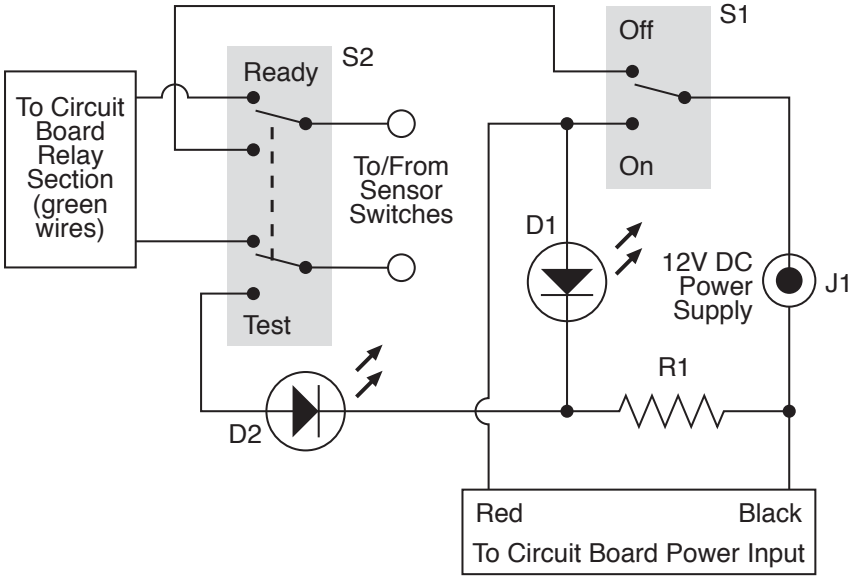

Figure 3-106. *This schematic suggests a convenient way to add an on/off switch, a continuity testing feature, and a noisemaker testing feature to the alarm.*

Now if S1 is turned to its On position, it sends power to the components on the perforated board. The transistor circuit sends power out along the green wires to S2, and as long as the button is not being pressed, the power goes out through the switch network and back through S2, to the transistor, keeping its base relatively negative. So the alarm remains silent. But as soon as a sensor switch is opened, the circuit is broken and the alarm sounds. The only way to stop it will be by switching S1 into its Off position.

Finally, if you press S2, the pushbutton, while S1 is in its On mode, you interrupt the network of switches and activate the noisemaker. In this way, S2 does dual duty: when S1 is off, pushbutton S2 tests the sensor switches for continuity. When S1 is on, S2 tests the noisemaker to make sure it creates a noise. I think this is the simplest possible way to implement these features.

Installing the Switches

If you bought a project box from RadioShack, it may have come with two optional top panels: one made of metal, the other made of plastic. I'll assume that you'll use the plastic one, as you'll have more trouble drilling holes in metal. The type of plastic used by RadioShack is ABS, which is very easy to shape with the tools that I have recommended.

You have to choose a layout for the switches and other components that will share the top panel of the project box. I like a layout to be neat, so I take the trouble to draw it using illustration software, but a full-size pencil sketch is almost as good. Just make sure there's room for the components to fit together, and try to place them similarly to the schematic, to minimize the risk of confusion.

Figure 3-107. *A printed layout for the switches, LEDs, and other components has been taped to the underside of the lid of the project box. An awl is pressed through the paper to mark the center of each hole to be drilled in the lid.*

Tape your sketch to the inside of the top panel, as shown in Figure 3-107, and then use a sharp pointed tool, such as a pick, to press through and mark the plastic at the center of each hole. The indentations will help to center your bit when you drill the holes. Remember that you'll need to make multiple holes to vent the sound from the loudspeaker, which will be beneath the top panel of the box. The result is shown in Figure 3-108.

Figure 3-108. *The exterior of the panel after drilling. A small handheld cordless drill can create a neat result if the holes were marked carefully.*

I placed all the components on the top panel, with the exception of the power input jack, which I positioned at one end of the box. Naturally, each hole has to be sized to fit its component, and if you have calipers, they'll be very useful for taking measurements and selecting the right drill bit. Otherwise, make your best guess, too small being better than too large. A deburring tool is ideal for slightly enlarging a hole so that a component fits snugly. This may be necessary if you drill 3/16-inch holes for your 5-inch mm LEDs. Fractionally enlarge each hole, and the LEDs should push in very snugly.

If your loudspeaker lacks mounting holes, you'll have to glue it in place. I used five-minute epoxy to do this. Be careful not to use too much. You don't want any of the glue to touch the speaker cone.

Drilling large holes in the thin, soft plastic of a project box can be a problem. The drill bit tends to dig in and create a mess. You can approach this problem in one of three ways:

1. Use a Forstner drill bit if you have one. It creates a very clean hole.
2. Drill a series of holes of increasing size.
3. Drill a smaller hole than you need, and enlarge it with a deburring tool.

Regardless of which approach you use, you'll need to clamp or hold the top panel of the project box with its outside surface face-down on a piece of scrap wood. Then drill from the inside, so that your bit will pass through the plastic and into the wood.

Finally, mount the components in the panel, as shown in Figure 3-109, and turn your attention to the underneath part of the box.

The circuit board will sit on the bottom, held in place with four #4-size machine screws (bolts) with washers and nylon-insert locknuts. You need to use locknuts to eliminate the risk of a nut working loose and falling among components where it can cause a short circuit.

You'll have to cut the perfboard to fit, taking care not to damage any of the components on it. Also check the underside the board for loose fragments of copper traces after you finish cutting.

Drill bolt holes in the board, if necessary, taking care again not to damage any components. Then mark through the holes to the plastic bottom of the box, and drill the box. Countersink the holes (i.e., bevel the edges of a hole so that a flat-headed screw will fit into it flush with the surrounding surface), push the little bolts up from underneath, and install the circuit board. Be extremely careful not to attach the circuit board too tightly to the project box. This can impose bending stresses, which may break a joint or a copper trace on the board.

I like to include a soft piece of plastic under the board to absorb any stresses. Because you're using locknuts, which will not loosen, there's no need to make them especially tight.

Test the circuit again after mounting the circuit board, just in case.

Figure 3-109. *Components have been added to the control panel of the project box (seen from the underside). The loudspeaker has been glued in place. Spare glue was dabbed onto the LEDs, just in case. The SPDT on/off switch is at the top right, the DPDT pushbutton is at top left, and the binding posts, which will connect with the network of magnetic sensor switches, are at the bottom.*

Soldering the Switches

Figure 3-110 shows how the physical switches should be wired together. Remember that S1 is a toggle switch and S2 is a DPDT pushbutton. Your first step is to decide which way up they should be. Use your meter to find out which terminals are connected when the switch is flipped, and when the button is pressed. You'll probably want the switch to be on when the toggle is flipped upward. Be especially careful with the orientation of the pushbutton, because if you wire it upside-down, it will constantly have the alarm in "test" mode, which is not what you want.

Remember, the center terminal of any double-throw switch is almost always the pole of the switch, connecting with the terminals immediately above it and below it.

Stranded wire is appropriate to connect the circuit board with the components in the top panel, because the strands flex easily and impose less stress on solder joints. Twisting each pair of wires together helps to minimize the mess.

Remember to install the LEDs with their short, negative wires connected with the resistor. This will entail some wire-to-wire soldering. You may want to protect some of these bare leads and joints with thin heat-shrink tubing, to minimize the risk of short circuits when you push all the parts into the box.

When you connect wires or components with the lugs on the switches, your pencil-style soldering iron probably won't deliver enough heat to make good joints. You can use your higher-powered soldering iron in these locations, but you absolutely must apply a good heat sink to protect the LEDs when you

attach them, and don't allow the iron to remain in contact with anything for more than 10 seconds. It will quickly melt insulation, and may even damage the internal parts of the switches.

In projects that are more complex than this one, it would be good practice to link the top panel with the circuit board more neatly. Multicolored ribbon cable is ideal for this purpose, with plug-and-socket connectors that attach to the board. For this introductory project, I didn't bother. The wires just straggle around, as shown in Figure 3-111.

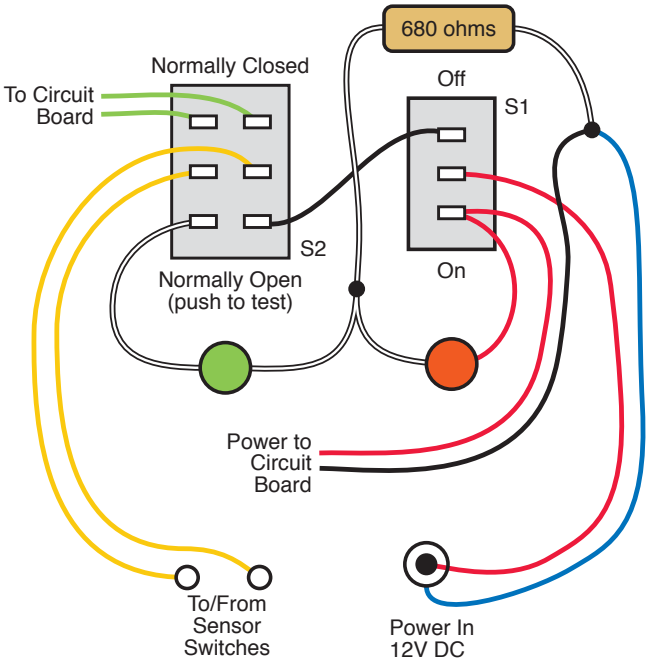

Figure 3-110. *The components can be wired together like this to replicate the circuit shown in The red and green circles are LEDs. Small, solid black circles indicate wire-to-wire solder joints.*

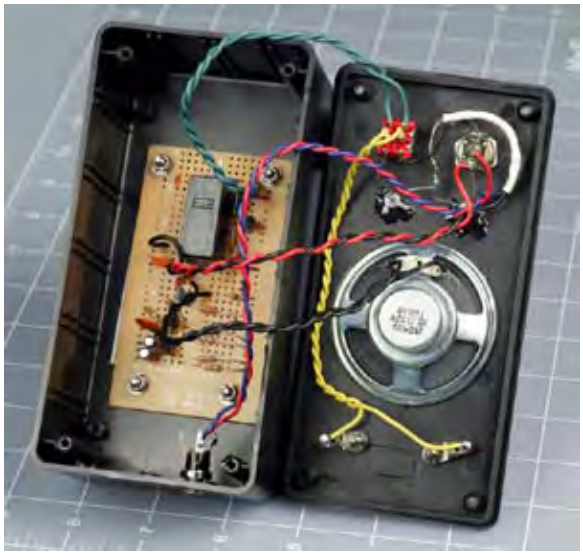

Figure 3-111. *The circuit board has been installed in the base of the project box, and the power input jack has been screwed into the end of the box. Twisted wire-pairs have been connected on a point-to-point basis, without much concern over neatness, as this is a relatively small project. The white insulation at the top-right corner of the front panel is heat-shrink tube that encloses a solder joint and the 680Ω load resistor. Soldering wires to the pushbutton switch requires care and precision, as the contacts are closely spaced.*

Final Test

When you've completed the circuit, test it! If you don't have your network of magnetic sensor switches set up yet, you can just use a piece of wire to connect the two binding posts. Make sure that S1 is in its Off position, then solder the appropriate plug to your 12-volt power source, and plug it into the power jack. When you press the button, the green LED should light up to show continuity between the two binding posts. Now disconnect the wire between the binding posts, press the button again, and the green LED should remain dark.

Reconnect the binding posts, flip S1 to its On position, and the red LED should light up. Press the button, and the alarm should start. Reset it by turning S1 off and then on again; then disconnect the wire between the binding posts. Again, the alarm should start, and it should continue even if you reconnect the wire.

If everything works the way it should, it's time to screw the top of the box in place, pushing the wires inside. Because you're using a large box, you should have no risk of metal parts touching each other accidentally, but still, proceed carefully.

Alarm Installation

Before you install your magnetic sensor switches, you should test each one by moving the magnetic module near the switch module and then away from it, while you use your meter to test continuity between the switch terminals. The switch should close when it's next to the magnet, and open when the magnet is removed.

Now draw a sketch of how you'll wire your switches together. Always remember that they have to be in series, not in parallel! Figure 3-112 shows the concept in theory. The two terminals are the binding posts on top of your control box (which is shown in green), and the dark red rectangles are the magnetic sensor switches on windows and doors. Because the wire for this kind of installation usually has two conductors, you can lay it as I've indicated but cut and solder it to create branches. The solder joints are shown as orange dots. Note how current flows through all the switches in series before it gets back to the control box.

Figure 3-113 shows the same network as you might actually install it in a situation where you have two windows and a door. The blue rectangles are the magnetic modules that activate the switch modules.

You'll need a large quantity of wire, obviously. The type of white, stranded wire that is sold for doorbells or furnace thermostats is good. Typically, it is 20-gauge or larger.

After you install all the switches, clip your meter leads to the wires that would normally attach to the alarm box. Set your meter to test continuity, and open each window or door, one at a time, to check whether you're breaking the continuity. If everything is OK, attach the alarm wires to the binding posts on your project box.

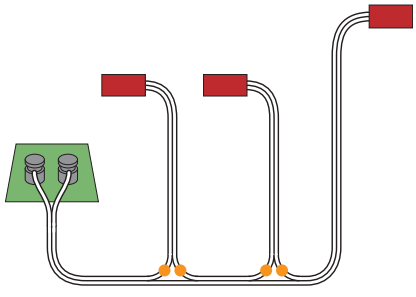

Figure 3-112. *Dual-conductor, white insulated wire can be used to connect the terminals on the alarm control box with magnetic sensors (shown in dark red). Because the sensors must be in series, the wire is cut and joined at positions marked with orange dots.*

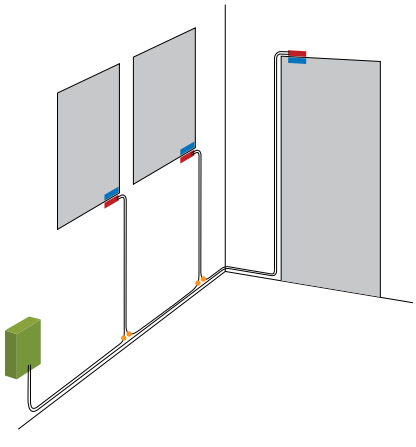

Figure 3-113. *In an installation involving two windows and a door, the magnetic components of the sensors (blue rectangles) could be placed as shown, while the switches (dark red) are located alongside them.*

Figure 3-114. *The intrusion alarm completed and in its project box.*

Now deal with the power supply. Use your AC adapter, set to 12 volts, hooked up to your type N power plug, or attach the power plug to a 12-volt alarm battery.

If you use a battery, be especially careful that the wire leading to the center terminal of your power plug is positive! A 12-volt battery can deliver substantial current, which can fry your components if you connect it the wrong way around. It would be a shame to destroy your entire project at the very last step.

The only remaining task is to label the switch, button, power socket, and binding posts on the alarm box. You know that the switch turns the power on and off, and the button tests the circuit and the noisemaker, but no one else knows, and you might want to allow a guest to use your alarm while you're away. For that matter, months or years from now, you may forget some details. Will you remember that the power source for this unit should be 12 volts?

Labeling really is a good idea. But as you can see in Figure 3-114, I haven't quite gotten around to it for the box that I built.

Conclusion

The alarm project has taken you through the basic steps that you will usually follow any time you develop something:

1. Draw a schematic and make sure that you understand it.
2. Modify it to fit the pattern of conductors on a breadboard.
3. Install components on the breadboard and test the basic functions.
4. Modify or enhance the circuit, and retest.
5. Transfer to perforated board, test, and trace faults if necessary.
6. Add switches, buttons, power jack, and plugs or sockets to connect the circuit with the outside world.
7. Mount everything in a box (and add labeling).

While going through this sequence, I hope you've learned the basics of electricity, along with some simple electrical theory, and fundamentals about electronic components. This knowledge should enable you to move on to the much more powerful realm of integrated circuit—which I'll cover in Chapter 4.

4

Chips, Ahoy!

Before I get into the fascinating topic of integrated circuit (IC) chips, I have to make a confession: some of the things I asked you to do in Chapter 3 could have been done a bit more simply. Does this mean you have been wasting your time? No, I firmly believe that by building circuits with old-fashioned components—capacitors, resistors, and transistors—you acquire the best possible understanding of the principles of electronics. Still, you are going to find that integrated circuit chips, containing dozens, hundreds, or even thousands of transistor junctions, will enable some shortcuts.

IN THIS CHAPTER

Shopping List: Experiments 16 Through 24
Experiment 16: Emitting a Pulse
Experiment 17: Set Your Tone
Experiment 18: Reaction Timer
Experiment 19: Learning Logic
Experiment 20: A Powerful Combination
Experiment 21: Race to Place
Experiment 22: Flipping and Bouncing
Experiment 23: Nice Dice
Experiment 24: Intrusion Alarm Completed

Shopping List: Experiments 16 Through 24

Tools

The only new tool that I recommend using in conjunction with chips is a logic probe. This tells you whether a single pin on a chip has a high or low voltage, which can be helpful in figuring out what your circuit is doing. The probe has a memory function so that it will light its LED, and keep it lit, in response to a pulse that may have been too quick for the eye to see.

Search online and buy the cheapest logic probe you can find. I don't have any specific brand recommendations. The one shown in Figure 4-1 is fairly typical.

Figure 4-1. *A logic probe detects the high or low voltage on each pin of a chip, and reveals pulses that may occur too quickly for you to perceive them with the unaided eye.*

Supplies

Integrated circuit chips

If you buy everything on this shopping list, and you bought basic parts such as resistors and capacitors that were listed previously, you should have everything you need for all the projects in this chapter.

As chips are quite cheap (currently around 50 cents apiece), I suggest you buy extras. This way, if you damage one, you'll have some in reserve. You'll also have a stock for future projects.

Please read the next section, "Fundamentals: Choosing chips," before you begin chip-shopping. Chips should be easily obtainable from all the major electronics retail suppliers, and sometimes are found on eBay shops. Look in the appendix for a complete list of URLs.

FUNDAMENTALS

Choosing chips

Figure 4-2 shows what is often referred to as an integrated circuit (IC). The circuit is actually etched onto a tiny wafer or "chip" of silicon, embedded in a black plastic body, which is properly referred to as the "package." Tiny wires inside the package link the circuit with the two rows of pins on either side. Throughout this book, I will use the word "chip" to refer to the whole object, including its pins, as this is the most common usage.

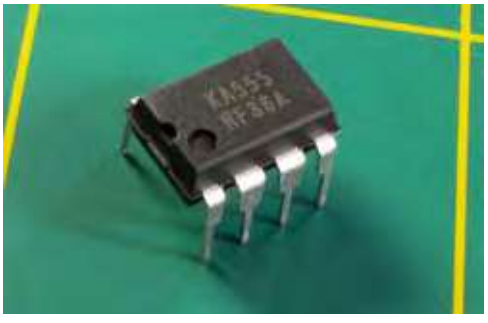

Figure 4-2. *An integrated circuit chip in Plastic Dual-Inline Pin package, abbreviated PDIP, or, more often, DIP.*

The pins are mounted at intervals of 1/10 inch in two rows spaced 3/10 inch apart. This format is known as a Plastic Dual Inline Package, abbreviated PDIP, or, more often, just DIP. The chip in the photograph has four pins in each row; others may have many more. The first thing you need to know, when shopping for chips, is that you'll only be using the DIP package. This book will not be featuring the more modern type, known as "surface-mount," because they're much smaller, more difficult to handle, and require special tools that are relatively expensive. Figure 4-3 shows a size comparison between a 14-pin DIP package and a 14-pin surface-mount package. Many surface-mount chips are even smaller than the one shown.

Just about every chip has a part number printed on it. In Figure 4-2, the part number is KA555. In Figure 4-3, the DIP chip's part number is M74HC00B1, and the surface-mount chip is a 74LVC07AD. You can ignore the second line of numbers and/or letters on each chip, as they are not part of the part number.

Notice in Figure 4-3 that even though the chips look quite different from each other, they both have "74" in their part numbers. This is because both of them are members of the "7400" family of logic chips, which originally had part numbers from 7400 and upward (7400, 7401, 7402, 7403, and so on).

Often they are now referred to as "74xx" chips, where "xx" includes all the members of the family. I'll be using this family a lot, so you need to know how to buy them. I'll give you some advice on that without going into details yet about what the chips actually do.

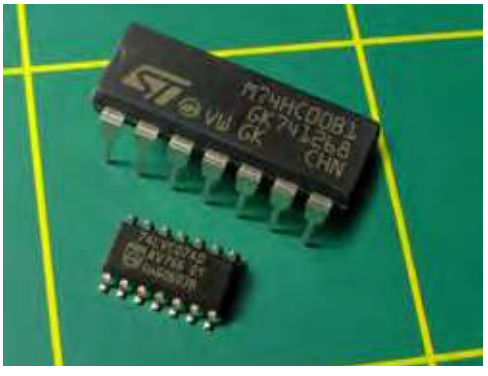

Figure 4-3. *The DIP chip, at the rear, has pins spaced 1/10 inch apart, suitable for insertion in a breadboard or perforated board. It can be soldered without special tools. The small-outline integrated circuit (SOIC) surface-mount chip (foreground) has solder tabs spaced at 1/20 inch. Other surface-mount chips have pins spaced at 1/40 inch or even less (these dimensions are often expressed in millimeters). Surface-mount chips are designed primarily for automated assembly and are difficult to work with manually. In this photo, the yellow lines are 1 inch apart to give you an idea of the scale.*

Take a look at Figure 4-4, which shows how to interpret a typical part number in a 74xx family member. The initial letters identify the manufacturer (which you can ignore, as it really makes no difference for our purposes). Skip the letters until you get to the "74." After that, you find two more letters, which are important. The 74xx family has evolved through many generations, and the letter(s) inserted after the "74" tell you which generation you're dealing with. Some generations have included:

- 74L
- 74LS
- 74C
- 74HC
- 74AHC

And there are more. Generally speaking, subsequent generations tend to be faster or more versatile than previous generations. In this book, for reasons I'll explain later, we are mostly using the HC generation.

FUNDAMENTALS

Choosing chips (continued)

After the letters identifying the generation, you'll find two (sometimes more) numerals. These identify the specific function of the chip. You can ignore any remaining letters and numerals. Looking back at Figure 4-3, the DIP chip part number, M74HC00B1 tells you that it is a chip in the 74xx family, HC generation, with its function identified by numerals 00. The surface-mount chip number, 74LVC07AD, tells you that it is in the 74xx family, LVC generation, with function identified by numerals 07. For convenience we could refer to the first chip as a "74HC00" and the second chip as a "74HC07" because, regardless of their different manufacturers and package sizes, the fundamental behavior of the circuit inside remains the same.

The purpose of this long explanation is to enable you to interpret catalog listings when you go chip shopping. You can search for "74HC00" and the online vendors are usually smart enough to show you appropriate chips from multiple manufacturers, even though there are letters preceding and following the term that you're searched for.

Suppose a circuit requires a 74HC04 chip. If you search for "74HC04" on the website of a parts supplier, you may find versions such as the CD74HC04M96 by Texas Instruments, the 74HC04N by NXP Semiconductors, or MM74HC04N by Fairchild Semiconductor. Because they all have "74HC04" in the middle, any of them will work.

Just be careful that you buy the larger DIP-style package, not the surface-mount package. If the part number has an "N" on the end, you can be sure that it's a DIP package. If there is no "N" on the end, it may or may not be a DIP package, and you will have to check a photo or additional description to make sure. If the part number begins with SS, SO, or TSS, it's absolutely definitely surface-mount, and you don't want it. Many catalogs show photographs of the chips to assist you in buying the right package style.

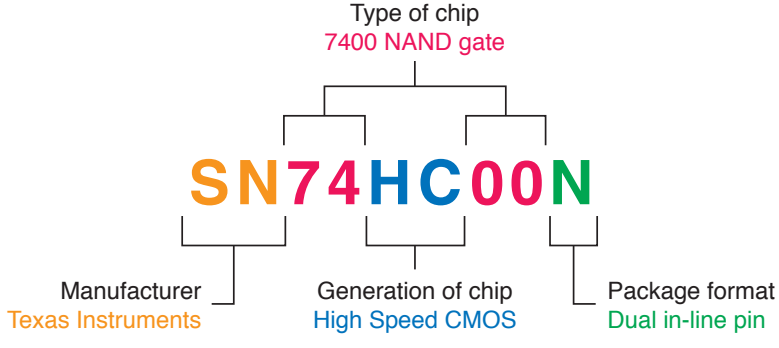

Figure 4-4. *Look for the chip family (74xx, in this case) with the correct generation (HC, in this case) embedded in the number. Make sure you buy the DIP version, not the surface-mount version. The manufacturer is unimportant.*

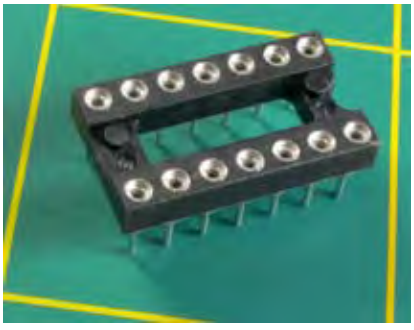

Figure 4-5. *When you're soldering a circuit onto perforated board, sockets eliminate the risk of overheating integrated circuit chips and reduce the risk of zapping them with static electricity, and enable easy replacement.*

Figure 4-6. *An HC series logic chip is rated to deliver only 4mA at each pin. This is inadequate to drive a typical 5 mm LED (right), which is rated for 20mA forward current. Miniature, low-current LEDs (left) will use as little as 1mA in series with a suitable resistor, and are ideal for test circuits in which you want to see the output with a minimum of hassle.*

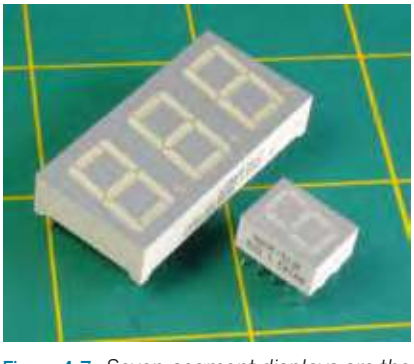

Figure 4-7. *Seven-segment displays are the simplest way to show a numeric output and can be driven directly by some CMOS chips. For finished projects, they are typically mounted behind transparent red acrylic plastic panels.*

Here's your chip list:

- 555 Timer. STMicroelectronics SA555N, Fairchild NE555D, RadioShack TLC555, or similar. Do not get the "CMOS" version of this chip, or any fancy versions such as those of high precision. Buy the cheapest you can find. Quantity: 10. The chip in Figure 4-2 is a 555 timer.
- Logic chips types 74HC00, 74HC02, 74HC04, 74HC08, 74HC32, and 74HC86. Actual part numbers could be M74HC00B1, M74HC02B1, M74HC04B1, and so on, by STMicroelectronics, or SN74HC00N, SN74HC02N, SN74HC04N, and so on, by Texas Instruments. Any other manufacturers are acceptable.
- Remember, each part number should have "HC" in the middle of it, and you want the DIP or PDIP package, not surface-mount. Quantity of each: At least 4.
- 4026 Decade Counter (a chip that counts in tens). Texas Instruments CD-4026BE or similar. Quantity: 4 (you'll need 3, but because this is a CMOS chip sensitive to static electricity, you should have at least one in reserve). Any chip with "4026" in its part number should be OK.
- 74LS92 counter chip, 74LS06 open-collector inverter chip, and 74LS27 triple-input NOR chip. Quantity: 2 of each. Note the "LS" in these part numbers! There will be one experiment in which I want you to use the LS generation instead of the HC generation.

IC sockets

I suggest that you avoid soldering chips directly onto perforated board. If you damage them, they're difficult to remove. Buy some DIP sockets, solder the sockets onto the board, and then plug the chips into the sockets. You can use the cheapest sockets you can find (you don't need gold-plated contacts for our purposes). You will need 8-pin, 14-pin, and 16-pin DIP sockets, such as parts 276-1995, 276-1999, and 276-1998 from RadioShack. See Figure 4-5. Quantity of each: 5 minimum.

Low-power LEDs

The logic chips that you'll be using are not designed to deliver significant power. You'll need to add transistors to amplify their output if you want to drive bright LEDs or relays. Because adding transistors is a hassle, I suggest an alternative: Special low-power LEDs that will draw as little as 1mA, such as the Everlight model T-100 Low Current Red, part number HLMPK150. Figure 4-6 shows a size comparison with a regular 5mm LED. Quantity: 10 (at a minimum).

LED numeric displays

In at least one of our projects, you'll want to illuminate some seven-segment LED numerals. You'll need either three individual numerals, or one package containing three numerals, such as the Kingbright High Efficiency Red Diffused, part number BC56-11EWA, which will be specifically referred to in schematics in this book. If you buy a different seven-segment display, it must be an LED with a "common cathode." (Don't buy liquid-crystal LCD numerals; they require different electronics to drive them.) If you have a choice of power consumption, buy whichever product consumes the least current. See Figure 4-7.

Latching relays

You're going to need a 5-volt latching relay that has two coils, instead of one. The first coil flips the relay one way; the second coil flips it back. The relay consumes no additional power while remaining passively in each state. I suggest the Panasonic DS2E-SL2-DC5V relay. If you buy a different relay, it must be dual-coil latching to run off 5 volts DC, switching at least 1 amp, in a "2 form C" package, to fit your breadboard.

Potentiometers

You'll need 5K, 10K, and 100K linear potentiometers (one of each). Also, a 10K trimmer potentiometer (which you may find described just as a "trimmer"). The manufacturer is unimportant.

Voltage regulators

Because many logic chips require precisely 5 volts DC, you need a voltage regulator to deliver this. The LM7805 does the job. Here again, the chip number will be preceded or followed with an abbreviation identifying the manufacturer and package style, as in the LM7805CT from Fairchild. Any manufacturer will do, but the package should look like the one in Figure 4-8, and if you have a choice, buy a regulator that can deliver at least 1 amp.

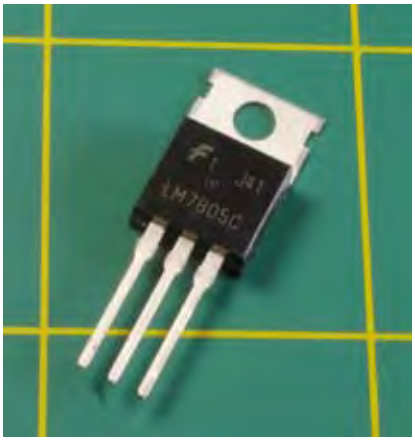

Figure 4-8. *Many integrated circuit chips require a controlled power supply of 5 volts, which can be delivered by this regulator when you apply 7.5 to 9 volts to it. The lefthand pin is for positive input, the center pin is a common ground, and the righthand pin is the 5V output. For currents exceeding 250mA, you should bolt the regulator to a metal heat sink using the hole at the top.*

Tactile switches

These are SPST pushbuttons (momentary switches), usually with four legs. Look for the ALPS part number SKHHAKA010 or any similar item that has pins to fit your breadboard or perforated board. See Figure 4-9.

Figure 4-9. *A tactile switch delivers tactile feedback through your fingertip when you press it. They are almost always SPST pushbuttons designed for mounting in circuit boards with standard 1/10-inch hole spacing.*

12-key numeric keypad

Velleman "12 keys keyboard with common output" (no part number, but has been available through All Electronics under catalog code KP-12). Quantity: 1.

This type of keypad has the same layout as an old-fashioned touchtone phone. It should have at least 13 pins or contacts, 12 of which connect with individual pushbuttons, the thirteenth connecting with the other side of all the pushbuttons. In other words, the last pin is "common" to all of them, and this type of keypad is often described as having a "common output." The type of keypad that you don't want is "matrix-encoded," with fewer than 13 contacts, requiring additional external circuitry. See Figures 4-10 and 4-11. If you can't find the Velleman keypad that I suggest, look carefully at keypad descriptions and photographs to make sure that the one you buy is not matrix-encoded and has a common terminal.

Alternatively, you may substitute 12 cheap SPST NO pushbuttons and mount them in a small project box.

Figure 4-10. *When shopping for a numeric keypad, it should have 12 keys in "touch-tone phone" layout, and should have at least 13 contacts for input/output. The contacts are visible here along the front edge.*

Figure 4-11. *This keypad has insufficient pins and will not work in the circuit in this book.*

BACKGROUND

How chips came to be

The concept of integrating solid-state components into one little package originated with British radar scientist Geoffrey W. A. Dummer, who talked about it for years before he attempted, unsuccessfully, to build one in 1956. The first true integrated circuit wasn't fabricated until 1958 by Jack Kilby, working at Texas Instruments. Kilby's version used germanium, as this element was already in use as a semiconductor. (You'll encounter a germanium diode when I deal with crystal radios in the next chapter of this book.) But Robert Noyce, pictured in Figure 4-12, had a better idea.

Born in 1927 in Iowa, in the 1950s Noyce moved to California, where he found a job working for William Shockley. This was shortly after Shockley had set up a business based around the transistor, which he had coinvented at Bell Labs.

Noyce was one of eight employees who became frustrated with Shockley's management and left to establish Fairchild Semiconductor. While he was the general manager of Fairchild, Noyce invented a silicon-based integrated circuit that avoided the manufacturing problems associated with germanium. He is generally credited as the man who made integrated circuits possible.

Early applications were for military use, as Minuteman missiles required small, light components in their guidance systems. These applications consumed almost all chips produced from 1960 through 1963, during which time the unit price fell from around $1,000 to $25 each, in 1963 dollars.

In the late 1960s, medium-scale integration chips emerged, each containing hundreds of transistors. Large-scale integration enabled tens of thousands of transistors on one chip by the mid-1970s, and today's chips can contain as many as several billion transistors.

Robert Noyce eventually cofounded Intel with Gordon Moore, but died unexpectedly of a heart attack in 1990. You can learn more about the fascinating early history of chip design and fabrication at *http://www.siliconvalleyhistorical.org*.

Figure 4-12. *This picture of Robert Noyce, late in his career, is from the Wikimedia Commons.*

Experiment 16: Emitting a Pulse

I'm going to introduce you to the most successful chip ever made: the 555 timer. As you can find numerous guides to it online, you might question the need to discuss it here, but I have three reasons for doing so:

1. It's unavoidable. You simply have to know about this chip. Some sources estimate that more than 1 billion are still being manufactured annually. It will be used in one way or another in most of the remaining circuits in this book.
2. It provides a perfect introduction to integrated circuits, because it's robust, versatile, and illustrates two functions that we'll be dealing with later: comparators and a flip-flop.
3. After reading all the guides to the 555 that I could find, beginning with the original Fairchild Semiconductor data sheet and making my way through various hobby texts, I concluded that its inner workings are seldom explained very clearly. I want to give you a graphic understanding of what's happening inside it, because if you don't have this, you won't be in a good position to use the chip creatively.

You will need:

- 9-volt power supply.
- Breadboard, jumper wires, and multimeter.
- 5K linear potentiometer. Quantity: 1.
- 555 timer chip. Quantity: 1.
- Assorted resistors and capacitors.
- SPST tactile switches. Quantity: 2.
- LED (any type). Quantity: 1.

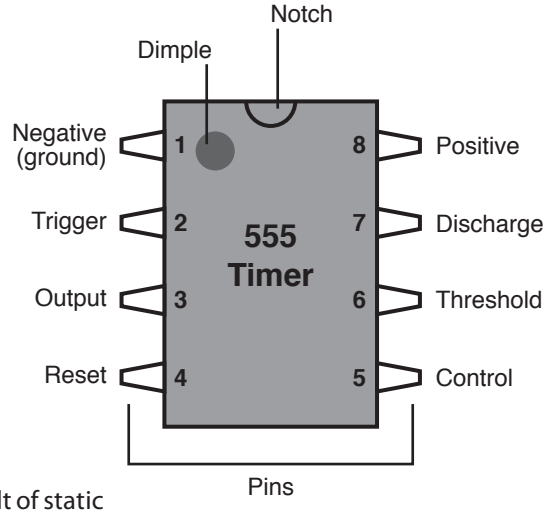

Figure 4-13. *The 555 timer chip, seen from above. Pins on chips are always numbered counterclockwise, from the top-left corner, with a notch in the body of the chip uppermost, or a circular indentation at top-left, to remind you which end is up.*

Procedure

The 555 chip is very robust, but still, in theory, you can zap it with a jolt of static electricity and kill it. Therefore, to be on the safe side, you should ground yourself before handling it. See the "Grounding yourself" warning on page 172 for details. Although this warning primarily refers to the type of chips known as CMOS, which are especially vulnerable, grounding yourself is always a sensible precaution.

Look for a small circular indentation, called the *dimple*, molded into the body of the chip, and turn the chip so that the indentation is at the top-left corner with the pins pointing down. Alternatively, if your chip is of the type with a notch at one end, turn the chip so that the notch is at the top.

The pins on chips are always numbered counterclockwise, starting from the top-left pin (next to the dimple). See Figure 4-13, which also shows the names of the pins on the 555 timer, although you don't need to know most of them just yet.

Insert the chip in your breadboard so that its pins straddle the channel down the center. Now you can easily feed voltages to the pins on either side, and read signals out of them. See Figure 4-14 for a precise guide to placement, in the first project. The timer is identified as "IC1," because "IC" is the customary abbreviation for "Integrated Circuit."

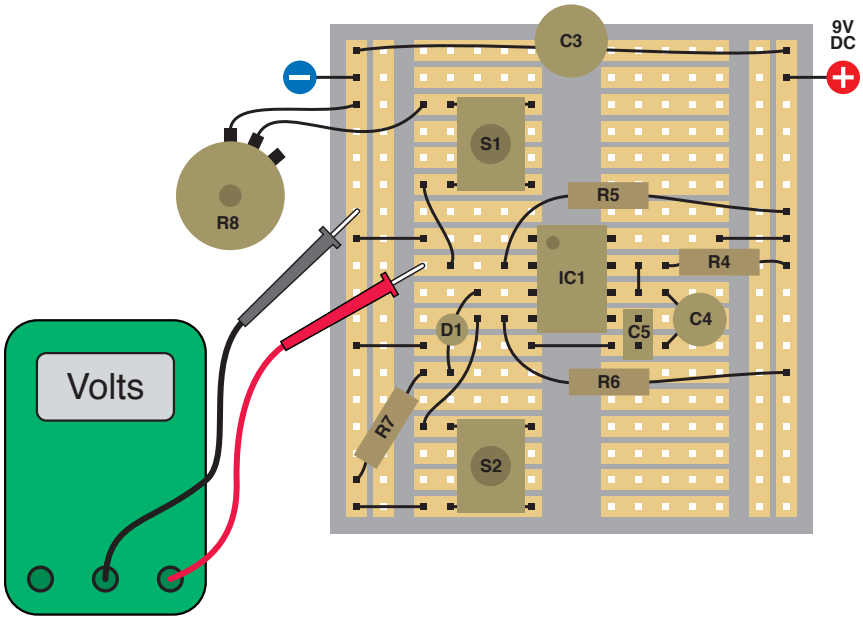

Figure 4-14. *This circuit allows you to explore the behavior of the 555 timer chip. Use your meter to monitor the voltage on pin 2 as shown. There are no resistors labeled R1, R2, or R3 and no capacitors labeled C1 or C2, because they'll be added in a later schematic. Component values in this schematic:*

R4: 100K
R5: 2K2
R6: 10K
R7: 1K
R8: 5K linear potentiometer
C3: 100 µF electrolytic
C4: 47 µF electrolytic
C5: 0.1 µF ceramic
IC1: 555 timer
S1, S2: SPST tactile switches (pushbuttons)
D1: Generic LED

R5 holds the trigger (pin 2) positive until S1 is pressed, which lowers the voltage depending on the setting of potentiometer R8. When the trigger voltage falls below 1/3 of the power supply, the chip's output (pin 3) goes high for a period determined by the values of R4 and C4. S2 resets (zeros) the timer, by reducing the voltage to pin 4, the Reset. C3 smoothes the power supply, and C5 isolates pin 5, the control, so that it won't interfere with the functioning of this test circuit. (We'll use the control pin in a future experiment.)

All integrated circuit chips require a power supply. The 555 is powered with negative voltage applied to pin 1 and positive to pin 8. If you reverse the voltage accidentally, this can permanently damage the chip, so place your jumper wires carefully.

Set your power supply to deliver 9 volts. It will be convenient for this experiment if you supply positive down the righthand side and negative down the lefthand side of the breadboard, as suggested in Figure 4-14. C3 is a large capacitor, at least 100 µF, which is placed across the power supply to smooth it out and provide a local store of charge to fuel fast-switching circuits, as well as to guard against other transient dips in voltage. Although the 555 isn't especially fast-switching, other chips are, and you should get into the habit of protecting them.

Begin with the potentiometer turned all the way counterclockwise to maximize the resistance between the two terminals that we're using, and when you apply the probe from your meter to pin 2, you should measure about 6 volts when you press S1.

Now rotate the potentiometer clockwise and press S1 again. If the LED doesn't light up, keep turning the potentiometer and pressing and releasing the button. When you've turned the potentiometer about two-thirds of the way, you should see the LED light up for just over 5 seconds when you press and release the button. Here are some facts that you should check for yourself:

- The LED will keep glowing after you release the button.
- You can press the button for any length of time (less than the timer's cycle time) and the LED always emits the same length of pulse.
- The timer is triggered by a fall in voltage on pin 2. You can verify this with your meter.
- The LED is either fully on or fully off. You can't see a faint glow when it's off, and the transition from off to on and on to off is very clean and precise.

Check Figure 4-16 to see how the components should look on your breadboard, and then look at the schematic in Figure 4-15 to understand what's happening. I will be adding more components later, which I will be labeling R1, R2, C1, and C2 to be consistent with data sheets that you may see for the 555 timer. Therefore, in this initial circuit the resistors are labeled R4 and up, and capacitors C3 and up.

When S1 (the tactile switch) is open, pin 2 of the 555 timer receives positive power through R5, which is 2K2. Because the input resistance of the timer is very high, the voltage on pin 2 is almost the full 9 volts.

When you press the button, it connects negative voltage through R8, the 5K potentiometer to pin 2. Thus, R8 and R5 form a voltage divider with pin 2 in the middle. You may remember this concept from when you were testing transistors. The voltage between the resistances will change, depending on the values of the resistances.

If R8 is turned up about halfway, it is approximately equal to R5, so the midpoint, connected to pin 2, has about half the 9-volt power supply. But when you turn the potentiometer so that its resistance falls farther, the negative voltage outweighs the positive voltage, so the voltage on pin 2 gradually drops.

If you have clips on your meter leads, you can hook them onto the nearest jumper wires and then watch the meter while you turn the potentiometer up and down and press the button.

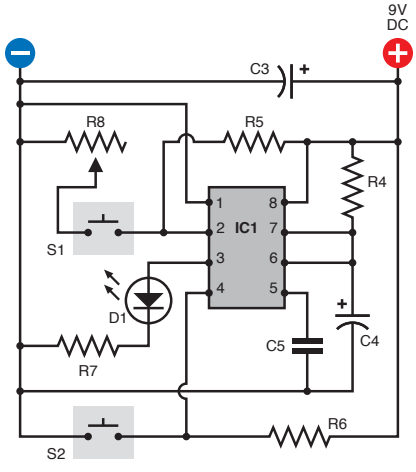

Figure 4-15. *A schematic view of the circuit shown in Figure 4-14. Throughout this chapter, the schematics will be laid out to emulate the most likely placement of components on a breadboard. This is not always the simplest layout, but will be easiest for you to build. Refer to Figure 4-14 for the values of the components.*

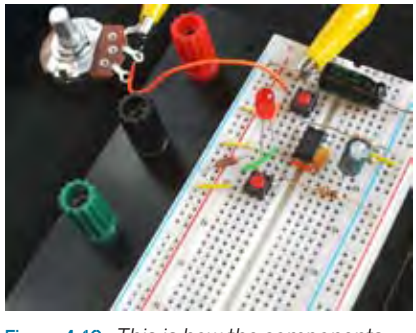

Figure 4-16. *This is how the components look when installed on the breadboard. The alligator clips are attached to a patch cord that links the 100 µF capacitor to the potentiometer. The power supply input is not shown.*

The graphs in Figure 4-17 illustrate what is happening. The upper graph shows the voltage applied to pin 2 by random button-presses, with the potentiometer turned to various values. The lower graph shows that the 555 is triggered if, and only if, the voltage on pin 2 actively drops from above 3 volts to below 3 volts. What's so special about 3 volts? It's one-third of our 9-volt power supply.

Here's the take-home message:

- The output of the 555 (pin 3) emits a *positive* pulse when the trigger (pin 2) drops *below* one-third of the supply voltage.
- The 555 delivers the *same duration* of positive pulse every time (so long as you don't supply a prolonged low voltage on pin 2).
- A *larger* value for R4 or for C4 will *lengthen* the pulse.
- When the output (pin 3) is high, the voltage is almost equal to the supply voltage. When the output goes low, it's almost zero.

The 555 converts the imperfect world around it into a precise and dependable output. It doesn't switch on and off absolutely instantly, but is fast enough to *appear* instant.

Now here's another thing to try. Trigger the timer so that the LED lights up. While it is illuminated, press S2, the second button, which grounds pin 4, the reset. The LED should go out immediately.

When the reset voltage is pulled *low*, the output goes *low*, regardless of what voltage you apply to the trigger.

There's one other thing I want you to notice before we start using the timer for more interesting purposes. I included R5 and R6 so that when you first switch on the timer, it is not emitting a pulse—but is ready to do so. These resistors apply a positive voltage to the trigger and the reset pin, to make sure that the 555 timer is ready to run when you first apply power to it.

As long as the *trigger* voltage is *high*, the timer *will not* emit a pulse. (It emits a pulse when the trigger voltage drops.)

As long as the *reset* voltage is *high*, the timer is *able* to emit a pulse. (It shuts down when the reset voltage drops.)

R5 and R6 are known as "pull-up resistors" because they pull the voltage up. You can easily overwhelm them by adding a direct connection to the negative side of the power supply. A typical pull-up resistor for the 555 timer is 10K. With a 9-volt power supply, it only passes 0.9mA (by Ohm's Law).

Finally, you may be wondering about the purpose of C5, attached to pin 5. This pin is known the "control" pin, which means that if you apply a voltage to it, you can control the sensitivity of the timer. I'll get to this in more detail a little later. Because we are not using this function right now, it's good practice to put a capacitor on pin 5 to protect it from voltage fluctuations and prevent it from interfering with normal functioning.

Make sure you become familiar with the basic functioning of the 555 timer before you continue.

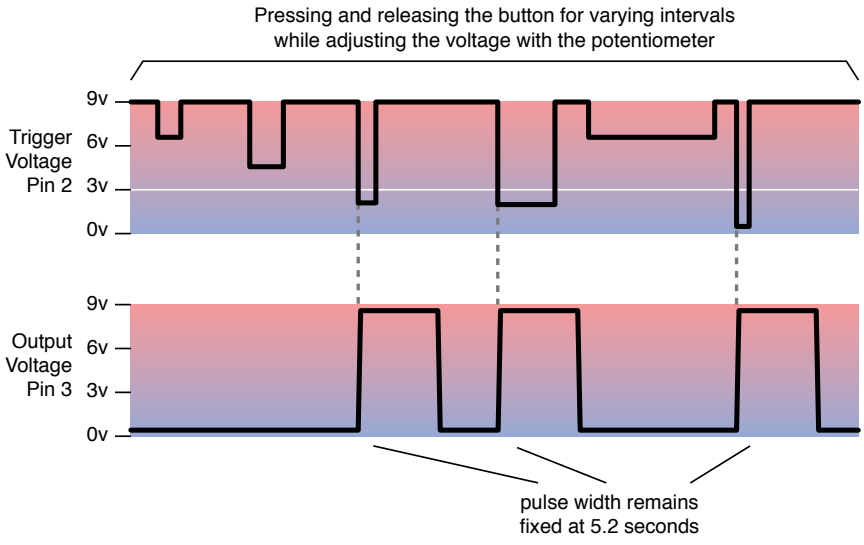

Figure 4-17. *The top graph shows voltage on the trigger (pin 2) when the pushbutton is pressed, for different intervals, at different settings of the potentiometer. The lower graph shows the output (pin 3), which rises until it is almost equal to the power supply, when the voltage on pin 2 drops below 1/3 the full supply voltage.*

FUNDAMENTALS

The following table shows 555 pulse duration in monostable mode:

- Duration is in seconds, rounded to two figures.
- The horizontal scale shows common resistor values between pin 7 and positive supply voltage.
- The vertical scale shows common capacitor values between pin 6 and negative supply voltage.

To calculate a different pulse duration, multiply resistance × capacitance × 0.0011 where resistance is in kilohms, capacitance is in microfarads, and duration is in seconds.

47 µF	0.05	0.11	0.24	0.52	1.1	2.4	5.2	11	24	52
22 µF	0.02	0.05	0.11	0.24	0.53	1.1	2.4	5.3	11	24
10 µF	0.01	0.02	0.05	0.11	0.24	0.52	1.1	2.4	5.2	11
4.7 µF		0.01	0.02	0.05	0.11	0.24	0.52	1.1	2.4	5.2
2.2 µF			0.01	0.02	0.05	0.11	0.24	0.53	1.1	2.4
1.0 µF				0.01	0.02	0.05	0.11	0.24	0.52	1.1
0.47 µF					0.01	0.02	0.05	0.11	0.24	0.52
0.22 µF						0.01	0.02	0.05	0.11	0.24
0.1 µF							0.01	0.02	0.05	0.11
0.047 µF								0.01	0.02	0.05
0.022 µF									0.01	0.02
0.01 µF										0.01
	1K	2K2	4K7	10K	22K	47K	100K	220K	470K	1M

THEORY

Inside the 555 timer: monostable mode

The plastic body of the 555 timer contains a wafer of silicon on which are etched dozens of transistor junctions in a pattern that is far too complex to be explained here. However, I can summarize their function by dividing them into groups, as shown in Figure 4-18. An external resistor and two external capacitors are also shown, labeled the same way as in Figure 4-15.

The negative and positive symbols inside the chip are power sources which actually come from pins 1 and 8, respectively. I omitted the internal connections to those pins for the sake of clarity.

The two yellow triangles are "comparators." Each comparator compares two inputs (at the base of the triangle) and delivers an output (from the apex of the triangle) depending on whether the inputs are similar or different. We'll be using comparators for other purposes later in this book.

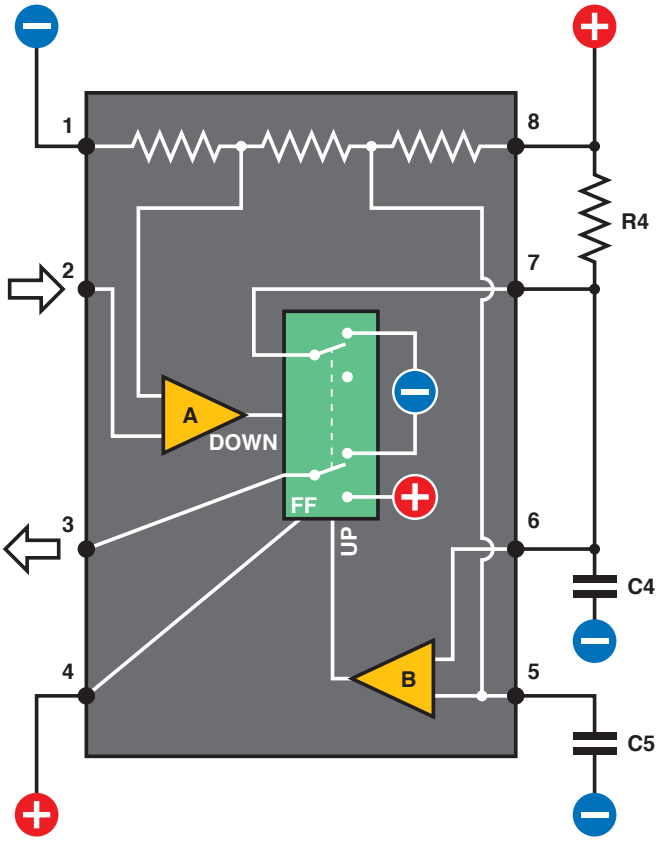

Figure 4-18. *Inside the 555 timer. White lines indicate connections inside the chip. A and B are comparators. FF is a flip-flop which can rest in one state or the other, like a double-throw switch. A drop in voltage on pin 2 is detected by comparator A, which triggers the flip-flop into its "down" position and sends a positive pulse out of pin 3. When C4 charges to 2/3 of supply voltage, this is detected by comparator B, which resets the flip-flop to its "up" position. This discharges C4 through pin 7.*

THEORY

Inside the 555 timer: monostable mode (continued)

The green rectangle, identified as "FF," is a "flip-flop." I have depicted it as a DPDT switch, because that's how it functions here, although of course it is really solid-state.

Initially when you power up the chip, the flip-flop is in its "up" position which delivers low voltage through the output, pin 3. If the flip-flop receives a signal from comparator A, it flips to its "down" state, and flops there. When it receives a signal from comparator B, it flips back to its "up" state, and flops there. The "UP" and "DOWN" labels on the comparators will remind you what each one does when it is activated.

Flip-flops are a fundamental concept in digital electronics. Computers couldn't function without them.

Notice the external wire that connects pin 7 with capacitor C4. As long as the flip-flop is "up," it sinks the positive voltage coming through R4 and prevents the capacitor from charging positively.

If the voltage on pin 2 drops to 1/3 of the supply, comparator A notices this, and flips the flip-flop. This sends a positive pulse out of pin 3, and also disconnects the negative power through pin 7. So now C4 can start charging through R4. While this is happening, the positive output from the timer continues.

As the voltage increases on the capacitor, comparator B monitors it through pin 6, known as the threshold. When the capacitor accumulates 2/3 of the supply voltage, comparator B sends a pulse to the flip-flop, flipping it back into its original state. This discharges the capacitor through pin 7, appropriately known as the discharge pin. Also, the flip-flop ends the positive output through pin 3 and replaces it with a negative voltage. This way, the 555 returns to its original state.

I'll sum up this sequence of events very simply:

1. Initially, the flip-flop grounds the capacitor and grounds the output (pin 3).
2. A drop in voltage on pin 2 to 1/3 the supply voltage or less makes the output (pin 3) positive and allows capacitor C4 to start charging through R4.
3. When the capacitor reaches 2/3 of supply voltage, the chip discharges the capacitor, and the output at pin 3 goes low again.

In this mode, the 555 timer is "monostable," meaning that it just gives one pulse, and you have to trigger it again to get another.

You adjust the length of each pulse by changing the values of R4 and C4. How do you know which values to choose? Check the table on page 157, which gives an approximate idea and also includes a formula so that you can calculate values of your own.

I didn't bother to include pulses shorter than 0.01 second in the table, because a single pulse of this length is usually not very useful. Also I rounded the numbers in the table to 2 significant figures, because capacitor values are seldom more accurate than that.

BACKGROUND

How the timer was born

Back in 1970, when barely a half-dozen corporate seedlings had taken root in the fertile ground of Silicon Valley, a company named Signetics bought an idea from an engineer named Hans Camenzind. It wasn't a huge breakthrough concept—just 23 transistors and a bunch of resistors that would function as a programmable timer. The timer would be versatile, stable, and simple, but these virtues paled in comparison to its primary selling point. Using the emerging technology of integrated circuits, Signetics could reproduce the whole thing on a silicon chip.

This entailed some trial and error. Camenzind worked alone, building the whole thing initially on a large scale, using off-the-shelf transistors, resistors, and diodes on a breadboard. It worked, so then he started substituting slightly different values for the various components to see whether the circuit would tolerate variations during production and other factors such as changes in temperature when the chip was in use. He made at least 10 different versions of the circuit. It took months.

Next came the crafts work. Camenzind sat at a drafting table and used a specially mounted X-Acto knife to scribe his circuit into a large sheet of plastic. Signetics then reduced this image photographically by a ratio of about 300:1. They etched it into tiny wafers, and embedded each of them in a half-inch rectangle of black plastic with the product number printed on top. Thus, the 555 timer was born.

It turned out to be the most successful chip in history, both in the number of units sold (tens of billions and counting) and the longevity of its design (unchanged in almost 40 years). The 555 has been used in everything from toys to spacecraft. It can make lights flash, activate alarm systems, put spaces between beeps, and create the beeps themselves.

Today, chips are designed by large teams and tested by simulating their behavior using computer software. Thus, chips inside a computer enable the design of more chips. The heyday of solo designers such as Hans Camenzind is long gone, but his genius lives inside every 555 timer that emerges from a fabrication facility. (If you'd like to know more about chip history, see *http://www.semiconductormuseum.com/Museum_Index.htm*.)

Figure 4-13. *Hans Camenzind, inventor and developer of the 555 timer chip for Signetics.*

FUNDAMENTALS

Why the 555 is useful

In its monostable mode (which is what you just saw), the 555 will emit a single pulse of fixed (but programmable) length. Can you imagine some applications? Think in terms of the pulse from the 555 controlling some other component. A motion sensor on an outdoor light, perhaps. When an infra-red detector "sees" something moving, the light comes on for a specific period—which can be controlled by a 555.

Another application could be a toaster. When someone lowers a slice of bread, a switch will close that triggers the toasting cycle. To change the length of the cycle, you could use a potentiometer instead of R4 and attach it to the external lever that determines how dark you want your toast. At the end of the toasting cycle, the output from the 555 would pass through a power transistor, to activate a solenoid (which is like a relay, except that it has no switch contacts) to release the toast.

Intermittent windshield wipers could be controlled by a 555 timer—and on earlier models of cars, they actually were.

And what about the burglar alarm that was described at the end of Chapter 3? One of the features that I listed, which has not been implemented yet, is that it should shut itself off after a fixed interval. We can use the change of output from a 555 timer to do that.

The experiment that you just performed seemed trivial, but really it implies all kinds of possibilities.

555 timer limits

1. The timer can run from a stable voltage source ranging from 5 to 15 volts.
2. Most manufacturers recommend a range from 1K to 1M for the resistor attached to pin 7.
3. The capacitor value can go as high as you like, if you want to time really long intervals, but the accuracy of the timer will diminish.
4. The output can deliver as much as 100mA at 9 volts. This is sufficient for a small relay or miniature loudspeaker, as you'll see in the next experiment.

Beware of Pin-Shuffling!

In all of the schematics in this book, I'll show chips as you'd see them from above, with pin 1 at top left. Other schematics that you may see, on websites or in other books, may do things differently. For convenience in drawing circuits, people shuffle the pin numbers on a chip so that pin 1 isn't necessarily shown adjacent to pin 2.

Look at the schematic in Figure 4-20 and compare it with the one in Figure 4-15. The connections are the same, but the one in Figure 4-20 groups pins to reduce the apparent complexity of the wiring.

"Pin shuffling" is common because circuit-drawing software tends to do it, and on larger chips, it is necessary for functional clarity of the schematic (i.e., logical groupings of pin names versus physical groupings on memory chips, for example). When you're first learning to use chips, I think it's easier to understand a schematic that shows the pins in their actual positions. So that's the practice I will be using here.

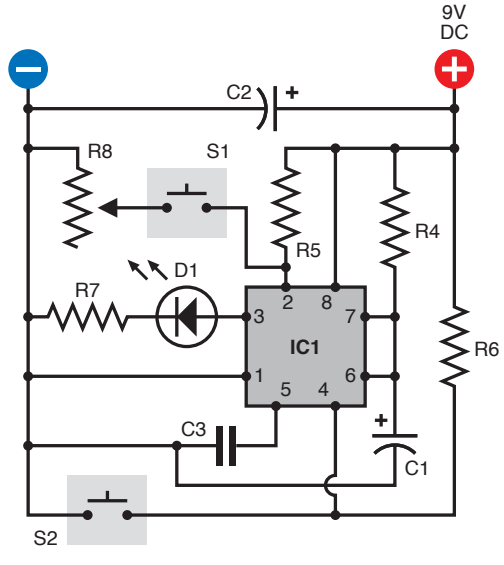

Figure 4-20. *Many people draw schematics in which the pin numbers on a chip are shuffled around to make the schematic smaller or simpler. This is not helpful when you try to build the circuit. The schematic here is for the same circuit as in Figure 4-15. This version would be harder to recreate on a breadboard.*

Experiment 17: Set Your Tone

I'm going to show you two other ways in which the 555 timer can be used.

You will need the same items as in Experiment 16, plus:

- Additional 555 timer chip. Quantity: 1.
- Miniature loudspeaker. Quantity: 1.
- 100K linear potentiometer. Quantity: 1.

Procedure

Leave the components from Experiment 16 where they are on the breadboard, and add the next section below them, as shown in Figures 4-21 and 4-22. Resistor R2 is inserted between pins 6 and 7, instead of the jumper wire that shorted the pins together in the previous circuit, and there's no external input to pin 2 anymore. Instead, pin 2 is connected via a jumper wire to pin 6. The easiest way to do this is by running the wire across the top of the chip.

I have omitted the smoothing capacitor from the schematic in Figure 4-22, because I'm assuming that you're running this circuit on the same breadboard as the first, where the previous smoothing capacitor is still active.

A loudspeaker in series with a 100Ω resistor (R3) has been substituted for the LED to show the output from the chip. Pin 4, the reset, is disabled by connecting it to the positive voltage supply, as I'm not expecting to use the reset function in this circuit.

Now what happens when you apply power? Immediately, you should hear noise through the loudspeaker. If you don't hear anything, you almost certainly made a wiring error.

Notice that you don't have to trigger the chip with a pushbutton anymore. The reason is that when C1 charges and discharges, its fluctuating voltage is connected via a jumper wire across the top of the chip to pin 2, the trigger. In this way, the 555 timer now triggers itself. I'll describe this in more detail in the next section "Theory: Inside the 555 timer: astable mode," if you want to see exactly what is going on.

In this mode, the chip is "astable," meaning that it is not stable, because it flips to and fro endlessly, sending a stream of pulses for as long as the power is connected. The pulses are so rapid that the loudspeaker reproduces them as noise.

In fact, with the component values that I specified for R1, R2, and C1, the 555 chip is emitting about 1,500 pulses per second. In other words, it creates a 1.5 KHz tone.

Check the table on page 166 to see how different values for R2 and C1 can create different pulse frequencies with the chip in this astable mode. Note that the table assumes a fixed value of 1K for R1!

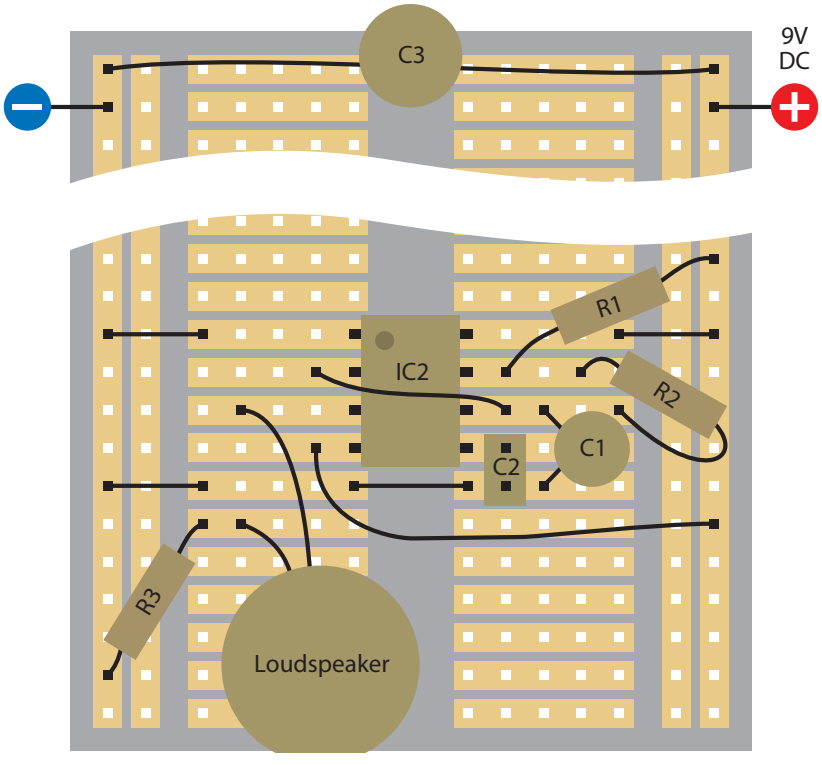

Figure 4-21. *These components should be added on the same breadboard below the components shown in Figure 4-14. Use the following values to test the 555 timer in its astable mode:*

R1: 1K
R2: 10K
R3: 100Ω
C1: 0.047 µF ceramic or electrolytic
C2: 0.1 µF ceramic
IC2: 555 timer

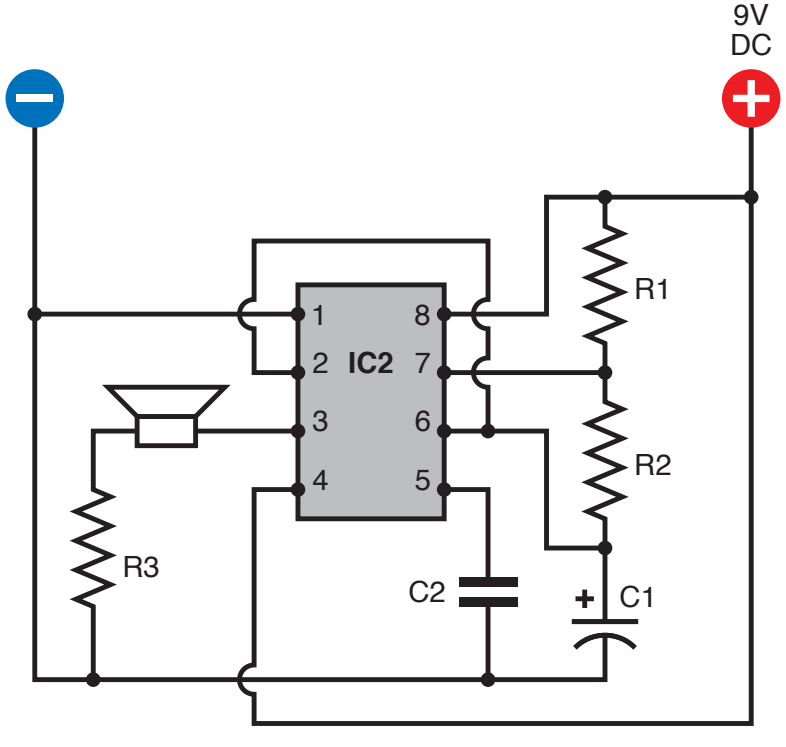

Figure 4-22. *This is the schematic version of the circuit shown in Figure 4-21. The component values are the same.*

THEORY

Inside the 555 timer: astable mode

Here's what is happening now, illustrated in Figure 4-23. Initially, the flip-flop grounds C1 as before. But now the low voltage on the capacitor is connected from pin 7 to pin 2 through an external wire. The low voltage tells the chip to trigger itself. The flip-flop obediently flips to its "on" position and sends a positive pulse to the loudspeaker, while removing the negative voltage from pin 7.

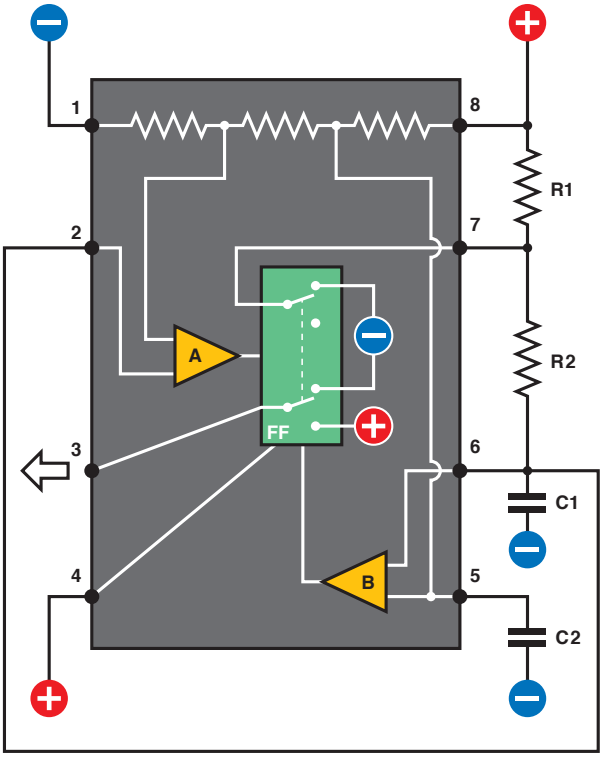

Figure 4-23. *When the 555 timer is used in astable mode, resistor R2 is placed between pin 6 and pin 7, and pin 6 is connected via an external wire to pin 2, so that the timer triggers itself.*

Now C1 starts charging, as it did when the timer was in monostable mode, except that it is being charged through R1 + R2 in series. Because the resistors have low values, and C1 is also small, C1 charges quickly. When it reaches 2/3 full voltage, comparator B takes action as before, discharging the capacitor and ending the output pulse from pin 3.

The capacitor takes longer to discharge than before, because R2 has been inserted between it and pin 7, the discharge pin. While the capacitor is discharging, its voltage diminishes, and is still linked to pin 2. When the voltage drops to 1/3 of full power or less, comparator A kicks in and sends another pulse to the flip-flop, starting the process all over again.

Summing up:

1. In astable mode, as soon as power is connected, the flip-flop pulls down the voltage on pin 2, triggering comparator A, which flips the flip-flop to its "down" position.
2. Pin 3, the output, goes high. The capacitor charges through R1 and R2 in series.
3. When the capacitor reaches 2/3 of supply voltage, the flip-flop goes "up" and the output at pin 3 goes low. The capacitor starts to discharge through R2.
4. When the charge on the capacitor diminishes to 1/3 of full voltage, the pull-down on pin 2 flips the flip-flop again and the cycle repeats.

Unequal on/off cycles

When the timer is running in astable mode, C1 charges through R1 and R2 in series. But when C1 discharges, it dumps its voltage through R2 only. This means that the capacitor charges more slowly than it discharges. While it is charging, the output on pin 3 is high; while it is discharging, the output on pin 3 is low. Consequently the "on" cycle is always longer than the "off" cycle. Figure 4-24 shows this as a simple graph.

If you want the on and off cycles to be equal, or if you want to adjust the on and off cycles independently (for example, because you want to send a very brief pulse to another chip, followed by a longer gap until the next pulse), all you need to do is add a diode, as shown in Figure 4-25.

Now when C1 charges, the electricity flows through R1 as before but takes a shortcut around R2, through diode D1. When C1 discharges, the diode blocks the flow of electricity in that direction, and so the discharge goes back through R2.

THEORY

Inside the 555 timer: astable mode (continued)

R1 now controls the charge time on its own, while R2 controls the discharge time. The formula for calculating the frequency is now:

Frequency = 1440 / ((R1 + R2) × C1)

If you set R1 = R2, you should get almost equal on/off cycles ("almost" because the diode itself imposes a small internal voltage drop of about 0.6V). The exact value depends primarily on the manufacturing process used to make the diode.

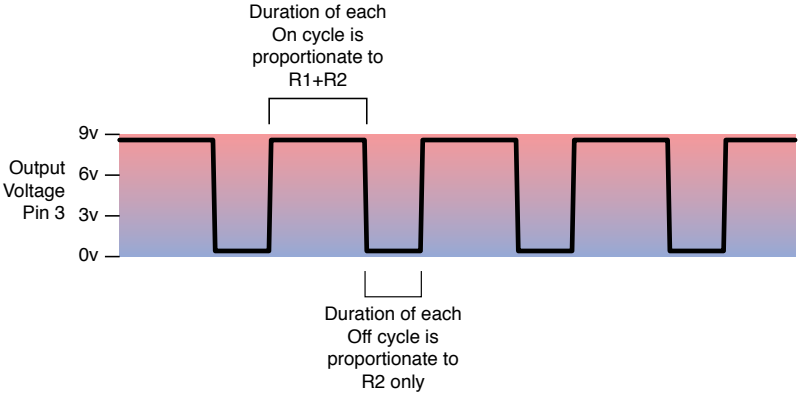

Figure 4-24. *In its usual astable configuration, the timer charges a capacitor through R1+R2 and discharges the capacitor through R2 only. Therefore its output on cycles are longer than its output off cycles.*

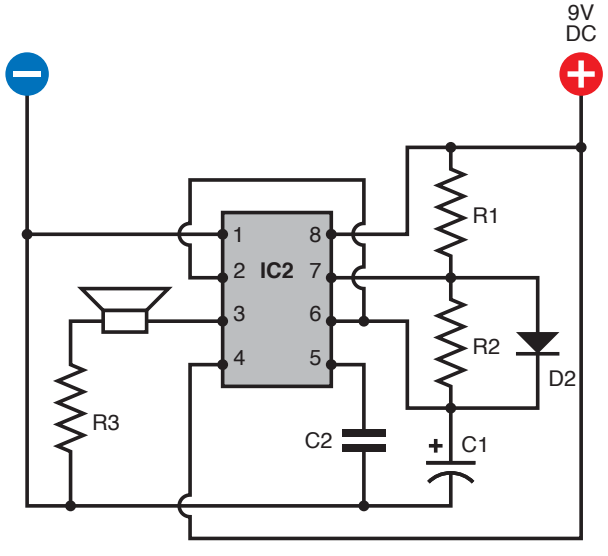

Figure 4-25. *This is a modification of the schematic shown in Figure 4-22. By adding a diode to a 555 timer running in astable mode, we eliminate R2 from the charging cycle of capacitor C1. Now we can adjust the output on cycle with the value of R1, and the output off cycle with the value of R2, so that the on and off durations are independent of each other.*

FUNDAMENTALS

The following table shows 555 timer frequency in astable mode:

- Frequency is in pulses per second, rounded to two figures.
- The horizontal scale shows common resistor values for R2.
- The vertical scale shows common capacitor values for C1. Resistor R1 is assumed to be 1K.
- Resistor R1 is assumed to be 1K.

To calculate a different frequency: double R2, add the product to R1, multiply the sum by C1, and divide the result into 1440. Like this:

Frequency = 1440 / ((R1 + 2R2) × C1) cycles per second

In this formula, R1 and R2 are in kilohms, C1 is in microfarads, and the frequency is in hertz (cycles per second). Note that the frequency is measured from the start of one pulse to the start of the next. The duration of each pulse is not the same as the length of time between each pulse. This issue is discussed in the previous section.

47 µF	10	5.7	3.0	1.5	0.7	0.3	0.2	0.1		
22 µF	22	12	6.3	3.1	1.5	0.7	0.3	0.2	0.1	
10 µF	48	27	14	6.9	3.2	1.5	0.7	0.3	0.2	0.1
4.7 µF	100	57	30	15	6.8	3.2	1.5	0.7	0.3	0.2
2.2 µF	220	120	63	31	15	6.9	3.3	1.5	0.7	0.3
1.0 µF	480	270	140	69	32	15	7.2	3.3	1.5	0.7
0.47 µF	1,000	570	300	150	68	32	15	7	3.3	1.5
0.22 µF	2,200	1,200	630	310	150	69	33	15	7	3.3
0.1 µF	4,800	2,700	1,400	690	320	150	72	33	15	7.2
0.047 µF	10,000	5,700	3,000	1,500	680	320	150	70	33	15
0.022 µF	22,000	12,000	6,300	3,100	1,500	690	330	150	70	33
0.01 µF	48,000	27,000	14,000	6,900	3,200	1,500	720	330	150	72
	1K	2K2	4K7	10K	22K	47K	100K	220K	470K	1M

Astable Modifications

In the circuits shown in Figures 4-22 or 4-25, if you substitute a 100K potentiometer for R2, you can adjust the frequency up and down by turning the shaft.

Another option is to "tune" the timer by using pin 5, the control, as shown in the Figure 4-26. Disconnect the capacitor that was attached to that pin and substitute the series of resistors shown. R9 and R11 are both 1K resistors, either side of R10, which is a 100K potentiometer. They ensure that pin 5 always has at least 1K between it and the positive and negative sides of the power supply. Connecting it directly to the power supply won't damage the timer, but will prevent it from generating audible tones. As you turn the potentiometer to and fro, the frequency will vary over a wide range. If you want to generate a very specific frequency, a trimmer potentiometer can be used instead.

A primary advantage of using pin 5 to adjust frequency is that you can control it remotely. Take the output from pin 3 of another 555 timer running slowly in astable mode, and pipe it through a 2K2 resistor to pin 5. Now you get a two-tone siren effect, as one timer controls the other. If, in addition, you add a 100 µF capacitor between pin 5 and ground, the charging and discharging of the capacitor will make the tone slide up and down instead of switching abruptly. I'll describe this in more detail shortly. This leads me to the whole topic of one chip controlling another chip, which will be our last variation on this experiment.

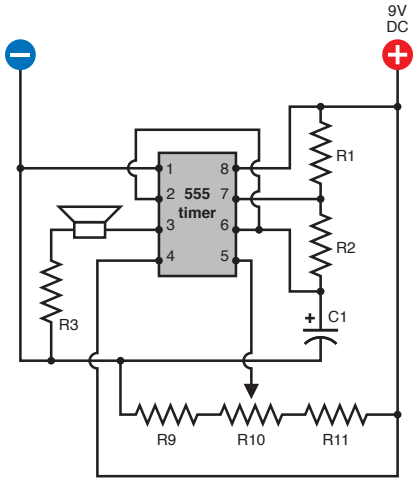

Figure 4-26. *The control (pin 5) is seldom used but can be useful. Varying the voltage on it will adjust the speed of the timer. This circuit enables you to test the behavior of it. Component values:*

R1: 1K
R2: 10K
R3: 100 ohms
R9, R11: 1K
R10: 100K linear potentiometer
C1: 0.047 µF

Chaining Chips

Generally speaking, chips are designed so that they can talk to each other. The 555 couldn't be easier in this respect:

- Pin 3, the output, from one 555 can be connected directly to pin 2, the trigger, of a second 555.
- Alternatively, the output can be sufficient to provide power to pin 8 of a second 555.
- The output is appropriate to control or power other types of chips too.

Figure 4-27 shows these options.

When the output from the first 555 goes high, it is about 70 to 80% of its supply voltage. In other words, when you're using a 9V supply, the high output voltage is at least 6 volts. This is still above the minimum of 5V that the second chip needs to trigger its comparator, so there's no problem.

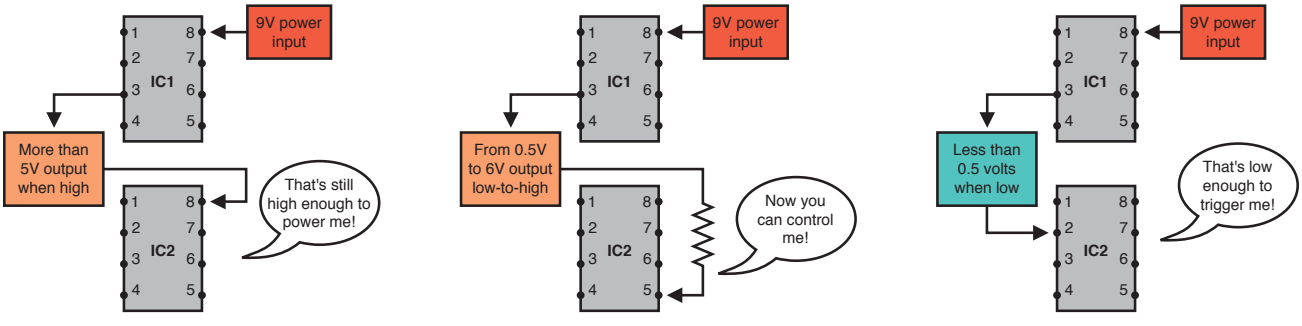

Figure 4-27. *Three ways to chain 555 timers together. The output of IC1 can power a second timer, or adjust its control voltage, or activate its trigger pin.*

You can chain together the two 555 timers that you already have on your breadboard. Figure 4-28 shows how to connect the two circuits that were shown previously in Figures 4-15 and 4-22. Run a wire from pin 3 (the output) of the first chip to pin 8 (the positive power supply) of the second chip, and disconnect the existing wire connecting pin 8 to your power supply. The new wire is shown in red. Now when you press the button to activate the first chip, its output powers the second chip.

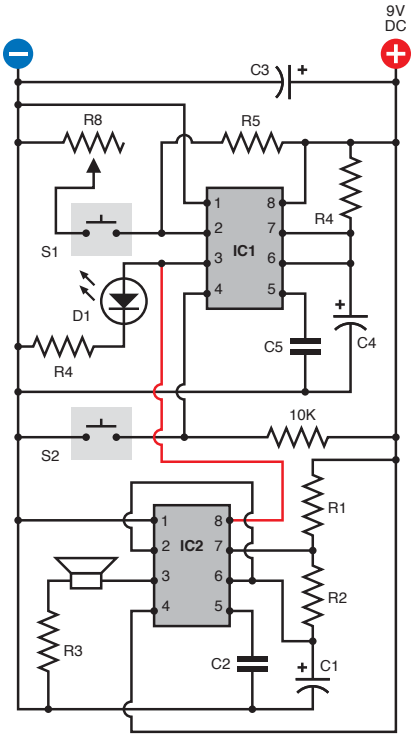

Figure 4-28. *You can combine the two circuits shown in Figures 4-15 and 4-22 simply by disconnecting the wire that provides power to pin 8 of the second timer, and running a substitute wire (shown in red).*

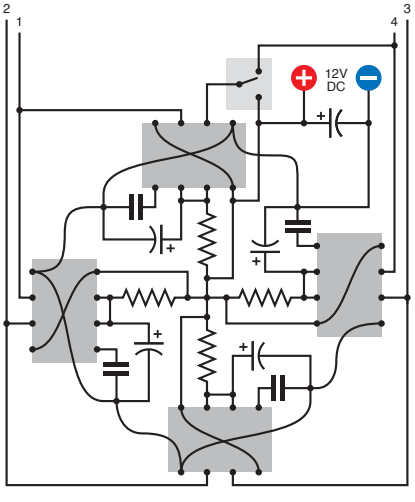

Figure 4-29. *Four 555 timers, chained together in a circle, can flash a series of four sets of LEDs in sequence, like Christmas lights or a movie marquee.*

You can also use the output from one chip to trigger another (i.e., you can connect pin 3 from the first chip to pin 2 of the second). When the output from the first chip is low, it's less than half a volt. This is well below the threshold that the second chip requires to be activated. Why would you want to do this? Well, you might want to have both timers running in monostable mode, so that the end of a high pulse from the first one triggers the start of a high pulse in the second one. In fact, you could chain together as many timers as you like in this way, with the last one feeding back and triggering the first one, and they could flash a series of LEDs in sequence, like Christmas lights. Figure 4-29 shows how four timers could be linked this way, in a configuration that would occupy minimal space (and would be wired point-to-point on perforated board, not on breadboard-format board). Each of the outputs numbered 1 through 4 would have about enough power to run maybe 10 LEDs, if you used relatively high load resistors to limit their current.

Incidentally, you can reduce the chip count (the number of chips) by using two 556 timers instead of four 555 timers. The 556 contains a pair of 555 timers in one package. But because you have to make the same number of external connections (other than the power supply), I haven't bothered to use this variant.

You can even get a 558 timer that contains four 555 circuits, all preset to function in astable mode. I decided not to use this chip, because its output behaves differently from a normal 555 timer. But you can buy a 558 timer and play with it if you wish. It is ideal for doing the "chain of four timers" that I suggested previously. The data sheet even suggests this.

Lastly, going back to the idea of modifying the frequency of a 555 timer in astable mode, you can chain two timers, as shown in Figure 4-30. The red wire shows the connection from the output of the first timer to the control pin of the second. The first timer has now been rewired in astable mode, so that it creates an oscillating on/off output around four times per second. This output flashes the LED (to give you a visual check of what's going on) and feeds through R7 to the control pin of the second timer.

But C2 is a large capacitor, which takes time to charge through R7. While this happens, the voltage detected by pin 5 slowly rises, so that the tone generated by IC2 gradually rises in pitch. Then IC1 reaches the end of its on cycle and switches itself off, at which point C2 discharges and the pitch of the sound generated by IC2 falls again.

You can tweak this circuit to create all kinds of sounds, much more controllably then when you were using PUT transistors to do the same kind of thing. Here are some options to try:

- Double or halve the value of C2.
- Omit C2 completely, and experiment with the value of R7.
- Substitute a 10K potentiometer for R7.
- Change C4 to increase or decrease the cycle time of IC1.

- Halve the value of R5 while doubling the value of C4, so that the cycle time of IC1 stays about the same, but the On time becomes significantly longer than the Off time.
- Change the supply voltage in the circuit from 9 volts to 6 volts or 12 volts.

Remember, you can't damage a 555 timer by making changes of this kind. Just make sure that the negative side of your power supply goes to pin 1 and the positive side to pin 8.

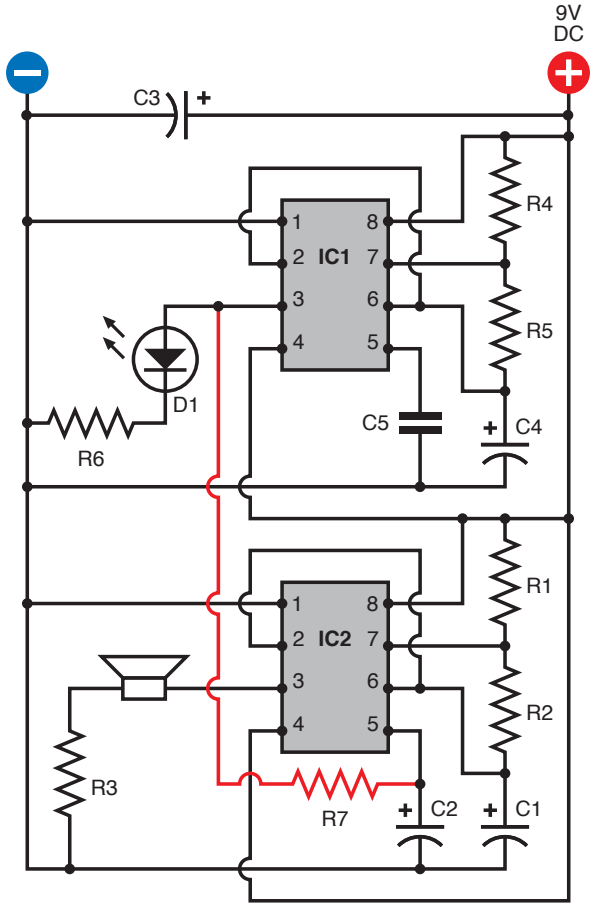

Figure 4-30. *When both timers are astable, but IC1 runs much more slowly than IC2, the output from IC1 can be used to modulate the tone generated by IC2. Note that as this is a substantial modification to the previous schematics, several components have been relabeled. To avoid errors, you may need to remove the old circuit from your breadboard and build this version from scratch. Try these values initially:*

R1, R4, R6, R7: 1K
R2, R5: 10K
R3: 100 ohms
C1: 0.047 µF
C2, C3: 100 µF
C4: 68 µF
C5: 0.1 µF

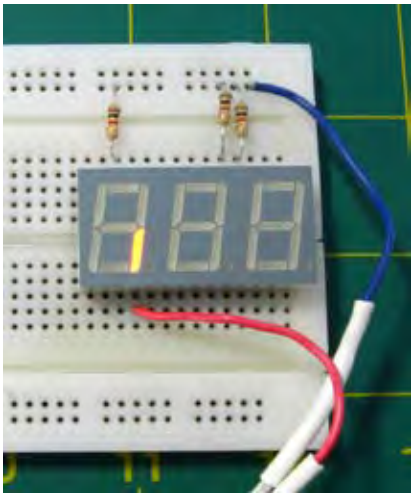

Figure 4-31. *After putting a 1K resistor between the common cathode of the display and the negative supply voltage, you can use the positive supply voltage to illuminate each segment in turn.*

Experiment 18: Reaction Timer

Because the 555 can easily run at thousands of cycles per second, we can use it to measure human reactions. You can compete with friends to see who has the fastest response—and note how your response changes depending on your mood, the time of day, or how much sleep you got last night.

Before going any further, I have to warn you that this circuit will have more connections than others you've tackled so far. It's not conceptually difficult, but requires a lot of wiring, and will only just fit on a breadboard that has 63 rows of holes. Still, we can build it in a series of phases, which should help you to detect any wiring errors as you go.

You will need:

- 4026 chip. Quantity: 4 (really you need only 3, but get another one in case you damage the others).
- 555 timers. Quantity: 3.
- Tactile switches (SPST momentary switches). Quantity: 3.
- Three numeric LEDs, or one 3-digit LED display (see the shopping list at the beginning of this chapter). Quantity: 1.
- Breadboard, resistors, capacitors, and meter, as usual.

Step 1: Display

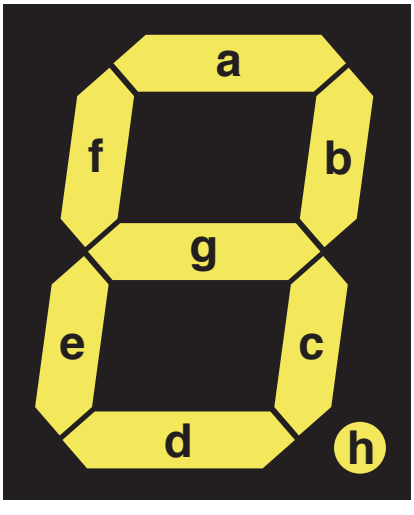

Figure 4-32. *The most basic and common digital numeral consists of seven LED segments identified by letters, as shown here, plus an optional decimal point.*

You can use three separate LED numerals for this project, but I suggest that you buy the Kingbright BC56-11EWA on the shopping list at the beginning of this chapter. It contains three numerals in one big package.

You should be able to plug it into your breadboard, straddling the center channel. Put it all the way down at the bottom of the breadboard, as shown in Figure 4-31. Don't put any other components on the breadboard yet.

Now set your power supply to 9 volts, and apply the *negative* side of it to the row of holes running up the breadboard on the *righthand* side. Insert a 1K resistor between that negative supply and each of pins 18, 19, and 26 of the Kingbright display, which are the "common cathode," meaning the negative connection shared by each set of LED segments in the display. (The pin numbers of the chip are shown in Figure 4-33. If you're using another model of display, you'll have to consult a data sheet to find which pin(s) are designed to receive negative voltage.)

Switch on the power supply and touch the free end of the positive wire to each row of holes serving the display on its left and right sides. You should see each segment light up, as shown in Figure 4-31.

Each numeral from 0 to 9 is represented by a group of these segments. The segments are always identified with lowercase letters *a* through *g*, as shown in Figure 4-32. In addition, there is often a decimal point, and although we won't be using it, I've identified it with the letter *h*.

Check Figure 4-33 showing the Kingbright display, and you'll see I have annotated each pin with its function. You can step down the display with the positive wire from your power supply, making sure that each pin lights an appropriate segment.

Incidentally, this display has two pins, numbered 3 and 26, both labeled to receive negative voltage for the first of the digits. Why two pins instead of one? I don't know. You need to use only one, and as this is a passive chip, it doesn't matter if you leave the unused one unconnected. Just take care not to apply positive voltage to it, which would create a short circuit.

A numeric display has no power or intelligence of its own. It's just a bunch of light-emitting diodes. It's not much use, really, until we can figure out a way to illuminate the LEDs in appropriate groups—which will be the next step.

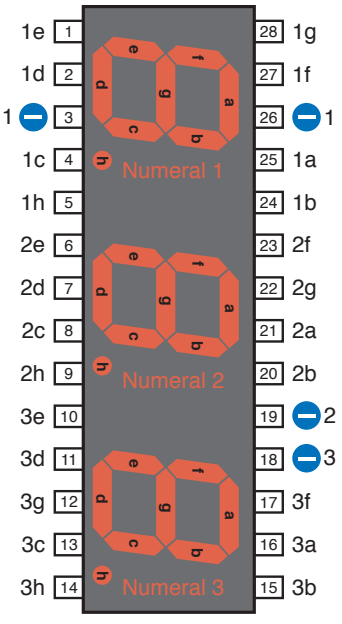

Figure 4-33. *This Kingbright unit incorporates three seven-segment numeric displays in one package, and can be driven by three chained 4026 decade counters. The pin numbers are shown close to the chip. Segments a through g of numeral 1 are identified as 1a through 1g. Segments a through g of numeral 2 are identified as 2a through 2g. Segments a through g of numeral 3 are identified as 3a through 3g.*

Step 2: Counting

Fortunately, we have a chip known as the 4026, which receives pulses, counts them, and creates an output designed to work with a seven-segment display so that it shows numbers 0–9. The only problem is that this is a rather old-fashioned CMOS chip (meaning, Complementary Metal Oxide Semiconductor) and is thus sensitive to static electricity. Check the caution on page 172 before continuing.

Switch off your power supply and connect its wires to the top of the breadboard, noting that for this experiment, we're going to need positive and negative power on both sides. See Figure 4-34 for details. If your breadboard does not already have the columns of holes color-coded, I suggest you use Sharpie markers to identify them, to avoid polarity errors that can fry your components.

The 4026 counter chip is barely powerful enough to drive the LEDs in our display when powered by 9 volts. Make sure you have the chip the right way up, and insert it into the breadboard immediately above your three-digit display, leaving just one row of holes between them empty.

The schematic in Figure 4-35 shows how the pins of the 4026 chip should be connected. The arrows tell you which pins on the display should be connected with pins on the counter.

Figure 4-36 shows the "pinouts" (i.e., the functions of each pin) of a 4026 counter chip. You should compare this with the schematic in Figure 4-35.

Include a tactile switch between the positive supply and pin 1 of the 4026 counter, with a 10K resistor to keep the input to the 4026 counter negative until the button is pressed. Make sure all your positives and negatives are correct, and turn on the power. You should find that when you tap the tactile switch lightly, the counter advances the numeric display from 0 through 9 and then begins all over again from 0. You may also find that the chip sometimes misinterprets your button-presses, and counts two or even three digits at a time. I'll deal with this problem a little further on.

The LED segments will not be glowing very brightly, because the 1K series resistors deprive of them of the power they would really like to receive. Those resistors are necessary to avoid overloading the outputs from the counter.

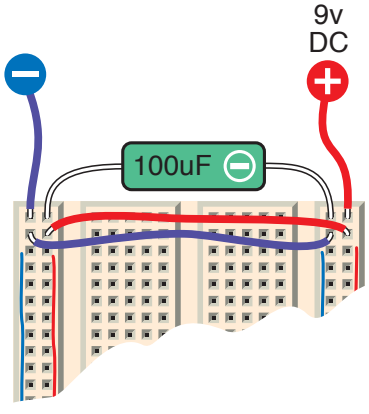

Figure 4-34. *When building circuits around chips, it's convenient to have a positive and negative power supply down each side of your breadboard. For the reaction timer circuit, a 9V supply with a 100 µF smoothing capacitor can be set up like this. If your breadboard doesn't color-code the columns of holes on the left and right sides, I suggest you do that yourself with a permanent marker.*

Grounding Yourself

To avoid the frustration that occurs when you power up a circuit and nothing happens, be sure to take these precautions when you use the older generation of CMOS chips (which often have part numbers from 4000 upward, such as 4002, 4020, and so on):

Chips are often shipped with their legs embedded in black foam. This is electrically conductive foam, and you should keep the chips embedded in it until you are ready to use them.

If the chips are supplied to you in plastic tubes, you can take them out and poke their legs into pieces of conductive foam or, if you don't have any, use aluminum foil. The idea is to avoid one pin on a chip acquiring an electric potential that is much higher than another pin.

While handling CMOS components, grounding yourself is important. I find that in dry weather, I accumulate a static charge merely by walking across a plastic floor-protecting mat in socks that contain some synthetic fibers. You can buy a wrist strap to keep yourself grounded, or simply touch a large metal object, such as a file cabinet, before you touch your circuit board. I am in the habit of working with my socked foot touching a file cabinet, which takes care of the problem.

Never solder a CMOS chip while there is power applied to it.

Grounding the tip of your soldering iron is a good idea.

Better still, don't solder CMOS chips at all. When you're ready to immortalize a project by moving it from a breadboard into perforated board, solder a socket into your perforated board, then push the chip into the socket. If there's a problem in the future, you can unplug the chip and plug in another.

Use a grounded, conductive surface on your workbench. The cheapest way to do this is to unroll some aluminum foil and ground it (with an alligator clip and a length of wire) to a radiator, a water pipe, or a large steel object. I like to use an area of conductive foam to cover my workbench—the same type of foam that is used for packaging chips. However, this foam is quite expensive.

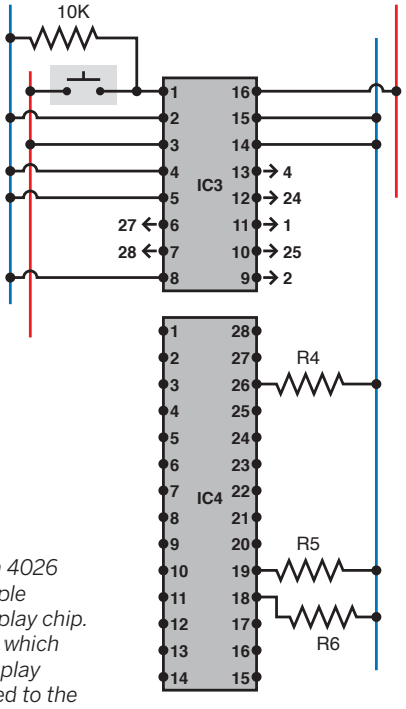

Figure 4-35. *IC3 is a 4026 counter. IC4 is a triple seven-segment display chip. The arrows tell you which pins on the LED display should be connected to the pins on the counter.*

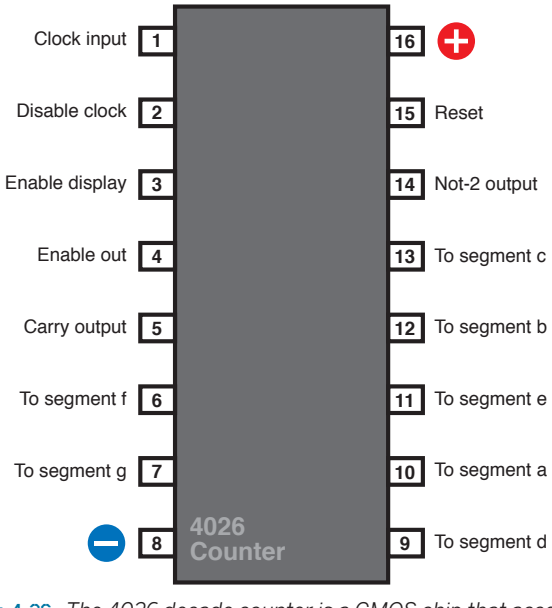

Figure 4-36. *The 4026 decade counter is a CMOS chip that accepts clock pulses on pin 1, maintains a running total from 0 to 9, and outputs this total via pins designed to interface with a seven-segment LED numeric display.*

FUNDAMENTALS

Counters and seven-segment displays

Most counters accept a stream of pulses and distribute them to a series of pins in sequence. The 4026 decade counter is unusual in that it applies power to its output pins in a pattern that is just right to illuminate the segments of a 7-segment numeric display.

Some counters create positive outputs (they "source" current) while others create negative outputs (they "sink" current). Some seven-segment displays require positive input to light up the numbers. These are known as "common cathode" displays. Others require negative input and are known as "common anode" displays. The 4026 delivers positive outputs and requires a common cathode display.

Check the data sheet for any counter chip to find out how much power it requires, and how much it can deliver. CMOS chips are becoming dated, but they are very useful to hobbyists, because they will tolerate a wide range of supply voltage—from 5 to 15 volts in the case of the 4026. Other types of chips are much more limited.

Most counters can source or sink only a few milliamps of output power. When the 4026 is running on a 9-volt power supply, it can source about 4mA of power from each pin. This is barely enough to drive a seven-segment display.

You can insert a series resistor between each output pin of the counter and each input pin of the numeric display, but a simpler, quicker option is to use just one series resistor for each numeral, between the negative-power pin and ground. The experiment that I'm describing uses this shortcut. Its disadvantage is that digits that require only a couple of segments (such as numeral 1) will appear brighter than those that use many segments (such as numeral 8).

If you want your display to look bright and professional, you really need a transistor to drive each segment of each numeral. An alternative is to use a chip containing multiple "op amps" to amplify the current.

When a decade counter reaches 9 and rolls over to 0, it emits a pulse from its "carry" pin. This can drive another counter that will keep track of tens. The carry pin on that counter can be chained to a third counter that keeps track of hundreds, and so on. In addition to decade counters, there are hexadecimal counters (which count in 16s), octal counters (in 8s), and so on.

Why would you need to count in anything other than tens? Consider that the four numerals on a digital clock each count differently. The rightmost digit rolls over when it reaches 10. The next digit to the left counts in sixes. The first hours digit counts to 10, gives a carry signal, counts to 2, and gives another carry signal. The leftmost hours digit is either blank or 1, when displaying time in 12-hour format. Naturally there are counters specifically designed to do all this.

Counters have control pins such as "clock disable," which tells the counter to ignore its input pulses and freeze the display, "enable display," which enables the output from the chip, and "reset," which resets the count to zero.

The 4026 requires a positive input to activate each control pin. When the pins are grounded, their features are suppressed.

To make the 4026 count and display its running total you must ground the "clock disable" and "reset" pins (to suppress their function) and apply positive voltage to the "enable display" pin (to activate the output). See Figure 4-36 to see these pins identified.

Assuming that you succeed in getting your counter to drive the numeric display, you're ready to add two more counters, which will control the remaining two numerals. The first counter will count in ones, the second in tens, and the third in hundreds.

In Figure 4-37, I've continued to use arrows and numbers to tell you which pins of the counters should be connected to which pins of the numeric display. Otherwise, the schematic would be a confusing tangle of wires crossing each other.

At this point, you can give up in dismay at the number of connections—but really, using a breadboard, it shouldn't take you more than half an hour to complete this phase of the project. I suggest you give it a try, because there's

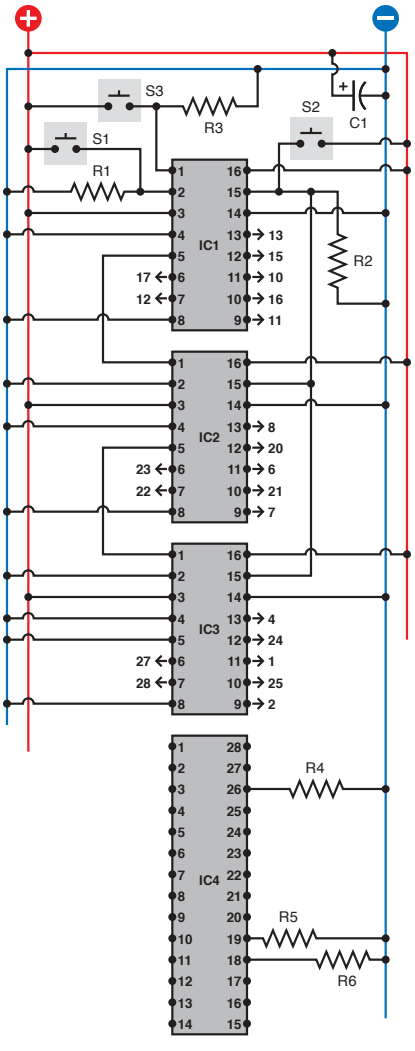

Figure 4-37. *This test circuit, laid out as you would be likely to place it on a breadboard, allows you to trigger a counter manually to verify that the display increments from 000 upward to 999.*

Component values:

All resistors are 1K.
S1, S2, S3: SPST tactile switches, normally open
IC1, IC2, IC3: 4026 decade counter chips
IC4: Kingbright 3-digit common-cathode display
C1: 100 µF (minimum) smoothing capacitor

Wire the output pins on IC1, IC2, and IC3 to the pins on IC4, according to the numbers preceded by arrows. The actual wires have been omitted for clarity. Check for the pinouts of IC4.

something magical about seeing a display count from 000 through 999 "all by itself," and I chose this project because it also has a lot of instructional value.

S1 is attached to the "clock disable" pin of IC1, so that when you hold down this button, it should stop that counter from counting. Because IC1 controls IC2, and IC2 controls IC3, if you freeze IC1, the other two will have to wait for it to resume. Therefore you won't need to make use of their "clock disable" features.

S2 is connected to the "reset" pins of all three counters, so that when you hold down this button, it should set them all to zero.

S3 sends positive pulses manually to the "clock input" pin of the first counter.

S1, S2, and S3 are all wired in parallel with 1K resistors connected to the negative side of the power supply. The idea is that when the buttons are not being pressed, the "pull-down" resistors keep the pins near ground (zero) voltage. When you press one of the buttons, it connects positive voltage directly to the chip, and easily overwhelms the negative voltage. This way, the pins remain either in a definitely positive or definitely negative state. If you disconnect one of these pull-down resistors you are likely to see the numeric display "flutter" erratically. (The numeric display chip has some unconnected pins, but this won't cause any problem, because it is a passive chip that is just a collection of LED segments.)

Always connect input pins of a CMOS chip so that they are either positive or negative. See the "No Floating Pins" warning on the next page.

I suggest that you connect all the wires shown in the schematic first. Then cut lengths of 22-gauge wire to join the remaining pins of the sockets from IC1, IC2, and IC3 to IC4.

Switch on the power and press S2. You'll see three zeros in your numeric display.

Each time you press S3, the count should advance by 1. If you press S2, the count should reset to three zeros. If you hold down S1 while you press S3 repeatedly, the counters should remain frozen, ignoring the pulses from S3.

FUNDAMENTALS

Switch bounce

When you hit S3, I think you'll find that the count sometimes increases by more than 1. This does not mean that there's something wrong with your circuit or your components; you are just observing a phenomenon known as "switch bounce."

On a microscopic level, the contacts inside a pushbutton switch do not close smoothly, firmly, and decisively. They vibrate for a few microseconds before settling; the counter chip detects this vibration as a series of pulses, not just one.

Various circuits are available to "debounce" a switch. The simplest option is to put a small capacitor in parallel with the switch, to absorb the fluctuations; but this is less than ideal. I'll come back to the topic of debouncing later in the book. Switch bounce is not a concern in this circuit, because we're about to get rid of S3 and substitute a 555 timer that generates nice clean bounceless pulses.

Pulse Generation

A 555 timer is ideal for driving a counter chip. You've already seen how to wire a 555 to create a stream of pulses that made noise through a loudspeaker. I'm reproducing the same circuit in Figure 4-38 in simplified form, using the positive and negative supply configuration in the current project. Also I'm showing the connection between pins 2 and 6 in the way that you're most likely to make it, via a wire that loops over the top of the chip.

For the current experiment, I'm suggesting initial component values that will generate only four pulses per second. Any faster than that, and you won't be able to verify that your counters are counting properly.

Install IC5 and its associated components on your breadboard immediately above IC1. Don't leave any gap between the chips. Disconnect S3 and R3 and connect a wire directly between pin 3 (output) of IC5 and pin 1 (clock) of IC1, the topmost counter. Power up again, and you should see the digits advancing rapidly in a smooth, regular fashion. Press S1, and while you hold it, the count should freeze. Release S1 and the count will resume. Press S2 and the counter should reset, even if you are pressing S1 at the same time.

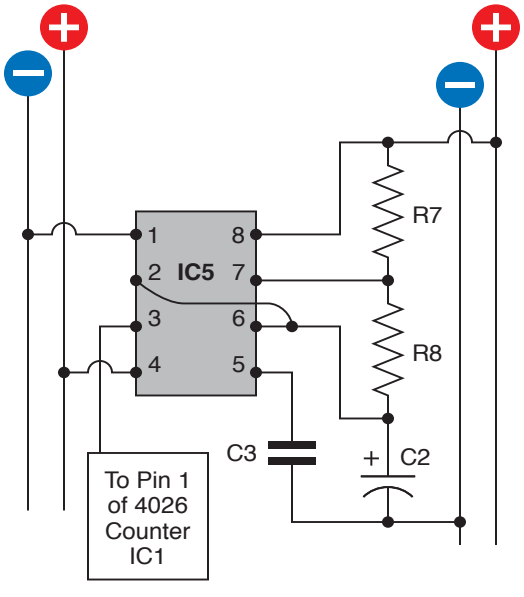

Figure 4-38. *A basic astable circuit to drive the decade counter in the previous schematic. Output is approximately 4 pulses per second.*

R7: 1K
R8: 2K2
C2: 68 µF
C3: 0.1 µF
IC5: 555 timer

No Floating Pins!

A CMOS chip is hypersensitive. Any pin that is not wired either to the supply voltage or to ground is said to be "floating" and may act like an antenna, sensitive to the smallest fluctuations in the world around it.

The 4026 counter chip has a pin labeled "clock disable." The manufacturer's data sheet helpfully tells you that if you give this pin a positive voltage, the chip stops counting and freezes its display. As you don't want to do that, you may just ignore that pin and leave it unconnected, at least while you test the chip. This is a very bad idea!

What the data sheet doesn't bother to tell you (presumably because "everyone knows" such things) is that if you want the clock to run normally, the clock-disable feature itself has to be disabled, by wiring it to negative (ground) voltage. If you leave the pin floating (and I speak from experience), the chip will behave erratically and uselessly.

All input pins must be either positively or negatively wired, unless otherwise specified.

Refinements

Now it's time to remember that what we really want this circuit to do is test a person's reflexes. When the user starts it, we want an initial delay, followed by a signal—probably an LED that comes on. The user responds to the signal by pressing a button as quickly as possible. During the time it takes for the person to respond, the counter will count milliseconds. When the person presses the button, the counter will stop. The display then remains frozen indefinitely, displaying the number of pulses that were counted before the person was able to react.

How to arrange this? I think we need a flip-flop. When the flip-flop gets a signal, it starts the counter running—and keeps it running. When the flip-flop gets another signal (from the user pressing a button), it stops the counter running, and keeps it stopped.

How do we build this flip-flop? Believe it or not, we can use yet another 555 timer, in a new manner known as bistable mode.

FUNDAMENTALS

The bistable 555 timer

Figure 4-39 shows the internal layout of a 555 timer, as before, but the external components on the righthand side have been eliminated. Instead, I'm applying a constant negative voltage to pin 6. Can you see the consequences? Suppose you apply a negative pulse to the trigger (pin 2). Normally when you do this and the 555 starts running, it generates a positive output while charging a capacitor attached to pin 6. When the capacitor reaches 2/3 of the full supply voltage, this tells the 555 to ends its positive output, and it flips back to negative.

Well, if there's no capacitor, there's nothing to stop the timer. Its positive output will just continue indefinitely. However, pin 4 (the reset) can still override everything, so if you apply negative voltage to pin 4, it flips the output to negative. After that, the output will stay negative indefinitely, as it usually does, until you trigger the timer by dropping the voltage to pin 2 again. This will flip the timer back to generating its positive output.

Here's a quick summary of the bistable configuration:

- A negative pulse to pin 2 turns the output positive.
- A negative pulse to pin 4 turns the output negative.
- The timer is stable in each of these states. Its run-time has become infinite.

It's OK to leave pins 5 and 7 of the timer unconnected, because we're pushing it into extreme states where any random signals from those pins will be ignored.

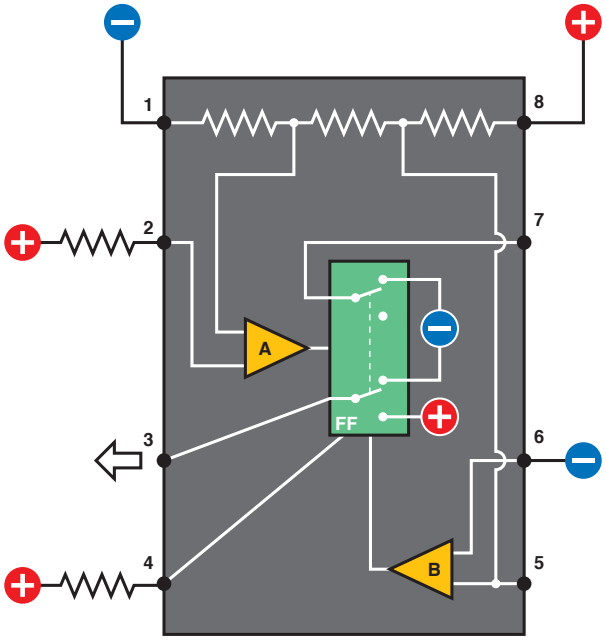

Figure 4-39. *In the bistable configuration, pin 6 of a 555 timer is perpetually negative, so the timer cycle never ends, unless you force it to do so by applying a negative pulse to pin 4 (the reset).*

In bistable mode, the 555 has turned into one big flip-flop. To avoid any uncertainty, we keep pins 2 and 4 normally positive via pull-up resistors, but negative pulses on those pins can overwhelm them when we want to flip the 555 into its opposite state. The schematic for running a 555 timer in bistable mode, controlled by two pushbuttons, is shown in Figure 4-40. You can add this above your existing circuit. Because you're going to attach the output from IC6 to pin 2 of IC1, the topmost counter, you can disconnect S1 and R1 from that pin. See Figure 4-41.

Now, power up the circuit again. You should find that it counts in the same way as before, but when you press S4, it freezes. This is because your bistable 555 timer is sending its positive output to the "clock disable" pin on the counter. The counter is still receiving a stream of pulses from the astable 555 timer, but as long as pin 2 is positive on the counter, the counter simply ignores the pulses.

Now press S5, which flips your bistable 555 back to delivering a negative output, at which point the count resumes.

We're getting close to a final working circuit here. We can reset the count to zero (with S3), start the count (with S5), and wait for the user to stop the count (with S4). The only thing missing is a way to start the count unexpectedly.

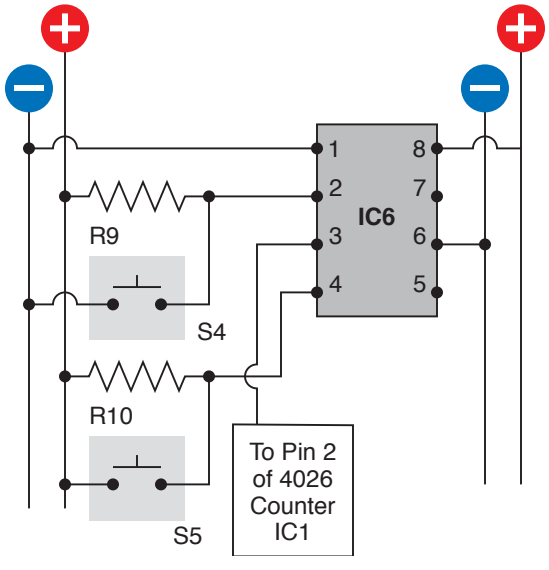

Figure 4-40. *Adding a bistable 555 timer to the reflex tester will stop the counter with a touch of a button, and keep it stopped.*

R9, R10: 1K
IC6: 555 timer

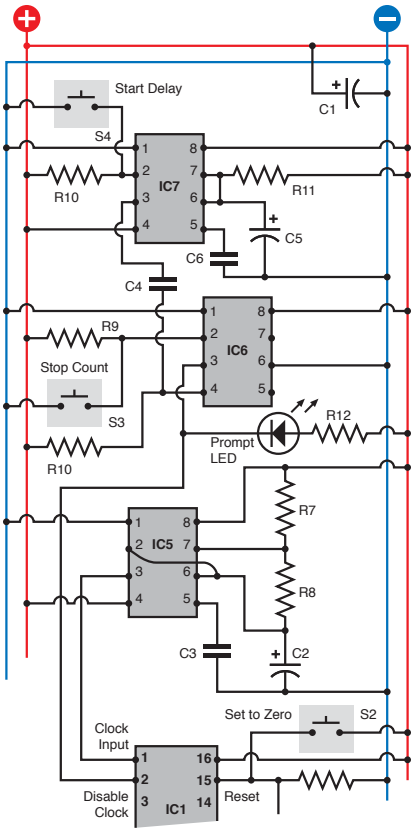

Figure 4-41. *The completed control section of the circuit, to be added above these timers.*

R7, R9, R10, R12: 1K
R8: 2K2
R11: 330K
C1: 100 µF
C2: 68 µF
C3, C4, C6: 0.1 µF
C5: 10 µF
S1, S2, S3: tactile switches
IC5, IC6, IC7: 555 timers

The Delay

Suppose we set up yet another 555 in monostable mode. Trigger its pin 2 with a negative pulse, and the timer delivers a positive output that lasts for, say, 4 seconds. At the end of that time, its output goes back to being negative. Maybe we can hook that positive-to-negative transition to pin 4 of IC6. We can use this instead of switch S5, which you were pressing previously to start the count.

Check the new schematic in Figure 4-41 which adds another 555 timer, IC7 above IC6. When the output from IC7 goes from positive to negative, it will trigger the reset of IC6, flipping its output negative, which allows the count to begin. So IC7 has taken the place of the start switch, S4. You can get rid of S4, but keep the pull-up resistor, R9, so that the reset of IC6 remains positive the rest of the time.

This arrangement works because I have used a capacitor, C4, to connect the output of IC7 to the reset of IC6. The capacitor communicates the sudden change from positive to negative, but the rest of the time it blocks the steady voltage from IC7 so that it won't interfere with IC6.

The final schematic in Figure 4-41 shows the three 555 timers all linked together, as you should insert them above the topmost counter, IC1. I also added an LED to signal the user. Figure 4-42 is a photograph of my working model of the circuit.

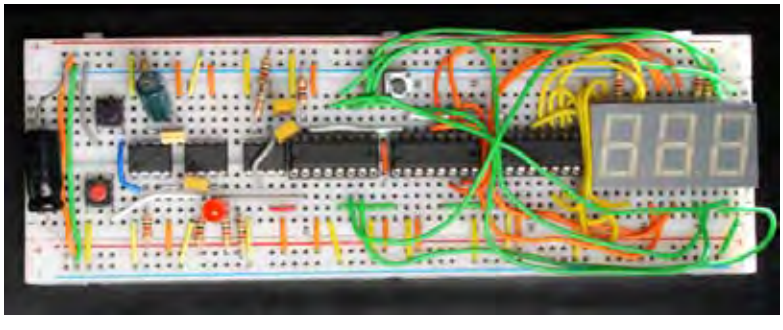

Figure 4-42. *The complete reaction-timer circuit barely fits on a 63-row breadboard.*

Because this circuit is complicated, I'll summarize the sequence of events when it's working. Refer to Figure 4-41 while following these steps:

1. User presses Start Delay button S4, which triggers IC7.
2. IC7 output goes high for a few seconds while C5 charges.
3. IC7 output drops back low.
4. IC7 communicates a pulse of low voltage through C4 to IC6, pin 4.
5. IC 6 output flips to low and flops there.
6. Low output from IC6 sinks current through LED and lights it.
7. Low output from IC6 also goes to pin 2 of IC1.

8. Low voltage on pin 2 of IC1 allows IC1 to start counting.
9. User presses S3, the "stop" button.
10. S3 connects pin 2 of IC6 to ground.
11. IC6 output flips to high and flops there.
12. High output from IC6 turns off the LED.
13. High output from IC6 also goes to pin 2 of IC1.
14. High voltage on pin 2 of IC1 stops it from counting.
15. After assessing the result, user presses S2.
16. S2 applies positive voltage to pin 15 of IC1, IC2, IC3.
17. Positive voltage resets counters to zero.
18. The user can now try again.
19. Meanwhile, IC5 is running continuously throughout.

In case you find a block diagram easier to understand, I've included that, too, in Figure 4-43.

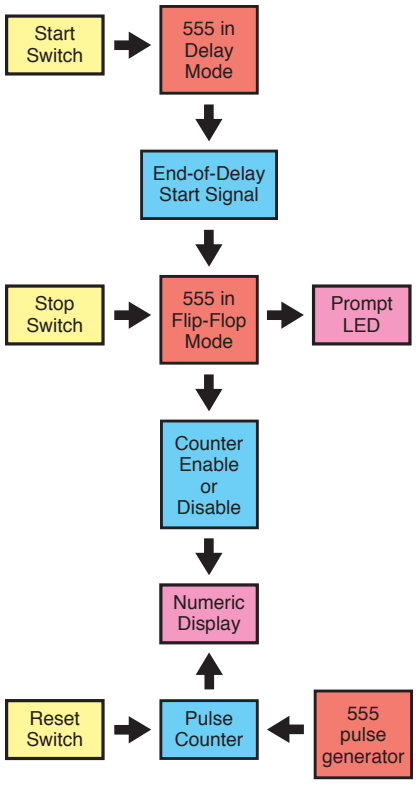

Figure 4-43. *The functions of the reflex tester, summarized as a block diagram.*

Using the Reflex Tester

At this point, you should be able to test the circuit fully. When you first switch it on, it will start counting, which is slightly annoying, but easily fixed. Press S3 to stop the count. Press S2 to reset to zero.

Now press S4. Nothing seems to happen—but that's the whole idea. The delay cycle has begun in stealth mode. After a few seconds, the delay cycle ends, and the LED lights up. Simultaneously, the count begins. As quickly as possible, the user presses S3 to stop the count. The numerals freeze, showing how much time elapsed.

There's only one problem—the system has not yet been calibrated. It is still running in slow-motion mode. You need to change the resistor and capacitor attached to IC5 to make it generate 1,000 pulses per second instead of just three or four.

Substitute a 10K trimmer potentiometer for R8 and a 1 µF capacitor for C2. This combination will generate about 690 pulses per second when the trimmer is presenting maximum resistance. When you turn the trimmer down to decrease its resistance, somewhere around its halfway mark the timer will be running at 1,000 pulses per second.

How will you know exactly where this point is? Ideally, you would attach an oscilloscope probe to the output from IC5. But, most likely, you don't have an oscilloscope, so here are a couple other suggestions.

First remove the 1 µF capacitor at C2 and substitute a 10 µF capacitor. Because you are multiplying the capacitance by 10, you will reduce the speed by 10. The leftmost digit in your display should now count in seconds, reaching 9 and rolling over to 0 every 10 seconds. You can adjust your trimmer potentiometer while timing the display with a stopwatch. When you have it right, remove the 10 µF capacitor and replace the 1 µF capacitor at C2.

The only problem is, the values of capacitors may be off by as much as 10%. If you want to fine-tune your reflex timer, you can proceed as follows.

Disconnect the wire from pin 5 of IC3, and substitute an LED with a 1K series resistor between pin 5 and ground. Pin 5 is the "carry" pin, which will emit a positive pulse whenever IC3 counts up to 9 and rolls over to start at 0 again. Because IC3 is counting tenths of a second, you want its carry output to occur once per second.

Now run the circuit for a full minute, using your stopwatch to see if the flashing LED drifts gradually faster or slower than once per second. If you have a camcorder that has a time display in its viewfinder, you can use that to observe the LED.

If the LED flashes too briefly to be easily visible, you can run a wire from pin 5 to another 555 timer that is set up in monostable mode to create an output lasting for around 1/10 of a second. The output from that timer can drive an LED.

Enhancements

It goes without saying that anytime you finish a project, you see some opportunities to improve it. Here are some suggestions:

1. No counting at power-up. It would be nice if the circuit begins in its "ready" state, rather than already counting. To achieve this you need to send a negative pulse to pin 2 of IC6, and maybe a positive pulse to pin 15 of IC1. Maybe an extra 555 timer could do this. I'm going to leave you to experiment with it.
2. Audible feedback when pressing the Start button. Currently, there's no confirmation that the Start button has done anything. All you need to do is buy a piezoelectric beeper and wire it between the righthand side of the Start button and the positive side of the power supply.
3. A random delay interval before the count begins. Making electronic components behave randomly is very difficult, but one way to do it would be to require the user to hold his finger on a couple of metal contacts. The skin resistance of the finger would substitute for R11. Because the finger pressure would not be exactly the same each time, the delay would vary. You'd have to adjust the value of C5.

Summing Up

This project demonstrated how a counter chip can be controlled, how counter chips can be chained together, and three different functions for 555 timers. It also showed you how chips can communicate with each other, and introduced you to the business of calibrating a circuit after you've finished building it.

Naturally, if you want to get some practical use from the circuit, you should build it into an enclosure with heavier-duty pushbuttons—especially the button that stops the count. You'll find that when people's reflexes are being tested, they are liable to hit the stop button quite hard.

Because this was a major project, I'll follow it up here with some quicker, easier ones as we move into the fascinating world of another kind of integrated circuit: logic chips.

Experiment 19: Learning Logic

You will need:

- Assorted resistors and capacitors.
- 74HC00 quad 2-input NAND chip, 74HC08 quad 2-input AND chip, and LM7805 voltage regulator. Quantity: 1 of each.
- Signal diode, 1N4148 or similar. Quantity: 1.
- Low-current LED. Quantity: 1.
- SPST tactile switches. Quantity: 2.

You're going to be entering the realm of pure digital electronics, using "logic gates" that are fundamental in every electronic computing device. When you deal with them individually, they're extremely easy to understand. When you start chaining them together, they can seem intimidatingly complex. So let's start with them one at a time.

Logic gates are much fussier than the 555 timer or the 4026 counter that you used previously. They demand an absolutely precise 5 volts DC, with no fluctuations or "spikes" in the flow of current. Fortunately, this is easy to achieve: just set up your breadboard with an LM7805 voltage regulator, as shown in the schematic in Figure 4-44 and the photograph in Figure 4-45. The regulator receives 9 volts from your usual voltage supply, and reduces it to 5 volts, with the help of a couple of capacitors. You apply the 9 volts to the regulator, and distribute the 5 volts down the sides of your breadboard instead of the unregulated voltage that you used previously. Use your meter to verify the voltage, and make sure you have the polarity clearly marked.

After installing your regulator, take a couple of tactile switches, two 10K resistors, a low-current LED, and a 1K resistor, and set them around a 74HC00 logic chip as shown in Figure 4-46. You may notice that many of the pins of the chip are shorted together and connected to the negative side of the power supply. I'll explain that in a moment.

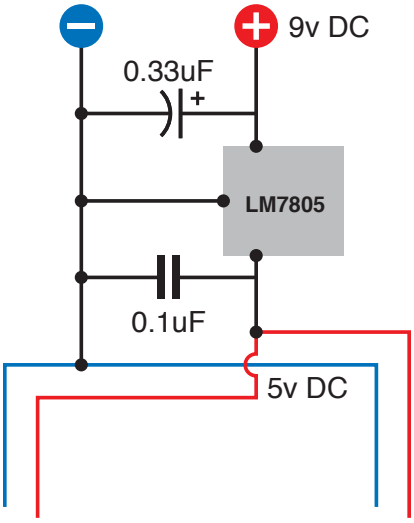

Figure 4-44. *This simple circuit is essential to provide a regulated 5V DC supply for logic chips.*

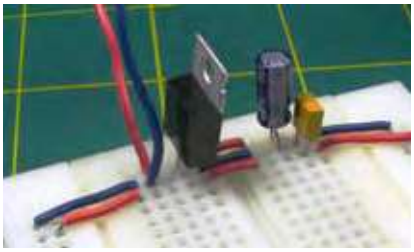

Figure 4-45. *The voltage regulator and its two capacitors can fit snugly at the top of a breadboard. Remember to apply the 9V input voltage at the left pin of the regulator, and distribute the 5V output down the sides of the breadboard.*

FUNDAMENTALS

Voltage regulators

The simplest versions of these little semiconductors accept a higher DC voltage on one pin and deliver a lower DC voltage on another pin, with a third pin (usually in the middle) serving as a common negative, or ground. You should also attach a couple of capacitors to smooth the current, as shown in Figure 4-46.

Typically you can put a 7.5-volt or 9-volt supply on the "input" side of a 5-volt regular, and draw a precise 5 volts from the "output" side. If you're wondering where the extra voltage goes, the answer is, the regulator turns the electricity into heat. For this reason, small regulators (such as the one in Figure 4-8) often have a metal back with a hole in the top. Its purpose is to radiate heat, which it will do more effectively if you bolt it to a piece of aluminum, since aluminum conducts heat very effectively. The aluminum is known as a heat sink, and you can buy fancy ones that have multiple cooling fins.

For our purposes, we won't be drawing enough current to require a heat sink.

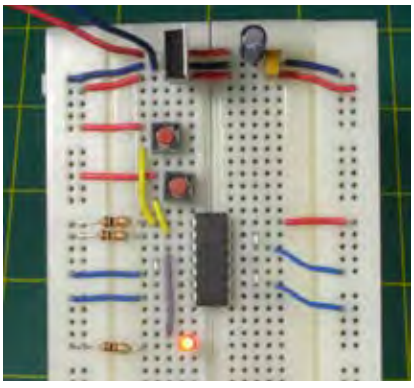

Figure 4-47. *This breadboard layout is exactly equivalent to the schematic in Figure 4-46.*

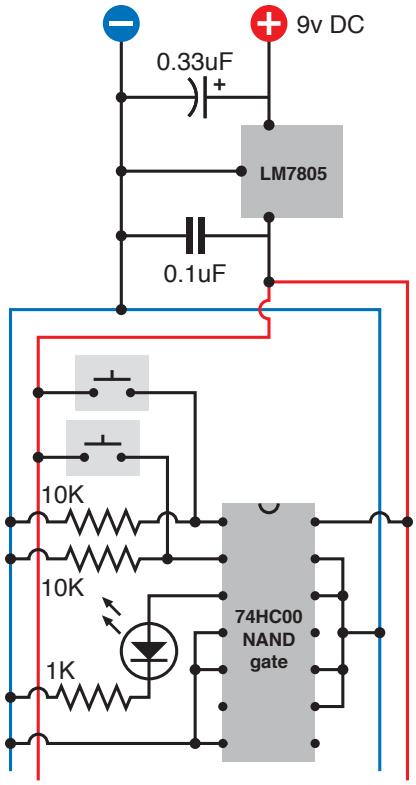

Figure 4-48. *By observing the LED when you press either, both, or neither of the buttons, you can easily figure out the logical function of the NAND gate.*

When you connect power, the LED should light up. Press one of the tactile switches, and the LED remains illuminated. Press the other tactile switch, and again the LED stays on. Now press both switches, and the light should go out.

Pins 1 and 2 are logic inputs for the 74HC00 chip. Initially they were held at negative voltage, being connected to the negative side of the power supply through 10K resistors. But each pushbutton overrides its pull-down resistor and forces the input pin to go positive.

The logic output from the chip, as you saw, is normally positive—but *not* if the first input *and* the second input are positive. Because the chip does a "Not AND" operation, it's known as a NAND logic gate. You can see the breadboard layout in Figure 4-47. Figure 4-48 is a simplified version of the circuit. The U-shaped thing with a circle at the bottom is the logic symbol for a NAND gate. No power supply is shown for it, but in fact all logic chips require a power supply, which enables them to put out more current than they take in. Anytime you see a symbol for a logic chip, try to remember that it has to have power to function.

The 74HC00 actually contains four NAND gates, each with two logical inputs and one output. They are arrayed as shown in Figure 4-49. Because only one gate was needed for the simple test, the input pins of the unused gates were shorted to the negative side of the power supply.

Pin 14 supplies positive power for the chip; pin 7 is its ground pin. Almost all the 7400 family of logic chips use the same pins for positive and negative power, so you can swap them easily.

In fact, let's do that right now. First, disconnect the power. Carefully pull out the 74HC00 and put it away with its legs embedded in conductive foam. Substitute a 74HC08 chip, which is an AND chip. Make sure you have it the right way up, with its notch at the top. Reconnect the power and use the pushbuttons as you did before. This time, you should find that the LED comes on if the first input AND the second input are both positive, but it remains dark otherwise. Thus, the AND chip functions exactly opposite to the NAND chip. Its pinouts are shown in Figure 4-50.

You may be wondering why these things are useful. Soon you'll see that we can put logic gates together to do things such as create an electronic combination lock, or a pair of electronic dice, or a computerized version of a TV quiz show where users compete to answer a question. And if you were really insanely ambitious, you could build an entire computer out of logic gates.

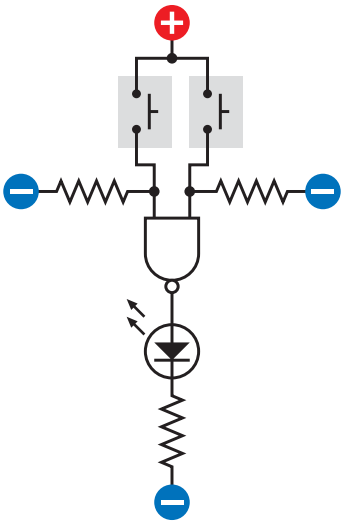

Figure 4-48. *The structure and function of the NAND gate is easier to visualize with this simplified schematic that omits the power supply for the chip and doesn't attempt to place the wires to fit a breadboard layout.*

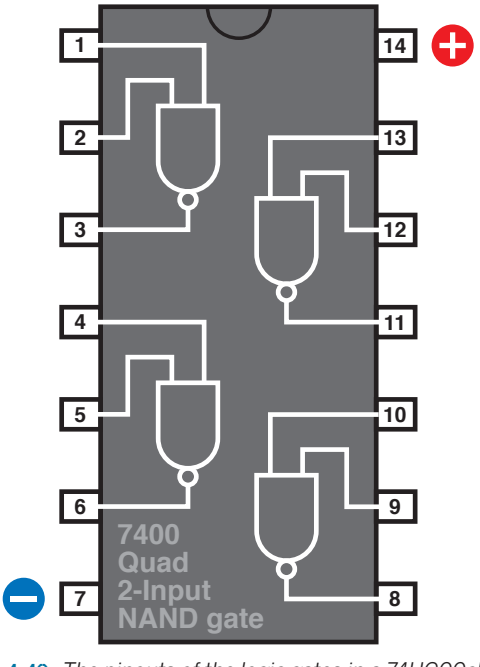

Figure 4-49. *The pinouts of the logic gates in a 74HC00chip.*

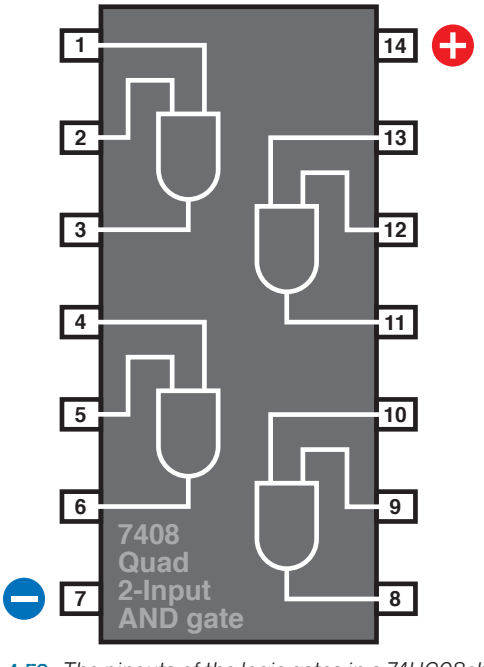

Figure 4-50. *The pinouts of the logic gates in a 74HC08chip.*

BACKGROUND

From Boole to Shannon

George Boole was a British mathematician, born in 1815, who did something that few people are ever lucky enough or smart enough to do: he invented an entirely new branch of mathematics.

Interestingly, it was not based on numbers. Boole had a relentlessly logical mind, and he wanted to reduce the world to a series of true-or-false statements which could overlap in interesting ways. For instance, suppose there is a couple named Ann and Bob who have so little money, they only own one hat. Clearly, if you happen to run into Ann and Bob walking down the street, there are four possibilities: neither of them may be wearing a hat, Ann may be wearing it, or Bob may be wearing it, but they cannot both be wearing it.

The diagram in Figure 4-51 illustrates this. All the states are possible except the one where the circles overlap. (This is known as a Venn diagram. I leave it to you to search for this term if it interests you and you'd like to learn more.) Boole took this concept much further, and showed how to create and simplify extremely complex arrays of logic.

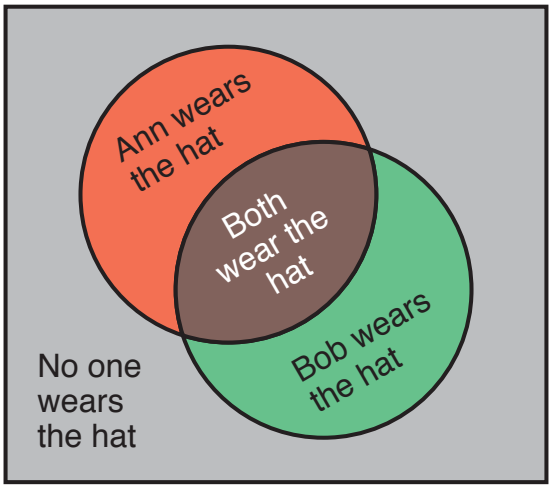

Figure 4-51. *This slightly frivolous Venn diagram illustrates the various possibilities for two people, Ann and Bob, who own only one hat.*

Another way to summarize the hat-wearing situation is to make the "truth table" shown in Figure 4-52. The rightmost column shows whether each combination of propositions can be true. Now check the table in Figure 4-53. It's the same table but uses different labels, which describe the pattern you have seen while using the NAND gate.

Boole published his treatise on logic in 1854, long before it could be applied to electrical or electronic devices. In fact, during his lifetime, his work seemed to have no practical applications at all. But a man named Claude Shannon encountered Boolean logic while studying at MIT in the 1930s, and in 1938 he published a paper describing how Boolean analysis could be applied to circuits using relays. This had immediate practical applications, as telephone networks were growing rapidly, creating complicated switching problems.

BACKGROUND

From Boole to Shannon (continued)

Ann is wearing the hat	Bob is wearing the hat	This combination can be
NO	NO	TRUE
NO	YES	TRUE
YES	NO	TRUE
YES	YES	FALSE

Figure 4-52. *The hat-wearing possibilities can be expressed in a "truth table."*

Input A	Input B	Output
OFF	OFF	ON
OFF	ON	ON
ON	OFF	ON
ON	ON	OFF

Figure 4-53. *The truth-table from can be relabeled to describe the inputs and outputs of a NAND gate.*

A very simple telephone problem could be expressed like this. Suppose two customers in a rural area share one telephone line. If one of them wants to use the line, or the other wants to use it, or neither of them wants to use it, there's no problem. But they cannot both use it at once. You may notice that this is exactly the same as the hat-wearing situation for Ann and Bob.

We can easily draw a circuit using two normally closed relays that creates the desired outcome (see Figure 4-54), but if you imagine a telephone exchange serving many thousands of customers, the situation becomes very complicated indeed. In fact, in Shannon's time, no logical process existed to find the best solution and verify that it used fewer components than some other solution.

Shannon saw that Boolean analysis could be used for this purpose. Also, if you used an "on" condition to represent numeral 1 and an "off" condition to represent numeral 0, you could build a system of relays that could count. And if it could count, it could do arithmetic.

When vacuum tubes were substituted for relays, the first practical digital computers were built. Transistors took the place of vacuum tubes, and integrated circuit chips replaced transistors, leading to the desktop computers that we now take for granted today. But deep down, at the lowest levels of these incredibly complex devices, they still use the laws of logic discovered by George Boole. Today, when you use a search engine online, if you use the words AND and OR to refine your search, you're actually using Boolean operators.

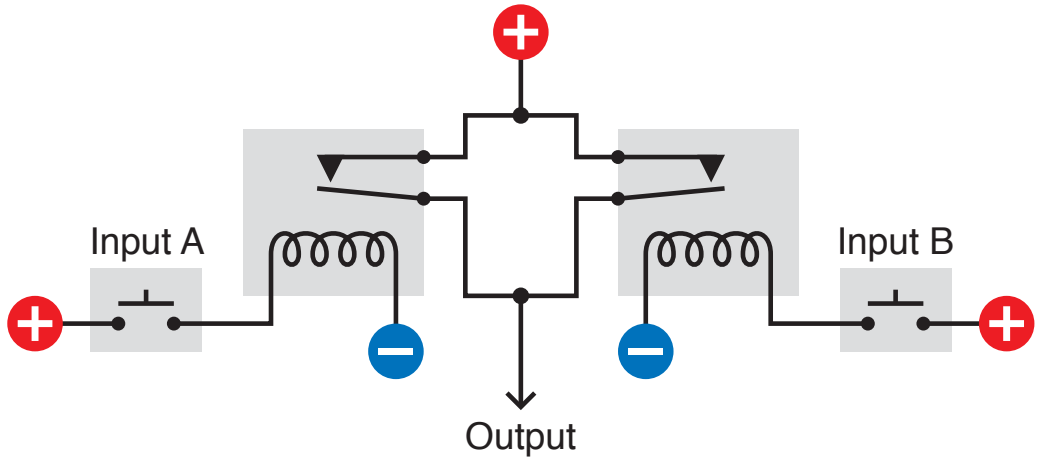

Figure 4-54. *This relay circuit could illustrate the desired logic for two telephone customers wanting to share one line, and its behavior is almost identical to that of the NAND schematic shown in Figure 4-48.*

Figure 4-55. *Ann and Bob attempt to overcome the limitations of Boolean logic.*

ESSENTIALS

Logic gate basics

The NAND gate is the most fundamental building block of digital computers, because (for reasons which I don't have space to explain here) it enables digital addition. If you want to explore more try searching online for topics such as "binary arithmetic" and "half-adder."

Generally, there are seven types of logic gates:

- AND
- NAND
- OR
- NOR
- XOR
- XNOR
- NOT

Of the six two-input gates, the XNOR is hardly ever used. The NOT gate has a single input, and simply gives a negative output when the input is positive or a positive output when the input is negative. The NOT is more often referred to as an "Inverter." The symbols for all seven gates are shown in Figure 4-56.

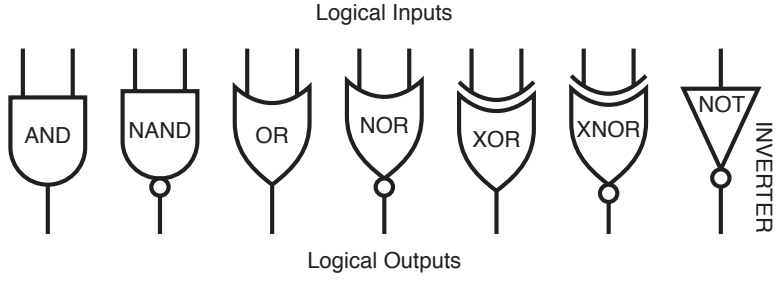

Figure 4-56. *American symbols for the six types of two-input logic gates, and the single-input inverter.*

I've shown the American symbols. Other symbols have been adopted in Europe, but the traditional symbols shown here are the ones that you will usually find, even being used by Europeans. I also show the truth tables, in Figure 4-57, illustrating the logical output (high or low) for each pair of inputs of each type of gate.

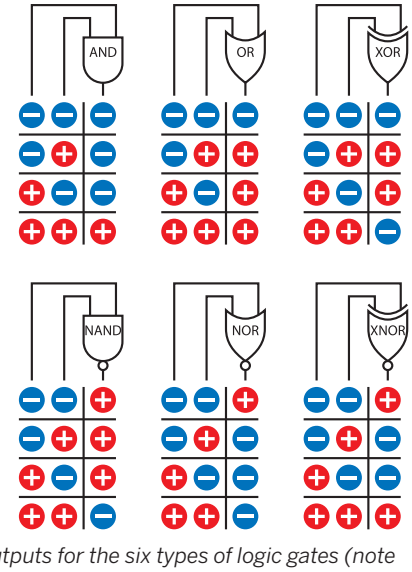

Figure 4-57. *Inputs and corresponding outputs for the six types of logic gates (note that the XNOR gate is seldom used). The minus signs indicate low voltage, close to ground potential. The plus signs indicate higher voltage, close to the positive potential of the power supply in the circuit. The exact voltages will vary depending on other components that may be actively connected.*

ESSENTIALS

Logic gate basics (continued)

If you have difficulty visualizing logic gates, a mechanical comparison may help. You can think of them as being like sliding plates with holes in them, in a bubblegum machine. Two people, A and B, can push the plates. These people are the two inputs, which are considered positive when they are doing something. (Negative logic systems also exist, but are uncommon, so I'm only going to talk about positive systems here.)

The flow of bubblegum represents a flow of positive current. The full set of possibilities is shown in Figures 4-58 through 4-63.

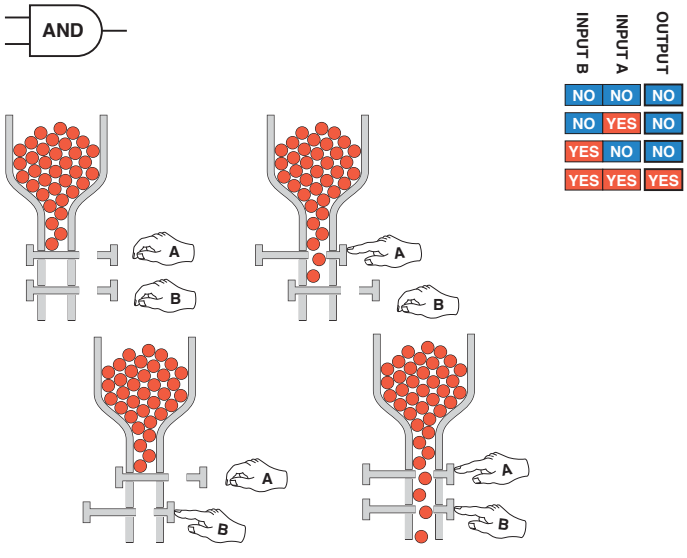

Figure 4-58

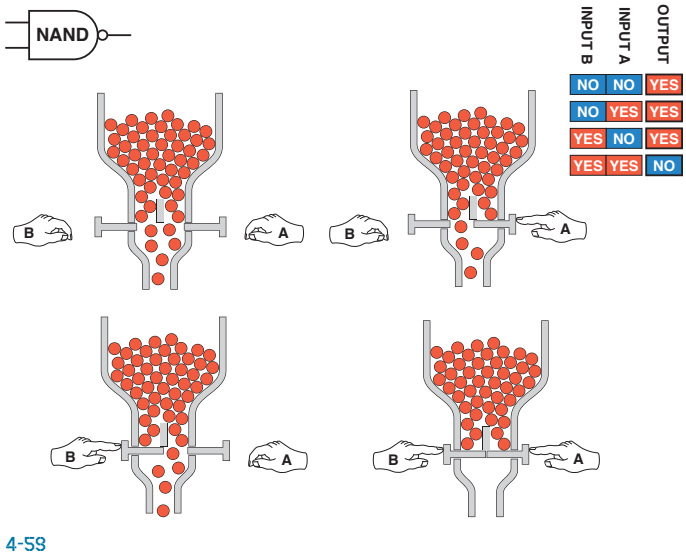

Figure 4-59

ESSENTIALS

Logic gate basics (continued)

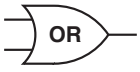

INPUT B	INPUT A	OUTPUT
NO	NO	NO
NO	YES	YES
YES	NO	YES
YES	YES	YES

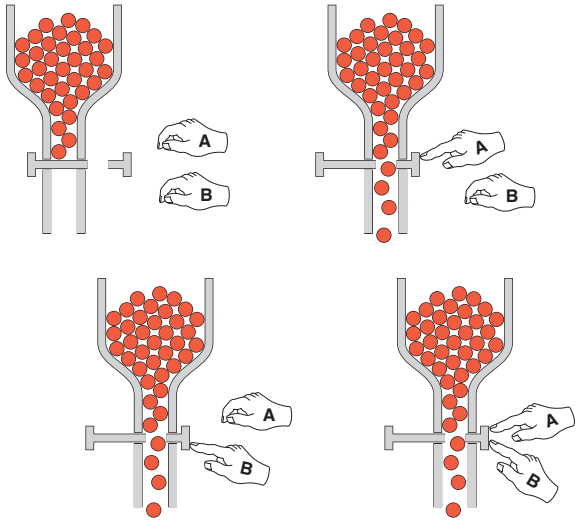

Figure 4-60

INPUT B	INPUT A	OUTPUT
NO	NO	YES
NO	YES	NO
YES	NO	NO
YES	YES	NO

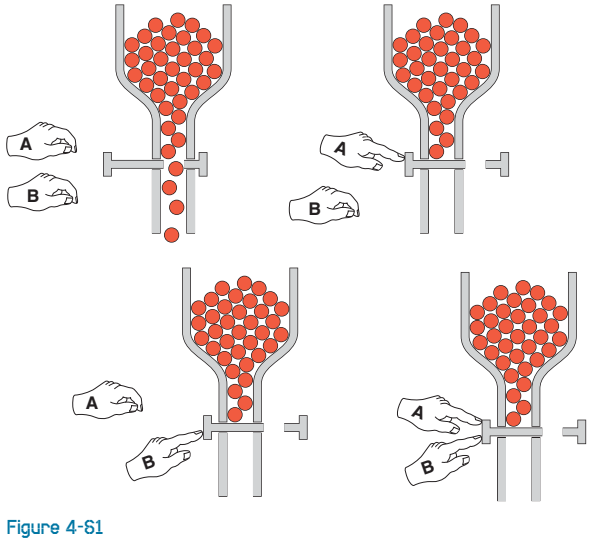

Figure 4-61

ESSENTIALS

Logic gate basics (continued)

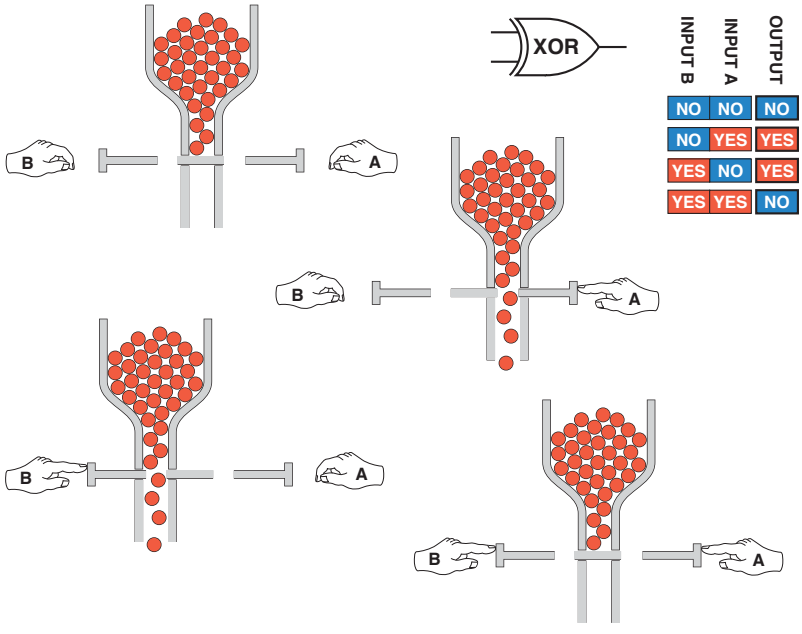

Figure 4-62

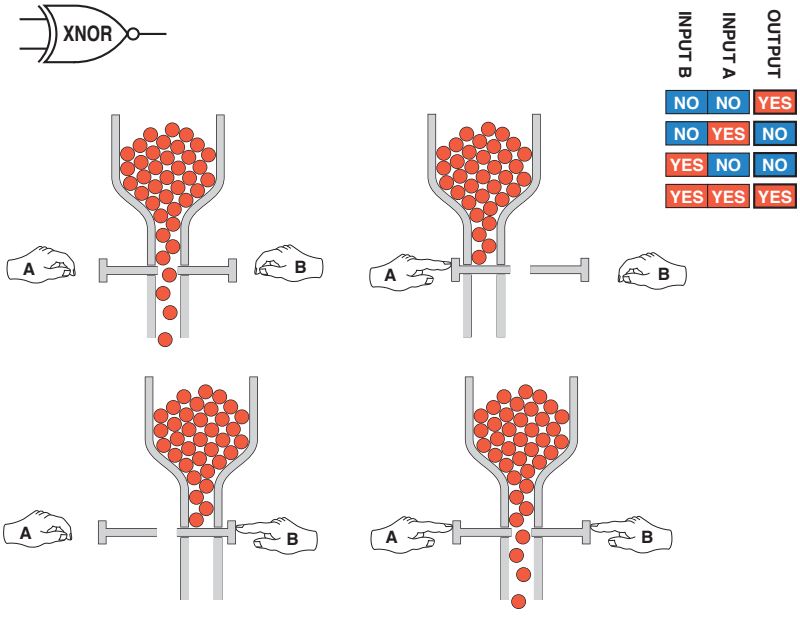

Figure 4-63

BACKGROUND

The confusing world of TTL and CMOS

Back in the 1960s, the first logic gates were built with Transistor-Transistor Logic, abbreviated TTL, meaning that tiny bipolar transistors were etched into a single wafer of silicon. Soon, these were followed by Complementary Metal Oxide Semiconductors, abbreviated CMOS. Each of these chips was a collection of metal-oxide field-effect transistors (known as MOSFETs). The 4026 chip that you used earlier is an old CMOS.

You may remember that bipolar transistors amplify current. TTL circuits are similar: they are sensitive to current, rather than voltage. Thus they require a significant flow of electricity, to function. But CMOS chips are like the programmable uni-junction transistor that I featured previously. They are voltage-sensitive, enabling them to draw hardly any current while they are waiting for a signal, or pausing after emitting a signal.

The two families named TTL and CMOS still exist today. The table in Figure 4-64 summarizes their basic advantages and disadvantages. The CMOS series, with part numbers from 4000 upward, were easily damaged by static electricity but were valuable because of their meager power consumption. The TTL series, with part numbers from 7400 upward, used much more power but were less sensitive and very fast. So, if you wanted to build a computer, you used the TTL family, but if you wanted to build a little gizmo that would run for weeks on a small battery, you used the CMOS family.

From this point on everything became extremely confusing, because CMOS manufacturers wanted to grab market share by emulating the advantages of TTL chips. Newer generations of CMOS chips even changed their part numbers to begin with "74" to emphasize their compatibility, and the functions of pins on CMOS chips were swapped around to match the functions of pins on TTL chips. Consequently, the pinouts of CMOS and TTL chips are usually now identical, but the meaning of "high" and "low" states changed in each new generation, and the maximum supply voltages for CMOS chips were revised downward. Note I have included question marks beside two categories in the CMOS column, as modern CMOS chips have overcome those disadvantages—at least to some extent.

Here's a quick summary, which will be useful to you if you look at a circuit that you find online, and you wonder about the chips that have been specified.

Where you see a letter "x," it means that various numbers may appear in that location. Thus "74xx" includes the 7400 NAND gate, the 7402 NOR gate, the 74150 16-bit data selector, and so on. A combination of letters preceding the "74" identifies the chip manufacturer, while letters following the part number may identify the style of package, may indicate whether it contains heavy metals that are environmentally toxic, and other details.

		TTL	CMOS
Part number series		7400	4000 (Later adopted 7400 numbering)
Vulnerable to static electricity		Less	More?
Speed		Faster	Slower?
Power Consumption	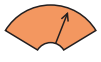	Higher	Very Low
Power Supply Range		Narrow 5v	Wider 3v-6v
Input Impedance		Low	Very High

Figure 4-64. *The basic differences between the two families of logic chips. In successive generations, these differences have gradually diminished.*

TTL family:

74xx
The old original generation, now obsolete.

74Sxx
Higher speed "Schottky" series, now obsolete.

74LSxx
Lower power Schottky series, still used occasionally.

74ALSxx
Advanced low-power Schottky.

74Fxx
Faster than the ALS series.

BACKGROUND

The confusing world of TTL and CMOS (continued)

CMOS family:

40xx
The old original generation, now obsolete.

40xxB
The 4000B series was improved but still susceptible to damage from static electricity. Many hobby circuits still use these chips because they will run from relatively high voltages and can power LEDs and even small relays directly.

74HCxx
Higher-speed CMOS, with part numbers matching the TTL family, and pinouts matching the TTL family, but input and output voltages not quite the same as the TTL family. I've used this generation extensively in this book, because it's widely available, and the circuits here have no need for greater speed or power.

74HCTxx
Like the HC series but matching the TTL voltages.

74ACxx
Advanced version of HC series. Faster, with higher output capacity.

74ACTxx
Like the AC series but with the same pin functions and voltages as TTL.

74AHCxx
Advanced higher-speed CMOS.

74AHCTxx
Like the AHC series but with the same pin functions and voltages as TTL.

74LVxx
Lower voltage (3.3v) versions, including LV, LVC, LVT, and ALVC series.

As you can see, these days you have to interpret part numbers very carefully. But which family and generation of chips should you use? Well, that depends! Following are some guidelines.

What you don't need:

1. Speed differences are irrelevant from our point of view, as we're not going to be building circuits running at millions of cycles per second.
2. Price differences are so small as to be inconsequential.
3. Lower-voltage (LV) CMOS chips are not very interesting for our small experimental circuits.
4. Try to avoid mixing different families, and different generations of the same family, in the same circuit. They may not be compatible.
5. Some modern chip varieties may be only available in the surface-mount package format. Because they're so much more difficult to deal with, and their only major advantage is miniaturization, I don't recommend them.
6. In the TTL family, the LS and ALS series cannot handle as much output current as the S series and the F series. You don't need them.

What you should use:

1. The old 74LSxx series of TTL chips was so popular, you'll still find schematics that specify these chips. You should still be able to buy them from sources online, but if not, you can substitute the 74HCTxx chips, which are designed to function identically.
2. The old 4000B series of CMOS chips are still used by hobbyists because their willingness to tolerate high voltages is convenient. While TTL or TTL-compatible chips require a carefully regulated 5 volts, the 4000B chips would handle 15 volts—and also delivered enough power to energize LEDs or even very small relays. Some hobbyists also have a nostalgic affection for the 74Cxx series of chips, which had the same pin connections as the TTL chips but could still tolerate higher voltages and higher output current. The trouble is, some of the 74Cxx chips are almost extinct, and while the 4000B chips are still available, they are considered almost obsolete.

BACKGROUND

The confusing world of TTL and CMOS (continued)

Bottom line: I suggest you use the 4000B chips only if you want to replicate an old circuit, or if a modern equivalent is unavailable (which is why I specified the 4026B chip for the reaction timer—I could not find a modern equivalent that will drive seven-segment numeric displays directly, and I didn't want you to have to deal with more parts than necessary).

If you check online suppliers such as *Mouser.com* you'll find that the HC family is by far the most popular right now. They are all available in through-hole format (to fit your breadboard and perforated board). They have the high input impedance of CMOS (which is useful) and they have the same pin identities as the old 74LSxx series.

Abbreviations

When looking at data sheets, you are likely to encounter some or all of these abbreviations:

- VOH min: Minimum output voltage in high state
- VOL max: Maximum output voltage in low state
- VIH min: Minimum input voltage to be recognized as high
- VIL max: Maximum input voltage recognized as low

BACKGROUND

Logic gate origins

The 7400 family of integrated circuits was introduced by Texas Instruments, beginning with the 7400 NAND gate in 1962. Other companies had sold logic chips previously, but the 7400 series came to dominate the market. The Apollo lunar missions used a computer built with 7400 chips, and they were a mainstay of minicomputers during the 1970s.

RCA introduced its 4000 series of logic chips in 1968, built around CMOS transistors; Texas Instruments had chosen TTL. The CMOS chips used less power, thus generating much less heat and enabling flexible circuit design, as each chip could power many others. CMOS was also tolerant of wide voltage ranges (from 3 to 15 volts) but prohibited switching speeds faster than around 1MHz. TTL was 10 times faster.

Design tweaks gradually eradicated the speed penalty for CMOS, and TTL chips have become relatively rare. Still, some people retain a special nostalgic loyalty to "the logic gates that went to the moon." A hardcore enthusiast named Bill Buzbee has built an entire web server from TTL-type 7400 chips, currently online at *http://magic-1.org*. Figure 4-65 shows just one of the handmade circuit boards that Bill assembled to run his computer.

Figure 4-65. *Hobbyist Bill Buzbee built himself a web server entirely from 7400 series logic chips, the oldest of which was fabricated back in 1969. The web server can be found online at http://magic-1.org, displaying pictures of itself and details of its construction. The picture here that Bill took shows just one of the circuit boards of this remarkable project.*

FUNDAMENTALS

Common part numbers

Each 14-pin chip can contain four 2-input gates, three 3-input gates, two 4-input gates, one 8-input gate, or six single-input inverters, as shown in the following table.

	2 input	3 input	4 input	8 input
AND	7408	7411	7421	
NAND	7400	7410	7420	7430
OR	7432			744078*
NOR	7402	7427		744078*
XOR	7486			
XNOR	747266			
Inverter	(1 input) 7404			

*The 744078 has an OR output and a NOR output on the same chip.

Figures 4-66 through 4-74 show the internal connections of the logic chips that you are most likely to use. Note that the 7402 NOR gate has its logical inputs and outputs arranged differently from all the other chips.

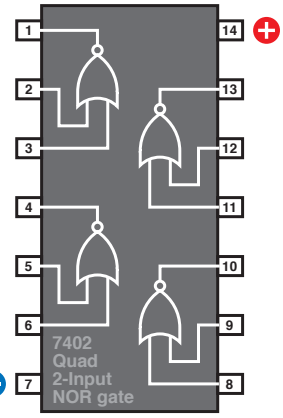

Figure 4-66. *Figures 4-66 through 4-74 show pinouts for some of the most widely used logic chips. Note that the inputs of the 7402 are reversed compared with the other chips.*

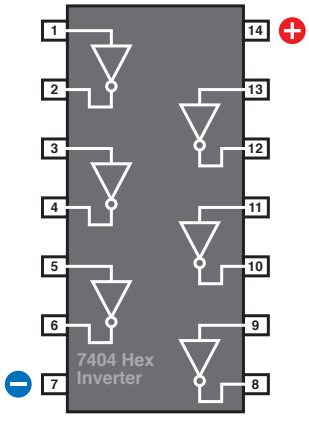

Figure 4-67

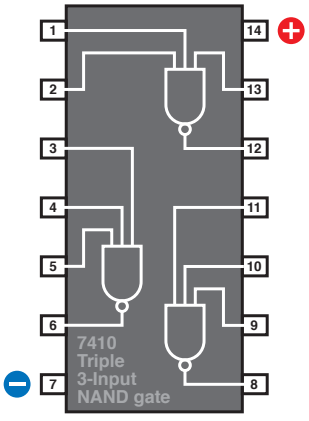

Figure 4-68

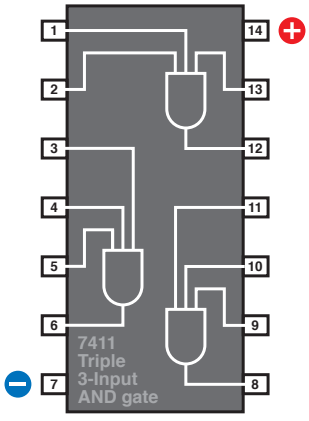

Figure 4-69

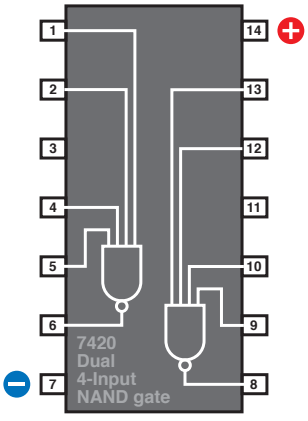

Figure 4-70

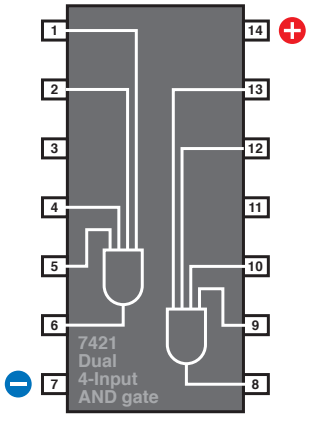

Figure 4-71

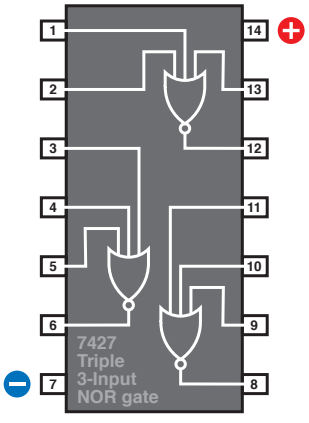

Figure 4-72

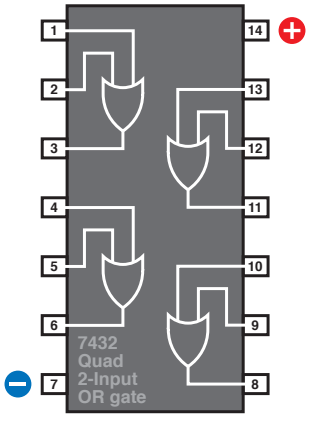

Figure 4-73

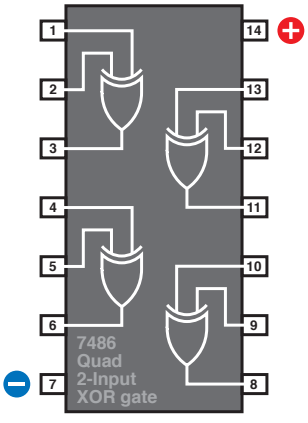

Figure 4-74

FUNDAMENTALS

Rules for connecting logic gates

Permitted:

- You can connect the input of a gate directly to your regulated power supply, either positive side or negative side.
- You can connect the output from one gate directly to the input of another gate.
- The output from one gate can power the inputs of many other gates (this is known as "fanout"). The exact ratio depends on the chip, but you can always power at least ten inputs with one logic output. The output from a logic chip can drive the trigger (pin 3) of a 555 timer. The output from the timer can then deliver 100mA, easily enough for half-a-dozen LEDs or a small relay.
- Low input doesn't have to be zero. A 74HCxx logic gate will recognize any voltage up to 1 volt as "low."
- High input doesn't have to be 5 volts. A 74HCxx logic gate will recognize any voltage above 3.5 volts as "high."

See Figures 4-75 and 4-76 for a comparison of permitted voltages on the input and output side of 74HCxx and 74LSxx chips.

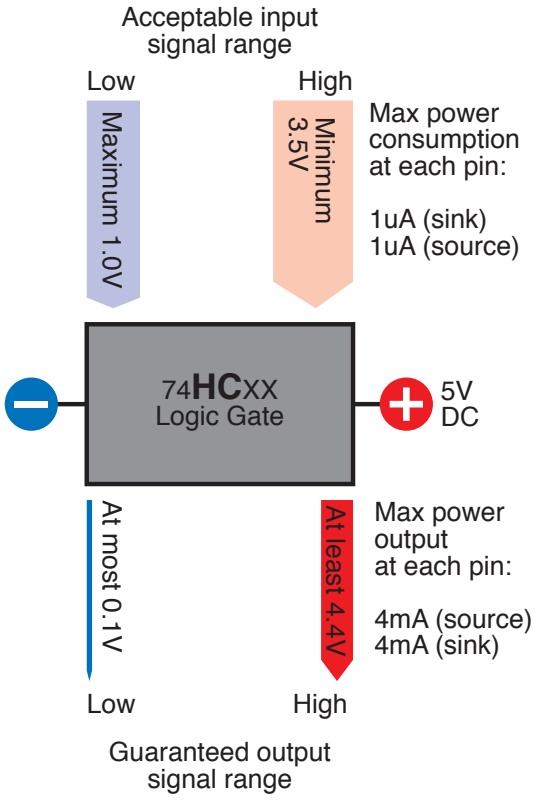

Figure 4-75. *Each family of logic chips, and each generation in each family, has different standards for input and output minimum and maximum voltages. This diagram shows the standards used by the HC generation of the CMOS family, which was chosen for most of the projects in this book. Note that the current required for input is minimal compared with the current available for output. The power supply to the chip makes up the difference.*

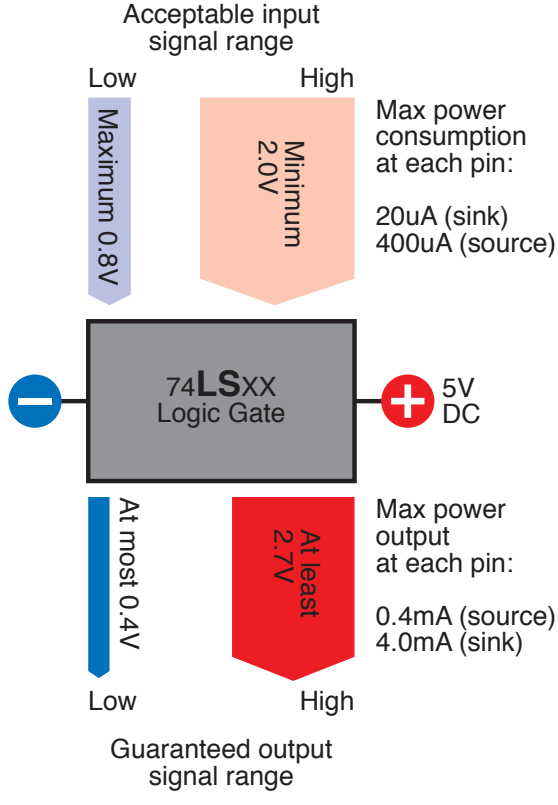

Figure 4-76. *Because the LS generation of the TTL family has such different tolerances for input voltages and different standards for output voltages, the LS generation of TTL chips should not be mixed in the same circuit as the HC generation of CMOS chips, unless pull-up resistors are used to bring the LS chips into conformance with standards expected by the HC chips. See Experiment 21 for a case study in using LS chips.*

FUNDAMENTALS

Rules for connecting logic gates (continued)

Not permitted:

- No floating-input pins! On CMOS chips such as the HC family, you must always connect all input pins with a known voltage, even if they supply a gate on the chip that you're not using. When you use a SPST switch to control an input, remember that in its "off" position, it leaves the input unconnected. Use a pull-up or pull-down resistor to prevent this situation. See Figure 4-77.
- Don't use an unregulated power supply, or more than 5 volts, to power 74HCxx or 74LSxx logic gates.
- Be careful when using the output from a logic gate to power even a low-current LED. Check how many milliamps are being drawn. Also be careful when "sharing" the output from a logic gate with the input of another gate, at the same time that it is driving an LED. The LED may pull down the output voltage, to a point where the other gate won't recognize it. Always check currents and voltages when modifying a circuit or designing a new one.
- Never apply a significant voltage or current to the output pin of a logic gate. In other words, don't force an input into an output.
- Never link the outputs from two or more logic gates. If they must share a common output wire, use diodes to protect them from each other. See Figure 4-78.

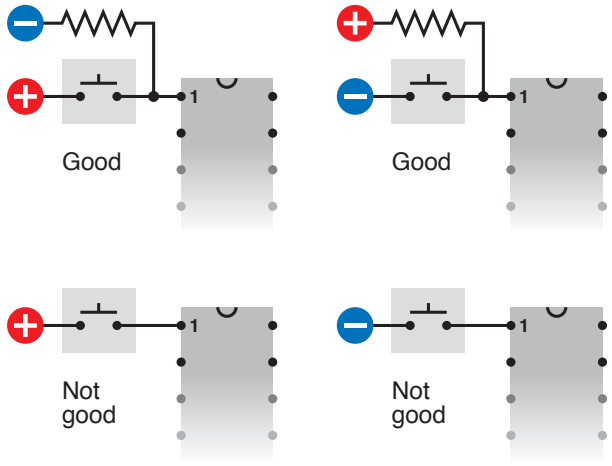

Figure 4-77. *Because a CMOS chip is so sensitive to input fluctuations, a logical input should never be left "floating," or unattached to a defined voltage source. This means that any single-throw switch or pushbutton should be used with a pull-up or pull-down resistor, so that when the contacts are open, the input is still defined.*

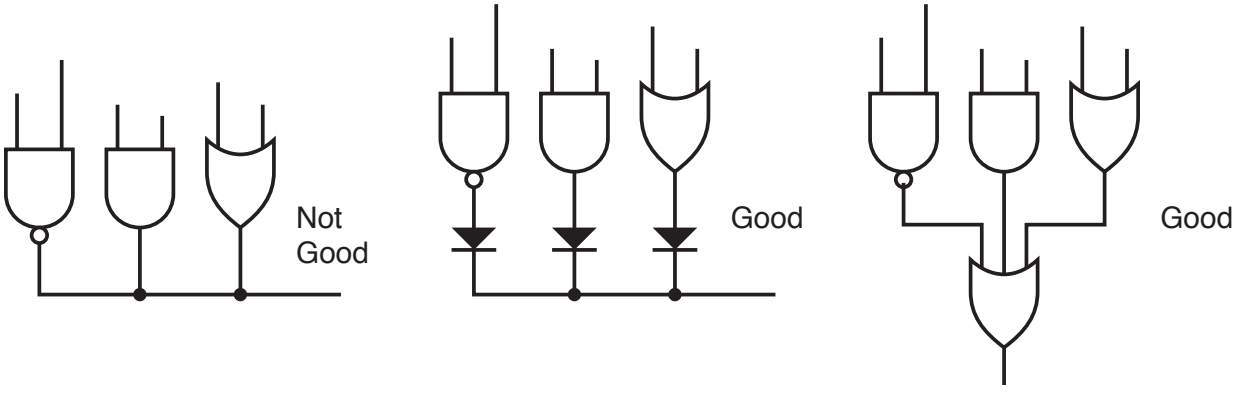

Figure 4-78. *The output from one logic gate must not be allowed to feed back into the output from another logic gate. Diodes can be used to isolate them, or they can be linked via another gate.*

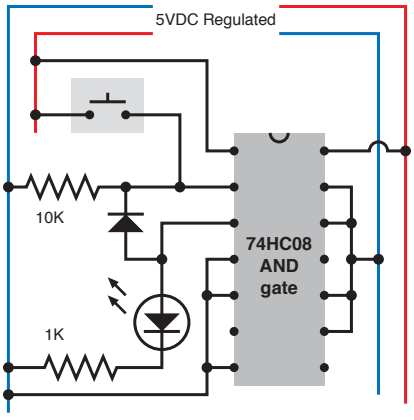

Figure 4-79. *Using a diode, the logical output from a gate can be allowed to feed back to one of its inputs, so that the gate latches after receiving a brief logical input pulse.*

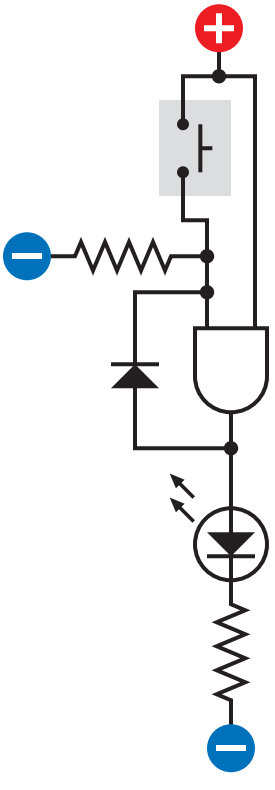

Figure 4-80. *The breadboard-format schematic in is simplified here to show more clearly the way in which a gate can latch itself after receiving an input pulse.*

In the 74HCxx logic family, each input of a logic gate consumes just a microamp, while the output can source 4 milliamps. This seems paradoxical: how can the chip give out more than it takes in? The answer is that it also consumes power from the power supply attached to pins 7 and 14. That's where the additional electricity comes from.

Because the logical output from a chip can be greater than the logical input, we can put the chip in a state where it keeps itself "switched on" in a way which is similar to the way the relay in the alarm project was wired to lock itself on. The simplest way to do this in a logic chip is by feeding some of the output back to one of the inputs.

Figure 4-79 shows an AND gate with one of its inputs wired to positive and its other input held low by a pull-down resistor, with a pushbutton that can make the input high. A signal diode connects the output of the chip back to the pushbutton-controlled input. Remember that the diode has a mark on it indicating the end which should be connected to the *negative* side of the power supply, which in this case will be the end of the 10K resistor.

The schematic in Figure 4-79 shows how the circuit should look in breadboard format. Figure 4-80 shows it in a simpler format.

> *From this point on, I won't bother to show the power regulator and the capacitors associated with it. Just remember to include them every time you see the power supply labeled as "5V DC Regulated."*

When you switch on the power, the LED is dark, as before. The AND gate needs a positive voltage on both of its logical inputs, to create a positive output, but it now has positive voltage only on one of its inputs, while the other input is pulled down by the 10K resistor. Now touch the pushbutton, and the LED comes on. Let go of the pushbutton, and the LED stays on, because the positive output from the AND gate circulates back through the diode and is high enough to overcome the negative voltage coming through the pull-down resistor.

The output from the AND gate is powering its own input, so the LED will stay on until we disconnect it. This arrangement is a simple kind of "latch," and can be very useful when we want an output that continues after the user presses and releases a button.

You can't just connect the output from the gate to one of its inputs using an ordinary piece of wire, because this would allow positive voltage from the tactile switch to flow around and interfere with the output signal. Remember, you must never apply voltage to the output pin of a logic gate. The diode prevents this from happening.

If you've grasped the basics of logic gates, you're ready now to continue to our first real project, which will use all the information that I've set out so far.

Experiment 20: A Powerful Combination

Suppose you want to prevent other people from using your computer. I can think of two ways to do this: using software, or using hardware. The software would be some kind of startup program that intercepts the normal boot sequence and requests a password. You could certainly do it that way, but I think it would be more fun (and more relevant to this book) to do it with hardware. What I'm imagining is a numeric keypad requiring the user to enter a secret combination before the computer can be switched on.

You will need:

- Numeric keypad. As specified in the shopping list at the beginning of this chapter, it must have a "common terminal" or "common output." The schematic in Figure 4-82 shows what I mean. Inside the keypad, one conductor (which I have colored red to distinguish it from the others) connects with one side of every pushbutton. This conductor is "common" to all of them. It emerges from the keypad on an edge connector or set of pins at the bottom, which I've colored yellow.

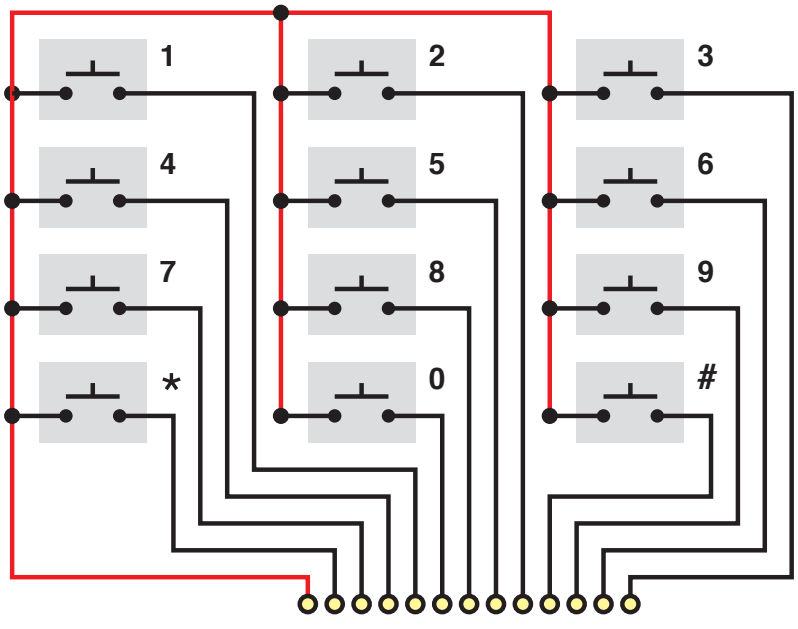

Figure 4-82. *A keypad of the type required for Experiment 20 incorporates a common terminal connected to one side of each of the 12 pushbuttons. The wire from the common terminal is shown red, here, to make it more easily identifiable.*

- Keypads that use "matrix encoding" won't work with the circuit that I'm going to describe. If the Velleman keypad, which I recommend, is unavailable, and you can't find another like it, you can use 12 separate SPST pushbuttons. Of course, that will cost a little more.
- 74HC08 logic chip containing four AND gates. Quantity: 1.
- 74HC04 logic chip containing six inverters. Quantity: 1.
- 555 timer chip. Quantity: 1.

The Warranty Issue

If you follow this project all the way to its conclusion, you'll open your desktop computer, cut a wire, and saw a hole in the cabinet. Without a doubt, this will void your warranty. If this makes you nervous, here are three options:

1. Breadboard the circuit for fun, and leave it at that.

2. Use the numeric keypad on some other device.

3. Use it on an old computer.

Figure 4-81. *Caution: This just might void your warranty.*

- Latching relay, 5 volt, DPST or DPDT, "2 form C" package, Panasonic DS2E-SL2-DC5V or similar. Must have two separate coils (one to latch, one to unlatch) with separate inputs. Quantity: 1.
- LEDs, 5mm generic, your choice of colors. Quantity: 3.
- Ribbon cable, with six conductors minimum, if you want to do a really neat job. You can use a cable of the type sold for hard drives, and split off the six conductors that you need, or shop around on eBay.
- Tools to open your computer, drill four holes, and make saw cuts between the holes, to create a rectangular opening for the keypad (if you want to take this project to its conclusion). Also, four small bolts to attach the keypad to the computer cabinet after you create the opening for it.

The Schematic

This time I'd like you to study the schematic before building anything. Let's start with the simplified version, shown in Figure 4-83.

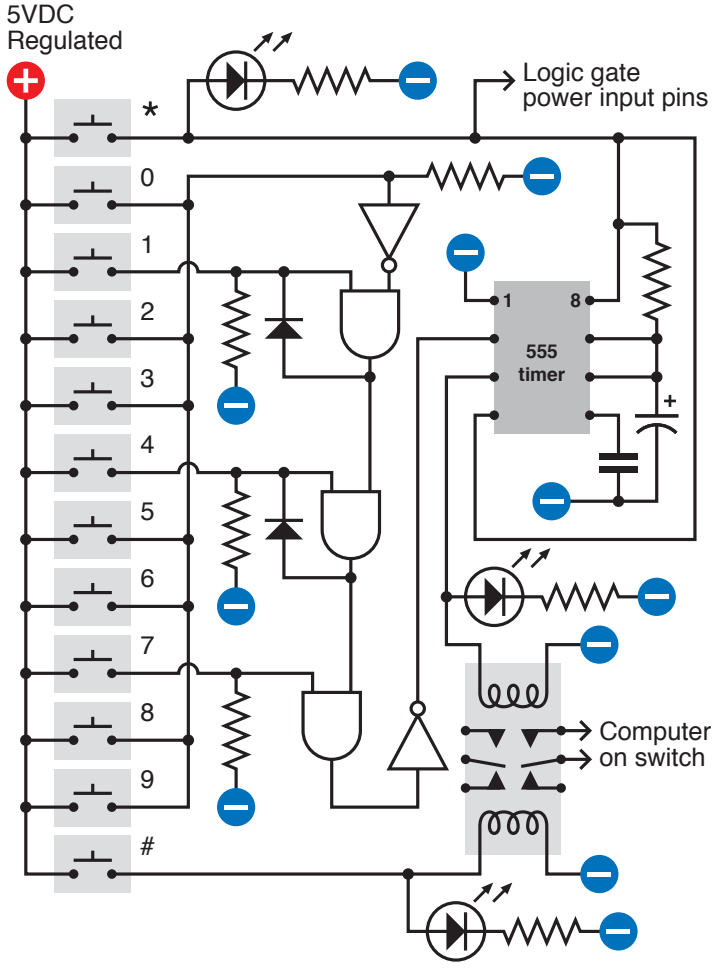

Figure 4-83. *A simplified schematic showing the basic structure of the combination lock circuit.*

I want this to be a battery-powered circuit, so that you don't have to run a separate power supply to it or (worse) try to tap into your computer's 5-volt bus. Battery power means that the circuit has to be "off" most of the time, to prevent the battery from running down. Because the keypad has two spare buttons (the asterisk and the pound sign), I'm going to use the asterisk as the "power on" button. When you press it, the LED at the top of the schematic lights up to confirm that everything's working, and the button sends power to the two logic chips and the 555 timer. You have to hold down the asterisk button while you punch in a three-digit code to unlock the computer.

Arbitrarily, I've chosen 1-4-7 as the three-digit code. Let's track what happens when you enter this sequence. (Naturally, if you build the circuit, you can wire it to choose any three digits you prefer.)

Pressing the 1 button sends positive power to one logical input of the first AND gate. The other logical input of this gate is also positive, because an inverter is supplying it, and the input of the inverter is being held negative by a pull-down resistor. When an inverter has a negative input, it gives a positive output, so pressing the 1 button activates the AND gate, and makes its output positive. The AND gate locks itself on, as its output cycles back to its switched input via a diode. So the gate output remains high even after you let go of the 1 button.

The output from the first AND gate also supplies one logical input of the second AND gate. When you press the 4 button, you send positive voltage to the other logical input of this AND gate, so its output goes high, and it locks itself on, just as the first gate did.

The second AND gate feeds the third AND gate, so when you press the 7 button, the third AND gate changes its output from low to high. This passes through an inverter, so the output from the inverter goes from high to low. This in turn goes to the trigger of a 555 timer wired in monostable mode.

When the trigger of a 555 timer goes from high to low, the timer emits a positive pulse through its output, pin 3. This runs down to the upper coil of the latching relay, and also flashes an LED to confirm that the code has been accepted and the relay has been activated.

Two of the contacts in the relay are wired into the power-up button of your computer. A little later in this description I'll explain why this should be safe with any modern computer.

Because we're using a latching relay, it flips into its "on" state and remains there, even when the power pulse from the timer ends. So now you can let go of the asterisk button to disconnect the battery power to your combination lock, and press the power-up button that switches on your computer.

At the end of your work session, you shut down your computer as usual, then press the pound button on your keypad, which flips the relay into its other position, reactivating the combination lock.

Incorrect Inputs

What happens if you enter the wrong code? If you press any button other than 1, 4, or 7, it sends positive voltage to the inverter near the top of the schematic. The positive voltage overwhelms the negative voltage being applied to the inverter through a pull-down resistor, and causes the inverter to output a negative voltage, which it applies to one of the logical inputs of the first AND gate. If the AND gate was locked on, the negative input will switch it off. If it was supplying the second AND gate, it'll switch that one off too.

Thus, any error when entering the first, second, or third digit of the secret code will reset the AND gates, forcing you to begin the sequence all over again.

What if you enter 1, 4, and 7 out of their correct sequence? The circuit won't respond. The third AND gate needs a high input supplied by the second AND gate, and the second AND gate needs a high input supplied by the first AND gate. So you have to activate the AND gates in the correct sequence.

Questions

Why did I use a 555 timer to deliver the pulse to the relay? Because the logical output from an AND gate cannot deliver sufficient power. I could have passed it through a transistor, but I liked the idea of a pulse of a fixed length to flip the relay and illuminate an LED for about 1 second, regardless of how briefly the user presses the 7 button.

Why do I need three LEDs? Because when you're punching buttons to unlock your computer, you need to know what's going on. The Power On LED reassures you that your battery isn't dead. The Relay Active LED tells you that the system is now unlocked, in case you are unable to hear the relay click. The System Relocked LED reassures you that you have secured your computer.

Because all the LEDs are driven either directly from the 5-volt supply or from the output of the 555 timer, they don't have to be low-current LEDs and can be used with 330Ω series resistors, so they'll be nice and bright.

How do you connect the keypad with the circuit? That's where your ribbon cable comes in. You carefully strip insulation from each of the conductors, and solder them to the contact strip or edge connector on your keypad. Push the conductors on the other end of the cable into your breadboard (when you're test-building the circuit) or solder them into perforated board (when you're building it permanently). Find a convenient spot inside your computer case where you can attach the perforated board, with double-sided adhesive or small bolts or whatever is convenient. Include a 9-volt battery carrier, and don't forget your power regulator to step the voltage down to 5 volts.

Breadboarding

No doubt you have realized by now that breadboards are very convenient as a quick way to push in some components and create connections, but the layout of their conductors forces you to put components in unintuitive configurations. Still, if you carefully compare the breadboard schematic in Figure 4-83 with the simplified schematic in Figure 4-84, you'll find that the connections are the same.

To help it make sense, I've shown the logic gates that exist inside the chips. I've also colored the power supply wires, as before, to reduce the risk of confusion. The positive side of the supply goes only to the common terminal on your keypad, and you have to press the asterisk key to send the power back down the ribbon cable, to supply the chips.

If you build the circuit and you can't understand why everything's dead, it's most likely because you forgot to hold down the asterisk button.

Note that the "wrong" numbers on the keypad are all shorted together. This will create some inconvenience if you want to change the combination in the future. I'll suggest a different option in the "enhancements" section that follows. For now, ideally, you should run a wire from every contact on your keypad, down to your circuit on its breadboard, and short the "wrong" keypad numbers together with jumper wires on the breadboard.

Also note that if you use a meter to test the inputs to the AND gates, and you touch your finger against the meter probe while doing so, this can be sufficient to trigger the sensitive CMOS inputs and give a false positive.

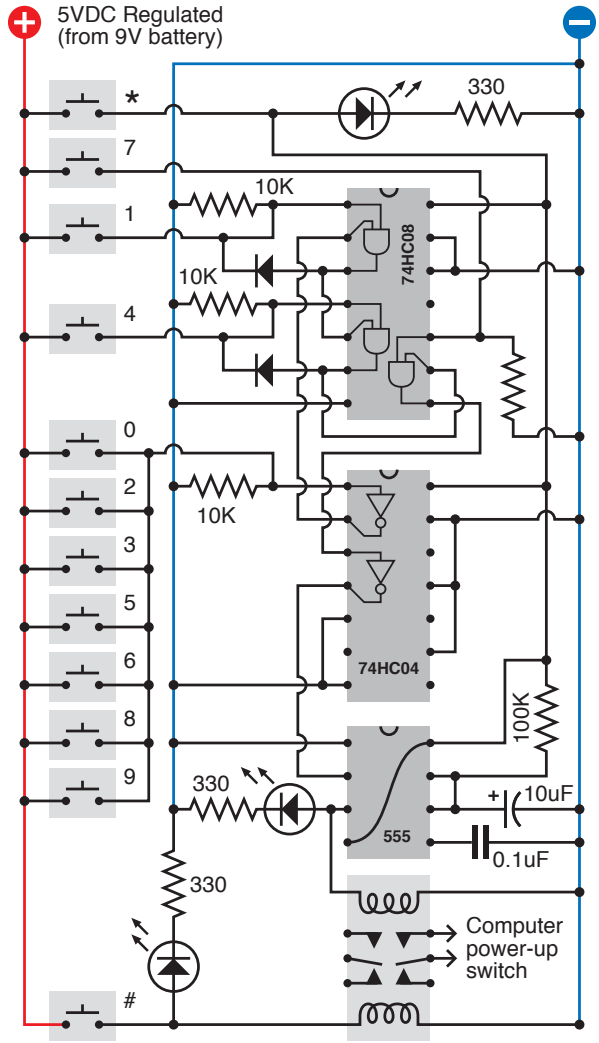

Figure 4-84. *The combination lock schematic redrawn to show how the components can be laid out on a breadboard.*

One Little Detail: The Computer Interface

Old computers used to have a big switch at the back, attached to the heavy metal box inside the computer, that transformed house current to regulated voltages that the computer needs. Most modern computers are not designed this way; you leave the computer plugged in, and you touch a little button on the box (if it's a Windows machine) or the keyboard (if it's a Mac), which sends a low-voltage pulse to the motherboard.

This is ideal from our point of view, because we don't have to mess with high voltages. Don't even think of opening that metal box with the fan mounted in it, containing the computer power supply. Just look for the wire (usually containing two conductors, on a Windows machine) that runs from the "power up" button to the motherboard.

To check that you found the right one, *make sure that your computer is unplugged*, ground yourself (because computers contain CMOS chips that are sensitive to static electricity) and very carefully snip just one of the two conductors in the wire. Now plug in your computer and try to use the "power up" button. If nothing happens, you've probably cut the right wire. Even if you cut the wrong wire, it still prevented your computer from booting, which is what you want, so you can use it anyway. Remember, we are not going to introduce any voltage to this wire. We're just going to use the relay as a switch to reconnect the conductor that you cut. You should have no problem if you maintain a cool and calm demeanor, and look for that single wire that starts everything. Check online for the maintenance manual for your computer if you're really concerned about making an error.

After you find the wire and cut just one of its conductors, unplug your computer again, and keep it unplugged during the next steps.

Find where the wire attaches to the motherboard. Usually there's a small unpluggable connector. First, mark it so that you know how to plug it back in the right way around, and then disconnect it while you follow the next couple of steps.

Strip insulation from the two ends of the wire that you cut, and solder an additional piece of two-conductor wire, as shown in Figure 4-85, with heat-shrink tube to protect the solder joints. (This is very important!)

Run your new piece of wire to the latching relay, making sure you attach it to the pair of contacts which close, inside the relay, when it is energized by the unlocking operation. You don't want to make the mistake of unlocking your computer when you think you're locking it, and vice versa.

Reconnect the connector that you disconnected from your motherboard, plug in your computer, and try to power it up. If nothing happens, this is probably good! Now enter the secret combination on your keypad (while holding down the asterisk button to provide battery power) and listen for the click as the relay latches. Now try the "power up" button again, and everything should work.

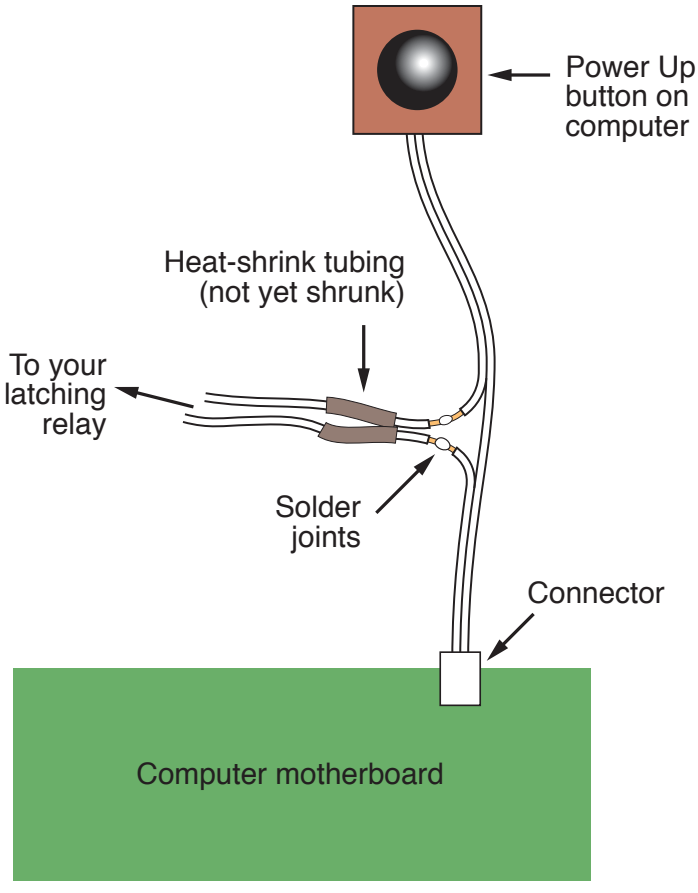

Figure 4-85. *The combination lock project can be interfaced with a typical desktop computer by cutting one conductor in the wire from the "power up" pushbutton, soldering an extension, and covering the joints with heat-shrink tube.*

Enhancements

At the end of any project, there's always more you can do.

To make this setup more secure, you could remove the usual screws that secure the case of the computer, and replace them with tamper-proof screws. Check any online source for "tamper-proof screws," such as *http://www.mcmaster.com*. Naturally, you will also need the special tool that fits the screws, so that you can install them (or remove them, if your security system malfunctions for any reason).

Another enhancement could be an additional 555 timer that is activated by the asterisk button, and delivers power to the other chips for, say, a limited period of 30 seconds, allowing you that much time to unlock the system. This would eliminate the need to hold down the asterisk button while you enter the unlocking code. A 555 timer can supply power to all the other chips, because they don't use very much. I omitted this feature for the sake of simplicity.

Yet another enhancement, if you are security-crazed, is to go for a four-button code. After all, the 74HC08 chip still has one unused AND gate. You could insert that into the chain of the existing AND gates and wire it to another keypad button of your choice.

Still another enhancement would be a way to change the code without unsoldering and resoldering wires. You can use the miniature sockets that I suggested in the heartbeat flasher project. These should enable you to swap around the ends of your wires from the keypad.

And for those who are absolutely, positively, totally paranoid, you could fix things so that entering a wrong code flips a second high-amperage relay which supplies a massive power overload, melting your CPU and sending a big pulse through a magnetic coil clamped to your hard drive, instantly turning the data to garbage (Figure 4-86). Really, if you want to protect information, messing up the hardware has major advantages compared with trying to erase data using software. It's faster, difficult to stop, and tends to be permanent. So, when the Record Industry Association of America comes to your home and asks to switch on your computer so that they can search for illegal file sharing, just accidentally give them an incorrect unlocking code, sit back, and wait for the pungent smell of melting insulation.

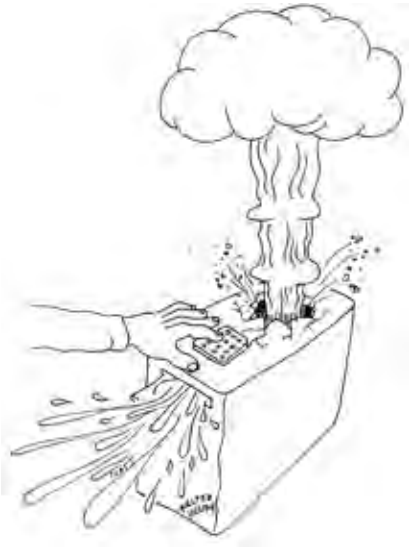

Figure 4-86. *For those who are absolutely, positively, totally paranoid: a meltdown/self-destruct system controlled by a secret key combination provides enhanced protection against data theft or intrusions by RIAA investigators asking annoying questions about file sharing.*

If you pursue this option, I *definitely* take no responsibility for the consequences.

On a more realistic level, no system is totally secure. The value of a hardware locking device is that if someone does defeat it (for instance, by figuring out how to unscrew your tamper-proof screws, or simply ripping your keypad out of the computer case with metal shears), at least you'll know that something happened—especially if you put little dabs of paint over the screws to reveal whether they've been messed with. By comparison, if you use password-protection software and someone defeats it, you may never know that your system has been compromised.

Experiment 21: Race to Place

The next project is going to get us deeper into the concept of feedback, where the output is piped back to affect the input—in this case, blocking it. It's a small project, but quite subtle, and the concepts will be useful to you in the future.

You will need:

- 74HC32 chip containing four OR gates. Quantity: 1.
- 555 timers. Quantity: 2.
- SPDT switch. Quantity: 1.
- SPST tactile switches. Quantity: 2.
- Various resistors.
- 5V supply using power regulator as before.

The Goal

On quiz shows such as *Jeopardy*, contestants race to answer each question. The first person who hits his answer button automatically locks out the other contestants, so that their buttons become inactive. How can we make a circuit that will do the same thing?

If you search online, you'll find several hobby sites where other people have suggested circuits to work this way, but they lack some features that I think are necessary. The approach I'm going to use here is both simpler and more elaborate. It's simpler because it has a very low chip count, but it's more elaborate in that it incorporates "quizmaster control" to make a more realistic game.

I'll suggest some initial ideas for a two-player version. After I develop that idea, I'll show how it could be expanded to four or even more players.

A Conceptual Experiment

I want to show how this kind of project grows from an idea to the finished version. By going through the steps of developing a circuit, I'm hoping I may inspire you to develop ideas of your own in the future, which is much more valuable than just replicating someone else's work. So join me in a conceptual experiment, thinking our way from a problem to a solution.

First consider the basic concept: two people have two buttons, and whoever goes first locks out the other person. I always find it helps me to visualize this kind of thing if I draw a sketch, so that's where I'll begin. In Figure 4-87, the signal from each button passes through a component that I'll call a "button blocker," activated by the other person's button. I'm not exactly sure what the button blocker will be or how it will work, yet.

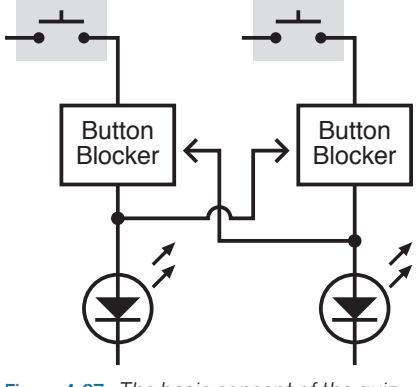

Figure 4-87. *The basic concept of the quiz project is that the output from one button should feed back to intercept the output of another button. At this point, the way in which the "button blocker" circuit works has not been figured out.*

Now that I'm looking at it, I see a problem here. If I want to expand this to three players, it will get complicated, because each player must activate the "button blockers" of *two* opponents. Figure 4-88 shows this. And if I have four players, it's going to get even more complicated.

Anytime I see this kind of complexity, I think there has to be a better way.

Also, there's another problem. After a player lets his finger off the button, the other players' buttons will be unblocked again. I need a latch to hold the signal from the first player's button and continue to block the other players.

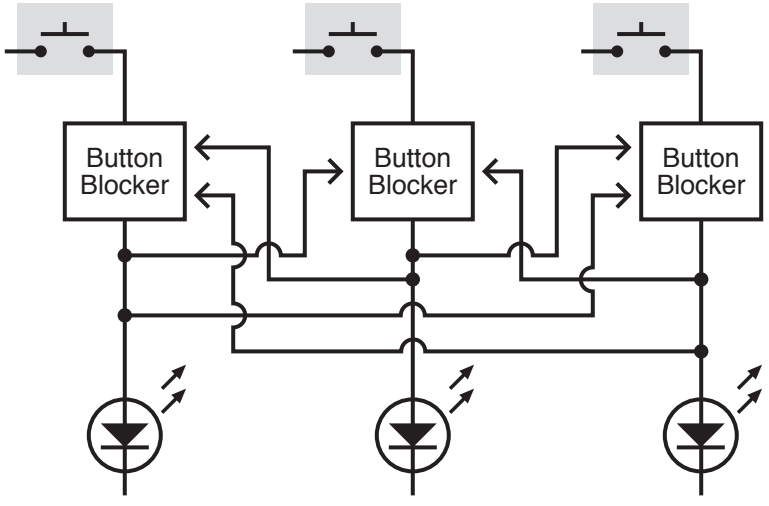

Figure 4-88. *The quiz concept becomes more complicated when an additional pushbutton is added. Now each button must block two other buttons. If a fourth button is added, the circuit will become unmanageably complex. There has to be a better way.*

This now sounds even more complicated. But wait a minute, if I have a latch which allows the winning player to take his finger off his button, I don't care if any of the buttons are being pressed anymore—including the button of the winning player. As soon as his signal is latched, *all* the buttons can be blocked. This makes things much simpler. I can summarize it as a sequence of events:

1. First player presses his button.
2. The signal is latched.
3. The latched signal feeds back and blocks all the buttons.

The new sketch in Figure 4-89 shows this. Now the configuration is modular, and can be expanded to almost any number of players, just by adding more modules.

There's something important missing, though: a reset switch, to put the system back to its starting mode after the players have had time to press their buttons and see who won. Also, I need a way to prevent players from pressing their buttons too soon, before the quizmaster has finished asking the question. Maybe I can combine this function in just one switch, which will be under the quizmaster's control. In its Reset position, the switch can reset the system and remove power to the buttons. In its Play position, the switch stops holding the system in reset mode, and provides power to the buttons. Figure 4-90 shows this. I've gone back to showing just two players, to minimize the clutter of lines and boxes, but the concept is still easily expandable.

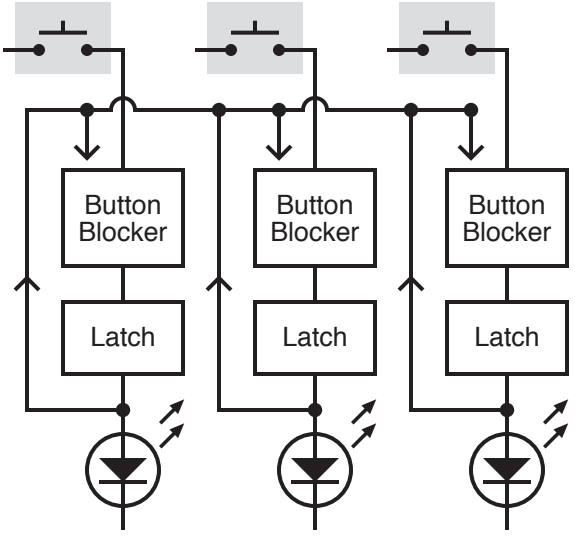

Figure 4-89. *If a latch is added below each button, it can retain one input and then block all inputs from all buttons. This simplifies the concept.*

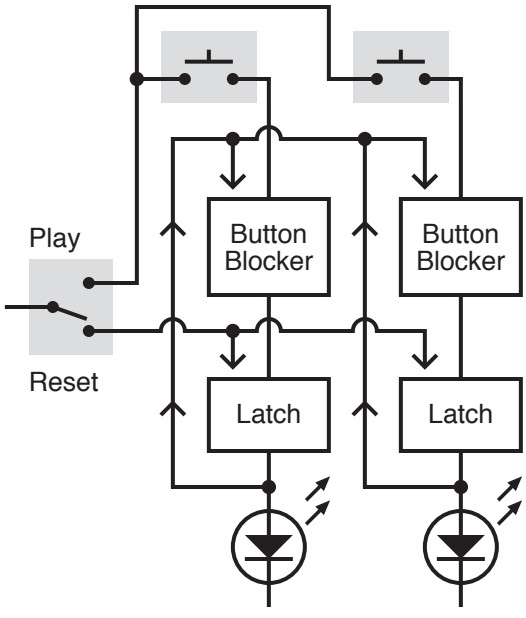

Figure 4-90. *A quizmaster switch will be needed to activate the buttons initially and then reset the circuit after a winning input has been recorded.*

Now I have to deal with a logic problem in the diagram. The way I've drawn it, after the output from the lefthand latch goes up to the "button blockers," it can also run down the wire to the other half of the circuit (against the direction to the arrows), because everything is joined together. In other words, if the lefthand LED lights up, the righthand LED will light up, too. How can I stop this from happening?

Well, I could put diodes in the "up" wires to block current from running down them. But I have a more elegant idea: I'll add an OR gate, because the inputs to an OR gate are separated from each other electrically. Figure 4-91 shows this.

Usually an OR gate has only two logical inputs. Will this prevent me from adding more players? No, because you can actually buy an OR that has eight inputs. If any one of them is high, the output is high. For fewer than eight players, I can short the unused inputs to ground, and ignore them.

Looking again at Figure 4-91, I'm getting a clearer idea of what the thing I've called a "button blocker" should actually be. I think it should be another logic gate. It should say, "If there's only one input, from a button, I'll let it through. But if there is a second input from the OR gate, I won't let it through."

That sounds like a NAND gate, but before I start choosing chips, I have to decide what the latch will be. I can buy an off-the-shelf flip-flop, which flips "on" if it gets one signal and "off" if it gets another, but the trouble is, chips containing flip-flops tend to have more features than I need for a simple circuit like this. Therefore I'm going to use 555 timers again, in flip-flop mode. They require very few connections, work very simply, and can deliver a good amount of current. The only problem with them is that they require a negative input at the trigger pin to create a positive output. But I think I can work with that.

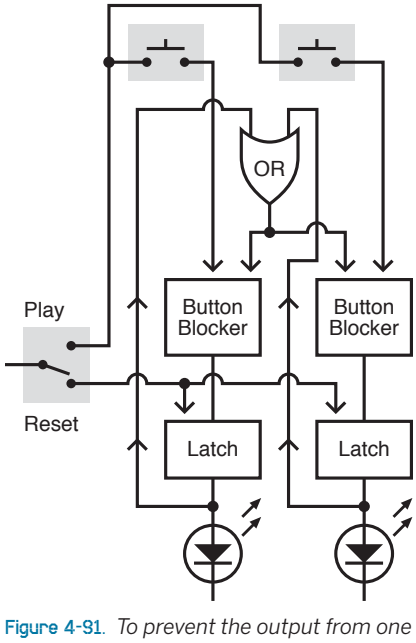

Figure 4-91. *To prevent the output from one latch feeding back around the circuit to the output from another latch, the outputs can be combined in an OR gate.*

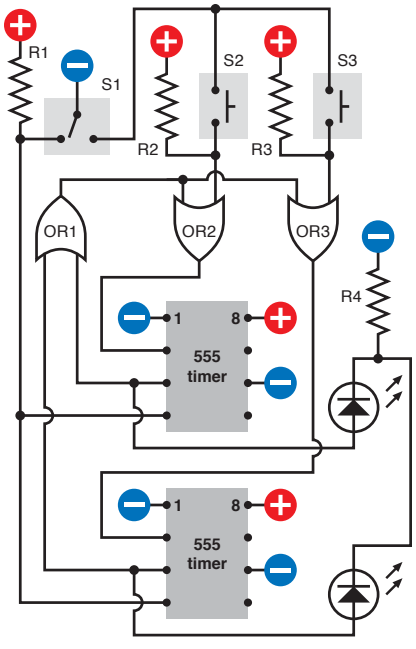

Figure 4-92. *Now that the basic concept of the quiz circuit has been roughed out, specific components can be inserted, with compatible inputs and outputs.*

So now, finally, here's a simplified schematic, in Figure 4-92. I like to show the pins of the 555 timers in their correct positions, so I had to move the components around a little to minimize wire crossovers, but you can see that logically, it's the same basic idea.

Before you try to build it, just run through the theory of it, because that's the final step, to make sure there are no mistakes. The important thing to bear in mind is that because the 555 needs a negative input on its trigger pin to create its output, when any of the players presses a button, the button has to create a negative "flow" through the circuit. This is a bit counterintuitive, so I'm including a three-step visualization in Figure 4-93, showing how it will work.

In Step 1, the quizmaster has asked a question and flipped his switch to the right, to supply (negative) power to the players' buttons. So long as no one presses a button, the pull-up resistors supply positive voltage to OR2 and OR3. An OR gate has a positive output if it has any positive input, so OR2 and OR3 keep the trigger inputs of the 555 timers positive. Their outputs remain low, and nothing is happening yet.

In Step 2, the lefthand player has pressed his button. Now OR2 has two negative inputs, so its output has gone low. But IC1 hasn't reacted yet.

In Step 3, just a microsecond later, IC1 has sensed the low voltage on its trigger, so its output from pin 3 has gone high, lighting the LED. Remember, this 555 timer is in flip-flop mode, so it locks itself into this state immediately. Meanwhile its high output also feeds back to OR1. Because OR1 is an OR gate, just one high input is enough to make a high output, so it feeds this back to OR2 and OR3. And now that they have high inputs, their outputs also go high, and will stay high, regardless of any future button-presses.

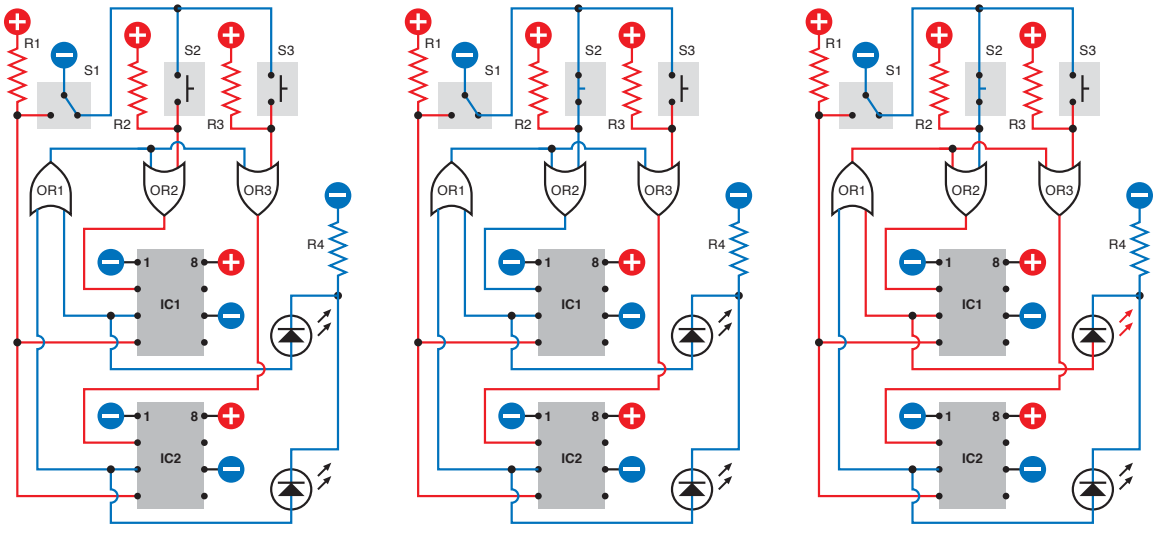

Figure 4-93. *These three schematics show the prevalence of higher and lower voltages (red and blue lines) through the quiz circuit when a pushbutton is pressed.*

Because OR2 and OR3 now have high inputs and outputs, IC1 and IC2 cannot be triggered. But IC1 is still locked into its "on" state, keeping the LED illuminated.

The only way to change IC1 is if the quizmaster flips his switch back to the left. That applies negative power to the reset pins of both the timers. Consequently their outputs go low, the LED goes out, and the circuit goes back into the same state as where it started. Having reset it, the quizmaster can ask another question, but the players' buttons are not activated until the quizmaster flips the switch back to the right again.

There's only one situation that I haven't addressed: what if both players press their buttons absolutely simultaneously? In the world of digital electronics, this is highly unlikely. Even a difference of a microsecond should be enough time for the circuit to react and block the second button. But if somehow both buttons are pressed at the same instant, both of the timers should react, and both of the LEDs will light up, showing that there has been a tie.

In case you feel a little uncertain about the way in which a two-player circuit can be upgraded to handle extra players, I've included a simplified three-player schematic in Figure 4-94.

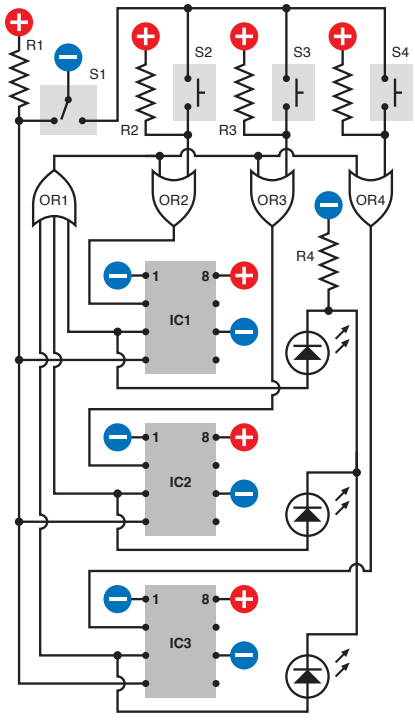

Figure 4-94. *The two-player schematic in can be easily upgraded to a three-player version, as shown here, provided the first OR gate can handle three inputs.*

Breadboarding It

Now it's time to create a schematic that's as close to the breadboard layout as possible, so that you can build this thing easily. The schematic is shown in Figure 4-95 and the actual components on a breadboard are in Figure 4-96. Because the only logic gates that I've used are OR gates, and there are only three of them, I just need one logic chip: the 74HC32, which contains four 2-input OR gates. (I've grounded the inputs to the fourth). The two OR gates on the left side of the chip have the same functions as OR2 and OR3 in my simplified schematic, and the OR gate at the bottom-right side of the chip works as OR1, receiving input from pin 3 of each 555 timer. If you have all the components, you should be able to put this together and test it quite quickly.

You may notice that I've made one modification of the previous schematic. A 0.01 µF capacitor has been added between pin 2 of each 555 timer (the Input) and negative ground. Why? Because when I tested the circuit without the capacitors, sometimes I found that one or both of the 555 timers would be triggered simply by flipping S1, the quizmaster switch, without anyone pressing a button.

At first this puzzled me. How were the timers getting triggered, without anyone doing anything? Maybe they were responding to "bounce" in the quizmaster switch. Sure enough, the small capacitors solved the problem. They may also slow the response of the 555 timers fractionally, but not enough to interfere with slow human reflexes.

As for the buttons, it doesn't matter if they "bounce," because each timer locks itself on at the very first impulse and ignores any hesitations that follow.

You can experiment building the circuit, disconnecting the 0.01 µF capacitors, and flipping S1 to and fro a dozen times. If you have a high-quality switch, you may not experience any problem. If you have a lower-quality switch, you may see a number of "false positives." I'm going to explain more about "bounce," and how to get rid of it, in the next experiment.

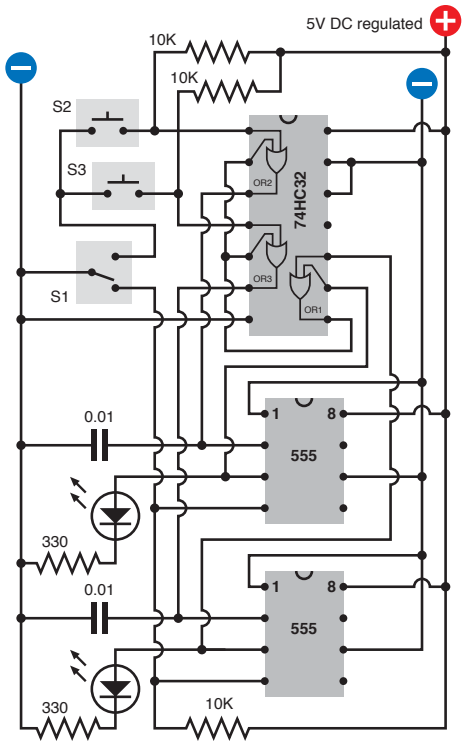

Figure 4-95. *Applying the simplified schematic to a breadboard inevitably entails a wiring layout that is less intuitively obvious and appears more complex. The connections are the same, though.*

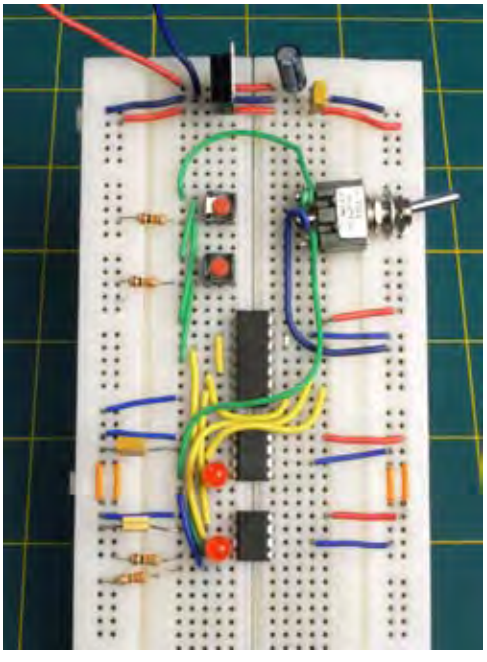

Figure 4-96. *The quiz schematic applied to a breadboard, to test the concept prior to full-scale implementation.*

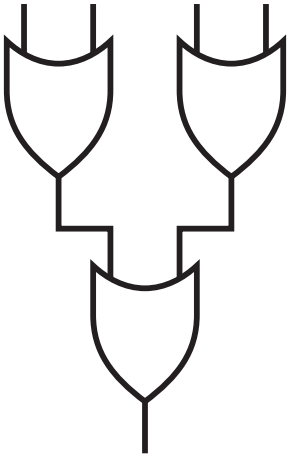

Figure 4-97. *Although a four-input OR gate is not manufactured, its functionality can be achieved easily by linking three 2-input OR gates together.*

Enhancements

After you breadboard the circuit, if you proceed to build a permanent version, I suggest that you expand it so that at least four players can participate. This will require an OR gate capable of receiving four inputs. The 74HC4078 is the obvious choice, as it allows up to eight. Just connect any unused inputs to negative ground.

Alternatively, if you already have a couple of 74HC32 chips and you don't want to bother ordering a 74HC4078, you can gang together three of the gates inside a single 74HC32 so that they function like a four-input OR. Look at the simple logic diagram in Figure 4-97 showing three ORs, and remember that the output from each OR will go high if at least one input is high.

And while you're thinking about this, see if you can figure out the inputs and output of three ANDs in the same configuration.

For a four-player game, you'll also need two additional 555 timers, of course, and two more LEDs, and two more pushbuttons.

As for creating a schematic for the four-player game—I'm going to leave that to you. Begin by sketching a simplified version, just showing the logic symbols. Then convert that to a breadboard layout. And here's a suggestion: pencil, paper, and an eraser can still be quicker, initially, than circuit-design software or graphic-design software, in my opinion.

Experiment 22: Flipping and Bouncing

I mentioned in the previous experiment that "bounce" from the buttons in the circuit wouldn't be a problem, because the buttons were activating 555 timers that were wired in bistable, flip-flop mode. As soon as the timer receives the very first pulse, it flips into its new state and flops there, ignoring any additional noise in the circuit. So can we debounce a switch or a button using a flip-flop? And as some 74HCxx chips are available containing flip-flops, can we use them?

The answers are yes, and yes, although it's not quite as simple as it sounds.

You will need:

- 74HC02 logic chip containing 4 NOR gates. 74HC00 logic chip containing 4 NAND gates. Quantity: 1 of each.
- SPDT switch. Quantity: 1.
- LEDs, low-current. Quantity: 2.
- 10K resistors and 1K resistors. Quantity: 2 of each.

Assemble the components on your breadboard, following the schematic shown in Figure 4-98. When you apply power (through your regulated 5-volt supply), one of the LEDs should be lit.

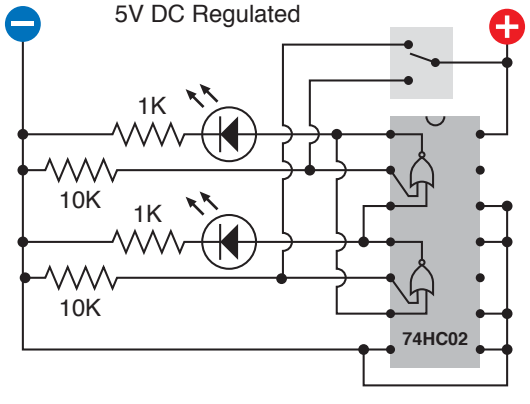

Figure 4-98. *A simple circuit to test the behavior of two NOR gates wired as a simple flip-flop that retains its state after an input pulse ceases.*

Now I want you to do something odd. Please disconnect the SPDT switch by taking hold of the wire that connects the positive power supply to the pole of the switch, and pulling the end of the wire out of the breadboard. When you do this, you may be surprised to find that the LED remains lit.

Push the wire back into the breadboard, flip the switch, and the first LED should go out, while the other LED should become lit. Once again, pull out the wire, and once again, the LED should remain lit.

Here's the take-home message:

- A flip-flop requires only an initial pulse.
- After that, it ignores its input.

How It Works

Two NOR gates or two NAND gates can function as a flip-flop:

- Use NOR gates when you have a positive input from a double-throw switch.
- Use NAND gates when you have a negative input from a double-throw switch.

Either way, you have to use a double-throw switch.

I've mentioned the double-throw switch three times (actually, four times if you count this sentence!) because for some strange reason, most introductory books fail to emphasize this point. When I first started learning electronics, I went crazy trying to understand how two NORs or two NANDs could debounce a simple SPST pushbutton—until finally I realized that they can't. The reason is that when you power up the circuit, the NOR gates (or NAND gates) need to be told in which state they should begin. They need an initial orientation, which comes from the switch being in one state or the other. So it has to be a double-throw switch. (Now I've mentioned it five times.)

I'm using another simplified multiple-step schematic, Figure 4-99, to show the changes that occur as the switch flips to and fro with two NOR gates. To refresh your memory, I've also included a truth table showing the logical outputs from NOR gates for each combination of inputs.

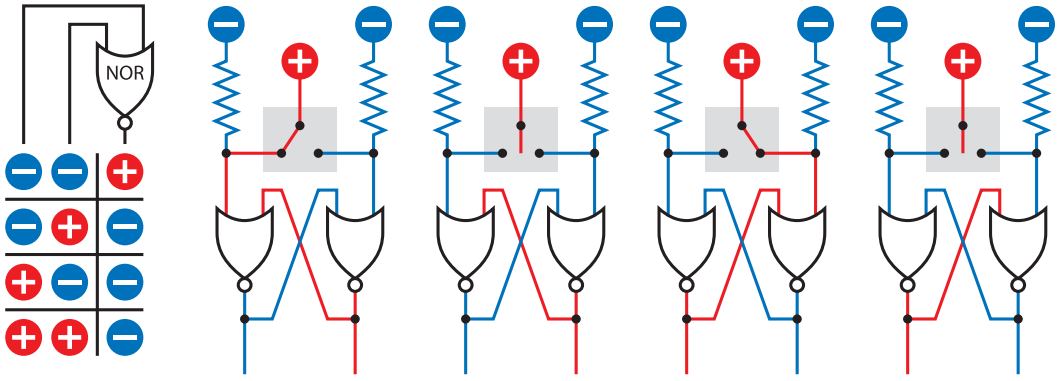

Figure 4-99. *Using two NOR gates in conjunction with a positive input through a SPDT switch, this sequence of four diagrams shows how a flip-flop circuit responds.*

Suppose that the switch is turned to the left. It sends positive current to the lefthand side of the circuit, overwhelming the negative supply from the pull-down resistor, so we can be sure that the NOR gate on the left has one positive logical input. Because any positive logical input will make the NOR give a negative output (as shown in the truth table), the negative output crosses over to the righthand NOR, so that it now has two negative inputs, which make it give a positive output. This crosses back to the lefthand NOR gate. So, in this configuration everything is stable.

Now comes the clever part. Suppose that you move the switch so that it doesn't touch either of its contacts. (Or suppose that the switch contacts are bouncing, and failing to make a good contact. Or suppose you disconnect the switch entirely.) Without a positive supply from the switch, the lefthand input

of the left NOR gate goes from positive to negative, as a result of the pull-down resistor. But the righthand input of this gate is still positive, and one positive is all it takes to make the NOR maintain its negative output, so nothing changes. In other words, the circuit has "flopped" in this state.

Now if the switch turns fully to the right and supplies positive power to the righthand pin of the right NOR gate, quick as a flash, that NOR recognizes that it now has a positive logical input, so it changes its logical output to negative. That goes across to the other NOR gate, which now has two negative inputs, so its output goes positive, and runs back to the right NOR.

In this way, the output states of the two NOR gates change places. They flip, and then flop there, even if the switch breaks contact or is disconnected again. The second set of drawings in Figure 4-100 shows exactly the same logic, using a negatively powered switch and two NAND gates. You can use your 74HC00 chip, specified in the parts list for this experiment, to test this yourself.

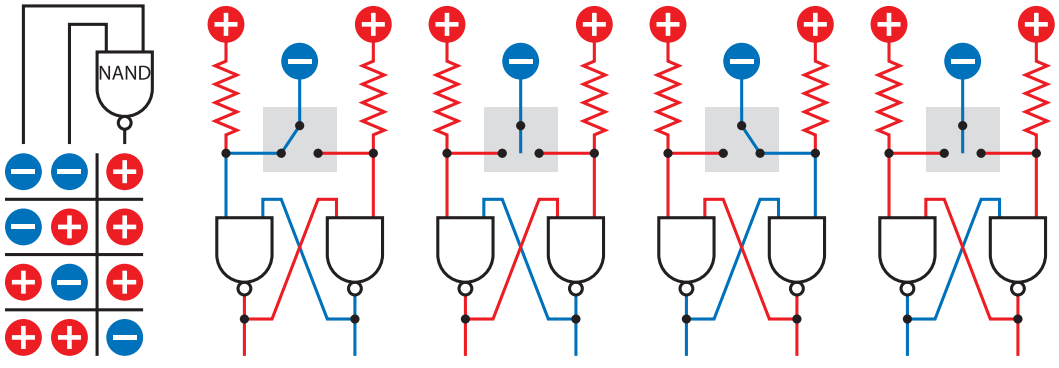

Figure 4-100. *The schematic from Figure 4-99 can be rewired with NAND gates and a negative switched input.*

Both of these configurations are examples of a jam-type flip-flop, so called because the switch forces it to respond immediately, and jams it into that state. You can use this circuit anytime you need to debounce a switch (as long as it's a double-throw switch).

A more sophisticated version is a clocked flip-flop, which requires you to set the state of each input first and then supply a clock pulse to make the flip-flop respond. The pulse has to be clean and precise, which means that if you supply it from a switch, the switch must be debounced—probably by using another jam-type flip-flop! Considerations of this type have made me reluctant to use clocked flip-flops in this book. They add a layer of complexity, which I prefer to avoid in an introductory text.

What if you want to debounce a single-throw button or switch? Well, you have a problem! One solution is to buy a special-purpose chip such as the 4490 "bounce eliminator," which contains digital delay circuitry. A specific part number is the MC14490PG from On Semiconductor. This contains six circuits for six separate inputs, each with an internal pull-up resistor. It's relatively expensive, however—more than 10 times the price of a 74HC02 containing NOR gates. Really, it may be simpler to use double-throw switches that are easily debounced as described previously.

Experiment 23: Nice Dice

This is the one experiment where I want you to use the 74LSxx generation of the TTL logic family, instead of the 74HCxx family of CMOS. Two reasons: first, I need to use the 7492 counter, which is unavailable in the HC family. And second, you should know the basic facts about the LS series of TTL chips, as they still crop up in circuits that you'll find in electronics books and online.

In addition, you'll learn about "open collector" TTL chips such as the 74LS06 inverter, which can be a convenient substitute for transistors when you want to deliver as much as 40mA of current.

The idea of this circuit is simple enough: run a 555 timer sending very fast pulses to a counter that counts in sixes, driving LEDs that are placed to imitate the spots on a die. (Note that the word "die" is the singular of "dice.") The counter runs so fast, the die-spots become a blur. When the user presses a button, the counter stops arbitrarily, displaying an unpredictable spot pattern.

Dice simulations have been around for many, many years, and you can even buy kits online. But this one will do something more: it will also demonstrate the principles of binary code.

So, if you're ready for the triple threat of TTL chips, open collectors, and binary, let's begin.

You will need:

- 74LS92 counter such as SN74LS92N by Texas Instruments. Quantity: 1 if you want to create one die, 2 to make two dice.
- 74LS27 three-input NOR gate such as SN74LS27N by Texas Instruments. Quantity: 1.
- 555 timers. Quantity: 1 if you want to make one die, 2 to make two dice.
- Signal diodes, 1N4148 or similar. Quantity: 4, or 8 to make two dice.

Seeing Binary

The counter that we dealt with before was unusual, in that its outputs were designed to drive seven-segment numerals. A more common type has outputs that count in binary code.

The 74LS92 pinouts are shown in Figure 4-101. Plug the chip into your breadboard and make connections as shown in Figure 4-102. Initially, the 555 timer will drive the counter in slow-motion, at around 1 step per second. Figure 4-103 shows the actual components on a breadboard.

Note that the counter has unusual power inputs, on pins 5 and 10 instead of at the corners. Also four of its pins are completely unused, and do not connect with anything inside the chip. Therefore, you don't need to attach any wire to them on the outside.

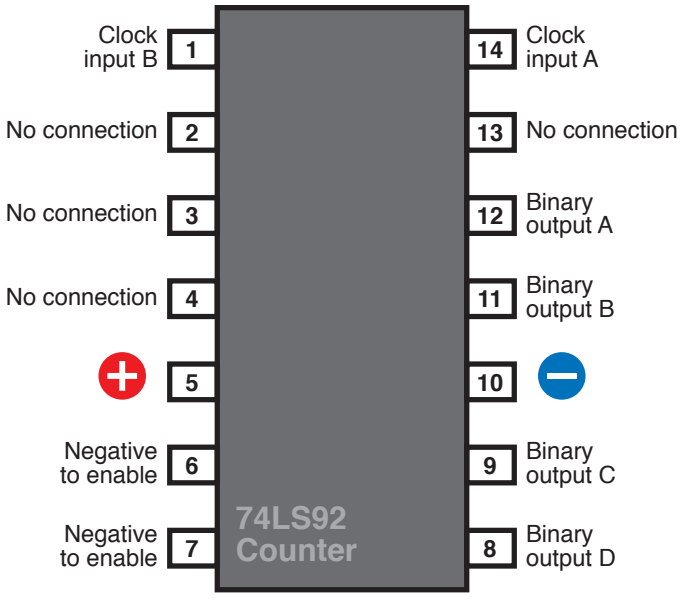

Figure 4-101. *The unusual pin assignments include four that have no connection of any kind inside the chip, and can be left unattached.*

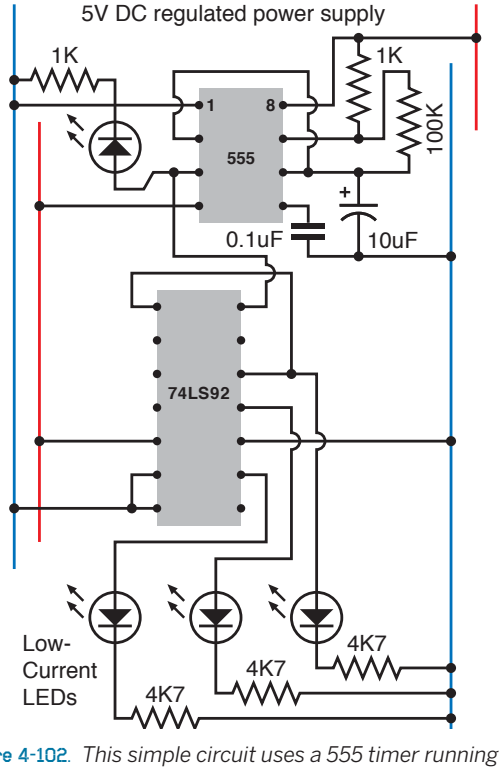

Figure 4-102. *This simple circuit uses a 555 timer running slowly to control the 74LS92 binary counter and display the succession of high states from its outputs.*

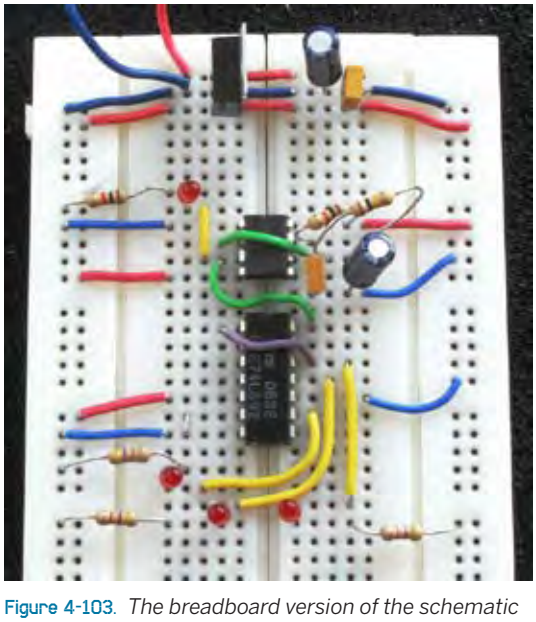

Figure 4-103. *The breadboard version of the schematic in Figure 4-102 to display the outputs from a 74LS92 counter.*

Now we come to the first new and difficult fact about the 74LSxx generation of TTL chips that makes them less desirable, for our purposes, than the 74HCxx generation of CMOS chips that I have recommended in previous projects. The modern and civilized HC chips will source 4mA or sink 4mA at each logical output, but the older LS generation is fussier. It will sink around 8mA into each output pin from a positive source, but when its output is high, it hardly gives you anything at all. This is a very basic principle:

- Outputs from TTL logic chips are designed to sink current.
- They are not designed to source significant current.

In fact, the 74LS92 is rated to deliver less than half a milliamp. This is quite acceptable when you're just connecting it with another logic chip, but if you want to drive an external device, it doesn't provide much to work with.

The proper solution is to say to the chip, "All right, we'll do it your way," and set things up with a positive source that flows through a load resistor to the LED that you want to use, and from there into the output from the chip. This is the "better" option shown in Figure 4-104.

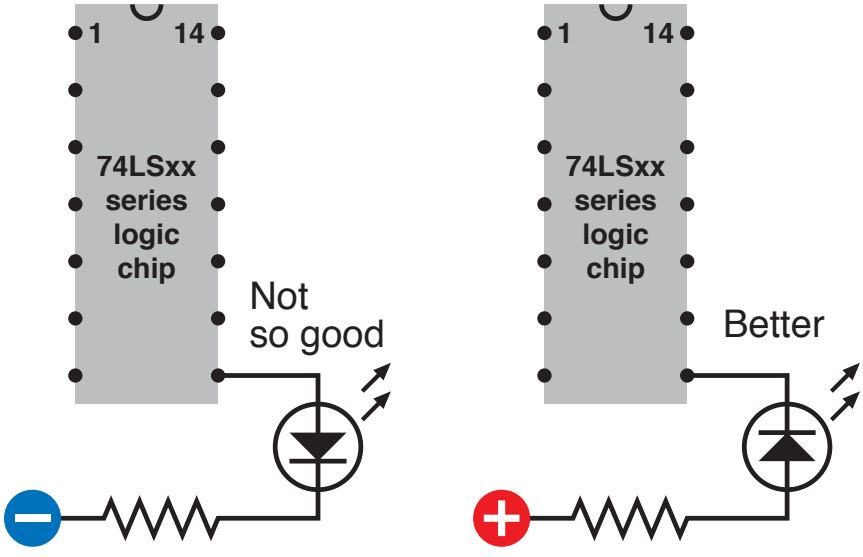

Figure 4-104. *Most TTL chips, including those in the LS generation, are unable to source much current from their logical output pins (left) and should usually be wired to sink current from a positive source (right).*

The only problem is that now the LED lights up when the counter's output is low. But the counter is designed to display its output in high pulses. So your LED is now off when it should be on, and on when it should be off.

You can fix this by passing the signal through an inverter, but already I'm getting impatient with this inconvenience. My way around the problem, at least for demo purposes, is to use the "Not so good" option in Figure 4-104 and make it work by connecting a very-low-current LED with a large 4K7 load resistor. This will enable us to "see" the output from the counter without asking it to give more than its rated limit, and if you want to create a more visibly powerful

display for a finished version of the dice circuit, I'll deal with that later. According to my meter, the 4K7 resistor holds the current between 0.3mA and 0.4mA, which is the counter's rated maximum.

Set up your initial version of the circuit as shown in Figures 4-102 and 4-103. Be careful when you wire the positive and negative power supply to the counter chip, with its nonstandard pin assignments.

The 555 will run in astable mode, at about 1 pulse per second. This becomes the clock signal for the counter. The first three binary outputs from the counter then drive the three LEDs.

The counter advances when the input signal goes from *high* to *low*. So when the LED beside the 555 timer goes out, that's when the counter advances.

If you stare at the pattern generated by the outputs for long enough, you may be able to see the logic to it, bearing in mind that its zero state is when they are all off, and it counts up through five more steps before it repeats. The diagram in Figure 4-105 shows this sequence. If you want to know why the pattern works this way, check the following section, "Theory: Binary arithmetic."

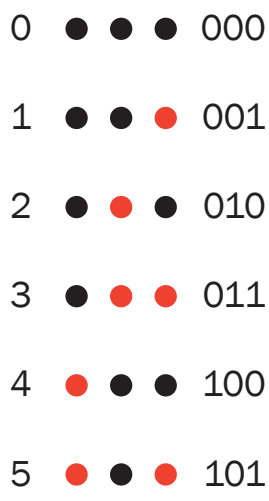

Figure 4-105. *The three output pins of the 74LS92 counter have high states shown by the red circles as the counter steps from 000 to 101 in binary notation.*

THEORY

Binary arithmetic

The rule for binary counting is just a variation of the rule that we normally use for everyday counting, probably without thinking much about it. In a 10-based system, we count from 0 to 9, then carry 1 over to the next position on the left, and go from 0 to 9 again in the right-most position. We repeat this procedure until we get to 99, then carry a 1 over to a new position to make 100, and continue counting.

In binary we do the same thing, except that we restrict ourselves to digits 0 and 1 only. So begin with 0 in the rightmost position, and count up to 1. As 1 is our limit, to continue counting we carry 1 over to the next place on the left, and start again from 0 in the right-most position. Count up to 1, then add 1 to the next place on the left—but, it already has a 1 in it, so it can't count any higher. So, carry 1 from there one space further, to the next place beside that—and so on.

If a glowing LED represents a 1, and a dark LED represents a 0, the diagram in Figure 4-105 shows how the 74LS92 counts up from 0 to (decimal) 6 or (binary) 101 in its inimitable fashion. I've also included a diagram in Figure 4-106 showing how a counter with four binary outputs would display decimal numbers from 0 through 15, again using the LEDs to represent 1s and 0s.

Here's a question for you: how many LEDs would you need to represent the decimal number 1024 in binary? And how many for 1023?

Obviously binary code is ideally suited to a machine full of logic components that either have a high or a low state. So it is that all digital computers use binary arithmetic (which they convert to decimal, just to please us).

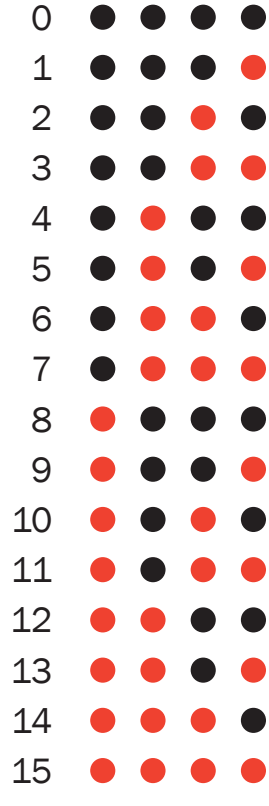

Figure 4-106. *A hexadecimal (16-based) binary counter would generate this succession of high states from its four output pins as it counts from 0 through 15 in decimal notation.*

Getting back to our project: I want to take the three binary outputs and make them create patterns like the spots on a die. How can I do this? Quite easily, as it turns out.

I'm assuming that I'll use seven LEDs to simulate the patterns of spots on a die. These patterns can be broken down into groups, which I have assigned to the three outputs from the counter in Figure 4-108. The first output (farthest to the right) can drive an LED representing the dot at the center of the die face. The second (middle) output can drive two more diagonal LEDs. The third output must switch on all four corner LEDs.

This will work for patterns 1 through 5, but won't display the die pattern for a 6. Suppose I tap into all three outputs from the counter with a three-input NOR gate. It has an output that goes high only when all three of its inputs are low, so it will only give a high output when the counter is beginning with all-low outputs. I can take advantage of this to make a 6 pattern.

Note that it's bad practice to mix the LS generation of TTL chips with the HC generation of CMOS chips, as their input and output ranges are different; so, the NOR chip has to be a 74LS27, not a 74HC27.

We're ready now for a simple schematic. In Figure 4-107 I've colored some of the wires just to make it easier for you to distinguish them. The colors have no other significance.

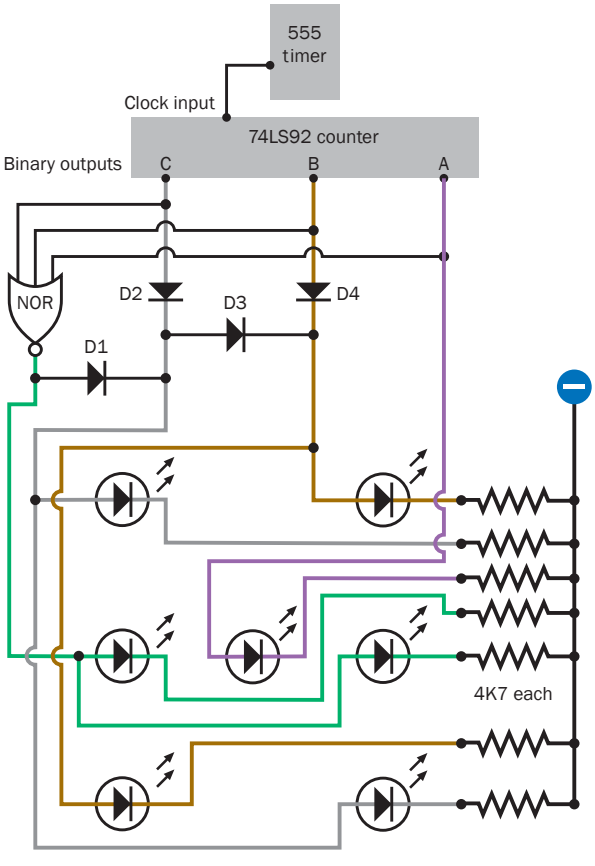

Figure 4-107. *A simplified schematic shows how outputs from the 74LS92 counter can be combined, with signal diodes and a single three-input NOR gate, to generate the spot patterns on a die. The wire colors have no special meaning and are used just to distinguish them from each other.*

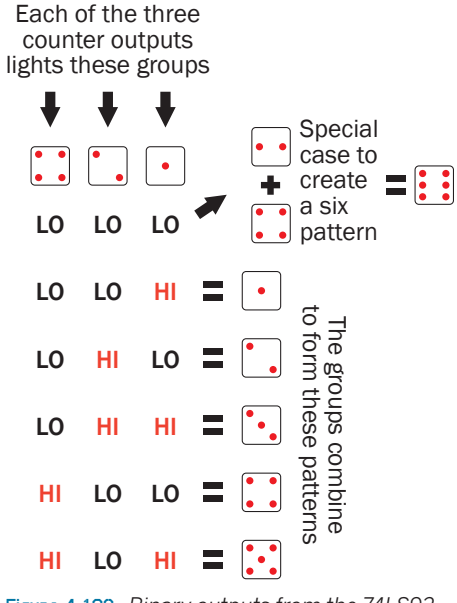

Figure 4-108. *Binary outputs from the 74LS92 counter can be used to power LEDs arrayed in groups to simulate the pattern of spots on a die.*

Each of the LEDs is grounded through a separate 4K7 load resistor. Unfortunately, this means that when they are displaying the pattern for a 6, all of them are running in parallel from the output of the NOR gate, which overloads it. As long as you don't leave the display in this mode for very long periods, it shouldn't cause a problem. You could compensate by increasing the load resistors, or by running pairs of the LEDs through one resistor, but this will make them so dim that they'll be difficult to see, as they're so close to their lower limit for current already.

Notice how I have added four signal diodes, D1 through D4. When Output C goes high, it has to illuminate all four corner LEDs, and so its power goes into the brown wire as well as the gray wire. But we must never allow one output to feed back into another, so D4 is needed to protect Output B when Output C is high.

Because there is now a connection between B and C, we need D2 to protect Output C when Output B is high. And because Output B must only feed two of the corner LEDs, we also need D3 to stop it from illuminating the other two. And, we have to protect the output from the NOR gate when either Output C or Output B is high. This requires D1.

Figure 4-109 shows everything that I've described so far assembled in breadboard format, while Figure 4-110 shows the test version that I built. Note that the unused logical inputs on the 74LS27 chip are shorted together and connected to the *positive* side of the power supply. Here's the rule:

- When using CMOS chips (such as the HC series), connect unused logical inputs to the negative side of the power supply.
- When using TTL chips (such as the LS series), connect unused logical inputs to the positive side of the power supply.

I assume that you have had enough fun watching the LEDs count slowly, so I've changed the capacitor and resistor values for the 555 to increase its speed from approximately 1 pulse per second to about 50,000 pulses per second. The counter could run much faster than this, but I just want it to cycle fast enough so that when the user presses and releases a button, the count will stop at an unforeseeable number.

The button starts and stops the 555 timer by applying and releasing power to the timing circuit only. This is the equivalent of shaking and then throwing the die.

While the counter is running fast, the LEDs are flashing so fast that all of them will seem to be on at once. At the same time, the circuit charges a new 68 µF capacitor, which I have added between the pushbutton and ground. When you release the button, this capacitor discharges itself through the 1K timing resistor. As the charge dissipates, the timing capacitor will take longer and longer to charge, and discharge, and the frequency of the 555 will gradually diminish. Consequently the LED display will also flash slower, like the reel on a Las Vegas slot machine gradually coming to a stop. This increases the tension as players can see the die display counting to the number that they're hoping for—and maybe going one step beyond it.

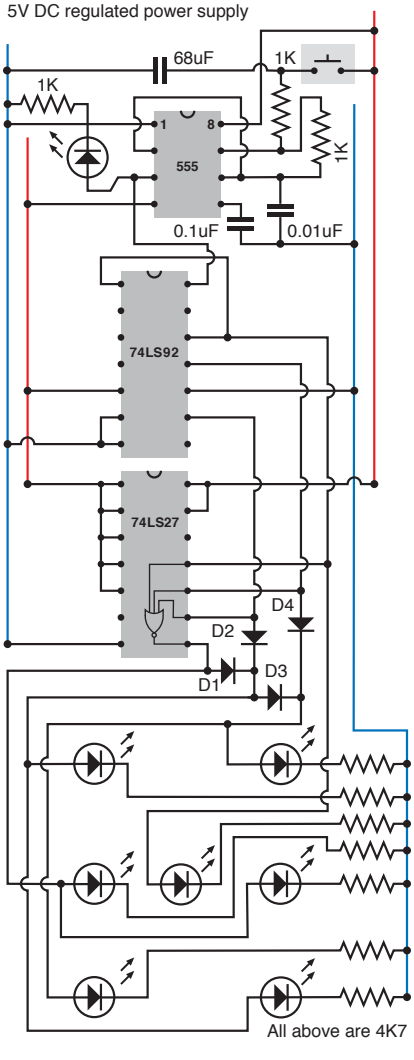

Figure 4-109. *With some extra components, the schematics from Figures 4-102 and 4-107 can be combined to make the working dice simulation.*

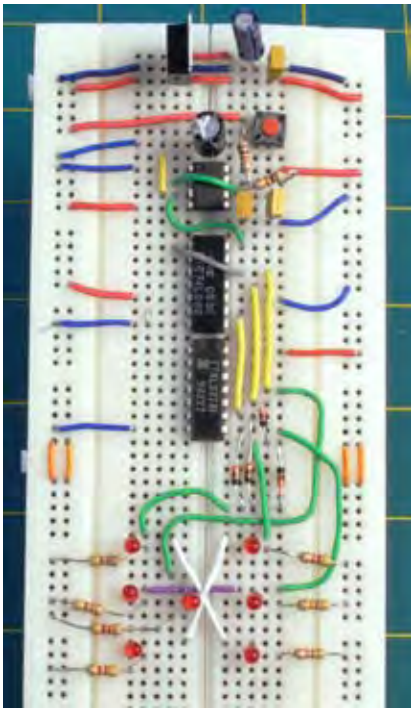

Figure 4-110. *The electronic dice schematic applied to a breadboard, with a pushbutton at the top to start and stop the counter, and 7 LEDs at the bottom to display the output.*

Note that to maximize this effect, the button has to be held down for a full second or more, so that the 68 µF capacitor becomes fully charged before the button is released.

So, this circuit now fulfills the original goal. But can it be better? Of course it can.

Enhancements

The main thing I want to improve is the brightness of the LEDs. I could add a transistor to amplify the current to each one, but there's a simpler alternative: a TTL "open collector" inverter.

I want to use an inverter because in the world of TTL, as I mentioned earlier, we can sink much more power into the output pin of a chip than we can source from it. So, I'm going to turn each LED the other way around and connect their load resistors to the positive side of the power supply. This way, they'll sink their power into the outputs of the inverter.

And the great advantage of an "open collector" version of the inverter chip is that it is designed to sink much more current than a normal TTL logic chip. It is rated for 40mA per pin. The only disadvantage is that it cannot source any current at all; instead of its output going high, it just behaves like an open switch. But that's OK for this circuit.

So the next and final schematic, in Figure 4-111, includes the 74LS06 inverter, which has also been added to the breadboarded version shown in Figure 4-112. I suggest that you put aside the little low-current LEDs and substitute some normal-size ones. Using Kingbright "standard" WP15031D 5mm LEDs, I find that each draws almost exactly 20mA with a voltage drop of about 2V with a 120 ohm series resistor. Because each output pin from the 74LS06 inverter powers no more than two LEDs at a time, this is exactly within its specification. I suggest that if you build this circuit, you check the consumption of your particular choice of LEDs and adjust the resistors if necessary.

Remember: to measure the voltage drop across an LED, simply touch the probes of your meter across it while it is illuminated. To measure the current, disconnect one side of the LED and insert the meter, in milliamp mode, between the leg of the LED and the contact that it normally makes in the circuit.

For a really dramatic display, you can get some 1 cm diameter LEDs (Figure 4-113). Check the specification, and you should find that many of these don't use more power than the usual 5 mm type. But whatever kind you use, don't forget to turn them around so that their negative sides face toward the inverter, and their positive sides face the resistors, which are connected to the positive side of the power supply.

One last detail: I had to add two 10K resistors to this version of the circuit. Can you see why? Diodes D1 through D4 are designed to transmit positive voltage through to the inverter when appropriate, but they prevent the inputs of the inverter from "seeing" the negative side of the power supply when the counter outputs are low. These inverter inputs require pull-down resistors to prevent them from "floating" and producing erroneous results.

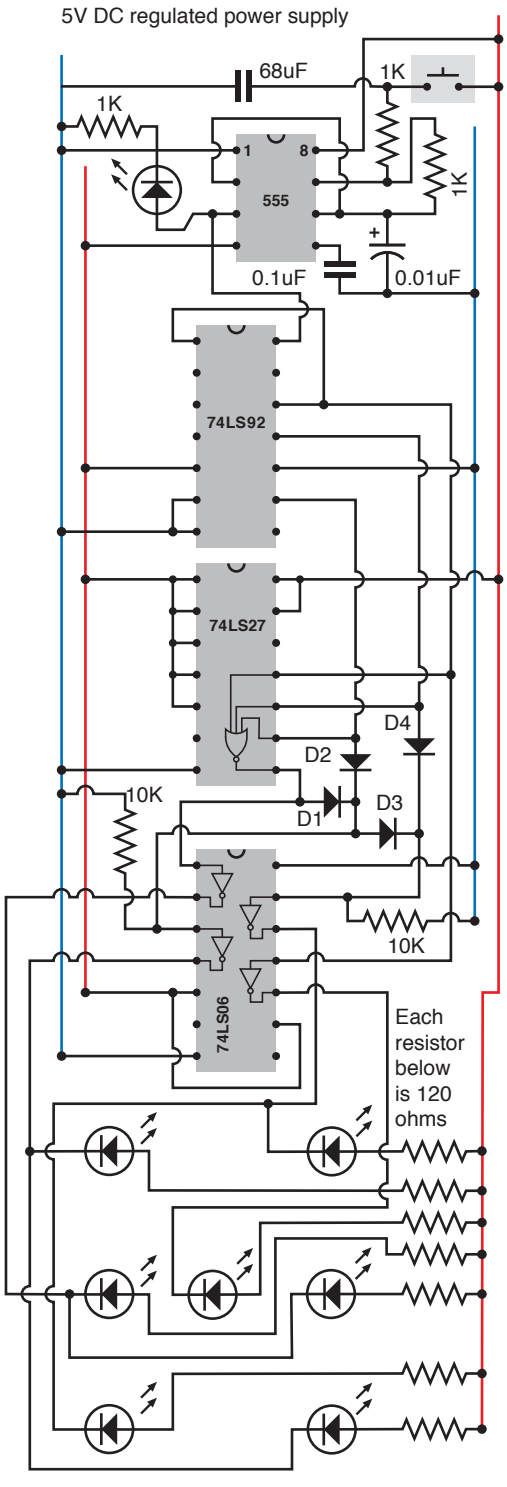

Figure 4-111. *If open-collector inverters are added to the dice schematic, it can drive full-size LEDs with up to 40mA, as long as the LEDs are turned around to sink current into the TTL output stage instead of trying to source current from it.*

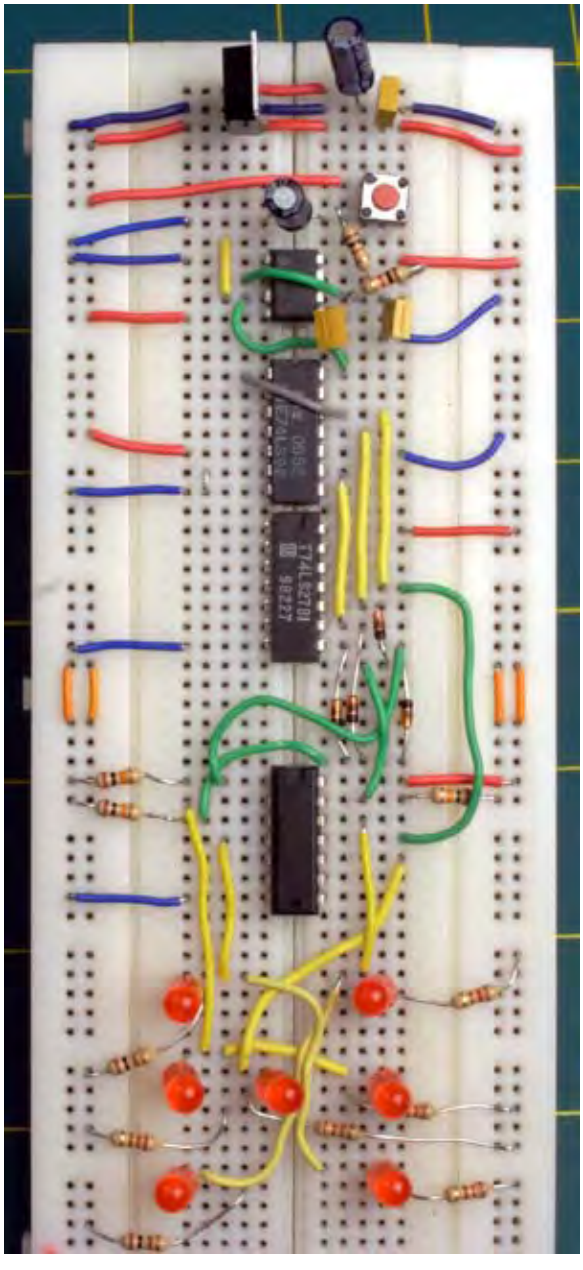

Figure 4-112. *The completed circuit using an open-collector inverter to drive full-size LEDs.*

The final enhancements are up to you. Most obviously, you can add a second die, as many games require two dice. The 74LS27 chip still has a couple of spare NOR gates in it, one of which you can make use of, but you will need an additional 555 timer, running at a significantly different speed to ensure randomness, and it will have to drive a second counter.

After you get your dice up and running, you may want to test them for randomness. Because the pulses from a 555 timer are of equal length, every number has an equal chance of coming up; but the longer you hold down the Start button, the better your odds are of interrupting the counting process at a truly random moment. Anyone using your electronic dice should be told that "shaking" them for a full second is mandatory.

Of course, I could have simulated dice more easily by writing a few lines of software to generate random numbers on a screen, but even a fancy screen image cannot have the same appeal as a well-made piece of hardware. Figure 4-113 shows white 1 cm LEDs mounted in a sanded polycarbonate enclosure for dramatic effect.

Most of all, I derived satisfaction from using simple, dedicated chips that demonstrate the binary arithmetic that is fundamental in every computer.

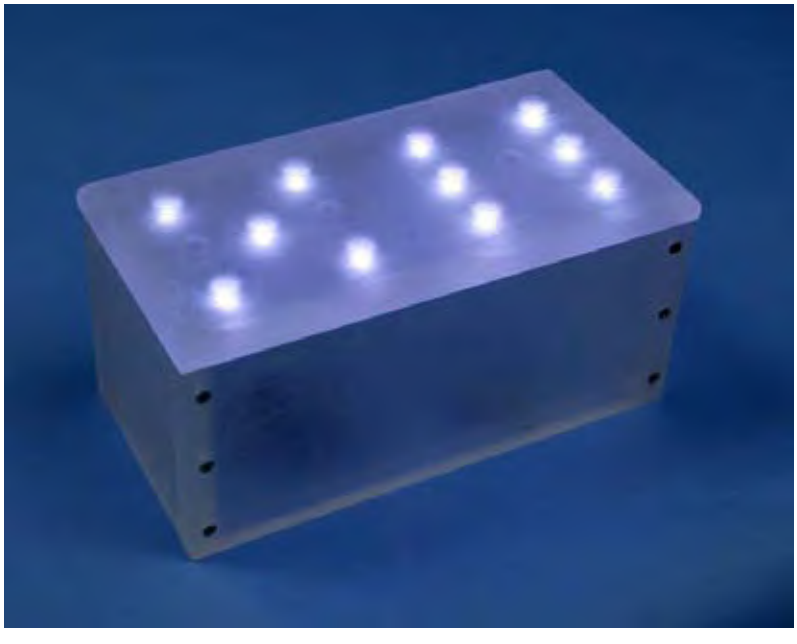

Figure 4-113. *The open-collector inverter chip in the dice circuit is sufficiently powerful to drive 1-cm white LEDs that draw about 20mA each, using a potential of 2V. In this finished version, the LEDs were embedded in cavities drilled from the underside of half-inch polycarbonate, which has been treated with an orbital sander to create a translucent finish.*

Experiment 24: Intrusion Alarm Completed

Now let me suggest how you can apply the knowledge from this chapter of the book to upgrade the burglar alarm project that was last modified in Experiment 15. You'll probably need to check Chapters 2 and 3 to refamiliarize yourself with some features of the alarm.

Upgrade 1: Delayed Activation

The biggest flaw in the alarm was that as soon as it was activated, it would immediately respond to any signal from the door and window sensors. It needed a feature to delay activation to give you a chance to exit from the building before the alarm armed itself. A 555 timer can provide this functionality, probably in conjunction with a relay. The power to the alarm should pass through the contacts of the relay, which are normally closed. When you press a button on the timer, it sends a positive pulse to the relay lasting for around 30 seconds, holding the relay open for that period. You could mount the timer in its own little box with a button on it, which you press when you're ready to leave the building. The 12-volt power supply to the burglar alarm passes through the box containing the delay circuit. For 30 seconds, the 555 interrupts power to the alarm, and then restores it, ready for action.

Upgrade 2: Keypad Deactivation

This is now really simple. You can substitute a latching relay instead of the switch, S1, on the alarm box (shown in Figure 3-110), and use a keypad to set and reset the relay in exactly the same way as in the combination lock in Experiment 20. You'll have to run an additional three wires from the relay, out of the alarm box, to the keypad (one supplying power to the "on" relay coil, another supplying power to the "off" coil, the third being a common ground). You can either use a 9-volt battery to power the electronics in association with the keypad, or run an additional fourth wire from the alarm box, to carry positive power to the logic chips, bearing in mind that you have to insert a voltage regulator at some point, to drop the 12 volts that the alarm uses to the 5 volts that the logic gates require. As the gates consume so little power, the 12-to-5 drop should be OK for the voltage regulator; it won't have to dissipate too much heat.

With this additional feature, you can use the alarm like this:

- Press the pound key on the keypad to flip the latching relay into its "on" mode, so that it passes power to the alarm box, which is now armed.
- If you want to leave the house, push the button on the delay unit to give you 30 seconds in which to do so.
- If the alarm is triggered, enter your secret code on the keypad to deactivate it by flipping the latching relay to its "off" position and cutting power to the alarm box.

These modifications are so simple that I think the block diagram in Figure 4-114 should be all you need. I don't think I need to give you any schematics. The only change you have to make to the existing alarm is to substitute the latching relay for the on/off switch.

But, there is still one obvious necessary enhancement needed: how can you get back into the house without instantly triggering the alarm?

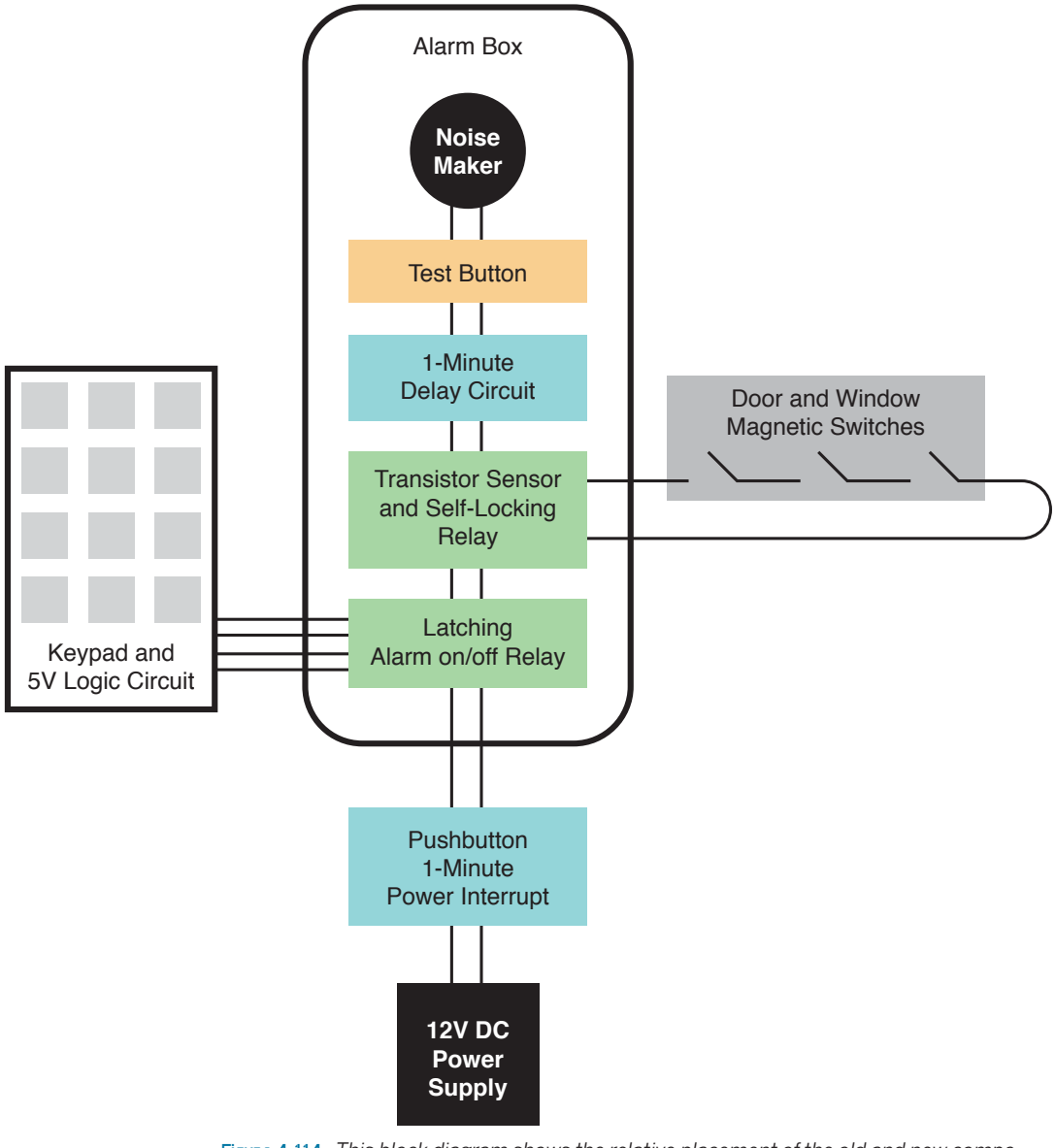

Figure 4-114. *This block diagram shows the relative placement of the old and new components. The pushbutton power interrupt (which allows you to leave the house before the alarm switches itself back on) goes between the power supply and everything else. The latching relay substitutes for the DPDT switch on the previous version of the alarm. The transistor and self-locking relay, connected with the door and window magnetic switches, remain unchanged. The new delay circuit is inserted between the self-locking relay and the noisemaker. The test button is wired with the latching relay in the same way that it was wired previously with the DPDT switch.*

Upgrade 3: Delay Before Deactivation

Typically, alarms include another delay feature. When you open a door on your way into the building and it triggers the alarm, you have 30 seconds to deactivate it, before it starts making a noise.

How can we implement this delay feature? If I try to use another 555 timer to generate a pulse to inhibit the noise, that won't work, because the output from either the transistor or the relay can continue indefinitely. The relay locks itself on, and the transistor can continue passing voltage for as long as someone leaves a door open. If either of these signals activates a timer in monostable mode, the pulse from the timer will never end, and it will suppress the alarm indefinitely.

I think what I have to do is use a resistor and a capacitor to create a delay. I'll power them through the existing relay, so that I can be sure that they'll receive the full voltage of the power supply, after beginning from zero. Gradually the capacitor will acquire voltage—but I can't connect this directly to the noisemaker, because the noisemaker will gradually get louder as the voltage increases.

I have to insert a device that will be triggered to give full voltage when the input rises past a certain point. To do this, I'll use a 555 timer that's wired in bistable mode. This kind of modification is generally known as a "kludge," because it's not elegant, uses too many components, and does not use them appropriately. What I really need is a comparator, but I don't have space to get into that topic. So, using the knowledge that you have so far, the schematic in Figure 4-115 shows how a delay can be added to the alarm—not elegantly, but reliably.

The only problem is that if you power up a 555 timer in bistable mode, there's a 50-50 chance that the timer starts itself with its output high or low. So I need to pull the voltage low on the reset pin (to start the timer with its output inhibited) and gradually let it become positive (to permit the output). At the same time, I want to start with the voltage high on the trigger pin and gradually lower it, until it falls below 1/3 of the power supply and triggers the output.

So there are two timing circuits. The one for the reset pin works faster than the one on the trigger pin, so that at the point when the timer is triggered, the reset won't stop it.

The schematic shows component values that will do this. The 10 µF capacitor starts low but is charged through the 10K resistor in a couple of seconds. The timer is now ready to be triggered. But the 68 µF capacitor starts high (being connected with the positive side of the power supply) and takes a full minute to be pulled down to 1/3 of supply voltage through the 1M resistor. At that point, its voltage is low enough to trigger the 555. The timer output goes high and supplies the noisemaker.

You should be able to insert this little delay module in your alarm box, between the output from the relay and the input to the noisemaker without too much trouble. And if you want to adjust the delay, just use a higher or lower value resistor than 1M.

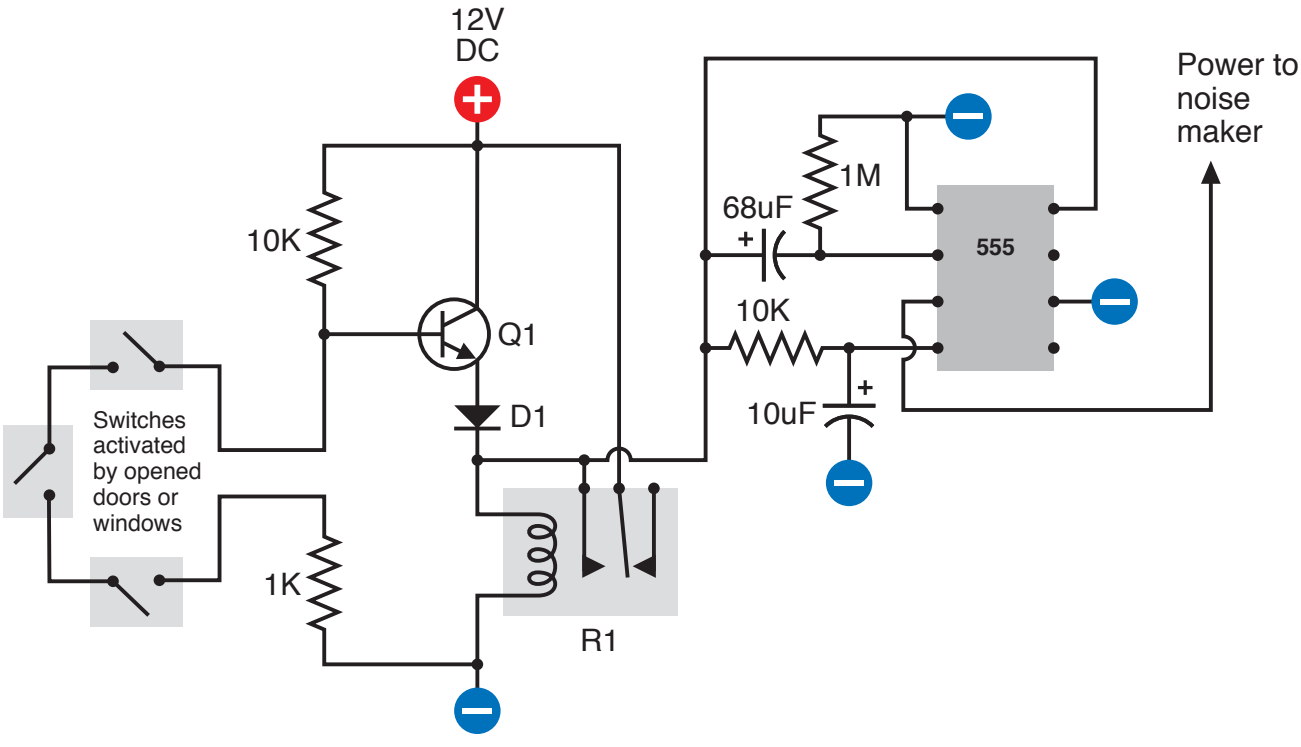

Figure 4-115. *This addition to the original alarm circuit imposes a one-minute delay before the alarm sounds. The 555 timer (wired in bistable mode) receives power through relay R1. The lower timing circuit initially applies negative voltage to the reset, ensuring that the 555 powers up with its output suppressed. This voltage quickly rises. Meanwhile the upper timing circuit applies a voltage to the trigger that gradually diminishes as the 68 µF capacitor equalizes its charge through the 1M resistor. When the voltage diminishes to 1/3 of the supply, the timer's output goes high and starts the noisemaker. If the power to the circuit is interrupted at any time before this, the relay relaxes, the capacitors gradually discharge, and the alarm does not sound.*

The Wrap-Up

If you add these three enhancements, your alarm will have all the features on my original wish list. Of course, if I were designing it from scratch, with all the information that has been added in this chapter of the book, it could be more elegant. But the modifications have not entailed making destructive changes to our original project, and all the design goals have been met.

What Next?

5

At this point, we can branch out in numerous directions. Here are some possibilities:

Audio electronics
: This is a field in itself, including hobby projects, such as simple amplifiers and "stomp boxes," to modify guitar sound.

Radio-frequency devices
: Anything that receives or transmits radio waves, from an ultra-simple AM radio to remote controllers.

Motors
: The field of robotics has encouraged the growth of many online sites selling stepper motors, gear motors, synchronous motors, servo motors, and more.

Programmable microcontrollers
: These are tiny computers on a single chip. You write a little program on your desktop computer, which will tell the chip to follow a series of procedures, such as receiving input from a sensor, waiting for a fixed period, and sending output to a motor. Then you download your program onto the chip, which stores it in nonvolatile memory. Popular controllers include the PICAXE, BASIC Stamp, Arduino, and many more. The cheapest ones retail for a mere $5 each.

Obviously, I don't have space to develop all of these topics fully, so what I'm going to do is introduce you to them by describing just one or two projects in each category. You can decide which interests you the most, and then proceed beyond this book by reading other guides that specialize in that interest.

I'm also going to make some suggestions about setting up a productive work area, reading relevant books, catalogs, and other printed sources, and generally proceeding further into hobby electronics.

IN THIS CHAPTER

Shopping List: Experiments 25 Through 36
Customizing Your Work Area
Reference Sources
Experiment 25: Magnetism
Experiment 26: Tabletop Power Generation
Experiment 27: Loudspeaker Destruction
Experiment 28: Making a Coil React
Experiment 29: Filtering Frequencies
Experiment 30: Fuzz
Experiment 31: One Radio, No Solder, No Power
Experiment 32: A Little Robot Cart
Experiment 33: Moving in Steps
Experiment 34: Hardware Meets Software
Experiment 35: Checking the Real World
Experiment 36: The Lock, Revisited
In Closing

Shopping List: Experiments 25 Through 36

Tools

You won't need any new tools for this section of the book.

Supplies and Components

As we have progressed to the point where you may want to pick and choose which projects you attempt, I will list the supplies and components at the beginning of each experiment.

Customizing Your Work Area

At this point, if you're getting hooked on the fun of creating hardware but haven't allocated a permanent corner to your new hobby, I have some suggestions. Having tried many different options over the years, my main piece of advice is this: don't build a workbench!

Many hobby electronics books want you to go shopping for 2×4s and plywood, as if a workbench has to be custom-fabricated to satisfy strict criteria about size and shape. I find this puzzling. To me, the exact size and shape of a bench is not very important. I think the most important issue is storage.

I want tools and parts to be easily accessible, whether they're tiny transistors or big spools of wire. I certainly don't want to go digging around on shelves that require me to get up and walk across the room.

Figure 5-1. *The ideal work area: surrounded by storage. Never again will you need to get out of your chair!*

This leads me to two conclusions:

1. You need storage above the workbench.
2. You need storage below the workbench.

Many DIY workbench projects allow little or no storage underneath. Or, they suggest open shelves, which will be vulnerable to dust. My minimum configuration would be a pair of two-drawer file cabinets with a slab of 3/4-inch plywood or a Formica-clad kitchen countertop placed across them. File cabinets are ideal for storing all kinds of objects, not just files.

Of all the workbenches I've used, the one I liked best was an old-fashioned steel office desk—the kind of monster that dates back to the 1950s. They're difficult to move (because of their weight) and don't look beautiful, but you can buy them cheaply from used office furniture dealers, they're generous in size, they withstand abuse, and they last forever. The drawers are deep and usually slide in and out smoothly, like good file-cabinet drawers. Best of all, the desk has so much steel in it that you can use it to ground yourself before touching components that are sensitive to static electricity. If you use an antistatic wrist strap, you can simply attach it to a sheet-metal screw that you drive into one corner of the desk.

What will you put in the deep drawers of your desk or file cabinets? Some paperwork may be useful, perhaps including the following documents:

- Product data sheets
- Parts catalogs
- Sketches and plans that you draw yourself

The remaining capacity of each drawer can be filled with plastic storage boxes. The boxes can contain tools that you don't use so often (such as a heat gun or a high-capacity soldering iron), and larger-sized components (such as loudspeakers, AC adapters, project boxes, and circuit boards). You should look for storage boxes that measure around 11 inches long, 8 inches wide, and 5 inches deep, with straight sides. Boxes that you can buy at Wal-Mart will be cheaper, but they often have tapering sides (which are not space-efficient).

The boxes that I like best are Akro-Grids, made by Akro-Mils (see Figures 5-2 and 5-3). These are very rugged, straight-sided, with optional transparent snap-on lids. You can download the full Akro-Mills catalog from *http://www.akro-mils.com* and then search online for retail suppliers. You'll find that Akro-Mils also sells an incredible variety of parts bins, but I don't like open bins because their contents are vulnerable to dust and dirt.

For medium-size components, such as potentiometers, power connectors, control knobs, and toggle switches, I like storage containers measuring about 11 inches long, 8 inches wide, and 2 inches deep , divided into four to six sections. You can buy these from Michaels (the craft store), but I prefer to shop online for the Plano brand, as they seem more durably constructed. The Plano products that are most suitable for medium-size electronic parts are classified as fishing-tackle boxes, and you'll see them at *http://www.planomolding.com/tackle/products.asp*.

Figure 5-2. *Akro-Grid boxes contain grooves allowing them to be partitioned into numerous compartments for convenient parts storage.*

Figure 5-3. *Lids are sold separately for Akro-Grid boxes to keep the contents dust-free. The height of the box in Figure 5-2 allows three to be stacked in a typical file-cabinet drawer. The box shown here allows two to be stacked.*

Figure 5-4. *This Plano brand box is undivided, making it useful for storing spools of wire or medium-size tools. When stacked upright on its long edge, three will fit precisely in a file-cabinet drawer.*

For undivided, flat-format storage boxes, the Prolatch 23600-00 is ideally sized to fit a file-cabinet drawer, and the latches are sufficiently secure that you could stack a series of them on their long edges. See Figure 5-4.

Plano also sells some really nicely designed toolboxes, one of which you can place on your desktop. It will have small drawers for easy access to screwdrivers, pliers, and other basics. Because you need a work area that's only about three feet square for most electronics projects, surrendering some desk space to a toolbox is not a big sacrifice.

If you have a steel desk with relatively shallow drawers, one of them can be allocated for printed catalogs. Don't underrate the usefulness of hard copy, just because you can buy everything online. The Mouser catalog, for instance, has an index, which is better in some ways than their online search feature, and the catalog is divided into helpful categories. Many times I've found useful parts that I never knew existed, just by browsing, which is much quicker than flipping through PDF pages online, even with a broadband connection. Currently, Mouser is still quite generous about sending out their catalogs, which contain over 2,000 pages. McMaster-Carr will also send you a catalog, but only after you've ordered from them, and only once a year.

Now, the big question: how to store all those dinky little parts, such as resistors, capacitors, and chips? I've tried various solutions to this problem. The most obvious is to buy a case of small drawers, each of which is removable, so you can place it on your desk while you access its contents. But I don't like this system, for two reasons. First, for very small components, you need to subdivide the drawers, and the dividers are never secure. And second, the removability of the drawers creates the risk of accidentally emptying the contents on the floor. Maybe you're too careful to allow this to happen, but I'm not!

Figure 5-5. *Darice Mini-Storage boxes are ideal for components such as resistors, capacitors, and semiconductors. The boxes can be stacked stably or stored on shelves, with their ends labeled. The brand sticker is easily removed after being warmed with a heat gun.*

My personal preference is to use Darice Mini-Storage boxes, shown in Figure 5-5. You can find these at Michaels in small quantities, or buy them more economically in bulk online from suppliers such as *http://www.craftamerica.com*. The blue boxes are subdivided into five compartments that are exactly the right size and shape for resistors. The yellow boxes are subdivided into ten compartments, which are ideal for semiconductors. The purple boxes aren't divided at all, and the red boxes have a mix of divisions.

The dividers are molded into the boxes, so you don't have the annoyance associated with removable dividers that slip out of position, allowing components to mix together. The box lids fit tightly, so that even if you drop one of the boxes, it probably won't open. The lids have metal hinges, and a ridge around the edge that makes the boxes securely stackable.

I keep my little storage boxes on a set of shelves above the desk, with a gap of 3 inches between one shelf and the next, allowing two boxes to be stacked on each shelf. If I want to work with a particular subset of boxes, I shift them onto the desktop and stack them there.

Labeling

No matter which way you choose to store your parts, labeling them is essential. Any ink-jet printer will produce neat-looking labels, and if you use peelable (nonpermanent) labels, you'll be able to reorganize your parts in the future, as always seems to become necessary. I use color-coded labels for my collection of resistors, so that I can compare the stripes on a resistor with the code on the label, and see immediately if the resistor has been put in the wrong place. See Figure 5-6.

Figure 5-6. *To check that resistors are not placed in the wrong compartments, print the color code on each label.*

Even more important: you need to place a second (non-adhesive) label inside each compartment with the components. This label tells you the manufacturer's part number and the source, so that reordering is easy. I buy a lot of items from Mouser, and whenever I open their little plastic bags of parts, I snip out the section of the bag that has the identifying label on it, and slide it into the compartment of my parts box before I put the parts on top of it. This saves frustration later.

If I were *really* well organized, I would also keep a database on my computer listing everything that I buy, including the date, the source, the type of component, and the quantity. But I'm not that well organized.

On the Bench

Some items are so essential that they should sit on the bench or desktop on a permanent basis. These include your soldering iron(s), helping hands with magnifier, desk lamp, breadboard, power strip, and power supply. For a desk lamp, I prefer the type that has a daylight-spectrum fluorescent bulb, because it spreads a uniform light and helps me to distinguish colors of adjacent stripes on resistors.

The power supply is a matter of personal preference. If you're serious about electronics, you can buy a unit that delivers properly smoothed current at a variety of properly regulated and calibrated voltages. Your little wall-plug unit from RadioShack cannot do any of these things, and its output may vary depending on how heavily you load it. Still, as you've seen, it is sufficient for basic experiments, and when you're working with logic chips, you need to mount a 5-volt regulator on your breadboard anyway. Overall, I consider a good power supply optional.

Another optional item is an oscilloscope. This will show you, graphically, the electrical fluctuations inside your wires and components, and by applying probes at different points, you can track down errors in your circuit. It's a neat gadget to own, but it will cost a few hundred dollars, and for our tasks so far, it has not been necessary. If you plan to get seriously into audio circuits, an oscilloscope becomes far more important, because you'll want to see the shapes of the waveforms that you generate.

You can try to economize on an oscilloscope by buying a unit that plugs into the USB port of your computer and uses your computer monitor to display the signal. I have tried one of these, and was not entirely happy with the results. It worked, but did not seem accurate or reliable for low-frequency signals. Maybe I was unlucky; I decided not to try any other brands.

The surface of your desk or workbench will undoubtedly become scarred by random scuffs, cut marks, and drops of molten solder. I use a piece of half-inch plywood, two feet square, to protect my primary work area, and I clamp a miniature vise to its edge. To reduce the risk of static electricity when working with sensitive components, I cover the plywood with a square of conductive foam. This is not cheap, but offers advantages in addition to protecting chips from being zapped. Instead of scattering stray components, I can stick them into the foam, like plants growing in a garden. And like a garden, I can divide it into sections, with resistors on one side, capacitors on the other, and chips straight ahead.

Inevitably, during your work you'll create a mess. Little pieces of bent wire, stray screws, fasteners, and fragments of stripped insulation tend to accumulate, and can be a liability. If metal parts or fragments get into a project that you're building, they can cause short circuits. So you need a trash container. But it has to be easy to use. I use a full-size garbage pail, because it's so big that I can't miss it when I throw something toward it, and I can never forget that it's there.

Last, but most essential: a computer. Now that all data sheets are available online, and all components can be ordered online, and many sample circuits are placed online by hobbyists and educators, I don't think anyone can work efficiently without quick Internet access. To avoid wasting space, I suggest you use a small, cheap laptop that has a minimal footprint. A possible workbench configuration, using a steel desk, is shown in Figure 5-7.

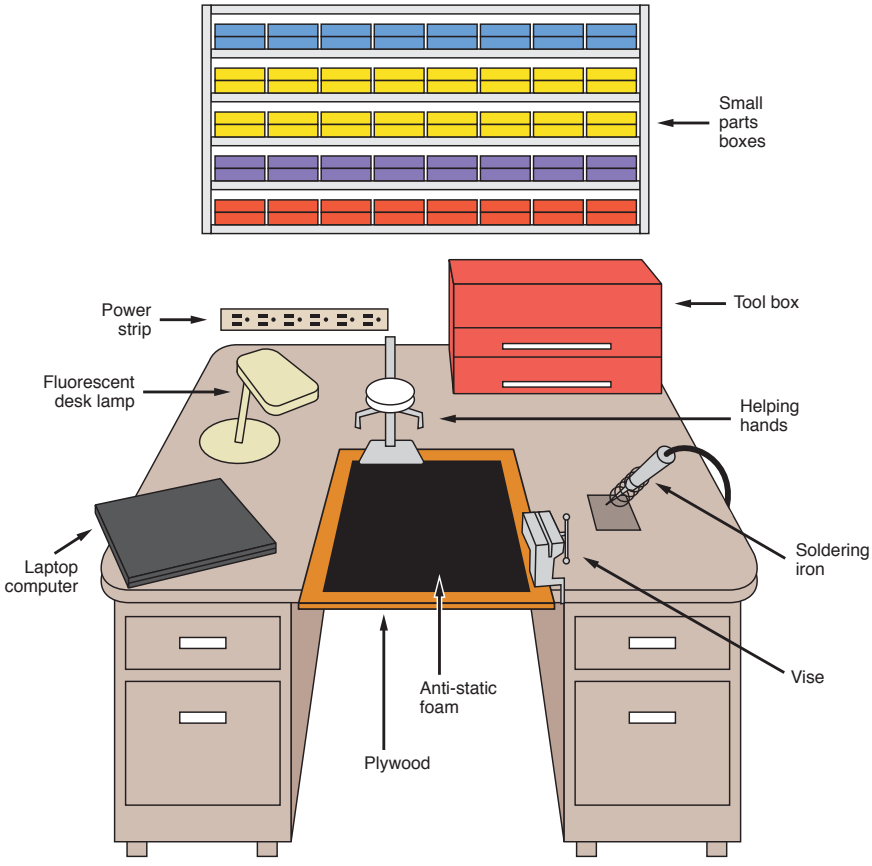

Figure 5-7. *An old steel office desk can be as good as, if not better than, a conventional workbench when building small electronics projects. It provides a large work area and ample storage, and has sufficient mass for you to ground yourself when dealing with components that are sensitive to static electricity.*

Reference Sources

Online

My favorite educational and reference site is Doctronics (*http://www.doctronics.co.uk)*. I like the way they draw their schematics, and I like the way they include many illustrations of circuits on breadboards (which most sites don't bother to do). They also sell kits, if you're willing to pay and wait for shipping from the UK. Part of a page from the doctronics website is reproduced in Figure 5-8.

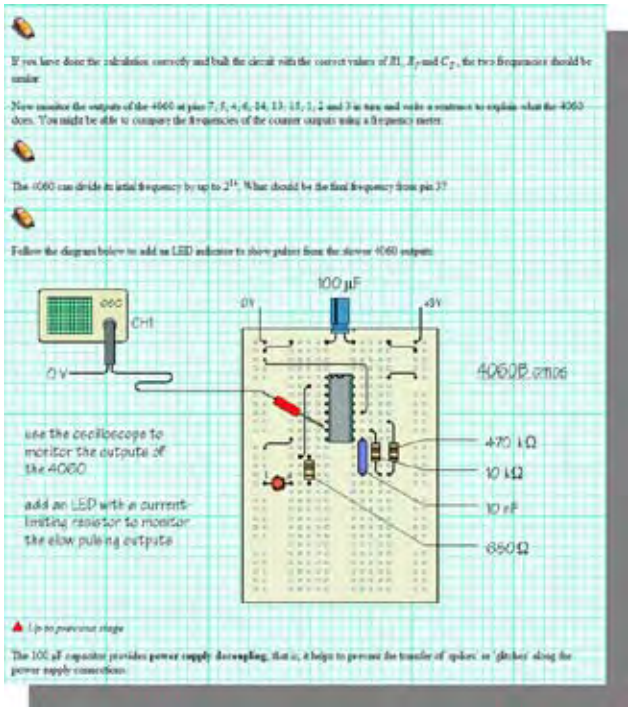

Figure 5-8. *A sample page from http://www.doctronics.co.uk shows their detailed instructional approach. This is a valuable free online resource.*

My next favorite hobby site is also British-based: the Electronics Club (*http://www.kpsec.freeuk.com)*. It's not as comprehensive as Doctronics, but very friendly and easy to understand.

For a more theory-based approach, try *http://www.electronics-tutorials.ws*. This will go a little farther than the theory sections I've included here.

For an idiosyncratic selection of electronics topics, try Don Lancaster's Guru's Lair (*http://www.tinaja.com*). Lancaster wrote *The TTL Cookbook* more than 30 years ago, which opened up electronics to at least two generations of hobbyists and experimenters. He knows what he's talking about, and isn't afraid of getting into some fairly ambitious areas such as writing his own PostScript drivers and creating his own serial-port connections. You'll find a lot of ideas there.

Books

Yes, you do need books. As you're already reading this one, I won't recommend other beginners' guides. Instead, in keeping with the orientation of this chapter, I'll suggest some titles that will take you farther in various directions, and can be used for reference. I own all of these myself, and find them valuable:

Practical Electronics for Inventors, by Paul Scherz (McGraw-Hill, Second Edition, 2007)

This is a massive, comprehensive book, well worth the $40 cover price. Despite its title, you won't need to invent anything to find it useful. It's my primary reference source, covering a wide range of concepts, from the basic properties of resistors and capacitors all the way to some fairly high-end math. If you buy only one book (in addition to this one, of course!), this would be my recommendation.

Getting Started with Arduino, by Massimo Banzi (Make: Books, 2009)

If you enjoy the simplicity and convenience of the PICAXE programmable microcontroller that I describe later in this chapter, you'll find that the Arduino can do a lot more. *Getting Started* is the simplest introduction around, and will help to familiarize you with the Processing language used in Arduino (similar to the C language, not much like the version of BASIC used by the PICAXE).

Making Things Talk, by Tom Igoe (Make: Books, 2007)

This ambitious and comprehensive volume shows how to make the most of the Arduino's ability to communicate with its environment, even getting it to access sites on the Internet.

TTL Cookbook, by Don Lancaster (Howard W. Sams & Co, 1974)

The 1974 copyright date is not a misprint! You may be able to find some later editions, but whichever one you buy, it will be secondhand and possibly expensive, as this title now has collectible value. Lancaster wrote his guide before the 7400 series of chips was emulated on a pin-for-pin basis by CMOS versions, but it's still a good reference, because the concepts and part numbers haven't changed, and his writing is so accurate and concise.

CMOS Sourcebook, by Newton C. Braga (Sams Technical Publishing, 2001)

This book is entirely devoted to the 4000 series of CMOS chips, not the 74HC00 series that I've dealt with primarily here. The 4000 series is older and must be handled more carefully, because it's more vulnerable to static electricity than the generations that came later. Still, the chips remain widely available, and their great advantage is their willingness to tolerate a wide voltage range, typically from 5 to 15 volts. This means you can set up a 12-volt circuit that drives a 555 timer, and use output from the timer to go straight into CMOS chips (for example). The book is well organized in three sections: CMOS basics, functional diagrams (showing pinouts for all the main chips), and simple circuits showing how to make the chips perform basic functions.

The Encyclopedia of Electronic Circuits, by Rudolf F. Graf (Tab Books, 1985)

A totally miscellaneous collection of schematics, with minimal explanations. This is a useful book to have around if you have an idea and want to see how someone else approached the problem. Examples are often more valuable than general explanations, and this book is a massive compendium of examples. Many additional volumes in the series have been published, but start with this one, and you may find it has everything you need.

The Circuit Designer's Companion, by Tim Williams (Newnes, Second Edition, 2005)

Much useful information about making things work in practical applications, but the style is dry and fairly technical. May be useful if you're interested in moving your electronics projects into the real world.

The Art of Electronics, by Paul Horowitz and Winfield Hill (Cambridge University Press, Second Edition, 1989)

The fact that this book has been through 20 printings tells you two things: (1) Many people regard it as a fundamental resource; (2) Secondhand copies should be widely available, which is an important consideration, as the list price is over $100. It's written by two academics, and has a more technical approach than *Practical Electronics for Inventors*, but I find it useful when I'm looking for backup information.

Getting Started in Electronics, by Forrest M. Mims III (Master Publishing, Fourth Edition, 2007)

Although the original dates back to 1983, this is still a fun book to have. I think I have covered many of its topics here, but you may benefit by reading explanations and advice from a completely different source, and it goes a little farther than I have into some electrical theory, on an easy-to-understand basis, with cute drawings. Be warned that it's a brief book with eclectic coverage. Don't expect it to have all the answers.

Figure 5-9. *These books from MAKE provide guidance if you want to go beyond basic microcontrollers into the more exotic realms of the Arduino chip.*

Figure 5-10. *A sun-damaged copy of the Don Lancaster's classic TTL Cookbook, a 2,000-page catalog from the Mouser Electronics supply company, and two comprehensive reference books that can provide years of additional guidance in all areas of electronics.*

Experiment 25: Magnetism

This experiment should be a part of any school science class, but even if you remember doing it, I suggest that you do it again, because setting it up takes only a matter of moments, and it's going to be our entry point to a whole new topic: the relationship between electricity and magnetism. Quickly this will lead us into audio reproduction and radio, and I'll describe the fundamentals of self-inductance, which is the third and final basic property of passive components (resistance and capacitance being the other two). I left self-inductance until last because it's not very relevant to the experiments that you've done so far. But as soon as we start dealing with analog signals that fluctuate, it becomes essential.

You will need:

- Large screwdriver.
- 22-gauge wire (or thinner). Quantity: 6 feet.
- AA battery.

Procedure

This couldn't be simpler. Wind the wire around the shaft of the screwdriver, near its tip. The turns should be neat and tight and closely spaced, and you'll need to make 100 of them, within a distance of no more than 2 inches. To fit them into this space, you'll have to make turns on top of previous turns. If the final turn tends to unwind itself (which will happen if you're using stranded wire), secure it with a piece of tape. See Figure 5-11.

Now apply a battery, as shown in Figure 5-12. At first sight, this looks like a very bad idea, because you're going to short out your battery just as you did in Experiment 2. But by passing the current through a wire that's coiled instead of straight, we'll get some work out of it before the battery expires.

Put a small paper clip near the screwdriver blade, on a soft, smooth surface that will not present much friction. A tissue works well. Because many screwdrivers are already magnetic, you may find that the paper clip is naturally attracted to the tip of the blade. If this happens, move the clip just outside the range of attraction. Now apply the 1.5 volts to the circuit, and the clip should jump to the tip of the screwdriver. Congratulations: you just made an electromagnet.

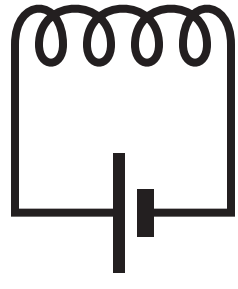

Figure 5-12. *A schematic can't get much simpler than this.*

FUNDAMENTALS

A two-way relationship

Every electric motor that was ever made uses some aspect of the relationship between electricity and magnetism. It's absolutely fundamental in the world around us. Remember that electricity can create magnetism:

When electricity flows through a wire, it creates a magnetic force around the wire.

The principle works in reverse: magnetism can create electricity.

When a wire moves through a magnetic field, it creates a flow of electricity in the wire.

This second principle is used in power generation. A diesel engine, or a water-powered turbine, or a windmill, or some other source of energy either turns coils of wire through a powerful magnetic field, or turns magnets amid some massive coils of wire. Electricity is induced in the coils. In the next experiment, you'll see a dramatic mini-demo of this effect.

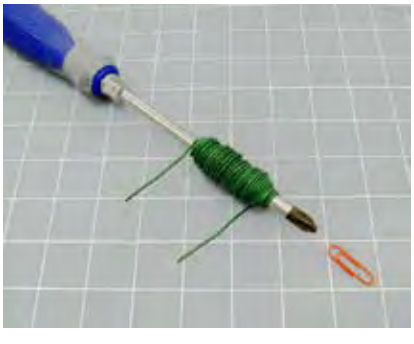

Figure 5-11. *Anyone who somehow missed this most basic childhood demo of electromagnetism should try it just for the fun of proving that a single AA battery can move a paper clip.*

THEORY

Inductance

When electricity flows through a wire, it creates a magnetic field around the wire. Because the electricity "induces" this effect, it is known as *inductance*. The effect is illustrated in Figure 5-13.

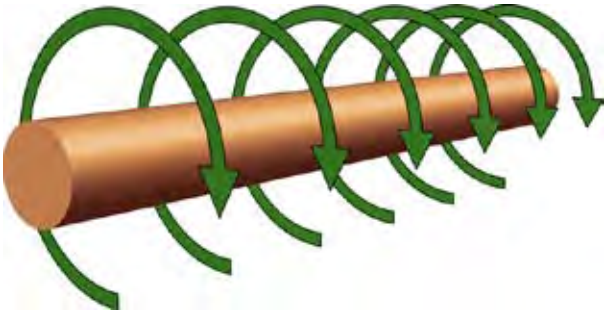

Figure 5-13. *When the flow of electricity is from left to right along this conductor, it induces a magnetic force shown by the green arrows.*

The field around a straight wire is very weak, but if we bend the wire into a circle, the magnetic force starts to accumulate, pointing through the center of the circle, as shown in Figure 5-14. If we add more circles, to form a coil, the force accumulates even more. And if we put a magnetic object (such as a screwdriver) in the center of the coil, the effectiveness increases further.

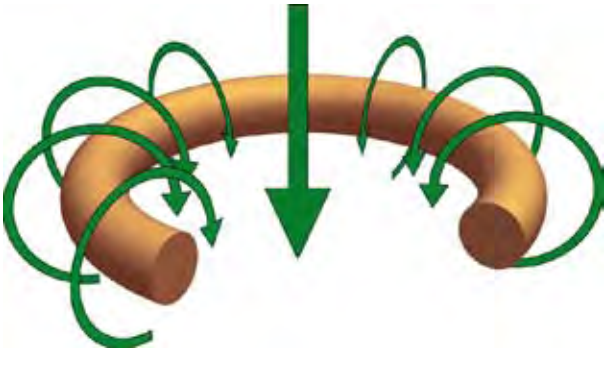

Figure 5-14. *When the conductor is bent to form a circle, the cumulative magnetic force acts through the center of the circle, as shown by the large arrow.*

Here's an approximated formula showing the relationship between the diameter of the coil, the width of the coil from end to end, the number of turns, and its inductance. The letter L is the symbol for inductance, even though the unit is the Henry, named after an American electrical pioneer named Joseph Henry:

L (in microHenrys) =
[(D × D) × (N x N)] / [(18 × D) + (40 × W)]
(Approximately)

In this formula, D is the diameter of the coil, N is the number of turns, and W is the width of the coil from end to end. See Figure 5-15. Here are three simple conclusions from this formula:

- Inductance increases with the diameter of the coil.
- Inductance increases with the square of the number of turns. (In other words, three times as many turns create nine times the inductance.)
- If the number of turns remains the same, inductance is lower if you wind the coil so that it's slender and long, but is higher if you wind it so that it's fat and short.

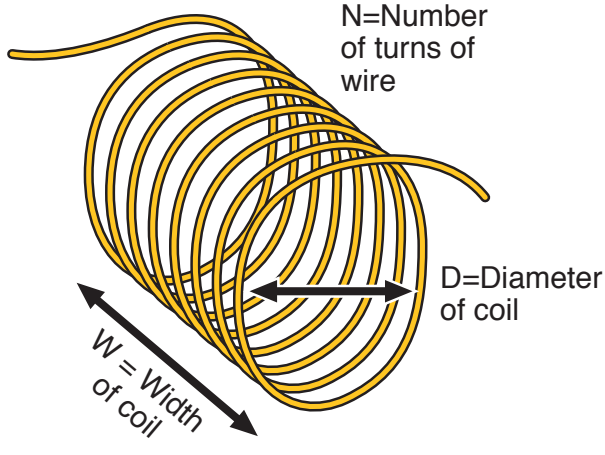

Figure 5-15. *The inductance of a coil increases with its diameter and with the square of its number of turns. If all other parameters remain the same, reducing the width (the distance from end to end) by packing the turns more tightly will increase the inductance.*

FUNDAMENTALS

Coil schematics and basics

Check the schematic symbols for coils in Figure 5-16. Note that if a coil has an iron core, this is shown with an extra couple of lines (sometimes only one line). If it has a ferrite core, the line is sometimes shown with dashes.

An iron core will add to the inductance of a coil, because it increases the magnetic effect.

A coil in isolation does not generally have any polarity. You can connect it either way around, but the magnetic force will be reversed accordingly (coils that interact with stuff—such as in transformers and solenoids—do have polarity).

Perhaps the most widespread application of coils is in transformers, where alternating current in one coil induces alternating current in another, often sharing the same iron core. If the primary (input) coil has half as many turns as the secondary (output) coil, the voltage will be doubled, at half the current—assuming hypothetically that the transformer is 100% efficient.

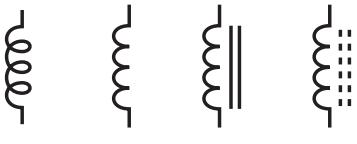

Figure 5-16. *Schematic diagrams represent coils. At far right is the older style. The third and fourth symbols indicate that the coil is wound around a solid or powdered magnetic core, respectively.*

BACKGROUND

Joseph Henry

Born in 1797, Joseph Henry was the first to develop and demonstrate powerful electromagnets. He also originated the concept of "self-inductance," meaning the "electrical inertia" that is a property of a coil of wire.

Henry started out as the son of a day laborer in Albany, New York. He worked in a general store before being apprenticed to a watchmaker, and was interested in becoming an actor. Friends persuaded him to enroll at the Albany Academy, where he turned out to have an aptitude for science. In 1826, he was appointed Professor of Mathematics and Natural Philosophy at the Academy, even though he was not a college graduate and described himself as being "principally self-educated." Michael Faraday was doing similar work in England, but Henry was unaware of it.

Henry was appointed to Princeton in 1832, where he received $1,000 per year and a free house. When Morse attempted to patent the telegraph, Henry testified that he was already aware of its concept, and indeed had rigged a system on similar principles to signal his wife, at home, when he was working in his laboratory at the Philosophical Hall.

Henry taught chemistry, astronomy, and architecture, in addition to physical science, and because science was not divided into strict specialties as it is now, he investigated phenomena such as phosphorescence, sound, capillary action, and ballistics. In 1846, he headed the newly founded Smithsonian Institution as its secretary.

Figure 5-17. *Joseph Henry was an American experimenter who pioneered the investigation of electromagnetism. This photograph is archived in Wikimedia Commons.*

Experiment 26: Tabletop Power Generation

If you have just three components, you can see magnetism generating electricity right in front of you, right now.

You will need:

- Cylindrical neodymium magnet, 3/4-inch diameter, axially magnetized. Quantity: 1. (Obtainable online at sites such as *http://www.kjmagnetics.com*.)
- Spool of hookup wire, 26-gauge, 100 feet. Quantity: 1.
- Spool of magnet wire, quarter-pound, 26-gauge, about 350 feet. Quantity: 1. (Search online for sources for "magnet wire.")
- Generic LED. Quantity: 1.
- 100 µF electrolytic capacitor. Quantity: 1.
- Signal diode, 2N4001 or similar. Quantity: 1.
- Jumper wires with alligator clips on the ends. Quantity: 2.

Procedure

You may be able to make this experiment work with the spool of hookup wire, depending on the size of the spool relative to the size of your magnet, but as the results are more likely to be better with the magnet wire, I'll assume that you're using that—initially, at least. The advantage of the magnet wire is that its very thin insulation allows the coils to be closely packed, increasing their inductance.

First peek into the hollow center of the spool to see if the inner end of the wire has been left accessible, as is visible in Figures 5-18 and 5-19. If it hasn't, you have to unwind the wire onto any large-diameter cylindrical object, then rewind it back onto the spool, this time taking care to leave the inner end sticking out.

Scrape the transparent insulation off each end of the magnet wire with a utility knife or sandpaper, until bare copper is revealed. To check, attach your meter, set to measure ohms, to the free ends of the wire. If you make a good contact, you should measure a resistance of 30 ohms or less.

Place the spool on a nonmagnetic, nonconductive surface such as a wooden, plastic, or glass-topped table. Attach the LED between the ends of the wire using jumper wires. The polarity is not important. Now take a cylindrical neodymium magnet of the type shown in Figure 5-20 and push it quickly down into the hollow core, then pull it quickly back out. See Figure 5-21. You should see the LED blink, either on the down stroke or the up stroke.

The same thing may or may not happen if you use 100 feet of 26-gauge hookup wire. Ideally, your cylindrical magnet should fit fairly closely in the hollow center of the spool. If there's a big air gap, this will greatly reduce the effect of the magnet. Note that if you use a weaker, old-fashioned iron magnet instead of a neodymium magnet, you may get no result at all.

Figure 5-18. *An everyday 100-foot spool of hookup wire is capable of demonstrating the inductive power of a coil.*

Figure 5-19. *Magnet wire has thinner insulation than hookup wire, allowing the turns to be more densely packed, inducing a more powerful magnetic field.*

Blood Blisters and Dead Media

Neodymium magnets can be hazardous. They're brittle and can shatter if they slam against a piece of magnetic metal (or another magnet). For this reason, many manufacturers advise you to wear eye protection.

Because a magnet pulls with increasing force as the distance between it and another object gets smaller, it closes the final gap very suddenly and powerfully. You can easily pinch your skin and get blood blisters.

If there's an object made of iron or steel anywhere near a neodymium magnet, the magnet will find it and grab it, with results that may be unpleasant, especially if the object has sharp edges and your hands are in the vicinity. When using a magnet, create a clear area on a nonmagnetic surface, and watch out for magnetic objects underneath the surface. My magnet sensed a steel screw embedded in the underside of a kitchen countertop, and slammed itself into contact with the countertop unexpectedly.

Be aware that magnets create magnets. When a magnetic field passes across an iron or steel object, the object picks up some magnetism of its own. Be careful not to magnetize your watch!

Don't use magnets anywhere near a computer, a disk drive, credit cards with magnetic stripes, cassettes of any type, and other media. Also keep magnets well away from TV screens and video monitors (especially cathode-ray tubes). Last but not least, powerful magnets can interfere with the normal operation of cardiac pacemakers.

Figure 5-20. *Three neodymium magnets, 1/4-, 1/2-, and 3/4-inch in diameter. I would have preferred to photograph them standing half-an-inch apart, but they refused to permit it.*

Figure 5-21. *By moving a magnet vigorously up and down through the center of a coil, you generate enough power to make the LED flash brightly.*

Here's another thing to try. Disconnect the LED and connect a 100 µF electrolytic capacitor in series with signal diode, as shown in Figure 5-23. Attach your meter, measuring volts, across the capacitor. If your meter has a manual setting for its range, set it to 20V DC. Make sure the positive (unmarked) side of the diode is attached to the negative (marked) side of the capacitor, so that positive voltage will pass through the capacitor and then through the diode.

Now move the magnet vigorously up and down in the coil. The meter should show that the capacitor is accumulating charge, up to about 10 volts. When you stop moving the magnet, the voltage reading will gradually decline, mostly because the capacitor discharges itself through the internal resistance of your meter.

This experiment is more important than it looks. Bear in mind that when you push the magnet into the coil, it induces current in one direction, and when you pull it back out again, it induces current in the opposite direction. You are actually generating alternating current.

The diode only allows current to flow one way through the circuit. It blocks the opposite flow, which is how the capacitor accumulates its charge. If you jump to the conclusion that diodes can be used to change alternating current to direct current, you're absolutely correct. We say that the diode is "rectifying" the AC power.

Experiment 24 showed that voltage can create a magnet. Experiment 25 has shown that a magnet can create voltage. We're now ready to apply these concepts to the detection and reproduction of sound.

Figure 5-22. *Because inductance increases with the diameter of a coil and with the square of the number of turns, your power output from moving a magnet through the coil can increase dramatically with scale. Those wishing to live "off the grid" may consider this steam-powered configuration, suitable for powering a three-bedroom home.*

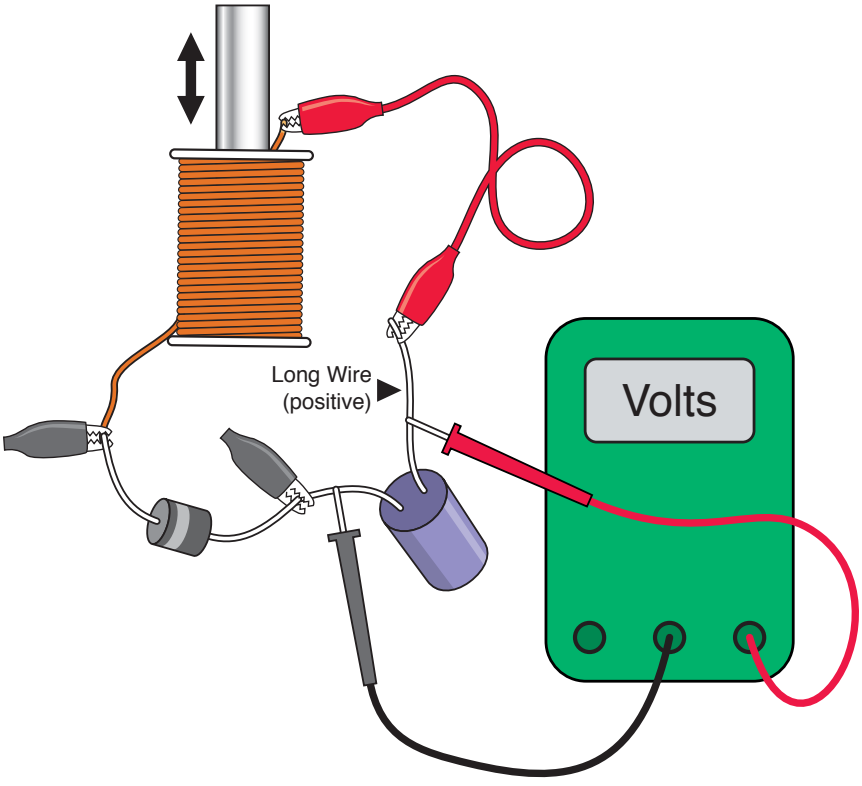

Figure 5-23. *Using a diode in series with a capacitor, you can charge the capacitor with the pulses of current that you generate by moving the magnet through the center of the coil. This demo illustrates the principle of rectifying alternating current.*

Figure 5-24. *A 2-inch loudspeaker can be instructively destroyed with a utility knife or X-Acto blade.*

Experiment 27: Loudspeaker Destruction

I'd like you to sacrifice a 2-inch loudspeaker, even though it means wasting the $5 or so that it probably costs. Actually, I don't consider this a waste, because if you want to learn how a component works, there's no substitute for actually seeing inside it. You might also have such a speaker already, part of a piece of cast-off personal electronics or toy you have in your basement.

You will need:

- Cheapest possible 2-inch loudspeaker. Quantity: 1. Figure 5-24 shows a typical example.

Procedure

Turn the loudspeaker face-up (as shown in Figure 5-25) and cut around the edge of its cone with a sharp utility knife or X-Acto blade. Then cut around the circular center and remove the ring of black paper that you've created. The result should look like Figure 5-26: you should see the flexible neck of the loudspeaker, which is usually made from a yellow weave. If you cut around its edge, you should be able to pull up the hidden paper cylinder, which has the copper coil of the loudspeaker wound around it. In Figure 5-27, I've turned it over so that it is easily visible. The two ends of this copper coil normally receive power through two terminals at the back of the speaker. When it sits in the groove visible between the inner magnet and the outer magnet, the coil reacts to voltage fluctuations by exerting an up-and-down force in reaction to the magnetic field. This vibrates the cone of the loudspeaker and creates sound waves.

Large loudspeakers in your stereo system work exactly the same way. They just have bigger magnets and coils that can handle more power (typically, as much as 100 watts).

Whenever I open up a small component like this, I'm impressed by the precision and delicacy of its parts, and the way it can be mass-produced for such a low cost. I imagine how astonished the pioneers of electrical theory (such as Faraday and Henry) would be, if they could see the components that we take for granted today. Henry spent days and weeks winding coils by hand to create electromagnets that were far less efficient than this cheap little loudspeaker.

Figure 5-25. *Loudspeaker ready for creative destruction.*

Figure 5-26. *The cone has been removed.*

Figure 5-27. *The neck of the cone has been pulled out. Note the coil of copper wire, which fits precisely in the groove between two magnets in the base of the speaker.*

BACKGROUND

Origins of loudspeakers

Loudspeakers utilize the fact that if you run a varying electrical current through a coil situated in a magnetic field, the coil will move in response to the current. This idea was introduced in 1874 by Ernst Siemens, a prolific German inventor. (He also built the world's first electrically powered elevator in 1880.) Today, Siemens AG is one of the largest electronics companies in the world.

When Alexander Graham Bell patented the telephone in 1876, he used Siemen's concept to create audible frequencies in the earpiece. From that point on, sound-reproduction devices gradually increased in quality and power, until Chester Rice and Edward Kellogg at General Electric published a paper in 1925 establishing basic principles that are still used in loudspeaker design today.

At *http://www.radiolaguy.com/Showcase/Gallery-HornSpkr.htm* you'll find photographs of very beautiful early loudspeakers, which used a horn design to maximize efficiency. As sound amplifiers became more powerful, speaker efficiency became less important compared with quality reproduction and low manufacturing costs. Today's loudspeakers convert only about 1% of electrical energy into acoustical energy.

Figure 5-28. *This beautiful Amplion AR-114x illustrates the efforts of early designers to maximize efficiency in an era when the power of audio amplifiers was very limited. Photos by "Sonny, the RadiolaGuy." Many early speakers are illustrated at www.radiolaguy.com. Some are for sale.*

THEORY

Sound, electricity, and sound

Time now to establish a clear idea of how sound is transformed into electricity and back into sound again.

Suppose someone bangs a gong with a stick. The flat metal face of the gong vibrates in and out, creating sound waves. A sound wave is a peak of higher air pressure, followed by a trough of lower air pressure.

The wavelength of the sound is the distance (usually ranging from meters to millimeters) between one peak of pressure and the next peak.

The frequency of the sound is the number of waves per second, usually expressed as hertz.

Suppose we put a very sensitive little membrane of thin plastic in the path of the pressure waves. The plastic will flutter in response to the waves, like a leaf fluttering in the wind. Suppose we attach a tiny coil of very thin wire to the back of the membrane so that it moves with the membrane, and let's position a stationary magnet inside the coil of wire. This configuration is like a tiny, ultra-sensitive loudspeaker, except that instead of electricity producing sound, it is configured so that sound produces electricity. Sound pressure waves make the membrane move to and fro along the axis of the magnet, and the magnetic field creates a fluctuating voltage in the wire.

This is known as a *moving-coil* microphone. There are other ways to build a microphone, but this is the configuration that is easiest to understand. Of course, the voltage that it generates is very small, but we can amplify it using a transistor, or a series of transistors. Then we can feed the output through the coil around the neck of a loudspeaker, and the loudspeaker will recreate the pressure waves in the air. Figures 5-29 through 5-32 illustrate this sequence.

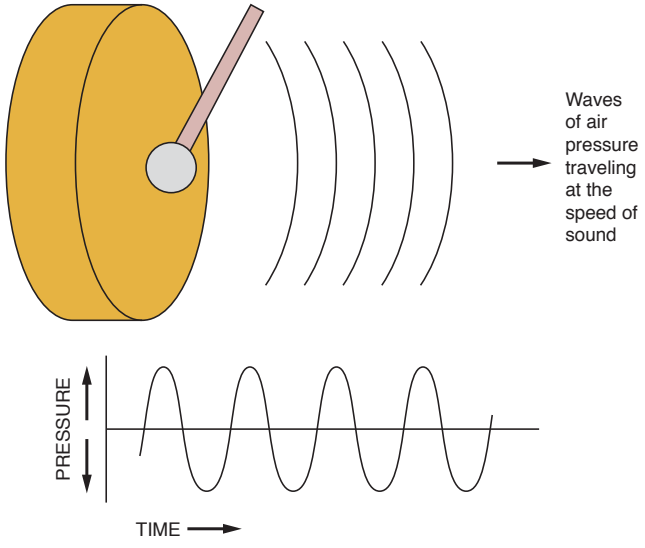

Figure 5-29. *Step 1 in the process of converting sound to electricity, and back again. When the hammer hits the gong, the face of the gong vibrates, creating pressure waves that travel through the air.*

THEORY

Sound, electricity, and sound (continued)

Somewhere along the way, we may want to record the sound and then replay it. But the principle remains the same. The hard part is designing the microphone, the amplifier, and the loudspeaker so that they reproduce the waveforms *accurately* at each step. It's a significant challenge, which is why accurate sound reproduction can be elusive.

Time now to think about what happens inside the wire when it generates a magnetic field. Obviously, some of the power in the wire is being transformed into magnetic force. But just what exactly is going on?

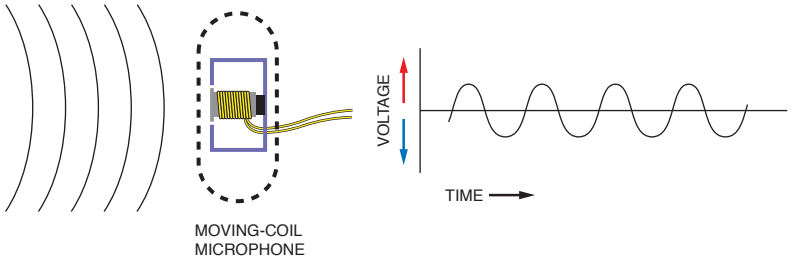

Figure 5-30. *Step 2: the pressure waves penetrate the perforated shell of a microphone and cause a diaphragm to vibrate in sympathy. The diaphragm has a coil attached to it. When the coil vibrates to and fro, a magnet at its center induces alternating current.*

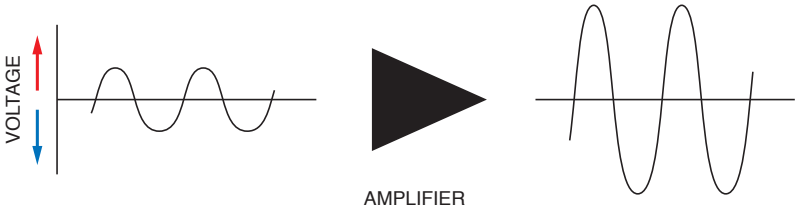

Figure 5-31. *Step 3: the tiny signals from the microphone pass through an amplifier, which enlarges their amplitude while retaining their frequency and the shape of their waveform.*

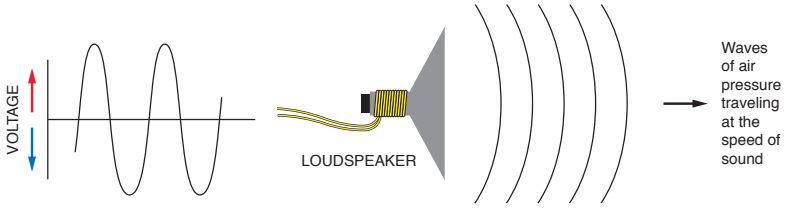

Figure 5-32. *Step 4: the amplified electrical signal is passed through a coil around the neck of a loudspeaker cone. The magnetic field induced by the current causes the cone to vibrate, reproducing the original sound.*

Experiment 28: Making a Coil React

A capacitor will absorb some DC current until it is fully charged, at which point it blocks the flow. There's another phenomenon that I haven't mentioned so far, which is the exact opposite of capacitance. It's known as *self-inductance*, and you find it in any coil of wire. Initially it blocks DC current (it reacts against it), but then its opposition gradually disappears. Here are a few definitions:

Resistance
: Constrains current flow and drops voltage.

Capacitance
: Allows current to flow initially and then blocks it. This behavior is properly known as capacitive reactance.

Self-Inductance
: Blocks the flow of current initially and then allows it. This is also often referred to as *inductive reactance*. In fact, you may find the term "reactance" used as if it means the same thing, but since self-inductance is the correct term, I'll be using it here.

In this experiment, you'll see self-inductance in action.

You will need:

- LEDs, low-current type. Quantity: 2.
- Spool of hookup wire, 26-gauge, 100 feet. Quantity: 1.
- Resistor, 220Ω, rated 1/4 watt or higher. Quantity: 1.
- Capacitor, electrolytic, 2,000 µF or larger. Quantity: 1.
- SPST tactile switch. Quantity: 1.

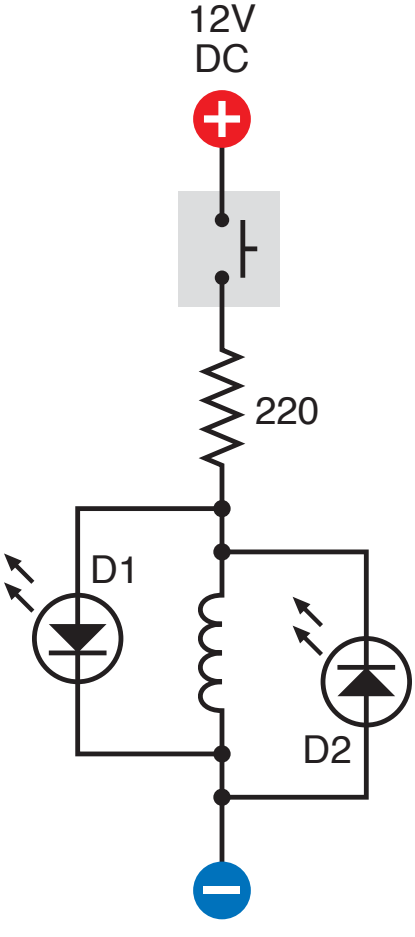

Figure 5-33. *In this demonstration of self-inductance, D1 and D2 are light-emitting diodes. When the switch is closed, D1 flashes briefly because the coil obstructs the initial flow of electricity. When the switch is opened, D2 flashes as the collapsing magnetic field induced by the coil releases another short burst of current.*

Procedure

Take a look at the schematic in Figure 5-33. At first it may not make much sense. The curly symbol is a coil of wire—nothing more than that. So apparently the voltage will pass through the 220Ω resistor, and then through the coil, ignoring the two LEDs, because the coil obviously has a much lower resistance than either of them (and one of them is upside-down anyway).

Is that what will happen? Let's find out. The coil can be a spool of 100 feet of 26-gauge (or smaller) hookup wire, although the spool of magnet wire listed in Experiment 25 will work better, if you have that. Once again, you will need access to both ends of the wire, and if the inner end is inaccessible, you'll need to rewind the coil, leaving the end sticking out.

Now that you have a coil, you can hook it up on your breadboard as shown in Figure 5-34, where the green circle is a tactile switch and the two circular red objects are LEDs. Make sure that you use low-current LEDs (otherwise, you may not see anything) and make sure that one of them is negative-side-up, positive-side-down and the other is positive-side-up, negative-side-down. Also, the 220Ω resistor should be rated at 1/4 watt or higher, if possible (see the following caution).

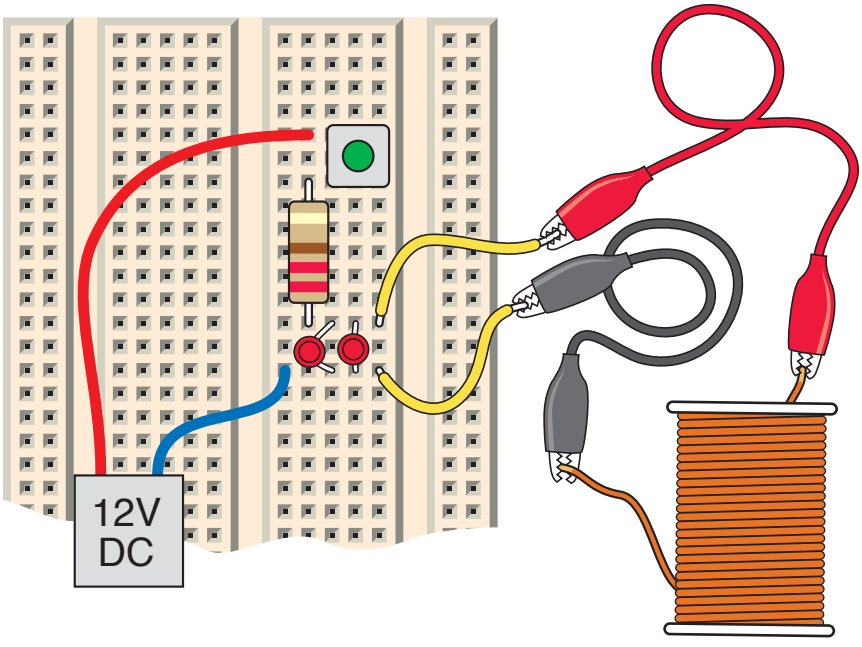

Figure 5-34. *The breadboarded version of the schematic in Figure 5-33 shows a simple way to set it up for a quick demo. The green button is a tactile switch. The two red LEDs should be placed so that the polarity of one is opposite to the polarity of the other.*

Hot Resistors

You'll be passing about 50mA through the 220Ω resistor, while the current is flowing. At 12 volts, this works out at 0.6 watts. If you use a 1/8-watt resistor, you will be overloading it, and it will get quite hot and may burn out. If you use a 1/4-watt resistor, it will still get hot, but is unlikely to burn out, as long as you don't press the button for more than a second or two.

Don't run the circuit without the coil of wire; you'll be trying to pass more than 50mA through the LEDs.

When you press the button, one LED should flash briefly. When you release the button, the other LED should flash.

What's happening here? The coil possesses self-inductance, which means that it reacts against any sudden change in the flow of electricity. First it fights it, and during that brief moment, it blocks most of the current. Consequently, the current looks for an alternative path and flows through D1, the lefthand LED in the schematic. (D2 doesn't respond, because it can pass current only in the opposite direction.)

Meanwhile, the voltage pressure overcomes the coil's self-inductance. When the self-inductance disappears, the resistance of the coil is no more than 10 ohms—so now the electricity flows mostly through the coil, and because the LED receives so little, it goes dark.

When you disconnect the power, the coil reacts again. It fights *any* sudden changes. After the flow of electricity stops, the coil stubbornly sustains it for a moment, because as the magnetic field collapses, it is turned back into electricity. This residual flow of current depletes itself through D2, the LED on the right.

In other words, the coil stores some energy in its magnetic field. This is similar to the way a capacitor stores energy between two metal plates, except that the coil blocks the current initially and then lets it build up, whereas the capacitor sucks up current initially, and then blocks it.

The more turns of wire you have in your coil, the more self-inductance the coil will have, causing your LEDs to flash more brightly.

Here's one last variation on this experiment to test your understanding of electrical fundamentals. Remove the 220Ω resistor, and substitute a 1K resistor (to protect your LED from sustained current). Remove the coil, and substitute a very large capacitor—ideally, about 4,700 µF. (Be careful to get its polarity the right way around.) What will you see when you press the button? Note that you will have to hold it down for a couple of seconds to get a result. And what will you see when you release the button? Remember: the behavior of capacitance is opposite to the behavior of self-inductance.

THEORY

Alternating current concepts

Here's a simple thought experiment. Suppose you set up a 555 timer to send a stream of pulses through a coil. This is a primitive form of alternating current.

We might imagine that the self-inductance of the coil will interfere with the stream of pulses, depending how long each pulse is, and how much inductance the coil has. If the pulses are too short, the self-inductance of the coil will tend to block them. Maybe if we can time the pulses exactly right, they'll synchronize with the time constant of the coil. In this way, we can "tune" a coil to allow a "frequency" to pass through it.

What happens if we substitute a capacitor? If the pulses are too long, compared with the time constant of the capacitor, it will tend to block them, because it will have enough time to become fully charged. But if the pulses are shorter, the capacitor can charge and discharge in rhythm with the pulses, and will seem to allow them through.

I don't have space in this book to get deeply into alternating current. It's a vast and complicated field where electricity behaves in strange and wonderful ways, and the mathematics that describe it can become quite challenging, involving differential equations and imaginary numbers. However, we can easily demonstrate the audio filtering effects of a loudspeaker and a coil.

Experiment 29: Filtering Frequencies

In this experiment, you'll see how self-inductance and capacitance can be used to filter audio frequencies. You're going to build a crossover network: a simple circuit that sends low frequencies to one place and high frequencies to another.

You will need:

- Loudspeaker, 8Ω, 5 inches in diameter. Quantity: 1. Figure 5-35 shows a typical example.
- Audio amplifier, STMicroelectronics TEA2025B or similar. Quantity: 1. See Figure 5-36.

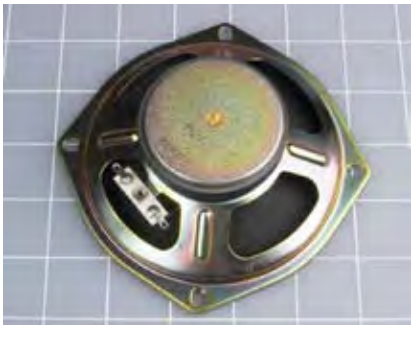

Figure 5-35. *To hear the effects of audio filters using coils and capacitors, you'll need a loudspeaker capable of reproducing lower frequencies. This 5-inch model is the minimum required.*

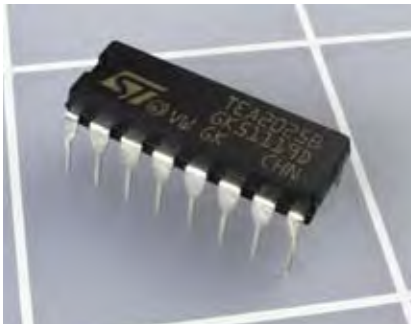

Figure 5-36. *This single chip contains a stereo amplifier capable of delivering a total of 5 watts into an 8Ω speaker when the two channels are combined.*

Figure 5-37. *A nonpolarized electrolytic capacitor, also known as a bipolar capacitor, looks just like an electrolytic capacitor, except that it will have "NP" or "BP" printed on it.*

- Nonpolarized electrolytic capacitors (also known as bipolar). 47 µF. Quantity: 2. A sample is shown in Figure 5-37. They should have "NP" or "BP" printed on them to indicate "nonpolarized" or "bipolar."
- Nonpolarized electrolytic capacitors (also known as bipolar). 100 µF. Quantity: 5. (Because you'll be working with audio signals that alternate between positive and negative, you can't use the usual polarized electrolytic capacitors. If you want to avoid the trouble and expense of ordering nonpolarized capacitors, you can substitute two regular electrolytics in series, facing in opposite directions, with their negative sides joined in the middle. Just remember that when you put capacitors in series, their total capacitance is half that of each individual component. Therefore, you would need two 220 µF electrolytics in series to create 110 µF of capacitance. See Figure 5-38.)
- Potentiometer, with audio taper if possible. 100K. Quantity: 1.
- Coil, for crossover network. Quantity: 1. You can search a source such as eBay for keywords "crossover" and "coil," but if you can't find one at a reasonable price, you can make do with a spool of 100 feet of 20-gauge hookup wire.
- Plastic shoebox. Quantity: 1.

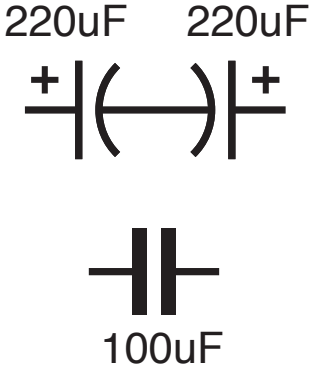

Figure 5-38. *You can make a nonpolarized electrolytic capacitor by putting two regular electrolytics in series. (In fact, that's what you'd find if you opened a real nonpolarized capacitor.) The symbol at the bottom is roughly equivalent to the pair of symbols at the top; bear in mind that two capacitors in series have a total capacitance that is half that of each of them.*

Figure 5-39. *A resonant enclosure is necessary if you want to hear some bass (lower frequencies) from your speaker. A cheap plastic shoebox is sufficient for demo purposes.*

Figure 5-40. *Drill some half-inch holes in the bottom of the box, then bolt the speaker in place, running a wire out through a hole in one end. Snap on the lid, and you're ready for not-quite-high-fidelity audio.*

Procedure

The purpose of the audio amplifier chip is to provide enough power to get a decent amount of sound out of your loudspeaker. The purpose of using a 5-inch speaker is to enable you to hear lower-frequency sounds than the baby speakers that we have used previously. Bass notes have long wavelengths that small speakers are not able to generate effectively.

Maybe you remember from building the intrusion alarm that a speaker makes much more noise if you prevent the sound waves from the back of the cone from cancelling the sound waves from the front of the cone. The obvious way to achieve this is by enclosing the speaker in a box. I suggest a plastic box, because they're cheap, and we don't care too much about sound quality as long as we can hear at least some of the low frequencies. Figure 5-39 shows the speaker bolted into the bottom of a plastic box, and Figure 5-40 shows the box turned upside-down after snapping its lid into place.

Normally, a speaker should be mounted in a cabinet of heavy, thick material that has a very low resonant frequency—below the limits of human hearing. To minimize the resonance of the shoebox, you can put some soft, heavy fabric inside it before you snap the lid on. A hand towel or some socks should be sufficient to absorb some of the vibration.

Adding an Amplifier

Back in the 1950s, you needed vacuum tubes, transformers, and other power-hungry heavyweight components to build an audio amplifier. Today, you can buy a chip for about $1 that will do the job, if you add a few capacitors around it, and a volume control. The TEA2025B that I'm recommending is intended for use in cheap portable cassette players and CD players, and can work in stereo or mono mode, from a power supply ranging from 3 to 9 volts. With 9 volts and the two sides of the chip bridged together to drive one 8Ω speaker, it can generate 5 watts of audio power. That doesn't sound much compared with a typical home theater system rated at 100 watts per channel, but because loudness is a logarithmic scale, 5 watts will be quite enough to irritate any family members in the same room—and possibly even in other rooms.

If you can't find the TEA2025B chip, you can use any alternative listed as an audio amplifier. Try to find one that is designed to drive an 8Ω speaker with up to 5 watts in mono mode. Check the manufacturer's data sheet to see where you attach capacitors around it. Note carefully whether some of the capacitors have no polarity marked, even though they have fairly high values, such as 100 µF. These capacitors must function regardless of which way the alternating current is flowing, and I've marked them "NP" in my schematic in Figure 5-41, meaning "nonpolarized." (You may find them identified as "bipolar" or "BP" in parts catalogs.) As noted in the shopping list, you can put two 220 µF capacitors in series, negative-to-negative, to get the same effect as a single 100 µF nonpolarized capacitor.

For this project, it's essential to include the regular 100 µF electrolytic smoothing capacitor across the power supply. Otherwise, the amplifier will pick up and—yes, amplify—small voltage spikes in the circuit.

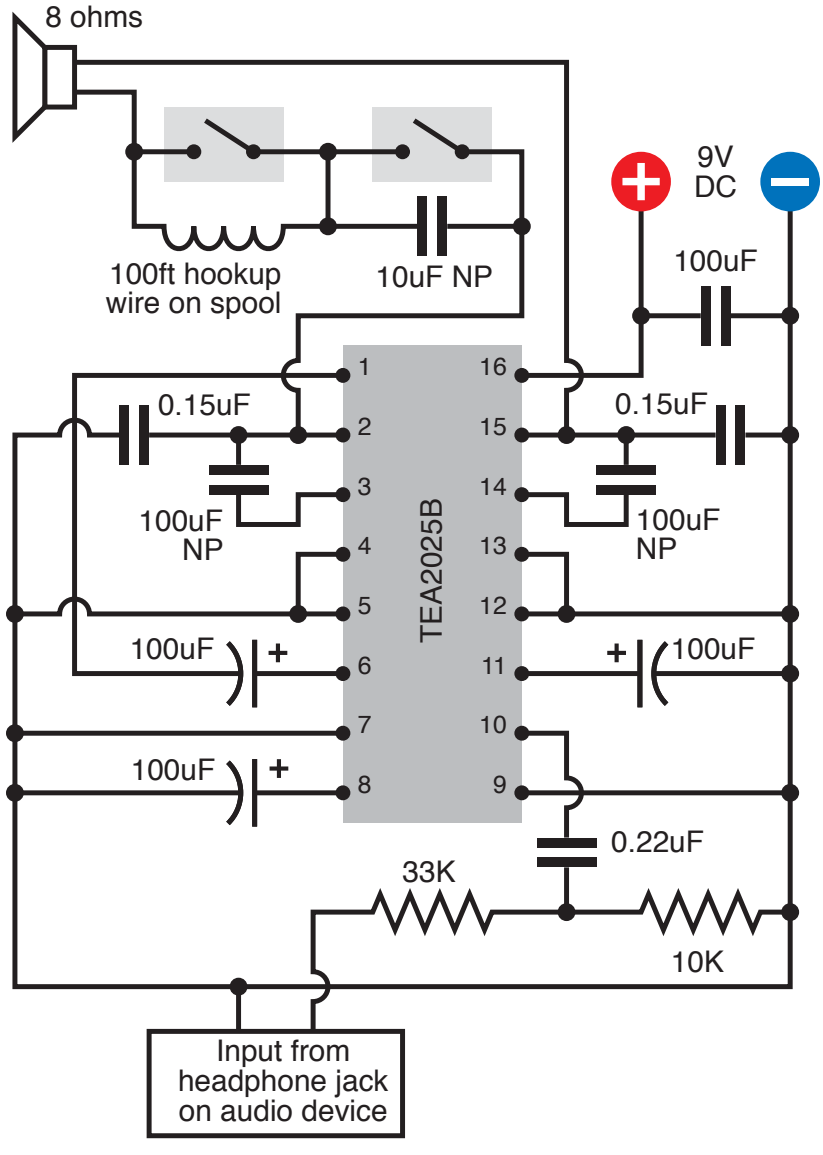

Figure 5-41. *The audio amplifier chip should be wired with capacitors around it as shown, "NP" denoting the ones that are not polarized. The acronym "BP," meaning bipolar, is also often used to mean the same thing. The output from pins 2 and 15 of the chip can be passed through a coil or a 10 µF capacitor to demonstrate audio filtering.*

The input shown in the schematic can receive a signal from a typical media player, such as a portable MP3 player, CD player, or cassette player. To connect its headphone jack to the breadboard, you can use an adapter that converts it to a pair of RCA-type audio jacks, and then stick a wire into one of them as shown in Figure 5-42. The wire will connect to the 33K resistor on the breadboard circuit. The chromed neck of the RCA jack (which is sometimes gold-plated, or at least gold-colored) *must* be connected with the negative side of your power supply on the breadboard; otherwise, you won't hear anything. You can ignore the second output on the adapter, because we're working in mono, here, not stereo.

Figure 5-42. *To sample the output from the headphone socket of a music player, you can use this adapter and push the stripped end of a piece of hookup wire into one of the sockets. Then use alligator clips on a jumper wire to connect the audio to your breadboarded circuit. Don't forget to use an additional jumper wire to connect the outside of the socket to the negative side of the power supply on the breadboard. Because we're only using one speaker, the amplifier is connected to only one of the stereo outputs from your player. The other is ignored.*

The 33K resistor is necessary to protect the amplifier from being overdriven. If you don't get enough volume using your music player, decrease the 33K value. If the music is too loud and distorted, increase the value. You can also try omitting or increasing the 10K resistor next to it, which is included in an effort to reduce background hum noise.

I've shown two switches at the top of the schematic: one to bypass a coil, the other to bypass a capacitor. You can use alligator clips instead, as long as you can easily compare the sound when each of the components is inserted into the circuit.

Figure 5-43. *The red and black alligator clips, lying on top of the shoebox, should connect with the output from your amplifier chip. The red jumper wire passes the signal through a coil of hookup wire on its way to the speaker. Note the change in sound when you short out the coil.*

Figure 5-43 shows a coil consisting of a spool of hookup wire being used. The red and black alligator clips resting loose on top of the shoebox will go to the output from the chip (on pins 2 and 15). There is no polarity; it doesn't matter which clip goes to which pin.

Begin by turning the volume control on your music source *all the way down* before you apply power. Don't be surprised if you hear humming or crackling noises when you activate the amplifier; it will pick up any stray voltages, because in this simple experiment, I haven't suggested that you should shield the input, and the amplifier circuit can pick up noise, as its wires can act like antennas.

Note that you may also get additional unwanted sound if you use the amplifier on a conductive desktop surface. Remove any aluminum foil or conductive foam for this project.

Make sure that your player is playing music, and slowly turn up its volume control until you hear it. If you don't hear anything, you'll have to check for circuit errors.

Now comes the interesting part. Insert the 100-foot spool of hookup wire between one output from the amplifier, and one input of the speaker (it doesn't matter which one), or if you used switches, open the switch that bypasses the coil. You should find that the music loses all its high-end response. By comparison, if you disconnect the coil and substitute a 10 µF capacitor, you should find that the music sounds "tinny," meaning that it loses all its low range, leaving only the high frequencies.

You've just tested two very simple filters. Here's what they are doing:

- The coil is a low-pass filter. It passes low frequencies but blocks high frequencies, because brief audio cycles don't have time to overcome the coil's self-inductance. A bigger coil eliminates a wider range of frequencies.
- The capacitor is a high-pass filter. It passes high frequencies and blocks low frequencies because longer audio cycles can fill the capacitance, at which point the capacitor stops passing current. A smaller capacitor eliminates a wider ranger of frequencies.

You can go a lot farther into filter design, using complex combinations of coils and capacitors to block frequencies at any point in the audible spectrum. Search online for audio filter schematics—you'll find hundreds of them.

Crossover Networks

In a traditional audio system, each speaker cabinet contains two drivers—one of them a small speaker called a *tweeter*, which reproduces high frequencies, the other a large speaker known as a *woofer*, which reproduces low frequencies. (Modern systems often remove the woofer and place it in a separate box of its own that can be positioned almost anywhere, because the human ear has difficulty sensing the direction of low-frequency sounds.)

The schematic that you just looked at and may have constructed is known as a "crossover network," and truly hardcore audiophiles have been known make their own (especially for use in car systems) to go with speakers of their choice in cabinets that they design and build themselves.

If you want to make a crossover network, you should use high-quality polyester capacitors (which have no polarity, last longer than electrolytics, and are better made) and a coil that has the right number of turns of wire and is the right size to cut high frequencies at the appropriate point. Figure 5-44 shows a polyester capacitor.

Figure 5-45 shows an audio crossover coil that I bought on eBay for $6. I was curious to find out what was inside it, so I bought two of them, and took one apart.

First I peeled away the black vinyl tape that enclosed the coil. Inside was some typical magnet wire—copper wire thinly coated with shellac or semitransparent plastic, as shown in Figure 5-46. I unwound the wire and counted the number of turns. Then I measured the length of the wire, and finally used a micrometer to measure the diameter of the wire, after which I checked online to find a conversion from the diameter in mils (1/1,000 of an inch) to American wire gauge.

As for the spool, it was plain plastic with an air core—no iron or ferrite rod in the center. Figure 5-47 shows the spool and the wire.

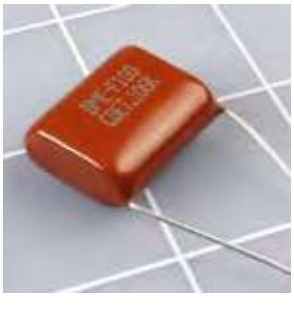

Figure 5-44. *Some nonelectrolytic capacitors have no polarity, such as this high-quality polyester film capacitor. However, they tend to be much more expensive, and are hard to find in values higher than 10 µF.*

Figure 5-45. *What exotic components may we find inside this high-end audio component that's used with a subwoofer to block high frequencies?*

Figure 5-46. *The black tape is removed, revealing a coil of magnet wire.*

Figure 5-47. *The audio crossover coil consists of a plastic spool and some wire. Nothing more.*

So here's the specification for this particular coil in an audio crossover network. Forty feet of 20-gauge copper magnet wire, wrapped in 200 turns around a spool of 1/16–inch-thick plastic with a hub measuring 7/8 inch in length between the flanges and 1/2-inch external diameter. Total retail cost of materials if purchased separately: probably about $1, assuming you can find or make a spool of the appropriate size.

Conclusion: there's a lot of mystique attached to audio components. They are frequently overpriced, and you can make your own coil if you start with these parameters and adjust them to suit yourself.

Suppose you want to put some thumping bass speakers into your car. Could you build your own filter so that they only reproduce the low frequencies? Absolutely—you just need to wind a coil, adding more turns until it cuts as much of the high frequencies as you choose. Just make sure the wire is heavy enough so that it won't overheat when you push 100 or more audio watts through it.

Here's another project to think about: a color organ. You can tap into the output from your stereo and use filters to divide audio frequencies into three sections, each of which drives a separate set of colored LEDs. The red LEDs will flash in response to bass tones, yellow LEDs in response to the mid-range, and green LEDs in response to high frequencies (or whatever colors you prefer). You can put signal diodes in series with the LEDs to rectify the alternating current, and series resistors to limit the voltage across the LEDs to, say, 2.5 volts (when the music volume is turned all the way up). You'll use your meter to check the current passing through each resistor, and multiply that number by the voltage drop across the resistor, to find the wattage that it's handling, to make sure the resistor is capable of dissipating that much power without burning out.

Audio is a field offering all kinds of possibilities if you enjoy designing and building your own electronics.

THEORY

Waveforms

If you blow across the top of a bottle, the mellow sound that you hear is caused by the air vibrating inside the bottle, and if you could see the pressure waves, they would have a distinctive profile.

If you could slow down time and draw a graph of the alternating voltage in any power outlet in your house, it would have the same profile.

If you could measure the speed of a pendulum swinging slowly to and fro in a vacuum, and draw a graph of the speed relative to time, once again it would have the same profile.

That profile is a *sine wave*, so called because you can derive it from basic trigonometry. In a right-angled triangle, the sine of an angle is found by dividing the length of the side opposite the angle by the length of the hypoteneuse (the sloping side of the triangle).

To make this simpler, imagine a ball on a string rotating around a center point, as shown in Figure 5-48. Ignore the force of gravity, the resistance of air, and other annoying variables. Just measure the vertical height of the ball and divide it by the length of the string, at regular instants of time, as the ball moves around the circular path at a constant speed. Plot the result as a graph, and there's your sine wave, shown in Figure 5-49. Note that when the ball circles below its horizontal starting line, we consider its distance negative, so the sine wave becomes negative, too.

Why should this particular curve turn up in so many places and so many ways in nature? There are reasons for this rooted in physics, but I'll leave you to dig into that topic if it interests you. Getting back to the subject of audio reproduction, what matters is this:

- Any sound can be broken down into a mixture of sine waves of varying frequency and amplitude.

Or, conversely:

- If you put together the right mix of audio sine waves, you can create *any sound at all*.

Suppose that there are two sounds playing simultaneously. Figure 5-50 shows one sound as a red curve, and the other as pale blue. When the two sounds travel either as pressure waves through air or as alternating electric currents through a wire, the amplitudes of the waves are added together to make the more complex curve, which is shown in black. Now try to imagine dozens or even hundreds of different frequencies being added together, and you have an idea of the complex waveform of a piece of music.

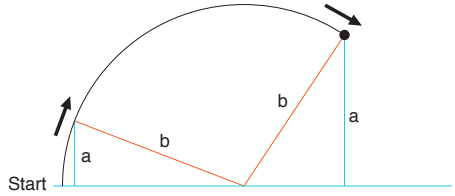

Figure 5-48. *If a weight on the end of a string (length b, in the diagram) follows a circular path at a steady speed, the distance of the weight from a horizontal center line (length a, in the diagram) can be plotted as a graph relative to time. The graph will be a sine wave, so called because in basic trigonometry, the ratio of a/b is the sine of the angle between line b and the horizontal baseline, measured at the center of rotation. Sinewaves occur naturally in the world around us, especially in audio reproduction and alternating current.*

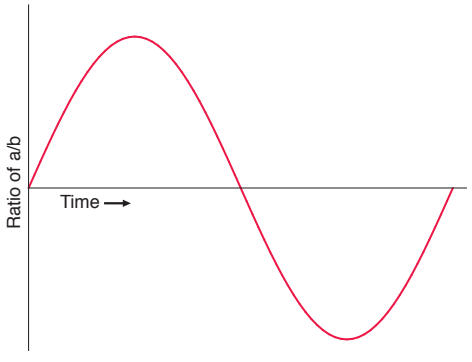

Figure 5-49. *This is what a "pure" sinewave looks like.*

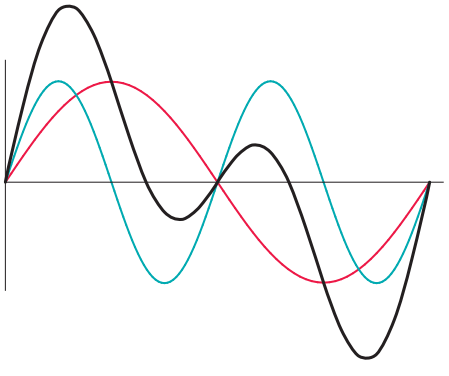

Figure 5-50. *When two sinewaves are generated at the same time (for instance, by two musicians, each playing a flute), the combined sound creates a compound curve. The blue sinewave is twice the frequency of the red sinewave. The compound curve (black line) is the sum of the distances of the sinewaves from the baseline of the graph.*

THEORY

Waveforms (continued)

You can create your own waveform as an input for your audio amplifier with the basic astable 555 timer circuit shown in Figure 5-51. You have to be careful, though, not to overload the amplifier input. Note the 680K series resistor on the output pin of the timer. Also note the 500Ω potentiometer.

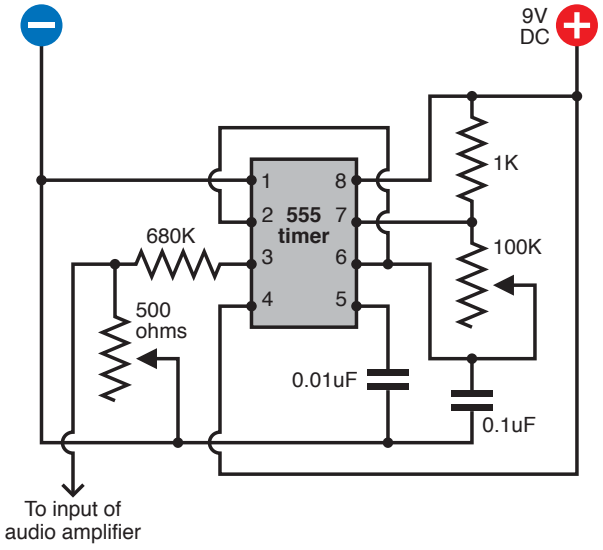

Figure 5-51. *A 555 timer is wired in astable mode using the component values shown here to generate a wide range of audible frequencies when the 100K potentiometer is adjusted. After the output is reduced in power, it can feed into the amplifier chip that was used previously.*

Disconnect your music player and connect the output from the 555 circuit to the input point (the 33K resistor) in the amplifier circuit shown earlier in Figure 5-41. You don't have to worry about a separate connection on the negative side as long as the 555 timer shares the same breadboard and the negative side of its power supply.

Make sure that the 500Ω potentiometer is turned all the way to short the output from the timer to the negative side of the power supply. This functions as your volume control. Also make sure the 100K potentiometer is in the middle of its range. Switch on the power and slowly turn up the 500Ω potentiometer until you hear a tone.

Now adjust the 100K potentiometer to create a low-pitched note. You'll find that it doesn't have a "pure" sound. There are some buzzing overtones. This is because the 555 timer is generating square waves such as those shown in Figure 5-52, not sine waves, and a square wave is actually a sum of many different sine waves, some of which have a high frequency. Your ear hears these harmonics, even though they are not obvious when you look at a square-shaped waveform.

Route one of the connections to your loudspeaker through your spool of hookup wire, and now you should hear a much purer tone, as the buzzing high frequencies are blocked by the self-inductance of the coil. Remove the coil and substitute the 10 µF capacitor, and now you hear more buzzing and less bass.

You've just taken a small step toward sound synthesis. If this subject interests you, you can go online and search for oscillator circuits. For a thorough understanding of the relationship between waveforms and the sounds you hear, you'll really need an oscilloscope, which will show you the shape of each waveform that you generate and modify.

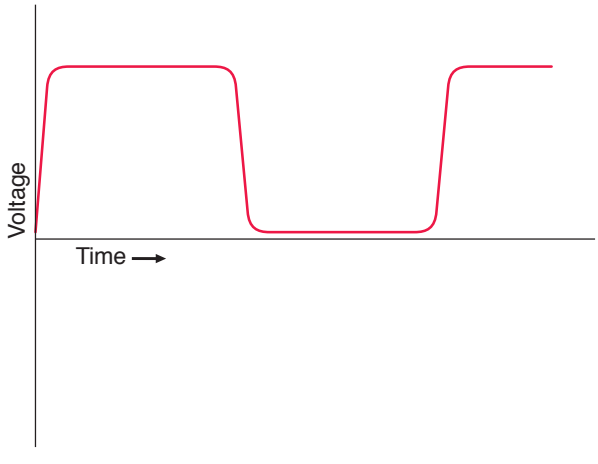

Figure 5-52. *The output from a 555 timer is either "on" or "off," with a very fast transition between those two states. The result is an almost perfect square wave. Theoretically, this can be disassembled into a complex set of sine waves that have many different frequencies. The human ear hears the high frequencies as harsh overtones.*

Experiment 30: Fuzz

Let's try one more variation on the circuit in Experiment 28. This will demonstrate another fundamental audio attribute: distortion.

You will need:

- One more 100K potentiometer.
- Generic NPN transistors: 2N2222 or similar. Quantity: 2.
- Various resistors and capacitors.

BACKGROUND

Clipping

In the early days of "hi-fi" sound, engineers labored mightily to perfect the process of sound reproduction. They wanted the waveform at the output end of the amplifier to look identical with the waveform at the input end, the only difference being that it should be bigger, so that it would be powerful enough to drive loudspeakers. Even a very slight distortion of the waveform was unacceptable.

Little did they realize that their beautifully designed tube amplifiers would be abused by a new generation of rock guitarists whose intention was to create as much distortion as possible.

The most common form of waveform abuse is technically known as "clipping." If you push a vacuum tube or a transistor to amplify a sine wave beyond the component's capabilities, it "clips" the top and bottom of the curve. This makes it look more like a square wave, and as I explained in the section on waveforms, a square wave has a harsh, buzzing quality. For rock guitarists trying to add an edge to their music, the harshness is actually a desirable feature.

Figure 5-53. *This Vox Wow-Fuzz pedal was one of the early stomp boxes, which deliberately induced the kind of distortion that audio engineers had been trying to get rid of for decades.*

The first gadget to offer this on a commercial basis was known as a "fuzz box," which deliberately clipped the input signal. An early fuzz box is shown in Figure 5-53. The clipping of a sine wave is shown in Figure 5-54.

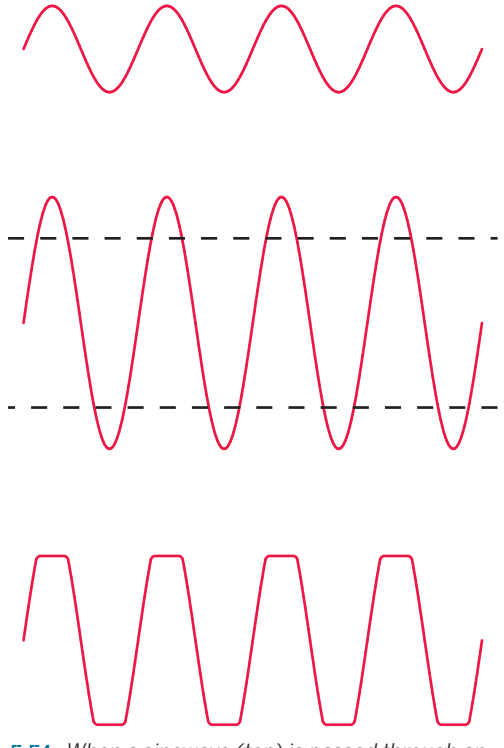

Figure 5-54. *When a sinewave (top) is passed through an amplifier which is turned up beyond the limit of its components (shown as dashed lines, center), the amplifier chops the wave (bottom) in a process known as "clipping." The result is close to a square wave and is the basic principle of a fuzz box commonly used to create a harsh guitar sound.*

Schematic

The output from the 555 timer is a square wave, so it already sounds quite "fuzzy," but we can make it more intense to demonstrate the clipping principle. I've redrawn the whole circuit in Figure 5-55, as several components have changed. The principal alteration is the addition of two NPN transistors.

If you assemble this circuit on your breadboard, note carefully that the 33K and 10K resistors at the bottom of the amplifier chip have been removed, and there's now just an 820Ω resistor in that location. The bottom of the adjacent 0.22 µF capacitor is still the input point for the amplifier, and if you follow the connection around to the middle of the schematic, you'll find it leading to a 100K potentiometer. This is your "fuzz adjuster."

The two NPN transistors are arranged so that the one on the left receives output from the 555 timer. This signal controls the flow of electricity through the transistor from a 33K resistor. This flow, in turn, controls the base of the righthand transistor, and the flow of current through that is what ultimately controls the amplifier.

When you power up the circuit, use the 100K potentiometer attached to the 555 timer to adjust the frequency (as before) and crank the "fuzz adjuster" potentiometer to hear how it adds increasing "bite" to the sound until ultimately it becomes pure noise.

The two transistors act as amplifiers. Of course, we didn't need them for that purpose—the input level for the amplifier chip was already more than adequate. The purpose of the lefthand transistor is simply to overload the righthand transistor, to create the "fuzz" effect. And when you turn up the output from the transistors with the "fuzz adjuster," eventually they overload the input of the amplifier chip, creating even more distortion.

If you want to tweak the output, try substituting different values for the 1K resistor and the 1 µF capacitor that are positioned between the emitter of the righthand transistor and the negative side of the power supply. A larger resistor should overload the transistor less. Different capacitor values should make the sound more or less harsh.

You can find literally thousands of schematics online for gadgets to modify guitar sound. The circuit I've included here is one of the most primitive. If you want something more versatile, you should search for "stomp box schematics" and see what you can find.

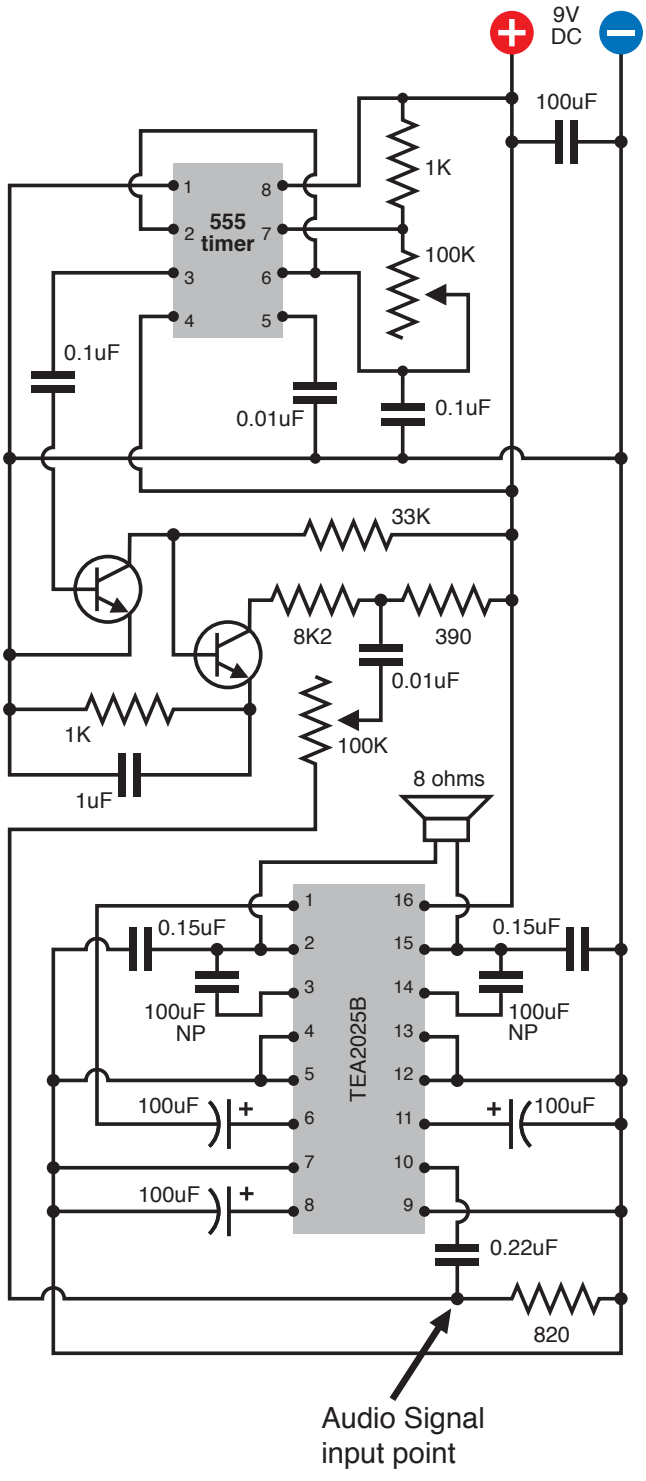

Figure 5-55. *For a quick demo of clipping, insert a couple of transistors between the output from the 555 timer and the input of the amplifier chip. One transistor overdrives the other, so that when you adjust the potentiometer at the center of the circuit, you hear an increasingly harsh, distorted sound.*

BACKGROUND

Stomp-box origins

The Ventures recorded the first single to use a fuzz box, titled "The 2,000 Pound Bee," in 1962. Truly one of the most awful instrumentals ever made, it used distortion merely as a gimmick and must have discouraged other musicians from taking the concept seriously.

Ray Davies of the Kinks was the first to embody distortion as an integral part of his music. Davies did it initially by plugging the output from one amp into the input of another, supposedly during the recording of his hit "You Really Got Me." This overloaded the input and created clipping—the basic fuzz concept. From there it was a short step to Keith Richards using a Gibson Maestro Fuzz-Tone when the Rolling Stones recorded "(I Can't Get No) Satisfaction" in 1965.

Today, you can find thousands of advocates promoting as many different mythologies about "ideal" distortion. In Figure 5-56, I've included a schematic from Flavio Dellepiane, a circuit designer in Italy who gives away his work (with a little help from Google AdSense) at *http://www.redcircuits.com*. Dellepiane is self-taught, having gained much of his knowledge from electronics magazines such as the British *Wireless World*. In his fuzz circuit, he uses a very high-gain amplifier consisting of three field-effect transistors (FETs), which closely imitate the rounded square-wave typical of an overdriven tube amp.

Dellepiane offers dozens more schematics on his site, developed and tested with a dual-trace oscilloscope, low-distortion sinewave oscillator (so that he can give audio devices a "clean" input), distortion meter, and precision audio volt meter. This last item, and the oscillator, were built from his own designs, and he gives away their schematics, too. Thus his site provides one-stop shopping for home-audio electronics hobbyists in search of a self-administered education.

Before fuzz, there was tremolo. A lot of people confuse this with vibrato, so let's clarify that distinction right now:

- Vibrato applied to a note makes the frequency waver up and down, as if a guitarist is bending the strings.
- Tremolo applied to a note makes its volume fluctuate, as if someone is turning the volume control of a guitar up and down very quickly.

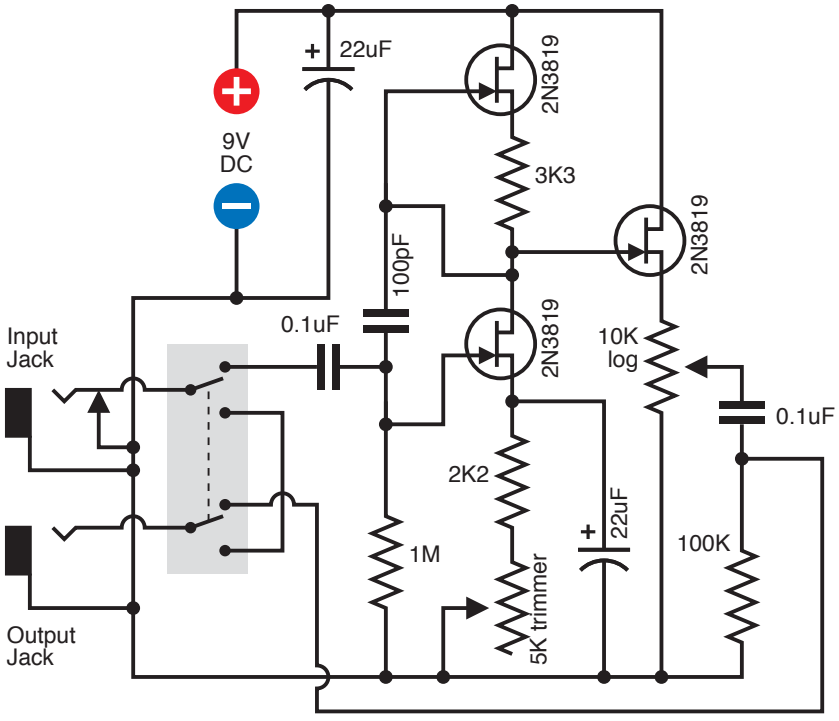

Figure 5-56. *This circuit designed by Flavio Dellepiane uses three transistors to simulate the kind of distortion that used to be created by overloading the input of a tube amplifier.*

BACKGROUND

Stomp-box origins (continued)

Harry DeArmond sold the first tremolo box, which he named the Trem-Trol. It looked like an antique portable radio, with two dials on the front and a carrying handle on top. Perhaps in an effort to cut costs, DeArmond didn't use any electronic components. His steam-punkish Trem-Trol contained a motor fitted with a tapered shaft, with a rubber wheel pressing against it. The speed of the wheel varied when you turned a knob to reposition the wheel up and down the shaft. The wheel, in turn, cranked a little capsule of "hydro-fluid," in which two wires were immersed, carrying the audio signal. As the capsule rocked to and fro, the fluid sloshed from side to side, and the resistance between the electrodes fluctuated. This modulated the audio output.

Today, Trem-Trols are an antique collectible. When industrial designer Dan Formosa acquired one, he put pictures online at *http://www.danformosa.com/dearmond.html*. And Johann Burkard has posted an MP3 of his DeArmond Trem-Trol so you can actually hear it: *http://johannburkard.de/blog/music/effects/DeArmond-Tremolo-Control-clip.html*.

The idea of a mechanical source for electronic sound mods didn't end there. The original Hammond organs derived their unique, rich sound from a set of toothed wheels turned by a motor. Each wheel created a fluctuating inductance in a sensor like the record head from a cassette player.

It's easy to think of other possibilities for motor-driven stomp boxes. Going back to tremolo: imagine a transparent disc masked with black paint, except for a circular stripe that tapers at each end. While the disc rotates, if you shine a bright LED through the transparent stripe toward a light-dependent resistor, you would have the basis for a tremolo device. You could even create never-before-heard tremolo effects by swapping discs with different stripe patterns. Figures 5-57 and 5-58 show the kind of thing I have in mind. For a real fabrication challenge, how about an automatic disc changer?

Today's guitarists can choose from a smorgasbord of effects, all of which can be home-built using plans available online. For reference, try these special-interest books:

- *Analog Man's Guide to Vintage Effects* by Tom Hughes (For Musicians Only Publishing, 2004). This is a guide to every vintage stomp box and pedal you can imagine.
- *How to Modify Effect Pedals for Guitar and Bass* by Brian Wampler (Custom Books Publishing, 2007). This is an extremely detailed guide for beginners with little or no prior knowledge. Currently it is available only by download, from sites such as *http://www.openlibrary.org*, but you may be able to find the previous printed edition from secondhand sellers, if you search for the title and the author.

Of course, you can always take a shortcut by laying down a couple hundred dollars for an off-the-shelf item such as a Boss ME-20, which uses digital processing to emulate distortion, metal, fuzz, chorus, phaser, flanger, tremolo, delay, reverb, and several more, all in one convenient multi-pedal package. Purists, of course, will claim that it "doesn't sound the same," but maybe that's not the point. Some of us simply can't get no satisfaction until we build our own stomp box and then tweak it, in search of a sound that doesn't come off-the-shelf and is wholly our own.

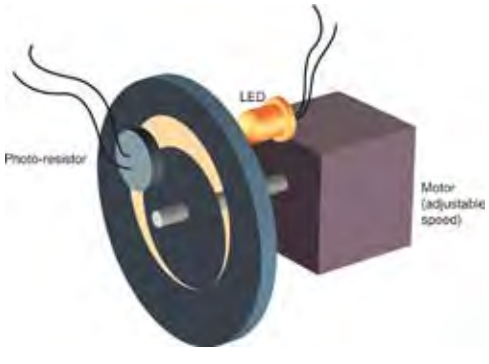

Figure 5-57. *Although electromechanical audio devices are obsolete now, some unexplored possibilities still exist. This design could create various tremolo effects, if anyone had the patience to build it.*

Figure 5-58. *Different stripe patterns could be used in conjunction with the imaginary electromechanical device in Figure 5-57 to create various tremolo effects.*

Experiment 31: One Radio, No Solder, No Power

Time now to go back one more time to inductance and capacitance, and demonstrate an application which also makes use of the way that waveforms can be added to each other. I want to show you how a simple circuit with no power supply at all can receive AM radio signals and make them audible. This is often known as a crystal radio, because the circuit includes a germanium diode, which has a crystal inside it. The idea dates back to the dawn of radio, but if you've never tried it, you've missed an experience that is truly magical.

Figure 5-59. *Just add wire and a coil, and this is all you need to receive AM radio signals. The black disc becomes the tuning dial, after it is screwed onto the variable capacitor (right). This is actually an optional extra. A germanium diode (center) rectifies the radio signal. The high-impedance earphone (top) creates a barely audible sound.*

You will need:

- Rigid cylindrical object, such as a vitamin bottle. Quantity: 1.
- 22-gauge hookup wire, solid-core. Quantity: 60 feet.
- 16-gauge wire, stranded. Quantity: 100 feet.
- Polypropylene rope ("poly rope") or nylon rope. Quantity: 10 feet.
- Germanium diode. Quantity: 1.
- High-impedance headphone. Quantity: 1.

The diode and headphone can be ordered from *http://www.scitoyscatalog.com*. You cannot use a modern headphone of the type you wear with an MP3 player.

Some of these items are shown in Figure 5-59.

First, you need to make a coil. It should be about 3 inches in diameter, and you can wind it around any empty glass or plastic container of that size, so long as it's rigid. A soda bottle or water bottle isn't suitable, because the cumulative squeezing force of the turns of wire can deform the bottle so that it isn't circular anymore.

Figure 5-60. *A large, 3-inch diameter empty vitamin bottle makes an ideal core for a crystal radio coil. The drilled holes will anchor wire wrapped around the bottle.*

I chose a vitamin bottle that just happened to be exactly the right size. To remove the label, I softened its adhesive with a heat gun (lightly, to avoid melting the bottle) and then just peeled it off. The adhesive left a residue, which I removed with Xylol (also known as Xylene). This is a handy solvent to have around, as it can remove "permanent" marker stains as well as sticky residues, but you should always use latex or nitrile gloves to avoid getting it on your skin, and minimize your exposure the fumes. Because Xylol will dissolve some plastics, clearly it's not good for your lungs.

After you prepare a clean, rigid bottle, drill two pairs of holes in it, as shown in Figure 5-60. You'll use them to anchor the ends of the coil.

Now you need about 60 feet of 22-gauge solid-core wire. If you use magnet wire, its thin insulation will allow the turns of the coil to be more closely spaced, and the coil may be slightly more efficient. But everyday vinyl-insulated wire will do the job, and is much easier to work with.

Begin by stripping the first 6 inches of insulation from the end of the wire. Now measure 50 inches along the insulated remainder and apply your wire strippers at that point, just enough to cut the insulation without cutting the

wire. Use your two thumb nails to pull the insulation apart, revealing about a half-inch of bare wire, as shown in Figure 5-61. Bend it at the center point and twist it into a loop, as shown in Figure 5-62.

You just made a "tap," meaning a point where you will be able to tap into the coil after you wind it. You'll need another 11 of these taps, all of them spaced 50 inches apart. (If the diameter of the bottle that you'll be using as the core of your coil is not 3 inches, multiply its diameter by 16 to get the approximate desired spacing of taps.)

After you have made 12 taps, cut the wire and strip 6 inches off that end. Now bend the end into a U shape about a half-inch in diameter, so that you can hook it through the pair of holes that you drilled at one end of the bottle. Pull the wire through, then loop it around again to make a secure anchor point.

Now wind the rest of the wire around the bottle, pulling it tightly so that the coils stay close together. When you get to the end of the wire, thread it through the remaining pair of holes to anchor it as shown in Figure 5-63. The completed coil is shown in Figure 5-64.

Figure 5-61. *Wire strippers expose the solid conductor at intervals along a 22-gauge wire.*

Figure 5-62. *Each exposed section of wire is twisted into a loop using sharp-nosed pliers.*

Figure 5-63. *The stripped end of the wire is secured through the holes drilled in the bottle.*

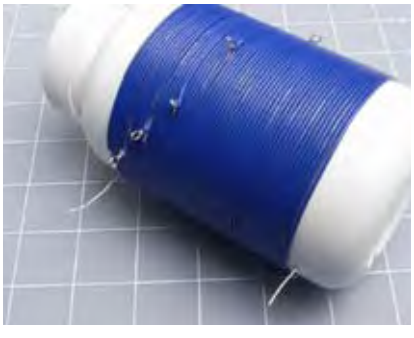

Figure 5-64. *The completed coil, wrapped tightly around the bottle.*

Your next step is to set up an antenna. If you live in a house with a yard outside, this is easy: just open a window, toss out a reel of 16-gauge wire while holding the free end, then go outside and string up your antenna by using polypropylene rope ("poly rope") or nylon rope, available from any hardware store, to hang the wire from any available trees, gutters, or poles. The total length of the wire should be about 100 feet. Where it comes in through the window, suspend it on another length of poly rope. The idea is to keep your antenna wire as far away from the ground or from any grounded objects as possible.

If you live in an apartment where you don't have access to a yard outside, you can try stringing your antenna around the room, hanging the wire from more pieces of poly rope. The antenna should still be about 100 feet long, but obviously it won't be in a straight line.

Hook the free end of your antenna to one end of your coil. At this point, you also need to add a germanium diode, which functions like a silicon-based diode but is better suited to the tiny voltages and currents that we'll be dealing with. The other end of the diode attaches to one of the wires leading to a high-impedance

High Voltage!

The world around us is full of electricity. Normally we're unaware of it, but a thunderstorm is a sudden reminder that there's a huge electrical potential between the ground below and the clouds above.

If you put up an outdoor antenna, never use it if there is any chance of a lightning strike. This can be extremely dangerous. Disconnect the indoor end of your antenna, drag it outside, and push the end of the wire into the ground to make it safe.

earphone. *A normal modern earphone or headphone will not work in this circuit.* The return wire from the headphone is connected to a jumper wire, the other end of which can be clipped to any of the taps in your coil.

One last modification, and you'll be ready to tune in. You have to ground the jumper wire. By this I mean connect it to something that literally goes into the ground. A cold-water pipe is the most commonly mentioned option, but (duh!) this will work only if the pipe is made of metal. Because a lot of plumbing these days is plastic, check under the sink to see if you have copper pipes before you try using a faucet for your ground.

Another option is to attach the wire to the screw in the cover plate of an electrical outlet, as the electrical system in your house is ultimately grounded. But the sure-fire way to get a good ground connection is to go outside and hammer a 4-foot copper-clad grounding stake into reasonably moist earth. Any wholesale electrical supply house should be able to sell you a stake. They're commonly used to ground welding equipment.

Figure 5-65. *The simple pleasure of picking up a radio signal with ultra-simple components and no additional power.*

Figures 5-66 and 5-67 show the completed radio.

If you've managed to follow these instructions (one way or another), it's time to tune your radio to the nearest station. Move the alligator clip at the end of your patch cord from one tap to another on your coil. Depending on where you live, you may pick up just one station, or several, some of them playing simultaneously.

It may seem that you're getting something for nothing here, as the earphone is making noise without any source of power. Really, though, there is a source of power: the transmitter located at the radio station. A large amplifier pumps power into the broadcasting tower, modulating a fixed frequency. When the combination of your coil and antenna resonates with that frequency, you're sucking in just enough voltage and current to energize a high-impedance headphone.

The reason you had to make a good ground connection is that the radio station broadcasts its signal at a voltage relative to ground. The earth completes the circuit between you and the transmitter. For more information on this and other concepts relating to radio, see the upcoming section "Theory: How radio works."

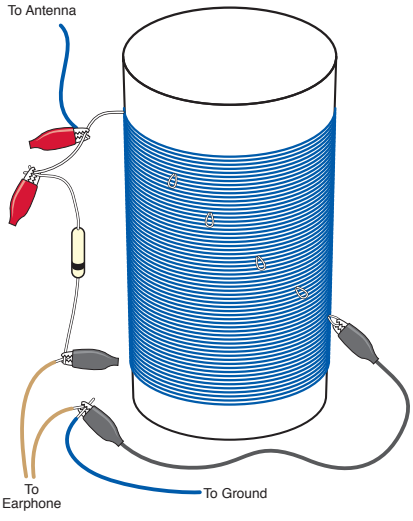

Figure 5-66. *A signal from the antenna can pass through the coil to ground. If the jumper wire is attached to an appropriate tap on the coil, it resonates with the radio signal, just powerfully enough to energize the earphone which is wired in series with a diode.*

Enhancements

The higher your antenna is, the better it should work. In my location, this is a major problem, as I live in a desert area without any trees. Still, just stringing the wire out of my window and tethering it (with rope) to the front bumper of my car enabled me to pick up a faint radio signal.

To improve the selectivity of your radio, you can add a variable capacitor, as shown in the following section. This allows you to "tune" the resonance of your circuit more precisely. Variable capacitors are uncommon today, but you can find one at the same specialty source that I recommended for the earphone and the germanium diode: the Scitoys Catalog (*http://www.scitoyscatalog.com)*.

This source is affiliated with a smart man named Simon Quellan Field, whose site suggests many fun projects that you can pursue at home. One of his clever ideas is to remove the germanium diode from your radio circuit and substitute a low-power LED in series with a 1.5-volt battery. This didn't work for me, because I live 40 miles from the nearest AM broadcaster. If you're closer to a transmitter, you may be able to see the LED varying in intensity as the broadcast power runs through it.

Figure 5-67. *The real-life version of Figure 5-66.*

THEORY

How radio works

When electrical frequencies are very high, the radiation they create has enough energy to travel for miles. This is the principle of radio transmission: A high-frequency voltage is applied to a broadcasting antenna, relative to the ground.

When I say "ground" in this instance, I literally mean the planet beneath us. If you set up a receiving antenna, it can pick up a faint trace of the transmission relative to the ground—as if the earth is one huge conductor. Actually the earth is so large and contains so many electrons, it can function as a common sink, like a gigantic version of the file cabinet that I suggested you should touch to get rid of static electricity in your body before touching a CMOS logic chip.

To make a radio transmitter, I could use a 555 timer chip running at, say, 850 kHz (850,000 cycles per second), and pass this stream of pulses through an amplifier to a transmission tower; if you had some way to block out all the other electromagnetic activity in the air, you could detect my signal and reamplify it.

This was more or less what Marconi (shown in Figure 5-68) was doing in 1901, after he had purchased rights to Edison's wireless telegraphy patent, although he had to use a primitive spark gap, rather than a 555 timer, to create the oscillations. His transmissions were of limited use, because they had only two states: on or off. You could send Morse code messages, and that was all.

Figure 5-68. *Marconi, the great pioneer of radio (photograph from Wikimedia Commons).*

Five years later, the first true audio signal was transmitted by imposing lower audio frequencies on the high-frequency carrier wave. In other words, the audio signal was "added" to the carrier frequency, so that the power of the carrier varied with the peaks and valleys of the audio.

At the receiving end, a very simple combination of a capacitor and a coil detected the carrier frequency out of all the other noise in the electromagnetic spectrum. The values of the capacitor and the coil were chosen so that their circuit would "resonate" at the same frequency as the carrier wave. Figures 5-69 and 5-70 illustrate these concepts.

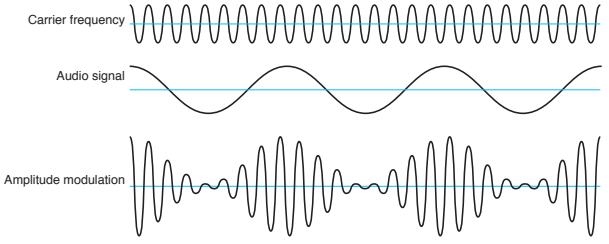

Figure 5-69. *When an audio signal (middle) is combined electronically with a high carrer frequency (top), the result looks something like the compound signal at the bottom. In actuality, the carrier frequency would be much higher compared with the audio frequency, by a radio of perhaps 1,000:1.*

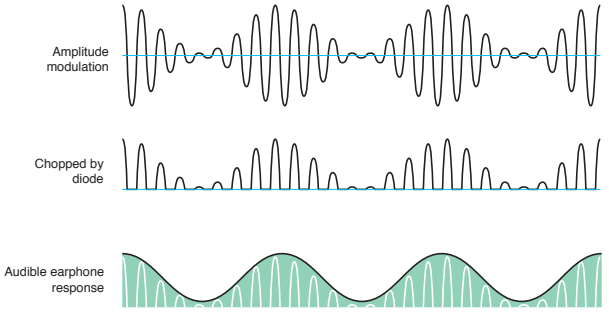

Figure 5-70. *When the compound signal is passed through a diode, only the upper half remains. An earphone cannot react fast enough to reproduce the high carrier frequency, so it "rides" the peaks and thus reproduces the audio frequency.*

The schematic in Figure 5-71 shows the simple circuit that you built by wrapping a coil around an empty vitamin bottle. When a positive pulse was received by the antenna, it resonated with the antenna and the coil, provided that the antenna was long enough and the coil was tapped at the appropriate number of turns.

THEORY

How radio works (continued)

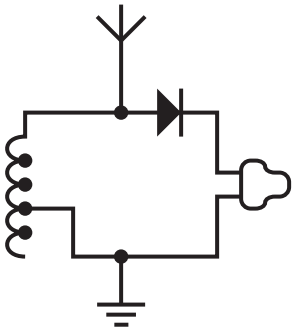

Figure 5-71. *An antenna at the top of the schematic picks up faint electromagnetic radiation from a distant transmitter. The coil at the left side is tapped at intervals so that its resonance can be adjusted to match the carrier frequency of the radio signal. Other frequencies are grounded (at the bottom of the schematic). The diode passes the "top half" of the signal to the earphone at the right, which is incapable of responding fast enough to reproduce the carrier frequency, and thus filters it out, leaving only the audio frequencies that were superimposed on it.*

By adding a capacitor, you can tune the circuit. Now an incoming pulse from the transmitter is initially blocked by the self-inductance of the coil, while it charges the capacitor. If an equally negative pulse is received after an interval that is properly synchronized with the values of the coil and the capacitor, it coincides with the capacitor discharging and the coil conducting. In this way, the right frequency of carrier wave makes the circuit resonate in sympathy. At the same time, audio-frequency fluctuations in the strength of the signal are translated into fluctuations in voltage in the circuit.

What happens to other frequencies pulled in by the antenna? The lower ones pass through the coil to ground; the higher ones pass through the capacitor to ground. They are just "thrown away."

The righthand half of the circuit samples the signal by passing it through a germanium diode and an earphone. The power from the transmitter is just sufficient to vibrate the diaphragm in the earphone, after the diode has subtracted the negative half of the signal.

Look back at the diagram of the amplitude-modulated signal. You'll see that it fluctuates up and down so rapidly, the earphone cannot possibly keep up with the positive-negative variations—hence the need for the diode. It will remain hesitating at the midpoint between the highs and lows, producing no sound at all. The diode solves this problem by subtracting the lower half of the "audio envelope," leaving just the positive spikes of voltage. Although these are still very small and rapid, they are now all pushing the diaphragm of the earphone in the same direction, so that it averages them out, approximately reconstructing the original sound wave.

Figure 5-72 shows how the circuit can be enhanced with a variable capacitor, to tune it without needing to tap the coil at intervals.

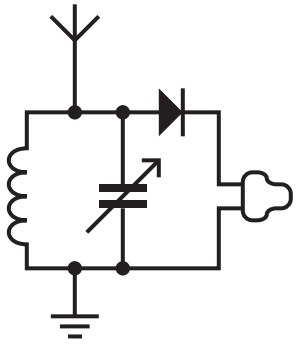

Figure 5-72. *By adding a capacitor to the circuit, its resonance can be tuned more precisely. The diagonal arrow indicates that a variable capacitor is used.*

The radio can pull in the stations on the AM (amplitude-modulated) waveband that happen to be most powerful in your area. The waveband ranges from 300 kHz to 3 MHz. If you find yourself interested in radio, your next step could be to build a powered radio using a couple of transistors. Alternatively you could build your own (legal) low-power AM transmitter. There's an ultra-simple kit available from *http://www.scitoys.com* consisting of just two principal components: a crystal oscillator, and a transformer, shown in Figure 5-73. That's all it takes.

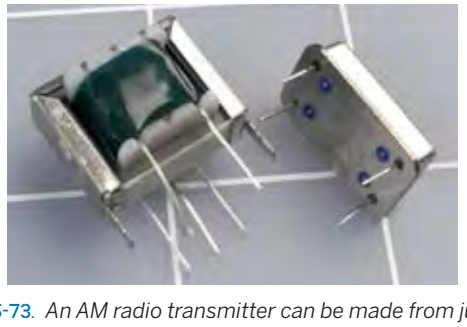

Figure 5-73. *An AM radio transmitter can be made from just two components: a transformer (left) and a crystal oscillator (right), available from http://www.scitoys.com.*

Figure 5-74. *A microswitch has a small button (at the front, righthand side in this picture) that is often actuated by a pivoted metal lever. The switch can respond to a very light pressure, but can handle relatively high currents.*

Figure 5-75. *For the Little Robot Cart, I found this 5-volt motor, which is supplied with a disc that fits its output shaft. The combination cost less than $10.*

Experiment 32: A Little Robot Cart

Robotics is another application of electronics that deserves a book in itself—or several books. So, once again, I'm going to give you an introduction followed by some points that you can follow if you want to go further. As always, I will start with the simplest possible device, which in the world of robotics is a cart that finds its way around your living room.

You will need:

- SPST or SPDT microswitches requiring minimal pressure to activate them. A force between 0.02 and 0.1 newtons would be ideal. Quantity: 2. See Figure 5-74.
- DC gear-motor, rated for any voltage between 5 and 12, drawing a maximum of 100mA in its free-running state, output shaft turning between 30 and 60 RPM. Quantity: 1. A motor is shown in Figure 5-75.
- Disc or arm that fits securely onto your motor shaft. Quantity: 1.
- 555 timer. Quantity: 1.
- DPDT nonlatching relay rated for the same voltage as your motor. Quantity: 1.
- 1/4-inch plywood or plastic, one piece about 2 feet square.
- #4 sheet-metal screws, 5/8 inch or 3/4 inch long. Quantity: 2 dozen.
- #6 bolts, 3/4 inch long, with nylon-insert lock nuts. Quantity: 2 dozen.
- 1/4-inch bolts, 1 inch long, with nuts, to mount the wheels. Quantity: 4.

I'm not specifying one particular motor, because if I did, it might not be available by the time you read this. Motors aren't like logic chips, which have retained their basic function throughout various improvements over a period of several decades. Motors come and go, and many that you may run across will be surplus parts that will never been seen again. Search online for "gear-motor" or "gearhead motor" and find one as close as possible to the specification that I have provided. The mechanical power output of the motor shouldn't be important, because we won't be requiring it to do much work.

The important consideration when you buy your motor is that you should also obtain something that fits onto its output shaft. Typically, this will be a disk or arm that can be screwed into place. To this you can then add a larger wheel of your own, which you can cut with a hole saw or make from the screw-on lid of a jar, or anything else circular that you may find in the house.

A larger wheel will make your cart move faster than a smaller wheel, but will reduce its torque, thus limiting its power to overcome obstacles.

This brings me to my next topic: fabrication. Although this is an electronics book, motors are electromechanical devices, and you have to be able to install them in some kind of a machine to get any interesting results. You can use

plywood to complete the two little robotics projects here (ideally, the kind of thin, high-quality plywood sold by hobby stores) but I recommend something that looks better and is easier to work with: ABS plastic. Before you start on the robotic cart, you may want to check the section "Fundamentals: All about ABS."

FUNDAMENTALS

All about ABS

Unless you think the steampunk movement isn't going back far enough, you probably don't want your autonomous robot cart to resemble a relic from before the 1800s. Therefore, wood may not be the best construction material. Metal can look nice, but is not easy to work with. For quick results that have a twentieth-century look (maybe even a 21st-century look), plastic is the obvious choice, and I feel that ABS is the best type of plastic to use, because it provides such quick, easy results. ABS stands for "acrylonitrile butadiene styrene." Lego® blocks are made of ABS. Car-stereo installers and model-railroad buffs use it. You can use it, too. You can saw it, drill it, sand it, whittle it, and drive screws into it, and it won't warp, split, or splinter. It's washable, doesn't need to be painted, and will last almost forever.

Delrin is another type of plastic, but tends to cost more and is a little tougher to drill and cut. It's a matter of personal preference. ABS machines fairly well, but when you drill it, for example, it can "catch" on the bit and the piece will spin with the bit due to the way that plastic chips off with the bit. Delrin is self-lubricating and has better melting properties under the heat of machining, so it drills and cuts much more cleanly and easily than ABS.

Where to find ABS

Pieces of ABS a couple of feet square are available from online sources such as *http://hobbylinc.com* or estreetplastics (an eBay store), but you'll save money if you can truck on down to your nearest plastic supply house and buy it like plywood, in sheets measuring 4 by 8 feet. To discover whether you have a nearby plastic supply house, search for "plastic supply" in your yellow pages or Google Local.

Piedmont Regal Plastics has many supply centers around the nation, but you'll have to collect it yourself, and they may not be willing to cut small pieces. You can check online at *http://www.piedmontplastics.com* for their locations.

Stock colors of ABS include black, white, and "natural," which is beige. Sheets usually are textured on one side, which is the side that should face outward, as it is more scratch-resistant than the smooth side.

Because you won't be adding paint or other finishes, you'll have to be careful not to scuff the plastic or scratch it while working. Clean your bench thoroughly before you begin, taking special care to remove any metal particles, which tend to become embedded in the plastic. Use wooden shims in the jaws of your vise, and avoid resting the plastic accidentally on any sharp tools or screws. Working with ABS requires a clean environment and a very gentle touch.

Cut with Care

You can saw ABS, but if you use a table saw, the plastic will tend to melt and stick to the blade. These smears will get warm and sticky when you feed the next piece of plastic into the saw, and the result will be extremely unpleasant. The whirling blade will grab the plastic and hurl it at you powerfully enough to break bones. This is known as "kickback" and is a very serious risk when sawing plastic.

If you have extensive experience using a table saw, you are actually more vulnerable, because the reflexes and cautions you have developed while dealing with wood will not be adequate for working with plastic. Please take this warning seriously!

Your first and most obvious precaution is to use a plastic-cutting blade, which has a larger number of thicker teeth to absorb the heat. The blade I have used is a Freud 80T, but there are others. If you use a blade that is not suitable, you will see it starting to accumulate sticky smears. This is the only warning you will get. Clean that blade with a solvent such as acetone, and never use it for ABS again.

Regardless of other precautions, always wear gloves and eye protection when using a table saw, and stand to one side when feeding materials into it. Personally, after one episode of kickback that I thought had broken my arm, I prefer not to use a table saw on plastic at all.

For long, straight cuts, the alternatives include:

- *Panel saw (big and expensive, but safe and accurate).*
- *Miniature handheld circular saw with a blade around 4 inches in diameter, guided with a straight edge clamped to the sheet.*
- *Hand saw. This is my old-school preference. My favorite is a Japanese pull-to-cut saw, which makes very clean cuts: the Vaughan Extra-Fine Cross-Cut Bear Saw, 9-1/2 inches, 17 tpi (teeth per inch). If you use one of these, be careful to keep your free hand out of the way, as the saw can easily jump out of the cut. Because it is designed to cut hard materials such as wood, it has no difficulty cutting soft flesh. Gloves are strongly recommended.*

Figure 5-78. *The perils of kickback. Plastic easily sticks to the blade of a table saw, which will hurl it at you unexpectedly. Use other tools to cut plastic.*

Curving Cuts

Curving cuts involve relatively little danger, although eye protection and gloves are still advisable. My preferred tools:

- Band saw with a 3/8- or 1/4-inch blade designed for thin wood or plywood.
- Jigsaw. I have a special liking for the DeWalt XRP using Bosch blades that are designed for hardwood or plastic. This will cut complex curves in ABS as easily as scissors cutting paper.

No matter what type of saw you use, you'll have to clean ragged bits of plastic off the cut afterward, and the absolutely necessary item for this purpose is a deburring tool, available from *http://www.mcmaster.com* and most other online hardware sources. A belt sander or disc sander is ideal for rounding corners, and a metal file can be used to remove bumps from edges that are supposed to be straight.

Figures 5-77 through 5-80 show various cutting tools. Figure 5-81 shows a deburring tool, and Figure 5-82 shows a disc sander.

Figure 5-77. *A band saw is an ideal tool for cutting complex shapes out of ABS plastic. You can often find them secondhand for under $200.*

Figure 5-78. *A handheld circular saw, running along a straight-edge, is much safer than a table saw for cutting plastic, and can produce comparable results.*

Figure 5-79. *This Japanese-style saw cuts when you pull it, rather than when you push it. After some practice, you can use it to make very accurate cuts. Because ABS is so soft, minimal muscle-power is required.*

Figure 5-80. *This DeWalt jigsaw can run at very slow speeds, enabling precise and careful work with plastic.*

Figure 5-81. *A deburring tool will clean and bevel the sawn edge of a piece of plastic in just a couple of quick strokes.*

Figure 5-82. *A belt sander or disc sander is the ideal tool for rounding corners when working with ABS plastic.*

Figure 5-83. *A Forstner drill bit makes clean, precise holes; a large regular drill bit will chew up ABS plastic and make a mess.*

Making Plans

I like to use drawing software to create plans, and I try to print them at actual scale. I tape them to the smooth side of a piece of white or natural-color ABS, then use an awl to prick through the plan into the soft surface beneath. I remove the paper and connect the awl marks by drawing onto the plastic using a pencil or a fine-point water-soluble pen. Its lines can be wiped away later with a damp cloth. Don't use a permanent marker, as the solvents that you will need to clean it may dissolve the plastic.

Because ABS will tend to open a fissure when you bend it at any inside corner where you don't have a smooth radius, you need to drill holes at these locations, as shown in the cart plans in Figure 5-92 on page 275.

A regular half-inch drill bit is too aggressive; it will tend to jam itself into the plastic within one turn of the drill. Use Forstner bits (shown in Figures 5-83 and 5-84) to cut nice smooth circles.

Note that the heat from bending will tend to make any marks on the plastic permanent.

Figure 5-84. *By drilling holes at any location where two bends intersect, you reduce the risk of the plastic fissuring.*

Figure 5-85. *Making clean, precise bends in ABS is simply a matter of resting the plastic over a bender that consists of an electric heating element.*

Bending It

A big advantage of plastic over wood is that you can make complex shapes by bending them, instead of cutting separate pieces and joining them with nails, screws, or glue. Unfortunately, bending does require an appropriate bender: an electric heating element mounted in a long, thin metal enclosure that you place on your workbench. The bender I use is made by FTM, a company that offers all kinds of neat gadgets for working with plastic. Their cheapest bender, shown in Figure 5-85, is just over $200 with a 2-foot element. You can get a 4-foot model for about $50 more. Check them out at *http://thefabricatorssource.com*.

Avoid Burns While Bending

A plastic bender will inflict serious burns if you happen to rest your hand on it accidentally, and because it has no warning light, you can easily forget that you have left it plugged in. Use gloves!

To bend plastic, lay it over the hot element of a plastic bender for a brief time (25 to 30 seconds for 1/8-inch ABS, 40 to 45 seconds for 3/16-inch, and up to a minute for 1/4-inch). If you overheat the plastic, you'll smell it, and when you turn it over you'll find it looks like brown melted cheese. Naturally you should learn to intervene before the plastic reaches that point.

ABS is ready to bend when it yields to gentle pressure. Take it off the bender and bend it *away* from the side that you heated. If you bend it toward the hot side, the softened plastic will bunch up inside the bend, which doesn't look nice.

You can work with it for about half a minute, and when you have it the way you want it, spray or sponge water onto it to make it set quickly. Alternatively, if you need more time, you can reheat it. The amount of force necessary to bend the sheet increases in proportion with the length of the bend, so a long bend can be difficult, and I usually insert it into a loose vise, push it a bit, move it along to the next spot, and push it again.

Because plastic bending is very similar to making shapes in origami, it's a good idea to model your projects in paper before you commit yourself to ABS.

If you decide that you don't want to spend money on a bender, don't abandon plastic just yet—you can use screws to assemble separate sections with greater ease and convenience than if you were working with wood.

Making 90-Degree Joints

Driving screws into the edge of a piece of plywood will almost always separate its layers, but ABS has no layers (or grain, either), and never splits or shatters. This means that you can easily join two pieces at 90° using small screws (#4 size, 5/8-inch long).

Figures 5-86 through 5-90 show the procedure for joining 1/8-inch (or thicker) ABS to 1/4-inch ABS, which I regard as the minimum thickness when you're inserting screws into its edge:

1. Mark a guideline on the thinner piece of plastic, 1/8 inch from its edge. For #4 screws, drill holes using a 7/64-inch bit. If you're using flat-headed screws, countersink the holes very gently.

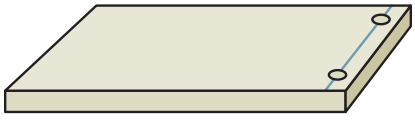

Figure 5-86

2. Hold or clamp the pieces in place and poke a pen or pencil through the holes to mark the edge of the 1/4-inch plastic beneath.
3. Remove the thin plastic, clamp the 1/4-inch plastic in a vise, and drill guide holes for the screws at each mark, centered within the thickness of the plastic. Because ABS does not compress like wood, the holes must be larger than you may expect; otherwise, the plastic will swell around the screw. A 3/32-inch bit is just right for a #4 screw.
4. Assemble the parts. Be careful not to overtighten the screws; it's easy to strip the threads that they cut in the soft plastic.

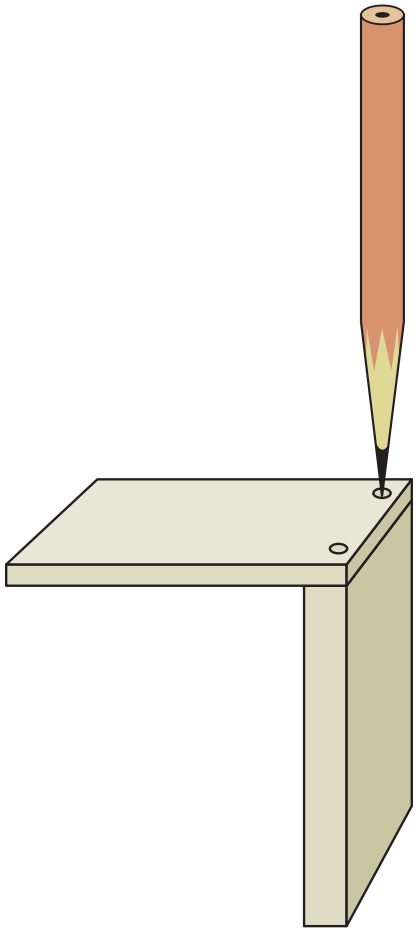

Figure 5-87

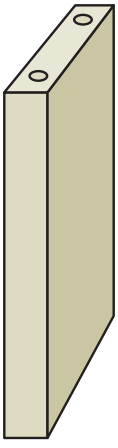

Figure 5-88

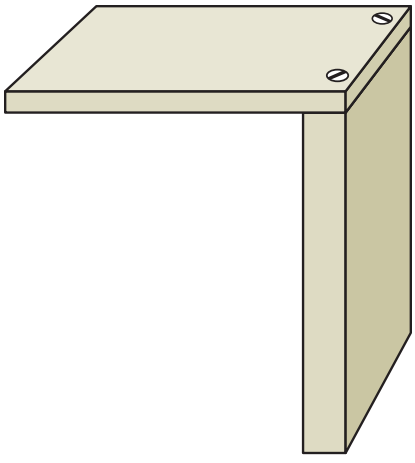

Figure 5-89. *Figures 5-86 through 5-89 illustrate four steps to join two pieces of ABS using #4 sheet-metal screws. Cut 7/64-inch holes on a line 1/8 inch from the edge of the first piece, then mark through the holes to the edge of the second piece. Drill 3/32-inch holes that are precisely centered in the edge, then screw the pieces together.*

Figure 5-90. *Three #4 screws driven into the edge of ABS, using a 1/16-inch guide hole, a 5/64-inch guide hole, and a 3/32-inch guide hole. respectively Because the first two guides holes were too small, the plastic swelled around the screw (but did not break).*

Framing Your Cart

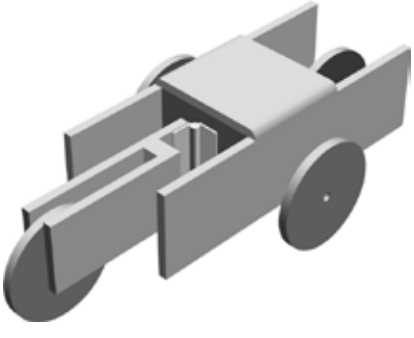

Figure 5-91. *If you have 3D rendering software, it can be a great way to test the feasibility of a construction project before you start cutting materials and trying to fit pieces together. This rendering was a proof-of-concept for the Little Robot Cart.*

For reasons that will soon be apparent, I've chosen an unusual diamond-shaped configuration of wheels. In the rendering shown in Figure 5-91, the front wheel (at the far end of the cart) applies power, the rear wheel (at the near end of the cart) steers the cart when backing up, and the side wheels prevent it from falling over.

Depending on the type of motor that you buy, you'll have to improvise a way to mount it in the front section of the cart. Don't be afraid to use kludges such as cable ties, duct tape, or even rubber bands to attach the motor to the frame. We're making a rough prototype, here, not a thing of beauty (although if you decide you like the cart, you can always rebuild it beautifully later).

The plan in Figure 5-92 shows the pieces that you will need. Part A is the body of the cart. If you're going to bend it from ABS, you should drill half-inch holes, with a forstner bit, at the four inside corners, so that these corners have rounded edges. If you simply saw the plastic to make sharp 90° corners, the plastic may develop fissures at the corners when you bend it. If you don't have a plastic bender and don't feel inclined to buy one, you can make Part A from three separate rectangles and then screw them together.

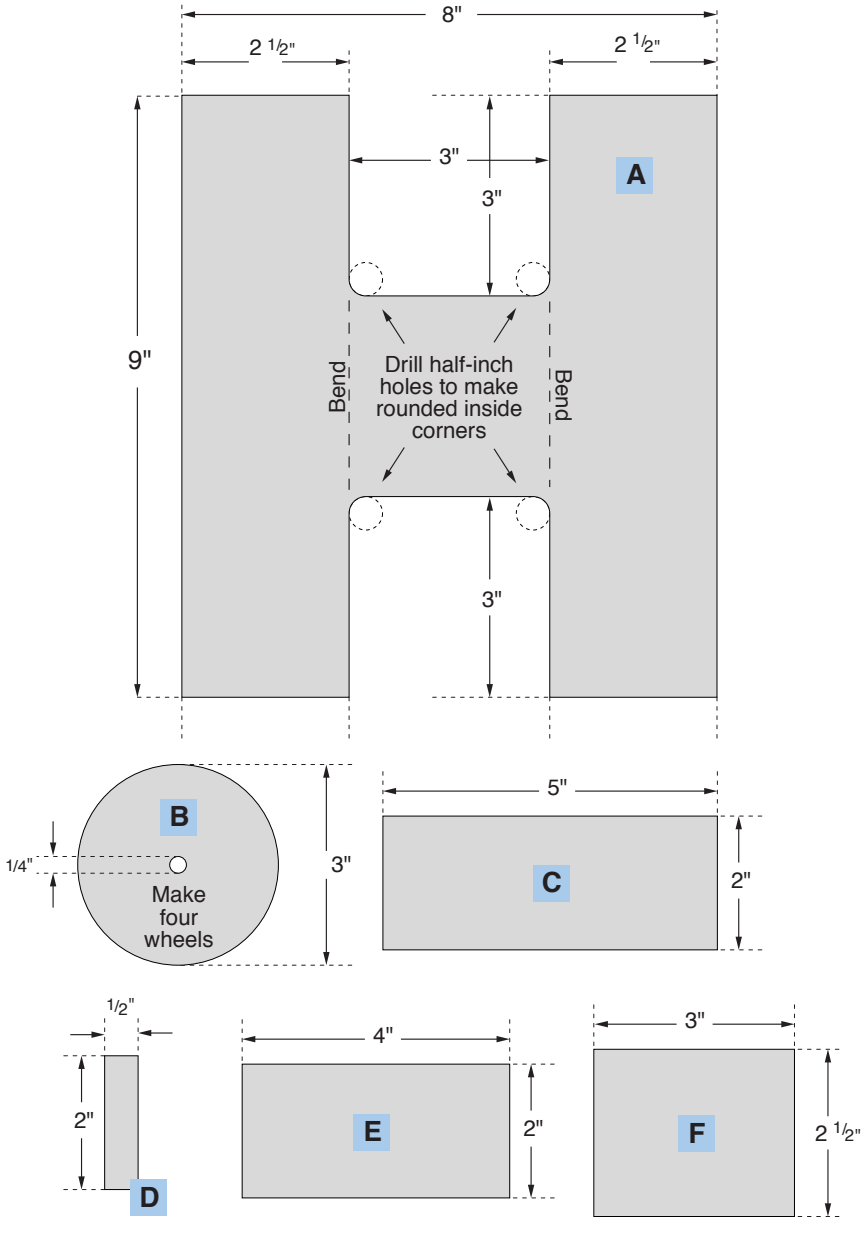

Figure 5-92. *These sections of 1/4-inch plastic can be assembled to create the simple cart described in Experiment 31.*

Part B is a wheel, of which you will need four. I cut them using a 3-inch hole saw. The front wheel is screwed to whatever disc or arm you obtained to mate with the shaft of your motor. See Figure 5-93.

Parts C, D, and E assemble to form a yoke in which the rear wheel is mounted. I used a 2-inch hinge to pivot the yoke. The hinge is mounted on Part F, which is a partition located midway in the frame of the cart. The photographs in Figures

Figure 5-93. *A 3-inch wheel is screwed to the disc that mates with the drive shaft of the motor.*

Figure 5-94. *The assembled body of the cart, before adding control electronics. The wheel at the righthand end will pull the cart from left to right. The hinged trailing wheel will allow the cart to move in a relatively straight line when it moves forward, but will tend to turn it when it backs up.*

Figure 5-95. *A closeup of the hinged trailing wheel, which rotates freely and can flip from side to side with minimal friction.*

5-94 and 5-95 will help to make this clear. Initially, when you install Part F, use only two screws, one each side, so that you can adjust its angle a little. This will be necessary to optimize the contact of the wheels with the floor.

The side wheels and rear wheel must spin freely, but on the other hand, they shouldn't wobble. I simply tightened the nuts on the bolts that serve as axles for the wheels, until there was maybe half a millimeter of clearance. I added a drop of Loctite to stop the nuts from getting loose.

The plans don't show precisely where to drill holes for the axle bolts, because the location will depend on the size of your wheels. You can figure this out as you go along. Just make sure that the side wheels aren't mounted too low. We don't want them to lift the front wheel or the rear wheel off the floor. If the side wheels are a fraction higher off the ground than the front and rear wheels, that's good.

If you have tile or wood floors, your cart may acquire better traction if you wrap a thick rubber band around each disc that you use for the drive wheel and the steering wheel.

The most important aspect of the construction is to place microswitches where they'll be triggered when the cart runs into something. I placed mine at the front corners, as shown in Figures 5-96 and 5-97. And that brings me to the electronics.

Figure 5-96

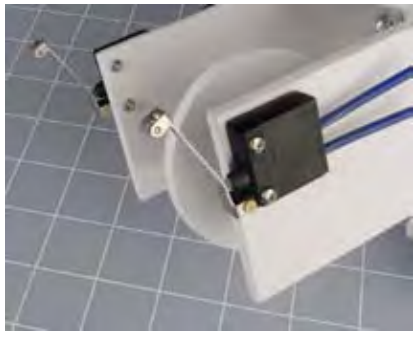

Figure 5-97. *Two microswitches with metal arms are mounted on each side of the cart, where they will sense any obstacle.*

The Circuit

The schematic is very, very simple, with only four principal components: two microswitches that sense obstacles in front of the cart, one relay, and one 555 timer. You will also need a small power switch, a battery or battery pack, and a resistor, and capacitors to go with the timer. A trimmer potentiometer will allow you to adjust the "on" time of the 555 timer, which will determine how long the cart takes to back up. See Figure 5-98.

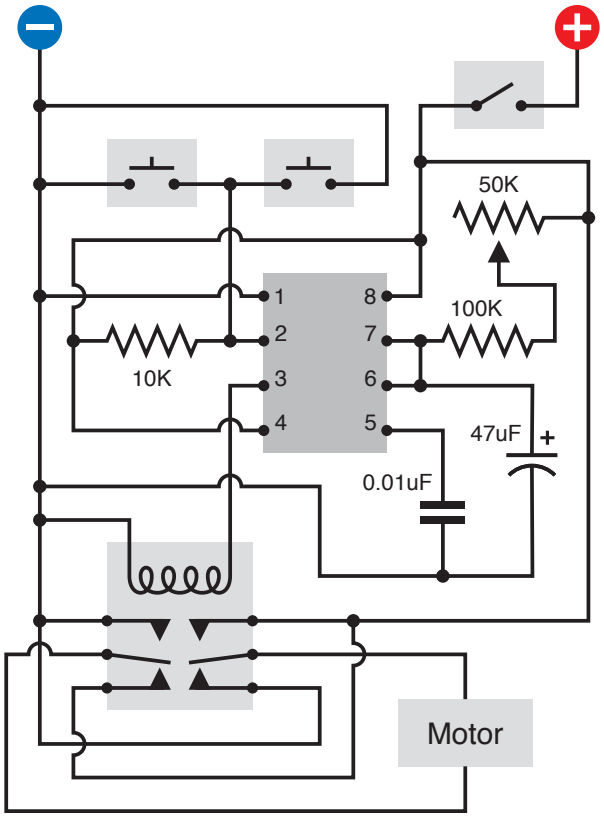

Figure 5-98. *This ultrasimple schematic is all the cart needs to enable it to back up when it hits an obstacle.*

The motor I chose requires 5 volts, so I had to use a voltage regulator with a 9-volt battery. If your motor uses 6 volts, you can wire four AA batteries to it directly. If you have a 12-volt motor, you can use two 9-volt batteries in series, supplying power through a 12-volt voltage regulator.

Assemble the components, mount them on the cart, and switch it on, and it should move forward slowly in a more-or-less straight line. If it moves backward, reverse your connection to the terminals on the motor.

When the cart bumps into something, either of the microswitches will connect negative voltage to the input pin of the 555 timer. This triggers the timer, which runs in monostable mode, generating a single pulse lasting about 5 seconds, which closes the relay, which is wired so that it reverses the voltage to the motor.

When the voltage is reversed to a simple DC motor, it runs backward. So the cart backs up. Because the rear wheel is mounted in a yoke that pivots, the yoke will tend to flip one way or the other, causing the cart to describe an arc as it moves backward. At the end of the timer cycle, the relay relaxes and the cart starts moving forward again. In forward mode, the rear wheel just follows along without applying any steering force, so the cart tends to follow a straight line—until it hits another obstacle, at which point it backs up, and tries another path.

FUNDAMENTALS

All about limit switches

The most obvious enhancement for your cart would be a better steering mechanism. You could use another motor to take care of this, with a pair of limit switches. Because limit switches are a basic, important idea in conjunction with motors, I'll explain them in detail.

Figure 5-99 shows three successive views of a motor with an arm attached to it, which can press either a lower pushbutton or an upper pushbutton. Both of the pushbuttons are normally closed, but will open when pressed by the motor arm. These buttons are the limit switches. Typically you would use microswitches for this purpose, just like the ones that I suggested as barrier-sensors at the front of the cart.

In addition, there's a DPDT relay that is activated by a simple on/off switch at the righthand side. On the cart, the 555 timer takes the place of the on/off switch, by feeding power to the relay.

Suppose that the motor begins with the arm pointing downward, as shown in the top view in Figure 5-99, and the motor is wired so that when it receives negative voltage at its lower terminal and positive at its upper terminal, it rotates counter-clockwise. This is what happens when the on/off switch closes and sends power to the DPDT relay. Positive voltage from the relay contacts cannot pass through the upper diode, but can pass through the upper limit switch, which is closed. Negative voltage cannot pass through the lower limit switch, because it's open, but can pass through the lower diode. So, the motor starts to turn counterclockwise. During the midpoint of its arc, it receives power through both of the limit switches.

Finally, the motor arm reaches the upper switch, and opens it. This prevents positive voltage from reaching the motor through that switch, and the positive voltage is also blocked by the upper diode. So, at this time, the motor stops.

Now suppose that the on/off switch is opened, as in the top view in Figure 5-100. The relay loses its power, so its contacts relax. The voltage to the motor is now reversed. Negative voltage passes through the upper diode, while positive voltage reaches the motor through the lower limit switch. The motor starts running clockwise, until its arm hits the lower switch, opening it and cutting off power to the motor.

Limit switches are necessary, because if you continue to apply voltage to a simple DC motor that is unable to turn, the motor sucks more current, gets hot, and may burn out.

You can easily see how this kind of system could be used to control the cart's steering. Even though the motor has only two positions, these are sufficient to make the cart turn when going backward, and proceed straight ahead when going forward.

To reduce power consumption, the DPDT relay could be replaced with a two-coil latching relay. The circuit would then have to be revised so that the relay is flipped to and fro by a pulse to each of its coils.

FUNDAMENTALS

All about limit switches (continued)

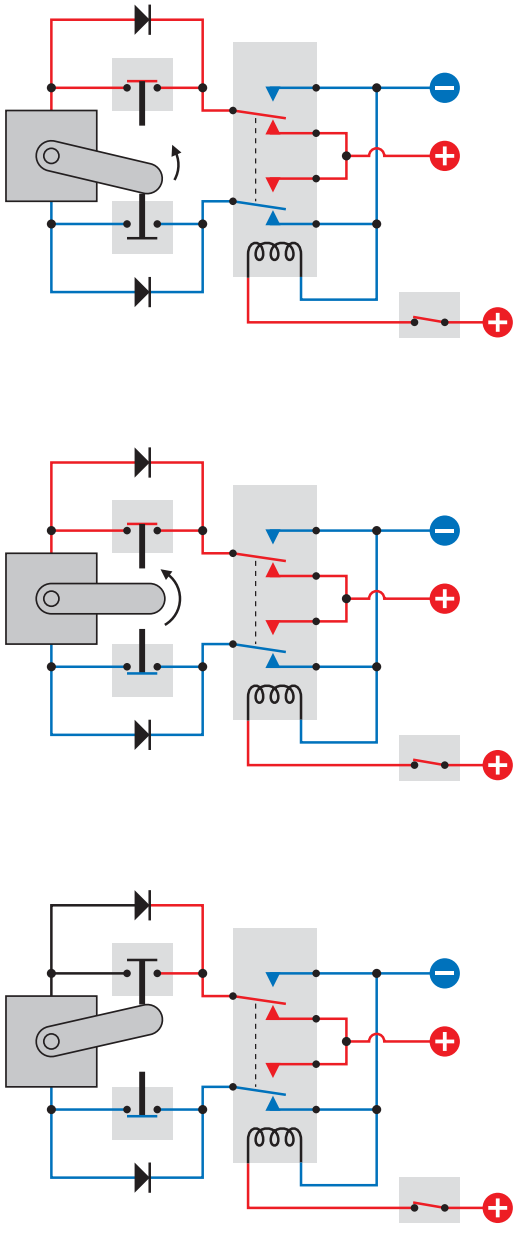

Figure 5-99. *The three diagrams, from top to bottom, show three snapshots of a motor controlled by a DPDT relay and two limit switches. When the on/off switch at bottom-right sends power to the relay, the lower relay contacts cause the motor to run counterclockwise until it stops itself as its arm opens the upper limit switch.*

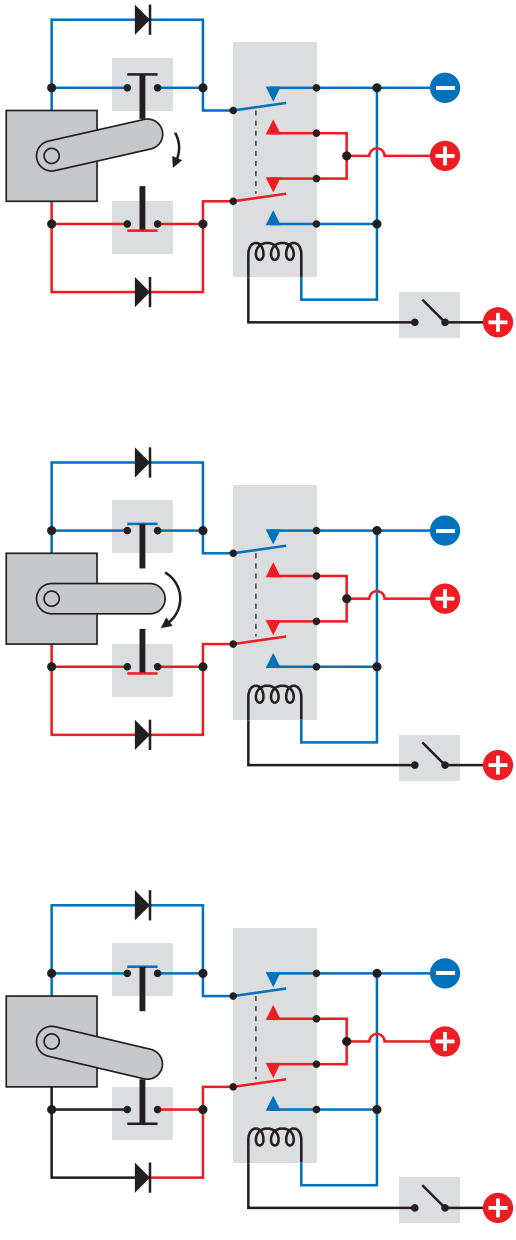

Figure 5-100. *When the on/off switch at bottom-right opens, the relay connects its upper contacts. This causes the motor to run clockwise until its arm opens the lower limit switch. Limit switches avoid the overheating and possible damage that are likely when power is delivered to a motor that is prevented from turning.*

FUNDAMENTALS

All about motors

Brushed DC motor

This is the oldest, simplest design for an electric motor, shown in very simplified form in Figure 5-101. Coils are attached to a shaft where they can interact with stationary magnets around them. The magnetic attraction turns the shaft a little, at which point the next coil on the shaft is energized to turn the shaft a little more, and then the next coil—and so on. To make this happen, electricity has to be fed into the coils by "brushes," often consisting of soft carbon pads that conduct power to a hub, known as a commutator, divided into sections, each of which is connected to a separate coil.

This basic design has several advantages if we want to build a small motorized gadget, such as a miniature robot or even a model airplane:

- Widely available
- Low cost
- Simple
- Reliable
- Will run in reverse when voltage reverses

In addition, brushed motors are often sold with reduction gearing built in. Such units are known as *gearhead motors* or *gear motors*. They free you from the need to use your own gears or belts to adjust the output speed yourself. You simply choose the motor that fits your specification.

DC stepper motor

This requires a controller, consisting of some electronics to tell the motor to rotate its shaft in small, discrete steps. The advantages of a stepper motor are:

- Precise positioning of the shaft
- Precise speed adjustment

Stepper motors are ideal for devices such as computer printers, where the paper has to roll up by a precise distance and the print head has to move laterally by an equally precise distance, but they are also useful in robots. If the motor is small enough to draw less than 200mA and will run on 12 volts or less, you can control it with pulses from a 555 timer. I'll describe stepper motors in more detail in Experiment 33.

Servo motor

This is generally used in conjunction with a programmable microcontroller, which sends instructors to rotate the motor shaft to a specific position and then hold it there. I'll mention servo motors when I introduce you to microcontrollers, but we won't be dealing with them in detail.

Other types of motors exist, including brushless DC motors (which require a different type of controller and are found in computer disk drives and CD players), and AC motors (including synchronous motors, which synchronize their rotation with the frequency of AC voltage, and were used extensively in clocks, before clocks mostly became digital).

In this book, I'll be talking mostly about brushed DC motors and DC stepper motors.

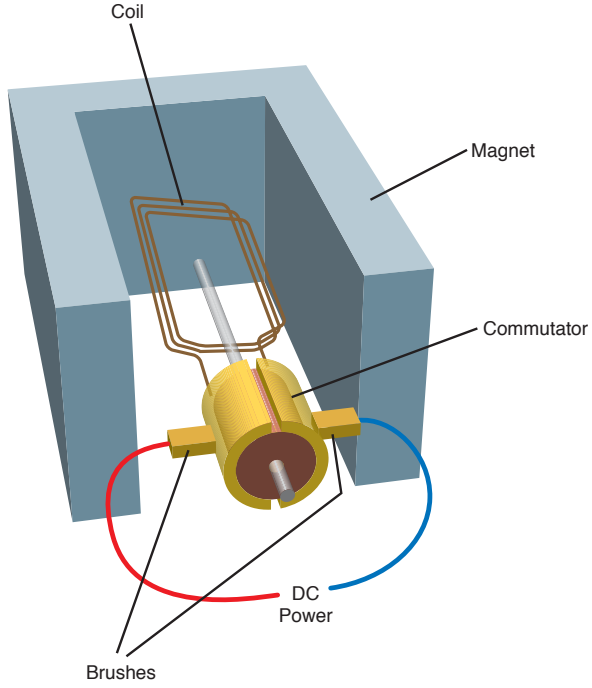

Figure 5-101. *The basic principle of a simple DC motor. The commutator passes electricity through a coil, creating a magnetic field that interacts with a magnet around the motor. The coil turns, and the commutator turns with it, until the electric field through the coil is reversed. This causes the process to repeat. In reality, a motor is likely to have a commutator formed from multiple segments, connected with multiple coils. The principle, however, remains the same.*

Take-home messages from this experiment include the following:

- You can buy simple DC motors with reduction gearing built in, providing your choice of RPM. Literally hundreds of websites will sell you small motors for robotics projects.
- When you reverse the voltage to a DC motor, the motor runs in reverse.
- A DPDT relay can be wired so that when it closes its contacts, it reverses a power supply to a motor.
- You can use two limit switches and a pair of diodes to stop a motor at two positions. In each of its stopping positions, the motor consumes no power and you won't have the risk of it burning out.

What other projects can you imagine using this simple set of techniques?

Mechanical Power

In the United States, the turning force, or torque, of a motor is usually measured in pound-feet or ounce-inches. In Europe, the metric system is used to measure torque in dynes.

A pound-foot is easy to understand. Imagine a lever pivoted at one end, as shown in Figure 5-102. If the lever is one foot long, and you hang a one-pound weight at the end of it, the turning force is one pound-foot.

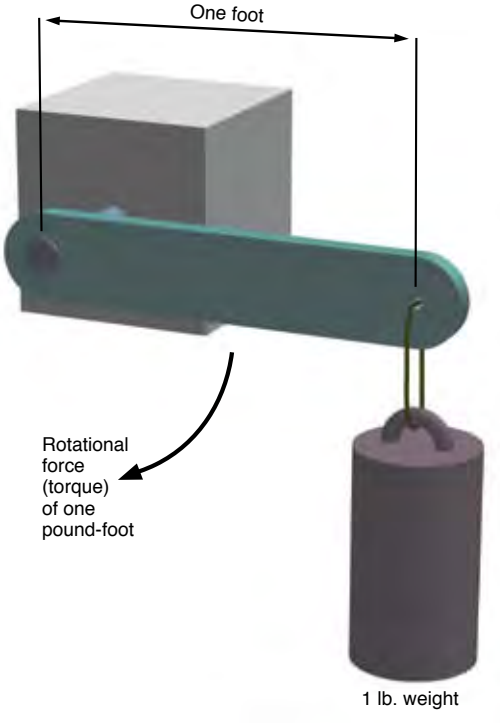

Figure 5-102. *The rotational force created by a motor is known as "torque," and in the United States it is measured in pound-feet (or ounce-inches, for small motors). In the metric system, torque is measured in dynes. Note that the torque created by a motor will vary according to the speed at which the motor is running.*

FUNDAMENTALS

Wire gauges

If you're going to power larger motors, or other components that take more current than LEDs or small relays, you really need to know about wire gauges. In particular, what's the relationship between wire thickness and AWG (American Wire Gauge)? And what gauge of wire should you use for any given current?

You can find numerous charts and tables if you go online, but many of these sources contradict each other, especially on the topic of how much current is safe to run through each gauge of wire.

After making several comparisons (and testing some wire samples myself), I've compiled the table in Figure 5-103, which I recommend as a compromise. Note the following:

- This table applies to solid-core copper wire.
- For stranded wire, or copper that has been tinned (giving it a silver appearance), the number of ohms per foot will *increase*, the number of feet per ohm will *decrease*, and the maximum amperage will *decrease*, probably by around 20%.

The maximum amperage assumes that the wire is insulated, preventing it from radiating heat as effectively as a bare conductor. I am also assuming that the wire is likely to be at least partially enclosed, inside a box or cabinet. At the amperages listed for each gauge of wire, you should expect the wire to become noticeably warm, and personally I would tend to use thicker wire instead of the maximums indicated in the table.

Most tables of this type only tell you the resistance of each gauge of wire in ohms per 1,000 feet. I have included that number but have also expressed the function the other way around, as the number of feet per ohm, as this doesn't require you to do so much arithmetic with decimals.

AWG		Diameter in inches	Ohms per 1,000 ft	Feet per ohm	Maximum amps (insulated)
0000		0.46	0.049	20,400	225
000		0.41	0.062	16,200	200
00		0.365	0.078	12,800	175
0		0.325	0.098	10,200	150
1		0.289	0.124	8,070	125
2		0.258	0.156	6,400	100
3		0.229	0.197	5,080	90
4		0.204	0.249	4,020	80
5		0.182	0.313	3,190	70
6		0.162	0.395	2,510	60
7		0.144	0.498	2,010	51
8		0.128	0.628	1,590	44
10		0.102	0.999	1,000	32
12		0.081	1.59	630	23
14		0.064	2.53	396	17
16		0.051	4.02	249	13
18		0.04	6.39	157	10
20		0.032	10.2	99	8
22		0.025	16.1	62	5
24		0.02	25.7	39	2.5
26		0.016	40.1	25	1.5
28		0.013	64.9	15	1.0
30		0.010	103.2	10	0.5

Figure 5-103. *American wire gauges (AWG) and their properties.*

THEORY

Calculating voltage drop

Another fact that you often need to know is how much of a voltage drop a particular length of wire will introduce in a circuit. If you want to get maximum power from a motor, you don't want to lose too much voltage in the wires that go to and from the motor.

Voltage drop is tricky, because it depends not only on the wire, but also on how heavily the circuit is loaded. Suppose that you are using 100 feet of 22-gauge wire, which has a resistance of about 1.5 ohms. If you attach it to a 12-volt battery and drive an LED and a series resistor offering a total effective resistance of about 1,200 ohms, the resistance of the wire is trivial by comparison. According to Ohm's Law:

amps = volts / ohms

so the current through the circuit is only about 10mA.

Again, by Ohm's Law:

volts = ohms × amps

so the wire with resistance of 1.5 ohms imposes a voltage drop of 1.5 × 0.01 = 0.015 volts.

Now suppose you're running a motor. The coils in the motor create impedance, rather than resistance, but still if we measure how much current is going through the circuit, we can establish its effective resistance. Suppose the current is 1 amp. Repeating the second calculation:

volts = ohms × amps

So the voltage drop in the wire is now 1.5 × 1 = 1.5 volts! This is illustrated in Figure 5-104.

Bearing these factors in mind, I have compiled a table for you. I've rounded the numbers to just two digits, as variations in the wire that you use make any pretense of greater accuracy unrealistic.

To use this table, you need to know how much current is passing through your circuit. You can calculate it (by adding up all the resistances and dividing it into the voltage that you are applying) or you can simply measure the current with a meter. Just make sure that your units are consistent (all in ohms, amps, and volts, or milliohms, milliamps, and millivolts).

In the table, I have arbitrarily assumed a length of 10 feet of wire. Naturally you will have to make allowances for the actual length of wire in your circuit. The shorter the wire, the less the loss will be. A circuit with only 5 feet of wire, and the same amperage and voltage, will suffer half of the percentage loss shown in the table. A circuit with 15 feet of wire, and the same amperage and voltage, will suffer 1.5 times the percentage loss. So, to use the table:

1. Divide your length of wire by 10. (Make sure that you measure the length in feet.)
2. Use the result to multiply the number in the table.

The table also arbitrarily assumes that you have a 12-volt supply. Again, you will have to make allowances if you are using a different voltage. So, to use the table:

1. Divide 12 by the actual voltage of your power supply.
2. Use the result to multiply the number in the table.

I can summarize those two steps like this:

Percent voltage lost = P × (12 / V) × (L / 10)

where P is the number from the table, V is your power-supply voltage, and L is the length of your wire.

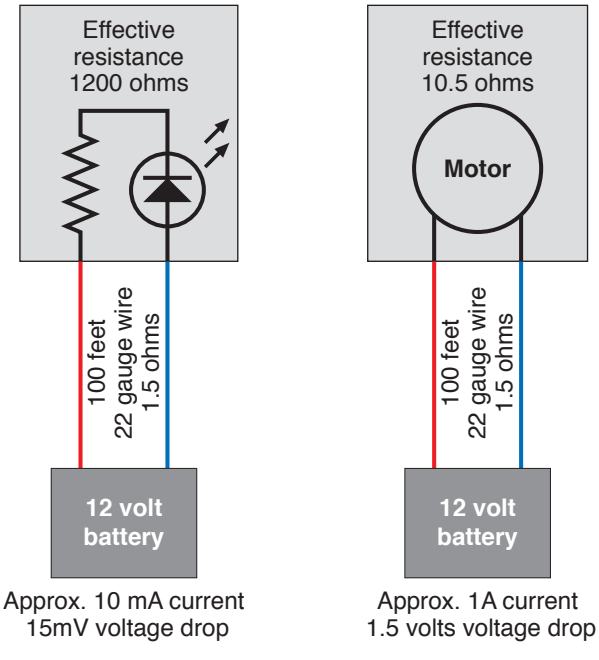

Figure 5-104. *The voltage drop imposed by wiring will depend on the current and the resistance in the circuit. The drop will be greatest when the resistance of the circuit is low and the amperage is high.*

THEORY

Calculating voltage drop (continued)

This table shows the percent voltage lost in a circuit with 10-foot wire at 12 volts.

Wire Gauge	Amperes									
	1	2	3	4	5	6	7	8	9	10
10	0.08	0.17	0.25	0.33	0.42	0.50	0.58	0.67	0.75	0.83
12	0.13	0.27	0.40	0.53	0.66	0.80	0.93	1.1	1.2	1.3
14	0.21	0.42	0.63	0.84	1.1	1.3	1.4	1.5	1.9	2.1
16	0.33	0.67	1.0	1.3	1.7	2.0	2.3	2.7	3.0	3.4
18	0.53	1.1	1.6	2.1	2.7	3.2	3.7	4.3	4.8	5.3
20	0.85	1.7	2.6	3.4	4.3	5.1	6.0	6.8	7.7	8.5
22	1.3	2.7	4.0	5.4	6.7	8.1	9.4	11	12	13
24	2.1	4.3	6.4	8.6	11	13	15	17	19	21
26	3.4	6.8	10	14	17	20	24	27	31	34
28	5.4	11	16	22	27	32	38	43	49	54
30	8.6	17	26	34	43	52	60	69	77	86

Remember, though, that the wire resistance will be higher if you are using stranded copper wire or tinned copper wire, and this will increase the percentage of voltage lost.

Experiment 33: Moving in Steps

Time now to build something more sophisticated: a cart that orients itself toward a light source. I'm going to tell you all you need to get started on this project, but this time I won't go all the way to the end in exhaustive detail. I want you to get into the habit of figuring out the details, improving on plans, and eventually inventing things for yourself.

You will need:

- 555 timers. Quantity: 8.
- Trimmer potentiometer, 2K linear. Quantity: 2.
- LEDs. Quantity: 4. If you get tired of using series resistors to protect LEDs in a 12-volt circuit, consider buying 12-volt LEDs such as Chicago Miniature 606-4302H1-12V, which contain their own resistors built in. However, the schematic in Figure 5-108 assumes that you will use regular 2V or 2.5V LEDs.
- Stepper motor: Unipolar, four-phase, 12-volt. Parallax 27964 or similar, consuming 100mA maximum. Quantity: 2.
- Photoresistors, ideally 500 to 3,000Ω range. Quantity: 2.

- ULN2001A or ULN2003A Darlington arrays by STMicroelectronics. Quantity: 2.
- CMOS octal or decade counter. Quantity: 2.
- Various resistors and capacitors.

Exploring Your Motor

I've specified a unipolar, four-phase, 12-volt motor because this is a very common type. A typical sample is shown in Figure 5-105. If you can't easily find the one that I've listed, you should feel safe in buying any other that has the same generic description. "Unipolar" means that you don't have to switch the power supply from positive to negative and back to positive again, to run the motor. Four-phase means that the pulses that run the motor must be applied in sequence to four separate wires. Because you will be running your motor directly from 555 timers, the lower its power consumption, the better.

Figure 5-105. *A typical stepper motor. The shaft rotates in steps when negative pulses are applied to four of the wires in sequence, the fifth wire being common-positive.*

First, though, we can apply voltage to the motor without using any other components at all. Most likely it will have five wires already attached, with the ends stripped and tinned, so that you can easily insert them into holes in a breadboard, as shown in Figure 5-106. Check the data sheet for your motor; you should find that four of the wires are used to energize the motor and turn it in steps, while the fifth is the common connection. In many cases, the common connection should be hooked to the positive side of your power supply, while you apply negative voltage to the other four wires in sequence, one step at a time.

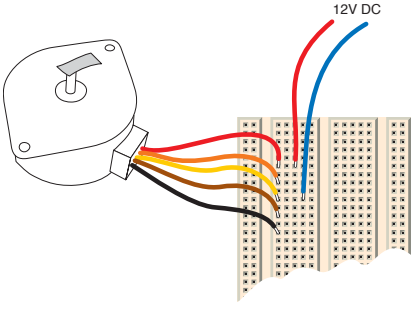

Figure 5-106. *The simplest test of a stepper motor is to apply voltage manually to each of its four control wires, while a piece of duct tape, attached to the output shaft, makes it easy to see how the motor responds.*

The data sheet will tell you in what sequence to apply power to the wires. You can figure this out by trial and error if necessary. One thing to bear in mind: a stepper motor is very tolerant. As long as you apply the correct voltage to it, you can't burn it out.

To see exactly what the motor is doing, stick a piece of duct tape to the end of the shaft. Then apply voltage to wires, one at a time, by moving your negative power connection from one to the next. You should see the shaft turning in little steps.

Inside the motor are coils and magnets, but they function differently from those in a DC motor. You can begin by imagining the configuration as being like the diagram in Figure 5-107. Each time you apply voltage to a different coil, the black quadrant of the shaft turns to face that coil. In reality, of course, the motor turns less than 90° from one coil to the next, but this simplified model is a good way to get a rough idea of what's happening. For a more precise explanation, see the upcoming section "Theory: Inside a stepper motor."

Bear in mind that as long as any of the wires of the motor are connected, it is constantly drawing power, even while sitting and doing nothing. Unlike a regular DC motor, a stepper motor is designed to do nothing for much of the time. When you apply voltage to a different wire, it steps to that position and then resumes doing nothing.

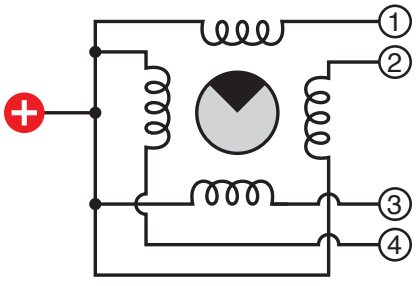

Figure 5-107. *This greatly simplified diagram helps in visualizing the way in which a stepper motor works. In reality, almost all motors rotate by less than 90° in response to each pulse.*

The coil inside the motor is holding the shaft in position, and the power that the motor draws will be dissipated as heat. It's quite normal for the motor to get warm while you're using it. The trouble is, if you use a battery to power it, and you forget that you have it connected, the battery will not hold its charge for long.

Quick Demo

Now that you've proved that your motor is functional, how can you actually run it? You need to send a pulse to each of the four wires in turn, in a rapidly repeating sequence. If you can also adjust the speed of the pulses, so much the better. I'm thinking that for a quick and simple demo, you can handle the challenge simply by using four 555 timers, all of them in monostable mode, with each one triggering the next.

The schematic in Figure 5-108 shows what I have in mind. It looks more complex than it really is. Each timer has the same pattern of components around it, so after you create the first module, you just make three copies of it.

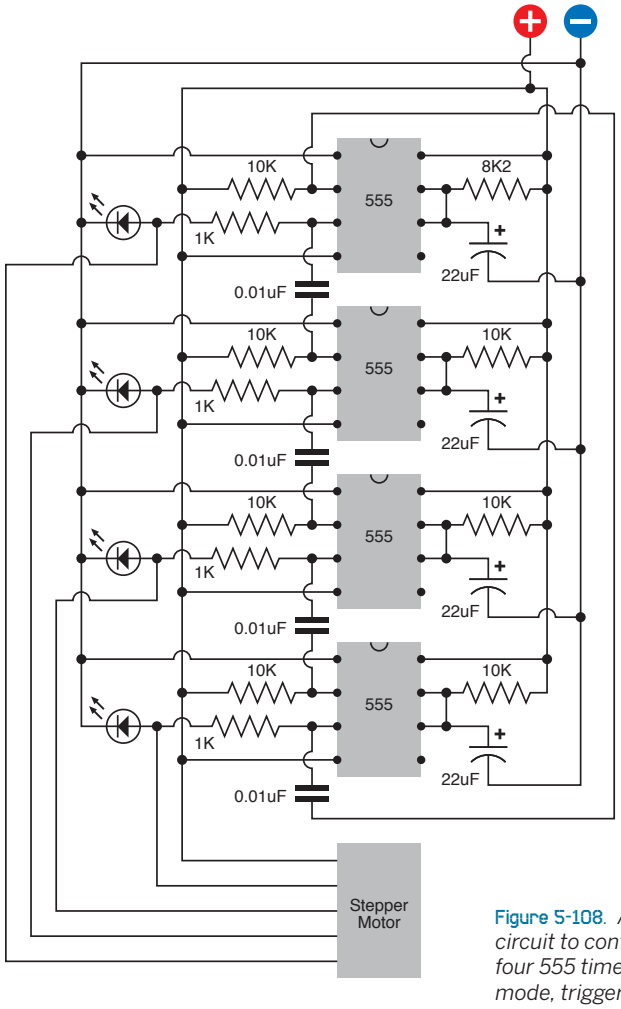

Figure 5-108. *A very quick and simple circuit to control a stepper motor uses four 555 timers, each in monostable mode, triggering each other in a repeating sequence.*

I've used a 10K resistor to pull up the input to each 555, so that the timers are naturally in their quiescent state. A 0.01 µF capacitor links the output from one timer to the input of the next so that they are electrically isolated from each other, and the capacitor just conveys a "spike" of voltage when one timer finishes its "on" cycle, and its output goes low, which triggers the next.

On the righthand side, I've used 10K resistors and 22 µF capacitors to generate a cycle of about a quarter of a second—except that the topmost timer has a 8K2 timing resistor. The reason for this is that when power is first applied, the timers will all be waiting for each other to begin, and timers 2 and 4 or 1 and 3 may fire together. By giving one timer a shorter cycle than the others, I minimize this problem.

The LEDs are included just to give you some visual verification of what's happening. Without them, if you make a wiring error, the motor may turn to and fro erratically, and you won't know why. Initially you can run your circuit with only the LEDs connected, just to make sure it works. Figure 5-109 shows the breadboarded circuit before the motor is plugged in. Then add the motor by plugging its wires into the breadboard, where you'll make connection with the outputs (pins 3) of the timers. See Figure 5-110.

Apply power, and you should see the motor turning in steps, in sequence with the LEDs. If the LED sequence isn't stable:

1. Connect a wire directly from the input (pin 2) of the topmost timer to the positive side of the voltage supply, and wait for the timers to calm down.
2. Restart the sequence by disconnecting the free end of this wire, or (if necessary) touch the free end of it briefly to the negative side of the supply, to trigger the first timer.

One thing you may have noticed, if you're paying very close attention: the common terminal of the motor is connected to positive. Therefore, when each timer flashes positive, that positive signal isn't actually powering the motor. The *low* outputs from the three timers that are *not* firing at any given moment are sinking current from the motor. It seems quite happy with this arrangement. You'll need some theory to understand why.

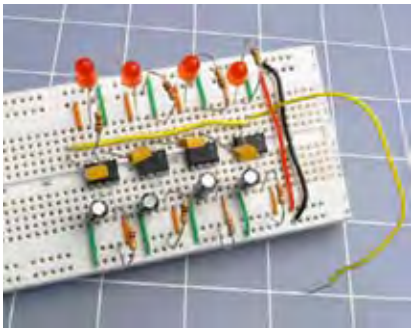

Figure 5-109. *To test the control circuit for errors, four LEDs show the outputs from the four 555 timers. The loose yellow wire at the righthand side connects to pin 2 of the first timer. Touch the free end of this wire to the positive side of the power supply to reset the timers, and then, if necessary, make a brief negative connection with the free end of the wire to restart their sequence.*

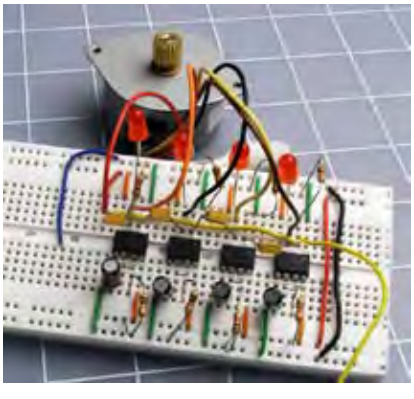

Figure 5-110. *After the circuit has been tested, the motor can be added by hooking its control wires to the outputs of the four 555 timers.*

THEORY

Inside a stepper motor

If you check the Wikipedia entry for stepper motors, you may see a very nice 3D rendering showing a toothed rotor and four coils arrayed around it. Maybe stepper motors used to be manufactured like this once upon a time, but not anymore.

Imagine two horizontal rows of coils. In the space between them is a series of little magnets, like a freight train, that can move left or right, as shown in Figures 5-111 and 5-112. Each coil has two windings, in opposite directions, so that current through one winding will create an upward magnetic force while current through the other will create a downward force. Each row of windings is connected in parallel, so that they switch on and off simultaneously.

In Step 1, the negative connection energizes the upper windings of the upper coils, which creates an upward magnetic force. I've shown this force using blue-green arrows so that you won't mistake it for a flow of electricity. It so happens that this force attracts the north poles of the magnets and repels the south poles, so if the magnets begin in the position shown in Step 1, they will want to move one step to the right.

This brings them to the position shown in Step 2. Now the upper windings of the lower coils are energized, and again, this produces an upward force, which again attracts the north poles and repels the south poles.

This advances the magnets to their location in Step 3. Now the lower windings of the upper coils are energized, producing a downward force. This repels the north poles of the magnets and attracts their south poles. So the magnets keep moving.

They reach the position shown in Step 4. The lower windings of the lower coils are energized, producing a downward force which continues to attract the south poles while repelling the north poles. So the magnets move a final step to the right—which leaves them in the same orientation shown in Step 1. And the process can repeat all over again.

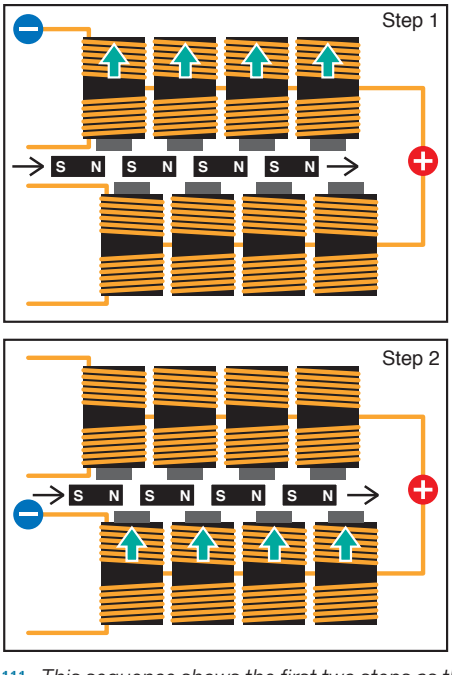

Figure 5-111. *This sequence shows the first two steps as the rotor of a stepper motor (shown as a series of north-south magnets) moves in response to pulses through electromagnets.*

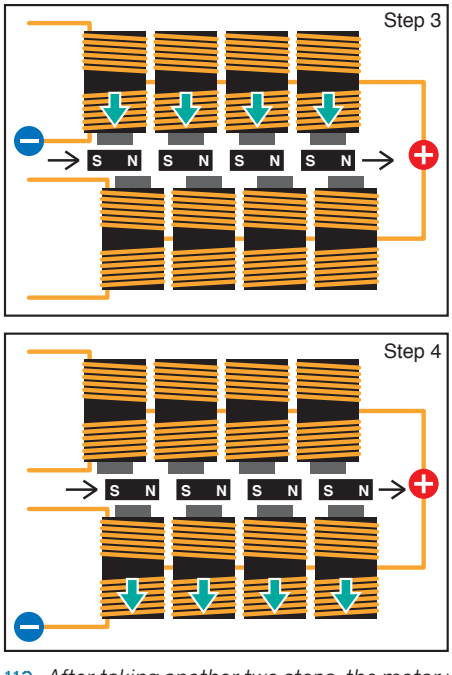

Figure 5-112. *After taking another two steps, the motor will be back where it started at Step 1 in Figure 5-111.*

THEORY

Inside a stepper motor (continued)

In reality, the magnets are not separate from each other. The edge of a rotor is magnetized in zones that alternate between south and north polarity. And instead of multiple coils, there are just four windings that go around all the magnetic cores. But the principle is exactly the same. The 3D rendering gives a general idea, and the photograph shows what I found when I cracked open a typical stepper motor.

Now bear in mind that when this device is driven by a set of 555 timers, we don't just connect negative to one wire at a time on the left, leaving the others floating. In reality, at any given moment, three of the timers have a negative output and the fourth has a positive output. The last diagram in Figure 5-112 shows this situation.

Suppose the top wire is positive while the other three are negative, as shown in Figure 5-113. The positive output does nothing, because it is balanced by the positive power on the other end of the coils. The two negatives attached to the bottom set of coils create equal and opposite forces that cancel each other out (while wasting some power). So the net result is the same as in Step 3.

In fact, you should find that you can disconnect the common wire completely while using the stepper motor with 555 timers, and the motor will still turn, because one of the timers is providing positive power while the others are negative. In fact, you'll be running them more efficiently this way.

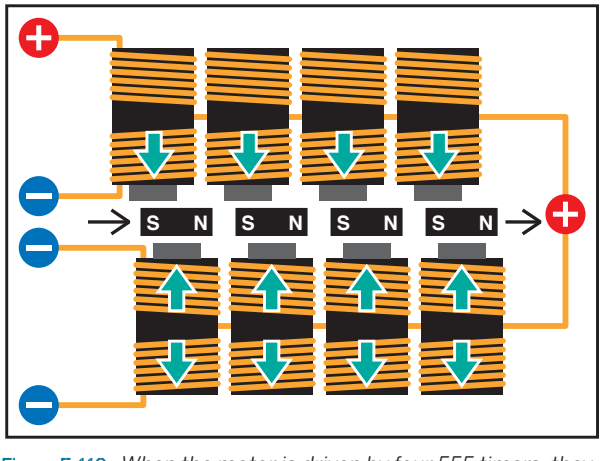

Figure 5-113. *When the motor is driven by four 555 timers, they are activating it by sinking positive voltage from it. The interior workings of the motor look something like this. It's not the most efficient way to do the job.*

Figures 5-114 and 5-115 may help to give you a clearer idea of what the motor actually looks like inside.

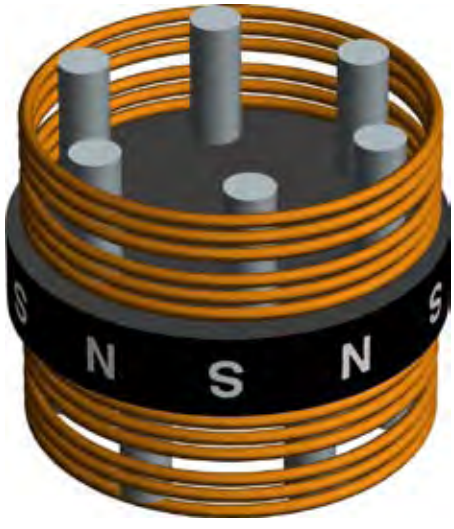

Figure 5-114. *This 3D rendering gives a better idea of what a typical stepper motor looks like inside. The copper coils and gray cylinders are stationary, while the black disc rotates between them.*

Figure 5-115. *When a stepper motor is broken open, this is what you're likely to find. On the left, the rotor of the motor, which has a magnetized band around its circumference, is still attached to the lower half of the casing. On the right, the upper half of the casing has been opened, and the coil has been removed (actually the winding you can see consists of two coils, wound in opposite directions). The spikes are the magnetic cores that exert force on the rotor.*

Speed Control

If you are a truly exceptionally observant, you may have noticed that I left pin 5 of each of the timers unconnected in the schematic for driving the stepper motor in Figure 5-108. Normally, pin 5 should be grounded through a capacitor to prevent it from picking up stray voltages which can affect the accuracy of the chip.

I left the pins unconnected because I had a plan for them. In fact, changing the timing of the chip is exactly what we want to do now, as a way to change the speed of the stepper motor.

If you tie pin 5 of all four timers together, as shown in Figure 5-116, and put a 2K trimmer potentiometer (shown in Figure 5-117) between them and the negative side of the power supply, you'll find that as you turn the trimmer to reduce its resistance, the timers start to run faster. Figure 5-118 shows the breadboard layout. Eventually, when the resistance goes below around 150 ohms, everything stops. The LEDs go dark, because you've reduced the voltage on pin 5 below the threshold level that the 555 timer finds acceptable.

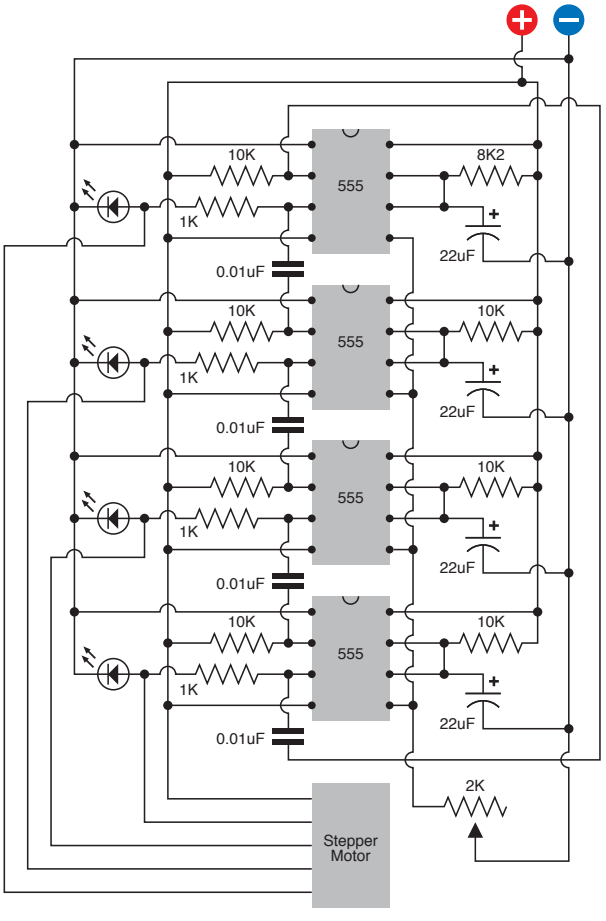

Figure 5-116. *To adjust the speed of the sequence of 555 timers, their control pins (pin 5 on each timer) are linked together and attached to a trimmer potentiometer that adjusts the resistance between the pins and the negative side of the power supply.*

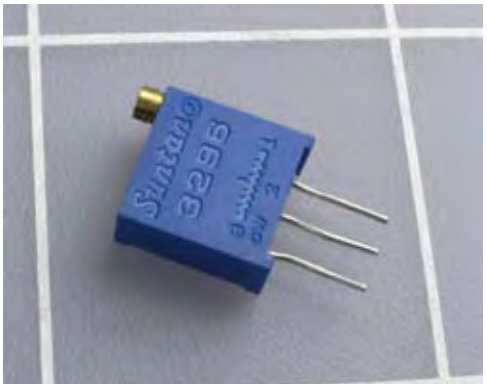

Figure 5-117. *Close-up of a trimmer potentiometer with pins spaced at 1/10 inch for insertion in a breadboard or perforated board. The brass screw, at top-left, turns a worm gear inside the unit, allowing precise adjustment of internal resistance.*

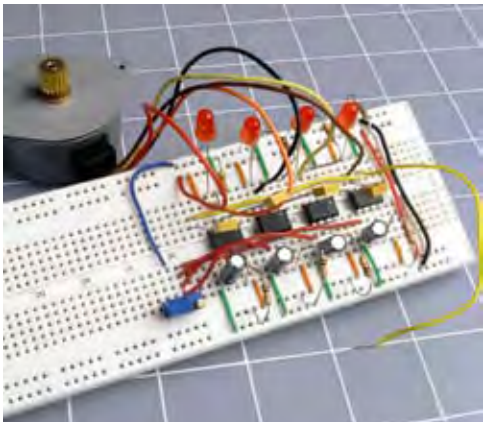

Figure 5-118. *The trimmer potentiometer has been added to the circuit, allowing motor speed control.*

Initially I suggested a step time of 1/4 second just so that you could see what was happening. When you're actually using this circuit, you'll never need it to run as slowly as that. So you can increase the entire range of speeds. Remove the 22 µF timing capacitors and substitute, say, 4.7 µF capacitors, or smaller. Now when you adjust the potentiometer, you'll get a useful range of speed.

Adding Autonomy

Currently, the circuit simply does what you tell it to do. The next step is to make it autonomous—in other words, give it the illusion of making up its own mind. I'm thinking that instead of a trimmer potentiometer, we could substitute a photocell, properly known as a photoresistor. Typically, the resistance of a cadmium sulfide photo resistor is highest in the dark, and lowest when light shines on it.

One problem with photoresistors is that they're not as widely available as many other types of electronic components. If you search Mouser.com, for instance, you'll find virtually nothing. Partly this is because the online search function at Mouser is the weakest feature of the site, and partly it's because Mouser is not oriented toward hobbyists. What you need to do is conduct a "product search." Go to *http://www.google.com/products*, enter the search terms "CdS" and "photocell," and you'll find a bunch of cheap cadmium sulfide components from places you may never have heard of.

Because photoresistors seem to come and go as erratically as DC motors, I am not offering any part numbers. You can buy any product that has an appropriate minimum resistance (in bright light) and maximum resistance (in the dark). If you find a component that ranges from 500 to 3,000Ω, that would be a good choice. If the only ones you can find have a higher minimum than 500Ω, you could consider putting a couple of them in parallel.

Setting Up Your Light Seeking Robot

Why would you want to control the speed of a stepper motor by using a photo resistor? Because the original objective was to build a robot that is attracted to light.

The idea is simple enough: use two stepper motors, each controlling the speed of one wheel of the cart. Use two photoresistors, each controlling the speed of the opposite stepper motor. When the righthand photoresistor picks up more light, its resistance lowers, causing the lefthand set of timers to run faster, which will make the lefthand wheel run faster. Thus, the cart will turn toward the light. Figure 5-119 illustrates the concept.

Before you start wiring more 555 timers, though, you might consider doing the job with a more appropriate component. The ULN2001A and ULN2003A are chips containing Darlington amplifiers specifically designed to deliver current to inductive loads such as solenoids, relays, and (you guessed it) motors. Each chip has seven inputs that require very little current, and seven outputs that can deliver 500mA each. The inputs are TTL and CMOS compatible (the 2001A has a wider tolerance for voltages than the 2003A) and each channel of

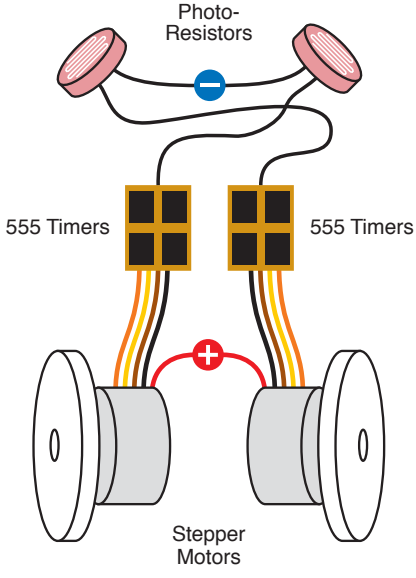

Figure 5-119. *If two photoresistors control the speed of two 555-timer arrays, the difference in speed between one wheel and the other can turn the cart toward a light source.*

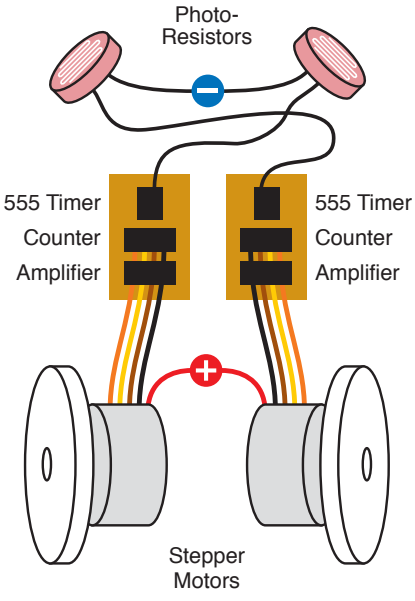

Figure 5-120. *A more efficient way to drive the motors is to use just one timer to set the speed of each, with a counter and amplifier (such as a Darlington array chip) sending the pulses down the wires. The principle is still the same, though.*

Figure 5-121. *This 3D rendering shows a possible configuration of the light-seeking cart, with two photoresistors enclosed in small tubes to restrict their response to light.*

the chip functions as an inverter, so that when the input goes high, the output goes low and sinks current. This is of course just what we need for our stepper motor that has a common positive connection.

The ULN2001A is only an amplification device, so you have to precede it with a counter that runs from 1 to 4 and then repeats. You can stick with your 555 timers, as you've already assembled them, or substitute almost any CMOS octal or decade counter that sends its output pulses to a series of pins. Just use the output from the fifth pin as the "carry" output to restart the counting sequence. I suggest a CMOS counter simply because it will run on 12 volts, so you can use the same power supply that suits your stepper motors.

If you switch to CMOS counters, you will still need a pair of 555 timers sending pulses to the counters. The timers will be free-running in astable mode, and your photoresistors will control their speed. Figure 5-120 shows the configuration.

One last item: you'll need a 12-volt battery. You can of course put eight AA cells together, but I think you should consider a rechargeable pack from a source such as *http://www.all-battery.com*, which has a section entirely devoted to "robot batteries."

If you put it all together, you should find that when you place your robot cart in a very dimly lit room, it will turn toward the beam from a bright, well-focused flashlight. To get reliable results, you may have to recess each of the photoresistors in little tubes, so that they receive much more light when they face your flashlight than when they face away from it. Figure 5-121 is a 3D rendering of the concept.

Another idea is to rewire your cart so that it actually runs away from the light. Can you imagine how this might be done?

Just one more thought: if you use infrared photoresistors, you can control your cart with beams from infrared LEDs, in normal room lighting. If you and a couple of friends all have infrared transmitters, you can get your cart to run from one of you to the next, like an obedient dog.

This takes us about as far as I'm going to go into robotics. I urge you to check out the sites online if you want to pursue the topic further. You can also buy a wide variety of robot kits, although of course I feel that it's more fun to invent or develop things for yourself.

All that's left now is to perform one last introduction: to a device that should make your life much easier, even though the device is much more complicated than anything we have dealt with so far.

Experiment 34: Hardware Meets Software

Throughout this book, in accordance with the goal of *learning by discovery*, I have asked you to do an experiment first, after which I've suggested the general principles and ideas that we can learn from it. I now have to change that policy, because the next experiment involves so much setup that it's only fair to tell you what to expect before you begin the preparations.

We are about to enter the realm of controller chips, often known as MCUs, which is an acronym for micro controller unit. An MCU contains some flash memory, which stores a program that you write yourself. The flash memory is like the memory in a portable media player, or the memory card that you use in a digital camera. It needs no electricity to power it. In addition, the chip has a processor which carries out the instructions in your program. It has RAM to store the values of variables on a temporary basis, and ROM, which tells it how to perform tasks such as sensing a varying voltage input and converting it into digital form for internal use. It also contains an accurate oscillator, so that it can keep track of time. Put it all together, and it's a tiny computer that you can buy for under $5.

Let's suppose that you have a greenhouse where the temperature must never fall below freezing. You set up a temperature sensor, and you have two different heaters. You want to switch on the first heater if the temperature falls below 38° Fahrenheit. But if, for some reason, that heater is broken, you want to switch on the second, backup heater when the temperature goes below 36° Fahrenheit.

Programming a MCU to take care of this can be very simple indeed. You could even add extra features, such as a second temperature sensor, just in case the first one fails, and you could tell the chip to use whichever sensor gives a lower reading.

Another application for a MCU would be in a fairly elaborate security system. The chip could monitor the status of various intrusion sensors, and can take various preprogrammed steps, depending on the sensors' status. You could include delay intervals, too.

Many MCUs have additional useful features built in, such as the ability to control servo motors that turn to a specific angle in response to a stream of pulses. Servos are widely used in radio-controlled model boats, airplanes, and hobby robotics.

Perhaps you are now wondering why, if MCUs can do all this, haven't we been using them all along? Why did I spend so much time describing the development of an alarm system using discrete components, if one chip could have done everything?

There are three answers:

1. MCUs cannot do everything. They need other components to help them interact with the world, such as transistors, relays, sensors, and amplifiers. You need to know how those things work, so that you can make intelligent use of them.
2. MCUs can introduce their own kinds of problems and errors, associated with using software in addition to hardware. I'll have more to say about this later.
3. MCUs have limits and restrictions, most obviously their requirement for a 5-volt regulated power supply, and their inability to source or sink much current from each pin. They also demand that you learn a programming language (which differs from one brand of MCU to the next). And to get the program into the chip, you have to be able to plug it into a computer and do a download, which is not always convenient.

In this experiment, you'll learn how to write a program for a small and simple MCU, and you'll transfer the program into it and see how it works.

BACKGROUND

Origins of programmable chips

In factories and laboratories, many procedures are repetitive. A flow sensor may have to control a heating element. A motion sensor may have to adjust the speed of a motor. Microcontrollers are perfect for this kind of routine task.

A company named General Instrument introduced an early line of MCUs in 1976, and called them PICs, meaning Programmable Intelligent Computer—or Programmable Interface Controller, depending which source you believe. General Instrument sold the brand to another company named Microchip Technology, which owns it today.

"PIC" is trademarked, but is sometimes used as if it's a generic term, like Scotch tape. In this book, I've chosen a range of controllers based on the PIC architecture. They are licensed by a British company named Revolution Education Ltd., which calls its range of chips the PICAXE, for no apparent logical reason other than that it sounds cool.

I like these microcontrollers because they were developed originally as an educational tool and because they are very easy to use. They're cheap, and some of them are quite powerful. Despite their odd name, I think they're the best way to get acquainted with the core concepts of MCUs.

After you play with the PICAXE, if you want to go farther into MCUs, I suggest the BASIC Stamp (which uses a very similar language, but with additional powerful commands) and the very popular Arduino (which is a more recent design, packed with powerful features, but requires you to learn a variant of C language to program it). I'll say more about these chips later.

If you search for "picaxe" on Wikipedia, you'll find an excellent introduction to all the various features. In fact, I think it's a clearer overview than you'll get from the PICAXE website.

Supplies

Figure 5-122 shows some of the chips in the PICAXE range. I'll be telling you how to use the smallest—the 08M—which costs less than $5 and is cheaper than any other MCU that I've found. It has only 256 bytes of memory to store a program (not gigabytes, megabytes, or kilobytes, just 256 bytes!), but you'll be surprised how many possibilities this amount allows for. Figure 5-123 shows a closeup of the 08M with its legs safely embedded in a piece of conductive foam.

In the United States, there are three distributors of this chip:

- *http://www.advancedmicrocircuits.com*
- *http://www.phanderson.com/picaxe*
- *http://www.sparkfun.com*

I like P. H. Anderson for its grass-roots hobbyist approach, and they have good prices if you want to buy multiple chips. But SparkFun Electronics offers other associated products that you may find interesting.

All the distributors will want to sell you "starter kits," such as the one in Figure 5-124, perhaps because the PICAXE itself is so cheap that it doesn't offer much of a profit margin. Still, for our purposes, you should buy the chip as a stand-alone item. And buy two of them, just in case you damage one (for example, by connecting voltage to it incorrectly).

Figure 5-122. *A page from the PICAXE catalog lists only some of the chips that are available. What began as an educational aid has become a useful prototyping tool.*

Figure 5-123. *When supplied by one of its American distributors, a PICAXE 08M arrives embedded in a little square of conductive foam. The chip is the same size as a 555 timer but has the power of a tiny computer.*

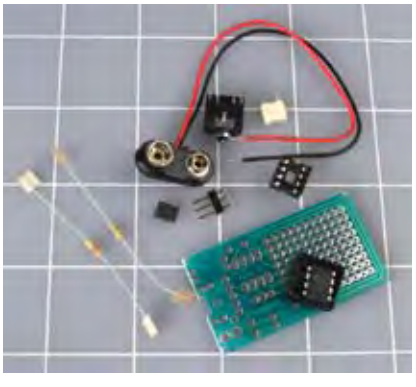

Figure 5-124. *A typical PICAXE kit includes a printed circuit board, which you may not really need, and some other not-entirely-essential items. But the 3.5-mm stereo jack socket (top, center) is absolutely necessary.*

To download your programming instructions into the chip, first you'll type the instructions on a computer, and then you'll feed them through a cable into the PICAXE memory. So you'll need to buy a cable, and you'll need software to help you to write the program.

Figure 5-125. *The USB download cable made for use with the PICAXE terminates in a 3.5-mm audio plug. This should not be inserted in any audio device. It establishes a serial connection with a computer, allowing program code to be downloaded into the chip.*

Figure 5-126. *Closeup of the 3.5-mm stereo socket that is used with the USB download cable.*

You can use the PICAXE with a serial cable, but I don't recommend it. The old RS-232 serial communications standard on PCs is pretty much obsolete, and PICAXE has recognized this by offering a USB cable (which contains a serial converter inside its plug). The USB cable is a little more expensive, but is also simpler and compatible with Apple computers. From any of the U.S. distributors, buy USB cable part AXE027, also sold as part PGM-08312 by *http://www.sparkfun.com* (quantity: 1). The cable is shown in Figure 5-125.

To write your software and send it down the wire to the chip, the PICAXE Programming Editor is the tool of choice. It comes in only a Windows version. For those who prefer Mac OS or Linux, you can get a free download of another piece of software known as AXEpad, which has fewer features, but will do the job. All the downloadable software is freely available from *http://www.rev-ed.co.uk/picaxe/software.htm*.

Finally, you need a 3.5-mm stereo audio socket with solder connections. The reason for this is that the manufacturers of the PICAXE have used a stereo audio plug on the free end of their USB cable, and you have to be able to plug it into something. The PICAXE breadboard adapter, SparkFun stock number DEV-08331, contains the necessary stereo socket in addition to a few other little items. Quantity: 1. See Figure 5-126.

Oddly enough, the USB cable is the most expensive item on the list, because of the electronics hidden inside it.

Software Installation and Setup

Now you have to go through a setup procedure. There is no way around this. Here is what you will be doing:

1. Install a driver so that your computer will recognize the special USB cable.
2. Install the Programming Editor software (or AXEpad for Mac/Linux) so that your computer will help you to write programs and then download them into the chip.
3. Mount the PICAXE on your breadboard and add the socket to receive downloads.

These steps are explained in the following sections.

The USB driver

Fair warning: If you go to the PICAXE website and try to use its search function, it probably won't find what you want. Search for "USB Driver," for instance, and it will pretend it has never heard of such a thing.

The PICAXE home page also has irritating drop-down menus that tend to disappear just when you're about to click on them, but at the time of writing, you can bypass these issues by going straight to the Software Downloads section at *http://www.rev-ed.co.uk/picaxe/software.htm*.

Scroll down past all the software until you get to Additional Resources. Look for the AXE027 PICAXE USB Download Cable. At first glance, it looks as if they want to sell you a cable, but in fact this is the list of drivers. Double-click the one appropriate to your computer, and choose a destination on your computer for the download—a place where you will find it easily, such as your desktop.

Be careful not to download the driver for the USB010 USB-Serial adapter by mistake. The USB-Serial adapter is something else entirely.

The download will leave you with a zipped file folder. You will have to unzip it. On Windows XP, right-click the folder and choose "Extract all." View the extracted files and you will find a PDF installation guide. Linux and Mac users can find instructions currently stashed at *http://www.rev-ed.co.uk/docs/AXE027.pdf*.

When installing the driver on a Windows platform, here are a few tips to minimize your exasperation level:

1. Remember, the special USB cable contains some electronics. It is not just a cable, but a device designed for interacting with a PICAXE chip. *Don't try to use it for anything else!*
2. You have to plug the cable into a USB port *before* you install the driver, because your computer will need to verify that the driver matches the cable.
3. You must not attach the PICAXE to the other end of the cable until *after* you have installed the driver.
4. Every USB port on your computer has a separate identity. Whichever one you choose when you first plug in the cable, you should use that port *every time in the future*. Otherwise, you will have to repeat the process of telling your computer what the cable is.
5. Bearing in mind Tip #4, you should avoid using the cable in a standalone USB hub.
6. The cable is fooling the PICAXE into thinking that it's talking to a serial port on your computer. Those "communication" ports are known as COM1, COM2, COM3, or COM4. When you install the driver, the installer will choose one of those COM ports for you, and later you will have to know which one it is. The PDF guide should help you through this procedure. Unfortunately, you cannot skip it.

The Programming Editor software

If you have come this far, you're ready for the next big step, which is much easier. You need the PICAXE Programming Editor, available for free on the Software Downloads web page where you found the USB driver. (If you are using a Mac or Linux, you will need AXEpad, which is on the same web page.)

Downloading and installing the Programming Editor should be simple and painless. Once you have done that, you should find that it has placed a shortcut on your desktop. Double-click it, go to View→Options, and in the window that opens (shown in Figure 5-127), click the Serial Port tab. You should see a dialog box like the one in Figure 5-128. Now make sure that the Programming Editor is looking at the same COM port that was chosen by the USB driver. Otherwise, the Programming Editor won't know where to find your PICAXE chip.

In the Programming Editor, go to View→Options and click the Mode tab, then click the button to select the 08M chip.

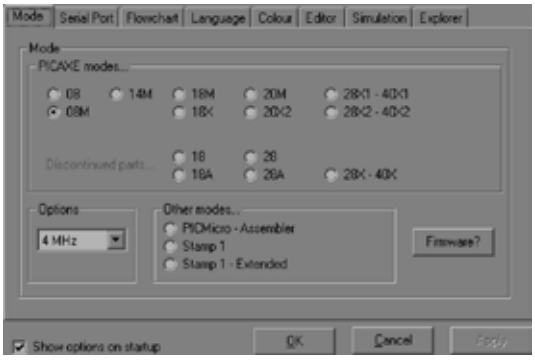

Figure 5-127. *This screenshot shows the options window of the PICAXE Program Editor, which you must use to select the type of chip that you intend to program (in our case, the 08M).*

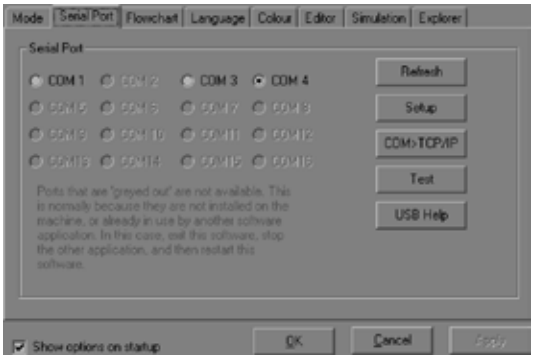

Figure 5-128. *Another screenshot of the options window shows the second essential choice that you must make: selection of the COM port that the installer chose on your computer.*

Are we having fun yet? Obviously not, but you're through with software hassles for the time being. The last step before you're ready to use the PICAXE is to mount it, and its socket, on your breadboard.

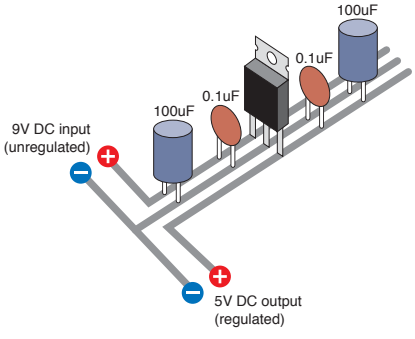

Figure 5-129. *PICAXE documentation specifies a 100 µF and 0.1 µF capacitor on the input side of a 5-volt regulator, and a similar pair of capacitors on its output side. On a breadboard, they can be arrayed like this.*

Setting up the hardware

The PICAXE 08M looks like a 555 timer. (Other chips in the PICAXE range have more pins and more features.) It requires a properly regulated 5 volts, just like the logic chips you dealt with previously. In fact, the PICAXE people are rather emphatic about protecting it from voltage spikes. They want you to use two capacitors (one 100 µF, one 0.1 µF) on either side of an LM7805 regulator. This seems like overkill, but the PICAXE is more inconvenient to replace than a 555 timer. You certainly can't run down to RadioShack to buy one. So let's do what the manufacturer says, just in case, and set up a breadboard as shown in Figures 5-129 and 5-130.

Now for the chip itself. Note that the pins for positive and negative power are *exactly opposite* to those for the 555 timer, so be careful!

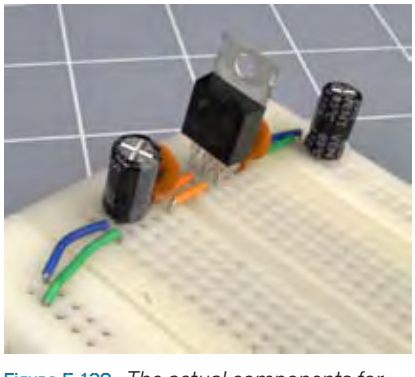

Figure 5-130. *The actual components for power regulation, applied to a breadboard, delivering 5 volts (positive and negative) down each side.*

Set up your breadboard following the schematic shown in Figure 5-131. Note that I am showing the stereo socket on its underside, because I think that's how you'll have to use it with the breadboard. If you try to stick its pins into the holes in the board, they will fit, but when you insert the plug into the socket, the thickness of the plug will tend to raise the socket up so that it loses contact. I really think the way to go is to solder wires to the pins on the socket and push the wires into the breadboard. See Figure 5-133.

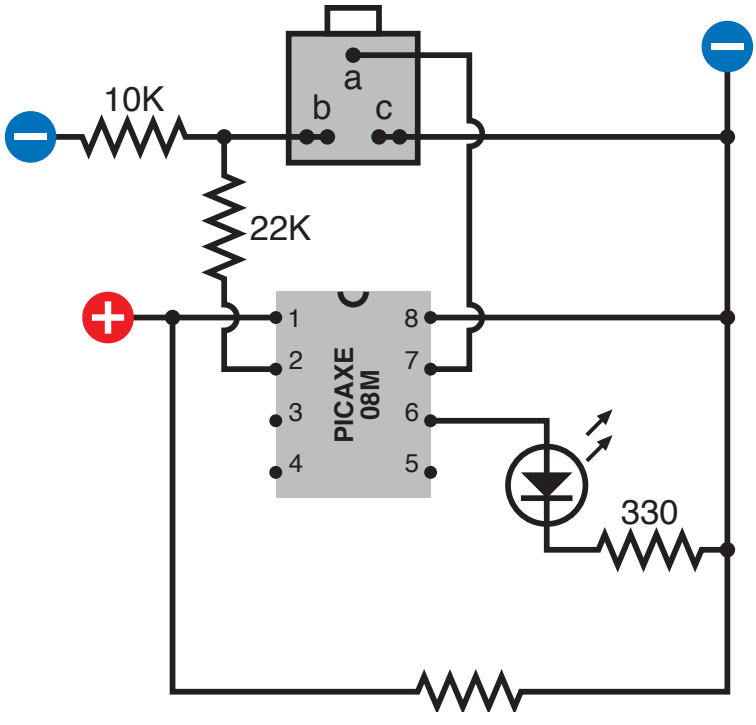

Figure 5-131. *The schematic of a test circuit for the PICAXE 08M shows the underside of the stereo socket, the essential 10K and 22K resistors on the input pin, and an LED to show an output from the chip.*

Be aware that the PICAXE manual shows things differently (although I have retained their labeling convention for the parts of the socket and the parts of the plug, identified as a, b, and c).

One little detail about the socket that is commonly supplied for use with the PICAXE: typically it has two *pairs* of contacts for the connections labeled b and c in the manual, and in my diagram. When you solder a connection, your solder joint should include *both* of the contacts in each pair, as shown in Figure 5-132.

Remember that the PICAXE must have 5 volts DC, and remember that your voltage regular will deliver this voltage reliably only if you give it extra voltage on its input side. If you provide it with 9 volts, that will provide a good amount of headroom.

The 22K and 10K resistors are essential for using the chip; see the following warning note for an explanation. My schematic also includes an LED and a 330Ω resistor, but they are needed only for the test that we'll be making momentarily.

Pin 2 Pull-Down

Always include the 22K resistor and the 10K resistor in the configuration shown in Figure 5-131. These resistors apply correct voltage to the serial connection, and when you're using the PICAXE on its own, they pull down the voltage on pin 2.

If pin 2 is left unconnected (floating), it may pick up random voltages, which the chip can misinterpret as a new program or other instructions, with unpredictable and undesirable results.

The 22K and 10K resistors should be regarded as permanent items accompanying your PICAXE regardless of whether you have it attached to your computer.

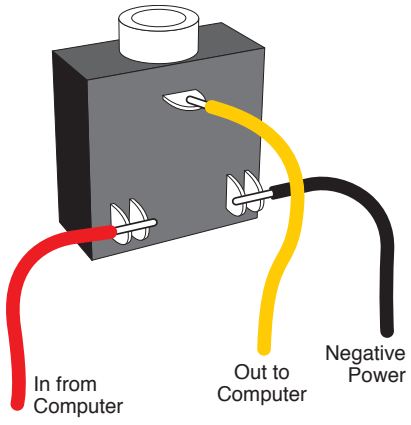

Figure 5-132. *Correct wiring of the socket is essential. When soldering wires to the lower terminals, make sure that you attach the wires to both of the terminals in each pair.*

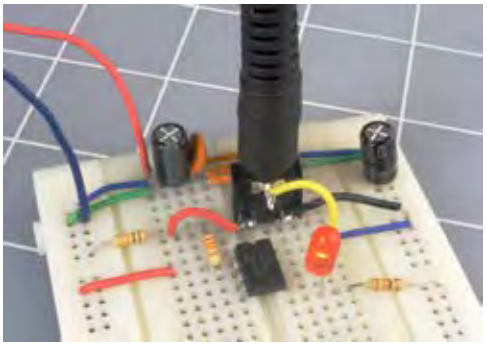

Figure 5-133. *The breadboard version of the test schematic, with the plug of the USB download cable inserted in the socket on the board. The PICAXE chip can now receive a downloaded program, and will immediately start to execute it.*

Verifying the Connection

Follow these steps carefully every time you want to program or reprogram your PICAXE chip:

1. Insert the USB plug of your PICAXE cable into the same USB port that you used before.
2. Start the Programming Editor (or AXEpad if you are using a Mac OS or Linux).
3. In the Programming Editor, select View→Options to verify that the editor is using the right COM port and is expecting the 08M PICAXE chip.
4. Plug the stereo plug on the free end of the USB cable into the stereo socket that is now wired into your breadboard. See Figures 5-133 and 5-134.
5. Check your wiring, and then connect your power supply to the breadboard.
6. Click the button labeled "program" in the Program Editor window to tell the software to look for the PICAXE.

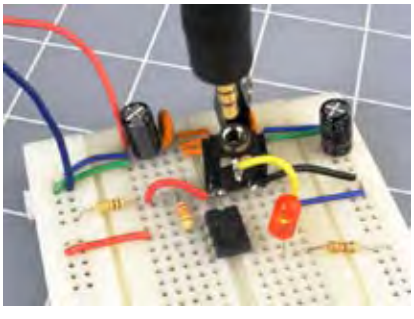

Figure 5-134. *After the program has been downloaded, the plug can be removed, and the program will continue to run, causing the LED to continue flashing.*

What If It Doesn't Work?

The first thing to do is pull out the plug of the USB cable from the PICAXE breadboard, leaving the other end of the cable attached to your computer. Set your multimeter to measure DC volts, and attach its probes to sections b and c of the plug. See Figure 5-135. Now click the "program" button again, and your meter should show 5 volts briefly coming out of your computer to the plug on the end of the cable.

If you detect the voltage, the software is installed and working properly. In that case, there's a problem on your breadboard, either in the chip or in the wiring around it.

If you cannot detect any voltage, the software probably wasn't installed properly, or is looking for the wrong serial port. Try uninstalling it and reinstalling it.

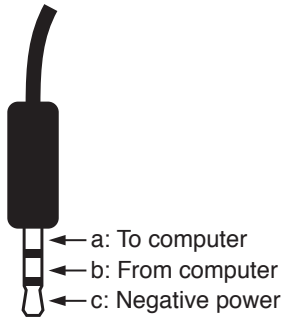

Figure 5-135. *The stereo plug on the end of the USB download cable can be used for fault tracing. A multimeter set to measure DC volts can be attached to sections b and c of the plug to establish whether the Programming Editor is sending data through the serial connection.*

Your First Program

Finally you're ready to create your first program. Type the following code into the Programming Editor window:

```
main:
    high 1
    pause 1000
    low 1
    pause 1000
    goto main
```

Be sure to include the colon after the word "main" on the first line. See Figure 5-136 for a screenshot. The indents are created by pressing the Tab key. Their only purpose is to make program listings more legible. The software ignores them.

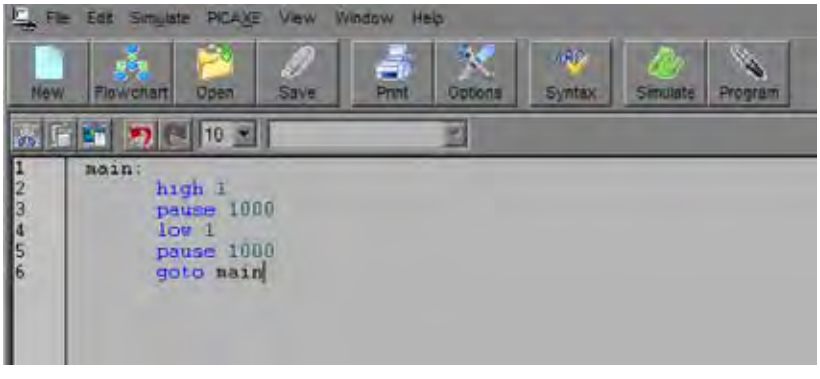

Figure 5-136. *This screenshot shows the first test program as it should be displayed by the Programming Editor (on a Windows computer).*

Click the Program button in the Programming Editor to download this program into the chip. As soon as the download is complete, the chip should start flashing the LED, lighting it for 1 second and then switching it off for 1 second. Figure 5-137 shows the steps that you should have followed to program the chip.

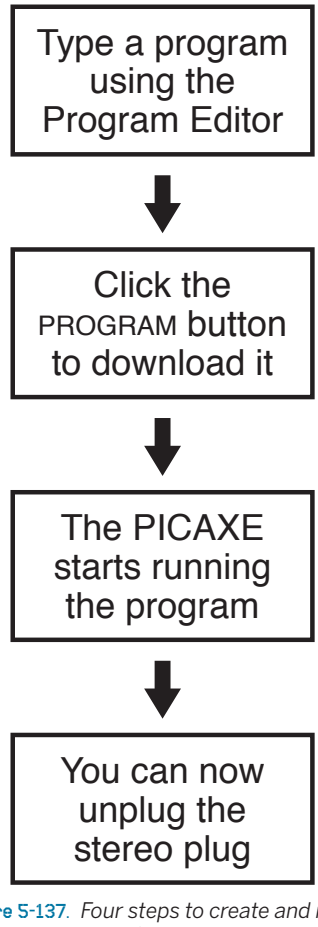

Figure 5-137. *Four steps to create and run a program on the PICAXE controller chip.*

Now for the interesting part: disconnect the USB cable from the breadboard. The chip should continue flashing.

Disconnect the power supply from the breadboard and wait a minute or two for the capacitors to lose their charge. Reconnect the power, and the chip will start flashing again.

The program that you downloaded to the chip will remain in the memory inside the chip and will begin running every time power is applied to the chip.

Decoding the Code

The program doesn't use the usual pin numbers on the chip. It uses what I will call "logic pin numbers." Figure 5-138 shows how they are numbered. Figure 5-139 shows their multiple functions. I have put Logic Pin 0 in parentheses because its main purpose is to send data to the computer through the USB cable. It can do double duty as a digital output, but you have to disconnect it from the USB cable first. It's easy to forget to do this. It's a hassle that I prefer to avoid.

Let's take a look at the little program that you typed in. The first line identifies a section of the program. This program only has one section, and we're calling it "main." Any word with a colon after it is the name of a section of a program:

```
main:
```

The second line tells the chip to send a high output from Logic Pin 1:

```
high 1
```

The third line of the program tells the chip to wait for 1,000 milliseconds. This of course is the same as one second:

```
pause 1000
```

The fourth line tells the chip to change Logic Pin 1 back to its low state:

```
low 1
```

The fifth line tells the chip to wait for another 1,000 milliseconds:

```
pause 1000
```

The last line tells the chip to go back to the beginning of the "main" section:

```
goto main
```

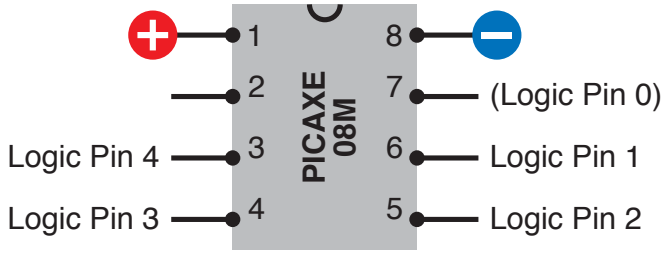

Figure 5-138. *The conventional pin numbers of the PICAXE chip are incompatible with the numbering system that is used in the PICAXE programming language. To minimize confusion, this guide refers to "Logic Pins" when using the numbering system that is required for programming the chip.*

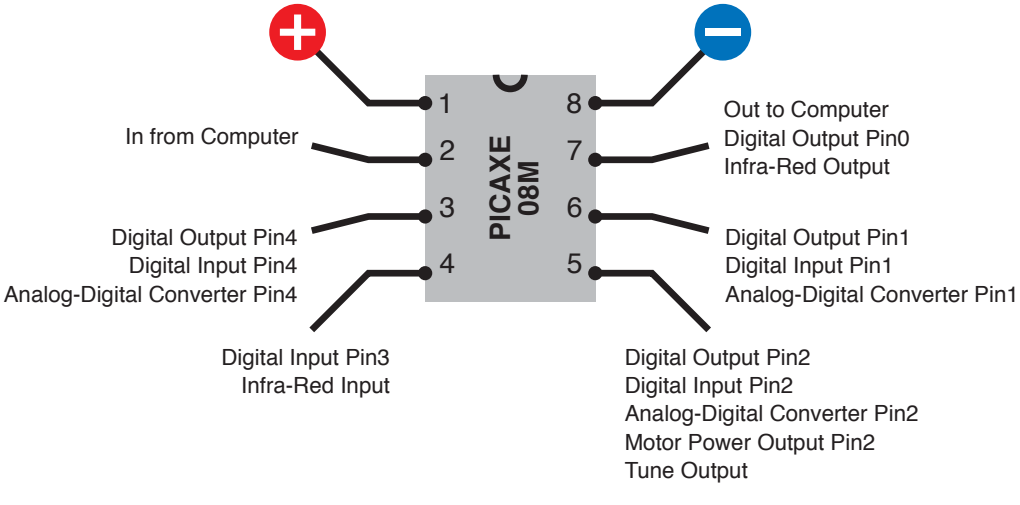

Figure 5-139. *Many of the pins on the PICAXE 08M have multiple functions, which can be selected by appropriate program instructions.*

Editing

What if you want to change the program? No problem! Use the Programming Editor to change one of the lines in the program. Substitute 100 instead of 1000 milliseconds, for instance. (The pause command can be followed by any number up to 65535.) In your program, don't use a thousands comma in any of the numbers that you specify.

Plug the USB cable into the breadboard again, hit the Program button on the screen, and the new version of the program will be automatically downloaded to the chip, overwriting the old version.

What if you want to save the program for future use? Just go to the File menu in the Programming Editor and save the program onto your computer's hard drive. Because the PICAXE uses a variant of the BASIC computer language, it adds a *.bas* filename extension.

Simulation

If you make a simple typing error, the Programming Editor will find it and stop you from downloading your program. It will leave you to figure out how to fix the line that contains the error.

Even if all the statements in your program are correctly typed, it's a good idea to run a simulation of what they'll do, before you download them. This is easily done: click the "simulate" button on the menu bar of the Programming Editor. A new window will open, displaying a diagrammatic view of the PICAXE chip and showing you the states of its pins. (Note that if you use very short pause commands, the simulation won't run fast enough to display the time accurately.) A simulation screenshot is shown in Figure 5-140.

The >> button at the bottom-right corner of the simulation window will open up a list of all the variables in your program. So far, it doesn't have any variables, but it soon will. All the zeros on the righthand side are binary numbers, which you can ignore for now.

You'll need to check the second part of the PICAXE documentation, which contains all the programming statements and their correct syntax. At the time of writing, this is stored at http://www.rev-ed.co.uk/docs/picaxe_manual2.pdf.

Figure 5-140. *This screenshot shows the simulation window that can be opened in the Program Editor to test program code before it is downloaded to the chip. The values of variables are shown in the section on the right. The pin states are shown on the left.*

Loops

Here's another thing I'd like you to try. Rewrite your program code as shown here and download it onto the PICAXE:

```
main:
    for b0 = 1 to 5
        high 1
        pause 200
        low 1
        pause 200
    next
    wait 2
    goto main
```

Note that `b0` is letter b followed by a zero, not letter b followed by letter O. The extra indents once again are added to make the listing easier to understand. The four lines beginning "high 1" and ending "pause 200" will be executed repeatedly. It's helpful to see them as a block.

Watch the light and see what happens. It should flash five times quickly, then wait for two seconds, and then repeat. You just added a *loop* to your program. You can use a loop if you want something to happen more than once.

Figure 5-141. *To understand how a program works, visualize a variable as being like a "memory box" with its name on the outside and a number stored on the inside.*

b0 is known as a *variable*. Think of it as being like a little "memory box" with its name, b0, on a label on the outside. Figure 5-141 illustrates this concept. This particular memory box can contain any number from 0 through 255. The loop begins by telling the computer to put number 1 in the box, then process the remaining statements, until the word "next" sends the processor back to the first line, at which point it adds 1 to the contents of b0. If the value of b0 is 5 or less, the loop repeats. If the value is 6, the loop has run five times, so it's over, and the PICAXE skips down to the "wait 2" statement after "next." See Figure 5-142 for an annotated version of the program listing.

"Wait" is a PICAXE command that is measured in whole seconds, so "wait 2" waits for 2 seconds. Then "goto main" begins the procedure all over again.

If your flashing-light demo worked out as planned, it's time to take the next step and make the chip do something more useful.

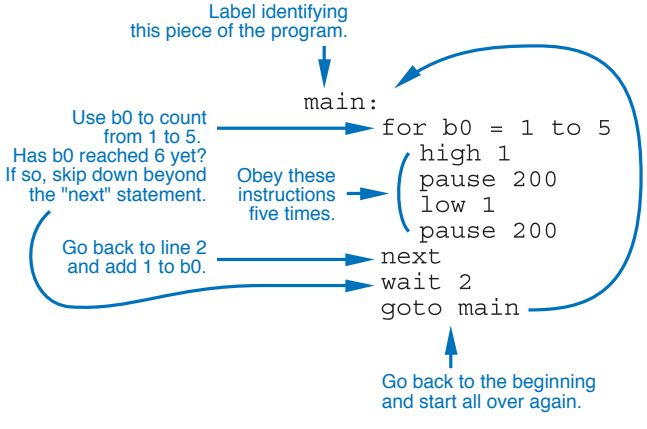

Figure 5-142. *The blue annotations explain what the program, on the right, is telling the PICAXE to do.*

FUNDAMENTALS

Basic PICAXE parameters

Here are some of the most useful parameters of the PICAXE:

- The PICAXE requires 5 volts DC, regulated.
- The inputs and outputs of the PICAXE are compatible with 5-volt logic chips. You can attach them directly.
- Each PICAXE pin can sink or source up to 20mA. The whole chip can deliver up to 90mA. This means that you can run LEDs directly from the pins, or a piezo noisemaker (which draws very little current), or a transistor.
- You can use a chip such as the ULN2001A Darlington array (mentioned in the previous experiment) to amplify the output from the PICAXE and drive something such as a relay or a motor.
- The chip executes each line of your program in about 0.1 milliseconds.
- The 08M chip has enough flash memory for about 80 lines of program code. Other PICAXE chips have more memory.
- The PICAXE provides 14 variables named b0 through b13. The "b" stands for "byte," as each variable occupies a single byte. Each can hold a value ranging from 0 through 255.
- No negative or fractional values are allowed in variables.
- You also have 7 double-byte variables, named w0 through w6. The "w" stands for "word." Each can hold a value ranging from 0 through 65535.
- The "b" variables share the same memory space as the "w" variables. Thus:
  - b0 and b1 use the same bytes as w0.
  - b2 and b3 use the same bytes as w1.
  - b3 and b4 use the same bytes as w2.
  - b5 and b6 use the same bytes as w3.
  - b7 and b8 use the same bytes as w4.
  - b9 and b10 use the same bytes as w5.
  - b11 and b12 use the same bytes as w6.
  - b13 and b14 use the same bytes as w7.

  Therefore, if you use w0 as a variable, do not use b0 or b1. If you use b6 as a variable, do not use w3, and so on.
- Variable values are stored in RAM, and disappear when the power is switched off.
- The program is stored in nonvolatile memory, and remains intact when the power is off.
- The manufacturer's specification claims that the nonvolatile memory is rewritable up to about 100,000 times.
- If you want to attach a switch or pushbutton to a pin and use it as an input, you should add a 10K pull-down resistor between the pin and the negative side of the power supply to hold the pin in a low state when the switch is open. Figure 5-143 shows how pull-down resistors should be used in conjunction with a SPST switch or a pushbutton.
- On the 08M chip, if you apply a varying resistance between Logic Pins 1, 2, or 4, and the negative side of the power supply, the chip can measure it and "decide" what to do. This is the "Analog-Digital Conversion" feature—which leads to our next experiment.

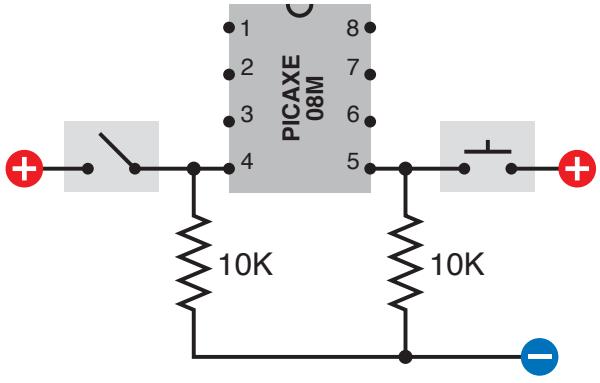

Figure 5-143. *The PICAXE can respond to the state of a switch or button attached to any of its input-capable pins. A 10K resistor must be used to pull down the state of the pin when the contact of the switch or button is open. Otherwise, you may get unpredictable results.*

Experiment 35: Checking the Real World

Often we want a microcontroller to measure something and respond in an appropriate way. For instance, it can measure a low temperature and sound an alarm, as I suggested in the example that I gave earlier.

The PICAXE has three analog-to-digital converters (ADCs) built in, accessible via logic pins 1, 2, and 4, as shown in Figure 5-139. The best way to use them is by applying a potential somewhere between 0 and 5 volts. In this experiment, I'll show you how to calibrate the response of the chip.

You will need:

- Trimmer potentiometer, 2K. Quantity: 1.
- PICAXE 08M chip and associated USB cable and socket. Quantity: 1 of each.

Procedure

Take the same trimmer potentiometer that you used in Experiment 32 and wire its center terminal to Logic Pin 2 of the PICAXE (which is hardware pin 5). The other two terminals of the 2K trimmer go to positive and to negative, respectively. So depending how you set the trimmer, the pin of the PICAXE is directly connected to positive (at one end of the scale), or directly connected to negative (at the other end of the scale), or somewhere in between. See Figure 5-144 for the revised schematic, and Figure 5-145 for a photograph of the breadboarded circuit.

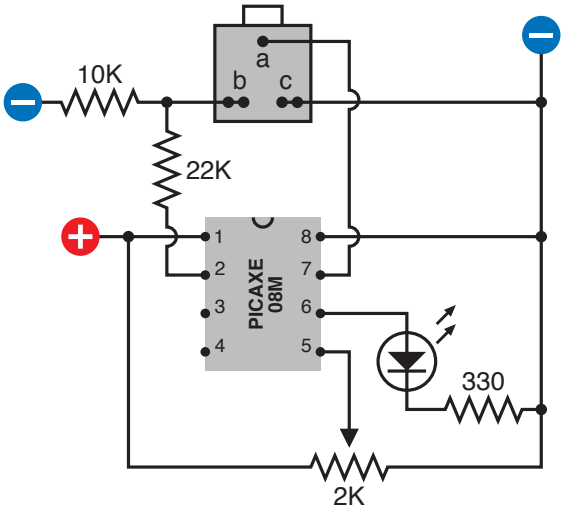

Figure 5-144. *This schematic, drawn in a layout suitable for breadboarding, shows how a 2K potentiometer can be used to apply a varying voltage to one of the pins of the PICAXE that is capable of converting an analog signal to a digital value.*

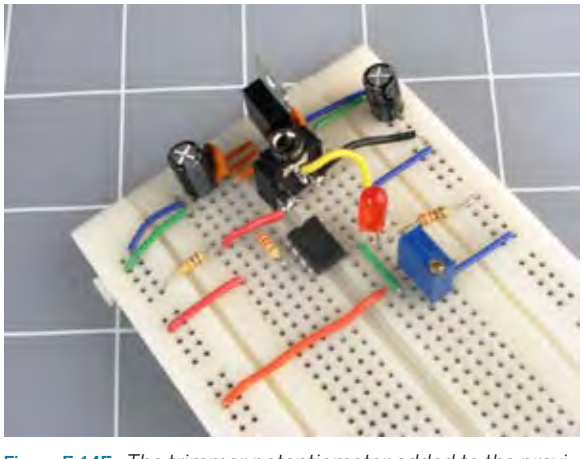

Figure 5-145. *The trimmer potentiometer added to the previously breadboarded circuit.*

Now we need a program to tell the chip what to do. Using the Programming Editor, start a new document. The code should look like this:

```
main:
    readadc 2,b0
    debug b0
    goto main
```

The command "readadc 2,b0" means "read the analog input on Logic Pin 2, convert from analog to digital, and store the result in b0."

The command "debug b0" tells the chip to go into program debugging mode, in which it uses its USB cable to tell the Programming Editor the values of all the variables while the program is running. The variables are displayed in a debugging window.

Download the program, and as the program starts to execute, the debugging window should open. Start adjusting the trimmer while looking at the value of b0, and you'll see b0 change its value.

You can make a table and draw a graph showing the relationship between the resistance between Logic Pin 2 and ground, and the value of b0. Just pull the trimmer off the breadboard, measure its resistance with a meter, then increase its resistance by, say, 200Ω, put it back into the breadboard, and look at the value of b0 again.

This is laborious, but calibrating equipment is always laborious—and in any case, I decided to do it for you. The graph is shown in Figure 5-146. You can also see the raw data numbers in the following table. I was pleased to find that the PICAXE gives a very precise, linear response to the input voltage. In other words, the graph is a straight line.

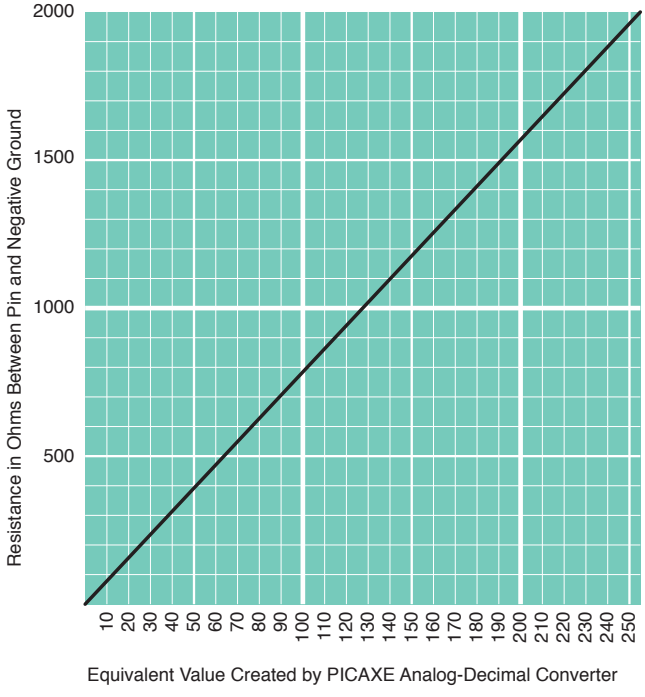

Figure 5-146. *When an ADC input pin is hooked up to a 2K potentiometer, which is connected across the same voltage that powers the chip, you should find that the resistance between the input pin and the negative side of the power supply generates the series of digital values shown on the graph. Note that the potentiometer must have a 2K value, and the power supply is assumed to be precisely 5 volts.*

This table shows measurements made with PICAXE 08M controller.

Resistance (in ohms) between the ADC pin and the negative supply	Equivalent digital value
2000	255
1900	243
1800	230
1700	218
1600	205
1500	192
1400	179
1300	166
1200	154
1100	141
1000	128
900	115
800	102
700	90
600	77
500	64
400	51
300	38
200	26
100	13
0	0

Now we can modify the program to make it do something with the information that it's taking in:

```
main:
    readadc 2,b0
    let w1 = 5 * b0
    high 1
    pause w1
    low 1
    pause w1
    goto main
```

Notice what's happening here. First we get a value in b0, and then on the next line, we do some arithmetic with it. The asterisk means "multiply." So the statement says, "Take whatever value is in b0, multiply by 5, and transfer it to another variable, w1." We have to use a w variable, because when we multiply the value of b0 by 5, we may get a number that is bigger than 255—too big to fit into a byte variable.

Finally, we take variable w1 and use it with a "pause" statement instead of a fixed number value. We're saying to the PICAXE, "pause for whatever number of microseconds you get by checking the value of w1."

So the software checks a variable resistance, turns it into a number, and applies that number to adjust the flashing speed of the LED.

Think back to the need of the cart powered by stepper motors. It was supposed to check two photoresistors, and adjust the speed of each motor accordingly. Well, this PICAXE program is a step in that direction. It can measure voltage on a pin and change the output frequency on another pin. If you had two PICAXE chips, you could wire each of them to a photoresistor and a motor. Then you could adjust the behavior of your cart by editing the second line in the program, where it converts the value of b0 to the value of w1 which will be used in the "pause" command to determine the number of pulses per second. Instead of multiplying by 5 you could multiply by 7 or whatever number gives you the result you need. This leads to an important conclusion: *a big advantage of a programmable chip is that you can make adjustments in software*.

Because the PICAXE 08M actually has more than one ADC input, and has three pins that can be used for output, you might wonder whether you could use just the one chip to control both motors in response to inputs from two sensors. The problem is that the three output pins on the 08M also function as the three ADC input pins. You'd do better to buy one of the more advanced PICAXE chips, such as the 18M, which has more pins to choose from. It uses the same basic set of programming instructions, and doesn't cost much more money.

Also, you should read the PICAXE documentation and look up the "pwmout" command, which is short for "pulse-width modulation output," but you can think of as meaning "power motor output." This is specifically intended to run stepper motors. It establishes an output frequency of pulses that will continue while the chip obeys other instructions in its program.

FUNDAMENTALS

Extra features

A complete guide to the 08M would fill a book of its own, and of course such books already exist (just search the books section of Amazon.com for keyword "picaxe"). But I'll finish my introduction to the controller by listing some of its extra capabilities, leaving you to look them up and explore them. Then I'm going to suggest one last experiment.

Interrupts

The PICAXE 08M allows you to set one "interrupt." This feature tells the chip to make a mental note that if a particular event occurs—such as a switch applying voltage to one pin—it should stop doing whatever else it was doing, and respond to the interruption.

Infrared

One pin on the PICAXE 08M can be used to receive infrared signals from a TV-style remote that you can buy from the same suppliers that sell the PICAXE itself. With an infrared sensor attached to the chip, you can issue commands remotely. If you want to build a remote-controlled robot, the chip is specifically designed with this in mind.

Servo motors

Every PICAXE chip has at least one pin that can send a stream of pulses to control a typical servo motor. On the 08M chip, it's Logic Pin 2. The width of each pulse tells the motor how far to rotate from its center position before stopping. A 555 timer can send this stream, but the PICAXE makes it easier. You can search online for more information about servo motors, which are especially useful for applications such as steering model vehicles, adjusting the flaps on model airplanes, and actuating robots.

Music

The PICAXE has an onboard tone generator that can be programmed with a "tune" command to play tunes that you write using a simple code.

Alphanumeric input/output

The "kbin" programming command is available in the PICAXE models 20X2, 28X1 and 28X2, and 40X1 and 40X2. You can plug a standard computer keyboard into the chip, and it will read the keypresses. You can also attach alphanumeric displays, but these procedures are nontrivial. For instance, when you're trying to figure out which key someone has pressed on a keyboard, your program has to contain a list of the special hexadecimal codes that the keyboard creates.

Pseudorandom number generation

All PICAXE models can generate pseudorandom numbers using a built-in algorithm. If you initialize the number generator by asking the user to press a button, and you measure the arbitrary time that this takes, you can seed the pseudorandom number generator with the result, and the pseudorandom number generator will have a less repeatable sequence.

Visit *http://www.rev-ed.co.uk/docs/picaxe_manual1.pdf* to learn more.

Experiment 36: The Lock, Revisited

The combination lock that I described in Experiment 20 is especially appropriate for a microcontroller, because it requires a series of operations that resemble a computer program. I'm going to show how this project can be redesigned using a PICAXE 08M, and then leave it to you to consider how some of the other projects in this book could be converted.

You will need:

- The same type of keypad and relay recommended in Experiment 20.
- A transistor or Darlington array to amplify the output from the PICAXE so that it can drive the relay.

Getting the User Input

Any of the input pins on the PICAXE can sense a switch closing. The trouble is that we only have three pins capable of doing this, and even the most advanced PICAXE chip has fewer than 10 such pins. So how can we attach a 10-key keypad to the 08M?

I have a suggestion: attach various resistors to the keypad, so that each key applies a different voltage to one of the ADC pins. Then use the ADC feature to convert the voltage to a number, and use a table of possible numbers to figure out which key is being pressed. This may not be the most elegant solution, but it works!

The keypad can be wired as shown in Figure 5-147. The asterisk key is still being used to supply power, as in the original experiment, while the pound key resets the relay at the end of your computing session, as before.

Current flows through a series of resistors, beginning with one that has a value of 500Ω. Because this is not a standard value, you will either have to make it by combining other resistors in series, or by presetting a trimmer potentiometer. After that, each button is separated from the next button by a 100Ω resistor. Finally, at the end of the chain, a 600Ω resistor separates the last button from the negative side of the power supply. Again, this is not a standard value, and you may have to use a trimmer.

Add up all the resistances and you have 2K, which is the range that the PICAXE wants us to use. When you press a button, you tap into the chain of resistances. Button 9 puts 600Ω between the PICAXE ADC pin and ground. Button 6 is 700Ω, button 3 is 800Ω, and so on. (You may prefer to lay out the buttons so that the resistance progresses in a more logical fashion. That's up to you. I chose to lay them out in the way that would be easiest to visualize on a keypad.)

Now look back at the ADC values that I supplied in the table on page 308. These are the values that you should get when you press various keypad buttons—but you cannot count on them being absolutely precise, because they may vary if your resistor values are not quite accurate, or if your power supply isn't exactly 5 volts. It's not safe to say, for example, that the PICAXE will deliver an ADC conversion value of precisely 77 when the resistance is 600Ω. It's safer to

say that the value will be between 71 and 83. If we specify a range as shown in the following table, we have a much better chance of interpreting each button correctly.

Button number		Range
9	600	71–83
6	700	84–96
3	800	97–108
0	900	109–121
8	1000	122–134
5	1100	135–147
2	1200	148–160
7	1300	161–172
4	1400	173–185
1	1500	191–198

Suppose you attach the common pin of your keypad to ADC Logic Pin 2 of the PICAXE. You can now use the Program Editor to write a program that looks like this:

```
getkey:
    readadc 2,b0
    let b1 = 9
    if b0 < 84 then finish
    let b1 = 6
    if b0 < 97 then finish
    let b1 = 3
    if b0 < 109 then finish
    let b1 = 0
    if b0 < 122 then finish
    let b1 = 8
    if b0 < 135 then finish
    let b1 = 5
    if b0 < 148 then finish
    let b1 = 2
    if b0 < 161 then finish
    let b1 = 7
    if b0 < 173 then finish
    let b1 = 4
    if b0 < 186 then finish
    let b1 = 2

finish:
    return
```

What does the word "return" mean at the end? I'll get to that in a second. I want to explain the rest of the routine first.

b0 receives the value supplied by the analog-digital converter when it looks at the keypad. After storing the number in b0, the routine has to figure out which keypad key it matches. The key identity (0 through 9) will be stored in another variable, b1.

The program starts by assigning value 9 to b1. Then it checks to see whether b0 < 84. This means "if b0 is less than 84." If it is, then the routine tells the PICAXE to "finish," which means "jump to the finish: label." But if b0 is *not* less than 84, by default the PICAXE continues on to the next line, which makes a second attempt at guessing which key has been pressed. It assigns number 6 to b1. Now there's another if-then test—and so on. This process of reassigning values to b1 stops only when it gets to the point where b0 is greater than a number in the table.

If you're familiar with other dialects of BASIC, this may seem a bit laborious to you. You may wonder why we can't use a statement such as this:

```
if b0 > 70 and b0 < 84 then b1 = 9
```

The answer is that PICAXE BASIC isn't sufficiently sophisticated to allow this. An if-then statement has to result in a jump to another section of the program. That's the only permitted outcome.

If you don't have any prior programming experience, the routine may still seem laborious to you, and perhaps a bit puzzling, too. This is understandable, because you're getting a crash course in software design without any formal preparation. Still, the PICAXE Programming Editor can be a big help, because it has its simulation feature. Before you can use this, though, you have to precede the routine that I just supplied with a control routine that you must type above it. The screenshot in Figure 5-148 shows you how it should look.

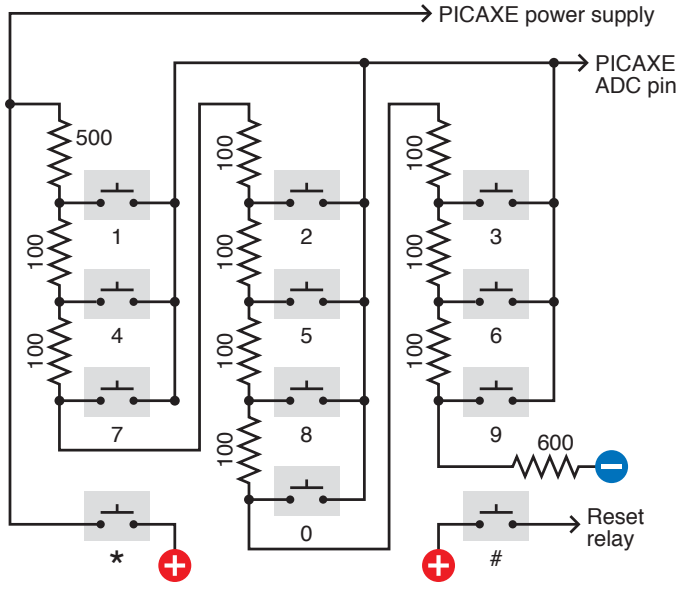

Figure 5-147. *A quick and simple way of attaching a keypad to provide numeric input to the PICAXE uses a chain of resistors totalling 2,000Ω. When a button is pressed, it connects the ADC input pin to a point in the chain. The resistance detected by the input pin can then be converted by the program in the chip to determine which key has been pressed.*

I have chosen an arbitrary combination of 7-4-1 for our combination lock. Using these numbers, the main section of the program looks like this:

```
main:
    low 1
    gosub getkey
    if b1<>7 then main
    gosub getkey
    if b1<>4 then main
    gosub getkey
    if b1<>1 then main
    high 1
    end
```

I should explain that the <> pair of symbols mean "is not equal to." So the fourth line of the program means, "if b1 is not equal to 7."

The value of b1 is supposed to be 7 if the user is putting in the correct combination. So if it's not 7, the user has entered the wrong value, and the if-then statement sends the PICAXE back to the beginning. In fact anytime the user inputs a number that is not in the correct 7-4-1 sequence, the program sends the PICAXE back to the beginning. This is the way the pure-hardware version of this experiment was set up.

But what is this word "gosub"? It means "go to a subroutine." A subroutine is any sequence of program statements that ends with the instruction to "return." So "gosub getkey" tells the PICAXE to mark its current place in the program while it skips to the `getkey:` section of code, which it obeys, until it finds the word "return," which returns it to the place from where it came.

The PICAXE continues in this fashion until it reaches the word "end." I had to insert the word "end" because otherwise the PICAXE will continue executing the program and will fall into the subroutine. "End" stops it from doing so. Figure 5-148 shows a screenshot of the complete listing.

So—is that all? Yes, that's it. If you enter the code into the Programming Editor exactly as I have supplied it, you should be able to run it in simulation mode, and in the simulation window, click the right-arrow beside Logical Pin A2 to increase its value in steps. Each time you pass one of the values in the `getkey:` subroutine, you should see the value for variable b1 change in the display.

This is really all you need to perform the functions of the combination lock. When the PICAXE runs this program, it waits for the correct combination. If it receives the combination, it sends the output from logical pin 1 high; otherwise, logical pin 1 stays low.

The only additional item you need is a transistor or CMOS gate between logical pin 1 and the relay that unlocks the computer, because the PICAXE cannot deliver enough current to operate the relay by itself.

Putting this procedure into a controller chip not only simplifies the circuit, but offers another advantage: you can change the combination simply by rewriting the program and downloading the new version into the chip.

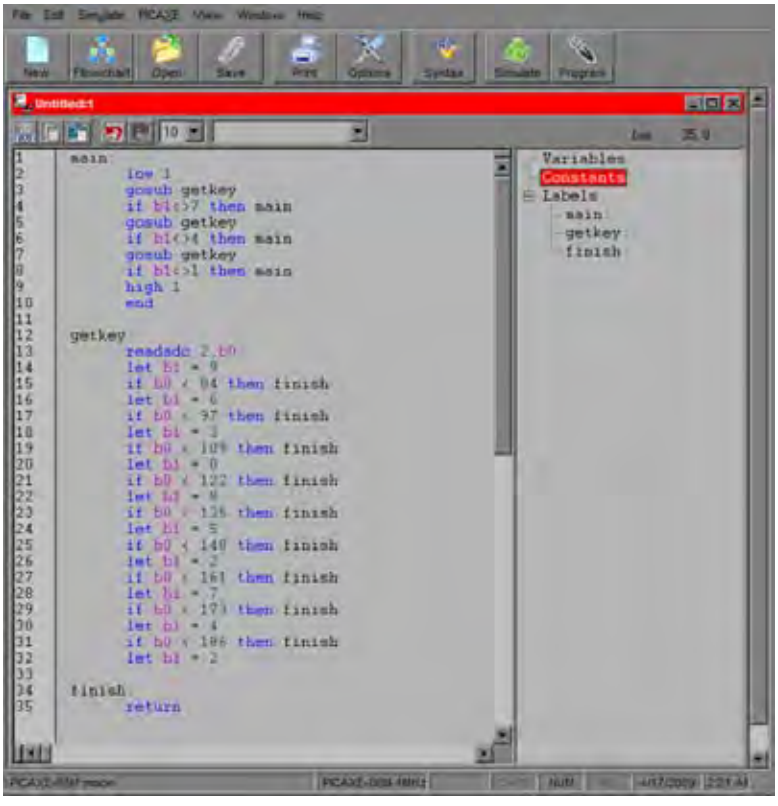

Figure 5-148. *This screenshot shows the complete listing of a program to read a sequence of three keypresses in conjunction with a combination lock. If the sequence is correct, the PICAXE sends a high output from one of its pins. If the sequence is incorrect, the program loops back to the beginning.*

FUNDAMENTALS

Limitations of MCUs

The PICAXE does have some disadvantages. Its voltage requirements alone restrict you from using it with the kind of freedom of a 555 timer.

Also, although I can get an instant result by plugging a 555 timer into a breadboard and adding a couple of resistors and a couple of capacitors, the PICAXE requires me to add a download socket, hook it up to my computer, write a program in the Programming Editor, and download the program.

Some people don't like writing software, or they have difficulty thinking in the relentlessly left-brain way that computer programming requires. They may prefer the hands-on process of assembling hardware.

Other people may have the opposite preference. This of course is a matter of taste, but one thing we know beyond all doubt is that computer programs often contain errors that may not reveal themselves until weeks or months later.

The PICAXE, for instance, doesn't protect you if a number is assigned to a variable that exceeds the limit for that type of variable. Suppose b1=200 and b2=60 and your program tells the PICAXE:

```
let b3 = b1 + b2
```

The result should be 260, but byte-size variables can only count up to 255. What happens? You will find that b3 acquires a value of 4, without any warning or explanation. This is known as an "overflow error," which can be very difficult to predict, because it happens at runtime, when external factors are in control. The code looks perfectly good; the Programming Editor doesn't find any syntax errors; the simulation behaves properly. But in the real world, days or even months later, an unexpected set of circumstances results in an input that causes the overflow, and because the code is residing inside the chip at this point, you may have a hard time figuring out what on earth went wrong.

Software has its problems. Hardware has its advantages.

FUNDAMENTALS

Unexplored territory

If you've taken the time to complete most of the projects in this book with your own hands, you have gained a very rapid introduction to the most fundamental areas of electronics.

What have you missed along the way? Here are some topics that remain wide open for you to explore. Naturally you should search online if they interest you.

The informal, learning-by-discovery approach that I have used in this book tends to be light on theory. I've avoided most of the math that you'd be expected to learn in a more rigorous course on the subject. If you have mathematical aptitude, you can use it to gain a much deeper insight into the way in which circuits work.

I didn't deal much with computer architecture, either. We didn't go very far into binary code, and you didn't build a half-adder, which is a great way to learn how computers function on the most fundamental level. Perhaps you should think about assembling one.

I avoided going deeply into the fascinating and mysterious properties of alternating current. Here again, some math is involved, but just the behavior of current at high frequencies is an interesting topic in itself.

For reasons already stated, I avoided surface-mount components—but you can still go into this area yourself for a relatively small investment, if you like the idea of creating fascinatingly tiny devices. This may be the future of hobby electronics, so if you stick with it, you'll probably end up in the world of surface-mount.

Vacuum tubes were not mentioned, because at this point, they are mainly of historical interest. But there's something very special and beautiful about tubes, especially if you can enclose them in fancy cabinetwork. In the hands of a skilled craftsperson, tube amplifiers and radios become art objects.

I didn't show you how to etch your own printed circuit boards. This is a task that appeals to only certain people, and the preparation for it requires you to make very neat drawings or use computer software for that purpose. If you happen to have those resources, you might want to do your own etching. It could be a first step toward mass-producing your own devices.

I didn't cover static electricity at all. High-voltage sparks don't have any practical applications, and they entail some safety issues—but they are stunningly impressive, and you can easily obtain the necessary information to build the equipment. Maybe you should try.

Other Controllers

If you want something more powerful, a BASIC Stamp is the logical next step after a PICAXE. the BASIC Stamp is so called because it originally looked like a postage stamp. The BASIC Stamp has a larger vocabulary of commands and a bigger range of add-on devices (including displays with graphical capability, and a little keyboard that is specifically designed for use with the controller). The BASIC Stamp is shown in Figure 5-149.

On the downside, you'll find that everything associated with the BASIC Stamp is a bit more expensive than in the PICAXE world, and the download procedure isn't quite as simple.

One of the more recent developments in the world of MCUs is the Arduino, which is both sophisticated and powerful. It does require programming in the C language. This language is a little more difficult to understand, and has only the vaguest similarity to the syntax that is used in the PICAXE and BASIC Stamp. On the other hand, because C dominates the larger world of computing, learning it might not be such a bad idea—and the Arduino offers some truly amazing capabilities. Because it is so popular, there are also many software tools, documentation, user forums, and many enthusatic hobbyists to help you. Two other Make: Books titles that I mentioned previously, *Getting Started with Arduino* and *Making Things Talk*, provide a great introduction.

Figure 5-149. *The BASIC Stamp controller consists of surface-mounted components on a platform that has pins spaced at 1/10-inch intervals, for insertion in a breadboard or perforated board. This component uses a version of BASIC that is similar to the programming language of the PICAXE, but has many more extensions. The BASIC Stamp is available for use with a wide range of peripheral devices, including many alphanumeric dot-matrix displays.*

In Closing

I believe that the purpose of an introductory book is to give you a taste of a wide range of possibilities, leaving you to decide for yourself what you want to explore next. Electronics is ideal for those of us who like to do things ourselves, because almost any application—from robotics, to radio-controlled aircraft, to telecommunications, to computing hardware—allows opportunities that we can explore at home, with limited resources.

As you delve deeper into the areas of electronics that interest you most, I trust you'll have a satisfying learning experience. But most of all, I hope you have lots of fun along the way.

Online Retail Sources and Manufacturers

This appendix contains URLs for companies mentioned as retail sources or manufacturers, along with the commonly used name of the source and the company name.

Colloquially used name	Actual corporate or company name	URL
3M	Minnesota Mining and Manufacturing Co.	*http://solutions.3m.com/en_US/*
Ace Hardware	Ace Hardware Corporation	*http://www.acehardware.com*
Advanced Micro Circuits	Advanced Micro Circuits Corp	*http://www.advancedmicrocircuits.com*
Akro-Mils	Myers Industries, Inc.	*http://www.akro-mils.com*
Alcoswitch	Division of Tyco Electronics Corporation	*http://www.tycoelectronics.com/catalog/menu/en/18025*
All Electronics	All Electronics Corporation	*http://www.allelectronics.com*
All Spectrum Electronics	All Spectrum Electronics	*http://www.allspectrum.com*
All-Battery.com	Tenergy Corporation	*http://www.all-battery.com*
Alpha potentiometers	Alpha Products Inc.	*http://www.alphapotentiometers.net*
ALPS pushbutton	ALPS Electric Co., Ltd.	*http://www.alps.com*
Amazon	Amazon.com, Inc.	*http://www.amazon.com*
Amprobe	Amprobe Test Tools	*http://www.amprobe.com*
Arduino	No corporate identity	*http://www.arduino.cc*
ArtCity	ArtCity	*http://www.artcity.com*
AutoZone	AutoZone, Inc.	*http://www.autozone.com*
Avago	Avago Technologies	*http://www.avagotech.com*
BASIC Stamp	Brand owned by Parallax, Inc.	*http://www.parallax.com*
BI Technologies	BI Technologies Corporation	*http://www.bitechnologies.com*
BK Precision	B&K Precision Corp.	*http://www.bkprecision.com*
Bussmann fuses	Cooper Bussman, Inc.	*http://www.cooperbussmann.com*
C&K switch	CoActive Technologies, Inc.	*http://www.ck-components.com*
Chicago lighting	CML Innovative Technologies	*http://www.cml-it.com*
CraftAmerica	Cardinal Enterprises	*http://www.craftamerica.com*
Darice	Darice Inc.	*http://www.darice.com*

Colloquially used name	Actual corporate or company name	URL
DeWalt	DeWalt Industrial Tool Company	*http://www.dewalt.com*
Digi-Key	Digi-Key Corporation	*http://www.digikey.com*
Directed switches	Directed Electronics Inc.	*http://www.directed.com*
Doctronics	Doctronics Educational Publishing	*http://www.doctronics.co.uk*
eBay	eBay Inc.	*http://www.ebay.com*
Elenco	Elenco Electronics Inc.	*http://www.elenco.com*
Everlight	Everlight Electronic Co. Ltd.	*http://www.everlight.com*
Extech	Extech Instruments Corporation	*http://www.extech.com*
Fairchild	Fairchild Semiconductor Incorporated	*http://www.fairchildsemi.com*
FTM	FTM Incorporated	*http://thefabricatorssource.com*
Fujitsu	Fujitsu America, Inc.	*http://www.fujitsu.com/us/*
GB wire strippers	Gardner Bender Inc.	*http://www.gardnerbender.com*
Hobbylinc	Hobbylinc Hobbies	*http://www.hobbylinc.com*
Home Depot	Homer TLC, Inc.	*http://www.homedepot.com*
Ideal wire strippers	Ideal Industries Inc.	*http://www.idealindustries.com*
Jameco	Jameco Electronics	*http://www.jameco.com*
K&J Magnetics	K&J Magnetics Inc.	*http://www.kjmagnetics.com*
Kingbright	Kingbright Corporation	*http://www.kingbrightusa.com*
Kobiconn	No web page found; use mouser.com	
KVM Tools	KVM Tools Inc.	*http://www.kvmtools.com*
Lowe's hardware	LF, LLC	*http://www.lowes.com*
Lumex	Lumex Inc.	*http://www.lumex.com*
McMaster-Carr	McMaster-Carr Supply Company	*http://www.mcmaster.com*
Megahobby	Megahobby.com	*http://www.megahobby.com*
Meter Superstore	Division of SRS Market Solutions Inc.	*http://www.metersuperstore.com*
Michaels craft stores	Michaels Stores, Inc.	*http://www.michaelscrafts.com*
Mill-Max	Mill-Max Manufacturing Corp.	*http://www.mill-max.com*
Mitutoyo	Mitutoyo America Corporation	*http://www.mitutoyo.com*
Motorola	Motorola, Inc.	*http://www.motorola.com/us*
Mouser electronics	Mouser Electronics, Inc.	*http://www.mouser.com*
Mueller alligator clip	Mueller Electric Company	*http://www.muellerelectric.com*
Newark	Subsidiary of Premier Farnell plc	*http://www.newark.com*
NKK switches	Nihon Kaiheiki Industry Co. Ltd.	*http://www.nkkswitches.com*
NXP semiconductors	NXP Semiconductors	*http://www.nxp.com*
Omron	Omron Corporation	*http://www.omron.com*
On Semiconductor	Semiconductor Components Industries, LLC	*http://www.onsemi.com*
Optek	Subsidiary of TT Electronics plc	*http://www.optekinc.com*
Panasonic	Panasonic Electric Works Corporation	*http://pewa.panasonic.com*

Colloquially used name	Actual corporate or company name	URL
PanaVise	Panavise Products, Inc.	*http://www.panavise.com*
Parallax	Parallax, Inc.	*http://www.parallax.com*
Pep Boys	Pep Boys-Manny, Moe and Jack	*http://www.pepboys.com*
Philips	Koninklijke Philips Electronics N.V.	*http://www.usa.philips.com*
PICAXE	Revolution Education Ltd.	*http://www.rev-ed.co.uk*
Piedmont Plastics	Piedmont Plastics, Inc.	*http://www.piedmontplastics.com*
Plano storages boxes	Plano Molding Company	*http://www.planomolding.com*
Pomona test equipment	Pomona Electronics Inc.	*http://www.pomonaelectronics.com*
RadioShack	RadioShack Corporation	*http://www.radioshack.com*
Sears	Sears Brands, LLC	*http://www.sears.com*
SparkFun Electronics	Sparkfun Electronics	*http://www.sparkfun.com*
Stanley tools	The Stanley Works	*http://www.stanleytools.com*
STMicroelectronics	STMicroelectronics Group	*http://www.st.com*
Texas Instruments	Texas Instruments Incorporated	*http://www.ti.com*
Tower Hobbies	Tower Hobbies	*http://www.towerhobbies.com*
Twin Industries	Twin Industries	*http://www.twinind.com*
Tyco	Tyco Electronics Corporation	*http://www.tycoelectronics.com*
Vaughan	Vaughan & Bushnell Mfg.	*http://hammernet.com/vaughan/*
Velleman keyboards	Velleman nv	*http://www.velleman.eu*
Vishay	Vishay Intertechnology Inc.	*http://www.vishay.com*
Wal-Mart	Wal-Mart Stores, Inc.	*http://www.walmart.com*
Weller	Division of Cooper Industries, LLC	*http://www.cooperhandtools.com/brands/weller/*
X-Acto	Division of Elmer's Products, Inc.	*http://www.xacto.com*
Xcelite	Division of Cooper Industries, LLC	*http://www.cooperhandtools.com/brands/xcelite/*
Xytronic	Xytronic Industries Ltd.	*http://www.xytronic-usa.com*

Secrets of Building Electrostatic

LIGHTNING BOLT GENERATORS

including high voltage test equipment, experiments, motors and more!

by Walt Noon

Lindsay Publications Inc

Secrets of Building
Electrostatic

LIGHTNING BOLT GENERATORS

including
high voltage test equipment,
experiments, motors and more!

by Walt Noon

Lindsay Publications Inc

Copyright ©1992 by Lindsay Publications Inc

All rights reserved.

Lindsay Publications Inc
PO Box 12
Bradley IL 60915-0012

ISBN 1-55918-090-0

2 3 4 5 6 7 8 9 0

To my Mom and Dad who
always took the time to answer
my questions

Original CAD drawings
and photographs by
Matthew J. Roddy

Cartoon drawings by
Mike Noon

Special thanks to
Kevin E. Curtin
Matthew J. Roddy
Mike Noon

WARNING

The author of this book is not a professional engineer nor has he had formal training in the design or operation of high voltage devices. The author is an amateur but has been successful in building and operating the devices discussed herein.

The methods that he used and describes are presented merely as guidelines for other amateurs in developing similar devices. These devices can be dangerous, possibly even lethal, and dangers have been pointed out wherever possible. Since the author is not a professional in this field, there may well be other dangers involved in the building and operation of the devices described.

The author hereby disclaims any liability for injury to persons or property that may result while using this project book, and the author does not intend by this publication to explain all dangers known or unknown that may exist in the building and operation of this project.

Lindsay Publications Inc has not built this project nor does it endorse the methods described. Lindsay Publications Inc assumes no liability for injury to person or property that may result form used of this information.

Contents

Electrophorus 4
Rotostatic Generator 9
"Cat-O-Static" Generator 17
Motor Control 18
External Van de Graaff Generator 23
Classic Van de Graaff Generator 31
Extremely High Power Van de Graaff Generator 39
Inductive Electrostatic Generator 42
High Voltage Measurements 46
FET Electroscope 47
Mechanical Electroscope 50
Neon Lamp Blank 51
Spark Gap 53
Leyden Jar 58
Water Capacitor 61
Plate Capacitor 62
Experiments 67
Ion Blower 76
Franklin Motor 78
Corona Motor 80
Atmospheric Electricity 81
Bibliography 86
Electroplating Terminals 87

Every text I've seen on the subject of electrostatics seems to begin with a history of the subject. A. D. Moore, one writer whose works I particularly enjoy, said that if cavemen had cats that rubbed up against them then they must certainly have been aware of the presence of static electricity. There are theories now going around the scientific community that claim lightning triggered the formation of the first chains of DNA. I'll take that one step further and guess that lightning began the evolutionary process that created our species.

Static electricity is one of the most fascinating and possibly most overlooked fields of modern electronics. We all take static for granted. Before I began experimenting with static electricity it would have been very difficult to convince me that it was easy to get 3500 volts from an old plastic bottle or 10,000 volts and more from a rubber band! Even now as I watch one of these tiny generators in action it is difficult to imagine that it is producing these voltages.

As you learn about electrostatics you will find many strange and wonderful experiments to perform. For example, it is possible to mysteriously levitate objects, blow a candle flame to one side with an invisible wind, and to light neon bulbs without wires.

There are motors that can be built to run on static electricity! Well-made electrostatic motors are so sensitive that they have been powered by the earth's natural electrical charge alone! Connect your motor to an antenna, and off it goes!

In addition to the many curiosities static electricity makes possible, there is also the potential for serious research with many astounding possibilities.

Consider the work of Professor John G. Trump, formerly of the Massachusetts Institute of Technology. Professor Trump points out that electrostatic forces are the most powerful forces known in nature – stronger by far than gravity or magnetism. Professor Trump demonstrates the practical application of electrostatic generators with the following illustration:

Consider two conductive plates, 100 square inches in area, facing each other and separated by an insulator. If the plates are each charged oppositely to 300 volts per centimeter the force of attraction between them will be one 2,000th of a pound. Increase this charge to 30,000 volts per centimeter and the attraction escalates to half a pound. Now increase this voltage to the order of three million volts per centimeter and the force of attraction jumps to 5,700 pounds! As Trump has said "Force of this order has more than a passing interest for power engineers." Trump and his colleagues had been pursuing the creation of electrostatic generators they hoped would one day rival modern electromagnetic generators.

Just how much electrostatic energy is theoretically possible? Consider an aluminum cube only one centimeter square. Imagine that all the electrons in that cube were removed and kept one meter away. The cube has only positive charges, and the electrons one meter away only negative charges. Since positive and negative charges attract, what would be the force of attraction generated between them? The answer turns out to be an astounding thirty-two million million million pounds! Professor A.D. Moore, an expert in electrostatics, points out that this force would be equal to the weight of a steel cube 76 miles high!

Of course, as much fun and as inspiring as it is to ponder the theoretical world of electrostatics, back in the real world we find that electrons don't leave home so easily. The most useful electrostatic inventions to date make use of the 'little' forces of electrostatics. But keep that cube in mind and let everyone wonder why you have that curious smirk on your face whenever you run your generator.

What voltages are possible for the experimenter? The four easily assembled generators shown in the following text will give you an idea. Each one intentionally operates on a slightly different principal of gathering an electrostatic charge. If you build them, or just simply become familiar with them, you will develop a understanding of the most popular ways of generating static electricity.

I am confident that if you become acquainted with these machines you will have no difficulty at all in constructing many others of your own design. The reason that I am so confident is that I designed and constructed all of these machines to teach myself about electrostatics! Each machine represents the best of my thoughts at the time I con-

structed it.

You will soon find that it is easily possible to construct a static generator capable of producing 50 to 100 thousand volts! If you are a craftsman, 200 thousand volts and more can be obtained by optimizing the designs of the higher power generators such as the Van De Graaff shown later in the text.

Electrostatic generators are also remarkably inexpensive. With a little foraging through the surplus bins, no generator in this text cost me more than $30 to build! I know of no other way to approach these voltages for such a low cost.

A Little History of the First Practical Generators

The first electrostatic generators produced their voltage with friction. Towards the end of the 17th century Otto von Guericke, an amateur physicist from Magdeburg, developed the first practical electrical machine – an electrostatic generator. What follows are his own instructions for building one:

"Secure one of the glass globes which are called phials, about the size of a youngster's head; fill it with sulfur, ground in a mortar and melted by the application of flame. After it freezes, break the phial, take out the sulfur globe and keep it in a dry place, not a moist one. Perforate it with a hole so that it can spin upon an iron axle. Thus the globe is prepared.

"To demonstrate the power developed by this globe, place it with its axis on two supports in the machine – a hand's breadth above the baseboard – and spread under it various sorts of fragments such as bits of leaves, gold dust, silver filings, snips of paper, hairs, shavings, etc. Apply a dry hand to the globe so that it is stroked or grazed two or three times or more. Now it attracts the fragments and, as it turns on its axis, carries them around with it.

"When a feather is in contact with the globe, and afterwards in the air, it puffs itself out and displays a sort of vivacity ... and if someone places a lighted candle on the table and brings the feather to within a hand's breadth of the flame, the feather regularly darts back suddenly to the globe and, as it were, seeks sanctuary there."

Otto Von Guericke goes on to describe experiments by which he produced both light and sound from his amazing globe!

The instructions for von Guericke's globe are simple enough for any experimenter today to follow. The only note that I would add is

that in casting my own globe I found that large quantities of sulfur would become much smaller pools when melted, and that if the globe were not filled on the first pouring it would not appear nearly as attractive when finished. So, remember to begin with a large amount of sulfur.

THE ELECTROPHORUS

Many generations passed and many ingenious machines were developed without great change using materials and processes similar to von Guericke's globe. The most important historically was Alessandro Volta's *electro perpetuo* known now as the electrophorus. With it we can dramatically demonstrate that electrostatic charges are much like magnetic forces in that like charges repel one another while opposite charges attract.

An electrophorus is very easily assembled. It consists simply of a rectangular block of insulating material such Lucite or, better yet, polyethylene and a metal disk which is attached to an insulating handle (Figure 1).

When the Lucite is rubbed with a woolen cloth, electrons are removed from the cloth and held on the Lucite. This happens because the cloth will hold its electrons less tightly than the Lucite. An insulating material, in this case Lucite, by its nature, will not allow the electrons to move around freely. The charges are therefore 'static' or held in place by the insulating material. The Lucite will now have a negative charge, and the wool will pick up a positive charge, respectively.

Next, the metal disk with the handle is set on top of the Lucite. The negative charges on the Lucite are attracted to positive charges on the metal disk, so, the positive charges in the metal disk move to the side of the metal plate facing the Lucite. The negative charges are similarly repelled to the back of the metal disk. Now, your hand or, better yet, a ground wire are touched briefly to the top (handle side) of the metal disk and then removed. In this way the negative charge is transferred to your hand (or ground) leaving only a positive charge. The metal plate will now have a positive charge, and the plastic negative.

If you have achieved a large enough charge, the Lucite can be picked up by the metal disk!

1 The Lucite block is rubbed with a piece of wool.

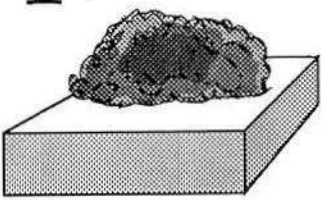

The plate and handle assembly is placed on the the Lucite.

2

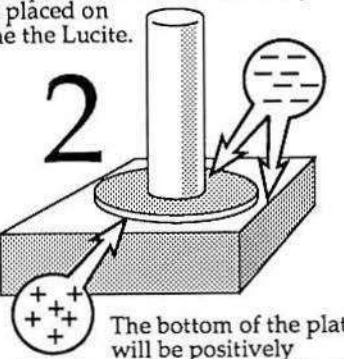

The bottom of the plate will be positively charged. The top of the plate and Lucite block will acquire a negative charge.

The top of the plate is grounded to remove the negative charge.

3

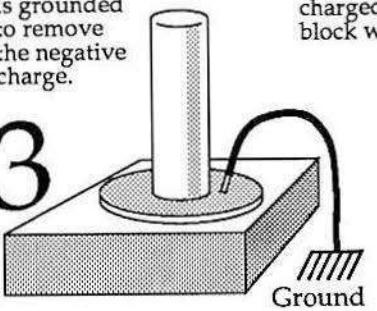

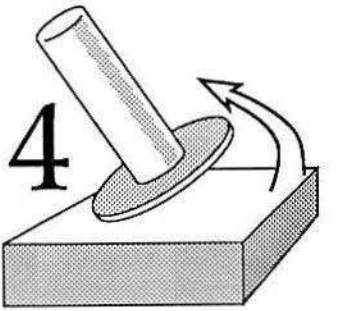

4

The plate and handle assembly is removed at an angle by lifting one side of the plate away from the block without breaking contact on the other side.

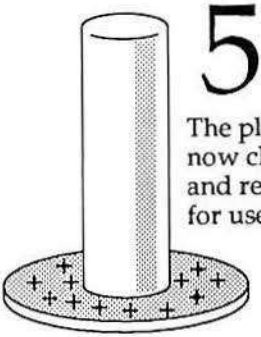

5

The plate is now charged and ready for use.

The Electrophorus

Figure 1

Slowly remove the metal plate by the handle, drawing it away from the Lucite at an angle. The metal plate now holds the charge you seek. Having charged your electrophorus, you can perform the experiments with Von Guericke's globe mentioned above including attracting hair, styrofoam and other small objects.

Because the charged surface of the electrophorus is flat, a startling demonstration can be performed wherein the electrophorus disk is actually floated above the Lucite by electrostatic forces. Performing this trick takes some practice. Make a second metal plate and handle. Remember that if the plate is to float above the other it must be very light weight. (Figure 2)

Now, we have the challenge of charging both the disk and the Lucite with a like charge so that they will repel each other. Charge your first disk with a positive charge as described above, and then bring it close to, but not touching, the second disk. This will charge the second disk by attracting a negative charge to the front of the disk. Next, ground the handle side of the second disk to bleed off the positive charge. The second disk is now negatively charged. The Lucite is also negatively charged, so, provided everything has been accomplished and the weight is not too great, the second disk will now float above the Lucite block!

Electrophoruses act a great deal like capacitors discussed later on and can be used for many surprising experiments including charging a Leyden jar and flickering a neon bulb in a darkened room!

Special Notes on Friction Generators

Before we move on to the more powerful friction generators, there are a number of things you should be aware of that will help you in both troubleshooting and designing generators.

My first bit of advice is to avoid humidity. It makes air more conductive. Moisture in the air can have a devastating effect on the charges stored by electrostatic devices.

I was given a first rate example of this shortly after building my first two generators. Both machines, only days old in their construction, were whirling away in my shop. I was doing "careful scientific study" – in other words, I was zapping everything in sight to see what would happen. Suddenly, and most mysteriously, both generators

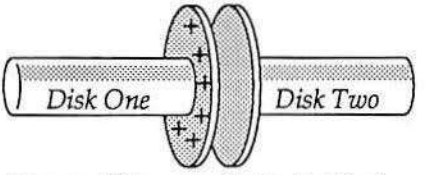

Charge disk one on the Lucite block.
Then bring it close to a second disk.

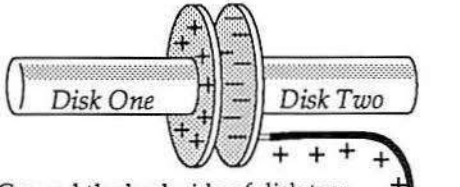

Ground the back side of disk two to neutralize its positive charge. The front side of disk two remains negatively charge.

Ground

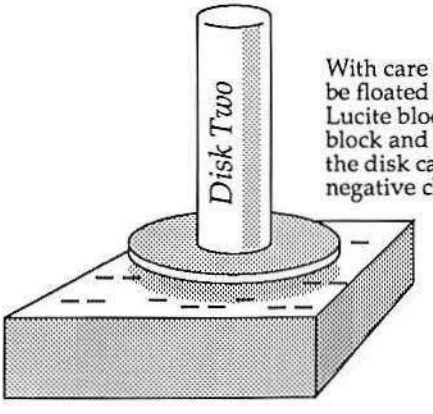

With care disk two can be floated above the Lucite block. Both the block and bottom of the disk carry repelling negative charges.

Floating the Electrophorus

Figure 2

stopped producing a charge. I couldn't imagine why both, each being very different in construction, might fail at exactly the same time. Then the culprit made itself known! Just outside the door the automatic lawn sprinklers had come on and extremely humid air was coming through my door!

Another good example of this problem is demonstrated by walking across a padded carpet. When the relative humidity is 20% or less, charges of up to 35,000 volts can be obtained by shuffling one's feet along the carpet. However, raise the humidity to 60% or more, and the maximum charge will plummet to a mere 1,500 volts! If you live in a humid region, you may not be able to get the same performance from a generator that someone living in the desert might. Hopefully, humidity will only be a seasonal problem for you. Dry winter days are best.

There are fascinating static generators which are more or less immune to humidity. These rely on generating a charge by induction rather than by friction. These machines will also be discussed in detail later on.

Be careful in selecting paint for your generator. I have found that many spray paints contain ingredients that will conduct static electricity. For the most part I have had few problems with this, although in a darkened room I have seen the telltale blue corona glow of escaping electrons coming from painted plastic surfaces on a generator. To correct the problem I simply coated the nearby metal surfaces that were losing their charges to the paint with high resistance "corona dope" sold in T.V. and better electronic stores.

Avoid using wood to build generators. Although we think of wood as an insulator, in reality it becomes an excellent conductor of very high voltages. In the machines that follow, you'll see polyvinyl chloride (pvc) pipe used extensively. If you can get acrylic or phenolic tubing, use it. It offers much better dielectric strength.

Dust can bleed away a charge. Dust on a high potential terminal can reduce your generator's efficiency by a whopping 40%. Because your high potential terminal carries a charge, dust will be attracted to it in much the same way that dust accumulates on the front of a T.V. screen. I have actually seen a tiny particle of dust prevent an eighth inch spark from arcing. Keeping your terminal clean is important.

On the other hand, the attraction of dust to your generator can be

quite entertaining. One way that I enjoy cleaning my generator is to ground myself and then pass my hand over the high potential terminal. The dust which has been sitting there has acquired a high voltage charge and jumps to your hand which it sees as ground. The effectiveness of this method for really getting your generator clean is doubtful since after a few seconds the dust in your hand looses its charge and heads back for the generator, but it's lots of fun.

Once during a rare Southern California thunderstorm I observed a particularly confused particle of dust. Apparently the storm had charged the air, and my generator had charged a large particle of fluff. The fluff couldn't decide where it wanted to be and would repeatedly fly around my bench only to return to the generator and then again off into the air. It was an astounding sight.

SUPER FRICTION GENERATOR – ROTOSTATIC

Now that you understand the basics of how a charge is picked up by friction, doesn't it seem that it would be possible to design a mechanical means to make and store a charge automatically and continuously? One solution to the problem is what I call a "rotostatic" generator, so named for an old magazine article that called a similar device a "rotostat." I said earlier that it was possible to get 3500 volts from an old plastic bottle, and I wasn't kidding. All you have to do is build the "rotostat".

These generators are extremely simple to build and may be hand cranked or operated by a small electric motor. They consist simply of a plastic drum – an old plastic jar works great – and a rubbing block – wool, nylon, asbestos, leather. When the bottle is rotated against the rubbing block a charge is developed on the plastic and on the block.

We need to attach some metallic brushes to the side of the plastic drum opposite the block to pick up the charges as they are generated. The brushes are attached to a metal sphere where the charges can be stored. A complete schematic of a rotostatic generator is shown in figure 3.

There is an infinite variety of possible configurations for such a generator, but keep in mind in designing yours that for static voltages even wood is a good conductor. It is most important to remember to keep your high potential components well insulated from ground.

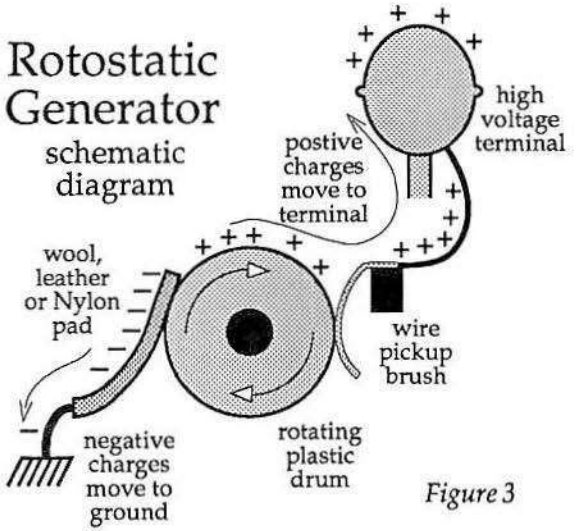

Figure 3

If your generator is well made it will generate enough power to light a neon bulb (Ne2 type), levitate styrofoam, and arc a spark perhaps as long as 1/16 to 1/8 inch – all of this while still being perfectly safe to touch. When touched, your generator will give your finger only a very light "pop" much like a very small static discharge from a doorknob. As an interesting side note, if you can feel a static charge at all, it will be at least 3,500 volts!

Though static machines deliver these high voltages, their rapid, low current discharges make them unusually safe. Even generators producing 100,000 volts or more rarely present a danger, though I for one would not intentionally take a shock from one. A later chapter on capacitors (energy storage devices) will give you an equation for finding out when a charge has become dangerous.

Building a Film Case Rotostatic Generator

In my rotostatic generator design I have attempted to maximize the output and storage capacity of this type of machine. I am sure that there are still many improvements that can be made. This device works extremely well, is reliable, and very easy to construct. A schematic and a photograph are shown in figure 4.

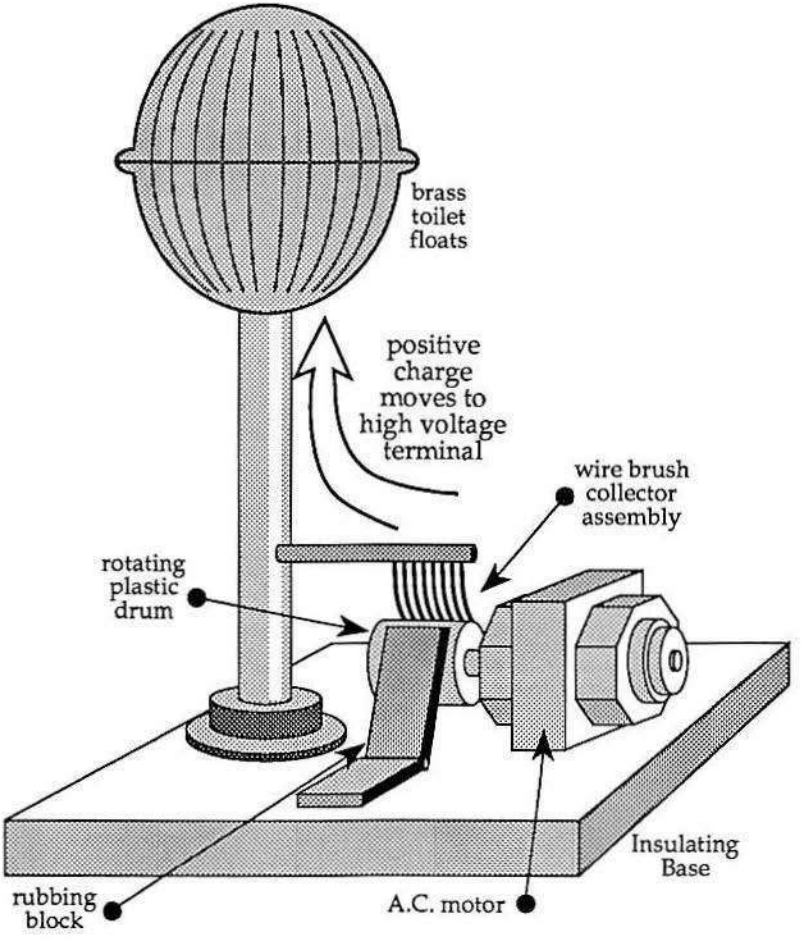

Rotostatic Generator

Figure 4

I used a surplus AC tape recorder motor to drive the unit. I like to use tape recorder motors in many projects because they are quiet and often have threaded axles that are very easy to mount components onto. In this case, I wanted to be able to switch plastic drums easily so I could experiment with a wide variety of materials. If you are unable to find such a motor, something similar can be used. A breakdown of

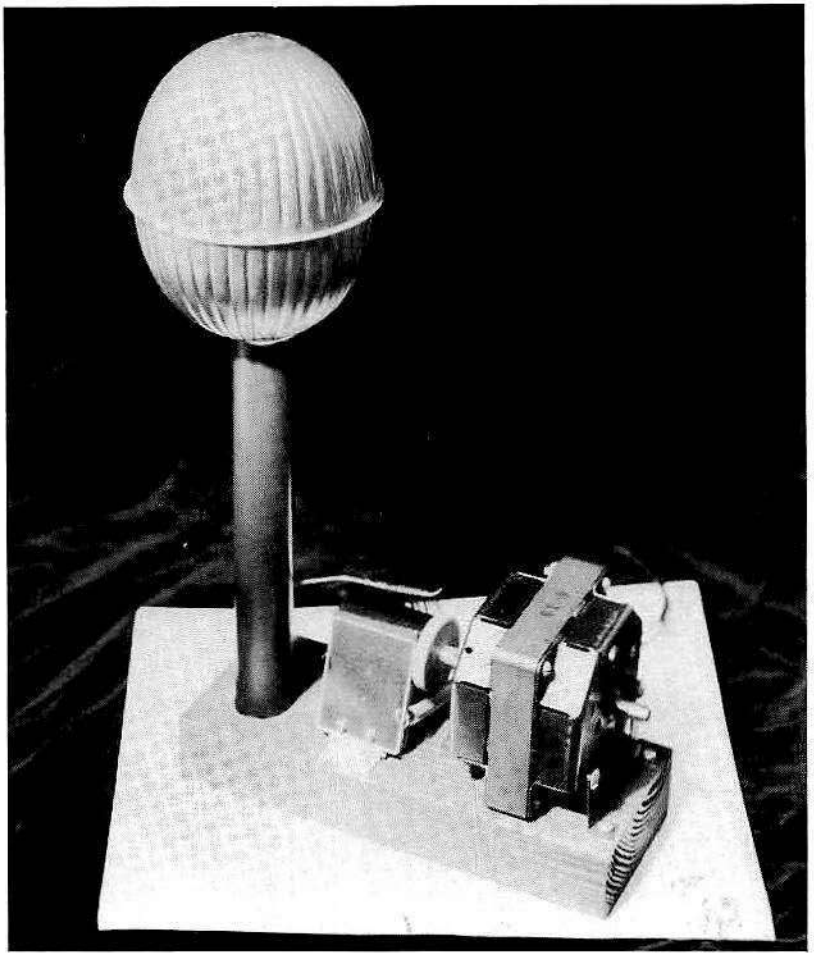

Fig. 5 – The complete Rotostatic Generator uses only a small plastic drum and a few common parts, and yet will light a hand-held 90 volt neon lamp!

AC and DC motors and their suggested hookups are shown in detail in the next chapter.

Assembly is straightforward and simple. The motor is mounted securely with wood screws to the base – in this case a section of 2x4. Make sure this connection is secure since in experimenting with different drums you will undoubtedly have some which will wobble due to imbalances in the drum or in the mounting. Also, remember to

select a motor with plenty of power. Tiny D.C. toy motors can work, but they have little torque and can stall, and that can be frustrating.

The drum can be mounted to the motor in a variety of ways. If the motor axle is hollow as the tape recorder axles are, you can simply use a screw to secure the bottle cap directly to the motor axle. If the axle is solid, you will probably want to extend the axle all the way through the drum.

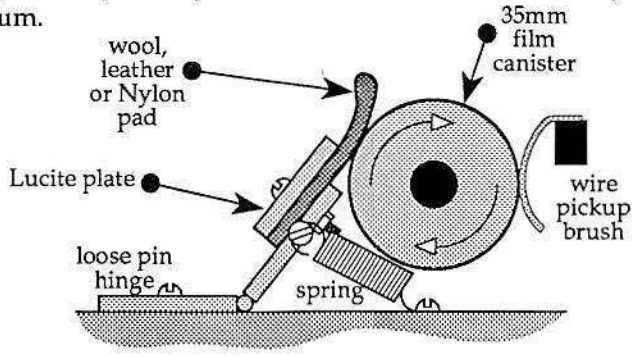

Wiper Assembly
for Roto Static Generator

Figure 6

To mate the motor axle to the axle running through your drum, glue progressively larger pieces of plastic tubing to the smaller axle until the tubing size matches that of the larger axle, then slip the tubing over both axles. Tubing used as fuel line on model airplanes, aquarium tubing, compressor hose, and the insulation stripped from wire can be used to make excellent adapters. Heat shrink tubing can also be used, however, after it has been shrunk it tends to become somewhat brittle.

As long as the pieces of tubing fit tightly over one another, any glue can be used to hold them together. I like cyanoacrylate (Super Glue) because it seems to hold rubber tubing nearly as well as it does skin. If you have used "Super Glue" for any length of time will know what I mean by this.

This method of connecting a motor to an axle also has the beneficial effect of acting as a "universal" joint. That is, your motor can actually power your axle from a variety of angles since the tubing will flex without difficulty. This is useful when using a variety of motors

to drive a variety of unusual drums.

The drum must be very well centered on the motor axle, but fortunately, this is surprisingly easy to do. Most plastic pill bottles, film cases etc. already have a little nub right on the center of the lid. I assume this is some natural artifact of the process by which they are formed. Just hunt around a bit and use a bottle with this built-in center mark, and you'll have no difficulty here.

Personally, I like to mount the lid from the bottle to the axle so that the bottle can be easily removed and replaced.

The rubbing block shown in figure 6 turned out to be a very handy design. By looping a piece of wool against the Lucite as shown, the block makes excellent contact with the drum. A variety of rubbing materials can be tried by simply slipping them in between the block and the drum. I think that leather or nylon probably provided the best results when used with the film case. To make these experiments easier, use "loose pin" hinges for mounting the rubbing block.

Rather than use steel brushes to collect the charge from the drum, I came up with what I call "riders." These are formed by wrapping a short length of wire around the copper wire conductor coming from the globe. These wires should be loose enough to dangle down onto the drum and "ride" along its surface. Riders have many advantages. They are very tolerant of wobble in the drum. You may be able to change drum types and sizes without adjusting them in any way. You can improve the efficiency of "riders" by coating unusued surfaces with corona dope.

The PVC tube and collecting ball are easily mounted by drilling a tight hole in the 2x4 to accommodate the PVC tubing, by applying a little Silicone glue to the base, and by tapping it into place with a hammer. A large copper wire is run through the tubing as shown and is connected to the collecting ball with a brass screw. The ball, itself, is then mounted with a bead of Silicone glue.

Testing and Operation

Turn on the static generator's motor and allow it to run for 20 to 30 seconds. It takes some time to build up a charge. Next, hold one lead of a Ne2 neon bulb, available at electronics stores for about 49 cents, and bring the other lead near the brass bulb. When the free lead is

nearly touching the bulb, the lamp should flicker or flash. Though the shock from this tiny generator can barely be felt, keep in mind that it takes nearly 90 volts to light the bulb!

Next spread some small, dry, pieces of styrofoam on the top of the ball. By bringing your hand close to the styrofoam you can actually cause them to move mysteriously toward your hands.

Touching this generator is perfectly safe. Under good conditions you should feel and hear a light static "pop" when you touch the fully charged top terminal. If you have trouble feeling the "pop" with your fingers try using your nose. I don't know why, but bringing your nose near the ball brings on a very subtle and strange electric sensation.

With this generator you can do many of the experiments mentioned later including charging up capacitors and energizing spark gaps. So experiment and enjoy.

REMEMBER!

If you are using yourself as ground, as described in the above experiments, you might find that generator performance seems to decrease after several experiments have been performed. What has actually happened is that by repeatedly touching the ball, you have charged yourself up to the same degree of charge as that of the ball, giving the electricity no desire to jump to you! This is simply remedied. Just touch a cold water pipe or other ground from time to time while you experiment.

One minor problem that can pop up is motor speed. Your motor may run too fast. We'll discuss a motor speed control a little later on. Don't worry if the riders hop around a bit. This is usually OK and won't cause problems.

Although a plastic film canister appears in the photos, jars with semi-transparent finishes perform. PVC might also make an exellent drum. Experiment!

A Useful List of Materials for Friction Generators

What follows is a useful list of materials that have a predisposition for taking on a negative or positive charge. By choosing materials that are far apart on this list you can increase the efficiency of a generator.

This list is excerpted from *Nature's Electricity* TAB books No. 2769 and is called "The TriboElectric Series."

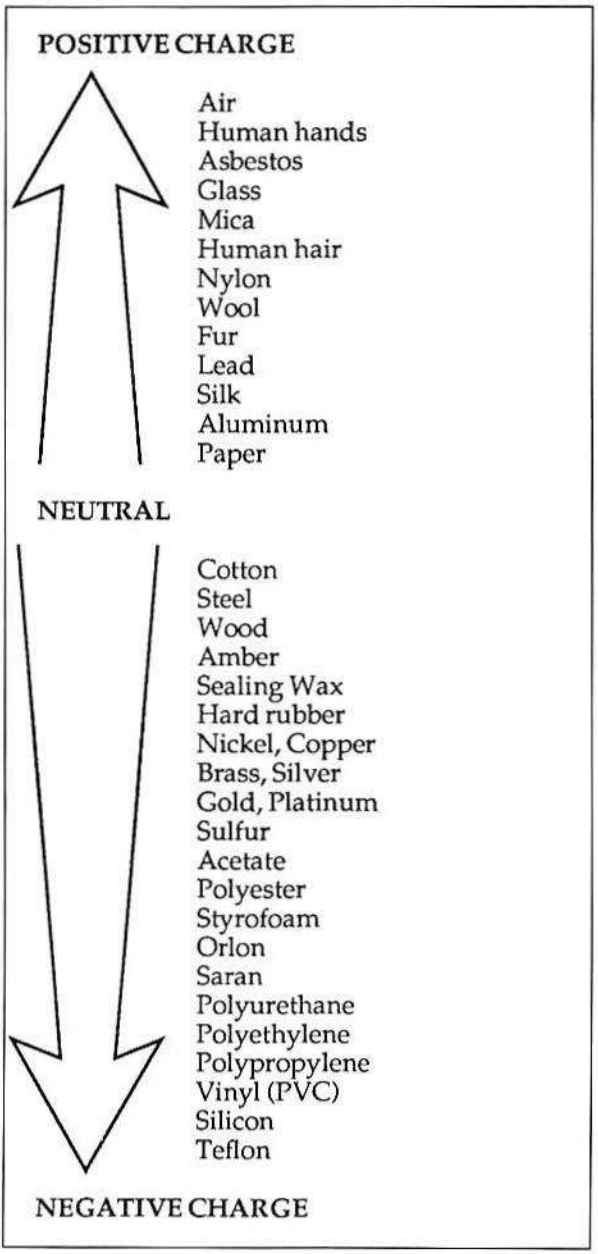

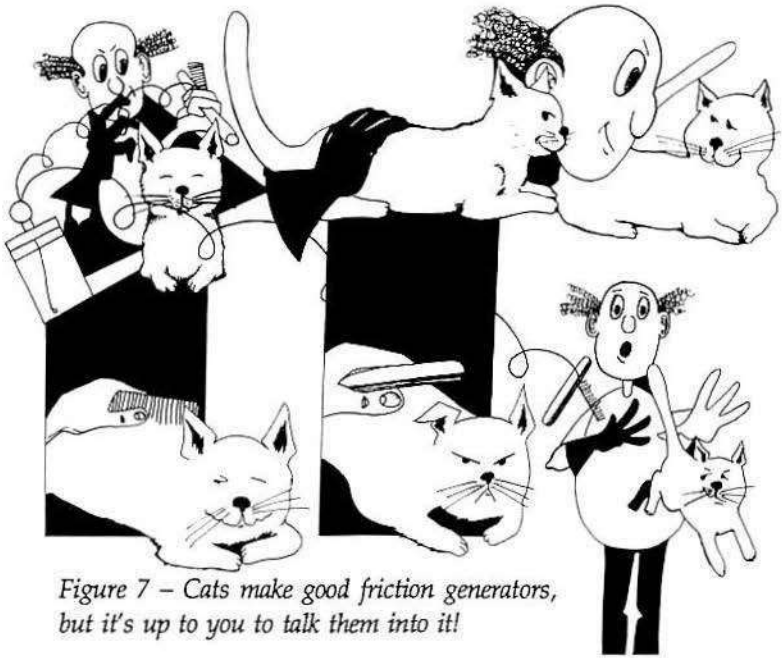

Figure 7 – Cats make good friction generators, but it's up to you to talk them into it!

THE "CAT-O-STATIC" GENERATOR

The last friction generator that I want to mention is what I call my Cat-O-Static generator. From the name you can probably already guess that the key component to this generator is your cat. I really would not mention this as a generator if it didn't work so remarkably well!

For the most part cats enjoy being electrostatic generators, the trick is to make them think they are being petted, and not used as a science experiment. (The cat commandments state somewhere: "Thou shalt allow thyself to be petted only when it suits your purposes and not those of another.")

First, you will need a rubbing material. The very best material I found for this purpose was the artificial leather used in cheap motorcycle gloves. It's actually a type of vinyl. You can secure a pair of these gloves for 5 or 10 dollars at any motorcycle shop. Some are called "man-made leather."

The next thing you will need is a metal flea comb and a length of PVC tubing. You will also need a Leyden jar to store the charge built up by your Cat-o-stat. Leyden jar construction is described in detail later on. The metal flea comb is held at the end of the PVC tubing by a slit cut in the tubing and some glue. A wire is attached from the flea comb to the top of the Leyden jar.

Put a glove on one hand and hold the PVC tubing with the other. Coax you cat into your lap, and tell him wonderful things about himself. This never fails to distract them. Pet him with the glove, and follow the glove with the metal comb to pick up the charge.

With my cat's fur and my particular gloves I am able to build up a charge so large that it will penetrate my vinyl gloves with a strong prickling! However, keep in mind that this type of generator will usually run off and hide before a large Leyden jar can be fully charged. Of course, if you have several cats, use them all to the charge the jar!

AC vs DC Motors and Controls

As we move on to the higher power generators, a little discussion is in order with regards to AC (alternating current) and DC (direct current) motors, and some good ways to control them.

In the generators I've built and discuss here, I have used both AC and DC motors. AC motors have advantages in that usually no external transformers or circuitry are required. They develop plenty of torque – so much so in fact, that you rarely have to worry about stalling the motor. Most AC motors have no brushes or other components to short or wear. They will generally run for years and years, often until the bearings themselves wear out! In general, I prefer using AC motors over DC motors whenever possible.

The major shortcoming of an AC motor is low rpm. The high performance Van-De-Graaff-type generators describe below work best at around 5,000 rpm. If the motor runs faster than this, electrons can literally be "blown" off of the carrying belt, and performance suffers. At lower rpm, leakage can impede the build up of high voltage. Since AC motors do not usually develop high rpm, DC motors should be considered for these high performance generators.

Unlike AC motors, DC motors are portable when battery powered and achieve high rpm easily. Keep in mind that a DC motor rated at

6500 rpm may not achieve that speed when driving your device. The rpm rating is usually the maximum no load speed of the motor.

Although not always necessary, you will probably find that you will want a motor with speed control as part of your DC static generator design. A number of dependable methods are shown in figures 8 through 12.

Figure 8 shows a piece of high resistance wire soldered or tied

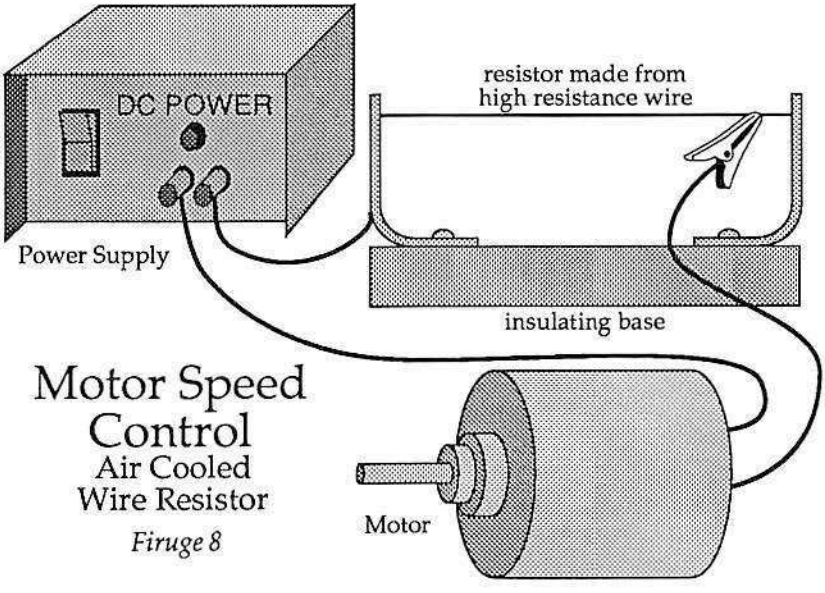

Motor Speed Control
Air Cooled
Wire Resistor
Firuge 8

between two copper posts. One side of the wire is tied to a 12v (or similar) power supply. A wire coming from your motor is attached to an alligator clip which can be moved along the wire to increase or decrease the motor speed. This method works extremely well. However, be aware that the wire can become red hot when supplying current to the motor! Make sure to house it safely.

High resistance wire is easily obtained from a variety of sources. You can use the NiChrome wire that comprises the heating coils in an old toaster, hair dryer, or similar heating device. You can also purchase NiChrome wire from any well-stocked hardware store. Keep in mind that a fairly long piece may be required. Another variation that can be tried is to use a high wattage rheostat, or even the speed control

handle from a "slot car" set.

Figure 9 shows the use of power resistors to slow a DC motor.

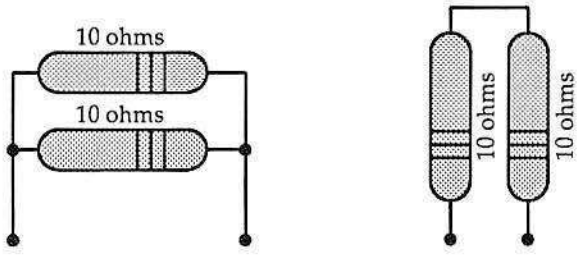

Parallel Connection
Total Resistance is 5 ohms

Series Connection
Total Resistance is 20 ohms

Figure 9

Power resistors are inexpensive, and if you buy a handful of different values you can connect them in parallel or series to get a wide variety of different values. Keep in mind that resistors have two ratings, the power handling capacity measured in Watts, and the resistance measured in Ohms.

An Ohm is a measure of the opposition to current flow. A resistor of 10 Ohms will oppose current flowing through it twice as much as a resistor of five Ohms.

Wattage is simply the amount of power your resistor can handle without being destroyed by overheating. In general, I'd say the higher the wattage rating the better. The Winter's Ring generator shown next required a 25 watt, 10 Ohm resistor, but had to be water cooled to increase its power handling capacity above the 25 watt air cooled rating.

Resistors oppose current flow and in doing so, convert electrical energy into heat. It's normal for them to become very warm. If your resistor gets too hot, its resistance can increase well above its stated value. A change in resistance can cause your motor to run at uneven speeds. You will either need to buy a resistor of a larger wattage, or use some means to cool it such as water (shown and discussed later). As a rule-of-thumb, don't use a resistor of less than 10 watts unless you have a very small or efficient motor.

Figure 10

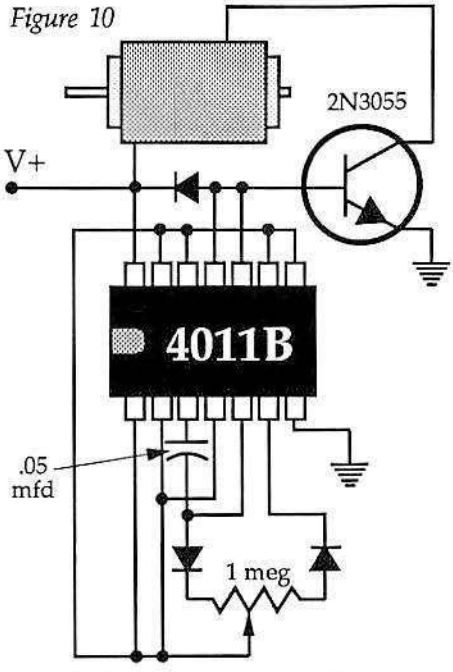

Motor Speed Control
Solid State

Figure 10 shows a very accurate and stable means of controlling a DC motor. An integrated circuit and power transistor are used to send a stream of pulses to the motor. As the pulse rate increases, the motor speed also increases. By simply turning the potentiometer, you can adjust motor speed at any time. For mid-sized DC motors a very large heat sink or water cooling is required for the transistor.

I have found that DC motors operating at high speeds can behave strangely. Slight variances in the motor's speed can set up an oscillation within the belt being driven. Because one side of the belt is being "pulled" and the other

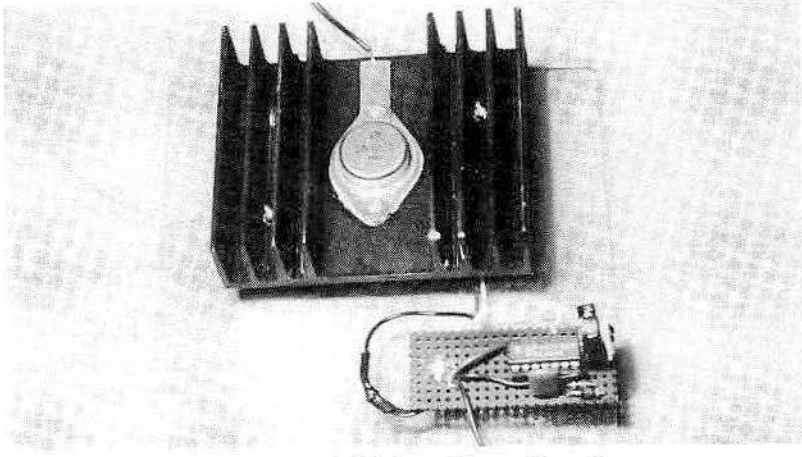

Figure 11 – Solid State Motor Control

is being "pushed", uneven tensions react with the belt's flexibility to produce a "flying" belt that makes only intermittent contact with the rollers or pulleys. This can cause a belt to fly off, bend brushes, or just make a lot of noise. Also, if ball bearings are not used in the rollers, an oscillation can occur among the bushings of the upper roller, the axle, and the belt. All of these problems can be easily solved by using a versatile speed control.

Component Cooling

You may to have to improvise methods of keeping electrical components cool. If you are using a fairly large, high RPM, DC motor which will need sizeable amounts of electrical power, components in the speed control are going to get hot. It may seem a little unorthodox, but water makes a fantastic heat sink for electrical components! Power resistors and even power transistors can be run well beyond ordinary

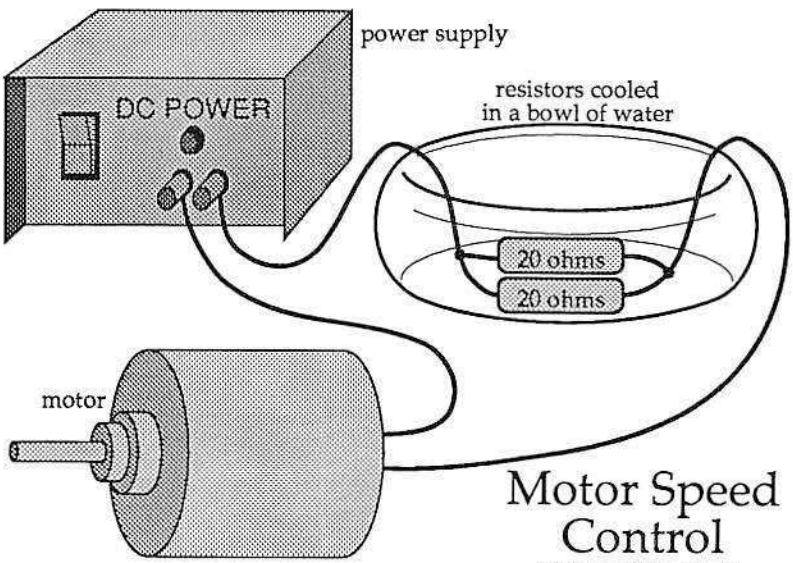

Figure 12

heat sink tolerances when submerged in water. (Figure 12)

Distilled water is a very poor conductor of electricity and will not

short out most components. Tap water is usually OK for resistors, but minerals and other gunk will cloud the water after a short time.

As long as the circuit is submerged in water, you know that the temperature of the water must be below 212 degrees Fahrenheit (100 Celsius) at normal atmospheric pressures. Above this temperature the water will boil away. Many electronic components work quite well up to 212 degrees. Just remember to add a little water now and then to compensate for evaporation.

AN EXTERNAL VAN DE GRAAFF USING "WINTER'S RING"

If you built the last generator described, you know that I wasn't exaggerating when I said you could get 3500 volts (or more) from an old film canister. Although interesting, this simple rotostatic generator won't keep you satisfied for long. There are higher voltages to conquer! So let's move on to the next type of generator and try for 10,000 volts (and possibly several times that amount) from a rubber band.

I call the following generator an "external" generator because all of the components of the generator have been mounted externally in such a way as to make construction and experimental modifications fast and easy. Since all of the workings are exposed, this generator is great for the experimenter who wants to quickly try different materials and configurations in developing his own generator design, or for someone who wants to whip together a simple generator to demonstrate.

The high voltage terminal of this generator consists of a metal ring, or toroid, of exceptional efficiency. I call it a "Winter's Ring" although such rings have been traditionally made of wood. They're rarely used anymore. As with other parts of this generator, the Winter's Ring may be quickly replaced by a more traditional spherical-shaped terminal or many others you might wish to try. Why not keep several on hand for demonstration?

Despite the fact that, as we've discussed, electrostatic principles have been well know for thousands of years, it was not until as recently as 1928 that a truly practical machine for generating high static voltages was perfected. Robert J. Van de Graaff, a young Rhodes

scholar working at Princeton, designed his first machine to generate the high potential needed to power a particle accelerator to bombard atomic nuclei as part of his experiments in nuclear research.

Although it can be difficult, it is not impossible for the home experimenter to make his own atom smasher! A Van de Graaff generator such as described here is an integral part of such an apparatus. If you are interested in taking on a project of epic proportions, find a copy *"The Amateur Scientist"* by C. L. Stong which is now out of print and very difficult to find, but worth the effort. Or write for similar information from Information Unlimited, P. O. Box 716, Amherst NH 03031.

The Van de Graaff is so simple and obvious in design that it amazes me that is wasn't developed sooner. I have always thought that this is a good example of just how inventions don't have to be extremely complex to have a significant impact on society. How many other simple devices are there waiting to be designed and built? It could be you that dramatically changes the world!

The easiest way to understand the Van de Graaff is to refer to the schematic diagram in figure 13. A Van de Graaff generator consists of a belt, two pulleys, a motor, brushes, a high and a low potential terminals.

In newer machines the bottom pulley is plastic while older machines used an insulator covered by wool or similar rubbing material. The top pulley must be of a conductive material such as metal or even wood which is not a good insulator at high voltages.

When the machine is in operation, a small motor attached to the bottom pulley drives the belt that is lightly stretched between the pulleys. Friction occurs between the surfaces of the belt and the plastic wheel, putting an electrostatic charge on the belt. The charge is carried by the belt toward the upper terminal. A grounded wire brush makes contact with the lower portion of the belt and bleeds off some of the negative charge. The brush at the top of the belt accepts the positive charge remaining and distributes it on the high potential terminal. (Note: It is possible to make a Van de Graaff generator that develops a negative charge on the high potential terminal.)

As the belt moves, charge builds up on the high potential terminal. Theoretically, this charge could increase forever. However, leakage into the air from the upper terminal limits the maximum potential to

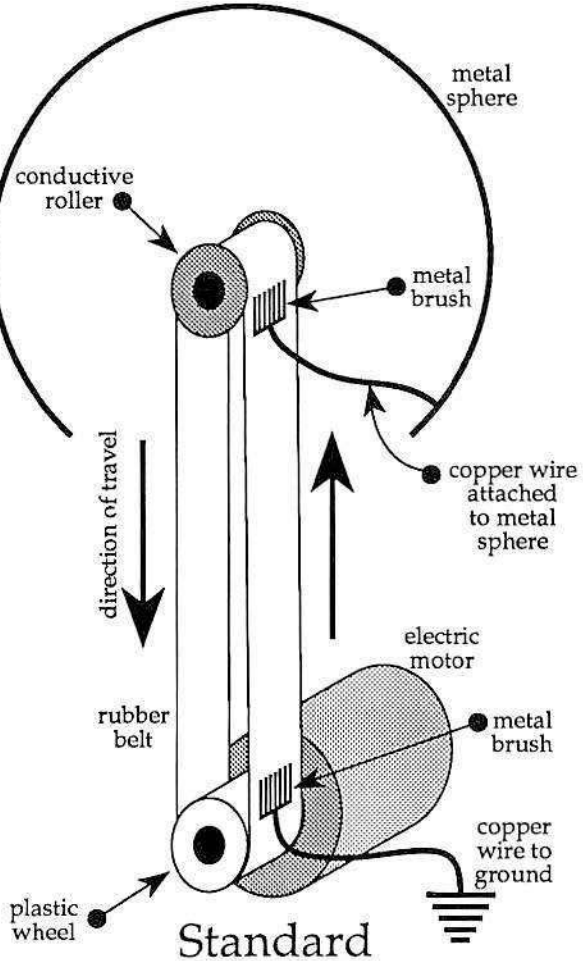

Figure 13

about 50 to 100 thousand volts typically.

A simple way to calculate the theoretical maximum for a "perfect" spherical top potential is to figure a voltage 70,000 times the smallest radius of the curvature of the high potential terminal. For example– most spheres are sold with reference to their diameter. For a 12 inch diameter sphere, we divide 12 by 2 to get the radius, or 6 inches. We

multiply 6 by 70,000 to get a theoretical voltage of 420,000 volts.

Because your terminal will never be a perfect sphere, and because there will be leakage into the atmosphere, theoretical voltages won't be reached. You might find these ball-park calculations interesting, nonetheless.

A photograph of my external Van De Graaff and its schematic are shown in figures 14 and 15. I found this to be an extremely simple and inexpensive design. In operation it will produce a reliable voltage in the range of 10 to 30 thousand volts using an ordinary rubber band. It will produce a solid and exhilarating "pop" when it discharges to your hand. It can throw sparks to ground more than an inch in length. Neon bulbs such as a Ne2 will glow brightly and continuously when near the generator. A blue corona glow can be readily observed from the collecting brushes in a darkened room once your eyes have adjusted to the dark. Negative and positive corona can also be identified by their appearance using this device as discussed later.

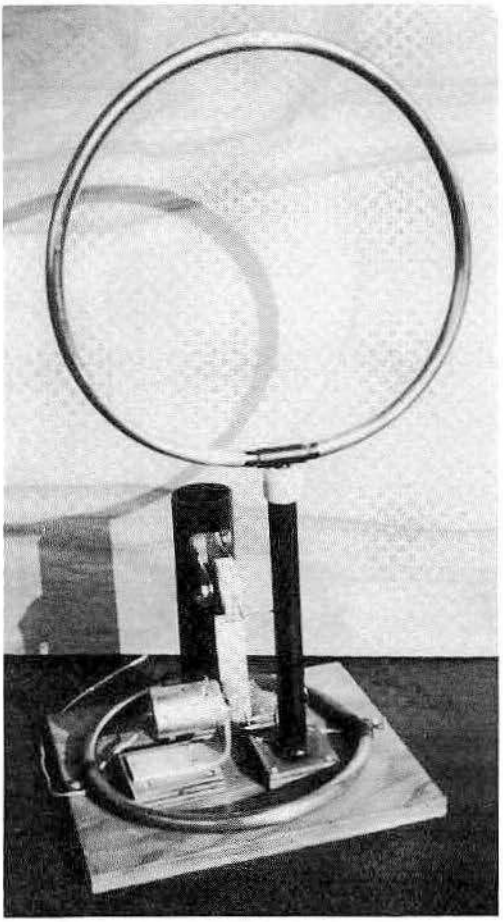

Figure 14 – External Van de Graaff Generator

The external Van De Graaff shown has some minor performance limitations due to the relatively high friction of the top wheel (no ball bearings) and excessive flexing of the rubber band. A rubber band should be used as a belt only for demonstration purposes. For more

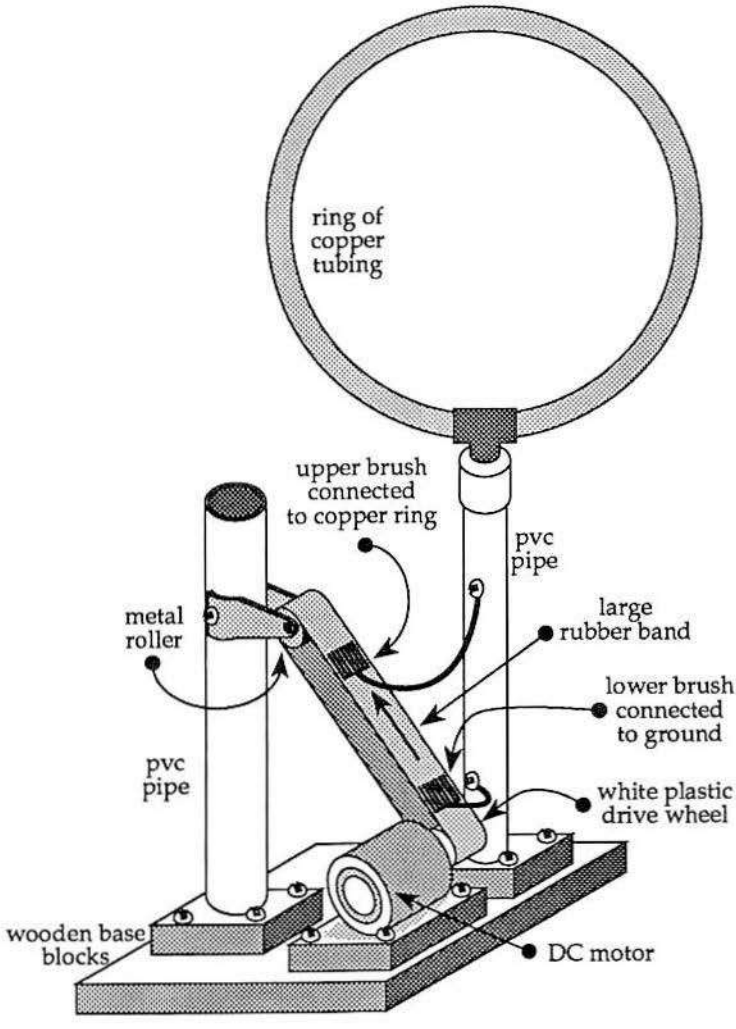

External
Van de Graaff Generator

Figure 15

serious experimenting, replace the belt with a less flexible belt such as made from a bicycle inner tube or, ideally, neoprene. Also, without ball bearings, the top wheel required occasional lubrication that frequently brought about the risk of oil contamination. Except for these minor problems, this generator has proven to be an excellent and reliable performer. It still remains the most easily modified and observed of the Van de Graaff designs I'll describe.

The construction of the external Van De Graaff is so simple and straightforward that little description is required outside of the drawing. A few tricks can simplify and improve construction.

An easy way to get your motor, roller and belt in alignment is to run your generator while holding the motor with your hand, experimenting until you find the right position for it. If your belt slips off, shift the motor slightly to change its attack or grip on the belt.

When connecting a belt between two rollers in any Van De Graaff type generator, it is natural to assume that pulleys should have flanges on their edges to provide a groove in which the belt will run preventing it from slipping off the driving wheel. Surprisingly enough, the belt will have a tendency to stay centered on the pulleys even when they are somewhat out of alignment! I assume this has something to do with the way the pressures change in the belt as it approaches the edge of a pulley. You may find that a small "hump" in the drive wheel can even be helpful at high rpm. Once aligned, you should have no problems at all with belts slipping off.

Use the largest diameter of copper tubing that you conveniently can for the top terminal. The problem is that when larger diameter copper tubing is bent into small diameter circles, undesireable ripples form. Larger gauge tubing must be bent into larger diameter circles forcing you to compromise between size and efficiency.

When soldering the two ends of the copper tube into the "T" connector, first clean them with extra fine steel wool, then coat (tin) them with a little solder before inserting them. This will give an exceptionally strong and smooth bond. You can use any ordinary propane torch for heating and soldering the tube.

If you use the same type of brushes as shown in the drawing, it might be tempting to shorten the copper wires leading to them from the PVC tubing or otherwise alter this mounting. Don't do it! It is the flexibility in these long copper wires that provides the "spring"

needed to keep the brushes flat against the belt.

The plastic bottom pulley is simply one of the white plastic wheels used on cheap furniture casters. It is attached to the motor shaft by carefully drilling out the wheel's center hole to a size slightly smaller than the diameter of the motor axle. You then apply a few drops of super glue to the axle and press or tap the wheel into place.

If the hole in the wheel is larger than the diameter of the axle, glue progressively larger diameter pieces of rubber tubing to the motor axle until the wheel fits snugly in place.

One last note: Since your top terminal is copper which quickly tarnishes, you might want to apply a little Silicone cleaner/protectant such as that sold for cleaning chrome automotive parts. This will keep your top terminal bright and shiny at all times. It also seems to limit leakage and produce an interesting double "pop" when touched.

The Evils of Oil

The only major problem that I encountered in building and operating Van De Graaff generators regardless of design is oil contamination. Since a Van De Graaff generator relies on friction between the plastic wheel and rubber belt to produce a charge, you can imagine the devastating effect oil or any lubricant can have on belt performance. Even the oil from your fingers can reduce the charge carried by the belt. Handle your belts sparingly, and hold them only from the outside edges as you might a record album.

The worst lubricant is a petroleum-based oil such as used to lubricate motor axles and bearings. Angular momentum from the motor axle can actually pull a drop of oil all the way along the axle, along the side of a wheel, and out onto a belt. *Therefore, **Do not oil your motor or bearings excessively.***

If you want a graphic demonstration of this effect, place a drop of fast drying super glue on your motor's axle. Before it has a chance to dry, run your motor for several seconds. If your motor is like mine, you will have a little trail of super glue from the axle to the outside of the wheel where it will form a little blob.

Once your belt and wheels are contaminated, they can be very difficult to clean. The best way to clean the belt is not to clean it all, but to throw it in the trash and get another belt.

The conductive metal top roller can be cleaned with a residue-free cleaner like ammonia, followed by a light sanding with extra fine sand paper and then by another ammonia cleaning.

Cleaning the plastic wheel is the most difficult. The plastic wheel usually builds up a static charge of its own during the time the generator is run. This charge seems to act like a sponge for oil! The only way I have found to remove it is it by attaching a wire to ground and running the motor while dragging the wire along the outside of the wheel. After discharging the pulley in this way, ground a piece of metallic sand paper and again run the motor while sanding away some of the outside of the wheel. This is accompanied with or followed by ammonia cleanings. Other solvents may work, but watch out for those that may dissolve the plastic. I realize this procedure may sound extreme, but I have even tried soaking the plastic wheels in industrial degreasers not available to the general public and have had no luck at removing this oil in any other fashion. If you are careful in your use of oil you will never encounter this problem.

A Few Words On Brushes

In both of the Van De Graaff generator designs described in this book, I used a simple tuft of wire soldered to the end of a thicker solid copper wire spring which provides the force necessary to keep the brush riding firmly against the belt. By far the biggest problem you are likely to encounter will be in keeping the brush riding solidly on the belt. If your brushes are not well placed, or your belt has undue flexibility, the brushes may have to be readjusted frequently.

Many configurations, some very elaborate, have been tried in an attempt to perfect a fool-proof brush assembly. I haven't found one yet. You may want to try a hinge, a spring, a piece of metal screen, or even a conductive rubber or foam such as those use to package integrated circuits. In designing a brush assembly, keep in mind that, ideally, it should be comprised of many fine points like the ends of wires because the density of electrons in a fine point is higher and electron transfer is more likely. Nevertheless I have had very good luck with non-pointed objects such as conductive foams. Most texts, and my own experience has shown that a good old tuft of wire usually wins out, but, as mentioned, this is not a perfect solution to the

problem. So, experiment. And have fun!

A Few Words On Belts

A good belt can be made from virtually any insulating material. Rayon, Dacron, rubber, paper, silk, plastic and even ordinary cloth have been used with success. Wear is probably the most important factor to consider in choosing a material. Rubber, for instance, rots in my home town due to the ozone contained in the smog here. Cloth will fray at high speed, although I have coated cloth with an extremely thin coating of Silicone rubber and have made good belts. Neoprene, joined with a diagonal splice is a long-time favorite.

In my opinion, the easiest all-around belt is made from an old bicycle inner tube, or even better, the rubber "liner" that covers the heads of spokes under the rim. One of these belts can be carefully spliced with inner tube cement from a tire patch kit. Even a little "Super Glue" will work if the splice is clamped.

In fabricating a belt also remember that the wider the belt, the faster a charge accumulates (within reason). And, you may also want to give a little thought to the noise generated by certain materials. At 5000 rpm a poorly made belt will make considerable noise.

One last belt option is to purchase a ready made belt from a scientific supply house such as Analytical Scientific, Post Box 675, Helotes, TX 78023. Such companies can often supply many different sizes and types of belts. I would suggest ordering the thickest, and strongest belt offered for a home-made generator. I find the price of commercial belts a bit too expensive for my bank account, but you might find their prices more acceptable depending on your project.

THE HIGH POWER "CLASSIC" VAN DE GRAAFF

Although these voltages are impressive, keep in mind that the classic Van De Graaff will easily produce 60 to 100 thousand volts or more and is only slightly more difficult to build.

The classic design for the Van De Graaff is shown in photograph 16. The one minor concession I made in my design was to use two stainless steel bowls for the high potential collector instead of the traditional sphere. I did this simply because I could not readily find a

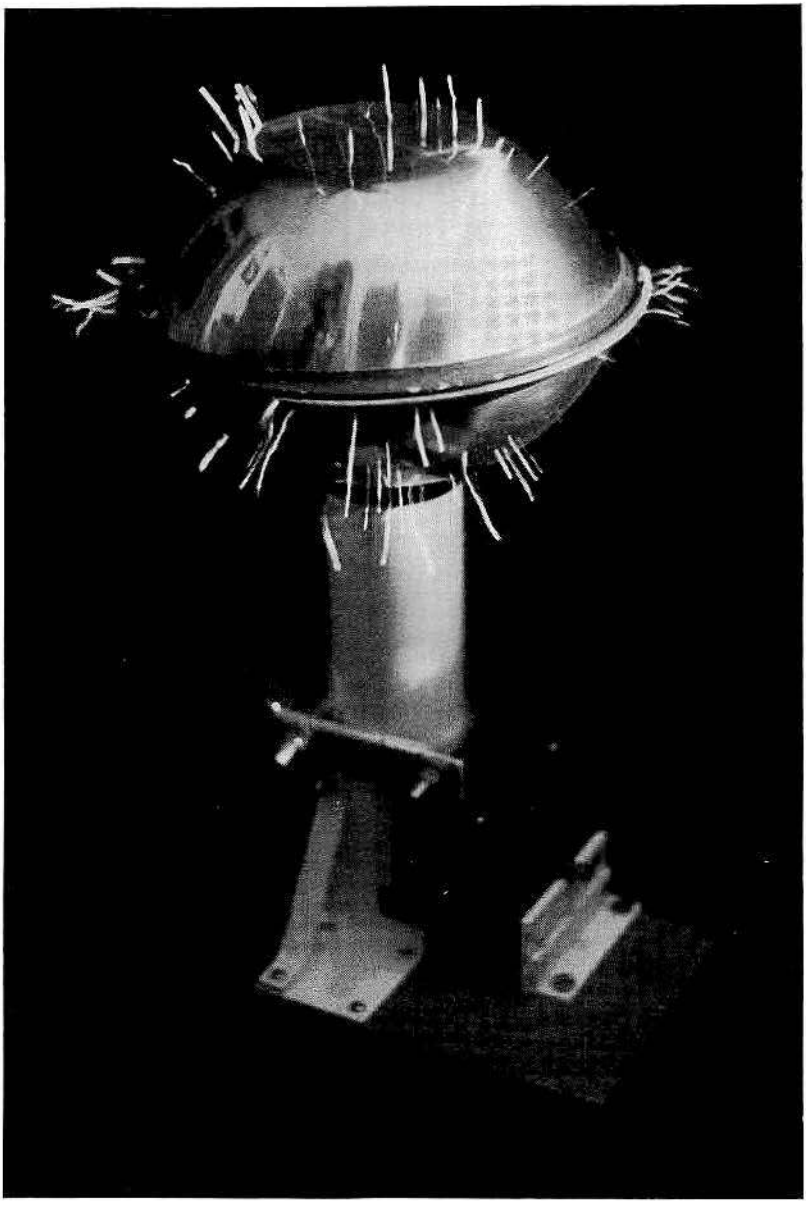

Figure 16 – Classic Van de Graaff Generator in Operation – This long-exposure photograph clearly shows the remarkable energy generated by this simple device.

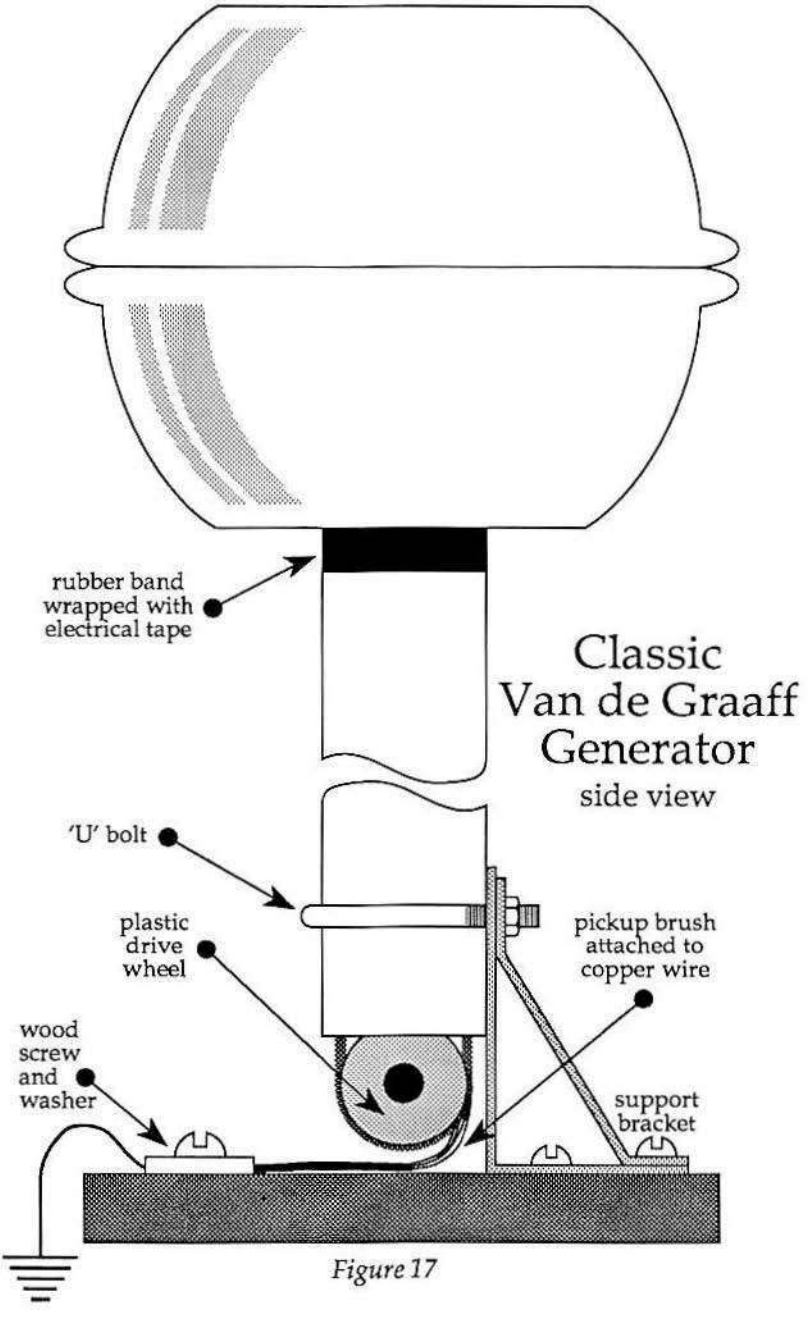
rubber band
wrapped with
electrical tape
Classic
Van de Graaff
Generator
side view
'U' bolt
plastic
drive
wheel
pickup brush
attached to
copper wire
wood
screw
and
washer
support
bracket

Figure 17

sphere of the proper dimensions. Besides, two bowls allow easy access to the top roller and brushes, and I wanted to test my hunch that almost as much power could be obtained from the bowls if the edges were heavily doped and insulated as could be obtained from a traditional spherical terminal.

All of the experiments to be described can be performed with this unit. It is an all-around solid machine and is fun to operate. If you plan to build only one generator from this book, and are wondering which generator to select, this machine is the best all-around performer. If carefully built, this design will exceed a voltage of 100,000 volts. It will arc thick, blue sparks well over four inches to an outstretched hand and deliver an invigorating, if not slightly uncomfortable, shock.

This generator is capable of charging up a person's body to a high voltage. It makes possible many experiments such as causing a person's hair to stand on end, or the rapid charging of large capacitors. The device will even produce an ominous "crackling" as your hand approaches the high potential terminal.

By standing on a large plastic insulator such as an overturned detergent bucket, a friend of mine was able to charge her body to such a high potential that her hands would "crackle" any time she pointed to a person nearby in the room. I think a physics or chemistry teacher would have little trouble keeping his/her students attention if the mere pointing of their hands produced this ominous cracking!

Though I am certainly not recommending the following approach, this generator was also inadvertently useful in training a dog in a single lesson not to jump on people. My dog, Merfi, had the bad habit of greeting people by jumping all over them. Nothing, it seemed, could discourage this behavior. One afternoon some friends and I were standing around a completed Van De Graaff and commenting on what an unusually large charge we had managed to bestow upon a person. Suddenly Merfi bounded into the shop. Despite our pleas, Merfi shot across the shop with his usual enthusiasm and leapt nose first into my highly charged friend, no doubt, intending to bestow upon him his traditional greeting.

We could do nothing but watch as a large blue spark jumped to Merfi's moist, waiting nose. Merfi stumbled back, temporarily lost control of his bladder, and then slunk out the door. A few moments later everyone was petting and reassuring Merfi, yet, to this day we

have had virtually no problems with Merfi's traditional greetings. He still eyes the friend from whom he received the shock with suspicion. And with good reason!

I suppose it is needless to say that it is wise to keep any and all pets a safe distance from your experiments. As with the external Van De Graaff generator, very little description outside of the drawings is required for constructing the classic Van De Graaff design.

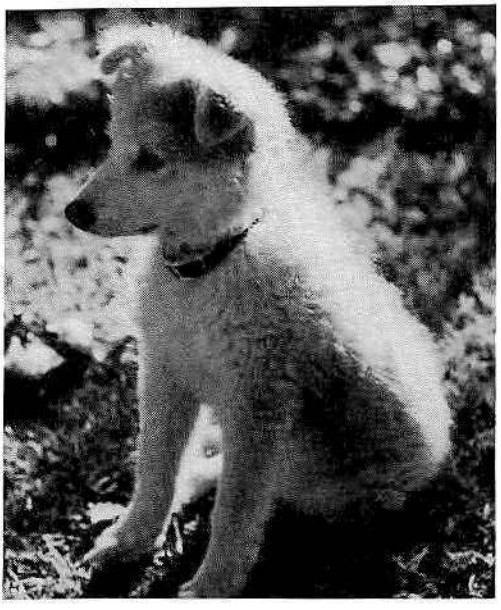

Figure 18 - "Merfi" – (An accidental electrostatic participant)

Things to keep in mind

The edges of the bowls are relatively sharp, even though the edges have been folded over. To prevent the charge from leaking through these sharp edges, they are coated with a special paint called "corona dope" which can be purchased in most T.V. and well-stocked electronic stores. It is available in both spray and brush-on forms. Corona dope has a high dielectric strength, and will prevent a charge from leaking off into the air. It can be used on any spots suspected of leakage on any of your high voltage projects. Keep in mind that the thicker the coating of corona dope, the better it will shield. I used around eight thick coats on my Van De Graaff and should have used more. Sparks fly right through it!

As with the last generator, the lower pulley is a white plastic wheel taken from an inexpensive furniture caster. It was mounted in the same way as was done in the external Van de Graaff.

The upper pulley is the front hub of a 10 speed bicycle wheel. I tried several different methods to reduce the friction of the hub bearings to make it turn more freely. I tried a variety of lighter oils and even

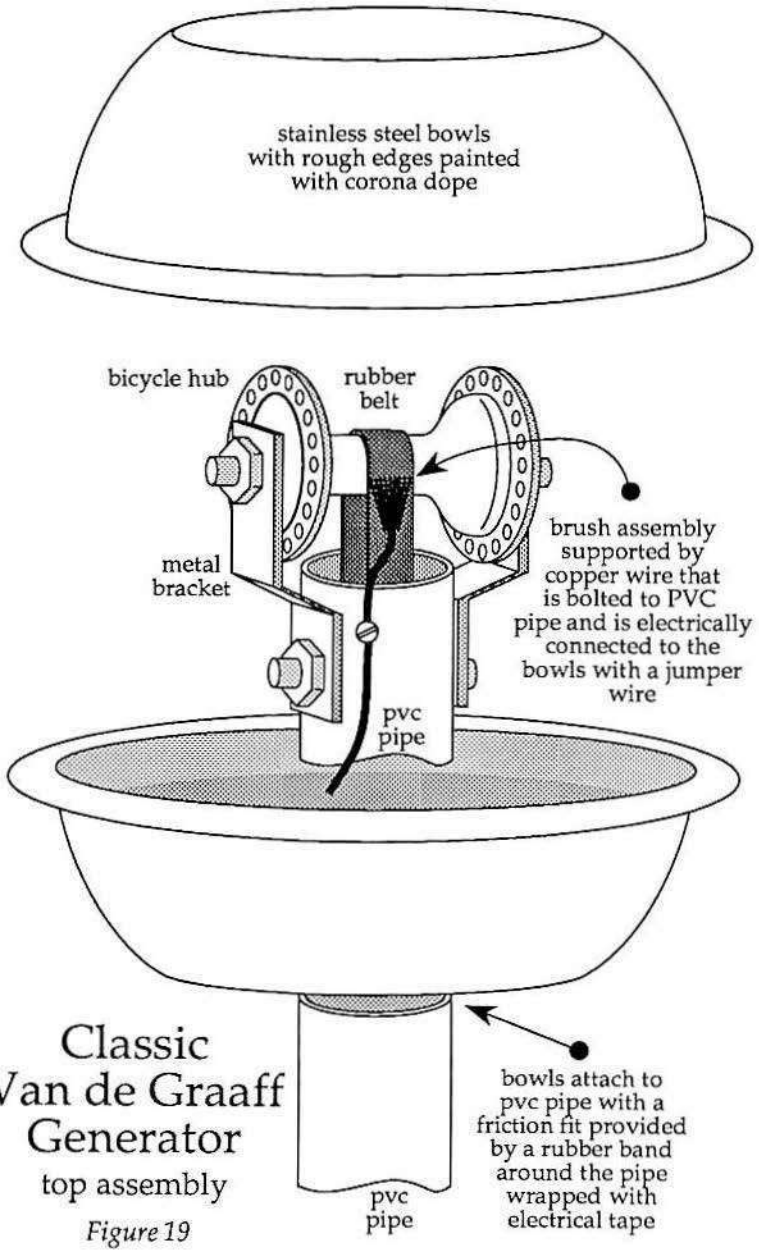

Classic Van de Graaff Generator

top assembly

Figure 19

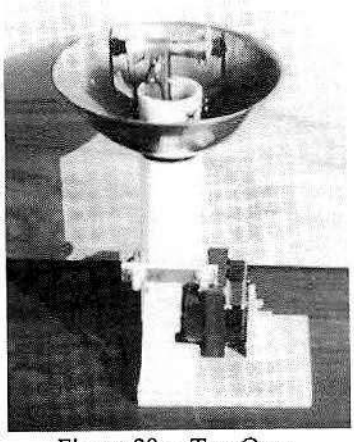

Figure 20 – Top Open

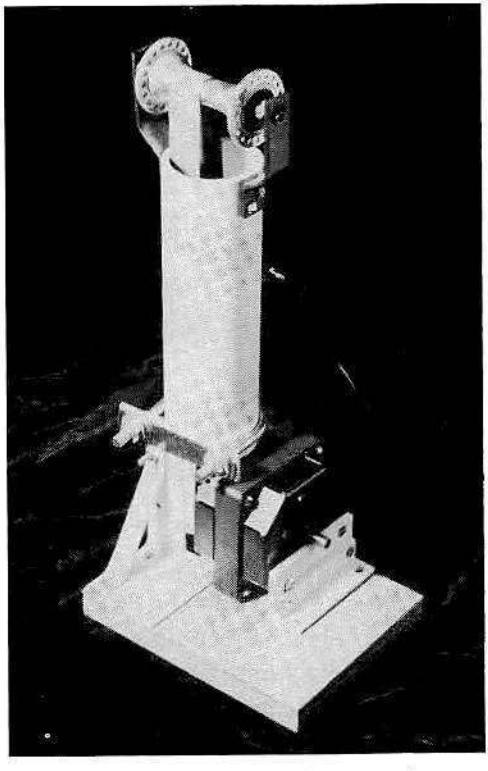

Figure 21 – Terminal Removed

removed the rubber covers that protect the ball bearings from dirt contamination. I found that lighter oil works well, but because of the risk of oil contamination as discussed earlier, I ended up using grease. Removing the covers also helps, but when the generator is running and the roller is spinning, a sizable charge builds up on its surface, and every dust particle in the area is attracted to it! Although you may want to experiment, I have come to the conclusion that the hub should be left pretty much as it is when it comes off the bike.

The two top bowls can be hinged together from the inside with a wide strip of black tape, or can be bolted together by some nylon screws through the lip. Keep in mind that you want the surface of these bowls to remain as smooth as possible to prevent electrons from leaking off. Don't use metal hinges or any sharp objects in attaching them.

The main body tube is fabricated from three-inch diameter PVC drain pipe. (Remember that acrylic or phenolic pipe might be superior to

Figure 22

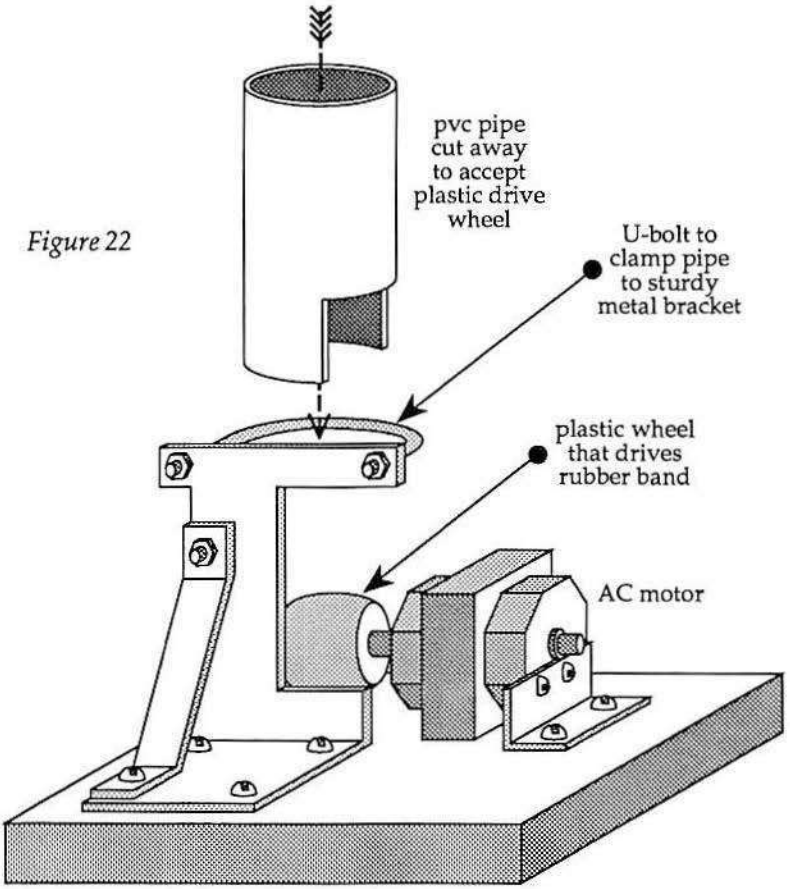

Classic Van de Graaff Generator

bottom assembly

PVC.) A slot is cut into the lower portion of the tube to allow the motor and plastic drive wheel to be inserted through wall. The PVC pipe is supported by a metal L-bracket and a U-bolt. Depending on the size of your motor, you may want to cut a notch into one side of the L-bracket to provide enough clearance for the motor to fully enter the bottom of the tube. Since this "L" bracket will support your whole generator, make sure it is sturdy and of a heavy gauge. You may even wish to add a metal brace as I did to increase rigidity.

When you have completed this generator, you will be able to perform any of the experiments that follow. This easy-to-build, high performance generator is a very exciting machine to own!

AN EXTREMELY HIGH POWER VAN DE GRAAFF

Before we move on to other types of static generators, I'd like to briefly describe one of the highest performance Van De Graaff generators I have ever seen. Shown in figure 24 is a design for an extremely high power Van De Graaff generator. I have not constructed this unit. I am providing details on this machine should you want to explore machines beyond the limits of my humble designs. This schematic will provide the essential design details.

At maximum efficiency this design could generate voltages exceeding 1,000,000 volts without using an auxiliary storage capacitor!

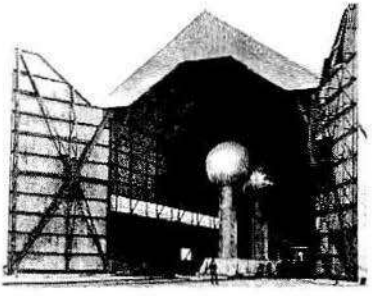

Figure 23 – Ten million volt Van de Graaff generators were built in the 1930's. One generator here is negatively charged, and the other is positive. Generators of this size are not recommended as a first project. (Perhaps not even as a second! ...but call me if you build one!)

Voltages of this order can be dangerous, possibly lethal. This is not a toy and should only be constructed by a serious and cautious experimenter. Because of its high output, I think this unit would make an outstanding laboratory power source for a homemade atom smasher.

The high power unit uses an external high voltage power supply to "spray" an initial charge on the rubber belt. Notice in the schematic that the ends of the spray wires are pointed. A rectified high voltage source between 5,000 to 10,000 volts is ideal. For low cost and ease of assembly you may want to try using an automotive coil as a transformer. For details see Lindsay Publications *"Build a 40,000 Volt Induction Coil."* (Written by an author who is generally a good sort.)

In this design, both top and bottom rollers are metal. The top roller itself is insulated from the high potential sphere. Charge is sprayed

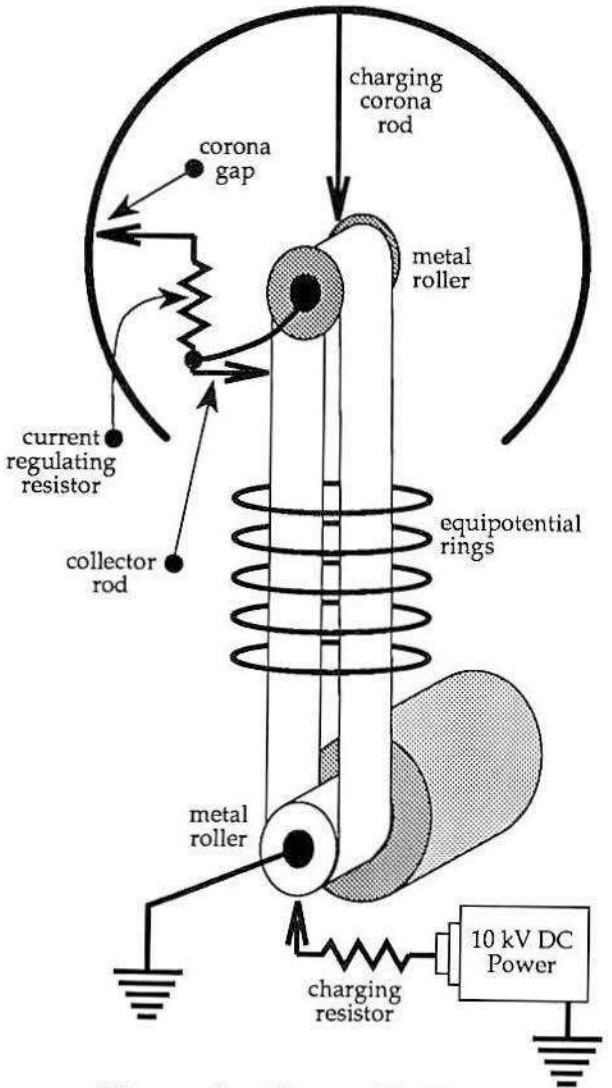

Van de Graaff Generator
high power configuration
using external excitation
(schematic diagram)

Figure 24

Figure 25

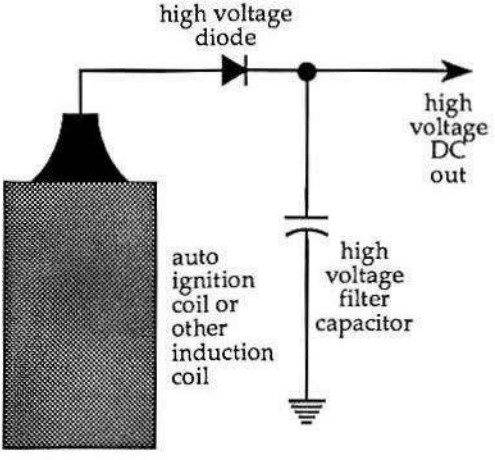

Induction Coil Exciter
for Van de Graaf Generator
output must be recitified
and filtered

onto the carrying belt as it passes through the corona discharge between the high voltage power supply and the lower roller which is grounded. A second set of points located just inside the upper high potential terminal picks up the charge and conducts it to the upper pulley. Once highly charged, current flows to the high potential terminal through the current regulating resistor. This configuration can also include a corona gap as shown near the inside surface of the high potential terminal.

An additional set of spray points, labeled "charging corona rod" on drawing, connect directly to the high potential terminal and are situated directly above the pulley.

According to *The Amateur Scientist, "The difference in potential between the upper pulley, made 'live' by the voltage drop across the current regulating resistor and corona gap, and the high-voltage terminal causes these points to 'spray a charge of opposite sign onto the downward run of the belt.' "*

The value of the current-regulating resistor can be computed roughly by Ohm's law. In small machines it is usually on the order of

40 megOhms.

Optimum belt speed for a high power unit is between 4,000 and 6,000 feet per minute. Most high power units use belts made from rubberized fabric.

If your design is to exceed 200,000 volts, charge distribution along the insulating column becomes important. Machines using belts more than four inches wide should be equipped with equipotential rings as shown spaced every two inches.

A large Van De Graaff generator intended to reach the million volt range is often sealed in a steel tank containing inert gases such as carbon dioxide and kept at many atmospheres of pressure. Keeping the gases at high pressure serves to increase their insulating properties and improves both the voltage and current output of the generator.

Owning a generator of this size would be incredible!

INDUCTIVE ELECTROSTATIC GENERATORS

Wouldn't it be wonderful to have a generator that could produce almost 90,000 volts while being virtually immune to changes in humidity? What if that same generator could be run extensively without concern for wear or maintenance? What if the same generator could be "daisy chained" to other generators to increase their output? What if it could be run as a motor, operating on electrostatic charges, just as a common D.C. generator can also by run as a motor? Well, what we would certainly have is a Dirod generator.

The Dirod generator is another invention of Mr. A. D. Moore. The Dirod gets its name from the main components of the generator: a high grade Plexiglas disk and a series of metal rods. "Dirod" is short for disk and rods. Its operation is most easily understood by observing a schematic representation of its workings.

Figure 26 shows a schematic of a basic Dirod generator. A number of metal rods are attached to an insulating disk (Lucite, glass, plastic, etc.) which is mounted on a bearing that allows it to rotate. In the center of the disk is an axle which is stationary, and attached to this axle is a wire with two brush ends as shown. As the disk rotates, each pair of metal rods is momentarily electrically connected to the stationary brushes as the rods pass by them.

Outside of the wheel we have two smooth metal plates each with

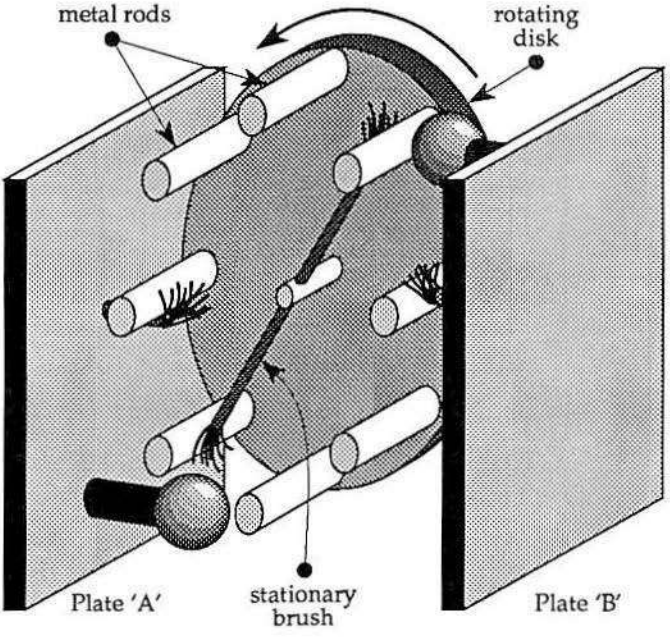

Induction Generator

schematic diagram

Figure 26

an electrode attached as shown and each having a pair of metal brushes as well. Positive and negative charges will form on these plates in the following manner. When the wheel begins its rotation, plate A and plate B will have similar amounts of negative and positive charges – similar, but of course, not exactly the same! Let's say that plate B has a slightly negative charge, and plate A has a slightly positive charge. Now, as a metal rod moves by the electrode from plate A, it is momentarily connected to the rod moving past the electrode from plate B, connected by the stationary brushes from the center axle as shown in figure 27a. At this point, since plate B has a slightly negative charge, the positive charges in the two bars rush into the bar closest to plate B (negative and positive charges attract), and the negative charges rush into the bar closest to plate A. This is comparable to one electrophorus charging the other without having them

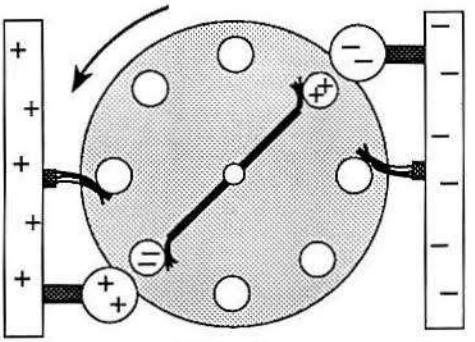

Figure 27a

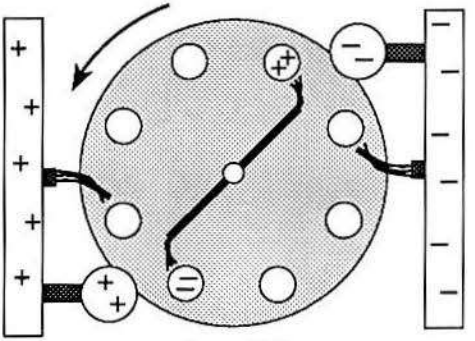

Figure 27b

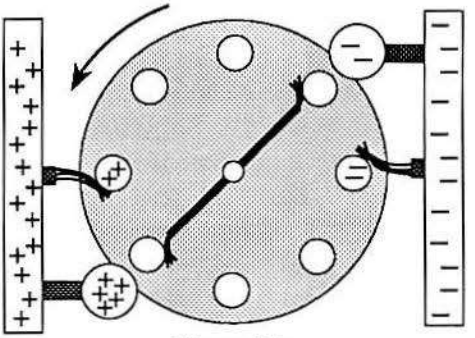

Figure 27c

Induction Generator Operation

actually touch.

As the disk continues to rotate, the two bars move past the brushes and break electrical contact. Now we have one bar with a mostly positive charge and one with a mostly negative charge. Figure 27b

As the bars continue to revolve around to the opposite plate, they briefly make a connection with the brushes from that opposite plate and bestow upon that plate their charge. Figure 27c. Now the plate has an even higher charge than it did originally. It charges the next rod passing by it even more forcefully. In this fashion the plates rapidly build up a larger and larger charge.

When you consider how fast these rods can be spun, and how fast these charges double, you realize how quickly this generator can produce high voltage!

To be a little more technical in describing the difference between our previous friction generators and an induction generator of this type, remember that friction generators charge by contact between two bodies and by the sharing of electrons from the resulting contact. Inductive generators make no demand on free electrons, but on the field they produce. This field causes electrons in the charging material to veer from their orbits. This displacement sets up or induces a charge in the formerly uncharged material. The series of figures 27a through 27c show not only how the machine moves but also how charges are built up during each step of the charging process described.

It is important to understand these simple principles of induction since they are critical to understanding and building the electrostatic motors that follow.

It is interesting to note that the Dirod generator is virtually the same as the world's first electric motor known as the "Franklin" motor for its inventor, Benjamin Franklin, and discussed later on.

Construction of the Dirod Generator

Construction of the Dirod generator is, again, straightforward and simple when viewing the drawings. Keep in mind that the metal rods can be mounted horizontally as shown or vertically, radiating out from the center. Vertical mounting is much trickier. However it is much less stressful on the Lucite disk allowing higher rotational speed to be achieved.

Also very important in achieving maximum voltages is a corona shield which is not shown in the drawing. A corona shield can be fabricated simply by placing a small sheet of Plexiglas between the metal spheres and the rotating rods. I would suggest that you first try your generator without a corona shield, and then with. If your design is optimum, your voltages will increase with the shield.

Because the brushes in this type of design can really take a beating I strongly suggest using a conductive foam such as the foam integrated circuits are packaged in or a conductive rubber brush. If forced to use a metal brush, use a metal that is very springy.

I built an induction generator by modifying the Franklin motor shown later on. By adding brushes and two stainless steel collectors to the Franklin motor, I had both an electrostatic motor and generator! Although I plan to build a much larger, more traditional Dirod machine, this small motor/generator still holds my fascination and continues to teach me the principles I will need to employ in devising the larger unit.

MEASURING VOLTAGES AND POLARITY

WARNING: As mentioned before, the electrostatic voltages produced by the generators in this text are generally safe for the experimenter even should he be accidentally shocked. The operation of the following devices is described for use with electrostatic devices. Should you choose to measure the voltage of other devices, more stringent safety precautions should be taken. Use extreme caution at all times.

Information in this chapter is useful not only in the field of electrostatics, but can also be valuable to those who work with Tesla coils, Oudin coils, induction coils, or other high voltage power generators. One of the most surprisingly difficult things to do with a high voltage is to accurately measure it. I was frustrated to find that text after text said simply that measurement of high voltages was impossible for the amateur. As a result of experimentation and having studied the writings of extraordinary experimenters such as Professor A.D. Moore, I can show you several methods of measuring high voltage that seem quite dependable and accurate. You can also use one of several means to determine the polarity of a high DC voltage – something which is rarely mentioned in any text.

Finding Polarity and Simple Voltage

There are several very simple means for determining the polarity of a high potential. The first, and by far the most sensitive is an FET based "electroscope." Figure 45 shows an electroscope of my own design. The device is simple to assemble and is shown in both schematic and component layout forms. The device works extremely well.

I highly recommend that you build one of these. It can show you the polarity of both very high voltages as well as low electrostatic

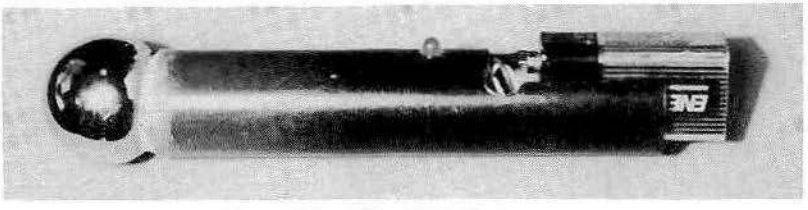

Figure 45 – The FET Electroscope

voltages. In fact, this electroscope will respond to the static build up found in clothes taken from a dryer, or the charge that builds up on a hard rubber comb.

You may want to modify my design. You should consider replacing the 10 megohm resistor with one of a smaller or larger value. It controls the sensitivity of the circuit. The larger the resistor used, the more sensitive the device becomes, the smaller the resistor, the less

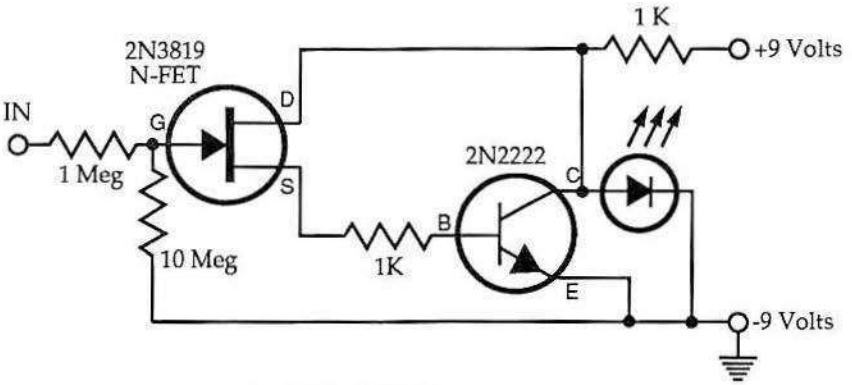

FET Electroscope
Schematic Diagram
Figure 29

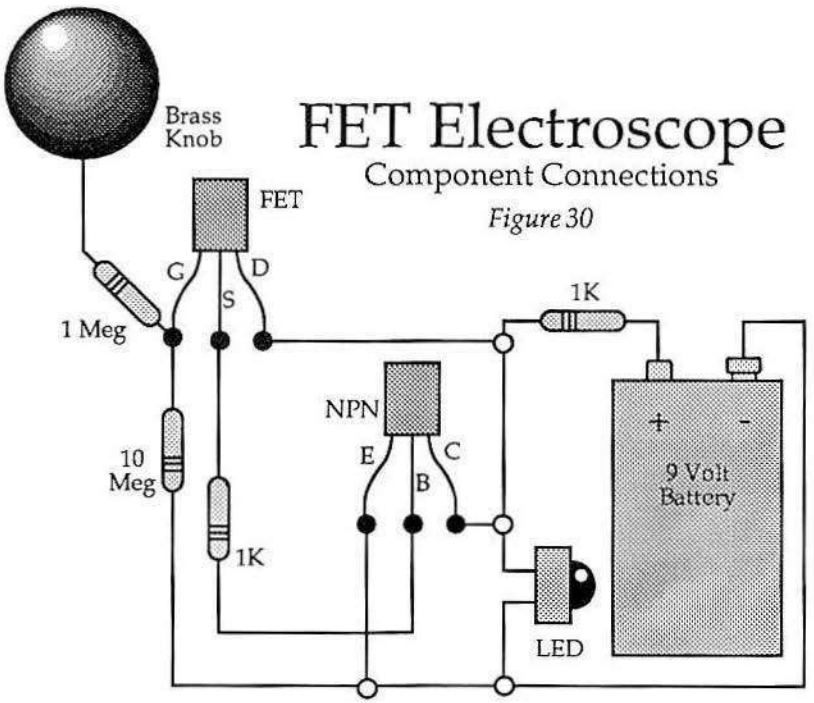

FET Electroscope
Component Connections
Figure 30

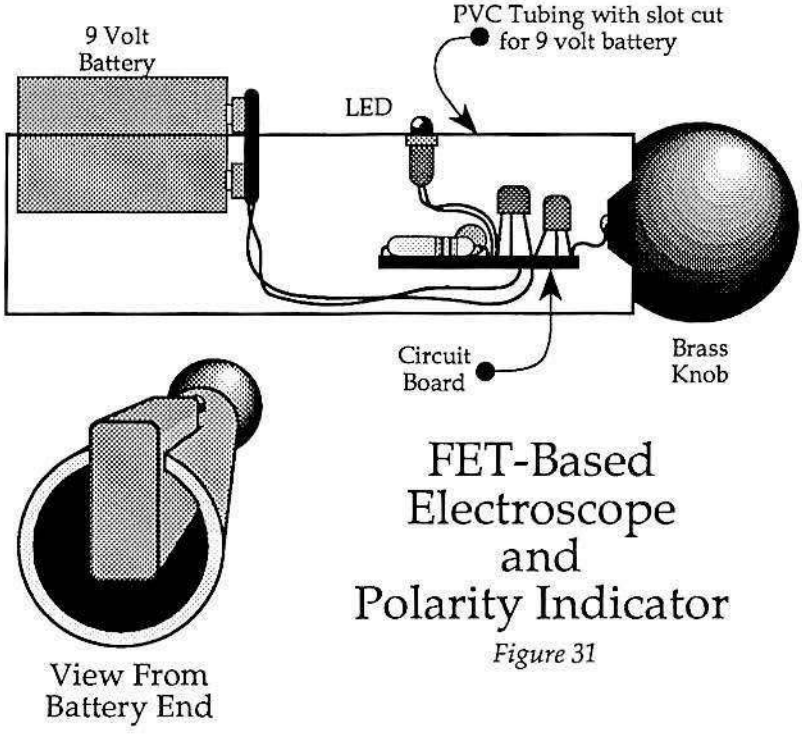

FET-Based Electroscope and Polarity Indicator

Figure 31

sensitive – within reason, of course. The resistor can also be removed all together for maximum sensitivity, but the device becomes unreliable because even stray radio emissions will be picked up.

When properly adjusted, the FET scope will light when placed in contact with a positive static charge. Keep in mind that the FET transistor, which is the heart of the circuit, could be damaged by an extremely high voltage, however, I have used my scope without difficulty to more than 30 thousand volts (30 Kv). This voltage was measured by placing the scope directly against the Van de Graaff with an appropriate spark gap.

A MECHANICAL ELECTROSCOPE

A mechanical version of the electroscope can be made quite easily from a glass jar, a little wire, and some aluminum foil. A mechanical electroscope is shown in figure 32.

When the top electrode on this scope is touched to a static voltage source, the aluminum leaves in the jar will separate. This happens because the foil in the jar takes on a uniform charge. Since like charges repel each other, the two leaves of foil are forced apart.

The demonstration of an electroscope can be quite impressive. Although it would be difficult, if not impossible, to calibrate, a

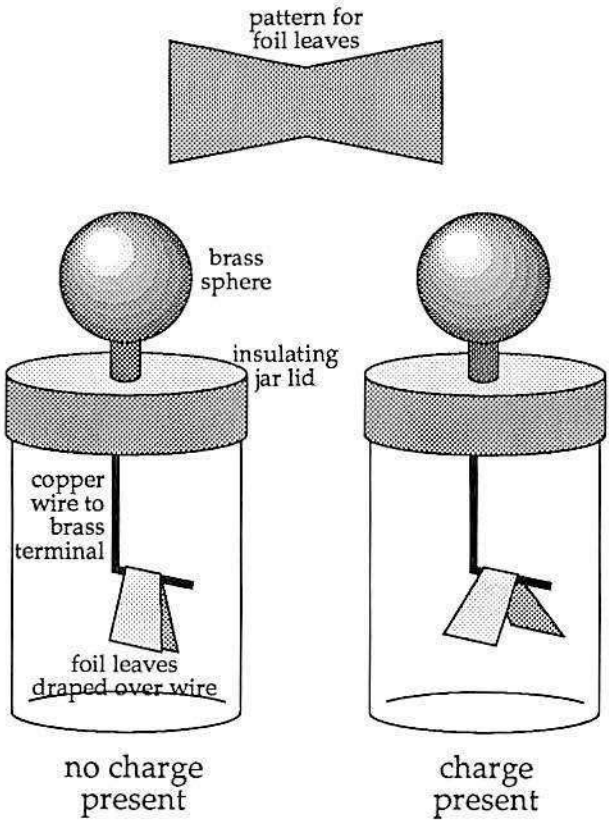

Mechanical Electroscope

Figure 32

mechanical electroscope of this type can also be used to measure voltage. Heavier leaves require greater voltages to separate them. Therefore, the distance the leaves move away from one another indicates a relative voltage.

The Neon Lamp Bank

Another less sensitive but much simpler way to measure low electrostatic voltages is with the use of a neon lamp bank. Figure 33 shows the assembly of such a bank. Ne2 neon lamps are wired in series along a Plexiglas panel as shown in the drawing. Since each lamp fires at about 70 volts, five bulbs wired in series will read a voltage of up to 350 volts. You can quickly see how larger or smaller banks can be easily built. The cost of these bulbs is quite low, so even fairly large banks can be built without great cost.

When connected to a source of high voltage, it is quite easy to see which bulbs are lit. Sometimes, however, you may have to darken the room to get a more accurate reading. Neon lamps are not always easy to see.

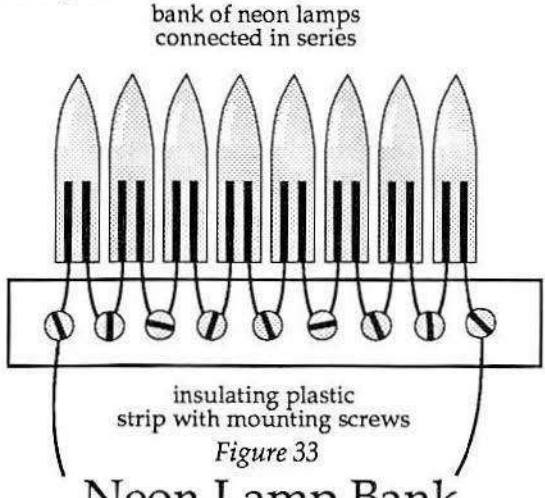

Figure 33
Neon Lamp Bank

You can increase visibility by leaving a small gap between the lamp bank and your high voltage source. Letting a spark periodically jump the gap will trigger the lamp bank. Attaching the bank directly to generator can draw enough current from the generator (load it down) such that it never reaches peak voltage. With a small Van de Graaff a steady stream of bright flashes will occur every two or three seconds.

Though this means of voltage measurement is crude, you could improve it somewhat by using bulbs with very close firing voltages.

The best way to find such bulbs is with the circuit such as shown in figure 34. Note that a volt-ohm meter can also be connected across the leads shown in order to gauge the exact voltage at which the bulbs will fire. By slowly bringing up the input voltage to a set of bulbs wired in parallel you can find which bulbs fire together and at what voltage.

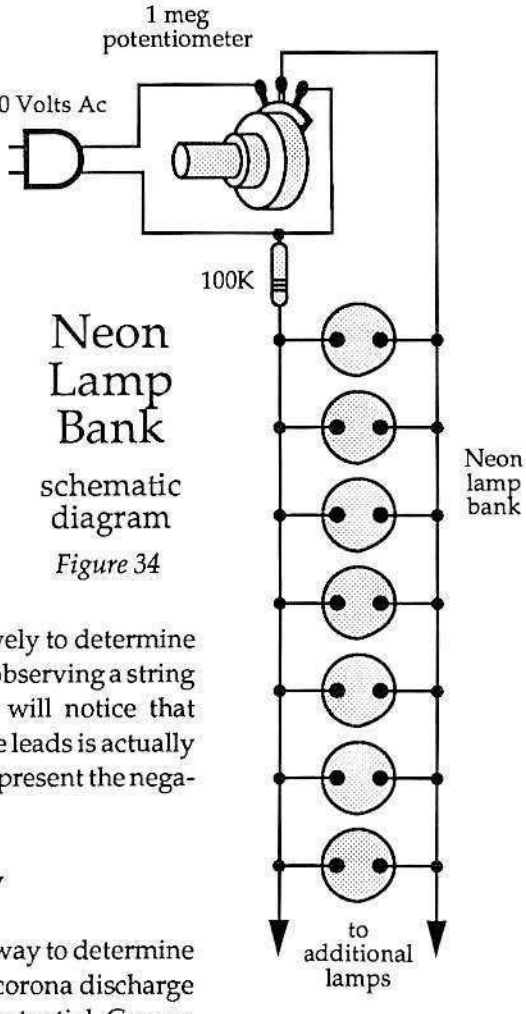

Neon Lamp Bank

schematic diagram

Figure 34

A neon bank can also be used very effectively to determine polarity. After carefully observing a string of flickering bulbs you will notice that only one of the two inside leads is actually lighting. This lead will represent the negative electrode.

Corona and Polarity

Another interesting way to determine polarity is by observing corona discharge from your high voltage potential. Corona discharge is that strange very faint blue glow that surrounds portions of your high potential terminal. To observe it, you will need to be in a darkened room with your eyes fully adjusted to the dark and your generator running.

One might assume that positive corona and negative corona look the same, but this is not true! Positive corona is even and uniform in appearance while negative corona is bushy, often with streaks or streamers that move around.

I first noticed this while using my external Van de Graaff, the same one described earlier. Not having had much experience with this generator, I immediately assumed that the light blue glow I was seeing in the darkness was due to arcing in the D.C. motor. It was too dark to see where the corona was coming from. Fearing the contacts in the motor would eventually be damaged, I tried every method I could think of to stop motor arcing, but the pesky blue glow went on unabated. Finally, I reached out in the darkness thinking I was going to touch the motor, but much to my surprise ended up touching the top of the generator! I had not expected to observe a corona discharge on this machine.

Another interesting fact is that negative corona can be heard! If you find that a hissing sound is coming from your generator, this will be generated by the negative corona discharges!

Using Spark Gaps To Determine Voltage

A spark gap is the best way I know of to accurately measure high voltage without having to resort to very expensive laboratory equipment.

Figure 35 shows the basic configuration of a "sphere gap" capable of accurately measuring up to 90,000 volts. A sphere gap consists simply of two hollow stainless steel spheres 1/2 inches in diameter which are attached to a length of threaded rod with epoxy glue that has

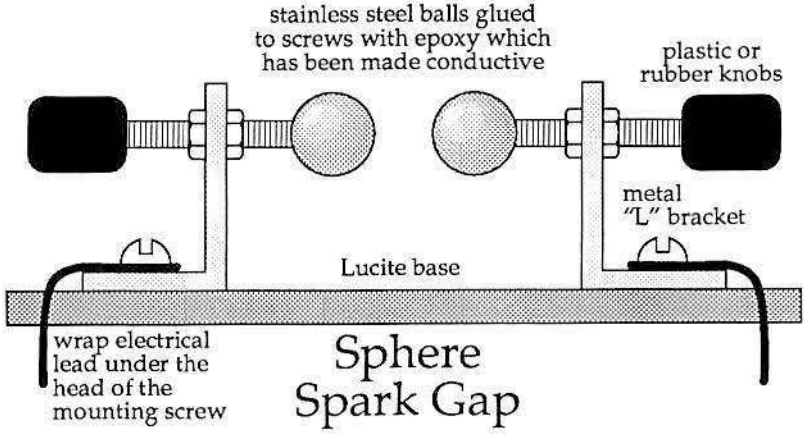

Figure 35

been made conductive by some additive or has been coated with a little silver paint in order to make electrical contact between the sphere and the rod. The rod is threaded through a metal stand, and plastic handles are added to allow the spheres to be turned while the device is operating. The spheres must be at least 3 sphere diameters above the base to prevent distortion of the electrical field which can give inaccurate results.

Another type of gap you can build is a rod gap consisting of two aluminum rods 3/4 inch in diameter. The rods are lined up with each other just like the sphere gap. The ends of the rods are rounded by turning on a lathe. Precision is important. The ends of the finished rods must be as close to hemispherical in shape as possible and must be highly polished. A rod gap of this type will give fairly accurate measurements up to 60,000 volts.

Unfortunately, there are too many variables to give a simple equation for determining at what voltage a spark will bridge a given gap. The only practical solution is to either calibrate your gap by using devices that generate known voltages, or to use a set of measurements which have already been taken.

What follows is a chart of known values for the apparatus described. These charts are excerpts from *Electrostatics* by A.D. Moore.

kV	Rod gap	Sphere gap
5	0.056	
10	0.112	
15	0.170	
20	0.228	0.234
25	0.288	
30	0.355	0.370
35	0.430	
40	0.520	0.531
45	0.625	
50	0.750	0.710
55	0.903	
60	1.122	0.950
70	.	1.102
80	.	1.380
90	.	1.700

Note: Gaps listed are in inches.

One limitation of measuring high voltages with a sphere gap is that you will loose accuracy dramatically if the gap between the spheres becomes larger than the diameter of one sphere. Because of this, you might need a general way to calculate voltages for spheres of different sizes. Also, you may not be able to find a sphere of the exact size mentioned and will need to have a reference for adjusting your figures.

What follows is a listing of spark gaps for spheres of several different sizes. By using these numbers and plotting along a curve, you can remain fairly accurate in determining the characteristics of spheres whose sizes fall between those shown.

Gap Distances in Inches
for a variety of voltages and sphere sizes

	sphere sizes in cm				
kV	2.5	3	4	5	10
10	0.30	0.30	0.30	0.30	0.30
20	0.61	0.61	0.61	0.61	0.61
30	0.95	0.95	0.95	0.95	0.95
40	1.40	1.32	1.30	1.30	1.30
50	2.00	1.82	1.73	1.71	1.65
60	2.81	2.40	2.21	2.16	2.02
70	4.05	3.16	2.80	2.68	2.41
80	.	4.40	3.50	3.26	2.82
90	.	.	4.40	3.93	3.28
100	.	.	.	4.76	3.75

THE "NOON" ION HIGH VOLTAGE METER

OK, I have to admit that it is terribly arrogant for me to name one of my devices after myself, but what the heck. For the record, I won't complain if you affix your name to one of your inventions! I think that you will find this meter which has solved so many of my voltage measuring problems to be an extremely useful tool in experimenting with high voltage.

As we have discussed, the surfaces of a high potential terminal should be smooth and round, ideally spherical, in order to prevent electrons from flying off into space. If we intentionally direct these electrons onto a sharply pointed terminal, the density of electrons will increase to the point where they begin to jump out into the atmosphere that surrounds the terminal. As these electrons stream away, the pointed terminal moves in an opposite direction by virtue of Newton's second law of physics (ie. for every action there is an equal and opposite reaction.)

This reaction is extremely small. However, it is measurable, and can even drive a small motor (described later) or, as I have discovered, push the pointer on a standard panel meter! Since the strength of the reaction is directly related to the voltage accelerating the electrons, it is possible to construct a meter capable of measuring high voltage.

One difficulty with this meter is that, if constructed from off-the-shelf parts, no two meters will read exactly the same due to variations in the exact dimensions of the pointed terminal and the meter itself. It is necessary to use other methods to initially calibrate your meter such as comparing meter readings to voltages ascertained by the spark gap method.

When using your meter remember to keep it well clear of ground or any object that might attract the ions streaming off your high voltage generator. Anything that upsets the stream of electrons can affect the meter reading.

HIGH VOLTAGE AND SAFETY

Because storage devices can accumulate enough electrical charge to be lethal, we must discuss safety.

Most texts simply warn the experimenter to stay away from a high voltage discharge, and, of course, this is a good idea. No shock is completely safe, and people have been injured and even killed by remarkably small voltages.

Even low voltage can deliver high damaging current. A capacitor carrying just a few volts has been known to melt the end of a screwdriver that accidentally bridged its terminals!

If your experiences with electricity are anything like mine, no matter how careful you try to be, electricity will occasionally find

some clever way to zap you when you aren't looking. Because of this, you should know how to determine when any source of high voltage you are experimenting with is safe.

The U.S. Atomic Energy Commission helps us by telling us that a discharge to the human body of 10 joules is known to be hazardous to life. A discharge of a mere 1/4 joules will deliver a heavy shock.

Use the following equation for figuring the charge in Joules:

$$\text{Joules} = \frac{1}{2}CV^2$$

where:

C = Capacitance in Farads
V = Voltage in Volts

What follows (again from A. D. Moore) is a short list of capacitors and the number of kilovolts needed to store up a dangerous 10 joule charge.

microfarads (uF)	kilovolts (kV)
0.002	100
0.20	10
20	1
80	.5
320	.25
2000	.1

From this you'll see that even small capacitors can store lethal amounts of electrical charge. Just because you may be dealing with less than 10 Joules does NOT mean you are safe! Again, remember that no shock is completely safe. If you are careful and use good judgement, you will have little to fear from electricity.

Most of the generators in this book will produce more than enough power to run any of the experiments outlined directly. High voltage static electricity is safe because there is so little current available. A Van de Graaff machine moving 50 square inches of belt per second generates only one microampere. Although the voltage (the pressure behind current) can be very high, there is very little current to be accelerated. Power is the product of voltage times current. One

microampere would have to be accelerated by one million volts to be able to deliver one watt of power. With such low current levels, power levels are necessarily low and relatively safe.

If, however, small currents accelerated by high voltage are stored in a capacitor or bank of capacitors, it is possible to accumulate enough charge at high voltage that when it quickly discharges it can produce deadly levels of current. Some commercial high power static generators go as far as to present the warning "Do not attach capacitors." If you are experimenting with larger capacitors than those described, remember that it is no longer safe to verify static charges by touching terminals! Capacitors can store charges from *minutes to months* depending on the dielectric! Careless or thoughtless use can prove fatal!

Electrostatic generators are unusually safe. Most generators will produce no worse a shock than a good jolt resulting from shuffling across the carpet. However, in coupling your generators to energy storage capacitors you're moving into dangerously high voltages. Be very careful!

ENERGY STORAGE WITH THE LEYDEN JAR

A Leyden jar is simply a capacitor, that is, a device that stores electrical energy. Like all capacitors it consists of two conducting metal plates separated by an insulator. Figure 36

A brass knob such as those used on the handles of bathroom drawers is attached to an insulator, in this case, a flat piece of Lucite. You could also use cork, plastic, wax, or almost any insulator. The Lucite is cemented to the lid of a jar with a little Silicone glue. A large hole cut in the lid of the jar allows a wire to pass from the bottom of the knob to the bottom of the jar. The inside and outside of the jar are coated with a layer of aluminum foil. The foil should be worked with your fingers until it smoothly conforms to the sides of the jar. A wire is attached to the outside foil, and the entire outside is then wrapped with black tape.

To use the Leyden jar, the wire lead coming from the outside foil is attached to ground. A cold water pipe makes an excellent ground. The brass knob is connected to the output terminal of your generator.

Leyden jars can be assembled in any size, larger jars having larger capacitance. My personal favorite Leyden jar was made from a 5

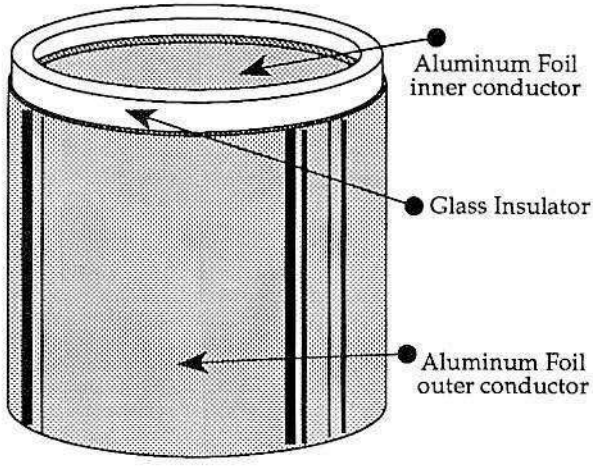

Leyden Jar & Other Capacitors
showing the
conductor-insulator-conductor layers

Figure 36

gallon white plastic pail that had contained detergent. This huge capacitor has been charged by the "Classic Van de Graaff" generator. Under good conditions it yields a very heavy, thick, multi-colored, spark of more than 4 inches accompanied by a "crack" that could be heard for some distance.

A word of warning: I made the error of touching this capacitor when I had thought it fully discharged, and though it was partially discharged at the time, I received a remarkably painful shock. This capacitor should be treated with respect. You can never be too careful.

Leyden Jar Tool

One tool you should build for your Leyden jar is a discharge rod. After experimenting with your Leyden jar, you will always want to be sure that it is fully discharged before handling or storing it. This is a very good habit to get into to avoid getting zapped when you are in a forgetful mood.

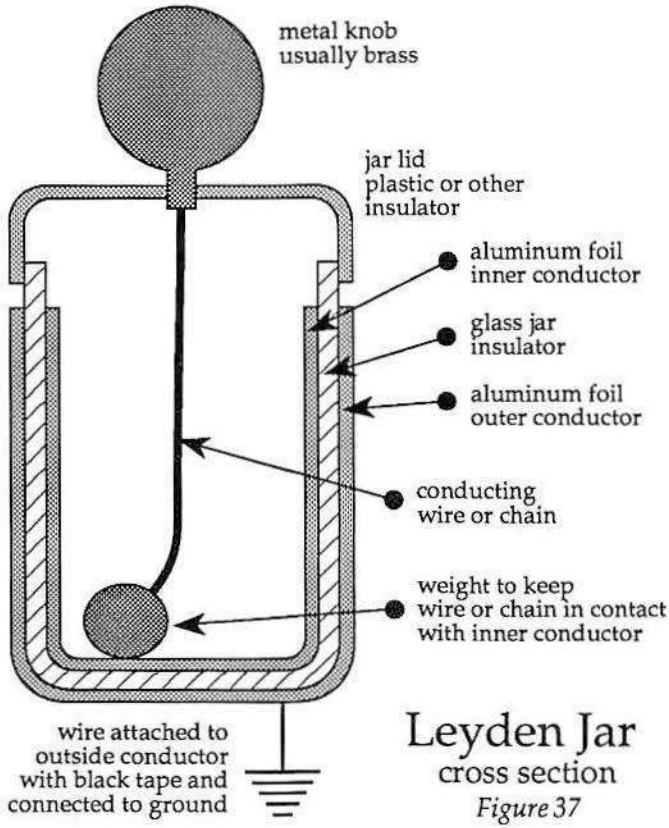

Leyden Jar
cross section
Figure 37

Electricity often seems to find some way to get into the jar without telling you. I was once shocked by a Leyden jar that was standing a few feet from a generator. It was not until I observed the generator and Leyden jar in a completely darkened room that I noticed a blue glow around a length of wire which had been acting as an aerial above the Leyden jar and had partially charged it although it was not even directly connected to the generator!

To make a discharge rod, simply take a length of heavy copper wire and bend it in a "U" shape. This "U" should cover the distance between the brass ball and the aluminum side of your Leyden jar. Attach an insulating handle to the center of the "U". Make sure this handle is long enough that a spark won't find its way along the handle

to your hand. Holding it by the plastic handle, you can bridge the gap between the brass ball and side of the Leyden jar, and safely discharge it.

Discharging a large Leyden jar with this tool can be lots of fun since a large noisy spark can be safely produced. This provides a terrific demonstration for those who doubt the power of static electricity!

THE WATER CAPACITOR

Believe it or not, ordinary water and plastic bowls can be used to form an extraordinarily high dielectric, and make a good capacitor. Figure 38. A water capacitor is nothing more than two plastic bowls set inside one another each being partially filled with tap water. Any tap water will be somewhat conductive like the metal plates of the Leyden jar because of impurities. Dissolved salts in the water form positive and negative ions which move readily. The plastic wall of the inside bowl forms the dielectric while the water in each bowl forms the electrodes. A small capacitor of this type having 53 inches of useful surface area has a capacitance of approximately 100 pF.

This type of capacitor was supposed to have been a favorite of inventor, Nikola Tesla. Tesla, it is said, would wire together banks of

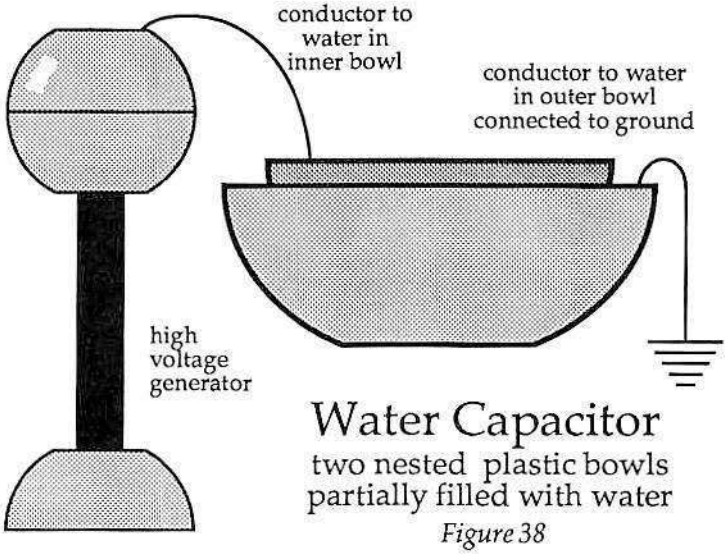

Water Capacitor
two nested plastic bowls
partially filled with water
Figure 38

insulated metal trays which were filled partially with water. By connecting these water capacitors in parallel, Tesla could reach very large storage potentials with a minimum of effort.

Plate Capacitors

As you have undoubtedly gathered, all that is required for a simple capacitor to hold a charge are two conductive plates with an insulator (dielectric) in between. There are an infinite number of configurations to be experimented with. Figure 39 shows what is probably the simplest useful capacitor possible.

The largest plate capacitor I attempted during the writing of this text was one made from aluminum foil and my sliding glass door. As soon as I became interested in electrostatics, and making high voltage capacitors, I started seeing the makings of capacitors everywhere. Every day I looked at my sliding glass door, and every day it looked less like a door and more like a capacitor. Finally I broke down and

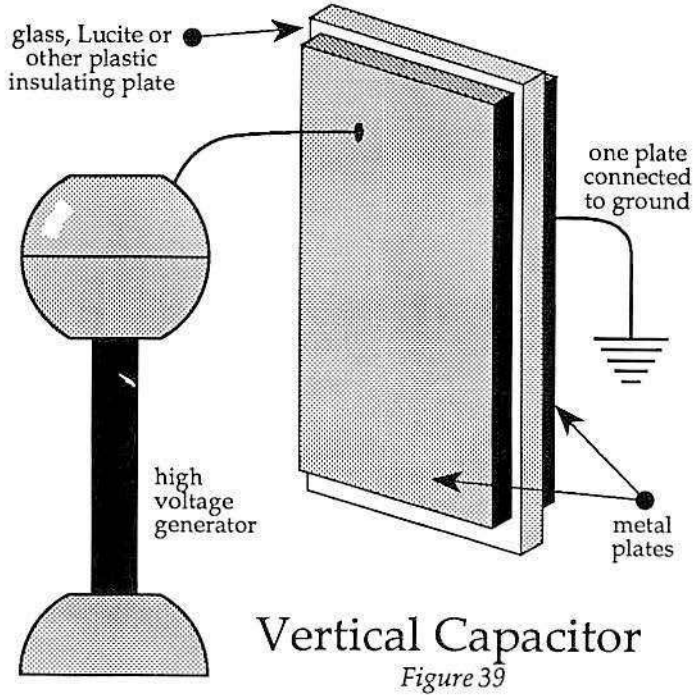

Vertical Capacitor
Figure 39

bought a large roll of aluminum foil and some tape. After a thorough cleaning, I transformed my door into a giant capacitor, by taping sheets of foil to each side of the glass. But alas! The results were disappointing. Temperature differences between the inside and outside of the glass caused condensation and all the problems that moisture brings, and the large sharp edges of the foil which I attempted to insulate bled off charge rapidly into the air. The foil did odd things such as crinkling and making sounds when charged, but failed to yield an interesting spark or hold a charge for any length of time at all.

I'm sure you'll come up with as many ideas as I do. Most recently, a television special showed the huge metal domes on buildings in Moscow square giving me visions of tremendous high potentials. As I watched, the buildings kept looking more and more like high potential tops of Van de Graaff generators and less and less like buildings. I think this high voltage stuff is affecting my mind! I think it's a good thing that I don't live in Moscow.

Calculating Capacitance

Once you begin designing and building capacitors, you will undoubtedly want to know what charges they are capable of storing. Capacitance is fairly easy to calculate, although homemade capacitors will be much less than perfect and probably perform more poorly than calculations might indicate. The following equations will give you a good idea of what can be expected from your designs.

Air is a good dielectric, and is accounted for in calculations. If we have two metal plates standing parallel to one another with air between, the equation for finding capacitance in picofarad is:

$$C = .08854 \frac{A}{S}$$

Where

A is the area of one side of one plate in square centimeters

S is the distance between plates in centimeters.

The same equation can also be revised for inches:

$$C = .2249 \frac{A}{S}$$

Note that these equations remain fairly accurate as long as the smallest dimension of the plate is ten or more times "S". In other words, the area of the plate should be much, much larger than the distance between them.

Different materials have different insulating capabilities which are reflected in their dielectric constant. Since you will want to use materials other than air as a dielectric, you will need to look up the dielectric constant from standard tables. You'll find that Plexiglas provides about four times the dielectric strength of air. A capacitor built from two conducting plates would have four times the capacitance of an air capacitor.

Another example: We might calculate from the equation above that a capacitor with a desired plate size has a capacitance of 100 pF using air as the dielectric. Using the chart below we see that if dry paper were substituted for air, the capacitance will be raised to 200 pF.

Shown below are some typical dielectrics relative to air borrowed from Attwood's book *Electric and Magnetic Fields:*

Dielectric Constant	Material
1	Air
25	Ethyl alcohol
2.5	Transformer oil
4.5 - 7	Various types of glass
6.8-8.4	Plate Glass
8.0	Window Glass
4.1-6.1	Pyrex
5.4-5.8	Bakelite
2	Dry paper
2.3	Paraffin
4	Plexiglas
2.5	Pure rubber
4	Wood

Capacitors can be connected in parallel or in series. Parallel connection increases total capacity. The total capacity is the sum of the individual capacities.

$$C_{Total} = C_1 + C_2 + C_3 + \ldots$$

For example, three capacitors having capacity of 10, 20 and 30 pF each would act as one capacitor having 60 pF when connected in parallel. The breakdown voltage of the combined capacitors is only as great as the lowest breakdown voltage of any single capacitor.

Calculating the capacitance of capacitors connected in series is more complicated, being the reciprocal of the sum of the reciprocals of the individual capacitances.

In series you would figure:

$$C_{Total} = \frac{1}{\frac{1}{C_1} + \frac{1}{C_2} + \frac{1}{C_3} + \ldots}$$

For example, three capacitors have capacitance of of 2, 4 and 4 pF. When connected in series, the total capacitance would be 1 pF. Although capacitance has decreased, the maximum working voltage has increased. If each capacitor had a maximum working voltage of 10,000 volts, the series connection would have a maximum working limit of 30,000 volts.

Power Capacitors

You can build a very powerful capacitor by creating a stack of alternating sheets of dielectric material and metal plates. On a large sheet of dielectric place a metal plate, then another sheet of dielectric, another metal plate and so on. The plates must be absolutely clean and free of even the tiniest contaminant or the capacitor will not work. To complete the capacitor connect alternating metal plates to one lead and the remaining metal plates to another.

For your first attempt, build a power capacitor with 5 sheets of dielectric and 3 metal plates. Connect the top and bottom metal plate to one lead, and the middle metal plate to another lead.

Benjamin Franklin — The Turkey Killer

Benjamin Franklin, an incurable prankster, was an ardent experimenter with electrostatic machines. Amazing as it may seem, according to his biography, the major reason Ben Franklin tried his dangerous kite experiment was that he was tired of charging his Leyden jar by hand cranking his static electricity generator. He wanted to charge it with lightning which he was able to do without getting himself killed! (Note: this method of charging a Leyden jar is not recommended for those other than "founding fathers" and other experimenters who seem to have a supernatural gift for avoiding harm. In other words, don't you try it.)

Franklin's hand-cranked static machine was large enough when coupled to Leyden jars to produce a lethal voltage. In fact, Franklin often used his static machine to kill his Thanksgiving turkey. In his own words *"... to the amazement of many... A turkey is to be killed for our dinner by electrical shock, and roasted by the electric jack, before a fire kindled by the electric bottle..."*

Franklin's pranks were not without risk. Just a short time before his famous kite experiment Franklin accidentally took the full force of his turkey killing device. He wrote, *"Being about to kill a turkey by the shock from two large glass jars, containing as much electrified fire as forty common phials, I inadvertently took the whole through my own arms and body, by receiving the fire from the united top wires with one hand while the other held a chain connected with the outside of both jars. The company present (whose talking to me, and to one another, I suppose occasioned my inattention to what I was about) say that the flash was very great and the crack as loud as a pistol; yet, my senses being instantly gone, I neither saw the one nor heard the other; nor did I feel the stroke of my hand.... I then felt what I know not well how to describe: a universal blow throughout my body from head to foot, which seemed within as well as without; after which the first thing I took notice of was a violent quick shaking of my body, which gradually remitting, my sense gradually returned.... That part of my hand and fingers that held the chain was left white, as though the blood had been driven out, and remained so eight to ten minutes after, feeling like dead flesh; and I had a numbness in my arms and the back of my neck that continued till the next morning..."*

Franklin's account of his own mishap should certainly give thought to those who do not take the dangers of static electricity seriously!

ELECTROSTATIC EXPERIMENTS

The experiments here are divided into two categories. The first group describes electrostatic experiments that can be performed for an audience. In other words they're merely for entertainment.

The second section features experiments which possible useful applications of electrostatics which are not often discussed. Many of these "useful" experiments could be or are being developed into very real, marketable industries and should be particularly interesting to the serious experimenter.

Hair Raising Experiences

Using electrostatic voltages to make a person's hair stand on end is a classic experiment every audience should see. It can be done in a number of ways. Find a subject with hair that is light and clean. With some experience you will be able to recognize the best subjects immediately. Next, convince the subject that the ominous apparatus that they have just seen throwing four inch sparks will not harm them.

You may want to explain why the experiment is perfectly safe by describing the "skin effect" of high voltages. This effect refers to the strange fact that voltages of this order travel only on the outside or "skin" of the object they pass over and will not travel through the inside of a body where they could do any harm. For alternating currents this is a true skin effect, but for direct currents there is a similar effect that occurs probably because of the repulsion of like charges rather than due to a true skin effect.

The subject should stand within reach of the generator and should be well insulated from any ground. This is accomplished by having the subject stand on a large insulator such as an overturned plastic bucket, or, as a joke, a stack of college text books since they are usually very dry. Instruct the subject to place one hand on the high potential terminal, and then turn the generator on. Remember to remind a nervous subject not to remove his hand from the terminal until the experiment is completed since removing his hand could provide a

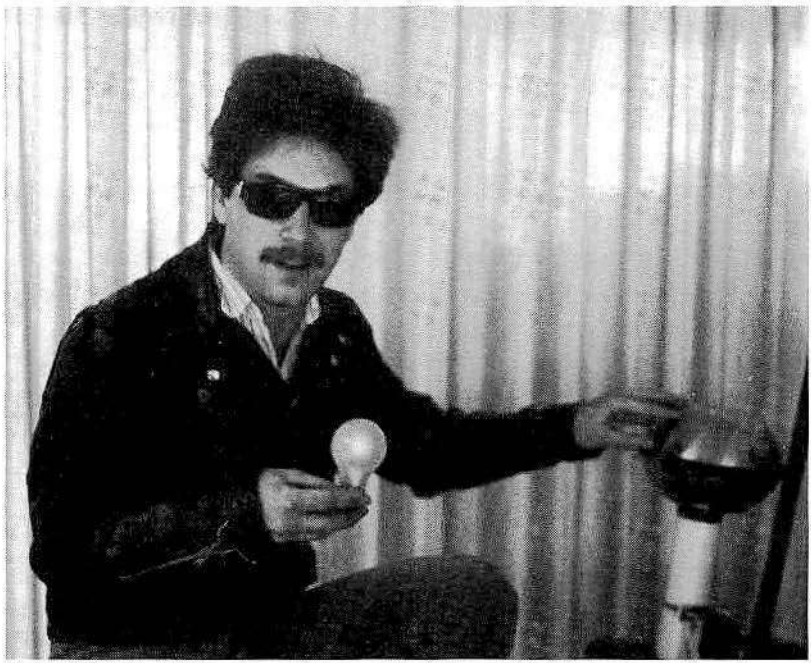

Figure 40 – The author's hair is usually flat and combed somewhat back. After a few minutes connected to a running Van de Graaff generator, and he's ready for a punk-rock concert!

shock. Depending on the output of your generator you may need to allow it to run for several minutes before your subjects hair will begin to rise. Having your subject shake his head occasionally with speed up the process.

During this whole procedure the subject will not feel the electricity passing over him other than perhaps a light tickling as his hairs stand on end. What is happening is that the subject's hair and whole body is taking on a charge from the generator. Since all of the hairs have the same charge whether it be positive or negative, and because like charges repel each other, every hair is repelled from every other hair and any nearby parts of the body. Warnings: **1) Don't use capacitors. 2) Hairspray is flammable. 3) Voltages over 500,000 are unsafe.**

Strangely enough, your generator will actually have a higher potential with someone is touching it than when it is operated alone

since it can now use the person's body as a high potential collector. The success of this experiment depends largely on the subject's hair. Some women with short frizzy hair will have their hair stand out nearly straight from their head!

After the experiment is complete, have your subject remain standing on the insulator. This will allow the charge accumulated in their body to bleed off and will reduce the possibility of a large spark occurring when they eventually touch something that is grounded.

There are a few simpler although perhaps less dramatic ways to perform the same experiment. One is to make a wig out of fuzzy yarn and to place it over the generator's high potential terminal. You can place it on the spherical terminal of a Van de Graaff generator to simulate a person's head. Some Mr. Wizard impersonators even like to put a pair of plastic sun glasses under the wig to give the generator a little character. After the generator has run for a time, the hairs of the wig will stand on end.

A very quick way to demonstrate this effect is to simply take a few hairs from an old hair brush and place them on the generator's surface. They will immediately stand on end, and will often fly off the generator all together! Many different light weight materials can be used for these type of experiments. Bits of styrofoam work extraordinarily well.

The Magic Wand

As discussed, smooth, round objects tend to hold their charges while sharp pointed objects will allow electrons to fly off in a stream sometimes referred to as an "electric wind." The effects of this wind can easily be seen. Connect a short length of wire to your high potential terminal and hold the free end of the wire with a handle made of an insulating materials such as plastic. Point the end of the wire toward a lighted candle, and observe the flame. The flame will bend mysteriously away from the invisible "electric wind." In a well darkened room with ones eyes well adjusted the "wind" may actually be visible.

Another interesting experiment is to use the wand to chase a soap bubble. Because there are two forces acting on the bubble, the outcome of the experiment may be unpredictable. One force is the charge of the generator itself which draws the bubble toward the wand. The other

force is the electric wind from the wand that pushes the bubble away. How the bubble will act is anyone's guess! It depends on which force is dominant.

A little later on we'll use this surprisingly powerful wind to create a small pinwheel motor.

Levitation

There are a number of ways that you can levitate lightweight materials using your generator. The easiest ways to demonstrate this is to simply spread very small shavings of styrofoam along the top of your generator. When the power is on, the pieces will take on the same charge as the surface of your generator and be repelled by it since like charges repel one another. The bits of styrofoam will levitate off into the air after the generator has been on a few seconds.

An entertaining experiment can be done by placing a number of tiny styrofoam balls in a short section of clear glass or plastic tubing about 2 1/2 inches in diameter and a few inches in length setting on your high potential terminal. Cover the top of the tubing with a metal plate, and connect it to ground. When your generator is turned on, the balls become charged and levitate to the top of the plastic tube. When they touch the metal plate at the top of the tube they lose their charge to ground and fall back to the generator again. The balls will oscillate between the ends of the tube until the generator is shut off. You should coat these balls with a conductive paint for a more complete charge transfer.

If you enjoy reproducing electrostatic experiments as they were originally done, you might want to try making your own old-fashioned pith balls instead of using styrofoam. Pith balls were used for these experiment before modern products like styrofoam were available. Pith balls are made by removing, shaping, and drying the insides of certain plants such as dandelions. Details can be found in old physics textbooks before 1900. I'll stick with good old styrofoam.

Place larger bits of styrofoam on your generator, and turn your generator on while touching the bits with your hand. The styrofoam will assume that you are ground and that your generator is a high voltage source. One side of the styrofoam will be charged one way, and the other side of the styrofoam the other. After removing your

hand, a number of things can happen. The styrofoam may flip over and be stuck to your generator like a magnet. The styrofoam may stick to your hand like a magnet. Or you may find the styrofoam floating on end as the hair did in the last experiment.

An interesting trick can be performed by passing your hand over the styrofoam remaining on your generator terminal. As you do so, the electrical charges in the foam and in your hand will cause the styrofoam to jump about.

I have meant for some time to place a metal plate on a table underneath a table cloth and to energize that plate from a hidden electrostatic machine. I could then sit at the table and "mysteriously" move light weight objects such as bits of hair, sawdust, styrofoam or other similar materials around the table simply by passing my hands over them. I think this would make a very convincing illusion of mental telekinesis. Try it.

Lighting Without Wires

If you or your friends doubt the power of your generator, have on hand a supply of Ne2 neon bulbs which are available for less than a dollar at any electronics store. Remind those onlooking that it takes at least 70 volts to light a neon bulb. Hold one lead of the neon bulb in your hand and move the bulb toward your generator. Within inches, or even feet, the bulb will flicker or light. I have seen some experimenters hold the bulb in their mouth while reaching toward a generator with their hand. Seeing a 70 volt bulb light in a persons mouth with no wires attached is an impressive demonstration.

You may want to try large florescent bulbs as well. When my generator has been running I have seen flickers in the florescent lights in the ceiling of my home. These bulbs are many feet above the top of my generator yet respond well in a darkened room.

Perpetual Motion

Anything that people assume can't be done interests me. Many of the greatest inventions of all time would never have come into being if their inventors hadn't at one point been told that it couldn't be done. Currently, perpetual motion qualifies as such.

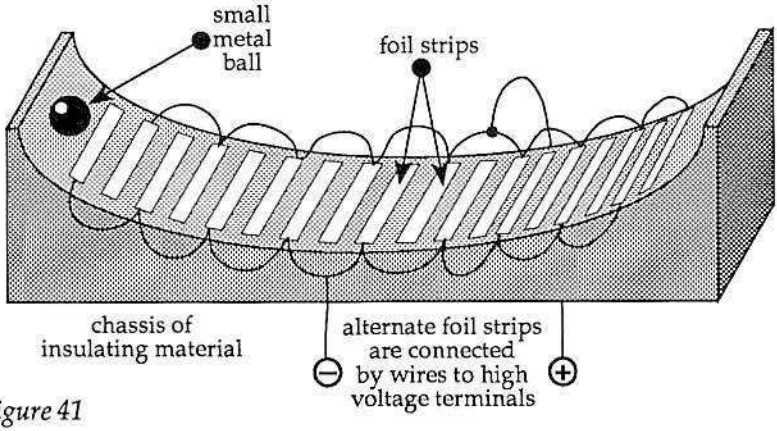

Figure 41

"Perpetual Motion"

The following device doesn't really qualify as perpetual motion, but it appears to be! Figure P1 shows the device. The idea is simple. A few light-weight conductive balls are released onto a U-shaped track on which the balls rock back and forth. It is normal to assume that the balls will slowly lose their energy and come to a stop in the center of the track. Instead, because of the electrodes in the track,the balls continue back and forth indefinitely and even pick up some speed along the way.

What has happened is that you have constructed simple electrostatic motor. As the balls pass over the foil strips they pick up the charge from that strip. Having the same charge as the strip, they are repelled by that strip and are simultaneously attracted to the next strip which has a dissimilar charge. Inertia will cause the balls to roll over the dissimilarly charged strip and on to the next. The electrostatic forces replace the energy lost in rolling friction. In this manner the balls will remain in motion for as long as power is supplied.

If you wish to really complete the illusion given by this device you will naturally want to hide the foil strips from view. To do this you could either use a conductive material other than foil that blends into the background, or, if your generator is powerful enough, you could probably bury the foil strips under the ramp material and still transfer a sufficient charge.

Trick Gun

We know that like charges repel one another. This has been demonstrated with the 'hair' experiments and others. What would happen if we introduced a charge into a liquid, and then shot that liquid out in a stream? We can find out with the use of a squirt gun. Purchase an inexpensive water gun that stores its water in the handle. Drill a small hole into the handle and twist a brass sheet metal screw into the hole. You may want to put a little Silicone glue around the top of the screw to make sure that this point will not leak when the gun is later filled with water. The brass screw provides electrical contact between your hand and the water.

Fill the gun with water, and pump out a few squirts. The water will come out in its customary straight stream probably covering the length of the room. Then stand on an insulator and charge yourself up as described earlier. When you squeeze the trigger, a stream of scattered droplets will be ejected only a few feet. What has happened is that all water droplets have a similar charge so each droplet is repelled by every other droplet. Other than being just an interesting way to get an unsuspecting friend wet, this mechanism can be applied anywhere that a liquid must be atomized.

I've wondered about making an electrostatic chamber on the carburetor of my car to see if better atomization of the fuel would result in better combustion. But first I need to check into the dangers of a spark occurring! I don't really want to blow myself up!

An Ion Motor

There are several different electrostatic motors that can be run by your generator, the simplest being an ion motor. You can make one by simply bending a length of light weight wire into a "Z". At the center of the "Z" shape, place a conductive bearing. Nothing fancy is required. In fact, just looping the center of the Z around an axle may work. Make sure however, that the Z will rotate very easily. A simple schematic of the ion motor can be seen in figure 42.

When power is applied to ion motor electrons stream off the pointed ends of the wire creating an electric wind. The force of the wind pushes the wire in the opposite direction. Again, for every action

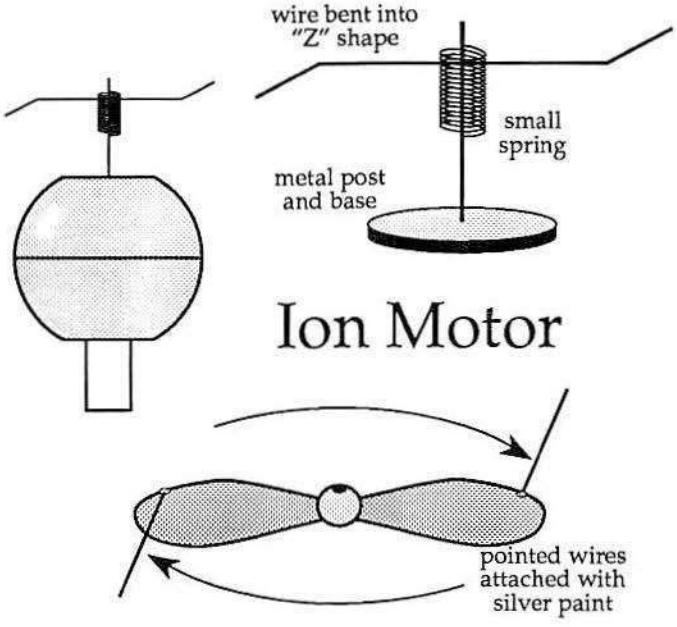

Plastic Toy Airplane Propellor

Figure 42

there is an equal and opposite reaction. If your rotor is well balanced and the bearing friction is very low, your motor can and will achieve speeds of several thousands revolutions per minute! Of course, the torque generated by this motor will be very, very small. Nevertheless, it is fascinating to watch a motor propelled by a stream of electrons!

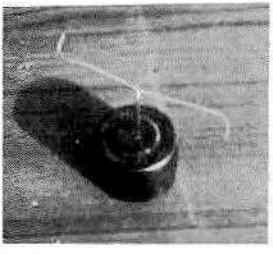

Figure 43 –Simple Ion Motor

Although the thrust of this motor is very small, I am certainly not the type of experimenter to let this hard-earned stream of electrons get away without doing some useful work along the way. I have attached one of my pinwheel motors to a tiny plastic airplane propeller as shown to blow a little air cool air my way. I think this is probably one of the few fans that I know of that must be connected to 100,000 volts or so to operate!

Another thought that I had for this fan was to drive it with a negative charge. Negative ions are thought to have many health benefits, and to cut down on pollutants in the air. Negative ions apparently attach themselves to specks of airborne dust and cause them to fall from the air. There are a number of negative ion generators being marketed for this purpose. I thought that a spinning propeller of this sort would be an absolutely outstanding way of both distributing and producing negative electrons in a room environment.

Ion motors also have serious applications in space travel. The Soviets have used ion motors to propel some of their long range probes. The problem with these motors is that the thrust is very small. However, ion motors offer at least two enormous advantages. First, they can be powered by a nuclear or solar electrical source which can provide power far longer than conventional chemical rockets. Second, an ion motor can provide higher velocity thrust than current chemical rockets because the nozzle velocity of a rocket is limited by the internal pressures that can be safely generated inside the rocket motor. An efficient ion motor can accelerate ions to speeds approaching the speed of light! Although the thrust is small, over time the space craft could itself approach the speed of light, at least, in theory.

A few tips for getting the best operation out of your ion motor—Make sure that your rotor is well balanced especially if you want your motor to be self-starting. Your rotor should spin easily for several seconds when tapped lightly by your finger. The more freely your rotor can spin, the faster it will revolve. The bearing used in a radiometer would make an excellent ion motor bearing.

Run your generator/motor in an area free of objects that might provide sources of ground. My first ion motor was well built and carefully balanced, yet it refused to spin. When I reached down to give it a tap to get it started, it refused to move. In fact it felt as though it were being held in place by a magnet. It was then that I realized that one of the arms of the rotor must have been attracted to an object with an opposite charge. That object turned out to be me! When I moved a short distance away, the ion motor sprang to life and immediately whirled up to several hundred RPM.

For this motor, voltage is more important than current. The motor will run and do useful work on currents under a microampere. Electrostatic motors have been run with currents of less than .001

microamperes, and have even from the earth's electrical charge itself.

Another interesting use that I have found for an ion motor is that of a primitive high voltage meter. The higher the voltage, the greater the thrust from the motor. This may be used to move a pointer such as in a panel meter or may be used simply to a relative indication of voltage.

I like to place a small ion motor on top of my Van de Graaff generator when I am charging capacitors. When the capacitors are charging, the motor will not move since the charge is being bled off from the generator to the capacitors. When the capacitors are fully charged, they stop drawing current from the generator. The terminal voltage rises, and the motor begins to spin. This is a very useful application of the ion motor since it is usually impossible to tell when a capacitor is fully charged any other way.

I am told that ion motors have been used in scientific toys such as those that can influence a balsa airplane in flight. Gustave LeBon's electrified rocket was a small aluminum foil rocket that could actually fly on electrostatic forces (Patent No. 2,018,585). I have not seen these devices, but they sound like something worth investigating.
Experimenting with "micro" sources of power can bring out the engineer in everyone.

An Ion Blower

The last experiment uses a stream of ions to propel a small rotor. Since in essence what we really have is a little jet engine, why not put our blower into a tube and see if we can pull a little air along with it. Figure 44 shows one possible configuration.

One end of a small, clear tube such of glass, Plexiglas, or other insulating material is fitted with a sharp metal point. A metal screen covers the other end. Electrons reach a high density at the metal point, break free into the air, and stream through the tube to the screen at the far end. As they move rapidly through the tube, they pull some of the air inside the tube with them. Obviously, a blower of this type has very low efficiency probably in the neighborhood of 1% under ideal conditions, Nevertheless, a puff of smoke at the intake side of the tube will easily be drawn through.

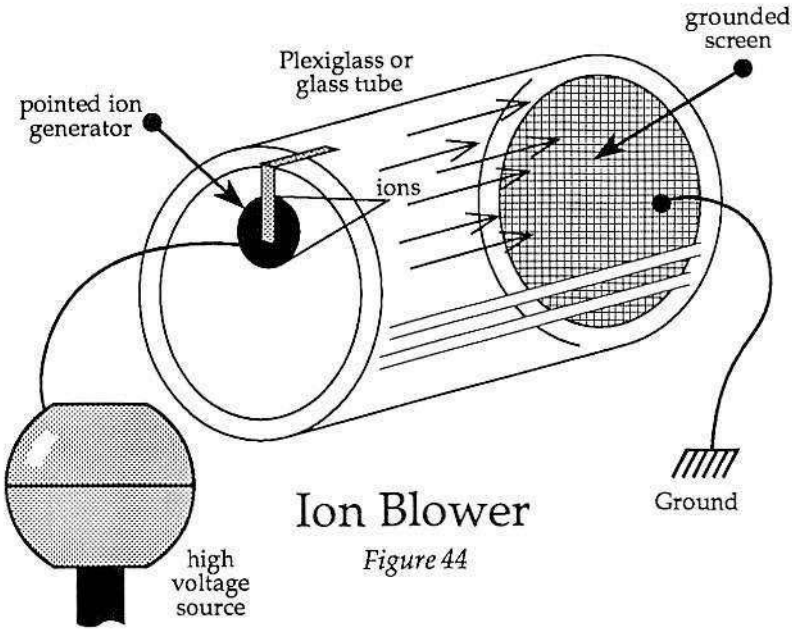

Ion Blower

Figure 44

Clearing The Air

Before moving on, here's another interesting smoke experiment you can try. Get a clear plastic or glass jar having no metal parts. Drive a pointed nail through the center of the lid. Blow a little smoke into the jar, and seal the jar with the lid. Next, connect the head of the nail to the output terminal of one of your high voltage generators.

As charge is applied to the smoke, it will begin to swirl. Soon the smoke will seem to disappear, although in reality it has been redistributed along the sides of the jar.

Variations of this effect are used in industry to place very fine films on surfaces. Similar electrostatic methods are being used to make sandpaper. When the tiny metallic abrasive particle are distributed along the surface of the sand paper they are given a charge that causes them to stand on end creating sandpaper with a better abrasive action.

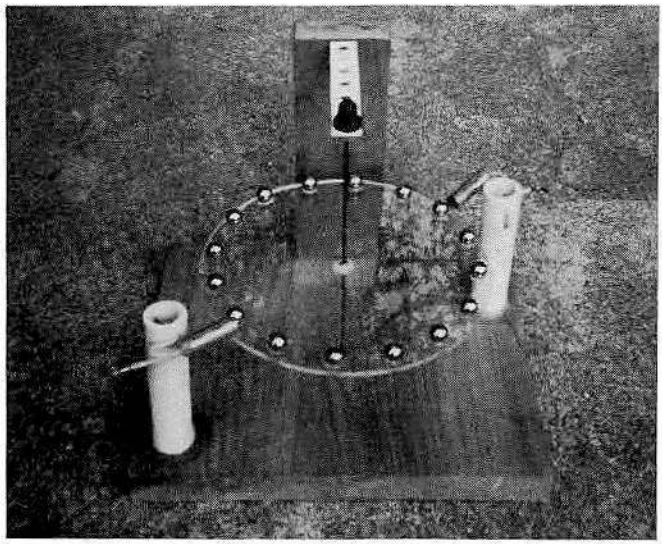

Figure 45 - Franklin Motor – Using large sling-shot balls and a simple Lucite disk, this little motor quickly speeds to over 600 rpm on less than 1 microampere of current!

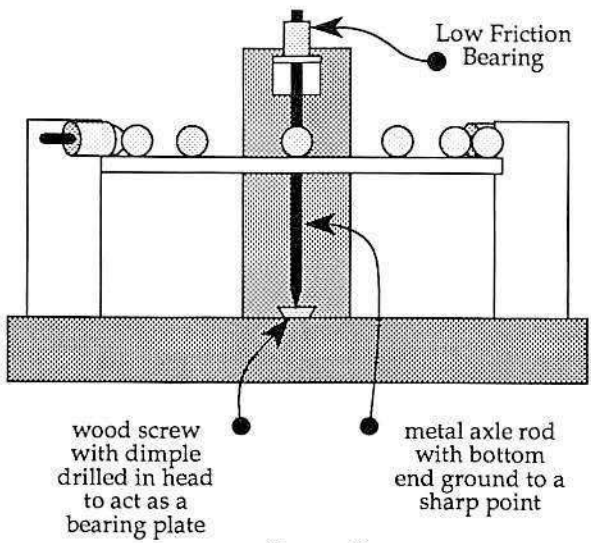

Figure 46

Franklin Motor

Front View

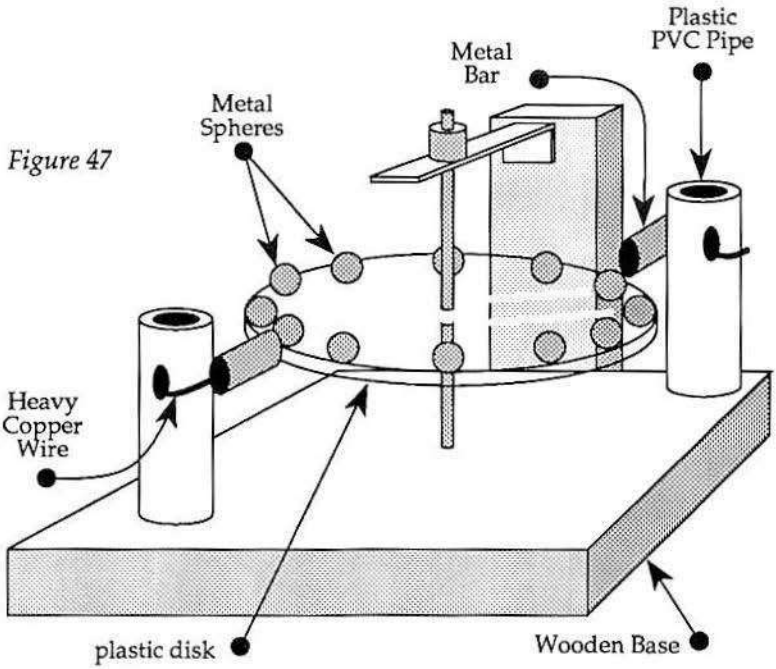

Figure 47

Franklin Motor

THE FRANKLIN ELECTROSTATIC MOTOR

The Franklin motor, named after its inventor Benjamin Franklin, is often said to be the first electric motor ever made. Its construction is simple, and, in fact, it is very similar in operation to the Dirod generator described earlier which can be run as a motor although inefficiently. Figure 47 shows the basic Franklin motor.

A series of lightweight spheres is glued in place along the outside of an insulating disk of Plexiglas, glass, etc. As these spheres rotate, they pass through the corona emanating from a highly charged high potential terminal at each side of the disk. One terminal is charged negatively and the other positively. As a sphere passes a terminal, it picks up a charge that will be attracted to other terminal causing the whole assembly to turn until the high voltage is removed.

One modification that you might like to experiment with is to

make the Franklin motor self-starting. This can be accomplished by adding points on the high potential sources to create an electric wind that gives the spheres just enough of a nudge to start the rotor revolving.

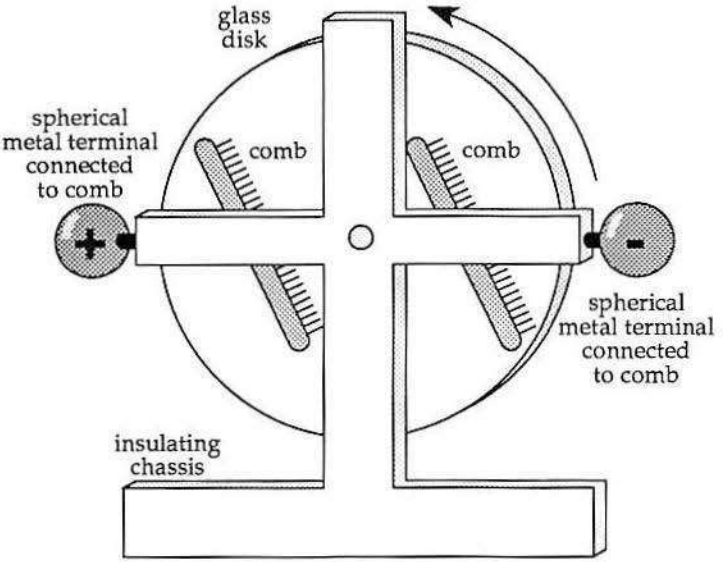

Corona Motor
schematic diagram
Figure 48

Poggendorff's Corona Motor

Franklin's motor works by charging a series of spheres as they pass by alternating high potentials. It is also possible to alternately charge an insulating surface as it passes near high potential terminals. Plexiglas, glass, and probably other materials will work. A drawing of Poggendorff's motor is shown in figure 48.

Here is how it works. Notice that there are two sets of brushes or combs with sharply pointed ends mounted at an angle. One brush sprays a negative charge onto the disk and the other a positive charge. As the disk continues to revolve, the charges on its surface find themselves attracted to the entire oppositely charged comb – not just

the tiny spray points. It is important that the brushes be mounted at an angle, so that charges on the disk may be attracted to the comb of opposite polarity before they are replaced with an opposite charge as the disk rotates under the points of the comb. Understanding how a motor like this works is simple. Getting one balanced well enough to be self-starting and smoothly running takes quite a bit of patience. It is nonetheless an exciting and interesting project.

Atmospheric Electricity

The earth itself is a huge electrostatic generator. In the air at any time there are some 200 volts of electricity encircling you all of the time. The reason that we aren't being zapped all the time is simply that we are all at roughly the same potential. That is we all have the same level of charge, so, the electricity has no reason to move from one point to another.

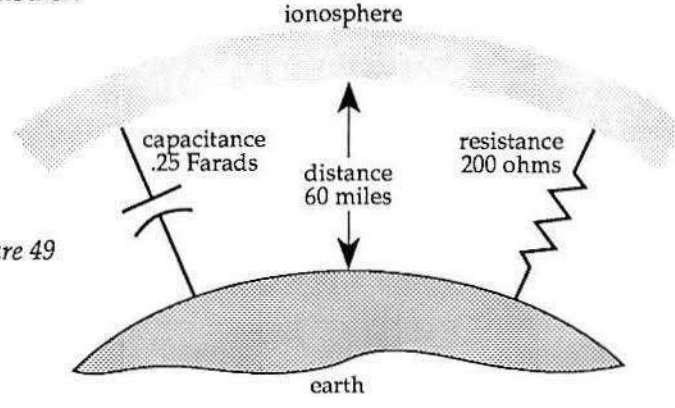

Figure 49

Earth's Atmosphere
electrical parameters

Between the earth and the electrically conductive ionosphere, both of which store electrical charge, exists an electrical potential. The same sort of buildup exists between clouds and the earth. When the potential builds to a level great enough, the air ionizes, loses its insulating capacity and becomes an excellent conductor. The result is a huge arc of static electricity we call lightning. As current flows between the cloud and the earth, the potential is reduced until the arc

can no longer be sustained, and the lightning bolt is extinguished. It fascinates me to think that I live on one of two highly charged electrodes.

As an electrostatic generator the earth is fairly impressive. Between two and six thousand thunderstorms are in progress at any one time. Worldwide, a hundred bolts of lightning strike the earth every second. It is estimated that this gives the earth a high voltage potential of approximately 360,000 volts between ground and ionosphere with an average lightning bolt conducting 1800 amperes. The density of the electric field decreases as altitude increases. Near the earth's surface, however, the field is estimated to be approximately 100 volts per yard of height.

I say that the earth is fairly impressive because for all its size it is limited to these voltages by the fact that the atmosphere is relatively conductive having a resistance of approximately 200 Ohms. This is a relatively low resistance which quickly bleeds away charges.

Although it can take a significant amount of time depending on weather conditions, any conductive material insulated from ground can acquire charge from the surrounding air, and become charged to a high potential. Although the charge accumulated is usually negative in polarity, thunderstorms and other atmospheric conditions may create a positive potential with respect to ground. Radio antennas and flag poles insulated from ground have been known to throw hefty sparks and even start fires.

Plugging In To The Earth's Charge

If you're as curious as I am, you're asking yourself, "Can I tap into this charge?" The answer is yes! The first order of business is to measure and verify that a charge is present. If you are a skeptic like me, you've "gotta see that needle move" before you are going to believe there is something there!

The best antenna for capturing atmospheric charge is a metal structure, insulated from ground, pointing straight up into the air. The simplest, and probably easiest way to accomplish this is to simply attach a length of very light, bare, copper wire to a large helium balloon. This can be dangerous! Remember to avoid power lines and airports if you plan to launch such an energy-gathering balloon!

Having your bare copper wire come in contact with a high-tension power line is not a pleasant way to die! Thunderstorms are extremely dangerous. (Ben Franklin was lucky to have survived his experiment.)

The bottom of the wire should be attached to a high quality insulator well above ground. Attach one lead of a extremely sensitive meter to ground. Occasionally attach the other lead to the vertical metal conductor. Be careful! Do not take for granted that the potential will be harmless! If left unchecked it could easily reach a level that will bite you. You may find that it can take an hour or more to build up a significant charge, however.

At one time I tried using a kite flown with bare copper wire but had mixed results. I experienced significant difficulty with the wire kinking as I let it out and reeled it in, in response to changing winds.

Another time I hooked a diode into the line and got surprising voltages, but I had been fooled. The diode and coil in the meter had made a primitive crystal radio. I was extracting power from the atmosphere that had been placed there by radio broadcasting stations. Although this is not static electricity, it is nonetheless interesting because it is a demonstration of wireless transmission of power that Tesla was trying to perfect.

An antenna of this type has been used quite adequately to run a corona motor from the natural potential that exists between the earth and its atmosphere! A motor of this type must be extremely well built having great sensitivity and very low friction bearings. I have seen such a motor run, but I have not run one of my motors from this charge.

Because of weather, it can take a long time to build the potential up to a level capable of doing useful work such as moving a sensitive meter or a small corona motor. Several methods have been devised to speed up the charging process. Early experiments devised by Lord Kelvin used an insulated metal tank filled with water suspended above the ground constructed in such a way so as to allow a steady stream of water droplets to reach the ground. Appropriately, he called the setup a "water dropper." He reasoned that the surface of each water drop would be an extension of the surface of the water in the tank at the moment it dropped away. As it did, the drop would carry charges away with it. This continues until equilibrium was reached between the tank and the air.

Using this same idea, charging time can also be reduced by

spraying a fine mist of water along a bare copper wire a hundred feet or more in length which is insulated from and suspended above ground. The falling water droplets can help to charge this wire to a measurable level in less than a minute's time.

Another method of speeding up the charging process is to increase the number of ions in the vicinity of the wire itself. A flame applied to the wire will increase the number of ions in the area of the flame and can bring a wire up to the same potential as the air around it in a matter of seconds. To accomplish this easily, wrap the wire with a flammable substance such as string or paper soaked in lead nitrate, and ignite it. It is also possible to get good results by simply waving a torch lightly across the wire.

In Conclusion

I hope that you will enjoy experimenting with electrostatics as much as I have! I find few subjects more fascinating than high voltage and its generation. As a technically minded person, you will undoubtedly see many improvements that can be made in my designs. I know that this is true because at times it seemed I might never complete this text because there was always one more improvement to make and one more experiment to try. No doubt, you will conceive of dozens of new ways to apply the basic principles of electrostatics. Like all experimentation, every change, every test, every improvement will suggest many more questions to be answered and new improvements to be made. You'll probably devise many new inventions!

Electrostatics is also a subject that everyone is absolutely fascinated by – even those who can't change flashlight batteries,. When I was experimenting with different friction generator materials, I purchased quite a number of little swatches of material from a local fabric store. The young ladies working in the store demanded to know what the fabric was for, and, were so fascinated by the idea of generating a spark that I emerged from the store piled high with swatches of material which they insisted be tried on the generator.

My own mother, who despises anything technical, shocked me to no end by demanding that I explain to her the workings of the atom immediately after seeing the classic Van De Graaff in operation. I do not think anyone can watch a powerful Van De Graaff generator at

work and not be curious about the forces at work. (And you and I will always want control of those forces!)

So dig in, get to work! Mysteries await!

SELECTED BIBLIOGRAPHY

B.I. Bleaney & B. Bleaney, *Electricity and Magnetism.* 1957 p.762

Tricker, R.A.R., *The Contributions of Faraday & Maxwell to Electrical Science.* 1966

Moore, Arthur Dearth, *Electrostatics.* 1968 p.240

Simon and Schuster, *The Way Things Work.* 1967 p.590

R.A. Ford, *Tesla Coil Secrets.* 1985 p.74

Lodge, Oliver, Sir, *The Nature and Properties of Negative Electricity.* 1906

Adams, Charles K., *Nature's Electricity.* 1987 p.147

Sootin, Harry, *Experiments With Static Electricity.* 1969 p.85

Van Doren, Carl, *Benjamin Franklin.* 1938 p.845

Ammen, C. W., *The Electroplater's Handbook,* 1986, p. 213

ADDENDUM

Electroplating High Potential Terminals

As you have certainly realized by now, a tremendous amount of your generator's efficiency rests in the quality of your high potential terminal and in your ability to effectively store the charges produced. I think you will be very happy with the performance of any of the classic generators and storage devices described earlier. However, for those of you seeking to go beyond these boundaries of performance, I'd like to let you in on new area of experimentation: electroplating.

Electroplating is simply a process wherein metal salts such as copper sulfate or nickel ammonium sulfate dissolved in an acidic aqueous solution can be deposited as elemental metal on conductor by applying an electrical current. This means simply that any conductive object can be covered through the process of electrodeposition with a layer of metal!

Since electrostatic charges can be distributed quite nicely on even very thin conductive surfaces, this is a perfect system for making a flawless Leyden jar or a huge high potential terminal. I am currently working on creating very large, near-perfect high potential terminals by plating large plastic globes sold in many lighting stores for under $15.00!

Anything can be plated – plastic, glass, pvc, etc. The only trick is in making their surface conductive initially so that a current can be applied.

The basic procedure for producing a perfect Leyden jar is as follows.

Begin by making the glass jar extremely clean. No fingerprints, water, or oil of any kind can remain. Use masking tape to cover the top 20% of the jar to prevent plating in this area and to preserve a well-proportioned jar. Paint the exposed glass with a resin such as white shellac thinned with denatured alcohol, if necessary. I've even used a spray lacquer.

From here there are several routes that you can take. The easiest method is to take a finely powered metal such as iron or aluminum (something around 400 mesh) and sprinkle it on the sticky, wet shellac. Since these finely powdered metals will float in the air much like

talcum powder, I usually put the metal powder and jar in a box and shake the two around around. Remember! These metals SHOULD NOT BE INHALED! Wear a safety mask, and if working with heavy metals, wearing protective clothing is a good idea. The metal powder should create a beautiful, even, light coating over the painted surface of the jar. Allow the paint to fully dry, and repeat the procedure on the inside of the jar. This is a little trickier, but not impossible.

At this point you can actually stop, and use the jar quite successfully. The tiny sandpaper edges of this powder metal coating will bleed off a stored charge when the jar is not in use. This makes a good natural safety feature.

The only drawback to the powdered-metal approach is that if you choose to copper plate it, the copper plating will be just as bumpy as the powdered metal surface itself. As a result, this method will always allow some leakage.

Another simple method of making the jar conductive is to cover the shellac with powdered graphite. This can be rubbed smoothly onto the surface when the shellac is partially dry and will provide a smoother surface which in turn will produce smoother plating. On the other hand, graphite surfaces often require considerably longer plating times and the process is less reliable.

Although both of the above methods work well and have merits, the very best way to make the jar or any non-conductor conductive is to allow the shellac to dry completely, then paint or dip it in a solution of

1/2	ounce	silver nitrate
4	ounces	distilled water
6	ounces	alcohol

While this is still wet, suspend the jar inside a larger jar or other acid-proof non-metallic vessel, and place a few lumps of potassium sulfite or iron pyrite in the bottom of the larger jar. Cover this with a solution made up of one part sulfuric acid and eight parts distilled water, and close the lid. You now have a jar covered with silver nitrate solution hanging above the potassium sulfite-acid solution in a sealed vessel. This will produce hydrogen sulfide fumes that will convert the nitrate to a sulfide which is a conductive coating for you jar. Within a

A glass jar for the Leyden jar capacitor is selected and thoroughly cleaned.

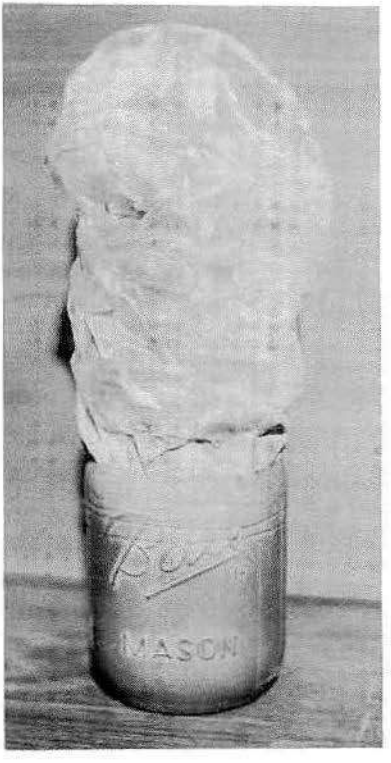

The jar is masked off and coated with conductive graphite.

few minutes the chemical reaction will stop, and your jar will be ready to be plated.

Now that the outside of the jar has been made conductive, it can easily be plated with copper. In an appropriate acid-proof vessel, make a solution of

25	ounces copper sulfate
6	ounces sulfuric acid
1	gallon distilled water

Use warm water when mixing to dissolve the copper sulfate more quickly. Do not allow this solution to touch your skin or clothes.

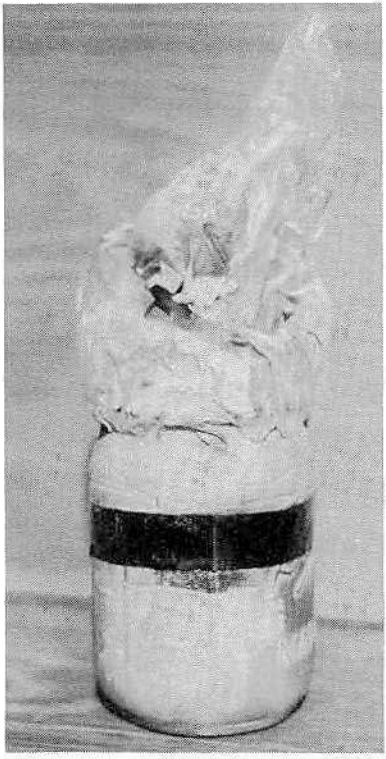

After a few hours, the deposit of copper is easily seen.

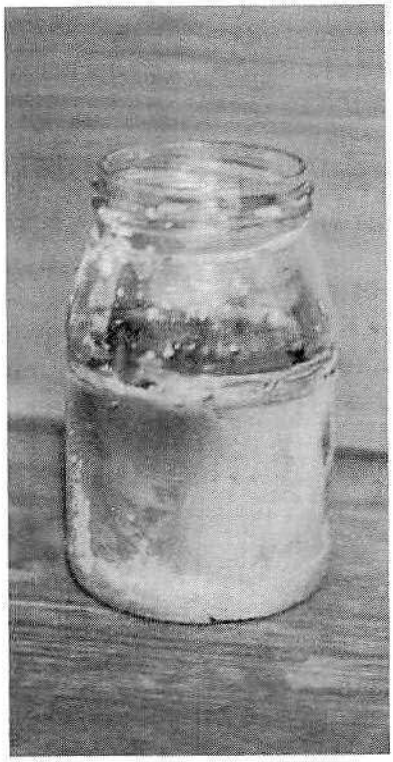

The plated jar is ready to be cleaned up and put into use.

Attach a wire from the negative lead of a 2 to 5 volt battery or transformer to the conductive part of your jar. A rubber band works well for this. Immerse the portion of your jar to be plated in the copper sulfate solution. Finally, attach a wire from the positive lead of your power source to a copper electrode having a large surface area such as a thin copper sheet. Set this electrode in your solution.

All that you have to do now is watch the jar as the plating takes place. Be sure you keep the solution warm, or the plating will proceed very slowly. I like a thick copper coat and usually allow my plating to take place overnight. However in a fairly short period of time you should see a reddish copper coating forming on the outside of your jar! Simply repeat this process for the inside of your jar.

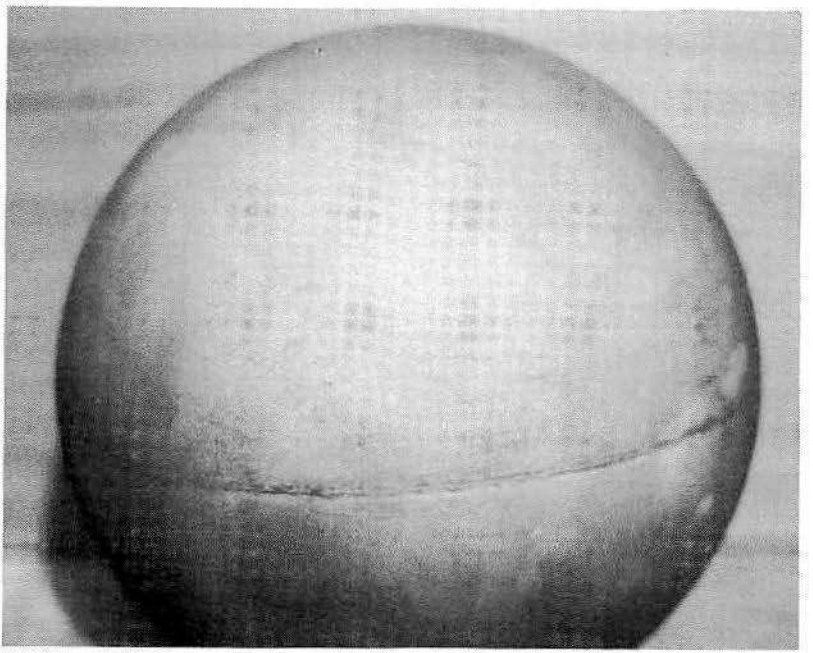

A twelve inch plastic sphere has been coated with graphite and is ready to be plated.

Very large spheres and other shapes can also be plated by scaling up this process. I have seen many inexpensive large glass and plastic globes since I began experimenting with this process that would lend themselves to this technique. For more information, refer to books on electroplating and electroforming that can give you advanced details on plating superior finishes.

As you can see, simple electroplating can make possible a vast number of new shapes and designs for high voltage terminals!